

Annual Cumulated Index

ACCESSION NOS. A69-10001 to A69-43818

INTERNATIONAL AEROSPACE ABSTRACTS

143
U. of ILL. LIBRARY

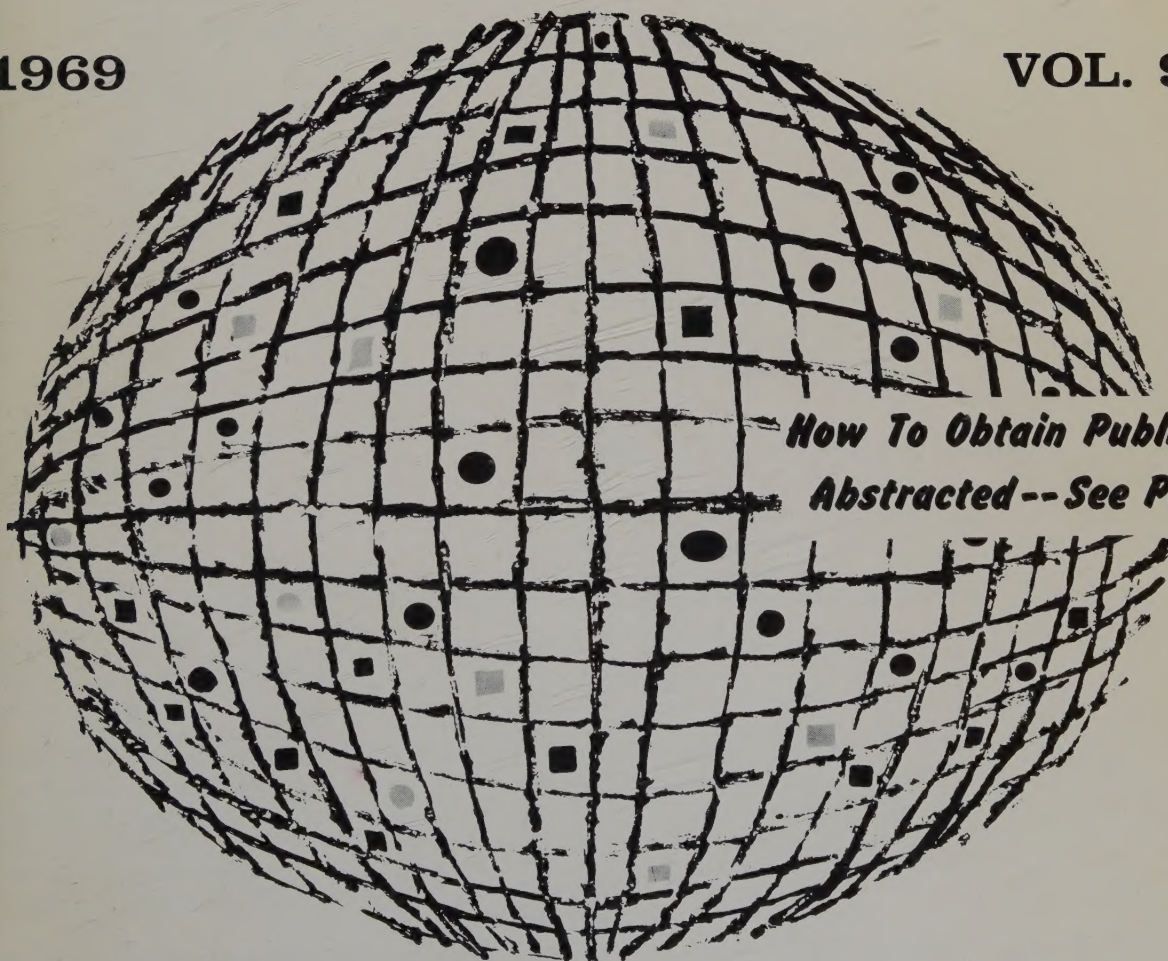
JAN 9 1970

CHICAGO CIRCLE

PART 1, PERIODICALS SCANNED, SUBJECT INDEX, A - L

1969

VOL. 9



*How To Obtain Publications
Abstracted -- See Page IV*

PUBLISHED BY THE TECHNICAL INFORMATION SERVICE
AMERICAN INSTITUTE OF AERONAUTICS AND ASTRONAUTICS

INTERNATIONAL AEROSPACE ABSTRACTS

ANNUAL

CUMULATED

INDEX

PART 1

PERIODICALS SCANNED, SUBJECT INDEX, A - L

VOLUME 9

JANUARY-DECEMBER

1969

ACCESSION NUMBERS A69-10001 to A69-43818

INTERNATIONAL AEROSPACE ABSTRACTS is prepared and published semimonthly (except March, June, September, and December, which have three issues) by the Technical Information Service, American Institute of Aeronautics and Astronautics, Inc., for the Institute and the National Aeronautics and Space Administration under Contract No. NSR 33-003-009. Editorial and Subscription Offices: 750 Third Avenue, New York, N. Y. 10017. Copyright © 1969 by the American Institute of Aeronautics and Astronautics, Inc.
Telephone: 212 TN-7-8300 TWX: 212 867-7265

SUBSCRIPTION INFORMATION. Semimonthly issues: United States and Possessions, 1 year, \$54 postpaid; Foreign Countries, 1 year, \$68.25 postpaid. Cumulated Index Volumes: United States and Possessions, 1 year, \$30 postpaid; Foreign Countries, 1 year, \$35 postpaid. Second-class postage paid at Phillipsburg, N.J.

CONTENTS

Pages

PART 1

INTRODUCTION	iii
HOW TO OBTAIN PUBLICATIONS ABSTRACTED	iv
CROSS REFERENCES	iv
LIST OF PERIODICALS SCANNED	v
SUBJECT INDEX, A - L	A1 - A1057a

PART 2

SUBJECT INDEX, M - Z

PART 3

PERSONAL AUTHOR INDEX

CONTRACT NUMBER INDEX

MEETING PAPER AND REPORT NO. INDEX

ACCESSION NUMBER INDEX

STAFF, AIAA Administrator—Technical Information Programs, Robert R. Dexter
STAFF, TECHNICAL INFORMATION SERVICE Director, John J. Glennon • **Associate Director—Administrative**, Thomas J. Meskel • **Associate Director—Technical**, Irene W. Bogolubsky • **Manager—Information Systems**, William T. Morris, Jr. • **Chief Librarian**, Patricia M. Marshall

Sheridan Printing Company, Inc.
Phillipsburg, N. J.

INTRODUCTION

INTERNATIONAL AEROSPACE ABSTRACTS (IAA) is an abstracting and indexing service covering the world's published literature in the field of aeronautics and space science and technology. IAA is issued semimonthly, on the 1st and 15th of each month (except March, June, September, and December, which have three issues).

Coverage of Published Literature

The following types of publications are covered in IAA:

- Periodicals (including government-sponsored journals) and books.
- Meeting papers and conference proceedings issued by professional societies and academic organizations.
- Translations of journals and journal articles.

Coverage of Reports ("Unpublished" Literature)

Abstracts and indexes of report literature are issued in SCIENTIFIC AND TECHNICAL AEROSPACE REPORTS (STAR), which is published by the Scientific and Technical Information Division, National Aeronautics and Space Administration.

By special arrangement between NASA and the American Institute of Aeronautics and Astronautics, IAA is issued in coordination with the twice-monthly schedule of STAR, which appears on the 8th and 23rd of each month.

IAA and STAR both utilize identical subject categories and indexes, which are described below.

Thus the two services provide comprehensive access to the national and international unclassified report and published literature of current significance to aerospace science and technology.

Arrangement of the Semimonthly Issues

IAA is arranged in two major sections:

- (1) Abstracts Section. This section contains complete bibliographic citations with informative abstracts, arranged by appropriate subject categories to facilitate scanning. The subject categories are numbered from 01 to 34, and the scope of each category is outlined in the Table of Contents and again at the beginning of each category in the Abstracts Section. Each abstract is prefixed by the IAA accession number.
- (2) Index Section. Five indexes are contained in this section: Subject, Personal Author, Contract Number, Meeting Paper and Report Number, and Accession Number. Each index is prefaced by explanatory notes to guide the user to the desired abstract.

Cumulated Indexes

Cumulated indexes are prepared and issued promptly at the end of each quarter year, with the 4th quarterly being the Annual Index.

Each cumulated index contains the following sections: A—Subject Index, B—Personal Author Index, C—Contract Number Index, D—Meeting Paper and Report Number Index, and E—Accession Number Index.

Indexing Vocabulary

The Preliminary Edition of the NASA THESAURUS (December 1967) (NASA SP-7030) is the authority for the indexing vocabulary that appears in the subject indexes to STAR and IAA. The NASA Thesaurus should be consulted for a total picture of the current indexing vocabulary and associated cross-reference structure. Copies of the NASA Thesaurus may be obtained from the Clearinghouse for Federal Scientific and Technical Information or the U.S. Government Printing Office at a price of \$8.50 for the three-volume set.

Information regarding SCIENTIFIC AND TECHNICAL AEROSPACE REPORTS and the availability of INTERNATIONAL AEROSPACE ABSTRACTS to organizations having contractual arrangements with NASA may be obtained from the following address:

National Aeronautics and Space Administration
Scientific and Technical Information Division
Attention: Code USI
Washington, D.C. 20546

how to obtain publications abstracted

Address all inquiries and requests to:

Technical Information Service
American Institute of Aeronautics
and Astronautics, Inc.
750 Third Avenue, New York, N. Y. 10017

Telephone: 212 TN-7-8300
TWX: 212 867-7265

All documents abstracted are available from the AIAA Technical Information Service as follows:

- Paper copies of accessions announced in IAA and of other published articles in the TIS library are available at \$3.00 per document up to a maximum of 20 pages. The charge for each additional page is \$0.25.
- Paper copies of accessions announced in *Scientific and Technical Aerospace Reports* (STAR) and of similar unpublished reports in the TIS library are available at the rate of \$0.25 per page, minimum order \$3.00.
- Microfiche of documents announced in IAA are available at the rate of \$0.50 per microfiche on demand. Documents available in this manner are identified by the symbol # following the accession number in the Abstracts Section and in the Meeting Paper and Report Number and the Accession Number Indexes.
- Minimum air-mail postage to foreign countries is \$1.00.
- A number of publications, because of their special characteristics, are available only for reference in the library.

**PLEASE REFER TO THE ACCESSION NUMBER WHEN
REQUESTING PUBLICATIONS**

CROSS REFERENCES

The subject index includes two types of cross references to aid the user of the index in locating the material being sought:

1. "USE" references (U) direct the user to alternate headings under which material on the subject will be found, for example

COLUMBIUM
U NIOBIUM

2. "NARROWER TERM" references (NT) refer the user to more specific headings in the same subject area, for example

LUMINESCENCE
NT ELECTROLUMINESCENCE

The periodicals listed in this section were scanned for material to be announced in *International Aerospace Abstracts* in 1969. The periodicals were received regularly throughout the year in all but a few instances. In the case of titles preceded by an asterisk, only the articles abstracted in *International Aerospace Abstracts* are available. All abstracted articles can be obtained from the AIAA Technical Information Service (see page iv).

BM — Bimonthly
BW — Biweekly
Irreg. — Irregular
M — Monthly

Q — Quarterly
SA — Semiannual
SM — Semimonthly
W — Weekly

A

Abastumanskaia Astrofizicheskaia Observatoriia, Biulleten'. Akademiia Nauk Gruzinskoi SSR, Tbilisi. Irreg.

Académie des Sciences (Paris), Comptes Rendus, Série A — Sciences Mathématiques, Série B — Sciences Physiques. Académie des Sciences; Gauthier-Villars & Cie., Paris. W

Académie des Sciences (Paris), Comptes Rendus, Série C — Sciences Chimiques. Académie des Sciences; Gauthier-Villars & Cie., Paris. W

Académie des Sciences (Paris), Comptes Rendus, Série D — Sciences Naturelles. Académie des Sciences; Gauthier-Villars & Cie., Paris. W

Académie Polonaise des Sciences, Bulletin, Série des Sciences Mathématiques, Astronomiques et Physiques. Académie Polonaise des Sciences; Państwowe Wydawnictwo Naukowe, Warsaw. M

Académie Polonaise des Sciences, Bulletin, Série des Sciences Techniques. Académie Polonaise des Sciences; Państwowe Wydawnictwo Naukowe, Warsaw. M

Académie Royale de Belgique, Classe des Sciences, Bulletin. Académie Royale de Belgique; Office International de Librairie, Brussels. M

Academy of Management, Journal. Academy of Management, Indiana University, Graduate School of Business, Bloomington, Ind. Q

Academy of Sciences, USSR, Bulletin, Physical Series (Akademiia Nauk SSSR, Izvestiia, Serii Fizicheskaia). Columbia Technical Translations, White Plains, N.Y. M

Academy of Sciences, USSR, Izvestiya, Atmospheric and Oceanic Physics (Akademiia Nauk SSSR, Izvestiia, Fizika Atmosfery i Okeana). American Geophysical Union, Washington, D.C. M

Accademia Nazionale dei Lincei, Atti, Rendiconti — Classe di Scienze Fisiche, Matematiche e Naturali. Accademia Nazionale dei Lincei, Rome. M

Accademia di Scienze e Lettere, Istituto Lombardo, Memorie. Istituto Lombardo di Scienze e Lettere, Milan. Irreg.

**Accounts of Chemical Research*. American Chemical Society, Washington, D.C. Irreg.

ACM, Communications. Association for Computing Machinery, New York. M

Acoustical Society of America, Journal. Acoustical Society of America; American Institute of Physics, Inc., New York. M

**Acta Anatomica*. S. Karger AG, Basel, Switzerland. 3 vols. per year

Acta Astronomica. Państwowe Wydawnictwo Naukowe, Warsaw. Q

Acta Biologica et Medica Germanica. Akademie-Verlag GmbH, Berlin. M

**Acta Chemica Scandinavica*. Copenhagen. 10 issues per year

Acta Geophysica Polonica. Polska Akademia Nauk; Państwowe Wydawnictwo Naukowe, Warsaw. Q

**Acta Histochemica*. VEB Gustav Fischer Verlag, Jena. SM

Acta Mechanica. Springer Verlag, Vienna. 8 issues per year

Acta Metallurgica. Pergamon Press, Ltd., Oxford. M

Acta Physica. Academiae Scientiarum Hungaricae, Budapest. BM

Acta Physica Austriaca. Österreichische Akademie der Wissenschaften; Springer Verlag, Vienna. Q

Acta Physica Polonica. Polska Akademia Nauk, Instytut Fizyki and Polskie Towarzystwo Fizyczne, Warsaw. M

Acta Physiologica Polonica. Polska Akademia Nauk; Państwowy Zakład Wydawnictw Lekarskich, Warsaw. BM

Acta Polytechnica, Series IV. České Vysoké Učení Technické, Prague. Q

Acta Polytechnica Scandinavica, Civil Engineering and Building Construction Series. Scandinavian Council for Applied Research, Stockholm. Irreg.

Acta Polytechnica Scandinavica, Mechanical Engineering Series. Scandinavian Council for Applied Research, Stockholm. Irreg.

Acta Polytechnica Scandinavica, Physics Including Nucleonics Series. Scandinavian Council for Applied Research, Stockholm. Irreg.

Acta Technica. Hungarian Academy of Sciences, Budapest. 4 vols. per year

Acta Technica ČSAV. Československá Akademie Věd, Prague. BM

Acta Universitatis Lundensis, Sectio II - Medica, Mathematica, Scientiae Rerum Naturalium. Kungl. Fysiografiska Sällskapet, Lund, Sweden. Irreg.

**Acta Universitatis Upsaliensis.* Almqvist & Wiksells, Uppsala. Irreg.

Acustica. S. Hirzel Verlag, KG, Stuttgart. M

Administrative Science Quarterly. Cornell University, Graduate School of Business and Public Administration, Ithaca, N.Y. 4 issues per year

Advances in Physics. Taylor & Francis, Ltd., London. Q

**Advances in Polymer Science.* Springer Verlag, Berlin. Irreg.

Aero-Revue. Aero-Club der Schweiz, Zurich. M

Aero Medical Society of India, Journal. Institute of Aviation Medicine, Bangalore. A

Aeronautical Journal. Royal Aeronautical Society, London. M

Aeronautical Quarterly. Royal Aeronautical Society, London. Q

Aeronautical Society of India, Journal. Aeronautical Society of India, New Delhi. Q

L'Aéronautique et l'Astronautique. Association Française des Ingénieurs et Techniciens de l'Aéronautique et de l'Espace and Société Française de l'Astronautique; Edition Air & Cosmos, Paris. M

**Aeronomica Acta - A.* Institut d'Aéronomie Spatiale de Belgique, Brussels. Irreg.

Aerospace Medicine. Aerospace Medical Association, Washington, D.C. M

L'Aeroteca. Associazione Italiana di Aerotecnica, Rome. BM

AIAA Journal. American Institute of Aeronautics and Astronautics, Inc., New York. M

AIAA Student Journal. American Institute of Aeronautics and Astronautics, Inc., New York. Q

AIChE Journal. American Institute of Chemical Engineers, New York. BM

AIME, Transactions. American Institute of Mining, Metallurgical and Petroleum Engineers, Inc., New York. M

Air BP. British Petroleum Co., Ltd.; Britannic House, London. 3 issues per year

Air et Cosmos. Société Française d'Astronautique, Paris. W

Air Line Pilot. Air Line Pilots Association/International, Chicago. M

Air University Review. Aerospace Studies Institute, Maxwell Air Force Base, Ala. BM

Aircraft Engineering. Bunhill Publications, Ltd., London. M

Akademiia Nauk Armianskoi SSR, Doklady. Akademiia Nauk Armianskoi SSR, Yerevan. 10 issues per year

Akademiia Nauk Armianskoi SSR, Izvestiia, Fizika. Akademiia Nauk Armianskoi SSR, Yerevan. BM

Akademiia Nauk Armianskoi SSR, Izvestiia, Mekhanika. Akademiia Nauk Armianskoi SSR, Yerevan. BM

Akademiia Nauk Armianskoi SSR, Izvestiia, Seriiia Tekhnicheskikh Nauk. Akademiia Nauk Armianskoi SSR, Yerevan. BM

Akademiia Nauk Azerbaidzhanskoi SSR, Doklady. Akademiia Nauk Azerbaidzhanskoi SSR, Baku. M

Akademiia Nauk Azerbaidzhanskoi SSR, Izvestiia, Seriiia Fiziko-Tekhnicheskikh i Matematicheskikh Nauk. Akademiia Nauk Azerbaidzhanskoi SSR, Baku. BM

Akademiia Nauk BSSR, Doklady. Akademiia Nauk Belorusskoi SSR, Minsk. M

Akademiia Nauk Gruzinskoi SSR, Soobshcheniia. Akademiia Nauk Gruzinskoi SSR, Tiflis. M

Akademiia Nauk Kazakhskoi SSR, Izvestiia, Seriiia Fiziko-Matematicheskakaia. Akademiia Nauk Kazakhskoi SSR, Alma Ata. BM

Akademiia Nauk Kazakhskoi SSR, Vestnik. Akademiia Nauk Kazakhskoi SSR, Alma Ata. M

Akademiia Nauk Latviiskoi SSR, Izvestiia, Seriiia Fizicheskikh i Tekhnicheskikh Nauk. Akademiia Nauk Latviiskoi SSR, Riga. BM

Akademiia Nauk SSSR, Doklady. Akademiia Nauk SSSR, Moscow. 36 issues per year

Akademiia Nauk SSSR, Izvestiia, Energetika i Transport. Akademiia Nauk SSSR, Moscow. BM

Akademiia Nauk SSSR, Izvestiia, Fizika Atmosfery i Okeana. Akademiia Nauk SSSR, Moscow. M

Akademiia Nauk SSSR, Izvestiia, Mekhanika Tverdogo Tela. Akademiia Nauk SSSR; Izdatel'stvo Nauka, Moscow. BM

Akademiia Nauk SSSR, Izvestiia, Mekhanika Zhidkosti i Gaza. Akademiia Nauk SSSR, Moscow. BM

Akademiia Nauk SSSR, Izvestiia, Metally. Akademiia Nauk SSSR, Moscow. BM

**Akademiia Nauk SSSR, Izvestiia, Neorganicheskie Materialy.* Akademiia Nauk SSSR, Moscow. M

Akademiia Nauk SSSR, Izvestiia, Seriiia Biologicheskakaia. Akademiia Nauk SSSR, Moscow. BM

Akademiia Nauk SSSR, Izvestiia, Seriiia Fizicheskakaia. Akademiia Nauk SSSR, Moscow. M

Akademiia Nauk SSSR, Izvestiia, Seriiia Matematicheskakaia. Akademiia Nauk SSSR, Moscow. BM

Akademiia Nauk SSSR, Izvestiia, Tekhnicheskakaia Kibernetika. Akademiia Nauk SSSR, Moscow. BM

Akademiia Nauk SSSR, Sibirskoe Otdelenie, Izvestiia, Seriiia Tekhnicheskikh Nauk. Akademiia Nauk SSSR, Sibirskoe Otdelenie, Novosibirsk. 3 issues per year

Akademiia Nauk SSSR, Vestnik. Akademiia Nauk SSSR, Moscow. M

Akademiia Nauk Tadzhikskoi SSR, Doklady. Akademiia Nauk Tadzhikskoi SSR, Dushanbe. M

Akademiia Nauk Tadzhikskoi SSR, Otdelenie Fiziko-Matematicheskikh i Geologo-Khimicheskikh Nauk, Izvestiia. Akademiia Nauk Tadzhikskoi SSR; Izdatel'stvo Donish, Dushanbe. Q

Akademiia Nauk Turkmeniskoi SSR, Izvestiia, Seriiia Fiziko-Tekhnicheskikh, Khimicheskikh i Geologicheskikh Nauk. Akademiia Nauk Turkmeniskoi SSR, Ashkhabad. BM

Akademiia Nauk Ukrain'skoi RSR, Dopovidi, Seriiia A - Fiziko-Tekhnichni i Matematichni Nauki. Akademiia Nauk Ukrain'skoi RSR; Naukova Dumka, Kiev. M

Akademiia Nauk Ukrain'skoi RSR, Dopovidi, Seriiia B - Geologiiia, Geofizika, Khimiiia i Biologiiia. Akademiia Nauk Ukrain'skoi RSR; Naukova Dumka, Kiev. M

Akademiia Nauk Uzbekskoi SSR, Doklady. Akademiia Nauk Uzbekskoi SSR, Tashkent. M

Akademiia Nauk Uzbekskoi SSR, Izvestiia, Seriiia Fiziko-

- Matematicheskikh Nauk.* Akademiia Nauk Uzbekskoi SSR, Tashkent. BM
- Akademiia Nauk Uzbekskoi SSR, Izvestiia, Seriya Tekhnicheskikh Nauk.* Akademiia Nauk Uzbekskoi SSR, Tashkent. BM
- Akademiia Navuk BSSR, Vestsy, Seriya Fizika-Tekhnichnykh Navuk.* Akademiia Navuk Belaruskai SSR, Minsk. Q
- Akusticheskii Zhurnal.* Akademiia Nauk SSSR, Moscow. Q
- Alata Internazionale.* Etas Kompass, Milan. M
- Alta Frequenza.* Associazione Elettrotecnica Italiana, Milan. M
- Aluminium.* Aluminium-Zentrale e.V.; Aluminium-Verlag GmbH, Düsseldorf. M
- American Ceramic Society, Bulletin.* American Ceramic Society, Inc., Columbus, Ohio. M
- American Ceramic Society, Journal.* American Ceramic Society, Inc., Columbus, Ohio. M
- American Chemical Society, Journal.* American Chemical Society, Washington, D.C. SM
- American Heart Journal.* C. V. Mosby, St. Louis, Mo. M
- American Helicopter Society, Journal.* American Helicopter Society, Inc., New York. Q
- American Industrial Hygiene Association, Journal.* American Industrial Hygiene Association, Cincinnati. BM
- *American Journal of Botany.* Botanical Society of America, Inc., New York. M
- American Journal of Cardiology.* American College of Cardiology; Reuben H. Donnelley Corp., New York. M
- *American Journal of Clinical Nutrition.* Reuben H. Donnelley Corp., New York. M
- *American Journal of Obstetrics and Gynecology.* American Gynecological Society; C. V. Mosby, St. Louis, Mo. SM
- American Journal of Physics.* American Institute of Physics, Inc., New York. M
- *American Journal of Physiology.* American Physiological Society, Washington, D.C. M
- American Journal of Psychiatry.* American Psychiatric Association, Washington, D.C. M
- *American Journal of Psychology.* University of Texas, Austin. Q
- *American Mathematical Society, Bulletin.* American Mathematical Society, Providence, R.I. BM
- American Mathematical Society, Memoirs.* American Mathematical Society, Providence, R.I. Irreg.
- American Mathematical Society, Transactions.* American Mathematical Society, Providence, R.I. M
- American Meteorological Society, Bulletin.* American Meteorological Society, Boston. M
- *American Mineralogist.* Mineralogical Society of America c/o U.S. Geological Survey, Washington, D.C. BM
- American Scientist.* Scientific Research Society of America, New Haven, Conn. Q
- American Society of Civil Engineers, Aero-Space Transport Division, Journal.* American Society of Civil Engineers, New York. BM
- American Society of Civil Engineers, Engineering Mechanics Division, Journal.* American Society of Civil Engineers, New York. BM
- American Society of Civil Engineers, Structural Division, Journal.* American Society of Civil Engineers, New York. BM
- *American Statistical Association, Journal.* American Statistical Association, Washington, D.C. Q
- *Analytical Biochemistry.* Academic Press, Inc., New York. M
- *Analytical Chemistry.* American Chemical Society, Washington, D.C. M
- *Anesthesiology.* American Society of Anesthesiologists; J. B. Lippincott Co., Philadelphia. BM
- Annalen der Meteorologie.* Deutscher Wetterdienst, Offenbach/Main. Irreg.
- Annalen der Physik.* Johann Ambrosius Barth Verlag, Leipzig. Irreg.
- Annales d'Astrophysique.* Centre National de la Recherche Scientifique, Paris. BM
- Annales de Géophysique.* Centre National de la Recherche Scientifique, Paris. Q
- Annales de Physique.* Centre National de la Recherche Scientifique; Masson & Cie., Paris. BM
- Annales de Radioélectricité (see Revue Technique Thomson - CSF).*
- Annales des Télécommunications.* Centre National d'Etudes des Télécommunications, Issy-les-Moulineaux (Seine), France. BM
- Annali di Geofisica.* Istituto Nazionale di Geofisica, Rome. Q
- *Annals of Mathematical Statistics.* Institute of Mathematical Statistics; Stanford University, Dept. of Statistics, Stanford. Q
- Annals of Physics.* Academic Press, Inc., New York. 15 issues per year
- *Annals of Surgery.* American Surgical Association; J. B. Lippincott Co., Philadelphia. M
- Annals of the International Geophysical Year.* Pergamon Press, Ltd., Oxford. Irreg.
- APL Technical Digest.* Applied Physics Laboratory, Silver Spring, Md. BM
- Aplikace Matematiky.* Československá Akademie Věd, Matematický Ústav, Prague. BM
- Applied Electrical Phenomena (Elektronnaiia Obrabotka Materialov).* Consultants Bureau, New York. BM
- Applied Mechanics Reviews.* American Society of Mechanical Engineers, New York. M
- *Applied Microbiology.* American Society for Microbiology, Baltimore. BM
- Applied Optics.* Optical Society of America; American Institute of Physics, Inc., New York. M
- Applied Physics Letters.* American Institute of Physics, Inc., New York. SM
- Applied Scientific Research.* Martinus Nijhoff, The Hague. Irreg.
- Applied Solar Energy (Geliotekhnika).* The Faraday Press, Inc., New York. BM
- Applied Spectroscopy.* Society for Applied Spectroscopy, Boston College, Mass.; American Institute of Physics, Inc., New York. BM
- Archiv der elektrischen Übertragung.* S. Hirzel Verlag, KG, Stuttgart. M
- Archiv für Elektrotechnik.* Springer Verlag, Berlin.
- Archiv für Meteorologie, Geophysik und Bioklimatologie, Serie A - Meteorologie und Geophysik.* Springer Verlag, Vienna. Irreg.

- Archiv für Mikrobiologie*. Springer Verlag, Berlin. 3 vols. per year
- Archiv für technisches Messen und industrielle Messtechnik*. Verlag R. Oldenbourg, Munich. M
- Archive for Rational Mechanics and Analysis*. Springer Verlag, Berlin. Irreg.
- **Archives of Biochemistry and Biophysics*. Academic Press, Inc., New York. M
- Archives of Environmental Health*. American Medical Association, Chicago. M
- **Archives of Neurology*. American Neurological Association; American Medical Association, Chicago. M
- Archiwum Automatyki i Telemekhaniki*. Polska Akademia Nauk; Państwowe Wydawnictwo Naukowe, Warsaw. Q
- Archiwum Budowy Maszyn*. Polska Akademia Nauk, Komitet Budowy Maszyn; Państwowe Wydawnictwo Naukowe, Warsaw. Q
- Archiwum Elektrotechniki*. Polska Akademia Nauk; Państwowe Wydawnictwo Naukowe, Warsaw. BM
- Archiwum Mechaniki Stosowanej*. Polska Akademia Nauk; Państwowe Wydawnictwo Naukowe, Warsaw. BM
- Arkiv för Astronomi*. Kungliga Svenska Vetenskapsakademien; Almqvist & Wiksells Boktryckeri AB, Stockholm. Irreg.
- Arkiv för Fysik*. Kungliga Svenska Vetenskapsakademien; Almqvist & Wiksells Boktryckeri AB, Stockholm. Irreg.
- Arkiv för Geofysik*. Kungliga Svenska Vetenskapsakademien; Almqvist & Wiksells Boktryckeri AB, Stockholm. Irreg.
- Arkiv för Matematik*. Kungliga Svenska Vetenskapsakademien; Almqvist & Wiksells Boktryckeri AB, Stockholm. BM
- Artificial Satellites*. Polish Academy of Sciences, Warsaw. Q
- Ärztliche Praxis*. Werk-Verlag, Munich. W
- ASCE, Transportation Engineering Journal*. American Society of Civil Engineers, New York. BM
- ASLE Transactions*. American Society of Lubrication Engineers; Academic Press, Inc., New York. Q
- ASM Transactions Quarterly*. American Society for Metals, Metals Park, Ohio. Q
- ASME, Transactions, Series A - Journal of Engineering for Power*. American Society of Mechanical Engineers, New York. Q
- ASME, Transactions, Series B - Journal of Engineering for Industry*. American Society of Mechanical Engineers, New York. Q
- ASME, Transactions, Series C - Journal of Heat Transfer*. American Society of Mechanical Engineers, New York. Q
- ASME, Transactions, Series D - Journal of Basic Engineering*. American Society of Mechanical Engineers, New York. Q
- ASME, Transactions, Series E - Journal of Applied Mechanics*. American Society of Mechanical Engineers, New York. Q
- ASME, Transactions, Series F - Journal of Lubrication Technology*. American Society of Mechanical Engineers, New York. Q
- **Association for the Advancement of Medical Instrumentation, Journal*. Association for the Advancement of

- Medical Instrumentation, Cambridge, Mass. BM
- Association for Computing Machinery, Journal*. Association for Computing Machinery, New York. Q
- Association Technique Maritime et Aéronautique, Bulletin*. Paris. A
- Astrofizika*. Akademiia Nauk Armianskoi SSR, Yerevan. Q
- Astronautica Acta*. International Academy of Astronautics, International Astronautical Federation; Pergamon Press, Ltd., Oxford. BM
- Astronautics and Aeronautics*. American Institute of Aeronautics and Astronautics, Inc., New York. M
- Astronautik*. Hermann Oberth-Gesellschaft, Hannover. BM
- Astronautyka*. Polskie Towarzystwo Astronautyczne, Warsaw. Q
- Astronomical Institutes of Czechoslovakia, Bulletin*. Československá Akademie Věd, Prague. BM
- Astronomical Institutes of the Netherlands, Bulletin*. Astronomical Institutes of the Netherlands; North-Holland Publishing Co., Amsterdam. 5 issues per year
- Astronomical Institutes of the Netherlands, Bulletin, Supplement Series*. Astronomical Institutes of the Netherlands; North-Holland Publishing Co., Amsterdam. Irreg.
- Astronomical Journal*. American Astronomical Society; American Institute of Physics, Inc., New York. 10 issues per year
- Astronomical Society of Australia, Proceedings*. Astronomical Society of Australia; Sydney University Press, Sydney. SA
- Astronomical Society of Japan, Publications*. Astronomical Society of Japan, Tokyo. Q
- Astronomical Society of the Pacific, Publications*. Astronomical Society of the Pacific, San Francisco. BM
- Astronomicheskii Vestnik*. Vsesoiuznoe Astronomo-Geodezicheskoe Obshchestvo; Izdatel'stvo Nauka, Moscow. Q
- Astronomicheskii Zhurnal*. Akademiia Nauk SSSR, Moscow. BM
- L'Astronomie*. Société Astronomique de France, Paris. M
- Astronomie und Raumfahrt*. Deutsche Astronautische Gesellschaft, Berlin. 5 issues per year
- Astronomische Gesellschaft, Mitteilungen*. Hamburg. Irreg.
- Astronomische Nachrichten*. Akademie Verlag GmbH, Berlin. Irreg.
- Astronomy and Astrophysics*. Springer Verlag, Berlin. M
- Astrophysical Journal*. University of Chicago Press, Chicago. M
- Astrophysical Journal Supplement Series*. University of Chicago Press, Chicago. Irreg.
- Astrophysical Letters*. Gordon and Breach, London. BM
- Astrophysics (Astrofizika)*. The Faraday Press, Inc., New York. Q
- Astrophysics and Space Science*. D. Reidel Publishing Co., Dordrecht, Netherlands. 8 issues per year
- **Atomnaia Energiia*. Akademiia Nauk SSSR, Moscow. M
- **Australian and New Zealand Journal of Surgery*. Royal Australian College of Surgeons; Australasian Medical Publishing Co., Glebe, N.S.W., Australia. Q

- Australian Journal of Chemistry.* Commonwealth Scientific and Industrial Organization, Melbourne. M
- Australian Journal of Physics.* Commonwealth Scientific and Industrial Research Organization, Melbourne. BM
- Australian Journal of Physics, Astrophysical Supplement.* Commonwealth Scientific and Industrial Research Organization, Melbourne. Irreg.
- Australian Mathematical Society, Journal.* Australian Mathematical Society; - P. Noordhoff N. V., Groningen, Netherlands. Q
- Australian Meteorological Magazine.* Bureau of Meteorology, Melbourne.
- **Australian Physicist.* Australian Institute of Physics, Chippendale, N.S.W., Australia. M
- **Australian Surveyor.* Institution of Surveyors, Sydney. Q
- Automatic Welding (Avtomaticheskaia Svarka).* British Welding Research Association, Cambridge. M
- Automatica.* Pergamon Press, Ltd., Oxford. BM
- Automation and Remote Control (Avtomatika i Telemekhanika).* Consultants Bureau, New York. M
- Automatisme.* Association Française de Régulation et d'Automatisme, Paris. M
- Automatizace.* Czechoslovak Scientific Society, Special Group for Automation, Prague. M
- Aviation Review.* Smiths Industries, Ltd., Aviation Division, Wembley, Middx., England. Irreg.
- Aviation Week and Space Technology.* McGraw-Hill, Inc., New York. W
- Aviatsiia i Kosmonavtika.* Voennoe Izdatel'stvo Ministerstva Oborony SSSR, Moscow. M
- Aviatsionnaia Tekhnika.* Ministerstvo Vysshego i Srednego Spetsial'nogo Obrazovaniia SSSR; Kazanskii Aviatsionnyi Institut, Kazan. Q
- Aviazione di Linea - Aeronautica e Spazio.* Rome. BM
- Avtomatika.* Akademiia Nauk Ukrainkoi SSR, Kiev. BM
- Avtomatika i Telemekhanika.* Akademiia Nauk SSSR, Moscow. M
- Avtomatika i Vychislitel'naia Tekhnika.* Akademiia Nauk Latvinskoi SSR, Riga. BM

B

- Babeş-Bolyai, Universitas, Studia, Series Mathematica-Physica.* Babeş-Bolyai, Universitas, Cluj, Rumania. SA
- Battelle Information.* Battelle Institute, Columbus, Ohio. Irreg.
- Behavioral Science.* Mental Health Research Institute, University of Michigan, Ann Arbor. BM
- Beiträge aus der Plasmaphysik.* Deutsche Akademie der Wissenschaften, Berlin. BM
- Beiträge zur Physik der Atmosphäre.* Akademische Verlagsgesellschaft mbH, Frankfurt/Main. Q
- Beiträge zur Radioastronomie.* Max-Planck-Institut für Radioastronomie; Ferd. Dümmlers Verlag, Bonn. Q
- Bell Laboratories Record.* Bell Telephone Laboratories, Inc., Murray Hill, N.J. M

- Bell System Technical Journal.* American Telephone and Telegraph Co., New York. 10 issues per year
- Bendix Technical Journal.* Detroit. Q
- Bildmessung und Luftbildwesen.* Herbert Wichmann Verlag, Karlsruhe. Q
- Biochemical and Biophysical Research Communications.* Academic Press, Inc., New York. SM
- **Biochemical Pharmacology.* Pergamon Press, Ltd., Oxford. M
- **Biochemistry.* American Chemical Society, Washington, D.C. M
- **Biochimica et Biophysica Acta.* Elsevier Publishing Co., Amsterdam. W
- **Biological Reviews.* Cambridge University Press, London. Q
- **Biophysical Journal.* Biophysical Society; Rockefeller University Press, New York. BM
- **BioScience.* American Institute of Biological Sciences, Washington, D.C. M
- Biotechnology and Bioengineering.* Interscience Publishers, New York. Q
- B'lgarska Akademiia na Naukite, Fizicheski Institut s ANEB, Izvestiia.* B'lgarska Akademiia na Naukite, Sofia. Irreg.
- B'lgarska Akademiia na Naukite, Institut po Tekhnicheska Mekhanika, Izvestiia.* B'lgarska Akademiia na Naukite, Sofia. Irreg.
- B'lgarska Akademiia na Naukite, Izvestiia na Geofizichniia Institut.* B'lgarska Akademiia na Naukite, Sofia. Irreg.
- **Blood.* Grune and Stratton, Inc., New York. M
- Bolgarskaia Akademiia Nauk, Doklady.* B'lgarska Akademiia na Naukite, Sofia. M
- Bollettino di Geofisica Teorica ed Applicata.* Osservatorio Geofisico Sperimentale, Trieste. Q
- **Botanical Gazette.* University of Chicago Press, Chicago. Q
- **Brain Research.* Elsevier Publishing Co., Amsterdam. M
- **Brennstoff-Chemie.* Verlag W. Girardet, Essen. M
- British Astronomical Association, Journal.* British Astronomical Association, Hounslow West, Middx., England. 8 issues per year
- British Interplanetary Society, Journal.* British Interplanetary Society, London. Q
- British Welding Journal* (see *Metal Construction and British Welding Journal*).
- Brno, Vysoké Učení Technické, Sborník.* Polytechnical Institute, Brno. M
- Brüel and Kjaer Technical Review.* B & K Instruments, Inc., Cleveland. Q
- Bucureşti, Institutul Politehnic Gheorghe Gheorghiu-Dej, Buletinul.* Bucharest. Q
- Bulletin Astronomique.* Centre National de la Recherche Scientifique, Service des Publications; Gauthier-Villars & Cie., Paris. Q
- Bulletin d'Informations Scientifiques et Techniques.* Dunod Editeur, Paris. M
- Bulletin Mathématique.* Societatea de Stiinte Matematice, Bucharest. Q
- **Bulletin of Mathematical Biophysics.* Mental Health Research Institute, University of Michigan, Ann Arbor, Mich. Q

C

- California Management Review*. University of California Press, Berkeley. Q
- Cambridge Philosophical Society, Proceedings*. Cambridge University Press, London. Q
- Canada, National Research Council, Division of Mechanical Engineering and National Aeronautical Establishment, Quarterly Bulletin*. National Research Council of Canada, Ottawa. Q
- Canadian Aeronautics and Space Journal*. Canadian Aeronautics and Space Institute, Ottawa. 10 issues per year
- Canadian Journal of Chemistry*. National Research Council of Canada, Ottawa. M
- Canadian Journal of Physics*. National Research Council of Canada, Ottawa. SM
- Canadian Journal of Physiology and Pharmacology*. National Research Council of Canada, Ottawa. BM
- Canadian Metallurgical Quarterly*. Canadian Institute of Mining and Metallurgy, Dept. of Mines and Technical Surveys, Ottawa. Q
- Canadian Operational Research Society, Journal*. Canadian Operational Research Society, Ottawa. 3 issues per year
- **Carbon*. Pergamon Press, Ltd., Oxford. Q
- CASI Transactions*. Canadian Aeronautics and Space Institute, Ottawa. SA
- Celestial Mechanics*. D. Reidel Publishing Co., Dordrecht, Netherlands. Q
- Československý Časopis pro Fysiku*. Československá Akademie Věd, Prague. BM
- Challenge*. General Electric Co., Missile and Space Div., Philadelphia. Q
- Chemical Engineering Progress, Symposium Series*. American Institute of Chemical Engineers, New York. M
- **Chemical Geology*. Elsevier Publishing Co., Amsterdam. Q
- Chemical Physics Letters*. North-Holland Publishing Co., Amsterdam. M
- **Chemical Society, Journal, Section C - Organic Chemistry*. London. M
- Chemie-Ingenieur-Technik*. Verlag Chemie GmbH, Weinheim. M
- Chile, Universidad, Departamento de Astronomia, Publicaciones*. Observatorio Astronomico Nacional, Santiago de Chile.
- **Chimie et Industrie*. Société de Productions Documentaires, Paris. M
- Chubu Institute of Technology, Memoirs*. Chubu Institute of Technology, Nagoya. Irreg.
- Ciel et Terre*. Société Belge d'Astronomie, de Météorologie et de Physique du Globe, Brussels. BM
- **Circulation Research*. American Heart Association, New York. M
- **Clays and Clay Minerals*. National Conference on Clays & Clay Minerals, Calif. A
- Cobalt*. Centre d'Information du Cobalt, Brussels. Q
- **Coelum*. Osservatorio Astronomico Università, Bologna. Irreg.
- **Color Engineering*. Chromatic Publishing Co., Inc., New York. BM

- Combustion, Explosion, and Shock Waves (Fizika Goreniia i Vzryva)*. The Faraday Press, Inc., New York. Q
- Combustion and Flame*. Combustion Institute; Butterworth & Co., Ltd., London. BM
- Comments on Astrophysics and Space Physics*. Gordon and Breach Science Publishers, Ltd., London. BM
- **Communications in Behavioral Biology*. Academic Press, Inc., New York. M
- **Communications in Mathematical Physics*. Springer Verlag, Berlin. Irreg.
- Communications on Pure and Applied Mathematics*. New York University, Institute of Mathematical Sciences; Interscience Publishers, New York. Q
- **Comparative Biochemistry and Physiology*. Pergamon Press, Ltd., Oxford. M
- Computer Journal*. British Computer Society, London. Q
- **Computing*. Springer Verlag, Vienna. Q
- Computing Surveys*. Association for Computing Machinery, New York. Q
- Contamination Control*. American Association for Contamination Control; Blackwell Publishing Co., Inc., Los Angeles. M
- Contemporary Physics*. Taylor & Francis, Ltd., London. BM
- Control*. Morgan Brothers (Publishers), Ltd., London. Q
- Control and Instrumentation*. Morgan-Grampian (Publishers), Ltd., London. M
- Control Engineering*. McGraw-Hill Publishing Co., Inc., New York. M
- Convair Traveler*. General Dynamics Corporation, Convair Division, San Diego. BM
- Coopération Méditerranéenne pour l'Energie Solaire, Bulletin*. Coopération Méditerranéenne pour l'Energie Solaire (COMPLES), Madrid. SA
- Corrosion*. National Association of Corrosion Engineers, Houston. M
- Corrosion Science*. Pergamon Press, Ltd., Oxford. M
- Cosmic Research (Kosmicheskie Issledovaniia)*. Consultants Bureau, New York. BM
- COSPAR Information Bulletin*. COSPAR Secretariat, Paris. Irreg.
- Cryogenic Technology*. Cryogenic Society of America; Technical Economics Associates, Inc., Wauconda, Ill. BM
- **Cryogenics*. Heywood-Temple Publications, London. BM
- Current Science*. Current Science Association, Bangalore, India. SM
- **Currents in Modern Biology*. North-Holland Publishing Co., Amsterdam. M
- Czechoslovak Journal of Physics, Series B*. Československá Akademie Věd, Prague. M

D

- Defense Management Journal*. Directorate for Cost Reduction and Management Improvement Policy, Office of the Assistant Secretary for Defense; USGPO, Washington, D.C. Q
- Deutscher Aerokurier*. Deutscher Aero-Club e.V., Frankfurt/Main. M

- DFL-Mitteilungen.** Deutsche Forschungsanstalt für Luft- und Raumfahrt, Braunschweig. Irreg.
- DGLR Mitteilungen.** Deutsche Gesellschaft für Luft- und Raumfahrt e.V., Köln. BM
- Differential Equations (Differentsial'nye Uravneniia).** The Faraday Press, Inc., New York. M
- Differentsial'nye Uravneniia.** Izdatel'stvo Nauka i Tekhnika, Minsk. M
- Doc-Air-Espace.** Service de Documentation Scientifique et Technique de l'Armement, Paris. BM
- Dominion Observatory, Publications.** Canada, Department of Energy, Mines and Resources, Observatories Branch, Ottawa.
- Dornier-Post.** Dornier-Werke GmbH, Munich. Q
- Dornier-Post (English Edition).** Dornier-Werke GmbH, Munich. Q
- DVL-Nachrichten.** Deutsche Versuchsanstalt für Luft- und Raumfahrt e.V., Porz-Wahn, West Germany. Irreg.

E

- Earth and Extraterrestrial Sciences.** Gordon & Breach Science Publishers, Ltd., London. Irreg.
- Earth and Planetary Science Letters.** North-Holland Publishing Co., Amsterdam. BM
- *EBU Review.** European Broadcasting Union, Brussels. BM
- L'Echo des Recherches.** Centre National d'Etudes des Télécommunications, Issy-les-Moulineaux, France. Q
- *Ecology.** Ecological Society of America; Duke University Press, Durham, N.C. BM
- EEE — The Magazine of Circuit Design Engineering.** Mactier Publishing Corporation, New York. M
- Eesti NSV Teaduste Akadeemia, Toimetised, Füüsika-Matemaatika.** Tallin. Q
- Electrical Communication.** International Telephone and Telegraph Corporation, New York. Q
- Electrical Engineering in Japan (Denki Gakkai Zasshi).** Institute of Electrical and Electronics Engineers, Inc., New York. M
- Electrochemical Society, Journal.** Electrochemical Society, Inc., New York. M
- *Electroencephalography and Clinical Neurophysiology.** International Federation of Societies for Electroencephalography and Clinical Neurophysiology; Elsevier Publishing Co., Amsterdam. 2 vols. per year
- Electronic Age.** Radio Corporation of America, New York. Q
- Electronic Design.** Hayden Publishing Co., Inc., New York. BW
- Electronic Engineer.** Chilton Co., Philadelphia. M
- Electronic Engineering.** Morgan Brothers, Ltd., London. M
- Electronic Packaging and Production.** Milton S. Kiver Publications, Inc., Chicago. M
- Electronic Progress.** Raytheon Co., Lexington, Mass. Q
- Electronics.** McGraw-Hill Publishing Co., Inc., New York. BW
- Electronics and Communications in Japan.** Institute of Electrical and Electronics Engineers, Inc., New York. M
- Electronics and Power.** Institution of Electrical Engineers, London. M
- Electronics Letters.** Institution of Electrical Engineers, London. M
- Electro-Technology.** Conover-Mast Technical Publications Corp., New York. M
- Elektromekhanika.** Ministerstvo Vysshego i Srednego Spetsial'nogo Obrazovaniia SSSR, Novocherkassk. M
- Elektronik.** Franzis-Verlag, Munich. M
- Elektronische Datenverarbeitung.** Friedr. Vieweg & Sohn GmbH, Braunschweig. BM
- Elektronische Rechenanlagen.** Verlag R. Oldenbourg, Munich. BM
- Elektrosviaz'.** Ministerstvo Sviazi SSSR, Moscow. M
- *Endocrinology.** Endocrine Society; J. B. Lippincott Co., Philadelphia. M
- Energomashinostroenie.** Gosudarstvennyi Komitet Tiazhelogo, Energeticheskogo i Transportnogo Mashinoostroeniia pri Gosplane SSSR, Leningrad. M
- Energy Conversion.** Pergamon Press, Ltd., Oxford. Q
- The Engineer.** Morgan Brothers (Publishers), Ltd., London. W
- Engineering Bulletin.** Motorola, Inc., Government Electronics Division, Scottsdale, Ariz. Irreg.
- Engineering Cybernetics (Akademiia Nauk SSSR, Izvestiia, Tekhnicheskaiia Kibernetika).** Institute of Electrical and Electronics Engineers, Inc., New York. BM
- Engineering Fracture Mechanics.** Pergamon Press, Ltd., Oxford. Q
- Entropie.** Editions Barthélemy & Cie., Paris. BM
- Environmental Engineering.** Society of Environmental Engineers; Kenneth Mason Publications, Ltd., London. BM
- Environmental Quarterly.** Environmental Publications, Inc., Little Neck, N.Y. Q
- Environmental Space Sciences (Kosmicheskaiia Biologiia i Meditsina).** Plenum Publishing Corp., New York. BM
- EOS.** American Geophysical Union, Washington, D.C. M
- Ergonomics.** Ergonomics Research Society; Taylor & Francis, Ltd., London. Q
- Ericsson Technics.** Telefonaktiebolaget L/M Ericsson, Stockholm. Q
- ESRO/ELDO Bulletin.** European Space Research Organization, Neuilly sur Seine, France. Q
- ESSO Air World.** ESSO International, Inc., New York. BM
- Eurocontrol.** Eurocontrol Organization, Public Relations Division, Brussels. SA
- Evaluation Engineering.** A. Verner Nelson Associates, Chicago. BM
- Experientia.** Birkhäuser Verlag, Basel. M
- Experimental Brain Research.** Springer Verlag, Berlin. Irreg.
- *Experimental Cell Research.** International Society for Cell Biology; Academic Press, Inc., New York. M
- Experimental Mechanics.** Society for Experimental Stress Analysis, Westport, Conn. M
- Explosifs.** Association des Fabricants Belges d'Explosifs et de Recherches Scientifiques, Brussels. Q
- Explosivstoffe.** Erwin Barth Verlag, KG, Mannheim, Germany. M

F

- Facilities for Atmospheric Research.* National Center for Atmospheric Research, Boulder, Colo. Q
- **Faraday Society, Discussions.* Butterworth & Co. (Publishers), Ltd., London. SA
- **Faraday Society, Transactions.* Aberdeen University Press, Ltd., Aberdeen, Scotland. M
- Finommechanika.* Lapkiadó Vállalat, Budapest. M
- Fizika.* Ministerstvo Vysshego i Srednego Spetsial'nogo Obrazovaniia SSSR; Tomskii Universitet, Tomsk. M
- Fizika Gorenii i Vzryva.* Akademiia Nauk SSSR, Sibirskoe Otdelenie; Izdatel'stvo Nauka, Novosibirsk. Q
- **Fizika i Khimiia Obrabotki Materialov.* Mezhdunarodnaia Kniga, Moscow. BM
- Fizika i Tekhnika Poluprovodnikov.* Akademiia Nauk SSSR, Leningrad. M
- Fizika Metallov i Metallovedenie.* Akademiia Nauk SSSR, Sverdlovsk. M
- Fizika Tverdogo Tela.* Akademiia Nauk SSSR, Moscow. M
- Fiziko-Khimicheskaiia Mekhanika Materialov.* Akademiia Nauk SSSR, Moscow. BM
- Fiziologichnii Zhurnal.* Akademiia Nauk Ukrainskoi SSR, Institut Fiziologii, Kiev. BM
- Flight International.* Iliffe Transport Publications, Ltd., London. W
- Flight Safety.* Pergamon Press, Ltd., Oxford. Q
- **Florida Academy of Sciences, Quarterly Journal.* Florida, University, Dept. of Biology, Gainesville. Q
- Flugrevue/Flugwelt International.* Vereinigte Motor-Verlag GmbH, Stuttgart. M
- Fluid Dynamics (Akademiia Nauk SSSR, Izvestiia, Mekhanika Zhidkosti i Gaza).* The Faraday Press, Inc., New York. BM
- Fluidics Quarterly.* Fluid Amplifier Associates, Ann Arbor, Mich. Q
- FOA Reports.* Försvarets Forskningsanstalt, Stockholm. Irreg.
- Forces Aériennes Françaises.* Comité d'Etudes Aéronautiques Militaires, Paris. M
- Forschung im Ingenieurwesen.* VDI-Verlag GmbH, Düsseldorf. BM
- Fortune.* Time, Inc., Chicago. M
- France, Ministère de l'Air, Publications Scientifiques et Techniques.* Service de Documentation Scientifique et Technique de l'Armement, Paris. Irreg.
- France, Ministère de l'Air, Publications Scientifiques et Techniques, Notes Techniques.* Service de Documentation Scientifique et Technique de l'Armement, Paris. Irreg.
- Franklin Institute, Journal.* Franklin Institute, Philadelphia. M
- Frequency* (see *Frequency Technology*).
- Frequency Technology* (formerly *Frequency*). Norwood, Mass. BM
- Frequenz.* Fachverlag Schiele und Schön, Berlin. M
- Fujitsu Scientific and Technical Journal.* Fujitsu, Ltd., Kanagawa, Japan. SA
- Fyzikálny Časopis.* Slovenska Akademia Vied, Bratislava. Q

G

- GEC-AEI Journal of Science and Technology* (see *Journal of Science and Technology*).
- Geliotekhnika.* Akademiia Nauk Uzbekskoi SSR, Tashkent. BM
- Genève, Société de Physique et d'Histoire Naturelle, Compte Rendu des Séances.* Irreg.
- **Génie Chimique* (Supplement to *Chimie et Industrie*), Paris. M
- Geochimica et Cosmochimica Acta.* Pergamon Press, Ltd., Oxford. M
- Geodesy and Aerophotography (Geodeziia i Aerofotos'emka).* American Geophysical Union, Washington, D.C. BM
- Geodeziia i Aerofotos'emka.* Moskovskii Institut Inzhenerov Geodezii, Aerofotos'emki i Kartografii, Moscow. BM
- Geodeziia i Kartografiia.* Gosudarstvennyi Geologicheskii Komitet SSSR, Moscow. M
- Geodezja i Kartografia.* Polska Akademia Nauk, Komitet Geodezji; Państwowe Wydawnictwo Naukowe, Warsaw. Q
- Geofisica e Meteorologia.* Società Italiana di Geofisica e Meteorologia, Genoa. 3 issues per year
- Geofizicheskii Biulleten'.* Akademiia Nauk SSSR, Moscow. Irreg.
- Geofysikální Sborník.* Československá Akademie Věd, Geofysikální Ústav, Prague. Annual
- **Geological Society of America, Bulletin.* Geological Society of America, New York. M
- Geomagnetism and Aeronomy (Geomagnetizm i Aeronomiia).* American Geophysical Union, Washington, D.C. BM
- Geomagnetizm i Aeronomiia.* Akademiia Nauk SSSR, Moscow. BM
- Geophysical Journal.* Royal Astronomical Society; Blackwell Scientific Publications, Ltd., London. M
- George Washington University Law Review.* Washington, D.C. Irreg.
- Gerlands Beiträge zur Geophysik.* Akademische Verlagsgesellschaft Geest & Portig, KG, Leipzig. BM
- Gidraeromekhanika i Teoriia Uprugosti.* Izdatel'stvo Khar'kovskogo Universiteta, Kharkov. Irreg.
- Göttingen, Akademie der Wissenschaften, Nachrichten, Mathematisch-physikalische Klasse.* Göttingen. Irreg.
- **Growth.* Southern Bio-Research Institute, Florida Southern College, Lakeland, Fla. Q

H

- **Harvard Business Review.* Harvard Business School, Des Moines, Iowa. BM
- Hawker Siddeley Review.* Hawker Siddeley Group, London. Q
- Heat Transfer — Soviet Research.* American Society of Mechanical Engineers, New York. BM
- **Heating, Piping and Air Conditioning.* Reinhold Publishing Corp., Chicago. M

Helvetica Physica Acta. Societas Physicae Helveticae; Birkhäuser Verlag, Basel. Irreg.

High Temperature (Teplofizika Vysokikh Temperatur). Consultants Bureau, New York. BM

**High Temperature Science*. Academic Press, Inc., New York.

Hiroshima University, Journal of Science, Series A - II. Hiroshima University, Hiroshima. 3 issues per year

**Histochemie*. Springer Verlag, Berlin.

Hochfrequenztechnik und Elektroakustik. Akademische Verlagsgesellschaft Geest & Portig, KG, Leipzig. BM

Hokkaido University, Faculty of Engineering, Bulletin. Hokkaido University, Sapporo, Japan.

Hokkaido University, Research Institute of Applied Electricity, Bulletin. Hokkaido University, Sapporo, Japan.

Hovering Craft and Hydrofoil. Kalerghi Publications, London. M

Human Factors. Human Factors Society of America, Santa Monica, Calif.; The Johns Hopkins Press, Baltimore. BM

Hydraulics and Pneumatics. Industrial Publishing Corp., Cleveland. M

I

Iași, Institutul Politehnic, Buletinul. Iași, Institutul Politehnic, Iași, Rumania. SA

IBM Journal of Research and Development. International Business Machines Corp., Armonk, N.Y. BM

IBM Systems Journal. International Business Machines Corp., Armonk, N.Y. Q

Icare. Société Nationale des Pilotes de Ligne; Orly Aéroport, France.

Icarus. Academic Press, Inc., New York. BM

I & EC — Industrial and Engineering Chemistry. American Chemical Society, Washington, D.C. M

I & EC — Industrial and Engineering Chemistry, Fundamentals. American Chemical Society, Washington, D.C. Q

I & EC — Industrial and Engineering Chemistry, Process Design and Development. American Chemical Society, Washington, D.C. Q

I & EC — Industrial and Engineering Chemistry, Product Research and Development. American Chemical Society, Washington, D.C. Q

IEEE, Proceedings. Institute of Electrical and Electronics Engineers, Inc., New York. M

IEEE Electrolatina. Institute of Electrical and Electronics Engineers, Inc., New York. Q

IEEE Journal of Quantum Electronics. Institute of Electrical and Electronics Engineers, Inc., New York. M

IEEE Journal of Solid State Circuits. Institute of Electrical and Electronics Engineers, Inc., New York. Q

IEEE Spectrum. Institute of Electrical and Electronics Engineers, Inc., New York. M

IEEE Transactions on Aerospace and Electronic Systems. Institute of Electrical and Electronics Engineers, Inc., New York. BM

IEEE Transactions on Antennas and Propagation. Institute of Electrical and Electronics Engineers, Inc., New York. BM

IEEE Transactions on Audio and Electroacoustics. Institute of Electrical and Electronics Engineers, Inc., New York. Q

IEEE Transactions on Automatic Control. Institute of Electrical and Electronics Engineers, Inc., New York. BM

IEEE Transactions on Bio-Medical Engineering. Institute of Electrical and Electronics Engineers, Inc., New York. Q

IEEE Transactions on Broadcasting. Institute of Electrical and Electronics Engineers, Inc., New York. Q

IEEE Transactions on Circuit Theory. Institute of Electrical and Electronics Engineers, Inc., New York. Q

IEEE Transactions on Communication Technology. Institute of Electrical and Electronics Engineers, Inc., New York. BM

IEEE Transactions on Computers. Institute of Electrical and Electronics Engineers, Inc., New York. M

IEEE Transactions on Education. Institute of Electrical and Electronics Engineers, Inc., New York. Q

IEEE Transactions on Electromagnetic Compatibility. Institute of Electrical and Electronics Engineers, Inc., New York. Irreg.

IEEE Transactions on Electron Devices. Institute of Electrical and Electronics Engineers, Inc., New York. M

IEEE Transactions on Engineering Management. Institute of Electrical and Electronics Engineers, Inc., New York. Q

IEEE Transactions on Geoscience Electronics. Institute of Electrical and Electronics Engineers, Inc., New York. Irreg.

IEEE Transactions on Industrial Electronics and Control Instrumentation. Institute of Electrical and Electronics Engineers, Inc., New York. Irreg.

IEEE Transactions on Information Theory. Institute of Electrical and Electronics Engineers, Inc., New York. Q

IEEE Transactions on Instrumentation and Measurement. Institute of Electrical and Electronics Engineers, Inc., New York. Q

IEEE Transactions on Magnetics. Institute of Electrical and Electronics Engineers, Inc., New York. Q

IEEE Transactions on Man-Machine Systems. Institute of Electrical and Electronics Engineers, Inc., New York. Q

IEEE Transactions on Microwave Theory and Techniques. Institute of Electrical and Electronics Engineers, Inc., New York. M

IEEE Transactions on Nuclear Science. Institute of Electrical and Electronics Engineers, Inc., New York. BM

IEEE Transactions on Parts, Materials and Packaging. Institute of Electrical and Electronics Engineers, Inc., New York. Q

IEEE Transactions on Reliability. Institute of Electrical and Electronics Engineers, Inc., New York. Irreg.

IEEE Transactions on Sonics and Ultrasonics. Institute of Electrical and Electronics Engineers, Inc., New York. Q

IEEE Transactions on Systems Science and Cybernetics. Institute of Electrical and Electronics Engineers, Inc., New York. Irreg.

Indian Academy of Sciences, Proceedings, Section A.

INTERNATIONAL AEROSPACE ABSTRACTS

- Indian Academy of Sciences, Bangalore. M
- Indian Institute of Science, Journal.* Indian Institute of Science, Bangalore. Q
- Indian Journal of Mathematics.* Allahabad Mathematical Society, Allahabad. SA
- Indian Journal of Meteorology and Geophysics.* India Meteorological Department, New Delhi. Q
- Indian Journal of Pure and Applied Physics.* Council of Scientific and Industrial Research, New Delhi. M
- Indian Journal of Technology.* Council of Scientific and Industrial Research, New Delhi. M
- Industrial Laboratory (Zavodskaja Laboratorii).* Consultants Bureau, New York. M
- Industrial Management Review.* School of Industrial Management, Massachusetts Institute of Technology, Cambridge, Mass. Irreg.
- Information and Control.* Academic Press, Inc., New York. M
- Information Display.* Information Display Publications, Inc., Los Angeles. BM
- *Information Sciences.* American Elsevier Publishing Co., Inc., New York. Q
- Infrared Physics.* Pergamon Press, Ltd., Oxford. Q
- Ingegneria Meccanica.* Etas Kompass, Milan. M
- Ingeniería Aeronáutica y Astronáutica.* Asociación de Ingenieros Aeronáuticos, Madrid. BM
- Ingenieur-Archiv.* Springer Verlag, Berlin. BM
- Innovation.* Technology Communication, Inc., Crawfordsville, Ind. M
- *Inorganic Chemistry.* American Chemical Society, Washington, D.C. M
- Inorganic Materials (Akademiia Nauk SSSR, Izvestiia, Neorganicheskie Materialy).* Consultants Bureau, New York. M
- Institut Fourier, Annales.* Centre National de la Recherche Scientifique, Paris.
- Institut Royal Météorologique de Belgique, Publications, Série B.* Institut Royal Météorologique de Belgique, Brussels. Irreg.
- Institut Teoreticheskoi Astronomii, Biulleten'.* Izdatel'stvo Nauka, Leningrad. Irreg.
- Institut Teoreticheskoi Astronomii, Trudy.* Akademiia Nauk SSSR, Institut Teoreticheskoi Astronomii, Leningrad. Irreg.
- Institute of Mathematics and Its Applications, Journal.* Academic Press, Ltd., London. Q
- *Institute of Metals, Journal.* Institute of Metals, London. Annual
- Institute of Navigation, Journal.* Institute of Navigation, London. Q
- Institute of Physical and Chemical Research, Reports.* Rikagaku Kenkyusho, Tokyo. Q
- Institution of Electrical Engineers, Proceedings.* Institution of Electrical Engineers, London. M
- Institution of Engineers (Australia), Mechanical and Chemical Engineering Transactions.* Science House, Sydney. SA
- Institution of Engineers (India), Journal, Electronics and Telecommunication Engineering Division.* Institution of Engineers, Calcutta. 3 issues per year
- Institution of Engineers (India), Journal, Mechanical Engineering Division.* Institution of Engineers, Calcutta. BM
- Institution of Mechanical Engineers, Proceedings.* Institution of Mechanical Engineers, London. Irreg.
- *Institution of Radio and Electronics Engineers (Australia), Proceedings.* Institution of Radio and Electronics Engineers, Sydney. M
- Institution of Telecommunication Engineers, Journal.* Institution of Telecommunication Engineers, New Delhi. M
- Instituto de Matemática, Astronomía y Física, Boletín.* Cordoba, Universidad Nacional, Cordoba, Argentina. Irreg.
- Instruments and Control Systems.* Rimbach Publications, Philadelphia. M
- Instruments and Experimental Techniques (Pribory i Tekhnika Eksperimental').* Instrument Society of America, Pittsburgh; Consultants Bureau, New York. BM
- Instytut Lotnictwa, Biuletyn Informacyjny.* Instytut Lotnictwa, Warsaw. BM
- Instytut Lotnictwa, Prace.* Instytut Lotnictwa; Wydawnictwo Naukowo-Techniczne, Warsaw. Irreg.
- Instytut Maszyn Przepływowych, Prace.* Polska Akademia Nauk, Instytut Maszyn Przepływowych, Gdansk; Państwowe Wydawnictwo Naukowe, Warsaw. Irreg.
- Inter-Electronique.* Editions LEPS, Paris. 10 issues per year
- Interavia.* Interavia S.A., Geneva. M
- International Journal of Biometeorology.* Leiden. 3 issues per year
- International Journal of Computer Mathematics.* Gordon & Breach Science Publishers, New York.
- International Journal of Control, First Series.* Taylor & Francis, Ltd., London. M
- International Journal of Electronics, First Series.* Taylor & Francis, Ltd., London. M
- International Journal of Engineering Science.* Pergamon Press, Ltd., Oxford. M
- International Journal of Fracture Mechanics.* P. Noordhoff, Ltd., Groningen, Netherlands. Q
- International Journal of Heat and Mass Transfer.* Pergamon Press, Ltd., Oxford. M
- International Journal of Man-Machine Studies.* Academic Press, Inc. (London), Ltd., London. BM
- *International Journal of Mass Spectrometry and Ion Physics.* Elsevier Publishing Co., Amsterdam. BM
- International Journal of Mechanical Sciences.* Pergamon Press, Ltd., Oxford. M
- International Journal of Nondestructive Testing.* Gordon & Breach Science Publishers, London.
- International Journal of Non-Linear Mechanics.* Pergamon Press, Ltd., Oxford. Q
- International Journal for Numerical Methods in Engineering.* John Wiley & Sons, Ltd., Chichester, Sussex, England. Q
- International Journal of Powder Metallurgy.* American Powder Metallurgy Institute, New York. Q
- *International Journal of Quantum Chemistry, Interscience Scientific Journals.* John Wiley & Sons, Inc., New York. BM
- International Journal of Radiation Biology.* Taylor & Francis, Ltd., London. M
- International Journal of Solids and Structures.* Pergamon Press, Ltd., Oxford. Q

- Internationale Elektronische Rundschau.* Verlag für Radio-Foto-Kinotechnik GmbH, Berlin. M
- **Internationale Zeitschrift für angewandte Physiologie einschliesslich Arbeitsphysiologie.* Springer Verlag, Berlin. 3 issues per year
- **Inventiones Mathematicae.* Springer Verlag, Heidelberg. 5 issues per year
- Inzhenerno-Fizicheskii Zhurnal.* Akademiia Nauk BSSR, Minsk. M
- Inzhenernyi Zhurnal — Mekhanika Tverdogo Tela.* Akademiia Nauk SSSR, Moscow. BM
- Iowa State University, Engineering Research Institute, Engineering Research Report.* Iowa State University, Ames.
- Irish Astronomical Journal.* Irish Astronomical Society, Armagh, Northern Ireland. M
- ISA Transactions.* Plenum Press, New York. Q
- Ishikawajima-Harima Engineering Review.* Ishikawajima-Harima Heavy Industries Co., Ltd., Tokyo. BM
- Israel Journal of Mathematics.* Weizmann Science Press of Israel, Jerusalem. Q
- Israel Journal of Technology.* Weizmann Science Press of Israel, Jerusalem. Q
- Istanbul Üniversitesi, Fen Fakültesi Mecmuası, Seri C — Astronomi-Fizik-Kimya.* Istanbul Üniversitesi, Istanbul. Q
- **Istituto Lombardo di Scienze e Lettere, Rendiconti.* Milan. 9 issues per year
- ITU Telecommunication Journal.* International Telecommunication Union, Geneva. M

J

- Japan Air Self Defence Force, Aeromedical Laboratory, Reports.* Aeromedical Laboratory, Tachikawa. Q
- Japan Defense Academy, Memoirs.* Defense Academy, Yokosuka, Japan. Irreg.
- Japan Institute of Light Metals, Journal.* Japan Institute of Light Metals, Tokyo. BM
- Japan Institute of Metals, Transactions.* Japan Institute of Metals, Sendai. Q
- Japan Society for Aeronautical and Space Sciences, Journal.* Japan Society for Aeronautical and Space Sciences, Tokyo. M
- Japan Society for Aeronautical and Space Sciences, Transactions.* Japan Society for Aeronautical and Space Sciences, Tokyo. Irreg.
- Japan Society of Lubrication Engineers, Journal.* Japan Society of Lubrication Engineers, Tokyo. M
- Japan Society of Materials Science, Journal.* Society of Materials Science, Kyoto. M
- Japanese Journal of Applied Physics.* Physical Society of Japan and Japan Society of Applied Physics, Tokyo. M
- **Japanese Journal of Genetics.* Japan Publications Trading Co., Ltd., Tokyo. BM
- Jemná Mechanika a Optika.* Ministerstvo Těžkého Průmyslu; Státní Nakladatelství Technické Literatury, Prague. M
- Jena Review.* VEB Verlag Technik, Berlin. BM
- JETP Letters (ZHETF Pis'ma v Redaktsiiu).* American

- Institute of Physics, Inc., New York. SM
- Journal de Mécanique.* Gauthier-Villars & Cie., Paris. Q
- Journal de Physique.* Société Française de Physique, Paris. 8 issues per year
- Journal de Recherches Atmosphériques.* Université de Clermont-Ferrand, Institut et Observatoire de Physique, Clermont-Ferrand, France. Q
- Journal des Observateurs.* Centre National de la Recherche Scientifique, Paris. Q
- Journal of Abnormal Psychology.* American Psychological Association, Washington, D.C. BM
- Journal of Air Law and Commerce.* Southern Methodist University, School of Law, Dallas. Q
- Journal of Air Traffic Control.* Air Traffic Control Association, Washington, D.C. BM
- Journal of Aircraft.* American Institute of Aeronautics and Astronautics, Inc., New York. BM
- Journal of Applied Mechanics and Technical Physics (PMTF — Zhurnal Prikladnoi Mekhaniki i Tekhnicheskoi Fiziki).* The Faraday Press, Inc., New York. BM
- Journal of Applied Meteorology.* American Meteorological Society, Boston. Q
- Journal of Applied Physics.* American Institute of Physics, Inc., New York. 13 issues per year
- **Journal of Applied Physiology.* American Physiological Society, Washington, D.C. BM
- Journal of Applied Polymer Science.* Interscience Publishers, New York. M
- Journal of Applied Psychology.* American Psychological Association, Inc., Washington, D.C. BM
- Journal of Atmospheric and Terrestrial Physics.* Pergamon Press, Ltd., Oxford. M
- **Journal of Bacteriology.* American Society of Microbiology, Baltimore. M
- **Journal of Biological Chemistry.* American Society of Biological Chemists, Baltimore. M
- Journal of Biomechanics.* Pergamon Press, Ltd., Oxford. Q
- **Journal of Catalysis.* Academic Press, Inc., New York. BM
- **Journal of Cellular Physiology.* Wistar Institute of Anatomy and Biology, Philadelphia. BM
- Journal of Chemical Physics.* American Institute of Physics, Inc., New York. SM
- Journal of Chromatographic Science* (formerly *Journal of Gas Chromatography*). Preston Technical Abstracts Co., Evanston, Ill. M
- **Journal of Chromatography.* Elsevier Publishing Co., Amsterdam. M
- **Journal of Colloid and Interface Science.* Academic Press, Inc., New York. M
- **Journal of Comparative and Physiological Psychology.* American Psychological Association, Inc., Washington, D.C. BM
- Journal of Composite Materials.* Technomic Publishing Co., Inc., Stamford, Conn. Q
- Journal of Computational Physics.* Academic Press, Inc., New York. Q
- Journal of Computer and System Sciences.* Academic Press, Inc., New York. Q
- Journal of Differential Equations.* Academic Press, Inc., New York. Q
- Journal of Engineering Mathematics.* P. Noordhoff, Ltd.,

INTERNATIONAL AEROSPACE ABSTRACTS

- Groningen, Netherlands. Q
- Journal of Engineering Physics (Inzhenerno-Fizicheskii Zhurnal)*. The Faraday Press, Inc., New York. M
- Journal of Environmental Sciences*. Institute of Environmental Sciences, Mt. Prospect, Ill. BM
- **Journal of Experimental Psychology*. American Psychological Association, Washington, D.C. M
- Journal of Fluid Mechanics*. Cambridge University Press, London. M
- **Journal of Gas Chromatography* (see *Journal of Chromatographic Science*).
- **Journal of General Microbiology*. Society for General Microbiology; Cambridge University Press, London.
- **Journal of Geology*. University of Chicago Press, Chicago. BM
- Journal of Geomagnetism and Geoelectricity*. Society of Terrestrial Magnetism and Electricity; Kyoto University, Geophysical Institute, Kyoto, Japan. Q
- Journal of Geophysical Research*. American Geophysical Union, Washington, D.C. SM
- **Journal of Gerontology*. Gerontological Society, St. Louis, Mo. Q
- Journal of Heterocyclic Chemistry*. Albuquerque, New Mexico. Q
- **Journal of Higher Education*. Ohio State University Press, Columbus, Ohio. M
- Journal of Hydronautics*. American Institute of Aeronautics and Astronautics, Inc., New York. Q
- **Journal of Invertebrate Pathology*. Academic Press, Inc., New York. Q
- **Journal of Macromolecular Science, Series A - Chemistry*. Marcel Dekker, New York. Q
- **Journal of Macromolecular Science, Series B - Physics*. Marcel Dekker, New York. Q
- **Journal of Macromolecular Science, Part C - Reviews of Macromolecular Chemistry*. Marcel Dekker, New York. Q
- Journal of Materials*. American Society for Testing and Materials, Philadelphia. Q
- Journal of Materials Science*. Chapman & Hall, Ltd., London. BM
- Journal of Mathematical Analysis and Applications*. Academic Press, Inc., New York. M
- **Journal of Mathematical and Physical Sciences*. Indian Institute of Technology, Madras, India.
- Journal of Mathematical Physics*. American Institute of Physics, Inc., New York. M
- Journal of Mathematics and Mechanics*. Indiana University, Dept. of Mathematics, Bloomington, Ind. M
- Journal of Mathematics and Physics* (see *Studies in Applied Mathematics*).
- Journal of Mechanical Engineering Science*. Institution of Mechanical Engineers, London. 5 issues per year
- Journal of Metals*. American Institute of Mining, Metallurgical and Petroleum Engineers, Inc., New York. M
- Journal of Microwave Power*. International Microwave Power Institute, Vancouver. Q
- **Journal of Molecular Biology*. Academic Press, Inc., New York. M
- **Journal of Molecular Spectroscopy*. Academic Press, Inc., New York. M
- **Journal of Neurochemistry*. Pergamon Press, Ltd., Oxford. M
- **Journal of Nuclear Medicine*. Society of Nuclear Medicine, Chicago. M
- **Journal of Nutrition*. American Institute of Nutrition; Wistar Institute of Anatomy and Biology, Philadelphia. M
- Journal of Occupational Medicine*. Industrial Medical Association, Pittsburgh. M
- Journal of Optimization Theory and Applications*. Plenum Press, New York. BM
- **Journal of Organic Chemistry*. American Chemical Society, Washington, D.C. M
- **Journal of Paint Technology*. Federation of Societies for Paint Technology, Philadelphia. M
- Journal of Paleontology*. Society of Economic Paleontologists and Mineralogists; Paleontological Society, Tulsa. BM
- **Journal of Pharmacology and Experimental Therapeutics*. American Society for Pharmacology and Experimental Therapeutics; Williams & Wilkins Co., Baltimore. M
- Journal of Photographic Science*. Royal Photographic Society of Great Britain, London. BM
- Journal of Physical Chemistry*. American Chemical Society, Washington, D.C. M
- Journal of Physics, Part A - Physical Society, Proceedings (General)*. Institute of Physics and The Physical Society, London. BM
- Journal of Physics, Part B - Atomic and Molecular Physics*. Institute of Physics and The Physical Society, London. M
- Journal of Physics, Part D - British Journal of Applied Physics*. Institute of Physics and The Physical Society, London. M
- Journal of Physics, Part E - Journal of Scientific Instruments*. Institute of Physics and The Physical Society, London. M
- **Journal of Physics and Chemistry of Solids*. Pergamon Press, Ltd., Oxford. M
- **Journal of Physics of the Earth*. Seismological Society of Japan, Geodetic Society of Japan, and the Volcanological Society of Japan, Tokyo. SA
- Journal of Plasma Physics*. Cambridge University Press, London. Q
- **Journal of Polymer Science, Part B - Polymer Letters*. Interscience Publishers, Inc., New York. M
- **Journal of Protozoology*. Society of Protozoologists, University of Illinois, Urbana. Q
- Journal of Quality Technology*. American Society for Quality Control, Inc., Milwaukee, Wis. Q
- **Journal of Quantitative Spectroscopy and Radiative Transfer*. Pergamon Press, Ltd., Oxford. Q
- Journal of Research, Section A - Physics and Chemistry*. National Bureau of Standards; Supt. of Documents, Washington, D.C. BM
- Journal of Research, Section B - Mathematical Sciences*. National Bureau of Standards; Supt. of Documents, Washington, D.C. BM
- Journal of Research, Section C - Engineering and Instrumentation*. National Bureau of Standards; Supt. of Documents, Washington, D.C. Q
- Journal of Science and Engineering Research*. Indian

- Institute of Technology, Kharagpur, West Bengal, India. SA
- Journal of Science and Technology* (formerly *GEC-AEI Journal of Science and Technology*). The General Electric and English Electric Companies Limited, London. Q
- Journal of Scientific and Industrial Research*. Council of Scientific and Industrial Research, New Delhi. M
- Journal of Sound and Vibration*. Academic Press, Inc., New York. BM
- Journal of Spacecraft and Rockets*. American Institute of Aeronautics and Astronautics, Inc., New York. M
- **Journal of Sports Medicine and Physical Fitness*. Fédération Internationale de Médecine Sportive; Edizioni Minerva Medica, Turin. Q
- Journal of Strain Analysis*. Joint British Committee for Stress Analysis; Institution of Mechanical Engineers, London. Q
- Journal of Systems Engineering*. Tinnon-Brown, Inc., Book Publishers, Los Angeles. Q
- Journal of Technology*. Bengal Engineering College, Howrah, India. Q
- Journal of the Astronautical Sciences*. American Astronautical Society, Inc., Washington, D.C. BM
- Journal of the Atmospheric Sciences*. American Meteorological Society, Boston. BM
- **Journal of the Experimental Analysis of Behavior*. Society for the Experimental Analysis of Behavior, Inc., Bloomington, Ind. Q
- Journal of the Less-Common Metals*. Elsevier Publishing Co., Amsterdam. M
- Journal of the Mechanics and Physics of Solids*. Pergamon Press, Ltd., Oxford. BM
- **Journal of Theoretical Biology*. Academic Press, Inc., New York. Q
- **Journal of Ultrastructure Research*. Academic Press, Inc., New York. 9 issues per year
- Journal of Vacuum Science and Technology*. American Vacuum Society; American Institute of Physics, Inc., New York. BM
- **Journal of Verbal Learning and Verbal Behavior*. Academic Press, Inc., New York. BM
- **Journal of Virology*. American Society for Microbiology; Williams and Wilkins, Baltimore, Md. BM
- JSME, Bulletin*. Japan Society of Mechanical Engineers, Tokyo. BM

K

- Kazanskii Aviatsionnyi Institut, Trudy, Raboty Aspirantov i Soiskatelei*. Kazanskii Aviatsionnyi Institut, Kazan. Irreg.
- Kazanskii Aviatsionnyi Institut, Trudy, Seriya Aviatsionnaia Tekhnologiya i Organizatsiya Proizvodstva*. Kazanskii Aviatsionnyi Institut, Kazan. Irreg.
- Kazanskii Aviatsionnyi Institut, Trudy, Seriya Matematika i Mekhanika*. Kazanskii Aviatsionnyi Institut, Kazan. Irreg.
- Kazanskii Aviatsionnyi Institut, Trudy, Seriya Prikladnaia Mekhanika*. Kazanskii Aviatsionnyi Institut, Kazan. Irreg.

- Kerntechnik*. Verlag Karl Thieme, KG, Munich. M
- Khar'kovskii Politekhnikeskii Institut, Vestnik, Preobrazovatel'naia Tekhnika*. Ministerstvo Vysshego i Srednego Spetsial'nogo Obrazovaniia USSR; Izdatel'stvo Khar'kovskogo Gosudarstvennogo Universiteta, Khar'kov. Irreg.
- Khimiia i Tekhnologiya Topliv i Masel*. Ministerstvo Neftepererabatyvaiushchei i Neftekhimicheskoi Promyshlennosti SSSR, Akademiia Nauk SSSR, and Nauchno-Tekhnicheskoe Obshchestvo Neftianoi i Gazovoi Promyshlennosti; Izdatel'stvo Khimiia, Moscow. M
- Kitt Peak National Observatory, Contribution*. Association of Universities for Research in Astronomy, Inc.
- **Kleinheubacher Berichte*. Fernmeldetechnisches Zentralamt der Deutschen Bundespost, Darmstadt. Irreg.
- **Kongelige Danske Videnskabernes Selskab, Matematisk-Fysiske Skrifter*. Munksgaard, Copenhagen. Irreg.
- Koninklijke Nederlandse Akademie van Wetenschappen, Proceedings, Series B - Physical Sciences*. North-Holland Publishing Co., Amsterdam. 5 issues per year
- Konstruktion* (see *Konstruktion im Maschinen-, Apparate und Gerätebau*).
- **Konstruktion im Maschinen-, Apparate- und Gerätebau*. Springer Verlag, Berlin. M
- Kosmicheskaya Biologiya i Meditsina*. Ministerstvo Zdravookhraneniia SSSR; Izdatel'stvo Meditsina, Moscow. BM
- Kosmicheskii Issledovaniia*. Akademiia Nauk SSSR, Moscow. BM
- Kovové Materiály*. Slovenská Akademia Vied, Bratislava. BM
- Kristallografiia*. Akademiia Nauk SSSR, Moscow. BM
- Krymskaia Astrofizicheskaia Observatoriia, Izvestiia*. BM
- Kybernetika*. Československá Akademie Ved, Prague. BM
- **Kyoto University, College of Science, Memoirs, Series A* (see *Kyoto University, Faculty of Science, Memoirs, Series - Physics, Astrophysics, Geophysics and Chemistry*).
- Kyoto University, Faculty of Engineering, Memoirs*. Kyoto University, Faculty of Engineering, Kyoto. Q
- Kyoto University, Faculty of Science, Memoirs, Series - Physics, Astrophysics, Geophysics and Chemistry* (formerly *Kyoto University, College of Science, Memoirs, Series A*). Kyoto University, Kyoto.
- Kyoto University, Institute of Astrophysics and Kwasan Observatory, Contributions*. Kyoto. Irreg.
- Kyushu University, Faculty of Engineering, Memoirs*. Kyushu University, Faculty of Engineering, Fukuoka, Japan. Q
- Kyushu University, Research Institute for Applied Mechanics, Reports*. Kyushu University, Fukuoka, Japan. Irreg.

L

- Leningradskii Gosudarstvennyi Universitet, Astro-nomicheskaya Observatoriia, Trudy*. Leningradskii

INTERNATIONAL AEROSPACE ABSTRACTS

- Gosudarstvennyi Universitet, Leningrad.
Leningradskii Universitet, Vestnik, Matematika, Mekhanika, Astronomiia. Leningradskii Universitet, Leningrad. Q
Lietuvos Fizikos Rinkiny. Akademiia Nauk Litovskoi SSR, Vilnius. Q
Lietuvos Matematikos Rinkiny. Akademiia Nauk Litovskoi SSR, Vilnius. Q
Life Sciences. Pergamon Press, Ltd., Oxford. BW
Lockheed-Georgia Quarterly. Lockheed-Georgia Co., Marietta, Ga. Q
Lockheed Horizons. Lockheed-California Co., Burbank, Calif.
Lubrication Engineering. American Society of Lubrication Engineers, Park Ridge, Ill. M
Luftfahrttechnik Raumfahrttechnik. Verlag Deutscher Ingenieure, Düsseldorf. M

M

- Machine Design.** Penton Publishing Co., Cleveland. BW
***Macromolecules.** American Chemical Society, Washington, D.C. BM
Magnetohydrodynamics (Magnitnaia Gidrodinamika). The Faraday Press, Inc., New York. Q
Magnitnaia Gidrodinamika. Akademiia Nauk Latvinskoi SSR, Riga. Q
Management Services. American Institute of Certified Public Accountants, New York. BM
Marconi Review. Marconi Co., Ltd., Chelmsford, Essex, England. Q
Mashinostroenie. Izdanie Moskovskogo Vysshogo Tekhnicheskogo Uchilishcha imeni N. E. Bauman, Moscow. M
Matematicheskii Sbornik. Akademiia Nauk SSSR and Moskovskoe Matematicheskoe Obshchestvo; Izdatel'stvo Nauka, Moscow. M
Matematichki Vesnik. Institut Mathématique, Belgrade. Q
Matematika. Kazanskii Gosudarstvennyi Universitet, Kazan. M
Materials Evaluation. Society for Nondestructive Testing, Evanston, Ill. M
Materials Protection. National Association of Corrosion Engineers, Inc., Houston. M
Materials Research and Standards. American Society for Testing and Materials, Philadelphia. M
Materials Research Bulletin. Pergamon Press, Ltd., Oxford. M
Materials Science and Engineering. Elsevier Publishing Co., Amsterdam. BM
Mathematics of Computation. American Mathematical Society, Providence. Q
***Mathematische Zeitschrift.** Springer Verlag, Berlin. 4 vols. per year
Max-Planck-Institut für Aeronomie, Mitteilungen. Springer Verlag, Berlin. Irreg.
Measurement and Control. Institute of Measurement and Control, London. M
Meccanica. Italian Association of Theoretical and Applied Mechanics; Tamburini Editore, Milan. Q

- Mechanical Engineering.** American Society of Mechanical Engineers, New York. M
Mechanics of Solids (Inzhenernyi Zhurnal - Mekhanika Tverdogo Tela) (formerly *Soviet Engineering Journal /Inzhenernyi Zhurnal/*). The Faraday Press, Inc., New York. BM
Mechanika Teoretyczna i Stosowana. Polskie Towarzystwo Mechaniki Teoretycznej i Stosowanej; Państwowe Wydawnictwo Naukowe, Warsaw. Q
Medical and Biological Engineering. International Federation for Medical and Biological Engineering; Pergamon Press, Ltd., Oxford. BM
Medical Research Engineering. Medical Research Technology, Little Falls, N.J. Q
Mekhanika Polimerov. Akademiia Nauk Latvinskoi SSR, Riga. BM
Mérés és Automatika. Budapest. M
Messerschmitt-Bölkow Mitteilungen. Messerschmitt-Bölkow GmbH, Munich. Irreg.
Messtechnik. Friedr. Vieweg & Sohn GmbH, Braunschweig. M
Metal Construction and British Welding Journal (formerly *British Welding Journal*). The Welding Institute, London. M
Metal Progress. American Society for Metals, Metals Park, Ohio. M
Metal Science and Heat Treatment (Metallovedenie i Termicheskaiia Obrabotka Metallov). Consultants Bureau, New York. BM
Metallovedenie i Termicheskaiia Obrabotka Metallov. Ministerstvo Tiazhelogo Mashinostroeniia and Tsentral'nyi Nauchno-Issledovatel'skii Institut Tekhnologii i Mashinostroeniia, Moscow. M
Metals Engineering Quarterly. American Society for Metals, Metals Park, Ohio. Q
Metalscope. Brooks & Perkins, Inc., Detroit. Q
Meteor-Forschungsergebnisse, Reihe B — Meteorologie und Aeronomie. Gebrüder Borntraeger, Berlin. Irreg.
Meteoritics. Meteoritical Society, New Haven, Conn. Irreg.
Meteoritika. Akademiia Nauk SSSR, Komitet po Meteoritam; Izdatel'stvo Nauka, Moscow. Irreg.
Meteorological Magazine. Meteorological Office; Her Majesty's Stationery Office, London. M
Meteorological Society of Japan, Journal. Japan Publications Trading Co., Tokyo. BM
***Meteorologiya i Gidrologiia.** Glavnoe Upravlenie Gidrometeorologicheskoi Sluzhby SSSR, Moscow. M
Meteorologische Abhandlungen. Freie Universität Berlin, Institut für Meteorologie und Geophysik; Verlag Dietrich Reimer, Berlin. Q
Meteorologische Rundschau. Springer Verlag, Berlin. BM
Microelectronics and Reliability. Pergamon Press, Ltd., Oxford. Q
Microwave Journal. Horizon House, Inc., Dedham, Mass. M
Microwaves. Hayden Microwaves Corp., New York. M
Middle East Technical University Journal of Pure and Applied Sciences. Middle East Technical University, Ankara. 3 issues per year
***Mikrochimica Acta.** Springer Verlag, Vienna. BM
Milano, Seminario Matematico e Fisico, Rendiconti.

- Milano, Università, Milan. Annual
- Missili e Spazio*. Associazione Italiana Razzi, Rome. BM
- Mitsubishi Denki Laboratory Reports*. Mitsubishi Electric Corp., Central Research Laboratories, Amagasaki, Kyogo Prefecture, Japan.
- Mitsubishi Heavy Industries Technical Review (English Edition)*. Mitsubishi Heavy Industries, Ltd., Tokyo.
- **MNASSA*. Astronomical Society of Southern Africa, Cape Town. M
- **Molecular Physics*. Taylor & Francis, Ltd., London. M
- Monthly Weather Review*. U.S. Weather Bureau, Washington, D.C. M
- **Moskovskii Universitet, Gosundarstvennyi Astronomicheskii Institut, Trudy*. Moskovskii Universitet, Moscow.
- Moskovskii Universitet, Vestnik, Seriya I — Matematika, Mekhanika*. Moskovskii Universitet, Moscow. BM
- Moskovskii Universitet, Vestnik, Seriya III — Fizika, Astronomiia*. Moskovskii Universitet, Moscow. BM
- Motorola Monitor*. Motorola Semiconductor Products, Inc., Phoenix. BM
- Mullard Technical Communications*. Mullard, Ltd., London. Irreg.

N

- Nachrichtentechnische Zeitschrift*. Nachrichtentechnische Gesellschaft; Friedr. Vieweg & Sohn GmbH, Braunschweig. M
- Nagoya University, Faculty of Engineering, Memoirs*. Nagoya University, Nagoya. Irreg.
- Nagoya University, Research Institute of Atmospheric, Proceedings*. Nagoya University, Nagoya. Irreg.
- Napoli, Istituto Universitario Navale, Annali*. Naples. Annual
- **National Academy of Sciences, Proceedings*. National Academy of Sciences, Washington, D.C. M
- **National Contract Management Journal*. National Contract Management Association, Inglewood, Calif. SA
- National Institute of Sciences of India, Proceedings*. Bahadur Shah Zafar Marg, New Delhi. BM
- Nature*. Macmillan & Co., Ltd., London. W
- **Naturwissenschaften*. Max-Planck-Gesellschaft zur Förderung der Wissenschaften; Springer Verlag, Berlin. SM
- **Naturwissenschaftliche Rundschau*. Wissenschaftliche Verlagsgesellschaft mbH, Stuttgart. M
- Naval Research Logistics Quarterly*. U.S. Navy, Office of Naval Research; Supt. of Documents, Washington, D.C. Q
- Naval Research Reviews*. U.S. Navy, Office of Naval Research; Supt. of Documents, Washington, D.C. M
- Navigation*. Institute of Navigation, Washington, D.C. Q
- Navigation* (Paris). Institut Français de Navigation, Paris. Q
- NEC Research and Development*. Nippon Electric Co., Ltd., Tokyo. SA
- Neue Physik*. Verlag Neue Physik, Vienna. 4 issues per year
- **Neues Jahrbuch für Geologie und Paläontologie, Monatshefte*. Schweizerbart'sche Verlagsbuchhandlung, Stuttgart. M

- **New England Journal of Medicine*. Massachusetts Medical Society, Boston. W
- New Scientist*. New Science Publications, Ltd., London. W
- New York Academy of Sciences, Annals*. New York Academy of Sciences, New York. Irreg.
- New York Academy of Sciences, Transactions, Series 2*. New York Academy of Sciences, New York. 8 issues per year
- New Zealand Journal of Science*. Department of Scientific and Industrial Research, Wellington, New Zealand. Q
- Nihon University, Research Institute of Science and Technology, Journal*. Nihon University, Tokyo. Irreg.
- NLL Translation Bulletin*. National Lending Library for Science and Technology, Boston Spa, Yorks., England. M
- Non-Ionizing Radiation*. Iliffe Science and Technology Publications, Ltd., Guildford, Surrey, England. Q
- **Nordisk Tidsskrift for Informationsbehandling*. Regnecentralen, Copenhagen. Q
- Nordrhein-Westfalen, Forschungsberichte*. Westdeutscher Verlag, Cologne. Irreg.
- **Notre Dame Lawyer*. Notre Dame, Ind. Irreg.
- NTZ-Communications Journal*. Friedr. Vieweg & Sohn GmbH, Braunschweig. BM
- Nuclear Applications* (see *Nuclear Applications and Technology*).
- Nuclear Applications and Technology* (formerly *Nuclear Applications*). American Nuclear Society, Inc., Hinsdale, Ill. M
- Nuclear Engineering and Design*. North-Holland Publishing Co., Amsterdam. BM
- Nuclear Fusion*. International Atomic Energy Agency, Vienna. Q
- Nuclear Instruments and Methods*. North-Holland Publishing Co., Amsterdam. M
- **Nuclear Physics*. North-Holland Publishing Co., Amsterdam. BW
- Nuclear Science and Engineering*. American Nuclear Society, Inc., Hinsdale, Ill. M
- Nukleonika*. Polska Akademia Nauk, Komitet do Spraw Pokojowego Wykorzystania Energii Jądrowej, Warsaw. M
- Numerische Mathematik*. Springer Verlag, Berlin. Irreg.
- Nuovo Cimento*. Società Italiana di Fisica, Bologna. 36 issues per year
- Nuovo Cimento, Lettere*. Società Italiana di Fisica, Bologna. 3 issues per month
- Nuovo Cimento, Rivista*. Società Italiana di Fisica, Bologna. Q
- Nuovo Cimento, Supplemento*. Società Italiana di Fisica, Bologna. Irreg.

O

- **Observatoire de Haute-Provence, Publications*. Saint-Michel, France. Irreg.
- Observatorio de Madrid, Boletín Astronómico*. Instituto Geográfico y Catastral, Madrid.
- Observatorios Tonantzintla y Tacubaya, Boletín*.

INTERNATIONAL AEROSPACE ABSTRACTS

- Universidad Nacional Autonoma de Mexico, Observatorio Astronomico, Mexico City. Irreg.
- The Observatory.* Royal Greenwich Observatory, Hailsham, Sussex, England. BM
- Obzornik za Matematiko in Fiziko.* Izdaja Drustvo Matematikov Fizikov in Astronomov SR Slovenije, Ljubljana, Yugoslavia. Q
- *Ole Rømer Observatoriet, Meddelelser.* Aarhus, Denmark. Irreg.
- L'Onde Electrique.* Société Française des Electroniciens et des Radioélectriciens; Editions Chiron S.A., Paris. M
- ONERA, TP.* Office National d'Etudes et de Recherches Aéropatiales, Chatillon-sous-Bagneux (Seine), France. Irreg.
- Optica Acta.* Taylor & Francis, Ltd., London. Q
- Optical Sciences Newsletter.* Optical Sciences Center, University of Arizona, Tucson. Irreg.
- Optical Society of America, Journal.* Optical Society of America, Inc., Washington, D.C. M
- Optical Spectra.* Optical Publishing Co., Inc., Pittsfield, Mass. Q
- Optics and Spectroscopy (Optika i Spektroskopiia).* Optical Society of America, Inc., Washington, D.C. M
- Optics Communications.* North-Holland Publishing Co., Amsterdam. M
- Optika i Spektroskopiia.* Akademiia Nauk SSSR, Leningrad. M
- Oregon State University, Engineering Experiment Station, Bulletin.* Oregon State University, Corvallis, Ore.
- *Organic Mass Spectrometry.* Heyden & Son, Ltd., London.
- *Organizational Behavior and Human Performance.* Academic Press, Inc., New York. Q
- Osaka City University, Faculty of Engineering, Memoirs.* Osaka City University, Osaka.
- Osaka Prefecture, University, Bulletin, Series A — Engineering and Natural Sciences.* Osaka Prefecture, University, Osaka. Irreg.
- Osaka University, Technology Reports.* Osaka University, Osaka. SA
- Österreichische Akademie der Wissenschaften, Mathematisch-naturwissenschaftliche Klasse, Sitzungsberichte, Abteilung 2.* Österreichische Akademie der Wissenschaften; Springer Verlag, Vienna. Irreg.

P

- The Pacer.* Scranton, Pa. BM
- Pacific Journal of Mathematics.* Berkeley, Calif. M
- Papers in Meteorology and Geophysics.* Meteorological Research Institute, Tokyo. Q
- *Pennsylvania Academy of Science, Proceedings.* Pennsylvania Academy of Science, Harrisburg. SA
- *Perception and Psychophysics.* Psychonomic Press, Goleta, Calif. M
- *Perceptual and Motor Skills.* Southern Universities Press, Missoula, Mont. BM
- Periodica Polytechnica, Electrical Engineering Series.* Budapest, Polytechnical University, Budapest. Q
- Periodica Polytechnica, Engineering Series.* Budapest, Polytechnical University, Budapest. Q
- Perspective.* Cornell Aeronautical Laboratory, Inc., Buffalo, N.Y. Q
- Pflügers Archiv.* Springer Verlag, Berlin.
- *Pflügers Archiv für die gesamte Physiologie des Menschen und der Tiere* (see *Pflügers Archiv*).
- Philips Research Reports.* N.V. Philips' Gloeilampenfabrieken, Research Laboratories, Eindhoven. BM
- Philips Research Reports Supplements.* N. V. Philips' Gloeilampenfabrieken, Research Laboratories, Eindhoven. Irreg.
- Philips Technical Review.* N.V. Philips' Gloeilampenfabrieken, Research Laboratories, Eindhoven. M
- Philosophical Magazine, 8th Series.* Taylor & Francis, Ltd., London. M
- Photochemistry and Photobiology.* Pergamon Press, Ltd., Oxford. M
- Photogrammetria.* Elsevier Publishing Co., Amsterdam. BM
- Photogrammetric Engineering.* American Society of Photogrammetry, Falls Church, Va. M
- Photographic Science and Engineering.* Society of Photographic Scientists and Engineers, Washington, D.C. BM
- Physica.* Physica Foundation, Amsterdam; Martinus Nijhoff, The Hague. Irreg.
- Physica Status Solidi.* Akademie Verlag GmbH, Berlin. M
- Physical Review, 2nd Series.* American Institute of Physics, Inc., New York. 60 issues per year
- Physical Review Letters.* American Institute of Physics, Inc., New York. SM
- Physical Society of Japan, Journal.* Physical Society of Japan, Tokyo. M
- Physics Letters.* North-Holland Publishing Co., Amsterdam. W
- Physics of Fluids.* American Institute of Physics, Inc., New York. M
- Physics of Metals and Metallography (Fizika Metallov i Metallovedenie).* Pergamon Press, Ltd., Oxford. M
- Physics of the Earth and Planetary Interiors.* North-Holland Publishing Co., Amsterdam. BM
- Physics Today.* American Institute of Physics, Inc., New York. M
- Physikalische Blätter.* Physik Verlag GmbH, Mosbach, Germany. M
- Physiologia Plantarum.* Scandinavian Society for Plant Physiology, Copenhagen. 4 vols. per year
- *Physiological Reviews.* American Physiological Society, Bethesda, Md. Q
- *Physiology and Behavior.* Pergamon Press, Ltd., Oxford. Q
- Pisa, Scuola Normale Superiore, Annali, Scienze Fisiche e Matematiche.* Pisa, Scuola Normale Superiore, Pisa. Q
- Planetarium.* Planet Publications, London. Q
- Planetary and Space Science.* Pergamon Press, Ltd., Oxford. M
- Planseeberichte für Pulvermetallurgie.* Reutte, Austria. 3 issues per year
- *Plant Physiology.* American Society of Plant Physiology, Washington, D.C. BM
- *Planta.* Springer Verlag, Berlin. Q

Plasma Physics. Pergamon Press, Ltd., Oxford. BM

PMM — Journal of Applied Mathematics and Mechanics (Prikladnaia Matematika i Mekhanika). Pergamon Press, Ltd., Oxford. BM

PMTF — Zhurnal Prikladnoi Mekhaniki i Tekhnicheskoi Fiziki. Akademiia Nauk SSSR, Sibirskoe Otdelenie, Novosibirsk. BM

Point to Point Telecommunications. Marconi Co., Ltd., Communications Division, Chelmsford, England. Q

Pokroky Matematiky, Fysiky a Astronomie. Československôa Akademie Véd, Prague. BM

Politechnika Czeŝochowska, Zeszyty Naukowe, Mechanika. Politechnika Czeŝochowska, Czeŝochowa, Poland. Irreg.

Politechnika Œlaska, Zeszyty Naukowe, Matematyka - Fyzyka. Politechnika Œlaska, Gliwice. Irreg.

Politechnika Œlaska, Zeszyty Naukowe, Mechanika. Politechnika Œlaska, Gliwice, Poland. Irreg.

Politechnika Warszawska, Prace Naukowe, Mechanika. Wydawnictwa Politechniki Warszawskiej, Warsaw. Irreg.

Politechnika Warszawska, Zeszyty Naukowe, Matematyka. Wydawnictwo Politechniki Warszawskiej, Warsaw. Irreg.

Politechnika Warszawska, Zeszyty Naukowe, Mechanika. Politechnika Warszawska, Warsaw. Irreg.

Polska Akademia Nauk, Instytut Automatyki, Prace. Polska Akademia Nauk, Warsaw.

**Polymer Engineering and Science*. Society of Plastics Engineers, Stamford, Conn. Q

Pomiary, Automatyka, Kontrola. Naczelna Organizacja Techniczna, Warsaw. M

Poroshkovaia Metallurgii. Akademiia Nauk Ukrainskoi SSR, Kiev. BM

Postępy Astronomii. Polskie Towarzystwo Astronomiczne; Państwowe Wydawnictwo Naukowe, Warsaw. Q

Postępy Astzonautyki. Polskie Towarzystwo Astronautyczne, Lodz. Q

Postępy Fyzyki. Polskie Towarzystwo Fizyczne; Państwowe Wydawnictwo Naukowe, Warsaw. BM

Powder Technology. Elsevier Publishing Co., Amsterdam. BM

Priboroŝtroenie. Leningradskii Institut Tochnoi Mekhaniki i Optiki, Leningrad. M

Pribory i Tekhnika Eksperimenta. Akademiia Nauk SSSR, Moscow. BM

Prikladnaia Matematika i Mekhanika. Akademiia Nauk SSSR, Otdelenie Tekhnicheskikh Nauk, Institut Mekhaniki, Moscow. BM

Prikladnaia Mekhanika. Akademiia Nauk Ukrainskoi SSR, Otdelenie Matematiki, Mekhaniki i Kibernetiki, Kiev. M

**Priroda*. Akademiia Nauk SSSR, Moscow. M

Priboroŝtroenie (Kiev). Ministerstvo Vysshego i Srednego Spetsial'nogo Obrazovaniia USSR; Izdatel'stvo Tekhnika, Kiev. Irreg.

Problemy Bioniki. Khar'kovskii Gosudarstvennyi Universitet, Kharkov. Irreg.

Problemy Peredachi Informatsii. Akademiia Nauk SSSR; Izdatel'stvo Nauka, Moscow. Q

Proceedings of Vibration Problems. Polska Akademia Nauk; Państwowe Wydawnictwo Naukowe, Warsaw. Q

Progress of Theoretical Physics. Research Institute for Fundamental Physics and The Physical Society of Japan; Kyoto University, Kyoto, Japan. M

Przegląd Elektoniki. Polska Akademia Nauk, Komitet Elektoniki i Telekomunikacji and Stowarzyszenie Elektrykow Polskich, Sekcja Elektoniki i Telekomunikacji, Warsaw. M

**Psychological Bulletin*. American Psychological Association, Washington, D.C. M

**Psychological Reports*. American Psychological Association, Washington, D.C.; Southern Universities Press, Missoula, Mont. BM

**Psychonomic Science*. Goleta, Calif. M

Public Administration Review. American Society for Public Administration, Washington, D.C. BM

Pulkovo, Glavnaia Astronomicheskaiia Observatoriia, Izvestiia. Izdanie Glavnoi Astronomicheskoi Observatorii, Leningrad. Irreg.

Pure and Applied Geophysics. Birkhäuser Verlag, Basel. 3 issues per year

Pyrodynamics. Gordon and Breach Science Publishers, Inc., New York. Q

Q

Quality Progress. American Society for Quality Control, Inc., Milwaukee. M

Quarterly of Applied Mathematics. Brown University, Providence. Q

Quarterly Journal of Mechanics and Applied Mathematics. Oxford University Press, London. Q

R

**Radiation Research Supplement*. Academic Press, Inc., New York. M

Radio and Electronic Engineer. British Institute of Radio Engineers, London. M

Radio Engineering and Electronic Physics (Radiotekhnika i Elektronika). Institute of Electrical and Electronics Engineers, Inc., New York. M

Radio Research Laboratories, Journal. Ministry of Posts and Telecommunications, Radio Research Laboratories, Tokyo. BM

Radio Research Laboratories, Review. Ministry of Posts and Telecommunications, Radio Research Laboratories, Tokyo. 4 issues per year

Radio Science. Environmental Science Services Administration; Supt. of Documents, Washington, D.C. M

Radioelektronika. Ministerstvo Vysshego Obrazovaniia, Kiev. M

Radiofizika. Gor'kovskii Universitet, Gorki. M

**Radiology*. Radiological Society of North America, Syracuse. M

Radiotekhnika. Nauchno-Tekhnicheskoe Obshchestvo Radiotekhniki i Elektrosviazi, Moscow. M

Radiotekhnika i Elektronika. Akademiia Nauk SSSR, Moscow. M

Raumfahrtforschung. Deutsche Gesellschaft für Rake-

INTERNATIONAL AEROSPACE ABSTRACTS

- tentechnik und Raumfahrt, e.V., Stuttgart. Q
- RCA Review*. RCA Laboratories, Princeton, N.J. Q
- La Recherche Aérospatiale*. Office National d'Etudes et de Recherches Aérospatiales, Chatillon-sous-Bagneux (Seine), France. BM
- La Recherche Spatiale*. Centre National d'Etudes Spatiales; Dunod Editeur, Paris. M
- Remote Sensing of Environment*. American Elsevier Publishing Co., Inc., New York. Q
- Report of Ionosphere and Space Research in Japan*. Science Council of Japan, Ionosphere Research Committee, Tokyo. Q
- Research/Development*. F. D. Thompson Publications, Inc., Chicago. M
- Research Management*. Wiley-Interscience, Inc., New York. BM
- Research Trends*. Cornell Aeronautical Laboratory, Inc., Buffalo. Q
- Respiration Physiology*. North-Holland Publishing Co., Amsterdam. 5 issues per year
- Review of Scientific Instruments*. American Institute of Physics, Inc., New York. M
- Reviews of Geophysics*. American Geophysical Union, Washington, D.C. Q
- Reviews of Modern Physics*. American Physical Society; American Institute of Physics, Inc., New York. Q
- Revista de Aeronáutica y Astronáutica*. Ministerio del Aire, Madrid. M
- Revista Transporturilor*. Ministerul Transporturilor Auto, Navale si Aeriene and Consiliul National al Inginerilor si Technicienilor, Bucharest. M
- Revue de Médecine Aéronautique et Spatiale*. Société Française de Physiologie et de Médecine Aéronautique et Cosmonautique; Masson et Cie., Paris. Q
- Revue de Métallurgie*. Paris. M
- Revue de Physique Appliquée*. Société Française de Physique and Centre National de la Recherche Scientifique, Paris. Q
- Revue des Corps de Santé des Armées*. Centre de Recherches du Service de Santé, Paris. BM
- Revue d'Optique*. Institut d'Optique Théorique et Appliquée and Syndicat Général de l'Optique et des Instruments de Précision, Paris. M
- Revue Energie Primaire*. Union des Ingénieurs de Louvain, Brussels. Q
- Revue Française de Droit Aérien*. Société Française de Droit Aérien, Paris. Q
- Revue Française de Mécanique*. Société Française des Mécaniciens, Paris. Q
- Revue Générale de l'Air et de l'Espace*. Editions Internationales, Paris. Q
- Revue Générale de l'Electricité*. Comité Electrotechnique Français et de l'Union Technique de l'Electricité, Paris. M
- Revue Générale de Thermique*. Institut Français des Combustibles et de l'Energie and Société Française des Thermiciens, Paris. M
- Revue Internationale des Hautes Températures et des Réfractaires*. Société Nationale Française des Hautes Températures et des Réfractaires; Masson & Cie., Paris. Q
- Revue mble*. Société Anonyme MBL, Brussels. Q
- Revue Roumaine de Mathématiques Pures et Appliquées*. Académie de la République Socialiste Roumaine, Bucharest. 10 issues per year
- Revue Roumaine de Physique*. Académie de la République Socialiste Roumaine, Bucharest. BM
- Revue Roumaine des Sciences Techniques, Série de Mécanique Appliquée*. Académie de la République Socialiste Roumaine, Bucharest. BM
- Revue Technique CECLES* (see *Revue Technique CECLES/CERS*).
- Revue Technique CECLES/CERS* (formerly *Revue Technique CECLES*). Gauthier-Villars & Cie., Paris. Q
- Revue Technique Thomson - CSF* (formerly *Annales de Radioélectricité*). Thomson - CSF, Service de Documentation Technique, Versailles, France. Q
- Ricerca Scientifica*. Consiglio Nazionale delle Ricerche, Rome. M
- Ricerche Astronomiche*. Specola Vaticana, Vatican City.
- Rivista Aeronautica*. Ministero Difesa Aeronautica, Rome. M
- Rivista di Ingegneria*. Editore Ulrico Hoepli, Milan. M
- Rivista di Medicina Aeronautica e Spaziale*. Rome. Q
- Rivista di Meteorologia Aeronautica*. Servizio Meteorologico d'Aeronautica, Rome. Q
- Rolls-Royce Journal*. Rolls-Royce, Ltd., Bristol Engine Division, Bristol.
- Roma, Osservatorio Astronomico, Contributi Scientifici*. Osservatorio Astronomico, Rome. Irreg.
- Royal Astronomical Society, Memoirs*. Royal Astronomical Society, London; Blackwell Scientific Publications, Oxford. Irreg.
- Royal Astronomical Society, Monthly Notices*. Royal Astronomical Society, London; Blackwell Scientific Publications, Oxford. M
- Royal Astronomical Society, Quarterly Journal*. Royal Astronomical Society, London; Blackwell Scientific Publications, Oxford. Q
- Royal Astronomical Society of Canada, Journal*. Royal Astronomical Society of Canada, Toronto. BM
- Royal Meteorological Society, Quarterly Journal*. Royal Meteorological Society, London. Q
- Royal Observatory Bulletins*. Royal Greenwich Observatory, Herstmonceux; Royal Observatory, Cape of Good Hope; H.M.S. Office, London. Irreg.
- Royal Society (Edinburgh), Proceedings, Section A*. Royal Society of Edinburgh, Edinburgh. Irreg.
- Royal Society (London), Philosophical Transactions, Series A*. Royal Society, London. Irreg.
- Royal Society (London), Proceedings, Series A*. Royal Society, London. Irreg.
- Rozprawy Inżynierskie*. Polska Akademia Nauk, Instytut Podstawowych Problemów Techniki; Państwowe Wydawnictwo Naukowe, Warsaw. Q
- Ruimtevaart*. Nederlandse Vereniging voor Ruimtevaart; Heemstede, Netherlands. Q
- Russian Engineering Journal (Vestnik Mashinostroeniia)*. Production Engineering Research Association of Great Britain, Melton Mowbray, Leics., England. M
- Russian Journal of Physical Chemistry (Zhurnal Fizicheskoi Khimii)*. Chemical Society, London. M
- Russian Mathematical Surveys (Uspekhi Matematicheskikh Nauk)*. London Mathematical Society; Macmillan & Co., Ltd., London. BM
- Ryan Reporter*. Ryan Aeronautical Co., San Diego. Q

S

- Safe Engineering.** Survival and Flight Equipment Engineers Society, Los Angeles. BM
- SAIT Electronics Review.** SAIT Electronics, Brussels. Q
- SAMPE Journal.** Society of Aerospace Material and Process Engineers, Azusa, Calif. BM
- SAWE Journal.** Society of Aeronautical Weight Engineers, Inc., Los Angeles. Irreg.
- Schweizer Archiv** (see *Schweizer Archiv für angewandte Wissenschaft und Technik*).
- Schweizer Archiv für angewandte Wissenschaft und Technik.** Verlag Vogt-Schild AG, Solothurn, Switzerland. M
- Schweizerische Technische Zeitschrift.** Zurich. M
- Science.** American Association for the Advancement of Science, Washington, D.C. W
- Science and Technology.** Conover-Mast Publications, Inc., New York. M
- Science Journal.** Associated Iliffe Press, Ltd., London. M
- *Science of Light.** Kyoiku University, Institute for Optical Research, Tokyo. 3 issues per year
- Science Progress.** Edward Arnold (Publishers), Ltd., London. Q
- Sciences et Industries Spatiales.** SADESI — Société Anonyme d'Éditions Scientifiques et Industrielles, Geneva. BM
- Sciences et Techniques.** Société des Ingénieurs Civils de France, Paris. M
- Scientific American.** Scientific American, Inc., New York. M
- Scripta Metallurgica.** Pergamon Press, Ltd., Oxford. M
- Secrétariat Général à l'Aviation Civile, Revue.** Secrétariat Général à l'Aviation Civile, Paris. Irreg.
- *Sedimentology.** International Association of Sedimentologists; Elsevier Publishing Co., Amsterdam. 8 issues per year
- *Seismological Society of America, Bulletin.** Seismological Society of America; Waverly Press, Inc., Baltimore. BM
- Sheffield University Fuel Society Journal.** Dept. of Chemical Engineering and Fuel Technology, University of Sheffield, Sheffield. Annual
- Shell Aviation News.** Shell Oil Co., London. M
- SIAM Journal on Applied Mathematics.** Society for Industrial and Applied Mathematics, Philadelphia. BM
- SIAM Journal on Control.** Society for Industrial and Applied Mathematics, Philadelphia. Q
- SIAM Journal on Numerical Analysis.** Society for Industrial and Applied Mathematics, Philadelphia. Q
- SIAM Review.** Society for Industrial and Applied Mathematics, Philadelphia. Q
- Siberian Mathematical Journal (Sibirskii Matematicheskii Zhurnal).** Consultants Bureau, New York. BM
- Sibirskii Matematicheskii Zhurnal.** Akademiia Nauk SSSR, Sibirskoe Otdelenie, Novosibirsk. BM
- *SID Proceedings.** Western Periodicals Company, North Hollywood, Calif. Q
- Siemens Review.** Siemens und Halske AG, Erlangen, W. Germany. M
- Signal.** Armed Forces Communications and Electronics Association, Washington, D.C. M
- Simulation.** Simulation Councils, Inc., La Jolla, Calif. M
- Sky and Telescope.** Sky Publishing Corp., Cambridge, Mass. M
- Skyline.** North American Aviation, Inc., El Segundo, Calif. Q
- Slaboproudý Obzor.** Státní Nakladatelství Technické Literatúry, Prague. M
- SMPTE, Journal.** Society of Motion Picture and Television Engineers, Inc., New York. M
- Società Astronomica Italiana, Memorie.** Gia Società degli Spettroscopisti Italiani, Milan. Q
- Société Royale des Sciences de Liège, Bulletin.** Université de Liège, Liège. Irreg.
- Société Royale des Sciences de Liège, Mémoires.** Université de Liège, Liège. Q
- *Society for Experimental Biology and Medicine, Proceedings.** Society for Experimental Biology and Medicine, New York. 11 issues per year
- Society of Experimental Test Pilots, Technical Review.** Society of Experimental Test Pilots, Lancaster, Calif. SA
- *Society of Rheology, Transactions.** John Wiley & Sons, Inc., New York. SA
- *Soil Biology and Biochemistry.** Pergamon Press, Ltd., Oxford.
- *Soil Science Society of America, Proceedings.** Madison, Wis. BM
- Solar Energy.** Solar Energy Society, Arizona State University, Tempe; Pergamon Press, Ltd., Oxford. Q
- Solar Physics.** D. Reidel Publishing Co., Dordrecht, Netherlands. 8 issues per year
- Solar System Research (Astronomicheskii Vestnik).** Consultants Bureau, New York. Q
- *Solid-State Communications.** Pergamon Press, Ltd., Oxford. M
- Solid-State Electronics.** Pergamon Press, Ltd., Oxford. M
- Solid State Technology.** Cowan Publishing Corp., New York. M
- Soprotivlenie Materialov i Teoriia Sooruzhenii.** Izdatel'stvo Budivel'nik, Kiev. Irreg.
- Sound and Vibration.** Acoustical Publications, Inc., Cleveland, Ohio. M
- Soviet Aeronautics (Aviatsionnaia Tekhnika).** The Faraday Press, Inc., New York. Q
- Soviet Applied Mechanics (Prikladnaia Mekhanika).** The Faraday Press, Inc., New York. M
- Soviet Astronomy (Astronomicheskii Zhurnal).** American Institute of Physics, Inc., New York. BM
- Soviet Automatic Control (Avtomatika).** Institute of Electrical and Electronics Engineers, Inc., New York. Q
- Soviet Engineering Journal (Inzhenernyi Zhurnal)** (see *Mechanics of Solids /Inzhenernyi Zhurnal - Mekhanika Tverdogo Tela/*).
- Soviet Journal of Nondestructive Testing (Defektoskopiia).** Consultants Bureau, New York. BM
- Soviet Journal of Optical Technology (Optiko-Mekhanicheskaiia Promyshlennost').** Optical Society of America, Inc., Washington, D.C. BM
- Soviet Materials Science (Fiziko-Khimicheskaiia Mekhanika**

- Materialov*. The Faraday Press, Inc., New York. BM
- Soviet Mathematics (Akademiia Nauk SSSR, Doklady)*. American Mathematical Society, Providence, R.I. BM
- Soviet Physics — Acoustics (Akusticheskii Zhurnal)*. American Institute of Physics, Inc., New York. Q
- Soviet Physics — Crystallography (Kristallografiia)*. American Institute of Physics, Inc., New York. BM
- Soviet Physics — Doklady (Akademiia Nauk SSSR, Doklady)*. American Institute of Physics, Inc., New York. M
- Soviet Physics — JETP (Zhurnal Eksperimental'noi i Teoreticheskoi Fiziki)*. American Institute of Physics, Inc., New York. M
- Soviet Physics — Semiconductors (Fizika i Tekhnika Poluprovodnikov)*. American Institute of Physics, Inc., New York. M
- Soviet Physics — Solid State (Fizika Tverdogo Tela)*. American Institute of Physics, Inc., New York. M
- Soviet Physics — Technical Physics (Zhurnal Tekhnicheskoi Fiziki)*. American Institute of Physics, Inc., New York. M
- Soviet Physics — Uspekhi (Uspekhi Fizicheskikh Nauk)*. American Institute of Physics, Inc., New York. BM
- Soviet Physics Journal (Fizika)*. The Faraday Press, Inc., New York. BM
- Soviet Plastics (Plasticheskie Massy)*. Rubber and Technical Press, Ltd., London. M
- Soviet Powder Metallurgy and Metal Ceramics (Poroshkovaia Metallurgiiia)*. Consultants Bureau, New York. M
- Soviet Radiophysics (Radiofizika)*. The Faraday Press, Inc., New York. BM
- Space/Aeronautics*. Conover-Mast Publications, Inc., New York. M
- Space Life Sciences*. D. Reidel Publishing Co., Dordrecht, Netherlands. Irreg.
- Space Science Reviews*. D. Reidel Publishing Co., Dordrecht, Netherlands. 9 issues per year
- Spaceflight*. British Interplanetary Society, London. M
- SPARMO Bulletin*. Solar Particles and Radiation Monitoring Organization, Meudon, France. Q
- SPE Journal*. Society of Plastics Engineers, Inc., Stamford, Conn. M
- *Spectrochimica Acta*. Pergamon Press, Ltd., Oxford. M
- *Spectroscopy Letters*. Marcel Dekker, Inc., New York. M
- Sperry Rand Engineering Review*. Sperry Gyroscope Co., Great Neck, N.Y. Q
- SPIE-Glass*. Society of Photo-Optical Instrumentation Engineers, Redondo Beach, Calif. BM
- SPIE Journal*. Society of Photo-Optical Instrumentation Engineers, Redondo Beach, Calif. BM
- Srpska Akademija Nauka i Umetnosti, Glas, Odelenje Tekhnichkikh Nauka*. Srpska Akademija Nauka i Umetnosti; Nauchno Delo, Belgrade. Irreg.
- *Stain Technology*. Biological Stain Commission; Williams & Wilkins Co., Baltimore. BM
- Sterne und Weltraum*. Verlag Bibliographisches Institut AG, Mannheim. M

- Strain*. British Society for Strain Measurement, London. Q
- Studia Geophysica et Geodaetica*. Československá Akademie Věd, Prague. Q
- Studia Scientiarum Mathematicarum Hungarica*. Hungarian Academy of Sciences, Budapest. SA
- Studies in Applied Mathematics (formerly Journal of Mathematics and Physics)*. MIT Press, Cambridge, Mass. Q
- Studii și Cercetări de Astronomie*. Akademia Republicii Socialiste Române, Bucharest. SA
- Studii și Cercetări de Fizică*. Akademia Republicii Socialiste Române, Bucharest. 10 issues per year
- Studii și Cercetări de Mecanică Aplicată*. Akademia Republicii Socialiste Române, Bucharest. BM
- Studii și Cercetări Matematice*. Akademia Republicii Socialiste Române, Institutul de Matematica, Bucharest. 10 issues per year
- Surface Science*. North-Holland Publishing Co., Amsterdam. M
- System*. Messerschmitt-Bölkow GmbH, Munich.

T

- *Tamagawa University, Faculty of Engineering, Memoirs*. Tamagawa University, Tokyo.
- Tech Air*. Society of Licensed Aircraft Engineers and Technologists, Kingston-upon-Thames, England. M
- Technika Lotnicza i Astronautyczna*. Stowarzyszenie Inżynierów i Mechaników Polskich, Sekcja Lotnicza; Naczelna Organizacja Techniczna, Warsaw. M
- Technische Mitteilungen AEG-Telefunken*. AEG-Telefunken, Berlin. BM
- Technische Mitteilungen PTT*. Generaldirektion PTT, Bern. M
- *Technology and Culture*. Society for the History of Technology; University of Chicago Press, Chicago. Q
- Technology Review*. Massachusetts Institute of Technology, Cambridge, Mass. 9 issues per year
- Technometrics*. American Statistical Association, Washington, D.C. Q
- Tecnica Italiana*. Trieste. M
- Teknisk Tidskrift*. Svenska Teknologföreningen, Stockholm. W
- Telecommunication Journal*. Union Internationale des Telecommunications, Geneva. M
- Telecommunications*. Horizon House, Dedham, Mass. M
- Telecommunications and Radio Engineering. Part I — Telecommunications, Part II — Radio Engineering (Elektrosviaz', Radiotekhnika)*. Institute of Electrical and Electronics Engineers, Inc., New York. M
- Telemetry Journal*. International Foundation for Telemetry, Los Angeles. BM
- Tellus*. Svenska Geofysiska Föreningen, Stockholm. Q
- Teoriia Funktsii, Funktsional'nyi Analiz i ikh Prilozheniia*. Khar'kovskii Gosudarstvennyi Universitet, Kharkov. Irreg.
- Teoriia Veroiatnostei i ee Primeneniia*. Akademiia Nauk SSSR; Izdatel'stvo Nauka, Moscow. Q

U

Teplotfizika Vysokikh Temperatur. Akademiia Nauk SSSR, Moscow. BM

**Tetrahedron.* Pergamon Press, Ltd., Oxford. M

**Tetrahedron Letters.* Pergamon Press, Ltd., Oxford. W

Texas Journal of Science. Texas Academy of Science, Denton, Texas. Q

Theory of Probability and its Applications (Teoriia Veroiatnostei i ee Primeneniia). Society for Industrial and Applied Mathematics, Philadelphia. Q

**Therapeutische Berichte.* Interessengemeinschaft Farbenindustrie Aktiengesellschaft, Leverkusen, W. Germany.

Thin Solid Films. Elsevier Publishing Co., Amsterdam. BM

Tohoku University, Research Institute for Strength and Fracture of Materials, Reports. Tohoku University, Sendai. Irreg.

Tohoku University, Research Institute of Electrical Communication, Reports. Tohoku University, Sendai.

Tokyo, University, Earthquake Research Institute, Bulletin. Tokyo, University, Earthquake Research Institute, Tokyo. Q

Tokyo, University, Faculty of Engineering, Journal, Series A. Tokyo, University, Faculty of Engineering, Tokyo. Annual

Tokyo, University, Faculty of Engineering, Journal, Series B. Tokyo, University, Faculty of Engineering, Tokyo. Irreg.

Tokyo, University, Institute of Space and Aeronautical Science, Bulletin. Tokyo, University, Institute of Space and Aeronautical Science, Tokyo. Q

Tokyo, University, Institute of Space and Aeronautical Science, Report. Tokyo, University, Institute of Space and Aeronautical Science, Tokyo. Irreg.

Tokyo, University, Tokyo Astronomical Observatory, Annals, Second Series. Tokyo, University, Tokyo.

Tokyo Astronomical Observatory, Tokyo Astronomical Bulletin, Second Series. Tokyo Astronomical Observatory, Tokyo. Q

Tokyo Institute of Technology, Bulletin. Tokyo Institute of Technology, Tokyo. Irreg.

Tool and Manufacturing Engineer. American Society of Tool and Manufacturing Engineers, Dearborn, Mich. M

**Torino, Accademia delle Scienze, Atti.* Torino, Accademia delle Scienze, Turin. Irreg.

Toshiba Review. Tokyo Shibaura Electric Co., Ltd., Tokyo. Q

Trend in Engineering. Washington, University, Engineering Experiment Station, Seattle. Q

TRW Space Log. TRW Systems, Redondo Beach, Calif. Q

Tsvetnaia Metallurgii. Ministerstvo Vysshego i Srednego Spetsial'nogo Obrazovaniia; Severokavkazskii Gornometallurgicheskii Institut, Ordzhonikidze. BM

**Tucuman, Universidad Nacional, Revista, Serie A — Matematica y Fisica Teorica.* Tucuman, Argentina. Irreg.

Ukrainian Physics Journal (Ukrains'kii Fizichnii Zhurnal).

American Institute of Physics, Inc., New York. M

Ukrains'kii Fizichnii Zhurnal. Akademiia Nauk Ukrains'koi RSR, Kiev. M

Ukrainskii Matematicheskii Zhurnal. Akademiia Nauk Ukrainskoi SSR, Kiev. BM

Ultrasonics. Iliffe Scientific and Technical Publications, Guildford, Surrey, England. Q

Umschau in Wissenschaft und Technik. Umschau Verlag, Frankfurt/Main. SM

Unione Matematica Italiana, Bollettino. Nicola Zanichelli Editore, Bologna. Q

Universidad Industrial de Santander, Revista. Universidad Industrial de Santander, Bucaramanga, Colombia. SA

University of Electro-Communications, Reports. Tokyo. Irreg.

Urania (Madrid). Sociedad Astronómica de España y America, Barcelona; Union Nacional de Astronomia y Ciencias Afines, Madrid. SA

URSI Bulletin d'Information. URSI, Secrétaire Général, Brussels. BM

Uspekhi Fizicheskikh Nauk. Akademiia Nauk SSSR, Moscow. M

USSR Computational Mathematics and Mathematical Physics (Zhurnal Vychislitel'noi Matematiki i Matematicheskoi Fiziki). Pergamon Press, Ltd., Oxford. BM

V

**Vakuum-Technik.* Deutsche Arbeitsgemeinschaft Vakuum; Rudolf A. Long, Wiesbaden. 10 issues per year

VDI Zeitschrift. VDI-Verlag GmbH, Düsseldorf. 36 issues per year

Vectors. Hughes Aircraft Co., Culver City, Calif. Q

Verkehrsmedizin und ihre Grenzgebiete. Transpress VEB Verlag für Verkehrswesen, Berlin. M

Vertical World. Press-Tech, Inc., Evanston, Ill. M

VertiFlight. American Helicopter Society, Inc., New York. M

Vibrotechnika. Leidykla "Mintis," Vilnius. Irreg.

Le Vide. Société Française des Ingenieurs et Techniciens du Vide, Nogent-sur-Marne (Seine), France. BM

Vilnius, Astronomijos Observatorijos, Biuletenis. Vilnius. Irreg.

Vision Research. Pergamon Press, Ltd., Oxford. BM

Vychislitel'naia i Prikladnaia Matematika. Izdatel'stvo Kievskogo Universiteta, Kiev. Irreg.

W

Wärme- und Stoffübertragung. Lange & Springer, Berlin. Q

Wear. Elsevier Publishing Co., Amsterdam. M

- Wehr und Wirtschaft.* Munich. M
Wehrmedizinische Monatsschrift. J. F. Lehmanns Verlag, Munich. M
Welding Journal. American Welding Society, New York. M
Welding Production (Svarochnoe Proizvodstvo). British Welding Research Association, Cambridge. M
Weltraumfahrt Raketentechnik. Umschau Verlag, Frankfurt/Main. BM
**Western Economic Journal.* University of Utah, Salt Lake City, Utah. 3 issues per year
Westinghouse Engineer. Westinghouse Electric Corp., Pittsburgh. BM
Wissenschaftliche Berichte AEG-Telefunken. Allgemeine Elektrizitäts-Gesellschaft, Berlin. Q
Wissenschaftliche Zeitschrift. Dresden, Technische Universität, Dresden. BM

Y

- *Yale Scientific Magazine.* New Haven, Conn. M
Yamagata University, Bulletin (Engineering). Yamagata University, Yamagata, Japan.

Z

- Zagadnienia Drgán Nieliniowych.* Polska Akademia Nauk, Instytut Podstawowych Problemów Techniki; Państwowe Wydawnictwo Naukowe, Warsaw. Irreg.
**Zeitschrift für analytische Chemie.* Springer Verlag, Berlin.
Zeitschrift für angewandte Mathematik und Mechanik. Akademie-Verlag GmbH, Berlin. M
Zeitschrift für angewandte Mathematik und Physik. Birkhäuser Verlag, Basel. BM
Zeitschrift für angewandte Physik. Springer Verlag, Berlin. M
Zeitschrift für Astrophysik. Springer Verlag, Berlin. Irreg.
Zeitschrift für Flugwissenschaften. Deutsche Gesellschaft

- für Luft- und Raumfahrt, e.V., and Deutsche Gesellschaft für Flugwissenschaften, e.V.; Friedr. Vieweg & Sohn GmbH, Braunschweig. M
Zeitschrift für Geophysik. Deutsche geophysikalische Gesellschaft, Hamburg; Physica-Verlag, Würzburg. BM
Zeitschrift für Luftrecht und Weltraumrechtsfragen. Köln, Universität, Institut für Luftrecht und Weltraumrechtsfragen; Carl Heymanns Verlag, KG, Cologne. Q
Zeitschrift für Metallkunde. Deutsche Gesellschaft für Metallkunde, e.V.; Riederer-Verlag GmbH, Stuttgart. M
Zeitschrift für Meteorologie. Akademie-Verlag GmbH, Berlin. M
Zeitschrift für Naturforschung, Ausgabe A. Verlag der Zeitschrift für Naturforschung, Tübingen. M
Zeitschrift für Naturforschung, Teil b. Verlag der Zeitschrift für Naturforschung, Tübingen. M
Zeitschrift für Physik. Deutsche physikalische Gesellschaft; Springer Verlag, Berlin. Irreg.
Zeitschrift für Vermessungswesen. Deutscher Verein für Vermessungswesen; Verlag Konrad Wittwer, Stuttgart. M
**Zemlia i Vselennaia.* Akademiia Nauk SSSR, Prezidium, Sektsiia Fiziko-Tekhnicheskikh i Matematicheskikh Nauk; Mezhdunarodnaia Kniga, Moscow. BM
Zentralblatt für Verkehrs-Medizin, Verkehrs-Psychologie, Luft- und Raumfahrt-Medizin. J. F. Lehmanns Verlag, Munich. Irreg.
Zhurnal Eksperimental'noi i Teoreticheskoi Fiziki. Akademiia Nauk SSSR, Moscow. M
Zhurnal Nauchnoi i Prikladnoi Fotografii i Kinematografii. Akademiia Nauk SSSR, Moscow. BM
Zhurnal Prikladnoi Spektroskopii. Akademiia Nauk Belorusskoi SSR, Institut Fiziki, Minsk. M
Zhurnal Tekhnicheskoi Fiziki. Akademiia Nauk SSSR, Moscow. M
Zhurnal Vychislitel'noi Matematiki i Matematicheskoi Fiziki. Akademiia Nauk SSSR, Moscow. BM
Zpráva VZLÚ. Výzkumný a Zkusební Letecký Ústav, Prague. Irreg.
Zpravodaj VZLÚ. Výzkumný a Zkusební Letecký Ústav, Prague. BM

A Notation of Content, rather than the title of the publication, appears under each subject heading; it is listed under several subject headings which provide multiple access to the subject content of each accession. The IAA accession number is located under and to the right of the Notation of Content. It is preceded by numbers identifying the issue and page of *International Aerospace Abstracts* where the abstract is located.

To illustrate:

Issue Number	Page Number	Accession Number
01	p0006	A69-11016

A

A STARS

Hydrogen alpha line strength in 951 O, B and early A stars from narrow band photoelectric measurements for stellar luminosity

03 p0511 A69-13435

Evolution of close spectroscopic binaries and Am stars

05 p0822 A69-15855

Element abundances in two horizontal branch A stars through coarse and fine spectroscopic analysis, noting metal deficiencies with respect to sun

08 p1385 A69-20061

Curve-of-growth abundance analysis for main sequence lambda Bootis stars, suggesting type Ap star characteristics

08 p1385 A69-20062

Brightness in blue light and radial velocity variability of metallic line star 28 Andromedae

08 p1395 A69-20637

Radial velocity, light and magnetic variations of HD 10783 from concurrent UVB photometric and Zeeman spectroscopic observations

09 p1600 A69-22197

Element abundances of sharp lined field early A stars using model atmosphere

09 p1600 A69-22198

Spectroscopic study of A stars with large Stromgren m sub one indices, discussing rotational velocity, spectral intensity and type

09 p1602 A69-22215

Effects of opacity arising from silicon bound-free transition on emergent fluxes and hydrogen line profiles for A and late B stellar atmospheres

09 p1604 A69-22403

A and B stars near North Galactic Pole and with magnitudes from 5 to 14.5, noting photoelectric UVB and four color photometric measurements

10 p1773 A69-22963

Surface gravities and detection of metallic line early A stars from spectral classification using equivalent line widths

12 p2171 A69-27151

Short period variability of B, A and F stars observed in photometry of New Delta Scuti stars

13 p2348 A69-27803

Positions, spectral types and B magnitudes for possible field horizontal-branch stars at high galactic latitudes, selected from faint A star list

13 p2348 A69-27807

Magnetic A star HD 152107 anomalous intensification of Balmer series H lines observed by spectrograms

13 p2352 A69-27873

Heavy element abundances in peculiar A stars, investigating nucleosynthesis during massive stars evolution

14 p2527 A69-29945

Canum Venaticorum variable A star spectrum, listing all lines observed between 5000 and 6650 A

15 p2692 A69-30773

Zeeman spectroscopy and UVB photometry of 17 Com and kappa Cnc, observing periodic magnetic and light variations

15 p2692 A69-30774

Metallic line /Am/ stars Zeeman observations, showing 16 Ori as spectroscopic binary, dubious binary nature of 15 Vul and doubtful presence of magnetic fields

15 p2692 A69-30775

Spectral Pt II lines in Ap stars of Hg class observed during analysis of double lined spectroscopic binary HR 4072

15 p2695 A69-30891

Two dimensional spectral classifications for bright A stars including magnitudes and colors

16 p2860 A69-32233

Effective temperature and gravity values for Mn Ap stars by comparing spectrum scans and H line profiles with predictions from atmospheric models

17 p3038 A69-33724

Spectrophotometric characteristics of Serpenteis, high metallicity A2 star and standard F zero V 9 Aurigae, analyzing chemical composition, microturbulence velocity and abundance by detailed differential growth curve

17 p3039 A69-33728

Microturbulent velocities of A and F stars observed for reciprocal effective temperature range

17 p3039 A69-33729

Galactic rotation in Cassiopeia region, studying O, B and A stars circular velocities as function of distance from galactic center

18 p3201 A69-35142

Southern stars of spectral types between O5 and A3 analyzed for equivalent widths and equatorial rotation velocity from direct intensity spectrogram tracings

20 p3600 A69-37491

Calcium K line strengths in A stars measured by narrow band spectrometer compensated for seeing and transparency variations

22 p4015 A69-40154

MK system spectral types determination for B, A and F type stars from slit spectrograms near NGC 2264

23 p4211 A69-41487

A-type stars investigation for anomalous spectral line intensities, discussing Hertzsprung-Russell diagrams, rotational velocities, magnetic fields and abundances

23 p4218 A69-42322

Model atmosphere analysis of line identifications and equivalent width data for relatively cool Ap star HD 204411, discussing atmospheric composition

24 p4376 A69-42664

A- 1 AIRCRAFT

Night vision requirements of Vietnam combat pilots investigated for relationship to Skyraider fatal crash during target strafing and H-34 helicopter crash landing

23 p4107 A69-41807

A- 6 AIRCRAFT

Low altitude atmospheric turbulence model evaluated from analysis of A-6A aircraft gust load data, comparing model estimates with aircraft response characteristics

01 p0056 A69-11053

A- 7 AIRCRAFT

A-7 Corsair 2 introduction to fleet and combat operations in Southeast Asia

06 p0867 A69-17660

TC-2 general purpose digital avionics computer in A-7D/E avionics system performing tasks in weapon delivery, navigation and guidance, display updating, self testing, etc

17 p2933 A69-34059

A-11 SATELLITE

U ECHO 1 SATELLITE

A- 300 AIRCRAFT

European A-300B airbus design, considering aerodynamics, fuselage, power plant, structure, systems, maintenance cost and autoland

11 p1822 A69-24464

A 300B twin engine short haul giant transport aircraft, discussing engines, aircraft performance and systems reliability

[RAES PAPER 11] 22 p3863 A69-40491

ABBREVIATIONS

U SYMBOLS

ABDOMEN

Decreasing barometric pressure effects on abdominal gas volume in military men under simulated flight conditions, noting abdominal fullness and pain

23 p4076 A69-41291

ABERRATION

Hologram chromatic aberration compensation by two lens system

01 p0080 A69-10430

Sectoral hoghorn as line feed for correcting spherical aberration in offset spherical reflector antennas

06 p0898 A69-17823

Escherichia coli WWU multiautotrophic revertants with nonsense suppression, noting role in aberrant morphology and in catabolizing thymidine for energy and carbon

07 p1069 A69-19503

Aberration of dielectric patches and rings attached to radome surface described by insertion phase

07 p1111 A69-19530

Single and double mirror systems geometrical optical image aberrations noting focal number, angle of field, secondary magnification and mutual position tolerances

11 p1918 A69-24836

Diffraction images of coherently illuminated objects in presence of aberrations stressing images of edges, disks and bars

13 p2297 A69-27451

Lenses spherical aberration role in studying laser induced breakdown of gases, considering intense ionization collinear regions multiplicity along optic axis

15 p2634 A69-30878

Aberrations of Fabry-Perot interferometers with small nonuniformities in plate spacing used as spectral and optical filters

17 p2972 A69-33081

Spherical aberration effect on atomic beam focusing in six pole magnetic system

19 p3380 A69-36602

ABIOTENESIS

NASA Planetary Exploration Program to gather data on origin of solar system and life, discussing planetary evolution and extraterrestrial life

02 p0200 A69-12804

Abiogenic synthesis of prebiological membranes under assumed primitive earth conditions by UV radiation of alkanes on phosphate and Mg ions aqueous solutions

11 p1828 A69-25462

Self assembly relation to origin of life and spontaneous generation applied to precellular polymers, biopolymers and cellular structures

12 p2018 A69-25776

Origin of microbial life on earth and implications for extraterrestrial forms

17 p2907 A69-32972

ABLATION

Soviet book on theories of origin, nature and evolution of life from viewpoint of dialectic materialism, covering evolution trends, cell differentiation, etc
19 p3259 A69-36746

Evolution of life as creation of order from chaos, noting molecules self ordering capability
21 p3651 A69-38577

Cell origin in self organizing natural polymers in terms of molecular evolutionary priority of polynucleotides and poly alpha amino acids
22 p3896 A69-40781

Pyrimidine polyribonucleotides or purine polyribonucleotides binding to lysine- or arginine-rich proteinoids considered for abiogenesis
23 p4113 A69-41509

Prebiological chemical evolution, studying synthesis and degradation rates relationship at primitive environment energy levels
24 p4269 A69-43514

ABLATION

Sikhote-Alin iron meteorite high temperature oxidation and ablation and simulation with Fe-Ni alloy, noting phase compositions and structure
01 p0025 A69-11373

Minerals in ablated crust of Saratov meteorite using X ray analysis
01 p0160 A69-11385

Thermal and ablative lag induced by periodic heat input to oscillating flat plate in high velocity flow, showing crossover from dynamically stabilizing to destabilizing condition as oscillation frequency increases
04 p0685 A69-14720
[AIAA PAPER 67-336]

Graphite ablation in high pressure environments, extending existing analysis of thermochemical and thermomechanical behavior to include allotropic features
04 p0686 A69-14873
[AIAA PAPER 68-1153]

Ablation surface patterns and resulting roll torques and roll behavior of hypervelocity vehicles
06 p1036 A69-18051
[AIAA PAPER 69-180]

Charring phenolic nylon ablator material pyrolysis and surface recession for cyclic and constant combined convective and radiative heating
06 p1036 A69-18055
[AIAA PAPER 69-151]

Low temperature simulation of hypersonic melting ablation and wave patterns of gas-liquid interface
06 p0907 A69-18064

Dynamic stability loss on ablating vehicles ascribed to boundary layer transition effect from turbulent aft body heating
06 p1037 A69-18087
[AIAA PAPER 69-106]

Graphite ablation in air, N, Ar and He assuming chemical equilibrium, equal diffusion coefficients and steady state ablation
06 p0947 A69-18155
[AIAA PAPER 69-148]

Ablation rate of Saint-Severin amphoterite based on heavy primary cosmic ray track densities in surface samples
08 p1406 A69-20933

Current sheet velocity in coaxial plasma accelerator, noting drag due to insulator ablation and degassing
09 p1566 A69-21258
[AIAA PAPER 69-265]

Oxygen depletion effect in chemical reactions between pyrolysis gases and air stream on surface recession of charring ablators
09 p1622 A69-21982
[AIAA PAPER 68-302]

Sample data reduction methods combined in special purpose computer for measuring ablation in reentry vehicle heat shields
10 p1660 A69-23290

Iron and stone meteorites ablation using electrodeless plasmatron and filmed onto IR films
15 p2697 A69-31252

Subliming ablation effects on boundary layer transition for cones in hypersonic flow, discussing Reynolds numbers measured in wind tunnel tests
16 p2732 A69-31881
[AIAA PAPER 68-40]

Steady inviscid compressible flow past wavy wall with simulated ablation, studying reflections effect on relationship between surface pressure and wall geometry
16 p2770 A69-31909

Saint-Severin amphoterite geometrically reconstructed from fragments in form prior to atmospheric breakup, noting agreement with track densities of iron ions
19 p3416 A69-36128

Polytetrafluoroethylene ablation in high temperature argon, nitrogen, air and oxygen jets, discussing electric heater and heat flux measurement
20 p3632 A69-37522

Dynamic model of ablation pitching moment derivative and time lag effect on spinning reentry vehicle applied to Black Knight flight results
24 p4245 A69-43249

Solid fuel ablation by nitric acid, controlling reaction interface displacement rate by mass and heat transfer phenomena
24 p4363 A69-43568

Solid fuel ablation and supersonic combustion processes for various propulsion configurations, testing plastic models in wind tunnel
24 p4414 A69-43569

Apollo afterbody heat transfer, studying ablation effects for various reentry angles of attack
24 p4415 A69-43680

ABLATIVE MATERIALS

Ablative heat shield materials for Mars and Venus atmospheric entries
02 p0333 A69-11750

Thermal protection by ablation calculated, emphasizing blocking phenomenon and effectiveness of laminated and reinforced resins
02 p0351 A69-11890

Ground simulation of reentry observables with ablation, studying ablation products interaction with flow-field of wave superheater hypersonic tunnel
02 p0229 A69-12502

Rapidly heated ablative reinforced plastics strength and stress-strain properties, considering heat shield designs
02 p0347 A69-12512

Apollo thermal protection system, noting low density ablation, flight and ground tests
03 p0519 A69-13558
[AIAA PAPER 68-1142]

Make wire, light pipe and spring wire ablation sensors development for measuring parameters of heat shield materials for reentry vehicles
04 p0602 A69-15428

High temperature directional reflectance measurements of ablative materials as function of sample temperature using paraboloid reflectometer
04 p0604 A69-15512
[AIAA PAPER 68-25]

Low density polyurethane foam with and without honeycomb as ablative material for reentry vehicles, discussing oxidation resistance
04 p0688 A69-15513

Ballistic range tests to study ablation effects on aerodynamic characteristics of ablating and nonablating slender cones
06 p1036 A69-18083
[AIAA PAPER 69-179]

Radiation profiles in ablating flat plate air- Teflon laminar boundary layer, discussing visible, UV and IR wavelengths
06 p1037 A69-18086
[AIAA PAPER 69-99]

Ablative and insulative performance of reference heat shield materials under transient heating simulating ballistic vehicle reentry trajectory, using plasma jet facility
06 p0907 A69-18110
[AIAA PAPER 69-150]

Thermal radiative reflectance characteristics of low density charring ablators subjected to planetary entry environment simulation
06 p0947 A69-18148
[AIAA PAPER 69-61]

Thermochemical and mechanical ablation mechanisms for Apollo heat shield material, comparing surface thermochemistry computer program and arc plasma tunnel data
06 p1038 A69-18149
[AIAA PAPER 69-98]

Pyrolytic carbon felt composite development and properties, measuring and tabulating mechanical, thermal and ablation properties
09 p1530 A69-22364

Stagnation point heat transfer for thin ablative coatings on sounding rockets in continuum supersonic and hypersonic flight regimes
10 p1808 A69-22934

Nozzle ablations based on chemical mechanism, discussing pure or reinforced phenolic resin
11 p1999 A69-24908

Ablation cooling application to aerodynamic heat shielding, discussing various materials, sublimation, rocket probe ascents, satellites and experimental aircraft
12 p2011 A69-25854

Nozzle erosion profile, char penetration and temperature response predicted for nozzle material for 260 SL-3 motor
12 p2118 A69-26784
[AIAA PAPER 68-504]

Ablation characteristics of heat shield materials measured in arc heated wind tunnels, considering influence of model scale, heating rate and pressure level
12 p2119 A69-26813

Ablation performances of asbestos phenolic and silica phenolic compared at higher stagnation pressures in wave-superheater hypersonic tunnel
12 p2119 A69-26814

Ablation test specimen environment at high temperature, analyzing laboratory heating, pyrolysis gas
12 p2119 A69-26814

diffusion, convective heating, critical stress and temperature profiles, etc
12 p2191 A69-26815

Ablation wedge model design for testing in wave superheater under controlled pressure gradients and constant temperature
12 p2059 A69-26816

Heating facility for testing ablative heat shield material models in combined convective and radiative heating environment with constant or transient heating conditions
13 p2243 A69-28278
[AIAA PAPER 69-342]

Passive temperature indicators for maximum temperatures attained within rocket nozzle ablative materials
15 p2613 A69-31271

Ablation injectants effect on supersonic stream pressure distribution inside cavity and upstream boundary layer velocity profiles
16 p2770 A69-31902

Ablative materials in hydrogen/oxygen thrust chamber using expansion nozzle to substitute regenerative thrust chamber assembly
16 p2747 A69-32702
[AIAA PAPER 69-442]

Nozzle throat ablative materials for controlled high regression rates in tactical rocket motors, primarily nylon reinforced thermosetting resins
16 p2804 A69-32710
[AIAA PAPER 69-423]

Metallic aerosol generator application in shock tube spectrometric measurements of radiation by molecules occurring as solids before decomposition to vapor phase
18 p3099 A69-34461

Glass overlaid B filament laminates interleaved with C and silica fabrics, evaluating ablative properties in solid rocket motor tests
19 p3354 A69-35515

Ablative materials thermal protection characteristics at low heating rates evaluated by convective heating tests, stressing polyurethane foam composite
19 p3557 A69-35536
[AIAA PAPER 69-151]

Ablative materials for solid rocket nozzles, discussing static firing tests, rating system, equipment design and cost reduction
19 p3357 A69-35537

Ablation heat shields, emphasizing dielectric low cost fabrication and application to entry vehicles
19 p3318 A69-35538

Flash X ray unit with special film transport devices to obtain sequenced dynamic radiographs of ablating models during reentry simulation tests
19 p3291 A69-35720

Ablating sphere viscous wake using image converter camera, computing luminance radial distribution by unit volume
19 p3306 A69-35739

Microwave-plasma interaction instrumentation for supersonic channel constructed to investigate turbulent boundary layers formed over ablating heat shield materials
19 p3294 A69-35754

High temperature materials for aerospace and spacecraft applications, considering carbon/carbon composites, oxides, carbides, fibers and ablative systems
19 p3346 A69-36320

Spectral emissivity measurement of ablating phenolic graphite heated by subsonic air stream to high temperature to simulate reentry condition
20 p3565 A69-37187

Ablation effect on heat transfer coefficient of carbon, silica and ceramic cloths impregnated with phenolic resin subjected to torch testing and motor firing
21 p3753 A69-39800

Speed conditions of environmental simulation of thermal scale models of reentry vehicles, considering ablative with phase-change and involved chemical reaction
22 p3922 A69-40384
[AIAA PAPER 69-1011]

Line source technique for ablative heat shield materials thermal conductivity measurements, comparing vacuum and atmospheric test results
22 p3922 A69-40386
[AIAA PAPER 69-1013]

Low density polybenzimidazole composites as ablative heat shields, discussing arc-heated wind tunnel tests of linear and crosslinked structures
23 p4179 A69-41715

Diamond shaped surface ablation patterns development mechanism for several ablation materials of ground test and recovered flight vehicles
23 p4059 A69-41891
[AIAA PAPER 68-671]

Carbon fibers and resin composites used as rocket motor systems ablative liners and structures, noting role in motor weight reduction

24 p4336 A69-43210

Dry ice ablating models for unheated supersonic and hypersonic wind tunnel tests, noting mass addition rate extension

24 p4297 A69-43255

Charring ablator char zone nonequilibrium flow and chemical reaction kinetics as function of temperature, using thermal environment simulator

24 p4409 A69-43512

Solid fuel ablation by nitric acid, controlling reaction interface displacement rate by mass and heat transfer phenomena

24 p4363 A69-43568

Diamond shaped striations development mechanism on ablative heat shield materials exposed to supersonic flow and turbulent boundary layers

24 p4248 A69-43598

ABLATIVE NOSE CONES

Ablation rate optical measurement near stagnation point of Teflon cylinder models, noting effect of nose curvature and temperature at supersonic speed

01 p0006 A69-10758

Unsteady aerodynamics of ablating flared reentry body, noting complications due to blunted nose shear flow and entropy gradient effects

02 p0189 A69-12524

Nosetip cooling system based on discrete subsonic forward liquid injection through ablative nosetip opening of blunted reentry vehicle

03 p0532 A69-13559

Charring phenolic nylon ablator material pyrolysis and surface recession for cyclic and constant combined convective and radiative heating

06 p1036 A69-18055

Nose cone reentry simulation under low temperature subliming ablators, discussing dry ice, camphor and steel calibrations models fabrication, instrumentation and boundary layer measurements

06 p0929 A69-18098

Ballistic reentry vehicle roll-pitch coupling, showing influence of nose asymmetries

06 p1018 A69-18156

Heat and mass transfer conditions in ablation of shear thinning and thickening fluids at stagnation point

13 p2374 A69-27778

Shape and surface roughness effects on turbulent ablation of reentry body nose tip, noting recession rate

17 p2952 A69-33435

ABNORMALITIES

NT MAGNETIC ANOMALIES

Boundary value problem solved for free air geoid, developing expressions for height anomaly from free air anomalies

07 p1129 A69-19396

Isotropic ideal bidimensional filter in interpretation of anomalous gravity fields, especially for separating local and regional effects

21 p3724 A69-39246

Statistical characteristics of linear transformations of gravity field anomalies by linear operators, noting computation of covariance function

21 p3716 A69-39247

Anomalies of isotropic cosmic ray secular variations at high latitudes based on supermonitor neutron data

23 p4206 A69-41854

ABORT APPARATUS

Crew survival insurance under emergency situations during manned space flight, discussing Apollo abort system refinements

24 p4272 A69-42848

ABORT TRAJECTORIES

Moon to earth trajectories analyzed numerically to determine effect of specified earth entry conditions on hyperbolic elements near moon for abort

20 p3595 A69-37174

ABORTED MISSIONS

Agreement on Rescue and Return of Astronauts and Return of Objects Launched into Outer Space, discussing unintended landing

20 p3636 A69-37113

Moon to earth trajectories analyzed numerically to determine effect of specified earth entry conditions on hyperbolic elements near moon for abort

20 p3595 A69-37174

Abort capability mission selection criterion, evaluating energy requirements, Mars flyby and velocity contours

21 p3805 A69-39209

Secondary or abort mission maximized subject to primary mission constraints by variational treatment of optimal branched trajectories

[AAS PAPER 68-138] 21 p3819 A69-39210

ABRASION

Hydrogen effects on ELI Ti-Al-Sn alloy, conducting tensile, fretting and abrasion tests on stressed and thermal cycled specimens

[AIAA PAPER 69-585] 16 p2803 A69-32760

ABRASION RESISTANCE

Yielding of matrix material and cell size of substructure relationship to dry abrasion resistance of SAP type aluminum alloy at room temperature

08 p1319 A69-19995

Abrasive wear model leading to abrasive wear equation and empirical findings on relative abrasive wear resistances

13 p2265 A69-27233

Friction wear of solid bodies based on microscopic contact system model, deriving particle distribution law from physicochemical analysis

13 p2268 A69-28051

Abrasion and corrosion resistant Cr-Co-B cast alloys in aggressive media, concluding resistance is due to chromium boride and fine dendritic structure

19 p3347 A69-36742

ABRASIVES

Abrasive wear model leading to abrasive wear equation and empirical findings on relative abrasive wear resistances

13 p2265 A69-27233

Lamellar solids abrasiveness, effects of particle shape in graphite and molybdenite samples

22 p3966 A69-39877

ABSCISSAS

U COORDINATES

ABSOLUTE TEMPERATURE SCALES

U TEMPERATURE SCALES

ABSORBERS [EQUIPMENT]

Parallel damped dynamic vibration absorbers, modifying conventional absorber by adding subsidiary undamped absorber mass

[ASME PAPER 68-WA/DE-6] 05 p0839 A69-16171

Parallel damped dynamic vibration absorbers, modifying conventional absorber by adding subsidiary undamped absorber mass

[ASME PAPER 68-WA/DE-6] 13 p2360 A69-27422

ABSORBERS [MATERIALS]

NT SOLAR ENERGY ABSORBERS

Optical pulse generator consisting of solid state laser with saturable absorber at cavity end using perturbation theory and Maxwell equations

01 p0089 A69-10179

Scattering from coated absorbing conducting bodies, considering flat plane and curved surfaces in Rayleigh region

03 p0384 A69-12908

Amino alcohol regenerable absorbers of carbon dioxides toxicological characteristics, discussing absorbing ability in rats

10 p1646 A69-23502

Traveling wave passive Q switched laser with bleachable absorber filter, analyzing unsteady processes without expanding field along natural resonator modes

10 p1705 A69-23949

Q switched carbon dioxide laser power increased by placing bleachable /boron tetrachloride/ filter in resonator

11 p1894 A69-24454

Absorption characteristics of thin metallic films in standing light wave for mode selection and conversion in lasers

12 p2104 A69-26024

Cosmic ray postinteraction nuclear active particle energy spectrum measurements with ionization calorimeter, noting energy underrating

13 p2331 A69-28392

Passive mode locking of pulsed Nd-YAG laser using saturable absorber, noting two photon fluorescence contrast ratio

16 p2797 A69-32019

Ruby laser resonator losses resulting from changes in mirror transmittance or inclination, or introduction of bleachable absorbers

19 p3331 A69-35863

Emission kinetics of passive Q switched laser without constraints on relaxation time and switching characteristics of absorption centers and medium

21 p3740 A69-39550

ABSORPTANCE

Solar absorptance, total hemispherical emittance and absorptance/emittance ratio for metals at cryogenic temperatures measured simultaneously with sinusoidally perturbed incident radiation

01 p0176 A69-10847

Energy characteristics of laser with passive Q switch, taking into account internal reflections

02 p0256 A69-11999

Aircraft measurements of stratus cloud absorption and albedo and earth surface albedo

04 p0627 A69-14914

Solar absorptance and hemispherical emittance of metals at space conditions determined with cyclic incident radiation technique

[AIAA PAPER 69-60] 06 p0945 A69-18154

IR absorptance of CO below room temperature, determining strength and half widths of lines in R branch of fundamental band

07 p1183 A69-19644

Optimal thickness of inhomogeneous absorption layer subjected to normally incident plane monochromatic wave treated as Mayer-Boltz variational problem

13 p2297 A69-27381

ABSORPTION COEFFICIENT

U ABSORPTIVITY

ABSORPTION CROSS SECTIONS

Absorption cross section for 68 Mev positive pion absorption by $1p\ 3/2$ neutron in C^{12} nucleus followed by single proton emission at 11 degrees

02 p0282 A69-11460

Radiation attenuation cross sections of monatomic and diatomic xenon gas from UV absorption measurements near resonance line

02 p0284 A69-12551

Very thin short metallic filament scattering and absorption cross sections for various values of filament conductivity

03 p0395 A69-13623

Pulsed electromagnetic signal reflection from plane boundary of absorbing medium

03 p0397 A69-13711

Photodissociation and photoionization of diatomic molecules at high temperatures with calculation of absorption cross sections

03 p0473 A69-14147

Autoionizing states effects on absorption cross sections for ejection of outer subshell electron from atomic oxygen

04 p0633 A69-15127

Transmittance and absorption cross sections of carbon particles suspended in flowing stream of nitrogen gas

06 p1034 A69-17804

Hydrogen molecule spectroscopy in vicinity of ionization limit, determining absorption and ionization cross sections and fluorescence

07 p1184 A69-18490

Hydrogenic approximation validity in evaluation of atomic energy levels and radiative absorption cross sections for computation of stellar opacity

07 p1223 A69-19626

Effective cross sections of UV radiation absorption by molecular oxygen in Schumann-Runge bands at high temperatures

11 p1921 A69-24617

Boron 10 absorption cross sections from counting ratios measurements of boron trifluoride proportional counter used to monitor neutron fluxes

17 p3008 A69-33753

Atmospheric ionization rates due to attenuation of 1-100 A nonflare solar X rays, giving solar fluxes and absorption cross sections

22 p4004 A69-40447

Cross sections of charge carrier capture by ions in gamma irradiated P-Al-Si glass with metal oxides additions measured for evaluating radiation stability improvement

23 p4180 A69-42470

ABSORPTION SPECTRA

NT FRAUNHOFER LINES

NT HERZBERG BANDS

NT TELLURIC LINES

Intrinsic absorption temperature dependence in doped p-InSb, discussing forbidden transitions

01 p0136 A69-10255

Methane IR absorption band centered near wavenumber 9050, noting R branch features and fine structure

01 p0023 A69-10289

Continuous and time-resolved absorption and emission spectra studies produced by exploding wires in

gases, discussing effects of environment, pressure and electrical energy

01 p0118 A69-10664

Copper exploding wire Kerr-cell time-resolved absorption spectra analysis, considering copper atom transition

01 p0118 A69-10665

Statistical band model and line by line calculations of transmittance for IR bands in absorption spectra of ozone and water vapor

[AFCLR-68-0505] 01 p0124 A69-10919

Spectral absorption curves of hematoxylin stains in stained tissue sections of rat thyroid

01 p0015 A69-10924

Total atmospheric moisture content by measuring radio wave absorption at water vapor molecule rotational spectrum absorption line

02 p0274 A69-11438

Atmospheric water vapor content from summer-fall 1966 measurements of atmospheric radio wave absorption of thermal radio emission, describing experimental apparatus

02 p0274 A69-11439

Nitrous oxide absorbance, deriving analytical expressions for transmission spectra

02 p0236 A69-11452

Ebert spectrometric experiment during Mars flyby aimed at detecting upper atmosphere atoms, ions and molecules in 1100-4300 angstrom spectral range

[AAS PAPER 68-184] 02 p0311 A69-11469

Absorption oscillator strengths of Ba 2 lines in UV and visible spectral regions, using cascade arc in argon with barium vapor

02 p0242 A69-11872

Absorption and emission redshift distribution in quasars, N systems and similar compact and radio galaxies

02 p0325 A69-12591

Stellar spectra observed with 2.8-14 micron IR spectrometer, noting broad absorption feature near 5 and 8 microns

02 p0327 A69-12713

Oscillator strength determination for Schumann-Runge band system in molecular oxygen

02 p0284 A69-12832

Molybdenum interband transitions noting low energy optical property anomalies and origin of two absorption bands

03 p0442 A69-12986

Radiation absorption variations in KC-19 CdSe glass during ruby laser radiation, noting microcrystals and nonlinear effects role in determining optical properties

03 p0436 A69-13036

Rapid recording microspectrophotometer for IR to UV absorption spectra of living cells, cell organelles and half micron diameter particles

03 p0428 A69-13109

Astronomical needs for atomic spectra, discussing emissions in Wolf-Rayet lines and Of stars and forbidden lines in absorption in sun and F-K stars

03 p0508 A69-13172

Molecular O 0.7620 micron absorption band in pure O and air, noting rotational lines mean half width and lower atmosphere transmission function

03 p0458 A69-13272

Telluric lines halfwidth and depth dependence on observation point altitude and intervening air mass, determining absorption line contours for isothermal atmosphere

03 p0512 A69-13695

Absorption and IR emission of nickel and cobalt doped alkali halides

03 p0490 A69-13941

Empirical growth curve determined by using equivalent widths of absorption lines of quasar 3C 191, concluding ionization is mainly due to collisional processes

03 p0514 A69-13962

Absorption oscillator strengths of S 1 and S 2 lines between 1100 and 2000 A, using arc burning light source

03 p0479 A69-13968

Optical absorption of thin film cesium between 2300 and 11000 A

03 p0491 A69-14060

Optical absorption of vacuum deposited thin rubidium films, noting similarity to sodium and potassium

03 p0491 A69-14114

Energy structure parameters for ZnTe-CdTe and ZnSe-ZnTe crystals, obtaining forbidden bandwidth dependence on composition

03 p0492 A69-14173

Mossbauer spectra of shocked and unshocked iron meteorite and fayalite

03 p0517 A69-14231

Atmospheric refractive index for IR radiation in one to six micron region

04 p0591 A69-14300

Inner corona Fraunhofer lines invisibility at solar eclipses, emphasizing uncertainty of photospheric absorption lines appearance as electron scattering

04 p0654 A69-14628

Dark equatorial belt of Jupiter atmosphere in 1962 and 1963, noting photometric contrasts, molecular absorption and possible structure

04 p0658 A69-14961

Taurus A 21 cm absorption line frequency decrease during optical path approach to sun, discussing gravitational and electromagnetic origin

04 p0661 A69-15148

Emission lines structure in quasar spectra, analyzing problem of weak absorption lines identification

04 p0662 A69-15236

Nanosecond range flash photolysis technique and application to absorption spectra of excited singlet states

05 p0760 A69-15608

Laser photolysis and spectroscopy for photographic recording of absorption spectra of transient intermediates in nanosecond reactions

05 p0772 A69-16025

Photoelectric absorption studies on molecular nitrogen indicate predissociation contributing to atomic nitrogen production in upper atmosphere

05 p0756 A69-16282

Upper limit of nonradiative relaxation time between specific states of absorption bands and fluorescence state emitting R lines in ruby laser

05 p0777 A69-16335

Continuum position location and total line absorption in solar spectrum, using Houtgast high dispersion intensity measurements of UV region

05 p0828 A69-16611

IR radiation attenuation in transparency windows of atmosphere, using searchlights as radiation sources

05 p0760 A69-16695

Oxygen absorption coefficients for atomic silicon in spectral range of Schumann-Runge bands

06 p0960 A69-17090

Oxygen line absorption at elevated temperatures in Schumann-Runge system, estimating line widths

06 p0962 A69-17803

Lunar occultations of galactic center region observed at 1667 MHz indicating OH absorption origin in uniform rotating cloud

06 p1009 A69-17961

Semiconductor lasers, discussing electron transitions, radiative band-band transitions, emission and absorption spectra, recombination rates, carrier lifetime and lasing conditions

06 p0937 A69-18009

Water vapor absorption line for nitrogen and oxygen mixtures with frequency measurements at various pressures and temperatures, discussing attenuation and line breadth

07 p1184 A69-18911

Organic dye lasers characteristics, describing broad continua production for nanosecond absorption spectroscopy

[IEEE PAPER A-3] 07 p1150 A69-19047

He-Ne laser self locking of modes and spectrum weeding out at small absorption

[IEEE PAPER G-13] 07 p1151 A69-19059

Absorption and emission spectra of ruthenium 2 complexes dissolved in rigid glasses, discussing crystal field theory and luminescence

07 p1200 A69-19219

Ce activated garnet crystals optical properties, noting IR and near UV absorption spectra and room and low temperature fluorescence

07 p1201 A69-19647

Equivalent widths of K line of single ionized calcium and central depths of unidentified broad absorption in O and B stars spectra

08 p1389 A69-20250

Carbon dioxide absorption and emission in mesosphere, discussing vibrational relaxation time and radiative heating rate

08 p1308 A69-20308

Low latitudes observations of 21 cm line of H I in galactic center direction, giving contours maps of brightness temperature

08 p1392 A69-20562

Diffuse interstellar absorption bands and doublet line, noting large intensities of forbidden transitions

08 p1395 A69-20639

Doublet structure suppression in mixtures of cesium and foreign gases, discussing absorption observations

08 p1356 A69-20736

Optical depth determination in absorption lines of interstellar neutral hydrogen clouds by spectral observation of variable intensity radio sources

08 p1398 A69-20774

Atmospheric molecular oxygen temperatures from photoelectric recordings of absorption bands, analyzing relaxation process and photoeffects in oxygen molecules

09 p1490 A69-21863

Lowest valence and Rydberg states assigned to ungerade singlet states in dipole allowed absorption spectrum of molecular nitrogen

09 p1542 A69-21916

Absorption red shifts in quasi-stellar source due to dead galaxies in cosmologically flat model of universe

09 p1602 A69-22228

Absorption red shifts in quasar spectra from spectroscopic observations of PHL 5200 and B194

09 p1604 A69-22271

Line blanketing for two level atom with spectral line formed in pure absorption and noncoherent scattering, studying wavelength and depth dependence

09 p1606 A69-22424

Fourth positive carbon monoxide system observed in absorption in vacuum UV region, discussing rotational and vibrational band structure

09 p1607 A69-22429

Intrinsic absorption temperature dependence in doped p-InSb, discussing forbidden transitions

09 p1559 A69-22648

Luminescence quantum yield in neodymium glass, noting independence to stimulating light frequency

10 p1702 A69-23211

Transitions between heavy hole and spin orbit split bands in uniaxially stressed Ge and GaAs, noting spectra for various temperatures and valence band parameters

10 p1745 A69-23359

Asymmetrical profiles of 4430 A interstellar absorption band, discussing stellar and electronographic spectra

10 p1781 A69-23676

Interstellar diffuse absorption bands due to resonance lines of impurity atoms trapped in low temperature hydrocarbon matrices

10 p1781 A69-23677

Reddened M supergiant 119 Tauri IR spectra and IR absorption by CO and SiO molecules in stellar atmosphere and silicate mineral in interstellar grains

10 p1786 A69-24104

Interstellar formaldehyde detection in absorption against galactic and extragalactic radio sources, discussing chemical evolution

10 p1786 A69-24108

Optical depth at under 110 A due to continuous absorption by N, O and Ne ions estimated in high excitation planetary nebulae

10 p1790 A69-24140

Tunable Fabry-Perot interferometer for photoelectric measurements of absorption and emission line contours and line center particle concentrations

10 p1698 A69-24212

Monograph on laser spectroscopy in megahertz range covering spark photography comparison, concept of modes, resonators, applications, etc

11 p1893 A69-24368

Methane absorption distribution in 6190 A band over Jupiter disk based on spectrograms, noting center to limb variations

11 p1960 A69-24730

Methane absorption distribution in 6190 A band over Saturn disk at center and polar latitudes based on spectrograms

11 p1960 A69-24731

Balloon-borne IR spectrometry to study atmospheric nitric acid vapor compared with absorption by ozone and methane

11 p1879 A69-25407

Image tube spectra observations of interstellar absorption band at 4430 A, noting emission band at 4400 A

11 p1965 A69-25658

Calcite IR absorption dependence on pressure, discussing calcite-aragonite transformation

12 p2141 A69-25783

Cyanogen band absorption in nuclei of elliptical and spiral galaxies derived from photoelectric measurements indicating rich metal content in central cores

12 p2153 A69-25803

IR absorption spectrum of Br-doped n-CdTe specimen, considering donor level transfer mechanism

12 p2142 A69-25979

IR absorbance data for atmospheres of ammonia and ammonia nitrogen mixtures at various wavelengths

- indicating absorption in strong line region for gas pressures used
12 p2132 A69-26247
- Shapes of extreme wings of collision-broadened carbon dioxide lines, noting absorption deviation from Lorentz-shaped lines
12 p2132 A69-26248
- Vibration and absorption bands in IR spectra of diborene hydrazine stabilized by boiling in benzene
12 p2027 A69-26917
- Quasar spectra, discussing 3C 345, 3C 191 absorption lines and model explaining quasar spectra
12 p2167 A69-27046
- Absorption line spectrum of quasar Ton 1530, discussing line widths and red shifts
13 p2334 A69-27306
- Statistical tests for cosmological hypothesis for origin of absorption lines in spectra of quasars, considering red shifts
13 p2334 A69-27307
- Rocket spectrographic observations of Alpha Virginis noting hydrogen Lyman absorption lines
13 p2338 A69-27555
- High dispersion classification of early K2-M6 giants of high and low velocity, using titanium oxide band strengths criteria tested by atomic lines estimation
13 p2338 A69-27556
- Line absorption effect on opacity and main sequence model stars noting luminosity, radius and mass of convective core
13 p2340 A69-27578
- Fine structure of absorption lines of circumstellar Ca ejected from Nova Delphini 1967, determining ejection dates and photospheric radius
13 p2346 A69-27709
- GaSe, GaSe and InSe crystals band structure from analyzing reflection spectra, noting sensitivity to visible, IR and hard radiation
13 p2317 A69-27883
- Supplementary absorption and Hall effect temperature dependence in solid solutions of gallium arsenic phosphide
13 p2318 A69-27894
- Molecular O 0.7620 micron absorption band in pure O and air, noting rotational lines mean half width and lower atmosphere transmission function
14 p2487 A69-28780
- CdS single crystals spectral dependence of photocurrent, photoconductivity quantum yield and photoelectromotive force in exciton absorption region
14 p2504 A69-28990
- Ruby laser beam effects on CdS crystals optical properties, measuring absorption spectrum and light dispersion in crystal
14 p2457 A69-28999
- Absorption band observation near 0.43 μ in solar spectra and scattered radiation of sky, determining nonelluric origin
14 p2441 A69-29407
- Absorption band edge position in p type indium antimonide thin films after heating, showing forbidden bandwidth function relationship to film thickness
15 p2666 A69-30044
- Spectral distribution of photosensitivity for p-n junctions in silicon doped GaAs, showing agreement with state density model and absorption data
15 p2666 A69-30067
- Spin temperature of interstellar neutral hydrogen calculated from 21 cm absorption spectra line profiles
15 p2681 A69-30411
- Cyanogen molecules increase attributed to nova shell compression from analyzing absorption spectrum of DQ Herculis 1934 after brightness maximum
15 p2688 A69-30558
- Submillimeter atmospheric absorption spectra, emphasizing absorption by isotopic and vibrationally excited forms of water molecules
15 p2568 A69-30699
- Quasar multiple absorption red shift lines caused by gas in extended galaxy halos, assuming broadened galactic cross section area
15 p2695 A69-30884
- Atomic H Lyman-alpha interstellar absorption line in theta Orionis spectrum, showing equivalent width relations to H column density and spin temperature
15 p2695 A69-30890
- Quasi-stellar and related objects emission and absorption red shifts tabulation suggesting absorption lines origin
15 p2701 A69-31532
- Supernovae spectra observation suggesting tracing as broad band interstellar absorption rather than emission features on continuum
15 p2701 A69-31534
- Calorimetric measurement of source and broadband spectral absorbances of spacecraft thermal control coatings during exposure to UV in vacuum environment
16 p2789 A69-31815
- Radio emission and absorption of cumulus and stratus clouds at millimeter and centimeter wavelengths, giving maximum SNR defined by brightness temperature
16 p2807 A69-32270
- Vertical ozone distribution from emission and absorption in 9.6 μ band determined during IGY in Switzerland
16 p2785 A69-32625
- Polymethine dyes in passive Q switches of neodymium lasers, noting effects of absorption band intensity, width and position on single pulse laser energy yield
17 p2983 A69-33968
- Quantitative IR spectral emissivity measurements of NO between 300-800 K made in absorption, correlating observed absorbance with optical path length and gas pressure
17 p3009 A69-34156
- Red shift table for six galaxies near Coma Cluster from spectrograms of absorption lines
17 p3044 A69-34182
- Absolute gf values for Fe I and Fe II lines between 3190 and 3315 Å measured by spectral absorption through shock heated gas containing Fe
18 p3175 A69-34304
- Dark equatorial belt of Jupiter atmosphere in 1962 and 1963, noting photometric contrasts, molecular absorption and possible structure
18 p3197 A69-34724
- Variation influence of total absorption to color excess ratio on galactic spiral structures indicating ineffective application of variable-extinction method to Q spectra
18 p3199 A69-34914
- High temperature air spectral absorption indices determined at different pressures and temperatures
18 p3231 A69-35122
- Fourier transform laboratory spectroscopy for absorption near earth atmosphere millimeter wave spectrum, discussing integrated absorption strength and dimeric effect
18 p3177 A69-35240
- Cloud layer multiple scattering in Jovian atmosphere, discussing influence on Lorentzian contour of planetary absorption lines
18 p3203 A69-35332
- Atomic and molecular absorption lines and width measurement in spectrum of WZ Cassiopeiae carbon star in visual and IR region
18 p3204 A69-35350
- Tau-luminescence in thin gamma-colored and uncolored ruby crystals containing Cr ions measured, discussing ions absorption spectrum changes
19 p3335 A69-36166
- Forbidden transitions in absorption spectra of sun and normal and peculiar stars
19 p3422 A69-36215
- Cadmium sulfide-selenide single crystals reflection coefficient polarimetric measurement, observing reflection peaks relationship to absorption spectral temperature dependence
19 p3391 A69-36607
- Spectral absorption coefficients and emissivities of thermodynamic equilibrium mixture of various combustion products at high temperatures, based on graphs
19 p3266 A69-36840
- Modular Michelson interferometer used as IR spectrometer for absorption and dispersion studies, describing instrument construction, range and accuracy
20 p3538 A69-37297
- Intensities of translational lattice mode absorptions of alpha phase solid molecular nitrogen in far IR, noting temperature dependence
20 p3579 A69-37346
- WY Gem star spectroscopic observation showing peculiarity about forbidden and absorption spectra superposition
20 p3598 A69-37464
- HD 200775 spectrum analyzed for absorption lines wavelengths and equivalent widths, noting role for NGC 7023
20 p3599 A69-37469
- Satellite onboard transmission measurements determining atmospheric water vapor influence on integrated refractivity at specific absorption line resonant frequency
20 p3545 A69-38097
- Ce II line reversal from absorption to emission in solar spectrum, noting reversal position dependence on wavelength and line source function scattering term
20 p3613 A69-38168
- Absorption spectrum of diatomic oxygen excited by AC silent discharge photographed with vacuum spectrograph, associating lines with Schumann-Runge band
20 p3581 A69-38276
- Atmospheric transmission determined in submillimeter solar radiation spectra using Bouguer law, identifying absorption lines in nocturnal and diurnal spectra
21 p3796 A69-38472
- Intensity integral inversion for Doppler core of strong solar absorption lines to obtain line source function for solar atmosphere
21 p3796 A69-38478
- Line statistics for representation of line absorption coefficient distribution for solar type stars
21 p3811 A69-38762
- Equivalent absorption line widths of supergiant B1 IA /kappa Cassiopeia/ tabulated with log NH content of atmosphere for various elements
21 p3803 A69-38844
- Spectral transmittance of mixture of carbon monoxide and nitrous oxide for overlapping absorption bands [AIAA PAPER 67-600]
21 p3819 A69-39013
- Nonograms for spectral transparency of atmosphere at 2.8-5.6 microns
21 p3759 A69-39117
- Absorption spectroscopy using resonance broadened atomic lines for two phase mixtures study
21 p3774 A69-39239
- Spectrophotometric analysis of interstellar absorption in direction of IC 1805 cluster, noting anomalies
21 p3814 A69-39576
- Absorption spectra from excited metastable states in tunable dye laser pumped atomic Ca, using fast flashlamp continuum
21 p3775 A69-39740
- Planetary spectroscopy with McDonald 107 inch telescope, discussing role of molecular and atomic absorption lines, line broadening, Doppler shifts and Rayleigh criterion
21 p3727 A69-39786
- Ti emission and absorption K spectra in Ti-Al intermetallics, suggesting hypothesis concerning long wave and fundamental subbands origin
21 p3749 A69-39787
- Singlet-singlet energy transfer kinetics dependence on emission and absorption spectra overlap via dipole-dipole interaction
22 p3895 A69-40056
- Total band absorbance of nonisothermal IR radiating gas, using wideband formulation of Curtis-Godson approximation and series expansion formulation
22 p3983 A69-40101
- Solar Zeeman triplet pseudo-pi-component at 5250 Å /Fe I/, using Unno theory to calculate visibility, contrast and displacement
22 p4019 A69-40289
- Absorption spectrum of CS atoms excited by electrical discharge and irradiated by monochromatic light and ionized by electron collisions
22 p3984 A69-40418
- King furnace absorption source used with spectrometer in relative oscillator strength measurement, with experiments on lines of Fe I
22 p4022 A69-40466
- Absorption and fluorescent spectra, relaxation times and quantum efficiencies measured for glasses doped with trivalent erbium, reviewing spectroscopic parameters involved with laser effect
22 p3962 A69-40476
- Absorption spectrum of NO molecule, analyzing f complexes electron structure, ionization potential and quadrupole moment
22 p3984 A69-40477
- Forbidden absorption bands of diatomic O in Ar continuum region, determining rotational constants of upper electronic states
22 p3896 A69-40479
- Jupiter spectrum observations in 2.8-14 micron range, describing absorption strength and brightness temperature, basing analysis on ammonia, methane and hydrogen absorption
22 p4028 A69-40662
- Molecular N UV spectrum at various pressures, showing absorption band dependence on pressure induced dipole transitions
22 p3986 A69-40723
- Amplification coefficient, luminescence power and spacing between Fermi quasi-levels in GaAs diode injection lasers, using spectral absorption dependence
22 p3965 A69-40801
- Absorption features of 21 cm neutral hydrogen line in part of Cygnus X and of W 49, showing equal velocity contour diagrams from right ascension scans
22 p4034 A69-41200

ABSORPTIVE INDEX

Absorption coefficient measurement for hydrocarbon gases for He-Ne laser beam at 3.39 microns, tabulating coefficients, noting variations from spectroscopic data
23 p4174 A69-42192

Absorption lines in stellar spectra and significance in cosmogony, discussing ionized Ca K line detection during delta Orionis study, K and H lines components, etc
24 p4383 A69-42999

Radiative transport in nongray cylindrical medium using total band absorptance
[ASME PAPER 69-HT-38] 24 p4411 A69-43534

Donor and acceptor impurity effect on absorption and reflection spectra of CdTe single crystals, analyzing In, Ga, S and Se
24 p4362 A69-43735

Optical properties of neodymium-doped YAG and glass laser materials including fluorescence lifetime and conversion efficiency, absorption spectra, sensitization effects, etc
24 p4329 A69-43751

Polycrystalline ammonium cyanide IR absorption spectrum as function of temperature, discussing ammonium ion hydrogen bonding to C or N atoms
24 p4280 A69-43809

ABSORPTIVE INDEX

U ABSORPTIVITY

ABSORPTIVITY

Optical absorption coefficients for triphenyl-methylarsonium tetracyanoquinodimethan complex single crystal, evaluating reflectance
01 p0140 A69-10934

Absorption coefficients of molecular oxygen at Lyman alpha line and vicinity measured by vacuum spectroscopy
01 p0076 A69-11230

Absorption coefficient of hydrazine and hydrogen peroxide determined with 2.5 angstrom bandwidth monochromator, giving results in graphical form
02 p0205 A69-11873

Thermal noise from passive linear multiports, noting influence of temperature and absorption coefficients
02 p0211 A69-12443

Linear absorption coefficient of semiinsulating Cr doped GaAs for IR carbon dioxide laser radiation, discussing lattice absorption mechanism
02 p0258 A69-12619

Ruby laser radiation nonlinear absorption coefficient measurement in CdS, ZnS and SiC semiconductor crystals, noting light limiting effects
03 p0436 A69-13038

Absorption coefficients of plasmas in capillary discharge tubes, discussing measurement using gas laser light source
03 p0442 A69-14218

Hydrogen spectral line broadening under combined action of ions and electrons, tabulating values for calculation of absorption coefficient
04 p0651 A69-14373

Continuous absorption of coefficient hydrogen-carbon plasma at 40,000 degrees K and 70 atm in 230-460 mm spectral range
04 p0639 A69-15371

Gas laser pulse induced attenuated and nonattenuated plasma radiation recording, determining absorption coefficients
05 p0762 A69-15900

Radiative heat transfer between parallel plates separated by nongray gas with picket fence absorption coefficient using integral equations
06 p1033 A69-17554

Radio wave absorption measurements in atmosphere at superhigh frequencies, considering earth radiation, antenna sidelobe anisotropy, instrument effects, etc
07 p1076 A69-18518

Hydrogen absorption coefficients, giving number densities in hydrogen gas or plasma for wide range of temperature and pressure
07 p1184 A69-19165

Stellar atmospheres radiative opacity, computing metal absorption coefficients
07 p1220 A69-19392

Ligand field transitions in tertiary phosphine and arsine complexes of ruthenium and osmium
07 p1075 A69-19483

Ruby absorption, fluorescence and lasing properties, calculating polarization effect on relative intensities and forms of R1 and R2 bands in macroscopic theory
07 p1201 A69-19646

Optical absorption index for molten beryllium oxide based on measurements of small beryllium/ solid propellant rocket motor exhaust plumes
08 p1351 A69-20149

Rational approximation for coefficients used in calculating hydrogenic photoionization Gaunt factors
08 p1354 A69-20153

Galactic clusters absorption, discussing optical thickness in blue and red light
09 p1587 A69-21356

Photocell base thickness for optimal power to weight ratio, noting photons spectral distribution and absorption coefficient dependence on frequency
09 p1443 A69-22719

Modified nonstationary method for determining materials absorptivity with respect to incident solar radiation through heating and cooling rate measurements
09 p1528 A69-22720

Plane and spherical albedos of planet surrounded by infinite optical thickness atmosphere, with application to Venusian atmosphere
10 p1776 A69-23210

Diffusion pump oil reflectance and absorption coefficients measured in three thicknesses using light source, monochromator and detector
10 p1725 A69-23647

Silicon dioxide coated Al reflectance, solar absorptivity and total normal and hemispherical thermal emissivity, noting application to satellite temperature control
11 p1918 A69-24835

Optical absorption cell with variable path length and temperature for measuring absorption coefficients of gases at low and high temperatures
12 p2093 A69-26482

Nuclear active cosmic ray component energy spectrum determined from calorimetric ionization burst measurements, discussing nuclear particle interactions absorption coefficients
13 p2331 A69-28393

Reflection and absorption coefficients analyzed for obliquely incident electromagnetic wave from magnetoactive plasma in constant parallel magnetic field
14 p2411 A69-28997

Reflection of electromagnetic wave from magnetoactive plasma at inclined incidence, finding reflection and absorption coefficients
14 p2417 A69-29661

Absorption coefficient in three microwave lines of O with different rotational quantum numbers calculated, examining Zeeman effect in geomagnetic field
15 p2597 A69-30941

Magneto-optical oscillation of absorption coefficient in semiconductors during direct electron transitions
16 p2824 A69-31574

Balmer line H alpha emission and absorption coefficients measured with hydrogen plasma generated in high current low voltage free burning arc
16 p2822 A69-32040

Continuous absorption of coefficient hydrogen-carbon plasma at 40,000 degrees K and 70 atm in 230-460 mm spectral range
16 p2822 A69-32118

Ozone absorption coefficients in vicinity of Hartley band maximum verified by photographic spectrophotometry
16 p2785 A69-32626

Normal and directional emittance for two dimensional emitting, absorbing and scattering semiinfinite plane slab based on Monte Carlo method compared with Bobco approximation
[AIAA PAPER 69-625] 17 p3005 A69-33301

Radio wave absorption in interstellar H I regions, considering mean absorption coefficient dependence on height above galactic plane, evaluating planar electron density
17 p3034 A69-33608

Energy dissipation in bonded structures, analyzing vibration damping, hysteresis loop and absorption coefficient dependence on deformation energy
17 p3066 A69-33943

Molecular gas absorption coefficient dependence on laser emission energy density, considering disturbed equilibrium distribution of molecules
17 p2983 A69-33973

Laser action in quantum system, analyzing absorption constant relation to spontaneous/ stimulated emission constants, energy level population inversion, pumping, etc
17 p2984 A69-34150

Galactic clusters absorption, discussing optical thickness in blue and red light
18 p3197 A69-34746

Hypersonic gas flow past blunt bodies valid for any optical thickness of gas, allowing for absorption coefficients dependence on temperature, pressure and frequency
20 p3457 A69-36993

Maser submillimeter emission lines used to determine atmospheric and water vapor absorption, noting role of pressure
20 p3553 A69-37296

Radiative energy transport quantities for hydrogen plasma including Plank and Rosseland mean absorption coefficients, discussing line and continuum radiation and optical limits
20 p3581 A69-37306

Bubble size and blood perfusion effect on gas bubbles absorption in tissues, noting decompression sickness
21 p3651 A69-38389

Line statistics for representation of line absorption coefficient distribution for solar type stars
21 p3801 A69-38762

Absorption constant and reflectivity coefficient on semiconductor samples with nonideally prepared surfaces, calculating measurement errors
21 p3782 A69-39240

Photoelectric measurements of UV absorption coefficients of high temperature air at specific temperature and wavelength ranges in pressure-driven shock tube
22 p4049 A69-40098

Absorptivity of nonuniformly heated thin walled cylindrical radiator with central radiating hole, calculated by forward-reverse and integral methods
23 p4238 A69-41332

Absorption coefficient measurement for hydrocarbon gases for He-Ne laser beam at 3.39 microns, tabulating coefficients, noting variations from spectroscopic data
23 p4174 A69-42192

Ionospheric radio waves constant absorption term obtained from sunrise and sunset data
23 p4127 A69-42424

ABSTRACTS

NASA scientific and technical information program for building technical data and literature repository for scientists, engineers and technical managers, describing IAA and STAR
[UN PAPER 68-95317] 06 p1043 A69-17068

World literature on boundary lubrication for machine design, giving 2711 abstracts and extensive bibliographies
11 p1891 A69-24925

ABUNDANCE

Age and initial helium abundance of stars in M15 globular clusters estimated from stellar evolution lifetime ratio
01 p0149 A69-10135

Solar copper abundance determined from measuring Cu I and 2 and resonance lines transition probabilities in electric arc emission under LTE conditions
02 p0204 A69-11456

Fraunhofer lines hyperfine structure effect on solar abundances of V, Mn, Co, Cu and Ba, calculating equivalent line widths by ALGOL program
02 p0311 A69-11458

Growth curve for analysis of stellar spectra, determining relative f values and abundance
03 p0508 A69-13174

Solar Fe abundance from photospheric permitted Fe and forbidden Fe II lines, noting equivalent widths of two Fe II lines
03 p0515 A69-14036

Solar wind abundance measurements at earth orbit related to solar corona
03 p0503 A69-14047

Spectra of close binary systems, analyzing abundance anomalies, noting metallicity results
05 p0822 A69-15854

Nitrogen abundances in chondritic meteorites determined by carrier gas fusion extraction
05 p0825 A69-16301

Stellar element abundance ratios determination using relative strengths of molecular lines or bands
06 p1003 A69-17320

Beryllium abundance in solar atmosphere from spectra observed at Oslo Solar Observatory
06 p1010 A69-17971

Metastable helium abundance in interstellar and intergalactic space, inferring low energy cosmic ray concentration
06 p1010 A69-17973

Element synthesis in stars of galactic halo as possible explanation for heavy elements presence in supermassive objects
07 p1219 A69-19296

Photoelectric observations for stars in and near galactic cluster NGC 3680, discussing age and metal abundance
08 p1384 A69-20054

- Element abundances in two horizontal branch A stars through coarse and fine spectroscopic analysis, noting metal deficiencies with respect to sun
08 p1385 A69-20061
- Curve-of-growth abundance analysis for main sequence lambda Bootis stars, suggesting type Ap star characteristics
08 p1385 A69-20062
- Cosmic ray nuclei energy spectra and abundances above 20 MeV/nucleon determined by OGO-1 satellite experiment, considering He, B, C, N, O, Ne, Mg, Si, Mn, Fe, Co and Ni
08 p1378 A69-20067
- Solar photosphere abundances of various heavy elements from photoelectric spectrometer measurements of equivalent width of known Fraunhofer lines
08 p1390 A69-20393
- Pu 244 and I 129 abundances in early solar system and continuous galactic synthesis model of element formation in stars
08 p1397 A69-20695
- Origin and distribution of elements - Conference, Paris, May 1967
08 p1398 A69-20892
- Galaxy formation from elements primeval abundance viewpoint stressing initial helium abundance
08 p1400 A69-20894
- S-process nucleosynthesis and temperature averaged neutron capture cross sections studied in relation to solar system, considering elemental and specific isotopic abundances
08 p1357 A69-20896
- Lead isotopes nucleosynthesis by three mechanisms and contribution of mechanisms to abundances, noting chronology in nucleosynthesis
08 p1357 A69-20897
- Formation ratios of light isotopes in spallation reactions compared to observed stellar and solar abundances of lithium, beryllium and boron, discussing astrophysical implications
08 p1401 A69-20902
- Solar system elements abundance compilation based on carbonaceous chondrites and nucleosynthesis in stars
08 p1401 A69-20903
- Chemical composition and element abundance in solar atmosphere and photosphere, noting solar absorption and emission and energy spectrum data
08 p1402 A69-20905
- Solar element abundances from nucleosynthesis standpoint, discussing measurements with high resolution spectrometer used in double pass with intermediate slit
08 p1402 A69-20906
- Present state of abundance determination in solar corona, discussing forbidden and UV lines analysis
08 p1402 A69-20907
- Chemical composition of atmospheres of oldest Galactic stars, considering element abundances, metal and helium content and nuclear activity of massive stars
08 p1402 A69-20909
- Abundance determinations and spectrum intercomparisons in late type peculiar stars, discussing carbon and heavy metal star classes
08 p1403 A69-20910
- Element abundances in magnetic stars, discussing Zeeman effect and anomalies in spectra
08 p1403 A69-20911
- Stellar abundances of lithium, deuterium, beryllium and boron indicating nonthermal atmospheric origin
08 p1403 A69-20912
- Primitive elemental abundances in solar system, discussing composition of sun, meteorites and lunar maria
08 p1403 A69-20914
- Antimony bromine and mercury abundances in meteoritic materials determined by neutron activation analysis
08 p1404 A69-20919
- Cometary origin of meteors and element abundance in primitive solar nebula, discussing neutron capture products in chondrites
08 p1406 A69-20930
- Chemical abundances in planetary atmospheres based on spectroscopic determinations, considering terrestrial and Jovian planets
08 p1406 A69-20934
- Geochemistry and element abundances for Henbury impact glass, Darwin glass and australites, noting evidence for meteorite impact on sandstone
08 p1407 A69-20937
- Statistical distribution of chemical elements average abundances in earth crust and meteorites and nucleosynthesis of elements under specific astral conditions
08 p1310 A69-20941
- Rare earths relative and absolute terrestrial abundances in shales, basalts, rhyolites and granites
08 p1310 A69-20942
- Earth crust transition elements distribution and abundance compared to rare earths
08 p1310 A69-20943
- Continental diabases and oceanic tholeiites in light of rare earth and barium abundances and partition coefficients indicating fusion process
08 p1310 A69-20945
- Abundance analysis of B3 V star in Orion association, noting titanium and strontium overabundance and oxygen underabundance
08 p1407 A69-21133
- Stellar abundance and origin of elements, discussing stellar atmospheres and gaseous nebulae spectral determination, chronology of galactic halo, etc
09 p1587 A69-21306
- Atmospheric models for metal deficient stars of K and G spectral type, studying reduced metal abundance effect on atmospheric structure
09 p1596 A69-22055
- Element abundances of sharp lined field early A stars using model atmosphere
09 p1600 A69-22198
- Primordial helium and horizontal branch star luminosity, obtaining luminosities in He burning phase for different He and metal abundances from models
09 p1601 A69-22211
- Hyperfine transition line of He 3 II for abundance in Messier 17 source by radio telescope
10 p1785 A69-24098
- Early F stars Li/Be abundance ratios estimation from change in solar Be abundance, discussing stellar Li isotopes ratios
10 p1785 A69-24099
- Nebular abundances allowing for temperature variations in nebula along line of sight, correcting changes in electron temperature along path of observation
10 p1787 A69-24116
- Models for emission line region of 3C 273, considering ionization distributions for estimation of relative abundances
10 p1790 A69-24137
- Initial Sr isotopic composition at time of planetary objects formation in solar system and precision measurements for age determination of basaltic achondrites
11 p1953 A69-24357
- Stellar evolution model for primeval He abundance in population II stars in globular clusters for big bang confirmation
12 p2156 A69-26228
- Atmospheric element contents of F stars of Cyg, Her and Boo, using Planckian gradients and computer calculations for growth curves of atmospheric models
12 p2157 A69-26335
- Element contents of supergiant HD 190603 atmosphere based on spectrophotometric analysis including temperatures, turbulent velocity, gravity acceleration and electron concentration
12 p2157 A69-26336
- Relative transition probabilities for visible Si atom lines, noting disagreement with LS coupling predictions and solar Si abundance determination
13 p2340 A69-27580
- Relative element abundances in Cyg, Her and Boo atmospheres, calculating curves of growth by Planck gradient method for stellar spectra
14 p2519 A69-29356
- Arcturus and solar rubidium abundance compared using Mount Wilson photographic spectrograms of Arcturus
14 p2522 A69-29589
- Heavy element abundances in peculiar A stars, investigating nucleosynthesis during massive stars evolution
14 p2527 A69-29945
- Supergiant HD-33579 in Magellanic cloud by model atmospheres, discussing abundances
14 p2529 A69-29979
- Validity range of nuclear quasi-equilibrium approximation for stellar silicon burning, discussing time rates of nuclear abundance changes and temperature effect
14 p2529 A69-29984
- Fe II forbidden lines profiles and equivalent widths prediction for solar photospheric spectrum, deducing photospheric Fe abundance
16 p2854 A69-31652
- Solar chromosphere metal abundance determined taking into account local thermodynamic equilibrium departures
16 p2855 A69-31657
- Stellar light element abundances, discussing evolution models for various star types
16 p2866 A69-32816
- Spectrophotometric characteristics of Serpents, high metallicity A2 star and standard F zero V 9 Aurigae, analyzing chemical composition, microturbulence velocity and abundance by detailed differential growth curve
17 p3039 A69-33728
- Photoelectric photometric stellar spectroscopy for calculating metal abundance from Fraunhofer absorption lines, relating results to star age
17 p3043 A69-34140
- Heavy nuclei origin based on empirical abundance distribution, discussing stellar, galactic and cosmic events for nuclear genesis
17 p3009 A69-34190
- RF recombination lines measurement of helium for abundance in nebulas, comparing optical and radio values for H II regions
18 p3190 A69-34293
- Ionization stratification and chemical abundances in planetary nebula NGC 7662, discussing density fluctuations effect on N II and O II lines
18 p3191 A69-34294
- Curve of growth analysis for close binary HR 5317 indicating Mg, Mn, Ca and Sr overabundance respecting standard star 110 Her
18 p3191 A69-34297
- Alpha Serpents spectrum study from model atmosphere and growth curves, finding metal abundance ratios five times as great as in Arcturus
18 p3200 A69-35130
- Meteorite and primordial matter composition related to possible fractionation processes influence, discussing nuclear species abundance
19 p3406 A69-36073
- Fractionation of abundant lithophile element ratios of Si, Mg, Ca, Al and Ti in carbonaceous, common and enstatite chondrites
19 p3409 A69-36087
- IR spectra of Eta Carinae, confirming nitrogen and sulfur abundance
19 p3423 A69-36229
- Atmospheric models for specified effective temperatures, hydrogen-to-metal ratios and surface gravities in studying metal deficiency effect on stellar atmosphere
19 p3425 A69-36338
- Solar rare earth abundances determined from high resolution tracings of solar spectrum, comparing results with nucleosynthesis theories
20 p3602 A69-37539
- Methane abundance and rotational temperature of Jupiter, considering effects of line saturation
20 p3613 A69-38174
- Revised solar iron abundance by photospheric Fe I lines analysis using Garz and Kock f values, noting influence on solar photospheric model
21 p3796 A69-38475
- Abundance compilations of elements due to nuclear processes, discussing carbonaceous chondrites character
21 p3789 A69-38812
- Stellar lithium and beryllium, discussing production and destruction processes in stellar atmospheres and abundance in various stars
21 p3810 A69-39505
- Chemical composition of galactic and solar cosmic rays, discussing differences from universal cosmic abundances, using Cerenkov counters, emulsions, etc
22 p4002 A69-40090
- Cometary nuclei composition as last samples of early solar system composition, discussing dirty snowball model and radical lifetime problem
22 p4013 A69-40097
- Neutrons, protons and alpha particles abundance resulting from nuclear evolution of nondegenerate matter exploding at very high temperatures
22 p3980 A69-40148
- C, N and O abundances in K giants alpha Boo, beta Gem and epsilon Peg, noting stellar nuclear burning and evolution
22 p4026 A69-40653
- Relative abundances U-235/U-238, Th-232/U-238, Pu-244/U-238 and I-129/I-127 at solar system formation time to obtain time evolution of gamma process nuclei
22 p3986 A69-40766

AC [CURRENT]

Extraterrestrial objects composition in defining cosmic abundance curve, including solar and meteoritic data

22 p4032 A69-40982

A-type stars investigation for anomalous spectral line intensities, discussing Hertzsprung-Russell diagrams, rotational velocities, magnetic fields and abundances

23 p4218 A69-42322

Galactic evolution using concept of stellar populations and correlation with metal and He abundances

23 p4218 A69-42323

Photoelectric measurements of emission line intensities for low density planetary nebula with moderate excitation located near north galactic pole, deriving abundances

24 p4376 A69-42662

Fe abundance in sun and carbonaceous chondrites, noting agreement between solar and meteorite abundances of Ni, Mg, Si and Li

24 p4385 A69-43223

Nuclear theory of elements origin, discussing nucleosynthesis to interpret abundances

24 p4386 A69-43334

AC [CURRENT]

U ALTERNATING CURRENT

AC GENERATORS

Final stage of three phase DC/AC converter, noting three phase control circuit for power stages with germanium transistors

08 p1285 A69-20381

Sun-like alternating field generators, discussing dynamo theory of stellar and planetary magnetic fields based on nonmirror symmetrical turbulent motion in conducting fluid

10 p1782 A69-23703

Airborne static inverter, called Digital Inverter, for conversion of DC to AC, single phase and/or three phase, noting precise frequency control

[SAE PAPER 690339] 11 p1824 A69-24495

Liquid flow MHD alternating current generator design, considering induced current in rotor and resulting magnetic field in pole gap

13 p2206 A69-27495

Spray oil cooling to reduce aircraft generator weight, enhance reliability and lengthen overhaul intervals

15 p2552 A69-30326

Transient characteristics of three phase AC alternators with rectified outputs

17 p2905 A69-34089

Cost optimization in converting brush type to brushless aircraft AC power systems, using analog computer to determine modifications

17 p2905 A69-34109

Argon turboalternator design and testing for Brayton cycle space power system, discussing inlet operating temperature and shaft bearings and rotation

23 p4071 A69-42279

ACCELERATED LIFE TESTS

Accelerated reliability tests of electronic capacitors using voltage as main forcing factor, establishing correlations between lifetimes in accelerated and long term tests

09 p1464 A69-22244

Shock testing methods using shock spectrum concept and description testing machines and instrumentation

11 p1862 A69-24408

Accelerated structural tests under creep conditions, noting isothermal structures subjected to uniaxial and complex stress loads

12 p2186 A69-26838

Third generation computer reliability including preparation and test of integrated logic circuits

15 p2626 A69-30832

Accelerated temperature tests, calculating temperature behavior of hazard rates and activation energy from failure data using computer simulation

18 p3117 A69-34509

Accelerated test parameters estimated maximum intensity, studying temperature effects on test results

[AIAA PAPER 69-1036] 22 p3925 A69-40403

ACCELERATION [PHYSICS]

NT ANGULAR ACCELERATION

NT ARTIFICIAL GRAVITY

NT DECELERATION

NT GRAVITATION

NT HIGH GRAVITY ENVIRONMENTS

NT IMPACT ACCELERATION

NT LUNAR GRAVITATION

NT LUNAR GRAVITATIONAL EFFECTS

NT PARTICLE ACCELERATION

NT PHYSIOLOGICAL ACCELERATION

NT PLANETARY GRAVITATION

NT PLASMA ACCELERATION

NT REDUCED GRAVITY

NT SOLAR GRAVITATION
NT SPIN REDUCTION

Spacecraft motion parameters determination under controlled acceleration using information from inertial sensors

01 p0161 A69-10569

Growth rate of wave instability in conducting liquid jet in perpendicular electric field and accelerating under gravity

01 p0062 A69-11207

Nonstationary wing motion in gas stream near solid surface, analyzing differential equation for acceleration potential

02 p0188 A69-12134

Accelerated plate motion effect on flow of electrically conducting viscous incompressible fluid past infinite flat plate in uniform magnetic field

02 p0289 A69-12237

Symmetric baroclinic instability role in Jupiter equatorial acceleration

03 p0508 A69-13347

Lunar high density mass concentrations effect on Lunar Orbiters accelerations, discussing lunar gravity field determination

04 p0661 A69-15145

Acceleration wave propagation and growth in elastic materials, discussing thermodynamic influences

05 p0836 A69-15931

Axisymmetric vortex free motion of ideal fluid in conical container with spherical bottom under axial acceleration

06 p0910 A69-17335

Spacecraft trajectory during atmospheric reentry determined from projections of longitudinal acceleration onto coordinate axes connected with spacecraft

06 p1014 A69-17581

Motion of gyroscopic integrator of linear accelerations, analyzing nutational vibrations imposed on precession

06 p0927 A69-17688

Incompressible laminar Falkner-Skan boundary layer suffering sudden acceleration by moving belt, noting boundary layer separation

[AIAA PAPER 69-40] 06 p0912 A69-18049

Photographic study of burning metalized composite propellant under acceleration, noting burning rate augmentation by heat transfer from alumina particles retained on propellant surface

[AIAA PAPER 69-173] 06 p0983 A69-18151

Bow shock wave position and shape in rectilinear flight with constant acceleration

09 p1433 A69-21386

Acceleration effects on forced convection in turbulent boundary layer, noting heat transfer history and rates prediction

09 p1480 A69-21480

Earth ellipsoid fundamental parameters for calculation of earth flattening and normal acceleration due to gravity

09 p1487 A69-21633

Formation and acceleration of luminescent current layer in Z pinch discharge, noting density and electron mean free path in cold gas

09 p1552 A69-22397

Space flight fuel consumption optimization as function of acceleration of nozzle control

10 p1666 A69-22919

Combustion rates of condensed systems under positive and negative accelerations at atmospheric pressure

11 p2001 A69-25195

Inertial navigation platform principles including acceleration and position of vehicle, single axis platforms and stabilized element coordination

12 p2078 A69-25872

Optimal control for minimization of heating and acceleration forces to reduce kinetic energy of reentry vehicle in space missions

13 p2352 A69-27960

Optimal linear space navigation policies including integrated nongravitational acceleration output from inertial measuring unit

14 p2479 A69-29487

Parametric resonance motion in viscous fluid column in communicating vessels during vertical oscillations, calculating critical accelerations over viscosity range

14 p2432 A69-29628

Spacecraft motion parameters determination under controlled acceleration using information from inertial sensors

15 p2702 A69-30739

Shock waves from accelerated, decelerated and stationary axisymmetric bodies flying at supersonic velocities in stratified isothermal atmosphere

15 p2551 A69-31171

Doppler tracking data from Lunar Orbiter missions for studying lunar gravity anomalies, plotting acceleration on lunar surface Mercator projection

15 p2697 A69-31313

Equations for gradually changing motion by differentiating momentum and energy equations with respect to abscissa noting wall resistance, viscosity, turbulence and Coriolis coefficients

15 p2593 A69-31489

Accelerated boundary layers classified in terms of integral balance of pressure, inertia, wall friction forces and entrainment momenta

[AIAA PAPER 69-666] 17 p2955 A69-33462

Controlled-variable prediction display based on Taylor series computation, describing acceleration system simulator and human operator performance

19 p3313 A69-36414

Stratified fluid flow past obstacle, considering steady inviscid flow with nonlinear convection and vertical acceleration

19 p3240 A69-36474

Newton gravitational constant determination from measured acceleration and known magnitude of masses, describing control system

20 p3537 A69-37140

Geotropic response reciprocity in oat seedlings grown in two axis clinostat compared with acceleration constraints of biosatellites, considering imposition of centrifugal force

20 p3477 A69-37620

Hot star photogravitational acceleration determined from difference between apex and antiapex brightness, noting constant magnitude and direction of principal component of apex force

20 p3608 A69-38046

Fluid motion in free falling partially filled cylindrical vessel due to sudden vertical velocity change, considering free surface disturbances

21 p3692 A69-38684

Acceleration effects on solid propellant rocket motors combustion characteristics

[AIAA PAPER 68-530] 21 p3786 A69-39217

Field equations for electromagnetic radiation propagation in accelerated systems including dispersive and nonisotropic media

21 p3772 A69-39466

Boundary layer development on body accelerating in viscous incompressible fluid, using straight lines approximation and asymptotic expansions

22 p3929 A69-40110

Cumulative error in flight vehicle position determination by inertial navigation system, showing dependence on constant acceleration components

22 p3978 A69-40252

Gyroscopic motion with center of mass displaced along suspension axes and kinetic moment varying as power law under linear accelerations

23 p4163 A69-41552

Accelerated motion influence on onboard vertical gyro with design based on free astatic gyro with electromagnetic compensation

23 p4163 A69-41553

One dimensional shock waves and acceleration fronts in nonlinear isotropic viscoelastic materials using constitutive equations

23 p4235 A69-42463

Stress analysis of incompressible solid propellant rocket charges by point matching technique, considering differential thermal shrinkage and axial acceleration cases

24 p4402 A69-43263

Circulatory reactions of humans under g forces in centrifuge for various periods, with or without anti-g suit

24 p4267 A69-43385

ACCELERATION PROTECTION

G suit inflation acute and prolonged effects on cardiovascular dynamics in recumbent and passively tilted individuals

06 p0883 A69-17843

Active broadband vibration isolation of human subjects from severe vertical dynamic excitations experienced in low level high speed flight

[ASME PAPER 69-VIBR-65] 10 p1650 A69-24157

Vibratory acceleration limiting equipment attachment for resonance conditions, utilizing attachment stiffness reduction above predetermined value

[ASME PAPER 69-VIBR-23] 10 p1806 A69-24170

Antihypoxic preparations protective effect on white mice and rats subjected to gravitational accelerations

17 p2906 A69-32931

ACCELERATION STRESSES [PHYSIOLOGY]
NT CENTRIFUGING STRESS

Human body dynamic response to vibration combined with linear acceleration, noting changes in body mechanical impedance and resonance
 01 p0022 A69-11335

Physiologic and psychomotor changes during various acceleration stresses
 01 p0019 A69-11340

Insignificant or recoverable changes observed in blood acetylcholine content and cholinesterase activity of rabbits subjected to 8 g acceleration
 02 p0197 A69-11491

Hypokinesia and transverse accelerations combined effect on human cardiovascular system and regional blood circulation
 02 p0197 A69-11495

Human nervous system and vestibular and auditory analyzers functional changes under combined hypokinesia and radial accelerations effects
 02 p0197 A69-11496

Physiological studies of centripetal and Coriolis accelerations effects on vestibular function of humans in rotating chamber
 02 p0197 A69-11498

Control mechanisms of hemodynamic shifts from dogs subjected to acceleration under anesthesia
 02 p0198 A69-11503

Cerebellar cortex function disorders of rats subjected to 10 g acceleration under weak anesthesia
 02 p0198 A69-11504

1.5 g angular acceleration effects on acetylcholine metabolism in guinea pig brains and hearts
 02 p0198 A69-11505

Lateral acceleration effects on human kidney functions, noting increase in diuresis and erythrocytes in urine
 02 p0198 A69-11514

Neutral buoyancy microelectrode for prolonged recording from single nerve units
 02 p0202 A69-11865

X ray investigation of repeated simulated exposures to altitude and acceleration on healthy professional flyers
 03 p0378 A69-14208

Coriolis acceleration dosages applied in vestibulometric tests of male subjects inclined in rotating chair
 05 p0710 A69-16521

X ray study of biomechanics of respiratory act under long term acceleration stresses
 05 p0710 A69-16522

Cerebral circulation under longitudinal acceleration, discussing rheoplethysmographic measurements of heart rate
 05 p0710 A69-16625

Blood circulation in brain during acceleration analyzed by tensometric sensors and electroplethysmography, noting intracranial sensitivity to gravitational changes
 06 p0874 A69-17646

Cardiac arrhythmias during positive G sub x acceleration, treadmill exercise and tilt table testing
 06 p0874 A69-17834

Increased gravitational stress effects on esophageal sphincter pressures and gastroesophageal reflux in rhesus monkeys, noting cardia competence
 06 p0874 A69-17838

Sympathoadrenal activity during and after impact stress measured from urinary excretion of catecholamines and 17-hydroxycorticosteroids
 06 p0875 A69-17839

Autonomic nervous system in control of heart rate in acceleratively stressed monkeys, discussing sympathetic, parasympathetic and bradycardiac influence
 06 p0875 A69-17844

Manual performance of aircraft pilots under sustained acceleration using measurements of hand-writing pressure
 06 p0884 A69-18030

Abrupt deceleration effects on monkey heart rate, noting occurrence of relative bradycardia
 06 p0876 A69-18031

Rules for selecting Soviet cosmonauts and physiological studies concerning heart and respiratory reactions to accelerations and weightlessness during preparation
 07 p1060 A69-18569

Gravitational effects during physiological functions formation of human organism, noting myogenic tonus rearrangement as primary response
 07 p1060 A69-18572

Physiological reactions of dogs during acceleration and weightlessness in suborbital flights of ballistic rockets
 07 p1061 A69-18577

Human vestibular reactions during weightlessness preceded and followed by acceleration
 07 p1061 A69-18581

Vestibular-vegetative reactions during angular and Coriolis accelerations alternating with weightlessness, noting increased parasympathetic and sympathetic activity
 07 p1062 A69-18587

Oculomotor muscular tonus of rabbit during rocket flight acceleration and weightlessness
 07 p1062 A69-18590

Overt motion sickness prevention by incremental exposure to Coriolis accelerations
 07 p1067 A69-19425

Viscoelastic rod model of human spine subjected to accelerations
 07 p1072 A69-19725

Clinicomorphological changes in rabbit eyes vascular system by exposing transverse accelerations
 08 p1262 A69-19832

Transverse acceleration effect on male rabbit frontal hypothalamus nuclei neurosecretory function, noting blood plasma antidiuretic activity
 08 p1262 A69-19930

Long time physiological effects of rotating systems, surveying acceleration effects and rotation experiments on humans and rats
 08 p1265 A69-21183

Coriolis acceleration in rotating environment, discussing origins and role in human existence in rotating space station
 09 p1540 A69-21891

High gradient headward acceleration effects on acid base balance of baboons and human subjects, noting arterial changes
 09 p1444 A69-22540

Mathematical, physical and physiological modeling for analysis of functional changes during varying gravity conditions
 09 p1444 A69-22541

Increased chronic acceleration physiological effects on chickens, comparing hematological observations with exercise capacity, survival and sexual development
 10 p1641 A69-23041

Acceleration effects on cellular and subcellular structures enzyme activity in humans and animals, noting changes resulting from changed permeability of membranes
 10 p1645 A69-23496

Rats sensitivity to accelerations found dependent on excitation-inhibition ratio in central nervous system and hypophyseal-adrenal system reactions during acoustic excitation
 10 p1645 A69-23497

Transverse accelerations effect on dogs gastrointestinal tract secretory activity, noting central nervous system role
 10 p1645 A69-23498

Combined effect of prolonged bed rest and acceleration exposure on human blood circulation, noting increased heart rate and arterial blood pressure
 10 p1646 A69-23584

Chronic acceleration effects on erythrocyte number, plasma volume, globulin fractions, erythrocyte size and plasma A/G ratio in chickens
 11 p1828 A69-25458

Blind goldfish behavioral responses to short lowered gravitational force cycles during vertical flight classified as vestibular reflexes resulting from otolith displacement
 11 p1828 A69-25464

Motion sickness studied with slow rotation room having controlled Coriolis accelerations, discussing oculogyril illusion, nystagmus, dizziness and neuromuscular incoordination
 12 p2019 A69-26547

Prolonged iterative accelerations and decelerations on vestibular apparatus, discussing nystagmus measurement attempt and centrifugation tests on guinea pigs
 13 p2211 A69-28592

Posture role in physiological effects of acceleration on motor activity, discussing gravitational importance to vital processes
 13 p2211 A69-28593

Acceleration component in pelvis to head direction found influencing hyperemia of brain at various g forces
 13 p2212 A69-28626

Human motion coordination under acceleration followed by weightlessness during jet flights along Keplerian orbits, discussing initial disturbance and subsequent subsiding
 17 p2907 A69-32938

High positive g sub x acceleration effects on red cells destruction rate, measuring endogenous CO production of Gemini astronauts
 17 p2908 A69-33176

Transverse acceleration overstrain effect on mice sensitivity to cystamine
 17 p2909 A69-33386

Coriolis acceleration dosages applied in vestibulometric tests of male subjects inclined in rotating chair
 18 p3096 A69-34740

X ray study of biomechanics of respiratory act under long term acceleration stresses
 18 p3096 A69-34741

Combined angular and centrifugal acceleration effects on human and animal eyes motion studied to explain weightlessness effects on humans
 20 p3471 A69-37257

Vestibular analyzer dynamic characteristics under Coriolis acceleration, measuring heart beat rate, arterial pressure, head bending aftereffects, etc
 20 p3472 A69-37262

Motion sickness prophylactic action of sodium hydrocarbonate in dogs subjected to vertical accelerations, using intravenous administration
 20 p3473 A69-37269

Electrocardiographic changes during gravitational stresses
 21 p3660 A69-39178

Cerebellar cortex reactions to sciatic nerve stimulation in rats under transverse accelerations in centrifuge
 22 p3877 A69-40279

Human heart chronotropic reactions during centrifuge acceleration tests up to tolerance limit, establishing sinus tachycardia in various degrees
 22 p3877 A69-40283

Physical training effects under normal atmospheric pressure on high altitude hypoxia and acceleration resistance in rats, including survival times
 23 p4079 A69-41383

Sequential lung emptying at varying expiratory flow rates at increasing acceleration levels using expired nitrogen analysis
 23 p4083 A69-41448

Human angular acceleration sensitivity using rotation and oculogyril illusion perception as indicators, relating to spatial orientation and flight control task precision
 23 p4101 A69-41674

Jet pilot blood pressure response during positive acceleration in actual flight measured by telemetry compared with centrifuge test
 23 p4089 A69-41822

Acceleration effect on greyhound cardiac output and regional blood flow from Sapirstein radioisotope uptake technique, studying blood, skin, skeletal muscle, etc
 23 p4089 A69-41823

M-1 Valsalva maneuver induced cardiovascular stresses effect on oculobulbar vergence of subjects observing Thorington scale, discussing probable physiological mechanisms
 24 p4266 A69-43373

High intensity and short duration acceleration effects on human beings, discussing mechanical resistance of spinal column and circulatory aspects
 24 p4266 A69-43380

Stillbirth and neonatal death in stressed rats exposed to mild and acute gravitational loads in automobile ride and aircraft flight
 24 p4266 A69-43381

Radioisotopic determination of haemodynamic and bioelectric disturbances of rat striated muscles subjected to acceleration and hypokinesia
 24 p4268 A69-43409

ACCELERATION TOLERANCE

Space environment barriers to man due to biological evolution and transition from land to space in single generation, noting orientation problems
 03 p0380 A69-14067

Organic reaction and adaptation of rabbits and dogs to simulated weightlessness and acceleration compared with orbital flight data of human responses
 03 p0376 A69-14192

Impact/injury data used to estimate human tolerance to instantaneous accelerations
 04 p0552 A69-14469

Orthostatic intolerance, with assessment of circulatory problem of weightlessness in prolonged space flight
 06 p0873 A69-17016

Human acceleration tolerance dependence on age, profession and physical training from investigation of reactions to repeated centrifugal accelerations
 07 p1065 A69-18980

Human acceleration tolerance under reduced pressures corresponding to various high altitudes, noting visual disorders

07 p1065 A69-18982

Tilt-table and acceleration tolerance of athletes and inactive students, comparing cardiovascular responses, heart rate and blackout level
[DVL-834]

09 p1444 A69-21304

Dogs orthostatic tolerance and resistance to transverse acceleration after 14-day hypodynamia, studying tachycardia and arterial pressure

10 p1645 A69-23499

Rats tolerance to impact accelerations from blood enzyme activity providing safety limits for living organisms

10 p1645 A69-23500

Human resistance to short duration high accelerations applied to aircraft ejection studies, noting bone damage, consciousness retention, etc

13 p2215 A69-28591

Physical exercises to increase cosmonaut space environment tolerance, discussing effects of acceleration, altitude and hypoxia

15 p2560 A69-31460

Antihypoxic preparations protective effect on white mice and rats subjected to gravitational accelerations

17 p2906 A69-32931

Space research centrifuge counteracting null gravity physiological deconditioning, discussing linear and angular accelerations sensitivity and deconditioning effect on reentry task performance

18 p3114 A69-34368

Threshold variations in caloric nystagmus in pigeons subjected to accelerations in head to tail direction in centrifuge at various temperatures

20 p3471 A69-37252

Vestibulo-somatic, vegetative and sensory reactions to angular acceleration, deceleration and tilting, evaluating functional state of vestibular analyzer

20 p3481 A69-37270

Vestibular function tested with angular acceleration, applying semicircular canal reflexes for flight crew selection and appraisal

20 p3481 A69-37271

Human acceleration tolerance dependence on age, profession and physical training from investigation of reactions to repeated centrifugal accelerations

20 p3479 A69-38228

Human acceleration tolerance under reduced pressures corresponding to various high altitudes noting visual disorders

20 p3480 A69-38230

Healthy, physically untrained students compared with trained athletes for differences in working capacity concerning orthostatic tolerance and blood pressure responses

22 p3889 A69-39940

Healthy, physically untrained students compared with trained athletes for differences in working capacity concerning orthostatic tolerance and blood pressure responses

23 p4108 A69-41821

ACCELERATORS

Mechanical linear accelerator simulating acceleration, shock and weightlessness, noting data acquisition and interpretation

17 p2945 A69-33423

ACCELEROMETERS

Fluidic acceleration sensor based on vibrating string principle, discussing design, suspension system, driving-oscillator circuit, beat frequency circuit and detection circuits

02 p0249 A69-12091

Nonorthogonal multisensor strapdown inertial reference unit providing redundant capabilities and optimal performance

03 p0429 A69-13211

Controlled transient signal distortion by shock monitoring instrumentation circuits using piezoelectric accelerometers

04 p0603 A69-15430

Low g accelerometers including air-film, electrically suspended, vibrating string, semiconductor and ONERA [ONERA-TP-449]

05 p0766 A69-16749

Self contained electrically servoed transducers for flight control, noting angle of attack transducer and force

05 p0766 A69-16750

Equations for instability of stabilized platform of inertial navigation system with viscous friction in accelerometers

06 p0954 A69-16824

Thermal performance of pressure transducers, accelerometers, displacement transducers, resistance

thermometers and control mechanisms for NERVA reactor

06 p0956 A69-16885

Velocity meter for precision adjustment of orbits of vehicles in space for long periods using digital integrating accelerometer

08 p1348 A69-21063

Wideband acceleration instrumentation for Rover ground test facility liquid hydrogen turbopumps to study structural and flow induced vibrations

10 p1692 A69-23250

Fluid rotor angular accelerometer design for stabilization and control, noting applications to centrifuge speed and thruster gas consumption

10 p1633 A69-23273

FM/AM telemetry circuits with three axis piezoelectric accelerometer for measurements during impact tests of soft landing models

10 p1654 A69-23279

Optimal control algorithm for spacecraft descent in atmosphere based on nominal trajectory and acceleration measurements

13 p2355 A69-27683

Accelerometer force balance used in measuring forces and moments acting on models in short duration rocket plume tests at simulated high altitude
[AIAA PAPER 69-351]

13 p2264 A69-28285

Reliability of high resolution accelerometer composed of semiconductor integrated circuits

15 p2627 A69-30843

Reciprocity method for absolute calibration of piezoelectric accelerometer mounted on electrodynamic shaker table

15 p2615 A69-31283

Atmospheric density measurements by triaxial accelerometer system, ionization gauges and orbital decay of OV1-15 satellite

15 p2602 A69-31384

Low altitude atmospheric density satellite OV1-16 measurements, showing agreement between onboard accelerometer and orbital drag data

15 p2602 A69-31385

Drag measuring requirements and comparison of accelerometer or drag-free satellite control systems usage for atmospheric density determination

16 p2788 A69-31722

Inertial navigation system theory that uses increased numbers of newtonometers /force measuring devices/ in place of gyroscopic sensitive elements

16 p2791 A69-32283

Electromagnetic accelerometer with symmetrically placed photocells detecting small steel ball position

17 p2971 A69-32897

Portable piezoelectric acceleration sensor, describing characteristics and principles of operation

17 p2975 A69-33594

Accelerometer force balance method for measuring aerodynamic rocket plume forces acting on flat plate model in short duration shock tunnel test environments

19 p3292 A69-35737

Telemetry by reflex klystron accelerometer and seismometer with on air or coaxial cable signal transmission

19 p3272 A69-36255

Charge amplifier for piezoelectric transducer used in acceleration measurements

20 p3508 A69-37913

Navigation state vector update effect on lunar mission completion capability for Saturn 5, emphasizing hardware and scheme errors and accelerometer failure
[AIAA PAPER 69-883]

21 p3764 A69-39409

Flotation technique for laboratory calibration of low level accelerometers, noting accuracy dependence on flotation fluid density stability
[AIAA PAPER 68-874]

24 p4315 A69-43242

ACCEPTOR MATERIALS

Interactions between intermediate fluorescence quenching trapping center and associated electron acceptor of oxygen evolving photosynthetic spinach chloroplast photosystem

01 p0024 A69-10928

Acceptor defect levels in cadmium telluride crystals prepared under various cadmium vapor pressures, demonstrating ionization energy variation by electrical measurements

02 p0294 A69-11546

Trapping parameters of Fe doped GaAs-GaP, measuring thermally stimulated conductivity and space charge limited currents

02 p0296 A69-11789

Electron scattering by neutral acceptors in semiconductors, noting relaxation time for Ge at very low temperatures

03 p0484 A69-13280

Photoluminescence measurements of p-type thermal conversion in GaAs grown from silica boats, noting compensation by copper and shallow acceptors

04 p0639 A69-14434

Strong p-type conductivity of silicon doped with beryllium by thermal diffusion, giving electrical and optical measurements

09 p1556 A69-21652

Electronic properties of beryllium doped silicon studied with IR absorption spectroscopy and electrical measurements, describing Be thermal diffusion

10 p1747 A69-23989

Electron scattering by neutral acceptors in semiconductors, noting relaxation time for Ge at very low temperatures

14 p2508 A69-29653

Electronic states of semiconductor acceptor centers at forbidden band deep levels, considering inner electron shell excitation in impurity ion

15 p2665 A69-30039

Energy levels of multicharge acceptor centers and level splitting in InSb and GaAs deformed crystals, using multizone approximation

21 p3781 A69-39067

Lithium doped silicon acceptor concentration resulting from electron irradiation damage decreased by annealing at 300 degrees K

23 p4197 A69-41498

Ultrahigh vacuum cleaved GaAs-Cs and GaAs-cesium monoxide photoemission acceptor densities, noting crystal parameters role

23 p4198 A69-41548

Donor and acceptor impurity effect on absorption and reflection spectra of CdTe single crystals, analyzing In, Ga, S and Se

24 p4362 A69-43735

ACCESSORIES

Aircraft engine accessories for engine control, monitoring and protection, discussing transducer redesign, equipment range for Concorde, small engine design, etc

16 p2789 A69-31813

ACCIDENT INVESTIGATION

NT AIRCRAFT ACCIDENT INVESTIGATION

Alcohol role in pilot victims of aircraft accidents

01 p0022 A69-11345

Apollo spacecraft fire, presenting recommendations for power supply, cabin atmosphere and safety measures

07 p1071 A69-18970

Epidemiology of aerial application accidents analyzed in groups of high and low wing monoplanes, biplanes and helicopters

09 p1447 A69-22554

Apollo spacecraft fire, presenting recommendations for power supply, cabin atmosphere and safety measures

20 p3483 A69-38218

ACCIDENT PREVENTION

Prevention of and protection against accidental explosion of munitions, fuels and other hazardous mixtures - Conference, New York, October 1966

04 p0644 A69-14467

Mixing function vs time relationship for liquid propellant explosion hazards prediction, noting thermocouple grid for maximum information

04 p0646 A69-14478

Government role in air transportation policy, considering growing demands on air traffic control

06 p1040 A69-16835

Ideal safety system for accident prevention, considering foreseeable and unforeseeable aspects to eliminate individual or collective human error

06 p1040 A69-16836

Air safety, emphasizing misunderstandings or unresolved problems in accident prevention connected with law/safety interface

06 p1040 A69-16837

FAA aviation safety program design standards, maintenance and inspection procedures and assessment of accidents

06 p1041 A69-16839

Aviation safety information dissemination to improve accident and incident prevention

06 p1041 A69-16841

Accident prevention and investigation procedures of National Transportation Safety Board /NTSB/, discussing management patterns

06 p1041 A69-16842

USAF accident information, reporting and retrieving, describing Directorate of Aerospace Safety structure and functioning

06 p1041 A69-16843

Aircraft accident prevention and damage control

06 p0878 A69-16961

Characteristics of accident experienced pilots based on personality and psychological tests

06 p0876 A69-18033

Qualitative and quantitative hazards analysis of potential accidents/incidents in Post Boost Propulsion System with hypergolic propellants, considering recovery

10 p1753 A69-22972

Aeromedical investigation of civil aircraft accidents by National Transportation Safety Board, noting post-mortem legal aspects and need for human factors investigation

12 p2021 A69-25840

Preventive medicine in handling airline pilots to avoid accidents attributable to disability and death from natural causes

12 p2024 A69-26559

Accident record of general aviation pilots over age 60/1965/

14 p2541 A69-29308

Jumbo jet instrument landing difficulties, suggesting specific improvements in aircraft and airport equipment

15 p2549 A69-30189

Accidental ignition during solid propellant processing in terms of hazard to facilities and personnel, emphasizing mixing operation

16 p2829 A69-31993

Aviation health service for flight safety problems with emphasis on accident prevention, emphasizing physician role in man-machine relationship of personnel surveillance

18 p3098 A69-35305

Accident prevention program of Bureau of Aviation Safety, discussing probable cause analysis and function in feedback loop, hazard analysis and accident data center

22 p3867 A69-41140

Third generation jet aircraft safety, discussing accident prevention and survival

22 p4054 A69-41142

Aircraft fuel vent line sensitivity to lightning hazards, using flame propagation and arrester experiments with high voltage and high current facilities [SAE PAPER 690434]

23 p4062 A69-41651

Aviation accidents medical aspects, discussing accident causes and remedies, training and regulation proposals, etc

23 p4106 A69-41792

ACCIDENT PRONENESS

Accident record of general aviation pilots over age 60/1965/

14 p2541 A69-29308

ACCIDENTS

NT AIRCRAFT ACCIDENTS

NT AUTOMOBILE ACCIDENTS

Deficiencies in two hazard classification system for detonating and fire producing materials from analysis of chemical industry accident fatality statistics

04 p0645 A69-14471

Air evacuation of maxilla-facially wounded persons from place of accident, noting helicopter use

24 p4270 A69-42603

ACCLIMATIZATION

NT ALTITUDE ACCLIMATIZATION

NT COLD ACCLIMATIZATION

Noise level criteria for acceptable voice communications in office environment, noting acclimatization

11 p1830 A69-24797

Artificial heat acclimatization effect on orthostatic tolerance in man exposed to stresses of heat, exercise and dehydration

16 p2746 A69-32810

Time required for acclimatization to work in high temperatures, noting rectal temperature and heart rate changes

21 p3654 A69-38905

Calorimetry-thermometry discrepancy during prolonged exercise in hot dry environment, measuring rectal temperature with increasing exposure time

23 p4098 A69-42104

Blood flow, volume and venous pressure measurements in right hand at low and high altitudes in residents and newcomers

23 p4098 A69-42106

ACCOMMODATION COEFFICIENT

Accommodation coefficient effect on linearized heat transfer in rarefied gas between parallel plates and concentric cylinders

01 p0177 A69-11405

Interaction of rarefied gas with solid surface, analyzing accommodation coefficients, energy and impulse exchange as function of atomic bulk size

04 p0632 A69-14991

Surface parameters influence on energy transfer to arc jet anode, discussing work function, accommodation coefficient and diffuse reflection coefficient of electrons [AIAA PAPER 69-107]

06 p1039 A69-18185

Thermal accommodation coefficient and critical supersaturation for nucleation of mercury vapor on pyrex glass

13 p2321 A69-28005

Low temperature thermal expansion coefficients and linear contraction of metal alloys from liquid hydrogen to room temperature tabulated as function of temperature

14 p2464 A69-29400

Disaccommodation component of magnetic aftereffect causing dynamic absorption of HF magnetic energy in ferrites

15 p2665 A69-30038

Thermal accommodation coefficients determination, comparing techniques based on free molecule flow heat flux data

18 p3230 A69-35071

ACCRETION

U DEPOSITION

ACCUMULATORS

NT DUST COLLECTORS

NT SOLAR COLLECTORS

NT SOLAR REFLECTORS

Water removal unit design for electrolyte reaction accumulation in hydrogen oxygen fuel cell systems

04 p0552 A69-15316

Collection efficiency of continuous dynode electron multiplier arrays, discussing incident electron current

06 p0897 A69-17699

Flux collectors and field imagers for IR astronomy, discussing design, construction and dimensions

13 p2239 A69-27605

Thermionic converter performance measured using test vehicles with guard ringed collectors and variable emitter-collector spacing

14 p2398 A69-29177

Close coupled accumulators for suppressing missile longitudinal oscillations (POGO) developed for Gemini and Titan 3, including pump interaction [AIAA PAPER 69-547]

16 p2869 A69-32729

ACCUMULATORS [COMPUTERS]

Large scale integrated circuit accumulator chip as control element for design of digital system by design automated techniques

12 p2037 A69-25942

ACCURACY

Laser application to machine tool accuracy and alignment [ASTME PAPER MR68-407]

02 p0252 A69-11797

Mean temperature values accuracy determined from fixed period values by frequency graphs, discussing deviations from mean

09 p1534 A69-21511

Calibration and accuracy check of measuring instruments at National Center of Space Studies in France, emphasizing reference instruments

12 p2080 A69-26123

Accuracy and variance of nonergodicity estimates for random processes associated with radiophysical applications

15 p2582 A69-30946

Satellite orbits obtained by tracking by synchronous satellites, discussing accuracy for low altitude satellites

15 p2698 A69-31340

Radar signal reflectivity and precipitation relationship revised on basis of radio signal damping for improved measurement accuracy

23 p4185 A69-42494

Gravitational constant G determination, describing accuracy enhancement

24 p4350 A69-42944

ACETATES

NT LEAD ACETATES

Acetate carbon 14 utilization in centrifuged rats, analyzing metabolism by measuring plasma glucose, FFA and lipids synthesis

07 p1067 A69-19429

Acetate-2-C 14 conversion to C 14 carbon dioxide and C 14 fatty acids in rats with 2/3 of liver removed

19 p3257 A69-35976

ACETIC ACID

Optically active alanine synthesis from oxaloacetic acid by hydrogenolytic asymmetric transamination, noting role of decarboxylation

12 p2026 A69-25780

ACETONE

Methyl alcohol, ether and acetone vapors decomposition in microwave discharge, obtaining H and CO in addition to solid polymeric films

22 p3895 A69-40103

ACETYL COMPOUNDS

Insignificant or recoverable changes observed in blood acetylcholine content and cholinesterase activity of rabbits subjected to 8 g acceleration

02 p0197 A69-11491

1.5 g angular acceleration effects on acetylcholine metabolism in guinea pig brains and hearts

02 p0198 A69-11505

Quantitative analysis for N-acetylneuraminic acid by gas-liquid chromatography using trimethylsilyl derivative

13 p2217 A69-28315

Mechanical vibrations and noise effects on acetylcholine concentration, esterase activity and synthesis ability in rat brain

23 p4079 A69-41381

Regression process in acetylcholine level in rats after mechanical vibrations and noise exposure

23 p4079 A69-41382

Optic nerve spikes elicited by acetylcholine application on isolated perfused retina of frog, varying response by prostigmine and atropine

23 p4084 A69-41465

ACETYLENE

Diacetylene burning and spontaneous combustion regularities, determining reaction kinetics at moderate temperature

02 p0351 A69-11981

Ignition time of methane and acetylene, considering concentration and thermodynamic properties during reaction [WSCI PAPER 68-41]

07 p1240 A69-18356

ACHONDRITES

NT KAPOETA ACHONDRITE

Indium abundances in chondritic and achondritic meteorites and terrestrial rocks determined by radiochemical neutron activation analysis

08 p1404 A69-20917

Initial Sr isotopic composition at time of planetary objects formation in solar system and precision measurements for age determination of basaltic achondrites

11 p1953 A69-24357

Quality assessment of quantitative data on chemical composition of stony meteorites, considering precision and accuracy

11 p1953 A69-24359

Lithophile elements relationship in chondrites and basaltic achondrites, tabulating Ca-Al ratios and Ca, Al, Ti, Zr, Sr, Ba and Sc percentages

11 p1954 A69-24360

Cosmogenic Al 26 in achondrites and chondrites measured by nondestructive gamma-gamma coincidence counting

17 p3034 A69-33584

Ca-rich achondrites genesis implied from rare earth and Ba absolute and relative concentrations

19 p3409 A69-36091

Calcium-rich achondrites age distribution determined from inert gas measurements and existing data of eucrites, shergottites and howardites

19 p3413 A69-36107

Alpha-scattering experiments by Surveyor missions, studying hypothesis regarding lunar origin of eucrites and howardites

20 p3597 A69-37341

Calcium rich achondrites radiation ages determined from measuring He, Ne and Ar in howardites, nakhlites and angrite

20 p3602 A69-37535

Chemical composition of basaltic achondrites /eucrites and howardites/, indicating dominant role of physical process over magmatic differentiation

24 p4382 A69-42928

Halogen concentrations in basaltic achondritic meteorites, discussing applications to rare gas and lunar surface studies

24 p4382 A69-42929

ACID BASE EQUILIBRIUM

High gradient headward acceleration effects on acid base balance of baboons and human subjects, noting arterial changes

09 p1444 A69-22540

ACIDITY

Relative gas phase acidities of simple aliphatic alcohols, considering effects of alkyl groups

19 p3265 A69-36289

ACIDOSIS

Relative gas phase acidities of carbon acids determined using ion cyclotron resonance spectroscopy
19 p3265 A69-36291

Relative gas phase acidities of simple aliphatic amines and ammonia noting increase in large alkyl groups substitution
19 p3265 A69-36293

ACIDOSIS

Dogs cardiovascular responses to histamine liberator /compound 48/80/, describing shock and acidosis with elevated histamine levels
22 p3873 A69-40206

ACIDS

NT ACETIC ACID
NT ADENINES
NT ALANINE
NT AMINO ACIDS
NT ASCORBIC ACID
NT BORIC ACIDS
NT BUTYRIC ACID
NT COENZYMES
NT CYSTEINE
NT DEOXYRIBONUCLEIC ACID
NT DICARBOXYLIC ACIDS
NT FATTY ACIDS
NT FORMIC ACID
NT GLUTAMIC ACID
NT GLYCINE
NT HYDROBROMIC ACID
NT HYDROCHLORIC ACID
NT HYDROFLUORIC ACID
NT LACTIC ACID
NT LEUCINE
NT LYSINE
NT METHIONINE
NT NITRIC ACID
NT NUCLEIC ACIDS
NT OXIDASE
NT PEPTIDES
NT PYRIDINE NUCLEOTIDES
NT RIBONUCLEIC ACIDS
NT TRYPTOPHAN
NT URIC ACID
NT URIDYLIC ACID

Acid fraction extraction of Green River shale identified by gas chromatography-mass spectrometry-computer system, noting trimethyl pentadecanoic acid
21 p3669 A69-38983

ACOUSTIC ATTENUATION

NT SHOCK WAVE ATTENUATION

Dispersion relation of internal acoustic gravity wave motion in compressible nonviscous and nonheatconducting atmosphere
02 p0242 A69-11868

Electronic attenuation of 10 to 130 MHz longitudinal ultrasonic waves in superconducting high purity Ti, noting energy gap anisotropy
03 p0485 A69-13293

Electronic attenuation of 10 to 130 MHz longitudinal ultrasonic waves in nonsuperconducting high purity Ti, noting anisotropy and measurements below 4.2 K
03 p0485 A69-13294

Constrained layer damping and conventional techniques combination for vibration and noise control
04 p0606 A69-14691

Absorption and amplification of sound in many valley semiconductors in strong electric field, noting dependence on electron heating and relaxation times
07 p1199 A69-18681

Field noise reduction frequency spectra afforded by spacecraft shroud, basing estimating criterion on flight test data
09 p1609 A69-21892

Ultrasonic pulse velocity and attenuation measurement in presence of noise, using coherent detection and signal averaging
14 p2449 A69-29564

Ultrasonic pulse-echo-overlap method modified for simultaneous measurement of time delay and relative voltages in determining sound velocities and attenuation of solids
14 p2450 A69-29567

Magnetoquantum-electric effect, analyzing center motion of cyclotron orbit during photon and phonon absorption and current quantity
16 p2826 A69-31823

Nonlinear response of single Helmholtz resonator subjected to finite amplitude pressure oscillations, detailing entrance, orifice and cavitation flow [AIAA PAPER 69-481]
16 p2844 A69-32719

MHD waves attenuation in ionosphere due to gyrorelaxation, reducing analysis to determination of anomalous absorption of acoustic waves
23 p4155 A69-41841

Welded honeycomb sandwich structures of Ti, steel and similar materials for use in extreme thermal and acoustical environments [AIAA PAPER 68-973]
24 p4326 A69-43716

ACOUSTIC COMBUSTION

U COMBUSTION STABILITY

ACOUSTIC DELAY LINES

Acoustic surface waves on thin film for pulse compression radar dispersive delay line, describing delay characteristic synthesis and control
19 p3267 A69-35929

Al and Mg alloys as ultrasonic wave acoustic lines, considering sound velocity, damping factor, grain size, chemical composition, etc
20 p3564 A69-38290

Ultrasonic diffraction delay lines technique to extend radar systems range without affecting target pinpointing capability
24 p4286 A69-42901

RF and microwave signal variable delay and processing using laser-acoustic interactions, photodetector and electrical-to-acoustical transducer
24 p4283 A69-43027

ACOUSTIC EXCITATION

Bounds from asymptotic behavior of solutions of nonlinear integrodifferential equation arising from nonlinear oscillators in acoustics
01 p0103 A69-10001

Threshold velocities of acoustoelectric current oscillations in elemental piezo- and nonpiezoelectric semiconductors, taking into account amplification and losses of phonons
05 p0807 A69-15956

Fatigue crack propagation and crack tip stresses measurements in tensioned cracked panels subjected to acoustic loading
10 p1797 A69-23078

Rats sensitivity to accelerations found dependent on excitation-inhibition ratio in central nervous system and hypophyseal-adrenal system reactions during acoustic excitation
10 p1645 A69-23497

Sound amplification role in increasing spread of bounded two dimensional smoke jet studied for application to fluid amplifiers [ASME PAPER 69-VIBR-3]
10 p1640 A69-24161

Cylindrical shells spectral response to random acoustic pressure excitation, noting natural modes and inner air column effects
11 p1990 A69-25506

Acoustic power transferred to plane homogeneous elastic structures and cylindrical shells by neighboring sound sources
13 p2363 A69-28186

SST fuselage response to reverberant and turbulent boundary layer noise calculated for computing equivalent reverberant acoustic fields
15 p2549 A69-30302

Sound effects on turbulent flame in gasoline-air mixture jet in Toepfer device with pulsed light source, measuring ionization in combustion zone
17 p3069 A69-33141

Response of three level particles system with equidistant spectrum under resonant action of acoustic and electromagnetic pulses sequence with different frequencies
21 p3737 A69-39068

Collisionless damping of large amplitude ion acoustic waves excited externally in thermally ionized Cs plasma
22 p3991 A69-41008

Topography of potentials induced by acoustic clicks in auditory cortex of dogs, including ectosylvian gyrus distribution
22 p3888 A69-41269

Cortical biopotentials in cats induced by strychnine under acoustic click stimuli of increasing intensity
22 p3888 A69-41270

Structural differences effect of gyrus and sulcal areas of acoustic projection cortex on primary induced acoustic responses
23 p4079 A69-41380

ACOUSTIC FATIGUE

Differential and threshold sensitivity of acoustic analyzer of humans under space flight factors
02 p0197 A69-11500

Collection of articles on noise and acoustic fatigue in aeronautics sponsored by Ministry of Aviation and USAF
05 p0703 A69-16800

ACOUSTIC GENERATORS

U SOUND GENERATORS

ACOUSTIC IMPEDANCE

Specific acoustic admittance of solid propellant burning surface for determining burning instability under rocket motor conditions
02 p0302 A69-11521

Acoustic absorbers for combustion stabilization, discussing analytical model based on temporal damping coefficient for oscillation modes and allowance for nonuniform distribution
03 p0532 A69-13133

Piezoelectric transducer theory, discussing acoustically matched sandwich type damper and calculating frequency characteristics
10 p1697 A69-24071

ACOUSTIC INSTABILITY

Doppler effect in ionospheric acoustic perturbations caused by strong ground explosion, noting accord with nonlinear acoustic wave propagation theory
09 p1488 A69-21694

Low pressure arc discharge plasma, studying ion-acoustic oscillations development in magnetic field
12 p2136 A69-26527

Pressure waves interaction with solid fuel hot surface at HF based on linear theory of acoustic instability in condensed systems
13 p2371 A69-27383

ACOUSTIC MEASUREMENTS

Noise and relations between environment and man, discussing sound perception, measurement and judgment of noise annoyance and harm
01 p0020 A69-10741

Acoustic probe for measuring pressure fluctuations on hypersonic reentry vehicle, discussing flow characteristics and heat shield ablation effects on frequency response
01 p0008 A69-11278

Differential and threshold sensitivity of acoustic analyzer of humans under space flight factors
02 p0197 A69-11500

Waveguide band transition noise of gas discharge source, discussing measurement methods for establishing excess noise ratio
02 p0212 A69-12461

Level crossing rate meter correction for boxcar-ed and receiver noise readings in incoherent weather radars
04 p0557 A69-14915

Noise signal mean square value measurement in pulse noise conditions by using noise amplitude limiter with limitation threshold in receiver
05 p0719 A69-16086

Anomalous infrasonic signals observed during launching of space vehicles with thrust greater than 200,000 lb, noting supersonic and subsonic group velocity spreads
07 p1078 A69-18853

Impulse noise damage risk criteria, discussing maximum tolerable exposure, hazardous exposure and methods of impulse noise measurement
07 p1066 A69-19171

Acoustical measurements on MD-12 passenger aircraft before and after application of insulation for noise suppression
07 p1057 A69-19704

Noise-signal receiver amplitude-limitation effect on noise measurement in presence of pulsed interference
07 p1088 A69-19754

Microwave converters structural characteristics, calculating noise figure
08 p1285 A69-20594

Interference capability of noise of different frequency bandwidths, comparing weighted sound pressure to loudness level
08 p1276 A69-20857

Modulus of elasticity changes and stress relaxation spectra of viscoelastic liquids measured by acoustic methods
11 p1887 A69-25206

Procedures and facilities applicable to sonic environmental testing of flight vehicles, discussing sonic energy sources in vehicles and potential failure modes
12 p2060 A69-26939

Supersonic boundary layer acoustic characteristics measured in wind tunnel on cylindrical model with several forebody configurations [AIAA PAPER 69-344]
13 p2249 A69-28279

Annoyance caused by noise near airports, discussing PNdB /perceived noise dB/, evaluation criteria, and French, British, American and German methods
13 p2214 A69-28588

Aircraft noisiness estimation methods
13 p2216 A69-28660

Noise measurement and scales in studying psychological and nonauditory physiological effects on human functioning
14 p2485 A69-29150

Acoustic sounding of atmospheric structure, utilizing energy backscattered from temperature fluctuations in turbulent regions
14 p2448 A69-29527

Noise sources in S band parametric amplifier with GaAs varactor diode measured at liquid nitrogen temperature, considering noise reduction
15 p2578 A69-30636

Near field flow noise generated in boundary layer of water vehicle measured for rotating cylinder, ship and buoyant unit using hydrophone
17 p3004 A69-32953

Noise intensity measurements in far field of circular nozzle for jet noise composition
17 p2957 A69-33602

Microphonic noise measuring systems for airborne radar system design for noise reduction
17 p2937 A69-33628

Acoustic spectrum averager for Mariner spacecraft environmental tests, calculating rms average 1/3 octave spectrum bands in real time [JPL-TR-32-1442]
17 p2946 A69-33658

Helicopter rotors forward-flight noise characteristics determined by wind tunnel tests compared to rotor noise during flyover
18 p3119 A69-35225

Acoustic measurements at room temperature for determining losses in rocket chamber during combustion instability, using small scale model
19 p3394 A69-35946

Crack growth in steel tested in hydrogenated condition, distilled water and in combination by acoustic emission, relating time intervals to hydrogen diffusion
19 p3350 A69-36893

Acoustic filters performance determination, standing wave tube and anechoic termination methods
20 p3464 A69-37321

Scanned receiver acoustical holography for mapping or imaging sources of radiated acoustic energy on complex vibrator in water, noting application in air
20 p3576 A69-37323

Real time analyzers of acoustic signals for aircraft engine noise, noting automatic test
20 p3462 A69-37756

Acoustic frequency response of unsteady turbulent flow in transmission lines, considering effects of small amplitude disturbances and heat transfer [ASME PAPER 69-FE-11]
20 p3516 A69-37988

Acoustic emission signals for nondestructive testing and material evaluation, determining critical stress intensity factor for stress corrosion cracking
20 p3512 A69-38270

Noise and vibration levels measured in An-24 Polish passenger aircraft indicating excess noise in crew compartment
22 p3862 A69-40005

Digital systems for acoustical or vibrational measurements reception and evaluation
22 p3945 A69-40168

Helicopter main rotor noise from square tipped blades determined as function of tip speed, blade area and thrust
22 p3864 A69-40676

Robbins-Monro stochastic approximation method using algorithms for identifying finite memory time-discrete time-stationary linear system from noisy input-output measurements
22 p3918 A69-41013

Speech interference aspects of noise measured as function of level and spectrum of speech and noise at listener ear, using simplifying nomogram
23 p4101 A69-41495

Distortion processes in ear, discussing sound pressure level /SPL/ measurements in rigid-walled couplers
23 p4085 A69-41573

Hearing adaptation measurements after aircraft noise stresses for estimation of induced noise damage
23 p4110 A69-42051

Retarded voice tests apparatus using graphical recording to determine intensity of deformations by autoaudition, considering application to recruitment investigation
24 p4270 A69-42604

Optimal focusing of acoustic system for tube defectoscopy with circular normal waves
24 p4296 A69-42655

Sonic diagnostic engine analyzer for detecting jet engine malfunctions prior to failure
24 p4312 A69-42758

Acoustic analyzer response of man during prolonged noise effect of varying pitch and intensity
24 p4278 A69-43408

ACOUSTIC PROPAGATION

Vertical propagation of acoustic waves in atmosphere without gravitational waves and with height varying atmospheric shear viscosity
02 p0274 A69-11440

Acoustic plasma waves propagation in thin films in case of film quantization, showing phase velocities close to Fermi velocities of electrons
02 p0300 A69-12649

Acoustoelectric domain propagation in N-type GaAs, noting flux influence on peak acoustic density
05 p0806 A69-15815

Acoustic and electromagnetic energy propagation in lower ionosphere and atmosphere for energy pulse generation by chemical explosion
07 p1078 A69-18844

Dispersion and average monthly numbers of whistlers for propagation trajectories during solar activity minimum, discussing electron concentrations in magnetosphere
09 p1485 A69-21531

Ion-acoustic wave experiments for disturbance travel in plasma sheath, obtaining ion number density
11 p1929 A69-25272

Acoustic waves in ionosphere relation to electron content fluctuations detected from beacon satellite BE-B signals [AFCRL-69-0291]
12 p2065 A69-26104

Turbulent boundary layer sound emission effect on elastic plate, discussing pressure pulsation spectrum reflection
13 p2246 A69-27538

Sound generation by unsteady rotational flow as singular perturbation problem solved by matched asymptotic expansions, discussing flow and radiation fields
13 p2299 A69-28187

Ion drag effects on acoustic gravity waves propagation in isothermal F region, discussing indicated wave damping
14 p2434 A69-28944

Dispersion and average monthly numbers of whistlers for propagation trajectories during solar activity minimum, discussing electron concentrations in magnetosphere
16 p2783 A69-32526

Hydrodynamic stability of solid fuel combustion in presence of acoustic disturbances in gas phase, considering material erosion and particle dispersion
18 p3231 A69-35150

Nondestructive test method using transducer action of flaw in stress field causing plastic deformation with energy release as acoustic emission
19 p3314 A69-36634

Turbulent boundary layer sound emission effect on elastic plate, discussing pressure pulsation spectrum reflection
20 p3518 A69-38204

Acoustic wave propagation in plasma, analyzing ionic and electron sound caused by oscillation and relaxation processes using Landau and Vlasov kinetic equations
23 p4196 A69-41726

Saturn F-1 rocket engine as generator of infrasonic waves and magnetic fluctuations, noting ignition and cut-off signal characteristics
24 p4365 A69-43415

ACOUSTIC PROPERTIES

NT REVERBERATION

NT SOUND INTENSITY

Acoustic paramagnetic resonance in arsenic doped germanium, measuring spin-lattice relaxation
02 p0296 A69-11835

Acoustical Bragg reflection and Debye-Sears effect with application to light and ultrasonics interaction
07 p1144 A69-18285

Hydraulic analog for determining acoustic behavior of baffle cell used in liquid rocket engines, comparing ring and spoke type baffles
09 p1570 A69-22004

Entrainment and acoustothermal effect in piezoelectric semiconductors having electrons with different energy
10 p1746 A69-23573

Acoustic effects in piezoelectric semiconductors due to sound-electrons interaction including sound absorption, sound velocity changes, electroacoustic effect, etc
14 p2503 A69-28786

Random oscillations of elastoacoustic systems, obtaining solution for spherical shell containing acoustic medium
17 p3057 A69-33199

Fluid-shell interactions, using piston theory and cylindrical-wave approximations
18 p3223 A69-35174

Acoustics and optics in terms of acoustic holography, seismic signal optical processing, acoustic and electromagnetic waveguides, etc
23 p4191 A69-42179

ACOUSTIC RADIATION

U SOUND WAVES

ACOUSTIC SCATTERING

NT REVERBERATION

Steady longitudinal motion of insulating cylinder in conducting fluid, discussing analog between steady MHD and acoustic scattering
04 p0638 A69-15192

Quasi-phonon model for acoustic scattering and diffraction from rigid real obstacle in fluid medium
05 p0797 A69-16649

Hole mobilities in InSb due to phonon and ionized impurities scattering on basis of strain potential constants
16 p2824 A69-31575

Airfield bird scaring methods including Very pistol shell cracker firing and broadcast calls on civilian and military airfields
17 p2915 A69-33365

ACOUSTIC SIMULATION

Finite amplitude standing transverse resonant acoustic field effects upon flow behavior of viscous fluid in cylindrical enclosure to acoustically model combustion instability [AIAA PAPER 69-667]
17 p2954 A69-33457

ACOUSTIC STABILITY

U FREQUENCY STABILITY

ACOUSTIC STREAMING

Acoustic streaming near small spherical obstacles, obtaining stream functions
04 p0631 A69-14904

Intense transverse resonant acoustic field interaction with viscous fluid flows [ASME PAPER 68-WA/FE-8]
05 p0748 A69-16091

Acoustic streaming near small spherical obstacles, obtaining stream functions
12 p2131 A69-26657

Intense transverse resonant acoustic field interaction with viscous fluid flows [ASME PAPER 68-WA/FE-8]
14 p2430 A69-29444

ACOUSTIC VELOCITY

Acoustic resonance excitation in axial flow compressor annulus by wake shedding from blades
01 p0142 A69-10058

Flow characteristics and sound velocity in two temperature plasma
05 p0802 A69-15796

Velocity of 1 MHz sound waves in He 4 along isotherms just above critical temperature, noting specific heat ratio for 4.5 and 5 K isotherms
06 p0957 A69-17142

Ultrasonic thermometry for nuclear reactors based on temperature dependence of sound velocity in solids, discussing simulation experiments [IEEE PAPER IC-4]
07 p1134 A69-19186

Speed of sound and shock waves in two phase flows of liquid metal MHD generators, considering droplets uniformly dispersed in gaseous phase
13 p2245 A69-27475

Ultrasonic pulse-echo-overlap method modified for simultaneous measurement of time delay and relative voltages in determining sound velocities and attenuation of solids
14 p2450 A69-29567

Weak shock waves relaxation time and amplitude and acoustic velocity as functions of thermorelaxing media
15 p2590 A69-30103

Small perturbations propagation in plasma at Newtonian acoustic velocity, determining temperature, pressure and current densities
15 p2663 A69-30993

Acoustic velocities in polymethylmethacrylate measured as functions of frequency, temperature and pressure, comparing data obtained with equation of state high pressure determinations
16 p2825 A69-31695

Polycrystalline BeO sound velocities determined as function of pressure and temperature using pulse superposition method
16 p2802 A69-32338

Flight velocity changes from sonic to supersonic through turbojet/ramjet combination possibility
17 p3020 A69-33348

Vertical structure concepts for air density, wind and sound velocity profiles in rocket climatology, discussing vertical relationship of wind shear statistics
17 p3000 A69-33794

Water jets with greater than half sound speed created by shock wave impinging on cavity within liquid, discussing mechanism, maximum speed, shape, etc
19 p3301 A69-36815

ACOUSTIC VIBRATIONS

U SOUND WAVES

ACOUSTICS

NT BIOACOUSTICS
NT LAMB WAVES
NT LAME WAVE EQUATIONS
NT MAGNETOACOUSTICS

Sonic bang intensities in stratified atmosphere obtained by geometrical acoustics and linear theory modifications to take account of nonlinear effects
01 p0008 A69-10056

Acoustical holography - Conference, Huntington Beach, California, December 1967, Volume 1
10 p1694 A69-23540

Physical principles and practical methods in light and sound holography, comparing advantages and limitations
10 p1694 A69-23541

Holographic techniques for acoustic imaging to obtain three dimensional images of opaque objects encountered in nondestructive testing
10 p1695 A69-23544

Quantitative analysis of plane waves for weak interaction of two dimensional sound and light fields in acoustical imaging by diffracted light
10 p1695 A69-23545

Acoustical transparencies illuminated by sound waves for optical imaging and ultrasonic diffraction, noting application to visualization of inhomogeneities in samples
10 p1695 A69-23546

Digital reconstruction of images from optical holograms for acoustical data, discussing image degradations
10 p1695 A69-23547

Qualitative analysis of recording phase only acoustic holograms of object wave instead of both phase and amplitude, considering fringe patterns and conjugate image
10 p1695 A69-23548

Matrix method for acoustical holograms and optical reconstruction of virtual and conjugate images using laser light of 6328 Å wavelength
10 p1696 A69-23549

Typographical spatial correlation filtering methods for reconstructing holographic images with ultrasonic waves, noting application to flaw recognition
10 p1696 A69-23551

Alphabetical listing of references and abstracts of papers on acoustical holography
10 p1696 A69-23552

Intracavity acoustooptic devices based on isotropic and anisotropic acoustic Bragg diffraction, discussing efficiency, bandwidth and acoustic column width
10 p1697 A69-23871

Acoustic holography free surface and scanning methods, noting acoustical intensity role in phase stability
11 p1883 A69-24687

Linear recording of object wave phase to produce acoustic holograms
13 p2259 A69-27243

CdS acoustoelectric oscillator steady state oscillation frequency dependence on voltage and conductivity compared with linear acoustoelectric amplification theory
13 p2227 A69-27244

Monograph on sound generation by turbulence and surfaces in arbitrary motion, discussing sound and multiple fields and governing equations
13 p2247 A69-27974

Acoustic hologram recorded by laser flying spot scanner
13 p2265 A69-28662

Magnetoelastic resonant interaction of microwave longitudinal phonons propagating at right angles to magnetic bias applied to YIG rod axis
15 p2565 A69-30184

Acoustic flow calorimeter for evaluating power transducers under loaded conditions
16 p2790 A69-32079

Systems approach in turbofan engine design acoustic evaluation, discussing noise sources and radiation patterns
[AIAA PAPER 69-491] 16 p2839 A69-32667

Machine recognition of continuous speech at acoustic level, noting low bit rate speech communication system
17 p2932 A69-34119

Acoustic visualization for nondestructive testing, describing image formation by lenses, reflectors, holography, Bragg diffraction and phase contrast
20 p3512 A69-38269

Frequency and space averaging effect on variability and standard deviation of multimode media transmission responses, with application to reverberant media
23 p4115 A69-41576

Acoustics and optics in terms of acoustic holography, seismic signal optical processing, acoustic and electromagnetic waveguides, etc
23 p4191 A69-42179

Acoustical holograms phase recording, combining external phase locked electronic reference beams
23 p4166 A69-42180

Temporal reference acoustical holography with Sokolov ultrasound camera system using double pulsed ruby or scanning CW laser
23 p4166 A69-42182

Phase and amplitude acoustical holography in opaque media, discussing medical diagnosis and underwater viewing
23 p4167 A69-42198

Acoustical holography principles and reconstruction techniques, noting advantages of liquid-surface and temporal reference holography over optical counterpart
23 p4167 A69-42199

ACQUISITION

U DATA ACQUISITION
U TARGET ACQUISITION

ACROBATICS

Differential equation for dynamic behavior of acrobatic flight navigation instruments in steep flight, considering vertical gyroscopes, gimbal platforms and time optimal control
11 p1880 A69-24328

ACRYLATES

Explosive acrylic polymers properties and preparation methods, noting chemical reactions and structure
08 p1376 A69-21152

Methyl 2-cyanoacrylate adhesive bonding characteristics, noting importance of film thickness
09 p1529 A69-22316

ACRYLIC RESINS

NT POLYMETHYL METHACRYLATE

Microbial contamination release from impact-fractured tubes, examining bacterial spores growth in fractured methyl methacrylate plastic for application to space exploration
20 p3475 A69-37614

ACRYLONITRILES

Electron beam radiation curing of mercaptan terminated butadiene-acrylonitrile liquid copolymers at ambient temperatures in air
09 p1512 A69-22368

ACTH

U ADRENOCORTICOTROPIN [ACTH]

ACTINIDE SERIES

NT PLUTONIUM ISOTOPES
NT PLUTONIUM 238
NT RADIUM 226
NT THORIUM
NT THORIUM ISOTOPES
NT URANIUM
NT URANIUM ISOTOPES
NT URANIUM 235

Superconductor research noting pressure effects, graphs and tables illustrate behavior of materials considered
20 p3584 A69-38015

ACTINIDE SERIES COMPOUNDS

U THORIUM COMPOUNDS
U THORIUM OXIDES
U URANIUM COMPOUNDS
U URANIUM FLUORIDES
U URANIUM OXIDES

ACTINOGRAPHS

U ACTINOMETERS

ACTINOMETERS

NT DICKE RADIOMETERS
NT ELECTROPHOTOMETERS
NT INFRARED DETECTORS
NT INFRARED SCANNERS
NT INFRARED SPECTROMETERS
NT INFRARED SPECTROPHOTOMETERS
NT MICROWAVE RADIOMETERS
NT PHOTOMETERS
NT PYRANOMETERS
NT RADIOMETERS
NT SOLAR SPECTROMETERS

NT SPECTROHELIOGRAPHS
NT SPECTROPHOTOMETERS
NT SPECTORADIOMETERS
NT ULTRAVIOLET SPECTROMETERS
NT ULTRAVIOLET SPECTROPHOTOMETERS

Satellite actinometric data computerized reduction in U.S.S.R., examining computer program features
[UN PAPER 68-95763] 06 p0916 A69-17038

Narrow and wide angle actinometric instruments on-board Cosmos 122, 144 and 156, describing optical and data acquisition systems
06 p0929 A69-17977

Calibrating long wave actinometric instruments designed for Soviet meteorological satellites
06 p0929 A69-17978

Vertical distribution of ascending long wave radiation, employing actinometric radio sondes
06 p0953 A69-17990

Computer program for processing actinometric data transmitted from Cosmos 122 satellite
11 p1913 A69-24831

Solar radiation actinometric and pyranometric observations during 20 May 1966 eclipse, examining IR component and spectral radiation energies
15 p2697 A69-31257

ACTIVATION

NT NEUTRON ACTIVATION ANALYSIS

Energy exchange between active centers in silicate and phosphate glass, comparing luminescent and lasing properties
15 p2632 A69-30053

ACTIVATION (BIOLOGY)

Biological experiments on cells with/without suppressors, discussing RNA, DNA, enzymatic and UAA codon activities
20 p3480 A69-38265

ACTIVATION ANALYSIS

NT NEUTRON ACTIVATION ANALYSIS

Silicon in iron meteorites and earth core determined by activation analysis on octahedrites, hexahedrites and ataxites
16 p2865 A69-32807

Oxygen 18 adsorption on silicon activation analysis measurements used to obtain kinetic curve for chemisorption from monolayers
18 p3183 A69-35107

Ti and Zr diborides sintering with Cr, Mo, W and Re additions, discussing activation, pressure effects and density
22 p3968 A69-39888

ACTIVATION ENERGY

Temperature dependence of semiconductivity of sintered polycrystalline EuO from current-voltage characteristics, measuring activation energy
02 p0296 A69-11875

Impurity-dislocation interaction in Al alloy by vacancy mechanism and repeated yielding phenomenon, establishing activation energy
04 p0613 A69-14440

Uniaxial compression load effect on activation energy in p-type GaSb single crystals
04 p0644 A69-15269

Activation energies in baffle stabilized flame deduced from reaction zone using gas chromatography
06 p1035 A69-17930

Finite kinetics calculations by computer programs to generate reactions among prescribed reactants
[WSCI PAPER 68-54] 07 p1072 A69-18314

Activation energies of bimolecular multivalent transfer reactions of gaseous compounds, considering bond dissociation energy, length and order
[WSCI PAPER 68-48] 07 p1239 A69-18321

Transfer coefficients for inhomogeneous systems characterized by constant density, mean free path and activation energy of carriers at each point
07 p1193 A69-19024

Oxidation kinetics of niobium titanium alloy in air and oxygen between 650 and 1000 C, analyzing activation energies and nitrogen effects
08 p1331 A69-20194

Creep of high purity Nb-Mo alloys in 800-1300 C range and at 1500-13000 lb/square inch stresses, giving activation energy for creep
10 p1711 A69-23375

Summation curves method for development of active region and time dependence of energy loss during proton flare
10 p1764 A69-23743

Alloying additions effect on plastic deformation anisotropy in GaAs single crystals, determining dislocation activation energies from creep tests
11 p1936 A69-24537

Reaction between nickel-base alloy and hydrogen sulphide at high temperatures under atmospheric pressure, discussing activation energy

12 p2115 A69-26617

Se activation energy dependence on crystals composition and Se concentration, based on Hall coefficient temperature dependence in gallium arsenic phosphides

13 p2317 A69-27875

GaAs photoelectric emission at different activation degrees by adsorbed Cs and BaO layers, noting spectral response characteristics differences and causes

14 p2504 A69-28993

Reaction rate constants of ion-molecule interchange reaction as function of temperature, flow velocity, activation energy and constant part of steric factor P

16 p2747 A69-32312

High temperature creep, discussing creep curves and activation energy

17 p2986 A69-32911

Activation energy of annealing of lattice defects in Au films deposited under irradiation with Au ions

18 p3182 A69-34349

Chemical reactions activation energy at high temperature, noting cross section shape role for deducing activation energy from rate data

18 p3099 A69-34443

Accelerated temperature tests, calculating temperature behavior of hazard rates and activation energy from failure data using computer simulation

18 p3117 A69-34509

Single and two mode laser emission dependence on pumping power distribution between four level active centers of different types

19 p3333 A69-35878

Thermal rare gas release from mineral separates of Mocs meteorite, using method giving activation energies as function of temperature

19 p3419 A69-36141

Finite chemical reaction rate detonation wave interaction with rarefaction wave, noting mixture activation energy and heating power influence

19 p3298 A69-36384

Molybdenum disilicide oxidation kinetics at various temperatures by thermal conductivity method, determining oxidation rates and activation energy

20 p3567 A69-37780

Se activation energy dependence on crystals composition and Se concentration, based on Hall coefficient temperature dependence in gallium arsenic phosphides

21 p3782 A69-39141

Einstein development of theory of fluctuations applied to homogeneous nucleation, calculating activation energy, liquid drop-vapor system equilibrium state peculiarity, etc

22 p3938 A69-40448

Antimony trisulfide single crystals spectral dependence of impurity and stimulated impurity photoconductivities, comparing optical and thermal activation energies

22 p3994 A69-41042

Mean adsorption lifetimes and activation energies of Ag and Au on polycrystalline tungsten substrate in ultrahigh vacuum system free of hydrocarbon contamination

23 p4198 A69-41542

ACTIVE SATELLITES

NT EARLY BIRD SATELLITES

NT SYNCOM SATELLITES

Experimental communication satellites Score, Courier, Telstar, Relay, Syncom, Intelsat 1 and Molniya 1, discussing equipment, results, and ATS program

09 p1608 A69-21272

Preemphasis applications compared in active communication satellite systems for frequency division multiplex telephony and for TV

09 p1449 A69-21275

ACTIVITY [BIOLOGY]

Information theory application to study of biologically stimulating effects of low ionizing radiation doses, thermal energy and other environmental factors

03 p0369 A69-13434

Sensory and motor activity of human subjects exposed to reduced gravitation during aircraft motions along parabolic trajectories

07 p1062 A69-18592

Human postural muscle activity, motor reactions and dexterity during gravitational changes

07 p1063 A69-18593

Myocardial repolarization changes in healthy persons with restricted motor activity

07 p1066 A69-18984

Hypokinesia effects on rats noting body and organ weights, liver glycogen and N content and tissue proteolysis of skeletal muscles

08 p1262 A69-19928

Prolonged hypokinesia effects on white rats resistance to convulsions induced by high altitude simulation

08 p1262 A69-19929

Stability of male cardiovascular, respiratory and motor systems functional conditions after physical activity in pure O medium at high altitude pressure

08 p1262 A69-19931

Motion sickness inhibitive effect on stomach motor activity, measuring biopotential of stomach wall, pyloric sphincter and ganglions

08 p1263 A69-19935

Corticosteroid and catecholamine metabolism change in rabbits during sharp limitation of motor activity

12 p2021 A69-26973

Integrated device to detect biological growth and catabolic and anabolic activity in extraterrestrial exploration

15 p2556 A69-31306

Biological material flow phenomena, discussing rheological approach, microcirculation, macrocirculation, instrumentation and mathematical model for quantitative observation

20 p3473 A69-37602

Myocardial repolarization changes in healthy persons with restricted motor activity

20 p3480 A69-38232

Neuronal organization of initial afferent inflow in thalamic visual center /lateral geniculate body /LGB/ of unanesthetized cats/, noting unit activity

22 p3879 A69-40845

Temperature dependence of afferent and efferent spontaneous activity of spinal cord, using filament recordings from ventral and dorsal roots in anesthetized cats

23 p4093 A69-42066

ACTIVITY CYCLES [BIOLOGY]

Latent desynchronization, discussing life system and distortion, body rhythms coordination, circadian rhythms and adaptation to new system of time

15 p2557 A69-31457

Biological clocks, discussing circadian rhythms of organisms using animal experiments and physical oscillator model

21 p3653 A69-38895

Desynchronization and resynchronization of human circadian rhythms of activity, body temperature and urine excretion during isolation in underground bunker in various conditions

21 p3660 A69-39173

ACTUATION

Jet pump actuation of intermittently operating variable density closed circuit subsonic wind tunnels, measuring wind tunnel power factor

11 p1892 A69-25371

ACTUATOR DISKS

Rotary actuator to create realistic control effects in hydraulic loading system of jet flight-training simulators

20 p3511 A69-38182

Actuator disk model for study of azimuthally nonuniform MPD arc plasma dynamics [AIAA PAPER 68-714]

24 p4359 A69-43570

ACTUATORS

NT ACTUATOR DISKS

Solid propellant cartridges, discussing uses for starting large engines and providing auxiliary power in missiles or actuating devices

02 p0302 A69-11524

Pneumatic stepping motor actuation system with pure fluid valves and signal processing and minimum number of moving mechanical parts for high g and temperature environments

02 p0196 A69-12086

Gas servo design utilizing floating flap disk switching valves and pulse-length modulated pressure waves to actuate on-off switch [AGARDOGRAPH-118]

08 p1257 A69-20950

Inertial servomechanisms actuators, discussing dynamic characteristics, power, vibration damping, matching, couplers, etc

11 p1826 A69-25119

Optimal controllers analytical design for closed loop systems with pure time delay in actuating mechanism using differential equations

12 p2045 A69-25959

Hydraulic servo actuators load effect included in control loop actuator simulation

12 p2016 A69-26266

Working fluids elastic characteristics variability effect on hydraulic actuator dynamics, studying adiabatic and isothermal conditions

14 p2405 A69-29423

Hydraulic regenerative servomechanism system for electrohydraulic actuator design, discussing specifications and test results

15 p2553 A69-31294

Detonation system for exploding missile warheads, discussing trigger detonation and safety release elements

17 p3050 A69-33698

Duplex servomechanism package sized for stabilator channel of F-4 aircraft providing compact integrated control surface positioning [AIAA PAPER 69-788]

19 p3249 A69-35640

Multilevel mathematical model of oculomotor apparatus using neuron networks and complex activators, including computer analysis

20 p3470 A69-37245

Design concepts and principles of systems for monitoring of Concorde flight control actuators, considering servo control, control interconnections and control input system

20 p3467 A69-38190

Motion stability of hydraulic actuators with open loop control system in presence of nonlinear negative resistance damping

21 p3650 A69-39716

Triple redundant actuator for fly-by-wire control system, noting electrohydraulic servomechanisms in side-by-side arrangement

22 p3870 A69-41242

All-electric nonlinear actuator steering advanced tactical missiles, noting 99.29 percent delivered unit reliability during mass production

23 p4225 A69-42458

Undissolved air effects on working fluids elastodynamics in aircraft hydraulic actuators

24 p4255 A69-43076

ACUITY

U VISUAL ACUITY

ADAPTATION

NT ACCLIMATIZATION

NT ALTITUDE ACCLIMATIZATION

NT COLD ACCLIMATIZATION

NT DARK ADAPTATION

NT DESERT ADAPTATION

NT LIGHT ADAPTATION

NT RETINAL ADAPTATION

Dog adaptation to 60 or 90 mm Hg carbon dioxide in 260 mm Hg total pressure environment, noting arterial pH and bicarbonate level

03 p0375 A69-14071

Organic reaction and adaptation of rabbits and dogs to simulated weightlessness and acceleration compared with orbital flight data of human responses

03 p0376 A69-14192

Physiological mechanisms of weightlessness on human organism, discussing adaptation to weightlessness

03 p0377 A69-14197

Human physiology advances in connection with space exploration, discussing internal medium adaptation to space environment

[UN PAPER 68-95729]

06 p0873 A69-17061

Overt motion sickness prevention by incremental exposure to Coriolis accelerations

07 p1067 A69-19425

Work capacity and adaptation characteristics of humans confined in small chamber and experiencing effects of isolation and sensory deprivation

08 p1262 A69-19838

Compensatory reactions to prolonged weightlessness in human and animal organisms emphasizing blood circulation, heart, metabolism, digestive and nervous systems

17 p2909 A69-33577

Human performance and adaptation to space flight effects under low calorie diet including optimal proportion of basic nutrients and amino acids

20 p3482 A69-37621

Colpoda maupasis resistance to Martian atmospheric pressure and oxygen partial pressure noting adaptation, reproduction and existence

20 p3478 A69-37627

Ear-hand coordination adaptability tested by exposure to auditory rearrangement entailing 30 degree rotation of interaural axis produced by electronic pseudophones

21 p3663 A69-38899

Human hearing and vision mathematical simulation, relating signal perception parameters to corresponding adaptation processes

23 p4109 A69-41979

ADAPTERS

Nonorientable five channel adapter with spherical measuring head for three dimensional gas flow measurement, noting sensitivity to mechanical disturbances in calibration

11 p1888 A69-25340

Adapter between dielectrically loaded waveguides with different cut-off frequencies and sizes for pulse compression systems

14 p2423 A69-29760

Adaptor for Debye-Scherrer powder camera to take high quality photographs even at liquid N temperature

19 p3313 A69-36493

ADAPTIVE CONTROL

NT LEARNING MACHINES

NT SELF ADAPTIVE CONTROL SYSTEMS

Adaptive detection mode for surveillance radar, using detection threshold proportional to spatially sampled clutter level estimates for regulation of false alarm probability

01 p0026 A69-10178

Comparative analysis of variable structure adaptive systems and time optimal system for control of plant described by differential equation

01 p0052 A69-10795

Multidimensional nonlinear plants adaptive control by direct integration, identifying differential equations coefficients

01 p0053 A69-10875

Optimum linear filters for signal detection against background noise using Hodges-Lehmann method

02 p0223 A69-11565

Optimal adaptive control of discrete linear systems with unknown gain, considering Gaussian distribution functions and random disturbances

02 p0224 A69-11962

Dynamic flight simulators fidelity assessment, discussing hybrid method based on pilot psychomotor responses

02 p0203 A69-12215

Gradual memory system for noise reduction in adaptive control system

02 p0212 A69-12606

Adaptive multiplex telemetry use in scientific satellite data management

02 p0212 A69-12817

Adaptive compression system for predicting and encoding video data for transmission in noiseless channel

03 p0427 A69-12869

Optimal adaptive systems synthesis by statistical theory

03 p0409 A69-12977

Adaptive processing limited memory receiver for synchronous detection of signals of unknown amplitude

03 p0400 A69-13228

Sensitivity models for adaptive and self adaptive systems design

04 p0582 A69-14797

Servosystems and control, discussing open and closed loops and parallel, decoupling, multivariable and adaptive control

04 p0550 A69-15180

Digital controller weighting function sectionalization to simplify logic in developing adaptive control system

05 p0739 A69-16386

Bayes estimator in decision directed adaptive detection problem, noting allowance for decision errors

05 p0740 A69-16583

Digital adaptive recording system /DARS/ 12 channel flight recorder

05 p0766 A69-16754

Adaptive processes - IEEE Conference, University of California, Los Angeles, December 1968

06 p0899 A69-17350

Design algorithm for adaptive control of systems using nonlinear integral equations with bounded input functions, formulating optimization as conditional minimization problem

06 p0900 A69-17351

Adaptive modeler to estimate state and future trajectory of unknown plant having automatically synthesized control

06 p0900 A69-17353

Adaptive control of reflective satellite communication system

06 p0887 A69-17356

Stochastic approximation algorithms for adaptive linear discrete time system identification using noisy input

06 p0904 A69-17940

Adaptive pattern recognition, discussing classification techniques and merging into other aspects of artificial intelligence research

07 p1088 A69-18381

Self organizing and learning control systems, adaptive systems theory and defining self organizing control systems

07 p1114 A69-18382

Learning matrices applied to mathematical relationship establishment during adaptation stage between input and output of adaptive systems

07 p1088 A69-18387

Adaptation process of management systems from point of view of control system philosophy

08 p1422 A69-20197

Function generator for approximating function of many variables without recourse to multiplication, providing continuous functions representation

08 p1278 A69-20235

Stability analysis of model reference adaptive control system with sinusoidal inputs, using reformulation of fourth order Runge-Kutta method

08 p1297 A69-20357

Welding current pulsation techniques for adaptive control of gas tungsten arc welding processes

09 p1508 A69-22334

Adaptive control algorithm operating on-line to make discrete time adjustments in controller parameters of continuous time control system

09 p1474 A69-22441

Microelectronics for digital adaptive controls, discussing digital filter design and chips required in fabrication

09 p1474 A69-22453

Adaptive logic trees with two input gates for mechanization of any desired function of variable set, deriving multilevel representations of functions

09 p1475 A69-22583

Estimation system distinction from adaptive system, discussing network of adaptive estimation systems

11 p1858 A69-24937

Spontaneous decomposition of image space into compact sets /images or classes/ using adaptive dispersion method to reduce system learning time

11 p1859 A69-24964

Kalman sequential estimation adaptation to target maneuvers without sacrificing tracking accuracy in nonmaneuvering portions of trajectory

11 p1861 A69-25455

Aircraft stability derivatives determined by adaptive method, emphasizing physical and mathematical characteristics of learning model

11 p1824 A69-25671

Passive adaptive sampled data control system with conditional feedback, discussing transfer function role and minimization of external disturbances and internal parameter variations effects

13 p2238 A69-27394

Extremal system of adaptive circuits adjusted by random search with varying random step distribution function

14 p2425 A69-28824

Adaptive signal pattern dependent feedback delta modulation for improved signal/quantization-noise ratio

15 p2565 A69-30177

Adaptive filter for estimating system noise inputs from actual residuals developed to control Kalman filter in satellite orbit estimation

18 p3110 A69-34676

State space structure of model reference adaptive control and parameter tracking systems subject to noise

18 p3111 A69-34686

Adaptive control for Mars entry based on sensitivity analysis

20 p3573 A69-37193

Adaptive compensation to minimize human task in continuous manual control system using various models

20 p3482 A69-37721

Dynamic system absolute stability and sensitivity to parameter variations in linear part of system calculated by graphical and analytical techniques

21 p3685 A69-38729

Adaptive control system for aerospace vehicles, describing model reference network for control parameter determination

21 p3688 A69-39857

Nonlinear adaptive reaction jet attitude control for long life space vehicles, providing optimal performance over bias acceleration disturbances

22 p4036 A69-40328

Adaptive control system synthesis for reducing computation labor for controlled inertialess plant, reproducing probability density function to describe unknown parameters

22 p3918 A69-40739

Optimum linear adaptive design of dominant-type systems with large parameter variations assuring system response within prescribed bounds by reducing internal noise sensitivity

22 p3918 A69-41011

Performance characteristics of multivariable model reference adaptive systems synthesized by Liapunov method analyzed using computer simulation

22 p3919 A69-41201

Flexible format adaptive telemetry encoder design, discussing system design and implementation technique with modular units

23 p4119 A69-41748

Absolute invariance of perturbations affecting dynamic plant achievable by inertial measurement of highest derivatives

23 p4145 A69-42369

Adaptive cost equations in computer programs supporting launch vehicle long range planning, based on launch vehicle anticipated usage

24 p4392 A69-42815

Adaptive control systems analysis and application, noting off-line and on-line optimization, dynamic programming, linear systems, etc

24 p4289 A69-42946

Adaptive manual control rapid variation determined by input, controlled element, task and programmed adaptation systems, discussing human strategy changes

24 p4274 A69-43022

Adaptive multicategory pattern classification system, using independent samples to form mean-square approximations to Bayes discriminant functions

24 p4285 A69-43134

Optimal hinged two body satellite configurations in circular and elliptical orbits, discussing need for adaptive attitude control for transient and steady state operation

24 p4393 A69-43247

Adaptive control function technique to design lateral stability augmentation system for hypothetical manned, lifting body entry vehicle

24 p4394 A69-43301

Adaptive model of human operator control strategy in response to sudden changes in plant dynamics and transient disturbances

24 p4276 A69-43325

ADAPTIVE FILTERS

Self adaptive systems stability analyzed using filter and correlation methods, considering higher harmonics at rectifier and synchronous detectors output

04 p0582 A69-14796

Adaptation in nonstationary environment formulated for tapped delay line filters with adjustable time varying gains

05 p0737 A69-15806

Identification of finite memory, time discrete linear systems by Kiefer-Wolfovitz stochastic approximation procedures, presenting two algorithms for sequential identification

06 p0900 A69-17359

Microelectronics for digital adaptive controls, discussing digital filter design and chips required in fabrication

09 p1474 A69-22453

Digital signal tracking module operation and stability, considering use of interconnecting modules to achieve adaptive tracking

09 p1459 A69-22477

Adaptive optimal estimation of sampled stochastic process with finite state unknown parameters, using separation technique

11 p1858 A69-24935

Polyharmonic predictive and self tunable filters synthesis based on signal periodic components detection, noting role in information transmission and processing systems

11 p1849 A69-24966

Adaptive filtering to prevent divergence observed in application of Kalman filter to orbit determination

12 p2045 A69-26059

Threshold signal gain estimated in Glaser frequency filter self adaptation process during transformation from square law summator into matched filter

15 p2576 A69-30344

Adaptive filter with operational amplifier and digital to analog converters for bandpass characteristics, discussing pattern recognition application

17 p2942 A69-34093

Adaptive filter for estimating system noise inputs from actual residuals developed to control Kalman filter in satellite orbit estimation

18 p3110 A69-34676

Adaptive predicting filter mathematical model based on information probability, using adaptive systems latent memory

19 p3287 A69-36665

Weighting coefficients calculations by recursive algorithm for designing optimal discrete adaptive Kalman filter

20 p3509 A69-37142

Adaptive tracking filter for bending mode stabilization of large flexible boosters [AIAA PAPER 69-874]

21 p3823 A69-39400

Optimum filter design for noisy analog feedback system with forward and feedback disturbances, using mean square error criterion between signal and data

21 p3687 A69-39449

Adaptive filtering to prevent divergence observed in application of Kalman filter to orbit determination

23 p4146 A69-42446

Adaptive signal processing interference rejection technique for suppression of cochannel AM interference in congested VHF tracking receiver

23 p4128 A69-42503

Microcircuit phased array electronic countermeasures system design and hardware techniques for aerospace applications, analyzing adaptive, retrodirective and combination array systems

24 p4287 A69-43110

ADDERS [CIRCUITS]

U ADDING CIRCUITS

ADDING CIRCUITS

Miniaturized adding sample and hold device with adjustable delay applied to digital filters

04 p0574 A69-14350

Weak periodic signal separation from noise using single and multichannel analog adders

04 p0597 A69-14848

Weak periodic signal separation from noise using single and multichannel analog adders

15 p2607 A69-30241

Subtractor performance for processing correlated random signals with different spectral widths in signal delay time indicator, discussing errors

15 p2572 A69-30346

ADDITION RESINS

U ACRYLIC RESINS

U POLYMETHYL METHACRYLATE

ADDITION THEOREM

Bessel functions new addition theorem suggested from mathematical investigation of ideal discriminator output voltage

19 p3266 A69-35767

ADDITIVES

NT ADMIXTURES

NT ANTIOXIDANTS

NT OIL ADDITIVES

NT OPACIFIERS

NT PLASTICIZERS

NT PROPELLANT ADDITIVES

NT PROPELLANT BINDERS

NT SOLID ROCKET BINDERS

N- and p-type InSb and GaSb single crystals microhardness, noting decrease after doping is limited to thin surface layer

01 p0139 A69-10832

Silicon doped p-n GaAs single crystals and epitaxial layers energy spectrum, studying shift in position of emission band maximum

01 p0139 A69-10833

Indium phosphide p-n junction current-voltage characteristics various temperatures, considering degree of doping effect

01 p0139 A69-10885

Tellurium-doped gallium arsenides stacking-faults transmission electron microscopic study

03 p0486 A69-13614

Absorption and IR emission of nickel and cobalt doped alkali halides

03 p0490 A69-13941

Temperature drop in combustion chamber of open cycle MHD power plant due to added potassium carbonate as function of various parameters

03 p0369 A69-14162

Temperature dependence of Hall coefficient, conductivity and carrier mobility in manganese doped indium antimonides

04 p0643 A69-15257

Nonuniform distribution and concentration of doping materials in semiconductors determined by measuring optical reflection coefficient

05 p0764 A69-16664

Active region doping effect on laser diode threshold current, noting current dependence on loss coefficient in interband transition model without selection rule

06 p0933 A69-17257

Combustion mixture composition dependence on electrical conductivity of products with potassium additive, discussing hydrocarbon fuels

06 p0870 A69-17908

Automatic test set for measuring dopant concentration profiles in epitaxial films

07 p1130 A69-18245

Adiabatic kinetic calculations of chemical additive effects on ignition delay of hydrogen-oxygen-argon gas mixtures [WSCIPAPER 68-52]

07 p1239 A69-18316

Doped silicon dioxide films as controlled reproducible diffusion sources for silicon devices fabrication

07 p1198 A69-18620

Additive processing technique for fabrication of single sided, double sided and multilayer printed circuit boards

07 p1100 A69-18621

Impurities effect on electron energy spectrum in semiconductors at zone boundary and arbitrary doping levels, using Green function

09 p1554 A69-21467

Strongly doped n-type indium antimonide, determining dependence of limiting electron concentration on dopant impurity nature

09 p1558 A69-21869

Face effect in p- and n-type gallium antimonide single crystals doped with zinc and tellurium

09 p1558 A69-21870

Noble gas additives for triggering stability of pulsed argon ion lasers, discussing repetition rate and power loss

10 p1702 A69-23341

Soviet book on highly doped semiconductors covering energy spectrum analysis, kinetic effects, optical properties, fabrication and applications

10 p1746 A69-23522

Alloying additions effect on plastic deformation anisotropy in GaAs single crystals, determining dislocation activation energies from creep tests

11 p1936 A69-24537

Gaussian summation for ion implantation profile control in semiconductors, describing computer program selecting optimum energies to fit predetermined profiles

11 p1857 A69-24546

Monograph on effect of boron, zirconium and titanium on austenite transformation of CrMo steels bainite and martensite covering carbides, nitrides, mechanical properties, etc

11 p1903 A69-24634

Molybdenum and vanadium effects on nickel steel properties, stressing brittleness avoidance and quenchability

11 p1904 A69-24642

Molybdenum, titanium and cobalt effects on nickel maraging steel strength and ductility

11 p1904 A69-24643

N and p type InSb and GaSb single crystals microhardness, noting decrease after doping is limited to thin surface layer

11 p1936 A69-24699

Silicon doped p-n GaAs single crystals and epitaxial layers energy spectrum, studying shift in position of emission band maximum

11 p1936 A69-24700

Aluminum additive effects on copper-titanium alloy decomposition, discussing Guinier complexes, heterogeneous nucleation, plastic deformation and low temperature aging

11 p1905 A69-24922

Structural imperfections of CdSb single crystals undoped and doped with tellurium and indium noting etching techniques, grain boundaries and impurities

11 p1938 A69-25030

Surface-active additives effect on crystallization kinetics of sial type glasses, discussing surface tension

11 p1907 A69-25032

Sb addition effect on electrical conductivity and Hall effect in PbTe single crystals over temperature range

11 p1939 A69-25706

Tellurium doping effect on phonon diffusion in GaSb, discussing thermal conductivity at low temperatures

12 p2142 A69-26294

Molybdenum additive role in deformed carbonylic nickel recrystallization process

12 p2114 A69-26454

Bismuth doped lead tin telluride diode lasers with low threshold currents at cryogenic temperatures, discussing doping effect

12 p2109 A69-26641

Indium phosphide p-n junction current-voltage characteristics at various temperatures, considering degree of doping effect

12 p2144 A69-26649

Thermionic converter improvements by electronegative additives and emitter surface finishes, noting cesium oxide, heat treatments with electropolishing, electroetching, etc

14 p2397 A69-29173

Polyurethane with additives for fuel fire control in aircraft structures, achieving desired protection without impairing foams mechanical properties

15 p2561 A69-30311

Impurities effect on electron energy spectrum in semiconductors at zone boundary and arbitrary doping levels, using Green function

15 p2669 A69-30712

Additives effect on flame propagation velocity and stability in N diluted hydrogen-chlorine propellants, noting entrained air role [WSCIPAPER 69-13]

16 p2831 A69-32353

Doped recrystallized ammonium perchlorate effects on composite propellant burning rates [WSCIPAPER 69-18]

16 p2831 A69-32356

Decomposition of ammonium perchlorate containing additives introduced by spray drying [AIAA PAPER 69-502]

16 p2834 A69-32752

German monograph on yttrium addition effects on tension and compression behavior of Nb and Mo at high temperature in vacuum

17 p2990 A69-33570

Lithium-doped silicon solar cells development for radiation environments, discussing contractor functions, dopants, etc

19 p3251 A69-35692

Ni base superalloy stacking fault energy, studying effects of various solute additions

19 p3343 A69-35925

InSb single crystals impurities incorporation and distribution, concluding electrical properties vary with homogeneity or heterogeneity of dopant microdistribution

19 p3389 A69-36547

Aluminum alloying additives effects on tungsten disilicide corrosion resistance, studying plasticity properties and oxidation rate

20 p3561 A69-37376

Aluminum doped silicon solar cell energy loss coefficient under proton and high energy electron irradiation

20 p3465 A69-37911

Silicon dioxide film doped with Al to increase MOS structure radiation resistance

20 p3584 A69-38070

Bcc metals strengthening and alloy softening mechanisms, studying temperature and additives effects

22 p3970 A69-40166

Strong doping criterion for Si with deep level impurity centers based on electron spectra of fast surface traps

22 p3992 A69-40604

Compactibility dependence of Fe, Co and Ni powders with Zr, Nb and Mo carbide additives on pressure, carbide content and lubricant

22 p3970 A69-40634

Doped silver carbonate defect structure and doping effect on reaction kinetics by X rays and electron paramagnetic resonance, finding new crystal structure

22 p3993 A69-40720

Defect structure of ceramic Ba titanate doped with Cr ions, evaluating visible, IR and EPR spectra

22 p3996 A69-41160

Ba titanate modifiers, classifying cations replacing Ti and Ba ions

22 p3996 A69-41161

Critical transition temperature of vanadium oxide semiconductors as function of doping element content and lattice constant, using X ray diffraction

23 p4198 A69-41564

N or He additions effects on carbon dioxide laser design and power output

24 p4327 A69-42640

ADDRESSING

Block structures and indirect addressing, discussing SNOBOL modifications and naming constraints

19 p3280 A69-36207

Digital data compression system transmission error statistical analysis, emphasizing addressing schemes effect on compression ratio

19 p3272 A69-36261

ADDUCTS

Enthalpies determination of adduct formation of sulfonides, sulfanilamides and thionylamides with

trimethylalane, noting replacement effect on electron donating ability of oxygen 07 p1074 A69-18631

ADENINES

Electron spin resonance spectra of gamma irradiated single crystals of 9-methyladenine, analyzing H abstraction radical and temperature effects 19 p3264 A69-35974

Adenylates condensation in protein-associated amino acids as clue to peptide bond synthesis within proto cellular structures 22 p3895 A69-40048

ADENOSINE TRIPHOSPHATE [ATP]

NADH stimulation of ATP dependent carbon dioxide fixation in crude extracts of *Hydrogenomonas facilis*, considering allosteric regulation of phosphoribulokinase activity 15 p2554 A69-30036

Adenosine triphosphate /ATP/ content of terrestrial soils, based on firefly bioluminescent reaction, for Mars soil problems 20 p3473 A69-37567

Adenosine triphosphate /ATP/ production in normal cells and sporulation mutants of *Bacillus subtilis*, discussing applications of ATP synthesis response to C sources 22 p3886 A69-41076

Cardiac myosin characteristics obtained from dogs with naturally occurring heart failure, showing reduced adenosinetriphosphatase activity as compared with normal dogs 24 p4258 A69-42630

ADENOSINES

U ADENOSINE TRIPHOSPHATE [ATP]

ADHEROMETERS

U ADHESION TESTS

ADHESION

Glow discharge technique for dielectric layer deposition between metal interconnection patterns in multilayer integrated circuits, noting adhesion and feedthrough problems 06 p0931 A69-17201

Fracture toughness of laminated adhesive bonded structures and monolithic aluminum, considering fracture stresses and ductile and brittle failure 09 p1526 A69-22318

Gold-underlayer film combinations adhesion to oxide substrates, describing adhesion changes as function of Au and underlayer film thickness, time, environment, etc 13 p2321 A69-28007

Friction resistance between steel and ground basal in ultrahigh vacuum, showing increase by adhesion 13 p2298 A69-28014

Collection of articles on adhesion and adhesives, Volume 2, Materials 14 p2468 A69-29338

Fiber reinforced adhesives, discussing adhesion definition and variables separation, applications and testing 14 p2455 A69-29343

Glass finish and glass resin chemical bond adhesion roles in filament wound structures response, failure and filament strength 14 p2468 A69-29345

Polyvinyl acetate and polyvinyl alcohol thermoplastic adhesives, discussing gluing properties, chemical properties, preparation, polymerization methods 14 p2469 A69-29347

Interface friction and adhesion of alloys workpieces and die materials under pressure and temperatures typical of plastic deformation 15 p2629 A69-30902

Adhesive pressure welded joints tightness and fabrication stability analyzed on duraluminum sheet samples 17 p2978 A69-32949

Quartz fiber adhesion to Re measured in LEED /low energy electron diffraction/ apparatus for clean and O layer surfaces, noting brittle fracture 18 p3156 A69-35182

Room temperature vulcanizing silicone rubber adhesive sealants strength and self bonding, describing primerless adhesion to Ti and Al alloys, Al, Ni and stainless steels 19 p3356 A69-35532

Metal fiber reinforced thermoplastic composites, analyzing unidirectional, crossed and random orientation cases taking into account adhesion efficiency between fiber and matrix 20 p3559 A69-37083

Plasma metal spray coating for Al and Mg alloy aircraft components adhesive bonding repair technique compared to welding and electroplating 21 p3728 A69-38462

Silico-organic liquid water repellant coatings for increasing binder adhesion to glass fiber in glass fiber reinforced plastic materials of aircraft components 21 p3752 A69-38876

Dynamic equilibrium of making and breaking adhesion bonds between polymer segments and dissimilar surfaces through water, allowing thermal stresses relaxation 24 p4326 A69-43458

ADHESION TESTS

Book on adhesive bonding techniques covering chemical types, mechanical and handling characteristics, application and mixing, joint design, non-destructive testing, documentation tooling, etc 01 p0084 A69-10130

Static adhesion of metals in hot oxidizing gas environment, considering dry lubrication to prevent adhesion [IME PAPER 4] 07 p1139 A69-18567

Microwave techniques for bondline defects and thickness of reentry elastomeric heat shield material bonded to titanium alloy 09 p1499 A69-22306

Pulse echo ultrasonic nondestructive testing of C-5 adhesive bonded aluminum composites with multiple bond lines 10 p1698 A69-23047

Pressure sensitive adhesives composition, tapes tacking and peeling theory and tests including electrolytic corrosion and insulation evaluation 14 p2468 A69-29342

Ultrasonic inspection systems to determine and record bond quality on all adhesive bonded assemblies of Saturn S-2 booster and Apollo Command and Service Modules 15 p2632 A69-31515

Mathematical model of yielding of adhesive bonds in form of viscous threads between elastic bodies, obtaining solution to two dimensional problem 18 p3215 A69-34569

Plating wear resistant electrodeposits of Ag, Cu, Ni and Cr on Ti, noting adhesion tests 18 p3148 A69-34654

Low temperature adhesive shear tests to measure force to break ice away from stainless steel surfaces coated with various bonded solid lubricants 19 p3323 A69-35581

Vacuum apparatus for measuring uniaxially loaded metal surfaces interfacial adhesion, showing surface oxide removal effectiveness influence in adhesion strength 21 p3689 A69-38594

Adhesive bonding of optical components, discussing material types, test methods, problem of operation at cryogenic temperature, etc 24 p4326 A69-43465

ADHESIVES

NT GLUES

NT PASTES

Phenolic and epoxy adhesives for metal-metal and honeycomb bonding, discussing cold cure adhesives for aircraft structures and aircraft floor sandwich design optimization 04 p0606 A69-14845

Bioadhesive investigation in echinoderms extended to class Holothuroidea, using electron microscope with correlative light microscopy for tube feet of sea cucumbers 05 p0708 A69-15984

Cryogenic behavior of adhesive materials used in fabrication of liquid hydrogen/liquid oxygen powered Saturn S-4B stage 05 p0784 A69-16487

Helicopter rotor blades in metal sandwich bonding, discussing component parts assembly by adhesive films 07 p1143 A69-19731

Spacecraft component heat sterilization, discussing heat effects on electrical connections, polymers and adhesives 08 p1284 A69-20267

Inhomogeneous half planes equilibrium bonded by elastic layer, noting tangential stresses at interfaces 09 p1611 A69-21482

Capacitance methods for measuring adhesives mechanical properties in thin film bonded joints, noting results for tension, compression and shear loading 09 p1500 A69-22309

Methyl 2-cyanoacrylate adhesive bonding characteristics, noting importance of film thickness 09 p1529 A69-22316

Adhesive bonded lap joint strength dependence on adherend mechanical properties under conditions of homogeneous adherend and cohesive failure 09 p1530 A69-22317

Thermoplastic resins as matrices for glass reinforced plastics and aerospace structural and nonstructural adhesives 09 p1530 A69-22365

Controlled expansion of captive silicone rubber used to achieve pressure control for adhesive bonding interface 09 p1512 A69-22367

Quality control tests for adhesives used in structural parts including ultrasonic and nondestructive tests 09 p1513 A69-22564

Aluminum bonded structures corrosion resistance through adhesive primers and surface treatments 10 p1700 A69-24088

Monograph on molecular structure and polymer properties, covering coherent adhesive layer of polymeric material for paint film in protective coatings 10 p1717 A69-24187

Metal adhesive bonding strength behavior in satellite and space vehicle applications, noting effects of various space environment factors 12 p2101 A69-25858

Metal bonded and sandwich structures application to space vehicles, launch vehicles, rocket motors, ground equipment and balloon gondolas, noting inspection methods 12 p2101 A69-25859

Adhesive metal bonding methods including continuous surface bonds, core to face bonds, lap joints and structural adhesive materials 14 p2454 A69-28847

Collection of articles on adhesion and adhesives, Volume 2, Materials 14 p2468 A69-29338

Epoxy adhesives physical chemistry, curing processes, formulation, surface application methods, testing and health hazards 14 p2468 A69-29339

Thermosetting adhesives properties and structural applications in aircraft, space and automotive use, discussing polymer systems, moisture, surface preparation, aging, etc 14 p2468 A69-29340

Elastomeric adhesives diffusion theory, tack increasing methods, cast polymer films, properties and applications in shoe manufacturing and sealants 14 p2468 A69-29341

Pressure sensitive adhesives composition, tapes tacking and peeling theory and tests including electrolytic corrosion and insulation evaluation 14 p2468 A69-29342

Fiber reinforced adhesives, discussing adhesion definition and variables separation, applications and testing 14 p2455 A69-29343

Heterocyclic-aromatic organic polymer adhesives used for high temperature structural purposes, discussing processing, testing, formulating and impact on basic research 14 p2469 A69-29346

Polyvinyl acetate and polyvinyl alcohol thermoplastic adhesives, discussing gluing properties, chemical properties, preparation, polymerization methods 14 p2469 A69-29347

High temperature structural adhesives at temperatures of 350 F and higher including epoxies, polyimides, amide-imides and polybenzimidazoles 15 p2642 A69-30329

High temperature structural adhesives developed from thermoplastic aromatic-heterocyclic polymers 19 p3357 A69-35560

Low temperature bond failures of room temperature vulcanizing methyl-phenyl adhesive bonds attributed to thermal stress cracking of primer, presenting in-process tests 19 p3321 A69-35563

Adhesives and adhesive resin bonding, describing internal stresses in joints, joints design for bonding, strength, bonding processes and testing 21 p3752 A69-38932

Load transfer to sheet metal plate from bonded strip axially loaded by single force, assuming linear viscoelastic adhesive layer 22 p4038 A69-39896

Outdoor aging effects on unstressed adhesive-bonded Al to Al lap shear joints 24 p4319 A69-42932

Adhesive joints design with uniform shear stress for prestressing wood beams 24 p4323 A69-43425

RTV silicone rubber for corrosion control coatings, high strength adhesives and low density sealants in aircraft structures

24 p4338 A69-43457

Real shear modulus and mechanical damping characteristics of cured adhesives measured for temperature effect, using torsion pendulum apparatus

24 p4338 A69-43460

Adhesive bonded joints for glass resin composite sandwich helicopter structures, describing aircraft applications

24 p4403 A69-43462

Gel permeation chromatography to measure rate of adhesive aging and curing in one shot epoxy tapes, noting handling techniques and space applications

24 p4338 A69-43463

Anaerobic adhesives for aircraft bonding tested for mechanical properties, noting advantages over epoxy adhesives

24 p4338 A69-43464

ADIABATIC CONDITIONS

Nonlinear adiabatic pulsations of sequence of massive stars of uniform composition, allowing for radiation pressure variations

01 p0149 A69-10266

Rotating star adiabatic axisymmetric motion solved numerically for small initial deviation from hydrostatic equilibrium

02 p0317 A69-11955

Adiabatic stirred reactor, discussing steady state nonlinear equations of reactant gases combustion

02 p0352 A69-12316

Short term weather forecasts by means of hydrodynamic equations in adiabatic approximation, noting atmospheric motions and processes, adiabatic invariants and meteorological fields

03 p0459 A69-13332

Thermal nonequilibrium of unsteady adiabatic gas flow in nonheat conducting tube with open ends

06 p0911 A69-17813

Radio wave propagation in unstable inhomogeneous medium with space-time dispersion, showing adiabatic compression or expansion of wave packet spectrum

10 p1658 A69-23955

Transport processes under adiabatic conditions between external magnetic field and thermal and electrical gradients in solid, defining galvanomagnetic and thermomagnetic effects

13 p2299 A69-28129

Climate studies with allowance for radiative heat inputs, constructing nonadiabatic motions model for improving prognosis

14 p2477 A69-29827

Conical shock wave-turbulent boundary layer interaction data obtained for adiabatic wall conditions at supersonic free stream Mach numbers, including suction effects

[AIAA PAPER 69-450] 16 p2773 A69-32754

Adiabatic and diabatic processes contributions to vertical atmospheric motions profile and IR cooling components comparison

17 p2962 A69-33689

Vibrational deexcitation shocks in expanding nonequilibrium nozzle flows extended to include embedded adiabatic shock

18 p3089 A69-35386

Solar protons captured in earth dipole trap, discussing conditions for nonadiabatic escape

20 p3587 A69-37042

Computer calculation of adiabatic expansion of air, allowing for specific heat ratio and compressibility factor changes

24 p4244 A69-43088

Adiabatic model deflagration limits for steady linear monopropellant burning at Lewis number of unity and one step gas phase reaction

24 p4415 A69-43670

ADIABATIC EQUATIONS

Equation describing statistically trapped particle motion under influence of fields varying in time and space

07 p1209 A69-19375

Double adiabatic MHD fluid equations for electrons and ions with pressure gradients for collisionless plasma in magnetic field

08 p1369 A69-20815

Adiabatic theory of charged particle motion in electromagnetic field, applying asymptotic methods of nonlinear oscillations theory

11 p1948 A69-24857

Group properties of adiabatic motion equations of medium in relativistic hydrodynamics, including solutions of subgroups applicable to multiple particle production

19 p3301 A69-36843

ADIABATIC FLOW

Nonisentropic simple waves in two dimensional steady flow of ideal gas

05 p0752 A69-16687

Sonic transmission of diatomic nitrogen during nozzle flow, presenting density dependence of natural oscillation energies and temperature

10 p1632 A69-22912

Dense plasma flow across transverse inhomogeneous magnetic field, proving adiabatic nature of motion

12 p2137 A69-26528

Two dimensional adiabatic transverse normal modes of inviscid compressible uniformly rotating fluid, discussing harmonic wave propagation in opposite directions and rotation effects

14 p2431 A69-29581

Turbulent base flowfields in multinozzle configurations, considering adiabatic flow and determining base pressure distribution from reverse jet impingement

[AIAA PAPER 69-570] 16 p2733 A69-32751

Adiabatic compressible turbulent boundary layer equations for two dimensional and axisymmetric flows, discussing methods of solution based on eddy viscosity formulation

[AIAA PAPER 69-687] 17 p2955 A69-33470

Adiabatic compressible turbulent equilibrium boundary layer integral method analysis extended to study nonequilibrium laminar flows, deriving dissipation integrals, presenting numerical solutions

[AIAA PAPER 69-689] 17 p2955 A69-33481

Constant pressure adiabatic turbulent boundary layer characteristics measurements correlated in incompressible reference frame, using modified Mager compressibility transformation

17 p2958 A69-34051

Film cooling slot adiabatic wall effectiveness measurement in two dimensional constant property flow, showing role of lip thickness and injection angle

20 p3585 A69-37082

Propagation characteristics of steady adiabatic one dimensional laminar flames in premixed gases, considering activation energy and Lewis number

21 p3849 A69-38802

ADIPOSE TISSUES

Nomogram for estimating body fat and specific gravity from height and weight, considering two component model of body composition and lean body weight

07 p1067 A69-19428

Norepinephrine, dinitrophenol and dicumaryl effect on brown adipose tissue of cold exposed rats

19 p3258 A69-36294

Brown adipose tissue providing internal heating jacket and metabolic heater overlying systemic vasculature, noting cold survival role

23 p4091 A69-42013

ADJOINTS

Energy transfer in circulatory force fields, noting mechanism changes for simultaneously operative original field and adjoint field energy sources

04 p0671 A69-14415

Trajectory terminal state error analysis using adjoint-generated sensitivities in nonlinear time-varying systems

13 p2296 A69-27940

Trajectory differential equations in state-variable form, presenting compatible difference equation adjoint scheme for trajectory integration

15 p2645 A69-31236

Adjoint system for determining equilibrium stability of elastic continuum subjected to follower type surface tractions

19 p3446 A69-36835

ADMINISTRATION

U MANAGEMENT

ADMITTANCE

U ELECTRICAL IMPEDANCE

ADMIXTURES

Concentration distribution of admixture in semibounded jet propagating along nonheat conducting plate, obtaining concentration profiles for various thermal and diffusion Prandtl numbers

21 p3854 A69-39844

ADRENAL GLAND

High altitude environmental effects on adrenal glands and hypothalamic neurosecretion in rats

13 p2211 A69-28615

Constant light/darkness effects on stress response rhythm of hypothalamic-pituitary-adrenocortical system in female rats

15 p2556 A69-31330

Vestibular stimulation effect on human blood composition during rocking test indicating blood eosinophil content as function of hypophysis and adrenal cortex reactions

20 p3473 A69-37268

Increased oxygen tension adaptation and effects on adrenocortical and sympatho-adreno-medullary activity in rats, indicating toxic conversion of epinephrine to indoles

23 p4087 A69-41791

Positive pressure breathing effects on cerebral arterial and venous blood pressure, hypothalamus and adrenal glands catecholamine content and cerebrum histological changes in dogs

24 p4265 A69-43371

ADRENAL METABOLISM

Brain norepinephrine effect on daily rhythmic changes in activity of tyrosine transaminase in livers of starved adrenalectomized rats

05 p0707 A69-15582

Sympathoadrenal activity during and after impact stress measured from urinary excretion of catecholamines and 17-hydroxycorticosteroids

06 p0875 A69-17839

Adrenal epinephrine and phenylethanolamine n-methyl transferase (PNMT) activity in rat bearing transplantable pituitary tumor

08 p1263 A69-20374

Corticosteroid and catecholamine metabolism change in rabbits during sharp limitation of motor activity

12 p0201 A69-26973

Aldosterone and hydrocortisone introduced into bladders of adrenalectomized dogs to restore sodium metabolism contributing to normal water-salt homeostasis

21 p3656 A69-38965

Rats adrenal corticosterone concentrations changes in response to ACTH, determining response sensitivity dependence on time after hypophysectomy

22 p3870 A69-39871

Aminazine and adrenaline effects on adrenocortical function in patients with diencephalic syndrome

22 p3888 A69-41272

Compensatory hypertrophy effects on adrenal phenylethanolamine n-methyl transferase (PNMT) activity in rats

23 p4080 A69-41404

Pituitary-adrenocortical axis of rats in oxygen atmosphere at low pressure, finding depressed norepinephrine excretion

23 p4087 A69-41790

ADRENALINE

U EPINEPHRINE

ADRENERGICS

Central adrenergic mechanisms role in neurosecretory function of hypothalamo-hypophyseal system of rabbits under transverse accelerations in centrifuge

15 p2554 A69-30055

Beta adrenergic blockade in differential diagnosis of cardiovascular changes produced by stress induced catecholamine liberation and organic disease

17 p2909 A69-33184

Olfactory bulb removal effects on uptake decline of telencephalic norepinephrine, noting use for mapping adrenergic pathways

22 p3871 A69-40055

Sotalol and propranolol cardiovascular effects, comparing toxicity and blocking action against circulatory and cardiac effects of catecholamines

23 p4080 A69-41403

Coronary circulation response to hyperoxia after vagotomy and combined alpha and beta adrenergic receptors blockade in anesthetized intact dog

23 p4096 A69-42088

Receptor and adrenergic blockade effects on blood loss, tolerated period and metabolic sequelae of hypotension in dogs

23 p4098 A69-42102

Adrenosympathetic reaction in flight, studying contributions of physical and nervous stresses in physically trained and untrained persons

23 p4099 A69-42363

ADRENOCORTICOTROPIN [ACTH]

Rats adrenal corticosterone concentrations changes in response to ACTH, determining response sensitivity dependence on time after hypophysectomy

22 p3870 A69-39871

ADSORPTION

NT CHEMISORPTION

Electron paramagnetic resonance study of interaction between adsorbed nitric oxide and NaY and deca-

tionized Y zeolites surfaces, considering catalytic activity

02 p0205 A69-11900

Liquid metal adsorption induced embrittlement, noting bond strength reduction and grain boundaries penetration

03 p0448 A69-13872

Lunar surface gas adsorption mechanism for lunar atmosphere absence

05 p0824 A69-16062

Barium, oxygen and BaO adsorption influence on Mo and Ti thin films conductivity and work functions

06 p0978 A69-16900

Gas adsorption on solids, discussing statistical mechanical theory assuming localized adsorption for first adlayer and nonlocalized mobile layer adsorption on top

06 p0980 A69-17387

Gas adsorption of molecular oxygen and hydrogen on molybdenum surface using collector section of field emission retarding potential analyzer

08 p1268 A69-20179

Adsorption kinetics of hydrocarbon oxidation on platinum electrode

08 p1268 A69-21052

Adsorption process limits when used as Cs reserve in thermionic converter

09 p1441 A69-21839

Digital computer program for heat and mass transfer characteristics of spacecraft carbon dioxide adsorption beds, discussing surface pressure of adsorbent material [AICHE PAPER 19C]

09 p1446 A69-21931

Molar heat and entropy of adsorption and activity coefficient of adsorbed phase for methane-ethane-silica gel system

10 p1652 A69-23370

Adsorption of N, H, O and CO on thick vapor deposited Be films at room temperature

13 p2322 A69-28017

CO adsorption on tungsten, determining work function changes and Fowler-Nordheim preexponentials on field emitter single crystal faces

14 p2409 A69-29093

Nuclear type cylindrical thermionic converter with porous adsorbent structure and liquid cesium tank

14 p2397 A69-29174

Langmuir S curves for tungsten single crystals in presence of adsorbed cesium, discussing orientation, theoretical and experimental correlation and instrumentation

14 p2506 A69-29271

Work function changes of tungsten single crystals as function of oxygen and CO gas pressure at high temperatures, using emission microscope

14 p2506 A69-29272

Lunar surface gas adsorption mechanism for lunar atmosphere absence

15 p2680 A69-30261

Kinetic theory and gas-surface interactions for upper atmospheric density measurements by mass spectrometers, pressure gages and satellite drag, detailing adsorption effect

16 p2776 A69-32089

Oxygen adsorption on Mo single crystals /100/ surface as function of temperature using low energy electron diffraction

16 p2748 A69-32795

Stress corrosion cracking mechanisms in liquid-solid metal combinations and solvent exposed plastics, discussing adsorption processes and cathodic polarization inhibition

19 p3349 A69-36887

Heats of adsorption of carbon dioxide on silver /I/ oxide and copper /II/ oxide by gas chromatography

20 p3485 A69-38277

Mean adsorption lifetimes and activation energies of Ag and Au on polycrystalline tungsten substrate in ultrahigh vacuum system free of hydrocarbon contamination

23 p4198 A69-41542

ADVECTION

Time dependent model of photochemical, advective and turbulent effects on meridional ozone distribution

07 p1122 A69-18253

Temperature advection dependence on local temperature changes, discussing variation with atmospheric layer thickness

09 p1534 A69-21509

Atmospheric ozone distribution as function of photochemical reactions, advection and vertical motions

16 p2787 A69-32643

Numerical wind field prediction based on advection equations and quasi-geostrophic wind assumption, considering equatorial belt in case of zonal pressure field

19 p3364 A69-36506

AEOLOTROPISM

Small twist of elastic circular cylindrical tube with nonorthogonal cylindrical aeolotropy, noting zero and nonzero warping conditions effects

05 p0831 A69-15580

Inhomogeneities in materially uniform simple bodies described in terms of third order tensor field, treating contorted aeolotropy

05 p0833 A69-15728

AERATION

Gas turbine engines smoke reduction, aerated fuel sprays for smoke control on engine design and factors affecting visibility of exhaust plumes

17 p3020 A69-33350

AERIAL EXPLOSIONS

Airplane explosion evidence, discussing examination of plastic seat cushion surface and metallic fragments

02 p0193 A69-12688

Hazards model for probabilistic prediction of casualties by exploding solid propellant rockets, deriving casualty expectation equation [AIAA PAPER 69-461]

16 p2869 A69-32749

High altitude nuclear explosions detected by distinguishing artificial from natural sudden enhancement of atmospheric /SEA/ phenomena

20 p3492 A69-37701

Radiation effects due to high altitude thermonuclear explosion measured by satellite, estimating fragments longitudinal drift velocity, plasma cloud expansion rate and fragment distribution

20 p3532 A69-37960

Photographic studies of explosive reactions with description of ultrahigh speed cameras

21 p3719 A69-38446

AERIAL PHOTOGRAPHY

Aerial color photography for terrain analysis noting development of cameras, filters, high speed emulsions and processing equipment

01 p0077 A69-10023

Avionics in forest resource inventories management, noting design of radar altimeter for low level aerial photography

01 p0080 A69-10352

Global cloud models construction techniques, discussing vertically pointing radars, airborne panoramic cameras, radiometry, meteorological satellites and light detection and ranging

02 p0275 A69-12381

Relative orientation elements of aerial photographs determined by iteration method

05 p0765 A69-16708

Individual differences and relation to Witkin concept of perceptual style in target identification in aerial photographs

06 p0880 A69-17211

Horizontal aerotriangulation by independent models using photogrammetric extension of horizontal control for small scale superwide angle photography, horizon photography and B 8 plotter

06 p0925 A69-17468

Aerial photography history, photographer qualities, airborne platforms, pilot briefing, air to air sortie, aerobatics, parachutes, etc

08 p1314 A69-20307

Aerial chronophotography of Southern Hemisphere conducted on around world polar flight analyzed for meteorological and geographical aspects and compared with satellite data

09 p1534 A69-21405

Aerial panoramic camera with instantaneous exposure using combined Bouwers concentric lens system and between lens shutter

09 p1499 A69-22246

Large scale color and color IR aerial photography evaluation to determine interpretability for improving range resource inventories

11 p1880 A69-24265

Multispectral photographic determination of reflectance of environmental features from aerial spectral photographs, noting EROS program application

11 p1880 A69-24266

Photogrammetric networks equalization by method of least squares, using external orientation elements of aerial photographs

12 p2079 A69-26032

Green flash photographed at sunset by aircraft at 10.6 km over Pacific, noting correspondence with visual observation

12 p2066 A69-26232

Photography for remote sensing, discussing aerial photography, side-looking radar and photography for recording, storing and retrieving data

12 p2096 A69-26975

Remote sensing and forest survey sampling designs, discussing nonstereo stratification, conventional photography and IR or radar imagery

12 p2097 A69-26991

Previsual detection of vigor loss and mortality signs in ponderosa pine trees subject to bark beetle attack

12 p2098 A69-26993

Multispectral and calibrated Alaskan Arctic aerial survey of sea ice, thaw lakes and polygonal soils

12 p2075 A69-26996

Remote oceanographic sensing from ships, aircraft and spaceborne platforms, using active /radar and laser/ and passive sensors in visible, IR and microwave regions

12 p2075 A69-26997

Terrain photography applications and analysis including remote sensing of photographic systems and photointerpretation

12 p2098 A69-27006

Airborne and satellite IR survey over active effusive eruption at Surtsey, Iceland, comparing thermal energy yield and radiant emission to ground measurements

12 p2076 A69-27011

Multiband aerial photography utilization for evaluating urban housing quality compared with present data collection methods

13 p2260 A69-27607

Computer based data handling and display for relating remote sensor signals to ground truth information derived from aerial photographs

14 p2416 A69-29534

Image quality of color disks in aerial photographs using panchromatic, color positive, color negative and false color films, measuring reflected sunlight

14 p2450 A69-29600

Apollo 9 multispectral photography compared with photographs taken simultaneously by aircraft using same film filter combinations

15 p2608 A69-30452

Color IR film improvement for high altitude remote sensor, using auxiliary minus-visual filters

15 p2609 A69-30457

Regional slope measurement from two monoscopic radar images of same terrain area, discussing accuracy and applications to geomorphology and hydrology

15 p2610 A69-30710

Earth resource satellites, discussing mapping, land evaluation, geological observation, agricultural and hydrological applications, electromagnetic spectrum information, sensors and photographs

16 p2881 A69-31763

Automated crop surveys from integrating observations made at different times /time dimensioning/ during growing season, noting earth resources satellites role

18 p3126 A69-34337

Aerospace images information suppressing and enhancing methods to aid interpreter in making more accurate recognition and measurement of earth resources subjects

18 p3133 A69-34338

Topographic mapping by high altitude jet aircraft photography

18 p3134 A69-34339

Aerial camera AFA-TES-10, discussing mean square aiming error, photogrammetric distortion and contrast

18 p3139 A69-35328

Aerial photography in geomorphological interpretations, noting advantages over conventional maps in slope microreliefs, soil erosion network and karst, glacial, aeolian and shore features

20 p3539 A69-37512

Errors in sighting and identifying geodetic contour points on aerial photographs, considering stereocomparators parallaxes effect

21 p3719 A69-38404

Image intensifiers and orthicons, plumbicons, vidicons as photoelectric devices in TV auroral observation from ground stations and jet aircraft

21 p3706 A69-38484

Comparative photointerpretation from panchromatic, color and Ektachrome IR aerial photography

22 p3944 A69-40039

Photogrammetric contours plotting from aerial color films

22 p3944 A69-40045

Superwide angle camera with aerial photogrammetric lens system, discussing light distribution, rotary disk shutter, etc

22 p3944 A69-40047

Surveying earth resources from space, covering orbital height photography in cartographic programs, hydrologic engineering, pollution control and geology
22 p3936 A69-40170

Tethered polyethylene balloon carrying radio controlled camera for time lapse photographs of wave generated near shore currents
22 p3865 A69-40808

Photographic platform applications of tethered balloons, discussing powered systems for low and high altitudes and free balloons
22 p3865 A69-40811

Color aerial photography - Conference, New York, June 1969
22 p3948 A69-40985

Glass filter systems for aerial color photography developed from spectral studies of sunlight, skylight and airlight in Rayleigh atmosphere
22 p3948 A69-40986

Multispectral processing of Apollo 6 earth photographs, evaluating geologic, vegetative and cultural features from red, green and blue portions of visible spectrum
22 p3941 A69-40987

Photographic properties of Cibachrome silver dye bleach materials for yielding color reflection prints directly from color transparencies, discussing applications to aerial photography
22 p3949 A69-40991

Aerial color film processing systems
22 p3949 A69-40992

Color and color IR aerial photography compared for estuarine and marshland research, considering detection of turbidity, pollution, salinity, etc
22 p3942 A69-40993

Aerial photography for near-shore ecology, noting biological cover on ocean floor, submarine biological communities and human activities on submarine life
22 p3894 A69-40995

Optical engineering and quality control of photogrammetric instruments for aerial color photography, discussing lenses, filters, projectors, plotters, electro-optical rectifier, etc
22 p3949 A69-40996

Multispectral color aerial photography using broadband spectral filters for detecting and identifying small environmental features of earth surface
22 p3949 A69-40997

Orthophotography as technique for eliminating distortions in vertical aerial photographs during conversion into uniform scale reproductions
22 p3949 A69-40998

Camera lenses and techniques for aerial color photography, discussing atmospheric influences, filters, films and exposure times
22 p3950 A69-40999

Xenon plasma continuous illumination sources design and operation for night and color aerial photography covering photogrammetric resource surveys, ground traffic, flight paths, etc
22 p3950 A69-41000

Orthophoto maps production, discussing scales, aerial photography, control points, orthoprojection, cartography and printing
22 p3951 A69-41246

Automated air photo identification of crop types, utilizing stereo height as discriminating variable
23 p4155 A69-41721

Earth orbital remote sensing applications to forest and range resources management, discussing conventional aerial photography
[AAS PAPER 69-059] 24 p4307 A69-42823

AERIAL RECONNAISSANCE

Military forward air control aircraft conversion from lightweight commercial tandem engine aircraft noting visibility, communication and navigation equipment
[SAE PAPER 690313] 11 p1822 A69-24511

Aerial multiband remote sensors for wildland resources, considering multiens photographic systems, optical mechanical scanners and radar devices
15 p2609 A69-30458

Equations derived for radar image coordinate transition to geodetic coordinates in aerial surveying by side-looking airborne radar
15 p2596 A69-30574

Satellite and aircraft use compared for earth resource surveys, discussing proposed aircraft data collection system
16 p2881 A69-31632

Spectral reflectances of objects and vegetative backgrounds to generate color photographic technique increasing detection sensitivity and rate
18 p3133 A69-34247

Aerial surveys flight functions cost plotted against degree of performance, allowing for obtainable accuracies
22 p3863 A69-40041

Instruments for obtaining auxiliary data in aerial triangulation, describing stratoscope, profile recorder, radar altimeter, horizon camera, etc
22 p3944 A69-40042

AERIAL RUDDERS

Nomogram for aircraft rudder pedals design and construction, considering thigh and knee angles
10 p1649 A69-23377

AEROBEE ROCKET VEHICLE

Conductive heat transfer between aerodynamically heated skin and barrel of Aerobee 150 sounding rocket telescope, noting effect of residual gas pressure
09 p1610 A69-22005

Aerobee rocket-borne liquid helium cooled telescope for IR night sky observations
11 p1885 A69-24852

Micrometeoroid collections, describing Gemini satellite and Aerobee rocket-borne equipment and experimental results
15 p2700 A69-31440

Artificial aurora generated at 100 km altitude by electron beam fired downward from aerobee 350 rocket above 230 km along earth magnetic field lines
18 p3127 A69-34365

AEROBES

Cellular localization of acetyl-coenzyme A synthetase in yeast, noting enzyme distribution during aerobic growth on glucose
04 p0554 A69-15333

B Coli commune cultivated on various substrates, studying oxygen consumption under aerobic/ anaerobic conditions
18 p3097 A69-35302

AEROBIOLOGY

Human intolerance to bacteria as food, considering response to Hydrogenomonas eutropha and Aerobacter aerogenes
13 p2213 A69-27265

AERODYNAMIC BALANCE

Swing wings on combat aircraft and SST, discussing suitability for aircraft carriers and problems in aerodynamic balance
03 p0367 A69-13677

Concorde fuel management, discussing trim, fuel as coolant and booster pumps
07 p1057 A69-19705

Stabilizing methods for supersonic aircraft, noting effect of aircraft characteristic parameters on magnitude of balancing coefficients of lifting force
16 p2735 A69-32127

Aerodynamic control surface/trim tab coupling coefficients in subsonic two dimensional unsteady flow using matrix method valid for motion involving harmonic oscillations
17 p2895 A69-33597

Aerospace vehicle mass property limits and dynamic balancing related, noting errors
[SAWE PAPER 772] 18 p3208 A69-34875

Mechanics of missile dispersion due to dynamic unbalance and rocket spin stabilization problems
[SAWE PAPER 741] 18 p3208 A69-34886

Dynamic balance for rotating aerospace vehicles, discussing error in principal axis location between rotor on machine and free body in space
[SAWE PAPER 740] 18 p3137 A69-34887

PDP8 digital computer and Trebel vertical balancing machine combined for real time presentation of trim weights and positions, noting noise in force components
[SAWE PAPER 738] 18 p3220 A69-34888

Moment of inertia measurements facility for spacecraft dynamic balancing operations at low angular rates
[SAWE PAPER 739] 18 p3118 A69-34889

Skin friction balance in Mach 5 wind tunnel with high heat transfer, measuring shear forces
19 p3292 A69-35734

Accelerometer force balance method for measuring aerodynamic rocket plume forces acting on flat plate model in short duration shock tunnel test environments
19 p3292 A69-35737

Wing flaps and blow-off and suction effect on longitudinal balance of landing TU-104 aircraft, noting air suction at wing leading edge
19 p3247 A69-35818

Wind tunnel model one component magnetic support and balance system for sphere drag investigation at subsonic Mach numbers
[AIAA PAPER 68-401] 24 p4298 A69-43714

AERODYNAMIC BRAKES

NT DRAG CHUTES
NT LEADING EDGE SLATS
NT TRAILING-EDGE FLAPS
NT WING FLAPS

Deceleration control system for aerobraking and skipout to orbit at Mars
[AIAA PAPER 68-1146] 03 p0520 A69-13564

Cost effective aerodynamic deceleration and retardation systems for military and space programs, noting technical research and development areas in need of advancement
03 p0364 A69-13854

Approximate method for calculating vertical velocity distribution in atmospheric braking of bodies along ballistic trajectories
04 p0541 A69-14485

Venus and Mars atmospheric braking entry and associated equipment, discussing potential cost savings
11 p1968 A69-25722

Structural and aerodynamic developments in attached inflatable decelerators for deployment of payload at supersonic speeds
[AIAA PAPER 68-929] 21 p3647 A69-39015

Deceleration control system for aerobraking and skipout to orbit at Mars
[AIAA PAPER 68-1146] 21 p3828 A69-39761

Aerodynamic deceleration systems for space missions, considering deployment of subsonic parachute and inflatable configuration following atmospheric entry
[AIAA PAPER 68-1081] 22 p4036 A69-40542

Flexible parawing lifting decelerator research data from wind tunnel and flight tests, noting manned space vehicle recovery and aircraft escape systems
[AIAA PAPER 68-967] 24 p4254 A69-43715

AERODYNAMIC BUZZ
U FLUTTER

AERODYNAMIC CHARACTERISTICS
NT INTERFERENCE LIFT
NT JET LIFT
NT LIFT
NT ROTOR LIFT
NT STATIC AERODYNAMIC CHARACTERISTICS
NT SUPERSONIC DRAG

Vortex method within slender body theory for aerodynamic interference between missile in both captive and dropped positions and carrying aircraft
01 p0007 A69-11026

One and two lobed conical, cylindrical and all-flexible parawing lift, drag and pitching moment and canopy shape
[AIAA PAPER 68-10] 01 p0007 A69-11027

Aerodynamic characteristics of delta wings for supersonic flow at large angles of attack, showing sweep-back angle influence on drag coefficient
02 p0191 A69-12585

V/STOL aircraft characteristics, emphasizing propeller, ducted fan and turbojet types
05 p0701 A69-15563

NASA research on flexible and stiffened flexible wings, discussing range of applicability, aerodynamic characteristics and wind tunnel results
05 p0701 A69-15568

Aerodynamic technology applied to takeoff and landing, discussing STOL airplanes in descent and boundary layer control/BLC/ flap system
05 p0696 A69-15569

Factors influencing development of both wind tunnel and flight test technology for determining aerodynamic derivatives of aircraft motions
05 p0741 A69-15572

Peculiarities of aerodynamic characteristics of flow past plate and pointed and blunt slender cones in viscous hypersonic thermodynamically ideal gas
05 p0699 A69-16673

Random search and multiple integral based Monte Carlo method for computer solution of nonlinear aerodynamic problems
06 p0858 A69-17334

Reciprocal interaction of combustion wave and field of turbulence, discussing aerodynamic principles, turbulence effect on flame propagation speed and measuring methods
06 p1032 A69-17420

Aircraft aerodynamic characteristics determination from numerical computer solution of supersonic gas flow past blunt body with broken generatrix
06 p0859 A69-17582

Lifting reentry spacecraft performance examined in context of realistic aerodynamic characteristics at low flight Reynolds numbers
06 p0860 A69-17634

Rolling ballistic vehicles mass and aerodynamic characteristics determined from dynamic motion data by performing Fourier analysis on roll axis equation of motion

[AIAA PAPER 69-102] 06 p0862 A69-18039

Ballistic range tests to study ablation effects on aerodynamic characteristics of ablating and nonablating slender cones

[AIAA PAPER 69-179] 06 p1036 A69-18083

Longitudinal dynamics of VTOL aircraft during hover-forward flight transition, using multiple time scale analysis

[AIAA PAPER 69-130] 06 p0869 A69-18157

Subsonic lifting surface theory including leading edge, discussing singularities in solution of integral equation for determination of aerodynamic properties

[AIAA PAPER 69-37] 06 p0865 A69-18167

Thermodynamic and aerodynamic characteristics of organic Rankine cycle working fluids for ideal applicability to manufacturing

[SAE PAPER 690063] 07 p1057 A69-18308

Aircraft propelled at Mach 7, discussing low speed and transonic characteristics, stability, power plant integration and ONERA wind tunnel experiments

[ONERA-TP-657] 07 p1052 A69-18414

Radomes design and manufacture for high speed flight vehicles, discussing interactions between aerodynamic and electrical requirements with reference to mechanism of aberration

07 p1141 A69-19510

Engineering testing of aerodynamic efficiency of helicopter rotors during hovering with and without ground effect

08 p1254 A69-20169

Variable geometry intake and convergent-divergent nozzle design for supersonic aircraft, noting subsonic installations

08 p1253 A69-21164

Complex bodies aerodynamic characteristics in free molecular gas flow by applying Monte Carlo method

09 p1430 A69-21793

Aerodynamic characteristics of propeller-wing-flap systems used on deflected slipstream STOL aircraft

09 p1431 A69-22278

Hypersonic: drag and shock wave characteristics of blunt bodies including cones, spherical nose and concave nose bodies

09 p1433 A69-22568

External burning ramjets in hypersonic stream noting applications to drag reduction, lift-drag ratio and attitude control

11 p1941 A69-24261

Flat plate in two dimensional low density hypersonic flow wind tunnel tested for aerodynamic effects on spacecraft reentry

11 p1819 A69-25424

Aerodynamic characteristics of flat plate in viscous hypersonic flow incident at zero or small angle of attack, using numerical integration

11 p1820 A69-25471

Concorde design problems due to kinetic heating, aerodynamic characteristics, structure, equipment, modified delta wing planform, etc

12 p2012 A69-26358

Apollo spacecraft command module aerodynamic characteristics during entry compared with wind tunnel test predictions

[AIAA PAPER 68-1008] 12 p2012 A69-26789

Linear and second order theory for maximum lift to drag ratio airfoils at moderate supersonics speed, considering length, thickness and area

13 p2199 A69-28214

Multirecompression heater for pure airflow tests of ballistic vehicles and hypersonic aircraft

[AIAA PAPER 69-332] 13 p2242 A69-28268

Longshot free piston gun tunnel for high Reynolds number hypersonic flow tests

[AIAA PAPER 69-333] 13 p2249 A69-28269

Hypersonic wind tunnel for erosion test of multiple particle impacts, considering dust on cork, carborazole and silicone rubber

[AIAA PAPER 69-341] 13 p2243 A69-28277

Angle of attack and blunting effect on aerodynamic lift and drag coefficients of flat plates in hypersonic flow at low Reynolds number

13 p2200 A69-28358

Diffusion characteristics of turbulent flow produced by square mesh grid in low speed wind tunnel

13 p2250 A69-28496

Supersonic aerodynamic characteristics of wings with complex planar geometry and subsonic leading and trailing edges, discussing varying geometry

14 p2391 A69-29624

Aerodynamic properties calculations of arbitrary slender supersonic wings using sum of simple integrals

15 p2548 A69-31170

Spoiler effect on aerodynamic characteristics of airfoil with hinged flap in inviscid fluid plane flow

15 p2549 A69-31223

Aeroelastic divergence and stability range for cantilevered and end supported structures computed as function of forward resistance and lift caused by wind

16 p2870 A69-31557

Perturbation solutions for planar cylindrical and spherical blast waves in air, considering third and fourth order approximations

16 p2770 A69-31900

Aerodynamic problems in future civil aircraft design, emphasizing Concorde development possibilities, discussing VTOL intercity transport, subsonic swept wing and hypersonic aircraft, all-wing airbus, etc

16 p2732 A69-32023

Turbomachinery two mode blade vibrations with emphasis on aerodynamic damping, noting shifts in natural frequencies

[ONERA-TP-678] 16 p2733 A69-32333

High temperature radial turbine design for small gas turbine engines, discussing aerodynamic, structural and thermal analyses

[AIAA PAPER 69-524] 16 p2838 A69-32662

Running test facility for study of aerodynamics and flight dynamics of V/STOL aircraft models

17 p2944 A69-32851

Aerodynamic characteristics of cone/cylinder and cone/cylinder/cone configurations with blunted cones in hypersonic flows at small angles of attack

17 p2889 A69-33122

Aerodynamic characteristics of power plant installation, discussing nacelle design from viewpoint of aircraft performance and economic efficiency

17 p2898 A69-33215

Flow simulation on wind tunnel test models for aerodynamic characteristics of aircraft design, discussing boundary layer and external flow coupling

[AIAA PAPER 69-660] 17 p2945 A69-33471

Aerodynamic interactions between two wing configurations with same aspect ratio located in same plane, discussing testing principles and initial experimental results

17 p3061 A69-33595

Drag and lift coefficients of moderate aspect ratio prismatic bodies analyzed as function of angle of attack, Reynolds number and aspect ratio

17 p2896 A69-33717

Soviet book on practical aerodynamics of An-2 aircraft covering aerodynamic characteristics, equilibrium, stability and control for various flight conditions, including icing

18 p3090 A69-34340

Aerodynamic characteristics of elliptical airfoils with jet circulation control for VTOL rotors including dual jets and cyclic results

[AIAA PAPER 69-741] 18 p3084 A69-34406

Aerodynamic and flight characteristics of variable geometry entry spacecraft during subsonic wing deployment and landing

[AIAA PAPER 69-742] 18 p3084 A69-34407

Hover and forward speed aerodynamic characteristics of tracked air cushion vehicle (TACV) models, discussing wind tunnel tests

[AIAA PAPER 69-750] 18 p3084 A69-34410

Stationary elliptic cylinders in subcritical flow, determining Strouhal number, pressure fluctuations and wake geometry as functions of angle of attack

[AIAA PAPER 69-745] 18 p3084 A69-34412

Aerodynamic characteristics of ballistic reentry vehicles from flight test dynamic measurements, illustrating results

18 p3085 A69-34670

Aerodynamic characteristics of sphere and blunt cone in highly rarefied gas flow, noting molecular collision effect

18 p3086 A69-34708

Air data system consisting of aerodynamic and thermodynamic sensors and computer calculating flight parameters for automatic flight control

18 p3169 A69-34854

Aircraft preliminary design weight and volume characteristics relation to aircraft density

[SAWE PAPER 813] 18 p3221 A69-34897

Computer programs determining gaseous properties and aerodynamic characteristics for missiles, reentry vehicles and spacecraft at angles of attack

18 p3107 A69-35068

Aerodynamic behavior of airfoil oscillating in reverse flow defined for various angles of attack and oscillatory amplitudes at low Mach numbers

18 p3087 A69-35219

Aerodynamic characteristics of two dimensional nonexpandable flexible sail in hypersonic inviscid flow discussing roles of sail length and chord and angle of attack

19 p3237 A69-35811

Aerodynamic characteristics of plane inviscid flow jets expanding over curvilinear surface, deriving force equations for surfaces in jet and rocket engines

19 p3296 A69-35812

Supersonic aerodynamic characteristics of flared cones with various flare angles studied by schlieren photography, showing geometrical parameters influence on flow patterns

19 p3239 A69-36385

Stream surface characteristics as criteria for hypersonic lifting bodies shapes for optimal aerodynamic fuel performance

19 p3248 A69-36399

VTOL aircraft lift systems, propulsion, airframe aerodynamic and aerodynamic characteristics, control systems, missions, safety, configurations and environment

[AIAA PAPER 68-977] 20 p3461 A69-37149

Aerodynamic performance tests of autorotative unpowered rotor entry vehicle model at various Mach numbers and angles of attack

[AIAA PAPER 68-950] 20 p3458 A69-37155

Vortex lattice method correlation on rotor/wing configurations for aerodynamic characteristics, noting triangular and circular hub and blades

20 p3458 A69-37163

Supersonic blowdown wind tunnel operating at Mach numbers obtained by fixed nozzles for aerodynamic optimization of wings and bodies

20 p3510 A69-37422

Nervous system relations to insect flight musculature of lift and thrust mechanism

21 p3651 A69-38780

Aircraft propelled at Mach 7, discussing low speed and transonic characteristics, stability, power plant integration and ONERA wind tunnel experiments

21 p3644 A69-39164

Reentry cones with mass and configuration asymmetries, studying nonlinear aerodynamic characteristics by wind tunnel and full scale flight tests

[AIAA PAPER 69-867] 21 p3823 A69-39393

Hypersonic lifting bodies with high lift-drag ratio, presenting flat-top wing-body combination aerodynamic characteristics

21 p3645 A69-39793

Hypersonic wave riders lift and drag coefficients, lift drag ratio, shock profile and pressure distribution, discussing wind tunnel measurements of caret wings

21 p3645 A69-39802

Aerodynamic characteristics of turbulent twisted jet in slipstream in open jet wind tunnel, determining static pressure, temperature and velocity component profiles

21 p3645 A69-39848

Internal aerodynamics of centrifugal compressor impeller, discussing impeller channel airflow model, impeller exit flow, rotating channel flow, etc

[RAES PAPER 19] 22 p3859 A69-40498

Flexible string extraction from bobbin through nozzle, solving equations of motion by neglecting bending rigidity, extensibility, drag, internal friction, etc

22 p3930 A69-40585

Aerostatic and aerodynamic characteristics of Dart Vee tethered balloon system

22 p3865 A69-40813

Proton 2 satellite orientation and motion about center of mass determined from telemetric data analysis under aerodynamic moment

22 p4037 A69-41090

Satellite aerodynamic characteristics, considering orbital position and attitude of cylindrical body and separate plate

22 p4037 A69-41102

Air mass mechanics, local lifting surface element aerodynamic response and aeroelastic blade response problems in lifting rotor technology

23 p4061 A69-41370

V/STOL propeller aerodynamics, considering thrust efficiency, roll and yaw control, flow visualization methods, etc

23 p4062 A69-41375

Rheoelectrical analog technique for low speed aerodynamic characteristics of finite wings in incompressible flow, using deep electrolytic tank for lifting surface calculations

23 p4061 A69-42351

Aerodynamic characteristics of moving and rotating bodies of revolution in free molecular rarefied gas flow assuming Maxwellian thermal velocity distribution and diffuse specular interaction

24 p4243 A69-42582

Subsonic wind tunnel balance and holders investigated for effects on lift, drag and stability of models of body of revolution
24 p4297 A69-43084

Aerodynamic frequency response calibration measurements of wind anemometer by input velocity and output drag values under unsteady flow conditions
24 p4315 A69-43262

AERODYNAMIC CHORDS

U AIRFOIL PROFILES
U CHORDS [GEOMETRY]

AERODYNAMIC COEFFICIENTS

Wing-body combinations analysis and design at supersonic and subsonic speeds by aerodynamic influence coefficients method
[AIAA PAPER 68-55] 01 p0006 A69-11016

Low Mach number airfoil profile drag calculation for various angles of attack and Reynolds numbers, noting effects of transition and airfoil thickness
01 p0006 A69-11017

Supercritical flow effects on unsteady aerodynamic coefficients used for subsonic aircraft flutter analysis, emphasizing changes due to shock and flow separation
01 p0007 A69-11020

Reattachment pressure correlated for any type of two dimensional turbulent supersonic separated flow
04 p0588 A69-14727

Blunt cone hypersonic roll damping derivative, using Mach number distribution and graphical integration
04 p0542 A69-14739

Ground effects influence on VTOL aircraft secondary forces during hovering and transitional flight, discussing component dynamic coefficients in wind tunnel
[DVL-851] 04 p0547 A69-14813

Vortex breakdown effect on aerodynamic coefficients of small aspect ratio delta wings during yawing
04 p0543 A69-14821

Wind tunnel wall constraints effects at extreme force coefficients during V/STOL testing shown different from effects in conventional aircraft testing
05 p0741 A69-15574

Lift and drag coefficients for circular cylinder immersed in time dependent flow analyzed using potential flow model
[ASME PAPER 68-FE-15] 05 p0747 A69-16072

Nonlinear equations of motion approximate solution, determining ordnance weapons aerodynamic stability coefficients from angular motion as functions of angle of attack
[AIAA PAPER 69-135] 06 p0863 A69-18120

Aerodynamic coefficients from observed motion of body in flight, eliminating need for closed form solutions by employing numerical solutions to equations of motion
[AIAA PAPER 69-134] 06 p0864 A69-18161

Bulk aerodynamic method for heat and water vapor fluxes from data obtained at Chiba /1966/, introducing modified integral diffusivity
07 p1176 A69-18965

Skin friction drag coefficient for right circular cylinder calculation coefficient on basis of Blasius solution for flow
11 p1819 A69-25384

Skin friction coefficient relation to pressure distribution in turbulent flow and development of momentum thickness along flow
11 p1819 A69-25385

Initial flow turbulence effects on drag coefficient for prismatic bodies in low velocity gas flow determined by wind tunnels
14 p2391 A69-29625

Drag and friction coefficients for laminar pulsating incompressible fluid flow in circular tubes obtained from Navier-Stokes equation
15 p2592 A69-30988

Atmospheric density determination based on long period variations of drag coefficients from satellite Proton 2, considering satellite orientation
15 p2602 A69-31392

Stabilizing methods for supersonic aircraft, noting effect of aircraft characteristic parameters on magnitude of balancing coefficients of lifting force
16 p2735 A69-32127

Blockage effects of flat plates and solid bluff bodies in closed wind tunnels compared concerning drag coefficient values
17 p2890 A69-33245

Drag measurements for sharp and blunt-nosed bodies shot into wind tunnel supersonic gas counterflows, discussing shock waves for different configurations
19 p3239 A69-36401

Lift coefficients of idealized tunnel type ram wing consisting of truncated semiconical shell computed by lifting surface theory
22 p3860 A69-40819

Stagnation point Mach number gradient, sonic point location and drag coefficient of hemisphere at zero angle of incidence
23 p4060 A69-41910

Aerodynamics of twisted jet propagating in same fluid by asymptotic expansion, analyzing twist influence on heat transfer
24 p4244 A69-43057

Optimum climb trajectories at constant lift coefficient, using variational methods with final altitude and final flight path angle as end point constraints
24 p4254 A69-43727

AERODYNAMIC CONFIGURATIONS

Aerodynamic configurations to reduce sonic boom at supersonic speeds
01 p0007 A69-11028

Supersonic interference on lateral stability of planar configurations analyzed using wind tunnel data
[AIAA PAPER 68-21] 02 p0189 A69-12377

Hypersonic lifting body configurations for maximum lift drag ratios and subject to volumetric efficiency, nose heating limit and skin friction constraints
02 p0189 A69-12378

Monte Carlo direct simulation for treating rarefied supersonic flows about bodies in transitional regime between continuum and free molecular flow
02 p0189 A69-12523

Scattering matrices of complex configuration specified by cross polarized radar cross sections based on Green function, noting wire loop and wedge scatterers
03 p0384 A69-12904

Hypersonic lifting body optimization under single and combined constraints of volumetric efficiency, heating and skin friction, using numerical search routine
[AIAA PAPER 68-1157] 03 p0362 A69-13557

Prandtl three main problems of airfoil theory interpreted and applied, discussing slender aircraft and hypothetical waverider aircraft
04 p0543 A69-14802

Conventional fuselage and streamline body shapes effect on drag at subsonic speeds, noting boundary layer development
05 p0697 A69-15827

Blockage correction for blunt based bodies of revolution in wind tunnels at low Mach numbers
05 p0699 A69-16395

Low drag three dimensional body configurations from tabulated low drag airfoil coordinates
06 p0857 A69-17000

Hypersonic body shaping for minimum drag and improved performance from view of flight regimes, discussing implications of pressure laws
[AIAA PAPER 69-181] 06 p0863 A69-18052

Aerobell extendible nozzle rocket engine design and performance, cold flow and simulated hot flow test results
[AIAA PAPER 69-4] 06 p0985 A69-18195

Optimum aerodynamic shapes theory, considering linearized and nonlinearized supersonic flow, Newton-Busemann hypersonic flow, free molecular flow, mathematical models and variational problems
08 p1253 A69-21127

Complex bodies aerodynamic characteristics in free molecular gas flow by applying Monte Carlo method
09 p1430 A69-21793

Lifting pressure distributions on oscillating surfaces in subsonic flows using doublet lattice method for various surface geometries
[AIAA PAPER 68-73] 09 p1430 A69-21946

Axissymmetric bodies longitudinal contours for hypersonic flow minimum drag, considering Newtonian pressure distribution and skin friction
10 p1632 A69-23886

Aerodynamic design of subsonic and transonic axial flow compressors, discussing blade configurations and computerized design of turbomachinery
12 p2147 A69-25792

Small gas turbine Brayton cycle analysis treating component efficiencies as dependent variables in examining single stage radial compressor and turbine aerodynamic configuration
[IME PAPER 5] 12 p2147 A69-25794

Book on hovercraft design and construction covering aerostatic and aerodynamic craft, cushion performance, ducting, fans, compressors, drag, propulsion, control, stability, economics
12 p2013 A69-26633

Ablation wedge model design for testing in wave superheater under controlled pressure gradients and constant temperature
12 p2059 A69-26816

Inviscid supersonic flow in right angle corner of varied angular intersecting wedges with bow waves remaining planar up to intersection line
13 p2200 A69-28251

Aerodynamic interactions between two wing configurations with same aspect ratio located in same plane, discussing testing principles and initial experimental results
17 p3061 A69-33595

Economics evaluation for operation of commercial fixed wing aircraft at aft center of gravity position, noting fuel saving from drag reduction
[SAWE PAPER 806] 18 p3091 A69-34902

Aerodynamic optimal shaping by multivariable search technique, comparing results with variational solutions for airfoil profiles
20 p3459 A69-37527

Optimum form for hypersonic profile with minimum drag for given bending strength solved by variational method
21 p3644 A69-39099

Book on optimal aerodynamic shapes by means of variational method, covering conventional and triangular thick wing lift systems in supersonic flow
21 p3644 A69-39667

Hypersonic wave riders lift and drag coefficients, lift drag ratio, shock profile and pressure distribution, discussing wind tunnel measurements of caret wings
21 p3645 A69-39802

Modified tailed delta configuration selection for U.S. SST, discussing power plant installation choice
[RAES PAPER 17] 22 p3863 A69-40496

Hypersonic turbulent boundary layer separation over cone-cylinder flare configuration at zero angle of attack and high Reynolds number
22 p3930 A69-40557

Transonic flows behind separated shock waves of ideal gases past bodies of various geometries
23 p4151 A69-41526

AERODYNAMIC DRAG

NT SUPERSONIC DRAG

Soviet monograph on laminar boundary layer in presence of suction covering incompressible flow through porous surface, drag reduction and optimal suction at high velocities
01 p0060 A69-10615

Low Mach number airfoil profile drag calculation for various angles of attack and Reynolds numbers, noting effects of transition and airfoil thickness
01 p0006 A69-11017

Lift efficiency of and stabilization by square flare on high speed missile, comparing wind tunnel measurements with circular conical flare
02 p0190 A69-12544

Minimum drag configurations with low heat transfer for hypersonic bodies of revolution, noting performance at supersonic speeds
02 p0191 A69-12578

Accelerometric measurement of atmospheric drag with satellite 1968-59B, obtaining upper atmosphere density profile at 130-160 km
02 p0245 A69-12728

Lift and drag parameters of axisymmetric bodies in Newtonian flow at random incidence by summation of appropriate portions
04 p0542 A69-14745

Heat transfer and drag of cylinders with cavities at hypersonic speeds measured by platinum film thermometer and strain gauge balance in gun tunnel
[DVL-850] 04 p0543 A69-14822

Flow field of impulsively started circular cylinder, noting drag due to nonlinear convection
04 p0544 A69-14897

Airplane drag prediction by wind tunnel tests
05 p0695 A69-15543

Laminar flow on swept low drag suction wings at high Reynolds numbers
05 p0696 A69-15557

Conventional fuselage and streamline body shapes effect on drag at subsonic speeds, noting boundary layer development
05 p0697 A69-15827

Low drag three dimensional body configurations from tabulated low drag airfoil coordinates
06 p0857 A69-17000

Polyvinyl chloride coating for reducing aerodynamic skin friction drag, noting water saturation effect on polyurethane foam
[AIAA PAPER 69-165] 06 p0912 A69-18043

AERODYNAMIC FORCES

MHD flow in channels with abruptly widening sections and finned walls under transverse magnetic field, discussing effects on drag
07 p1192 A69-19016

Equivalent cross section theory relating air resistance of randomly tumbling bluff objects to resistance of equivalent spheres
09 p1431 A69-22000

Small body drag in wake of large satellite using two dimensional model noting methods for calculating distribution function moments in wake regions
12 p2012 A69-26798

Mass transfer cooling data correlation for estimating mass injection effect on slender cone drag
13 p2199 A69-28224

Three dimensional effects on Stanton tube data for skin friction determination for small protruberances drag immersed in turbulent boundary layer
16 p2771 A69-31920

Trajectory calculation of axisymmetrical body during ballistic and vertical flight, assuming air drag proportional to square of velocity
17 p2889 A69-32950

Base flow component of total drag for axisymmetric supersonic afterbody with single exhaust jet, considering turbulent mixing
[AIAA PAPER 69-650] 17 p2956 A69-33485

Stratospheric winds effect on instrument package suspended from high altitude balloon, discussing package displacements, yarn shapes and air drag characteristics
17 p2961 A69-33612

Economics evaluation for operation of commercial fixed wing aircraft at aft center of gravity position, noting fuel saving from drag reduction
[SAWE PAPER 806] 18 p3091 A69-34902

Computer-generated airline fleet performance data on B-720, B-727 and DC-8 aircraft, attributing deterioration to increased drag and fuel consumption
[AIAA PAPER 69-770] 19 p3245 A69-35651

Drag influence on mission performance of hypersonic aircraft during climb and cruise, noting payload capacity
20 p3461 A69-37154

Schweikhard method for measuring changes in lift, drag and pitching moment of fixed wing aircraft as function of distance from ground
20 p3462 A69-37423

F region atmospheric density measurements obtained from aerodynamic drag on San Marco 2 satellite in equatorial orbit, comparing data with San Marco 1
21 p3704 A69-38369

Structural and aerodynamic developments in attached inflatable decelerators for deployment of payload at supersonic speeds
[AIAA PAPER 68-929] 21 p3647 A69-39015

Satellite orbits calculation in nonrotating atmospheres, considering atmospheric drag and zonal harmonics coupled effects
[AIAA PAPER 69-925] 21 p3808 A69-39352

Shear stress and free molecular drag for gas flow along concave cylindrical surface oriented at angle of attack, analyzing multiple surface collisions effect
24 p4249 A69-43660

AERODYNAMIC FORCES

- NT BLAST LOADS
- NT GUST LOADS
- NT HYPERSONIC FORCES
- NT INTERFERENCE LIFT
- NT JET LIFT
- NT LIFT
- NT ROTOR LIFT
- NT SUPERSONIC DRAG
- NT WING LOADING

Velocity field excited by wing vibrations propagating over elastic surface at supersonic velocities, considering nonvertical motion and absence of external forces
02 p0188 A69-11976

Unsteady aerodynamic forces on coplanar lifting surfaces in subsonic flow induced by wing/ horizontal tail interference
04 p0543 A69-14819

Calculation method for surface aircraft structures by treating normal forces and bending moments as unknown values
04 p0677 A69-14839

Wind tunnel wall constraints effects at extreme force coefficients during V/STOL testing shown different from effects in conventional aircraft testing
05 p0741 A69-15574

Satellite relative equilibrium stability under action of gravitational and aerodynamic moments
05 p0830 A69-16503

Aerodynamic torque on spinning spherical satellite, noting applications to accommodation coefficient measurement and study of aerodynamic gas-surface interactions
09 p1611 A69-22087

Aerodynamic stick force and speed characteristics of various horizontal tails and elevator trimmers, noting zero stick force case
09 p1434 A69-22597

Subsonic channel flow of frictionless barotropic gas through oscillating grid, investigating perturbation velocity field and aerodynamic forces on airfoils
10 p1631 A69-22905

Velocity, lifting force, pressure moment and circulation around linear array of thin foils with direction normal to profile chords calculated by Birnbaum-Glauret method
11 p1817 A69-24348

Aerodynamic forces causing deformation and breakup of liquid droplet with ellipsoid of revolution form in constant velocity gas flow
11 p1875 A69-25466

Mathematical model with straight wake airfoil to determine aerodynamic forces on oscillating rotor blades in hovering flight
11 p1821 A69-25514

External perturbation effects of near earth environment on dynamics and attitude of slowly spinning multibody satellite
[AIAA PAPER 68-856] 12 p2174 A69-26795

Accelerometer force balance used in measuring forces and moments acting on models in short duration rocket plume tests at simulated high altitude
[AIAA PAPER 69-351] 13 p2264 A69-28285

Skin friction measurement in aerodynamic tests using thin liquid crystal coatings with changes in maximum light scattering wavelength in response to shearing forces
14 p2427 A69-29029

Velocity field excited by wing vibrations propagating over elastic surface at supersonic velocities, considering nonvertical motion and absence of external forces
15 p2547 A69-30259

Atmospheric density measurement above 50 km by aerodynamic and atmosphere excitation probes, emphasizing beta ray, bremsstrahlung and molecular fluorescence densitometers
15 p2615 A69-31284

Jet influence and aerodynamic force changes on V/STOL aircraft in transitional and high speed flight investigated in wind tunnel tests for fighter aircraft
16 p2734 A69-31937

Aerodynamic forces acting on harmonically oscillating thin profile in stalled plane parallel flow of ideal incompressible fluid
16 p2732 A69-32142

Stability analysis of missile lateral supersonic flutter based on Lagrange equations, considering conservative thrust, control deviation and aerodynamic forces
17 p3045 A69-32946

Leading edge flap angle and planform effects on low speed vortex patterns of flat plate double delta wings, measuring aerodynamic forces
17 p2890 A69-33246

Hypersonic aircraft induced changes in chemical and thermodynamic properties of air influencing aerodynamic forces on vehicle
17 p2895 A69-33576

Test facility to determine factors influencing aerodynamic energy dissipation of cantilever rods oscillating in airstream
17 p2947 A69-33928

Aerodynamic energy dissipation during vibrations of bars in airstreams characterized by energy loss per cycle and logarithmic decrement
17 p3066 A69-33948

Additional yawing by gyroscopic moment of power plant and effect on aircraft maneuver during curvilinear flight, noting compensation by automatic control
18 p3092 A69-34973

Accelerometer force balance method for measuring aerodynamic rocket plume forces acting on flat plate model in short duration shock tunnel test environments
19 p3292 A69-35737

Aircraft wing aerodynamic forces and moments due to lifting engine air intake simulated by wind tunnel experiment
19 p3239 A69-36400

Finite difference scheme for primitive equation model, emphasizing two grid internal noise suppression to improve gradient force expression accuracy
19 p3364 A69-36507

Atmospheric entry-capsule dynamics, considering angle of attack motion under gravity forces influence and aerodynamic normal force stability relations
20 p3617 A69-37197

Rotary derivatives of aerodynamic forces and moments in subsonic and supersonic flow, emphasizing kinematic and dynamic oscillations
21 p3647 A69-38733

Theoretical nonlinear method for calculating aerodynamic forces on low aspect ratio wings at high angles of attack and wide range of Mach numbers
21 p3644 A69-39084

Aerodynamic and gravitational torque effects on orbiting satellites attitude stability, applying Liapunov direct method in case of conservative aerodynamic torque
[AIAA PAPER 69-832] 21 p3821 A69-39363

Flight vehicle motion in high density medium reacting with static, vortex and dynamic forces analyzed for optimal regime via Lagrange-Euler equation
21 p3768 A69-39824

Aerodynamic forces under space-like conditions measured by swing balance, using large scale molecular beams for rarefied hypersonic gas flow simulation
[AIAA PAPER 69-1032] 22 p3924 A69-40400

Mach 8 flow field effects and forces on small delta tail surfaces mounted on body of revolution at various angles of attack
[AIAA PAPER 68-891] 22 p3859 A69-40539

Helicopter main rotor noise from square tipped blades determined as function of tip speed, blade area and thrust
22 p3864 A69-40676

Forces on aircraft during ground roll with slick runway surface and cross wind for deceleration and control on ground
[SAE PAPER 690375] 23 p4062 A69-41652

Aerodynamic forces on hypersonic vehicle surfaces, deriving relations for weak interaction pressures induced in unsteady flow
24 p4306 A69-43676

LF approximation in predicting unsteady aerodynamic forces affecting large aircraft stability, analyzing velocity potential of oscillating wings
24 p4250 A69-43729

AERODYNAMIC HEAT TRANSFER

- NT HYPERSONIC HEAT TRANSFER
- NT SUPERSONIC HEAT TRANSFER

Stagnation point heat transfer for thin ablative coatings on sounding rockets in continuum supersonic and hypersonic flight regimes
10 p1808 A69-22934

Heat transfer at plate in hydrodynamically stabilized turbulent boundary layer region, obtaining formulas for calculating transfer coefficients
10 p1809 A69-23427

Local film heat transfer coefficients variations effect on longitudinal constant area fin surface under turbulent flow
[ASME PAPER 68-HT-20] 13 p2373 A69-27770

Surface pressure and heat transfer over blunt conical body in hypersonic flow with uniform mass addition of various gases
[AIAA PAPER 69-716] 17 p2891 A69-33463

Radiative energy emission by blunt vehicle shock layer under severe entry conditions, discussing flow properties and radiative transfer coupling
[AIAA PAPER 69-719] 18 p3084 A69-34416

Heat exchange in stagnation point region of blunt body, using shock test simulation of high speed flight
18 p3086 A69-35118

Transonic flow around profiles with heat input, showing drag reduction in supersonic part of flow field
23 p4061 A69-42414

Aerodynamics of twisted jet propagating in same fluid by asymptotic expansion, analyzing twist influence on heat transfer
24 p4244 A69-43057

Apollo afterbody heat transfer, studying ablation effects for various reentry angles of attack
24 p4415 A69-43680

AERODYNAMIC HEATING

Heat transfer efficiency of triangular radiating fin in diathermal medium producing aerodynamic heating
02 p0354 A69-12490

Boundary layer transition to turbulence shown to have influence on magnitude of lifting reentry body heating rate
[AIAA PAPER 68-1155] 03 p0416 A69-13674

Kinetic heating of aircraft, discussing aerodynamic boundary layer, relationship between heat transfer coefficient or boundary layer energy turbulence and skin friction
03 p0534 A69-14087

- Heat transfer and drag of cylinders with cavities at hypersonic speeds measured by platinum film thermometer and strain gauge balance in gun tunnel [DVL-850] 04 p0543 A69-14822
- Dynamic stability loss on ablating vehicles ascribed to boundary layer transition effect from turbulent aft body heating [AIAA PAPER 69-106] 06 p1037 A69-18087
- Ablative and insulative performance of reference heat shield materials under transient heating simulating ballistic vehicle reentry trajectory, using plasma jet facility [AIAA PAPER 69-150] 06 p0907 A69-18110
- Limiting speed for target tracking hypersonic vehicle due to electrons formation through aerodynamic heating, calculating allowable flow conditions, maximum speeds and electron distribution 07 p1086 A69-19509
- Hypersonic slipper bearing problem in rocket boosted sleds, discussing flow model consisting of laminar stagnation region and boundary layers [AIAA PAPER 68-736] 09 p1477 A69-22003
- Conductive heat transfer between aerodynamically heated skin and barrel of Aerobee 150 sounding rocket telescope, noting effect of residual gas pressure 09 p1610 A69-22005
- Radiant heat transfer in hypersonic aerodynamic heating, discussing radiant flux and carbon dioxide concentration in reentry problems 11 p2002 A69-25233
- Aerodynamic heating of ELDO-A booster rocket, calculating flow field, heat transfer and conduction by method of characteristics and thermal models 11 p1966 A69-25433
- Configuration, trajectory planning, instrumentation, calorimetry and aerodynamic heating for planetary atmosphere entry 11 p1968 A69-25719
- Ablation cooling application to aerodynamic heat shielding, discussing various materials, sublimation, rocket probe ascents, satellites and experimental aircraft 12 p2011 A69-25854
- Thin multiple layer superinsulation protection against reentry heat, discussing composite design considerations and refractory materials selection 12 p2060 A69-26817
- Optimal control for minimization of heating and acceleration forces to reduce kinetic energy of reentry vehicle in space missions 13 p2352 A69-27960
- Ceramic heat transfer gage for supersonic wind tunnel investigation of blunt swept wing leading edges aerodynamic heating 15 p2613 A69-31272
- Spacecraft sterilization by destructive heating with thermite or high velocity entry friction before entering planet atmosphere 15 p2560 A69-31472
- Nonuniform heating rates during laminar boundary layer transition on slender cone at hypersonic speeds 18 p3085 A69-34435
- Unsteady temperature field in plane skin of aerodynamic body in case of temperature dependent thermophysical characteristics of skin material 18 p3092 A69-34982
- Aerodynamic skin heating at high Mach numbers affecting structural design, noting use of high temperature materials, insulation systems and shell construction method 21 p3646 A69-38460
- Radiation self absorption effects on heating loads of blunt body during hyperbolic entry 21 p3644 A69-39040
- Arc-heated hypersonic wind tunnel for simulated spacecraft reentry environment, aerodynamic heating characteristics and research applications 22 p3927 A69-40595
- Unsteady aerodynamic heating at stagnation region including surface combustion in arc heated high enthalpy wind tunnel 22 p3860 A69-40597
- Structural aircraft design requirements for high flight speeds stressing aerodynamic heating, heat resistant materials, weight and geometry problems 23 p4233 A69-42164
- Boundary layer transition to turbulence shown to have influence on magnitude of lifting reentry body heating rate [CIAA PAPER 68-1155] 24 p4300 A69-43251
- AERODYNAMIC LIFT**
U LIFT
- AERODYNAMIC LOADS**
NT BLAST LOADS
NT GUST LOADS
NT WING LOADING
- Nonstationary aerodynamic load for harmonically oscillating body in fluid flow with constant mean velocity measured, determining errors as functions of system parameters 07 p1050 A69-18752
- Spherical sandwich radomes designs, discussing aerodynamic loads, wind pressure effect, electrical properties and mountings 07 p1112 A69-19538
- Disturbed index of refraction scattering cross sections and aircraft acceleration increments for clear air turbulence, deriving correlation for measurements 10 p1656 A69-23651
- Spectral model used for analysis of atmospheric turbulence as related to loads on gliders 12 p2127 A69-26931
- External and internal energy dissipation coefficients in vibrating aerodynamic rod structures 14 p2537 A69-29748
- Maximum helicopter level flight speed loads spectrum shape and severity related to rotor component fatigue design strength [AHS PAPER 372] 17 p3059 A69-33516
- Two dimensional airfoil data application to three dimensional rotor blade element environment, predicting stall induced structural loads [AHS PAPER 322] 17 p2895 A69-33536
- Shock tube calibration for aerodynamic loading, determining flow parameters by observing particle trajectories with high speed photography of smoke tracers 18 p3085 A69-34469
- Flow breakdown in wind tunnel tests of high disk loading systems at low forward speeds, investigating downwash distribution effect using disk loading and airfoil models 18 p3119 A69-35230
- Helicopter rotor blades instabilities during starting and stopping cycles, predicting aerodynamic loads by wind tunnel tests, determining negative/positive angles of attack 20 p3463 A69-37804
- Dynamic stall effect on helicopter rotor blades air-loading and blade pitching motion at high advance ratio 20 p3463 A69-37809
- Air launched sounding rockets design, development and testing noting aerodynamic loading and surface, propulsion unit, cost effectiveness, etc 21 p3820 A69-39218
- Rotor operating limits, loads, performance prediction and airfoil development in rotary wing aerodynamics research 23 p4057 A69-41371
- Numerical integration of double integral with Cauchy type singularity for calculation of aerodynamic or hydrodynamic load on lifting body 23 p4182 A69-41913
- High speed compound helicopter rotor loads flight test program, discussing measured parametric effects [AIAA PAPER 68-980] 24 p4250 A69-43712
- AERODYNAMIC MOMENTS**
U STABILITY DERIVATIVES
- AERODYNAMIC NOISE**
- Pressure fluctuations in separated flow region behind thin fence, determining recombination point position, noise sources and frequency spectra variations 04 p0544 A69-14868
- Collection of articles on noise and acoustic fatigue in aeronautics sponsored by Ministry of Aviation and USAF 05 p0703 A69-16800
- Sonic boom reduction devices, discussing supersonic electroaerodynamic flow with shock waves, gas discharge one dimensional continuum analysis, power expenditure and aerodynamic interaction [AIAA PAPER 69-38] 06 p0869 A69-18150
- Broadband sound field generated aerodynamically by relatively smooth disk rotating in own plane, noting turbulent boundary layer flow and surface roughness effect 09 p1539 A69-21718
- Radiated aerodynamic noise effects on boundary layer transition on sharp leading edge hollow cylinders in wind tunnels, noting Reynolds numbers correlation [AIAA PAPER 68-375] 13 p2241 A69-28211
- Fluctuating turbulent stress measurements in mixing layer of two dimensional jets including intensity, spatial correlation and wave-number fluctuating stress frequency spectra 14 p2431 A69-29577
- SST fuselage response to reverberant and turbulent boundary layer noise calculated for computing equivalent reverberant acoustic fields 15 p2549 A69-30302
- Sonic boom theory for steady flight in atmosphere without winds, discussing sonic boom reduction by aerodynamic means 17 p2902 A69-34017
- Discrete sound radiation theory considering rotational noise as dominant rotor noise and stressing fluctuating forces as typical of helicopter rotor 18 p3090 A69-34323
- Axial flow fan blade row noise generation, discussing equation linearization, acoustic energy prediction and effects of flowing medium [ASME PAPER 69-FE-12] 20 p3460 A69-37989
- AERODYNAMIC STABILITY**
- Active control system augmentation of inherent aerodynamic damping assuring acceptable limits on oscillatory rotational motion during hypersonic Martian atmospheric entry 02 p0333 A69-11742
- Lift efficiency of and stabilization by square flare on high speed missile, comparing wind tunnel measurements with circular conical flare 02 p0190 A69-12544
- Aeroelastic rotor and nonsteady rotor aerodynamics 05 p0695 A69-15549
- Aerodynamic interference effects arising from jet efflux of V/STOL aircraft, developing vortex sheet theory for jet interference 05 p0696 A69-15566
- Rotating turbomachinery design to minimize fluctuating lift on isolated airfoils, presenting cascade geometry by quasi-steady analysis [ASME PAPER 68-WA/FE-12] 05 p0698 A69-16092
- Roll acceleration influence on angle of attack convergence and windward meridian rotation rate of rolling reentry vehicles [AIAA PAPER 69-100] 06 p1018 A69-18089
- Nonlinear equations of motion approximate solution, determining ordnance weapons aerodynamic stability coefficients from angular motion as functions of angle of attack [AIAA PAPER 69-135] 06 p0863 A69-18120
- Dynamic stability derivatives of large angle blunted conical spacecraft near transonic speed in simulated Mars environment for various angles of attack [AIAA PAPER 69-104] 06 p1019 A69-18210
- V/STOL rotary wing and propeller aircraft dynamic and aeroelastic problems emphasizing instabilities [AIAA PAPER 69-202] 08 p1419 A69-21031
- Self excited aeroelastic galloping oscillations of long prismatic bodies subjected to wind velocity, noting effect of aerodynamically unstable cross sections 09 p1615 A69-21923
- Computer implemented analysis of aeroelastic stability for elapsed data reduction time, discussing frequency modes and digital filters 10 p1634 A69-23274
- Optimization of control systems with allowance for failures of elements in parallel operation, noting application to vehicle with clustered propulsion system 11 p1966 A69-25331
- Mechanical engineering applications to aerospace flight, discussing stability and piloting problems and experimental methods 11 p1824 A69-25672
- Membrane flutter and panel stability in supersonic flow, considering infinite aspect ratio equation solution through Galerkin method 13 p2365 A69-28236
- Analog computer simulation of helicopter dynamics after main and tail rotor blades partial loss, showing banking and controllability 14 p2393 A69-29744
- Aerodynamic failure investigation of Black Brant 2 single stage sounding rockets 15 p2703 A69-31545
- Aeroelastic nonlinear panel stability in supersonic gas stream, defining hazardous conditions of critical flutter boundary 15 p2716 A69-31549
- Reentry flight test vehicle development for West German space program, using hypersonic model to determine controllability and aerodynamic stability 16 p2867 A69-31934
- Critique of paper on comparison of dynamically scaled model rotor test data with discrete azimuth aeroelastic stability theory [AHS PAPER 341A] 17 p3059 A69-33505
- Gyro controlled rigid rotor dynamic stability studied for stoppable rotor operation, developing analytical expressions for determining stability boundary of constant and rotor speed gyros [AHS PAPER 343] 17 p2899 A69-33508

Vortex breakdown on slender sharp edged and modified delta wings with varying sweep angles investigated in wind tunnel using schlieren system for flow visualization

[AIAA PAPER 69-778] 19 p3237 A69-35644

Rotating turbomachinery design to minimize fluctuating lift on isolated airfoils, presenting cascade geometry by quasi-steady analysis

[ASME PAPER 68-WA/FE-12] 19 p3240 A69-36419

Sounding rocket aerodynamic stability as function of nose length and mass, discussing wind tunnel test data

19 p3432 A69-36761

Cylindrical concentric detonation front and stability mechanism space-time measurement

20 p3632 A69-37215

Flight control and stability of STOL transport aircraft with powered-lift boundary layer control system augmented lift

20 p3462 A69-37513

V/STOL aircraft aerodynamic roll motion control requirements at low speeds

20 p3574 A69-37514

Aeroelastic instabilities of aircraft in flight by representing motion in space function base, using natural vibration mode

[ONERA-TP-697] 20 p3626 A69-37755

Helicopter rotor blades instabilities during starting and stopping cycles, predicting aerodynamic loads by wind tunnel tests, determining negative/positive angles of attack

20 p3463 A69-37804

Passive helicopter rotor isolation for alleviating rotor induced vibration, using dynamic antiresonant vibration isolator

20 p3463 A69-37807

Dynamic stall effect on helicopter rotor blades air-loading and blade pitching motion at high advance ratio

20 p3463 A69-37809

Aerodynamic pitch-roll coupling in spinning vehicles, showing unsteady components complicating data reduction

21 p3647 A69-39038

Dynamic stability derivatives of large angle blunted conical spacecraft near transonic speed in simulated Mars environment for various angles of attack

22 p4036 A69-40550

AERODYNAMIC STALLING

Fluidic compressor bleed control unit for TF-30 jet engine to prevent stall at low rpm operation

10 p1753 A69-23559

Dynamic stall data for helicopter rotor blade analyses obtained by oscillatory tests in pitch and in vertical translation at full scale Reynolds number

11 p1819 A69-25374

Inlet produced dynamic distortion and effects on stall margin of J-85 turbojet engine from supersonic wind tunnel tests

[AIAA PAPER 69-487] 16 p2840 A69-32676

Critique of paper on comparison of dynamically scaled model rotor test data with discrete azimuth aeroelastic stability theory

[AHS PAPER 341A] 17 p3059 A69-33505

Steady state and dynamic distortion influence on performance and stall of turbofan engine, discussing compressor instrumentation, tests and simulation data

18 p3185 A69-35175

Dynamic stall effect on helicopter rotor blades air-loading and blade pitching motion at high advance ratio

20 p3463 A69-37809

Computerized pressure distribution estimation for stalled airfoil with arbitrary wake geometry

24 p4250 A69-43726

AERODYNAMICS

NT AEROTHERMODYNAMICS

NT HYPERSONICS

NT ROTOR AERODYNAMICS

Aerodynamic moments related to turbfans of subsonic transport aircraft

[ONERA-TP-629] 02 p0187 A69-11622

Wind tunnel measurement of rear parts drag of small scale aircraft models

[ONERA-TP-633] 02 p0226 A69-11624

Flight vehicle dynamics, discussing classical mechanics, fluid dynamics, structural dynamics and thermodynamics

02 p0193 A69-11985

Unsteady aerodynamics of ablating flared reentry body, noting complications due to blunted nose shear flow and entropy gradient effects

02 p0189 A69-12524

Unsteady pressure field in zone of aerodynamic proximity of free moving airscrew investigated with propeller blades replaced by surface singularities

02 p0192 A69-12827

Entry phase flight data of Missions AS-202, Apollo 4 and 6 compared with wind tunnel aerodynamics data

[AIAA PAPER 68-1143] 03 p0519 A69-13556

Nonlinear aerodynamic problems of plane and asymmetric flows solved by digital computer, using modified Monte Carlo method

03 p0364 A69-13921

Book on transonic aerodynamics, emphasizing two dimensional and three dimensional problems involving transonic flow about airfoils with and without shocks

04 p0541 A69-14580

Aerodynamics of bodies of revolution in nonplanar motion using nonlinear functional analysis of moments for motion about center of gravity

[AIAA PAPER 68-20] 04 p0542 A69-14714

Airframe subsonic aerodynamic problems for fixed wing aircraft under low speed/high lift conditions

05 p0695 A69-15542

Tensiometric aerodynamic balances in great velocity ranges, discussing measurements, elastic elements and tensiometric balance construction and measuring errors nature

05 p0762 A69-15922

Propeller at static working state using vortex theory assuming infinite blade number, discussing thrust and torque coefficients

06 p0857 A69-17194

Fifty years of N. E. Zhukovski Central Aerohydrodynamic Institute in U.S.S.R.

06 p1043 A69-17390

Flow fields about upswept rear fuselages of rear loading cargo transport aircraft

06 p0859 A69-17492

Free fall vehicle dynamics for wind tunnel measurements of research shapes used in computer simulation of vehicle trajectories

[AIAA PAPER 69-229] 06 p0864 A69-18130

Solar wind flow past earth and magnetosphere correspondence to external aerodynamics of round nosed bodies in supersonic stream

07 p1128 A69-19360

Book on wing theory in supersonic flow covering simple and cruciform wings, wings with vertical plane tail, etc

08 p1251 A69-20523

Aerodynamic design, discussing research in aeronautical engineering and European organization

09 p1433 A69-22774

Book on aerodynamics of aircraft flight covering air flow, wing geometry, forces on wings, etc

11 p1817 A69-24583

Holography for optical analysis of hypersonic aerodynamics in single shot firing tunnel

12 p2087 A69-26176

Aerodynamic field around symmetric profile two dimensional plates, visualizing velocity fields with Al particles

12 p2011 A69-26288

Potential error source in VTOL aircraft dynamics analysis suggested by dual function of symbol used in perturbation equations of motion

12 p2014 A69-26776

Shadow, schlieren and interferometric methods for study of transonic, supersonic and hypersonic fields of aerodynamics, using refractivity variations in heterogeneous medium

12 p2060 A69-26934

Equations of motion of compressible fluid with non-zero resistivity near thin foil, solving supersonic and subsonic flow by Fredholm integral equations

13 p2200 A69-28360

Aerodynamic lift and moment fluctuations of sphere at supercritical Reynolds numbers measured by hot-wire anemometers, noting dependence on time

14 p2390 A69-29573

Unsteady aerodynamic processes in centrifugal compressor stage with impeller, vaneless diffuser and annular receiver chamber

15 p2547 A69-30073

Aerodynamic losses and stage efficiency in partial admission turbines, using flat bladed rotor experiments and rotors of different blade pitch

15 p2547 A69-30290

Mechanical construction device for Carafoli profile in aerodynamics and hydraulics, establishing mechanism for tracing rounded and sharp trailing edges profiles

15 p2549 A69-31264

Aerodynamic problems posed by hypersonic flight from Mach 3 to 20, considering relationship to half cone with flat base

16 p2867 A69-31761

Slender body aerodynamics combined with wave propagation theory for sonic booms of aircraft configurations, propeller and helicopter noise, sonic boom alleviation, etc

16 p2732 A69-31867

Soviet book on rocket aerodynamics covering configurations, lifting, stabilizing and control surfaces, friction and heat transfer characteristics

17 p2889 A69-32829

Soviet collection of articles on hydroaeromechanics and elasticity theory, number 7

17 p3054 A69-33121

Book on experimental aerodynamics covering subsonic and supersonic wind tunnels, wall measurements, airfoils, aerodynamic characteristics of propellers, fixed and rotary wing aircraft

17 p2891 A69-33318

Statistical analysis in inlet air flow dynamics, discussing inlet duct design and pressure variations

[AIAA PAPER 68-649] 17 p2896 A69-34020

Turbomachinery aerodynamics, discussing secondary flow in blading and digital computer applications to annulus flow field

18 p3086 A69-34925

Aerodynamics of rotary wing and V/STOL aircraft - Conference, Buffalo, June 1969, Volume 2, Wind tunnel testing, New concepts in rotor control

18 p3088 A69-35226

Air and space research at Goettingen Aerodynamic Testing Institute

19 p3295 A69-36684

Pade method applied in aerodynamics for determining detached shock wave shapes and shock waves attached at vertex of cone

19 p3241 A69-36778

Linearized theory of subsonic gas flow past profile compared with methods based on approximations of relationship between density and pressure

19 p3241 A69-36782

Sedov formula for complex velocity of arbitrary circulation in two dimensional theory of small curvature thin wings

19 p3242 A69-36795

Drag minimization as extremization of products integrals powers, noting application to optimum wings and fuselages

19 p3242 A69-36800

Algorithm using Biot-Savart law for determining induced velocity of curved vortex lines in aerodynamics, noting required line integration method

20 p3458 A69-37169

Soviet book on theory and design of turbocompressors covering gas dynamic cascade theory, thermodynamics and aerodynamics, viscous gas flow, etc

20 p3459 A69-37238

Flow stability regions at surface of flight vehicle, considering boundary layer flow of incompressible fluid

21 p3645 A69-39827

Monograph on aerodynamic studies of effusion cooled turbine blades covering turbulent boundary layers, gas turbine performance, experimental design, etc

[AIAA PAPER 69-871] 21 p3786 A69-39867

Aerodynamics of rotary wing and V/STOL aircraft - Conference, Buffalo, June 1969, Volume 3

23 p4057 A69-41369

Aerodynamic research for rotary wing and V/STOL aircraft, suggesting analytical techniques with software packages designed around standard input/output formats

23 p4146 A69-41373

Aerodynamic research in VTOL field including rotor wake, noise reduction, airfoil sections, lift coefficient, drag, wind tunnels, etc

23 p4058 A69-41374

AEROELASTICITY

NT AEROTHERMOELASTICITY

Root locus method applied to longitudinal and lateral stability of aircraft with flexible fuselage and wing

04 p0677 A69-14835

Aeroelastic rotor and nonsteady rotor aerodynamics

05 p0695 A69-15549

Longitudinal stability derivatives prediction for rigid and elastic airplanes, using influence coefficient method

[AIAA PAPER 69-131] 06 p0868 A69-18134

V/STOL rotary wing and propeller aircraft dynamic and aeroelastic problems emphasizing instabilities

[AIAA PAPER 69-202] 08 p1419 A69-21031

Self excited aeroelastic galloping oscillations of long prismatic bodies subjected to wind velocity, noting effect of aerodynamically unstable cross sections
09 p1615 A69-21923

Computer implemented analysis of aeroelastic stability for elapsed data reduction time, discussing frequency modes and digital filters
10 p1634 A69-23274

Graphite and B filament-epoxy resin composites application to aeroelastic scaled dynamic models, analyzing weight savings, fabrication and component stiffness
11 p1990 A69-25508

Dynamic systems stability with periodically varying parameters analyzed by Hill type infinite determinant, exemplifying helicopter rotor aeroelastic stability in forward flight
11 p1990 A69-25510

Servocontrol to delay flutter onset of aeroelastic structures, discussing rapid amplitude and phase changes near instability point, wind tunnel models, instrumentation, analog simulation
11 p1992 A69-25518

Sailplanes design, discussing structural flexibility, deformations, aeroelastic effects and plastics and man-made fibers
15 p2551 A69-30899

Aeroelastic nonlinear panel stability in supersonic gas stream, defining hazardous conditions of critical flutter boundary
15 p2716 A69-31549

Aeroelastic divergence and stability range for cantilevered and end supported structures computed as function of forward resistance and lift caused by wind
16 p2870 A69-31557

Cylindrical shell aeroelastic dynamic stability subjected to supersonic flow field, considering geometric imperfections, edge constraint and prestability deformation
[AIAA PAPER 68-285] 16 p2874 A69-32159

Critical review of paper on tail rotor structural design principles covering sizing, blade frequency and response and aeroelasticity
[AHS PAPER 342A] 17 p3059 A69-33503

Dynamically scaled model rotor tested in wind tunnel to evaluate blade aeroelastic limits constructed with realistic mass and stiffness distributions
[AHS PAPER 341] 17 p3059 A69-33506

Aerodynamic interactions between two wing configurations with same aspect ratio located in same plane, discussing testing principles and initial experimental results
17 p3061 A69-33595

Structural damping effects on semiinfinite panel boundary aeroelastic limit by Galerkin variational method
19 p3437 A69-36148

Aeroelastic instabilities of aircraft in flight by representing motion in space function base, using natural vibration mode
[ONERA-TP-697] 20 p3626 A69-37755

Aeroelasticity of supersonic aircraft in flight, discussing buffeting, wing flutter and control surface flutter
22 p3862 A69-40003

Air mass mechanics, local lifting surface element aerodynamic response and aeroelastic blade response problems in lifting rotor technology
23 p4061 A69-41370

Aeroelastic stability of thin plates exposed to supersonic flow using singular perturbation methods, obtaining flutter boundary and membrane solution
24 p4403 A69-43573

AEROGYRO HELICOPTERS
U XH-51 HELICOPTER

AEROLOGY
Meteorological effects on anomalous radio echo determined from simultaneous aerological and radar observations, noting maximum signal amplitude during high humidity and low wind speeds
16 p2808 A69-32277

Optimum aerological network design, discussing atmospheric model, numerical analysis, data acquisition, weather forecasts, rms measurement error, etc
19 p3364 A69-36505

Cirrus clouds occurrence, position and wind velocities on jetstream axes based on statistical analysis of aerological data and satellite TV pictures
19 p3366 A69-36669

AEROMAGNETISM
U GEOMAGNETISM

AEROMAGNETO FLUTTER
U FLUTTER

AERONAUTICAL ENGINEERING

Human factors in aviation - Conference, Los Angeles, June 1968
01 p0010 A69-10448

Boeing 747 performance, propulsion, structural and circuit characteristics, mass production and airport passenger installations
01 p0011 A69-11067

CF6 turbofan engine technology program for improvement in performance, weight, durability, noise, etc
[SAE PAPER 680691] 03 p0496 A69-13446

Competition and aeronautical progress in aircraft industry, examining costs and effects of government limits on Boeing 707 and Douglas DC-8
03 p0536 A69-14110

Statistical analysis of aircraft programs engineering man hours, aircraft performance and weight, avionics systems, schedules, etc, as estimating standards
05 p0769 A69-16239

High turbine inlet temperature technology using thermosiphon cooling for gas turbine, possibly doubling specific horsepower of aircraft
[SAE PAPER 690034] 07 p1203 A69-18311

National tasks in civil aeronautical research and development noting technological and social factors
08 p1422 A69-20171

Composite materials based on carbon and boron filaments, discussing application in turbine blades, propeller and helicopter rotor blades and airframe components
08 p1341 A69-20601

Environmental simulation in aircraft engineering, tests concerning aerodynamic conditions and simulator design
08 p1301 A69-20603

Maritime and aeronautical engineering - Conference, Paris, May 1968
08 p1255 A69-20652

Aircraft electrohydraulic primary control systems including electrical signal transmission, engine failure detection, signal structure and digital systems
08 p1347 A69-20872

Airport evolution in London, discussing transportation, safety, international trade, economics, aircraft types and noise spectra
09 p1479 A69-22582

Aerodynamic design, discussing research in aeronautical engineering and European organization
09 p1433 A69-22774

V/STOL aircraft future, discussing Federal Government policies, economics, airport planning, engineering problems, etc
10 p1811 A69-23221

Aircraft technology for hypersonic speed range including swept wing, engine design, composite materials, lift-drag ratio, considering weight, efficiency, STOL requirements
10 p1634 A69-23598

Design management in next century covering computer methods, market needs, etc
11 p2004 A69-24371

Competition and aeronautical progress in aircraft industry, examining costs and effects of government limits on Boeing 707 and Douglas DC-8
11 p2004 A69-24372

Computerized design of optimal direct lift controller for aircraft and aerodynamic surfaces, using Kalman linear state regulator theory
12 p2014 A69-26765

CF6 turbofan engine technology program for improvement in performance, weight, durability, noise, etc
13 p2324 A69-27331

Engineering assessment and flight testing of aircraft systems in UK, discussing operational reliability, etc
13 p2201 A69-27539

Galaxy C-5A aircraft Value Control Program stressing design organization, upper management authority, budgetary adjustments, etc
13 p2383 A69-28095

Weight and cost control program for Boeing 747 aircraft through combined value and weight engineering methods
13 p2383 A69-28096

Pressure, temperature, vibrations and structural stresses data acquisition system for aeronautical applications
14 p2450 A69-29686

Turbofan engines impact on aircraft engineering development emphasizing large performances, high fan flow rates and low fuel consumption
15 p2550 A69-30322

Next generation subsonic aircraft, discussing basic concerns, aerodynamic factors, materials, noise reduction, cost effectiveness, titanium techniques, etc
15 p2550 A69-30590

Aerodynamic problems in future civil aircraft design, emphasizing Concorde development possibilities, discussing VTOL intercity transport, subsonic swept wing and hypersonic aircraft, all-wing airbus, etc
16 p2732 A69-32023

CF6 turbofan engine technology program for improvement in performance, weight, durability, noise, etc
[SAE PAPER 680691] 16 p2837 A69-32367

Airworthiness objectives for civil powered lift aircraft, discussing safety, traffic growth and accident rates
17 p2897 A69-33211

Aircraft structural weight optimization based on design consideration of grouped related elements, noting application to Boeing 747 trailing edge flap driver
[SAE PAPER 757] 18 p3220 A69-34881

Elastomeric and coating materials for aerospace systems, considering temperature, rain, sand erosion, propellant and radiation resistant properties
19 p3357 A69-35586

Aircraft directional stability in terms of ideal non-holonomic coupling on mechanical system, noting servosystem role
21 p3830 A69-39836

Wind information obtained for design and operation of tethered or hovering free floating balloon systems
22 p3864 A69-40804

Analog and digital computer elements combined in hybrid technique for aeronautic simulation
23 p4146 A69-41603

Nondestructive thermal method of measuring wall thickness and channel blockage in investment castings used in aircraft parts production
24 p4312 A69-42754

Supersonic aircraft design data, costs and benefits, discussing origin and significance of sonic boom
24 p4252 A69-42997

Elastomers for SST aircraft applications, discussing properties evaluation, material selection, sealant requirements, etc
24 p4338 A69-43455

AERONAUTICS
Maritime and aeronautical developments - Conference, Paris, April 1967
02 p0192 A69-11886

1967 yearbook on air and space travel covering airbus, astronautics, V/STOL, aerodynamics, flight mechanics, simulation and aeroelasticity
04 p0545 A69-14801

Subsonic aeronautics - Conference, New York, April 1967
05 p0699 A69-15541

Aeronautic electronics - Conference, Washington, D.C., September 1968
05 p0789 A69-16716

Soviet collection of papers on aviation climatology covering cloud covers, tropopause characteristics, icing conditions, etc
12 p2127 A69-26898

Aviation and astronautics - Conference, Tel-Aviv and Haifa, March 1969
14 p2429 A69-29011

Bibliographies for aeronautics and astronautics /AIAA/ technical disciplines
14 p2542 A69-29510

Soviet collection of articles on aviation forecasting of cloud cover, high altitude wind and turbulence
14 p2473 A69-29734

Professional programs for aeronautics, rocketry and astronautics development
18 p3233 A69-34552

Plastics applications in naval air systems command, discussing polymer families, nonstructural glass fiber-based products, radomes, electromagnetically transparent bodies, advanced composites, etc
21 p3751 A69-38532

NASA computer language CLASP coordinated with evolution of SPL /Space Programming Language/ for aeronautics and space programming
[AIAA PAPER 69-957] 22 p3905 A69-40339

AERONOMY
Upper atmosphere structure, phenomena and composition, discussing interactions between photons, electrons, atoms and molecules
02 p0242 A69-11902

Meteorological rockets for space meteorology, aeronomy and weather forecasting, noting international programs involving U.S.S.R.
06 p1043 A69-17056

Collisional processes relevant to daytime and nighttime models of upper atmosphere neutral density and temperature

07 p1130 A69-19654

Aeronomics parameters effect on ionospheric effect of SC magnetic storm, calculating maximum ionization levels, F layer ionization and vertical ionization profile parameters

09 p1486 A69-21546

Aeronomics phenomena observed near Altair and theta Aquila ascribed to Apollo 8 lunar flight

11 p1957 A69-24411

Space experiments analysis involving standardization for economy and mission thesis compromise, detailing aeronomics satellite project with integrated utilization

12 p2173 A69-26128

Photoionizing effect of hydrogen and helium UV glow in nighttime ionosphere compared with ground based IF ionosonde and sounding rocket observations

15 p2605 A69-31436

Aeronomics parameter effect on ionospheric effect of SC magnetic storm, calculating maximum ionization levels, F layer ionization and vertical ionization profile parameters

16 p2783 A69-32541

Time distribution of commencements of substantial intensity increases of geomagnetic and aeronomics phenomena

17 p2964 A69-33958

Nighttime F region time-altitude variations in aeronomics parameters calculated under conditions close to solar activity maximum

23 p4156 A69-41844

Equatorial aeronomy - Conference, Ahmedabad, India, February 1969

23 p4159 A69-42422

AEROPHYSICS

U. ATMOSPHERIC PHYSICS

AEROSOLS

NT FOG

Light polarization properties in atmosphere noting aerosols effect

01 p0075 A69-11189

Aerosol scattering indicatrix of atmospheric ground layer theoretical estimation to make up for lack of experimental values

02 p0274 A69-11443

Aerosol size distribution and variation with humidity effects on visual range, comparing computations with transmissometer and scattering recorder measurements

02 p0276 A69-12760

Mie total and differential backscattering cross sections at laser wavelengths for Junge size distribution aerosol models

04 p0609 A69-14290

Stratospheric aerosol investigation by IR and lidar, applying Mie theory to model aerosol size distribution

04 p0592 A69-14654

Terrestrial and Martian aerosols estimation based on carbon dioxide spectral and Mariner 4 RF occultation measurements

[AIAA PAPER 69-52] 06 p1011 A69-18199

Dayglow determination from aerosol spectrum obtained through data of brightness and polarization of day sky

07 p1211 A69-18545

Spatial size and velocity distributions for liquid or solid aerosols suspended in air flow using Q spoiled ruby laser and holography

09 p1492 A69-21418

Automatic counter for concentration of cloud condensation nuclei in thermal diffusion chamber, measuring light scattering coefficient of cloud

09 p1494 A69-21640

Daytime clear sky light polarization in UV and visual spectral regions calculated with considerations for aerosol components polarization effect

09 p1491 A69-22708

Scattered light mean intensity determination in twilight aerosol atmosphere from satellite observations, formulating boundary value problem

10 p1689 A69-23970

Atmospheric optics by spacecraft and high altitude probes concerning ozone and aerosol distributions, scattering indicatrix polarization and dust cloud inhomogeneities

12 p2055 A69-25815

Stratospheric aerosol attenuation factor vertical distribution statistical structure, tabulating normalized correlation matrices, eigenvectors and eigenvalues

12 p2125 A69-25956

Charged aerosols production for electrohydrodynamic processes by spraying liquids through capillary at high electric field strengths into high pressure air flows

12 p2138 A69-26631

Trapped aerosols below temperature inversions causing lidar echoes in troposphere layers, discussing simultaneous balloon refractometer, thermometer and ground based lidar soundings

13 p2254 A69-28475

Ion pair annihilation average rate by single aerosol particle action in lower ionosphere noctilucent clouds

14 p2434 A69-28941

Aerosol content of mesosphere with noctilucent clouds measured with optical radar in Norway

14 p2444 A69-29877

Polarization and angular distribution of 6328 Å He-Ne laser light scattered by latex-sphere hydrosols, comparing coherent and incoherent scattering patterns

15 p2595 A69-30223

Atmospheric aerosols influence on electric field in ground layer to account for ionization, demonstrating number and turbulent exchange coefficient relationship

17 p2996 A69-33036

Continental and maritime hygroscopic particles associated with increasing relative humidity, determining effect on backscattered power from laser beam using Mie scattering equations

17 p2981 A69-33160

Self contained hand held battery operated aerosol particle analyzer, measuring aerosol concentration and size distribution for laboratory and space flight applications

18 p3136 A69-34691

Atmospheric aerosols influence on ion density profile in stratosphere obtained from numerical solution of equilibrium ionization equation

18 p3129 A69-34962

Vertical distribution of concentration, microstructure and chemical composition of solid aerosol in troposphere and stratosphere from high altitude balloon measurements

18 p3132 A69-35340

Scattered light mean intensity determination in twilight aerosol atmosphere from satellite observations, formulating boundary value problem

21 p3717 A69-39656

Aerosol attenuation coefficients vs altitude in troposphere and stratosphere, noting seasonally dependent surface convective dust layer and temperature dependent aerosol maximum altitude

21 p3718 A69-39773

Normalized phase function and scattering coefficient of aerosols prediction from measurements of particle size distribution, density and refractivity based on Mie solution

21 p3719 A69-39774

Detonation wave instability and damping in gas containing liquid or solid inflammable aerosol, considering atomized propellants

23 p4240 A69-42339

Radiation contribution to large scale atmospheric mass circulation simulation, considering short wave radiation, temperature variations, exponential and aerosol attenuation

23 p4184 A69-42487

Scattered light meter accuracy as function of aerosol particles atmospheric distribution according to size, analyzing measurement errors

24 p4343 A69-42966

AEROSPACE ENGINEERING

NT AERONAUTICAL ENGINEERING

Aerospace technology role in economic and social benefits

[UN PAPER 68-95321] 01 p0178 A69-10467

Space program effects in education, science and engineering, noting impact of first satellite on U.S. research and technology

01 p0179 A69-10500

Inner and outer meteorological balloon assembly for fast rising and high altitude sounding

01 p0010 A69-10541

Hot pressed boron nitride properties and fabrication, noting low moisture absorptivity and aerospace applications

02 p0270 A69-11802

Rocket motor integration into Scout vehicle to improve performance

02 p0335 A69-12384

Canadian program of scientific rocket sounding of auroral phenomena, outlining systems approach, engineering and scientific cooperation requirements, etc

02 p0335 A69-12689

Automatic checkout of space systems, discussing cost effectiveness tradeoffs, ground and onboard equipment utilization, vehicle design and mission success risk

03 p0411 A69-13392

Aerospace company engineering administration criteria and functions for chief project engineer

[SAE PAPER 680682] 03 p0535 A69-13447

Astronaut safety considerations impact on design of Apollo Lunar Surface Experiments Package /ALSEP/

[SAE PAPER 680721] 03 p0433 A69-13448

Aerospace manufacturing contribution to engineering in design development

[SAE PAPER 680668] 03 p0433 A69-13451

Beryllium assemblies for aerospace and nuclear requirements, emphasizing braze joining structural components and effective manufacturing methods

[SAE PAPER 680651] 03 p0433 A69-13454

Beryllium aerospace applications, considering advantages vs disadvantages in systems engineering

[SAE PAPER 680648] 03 p0444 A69-13456

Systems analysis in aerospace engineering by adding motion pictures and TV techniques

[SMPT PAPER 104-17] 04 p0596 A69-14359

Reliability in air and space travel, quality/ quantity aspects, problems and cooperation

04 p0606 A69-14803

Permissible development direction for space research, discussing space station, required systems and cost estimates

05 p0829 A69-15920

Aerospace instrumentation - Conference, Cranfield, Beds., England, March 1968

05 p0765 A69-16747

Materials compatibility for space requirements, discussing shape retention, ductility, tensile strength, dissimilar materials stability, etc

06 p0945 A69-17872

Aircraft and spacecraft guidance and control technology including computers, optimum and Kalman filtering, strapdown inertial navigation, sensors and test pads

[AIAA PAPER 69-72] 06 p0956 A69-18136

U.S. aerospace programs, reviewing manned space missions, space applications, space science, transportation, strategic and tactical warfare and influence on aerospace industry

07 p1243 A69-18376

Aircraft communications, navigation and identification, discussing role of satellites, common waveform modulation and electronics technology

07 p1085 A69-19178

Aircraft and spacecraft guidance and control technology including computers, optimum and Kalman filtering, strapdown inertial navigation, sensors and test pads

[AIAA PAPER 69-72] 07 p1177 A69-19179

Reliability in aeronautics and astronautics, discussing safety, economic cost of technical delays and effect on public, air transport, design, development, testing, utilization, etc

07 p1053 A69-19287

Aluminum coatings compared with cadmium coatings for aerospace fasteners, discussing plating methods

[ASM PAPER D8-5.2] 07 p1142 A69-19663

Strength increase in steel components of aircraft, missiles and subsurface in relation to chronological application sequence, discussing ultimate strength

[ASM PAPER GG8-9.4] 07 p1169 A69-19675

Development of materials in aerospace structures and propulsion systems, discussing superelastic alloys, graphite fibers, composites, refractory metals and processing techniques

08 p1332 A69-20306

Flight research testing facilities at Arnold Engineering Development Center for rockets, turbojets, ramjet engines, aircraft, missiles, satellites and spacecraft

08 p1302 A69-20883

Collection of papers on applications of microelectronics to aerospace equipment, noting design and reliability of circuits and computers

[AGARDOGRAPH-114] 08 p1291 A69-20981

Electrochemical generators for space applications - Conference, Paris, December 1967

08 p1258 A69-21034

Optimum integration of aircraft equipment, subsystems and computer mechanizations for low cost navigation system consistent with mission requirements

08 p1348 A69-21065

Development and fabrication of fiber-resin and fiber-metal composites, discussing application to aerospace technology

09 p1524 A69-22069

Aerospace material investigation and fabrication techniques - Conference, Cocoa Beach, November 1968

09 p1504 A69-22301

- Friction welding of aerospace materials, discussing joint strength and dissimilar materials
09 p1508 A69-22335
- Compressive behavior of uniaxial filament reinforced epoxy tubes for aerospace structures, using hand layup method with Teflon mandrel and sleeve
09 p1508 A69-22339
- Technology Feasibility Spacecraft /TFS/ sterilization and bioassay program during assembly, analyzing sampling and cleaning procedures
09 p1446 A69-22358
- Thermoplastic resins as matrices for glass reinforced plastics and aerospace structural and nonstructural adhesives
09 p1530 A69-22365
- Electrical devices for detonation initiation in pyrotechnic equipment for space applications, tabulating characteristics
10 p1749 A69-23006
- Silver and cadmium nitrides, copper chlorotetrazolate and barium and potassium dinitrobenzofuroxannates compared for priming explosive applications
10 p1750 A69-23011
- Neutron radiography facility for production non-destructive testing inspection of aerospace components, noting collimation, neutron/gamma ray ratio optimization and neutron source
[AGN-TP-229] 10 p1699 A69-23051
- True position dimensioning and tolerancing /TPDT/ system usage in aerospace industry
10 p1700 A69-23355
- Frequency response dynamics of beam type periodic structures on elastic supports typical in flight vehicle designs
[ASME PAPER 69-VIBR-17] 10 p1804 A69-24150
- Aluminum alloys role in aerospace technology, discussing temperature characteristics, gas absorption, weldability, purity, etc
11 p1903 A69-24518
- Spray cooling techniques for thermal protection of aerospace structures including lithium spray cooling, vapor collection and condensation, etc
11 p1966 A69-24532
- Mechanical engineering applications to aerospace flight, discussing stability and piloting problems and experimental methods
11 p1824 A69-25672
- Thermally stable polymers for high stress aerospace applications, noting chemical stability and structure of high polymers
12 p2117 A69-25853
- Metal bonded and sandwich structures application to space vehicles, launch vehicles, rocket motors, ground equipment and balloon gondolas, noting inspection methods
12 p2101 A69-25859
- Aerospace applications of electric discharge interaction with fluid motion including sonic boom reduction, high lift devices, reentry vehicle pitch control, etc
12 p2136 A69-26405
- Dynamic analysis methods for airframe flight control design noting equations of motion, system criteria and analysis and synthesis methods
[AIAA PAPER 68-832] 12 p2174 A69-26758
- Thermostructural simulation of lifting vehicle panel design, considering safety and trajectory shaping of flying laboratory
12 p2060 A69-26836
- Materials rating method in pressure vessel applications, considering impact on design of minimum cost space launch vehicle
12 p2175 A69-26844
- Ballistically effective atmospheric parameters for rocket vehicle design manuals involving application of climatological concepts of meteorology
12 p2175 A69-26874
- Soviet book on solid propellant guided/unguided rocket design with emphasis on thrust control, including trajectory calculations, optimal parameters and components estimation by weight analysis
12 p2175 A69-27077
- Boosters and space vehicles including earth satellites, lunar probes and interplanetary spacecraft
13 p2356 A69-27914
- NASA manned aerospace simulation techniques and equipment as used at Ames Research Center, noting applications to various types of manned vehicles
[ASME PAPER 69-DE-56] 14 p2427 A69-28844
- Computer driven graphical techniques for aerospace design and analysis
[ASME PAPER 69-DE-27] 14 p2454 A69-28854
- Space technology difficulties, achievements and applications
14 p2527 A69-29895
- Remote manipulators applications in space, discussing joint configurations, master-slave systems design, control systems, etc
15 p2558 A69-30187
- Leak detection for aerospace hardware, discussing equipment, operations, checkout, etc
15 p2618 A69-30315
- Aerospace structures modal vibration tests data acquisition including multishake excitation methods
15 p2585 A69-30358
- Rocket motors with combustion chambers of variable geometry for hybrid propellants, stressing toroidal chamber
15 p2671 A69-30600
- Variational principles and differential equations of thin elastic panels mechanics for aerospace structures
15 p2712 A69-30974
- Centro Ricerche Aerospaziali objectives, equipment and activities in aerospace research, including space flight simulation facilities and scientific satellite launching range
15 p2724 A69-31456
- Manned space stations role in future space plans, discussing prototypes and conceptual design
16 p2866 A69-31736
- Computer programs for space engineering analytical and scientific computation using digital computers
16 p2756 A69-32555
- Design philosophy for cost reductions on future space transportation systems, exemplifying application to booster system for earth orbital logistics
[AIAA PAPER 69-439] 16 p2882 A69-32654
- Cost reduction criteria for rocket propulsion systems and components, discussing literature searches, engineering criteria, total program cost vs mission accomplished, etc
[AIAA PAPER 69-440] 16 p2883 A69-32748
- Electroforming methods in design and fabrication of liquid propellant rocket motor injectors and composite thrust chambers
[AIAA PAPER 69-583] 16 p2794 A69-32757
- General technology history, stressing space technology and programs influencing developments in other fields
17 p3076 A69-34045
- Flight performance analysis of space systems, discussing preparation, implementation and communication
18 p3206 A69-34501
- Aerospace balancing system with hydrostatic spindle, describing component construction and functions
[SAWE PAPER 737] 18 p3118 A69-34890
- Computer program for weight and center of gravity tolerance data for assembly aerospace vehicle
[SAWE PAPER 734] 18 p3221 A69-34892
- Aerospace structures optimization, discussing weight considerations and finite element techniques
[SAWE PAPER 814] 18 p3221 A69-34896
- Large solar array systems in space, discussing design and operation
18 p3094 A69-35056
- Space, technology and society - Conference, Cocoa Beach, Florida, March 1969, Volume 1
18 p3234 A69-35070
- Technological possibilities of gravity free production in space environment, discussing containerless manufacture of glass, liquid metal manipulation and defect free fibers
18 p3206 A69-35490
- Materials and processes for aerospace applications in 70s - Conference, Los Angeles, April-May 1969
19 p3315 A69-35501
- Forming, machining and joining characteristics of B-Al composite sheet metal material for space structures
19 p3318 A69-35507
- Tape placement machines to fabricate composite high modulus filamentary tape reinforced aerospace structures, anticipating future generations evolution into automatic control
19 p3323 A69-35584
- Minimum cost design /MCD/ of space launch vehicle, discussing material and process selection based on fracture-safe conditions
19 p3433 A69-35587
- Differential synthesis technique application to design of multiaxis stability augmentation systems for aerospace vehicles
[AIAA PAPER 68-834] 20 p3616 A69-37156
- Computerized optimization and testing of aerospace vehicle designs, describing simulation techniques, algorithm and computer selection, display devices, etc
20 p3498 A69-37292
- Automation application to rocketry, discussing process control in installations including control circuits and electronic direct digital control system
20 p3617 A69-37340
- Ionospheric satellite series Alouette-ISIS, discussing successive engineering and management constraints leading to ISIS-C design
20 p3618 A69-37856
- Avionics system analysis, engineering, design, fabrication and testing problems
20 p3545 A69-37929
- Precipitation hardening stainless steels applications in aerospace industry, discussing steel selection and heat treatment
20 p3563 A69-37931
- Landing shock struts of Surveyor 6, emphasizing silicone liquid springs role as absorbers and stabilizers
20 p3466 A69-38180
- Satellite Airborne Communications /STAIRCOM/ design constraints
20 p3497 A69-38314
- JR 100 F lift jet engines for Japanese national aerospace laboratory produced as part of VTOL developing program
21 p3785 A69-38608
- Thermally stable polymers chemical and structural properties, discussing polymer use in aerospace technology
21 p3751 A69-38789
- Hydrodynamic conical and spherical spiral grooved grease bearings replacement of gyro ball bearings for extended space missions
[AIAA PAPER 69-836] 21 p3732 A69-39367
- Aerospace and marine corrosion technology - Conference, Los Angeles, July 1968
21 p3747 A69-39484
- Stress corrosion cracking in aerospace situations, discussing corrective measures emphasizing fracture toughness criteria
21 p3748 A69-39491
- Filament wound composites for structures, discussing fabrication, properties and aerospace applications
21 p3753 A69-39496
- Scattered light mean intensity determination in twilight aerosol atmosphere from satellite observations, formulating boundary value problem
21 p3717 A69-39656
- Technical and economic factors of program to provide communications services via satellite facilities in continental U.S.
[AIAA PAPER 68-412] 21 p3678 A69-39762
- Aerodynamic deceleration systems for space missions, considering deployment of subsonic parachute and inflatable configuration following atmospheric entry
[AIAA PAPER 68-1081] 22 p4036 A69-40542
- Carbon materials manufacture, properties and applications in space technology, discussing carbon fibers, textiles, graphite, pyrolytic carbon, composites and vitreous carbon
23 p4180 A69-42160
- Optimum integration of aircraft equipment, subsystems and computer mechanizations for low cost navigation system consistent with mission requirements
23 p4186 A69-42538
- Technological forecasting as aid to aerospace planner in optimizing R and D resources allocation
[AAS PAPER 69-105] 24 p4417 A69-42819
- Apollo Applications Program /AAP/ spacecraft, describing contributions to space station engineering
[AAS PAPER 69-491] 24 p4392 A69-42838
- Space nuclear electric power systems applications and development, summarizing current status and near future programs
[AAS PAPER 69-305] 24 p4364 A69-42865
- Cost analysis in low cost launch vehicle studies emphasizing sustaining engineering and plant economics
24 p4393 A69-43120
- Materials in space technology - Conference, Bristol, England, April 1969
24 p4332 A69-43206
- Metallic and nonmetallic materials for space applications with launch and orbit condition requirements, examining finishes and lubricants
24 p4332 A69-43207
- Carbon fiber reinforced plastic components aerospace applications, discussing honeycomb sandwich satellite structure for investigating lamination methods, shapes, bonding and machining
24 p4336 A69-43209
- Silicon nitride ceramics fabrication technology and dimensional stability during nitridation, discussing ap-

plicability to aerospace precision or joined ceramic shapes

24 p4336 A69-43211

Design criteria for antenna control equipment for earth tracking from landing site on Martian surface [AIAA PAPER 68-868]

24 p4348 A69-43246

Aircraft Structures and Materials Application - Conference, Seattle, September 1969

24 p4321 A69-43416

Flame resistant organic fiber in cross linked polymer structure, discussing properties and aerospace applications

24 p4337 A69-43424

Aero-space pressure vessel materials selection and construction, applying Apollo program experience to future programs

24 p4324 A69-43430

Gel permeation chromatography to measure rate of adhesive aging and curing in one shot epoxy tapes, noting handling techniques and space applications

24 p4338 A69-43463

AEROSPACE ENVIRONMENTS

NT Cislunar Space

NT Deep Space

NT Interplanetary Space

NT Interstellar Space

Book on material and design problems encountered in construction of high performance missiles, rockets and spacecraft, considering influence of space environment

01 p0084 A69-10021

Electronic packaging techniques for long life spacecraft, discussing effects of mechanical and electrical stress, temperature cycling, vacuum, radiation and contamination

01 p0038 A69-10145

Space biology, discussing U.S. research program, emphasizing gravity/organism reactions, biochemistry and exobiology [UN PAPER 68-95345]

01 p0014 A69-10486

Environmental effects on aircraft and propulsion systems - Conference, Bordentown, New Jersey, October 1968

01 p0055 A69-11043

Cytological analysis of *Tradescantia paludosa* microspores for space flight influence onboard Cosmos 110

01 p0018 A69-11317

French applied and basic research in space biology including manned space flight, deep space problems, weightlessness and cosmic heavy ion radiation effects

02 p0199 A69-11909

Technological requirements for solar probe with close perihelion, discussing solar approach and space environment problems

03 p0519 A69-12855

Space environment barriers to man due to biological evolution and transition from land to space in single generation, noting orientation problems

03 p0380 A69-14067

Charged particle environment in synchronous orbit region, discussing electrons and protons under influence of geomagnetic field

07 p1204 A69-18340

European research on ultrahigh vacuum lubrication in space environments, emphasizing friction of materials under various loadings and temperatures [IME PAPER 10]

07 p1138 A69-18564

Plants growth from seeds exposed to space environment onboard Cosmos 110 biological satellite compared with control plants

07 p1064 A69-18972

Environmental simulation in aircraft engineering, tests concerning aerodynamic conditions and simulator design

08 p1301 A69-20603

Arc jet generation and control noting application to hyperthermal aerospace environment studies, wind tunnels and materials heating and fabrication

08 p1371 A69-21128

Electroexplosive element design for safe reliable devices in liftoff and space environment, considering stray electric currents, RF fields and electrostatic discharges

10 p1752 A69-23022

Human adaptation to various environments, emphasizing experimental space psychoneurology role in human behavior examinations during space missions

10 p1647 A69-23587

Soviet book on space radiobiology, discussing somatic effects, influence of flight factors, relative biological effectiveness of various radiations and radiation safety

11 p1827 A69-24263

Calculation of radiation doses in space - Conference, Toulouse, France, February 1968

11 p1947 A69-24854

Electronic systems and component reliability in space, considering electric parameter variation effects

11 p1848 A69-24867

Solar cells degradation by charged particles in space, considering protection by filter, silicon properties and use of cadmium cells

11 p1825 A69-24870

Planar transistor gain degradation under weak ionizing radiation, considering operating voltage and temperature conditions

11 p1848 A69-24874

Second tacite sounding rocket test for measuring UV radiation in transition zone between upper ionosphere and space

11 p1887 A69-25213

Microorganism survival in space for exposure to solar UV radiation on balloons, rockets and satellites

11 p1828 A69-25457

Environmental problems of entry vehicle returning from lunar or planetary mission, discussing heat protection system efficiency

11 p1968 A69-25721

Metal adhesive bonding strength behavior in satellite and space vehicle applications, noting effects of various space environment factors

12 p2101 A69-25858

Space mission medical heat problems covering thermal characteristics and heat control, protection and resistance of space vehicle and astronaut adaptation

12 p2023 A69-26493

Vacuum effects on resistance spot welds in aluminum, stainless steel and titanium alloys, noting X ray and tensile shear test results

12 p2103 A69-26622

Book on earth atmosphere and outer space influence on human physiology for life support systems design

12 p2024 A69-27074

Traveling wave tubes for high efficiency and extreme environments, discussing power output and RF drive

13 p2232 A69-28055

Spacecraft surfaces bidirectional reflectance flux distribution applications to space thermal control computations

[AIAA PAPER 68-26]

13 p2222 A69-28216

Weightlessness, increased gravitational fields and radiation effects on biological systems at organismal, cellular and subcellular levels, discussing biosatellite experiments

14 p2406 A69-29097

Military aircraft operating in various environments with low support costs emphasizing improved design, development and manufacturing standards

14 p2392 A69-29503

Reliability of electronic components for space - Conference, Grenoble, November 1968

15 p2622 A69-30816

Transient and long lasting space environment stresses, discussing accelerations, vibrations, shocks, rapid descent in vacuum, temperature variations, gravity, etc

15 p2625 A69-30824

Radiobiology of *Tradescantia* clone orbited in Biosatellite 2, analyzing space effects on spontaneous and radiation induced mutation and cytological changes

15 p2556 A69-31321

Thin foil penetration measurements for Fe microparticle impacts on metal and Mylar foils in space

15 p2641 A69-31339

Impingement pressure analysis associated with two phase cryogenic propellant venting to space environment

[AIAA PAPER 69-571]

16 p2869 A69-32753

Temperature determination of thick flat plate rotating in space in solar flux with one surface insulated compared with Apollo heat shield results

[AIAA PAPER 69-614]

17 p3071 A69-33266

Two dimensional airfoil data application to three dimensional rotor blade element environment, predicting stall induced structural loads

[AHS PAPER 322]

17 p2895 A69-33536

Gas particle concentrations on moon due to solar wind, surface emissions and atmospheric contamination by lunar operations and rocket motor products

18 p3189 A69-34236

Environmental studies using orbital photography, discussing color, color IR, black and white applications from Gemini and Apollo programs

18 p3132 A69-35275

Technological possibilities of gravity free production in space environment, discussing containerless manu-

facture of glass, liquid metal manipulation and defect free fibers

18 p3206 A69-35490

Resistance spot welds in Al, Ti and stainless steel in air and hard vacuum, showing feasibility for space assembly

19 p3319 A69-35554

Materials and products fluid state processing in space, discussing g, zero-g and induced forces effect on fluid matter and process, cost and operational effectiveness

19 p3324 A69-35588

Materials processing in space, suggesting electronic single crystals preparation, materials melting and utilization of low g earth orbit environment

19 p3324 A69-35589

Surveyor thermal vacuum test data comparison with flight results indicating performance prediction reliability of earth-based tests for vacuum and lunar environments

19 p3430 A69-36016

Boundary layer formed in miniature nozzle studied for effect on jet spreading discharged into space at high Mach numbers

19 p3395 A69-36760

Plants growth from seeds exposed to space environment onboard Cosmos 110 biological satellite compared with control plants

20 p3479 A69-38220

Vacuum integrating sphere for measuring solar absorptance in space environment to determine thermal control coatings qualifications

[AIAA PAPER 69-1021]

22 p3923 A69-40392

Space attenuation at VHF and UHF telemetry frequencies

24 p4281 A69-42622

High reliability of solenoid and pressure regulating valves under long duration space missions, considering design, tests and controls

[AAS PAPER 69-238]

24 p4319 A69-42854

Environmental stress effects on medical leech studied to determine tolerance to spacecraft launching, orbiting and reentry

24 p4268 A69-43403

AEROSPACE INDUSTRY

NT Aircraft Industry

Book on material and design problems encountered in construction of high performance missiles, rockets and spacecraft, considering influence of space environment

01 p0084 A69-10021

Fabrication of large parts in aircraft and space industry, discussing extrusion, forging, explosive forming and diffusion bonding

01 p0088 A69-11400

Stabilization and control techniques for future unmanned commercial space vehicles, emphasizing application of projected technological advances in instrumentation

[AIAA PAPER 67-878]

02 p0334 A69-12367

Aerospace research and development projects selection and planning for success in manufacturing competition

03 p0393 A69-13252

Aerospace company engineering administration criteria and functions for chief project engineer [SAE PAPER 680682]

03 p0535 A69-13447

Aerospace manufacturing contribution to engineering function in design development

[SAE PAPER 680668]

03 p0433 A69-13451

High strength carbon fibers development and applications in reinforced composite materials and aerospace industry

06 p0947 A69-18236

Tests and quality control equipment used in German aeronautical and astronautical industries

09 p1513 A69-22565

Cost-profit sharing agreement with aerospace manufacturing companies involved in Boeing 747 construction, detailing final assembly building

09 p1514 A69-22713

Instrumentation in the aerospace industry - Conference, Boston, June 1968, Volume 14

10 p1670 A69-23245

Government flight recorder regulations, detailing approved systems

10 p1691 A69-23246

Space electronic component reliability, considering suppliers and laboratory-workshop partnership

15 p2624 A69-30822

German rocket engine industry reliability and performance, discussing solid fuel, two component fuel, single fuel hydrazine, mixed fuel and ramjet engines

17 p3021 A69-33361

Life cycle maintenance costs reduction in aerospace industry by computers, describing on-line and off-line test systems

17 p2979 A69-33649

Aerospace electronics - IEEE Conference, Dayton, May 1969

17 p2939 A69-34056

Aerospace R and D marketing decisions, considering capability identification, business opportunities, strategies and independent program funding

17 p3077 A69-34127

Quantitative and qualitative reliability programs for commercial and aerospace products, considering Failure Effect Management System

18 p3143 A69-34486

Aerospace management technology transfer, discussing conceptual contributions, planning, administrative and evaluation methods

18 p3236 A69-35086

Collection of papers on aircraft construction and air fleet equipment covering aerospace vehicles theory, engines, automation, design and production

19 p3246 A69-35813

Optimized contracting for systems engineering management, discussing industry views, scope, application, depth, procurement and performance measurement

19 p3454 A69-36005

Composite materials application in aerospace industry, discussing boron and carbon filament properties, epoxy resins, etc

20 p3563 A69-37930

High quality castings unified standards for European aerospace industry

20 p3551 A69-38029

U.S. aerospace technological forecasting involving space flight, air transport and V/STOL aircraft

22 p4052 A69-39930

Management activities related to economics of failure in aerospace industry

24 p4416 A69-42777

Molded fiber composites in aerospace components applications, considering weight, stiffness, production and cost

24 p4326 A69-43448

AEROSPACE MEDICINE

Medicinal therapy and flight safety of pilots and astronauts, discussing drug use, self treatment, tolerance and environmental factors

01 p0014 A69-10583

Soviet book on space physiology covering space flight and laboratory data on cerebral cortex function, digestive system, tissue changes, etc

01 p0014 A69-10743

Gemini and Mercury space flights medical results, summarizing physiological effects noted on body systems

01 p0017 A69-11074

French applied and basic research in space biology including manned space flight, deep space problems, weightlessness and cosmic heavy ion radiation effects

02 p0199 A69-11909

Clinical problems during interplanetary flights, stressing need for diagnostic algorithms and automated medical equipment

02 p0202 A69-12121

Space biomedical research trends, noting gastroenterology and lack of research on disease processes during space travel and overemphasis on space physiology

03 p0369 A69-12859

Biological space research, discussing microecology and weightlessness effects on human space flight [DVL-847]

04 p0553 A69-14811

German Air Force Center of Aeronautical Medicine, discussing organization, work projects and proposed mutual cooperation with French counterpart

05 p0850 A69-16629

Retinal lacerations and detachment in jet pilots, discussing pathogenesis, diagnosis and surgical reattachment methods

05 p0710 A69-16630

Corneal greyish opaque arc as warning of atheromatosis in flight crews

05 p0711 A69-16631

Book on space clinical medicine covering hypoxia, ebullism, decompression, aerotitis, dehydration, hypothermia, cabin atmosphere contamination, urinary calculus, etc

05 p0711 A69-16801

Therapeutic potential of dimethyl sulfoxide in aerospace medicine

06 p0883 A69-17851

Optimum physiological parameters selection criteria for medical control of crew during space flights

07 p1071 A69-18978

Medical factors as probable cause of aircraft accidents, discussing psychological factors, CO poisoning, hypoxia, alcohol, etc

07 p1067 A69-19433

Biomedical experiment onboard Cosmos 110 concerning nonpathological changes

08 p1261 A69-19827

Collection of papers on thermal problems in aerospace medicine covering intense heat, cutaneous vasomotor and sudomotor control, water immersion, etc

08 p1263 A69-20667

High gradient headward acceleration effects on acid base balance of baboons and human subjects, noting arterial changes

09 p1444 A69-22540

Mathematical, physical and physiological modeling for analysis of functional changes during varying gravity conditions

09 p1444 A69-22541

Computer program for onboard medical checkups of spacecraft crews during extended space flights, discussing tests and intervals

10 p1649 A69-23505

Soviet space biology and medicine, discussing ecological physiology, closed system ecology, exobiology and medical tests on cosmonauts

13 p2209 A69-27356

Space travel and lunar exploration medical problems

13 p2210 A69-27909

Pharmacology for long term manned space flights

13 p2211 A69-28613

Visual, auditory and reaction-time responses in aging pilots, determining continuing capacity for choice and discrimination with advancing age

14 p2408 A69-29307

Medicinal therapy and flight safety of pilots and astronauts, discussing drug use, self treatment, tolerance and environmental factors

15 p2555 A69-30753

Aerospace medical association - Conference, San Francisco, May 1969

16 p2742 A69-32008

Aeromedical developments by NASA biomedical applications program applied to general medical equipment including cardiac sensors, surgical sterilization, ballistocardiograph, etc

16 p2882 A69-32430

Aerospace biomedical technology transfer analysis, discussing spinoff, popular interest, transfer barriers, etc

18 p3236 A69-35104

Medical and biological laboratory ground experiments role in development of life support systems and suitable environments for prolonged manned space flights

18 p3098 A69-35165

Space medicine to characterize nature and degree of changes in human functional capabilities due to space flight environment prolonged exposure

19 p3456 A69-36460

Clinical data on ambulant airmen with complete left bundle branch block discovered on electrocardiogram, finding majority with evidence of organic heart disease

19 p3263 A69-36463

Optimum physiological parameters selection criteria for medical control of crew during space flights

20 p3483 A69-38226

Aircraft pilots medical disabilities as potential flight safety hazard, discussing aerospace medical specialist role and pilot education in symptoms evaluation

22 p3894 A69-41146

Space physiology, describing laboratory and onboard experiments

23 p4086 A69-41686

Aviation and space medicine - Conference, Oslo, August 1968

23 p4103 A69-41783

Aviation accidents medical aspects, discussing accident causes and remedies, training and regulation proposals, etc

23 p4106 A69-41792

Blood pressure measurements of pilots at rest during tests under stress on bicycle ergometer revealing transient hypertension

23 p4087 A69-41795

Dynamic roentgenology of cervical spine noting ease of use in neutral profile, hyperflexion and hyperextension for aeronautical medicine

23 p4087 A69-41797

Aerospace medical educational programs for MD, post-MD and practicing physicians at medical faculties in U.S. and at Ohio State University

23 p4106 A69-41799

Space medicine to characterize nature and degree of changes in human functional capabilities due to space flight environment prolonged exposure

23 p4087 A69-41803

Nonsurgical methods of cardiac output measurement in aerospace medicine, considering simultaneous recording of carotid and femoral pulses and impedance plethysmography

23 p4088 A69-41813

Aerospace medicine - Conference, Amsterdam, September 1969

24 p4263 A69-43369

Radiology diagnosis of military jet pilots injuries during ejection and touchdown, discussing fractures, spine injuries and ejection seat spine position

24 p4266 A69-43379

Medical wastage of military and civil aviators in Great Britain /1963-1968/, discussing cardiovascular disease, fatal flying accidents and psychiatric disease

24 p4277 A69-43391

Unscheduled aircraft landing to deplane passenger for medical reasons, discussing costs, time consumption and avoidance methods

24 p4278 A69-43393

Interplanetary space travel medical problems during long duration missions, noting earth diagnostic and therapeutic methods adaptation, drugs selection, astronaut medical training, etc

24 p4278 A69-43396

White mice survival rates and blood morphology and sedimentation rates in low ambient pressure confinement following infectious bacteria injection

24 p4267 A69-43397

AEROSPACE SCIENCES

Space system engineering courses background, objectives and results at MIT and Stanford University dealing with applications of space technology [UN PAPER 68-95870]

01 p0178 A69-10485

Space techniques for application to civil aviation, discussing air to ground communications, air traffic monitoring and navigation and weather forecasting by satellite

[UN PAPER 68-95349]

01 p0179 A69-10490

Space research practical benefits in solar physics, radio astronomy, meteorology, radio physics, communications, etc [UN PAPER 68-11608]

01 p0179 A69-10496

Scientific advances from space research in communications astronomy, electronics, transportation, etc

01 p0151 A69-10498

Space program effects in education, science and engineering, noting impact of first satellite on U.S. research and technology

01 p0179 A69-10500

Science education and training, discussing student motivation [UN PAPER 68-95809]

01 p0179 A69-10515

Handbook on Soviet space science research covering rockets, satellites, space probes, biomedical investigations, atmospheric composition

01 p0154 A69-10935

Soviet literature on extraterrestrial life and civilization emphasizing establishment of contact by radio and laser sources

01 p0016 A69-10953

Space projections - Conference, Denver, July 1968, Volume 2

02 p0332 A69-11734

Space projections - AIAA-AAS Conference, Denver, July 1968, Volume 3

02 p0226 A69-11755

Space projections - Conference, Denver, July 1968, Volume 1

02 p0330 A69-12801

Space science and technology - Conference, London, February 1968

06 p0997 A69-16852

UK space research in 1970s emphasizing solar observations in UN, cosmic X ray astronomy, solar space astronomy and ionospheric investigation

06 p0997 A69-16853

Space sciences - USAF Conference, Albuquerque, June 1968

08 p1423 A69-21123

Scientific report of Rockwell polar flight, November 14-17, 1965

09 p1484 A69-21401

Auroral French rocket probe in Norway, studying low energy particles, relations between electron showers and high altitude electric fields, etc

09 p1498 A69-22160

Bibliography of reports and papers on space sciences and research activities of national institutions of COSPAR members /1966-1967/

10 p1784 A69-24001

Solar flares theories, discussing data acquisition by space research and solar radio astronomy

11 p1946 A69-24516

Minimum height of monochromatic radiation ionization in atmosphere assuming spherical earth for space science applications

13 p2256 A69-28653

Radio propagation in upper atmosphere and ionosphere noting rocket and satellite experiments including plasma physics research, tropospheric studies and space science services

14 p2526 A69-29854

Space technology difficulties, achievements and applications

14 p2527 A69-29895

Space exploration influence on science education, showing NASA instructional materials for teachers in biology, chemistry, physics, mathematics, industrial arts, etc

18 p2325 A69-35077

Air and space research at Goettingen Aerodynamic Testing Institute

19 p2395 A69-36684

Life sciences and space research on biological effects of radiation in space - COSPAR Conference, Tokyo, May 1968

20 p3474 A69-37612

Space research - COSPAR Conference, Tokyo, May 1968

21 p3698 A69-38334

Manned space flight history and spacecraft development [AAS PAPER 69-501]

24 p4380 A69-42852

Solar flare and space research - COSPAR Conference, Tokyo, May 1968

24 p4369 A69-43603

AEROSPACE SYSTEMS

Electronics and aerospace systems - IEEE Conference, Washington, D.C., September 1968

03 p0385 A69-13176

Space systems use for planetary geology and geophysics - Conference, Boston, May 1967

03 p0509 A69-13390

Automatic checkout of space systems, discussing cost effectiveness tradeoffs, ground and onboard equipment utilization, vehicle design and mission success risk

03 p0411 A69-13392

Manned reusable space transportation systems development, discussing requirements for future space mission planning

03 p0519 A69-13395

Beryllium aerospace applications, considering advantages vs disadvantages in systems engineering [SAE PAPER 680648]

03 p0444 A69-13456

Aerospace sensor systems, discussing adaptive multimode sensors and multispectral sensing, electronic recognition of image components, laser radar and Raman scattering technique

03 p0431 A69-13851

Flight test support design, developing measure of performance of test environments stated in weapon or space system terms

05 p0742 A69-15804

Orbital station projects, concepts and future uses

06 p1013 A69-17266

Spacecraft systems, education - Conference, Belgrade, September 1967

06 p1015 A69-17596

Weightless simulators effectiveness for obtaining space systems maintainability criteria, using non-parametric experimental design for performance data

06 p0882 A69-17648

Microminiature system mechanical design for aerospace environment, considering guidelines for implementation of requirements [AGARDOGRAPH-114]

08 p1291 A69-20986

Microelectronic equipment for aerospace application and integrated circuit production in UK [AGARDOGRAPH-114]

08 p1292 A69-20992

Space flight trajectory analysis of aerospace systems, discussing Analytical Trajectory Optimization Model

09 p1585 A69-21207

Space systems and radio astronomy - Conference, Geneva, September-October 1968

09 p1448 A69-21268

Radio location system based on measuring distance between object and two stationary satellites, noting application to air traffic over North Atlantic

09 p1537 A69-21269

Domestic satellite system for carrying maximum traffic by full use of rocket technology including Saturn 5 type propulsion systems, antennas, frequencies, etc

09 p1458 A69-22467

Heat resistant DIPAM and HNS explosives in aerospace applications, considering mild detonating fuse and core loading

10 p1750 A69-23014

Computerized design of optimal direct lift controller for aircraft and aerodynamic surfaces, using Kalman linear state regulator theory

12 p2014 A69-26765

Spaceborne optical telescopes requirements and development including mirror material and construction, optical design, servocontrol, etc

13 p2261 A69-27946

Book on calculus of variations and optimal control theory, discussing functional analysis for use in space science

13 p2289 A69-28054

Scientific aims, optical design, instrument data, control and orbit operation of European Large Astronomical Satellite used in UV observations

13 p2264 A69-28477

Systems engineering approach to aerospace product defects minimization, discussing scope, contract development, mainstream functions, component development, design data and subsystem integration

15 p2719 A69-30085

Leak detection for aerospace hardware, discussing equipment, operations, checkout, etc

15 p2618 A69-30315

Program stretchout in aerospace procurement, discussing costs effect in relation to incentive contracts

15 p2721 A69-31071

Demand assigned frequency division multiple access-PCM system designed by COMSAT for satellite communication

16 p2749 A69-31602

Satellite gravitational stabilization system with maximum damping rate, discussing orbital plane oscillations

16 p2867 A69-31738

Computerized Markov effectiveness models of repairable and nonrepairable complex aerospace systems

18 p3195 A69-34527

Attitude control system for Apollo Telescope Mount, discussing selection features based on manned orbital space platform requirements

18 p3168 A69-34683

Momentum control system for satellite maneuvering and pointing in pitch and roll developed by modifying existing libration damping gyrostatizer

18 p3207 A69-34684

Aerospace technology application to commercial aviation system for cost effectiveness in functions expansion, phase-over, installation, maintenance and operation, discussing added information functions

18 p3108 A69-35069

Elastomeric and coating materials for aerospace systems, considering temperature, rain, sand erosion, propellant and radiation resistant properties

19 p3357 A69-35586

Cost model to trade off competing systems designs for space communications, navigation, operational availability and ballistic missile defense

19 p3454 A69-36007

Software support package for aerospace digital computer emulation, consisting of symbolic assembly program and interpretive simulator program and subprogram [AIAA PAPER 69-974]

22 p3907 A69-40354

Flexible format generator for manned spacecraft data management system designed with memory for data sampling formats, emphasizing software counters and power strobing

23 p4133 A69-41762

Flammability control for aerospace avionics systems safety, considering risk, test method, acceptability criteria, confidence level and ignition source

24 p4336 A69-43422

Aerospace systems failures caused by stress corrosion, fatigue, overload, improper designing or inadequate processing control

24 p4323 A69-43428

AEROSPACE VEHICLES

Spacecraft illuminance by reflected solar radiation calculated by computer method

01 p0151 A69-10576

Computer program for predicting temperature distribution and heat transfer through coated and uncoated window systems of aerospace vehicles [AIAA PAPER 69-28]

06 p1038 A69-18178

Ceramic radomes for hypervelocity aerospace vehicles, considering wide temperature environment effects on stability and properties

07 p1171 A69-19511

Aerospace structures modal vibration tests data acquisition including multishake excitation methods

15 p2585 A69-30358

Spacecraft illuminance by reflected solar radiation calculated by computer method

15 p2691 A69-30746

Dynamic balance for rotating aerospace vehicles, discussing error in principal axis location between rotor on machine and free body in space [SAWE PAPER 740]

18 p3137 A69-34887

Computer program for weight and center of gravity tolerance data for assembly aerospace vehicle [SAWE PAPER 734]

18 p3221 A69-34892

Collection of papers on aircraft construction and air fleet equipment covering aerospace vehicles theory, engines, automation, design and production

19 p3246 A69-35813

Nondestructive testing for aerospace corrosion, discussing light, penetrants, X rays, sound, ultrasounds, electrical conductivity, magnetic reaction and radiation backscatter methods

21 p3733 A69-39495

AEROSPACEPLANES

Lifting body type M2-F1 and M2-F2 aircraft enabling astronauts to make own landings at choice airport

03 p0366 A69-13367

AEROTHERMOCHEMISTRY

Thermodynamics of combustion products and aerothermochemistry noting temperature calculation, heat, mass and momentum transfer in gases and deflagration wave propagation

06 p1031 A69-17414

Flame establishment and propagation in gas phase taking into account aerodynamic and chemical kinetics

06 p1031 A69-17418

Combustion in liquid propellant rockets, discussing aerothermochemical steady state and nonsteady behavior analysis and experiments

16 p2835 A69-31732

AEROTHERMODYNAMICS

Book on combustion covering aerodynamic and chemical aspects, combustion instability, detonation and rocket propellant combustion

01 p0176 A69-10906

Mission requirements influence on aerothermodynamic environment for vehicle entering Venus atmosphere, considering different entry modes

02 p0332 A69-12823

Aerothermodynamics of subsonic-aircraft propulsion, analyzing performance of bypass engine, fuel consumption and specific weight

05 p0695 A69-15551

Thermodynamics of combustion products and aerothermochemistry noting temperature calculation, heat, mass and momentum transfer in gases and deflagration wave propagation

06 p1031 A69-17414

Flame establishment and propagation in gas phase taking into account aerodynamic and chemical kinetics

06 p1031 A69-17418

Thermodynamics and aerothermodynamics for propulsion problems noting thermodynamic laws and quantities, steady flow, shock waves, nozzles, inlet and thermodynamic cycles

11 p1821 A69-25583

Aerodynamic design of axial flow compressors and turbines, using aerothermodynamic equations for compressible flow analysis

11 p1821 A69-25585

Aerothermodynamic problems during transition after activation of thrust inverter in solid propellant rocket engines

17 p3018 A69-33327

AEROTHERMOELASTICITY

Aerothermoelasticity problems for Mars entry vehicles, discussing deceleration loads, separated hot gas flow, shield thermal gradients and oscillatory body motion [AIAA PAPER 68-283]

09 p1610 A69-21991

Heated three layer plates stability under finite deflections in supersonic gas flow, deriving aerothermoelasticity equations

24 p4395 A69-42590

AEROZINE

Bipropellant propulsion systems using Aerozine 50 and nitrogen tetroxide for Symphonie telecommunications satellite

16 p2828 A69-31733

Halon 1301 /bromotrifluoromethane/ concentration for inerting Aerozine-50 spills or extinguishing fires, noting joint use of carbon dioxide and water
18 p3094 A69-35090

AFC [CONTROL]
U AUTOMATIC FREQUENCY CONTROL

AFCs [CONTROL SYSTEM]
U AUTOMATIC FLIGHT CONTROL

AFFERENT NERVOUS SYSTEMS
Visceral afferent pathways influence on vasopressin secretion, ADH levels and urinary excretory patterns of dogs during surgical stress
05 p0708 A69-15970

Ventral posterolateral potentials in anesthetized immobilized cats in response to electric stimulation of mesenteric nerves and mechanoreceptors, studying thalamus nucleus role
12 p2020 A69-26562

Labyrinth polarization effect on stimulation and neuron activity in visual cortex of cats, using electroencephalograph
20 p3469 A69-37244

Rapid component of nystagmus using photostagmography, noting dependence on afferent pulse of ampullar apparatus
20 p3481 A69-37272

Sympathetic nerve activity inhibition due to afferent baroreceptor nerves reflexes, studying carotid sinus and aortic nerves as pathways to vasomotor center
20 p3479 A69-38073

Neuronal organization of initial afferent inflow in thalamic visual center /lateral geniculate body /LGB/ of unanesthetized cats/, noting unit activity
22 p3879 A69-40845

Information transfer capacity of afferent and efferent cell system and fiber tracts of human cerebellum numerically defined with regard to cybernetics
23 p4084 A69-41467

Temperature dependence of afferent and efferent spontaneous activity of spinal cord, using filament recordings from ventral and dorsal roots in anesthetized cats
23 p4093 A69-42066

Efferent innervation influence of one ear to another in feline auditory system, based on afferent neurons responses to contralateral and binaural stimulation
23 p4094 A69-42073

Primary muscle spindle afferents from gastrocnemius muscle of cat before, during and after cold shivering, utilizing ramp stretches of same muscle
23 p4096 A69-42091

AFRICA
Geomagnetic pulsations recorded in equatorial regions of Africa found continuous and not pearl modulated
09 p1491 A69-22051

AFTERBODIES
Shoulder pressure on slender cone/afterbody combinations in hypersonic inviscid flow of perfect gas
04 p0542 A69-14735

Pressure distribution measurement over sphere with cylindrical afterbody in magnetofluid dynamic flow, showing drag decrease at large magnetic field
11 p1873 A69-25136

Free flight telemetry base pressure measurements on slender cones and domed afterbodies in hypersonic laminar flow, using shock tunnel test facility [AIAA PAPER 68-698]
24 p4249 A69-43675

Apollo afterbody heat transfer, studying ablation effects for various reentry angles of attack
24 p4415 A69-43680

AFTERBURNERS
U AFTERBURNING

AFTERBURNING
Fluorid light-off detector /FLOD/ for sensing and indicating minimum light-off or blow out conditions in turbojet engine afterburner [ASME PAPER 69-GT-36]
09 p1501 A69-22488

Acoustic frequency of longitudinal self oscillations during vibrational fuel combustion in afterburner, taking into account nonlinear properties of heat supply zone
11 p2002 A69-25339

AFTERGLOWS
NT HELIUM AFTERGLOW

Two body rate coefficients for charge transfer reactions of nitrogen, oxygen and NO positive ions to Na atoms measured using flowing afterglow system
07 p1185 A69-19303

Free fall theory for afterglow decay of average electron density and temperature in pulsed cylindrical mercury vapor discharge plasma
08 p1358 A69-19811

Ion number densities time dependence in pink afterglow of N measured with quadrupole mass spectrometer
08 p1308 A69-20292

Argon afterglow microwave and spectroscopic studies, monitoring time-varying electron density and temperature and extracting electron-ion recombination coefficients
15 p2658 A69-30173

Microwave reflection and noise emission from cylindrical rare gas afterglow plasmas in axial magnetic field measured near electron cyclotron resonance
18 p3127 A69-34436

Air afterglows electron loss mechanisms, measuring electron densities decay rates after microwave ionization
22 p4006 A69-40527

Mechanism for pink afterglow accompanying microwave discharge in pure nitrogen, emphasizing gas kinetic temperature role
24 p4353 A69-43749

AFTERIMAGES
Visual long term storage capability demonstration, describing negative aftereffect of motion perceived after fixation of moving spiral pattern
21 p3661 A69-39332

AGC [CONTROL]
U AUTOMATIC GAIN CONTROL

AGE DETERMINATION
U CHRONOLOGY

AGE FACTOR
Ophthalmic 2 percent pilocarpine effect on normal ocular dynamics of various age groups, influencing visual acuity, accommodation and refraction
01 p0022 A69-11347

Physiological functions of aged Japanese pilots, discussing height, weight, Rohrer index, obesity, vision deterioration and hearing disturbances
06 p0876 A69-18028

Period-age relations for delta Cephei stars based on stellar evolution theory and initial abundance of hydrogen
08 p1392 A69-20564

Accident record of general aviation pilots over age 60/1965/
14 p2541 A69-29308

O uptake of middle aged men, comparing short and long term endurance running effects
21 p3654 A69-38904

Age and carbon dioxide tension effects on EEG of adolescents and adults, discussing end-tidal carbon dioxide during routine hyperventilation
22 p3872 A69-40162

Subjective and objective thresholds of darkness adaptation in human subjects grouped from infancy to adulthood, using same variable intensity light source equipment
22 p3881 A69-40861

Globular cluster star age and initial He abundance from main sequence, horizontal branch and red giant tip models using radiative opacities
22 p4035 A69-41205

Pulsars turn off time compared to Galaxy age, discussing physical theory and pulsar models
24 p4389 A69-43745

AGE HARDENING
U PRECIPITATION HARDENING

AGENA ROCKET VEHICLES
Agena propulsion system performance model for predicting propellant flow rate, mixture ratio, thrust time and specific impulse [AIAA PAPER 69-453]
16 p2841 A69-32683

Agena rocket vehicle production reliability evaluation program, testing specific representative equipment randomly selected from production stores
18 p3146 A69-34510

AGGLOMERATION
Liquid alumina particles agglomeration in convergent and throat region of nozzle leading to performance decrease by increasing velocity and temperature difference between phases
22 p4001 A69-40929

AGING
Glass fiber reinforced plastics aging behavior under heat and weathering influence
03 p0454 A69-13823

Polymeric insulation materials, discussing intrinsic properties dependence on temperature and atmosphere, stressing effect on aging
13 p2285 A69-27985

Artificial aging effect on spinel structure and properties of ferrites using X ray analysis, neutron diffraction and electron microscopy
13 p2320 A69-27997

AGING [BIOLOGY]
Cardiovascular disease incidence among airline flight deck personnel in relation to increase in average age of personnel
06 p0875 A69-17848

Visual, auditory and reaction-time responses in aging pilots, determining continuing capacity for choice and discrimination with advancing age
14 p2408 A69-29307

Physiologic and psychologic aging in professional pilots analyzed on basis of cardiovascular, pulmonary, exercise tolerance and sense testing
14 p2408 A69-29309

Mortality kinetics of Drosophila melanogaster, comparing effects of gamma radiation-induced life shortening and natural aging
15 p2555 A69-30444

AGING [METALLURGY]
Natural aging effects on fracture characteristics of aluminum weldments, investigating precracked Charpy impact toughness
01 p0086 A69-10537

Deformation in aged Fe-Cr alloy studied for rate-controlling solid solution mechanism as function of stress
01 p0095 A69-10601

Atmospheric stress corrosion tests of aluminum alloys in various environments, comparing aging results with accelerated laboratory tests
01 p0100 A69-11352

Cooling rate effect during aging on heat resistance of forged blanks of nickel based chromium alloy
02 p0266 A69-12125

Superconductivity of niobium-titanium-oxygen alloy wires containing 40 percent minimum niobium weight, noting thermomechanical aging effect on critical current density
03 p0484 A69-13118

Al/Zn/Mg alloys preprecipitation, discussing Guinier-Preston and critical zone sizes and reversible vacancy trap
03 p0447 A69-13613

Alloying elements effect on mechanical and refractory properties and structure of forging of age hardenable Ni base alloys
03 p0452 A69-14122

Properties of Ni-Mo-Al age hardening steels, discussing data confirming validity of low carbon low aluminum approach
04 p0613 A69-14527

Low temperature aging prior to higher temperature artificial aging increases Al alloys strength
04 p0614 A69-14634

Ferrite-austenitic stainless steels with Ti analyzed during aging at 450-600 C for excess phase nature
04 p0615 A69-14641

High strength martensitic aging steels alloying effects, phase transformation and aging
04 p0615 A69-14644

Maraging steel with reduced Co, establishing optimal temperature range for short aging
04 p0616 A69-14650

Precipitation hardening effects on Al-Zr recrystallization with Fe and Si additions, noting peak hardness increment with decrease in aging temperature
04 p0617 A69-14931

Plastic deformation effect on structure, yield point and tensile strength of aged austenitic alloy containing Ni, Cr and Ti
04 p0618 A69-15177

Electron microscopic and microdiffraction study of structure of quenched and annealed titanium alloy foils at high temperatures
05 p0783 A69-16810

Aging and recovery effect on structure and hardness of Ag and Be doped Al-Mg alloys
05 p0783 A69-16811

Electron microscopic study of structural changes occurring during aging of martensite in Fe-Ni-Ti alloy
05 p0783 A69-16813

Plastic deformation, aging, heat treatment and machining effect on structure of thin films of AlMg11 alloy
05 p0783 A69-16814

Edge dislocations effect in perpendicular slip planes on work hardening and strain aging, calculating dilatation centers absorbed
07 p1238 A69-19695

Solution annealing and aging time and temperature effects on precipitation in quenched and aged beryllium
08 p1330 A69-20008

Retained austenite content control, strain aging and ausforming to improve toughness of high strength martensitic stainless steel without strength loss
08 p1330 A69-20010

Initial aging stage in Fe-Ni-Ti alloys using diffuse X ray scattering with electron microscopy of thin foils
10 p1712 A69-23720

Near boundary zones in VT15 Ti alloy not involved in beta phase decomposition during aging below 500 C attributed to vacancy concentration decrease
11 p1902 A69-24275

Preliminary natural aging effects on maximum strength properties obtained at various artificial aging temperatures for aluminum ternary alloy
11 p1905 A69-24921

Aging effects on hardness and tensile strength of nickel-chromium steels at various high temperatures and time periods
11 p1906 A69-25439

Heat treatment effect on Ti-Mn alloy microstructure, discussing fcc martensite transformation into alpha, beta and intermediate phases as function of aging
11 p1906 A69-25578

Precipitated phase composition and structure of Co-Ti solid solution during aging
12 p2112 A69-26037

Electrical resistivity decrease in niobium-hydrogen alloys during isothermal aging at low temperature attributed to hydride precipitation, noting reaction rate and activation energy
14 p2463 A69-29288

Growth kinetics, lattice constant changes and hardness during aging of nimonic alloy from X ray diffraction diagrams
14 p2463 A69-29310

Temperature dependent aging mechanisms in deformed Mo alloys during annealing, using transmission electron microscope
14 p2463 A69-29312

Maximum strengthening due to second phase precipitation within operating temperatures maintainable to 20 hr during aging of Nb-Hf-O and Nb-Zr-O alloys
15 p2640 A69-30632

Fatigue crack propagation in thin aluminum alloy plates under plane bending using microscopic surface observation and electron fractography, noting role of aging conditions
17 p3061 A69-33677

Ti-Al-V sheets quenched from alpha plus beta field into salt bath at various high temperatures, studying effects of bath temperature and holding time on aging and mechanical properties
21 p3730 A69-38667

Plastic deformation combined effect with aging on mechanical properties of phase-hardened austenitic Fe-Ni-Ti alloys
21 p3746 A69-38956

Coherent matrix precipitates observation in Fe-Ni-Cr alloy by transmission electron microscopy, discussing yield strength and elongation dependence on aging conditions
23 p4176 A69-41508

Cold working and aging effects on mechanical properties of TiAl-V including creep and temperature effects [DGLR-69-002]
23 p4177 A69-42163

Outdoor aging effects on unstressed adhesive-bonded Al to Al lap shear joints
24 p4319 A69-42932

AGITATION

U ULTRASONIC AGITATION

AGREEMENTS

Interpretation of term peaceful in Space Treaty and use of outer space including celestial bodies
07 p1244 A69-19234

AGRICULTURE

Aerospace research applications in agriculture and forestry, discussing information acquisition for worldwide coverage [UN PAPER 68-95393]
01 p0065 A69-10504

Agricultural remote sensing information system composed of data acquisition, processing and information extraction and interpretation phases, providing knowledge of earth resources
03 p0400 A69-13195

Radar imagery for agricultural land mapping, noting field and crop discrimination and parameters influencing radar return
12 p2097 A69-26986

Adaptive pattern recognition system simulated and tested with agricultural radar images, describing predictive environmental model mathematically
12 p2097 A69-26990

Carrot plants growing during 374 days in conveyor type aeroponic assembly, noting yield and morphological features
17 p2912 A69-32943

Agricultural and forestry applications of tethered balloons, discussing observation angle effect on spectral signature response and signal preprocessing
22 p4053 A69-40805

AILERONS

Differential gearing of aileron movements to reduce control forces in aircraft
03 p0367 A69-13786

AIR

NT ALVEOLAR AIR
NT COMPRESSED AIR
NT HIGH TEMPERATURE AIR

Sparks four meters long in atmospheric air, noting image converter photographs, electrical measurements, light output, spectra and energy balance
02 p0281 A69-12406

Air cushion effect in explosive forming of metal sheets, considering simple geometrical shape
06 p0931 A69-17526

HF breakdown of air using Boltzmann equation to determine net ionization frequency relation with electric field strength
08 p1357 A69-20810

Multicomponent diffusion coefficients of dissociated air as function of pressure, temperature and concentration, based on simplified model of binary diffusion
09 p1623 A69-22098

Kinetics of air plasma formation in wake of shock wave propagating in air, taking into account nonequilibrium ionization
12 p2062 A69-26674

Probable sign-invariant periods of air temperature anomalies based on random Gaussian processes
13 p2294 A69-27855

Corrosive wear by atmospheric air and moisture under nonsufficing conditions, noting control by dry nitrogen blanketing and oil additives [ASLE PAPER 68-LC-10]
15 p2622 A69-30608

Hypersonic aircraft induced changes in chemical and thermodynamic properties of air influencing aerodynamic forces on vehicle
17 p2895 A69-33576

Analytical, graphical and graph-analytical methods for synthesis of passive circuits ensuring air removal from chambers of pneumatic logic control and servomechanisms
18 p3093 A69-34831

Pubertal puppy and adult dog cardiovascular system during inhalation of various nitrogen-oxygen mixtures, comparing heart beat rates, minute blood volumes, etc
19 p3257 A69-36169

Emissivity of nitrogen, oxygen and air plasmas in vacuum UV region of spectrum by photographic measurement, using He recombination radiation as brightness standard
21 p3774 A69-38944

Respiratory gas exchange during workloads, comparing values for ventilation, oxygen uptake and carbon dioxide output measured in air and in helium-oxygen mixture
22 p3891 A69-40221

Differential capacitance transducer measuring small displacements in heated transformer oil, air, castor oil or glycerin
22 p3946 A69-40439

Hydrogen-air reaction kinetics analyzed using standing wave normal shock noting wall effects, ignition delay and recombination [AIAA PAPER 67-479]
23 p4239 A69-41893

Air density determination using transit time method involving microwave phase measurements
24 p4313 A69-42898

Air bubbles rise velocity and path in water based on time measurement of bubble traversing two light beams, describing electronic recording system
24 p4299 A69-42918

AIR BEARINGS

U GAS BEARINGS

AIR BLASTS

U AERIAL EXPLOSIONS

AIR BREATHING ENGINES

NT JET ENGINES

Blow-down facility for hypersonic testing of air breathing engines, describing test cell, air heating system, exhausters and data system
02 p0227 A69-11756

Supersonic ramjet propelled air breathing booster for speeds up to Mach 12, discussing flight mechanics, aerodynamics, propulsion, heating and air intake design
09 p1573 A69-22608

UV, visible and near IR spectral characteristics of hydrocarbon-air flames with particulate Al, Mg and B, noting hot metal continuum and oxide emissions
11 p1940 A69-24483

Thermodynamic cycle analysis of various gas turbines and air breathing propulsion systems noting regenerators, heat exchangers and pulsejet engine
11 p1943 A69-25584

Ramjets and air augmented rockets as propulsion systems for supersonic atmospheric flight, noting inlet design, combustors and nozzles
11 p1943 A69-25586

Supersonic combustion technology, noting air breathing propulsion systems for application to hypersonic flight
11 p2003 A69-25596

Vitiated air contamination effects on combustion and hypersonic air breathing engine ground tests [AIAA PAPER 69-338]
13 p2325 A69-28274

Boron combustion for air augmented rocket applications, discussing single boron particle ignition and combustion characteristics
16 p2828 A69-31737

Air breathing engines performance possibilities, describing design and testing difficulties, stability requirements, etc
18 p3185 A69-35139

Technology trends in airbreathing propulsion, discussing noise control for subsonic jet transports, turbine blade cooling, etc [AIAA PAPER 69-774]
19 p3244 A69-35648

Liquid, solid, hybrid propellant and nuclear, electric and air breathing rocket engines, discussing orbiting payload cost, controllability, operating environments, velocity, etc
19 p3395 A69-36321

Vitiated contamination effect on airbreathing engine ground testing, considering equilibrium, vibrational and chemical relaxation, condensation, combustion, mixing and engine performance [AIAA PAPER 69-456]
19 p3448 A69-36333

Airbreathing gas turbines construction materials including composites and Ti and austenitic alloys [ASM PAPER D8-25.2]
20 p3586 A69-38133

Thrust increase methods for air breathing turbojet engines analyzed with respect to effectiveness, taking into account environmental supporting mass and fuel expenditures
23 p4199 A69-41578

Combustion considerations in fuel rich solid and hybrid propellant systems in air breathing propulsion for comparison with metal ignition requirements
23 p4199 A69-41894

NASA programs for development of high temperature alloys for advanced air breathing engines emphasizing cast Ni-base alloy [ICAS PAPER 68-26]
24 p4335 A69-43718

AIR CARGO

Air cargo traffic increase, discussing technical and economical prospects, use of intermodal containers and transportation automation tendency
01 p0008 A69-10030

Containerized freight, discussing means of transport, methods of distribution, suitable aircraft for carriage, economic and social effects and combined air-water-land transport
02 p0228 A69-11887

Air freight transport development, characteristics and economics
02 p0356 A69-11888

Air cargo and world trade, discussing economics, cargo tariffs, customs procedures, cargo airports and convertible aircraft
03 p0536 A69-14088

Air cargo transportation in 1970s, discussing Boeing 747 and Lockheed 500 super airfreighters, terminals, rates, marketing, etc
13 p2381 A69-27336

Air cargo terminal materials handling, discussing computer control, off-airport consolidation, packaging, etc
13 p2239 A69-27337

Airport planning for large aircraft loading of passengers, baggage and cargo containers
17 p2948 A69-34208

Jumbo aircraft production technology causing economic setback, recommending added emphasis on passenger/cargo requirements and operating environments for greater profitability
18 p2322 A69-34542

Air cargo traffic, discussing planload lots, aircraft types suitable for freight transport, difficulties and solution
22 p4052 A69-40426

Civil cargo aircraft characteristics and development trends, discussing cargo and passenger traffic management, communications network, etc
22 p3863 A69-40427

Handling and processing function in air freight transportation, discussing system design approaches, cargo terminals, materials handling systems and containerization
22 p4053 A69-40483

General aviation airport application as freight consolidation terminals to reduce ground handling costs, circumvent air and ground traffic problems, etc
24 p4419 A69-43047

AIR CONDITIONING

Mathematical simulation of temperature and humidity changes in compartments of hermetically sealed space vehicle cabins
02 p0200 A69-11489

Personal cooling in inadequately air conditioned cockpits, considering dry air, air ventilated suits and liquid circulated tubes near skin
[AGARDOGRAPH-111] 08 p1267 A69-20684

Trident 2E aircraft, discussing fuel system, electric power installation, hydraulic system, air conditioning, pressurization and flying controls
13 p2202 A69-27973

Heat tolerance in case of SST aircraft air conditioning failure, discussing physiological and psychomotor reactions and time curves for metabolic activity levels
24 p4277 A69-43382

AIR CONDITIONING EQUIPMENT

Air conditioning system for transport airplane using combined simple/bootstrap cycle refrigeration unit, discussing thermodynamic performance and hardware implementation
[AIAA PAPER 69-787] 19 p3243 A69-35641

AIR CONDUCTIVITY

Air-earth current and conductivity measurements, noting greater conduction current at one mile altitude
05 p0758 A69-16419

Solar flare influence on potential gradient and air-earth current properties at high mountain stations
05 p0759 A69-16634

Electrical conductivity of air behind incident and reflected shock wave fronts as function of temperature and Mach numbers determined by electrode method
11 p1888 A69-25220

Air plasma electrical and thermal conductivity coefficients measured in wall stabilized DC arc at atmospheric pressure and high temperatures
15 p2663 A69-30979

Air electrical conductivity reduction in fog ascribed to small ions concentration, increase in droplets capture efficiency and particle concentration
24 p4347 A69-43509

AIR COOLING

Transpiration cooling of porous flat plate by injection of carbon dioxide or air into carbon dioxide and air free streams
03 p0413 A69-12996

Air film cooling of rotating turbine disk, suggesting applicability to gas flows
06 p1034 A69-17814

Gas turbine blade cooling by longitudinal air flow, discussing cooling efficiency of guide and impeller blades and blade ring
11 p1942 A69-25337

High power ferrite latching switch with forced air cooling, discussing nonreciprocal phase shifter materials and configurations
13 p2229 A69-27674

Internal heat transfer coefficients for impingement cooling of gas turbine airfoil leading edge
[AIAA PAPER 68-564] 17 p3022 A69-34021

Working fluid flow parameters compensation by expelled cooling air in air-gas flow area of turbine stage
18 p3184 A69-34985

Vortex flow air cooling system for lasers using vortex effect of gas separation, resulting in minimum weight and dimensions and high cooling efficiency
21 p3734 A69-38399

Cooling air from blades discharged into flow-through part of gas turbine, examining gas mixing with air from blade and effect on turbine efficiency
21 p3785 A69-39090

Natural convective heat transfer to gas turbine rotor blade and thermal resistance of cooling system using centrifugal pump
21 p3785 A69-39103

Temperature field in deflector cooled turbine blades for nonstationary regimes, considering heating of cooling air, thermal conductivity and thermophysical coefficient changes
21 p3786 A69-39718

Thermal design of power amplifier for airborne HF transceiver, discussing component layout, air cooling and materials
22 p3909 A69-39942

Electronic equipment environmental cooling by controlled airflow systems, reviewing systems designs, control problems, etc
22 p3954 A69-40035

Internally air cooled turbine blades and vanes emphasizing coolant aerodynamics, heat transfer and blade life, high temperature in jet engines, etc
[RAES PAPER 22] 22 p4000 A69-40500

Turbine rotors temperature reducible by increasing air cooling system flow rate
24 p4364 A69-43081

Turbine blade edge cooling efficiency, investigating Reynolds number and gas temperature to cooling air ratio influence
24 p4364 A69-43082

Edge effects in efficiency of air cooled turbine blade cascades with cooling air ejection from blade trailing edges into gas flow
24 p4364 A69-43090

AIR CURRENTS

NT JET STREAMS [METEOROLOGY]
NT MERIDIONAL FLOW
NT VERTICAL AIR CURRENTS

Air movements in lower stratosphere analyzed on basis of ozone measurements, showing correlation with north-south gradient of total ozone amount
02 p0246 A69-12762

Wind changes calculated from Doppler data and inertial system, noting role of heading and air speed
08 p1346 A69-20317

Acoustic sounding of atmospheric structure, utilizing energy backscattered from temperature fluctuations in turbulent regions
14 p2448 A69-29527

Zonal and meridional components of air circulation in troposphere and lower stratosphere for Northern Hemisphere
14 p2477 A69-29829

Ion-neutral air motion in F region under time dependent electric and constant magnetic field effect, using partial differential equations
16 p2777 A69-32181

AIR CUSHION VEHICLES
U GROUND EFFECT MACHINES

AIR DEFENSE

Helicopter self defense armament for fire support of British Army operations, discussing vulnerability, weapons selection and tactics, logistics, etc
01 p0010 A69-10869

Automated programmed instruction /API/ for training backup interceptor control personnel to conduct air defense operations
[AIAA PAPER 69-956] 22 p3905 A69-40338

AIR DUCTS

Dust particle separation from inlet flow with S-bend duct to minimize engine dust ingestion, determining particle trajectories
[AHS PAPER 211] 01 p0006 A69-10409

Turbine powered helicopter engine inlet air filtration system utilizing direct-connect S-bend duct
01 p0143 A69-11054

Air deflection and modulation /ADAM/ turbobfan propulsive wing V/STOL design
[AIAA PAPER 69-201] 07 p1056 A69-19573

Peak acoustic attenuation frequency shifts and peak power insertion losses in air flow ducts related to air specific weight changes
07 p1117 A69-19700

Monte Carlo method application to neutron streaming in hemispherical air-filled ducts in water tank to determine leakage through nuclear reactor shields
18 p3171 A69-35178

AIR FILTERS

Dust particle separation from inlet flow with S-bend duct to minimize engine dust ingestion, determining particle trajectories
[AHS PAPER 211] 01 p0006 A69-10409

Turbine powered helicopter engine inlet air filtration system utilizing direct-connect S-bend duct
01 p0143 A69-11054

Protective filter for inspiration valve of oxygen masks in high performance aircraft, reducing respiratory volume exchange with given pressure amplitude
17 p2916 A69-33773

AIR FLOW

NT JET STREAMS [METEOROLOGY]
NT MERIDIONAL FLOW
NT VERTICAL AIR CURRENTS

Heat exchange and hydraulic resistance in turbulent heat exchangers in longitudinal air flow calculated by criteria equations
01 p0173 A69-10092

Supersonic air flow around blunt body studied near critical line with allowance for viscosity, thermal conductivity and radiant energy transfer, assuming thermodynamic equilibrium
01 p0006 A69-10378

Very high temperature air flow laminar boundary layers on rotating bodies with unsteady chemical reactions, determining flow dynamic behavior
01 p0060 A69-10725

Group invariant solutions of differential equation systems applied to quasi-linear partial differential equations of motion of air masses
02 p0274 A69-11444

Arc discharge in axially turbulent airflow producing equilibrium air plasma
02 p0285 A69-11571

Numerical solution for ambipolar diffusion and kinetic decomposition of rotating body of complex chemical composition in ionized airstream
02 p0191 A69-12580

Longitudinal correlation lengths in grid turbulence air flow transport subjected to planar deformation measured from energy spectra of velocity fluctuations
02 p0192 A69-12626

Heat transfer in cooled portion of air gas flow area of high temperature gas turbines
03 p0495 A69-12957

Airflow and power requirements of compressible hovercraft jet operating under equilibrium conditions
05 p0697 A69-15708

Equations describing chemical kinetics and conservation law derived for ionization relaxation processes behind shock wave front in air
05 p0746 A69-15891

Asymmetric supersonic air flow at 60 degree angle of attack past ellipsoid with frontal spike creating separation area
06 p0858 A69-17337

Parasitic eigenvalue in integration of equations governing one dimensional flow of chemically reactive gas
07 p1118 A69-18317

Air backflow in nuclear exhaust system duct for ground testing of NERVA engines, noting overpressure effect
[AIAA PAPER 69-325] 09 p1479 A69-22390

High enthalpy air flow in hypersonic conical nozzle, calculating chemical and thermodynamic nonequilibrium effects with computer program
09 p1433 A69-22610

Combustion chamber design for advanced gas turbines, noting influence of fuel air mixing and air flow distribution
09 p1573 A69-22612

Performance analysis of combustion chambers with continuous air admission along flame tube, deriving governing equation from reaction kinetics
09 p1624 A69-22618

Airflow through open foam cellular structure, discussing mathematic model for predicting pressure buildup and foam response in shock and vibration isolation
[ASME PAPER 69-VIBR-46] 10 p1803 A69-24144

Book on aerodynamics of aircraft flight covering air flow, wing geometry, forces on wings, etc
11 p1817 A69-24583

Air flow distribution and wind velocities in cyclones constructed from Cosmos 122 TV cloud images
11 p1912 A69-24825

Statistical analysis of lee wave clouds from satellite TV pictures, determining lengths and air flow direction
11 p1912 A69-24828

Forced heat convection in steady turbulent air flow in circular cross sectioned tubes, noting laminar sublayer in wall regions
11 p2000 A69-25096

Fuel jet shape in air stream/mechanical atomization calculated as function of stream and fuel injection parameters
11 p2002 A69-25336

Gas turbine blade cooling by longitudinal air flow, discussing cooling efficiency of guide and impeller blades and blade ring
11 p1942 A69-25337

Supersonic air flow past blunt body of revolution in presence of nonequilibrium chemical reactions, ionization and molecular excitation
11 p1820 A69-25474

AIR INTAKES

Charged aerosols production for electrohydrodynamic processes by spraying liquids through capillary at high electric field strengths into high pressure air flows
12 p2138 A69-26631

Supersonic air flow around blunt body studied near critical line with allowance for viscosity, thermal conductivity and radiant energy transfer, assuming thermodynamic equilibrium
12 p2012 A69-26669

Velocity potential function for flow over disk shaped wing near screen, noting aerodynamic lift and drag
13 p2199 A69-27524

Multirecompression heater for pure airflow tests of ballistic vehicles and hypersonic aircraft
[AIAA PAPER 69-332] 13 p2242 A69-28268

Westerly air flow frequency decline resulting in lower seasonal temperatures, tabulating Lamb categories daily maximum and minimum temperatures
13 p2222 A69-28474

Heat transfer at gas flow stagnation point past blunt body under radiation from air layer in shock wave wake, using gray gas model
14 p2390 A69-29614

Finite difference method for turbulent mixing and combustion of hydrogen injected parallel to supersonic air stream, considering vitiated and unvitiated air
[AIAA PAPER 69-539] 16 p2777 A69-31844

Multiple function combination probe design for compressor and turbine air flow research
16 p2766 A69-31917

Radial blade tip clearance effect on isentropic efficiency and air delivery in axial flow compressor with allowance for casing deformations and rotor displacements
16 p2837 A69-32004

Shock tunnel facility generating short duration high velocity high density air flow with equilibrium chemical simulation of free stream flight conditions
[AIAA PAPER 68-17] 16 p2766 A69-32167

Planetary zonal flows hydrodynamic instability characteristics analysis, using quasi-geostrophic numerical model to study earth atmospheric cyclone wave role
17 p2960 A69-33149

Noise transmission from turbulent boundary layer through flexible plate into closed cavity, emphasizing nonlinear plate stiffness and mutual interaction between plate and airflow
17 p3006 A69-33409

Test facility to determine factors influencing aerodynamic energy dissipation of cantilever rods oscillating in airstream
17 p2947 A69-33928

Air resistance effect on transverse vibration damping of flat specimens of heat resistant alloy, duralumin, Ti, Mo and Nb
17 p2991 A69-33947

Aerodynamic energy dissipation during vibrations of bars in airstreams characterized by energy loss per cycle and logarithmic decrement
17 p3066 A69-33948

Normal and negative Magnus force experienced by rotating cylinder in air flow, discussing wind tunnel tests, laminar and turbulent boundary layers separation, pressure distribution, etc
17 p2958 A69-34213

Flow structure in wake of blunt bodies placed perpendicular in parallel airstream determined from hot-wire anemometry
[AIAA PAPER 69-746] 18 p3084 A69-34409

Ducted fan engine turbine air flow rate and frontal gas temperature determined from air temperature/pressure measurements behind compressor and engine fuel flow
18 p3086 A69-34986

Double knife-edged double-crossing schlieren apparatus analyzed for operation principle and applied to measure hypersonic wake characteristics in hotshot tunnel
19 p3293 A69-35740

Wall influence on thermoanemometer readings in incompressible air stream measured with wedge shaped film sensors
19 p3308 A69-35857

Nonequilibrium laminar boundary layer of dissociating air on axisymmetric body determined using concentration profiles of oxygen and nitrogen components
19 p3239 A69-36395

Cloud bank structure formation physical mechanism relationship with airflow using differential equations
20 p3569 A69-36985

Electron density distribution in laminar air boundary layer on sharp wedges and cones predicted by reducing

chemical kinetic model to ordinary differential equations
[AIAA PAPER 68-733] 20 p3458 A69-37181

Cloud physics problems of precipitation release from interaction of air motions and microphysical events, discussing raindrop growth initiation, artificial cloud modification, etc
20 p3572 A69-37906

Monograph on aerodynamic studies of effusion cooled turbine blades covering turbulent boundary layers, gas turbine performance, experimental design, etc
[AIAA PAPER 69-871] 21 p3786 A69-39867

Internal aerodynamics of centrifugal compressor impeller, discussing impeller channel airflow model, impeller exit flow, rotating channel flow, etc
[RAES PAPER 19] 22 p3859 A69-40498

Recirculation concept for air cushion vehicle air curtain evaluated by two dimensional and circular models, discussing optimum cushion area/jet exit area ratio
22 p3866 A69-40816

Heat transfer coefficient of turbulent air flow found independent of temperature head during cooling
22 p4051 A69-41026

Proportional fluid amplifiers analysis in cascade and with feedback by extended lumped parameter method, discussing dynamic characteristics of analog amplifiers with air
24 p4255 A69-43268

Molecular vibrational relaxation effect on dissociating airflow behind shock wavefront, giving relations to chemical reaction rates in diffusion approximation
24 p4302 A69-43486

AIR INTAKES

NT ENGINE INLETS

NT HYPERSONIC INLETS

NT SUPERSONIC INLETS

Engine air intake design and development for Concorde aircraft, discussing design constraints
[AIAA PAPER 67-752] 01 p0006 A69-11014

Wind tunnel pressure tests of Concorde air intake mockups in presence of aircraft wing and nose for Mach numbers 2, 2.2 and 2.35
03 p0361 A69-12879

Supersonic compressors for supersonic and subsonic air intakes, studying wave configuration at entry of circular cascade of blades with hydraulic analogy
[ONERA-TP-669] 05 p0699 A69-16340

Engine air intake for operational Harrier V/STOL strike/reconnaissance fighter, describing intake instrumentation ring, temperature and pressure probe development and pressure recording
05 p0767 A69-16673

Air intakes for fixed exhaust throat hypersonic ramjet engines, discussing configuration dependence on Mach number at beginning of combustion
[ONERA-TP-658] 07 p1203 A69-18418

V/STOL air intakes and jets simulation in wind tunnel tests, noting thrust simulation possibilities
11 p1866 A69-25431

AIR JETS

Heat transfer near stagnation point in axisymmetric turbulent jet impinging on circular disk
02 p0354 A69-12491

Air jet high temperature and low pressure influence on combustion stability in ramjet engine
03 p0531 A69-12968

Round air jet projected parallel to wall, analyzing velocity profiles, decay and growth rate
04 p0591 A69-15487

Heat transfer characteristics of single lines of circular air jets impinging on concave cylindrical surfaces, discussing nozzle target spacing effect
[ASME PAPER 68-WA/GT-1] 05 p0848 A69-16137

Jet perpendicular penetration prediction from holes or tubes, discussing resultant gas stream mixing and temperature profiles
[ASME PAPER 68-WA/GT-8] 05 p0750 A69-16143

Nickel structure alterations during interaction with high speed air flow at elevated temperatures
05 p0783 A69-16812

Soviet collection of papers on turbulent jets of air, plasma and real gas
07 p1049 A69-18392

Thin jet-flapped airfoil flow analysis in ground proximity at small angle of incidence, assuming inviscid incompressible flow
09 p1431 A69-22275

Tangential air jet for separation control of two dimensional incompressible flow along circular cylindrical wall
09 p1431 A69-22277

Turbulent circular wall air jet trajectory and spreading in perpendicular crossflow of constant and varying velocities
[ASME PAPER 69-GT-33] 09 p1483 A69-22491

Air powered fluid jet engine compressor bleed control stressing closing, reset and override operations
[ASME PAPER 69-GT-19] 09 p1571 A69-22498

Surface heat transfer coefficients under perforated plate of multiple square array round impinging air jets
[ASME PAPER 69-GT-4] 09 p1624 A69-22508

Cavity formation on water and wet cement surfaces by impingement of axisymmetric air jet noting cavity shape, depth and diameter
11 p1869 A69-24888

Ingestion and flow field characteristics of interaction of two heated parallel air jets, discussing VTOL exhaust ingestion tests
[AIAA PAPER 68-79] 12 p2012 A69-26761

Ambient air pressure effects on fatigue crack growth rate in strain hardened aluminum
13 p2276 A69-27393

Air-hydrogen supersonic mixing and combustion, characterizing hot hydrogen jet discharging into supersonic concentric air stream at atmospheric pressure
[AIAA PAPER 69-339] 13 p2378 A69-28275

Airstream parameters /temperature and velocity/ of turbulence intensity in jet core at tube exit and behind grids measured by He diffusion method
16 p2771 A69-31959

Ejector driven wind tunnel for turbulent flow generation with arbitrary velocity profile, using jet arrays
[AIAA PAPER 69-743] 18 p3114 A69-34408

Subsonic and supersonic turbulent air jets expansion over perpendicularly positioned plane disk obstacle, deriving equations for pressure distribution and stagnation temperature
18 p3123 A69-34990

Forced and periodic motion of air or water jets impinging in double input vortex chamber described in terms of oscillator deriving energy from hydrodynamic instability
[ASME PAPER 69-FLCS-19] 20 p3465 A69-37981

Integral relations method applied to air jet flow along cylinder with boundary layer control by suction or blowing
21 p3698 A69-39845

AIR LAUNCHING

Air launched sounding rockets design, development and testing noting aerodynamic loading and surface, propulsion unit, cost effectiveness, etc
21 p3820 A69-39218

AIR LOCKS

Expandable D 21 airlock scheduled for testing on NASA Orbital Workshop Flight based on elastic materials technique, noting more complex chemically rigidized concept
[IAF PAPER SD-49] 02 p0334 A69-11949

Portable multiunit low pressure chamber with locks, permitting water replenishment, feeding of animals under continuous pressure and gas mixtures
22 p3891 A69-40217

AIR MASSES

Thermodynamics of nonadiabatic vertical ascent of overheated individual air volumes in stably stratified atmosphere
02 p0274 A69-11441

Group invariant solutions of differential equation systems applied to quasi-linear partial differential equations of motion of air masses
02 p0274 A69-11444

Air mass cumulus cloud growth stimulation by means of vertical updrafts capable of perforation of retaining layers
03 p0461 A69-13409

Telluric lines halfwidth and depth dependence on observation point altitude and intervening air mass, determining absorption line contours for isothermal atmosphere
03 p0512 A69-13695

Air mass displacements and diurnal variations in potential temperature at tropopause level
13 p2252 A69-27608

Air mass analysis, discussing homogeneity, quasi-barotropic fluids, noise elimination to arrive at smooth flow pattern, etc
15 p2647 A69-30193

Air masses transformation, solving nonlinear simultaneous system of equations of motion, heat influx and turbulent energy balance
15 p2649 A69-30647

Nocturnal development of air mass stratus clouds in Texas and mechanism of formation, discussing turbulent mixing theory
15 p2649 A69-30893

Lagrangian solution for air mass element trajectory in free atmosphere using vortex invariant, noting application to atmospheric transport of contamination 16 p2805 A69-31611

Lateral mixing of air masses in jet stream by water fluid model experiments, discussing steady and non-steady state turbulent momentum exchange 17 p3000 A69-33759

Mean patterns of meridional interhemispheric flow for 40 degree equatorial sector, calculating mean air mass transport in lower troposphere over western Indian Ocean 18 p3166 A69-34420

Solar constant and spectral irradiance curve for zero air mass obtained from aircraft measurements 23 p4216 A69-42191

Cloud cover forms in circulatory-climatic zones of earth based on Zond 5 picture analysis, discussing air-mass exchanges and motions direction 23 p4184 A69-42486

Radiation contribution to large scale atmospheric mass circulation simulation, considering short wave radiation, temperature variations, exponential and aerosol attenuation 23 p4184 A69-42487

AIR NAVIGATION

NT ALL-WEATHER AIR NAVIGATION
NT TACAN

Navigational instruments developments during past fifty years emphasizing land, marine and air navigation aids 01 p0112 A69-10311

Airline area navigation system functions for developing map type pictorial display system including digital computer, cockpit control unit and microfilm charts 01 p0112 A69-10453

Navigation Service Satellite System for aiding aircraft and ships at sea in Pacific Ocean, noting equipment and functions [UN PAPER 68-95251] 01 p0112 A69-10470

Space techniques for application to civil aviation, discussing air to ground communications, air traffic monitoring and navigation and weather forecasting by satellite [UN PAPER 68-95349] 01 p0179 A69-10490

Aircraft navigation using synchronous satellites based on position location by intersection of two circles with centers below satellites 01 p0114 A69-11011

Vertical flight path navigation requirements for supersonic aircraft based on computer simulated flights of Mach 2 Concorde 02 p0277 A69-11590

Great circle route determination based on celestial spherical triangulation 02 p0278 A69-12360

Transatlantic aircraft cross-track air navigation error reducible by augmenting Doppler system with satellite ranging system 03 p0464 A69-13237

Navigational and tactical data with correlative map information provided on single CRT display in aircraft, storing map data on video tape 03 p0464 A69-13246

Navigation computer utilizing current integrators and step motors to record flight path 03 p0404 A69-13431

STOL and VTOL aircraft characteristics in operation, considering impact on terminal navigation and air traffic control [SAE PAPER 680666] 03 p0465 A69-13452

ASTRE programming language applicability to maximum memory information treatment in aerial navigation 03 p0401 A69-14180

Aerial navigation regulation and international law, discussing 1944 Chicago convention for international cooperation 05 p0849 A69-15681

Area navigation implementable by airborne course line computers, pictorial displays, Doppler radars and inertial platforms for use in ATC systems 05 p0790 A69-16720

Dioscures system for international air traffic control and navigation over North Atlantic by means of two geostationary satellites [UN PAPER 68-95832] 06 p0954 A69-17063

Air navigation and economics, discussing air traffic control and traffic density effects on fuel consumption and engine life 07 p1052 A69-18661

Aircraft communications, navigation and identification, discussing role of satellites, common waveform modulation and electronics technology 07 p1085 A69-19178

Sensor data acquisition and processing and required levels of navigation integration for increasing air space capacity 07 p1177 A69-19211

Most probable position (MPP) choosing methods accuracy, investigating relative effects of dead reckoning (DR) and celestial lines of position (LOP) errors 07 p1177 A69-19214

Airborne area navigational capability achieved by course line computer processing VOR information 07 p1178 A69-19763

Air traffic development related to control systems advances, discussing telecommunications effect and radio navigation systems enabling pilot to determine position 08 p1347 A69-20598

Long range subsonic transport navigation systems accounting for reductions in horizontal separation on high density oceanic routes 08 p1348 A69-21062

Optimum integration of aircraft equipment, subsystems and computer mechanizations for low cost navigation system consistent with mission requirements 08 p1348 A69-21065

National plan for air navigation covering R and D and operational aspects 08 p1348 A69-21192

Satellite navigation system feasibility for accurate and continuous navigation capability for Army tactical aircraft 08 p1349 A69-21193

Integrated inertial aircraft navigation with velocity and position aids, discussing in-flight calibration capabilities, performance under quick-reaction constraints and digital simulation results 08 p1349 A69-21196

Marine and aircraft satellite navigation techniques, discussing equipment requirements, related performance characteristics and limitations 08 p1349 A69-21198

Range difference air navigation equations solution, discussing error updating of satellite position and constellation geometry 09 p1538 A69-21996

Subjective and objective upper air forecasts compared for error analysis of headwinds, noting influence of geographical location 09 p1536 A69-22074

International air traffic regulations for reciprocity and conventions between contracting states 09 p1626 A69-22092

Navigation accuracy and telecommunications system capacity interrelationships in economical improvement of air traffic control system over North Atlantic 10 p1723 A69-23704

VOR/DME ground facilities accuracy improvement by complementing navigation computation with signals from inertial navigation system [SAE PAPER 690338] 11 p1914 A69-24499

Monograph on computer aided air traffic control systems design, discussing air navigation, man-machine relations, equipment requirements, programs, plan position color display, etc 11 p1914 A69-25085

Pure inertial navigation system support by supplying additional or redundant navigational information, considering space flight applications and earth related problems 12 p2128 A69-25873

Soviet book on radio navigation of flight vehicles covering systems classification, operational characteristics, satellite navigation, etc 12 p2129 A69-27076

Hyperbolic marine and air navigation including TACAN, pulse modulation, rotating hyperbolic fields, sector beacons and all-weather landing aids 13 p2296 A69-27334

Pictorial display techniques aiding air traffic and aircraft control, discussing projection and directly viewed display 13 p2296 A69-27335

Navy Navigation Satellite System (NAVSAT) applications, considering nonmilitary marine and air all-weather navigation and positioning 14 p2479 A69-29856

National plan for air navigation covering R and D and operational aspects 14 p2480 A69-29858

Optimal navigation system for supersonic Concorde aircraft, discussing in-flight and terminal navigation methods 14 p2480 A69-29859

Aircraft constant altitude-pressure flight navigation attained using Bellamy formula and loxodromic route for drift compensation 15 p2651 A69-30294

Bearing errors from radio beacons with rotating or multilobe radiation patterns 15 p2567 A69-30343

Dioscures project for telecommunication, ATC and navigation by satellites to provide continuous position determination 15 p2651 A69-30691

Doppler and inertial self contained systems for long range navigation, considering air traffic control separation standards 15 p2651 A69-31544

North Atlantic aircraft navigation and traffic control system using satellites 16 p2809 A69-32054

Airborne digital computer and display devices role in navigation management, discussing data processing and hybrid navigation systems 16 p2809 A69-32260

Aircraft electromagnetic position finding system based on Doppler shift of CW carriers 17 p3002 A69-34078

Navigation and guidance systems for low altitude aircraft flight safety noting position determination, cockpit environment and fail-safe operation 17 p3002 A69-34080

Collection of articles on avionics navigation systems covering navigation equations, airborne digital and analog computers, radio, Doppler and inertial navigation, etc 18 p3168 A69-34843

Reliability and component relationships of aircraft navigation systems, describing dead reckoning, position fixing, guidance and vertical navigation 18 p3168 A69-34844

Inertial aircraft navigation, describing instruments and error analyses with regard to simulation, error propagation and total system error 18 p3169 A69-34850

Attitude and heading reference devices for aircraft navigation, describing instruments, gyroscopes and gravity sensors 18 p3169 A69-34853

Situation displays and flight instrument development including head-up, vertical tape and map systems 18 p3170 A69-34858

Inertial navigation systems technology, discussing man machine dialog, alignment, etc 19 p3371 A69-36703

IR equipment to aid air navigation, discussing detection cells, temperature direction finding, mobile source tracking, etc 19 p3371 A69-36705

Subsonic civil air transport navigation systems, discussing flight routes redistribution across North Atlantic to meet increased traffic 20 p3574 A69-37417

Guidance and navigation flight tests, demonstrating system performance improvements by onboard inertial system communicating with external navigation aid [AIAA PAPER 69-842] 21 p3765 A69-39429

Moving map pictorial display system for on board capability of area navigation, noting crew reaction [SAE PAPER 690393] 23 p4186 A69-41663

Maritime navigation hyperbolic charts for aircraft position determination 23 p4186 A69-42026

Optimum integration of aircraft equipment, subsystems and computer mechanizations for low cost navigation system consistent with mission requirements 23 p4186 A69-42538

Omega aircraft navigation, discussing digital computer applications, SNR environment, carrier interference and accuracy requirements for signal reception 23 p4186 A69-42539

Aircraft navigation by geostationary satellites, discussing Dioscures project 24 p4280 A69-42568

Illumination effect on air navigation chart reading during flight, using questionnaire data 24 p4271 A69-42605

Surface and aerospace navigation by VLF radio network, discussing Omega transmitting station location, operational modes and daytime-nighttime accuracies [AAS PAPER 69-405] 24 p4347 A69-42834

AIR POLLUTION

Jet engine exhaust composition and methods for reducing smoke emission through burner design changes, noting primary zone fuel and airflow pattern [SAE PAPER 680348] 03 p0495 A69-13350

Control methods and designs for limiting atmospheric pollution emitted by aircraft gas turbine engines [SAE PAPER 680347] 07 p1204 A69-19729

Pollution control forecast, contamination control specialist and systems approach 08 p1265 A69-19808

Exchange coefficient of energy balance of earth surface for propagation studies of entrained atmospheric contaminants 09 p1535 A69-21514

Control methods and designs for limiting atmospheric pollution emitted by aircraft gas turbine engines 12 p2147 A69-26236

Correlation spectrometer for air pollution surveillance from airborne and spaceborne platforms, noting scanning satellite system for continuous global coverage 12 p2096 A69-26981

Vitiated air contamination effects on combustion and hypersonic air breathing engine ground tests [AIAA PAPER 69-338] 13 p2325 A69-28274

Remote optical heterodyne measurement of Doppler shift as method for determining vector wind velocity, noting influence of air pollution 14 p2448 A69-29523

Lagrangian solution for air mass element trajectory in free atmosphere using vortex invariant, noting application to atmospheric transport of contamination 16 p2805 A69-31611

Atmospheric aerosols influence on electric field in ground layer to account for ionization, demonstrating number and turbulent exchange coefficient relationship 17 p2996 A69-33036

Vitiated contamination effect on airbreathing engine ground testing, considering equilibrium, vibrational and chemical relaxation, condensation, combustion, mixing and engine performance [AIAA PAPER 69-456] 19 p3448 A69-36333

Airborne correlation spectrometer for air pollution remote sensing, describing applications [RAES PAPER 7] 22 p3896 A69-40488

Sulfur dioxide, nitrogen dioxide and Aitken nuclei washout by artificial rain of known intensity and droplet size distribution 24 p4345 A69-43146

Mixing spread of hydrogen plumes and air pollutants exhausted into open atmosphere, predicting subsonic free round jets air entrainment 24 p4300 A69-43257

AIR SAMPLING

Extraterrestrial life detection methods based on soil or atmospheric sampling, discussing enzyme activity, DNA determination, microbial growth, etc 01 p0021 A69-11093

Control and sampling in sterile rooms, noting worker introduction of contaminants 05 p0714 A69-15953

Stratospheric air sampling reliability instrumentation as part of radioactivity fallout detection program 05 p0766 A69-16751

AIR TO AIR MISSILES

Onboard radar for light interceptor aircraft /Aida III/, discussing navigation, low altitude penetration and air to air missile interception 19 p3278 A69-36701

Thermal protection for air-launched missile electronics during carry and free flight, considering active, passive and combination systems and weight penalties 22 p4049 A69-39943

AIR TO SURFACE MISSILES

Kormoran airborne missile weapon system for attacking sea-going targets, discussing navigation guidance, radar tracking and homing system 17 p3050 A69-33697

Thermal protection for air-launched missile electronics during carry and free flight, considering active, passive and combination systems and weight penalties 22 p4049 A69-39943

AIR TRAFFIC

Air cargo traffic increase, discussing technical and economical prospects, use of intermodal containers and transportation automation tendency 01 p0008 A69-10030

Ship and aircraft traffic conditions in Japan and neighboring areas and requirements for navigation satellite system [UN PAPER 68-95226] 01 p0113 A69-10520

Air traffic prediction based on mathematical econometric methods 03 p0536 A69-14105

Passenger aircraft design to cope with air traffic volume increase in 1970s, discussing economic aspects of high capacity aircraft 04 p0546 A69-14804

Elasticity of demand theory applied to fare changes effect on passenger volume, noting interdependence of aircraft size and fare formulation 04 p0689 A69-14805

Fitting airport interfaces to air traffic, considering bottleneck elimination 05 p0742 A69-15918

Aeronautic electronics - Conference, Washington, D.C., September 1968 05 p0789 A69-16716

V/STOL operations in intercity and intracity service, discussing technical feasibility and need for steep approach instrument landing system 05 p0703 A69-16723

STOL and V/STOL role in eliminating air traffic congestion at U.S. and West European airports and in short haul and municipal routes 08 p1254 A69-20093

Mathematical models for outgoing traffic flow in airport terminal used for determining service requirements 09 p1476 A69-21439

Complex climatological cloud profiles structural characteristics along given air traffic routes prepared for practical aviation problems 12 p2127 A69-26899

U.S.-Europe air traffic, attributing European lag to dense air route duplication, load factors, etc 13 p2381 A69-27338

Air transportation problems in connection with rapid aviation growth noting crisis in near future 15 p2720 A69-30588

Ground facilities long term planning, considering factors to determine air transport growth and changing commercial aviation pattern 16 p2766 A69-32020

Gate arrival approach to Kansas City airport terminal planning for facilities and operations decentralization, congestion reduction and passenger walk distance minimization 16 p2766 A69-32327

Space criteria for aircraft parking positions noting radial wedges configuration 16 p2766 A69-32328

Space requirements of departure lounges in airport buildings for large aircraft loading, discussing entry doors, boarding times, etc 16 p2766 A69-32330

Los Angeles International Airport development planning, discussing airfield improvement, tunnel reconstruction, terminal layouts, parking, roads and access, etc [AIAA PAPER 69-806] 19 p3288 A69-35590

Air terminals plans for 1975 aircraft and air traffic based on runway configurations [AIAA PAPER 69-805] 19 p3288 A69-35591

Problems caused by air traffic rate growth in London Terminal area, examining runway limits, safety and noise restrictions 19 p3371 A69-36736

STOL aircraft to serve traffic needs of northeast corridor, discussing decision making regarding size, type, cost, speed and strip-length 20 p3462 A69-37352

Air passenger traffic growth to 1980 in major sectors of air transport industry, emphasizing traffic volumes 22 p4052 A69-40425

Air cargo traffic, discussing payload lots, aircraft types suitable for freight transport, difficulties and solution 22 p4052 A69-40426

Civil cargo aircraft characteristics and development trends, discussing cargo and passenger traffic management, communications network, etc 22 p3863 A69-40427

Air traffic problems due to tourism, suggesting service modifications to meet future needs 22 p4053 A69-40434

Planning for safety of future supersonic air traffic including financing and coordination activity of government and industry 22 p4054 A69-41131

Air traffic safety enhanced through flight crew awareness of hazards, clear air turbulence detection and avoidance, collision avoidance, etc 22 p3868 A69-41151

Air traffic growth forecasting, describing various mathematical econometric models [AAS PAPER 69-329] 24 p4417 A69-42807

AIR TRAFFIC CONTROL NT RADAR APPROACH CONTROL

Space techniques for application to civil aviation, discussing air to ground communications, air traffic monitoring and navigation and weather forecasting by satellite [UN PAPER 68-95349] 01 p0179 A69-10490

Satellites and ocean platforms for civil aviation operations over North Atlantic, noting cost justification dependence on supersonic traffic increase [UN PAPER 68-95887] 01 p0113 A69-10521

Air traffic control at Los Angeles International Airport, discussing simultaneous parallel ILS approaches and departures and STOL problems 01 p0057 A69-11356

Interim radar improvement program for air route traffic control centers pending development of automated terminal radar programs 01 p0114 A69-11357

Satellite monitoring application to air traffic control in parallel track system, discussing lateral and longitudinal separation control 02 p0277 A69-11591

Navigation by satellite systems, discussing vehicle position determination and communications link for traffic control with comment on French space program 02 p0278 A69-11912

Avionics technology and systems for future SST aircraft noting improved air traffic control systems 02 p0279 A69-12364

SPOT /Speed, Position and Track/ transoceanic traffic surveillance and navigation system for aircraft and marine users 03 p0463 A69-13234

Transoceanic air traffic control system with independent surveillance of aircraft positions, decision making agency and undelayed communications, using satellites 03 p0464 A69-13236

International satellite system for commercial aircraft communications and air traffic control 03 p0464 A69-13238

STOL and VTOL aircraft characteristics in operation, considering impact on terminal navigation and air traffic control [SAE PAPER 680666] 03 p0465 A69-13452

Application satellites for air traffic control, meteorology and earth resources, considering European participation 03 p0520 A69-13587

Telecommunications network for air traffic in Central America to attain higher degree of reliability 03 p0399 A69-14182

Simulation design of multiprocessing system to provide air traffic control capabilities through use of real time operations 04 p0629 A69-15365

FAA coded broadcasting to transponder equipped aircraft for air traffic control, navigation, collision avoidance and airfield approach 04 p0629 A69-15478

Integrated guidance and traffic control system to handle VTOL traffic in Northeast Corridor 05 p0789 A69-15560

FAA research and development responsibility to National Airspace System, examining programs for ATC automation, solid state technology application, communications, etc 05 p0850 A69-16717

Air traffic control /ATC/ automation, discussing display, data acquisition, automated radar terminal systems /ARTS/, etc 05 p0790 A69-16719

Area navigation implementable by airborne course line computers, pictorial displays, Doppler radars and inertial platforms for use in ATC systems 05 p0790 A69-16720

Digital communications between aircraft and flow control computers on ground to avoid runway saturation and automating routing functions 05 p0721 A69-16722

Government role in air transportation policy, considering growing demands on air traffic control 06 p1040 A69-16835

International problems of air traffic control, discussing legal and political basis for organization and ATC liability 06 p1042 A69-16846

Automatic air traffic control systems design, development and application to civil and military aviation 06 p0955 A69-17858

Aircraft traffic control with cockpit self sufficiency for accurate and reliable navigation capability, discussing radar vector navigation and communication 07 p1177 A69-19210

Sensor data acquisition and processing and required levels of navigation integration for increasing air space capacity

07 p1177 A69-19211

Navigation satellites system designed for ATC without requirement for onboard transmitter, discussing spectrum occupancy, satellite power, lane ambiguities and computational procedures

07 p1177 A69-19212

Aircraft position and velocity in directions normal to ILS reference path by correlation with inertial navigation system, noting minimal time controller

07 p1177 A69-19213

Qualitative V/STOL air traffic control requirements, discussing airborne and ground data, procedures and equipment categories

[AIAA PAPER 69-211] 07 p1177 A69-19552

Optimum approach and departure paths for VTOL aircraft simulated by hybrid computer under constraints

[AIAA PAPER 69-209] 07 p1178 A69-19570

Aircraft separation standards, considering separate space for VTOL in automated high density airways system

[AIAA PAPER 69-210] 07 p1178 A69-19579

Air traffic development related to control systems advances, discussing telecommunications effect and radio navigation systems enabling pilot to determine position

08 p1347 A69-20598

Monograph on mathematical model for aircraft separation in air traffic safety control, analyzing aircraft motions and collision avoidance

08 p1347 A69-20712

Project Dioscures for permanent air traffic control centers, positive telecommunication links and satellite navigation

08 p1347 A69-20779

Control and recording device for parameters and information relating to takeoff and landing, using detection elements and cross wire on runway

08 p1347 A69-20780

Vector analog computer functions and applications in air traffic control, discussing area navigation equipped aircraft

08 p1349 A69-21195

Air traffic lateral separation assurance over North Atlantic for increased routes capacity without safety reduction

08 p1349 A69-21200

Radio location system based on measuring distance between object and two stationary satellites, noting application to air traffic over North Atlantic

09 p1537 A69-21269

Transponder design with planar triode for aircraft identification and air traffic control

09 p1462 A69-21411

Alphanumeric characters to identify radar targets on PPI display for air traffic control, considering technique for reducing smear

09 p1495 A69-21675

Navigation accuracy and telecommunications system capacity interrelationships in economical improvement of air traffic control system over North Atlantic

10 p1723 A69-23704

Secondary radar for air traffic control automation in France, discussing onboard equipment

10 p1723 A69-23705

Monograph on computer aided air traffic control systems design, discussing air navigation, man-machine relations, equipment requirements, programs, plan position color display, etc

11 p1914 A69-25085

Visual simulation for critical maneuvers of aircraft takeoff and landing, noting method based on limited corridor simulation and maneuver freedom

[AIAA PAPER 68-255] 11 p1866 A69-25376

Designs and capabilities of digital processing systems for automatic air traffic control radar information stressing future use of display for computerized control

13 p2295 A69-27332

Pictorial display techniques aiding air traffic and aircraft control, discussing projection and directly viewed display

13 p2296 A69-27335

Satellite networks for air traffic control and aircraft communications in North Atlantic

13 p2296 A69-27831

Aircraft noise control at source through high bypass ratio engine modification, FAA decibel standards and higher capacity aircraft for increased traffic density

14 p2509 A69-29156

Computer uses for air traffic control in Germany including flight plans and weather report data processing

15 p2650 A69-30230

Air lane longitudinal separation distance reduction for accommodating increased traffic using airborne computers for single file system

15 p2651 A69-30293

Airport problems in increasing air traffic, discussing passenger delays, runway capacity, instrument controlled takeoff and landing, fog dispersal, baggage flow, etc

15 p2589 A69-30589

Dioscures project for telecommunication, ATC and navigation by satellites to provide continuous position determination

15 p2651 A69-30691

Primary-secondary radar /SECAR/ integration for air traffic control, discussing problems of simultaneous display, transmission synchronization, signal multiplexing, etc

15 p2570 A69-31222

Economics of airport use, congestion and safety, discussing differentiated pricing systems

15 p2723 A69-31241

Secondary radar system chosen by EUROCONTROL Agency for civil air traffic control at Shannon and Brussels airports

15 p2571 A69-31501

Doppler and inertial self contained systems for long range navigation, considering air traffic control separation standards

15 p2651 A69-31544

Dioscures project for worldwide telecommunications, air traffic control and navigation by satellites, discussing technical, operational and economic characteristics

16 p2749 A69-31601

North Atlantic aircraft navigation and traffic control system using satellites

16 p2809 A69-32054

CAB decisions regarding subsidy reduction, carrier mergers, and dense route certification requiring improved clarity and timeliness

16 p2882 A69-32336

Color signal light gun for aircraft control at airport towers, noting pilot tests for familiarity with signal code

17 p2914 A69-33185

Terminal area navigation and landing guidance systems for V/STOL intercity transport aircraft, considering radio guidance, aircraft control and system interaction

17 p2897 A69-33210

Tacan navigation system developments including data transmission, links to airborne computers and air traffic control transponders

17 p3003 A69-34101

Experimental SST terminal for satellite L band communications/surveillance ATC system, establishing terminal requirements for NASA and FAA studies

17 p2932 A69-34118

Future navigation systems and ATC, discussing traffic flow factors and approach and landing systems

17 p3004 A69-34201

Air traffic control and airline operators liaison with reference to air transport priorities, considering relationship to aircraft and airport development

17 p3004 A69-34204

All-weather operations, aircraft size, air traffic and noise as airport design factors, discussing financing priorities for runway construction, facilities and personnel

17 p3004 A69-34207

Air traffic control/electronics automation developments and controllers responsibilities in Great Britain and Netherlands

18 p3168 A69-34805

Air traffic control ground equipment developments including radio direction finders, surveillance radar, interconsole marking, etc

18 p3168 A69-34806

Air traffic control, discussing objectives, governmental responsibilities and airspace organization, including U.S. system

18 p3170 A69-34859

Satellite systems for air traffic control, navigation, communications and telemetry in view of regulations of frequency allocations

18 p3103 A69-35089

Airport alternate facilities, restrictive flight schedules and fee schedules for relieving airport congestion during peak traffic hours

[AIAA PAPER 69-820] 19 p3453 A69-35595

Pictorial display area navigation system for air traffic control in terms of cockpit utilization, interface with ground navigation aids, parallel multiple routes, etc

[AIAA PAPER 69-798] 19 p3367 A69-35632

Time/frequency technology using time-ordered reporting digital data for air traffic control to avoid airborne collision

[AIAA PAPER 69-795] 19 p3367 A69-35635

FAA ARTS-III terminal air traffic control system reliability and maintainability, discussing module addition

19 p3370 A69-36000

Computerized clock sequenced ATC system, area navigation /R Nav/ systems and STOL flight control

19 p3370 A69-36317

Supersonic transport aircraft impact on air traffic control in Eurocontrol area, discussing climb, acceleration, cruise and descent

19 p3370 A69-36653

Eurocontrol Experimental Data Processor for automation in air traffic control, discussing system size configuration and environment

19 p3280 A69-36654

Transport aircraft automatic altitude transmission requirements, discussing altimeter-transponder radar system to aid air traffic control

19 p3371 A69-36700

Airborne collision avoidance system based on time-frequency techniques for use within ground based control systems, showing air/ground synchronization and collision geometry

19 p3371 A69-36735

Short haul air transportation traffic congestion problems in Northeast corridor, emphasizing STOL solution for economy

19 p3248 A69-36865

ATC systems analysis including airports, ground access and air transportation

19 p3371 A69-36866

Terminal air traffic management in future noting transition airspace, approach and departure paths and airport capacity

[AIAA PAPER 68-1101] 20 p3573 A69-37160

Subsonic civil air transport navigation systems, discussing flight routes redistribution across North Atlantic to meet increased traffic

20 p3574 A69-37417

ATC medium range radar /SRE-LL1/, describing reflectors positions, information rate, installation, antenna parameters, etc

20 p3496 A69-37932

Radar digital processing and display system for air traffic control with IC central processor and discrete data transmission over telephone lines from remote sites

21 p3760 A69-38328

STOL airline operation test programs involving aircraft, navigation equipment, systems and ATC

21 p3646 A69-38731

Correlation protected ILS implementing conventional ILS with no operational restrictions on air traffic control, taking into account changing terminal conditions

22 p3978 A69-39963

Air traffic systems and diminishing airspace capacity problems requiring additional airport facilities and STOL aircraft

22 p3925 A69-40428

Air traffic control transoceanic satellite system for minimizing navigation errors forcing wide separations, providing VHF voice communication and position surveillance

22 p3901 A69-41147

Air traffic interfaces of VTOL, STOL and CTOL aircraft serving same metropolitan terminal, emphasizing navigation systems, geographical positions, ground communication, etc

[SAE PAPER 690422] 23 p4185 A69-41646

Airline area navigation test programs involving use of VOR/DME signals and inertial navigation system within air traffic control system

23 p4185 A69-41662

Human factors in air traffic control, considering personnel, equipment, environmental and social factors

23 p4108 A69-41828

Short range aviation terminal weather predictions concerning runway visual range, cloud-base height and wind, using FAA mesometeorological network

24 p4342 A69-42892

AIR TRANSPORTATION

Air freight transport development, characteristics and economics

02 p0356 A69-11888

Air cushion landing gear in civil air transport, discussing system concept, advantages and LA 4 aircraft experimental application

02 p0193 A69-12690

Business jet aircraft use for air transport pilot training instead of simulating devices, noting pilot cabins
03 p0366 A69-13643

1967 yearbook on air and space travel covering airbus, astronautics, V/STOL, aerodynamics, flight mechanics, simulation and aeroelasticity
04 p0545 A69-14801

French air transport and airports covering aviation enterprises, air traffic density, airport activities, traffic flow, etc
04 p0689 A69-15479

Subsonic aircraft potential for short haul transportation, discussing technical problems
05 p0701 A69-15559

Fitting airport interfaces to air traffic, considering bottleneck elimination
05 p0742 A69-15918

Government role in air transportation policy, considering growing demands on air traffic control
06 p1040 A69-16835

LR-1 prototype design criteria and flight testing, discussing Model 99 airliners for commuter airlines
06 p0867 A69-17668

Future commercial VTOL transportation, considering technical, political and socio-economic problems [AIAA PAPER 69-198]
07 p1056 A69-19567

STOL and V/STOL role in eliminating air traffic congestion at U.S. and West European airports and in short haul and municipal routes
08 p1254 A69-20093

Single stage rocket vehicle design for rapid global air transportation noting size, range and economics
09 p1433 A69-21303

Airport evolution in London, discussing transportation, safety, international trade, economics, aircraft types and noise spectra
09 p1479 A69-22582

V/STOL aircraft future, discussing Federal Government policies, economics, airport planning, engineering problems, etc
10 p1811 A69-23221

Airport operation and administration, discussing supply, costs, tariffs, etc
10 p1811 A69-23602

Air carrier liability for nuclear weapons damage, discussing international agreements
11 p2003 A69-24260

Supersonic transport airline operations including safety, noise, traffic control, routing, etc
11 p2004 A69-24373

Multiengine helicopter scheduled passenger service operations in Europe
11 p2004 A69-24378

Air transport prediction for West Europe by 1980
11 p2004 A69-25216

V/STOL aircraft in commercial aviation, discussing costs, noise reduction, propulsion systems, projected routes, etc
13 p2203 A69-28039

FAA additional airworthiness standards for small aircraft in air taxi and commercial operations, noting safety levels [SAE PAPER 690320]
15 p2549 A69-30090

Space flight cost analysis, relative costs of various types of transportation and need for reusable single stage to orbit vehicles
15 p2719 A69-30186

Air transport industry safety record and variable stability research planes to simulate aircraft airborne behavior and handling qualities
15 p2558 A69-30453

Air transportation problems in connection with rapid aviation growth noting crisis in near future
15 p2720 A69-30588

Airport problems in increasing air traffic, discussing passenger delays, runway capacity, instrument controlled takeoff and landing, fog dispersal, baggage flow, etc
15 p2589 A69-30589

Book on competition in North Atlantic commercial air transport covering passengers, freight and mail from supply, demand and market point of view
16 p2881 A69-31866

Aircraft role in future transport systems for passengers and goods, emphasizing shorter distances, intercity and interurban communication, etc
16 p2881 A69-31932

Ground facilities long term planning, considering factors to determine air transport growth and changing commercial aviation pattern
16 p2766 A69-32020

Civil aircraft requirements from 1975 onward, discussing classes, categories and R and D
16 p2882 A69-32022

Airport planning, discussing air transportation and city planning problems for Hannover air terminal
16 p2882 A69-32329

Long distance air flights through different time zones, discussing circadian physiological cycles, light-dark ratio shifts effects and methods of lessening desynchronization effects
16 p2745 A69-32444

Short range transport - Royal Aeronautical Society Conference, London, May 1969
17 p2897 A69-33206

Air transport systems aspects including efficiency, performance and economics interplay for subsonic and supersonic aircraft
17 p3018 A69-33218

Skyvan 3 light passenger/freight carrier design, detailing power plant, installation and power management
17 p2902 A69-34192

Air traffic control and airline operators liaison with reference to air transport priorities, considering relationship to aircraft and airport development
17 p3004 A69-34204

Air travel and population growth requiring larger structures for office buildings, airport passenger terminals and aircraft servicing facilities [AIAA PAPER 69-809]
19 p3289 A69-35622

General aviation missions in national transportation system /1968, 1975, 1980/, considering fuel taxes, overall system economics, ground facilities, etc [AIAA PAPER 69-818]
19 p3453 A69-35624

Article 8 /I/ of Carriage by Air Act, 1932 compared to Warsaw Convention Article 8 /I/, noting definition of legal liability of carrier
19 p3455 A69-36331

Air transport development relationship to city regional planning, including analysis of Heathrow airport design
19 p3296 A69-36850

Short haul air transportation traffic congestion problems in Northeast corridor, emphasizing STOL solution for economy
19 p3248 A69-36865

ATC systems analysis including airports, ground access and air transportation
19 p3371 A69-36866

VSTOL and conventional transport aircraft compared for short haul air transport services
20 p3461 A69-37281

Subsonic civil air transport navigation systems, discussing flight routes redistribution across North Atlantic to meet increased traffic
20 p3574 A69-37417

Electronic stethoscopes for use in high background noise environments for patients on air evacuation flights
21 p3667 A69-39444

Commercial supersonic and subsonic air traffic growth forecast
22 p3862 A69-39934

Air passenger traffic growth to 1980 in major sectors of air transport industry, emphasizing traffic volumes
22 p4052 A69-40425

VTOL, STOL and CTOL transportation systems cost effectiveness comparison for Northeast Corridor operation, considering ground facilities, access time, etc [SAE PAPER 690417]
23 p4147 A69-41642

Compound helicopter transport for short haul transportation system for Northeast Corridor, discussing terminals near origin and destination, takeoff and landing patterns, etc [SAE PAPER 690419]
23 p4062 A69-41643

STOL program in Northeast Corridor demonstrating significant city-to-city block time reduction by STOL transportation system [SAE PAPER 690420]
23 p4185 A69-41644

Patient transportation and evacuation system at disposal of Paris hospital, using short and long haul aircraft, turbojets and helicopters
23 p4105 A69-41785

Jumbo jet role in air transportation, discussing future traffic growth, pilot problems and aircraft size limitations
23 p4063 A69-41819

Intercity air transportation compared with automobile and train travel, attributing air travel dead time to ground route and airspace congestion
24 p4416 A69-42561

VTOL transport aircraft to solve short haul travel problems, examining lateral and horizontal maneuvering and vertical to horizontal flight transition
24 p4250 A69-42564

Air evacuation of maxilla-facially wounded persons from place of accident, noting helicopter use
24 p4270 A69-42603

Algorithm for aeromedical airlift system stop selection and sequencing, minimizing patient in-system time and aircraft flight distance [AAS PAPER 69-385]
24 p4251 A69-42804

Operational and economical aspects of V/STOL air transportation reevaluated for civil aviation promotion [AAS PAPER 69-325]
24 p4418 A69-42870

Demand curves for VTOL intercity transportation, discussing conventional helicopters, compound helicopters, tilt rotor, tilt wing, stored rotor and fan or jet lift
24 p4254 A69-43721

AIRBORNE EQUIPMENT

Aerial radiation temperature measurement, damping factor of atmosphere and determination of ground and water surface temperatures by radiometry
01 p0110 A69-10693

Analytical reliability ratio to operational reliability for airborne equipment taking into account electrical and thermal aspects
01 p0011 A69-11069

Aircraft cockpit displays design for flight control and navigation, discussing integration, pictorial realism, moving part, pursuit tracking, frequency separation and optimum scaling
02 p0203 A69-12213

Microwave radiometer with two reference temperatures, discussing overall stability of design, sensitivity and airborne design for operation in X band [DVL-895]
02 p0220 A69-12435

Digital modified discrete Fourier transform Doppler radar processor for tactical aircraft
03 p0389 A69-13196

Radar return signal generation for computer simulations of airborne radar systems, using digital computer program for time varying radar backscatter
03 p0429 A69-13199

Navigational and tactical data with correlative map information provided on single CRT display in aircraft, storing map data on video tape
03 p0464 A69-13246

Satellite traveling wave tube for X band duplicating C and S band performance
03 p0405 A69-13678

Avionics, discussing use of electronics in control of aerospace vehicles
03 p0431 A69-14085

Airborne radiometric /8 to 14 micron/ temperature measurements, determining emissivities of ocean, stratus clouds, desert and snow
04 p0592 A69-14653

Jaguar aircraft equipment conformity to maximum standardization with equipment for other programs
04 p0550 A69-15063

He refrigerators, noting 4 K design for large scale fixed installations and 20 K small scale design for airborne applications
05 p0704 A69-15671

Multielectrode analyzers for measuring properties of ionospheric charged particles
05 p0761 A69-15702

Balloon-borne SPARMO detector SC 67 used for measuring radiation at high altitudes
05 p0762 A69-15823

Balloon-borne instrumentation X ray measurements, discussing detector electronics, telemetry, pressure transducer, power supply, environmental tests, energy limit and calibration
05 p0762 A69-15824

Industry airborne collision avoidance systems /CAS/ development program, discussing cooperative devices in aircraft
05 p0790 A69-16725

Pilot warning indicators to equip all aircraft at low cost, discussing Doppler system
05 p0790 A69-16726

Airborne polarimeter to measure Stokes parameters of linearly polarized visible atmospheric radiation in four narrow spectral regions
06 p0923 A69-16924

Arizona-NASA atlas of IR solar spectrum, reproducing photometric tracings obtained from CV-990 aircraft flights
06 p1008 A69-17808

Life raft thermal protection against exposure of aircrews to cold, noting chemically fueled heaters and IR reflective liners
06 p0883 A69-17841

Atmospheric microwave radiation and sensitivity of airborne radiometric sounding in water and moisture contents determination
06 p0954 A69-18001

Atmospheric measurements and experiments using aircraft as platforms, noting aircraft operation in severe

- weather, electrical supply problem and aircraft wake problem
[AIAA PAPER 69-157] 06 p0869 A69-18153
- Satellite and aircraft radiation measurements in cm and mm wavelength range to provide information on underlying surfaces
07 p1130 A69-18257
- Minimum operational characteristics for airborne VHF communication systems, discussing FCC requirements and system performance
07 p1077 A69-18638
- Ferrite Y junction E plane circulator for airborne high power X band radar
07 p1100 A69-18639
- High reliability magnetic tape recorders for satellite, aircraft and drone applications
07 p1133 A69-19104
- Airborne S-band telemetry antennas for omnidirectional patterns of polarization component, discussing design, pattern measurements and application
07 p1106 A69-19112
- Adaptive airborne VHF/UHF transmitter system, discussing design, ground isolation, current limiting, internal telemetry, wideband frequency response, real time video signals, etc
07 p1106 A69-19114
- Double sideband suppressed carrier FM telemetry system as airborne data recorder, discussing noise, environmental conditions, laboratory and flight tests
07 p1084 A69-19132
- Mathematical model of radar display, considering radar construction tube resolution, environment and eye perception parameters
07 p1136 A69-19504
- Radomes developments for supersonic/hypersonic aircraft and missiles, considering conditions imposed by speed and by electronic requirements
07 p1171 A69-19508
- Radomes design and manufacture for high speed flight vehicles, discussing interactions between aerodynamic and electrical requirements with reference to mechanism of aberration
07 p1141 A69-19510
- Wind tunnel investigation of damage to aircraft radomes by water droplet encounter during cloud passage and gaseous molecule friction in air
07 p1054 A69-19541
- Thermal stabilization and ethylene oxide effect on spaceborne electronic component sterilization and decontamination
08 p1283 A69-20266
- Hertzian radiometric antennas and signal processing techniques for aerial mapping project for sun
08 p1290 A69-20976
- Microelectronic multimode airborne radar system with modular construction, discussing system design, development, flight testing and operational results
[AGARDOGRAPH-114] 08 p1277 A69-20989
- Airborne ILS marker beacon receivers and secondary surveillance radar transponder using microelectronic equipment, noting thermal dissipation problems
[AGARDOGRAPH-114] 08 p1292 A69-20991
- Microelectronic studies in France noting semiconductor integrated circuits, thin film devices and application to airborne apparatus and small computer
[AGARDOGRAPH-114] 08 p1292 A69-20993
- Ion exchange fuel cells for emitter-receiver on atmospheric constant ceiling balloon, stressing pressure effect on operation and fuel storage
08 p1260 A69-21042
- Flight test performance of airborne Omega radio navigation system capable of worldwide coverage, discussing diurnal variations effects in phase velocity
08 p1348 A69-21191
- Error analysis of high resolution balloon-borne temperature sensor and comparison of temperature data with simultaneous rawinsonde measurements
09 p1494 A69-21642
- Soviet book on electronics and radio instruments of flight vehicles, covering radars and antennas, automatic pilots and design
09 p1463 A69-21930
- Flight test evaluation program for airborne multisensor electro-optical display systems performance in TV mode under variety of optical conditions
[AIAA PAPER 69-317] 09 p1500 A69-22387
- Airborne integrated in-flight data system to record and evaluate various engine parameters of operating jet engines
10 p1660 A69-23262
- Airborne integrated data acquisition and analysis systems to determine aircraft technical performance
10 p1660 A69-23264
- Flight test telemetry data processing system designed for C-5
10 p1660 A69-23269
- Secondary radar for air traffic control automation in France, discussing onboard equipment
10 p1723 A69-23705
- Airborne static inverter, called Digital Inverter, for conversion of DC to AC, single phase and/or three phase, noting precise frequency control
[SAE PAPER 690339] 11 p1824 A69-24495
- Airborne pulsed laser system for altimetry, determining height by measurement of transit time for pulse traveling to ground and back
11 p1885 A69-25035
- Apollo Range Instrumented Aircraft /ARIA/ telemetry antenna system for trajectory tracking, discussing computer program for simulation of behavior
11 p1840 A69-25309
- Airborne collision avoidance system /CAS/ performance and operational requirements
11 p1914 A69-25430
- Concorde SST equipment and systems noting microelectronics, automatic control, inertial navigation, head-up displays, linear instruments and hydraulic systems
12 p2091 A69-26360
- Barbados airborne dust collections showing metal fragments and black magnetic spherules contaminants from handling, discussing deep sea cosmic spherules and zodiacal cloud
12 p2075 A69-26964
- Electronic nonimaging polarimeter/photometer for aircraft observations of pure red pine stand, suggesting application to terrestrial, airborne and satellite remote sensing
12 p2096 A69-26983
- Airborne IR line scanning systems for latent forest fire detection, discussing discrimination module for automatic identification of hot targets
12 p2193 A69-26994
- Airborne IR remote sensing techniques for fire detection, considering marginal and submarginal targets
12 p2098 A69-26995
- Airborne magnetometer application for remote measurement of ocean wave spectra, obtaining wave noise power spectra and wave height profile
12 p2075 A69-26998
- Airborne scanning spectrometer for IR detection of clear air turbulence, presenting flight records
12 p2098 A69-26999
- Airborne IR surveys in engineering studies of terrain, discussing instrumentation technology, data interpretability, economic feasibility, etc
12 p2098 A69-27007
- Side-looking airborne radars /SLAR/ application to geological exploration of remote unmapped areas
12 p2099 A69-27009
- Connecting duct influence on slide wire vertical air-speed indicator operating on barometric principle during aerial gravimetric surveying
13 p2260 A69-27828
- Stratoscope II unmanned balloon-borne telescope design, detailing pointing, focusing and thermal characteristics
13 p2261 A69-27956
- Guiding system of Spectro-Stratoscope /balloon-borne solar telescope/, describing hydrostatic bearing and torque motor
13 p2262 A69-27957
- Atmospheric IR emission measured at high altitudes by interferometer spectrometers behind nitrogen cooled chopper
13 p2254 A69-28261
- Electronic boresight shift in space-borne monopulse radar system, expressing antenna and signal parameters in terms of equivalent branch and channel asymmetries
14 p2411 A69-28895
- A-New avionics system for carrier based VSX aircraft used in U.S. Navy aerial submarine hunting, discussing TV, lasers, sonobuoy system, radar, etc
14 p2392 A69-29430
- Solid state programmable avionics converter for signal processing, information conversion and aircraft control
14 p2405 A69-29687
- Unoccupied space utilization in aircraft compartments due to microminiaturization, considering reliability enhancement of electronic equipment
15 p2576 A69-30353
- Airborne pulsed lasers for near shore bathymetric measurements, discussing feasibility results
15 p2609 A69-30459
- Rescue locator beacons and airborne search equipment of VHF and UHF capabilities available to international civil aircraft operations
15 p2552 A69-30852
- Cadmium sulfides thin film solar cells for supplying power to instrumentation and data telemetry on longer lived balloons
15 p2553 A69-31287
- Power supplies for balloon-borne instruments, describing light flexible NiCd batteries and solar cells used in EOLE project
16 p2736 A69-31745
- Piloting errors due to false instrument readings during turbulent atmosphere flight
16 p2734 A69-32007
- Solar spectral irradiance measured by airborne instruments, discussing construction, calibration, etc, of photoelectric filter radiometer and Leiss monochromator
16 p2861 A69-32261
- Electromagnetic interference correction for airborne telemetry, illustrating actual and simulated data for interfering source signatures identification
16 p2754 A69-32575
- Ocean and water surface temperature measurement by IR remote sensing from aircraft and satellites, discussing accuracy and data correction
[AIAA PAPER 69-590] 17 p2973 A69-33286
- Onboard flight data recorder as integrated system for investigating aircraft accidents, describing German LEADS 200 model
17 p2974 A69-33429
- Airborne clock used to synchronize atomic clocks at different locations, discussing equipment and error sources
17 p2975 A69-33593
- Microphonic noise measuring systems for airborne radar system design for noise reduction
17 p2937 A69-33628
- Digital IC radiosonde system, discussing sampling, pulse width modulation, time multiplexing, follow-on subsystems, etc
17 p2937 A69-33675
- Airborne radomes reliability and high temperature environments, discussing missile nose cones, light weight ceramic techniques, circular polarization, etc
17 p2942 A69-34084
- Beam control of optically fed two axis airborne electronically scanned phased arrays by on-array and off-array processing
17 p2942 A69-34085
- Aircraft generator weight in relation to system performance requirements, using digital computer to study generator design
17 p2904 A69-34087
- Electric power quality effects on aircraft electronic utilization equipment, discussing characteristics of variable speed constant frequency /VSCF/ generating system
17 p2905 A69-34091
- Cost optimization in converting brush type to brushless aircraft AC power systems, using analog computer to determine modifications
17 p2905 A69-34109
- Airborne electric power systems maintenance aids, describing design and operation of annunciator for establishment and display of system failure causes
17 p2905 A69-34112
- Solid state broadband RF power amplifier for airborne HF radio, eliminating total servosystem and all higher voltage components
17 p2942 A69-34114
- Airborne communication receiver solid state interference blanker circuitry comprising black box insertable between antenna and RF input
17 p2943 A69-34132
- Automatic multichannel transient monitor for electrical transient detection and data processing, transmission and storage on aircraft
17 p2947 A69-34135
- Series 3 Skyvan design, describing controls, electric and electronics equipment, weather protection, environmental and fuel systems
17 p2906 A69-34194
- Midday aurora oval and polar cap region airborne observation, noting relation to sporadic E layer
18 p3126 A69-34258
- Soviet book on reliability of semiconductor radio devices of flight vehicles covering failures through production errors, power source instability, environmental induced changes, etc
18 p3108 A69-34350

Airborne radar navigation with emphasis on semiautomatic fixing, describing beacon mode, map matching and airborne weather radar

18 p3169 A69-34851

Laboratory and flight tests of airborne solid state UHF telemetry transmitter, discussing miniaturized coaxial hardware from RF power conservation viewpoint

19 p3267 A69-35996

Airborne astatic vertical gyro motion found dependent on aircraft motion along trajectory

19 p3311 A69-36194

NASA Earth Resources Survey Aircraft Program, describing aircraft and remote sensors characteristics

19 p3312 A69-36259

Airborne collision avoidance system based on time-frequency techniques for use within ground based control systems, showing air/ground synchronization and collision geometry

19 p3371 A69-36735

Geomagnetic field total vector modulus secular variations from airborne measurements

20 p3522 A69-37061

Airborne imaging radar motion compensation and sensing problems concerning perturbed signal correction, discussing spatial sensitivity measures and constraints

20 p3490 A69-37645

Phase and amplitude stability measurements in airborne pulse Doppler radar

20 p3492 A69-37711

Airborne imaging radar drawbacks and advantages, describing techniques to overcome defects

20 p3493 A69-37735

Solar IR spectrum recorded by LPL B spectrometer on NASA CV-990 aircraft using one micron grating, noting resolution

21 p3800 A69-38683

Gyroplatform to stabilize gravimetric equipment on aircraft, noting channel stabilization by electrohydraulic servomechanism

21 p3723 A69-38885

Thermal design of power amplifier for airborne HF transceiver, discussing component layout, air cooling and materials

22 p3909 A69-39942

Instruments for obtaining auxiliary data in aerial triangulation, describing stratoscope, profile recorder, radar altimeter, horizon camera, etc

22 p3944 A69-40042

Airborne electromagnetic systems measuring complex dielectric constant in earth crust for mineral and water resources exploration [RAES PAPER 8]

22 p3946 A69-40481

Airborne correlation spectrometer for air pollution remote sensing, describing applications [RAES PAPER 7]

22 p3896 A69-40488

Advances in geophysics, Volume 13, covering airborne geophysical methods, ball lightning structure, lidar, middle atmosphere energetics, etc

22 p3940 A69-40534

Tools and equipment for extra- and intravehicular activities in space and on lunar surface [AAS PAPER 69-438]

24 p4319 A69-42802

Heat pipe coupled to air cooled heat exchanger to cool high power airborne radio component by dissipating thermal load into ambient air [ASME PAPER 69-HT-16]

24 p4413 A69-43552

AIRBORNE/SPACEBORNE COMPUTERS

Channel identification coding for data compressors, deriving optimum code word length for bit compression ratio and overflow identification scheme

03 p0391 A69-13219

Onboard SDP-3 computer data system core for IMP spacecraft, considering payload

03 p0400 A69-13243

Navigation computer utilizing current integrators and step motors to record flight path

03 p0404 A69-13431

Aerospace digital computer design, discussing influence of data trends and reliability techniques

03 p0401 A69-14181

Instrument and rounding-off errors of aircraft computers as function of digital network dimensions

04 p0563 A69-14491

Space oriented programming languages and compilers for translating languages, discussing software generating tools under development for space missions

04 p0564 A69-15297

Stored program computer for small scientific spacecraft, noting program and data memory capacities

04 p0569 A69-15472

General purpose satellite computer, discussing onboard processor /OBP/ design, memory, central unit, input/output and software

05 p0725 A69-16710

Onboard digital computer evaluation of trigonometric functions for antenna pointing

07 p1089 A69-19745

Airborne area navigational capability achieved by course line computer processing VOR information

07 p1178 A69-19763

STOL aircraft intercity test flights emphasizing curved ILS approach, using onboard computer for altitude and distance data

08 p1347 A69-20602

Stellar identification system using onboard sighting equipment and computer mathematical methods

08 p1347 A69-20657

OMEGA airborne navigational computers, discussing earth ellipticity and phase variations problems for signal conversion into latitude and longitude coordinates

08 p1347 A69-20778

Collection of papers on applications of microelectronics to aerospace equipment, noting design and reliability of circuits and computers [AGARDOGRAPH-114]

08 p1291 A69-20981

Complex digital computers designed for Apollo spacecraft missions, discussing construction techniques [AGARDOGRAPH-114]

08 p1279 A69-20990

Airborne digital computers for optimization of aircraft control and monitoring functions, discussing avionics and circuit technology

08 p1349 A69-21194

Airborne computerized Omega Navigation set from combination of functional analysis of Airborne Omega Navigation Receiver with capabilities of current airborne computers

08 p1349 A69-21197

OMNITRAC general purpose airborne digital computer with permanent memory of 4096 words of 23 bits, noting modular construction

10 p1659 A69-22845

Optimum microcircuit analog to digital converter for aerospace environment by combining monolithic circuits and thin film resistors

10 p1636 A69-23282

Computer program for onboard medical checkups of spacecraft crews during extended space flights, discussing tests and intervals

10 p1649 A69-23505

Automatic computer processing of physiological data during space flights, discussing choice of computers and computer programs

10 p1649 A69-23509

Airborne computer controlled data acquisition system for real time fault detection and isolation in avionics

11 p1843 A69-25082

Computer design for booster/satellite control, discussing systems reliability, low power and tradeoffs

11 p1843 A69-25320

Apollo mission simulation, discussing Command Module Simulator /CMS/, onboard computer system and dynamic visual presentation via infinity-optics display [SMPTE PAPER 105-74]

12 p2055 A69-25768

Digital computer redundancy, analyzing triple modular redundancy in Saturn vehicles and quad design in primary processor and data storage for OAO

12 p2034 A69-26567

Air lane longitudinal separation distance reduction for accommodating increased traffic using airborne computers for single file system

15 p2651 A69-30293

Large scale integration /LSI/ and medium scale integration /MSI/ circuits evolution and requirements, noting onboard computers and space applications

15 p2625 A69-30825

Airborne digital computer and display devices role in navigation management, discussing data processing and hybrid navigation systems

16 p2809 A69-32260

Astronomical satellite direct digital attitude control using digital computer between sensor and actuator to achieve optimal filtering and stabilization

17 p3049 A69-33244

Flight command computer for V/STOL aircraft, discussing design concepts, operating modes, displays, etc [AHS PAPER 313]

17 p3001 A69-33543

TC-2 general purpose digital avionics computer in A-7D/E avionics system performing tasks in weapon delivery, navigation and guidance, display updating, self testing, etc

17 p2933 A69-34059

AN/ASN-24/V/ general purpose digital computer deployed in large worldwide jet transport fleet

17 p2933 A69-34061

Airborne data processing systems reliability, discussing software and hardware reconfiguration techniques and man-machine interface problems

17 p2977 A69-34072

Onboard hybrid computer for helicopter fire control system, generating turret pointing angles and corrections

17 p2934 A69-34074

VLF wave propagation phase velocity prediction for airborne Omega computer, using scatter model based on abnormal ionosphere

17 p3002 A69-34077

Doppler inertial system with remote attitude capability, detailing sensor operation by airborne computers

17 p3002 A69-34097

Tacan navigation system developments including data transmission, links to airborne computers and air traffic control transponders

17 p3003 A69-34101

Vertical path guidance computer, noting applications to feeder airlines and air taxi services operating from airports with VOR/TACAN only

17 p3003 A69-34104

Multisensor data processing technique for fail operational landing commands, using real time error analysis inherent in Kalman filter

17 p3003 A69-34106

Post Attack Command and Control System - Airborne Data Automation /PACCS-ADA/, describing components, operation, etc

17 p2977 A69-34116

Electromagnetic compatibility /EMC/ hardware design, discussing NDC 1060 computer configuration, requirements and service environment

17 p2947 A69-34136

Avionics of Naval E-2C airborne sentry and command and control system, discussing digital computer, search radar, etc

18 p3108 A69-34811

Airborne digital computers techniques in avionics stressing memory design, packaging, reliability and maintainability

18 p3106 A69-34846

Navigational equations solution by airborne analog computer techniques, describing electronic, electromechanical, digital reset and mechanical integrations with respect to time

18 p3107 A69-34847

Air data system consisting of aerodynamic and thermodynamic sensors and computer calculating flight parameters for automatic flight control

18 p3169 A69-34854

Aircraft terrain-following algorithm for use with airborne general purpose digital computer, discussing simulation techniques and test results [AIAA PAPER 69-817]

19 p3366 A69-35625

Real time terrain following computer for C-5A transport, discussing automatic throttle system and speed bleedoff utilization [AIAA PAPER 69-797]

19 p3367 A69-35633

Masking and standby redundancy approach to fault tolerance in space navigation computers with illustrations, discussing automatic maintenance

19 p3279 A69-35798

Strapdown electrostatic aerospace navigator /SEAN/ using electrostatically suspended gyros /ESG/ for inertial reference, including drift and computer tests

19 p3369 A69-35802

IMP-1 experiment, describing design and applications of SDP-3 computer

19 p3280 A69-36265

Onboard data processing and acquisition for aircraft and spacecraft problems based on integrated data management approach, discussing readout and display

19 p3280 A69-36315

Onboard computers on rockets and satellites - Conference, Paris, December 1968

20 p3498 A69-37377

Binary increment and residual class notation techniques for onboard spacecraft computer arithmetic

20 p3499 A69-37378

Onboard satellite computer design and programming language criteria, considering cost, reliability, weight, volume and energy requirements

20 p3499 A69-37379

Missile-borne and satellite-borne computers analogies, comparing design, operational conditions and functional requirements

20 p3500 A69-37380

Computer based onboard satellite PCM telemetry, showing improved adaptability, size and cost reduction

20 p3500 A69-37382

Spacecraft onboard processor for digital filtration and data compression, discussing prototype design, construction, sample memory, weight memory, arithmetic unit and programmer

20 p3500 A69-37383

Onboard spacecraft computer design, programming and operation based on dual bussing system

20 p3500 A69-37384

SDP-3-A general purpose stored program computer designed for small scientific spacecraft onboard data system, noting computerized simulation

20 p3500 A69-37385

Swedish satellite onboard computer for particle experiment, discussing functional design based on buffer unit for experimental data

20 p3501 A69-37386

Onboard data processor design for Swedish satellite to study spatial and temporal variations of auroral particles

20 p3501 A69-37387

Onboard satellite computer for project Roseau experiments for magnetosphere study, discussing program switches, monitors and data compilers

20 p3501 A69-37388

Roseau satellite onboard computer systems design, emphasizing simulator and assembly programs for real time operation verification

20 p3501 A69-37389

Data handling system design for large astronomical satellite /LAS/, discussing spacecraft configuration, basic aims, program functions, subsystems, signal flow, flight repair, etc

20 p3501 A69-37390

Microminiature Elliott MCS 920 M digital computer for inertial guidance of CECLES-ELDO launcher, discussing construction, code, interrupt, guidance system and functions

20 p3501 A69-37391

Microminaturized digital computers for missiles and aircraft, discussing characteristics, environmental conditions and transformation possibility for use in satellites

20 p3502 A69-37392

Spacecraft discrete automatic control system computerized simulation, discussing logic elements, applications to design, etc

20 p3502 A69-37393

Onboard computer and environment simulation for real time programs development, discussing instructions analysis, variables extraction and values and peripheral components

20 p3502 A69-37395

Roseau onboard computer simulation by IBM 360, discussing use of assembly language and FORTRAN

20 p3502 A69-37396

Symbolic language and assembly program for Roseau computer, discussing mnemonic code and program operation

20 p3502 A69-37397

Onboard navigation digital computer simulation to verify calculation principle and logic units during design and construction

20 p3502 A69-37398

Satellite onboard computers automatic reconfiguration and self repair

20 p3503 A69-37399

Onboard computer reliability, discussing missile computers and maintenance procedures

20 p3503 A69-37400

Wire type memory model for satellite onboard computers, discussing nondestructive readout, power requirements, marginal temperatures, material and volume

20 p3503 A69-37403

Digital autopilots for Apollo CSM and CSM/LM vehicles thrust vector control, describing modifications of onboard computers and programs

[AIAA PAPER 69-847] 21 p3762 A69-39377

Titan 3C launch vehicle digital flight control system using flight equations time-shared with guidance equations

[AIAA PAPER 69-878] 21 p3824 A69-39404

Strapdown gimballess inertial measurement unit with general purpose computer, describing hardware, software and test results

[AIAA PAPER 69-850] 21 p3765 A69-39426

Spacecraft atmospheric entry descent trajectory optimization by stochastic procedure, requiring onboard digital computer to realize optimal algorithms

21 p3767 A69-39648

Onboard processor servicing spacecraft sensors, programmable from ground, discussing functions and applications

22 p3903 A69-39921

Computer controlled TV cloud recognition equipment on meteorological satellites, discussing multistep process of automatic perspective distortion corrections by onboard computer

22 p3977 A69-40004

Programmatic constraints on onboard processing of data collected by payload sensors

[AIAA PAPER 69-942] 22 p3904 A69-40325

Centaur computer assimilating Centaur vehicle hardware functions performed by digital computer, discussing modules, flight control system, cost reduction, etc

[AIAA PAPER 69-943] 22 p3904 A69-40326

Kalman filter simulation for estimating aircraft position and velocity from airborne digital computer data in zero-zero landing system

[AIAA PAPER 69-944] 22 p3978 A69-40327

Spacecraft onboard computer for prelaunch targeting constants verification through checksum equation and error detection scheme, using generated number sequences

[AIAA PAPER 69-946] 22 p3974 A69-40329

Programming and checkout of computer for Eldo inertial guidance system, including flight simulation and autopilot tests

[AIAA PAPER 69-961] 22 p3978 A69-40342

LSI oriented cellular array implementation of complex arithmetic functions for aerospace computers, describing techniques of automatic switching-in of spare modules for failures

[AIAA PAPER 69-964] 22 p3906 A69-40345

Self testing and repairing /STAR/ aerospace computer for automatic maintenance of unmanned interplanetary spacecraft

[AIAA PAPER 69-966] 22 p3906 A69-40347

Computerized simulation for performance evaluation of System/4 Pi-EP multiprocessor for use in aerospace vehicle

22 p3907 A69-40353

Digital computer system for navigation, landing, fire control, monitoring and checkout aboard Saab 37 Viggen aircraft handling attack, reconnaissance and fighter missions

[AIAA PAPER 69-985] 22 p3908 A69-40365

Aircraft navigation system requiring computer and display for approach guidance to circular orbit over fixed ground area

[AIAA PAPER 69-986] 22 p3978 A69-40366

Booster digital guidance and control system, discussing communication device providing data transfer between airborne digital computer and control device

[AIAA PAPER 69-988] 22 p3978 A69-40368

Aircraft digital control hardware and applications including airborne computer proper, distributed systems, loop control, system integrity, etc

[RAES PAPER 4] 22 p3908 A69-40485

Programmable data handling and telemetry systems for scientific satellites, noting system checkout, spacecraft integration, software and ground data processing

23 p4132 A69-41735

Spaceborne stored program computer design for OAO-C, noting auxiliary command storage, spacecraft monitoring and malfunction reporting, etc

23 p4132 A69-41736

SDP-3 small serial computer for engineering experiment on IMP spacecraft, discussing design modifications to improve performance

23 p4133 A69-41737

Spacecraft onboard data handling system with MSI complementary MOS arrays, describing various components

23 p4133 A69-41739

Flexible format generator for manned spacecraft data management system designed with memory for data sampling formats, emphasizing software counters and power strobing

23 p4133 A69-41762

Spacecraft central data system for deep space solar probe data management

24 p4284 A69-42621

Digital computers effect on aircraft automatic power unit controls, discussing safety, reliability, self monitoring and redundant computer systems

24 p4253 A69-43113

On-board digital filtering applied to spectral estimation and data compression, discussing theory, techniques, computerized implementation and prototype design

[AIAA PAPER 69-969] 24 p4285 A69-43510

F-111D computer complex to provide selective functional redundancy and flexibility to accommodate mechanization changes

[AIAA PAPER 68-837] 24 p4285 A69-43719

AIRBORNE TERRAIN ANALYSIS U TERRAIN ANALYSIS

AIRCRAFT ACCIDENT INVESTIGATION

Aircraft accidents, discussing complexity analysis, wreckage, anomalies and investigator role

01 p0009 A69-10351

Airplane explosion evidence, discussing examination of plastic seat cushion surface and metallic fragments

02 p0193 A69-12688

Explosive devices to sabotage aircraft in flight, discussing evidence of sabotage in aircraft wreckage and detection of explosives before loading

04 p0549 A69-14943

Aircraft in-flight collision, discussing difficulties and procedures of medical board of inquiry

03 p0715 A69-16628

German Air Force Center of Aeronautical Medicine, discussing organization, work projects and proposed mutual cooperation with French counterpart

05 p0850 A69-16629

Accident prevention and investigation procedures of National Transportation Safety Board /NTSB/, discussing management patterns

06 p1041 A69-16842

USAF accident information, reporting and retrieving, describing Directorate of Aerospace Safety structure and functioning

06 p1041 A69-16843

Aircraft accident prevention and damage control

06 p0878 A69-16961

Commercial jet safety, analyzing aircraft accidents and accident rates

06 p0868 A69-17829

Fragments and markings produced on aircraft aluminum by explosion as means of detecting sabotage in crashes

06 p0868 A69-17833

Crash protection of flight data recorders, aircraft accident investigation, systems analysis, environment and enclosures

10 p1691 A69-23248

Medical investigation of aviation accidents - Conference, Washington, D.C., September 1966

12 p2021 A69-25837

Pathology and aircraft accident causes noting environmental factors, injuries and preexisting diseases

12 p2021 A69-25838

Aeromedical investigation of civil aircraft accidents by National Transportation Safety Board, noting post-mortem legal aspects and need for human factors investigation

12 p2021 A69-25840

Aviation pathology in aircraft accident investigation of accident survivability features and accident precipitation factors, noting cockpit structures and protective equipment

12 p2021 A69-25841

Aircraft accident toxicology, guidelines for collection, preservation, shipment and analysis of specimens and test result interpretation

12 p2022 A69-25842

FAA aircraft accident human factors investigation plan, discussing on-call pathologists, site organization and investigation, autopsy and result reporting

12 p2022 A69-25843

Civil aircraft accident investigation, discussing organization and procedures of Bureau of Aviation Safety of National Transportation Safety Board

12 p2191 A69-25844

Aircraft accident investigation procedures in Canada for routine/major accidents and public inquiries, outlining organization

13 p2201 A69-27540

Accident record of general aviation pilots over age 60 /1965/

14 p2541 A69-29308

Jet transport operation and accidents statistics, analyzing world data, accident causes and safety gap

22 p4054 A69-41130

Refused takeoff as critical maneuver in ground operations during jet transport accident investigation, emphasizing pilot anticipation of conditions and preplanning actions

[SAE PAPER 690378] 23 p4062 A69-41654

AIRCRAFT ACCIDENTS

Flight accident rate of U.S. physician pilots noting relation to number of takeoffs and landings

01 p0022 A69-11344

Alcohol role in pilot victims of aircraft accidents

01 p0022 A69-11345

Manufacturer and assembler liability for injuries caused by design defects resulting from engineering errors in aircraft products

01 p0180 A69-11392

Litigation for aircraft accidents, discussing legal and fiscal aspects and deterrent effect contributing to aviation safety

01 p0181 A69-11393

Occupant restraint systems for automobiles, aircraft and manned space vehicles, discussing cost, practicability, ease of use, acceptability and possible improvements

03 p0380 A69-13459

Coronary atherosclerosis in military pilot fatalities of aviation accidents, demonstrating irrelevance of amount of flying time and type of aircraft

03 p0376 A69-14080

Ideal safety system for accident prevention, considering foreseeable and unforeseeable aspects to eliminate individual or collective human error

06 p1040 A69-16836

Air safety, emphasizing misunderstandings or unresolved problems in accident prevention connected with law/safety interface

06 p1040 A69-16837

Aviation insurance function in providing risk capital in expanding aviation enterprises at fair and equitable rates, discussing air safety

06 p1041 A69-16845

Federal government legal liability for commercial air safety in aircraft accident suits

06 p1042 A69-16848

Aircraft parts manufacturer liability in air accidents, discussing litigation and warranties

06 p1042 A69-16849

Psychophysiologic factors in USAF aircraft mishaps involving ground egress

06 p0878 A69-16959

Airline pilot incapacitation by death or terminal collapse due to organic causes while on duty, noting incidence and resulting accidents

06 p0883 A69-17849

Characteristics of accident experienced pilots based on personality and psychological tests

06 p0876 A69-18033

Climatic factors affecting pilot vision and contributing to misjudgement during landing procedures, noting effect of downward slope in runway approach

06 p0884 A69-18036

System reliability influence on air accidents resulting from pilot errors, unforeseen obstacles, breakdowns and atmospheric effects

07 p1054 A69-19288

Spatial disorientation as factor in accidents in operational command, noting relatively high experience level of involved pilots

07 p1072 A69-19431

General aviation accidents and hazards presented by drugs, ethyl alcohol, pesticides and carbon monoxide

07 p1068 A69-19435

Passenger and crew members escape from aircraft following water accidents, discussing ditching, evacuation, survival and rescue facilities

08 p1254 A69-20453

Reaction vs time relations in accidental impact of large commercial aircraft against rigid surface, detailing stress analysis of nuclear power plants structures

09 p1613 A69-21677

Epidemiology of aerial application accidents analyzed in groups of high and low wing monoplanes, biplanes and helicopters

09 p1447 A69-22554

Air carrier liability for nuclear weapons damage, discussing international agreements

11 p2003 A69-24260

Human survivability in severe light plane slow speed accidents due to stalling, turning, takeoff or approach, discussing crash load vectors and magnitude

[SAE PAPER 690336] 11 p1822 A69-24492

Business aircraft injury protection and impact survival design considerations, stressing upper torso restraint installations

[SAE PAPER 690335] 11 p1829 A69-24493

Aircraft electronic proximity warning devices applications, discussing compatibility in ATA collision avoidance system

[SAE PAPER 690340] 11 p1914 A69-24496

Large and small fixed wing airplane crashworthiness requirements, noting occupant protection in survivable crash environment and rapid safe evacuation

[SAE PAPER 690321] 11 p2004 A69-24509

Airborne collision avoidance system /CAS/ performance and operational requirements

11 p1914 A69-25430

Pathology and aircraft accident causes noting environmental factors, injuries and preexisting diseases

12 p2021 A69-25838

Identifying human bodies torn apart or crushed in aircraft accidents, noting example of jet passenger plane crash

12 p2021 A69-25839

Preventive medicine in handling airline pilots to avoid accidents attributable to disability and death from natural causes

12 p2024 A69-26559

Air Canada flight safety system including company philosophy, safety activities, incident and accident handling and information schemes

13 p2201 A69-27541

Psychophysiologic factors in USAF aircraft mishaps involving ground egress

15 p2558 A69-30462

Crash helmet impact protection capability, considering helmet construction

17 p2913 A69-33169

Airworthiness objectives for civil powered lift aircraft, discussing safety, traffic growth and accident rates

17 p2897 A69-33211

Onboard flight data recorder as integrated system for investigating aircraft accidents, describing German LEADS 200 model

17 p2974 A69-33429

Light aircraft emergency downed position indicators installation program, discussing transmitter minimum performance standards, listening watch insurance, etc.

17 p2931 A69-34102

Aviation health service for flight safety problems with emphasis on accident prevention, emphasizing physician role in man-machine relationship of personnel surveillance

18 p3098 A69-35305

Annual general aviation aircraft accident rate variation related to annual variations in pilot flight training activity

19 p3262 A69-36448

Engine powered lift civil aircraft certification factors taking into account traffic growth, accident rates, learning rate and acceptable safety level

22 p3862 A69-39962

Statistics of jet aircraft accidents including worldwide data and safety trends

22 p4054 A69-41128

Background flying experience of tactical fighter aircraft pilots accident potential, comparing accident and nonaccident groups

23 p4103 A69-41685

Aviation accidents medical aspects, discussing accident causes and remedies, training and regulation proposals, etc.

23 p4106 A69-41792

Annual general aviation accident rate prediction from annual flight training variations

23 p4062 A69-41793

Passenger safety during aircraft accidents in Arctic, discussing survival equipment and methods

23 p4107 A69-41811

Medical aid organization after aircraft accidents at airports, examining injury probability by statistical methods

23 p4107 A69-41812

Medical aid, equipment and organization for injured passengers in large aircraft accidents at airports and immediate neighborhood

24 p4270 A69-42602

In-flight medical disorders sustained by crew members of various aircraft in French Air Force correlated with aircraft accidents, flight experience and age

24 p4277 A69-43383

AIRCRAFT ANTENNAS

Current antenna system technology, particularly airborne and spaceborne applications

04 p0576 A69-14767

Secondary radar equipment functions and features forming IFF-SIF chain, discussing displacement controller and minor lobe suppression functions technical problems

05 p0721 A69-16591

Telemetry and tracking antenna feed system in EC-135N instrumented aircraft for Apollo moon project

07 p1105 A69-19110

Aircraft radomes lightning protection, discussing evaluation by experimental methods and simulation

07 p1142 A69-19535

X band eight element matrix array construction, producing antenna suitable for aircraft

08 p1288 A69-20966

Self focusing aerial antenna arrays with full angular coverage for two way airborne communications

08 p1289 A69-20971

Siting two antennas for combining signals to obtain all-around coverage in aircraft communication

08 p1289 A69-20972

Apollo Range Instrumented Aircraft /ARIA/ telemetry antenna system for trajectory tracking, discussing computer program for simulation of behavior

11 p1840 A69-25309

Signal reflection elimination from underlying surface during aircraft flights by using two antenna array with identical radiation patterns

15 p2567 A69-30345

Mathematical model for aircraft antenna to antenna electromagnetic interference analysis, emphasizing techniques for propagation paths and shading factors

17 p2943 A69-34134

Aircraft antenna-coupled electromagnetic interference analysis, describing mathematical model for frequency coincidence, power levels and receiver thresholds

23 p4141 A69-42224

AIRCRAFT APPROACH INSTRUMENTS

U APPROACH INDICATORS

AIRCRAFT APPROACH SPACING

Satellite monitoring application to air traffic control in parallel track system, discussing lateral and longitudinal separation control

02 p0277 A69-11591

Aircraft separation standards, considering separate space for VTOL in automated high density airways system

[AIAA PAPER 69-210] 07 p1178 A69-19579

Monograph on mathematical model for aircraft separation in air traffic safety control, analyzing aircraft motions and collision avoidance

08 p1347 A69-20712

Long range subsonic transport navigation systems accounting for reductions in horizontal separation on high density oceanic routes

08 p1348 A69-21062

Air lane longitudinal separation distance reduction for accommodating increased traffic using airborne computers for single file system

15 p2651 A69-30293

Airport capacity increase in terms of operations delay, discussing computer aided approach systems and additional runways

22 p3925 A69-40429

STOL aircraft characteristics emphasizing ground and air space operations requirements and noise levels

22 p3863 A69-40430

AIRCRAFT BASES

U MILITARY AIR FACILITIES

AIRCRAFT BRAKES

NT LEADING EDGE SLATS

NT TRAILING-EDGE FLAPS

NT WING FLAPS

Soviet book on turbojet engine reverse thrust systems and systems for deflection of jet stream covering aircraft braking efficiency

04 p0647 A69-14934

HF brake excited vibration damping in aircraft landing gear, obtaining closed form solution

[AIAA PAPER 68-312] 11 p1823 A69-25370

Beryllium brake disks use on C-5A aircraft, comparing size, weight and peak temperature with steel structure

15 p2639 A69-3059

Sliding friction and wear properties of metal ceramic composites applied to aircraft brakes

17 p2987 A69-33375

Full circle Be brake disks in C-5 aircraft, discussing properties at elevated temperature and fastening of friction lining

18 p3095 A69-35424

Aircraft braking, discussing systems, brakes, tires, runway interface, heat sink materials, friction measurements, skid control, cooling and recovery equipment

[SAE PAPER 690376] 23 p4063 A69-41671

AIRCRAFT BREATHING APPARATUS

U BREATHING APPARATUS

AIRCRAFT CARRIERS

A-7 Corsair 2 introduction to fleet and combat operations in Southeast Asia

06 p0867 A69-17660

Aircraft carrier landing system performance, variations in pilot experience, aircraft types and environment, emphasizing night carrier recovery

17 p2916 A69-34012

Deterministic and statistical prediction techniques for aircraft carrier motions at sea for application to aircraft landing operations

[AIAA PAPER 68-123] 17 p2902 A69-34014

Landing guidance devices under difficult weather, discussing landing mechanics for land and carrier based aircraft
18 p3170 A69-34857

Wave-off Decision Device to define potential aircraft carrier-ramp-strike wave-off criteria for aircraft approach
20 p3573 A69-37161

Aircraft characteristics influence on longitudinal handling qualities during carrier approach from visual landings on moving base simulator
[AIAA PAPER 69-894] 21 p3648 A69-39418

Longitudinal flying qualities evaluation by pilots in carrier approach flight simulation, describing experiment apparatus, procedures and results
[AIAA PAPER 69-895] 21 p3648 A69-39419

Aircraft flying qualities research program, discussing Navy test pilot evaluations and longitudinal handling characteristics for simulated carrier landing task
[AIAA PAPER 69-897] 21 p3648 A69-39421

AIRCRAFT COMMUNICATION

Ground-air-ground communications system using pseudonoise through satellite and central ground based control facility, discussing system advantages, SNR and modulation schemes
01 p0033 A69-11009

Aeronautical satellite system to relay communications at VHF or L band frequencies from aircraft flying over oceanic routes
03 p0464 A69-13235

International satellite system for commercial aircraft communications and air traffic control
03 p0464 A69-13238

Telecommunications network for air traffic in Central America to attain higher degree of reliability
03 p0399 A69-14182

Aeronautical service satellites, considering communications, surveillance for navigation, traffic control, collision avoidance and search and rescue, weather and border control functions
04 p0666 A69-15295

Aeronautical satellite communications, discussing results with NASA ATS-1 satellite
05 p0790 A69-16721

Digital communications between aircraft and flow control computers on ground to avoid runway saturation and automating routing functions
05 p0721 A69-16722

Aircraft Searchmeter, discussing device fitted to locate emergency radio beacon signal
06 p0878 A69-16963

Aircraft communications, navigation and identification, discussing role of satellites, common waveform modulation and electronics technology
07 p1085 A69-19178

Siting two antennas for combining signals to obtain all-around coverage in aircraft communication
08 p1289 A69-20972

Satellite networks for air traffic control and aircraft communications in North Atlantic
13 p2296 A69-27831

Frequency hopping technique applied to multiple access air-to-air/ground communication for tactical fighters, noting additive recognition
17 p2931 A69-34117

Worldwide communication system via synchronous satellites for aeronautical, maritime and land mobile services
23 p4114 A69-41355

AIRCRAFT COMPARTMENTS

Aircraft cockpit and surface temperatures after solar radiation exposure in desert, showing inadequacies of meteorological data for thermal stress predictions
03 p0381 A69-14077

Synthesis of simulated aircraft cabin pure fluidic temperature control system
[ASME PAPER 68-WA/FE-30] 05 p0705 A69-16103

Convective heat exchange coefficients for human organism in aircraft surroundings under homogeneous temperature conditions, deriving acclimatization equations
[AGARDOGRAPH-111] 08 p1266 A69-20673

Bleed air environmental system utilizing air to jet pumps as flow multipliers for cabin pressurization air supply in commercial turbo-prop aircraft
[SAE PAPER 690331] 11 p1941 A69-24494

Pressurized Navajo aircraft environmental system, discussing ventilation, pressurization, heating and air cooling systems
[SAE PAPER 690330] 11 p1829 A69-24504

Passenger cabin windows on Convair liner type aircraft, describing construction, installation, strength, etc
17 p3061 A69-33667

Flight compartment and cabin layout of Skyvan 3 designed as freighter with passenger capability
17 p2903 A69-34195

Aircraft interior conversion for passenger or cargo service, discussing convertible aircraft and quick change concepts
[AIAA PAPER 69-784] 19 p3244 A69-35642

Manual extinguisher using bromochlorodifluoromethane (BCF) for aircraft cabin fire protection, discussing design and low toxicity, corrosiveness and cost
19 p3256 A69-36863

DC 3 tail wheeled single skin piston aircraft conversion into first class luxury passenger aircraft for short haul service
20 p3460 A69-36918

Technical problems in converting long service civil aircraft to obtain more volume, easier loading access or greater flexibility
20 p3461 A69-36919

Decompression study simulating supersonic aircraft cabin small structural failure at 60,000 ft, using monkeys as subjects
21 p3665 A69-39171

Autotransformer with static tap changer to provide varying power levels for controlled gradual heating of aircraft window to avoid thermal shock
22 p3869 A69-40414

Aircraft passenger cabins pressure safety limits estimating factors, discussing human respiratory gas exchange mechanism, pressure drop and smoking effects, etc
24 p4269 A69-43411

AIRCRAFT CONFIGURATIONS

Radar cross section of missile and aircraft configurations, comparing theoretical and experimental results for Convair 990 static test model
03 p0384 A69-12911

X V-4B Hummingbird 2, noting modification from XB-4A two engine ejector augmentation to six engine direct and diverted thrust configuration
03 p0366 A69-13112

Helicopter role, development and configurations, noting V/STOL competition impetus
05 p0700 A69-15547

Helicopter, compounds and composite aircraft design trends
05 p0700 A69-15548

Compound rotorcraft VTOL vehicle current programs
05 p0703 A69-16394

Lockheed 1011 Tristar with three turbofan engines for large capacity medium range service, noting configuration, aerodynamics, structure and cutaway drawings
08 p1255 A69-21143

Book on aircraft stability and control covering conventional, canard, variable sweep, slender delta wing, helicopter and other VTOL aircraft
11 p1821 A69-24370

Store separation from high speed aircraft via wind tunnel test techniques, discussing drop model, flowfield survey and captive trajectory testing
[AIAA PAPER 68-361] 11 p1819 A69-25373

Book on experimental aerodynamics covering subsonic and supersonic wind tunnels, wall measurements, airfoils, aerodynamic characteristics of propellers, fixed and rotary wing aircraft
17 p2891 A69-33318

Folding propotor V/STOL aircraft characteristics, showing configuration effects on performance and optimization of rotor, wing and propulsion systems
[AHS PAPER 302] 17 p2901 A69-33547

Weights study of V/STOL aircraft types for similar mission and payload requirements with different propulsion systems and flight profiles
[SAWE PAPER 783] 18 p3091 A69-34869

Gross weight and aircraft size estimates for configuration design of fighter aircraft
[SAWE PAPER 760] 18 p3220 A69-34880

Circulation control by blowing and application to stopped rotor aircraft, discussing data from model scale blade experiments
19 p3248 A69-36767

VTOL aircraft lift systems, propulsion, airframes, dynamic and aerodynamic characteristics, control systems, missions, safety, configurations and environment
[AIAA PAPER 68-977] 20 p3461 A69-37149

Schweikhard method for measuring changes in lift, drag and pitching moment of fixed wing aircraft as function of distance from ground
20 p3462 A69-37423

Gust absorber system configuration flight tests and analysis, emphasizing application to delta wing aircraft
[ONERA-TP-698] 20 p3462 A69-37753

Sonic boom signatures produced by diverse SST configurations during cruise, indicating aircraft length as overpressure limit factor
24 p4253 A69-43661

AIRCRAFT CONTROL

NT HELICOPTER CONTROL

Aircraft cockpit displays design for flight control and navigation, discussing integration, pictorial realism, moving part, pursuit tracking, frequency separation and optimum scaling
02 p0203 A69-12213

Advance indication based on extrapolation for aiding manual attitude control of VTOL aircraft in hovering flight, noting results on flight simulator
03 p0366 A69-13645

Differential gearing of aileron movements to reduce control forces in aircraft
03 p0367 A69-13786

Avionics, discussing use of electronics in control of aerospace vehicles
03 p0431 A69-14085

Two term and three term controllers for hovering rigs and VTOL aircraft, comparing stability, transient response and control force
04 p0547 A69-14814

Servolements and control methods for V/STOL aircraft, including lift and propulsion throttle configurations
04 p0547 A69-14815

Open class type glider design, discussing structural materials, dimensions and control
05 p0702 A69-16027

Optimum evasion tactics for aircraft pursued by missile, using steepest ascent method for maximization of distance of closest approach
06 p0866 A69-17401

Flight evaluation of direct lift control on DC-8 super 63 jet transport
06 p0867 A69-17666

Aircraft and spacecraft guidance and control technology including computers, optimum and Kalman filtering, strapdown inertial navigation, sensors and test pads
[AIAA PAPER 69-72] 06 p0956 A69-18136

Aircraft and spacecraft guidance and control technology including computers, optimum and Kalman filtering, strapdown inertial navigation, sensors and test pads
[AIAA PAPER 69-72] 07 p1177 A69-19179

Subjective pilot ratings based on Cooper scale compared with aircraft handling criterion based on Shannon information theory, discussing pilot error and accident probability
08 p1254 A69-20458

Control technique to make aircraft insensitive to parameter variations and to achieve desired response to control
08 p1255 A69-20719

Aircraft electrohydraulic primary control systems including electrical signal transmission, engine failure detection, signal structure and digital systems
08 p1347 A69-20872

Aircraft modal control systems synthesis to improve response characteristics by altering pairs of complex conjugate and real eigenvalues simultaneously
09 p1435 A69-22779

Manual control displays for instrument landing approach of large subsonic jet transport, evaluating closed loop system performance and scanning workload
10 p1650 A69-23877

Book on aircraft stability and control covering conventional, canard, variable sweep, slender delta wing, helicopter and other VTOL aircraft
11 p1821 A69-24370

Monograph on flight mechanics and control technology of low flight vehicles at high flight velocities, discussing altitude control design, power spectra, etc
11 p1823 A69-24638

Visual simulation for critical maneuvers of aircraft takeoff and landing, noting method based on limited corridor simulation and maneuver freedom
[AIAA PAPER 68-255] 11 p1866 A69-25376

VTOL aircraft flight control systems, considering computerization and automation approach with human pilot serving as monitor and emergency system
11 p1823 A69-25387

Pictorial display techniques aiding air traffic and aircraft control, discussing projection and directly viewed display
13 p2296 A69-27335

Trident 2E aircraft, discussing fuel system, electric power installation, hydraulic system, air conditioning, pressurization and flying controls
13 p2202 A69-27973

Ballistic deviations limits for aircraft vertical gyroscope taking into account aircraft vertical movements, using compensation in system

14 p2445 A69-28899

Runway roughness induced vibrations in highly flexible aircraft, noting effect on pilot control of aircraft and airframe structure

14 p2392 A69-29504

X-22A VSTOL aircraft testing, discussing control sensitivity, dutch roll mode period and performance test planning based on characteristics prediction

14 p2392 A69-29699

Digital computerized analysis and characteristics of variable stability aircraft, examining digital control system

15 p2549 A69-30229

Aircraft constant altitude-pressure flight navigation attained using Bellamy formula and loxodromic route for drift compensation

15 p2651 A69-30294

Motion equations for dynamics of aircraft control surface controlled by autopilot with rigid feedback

16 p2809 A69-32134

Color signal light gun for aircraft control at airport towers, noting pilot tests for familiarity with signal code

17 p2914 A69-33185

Book on flight mechanics of aircraft and missiles covering mass, propulsion and aerodynamic forces, TOL problems, optimization problems, etc

17 p2898 A69-33319

Lifting rotor dynamics and undesirable characteristics reduction, discussing feedback control systems for pitch and roll

[AHS PAPER 340A]

17 p2899 A69-33509

Analog correction method to suppress pilot maneuver effects during analysis of aircraft accelerations induced by atmospheric turbulence

[ICAS PAPER 68-39]

17 p2901 A69-33590

VTOL variable stability system /VSS/ for XV-4B lift jet for flight control and handling verification

17 p2902 A69-34066

Soviet book on practical aerodynamics of An-2 aircraft covering aerodynamic characteristics, equilibrium, stability and control for various flight conditions, including icing

18 p3090 A69-34340

Parametric approach for weight estimation of surface control systems of transonic and supersonic combat and subsonic transport aircraft

[SAWE PAPER 812]

18 p3221 A69-34898

Additional yawing by gyroscopic moment of power plant and effect on aircraft maneuver during curvilinear flight, noting compensation by automatic control

18 p3092 A69-34973

Aircraft terrain-following algorithm for use with airborne general purpose digital computer, discussing simulation techniques and test results

[AIAA PAPER 69-817]

19 p3366 A69-35625

Fighter aircraft higher order control system dynamics effects on longitudinal handling qualities evaluated by in-flight simulator for role of pilot induced oscillations tendencies

[AIAA PAPER 69-768]

19 p3245 A69-35655

VTOL aircraft lift systems, propulsion, airframes, dynamic and aerodynamic characteristics, control systems, missions, safety, configurations and environment

[AIAA PAPER 68-977]

20 p3461 A69-37149

Book on synchros application and design covering telemetry, torque and control systems, synchro circuits, resolvers as computer elements, etc

21 p3681 A69-38450

Analytical and graphical methods for characteristics of optima produced by quadratic performance index for VTOL prefilter model reference attitude control system

[AIAA PAPER 69-884]

21 p3764 A69-39411

Longitudinal flying qualities of aircraft, comparing attitude and altitude control data

[AIAA PAPER 69-898]

21 p3648 A69-39422

Adaptive control system for aerospace vehicles, describing model reference network for control parameter determination

21 p3688 A69-39857

Clear air turbulence /CAT/ causes effect on aircraft control, discussing monitoring device and aircraft position maintenance under CAT conditions

22 p3977 A69-40007

Aircraft digital control hardware and applications including airborne computer proper, distributed systems, loop control, system integrity, etc

[RAES PAPER 4]

22 p3908 A69-40485

Parameter optimization technique for aircraft control equipment design

22 p3919 A69-41051

Flight simulation requirements for reducing aircraft training flight time, discussing control system and instrument motion characteristics, visual simulation and critical maneuvers motion

22 p3928 A69-41139

Forces on aircraft during ground roll with slick runway surface and cross wind for deceleration and control on ground

[SAE PAPER 690375]

23 p4062 A69-41652

JT9D engine fuel and vane control systems for Boeing 747, noting computing system positioning of throttle valve for fuel flow control

[SAE PAPER 690405]

23 p4201 A69-41658

Manual vehicle control analysis based on feedback systems analysis and mathematical models for human operators engaged in control tasks

24 p4274 A69-43021

Optimal gain theory for input vector and application to regulator problem describing aircraft dynamics

24 p4293 A69-43305

AIRCRAFT DESIGN NT HELICOPTER DESIGN

Pneumatics for aircraft systems integration, proposing engine bleed air use for high power short term duties, heat recovery from cabin air conditioning, etc

01 p0012 A69-10594

Balsa wood laminates as aircraft structural material noting thermal properties, fire and fatigue resistance, weight savings, etc

01 p0101 A69-10595

Boeing 747 characteristics for passenger and cargo service noting economic gain, operational performance, control cabin, engine, etc

[AIAA PAPER 67-397]

01 p0010 A69-10636

Cost prediction equations used in perturbed environment of learning curves subjected to design change in industry

01 p0180 A69-10652

Structural testing in aircraft design, discussing costs, environmental conditions, test rigs and apparatus

01 p0170 A69-10864

Reliability and maintenance economics for jet transport operations of 1980s, discussing Aircraft Integrated Data System /AIDS/ sensors design

[AIAA PAPER 68-207]

01 p0011 A69-11022

Atmospheric turbulence power spectra for design criteria of future low altitude aircraft from LO-LOCAT program, analyzing turbulence scale lengths

[AIAA PAPER 68-216]

01 p0011 A69-11023

Emergency oxygen supply systems for aircraft, discussing simplicity, standardization, safety, reliability and maintenance

[AIAA PAPER 67-965]

01 p0013 A69-11025

Boeing 747 performance, propulsion, structural and circuit characteristics, mass production and airport passenger installations

01 p0011 A69-11067

Manufacturer and assembler liability for injuries caused by design defects resulting from engineering errors in aircraft products

01 p0180 A69-11392

Welding use in aircraft design, noting weight and cost advantages and problems of stressing, stress corrosion and inspection

02 p0253 A69-12062

Aircraft and engine parameters for maximum theoretical range of turbojet for given cruising speed

03 p0366 A69-12950

Minimum admissible spacing between supersonic jet expelled from VTOL aircraft nozzle and plane surface near nozzle exit

03 p0361 A69-12955

X V-4B Hummingbird 2, noting modification from XB-4A two engine ejector augmentation to six engine direct and diverted thrust configuration

03 p0366 A69-13112

Cost analysis techniques for aircraft design and development, considering passenger capacity, flight distances and flight frequencies for various aircraft types

03 p0366 A69-13646

VFX fighter aircraft, discussing U.S. Navy requirements influence in VFX-1 and VFX-2 design

03 p0367 A69-13675

Airframe/propulsion blending in high performance fighter aircraft, discussing thrust augmentation, fuel consumption, induction system and exhaust nozzle balance with airframe

03 p0364 A69-13676

Swing wings on combat aircraft and SST, discussing suitability for aircraft carriers and problems in aerodynamic balance

03 p0367 A69-13677

Differential gearing of aileron movements to reduce control forces in aircraft

03 p0367 A69-13786

Numerical method for explicit solution of aircraft mass problem based on linearization of equations describing individual aircraft section masses

03 p0367 A69-13790

Hovercraft range operating at constant speed as function of design efficiency, power apportionment, fuel consumption and initial specific resistance

03 p0367 A69-13909

Hovercraft and applications of air cushion principle, discussing large and small size vehicles, autobalancing, hybrids and ram wings

03 p0367 A69-14084

Soviet collection of papers on aircraft construction and air fleet equipment

04 p0672 A69-14483

Prandtl three main problems of airfoil theory interpreted and applied, discussing slender aircraft and hypothetical waverider aircraft

04 p0543 A69-14802

Passenger aircraft design to cope with air traffic volume increase in 1970s, discussing economic aspects of high capacity aircraft

04 p0546 A69-14804

Elasticity of demand theory applied to fare changes effect on passenger volume, noting interdependence of aircraft size and fare formulation

04 p0689 A69-14805

Maintainability and reliability affect utilization and operating costs of commercial aircraft

04 p0547 A69-14806

Design parameters optimization for V/STOL jet aircraft with lift engines mounted in wing pod, discussing wing loading and aspect ratio, power plant, etc

04 p0547 A69-14812

Early design stage flutter analysis for variable sweep aircraft, using subsonic flutter model

04 p0677 A69-14834

Boeing/Vertol Hybrid Facility for solving engineering problems in V/STOL design and research

04 p0567 A69-15352

Tactical support aircraft size, economy and flexibility requirements based on Vietnam experience

04 p0549 A69-15486

Airframe subsonic aerodynamic problems for fixed wing aircraft under low speed/high lift conditions

05 p0695 A69-15542

Airplane drag prediction by wind tunnel tests

05 p0695 A69-15543

Design of high lift devices in relation to fixed wing subsonic transport aircraft, considering lift, drag, stability and control

05 p0695 A69-15544

Stability derivative estimation at subsonic speeds for preliminary design engineer

05 p0700 A69-15545

Helicopter, compounds and composite aircraft design trends

05 p0700 A69-15548

Rotary wing handling qualities, discussing analytical tools, design and IFR capabilities for higher speed range

05 p0701 A69-15550

Tip turbine driven flush thin profile wing or platform lift fan design and operating considerations

05 p0696 A69-15554

Aircraft propulsion by wake regeneration, noting supersonic transport ogee layout with maximum drag fraction

05 p0811 A69-15555

Unified design approach for second generation air cushion craft based on existing first generation craft

05 p0701 A69-15567

Design parameters optimization techniques for V/STOL aircraft, noting necessary cooperation between engineering and computing facilities

05 p0701 A69-15570

Nimrod maritime reconnaissance aircraft, discussing high speed high altitude transit flights

05 p0702 A69-15885

Aircraft structure lightweight construction materials, reviewing Ti alloys and Be and Al-B bonded filament materials

05 p0779 A69-15917

Open class type glider design, discussing structural materials, dimensions and control

05 p0702 A69-16027

SST System Safety Program, discussing cosmic radiation and aerodynamic heating

06 p1041 A69-16838

Low drag three dimensional body configurations from tabulated low drag airfoil coordinates

06 p0857 A69-17000

Aircraft aerodynamic characteristics determination from numerical computer solution of supersonic gas flow past blunt body with broken generatrix
06 p0859 A69-17582

Boeing SST designs, discussing performance, flying qualities and operational characteristics of configurations
06 p0868 A69-17830

Helicopters and fixed wing STOL and VTOL aircraft for intertheater military logistics transportation, discussing C-5A role in 1970s
07 p1053 A69-19177

Small and full scale model tests for feasibility of retracted rotor aircraft for high speed flight [AIAA PAPER 69-219]
07 p1055 A69-19550

V/STOL commercial intercity jet aircraft design concept for high density short haul travel featuring low noise, high economy, reliability and tandem wing configuration [AIAA PAPER 69-200]
07 p1056 A69-19571

TRAC variable diameter rotor design based on jackscrew mechanism applied to compound helicopter [AIAA PAPER 69-221]
07 p1056 A69-19572

Air deflection and modulation /ADAM/ turbofan propulsive wing V/STOL design [AIAA PAPER 69-201]
07 p1056 A69-19573

Damage tolerance as design consideration for aircraft safety and reliability, discussing application of failed single principal member concept to airframe construction [AIAA PAPER 69-212]
07 p1056 A69-19574

Minimum drag wing flap profile design, discussing application for trailing edge flaps
08 p1251 A69-20441

Aircraft design, fabrication and finish techniques taking into account aircraft integral fuel tank corrosion due to contaminants associated with microbiological debris [NACE PAPER 49]
08 p1320 A69-20599

Environmental simulation in aircraft engineering, tests concerning aerodynamic conditions and simulator design
08 p1301 A69-20603

LFU 205 light aircraft design and construction with fiberglass reinforced plastic
08 p1321 A69-20867

Landing gear requirements for aircraft design, discussing tire pressure, wheel arrangement, brakes for loading and aircraft weight
08 p1255 A69-21161

Single stage rocket vehicle design for rapid global air transportation noting size, range and economics
09 p1433 A69-21303

Firebee 2 /BQM-34E/ turbojet-propelled recoverable supersonic aerial target construction, performance prediction and missions
09 p1434 A69-21901

Human engineering program at early design phase of SST aircraft to achieve maximum human efficiency and man machine compatibility
09 p1447 A69-22546

Boeing 747 aircraft, discussing weight and cost reduction, flap design, structural philosophy, powerplants, fuel system, flying controls, power systems, etc
09 p1435 A69-22714

Aerodynamic design, discussing research in aeronautical engineering and European organization
09 p1433 A69-22774

Buccaneer aircraft development, considering structure, air bleed, aerodynamics, controls, electric systems, flight refueling, aircrew escape, armament and weapons delivery
09 p1435 A69-22775

V/STOL undercarriage design, considering influence of aircraft operation, engine installation, rough/soft ground capability, etc
09 p1435 A69-22781

Lockheed XV-4B Hummingbird 2 VTOL aircraft propulsion, control, escape systems, with tests
10 p1634 A69-23597

Aircraft technology for hypersonic speed range including swept wing, engine design, composite materials, lift-drag ratio, considering weight, efficiency, STOL requirements
10 p1634 A69-23598

Titanium compared with aluminum in application to supersonic aircraft structures, considering tests and costs
10 p1700 A69-23600

Soviet supersonic transport Tu 144, describing wing unit, fuselage, passenger accommodation, tail unit, landing gear, power unit engine nacelle and navigation
10 p1634 A69-23838

Folding propotor VTOL aircraft configuration analytical and experimental investigations to study design requirements for cruise speeds to Mach 0.75 [AIAA PAPER 69-220]
10 p1635 A69-24087

Tilt wing executive transport aircraft designed by postgraduates at College of Aeronautics of UK, discussing costs, construction and marketability
11 p1821 A69-24321

European A-300B airbus design, considering aerodynamics, fuselage, power plant, structure, systems, maintenance cost and autoland
11 p1822 A69-24464

Light aircraft and helicopter manufacturing methods, design concepts and materials, discussing aluminum airframes, riveting, fiberglass, UV curing, etc [SAE PAPER 690341]
11 p1822 A69-24498

Aircraft and fuel supply system functional compatibility requirements and analysis noting gasolines, fuel tanks, valves, fuel transfer and metering [SAE PAPER 690308]
11 p1825 A69-24503

Military forward air control aircraft conversion from lightweight commercial tandem engine aircraft noting visibility, communication and navigation equipment [SAE PAPER 690313]
11 p1822 A69-24511

Compatibility effects of automatic test equipment on avionic hardware design
11 p1865 A69-25070

Douglas DC-10 medium range aircraft, discussing engine placement, passenger and cargo capacity, construction data, etc
11 p1823 A69-25211

Comparative evaluation of avionic installations in design stage, detailing parameters for civil aeronautical use
11 p1887 A69-25212

Minimum drag wing profile at zero angle of attack in supersonic flow, allowing for initial structural flaws and randomly varying parameters
11 p1818 A69-25328

Store separation from high speed aircraft via wind tunnel test techniques, discussing drop model, flowfield survey and captive trajectory testing [AIAA PAPER 68-361]
11 p1819 A69-25373

Aircraft structure geometry design for minimizing total mass concerning flutter requirements
11 p1989 A69-25493

Gust load predictions for aircraft design by treating aircraft load history as linear response to stationary Gaussian process excitation
11 p1823 A69-25504

Concorde design problems due to kinetic heating, aerodynamic characteristics, structure, equipment, modified delta wing planform, etc
12 p2012 A69-26358

Exhaust gas recirculation for VTOL aircraft [AIAA PAPER 67-439]
12 p2013 A69-26760

Systems design of airframe structures taking into account material characteristics noting structural stability, shell postbuckling, fail-safe designs, etc
12 p1816 A69-26833

Multicell air cushion vehicle technology based on 1/4 scale and full scale tests, noting comparison with plenum systems and costs
13 p2202 A69-27547

Trident 2E aspect ratio, wing area, high lift devices, fuel capacity, range improvement, etc
13 p2202 A69-27971

Spey 512 turbofan and RB.162 booster turbojet engines for Trident 2E and 3B power plant
13 p2325 A69-27975

Aircraft design cost control emphasizing engineering performance direct inclusion in design costs including tooling, testing, etc
13 p2382 A69-28094

Galaxy C-5A aircraft Value Control Program stressing design organization, upper management authority, budgetary adjustments, etc
13 p2383 A69-28095

Weight and cost control program for Boeing 747 aircraft through combined value and weight engineering methods
13 p2383 A69-28096

Turbofan V/STOL with separate lift units for takeoff and landing, discussing commercial and military applications, cost effectiveness and operational characteristics
13 p2203 A69-28354

Aircraft design synthesis requirement definition in hardware commitment, discussing error effects of weight, aerodynamics and propulsion
14 p2392 A69-29432

Military aircraft operating in various environments with low support costs emphasizing improved design, development and manufacturing standards
14 p2392 A69-29503

Fighter aircraft design and performance criteria including acceleration, maneuvering, interception and turning combat capabilities
14 p2393 A69-29700

Soviet book on partially liquid filled solid body dynamics from viewpoint of space and aircraft applications
14 p2530 A69-29815

Book on subdivision of aircraft structural design covering technology, economics, working conditions, performance, etc
14 p2456 A69-29860

Electron beam welding characteristics for aircraft components and design noting limitations [SAE PAPER 690318]
15 p2617 A69-30089

Helicopter weight analysis in preliminary design and proposal field
15 p2550 A69-30463

Next generation subsonic aircraft, discussing basic concerns, aerodynamic factors, materials, noise reduction, cost effectiveness, titanium techniques, etc
15 p2550 A69-30590

Beryllium brake disks use on C-5A aircraft, comparing size, weight and peak temperature with steel structure
15 p2639 A69-30591

German VFW 614 short haul commercial jet aircraft design, marketing, etc
16 p2734 A69-31805

Civil aircraft requirements from 1975 onward, discussing classes, categories and R and D
16 p2882 A69-32022

Aerodynamic problems in future civil aircraft design, emphasizing Concorde development possibilities, discussing VTOL intercity transport, subsonic swept wing and hypersonic aircraft, all-wing airbus, etc
16 p2732 A69-32023

Civil aircraft projected development regarding materials and structures, discussing new components and fuel contribution to weight and metals and composites for replacing Al
16 p2872 A69-32024

Medium range Tu-154 three jet transport aircraft, detailing fuselage, airfoil, tail unit, landing gear, propulsion unit and circuitry
16 p2735 A69-32073

Book on soviet An-24 aircraft-construction and exploitation covering fuselage, powerplant, controls, fire prevention, air conditioning, maintenance, etc
16 p2735 A69-32112

High bypass ratio engine influence on short range civil aircraft design, considering performance, noise, engine location, etc
17 p2897 A69-33212

Aircraft auxiliary power system influence on power plant installation and aerodynamic design
17 p3017 A69-33216

Heat transfer suppression techniques in high temperature low density fiberglass insulation for flight vehicles [AIAA PAPER 69-606]
17 p3072 A69-33279

Aircraft designers and operators problems with danger and damage caused by bird strikes, considering warning devices and protective windshield panels
17 p2899 A69-33363

Concorde design, discussing planform, wing twist and camber, hypersustentation, kinetic heating, aeroelasticity, R and D, tests, etc
17 p2899 A69-33380

German VTOL aircraft development excluding helicopters, discussing technical problems, safety and economy in civil application
17 p2899 A69-33381

Flow simulation on wind tunnel test models for aerodynamic characteristics of aircraft design, discussing boundary layer and external flow coupling [AIAA PAPER 69-660]
17 p2945 A69-33471

V/STOL fatigue design parameters, balancing fail-safe and safe-life design procedures [AHS PAPER 376]
17 p2900 A69-33512

Avionics systems with integration and federation applied to integrated light attack avionics system /ILAAS/ design to provide navigation, weapon delivery and flight control
17 p2976 A69-34057

Canadair CL-84 two propeller V/STOL utility tilt wing vehicle development program and flight tests to assess military potential of aircraft
17 p3077 A69-34065

Skyvan 3 light passenger/freight carrier design, detailing power plant, installation and power management
17 p2902 A69-34192

Skyvan 2 aircraft aerodynamic design, describing modifications to increase fuel capacity, directional stability and range capability

17 p2896 A69-34193

Series 3 Skyvan design, describing controls, electric and electronics equipment, weather protection, environmental and fuel systems

17 p2906 A69-34194

Flight compartment and cabin layout of Skyvan 3 designed as freighter with passenger capability

17 p2903 A69-34195

Aircraft developments affecting international airport planning

17 p2948 A69-34203

Air traffic control and airline operators liaison with reference to air transport priorities, considering relationship to aircraft and airport development

17 p3004 A69-34204

Aircraft design determined by airport environment and facilities defined as pavement strength, passenger and baggage loading and aircraft handling, noting noise abatement

17 p2948 A69-34209

Airport performance, noise and aircraft utilization influence on aircraft design and operating costs, stressing takeoff distance, obstacle clearance and noise regulations

17 p2948 A69-34210

Fixed weight aircraft growth factor variation with location of initial weight penalty along fuselage station, using static stability margin and trim capability

[SAWE PAPER 796] 18 p3220 A69-34862

Advanced design weight analysis and fixed equipment and propulsion systems weight prediction, noting error probability

[SAWE PAPER 790] 18 p3220 A69-34867

Armor selection for advanced aircraft systems based on premium value concept and cost-weight considerations

[SAWE PAPER 764] 18 p3094 A69-34878

Statistical weight estimation equations developed by constrained regression analysis, noting application to vertical tail of cargo/transport aircraft

[SAWE PAPER 762] 18 p3220 A69-34879

Gross weight and aircraft size estimates for configuration design of fighter aircraft

[SAWE PAPER 760] 18 p3220 A69-34880

Aircraft structural weight optimization based on design consideration of grouped related elements, noting application to Boeing 747 trailing edge flap drive

[SAWE PAPER 757] 18 p3220 A69-34881

Design iteration loop calculations related to fighter aircraft weight growth factor, noting asymptotic aircraft performance and strength

[SAWE PAPER 732] 18 p3221 A69-34893

Synthesis and integration of cross discipline function for weight effective design of airplanes

[SAWE PAPER 730] 18 p3221 A69-34895

Aircraft preliminary design weight and volume characteristics relation to aircraft density

[SAWE PAPER 813] 18 p3221 A69-34897

Boeing 747 design and development, discussing aircraft characteristics, performance, inertial navigation system, production costs, etc

[SAWE PAPER 746] 18 p3091 A69-34907

Tupolev Tu-154 three jet transport featuring automatic flight control system with inertial and Doppler navigation inputs, low speed wing devices

18 p3092 A69-34933

Military aircraft design, discussing reduction of specialization bias and timely application of technical advances

18 p3092 A69-35137

Aircraft engine lubrication system design, discussing bearings reduction, oil compartment scavenging, sealing, cooling, pressurization, etc

18 p3185 A69-35244

Lockheed L-500 aircraft weight consideration in structural design as all cargo lifter, describing engine thrust, payload, options, etc

18 p3092 A69-35464

Cargo aircraft future design regarding engine development, structural flexibility, airport compatibility, cargo handling, etc

18 p3092 A69-35467

Air terminals plans for 1975 aircraft and air traffic based on runway configurations

[AIAA PAPER 69-805] 19 p3288 A69-35591

L-1011 Tri-Star aircraft systems and safety provisions, discussing automatic flight control system, propulsion, noise reduction, galley, coat storage and cabin window shades

[AIAA PAPER 69-828] 19 p3243 A69-35598

Aircraft Economic Design Evaluation /AEDE/ computerized model to estimate aircraft design performance differences economic impact to carriers

[AIAA PAPER 69-814] 19 p3289 A69-35626

Quiet military aircraft design factors, considering human hearing characteristics, noise suppression methods, propeller noise-performance relationships and jet engine noise nature

[AIAA PAPER 69-792] 19 p3243 A69-35637

YF-12A interceptor aircraft development and testing, discussing titanium alloys application, aerodynamics and thermodynamics, escape systems for high speed and altitude tests

[AIAA PAPER 69-757] 19 p3245 A69-35652

Flight control systems influence on military aircraft design and performance, discussing static stability, ride quality, flutter margin and maneuver load controls

[AIAA PAPER 69-767] 19 p3245 A69-35656

Concorde aerodynamic design compromise between high and low speed requirements, kinetic heat problems and materials selection

[AIAA PAPER 69-759] 19 p3245 A69-35661

Man machine interface problems in C-5 equipment and system design

19 p3261 A69-36024

DC 10 aircraft reliability program, discussing passenger attractiveness, dispatch reliability, maintenance cost, flight safety and computer simulation for reliability engineering

19 p3248 A69-36027

C-5 air force logistic transport, discussing structural design, configuration, payload, aerodynamics and flight testing

[AIAA PAPER 69-758] 19 p3248 A69-36295

DC 10 wing design, wind tunnel models, structural and systems testing, production and marketing

[AIAA PAPER 69-830] 19 p3248 A69-36296

Cost comparison of single and twin engined layouts for tactical strike/close support aircraft

19 p3248 A69-36855

DC 3 tail wheeled single skin piston aircraft conversion into first class luxury passenger aircraft for short haul service

20 p3460 A69-36918

Technical problems in converting long service civil aircraft to obtain more volume, easier loading access or greater flexibility

20 p3461 A69-36919

Random gust design requirement and gust load covariances to define boundaries of gust-loading region for airframes

20 p3621 A69-37167

STOL aircraft to serve traffic needs of northeast corridor, discussing decision making regarding size, type, cost, speed and strip-length

20 p3462 A69-37352

Tilt propotor composite aircraft design, discussing performance and mission potential

[AHS PAPER 202] 20 p3463 A69-37805

Jaguar aircraft design and operational characteristics, noting supersonic performance at high altitudes and during maneuvers

20 p3463 A69-37928

Avionics system analysis, engineering, design, fabrication and testing problems

20 p3545 A69-37929

Hydraulic power pack for automatically raising or lowering landing gear in small aircraft

20 p3467 A69-38183

Rain erosion problems in aircraft design, reviewing protective measures for all-weather aircraft

21 p3646 A69-38393

All-plastic light passenger aircraft with inflated tube construction for shell, discussing design and performance

21 p3728 A69-38461

Northrop F-5-21 fighter design, avionics, performance and operational existence

21 p3646 A69-38732

Tail plane shape for optimal damping of rotational motion and elastic torsional deformations of aircraft body around longitudinal axis using calculus of variations

21 p3647 A69-38845

Economic effectiveness determination methods for commercial transport aircraft design analyzed quantitatively, using four engine 100-seat turboprop aircraft

21 p3855 A69-38873

Economic effectiveness of design and fabrication changes in aircraft construction industry for profitable operation of commercial transport aircraft

21 p3855 A69-38874

NF106B-VST model follower flight control system, discussing design criteria/performance index,

rigid/elastic math model development, flight test evaluation, hardware design, etc

[AIAA PAPER 69-886] 21 p3764 A69-39412

Soviet book on flight vehicle design dynamics, discussing lift effectiveness and rigidity as function of internal stresses during ground and flight operations

21 p3825 A69-39533

Design criteria for Concorde SST servoflight control system reliability and safety

21 p3650 A69-39697

Turbofan engine influence on civil transport aircraft design as function of thrust, discussing engine ratings, number of engines, APU and thrust engine

22 p3862 A69-39961

Computerized crewstation geometry evaluation and design optimization using 23-pin-joint man-model

[AIAA PAPER 69-977] 22 p3892 A69-40357

Piloted ground-based flight simulators role in tactical and VTOL aircraft design, describing simulation devices, computer programs and design information

[RAES PAPER 10] 22 p3927 A69-40490

A 300B twin engine short haul giant transport aircraft, discussing engines, aircraft performance and systems reliability

[RAES PAPER 11] 22 p3863 A69-40491

Design and economic concepts of Lockheed L-1011 wide body trijets, discussing airport and airways congestion alleviation, passenger appeal, etc

[RAES PAPER 15] 22 p3863 A69-40494

Design of Concorde wing for Mach 2 cruising speed including fuselage/wing relations, wing planform and leading edge camber, etc

[RAES PAPER 18] 22 p3859 A69-40497

Boeing 747 design, fitting to operation, airline planning for flight training, airport facilities, ground equipment, service functions, etc

[RAES PAPER 12] 22 p3864 A69-40621

Safety engineering programs for aircraft design, discussing organizational relations, failure and operational safety analyses

22 p3867 A69-41132

Safety standards for DC 10 aircraft, considering cockpit design, hydraulic, electric power, autoland and direct lift control systems, structural safety and crash worthiness

22 p3867 A69-41133

Boeing 747 safety engineering program, discussing organization, design review, system safety, systems design-analysis and tests

22 p4054 A69-41136

SNECMA thrust reverser system design on Concorde prototype, discussing performance, safety, airworthiness, operational requirements, reliability and maintenance

[SAE PAPER 690412] 23 p4200 A69-41640

Douglas DC-10 aircraft design programs and methods stressing power plant reliability, maintainability and costs

[SAE PAPER 690391] 23 p4201 A69-41664

Structural aircraft design requirements for high flight speeds stressing aerodynamic heating, heat resistant materials, weight and geometry problems

23 p4233 A69-42164

Airplane structure electromagnetic compatibility engineering problem including bonding, electrointerference suppression and static control considerations

23 p4063 A69-42234

Rolls-Royce-Bristol/SNECMA M45H medium power turbojet for VFW 614 aircraft

24 p3463 A69-42566

V/STOL commercial intercity jet aircraft design concept for high density short haul travel featuring low noise, high economy, reliability and tandem wing configuration

[AIAA PAPER 69-220] 24 p4251 A69-42648

Aircraft engine lubrication system design, discussing bearings reduction, oil compartment scavenging, sealing, cooling, pressurization, etc

24 p4363 A69-42780

MIG-21 fighter aircraft development, characteristics and technical and operational data

24 p4251 A69-42795

Beriev Be-12 cranked wing seaplane design including technical and operational data

24 p4251 A69-42796

Aero L-39 low wing cantilever monoplane jet trainer developed in Czechoslovakia

24 p4251 A69-42797

Czechoslovak L-400 high wing short range STOL transport aircraft powered turboprop engines, discussing passenger and cargo version

24 p4251 A69-42799

Commercial aircraft environmental compatibility planning, considering problems of airport traffic growth and restrictive air traffic control regulations [AAS PAPER 69-326] 24 p4252 A69-42808

SST contribution to commercial aircraft transportation, discussing economic and operational aspects, decision making process leading to fixed wing design, etc [AAS PAPER 69-323] 24 p4252 A69-42869

Supersonic aircraft design data, costs and benefits, discussing origin and significance of sonic boom 24 p4252 A69-42997

Aerodynamics, transonic performance, airframe/propulsion, compatibility, structures and materials, flight controls, takeoff and landing capabilities and combat survivability of next generation military aircraft 24 p4252 A69-43046

Orthotropic aircraft materials plasticity theory, deriving stress-strain relationships in three mutually perpendicular symmetry planes for use in engineering calculations 24 p4400 A69-43083

Maximum admissible weight of structural elements required for conventional wing conversion into variable geometry wing without performance impairment 24 p4253 A69-43092

FAA power spectral gust methods for computing design limit loads on commercial aircraft, noting British investigations 24 p4253 A69-43111

Aircraft fastener corrosion control with emphasis on surrounding joint and structure, discussing test programs, Al coatings, etc 24 p4334 A69-43442

Damage tolerance design concepts required to obtain reliability, maintainability and operational safety of complex aircraft [ICAS PAPER 68-23] 24 p4254 A69-43717

Scramjet engine active cooling with regenerative system using superalloy heat exchangers and hydrogen fuel as coolant [AIAA PAPER 68-1091] 24 p4365 A69-43725

AIRCRAFT DETECTION

Airport surface traffic control system /STRACS/ for detection of aircraft, identification, guidance on taxiways, tower display, fail-safe alarm logic, priority routings, conflict protection, etc 05 p0790 A69-16724

Statistical distribution functions for radar cross section of flying aircraft 14 p2414 A69-29500

Very short pulses effect on aircraft echoes, noting echoing area reduction as resolution cell diminishes 21 p3672 A69-38755

Clear air turbulence detection in troposphere by multifrequency radiometric sensor, noting multibeam system for supersonic aircraft 23 p4144 A69-42536

AIRCRAFT ENGINES

NT BRISTOL-SIDDELEY OLYMPUS 593 ENGINE

NT DUCTED FAN ENGINES

NT HELICOPTER ENGINES

NT J-79 ENGINE

NT J-85 ENGINE

NT PULSEJET ENGINES

NT RAMJET ENGINES

NT SUPERSONIC COMBUSTION RAMJET ENGINES

NT T-53 ENGINE

NT TURBOFAN ENGINES

NT TURBOJET ENGINES

NT TURBOPROP ENGINES

Environmental effects on aircraft and propulsion systems - Conference, Bordentown, New Jersey, October 1968 01 p0055 A69-11043

Engine inlet thermal antiicing analysis, detailing computer programs to determine air flow velocity, water impingement and thermal requirements 01 p0055 A69-11045

Titanium alloy stress corrosion behavior in atmospheric salt environments at elevated temperatures related to aircraft engine part failures 01 p0099 A69-11056

Aircraft gas turbine compressor parts erosion tests 01 p0099 A69-11058

Steam ingestion tests on carrier aircraft gas turbine engines, analyzing inlet pressure and temperature distortion in steam-air environment 01 p0143 A69-11062

Cost factors in choosing single or twin-engine layout for tactical aircraft 02 p0193 A69-12066

Onboard electric power systems of transport aircraft, analyzing constant frequency systems for supersonic aircraft 02 p0196 A69-12166

Digital electronic computer technique for control of aircraft power plant, describing self adaptive control 03 p0496 A69-14091

Aerothermodynamics of subsonic-aircraft propulsion, analyzing performance of bypass engine, fuel consumption and specific weight 05 p0695 A69-15551

High bypass turbofan design, discussing JT9D engine combustion, materials and cooling 05 p0811 A69-15552

Soviet book on design of aircraft engine component and subsystem elements, emphasizing aligning, locking and sealing methods, torque transmission, etc 05 p0812 A69-15864

Similarity conditions in turbine engine tests, analyzing flight speed, Reynolds number, combustion efficiency, heat changes, inlet turbulence and outlet nozzle 05 p0742 A69-16028

Aircraft turbine engines operation and control, discussing technology, simulation and system developments 05 p0812 A69-16528

High turbine inlet temperature technology using thermosiphon cooling for gas turbine, possibly doubling specific horsepower of aircraft [SAE PAPER 690034] 07 p1203 A69-18311

Liquid and vapor phase microscale panel cokers applied to screening synthetic lubricants for aircraft turbine engines [ASLE PAPER 68-LC-22] 07 p1140 A69-19309

Control methods and designs for limiting atmospheric pollution emitted by aircraft gas turbine engines [SAE PAPER 680347] 07 p1204 A69-19729

Aircraft gas turbine engines control systems capabilities and future requirements, considering maximum propulsion system performance with minimum fuel consumption [ASME PAPER 68-GT-62] 08 p1376 A69-19846

Supercharged bypass engines for possible application in light aircraft, noting payload fractions and total takeoff weights values 08 p1254 A69-20168

Flight research testing facilities at Arnold Engineering Development Center for rockets, turbojets, ramjet engines, aircraft, missiles, satellites and spacecraft 08 p1302 A69-20883

Jet mixing applications to aircraft engines, discussing one dimensional calculation of coaxial streams mixing inside conduit 09 p1429 A69-21305

Power systems for future aircraft emphasizing growth in performance and reduction in weight 09 p1567 A69-21387

Composite materials and alloys for jet turbine components in 1970s, discussing anticipated temperatures and material properties 09 p1523 A69-22061

Design, metallurgical and manufacturing problems of titanium application in superjet C5 and SST engines 09 p1570 A69-22062

High recovery inlet design for Boeing 747 high bypass ratio fan engine, considering throat Mach number, lip losses and auxiliary passage losses [ASME PAPER 69-GT-41] 09 p1570 A69-22482

Nickel base superalloys for aircraft gas turbines, considering strengthening mechanisms for creep resistance [ASME PAPER 69-GT-7] 09 p1527 A69-22506

Baseline requirements for commercial aircraft propulsion systems, stressing engine installation in aircraft [ASME PAPER 69-GT-57] 09 p1572 A69-22514

Gas bearings for spool gas generator for aircraft turbine engines, noting rotor bearing stability and LP spool balancing and seal leakage [ASME PAPER 69-GT-60] 09 p1513 A69-22515

Cooled turbine performance evaluation methods, noting promise of analytical methods [ASME PAPER 69-GT-63] 09 p1572 A69-22517

Jet aircraft engines condition monitoring system for detecting malfunctions without engine disassembly [ASME PAPER 69-GT-66] 09 p1501 A69-22518

Film cooling injection slots number and position over flame tube and minimum cooling airflow in aircraft gas turbines 09 p1625 A69-22623

Aircraft engine instrument displays evaluated by human factors, noting vertical scale design [SAE PAPER 690328] 11 p1829 A69-24488

Explosive fabrication of aircraft components including turbine engine exhaust components, door seals, etc [SAE PAPER 690316] 11 p1890 A69-24510

Performance correction and nonstandard day performance prediction for analyzing turbocharged reciprocating aircraft engines in light aircraft applications [SAE PAPER 690309] 11 p1942 A69-24514

Turbine engine in-flight operating conditions simulated on test stand 11 p1942 A69-24528

Aircraft engines future specifications as affected by expanding market, noting speed requirements and thrusts 11 p1942 A69-25215

Frequency characteristics of flexible compensated manifolds for aircraft engines, considering axial force 11 p1826 A69-25332

Gas turbine fuel and control systems for two and three shaft engines in military and civilian aircraft including helicopters [IME PAPER 12] 12 p2147 A69-25796

Control methods and designs for limiting atmospheric pollution emitted by aircraft gas turbine engines 12 p2147 A69-26236

Concorde SST turbojet engine integrated assembly consisting of air inlet, gas generator, reheater and convergent-divergent nozzle 12 p2147 A69-26357

Aircraft engine spark plugs development, reviewing ceramic and mica insulated plugs and four pole electrode spark plugs 13 p2324 A69-27333

Temperature measurement for aircraft gas-turbine engine development 14 p2509 A69-28886

Digital computers for aircraft engines control, discussing economic assessment, advantages and basic control system 15 p2671 A69-30323

Aircraft gas turbine parts design and fabrication, discussing role of welding techniques 15 p2629 A69-30928

Propulsion system influence on aircraft reliability from viewpoint of engine manufacturer 15 p2629 A69-31122

Eddy current and ultrasonic applications to aircraft engine inspection, discussing electric and magnetic methods for quality control during fabrication 15 p2632 A69-31516

Variable bypass ratio lift/thrust engine arrangement in relation to safety and economic requirements, using scale model of V/STOL 15 p2672 A69-31542

Subsonic transport high bypass ratio engine evaluation in terms of fuel consumption, size, thrust-weight ratio, noise and price 16 p2835 A69-31803

Aircraft engine accessories for engine control, monitoring and protection, discussing transducer redesign, equipment range for Concorde, small engine design, etc 16 p2879 A69-31813

Location effect of power plants on aft-mounted supersonic cruise exhaust nozzles at transonic speeds in flight and wind tunnel [AIAA PAPER 69-427] 16 p2734 A69-32769

Self contained lift fan concept and circulation controlled rotor aircraft power plants for high speed VTOL transports 17 p2897 A69-33208

Civil transport aircraft power plant and auxiliary systems as sources of delays, presenting critical path analysis 17 p2898 A69-33213

Power plant installation on swept winged transport aircraft, discussing interference drag sources, high lift problems, unorthodox installations, nacelle effects, etc 17 p2898 A69-33214

Aircraft auxiliary power system influence on power plant installation and aerodynamic design 17 p3017 A69-33216

Aircraft auxiliary power systems, discussing weight and power requirements, component design, driving methods and influence on power plant design 17 p3018 A69-33217

Small turbine development for long life applications in helicopters and unpurssured aircraft, describing Artouste, Turmo, Astazou and Bastan series 17 p3020 A69-33346

Aircraft turbines mechanical parts reliability tests, discussing examples of blade fatigue rupture and rotor disk fatigue 17 p3020 A69-33347

AIRCRAFT EQUIPMENT

Turboshaft engines for military aircraft, discussing size, technology and environmental factors with respect to anticipated market [AHS PAPER 331] 17 p3022 A69-33530

Vertical takeoff aircraft propeller/rotor design and performance prediction, discussing vortex model, wake contraction, blade element aerodynamic properties, etc [AHS PAPER 325] 17 p2894 A69-33534

Digital computer for aircraft engine control covering in-flight health monitoring, automatic flight checkout, diagnostic failure routines, etc 17 p3022 A69-33603

Forced pressure fluctuations in hydraulic systems of aircraft fuselages and engines, taking into account square law of losses at resistance points 18 p3094 A69-34991

Aircraft engine lubrication system design, discussing bearings reduction, oil compartment scavenging, sealing, cooling, pressurization, etc 18 p3185 A69-35244

Mechanical components life or cycles to failure probability distributions determined by Monte Carlo method, comparing theory with aircraft engine parts field data 19 p3327 A69-36031

Low smoke emission combustors for aircraft turbine engines, discussing effects on ignition and exit temperature distribution [AIAA PAPER 69-493] 19 p3394 A69-36299

Concorde Olympus 593 engines electronic control and adjustment devices 19 p3395 A69-36706

Pressure sensors, strakes, removal of full length guide vanes indicate possible difficulties with thrust of NK-8-2 turbofans in Tu-154 19 p3395 A69-36757

Cost comparison of single and twin engine layouts for tactical strike/close support aircraft 19 p3248 A69-36855

Wankel aircraft engines compared to piston and turbine aircraft engines for performance, maintenance and reliability 19 p3395 A69-36872

Supersonic aircraft and power plant structural members operating under cyclic stress at elevated temperatures tested by various methods for interaction between creep and fatigue 20 p3620 A69-37001

Airbreathing gas turbine construction materials including composites and Ti and austenitic alloys [ASM PAPER D8-25.2] 20 p3586 A69-38133

Pneumatic Vernier engines in aircraft and spacecraft, discussing weight, gas expansion and gas temperature 21 p3785 A69-39093

Dornier R and D, discussing single and twin engine aircraft, utility aircraft, helicopter, VTOL transport, safety, etc 22 p3862 A69-39931

RB 202 self contained lift fan engine design for high speed interurban civil VTOL operations, considering weight, cost, noise and fuel consumption 22 p3862 A69-39933

Wakkel engine development in Poland for powered military gliders at 18 hp and 5500 rpm 22 p3999 A69-40006

Modified tailed delta configuration selection for U.S. SST, discussing power plant installation choice [RAES PAPER 17] 22 p3863 A69-40496

Aircraft engine technology, discussing turbine entry temperatures, reheat temperatures, high pressure spools, high temperature materials and small blades fabrication [RAES PAPER 20] 22 p4000 A69-40499

TF39 high bypass ratio engine design, development and tests, noting low smoke combustor [RAES PAPER 21] 22 p4000 A69-40622

Engine oil analysis applied to commercial airline operations, ensuring lubricating qualities retention and detecting oil-wetted component failures [SAE PAPER 690423] 23 p4169 A69-41647

Aircraft gas turbine engine lubricant evaluation and systems design from standpoint of effective oil life and lubricant stability requirements [SAE PAPER 690424] 23 p4200 A69-41648

Engine fuel and geometry control design for large high bypass aircraft turbofan engines used for airbus powering [SAE PAPER 690403] 23 p4201 A69-41659

Douglas DC-10 aircraft design programs and methods stressing power plant reliability, maintainability and costs [SAE PAPER 690391] 23 p4201 A69-41664

STOL transport aircraft propulsion requirements, discussing engine cycle selection, design variables effects, etc [SAE PAPER 690380] 23 p4201 A69-41668

Numerical control as manufacturing tool, with application to aircraft engine precision components 24 p4318 A69-42710

Aircraft engine lubrication system design, discussing bearings reduction, oil compartment scavenging, sealing, cooling, pressurization, etc 24 p4363 A69-42780

Digital computers effect on aircraft automatic power unit controls, discussing safety, reliability, self monitoring and redundant computer systems 24 p4253 A69-43113

Oil high temperature and oxidation conditions in aircraft piston engines, including physicochemical changes 24 p4321 A69-43141

AIRCRAFT EQUIPMENT

Collection of papers on aircraft construction and air fleet equipment covering aerospace vehicles theory, engines, automation, design and production 19 p3246 A69-35813

Soviet book on testing aircraft electrical equipment covering climatic and mechanical tests, malfunction detection, etc 20 p3464 A69-37237

Onboard aircraft computer design criteria, considering adaptability, maintainability, reliability, cost, prototype delivery time, weight and volume 20 p3500 A69-37381

Microminiaturized digital computers for missiles and aircraft, discussing characteristics, environmental conditions and transformation possibility for use in satellites 20 p3502 A69-37392

AIRCRAFT EXHAUST U EXHAUST GASES

AIRCRAFT FUEL SYSTEMS

Liquid nitrogen inertant for continuous suppression of pressurized fuel tank explosion 05 p0703 A69-16505

Low pressure fuel system and turbine rotor blade temperature measurement method for Concorde Olympus 593 engine [ASME PAPER 68-GT-63] 06 p0984 A69-17187

Concorde fuel management, discussing trim, fuel as coolant and booster pumps 07 p1057 A69-19705

Aircraft design, fabrication and finish techniques taking into account aircraft integral fuel tank corrosion due to contaminants associated with microbiological debris [NACE PAPER 49] 08 p1320 A69-20599

Aircraft and fuel supply system functional compatibility requirements and analysis noting gasolines, fuel tanks, valves, fuel transfer and metering [SAE PAPER 690308] 11 p1825 A69-24503

Aircraft integral fuel tanks corrosion causes and prevention, discussing microorganisms, maintenance and cleaning procedures, anticorrosion additives, etc 12 p2013 A69-25946

Trident 2E aircraft, discussing fuel system, electric power installation, hydraulic system, air conditioning, pressurization and flying controls 13 p2202 A69-27973

AIRCRAFT FUELS

JP-4 fuel emulsions properties, handling characteristics and safety performance, noting satisfactory shelf life and thermal stability [ASME PAPER 68-GT-24] 06 p0982 A69-17190

Fuel requirements for flights up to Mach 3.5, discussing heat stable mineral oil based SST fuels 11 p1941 A69-25422

Monograph on spreading of explosive vapor/air mixtures during aircraft fueling, covering underlying flow technology principles 15 p2551 A69-30930

Microbiological corrosion and degradation of aircraft metals and organic materials in fuel tanks 19 p3341 A69-35569

Aviation fuel development covering internal combustion engine, antiknock compounds, isooctane rating methods, gas turbines, jet fuels, etc [AIAA PAPER 69-779] 19 p3392 A69-35643

Film vaporization of fuel in combustion chambers of aircraft turbines, determining concentration and velocity distributions of fuel and air 20 p3633 A69-37921

AIRCRAFT GUIDANCE

Navigation system for American SST noting use of Doppler radar and inertial navigation 02 p0278 A69-12238

Inertial navigation for commercial aircraft, discussing Sagem-Ferranti and Litton systems 02 p0278 A69-12239

Error reduction in initial azimuth alignment and azimuth and level axis gyro drifts in long range air transport gyro accelerometer inertial systems 02 p0278 A69-12361

Laser gyro in future inertial navigation systems for Category 1 landing without position updating 03 p0463 A69-13210

Flight inspection positioning system, discussing microwave interferometer angle calibration for instrument landing 03 p0430 A69-13680

Aircraft and spacecraft guidance and control technology including computers, optimum and Kalman filtering, strapdown inertial navigation, sensors and test pads [AIAA PAPER 69-72] 06 p0956 A69-18136

Aircraft and spacecraft guidance and control technology including computers, optimum and Kalman filtering, strapdown inertial navigation, sensors and test pads [AIAA PAPER 69-72] 07 p1177 A69-19179

Monograph on mathematical model for aircraft separation in air traffic safety control, analyzing aircraft motions and collision avoidance 08 p1347 A69-20712

Polar flight navigation charts showing feasibility of three dimensional celestial positioning 09 p1538 A69-21406

Terminal area navigation and landing guidance systems for V/STOL intercity transport aircraft, considering radio guidance, aircraft control and system interaction 17 p2897 A69-33210

Vertical path guidance computer, noting applications to feeder airlines and airtaxi services operating from airports with VOR/TACAN/only 17 p3003 A69-34104

Artificial horizon indicator design modifications to facilitate maintaining horizontal aircraft position, discussing automatic pilot advantages in turbulence and flight simulators 17 p2903 A69-34214

Landing guidance devices under difficult weather, discussing landing mechanics for land and carrier based aircraft 18 p3170 A69-34857

Sensory physiology of pilot landing guided by runway lighting, stressing visibility influence 19 p3260 A69-35987

Aircraft navigation system requiring computer and display for approach guidance to circular orbit over fixed ground area [AIAA PAPER 69-986] 22 p3978 A69-40366

Takeoff indicator design based on solution of equilibrium equation for forces acting on aircraft along drag axis 24 p4253 A69-43085

AIRCRAFT HAZARDS

Environmental effects on aircraft and propulsion systems - Conference, Bordentown, New Jersey, October 1968 01 p0055 A69-11043

Drag and spray effects due to slush and water on runways during aircraft takeoffs 01 p0011 A69-11048

Light aircraft all-weather flight feasibility, discussing storm and clear air turbulence detection and icing prevention 01 p0111 A69-11049

Icing of airframes, discussing ice formation, deicing methods and protection of aircraft 02 p0192 A69-11889

Frequencies and natural oscillation modes in sporting gliders, demonstrating horizontal oscillation induced aileron suspension brackets destruction 04 p0549 A69-15416

Predictive scale of aircraft emergencies, analyzing human error rate under stress 06 p0880 A69-17208

Supersonic aircraft radiation hazard due to solar flare proton exposure, using Monte Carlo method to estimate dosage as function of tissue slab 11 p1949 A69-24864

Sonic boom damage to structures from supersonic aircraft overflights using inductive and deductive approaches 15 p2585 A69-30370

Ozone concentrations harmful to humans in atmosphere based on U.S. and Western European observations, emphasizing lower stratosphere 15 p2596 A69-30642

Monograph on spreading of explosive vapor/air mixtures during aircraft fueling, covering underlying flow technology principles

15 p2551 A69-30930

Birds as pests - Conference, London, September 1967

17 p2898 A69-33362

Aircraft designers and operators problems with danger and damage caused by bird strikes, considering warning devices and protective windshield panels

17 p2899 A69-33363

Interspecific synthetic signals research for effective bioacoustic bird scaring techniques including optical signals

17 p2914 A69-33364

Airfield bird scaring methods including Very pistol shell cracker firing and broadcast calls on civilian and military airfields

17 p2915 A69-33365

Habitat modification for airport bird population control, discussing draining of wet areas, waste control, etc

17 p2915 A69-33368

Bird hazard in aviation, discussing aircraft/bird collisions in France, protective measures and airport environment control against nesting and breeding

18 p3090 A69-34695

Electrical failures in aircraft due to static electrification of electrically heated windscreens, noting materials for reducing surface resistivity

19 p3256 A69-36769

Absorbed dose and dose equivalent radiation rates at various depths in atmosphere due to proton spectrum of energetic solar flare

23 p4204 A69-41337

Aircraft fuel vent line sensitivity to lightning hazards, using flame propagation and arrester experiments with high voltage and high current facilities

[SAE PAPER 690434] 23 p4062 A69-41651

Ignition of aircraft fluids leaked onto hot turbofan engine surfaces, considering cooling air direction, surface temperature, nacelle engine compartment ventilation, engine power, etc

[SAE PAPER 690436] 23 p4200 A69-41653

Solar flare radiation hazard to SST crew and passengers, discussing onboard and ground based warning systems and ICAO requirements

23 p4063 A69-41830

Heat tolerance in case of SST aircraft air conditioning failure, discussing physiological and psychomotor reactions and time curves for metabolic activity levels

24 p4277 A69-43382

Physical and physiological factors involved in determining aircraft passengers time of safe unconsciousness permissible after cabin decompression

24 p4278 A69-43398

AIRCRAFT HYDRAULIC SYSTEMS

Hydraulic powered flight control system for Jaguar supersonic military training aircraft

01 p0012 A69-10634

Compact hydraulic power transfer units in aircraft with common connecting shaft for pump/motor elements, discussing integrated power package

06 p0930 A69-17168

Flapper valves in high pressure hydraulic aircraft systems, with hydrodynamic equations and charts for design and performance characteristics

09 p1435 A69-21296

Modular hydraulic power source systems for general aviation aircraft, discussing design selection, phase in and customer acceptance problems

[SAE PAPER 690329] 11 p1825 A69-24505

Trident 2E aircraft, discussing fuel system, electric power installation, hydraulic system, air conditioning, pressurization and flying controls

13 p2202 A69-27973

Aircraft hydraulic equipment ultrafine filters effect on component life and system reliability

15 p2552 A69-30069

C-5A Galaxy military transport hydraulic system, considering applications for industrial hydraulics

20 p3466 A69-38177

Hydraulic power pack for automatically raising or lowering landing gear in small aircraft

20 p3467 A69-38183

Soviet book on fluid contamination influence on aircraft hydraulic systems operational reliability covering friction, particle size, filtration, etc

21 p3649 A69-39530

Protective layer material for high sludge capacity filters for fine purification of liquids used in aircraft hydraulic system

22 p3869 A69-40637

Undissolved air effects on working fluids elastodynamics in aircraft hydraulic actuators

24 p4255 A69-43076

AIRCRAFT INDUSTRY

Military aircraft procurement trends examined to forecast military aircraft market

01 p0009 A69-10147

Boeing 747 performance, propulsion, structural and circuit characteristics, mass production and airport passenger installations

01 p0011 A69-11067

Optimal transport aircraft, considering VTOL/STOL aircraft, construction requirements and flying distances

01 p0012 A69-11293

Manufacturer and assembler liability for injuries caused by design defects resulting from engineering errors in aircraft products

01 p0180 A69-11392

Welding use in aircraft design, noting weight and cost advantages and problems of stressing, stress corrosion and inspection

02 p0253 A69-12062

Competition and aeronautical progress in aircraft industry, examining costs and effects of government limits on Boeing 707 and Douglas DC-8

03 p0536 A69-14110

Aircraft parts manufacturer liability in air accidents, discussing litigation and warranties

06 p1042 A69-16849

Tort system of U.S. law effect on air safety promotion, discussing liability influence on government, manufacturers and airlines

06 p1042 A69-16850

Aviation industry passenger liability, discussing negligence litigation, compensation standards and roles of government, manufacturers and courts

06 p1042 A69-16851

Concorde equipment, summary of British companies activities in supplying components

07 p1057 A69-19706

Manufacturer-supplier relationship in helicopter industry

09 p1502 A69-21388

Baseline requirements for commercial aircraft propulsion systems, stressing engine installation in aircraft

[ASME PAPER 69-GT-57] 09 p1572 A69-22514

Competition and aeronautical progress in aircraft industry, examining costs and effects of government limits on Boeing 707 and Douglas DC-8

11 p2004 A69-24372

Aircraft design synthesis requirement definition in hardware commitment, discussing error effects of weight, aerodynamics and propulsion

14 p2392 A69-29432

Book on subdivision of aircraft structural design covering technology, economics, working conditions, performance, etc

14 p2456 A69-29860

Stress corrosion cracking prevention by shot peening, considering aircraft industry applications

14 p2466 A69-29937

Air transport industry safety record and variable stability research planes to simulate aircraft airborne behavior and handling qualities

15 p2558 A69-30453

Propulsion system influence on aircraft reliability from viewpoint of engine manufacturer

15 p2629 A69-31122

Soviet efforts to market civil aviation equipment in West

18 p3232 A69-34538

Jumbo aircraft production technology causing economic setback, recommending added emphasis on passenger/cargo requirements and operating environments for greater profitability

18 p3232 A69-34542

Aircraft structures design, discussing reinforced sandwiches and composites, failure mechanisms, non-destructive testing and fabrication

19 p3438 A69-36325

European cooperation in aircraft industry and application to Anglo-French helicopter program

19 p3456 A69-36849

Soviet book on interchangeability of structural elements in aircraft construction, discussing experiences in serial production of aircraft and helicopters

20 p3462 A69-37443

Precipitation hardening stainless steels applications in aerospace industry, discussing steel selection and heat treatment

20 p3563 A69-37931

Economic effectiveness of design and fabrication changes in aircraft construction industry for profitable operation of commercial transport aircraft

21 p3855 A69-38874

Commercial supersonic and subsonic air traffic growth forecast

22 p3862 A69-39934

AIRCRAFT INSTRUMENTS

NT ALTIMETERS
NT APPROACH INDICATORS
NT ATTITUDE INDICATORS
NT FLIGHT RECORDERS
NT RADIO ALTIMETERS

Orbiting satellite global all-weather oceanographic data acquisition to complement higher resolution data from ships, buoys and aircraft remote sensors

[UN PAPER 68-95878] 01 p0064 A69-10491

Aircraft instrumentation system for cloud nucleation studies measures and records ice nucleus and aerosol concentration/distribution, temperature, etc

01 p0080 A69-10542

Atmospheric optical data recorded by instrumented aircraft near Crater Lake, discussing surface spectral irradiance data

01 p0111 A69-10846

Cloud instrumentation for measurement of icing conditions of airplane flight tests

01 p0055 A69-11044

Vibrating rod automatic ice detection and control system for fixed and rotary wing aircraft

01 p0083 A69-11046

Low altitude atmospheric turbulence model evaluated from analysis of A-6A aircraft gust load data, comparing model estimates with aircraft response characteristics

01 p0056 A69-11053

Avionics technology and systems for future SST aircraft noting improved air traffic control systems

02 p0279 A69-12364

Fiat G.91Y subsonic light tactical fighter, discussing fixed armaments and weapons facilities

02 p0193 A69-12679

Slide wire aircraft vertical velocity meter for application during aerogrammetric mapping, discussing calibration and gravitational force measurement accuracy

03 p0429 A69-13261

Aircraft instrument lighting color effects on posture, scotopic absolute and acuity threshold and legibility for reading of instruments

03 p0380 A69-14073

Soviet collection of papers on aircraft construction and air fleet equipment

04 p0672 A69-14483

Aircraft measurements of stratus cloud absorption and albedo and earth surface albedo

04 p0627 A69-14914

Jaguar aircraft equipment conformity to maximum standardization with equipment for other programs

04 p0550 A69-15063

Aircraft instrumentation for measuring aircraft electrostatic charge, atmospheric electric field intensity and currents of aircraft

04 p0549 A69-15107

Aircraft charge measurements in stratus clouds, noting charge sign is independent of cloud space charge

04 p0549 A69-15108

Aircraft instrument panel lighting color and intensity preference by pilots for taxiing, takeoff, cruising flight and landing

05 p0715 A69-16622

Aircraft instrument panel lighting, comparing red and white colors for general and peripheral vision

05 p0715 A69-16623

Fluidic type temperature sensor for total temperature measurement for hypersonic aircraft in atmosphere

05 p0766 A69-16755

Aerodynamic instrumentation to improve helicopter takeoff and landing piloting performance under high gross weight conditions

05 p0767 A69-16776

Reading and reliability efficiency comparison in round vs vertical aircraft displays

06 p0883 A69-18025

Aircraft nose-mounted radome refraction errors influence on directional tracking and navigation, considering fire control and terrain following radars

07 p1086 A69-19512

Wind changes calculated from Doppler data and inertial system, noting role of heading and air speed

08 p1346 A69-20317

Aircraft head-up display systems emphasizing all-weather operations and equipment characteristics
08 p1315 A69-20451

All-weather head-up displays /HUD/, discussing operational usage, hardware availability and design philosophy
08 p1315 A69-20452

Optimum integration of aircraft equipment, subsystems and computer mechanizations for low cost navigation system consistent with mission requirements
08 p1348 A69-21065

Earth rotation and aircraft speed effects on vertical gyroscopes during banking, obtaining formulas for gyro errors
09 p1498 A69-22107

Kinematics of vertical gyroscope mounted in additional servo frame, determining kinematic errors due to rotor axis deviation
09 p1498 A69-22108

Skorsky HH-3F helicopters electronic equipment, discussing communication and navigation aids, search and recovery missions, etc
10 p1662 A69-23222

Onboard aircraft weighing system /OBAWS/ for accurate gross weight and CG measurements, describing axle shear deflection transducer system
10 p1693 A69-23276

Aircraft engine instrument displays evaluated by human factors, noting vertical scale design [SAE PAPER 690328]
11 p1829 A69-24488

Onboard test instrumentation for monitoring aircraft communication, navigation and identification systems, noting adaptive programming
11 p1866 A69-25080

Onboard magnetic anomaly detection system for Canadian helicopter, discussing magnetometer location, boom design and testing and equipment installation [AIAA PAPER 68-487]
12 p2094 A69-26771

Ballistic deviations limits for aircraft vertical gyroscope taking into account aircraft vertical movements, using compensation in system
14 p2445 A69-28899

A-New avionics system for carrier based VSX aircraft used in U.S. Navy aerial submarine hunting, discussing TV, lasers, sonobuoy system, radar, etc
14 p2392 A69-29430

Low cost inertial measurement unit /IMU/ for commercial and private aircraft, evaluating components and system [SAE PAPER 690337]
15 p2606 A69-30092

Navigational information display in aircraft, discussing moving map technique and mechanization
15 p2558 A69-30692

Fatigue life gauge on operational aircraft providing in situ monitoring of fatigue damage prior to and during propagation of running fatigue cracks
15 p2613 A69-31271

Satellite and aircraft use compared for earth resource surveys, discussing proposed aircraft data collection system
16 p2881 A69-31632

Vector airspeed measuring system /VAMS/ for helicopters and V/STOL aircraft utilizing gas discharge mass flowmeter to improve takeoff performance [AHS PAPER 350]
17 p2974 A69-33527

AN/ASN-24/V/ general purpose digital computer deployed in large worldwide jet transport fleet
17 p2933 A69-34061

Situation/command system displays and maneuvers for collision avoidance systems, discussing pilot preferences
17 p3002 A69-34096

Automatic flight control, discussing equipment, components and relationship between autopilot and navigation system
18 p3170 A69-34856

Situation displays and flight instrument development including head-up, vertical tape and map systems
18 p3170 A69-34858

STAN integral weight and balance system providing aircrews with takeoff gross weight and CG data [SAWE PAPER 755]
18 p3136 A69-34882

Aircraft nucleonic fuel gauging system, using radioactive gas to emit gamma rays for fuel mass sensing
18 p3139 A69-35468

Operational flight tests of IR atmospheric turbulence detection system [AIAA PAPER 69-799]
19 p3367 A69-35631

High altitude aircraft range requirements for airborne turbulence detector, taking into account passenger comfort, turbulence geometry, maneuverability and pilot decision making
20 p3537 A69-37164

Laser profilometer to measure sea wave profiles from airborne platform, describing transmitter, receiver and signal processor
21 p3739 A69-39461

Cockpit displays for transport aircraft noting digital techniques and flight control-navigation integration
22 p3946 A69-40486

Systems approach to avionics optimization, discussing instruments, devices, display and automation techniques [RAES PAPER 6]
22 p3946 A69-40487

SST flight crew operational requirements to achieve maximum human efficiency and man/machine compatibility, discussing pilot role, advanced flight instrumentation, etc
23 p4107 A69-41820

Solar constant and spectral irradiance curve for zero air mass obtained from aircraft measurements
23 p4216 A69-42191

Optimum integration of aircraft equipment, subsystems and computer mechanizations for low cost navigation system consistent with mission requirements
23 p4186 A69-42538

Takeoff indicator design based on solution of equilibrium equation for forces acting on aircraft along drag axis
24 p4253 A69-43085

AIRCRAFT LANDING

NT CRASH LANDING

NT DITCHING [LANDING]

NT SKID LANDINGS

Piloting aspects of jet V/STOL aircraft for poor weather operations without complicated ground aids, discussing deceleration transition, forward speed and final approach angle
01 p0010 A69-10868

Low visibility instrument landing of aircraft using ILAS and inertial guidance
01 p0114 A69-11012

Air traffic control at Los Angeles International Airport, discussing simultaneous parallel ILS approaches and departures and STOL problems
01 p0057 A69-11356

Low visibility landing, discussing problems of radio guidance geometry, visibility measurement, aircraft dynamics, pilot psychology, regulation and politics
01 p0114 A69-11391

Air cushion landing gear in civil air transport, discussing system concept, advantages and LA 4 aircraft experimental application
02 p0193 A69-12690

Flight inspection positioning system, discussing microwave interferometer angle calibration for instrument landing
03 p0430 A69-13680

Low visibility aircraft landing, discussing total system approach, modern electronic developments, collision avoidance, safety and air traffic control
03 p0465 A69-13853

Heligyro type takeoff and landing maneuvers, discussing M 211 takeoff jet thrust, pressure ratio, tip speed, etc
04 p0547 A69-14816

Aerodynamic technology applied to takeoff and landing, discussing STOL airplanes in descent and boundary layer control /BLC/ flap system
05 p0696 A69-15569

Maximum downwind and crosswind vertical wind shear in boundary layer, noting effect on swept wing jet aircraft landing
06 p0951 A69-17790

Approach light efficiency, discussing Calvert bar system and strobe flash on basis of pilot questionnaire polling
06 p0884 A69-18029

Climatic factors affecting pilot vision and contributing to misjudgment during landing procedures, noting effect of downward slope in runway approach
06 p0884 A69-18036

Qualitative V/STOL air traffic control requirements, discussing airborne and ground data, procedures and equipment categories [AIAA PAPER 69-211]
07 p1177 A69-19552

Scanning beam landing systems for VTOL aircraft
07 p1178 A69-19631

Helicopters operation from small ships, describing underside harpoon mooring technique for Alouette 2 and 3
08 p1255 A69-20654

Monograph on length requirements for takeoff and landing of jet transports covering airport classification, roll distance formulas and long range transport performance nomograms
08 p1301 A69-20717

Control and recording device for parameters and information relating to takeoff and landing, using detection elements and cross wire on runway
08 p1347 A69-20780

Electronic terminal guidance requirements for all-weather VTOL operations, suggesting future first generation landing system
08 p1348 A69-21064

Landing and takeoff demonstration tests of OV-10A aircraft through rough terrain, noting pilots excessive physiological stresses [AIAA PAPER 69-316]
09 p1434 A69-22391

All-weather landing including zero-zero, discussing planning in Europe and U.S.A.
10 p1722 A69-23698

Foam carpet and airport equipment to prevent fires and explosions from retracted gear landings
10 p1674 A69-23708

Stopping barriers for jet aircraft landing design and operation
11 p1862 A69-24354

HF brake excited vibration damping in aircraft landing gear, obtaining closed form solution [AIAA PAPER 68-312]
11 p1823 A69-25370

Trident category 3 automatic landing, discussing triplex pitch and roll control, duplex rudder, autothrottle and azimuth paravision display
13 p2296 A69-27976

Jumbo jet instrument landing difficulties, suggesting specific improvements in aircraft and airport equipment
15 p2549 A69-30189

Lidar data obtained at Hamilton AFB, Calif., computer analyzed for lidar operational utility, determining cloud ceiling and visibility for aircraft landing operations
15 p2651 A69-30895

Aircraft carrier landing system performance, variations in pilot experience, aircraft types and environment, emphasizing night carrier recovery
17 p2916 A69-34012

Deterministic and statistical prediction techniques for aircraft carrier motions at sea for application to aircraft landing operations [AIAA PAPER 68-123]
17 p2902 A69-34014

Direct lift controller design for aircraft approach and landing by computer program based on Kalman linear state regulator theory
17 p2902 A69-34027

Tire test machine for tire parameter determination in aircraft landing gear shimmy stability studies [AIAA PAPER 68-311]
17 p2902 A69-34029

Aircraft landing gear cylinder reinforcement rings design for minimum weight, using optimization iteration method for planar frames with elastic supports [AIAA PAPER 68-328]
17 p3066 A69-34030

Multisensor data processing technique for fail operational landing commands, using real time error analysis inherent in Kalman filter
17 p3003 A69-34106

Landing guidance devices under difficult weather, discussing landing mechanics for land and carrier based aircraft
18 p3170 A69-34857

Wind shear effects on jet aircraft approach, discussing airspeed and glide path position maintenance requirements [AIAA PAPER 69-796]
19 p3367 A69-35634

Wing flaps and blow-off and suction effect on longitudinal balance of landing TU-104 aircraft, noting air suction at wing leading edge
19 p3247 A69-35818

Wave-off Decision Device to define potential aircraft carrier-ramp-strike wave-off criteria for aircraft approach
20 p3573 A69-37161

All-weather landing in civil air operations, discussing ground/air systems in tracking, visual reference and aircraft performance required for safe landing capability
20 p3574 A69-38119

Aircraft characteristics influence on longitudinal handling qualities during carrier approach from visual landings on moving base simulator [AIAA PAPER 69-894]
21 p3648 A69-39418

Electronic terminal guidance requirements for all-weather VTOL operations, suggesting future first generation landing system
22 p3978 A69-39875

Correlation protected ILS implementing conventional ILS with no operational restrictions on air traffic control, taking into account changing terminal conditions
22 p3978 A69-39963

- Steep descent landing systems developmental phases for VTOL aircraft, discussing noise abatement, approach angle and descent rates 22 p3978 A69-40674
- Low visibility VSTOL instrument landing system and associated electronic structures, discussing instrument to visual flight transition 22 p3979 A69-40675
- Landing performance in T-33A aircraft with loss of binocular vision compared to performance with both eyes 23 p4102 A69-41675
- Quasi-optimum control law for aircraft landing control system design based on Friedland technique, evaluating effectiveness by computer simulation 24 p4253 A69-43280
- Unscheduled aircraft landing to deplane passenger for medical reasons, discussing costs, time consumption and avoidance methods 24 p4278 A69-43393
- AIRCRAFT LANDING INSTRUMENTS**
- U LANDING INSTRUMENTS**
- AIRCRAFT LAUNCHING DEVICES**
- Aircraft steam catapult test facilities, noting construction and operational requirements 10 p1674 A69-24068
- Reusable aircraft type satellite launchers, discussing first stage recovery by parachute, ballutes, flexible wings and gyroglider 24 p4250 A69-42562
- AIRCRAFT MAINTENANCE**
- Reliability and maintenance economics for jet transport operations of 1980s, discussing Aircraft Integrated Data System /AIDS/ sensors design [AIAA PAPER 68-207] 01 p0011 A69-11022
- Emergency oxygen supply systems for aircraft, discussing simplicity, standardization, safety, reliability and maintenance [AIAA PAPER 67-965] 01 p0013 A69-11025
- Aircraft flight safety, discussing structural and aerodynamic concepts, maintenance and operations 03 p0365 A69-12886
- Electrochemical grinding application to metal cutting of refractory alloys in aircraft jet engine overhaul [SAE PAPER 680662] 03 p0433 A69-13453
- Airline operators economic oriented airframe maintenance problems, discussing cost accounting improvement 03 p0434 A69-13698
- Maintainability and reliability affect utilization and operating costs of commercial aircraft 04 p0547 A69-14806
- Tactical airfield/aircraft system effectiveness in terms of ground support resources, aircraft reliability and maximum potential sorties 05 p0743 A69-16238
- Nondestructive testing methods for civilian transport aircraft production, overhaul and maintenance 07 p1143 A69-19702
- Transport aircraft fleet management and handling of mechanical and avionic machine defects using operations research 08 p1422 A69-20626
- Symptom pattern observation technique for flight data analysis, discussing in-flight symptoms and SPOT chart in aircraft maintenance 10 p1669 A69-22982
- Maintenance recording systems for aircraft fleet, discussing operations objectives and research, data collection and implementation using systems engineering 10 p1671 A69-23261
- Howell engine hot section analyzer /HSA/ developed to improve maintenance, flight safety and costs of jet aircraft engines 10 p1671 A69-23263
- Computer controlled testing of commercial aircraft avionic systems for automatic, semiautomatic and manual operation to perform repair and calibration tasks 11 p1864 A69-25061
- Optimized automated system for direct support maintenance of AH-56A subsystem equipment 11 p1865 A69-25075
- Integrated computerized reliability monitoring program for detecting aircraft systems and components performance trends and optimizing cost, utility and response 12 p2055 A69-25972
- Efficient allocation of maintenance resources in USAF, analyzing B-52 costs and substitution of capital for labor 13 p2382 A69-28041
- Instruction manual for maintenance personnel and pilots regarding clear vision and window integrity of Convair aircraft, discussing windshield installation and replacement 14 p2391 A69-28932
- Airline aircraft maintenance programs, discussing objectives, procedures and failure analysis models 15 p2549 A69-30209
- Defense integrated management engineering system at California Naval Air Rework Facility 15 p2588 A69-30427
- VFW H3 Sprinter autogyro maintenance, reliability and operating costs 16 p2735 A69-32056
- Maintenance system in Germany for F-104-G Starfighter planes noting disassembling, system testing and test flight 17 p2979 A69-33703
- Aircraft solid state electric system logic level tested functionally by built-in test equipment /BITE/ operated on ground during preflight tests 17 p2977 A69-34110
- Aircraft secondary power sources reliability dependence on electric loads, charge control and maintenance, discussing hermetically sealed batteries features 17 p2905 A69-34113
- C-141 aircraft reliability growth history, discussing fleet performance, aging trends and delivery vs production sequence 18 p3090 A69-34521
- C-141 engine health monitoring program, applying results to maintenance costs reduction [AIAA PAPER 69-775] 19 p3244 A69-35646
- Combat fielded cargo-carrying CH-54A Flying Crane helicopter industry-government reliability/maintainability field test evaluation 19 p3247 A69-36017
- Cost and maintenance calculations for inertial navigation system /INS/ based on three systems per aircraft, assuming 4000 hr/year aircraft utilization 19 p3371 A69-36734
- Relationship between chronological and fatigue life in airframes, showing fatigue life dependence on operating conditions, pilot techniques and maintenance and inspection quality 20 p3461 A69-36920
- Optical devices for nondestructive testing of large piston engined equipment 20 p3547 A69-36921
- Soviet book on testing aircraft electrical equipment covering climatic and mechanical tests, malfunction detection, etc 20 p3464 A69-37237
- C-5A transport modular valve design for improved maintenance and high reliability due to manifold- cartridge arrangement 20 p3466 A69-38178
- Fuselage corrosion effect on structure and skin of older aircraft with emphasis on pressurized aircraft 21 p3646 A69-38392
- Jet fleet engine performance monitoring program, discussing systems design and resultant management planning 22 p3999 A69-39922
- Lockheed 1011 propulsion system design relating to system and component maintainability, reliability, performance and noise [SAE PAPER 690390] 23 p4201 A69-41665
- Military aircraft service life problems solved by alternative replacement policies comparative present value analysis 24 p4253 A69-43058
- Damage tolerance design concepts required to obtain reliability, maintainability and operational safety of complex aircraft [ICAS PAPER 68-23] 24 p4254 A69-43717
- AIRCRAFT MODELS**
- Elastic wind tunnel models used for testing at full scale dynamic pressures, discussing scaling laws and manufacturing and testing problems [AIAA PAPER 68-56] 01 p0011 A69-11018
- Flight simulator based on analog computer simulating six linearized equations of motion and aircraft model, discussing design and applications 01 p0057 A69-11300
- Wind tunnel measurement of rear parts drag of small scale aircraft models [ONERA-TP-633] 02 p0226 A69-11624
- Aircraft squadron performance effectiveness model 03 p0367 A69-13911
- Simulation of flight dynamic equations of motion for fixed wing aircraft, using variable analog computer with gimbal and servocontrolled aircraft model 04 p0585 A69-14829
- Dynamic stability tests of tilt winged V/STOL aircraft model in ultralow speed range, discussing apparatus for stability derivatives 06 p0866 A69-17091
- V/STOL air intakes and jets simulation in wind tunnel tests, noting thrust simulation possibilities 11 p1866 A69-25431
- Aircraft stability derivatives determined by adaptive method, emphasizing physical and mathematical characteristics of learning model 11 p1824 A69-25671
- Exhaust gas recirculation for VTOL aircraft [AIAA PAPER 67-439] 12 p2013 A69-26760
- Exhaust gas reingestion and inlet flow distortion in V/STOL lift engines, discussing static and wind tunnel testing using fighter configuration models [AIAA PAPER 68-78] 12 p2012 A69-26762
- C-5A aircraft model high subsonic speed tests, correlating data from three transonic wind tunnels [AIAA PAPER 69-794] 19 p3237 A69-35636
- Aircraft simulation, discussing flight simulation, real time computer assembly operation, computer-auxiliary interfaces, etc 19 p3296 A69-36707
- STOL seaplane bottom pressure distribution from tests on scale model of PX-S seaplane, discussing boundary layer control effects 22 p3864 A69-40586
- AIRCRAFT NOISE**
- NT JET AIRCRAFT NOISE**
- NT SONIC BOOMS**
- Aircraft engine noise reduction in test runs by sound insulating hangar 01 p0054 A69-10033
- VTOL aircraft design for noise reduction, discussing localities tolerance, noise sources, operating cost, etc 01 p0009 A69-10421
- Human reaction to aircraft engine noise, evaluating effective perceived noise level and constraints on engine design 02 p0204 A69-12766
- Soviet MI-8 and MI-4 passenger helicopters noise characteristics with turboprop and piston engines and during landing takeoff and horizontal flight 03 p0366 A69-13417
- Helicopter rotor noise generation, propagation, reception and reduction, discussing design charts for rotational noise spectra as function of design and flight variables [AIAA PAPER 69-195] 07 p1055 A69-19563
- Mathematical formulation of Noy tables, noting more efficient programming and minimal disagreement with original tables 08 p1266 A69-20403
- Annoyance caused by noise near airports, discussing PNdB /perceived noise dB/, evaluation criteria, and French, British, American and German methods 13 p2214 A69-28588
- Aircraft noisiness estimation methods 13 p2216 A69-28660
- Aircraft noise alleviation through flight procedures improvement, home building modification and noise standards legislation 14 p2392 A69-29154
- Aircraft noise control at source through high bypass ratio engine modification, FAA decibel standards and higher capacity aircraft for increased traffic density 14 p2509 A69-29156
- Airport noise control responsibility for airport and community planners using perceived noise level, noise and number index and community annoyance index as planning criteria 14 p2541 A69-29506
- Aircraft created pressure patterns responsible for sonic boom, discussing design techniques for noise reduction 15 p2550 A69-30369
- Aircraft noise environmental problem, discussing improvement through source, transmission and receiver control options 15 p2585 A69-30373
- Human noise tolerance laboratory and community studies, discussing proposed tone corrections for aircraft noise 15 p2719 A69-30374
- Boeing 747 problems including noise and automatic landings in CAT-II conditions 16 p2734 A69-31631

Slender body aerodynamics combined with wave propagation theory for sonic booms of aircraft configurations, propeller and helicopter noise, sonic boom alleviation, etc
16 p2732 A69-31867

Aircraft noise assessment, discussing computer programmed formula, noise contours and duration calculation, with appendices presenting engine noise characteristics, air and ground attenuation, etc
16 p2735 A69-32021

Noise abatement and smoke emission reduction from aircraft engines
[AIAA PAPER 69-489] 16 p2746 A69-32764

High bypass ratio engine influence on short range civil aircraft design, considering performance, noise, engine location, etc
17 p2897 A69-33212

Helicopter noise characteristics, discussing effects of noise reduction measures on design and operations
[AHS PAPER 352] 17 p2915 A69-33525

Helicopter rotor vortex noise data analyzed for noise suppression, obtaining sound power equations
17 p2896 A69-34034

Aircraft design determined by airport environment and facilities defined as pavement strength, passenger and baggage loading and aircraft handling, noting noise abatement
17 p2948 A69-34209

Airport performance, noise and aircraft utilization influence on aircraft design and operating costs, stressing takeoff distance, obstacle clearance and noise regulations
17 p2948 A69-34210

Far field helicopter rotor noise radiation, analyzing blade slap, rotation noise, vortex noise effects and loading harmonics utilizing computer program
18 p3090 A69-34322

Aircraft noise acceptability tests based on listening in absence and presence of speech
18 p3097 A69-34325

Distributive loading rotational theory for helicopter rotor noise generation, considering steady and fluctuating force radiation and impulsive blade slap
18 p3088 A69-35222

Vortex shedding effects on helicopter rotor noise with and without blade slap, noting far and near field noise
18 p3088 A69-35223

Helicopter rotor rotational and vortex noises prediction methods and trends
18 p3088 A69-35224

Helicopter rotors forward-flight noise characteristics determined by wind tunnel tests compared to rotor noise during flyover
18 p3119 A69-35225

Aircraft noise abatement oriented toward compatibility between airports and adjacent metropolitan environments, analyzing results for theoretical and actual airports
[AIAA PAPER 69-800] 19 p3453 A69-35593

Quiet military aircraft design factors, considering human hearing characteristics, noise suppression methods, propeller noise-performance relationships and jet engine noise nature
[AIAA PAPER 69-792] 19 p3243 A69-35637

Problems caused by air traffic rate growth in London Terminal area, examining runway limits, safety and noise restrictions
19 p3371 A69-36736

Real time analyzers of acoustic signals for aircraft engine noise, noting automatic test
20 p3462 A69-37756

Noise and vibration levels measured in An-24 Polish passenger aircraft indicating excess noise in crew compartment
22 p3862 A69-40005

STOL aircraft characteristics emphasizing ground and air space operations requirements and noise levels
22 p3863 A69-40430

Airport design for noise reduction, considering aircraft noise, runway orientation and flight paths
22 p3926 A69-40433

Helicopter main rotor noise from square tipped blades determined as function of tip speed, blade area and thrust
22 p3864 A69-40676

Lockheed 1011 propulsion system design relating to system and component maintainability, reliability, performance and noise
[SAE PAPER 690390] 23 p4201 A69-41665

Cockpit noise intensity during normal cruising operations at various altitudes for 15 different single engine general aviation light aircraft
23 p4102 A69-41676

Commercial aircraft peak cockpit noise level during cruise and high speed descent, discussing damage risk criteria and inter-pilot speech interference
23 p4102 A69-41682

Hearing adaptation measurements after aircraft noise stresses for estimation of induced noise damage
23 p4110 A69-42051

Noise levels in twin engine general aviation light aircraft cockpits, discussing protection against possible hearing damage
24 p4252 A69-42902

AIRCRAFT PARTS

Wind tunnel measurement of rear parts drag of small scale aircraft models
[ONERA-TP-633] 02 p0226 A69-11624

Explosive forming process to shape aircraft structural parts, advantages and potentials
[ASM PAPER C7-2.4] 04 p0604 A69-14524

Soviet aircraft roller bearings design, operation, service life, defect testing, etc
04 p0606 A69-14936

Aircraft gas turbine component pressure data storage and scanning
05 p0726 A69-16768

Aircraft parts manufacturer liability in air accidents, discussing litigation and warranties
06 p1042 A69-16849

Wind tunnel rain erosion testing of components of aircraft or missiles flying at high speed
07 p1117 A69-19534

Concorde equipment, summary of British companies activities in supplying components
07 p1057 A69-19706

Composite materials based on carbon and boron filaments, discussing application in turbine blades, propeller and helicopter rotor blades and airframe components
08 p1341 A69-20601

Metal castings around ceramic cores for economic manufacture of jet engines
09 p1503 A69-21907

Giant landing gear steel parts fabrication for Boeing 747 aircraft, discussing material and processing problems including Cr and Cd-Ti coatings application
09 p1434 A69-22064

Organic quenchant additive for distortion free heat treatment of dip-brazed aluminum parts
09 p1504 A69-22065

Automatic fabrication process for boron reinforced composite structures, concerning orienting and laminating jet flap skins
09 p1507 A69-22329

Nomogram for aircraft rudder pedals design and construction, considering thigh and knee angles
10 p1649 A69-23377

Explosive fabrication of aircraft components including turbine engine exhaust components, door seals, etc
[SAE PAPER 690316] 11 p1890 A69-24510

Tempered glass plates strength nondestructive testing by scattered light photoelastic method, discussing application to aircraft windshield sandwich structures
[AIAA PAPER 68-323] 12 p2118 A69-26768

Nondestructive eddy current testing of chromium steel for early stage fatigue damage of aircraft components
18 p3136 A69-34777

Reliability and component relationships of aircraft navigation systems, describing dead reckoning, position fixing, guidance and vertical navigation
18 p3168 A69-34844

Machined fastened joints for airframe structural parts, discussing fatigue life, strength and fastener hole preparation
19 p3319 A69-35553

Silico-organic liquid water repellent coatings for increasing binder adhesion to glass fiber in glass fiber reinforced plastic materials of aircraft components
21 p3752 A69-38876

Computer programming procedures in automatic control of hole boring processes for aircraft components
21 p3731 A69-38881

Stress-strain state of thick and thin walled closed shells of variable thickness during elastoplastic torsion developing in aircraft component production
21 p3835 A69-38882

Aircraft fastening systems guidelines based on mechanical strength, weight, cost and joint efficiency, discussing hole preparation and expansion design
22 p3956 A69-40822

Mechanical properties of aircraft fasteners high temperature materials
22 p3956 A69-40823

Titanium alloys for strength and weight saving in aircraft fasteners operating at cryogenic or elevated temperatures, discussing corrosion and notch sensitivity
22 p3956 A69-40824

Galvanic corrosion prevention measures for airframe fasteners, discussing crevice sealants, primers, zinc chromate, cadmium and aluminum coatings
22 p3957 A69-40825

Aircraft fastener fatigue-acceptance criteria compared with actual tests, considering unusual service conditions
22 p4045 A69-40826

Nondestructive thermal method of measuring wall thickness and channel blockage in investment castings used in aircraft parts production
24 p4312 A69-42754

Cobalt-base superalloys analysis for temperature stability, corrosion resistance, creep, fatigue and strength in aircraft structures and parts applications
24 p4334 A69-43427

AIRCRAFT PERFORMANCE

NT HELICOPTER PERFORMANCE

Aircraft flight testing for determining airframe, engine and pilot degradation, examining flutter, handling characteristics, water ballast, propulsion, etc
01 p0054 A69-10292

CH-46 Sea-Knight and CH-47 Chinook transport helicopters experience in Vietnam war, discussing missions, payloads, speeds, operating ranges, etc
01 p0009 A69-10405

T63 regenerative helicopter engine program, noting operational performance and engine-aircraft compatibility
[AHS PAPER 212] 01 p0143 A69-10410

Boeing 747 characteristics for passenger and cargo service noting economic gain, operational performance, control cabin, engine, etc
[AIAA PAPER 67-397] 01 p0010 A69-10636

BAC Three-Eleven 220 seat airliner for short and middle distance routes, discussing operating costs, thrust and range
02 p0193 A69-12067

CF6 turbofan engine technology program for improvement in performance, weight, durability, noise, etc
[SAE PAPER 680691] 03 p0496 A69-13446

Aircraft squadron performance effectiveness model
03 p0367 A69-13911

Aerodynamic technology applied to takeoff and landing, discussing STOL airplanes in descent and boundary layer control /BLC/ flap system
05 p0696 A69-15569

Factors influencing development of both wind tunnel and flight test technology for determining aerodynamic derivatives of aircraft motions
05 p0741 A69-15572

Test facilities and techniques for low speed flight problems of aircraft handling qualities, stability, control and performance
05 p0741 A69-15575

Nimrod maritime reconnaissance aircraft, discussing high speed high altitude transit flights
05 p0702 A69-15885

A-7 Corsair 2 introduction to fleet and combat operations in Southeast Asia
06 p0867 A69-17660

C-5A transport flight test and progress report, discussing taxi runs, first flights and flight-flutter program
06 p0867 A69-17665

Boeing SST designs, discussing performance, flying qualities and operational characteristics of configurations
06 p0868 A69-17830

F-111 interdiction capability, discussing avionics subsystems for low level penetration flying and Vietnam performance
07 p1052 A69-18550

Mirage G supersonic swing wing two seater aircraft performance, discussing hinging of mobile wing on pivot, fluids for airfoil-fuselage transfer, landing gear, etc
07 p1053 A69-19230

Aerial photography history, photographer qualities, airborne platforms, pilot briefing, air to air sortie, aerobatics, parachutes, etc
08 p1314 A69-20307

Optimum cruise altitude, block time and fuel relations for Convair 600/640 aircraft for various temperatures, segment distances and weight
08 p1255 A69-21007

Landing and takeoff demonstration tests of OV-10A aircraft through rough terrain, noting pilots excessive physiological stresses
[AIAA PAPER 69-316] 09 p1434 A69-22391

- JT15D business aircraft turbofan engine, discussing low costs and fuel consumption, maintenance, reliability, installation, etc
[ASME PAPER 69-GT-119] 09 p1572 A69-22524
- Airborne integrated data acquisition and analysis systems to determine aircraft technical performance 10 p1660 A69-23264
- V/STOL aircraft performance characteristics related to civil aviation operations and certification requirements [ICAS PAPER 68-05] 11 p1822 A69-24463
- Integrated computerized reliability monitoring program for detecting aircraft systems and components performance trends and optimizing cost, utility and response 12 p2055 A69-25972
- Monograph on optimal design of free-running drag turbines for boundary layer suction in aircraft, emphasizing gliders performance 12 p2011 A69-26117
- X-15 research aircraft program piloting problems, ground facilities, heat transfer, space flight and steep reentry 12 p2014 A69-26872
- Short range passenger aircraft, considering payloads, weights and economical classification 13 p2201 A69-27294
- CF6 turbofan engine technology program for improvement in performance, weight, durability, noise, etc 13 p2324 A69-27331
- Boeing 747 operational and economic considerations including capacity, airport constraints, noise factors, landing gear, compatibility, etc 13 p2201 A69-27340
- TU-134 jet passenger aircraft performance characteristics noting similarity to BAC 111 13 p2202 A69-27931
- Trident 2E aspect ratio, wing area, high lift devices, fuel capacity, range improvement, etc 13 p2202 A69-27971
- Thrust, bank angle and angle of attack of aircraft minimum fuel lateral turns at constant altitude and specified velocities 13 p2203 A69-28245
- Short takeoff aircraft characteristics, discussing aircraft certification and airfield regulation in Great Britain 13 p2203 A69-28356
- Military aircraft operating in various environments with low support costs emphasizing improved design, development and manufacturing standards 14 p2392 A69-29503
- Inverted spin testing techniques using jet trainer, emphasizing entry variations and effect on spin characteristics 14 p2392 A69-29696
- Civilian transport aircraft operation realities vs theoretical performance certification 14 p2392 A69-29698
- Fighter aircraft design and performance criteria including acceleration, maneuvering, interception and turning combat capabilities 14 p2393 A69-29700
- C-141 Category IIIB all weather landing system, discussing system concept, components, operations and performance 14 p2479 A69-29701
- Turbofan engines impact on aircraft engineering development emphasizing large performances, high fan flow rates and low fuel consumption 15 p2550 A69-30322
- CF6 turbofan engine technology program for improvement in performance, weight, durability, noise, etc [SAE PAPER 680691] 16 p2837 A69-32367
- Air transport systems aspects including efficiency, performance and economics interplay for subsonic and supersonic aircraft 17 p3018 A69-33218
- Folding propurator V/STOL aircraft characteristics, showing configuration effects on performance and optimization of rotor, wing and propulsion systems [AHS PAPER 302] 17 p2901 A69-33547
- Interim revision of military flying qualities specifications according to experimental data and characteristics of existing aircraft [AIAA PAPER 68-245] 17 p2902 A69-34026
- Performance capabilities and handling quality characteristics of aircraft equipped for in-flight thrust reversing [AIAA PAPER 68-880] 17 p2902 A69-34031
- Skyvan 2 aircraft aerodynamic design, describing modifications to increase fuel capacity, directional stability and range capability 17 p2896 A69-34193
- Fixed weight aircraft growth factor variation with location of initial weight penalty along fuselage station, using static stability margin and trim capability [SAWE PAPER 796] 18 p3220 A69-34862
- Tail tip-evacuation limits, calculating aircraft balance effect of passenger relocations by graphical method [SAWE PAPER 765] 18 p3091 A69-34877
- Design iteration loop calculations related to fighter aircraft weight growth factor, noting asymptotic aircraft performance and strength [SAWE PAPER 732] 18 p3221 A69-34893
- Synthesis and integration of cross discipline function for weight effective design of airplanes [SAWE PAPER 730] 18 p3221 A69-34895
- Monograph on weight and performance tradeoff methodology for selection of high lift devices [SAWE PAPER 761] 18 p3091 A69-34906
- Boeing 747 design and development, discussing aircraft characteristics, performance, inertial navigation system, production costs, etc [SAWE PAPER 746] 18 p3091 A69-34907
- Avionics and electronic countermeasures equipment design, development, installation and application problems for high performance military aircraft to meet hostile electronic environment [AIAA PAPER 69-822] 19 p3243 A69-35599
- Aircraft Economic Design Evaluation (AEDE)/computerized model to estimate aircraft design performance differences economic impact to carriers [AIAA PAPER 69-814] 19 p3289 A69-35626
- Aircraft performance optimization using computationally oriented strategy for handling state variable inequality constraints [AIAA PAPER 69-812] 19 p3243 A69-35628
- Takeoff and landing analysis digital computer program (TOLA)/developed by Air Force Flight Dynamics Laboratory for quantitative performance analysis [AIAA PAPER 69-810] 19 p3289 A69-35630
- Computer-generated airline fleet performance data on B-720, B-727 and DC-8 aircraft, attributing deterioration to increased drag and fuel consumption [AIAA PAPER 69-770] 19 p3245 A69-35651
- Flight control systems influence on military aircraft design and performance, discussing static stability, ride quality, flutter margin and maneuver load controls [AIAA PAPER 69-767] 19 p3245 A69-35656
- Drag influence on mission performance of hypersonic aircraft during climb and cruise, noting payload capacity 20 p3461 A69-37154
- Stability augmentation system for B-52, noting flight test performance evaluation for structural vibrations and rigid body motions of aircraft [AIAA PAPER 68-1068] 20 p3461 A69-37157
- Manned aircraft air to air combat capabilities evaluated by simulator using two cockpits, digital computer and collimated displays [AIAA PAPER 68-253] 20 p3510 A69-37159
- Tilt propurator composite aircraft design, discussing performance and mission potential [AHS PAPER 202] 20 p3463 A69-37805
- Northrop F-5-21 fighter design, avionics, performance and operational existence 21 p3646 A69-38732
- Jet fleet engine performance monitoring program, discussing systems design and resultant management planning 22 p3999 A69-39922
- Kalman filter simulation for estimating aircraft position and velocity from airborne digital computer data in zero-zero landing system [AIAA PAPER 69-944] 22 p3978 A69-40327
- MIG-21 fighter aircraft development, characteristics and technical and operational data 24 p4251 A69-42795
- Simultaneous lower atmosphere clear air turbulence analysis by multiwavelength radar, jet aircraft and special rawinsondes 24 p4342 A69-42894
- Coronary atherosclerosis in military pilot fatalities of aviation accidents, demonstrating irrelevance of amount of flying time and type of aircraft 03 p0376 A69-14080
- Retinal lacerations and detachment in jet pilots, discussing pathogenesis, diagnosis and surgical reattachment methods 05 p0710 A69-16630
- Telemetric system for in-flight measurements of jet pilot heart and circulatory system to determine flight stresses leading to pilot failure 05 p0715 A69-16707
- Airline pilot incapacitation by death or terminal collapse due to organic causes while on duty, noting incidence and resulting accidents 06 p0883 A69-17849
- Essential hypertension in selection and evaluation of airline pilots, discussing use of thiazide therapy 06 p0875 A69-17850
- Pilot protection against laser hazards, discussing protective eyeglasses, fireproof clothing and materials 07 p1072 A69-19436
- Epilepsy acquired by 25 year old jet fighter pilot, noting cardiovascular abnormalities 09 p1446 A69-22728
- Blood pressure fluctuations in multiple extra systoles during tilt table studies for flying fitness of pilot 10 p1645 A69-23379
- Preventive medicine in handling airline pilots to avoid accidents attributable to disability and death from natural causes 12 p2024 A69-26559
- Personality characteristics of jet pilots measured by Edwards Personal Preference Schedule, including percentile norms table 14 p2408 A69-29294
- Accident record of general aviation pilots over age 60/1965/ 14 p2541 A69-29308
- Inflight spontaneous pneumothorax case of civilian pilot lung collapse experience during exposure to reduced ambient pressure, discussing etiology, incidence, treatment and disposition 17 p2909 A69-33183
- Pilots mental and physical welfare, discussing roles of mental hygiene and preventive medicine in flight surgeons programs 18 p3097 A69-35301
- Fighter pilot teeth loss prevention and curative treatments, describing various suitable dentures 21 p3661 A69-39277
- Flight performance analysis of airline pilot group related to flight recording monitoring system 22 p3868 A69-41145
- Aircraft pilots medical disabilities as potential flight safety hazard, discussing aerospace medical specialist role and pilot education in symptoms evaluation 22 p3894 A69-41146
- Airline management service to cockpit team for safe operation providing safety information sources and transmission channels and undesirable trend detection and correction 22 p4054 A69-41149
- Initial training and checking of airline pilots in new equipment to ensure competency, reduce nonrevenue flight time and use minimum airspace 22 p3894 A69-41150
- Commercial aircraft peak cockpit noise level during cruise and high speed descent, discussing damage risk criteria and inter-pilot speech interference 23 p4102 A69-41682
- Civil pilots medical certification after head trauma, evaluating current methods efficiency 23 p4086 A69-41687
- Blood pressure measurements of pilots at rest during tests under stress on bicycle ergometer revealing transient hypertension 23 p4087 A69-41795
- Military pilots cervical spine dynamic X ray studies, comparing spine curvature and rectitude of jet and nonjet pilots and nonflying personnel 23 p4087 A69-41798
- Exercise prescription for hypokinetic airline pilots to prevent physiological deterioration and maintain performance, discussing predictive tests, tolerance evaluation, training regimens, etc 23 p4106 A69-41800
- Indentation tonometry for occult pathology and glaucoma in commercial pilots 23 p4088 A69-41805
- Contact lenses hazards during high altitude aircraft piloting analyzed via bubble development 23 p4106 A69-41806

**AIRCRAFT PILOTS
NT TEST PILOTS**

- Alcohol role in pilot victims of aircraft accidents 01 p0022 A69-11345
- Glaucoma in commercial airline pilots noting value and safety of routine tonometry 03 p0376 A69-14078

Jet pilot blood pressure response during positive acceleration in actual flight measured by telemetry compared with centrifuge test

23 p4089 A69-41822

Pilots body images determined by inkblot tests, considering effects of aircraft type, pilots experience, etc

23 p4112 A69-42364

Measurement methods for quantitative character of aircraft pilot rating scales for vehicle flying qualities, considering wording ambiguity, dual mission character, etc

24 p4276 A69-43326

Radiology diagnosis of military jet pilots injuries during ejection and touchdown, discussing fractures, spine injuries and ejection seat spine position

24 p4266 A69-43379

Airline pilots simulated incapacitation involving myocardial infarction or cerebrovascular accident, discussing effect on crew behavior during flight task performance

24 p4277 A69-43386

Pilots myopia incidence statistical study after initiate medical examination, emphasizing skiagram value in prognosis

24 p4267 A69-43400

Physiological and psychological variables relationship in candidate pilots, noting age and educational level

24 p4268 A69-43406

AIRCRAFT PRODUCTION

Human factors in aircraft systems, discussing personnel selection throughout design and manufacturing phases

01 p0019 A69-10449

Human engineering program plans for Phase 3 of SST Development Program in accordance with airframe and engine contracts

01 p0019 A69-10451

Electrolytic marking process for aircraft component identification without use of stamping or engraving

02 p0253 A69-12065

Compressed air in aircraft manufacture, discussing versatility in production and testing of Concorde 002

02 p0253 A69-12069

Cost analysis techniques for aircraft design and development, considering passenger capacity, flight distances and flight frequencies for various aircraft types

03 p0366 A69-13646

Soviet book on press working of aviation materials, noting granulated and powdered materials and high strength and refractory materials

03 p0451 A69-14117

Statistical analysis of aircraft programs engineering man hours, aircraft performance and weight, avionics systems, schedules, etc, as estimating standards

05 p0769 A69-16239

Nondestructive testing methods for civilian transport aircraft production, overhaul and maintenance

07 p1143 A69-19702

Forming and processing facility for producing one million titanium alloy parts per month for Boeing 747 aircraft

09 p1504 A69-22063

Incentive contracts design covering cost estimates, technical performance, realistic programs and multiple incentive arrangements

09 p1626 A69-22776

Light aircraft and helicopter manufacturing methods, design concepts and materials, discussing aluminum airframes, riveting, fiberglass, UV curing, etc [SAE PAPER 690341]

11 p1822 A69-24498

Management and control techniques for aircraft product engineering changes [ASME PAPER 69-DE-67]

14 p2540 A69-28850

Jumbo aircraft production technology causing economic setback, recommending added emphasis on passenger/cargo requirements and operating environments for greater profitability

18 p3232 A69-34542

DC 10 wing design, wind tunnel models, structural and systems testing, production and marketing [AIAA PAPER 69-830]

19 p3248 A69-36296

French helicopter industry projected development for existing types, production models or final development and long range design programs

19 p3248 A69-36848

C-5A transport aircraft airframes manufacture, discussing Lockheed profits, contract disputes and Cheyenne helicopter contract cancellation

20 p3640 A69-37355

Electron beam welding machine modifications for welded airframe components production, discussing

work chamber, vacuum system and workpiece mounting [SBAC PAPER 13]

20 p3550 A69-37455

Optimum number of test aircraft in test program to predetermine endurance and service life of same aircraft in serial production

21 p3647 A69-39098

Ti alloy aircraft components and equipment production, considering roles of temperature, deformation rate and thermal conductivity in drop forging and extrusion processes [DGLR-69-003]

23 p4170 A69-42162

AIRCRAFT PROTUBERANCES U PROTUBERANCES

AIRCRAFT RELIABILITY

Helicopter structures design for maximum practicable crashworthiness and survivability, comparing load factors and deformations with indicated human impacts tolerance [AHS PAPER 225]

01 p0009 A69-10408

Structural testing in aircraft design, discussing costs, environmental conditions, test rigs and apparatus

01 p0170 A69-10864

Reliability and maintenance economics for jet transport operations of 1980s, discussing Aircraft Integrated Data System /AIDS/ sensors design [AIAA PAPER 68-207]

01 p0011 A69-11022

Reliability in air and space travel, quality/ quantity aspects, problems and cooperation

04 p0606 A69-14803

Maintainability and reliability affect utilization and operating costs of commercial aircraft

04 p0547 A69-14806

Test equipment for rapid automatic checkout and evaluation of automatic flight control systems on commercial and jet transport aircraft

05 p0742 A69-15883

Tactical airfield/aircraft system effectiveness in terms of ground support resources, aircraft reliability and maximum potential sorties

05 p0743 A69-16238

Aviation insurance function in providing risk capital in expanding aviation enterprises at fair and equitable rates, discussing air safety

06 p1041 A69-16845

Aircraft reliability under cyclic loads in flight taking into account stress fluctuations

08 p1322 A69-21106

Large and small fixed wing airplane crashworthiness requirements, noting occupant protection in survivable crash environment and rapid safe evacuation [SAE PAPER 690321]

11 p2004 A69-24509

Engineering assessment and flight testing of aircraft systems in UK, discussing operational reliability, etc

13 p2201 A69-27539

Helicopter airworthiness requirements, discussing need for international cooperation on safety regulations

13 p2202 A69-27837

Helicopter climatic testing, discussing component, systems and field tests and facilities

14 p2427 A69-29505

Aircraft hydraulic equipment ultrafine filters effect on component life and system reliability

15 p2552 A69-30069

FAA additional airworthiness standards for small aircraft in air taxi and commercial operations, noting safety levels [SAE PAPER 690320]

15 p2549 A69-30090

Spray oil cooling to reduce aircraft generator weight, enhance reliability and lengthen overhaul intervals

15 p2552 A69-30326

Propulsion system influence on aircraft reliability from viewpoint of engine manufacturer

15 p2629 A69-31122

VFW H3 Sprinter autogyro maintenance, reliability and operating costs

16 p2735 A69-32056

Fatigue life estimation for irregularly varying loads with emphasis on ground-air-ground stress cycles in aircraft

17 p3052 A69-32977

Airworthiness objectives for civil powered lift aircraft, discussing safety, traffic growth and accident rates

17 p2897 A69-33211

Spacecraft and aircraft components failure analysis for ensuring high reliability of final products

18 p3143 A69-34483

Ballistic missile and aircraft operational effectiveness, discussing data collection, reliability, availability and capability surveillance by computer

18 p3145 A69-34500

C-141 aircraft reliability growth history, discussing fleet performance, aging trends and delivery vs production sequence

18 p3090 A69-34521

Reliability and component relationships of aircraft navigation systems, describing dead reckoning, position fixing, guidance and vertical navigation

18 p3168 A69-34844

Aircraft on board weight and balance system, discussing operations and economics programs [SAWE PAPER 805]

18 p3091 A69-34900

Product reliability program for C-5A to provide high delay/abort reliability during operational usage

19 p3247 A69-36011

System engineering to select hydraulics subsystems for advanced fighter aircraft by cost effectiveness analysis, noting maintainability and reliability

19 p3254 A69-36012

Combat fielded cargo-carrying CH-54A Flying Crane helicopter industry-government reliability/maintainability field test evaluation

19 p3247 A69-36017

DC 10 aircraft reliability program, discussing passenger attractiveness, dispatch reliability, maintenance cost, flight safety and computer simulation for reliability engineering

19 p3248 A69-36027

Airworthiness certification of civil aircraft, discussing international cooperation on inspection, accident investigation, etc

19 p3456 A69-36688

Flight vehicle motion optimization taking into account random failures of sectioned power plant with limited capacity and independent parallel units

21 p3647 A69-38893

Optimum number of test aircraft in test program to predetermine endurance and service life of same aircraft in serial production

21 p3647 A69-39098

Soviet book on fluid contamination influence on aircraft hydraulic systems operational reliability covering friction, particle size, filtration, etc

21 p3649 A69-39530

Design criteria for Concorde SST servoflight control system reliability and safety

21 p3650 A69-39697

Engine powered lift civil aircraft certification factors taking into account traffic growth, accident rates, learning rate and acceptable safety level

22 p3862 A69-39962

Reliability prediction accuracy through reliability testing with reference to interplay between design, manufacture, test programs, environmental conditions, etc

22 p3952 A69-40023

Safety implications of technological developments in aviation, discussing standards and statistical data for supersonic transports and jumbo jets

22 p3867 A69-41134

Lockheed 1011 propulsion system design relating to system and component maintainability, reliability, performance and noise [SAE PAPER 690390]

23 p4201 A69-41665

AIRCRAFT SAFETY

Aircraft accidents, discussing complexity analysis, wreckage, anomalies and investigator role

01 p0009 A69-10335

Helicopter structures design for maximum practicable crashworthiness and survivability, comparing load factors and deformations with indicated human impacts tolerance [AHS PAPER 225]

01 p0009 A69-10408

Head-Up Display /HUD/ flight information applied to civil aviation, noting operational safety improvement and pilot work load reduction

01 p0020 A69-10635

In-flight measurement of shock and vibration effects on aircraft and propulsion systems

01 p0084 A69-11051

In-flight and flight line checkout techniques for foreign object damage to jet engines

01 p0056 A69-11055

Litigation for aircraft accidents, discussing legal and fiscal aspects and deterrent effect contributing to aviation safety

01 p0181 A69-11393

Safety problems of jumbo jet Airbus and SST, discussing operational safety procedures and techniques

03 p0365 A69-12882

Aircraft flight safety, discussing structural and aerodynamic concepts, maintenance and operations

03 p0365 A69-12886

- Lightning strikes to aircraft, discussing corona discharge, electric fields and meteorological measurements during thunderstorm in cumulonimbus
03 p0458 A69-13031
- Automatic all-weather landing system for scheduled civil passenger aircraft, discussing safety, display devices, Category 2 and 3 conditions
03 p0465 A69-13697
- Temperature stresses analysis for jet lift VTOL aircraft structure during takeoff and landing, discussing fire hazard in lift pod
04 p0548 A69-14841
- Soviet book on aeronautical climatology covering methodology of climatologic indices useful for airfields, pilots and flight routes evaluation
04 p0627 A69-14935
- Explosive devices to sabotage aircraft in flight, discussing evidence of sabotage in aircraft wreckage and detection of explosives before loading
04 p0549 A69-14943
- Liquid nitrogen inertant for continuous suppression of pressurized fuel tank explosion
05 p0703 A69-16505
- Ideal safety system for accident prevention, considering foreseeable and unforeseeable aspects to eliminate individual or collective human error
06 p1040 A69-16836
- Air safety, emphasizing misunderstandings or unresolved problems in accident prevention connected with law/safety interface
06 p1040 A69-16837
- SST System Safety Program, discussing cosmic radiation and aerodynamic heating
06 p1041 A69-16838
- FAA aviation safety program design standards, maintenance and inspection procedures and assessment of accidents
06 p1041 A69-16839
- Airline safety programs focused on developing reliable automatic landing system, realistic pilot training and airborne monitoring/recording system
06 p1041 A69-16840
- Aviation safety information dissemination to improve accident and incident prevention
06 p1041 A69-16841
- USAF accident information, reporting and retrieving, describing Directorate of Aerospace Safety structure and functioning
06 p1041 A69-16843
- Aviation insurance function in providing risk capital in expanding aviation enterprises at fair and equitable rates, discussing air safety
06 p1041 A69-16845
- Air carrier legal responsibility for commercial air safety as compared to liability in other transportation modes
06 p1042 A69-16847
- Federal government legal liability for commercial air safety in aircraft accident suits
06 p1042 A69-16848
- Tort system of U.S. law effect on air safety promotion, discussing liability influence on government, manufacturers and airlines
06 p1042 A69-16850
- Rain repellent system providing transparent film on aircraft windshield surface
06 p0877 A69-16954
- Small column insulated delay /SCID/ aircraft seat ejection systems, illustrating weight saving
06 p0877 A69-16957
- Aircraft accident prevention and damage control
06 p0878 A69-16961
- Supersonic aircraft fire detection using coherent fiber bundles
06 p0926 A69-17679
- Commercial jet safety, analyzing aircraft accidents and accident rates
06 p0868 A69-17829
- Aircraft radomes lightning protection, discussing evaluation by experimental methods and simulation
07 p1142 A69-19535
- Optimum approach and departure paths for VTOL aircraft simulated by hybrid computer under constraints
[AIAA PAPER 69-209] 07 p1178 A69-19570
- Damage tolerance as design consideration for aircraft safety and reliability, discussing application of failed single principal member concept to airframe construction
[AIAA PAPER 69-212] 07 p1056 A69-19574
- System safety analysis for V/STOL aircraft, discussing fault-tree technique role in fail-safe design
[AIAA PAPER 69-216] 07 p1056 A69-19575
- NASA flight safety research, discussing size effects on aircraft handling and built-in response to failure modes
07 p1057 A69-19764
- Air safety - Conference, Seattle, July 1968
08 p1315 A69-20449
- FAA regulations for improvements on crashworthiness and emergency evacuation from viewpoint of plastic applications and fire safety in aircraft
08 p1254 A69-20497
- Air traffic lateral separation assurance over North Atlantic for increased routes capacity without safety reduction
08 p1349 A69-21200
- Airport evolution in London, discussing transportation, safety, international trade, economics, aircraft types and noise spectra
09 p1479 A69-22582
- Business aircraft injury protection and impact survival design considerations, stressing upper torso restraint installations
[SAE PAPER 690335] 11 p1829 A69-24493
- Anticing for all-weather operation of business jets, discussing atmospheric conditions, ice formations, prevention and removal systems
[SAE PAPER 690335] 11 p1822 A69-24500
- Large and small fixed wing airplane crashworthiness requirements, noting occupant protection in survivable crash environment and rapid safe evacuation
[SAE PAPER 690321] 11 p2004 A69-24509
- Passenger aircraft flight readiness verification, discussing flaw and corrosion detection and rivet joint inspection methods
11 p1822 A69-24526
- Aircraft safety hazards due to birds, discussing radar role in plotting bird migrations
11 p1837 A69-25247
- Airborne collision avoidance system /CAS/ performance and operational requirements
11 p1914 A69-25430
- Aeromedical investigation of civil aircraft accidents by National Transportation Safety Board, noting post-mortem legal aspects and need for human factors investigation
12 p2021 A69-25840
- Aviation pathology in aircraft accident investigation of accident survivability features and accident precipitation factors, noting cockpit structures and protective equipment
12 p2021 A69-25841
- Civil aircraft accident investigation, discussing organization and procedures of Bureau of Aviation Safety of National Transportation Safety Board
12 p2191 A69-25844
- Monograph on physicochemical principles of takeoff monitoring systems for large aircraft covering taxiing, safety control systems design, analog simulation, etc
12 p2128 A69-26119
- Traditional flight crew organization relevance to current and developing flight systems, discussing inadequacies, anachronisms and safety threats
12 p2023 A69-26555
- Aircraft collision avoidance systems development, current status and future prospects, discussing basic requirements, criteria and prototypes
13 p2295 A69-27330
- Runway roughness induced vibrations in highly flexible aircraft, noting effect on pilot control of aircraft and airframe structure
14 p2392 A69-29504
- Safety measures for aircraft ditching at sea, discussing low wing configuration advantages and life rafts
14 p2392 A69-29697
- FAA additional airworthiness standards for small aircraft in air taxi and commercial operations, noting safety levels
[SAE PAPER 690320] 15 p2549 A69-30090
- Air lane longitudinal separation distance reduction for accommodating increased traffic using airborne computers for single file system
15 p2651 A69-30293
- Air transport industry safety record and variable stability research planes to simulate aircraft airborne behavior and handling qualities
15 p2558 A69-30453
- Turbulence and SST, discussing subsonic accidents, probability of encountering gust induced accelerations, turbulence at cruise altitudes, radar storm return and mountain waves
16 p2808 A69-32368
- Nuclear aircraft power plant, discussing safety, economy and obstacles
[AIAA PAPER 69-554] 16 p2811 A69-32761
- Protective helmet design effectiveness against concussion and skull fracture as function of dimension, weight, load spreading, etc
17 p2913 A69-33177
- Airworthiness objectives for civil powered lift aircraft, discussing safety, traffic growth and accident rates
17 p2897 A69-33211
- Airfield bird scaring methods including Very pistol shell cracker firing and broadcast calls on civilian and military airfields
17 p2915 A69-33365
- Navigation and guidance systems for low altitude aircraft flight safety noting position determination, cockpit environment and fail-safe operation
17 p3002 A69-34080
- L-1011 Tri-Star aircraft systems and safety provisions, discussing automatic flight control system, propulsion, noise reduction, galley, coat storage and cabin window shades
[AIAA PAPER 69-828] 19 p3243 A69-35598
- Air piracy legal aspects as determined by Swiss law and Treaty of Tokyo
19 p3454 A69-35979
- Descent device for emergency egress from jumbo jets based on centrifugal brake, including test data on C-5 fuselage section
19 p3255 A69-36146
- Problems caused by air traffic rate growth in London Terminal area, examining runway limits, safety and noise restrictions
19 p3371 A69-36736
- Concorde SST fire protection equipment, discussing fire and overheat detectors, fire extinguisher, crash fire protection, explosion suppression equipment, etc
19 p3256 A69-36864
- Electrohydraulic servosystem to counteract atmospheric turbulence effects on B-52 global bombers, noting reduction in aircraft fatigue and structural damage
20 p3467 A69-38184
- Design criteria for Concorde SST servoflight control system reliability and safety
21 p3650 A69-39697
- Custody, jurisdictional conflict and prosecution problems of in-flight crimes, discussing federal judicial jurisdiction and Tokyo Convention ratification
22 p4053 A69-40708
- Air safety - Conference, Anaheim, October 1968
22 p3866 A69-41127
- Reliability engineering application to aircraft safety, considering mathematical models involving safety, human errors and accident causes
22 p3867 A69-41129
- Planning for safety of future supersonic air traffic including financing and coordination activity of government and industry
22 p4054 A69-41131
- Safety engineering programs for aircraft design, discussing organizational relations, failure and operational safety analyses
22 p3867 A69-41132
- Safety standards for DC 10 aircraft, considering cockpit design, hydraulic, electric power, autoland and direct lift control systems, structural safety and crash worthiness
22 p3867 A69-41133
- Safety implications of technological developments in aviation, discussing standards and statistical data for supersonic transports and jumbo jets
22 p3867 A69-41134
- B-747 safety assurance program, discussing organization, management, hazard sources, accident statistics, night visual approach and maintainability
22 p3867 A69-41135
- Boeing 747 safety engineering program, discussing organization, design review, system safety, systems design-analysis and tests
22 p4054 A69-41136
- Third generation jet aircraft safety, discussing accident prevention and survival
22 p4054 A69-41142
- XB-70 aircraft test data as applied to SST safety, describing aircraft design, flight characteristics, instrumentation, takeoff and landing, etc
22 p3868 A69-41143
- Airport standards analysis for safe, efficient air carrier operations including airport funding, safety programs for runways and terminal facilities
22 p4054 A69-41144
- Vertebral column fracture resulting from aircraft ejection, studying ejection seat geometry and personal equipment design influence on spinal curvature relation to catapult thrust
23 p4102 A69-41681

Civil aircraft structural components failure analysis, discussing fatigue failures and fail-safe design for accident prevention

24 p4251 A69-42779

F-5 cockpit fogging during low flights and dive bombing in South Vietnam attributed to hot humid weather, recommending cockpit temperature control and pilot diet

24 p4277 A69-43376

Damage tolerance design concepts required to obtain reliability, maintainability and operational safety of complex aircraft

[ICAS PAPER 68-23] 24 p4254 A69-43717

AIRCRAFT SPECIFICATIONS

Wind gust simulation procedures, discussing high altitude clear air turbulence and simulation of air perturbations

03 p0461 A69-13647

Lockheed 1011 Tristar with three turbofan engines for large capacity medium range service, noting configuration, aerodynamics, structure and cutaway drawings

08 p1255 A69-21143

Large and small fixed wing airplane crashworthiness requirements, noting occupant protection in survivable crash environment and rapid safe evacuation

[SAE PAPER 690321] 11 p2004 A69-24509

Douglas DC-10 medium range aircraft, discussing engine placement, passenger and cargo capacity, construction data, etc

11 p1823 A69-25211

Aircraft engines future specifications as affected by expanding market, noting speed requirements and thrusts

11 p1942 A69-25215

Concorde SST industrial project in international cooperation and stage in transport history including supersonic boom, weight, fuel consumption rates and aerodynamic heating

12 p2013 A69-26356

Short range passenger aircraft, considering payloads, weights and economical classification

13 p2201 A69-27294

Dassault Mercure high speed twin turbojet aircraft, discussing capacity, range, propulsion, profitability threshold, etc

15 p2550 A69-30318

Military V/STOL aircraft flying qualities specification, considering structure, hover and low speed requirements, forward flight, transition maneuverability and control

[AHS PAPER 363] 17 p2900 A69-33520

Interim revision of military flying qualities specifications according to experimental data and characteristics of existing aircraft

[AIAA PAPER 68-245] 17 p2902 A69-34026

Airframe cost element prediction and application to cost control, considering government specifications

[SAWE PAPER 731] 18 p3221 A69-34894

Boeing 747 design and development, discussing aircraft characteristics, performance, inertial navigation system, production costs, etc

[SAWE PAPER 746] 18 p3091 A69-34907

Aircraft interior conversion for passenger or cargo service, discussing convertible aircraft and quick change concepts

[AIAA PAPER 69-784] 19 p3244 A69-35642

AIRCRAFT STABILITY

NT HOVERING STABILITY

Supercritical flow effects on unsteady aerodynamic coefficients used for subsonic aircraft flutter analysis, emphasizing changes due to shock and flow separation

01 p0007 A69-11020

Two term and three term controllers for hovering rigs and VTOL aircraft, comparing stability, transient response and control force

04 p0547 A69-14814

Aircraft stability during sideslip, discussing influence of fuselage/wing interference

04 p0548 A69-14824

Root locus method applied to longitudinal and lateral stability of aircraft with flexible fuselage and wing

04 p0677 A69-14835

Optimal flight stabilization of VTOL aircraft in hovering mode based on linear rotation dampers system

05 p0702 A69-16024

Modal response analysis of servocontrols as deduced from vibration test, for possible application to aircraft

[ONERA-TP-668] 06 p0869 A69-17100

Longitudinal stability derivatives prediction for rigid and elastic airplanes, using influence coefficient method

[AIAA PAPER 69-131] 06 p0868 A69-18134

Variable properties aircraft for flying simulator, discussing flight control system and stability behavior

07 p1052 A69-18254

Flying qualities considerations in design and development of Huey Cobra for helicopter attack mission, describing stability and control augmentation systems

[AHS PAPER 217] 07 p1053 A69-18871

Longitudinal stability of V/STOL aircraft at low speeds, discussing three tilt wings and quad ducted propeller configurations

[AIAA PAPER 69-194] 07 p1055 A69-19566

Control technique to make aircraft insensitive to parameter variations and to achieve desired response to control

08 p1255 A69-20719

Fluidic control systems for angular rate and attitude stabilization flight-tested, noting good impact and acceleration resistance

[AGARDGRAPH-118] 08 p1257 A69-20955

Helicopter instability on ground with propulsion system operating and inoperative, discussing overturning, restoring moments and pilot training

09 p1433 A69-21385

Lateral stability of glider towed by cable in steady rectilinear horizontal flight, deriving motion equations as ordinary differential equations

09 p1433 A69-21498

Aircraft gust alleviation system for minimizing weighted sum of normal acceleration and pitch rate response by limiting control surface deflections

09 p1434 A69-22279

Newton-Raphson technique development for determining stability derivatives from flight data, noting use of a priori wind tunnel information

[AIAA PAPER 69-315] 09 p1434 A69-22379

Helicopter all-weather flight control system, using autostabilization and artificial horizon

09 p1435 A69-22778

Root sensitivity of characteristic equation of linear automatic control system to system parameter changes applied to aircraft angular stabilization

10 p1666 A69-23610

Book on aircraft stability and control covering conventional, canard, variable sweep, slender delta wing, helicopter and other VTOL aircraft

11 p1821 A69-24370

Atmospheric turbulence effects on aircraft flight noting causes of turbulence

11 p1911 A69-24527

Optimum planform stabilizer selection for damping of rotational motion and elastic torsional stresses of aircraft fuselage about longitudinal axis

11 p1966 A69-25327

Aircraft dynamic response to three dimensional turbulence, establishing unique correspondence between spatial symmetry properties of ambient fields of turbulence and aircraft

11 p1823 A69-25503

Aircraft stability derivatives determined by adaptive method, emphasizing physical and mathematical characteristics of learning model

11 p1824 A69-25671

Computer aided design of linear multivariable control systems applied to VTOL aircraft stability augmentation

12 p2013 A69-26068

Monograph on rapid rotations of aircraft with fixed controls, covering spin and roll movements differential equations

12 p2013 A69-26118

Digital computerized analysis and characteristics of variable stability aircraft, examining digital control system

15 p2549 A69-30229

Air transport industry safety record and variable stability research planes to simulate aircraft airborne behavior and handling qualities

15 p2558 A69-30453

Aircraft neutral stability empirical and mathematical aspects, considering control stabilization, damping and phugoid motion

15 p2551 A69-31012

Stabilizing methods for supersonic aircraft, noting effect of aircraft characteristic parameters on magnitude of balancing coefficients of lifting force

16 p2735 A69-32127

Stability augmentation system for CX-84 tilt wing V/STOL aircraft, using redundancy techniques to achieve fail operational performance with two active channels

[AHS PAPER 310] 17 p2901 A69-33545

VTOL variable stability system /VSS/ for XV-4B lift jet for flight control and handling verification

17 p2902 A69-34066

Soviet book on practical aerodynamics of An-2 aircraft covering aerodynamic characteristics, equilibrium, stability and control for various flight conditions, including icing

18 p3090 A69-34340

STAN integral weight and balance system providing aircrews with takeoff gross weight and CG data

[SAWE PAPER 755] 18 p3136 A69-34882

Additional yawing by gyroscopic moment of power plant and effect on aircraft maneuver during curvilinear flight, noting compensation by automatic control

18 p3092 A69-34971

Angular velocity of aircraft rotation about longitudinal axis at arbitrary point of passive trajectory section, with assumptions on roll damping, momentum, etc

18 p3092 A69-34980

Higher harmonic pitch angle inputs to eliminate oscillatory helicopter blade root shear determined through teetering rotor model

18 p3089 A69-35233

Fighter aircraft higher order control system dynamics effects on longitudinal handling qualities evaluated by in-flight simulator for role of pilot induced oscillations tendencies

[AIAA PAPER 69-768] 19 p3245 A69-35655

Differential synthesis technique application to design of multi-axis stability augmentation systems for aerospace vehicles

[AIAA PAPER 68-834] 20 p3616 A69-37156

Stability augmentation system for B-52, noting flight test performance evaluation for structural vibrations and rigid body motions of aircraft

[AIAA PAPER 68-1068] 20 p3461 A69-37157

High altitude aircraft range requirements for airborne turbulence detector, taking into account passenger comfort, turbulence geometry, maneuverability and pilot decision making

20 p3537 A69-37164

Flight control and stability of STOL transport aircraft with powered-lift boundary layer control system augmented lift

20 p3462 A69-37513

Aeroelastic instabilities of aircraft in flight by representing motion in space function base, using natural vibration mode

[ONERA-TP-697] 20 p3626 A69-37755

Equations of motion for optimal attitude of suborbital aircraft regarding time and distance range

21 p3795 A69-38440

Flight control system providing variable stability in pitch axis of NF-8D Crusader, discussing flight evaluation of power approach short period configurations

[AIAA PAPER 69-896] 21 p3648 A69-39420

In-flight test to determine variation effects in bank angle control parameters on cruise flight handling qualities, considering spiral stability

[AIAA PAPER 69-893] 21 p3648 A69-39425

Aircraft directional stability in terms of ideal non-holonomic coupling on mechanical system, noting servosystem role

21 p3830 A69-39836

Noise and vibration levels measured in An-24 Polish passenger aircraft indicating excess noise in crew compartment

22 p3862 A69-40005

Fluidic servoactuator controlled by hydraulic vortex valves using mechanical signals for helicopter stability augmentation system

24 p4255 A69-42800

LF approximation in predicting unsteady aerodynamic forces affecting large aircraft stability, analyzing velocity potential of oscillating wings

24 p4250 A69-43729

AIRCRAFT STRUCTURES

NT AIRFRAMES

NT FUSELAGES

NT PLASTIC AIRCRAFT STRUCTURES

Structural vibration problems of SA 330 helicopter from test flight data, discussing natural frequency displacement of blades and dynamic response improvement of structure

01 p0009 A69-10158

Power spectral density method of random loads analysis applied to V/STOL aircraft structural analysis, discussing statistical distribution

01 p0168 A69-10407

Balsa wood laminates as aircraft structural material noting thermal properties, fire and fatigue resistance, weight savings, etc

01 p0101 A69-10595

Structural testing in aircraft design, discussing costs, environmental conditions, test rigs and apparatus

01 p0170 A69-10864

Fabrication of large parts in aircraft and space industry, discussing extrusion, forging, explosive forming and diffusion bonding

01 p0088 A69-11400

Concorde structural tests, discussing ground test program for simulating flight temperature and stress conditions at 2.6/2.7 station of wing-fuselage section

02 p0193 A69-11892

Strain multiplier device for fatigue sensors for totalizing resistance change from aircraft service load parameters

02 p0250 A69-12230

Book on flight structure theory and analysis covering methods for digital computers, differential equations for equilibrium boundary value problems, etc

03 p0525 A69-13266

Kinetic heating of aircraft, discussing aerodynamic boundary layer, relationship between heat transfer coefficient or boundary layer energy turbulence and skin friction

03 p0534 A69-14087

Skin panel stresses for random acoustic loading, determining aircraft structure responses

03 p0530 A69-14092

Soviet collection of papers on aircraft construction and air fleet equipment

04 p0672 A69-14483

Spar attachments of aircraft wings analyzed with respect to weight and applied loads, determining optimum bolt diameter ratio to lug width

04 p0673 A69-14496

Explosive forming process to shape aircraft structural parts, advantages and potentials

04 p0604 A69-14524

Ground vibration testing of flight and space vehicles, noting structural damping asymmetries and nonlinearities

04 p0585 A69-14833

Calculation method for surface aircraft structures by treating normal forces and bending moments as unknown values

04 p0677 A69-14839

Phenolic and epoxy adhesives for metal-metal and honeycomb bonding, discussing cold cure adhesives for aircraft structures and aircraft floor sandwich design optimization

04 p0606 A69-14845

Aircraft structure lightweight construction materials, reviewing Ti alloys and Be and Al-B bonded filament materials

05 p0779 A69-15917

Open class type glider design, discussing structural materials, dimensions and control

05 p0702 A69-16027

Statistical method to investigate time varying stresses in helicopter structures, considering service life evaluation

05 p0767 A69-16775

Turbulent boundary layer loading function for use with finite element structural analysis system applied to elastic aircraft structures random vibration

06 p0914 A69-18132

Static endurance of aircraft structural elements under single and multiple loading, based on real alloys and crystalline materials theories

07 p1231 A69-18554

Concorde testing program, detailing materials, structure, systems, engine, wind tunnel and flight tests

07 p1054 A69-19294

Fail-safe design principles and criteria for helicopter structures to prevent operational failure arising from undetected fatigue damage

07 p1054 A69-19549

Fabrication and processing techniques, tooling concepts and quality control for composite materials used in large aircraft, discussing honeycomb and sandwich structures

07 p1172 A69-19670

Titanium hot forming and sizing die fabrication concepts for aircraft structures

07 p1143 A69-19671

Technology of titanium for C-5A aircraft, discussing structural and functional components and machining, welding, forging, etc

07 p1143 A69-19672

Concorde equipment, summary of British companies activities in supplying components

07 p1057 A69-19706

Al alloys application to Concorde project and other aircraft structures, noting mechanical properties

08 p1335 A69-21141

Aircraft structural aluminum alloy fatigue life, considering atmospheric relative and absolute humidity

09 p1521 A69-21390

Forming and processing facility for producing one million titanium alloy parts per month for Boeing 747 aircraft

09 p1504 A69-22063

High strength room temperature vulcanizing silicone rubber for tooling and fabrication of aircraft and missile components

09 p1507 A69-22331

Ultrasonically assisted installation of fasteners for weight savings in aircraft/spacecraft structures

09 p1478 A69-22373

Fatigue strength and aircraft structural standards based on experimentally determined safety factors

09 p1619 A69-22571

Elastoplastic stress in notch as cause of decreased lifetime of aircraft components, analyzing stress reversal and displacement during takeoff and landing

09 p1620 A69-22576

Pulse echo ultrasonic nondestructive testing of C-5 adhesive bonded aluminum composites with multiple bond lines

10 p1698 A69-23047

Titanium compared with aluminum in application to supersonic aircraft structures, considering tests and costs

10 p1700 A69-23600

Cyclic stress-strain and fatigue behavior in aircraft structural metals, discussing hardening and softening in aluminum alloys, steels and titanium alloys

10 p1714 A69-23981

Active feedback control of distributed parameter systems including elastic airplane and missile structures, noting feedback loop coupling problem

10 p1668 A69-24145

Dynamic IR inspection to detect fatigue cracks in aircraft and missile structure from distance

11 p1861 A69-24262

Aircraft structures fatigue strength determination, discussing test procedures, sample preparation, strength prediction, etc

11 p1970 A69-24525

Aircraft structures fatigue life determination based on Kordonskii method, comparing steel tests result with linear summation theory

11 p1987 A69-25345

Permissible expenditures for decreasing aircraft structural weight

11 p2005 A69-25349

Variable and fixed weight growth factor effect on aircraft, showing coincidence of minimum weight

11 p1987 A69-25432

Aircraft structure geometry design for minimizing total mass concerning flutter requirements

11 p1989 A69-25493

Servocontrol to delay flutter onset of aeroelastic structures, discussing rapid amplitude and phase changes near instability point, wind tunnel models, instrumentation, analog simulation

11 p1992 A69-25518

Fabrication, machining and contouring of boron-epoxy composite for sandwich type aircraft structure, noting F-5 supersonic fighter main landing gear strut door

12 p2103 A69-26826

Diffusion bonded Ti honeycomb sandwich, demonstrating structural integrity, efficiency, low weight and cost effectiveness

12 p2115 A69-26828

Collection of papers on aerodynamic flutter covering airfoils, flow theory, aircraft structures, etc

13 p2358 A69-27234

Trident 2E and 3B structural design and fail-safe tests, noting difference in fuselage length

13 p2202 A69-27972

Book on subdivision of aircraft structural design covering technology, economics, working conditions, performance, etc

14 p2456 A69-29860

Electron beam welding characteristics for aircraft components and design noting limitations

15 p2617 A69-30089

Polyurethane with additives for fuel fire control in aircraft structures, achieving desired protection without impairing foams mechanical properties

15 p2561 A69-30311

Civil aircraft projected development regarding materials and structures, discussing new components and fuel contribution to weight and metals and composites for replacing Al

16 p2872 A69-32024

Book on soviet An-24 aircraft construction and exploitation covering fuselage, powerplant, controls, fire prevention, air conditioning, maintenance, etc

16 p2735 A69-32112

Starting weight increments in aircraft designs having various structural features and dimensions

16 p2735 A69-32144

Numerical procedure to optimize complex structures by determining relative proportions of selected elements attaining flutter speed with minimum total mass

16 p2874 A69-32163

Aircraft and missile dynamic characteristics for heavy loads and large heat flux, noting small harmonic vibrations of heated structures in plastic domain

17 p3061 A69-33589

Passenger cabin windows on Conqair liner type aircraft, describing construction, installation, strength, etc

17 p3061 A69-33667

Damping properties of multilayer coatings for aircraft structures analyzed on duralumin samples subjected to bending at room, elevated and low temperatures

17 p2993 A69-33941

Moldable plastic shim material for structural airframe components, discussing application requirements

19 p3319 A69-35551

Static dynamic and damage tolerant strengths of advanced materials for VTOL aircraft with emphasis on Ti, cryoformed 301 stainless steels and filamentary composites

19 p3433 A69-35658

Stress coining methods for improving aircraft structure fatigue life by controlling material yielding inside holes and materials surrounding holes and slots

19 p3433 A69-35659

Collection of papers on aircraft construction and air fleet equipment covering aerospace vehicles theory, engines, automation, design and production

19 p3246 A69-35813

Aircraft structures design, discussing reinforced sandwiches and composites, failure mechanisms, non-destructive testing and fabrication

19 p3438 A69-36325

Relationship between chronological and fatigue life in airframes, showing fatigue life dependence on operating conditions, pilot techniques and maintenance and inspection quality

20 p3461 A69-36920

Soviet monograph on metal fatigue in aircraft structures, discussing effects of temperature, loading, residual stresses, surface finish and contact corrosion

20 p3622 A69-37231

Supersonic blowdown wind tunnel operating at Mach numbers obtained by fixed nozzles for aerodynamic optimization of wings and bodies

20 p3510 A69-37422

Soviet book on interchangeability of structural elements in aircraft construction, discussing experiences in serial production of aircraft and helicopters

20 p3462 A69-37443

Al alloy application to welded primary airframe structures, discussing welding processes with emphasis on fusion welding

20 p3549 A69-37445

Weld defect data analysis in relation to aerospace structure performance, emphasizing effect on fatigue behavior and acceptance standard

20 p3550 A69-37450

Welding quality control in aircraft structures, considering weld design, process, weld and materials specifications, welding equipment and inspection

20 p3550 A69-37452

Seam welded Al alloy aircraft structure fabrication problems, emphasizing stress corrosion

20 p3550 A69-37454

Electron beam welding for fabrication of aircraft structures, discussing fatigue strength of Ti and Al alloys and margining and low alloy steels

20 p3550 A69-37456

Aircraft structures efficiency and weldability as function of application, welding procedures and metallurgical factors, considering high strength Al alloys, Ti and Ni alloys, etc

20 p3550 A69-37457

Eddy current machine /nondestructive testing device/ for aircraft structures surface cracks detection

21 p3719 A69-38391

Carbon fiber reinforced plastics application to aircraft metal components for weight reduction, low cost and high mechanical properties

21 p3750 A69-38428

Ti structural components for forgings, noting problems facing die-forging industry and machining equipment

21 p3728 A69-38459

Plasma metal spray coating for Al and Mg alloy aircraft components adhesive bonding repair technique compared to welding and electroplating

21 p3728 A69-38462

Design and processing tradeoffs for preventing stress corrosion cracking in Al alloy aircraft structural forgings
[ASM PAPER W9-14.4] 21 p3729 A69-38657

Computerized aircraft structural analysis system, adopting finite element technique /direct stiffness method/ based on COSMOS system
21 p3842 A69-39307

Creep buckling strength reduction of aircraft compression structure, discussing initial eccentricity and loading mode effects on supersonic aircraft operation mode
21 p3842 A69-39308

Al-B composite aircraft structure fabrication, discussing wingspan segment, resistance spot welding, hot forming of joggles, etc
[AIME PAPER S69-1] 21 p3732 A69-39471

Book on convergence in calculation of elastoplastically deformable aircraft structures and continua, covering matrix displacement method and stepwise linearized computational technique
22 p4044 A69-40619

Aircraft fastening systems guidelines based on mechanical strength, weight, cost and joint efficiency, discussing hole preparation and expansion design
22 p3956 A69-40822

Large diameter bolts in aircraft structures resisting hydrogen embrittlement and stress corrosion, noting fatigue properties
22 p3957 A69-40827

Interference fit fasteners role in improving aircraft structure fatigue life through preload barrier against fatigue stresses
22 p3957 A69-40830

Airplane structure electromagnetic compatibility engineering problem including bonding, electrointerference suppression and static control considerations
23 p4063 A69-42234

Civil aircraft structural components failure analysis, discussing fatigue failures and fail-safe design for accident prevention
24 p4251 A69-42779

Aircraft Structures and Materials Application - Conference, Seattle, September 1969
24 p4321 A69-43416

Aircraft structure fabrication combining unidirectional strength and stiffness of B composite with metal, including test and weight/cost data
24 p4323 A69-43419

Cobalt-base superalloys analysis for temperature stability, corrosion resistance, creep, fatigue and strength in aircraft structures and parts applications
24 p4334 A69-43427

Concorde elevons sandwich construction to meet sonic environment, discussing core, adhesive, design and fabrication
24 p4403 A69-43429

Ti and Ti alloys investment castings mechanical properties, dimensional control and corrosion resistance in aircraft and aerospace structural application
24 p4324 A69-43433

SST range-payload improvement by emphasizing Ti alloys honeycomb and trusscore sandwich panels fabrication for structural boxes in wing and empennage
24 p4324 A69-43436

Aerospace fastener systems standardization proposal to reduce inventories, simplify design and provide extended structural life
24 p4325 A69-43439

Aerospace fastening system requirements to lower in-place costs, extend service life and reduce weight of aircraft
24 p4325 A69-43440

Fastener materials selection for high temperature aircraft structures, considering various physical properties influence
24 p4325 A69-43441

Orthotropic fiberglass/epoxy faced honeycomb aircraft type sandwich structure elastic properties by edgewise compression test
24 p4403 A69-43443

Boron epoxy composites evaluation for use in aircraft dynamic components, considering fatigue failure mechanism identification
24 p4337 A69-43450

Polycarbonate and polysulfone thermoplastic bonding of Al and Ti in aircraft structures, discussing peel strength and stress crazing tests
24 p4326 A69-43459

F-111 sandwich structure adhesive joints glue lines, describing thickness measurement techniques and acceptance criteria
24 p4403 A69-43461

Adhesive bonded joints for glass resin composite sandwich helicopter structures, describing aircraft applications
24 p4403 A69-43462

Anaerobic adhesives for aircraft bonding tested for mechanical properties, noting advantages over epoxy adhesives
24 p4338 A69-43464

AIRCRAFT TIRES

Aircraft tire wear determination by measuring intensity of radiation originating from point source within thread, using thulium 170 isotope
07 p1143 A69-19703

Hertz impact theory application to aircraft tire in operation, considering imperfectly elastic body with impact expressible by Newton recovery factor of about one
10 p1633 A69-22887

Tire test machine for tire parameter determination in aircraft landing gear shimmy stability studies
[AIAA PAPER 68-311] 17 p2902 A69-34029

Runway grooving to improve aircraft tire traction in adverse weather tested by F-4D and Convair 990A under wet conditions
[AIAA PAPER 69-773] 19 p3244 A69-35649

Dynamic stability of dual wheel gears for aircraft applications, discussing shimmy, tire characteristics, velocity effects, etc
[AIAA PAPER 69-769] 19 p3245 A69-35654

Aircraft tire skidding on wet surfaces, measuring interstitial water pressure for various treads, velocities and surface textures
19 p3247 A69-35910

Aircraft braking, discussing systems, brakes, tires, runway interface, heat sink materials, friction measurements, skid control, cooling and recovery equipment
[SAE PAPER 690376] 23 p4063 A69-41671

AIRCRAFT WAKES

NT HELICOPTER WAKES
NT PROPELLER SLIPSTREAMS
NT SLIPSTREAMS

Flow fields about swept rear fuselages of rear loading cargo transport aircraft
06 p0859 A69-17492

Aircraft vortex wake development prediction for turbulent flow noting vortex size, strength and peak tangential velocity
11 p1819 A69-25377

Vertical takeoff aircraft propeller/rotor design and performance prediction, discussing vortex model, wake contraction, blade element aerodynamic properties, etc
[AHS PAPER 325] 17 p2894 A69-33534

Thin jet flapped airfoil analysis with wake fully developed from leading edge and jet flow reflected from ground
22 p3861 A69-41184

Computerized pressure distribution estimation for stalled airfoil with arbitrary wake geometry
24 p4250 A69-43726

AIRCRAFTS

U FLIGHT CREWS

AIRFIELD SURFACE MOVEMENTS

Tactical airfield/aircraft system effectiveness in terms of ground support resources, aircraft reliability and maximum potential sorties
05 p0743 A69-16238

Airport surface traffic control system /STRACS/ for detection of aircraft, identification, guidance on taxiways, tower display, fail-safe alarm logic, priority routings, conflict protection, etc
05 p0790 A69-16724

Runway development for increased airport capability, discussing computer simulation model of airport operations
06 p0906 A69-17166

Automatic ground traffic control of aircraft on airport taxiway without visual detection, noting induction loop detection in surface traffic control system /STRACS/
11 p1913 A69-24267

Aircraft design determined by airport environment and facilities defined as pavement strength, passenger and baggage loading and aircraft handling, noting noise abatement
17 p2948 A69-34209

Airport performance, noise and aircraft utilization influence on aircraft design and operating costs, stressing takeoff distance, obstacle clearance and noise regulations
17 p2948 A69-34210

Los Angeles International Airport development planning, discussing airfield improvement, tunnel

reconstruction, terminal layouts, parking, roads and access, etc
[AIAA PAPER 69-806] 19 p3288 A69-35590

Forces on aircraft during ground roll with slick runway surface and cross wind for deceleration and control on ground
[SAE PAPER 690375] 23 p4062 A69-41652

Refused takeoff as critical maneuver in ground operations during jet transport accident investigation emphasizing pilot anticipation of conditions and preplanning actions
[SAE PAPER 690378] 23 p4062 A69-41654

AIRFOIL CHARACTERISTICS

U AIRFOILS

AIRFOIL PROFILES

NT WING PROFILES
NT WING SPAN

Low Mach number airfoil profile drag calculation for various angles of attack and Reynolds numbers, noting effects of transition and airfoil thickness
01 p0006 A69-11017

Arbitrary phase shift vibrations of airfoil profiles in incompressible flow reduced to Fredholm equations, allowing for trailing vortices influence
02 p0190 A69-12574

Lift from unsteady flow past cascade of slender profiles with stagger angle reduced to solution of Fredholm integral equation
02 p0190 A69-12575

Aerodynamics of flap balanced swivel airfoils, discussing lift curve slope, incidence change response and application of control forces and movements
03 p0364 A69-13908

Thickness effects on flow past sweptback wings in supersonic flight noting influence of oscillatory motion
[ASME PAPER 68-FE-31] 05 p0698 A69-16078

Low drag three dimensional body configurations from tabulated low drag airfoil coordinates
06 p0857 A69-17000

Conical flow past cruciform wing-body and tail-body systems, considering various positions of leading edges with respect to Mach cone
15 p2548 A69-31002

Natural frequencies and vibration modal shapes of asymmetrical airfoil blades analyzed by differential equations of motion, noting flexure coordinates center variations effect
17 p3067 A69-34053

Optimum pressure distribution and airfoil profiles for maximum lift without separation in incompressible flow determined by second order theory
[AIAA PAPER 69-739] 18 p3083 A69-34401

Pressure distribution in two dimensional incompressible potential flow on Joukowski airfoils with normal upper surface spoilers, emphasizing potential flow theory
[AIAA PAPER 69-737] 18 p3083 A69-34402

Numerical solutions of thick cambered jet flap in ground effect for flat plate and diamond shaped airfoil
[AIAA PAPER 69-738] 18 p3083 A69-34404

Aerodynamic characteristics of elliptical airfoils with jet circulation control for VTOL rotors including dual jets and cyclic results
[AIAA PAPER 69-741] 18 p3084 A69-34406

Linearized theory of subsonic gas flow past profile compared with methods based on approximations of relationship between density and pressure
19 p3241 A69-36782

Potential flow theory applied to determination of airfoil separated vortex flow and maximum lift and Reynolds number dependence
20 p3459 A69-37421

Aerodynamic optimal shaping by multivariable search technique, comparing results with variational solutions for airfoil profiles
20 p3459 A69-37527

AIRFOILS

NT AERIAL RUDDERS
NT AILERONS
NT CAMBERED WINGS
NT CARET WINGS
NT CRUCIFORM WINGS
NT DELTA WINGS
NT ELEVATORS (CONTROL SURFACES)
NT ELEVONS
NT FIXED WINGS
NT FLAPS (CONTROL SURFACES)
NT FLEXIBLE WINGS
NT HORIZONTAL TAIL SURFACES
NT JET FLAPS
NT LAMINAR FLOW AIRFOILS
NT LEADING EDGE SLATS
NT LIFTING ROTORS
NT LOW ASPECT RATIO WINGS
NT PARAGLIDERS
NT PARAWINGS

NT PROPELLER BLADES
 NT RIGID ROTORS
 NT RIGID WINGS
 NT RING WINGS
 NT ROTARY WINGS
 NT SLENDER WINGS
 NT SPOILERS
 NT SUPERSONIC AIRFOILS
 NT SWEPT WINGS
 NT TABS [CONTROL SURFACES]
 NT THIN AIRFOILS
 NT THIN WINGS
 NT TILTING ROTORS
 NT TIP DRIVEN ROTORS
 NT TRAILING-EDGE FLAPS
 NT TRAPEZOIDAL WINGS
 NT TWISTED WINGS
 NT VARIABLE SWEEP WINGS
 NT WING FLAPS
 NT WINGS

Passive ice protection of aerodynamic surfaces by icephobic coating, measuring removal of ice under simulated conditions in tunnel tests

Reynolds and Mach numbers influence on loss coefficient magnitude at straight airfoil lattice

Wind tunnel and test equipment for studying flow in straight airfoil lattices at Reynolds numbers 50,000-1,200,000 and Mach numbers 0.1-1.0

Prandtl three main problems of airfoil theory interpreted and applied, discussing slender aircraft and hypothetical waverider aircraft

Ideal plane incompressible fluid flow past airfoil noting hydrodynamic effects, assuming presence of constant eddy

Trailing edge velocity and stagnation points for isolated and latticed airfoils using Zhukovskii and Weing transformations

Zhukovskii lifting force theorem application to slender wing profile and airfoil lattice in linearized supersonic flow

Lift fluctuation on airfoil due to transverse and chordwise gusts applied to rotating fan and compressor blade design

Rotating turbomachinery design to minimize fluctuating lift on isolated airfoils, presenting cascade geometry by quasi-steady analysis

Plane subcritical flow past lifting aerofoil analyzed using conformal mapping and difference scheme on angular mesh inside circle

Tandem airfoils wing-tail interaction flutter analysis, using three dimensional vortex lattice aerodynamic theory

Hodograph for lifting airfoil with subsonic velocity at infinity, using Chaplygin compressibility law for computation

Plane steady transonic flow of perfect fluid around airfoils with constant curvature using hodographic method, discussing various boundary conditions

Transonic flow around airfoils with constant curvature in uniform asymptotic stream, studying leading edges in exact form

Conformal mapping of regions with corners and large curvatures of boundary curves onto unit circle with digital computer, considering airfoil

Subsonic channel flow of frictionless barotropic gas through oscillating grid, investigating perturbation velocity field and aerodynamic forces on airfoils

Steady incompressible fluids flow around stationary wings and through rotating blades cascades based on Prandtl airfoil theory of bound vortices

Dynamic stall data for helicopter rotor blade analyses obtained by oscillatory tests in pitch and in vertical translation at full scale Reynolds number

Linear and second order theory for maximum lift to drag ratio airfoils at moderate supersonics speed, considering length, thickness and area

13 p2199 A69-28214

Book on experimental aerodynamics covering subsonic and supersonic wind tunnels, wall measurements, airfoils, aerodynamic characteristics of propellers, fixed and rotary wing aircraft

Two dimensional airfoil data application to three dimensional rotor blade element environment, predicting stall induced structural loads

Internal heat transfer coefficients for impingement cooling of gas turbine airfoil leading edge

Aerodynamic behavior of airfoil oscillating in reverse flow defined for various angles of attack and oscillatory amplitudes at low Mach numbers

Rotor airfoils design for helicopter performance optimization, noting hovering figure of merit and blade profile characteristics relationship

Flow breakdown in wind tunnel tests of high disk loading systems at low forward speeds, investigating downwash distribution effect using disk loading and airfoil models

Rotating turbomachinery design to minimize fluctuating lift on isolated airfoils, presenting cascade geometry by quasi-steady analysis

Monograph on interaction between primary and jet flapped secondary airfoils covering line-vortex use for lift augmentation, aerodynamic characteristics, etc

Dynamic stall characteristics of high speed symmetrical and cambered helicopter rotor blade airfoils from two dimensional wind tunnel determinations

Adiabatic plane ideal gas flow past airfoil, studying shock waves propagation effect on dynamic behavior

Airfoils and cascades design for incompressible flow by numerical methods

Linear small perturbation approximation for supersonic nonequilibrium flows past oscillating airfoil in two dimensional wind tunnel, noting Laplace transform solution

Incompressible fluid flow inhomogeneities effect on oscillations of airfoils cascade, noting occurrence of parametric resonance in turbine engine blades

Computerized pressure distribution estimation for stalled airfoil with arbitrary wake geometry

24 p4250 A69-43726

AIRFRAME MATERIALS

Balsa wood laminates as aircraft structural material noting thermal properties, fire and fatigue resistance, weight savings, etc

Airline operators economic oriented airframe maintenance problems, discussing cost accounting improvement

Soviet book on press working of aviation materials, noting granulated and powdered materials and high strength and refractory materials

Metal welding procedures for aircraft assembly, discussing weight, specific alloys and airframe components

Aircraft structure lightweight construction materials, reviewing Ti alloys and Be and Al-B bonded filament materials

VTOL aircraft materials for improved lightness, durability and cost, noting Be alloys, filamentary composite materials and future problems

Resin bonded glass cloth for large airframe structures rectification

Titanium fuselage skin contouring to shallow compound curvature of supersonic aircraft by elastic draping, shot peen forming and cold stretching, discussing residual stresses

Titanium compared with aluminum in application to supersonic aircraft structures, considering tests and costs

10 p1700 A69-23600

Light aircraft and helicopter manufacturing methods, design concepts and materials, discussing aluminum airframes, riveting, fiberglass, UV curing, etc

Composite materials for aerospace applications, discussing high modulus filaments, structural and non-structural design considerations, nondestructive testing techniques, etc

Systems design of airframe structures taking into account material characteristics noting structural stability, shell postbuckling, fail-safe designs, etc

Concorde aircraft and engine materials selection factors including mechanical properties of metals and nonmetals, corrosion resistance, service life, sealants, weight analysis, etc

Aircraft construction materials, discussing aluminum alloys use in Concorde project based on temperature tests, creep and fatigue properties and joint requirements

Composite ceramic armor systems for airborne vehicles and personnel, air cushion vehicles and ground troops, discussing weight and contour forming advantages

Moldable plastic shim material for structural airframe components, discussing application requirements

Structural aerospace materials development with emphasis on Be and Ti alloys, discussing material combinations and composites

Al alloy application to welded primary airframe structures, discussing welding processes with emphasis on fusion welding

Fusion welding for thin gauge corrugated core sandwich airframe structures capable of operating at high temperature, discussing equipment, techniques and quality control

Seam welded Al alloy aircraft structure fabrication problems, emphasizing stress corrosion

Aircraft structures efficiency and weldability as function of application, welding procedures and metallurgical factors, considering high strength Al alloys, Ti and Ni alloys, etc

Fracture toughness and crack propagation in annealed aircraft titanium alloys tested per ASTM procedure, comparing results with high strength steels and aluminum alloys

Orthotropic aircraft materials plasticity theory, deriving stress-strain relationships in three mutually perpendicular symmetry planes for use in engineering calculations

24 p4177 A69-42165

24 p4400 A69-43083

AIRFRAMES

Aircraft flight testing for determining airframe, engine and pilot degradation, examining flutter, handling characteristics, water ballast, propulsion, etc

Icing of airframes, discussing ice formation, deicing methods and protection of aircraft

Airframe/propulsion blending in high performance fighter aircraft, discussing thrust augmentation, fuel consumption, induction system and exhaust nozzle balance with airframe

Airframe subsonic aerodynamic problems for fixed wing aircraft under low speed/high lift conditions

Holographic interferometry, determining mechanical vibration amplitudes of compressor and turbine blades and airframe panel

Dynamic analysis methods for airframe flight control design noting equations of motion, system criteria and analysis and synthesis methods

Systems design of airframe structures taking into account material characteristics noting structural stability, shell postbuckling, fail-safe designs, etc

Exhaust nozzle/airframe interference test evaluation for twin engine supersonic fighter

16 p2733 A69-32730

Air Transport Total In-Flight Simulator-707 /AT/IFS-707/ concept for pilot training, stressing airframe and major flight systems [SAWE PAPER 747] 18 p3118 A69-34884

Airframe cost element prediction and application to cost control, considering government specifications [SAWE PAPER 731] 18 p3221 A69-34894

Machined fastened joints for airframe structural parts, discussing fatigue life, strength and fastener hole preparation 19 p3319 A69-35553

C-5A transport aircraft airframes manufacture, discussing Lockheed profits, contract disputes and Cheyenne helicopter contract cancellation 20 p3640 A69-37355

Quality control and dimensional accuracy in airframe structures fusion welding 20 p3549 A69-37446

Electron beam welding machine modifications for welded airframe components production, discussing work chamber, vacuum system and workpiece mounting [SBAC PAPER 13] 20 p3550 A69-37455

Airframe stability of VAK 191 examined by displacement method, using matrix calculations within Automatic System of Kinematic Analysis 20 p3462 A69-37515

Concorde structural tests emphasizing problems associated with thermal cycle, including fatigue test setup on complete airframe [RAES PAPER 16] 22 p4043 A69-40495

Mathematical method of processing test data airframe panels subjected to repeated static loads to obtain lifetime equations and statistical characteristics 24 p4400 A69-43086

Structural airframe fasteners, reviewing systems for fatigue critical wing/fuselage structures, honeycomb panel attachments and data on fatigue life 24 p4325 A69-43437

AIRGLOW

NT GEOCORONAL EMISSIONS

NT NIGHTGLOW

NT TWILIGHT GLOW

H alpha emission symmetrical spatial distribution of night airglow observed with high transmission diffraction spectrographs 01 p0062 A69-10128

Atmospheric temperature and airglow spectra from IR measurements noting OH bands, atmospheric structure between 10 and 200 km at midlatitude and atmospheric absorption [UN PAPER 68-95471] 01 p0108 A69-10464

Soviet rocket and satellite night, twilight, airglow and auroral studies, discussing day sky brightness, night airglow and atmospheric stratification 01 p0066 A69-10941

Tropical night F layer maintenance mechanism, noting airglow enhancement and ionization source association with plasma drifts 02 p0242 A69-11825

Fluorescence efficiency of air under electron bombardment measured at low pressure 02 p0284 A69-12734

Visible and IR nonequilibrium radiation from dilute gases of upper atmosphere, describing laboratory, ground, aircraft and rocket observations of reactions and interactions 02 p0247 A69-12810

Latitudinal distribution of auroral and airglow emissions in Northern Hemisphere photometrically surveyed by jet aircraft 05 p0754 A69-16258

IR zero one band of molecular O observed in day airglow with ground based scanning grating spectrometer 08 p1306 A69-20096

Cosmos 92 satellite observation of night airglow flare, discussing NO bands emission and origin 09 p1485 A69-21533

Daily observational results of solar phenomena, cosmic rays, geomagnetic variations, ionosphere, radio wave propagation and airglow arranged according to solar rotation number 10 p1771 A69-22808

Aeronomic phenomena observed near Altair and theta Aquila ascribed to Apollo 8 lunar flight 11 p1957 A69-24411

IR day and night airglow of upper atmosphere utilized for atmospheric energy content and reactions analysis 13 p2252 A69-27585

IR airglow spectra measured by two beam interferometer on balloon, noting carbon dioxide and OH emission bands 13 p2252 A69-27586

Dynamic Michelson interferometer equipped with Ge detector to obtain spectra of airglow from 1.2-1.6 microns 13 p2252 A69-27587

Night airglow variations observed during Cosmos 92 satellite orbits, determining atmospheric albedo wavelength dependence for solid and medium cloudiness and clear skies 14 p2435 A69-29042

Low energy electron and proton precipitation, discussing acceleration mechanisms and periodicity in relation to auroras and airglows 15 p2594 A69-30018

Airglow research, discussing emission features, observation methods and instruments, ground station network, etc 15 p2594 A69-30020

UV OGO observations of atomic hydrogen and oxygen in airglow, comparing results to exospheric models of hydrogen geocorona 15 p2603 A69-31400

Zenith and azimuthal photometric observations of red line atomic O airglow predawn enhancement over UK 16 p2775 A69-32086

Diurnal variations of IR atmospheric oxygen bands in airglow observed with filter photometer on balloon flights 16 p2776 A69-32091

Thermosphere neutral wind speed measured from observing Doppler shift in O I 6300 night airglow line with Fabry-perot interferometer 16 p2776 A69-32093

Portable photometer with red-sensitive photocathode and high SNR for O I 6300 airglow experiments 16 p2777 A69-32107

Solar corpuscular and UV radiation variation relationship to midlatitude airglow intensity in O I line 16 p2850 A69-32322

Cosmos 92 satellite observation of night airglow flare, discussing NO bands emission and origin 16 p2783 A69-32528

OGO 4 UV airglow spectrometer consisting of Ebert-Fastie monochromator and photomultipliers with cesium telluride and cesium iodide channels 19 p3315 A69-36682

Spectral intensity distribution of night airglow, noting visual spectra distribution difference from G2 stars 20 p3522 A69-37057

Upper atmosphere emission processes, comparing emission quenching lifetime with transition probability rates, plotting atomic and molecular states 21 p3711 A69-38513

Ionosphere characteristics in terms of airglow, describing daytime F/D layers formation model provided by photoionization, loss processes and ambipolar diffusion 21 p3712 A69-38517

Airglow and vertical eddy transport photochemical models, analyzing O green line and OH emission distribution 21 p3713 A69-38523

Conjugate regions 6300 A airglow enhancement during predawn, noting photoelectrons role in heating dark ionosphere region by producing fast electron flux 24 p4308 A69-43011

AIRLINE OPERATIONS

Airline crew training, requalification, recurrent, upgrading and aircraft transition training for crew and pilot 01 p0019 A69-10450

Airline area navigation system functions for developing map type pictorial display system including digital computer, cockpit control unit and microfilm charts 01 p0112 A69-10453

Redevelopment program for Newark airport noting runway construction, underground fuel system and passenger terminal complex 01 p0057 A69-11275

Aircraft high level cloud data to estimate vertical distribution of cirriform clouds and tropical tropopause levels on airline routes 03 p0458 A69-13032

Airline operators economic oriented airframe maintenance problems, discussing cost accounting improvement 03 p0434 A69-13698

Circadian rhythms disruption during long distance flights, discussing adverse effects on pilot and passenger performance 03 p0378 A69-14260

Response to technical, social and political criticism of U.S. SST program [AIAA PAPER 68-1024] 04 p0689 A69-14794

Passenger aircraft design to cope with air traffic volume increase in 1970s, discussing economic aspects of high capacity aircraft 04 p0546 A69-14804

Elasticity of demand theory applied to fare changes effect on passenger volume, noting interdependence of aircraft size and fare formulation 04 p0689 A69-14805

Maintainability and reliability affect utilization and operating costs of commercial aircraft 04 p0547 A69-14806

French air transport and airports covering aviation enterprises, air traffic density, airport activities, traffic flow, etc 04 p0689 A69-15479

FAA aviation safety program design standards, maintenance and inspection procedures and assessment of accidents 06 p1041 A69-16839

Airline safety programs focused on developing reliable automatic landing system, realistic pilot training and airborne monitoring/recording system 06 p1041 A69-16840

Medical fitness regulations for pilots, including federal and internal airline regulations 06 p1041 A69-16844

Air carrier legal responsibility for commercial air safety as compared to liability in other transportation modes 06 p1042 A69-16847

Tort system of U.S. law effect on air safety promotion, discussing liability influence on government, manufacturers and airlines 06 p1042 A69-16850

Flight deck equipment guidelines in aircraft, discussing pilots natural senses, visual information, displays, logic and memory capable computers and ground controller 08 p1266 A69-20450

Transport aircraft fleet management and handling of mechanical and avionic machine defects using operations research 08 p1422 A69-20626

Airport operation and administration, discussing supply, costs, tariffs, etc 10 p1811 A69-23602

Supersonic transport airline operations including safety, noise, traffic control, routing, etc 11 p2004 A69-24373

Operational research applications to management problems, discussing specific airlines operations cases 11 p1822 A69-24377

Multiengine helicopter scheduled passenger service operations in Europe 11 p2004 A69-24378

V/STOL aircraft performance characteristics related to civil aviation operations and certification requirements [ICAS PAPER 68-05] 11 p1822 A69-24463

Abbreviated Test Language for Avionics Systems /ATLAS/ as standard compiler input language for commercial airline automatic test equipment /ATE/ 11 p1842 A69-25064

Aircraft engines future specifications as affected by expanding market, noting speed requirements and thrusts 11 p1942 A69-25215

Traditional flight crew organization relevance to current and developing flight systems, discussing inadequacies, anachronisms and safety threats 12 p2023 A69-26555

U.S.-Europe air traffic, attributing European lag to dense air route duplication, load factors, etc 13 p2381 A69-27338

Airline ticket as international commodity, discussing regulations and agreements concerning appearance, loss, transferability, etc 13 p2381 A69-27530

Air Canada flight safety system including company philosophy, safety activities, incident and accident handling and information schemes 13 p2201 A69-27541

Litton LTN-51E inertial navigation system accuracy and reliability evaluated on basis of transpacific flights [SAE PAPER 680299] 13 p2296 A69-28103

Vertical takeoff aircraft role in British Government air industry program, noting applications to intercity passenger service 13 p2203 A69-28355

Deterministic economicomathematical models for optimum airline networks, considering transportation cost 14 p2540 A69-29141

Probabilistic forecasts in meteorological support of aviation, comparing economic implications of squall forecasting
14 p2474 A69-29739

Flight regularity and safety in complex meteorological situations, noting synoptic forecasting advantages over inertial forecasting
14 p2475 A69-29740

Airline aircraft maintenance programs, discussing objectives, procedures and failure analysis models
15 p2549 A69-30209

Airport problems in increasing air traffic, discussing passenger delays, runway capacity, instrument controlled takeoff and landing, fog dispersal, baggage flow, etc
15 p2589 A69-30589

Economics of airport use, congestion and safety, discussing differentiated pricing systems
15 p2723 A69-31241

Ground facilities long term planning, considering factors to determine air transport growth and changing commercial aviation pattern
16 p2766 A69-32020

Civil aircraft requirements from 1975 onward, discussing classes, categories and R and D
16 p2882 A69-32022

Gate arrival approach to Kansas City airport terminal planning for facilities and operations decentralization, congestion reduction and passenger walk distance minimization
16 p2766 A69-32327

Space criteria for aircraft parking positions noting radial wedges configuration
16 p2766 A69-32328

Space requirements of departure lounges in airport buildings for large aircraft loading, discussing entry doors, boarding times, etc
16 p2766 A69-32330

CAB decisions regarding subsidy reduction, carrier mergers, and dense route certification requiring improved clarity and timeliness
16 p2882 A69-32336

STOL and V/STOL short haul intercity airliners emphasizing propulsion systems, operational aspects and economics
17 p2898 A69-33356

Aircraft designers and operators problems with danger and damage caused by bird strikes, considering warning devices and protective windshield panels
17 p2899 A69-33363

Future navigation systems and ATC, discussing traffic flow factors and approach and landing systems
17 p3004 A69-34201

Air traffic control and airline operators liaison with reference to air transport priorities, considering relationship to aircraft and airport development
17 p3004 A69-34204

Large subsonic transport aircraft effect on economics of air operations with emphasis on airport facilities for Boeing 747
17 p3077 A69-34205

Technical and operational planning activities of airline resulting from airport restrictions in terms of congestion, performance and noise and runway strength
17 p2948 A69-34206

Edwards Inquiry Report into British Civil Air Transport based on cost effective economic study, involving airlines and regulatory system
18 p3231 A69-34311

Jumbo aircraft production technology causing economic setback, recommending added emphasis on passenger/cargo requirements and operating environments for greater profitability
18 p3232 A69-34542

Expected occurrences mathematical model for flight system availability under uncertainty
18 p3210 A69-35083

Los Angeles International Airport development planning, discussing airfield improvement, tunnel reconstruction, terminal layouts, parking, roads and access, etc
19 p3288 A69-35590

Aircraft Economic Design Evaluation (AEDE)/computerized model to estimate aircraft design performance differences economic impact to carriers
19 p3289 A69-35626

Aircraft interior conversion for passenger or cargo service, discussing convertible aircraft and quick change concepts
19 p3244 A69-35642

Accelerate-stop criteria examined from human engineering standpoint, discussing flight simulator study of pilot reaction times for transition to rejected takeoff configuration
19 p3244 A69-35650

Computer-generated airline fleet performance data on B-720, B-727 and DC-8 aircraft, attributing deterioration to increased drag and fuel consumption
19 p3245 A69-35651

Cost and maintenance calculations for inertial navigation system (INS)/based on three systems per aircraft, assuming 4000 hr/year aircraft utilization
19 p3371 A69-36734

Short haul air transportation traffic congestion problems in Northeast corridor, emphasizing STOL solution for economy
19 p3248 A69-36865

All-weather landing in civil air operations, discussing ground/air systems in tracking, visual reference and aircraft performance required for safe landing capability
20 p3574 A69-38119

STOL airline operation test programs involving aircraft, navigation equipment, systems and ATC
21 p3646 A69-38731

Cardiovascular illnesses incidence among airline flight personnel, discussing coronary insufficiency detection
21 p3661 A69-39271

Jet fleet engine performance monitoring program, discussing systems design and resultant management planning
22 p3999 A69-39922

Airport capacity increase in terms of operations delay, discussing computer aided approach systems and additional runways
22 p3925 A69-40429

Air traffic problems due to tourism, suggesting service modifications to meet future needs
22 p4053 A69-40434

Custody, jurisdictional conflict and prosecution problems of in-flight crimes, discussing federal judicial jurisdiction and Tokyo Convention ratification
22 p4053 A69-40708

Washington area airport efficient use plan from projections of passengers, aircraft operations and net revenue trends
22 p4053 A69-40709

Airport standards analysis for safe, efficient air carrier operations including airport funding, safety programs for runways and terminal facilities
22 p4054 A69-41144

Pilots and flight crews screening and training by supplemental air carriers
22 p4054 A69-41148

Airline management service to cockpit team for safe operation providing safety information sources and transmission channels and undesirable trend detection and correction
22 p4054 A69-41149

Telecommunication systems used in airline industry and reorganization requirements for efficient operation
23 p4114 A69-41356

Airline economics long term trends requiring management tools for cost control, operations simulation and monitoring, computer use and information data processing
23 p4241 A69-41641

VTOL, STOL and CTOL transportation systems cost effectiveness comparison for Northeast Corridor operation, considering ground facilities, access time, etc
23 p4147 A69-41642

Terminal facilities planning for STOL service to meet traffic demand, considering site selection, runway alignment, aircraft noise, ground accessibility, etc
23 p4147 A69-41645

Engine oil analysis applied to commercial airline operations, ensuring lubricating qualities retention and detecting oil-wetted component failures
23 p4169 A69-41647

Metropolitan downtown airports for STOL and VTOL aircraft stressing Los Angeles Metroport
23 p4147 A69-41660

Airline area navigation test programs involving use of VOR/DME signals and inertial navigation system within air traffic control system
23 p4185 A69-41662

Moving map pictorial display system for on board capability of area navigation, noting crew reaction
23 p4186 A69-41663

SST flight crew operational requirements to achieve maximum human efficiency and man/machine compatibility, discussing pilot role, advanced flight instrumentation, etc
23 p4107 A69-41820

Flight simulators role in airline pilot training, discussing skilled learning, performance measurements and future developments
23 p4112 A69-42366

Short haul transport aircraft development, discussing twin jet Mercure aircraft with low operation cost and Category III weather conditions landing
24 p4250 A69-42565

Component reliability effect on airline operation of VC 10 aircraft, investigating failure modes and maintenance
24 p4318 A69-42776

Air traffic growth forecasting, describing various mathematical econometric models
24 p4417 A69-42807

Commercial aircraft environmental compatibility planning, considering problems of airport traffic growth and restrictive air traffic control regulations
24 p4252 A69-42808

SST contribution to commercial aircraft transportation, discussing economic and operational aspects, decision making process leading to fixed wing design, etc
24 p4252 A69-42869

Operational and economical aspects of V/STOL air transportation reevaluated for civil aviation promotion
24 p4418 A69-42870

Unscheduled aircraft landing to deplane passenger for medical reasons, discussing costs, time consumption and avoidance methods
24 p4278 A69-43393

AIRLINERS
U COMMERCIAL AIRCRAFT
U PASSENGER AIRCRAFT

AIRPLANE PRODUCTION COSTS
Cost factors in choosing single or twin-engine layout for tactical aircraft
02 p0193 A69-12066

Deterministic model for cost effectiveness of avionics support programs based on subsystems support ability, test philosophy and test equipment design and manufacture
09 p1478 A69-22377

Effective cost improvement of product and profit planning activity in jet engines production stressing J47 and J79 engines
09 p1513 A69-22516

Cost-profit sharing agreement with aerospace manufacturing companies involved in Boeing 747 construction, detailing final assembly building
09 p1514 A69-22713

Galaxy C-5A aircraft Value Control Program stressing design organization, upper management authority, budgetary adjustments, etc
13 p2383 A69-28095

Weight and cost control program for Boeing 747 aircraft through combined value and weight engineering methods
13 p2383 A69-28096

Armor selection for advanced aircraft systems based on premium value concept and cost-weight considerations
18 p3094 A69-34878

Airframe cost element prediction and application to cost control, considering government specifications
18 p3221 A69-34894

Design and economic concepts of Lockheed L-1011 wide body trijets, discussing airport and airways congestion alleviation, passenger appeal, etc
22 p3863 A69-40494

AIRPORT LIGHTS
U RUNWAY LIGHTS

AIRPORT PLANNING
Airport warm fog dispersal, discussing full scale aircraft seeding of polyelectrolyte materials, noting ground dispenser
01 p0054 A69-10149

Boeing 747 performance, propulsion, structural and circuit characteristics, mass production and airport passenger installations
01 p0011 A69-11067

Redevelopment program for Newark airport noting runway construction, underground fuel system and passenger terminal complex
01 p0057 A69-11275

Air traffic control at Los Angeles International Airport, discussing simultaneous parallel ILS approaches and departures and STOL problems
01 p0057 A69-11356

Interim radar improvement program for air route traffic control centers pending development of automated terminal radar programs
01 p0114 A69-11357

Air cargo and world trade, discussing economics, cargo tariffs, customs procedures, cargo airports and convertible aircraft
03 p0536 A69-14088

Fitting airport interfaces to air traffic, considering bottleneck elimination

05 p0742 A69-15918

Runway development for increased airport capability, discussing computer simulation model of airport operations

06 p0906 A69-17166

Cost estimating relationships for vertiports and airports, comparing terminal costs per passenger for each facility

[AIAA PAPER 69-208] 07 p1245 A69-19564

Monograph on length requirements for takeoff and landing of jet transports covering airport classification, roll distance formulas and long range transport performance nomograms

08 p1301 A69-20717

Mathematical models for outgoing traffic flow in airport terminal used for determining service requirements

09 p1476 A69-21439

Airport evolution in London, discussing transportation, safety, international trade, economics, aircraft types and noise spectra

09 p1479 A69-22582

V/STOL aircraft future, discussing Federal Government policies, economics, airport planning, engineering problems, etc

10 p1811 A69-23221

Civil aviation statistical data and airport planning

10 p1634 A69-23601

Airport operation and administration, discussing supply, costs, tariffs, etc

10 p1811 A69-23602

All-weather landing including zero-zero, discussing planning in Europe and U.S.A.

10 p1722 A69-23698

Runways slipperiness and grooving, discussing influence of wetness, tire form and speed on friction coefficient

10 p1674 A69-23707

Stopping barriers for jet aircraft landing design and operation

11 p1862 A69-24354

Supersonic transport airline operations including safety, noise, traffic control, routing, etc

11 p2004 A69-24373

Monograph on computer aided air traffic control systems design, discussing air navigation, man-machine relations, equipment requirements, programs, plan position color display, etc

11 p1914 A69-25085

Comparative evaluation of avionic installations in design stage, detailing parameters for civil aeronautical use

11 p1887 A69-25212

Short takeoff aircraft characteristics, discussing aircraft certification and airfield regulation in Great Britain

13 p2203 A69-28356

Airport noise control responsibility for airport and community planners using perceived noise level, noise and number index and community annoyance index as planning criteria

14 p2541 A69-29506

Civil airports design standards development noting advisory circulars

15 p2588 A69-30408

Airport problems in increasing air traffic, discussing passenger delays, runway capacity, instrument controlled takeoff and landing, fog dispersal, baggage flow, etc

15 p2589 A69-30589

Economics of airport use, congestion and safety, discussing differentiated pricing systems

15 p2723 A69-31241

Ground facilities long term planning, considering factors to determine air transport growth and changing commercial aviation pattern

16 p2766 A69-32020

Gate arrival approach to Kansas City airport terminal planning for facilities and operations decentralization, congestion reduction and passenger walk distance minimization

16 p2766 A69-32327

Space criteria for aircraft parking positions noting radial wedges configuration

16 p2766 A69-32328

Airport planning, discussing air transportation and city planning problems for Hannover air terminal

16 p2882 A69-32329

Space requirements of departure lounges in airport buildings for large aircraft loading, discussing entry doors, boarding times, etc

16 p2766 A69-32330

Community planning and airport requirement interrelation, discussing land usage, satellite airport system for private aviation, etc

16 p2882 A69-32331

Habitat modification for airport bird population control, discussing draining of wet areas, waste control, etc

17 p2915 A69-33368

Future navigation systems and ATC, discussing traffic flow factors and approach and landing systems

17 p3004 A69-34201

Aircraft developments affecting international airport planning

17 p2948 A69-34203

Air traffic control and airline operators liaison with reference to air transport priorities, considering relationship to aircraft and airport development

17 p3004 A69-34204

Large subsonic transport aircraft effect on economics of air operations with emphasis on airport facilities for Boeing 747

17 p3077 A69-34205

Technical and operational planning activities of airline resulting from airport restrictions in terms of congestion, performance and noise and runway strength

17 p2948 A69-34206

All-weather operations, aircraft size, air traffic and noise as airport design factors, discussing financing priorities for runway construction, facilities and personnel

17 p3004 A69-34207

Airport planning for large aircraft loading of passengers, baggage and cargo containers

17 p2948 A69-34208

Airport performance, noise and aircraft utilization influence on aircraft design and operating costs, stressing takeoff distance, obstacle clearance and noise regulations

17 p2948 A69-34210

Airport runway surface construction materials requirements, taking into account factors different from highway pavement

17 p2948 A69-34215

Bird hazard in aviation, discussing aircraft/bird collisions in France, protective measures and airport environment control against nesting and breeding

18 p3090 A69-34695

Los Angeles International Airport development planning, discussing airfield improvement, tunnel reconstruction, terminal layouts, parking, roads and access, etc

[AIAA PAPER 69-806] 19 p3288 A69-35590

Air terminals plans for 1975 aircraft and air traffic based on runway configurations

[AIAA PAPER 69-805] 19 p3288 A69-35591

Shuttle VTOL airport access system analysis for New York area

[AIAA PAPER 69-804] 19 p3288 A69-35592

Airport alternate facilities, restrictive flight schedules and fee schedules for relieving airport congestion during peak traffic hours

[AIAA PAPER 69-820] 19 p3453 A69-35595

Mass transit rail service between Manhattan and Kennedy Airport using Long Island Railroad mainline route, discussing baggage handling and time schedules

[AIAA PAPER 69-803] 19 p3453 A69-35596

Air travel and population growth requiring larger structures for office buildings, airport passenger terminals and aircraft servicing facilities

[AIAA PAPER 69-809] 19 p3289 A69-35622

Airport facilities planning for conventional jet, STOL and SST aircraft ground handling, stressing facilities economy and transportation subsystems

[AIAA PAPER 69-808] 19 p3289 A69-35623

Problems caused by air traffic rate growth in London Terminal area, examining runway limits, safety and noise restrictions

19 p3371 A69-36736

Air transport development relationship to city regional planning, including analysis of Heathrow airport design

19 p3296 A69-36850

ATC systems analysis including airports, ground access and air transportation

19 p3371 A69-36866

Terminal air traffic management in future noting transition airspace, approach and departure paths and airport capacity

[AIAA PAPER 68-1101] 20 p3573 A69-37160

World airport planning - Conference, London, September 1969

22 p3925 A69-40424

Air cargo traffic, discussing paneload lots, aircraft types suitable for freight transport, difficulties and solution

22 p4052 A69-40426

Air traffic systems and diminishing airspace capacity problems requiring additional airport facilities and STOL aircraft

22 p3925 A69-40428

Airport capacity increase in terms of operations delay, discussing computer aided approach systems and additional runways

22 p3925 A69-40429

Airport location effect on facilities supply factors including atmospheric, environmental and economic conditions

22 p3926 A69-40431

Airport requirements in England, considering various sites, noise nuisance and integration into total transport system

22 p3926 A69-40432

Airport design for noise reduction, considering aircraft noise, runway orientation and flight paths

22 p3926 A69-40433

STOLport policy for New York City including travel time analysis, ground transport systems, political and community acceptance, aircraft noise, etc

[RAES PAPER 3] 22 p3927 A69-40484

Washington area airport efficient use plan from projections of passengers, aircraft operations and net revenue trends

22 p4053 A69-40709

Planning for safety of future supersonic air traffic including financing and coordination activity of government and industry

22 p4054 A69-41131

Airport standards analysis for safe, efficient air carrier operations including airport funding, safety programs for runways and terminal facilities

22 p4054 A69-41144

Terminal facilities planning for STOL service to meet traffic demand, considering site selection, runway alignment, aircraft noise, ground accessibility, etc

[SAE PAPER 690421] 23 p4147 A69-41645

Air traffic interfaces of VTOL, STOL and CTOL aircraft serving same metropolitan terminal, emphasizing navigation systems, geographical positions, ground communication, etc

[SAE PAPER 690422] 23 p4185 A69-41646

Metropolitan downtown airports for STOL and VTOL aircraft stressing Los Angeles Metroport

[SAE PAPER 690402] 23 p4147 A69-41660

Airport terminal planning, considering expansion, automation, backup measures, layout problems and solutions, etc

[SAE PAPER 690399] 23 p4147 A69-41661

Jet runway design, construction and operation, discussing surface texture, lightning, grooving, etc

[SAE PAPER 690377] 23 p4147 A69-41670

Air space saturation, urban surface transport network enlargement necessity and expeditious passenger processing and baggage handling

24 p4296 A69-42567

General aviation airport application as freight consolidation terminals to reduce ground handling costs, circumvent air and ground traffic problems, etc

24 p4419 A69-43047

AIRPORTS

NT HELIPORTS

Construction practice for hot-mix bituminous pavements covering production, composition, application and quality control

01 p0057 A69-11276

Soviet book on aeronautical climatology covering methodology of climatologic indices useful for airfields, pilots and flight routes evaluation

04 p0627 A69-14935

French air transport and airports covering aviation enterprises, air traffic density, airport activities, traffic flow, etc

04 p0689 A69-15479

Statistical method for determining accuracy of airfield weather reports on takeoff and landing conditions, visibility and cloud ceiling, correlating forecasts and actual conditions

11 p1913 A69-25205

Ground access routes between business districts and airports compared for passenger transport modes

[AIAA PAPER 68-1072] 12 p2059 A69-26773

Visibility changes in fog at London airport determined by transmissometer records

18 p3167 A69-35266

Aircraft noise abatement oriented toward compatibility between airports and adjacent metropolitan environments, analyzing results for theoretical and actual airports

[AIAA PAPER 69-800] 19 p3453 A69-35593

Private one doctor one nurse clinic at Sydney airport, discussing history, operating conditions, medical record and statistics

23 p4105 A69-41786

Short range aviation terminal weather predictions concerning runway visual range, cloud-base height and wind, using FAA mesometeorological network

24 p4342 A69-42892

AIRSPACE

Book on law of airspace covering property rights, legal aspects of airspace utilization, airspace transactions, courts role, damage suits, etc

07 p1244 A69-18709

Air traffic systems and diminishing airspace capacity problems requiring additional airport facilities and STOL aircraft

22 p3925 A69-40428

Intercity air transportation compared with automobile and train travel, attributing air travel dead time to ground route and airspace congestion

24 p4416 A69-42561

AIRSPEED

Low range airspeed system /LORAS/ on X-22A and P 1127 VTOL aircraft for accurate airspeed information

05 p0767 A69-16774

Aerodynamic stick force and speed characteristics of various horizontal tails and elevator trimmers, noting zero stick force case

09 p1434 A69-22597

Connecting duct influence on slide wire vertical airspeed indicator operating on barometric principle during aerial gravimetric surveying

13 p2260 A69-27828

Atmospheric stability influence on vertical spectra of refractive index and air velocity deduced from beam swinging experiments and compared with radiosondes data

17 p2960 A69-33157

Vector airspeed measuring system /VAMS/ for helicopters and V/STOL aircraft utilizing gas discharge mass flowmeter to improve takeoff performance [AHS PAPER 350]

17 p2974 A69-33527

VOR/DME information augmentation by air data /airspeed/ for positional accuracy improvement, describing error sources, optimum data filter and system sensitivity and performance [AIAA PAPER 69-841]

21 p3762 A69-39372

AIRWORTHINESS

U AIRCRAFT RELIABILITY

AIRWORTHINESS REQUIREMENTS

U AIRCRAFT RELIABILITY

AIRY FUNCTION

Asymptotic wave equation application conditions in describing field behavior near caustic surface, using Airy functions

07 p1076 A69-18520

Analytic integration of Langmuir equation for spherical space charge flow obtained in terms of Airy equation or Bessel functions solution

07 p1115 A69-18864

AJ-1000 ENGINE

U M-1 ENGINE

ALANINE

Metal oxides catalytic and inhibitory effects on photolysis of alanine by UV light

01 p0025 A69-11095

Optically active alanine synthesis from oxaloacetic acid by hydrogenolytic asymmetric transamination, noting role of decarboxylation

12 p2026 A69-25780

ALARMS

U WARNING SYSTEMS

ALBEDO

NT COSMIC RAY ALBEDO

NT EARTH ALBEDO

Gray tone differences between undisturbed lunar surface and darker ejecta observed around Surveyor 1 footpads, discussing possible albedo differences

04 p0660 A69-15124

Polarization-albedo relationship for selected lunar maria, highlands and mountains in five passbands suggest optical path length function of effective refractive index and particle size

05 p0829 A69-16663

Radiation field at optical depths within plane parallel Rayleigh scattering atmosphere subjected to generalized free surface boundary conditions

09 p1606 A69-22423

Plane and spherical albedos of planet surrounded by infinite optical thickness atmosphere, with application to Venusian atmosphere

10 p1776 A69-23210

Venus albedo dependence on wavelength in UV spectrum between 4500 and 3200 A from reflector observations

11 p1957 A69-24406

Radiation measurements by Cosmos 122 satellite over various regions, determining radiation temperature, long wave heat flux and albedo

13 p2291 A69-27726

Monograph on interstellar extinction computations covering theoretical curves for spherical metal and graphite particles, albedo, optical constants, normalization, temperature dependence, etc

14 p2516 A69-28901

Mars surface temperature calculated by applying Humphrey formula for planetary radiation energy, finding mean annual values of temperature for different albedo

17 p3034 A69-33412

Search for diffuse galactic light component between 2100-2800 A by rocket measurements of night sky brightness, showing low albedo of interstellar dust

18 p3202 A69-35210

Particle albedos and extinction cross sections computed by Mie theory showing dependence on refractivity, considering thermal radiation from cloudy planetary atmospheres

20 p3614 A69-38255

Stellar and diffuse galactic radiation intensity observations to obtain albedo values of interstellar dust particles

22 p4034 A69-41112

Venus albedo dependence on wavelength in UV spectrum between 4500 and 3200 A from reflector observations

24 p4391 A69-43796

ALBUMINS

Whole body X irradiation effect on protein degradation in mice, using radioactive I labeled albumin

23 p4099 A69-42151

ALCOHOLS

NT ETHYL ALCOHOL

NT GLYCOLS

NT METHYL ALCOHOLS

NT PHENOLS

Alcohol role in pilot victims of aircraft accidents

01 p0022 A69-11345

Amino alcohol regenerable absorbers of carbon dioxides toxicological characteristics, discussing absorbing ability in rats

10 p1646 A69-23502

Failure mechanism for intergranular stress corrosion cracking of vacuum annealed unalloyed Ti in alcohol iodine solutions

16 p2798 A69-31717

Relative gas phase acidities of simple aliphatic alcohols, considering effects of alkyl groups

19 p3265 A69-36289

ALDEHYDES

U FORMALDEHYDE

ALDOSTERONE

Aldosterone and hydrocortisone introduced into bladders of adrenalectomized dogs to restore sodium metabolism contributing to normal water-salt homeostasis

21 p3656 A69-38965

ALFVEN WAVES

U MAGNETOHYDRODYNAMIC WAVES

ALGAE

NT ANABAENA

NT BLUE GREEN ALGAE

NT CHLORELLA

NT SCENEDESMUS

Biological life support system based on continuous algae seaweed cultivation as link of closed ecological system, discussing design and performance

01 p0020 A69-11077

Biological life support system for regenerating closed atmosphere by photosynthesis, using gas exchange between man and microalgae

01 p0021 A69-11078

Chlorella and Scenedesmus unicellular algae mixture tested for biological protein value in humans for possible food source

01 p0021 A69-11079

Nutritive value of protein from discolored algae biomasses on groups of rats kept on algae biomass, casein and soybean diets

02 p0198 A69-11510

Hydrogen adaptation effect on fluorescence of normal and Mn deficient algae, noting system II photosynthesis

04 p0554 A69-15325

Algae diet more effective than soya-protein diet in recovering metabolic processes in protein deficient white rats

07 p1065 A69-18977

Manganese catalyst photoreactivation in photosynthetic oxygen evolution in Mn deficient algae Anacystis nidulans cells

13 p2210 A69-28257

Manganese deficiency effect on growth and chlorophyll content of algae with and without hydrogenase

15 p2558 A69-31551

Water purification through biological oxidation of organic wastes using controlled photosynthesis, discussing algae production and harvesting

21 p3668 A69-39711

Radiation damage in chlamydomonas, discussing dark repair activities

23 p4090 A69-41964

Gradually decreasing N concentration effects on composition, tissue production and oxygen yield of unicellular algae in continuous culture

24 p4263 A69-43201

ALGEBRA

NT ADJOINTS

NT BANACH SPACE

NT CANONICAL FORMS

NT CUBIC EQUATIONS

NT DETERMINANTS

NT DYADICS

NT EIGENVALUES

NT EIGENVECTORS

NT GROUP THEORY

NT HERMITIAN POLYNOMIAL

NT HILBERT SPACE

NT JORDAN FORM

NT LIE GROUPS

NT LINEAR EQUATIONS

NT LINEAR TRANSFORMATIONS

NT MATRICES [MATHEMATICS]

NT POLYNOMIALS

NT QUADRATIC EQUATIONS

NT SPINOR GROUPS

NT STATE VECTORS

NT STOKES THEOREM [VECTOR CALCULUS]

NT STRESS TENSORS

NT TENSORS

NT VECTOR SPACES

NT VECTORS [MATHEMATICS]

NT VORTICITY

Iterative method to solve large sets of algebraic equations in approximate solution of multidimensional partial differential equations by implicit numerical techniques

03 p0456 A69-13554

Conditional probabilities, definition and algebra

04 p0623 A69-14948

Hybrid loop properties determination using quadrupole algebra, noting frequency dependence of input impedance and voltage transmission

04 p0582 A69-15072

Volterra operator algebra for boundary value problems involving linear viscoelasticity with continuous relaxation time and delay time spectra

12 p2182 A69-26677

Algebra of quasi-homogeneous pseudodifferential operators applied to lateral boundary values of solutions of parabolic differential equations, discussing function spaces

17 p2994 A69-32842

Partially conserved axial vector currents and current algebra to obtain vertex functions at point having zero mass by extrapolations

17 p3008 A69-33004

Algebraic formulation of electromagnetic diffraction, discussing propagation of positive and negative time frequency components by dual operators

18 p3172 A69-35010

Eigenvalue conversion of second variation test for algebraic and differential constraints to Jacobi accessory minimum problem by introducing norm in coordinate perturbation space

19 p3400 A69-35672

Holor algebra with tensor notations applied to elastic structures /discrete systems/, discussing inertia and stiffness tensors

21 p3831 A69-38415

Algebraic decoding techniques, discussing channel models, errors correction, hardware and software, etc

23 p4119 A69-41746

General linear state estimation from algebraic viewpoint without probability theory concepts, establishing least squares parameter estimation

23 p4182 A69-41880

ALGOL

Computer program in ALGOL for computing satellite ephemerides applicable to satellites with direct or retrograde motion observed in Northern or Southern Hemispheres

12 p2159 A69-26448

Monograph on reduction of satellite data using fixed stars covering ALGOL programming for computing satellite direction from photographic model

14 p2446 A69-29286

ALGORITHMS

Error and sensitivity analysis of on-line algorithms for fixed point linear smoothing

01 p0050 A69-10238

Optimal rank algorithm construction for signal detection in noise investigated for use in information transmission systems

01 p0027 A69-10374

Algorithms for linear system of first order differential equations, emphasizing equations associated with computer oriented circuit design

01 p0036 A69-10708

Algorithms for three dimensional supersonic gas flow incident on bodies applied to calculating oxygen flow in asymmetric nozzle

01 p0060 A69-10724

Monte Carlo method used to construct optimal algorithms for simulating homogeneous Markov chains whose trajectories reach absorbing state with probability of one

01 p0105 A69-10726

Circuits with magnetic coupling, describing digital computer algorithms for assembly of loop current equations

01 p0036 A69-10745

Time optimal control design by algorithm method

01 p0052 A69-10794

Forced processes in continuous external control systems, proposing algorithm for designing dynamic model

01 p0052 A69-10798

Discrete time optimal control problems solved by second order variational algorithm, developing recurrence relations for perturbation equations

01 p0054 A69-11416

Atmospheric temperature profiles by regularizing algorithm, discussing influence of random errors in measured radiation and kernel of integral equation on interpretation accuracy

02 p0274 A69-11448

Reliability of eliminating multivaluedness in two scale phase measurement method resolved by algorithm formulated on white Gaussian noise interference

02 p0206 A69-11603

Algorithm for N/h ionospheric profiles calculations using both x and o magnetoionic components, taking into account interlayer and underlying ionization influence

02 p0239 A69-11687

Structure oriented parallel algorithms for matrix operations, noting applicability to real time calculations for discrete Kalman filter and control problems

02 p0224 A69-11743

Algorithms for error analysis, optimum filtering sensitivity and fixed interval smoothing solutions to linear estimation problems

02 p0224 A69-11961

Computational algorithm for determining piecewise-constant feedback gains for linear system optimal control

02 p0224 A69-11964

Algorithm minimizing performance index and sensitivity of controller design with and without saddle point

02 p0224 A69-11966

Clinical problems during interplanetary flights, stressing need for diagnostic algorithms and automated medical equipment

02 p0202 A69-12121

Algorithm for Orr-Sommerfield equation applied to stability of laminar flow, noting profile resembling mean velocity profile of turbulent flow in flat tube

02 p0233 A69-12573

Algorithm computing spherical harmonic coefficients for eccentric geomagnetic dipole potential

02 p0245 A69-12735

Equilibrium problem for fluid subjected to gravitational forces and surface tension, proposing algorithm for numerical solution

03 p0417 A69-13810

Algorithm for numerical solution of variational problems for functions of two independent variables

and boundary value problems using local variations method

04 p0622 A69-14616

Numerical algorithm for supersonic gas flow past blunt bodies with shock wave separation, using Dorodnitsyn method of integral correlation

04 p0587 A69-14621

Book on dynamic programming basic theory and standard computational algorithm and applications to optimization in diverse fields

04 p0563 A69-14652

Algorithm for Navier-Stokes and continuity equations used to derive curvilinear coordinate system

04 p0564 A69-14858

Fast Fourier transform, discussing algorithms for sampled Fourier spectra and FORTRAN programs

04 p0625 A69-15223

Algorithm for simultaneous nonlinear equations solution on computer, noting quadratic convergence for convex space

04 p0565 A69-15335

Algorithm for calculating discrete Fourier transform by computer

04 p0565 A69-15336

Functional optimization techniques for serial hybrid computer solution of partial differential equations, emphasizing algorithms handled on digital computer

04 p0566 A69-15344

Algorithm generating same stereogram for two or more selected surfaces by extending random dot stereogram technique

04 p0603 A69-15445

Algorithm for discriminating random signals with unknown mean values, discussing decision functions possible existence to minimize error probability

05 p0719 A69-16218

Pattern classification algorithms classified according to type of input information required

05 p0725 A69-16571

Design algorithm for adaptive control of systems using nonlinear integral equations with bounded input functions, formulating optimization as conditional minimization problem

06 p0900 A69-17351

Recursive algorithms for pattern classification using misclassified samples

06 p0891 A69-17357

Deterministic pattern classification algorithms, discussing abstraction problem, stochastic algorithms, minimum error scheme and modified least squares scheme

06 p0892 A69-17395

Trunk and tree searching properties of Fano sequential decoding algorithms

06 p0902 A69-17400

M measurement optimal feedback control algorithm for stochastic discrete time systems, considering nonlinear plant, constrained controls, nonquadratic cost and simulations

06 p0902 A69-17402

Nonlinear programming computational algorithm for recursive optimal estimates of constrained states of linear system

06 p0902 A69-17403

Synthesis of optimum linear antenna using algorithm

06 p0897 A69-17543

Algorithms construction for aerospace vehicle trajectory optimization, considering quasi-linearization method for computation of variable time optimum trajectories

06 p1006 A69-17569

Algorithms for polynomial results computation, considering extraneous factors, truncation errors, memory and computing speed

06 p0892 A69-17884

Stochastic approximation algorithms for adaptive linear discrete time system identification using noisy input

06 p0904 A69-17940

Digital computer algorithm for automatic processing of IR weather data transmitted by Cosmos 122 and 144 meteorological satellites

06 p0929 A69-17981

Fourier transform algorithm introduction leading to image coding technique with image transformed by Hadamard matrix operator

07 p1078 A69-18859

Algorithm for high speed digital computers to evaluate stellar radiative opacities

07 p1222 A69-19589

Algorithm for calculating Moore automaton or connected network channel capacity and source of input symbols for full capacity utilization

07 p1088 A69-19707

Space-time evolution of one Petrov type into another, obtaining algorithm, flow diagram and discontinuous hypersurfaces results

08 p1350 A69-19789

Algorithm with iterative technique for nonlinear minimax approximations

08 p1344 A69-20829

Linear shift register synthesis algorithm found to coincide with Berlekamp iterative algorithm for decoding BCH codes

09 p1470 A69-21317

Brightness curves of eclipsing systems under monotonicity of unknown functions, using stable algorithm

09 p1588 A69-21363

Differential dynamic programming algorithms of second and first order for optimal control, considering nonlinear unconstrained and constrained problems

09 p1531 A69-21415

Algorithms in electronic circuit analysis, establishing algebraic and topological analogs based on generation of fundamental relations

09 p1472 A69-21777

Linear systems analysis by generalized numbers method, discussing algorithms for manual or computer analysis

09 p1472 A69-21778

Linear electronic circuit canonical synthesis by computer, using algorithm based on linear and nonlinear programming

09 p1472 A69-21781

Specialized mathematical machine for expanding matrix determinants and solving combinatorial problems, discussing symbolic circuit

09 p1460 A69-21782

Digital computer algorithm for analyzing circuits represented as autonomous multiport networks

09 p1472 A69-21786

Nonlinear boundary value problem algorithm in shell theory, showing aid of numerical technique

09 p1614 A69-21887

Kutta-Merson algorithm for converting partial differential equation for two dimensional unsteady state heat conduction to simultaneous ordinary differential equations

09 p1623 A69-22280

Adaptive control algorithm operating on-line to make discrete time adjustments in controller parameters of continuous time control system

09 p1474 A69-22441

Algorithm for mean energy transmission coefficient of fundamental mode in beam guide with given inhomogeneities, discussing mode conversions

09 p1469 A69-22629

Reissner algorithms for displacements of bent plate represented in finite series form as solutions of Euler equations

10 p1793 A69-22883

Algorithm in fault detection and isolation, discussing test optimization for complex systems or structures subject to failure

10 p1698 A69-22978

Waveguide Y circulator electrodynamic parameters by design algorithm and computer programs

10 p1661 A69-23108

Nondifferential function minimization on entire vector space or bounded subset for application to minimax problems in function spaces, time optimal control, etc

10 p1721 A69-23863

Algorithm for determining readings dispersion during cosmic ray recording, considering cosmic rays variability, statistical nature and instrument errors

10 p1770 A69-23906

Statistical regularization for obtaining a priori probability distribution information on mathematically incorrect inverse geophysical problems, deriving algorithm

10 p1689 A69-23968

Algorithm for calculating Bayes estimates for unsteady Gaussian signals separation in presence of unsteady Gaussian noise by least squares method

11 p1833 A69-24443

Reliability of eliminating multivaluedness in two scale phase measurement method resolved by algorithm formulated on white Gaussian noise interference

11 p1835 A69-24710

Stochastic approximation procedure minimizing mean square error criterion for system identification, estimation and decomposition of mixtures

11 p1842 A69-24934

Hybrid matrix algorithm for electronic circuits analysis, showing applications to transistorized circuits

11 p1859 A69-24954

Pattern classification algorithms classified according to type of input information required

11 p1843 A69-25445

- Iterative algorithm to determine transition probability final distribution in Markov extremal systems
11 p1861 A69-25712
- Digital control algorithm based on self adaptive linear model of multivariable processes used for feed-forward control of output signals
12 p2046 A69-26063
- Minimal representation in state variables for multivariable control system, discussing algorithms, identification methods and flow graph techniques
12 p2047 A69-26070
- Load deflection equation solution based on row operations, involving three passes of coefficient matrix, using wavefront processing and modified Gauss algorithm
13 p2358 A69-27208
- Parallel processing in system of computers with identical output, including probability graph for algorithm
13 p2224 A69-27426
- Regional boundaries in control-parameter space constructed by computer algorithm, involving parameter vibration direction changes in parameter plane
13 p2225 A69-27967
- Finite difference Newton-Raphson algorithm extension to solve variational equations for simultaneous optimization of trajectories and associated parameters [AIAA PAPER 68-115]
13 p2353 A69-28203
- Independently fluctuating Poisson light signals detected by receiver with inertialess photodetector, developing algorithm for estimating amplitude of useful signals
13 p2223 A69-28552
- Algorithm for N/h/ ionospheric profiles calculations using both x and o magnetoionic components, taking into account interlayer and underlying ionization influence
13 p2258 A69-28718
- Automatic control circuit zero drift compensation during external disturbance, using algorithm for computer minimizing of losses caused by control and response inaccuracy
14 p2425 A69-29140
- Image recognition algorithm for determination of hyperplane separating two finite sets of elements in Euclidean space
14 p2418 A69-29353
- Algorithm for solving Dirichlet problem of nonlinear elliptical differential equations representing atmospheric dynamics balance equation
14 p2470 A69-29401
- Optimal control problems solved by dynamic programming algorithm based on successive approximations of elementary control operation in space of states
14 p2426 A69-29472
- Iterative solution for difference equations approximating displacement vector determination problem in theory of elasticity, investigating algorithm convergence
14 p2536 A69-29479
- Bayesian theory to determine maximum a posteriori estimation algorithms for optimum bit synchronization in digital communication systems
14 p2413 A69-29496
- Algorithm for enumerating all circuits of linear graph, noting suitability for computerization without large computer memory
14 p2421 A69-29541
- Fast folding algorithm for detection and correlation of digital data with weak noisy pulse trains of differing periods
14 p2416 A69-29548
- Error bounds for covariance matrix used in optimum filtering and smoothing algorithms for control and communications systems operation
14 p2416 A69-29549
- General algorithm for eruptive plasma instabilities in fusion plasmas, flares and novae, yielding time behavior and dissipative effects
14 p2499 A69-29850
- Hybrid computer system for real time optimum feedback controller using iterative algorithms with rapid convergence, discussing simulation and performance
15 p2582 A69-30071
- Digital simulation for radio systems nonlinear elements, outlining procedures to obtain algorithms
15 p2582 A69-30111
- Algorithms for optimal detection of signals on background of normal noise with time varying intensity
15 p2563 A69-30133
- Algorithm for processing binary-quantized echo signal packets, obtaining useful and noise signals relation
15 p2571 A69-30331
- Polygonal approximation to functional equation solution by using search algorithms, listing FORTRAN IV programs
15 p2644 A69-30424
- Algorithm for calculating recognition error by applying pattern vectors having two multivariate Gaussian distribution to optimum Bayes classifier
15 p2572 A69-31113
- Rapid convergence algorithms as second variation methods for dynamic optimization problems
15 p2645 A69-31235
- Independent operations optimum performing sequence determined for parallel machines differing in technological characteristics and with assigned time using algorithm
16 p2763 A69-31626
- Minimization algorithm for complex and switching functions using unique identifiers on Karnaugh map
16 p2764 A69-31710
- Solid propellants formulation quantitative predictability for algorithmic modeling of functional selection, discussing specific impulse and burning rate [AIAA PAPER 69-432]
16 p2828 A69-31845
- Continued fraction inversion to rational fraction of two polynomials based on state space formulation and Routh algorithm
16 p2805 A69-32470
- Quasi-linearization algorithm for solution of boundary value problems for ordinary differential equations, formulating representation and convergence theorems
17 p2994 A69-32835
- Gyrocompass differential equations of motion reduced to Volterra integral equation, proposing solution algorithm
17 p2995 A69-33617
- Adaptive random search algorithm utilizing boundary cost-function hypersurfaces measurement to implement Pontryagin maximum principle, discussing hybrid computer use, iterative solution and convergence properties
17 p2933 A69-33745
- Algorithm for assigning binary codes to inputs, internal states and outputs for sequential machines by threshold logic
18 p3105 A69-34618
- Algorithm for minimizing expected value of quadratic performance index in closed loop optimal control of linear time varying systems
18 p3111 A69-34688
- Numerical procedure for testing absolute stability and positive realness of free dynamic systems based on Routh algorithm
18 p3112 A69-34689
- Brightness curves of eclipsing systems under monotonicity of unknown functions, using stable algorithm
18 p3197 A69-34753
- Algorithm for minimum weight structures automated design, coupling strain energy criteria with linear interpolation search technique to cover stress and displacement constraints [SAWE PAPER 798]
18 p3219 A69-34861
- Plate dynamics generalized equations independent of plate theory hypotheses, discussing algorithm and initial and boundary conditions
18 p3226 A69-35376
- Parameters distinguishing analytic queueing models of time sharing algorithms, emphasizing techniques used for analyzing round-robin and multiple level queueing models
19 p3279 A69-35600
- Orbit computation by means of predictor-corrector algorithms based on nonpolynomial functions, including numerical results for two body elliptic motion
19 p3397 A69-35611
- Modified Newton-Raphson methods for preliminary orbit determination, showing fast convergence and short computation times
19 p3397 A69-35613
- Aircraft terrain-following algorithm for use with airborne general purpose digital computer, discussing simulation techniques and test results [AIAA PAPER 69-817]
19 p3366 A69-35625
- Ordinary differential equations integration method, presenting algorithm based on double constraint of maximum accuracy and stability
19 p3279 A69-35805
- Iterative algorithm applied to shell theory boundary value problem of stress concentrations at shallow shell holes
19 p3436 A69-35847
- Impulsive orbit transfer optimization using accelerated gradient program based on Newtonian algorithm for digital computer method
19 p3402 A69-35956
- Algorithms for equivalence equation to approximate transient processes in higher order linear system by transient processes of lower order linear models
19 p3286 A69-36191
- Algorithm for determining multidimensional random process from canonical representation of current state, noting minimum rms prediction error
19 p3287 A69-36663
- Perceptron probability algorithm for random events prediction based on previous histories, applying Bayes formulas, static solutions formulas and transition probability tables and graphs
19 p3287 A69-36664
- Computer-algorithm elements required for engineering design and invention problems including design requirements, selection of spaces for variables using computerized heuristics, etc
19 p3280 A69-36666
- Dispersive quadrupole network design using algorithm method
19 p3287 A69-36740
- Algorithm minimizing nonzero elements during Crout reduction of sparse matrices
20 p3497 A69-36946
- Algorithm for definite integrals evaluation, using Clenshaw-Curtis and Romberg quadratures combination in each subinterval
20 p3498 A69-36947
- Algorithm for Chernousko local variation method during application to solution of variational problems involving nonadditive functionals, assessing convergence
20 p3513 A69-36990
- Weighting coefficients calculations by recursive algorithm for designing optimal discrete adaptive Kalman filter
20 p3509 A69-37142
- Algorithm using Biot-Savart law for determining induced velocity of curved vortex lines in aerodynamics, noting required line integration method
20 p3458 A69-37169
- Failure test algorithm for sequential units with delay lines of control digital computers, detecting replacement of output terminals by sensitive paths
20 p3502 A69-37394
- Electronic computer for processing observational data from pilot balloons, utilizing algorithms of values in programming for accuracy and time saving
20 p3572 A69-37700
- Pulsar search signal processing and digital techniques, using fast folding /cross correlation/ or fast Fourier transform /FFT/ algorithms
20 p3605 A69-37824
- Brightness distribution over source, discussing regularization algorithms for radio astronomical data reduction from crossed telescope
20 p3606 A69-38033
- N strip algorithm of integral relations to analyze flow around circular cone at incidence in supersonic flow
20 p3460 A69-38128
- Discrete problems of optimal control solved by general minimum principle, proposing several algorithms for optimality problems
20 p3509 A69-38295
- Algorithms testing characteristic polynomials and differential equation classical stability relations
21 p3755 A69-38925
- Numerical algorithms for nonlinear optimal pursuit problems
21 p3757 A69-39536
- Algorithm for programming language grammars conversion into pushdown store automata translators
21 p3679 A69-39607
- Spacecraft descent trajectory optimization during atmospheric reentry, proposing algorithm for continuous trajectory determination
21 p3766 A69-39647
- Spacecraft trajectory control algorithm for hypersonic reentry, describing onboard equipment role and simulation results
21 p3767 A69-39649
- Optimal control system for earth satellite orbital transfer, using wandering ellipse technique to develop trajectory correction algorithm
21 p3767 A69-39652
- Statistical regularization for obtaining a priori probability distribution information on mathematically incorrect inverse geophysical problems, deriving algorithm
21 p3680 A69-39654
- Long range space flight trajectory correction problem, obtaining algorithm for determining minimum number of corrections
21 p3818 A69-39822

Heart electrical activity time sequence estimation based on multiple dipole binary model, deriving algorithm

21 p3668 A69-39865

Algorithmic approach to nonlinear signal estimation problem useful in fetal electrocardiography

21 p3668 A69-39866

Algorithm for numerical modeling by Monte Carlo method of diffusion bounded light beams in dispersive media, applying to light pulse in cloudlike medium

22 p3981 A69-40248

Computerized algorithm facilitating automatic synthesis of time invariant linear compensation for highly complex multiloop control systems

[AIAA PAPER 69-941]

22 p3917 A69-40324

Algorithms for close earth satellite orbit calculation developed by numerical integration methods, discussing solution efficiency

[AIAA PAPER 69-948]

22 p4021 A69-40331

Newton-Raphson function space algorithm for optimizing control systems with discontinuities and terminal constraints, discussing spacecraft examples

22 p3918 A69-41009

Robbins-Monro stochastic approximation method using algorithms for identifying finite memory time-discrete time-stationary linear system from noisy input-output measurements

22 p3918 A69-41013

Algorithm for optimal solution to secondary optimization problem in nonserial dynamic programming

22 p3976 A69-41037

Variable time of arrival (VTA)/guidance generalized, developing computational algorithms to supplement linear guidance method

22 p3979 A69-41186

Assignment algorithm for target recognition in multiradar tracking systems

22 p3902 A69-41250

Monotonic minimization algorithm for nonsmooth extremal problems of mathematical programming, game theory, approximations and optimal control in arbitrary Banach space

23 p4181 A69-41524

System: asymptotic motion stability for given parameter values using algorithms with aid of R functions

23 p4191 A69-41704

Image recognition algorithms estimated for effectiveness by formulas minimizing classification error probability

23 p4134 A69-41954

Algorithm for stress analysis of structurally orthotropic conical and cylindrical shells, resolving first order differential equations

23 p4229 A69-42000

N-terminal parent networks with symmetry constraints derived for nonredundant one port configurations through combinatorial functions test patterns, using computer algorithm

23 p4134 A69-42524

Minimization algorithm for switching systems synthesis, describing design of mass spectrometer curve function generator and autonomous shift register

23 p4146 A69-42535

Algorithm for aeromedical airlift system stop selection and sequencing, minimizing patient in-system time and aircraft flight distance

[AAS PAPER 69-385]

24 p4251 A69-42804

Algorithm minimizing personnel number and training costs to meet uncertain skill requirements, applying to army aviation contingency force training composition

[AAS PAPER 69-116]

24 p4271 A69-42818

Memory gradient algorithm for reducing computing time by minimizing quadratic function of unconstrained variables compared with Fletcher-Reeves algorithm

24 p4340 A69-42957

Nonparametric partitioning algorithm for pattern classification, discussing pattern recognition, classifiers structure, real data applications, etc

24 p4285 A69-43062

Nonblocking switching networks operating in ordinary and in simultaneous switching regime, including control algorithms for optimal space communication

24 p4289 A69-43138

Multidimensional approximation algorithm for parameter optimization of nonlinear stochastic systems, detailing application to space vehicle attitude controller

24 p4291 A69-43275

Optimal control for systems with discontinuities and terminal constraints using Newton-Raphson algorithm/successive sweep method/

24 p4294 A69-43306

Parameter identification algorithm identifying linear dynamic systems by digital computer used to identify human operator characteristics in closed loop control situation

24 p4276 A69-43320

ALIGNMENT

NT SELF ALIGNMENT

Laser application to machine tool accuracy and alignment

[ASTME PAPER MR68-407]

02 p0252 A69-11797

Astronomical alignment accuracy by rocket Cassiopeia system, discussing scientific payload rotation and orientation by celestial bodies

03 p0462 A69-12850

Rotation and orientation of cosmic dust particles due to collisions with interstellar gas particles

03 p0511 A69-13420

Optical sighting method for determining orientation of rocket on launch pad by laser collimator, noting lining up of Cassiopeia system

06 p0930 A69-17104

Optical alignment for lasers with electro-optical Q switching and mutually misaligned ruby rod, KDP crystal and polarizing prism

12 p2107 A69-26589

Fiber axis distribution resulting from mechanical working deformation of matrix containing initially randomly oriented fibers

12 p2188 A69-26933

Cosmic rays suggested as origin of interstellar grain alignment, discussing galactic central radiation, gas collisions and isotropic bombardment

13 p2333 A69-28469

Asymmetry method for precision alignment of rectilinear systems, using laser light diffraction behind misaligned target

21 p3742 A69-39781

Portable He-Ne laser design featuring positional adjustment for use in aligning optical systems

24 p4327 A69-42924

ALIPHATIC COMPOUNDS

NT ACETIC ACID

NT ACETONE

NT ACETYL COMPOUNDS

NT ACETYLENE

NT ACRYLATES

NT ACRYLONITRILES

NT ADENINES

NT ADENOSINE TRIPHOSPHATE [ATP]

NT ALKANES

NT ALKENES

NT ALKYL COMPOUNDS

NT ALLYL COMPOUNDS

NT BUTADIENE

NT BUTANES

NT CARBON TETRACHLORIDE

NT CELLULOSE

NT CHLOROFORM

NT CHLORPROMAZINE

NT CHOLINE

NT CYANOGEN

NT CYCLIC HYDROCARBONS

NT CYSTEINE

NT DICHLORODIPHENYLTRICHLOROETHANE

NT ETHANE

NT ETHYL ALCOHOL

NT ETHYLENE

NT FORMIC ACID

NT GLUCOSE

NT GLUTAMIC ACID

NT GLYCEROLS

NT GLYCOLS

NT HYDRAZINES

NT KETONES

NT LACTATES

NT LACTIC ACID

NT METHANE

NT METHYL ALCOHOLS

NT METHYL COMPOUNDS

NT METHYLHYDRAZINE

NT MONOSACCHARIDES

NT NUCLEOSIDES

NT PARAFFINS

NT PENTANES

NT PROPANE

NT PROPYL COMPOUNDS

NT PROPYLENE

NT STARCHES

NT SUGARS

NT TETRAFLUOROHYDRAZINE

NT THIOLS

NT TRIMETHYL COMPOUNDS

NT URETHANES

Photolysis of aliphatic amino acids by UV light in presence of salt ions forming ammonia, glyoxalic acid, acetaldehyde and formaldehyde

01 p0025 A69-11094

Metal oxides catalytic and inhibitory effects on photolysis of alanine by UV light

01 p0025 A69-11095

Halocarbon solvent for application of chlorosilane finish to heat cleaned glass fabric for reinforcement of plastic, noting relative humidity effect

08 p1341 A69-20513

Relative gas phase acidities of simple aliphatic alcohols, considering effects of alkyl groups

19 p3265 A69-36289

Relative gas phase acidities of simple aliphatic amines and ammonia noting increase in large alkyl groups substitution

19 p3265 A69-3629

Linear aliphatic polyesters preparation by acid chloride synthesis, acid exchange and ester exchange stressing products purification

19 p3265 A69-36372

Gel permeation chromatography of nominally linear aliphatic polyesters, using tetrahydrofuran solvent at 37 degrees C

21 p3670 A69-39806

DENDRAL program used to construct all possible acyclic structural isomers of C, H, N and O

23 p4114 A69-42214

Geochemical synthesis of branched chain acyclic polymers from irradiated isoprene

24 p4269 A69-43750

ALKALI HALIDES

NT CESIUM IODIDES

NT SODIUM CHLORIDES

Ruby laser light beam self focusing in sodium chloride and potassium bromide crystals

03 p0438 A69-13051

Absorption and IR emission of nickel and cobalt doped alkali halides

03 p0490 A69-13941

Halide salts, semiconductors and nonoxide glasses as materials for high power laser windows

07 p1144 A69-18401

Alkali halide crystals destruction by laser radiation for estimating optical strength, discussing impact ionization hypothesis

08 p1328 A69-21188

Alkali halide single crystals disintegration by laser radiation differs as function of crystal physicochemical properties and band structure

10 p1745 A69-23322

Alkali halide crystals destruction by laser radiation for estimating optical strength, discussing impact ionization hypothesis

18 p3152 A69-35157

F center formation and X ray and photostimulated F-band luminescence in europium ion-activated potassium halides as function of temperature and X ray dosage

19 p3383 A69-36164

Electron spin memory in optical pumping cycle of potassium halides F centers, measuring relaxed excited state g factors and spin resonance line widths

23 p4198 A69-42419

ALKALI METALS

NT CESIUM

NT CESIUM VAPOR

NT CESIUM 133

NT LIQUID POTASSIUM

NT LIQUID SODIUM

NT LITHIUM

NT LITHIUM ISOTOPES

NT POTASSIUM

NT POTASSIUM ISOTOPES

NT POTASSIUM 40

NT RUBIDIUM

NT RUBIDIUM ISOTOPES

NT RUBIDIUM 86

NT SODIUM

NT SODIUM ISOTOPES

NT SODIUM VAPOR

NT SODIUM 22

Vacuum distillation technique for isolation and recovery of alkali metal reaction products with Ta, Ni, V and oxygen

01 p0083 A69-10927

Alkali metal vapors thermal conductivity determination by temperature difference dilatometric measurement

02 p0247 A69-11579

Magnetic confinement of electric arc in alkali metal vapor containing gas flow, considering degree of ionization

02 p0286 A69-11585

Alkali metal ion sources noting cesium ion engine development for space propulsion

[ECS PAPER 170B]

03 p0478 A69-13859

Alkali metals thermoelectric power and energy dependence of Heine-Abarenkov pseudopotential, taking into account anisotropy effects
05 p0809 A69-16507

Alkali metals electrical resistivity variation with temperature calculated in free electron approximation with Kreh model for phonon spectrum
08 p1372 A69-20229

Rare gas-alkali plasma electrical conductivity dependence on gas temperature and preionization to determine optimum operating conditions for MHD generator
10 p1733 A69-23451

Fermi surface data of alkali metals interpreted in terms of interaction between conduction electrons and ionic lattice for deducing partial wave phase shifts
13 p2304 A69-28681

Alkaline metal adsorption on high work function metals with charge transfer, measuring polycrystalline Mo photoelectric emission as function of Cs coverage
14 p2507 A69-29275

Collisionless Ce and K plasmas measurements to determine steady state parameters and LF oscillations, noting noise relationship to drift instability
14 p2499 A69-29849

Ionization within intersecting alkali atomic and slow electron beams, observing ionization cross sections increment near ionization threshold
15 p2655 A69-30726

ALKALIES
U POTASSIUM HYDROXIDES

ALKALINE BATTERIES
Low temperature hydrogen fuel cells and basic-electrolyte batteries design, discussing electrolyte concentration regulation by elimination of water formed
08 p1258 A69-21027

Thermodynamics and polarization of zinc electrode in alkaline media, discussing anodic dissolution and passivation
08 p1268 A69-21048

Zinc oxidation in weakly alkaline media, discussing basic properties of electrochemical cells containing zinc
08 p1268 A69-21050

Thermodynamics and polarization of Zn electrode in alkaline medium for electric generators
16 p2739 A69-32419

Gamma radiation effects on behavior of nickel and cadmium electrodes in alkaline solution
20 p3466 A69-38072

ALKALINE EARTH OXIDES
U BARIUM OXIDES
U BERYLLIUM OXIDES
U CALCIUM OXIDES
U MAGNESIUM OXIDES

ALKALOIDS
U PILOCARPINE

ALKANES
NT BUTANES
NT ETHANE
NT METHANE
NT PARAFFINS
NT PENTANES
NT PROPANE

Chemical mechanism of two stage spontaneous ignition controlled by cool flames of alkane-air mixtures under engine conditions to avoid knocking
11 p1998 A69-24479

Isoprenoids and isomeric alkanes identification in carbonaceous chondrites by gas-chromatographic mass-spectrometric analyses, including results from troilite nodules
19 p3414 A69-36113

Benzines antidetonation properties improved by separating n-alkanes with synthetic zeolite
23 p4199 A69-42479

ALKENES
NT BUTADIENE
NT ETHYLENE
NT PROPYLENE

Olefins combustion studies, considering influence on hexane combustion at different oxidation stages leading to ignition
02 p0352 A69-12309

Mechanical relaxation of poly 4 methyl pentene 1 at cryogenic temperatures, discussing temperature dispersion curve and secondary absorption associated with thermal motion of side chains
05 p0785 A69-16492

Ion structure of keto and enol and McLafferty rearrangements determined by ion cyclotron resonance spectroscopy
19 p3265 A69-36288

ALKYD RESINS

High temperature organic sealants for repairing small gas leakages in vacuum devices, tabulating test results for alkyd, epoxy, silicone and polyimide resins
11 p1907 A69-24742

ALKYL COMPOUNDS

NT TRIMETHYL COMPOUNDS

Photolysis of t-butyl iodide at low temperatures as source of t-butyl peroxy radicals for synthesis of peroxides
07 p1073 A69-18375

Thermodynamic dissociation constants of alkyl phenols in aqueous and methanol media based on UV spectroscopic analysis, noting anticarcinogenic properties
11 p1831 A69-24539

Relative gas phase acidities of simple aliphatic alcohols, considering effects of alkyl groups
19 p3265 A69-36289

Relative gas phase acidities of simple aliphatic amines and ammonia noting increase in large alkyl groups substitution
19 p3265 A69-36293

ALKYNES

U ACETYLENE

ALL SKY PHOTOGRAPHY

Auroral observations from constant local time westward flights of jet plane
02 p0245 A69-12738

Irregular pulsations in morning sky brightness using all-sky photographic airborne auroral observations along auroral oval
09 p1594 A69-21666

Vilna meteorite bolide observation with all-sky camera noting seismic and analytic records
13 p2334 A69-27189

Auroral substorm westward traveling surge and poleward, eastward and equatorward motion analyzed from all sky photographs
15 p2595 A69-30214

Auroral displays observed in combined field of view of polar all sky camera networks, considering simultaneous geomagnetic disturbances over Alaska
15 p2595 A69-30215

ALL-WEATHER AIR NAVIGATION

All-weather landing factors for aircraft and pilots, describing instrument landing system, runway and visibility, pilot and crew procedures, etc
01 p0112 A69-10454

All-weather landing flight director systems and fault warning display simulator studies of Boeing 707-720B aircraft in Category 3-C environment
01 p0010 A69-10455

TRANSIT satellite navigation system for all-weather diurnal position fixing, noting Doppler frequency measurement and ionospheric signal refraction
01 p0112 A69-10457

Light aircraft all-weather flight feasibility, discussing storm and clear air turbulence detection and icing prevention
01 p0111 A69-11049

Navy Navigation Satellite System TRANSIT providing all-weather continuous worldwide service for military and civil users
02 p0277 A69-11753

Automatic all-weather landing system for scheduled civil passenger aircraft, discussing safety, display devices, Category 2 and 3 conditions
03 p0465 A69-13697

All weather wind profile monitoring system using FPS-16 radar/Jimsphere system and flight simulation for protection of space vehicle and missile launches
03 p0462 A69-13852

Military rotor blade radar antennas for all-weather low level flight and fire control
04 p0559 A69-15197

Aircraft position and velocity in directions normal to ILS reference path by correlation with inertial navigation system, noting minimal time controller
07 p1177 A69-19213

Aircraft head-up display systems emphasizing all-weather operations and equipment characteristics
08 p1315 A69-20451

All-weather head-up displays /HUD/, discussing operational usage, hardware availability and design philosophy
08 p1315 A69-20452

Electronic terminal guidance requirements for all-weather VTOL operations, suggesting future first generation landing system
08 p1348 A69-21064

Helicopter all-weather flight control system, using autostabilization and artificial horizon
09 p1435 A69-22778

All-weather landing including zero-zero, discussing planning in Europe and U.S.A.
10 p1722 A69-23698

C-141 Category IIIB all weather landing system, discussing system concept, components, operations and performance
14 p2479 A69-29701

All-weather operations, aircraft size, air traffic and noise as airport design factors, discussing financing priorities for runway construction, facilities and personnel
17 p3004 A69-34207

Landing guidance devices under difficult weather, discussing landing mechanics for land and carrier based aircraft
18 p3170 A69-34857

All-weather landing in civil air operations, discussing ground/air systems in tracking, visual reference and aircraft performance required for safe landing capability
20 p3574 A69-38119

Electronic terminal guidance requirements for all-weather VTOL operations, suggesting future first generation landing system
22 p3978 A69-39875

Head-Up Display /HUD/ incorporated with autopilot for human participation in flight control for all-weather operation
23 p4109 A69-41871

ALLOCATIONS

NT GRANTS

Efficient allocation of maintenance resources in USAF, analyzing B-52 costs and substitution of capital for labor
13 p2382 A69-28041

ALLOTROPY

Medium heating by explosion in presence of allotropic changes and thermochemical reactions concerning temperature field determination
03 p0534 A69-14159

Molybdenum disilicide allotropy influence on coating growth rate and morphology
[ONERA-TP-642] 08 p1335 A69-19967

Volumetric and allotropic changes during heating in electrolytic cobalt multiple phase transformations
12 p2114 A69-26455

ALLOYS

NT ALUMINUM ALLOYS

NT AUSTENITIC STAINLESS STEELS

NT BAINITIC STEEL

NT BEARING ALLOYS

NT BERYLLIUM ALLOYS

NT BINARY ALLOYS

NT BISMUTH ALLOYS

NT BORON ALLOYS

NT BRASSES

NT BRONZES

NT CARBON STEELS

NT CHROMIUM ALLOYS

NT CHROMIUM STEELS

NT COBALT ALLOYS

NT COPPER ALLOYS

NT EUTECTIC ALLOYS

NT GALLIUM ALLOYS

NT GERMANIUM ALLOYS

NT GOLD ALLOYS

NT HAFNIUM ALLOYS

NT HASTELLOY [TRADEMARK]

NT HEAT RESISTANT ALLOYS

NT HIGH STRENGTH ALLOYS

NT HIGH STRENGTH STEELS

NT INCONEL [TRADEMARK]

NT INDIUM ALLOYS

NT IRON ALLOYS

NT KAMACTITE

NT LEAD ALLOYS

NT LITHIUM ALLOYS

NT MAGNESIUM ALLOYS

NT MANGANESE ALLOYS

NT MANGANIN [TRADEMARK]

NT MARAGING STEELS

NT MARTENSITIC STAINLESS STEELS

NT MOLYBDENUM ALLOYS

NT NICHROME [TRADEMARK]

NT NICKEL ALLOYS

NT NICKEL STEELS

NT NIMONIC ALLOYS

NT NIOBIUM ALLOYS

NT PALLADIUM ALLOYS

NT PERMALLOYS [TRADEMARK]

NT PLATINUM ALLOYS

NT QUATERNARY ALLOYS

NT REFRACTORY METAL ALLOYS

NT RHENIUM ALLOYS

NT RHODIUM ALLOYS

NT SILICON ALLOYS

NT SILVER ALLOYS

NT STAINLESS STEELS
NT STEELS
NT TANTALUM ALLOYS
NT TELLURIUM ALLOYS
NT TERNARY ALLOYS
NT TIN ALLOYS
NT TITANIUM ALLOYS
NT TUNGSTEN ALLOYS
NT VANADIUM ALLOYS
NT WASPALOY
NT WROUGHT ALLOYS
NT YTTRIUM ALLOYS
NT ZINC ALLOYS
NT ZIRCALOY 2 [TRADEMARK]
NT ZIRCONIUM ALLOYS

Alloy elements effect on spreading of liquid titanium and zirconium alloys on graphite
03 p0446 A69-13573

Mechanical properties and stress concentration sensitivity of structural alloys at low temperature
04 p0614 A69-14574

Long term strength of Ni-Cr-Al-Ti alloys, studying gamma particles size and distribution effect
04 p0616 A69-14651

Chemical compatibility estimation of lead and tin tellurides thermoelectric materials with metallic alloys
04 p0551 A69-15315

Galvanic corrosion couples of metals and alloys tested in liquid fluorine, determining corrosion rates for possible missile components application
06 p0944 A69-17854

Transient heat evolution response to reapplied stress of alloys plastically preformed at 4.2 K attributed to thermally softened defect structures
07 p1165 A69-18906

Directional solidification of multicomponent metal alloys for matrix in fiber reinforced composites, using monovariant eutectic reactions
07 p1166 A69-19145

Atmospheric and alloying elements effects on casehardening by gas carburization of structural steels, noting carbon potential
07 p1167 A69-19344

Microstructural changes during liquid phase sintering of alloys, considering temperature effect on carbide grain growth and activation energies
07 p1168 A69-19599

Tensile strength of alloys under high pressure of hydrogen and helium, discussing embrittlement [ASM PAPER D8-14.2]
07 p1169 A69-19667

Composite materials and alloys for jet turbine components in 1970s, discussing anticipated temperatures and material properties
09 p1523 A69-22061

Pressure vessels burst tests for investigating alloys, fabrication processes and biaxial loading effects, noting vessel configurations and test temperatures
10 p1714 A69-23974

Temperature effect on amplification factor of box type dynode system of photoelectron multipliers made of alloy AMGK, using single electron method
11 p1846 A69-24626

Soviet collection of articles on atomic ordering effects on alloy properties
11 p1936 A69-24701

Order-disorder in alloys with several phase transition temperatures, discussing crystal lattices, interstitial alloys, atomic and magnetic ordering
11 p1936 A69-24702

Superstructures in multicomponent alloys, transition mode and temperature, ordered state and atomic interactions
11 p1937 A69-24703

Pressure effects on hcp crystalline lattice alloys order-disorder transformations
11 p1937 A69-24704

Laser radiation in vacuum effects on metals and alloys
11 p1906 A69-25684

Room temperature thermal conductivity of semiconducting alloys with stoichiometric distributions of vacancies in cation sublattice, discussing heat resistance
12 p2142 A69-25975

Grain size and deformation velocities effects on plasticity of dispersion hardened alloy
13 p2283 A69-28489

Ferrous and nonferrous metals shock tensile strength by elastic contact dynamometer, noting diagram shape dependence on stress growth rate
14 p2464 A69-29314

Low temperature thermal expansion coefficients and linear contraction of metal alloys from liquid hydrogen to room temperature tabulated as function of temperature
14 p2464 A69-29400

Amorphous semiconducting alloys single band model characteristics
15 p2667 A69-30199

Mechanical properties and stress concentration sensitivity of structural alloys at low temperature
15 p2638 A69-30275

Interface friction and adhesion of alloys workpieces and die materials under pressure and temperatures typical of plastic deformation
15 p2629 A69-30902

Ceramic phase reinforcement of metals and alloys, discussing interfacial energies, binding forces and elastic stress fields [ONERA-TP-661]
16 p2802 A69-32204

Alloying pairs of metal pellets to n and p type semiconducting GaAs, discussing photo effects
17 p3015 A69-32824

Structural modifications of metals and alloys accompanying various stages of creep, interpreting equations describing time-deformation relation
17 p2985 A69-32904

Alloying elements effects on low temperature metal fracture, considering changes in ductile-brittle transition flow due to solute
17 p2988 A69-33551

Electrode potential measurements for corrosion study of metals and alloys in aqueous solutions, molten salts and gaseous atmospheres
18 p3150 A69-35412

Heat resistance evaluation of ZrH₂-K alloy subjected to multicomponent surface diffusion alloying combinations of Al, B, Cr, Si, Zr
19 p3345 A69-36159

Nonferrous metals and alloys conductivity standards development program resulting in fabrication, calibration and certification of 16 primary reference standards
20 p3537 A69-37008

Qualitative interpolation formula for phonon frequency spectrum of mass disordered alloys three dimensional systems at high concentrations
20 p3583 A69-37279

Vacuum heat treating and joining process for various ferrous and nonferrous metals and alloys, discussing advantages, applications and economics [ASM PAPER D8-22.3]
20 p3551 A69-38132

Spectrographic analysis for ferrous and nonferrous alloys as nondestructive testing
20 p3551 A69-38133

Engineering alloys electrical resistivities measurement at various temperatures, noting temperature and heat treatment effects [NAS-NRC PAPER D-5]
22 p3970 A69-40633

Mounting elements alloys relaxation characteristics at various temperatures, considering effects of scale factor and stress concentrations
23 p4169 A69-41419

ALLYL COMPOUNDS

Polydiethylene glycol-bis-allyl carbonate /PBAC/ Hugoniot equation of state, reporting shock data, discussing applications to propellant testing
16 p2879 A69-32179

ALMUCANTAR

U ELEVATION ANGLE

ALOUETTE HELICOPTERS

NT SA-330 HELICOPTER

Helicopters operation from small ships, describing underside harpoon mooring technique for Alouette 2 and 3
08 p1255 A69-20654

ALOUETTE SATELLITES

Transpolar exospheric electron concentration distributions along earth-sun line parallel path of Alouette 1 satellite
03 p0425 A69-14018

Ionospheric conditions following solar proton flare observed with topside sounders of Alouette satellites, showing electron density depletion and hydromagnetic wave relationship
10 p1684 A69-23781

Ionospheric satellite series Alouette-ISIS, discussing successive engineering and management constraints leading to ISIS-C design
20 p3618 A69-37856

Alouette spacecraft design and dynamics emphasizing antenna characteristics
20 p3618 A69-37858

Sweep frequency ionospheric topside sounder design for Alouette and ISIS satellites, discussing influence of experiment requirements and spacecraft limitation and environments
20 p3507 A69-37859

Data acquisition and processing ionograms from Alouette satellites telemetered sweep frequency topside sounding data
20 p3503 A69-37860

Receiving and display telemetry system for obtaining direct ionospheric topside ionograms from Alouette 1 satellite, discussing video data tape recording cost
20 p3507 A69-37861

ALOUETTE 1 SATELLITE

Vertical incidence pulse dispersion with application to Alouette 1, discussing echo width, sounder system bandwidth and frequency gradient of ionospheric virtual height
16 p2750 A69-31977

Magnetic activity effect on electron density in topside ionospheres determined from Alouette 1 data statistical analysis
23 p4156 A69-41856

ALOUETTE 2 SATELLITE

Conjugate echoes in Alouette 2 topside sounder ionograms explained by multiple reflections between conjugate points of field line, noting magnetospheric waveguides role
08 p1274 A69-20045

Cylindrical electrostatic probes on Alouette 2 and Explorer 31 satellites used in intersatellite comparison of directly measured ionospheric electron temperature and density
20 p3544 A69-37876

Cylindrical electrostatic probe measurements on Alouette 2 and Explorer 31, considering implications for future missions
20 p3544 A69-37877

Alouette 2 ionograms secondary resonances data indicating day-night effect in relative frequency of occurrence
20 p3496 A69-37889

Two-hop signals observed on high latitude Alouette 2 topside ionograms found propagating in field aligned cylindrical ionospheric ducts
20 p3531 A69-37890

Topside ionospheric structure from Alouette 2 data, discussing thermopause temperature, plasma temperature, electron density profiles, satellite plasma frequency, etc
20 p3532 A69-37895

Plasma temperature and ion concentration profiles determined from simultaneous measurements by Alouette 2 and Explorer 31 satellites of electron density, temperature and ion abundance
20 p3532 A69-37896

ELF noise band observed by Alouette 2 receiver in interpreted in terms of electrostatic proton cyclotron harmonic waves, using digital power spectrum techniques
20 p3497 A69-38079

ALPHA PARTICLES

Angular correlation of inelastically scattered alpha particles and gamma rays emitted from 2-plus state of Sn 120
03 p0469 A69-13098

Angular correlation between inelastically scattered 42 Mev alpha particles and emitted gammas from 2-plus Ni 58
03 p0470 A69-13100

Absolute cross sections for coincidence detection of deuteron breakup by 42 Mev alpha particles, showing He 5 and Li 5 final state interaction peaks
03 p0472 A69-13469

Electrical resistance temperature dependence below room temperature for polycrystalline epitaxially grown Au and Ag films, noting effects of alpha irradiation
03 p0486 A69-13582

Asymmetry of polarized protons scattered from He 4 at 540 Mev for laboratory angles between 4 and 42 degrees
04 p0632 A69-14966

Spectra analysis of proton and He nuclei having different charge-to-mass ratios to obtain information on solar modulation and injection spectra
06 p0988 A69-17272

Helium component flux in primary cosmic rays determined, using corrected alpha particles number
06 p0988 A69-17275

Oriented nuclear emulsion stack for determining differential rigidity spectrum of primary He nuclei between 12 and 35 bv
06 p0988 A69-17276

Permanent magnet and nuclear emulsion for measuring He nuclei momentum spectra up to 100 gv rigidity
06 p0989 A69-17277

Distribution characteristics of radiation defects in materials irradiated by monoenergetic beams of protons and alpha particles
06 p0981 A69-17878

Differential energy spectrum of protons and helium nuclei using lithium drifted silicon detectors and scintillator-Cerenkov counter
07 p1204 A69-18833

Energy spectrum of primary cosmic ray helium nuclei from nuclear emulsion stacks exposed in sounding rocket flights

08 p1378 A69-20264

Time histories of Mev proton and alpha particle intensities during and after July 7, 1966 solar flare, noting abundance ratio and geophysical effects

10 p1768 A69-23768

Energetic particles observed during proton flare noting relativistic electrons, protons to alpha particles ratio, low energy particles and bidirectional proton stream

10 p1768 A69-23785

Distribution characteristics of radiation defects in materials irradiated by monoenergetic beams of protons and alpha particles

14 p2503 A69-28787

Proton and alpha particle fluxes above specified vertical geomagnetic cut-off rigidity measured by balloon-borne Cerenkov scintillation counter telescope

14 p2511 A69-28951

Earth radiation belt data, discussing origin, density, distribution, etc. of protons, electrons and alpha particles

15 p2674 A69-30016

Rocket observations of protons and alpha particles energy spectra after solar flares, noting riometer and magnetometer recordings

15 p2677 A69-31329

Low energy solar protons and alpha particles from 28 May 1967 solar flare used as probes of interplanetary medium

16 p2847 A69-31965

Solar wind model for studying long wavelength turbulence as heat source for alpha particles and protons in solar plasma

18 p3186 A69-34299

Alpha-scattering experiments by Surveyor missions, studying hypothesis regarding lunar origin of eucrites and howardites

20 p3597 A69-37341

Interplanetary proton and alpha particle radial gradients determined from Mariner data, considering Forbush decrease, particle solar origin, galactic cosmic radiation, etc

20 p3592 A69-38096

Chemical analysis of lunar surface by devices exploiting alpha particle backscattering and proton production by alphas placed by Surveyor 5, 6 and 7

22 p4012 A69-40088

Angular distributions for Sc 45-Ti 46 nuclear reactions involving 41 Mev alpha particles bombardment described by Born approximation

22 p3988 A69-41044

Geomagnetically trapped protons and alpha particles, analyzing OGO 4 data

24 p4368 A69-43184

Solar protons and alpha particles measurements at synchronous orbit altitudes providing data for solar cell shield design to prevent radiation damage

24 p4369 A69-43265

ALPHANUMERIC CHARACTERS

NT BINARY DIGITS

Alpha numerical and symbolic information combined for head up display /HUD/ systems, providing pilot with takeoff director

03 p0379 A69-12885

Alphanumeric characters to identify radar targets on PPI display for air traffic control, considering technique for reducing smear

09 p1495 A69-21675

Pattern recognition as part of statistical communication theory, using Karhunen-Loeve expansion to minimize root-mean-square errors, showing application to handwritten numerals

09 p1461 A69-22292

Alphanumeric listing and digital data x-y plotting by high speed printer, describing equipment modifications and control software

17 p2932 A69-33108

ALSEP

U APOLLO LUNAR SURFACE EXPERIMENTS PACKAGE

ALTERNATING CURRENT

Surface structure effect on flux penetration and AC losses in superconductive niobium

02 p0298 A69-12031

Current oscillations or instabilities in semiconductor wafer with one electromagnetic mode and one carrier mode, investigating resonant frequencies

03 p0408 A69-14049

Transient stability of AC generator analyzed by Liapunov direct method, considering effects of flux decay, speed governor and voltage regulator

07 p1058 A69-18644

Final stage of three phase DC/AC converter, noting three phase control circuit for power stages with germanium transistors

08 p1285 A69-20381

Welding current pulsation techniques for adaptive control of gas tungsten arc welding processes

09 p1508 A69-22334

AC diode switching circuits employed as threshold elements in functional rectifiers for approximating nonlinear functions

11 p1857 A69-25717

Single phase bidirectional AC/DC power convertor based on back-to-back SCR hybrid bridge

13 p2209 A69-28178

Charged colloids generation by electrostatic spraying for thruster concept, subjecting metal capillary needles to AC voltage

[AIAA PAPER 69-495]

16 p2846 A69-32773

Triple probes behavior in plasmas under AC electric field perturbations

17 p2920 A69-33592

Amplitude ratio measurement for two AC signals of given relative phase shift and same frequency

17 p2975 A69-33615

AC technique using lock-in power amplifier SNR for measuring galvanomagnetic and Shubnikov-de Haas effects, noting error reduction

19 p3312 A69-36375

Two dimensional analysis of junction transistor electrical behavior, analyzing DC and AC crowding effects, conduction and impedance of base and collector

22 p3911 A69-40011

Ionospheric perturbations generation by time variable alternating electrical currents at polar latitudes, constructing radiation patterns for gravitational waves

23 p4155 A69-41842

Coil under alternating current interacting with laminated conducting structure, giving recurrence formula for calculating deflector voltage

24 p4296 A69-42653

ALTERNATING CURRENT GENERATORS

U AC GENERATORS

ALTERNATIVES

Systems design value analysis including alternate solutions to cost effectiveness for design development and production phases

13 p2383 A69-28097

ALTERNATORS [GENERATORS]

U AC GENERATORS

ALTIMETERS

NT RADIO ALTIMETERS

Pressure-altitude transducers for atmospheric pressure measurements on balloon flights including diaphragm, thermoconductivity, radioactive density and hypsometer gauges

07 p1132 A69-18873

Modern barometric altimeter evolution, discussing three pointer, radio, radar and servo altimeters, emphasizing Central Air Data Computer

08 p1313 A69-20123

Airborne pulsed laser system for altimetry, determining height by measurement of transit time for pulse traveling to ground and back

11 p1885 A69-25035

Barometric altimeters development, discussing servo and three pointer types, accuracy, Central Air Data Computer repeater function and future trends

15 p2610 A69-30859

Transport aircraft automatic altitude transmission requirements, discussing altimeter-transponder radar system to aid air traffic control

19 p3371 A69-36700

ALTITUDE

NT FLIGHT ALTITUDE

NT HIGH ALTITUDE

NT LOW ALTITUDE

NT SIMULATED ALTITUDE

Ekman-Okkerblom problem for electrically conducting atmosphere located in external magnetic field, obtaining altitude distribution for wind velocity components

03 p0461 A69-13510

Altitude effects on radar attenuation in nonequilibrium solid propellant afterburning rocket exhaust plumes

04 p0685 A69-14730

Light waves refractive index distribution from balloon sounding data found to decrease with height in winter regardless of time of day

09 p1536 A69-21917

Earth radar studies, relating echo behavior to rocket altitude and surface electrical characteristics

14 p2416 A69-29531

Dispersion relation for gravity waves propagating in atmosphere with horizontal background wind variable with altitude

18 p3128 A69-34801

Vertically moving ionospheric disturbances altitude estimated from geomagnetic pulsations in earth electromagnetic field

20 p3528 A69-37686

ALTITUDE ACCLIMATIZATION

Blood volume in rats exposed to high altitude and deacclimated at ambient pressure, noting changes and control level restoration

01 p0015 A69-10922

Lactodehydrogenase activity and LDG isoenzymes ratio in various tissues of rats during exposure to prolonged hypoxia at simulated heights

02 p0199 A69-11982

Thyroid gland role in resistance and myoglobin content of skeletal muscles of flat land and high altitude acclimatized white rats

05 p0709 A69-16517

Visual feedback mechanisms in simulated high altitude conditions, discussing physiology of ocular homeostasis adaptation

06 p0882 A69-17647

Acclimation to altitude hypoxia and duration of resistance to muscular effort in white Wistar rats on treadmill

09 p1445 A69-22725

Altitude climates effects on human performance, discussing oxygen consumption at moderate altitudes during vigorous physical activity

11 p1827 A69-24924

Irreversible blunted respiratory response to ventilation in high altitude natives, considering hypoxic and hypercapnic stimuli

12 p2018 A69-26130

High altitude acclimatization effects on cardiovascular system, external respiration, blood composition, optical and vestibular analyzers in human subjected to various stresses

13 p2212 A69-28623

Physical exercises to increase cosmonaut space environment tolerance, discussing effects of acceleration, altitude and hypoxia

15 p2560 A69-31460

Thyroid gland role in resistance and myoglobin content of skeletal muscles of flat land and high altitude acclimatized white rats

18 p3096 A69-34736

O conductance nonlinear equation solution applied to O uptake at sea level and at altitude, noting blood transport problems

21 p3654 A69-38906

Peripheral chemoreceptor carbon dioxide sensitivity, measuring human respiratory response to large carbon dioxide breath in oxygen at sea level and high altitude

22 p3890 A69-40207

Hypoxia tolerances in nitrogen dilution chamber of chickens at sea level and high altitudes, discussing role of hematocrit and heart mass

22 p3874 A69-40214

Human lung ventilation-perfusion scatter decreasing gas exchange efficiency during high altitude adaptation

22 p3875 A69-40227

Protein rates and RNA synthesis in cerebra of rats analyzed as factor of high altitude hypoxia adaptation

22 p3886 A69-41122

Physical training effects under normal atmospheric pressure on high altitude hypoxia and acceleration resistance in rats, including survival times

23 p4079 A69-41383

Hypoxia acclimatization studied by subjecting groups to bicycle exercise at simulated high altitude and at ground level

23 p4086 A69-41678

Exhaustion time extension in rats by altitude acclimation, noting adaptation loss resulting from physical exercise discontinuation

23 p4086 A69-41787

Arterial oxygen partial pressures and heart beat rates measured in humans during acute hypoxia after altitude and ergometer training, noting sensorimotor performance

23 p4086 A69-41788

Blood flow, volume and venous pressure measurements in right hand at low and high altitudes in residents and newcomers

23 p4098 A69-42106

ALTITUDE CONTROL

Satellite altitude stabilization by gravity gradient capture in earth elliptical orbit, showing effect of increase in damping

10 p1791 A69-22926

ALTITUDE SICKNESS

Multiple drone aircraft automatic control system, discussing preprogrammed mission path and controls of altitude, plan position and velocity

14 p2392 A69-29495

Supersonic flight altitude stability, studying effects of velocity, lift-drag ratio, thrust law, wind direction, engine unstarts, etc
[AIAA PAPER 69-813]

19 p3366 A69-35627

Maximum trajectory for glider entering earth atmosphere at supercircular velocity, subject to maximum altitude constraint

19 p3399 A69-35667

Thrust optimization for sounding rocket to reach maximum altitude with given initial and propellant weight, using polygonal time function and multiple-parameter numerical technique

22 p4037 A69-41050

ALTITUDE SICKNESS

Decreasing barometric pressure effects on abdominal gas volume in military men under simulated flight conditions, noting abdominal fullness and pain

23 p4076 A69-41291

Altitude decompression sickness in aviation, discussing physiological mechanisms underlying syndrome and treatment of conditions

24 p4269 A69-43412

ALTITUDE SIMULATION

Increasing hypoxia effects on rabbit EEG and light flash conditioned alimentary reflex for simulated altitude ascent, noting subcortical stimulation

02 p0197 A69-11492

Hypoxia effects on vestibular analyzer function of rats in pressure chambers at simulated altitudes from 11,000 to 12,000 m

02 p0198 A69-11506

Human acceleration tolerance under reduced pressures corresponding to various high altitudes, noting visual disorders

07 p1065 A69-18982

Neurological impairment in baboons exposed to prolonged decompression simulating high altitude aircraft cabin structural failure, noting neuropathological examination results

07 p1067 A69-19426

Speech intelligibility in air at ground level and in helium-oxygen mixture at 18,000 ft

12 p2019 A69-26548

Bird respirator function at simulated high altitude, noting adequate support in case of rapid decompression

14 p2406 A69-29290

Hypoxic hypoxia effect on catecholamine content and cytochemical changes in hypothalamus of cat exposed to simulated altitude, using Euler method

14 p2407 A69-29297

Solid rocket propellants tests, considering propulsion performance measurements, altitude simulation problems, internal flow patterns, nozzle geometry, etc

16 p2765 A69-31751

Human acceleration tolerance under reduced pressures corresponding to various high altitudes noting visual disorders

20 p3480 A69-38230

Hypoxia acclimatization studied by subjecting groups to bicycle exercise at simulated high altitude and at ground level

23 p4086 A69-41678

ALTITUDE TESTS

NT HIGH ALTITUDE TESTS

Upper atmospheric models, considering satellite orbital and solar panel torques, prediction, atmospheric density and composition measurements, etc
[AIAA PAPER 69-50]

06 p1011 A69-18085

Cosmic ray penetrating component properties identical to muon component at mountain level, indicating baryon passive nuclear state nonexistence

13 p2331 A69-28400

Exercise-temperature regulation in men under constant submaximal workload at various simulated altitudes, discussing exercise core temperature equilibrium level setting mechanisms

22 p3891 A69-40219

ALTITUDE TOLERANCE

Aircrew incapacitation during high altitude flying following partial gastrectomy, discussing aeromedical evaluation

10 p1645 A69-23381

Altitude effects on body chilling rate in rats noting hypoxia role in inducing hypothermia

13 p2210 A69-28532

High altitude environmental effects on adrenal glands and hypothalamic neurosecretion in rats

13 p2211 A69-28615

ALU [COMPUTER COMPONENTS]

U ARITHMETIC AND LOGIC UNITS

ALUMINA

U ALUMINUM OXIDES

ALUMINATES

Exchange interactions in lithium ferrite aluminates, measuring spontaneous magnetization by ballistic technique from 77 K to Curie point

13 p2320 A69-27995

ALUMINIZING

U ALUMINUM COATINGS

ALUMINUM

NT POWDERED ALUMINUM

NT SINTERED ALUMINUM POWDER

Slip band continuity across grain boundaries in aluminum bicrystals reexamined for geometrical criteria

01 p0095 A69-10607

Heat transfer principles analyzed in development of new quenchants for aluminum, noting properties of inversely water soluble polyalkylene glycols

01 p0087 A69-10900

Gas content and impurities in aluminum melts, analyzing oxides and hydrogen interactions

01 p0098 A69-10958

Plastic deformation wave propagation and heat generated near yield point of annealed aluminum

02 p0342 A69-12280

Aluminum deformation at various strain rates and temperatures under combined stress, comparing results with theoretical predictions

02 p0343 A69-12282

Electroerosion effect on fabrication of small disks for direct examination by electron microscopy, using refined and heat treated aluminum

03 p0427 A69-12880

Dynamic tensile stress-strain curves for annealed Al, Cu and Fe at constant strain rates, describing experimental method

03 p0524 A69-13065

Strain rate and temperature effect on flow stress of 7075 aluminum bars

03 p0443 A69-13120

Yield curve softening in hard Al subject to cyclic torsional loading, noting deformation resistance, surface hardness and yield strength

04 p0671 A69-14411

Thermal strengthening effect in aluminum due to temperature fluctuations

04 p0615 A69-14638

Aluminum corrosion by fungi isolated from jet fuel system with predominance of Cladosporium resiniae, noting protective coatings

04 p0616 A69-14765

Aluminum corrosion characteristics immersed in ion-exchanged water with trace impurities, determining corrosion rates

04 p0617 A69-14932

Sapphire whisker reinforced aluminum composites fabrication and evaluation

06 p0939 A69-16942

Fiber orientation and morphology effect on tensile behavior of aluminum-nickel whisker reinforced aluminum

06 p0939 A69-16943

Diffusion bonded aluminum-boron composite material, discussing mechanical, metallographic and radiographic properties

06 p0939 A69-16946

Micromechanics of boron filament reinforced aluminum composites

06 p0940 A69-16948

Aluminum-silica fiber reinforced metal composite, discussing mechanical behavior and effect upon engineering applications

06 p0940 A69-16949

Aluminum-stainless steel wire reinforced metal matrix composites, analyzing strain hardening and plastic deformation

06 p0940 A69-16950

Aluminum corrosion by fungus culture isolated from jet fuel system

06 p0941 A69-17123

Absolute short term current efficiency of aluminum electrolytic cell, stressing aluminum amount determination in cathode

06 p0869 A69-17233

Diffusion bonding of whisker reinforced aluminum in closed steel die in argon atmosphere

06 p0943 A69-17238

Theoretical and experimental results on annealed tapered aluminum rods to assess one-dimensional rate independent theory of plastic wave propagation from longitudinal impact

06 p1022 A69-17365

Fragments and markings produced on aircraft aluminum by explosion as means of detecting sabotage in crashes

06 p0868 A69-178338

Anodizing effect on flexural properties of Al-aluminum oxide sandwich composites, emphasizing properties of oxide coatings as function of thickness

07 p1159 A69-18722

Aluminum and aluminum alloys surface treatment prior to adhesive bonding, discussing degreasing, anodization, shear and bond strengths

07 p1141 A69-19312

Crystal growth and deformation induced recrystallization in pure aluminum
[ONERA-TP-671]

07 p1167 A69-19341

Surface environment effects on mode of microcrack formation during fatigue of Al single crystals, noting surface void formation mechanism

07 p1235 A69-19387

Subgrain diameter relation to misorientation in melt-grown aluminum single crystals from etch pitting and X ray techniques, discussing critical shear stress

08 p1330 A69-20011

Aluminum effect on ammonium percholate/polyformaldehyde mixtures combustion properties noting heat transfer decrease into k phase

08 p1375 A69-20338

Bonded Al-B metal matrix composite materials hot press fabrication and design, discussing temperature pressure time cycles and honeycomb sandwich structures

09 p1510 A69-22351

Aluminum plates bending fatigue tests, discussing mechanical properties, structural failure, grain size, strain hardening, stress-strain-time relations, heat treatment, etc

10 p1711 A69-23356

Titanium compared with aluminum in application to supersonic aircraft structures, considering tests and costs

10 p1700 A69-23600

Very low temperature dependence of thin single crystal Al plates electrical resistance, noting Umklapp processes contribution

10 p1711 A69-23620

Dislocations velocity in high purity aluminum single crystals determined as function of applied stress at 74 and 83 K

10 p1713 A69-23840

Aluminum abundances in stony meteorites measured using nondestructive instrumental neutron activation analysis

11 p1952 A69-24334

Silicon dioxide coated Al reflectance, solar absorptivity and total normal and hemispherical thermal emissivity, noting application to satellite temperature control

11 p1918 A69-24835

Dislocation structure and surface deformation markings correlation analyzed on fatigued Al electron microscope foils

11 p1905 A69-25184

Microwave analysis of plasmas produced by laser beam on aluminum spheres, noting expansion velocity and electron density

11 p1930 A69-25287

Spectrum analysis of aluminum plasma excited by giant pulse ruby laser radiation, discussing temperature and density

12 p2134 A69-26027

Aerodynamic field around symmetric profile two dimensional plates, visualizing velocity fields with Al particles

12 p2011 A69-26288

Cryogenic solenoids with pure Al conductor for production of strong magnetic fields, discussing softness and strain resistivity problems

12 p2016 A69-26497

Three dimensional network of closely spaced oxide particles for Al strengthening investigated by transmission electron microscopy and tensile tests

13 p2276 A69-27371

Ambient air pressure effects on fatigue crack growth rate in strain hardened aluminum

13 p2276 A69-27393

Copper and aluminum fatigue in vacuum and ultrahigh vacuum, discussing effects of hydrogen, nitrogen and oxygen pressures

13 p2280 A69-28088

Aluminum double sheet target penetration resistance determined by studying high velocity pyrex glass impact effects on front/rear sheets and spacing
[AIAA PAPER 69-375]

13 p2367 A69-28305

- Aluminum-boron metal matrix composite joining methods including electron beam, resistance spot, plasma arc and fusion welding
[ASM PAPER W9-23.4] 14 p2455 A69-29449
- X ray investigation of niobium, aluminum and niobium-aluminum systems to obtain K-spectra and L-spectra
14 p2508 A69-29664
- Aluminum corrosion in ethylene glycol-water systems, discussing protection mechanisms of adsorption-type inhibitors and additives effects on corrosion rate
14 p2466 A69-29932
- Flexible aluminum elliptical waveguide design, discussing installation, economy and electrical characteristics
15 p2578 A69-30798
- Multiple repair welding effects on AL welds tensile strength, using conductivity measurements to monitor strength
15 p2631 A69-31509
- Superconductive tunneling measurements on thin Al films, discussing enhanced transition temperatures, energy gap dependence on temperature, electron microscope observation of crystallites, etc
16 p2825 A69-31634
- Inert gas diffusion of Xe 133 in aluminum and titanium at various temperature ranges, showing effects of recrystallization, plastic deformation and phase transformations
16 p2800 A69-31775
- Ultrasonic and mechanical vibration effects on superpure Al and Al-Zn-Mg alloy, showing dependence of breaking stress on cycles
16 p2801 A69-31789
- Combustion of pulse heated single Al and Be particles in various oxidizers
[WSCIPAPER 69-2] 16 p2830 A69-32343
- Creep behavior of oriented Al bicrystals, emphasizing intergranular creep types and crystal orientation
17 p2985 A69-32906
- Microfractographic observations of Al, Al alloy, Nimonic 90 and austenitic steel 18/10 after creep rupture
17 p2986 A69-32910
- Plastic failure under internal pressure of aluminum spherical shells with single radial or oblique nozzle based on limit analysis theory
17 p3052 A69-32983
- Plane strain forging of pure Al and Al-Cu alloy at low strain rates and elevated temperatures, in constant velocity compression test
17 p2979 A69-34137
- Low endurance fatigue in aluminum, Nylon 66 and epoxy resin compared, considering stress-strain relationships, fatigue damage, failure mechanisms and crack propagation
18 p3155 A69-34633
- Al cryogenic quenching using liquid N for slow and uniform heat removal to eliminate distortion
18 p3150 A69-35419
- Forming, machining and joining characteristics of B-Al composite sheet metal material for space structures
19 p3318 A69-35507
- Manufacturing ultrahigh purity aluminum strip for cryogenic magnets, discussing ingot preparation, rolling, chemical milling and cleaning, arc welding, annealing and sampling
19 p3318 A69-35541
- Spray cleaning and deoxidizing of Al surfaces for structural bonding using sulfuric acid-sodium dichromate deoxidizer, noting tests with proprietary solutions
19 p3321 A69-35564
- Anisotropy coefficients obtained during annealed Al sheet tests based on stress-strain characteristics, noting fading memory effects
19 p3447 A69-36857
- Stress corrosion cracking model for 7075 Al, correlating macroscopic yield stress and corrosion time to failure
19 p3351 A69-36897
- Boron fiber reinforced Al matrix composite material for high performance aircraft gas turbine engine compressor blading
[AIAA PAPER 68-1037] 20 p3586 A69-37153
- Surface grains orientation effect on fatigue behavior in polycrystalline Al, noting strain hardening role in failure
20 p3561 A69-37597
- Low temperature predeformation and disorientation of mosaic blocks to strengthen aluminum
20 p3562 A69-37819
- Aluminum doped silicon solar cell energy loss coefficient under proton and high energy electron irradiation
20 p3465 A69-37911
- Diffusion bonding of Al and boron filament layers into continuous structural material, studying process variables including heat treatment and cross rolling effects
[AIME PAPER S69-6] 20 p3564 A69-38197
- Al-B composite aircraft structure fabrication, discussing wingspan segment, resistance spot welding, hot forming of joggles, etc
[AIME PAPER S69-1] 21 p3732 A69-39471
- BORSIC Al composites for propeller blades, discussing designs, fabrication methods and tensile test results
[AIME PAPER S69-4] 21 p3733 A69-39473
- Al discontinuous deformation noting role of intergranular boundary surface at low temperatures
21 p3750 A69-39789
- Outgassing rates of stainless steel and Al with different surface treatments, including glass bead shot blasting, electropolishing, baking and vacuum cleaning
22 p3958 A69-41215
- Step cathodic flux cleaning of furnace brazed Al assemblies used in combination with ultrasonic and chemical conversion coating techniques
24 p4319 A69-42938
- Redesigned Al wing structure using B-epoxy composite applied to pressurized fuel carrying section, including material, fabrication and test data
24 p4323 A69-43418
- Corrosion resistant bonding materials, discussing metal-to-metal adhesive primers, Al honeycomb core and foil finish
24 p4334 A69-43421
- Al brazed Ti honeycomb sandwich structures brazed in vacuum and Ar, analyzing mechanical properties and corrosion resistance as functions of temperature and pressure
24 p4324 A69-43435
- Tensile strength improvement in Al-B composites by heat treatment to T6 condition and subsequent cold rolling
24 p4334 A69-43449
- Al-B composites fracture toughness obtained by comparing notched tensile data with unnotched specimens
24 p4335 A69-43451
- ### ALUMINUM ALLOYS
- Low cycle fatigue life of aluminum alloy in reversed biaxial bending
01 p0093 A69-10116
- Chemical composition effect on duraluminum supersaturated solid solution stability, presenting time vs temperature C curves of isothermal decomposition
01 p0094 A69-10396
- Aluminum-Zn-Mg alloys weldability, discussing base metal composition and heat treatment influence during gas-shielded arc welding
01 p0086 A69-10536
- Natural aging effects on fracture characteristics of aluminum weldments, investigating precracked Charpy impact toughness
01 p0086 A69-10537
- Irradiation influence on yield stress of Ni-Al intermetallics noting temperature dependence and electron dosage
01 p0095 A69-10608
- Moisture effects on crack propagation in high strength aluminum alloys studied by fatigue tests
01 p0098 A69-10766
- Atmospheric stress corrosion tests of aluminum alloys in various environments, comparing aging results with accelerated laboratory tests
01 p0100 A69-11352
- Long term atmospheric corrosion test program for aluminum and magnesium base alloys, comparing tensile strength of exposed and control specimens
01 p0100 A69-11353
- Weathering tests on wrought aluminum alloys exposed at U.S. sites compared to British industrial atmospheric exposure results
01 p0101 A69-11354
- Nickel-rich region of Al-Ni-Y ternary system, emphasizing identification of solid phase equilibria through analysis of equilibrated alloy specimens
02 p0265 A69-12004
- Welding with aluminum-zinc-magnesium alloys, discussing stress corrosion, embrittlement, compositions, heat treatment, material production and fabrication
02 p0266 A69-12063
- Strain gage behavior on unstressed aluminum alloy under rapid heating using radiant heating, weld strength and high temperature test equipment
02 p0341 A69-12229
- Elastic-plastic wave profiles in Al alloy under uniaxial strain load, investigating sensitivity to various strain rates
02 p0344 A69-12289
- Aging and cold work hardening effect on deformability of aluminum-magnesium-silicon-copper alloy
02 p0254 A69-12677
- Fabrication of large arched bottoms for pressure vessels from aluminum alloys, discussing sheet cutting and welding, annealing, machining, etc
02 p0254 A69-12678
- Magnified image of Al-Mg specimen microanalyzed during examination by electron microscope, studying segregation and initial precipitation at grain boundaries
03 p0442 A69-12894
- Damping capacity and resistance to resonance fatigue of titanium and aluminum based steels and alloys
03 p0443 A69-13025
- Aluminum alloy with lithium and magnesium noting mechanical properties and electrical and corrosion resistance
03 p0443 A69-13026
- Fatigue and corrosion fatigue properties of aluminum alloys, noting elastic modulus, cyclic loading strength, corrosion resistance, etc
03 p0443 A69-13027
- Creep relaxation and kinking of aluminum-nickel whiskers at elevated temperature, noting permanent plastic deformation after heat treatment
03 p0443 A69-13119
- Strain induced deformational instability of aluminum alloys
03 p0447 A69-13818
- Powdering temperature effect on mesh size, structure and mechanical properties of pressed semifinished sintered Al-Cr and Al-Fe alloys
03 p0452 A69-14119
- Si and iron impurities effects on duraluminum alloy structure and mechanical and plastic properties for fabrication from granules and rolling from ingots
03 p0452 A69-14120
- Impurity-dislocation interaction in Al alloy by vacancy mechanism and repeated yielding phenomenon, establishing activation energy
04 p0613 A69-14440
- Large hydraulic press forgings for light metals, discussing 50,000 ton machine used for Al alloys, tooling and die considerations
04 p0604 A69-14521
- Al-Mg-Si alloy strain aging, noting effect of deformation stresses on kinetics and aging mechanism for prior and concurrent deformation
04 p0614 A69-14575
- Heat treatment and shot peening effects on Al alloy fatigue strength and fine crystallographic structure
04 p0614 A69-14576
- Low temperature aging prior to higher temperature artificial aging increases Al alloys strength
04 p0614 A69-14634
- Precipitation hardening effects on Al-Zr recrystallization with Fe and Si additions, noting peak hardness increment with decrease in aging temperature
04 p0617 A69-14931
- Phase equilibria, phase transformation temperatures and relation between resistivity and chemical composition for alloys of Ti-Al-Mo-Zr system
04 p0618 A69-15079
- Cold working considered for decreasing fatigue crack propagation rate in thin duraluminum sheets with various plastic deformations
04 p0681 A69-15170
- Flow stress of iron wire reinforced aluminum alloy composites
[ASME PAPER 68-WA/MET-10] 05 p0780 A69-16150
- Fatigue crack growth in notched samples of aluminum alloy subjected to cyclic compressive loading, noting residual tensile strength at notch root
[ASME PAPER 68-WA/MET-16] 05 p0838 A69-16154
- Interaction between point defects and magnesium atoms in aluminum irradiated by neutrons, analyzing magnesium concentration effect on recovery
05 p0781 A69-16613
- Aging and recovery effect on structure and hardness of Ag and Be doped Al-Mg alloys
05 p0783 A69-16811
- Plastic yielding and strain distribution in Al reinforced with stainless steel wires determined by electron microscopy
06 p0940 A69-16947
- Superimposed stress of higher frequency and rotating bending stress effects on aluminum alloy
06 p0941 A69-17121

Controlled microstructures of eutectic aluminum-copper aluminides produced for mechanical properties studies

06 p0942 A69-17227

Stress corrosion crack initiation in aluminum alloy observed by optical microscopy

06 p0944 A69-17855

Titanium aluminum alloys two stage direct production by aluminothermal reduction of titanium tetrachloride

07 p1159 A69-18536

Plastic fractures of age hardened aluminum alloys analyzed by tensile tests and electron fractography, considering stresses, surface and intergranular effects

07 p1166 A69-18961

GP zones study in aluminum alloys during fatigue process by electrical measurement, discussing resistivity, cyclic deformation, loading and unloading

07 p1166 A69-18962

Aluminum and aluminum alloys surface treatment prior to adhesive bonding, discussing degreasing, anodization, shear and bond strengths

07 p1141 A69-19312

Impact cyclic loading fatigue tests of smooth and notched duralumin, discussing increased impact strength resulting from initial underloading

07 p1167 A69-19317

Parameters interrelating time and temperature used to present creep-rupture data for Al alloys, providing direct readings of stresses

[ASM PAPER D8-9.7] 07 p1169 A69-19665

Yielding of matrix material and cell size of substructure relationship to dry abrasion resistance of SAP type aluminum alloy at room temperature

08 p1319 A69-19995

Al alloys application to Concorde project and other aircraft structures, noting mechanical properties

08 p1335 A69-21141

Aircraft structural aluminum alloy fatigue life, considering atmospheric relative and absolute humidity

09 p1521 A69-21390

Grain morphology and preferred orientation effects on direction and propagation of stress corrosion cracking of aluminum alloy plate

09 p1521 A69-21399

Plastic yielding of tensile V-notched aluminum alloys elements with intermediate thickness and various shoulder ratios, studying thickness effect on yield load

09 p1612 A69-21499

Spinodal decomposition effect on Al-Zn alloy mechanical properties noting strengthening, brittleness and work hardening capacity

09 p1522 A69-21501

Structure of spinodal decomposition in Al-Zn alloys by X ray diffraction noting anisotropy, periodicity and stability

09 p1522 A69-21502

Microstructure for spinodal decomposition in Al-Zn alloys noting Zn precipitation, fracture mechanics, dislocations and transmission electron microscopy results

09 p1522 A69-21503

Organic quenchant additive for distortion free heat treatment of dip-brazed aluminum parts

09 p1504 A69-22065

Fretting fatigue prevention in Al alloys, noting strength reduction due to fretting

09 p1526 A69-22148

Plastic strain intensity distribution in aluminum alloy specimen with central hole measured with marked orthogonal lattice

09 p1617 A69-22221

Primary silicon crystals content and grain size effect on wear of high silicon aluminum alloys

09 p1526 A69-22281

Weld discontinuities effects on fatigue strength of Al welds tested to determine unaffected defect size and severity of discontinuities

09 p1527 A69-22372

Diffusion bonding parameters for producing hollow Ti-Al compressor blades, discussing surface preparation, postbond heat treatment quality control and mechanical properties

[ASME PAPER 69-GT-46] 09 p1513 A69-22484

Unidirectionally solidified eutectic composite of Al and Cu-Al intermetallic, noting tensile properties at room and high temperatures

10 p1708 A69-22995

Stress corrosion of nonage-hardenable Al-Mg-Cr alloy investigated for failure in absence of grain boundary precipitate, using notched specimens

10 p1709 A69-23055

Aluminum alloy thin sheets with central transverse fatigue cracks subjected to increasing static loads to fracture, investigating crack tip deformation

10 p1709 A69-23056

Electron fractography of aluminum alloy fatigue for intermetallic particles and inclusions effects on crack growth

10 p1795 A69-23065

Aluminum alloy crack propagation and fracture patterns as function of temperature under high strain amplitude and low strain rate

10 p1709 A69-23071

Debonding mechanism role in fatigue crack development in notched aluminum alloy samples using optical and electron microscopy

10 p1710 A69-23076

Environment influence on fatigue crack propagation mechanisms in aluminum alloys in vacuum, ambient air and distilled and sea water

10 p1710 A69-23084

Elastic release wave and pressure drop measurement in 2024-T4 aluminum at 313 kb for dynamic yield strength, considering surface velocity and stress

10 p1712 A69-23665

Yield points compared for axial and biaxial tensile loading of aluminum alloy sheets

10 p1801 A69-23849

Silicon particle sizes in Al-Si system investigated for interactions with dislocations as function of strain and for effect in dispersion hardening

10 p1714 A69-23980

Cyclic stress-strain and fatigue behavior in aircraft structural metals, discussing hardening and softening in aluminum alloys, steels and titanium alloys

10 p1714 A69-23981

Cyclic deformation resistance and fatigue damage accumulation in aluminum alloys, aircraft steels and titanium alloys

10 p1715 A69-23983

Aluminum bonded structures corrosion resistance through adhesive primers and surface treatments

10 p1700 A69-24088

Aluminum alloys role in aerospace technology, discussing temperature characteristics, gas absorption, weldability, purity, etc

11 p1903 A69-24518

Stress corrosion cracking of Ti-6Al-4V alloy tensile tested in anhydrous methanol by electron fractography and diffraction, noting hydrogen embrittlement

11 p1903 A69-24576

Stress-strain relation in crystalline media for pure tension and elongation epsilon several times conventional elastic limit, verifying by testing Al alloy [ONERA-TP-695]

11 p1975 A69-24754

Aluminum alloy weld tensile strength increased by heat treatment, discussing weld porosity due to surface film of absorbed hydrogen

11 p1891 A69-24896

Aluminum additive effects on copper-titanium alloy decomposition, discussing Guinier complexes, heterogeneous nucleation, plastic deformation and low temperature aging

11 p1905 A69-24922

Arc welding aluminum to steel using bimetal transition insert piece

11 p1891 A69-24929

Plastic strains in aluminum alloy under biaxial tensile and combined tensile and torsion tests, discussing small elastoplastic deformation theory

11 p1905 A69-24948

Rectangular aluminum alloy rods carrying capacity under compression loads applied eccentrically to rod ends

11 p1986 A69-25326

Weld cracking sensitivity of Inconel 713C investigated for determining aluminum content effect on weldability of nickel base heat resistant alloys

11 p1906 A69-25577

Inclination effect of fatigue cracks on plane strain fracture toughness of 7075-T651 Al alloy, discussing cantilever bending

12 p2177 A69-25958

Corrosion resistance rate of duralumin sheet in aqueous superphosphate solutions dependence on concentration

12 p2113 A69-26124

Wetting and sessile drop contact angles between liquid binary Al alloys and solid Be, boron carbide and graphite under vacuum and in He

[ACS PAPER 15-C-68F] 12 p2114 A69-26301

Incipient stress corrosion damage detection in aluminum alloys, using Rayleigh wave attenuation

12 p2114 A69-26306

Electrical conductivity measurements combined with indentation hardness measurements for non-destructive evaluation of commercial precipitation hardenable aluminum alloys

12 p2114 A69-26307

Fatigue life of Al alloy thin laminated sheets, considering cyclic frequency and temperature effects

12 p2180 A69-26359

Fatigue crack propagation and fail-safe design for stiffened large Al alloy panels with crack stoppers, using residual strength analysis method

12 p2186 A69-26835

Fatigue crack initiation and propagation correlation with substructure formation by static and alternating stresses in Al

12 p2188 A69-26915

Fatigue fracture surfaces in cast steel and Al alloys studying fracture morphology, crack propagation rate and striation spacing with microfractographic methods

12 p2116 A69-26991

Creep behavior of aluminum-alumina alloys analyzed using rupture time to determine deformation speed influence on elongation and crack formation

12 p2120 A69-26938

Metal fatigue in Al alloys subjected to stress cycles, determining macrocracks propagation stages

13 p2359 A69-27291

Composition, gamma structure and mechanical properties of three unidirectionally solidified eutectics within Ni-Al-Cb, Ni-Al-Zr and Ni-Al-Ti systems

13 p2277 A69-27407

Plasma spray quenched Al-V alloys resulting in dispersion strengthening of material

13 p2277 A69-27409

Aluminum alloys ductile fatigue striations, considering dependence on grains crystallographic orientation and vacuum effect

13 p2278 A69-27415

Fatigue crack propagation in aged aluminum alloy sheets, studying specimen geometry and stress level variations effects

13 p2280 A69-27835

Aluminum alloys precipitation hardening types requiring solution heat treatment, quenching and artificial aging, noting advantages in strength and weldability

13 p2282 A69-28180

Crack behavior and toughness of aluminum alloy parent metal and weldments, noting temperature effect

14 p2462 A69-29003

Al-Mg-Si alloy strain aging, noting effect of deformation stresses on kinetics and aging mechanism for prior and concurrent deformation

15 p2638 A69-30276

Longitudinal internal cracks in deformed Al alloys initiated by elastic stress concentration in areas of highest flow rate gradient

15 p2638 A69-30277

Heat treatment and shot peening effects on Al alloy fatigue strength and fine crystallographic structure

15 p2638 A69-30278

Discontinuous yielding characteristics of 2024 Al alloy determined for different conditions of solution, heat treatment and age hardening

15 p2639 A69-30598

Annealed aluminum rods dynamically compressive impact loading used to study longitudinal plastic waves propagation velocity

15 p2709 A69-30677

Room temperature fatigue crack propagation rates for high strength aluminum alloy in heavy water environment compared with argon and distilled water

15 p2640 A69-30815

Aluminum nonheat-treatable alloys cryogenic vessels welding, considering TIG, pulsed arc and MIG processes with respect to plate thickness, joint and accessibility

15 p2630 A69-31210

Electrical conductivity, hardness, ultimate tensile strength and yield strength correlations of age hardenable Al alloys by eddy current methods

15 p2641 A69-31513

Electrochemical test predicting stress corrosion performance of 2219 aluminum alloy in T851 and T87 tempers

16 p2798 A69-31716

Strain hardening experiments on single crystals of AlZn and AlAg alloys noting plastic behavior

16 p2800 A69-31776

Ultrasonics for wrought and cast aluminum alloys nondestructive testing, discussing ultrasonic energy damping measurements

16 p2800 A69-31778

Stress corrosion resistance of AlZnMgCu and AlZnMg alloys, discussing combinations of alloy composition, heat treatment and stable precipitation conditions

16 p2800 A69-31779

Aluminum alloys high temperature creep effects distinguished from effects of long period at high temperature, discussing tensile test data and deformation-time curves

16 p2800 A69-31781

Creep rate and temperature effect on creep resistance shown in direct correlation with Al-Mg alloys strength by long term high temperature tests

16 p2801 A69-31782

Trace elements influence on precipitation process and properties of Al-Cu, Al-Zn-Mg and Al-Mg alloys, using X ray diffraction

16 p2801 A69-31783

Ultrasonic and mechanical vibration effects on superpure Al and Al-Zn-Mg alloy, showing dependence of breaking stress on cycles

16 p2801 A69-31789

Aircraft construction materials, discussing aluminum alloys use in Concorde project based on temperature tests, creep and fatigue properties and joint requirements

16 p2801 A69-31791

Microfractographic observations of Al, Al alloy, Nimonic 90 and austenitic steel 18/10 after creep rupture

17 p2986 A69-32910

Rotating bending fatigue tests on aluminum alloys based on statistical analysis for material strength

17 p3052 A69-32979

Fracture strength of Al alloy in biaxial stress field, considering strain rate influence on material toughness

17 p2986 A69-32985

Ti-Al base alloys brittleness and stress corrosion cracking, discussing diffusion mechanism, hydrogen mobility, dislocations, etc

17 p2987 A69-33372

Fracture strength of Al alloys, discussing tests for tensile properties, linear elastic fracture mechanics techniques, yield strength, corrosive media, etc

17 p2989 A69-33555

Fatigue crack propagation in thin aluminum alloy plates under plane bending using microscopic surface observation and electron fractography, noting role of aging conditions

17 p3061 A69-33677

Plane strain forging of pure Al and Al-Cu alloy at low strain rates and elevated temperatures, in constant velocity compression test

17 p2979 A69-34137

TiNi compound alloying with Al and Fe, considering effect on hot hardness at various temperatures

18 p3157 A69-35249

Alpha Ti-Al and Ti alloys plastic deformation at low temperatures, noting slip and twin mechanisms role

18 p3158 A69-35444

Recrystallization limit effects on coarse grain growth in aluminum alloys extruded sections, studying roles of additives, extruding temperature and heat treatment duration

18 p3160 A69-35472

Lightly loaded truss structures fabricated from Be, Be-Al alloy and uniaxial B filament reinforced epoxy tubing for unmanned spacecraft applications

19 p3340 A69-35504

Silicon carbide coated boron fibers in aluminum alloy matrix, discussing tensile and structural properties of braze bonded specimens

19 p3340 A69-35509

Electroforming of Al matrix composites by codeposition of short graphite fibers, obtaining increased strength and elastic modulus

19 p3318 A69-35510

Be/Al cast duplex alloy with Be embedded as discrete particles in Al matrix, detailing fabrication techniques and mechanical properties

19 p3340 A69-35524

Outdoor aging effects on unstressed Al-Al lap shear joints bonded by various polymeric adhesives

19 p3320 A69-35562

Adhesive bonding of Al sheets for honeycomb sandwich material, using electrical conductivity to measure sheets age hardening progress during high temperature curing

19 p3321 A69-35565

Exposure tests of corrosion resistant claddings for high strength Al alloys protection, finding higher purity alloy cladding superiority

19 p3322 A69-35571

Be and BeAl alloy stress corrosion behavior in aqueous NaCl solution, discussing metallography and electron fractography

19 p3341 A69-35572

Fatigue characteristics of Al alloys by fatigue tests with complex stress patterns, finding secondary stress wave effects

19 p3342 A69-35772

Stoichiometric NiAl slip line and dislocation structures during creep at high temperatures, considering possible creep mechanisms

19 p3343 A69-35923

Silicon carbide coated boron fiber reinforced /Bor-sic/ Al composites tensile strength and elastic properties

19 p3344 A69-35926

Ti-Al alloys yield and fracture characteristics as function of high exposure temperatures, studying causes of embrittlement

19 p3344 A69-35927

Surface alloying of high melting point metals in Al melts, noting prior oxidation enhancement and simplifying of calorizing techniques

19 p3328 A69-36158

Axial load fatigue crack propagation tests on Al alloy sheets for stress ratio effects

19 p3346 A69-36435

Fabrication effects on high strength Al alloy plate properties, comparing texture, plane strain fracture toughness, yield stress, ultimate tensile stress and elongation

19 p3346 A69-36437

Stress corrosion cracking mechanism in Al alloys, discussing requisites for stress corrosion cracking

19 p3350 A69-36895

Aluminum 7 percent Mg alloys stress corrosion cracking, presenting aging kinetics and depletion zone dislocations at grain boundaries

19 p3350 A69-36896

Precipitation hardening, microstructure and dislocation influence on intergranular stress corrosion cracking /SCC/ of high strength Al alloys examined by transmission electron microscopy

19 p3351 A69-36898

Electrochemical analysis of stress corrosion cracking in Al-Zn-Mg alloy, noting oxide film growth at grain boundary

19 p3351 A69-36899

Yield strength, deformation modes and fracture characteristics of Ti-Al alloys, examining strength and fracture characteristics as function of structure and chemical composition

20 p3557 A69-36959

Elements substitution for Al in gamma prime of Ni-Al alloy to change aged hardness by gamma prime mismatch and coherency strains

20 p3558 A69-36963

Aluminum alloying additives effects on tungsten disilicide corrosion resistance, studying plasticity properties and oxidation rate

20 p3561 A69-37376

Al alloy application to welded primary airframe structures, discussing welding processes with emphasis on fusion welding

[SBAC PAPER 4] 20 p3549 A69-37445

Seam welded Al alloy aircraft structure fabrication problems, emphasizing stress corrosion

[SBAC PAPER 5] 20 p3550 A69-37454

Boron fiber reinforced Al alloys spall failure and shock induced filament damage, using flyer plate technique

20 p3562 A69-37772

Large aperture Al alloy telescope mirrors consisting of Tenzalloy Al coated with Ni alloy, presenting performance data

20 p3546 A69-38193

Al and Mg alloys as ultrasonic wave acoustic lines, considering sound velocity, damping factor, grain size, chemical composition, etc

20 p3564 A69-38290

Design and processing tradeoffs for preventing stress corrosion cracking in Al alloy aircraft structural forgings

[ASM PAPER W9-14.4] 21 p3729 A69-38657

Shock hardening of Al alloys in annealed, solution heat treated and aged conditions compared with cold-rolled materials

[ASM PAPER W9-10.4] 21 p3729 A69-38664

Ti honeycomb sandwich panels, comparing properties of Ti and Al based brazing alloys

21 p3730 A69-38665

Inconel and aluminum tested in pressurized hydrogen at room temperature, using surface flawed fracture toughness specimens and preflawed pressure vessels

21 p3730 A69-38666

Al alloys properties evaluated to determine tensile and static fracture behavior

21 p3743 A69-38668

Al alloys sheet, plate and weldments crack behavior and fracture toughness at cryogenic temperatures, using notched and surface flawed plane strain specimens

[ASM PAPER W9-19.3] 21 p3743 A69-38669

Fatigue resistance of bimetallic sheets of steel and Al alloys by fatigue resonant machine, analyzing lifetime distribution and failure probability

21 p3835 A69-38773

Creep measurements in Al alloy during uniaxial tensile stresses between 200-350 C, determining deformation dependence on time and stress

21 p3744 A69-38871

Aluminum alloy laminates composed of two metal-lurgically bonded Al alloys of different composition

21 p3745 A69-38936

Melt cooling rates effect on supersaturated solid solutions in Al ternary systems

21 p3745 A69-38955

Deformation rates effect on failure of cast aluminum alloys under various loading rates for tension and compression

21 p3746 A69-38958

Bending creep tests on fabricated Al alloy box beams under constant load and temperature using continuous deflection and strain measurement

21 p3842 A69-39309

Creep accumulation under time varying stress of Al alloy sheet, using creep recovery analysis to determine anelastic strain growth

21 p3747 A69-39323

Corrosion and stress effects separation in stress corrosion of Al-Zn-Mg-Cu alloy, considering machined surface finishing role

21 p3747 A69-39435

Stress corrosion cracking of welded Al alloys in sea water solution, showing combined action of sustained stress, corrosive environment and heat treatment

21 p3748 A69-39492

Recovery process observation in pure binary Al-Cu alloy and commercial Al-Cu-Mg-Pb alloy, noting electron microscope applicability

22 p3968 A69-40062

Cu, Ni, Co, Cr and Ti effect on high temperature mechanical properties and stability after prolonged annealing of Al-Si alloy with added 1 percent Mg

22 p3968 A69-40063

Weld porosity in Al alloys as function of composition variations, discussing water vapor contamination of welding arc

22 p3956 A69-40461

Dual filler metals for increasing joint efficiency by changing fusion zone composition, discussing mechanical properties in Ti and Al plates welding

22 p3956 A69-40462

Solid solutions precipitation effect during deformation process on static and dynamic tensile tests of Al alloy by electric resistance measurement

22 p3972 A69-41082

Al-Ni-Co alloys precipitation mechanism effect on magnetic properties, including heat treatment and Ti alloying effects

23 p4175 A69-41298

Aluminum alloys fracture strength tabulated data showing trends regarding yield strength, specimen orientation effects and product size

23 p4175 A69-41476

Ingot dendrite arm spacing and thermomechanical treatment effects on fracture behavior and mechanical properties of Al alloy, finding ultimate and yield strengths

23 p4176 A69-41506

Ni plated 40-cm lightweight Al alloy telescope mirror, noting weldment stress relief by annealing

23 p4164 A69-41624

Stress corrosion cracks propagation from fatigue precrack in Al alloy exposed to organic liquid environments

23 p4178 A69-42452

Notch effect on corrosion fatigue behavior of high strength Al alloy under bending and direct stresses

24 p4330 A69-42553

Al-Mn-V ternary system equilibrium diagram at various aluminum concentrations determined by magnetic and microhardness measurements, microstructural observations and X ray analysis

24 p4330 A69-42601

Seam welding processes and power supply effects on control efficacy based on electrode displacement for Al-Mg alloys

24 p4319 A69-42919

Cyclic stress tests of stainless steel fiber Al alloy matrix composite, including strain hardening and stiffness characteristics

24 p4331 A69-42925

ALUMINUM CHLORIDES

Outdoor aging effects on unstressed adhesive-bonded Al to Al lap shear joints
24 p4319 A69-42932

Porosity and inclusions effects on Al arc weld fatigue properties at ambient and cryogenic temperatures
24 p4331 A69-42940

Fracture and tensile properties of electron beam welded Al alloy for pressure vessels compared to tungsten arc welding results
24 p4319 A69-42941

Sonic riveting of aircraft Al alloys, noting no evidence of forging bursts, cracking, splitting, tearing and springback
24 p4320 A69-43060

Lap-shear strengths of Mg-Al alloy bonded with nylon-epoxy adhesive, including anodized coating rolling schedule and honeycomb core fabrication
24 p4323 A69-43417

Ti-Al alloy structure manufacturing technology covering forming, cleaning, chem-milling, machining, fastening and welding
24 p4324 A69-43431

ALUMINUM CHLORIDES

Conditions for obtaining concentrated Ti-containing melts free of Al and V chlorides by cementing with metallic Ti and Ti-containing materials
22 p3957 A69-40918

ALUMINUM COATINGS

Aluminum plastic sandwich products production costs compatibility with conventional materials
02 p0348 A69-12749

Aluminum coatings compared with cadmium coatings for aerospace fasteners, discussing plating methods
[ASM PAPER D8-5.2] 07 p1142 A69-19663

Semiconducting films as collector work function in thermionic converters, with regard to I-V characteristics
09 p1558 A69-21825

Metallographic analysis techniques for high aluminum activity pack cementation coating on nickel-base alloy
13 p2282 A69-28163

Dielectric overcoating effects on electromigration Al interconnections, showing dependence on thickness and surface passivation
17 p2935 A69-32889

Al interconnections discontinuities at integrated circuit contact windows observed by scanning electron microscope, noting catastrophic failure and Si presence
17 p2936 A69-32893

Hypervelocity micrometeor impact sites identification on aluminized glass, using conchoidal pattern as criterion in analysis
18 p3199 A69-34952

Beryllium wire reinforced Al composites, discussing layup techniques and coated filament advantages
19 p3340 A69-35508

Cleaning, deoxidizing and chromating process effects on chromate coated Al, using salt spray corrosion tests
19 p3321 A69-35570

Ion beam sputtering, evaporation and electrical degradation of Al contacted Si solar cells observed in high temperature cyclic tests
19 p3250 A69-35686

Al effect on B and Cr diffusion in protective coating on Cr-Ni heat resistant alloy, noting thermochemical kinetics for homogeneous layers
19 p3345 A69-36157

Surface alloying of high melting point metals in Al melts, noting prior oxidation enhancement and simplifying of calorizing techniques
19 p3328 A69-36158

Fabry-Perot interferometer with Al coating reflecting surface deposited on unbacked thin films
20 p3536 A69-36933

Aluminizing and operational effects on surface layer and core of first and second stage turbine blades
20 p3561 A69-37370

Large aperture Al alloy telescope mirrors consisting of Tenzalloy Al coated with Ni alloy, presenting performance data
20 p3546 A69-38193

Anodic Al oxide films mechanical and fracture properties, studying roles of environmental water vapor and film thickness
[ECS PAPER 81] 22 p3973 A69-40736

Aircraft fastener corrosion control with emphasis on surrounding joint and structure, discussing test programs, Al coatings, etc
24 p4334 A69-43442

ALUMINUM COMPOUNDS NT ALUMINATES

NT ANDESITE
NT BERYL
NT CORDIERITE
NT CRYOLITE
NT FELDSPARS
NT LITHIUM ALUMINUM HYDRIDES
NT MONTMORILLONITE
NT NEPHELINE
NT ORGANIC ALUMINUM COMPOUNDS
NT SAPPHIRE

Ferromagnetic ordering effect on gadolinium dialuminate thermoelectric power, measuring temperature dependence of power and electrical resistivity
03 p0485 A69-13322

Cross slip model for work hardening of nickel aluminate crystals, discussing temperature dependence
05 p0779 A69-15760

Composites reinforcement with single crystal flakes of aluminum diboride
05 p0785 A69-16581

Injection characteristics of n-aluminum gallium arsenides-p-GaAs heterojunctions from recombination radiation spectra
06 p0979 A69-16993

Niobium aluminide-niobium germanide alloys superconductivity and heat treatment influence on critical temperature
13 p2316 A69-27659

Structural formula of slowly cooled Mg and Al-Mg microwave ferrites, noting ion mobility during cooling
15 p2670 A69-31184

ALUMINUM NITRIDES

Vacuum deposition of thin film microwave acoustic transducers of piezoelectric aluminum nitride
05 p0761 A69-15820

Nitrogen solubility measured in liquid Fe-Cr-Ni-Al alloys, noting solubility increase with increasing Al content
06 p0942 A69-17228

Resistivity, capacitance and dielectric loss measurements for diode reactive sputtering grown AlN films and film sandwich structures of Ta, Au and Al films
13 p2322 A69-28013

ALUMINUM OXIDES

NT SAPPHIRE
Polycrystalline corundum thermal conductivity coefficients determination, describing measuring procedures at low temperatures
01 p0101 A69-10108

Pressure and temperature dependence of isotropic elastic moduli of polycrystalline alumina, noting Grueneisen parameter, equation of state and Debye temperature
02 p0268 A69-12407

Reflection indicatrices of aluminum oxide, MgO, Au and Pt surfaces for normal irradiation noting temperature and surface treatment effects
03 p0534 A69-14161

Tank collection and spectrophotometric tests in determining aluminum oxide particle size produced by small rocket engine
[AIAA PAPER 69-146] 06 p0984 A69-18117

Potential barrier curvature influence in aluminum trioxide tunnel junctions, noting ionic space-charge effect on shape
07 p1196 A69-18243

Anodizing effect on flexural properties of Al-aluminum oxide sandwich composites, emphasizing properties of oxide coatings as function of thickness
07 p1159 A69-18723

Band profiles and emission spectra of shock heated AlO compared for self absorption of blue-green system, discussing electronic transition moment
07 p1184 A69-19163

Fiber reinforced plastic and metallic composites for longevity and endurance of materials at high temperatures and extreme loads, discussing alumina whiskers
07 p1167 A69-19290

Metal bath surface conditions for floating aluminum trioxide inclusions in pure iron and carbon steels
07 p1167 A69-19342

Alumina radomes manufacture by flame spraying process, discussing raw materials quality control, spraying operation, sintering and final inspection
07 p1142 A69-19529

Alumina radomes fabrication and control techniques to assure reproducibility of electrical and mechanical properties, detailing finished product inspection methods
07 p1142 A69-19529

Arc driven shock tube with alumina ceramic liner to reduce driver gas contamination, noting shock speed and test time increase
[AIAA PAPER 68-366] 09 p1570 A69-21957

Silicated alumina attachment for high temperature radomes and leading surface heat shields, discussing radome concentration and load transfer
09 p1477 A69-22370

Micromin alumina substrates design data, determining dielectric constant, impedance vs line width and wavelength vs frequency
09 p1460 A69-22792

Electrolytic hydrogen evolution reaction on Al covered by thin oxide in aqueous buffered acetate solutions
11 p1832 A69-25674

Creep behavior of aluminum-alumina alloys analyzed using rupture time to determine deformation speed influence on elongation and crack formation
12 p2120 A69-26938

Three dimensional network of closely spaced oxide particles for Al strengthening investigated by transmission electron microscopy and tensile tests
13 p2276 A69-27371

Optical measurement method for burning surface temperature of condensed systems, realizing radiation from surface of combustion by light guide of monocrystalline aluminum oxide
13 p2379 A69-28453

Oxygen K-shell X ray production cross section and stopping power of aluminum oxide thin films for 20-100 kev protons
14 p2489 A69-29994

MOS devices for radiation environments utilizing aluminum oxide as gate insulator for developing resistance to radiation damage
15 p2577 A69-30595

Microfibrous boehmite as binder for molybdenum disulfide in formation of ductile water resistant dry lubricant films
[ASLE PAPER 68-LC-14] 15 p2642 A69-30606

Electrical resistivity of aluminum oxide films deposited on tubular substrates by plasma and gas flame spraying, noting dependence on film thickness and substrate
15 p2630 A69-31179

Alpha alumina whiskers grown by vapor reaction examined by X ray microtopography and etching
16 p2802 A69-32341

Neutron bombardment and ionizing radiation resistance of aluminum oxide MOS devices using gate insulator fabricated by plasma anodization
17 p2935 A69-32888

Aluminum oxide relative grain boundary energy and surface diffusion coefficient, considering thermal grooving of bicrystals with symmetrical tilt boundaries
17 p2993 A69-34191

Andalusite crystals as active media in paramagnetic quantum amplifiers, discussing design and performance
19 p3333 A69-35881

Radiative heat transfer in polycrystalline corundum, studying photon thermal conductivity influence on lattice thermal resistivity
20 p3565 A69-36975

Aluminum oxide droplets condensation from atmosphere of metal vapor and oxygen, studying temperature and time effects on particle nucleation, growth and distribution
21 p3783 A69-38799

Anodic Al oxide films mechanical and fracture properties, studying roles of environmental water vapor and film thickness
[ECS PAPER 81] 22 p3973 A69-40736

Liquid alumina particles agglomeration in convergent and throat region of nozzle leading to performance decrease by increasing velocity and temperature difference between phases
22 p4001 A69-40929

Silicate glass impurity droplet formations on alumina single crystals polished surfaces analyzed by electron microprobe as function of high temperature
23 p4176 A69-41597

Static and cyclic tensile fatigue of alumina by ring test method, measuring time to failure
24 p4334 A69-43343

ALUMINUM SILICATES

NT ANDESITE
NT MONTMORILLONITE

Quantum paramagnetic amplifier using andalusite single crystal and operating with three level pumping system
04 p0577 A69-14780

ALUMINUM 26

Accretion rate of cosmic dust estimation from cosmogenic aluminum-26
03 p0514 A69-13935

Cosmogenic Al 26 in achondrites and chondrites measured by nondestructive gamma-gamma coincidence counting
17 p3034 A69-33584

ALVEOLAR AIR
Sampled data regulator for maintenance of constant alveolar carbon dioxide during steady state and transient ventilatory responses to hypoxic stimulation
07 p1072 A69-19480
Digital computer program for determining aveolar and capillary blood gas compositions corresponding to ventilation-perfusion values, considering dissolved oxygen and inert gas exchange
22 p3875 A69-40230

ALVEOLI
Gas vacuoles development in blue green algae by cell transfer from defined medium to distilled water
10 p1644 A69-23184
Blood sheet flow velocity distribution and pressure gradients in pulmonary alveolar septa determined, allowing for system elasticity
22 p3874 A69-40216
Alveolar and pleural pressures affecting pulmonary interstitial pressure in anesthetized dogs, applying Starling law of transcapillary exchange
24 p4257 A69-42627

AMBIENT TEMPERATURE
Temperature field calculation in infinite plate with heat transfer coefficient and ambient temperature arbitrary functions of time
10 p1809 A69-23430
Combined hypoxic hypoxia and high ambient temperature found relieving strain on humans by increasing heat release by evaporation
13 p2212 A69-28628
Human sweat glands reflex responses to diverse skin cooling rates in hot room, discussing bath temperature step decrease effect on lower limb
23 p4082 A69-41446

AMBIGUITY
Ambiguity function interaction with target scattering function in range-Doppler radar, discussing matched filtering application
20 p3490 A69-37641

AMBIPOLAR DIFFUSION
Numerical solution for ambipolar diffusion and kinetic decomposition of rotating body of complex chemical composition in ionized airstream
02 p0191 A69-12580
Interstellar gas field dynamic instability, discussing enhanced ambipolar diffusion in twisted field
02 p0326 A69-12707
Ambipolar motion of light injected photocarriers in cadmium-mercury-telluride in terms of diffusion and drift in electric fields
06 p0979 A69-17154
Ambipolar diffusion in electron concentration inhomogeneities of weakly ionized plasma in magnetic field analyzed by linearized quasi-hydrodynamic equations
08 p1362 A69-20426
Ions and electrons in ionosphere diffusion tensor components and ambipolar diffusion coefficient expressions derived for nonisothermal plasma
12 p2071 A69-26700
Ion cloud ambipolar diffusion and motion dependence on initial configuration and close magnetic field alignment above 95 km, discussing observations of meteor trails
12 p2074 A69-26961
Mass transfer due to plasma recombination, ambipolar diffusion and electrode erosion and resistance forces effects on electrodynamic accelerated plasma
13 p2315 A69-28555
Steady state density profile dependence on electron density dependence of net volume ionization rate by analyzing ambipolar diffusion in RF excited magnetized plasmas
16 p2818 A69-31672
Surface type airborne electrostatic probes in ambipolar diffusion flux, measuring ion saturation current, discussing electrode contamination and temperature and ablation tests
17 p2974 A69-33443
Equilibrium Couette flow of ionized multicomponent ideal gas from moving catalytic plates, obtaining thermal flow formulas and thermal conductivity coefficient
19 p3240 A69-36403
Electron-ion gas ambipolar diffusion effect on F 2 layer electron density vertical distribution variations
20 p3525 A69-37655

AMBIT
U FIELD THEORY [PHYSICS]

AMBULANCES

Helicopter evacuation role in mortality rate among wounded in battle in Korea and Vietnam, discussing air ambulance unit organization
23 p4107 A69-41809

AMIDES

NT POLYIMIDES
NT UREAS
Enthalpies determination of adduct formation of sulfoxides, sulfanimides and thionylamides with trimethylalane, noting replacement effect on electron donating ability of oxygen
07 p1074 A69-18631
Reaction kinetics between hydrazine and esters in benzene solution at 55 C, using amides as catalytic agents
14 p2409 A69-29033

AMINES

NT AMPHETAMINES
NT CATECHOLAMINE
NT CYSTEAMINE
NT DIAMINES
NT HYDROXYLAMINE SULFATE
NT TETRAFLUOROHYDRAZINE
NT TETRYL
NT TRYPTAMINES
IR and Raman spectra of solid and matrix isolated methylamine and deuterium derivatives, locating amine twisting vibration in solid phase IR spectra
01 p0023 A69-10287
Amino alcohol regenerable absorbers of carbon dioxides toxicological characteristics, discussing absorbing ability in rats
10 p1646 A69-23502
Solvent effect in catalytic hydrogenation reaction of Schiff bases of alpha-keto acids with optically active alpha-alkylbenzylamine
12 p2026 A69-25779
Jet fuel quality improvement by adding isopropylotadecylamine and other substances because of surface-active and sorptive qualities
16 p2828 A69-31562
Electric quadrupole coupling for N 14 in aminedisulfonite studied by observation of second order transitions in electron spin resonance spectra
18 p3178 A69-35474
Relative gas phase acidities of simple aliphatic amines and ammonia noting increase in large alkyl groups substitution
19 p3265 A69-36293
Electron transport chain of monovalent and divalent cations and of polyamines, studying effects on menadione reductase activity to determine salt dependence
22 p3886 A69-41077

AMINO ACIDS

NT ADENINES
NT ADENOSINE TRIPHOSPHATE [ATP]
NT ALANINE
NT COENZYMES
NT CYSTEINE
NT GLUTAMIC ACID
NT GLYCINE
NT LEUCINE
NT LYSINE
NT METHIONINE
NT PEPTIDES
NT PYRIDINE NUCLEOTIDES
NT TRYPTOPHAN
NT URIDYLIC ACID
Tyrosine transaminase activity estimation by radioactive isotopic assay method, discussing application to rat liver and other organs
01 p0014 A69-10902
Photolysis of aliphatic amino acids by UV light in presence of salt ions forming ammonia, glyoxalic acid, acetaldehyde and formaldehyde
01 p0025 A69-11094
Hypoxia effect on animal brain gamma-aminobutyric acid levels
04 p0552 A69-14482
Amino acid composition of organic matrix in modern and fossil calcareous oolites
04 p0553 A69-14978
Thermal reaction kinetics of pyrolytic products of proline, leucine, arginine and lysine in aqueous solution
05 p0716 A69-15627
Amino acid biosynthesis control in microorganisms by end product/feedback/ inhibition of enzyme action
06 p0876 A69-18238
Reagent menthyl chloroformate use in optical analysis of asymmetric amino and hydroxyl compounds by gas chromatography
07 p1075 A69-19499

Solvent effect in catalytic hydrogenation reaction of Schiff bases of alpha-keto acids with optically active alpha-alkylbenzylamine
12 p2026 A69-25779
Gas-liquid chromatography of natural protein amino acids in biological substances, noting separation characteristics
13 p2217 A69-28258
Quantitative gas-liquid chromatography of sulfur amino acids trimethylsilyl derivatives
13 p2217 A69-28259
Organosilicon-containing derivatives of 2-aminoethanethiols and 2-aminoethanethiosulphuric acids as radiation protective agents
13 p2210 A69-28486
Mice convulsions at varying hyperbaric oxygen pressures and carbon dioxide content correlated with decreasing brain alpha aminobutyric acid levels
19 p3257 A69-35972
Cations of sulphates photosensitizing role in photolysis of amino acids and peptides in various atmospheres
20 p3477 A69-37626
ESR comparative study of selenoamino acids and S analog radical formation and radiation resistance, noting selenium groups ability as acceptors for unpaired electrons
21 p3668 A69-38425
Amino acid components in paleozoic plant fossils and rock samples noting glycine, serine and glutamic acid
21 p3662 A69-39535
Adenylates condensation in protein-associated amino acids as clue to peptide bond synthesis within protocellular structures
22 p3895 A69-40048
NonDarwinian evolution of protein and DNA, comparing expectations of evolution models for protein and amino acid changes
22 p3871 A69-40060
Scenedesmus ferredoxin amino acid sequence
22 p3896 A69-40435
Cell origin in self organizing natural polymers in terms of molecular evolutionary priority of polynucleotides and poly alpha amino acids
22 p3896 A69-40781
DNA interaction with ribosomes enhancing amino acid incorporation into cell-free protein synthesizing system extracted from *Chlorella pyrenoidosa*
23 p4080 A69-41430
Tension effects on amino acid incorporation rate into proteins of cross-striated muscles of rats
23 p4083 A69-41458
Transesterification of amino acid peptide alkyl and fatty acid esters by treatment with anion-exchange resin
24 p4280 A69-43513

AMMONIA
NT LIQUID AMMONIA
Ammonia gas molecules in interstellar medium, discussing detection in direction of galactic center by means of microwave emission
03 p0518 A69-14258
Charge exchange cross sections in methane and ammonia, noting dissociative charge exchange role
06 p0884 A69-17114
Shock tube study of ammonia oxidation at high temperature, detecting molecular species in reaction zone by IR emission
06 p0885 A69-17936
Further microwave emission lines and ammonia clouds in Sagittarius region, tabulating relevant transitions in ammonia and water
09 p1597 A69-22150
Laser emission lines produced by pulsed electrical discharge through ammonia
10 p1704 A69-23666
IR absorptance data for atmospheres of ammonia and ammonia nitrogen mixtures at various wavelengths indicating absorption in strong line region for gas pressures used
12 p2132 A69-26247
Ammonia gas diffusion from line source in turbulent boundary layer, discussing concentration profile discrepancy due to eddy diffusivity and plume shear
13 p2250 A69-28343
Jupiter photochemistry above 1000 A, noting methane and ammonia photolysis zones, atmospheric pressures and hydrogen recombinations
17 p3032 A69-33165
Relative gas phase acidities of simple aliphatic amines and ammonia noting increase in large alkyl groups substitution
19 p3265 A69-36293

Ammonia inversion radiation in Sgr B2 region, observing distribution of density, velocity and rotational excitation

21 p3799 A69-38647

Turbulent premixed ammonia-air flame stabilization on flameholders, discussing secondary oxygen injection into circulation zone at blowoff limits

21 p3849 A69-38808

Ammonia addition effect on laminar flame speeds of propane-air mixtures

21 p3849 A69-38809

Ammonia resistojet thruster, describing ammonia physicochemical properties and systems characteristics of pulsed mode operation and continuous thrust resistojets

23 p4203 A69-41931

Chlorella enzymes activity in reducing nitrate to nitrite and nitrite to ammonia

24 p4263 A69-43136

AMMONIUM CHLORIDES

Polymethyl methacrylate burning rates in mixture with ammonium perchlorate or in hybrid systems when mixed with ammonium chloride

13 p2324 A69-28503

AMMONIUM COMPOUNDS

NT HYDROXYLAMMONIUM PERCHLORATES

Ammonium chlorate thermal decomposition by measuring formed noncondensable gas pressure and weight loss in solid state kinetic investigation

21 p3669 A69-38800

Polycrystalline ammonium cyanide IR absorption spectrum as function of temperature, discussing ammonium ion hydrogen bonding to C or N atoms

24 p4280 A69-43809

AMMONIUM NITRATES

Chromium oxide additions effects on reaction rates decrease during ammonium perchlorate and nitrate combustion

08 p1375 A69-20340

Ammonium nitrate thermal decomposition activation by dyes and halides, noting endothermic and exothermic reactions, proposing models to study impurities role

17 p3016 A69-32830

AMMONIUM PERCHLORATES

Ammonium perchlorate base propellant and polyurethane binder heat stability, dangers of aging under abnormal conditions and reaction products for components and tolylene diisocyanate

02 p0303 A69-11529

Thermal decomposition of ammonium perchlorate and ammonium perchlorate-copper chromite mixtures

02 p0304 A69-12312

Detonation capacity of mixture of ammonium perchlorate base and polymethyl methacrylate and polystyrene, noting critical particle size dependence on composition

02 p0305 A69-12674

Ammonium perchlorate thermal decomposition, studying point defects role

03 p0494 A69-12896

Rocket engine combustion mechanism of ammonium perchlorate composite propellants

03 p0532 A69-13002

Burning rate of composite propellant with gamma irradiated ammonium perchlorate, noting enhancement at atmospheric pressure

04 p0647 A69-15519

Unstable combustion of ammonium perchlorate/AP, discussing correlation between propellant particle diameter and frequency in burning rate

06 p1036 A69-18063

Ammonium perchlorate high temperature decomposition by using carbon dioxide laser pyrolysis/mass spectrometry

06 p0885 A69-18111

Ammonium perchlorate exothermic decomposition control noting effects of preheating and ammonium fluoroborate additives

07 p1202 A69-18363

Catalytic effect of potassium bichromate and chromic oxide additives on burning of ammonium perchlorate and mixtures

08 p1375 A69-19997

Aluminum effect on ammonium perchlorate/polyformaldehyde mixtures combustion properties noting heat transfer decrease into k phase

08 p1375 A69-20338

Ammonium perchlorate decomposition kinetics at high temperatures by measuring loss of weight in samples and gas evolution

08 p1375 A69-20339

Chromium oxide additions effects on reaction rates decrease during ammonium perchlorate and nitrate combustion

08 p1375 A69-20340

Vanadium pentoxide addition effect on combustion rates of mixtures of ammonium perchlorate and metallic fuels in nitrogen atmosphere

08 p1375 A69-20342

Pure ammonium perchlorate single crystal self deflagration, determining energy transfer mechanisms from pressure effects, combustion characteristics and subsurface profile

[AIAA PAPER 69-142] 09 p1560 A69-21900

Shock initiation and sensitivity of granular explosives, noting heterogeneity effect in ammonium perchlorate

10 p1751 A69-23016

Sublimation in ammonium perchlorate propellants combustion, discussing low temperature isothermal processes, linear regression rates measurements and low ambient pressure

11 p1940 A69-24481

Infinite diameter detonation velocity vs loading density curve for ammonium perchlorate, finding quadratic mean error

11 p1940 A69-24486

Critical diameter of ammonium perchlorate stable detonation as function of initial temperature, water content, density and particle size

11 p1940 A69-24553

Ionizing radiation effects on combustion of ammonium perchlorate compacts with and without fuel addition, considering X ray, electron and plasma radiation

11 p1941 A69-25194

Component ratio effect on pressure dependence of burning rate in ammonium and potassium perchlorate mixed with organic compounds, graphite and tungsten

12 p2027 A69-24744

Limiting pressure for deflagration related to initial solid temperature of single crystals and pressed pellets of ammonium perchlorate

13 p2324 A69-27364

Polyester/ammonium perchlorate combustion, determining degradation rate by loss in weight method at different intervals

13 p2324 A69-28234

Polymethyl methacrylate burning rates in mixture with ammonium perchlorate or in hybrid systems when mixed with ammonium chloride

13 p2324 A69-28503

Compressed ammonium perchlorate combustion rate and pressure requirements established from initial temperature effects

14 p2508 A69-28914

Solid rocket motor propellant burning rate increased by adding special fine ammonium perchlorate/SEAP/ to optimize particle size distribution

[AIAA PAPER 69-519] 16 p2793 A69-31850

Combustion bomb testing of propellants containing fluorocarbon binder and ammonium perchlorate, noting unique ignition, combustion and extinction properties

[WSCI PAPER 69-9] 16 p2831 A69-32349

Linear pyrolysis of thermoplastics during combustion of composite solid propellants and ammonium perchlorate solid propellant deflagration mechanism studied by loose granule analog

[WSCI PAPER 69-16] 16 p2831 A69-32354

Point defect structure to control ammonium perchlorate burning rate, discussing thermal analysis data correlations, isothermal decomposition, etc

[WSCI PAPER 69-17] 16 p2831 A69-32355

Doped recrystallized ammonium perchlorate effects on composite propellant burning rates

[WSCI PAPER 69-18] 16 p2831 A69-32356

Granular ammonium perchlorate thermal decomposition analyzed by cinematography, discussing sublimation role

[WSCI PAPER 69-20] 16 p2832 A69-32358

Ammonium perchlorate sublimation models, discussing low temperature decomposition influence on pressure dependence of sublimation rate

[WSCI PAPER 69-22] 16 p2832 A69-32360

Ammonium perchlorate pyrolysis by convective surface heating, monitoring IR emission as measure of surface temperature

[WSCI PAPER 69-23] 16 p2832 A69-32361

Ammonium and magnesium perchlorate mixture thermal stability study with differential scanning calorimetry, noting exothermic decomposition of AP

[AIAA PAPER 69-500] 16 p2833 A69-32661

Ammonium perchlorate grinding and blending facility, discussing process flow, machinery, etc

[AIAA PAPER 69-516] 16 p2767 A69-32664

Premature exothermic decomposition suppression in propellant grade ammonium perchlorate, using differential thermal analysis

[AIAA PAPER 69-503] 16 p2833 A69-32688

Compositional and oxidizer particle size effects on combustion instability of plastic propellant based on ammonium perchlorate and polyisobutene

[AIAA PAPER 69-478] 16 p2834 A69-32734

Decomposition of ammonium perchlorate containing additives introduced by spray drying

[AIAA PAPER 69-502] 16 p2834 A69-32752

Ammonium perchlorate linear pyrolysis by convective surface heating, discussing propellant deflagration models

[AIAA PAPER 69-501] 16 p2835 A69-32758

ELDO/PAS rocket motor for satellite launching from elliptic orbit apogee to synchronous orbit powered by ammonium perchlorate with organic binder and Al

17 p3022 A69-33604

Ammonium perchlorate melting point estimate taking into account theory of corresponding states encompassing two sets of experimental independent data

20 p3585 A69-37217

Ammonium perchlorate experimental heat capacity data significance for rotational freedom of ammonium ion

20 p3484 A69-37344

Proton transfer mechanism of copper chromite catalyzed thermal decomposition of ammonium perchlorate, noting electron transfer

21 p3783 A69-38810

Shock front reaction and detonation initiation in low density ammonium perchlorate

21 p3784 A69-39590

Ammonium perchlorate decomposition, discussing high and low temperature reactions, combustion, catalysts and gaseous environment effects

21 p3784 A69-39593

AMMONIUM PHOSPHATES

Electrooptical ADP modulator design for use with helium-neon laser, considering temperature stability and crystal faces parallelism

13 p2272 A69-28191

AMORPHOUS MATERIALS

Semiconductor devices development based on amorphous materials, reviewing solid state physics implications

23 p4198 A69-41560

AMORPHOUSNESS

U CRYSTALLINITY

AMPERAGE

U ELECTRIC CURRENT

AMPHETAMINES

Antimotion sickness drugs tested in slow rotation room with controlled Coriolis accelerations, noting summation effect of dextroamphetamine sulfate and scopolamine hydrobromide

03 p0381 A69-14079

D-amphetamine effect on single tectal neurons activity of cat optium recorded by steel microelectrodes before and after intravenous injection

23 p4084 A69-41466

AMPHIBIA

U FROGS

AMPHIBIOUS AIRCRAFT

Maritime and aeronautical engineering - Conference, Paris, May 1968

08 p1255 A69-20652

Helicopter seaworthiness, comparing full scale sea landing and flotation studies with model test results

08 p1255 A69-20653

HRV-1 navy research pusher amphibian aircraft, discussing hydrofoils and operational problems

10 p1633 A69-23223

AMPHIBIOUS VEHICLES

NT CAPTURED AIR BUBBLE VEHICLES

Semi-amphibious Vosper VT 1 hovercraft for passengers and cars, discussing design, water contact propulsion, peripheral skirt, supercavitating propellers, structure, performance, etc

04 p0549 A69-15187

Mountbatten class hovercraft for truly amphibious craft

06 p0867 A69-17664

U.S. policy for commercial surface effects ships regulation, discussing operational, construction and design requirements

08 p1254 A69-20199

AMPLIFICATION

NT POWER GAIN

NT SOUND AMPLIFICATION

Amplification process for VLF whistler mode radio signals observed in study of magnetosphere frequency shifting mechanism

01 p0077 A69-11241

Impedance and gain approximation in transistor configurations, noting gyrator circuit

02 p0213 A69-11532

Regenerative amplification stability in nonretarded wave helitron and traveling wave mitron type devices

02 p0214 A69-11610

Optimal adaptive control of discrete linear systems with unknown gain, considering Gaussian distribution functions and random disturbances

02 p0224 A69-11962

Gain and radiation pattern of conical horn excited by circular waveguide, using geometric theory of diffraction

02 p0218 A69-12327

Gain factor of offset-fed paraboloidal reflector as function of angular aperture and offset angle, noting phase error effects

02 p0218 A69-12329

Simultaneous measurement of gain and noise of linear two port device using noise generators as signal sources

02 p0210 A69-12430

Frequency and time dependent gains of dye solution lasers for pumping by lasers and flashlamps

02 p0257 A69-12616

Logarithmic variation criteria for stability of feedback systems with time varying gains

03 p0409 A69-13073

Traveling wave tube segmentation, analyzing effects of drift, grouping and selecting sections on efficiency and amplification

03 p0407 A69-13985

Emission amplification coefficients of gas laser using pure carbon dioxide, carbon dioxide/air mixtures and carbon dioxide/air/helium mixtures

04 p0611 A69-14426

Stimulated emission of cyanine dyes, discussing amplification coefficients

04 p0612 A69-15373

Adaptation in nonstationary environment formulated for tapped delay line filters with adjustable time varying gains

05 p0737 A69-15806

Pc 1 micropulsation and magnetospheric amplification of hydromagnetic waves

05 p0754 A69-16263

Double diffused Si transistors, discussing temperature dependence of gain, injection efficiency, emitter and base regions energy gaps and excess noise

05 p0733 A69-16558

Critical electron drift velocity threshold in surface wave amplification in semiconductor in magnetic field, noting partial effect of diffusion

05 p0810 A69-16648

He-Ne laser gain dependence on temperature noting influence of pumping conditions, discharge tube filling and geometry

06 p0934 A69-17260

Synthesized aperture method of measuring antenna gain and radiation patterns

06 p0894 A69-17452

Nonsaturated gain of laser radiation in gas discharge in carbon dioxide with N and He

07 p1151 A69-19060

Pulse generation in Q switched traveling wave laser, noting effect of field amplification [IEEE PAPER Q-5]

07 p1154 A69-19077

Amplification curve change of active substance due to saturation by self field of He-Ar laser, discussing axial operation modes instability

08 p1323 A69-19942

Large aperture satellite communication antenna gain measurement technique, using extraterrestrial radio wave source or satellite

09 p1456 A69-22116

Superdirective aerial endfire array of four unequally spaced half wave dipoles and only one fed element, calculating and measuring maximum gain

09 p1468 A69-22603

Telemetry data channel gain and phase correction with frequency response calibration technique using digital filtering

10 p1654 A69-23291

Atmospheric turbulence effect on linear antenna gain in direction of radiation pattern maximum determined together with antenna dimensions

11 p1844 A69-24435

Temperature effect on amplification factor of box type dynode system of photoelectron multipliers made of alloy AMGK, using single electron method

11 p1846 A69-24626

Regenerative amplification stability in nonretarded wave helitron and traveling wave mitron type devices

11 p1847 A69-24717

Planar transistor gain degradation under weak ionizing radiation, considering operating voltage and temperature conditions

11 p1848 A69-24874

Gain decrease due to saturation during amplification of pulses from Q switched carbon dioxide laser oscillator, noting rotational sublevels relaxation rate

11 p1899 A69-25055

Synchrotron radiation amplification by monoenergetic electron stream helically gyrating in static magnetic field of cold plasma, discussing amplification rate frequency dependence

11 p1931 A69-25361

Upconverter with gain and stabilized frequency, using sideband locking of IMPATT diode oscillator

12 p2036 A69-25909

Tracking system for gain and time delay parameter measurements of compensatory control crossover model

12 p2022 A69-25930

Statistical gain characteristics of radar antennas at very short Fresnel zone ranges compared to Fraunhofer zone

12 p2040 A69-26470

Collector supply voltage and base width effects on transistor amplification and frequency characteristics at microampere currents

12 p2042 A69-26879

Statistical linearization of strong nonlinearity in series with random-gain amplifier element, deriving formulas for statistical gain parameters

14 p2425 A69-28920

Threshold signal gain estimated in Glaser frequency filter self adaptation process during transformation from square law summator into matched filter

15 p2576 A69-30344

Stimulated emission of cyanine dyes, discussing amplification coefficients

16 p2797 A69-32120

Pulse height distributions, gain and counting rate characteristics of two magnetic strip multipliers and two channel multipliers in 1.5 to 44 A region of soft solar X-rays

17 p2972 A69-33082

Automatic radar station for meteor observations, discussing separate transmitting and receiving antennas directive gain and radio echo power

17 p2939 A69-33902

Electrostatically focused klystron /EFSK/ small signal gain calculations based on lens cell space charge wave analysis

18 p3109 A69-35294

Gallium arsenide junction lasers operating above threshold, showing resonant modes dependence of steady state gain function and frequency dependence of spatial gain distribution

19 p3338 A69-36691

Amplification stability region in overexcited regenerative traveling wave amplifier with respect to parasitic emission buildup

20 p3506 A69-37724

Synthesized aperture method of measuring antenna gain and radiation patterns

20 p3508 A69-37937

Amplification saturation in spatially inhomogeneous laser field, relating power to active medium and resonator parameters

21 p3740 A69-39549

Gain modification from spectral splitting of optical transition by incident light wave on higher frequency coupled transition

22 p3965 A69-41125

Carbon dioxide laser amplifier operation, showing photon-induced current changes dependence on amplifier gain

23 p4172 A69-41398

Weak magnetic field amplification in turbulent flow with velocity field as random function of space and time

24 p4375 A69-42657

Small signal amplitude/frequency response or transfer gain of volume-terminated pneumatic lines with circular and rectangular cross sections

24 p4301 A69-43288

AMPLIFIER DESIGN

Amplifier with logarithmic transfer function noting use as null detector

01 p0038 A69-10075

Monolithic sense amplifier for laminated-ferrite memories including provision for strobing, detecting, pulse forming and internal inversion logic using thermal feedback control

01 p0039 A69-10174

Microwave amplifier design with hybrid integrated circuits of thin film lumped elements, noting gain and efficiency of transistor circuits

01 p0039 A69-10190

Hybrid integrated parametric amplifier design considerations for fabrication in microstrip transmission line

01 p0040 A69-10193

Microwave transistor amplifier computerized design, discussing wide bandwidth and flat in-band gain response optimization on high dielectric substrates

01 p0040 A69-10194

Transistor distributed amplifier theory, noting effect of collector line and base line delay difference on gain and transient responses

01 p0041 A69-10203

Voltage tunable magnetron used in conjunction with ferrite circulator as phase locked amplifier

01 p0045 A69-10632

Signal to cross modulation noise ratio in TWT tube during amplification of sinusoidal signals

01 p0031 A69-10780

Transient process in n stage nonlinear amplifiers analyzed on basis of structural circuit

01 p0047 A69-10781

Punch-through microwave negative resistance diode explained and contrasted with similar Read and Shockley structures

02 p0215 A69-11938

Curved wall fluid amplifier performance under high or low supply pressure

02 p0196 A69-12083

RF feedback amplifier analytical design, deriving open and closed loop feedback noise figure expressions by use of equivalent noise model

02 p0217 A69-12150

Liquid helium cooled broadband parametric amplifier, discussing circuits and noise performance

02 p0221 A69-12458

CW klystron amplifiers design limitations at Ku and Ka bands, discussing operation characteristics

03 p0405 A69-13724

Low noise broadband parametric amplifier for communication satellite ground stations

03 p0406 A69-13733

Linear analysis of operation of multistage magnetron amplifiers using injected electron flux and stepwise varying dimensions of interaction space

03 p0407 A69-13977

Output power, efficiency and gain of two stage magnetron-type cascade amplifier

03 p0407 A69-13978

Transistorized two stage amplifiers with common feedback operating under steady conditions and for short times

04 p0575 A69-14466

258 GHz reflection amplifier with saturated gas resonance, analyzing amplification variation with gas pressure, pumping power, frequency, Q values and cavity tuning

04 p0557 A69-14754

Stability limits of regenerative echo amplifier during simultaneous variation of network capacitance and negative resistance

04 p0577 A69-14778

Servosystems components design, discussing detector, corrector, amplifier and motor

04 p0550 A69-15181

Reading amplifier for thin magnetic film memory stores permitting tunnel diode register positioning

04 p0579 A69-15319

Performance characteristics of variable geometry bistable fluid amplifiers [ASME PAPER 68-WA/FE-18]

05 p0748 A69-16094

Circuit with tunnel diodes and transistors for nonlinear amplification, noting current-voltage characteristics dependence on circuit parameters

05 p0730 A69-16221

Frequency and power stable backward wave oscillators as energy pumps for molecular and wideband parametric amplifiers used in satellite receivers

07 p1095 A69-18430

Design of coupled cavity extended interaction output resonators for klystron amplifiers

07 p1095 A69-18431

Double gap catchers for klystron amplifiers and oscillators

07 p1095 A69-18432

UHF high power klystron for DESY synchrotron, discussing design, short circuited load operation, phase variations and optimum RF outputs
07 p1096 A69-18434

Helium cooled low noise high gain parametric preamplifier for satellite communication by stagger tuning stages
07 p1098 A69-18460

Helium closed cycle cooled very low noise high gain parametric amplifier for investigating interstellar atomic hydrogen radiation
07 p1098 A69-18461

Helium cooled low noise high gain wideband parametric amplifier for spacecraft communication
07 p1099 A69-18462

Wideband uncooled two stage reflecting parametric amplifiers with low noise temperature, noting application to space stations for telecommunications by satellites
07 p1099 A69-18463

Tunnel diode amplifiers for amplifying weak microwave signals, discussing low noise wideband preamplifier for communication satellites
07 p1099 A69-18464

Precision monolithic circuits fabrication techniques, describing differential amplifier design incorporating emitter feedback and direct DC errors compensation
07 p1102 A69-18875

Monolithic operational amplifier design combining junction FET with n-p-n transistor
07 p1103 A69-18876

Multistage amplifier design with frequency compensation by eliminating stages in HF region
07 p1103 A69-18877

Monolithic planar process to fabricate DC coupled amplifiers having less than nanosecond risetime
07 p1103 A69-18878

Integrated four transistor bridge network used for self neutralized active element in tuned RLC amplifier design
07 p1103 A69-18884

Direct coupled monolithic IF amplifier with active gain control, analyzing large signal response, stability, available gain and noise behavior
07 p1104 A69-18885

Lithium niobate based parametric image converter for IR to visible operation, discussing design factors performance calculations
[IEEE PAPER B-3] 07 p1150 A69-19048

Miniature power amplifier stage for telemetry transmitters, discussing equipment size and weight reduction methods and hermetic envelope
07 p1106 A69-19115

Design criteria for pneumatic servo controls with fluidic elements stressing final transient, pilot circuits and amplifier elements
08 p1256 A69-20305

Flapper-nozzle type electrohydraulic amplifier design with emphasis on elements and subsystems
08 p1256 A69-20459

Noise properties of junction diodes and bipolar transistors as basis for low noise amplifiers design
08 p1286 A69-20839

Cascaded avalanche diodes in negative resistance amplifying mode for increased output power and extended dynamic range
09 p1462 A69-21408

Transistorized amplifier stage noise factor dependence on parameters and modes of operation of transistors
09 p1463 A69-21724

Multichannel microwave amplifier at L band frequencies, using several amplifiers in parallel
09 p1466 A69-22446

Discontinuous vortex power amplifier and diode design, noting supply regulator effects and load matching
09 p1443 A69-22737

Vortex amplifiers design and performance, noting nonvented and vented amplifiers and fluid valving applications
09 p1443 A69-22741

Signal to cross modulation noise ratio in TWT tube during amplification of sinusoidal signals
10 p1653 A69-23109

Transient process in n stage nonlinear amplifiers analyzed on basis of structural circuit
10 p1661 A69-23110

Signal conditioning amplifiers covering carrier and DC amplifiers, differential amplifiers, charge amplifiers and active filters
10 p1691 A69-23230

Fluidic jet beam deflection amplifier, discussing basic principles, operating characteristics and design criteria
10 p1638 A69-23554

High gain proportional and bistable fluidic amplifier design, noting high impedance role in pressure sensing and computer circuits in aircraft engine control
10 p1638 A69-23555

Parametric amplifying systems with lumped reactive nonlinear elements, emphasizing UHF systems
11 p1844 A69-24448

Thin film lumped passive elements for microwave power amplifier integrated circuits, discussing distributed reactances, element size and fabrication, etc
11 p1856 A69-25654

P-n-p planar epitaxial germanium microwave transistor used as amplifier in 1-4 GHz range and as high speed switch, summarizing design, fabrication and characterization
12 p2037 A69-25940

Bandwidth potential increase of parametric amplifier obtained by adding active filter elements to signal circuit, noting satellite communication band
12 p2039 A69-26380

Transistorized LF-HF RC filters and current amplifiers design, exhibiting polynomial type characteristics
12 p2040 A69-26488

Traveling wave tube for European communication satellite power amplifiers, showing nonlinear distortions dependence on RF input/output power and helix voltage
[AIAA PAPER 68-430] 12 p2041 A69-26786

Negative resistance parametric amplifier used as tracking filter, noting resonant frequency dependence on pumping frequency and input and idler circuits
13 p2225 A69-27183

Integrated S-band parametric amplifier design, combining low noise performance at room temperature with broadband flat gain and linear phase response
13 p2230 A69-27678

Two stage tunnel diode amplifier synthesis with gain stabilization circuit widening passband, discussing operating frequency and maximally flat amplitude frequency response
13 p2236 A69-28575

L-band parametric amplifier operated in liquid N for noise reduction, discussing measurement circuit for gain, bandwidth and noise figure
13 p2237 A69-28644

High gain broadband amplifiers with triple tuned coaxial resonators and gridded power tubes, discussing phase stability
14 p2418 A69-28892

Negative resistance amplifier with stabilizing resistor in compensating circuit for operation in microwave duct mismatched beyond amplifier passband range
15 p2573 A69-30118

Bulk negative resistance material stability, discussing amplifier skin effect limitation and instability beyond critical length
15 p2575 A69-30172

Automatic frequency control of laser and regenerative amplifier, considering frequency stability
15 p2633 A69-30238

Resonant fixtures used for mechanical amplification of vibrator output to desired test levels
15 p2588 A69-30404

Wideband tunnel diode amplifier design, discussing implementation to out-of-band circulator characteristics and VSWR suppression
15 p2578 A69-30804

Linear fluid amplifier with beam-deflection proportional active element, discussing optimum maximally flat frequency response
15 p2553 A69-31299

Fluidic operational amplifier design and applications
15 p2554 A69-31300

Fluidic digital position sensor consisting of fluidic monostable amplifier, analyzing operation by characteristics method
15 p2554 A69-31301

Servosystems' components design, discussing detector, corrector, amplifier and motor
16 p2741 A69-32431

Wideband selective amplifier design methods proposed by Martini and Schiaffino
16 p2761 A69-32442

Four terminal silicon planar p-n-p-n model operating as semiconductor small signal linear tetrode amplifier, discussing properties and mathematical models
18 p3109 A69-35293

Book on field effect and bipolar junction transistors and microcircuits, covering ideal and practical amplifiers, circuit characteristics, etc
20 p3505 A69-37147

One kw HF ground grid wideband untuned power amplifier in transformer coupled cascade stages
20 p3488 A69-37286

Transistorized amplifier stage noise factor dependence on parameters and modes of operation of transistors
20 p3505 A69-37460

Charge amplifier for piezoelectric transducer used in acceleration measurements
20 p3508 A69-37913

Fluidic direct impact modulator design, studying effects of pressure levels and nozzle geometries
[ASME PAPER 69-FLCS-38] 20 p3465 A69-37983

Proportional fluid jet amplifier with flat saturation characteristics, describing gain, differential output pressures and noise levels
[ASME PAPER 69-FLCS-21] 20 p3466 A69-37985

Solid state SHF transmission amplifiers design using rectangular waveguides and biased bulk GaAs
21 p3683 A69-39452

Thermal design of power amplifier for airborne HF transceiver, discussing component layout, air cooling and materials
22 p3909 A69-39942

Two loop resonant amplifiers design, considering mismatched, matched and optimally matched regimes
22 p3912 A69-40258

Carbon dioxide laser development, discussing gain, static amplifier and high pressure operations
22 p3962 A69-40474

Fluidic amplifiers development and logic applications, describing various elements and circuits
22 p3870 A69-41239

Design of vortex fluid amplifiers operating in incompressible flow regime, based on fluid properties and geometry effects on amplifier behavior
24 p4256 A69-43299

AMPLIFIERS

NT BEAM PLASMA AMPLIFIERS
NT BROADBAND AMPLIFIERS
NT CARCINOTRONS
NT CROSSED FIELD AMPLIFIERS
NT CURRENT AMPLIFIERS
NT DIFFERENTIAL AMPLIFIERS
NT DISTRIBUTED AMPLIFIERS
NT FEEDBACK AMPLIFIERS
NT FLUID AMPLIFIERS
NT INTERMEDIATE FREQUENCY AMPLIFIERS
NT JET AMPLIFIERS
NT LIGHT AMPLIFIERS
NT LIMITER AMPLIFIERS
NT MICROWAVE AMPLIFIERS
NT PARAMETRIC AMPLIFIERS
NT PHOTOMULTIPLIER TUBES
NT POWER AMPLIFIERS
NT PREAMPLIFIERS
NT PUSH-PULL AMPLIFIERS
NT SERVOAMPLIFIERS
NT TRANSISTOR AMPLIFIERS
NT TRAVELING WAVE AMPLIFIERS
NT VOLTAGE AMPLIFIERS

Amplifying channel processes of DC amplifier, discussing relations to couple channel with HF channels of operational operators and to synthesize amplifier frequency characteristics
01 p0053 A69-10802

Electromagnetic wave propagation and amplification in periodic structures, including travel wave and parametric amplifiers, reactance diodes, lasers and quantum amplification
03 p0396 A69-13701

Reflections from input and output ducts influence on gain of TWT strophotron amplifier with/without allowance for back radiation
03 p0407 A69-13980

Current mode amplifier circuit used with carbon resistors for measuring low flow rates of liquid hydrogen from small containers
04 p0577 A69-15025

Resonant amplifier response having stages identical to radio pulse with exponential envelope
05 p0720 A69-16444

Automatic phase control and transient processes in resonant amplifier in presence of phase discontinuities of input signal
05 p0721 A69-16533

Si IMPATT diode oscillator and amplifier for CW operation at 50 GHz noting fabrication, performance and phase locking properties
05 p0733 A69-16560

Noise measure formula for negative resistance amplifiers imbedded in lossy passive network
05 p0735 A69-16731

Frequency dependence of input impedance of voltage controlled bootstrap amplifier stages
07 p1090 A69-18294

Oscillators and amplifiers based on intervalley electron transfer in bulk GaAs
07 p1096 A69-18442

Tunnel diode amplifier operation in presence of noise
09 p1469 A69-22630

DC conversion amplifier commutation induced noise and signal ratio as function of shunt capacitance across vibrator load investigated for increased noise stability
11 p1845 A69-24555

Small signal, HF equivalent circuit for intrinsic metal oxide semiconductor field effect transistor, considering nonpinchoff and pinchoff modes
13 p2238 A69-28429

VHF surface acoustoelectric amplifier investigated in DC drift field using composite spatially adjacent structure of lithium niobate and silicon film
14 p2422 A69-29559

Equivalent circuits of dielectric loaded and unloaded rectangular waveguide Esaki diode reflection amplifier
15 p2578 A69-30801

Electronic-ultrasonic amplifiers with external electron stream and longitudinal or surface wave studied for damping influence, deriving dispersion equation
16 p2761 A69-32061

Automatic phase control and transient processes in resonant amplifier in presence of phase discontinuities of input signal
16 p2753 A69-32474

Resonant amplifier response having stages identical to radio pulse with exponential envelope
16 p2753 A69-32476

Amplifier working in conjunction with solid state phase sensitive detector replacing existing commutator in Dobson ozone spectrophotometer
16 p2792 A69-32641

Carrier frequency monitoring amplifier with automatic bridge tuning for coupling to passive sensors including strain gages, inductive transmitters, etc
22 p3915 A69-40937

Frequency and phase instability characteristics of negative resistance amplifier due to changes in circuit parameters
22 p3916 A69-40962

AMPLITRONS [TRADEMARK]
U PLANOTRONS

AMPLITUDE DISTRIBUTION ANALYSIS

Critical parameters for optimum design of Cassegrain antenna used in space communications
[UN PAPER 68-95280] 01 p0043 A69-10481

Reliability of binary message in Gaussian noise impaired by amplitude limiting in case of evaluation by integration
01 p0031 A69-10736

Phase and amplitude variation at output of tuned amplifier, noting graphs and formulas
01 p0047 A69-10786

Amplitude-frequency characteristics of rotor mounted on hydrostatic bearings calculated by equations of dynamic compliance method
03 p0432 A69-12961

Atmospheric noise amplitude distribution relation to rms phase errors in frequency components of VLF timing pulse
03 p0396 A69-13629

Atmospheric fine structure studied by amplitude distribution and autocorrelation functions for different heights of scatter volume in microwave range
04 p0628 A69-15306

Difference radiation patterns of circular aperture with axisymmetric amplitude distribution
05 p0717 A69-15636

Statistical theory of traveling wave antennas for random phase-amplitude distribution of current, discussing phase errors
06 p0898 A69-17797

Natural amplitude and phase fluctuations of originally monochromatic oscillations at output of regenerative frequency divider with thermal and shot noise
07 p1099 A69-18526

Reflected radio wave amplitude distributions related to distributions of curvature at reflector
07 p1086 A69-19225

Recursive method for estimating number, amplitudes and time delays of signals overlapping in time and in presence of additive white Gaussian noise
08 p1270 A69-19854

Atmospheric radio noise at 27 kc measured at European stations, showing field strength variations, latitude dependence and amplitude distribution
09 p1491 A69-22163

Microwave antennas optical simulation, discussing given phase amplitude distribution problems
09 p1469 A69-22625

Phase and amplitude variation at output of tuned amplifier, noting graphs and formulas
10 p1662 A69-23115

Dual reflector antenna design methods for obtaining necessary phase and amplitude illumination across secondary aperture in low noise applications
11 p1852 A69-25316

Angle of arrival in amplitude comparison monopulse radars in presence of internally generated thermal noise
13 p2220 A69-27942

Antenna system synthesis for amplitude distribution along linear emitter, considering radiation patterns
13 p2235 A69-28521

Large amplitude pulsations in magnetic field magnitude and proton fluxes observed by satellite during magnetic storm compared with various models
14 p2434 A69-28947

Amplitude and frequency spectra for Ipc pulsations during geomagnetic storms
14 p2441 A69-29417

Log amplitude fluctuations of laser beam in turbulent atmosphere, obtaining asymptotic expressions for near field of transmitter aperture
14 p2460 A69-29638

Log amplitude variance calculation methods compared in statistics of optical scintillation by application to measurements with laser
14 p2486 A69-29642

Logarithmic amplifiers amplitude characteristics accuracy obtained by gain variations or successive summation of voltages, plotting curves illustrating error variations vs gain
15 p2574 A69-30128

Waveform amplitude variation of phase modulation pulses affected by band limitation
15 p2569 A69-30803

Wave reflection in laser resonators with ferrite end faces, determining oscillation spectra and wave amplitudes
15 p2579 A69-30954

Amplitude distribution and correlation functions of signals reflected from precipitations at various polarizations of waves emitted and received
16 p2807 A69-32269

Gaussian amplitude distribution of 1/f noise by oscilloscope display and scanning with movable slit
16 p2752 A69-32383

Difference radiation patterns of circular aperture with axisymmetric amplitude distribution
16 p2754 A69-32494

Whistlers propagation in cold plasma in uniform magnetic field, considering amplitude dispersion effect
18 p3179 A69-34437

Modified pulse height analyzer /PHA/ for sample amplitude height occurrence frequency measurements obtaining amplitude probability distribution /APD/ and three moments of atmospheric noise
18 p3102 A69-34960

Amplitude and intensity distributions of plane periodic Fresnel diffraction grating calculated by Fraunhofer theory, noting applicability to spectrometric and meteorological instruments
19 p3372 A69-35906

Electron beam pumped semiconductor laser light beam amplitude and phase distribution, studying effects of inhomogeneous excitation by model
21 p3737 A69-39041

Satellite scintillating signals amplitude distribution, correlating observations and theoretical results
23 p4115 A69-41486

Cophase antenna aperture with shaded central region, considering sidelobe radiation reduction by varying field amplitude distribution
23 p4138 A69-41939

Dielectric materials permittivity determined by measuring amplitude ratios of reflected and transmitted plane electromagnetic waves
23 p4123 A69-41950

AMPLITUDE MODULATION

Amplitude modulation factors expressed as carrier and sideband power for sinusoid and square wave signals, considering negative clipping by modulator cut-off
01 p0028 A69-10419

Optimal reception methods noise stability for AM radio signals based on nonlinear filtration of information parameters of signals received on noise background
01 p0030 A69-10589

Optimal AM radio reception in presence of fluctuating noise and one AM interference signal with random initial phase of carrier oscillation
01 p0031 A69-10782

Zero memory frequency independent nonlinearities response to modulated input noting FM limiter, band-pass limiter and AC carrier control systems
01 p0034 A69-11142

Solar and galactic cosmic rays measurement data to investigate variation in time of relations between cosmic rays modulation amplitude and solar activity variations
02 p0306 A69-11658

Superposition of discrete number of collinear amplitude modulated harmonic oscillations
02 p0281 A69-12252

AM and FM noise in mutually synchronized oscillators
02 p0220 A69-12449

Microwave measurements of AM and FM noise spectra with video frequency and RF coverage flexibility and high sensitivity
02 p0221 A69-12455

Amplitude noise spectra of X band microwave oscillators with Si avalanche diodes, noting various contributions and dependence on circuit and operating parameters
02 p0221 A69-12456

AM/PM noise conversion in solid state FM microwave signal sources, relating baseband noise power contribution to PM baseband noise power
02 p0212 A69-12462

Phase input power characteristics of TWT, TDA and parametric amplifiers, noting crosstalk calculations and AM-PM conversion coefficients
04 p0573 A69-14336

Reflected radar signal random fluctuations suppressed by using antenna, receiving channels and logarithmic amplifiers
04 p0556 A69-14490

Single band millimeter wave amplitude modulator for phase meters with homodyne frequency conversion
04 p0577 A69-14850

Nonlinear demodulation of amplitude modulated wave propagating in plasma
04 p0559 A69-15210

Microwave generator of FM oscillations using two reflex klystrons and modified by wideband regenerative amplifier to minimize intrinsic AM
05 p0736 A69-16791

External and internal modulation methods in lasers noting phase, amplitude and frequency modulation, birefringence, electrooptics and Stark and Zeeman effects
06 p0937 A69-18010

Nonlinear computer analysis of TWT small amplitude compression and small AM to PM conversion, noting coupling and circuit breaker effects
07 p1094 A69-18422

Tape flutter and additive noise time base errors in coherent demodulation of suppressed carrier AM multiplex
07 p1082 A69-19119

Cross modulation of amplitude modulated wave propagating in nonlinear dispersive plasma, obtaining electric vector
07 p1086 A69-19228

Amplitude modulation of radiation pulses of two level paramagnetic maser as affected by inhomogeneous broadening and spinning of resonance line
07 p1158 A69-19751

Radio signal from magnetron transmitter, noting slow amplitude phase fluctuations distribution according to log-normal law
08 p1275 A69-20424

Noise power ratio at output of wideband amplifier with angle modulated multicarrier input, obtaining intermodulation products from Bessel functions expansion
08 p1285 A69-20595

Ionospheric scattered radio wave field amplitude and phase variations assessed for diffraction at regular phase screen
09 p1453 A69-21526

Thermal effects on modulation sensitivity and inherent AM percentage as functions of modulation frequency in IMPATT oscillators
09 p1468 A69-22588

Intrinsic amplitude and frequency fluctuations in transistor autooscillator, examining natural additive noise influence
09 p1469 A69-22632

Envelope shock waves transitions between modulated wave amplitude and frequency in dispersive medium with relaxing nonlinearity
09 p1483 A69-22660

Optimal reception methods noise stability for AM radio signals based on nonlinear filtration of information parameters of signals received on noise background
10 p1653 A69-23104

Optimal AM radio reception in presence of fluctuating noise and one AM interference signal with random initial phase of carrier oscillation
10 p1653 A69-23111

Analytic expressions for predicted widths of AM and FM mode locked pulses in homogeneous lasers
13 p2270 A69-27191

Signal strength of two beam interferometers with laser illumination, considering modulation depth of interference pattern
13 p2259 A69-27450

Solar and galactic cosmic rays measurement data used to investigate variation in time of relations between cosmic rays modulation amplitude and solar activity variations
13 p2333 A69-28689

Power spectrum analysis and linear filtering for 27 day variation amplitude of geomagnetic disturbance subject to semiannual amplitude modulation
14 p2434 A69-28955

Amplitude modulator with field effect tetrode transistor (FETT), discussing linear mode operation of modulator circuit
14 p2420 A69-29459

Amplitude modulation of electromagnetic waves by modulated magnetic fields for communications through rocket exhausts and reentry plasma sheaths during blackout
14 p2417 A69-29591

Noise parameters at output of logarithmic detector separating two AM signals with overlapping spectra
15 p2564 A69-30148

AM sinusoidal current pulse generator for semiconductor lasers, describing solid state circuit
15 p2633 A69-30235

Single band millimeter wave amplitude modulator for phase meters with homodyne frequency conversion
15 p2575 A69-30242

Spectral correlation characteristics of amplitude modulated signal with background noise at envelope detector output
15 p2576 A69-30348

General autocorrelation function for input signal composed of two amplitude modulated noise waves and background noise from detecting system composed of half wave element
15 p2569 A69-30805

Ionospheric scattered radio wave field amplitude and phase variations assessed for diffraction at regular phase screen
16 p2754 A69-32521

Oscillator without reactive components for integrated circuit biotelemetry, noting transmission in AM broadcast band
19 p3261 A69-36244

Baseband automatic gain control in AM/FM systems, determining time constant and steady state and tracking error
19 p3274 A69-36276

Receiving circuit for AM signal envelope separation in presence of AM interference and fluctuation noise, using converter cascades to effect input signal frequency spectrum symmetry
19 p3277 A69-36568

Phase and amplitude stabilization during phase modulated discrete data transmission
19 p3277 A69-36571

Array aperture amplitude and phase distortions effect on radiation field uniformity
23 p4138 A69-41940

AMPLITUDES

NT PULSE AMPLITUDE

NT SCATTERING AMPLITUDE

Quasi-sinusoidal tunnel diode oscillator studied for frequency and amplitude of harmonic voltage components
01 p0038 A69-10070

Vibrational characteristics of sonar transducer analyzed by optical holographic interferometry
04 p0598 A69-14871

Limiting amplitude of output shaft vibrations of servodrive operated in linear region as function of frequency
04 p0584 A69-15417

Blade oscillations in cascade flow of axial turbomachinery calculated as function of pitch ratio, stagger angle, angle of attack and camber
05 p0837 A69-16069

Amplitude fluctuations and line width of traveling wave and standing wave He-Ne laser, considering saturation effects
10 p1701 A69-23135

Qualitative analysis of recording phase only acoustic holograms of object wave instead of both phase and amplitude, considering fringe patterns and conjugate image
10 p1695 A69-23548

Phase and amplitude changes of arbitrary-Q self excited oscillator under external disturbance, using differential equations
13 p2300 A69-28574

Vortex breakdown in rotating fluids associated with wave motion along axis of rotation, considering effects of nonzero wave amplitude
17 p2892 A69-33478

Amplitude ratio measurement for two AC signals of given relative phase shift and same frequency
17 p2975 A69-33615

AN-24 AIRCRAFT

Book on soviet An-24 aircraft-construction and exploitation covering fuselage, powerplant, controls, fire prevention, air conditioning, maintenance, etc
16 p2735 A69-32112

ANABAENA

Blue green alga Anabaena flos-aquae A-37 growth limitation by absence of K or Na from culture medium
23 p4079 A69-41386

Electrodialysis method for depleting positive Na, K, Ca and Mg ions from Anabaena flos-aquae A-37, noting algae survival rate
23 p4079 A69-41387

ANAEROBES

B Coli commune cultivated on various substrates, studying oxygen consumption under aerobic/ anaerobic conditions
18 p3097 A69-35302

Anaerobic adhesives for aircraft bonding tested for mechanical properties, noting advantages over epoxy adhesives
24 p4338 A69-43464

ANALOG CIRCUITS

Mechanization of analog electrical-to-fluidic transducer using carrier circuit techniques and piezoelectric bender drive assembly
24 p4315 A69-43026

ANALOG COMPUTERS

Combustion chamber equation for liquid fuel rocket engine, considering time varying ignition lag
01 p0142 A69-10090

Semiautomatic computer for determining torsional oscillation natural frequency in multimass in-line systems
01 p0035 A69-10596

Flight simulator based on analog computer simulating six linearized equations of motion and aircraft model, discussing design and applications
01 p0057 A69-11300

Zener diode function generators used in analog computers for solution of complex problems involving nonlinear relationship
02 p0214 A69-11595

Hybrid computers, discussing analog and digital devices combination and distinction between use of computer for general purpose computation and control purposes
02 p0212 A69-11997

Vertical contact analog display (VCAD) design, emphasizing need for integrated and supplementary information to pilots in systematic way
03 p0379 A69-13361

Nonlinear system on-line identification in presence of noise, using stochastic methods and analog equipment
03 p0401 A69-13764

Baird-Hitchcock iterative method analog computer simulation by steepest descent
05 p0723 A69-15933

Semidiscrete approximate solution by analog computer of inverse problem of transient heat conduction [ASME PAPER 68-WA/HT-26]
05 p0848 A69-16127

Pontryagin maximum principle used to solve optimal control problems on analog computer
05 p0739 A69-16473

Analog to digital converter parameters, considering selection of conversion technique
05 p0726 A69-16760

Analog-hybrid computer configurations for average and rms values of signals with respect to time
06 p0891 A69-17220

Analog computer modeling of human systemic arterial tree, based on lump parameter circuit approximation
07 p1072 A69-19727

Single purpose analog computer with analog and hybrid elements for calculating Nyquist diagrams for feedback circuits
08 p1278 A69-20397

Analog study of periodic permanent magnet focusing, considering ray equation, beam radius dependence on distance, amplitude variations, etc
08 p1285 A69-20555

Analog video processor in omnidirectional radar system for flight safety, discussing construction, transistorization and circuitry
08 p1276 A69-20605

Vector analog computer functions and applications in air traffic control, discussing area navigation equipped aircraft
08 p1349 A69-21195

Analog multiplier with controlled current splitting devices and feedback technique for stabilization of transfer characteristics, noting implementation in bipolar transistor
09 p1475 A69-22584

Automatic plotting devices for graphic readouts in analog and digital computers
12 p2091 A69-26303

Digital differential analyzer as control element, analyzing performance limitations imposed by scaling constraints with canonical realization of transfer functions
12 p2053 A69-26509

Linear two dimensional partial differential equations solved by Laplace transforms on analog computer
12 p2123 A69-26717

Resonance circuit application to harmonic analysis of periodic functions on analog computer, considering transient period and sequential order
12 p2123 A69-26718

Dynamic multistable analog integrator capable of prolonged retention of integration, giving differential equation of device
13 p2224 A69-27427

Error analysis involved in calculating tangent functions defined by nonlinear differential equation solution, using digital differential analyzer
13 p2225 A69-27968

Computer model for avalanche transit time diode oscillator with single and double resonant circuit
15 p2577 A69-30615

Time delay errors compensation methods in analog-digital computation loops, finding digital scheme inferior to analog
15 p2572 A69-30618

Cantilever beam profile optimization methods using iterative analog computation to achieve minimum deflection, showing application of Pontryagin maximum principle
15 p2709 A69-30671

Universal transfer function computer based on synchronous spectrum analyzer having outputs combined in cross spectrum correlation computer to yield plot in Bode form
15 p2615 A69-31282

Analog computer for design of control systems used in nonnuclear testing of nuclear rocket engine components and subsystems
15 p2589 A69-31289

Automated patching system design for analog and hybrid computers to reduce number of switches required
16 p2756 A69-32551

Planar distributed function generator for analog computing scheme, considering operation, cosine circuit and temperature error
17 p2934 A69-34123

Automated analog scaling for in hybrid computer systems imposing magnitude and frequency constraints, using equations for amplifier input factors
18 p3105 A69-34617

Numerical methods using analog computer in linear one dimensional transient heat conduction
18 p3229 A69-34835

Navigational equations solution by airborne analog computer techniques, describing electronic, electromechanical, digital reset and mechanical integrations with respect to time
18 p3107 A69-34847

Analog device to compute running ten minute average and store latest ten minute peak of unipolar data input for wind speed sensors
19 p3312 A69-36278

HF direction finder for display of time varying multimode propagation phenomena, using analog computer and phase sensitive interferometer
21 p3677 A69-39456

Steady state digital-analog integrator for solving nonlinear heat conduction type equations
21 p3680 A69-39852

ANALOG DATA

Hybrid digital transmission systems, discussing joint optimization of analog and digital repeaters and information rate of coaxial cable systems
01 p0027 A69-10248

Quantizing noise effect on reconstructed analog signal at reception terminal of digital data transmission system
01 p0027 A69-10250

Analog to digital converter parameters, considering selection of conversion technique
05 p0726 A69-16760

Joint filter optimization in combination analog-digital hybrid multilevel transmission system
09 p1457 A69-22465

Magnetic tape recorder/reproducer for FM analog test data
10 p1691 A69-23233

Vortex amplifier as active element in analog circuits
10 p1639 A69-23556

Analog signal transmission through randomly fading channels, proposing pseudorandom phase reversals method for slowly varying multipath communication channels
11 p1834 A69-24552

Optimum recording conditions for analog recorders with continuous recording in rectangular coordinate system
12 p2091 A69-26332

Analog correlator performance interpreted as output SNR dependence on input signals and integrating system characteristics, covering filters and finite time integrators
14 p2413 A69-29485

Analog signal processing concepts based on models simulating mechanical function of ear cochlea
17 p2911 A69-34092

Analog telemetry signals generalizing frequency and pulse position modulations over coherent channels, noting added degrees of freedom function
20 p3492 A69-37713

Numerical and analog data acquisition system /CARINA/ for processing rocket, balloon and satellite data, describing distributor characteristics, control console, etc
20 p3511 A69-37914

Noiseless feedback schemes for digital and analog transmission over additive white Gaussian noise channels
21 p3671 A69-38405

Integrated adaptive data transmission system accepting analog inputs through information compressing sampler or digital inputs by sampling
23 p4121 A69-41760

Analog feedback system for digital data transmission, describing feedback channel, error rate and SNR effects
24 p4289 A69-42977

ANALOG SIMULATION

Efficiency curve for step recovery diode frequency multipliers, using analog computer simulation
02 p0215 A69-11947

Equalization of multiple electromagnetic shakers for environmental vibration testing, using analog computer [JPL-TR-32-1364]
02 p0229 A69-12374

Difference schemes for heat conduction analog simulation on electric integrators
03 p0410 A69-13300

Analog sampled data simulator using field effect transistors and single value of holding capacitor for covering sample frequency variation
03 p0405 A69-13600

Simulation of flight dynamic equations of motion for fixed wing aircraft, using variable analog computer with gimbaled and servocontrolled aircraft model
04 p0585 A69-14829

Engineering solution for integrodifferential equations of physical systems with electronic circuits
05 p0724 A69-16468

Mathematical model simulation of structures using building block approach
05 p0842 A69-16471

Analog simulation of water hammer type phenomena governed by linear constant coefficient partial differential equations
05 p0751 A69-16475

Error and noise sources in analog differentiators, discussing signal distortion minimization techniques and augmentation with linear phase filter
06 p0897 A69-17702

Analog simulation of chemically reacting system applied to thermal decomposition of oxygen difluoride [WSCI PAPER 68-49]
07 p1073 A69-18318

Hydraulic analog for determining acoustic behavior of baffle cell used in liquid rocket engines, comparing ring and spoke type baffles
09 p1570 A69-22004

Mathematical model, analog computer simulation and information comparison of closed Brayton cycle systems for power conversion [ASME PAPER 69-GT-50]
09 p1442 A69-22479

Bilinear hysteretic system undergoing random vibration, substantiating linearization analysis with analog computer simulation and comparing lifetime to linear system [ASME PAPER 69-VIBR-25]
10 p1806 A69-24173

Analog simulation of cylinder wake potential for hypersonic motion in collisionless plasma
11 p1926 A69-24756

Canonical transformations of unsteady control system motion equations, simplifying control process study and controller simulation on analog computer
12 p2045 A69-25960

Monograph on physicochemical principles of takeoff monitoring systems for large aircraft covering taxiing, safety control systems design, analog simulation, etc
12 p2128 A69-26119

Analog simulation of nonlinear functions of single independent variable compared digital to analog representation principles
13 p2224 A69-27531

Minimum vibration frequency and compressive force for freely supported rectangular, triangular and circular plates simulated on analog computer
15 p2708 A69-30665

Linear pyrolysis of thermoplastics during combustion of composite solid propellants and ammonium perchlorate solid propellant deflagration mechanism studied by loose granule analog [WSCI PAPER 69-16]
16 p2831 A69-32354

Numerical integration of Eole satellite attitude equations compared with results obtained by analog simulation or hybrid computation
17 p3048 A69-33232

Spinning satellite attitude perturbations due to oscillating mass in satellite rigid frame, discussing analytical approach and analog simulation results
20 p3618 A69-37912

Robot command and control by computer assembly, describing engineering analog of vertebrate nervous system
21 p3679 A69-39603

Computer assisted electrocardiography, discussing multidipole analog simulation of heart electrical activity and vectorcardiogram recording
23 p4105 A69-41784

Nerve and muscle tissues subthreshold reactions on analog model, discussing transient characteristics under various excitations
23 p4109 A69-41980

Human thermal regulatory mechanism using analog simulation compared with experimental results of resting subjects responses to climatic chamber
23 p4111 A69-42079

ANALOG TO DIGITAL CONVERTERS

Microwave carrier graycode analog to digital converter capable of 1200 megabits per second
01 p0044 A69-10627

Pneumatic analog to digital and digital to analog converters, noting diaphragm force balance capsules, converters using stepping motors and factors affecting accuracy [ASME PAPER 68-WA/AUT-16]
05 p0706 A69-16176

Computer programs and analysis methods for digitalization of continuous feedback network in missile control systems
05 p0725 A69-16470

Analog to digital converter parameters, considering selection of conversion technique
05 p0726 A69-16760

X ray proportional counter, analog to digital converter and power supply for gamma ray spectrometry used in satellite applications [IEEE PAPER 3A-7]
07 p1134 A69-19194

Delta modulation for analog to PCM encoding due to tapped binary shift register and up-down counter
09 p1455 A69-21844

Analog to digital conversion for data sampling systems including scanning, distributors, multiplexing, automatic ranging, noise reduction and data storage techniques
10 p1660 A69-23232

Optimum microcircuit analog to digital converter for aerospace environment by combining monolithic circuits and thin film resistors
10 p1636 A69-23282

High speed ten-bit analog to digital converter with medium scale integration (MSI) elements, considering conversion accuracy and time
11 p1845 A69-24520

Time-pulse function generator with piecewise parabolic approximation for converting value given by DC voltage or time interval into DC voltage for arbitrary functional relation
12 p2079 A69-25968

Digital method to produce radar reflectivity from analog audio frequency Doppler data extracted from terrain echo signal of CW scatterometer radar
15 p2572 A69-31111

Analog to digital conversion, describing successive approximation technique with built-in sample and hold and discrete analog amplitude modification
17 p2934 A69-34124

Integrated circuit ultrahigh speed analog to digital converter, considering interactions at high digital rates and video bandwidths
17 p2943 A69-34125

High speed analog to digital multiple channel wide-band data acquisition system designed for short pulse Doppler radar and probe measurements
19 p3307 A69-35745

Nonlinear encoding for picture transmission using nonlinear analog to digital converter
23 p4119 A69-41747

ANALOGIES

NT HYDRAULIC ANALOGIES

Jet line in rotational incompressible plane flows around shrouded propeller blade, using electrical analog
01 p0058 A69-10037

Electrohydrodynamic analogies to known MHD effects studied by differential equations for hydrodynamic and electric field energy relations
01 p0131 A69-10775

Hydrodynamics-electrodynamics analogies for electromagnetic flight
01 p0121 A69-11134

Lifting wing profiles in uniform transonic compressible fluid flow calculated by analog method, noting hodograph method simplification
02 p0187 A69-11536

Electrical analogs with passive elements in combination with stepping switches for simulation of plants with distributed parameters
09 p1471 A69-21436

Transient heat flow in isotropic solids by electrical analog modeling in orthogonal curvilinear coordinate system
09 p1477 A69-22241

Analogy between differential equations for skew isotropic plates and rectangular anisotropic plates
13 p2371 A69-28678

Linear passive electrical analog model of human systemic arterial tree, discussing artery segment modeling, vessels input impedance, wave travel, etc
17 p2908 A69-33007

Solid propellant motor extinction by depressurization, determining extinction conditions by electrical analogy
17 p3021 A69-33355

Side force problem for shallow helicoidal shell, shown as static geometric analog of pure bending problem, solved by applying analogy [ASME PAPER 69-APM-11]
18 p3213 A69-34387

Solid propellant motor extinction by depressurization, determining extinction conditions by electrical analogy [ONERA-TP-722]
18 p3184 A69-34637

Analog method for determining structural creep displacement by setting up boundaries for linear elasticity and perfect plasticity
20 p3628 A69-37915

Temperature-vorticity analogy for viscous two dimensional fluid flow extended to compressible flows, noting enthalpy and shear stress analogy
22 p3929 A69-39892

Coherent light focusing by helicoidal guide- extension to particle focusing, discussing analogy between index distribution for classical optics and potential distribution for electronic optics

22 p3981 A69-40475

Linear electrical analogs for two dimensional optical data processing systems, discussing diffraction field model, quadratic phase filters, thin lenses, photographic film applications, etc

24 p4286 A69-42619

ANALOGS

Mean seasonal atmospheric and synoptic circulation types examined by criterion for identifying analog types

13 p2295 A69-28652

Finite difference analogs with increasing error terms applied to simple differential Laplace operator for accuracy determination

19 p3365 A69-36510

Atmospheric predictability as revealed by naturally occurring analogs, noting superposed error

20 p3573 A69-38057

Analog problem solution for semiinfinite medium with Newtonian cooling at boundary, noting first term of asymptotic expansion in heat conduction equation

22 p4052 A69-41126

ANALYSIS [MATHEMATICS]

NT AIRY FUNCTION
NT ANALYTIC FUNCTIONS
NT APERIODIC FUNCTIONS
NT ASYMPTOTES
NT ASYMPTOTIC SERIES
NT BANACH SPACE
NT BESSEL FUNCTIONS
NT BIHARMONIC EQUATIONS
NT BINARY INTEGRATION
NT BLASIUS EQUATION
NT BOREL SETS
NT BURGER EQUATION
NT CALCULUS OF VARIATIONS
NT COLLINEARITY
NT COMPLEX VARIABLES
NT CONFORMAL MAPPING
NT CONJUGATES
NT CONTINUITY [MATHEMATICS]
NT CONVOLUTION INTEGRALS
NT COPLANARITY
NT CUBIC EQUATIONS
NT CURL [VECTORS]
NT DELTA FUNCTION
NT DEPENDENT VARIABLES
NT DIFFERENTIAL CALCULUS
NT DIFFERENTIAL EQUATIONS
NT DUFFING DIFFERENTIAL EQUATION
NT EINSTEIN EQUATIONS
NT ELLIPTIC DIFFERENTIAL EQUATIONS
NT ELLIPTIC FUNCTIONS
NT ENTIRE FUNCTIONS
NT EXISTENCE THEOREMS
NT EXPONENTIAL FUNCTIONS
NT EXTREMUM VALUES
NT FALKNER-SKAN EQUATION
NT FOKKER-PLANCK EQUATION
NT FOURIER ANALYSIS
NT FOURIER SERIES
NT FOURIER TRANSFORMATION
NT FREDHOLM EQUATIONS
NT FUNCTION SPACE
NT FUNCTIONAL ANALYSIS
NT FUNCTIONAL INTEGRATION
NT GAMMA FUNCTION
NT GAUSS EQUATION
NT GREEN FUNCTION
NT HALF PLANES
NT HALF SPACES
NT HANKEL FUNCTIONS
NT HARMONIC ANALYSIS
NT HARMONIC FUNCTIONS
NT HELMHOLTZ VORTICITY EQUATION
NT HILBERT SPACE
NT HILBERT TRANSFORMATION
NT HILL DETERMINANT
NT HYPERBOLIC FUNCTIONS
NT HYPERGEOMETRIC FUNCTIONS
NT HYPERPLANES
NT INTEGRAL CALCULUS
NT INTEGRAL EQUATIONS
NT INTEGRAL TRANSFORMATIONS
NT JACOBI INTEGRAL
NT JACOBI MATRIX METHOD
NT KERNEL FUNCTIONS
NT LAME WAVE EQUATIONS
NT LAPLACE TRANSFORMATION
NT LEGENDRE FUNCTIONS
NT LIAPUNOV FUNCTIONS
NT LIMITS [MATHEMATICS]
NT LINEAR EQUATIONS
NT LIOUVILLE EQUATIONS
NT LIPSCHITZ CONDITION
NT LOGARITHMS
NT MATHIEU FUNCTION

NT MEASURE AND INTEGRATION
NT MINIMA
NT NEUMANN PROBLEM
NT NONHOLONOMIC EQUATIONS
NT NONLINEAR EQUATIONS
NT NUMERICAL INTEGRATION
NT ORTHOGONAL FUNCTIONS
NT PADE APPROXIMATION
NT PARABOLIC DIFFERENTIAL EQUATIONS
NT PARTIAL DIFFERENTIAL EQUATIONS
NT PERIODIC FUNCTIONS
NT PHASE-SPACE INTEGRAL
NT POISSON EQUATION
NT POWER SERIES
NT QUADRATIC EQUATIONS
NT RATIONAL FUNCTIONS
NT REAL VARIABLES
NT RUNGE-KUTTA METHOD
NT SERIES [MATHEMATICS]
NT SINE SERIES
NT SINGULAR INTEGRAL EQUATIONS
NT SINGULARITY [MATHEMATICS]
NT SPHERICAL HARMONICS
NT STIELTJES INTEGRAL
NT STURM-LIOUVILLE THEORY
NT TANGENTS
NT TAYLOR SERIES
NT TESSERAL HARMONICS
NT TRIGONOMETRIC FUNCTIONS
NT VECTOR ANALYSIS
NT VLASOV EQUATIONS
NT VOLTERRA EQUATIONS
NT VORTICITY
NT WEIGHTING FUNCTIONS
NT WHITTAKER FUNCTIONS
NT WIENER HOPF EQUATIONS
NT ZONAL HARMONICS

Collection of Soviet papers on mathematical physics
11 p1916 A69-24770

Boltzmann H theorem and related mathematical topics, noting applications to subsonic gas flow and continuum flow around and over body

11 p1870 A69-25008

Stability of stationary motion, analyzing gyroscopically unstabilizable systems and extension to continuous spectrum case

11 p1919 A69-25437

Pattern recognition and analysis, discussing definitions, rules of image transformation, pure and deformed patterns, etc

14 p2470 A69-29360

Exact analytic solution for thermal conductance of two dimensional eccentric constriction in dimensionless numbers

18 p3228 A69-34375

Analytical relations in phenomenological model theories for turbulent flow near wall

21 p3695 A69-39010

Mathematical analysis of dendrite design of solid propellant grains for variant of modified wagon wheel design

22 p3997 A69-40553

ANALYTIC FUNCTIONS

NT ENTIRE FUNCTIONS

Eigenvalue problem for Laplace operator for two dimensional region with boundary composed of piecewise-analytic simple closed curves solved by finite difference method

02 p0271 A69-11650

Equilibrium problem of elastic medium with stress couples in linearized elasticity theory, representing biharmonic function with aid of analytical functions

02 p0340 A69-12035

One to one mappings of Fourier series of analytic almost periodic functions and Dirichlet series, discussing satisfaction of functional equation

05 p0786 A69-15882

Circle theorem extensions and applications to mechanics of continua, noting supersonic and subsonic compressible fluid flow

10 p1723 A69-22877

Sommerfeld type and Fermi type approximation analytical solutions of Thomas-Fermi differential equations for positive ions

10 p1726 A69-23525

Convergence of zeta function for flows and diffeomorphisms

10 p1720 A69-23639

Theory for approximation of analytic functions given on closed spaces with piecewise smooth boundaries

12 p2120 A69-26198

Analytic continuation of Appell hypergeometric series into linear combination of four infinite series

12 p2123 A69-26605

Quasi-L-analytic functions for ordinary linear operator L

13 p2290 A69-28484

Integral representation of p-analytic functions of complex variable, applying axisymmetric boundary value problems of elasticity theory for cylindrical surfaces and paraboloid of revolution

15 p2714 A69-31191

Nonlinear differential equations of mechanical systems with restoring forces approximated by odd power displacement functions and energy dissipation approximated by displacement and velocity functions

17 p3007 A69-33914

Reduction of partitioned submatrices functions for expediting calculations of hypercirculant and hyperhyper Jacobi analytic functions

18 p3163 A69-34330

Analytic functions representation and application to theory of singular integral equations in continuum mechanics, noting Cauchy kernels and boundary value problems

19 p3361 A69-36813

Solution procedure for torus with given surface loads or displacements, using series expansion of generalized analytical functions, discussing stress concentration near toroidal cavity

21 p3839 A69-39192

Inequalities for coefficients of univalent functions

22 p3975 A69-40453

Iterative integration method of numerical quadrature over finite interval for analytic function, taking into account simple nonanalytic singularities in integrand

24 p4341 A69-43229

ANALYTIC GEOMETRY

U CYCLOIDS
U ELLIPSES
U HYPERBOLAS
U LOCI
U MERCATOR PROJECTION
U OBLATE SPHEROIDS
U PARABOLAS
U PROLATE SPHEROIDS
U S CURVES
U SPHEROIDS
U TANGENTS
U TORUSES
U TRIGONOMETRY

ANALYZERS

NT ENGINE ANALYZERS
NT SIGNAL ANALYZERS

HF inductive analyzer of concentrations of electrically conducting solutions and nonconducting mixtures

05 p0763 A69-15994

Spherical, cylindrical and toroidal electrostatic analyzers with symmetrical angular characteristics for solar wind investigations

19 p3396 A69-36632

ANALYZING

U FAILURE ANALYSIS

ANATASE

South African octahedrite containing inclusions of troilite and graphite veined with kamacite

03 p0507 A69-13097

Shock histories of hexahedrites and Ga-Ge group III octahedrites based on metallographic and X ray diffraction analysis, noting meteorites shocked preterrestrially

19 p3418 A69-36136

ANATOMY

NT ADRENAL GLAND
NT AORTA
NT ARTERIES
NT BLADDER
NT BLOOD VESSELS
NT BONES
NT BRAIN
NT BRAIN STEM
NT CAPILLARIES [ANATOMY]
NT CARDIAC AURICLES
NT CARDIAC VENTRICLES
NT CARDIOVASCULAR SYSTEM
NT CARTILAGE
NT CEREBELLUM
NT CEREBRAL CORTEX
NT CEREBRUM
NT CHEMORECEPTORS
NT CHOROID MEMBRANES
NT CIRCULATORY SYSTEM
NT COCHLEA
NT COLLAGENS
NT CORNEA
NT CORTI ORGAN
NT CRANIUM
NT DIASTOLE
NT EAR
NT ERYTHROCYTES
NT ESOPHAGUS
NT EYE [ANATOMY]
NT FOREARM
NT FOVEA
NT GRAVIRECEPTORS

NT HAND [ANATOMY]
 NT HEAD [ANATOMY]
 NT HEART
 NT HIPPOCAMPUS
 NT HUMAN BODY
 NT KIDNEYS
 NT LABYRINTH
 NT LEG [ANATOMY]
 NT LEUKOCYTES
 NT LIMBS [ANATOMY]
 NT LIVER
 NT LUNGS
 NT LYMPHOCYTES
 NT MARROW
 NT MIDDLE EAR
 NT MUSCULOSKELETAL SYSTEM
 NT MYOCARDIUM
 NT OCCIPITAL LOBES
 NT OCULOMOTOR NERVES
 NT ORGANS
 NT OTOLITH ORGANS
 NT PHOTORECEPTORS
 NT PINEAL GLAND
 NT PITUITARY GLAND
 NT RESPIRATORY SYSTEM
 NT RETINA
 NT SCIATIC REGION
 NT SEMICIRCULAR CANALS
 NT SENSE ORGANS
 NT SKULL
 NT STOMACH
 NT SYSTOLE
 NT THERMORECEPTORS
 NT THYROID GLAND
 NT TRACHEA
 NT VASCULAR SYSTEM
 NT VEINS
 NT VERTEBRAL COLUMN
 NT VESTIBULES

Human taste perception mechanism and taste system anatomy
 21 p3652 A69-38783

ANDESITE

Trace element geochemistry of calc-alkaline andesites, discussing crustal composition models and trace elements distribution
 08 p1309 A69-20940

ANDROMEDA CONSTELLATION

Forbidden emission transition probabilities in high excitation symbiotic stars, novae, Cygni stars and peculiar binaries
 19 p3423 A69-36227

Omicron Andromedae radial velocity measurements /1961-1966/ during normal B star periods
 22 p4028 A69-40755

ANDROMEDA GALAXIES

Novas in M 31 on Tautenburg Schmidt photographs
 08 p1382 A69-19873

Andromeda M 31 galactic model, using luminosity and velocity data from optical and radio observations to construct nucleus, kernel, disk and flat component
 19 p3426 A69-36579

M 31 nebula radio continuum survey, describing discrete sources catalog and Andromeda nebula radiation distribution
 20 p3601 A69-37493

Andromeda galaxy brightness distribution, discussing nuclear region, energy distribution, surface brightness, brightness profile, etc
 20 p3610 A69-38141

ANECHOIC CHAMBERS

Acoustic filters performance determination, standing wave tube and anechoic termination methods
 20 p3464 A69-37321

ANELASTICITY

Creep accumulation under time varying stress of Al alloy sheet, using creep recovery analysis to determine anelastic strain growth
 21 p3747 A69-39323

High temperature anelastic effect in Mo single crystals ascribed to internal friction peak due to electronic interactions between dislocations and C interstitials
 24 p4332 A69-43031

ANEMOMETERS

NT HOT-WIRE ANEMOMETERS
 NT SONIC ANEMOMETERS

Laser Doppler velocity profile measurement at localized points in flow stream without disturbing flow
 01 p0090 A69-10298

Theoretical response of cup and vane anemometers to steady and varying flows derived analytically and by using analog computer
 08 p1314 A69-20315

Anemometer based on neon helium ring laser with four mirror resonator
 13 p2260 A69-27857

Aerodynamic frequency response calibration measurements of wind anemometer by input velocity and output drag values under unsteady flow conditions
 24 p4315 A69-43262

ANEMOMETRY

U VELOCITY MEASUREMENT

ANESTHETICS

NT CHLOROFORM

Energy cost of muscular exercise in gastrocnemius muscle of dogs anesthetized with morphine, chloralose and urethane
 23 p4093 A69-42065

ANGELS

Angel type radar echoes from coherent pulses in centimeter and decimeter wavelengths characterized by daytime convection and presence of inversion/ isothermal layers
 09 p1491 A69-22706

Depolarization degree of angel echo signals measured by radar station, indicating insects and other foreign particles in atmosphere as reflection sources
 16 p2779 A69-32274

Angle nature from backscattering patterns at radar station with one transmitting and two receiving antennas
 16 p2779 A69-32275

Angel sources rate of motion observed at automatic tracking coherent pulse station, obtaining coincidence with wind and insect velocities
 16 p2779 A69-32276

Angel type radar echoes from coherent pulses in centimeter and decimeter wavelengths characterized by daytime convection and presence of inversion/ isothermal layers
 16 p2753 A69-32486

ANGLE OF ATTACK

NT ZERO ANGLE OF ATTACK

Mach-Zehnder interferometer for studying temperature distribution and heat transfer in turbulent jets, noting temperature dependence on jet thickness at different angles of attack
 01 p0005 A69-10101

Propeller static performance calculations for infinite number of blades applied to four blade propeller at different blade angles
 02 p0188 A69-11957

Hypersonic perfect gas flow past delta wing with blunt edges at small angles of attack, noting constant drag coefficient
 02 p0191 A69-12584

Aerodynamic characteristics of delta wings for supersonic flow at large angles of attack, showing sweep-back angle influence on drag coefficient
 02 p0191 A69-12585

Soviet book on hypersonic flow past truncated cones at various angles of attack with allowance for physicochemical equilibrium transformations
 03 p0362 A69-13633

Three dimensional boundary layers on cones at small angle of attack, presenting numerical solutions with heat transfer effects for wind tunnel model
 [ASME PAPER 68-WA/APM-24]
 04 p0541 A69-14389

Angle of attack effect on motion throughout entry of spinning descending vehicle, noting effects of transverse angular velocity and spin rate
 04 p0666 A69-15522

Delta wing head wave at zero angle of attack in steady supersonic flow during transition from subsonic to supersonic leading edges
 [DVL-871]
 06 p0858 A69-17242

Asymmetric supersonic air flow at 60 degree angle of attack past ellipsoid with frontal spike creating separation area
 06 p0858 A69-17337

Roll acceleration influence on angle of attack convergence and windward meridian rotation rate of rolling reentry vehicles
 [AIAA PAPER 69-100]
 06 p1018 A69-18089

Anomalous roll behavior of spinning ballistic reentry vehicles with compound aerodynamic asymmetry consisting of lateral offset combined with trim angle of attack
 [AIAA PAPER 69-103]
 06 p1019 A69-18168

Three dimensional hypersonic steady flow around blunt and pointed cones at nonzero angles of attack calculated by method of characteristics
 [AIAA PAPER 69-187]
 06 p0865 A69-18176

Mixed three dimensional separation of boundary layer on ellipsoid of revolution at ten degree angle of attack, ignoring heat flux
 08 p1251 A69-19876

Angle of attack and bank angle for orbiting reentry glider, determining optimal trajectory for ground landing at given point
 [ICAS PAPER 68-41]
 11 p1966 A69-24750

Angle of attack and Reynolds number effect on hypersonic flow past circular cone, obtaining shock wave shape
 [ONERA-TP-692]
 11 p1818 A69-24751

Propeller performance prediction for nonnegligible angle of attack, determining tip loss factor with model similar to Prandtl model for axial flight
 11 p1819 A69-25375

Free transonic gas flow incident on symmetrical profile at angle of attack with given velocity at infinity calculated using difference scheme
 11 p1820 A69-25469

Aerodynamic characteristics of flat plate in viscous hypersonic flow incident at zero or small angle of attack, using numerical integration
 11 p1820 A69-25471

Supersonic and hypersonic flow of rarefied gas around blunted cylinders at various angles of attack, noting pressure distribution on model surface
 11 p1821 A69-25478

Laminar compressible subsonic boundary layer flow on symmetrical cylinder bounded by circular arcs noting zero/nonzero angle of attack
 12 p2062 A69-26272

Thrust, bank angle and angle of attack of aircraft minimum fuel lateral turns at constant altitude and specified velocities
 13 p2203 A69-28245

Angle of attack and blunting effect on aerodynamic lift and drag coefficients of flat plates in hypersonic flow at low Reynolds number
 13 p2200 A69-28358

Supersonic gas flow past wedge at zero angle of attack with separated shock wave, calculating velocity gradient at stagnation point and pressure and drag distribution
 14 p2390 A69-29615

Three dimensional periodic boundary layer on ellipsoid in harmonic motion at given angle of attack, using successive approximations
 15 p2548 A69-31008

Wall pressure and heat flux distribution in hypersonic flow on delta wings at variable angle of attack for low Reynolds numbers
 16 p2731 A69-31605

Aerodynamic characteristics of cone/cylinder and cone/cylinder/cone configurations with blunted cones in hypersonic flows at small angles of attack
 17 p2889 A69-33122

Drag and lift coefficients of moderate aspect ratio prismatic bodies analyzed as function of angle of attack, Reynolds number and aspect ratio
 17 p2896 A69-33717

Stationary elliptic cylinders in subcritical flow, determining Strouhal number, pressure fluctuations and wake geometry as functions of angle of attack
 [AIAA PAPER 69-745]
 18 p3084 A69-34412

Computer programs determining gaseous properties and aerodynamic characteristics for missiles, reentry vehicles and spacecraft at angles of attack
 18 p3107 A69-35068

Aerodynamic behavior of airfoil oscillating in reverse flow defined for various angles of attack and oscillatory amplitudes at low Mach numbers
 18 p3087 A69-35219

Inverse transformation method for plane subsonic flow extended to flow past cambered profiles at angle of attack, obtaining velocity distribution
 19 p3240 A69-36473

Theoretical nonlinear method for calculating aerodynamic forces on low aspect ratio wings at high angles of attack and wide range of Mach numbers
 21 p3644 A69-39084

Axisymmetric supersonic flow around spherically blunted body at small angles of attack, deriving equations for shock deformation perturbations and surface pressure
 22 p3861 A69-41179

Windward shock angle parameters on yawed cones correlated in single variable for hypersonic flow
 23 p4060 A69-41918

Second order differential equations of supersonic flows past bodies at small angles of attack, showing linearized characteristics method applicability for conical nose
 24 p4243 A69-42581

Pressure distribution correlation over blunted slender cone at various angles of attack by tangent cone method, describing hypersonic wind tunnel tests
 24 p4249 A69-43681

ANGLES [GEOMETRY]

NT BRAGG ANGLE

NT BREWSTER ANGLE

Reflection measurements in IR, investigating effect of angle of incidence and collimated beam on reflection spectra

01 p0120 A69-10891

Maximum probability technique for measuring angular coordinate with unknown signal and noise intensity

03 p0399 A69-14132

Angle of incidence influence on unpolarized and linear polarized light of solar cell short circuit current

04 p0551 A69-15312

Mechanical calculators for solving spherical triangle problem of navigation

07 p1135 A69-19207

Radar target detection and angular location estimation in amplitude comparison monopulse radar by simultaneous observation with group of antennas

09 p1452 A69-21312

Refraction angles for objects between 5-300 km and zenith distances between 1-88 degrees, describing calculation method for corrections

09 p1490 A69-21918

Optical sensing devices for angle measurement between celestial body and satellite axes

12 p2078 A69-25871

Fourth angle driving law for different four gimbal systems used for simulation display and inertial platform isolation

12 p2055 A69-26265

X-15 research aircraft program piloting problems, ground facilities, heat transfer, space flight and steep reentry

12 p2014 A69-26872

Angular dependence of ocean surface-cloudless atmosphere reflectance for solar radiation studied with digitized camera signals from ATS 1 satellite

21 p3704 A69-38372

Isoclinic angle errors effects on photoelastic fringe order measurements accuracy

22 p3945 A69-40082

Photomultiplier tubes performance enhancement by light incidence on photocathode at oblique angles explained by reflection

23 p4191 A69-42194

ANGULAR ACCELERATION

1.5 g angular acceleration effects on acetylcholine metabolism in guinea pig brains and hearts

02 p0198 A69-11505

Rotational velocity estimates by observers during angular acceleration, noting vestibular function interpretation

04 p0554 A69-15332

Strapdown gyros in back to back connection for reduction of component cross coupling errors

04 p0603 A69-15473

Psychophysical methods for determining perception threshold of angular acceleration in man during vertical rotation

05 p0708 A69-15969

Vestibular-vegetative reactions during angular and Coriolis accelerations alternating with weightlessness, noting increased parasympathetic and sympathetic activity

07 p1062 A69-18587

Fluidic control systems for angular rate and attitude stabilization flight-tested, noting good impact and acceleration resistance

[AGARDOGRAPH-118] 08 p1257 A69-20955

High sensitivity gyroscopic HF angular acceleration sensor using special differentiator, obtaining motion equations and dynamic response

09 p1498 A69-22109

Torsiograph systems analysis for rotors angular acceleration recording, discussing dynamic characteristics, system, environmental problems, etc

10 p1692 A69-23252

Fluid rotor angular accelerometer design for stabilization and control, noting applications to centrifuge speed and thrustor gas consumption

10 p1633 A69-23273

Optimal parameters of hydraulic sensor of angular accelerations for given dynamic and geometrical requirements

13 p2259 A69-27432

Dynamic stresses in case bonded cylinder due to transient angular accelerations, presenting numerical results for incompressible elastic cylinder

13 p2364 A69-28209

Vestibulo-somatic, vegetative and sensory reactions to angular acceleration, deceleration and tilting, evaluating functional state of vestibular analyzer

20 p3481 A69-37270

Human angular acceleration sensitivity using rotation and oculogyral illusion perception as indicators,

relating to spatial orientation and flight control task precision

23 p4101 A69-41674

Human physiological responses to angular acceleration during breath holding, MI, Valsalva and Mueller respiratory maneuvers in hollow spherical simulator

23 p4102 A69-41679

ANGULAR CORRELATION

Critical values of laser formed solid angle determined in plasma diagnostics of scattering spectrum density distribution

02 p0251 A69-12416

Angular correlation of inelastically scattered alpha particles and gamma rays emitted from 2-plus state of Sn 120

03 p0469 A69-13098

Angular correlation between inelastically scattered 42 Mev alpha particles and emitted gammas from 2-plus Ni 58

03 p0470 A69-13100

Ionizing electron collisions with He, determining energies and angular correlation distributions of scattered and ejected electrons

06 p0962 A69-17191

Angle of arrival in amplitude comparison monopulse radars in presence of internally generated thermal noise

13 p2220 A69-27942

ANGULAR DISTRIBUTION

Emission and frequency shift angles of antiStokes radiation from trapped filaments of laser light in liquids

01 p0114 A69-10012

Angular distribution of radiation scattered by microscopic polyvinyl toluene sphere monolayer, noting intensity distribution approximation using Mie theory [AIAA PAPER 68-30]

02 p0282 A69-12503

Glass pleats and cold cathodes in laser discharging tube, discussing angular displacements

03 p0435 A69-12981

Angular and spectral distribution of earth IR radiation near horizon from satellite observation and spectrograms

03 p0422 A69-13506

Directional intensity of radiation emerging from top and bottom of Rayleigh scattering atmosphere

03 p0426 A69-14026

Angular distribution of particles sputtered from GaAs and GaP single crystals, bombarding faces with Ar ions at low energy

04 p0640 A69-14452

Angular distribution of reactive elastic scattering by opacity function/reaction probability/

04 p0554 A69-14859

Histograms construction for azimuthal distribution of atmospheric from visual and photographic data obtained by CRT display goniometer

04 p0593 A69-15102

CRT direction finder with linear scanning to determine statistical data for azimuthal distribution of atmospheric

04 p0600 A69-15104

Expansion anisotropy in angular distribution of laser produced plasmas in terms of drifting and expanding sphere model, discussing particle velocities, currents and time integrated counts

05 p0804 A69-16460

Angular dependence of low energy electron impact excitation cross section of lowest molecular hydrogen triplet states

06 p0962 A69-17820

Angular distribution measurements of visible and near IR radiation reflected from carbon dioxide cryodeposits formed on liquid nitrogen cooled surface in vacuum

[AIAA PAPER 69-63] 06 p0959 A69-18131

Angular intensity distribution of corpuscular radiation in time independent geomagnetic field characterized by particle velocity distribution

07 p1210 A69-19619

Angular distribution of photon radiance of spherical satellite irradiated by Lambertian earth, assuming nonemissive satellite

08 p1311 A69-21095

Angular dependence of EPR line widths of trivalent Cr ions in zinc tungstate in rotating magnetic field, noting spin-phonon mechanism

10 p1743 A69-23131

Angular energy distribution in gamma quanta beam during collision between laser photons and relativistic electrons

10 p1701 A69-23132

Nonthermal cosmic radio emission spectral index angular variations during scanning of sky by receiver antenna, analyzing dependence on galactic latitude

10 p1784 A69-23940

Radio sources optical positions for independent calibration sources

11 p1958 A69-24465

Ruby laser light scattered at 90 degrees by dense plasma focus, analyzing signal detection

11 p1899 A69-25324

Angular distribution of electrons leaving plasma at electrode boundary, using kinetic Boltzmann equation with scattering function and specular reflection

11 p1933 A69-25544

Interplanetary scintillation and angular spectrum of radio waves scattered by solar plasma, noting magnetospheric tail and solar wind

12 p2161 A69-26942

Light scattering from high reflectivity dielectric mirrors, measuring angular power distribution from beam axis by scanning with narrow slit

13 p2298 A69-27663

Angular distribution of penetrating shower particles produced in nuclear interaction of cosmic rays with C, Sn, Cu and Pb

13 p2330 A69-28381

Angular distribution of nuclear particles dispersed during motion determined from photon energy and inelasticity coefficient

13 p2303 A69-28390

Angular distribution function calculations for avalanche electrons at various stages of cascade development, discussing electron energies and primary electron roles

13 p2303 A69-28414

Cosmic ray muons energy and angular distribution measurements, obtaining curve with respect to projection angles

13 p2332 A69-28420

Cosmic ray muons angular distribution measuring device for determining pion/kaon ratio

13 p2332 A69-28421

Double light scattering near critical point, examining angular distribution

14 p2482 A69-28738

Cosmic ray angular distribution spectrum and interplanetary magnetic field properties determined from semidiurnal cosmic ray variations data

14 p2512 A69-29046

Optophotoclectric pickup design for angular displacement measurements, considering application of moire pattern produced by radial diffraction gratings

14 p2447 A69-29327

Polarization and angular distribution of 6328 A He-Ne laser light scattered by latex-sphere hydrosols, comparing coherent and incoherent scattering patterns

15 p2595 A69-30223

Plasma three electrode source ion-optical characteristics, noting beam angular divergence dependence on spacing between discharge cavity and intermediate electrode

15 p2658 A69-30240

Plane electromagnetic wave refraction and scattering in solar corona during eclipsed observations of cosmic sources, calculating angular distribution of radiation intensity

15 p2688 A69-30555

Earth reflected solar radiation spatial, angular and spectral distributions measured by telephotometers onboard Cosmos 149

15 p2596 A69-30650

Resonance cones in angular distribution of short antenna RF electric field in anisotropic plasma noting variation with incident, cyclotron and plasma frequency

15 p2659 A69-30876

Noctilucent clouds thickness determinable from angular dimensions of visible edge

15 p2598 A69-31254

Angular structure of second optical harmonic for cylindrical lens focusing of ND laser beam into negative KDP crystal

17 p2981 A69-33110

Angular dependence of lunar nighttime IR radiation by invariant tensor techniques, noting surface roughness effect on radiation pattern

[AIAA PAPER 69-597] 17 p3032 A69-33276

Azimuth angle distribution of secondary particles forming cosmic ray diffused cone with high energy, showing asymmetry and deducing particle transverse momentum upper limit

17 p3024 A69-33763

Angular spectrum representation of diffracted wave fields expressible by plane wave expansions containing only homogeneous waves

17 p3007 A69-34153

Optical constants changes in germanium determined by modulation method of measuring light reflected at different angles

18 p3173 A69-35014

Velocity and angular distributions of KBr formed in reactive collisions between crossed molecular beams of K and thermal HBr/DBr/

18 p3178 A69-35476

Relation between angular divergence, spectral characteristics and kinetic behavior of laser operating in various pulsed modes

19 p3333 A69-35879

Thermal molecular beam sources fabricated from multichannel arrays, describing molecular flux leak rates and angular distributions

19 p3376 A69-36175

Auroral electron and proton fluxes precipitation measurements by satellite, studying data in terms of spatial, energy and angular distributions

21 p3709 A69-38500

Deposited beta active thallium isotope materials angular distribution after vaporization by Q switched laser beam determined by target fragment recoil

21 p3737 A69-38992

Cosmic ray electron recorder for measuring intensity, energy spectrum and angular distribution of electron fluxes within specific energy range

21 p3724 A69-39074

Accelerating electric field model to interpret energy and angular distribution of auroral particles, noting electric potential limitations

22 p3938 A69-40445

Angular distributions for Sc 45-Ti 46 nuclear reactions involving 41 Mev alpha particles bombardment described by Born approximation

22 p3988 A69-41044

Angular distribution of He-Ne laser beam scattered by artificial fog from data by light detection devices at various angles

24 p4328 A69-43503

Diffractive coupling of power from carbon dioxide laser, computing angular distribution of output light

24 p4329 A69-43753

ANGULAR MOMENTUM

Origin of binaries from angular momentum vectors orientation and separation distribution

05 p0822 A69-15856

Laminar flow stability parameter presenting coupling ratio between angular momentum change and loss rate by frictional drag

05 p0750 A69-16187

Equilibria of orbiting gyrostal satellite with internal angular momenta along principal axes

07 p1227 A69-18336

Interhemispheric transfer of atmospheric angular momentum, noting hemispheric angular momentum contents and annual variations

07 p1127 A69-19258

Galactic angular momentum of rotation, applying rotation theory to gravitational instability model of galactic formation

08 p1383 A69-20050

Meridional flow, angular momentum and energy flux in atmosphere calculated from IGY data

08 p1346 A69-20312

Stellar rotation braking due to mass loss from coronae through stellar wind based on calculation of acoustic energy generation from convective zone

08 p1396 A69-20644

Angular inertia of lubricant in MHD hydrostatic thrust bearings, obtaining critical angular speed of rotor

09 p1503 A69-21443

Angular momenta of stars, planets and asteroids, plot log of angular momentum per unit mass against log of mass of astronomical object

09 p1608 A69-22716

Binary eclipsing visual star systems angular momenta, discussing evolution

10 p1777 A69-23313

Penfield-Haus solution to magnetodynamic effect problem as inertial effect of orbital angular momentum, deriving Bohr magneton formula from Einstein equivalence principle

11 p1919 A69-25098

Spacecraft attitude control and stabilization by three degree of freedom control moment gyro with controllable gyro spin angular velocity

13 p2355 A69-27445

Isotropic and anisotropic dust cosmological models density perturbation growth, considering angular momentum conservation in expanding universe

13 p2343 A69-27619

Angular momentum-gravitational field coupling in collapsing star, applying rotational perturbation to spherically symmetric time dependent interior solution of Einstein field equation

14 p2520 A69-29374

Lunar origin theories, considering moon/earth mass ratio, earth-moon system angular momentum deficiency and differential volatilization in earth

14 p2527 A69-29882

Self maintenance of absolute angular momentum in atmosphere as explanation of subtropical jet stream origin

15 p2647 A69-30192

Plasma viscosity relation to stellar magnetic fields generation, taking into consideration angular momentum transfer

15 p2700 A69-31492

Regional distribution of relative angular momentum transport over equator, noting advective and turbulent transfer

16 p2773 A69-31793

Gimbal torquing as function of gimbal structure response resulting in free gyro erection system, using any angular momentum at any initial starting angle

16 p2792 A69-32553

Line widths of 48 galaxies at 21 cm and spectroscopic data, estimating masses and angular momenta, finding mass-angular momentum relation

16 p2866 A69-32818

Planetary systems interrelationship with binaries and rotating stars, emphasizing occurrence frequency study based on stellar angular momentum orientation

17 p3032 A69-33105

Solar wind phenomenon, discussing angular momentum loss to sun, fluctuations at earth orbit and wind conditions at terminus and regions unvisited by spacecraft

17 p3023 A69-33370

Turbulent boundary layer on disk rotating in free air, using circumferential and radial momentum integral equations and entrainment equation

17 p2957 A69-33601

Quiet solar wind model with magnetic field numerically calculated, obtaining coronal electron densities and angular momentum near earth

18 p3186 A69-34301

Time and fuel optimization of angular momentum alignment and nutation elimination of spin stabilized bodies with inertial reference direction

18 p3208 A69-34775

Protosun and solar system angular momentum losses analyzed from equations for convective star rotation change, noting almost total protosun initial momentum loss possibility

18 p3203 A69-35346

Finite electrical conductivity effect on sun angular momentum loss due to solar wind

18 p3189 A69-35398

Primitive solar nebula physical model considered under angular momentum conservation in collapsing fragment

19 p3406 A69-36074

Forbidden transitions in diatomic molecules with nonzero spin and zero orbital angular momentum, stressing application in outer planets and M stars hydrogen spectra

19 p3421 A69-36213

Time scale of diffusion of angular momentum estimated by model for disturbances occurring in star with secularly unstable angular velocity distribution

20 p3605 A69-37826

Earth polar wanderings attributed to rotation axis angular displacements generated by density redistribution on geologic time scale

20 p3535 A69-38192

Order-disorder transitions in solid hydrogen, discussing model to explain molecular rotation angular momentum operator fluctuations

24 p4350 A69-43119

ANGULAR RESOLUTION

Angular separation of two point sources measured through expressing antenna resolving power by a posteriori probability laws

08 p1288 A69-20961

Solar radio burst fringes at 21 cm observed with high angular resolution using two element E-W interferometers

17 p3040 A69-33809

Radiant heat transfer integral equations solutions accuracy determined from differences between geometric and resolving angular emission factors

18 p3230 A69-35119

Ring laser bias in angular rotation measurement using optical phase shifters

21 p3735 A69-38651

ANGULAR VELOCITY

Variable thickness circular annular disk bending in centrifugal force field, establishing dependence between angular velocity and axial pressure intensity

01 p0168 A69-10401

Gyrovibrator /angular rate measuring device/, discussing output signal and natural frequency dependence on moments of inertia

01 p0083 A69-11004

Solid body automatic orientation, discussing data units for angular error and angular velocity

01 p0122 A69-11302

Unsteady slow rotational motion of viscoelastic liquid contained between two concentric spheres rotating with constant angular velocities

02 p0230 A69-11563

Atmospheric circulation influence on earth rotation velocity, discussing estimation methods

02 p0236 A69-11641

Einstein equations obtained for axisymmetric distribution of masses in approximation of square of stellar rotation angular velocity in empty space

02 p0317 A69-11956

Angular motion during first stage cut-off of Europa 1 launch vehicle from flight tests compared with theoretical predictions

03 p0519 A69-12856

Relation between amplitude of light and radial velocity variations of beta Canis Majoris stars

03 p0517 A69-14126

Rotational velocity estimates by observers during angular acceleration, noting vestibular function interpretation

04 p0554 A69-15332

Vortex value and angular rate sensor based on amplification of tangential velocity component of swirl achieved by control jet or rotation

05 p0746 A69-16006

Liquid rise in partially filled circular cylinder with free surface accelerated from rest to constant angular velocity [ASME PAPER 68-FE-13]

05 p0747 A69-16065

Three axis attitude servomechanism design to adjust attitude and angular velocity of spacecraft

06 p0955 A69-17589

Angular velocity of rotation measurement using angular gas laser undergoing axial torsional vibrations

07 p1147 A69-18523

Galactic rotation constant calculated from radial velocities of O, B and A stars in Cassiopeia constellation, using Fehrenbach objective prism

07 p1214 A69-18664

Meteor angular velocities distribution over sky in showers, considering effect of altitude, night hour, season and azimuth

08 p1393 A69-20607

Magnetic field decay modes due to nonuniform rotation having angular velocity as increasing function of distance from axis in infinite circular conducting fluid cylinder

08 p1369 A69-20999

Gyrostatic moments effects on critical angular velocities of varying and constant cross section rigidly and elastically supported hinged rotors

09 p1567 A69-21384

Symmetrical body rotational motion with asymmetrical mass distribution about center of mass, determining minimum initial value of angular velocity

09 p1595 A69-21762

Bubble spiral path motion toward axis of rotation of liquid rotating at constant angular velocity

09 p1483 A69-22006

Radial velocities of stars near cluster NGC 7380, discussing discovered stars, double lined spectroscopic binaries and photometric information

09 p1597 A69-22060

Increasing rotation of axisymmetric body about velocity vector ascribed to asymmetry in mass distribution, defining conditions for occurrence

09 p1431 A69-22077

Self oscillations in angular velocity sensor using electric spring and potentiometric pickup, examining friction moment and inductance coil effects

09 p1497 A69-22106

ANIMALS

Solar interior rotational angular velocity influence on solar oblateness, noting reduction by turbulent mixing

09 p1600 A69-22201

Stellar model with magnetic field accelerating central core rotation to instability for determining rotating star energy and angular velocity distribution dependence

11 p1952 A69-24249

Solar quiescent prominences spectra with bright metallic lines, discussing turbulent angular velocity and kinematic temperature of filaments

11 p1945 A69-24387

Differential solar rotation noting strong quasi-kineticity effect on solar convective zone and rotation influence on viscosity tensor and rotation law

11 p1955 A69-24390

Rotor angular velocity and flexural strain interdependence at critical velocity

11 p1987 A69-25390

Thin liquid film equilibrium on rotating sphere, determining conditions for detachment as function of angular velocity

12 p2061 A69-25886

Torsional flow of incompressible anisotropic fluid between parallel circular plates rotating with constant angular velocity, showing resemblance to shear flow

12 p2062 A69-26277

Space vehicle angular velocities reduced to zero through linear and nonlinear optimal feedback control systems

12 p2054 A69-26516

Nonrelativistic theory of rotating configurations in terms of gravitational potential, center mass density and variable angular velocity

12 p2159 A69-26662

Viscous heat conducting compressible fluid response to abrupt change in circular cylinder angular velocity at stable temperature distribution, considering Boussinesq approximation

13 p2245 A69-27378

Triaxial gyrostabilizer systematic drifts during rocking at large platform displacement angles, analyzing drift direction and rate dependence

13 p2259 A69-27430

Arc plasma jets radial velocity profiles measured by two probes in cyclic movement between jet edge and middle, including error estimation

13 p2307 A69-27611

Planetary mantles thermal and nonthermal convection model, solving sphere density variations and radial velocity components due to internal time-independent motions

13 p2344 A69-27644

Messier 51 ionized hydrogen observations, discussing H II regions, radial velocities and galactic mass, rotation and noncircular nuclear motions

13 p2347 A69-27720

Astronomical unit determined by measuring radial velocity of radio wavelength spectral line source

13 p2350 A69-27822

Internal structure of rotating stars, analyzing physical changes, circulation influence on mixing during evolution and angular velocity

15 p2683 A69-30512

Self excited vibrations of rotors supported in gas bearings from analyzing solutions to equations of rotor motion

16 p2875 A69-32250

Turbopump weight minimization and low suction pressure requirements realized using high rotating speeds, hydraulic turbine driven upstream inducer and computer testing

16 p2741 A69-32747

Spectral lines radial velocities and profiles observed on 48 Librae from 1950-1962

17 p3038 A69-33722

Radial velocities differences as indicator of stellar atmospheric turbulence, applying method to sun

17 p3044 A69-34177

Mean rotational velocity of finite width gaseous ring in close binary system from rotational velocity measured on spectrograms

17 p3044 A69-34180

Angular velocity effects on meteors apparent brightness

17 p3045 A69-34222

Elastohydrodynamic solution for ball torque spinning without rolling in nonconforming groove, showing increase in torque with stress and spinning and decreasing conformity

18 p3140 A69-34381

Angular velocity of aircraft rotation about longitudinal axis at arbitrary point of passive trajectory section, with assumptions on roll damping, momentum, etc

18 p3092 A69-34989

Microwave background angular fluctuations investigated for relationship between whirl motion velocity and temperature dispersion, noting role of scattering by moving plasma

18 p3188 A69-35208

Vibrarotor gyroscope operated as rate gyro for simultaneously indicating two components of angular velocity by amplitude and phase of periodic output signal

18 p3139 A69-35299

Viscoelastic shaft stability rotating at harmonically variable angular velocity, considering internal and external damping

18 p3224 A69-35300

Angular velocity torsional oscillations of solid sphere under elastic force couple rotating in viscous liquid bounded by immobile concentric sphere

18 p3175 A69-35320

Asynchronous gyrostatt postimpact drift direction found orthogonal with respect to initial impulse by averaging method

19 p3311 A69-36192

Tangential and radial velocities in vortex boundary layer flow, relating diminishing amplitudes to increasing height using iterative method

19 p3363 A69-36499

Dimensionless radial and transverse velocity profiles for unsteady incompressible boundary layer on rotating disk in rotating fluid

19 p3300 A69-36720

Curved beams ultimate strength using angular velocity considerations for collapse load

20 p3629 A69-38031

Magnetic field fluctuations and radial velocity in undisturbed photosphere, discussing magnetic field relation to radial velocity, cross correlation asymmetry, etc

20 p3535 A69-38300

Gaseous rotating stars radial oscillations by perturbation method, considering angular velocity effects

21 p3795 A69-38470

Interferogram observations of central velocity of M 31 under constant rotational velocity assumption, noting galaxy inclination

21 p3797 A69-38481

Fluidic angular rate sensor, obtaining rate information by sensing laminar jet flow deflection from nozzle, discussing advantages over mechanical rate sensors

21 p3722 A69-38766

Rotating stratified fluid in thermally insulated cylinder, studying angular velocity abrupt change effects under stable temperature distribution

21 p3694 A69-38768

Satellite attitude stabilization synthesis by flywheels allowing independent control of angular motions, assessing perturbation type influence

21 p3768 A69-39831

Neutral exosphere model for nonrotating planet permitting barosphere uniform rotation at certain angular velocity, determining velocity distribution and density

22 p4023 A69-40524

Angular velocity of visual stimulus effect on human torsional eye movements using sectorized disks

22 p3883 A69-40874

Increasing rotation of axisymmetric body about velocity vector ascribed to asymmetry in mass distribution, defining conditions for occurrence

23 p4060 A69-41968

Carroll Fourier transform method applied to stellar spectra lines to determine small rotational velocities

23 p4222 A69-42404

Nadai and Zyczkowski stress analysis for Tresca yield condition reexamined for determination of critical angular velocity of solid elastic perfectly plastic disk

23 p4235 A69-42480

Pointing vector and angular rate relationships for various optical elements, discussing analytical models development for precision electro-optical stabilization systems

23 p4131 A69-42544

Solar quiescent prominences spectra with bright metallic lines, discussing turbulent angular velocity and kinematic temperature of filaments

24 p4375 A69-43777

Differential solar rotation noting strong quasi-kineticity effect on solar convective zone and rotation influence on viscosity tensor and rotation law

24 p4390 A69-43780

NT BEETLES
NT BIRDS
NT CATS
NT CHICKENS
NT CHIMPANZEES
NT CRABS
NT DOGS
NT DROSOPHILA
NT FISHES
NT FLAGELLATA
NT FLATWORMS
NT FROGS
NT GROUND SQUIRRELS
NT GUINEA PIGS
NT HAMSTERS
NT HETEROTROPHS
NT HOMEOTHERMS
NT HUMAN BEINGS
NT INSECTS
NT INVERTEBRATES
NT LIZARDS
NT MAMMALS
NT MICE
NT MICROSPORES
NT MONKEYS
NT PARAMECIA
NT PIGEONS
NT POCKET MICE
NT PRIMATES
NT PROTOZOA
NT PUPA
NT RABBITS
NT RATS
NT ROBENTS
NT SHEEP
NT SPORES
NT TURTLES
NT VERTEBRATES
NT WORMS

Pituitary-adrenocortical axis and neuro-endocrine functions in animals maintained in oxygen atmosphere, discussing norepinephrine and epinephrine excretion values, etc

01 p0019 A69-11343

Acceleration, hypoxia and stress effects on humans and animals, noting latent functional disorders of organisms requiring special techniques for detection

02 p0197 A69-11488

Physiological processes occurring in voluntary movements of animals under space flight weightlessness conditions

02 p0199 A69-11827

Organic reaction and adaptation of rabbits and dogs to simulated weightlessness and acceleration compared with orbital flight data of human responses

03 p0376 A69-14192

Weightlessness effect on blood circulation system of human beings and animals during suborbital/ orbital space flight

03 p0376 A69-14194

Hypoxia effect on animal brain gamma-aminobutyric acid levels

04 p0552 A69-14482

Bioadhesive investigation in echinoderms extended to class Holothuroidea, using electron microscope with correlative light microscopy for tube feet of sea cucumbers

05 p0708 A69-15984

High oxygen concentration influence on animal organisms noting respiration, pulmonary gas exchange, hypoxia, brain phosphorylation, immunological indices and morphological structure of rats and mice

05 p0709 A69-16512

Decrease in bioelectric activity of skeletal muscles in animals and man during intermittent acceleration and weightlessness

07 p1062 A69-18591

Telemetry with unrestrained animals, discussing radio tracking of game animals and instrumentation requirements for studying green sea turtle goal finding ability

07 p1071 A69-19136

Visceral lesions observed in mice and rats exposed to ultrashort waves indicating no pathological modification of physiology of reproduction

08 p1266 A69-20679

Animals in weightless state, noting vigilance, attention, sensorial and motor reaction time, muscular tone at rest and muscles electrical activity in movement

09 p1445 A69-22721

Hydrogenomonas eutropha as means of protein food source independent of conventional agriculture for animal feed supplement

10 p1644 A69-23306

Acceleration effects on cellular and subcellular structures enzyme activity in humans and animals, noting changes resulting from changed permeability of membranes

10 p1645 A69-23496

ANIMALS
NT BABOONS

Heart rate and bodily fluid changes in aestivating desert anurans, discussing weight loss and metabolism reduction
11 p1827 A69-24923

Space biological tests performed on lower animals and vegetables relating to higher organisms reactions during prolonged manned space flights, reviewing Nasa experiments
12 p2019 A69-26494

Circadian rhythm of optic nerve impulses in isolated eye of sea hare *Aplysia californica* in total darkness
14 p2406 A69-28870

Dynamic differential thermal analysis of dried plant and animal specimens and related substances yielding discrete decomposition peaks of exothermic type
15 p2555 A69-31000

Synaptic configurations in neuropil of planarian *Dugesia dorotocephala* brain, discussing neurotransmitters at phyletic level
16 p2741 A69-31555

Macromolecular ring shaped components corresponding to hemagglutinin studied in *Limulus polyphemus* hemolymph by electron microscopy
16 p2742 A69-31864

Compensatory reactions to prolonged weightlessness in human and animal organisms emphasizing blood circulation, heart, metabolism, digestive and nervous systems
17 p2909 A69-33577

Lateral hypothalamic stimulation bound eating motivation in animals, comparing electrical stimulation and hunger elicited eating
17 p2910 A69-33752

High oxygen concentration influence on animal organisms noting respiration, pulmonary gas exchange, hypoxia, brain phosphorylation, immunological indices and morphological structure of rats and mice
18 p3095 A69-34731

Toxic effects of Freon R FE 1301 on animals and human beings at different concentrations, assessing judgement, alertness and neuromuscular skill
18 p3098 A69-35061

Portable multiunit low pressure chamber with locks, permitting water replenishment, feeding of animals under continuous pressure and gas mixtures
22 p3891 A69-40217

Viscoelastic properties of lenses extracted from cats and dogs analyzed as function of displacement using computer simulation
22 p3883 A69-40875

Catalytic, physical and chemical properties of enzyme lactate dehydrogenase isolated from lobster tail muscle
22 p3897 A69-41069

Cardiovascular changes induced in animals by prolonged weightlessness, using implanting polyethylene cannulas in neck or head
23 p4108 A69-41824

Cardiopulmonary bypass developed for studies of long term weightlessness on cardiovascular system of mice, white rats and squirrel monkeys
24 p4278 A69-43394

ANIMATION
U MOTION

ANIONS

Ionospheric negative ion coefficient variations, analyzing formation microprocesses
01 p0066 A69-10599

Benzene anion radical in solid solution ESR spectrum, noting removal of orbital degeneracy at 4.2 degrees K
03 p0382 A69-13379

Ion pairing effects of cyclooctatetraene anion radical, studying electron spin resonance spectra temperature dependence
10 p1651 A69-22938

Negative ion influence on electrical conductivity of partially ionized multicomponent gas mixtures, basing analysis on thermodynamic calculations of composition
21 p3774 A69-38867

ANISOTROPIC FLUIDS

Stress field and force system within torsional flow of cylindrical mass of incompressible anisotropic fluid
02 p0229 A69-11558

Laminar flow of anisotropic Ericksen fluid near wall at large Reynolds numbers, discussing Newtonian behavior, viscosity coefficient and particle orientation
02 p0231 A69-12141

Torsional flow of incompressible anisotropic fluid between parallel circular plates rotating with constant angular velocity, showing resemblance to shear flow
12 p2062 A69-26277

Turbulent fluid flow analysis described by Navier-Stokes equations, introducing asymmetric tensors for anisotropic cases
13 p2297 A69-27289

Langmuir HF turbulence effect on anisotropic plasma oscillation spectra, determining instability conditions
13 p2315 A69-28448

Gupta stability solution extended to liquid anisotropic viscoelastic films, analyzing surface and shear wave perturbations in material structures
22 p3929 A69-39893

ANISOTROPIC MEDIA

Viscous effects of neutrinos in anisotropic cosmological models examined using Boltzmann equation with simple collision term
01 p0148 A69-10053

Quasi-monochromatic wave dispersion relation and energy transfer in inhomogeneous anisotropic medium
01 p0126 A69-10278

Energy function invariants for cubic and hexagonal systems of anisotropic media with coupled stresses
01 p0169 A69-10811

Numerical method for determining group velocity of waves in homogeneous anisotropic medium, using implicit function from dispersion relation
01 p0131 A69-11117

Anisotropic two component plasma relaxation taking into account dynamic shielding collective effects
01 p0134 A69-11419

Menabrea theorem for anisotropic elastic body with internal incompressibility constraint, discussing validity during thermoelastic transformation
02 p0341 A69-12194

Menabrea theorem for nonisothermal transformations of anisotropic elastic body with internal incompressibility constraint and initial stress
02 p0341 A69-12197

Plasma stability under anisotropic pressure in axisymmetric magnetic fields determined by quasi-hydrodynamic approximation
02 p0291 A69-12552

Wave structure for moving load on surface of anisotropic material in plane stress investigated for stable elastic wave propagation
02 p0348 A69-12609

Light-light interaction in homogenous media ascribed to multilevel atomic system simultaneous excitation by both fields
02 p0258 A69-12637

Electrodeless conductivity probe impedance in anisotropic plasma computed on basis of Maxwell equation
03 p0483 A69-14252

Anisotropic nonlinear wave propagation in arbitrarily moving ideal gas, using singular surface/ray combined theories
04 p0630 A69-14532

Stresses and displacements in anisotropic elastic solids under mechanical loading, determining general solution for treatment of time dependent boundary conditions
04 p0675 A69-14595

Electromagnetic wave propagation in uniform anisotropic plasma, considering wave vectors perpendicular to magnetic field
04 p0637 A69-15048

Equation for analyzing radiation produced by current passing through filament situated over anisotropically conducting plane in flat waveguide
05 p0718 A69-15647

Linear theory applied to anisotropic elastic materials, discussing transition from compressible to incompressible elastic materials
05 p0834 A69-15795

Potential functions to solve coupled wave equations for compressible anisotropic plasma with electric and magnetic current sources
05 p0803 A69-16350

Gravitational instability of rotating anisotropic plasma for longitudinal wave propagation mode, obtaining dispersion by using modified Chew-Goldberger-Low equation
05 p0827 A69-16596

Basic equations describing stress-strain state of anisotropic half planes and anisotropic planes with cuts
06 p0120 A69-16827

Stress-strain relations for laminar anisotropic medium from known mechanical properties of layers for application to fiber reinforced plastics
06 p1021 A69-17176

Geometrical optics approximation of Maxwell equations for electrodynamics of inhomogeneous anisotropic media
07 p1076 A69-18519

Anisotropic glass fiber reinforced epoxy resin composite under biaxial and uniaxial loads, noting isochromatics and isoclinics in photoelastic analysis
07 p1170 A69-18715

Sign conventions definition and importance for shear stress and strain analysis in laminated anisotropic composite materials, noting role in studying response
07 p1170 A69-18720

Axial loading of unidirectional composite with hexagonal array of isotropic circular filaments generalized for filament anisotropy, discussing matrix elastic modulus and Poisson ratio
07 p1170 A69-18724

Linearized simple beams and columns theory for anisotropic materials, discussing flexural and extensional effects coupling in tension test
07 p1171 A69-18727

Ray-optical description for point source excited surface waves in stratified anisotropic media
07 p1079 A69-18918

Anisotropic stress analysis of creep in theory of linear viscoelasticity
07 p1234 A69-19381

Scattering and diffraction of plane electromagnetic wave incident on conducting cylinder coated with moving anisotropic medium
07 p1086 A69-19469

Coupled wave equation solution based on spectral resolution for longitudinal components of electric and magnetic fields when source currents are present in compressible anisotropic plasma
08 p1274 A69-20031

Stress fields in Hertzian contact of parallel cylinders composed of anisotropic materials and transversely isotropic spherical bodies
08 p1414 A69-20524

Capacitance and lowest eigenvalue bounds for two dimensional anisotropic media as exemplified by transverse vibrations of stretched membrane
08 p1418 A69-20848

Transversely isotropic elastic solid approximation for oriented fibers of polyethylene, nylon, polyethylene terephthalate and polypropylene, measuring elastic compliances
09 p1528 A69-21504

Singular surface theory combined with ray theory for propagation of weak discontinuities in nonlinear anisotropic media applied to MGD
09 p1547 A69-21613

Plane deformation in nonorthotropic body composed of various anisotropic cylinders with different elastic constants
10 p1799 A69-23156

Electromagnetic wave transmission through anisotropic plasma, discussing incident wave field strength effects near cyclotron frequency
10 p1728 A69-23167

Weakly attenuated components of VLF mode spectrum associated with propagation below anisotropic ionospheres as function of frequency and azimuth
10 p1655 A69-23417

One dimensional nonlinear model of anisotropic plasma instability with respect to Alfvén waves growth, noting applicability to solar wind processes
10 p1741 A69-23961

Varying diameter anisotropic composite shafts torsion based on strain and stress functions
11 p1982 A69-24975

Anisotropic plasma density measurement by launching circularly polarized plane electromagnetic wave at small angles to magnetic field direction
11 p1930 A69-25286

Electromagnetic wave propagation in rectangular waveguide containing uniaxial anisotropic birefringent medium, deriving field equations
11 p1853 A69-25350

Input impedance of quarter wavelength antenna in anisotropic plasma, discussing plasma parameters role and use of probe antenna in plasma diagnostics
12 p2044 A69-27071

Controllable motions of compressible homogeneous isotropic solids, anisotropic solids and fluids with memory under constant body force
12 p2189 A69-27118

Radio wave propagation in anisotropic inhomogeneous medium, obtaining reflection and conversion coefficients and electromagnetic field distribution
13 p2218 A69-27182

Plane wave solution for wave propagation in inhomogeneous anisotropic time-varying media
13 p2219 A69-27397

Atomic and molecular spins dynamic orientation in anisotropic radiation field, examining medium properties and astrophysical consequences
13 p2350 A69-27861

Cerenkov radiation from point charge uniformly moving along external magnetostatic field in warm anisotropic plasma, noting excitation modes and propagation frequencies

13 p2307 A69-27964

Plasma stability under anisotropic pressure in axisymmetric magnetic fields determined by quasi-hydrodynamic approximation

15 p2658 A69-30249

Tissue-type fiberglass reinforced material properties as prototype of continuous anisotropic hereditary elastic media

15 p2642 A69-30584

Resonance cones in angular distribution of short antenna RF electric field in anisotropic plasma noting variation with incident, cyclotron and plasma frequency

15 p2659 A69-30876

Thermal radiation polarization in anisotropic and gyrotropic media described by Hermitian permittivity tensor, noting linearity

15 p2653 A69-30940

Electromagnetic wave propagation in anisotropic inhomogeneous media by geometric optics approximation, obtaining equations for beam trajectories in spherically symmetrical medium

15 p2569 A69-30949

Equation for analyzing radiation produced by current passing through filament situated over anisotropically conducting plane in flat waveguide

16 p2762 A69-32504

Wave propagation and scattering in anisotropic media, obtaining asymptotic expression for dyadic Green function for infinite space

17 p2924 A69-33835

Differential equations as Hamiltonian function for signal path, travel time and frequency variation in anisotropic nonpermanent absorbing medium

17 p2924 A69-33836

Ray methods application to partial differential equations for electromagnetic wave propagation in ionosphere, discussing strongly and weakly anisotropic inhomogeneous plasma

17 p2925 A69-33840

Wave propagation in two dimensional anisotropic media with several perturbation speeds, using Lundquist linear equations ensuring lacunas presence

17 p2925 A69-33841

Electromagnetic beam propagation in anisotropic media, discussing quasi-optical beam divergence

17 p2925 A69-33845

Electromagnetic wave propagation in anisotropic media analyzed for wave packet behavior function, stressing waveguide theories

17 p2926 A69-33847

Diffraction of skew incident plane electromagnetic wave by perfectly conducting right angled wedge embedded in uniaxially anisotropic medium

17 p2930 A69-33889

Plane anisotropic dielectric p-n junction layer waveguide properties, deriving characteristic equations for refraction indices

17 p2983 A69-33971

Electronically tunable lithium niobate optical filter utilizing collinear acousto-optic diffraction in anisotropic medium

17 p2943 A69-34157

Fiberglass reinforced plastics short and long term strength anisotropy, correlating stress and logarithm of time to rupture under tension along different directions

18 p3162 A69-35352

Yield condition of maximum constant distortion strain energy for anisotropic material without incompressibility assumption

18 p3227 A69-35494

Computed and experimental displacement distribution curves compared for anisotropic material concerning creep rate enhancement by small cracks

20 p3620 A69-36965

Radio wave propagation in anisotropic plasma consisting of oxygen ions and protons, deriving expressions for radio wave refractive index

20 p3486 A69-37052

Electromagnetic radiation in moving uniaxially anisotropic medium, obtaining time dependent solutions for oriented magnetic dipole current distribution density

20 p3576 A69-37578

Uniqueness theorems for wave propagation in homogeneous or inhomogeneous anisotropic media

20 p3578 A69-38196

Atomic sources local multipolar field in anisotropic dielectrics determined from magnetic dipole radiation spatial distribution measurements

21 p3779 A69-38531

Asymptotic method applied to nonlinear equations, determining thermal conductivity coefficient for temperature distribution in moving anisotropic media

21 p3848 A69-38642

Stress-strain state of homogeneous anisotropic elastic body under action of internal forces, deriving equations to generalize state

21 p3838 A69-39184

Approximate boundary conditions in electrodynamic of stratified tensor media estimated for ferrite layers

21 p3675 A69-39282

Green matrix for operator M governing steady state wave propagation in inhomogeneous anisotropic media obtained as solution of integral equations system

23 p4180 A69-41368

Radiative heat transfer in nonisothermal absorbing and emitting media without scattering and with anisotropic and isotropic scattering

23 p4239 A69-41632

Semiinverse method involving plane wave expansions to solve elliptical crack expansion and self similar phase transformation in anisotropic solid

24 p4397 A69-42749

ANISOTROPIC PLATES

Equations of linear theory of anisotropic elastic plates including Reissner-Green bending equations

01 p0168 A69-10387

Elastic stability equations solved in geometrical linearization for thin anisotropic plates under transverse shear, using variational method

03 p0525 A69-13130

Elastic equilibrium stress condition of anisotropic plates with circular isotropic inclusions

04 p0667 A69-14264

Soviet handbook on stress analysis of anisotropic three layer reinforced plates and shells and of thick walled cylinders, Volume 2

04 p0683 A69-15500

Piezooptical method applied to anisotropic bodies and reinforced plastics, deriving relation between dielectric tensors and stresses and strains

05 p0837 A69-16038

Stress-strain state of infinite plate with two holes of different diameter solved, using integral equation derived for two dimensional problem in elasticity theory for anisotropic medium

05 p0843 A69-16680

Stability of rectangular transversely isotropic plate hinged at three sides under uniform pressure applied to two opposite hinged sides

06 p1021 A69-17178

Optimal computer calculation procedure for medium thickness anisotropic laminar plates with shear applied to rectangular and hinged plates

06 p1026 A69-18015

Plane anisotropic rectangular plates with various boundary conditions, analyzing stability, natural frequencies, mode shapes and displacement under lateral loads

07 p1232 A69-18719

Unsymmetrically laminated simply supported plates approximate solutions, considering potential energy and reduced stiffness matrix

07 p1232 A69-18725

Linear viscoelastic bending of anisotropic plates based on equation for Voigt plate, considering elliptic and rectangular plates

10 p1793 A69-22881

Reduced modulus of elasticity dependence on form of plane stressed state, assuming initially anisotropic body with transversely isotropic elastic properties

11 p1986 A69-25182

Book on statics and dynamics of anisotropic and heterogeneous elastic structures covering thin heterogeneous anisotropic panels, elastic and sandwich plates, etc

11 p1986 A69-25236

Unsteady temperature field and thermal stresses for anisotropic and orthotropic plates heated by heat sources and having Newton law heat transfer

12 p2177 A69-25992

Clamped edge anisotropic elliptical plate bending under varying loads, assuming torsional rigidity bearing constant ratio to geometric mean of bending rigidities

12 p2180 A69-26269

Critical load for anisotropic right-angled isosceles triangular plate stability with large deflections obtained from differential equation

12 p2180 A69-26270

Simply supported laminated anisotropic rectangular plate with coupling occurring between bending and in-plane extension, discussing stiffness analysis by Fourier series method

12 p2184 A69-26808

Buckling loads for anisotropic fiber reinforced composite plates with strong bending membrane coupling terms

12 p2186 A69-26840

Free vibrations of laminated anisotropic rectangular plates with clamped edges analyzed by Rayleigh-Ritz energy method

13 p2371 A69-28673

Analogy between differential equations for skew isotropic plates and rectangular anisotropic plates

13 p2371 A69-28670

Rolling direction tensile tests of alloy steel plate displaying various fracture configurations over distinct temperature ranges, noting stress state, void formation and anisotropy

[ASME PAPER 68-WA/MET-1]

14 p2464 A69-29440

Elastic anisotropic panels mechanics analyzed using differential equations stressing transverse displacements, anisotropic thermal expansion, shape imperfections and slip deformations

15 p2711 A69-30904

Linear bending theory of elastic anisotropic sandwich plates with strong and weak cores

15 p2713 A69-31025

Bending problem of anisotropic /nonorthotropic/ plates solved by method of small parameter

16 p2875 A69-32294

Anisotropic elastic plate deflection weakened by circular hole with thin elastic ring reinforcement, assuming no load on ring and uniform stress-strain state of plate

17 p3055 A69-33128

Laminated anisotropic plate equations from thin plate theory including nonlinear terms, inertia and thermal stresses

[ASME PAPER 69-APM-15]

18 p3213 A69-34390

Stress conditions of anisotropic plate with soldered in circular isotropic aluminum disk in presence of notches at seam, assuming elastic symmetry of plate

18 p3218 A69-34602

Two dimensional theory for anisotropic plates motion derived, using asymptotic integration of three dimensional elasticity equations

18 p3224 A69-35292

Energy formulation extended for plane anisotropic rectangular plates, handling nonuniform properties and loadings

20 p3627 A69-37766

Buckling loads of homogeneous anisotropic plates of composite materials with simply supported boundary conditions, noting Kirchhoff-Love nondeformable normal hypothesis

20 p3628 A69-37776

Asymptotic integration method of nonlinear elasticity equations for first approximation theory of anisotropic plates moderately large deflections

20 p3630 A69-38129

ANISOTROPIC SHELLS

Boundary value bending problem for anisotropic shells of revolution under asymmetrical loading solved by finite difference technique

01 p0165 A69-10088

Asymptotic integration of three dimensional elasticity equations for thin anisotropic shells and plates, deriving variability exponent of stress under given load

01 p0170 A69-10878

Soviet handbook on stress analysis of anisotropic three layer reinforced plates and shells and of thick walled cylinders, Volume 2

04 p0683 A69-15500

Dynamic response of anisotropic circular cylinders to uniformly distributed pressure varying periodically with time analyzed using Laplace transformation

09 p1611 A69-21440

Bending theory for truncated multilayer anisotropic conical shells, defining relations between displacements and external forces

11 p1984 A69-25141

Anisotropic conical shells free vibrations analyzed by Galerkin and operator-matrix methods, neglecting transverse shear deformation and rotatory inertia effects

16 p2874 A69-32165

Free vibrational characteristics of thin walled circular cylindrical shells with layers of anisotropic elastic material laminated about middle surface

20 p3627 A69-37767

Yield condition and relation between stresses and strain rates for anisotropic body, allowing for influence of stressed state type

22 p3934 A69-41169

Dynamic response of anisotropic elastic cylindrical and spherical shells determined by application of Hankel transforms, considering time dependence of loads
23 p4235 A69-42481

ANISOTROPY

NT ELASTIC ANISOTROPY

NT PLASTIC ANISOTROPY

Weakly interacting neutrinos in anisotropic cosmological models with emphasis on equilibrium period, noting energy increment
01 p0123 A69-10348

Elastic anisotropy and polycrystalline orientations in cold rolled titanium sheets investigated by Fourier series method, discussing Young modulus values
01 p0094 A69-10431

Highly oriented graphite crystallites in pyrographites and composite materials, discussing preparation and anisotropy ratios in physical properties
01 p0102 A69-10978

Electromagnetic wave path emitted by artificial satellites across anisotropic ionosphere due to geomagnetic field determined by computer program
01 p0068 A69-11115

Linear stationary thermoelasticity equations for Cosserat continua, discussing static and kinematic conditions, anisotropy and centrosymmetric isotropy equations
02 p0336 A69-11557

Cosmic ray meson diurnal anisotropies direction calculated on basis of subtracted diurnal vectors
02 p0306 A69-11730

Superconductor energy spectrum gap, discussing temperature dependence, anisotropy, thermodynamic and kinetic properties and relation to Fermi surface and phonon spectrum
03 p0485 A69-13331

Magnetoconductance of nonequilibrium plasmas in indium antimonides, noting anisotropy effect of electric and magnetic field orientation
03 p0486 A69-13463

Anisotropically conducting spiral cone current phase distribution applied to frequency independent antennas analysis, discussing spiral motion and field azimuthal dependence effects
03 p0408 A69-14133

Electrical conductivity anisotropy in isotropic germanium and silicon semiconductors, noting effect of metallic contact insertion
05 p0808 A69-16216

Expansion anisotropy in angular distribution of laser produced plasmas in terms of drifting and expanding sphere model, discussing particle velocities, currents and time integrated counts
05 p0804 A69-16460

Transformation of differential mean and current densities and anisotropy of cosmic ray particles and photons observed in frames of reference relative to each other with isotropic flux
05 p0817 A69-16651

Temperature dependence of Josephson critical current in superconductor model having anisotropic energy gap
05 p0810 A69-16803

Galactic cosmic rays anisotropies due to density gradient perpendicular to ecliptic plane studied, using diurnal and semidiurnal component and intensity deficiency
06 p0990 A69-17289

Anisotropies in Forbush decreases in March 1966, noting dependence on interplanetary magnetic field structure
06 p0990 A69-17290

Variational coefficients for vertical and inclined meson telescopes, deriving primary cosmic rays anisotropy parameters from daily variations
06 p0924 A69-17293

Laser light scattering with orientation saturation of microsystems by electric field, noting application to optical anisotropy of macromolecules and colloidal particles
07 p1149 A69-18900

Soviet monograph on diurnal solar cosmic ray variations from maximum to minimum solar activity, discussing model based on anisotropic particle scattering theory
07 p1209 A69-19500

Relative free energies of crystal zones of tungsten using field electron microscope, determining surface energy anisotropy from Wulff construction
08 p1330 A69-20139

Lipshits-Khalatnikov law applicability to early stages anisotropy of cosmological expansion and relic emission
09 p1593 A69-21568

Cosmic ray anisotropy relation to scattering and sectorial structure of interplanetary magnetic field using neutron monitor data
10 p1758 A69-22834

Forbush effects energy spectra and cosmic ray anisotropy beyond magnetosphere analyzed during solar activity minimum, using data from neutron monitors global network
10 p1758 A69-22835

Ionospheric irregularities drift and anisotropy parameters variation with true reflection height during magnetically disturbed conditions
10 p1659 A69-24062

Three dimensional problem of elasticity for transversely isotropic medium with cylindrical anisotropy, using partial differential equations for unknown functions
11 p1983 A69-25091

Anisotropic fluxes of energetic particles in and near distant trapping region encountered by Explorer 33 satellite in outer magnetosphere
11 p1950 A69-25146

Neutron emission anisotropies in capacitor discharge produced plasma focus, detailing coaxial plasma gun energy spectrum and flux measurement
11 p1930 A69-25321

Calcite crystals stability anisotropy to ruby laser radiation, studying threshold power as function of beam polarization
11 p1900 A69-25553

Magnetic domain structure in supercritical ferromagnetic films with perpendicular anisotropy
12 p2143 A69-26458

Magnetic crystallographic anisotropy of Li-Ga ferrite single crystals at temperature range measured by ferromagnetic resonance techniques
12 p2144 A69-26721

Zeeman laser with one end mirror exhibiting x-y-type loss anisotropy, considering resonance condition for round trip pass and self consistent field equations
13 p2271 A69-27398

Polarization dependent gain saturation and nonlinearity induced anisotropy in He-Ne laser amplifier
14 p2457 A69-28931

Rocket observations of Lyman alpha anisotropic galactic radiation, noting distribution of neutral interstellar hydrogen near sun
14 p2516 A69-28952

Plasma instabilities due to anisotropic velocity distributions computer analyzed to study nonlinear phenomena and validity limits of linear theory
15 p2661 A69-30920

Magnetic anisotropy and porosity from approach to saturation of polycrystalline ferrites based on magnetization measurement
16 p2825 A69-31700

High strength fibers and composite materials for structural design, considering anisotropy and low ultimate tensile strain
16 p2802 A69-32380

Cavity linear phase anisotropy and axial magnetic field effect on single mode Zeeman gas laser
16 p2798 A69-32606

Microwave background anisotropy induced by gravitational effects interpreted using spatially flat Friedmann model for substratum
18 p3190 A69-34286

Cosmic ray diurnal anisotropy variations, correlating component annual means with magnetic activity
18 p3186 A69-34934

Friction coefficient increase caused by metal surface textures anisotropic effect on friction force
18 p3149 A69-35151

Solar cosmic ray anisotropies in terms of model with particles propagating along interplanetary magnetic field undergoing pitch-angle scattering
18 p3189 A69-35400

Source position of cosmic ray diurnal anisotropy relative to ecliptic plane from neutron monitor data at Mawson and Churchill stations
18 p3189 A69-35441

Heat conduction orientation anisotropy in linear amorphous high polymers due to uniaxial stretching, noting molecular weight distribution and temperature effects
19 p3359 A69-36443

Anisotropy of derivatives of transverse velocity fluctuations in grid turbulence subjected to plane deformation, determining dimensionless coefficient
19 p3299 A69-36647

Anisotropy coefficients obtained during annealed Al sheet tests based on stress-strain characteristics, noting fading memory effects
19 p3447 A69-36857

Electrical conductivity anisotropy in isotropic germanium and silicon semiconductors, noting effect of metallic contact insertion
20 p3584 A69-37786

Twenty year wave in diurnal anisotropy component of galactic cosmic rays arriving at earth from asymptotic direction east of sun interpreted as magnetic reconnection
20 p3592 A69-38098

Anisotropy of relativistic cosmic ray electrons, considering electron exposure time to synchrotron effects, energy loss from inverse Compton effect, etc
20 p3593 A69-38145

Magnetic crystallographic anisotropy of Li-Ga ferrite single crystals measured by ferromagnetic resonance techniques
21 p3781 A69-39134

Pitch angle distribution of cosmic ray electrons in decreasing magnetic field for waves in ionized plasma, noting anisotropy due to synchrotron radiation
22 p4006 A69-40642

Cosmic ray anisotropy direction during periodic intervals determination, noting application to event of December 1957
23 p4204 A69-41482

Homogeneous axisymmetric anisotropic cosmological models, analyzing magnetic fields and initial anisotropies effect on 3K radiation and primordial He production
23 p4222 A69-42402

Plasma microinstabilities due to ion and electron anisotropic velocity distributions, considering frequencies near harmonics of ion cyclotron frequency
24 p4355 A69-42686

Solar cosmic ray anisotropy measurement by Explorer 34 satellite during solar flare events
24 p4373 A69-43619

ANNA SATELLITES

Anna 1-B geodetic satellite design, instruments and data acquisition
[UN PAPER 68-96195] 06 p0917 A69-17082

ANNEALING

NT PULSE HEATING

Substructural void formation in tungsten powder metallurgy as function of annealing temperature for doped, undoped and electron beam melted material
01 p0093 A69-10061

Shock loading history effect on solid state response of iron meteorites to annealing at moderate temperatures permits deductions about thermal history
01 p0149 A69-10134

Molybdenum elasticity limit and rupturing stress dependence on structure for high temperature annealing, noting changes in solid solution interstitial impurity concentration
02 p0268 A69-12191

Cold rolling and annealing effects on tensile strength, heat resistance and ductility of sintered Al powder sheets
03 p0452 A69-14121

Nimonic alloys high temperature annealing effect on dislocation structure stability created by thermochemical treatment, using transmission microscopy
04 p0615 A69-14636

Electric field effects on thermal annealing of electron irradiation damage in p-channel MOSFET device
05 p0733 A69-16562

Isochronic annealing effect on coercive force of Mo Permalloy samples bombarded with neutrons in nuclear reactor
05 p0783 A69-16815

Recovery of carrier concentration and lifetime in n- and p-type Si during annealing after irradiation by 10 Mev electrons, noting impurities effects
06 p0974 A69-16865

Neutron irradiated Si transistors radiation and annealing characteristics determined for inverse configuration
06 p0975 A69-16872

Electron irradiation annealing and modification of 35 and 65 K defects in n-type Ge induced by 1 Mev electrons at low temperature
06 p0980 A69-17757

Structural defects in annealed niobium crystals observed by optical microscopy, discussing etch pits
07 p1169 A69-19603

Solution annealing and aging time and temperature effects on precipitation in quenched and aged beryllium
08 p1330 A69-20008

Repeated stepwise annealing process to obtain homogenized InSb-GaSb alloys continuous solid solutions
10 p1745 A69-23331

Annealing temperature of radiation defects in phosphorus doped silicon, discussing isochronal recovery characteristics of solar cells with different donor and oxygen concentrations
10 p1747 A69-24006

Diffusion processes during annealing of metals irradiated by electrons and neutrons, discussing crystal damage, recovery and recrystallization
11 p1891 A69-24800

Annealing effects on cold rolled titanium sheets, noting changes in Young modulus and characteristics of recrystallized titanium
11 p1904 A69-24899

Annealing effects on titanium oxidation kinetics, indicating no relation between oxide formation and diffusion anisotropy of oxygen
12 p2112 A69-26039

Lattice defects in annealed and plastically deformed cobalt, showing increase with increasing martensite transformations
12 p2113 A69-26042

Metallographic study of microstructure recrystallization of 50 Ni-50 Fe alloy during annealing using special etchants and methods
13 p2281 A69-28155

Temperature dependent aging mechanisms in deformed Mo alloys during annealing, using transmission electron microscope
14 p2463 A69-29312

Cold worked high purity Mo wire recovery after plastic deformation at room temperature, considering electrical resistivity decrease as function of annealing temperature
15 p2636 A69-30082

Electrical parameters measurement for homogeneous batches of planar silicon transistors subjected to cobalt 60 gamma rays, considering isochronal and isothermal annealing
15 p2625 A69-30827

In-process annealing and warm working temperature effects on long time creep rupture properties of Mo alloys tested in vacuum furnace
17 p2987 A69-33076

Activation energy of annealing of lattice defects in Au films deposited under irradiation with Au ions
18 p3182 A69-34349

Hydraulically extruded Mo properties after annealing, showing reduction in stability and hardness and varying nature of change in plasticity
18 p3156 A69-34719

Annealing temperature effect on Ni-Ti alloys internal friction, noting peak connected with solid solution grain boundaries
18 p3158 A69-35443

Annealing time effects on creep properties of Ni at various temperatures after work hardening
18 p3159 A69-35445

Annealing effect on transition zone cohesion strength in two layer steel-titanium sheet, investigating role of TiC formation
18 p3159 A69-35450

Bonded solderless solar cell panel prototype withstanding high annealing temperature and thermal shock without electrical or mechanical degradation
19 p3251 A69-35688

Imperfection photoconductivity in electron irradiated Li-doped Si annealed at room temperature, noting level rearrangement in O rich material
19 p3382 A69-35696

Cadmium sulfide solar cells and Kapton coverslides under proton irradiation, noting annealing of damage in samples exposed to air
19 p3253 A69-35705

Recrystallization in thorium dispersed Ni sheet as function of strain-anneal cycles, using electron transmission technique quantitative determination
20 p3557 A69-36958

Abnormal grain growth during secondary recrystallization of hydraulically extruded molybdenum as function of annealing
21 p3745 A69-38953

Dislocation structures in Nb-Ti alloys formed after annealing
21 p3747 A69-39163

Plasticity of tubular steel annealed in vacuum furnace and subjected to complex tension and torsion along deformation trajectories containing salient point
21 p3839 A69-39197

Lithium doped silicon acceptor concentration resulting from electron irradiation damage decreased by annealing at 300 degrees K
23 p4197 A69-41498

Cosmic gamma ray spectra from metagalactic proton-antiproton annihilation
09 p1574 A69-21459

Extragalactic gamma ray fluxes predicted, discussing collisions, matter-antimatter annihilation and cosmological implications
11 p1946 A69-24466

Annihilation gamma ray spectra from equilibrium spectra of secondary galactic positrons
14 p2514 A69-29948

Antimatter meteors detectability, considering annihilation and vaporization in earth atmosphere
17 p3034 A69-33579

Astrophysical ions acceleration model based on magnetic field annihilation theory
22 p3987 A69-41002

Antimatter motion in solar system and earth atmosphere, discussing vaporization and annihilation energy in collisions with interplanetary gas atoms
22 p4034 A69-41100

High energy negative kappa meson-nucleon interactions with respect to multiplicity distribution of charged pions in nucleon-antinucleon annihilation, showing binomial distribution
24 p4351 A69-42791

ANNUAL VARIATIONS

North-south ionospheric drift velocities near magnetic equator, noting marked seasonal characteristics and diurnal variations
01 p0062 A69-10138

Seasonal variation of evening-morning difference in maximum density heights of twilight sodium layer
01 p0063 A69-10275

Night ionosphere electron content changes in Southern Hemisphere, discussing diffusion from exosphere and corpuscular radiation as sources of ionization
01 p0063 A69-10423

Whistler rate and dispersion daily and annual variations derived relative to propagation conditions and magnetospheric behavior over North Italy
01 p0067 A69-11033

Gross behavior patterns of intense sporadic E including seasonal, diurnal and geographic variations and latitudinal and longitudinal effects
01 p0070 A69-11157

Seasonal variations in thickness of ionospheric E-F interlayer region during daylight and maximum integral ionization values
02 p0239 A69-11682

Sporadic E layer critical frequencies seasonal and diurnal periodic variations, noting independence of solar activity cycle
02 p0239 A69-11685

High sensitivity mercury vapor analysis automated to provide continuous monitoring of Hg in atmosphere, discussing winter and summer concentrations
02 p0244 A69-12019

Seasonal mean vertical ozone distributions obtained with electrochemical ozone sondes over southeastern Australia
02 p0276 A69-12696

Refractivity distribution at ground level and at one km over India, correlating surface refractivity with difference, noting seasonal and diurnal variations
03 p0393 A69-13304

Ionospheric midday radio wave absorption as function of geomagnetic latitude, season and solar activity from pulsed vertical radar sounding data
03 p0394 A69-13521

Frequency of cold front passages during year in French part of Switzerland and times of occurrence during day
04 p0628 A69-15089

F region seasonal and magnetic storm behavior from region daily behavior showing global upper atmospheric circulation
05 p0757 A69-16404

Upper atmosphere semiannual density variations, using satellite drag analysis
06 p0918 A69-17380

Semiannual variations in exospheric density near 1100 km derived from Echo 2 orbit, noting phases during solar cycle
06 p0918 A69-17385

Twilight resonance emissions due to atmospheric sodium, lithium and potassium, noting similarity of annual sodium and lithium twilight abundance variations [AFCRL-69-0097]
06 p0918 A69-17494

Seasonal variations in auroral absorption zone position interpreted as consequence of asymmetric shape of magnetosphere
06 p0920 A69-17728

Nighttime equatorial Pi 2 micropulsations, noting seasonal and diurnal distributions and dependence on three hour index of magnetic activity
07 p1125 A69-18841

Long range prediction of zonal westerlies based on lunar cycles or quasi-biennial oscillations, considering aliasing problem
07 p1175 A69-18945

Annual temperature variation in lower tropical stratosphere, noting effect of equatorial upward motion
07 p1126 A69-19043

Tropospheric energy cycle interannual variability and quasi-biennial oscillation from geostrophic computations of eddy kinetic energy, energy transfer and internal redistribution
07 p1129 A69-19628

Seasonal maximum ozone concentration variations, discussing vertical ozone distribution
08 p1307 A69-20260

Mean tropospheric wind vectors periods compared to annual variations of earth rotation and pole latitude
08 p1309 A69-20854

Eleven year cyclicity of geomagnetic activity from Sverdlvsk Observatory data, noting possible relation with structural features of solar activity cycles
09 p1486 A69-21552

Air density at 470 km from orbit of satellite 1966-118 A, confirming large semiannual variation
09 p1488 A69-21659

Power spectral analysis of upper wind data of equatorial lower stratosphere noting quasi-biennial oscillation
09 p1537 A69-22297

Hibernation seasonality, protein synthesis during periodic awakenings and importance of awakenings to maintenance and evolution of thyroid activity
10 p1642 A69-23120

Nighttime ionospheric recombination studies by model reference heights varying diurnally, seasonally and with solar flux and geographic location
10 p1685 A69-23834

Secular variations distribution on earth surface, plotting isopore charts from mean annual values of magnetic elements /1960-1965/
10 p1687 A69-23920

Nonpolar LF latitude variations based on spectroscopic and harmonic analysis of zenith telescope and prismatic astrolabe observations
11 p1956 A69-24401

Statistical rules for seasonal forecasts based on temperature and precipitation deviations analysis in long term climatological records, considering sunspot cycle role
12 p2125 A69-25895

IR radiative temperature changes as function of latitude, season and height in region 30-110 km
12 p2064 A69-26008

Tropospheric zonal wind semiannual oscillations in Southern Hemisphere tropics with westerly maxima and easterly minima in May and November
12 p2064 A69-26011

Semiannual density variations in thermosphere and exosphere as function of mixotape height variations
12 p2064 A69-26012

Satellite 1968-5A orbit analyzed for atmospheric density at 140-180 km, noting semiannual variation
12 p2066 A69-26229

Diurnal and seasonal variations in drift velocity vector of small scale inhomogeneities in F 2 layer ionization
12 p2070 A69-26688

Mean annual characteristics of F 2 layer ionization state, using results of worldwide observation station system
12 p2071 A69-26701

Kelvin waves relation to quasi-biennial oscillation, using zonal wind and temperature variance data taken at Canton Island
13 p2290 A69-27391

Latitudinal and vertical variations in six-month zonal wind cycles in equatorial and tropical stratosphere and lower mesosphere, utilizing rocket observations
13 p2294 A69-27854

Soviet book on temperature regime of free atmosphere above Northern Hemisphere covering aerological data processing, statistical estimates, latitudinal and seasonal variations
13 p2294 A69-27934

Mean seasonal atmospheric and synoptic circulation types examined by criterion for identifying analog types
13 p2295 A69-28652

Seasonal variations in thickness of ionospheric E-F interlayer region during daylight and maximum integral ionization values
13 p2257 A69-28713

ANNIHILATION REACTIONS
NT POSITRON ANNIHILATION

Sporadic E layer critical frequencies seasonal and diurnal periodic variations, noting independence of solar activity cycle

13 p2258 A69-28716

Seasonal variation in ionospheric radiation absorption related to time variation between sunrise and constant angle attainment of sun

14 p2437 A69-29072

Seasonal variations of electron density profiles in lower ionosphere measured by differential absorption using partial reflections

14 p2438 A69-29109

Noon electron densities between 65-90 km from measurements of differential absorption of partial reflections, discussing seasonal variations at midlatitudes

14 p2439 A69-29110

F 2 region small scale inhomogeneities drift observations showing seasonal and diurnal velocity and direction changes

14 p2444 A69-29868

Ozonosphere inhomogeneities from UV spectra of reflected solar radiation, studying latitude dependence of seasonal behavior at different heights

15 p2597 A69-30654

Hydrogen and He ion distribution measurements, noting seasonal and local magnetic time variability

15 p2599 A69-31326

Seasonal and latitudinal models of atmospheric wind and temperature structure between 30 and 120 km altitude

15 p2600 A69-31367

Satellites orbits analysis for semiannual variation of air density in upper atmosphere

15 p2601 A69-31378

Intensity and rotational temperature seasonal variations of hydroxyl emission at different latitudes in upper atmosphere

16 p2775 A69-32081

Noctilucent clouds seasonal frequency, considering meteor shower effects and temperature dependence role

16 p2781 A69-32453

Semiannual variation in amplitude of solar daily quiet geomagnetic variation, discussing sunspot dependence of seasonal secondary minimum and maxima

16 p2782 A69-32459

Eleven year cyclicity of geomagnetic activity from Sverdrlovsk Observatory data, noting possible relation with structural features of solar activity cycles

16 p2784 A69-32547

Ozone vertical distribution variations over India observed by Brewer electrochemical ozonesonde, noting effects of dry and monsoon seasons

16 p2786 A69-32627

Vertical ozone distribution determination discrepancies between Brewer-Mast electrochemical sonde and Umkehr methods, discussing influence of seasonal and diurnal variations

16 p2786 A69-32630

Atmospheric density semiannual variation in thermosphere base, suggesting origin at lower heights in mesosphere or stratosphere

17 p2958 A69-32863

Upper atmospheric gas density and temperature distribution diurnal and seasonal variations calculated from satellites orbiting time changes

17 p2959 A69-32924

Radio waves ionospheric absorption dependence on equivalent frequency, showing marked difference for summer and winter conditions

17 p2918 A69-32927

Zonal winds in temperate latitude analyzed as function of latitude and month from GHOST balloon flights in Southern Hemisphere at 200 mb

17 p2997 A69-33163

Ozone concentration worldwide anomaly above 40 km in annual variations, noting dissimilarity in seasonal maximum and minimum with lower level

17 p2960 A69-33166

E region horizontal drift measurements at Ahmedabad from 1956 to 1966, noting solar activity and seasonal influences

17 p2962 A69-33678

Meteor trail drift radar observations in Kharkov, giving wind velocity diurnal and seasonal variations

17 p3041 A69-33897

Unsteady model taking into account photoionization, neutralization and diffusion, describing electron concentration diurnal and seasonal variations in ionosphere F 2 region at midlatitudes

17 p2966 A69-33978

Annual variations of postsunset altitude peak of equatorial F region noting correlation with solar activity

17 p2966 A69-33983

Ionospheric radio wave absorption measurements by A1 method at 2.2 MHz, showing height estimates of absorption region and winter anomaly

17 p2968 A69-33993

Annual general aviation aircraft accident rate variation related to annual variations in pilot flight training activity

19 p3262 A69-36448

Diurnal and seasonal phase-difference fluctuation measurement of radio waves propagating along ground layer caused by atmospheric turbulence

20 p3485 A69-36971

F 2 layer seasonal anomaly, discussing global distribution observed by network of ionospheric stations

20 p3526 A69-37666

Seasonal anomaly of F 2 layer critical frequency in Northern and Southern Hemispheres during high and low solar activity, discussing geomagnetic effect

20 p3526 A69-37667

Diurnal, seasonal and cyclic altitude and maximum ionization median value variations of undisturbed ionosphere from vertical sounding data obtained at Yakutsk, Siberia

20 p3527 A69-37668

Ionospheric radio wave absorption seasonal and diurnal variations over Tiflis from pulsed ionospheric sounding at 2.2 MHz

20 p3491 A69-37677

Diurnal and seasonal variations of primary atmospheric ions in topside ionosphere correlated with solar zenith angle, using ion mass spectrometer on Explorer 32

20 p3534 A69-38087

Distributions, seasonal variations and ionospheric implications of mesospheric nitric oxide concentration

21 p3703 A69-38364

Seasonal effects on energy expenditure during rest and exercise at controlled ambient temperatures, noting effects on heart rate

22 p3890 A69-40211

Spectral reflectivity curves for Mars light and dark areas and seasonal changes of dark area simulated in laboratory

23 p4209 A69-41319

Annual general aviation accident rate prediction from annual flight training variations

23 p4062 A69-41793

Amplitude and phase maps for annual global variations in atmospheric pressure based on harmonic data analysis, suggesting standing wave type distributions

23 p4185 A69-42493

Mesospheric circulation related to noctilucent cloud data, discussing seasonal variations

24 p4307 A69-42965

Upper atmosphere OH molecules vibrational temperature and total emission energy, measuring average seasonal variations

24 p4308 A69-43007

Nonpolar LF latitude variations based on spectroscopic and harmonic analysis of zenith telescope and prismatic astrolabe observations

24 p4391 A69-43791

ANNULAR FLOW

Tangential velocity profile growth in laminar axial flow through concentric annulus with rotating inner cylinder, using Navier-Stokes equations for prediction

01 p0058 A69-10143

Linear stability of parallel flow in concentric annulus for infinitesimal axisymmetric disturbances

01 p0061 A69-11201

Thin rigid radial wall effect on convective flow in heated rotating annulus

02 p0275 A69-12013

Second normal stress difference measurement by annular flows, giving approximate method for experimental data inversion

02 p0234 A69-12604

Thermal convection in rotating fluid annulus, discussing suppression of frictional constraint on lateral boundary

03 p0460 A69-13339

Gas flow rate predictions for long and short tubes and annuli and at densities between laminar continuum and free molecular regimes

[ASME PAPER 68-WA/PID-5]

05 p0750 A69-16166

Radial distribution of azimuthally averaged temperature and amplitude vacillation characteristics in rotating differentially heated fluid annulus determined by multiprobe technique

07 p1126 A69-19040

Corrected stability limit for Poiseuille flow in pipes, annuli and channels, discussing flow between cylinders

07 p1121 A69-19475

Semilogarithmic law of velocity and temperature for turbulent flow in circular channel, examining analogy between momentum and energy transfer

08 p1420 A69-19877

Stability of inviscid swirling flow with finite axial velocity components and nonvanishing radial density gradients, noting criterion for infinitesimal disturbances

08 p1305 A69-20851

Natural convective oscillatory three dimensional flow in cylindrical annuli, describing inception, amplitude, period and wavelength

09 p1481 A69-21902

Differential equation for laminar flow of nonNewtonian fluid in annulus with porous walls of nonuniform permeability, considering inelastic and suction Reynolds numbers

10 p1680 A69-23690

Reduction of noise from underexpanded axisymmetric jet flows using radial jet flow impingement

[AIAA PAPER 68-81]

13 p2248 A69-28212

One dimensional viscous magnetofluidynamic flow in annulus formed by concentric cylindrical electrodes, reducing problem to linear partial differential equation set

[AIAA PAPER 69-725]

17 p3012 A69-33493

Turbomachinery aerodynamics, discussing secondary flow in blading and digital computer applications to annulus flow field

18 p3086 A69-34925

Flow characteristics and wall heat transfer in separated flow region of annular cavity at free stream hypersonic speed and high gas temperature

[AIAA PAPER 68-672]

20 p3458 A69-37185

Slip ratios in annular two phase flow for case of laminar flow in film and no entrainment of liquid in vapor

[ASME PAPER 69-FE-43]

20 p3517 A69-37995

Density field surrounding leaking circular hatch of spacecraft treated as free molecular flow from annulus, superposing far field of effusive orifice flow

21 p3695 A69-39035

ANNULAR JETS

U JET FLOW

ANNULAR PLATES

Annular plate clamped at inner and outer boundaries and subject to point load, computing deflection

04 p0676 A69-14725

Axisymmetric problems in thermoviscous plasticity, discussing stress-strain state of annular disks and thick walled cylinders made of rate sensitive materials

10 p1802 A69-24025

Limit loads for circular and annular plates of smoothly varying profile under uniformly distributed transverse loads

11 p1982 A69-24946

Rigid plastic circular and annular plates dynamics taking into account yield point dependence on strain rate

12 p2177 A69-25994

Stress-strain state of circular annular plate with varying thickness subjected to concentrated axisymmetric load and shearing force applied to internal perimeter

13 p2369 A69-28563

Rigid supporting ribs effect on annular plate critical loading, stability loss and buckling

14 p2533 A69-28983

Stress-strain state determination for axisymmetric shells applied to design of circular/annular plates and rotating disks

17 p3057 A69-33194

Critical loads and stability loss forms of annular plates flexibly clamped at edges in uniform stress field

17 p3057 A69-33197

Ponderable annular region under symmetrically applied concentrated forces, obtaining solution for stress state by successive approximations

18 p3216 A69-34577

Stability loss nonaxisymmetric distribution in elastic annular plates under axisymmetric heating, using Ritz method to determine critical temperature

20 p3623 A69-37327

One dimensional numerical solution for steady state thermal behavior of trapezoidal profile annular fins transferring heat by conduction and radiation

[ASME PAPER 69-HT-6]

24 p4413 A69-43553

ANNULI

He/Ne ratio effect on performance of He-Ne laser in annular cavity

04 p0612 A69-15176

Velocity fields and wall shear stress distributions in eccentric annuli

[ASME PAPER 68-WA/FE-35]

05 p0750 A69-16108

- Wave motion onset and waveforms in rotating annulus with sinusoidally varying temperature differences
07 p1126 A69-19039
- Radial liquid flow between flat annular rings /face seals/, discussing film cavitation
13 p2267 A69-27365
- He/Ne ratio effect on performance of He-Ne laser in annular cavity
18 p3152 A69-34718
- Michell type optimum fiber arrangement for transferring torque across annulus, considering single straight, double and multiple annular arrays under single load system
19 p3447 A69-36851

ANODES

NT CELL ANODES

- Electron flow in stable negative electrostatic potential well produced by electronic injection at center of hollow open spherical anode
03 p0475 A69-13153
- Electrochemical oxidation of n-octane based fuels containing aromatic, olefinic and naphthenic components [ACS PAPER 93]
05 p0716 A69-16234
- Long term electrochemical oxidation performance of n-octane based fuels containing aromatic, olefinic and naphthenic components [ACS PAPER 94]
05 p0716 A69-16235
- Segmented anode current and heat distribution in MPD engine measured with current shunts and calorimetric methods [AIAA PAPER 69-244]
09 p1566 A69-21260
- Platinum based metal binary catalysts as anodes for hydrogen/carbon monoxide fuel mixtures oxidation, discussing alloy surface chemisorption of CO
12 p2026 A69-25937
- Thermionic converter cathode and anode temperatures difference during start-up heating and under normal operational conditions
14 p2400 A69-29226
- Mode transition characteristics of free burning argon electric arc with transpiration cooled anode, noting current blowing parameter [AIAA PAPER 69-696]
17 p3011 A69-33451
- Anode fall measurements with Langmuir probe in coaxial arcs in Ar compared with anode energy balance values
24 p4256 A69-43695

ANODIC COATINGS

- Anodizing effect on flexural properties of Al-aluminum oxide sandwich composites, emphasizing properties of oxide coatings as function of thickness
07 p1159 A69-18723
- Anodic Al oxide films mechanical and fracture properties, studying roles of environmental water vapor and film thickness [ECS PAPER 81]
22 p3973 A69-40736

ANODIZING

- N-type Si surface photopotential, conductivity and capacitance during anodic oxidation in absolute ethylene glycol
04 p0643 A69-15260
- Voltage drop measurement across plasma anodized germanium film to determine anodization constant
10 p1742 A69-24004
- Austenitic stainless steels nonreproducible passivating tendencies, determining electrochemical and corrosion characteristics, discussing critical anodic current density role
20 p3562 A69-37750

ANOMALIES

U ABNORMALITIES

ANOXIA

- Anoxia effect on succinic dehydrogenase and lactic dehydrogenase activities in digestive glands and organs sensitive to oxygen tension changes
22 p3887 A69-41193
- Anoxia effects on leucine-super 3 H incorporation by submandibular gland cells of neonatal rats, discussing cytoplasmic proteins synthesis impairment
22 p3887 A69-41195

ANTARCTIC REGIONS

- Ion formation rate in F 2 layer in southern polar cap, noting effect of season, latitude and solar activity
02 p0238 A69-11679
- Antarctic spread F irregularities, examining models and performing ray tracing
04 p0595 A69-15439
- Albedo over Antarctica, measuring solar radiation reflected by surface and atmosphere by Eppley radiometer
09 p1484 A69-21404

Irregular regions in Antarctic ionosphere from Polar Ionosphere Beacon Satellite S-66 recordings, obtaining irregularities density from nulls clarity
09 p1490 A69-21716

Graphs of ionospheric measurements by vertical incidence sounding during Antarctic expedition, describing instrumentation and sounding techniques
10 p1681 A69-23315

Gustaffson pattern for variations in position of quiet homogeneous arcs, noting diurnal variations from visual observations at antarctic station
12 p2073 A69-26951

Ion formation rate in F 2 layer in southern polar cap noting effect of season, latitude and solar activity
13 p2257 A69-28710

Solar flare effect on polar chorus variation determined by comparing Antarctica VLF data with low latitude magnetograms
14 p2514 A69-29385

H alpha line emission preceding auroral breakup by data analysis of Antarctica Meinel-type patrol spectrograph, noting magnetic activity role
14 p2441 A69-29386

Similarity and correlation methods for drift of ionospheric inhomogeneities in Antarctica
14 p2444 A69-29867

Sterile soil from Antarctica found to contain organic carbon, noting significance for biological exploration of Mars
16 p2746 A69-31552

Polar Ionosphere Beacon Satellite S-66 signals measured for large scale horizontal gradients in total electron content of Antarctic ionosphere at sunspot minimum and maximum
16 p2774 A69-31989

Ionization troughs below F 2 layer maximum due to ionospheric disturbances detected by Antarctica ionograms direction of arrival data
16 p2775 A69-32080

Irregularities distribution in antarctic ionosphere from polarization angle fluctuations of satellite S-66 radio signals, discussing diurnal magnetic and solar cycle effects
18 p3125 A69-34249

Antarctic VLF emissions observations at 12 kHz, showing dependence on geomagnetic disturbances, auroras and radio absorption in ionosphere
18 p3102 A69-34964

Antarctic VLF emissions polarization and direction determination, using combination of antennas with planes lying in geomagnetic E-W and N-S directions
18 p3102 A69-34965

Solar protons intensity increase observed by balloon-borne instruments over Antarctica, describing decay phases
20 p3589 A69-37556

Balloon-borne instrument for auroral X ray measurements at Antarctic station, discussing design requirements, circuit characteristics and improvement recommendations
23 p4166 A69-42011

ANTARCTICA

U ANTARCTIC REGIONS

ANTENNA ARRAYS

- NT ENDFIRE ARRAYS
- NT INERTIALESS STEERABLE ANTENNAS
- NT LINEAR ARRAYS
- NT STEERABLE ANTENNAS
- NT YAGI ANTENNAS

Nomograph for planning circular planar aperture antenna arrays, discussing element totalling and spacing, layout geometry, sidelobe suppression and scan loss from broadside
01 p0037 A69-10017

Planar arrays of linear antennas above stratified medium, showing antenna impedance and current distribution expressed in terms for free space environment
01 p0042 A69-10343

Antenna performance optimization, considering gain dependence on diameter, feed, tolerances, noise temperature, etc [UN PAPER 68-95813]
01 p0043 A69-10517

Tropospheric structure studied with high resolution antennas having small common volume
01 p0043 A69-10560

Dipole array antenna radiation pattern, gain and beamwidth as function of number of dipoles, noting case for main beam scanning
01 p0046 A69-10737

Specular component of ionospherically reflected radio waves between antenna array elements measured for statistical variations
01 p0032 A69-10968

Digital matched filtering technique for RF interferometer employing carrier modulated by pseudonoise sequence, discussing applications to antenna arrays
01 p0048 A69-11003

Low polarization error HF loop antenna array direction finder performance tests, comparing measured bearings with polarimeter and conventional crossed loops data
01 p0048 A69-11006

Phase, frequency and amplitude scanning, noting array design and applications
01 p0049 A69-11348

Phased array radar antennas emphasizing beam steering of transmitting linear array with number of phase shifters
01 p0049 A69-11390

Fourier transformation method for current distribution and driving point admittance of coupled antennas in dissipative medium
02 p0215 A69-11946

Radio telescope for Owens Valley Radio Observatory, noting interferometer array of steerable antennas and signal wavelength influence on telescope reflector accuracy
02 p0229 A69-11974

Technique for combining large numbers of solid state energy sources by using dense array of radiating elements
02 p0217 A69-12148

Reflected and transmitted radiation fields for dielectric loaded infinite phased array of parallel plate waveguides as function of scan angle
02 p0218 A69-12326

Helical log periodic and log periodic dipole arrays impedance and radiation patterns measurements have similar characteristics
02 p0219 A69-12337

Dynamic programming application to synthesis of unequally spaced symmetrical antenna arrays
02 p0219 A69-12338

Legendre polynomial description of radiation pattern of group of radiators, discussing design of linear radiators
02 p0209 A69-12341

96 element wide band scanning array measurements, considering array simulators usability at frequencies above operating frequencies
02 p0219 A69-12343

Retrodirective antenna array with switched Butler matrix feed
02 p0223 A69-12813

Subsurface radio propagation experiments determining feasibility of communication between vertical linear antennas located in drill holes and similar antennas on surface
03 p0395 A69-13622

Electrically small beamed receiving arrays in HF band and random noise
03 p0398 A69-13904

Current distribution in scanning rectangular array with all-directional constant sidelobe and narrowest beamwidth
04 p0570 A69-14302

Directivity and beamwidth determination of large scanning Dolph-Chebyshev arrays
04 p0570 A69-14303

Nonorthogonal beam steering commands for multielement two dimensional phased array antenna
04 p0570 A69-14305

Granularity of beam positions in digital phased arrays based on method of moments and phase distribution
04 p0570 A69-14306

Triangular lattice arrays radiation characteristics similarity to linear tapered arrays, noting sidelobe level
04 p0570 A69-14308

Planar array multiple beam generation and position determination using N-port Butler matrices
04 p0570 A69-14309

Complex power radiated by infinite planar array antenna, noting aperture field distribution influence on formula applicability
04 p0571 A69-14311

Impedance matching of volumetrically scanned waveguide arrays, stressing element spacing, surface wave impedance, etc
04 p0571 A69-14312

Linearly polarized waveguide phased array design, noting waveguide aperture size effect on admittance and minimization of zero radiation directions
04 p0571 A69-14313

Infinite phased dipole array, discussing integral equation, current distributions and active admittances
04 p0571 A69-14316

Phased array antenna radiator element design, emphasizing configuration selection and reflection loss for beam steering

04 p0572 A69-14321

Reflection coefficients of edge and center elements of large periodic two dimensional antenna array, noting TEM mode parallel plate horn arrays

04 p0572 A69-14322

Electronic scanning antenna system consisting of ceramic rod linear array, power distributor, electronic ferrite phase shift feed and driver

04 p0572 A69-14327

Two dimensional electronically scanned k-band phased array antenna design and performance, discussing radiometric system

04 p0572 A69-14328

Butler matrix-fed circular array for continuous 360 degree beam scanning

04 p0573 A69-14329

Radiation properties of spherical phased array of 16 flat spiral antennas and radiation field polarization characteristics

04 p0573 A69-14331

Book on cylindrical dipole arrays covering theory and programs for computational analysis and design with desired characteristics

04 p0574 A69-14353

Current antenna system technology, particularly airborne and spaceborne applications

04 p0576 A69-14767

Asymptotic estimates of radiation patterns of nonequidistant antenna array represented in integral form

04 p0576 A69-14772

Radiation pattern of linear phased antenna array calculated during commutated scanning

04 p0577 A69-14785

Corrugated impedance antennas synthesized, using model in impedance surface form

04 p0577 A69-14786

Electronic counterrotating antennas, developing turning model of antenna group of telecommunications satellite

04 p0578 A69-15065

Mathematical models relating gain, cost, diameter, frequency and rms surface tolerance of ground antennas for exposed and radome enclosed parabolic reflectors

04 p0561 A69-15449

Electronically scanned X band array used as receiving antenna for target recognition radar

04 p0562 A69-15476

Multielement antenna array radiators interaction taking into account edge effects

05 p0727 A69-15638

Directive gain optimization of antenna array during 90 degree radiation deflection

05 p0728 A69-15652

Commutation antenna arrays with arbitrary amplitude distribution, considering phase error effect

05 p0729 A69-16082

Ionospheric drift measurements made on adjacent antenna arrays during IQSY

05 p0757 A69-16409

Synthesized aperture method of measuring antenna gain and radiation patterns

06 p0894 A69-17452

Gunn effect pulse generator for antenna arrays operating at decimeter wavelengths with external power source

06 p0895 A69-17459

Slope optimization of antenna array difference radiation patterns coinciding with antenna directive gains

06 p0895 A69-17461

Synthesis of optimum linear antenna using algorithm

06 p0897 A69-17543

Circular antenna array consisting of identical center fed cylindrical dipoles placed tangential to and in plane of circle and with equal spacing

06 p0898 A69-17765

Multiring antenna arrays for space telemetry and communication, analyzing distant field, radiation resistance, directive gain and mutual impedance

06 p0899 A69-17827

Antenna transmission and receiving system effects on radio brightness temperature measurements by airborne equipment

06 p0929 A69-18000

Satellite communications antenna system at Fucino earth station, describing transmitting and receiving equipment, facilities, power supply, etc

07 p1075 A69-18493

Reflected radio wave amplitude distributions related to distributions of curvature at reflector

07 p1086 A69-19225

Cylindrical antenna in uniaxial resonant plasmas, calculating current distribution and input admittance on basis of Wiener-Hopf technique

07 p1107 A69-19227

Large aperture low noise aerial design for satellite communication earth stations, discussing expected performance of 85-ft antenna at 4 GHz

08 p1279 A69-19956

High gain-temperature ratios aerials design by radio modeling techniques for horn and planar antennas, prime feed paraboloids and Cassegrain systems

08 p1279 A69-19961

Backfire log periodic cavity-backed slot array, giving H plane power patterns with near field plots along array

08 p1281 A69-20035

Radiation pattern synthesis of circular arrays with many directive elements, deriving required excitations without matrix inversion for design purposes

08 p1282 A69-20036

Capacitance and effective height for VLF umbrella antennas using multiple wire structural members to increase effective antenna surface area

08 p1282 A69-20041

Current distribution of long thin cylindrical antenna driven at arbitrary point along length

08 p1282 A69-20043

TV transmission antenna radiation patterns measured with helicopter flown equipment and Decca navigation equipment

08 p1274 A69-20130

Wavefront Wilkins-Minnis, null selection and elevation scanning techniques for measuring radio signals elevation angles with vertical antenna arrays

08 p1275 A69-20293

Focusing effect on far field directional pattern shifting of array normal, noting electronic scanning properties

08 p1285 A69-20400

Radio interferometer antenna array spatial characteristics obtained as function of geographical coordinates of site for reducing observation errors

08 p1314 A69-20434

Center feed system for broadening frequency bandwidth in X-band edge slotted waveguide array antenna

08 p1286 A69-20836

Signal processing arrays - Conference, Dusseldorf, July 1966

08 p1287 A69-20957

Literature survey and critique of signal processing arrays, discussing synthetic, self phasing, retrodirective correlation and decision theoretic arrays

08 p1287 A69-20958

Signal processing arrays characterized by Fourier series radiation sources, time gating and signal smoothing by narrow band filtering

08 p1287 A69-20959

Wullenweber arrays with extended frequency ranges, discussing design considerations and performance characteristics

08 p1288 A69-20962

Broadband steerable arrays design, describing Wullenweber array with doublet aerials yielding good radiation patterns and low cost construction

08 p1288 A69-20963

Electronic beam-rotation systems operation using matrix network to feed circular arrays, noting applicability to direction finding or radar systems

08 p1288 A69-20964

Broadband multibeam antenna array with frequency independent beam directions, noting aperture gain limitation

08 p1288 A69-20965

X band eight element matrix array construction, producing antenna suitable for aircraft

08 p1288 A69-20966

Self focusing aerial antenna arrays with full angular coverage for two way airborne communications

08 p1288 A69-20971

Hemispherical scanning with small aperture monopoles, spirals, scimitars and wire antennas, discussing various types for multiple beam operations

08 p1290 A69-20973

Active microwave scattering antenna arrays at super-high frequencies, noting low bias power requirement

08 p1290 A69-20975

Space frequency filter antennas, using multiple terminals for signal processing as function of frequency and angle

08 p1290 A69-20977

Maxson multibeam antenna design for noninteracting beams, considering beam shapes and positions and applications

09 p1463 A69-21676

UHF telemetry conversion program at Pacific Missile Range, describing antenna, receive- record and separation display systems

09 p1454 A69-21800

Scattering matrix for pattern forming circuit for multiple beam antenna arrays with interacting elements, noting orthogonal pattern optimization

09 p1469 A69-22627

Ionospheric movements from sampling radio diffraction pattern at 89 points and conversion into visible pattern

09 p1492 A69-22756

Pseudodynamic programming for optimizing design of correlator supersynthesis antenna arrays used for radio source tracking

10 p1663 A69-23420

Waveguides mutual coupling in finite antenna arrays analyzed by integral equation method, noting coupling decrease correlation with wavelength and waveguides distance

10 p1663 A69-23421

Multipath fading reduction on line of sight microwave radio relay links by dual space diversity, noting effects of vertical antenna separation, frequency, etc [IEEE PAPER 68-TP-350-COM]

10 p1656 A69-23535

Antenna for lunar occultation observations at 81.5 MHz, detailing experimental procedure and data reduction

10 p1779 A69-23606

Resolving power increase in multibeam antenna, discussing signal demodulation through incident field breakdown

10 p1664 A69-23797

Antenna point and astigmatic sources due to phase centers and phase diagrams relations and antenna caustic curves

10 p1664 A69-23798

Scanning antenna array design utilizing element coupling and telescope type cylindrical optical system

10 p1664 A69-23800

Signal processing method for achievement of very rapid space scanning with antenna array noting application to radar system

10 p1657 A69-23801

Radiation field of log periodic dipole array calculated as function of observation point and dipole currents

10 p1664 A69-23802

Antenna array statistical synthesis, investigating signal detection capacity for large phase fluctuations

11 p1833 A69-24439

Antenna array models with different emitters to investigate characteristics of radiation patterns in near and far fields

11 p1844 A69-24451

Log periodic dipole array antennas simulated with simple RLC circuit loading uniform transmission line

11 p1850 A69-24977

Nested rhombic antenna spacing determined by measuring mutual coupling and interacting effect on radiation patterns

11 p1850 A69-24979

Self steered retrodirective antenna arrays with phase synthesizer, combining signals from individual elements at LF levels

11 p1850 A69-24983

Radiating collinear open ended waveguides and near field coupling analyzed using simultaneous integral equations and Fourier series expansion of aperture field

11 p1850 A69-24984

Vertical parabolic antenna array and receiving system for S band transhorizon signal phase and amplitude measurement

11 p1851 A69-24987

Slow waves contribution to image radiation from array of line sources above ground plane, determining optimum height of lowest element of array

11 p1837 A69-25002

Electrical servopositioning of telemetry reception antenna for tracking satellites, considering weight, stability, etc

11 p1852 A69-25118

Current distribution on elements of circular arrays of tangential dipoles, discussing large odd component in zeroth order approximation

11 p1853 A69-25318

Thinned arrays design based on array excitation autocorrelation function, considering element spacing

11 p1856 A69-25661

Constant amplitude current excitations superposed on uniformly spaced array for sidelobe reduction, comparing results to Chebyshev arrays
12 p2040 A69-26473

Antenna suspension height variation effects on HF signals in ionospheric scattering lines
12 p2032 A69-26705

Aesthetic preservation of visual amenities in countryside by proper antenna design without affecting performance or cost
12 p2044 A69-26924

Antenna circular array for synchronous communications satellites, discussing directional patterns, super-gain ratio, element spacing, etc
13 p2225 A69-27184

Antenna cross dipole array for vehicle tracking in VHF band, obtaining effect of local rotation by electrical phase shifting
13 p2226 A69-27185

Multiple beam HF receiving antenna system for directivity, azimuthal coverage and noise limitation
13 p2228 A69-27631

Radio emission of atmospheric cosmic ray showers observed with multiple wideband half wave dipole antenna system, obtaining radiation spatial distribution
13 p2332 A69-28407

Admittance of radiating elements in circular array with longitudinal slots on conducting cylinder, taking into account element interactions
13 p2234 A69-28505

Passive magnetic elements array calculation for radiation pattern, discussing emitter position
13 p2235 A69-28513

Antenna system synthesis for amplitude distribution along linear emitter, considering radiation patterns
13 p2235 A69-28521

Current distribution along linear antenna array taking into account interaction between neighboring elements and effect on antenna radiation characteristics
13 p2236 A69-28572

Stepped scanned ring monopulse array, discussing pattern analysis, directivity, co-phased and quasi-phased model
14 p2419 A69-28894

High resolution azimuth and elevation arrays sensing remote ionosphere and sea surface characteristics, discussing backscatter data for ionosphere and sea scatter
14 p2448 A69-29520

Two antenna radio direction finding system statistical synthesis, using quadratic linear process
15 p2562 A69-30110

Signal reflection elimination from underlying surface during aircraft flights by using two antenna array with identical radiation patterns
15 p2567 A69-30345

Orthonormalized partial radiation patterns for antenna array of N emitters developed by introducing scattering matrix
15 p2579 A69-30951

Three antenna interferometer angle measurement accuracy dependent on antenna spacing, deriving optimal spacing value
16 p2758 A69-31730

Multielement antenna array radiators interaction taking into account edge effects
16 p2762 A69-32496

Directive gain optimization of antenna array during 90 degree radiation deflection
16 p2762 A69-32509

Vertically polarized log periodic antenna consisting of unipole vertical radiators with side radiators for achieving minimum size
16 p2763 A69-32580

Antenna systems design for ISIS-A scientific satellite, discussing antenna array of 13 radiators for telemetry, command, beacon and experimental purposes
17 p2918 A69-33030

Antenna array construction for reception of weather satellite transmissions, noting automatic picture transmission systems/APT/
17 p2946 A69-33767

Seven helix antenna array components and operation mode at Berlin weather station, including biaxial rotator, preamplifier servoamplifier and VHF telemetry receiver
17 p2946 A69-33768

Driving point admittance of radiating aperture in infinite periodic phased array, determining Floquet series and coefficients of waveguide modal expansion
17 p2938 A69-33876

Van Atta array reflector retrograde effect, studying influence of transmission line length, interelement

spacing and line-dipole matching on incident reflected radiation phase correlation
17 p2929 A69-33878

Directional transmitting and receiving antenna arrays for short wave meteor studies in Kharkov
17 p2939 A69-33903

Phased arrays applied to inertialess electronic steering of satellite antennas, discussing digitally steered, retrodirective and hybrid matrix arrays
17 p2942 A69-34083

Mathematical model of fields reradiated by Huygen sources in front of array for glide path site analysis
17 p3003 A69-34107

Minimum weight design of tiltable enclosed antenna structure as subject to deformation constraints
18 p3211 A69-34341

Digital computer controlled antenna positioning system computing spacecraft tracking trajectory from given parameter input set
19 p3267 A69-35997

Backfire antenna radiation characteristics and physical dimensions for tracking and telemetry applications, including five element array model
19 p3271 A69-36251

Gain measurement of two element phased array aperture antenna during ATS-C tracking
19 p3272 A69-36254

Radio wave information transmission, discussing propagation in various media, antenna arrays, diffraction, scattering, plasmas, guided waves and periodic structures
19 p3276 A69-36431

Beam shape loss /BSL/ for electronically steerable array in search mode, determining optimum search beam locations from BSL computations
20 p3506 A69-37717

Analysis theory of shaped beam doubly curved reflector antenna, computing far field patterns by determining current density distribution on nonanalytic surface
20 p3506 A69-37835

T shaped radio astronomical array, discussing time sharing technique providing simultaneous observation capability and merits of T and cross configuration telescopes
20 p3507 A69-37837

Active admittance, realized gain and linear polarization degradation vs scan angle for infinite periodic phased arrays of circular apertures
20 p3507 A69-37844

Parallel wire antenna array design for specified pattern using matrix methods and method of moments for self and mutual impedances and required excitations
20 p3507 A69-37847

Synthesized aperture method of measuring antenna gain and radiation patterns
20 p3508 A69-37937

Gunn effect pulse generator for antenna arrays operating at decimeter wavelengths with external power source
20 p3508 A69-37942

Slope optimization of antenna array difference radiation patterns coinciding with antenna directive gains
20 p3508 A69-37944

Soviet book on antenna synthesis theory for application to antenna radiation patterns with allowance for Fourier transforms limitations
20 p3508 A69-38208

Antenna arrays subject to random excitation error analyzed by probability theory, noting relationship between antenna pattern and excitation distribution parameters
21 p3681 A69-38742

Antenna synthesis problems in mathematical physics, discussing radiation pattern, shape and source and optimal solution via operators spectral theory
21 p3682 A69-39124

Synthesis by differential equation technique for linear antenna arrays of identical radiators radiation patterns
21 p3682 A69-39125

Mutual impedances of radiators in periodic and doubly periodic rod antenna arrays with orthogonal harmonics current distribution, noting diffraction theory applications
21 p3682 A69-39126

Deployable cross log periodic dipole /LPD/ array on conducting cone as potential application to spacecraft or missile requiring frequency independence in VHF-UHF band
22 p3913 A69-40693

Prolate spheroidal antennas operation in isotropic plasmas, studying effects of collision frequency, elec-

tron temperature and antenna length on admittance, radiation and current distribution
22 p3914 A69-40702

Circular and spherical antenna arrays elements random distribution in three dimensional space using Monte Carlo method, considering arbitrary excitation and nonisotropic elements
22 p3914 A69-40704

Spacecraft phase array designed for use on synchronous communication satellite, discussing low structural weight packaging and unfurling problems and helix approach
22 p3915 A69-40705

Circular antenna arrays radiation pattern synthesis in moving medium relative to main beam, noting medium motion influence on pattern changes
22 p3915 A69-40706

Aperture efficiency, weight and control power requirements for hybrid matrix arrays in synchronous satellite applications, calculating residual array gains
22 p3915 A69-40707

Microwave power transmission to high or low altitude balloon systems for stationkeeping, describing flexible diode array rectifier antenna
22 p3870 A69-40809

Antenna array synthesis optimization for limited deviations of source distribution function from prescribed function
22 p3916 A69-40952

Antennas aperture radiation patterns optimal interpolation synthesis permitting confident control of main lobe shape
22 p3916 A69-40953

Redirection of time varying signal between specified points by arbitrarily spaced antenna array elements with condition involving time delays for validity of retrodirection
23 p4136 A69-41580

Kirchhoff equations for synthesis of passive dipole arrays, obtaining best approximation to radiation patterns
23 p4138 A69-41935

Synthesis of antenna arrays of longitudinal passive slot radiators on metallic cylinder excited by single active slot, including experimental patterns
23 p4138 A69-41936

Array aperture amplitude and phase distortions effect on radiation field uniformity
23 p4138 A69-41940

Electromagnetic wave diffraction normally incident on symmetrical five element metallic array
23 p4123 A69-42029

Linearly polarized electromagnetic wave diffraction during oblique incidence on crossed strip arrays, describing crossing angle effects on reflection, transmission and polarization conversion coefficients
23 p4124 A69-42030

Dispersion and resonant properties of electromagnetic waves propagating along plane metallic strip array with shield and dielectric
23 p4124 A69-42038

High sensitivity communication system design consisting of radome enclosed steerable antenna, 500 kw transmitter and microwave configuration compatible with low noise receivers
23 p4149 A69-42131

Antenna arrays for radio astronomy in meter-wavelength region including cross-polarized rhombics, steerable broadside collinear array and radio interferometer
23 p4143 A69-42353

Antenna design, based on helical beam radiator data, providing checking facility giving automatic alarm
24 p4312 A69-42573

Ground antenna array for ionospheric physics experiments, consisting of wire dipoles connected to receive circular or linear polarization
24 p4286 A69-42607

SNR improvement by antenna array optimization
24 p4287 A69-43140

Asymmetric metal flanges effect on beam tilt of aperture antennas
24 p4288 A69-43765

ANTENNA COUPLERS
NT COUPLING CIRCUITS

Asymptotic decay of coupling for infinite phased arrays proved valid for infinite parallel linear plate array immersed in magnetized cold plasma
04 p0571 A69-14314

Equivalent network representation of feedthrough lens array taking into account mutual coupling between elements to predict performance characteristics
08 p1280 A69-20014

Coupling between array antennas shown to reduce reflecting properties of Van Atta reflector consisting of linear half wave dipoles
08 p1282 A69-20037

Waveguides mutual coupling in finite antenna arrays analyzed by integral equation method, noting coupling decrease correlation with wavelength and waveguides distance
10 p1663 A69-23421

Scanning antenna array design utilizing element coupling and telescope type cylindrical optical system
10 p1664 A69-23800

Nested rhombic antenna spacing determined by measuring mutual coupling and interacting effect on radiation patterns
11 p1850 A69-24979

Synthesis for asymmetrical branch guide directional coupler-impedance transformers, noting application in antenna design
13 p2233 A69-28069

Interrelations among mutual coupling, element efficiency, active impedance and radiation patterns in linear arrays derived from infinite order difference equation
17 p2929 A69-33874

OGO 5 spacecraft detector instrumentation for measuring electrostatic and electromagnetic waves electric fields with coupled antennas, describing in-flight operation
19 p3315 A69-36683

Asymptotic approximation formulas to compute on-axis Fresnel region fields for coupling between two large aperture antennas
23 p4136 A69-41582

Directional couplers applied to excitation of non-protruding surface wave antennas, examining ridge slot system
23 p4139 A69-41946

ANTENNA FEEDS

Retrodirective antenna array with switched Butler matrix feed
02 p0223 A69-12813

Multiple beam electronically steerable retrodirective antenna array with automatic inertialess compensation for altitude or beacon location
02 p0212 A69-12816

Electronic scanning antenna system consisting of ceramic rod linear array, power distributor, electronic ferrite phase shift feed and driver
04 p0572 A69-14327

Butler matrix-fed circular array for continuous 360 degree beam scanning
04 p0573 A69-14329

Rear gain control of dielectric rod antenna in airborne Doppler system with choke at feed point
04 p0576 A69-14770

Feed support blockage loss in parabolic antennas evaluated by shadowgraph photography
04 p0576 A69-14771

Random phase errors in end-fed linear antenna arrays
04 p0578 A69-15211

Antennas with any mean surface, prescribed feeder and radiation pattern synthesized by microwave holography
05 p0734 A69-16574

Propagation constant and radiation of center fed linear antenna with feed points displaced transverse to antenna axis and immersed in warm compressible plasma
06 p0896 A69-17476

Sectoral hoghorn as line feed for correcting spherical aberration in offset spherical reflector antennas
06 p0898 A69-17823

Shot noise in dipole antenna immersed in hot plasma related to antenna input resistance, using Maxwellian velocity distribution
07 p1079 A69-18920

Telemetry and tracking antenna feed system in EC-135N instrumented aircraft for Apollo moon project
07 p1105 A69-19110

Adaptive primary feed system for wide angle beam scanning from parabolic reflector antenna, using Fourier transformation to obtain uniform power distribution
08 p1279 A69-19908

High gain-temperature ratios aeriads design by radio modeling techniques for horn and planar antennas, prime feed parabolooids and Cassegrain systems
08 p1279 A69-19961

Phasing of active region of log-periodic array antennas by modulated impedance feeders, discussing monopole and slot arrays
08 p1281 A69-20015

Center feed system for broadening frequency bandwidth in X-band edge slotted waveguide array antenna
08 p1286 A69-20836

Electronic beam-rotation systems operation using matrix network to feed circular arrays, noting applicability to direction finding or radar systems
08 p1288 A69-20964

Mode coefficients for geometrical optics field expansion at waveguide feed junction of sectoral horn
09 p1468 A69-22590

Superdirective aerial endfire array of four unequally spaced half wave dipoles and only one fed element, calculating and measuring maximum gain
09 p1468 A69-22603

Multimode tracking/SYMMTRAC I and II/ feeds for low noise antennas, noting feed performance
11 p1852 A69-25317

Coaxial radiator as feed for low noise paraboloid antennas, presenting pattern synthesis
11 p1856 A69-25635

Subtraction procedure for feedpoint singularity in current on axially symmetric antenna with slice generator
12 p2041 A69-26864

Horn exciter with fundamental and second mode in feeding waveguide of shallow paraboloid antennas
12 p2044 A69-27093

Soviet monograph on intrinsic noise emission in radio channels covering noise temperature at receiver input, thermal microwave radiation, etc
13 p2219 A69-27304

Input impedance measurement of radiating symmetrical HF and microwave antennas, using solid state oscillator for feeding
14 p2420 A69-29394

Corrugated cylindrical waveguides used as hybrid mode feeds for reflector antennas
15 p2575 A69-30175

Corrugated conical horn used as antenna feed, studying fields in horn and associated radiation patterns by spherical hybrid functions analysis
15 p2575 A69-30176

Vertically polarized log periodic antenna consisting of unipole vertical radiators with side radiators for achieving minimum size
16 p2763 A69-32580

Waveguide feeder for Goonhilly Downs satellite communication antenna reducing feeder loss for use with low elevation Intelsat 3 satellite
17 p2935 A69-32849

Beam control of optically fed two axis airborne electronically scanned phased arrays by on-array and off-array processing
17 p2942 A69-34085

Multiplicative feed system for monopulse angle tracking antennas, discussing influence of sidelobe and backlobe responses on control function slope determining antenna bearing angle
20 p3510 A69-37704

Waveguide fed rectangular aperture antenna with dielectric plug load, describing admittance resonant perturbation due to excited TE mode
23 p4136 A69-41589

Monopulse, high power, three channel antenna feed system design for communication satellites, noting orthogonal polarization of transmit and receive functions
23 p4120 A69-41750

Parabolic antenna properties generated by dual band circularly polarized focused two channel monopulse feed system, discussing tracking data from helicopter, Apollo 8 and Cassiopeia A
23 p4120 A69-41752

ANTENNA RADIATION PATTERNS

NT SIDELOBES

Nomograph for planning circular planar aperture antenna arrays, discussing element totalling and spacing, layout geometry, sidelobe suppression and scan loss from broadside
01 p0037 A69-10017

Atmospheric noise at millimeter wavelengths, discussing solar radiation and antenna near and far field patterns
01 p0028 A69-10420

Critical parameters for optimum design of Cassegrain antenna used in space communications [UN PAPER 68-95280]
01 p0043 A69-10481

Radiation pattern shaping from circular aperture antenna with constant illumination amplitude [UN PAPER 68-95756]
01 p0029 A69-10524

Dipole array antenna radiation pattern, gain and beamwidth as function of number of dipoles, noting case for main beam scanning
01 p0046 A69-10737

Radiation pattern, gain and polarization of omnidirectional antenna consisting of dipoles or monopoles arranged along circular cone
01 p0046 A69-10738

Far and near fringe radiation of asymmetrical mirror and horn antennas by method of boundary waves
02 p0214 A69-11601

Symmetric and asymmetric metal flanges effects on radiation patterns of H plane sectoral horns, noting theoretical explanation and applications
02 p0216 A69-12027

Asymmetric excitation of conducting flanges by primary aperture antenna and consequent radiation pattern
02 p0217 A69-12246

Variation method for optimal solution of antenna synthesis problem for given radiation pattern
02 p0217 A69-12260

Gain and radiation pattern of conical horn excited by circular waveguide, using geometric theory of diffraction
02 p0218 A69-12327

Horn antenna far field radiation pattern distortion by isotropic plasma slab, noting attenuation variation with electron density
02 p0218 A69-12335

Short backfire antenna radiation fields calculation by approximate method
02 p0219 A69-12339

Legendre polynomial description of radiation pattern of group of radiators, discussing design of linear radiators
02 p0209 A69-12341

Wave measurements of normal electric field and tangential magnetic field over microwave disk antenna surfaces
02 p0219 A69-12342

96 element wide band scanning array measurements, considering array simulators usability at frequencies above operating frequencies
02 p0219 A69-12343

Dual band shunt slot linear array for S and X band radiation patterns generated from single aperture
02 p0219 A69-12344

Aperture blockage by subreflector in Cassegrain antenna system, computing effects on far field radiation patterns
03 p0401 A69-12853

Antennas with vertical radiation patterns to measure frequency spectrum of distributed cosmic radio emission between 6.3-40 MHz
03 p0500 A69-13080

Balanced symmetrical four arm conical equiangular spiral antenna providing omnidirectional circularly polarized radiation pattern in azimuthal plane
03 p0404 A69-13471

Electric or magnetic dipole antenna radiated electromagnetic field for antenna orientation perpendicular to striations of periodically stratified dielectric medium
03 p0398 A69-13802

Advanced potentials method to determine electric field intensity tangential component on surface of cylindrical radiator
03 p0408 A69-14131

Current distribution in scanning rectangular array with all-directional constant sidelobe and narrowest beamwidth
04 p0570 A69-14302

Directivity and beamwidth determination of large scanning Dolph-Chebyshev arrays
04 p0570 A69-14303

Collimation of row and column steered phased arrays
04 p0570 A69-14304

Electronically steered and shaped beams for linear and ring phased array antennas by sampling element signals multiplexed into single channel
04 p0570 A69-14307

Triangular lattice arrays radiation characteristics similarity to linear tapered arrays, noting sidelobe level
04 p0570 A69-14308

Element pattern nulls in phased arrays and relation to guided waves supported by array face
04 p0570 A69-14310

Complex power radiated by infinite planar array antenna, noting aperture field distribution influence on formula applicability
04 p0571 A69-14311

Linearly polarized waveguide phased array design, noting waveguide aperture size effect on admittance and minimization of zero radiation directions
04 p0571 A69-14313

ANTENNA RADIATION PATTERNS

HAPDAR-TACOL phased array radar design, discussing array patterns and multitarget tracking performance
04 p0556 A69-14324

Two dimensional electronically scanned k-band phased array antenna design and performance, discussing radiometric system
04 p0572 A69-14328

Butler matrix-fed circular array for continuous 360 degree beam scanning
04 p0573 A69-14329

Radiation properties of spherical phased array of 16 flat spiral antennas and radiation field polarization characteristics
04 p0573 A69-14331

Directional properties of electric vibrator positioned at reflecting circular cylinder, discussing radiation patterns and cylindrical wave diffraction
04 p0574 A69-14459

Contour pattern analysis of AN/FQP-6 monopulse radar Cassegrainian antenna, giving three dimensional drawings
04 p0576 A69-14769

Rear gain control of dielectric rod antenna in airborne Doppler system with choke at feed point
04 p0576 A69-14770

Asymptotic estimates of radiation patterns of nonequidistant antenna array represented in integral form
04 p0576 A69-14772

Radiation pattern of linear phased antenna array calculated during commutated scanning
04 p0577 A69-14785

Statistical characteristics of radiation pattern of mirror antennas in region of irregular sidelobes
04 p0577 A69-14787

Dielectric sheath effect on far zone radiation characteristics of aperture bounded by perfectly conducting ground plane
04 p0579 A69-15450

Difference radiation patterns of circular aperture with axisymmetric amplitude distribution
05 p0717 A69-15636

Directive gain optimization of antenna array during 90 degree radiation deflection
05 p0728 A69-15652

Commutation antenna arrays with arbitrary amplitude distribution, considering phase error effect
05 p0729 A69-16082

Antennas with any mean surface, prescribed feeder and radiation pattern synthesized by microwave holography
05 p0734 A69-16574

Microwave antennas simulation by optical systems based on Huygens-Kirchhoff approximation, noting application to antenna analysis, synthesis and radiation patterns
05 p0736 A69-16780

Optical simulation of microwave antennas with variable profile reflectors, investigating radiation patterns by photometric scanning of photographs obtained with He-Ne laser
05 p0736 A69-16781

Optimum antenna radiation patterns during suboptimum scattered Gaussian signal detection in homogeneous interference level investigated with single channel antenna
05 p0736 A69-16782

Emission of thin metallic antenna in randomly inhomogeneous medium, determining effective impedance
06 p0894 A69-17451

Synthesized aperture method of measuring antenna gain and radiation patterns
06 p0894 A69-17452

Directional mirror antenna parameters measurement by finite focusing of radiating element
06 p0895 A69-17453

Linear antenna synthesis for optimal separation of plane waves providing maximum SNR with allowance for statistical phase distribution of field
06 p0895 A69-17460

Slope optimization of antenna array difference radiation patterns coinciding with antenna directive gains
06 p0895 A69-17461

Tuning of two mirror antennas in near zone with various mirror combinations, discussing field cophasing
06 p0895 A69-17462

Propagation constant and radiation of center fed linear antenna with feed points displaced transverse to antenna axis and immersed in warm compressible plasma
06 p0896 A69-17476

Circular antenna array consisting of identical center fed cylindrical dipoles placed tangential to and in plane of circle and with equal spacing
06 p0898 A69-17765

Airborne S-band telemetry antennas for omnidirectional patterns of polarization component, discussing design, pattern measurements and application
07 p1106 A69-19112

Measurement bases in general, discussing theoretical data justifying ground level base and measurements results
07 p1136 A69-19516

Radioelectric axis deviation of radome in front of monopulse radar antenna
07 p1111 A69-19524

Radiation pattern deformation due to sharp angle radome studied by analyzing diffraction in antenna dihedron system
07 p1112 A69-19539

Radiation pattern solved for antenna enclosed in radome, deriving exact formulas for scalar field
07 p1112 A69-19543

Object restoration, discussing data processing method for single variable functions with small signal to noise ratios
07 p1137 A69-19721

Antenna pattern loss factor for determination of average probability of detection vs SNR curves for three dimensional or pencil beam radars
08 p1270 A69-19858

Algebraic expression for field pattern of asymmetrically driven long antenna with multiple excitations, using Wiener-Hopf integral equation
08 p1281 A69-20016

Electromagnetic multipole left- and right-hand circularly polarized modal fields for multiarm log spiral antennas, discussing current distributions, multipole coefficients and field patterns
08 p1281 A69-20018

Bounds on electric field outside radiating system determined for application to UHF and VHF systems design, considering microwave breakdown
08 p1273 A69-20026

Log periodic antenna with vertically polarized omnidirectional radiation constant over bandwidth
08 p1281 A69-20033

Backfire log periodic cavity-backed slot array, giving H plane power patterns with near field plots along array
08 p1281 A69-20035

Radiation pattern synthesis of circular arrays with many directive elements, deriving required excitations without matrix inversion for design purposes
08 p1282 A69-20036

Pressure formed parabolic reflectors for millimeter waves, discussing electrical measurements at 30 GHz
08 p1282 A69-20039

Monopole antenna behavior over grounded metal hemisphere, noting application to spacecraft and broadcasting antennas erected on hill
08 p1282 A69-20040

Numerical double integral evaluation technique for antenna radiation patterns, discussing error data
08 p1282 A69-20042

TV transmission antenna radiation patterns measured with helicopter flown equipment and Decca navigation equipment
08 p1274 A69-20130

Antenna tolerances theory, discussing illumination correlation function analytical evaluation for uniform and tapered illuminations
08 p1284 A69-20294

Focusing effect on far field directional pattern shifting of array normal, noting electronic scanning properties
08 p1285 A69-20400

Lunar radio emission polarization characteristics, considering knife-edge type radiation pattern effect of antenna array
08 p1391 A69-20423

Radiation field patterns of linear antennas immersed in weakly ionized plasma evaluated for propagation constants of current distribution
08 p1285 A69-20551

Metal flanges position effect on radiation patterns of H-plane sectoral horn radiators
08 p1285 A69-20554

Duty cycle increase on meteor forward scatter radio communication paths by use of wide-beam transmitting antenna along great circle
08 p1394 A69-20609

Broadband steerable arrays design, describing Wullenweber array with doublet aeriels yielding good radiation patterns and low cost construction
08 p1288 A69-20963

Counterrotating antenna for spin stabilized satellite, noting linear phase shift influence on radiation pattern
08 p1289 A69-20968

Self focusing linear array for communication satellites, evaluating reradiated field taking into account mutual coupling between elements
08 p1289 A69-20970

Hemispherical scanning with small aperture monopoles, spirals, scimitars and wire antennas, discussing various types for multiple beam operations
08 p1290 A69-20973

Reciprocal and nonreciprocal electronically adjustable ferrite phase shifters and application in scanning leaky wave antennas
08 p1290 A69-20979

Frequency independent antenna far field radiation approximated for gain, polarization, field amplitude and phase, defining omnidirectional antenna with wide-band goniometry
08 p1295 A69-21149

Earth station antenna radiation patterns for studying mutual interference effects between radio relay stations and communication satellite earth stations
09 p1461 A69-21282

Magnetic field plane radiation patterns for tapered dielectric rod antennas computed by Schelkunoff principle, noting taper angle effect on lobes
09 p1464 A69-22097

Horizontal VLF cylindrical transmission antenna current distribution calculated with allowance for ground reaction, showing exponential decrease with distance
09 p1467 A69-22581

Microwave antennas optical simulation, discussing given phase amplitude distribution problems
09 p1469 A69-22625

Scattering matrix for pattern forming circuit for multiple beam antenna arrays with interacting elements, noting orthogonal pattern optimization
09 p1469 A69-22627

Ionospheric movements from sampling radio diffraction pattern at 89 points and conversion into visible pattern
09 p1492 A69-22756

Antenna gain increase, using matched pair of Cassegrain reflectors with one primary source
10 p1664 A69-23799

Radiation field of log periodic dipole array calculated as function of observation point and dipole currents
10 p1664 A69-23802

Conducting flanges effects on H plane radiation patterns of E plane sectoral horns, noting improved beam width and gain and H plane beam tilting
10 p1665 A69-24063

Atmospheric turbulence effect on linear antenna gain in direction of radiation pattern maximum determined together with antenna dimensions
11 p1844 A69-24435

Antenna array models with different emitters to investigate characteristics of radiation patterns in near and far fields
11 p1844 A69-24451

Far and near fringe radiation of asymmetrical mirror and horn antennas by method of boundary waves
11 p1846 A69-24708

Approximate method for calculating linear multidipole antennas parameters in terms of power requirement, considering equidistant/nonequidistant element antennas
11 p1849 A69-24969

Nested rhombic antenna spacing determined by measuring mutual coupling and interacting effect on radiation patterns
11 p1850 A69-24979

Yagi-Uda type antennas analysis based on radiated electric field equations, noting far field pattern dependence on phase velocity
11 p1850 A69-24980

Radiation fields induced by constant current in elliptic ring, discussing analysis results applicability to elliptic capacitive antennas and annular slot
11 p1850 A69-24981

Radiation field patterns from metal wall aperture in waveguide with rectangular cross section determined using elliptic cylinder
11 p1850 A69-24982

Two dimensional radiation from apertures in conducting cylinders of arbitrary cross section, solving current distribution, admittances and radiation patterns
11 p1836 A69-24985

Power transmission efficiency between arbitrarily focused circular antennas with Gaussian amplitude illumination in Fresnel region for various phase illuminations and Fresnel numbers
11 p1851 A69-24991

Conducting grill effect on E-plane radiation patterns of E-plane sectorial horns, giving data for various horns at different frequencies

11 p1836 A69-24992

Radiation pattern of axial slot on circular conducting cylinder based on wedge diffraction and creeping wave theory

11 p1836 A69-24993

Electric field vertical and radial components for time harmonic electric line sources with piecewise sinusoidal current distribution

11 p1836 A69-24995

Slow waves contribution to image radiation from array of line sources above ground plane, determining optimum height of lowest element of array

11 p1837 A69-25002

Radiation pattern as function of asymmetry in amplitude of secondary source excitation by primary aperture antenna

11 p1852 A69-25117

Microwave antenna testing on small indoor ranges, discussing reflectors and feeds for generation of approximately uniform plane waves for antenna illumination

11 p1852 A69-25314

Coaxial radiator as feed for low noise paraboloid antennas, presenting pattern synthesis

11 p1856 A69-25635

Thinned arrays design based on array excitation autocorrelation function, considering element spacing

11 p1856 A69-25661

Radiation pattern of circular cylindrical dielectric rod antenna excited in mixed magnetic and electric modes, discussing mode transducer

12 p2035 A69-25900

Far field radiation pattern, radiation resistance, power gain, directivity and effective aperture for center fed dipole antenna with feed points displaced arbitrarily

12 p2039 A69-26352

Constant amplitude current excitations superposed on uniformly spaced array for sidelobe reduction, comparing results to Chebyshev arrays

12 p2040 A69-26473

Dielectric coated finite cylindrical antennas, using numerical and Wiener-Hopf methods to obtain input admittance and current distribution

12 p2041 A69-26604

Atmospheric thermal radio emission fluctuations effects on radio telescope sensitivity, evaluating dispersion at low angles to horizon

12 p2031 A69-26643

Input impedance of quarter wavelength antenna in anisotropic plasma, discussing plasma parameters role and use of probe antenna in plasma diagnostics

12 p2044 A69-27071

Field patterns for wave radiation from electric dipole immersed in anisotropic plasma column excited by longitudinal DC magnetic field

12 p2034 A69-27103

Antenna circular array for synchronous communications satellites, discussing directional patterns, supergain ratio, element spacing, etc

13 p2225 A69-27184

Antenna cross dipole array for vehicle tracking in VHF band, obtaining effect of local rotation by electrical phase shifting

13 p2226 A69-27185

Gain optimization for dipole endfire array through orthogonalization of element directivity noting effects of element spacing, element gain and mutual coupling

13 p2226 A69-27186

Admittance of radiating elements in circular array with longitudinal slots on conducting cylinder, taking into account element interactions

13 p2234 A69-28505

Passive magnetic elements array calculation for radiation pattern, discussing emitter position

13 p2235 A69-28513

Antenna system synthesis for amplitude distribution along linear emitter, considering radiation patterns

13 p2235 A69-28521

Radiation pattern of electric and magnetic dipole on flat sem infinite impedance system edge found similar

13 p2236 A69-28546

Current distribution along linear antenna array taking into account interaction between neighboring elements and effect on antenna radiation characteristics

13 p2236 A69-28572

Radar antenna radiation effects on man and biological material dependent on absorption degree and emission characteristics including wavelength, peak and mean power

13 p2215 A69-28597

Antennas with vertical radiation patterns to measure frequency spectrum of distributed cosmic radio emission between 6.3-40 MHz

14 p2509 A69-28762

Directional properties of electric vibrator positioned at reflecting circular cylinder, discussing radiation patterns and cylindrical wave diffraction

14 p2418 A69-28830

Stepped scanned ring monopulse array, discussing pattern analysis, directivity, co-phased and quasi-phased model

14 p2419 A69-28894

Optical image diffraction method for analyzing radiation patterns of horn antenna sounding beams used in microwave measurement of expanding plasmods

14 p2497 A69-29793

Corrugated conical horn used as antenna feed, studying modes in horn and associated radiation patterns by spherical hybrid functions analysis

15 p2575 A69-30176

Binary-quantized signal packet center for target azimuth determination, discussing antenna radiation pattern role

15 p2566 A69-30332

Bearing errors from radio beacons with rotating or multilobe radiation patterns

15 p2567 A69-30343

Signal reflection elimination from underlying surface during aircraft flights by using two antenna array with identical radiation patterns

15 p2567 A69-30345

Theory of field distribution in antenna aperture extended to scanning with desired shape beam

15 p2578 A69-30634

Resonance cones in angular distribution of short antenna RF electric field in anisotropic plasma noting variation with incident, cyclotron and plasma frequency

15 p2659 A69-30876

Orthonormalized partial radiation patterns for antenna array of N emitters developed by introducing scattering matrix

15 p2579 A69-30951

Digital method to produce radar reflectivity from analog audio frequency Doppler data extracted from terrain echo signal of CW scatterometer radar

15 p2572 A69-31111

Radar calibration and precipitation measurements equation taking Gaussian approximation for antenna radiation pattern

16 p2806 A69-32264

Difference radiation patterns of circular aperture with axisymmetric amplitude distribution

16 p2754 A69-32494

Directive gain optimization of antenna array during 90 degree radiation deflection

16 p2762 A69-32509

Vertically polarized log periodic antenna consisting of unipole vertical radiators with side radiators for achieving minimum size

16 p2763 A69-32580

Spacecraft antennas properties, structure and problems including frequency ranges, external influences, omnidirectional radiation, input impedance, etc

16 p2763 A69-32584

Short backfire antenna based on yagi type equipped with end reflector, noting fewer elements and low sidelobe advantages

16 p2763 A69-32586

Plasma electroacoustic resonance in reentry sheath of Trailblazer 2 vehicle excited by nonradiating coaxial antenna, deducing electron density gradient at vehicle surface

17 p3010 A69-32915

Ground conductivity effects on MF sky wave transmission strength, discussing transmission over open sea

17 p2918 A69-33029

Horn antenna with parabolic reflector for 30 cm wavelength, calculating field distribution, main and sidelobe radiation patterns and aperture efficiency

17 p2937 A69-33147

Monograph on radiation zones and phase center of two arm conical logarithmic spiral antenna covering wideband design, near field measurements and far field integration

17 p2937 A69-33572

Radio map of Orion A region, resolving M 42 and M 43 nebulae at 1.94 cm wavelength, noting optical photographs comparison

17 p3035 A69-33609

Phased array blindness at inoperative scan angles explained in terms of elements excitation and termination caused by leaky wave

17 p2928 A69-33872

Interrelations among mutual coupling, element efficiency, active impedance and radiation patterns in linear arrays derived from infinite order difference equation

17 p2929 A69-33874

Linear array composed of dual mode elements radiating into parallel plate region, obtaining scan angle compensation of element impedance

17 p2929 A69-33875

Van Atta array reflector retrograde effect, studying influence of transmission line length, interelement spacing and line-dipole matching on incident reflected radiation phase correlation

17 p2929 A69-33878

Microwave holography for antenna synthesis, radiation patterns and visible images reconstruction

17 p2976 A69-33891

Radio antenna consisting of truncated confocal paraboloids, discussing pencil beam pattern, antenna parameters and experimental results

17 p2939 A69-33904

Antenna three dimensional radiation patterns, describing error analysis of various pattern measurement techniques

17 p2942 A69-34086

Mathematical model of fields reradiated by Huygen sources in front of array for glide path site analysis

17 p3003 A69-34107

Artificial plasma properties at microwave frequencies, determining plasma electron density and effects on horn antenna radiation characteristics

18 p3100 A69-34271

Reciprocal theorem for obtaining relations between transmitting antenna effective area, radiation pattern and aperture distribution

19 p3281 A69-35765

Backfire antenna radiation characteristics and physical dimensions for tracking and telemetry applications, including five element array model

19 p3271 A69-36251

Sounding rocket S band telemetry antenna operation, proposing quasi-isotropic pattern criterion to reduce effects of shadowing and interference

19 p3271 A69-36252

Active interferometer controlled telemetry tracking system for missile range, discussing automatic target acquisition, dish feed, costs and optimized data-channel antenna patterns

19 p3271 A69-36253

Radio wave information transmission, discussing propagation in various media, antenna arrays, diffraction, scattering, plasmas, guided waves and periodic structures

19 p3276 A69-36431

Field strength determination at reception point for long range short wave paths, taking into account multiple ray paths and antenna radiation patterns

20 p3520 A69-37035

Residue series representation of radiation fields for azimuthal leaky wave antenna on conducting cylinder, showing zeroth term correspondence to omnidirectional antenna

20 p3506 A69-37834

Analysis theory of shaped beam doubly curved reflector antenna, computing far field patterns by determining current density distribution on nonanalytic surface

20 p3506 A69-37835

Scattered field of linear array of center loaded cylindrical elements illuminated by plane electromagnetic wave

20 p3494 A69-37838

Radiation field produced by parasitic loop counterpoise antenna, obtaining far field from geometrical diffraction theory

20 p3507 A69-37840

Normalized SNR of aperture antennas determined in terms of random signal and noise fields correlation functions

20 p3494 A69-37845

Parallel wire antenna array design for specified pattern using matrix methods and method of moments for self and mutual impedances and required excitations

20 p3507 A69-37847

Emission of thin metallic antenna in randomly inhomogeneous medium, determining effective impedance

20 p3508 A69-37936

Synthesized aperture method of measuring antenna gain and radiation patterns

20 p3508 A69-37937

Directional mirror antenna parameters measurement by finite focusing of radiating element
20 p3508 A69-37938

Linear antenna synthesis for optimal separation of plane waves providing maximum SNR with allowance for statistical phase distribution of field
20 p3508 A69-37943

Slope optimization of antenna array difference radiation patterns coinciding with antenna directive gains
20 p3508 A69-37944

Tuning of two mirror antennas in near zone with various mirror combinations, discussing field cophasing
20 p3508 A69-37945

Soviet book on antenna synthesis theory for application to antenna radiation patterns with allowance for Fourier transforms limitations
20 p3508 A69-38208

Rotation of antenna pattern of radio telescope parabolic mirror subjected to thermoelastic deformations due to asymmetric solar heating
20 p3497 A69-38307

Radiation field of tapered dielectric rod antenna by Schelkunoff equivalence principle, investigating input impedance variation with axial length and taper angle
21 p3681 A69-38444

Antenna arrays subject to random excitation error analyzed by probability theory, noting relationship between antenna pattern and excitation distribution parameters
21 p3681 A69-38742

Antenna synthesis problems in mathematical physics, discussing radiation pattern, shape and source and optimal solution via operators spectral theory
21 p3682 A69-39124

Synthesis by differential equation technique for linear antenna arrays of identical radiators radiation patterns
21 p3682 A69-39125

Transistorized low noise reception antennas with built-in amplifying elements, discussing radiation patterns and noise problems
21 p3683 A69-39264

Microwave breakdown characteristics predictable for circular loop antennas from near electric field analysis
21 p3683 A69-39281

VHF cavity backed cylindrical gap antenna input tuning impedance and equatorial radiation patterns controlled by cavity adjustments
22 p3914 A69-40698

Radiation and impedance characteristics of spherically capped conical and monopole antennas protruding from spherical vehicle related to cone height, angle and vehicle diameter
22 p3908 A69-40699

Mars entry capsule ionized wake producing circularly polarized antenna radiation null region, noting effect on communication blackout time
22 p3914 A69-40701

Equatorial radiation pattern of parallel plate TEM mode axial slot on elliptical conducting cylinders, using wedge diffraction and creeping wave theory
22 p3914 A69-40703

Circular and spherical antenna arrays elements random distribution in three dimensional space using Monte Carlo method, considering arbitrary excitation and nonisotropic elements
22 p3914 A69-40704

Circular antenna arrays radiation pattern synthesis in moving medium relative to main beam, noting medium motion influence on pattern changes
22 p3915 A69-40706

Antennas aperture radiation patterns optimal interpolation synthesis permitting confident control of main lobe shape
22 p3916 A69-40953

Asymptotic approximation formulas to compute on-axis Fresnel region fields for coupling between two large aperture antennas
23 p4136 A69-41582

Edge diffraction effects in TEM axially slotted finite ground plane on elliptical radiation pattern in waveguides of different geometries
23 p4116 A69-41588

Simple antenna with good circular polarization over wide space sector, showing geometry, normalized orthogonal field distributions and beamwidth range, considering slot combinations
23 p4137 A69-41590

Slot antenna radiation patterns in presence of aperture RF plasma breakdown sheath measured for various gas pressures and breakdown power levels
23 p4116 A69-41595

Digital computer program for determining flight vehicle telemetry antenna performance from ground test readings
23 p4133 A69-41754

Kirchhoff equations for synthesis of passive dipole arrays, obtaining best approximation to radiation patterns
23 p4138 A69-41935

Synthesis of antenna arrays of longitudinal passive slot radiators on metallic cylinder excited by single active slot, including experimental patterns
23 p4138 A69-41936

Radiation characteristics of dipole on wedge edge with sinusoidal current, discussing spatial phase and polarization calculations by computer
23 p4138 A69-41937

Cophase antenna aperture with shaded central region, considering sidelobe radiation reduction by varying field amplitude distribution
23 p4138 A69-41939

Array aperture amplitude and phase distortions effect on radiation field uniformity
23 p4138 A69-41940

Statistical analysis of random production errors on phasing section polarization field of antenna with elliptical polarization
23 p4125 A69-42041

Antenna losses produced by metal space frame radome determined by considering end effects, member junctions circulating currents, mutual scattering and near field effects
23 p4149 A69-42127

Large reflector paraboloid antenna performance under environmental loads
23 p4231 A69-42132

Radiated interference and susceptibility prediction for unshielded wires in near field of vertical rod antenna
23 p4141 A69-42225

Near field effects on accuracy of LF shielded enclosure measurements compared to open field environment
23 p4141 A69-42226

ANTENNAS

NT AIRCRAFT ANTENNAS
NT CASSEGRAIN ANTENNAS
NT CYLINDRICAL ANTENNAS
NT DIPOLE ANTENNAS
NT DIRECTIONAL ANTENNAS
NT HELICAL ANTENNAS
NT HORN ANTENNAS
NT INERTIALESS STEERABLE ANTENNAS
NT LENS ANTENNAS
NT LOG PERIODIC ANTENNAS
NT LOG SPIRAL ANTENNAS
NT LOOP ANTENNAS
NT MICROWAVE ANTENNAS
NT MISSILE ANTENNAS
NT MONOPOLE ANTENNAS
NT MONOPULSE ANTENNAS
NT MULTIPLE BEAM INTERVAL SCANNERS
NT OMNIDIRECTIONAL ANTENNAS
NT PARABOLIC ANTENNAS
NT RADANT
NT RADAR ANTENNAS
NT RADIO ANTENNAS
NT RHOMBIC ANTENNAS
NT SATELLITE ANTENNAS
NT SLOT ANTENNAS
NT SPACECRAFT ANTENNAS
NT SPIRAL ANTENNAS
NT STEERABLE ANTENNAS
NT SUBREFLECTORS
NT TWO REFLECTOR ANTENNAS
NT WAVEGUIDE ANTENNAS
NT YAGI ANTENNAS

Design evolution of mechanically despun antenna systems from ATS to INTELSTAT, discussing RF and control systems
03 p0403 A69-13239

Residue contributions to integrals associated with admittance of plasma or dielectric covered circular aperture antenna used to calculate surface wave contribution to waveguides
06 p0896 A69-17477

Quasi-static theory of antenna in magnetoactive plasma subjected to resonance, solving boundary value problem
07 p1099 A69-18522

Antenna impedances in cold plasma with perpendicular static magnetic field
08 p1281 A69-20029

Induced EMF method for calculation of antenna impedance, discussing effects of approximations in calculation
11 p1851 A69-24997

Dual reflector antenna design methods for obtaining necessary phase and amplitude illumination across secondary aperture in low noise applications
11 p1852 A69-25316

Superconducting antenna factors and matching circuit equivalents developed for predicting efficiency and Q increase on basis of Pb surface resistance
17 p2937 A69-33784

Active antenna impedance matching network constituting low noise device for electromagnetic interference measurements useful for automatic or manual scanning
17 p2943 A69-34131

Equivalent circuit demonstrating noise reduction through input transistor integration into passive receiving antenna, stressing circuit loss control and preamplification role
19 p3281 A69-35764

Book on antennas in inhomogeneous media, discussing impedances for dielectric loading, reentry, ionosphere and buried environment, wire antennas in free space, etc
19 p3268 A69-36150

Electron beam welding for repair and production, discussing application to Ti VHF antennas, Concorde shuttles and nuclear reactor loading tubes [SBAC PAPER 14]
20 p3550 A69-37451

Q factors of ideal antenna enclosed in imaginary sphere with excited TE and TM modes
20 p3506 A69-37836

Antenna noise spectrum in collisionless isotropic plasma, considering plasma fluctuation theory and reciprocity theorem
21 p3683 A69-39284

Direction finding characteristics of nonlinear antenna, including current determination and optimal angle for sidelobe level
21 p3684 A69-39619

Waveguide fed rectangular aperture antenna with dielectric plug load, describing admittance resonant perturbation due to excited TE mode
23 p4136 A69-41589

ANTI-AIRCRAFT MISSILES

Optimum evasion tactics for aircraft pursued by missile, using steepest ascent method for maximization of distance of closest approach
06 p0866 A69-17401

ANTIBODIES

NT GAMMA GLOBULIN

Specific antibody formation to influenza A virus vaccine /strain PR sub s/ in hibernating ground squirrels /Citellus tridecemlineatus/
08 p1263 A69-20173

Sublethal ionizing radiation doses effect on hemolytic immunocompetent spleen cells in mice upon using chemical radiation protectors
13 p2210 A69-28334

Local stress effect on immunocompetent cells differentiation in guinea pigs lymphatic ganglia, showing antibody producing cells number increase
22 p3877 A69-40277

ANTICYCLONES

Horizontal ozone distribution at high cyclones and anticyclones in middle stratosphere
08 p1308 A69-20261

Equatorial anticyclones over eastern Pacific caused by large scale cross-equatorial flows determined by ATS-1 photographs, noting frictional convergence factor
24 p4342 A69-42895

ANTI-DIURETICS

Short latency antidiuresis following initiation of food ingestion by food deprived rats, noting possible signaling factor
01 p0014 A69-10860

Visceral afferent pathways influence on vasopressin secretion, ADH levels and urinary excretory patterns of dogs during surgical stress
05 p0708 A69-15970

Decreased antidiuretic activity measured in blood of chronically centrifuged rats, noting role of antidiuretic hormone /ADH/
14 p2407 A69-29301

Antidiuretic hormone /ADH/ and bradykinin effects on human thermal and cholinergic sweating after subdermal injection in forearm, abdomen and leg
23 p4077 A69-41311

ANTIDOTES

Antihypoxic preparations protective effect on white mice and rats subjected to gravitational accelerations
17 p2906 A69-32931

ANTIFERROMAGNETISM

- Figures of merit for polycrystalline uniaxial antiferromagnetic materials, for nonreciprocal devices at millimeter and submillimeter wavelengths, calculated from perturbation theory [IEEE PAPER 17.11] 01 p0045 A69-10720
- Antiferromagnetic semiconductor transformation into metal in magnetic field 09 p1556 A69-21672
- Anisotropic Heisenberg antiferromagnetism in spin wave approximation, calculating thermodynamic quantities in terms of elliptic integrals 12 p2144 A69-26500
- Electron magnon interaction in ferromagnetic and antiferromagnetic semiconductors, showing conduction band and electron effective mass and magnetic moment dependences on temperature and spin direction 14 p2504 A69-28991
- Theory of temperature dependent magnon energies in antiferromagnets based on spin wave operator expansion of Hamiltonian, taking into account dynamical interaction between waves 15 p2668 A69-30684

ANTIFRICTION BEARINGS

- NT BALL BEARINGS
- NT ROLLER BEARINGS
- Mechanical properties of free rolling contact surfaces subject to high loads, discussing effect of oil film separation and fatigue crack initiation 02 p0339 A69-11989
- Miniature ball and jewel bearings and gear lubrication in ultrahigh vacuum tests for space environment operation [IME PAPER 6] 07 p1138 A69-18562
- Bearing lubrication at low temperature, examining safety limits, working fluid in liquid or gaseous state [IME PAPER 9] 07 p1138 A69-18565
- Microstructural changes in 52100 steel bearing inner rings during cyclic stressing, obtaining thickening rate data on white-etching regions and lenticular carbides 08 p1319 A69-20004
- Plain and rolling metal bearings manufacture and use, discussing materials structure and properties, operating conditions, lubrication, etc 11 p1903 A69-24517
- Sliding behavior of nonmetallic bearing materials /plastics, ceramics and cermets/, discussing non-lubricated bearing application 14 p2454 A69-28851
- Self lubricating bearings lifetime calculated as function of lubricant in pores and consumption rate, noting temperature effects 15 p2618 A69-30281
- Radial clearance influence on self lubricating porous bearing friction coefficient and oil losses as function of operation duration 16 p2794 A69-32067
- Critical speeds of high speed turbine rotors running in friction bearings determined by varying natural frequencies of rotor and supports 18 p3147 A69-34545
- Friction bearing vibration recording device using light beam and photodiode 20 p3539 A69-37436
- Hydrodynamic conical and spherical spiral grooved grease bearings replacement of gyro ball bearings for extended space missions [AIAA PAPER 69-836] 21 p3732 A69-39367

ANTIGENS

- Tryptic pentapeptide Asp-Glu-Leu-Thr-Lys synthesis is showing relation to Gm/a/ antigen of human gamma g-globulin 24 p4279 A69-42712
- Inoculum dose effect on complement-fixing antigen production, heat lability and separation from BHK-21 cells infected with lymphocytic choriomeningitis virus 24 p4263 A69-43336

ANTIINFECTIVES AND ANTIBACTERIALS

- Antimicrobial spacecraft materials, discussing feasibility of impregnation or chemical combination of materials with bactericides 05 p0713 A69-15944

ANTIMATTER

- NT ANTINEUTRINOS
- NT ANTINUCLEONS
- NT ANTIPARTICLES
- NT ANTIPROTONS
- NT POSITRONS
- Galactic formation by massive matter cloud passage through antimatter cloud, discussing radio sources genesis 12 p2170 A69-27064

Symmetry between koinomatter and antimatter in universe, discussing koinonucleons production, big bang theory, protogalaxy model, quasi-stellar objects, galaxy evolution, etc 15 p2690 A69-30670

Antimatter in universe, presenting arguments for microscopic and macroscopic symmetries 17 p3006 A69-33578

Antimatter meteors detectability, considering annihilation and vaporization in earth atmosphere 17 p3034 A69-33579

Antimatter motion in solar system and earth atmosphere, discussing vaporization and annihilation energy in collisions with interplanetary gas atoms 22 p4034 A69-41100

ANTIMISSILE MISSILES

Hypersonic missile interceptor vibration characteristics in lower atmosphere, noting role of base pressure excitation 09 p1614 A69-21890

ANTIMONIDES

- U CADMIUM ANTIMONIDES
- U GALLIUM ANTIMONIDES
- U INDIUM ANTIMONIDES
- U ZINC ANTIMONIDES

ANTIMONY

- Antimony bromine and mercury abundances in meteoritic materials determined by neutron activation analysis 08 p1404 A69-20919
- Sb addition effect on electrical conductivity and Hall effect in PbTe single crystals over temperature range 11 p1939 A69-25706
- Chondritic meteorites arsenic, tin and antimony content determined by anion-exchange chromatography and neutron activation analysis 13 p2344 A69-27630

ANTIMONY COMPOUNDS

- NT CADMIUM ANTIMONIDES
- NT GALLIUM ANTIMONIDES
- NT INDIUM ANTIMONIDES
- NT ZINC ANTIMONIDES
- Space charge limited currents in SbSI single crystals with gallium electrodes during phase transition, discussing sticking probability and photoconductivity 01 p1337 A69-10258
- Space charge limited currents in SbSI single crystals with gallium electrodes during phase transition, discussing sticking probability and photoconductivity 09 p1559 A69-22651
- Antimony trisulfide natural light reflection and transmission in and near IR region, noting spectral temperature and time dependence peculiarities 19 p3384 A69-36481
- Antimony trisulfide single crystals spectral dependence of impurity and stimulated impurity photoconductivities, comparing optical and thermal activation energies 22 p3994 A69-41042

ANTINEUTRINOS

Neutrino and antineutrino emission by URCA process calculated, assuming nuclear reactions in static and beta processes in kinetic equilibrium 15 p2674 A69-30542

ANTINUCLEONS

High energy negative kappa meson-nucleon interactions with respect to multiplicity distribution of charged pions in nucleon-antinucleon annihilation, showing binomial distribution 24 p4351 A69-42791

ANTIOXIDANTS

Additions of dialkyl and diaryldithiophosphates of Ba, Ca, Zn, Pb and Ni as antioxidants and corrosion inhibitors for hydrocarbons 12 p2027 A69-27091

ANTIPARTICLES

- NT ANTINEUTRINOS
- NT ANTINUCLEONS
- NT ANTIPROTONS
- NT POSITRONS
- Universal dependence of density fluctuations on specific entropy derived from equation describing material composed of neutral particles and equal number of charged and antiparticles 21 p3771 A69-38995

ANTIPODES

- Earth ionosphere cavity model for atmospheric waveform shape, considering ELF pulse distortion after propagation through antipode 16 p2750 A69-31978
- Pulse propagation through antipode, calculating time domain response of fields near axial caustic 18 p3100 A69-34233

ANTIPROTONS

- Cosmic gamma ray spectra from metagalactic proton-antiproton annihilation 09 p1574 A69-21459
- Matter traversal of high energy primary galactic cosmic ray protons from antiproton flux and energy measurements 15 p2678 A69-31491
- Proton-antiproton high energy elastic scattering by bosons exchange, introducing vertex functions for non-local Lagrangian 21 p3775 A69-39467

ANTIRADIATION DRUGS

- Prophylactic and therapeutic vitamin and organic compounds complexes in radiation damage reduction and death prevention for dogs exposed to X rays 02 p0197 A69-11493
- Radiation structural and transcription damage to deoxyribonucleic acid (DNA), noting postirradiation repair on molecular level 03 p0372 A69-13489
- Sublethal ionizing radiation doses effect on hemolytic immunocompetent spleen cells in mice upon using chemical radiation protectors 13 p2210 A69-28334
- X ray radiation damage to white mice blood serum proteins disappearing following intraperitoneal administration of imidazole or benzimidazole 23 p4077 A69-41300

ANTISUBMARINE WARFARE AIRCRAFT

- NT CL-84 AIRCRAFT
- NT SH-3 HELICOPTER
- A-New avionics system for carrier based VSX aircraft used in U.S. Navy aerial submarine hunting, discussing TV, lasers, sonobuoy system, radar, etc 14 p2392 A69-29430

ANTISYMMETRY

Stress-strain state of circular disks with arbitrarily varying thickness along radius under antisymmetrical load calculated by integral equations method 22 p4047 A69-41168

ANTITANK MISSILES

- Antitank missile guidance system with tracker using two optical paths and pyrotechnic flare noting transmission ratios, visibility coefficients and improvement factors 23 p4164 A69-41625
- Extreme value statistics used to determine minimum acceptable tensile strength of wire command links in TOW antitank missiles 24 p4318 A69-42642

ANTONOV AIRCRAFT

- NT AN-24 AIRCRAFT
- Soviet book on practical aerodynamics of An-2 aircraft covering aerodynamic characteristics, equilibrium, stability and control for various flight conditions, including icing 18 p3090 A69-34340

ANTONOV AN-24 AIRCRAFT

- U AN-24 AIRCRAFT

AORTA

- Elastic behavior of large blood vessels in canine aorta by measuring dispersion and attenuation of artificially induced pressure waves 04 p0553 A69-14692
- Flow rate in ascending aorta, stroke volume and cardiac output determination by ballistocardiography, calculations based on Hagen-Poiseuille theory 17 p2915 A69-33772
- Sympathetic nerve activity inhibition due to afferent baroreceptor nerves reflexes, studying carotid sinus and aortic nerves as pathways to vasomotor center 20 p3479 A69-38073
- Aortic pressure effect on left ventricular function, emphasizing effect of heart rate hematocrit and oxygen consumption 23 p4092 A69-42061
- Spontaneous rhythmical activity and mean vascular tone dependence in isolated helical rat aorta strips on extracellular concentration of noradrenalin 23 p4093 A69-42069
- Vascular interface histological and chemical responses to acute mechanical stress in dog aorta 24 p4257 A69-42625
- Errors in estimating cardiac function from aortic and peripheral pulses, using cadaver experiments 24 p4262 A69-42728

APATITES

- U MINERALS

APERIODIC FUNCTIONS

Optimal control of open loop aperiodically modulated discrete time systems, discussing solution of associated two point boundary problem

02 p0226 A69-12732

Extrapolation of aperiodic step responses

12 p2051 A69-26237

Aperiodic feedback substitution for angular velocity component of control signal in stabilization systems of oriented satellites

21 p3829 A69-39832

APERTURES

NT IRISES [MECHANICAL APERTURES]

Radiation pattern shaping from circular aperture antenna with constant illumination amplitude [UN PAPER 68-95756]

01 p0029 A69-10524

Admittance of parallel plate waveguide aperture with infinite flange illuminating metal sheet, using wedge diffraction theory and integral transform method

02 p0218 A69-12328

Aperture effects in nonlinear optical processes associated with second harmonic and parametric generation of light

03 p0439 A69-13056

Optical imaging systems achieving aperture synthesis by lensless Fourier transform holography, noting X ray astronomy, ultrasonic and space applications

03 p0430 A69-13324

Diffraction coefficient for higher order edge-edge interaction terms in two dimensional diffraction by narrow slit and small circular aperture

03 p0396 A69-13631

Dielectric sheath effect on far zone radiation characteristics of aperture bounded by perfectly conducting ground plane

04 p0579 A69-15450

Difference radiation patterns of circular aperture with axisymmetric amplitude distribution

05 p0717 A69-15636

Dynamics of pulsed microwave breakdown in nonuniform field at waveguide fed mica aperture, noting electric field distribution change due to initial plasma configuration

07 p1107 A69-19448

Filled and unfilled aperture radio telescopes, noting uses in radar astronomy and for aperture synthesis antennas

10 p1674 A69-23866

Light flux intensity fluctuation dispersion and averaging effect for passage through circular receiving aperture

10 p1658 A69-23950

Statistical properties of electromagnetic field diffracted by illuminated plane aperture studied in Fresnel zone on basis of partial coherence theory

11 p1836 A69-24978

Radiation field patterns from metal wall aperture in waveguide with rectangular cross section determined using elliptic cylinder

11 p1850 A69-24982

Radiating collinear open ended waveguides and near field coupling analyzed using simultaneous integral equations and Fourier series expansion of aperture field

11 p1850 A69-24984

Two dimensional radiation from apertures in conducting cylinders of arbitrary cross section, solving current distribution, admittances and radiation patterns

11 p1836 A69-24985

Air gap tolerances effect on admittance of TEM mode dielectric and plasma coated slot antennas determined by variational method

11 p1851 A69-24986

Rapidly convergent series expansions for plane wave transmission coefficients for elliptical and rectangular apertures

11 p1837 A69-25001

Time harmonic electromagnetic waves diffraction by circular aperture in conducting plane screen between different media, using Hertz vector formulation

12 p2030 A69-26463

Irradiance distribution in far field diffraction patterns of partially coherent light diffracted by annular aperture, using Fourier transformation relationship of Schell

14 p2460 A69-29640

Recording arrangement aperture effect on plasma scattering spectrum during plasma parameter determination by light scattering technique

15 p2664 A69-30996

Difference radiation patterns of circular aperture with axisymmetric amplitude distribution

16 p2754 A69-32494

Double aperture problem with partially coherent incident field, noting application to microwave antenna-reflector combination

17 p2929 A69-33877

Mechanical collimator using random aperture arrays for celestial observation at extreme UV and X rays

19 p3313 A69-36489

Image deblurring and aperture synthesis using a posteriori processing by Fourier transform holographic spatial filtering

21 p3722 A69-38793

Synthetic aperture radio telescopes analysis, noting resolution and sensitivity at radio wavelengths for correlator array in supersynthesis mode operation

21 p3677 A69-39512

Stellar scintillation spectra theory extended to rectangular apertures, generalizing to planetary scintillation and effects of diffraction, atmospheric dispersion and seeing

21 p3773 A69-39771

Aperture efficiency, weight and control power requirements for hybrid matrix arrays in synchronous satellite applications, calculating residual array gains

22 p3915 A69-40707

Aperture distortions and spectral line shapes of electromagnetic radiation diffused by plasma

22 p3982 A69-40799

Cophase antenna aperture with shaded central region, considering sidelobe radiation reduction by varying field amplitude distribution

23 p4138 A69-41939

Array aperture amplitude and phase distortions effect on radiation field uniformity

23 p4138 A69-41940

APEXES

Series expansion for exponent of singularity of Laplace equation for flow near apex of plane delta wing

19 p3240 A69-36590

APNEA

U RESPIRATION

APOLLO APPLICATIONS PROGRAM

Space station design requirements, Apollo applications program and various experimental programs

01 p0163 A69-11395

Communications for Apollo Applications Program, considering extended duration manned missions in low earth orbit and Gemini, Saturn and Apollo hardware

07 p1083 A69-19124

Manned spacecraft developments, considering Apollo Applications Program, space station establishment, space shuttle operations and payload cost

10 p1791 A69-22866

Apollo telescope mount /ATM/ for solar experiments conducted from manned earth orbiting laboratory

10 p1791 A69-22871

AIAA view on Post-Apollo space program, considering multiple goals, unmanned application satellites and manned space flight objectives

18 p3236 A69-35136

Stored program data processor used as PCM telemetry data acquisition system for postApollo applications, considering format and bit rate changes

19 p3274 A69-36280

Fuel cell /battery and solar array/ battery systems for manned Apollo Applications Program /AAP/ space vehicles, considering mission and power requirements

23 p4069 A69-42244

Logistics management developed for Apollo Applications Program of NASA Manned Spacecraft Center [AAS PAPER 69-204]

24 p4417 A69-42812

Apollo Applications Program /AAP/ spacecraft, describing contributions to space station engineering

24 p4392 A69-42838

Orbital EVA, discussing technology associated with Apollo Applications Program [AAS PAPER 69-517]

24 p4272 A69-42841

APOLLO FLIGHTS

Entry phase flight data of Missions AS-202, Apollo 4 and 6 compared with wind tunnel aerodynamics data [AIAA PAPER 68-1143]

03 p0519 A69-13556

Apollo 4, 5 and 6 space missions, with preview of Apollo 7, 8 and 9 missions

06 p1017 A69-17672

Baker-Nunn photometry from Apollo tracking utilizing photographs for brightness, dynamics and duration of rocket exhausts and venting clouds

15 p2571 A69-31338

Data compression and transmission technique for real time system to monitor manned space missions, noting Apollo telemetry data [AIAA PAPER 69-970]

22 p3906 A69-40350

Mission simulation testing in thermal vacuum environment for Apollo Lunar Module, noting conformal skin heaters

[AIAA PAPER 69-991] 22 p3920 A69-40369

Multispectral processing of Apollo 6 earth photographs, evaluating geologic, vegetative and cultural features from red, green and blue portions of visible spectrum

22 p3941 A69-40987

APOLLO LUNAR SURFACE EXPERIMENTS PACKAGE

Astronaut safety considerations impact on design of Apollo Lunar Surface Experiments Package /ALSEP/ [SAE PAPER 680721]

03 p0433 A69-13444

Apollo 11 passive seismic experiment design and objectives, describing seismometer characteristics and lunar interior

20 p3539 A69-37516

SNAP 27 radioisotope thermoelectric generator system designed as prime power supply for Apollo lunar surface experiment package /ALSEP/

23 p4187 A69-42249

Lunar laser beam retroreflection observations, showing agreement with predicted ephemeris and signal strength

24 p4384 A69-43197

APOLLO PROJECT

PostApollo lunar passive seismic experiments, discussing probable results of present program, exploration sites and additional network stations and instruments [AAS PAPER 68-204]

02 p0312 A69-11479

Magnetometer experiment for Apollo project to measure lunar surface magnetic field, describing mission requirements and instrumentation [AAS PAPER 68-206]

02 p0312 A69-11481

Heat flow measurement from moon interior planned for Apollo missions to determine temperature increase rate with depth during lunar year [AAS PAPER 68-207]

02 p0313 A69-11482

Data acquisition program for Apollo crew motion disturbances experiment consisting of ground simulations and orbital experiment establishing mathematical model of human body

02 p0201 A69-11759

Communications system considerations for lunar libration point relay satellite to support Apollo lunar far side mission

03 p0388 A69-13180

Photographic control system requirements for Project Apollo manned launches, considering extreme heat, vibration and sound pressure environment [SMPT PAPER 104-20]

04 p0596 A69-14360

Post-telescopic lunar exploration, discussing Apollo program and development of selenology [JPL-TR-32-1399]

06 p1001 A69-17159

Systems engineering activities in manned space flight involving design, development, manufacture, test and operation of Mercury, Gemini and Apollo flight systems

06 p1016 A69-17602

Radiation protection plan for Apollo lunar mission based on real time monitoring of solar activity and radiation in spacecraft [AIAA PAPER 69-19]

06 p0996 A69-18113

Telemetry and tracking antenna feed system in EC-135N instrumented aircraft for Apollo moon project

07 p1105 A69-19111

Apollo lunar TV camera for real time pictures during all phases of Apollo lunar landing mission, describing camera tube, circuitry and optics

07 p1133 A69-19137

Caterpillar diesel electric sets for powering NASA tracking station in Australia during Apollo 8 flight

07 p1117 A69-19632

Intelsat 2 satellite structural design for Apollo communications

08 p1408 A69-19907

Complex digital computers designed for Apollo spacecraft missions, discussing construction techniques [AGARDOGRAPH-114]

08 p1279 A69-20990

Medium temperature fuel cells, noting reliability and high efficiency leading to selection for lunar exploration vehicle of Apollo project

08 p1260 A69-21046

Apollo/Saturn V automatic checkout test verification and debug program using real time computer simulation with digital space vehicle system model [AIAA PAPER 69-321]

09 p1478 A69-22378

Nondestructive testing methods for Saturn 5 space vehicle with emphasis on NDT equipment for Apollo program

10 p1699 A69-23050

Electrical, thermal and mechanical requirements in design of Landing Radar Electronic Assembly for Apollo Lunar Module

10 p1663 A69-23537

Schmidt all-reflecting telescope for UV imaging in Apollo Earth Orbital Scientific Experiment

11 p1887 A69-25101

Apollo Range Instrumented Aircraft /ARIA/ telemetry antenna system for trajectory tracking, discussing computer program for simulation of behavior

11 p1840 A69-25309

Apollo mission simulation, discussing Command Module Simulator /CMS/, onboard computer system and dynamic visual presentation via infinity-optics display

[SMPTE PAPER 105-74] 12 p2055 A69-25768

Thermal vacuum /TV/ manned test operations related to Apollo lunar module in simulated space environment

15 p2558 A69-30394

Apollo/Saturn 5 base at Kennedy Space Center and facilities and equipment supporting manned lunar mission, discussing site location choice and launch complex design concept

16 p2767 A69-32429

Photographic system for astronaut training in Apollo Mission Simulator, using fixed camera and moving earth model coincident with strip color film past exposure slit

16 p2792 A69-32787

Pivotal computer operations in Apollo NASA Communication Network, describing UNIVAC computers in use and design considerations

18 p3100 A69-34267

Project management of Apollo short stack testing project, discussing organization, planning, operations and procurement to cut testing time

18 p3233 A69-34616

Apollo project by-products, emphasizing NASA project management methods application to large R and D projects

18 p3233 A69-34649

Apollo 10 field sequential color TV system, describing camera modifications, systems design and equipment compatibility problems

18 p3101 A69-34810

Nondestructive testing methods for Saturn 5 space vehicle with emphasis on NDT equipment for Apollo program

19 p3431 A69-36329

NASA lunar survey and mapping for generating Apollo satellite landing navigation control, using analytic photogrammetry, camera position and altitude data of lunar topography

20 p3536 A69-36931

Plastics applications in Apollo-Saturn 5 program, considering foam, honeycomb, conformal coatings, embedment compounds, dielectrics, damping compounds, adhesives, sealants and gaskets

21 p3751 A69-38533

Apollo translunar injection burn simulation, analyzing polynomial solutions of optimum geometry and characteristic velocity

[AAS PAPER 68-150] 21 p3820 A69-39225

Apollo Guidance, Navigation and Control system prelaunch checkup, flight experience and error analysis

[AIAA PAPER 69-891] 21 p3824 A69-39416

Spectral reflectivity and emissivity observations of proposed Apollo landing sites compared with other lunar localities and unmanned lunar probe data

21 p3815 A69-39585

Visible and IR spectral reflectivity of Apollo lunar landing sites, attributing reflectivity differences to compositional and/or mineralogical differences

21 p3815 A69-39586

Lunar surface IR emissivity comparison spectra including proposed Apollo landing sites, indicating Si-O ratio difference for Plato crater

21 p3815 A69-39587

Real time targeting for Apollo lunar orbit insertion maneuver burn, discussing impulsive maneuvers for flight control

[AIAA PAPER 68-848] 21 p3828 A69-39760

Apollo lunar sample collection and analysis, discussing astronauts activity and equipment, sample types, laboratories for radioactive counting and gas analysis, etc

22 p3919 A69-40191

Real time orbit determination system at NASA manned space center for Apollo missions

[AIAA PAPER 69-938] 22 p4020 A69-40321

Operational reliability verification of Apollo real time mission program and testing structure, discussing

environment, processing, controls, response criteria, etc

[AIAA PAPER 69-981] 22 p3907 A69-40361

Lunar TV camera for Apollo missions, discussing operational requirements and design

23 p4162 A69-41478

Miniaturized seismic refraction system for manned lunar landings consisting of geophones, three channel amplifier, calibrator and logarithmic compressor

23 p4162 A69-41533

Apollo Extravehicular Communication Telemetry System for monitoring astronaut portable life support system, space suit performance and body functions on lunar surface

23 p4121 A69-41767

Crew survival insurance under emergency situations during manned space flight, discussing Apollo abort system refinements

[AAS PAPER 69-469] 24 p4272 A69-42848

Lunar landing decision, analyzing American space policy making process with aid of Huntington model

[AAS PAPER 69-500] 24 p4418 A69-42853

Apollo type reentry trajectory optimization numerical methods

24 p4386 A69-43281

Aerospace pressure vessel materials selection and construction, applying Apollo program experience to future programs

24 p4324 A69-43430

APOLLO SHORT STACK

Static structure ground test for Saturn-Apollo vehicle short stack, describing air pressure simulation, data acquisition and readout systems

15 p2589 A69-31079

APOLLO SPACECRAFT

Apollo landmark sighting by astronaut using Apollo onboard navigation system, simulating cloud cover effects with Monte Carlo technique

01 p0110 A69-10692

Apollo thermal protection system, noting low density ablation, flight and ground tests

[AIAA PAPER 68-1142] 03 p0519 A69-13558

Entry corridor thermal entry limits for Apollo spacecraft defined for design of thermal protection system

[AIAA PAPER 68-1144] 03 p0521 A69-13673

Apollo guidance, navigation, stabilization and control subsystems, detailing inertial, optical and computer units for data processing and collecting

04 p0665 A69-14881

Apollo 4, 5 and 6 space missions, with preview of Apollo 7, 8 and 9 missions

06 p1017 A69-17672

Thermochemical and mechanical ablation mechanisms for Apollo heat shield material, comparing surface thermochemistry computer program and arc plasma tunnel data

[AIAA PAPER 69-98] 06 p1038 A69-18149

Radiation measurements inside Apollo 4 and 6 command modules during passage through trapped radiation belts

[AIAA PAPER 69-17] 06 p0884 A69-18202

Apollo spacecraft fire, presenting recommendations for power supply, cabin atmosphere and safety measures

07 p1071 A69-18970

Apollo LM and CSM tracking systems boresight shift reducible by decreasing modulation indices or scaling factor alpha

10 p1672 A69-23277

Computerized shake test facility for Saturn 5 moon rocket, describing data acquisition, magnetic tape units, X-Y plotters, display devices, etc

10 p1672 A69-23285

Guidance and control concepts and hardware for atmospheric entry of Mercury, Gemini and Apollo spacecraft

11 p1914 A69-25724

Apollo spacecraft command module aerodynamic characteristics during entry compared with wind tunnel test predictions

[AIAA PAPER 68-1008] 12 p2012 A69-26789

Aerodynamic measurements on Apollo CM model at hypersonic flow simulating earth orbital reentry trajectory

12 p2012 A69-26800

Saturn 5 boost phase environment simulation on Apollo stages, discussing fixtures, load devices, instrumentation and ground test

15 p2588 A69-30405

Manned spacecraft fuel cell selection and design, discussing Gemini ion exchange membrane and Apollo Bacon cell systems

16 p2737 A69-32406

Attitude control system for Apollo Telescope Mount, discussing selection features based on manned orbital space platform requirements

18 p3168 A69-34683

Halon 1301 fire extinguisher for burning spilled hypergol on Apollo/Saturn LM adapter, discussing concentration requirements and exposure hazards

18 p3094 A69-35062

Apollo optics system ground and flight performance tests results, suggesting possible design changes for sunlit space environments

19 p3307 A69-35796

Apollo lunar module landing radar, discussing descent phases, operating modes, assemblies and Surveyor radar

19 p3267 A69-35797

Apollo navigation, guidance and control systems in command module and lunar module, discussing inertial, optical and computer hardware operation

19 p3369 A69-35799

Apollo spacecraft equipment qualification program for margin assurance, discussing ground and flight tests

19 p3430 A69-36015

Apollo spacecraft fire, presenting recommendations for power supply, cabin atmosphere and safety measures

20 p3483 A69-38218

Crawler-Transporter at Kennedy Space Center for moving ground support equipment, Apollo/Saturn space vehicle and mobile launcher, describing design and components

21 p3690 A69-38754

Digital autopilots for Apollo CSM and CSM/LM vehicles thrust vector control, describing modifications of onboard computers and programs

[AIAA PAPER 69-847] 21 p3762 A69-39377

Apollo-Saturn 5 propulsion and structure feedback loop, analyzing Pogo components and Nyquist plot application

[AIAA PAPER 69-877] 21 p3824 A69-39403

Apollo Guidance, Navigation and Control system prelaunch checkup, flight experience and error analysis

[AIAA PAPER 69-891] 21 p3824 A69-39416

Apollo 6 multisensor imagery of Wilcox Playa /prehistoric lake remnant/ in Arizona, using IR scanner, microwave radiometer, vidicon system and cameras

22 p3942 A69-40988

Telecommunications performance of two lunar relay satellite system /LRSS/, determining operation capabilities with Apollo communications system

23 p4129 A69-42508

Apollo 11 guidance and navigation systems involved in lunar landing, describing command and service modules design

24 p4295 A69-42550

Apollo afterbody heat transfer, studying ablation effects for various reentry angles of attack

24 p4415 A69-43680

APOLLO TELESCOPE MOUNT

Real time digital computer hardware simulation of Apollo Telescope Mount /ATM/ mission

[AIAA PAPER 69-940] 22 p3919 A69-40323

Apollo Telescope Mount /ATM/ solar cell module electrical performance testing using sunlight simulation

23 p4072 A69-42286

APOLLO 10 FLIGHT

Apollo 10 lunar landing module, detailing weight, shape, electronic system and rendezvous radar

18 p3207 A69-34629

APOLLO 11 FLIGHT

Lunar seismology, discussing Apollo 11 instrumentation and experiments, moonquakes and travel times measurements and lunar tides

19 p3315 A69-36765

Apollo 11 moon reflector-laser beam experiment, discussing range changes produced by axial rotation and orbital motion and use for earth-moon dynamics

19 p3339 A69-36766

Apollo 11 mission and future space exploration prospects including moon base, manned space station, reusable shuttle vehicles, etc

23 p4211 A69-41477

Apollo 11 observations of lunar surface glazing, considering radiation heating due to solar outbursts, rocket exhaust effects, shock heating or volcanism, erosion, etc

23 p4216 A69-42202

Lunar rocks and fines samples physical, chemical, mineralogical and biological preliminary analysis at Lunar Receiving Laboratory

24 p4382 A69-42935

APOLLO 7 FLIGHT

APOLLO 7 FLIGHT

Clinical report on Apollo 7 and 8 mission medical data, discussing preflight preventive medical activities, inflight treatment, radiation levels, etc
09 p1446 A69-22542

Apollo 7 and weather satellite observation photographs of hurricane Gladys and typhoon Gloria
10 p1722 A69-22944

APOLLO 8 FLIGHT

Clinical report on Apollo 7 and 8 mission medical data, discussing preflight preventive medical activities, inflight treatment, radiation levels, etc
09 p1446 A69-22542

Aeronomic phenomena observed near Altair and theta Aquila ascribed to Apollo 8 lunar flight
11 p1957 A69-24411

Moon pictures from Apollo 8 spacecraft including full moon, crater Tsiolkovsky and unidentified area showing volcanism
14 p2527 A69-29889

Apollo 8 photooptics, considering TV camera and broadcasts, photographic equipment and visual observation
15 p2609 A69-30469

Lunar photometric function near zero phase from Apollo 8 closeup photography, noting higher reflected brightness than at 1.5 degree phase angle
23 p4220 A69-42380

APOLLO 9 FLIGHT

Apollo 9 multispectral photography compared with photographs taken simultaneously by aircraft using same film filter combinations
15 p2608 A69-30452

APPEARANCE

Color and appearance properties of paint films and relations to amounts and properties of colorants, noting translucent plastics and metallized paint films
04 p0620 A69-14886

APPENDAGES

NT FOREARM
NT HAND [ANATOMY]
NT LEG [ANATOMY]

Deployable appendages of OGO attitude controlled spacecraft design
06 p1017 A69-17606

APPLICATIONS OF MATHEMATICS

Statistical characteristics of random phase quasi-harmonic process investigated for application of mathematical representation
02 p0208 A69-12263

Application of modern stability theory to solution of practical problems by means of comparison theorems, demonstrating effectiveness of method
03 p0467 A69-13747

Mathematical methodology for nonlinear equations of transport processes, discussing group concept and similarity, boundary value conversion to initial value, etc
[AICHE PAPER 31A] 08 p1302 A69-19849

Applied mathematics and mechanics - Conference, Prague, April 1968
10 p1675 A69-22874

Collection of papers on fracture, Volume 2, Mathematical fundamentals
11 p1974 A69-24667

Soviet collection of papers on mathematical physics
11 p1915 A69-24759

Applied function theory, Volume 6, Tables of theta functions and elliptical functions with examples, Part I
14 p2471 A69-29774

Book on Bessel functions with physical applications covering solution of Bessel and associated equations, integral representations, Fourier-Bessel series, Hankel transforms, etc
15 p2643 A69-30037

Uniform approximation mathematical theory applied to wave propagation problems, considering cylindrical waves and rainbows and glory scattering
15 p2653 A69-31165

Mathematical analysis of compaction process for powder mixtures of different metals assuming known characteristics of components
15 p2641 A69-31182

Book on mathematical methods in kinetic theory covering boundary value problems associated with Boltzmann equation, model equations, rarefied gas dynamics, etc
16 p2811 A69-31721

Book on estimation theory and applications covering stochastic processes, linear estimators and recursive formulations
16 p2764 A69-32386

Book on quasi-reversibility application to partial differential equations covering parabolic, nonparabolic, elliptic equations and boundary conditions control
17 p2994 A69-33205

Book on applicable mathematics covering areas of application in engineering and technology
17 p2995 A69-33618

Celestial mechanics, Part 1, covering almost periodic functions, relation to classical astronomy and modern mathematics, implicit function theorem, three body problem, etc
18 p3199 A69-34928

Mathematical methods for quantum mechanical problems caused by electromagnetic field interaction with matter
18 p3175 A69-35402

Negative absolute temperatures physical meaning confirmed mathematically using statistical physics
18 p3231 A69-35403

Scientific theories construction analyzed, including cognitive role of mathematics
20 p3575 A69-37012

Book on mathematical foundations of systems analysis covering calculus, linear algebra, linear and non-linear programming and major applications
21 p3754 A69-38576

Trajectories of roots of two channel systems with antisymmetric cross couplings using geometrical and analytical methods, noting hodograph
21 p3686 A69-38886

Antenna synthesis problems in mathematical physics, discussing radiation pattern, shape and source and optimal solution via operators spectral theory
21 p3682 A69-39124

Monotonic minimization algorithm for nonsmooth extremal problems of mathematical programming, game theory, approximations and optimal control in arbitrary Banach space
23 p4181 A69-41524

Mathematical flow graphs application in analysis and design of elastomechanical structural systems
[AAS PAPER 69-151] 24 p4339 A69-42816

APPLICATIONS PROGRAMS [COMPUTERS]
MACRO /methodology for allocating corporate resources to objectives/ for R and D, discussing program for optimal budget management
15 p2720 A69-30958

APPLICATIONS TECHNOLOGY SATELLITES
Space applications program including communications and navigation meteorology, earth resources survey and geodesy
[UN PAPER 68-95437] 01 p0178 A69-10472

Book on Demeter-earth resources satellite system covering design, instrumentation, cost estimates, economic benefits and political considerations
01 p0163 A69-11333

Ionospheric electron density determined from Faraday effect, using ATS-3 radio signals
02 p0237 A69-11660

Design evolution of mechanically despun antenna systems from ATS to INTELSAT, discussing RF and control systems
03 p0403 A69-13239

NASA Space Application Program strategy, discussing research and development trend toward complexity, versatility and multidisciplinary use of larger spacecraft
03 p0511 A69-13427

Mission analysis for applications satellites, discussing tradeoffs among mission objectives, launch vehicles, spacecraft and geopolitical considerations
03 p0511 A69-13428

Bibliography on applications satellites covering communication satellites, technology, astronomical science, photography, etc
03 p0535 A69-13429

Application satellites for air traffic control, meteorology and earth resources, considering European participation
03 p0520 A69-13587

Aeronautical satellite communications, discussing results with NASA ATS-1 satellite
05 p0790 A69-16721

Channel multiplier spectrometer for low energy electrons and protons at synchronous altitude on ATS-E satellite
[IEEE PAPER 3C-5] 07 p1135 A69-19199

Cosmic radio noise intensity measurements by ATS 2 satellite-borne radiometer
07 p1224 A69-19715

Ammonia resistojet stationkeeping subsystem on-board ATS 4 satellite, noting flight test data agreement with ground tests
[AIAA PAPER 69-296] 09 p1560 A69-21212

Cesium contact ion microthruster experiment on-board ATS 4, measuring emission currents and spacecraft potentials
[AIAA PAPER 69-297] 09 p1561 A69-21218

Experimental communication satellites Score, Courier, Telstar, Relay, Syncom, Intelsat 1 and Molniya 1, discussing equipment, results, and ATS program
09 p1608 A69-21272

Attitude determination and hydrogen peroxide control system for spacecraft orientation in Syncom, Early Bird and ATS
[AIAA PAPER 67-532] 09 p1610 A69-21988

ATS satellite distorted photographs conversion into normal and Mercator projections, using computer programs
10 p1689 A69-22945

Solar flare and magnetic storm signals from ATS 1 geostationary satellite on May 28, 1967, deriving total electron content
11 p1951 A69-25161

Meteorological application of ATS observations in form of time lapse movies of weather in motion, describing camera and data flow
[AIAA PAPER 68-1094] 12 p2174 A69-26804

Ionospheric electron density determined from Faraday effect, using ATS-3 radio signals
13 p2256 A69-28691

Solar proton flux in two energy intervals measuring by ATS detectors during January 1967 event compared with data from satellites outside magnetosphere
14 p2509 A69-28935

ATS 3 satellite reflectometer experiment carrying test samples to measure specular reflectance, noting silica shield effects
[AIAA PAPER 69-644] 17 p3071 A69-33270

Heat pipe application to thermal equalization around ATS-E solar cell mounting panels, comparing predicted and actual performance
[AIAA PAPER 69-630] 17 p3072 A69-33277

Meteorological satellite research, ATS-3 program earth color picture from oceanographic and geomorphological viewpoints and U.S.S.R. research
17 p3000 A69-33777

AIAA view on Post-Apollo space program, considering multiple goals, unmanned application satellites and manned space flight objectives
18 p3236 A69-35136

Solar cell radiation damage during 146.8 days in synchronous orbit on satellite ATS 1, discussing radiation shields
19 p3253 A69-35704

Gain measurement of two element phased array aperture antenna during ATS-C tracking
19 p3272 A69-36254

ATS 3 spacecraft ammonia-fueled resistojet engine test performance
[AIAA PAPER 68-553] 21 p3786 A69-39754

High voltage power supply electronic subsystem for electric propulsion of ATS-D satellite, describing packaging, temperature control and performance in simulated space environment
22 p3999 A69-39948

ATS 3 mechanically despun communications antenna, using parabolic cylindrical reflectors, in-line feed and vernier type stepping motor drive positioning
22 p3913 A69-40692

Intersatellite microwave laser communication system for ATS-F and ATS-G, discussing experiment, functional design and parameters
23 p4120 A69-41758

Short term frequency stability and spectral purity measurements of ATS 1 multiple access communication system
23 p4129 A69-42509

TDMA/PCM system for communication tests via Applications Technology Satellites, discussing time synchronization and bit and frame coherency
23 p4129 A69-42510

Cesium contact ion microthruster experiment on-board ATS 4, measuring emission currents and spacecraft potentials
[AIAA PAPER 69-297] 24 p4365 A69-43238

APPROACH
U INSTRUMENT APPROACH
RADAR APPROACH CONTROL

Piloting aspects of jet V/STOL aircraft for poor weather operations without complicated ground aids, discussing deceleration transition, forward speed and final approach angle
01 p0010 A69-10868

Low visibility instrument landing of aircraft using ILAS and inertial guidance
01 p0114 A69-11012

Approach light efficiency, discussing Calvert bar system and strobe flash on basis of pilot questionnaire polling
06 p0884 A69-18029

Manual control displays for instrument landing approach of large subsonic jet transport, evaluating closed loop system performance and scanning workload
10 p1650 A69-23877

Third phase dynamics of planetary approach of earth-Mars journey, computing approach trajectory on two body spacecraft-Mars assumption
11 p1968 A69-25725

Direct lift controller design for aircraft approach and landing by computer program based on Kalman linear state regulator theory
17 p2902 A69-34027

On-course monitoring for instrument landing system glide path operating with far field samples
17 p3003 A69-34105

Wind shear effects on jet aircraft approach, discussing airspeed and glide path position maintenance requirements
[AIAA PAPER 69-796] 19 p3367 A69-35634

Wave-off Decision Device to define potential aircraft carrier-ramp-strike wave-off criteria for aircraft approach
20 p3573 A69-37161

Subsonic glide landing approach guidance for unpowered lifting vehicles, using perturbation feedback and approximation of heading and position coordinates
[AIAA PAPER 69-865] 21 p3763 A69-39391

Longitudinal flying qualities evaluation by pilots in carrier approach flight simulation, describing experiment apparatus, procedures and results
[AIAA PAPER 69-895] 21 p3648 A69-39419

Aircraft navigation system requiring computer and display for approach guidance to circular orbit over fixed ground area
[AIAA PAPER 69-986] 22 p3978 A69-40366

Airport capacity increase in terms of operations delay, discussing computer aided approach systems and additional runways
22 p3925 A69-40429

B-747 safety assurance program, discussing organization, management, hazard sources, accident statistics, night visual approach and maintainability
22 p3867 A69-41135

V/STOL aircraft radar inertial navigation system, describing approach and landing phase flight test results
[AAS PAPER 69-401] 24 p4252 A69-42831

APPROACH INDICATORS

Flight inspection positioning system, discussing microwave interferometer angle calibration for instrument landing
03 p0430 A69-13680

APPROXIMATION

NT BORN APPROXIMATION
NT CHEBYSHEV APPROXIMATION
NT EDDINGTON APPROXIMATION
NT FINITE DIFFERENCE THEORY
NT HARTREE APPROXIMATION
NT LEAST SQUARES METHOD
NT NEWTON-RAPHSON METHOD
NT OSEEN APPROXIMATION
NT PADE APPROXIMATION
NT PARTICLE IN CELL TECHNIQUE
NT RAYLEIGH-RITZ METHOD
NT RELAXATION METHOD [MATHEMATICS]
NT RITZ AVERAGING METHOD
NT SOMMERFELD APPROXIMATION

Steady state problem of convective heat transfer in half space with boundary conditions of third kind
01 p0174 A69-10103

Book on approximate representation of regular functions of complex variable, discussing Faber polynomials, best approximation theorems, etc
01 p0104 A69-10616

Coulomb approximation for dipole and quadrupole transitions, calculating tables for radial matrix elements
01 p0124 A69-10901

Smoothing and prediction of satellite orbit elements by stochastic approximation method, solving nonlinear equations system
01 p0158 A69-11319

Exponential approximation with piecewise linear error criteria for continuous function over interval
01 p0107 A69-11415

Ultraspherical potential approximation in nonlinear symmetric free oscillations applied to systems with hardening and softening cubic nonlinearities
01 p0107 A69-11418

Germanium tunnel diode current-voltage characteristics, proposing expression for approximation of differential conductivity as function of voltage
02 p0214 A69-11613

Modified Galerkin method applied to approximate solutions of two dimensional elasticity equations of equilibrium
02 p0338 A69-11748

Approximate solution of linear functional, singular integral and integrodifferential equations by general theory of approximate methods
02 p0272 A69-12163

Mathematical analysis to determine complete characteristic of functions tolerating polynomial approximation in mean in crescent type noncaratheodory domains
02 p0272 A69-12164

Supersonic gas jet impingement on inclined plane barrier, calculating parameters by approximation
03 p0413 A69-12958

Approximation of correlation or transfer function obtained through exponential polynomial to determine stochastic process spectral density
03 p0409 A69-12976

Approximation for discretization error of discrete analog of Bergman harmonic kernel, discussing discretization error in Dirichlet and Neumann problems for Laplace equation
03 p0456 A69-13555

Cylindrical wave approximation modified to include axial effects, discussing time histories of deflection and applicability range
04 p0671 A69-14410

Approximate method for finding solution of weak free convection in partially filled vessel in gravitational field
04 p0685 A69-14619

Autoionizing states effects on absorption cross sections for ejection of outer subshell electron from atomic oxygen
04 p0633 A69-15127

Approximate method to determine nonstationary thermal fields in solid bodies with thermal capacity and thermoconductivity coefficient depending linearly on temperature
04 p0688 A69-15409

Approximate method for wave equation with dielectric variation in propagation direction
06 p1030 A69-17116

Double stochastic approximation algorithm for minimizing mean square error in finite expansion of unknown probability distribution functions
06 p0947 A69-17361

Approximate optimal control of nonlinear dynamical system with state dependent variables, using stochastic linearization of system
06 p0902 A69-17404

Optimal approximation of functional matrix, giving upper bounds for deviations of general matrices from closest special matrices
06 p0948 A69-17495

Hydromagnetic plasma stability in infinite electrical conductivity approximation applied to smooth closed systems, discussing ballooning instability mode
06 p0965 A69-17519

Approximate solution for determining satellite motion around axisymmetric planet
06 p1005 A69-17563

Successive approximation for iterative construction of near optimum guidance
06 p0954 A69-17573

Approximate expression for temperature distribution during heat transient in infinite solids of plane, cylindrical and spherical geometry
06 p1025 A69-17779

Approximate solution for hollow circular cylinder with fixed ends under axial displacement and cylindrical surfaces free from traction, using boundary layer technique
07 p1230 A69-18265

Soviet book on theory of approximate methods and applications to numerical solution of singular integral equations
07 p1174 A69-19580

Solution of equations of motion of charged particles in constant magnetic field and variable electric field
08 p1361 A69-20213

Approximate equations for transonic viscous heat conducting gas flow past finite body of revolution
08 p1251 A69-20322

Kinetic equations for polyatomic gases obtained by extending 13 moment approximation to solve inelastic Boltzmann equation, resulting in 17 moment approximation
08 p1357 A69-20784

Approximation method applied to closed viscous streamline flow in rectangular cavity, discussing constant shear stress boundary condition
08 p1304 A69-20811

Planckian stellar velocity distribution function, moduli and projections on coordinate planes determined by ellipsoidal approximation
09 p1589 A69-21370

Optimal control problem involving approximation by monotone functions
09 p1531 A69-21412

Mathematical model for improving statistical approximation convergence and accuracy in estimating structural components parameters
09 p1461 A69-21857

Optimum number of terms in Prandtl approximation of realizations of random process by polynomials
09 p1475 A69-22667

Approximate solution method for Navier-Stokes equations for incompressible viscous fluids
10 p1718 A69-22861

Second order system equations to approximate transfer function of homogeneous pneumatic instrumentation line terminated with pressure transducer
10 p1692 A69-23267

Similar boundary layers in Prandtl approximation determining similarity conditions for second order effects due to curvatures and outer vorticity
10 p1632 A69-23700

Periodic functions approximated by linear methods of Fourier series
11 p1908 A69-24697

Germanium tunnel diode current-voltage characteristics, proposing expression for approximation of differential conductivity as function of voltage
11 p1847 A69-24721

Physical data representation by approximation formulas for computer processing, considering polynomials, rational and spline functions and error curves
11 p1842 A69-24904

Unforced periodically varying systems, developing approximate solutions with Floquet theory
11 p1909 A69-25289

Theory for approximation of analytic functions given on closed spaces with piecewise smooth boundaries
12 p2120 A69-26198

Linear plate theory deficiency for large plate deflections, considering approximation of nonlinear behavior permitting changes in form without additional terms
12 p2185 A69-26822

Eigenvalue approximation for first order systems by introducing artificial periodicity through successive impulse functions of alternate sign
13 p2287 A69-27242

Integral equation solved by successive approximation procedure for determining mass distribution in galaxies on radial velocity basis, applying to NGC 7331
13 p2353 A69-28325

Satellite motion relative to center of mass and resonances by approximate solutions to motion equations, applying asymptotic methods
13 p2357 A69-28502

Linear approximation of electron temperature increment and electron mobility in nondegenerate polar semiconductor in crossed fields
14 p2508 A69-29662

Successive approximations method applied to system of independent equations describing electromagnetic wave propagation in space with gravitational wave metric
14 p2487 A69-29669

Polygonal approximation to functional equation solution by using search algorithms, listing FORTRAN IV programs
15 p2644 A69-30424

Electromagnetic wave propagation in anisotropic inhomogeneous media by geometric optics approximation, obtaining equations for beam trajectories in spherically symmetrical medium
15 p2569 A69-30949

Uniform approximation mathematical theory applied to wave propagation problems, considering cylindrical waves and rainbows and glory scattering
15 p2653 A69-31165

Plate bending problems, comparing various approximate analytical methods including point matching, Galerkin, Ritz, Kantorovich and least squares techniques
16 p2874 A69-32160

[AIAA PAPER 68-296] 16 p2874 A69-32160

Soviet monograph on projective-iterative methods of solving operator equations in generalized metric and structurally normalized spaces
16 p2805 A69-32366

Monograph on Navier-Stokes equations with integral relations approximate solution and application to flow around flat plate of finite length
17 p2949 A69-32993

Approximate equations for transonic viscous heat conducting gas flow past finite body of revolution
17 p2891 A69-33312

Analog to digital conversion, describing successive approximation technique with built-in sample and hold and discrete analog amplitude modification
17 p2934 A69-34124

Reliability prediction limited to approximations related to past experience on similar equipment
18 p3147 A69-34517

Convergence of discrete approximations of Navier-Stokes equations to solutions of corresponding differential equations
18 p3121 A69-34613

Three dimensional supersonic flow past pointed nonaxisymmetrical bodies characterized by great local surface curvature changes, using new approximation
18 p3086 A69-34705

Regularization method for maximum height ascent of rocket uniformly approximating control function by gradient projection method
18 p3164 A69-34706

Planckian velocity distribution function, moduli and projections on coordinate planes determined by ellipsoidal approximation
18 p3198 A69-34759

Heat transfer coefficient approximation under thermal instability conditions complicated by radiant heat exchange at plate surface, noting aircraft design applications
18 p3230 A69-34984

Simplification of linear equation of first kind with Tikhonov smoothing functionals
18 p3165 A69-35052

One degree of freedom systems nonlinear oscillations differential equations periodic solutions by successive approximations, obtaining proof for convergence
18 p3174 A69-35311

Free oscillation period of nonlinear oscillators with one degree of freedom, discussing approximation method
19 p3373 A69-36310

Large atmospheric motions analyzed by elliptic partial differential equation and hydrostatic and quasigeostrophic approximations
19 p3364 A69-36504

Singular perturbations and boundary layer theory for approximating solutions to simple ordinary differential equations
20 p3515 A69-37583

Partial differential equation initial value problems analyzed by ordinary differential equations via functional approximation method
21 p3756 A69-39132

Approximations for meson-nucleus scattering length from energy level measurements on mesonic atoms, emphasizing formula for negative pi mesonic atoms
22 p3987 A69-41004

Successive approximations method applied to boundary problem for quasi-linear parabolic equation in n dimensional Euclidean space
23 p4181 A69-41411

Equations governing cosmic ray modulation and approximate equations valid at high and low energies
24 p4367 A69-43169

Uniqueness theorem and successive approximations for delay functional differential equations, noting scalar problems
24 p4341 A69-43236

P-Q norms generalized inverse concept of matrix derived from extension of Penrose best approximate solution of linear equations
24 p4342 A69-43703

APSIDAL ANGLES
U ANGLES [GEOMETRY]

APSIDES
U PERIHELIONS

APT [PICTURE TRANSMISSION]
U AUTOMATIC PICTURE TRANSMISSION

ARC CHAMBERS
Arc driven shock tube with alumina ceramic liner to reduce driver gas contamination, noting shock speed and test time increase
[AIAA PAPER 68-366] 09 p1570 A69-21957

ARC DISCHARGES
Electron density in arc discharge between carbon electrodes and in discharge with Na vapor, noting relation to temperature and current
01 p0128 A69-10433

Arc discharge in axially turbulent airflow producing equilibrium air plasma
02 p0285 A69-11571

Capillary arc source spectroscopy, determining plasma temperature and pressure dependence on capillary geometry and discharge current
02 p0286 A69-11573

DC arc plasma torch as heat source in plasma tunnel, discussing nonuniformity of plasma flame
02 p0291 A69-12424

Pulsed arc source using plasma jet to obtain intense hydrogen ion beam
03 p0412 A69-13842

Equivalent pressure concept verification for arc discharge with incandescent cathode in mercury vapor
03 p0478 A69-13843

Arc and HF discharges in Ne-He lasers, comparing output power, spectral line intensities and reduced electric field vs reduced tube radius plots
03 p0441 A69-14139

Nonequilibrium ionization rate in arc discharge, studying perturbations effect in near cathode Langmuir layer
04 p0635 A69-14763

Fast response thin skinned calorimeters for high heat flux profiles of arc jet flows
04 p0602 A69-15427

Low voltage Knudsen arc in cesium argon mixture using tungsten electrodes, analyzing current voltage characteristics
06 p0963 A69-16920

Arc cloud thermal conductivity effects on discharge temperature and radiation intensity, solving energy balance equation
06 p0964 A69-17254

Arc phenomena and gas dynamic effects during shock heated plasma interaction with magnetic field
07 p1188 A69-18273

Spectroscopic analysis of hydrogen spark plasma discharge parameters at small PD values, discussing shock wave initiation accounting for transition to quasi-stable phases
08 p1360 A69-20100

Kine films of gas flows within highly luminous transient arc taken by laser schlieren technique
08 p1316 A69-20615

Behavior of bounded and free arc discharges under action of transverse magnetic fields and gas flows
08 p1366 A69-20767

Rotating spoke in unstable pulsed MPD arc, noting rotation frequency and resemblance to plasma rotation [AIAA PAPER 69-234] 09 p1561 A69-21219

Segmented anode, carbon dioxide-hydrogen performance and hollow cathode erosion tests on low power MPD arc thruster, noting current measurements [AIAA PAPER 69-242] 09 p1563 A69-21236

Low current arc discharge plasma diagnostics by light probe, analyzing deviation of resonance level population from equilibrium described by Saha equation
09 p1546 A69-21586

Device for producing high current high pressure arc discharge using water cooled chamber and Be bronze electrodes
09 p1547 A69-21593

Total radiation of dense low temperature argon arc discharge plasma measured by bolometer, showing increase with arc current and pressure
09 p1547 A69-21595

Nitrogen impurities effect on electron energy balance in DC arc burning in inert gas
10 p1732 A69-23442

Heat flux toward electrodes measured under high current discharge, showing conductive heat transfer and erosion effect
11 p1928 A69-25227

Chain mechanism of arc discharge development in crossed electric and magnetic fields explained by direct ionization of neutral particles by ions
11 p1932 A69-25540

Current-voltage characteristics and ionization equilibrium of low voltage arc plasma in narrow gap of thermionic converter at high current density
11 p1933 A69-25554

Multiple lens high speed camera with mechanical shutter for investigating AC arc in circuit breaker during zero current, noting framing rate and capacity
12 p2085 A69-26159

Low pressure arc discharge plasma, studying ion-acoustic oscillations development in magnetic field
12 p2136 A69-26527

High pressure arc discharge diagnostics with spectroscopic method relating spectral profiles to central temperature, pressure and temperature distribution
12 p2094 A69-26968

Laser light scattered from arc discharge, observing enhanced plasma oscillations
13 p2307 A69-27629

Screw instability in glowing discharge plasma column in longitudinal magnetic field generalized to instabilities in low pressure arc, Penning and high current discharges
13 p2315 A69-28526

Decaying arc discharge Cs plasma luminosity anomalous behavior due to combined effect of intrinsic monotonic and complex nonmonotonic emissions
14 p2490 A69-28996

Low voltage arc discharge characteristics in cesium vapor, considering energy balance, electron temperature, energy losses, volt-ampere characteristics, ignition, cathode temperatures, etc
14 p2401 A69-29234

Knudsen arcs kinetic theory with cesium/inert gas mixtures in narrow gap between parallel plate electrodes, discussing fast particle beams and electron scattering
14 p2491 A69-29245

Thermal emission converter, using Cs-Ba mixture in low voltage arc mode, detailing construction
14 p2403 A69-29247

Experimental and theoretical data correlation on low voltage arc in thermionic converters using cesium vapor, describing discharge plasma by solving differential equation system
14 p2404 A69-29254

Excited cyanide molecules concentration in arc discharge determined from spectral bands absolute intensities during electron transition
15 p2654 A69-30080

Spectroscopic determination of temperature fields in water and transpiration cooled constricted Ar arc jets at atmospheric pressure
15 p2657 A69-30155

H beta line for measuring radial temperature distribution in cylindrical hydrogen arc at one atm and to 150 A current in high temperature range
15 p2671 A69-31101

Longitudinal electric field, electron density and temperature in positive column of low pressure Cs-Ar DC arc discharge, discussing Cs vapor depletion
19 p3380 A69-36441

Light sources in 0.15-20 micron spectral range from published literature, unpublished reports, light source manufacturers and individuals
23 p4191 A69-42190

Low pressure arc discharge motion between concentric electrodes in transverse magnetic field, noting Lorentz, stationary and retrograde modes due to temperature nonequilibrium [AIAA PAPER 68-708] 24 p4359 A69-43644

ARC HEATING

Hydrogen arc in axially parallel magnetic field produces higher plasma temperatures by reduced thermal conductivity coefficient
07 p1189 A69-18489

Arc jet generation and control noting application to hyperthermal aerospace environment studies, wind tunnels and materials heating and fabrication
08 p1371 A69-21128

Enthalpy distribution in plasma tube arc heater inlet flow region with hot and cold gas core boundary in presence of electric field
09 p1553 A69-22538

High pressure AC arc heater system design criteria, discussing magnetic field, chamber gas flow, stabilizing elements, etc [AIAA PAPER 69-348] 13 p2243 A69-28283

Low voltage Knudsen arc in cesium-argon mixture for thermal emission converters
14 p2403 A69-29248

Multimegawatt arc heater for hypersonic continuous flow high enthalpy wind tunnel
15 p2586 A69-30378

Flow field of highly ionized arc heated supersonic free jet, using continuous flow test facility [AIAA PAPER 68-135] 16 p2772 A69-32153

He and Ar arc-heated flows into reservoir and expansion in converging-diverging supersonic nozzles, considering flow equilibrium effect on heat transfer and enthalpy
20 p3631 A69-37198

Operational characteristics of multiple arcjet wind tunnel for time varying mass flow rate programs, calculating isentropic core densities and velocities [AIAA PAPER 68-229] 22 p3927 A69-40541

Arc-heated hypersonic wind tunnel for simulated spacecraft reentry environment, aerodynamic heating characteristics and research applications
22 p3927 A69-40595

Arc-heated plasma jet wind tunnel flow properties in plenum chamber by spectroscopic techniques, measuring electron excitation, temperature and densities 22 p3990 A69-40596

Arc heating of shock tube driver gas, describing radiative energy transfer mechanism 23 p4147 A69-41895

ARC JET ENGINES

Surface parameters influence on energy transfer to arc jet anode, discussing work function, accommodation coefficient and diffuse reflection coefficient of electrons [AIAA PAPER 69-107] 06 p1039 A69-18185

Pulsed MPD arc jet electric propulsion system requirements, examining physical constraints, pulse duration, duty cycle, power network structural details, etc [AIAA PAPER 69-269] 09 p1560 A69-21215

Radiation cooled MPD arc thruster design and performance, noting specific impulse relation to arc spoke rotation frequencies [AIAA PAPER 69-245] 09 p1566 A69-21259

Electric propulsion systems for manned planetary exploration flights, discussing arc jet, ion and plasma engines 18 p3185 A69-35108

Rotational arc motion in MPD accelerators with strong axial fields predicted by plasma physics equations 23 p4201 A69-41909

ARC LAMPS

Xenon high wattage short arc lamps for space/solar simulators, describing seals, electrodes shapes and cooling, operating characteristics, etc [AIAA PAPER 69-998] 22 p3920 A69-40376

ARC MELTING

Titanium production, discussing two stage electrode vacuum arc melting furnace, control and cooling equipment 02 p0229 A69-12068

Vacuum arc melted W and W-Re alloys mechanical properties, noting Re additions effects 08 p1331 A69-20190

Molten high melting compounds obtained by arc furnace with consumable electrode and adjustable protecting atmosphere 12 p2055 A69-26264

ARC SPRAYING

Plasma arc welding, discussing transferred and non-transferred arc systems application to spraying and welding techniques, including automated microplasma welding 04 p0608 A69-15482

ARC WELDING

NT GAS TUNGSTEN ARC WELDING

NT PLASMA ARC WELDING

Aluminum-Zn-Mg alloys weldability, discussing base metal composition and heat treatment influence during gas-shielded arc welding 01 p0086 A69-10536

Cavities elongation in automatic inert gas shielded welds in titanium alloys 05 p0767 A69-15972

Approximate method for calculating subsonic gas flows in curvilinear channels for gas admission control in arc welding 06 p0908 A69-16828

Weldability of thermally stable titanium alloy, noting properties of electron beam and submerged arc welding 06 p0940 A69-17092

Surface treatment effect on weld porosity causes and removal in VT5-1 Ti alloy argon arc welding 06 p0945 A69-17897

Surface edge preparation of titanium alloy sheets for argon shielded arc welding 06 p0932 A69-17898

Welding methods used for Ti and Ti alloys and difficulties encountered 07 p1139 A69-18789

Arc welding aluminum to steel using bimetal transition insert piece 11 p1891 A69-24929

Narrow gap gas metal arc welding process in spray transfer range for narrow welds in thick plates, discussing equipment and applications 11 p1891 A69-24930

Bulk weld filler metals, discussing granular compositions, electrodes and iron, nickel and cobalt base deposits 11 p1891 A69-24931

Dynamic properties of supply sources in carbon dioxide shielded welding as function of short circuit

current statistical parameters, noting metal spatter correlation 11 p1892 A69-25667

Porosity sources in Ti alloy welds, discussing increased gas content and silica, edge surface finish and gas hose contaminants 11 p1892 A69-25668

Rare earths additives effects on arc instability and weld puddle fluidity of stainless steel bare wire electrodes 12 p2103 A69-26623

Capacitor discharge stud welding on Ti alloys, discussing weld zone microstructure, arc and mechanical properties 18 p3151 A69-35431

ARCHES

Equilibrium stability of elastic circular arch constrained in rigid cavity and subjected to uniformly distributed parallel loading 03 p0524 A69-13066

Stability against snap-through and final states of shallow arches on elastic foundations and subject to time varying loads [ASME PAPER 68-WA/APM-26] 04 p0669 A69-14394

Two point boundary value problems for determining buckling behavior of two hinged circular arches [ASME PAPER 68-WA/APM-18] 04 p0669 A69-14399

Large deflection behavior of shallow circular arch subjected to vertical point load by nonlinear Rayleigh-Ritz finite element method, discussing deformation path 08 p1411 A69-20140

Natural mode structural analysis matrix methods for small displacements, discussing curved local subbeam in space and circular arch 11 p1969 A69-24374

Deep circular arches undergoing large deflections and stability loss, determining buckling load variations 20 p3622 A69-37210

Damping influence on shallow arch static and dynamic snapping under step pressure load 24 p4405 A69-43654

ARCHITECTURE

Aesthetic preservation of visual amenities in countryside by proper antenna design without affecting performance or cost 12 p2044 A69-26924

ARCTIC OCEAN

Insulated one man life raft for sea survival in arctic or subarctic conditions, evaluating thermal protection with endurance time and rectal temperature 12 p2020 A69-26550

ARCTIC REGIONS

Wind data from Arctic upper mesosphere showing easterly winds increasing with height, resolving diurnal and semidiurnal oscillations 06 p0949 A69-17005

Polar cap sporadic E investigation with backscatter at 28 MHz, noting geographic distribution, annual and diurnal variations 12 p2069 A69-26464

Multispectral and calibrated Alaskan Arctic aerial survey of sea ice, thaw lakes and polygonal soils 12 p2075 A69-26996

Longitudinal variations of density, temperature and pressure distributions in stratosphere and mesosphere based on rocket observations, emphasizing arctic and subarctic regions 15 p2602 A69-31379

Auroral absorption distribution from arctic riometric observations mapped for evaluating radio communications reliability 17 p2967 A69-33990

Neutral components of arctic thermosphere measured with rocket-borne RF mass spectrometers, discussing origin of atomic hydrogen and water lines 21 p3704 A69-38367

Aircrew Arctic survival situation simulation experiments with survivors staying close to aircraft and walking across difficult terrain from emergency location 23 p4088 A69-41810

Passenger safety during aircraft accidents in Arctic, discussing survival equipment and methods 23 p4107 A69-41811

AREA

Gas turbine areas calculation of through flow cross sections for temperature deformations and blades elongation 18 p3184 A69-34987

ARENDE-ROLAND COMET

Comet Arend-Roland orbit, deducing interstellar origin from nongravitational orbital energy increase 04 p0660 A69-15036

Kepler hyperbolic sine equation calculated for Arend-Roland comet for case of constant residues by false position method 06 p0997 A69-16821

Comet Arend-Roland type-1 tail characteristics including accelerating disturbance, outward-moving waves, tail inclination, etc 13 p2349 A69-27816

Luminescent material density distribution in comet Arend-Roland 1956h head determined from observed brightness variation with distance 14 p2524 A69-29711

Surface brightness distribution in comet Arend-Roland tail from diffusion model and photometric investigation of photographs obtained by 40-cm astrograph 15 p2684 A69-30519

Comet Arend-Roland 1957 III orbit elements computer calculated and tabulated from worldwide observations, taking into account orbital perturbations caused by major planets 20 p3596 A69-37311

Arend-Roland comet head luminescence intensity, considering radiation scattering by dust component 21 p3804 A69-39080

ARGENTINA

Argentina space research report to COSPAR covering Orion II sounding rocket, balloon experiments, cosmic rays, X ray astronomy, international cooperative programs, etc 15 p2724 A69-31452

ARGON

Ar atom transition probabilities in 5000-6000 angstrom range, noting effect of nonuniform source temperature 01 p0125 A69-10963

Initial ionization rates and collision cross sections in shock heated argon in low pressure shock tube, using double electrostatic probes 01 p0132 A69-11206

DC argon arc electrical and thermal parameters and optical properties at high pressure, using spherical anode 02 p0291 A69-12482

Cylindrical afterbodies at free stream Mach 2 with hot argon gas ejection, discussing flow rate influence on base pressure 02 p0190 A69-12533

Excess radiogenic argon in deep sea basalts from crest of East Pacific Rise, noting relation to glass content 02 p0244 A69-12568

Tradeoffs among beam divergence, power output and mirror alignment tolerances of high power argon ion lasers operating in various low order transverse modes 03 p0440 A69-13549

Microwave excited argon discharge emission spectrum analysis, suggesting possible laser action in microwave discharges 04 p0609 A69-14346

Combination rate constants for H-F-O reactions, discussing expressions and relative efficiencies with Argon as third body 04 p0646 A69-14743

Lorentz force sustained energy discharge, discussing cesium added argon flow across magnetic field in disk channel 06 p0969 A69-17910

Stabilized frequency single mode ionized argon laser, discussing intensity of electric field in cavity and mode selector 07 p1145 A69-18475

Electron collisional excitation cross sections for upper states in Ar ion lasers 07 p1157 A69-19656

Forward scattering of metastable and ground state argon atoms after argon ion-atom charge transferring collisions, discussing excitation resonances 08 p1354 A69-19809

Vacuum UV perturbation spectroscopy compatibility with resonance transitions in Ar ion laser 08 p1324 A69-20161

Redistribution of potassium and argon in meteorites and rock samples, discussing thermal diffusion and grain size 08 p1405 A69-20926

Momentum transfer cross sections, recombination coefficients and ionization coefficients of working gases for MHD energy converter
10 p1733 A69-23446

Argon discharges in metal capillary cathodes noting effects of electron density, flow velocity, electrode phenomena and gas temperature
10 p1733 A69-23450

Shock front propagation in argon with electrode-drawn induced EMF, using shock tube with induced transverse magnetic field
10 p1737 A69-23469

Relaxation phenomena in ionization process in argon shock front structure, using EM and pressure driven shock tube to drive high speed shock waves
10 p1726 A69-23685

Single frequency Ar ion laser for deep field holography noting thermal compensation, servo stabilization, operating mode, high power and high coherence
11 p1895 A69-24689

Low order transverse modes in Ar ion lasers, analyzing beam divergence, output, mirror alignment and cavity configurations
11 p1896 A69-24841

Argon ion laser with water cooled mercury pool cathode shielded by U-bent section trap, considering advantages as compared to oxide cathodes
12 p2107 A69-26326

Spatial distribution patterns of gaseous argon atoms scattered from solid argon surface
13 p2300 A69-28658

Low voltage Knudsen arc in cesium-argon mixture for thermal emission converters
14 p2403 A69-29248

Argon afterglow microwave and spectroscopic studies, monitoring time-varying electron density and temperature and extracting electron-ion recombination coefficients
15 p2658 A69-30173

Electron excitation and phase shift method for radiative lifetimes of Ar II UV transitions
15 p2656 A69-31034

Monograph on ionization of Ar-CH mixtures during Townsend discharge, covering metastable Ar atoms lifetime in various pressure ranges
16 p2814 A69-31841

Electron concentration and mass density behind reflected shock in ionizing argon, using time resolved two wavelength interferometry
16 p2771 A69-31918

FM detecting resolution using free running multimode uniphase Ar laser with Doppler broadened bandwidth
17 p2981 A69-33091

Mode transition characteristics of free burning argon electric arc with transpiration cooled anode, noting current blowing parameter
[AIAA PAPER 69-696] 17 p3011 A69-33451

Interferometric study of electron concentration and mass density profiles through ionized argon thermal end-wall layer formed in shock tube
[AIAA PAPER 69-694] 17 p3074 A69-33477

Shock heated argon thermal conductivity studied by optical interferograms, deriving equation for measured mean value
18 p3228 A69-34459

Ar 39 and Cl 36 production rates and ratios in stone and stony-iron meteorites metal phases, discussing terrestrial age calculation
19 p3411 A69-36100

Ar-Kr integral collision cross sections based on density measurements of Ar beam passed through liquid nitrogen cooled Kr filled scattering chamber
19 p3378 A69-36185

Inductively coupled RF excited toroidal Ar ion laser, confining current discharge by strong axial magnetic field to reduce wall losses
19 p3338 A69-36690

Differential cross sections for elastic scattering of protons by Ar atoms in energy range 12.7-44.1 eV, estimating internuclear separation
20 p3580 A69-37499

Precursors ahead of pressure driven shock waves in Ar, considering electron diffusion, temperature a density
20 p3518 A69-38237

Equilibrium absorption and desorption rates of carbon dioxide-argon mixtures from silica gel measured as function of temperature using gas dynamics method
21 p3848 A69-38707

Electron temperature profile across shock wave in weakly ionized nonequilibrium argon by numerical integration of energy conservation equation, noting three body recombination
21 p3698 A69-39791

Scattering of high energy Ar beams by room-temperature Ar, He and H molecules, deriving interaction energies at internuclear distances
22 p3988 A69-41187

Flow and thermodynamic variables of Ar-Cs mixture behind normal shock in shock tube at various temperatures and pressures
23 p4150 A69-41335

ARGON ISOTOPES

Tritium and argon 39 measurements of stone and iron meteorites, discussing decay and production rates and cosmic ray intensity
09 p1604 A69-22398

Ar 39 content in chondrites interpreted for meteorite size, exposure age and orbital elements
19 p3411 A69-36101

Ar 39-Ar 40 method using neutron activation and inert gas mass spectrometry to investigate meteoritic thermal histories
19 p3412 A69-36105

K and Ar 40 determination in iron meteorites by neutron activation for K/Ar dating
19 p3412 A69-36106

ARGON LASERS

Argon ion laser single frequency output spectrum characteristics
21 p3738 A69-39140

Argon laser lower operating level decay probabilities, using spectrum analysis to study role of radiative decay
22 p3965 A69-40965

Photochromic film behavior under high power argon ion laser excitation studied for display and computer memory applications, using excitation model
23 p4173 A69-41629

ARGON PLASMA

Ion acoustic wave dispersion in highly ionized Ar plasma in longitudinal magnetic field, noting effects of several phenomena
01 p0133 A69-11216

Electric potential effects on heat transfer from plasma to solid wall, measuring heat input rates
02 p0290 A69-12423

Plasma decay at high pressure in helium and argon with cesium vapor admixture and pure cesium vapor, using Saha equation
03 p0480 A69-14052

Ion and atom temperature distribution for two fluid model of Ar plasma in cylindrically symmetrical wall stabilized electric arc column
03 p0481 A69-14155

Radial profile measurement technique for individual emission line intensities in plasma applied to populations of excited atomic and ionic Ar in capillary discharges
04 p0634 A69-14441

Elastic scattering of electrons from argon atoms in argon air plasmas by shock tube microwave reflection method, measuring power reflection coefficient
[AIAA PAPER 68-138] 04 p0632 A69-14701

Magnetic field effects on heat transfer between Ar plasma flow and channel wall, noting effects of temperature and Reynolds number
04 p0636 A69-14989

Argon-K plasma electrical conductivity as function of electric current density at 1400-2400 K
05 p0798 A69-15614

Reducing decarburization of titanium carbide in argon plasma by carbon containing atmosphere, obtaining stable spheroidal particles
05 p0767 A69-15976

Low voltage Knudsen arc in cesium argon mixture using tungsten electrodes, analyzing current voltage characteristics
06 p0963 A69-16920

Radial temperature profile in induction coupled argon plasmas at low and atmospheric pressures
06 p0964 A69-17193

Potassium seeded argon plasma conductivity in induced electric field at static gas temperature for MHD generator model
06 p0871 A69-17909

Electron bombardment ion source generated Ar plasma beam to study wakes of disks and spheres, considering plasma interaction with bodies
[AIAA PAPER 69-79] 06 p0865 A69-18200

Nonequilibrium of electron and gas temperatures and reaction process for force-free plasma parallel beam produced in burner by expansion of argon plasma [DVL-875] 07 p1188 A69-18277

Argon plasma composition in Saha equilibrium, using FORTRAN 4 program
07 p1193 A69-19168

Argon plasma characteristics calculated from 8 mm interferometer data, interpreting transmission coefficients of dielectric film with permittivity gradient
07 p1194 A69-193240

Spectral distribution and energy of luminous radiation emitted during theta pinch in Ar plasma, noting energy maximum as function of pressure
08 p1362 A69-202838

Boron crystalline modification during transit through induction coupled Ar plasma producing better crystallized spheroids
08 p1372 A69-206878

Partially ionized argon plasma stagnation flow past blunt body using multifluid theory, obtaining flow profiles
08 p1369 A69-208171

Magnetic pinch effect in thermal RF induction plasma in argon, developing theory for calculating excess magnetic pressure
09 p1544 A69-213411

Total radiation of dense low temperature argon arc discharge plasma measured by bolometer, showing increase with arc current and pressure
09 p1547 A69-215951

DC plasmatron for heating argon with potassium additions at high temperatures and at near atmospheric pressure to obtain argon flow
09 p1547 A69-215961

Local enthalpy measurements in atmospheric argon arc plasma jet at various arc currents, comparing calorimetric and spectrometric methods
09 p1547 A69-216021

Ionic species identification in argon-cesium discharges for thermionic converter design
09 p1440 A69-218301

Excitation and ionization relaxation of cesium seeded argon gas computed for stepwise increase of electron temperature
10 p1732 A69-234441

Ionization relaxation in atmospheric pressure Ar plasma, considering two and three body recombination and O impurity effects
10 p1733 A69-234451

Velocity and temperature influence on discharge characteristics of K seeded argon plasma flow at 1 atm pressure
10 p1733 A69-234491

Electron temperature distributions in Ar-K plasma of simulated Faraday type MHD generator for current distributions, determining current density distribution experimentally
10 p1734 A69-234531

Instabilities in K seeded Ar plasma in crossed electric and magnetic fields and with nonequilibrium ionization, noting effects on MHD generator characteristics
10 p1734 A69-234571

One dimensional analysis of stationary argon flow in linear Hall generator from continuity, momentum and energy equations, discussing electron heating and nonequilibrium ionization
10 p1736 A69-234651

Current-voltage characteristics of combustion driven shock tube generated argon plasma
10 p1737 A69-234661

MHD generator performance operating on nonequilibrium Ar plasma with K additions in presence of electric fields
10 p1637 A69-234801

Magnetic field induced nonequilibrium argon plasma ionization relaxation processes obtained with allowance for flow parameters change in relaxation zone
11 p1922 A69-242251

Positive column contraction in Ar and Ar-Cs mixtures, developing theory for nonisothermal local collision arc
11 p1932 A69-255391

Ar plasma diagnostics in pinch-discharge laser, determining electron temperature by spectroscopy and measuring plasma conductivity and ion concentration and temperature
11 p1933 A69-255481

Reflection of moving rarefied Ar plasma from surface of nickel cylinder inserted into gas discharge tube
11 p1934 A69-257101

Knudsen arcs in argon showing potential well presence with anode barrier and cathode potential drop, establishing slow electrons thermal equilibrium
12 p2137 A69-265361

Electron concentrations in steady Ar and Ar-He plasma jets measured with microwave Fabry-Perot interferometer and Stark broadening of H beta line
12 p2137 A69-265371

Aluminum, Cu, Ni and titanium oxides injection into axis of Ar thermal induction plasma, observing decomposition as function of distance traveled within plasma
13 p2315 A69-28458

Plasma scanner in obtaining current cross sections and current-voltage characteristics of hollow cathode magnetically confined arc plasma in argon
14 p2450 A69-29568

Balance equations for axial separation in anisothermic plasma columns with radial variation of neutral gas temperature applied to argon discharge with mercury vapor addition
14 p2493 A69-29690

Spectroscopic determination of temperature fields in water and transpiration cooled constricted Ar arc jets at atmospheric pressure
15 p2657 A69-30155

Argon electric arc axis temperature measurements, showing current and tube diameter ratio dependence
15 p2662 A69-30977

Electron temperature relaxation in shock heated Ar plasma, measuring plasma microwave radiation
15 p2663 A69-30995

Electron and ion density distributions in propagating current sheet in Z pinch discharge in argon obtained by microwave reflection interferometer
16 p2816 A69-31639

Wide argon plasma column by axial current density measurements, confirming existence of instability and determining critical magnetic field
16 p2819 A69-31680

Nonlinear mixing of Ar plasma ion wave and externally applied electromagnetic wave
16 p2820 A69-31769

High temperature ionized turbulent argon jet gasdynamics noting electron density
16 p2770 A69-31889

Correlation coefficient of light fluctuations measured in Ar plasma in positive column of glow discharge, noting ionization wave appearance at critical gas pressure
16 p2822 A69-32039

Test apparatus for determining radiative properties of Ar plasma as function of high temperature and pressure [AIAA PAPER 69-601]
17 p3010 A69-33310

Shock structure in RF heated partially ionized Ar plasma jet, using cylindrical free molecule Langmuir probe [AIAA PAPER 69-697]
17 p3011 A69-33466

Plasma decay at high pressure in helium and argon with cesium vapor admixture and pure cesium vapor, using Saha equation
18 p3181 A69-35045

Relative oscillator strengths of 3500-5600 Å Fe I lines in emission of arc burning in Ar with iron chloride admixture
20 p3581 A69-37823

Microwave absorption by Ar plasma of positive column discharge in waveguide under inhomogeneous magnetic field
21 p3778 A69-39547

Spectroscopic measurements of weakly ionized Ar plasma premixed with diatomic N in plenum chamber, demonstrating role of competitive reactions for metastable Ar atom
21 p3779 A69-39794

Ionized He and Ar plasmas nonequilibrium nozzle flows, noting temperature difference between electron gas and atom-ion gas, calculating flow parameters
22 p3861 A69-41047

Argon plasma jet spectral radiation properties, considering electron density, recombination, excitation, argon density, etc
22 p3991 A69-41052

DC argon plasma generator operation, studying effects of gas flow direction and rate
24 p4255 A69-43077

Electrothermal waves in nonequilibrium electrical discharge in potassium seeded argon plasma
24 p4359 A69-43645

ARGUMENTS [MATHEMATICS]
U INDEPENDENT VARIABLES

ARIEL 3 SATELLITE

Ariel 3 receiver for measuring galactic noise spectrum, discussing loop antenna use with swept receiver, false terrestrial signals, etc
03 p0404 A69-13581

Scientific results from Ariel 3 satellite - Conference, London, April 1968
21 p3716 A69-39254

Ariel 3 satellite management structure, responsibilities and orbit, stabilization, launch window, data acquisition and processing
21 p3856 A69-39255

Ariel 3 satellite shape and systems including heat balance, data storage and compatibility problems
21 p3820 A69-39256

Ariel 3 satellite observations, including topside ionospheric variations with time and solar activity, electron density, temperature measurements, etc
21 p3716 A69-39257

Ariel 3 satellite attempted background radiation measurement between 2-4 MHz to show absorption onset in Galaxy
21 p3806 A69-39258

Terrestrial radio noise from lightning discharges measured by Ariel 3 satellite to deduce sources distribution
21 p3759 A69-39259

Ariel 3 satellite attitude determination, using solar aspect sensors to define conical surface containing spin axis
21 p3820 A69-39260

Ariel 3 satellite spin axis direction determination by optical means from analyzing sunlight glints reflected from surfaces
21 p3820 A69-39261

Synoptic study of worldwide VLF electromagnetic wave fields distribution above ionosphere from Ariel 3 observations
21 p3717 A69-39262

Molecular O distribution in thermosphere from Ariel 3 observations of solar radiation attenuation, showing large and systematic variation with longitude
21 p3717 A69-39263

ARIP [IMPACT PREDICTION]
U COMPUTERIZED SIMULATION
U IMPACT PREDICTION

ARITHMETIC

Chebyshev polynomials maximum property, examining effect of roundoff errors in Horner scheme for floating point arithmetic
03 p0456 A69-13553

Classical and differential conditioning of eyelid response with correctness of solutions of arithmetic problems as discriminandum
07 p1064 A69-18637

Binary increment and residual class notation techniques for onboard spacecraft computer arithmetic
20 p3499 A69-37378

ARITHMETIC AND LOGIC UNITS

LSI oriented cellular array implementation of complex arithmetic functions for aerospace computers, describing techniques of automatic switching-in of spare modules for failures [AIAA PAPER 69-964]
22 p3906 A69-40345

ARM [ANATOMY]
U FOREARM

ARMED FORCES
NT NAVY

Coronary atherosclerosis in military pilot fatalities of aviation accidents, demonstrating irrelevance of amount of flying time and type of aircraft
03 p0376 A69-14080

ARMED FORCES [FOREIGN]

Beriev Be-12 cranked wing seaplane design including technical and operational data
24 p4251 A69-42796

ARMED FORCES [UNITED STATES]

Clinical analysis of combat and noncombat ejection experience of USAF
06 p0878 A69-16960

U.S. Army Materiel Command R and D planning structure and technical planning processes influence on decisions improvement
08 p1423 A69-21153

Efficient allocation of maintenance resources in USAF, analyzing B-52 costs and substitution of capital for labor
13 p2382 A69-28041

U.S. Navy Numerical Value Rating System computing method of selecting lowest cost design approach to accomplish specific function
13 p2383 A69-28098

Space Ground Link Subsystem as S-band communication link within Air Force Satellite Control Facility including unified telemetry, tracking and command systems
14 p2427 A69-28879

VHF to UHF telemetry bands transition implemented by Naval Weapons Center
14 p2411 A69-28880

Lidar data obtained at Hamilton AFB, Calif., computer analyzed for lidar operational utility, determining cloud ceiling and visibility for aircraft landing operations
15 p2651 A69-30895

Balloon flights with space available for secondary experiments, discussing launching agencies and experiment design restrictions
22 p3865 A69-40807

ARMOR

Boron carbide body armor fabrication by hot pressing in graphite molds
08 p1320 A69-20411

Fiber glass reinforced plastic backing phase of composite armor, noting test method for evaluation of performance
09 p1507 A69-22319

Armor selection for advanced aircraft systems based on premium value concept and cost-weight considerations [SAWE PAPER 764]
18 p3094 A69-34878

Composite ceramic armor systems for airborne vehicles and personnel, air cushion vehicles and ground troops, discussing weight and contour forming advantages
19 p3355 A69-35525

AROMATIC COMPOUNDS

Sulfur-organic compounds association with aromatic hydrocarbons, noting oxidation inhibiting effect on petroleum oil
03 p0494 A69-13800

Cross-linked polymers obtained by direct reaction of aryl polycarbonyls with aryl polyamines, studying char yields effect
08 p1269 A69-21059

Cross-links effect on char yields of azomethine polymers produced by aryl diamines with aryl diketones
08 p1269 A69-21060

Temperature effects on phosphorescence lifetimes and intensities of aromatic hydrocarbons in polymethyl methacrylate, estimating activation energy for thermally activated nonradiative decay mode
10 p1652 A69-23523

Interstellar extinction models of classical Mie particles and quantum mechanical polycyclic aromatic molecules
10 p1781 A69-23679

Normal, isoprenoid, dicarboxylic, keto and various aromatic acids isolated from controlled stepwise degradation of Green River kerosene by successive chromic acid oxidations
15 p2606 A69-31533

Molecular structure and uses of heat resistant plastics, discussing aromatic polyamides
18 p3161 A69-34279

Photochromic panel for flash blindness protection using epoxy plastic plates containing aromatic hydrocarbon compounds excited to triplet states
21 p3668 A69-39783

ARRAYS

NT ANTENNA ARRAYS

NT ENDFIRE ARRAYS

NT INERTIALESS STEERABLE ANTENNAS

NT LINEAR ARRAYS

NT PHASED ARRAYS

NT STEERABLE ANTENNAS

NT SYNTHETIC ARRAYS

NT YAGI ANTENNAS

Large scale integration /LSI/ arrays, discussing high yield manufacturing methods based on fixed nondiscretionary connections among components
02 p0254 A69-12467

Array radar technology development offering multifrequency operations from common aperture
03 p0388 A69-13182

Single crystal cells for construction of large deployable solar cell arrays
03 p0368 A69-13993

Reflection and absorption characteristics of two dimensional array of magnetic dipoles for microwaves, considering element orientation and distribution
12 p2035 A69-25901

Solar array energy performance as function of orbital parameters and spacecraft attitude
13 p2203 A69-27419

Orientation distribution of lineal and areal elements in space, expanding density function definition of two dimensional lineal array
14 p2470 A69-29363

Roll-up solar array based on erection of planar sandwich structure from two rolled constituent halves
16 p2762 A69-32559

Large area Si solar cell arrays design, considering environment, cell layout, thermal expansion, coverslides fabrication, costs, etc

19 p3253 A69-35708

Solar cell retractable array for spacecraft multikilowatt power generation

19 p3254 A69-35711

Plane electromagnetic wave diffraction by screened periodic metallic strips array with real ferrite transversely magnetized to saturation

23 p4124 A69-42032

Electromagnetic wave diffraction by multielement periodic metallic strips arrays positioned transversely in rectangular waveguide

23 p4124 A69-42035

Accuracy standards for diffraction measurements of electromagnetic waves incident on periodic arrays, using monochromatic field and plane wavefront

23 p4139 A69-42042

Plane polarized electromagnetic wave diffraction incident on skewed metal ribbons array

23 p4125 A69-42043

Spacecraft Si cell solar array using self rigidizing folded panels with flexible substrates for increased power/weight and power/stowage volume ratios

23 p4073 A69-42290

Lightweight large area solar cell arrays for space programs with multikilowatt predicted performance, noting rollup array orbital flight testing

23 p4073 A69-42291

ARRESTING GEAR

Exterior arresting devices for commercial aircraft full scale tests

03 p0367 A69-14104

Caravelle aircraft halting tests with barrier net

10 p1674 A69-23706

Stopping barriers for jet aircraft landing design and operation

11 p1862 A69-24354

ARRHYTHMIA

Cardiac arrhythmias during positive G sub x acceleration, treadmill exercise and tilt table testing

06 p0874 A69-17834

Arrhythmia diagnosis instruction aided by cardiac pacemaker digital simulation, discussing clinical electrocardiograms generation mechanisms

21 p3667 A69-39606

Supraventricular arrhythmias after acute myocardial infarction, noting benefit of early DC shock

24 p4262 A69-42729

ARSENIC

Temperature dependence of partial pressure of saturated As vapor over solid solutions of InAs-GaAs of different composition

04 p0642 A69-14938

Chondritic meteorites arsenic, tin and antimony content determined by anion-exchange chromatography and neutron activation analysis

13 p2344 A69-27630

ARSENIC COMPOUNDS

U ARSENIDES

U GALLIUM ARSENIDES

U INDIUM ARSENIDES

ARSENIDES

NT GALLIUM ARSENIDES

NT INDIUM ARSENIDES

Conduction band anisotropy in n-type cadmium tin arsenides, analyzing galvanomagnetic tensor and distribution of isoenergetic surfaces for electrons

03 p0488 A69-13888

Coherent emission in epitaxial structures with heterojunctions in AlAs-GaAs system

03 p0489 A69-13896

Conduction band anisotropy in n-type cadmium tin arsenides, analyzing galvanomagnetic tensor and distribution of isoenergetic surfaces for electrons

11 p1939 A69-25689

Coherent emission in epitaxial structures with heterojunctions in AlAs-GaAs system

11 p1939 A69-25697

Cadmium arsenide carriers effective mass under strong transverse magnetic field, noting restricted role of thermal EMF and Hall coefficients

13 p2318 A69-27897

Electronic properties changes in amorphous CdGeAs caused by long range order loss studied by measuring optical and transport properties

19 p3390 A69-36557

Thermal EMF in cadmium arsenide specimens with various electron concentrations determined to verify parabolic subband structure of conduction band

22 p3993 A69-40607

ARTERIES

NT AORTA

Axial waves in blood vessels, determining phase velocities and damping, noting anisotropic behavior of artery wall

[SESA PAPER 1350] 07 p1069 A69-19726

Analog computer modeling of human systemic arterial tree, based on lump parameter circuit approximation

07 p1072 A69-19727

Arterial tone and human muscular activity limitations, analyzing hypodynamic effects on aorta, arm and leg vessels constriction

10 p1647 A69-23586

Linear passive electrical analog model of human systemic arterial tree, discussing artery segment modeling, vessels input impedance, wave travel, etc

17 p2908 A69-33007

Transfer function in pulmonary ventilation and O tension in arterial blood analyzed by automatic control

19 p3260 A69-35897

Coronary angiography for evaluating cardiac problems of aircrew, giving case histories and clinical and laboratory findings

19 p3263 A69-36461

Cerebral circulation arterial system pulsatile flow flexible vessel digital simulation models distribution

19 p3264 A69-36867

Electromagnetic catheter flowmeter with flexible sensor suitable for branch and artery application to minimize surgical intervention

22 p3889 A69-40058

Arterial occlusion effects on retinal structure in cats, describing degrees of cell degeneration

22 p3884 A69-40883

Gilson cuvette densitometer used for blood flow measurement in canine forelimb and human forearm and hand during constant intrabrachial arterial dye infusion

23 p4077 A69-41294

Carbon dioxide inhalation and intravenous isoproterenol effects on hemorrhagic consolidation occurring after left pulmonary artery ligation in dogs

23 p4082 A69-41441

Mathematical formulation for relative values of cardiac output and peripheral resistance as two contributing factors to arterial pressure change

23 p4085 A69-41473

Pulsatile flow in coronary arteries simplified model compared with experiment in anesthetized dogs

23 p4098 A69-42103

Human arterial pressure reflex regulation during sleep, assessing baroreflex sensitivity

24 p4257 A69-42626

ARTERIOSCLEROSIS

Coronary atherosclerosis in military pilot fatalities of aviation accidents, demonstrating irrelevance of amount of flying time and type of aircraft

03 p0376 A69-14080

Corneal greyish opaque arc as warning of atherosclerosis in flight crews

05 p0711 A69-16631

ARTHROPODS

U BEETLES

U CRABS

U DROSOPHILA

U INSECTS

U PUPA

ARTICULATION

Speech intelligibility in air at ground level and in helium-oxygen mixture at 18,000 ft

12 p2019 A69-26548

ARTIFICIAL CLOUDS

Large convective clouds in superheated air generated by static tests of Saturn 5 first stage

03 p0462 A69-14125

Simulation experiments using artificial plasma for astrophysical rocket exploration, discussing experiments leading to barium-copper oxide mixture choice for plasma cloud

06 p0999 A69-16973

Temperature variability data for 120-km altitude from observations of grenade glow clouds, calculating molecular diffusion coefficients and atmospheric temperature and density

07 p1127 A69-19277

Space electric fields research by artificial clouds of vaporized barium launched by rockets, noting neutral atmosphere and ionospheric results

09 p1492 A69-22800

Artificial noctilucent clouds or meteor trails positions determined by transforming photogrammetric coordinates

12 p2154 A69-25822

Ground and metastable state photoionization cross sections of Ba to explain artificial Ba clouds, using many channel quantum defect method

18 p3177 A69-35238

Artificial ion plasma cloud experiment for studying auroral electric fields

21 p3710 A69-38507

Spectra and intensities of rocket releases for upper atmosphere composition, temperature and reaction kinetics, noting chemiluminescence and atomic and molecular emissions

21 p3712 A69-38522

Turbulent field structure between 90-120 km estimated from sodium clouds diameters variation ejected from rockets

21 p3713 A69-38524

Lower ionosphere vertical wind velocity profiles determined from rocket-released grenade glow cloud photographs, developing cloud buoyancy effect empirical model

23 p4154 A69-41305

ARTIFICIAL GRAVITY

Biological systems response to inertial environment, escape from earth gravity, planetary gravity and artificial gravity

06 p0872 A69-17011

Weightlessness simulation, discussing mechanics of biological effects, simulation of specific anticipated effects and concept of mechanical acceleration and gravity equivalent effects

06 p0879 A69-17012

Manned space stations for future space exploration, discussing earth-like environment, artificial gravity, human factors and time dependence

11 p1965 A69-25644

Weightlessness problems, discussing artificial gravitation on spacecraft and astronaut experiences

16 p2746 A69-31930

Rotational equations of motion for two body spacecraft on common spin axis required for simulated gravity environment or gyroscopic stability augmentation

17 p3047 A69-33227

Squirrel monkeys exposed to centrifugally generated artificial gravity trained to respond for food reinforcement at selected gravity levels

23 p4081 A69-41434

ARTIFICIAL INTELLIGENCE

Soviet book on electronic countermeasures and intelligence covering jamming methods for automatic systems

03 p0385 A69-12927

Artificial intelligence application to design of off-line and on-line learning control systems for controlling spacecraft attitudes

04 p0581 A69-14568

Adaptive pattern recognition, discussing classification techniques and merging into other aspects of artificial intelligence research

07 p1088 A69-18381

Cybernetic structural model for learning and mentation comprehending symbol systems, languages, homeostatic mechanisms, etc

07 p1070 A69-18385

Learning model of motor behavior in brain cortex of higher animals and man, discussing M automaton, information reception, correlation, memory, emotions, desires and actions

23 p4109 A69-41977

ARTIFICIAL RADIATION BELTS

Unique solution for radial diffusion coefficient applicable to equatorially trapped electrons in artificial radiation belt

05 p0816 A69-16279

ARTIFICIAL SATELLITES

NT ACTIVE SATELLITES

NT ALOUETTE SATELLITES

NT ALOUETTE 1 SATELLITE

NT ALOUETTE 2 SATELLITE

NT ANNA SATELLITES

NT APOLLO SPACECRAFT

NT APPLICATIONS TECHNOLOGY SATELLITES

NT ARIEL 3 SATELLITE

NT BEACON SATELLITES

NT BIOSATELLITE 2

NT BIOSATELLITES

NT COMMUNICATION SATELLITES

NT COSMOS SATELLITES

NT COSMOS 5 SATELLITE

NT COSMOS 6 SATELLITE

NT COSMOS 149 SATELLITE

NT D-1 SATELLITE

NT DIADEME SATELLITE

NT DODGE SATELLITE

NT EARLY BIRD SATELLITES

NT EARTH RESOURCES TECHNOLOGY
SATELLITES
NT ECHO SATELLITES
NT ECHO 1 SATELLITE
NT ELEKTRON SATELLITES
NT ELEKTRON 4 SATELLITE
NT ESRO 1 SATELLITE
NT ESRO 2 SATELLITE
NT ESRO SATELLITES
NT ESSA SATELLITES
NT EUROPEAN 1 SPACECRAFT
NT EXPLORER SATELLITES
NT EXPLORER 1 SATELLITE
NT EXPLORER 16 SATELLITE
NT EXPLORER 18 SATELLITE
NT EXPLORER 20 SATELLITE
NT EXPLORER 22 SATELLITE
NT EXPLORER 26 SATELLITE
NT EXPLORER 29 SATELLITE
NT EXPLORER 30 SATELLITE
NT EXPLORER 31 SATELLITE
NT EXPLORER 33 SATELLITE
NT EXPLORER 35 SATELLITE
NT EXPLORER 38 SATELLITE
NT EXPLORER 40 SATELLITE
NT GEODETIC SATELLITES
NT GEOPHYSICAL SATELLITES
NT GEOS 2 SATELLITE
NT GRAVITY GRADIENT SATELLITES
NT HEOS A SATELLITE
NT HEOS SATELLITES
NT IMP
NT INJUN SATELLITES
NT INTELSAT SATELLITES
NT ISIS-A
NT ISIS SATELLITES
NT LINCOLN EXPERIMENTAL SATELLITES
NT LUNAR ORBITER
NT LUNAR SATELLITES
NT METEOROLOGICAL SATELLITES
NT MICROMETEOROID EXPLORER SATELLITES
NT MOLNIYA SATELLITES
NT NAVIGATION SATELLITES
NT NIMBUS SATELLITES
NT NIMBUS 3 SATELLITE
NT OAO
NT OGO
NT OGO-D
NT OGO-E
NT OGO-F
NT ORBIS CAL SATELLITE
NT ORBITAL SPACE STATIONS
NT ORBITAL WORKSHOPS
NT OSO
NT OSO-3
NT OSO-C
NT PASSIVE SATELLITES
NT PROTON SATELLITES
NT PROTON 2 SATELLITE
NT RADIO ASTRONOMY EXPLORER SATELLITE
NT RELAY SATELLITES
NT SAN MARCO SATELLITE
NT SAN MARCO 2 SATELLITE
NT SYNCHRONOUS METEOROLOGICAL SATELLITE
NT SYNCHRONOUS SATELLITES
NT SYNCOM SATELLITES
NT TIROS SATELLITES
NT TIROS 9 SATELLITE
NT TRANSIT 4A SATELLITE
NT TRANSIT SATELLITES
NT VELA SATELLITES
NT VENERA SATELLITES
NT VENERA 4 SATELLITE

Soviet artificial earth satellites, discussing Sputnik, Polet, Elektron, Cosmos, Molniya and Vostok series
01 p0162 A69-10937
Thermal gradients in artificial satellites, considering heat exchange among various points of closed cavity surface by gray body diffuse radiation and reflection
08 p1421 A69-20157
Electron and proton radiation doses impinging on orbiting satellites computed using orbit calculation and B, L coordinates
11 p1949 A69-24862
Improved spheroidal method for calculation of almost polar orbit of artificial satellites, bypassing right ascension
12 p2152 A69-25799
Algorithm for solving autonomous artificial satellite orbital elements by using successive approximations
13 p2296 A69-27687
Photoelectric photometry of artificial satellites noting equipment, Pageos satellite observations and light curves from Cosmos 151, 192 and 220
15 p2616 A69-31391

Satellite motion about center of mass, discussing satellite stabilization and libratory motion in gravitational force field, planet resonances, etc
15 p2703 A69-31411
Legal principles observed for international telecommunication systems establishment by means of artificial satellites regarding states interests and rights
20 p3638 A69-37124
Near-polar circular orbiting satellite for calibrating and evaluating ground-based radars observing space objects
20 p3617 A69-37714
Radiative heat input to artificial satellite in orbit due to solar and earth radiations calculated and presented in graphs for satellite temperature calculation
22 p4006 A69-40589
Artificial satellite motion analysis and perturbation function, considering disturbances due to second satellite or sun
22 p4030 A69-40906
Planetary gravitational fields and artificial satellite orbits determined by using earth based range rate measurements
24 p4388 A69-43650

ARYL COMPOUNDS
U AROMATIC COMPOUNDS

ASBESTOS
High modulus graphite/asbestos reinforced laminates, noting improved transverse strength and thermal properties
24 p4337 A69-43447

ASCENT
NT CLIMBING FLIGHT
Inner and outer meteorological balloon assembly for fast rising and high altitude sounding
01 p0010 A69-10541
Bright fundamental stars right ascensions observed in Chile, discussing instruments, declination range, systematic errors, etc
10 p1777 A69-23388
Mathematical model for ascent and descent of high altitude tethered balloon, developing computer program and deriving differential equations of motion [AIAA PAPER 68-942]
24 p4254 A69-43722

ASCENT TRAJECTORIES
Aircraft takeoff airborne phase trajectory analysis, deriving expressions for projection angle, velocity, path length and instantaneous altitude
19 p3247 A69-35817
Lunar module motion during optimal ascent from moon surface into circular orbit of command module, noting descent maneuver similarity
19 p3431 A69-36617
Optimization of RF ion thruster cluster engines for ascending trajectory, discussing unfolding mechanism of solar cell panels [DGLR-69-022]
23 p4203 A69-41933

ASCORBIC ACID
Space flight factors, ionizing radiation and combined effects on vitamin C content in onion bulbs
05 p0708 A69-16510
Space flight factors, ionizing radiation and combined effects on vitamin C content in onion bulbs
18 p3095 A69-34729

ASPECT RATIO
NT HIGH ASPECT RATIO
NT LOW ASPECT RATIO
Model of auroral backscatter from E region including ionospheric refraction, comparing computations to experimental HF auroral backscatter data for aspect sensitivity
09 p1488 A69-21700
Wing geometry and wing lower surface boundary layer effects on rolled-up tip vortices geometry and strength
11 p1819 A69-25372
Membrane flutter and panel stability in supersonic flow, considering infinite aspect ratio equation solution through Galerkin method
13 p2365 A69-28236
Drag and lift coefficients of moderate aspect ratio prismatic bodies analyzed as function of angle of attack, Reynolds number and aspect ratio
17 p2896 A69-33717
Clamped uniformly loaded rectangular plate large deflection elastic behavior approximate analysis, using perturbation method
20 p3620 A69-36998
Vibration properties of cantilever parallelogram box beam, using existing static deformation equations under large aspect ratio condition
21 p3846 A69-39803

Wingtip mounted propellers effect on wing lift and induced drag, varying lift to drag ratio by changing in-flight aspect ratio
24 p4250 A69-43713

ASPHERICITY
Aspherical surfaces formation from spherical by removing part of substrate by means of tool mask for lapping nonuniform wear of surface
12 p2102 A69-26597
Eye optical system spherical aberration measured by knife-edge method derived from Foucault test, investigating retinal image quality
22 p3882 A69-40873

ASPIRATION
U VACUUM
ASSAULTING
U ATTACKING [ASSAULTING]
ASSAYING
Automatic devices to count bacterial colonies Petri dishes consisting of culture plate scanner and data processor
02 p1201 A69-11773

ASSEMBLER ROUTINES
Maintenance system in Germany for F-104-G Starfighter planes noting disassembling, system testing and test flight
17 p2979 A69-33703
Symbolic language and assembly program for Roseau computer, discussing mnemonic code and program operation
20 p3502 A69-37397

ASSEMBLIES
Fretting effect on fatigue of press fitted axle assemblies, analyzing relative slip amplitude dependence on size, shape, clamping pressure, nominal stress and cycles
01 p0167 A69-10305
Integrated logic circuits assembly for digital computers, considering high density, mechanical environment, reliability, accessibility and costs
20 p3505 A69-37401
Hybrid microwave IC assembly techniques, discussing active devices connection to substrate with thick or thin film metallizations
22 p3912 A69-40068

ASSEMBLING
NT ORBITAL ASSEMBLY
Metal welding procedures for aircraft assembly, discussing weight, specific alloys and airframe components
04 p0608 A69-15483
Quality control of high volume microelectronic circuit assembly of military computer emphasizing preventive action
15 p2580 A69-31129
Kennedy Space Center Vehicle Assembly Building construction, capacity and operation for manned spacecraft
19 p3288 A69-35500
Clamping and sealing fastener for single direction installation consisting of pin, collar and sealing collar with insert
22 p3957 A69-40831

ASSESSMENTS
Meteorological probability assessors, describing framework for evaluation consistent with subjective probability theory
01 p0110 A69-10690

ASSIGNMENT
U ALLOCATIONS
ASSOCIATIONS
U ORGANIZATIONS

ASTEROIDS
NT ICARUS ASTEROID
Gegenschein measurements for determining upper limit on asteroidal debris spatial density
02 p0324 A69-12545
Light curves for Vesta compared and rotation derived from aspect change effect on rotational period
04 p0657 A69-14677
Mare Orientale basin satellite photographs suggest asteroid impact formation
04 p0664 A69-15421
Icarus observation by Trepied-Metcalf method, tables show Icarus retreat and advance and velocities of eight asteroids neighboring earth
05 p0819 A69-15698
Orbit corrections for lost minor planets 457, 1038, 1161, 1297, determining new ephemerides for oppositions
05 p0829 A69-16704

Asteroidal and cometary orbits and origin of meteorites, discussing eccentricities, exposure ages and mass yield
08 p1406 A69-20929

Angular momenta of stars, planets and asteroids, plot log of angular momentum per unit mass against log of mass of astronomical object
09 p1608 A69-22716

Orbits of asteroids surrounding commensurabilities with Jupiter, discussing theory for origin of Kirkwood gaps
10 p1778 A69-23604

Solar radiation pressure on interplanetary dust particles calculated as function of radius and density, noting asteroidal origin of dielectric and absorbing particles
11 p1956 A69-24397

Comet Berbon and minor planet positions photographically recorded /1964-1967/
11 p1962 A69-25121

Quasi-stochastic nonlinear one dimensional oscillations in periodically disturbed field applied to celestial mechanics of planetoids
12 p2130 A69-26373

Provisional elliptic orbit computed for asteroid Floirac using Gauss-Encke and least squares method, tabulating residuals and ephemeris
14 p2521 A69-29585

Integrodifferential equation derived and solved for evolution of collisional model of asteroids and debris
14 p2526 A69-29879

Exact positions of Ceres, Pallas, Juno and Vesta from 1941 to 1995 determined taking into account planets influence
16 p2859 A69-32224

Asteroidal jet streams from Hirayama family Flora, difficult to reconcile with exploded planet view
17 p3030 A69-33070

Long range perturbations of satellites and asteroids with arbitrary inclination and eccentricity, illustrating motion around moon, oblate and spherical planets using energy integral
17 p3031 A69-33098

Epochs and ephemerides of asteroid Amor for 1916, 1924 and 1972, noting unfavorable observing conditions in future
17 p3038 A69-33723

Depth distribution of primary cosmic radiation fluxes and secondary nuclear-active particles in stone meteorites and surface layer of planets, moon and asteroids
19 p3410 A69-36092

Minor planets osculating elements computer calculated and tabulated
20 p3596 A69-37309

Minor planets positions computer calculated and tabulated from Tashkent 1963 and 1964 astrograph observations, stating time and equatorial coordinates
20 p3596 A69-37312

Minor planets positions computer calculated and tabulated from 1966 and 1967 Crimean astrograph observations, using Yale catalog reference stars
20 p3570 A69-37313

Hill method applied to motion theory for minor planet 11 Parthenope using computerized first order perturbations from principal planets
20 p3596 A69-37316

Jupiter mass determined from observations of four minor planets perturbations
22 p4013 A69-40121

Resonant asteroids in statistically underpopulated Kirkwood gaps, noting osculating mean motion distribution
22 p4013 A69-40122

Lightcurves for 624 Hektor with Radcliffe, Kitt Peak, Catalina and Cerro Tololo reflectors, noting asteroid shape and rotational axis
22 p4013 A69-40124

Harmonia and Parthenope /minor planets/ positions, establishing time dependence of relation between image diameter and planet magnitude
22 p4025 A69-40614

Cometary and asteroidal orbital differences and similarities, emphasizing limiting cases to study orbital evolution of meteors
23 p4208 A69-41284

Spacecraft probes design for mapping meteoroid environment and penetration hazard through asteroid belt
[AAS PAPER 69-321] 24 p4392 A69-42867

Asteroid exploration by solar photovoltaic powered ion propelled probe, discussing spacecraft design, mission and 1975 Mariner utilization
[AAS PAPER 69-322] 24 p4381 A69-42868

Solar radiation pressure on interplanetary dust particles calculated as function of radius and density, noting asteroidal origin of dielectric and absorbing particles
24 p4390 A69-43787

ASTHMA

Asthmatic attacks in military air crews, discussing flight stress factors including altitude, ventilation and insecurity as possible causes
05 p0710 A69-16624

ASTIGMATISM

Weightlessness and higher g values effects on caloric and rotational nystagmus
12 p2020 A69-26551

Human vestibular reactions at various bodily rotation rates and planes, including counterrotation illusion and nystagmic reaction
12 p2020 A69-26564

Human nystagmic reaction variations due to simultaneous rotation of head and body, studying coriolis couple in horizontal semicircular canals
12 p2020 A69-26565

Prolonged iterative accelerations and decelerations on vestibular apparatus, discussing nystagmus measurement attempt and centrifugation tests on guinea pigs
13 p2211 A69-28592

Single flash and rhythmic light stimuli effect on nystagmus of patients with tumoral posterior cranial fossa, recorded electroencephalographically
20 p3470 A69-37250

Threshold variations in caloric nystagmus in pigeons subjected to accelerations in head to tail direction in centrifuge at various temperatures
20 p3471 A69-37252

Motion sickness prophylaxis for rabbits subjected to rotation, investigating effects of adrenalin, ephedrine, sympatholitin, piperoxane and pyridoxyphenone on nystagmus and respiration
20 p3472 A69-37265

Nystagmus reactions in rabbits subjected to rotating vestibular tests, noting decrease following previous adaptation to stimulus
20 p3473 A69-37267

Rapid component of nystagmus using photostagnography, noting dependence on afferent pulse of ampullar apparatus
20 p3481 A69-37272

Focus broadening by astigmatism of large microwave parabolic antennas, discussing large span surface deformations caused by astigmatic aberration
23 p4140 A69-42188

Retinal eccentricity effects on horizontal-vertical illusion magnitude, considering eye flattening and astigmatic properties
24 p4263 A69-43117

ASTRONICS

Microelectronic equipment for aerospace application and integrated circuit production in UK
[AGARDOGRAPH-114] 08 p1292 A69-20992

Spacecraft electronics - Conference, Chicago, December 1968
09 p1465 A69-22433

Evaluation technique for astronics subsystems in automated spacecraft designed for interplanetary missions, considering operation times, navigation updating and midcourse correction
[AIAA PAPER 69-882] 21 p3764 A69-39408

ASTROBIOLOGY U EXOBIOLOGY

ASTRODYNAMICS

Book on planetocentric, lunar and interplanetary transfer techniques covering communications and coordinate system selection, minimum fuel and time transfer and rendezvous, etc
04 p0652 A69-14458

Single impulse noncoplanar orbital transfer with finite time of thrust action for satellite in elliptical orbit
05 p0823 A69-16044

Astrodynamic, guidance and control - Conference, Belgrade, September 1967, Volume I
06 p1004 A69-17560

Astrodynamic data compilation for use by system engineer for mission planning
[AIAA PAPER 69-124] 06 p1011 A69-18090

Mars imaging mission and astrodynamic interaction, discussing arrival geometry and orbit size effects
[AIAA PAPER 69-127] 06 p1011 A69-18169

Single impulse noncoplanar orbital transfer with finite time of thrust action for satellite in elliptical orbit
20 p3606 A69-37953

ASTROGRAPHY

Icarus positions from photographic observations with astrograph
01 p0159 A69-11331

Sunspot observations with astrograph telescope by tracing on projected image of solar disk
08 p1387 A69-20118

Proper motions and positions of X ray source Sco X-1 and surrounding stars derived from astrographic plates using overlap technique
12 p2152 A69-25798

Icarus asteroid observed at Royal Observatory of Belgium with 40-cm double astrograph, tabulating acquired data
14 p2521 A69-29584

Minor planets positions computer calculated and tabulated from Tashkent 1963 and 1964 astrograph observations, stating time and equatorial coordinates
20 p3596 A69-37312

Minor planets positions computer calculated and tabulated from 1966 and 1967 Crimean astrograph observations, using Yale catalog reference stars
20 p3570 A69-37313

ASTROMETRY

Photographic plates based parallax determinations of nearby stars weights, relative and absolute values, probable error and observation interval
04 p0663 A69-15381

Relative proper motions of stars measured by microscope projection technique
10 p1778 A69-23570

Satellite photographic astrometry and chronometry, determining spatial positions of satellites and observation stations by space triangulation
11 p1956 A69-24400

Cosmic triangulation by geometrical synchronization of astrometric satellite observation, with precise times unavailable
12 p2158 A69-26432

Flare star astrometric study to determine possible variable proper motion
13 p2348 A69-27810

Radial velocities of southern OB stars and supergiants noting tabulation of information
14 p2519 A69-29368

Transit instruments operational principles and practical experience
15 p2608 A69-30440

Pitch determination of micrometer screw by scalar star pairs derived from FK3 and Washington zenith catalog noting temperature and dampness effects
16 p2859 A69-32218

Soviet collection of articles on problems of astrometry covering nutation, earth pole motion, nighttime latitude, meridian observations, Mars observations, libration, etc
17 p3026 A69-32867

Lunar rotation elements determined from distances between Moesting A and limb craters, using Iakovkin position angle method
17 p3028 A69-32876

Azimuth error from observations of circumpolar stars at greatest elongation using transit instrument
17 p3028 A69-32878

Differences in latitude readings obtained with two zenith telescopes, showing Pearson distribution of type VII and influence of observation conditions
17 p2959 A69-32879

Electronic device utilizing scanning beam to evaluate limb photographs, reducing errors by introducing second generator with frequency proportional to deflecting potential variation
17 p2970 A69-32884

CP 0950 and CP 1133 pulsating stars position, using radio telescope at two frequencies
17 p3036 A69-33639

Light changes caused by distortion of binary components, computing theoretical brightness variations by numerical integration of emerging atmospheric intensities over visible surface
17 p3044 A69-34179

Satellite photographic astrometry and chronometry, determining spatial positions of satellites and observation stations by space triangulation
24 p4391 A69-43790

ASTRON THERMONUCLEAR REACTOR

Energy principle applied to Astron type device stability based on model with rigid E layer electrons, finding critical pressure expression for ballooning modes
16 p2821 A69-32035

ASTRONAUT LOCOMOTION

Lunar gravity simulation effect on human performance, discussing fidelity requirements, self locomotion, metabolic rate and psychomotor task decrement
02 p0203 A69-12217

- Astronaut extravehicular protection systems, discussing space suit, life support and thermal control subsystems and micrometeoroid protection
06 p0882 A69-17643
- Lurain simulator for metabolic studies, using BPMU for assessing O consumption of test subjects at rest and various speeds of ambulation
17 p2914 A69-33187
- Spacecraft rotation and astronaut head and body motion as stimuli for vestibular analyzer function study during weightlessness
20 p3473 A69-37275
- Real time servo driven simulator of human body in zero-g activity used to study self induced rotation and astronaut mobility under thruster forces
21 p3664 A69-39034
- Mathematical model of astronaut motion and spacecraft angular control during tethered reentry, discussing conditions preventing spinning and collisions
21 p3667 A69-39630
- Unstabilized astronaut, hand-held and integrated life support EVA maneuvering units tested in gimbaled six degree of freedom servo driven moving base simulator [AAS PAPER 69-516]
24 p4272 A69-42850
- ASTRONAUT PERFORMANCE**
- Medicinal therapy and flight safety of pilots and astronauts, discussing drug use, self treatment, tolerance and environmental factors
01 p0014 A69-10583
- Soviet book on human movements coordination during space flight covering space walks, lunar surface photographs, space docking, weightlessness, etc
01 p0018 A69-11180
- Physiological causes and prevention of motion sickness during space flight, emphasizing conditioned reflex, different analysors interactions and vestibular-vegetative changes during weightlessness
02 p0200 A69-12122
- Voskhod 1 and 2 crew performance, orientation and motor activity analysis indicating time increment for task performance, psychophysiological irregularities and visual analysors impaired functioning
02 p0203 A69-12123
- Cardiovascular system, respiratory system and metabolism of cosmonauts on three man flight of Voskhod, noting physiological and biochemical studies
03 p0377 A69-14195
- Cosmonauts cardiac activity and respiration changes during physical exertion in orbital flight on Voskhod spacecraft
03 p0377 A69-14196
- Lunar environment simulation, discussing space suit encumbrances on astronaut performance, gravity effects, surface texture, illumination, confinement and isolation
06 p0906 A69-17388
- Soviet cosmonauts physiological reactions during weightlessness, analyzing EKG, arterial pressure, heart and respiratory rates and motion coordination
07 p1060 A69-18570
- Pneumograms and EKG used to determine heart beat, respiration rates and systolic index of cosmonauts during Voskhod 2 flight
07 p1062 A69-18585
- Vestibular function of cosmonauts during preflight training and flight on Voskhod spacecraft, tabulating heart beat, respiration rates and writing test ratings
07 p1062 A69-18588
- Oculomotor activity of cosmonauts during orbital flight, analyzing electrooculograms taken during vestibular tests
07 p1063 A69-18594
- Human motor reactions during weightlessness based on parabolic or orbital space flight observations, noting cosmonaut writing performance
07 p1063 A69-18595
- Space flight crew efficiency during prolonged weightlessness, stressing preflight adaptation and space vehicle technology improvement
07 p1063 A69-18596
- Time perception capacity of astronauts and jet pilots during brief weightlessness, noting emotional state effects
07 p1065 A69-18981
- Human operator manual control of spacecraft under accelerations up to 18 g, noting performance and efficiency of males
08 p1265 A69-19936
- Heat susceptibility and tolerance in astronauts obtained by plot of skin and oral temperatures for subject under thermal stress
10 p1644 A69-23376
- Lunar visual environment effects on astronaut control manipulation task performance, discussing solar illumination simulation facility
12 p2059 A69-26554
- Weightlessness effects on human external respiration, gas exchange and energy expenditure indices during flight of Voskhod 2
12 p2020 A69-26563
- Lunar astronauts psychological problems, discussing isolation from outside world, gravitational and extreme light effects, protective space suits, etc
13 p2210 A69-27905
- Space travel and lunar exploration medical problems
13 p2210 A69-27909
- Circadian rhythms characteristics in humans, animals and plants, noting possible effects of rhythm disturbances on astronauts
13 p2211 A69-28614
- Medicinal therapy and flight safety of pilots and astronauts, discussing drug use, self treatment, tolerance and environmental factors
15 p2555 A69-30753
- Weightlessness problems, discussing artificial gravitation on spacecraft and astronaut experiences
16 p2746 A69-31930
- Cooling system control system for astronaut thermal equilibrium and work output maximization during extravehicular space missions
17 p2914 A69-33278
- Space research centrifuge counteracting null gravity physiological deconditioning, discussing linear and angular accelerations sensitivity and deconditioning effect on reentry task performance
18 p3114 A69-34368
- Microbiological influence on astronauts efficiency during and after long space flights, stressing simulated microclimates and confinement effects on flora
18 p3097 A69-35304
- Space crew performance subsequent to sudden sleep arousal, noting selection between simultaneous and staggered sleep schedules
19 p3263 A69-36453
- Astronaut vestibular and motor analyzer functions during flight and simulation tests, discussing illusory space orientation and role of cortical dynamics
20 p3469 A69-37241
- Weightlessness tests during parabolic flight to supplement vestibular tests in astronaut selection
20 p3481 A69-37276
- Time perception capacity of astronauts and jet pilots during brief weightlessness, noting emotional state effects
20 p3480 A69-38229
- Hard space suit temperature history during lunar operational task simulation
21 p3666 A69-39182
- Biological model describing spacecraft operator sensorimotor activity in response to various spacecraft control stimuli, outlining computer algorithm
22 p3892 A69-40281
- Real time metabolic rate analysis of suited astronaut using heart rate and O methods during thermal vacuum and extravehicular mobility tests
22 p3893 A69-40371
- Neutral buoyancy simulation of astronaut performing module replacement and repair task in zero-g environment
22 p3921 A69-40379
- Muscle function measurement in astronauts using electromyogram, electrocardiogram and isometric tension at fixed percentage of maximum voluntary contraction
23 p4103 A69-41684
- Apollo Extravehicular Communication Telemetry System for monitoring astronaut portable life support system, space suit performance and body functions on lunar surface
23 p4121 A69-41767
- Orbital biomedical laboratory for in-flight measurement to assure human safety and optimize astronauts performance in extended space mission
23 p4223 A69-41801
- ASTRONAUT TRAINING**
- Professional activity of cosmonauts, considering training, mental and physical qualities and engineering background
06 p0879 A69-17036
- Manned space flight safety, discussing astronaut exposure to danger on ground, in training and in space mission
06 p0882 A69-17650
- Aerospace research pilot school /ARPS/ to train experimental test and aerospace research pilots and Manned Orbiting Laboratory /MOL/ astronauts
06 p0882 A69-17670
- Sensory and physiological reactions experienced by cosmonauts during parabolic training flights, tabulating arterial pressure, heart beat and respiration rate
07 p1061 A69-18580
- Vestibular function of cosmonauts during preflight training and flight on Voskhod spacecraft, tabulating heart beat, respiration rates and writing test ratings
07 p1062 A69-18588
- Lunar astronauts psychological problems, discussing isolation from outside world, gravitational and extreme light effects, protective space suits, etc
13 p2210 A69-27905
- Astronauts physical training for space flight requirements
13 p2215 A69-28611
- Physical exercises to increase cosmonaut space environment tolerance, discussing effects of acceleration, altitude and hypoxia
15 p2560 A69-31460
- Photographic system for astronaut training in Apollo Mission Simulator, using fixed camera and moving earth model coincident with strip color film past exposure slit
16 p2792 A69-32787
- Interplanetary space travel medical problems during long duration missions, noting earth diagnostic and therapeutic methods adaptation, drugs selection, astronaut medical training, etc
24 p4278 A69-43396
- ASTRONAUTICS**
- 1967 yearbook on air and space travel covering airbus, astronautics, V/STOL, aerodynamics, flight mechanics, simulation and aerostatics
04 p0545 A69-14801
- Microelectronics in astronautics, discussing properties of thick and thin film electronic devices, integrated semiconductor circuits and hybrid circuits
07 p1089 A69-18256
- Book on reentry and planetary entry physics and technology covering entry dynamics, thermodynamics, radiation, ablation and heat transfer
11 p1967 A69-25573
- Astronautics - Conference, Braunschweig, West Germany, October 1968, Volume 3, Strength, material, methods of construction
12 p2176 A69-25850
- Aviation and astronautics - Conference, Tel-Aviv and Haifa, March 1969
14 p2429 A69-29011
- Bibliographies for aeronautics and astronautics /AIAA/ technical disciplines
14 p2542 A69-29510
- Professional programs for aeronautics, rocketry and astronautics development
18 p3233 A69-34552
- Space law as foreseen in light of expected scientific progress in astronautics
20 p3638 A69-37126
- ASTRONAUTS**
- Luminous particles in space observed by Vostok, Mercury and Voskhod astronauts, discussing distribution, trajectories and terrestrial origin
07 p1222 A69-19617
- Chemical and biological means of safeguarding body of astronaut against ionizing radiation and vibration
10 p1648 A69-23297
- Radiation dose and radioactive isotopes induced in astronaut body by cosmic rays of various energies
11 p1831 A69-25463
- Space mission medical heat problems covering thermal characteristics and heat control, protection and resistance of space vehicle and astronaut adaptation
12 p2023 A69-26493
- Astronaut selection and training in U.S. and U.S.S.R.
13 p2216 A69-28636
- Pre and postflight leukocyte chromosome aberration analyses of Gemini astronauts
17 p2908 A69-33173
- High positive g sub x acceleration effects on red cells destruction rate, measuring endogenous CO production of Gemini astronauts
17 p2908 A69-33176
- ASTRONAVIGATION**
- Spacecraft orientation from onboard stellar photographs, calculating absolute and relative elements, accuracy and camera parameters
13 p2296 A69-27696
- Soviet book on flight vehicles astronautavigation covering automatic equipment accuracy, changes in spherical coordinates, time measuring, etc
18 p3168 A69-34355
- Most probable position determination in astronomical navigation by tracing lines on nautical chart
23 p4186 A69-42025

ASTRONOMICAL COORDINATES

Geomagnetic field components measurements from moving object, investigating astronomical orientation applicability for three component geomagnetometer
02 p0277 A69-11674

Aurora displays distribution over earth, analyzing magnetosphere dependence on astronomical orientation of geomagnetic field in relation to solar wind
02 p0247 A69-12772

Intense discrete radio sources observation by antenna array with fan beam, determining right ascension and east-west structure
04 p0663 A69-15379

Galactic X ray sources noncoincident with conspicuous visible or radio objects, identifying visible and radio counterparts by determination of accurate celestial coordinates
05 p0813 A69-15845

Laboratory equipment for atomic and astronomical time and frequency measurement
05 p0827 A69-16582

Absolute coordinates of 906 lunar features derived and tabulated, eliminating errors due to atmospheric turbulence by using 120 lunar negatives
07 p1213 A69-18612

Spacecraft tracking network for determining spacecraft motion parameters, noting application to coordinates and velocities determination for terrestrial observers
07 p1087 A69-19609

Yerkes star trailed lunar photographs with ephemeris values of moon libration for selenodetic coordinates of secondary points, discussing errors and altitudes
07 p1225 A69-19773

Tucson selenodetic triangulation for coordinated points, considering measures on Yerkes star trailed plates
07 p1225 A69-19774

Pointing calibration of Haystack parabolic antenna by using radiometric measurements of cosmic ray sources
08 p1281 A69-20032

Geomagnetic field components measurements from moving object, investigating astronomical orientation applicability for three component geomagnetometer
13 p2257 A69-28705

Lunar coordinate corrections from solar ring coronagraphic observations of 20 May 1966 annular solar eclipse
15 p2686 A69-30532

Bright and faint stars absolute declinations compared in vertical circle systems used in Golosevov and Pul'kovo catalogs
17 p3027 A69-32872

Photographic observations of Mars position and surrounding stars, correcting coordinates for Mars phase by local desensitization of plate
17 p3027 A69-32873

Photomicroscope film plane inclination adjusted to improve circle readings measurement, noting instrument errors role in star declinations errors
17 p2970 A69-32881

Pulsars properties and distribution in galactic coordinates, deriving interstellar medium properties and physical nature of objects based on neutron star rotation
17 p3040 A69-33800

Soviet book on flight vehicles astronavigation covering automatic equipment accuracy, changes in spherical coordinates, time measuring, etc
18 p3168 A69-34355

Perturbations of planet motion in planetary coordinates, noting unperturbed motion
18 p3199 A69-34912

Minor planets positions computer calculated and tabulated from Tashkent 1963 and 1964 astrophot observations, stating time and equatorial coordinates
20 p3596 A69-37312

IC 4499 cluster variable stars coordinates in tabular form, showing high percentage of short period
20 p3598 A69-37462

Spherical trajectories control by star height maintenance, analyzing resulting cycloid and cartographic representations
23 p4186 A69-42023

ASTRONOMICAL MAPS

Changes in bands of Jupiter /1962-1965/ from astronomical synoptic mapping program, tabulating overall and chromatic intensities and longitudinal velocities
03 p0512 A69-13696

French atlas of planets covering ancient and modern planetary system and discoveries, physical nature and movement, etc
03 p0513 A69-13778

Relative number of galactic pairs and distribution of linear separation of components determined from Palomar Observatory maps
07 p1214 A69-18663

Contour map of southern Milky Way at 1410 MHz obtained using 210 ft radio telescope at Parkes, Australia
07 p1214 A69-18667

Southern Hemisphere galactic H II regions continuum thermal radiation at 6 cm, noting maps for 28 of 36 sources, peak temperatures and emission and half intensity widths
07 p1206 A69-19271

Contour maps of supernova remnants HB 9, Simeis 147 and IC 443, noting spectra showing radiation nonthermal
09 p1604 A69-22408

Radio brightness map at 22.25 MHz of galactic plane including H II regions IC 1805 and IC 1848, discussing LF absorption
10 p1787 A69-24115

Spectroheliograph technique, obtaining high resolution magnetic maps of solar magnetic fields directly in single image without photographic substructure
11 p1880 A69-24432

Sky mapping in IR, using IR photometer on TD1 ESRO satellite
13 p2260 A69-27606

Astronomical maps of integrated hydrogen density, dispersion and velocity of high galactic latitude neutral hydrogen concentration, discussing kinetic temperature
13 p2347 A69-27718

Contour maps of Milky Way continuum radiation at 1410 and 2650 MHz from low latitude survey, listing sources with estimates of flux density
14 p2526 A69-29772

Tachoheliograph /modified spectroheliograph/ for obtaining two dimensional solar velocity maps, discussing construction and theory of operation
17 p3030 A69-33061

Radio map of Orion A region, resolving M 42 and M 43 nebulae at 1.94 cm wavelength, noting optical photographs comparison
17 p3035 A69-33609

Galactic plane at 9.26 cm between longitudes of 32 to 49 degrees, tabulating contour map of antenna temperature and sources
18 p3195 A69-34426

Continuum survey at 1415-MHz between declinations of zero and 20 degrees N with radio telescope, noting flux densities and contour maps of sources
18 p3195 A69-34428

Milky Way continuum radiation at 4170 MHz using parabolic antenna, mapping discrete sources concentration at galactic equator
18 p3200 A69-34996

Book on Messier nebulae and star clusters covering current astronomical ideas, star maps, identification diagrams, telescope illustrations and astronomical data
18 p3206 A69-35471

Finding list of spectral type A7 stars and earlier in region at south galactic pole compiled from prism survey data
22 p4021 A69-40436

Orion nebula isophotal contours optical observation for three continuum colors /blue, yellow and IR/ and H alpha
22 p4031 A69-40942

Space vehicle multibeam Cassegrain antenna system design meeting radiometric mapping requirements in microwave frequency range, discussing mounting, degrees of freedom, etc
23 p4143 A69-42527

Milky Way hydrogen line survey with Parkes telescope, giving velocity-longitude control maps and tabulated data covering galactic equator
24 p4383 A69-42961

Radio emission from diffuse thermal radio sources in northern Milky Way, giving contour maps
24 p4388 A69-43641

ASTRONOMICAL MODELS

Viscous effects of neutrinos in anisotropic cosmological models examined using Boltzmann equation with simple collision term
01 p0148 A69-10053

Weakly interacting neutrinos in anisotropic cosmological models with emphasis on equilibrium period, noting energy increment
01 p0123 A69-10348

Open cosmological model containing radiation and matter, noting matter density relationship to visible matter average
01 p0150 A69-10371

Pulsars features explained by model based on binary system of neutron stars, discussing associated stellar plasmas as directional HF radio wave source
01 p0156 A69-10981

Second harmonic cosmic ray daily variation, discussing density gradient model with particle diffusion along field direction
02 p0305 A69-11422

Direct planetary atmosphere measurement by vehicles entering atmosphere, using Mars and Venus model atmospheres for accuracy expectation
[AAS PAPER 68-187] 02 p0311 A69-11472

Lunar electrical parameters range determination using models
[AAS PAPER 68-199] 02 p0312 A69-11477

Observable surface of part of Friedmann universe calculated using analytical continuation of Schwarzschild coordinate system, noting angular extent and angle of observation effect
02 p0314 A69-11644

Rotating star adiabatic axisymmetric motion solved numerically for small initial deviation from hydrostatic equilibrium
02 p0317 A69-11955

Earth structure model based on million random trials using eigenfrequencies, travel times of shear and compressional waves, mass and moments of inertia
02 p0243 A69-12009

Topochrone and generalized Hubble law considered for singular origin of universe with big bang explosions
02 p0321 A69-12195

Statistical mechanics and thermodynamics for molecular systems applied to gravitational systems, discussing collisionless Boltzmann equation and Chandrasekhar binary collision model
02 p0323 A69-12273

Computer models of one dimensional stellar problems, discussing fast relaxation of unsteady state to Fermi-Dirac distribution and slow relaxation to thermal equilibrium
02 p0323 A69-12274

Light fluctuations rise time, electron density, emission temperature and peak luminosity estimated for quasars powered by local gravitational collapse events
02 p0325 A69-12590

Red giants limiting helium core mass dependence on total stellar mass and initial composition from stellar evolutionary models
02 p0327 A69-12710

Force free magnetic fields and solar filaments, describing model for explaining filament characteristics
02 p0329 A69-12787

Solar flare model assuming open magnetic field configuration, discussing flare properties by application of tearing mode instability and nonlinear development
02 p0309 A69-12788

Plasma model of quasars and radio galaxies for observations of high energy radiation
02 p0329 A69-12794

Electromagnetic induction theory for spherical earth model involving conducting core with radial conductivity variation and concentric nonconducting mantle
03 p0423 A69-13523

Photosphere models comparison based on theoretical rotational temperatures of various diatomic molecular free radicals, using faint lines method
03 p0512 A69-13694

IR radiation of NML Cygnus with O/C ratio close to unity ascribed to circumstellar shell of graphite particles
03 p0513 A69-13775

Numerical calculation of trajectories of high energy cosmic rays in galactic disk, using quasi-longitudinal model of magnetic field
03 p0501 A69-13960

Scaled solar and gray-body temperature distribution models compared to determine stellar atmosphere
04 p0653 A69-14626

Mathematical density-depth model proposed for lunar outermost layer compared to Matveev model, noting Surveyor estimates
04 p0655 A69-14659

Asymptotic solutions of linear difference equations, discussing applications to eigenvalue problems of free oscillations of model galaxies
04 p0623 A69-14946

Cosmology, experiments on gravitation, space-time theory and model of universal history
04 p0661 A69-15157

Nonquadrupole nature of cosmological radio emission intensity distribution demonstrated for anisotropic homogeneous cosmological models without flat space
04 p0662 A69-15238

X ray astronomy, discussing sources associated with bremsstrahlung or synchrotron radiation, astrophysical models, black body radiation, relativistic electrons, etc
04 p0662 A69-15326

X ray emission from Seyfert galaxy nuclei, noting model with bremsstrahlung from hot source
04 p0649 A69-15387

Coronal structure predicted for September 22, 1968 solar eclipse by model constructed for large structure of coronal and interplanetary magnetic fields
05 p0818 A69-15602

Lithium abundance determination difficulties for undisturbed solar photosphere, noting Li I resonance line identification and model choice
05 p0821 A69-15849

Theoretical models explaining observed properties of radio galaxies and quasars, discussing quasar distance
05 p0821 A69-15851

MHD quasar model consisting of galaxy with super-massive plasma nucleus moving in magnetic field
05 p0822 A69-15853

Spinning neutron star model for pulsars based on slowing down of pulse rate, proposing emission mechanism for radio energy and relativistic gas
05 p0825 A69-16351

Homogeneous main sequence star models with convective cores, considering core chemical composition, size and energy generation ratio mechanism
05 p0829 A69-16777

Pressure stratification and transparency/geometrical depth expansion/ in Fricke-Elsasser and Zwaan sunspot models
06 p0999 A69-16976

Model for Evershed effect postulating unipolar symmetrical sunspot surrounded by magnetic knots of opposite polarity
06 p0999 A69-16977

Solar wind model for electrons and collisionless ions temperatures and anisotropies
06 p0986 A69-16983

Relativity and stellar model stability, discussing energetics of quasars and gravitational collapse of super-massive stars
06 p1002 A69-17315

Solar flares acceleration processes related to solar atmospheric currents
06 p0995 A69-17442

Model to account for flare and sunspot phenomena, discussing uni- and bipolar spots
06 p0995 A69-17443

Light variations of irregular eruptive variables known as RW Aurigae or T Tauri stars, discussing suitability of stochastic model
06 p0996 A69-17448

Carbon molecule photodissociation in cometary atmospheres, discussing intensity level distribution based on model
06 p1004 A69-17534

Planetary nebulae NGC 7662 and IC 418 forbidden line spectra compared with computer model predictions, noting evidence for dynamical effects and filamentary structure
06 p1009 A69-17963

Solar cosmic ray dose rate and total dose magnitude predictions based on Epeak and isotropic diffusion models
[AIAA PAPER 69-14] 06 p0997 A69-18160

Cosmology, discussing big bang and steady state models, arrow of time, red shift/distance relation, background radiation, etc
07 p1210 A69-18390

Cosmological model describing relation between red shift and magnitude of quasars
07 p1211 A69-18406

Permissible nonthermal convection modes in planetary interiors derived from conservation equations for self gravitating homogeneous nonrotating compressible fluid spheres
07 p1213 A69-18611

Convection in planetary interiors produced by combined thermal and nonthermal mechanisms, noting self gravitating homogeneous nonrotating compressible fluid spheres
07 p1214 A69-18613

High electron-proton temperature ratios effect on solar wind double shock wave structure, using one dimensional and two fluid models
07 p1205 A69-18849

Galactic model with differential rotation, discussing experiments on bar and cylindrical galaxy and spiral and loop structures formation
07 p1216 A69-19204

Quiescent solar prominences horizontal oscillations, explaining periods, damping times and prominence shape changes by model of freely oscillating prominence in corona
07 p1205 A69-19245

Solar flare initial development model assuming high temperature chromospheric point explosion, noting subsequent expansion and large density gradient effects
07 p1205 A69-19246

Luminosity distance, distance by apparent size, number counts, background radiation and apparent angular motion of sources in homogeneous anisotropic model universe
07 p1218 A69-19282

Redundant world models, discussing elimination through measurement of larger red shifts of galaxies and quasars
07 p1219 A69-19283

Cosmological models with antipole, determining models consistent with spatial distribution of quasars and radio galaxies
07 p1219 A69-19284

Dynamical stability in premain sequence stars, discussing adiabatic models for pure hydrogen composition and collapse initiation by low opacity
07 p1220 A69-19388

Rotating stellar models oscillation and stability approximated by virial equations
07 p1220 A69-19389

Soviet monograph on diurnal solar cosmic ray variations from maximum to minimum solar activity, discussing model based on anisotropic particle scattering theory
07 p1209 A69-19500

Plane symmetric perfect fluid cosmological model derived from class I considerations, evaluating scalar invariants for line element
07 p1222 A69-19586

Relativistic cosmological models with radiation and matter, analyzing conversion from radiation-like models to dust-like models
07 p1222 A69-19587

Critical density ratio concept introduced into cosmological models for matter concentration into galaxies in expanding universe
08 p1381 A69-19794

Emission line formation in homogeneous chromosphere for noncoherent scattering, considering various chromosphere models
08 p1381 A69-19800

Primordial magnetic field effects on spatially homogeneous cosmological models with anisotropic Euclidean metric
08 p1383 A69-20049

Galactic angular momentum of rotation, applying rotation theory to gravitational instability model of galactic formation
08 p1383 A69-20050

Neutrino emission and carbon burning onset in 1.45 solar mass stellar models with pure He envelope, He burning shell and degenerate C-O core
08 p1384 A69-20059

Interplanetary scintillations of 3C 279 and CTA 21 combined to derive solar wind density fluctuation model, using random thin screen theory
08 p1385 A69-20069

Isotropic Newtonian cosmological models symmetry shown to have velocity distribution obtainable from solution of Vlasov equation
08 p1386 A69-20073

Convection inhibition effects on premain sequence evolution of solar mass star, discussing largely radiative models
08 p1386 A69-20088

Preliminary model atmospheres for cepheid variable eta Aquilae, discussing mass loss processes
08 p1386 A69-20089

Martian structure theory, comparing mathematical model based on earth long term evolution and ad hoc models
08 p1387 A69-20092

Evolutionary cosmological models, relevant observational cosmology, quasar red shift, cosmic black body radiation, cosmic He abundance and universe temperature history
08 p1388 A69-20223

Number count formula in zero pressure model universe for extragalactic radio sources with arbitrary luminosity and evolution functions, discussing red shifts
08 p1390 A69-20388

Long term modulation of cosmic rays by solar activity explained by Parker solar wind model, noting confirmation by direct satellite measurements
08 p1397 A69-20533

Models for lunar density distribution consistent with available data on lunar physical properties
08 p1393 A69-20579

Diffusion model for propagation of solar cosmic rays in interplanetary space, obtaining injection spectra for solar flare protons
08 p1379 A69-20613

Close binaries evolution and Algol type systems origin, discussing hydrogen exhaustion in center
08 p1395 A69-20633

Wolf-Rayet star properties, model and mass loss
08 p1395 A69-20640

Solar wind model including effects of rotation, magnetic fields and anisotropic heat conduction
08 p1380 A69-20643

Carbon 12 stars to simulate core evolution of planetary nebulae precursors, discussing nuclear shell burning
08 p1396 A69-20649

Orbiter and rotator models of pulsating radio sources, considering relationship between lack of Faraday rotation and similar polarization in decametric radiation from Jupiter
08 p1397 A69-20688

Instability of stellar structures intermediate between white dwarfs and neutron stars shown by stellar models, discussing pulsar signals periodicities
08 p1397 A69-20770

Model for nucleosynthesis of Li, Be and B in solar system from mass spectrometric measurements of high energy proton production of light elements
08 p1401 A69-20901

Quasi-stellar radio sources (QSS) and radio galaxies structure and evolution, discussing nucleus nonuniform model
09 p1592 A69-21500

Poincare recurrence theorem applicable to collapsing gravitational system with particles velocity dispersion other than zero
09 p1593 A69-21567

Lipshits-Khalatnikov law applicability to early stages anisotropy of cosmological expansion and relic emission
09 p1593 A69-21568

Nighttime Venus ionosphere models compared with Mariner 5 observations, discussing implications with regard to He and H abundance consequences and nightglow
09 p1594 A69-21695

Subdwarf HD 25329 studied with model atmosphere approach, using H alpha, Na I and Mg I profiles for effective temperature
09 p1600 A69-22199

Optically thick planetary atmospheres in radiative-convective equilibrium investigated by models with adiabatic temperature gradient in troposphere, discussing gray stratospheric solution
09 p1600 A69-22200

Sco X-1 optical spectrum magnitude and color changes, proposing variable black body model
09 p1601 A69-22213

Stellar models for Population II lower main sequence stars, discussing uncertainties in radii and bolometric magnitude
09 p1601 A69-22214

Absorption red shifts in quasi-stellar source due to dead galaxies in cosmologically flat model of universe
09 p1602 A69-22228

Radiation fields of Lyman alpha to Lyman 10 calculated for model planetary nebulae with constant and exponential density distributions in spherical symmetry
09 p1604 A69-22407

Bolometric luminosity-red shift relations of Friedmann dust universes corrected for inhomogeneities, using locally inhomogeneous Swiss cheese models
09 p1605 A69-22411

General relativistic models of massive hot nonrotating stars with adiabatic temperature gradients consisting of ideal gas and radiation mixture
09 p1605 A69-22416

Gravitational waves emitted by relativistic, nonrotating, nonradially pulsating stellar model, discussing polarization and energy and momentum transport
09 p1605 A69-22417

Carbon rich star models with and without neutrinos, considering carbon burning, central stars of planetary nebulae and hot white dwarfs
09 p1606 A69-22419

Neutrino loss effects on evolution of pure iron stars, considering white dwarf, presupernova models and iron-helium transition
09 p1606 A69-22420

Structure and pulsational properties of massive stars with helium cores and thin hydrogen poor envelopes
09 p1606 A69-22421

ASTRONOMICAL MODELS

Uniformly rotating star models within first order perturbation theory in convective equilibrium and with radiation pressure, discussing radiative and gas pressure ratio
09 p1606 A69-22422

Collisionless plasma heating by damping hydromagnetic waves applied to solar wind qualitative model, discussing magnetoacoustic wave energy
09 p1607 A69-22426

Thermal models for Jupiter and Saturn corresponding to completely convective structure, using De Marcus state equations
09 p1607 A69-22428

Characteristic length constant in open cosmological model of large scale properties of real space-time, noting relation to other constants
09 p1608 A69-22528

Cosmology, reviewing Friedman and Lemaitre model, big bang model, primeval fireball hypothesis for residual black body radiation and galactic origin theories
09 p1608 A69-22715

Jupiter model /cyclotron/ of pulsar radiation generation
09 p1608 A69-22761

Homogeneous anisotropic cosmological models of pancake and cigar forms, discussing quasars and emission time effects on red shift and luminosity distance
10 p1771 A69-22856

Optical features of Sco-X-1, Tau-X-1 and Cyg-X-2 X ray sources, discussing optically thin hot plasma model for X ray emitter
10 p1682 A69-23327

Mass and velocity distribution of interstellar clouds from Oort model simulated by Monte Carlo method on computer, predicting rogue cloud existence
10 p1779 A69-23608

Zero point energy, evolutionary cosmology, negative kinematic pressure and space curvature, assuming physical vacuum as ground state of Bose field
10 p1780 A69-23649

Polarization to extinction ratio criterion to choose interstellar cloud model, discussing magnetic field strength requirements
10 p1781 A69-23673

Interstellar grain model consisting of elongated dielectric particles represented by infinite circular cylinders reproducing observed interstellar extinction in IF far UV spectra
10 p1781 A69-23674

Silicon carbide particle growth and motion in carbon star atmospheres
10 p1781 A69-23678

Interstellar extinction models of classical Mie particles and quantum mechanical polycyclic aromatic molecules
10 p1781 A69-23679

K coronameter observations used to construct electron density models of corona above proton flare region of July 1966
10 p1763 A69-23733

Steady state spherically symmetric model for solar plasma acceleration with distance, showing essential role of viscosity
10 p1769 A69-23899

Ionized meteor trails initial radii statistical characteristics determined for two models
10 p1783 A69-23917

Interstellar gas model based on calculations of heating by low energy cosmic rays, noting gravitational compression to form clouds
10 p1770 A69-24095

Density wave theory of galactic spirals, discussing hydrogen distribution, young star distribution, stellar migration, magnetic field structure, density waves in stellar formation, etc
10 p1786 A69-24109

Stochastic model of interstellar magnetic field to account for observed cosmic ray mean life
10 p1771 A69-24112

Stellar evolution, computing sequences to establish solar model of primordial composition, comparing models with spectroscopic observations
10 p1788 A69-24126

Stellar models for chemical compositions to explain gap above main sequence in color-magnitude diagram of NGC 188
10 p1789 A69-24127

Axisymmetric models for stable and unstable oscillations of rapidly rotating zero temperature white dwarfs, discussing kinetic and potential energy
10 p1789 A69-24129

Dynamical model for spherical inhomogeneity in mean mass density of universe to predict velocity dispersion observed for Coma Cluster
10 p1789 A69-24133

Radio sources log N-log S diagram, red shifts and luminosity functions in zero cosmological constant and Lemaitre type Friedmann universes
10 p1789 A69-24134

Radio nebula NRAO 591/593, discussing thermal and nonthermal source and models based on electron density distribution
10 p1790 A69-24136

Models for emission line region of 3C 273, considering ionization distributions for estimation of relative abundances
10 p1790 A69-24137

Radio astronomical observations of Venus at atmosphere interpreted noting agreement with model based on Venera 4 data
10 p1791 A69-24202

Absolute dimensions of 34 eclipsing variables having both components near main sequence, comparing mass luminosity and mass spectrum to homogeneous model stars
11 p1952 A69-24248

Stellar model with magnetic field accelerating central core rotation to instability for determining rotating star energy and angular velocity distribution dependence
11 p1952 A69-24249

Nongray models of atmospheres of early stars, giving Avrett-Krook method of correcting temperature distribution
11 p1954 A69-24361

Period variations, colors and light curve peculiarities of models of U Geminorum type stars
11 p1954 A69-24363

Astronomical model indicating thin radial filaments in planetary nebula NGC 7293 formed by envelope density fluctuations attributed to ionizing and shock waves
11 p1955 A69-24384

Equivalent line widths for solar disk Fe and Ti spectra determined for umbra models, noting role of sunspot location
11 p1955 A69-24388

Stability of spherically symmetrical nonrotating mass systems moving in self consistent gravitational Einstein field, considering quasar applicability
11 p1956 A69-24394

Green function solution to Maxwell equations for interplanetary and coronal magnetic fields above photosphere, considering field at source surface
11 p1958 A69-24429

Red shift hypothesis postulated on perfect cosmological principle and uniqueness of electromagnetic wavelength measurements, showing agreement with astronomical data
11 p1961 A69-25108

Physical structure of convective envelopes of population II main sequence stellar models by mixing length theory, emphasizing hydrogen molecule formation and pressure ionization
11 p1961 A69-25109

Optical and radio measurements of electron temperature of H II regions obtained from brightness ratio of hydrogen line and continuum, considering isothermal model
11 p1950 A69-25110

Einstein field equations solutions for homogeneous cosmological models, assuming perfect fluid gravitation source and existence of simply transitive surface motions
11 p1919 A69-25245

Theoretical models corresponding to initial phases in thermal-gravitational collapse of spherical clouds from interstellar gas for stellar formation
11 p1963 A69-25261

Test particle classical dynamics in closed expanding universe, discussing Newtonian inertial mass decrease and canonical methods for determining momentum, velocity and energy
11 p1920 A69-25561

Joule heating role in generating internal gravity wave energy in auroral electrojet region, using linear model
12 p2064 A69-26010

Radio emission of fast cosmic ions by plasma wave conversion to electromagnetic waves, using nonlinear mechanism in turbulent plasma
12 p2149 A69-26209

Computer program for model stellar envelopes of red supergiants with extended atmospheres
12 p2156 A69-26218

Stellar evolution model for primeval He abundance in population II stars in globular clusters for big bang confirmation
12 p2156 A69-26228

White dwarfs structure model for deriving formula for phase density in color-luminosity diagram
12 p2159 A69-26665

Galactic descriptive functions and empirical model construction methods for determining mass distribution
12 p2160 A69-26852

Unified model for spatial distribution of transplanetary exospheric electron density for polar plasma study
12 p2151 A69-26952

Quasar spectra, discussing 3C 345, 3C 191 absorption lines and model explaining quasar spectra
12 p2167 A69-27046

Isotropic 3 K black body radiation implications for hot cosmological model, formation of galaxies, existence of superdense bodies and density nonuniformity during prestellar stage
12 p2167 A69-27047

Coherent radio emission mechanism in quasars and supernova remnants, discussing magnetic effects
12 p2168 A69-27050

Magnetic models of pulsars and rotating neutron stars to explain narrowness of radiation beam in polar diagram
12 p2172 A69-27168

Linear oscillation modes of premain sequence star model of pure hydrogen composition with variable specific heats ratio, discussing dynamic instability of polytropes
13 p2336 A69-27449

Solar cycle kinematical model based on field amplification by solar differential rotation including fluctuations in eruption rate
13 p2337 A69-27548

Radiative relaxation of relativistic particle distribution undergoing synchrotron radiation and reabsorption, discussing self absorbed radio source model
13 p2327 A69-27572

Microwave background radiation by intense sources studied by homogeneous and isotropic Friedmann and steady state models
13 p2339 A69-27574

Quasar applications as gravitational lenses within Hoyle-Fowler quasar model
13 p2340 A69-27575

Line absorption effect on opacity and main sequence model stars noting luminosity, radius and mass of convective core
13 p2340 A69-27578

Isotropic and anisotropic dust cosmological models density perturbation growth, considering angular momentum conservation in expanding universe
13 p2343 A69-27619

Astronomical model explaining shell instability of Pleione /28 Tauri/ extended atmosphere, discussing magnetic field amplification by differential rotation to explosive dissipation in 9.16 years
13 p2347 A69-27716

Relativistic version of generalized gravitation theory, establishing models to describe gravitars having large gravitational mass defect and red shift
13 p2351 A69-27864

Photometric data and law of rotation in symmetry plane for constructing mathematical model of mass and luminosity distribution in M 31
13 p2351 A69-27870

Polytropic gas spheres static models integral characteristics by nonrelativistic generalized gravitation theory, noting central densities dependence on critical values
13 p2352 A69-27872

Diurnal hemisphere auroras assuming origins in magnetosphere tail with pressure responsible for tail formation, discussing tentative model and implications
13 p2256 A69-28654

Space-time interpretation of static Einstein universe model and Friedmann space with variable positive curvature
14 p2484 A69-28865

Vacuum chamber model for sinusoidal rilles on lunar surface produced by aqueous erosion under ice blanket
14 p2485 A69-28873

Solar wind quiet state thermal properties and chemical composition compared with coronal expansion hydrodynamic model predictions
14 p2513 A69-29098

Tentative solar photospheric model meeting Noyes and Withbroe criticism
14 p2518 A69-29131

Extinction efficiency of graphite core interstellar grains with solid hydrogen and ice mantles, using theoretical models
14 p2486 A69-29587

Pulsar model used to explain stellar shape oscillations as cause of radio emission intensity periodic variations
14 p2522 A69-29675

- Cometary tail diffusion model based on luminous particle number decrease with time and particle accelerated motion and diffusion in space
14 p2523 A69-29705
- Critical analysis of Oort cometary cloud existence, discussing stellar encounters of sun, planetary explosions, etc
14 p2524 A69-29714
- Sunspot equivalent line widths calculated using sunspot models, considering influence of light scatter correction
14 p2525 A69-29721
- Extragalactic background radiation intensity in isotropic world models as function of universe thermal history
14 p2514 A69-29769
- Integrodifferential equation derived and solved for evolution of collisional model of asteroids and debris
14 p2526 A69-29879
- Low density Friedmann universe models with non-zero cosmological constant and long ages, deducing galaxy evolution rates from magnitude-red shift relations
14 p2527 A69-29944
- Amplitude and scale of microscopic fluctuations of electron density within M8 from brightness ratios of O II lines, using multiple shell model
14 p2514 A69-29949
- Supergiant HD-33579 in Magellanic cloud by model atmospheres, discussing abundances
14 p2529 A69-29979
- Closed space cosmological model, discussing complex singularity behavior
15 p2680 A69-30200
- Convective neutral stability in Schwarzschild-Harm model for evolution of stars with large masses
15 p2681 A69-30422
- Solar corpuscular radiation characterization by stable four streamer structure at near minimum solar activity
15 p2674 A69-30517
- Surface brightness distribution in comet Arend-Roland tail from diffusion model and photometric investigation of photographs obtained by 40-cm astrograph
15 p2684 A69-30519
- Gasdynamic model of comet nucleus region, discussing molecular collisions, surface brightness distribution and dust particle motion
15 p2684 A69-30520
- Negative curvature electron energy spectrum of discrete radio source model, assuming acceleration by Fermi mechanism and energy loss by synchrotron radiation
15 p2687 A69-30540
- Spiral density waves formation in galaxy model with differentially rotating and nonrotating subsystems based on collective interactions
15 p2688 A69-30550
- Coronal structure during 22 September 1968 eclipse from photographs, showing agreement with prediction by model
15 p2690 A69-30696
- Einstein equations solution for empty space without singularities containing metric, with closed homogeneous space type hypersurfaces expanding anisotropically
15 p2690 A69-30732
- Hydrogen recombination in hot universe model, discussing emission of energetic quanta
15 p2690 A69-30734
- Solar neutrino fluxes sensitivity to localized changes in opacity and equation of state, discussing solar models
15 p2675 A69-30768
- Nova outburst dynamics investigation by time dependent hydrodynamics computer program including energy transport by radiation and convection
15 p2692 A69-30769
- Pure hydrogen stellar atmosphere nonLTE models, calculating surface temperature rise due to H alpha line effect on continuum energy balance
15 p2693 A69-30777
- Surface gravity and temperature model atmospheres for O-type stars with UV line blanketing
15 p2693 A69-30778
- Temperature and density models for coronal green line enhancements with and without magnetic field effects, using graded height spectrograms
15 p2693 A69-30782
- Distribution model for ionized interstellar gas over galactic disk for explaining radio emission absorption and depolarization from discrete sources
15 p2695 A69-30935
- Close binary system components approximated by two nonsimilar ellipsoids, obtaining interpretation of light curves
15 p2695 A69-30957
- Zodiacal light models /including spherical and nonspherical models/, discussing mechanisms for orientation of particles in solar orbits
15 p2698 A69-31366
- Inertial systems in homogeneous isotropic expanding universe model, giving expression for line element accounting for Hubble effect
15 p2654 A69-31495
- Mathematical solutions of Einstein cosmological equations for radiation universe, discussing model limitations for universes older than 5-6 billion years
15 p2700 A69-31496
- Interstellar cloud models, considering gas pressure, cosmic ray flux, magnetic field values, etc
16 p2853 A69-31599
- Electrostatic heating of solar wind ions from instability in two fluid solar wind model leading to preferential heating of protons over electrons
16 p2848 A69-31971
- Equilibrium models reliability for main sequence stars estimated from systematic applications of physical assumption sets and numerical methods
16 p2859 A69-32219
- Viscous and thermal generators applicability to production of spin generated galactic magnetic fields in primordial fireball
16 p2866 A69-32812
- Water bag spherically symmetrical universe model, discussing system stability, distribution function representation and polytrope equivalency
16 p2866 A69-32813
- Stellar light element abundances, discussing evolution models for various star types
16 p2866 A69-32816
- Evolutionary tracks along horizontal branch of models for Population II stars in postred giant phase
17 p3030 A69-33071
- Planetary free vibrations, discussing models for earth, moon, Venus and Mars, rotation and ellipticity effects and measurement on seismometers, gravimeters and magnetometers
17 p3031 A69-33097
- Directional characteristics of lunar IR radiation accounted for by crater model
[AIAA PAPER 69-598] 17 p3033 A69-33285
- Lunar photometric function determined using modified Hapke surface model and corrected Lommel-Seeliger law for surface roughness and crater distribution
[AIAA PAPER 69-596] 17 p3033 A69-33308
- Pulsed radio sources origin from models, emphasizing pulsating white dwarfs
17 p3037 A69-33640
- Radial oscillation periods of Hamada-Salpeter white dwarf models graphically compared with models by Harrison-Wheeler Wakano equation of state
17 p3037 A69-33642
- Magnetized solar wind model to evaluate temperature, density, velocity and magnetic field for various boundary conditions
17 p3041 A69-33812
- Red dwarf star YZ CMi corona structure showing possible estimation of additional carried energy by shock waves after flare
17 p3043 A69-34166
- Corrections to previous papers on extragalactic gamma rays, discussing effects on various cosmological models
17 p3025 A69-34168
- Cosmic ray propagation equilibrium model for rays origin and storage in galaxy, considering energy dependence of nuclei relative abundances
18 p3185 A69-34276
- Microwave background anisotropy induced by gravitational effects interpreted using spatially flat Friedmann model for substratum
18 p3190 A69-34286
- Quasars and intergalactic hydrogen density, using Schmidt law of increase in number density of quasars to construct plausible models
18 p3190 A69-34288
- Pure carbon 12 stellar models evolution studied to determine production mechanism of planetary nebulae, discussing shell burning and surface layers unbinding role
18 p3191 A69-34298
- Solar wind model for studying long wavelength turbulence as heat source for alpha particles and protons in solar plasma
18 p3186 A69-34299
- Quiet solar wind model with magnetic field numerically calculated, obtaining coronal electron densities and angular momentum near earth
18 p3186 A69-34301
- Particulate thermophysical lunar soil model for measuring lunation nighttime and eclipse cooling, noting applicability to IR surface brightness temperature of Mercury hot pole
18 p3191 A69-34303
- Solar Fe II lines theoretical equivalent widths calculations, estimating influence of photosphere model on iron abundance data
18 p3191 A69-34305
- Lunar temperature prediction with emphasis on variable property models, noting assumptions about physical properties appearing in heat conduction equations
18 p3194 A69-34374
- Thin disk galactic models small oscillations, discussing frequency spectra and types of continua
18 p3196 A69-34551
- Models for pulsars periodicity and period range due to nonradial gravity wave in almost adiabatic matter of degenerate neutron stars
18 p3196 A69-34645
- Oblique rotator model for pulsars, discussing difficulties arising from two asymmetrically spaced pulses during each stellar rotation
18 p3196 A69-34647
- Source requirements for cosmic radiation origin model, noting fluctuations in momentum changing process
18 p3188 A69-35005
- Alpha Serpentis spectrum study from model atmosphere and growth curves, finding metal abundance ratios five times as great as in Arcturus
18 p3200 A69-35130
- Comet-solar wind interaction model, determining contact discontinuity size and shape around comet nucleus and ion specular reflection
18 p3188 A69-35190
- X ray sources model, describing possible ring of matter around white dwarf near end of active evolution
18 p3188 A69-35204
- Jupiter decametric radio source analysis suggesting two component model of rotation at both constant and variable rotational periods
18 p3202 A69-35212
- Pulsar PSR 0833-45 polarization structure frequency dependence measurement leading to model implying radiation emanated from magnetic poles neighborhood
18 p3202 A69-35215
- Fluctuations evolution in density perturbations analyzed to obtain free fall and free expansion universe models, showing no difference between expanding and static Newtonian universes
18 p3203 A69-35347
- Molecular concentration-optical depth curves for combinations of two photospheric and two facular models, noting lines contrast dependence on dissociation energy
18 p3204 A69-35391
- Solar flare model based on force-free currents in solar atmosphere, noting rapid energy release due to exceeding current density critical limit
18 p3188 A69-35392
- Hydrodynamics of gas flow due to solar flares using point explosion model, determining shock wave travel time to earth orbit
18 p3189 A69-35397
- Solar cosmic ray anisotropies in terms of model with particles propagating along interplanetary magnetic field undergoing pitch-angle scattering
18 p3189 A69-35400
- Cosmological model based on inertia and relativity principles, considering scalar gravitational and electrostatic potential, light velocity, gravitational interaction and observed galactic red shift
18 p3206 A69-35470
- Primitive solar nebula physical model considered under angular momentum conservation in collapsing fragment
19 p3406 A69-36074
- Monte Carlo relaxation method for physically self consistent model stellar atmospheres, discussing stability, accuracy and convergence of solution
19 p3425 A69-36337
- Atmospheric models for specified effective temperatures, hydrogen-to-metal ratios and surface gravities in studying metal deficiency effect on stellar atmosphere
19 p3425 A69-36338
- Lunar interior chemical heterogeneity determined from model taking into account pressure, temperature and composition effects
19 p3425 A69-36421

Andromeda M 31 galactic model, using luminosity and velocity data from optical and radio observations to construct nucleus, kernel, disk and flat component 19 p3426 A69-36579

Proton satellites measurements reconciliation with diurnal stellar variation data and cosmic rays origin models 19 p3396 A69-36621

Mercury internal constitution and chemical composition, discussing models with iron cores and iron admixtures in mantle 20 p3597 A69-37331

Mercury and Venus thermal histories based on analogy to earth models 20 p3597 A69-37333

Thomas wave equation in fluid mechanics, examining coordinates system with normal hyperbolic metric of universe tube having given signature 20 p3598 A69-37430

Criteria to prove incorrectness of two column model for photospheric granulation proposed by Margrave and Swihart /1969/ 20 p3603 A69-37541

Stability analysis of Kippenhahn-Schluter model of solar corona filaments against arbitrary perturbations treated in MHD approximation using Bernstein energy principle 20 p3588 A69-37544

Radiation emission mechanism for NP 0532 associated with Crab Nebula, discussing shock- neutral sheet interaction 20 p3604 A69-37572

Sunspot umbra observed on 21 September 1966, computing transparency in model equalling photosphere transparency at same optical depth 20 p3605 A69-37825

Time scale of diffusion of angular momentum estimated by model for disturbances occurring in star with secularly unstable angular velocity distribution 20 p3605 A69-37826

Cosmological constant and elementary particle theory 20 p3606 A69-38013

Cold disk galactic models free short wavelength oscillations, obtaining asymptotic approximations for eigenfrequencies and eigenfunctions of bending and planar modes 20 p3611 A69-38151

Scorpius X-1 X ray star model based on relativistic electron distribution due to magnetic field fluctuations, considering role of Alfvén waves 20 p3593 A69-38154

Matter and radiation interaction in hot model universe, investigating residual radiation spectrum deviation from Planck curve 21 p3797 A69-38536

Galaxy model for spiral structure origin 21 p3797 A69-38537

LTE departure calculated for He I in hot star model atmospheres for effects on populations of singlet and triplet states 21 p3801 A69-38761

X rays and gamma rays extragalactic components, calculating background component intensity for given model of universe 21 p3789 A69-38818

Spherically symmetrical T models of dust matter yielding method for obtaining maximum total mass effect in general relativity theory different from Friedman closed model 21 p3803 A69-38994

Optimum midcourse impulses effects on heliocentric launch window, comparing two and three impulse delta 5 performance for two and three dimensional solar system models [AAS PAPER 68-095] 21 p3804 A69-39201

Quasi-stellar objects identification, distribution, emission lines interpretation, energy distribution, absorption spectra, radio properties, etc 21 p3811 A69-39515

Density fluctuations in universe during early stages, using hot big bang cosmological model 21 p3814 A69-39571

Cometary nuclei composition as last samples of early solar system composition, discussing dirty snowball model and radical lifetime problem 22 p4013 A69-40097

Spectrophotometric observations of delta Scuti short period variable stars compared with model atmospheres 22 p4015 A69-40150

Nongray models representing atmospheres of F and G supergiants computed and tabulated for 5400- 6600 K and various surface gravities 22 p4015 A69-40152

Sunspot penumbra model in hydrostatic equilibrium accounting for continuum and Fraunhofer lines observations 22 p4019 A69-40290

Type 3 solar radio bursts observed during April-October 1967 for two alternative models of active region streamers in outer corona 22 p4003 A69-40300

Hydrodynamic equations for radial solar wind expansion linearized and specialized to treat co-rotating perturbations 22 p4003 A69-40302

Variational principle for stability of galaxies models, developing perturbation potential in terms of operator similar to Hartree-Fock exchange operator 22 p4022 A69-40468

Time symmetric electrodynamics for various cosmological models, discussing position and negative space curvature 22 p4022 A69-40469

Photoionization model of Seyfert galaxy extended to calculate temperatures, luminosities and sizes of zones emitting forbidden Fe X /6374 Å/ and Fe XIV /5303 Å/ 22 p4024 A69-40581

Free-free intergalactic absorption at LF as function of red shift for uniform zero pressure cosmological models 22 p4025 A69-40640

Evolutionary dynamic model for H II region produced by massive stars within dense dust-laden clouds, discussing grain sputtering and time scales 22 p4025 A69-40646

Radiant energy diffusion from spherical expanding matter for masses and velocities of model supernova outbursts, discussing thermonuclear and neutron star origins of supernovae 22 p4026 A69-40649

Model atmospheres of late type stars with solar abundances, effective temperatures between 2000-4000 K and gravities corresponding to dwarf, giant and supergiant stars 22 p4027 A69-40654

Rotating neutron stars with magnetic fields symmetric about rotation axis considered for pulsar model 22 p4027 A69-40657

Universe expansion model, integrating Einstein gravitation equations with cosmological constant lambda to interpret Hubble effect 22 p4029 A69-40756

Relative abundances U-235/U-238, Th-232/U-238, Pu-244/U-238 and I-129/I-127 at solar system formation time to obtain time evolution of gamma process nuclei 22 p3986 A69-40766

Exact solution of macroscopic line transfer equation including electron scattering terms for Milne-Eddington model atmosphere, discussing electron scattering effect on growth curves 22 p4007 A69-40903

Pulsar magnetic models, coherent radio emission mechanisms, radiation polarization, data summary and astrophysical nature 22 p4030 A69-40905

Galactic mass model and interstellar dust scattering data used to examine high latitude nebulae illumination possibility by integrated galactic light 22 p4033 A69-41059

Globular cluster star age and initial He abundance from main sequence, horizontal branch and red giant tip models using radiative opacities 22 p4035 A69-41205

Main sequence star models for diverse solar masses, covering hydrogen burning phase in core and conditions for dynamic instability and mass exchange 23 p4208 A69-41286

Eclipsing binaries spectroscopic and photometric data compared to Iben and Horn models of main sequence stars, noting stellar mass effects 23 p4208 A69-41287

Spectral reflectivity curves for Mars light and dark areas and seasonal changes of dark area simulated in laboratory 23 p4209 A69-41319

Statistical model of cratered planetary surface slopes and elevation applied to radio wave scattering by moon and Venus 23 p4209 A69-41322

Martian surface mineralogical study of present state and past processes from rock analyses by unmanned spacecraft instruments to test planetary models 23 p4212 A69-41619

Pulsars models and radiation mechanism, noting neutron stars with rotating magnetospheres 23 p4218 A69-42326

Deceleration parameter lower and upper limits for zero pressure big bang cosmological Friedmann models imposed by density parameter, Hubble constant and universe age 23 p4219 A69-42373

Universe behavior in time, discussing expansion observed by red shift, closed universe with future contraction phase and unlimited expansion open model 23 p4221 A69-42391

Homogeneous axisymmetric anisotropic cosmological models, analyzing magnetic fields and initial anisotropies effect on 3K radiation and primordial He production 23 p4222 A69-42402

Model atmosphere analysis of line identifications and equivalent width data for relatively cool Ap star HD 204411, discussing atmospheric composition 24 p4376 A69-42664

Pulsar model with seat as rotating neutron star having dipolar magnetic field not parallel to rotation axis 24 p4377 A69-42666

Phenomenological sunspot model describing granules, supergranules, magnetic fields and photospheric convection 24 p4378 A69-42691

Model of moon accumulated at low temperatures, discussing lunar surface layer characteristics 24 p4383 A69-42936

Critique of magnetic response model for interaction of moon and interplanetary plasma magnetic field proposed by Blank and Sill 24 p4384 A69-43190

Model for accumulation of earth and planets from primitive solar nebula, implying inhomogeneous chemical composition of bodies in solar system 24 p4385 A69-43215

Rotating neutron stars, pulsars and cosmic X ray sources, accounting for large and small diameter sources by rotating neutron star losing mass in magnetic field 24 p4369 A69-43222

Solar flare models in terms of energy storage and release mechanisms 24 p4374 A69-43622

Outer solar convection zone structure dependence on change of parameters in mixing length theory examined to construct model 24 p4387 A69-43634

Circular arm with elliptical cross section used as magnetohydrodynamical model of helical magnetic field in spiral arms to demonstrate interstellar gas flow path 24 p4388 A69-43640

Astronomical model indicating thin radial filaments in planetary nebula NGC 7293 formed by envelope density fluctuations attributed to ionizing and shock waves 24 p4390 A69-43774

Equivalent line widths for solar disk Fe and Ti spectra determined for umbra models, noting role of sunspot location 24 p4390 A69-43778

Stability of spherically symmetrical nonrotating mass systems moving in self consistent gravitational Einstein field, considering quasar applicability 24 p4390 A69-43784

ASTRONOMICAL OBSERVATORIES
 NT OAO
 NT OSO
 NT OSO- 3
 NT OSO-C
 NT SOLAR OBSERVATORIES

Seismic refraction study of internal structure of volcanic cinder cone 02 p0236 A69-11465

Catalog of meridian program star observations made in Brorfelde, determining position relative to FK 4 stars by using impersonal photographic micrometer 02 p0315 A69-11815

Polarized radio emission from Jupiter, giving hypothesis of radiation belts deformation by solar wind 03 p0512 A69-13703

Meteorological observations of Mars northern polar cap and Southern Hemisphere from northern summer solstice to early autumn 05 p0825 A69-16302

Attitude stabilization for astronomical satellites 06 p1015 A69-17588

Royal Belgian Observatory studies on time, meridian, seismological and gravimetric services, latitude variation due to polar motion, terrestrial tides and geodetic satellites 08 p1306 A69-19992

Ballistics room of Royal Belgian Observatory for observation of geodetic satellites 08 p1272 A69-19993

Photoelectric observations of Aurigae during 1963-1964 eclipse, noting reliability of equipment and effect on observation series 08 p1388 A69-20242

Two pulsars discovered during search with transit telescope at U.S. National Radio Astronomy Observatory, tabulating pulsar parameters 09 p1592 A69-21484

Magnetograph in Italian observatory for weak solar magnetic field longitudinal components avoiding differential amplifier by electronic compensation 10 p1693 A69-23311

Bright fundamental stars right ascensions observed in Chile, discussing instruments, declination range, systematic errors, etc 10 p1777 A69-23388

Radiophysics Laboratory /Sidney/, discussing radio astronomy, radioheliographs, radio telescopes, cloud physics and research 10 p1784 A69-23988

Nonpolar latitude variations due to observation errors, discussing instrumental, computational and meteorological influence, particularly refraction resulting from climatic conditions 11 p1952 A69-24257

Galactic radio source W 49 /3C 398/ observed with Cambridge one-mile radio telescope 11 p1963 A69-25259

Computer program solving for station coordinates and dynamical parameters at Smithsonian Astrophysical Observatory from optical data, laser range and range rate 12 p2068 A69-26428

Observatory camera for satellite observation, discussing objective focusing and diameter and manual/automatic operation 12 p2092 A69-26450

Reflector radio telescope of Pulkovo astronomical observatory noting high resolution 15 p2679 A69-30102

Variable stars research and facilities in Tautenburg, East Germany 15 p2682 A69-30438

European Southern Observatory installation in Chile, discussing site, instruments, domes design, administrative structure, etc 15 p2589 A69-31098

Photoelectric observations program at Astronomical Observatory of Bucharest to determine smallest moments of several eclipsing stars 15 p2696 A69-31224

Uranus observations in 1964 by Algiers and Quito astrolabes compared with Washington transit results 16 p2853 A69-31620

Trieste astronomical observatory optical and radio solar photosphere observations in 1967, including solar cycle and north-south symmetry 16 p2858 A69-32206

Space station observations of stars, galaxies and quasars, stressing electromagnetic spectrum role in astronomy 18 p3194 A69-34370

Solar activity /Madrid 1967/, detailing Wolf numbers, sunspots, chromospheric faculae, H filaments and prominences 18 p3202 A69-35290

Supernovae observations at Palomar during 1968 made with Schmidt telescopes 19 p3403 A69-35963

Short region scanning of Arcturus spectrum with McMath solar spectrometer double pass system at Kitt Peak National Observatory compared to single pass system 21 p3721 A69-38697

Solar radio emission /S component/ observations with 22-m radio telescope at Crimean Astrophysical Observatory 22 p4020 A69-40295

ASTRONOMICAL PHOTOGRAPHY

Relative proper motion of blue star in field of pulsar CP 1919 determined from photographic data analysis 01 p0149 A69-10270

Icarus asteroid position measurements by astronomical photography, noting comparison for two South African observatories 01 p0150 A69-10373

Icarus positions from photographic observations with astrophotograph 01 p0159 A69-11331

Meteor photographic observation noting initial mass, motion, position and duration, disintegration in process of flaring, spectra and meteor flare classification scheme 01 p0159 A69-11372

Lunar rays nature from terrestrial observations and surface photographs by lunar probes, noting high crater concentration structure 02 p0236 A69-11642

Meteor masses and atmospheric density calculation inaccuracy by use of effective stellar magnitudes of meteors 02 p0314 A69-11695

Catalog of meridian program star observations made in Brorfelde, determining position relative to FK 4 stars by using impersonal photographic micrometer 02 p0315 A69-11815

Mercury rotation period determination by surface photography, correcting earlier interpretation 03 p0517 A69-14233

Photographic recording to produce spatial analog of temporal Fourier spectrum of astronomical source used for distinguishing weak periodic signal from background signal 04 p0556 A69-14294

IR object discovered during T Tauri objects and diffuse nebulae study, discussing peculiarity 04 p0655 A69-14665

High resolution H alpha line photographs of solar chromosphere, showing superpenumbra-like dark fibrils around isolated sunspots 04 p0664 A69-15526

Optical observations of radio galaxies and quasars, noting evidence for galactic explosions, surface distribution, physical properties, radio quiet quasars, etc 05 p0820 A69-15837

Variability in quasi-stellar objects, tabulating results of optical photographic survey 05 p0826 A69-16387

Photographic investigation of gegenschein and cloud satellites at L sub 5 earth-moon libration point, noting gegenschein intensity peak 07 p1212 A69-18602

Mars surface features identification from comparison of Mariner 4 and ground bases telescopic photographs 07 p1213 A69-18605

Jupiter Red Spot vorticity at perimeter indicated by interaction with dark spots circulating along south equatorial belt 07 p1213 A69-18606

Joint radio-optical observations of flare star UV Ceti in Australasia during September-October 1967 07 p1214 A69-18666

Novas in M 31 on Tautenburger Schmidt photographs 08 p1382 A69-19873

Photographic magnitudes of stars in various open clusters based on UB system and photoelectric sequence 08 p1389 A69-20245

Sky background light automatic compensation in stellar photography, using single or double channel photometer 08 p1313 A69-20247

Photographic magnitudes in UB system for southern open clusters, giving table of photographic plates 08 p1389 A69-20253

Photographic magnitudes in UB system based on photoelectric sequence for various open clusters stars, determining spectral classes for brighter stars 08 p1389 A69-20254

Design and operation of Polaroid camera for use with telescope, noting six exposures per negative 08 p1316 A69-20617

Galaxies classification using rectified images, noting pitch and inclination angles 08 p1408 A69-21135

Photographic and reflector observations of comets including orbit determinations and recoveries 08 p1408 A69-21140

Half intensity angular diameter upper limit of Seyfert galaxy NGC 4151 nucleus, considering nonthermal continuum 09 p1602 A69-22227

Multiple pinhole camera for X ray astronomy, suggesting cross correlation image recovery technique based on Fourier convolution theorem 09 p1502 A69-22768

Qualitative considerations of color indices grouping for Abell-1781 cluster of galaxies, table of data and identification charts 10 p1775 A69-23204

Relative proper motions of stars measured by microscope projection technique 10 p1778 A69-23570

Auroral H beta intensities determined from photographs by image intensifier, describing equipment and data reduction method 10 p1684 A69-23824

Atmospheric density analyzed on basis of photographic observations of meteors, comparing vertical profile with CIRA profile 10 p1688 A69-23936

Stars astronomical positions elimination from photographic plates because of errors, discussing elimination criteria and picture taking method 10 p1784 A69-24034

Far UV spectra of zeta Puppis and gamma super two Velorum with 1.6 A resolution photographed with all reflective objective spectrograph on Aerobee rocket 10 p1788 A69-24120

Flares development in form of loop tunnel, discussing role of filaments 11 p1945 A69-24238

Photoelectric and photographic observations in UVB system of open star clusters, analyzing dispersion in two color diagrams, noting absorbing material structure 11 p1951 A69-24247

Microphotometer for stellar magnitudes of galaxies determination from photographs 11 p1879 A69-24256

Satellite photographic astrometry and chronometry, determining spatial positions of satellites and observation stations by space triangulation 11 p1956 A69-24400

Martian polar caps dimensions as function of planet heliocentric longitude examined from photographic observations, noting compatibility with spectroscopic data 11 p1959 A69-24728

Rocket-borne spectroheliograph for monochromatic solar photography in Mg II 2802.7 A line noting filter bandwidth, film polarizers and temperature control 11 p1884 A69-24838

Characteristics of astronomical photography, considering cameras, photographs, color films, photoemulsions and processing, etc 11 p1885 A69-24973

Comet Berbon and minor planet positions photographically recorded /1964-1967/ 11 p1962 A69-25121

Crab Nebula pulsar detection by TV camera with image intensifier at focus of astronomical telescope, detailing instrumentation and observations 11 p1962 A69-25251

Mars photographic and radar data correlation indicating smoothness of dark areas and roughness of desert areas 11 p1964 A69-25406

Planetary imaging systems design problems illustrated by Mars orbiter reconnaissance, discussing radiation effect on film, shielding, stereo method comparisons, color bands, etc 12 p2078 A69-25770

Magellanic Clouds color composite photographs prepared from negatives taken in blue and IR light 12 p2152 A69-25801

Faint stars background exposure density and detection limit determined by astrosensitometer for Kodak Spectroscopic Plates 12 p2153 A69-25811

Astronomical wide field cameras of large aperture ratio to detect extended near UV light sources outside atmosphere 12 p2080 A69-26127

Photographic observations of Nova Her 1963 in 1967, showing nonreturn to prenova stage 12 p2156 A69-26223

Photographic magnitudes of galactic nuclei, presenting plots for stellar magnitude distribution of galactic nuclei 12 p2165 A69-27029

Photographic studies of unsteady features of galaxies, discussing spectra, color, spiral arm instability and extragalactic H II regions 12 p2170 A69-27063

H alpha line photograph in M 82 spectra, giving equivalent radiating area and total ionized hydrogen mass 12 p2171 A69-27067

Photographic observations of quasi-stellar objects for position determination 13 p2334 A69-27308

Spectrum analysis of radio galaxy M82 nucleus, noting H alpha emission lines from analysis of IR photograph 13 p2335 A69-27310

IR objective-prism survey along southern Milky Way for identifying high luminosity stars

13 p2335 A69-27314

Optical radiation detection from pulsar PSR 0833-45 associated with supernova remnant in Vela, noting UV excess from plates using U and B filters

13 p2337 A69-27516

Natural terrestrial satellites existence suggested by telescopic and photographic observations and artificial satellites orbital perturbations

13 p2344 A69-27642

Ionized hydrogen regions in NGC 4449 from H alpha photography through narrow band interference filter, obtaining radial velocities

13 p2347 A69-27714

Stratoscope II unmanned balloon-borne telescope design, detailing pointing, focusing and thermal characteristics

13 p2261 A69-27956

Meteor masses and atmospheric density calculation inaccuracy by use of effective stellar magnitudes of meteors

13 p2355 A69-28726

Monograph on reduction of satellite data using fixed stars covering ALGOL programming for computing satellite direction from photographic model

14 p2446 A69-29286

Comet Ikeya-Seki head and tail structure noting cloud ribbons at angle to tail axis

14 p2524 A69-29708

Visual, photographic and spectral observations of comets during IQSY, discussing comets Tomita-herber-Honda 1964c and Ikeya-Seki 1965f

14 p2525 A69-29716

Errors in magnitude equation and atmospheric dispersion calculated for 400 mm astrophotograph, emphasizing constant errors due to objective

15 p2646 A69-30162

Stellar image vibration dependence on zenith distances and terrain relief determined from stellar traces by 200 mm telescope

15 p2647 A69-30163

Stellar image vibration amplitude dependence on trace direction by comparison with traces of moving satellites

15 p2647 A69-30166

Coronal structure during 22 September 1968 eclipse from photographs, showing agreement with prediction by model

15 p2690 A69-30696

Extraterrestrial imagery, discussing earth based telescopes, IR imagery, moon mapping, lunar and planetary probes, Lunar Orbiter photos interpretation and sensors for detecting life

15 p2690 A69-30711

Activity in Crab Nebula from 200-inch continuum and polarization plates, discussing nature and motion of wisps

15 p2691 A69-30758

Lasers and holography applications in astronomy including high resolution spectrographic diffraction gratings manufacture and astronomical objects photographic pictures evaluation

15 p2610 A69-30880

Solar corona observations on eclipse day by Aerobee rocket launched in New Mexico correlated to Siberian total eclipse photograph

15 p2696 A69-31099

Photographically observed meteor orbits 1937-1963, noting overestimation of hyperbolic orbits due to observation errors

15 p2697 A69-31253

Photoheliographic data tabulation of sunspots positions and areas for 1961 obtained from various astronomical observatories

15 p2700 A69-31490

Quasi-stellar objects anomalous Hubble plot, suggesting explanation for steeper plot under assumption on red shift vs apparent magnitude relation

15 p2701 A69-31536

Nova Vulpeculae 1968 photographic observations analyzed for magnitudes, indicating 16 July 1968 explosion

16 p2855 A69-31659

Star chains around Eta Carinae, discussing nonrandom real groupings and probability criteria using ADH red sensitive plate without filter

16 p2856 A69-31931

Instrumental observations of Jupiter opposition in 1967 and 1968

16 p2858 A69-32205

Instrument for simultaneous observation of astronomical plate pairs for detection of stars with UV color excess

16 p2791 A69-32226

Photographic observations of Mars position and surrounding stars, correcting coordinates for Mars phase by local desensitization of plate

17 p3027 A69-32873

Finite resolution effect on solar granulation simulated by numerical experiments using two dimensional smeared pattern

17 p3029 A69-33046

Day sky brightness at altitude above 100 km obtained during rocket flight compared to night sky viewed from ground

17 p3037 A69-33664

Selection effects on comets discovery, comparing effectiveness of photographic and visual observation techniques

17 p3045 A69-34221

Metagalactic light measurements by lunar based night sky photography

18 p3189 A69-34242

Supernovae observations at Palomar during 1968 made with Schmidt telescopes

19 p3403 A69-35963

Comet observations and orbit determinations, noting eccentricity of comet Thomas

19 p3403 A69-35970

Butterfly diagram of sunspot distribution, concluding physical processes not yet clarified

19 p3426 A69-36583

Mars photographs from various observatories taken during 1969

20 p3598 A69-37424

Photographic and spectroscopic observation of Saturn at Cassegrain focus of 122 cm reflector during earth passage through ring plane, discussing Saturn satellites

20 p3600 A69-37481

Spectroscopic and photographic observations of compact galaxies, discussing distances, absolute magnitudes, linear dimensions, Hubble diagram position and correlations with objects showing similar characteristics

20 p3600 A69-37483

Solar photography at extreme UV wavelengths using pinhole camera instrumentation on stabilized Skylark rocket

20 p3539 A69-37545

Monochromatic coronal emission line photographs improved by composite technique

20 p3539 A69-37547

Tabulated results of photographic plate measurements of minor planets positions at Leiden observatory /1938-1964/

20 p3605 A69-37789

Magnetically focused electronographic image converters for far UV photography and spectroscopy from sounding rockets, discussing stellar observations

20 p3543 A69-37801

Cameras photogrammetric parameters determined from stellar photographs, considering distortion components, reference points, etc

20 p3545 A69-38054

Schmidt camera image quality examined with spot diagrams, emphasizing methods of color confusion reduction over wide wavelength range

20 p3546 A69-38272

TV-optical observations of asteroid Icarus, discussing installation, photographs and position

21 p3719 A69-38402

M 82 direct photographs sequence observation in optical IR region, noting small nucleus and unbroadened inclined emission lines

21 p3799 A69-38649

Mars TV pictures from Mariner 7, describing prominent surface features

21 p3806 A69-39330

Planetary nebulae imaging stratification effects on structural difference studies by slit and slitless spectrographs and narrow band photography

21 p3817 A69-39785

Atlas of H II regions in 20 nearby galaxies

22 p4015 A69-40153

Ephemeris calculations and lunar craters and reference stars coordinates measured from photographic plates, using digital computers

22 p4024 A69-40610

Photographic observations of supernovae including magnitudes, comparison star tables and instrument details

22 p4032 A69-40944

UBV magnitudes for open cluster NGC 559 stars determined from combined photoelectric and photographic measurements

23 p4211 A69-41490

Photographic observations of open cluster IC 4665 made on blue and yellow sensitive plates with Vatican refractor compared with photometric measurements

23 p4215 A69-42008

Satellite photographic astrometry and chronometry, determining spatial positions of satellites and observation stations by space triangulation

24 p4391 A69-43790

ASTRONOMICAL PHOTOMETRY NT STELLAR SPECTROPHOTOMETRY

Chromospheric flares photometric measurements during near minimum solar activity, discussing characteristics

01 p0149 A69-10127

Neptune mean diameter determination by photometric observations of stellar occultation by planet

01 p0150 A69-10386

Late type variable stars time dependent photometry and polarimetry in blue and violet, noting correlation for stellar brightness and degree of polarization

01 p0158 A69-11326

Eight color narrow band photometry of bright stars, discussing band system, instrumentation, data and calibration

02 p0313 A69-11487

Model spectra applied to carbon dioxide bands in Venus spectrophotometric measurements

02 p0319 A69-12107

Narrow band and UVB photometry of GX3 plus 1 and Wolf-Rayet stars /HD 50896 and HD 45166/

02 p0325 A69-12596

Photometric-polarimetric observations of planetary surfaces, discussing geological environment interpretation and spacecraft reconnaissance system mission planning

03 p0421 A69-13394

Revision of RGU photometry fundamental data, noting main sequence curve position of O-B5 and distinction between zero age main sequence and class V

03 p0514 A69-13963

Position of binary stars in photometric diagrams at Geneva observatory, discussing sequence profile of HR diagram

03 p0517 A69-14094

Dark equatorial belt of Jupiter atmosphere in 1962 and 1963, noting photometric contrasts, molecular absorption and possible structure

04 p0658 A69-14961

Solar image or spectrum focal plane scanning technique with output beam displaced but undeviated relative to input beam for solar spectrophotometry

04 p0602 A69-15378

Computer controlled photometric telescope, describing star setting, photometric measurements and data processing

04 p0602 A69-15380

Photoelectric photometry of Mercury, Venus, Mars, Jupiter and Saturn /1963-1965/, determining phase curves and monochromatic albedos

04 p0663 A69-15383

Seyfert galaxies nuclear regions, noting multicolor photometric measurements between 0.3 and 1.6 micron and measurements of M87 jet at 1.55 micron

04 p0663 A69-15386

Photometric investigation in UVB and H alpha of early B stars in Scorpio-Centaurus association, computing intrinsic colors and magnitudes corrected for interstellar absorption

06 p1001 A69-17195

Photoelectric observation of star occultation by Neptune for mean radius determination

06 p1007 A69-17693

Photoelectric observation of star occultation by Neptune for scale height determination

06 p1008 A69-17694

Photoelectric observation of Sco X-1 variations with 91-cm reflector, tabulating results and estimating accuracy

06 p1008 A69-17695

Mars surface photometric and spectrophotometric measurements, relating opposition effect details with corresponding laboratory sample measurements

07 p1212 A69-18601

Absolute isophotometry of hydrogen alpha photographs of bright galactic H II regions, attributing difference between theoretical and observed ratio to interstellar absorption

07 p1217 A69-19231

Saturn rings optical properties and thickness from edgewise photometric observations, noting luminance relationship to direct brightness

07 p1219 A69-19335

Photographic photometry of Saturn rings around times of disappearance /1966/

08 p1381 A69-19791

Three color photoelectric observations of stars near Orion Nebula, discussing gravitational contraction stars and color magnitude diagram

08 p1384 A69-20055

Three color RGU system photometry in Milky Way field in direction of anticenter, determining absolute brightness, luminosity and density of stars

08 p1387 A69-20119

Color excesses in Kapteyn Selected Area 4 using photovisual /yellow/ and photographic /blue/ magnitudes from catalog data

08 p1388 A69-20241

Photoelectric observations of Aurigae during 1963-1964 eclipse, noting reliability of equipment and effect on observation series

08 p1388 A69-20242

Photoelectric UVB photometry of stars in Puppis-Vela border region for associations of intermediate type stars

08 p1389 A69-20248

Scattered light reduction in sunspot photometry, noting eliminating effect when observing spectral lines or narrow spectral regions

08 p1389 A69-20251

Photoelectric observations of SRa variable CH Cygni reveal strong variability, discussing existence of hot companion

08 p1396 A69-20650

Isophotal wavelengths of U, B, V and R bright star systems for replacing spectrophotometry with broadband multicolor data

08 p1408 A69-21134

Polaris cepheid variable star system color index and absolute magnitude from photometric observations

08 p1408 A69-21138

Stellar absolute magnitudes recalibration for consistency with photometric distance moduli of clusters

08 p1408 A69-21139

Photoelectric observations of nuclei of planetary nebulae He 1-5 and NGC 1514, noting changes in color and brightness characteristics

09 p1590 A69-21379

Radial velocities of stars near cluster NGC 7380, discussing discovered stars, double lined spectroscopic binaries and photometric information

09 p1597 A69-22060

Distance of bright stars in Cepheus OB2 region by MK spectral classification and UVB photometry, noting early main sequence and supergiant stars

09 p1599 A69-22194

Rocket-borne photoelectric photometers for UV observations of Saturn, using interference filters

09 p1602 A69-22216

Photometric standard based on calibration of Vega by Hayes compared with six color magnitudes

09 p1603 A69-22233

A and B stars near North Galactic Pole and with magnitudes from 5 to 14.5, noting photoelectric UVB and four color photometric measurements

10 p1773 A69-22963

Eclipsing binary AU Puppis studied photoelectrically in yellow and blue light, noting period decrease by 1.3 sec in last 40 years

10 p1774 A69-22968

Starlight extinction by interplanetary medium evidenced from confirming correlation between star brightness on ecliptic and elongation

10 p1775 A69-23198

Photometric consequences of reflection effect in close binaries, tabulating light curves

10 p1776 A69-23218

Simultaneous photometric observations of coronal emission lines during July 1966 solar proton flare plotted on synoptic charts

10 p1763 A69-23731

Cometary nucleus dynamic center noncoincidence with photometric center, using computer calculations of Arend-Roland comet

10 p1784 A69-24035

Broadband photometry for circumstellar IR emission from cool stars, considering giant and carbon stars

10 p1786 A69-24102

Spectral lines relative intensities for bright medium excitation gaseous planetary nebula IC 3568, using photoelectric spectrum scanner and spectrophotometry technique

10 p1787 A69-24117

Six color stellar photometry of 159 field stars including subdwarfs, high velocity stars and 50 Hyades stars, tabulating color data

10 p1788 A69-24122

Faint blue objects in intermediate to high galactic latitudes, summarizing results of UVB photoelectric photometry

10 p1788 A69-24123

Power spectrum analysis of photometric observations of white dwarf stars for measuring variability of stellar luminosity

10 p1788 A69-24124

Isophot system characterizing photometric structure of elongated celestial objects constructed by equidensitometric method based on Sabatier photographic phenomenon

11 p1952 A69-24255

Brightness temperatures and spectra of Venus, Mars, Jupiter and moon measured from 8 to 14 microns by reflector and prismatic spectrometer

11 p1956 A69-24395

Photoelectric measurements of nightglow intensities during sunspot minima by zenith photometer, considering background continuum

11 p1877 A69-24584

Modified Diggelen photometric method in lunar topography, analyzing surface brightness and inclinations in mare regions and Korolev thalassoid

11 p1959 A69-24724

Optical characteristics of Martian atmosphere from photometric data for continent-mare contrasts, discussing transmittance and optical thickness

11 p1959 A69-24727

Atmospheric scintillation effect on planetary brightness distribution over disk from photometric measurements

11 p1960 A69-24729

Proper motions of low luminosity stars in Hyades cluster, noting photoelectric observations

12 p2152 A69-25797

Cyanogen band absorption in nuclei of elliptical and spiral galaxies derived from photoelectric measurements indicating rich metal content in central cores

12 p2153 A69-25803

Statistical analysis of photometric curves for meteors undergoing fragmentation at onset of vaporization

12 p2154 A69-25819

Photometric standardization and calibration of meteor spectrograms for real meteor masses determination using spectroensitometer

12 p2154 A69-25820

UVB photometry observations of eclipsing binary AG Persei at Mount Palomar with 51 cm reflector

12 p2156 A69-26220

Soviet satellites rotation periods from processing of photometric observations

12 p2069 A69-26440

Current to frequency converter for astronomical photometry, discussing oscillator drift, linearity characteristics and feedback pulse counting

12 p2040 A69-26479

Successive explosions produced two gas systems observed in six Seyfert galaxy nuclei by spectrophotometry, using diffraction spectrographs

12 p2164 A69-27022

Luminosity changes in quasar 3C 273, describing corrections introduced into luminosity curve obtained by iris photometer

12 p2167 A69-27044

Spectral energy distribution in quasars, using photoelectric spectral scanner in several wavelength ranges

12 p2168 A69-27051

Law of optical radiation and photometric characteristics of quasars, noting photometric effect of strong emission lines and color dependence on red shift

12 p2168 A69-27052

Galaxies NGC 4402 and NGC 4438 structure, luminosity and color from two color photometric study of Virgo cluster center

12 p2169 A69-27058

Photometric and spectroscopic analysis of southern peculiar galaxy NGC 6438, discussing isophotes, color distribution and radial velocity

12 p2169 A69-27059

Photometric and polarimetric properties of Mars, discussing powder covering, chemical composition and particle size of bright and dark areas and blue haze

12 p2171 A69-27145

Photoelectric observation of RR Lyrae stars in globular clusters to estimate reddening near galactic poles, considering color indices

12 p2172 A69-27157

IR observations of ETA Carinae to 20 microns, noting continued increase in flux density into IR

13 p2335 A69-27316

Spectral reflectivity differences of selected dark and bright regions of Mars observed with double beam photometer

13 p2338 A69-27553

Photoelectric scanning of CH Cygni spectrum calibrated and compared with 45 Arctis, discussing

high dispersion, excess blue and UV continua, H beta emission, etc

13 p2338 A69-27557

Multiband photoelectric photometer for near IR observations, tabulating magnitudes, colors, spectral irradiance, radii and effective temperatures of late type stars

13 p2342 A69-27592

Lunar surface light scattering data cataloged for various phase angles from photometric observations of lunar features brightness

13 p2344 A69-27648

Twelve color stellar photometry for studying galaxy synthesis, relating observations to temperature, luminosity and metal abundance

13 p2348 A69-27804

Spectrometric and photometric investigation of spectral characteristics of large sunspot 45 degrees from solar disk center, tabulating characteristics of 134 spectral lines

13 p2218 A69-28324

Photoelectric observations of NGC 1275, noting increase in nucleus brightness

14 p2517 A69-29086

Intermediate band photometry of G, K and M stars in IR indicating continuous stellar radiation deviant from black bodies

14 p2520 A69-29375

Photoelectric observation of passage of stars through meridian, detailing error sources and corrective technique

14 p2521 A69-29507

Comet Ikeya-Seki 1965f photometric investigation during perihelion, determining tail type according to Bredikhin classification

14 p2524 A69-29709

Variable stars in Large Magellanic Cloud from photoelectric measurements obtained in blue and violet, including periods of Cepheids and some period amplitude differences

14 p2526 A69-29853

IQSY night airglow photometric observations, summarizing zenith intensity and north/south intensity ratio data

15 p2594 A69-30019

Nova Delphini 1967 observational data and equipment including Cassegrain spectrograph, reflector telescope and photoelectric photometer

15 p2682 A69-30439

Surface brightness distribution in comet Arend-Roland tail from diffusion model and photometric investigation of photographs obtained by 40-cm astrograph

15 p2684 A69-30519

Polarimetric and photometric observations of comet Ikeya-Seki 1965f, plotting isophotes of head and polarized light distribution in tail

15 p2685 A69-30525

Photographic photometry of comet Ikeya-Seki during passage near sun, plotting isophotes of coma and tail and brightness distribution diagrams

15 p2685 A69-30527

Photographic observations of comet Kilsten 1966b, estimating brightness, absolute magnitude and color index

15 p2685 A69-30529

Seyfert galaxy NGC 4151 electrophotometric investigation in UVB, confirming nucleus optical variability observed in visible and IR

15 p2686 A69-30536

Radial brightness and color variation curves for Seyfert galaxies plotted from measurements with concentric diaphragm in UVB

15 p2686 A69-30537

Response color curves of U, B, V photometric system compatible for stellar observation, including U revision

15 p2689 A69-30562

Spectral classifications and UVB photometry for southern association Sco OB 1 containing cluster NGC 6231

15 p2692 A69-30771

Photoelectric /UVB/ photometry of Cepheids in Cygnus and Monoceros noting sequence stars near Nova Cyg 1948

15 p2692 A69-30772

Zeeman spectroscopy and UVB photometry of 17 Com and kappa Cnc, observing periodic magnetic and light variations

15 p2692 A69-30774

Coronal limb enhancement photometric study by spectroheliograms, comparing maximum brightness profiles in lines of different temperature in extreme UV

15 p2693 A69-30781

Photometric calibration correction for B-V and U-B colors taking into account hydrogen line blocking
15 p2694 A69-30786

Photometric observations of zodiacal light, noting dust in earth-moon environment
15 p2599 A69-31334

Spectrophotometry of elliptic galaxy NGC 1052 nucleus from 3400 to 6300 Å for relating radio properties and optical characteristics
16 p2853 A69-31610

Five color photometry of X ray source SCO X-1 in 1966-1968, discussing luminosity pulsations and flare activity
16 p2847 A69-31648

Stellar group Ba 6 distance measured using three color photometry in RGU system
16 p2854 A69-31650

Open galactic cluster NGC 2254 distance determined by three color photometry in RGU system
16 p2854 A69-31651

Portable photometer with red-sensitive photocathode and high SNR for O I 6300 airglow experiments
16 p2777 A69-32107

Photoelectric observations in B and V colors of binary system S Equ
16 p2858 A69-32212

Photoelectric visible radiation observations of binary star AH Vir
16 p2858 A69-32215

Iris microphotometer with measurement and reference beams traversing plate in neighboring regions designed for stellar images measurement
16 p2790 A69-32225

UBV photometry of southern quasars, radio galaxies and normal galaxies including two color diagrams, radio luminosity, brightness and color distribution
16 p2859 A69-32228

Four color photoelectric photometry of bright galaxies in Virgo Cluster, analyzing properties in nuclear regions
16 p2860 A69-32230

DQ Herculis photometric measurements synchronized with white dwarf component pulsation, discussing equipment, eclipse shape and binary period dependence on time
16 p2862 A69-32373

Epsilon CrA light and color curves analyzed from UVB photoelectric photometry observations
16 p2863 A69-32398

Photomicroscope film plane inclination adjusted to improve circle readings measurement, noting instrument errors role in star declinations errors
17 p2970 A69-32881

Photoelectric method to measure galactic reflection nebulae brightness, color and polarization used to explore interstellar grains physical nature
17 p3032 A69-33104

Lunar photometric function determined using modified Hapke surface model and corrected Lommel-Seeliger law for surface roughness and crater distribution
17 p3033 A69-33308

Optical spectrum of galaxy NGC 3031 nucleus, considering emission and absorption lines and continuum
17 p3034 A69-33396

13 color narrow band photometry of 1000 bright stars in tubular form, discussing sample points, Balmer discontinuity, absolute energy calibration, etc
17 p3038 A69-33692

Photoelectric observations of BD minus 17 degrees 4388 occultation by Neptune on 7 April 1968, studying light curves during immersion and emersion of star
17 p3041 A69-33815

Meteor dynamical and photometrical analyses compared quantitatively, determining mass loss value from fragmentation model
17 p3045 A69-34223

Four color photometry data of late F type stars in general catalog tabulated with columns for HD and GC numbers, apparent visual magnitude, etc
18 p3195 A69-34430

Dark equatorial belt of Jupiter atmosphere in 1962 and 1963, noting photometric contrasts, molecular absorption and possible structure
18 p3197 A69-34724

Photoelectric observations of nuclei of planetary nebulae He 1-5 and NGC 1514, noting changes in color and brightness characteristics
18 p3198 A69-34767

UBV photoelectric observation of OB and open cluster Tr 16 stars in Carina-Centaurus, suggesting no limit in depth distribution
18 p3200 A69-35133

Radial velocity measurements with objective prisms and results in SA8
18 p3201 A69-35143

Fornax clusters integrated V magnitudes and B-V and U-B colors measurement
18 p3201 A69-35205

Umbral chromosphere flashes visual and photometric observations at 5 sec intervals on K line filtergrams using Halle filter
18 p3204 A69-35390

Photometric evolution of Nova Delphini 1967 /HR Del/ in UPXYZVS seven color intermediate waveband system, showing position on QQ diagram
19 p3425 A69-36563

Nova Delphini 1967 /HR Del/ observations in UPX-YZV photometric system, tabulating color indices
19 p3426 A69-36564

Spectral energy distribution of gamma-Cas in 1967 based on observations in seven color photometric system
19 p3426 A69-36565

UBV photoelectric observations of Nova Delphini 1967 at Bologna Observatory
20 p3599 A69-37475

Lunar brightness variations during eclipse on 13 April 1968 measured photoelectrically, suggesting nonuniform diurnal distribution of atmospheric scatterers for observed asymmetry
20 p3601 A69-37510

Relative penumbral intensity independent of spot position from data by pinhole photometer of large sunspots
20 p3603 A69-37542

Photometric and spectral observations of Chuadze and Wild supernovae, showing type I classification
20 p3607 A69-38038

Andromeda galaxy brightness distribution, discussing nuclear region, energy distribution, surface brightness, brightness profile, etc
20 p3610 A69-38141

Photometric and spectroscopic observations analysis of Comet Honda 1968c
20 p3614 A69-38252

Sunspot size and shape in continuous spectrum regions from photometric observations in UV and red ranges
20 p3616 A69-38301

Neptune equatorial radius, diameter, flattening and upper atmosphere optical properties determined from photometric curves of star BD-17 occultation
21 p3796 A69-38471

Spectrophotometric analysis of interstellar absorption in direction of IC 1805 cluster, noting anomalies
21 p3814 A69-39576

Milky Way galactic diffuse radiation photometric study using Schmidt camera, stressing Northern Coal-sack commencement region
21 p3817 A69-39725

Photoelectric observation of EM Cygni eclipsing binary and old nova
22 p4015 A69-40151

Cepheid variable stars distance estimated from UVB three color photoelectric photometry data
22 p4031 A69-40943

Photoelectric photometer monitoring of flare star UV Cet, comparing time intervals between flares to those of YZ CMi
22 p4032 A69-40945

Photometric data for variable stars in Lyra and Cygnus including eclipsing variables
23 p4215 A69-42009

Photometric data for long period variable stars in Cygnus obtained from plates of various observatories
23 p4215 A69-42010

Optical detection of pulsars with emphasis on CP 1919, discussing optical variation
23 p4218 A69-42325

Law of optical radiation and photometric characteristics of quasars, noting photometric effect of strong emission lines and color dependence on red shift
24 p4375 A69-42552

Photoelectric measurements of emission line intensities for low density planetary nebula with moderate excitation located near north galactic pole, deriving abundances
24 p4376 A69-42662

Brightness temperatures and spectra of Venus, Mars, Jupiter and moon measured from 8 to 14 microns by reflector and prismatic spectrometer
24 p4390 A69-43785

Astronomical photoelectric photometry system, describing telescope and photometer, coldboxes, analog integrators, digital recording equipment and computer programs
24 p4318 A69-43805

ASTRONOMICAL SPECTROSCOPY

Model spectra applied to carbon dioxide bands in Venus spectrophotometric measurements
02 p0319 A69-12107

Spectral line identification in quasars, noting emission lines characteristic of emission nebulae and absorption lines of stellar atmospheres
03 p0508 A69-13173

Limiting conditions for gaseous atmospheres surrounding major and minor planets related to suitability for synoptic observation with optical telescopes and spectrometers
03 p0510 A69-13393

Light and radial velocity changes in close binary systems, including limb and gravity darkening of distorted stars in analysis of spectroscopic effects
04 p0653 A69-14612

Meteor spectrum from 1966 Leonid shower considered to be closer to comet nucleus spectra than previous spectra
04 p0655 A69-14664

Solar image or spectrum focal plane scanning technique with output beam displaced but undeviated relative to input beam for solar spectrophotometry
04 p0602 A69-15378

Fiber optic electrostatically focused image intensifier tube for recording star spectra with reduced exposure time [WERL-68-1C2-TAEC-P1]
04 p0603 A69-15444

Optical observations of radio galaxies and quasars, noting evidence for galactic explosions, surface distribution, physical properties, radio quiet quasars, etc
05 p0820 A69-15837

Crab Nebula and Cygnus XR-1 X ray spectra shown to have differential number power law spectra and same intensity
05 p0813 A69-15846

Telescope dispersion role in research projects, discussing techniques for spectral classification and radial velocities
07 p1074 A69-19202

Fe II lines relative intensities in eta Carinae spectrum, discussing possible intrinsic reddening of object and representation of visible and near IR continuum
07 p1217 A69-19253

Radio sources flux densities from fan beam survey using Molongo radio telescope compared to flux densities of Parkes catalog, presenting revised spectra
07 p1218 A69-19278

Electron temperatures and internal turbulence in H II regions of Sagittarius arm measured by high resolution interference method
08 p1392 A69-20566

Spectroscopic residual intensities variation of metallic and hydrogen lines of eclipsing system R Canis Majoris with phase, discussing surrounding gaseous matter
08 p1396 A69-20646

Spectroscopic evidence for mass loss from CH Cygni based on observations of chromospheric lines of high dispersion spectrograms
08 p1396 A69-20651

Solar element abundances from nucleosynthesis standpoint, discussing measurements with high resolution spectrometer used in double pass with intermediate slit
08 p1402 A69-20906

Multichannel photoelectric spectrometer design for Hale telescope, noting effectiveness in red and IR observations
08 p1318 A69-21131

Stellar abundance and origin of elements, discussing stellar atmospheres and gaseous nebulae spectral determination, chronology of galactic halo, etc
09 p1587 A69-21306

Radial velocities of stars near cluster NGC 7380, discussing discovered stars, double lined spectroscopic binaries and photometric information
09 p1597 A69-22060

Distance of bright stars in Cepheus OB2 region by MK spectral classification and UVB photometry, noting early main sequence and supergiant stars
09 p1599 A69-22194

Scor X-1 optical spectrum magnitude and color changes, proposing variable black body model
09 p1601 A69-22213

Spectroscopic study of A stars with large Stromgren m sub one indices, discussing rotational velocity, spectral intensity and type
09 p1602 A69-22215

Red shifts of radio sources obtained with Carnegie image tube spectrograph, noting quasi-stellar objects and galaxies
09 p1602 A69-22224

- Red shifts of quasi-stellar objects obtained with image tube spectrograph, noting photoelectric magnitudes and colors
09 p1602 A69-22225
- Spectroscopic observation of quasi-stellar objects noting red shifts
09 p1602 A69-22226
- Photoelectric spectrum scanning and IR photometric observations of Scorpius XR-1 X ray source
09 p1604 A69-22401
- Early type stars spectrophotometric parameters, discussing hydrogen beta, gamma and delta line widths, magnitude, etc
10 p1777 A69-23387
- Interstellar grain model consisting of elongated dielectric particles represented by infinite circular cylinders reproducing observed interstellar extinction in IF far UV spectra
10 p1781 A69-23674
- Spectroscopic observations of faint quasar near double galaxy NGC 3561, noting red shifts
10 p1785 A69-24092
- Spectra of low energy X ray source at position of Large Magellanic Cloud, noting flux
10 p1770 A69-24093
- Diffuse X radiation spectrum below 4 kev measured with beryllium window proportional counter at rocket altitudes
10 p1770 A69-24094
- Spectroscopic observations of optical object identified with X ray source Cygnus X-2 noting radial velocity in absorption and emission lines
10 p1785 A69-24097
- Spectrum of IR object NML Cygnus, discussing model based on circumstellar IR emission
10 p1785 A69-24101
- Quasar and radio galaxy spectra obtained on Cassegrainian focusing diffraction spectroscopy
11 p1951 A69-24236
- Flux densities and spectral indices of radio sources in 3C and 3 CR catalogs, noting measurements at 86 MHz frequency
11 p1951 A69-24237
- Spectroscopic, photometric and polarimetric observations of magnetic stars, discussing magnetic curves of periodic variables
11 p1954 A69-24362
- Martian polar caps dimensions as function of planet heliocentric longitude examined from photographic observations, noting compatibility with spectroscopic data
11 p1959 A69-24728
- Methane absorption distribution in 6190 A band over Jupiter disk based on spectrograms, noting center to limb variations
11 p1960 A69-24730
- Methane absorption distribution in 6190 A band over Saturn disk at center and polar latitudes based on spectrograms
11 p1960 A69-24731
- Spectroscopy and star classification on basis of spectra
12 p2155 A69-26122
- Spectrum analysis of Jupiter atmospheric composition, obtaining abundances of minor constituents
12 p2155 A69-26205
- Limits for Martian surface materials established by comparing visible and IR spectra with laboratory spectra
12 p2156 A69-26225
- Lallemand electronic camera application for spectroscopic observations of unsteady phenomena in galactic nuclei at 4000 A, noting radial velocities
12 p2163 A69-27017
- M 31 galaxy ionized gas region high resolution spectroscopy, emphasizing radial velocities in O II lines at various distances from nucleus
12 p2163 A69-27020
- Galactic and quasar radio sources distribution, discussing spectral indices
12 p2166 A69-27036
- Quasar spectra, discussing 3C 345, 3C 191 absorption lines and model explaining quasar spectra
12 p2167 A69-27046
- Red shift determinations and line identifications for quasars, using spectrograph with electro-optical converter
12 p2168 A69-27048
- Photometric and spectroscopic analysis of southern peculiar galaxy NGC 6438, discussing isophotes, color distribution and radial velocity
12 p2169 A69-27059
- NGC 4038-9 velocity field from spectrum obtained at McDonald Observatory, suggesting existence of two centers of matter ejection
12 p2169 A69-27060
- Photographic studies of unsteady features of galaxies, discussing spectra, color, spiral arm instability and extragalactic H II regions
12 p2170 A69-27063
- Spectroscopic and eclipsing binaries in zodiac tabulated for photometric studies at lunar occultations
12 p2171 A69-27152
- Absorption line spectrum of quasar Ton 1530, discussing line widths and red shifts
13 p2334 A69-27306
- IR spectroscopic observations of moon to interpret molecular vibration spectra in terms of molecular composition, discussing rock surface roughness effects
13 p2341 A69-27582
- Solar spectroscopic techniques, discussing instrumentation problems affecting photosphere line spectra, SNR in absorption spectra and near IR spectra
13 p2341 A69-27588
- Venus carbon dioxide spectral band analysis methods, discussing spectral lines and rotational temperatures obtained
13 p2344 A69-27649
- Venusian water vapor spectroscopic data indicating longitudinal and time dependent variations in abundance
13 p2345 A69-27650
- Fe III line profiles and equivalent widths from spectrograms of zeta Cas and gamma Peg for Fe abundance, using model atmospheres
13 p2347 A69-27715
- Markarian galaxies with strong UV continuum, observing emission lines differing from each other
13 p2351 A69-27866
- Goddard Experiment Package /automated spaceborne telescope design/ for stars and nebulae UV spectral emittance measurements
13 p2261 A69-27948
- Frequency selection, spectral index distributions and counts of extragalactic radio sources
14 p2518 A69-29134
- Interstellar gas radio and optical spectral lines of neutral H compared with Ca and neutral Na, discussing critically low velocity gas distribution
14 p2519 A69-29135
- Visual, photographic and spectral observations of comets during IQSY, discussing comets Tomita-herber-Honda 1964c and Ikeya-Seki 1965f
14 p2525 A69-29716
- Unidentified cometary spectra line emission possible interpretations, examining atomic hydrogen abundance in cometary atmosphere and ionic hydrogen recombination
15 p2685 A69-30523
- Zeeman spectroscopy and UVB photometry of 17 Com and kappa Cnc, observing periodic magnetic and light variations
15 p2692 A69-30774
- Photometric calibration correction for /B-V/ and /U-B/ colors taking into account hydrogen line blocking
15 p2694 A69-30786
- Virgo XR-1 rocket observations, presenting count rate histograms, differential photon spectrum and X ray and M87 core radio spectra
15 p2701 A69-31535
- Spectrophotometry of elliptical galaxy NGC 1052 nucleus from 3400 to 6300 A for relating radio properties and optical characteristics
16 p2853 A69-31610
- Wolf 359 flare spectra obtained with Palomar telescope, noting hydrogen and He line enhancement, broadening and violet shifting
16 p2852 A69-32817
- Magnetically focused electronographic image converters in far UV photography and spectroscopy in space astronomy applications
17 p2972 A69-33084
- Optical spectrum of galaxy NGC 3031 nucleus, considering emission and absorption lines and continuum
17 p3034 A69-33396
- Spectral lines radial velocities and profiles observed on 48 Librae from 1950-1962
17 p3038 A69-33722
- Alpha Serpentis spectrum study from model atmosphere and growth curves, finding metal abundance ratios five times as great as in Arcturus
18 p3200 A69-35130
- UBV photoelectric observation of OB and open cluster Tr 16 stars in Carina-Centaurus, suggesting no limit in depth distribution
18 p3200 A69-35133
- HD 217050 spectroscopic study, determining Balmer envelope temperature from comparison of homologous Balmer and Paschen lines intensities
18 p3201 A69-35144
- Pulsars measured parameter data tabulation including right ascension, declination pulse repetition period, showing sources distribution and clusters
18 p3202 A69-35211
- Celestial spectra forbidden lines tabulated by element and ionization stages, describing laboratory spectrum analysis programs
19 p3421 A69-36212
- Forbidden transitions in diatomic molecules with nonzero spin and zero orbital angular momentum, stressing application in outer planets and M stars hydrogen spectra
19 p3421 A69-36213
- Collisional excitation of forbidden lines in planetary nebulae from 5537/5517 intensity ratio measurements, noting density and intensity relationship
19 p3422 A69-36221
- Forbidden lines of O I, O II, S II, N II and A III in red and near IR spectra of NGC 1976, IC 418 and II 4997
19 p3422 A69-36222
- Monochromatic energy flux measurement in H and forbidden lines of planetary nebulae indicating ionization level and optical depth
19 p3423 A69-36223
- Forbidden emission lines in spectra of normal, radio and Seyfert galaxies and quasars, giving information about quasi-stellar mean densities; temperatures, ionization, etc
19 p3424 A69-36236
- Photometric evolution of Nova Delphini 1967 /HR Del/ in UPXZYVS seven color intermediate waveband system, showing position on QQ diagram
19 p3425 A69-36563
- Markarian galaxies with strong UV continua, discussing emission spectra, red shift, absolute magnitudes, etc
19 p3426 A69-36577
- Photographic and spectroscopic observation of Saturn at Cassegrain focus of 122 cm reflector during earth passage through ring plane, discussing Saturn satellites
20 p3600 A69-37481
- Spectroscopic and photographic observations of compact galaxies, discussing distances, absolute magnitudes, linear dimensions, Hubble diagram position and correlations with objects showing similar characteristics
20 p3600 A69-37483
- Radio source flux density values in revised 3C catalog determining spectrum, discussing effects of relativistic electron energy distribution, self absorption and spatial distribution
20 p3609 A69-38138
- Spectra of peculiar S zero galaxy NGC 7625 with irregular dust distribution, discussing central spheroid rotation and mass
20 p3610 A69-38142
- X ray spectra of Sco XR-1, Cyg XR-1 and Cyg XR-2 for proton energy range 1.5-13 kev from proportional counter measurements
20 p3593 A69-38152
- Photometric and spectroscopic observations analysis of Comet Honda 1968c
20 p3614 A69-38252
- Carbon dioxide band in Venus spectrum by dispersion analysis, deriving rotational temperature
20 p3614 A69-38254
- Cosmic X ray background spectral measurement from rocket flight near geomagnetic pole
21 p3787 A69-38351
- Spectroscopic orbital elements of eclipsing binary IZ Per determined from 22 spectra using Wilsing and Russell method
21 p3795 A69-38469
- Radio spectra of 136 sources determined at various declination ranges noting flattening at frequencies below 408 MHz
21 p3797 A69-38480
- Spectroscopic observations of optical pulsar NP 0532, using technique permitting phase resolution of spectra of main pulse and interpulse
21 p3799 A69-38646
- Trial and error procedure applied to instrumental profile of Liege Solar Atlas, convoluting instrumental profile with telluric A band profile
21 p3722 A69-38698
- First order profile of Utrecht Solar Atlas from second order profile and oxygen band refining procedure, deducing instrumental profile for first order spectra
21 p3722 A69-38699

Stellar IR spectroscopy, describing absorption and emission lines of various atoms and molecules, atmospheric composition, problems with variable stars, etc

21 p3811 A69-39510

Invalidity of Pagel method for intrinsic and interstellar reddening for peculiar objects, discussing excitation mechanism for forbidden lines of ionized Fe for Eta Carinae

21 p3815 A69-39616

Planetary nebulae imaging stratification effects on structural difference studies by slit and slitless spectrographs and narrow band photography

21 p3817 A69-39785

Planetary spectroscopy with McDonald 107 inch telescope, discussing role of molecular and atomic absorption lines, line broadening, Doppler shifts and Rayleigh criterion

21 p3727 A69-39786

Flux measurements of radio sources at 4.3 mm by 36 ft parabolic antenna, noting flux densities relative to Jupiter

22 p4014 A69-40126

Spectroscopic analysis of nebula NGC 6302 for identification as highly excited gaseous nebula, noting He-H ratio

22 p4026 A69-40647

Spectral and orbital evidence of connection among fireballs with orbit inclination, comets and carbonaceous meteorites

23 p4208 A69-41285

X ray spectra of four high energy sources near galactic center

23 p4206 A69-42114

Radial velocity errors in high dispersion astronomical spectrographs in terms of variable spectral shifts along plate produced by mirror surface irregularities

23 p4167 A69-42189

Galactic X ray sources observed in EM spectrum high energy region, discussing hot plasma cloud thermal radiation and electrons synchrotron radiation as emission sources

23 p4206 A69-42318

A-type stars investigation for anomalous spectral line intensities, discussing Hertzprung-Russell diagrams, rotational velocities, magnetic fields and abundances

23 p4218 A69-42322

Daylight observations of Comet Ikeya-Seki 1965-f at perihelion passage, discussing resulting emission line spectra within comet head

23 p4221 A69-42386

Red shift determinations and line identifications for quasars, using spectrograph with electro-optical converter

24 p4375 A69-42551

High radial velocity gas cloud near Seyfert type galaxy NGC 4939 nucleus investigated spectroscopically

24 p4375 A69-42609

Milky Way hydrogen line survey with Parkes telescope, giving velocity-longitude control maps and tabulated data covering galactic equator

24 p4383 A69-42961

ASTRONOMICAL TELESCOPES

NT HELIOMETERS

NT SPECTROSCOPIC TELESCOPES

NT STRATOSCOPE TELESCOPES

NT X RAY TELESCOPES

Optical space astronomy, discussing Large Space Telescope, intermediate scale telescopes and lunar systems

[AAS PAPER 68-218] 02 p0313 A69-11484

Limiting conditions for gaseous atmospheres surrounding major and minor planets related to suitability for synoptic observation with optical telescopes and spectrometers

03 p0510 A69-13393

Optical and mechanical design of Anglo-Australian 150 inch telescope for observations of southern sky at Siding Spring Observatory, Australia

03 p0411 A69-13466

22-m parabolic reflector radio telescope with 9525 mm focal length at Crimean Astrophysical Observatory, noting high performance in mm wavelength range

04 p0584 A69-14376

Computer controlled photometric telescope, describing star setting, photometric measurements and data processing

04 p0602 A69-15380

Astronomical two mirror telescope with aplanatic secondary focus, describing prime and secondary focus field correctors

05 p0761 A69-15733

Telescope dispersion role in research projects, discussing techniques for spectral classification and radial velocities

07 p1074 A69-19202

High dispersion IR image tube spectroscopy using telescope, discussing alpha Sco and alpha Boo spectral regions

07 p1074 A69-19203

Sunspot observations with astrophot telescope by tracing on projected image of solar disk

08 p1387 A69-20118

Coincidence error between star image and planet edge for entrance pupil and telescope magnification

08 p1314 A69-20383

Diffraction limited telescope fine guidance experiment to improve pointing stability in space, noting attitude control system and nonmechanical suspension

08 p1317 A69-21072

Multichannel photoelectric spectrometer design for Hale telescope, noting effectiveness in red and IR observations

08 p1318 A69-21131

Conductive heat transfer between aerodynamically heated skin and barrel of Aerobee 150 sounding rocket telescope, noting effect of residual gas pressure

09 p1610 A69-22005

Geomagnetic activity correlation to cosmic ray solar daily variation underground, observing primary cosmic ray flux with meson telescopes

09 p1583 A69-22755

Aerospace Corp. solar observatory /California/ compound telescope, vacuum spectroheliograph, instrumentation and applications

11 p1862 A69-24792

Aerobee rocket-borne liquid helium cooled telescope for IR night sky observations

11 p1885 A69-24852

Large astronomical mirrors support and testing - Conference, Tucson, December 1966

12 p2055 A69-26406

Lever support systems for telescopes noting tilt compensation, acceleration balance and problems of friction, pivot viscosity, thermal effects and weight

12 p2057 A69-26410

Optical tests of Hale telescope mirror and support system at Palomar, noting various maladjustments and malfunctions

12 p2057 A69-26411

Axial support systems for large astronomical mirrors, considering gas support system for flat mirror submerged and floating in isostatic liquid

12 p2057 A69-26412

Sinusoidal tension and compression radial support system for large solid disk primary mirror, noting pivot design and pad bonding adhesive

12 p2057 A69-26413

Large mirror support systems definition in terms of axial location and radial position

12 p2057 A69-26414

Lick telescope support system for 120 inch mirror, noting use of levers and counterweights concept

12 p2058 A69-26415

Isaac Newton telescope, describing support of 98 inch mirror, structure between fabricated cell steel surface and mirror and tests with air bag support

12 p2058 A69-26416

Support system for McDonald 107 inch telescope mirror, adopting Couder design using lily pad single lever supports for axial thrust

12 p2058 A69-26417

Axial support system for Canadian 150 inch telescope mirror, discussing flexural and shear analyses and ring supports repositioning for balancing shear

12 p2058 A69-26418

Axial counterweight lateral support system with ternary symmetry for European Southern Observatory telescope mirror

12 p2058 A69-26419

Axial support system for controlling thermal distortion of 82 inch heliostat mirror for Kitt Peak solar telescope

12 p2058 A69-26422

Active optics system for obtaining perfect mirror figure in orbiting astronomical telescope, using laser and white light sources, interferometers and data converter

12 p2092 A69-26423

Dynamic relaxation method for elastic deformation in mirrors, using tensor equations of elasticity in nonorthogonal curvilinear coordinates

12 p2187 A69-26890

Test-methods for telescope mirror, discussing polishing, monitoring by Hartmann test and visual null test

13 p2259 A69-27205

Submillimeter astronomy role for solar and atmospheric studies

13 p2343 A69-27604

Spaceborne optical telescopes requirements and development including mirror material and construction, optical design, servocontrol, etc

13 p2261 A69-27946

Goddard Experiment Package /automated spaceborne telescope design/ for stars and nebulae UV spectral emittance measurements

13 p2261 A69-27948

Mirror correctors used with paraboloidal spaceborne telescopes in far UV, yielding enlarged photographic field

13 p2261 A69-27949

Segmented active mirror optics design concept for lightweight optically stable primary reflector used in large orbiting astronomical telescopes

13 p2261 A69-27950

Control system for thin diffraction limited orbiting astronomical telescope mirror based on structural analysis of static deflections

13 p2261 A69-27951

Ultralightweight mirror blanks for astronomical telescopes, discussing weight saving low thermal expansion and fused monolithic core technology

13 p2261 A69-27953

Solar telescope imaging quality measured as function of atmospheric turbulence and temperature above land level

14 p2453 A69-29973

Reflector radio telescope of Pulkovo astronomical observatory noting high resolution

15 p2679 A69-30102

Stellar scintillation spectra for different zenith distances, correlating data with meteorological conditions at time of observation

15 p2647 A69-30165

Large telescope dome movements automatic control, considering central and eccentric telescope mounting

15 p2588 A69-30441

Astronomical UV radiation observation by OAO 2 satellite, discussing solar images, corona, chromosphere and UV spectrum, stellar evolution, etc

15 p2689 A69-30597

Solar telescope in Berlin observatory for prominences and other solar phenomena observations by public

15 p2611 A69-30881

European Southern Observatory installation in Chile, discussing site, instruments, domes design, administrative structure, etc

15 p2589 A69-31098

Close visual binaries separations for checking large aperture telescope resolution, listing binaries, orbits and ephemeris

16 p2855 A69-31662

Night sky far IR observation by rocket-borne telescope, discussing minimum signal detection and origin

16 p2781 A69-32445

Bamberg zenith telescope investigation, noting level constant dependence on level tube bubble length

17 p2970 A69-32882

Objective lens of AVR-2 refractor at Poltava Observatory measured for spherical aberration, astigmatism field curvature, coma and distortion

17 p2970 A69-32883

Manned space telescope attitude stabilization using counter-rotational triaxial gyro system

18 p3206 A69-34371

LASSO /modified S-4B/ IU/ vehicle mission to place in orbit two unmanned Lunar Modules for landing of radio and optical telescopes on lunar surface

18 p3136 A69-34813

Supernovae observations at Palomar during 1968 made with Schmidt telescopes

19 p3403 A69-35963

Prismatic Cassegrainian-focus spectrograph of telescope at Shemakha Observatory, discussing camera inclination, instrumental contour for yellow neon line, astigmatism, optical temperature effects, etc

19 p3313 A69-36582

Image converter camera and astronomical telescope arrangement for photographing metal diaphragm openings in shock tube

20 p3538 A69-37227

Astronomical data collection and evaluation, discussing digital distance measurement, photoelectric photometry, servocontrols and electronic computers suited for Schmidt telescope output

20 p3539 A69-37525

Rocket-borne IR astronomical telescope high altitude observations compared with balloon observations

20 p3605 A69-37800

Stellar systems observations using photometers with long narrow slits in identical telescopes

20 p3545 A69-38055

Large aperture Al alloy telescope mirrors consisting of Tenzalloy Al coated with Ni alloy, presenting performance data

20 p3546 A69-38193

Two channel TV Cassegrain telescope, describing color separation system for obtaining integral and monochromatic images of astronomical objects

20 p3547 A69-38309

Planetary spectroscopy with McDonald 107 inch telescope, discussing role of molecular and atomic absorption lines, line broadening, Doppler shifts and Rayleigh criterion

21 p3727 A69-39786

Vienna 60 inch telescope concept and design, discussing optical systems possible combinations under local conditions

24 p4314 A69-43000

Astronomical photoelectric photometry system, describing telescope and photometer, coldboxes, analog integrators, digital recording equipment and computer programs

24 p4318 A69-43805

ASTRONOMY

NT INFRARED ASTRONOMY

NT RADAR ASTRONOMY

NT RADIO ASTRONOMY

NT X RAY ASTRONOMY

Space research practical benefits in solar physics, radio astronomy, meteorology, radio physics, communications, etc

[UN PAPER 68-11608] 01 p0179 A69-10496

Soviet space astronomy including rocket, satellite and space probe measurements for solar, stellar, planetary and lunar studies

01 p0155 A69-10946

Solar gravitational field influence on annual trigonometric parallaxes within relativistic theory framework

03 p0506 A69-13091

Advances in astronomy and astrophysics, Volume 6, covering periodic orbits, binary stellar systems, interstellar molecules and lunar luminescence

04 p0652 A69-14610

Astronomy - Conference, Prague, August 1967

05 p0820 A69-15834

UV astronomy, discussing vehicle stabilization, unstabilized sounding rockets, scanning satellites, balloons, stabilized rockets, pointing satellites, optics and detectors

05 p0821 A69-15839

Astronomy - Conference, Nuremberg, September 1968

06 p0998 A69-16967

Soviet book on theoretical astronomy covering evolution from Ptolemy to Einstein, universal gravitation and principles of celestial mechanics

07 p1211 A69-18544

Visual and photographic comet observations, including perihelion passage of P/Perrine-Mrkos in 1968

07 p1216 A69-19205

Astronomical unit determined by measuring Doppler shift of spectral features of galactic hydrogen

07 p1222 A69-19590

Bibliography of astronomical literature, Volume 67

09 p1602 A69-22223

Book on relativity and cosmos, space and time in physics, astronomy and cosmology covering theoretical and empirical research

10 p1784 A69-24019

Brightness temperature distributions from intensity interferometric measurements reconstructed by computation

11 p1888 A69-25256

Astronomical unit determined by measuring radial velocity of radio wavelength spectral line source

13 p2350 A69-27822

Earth orbital manned space astronomy, discussing long range program, instruments, facilities and data processing

13 p2240 A69-27947

Solar gravitational field influence on annual trigonometric parallaxes within relativistic theory framework

14 p2516 A69-28773

Q switched ruby laser designed for lidar probing of cosmic bodies and earth atmosphere

14 p2460 A69-29660

Book on New Cosmos covering classical astronomy concepts, stellar astrophysics and galaxies

14 p2522 A69-29684

Pulsar NP 0532 in Crab Nebula observed by rocket and telescope showing strong pulsed X ray signal

15 p2679 A69-31529

Astronomical and geophysical observations, selecting degree of smoothing via Whittaker method for curve construction

17 p3028 A69-32877

Collection of papers on astronomy covering orbit calculation, stellar photometry, interstellar matter and equipment characteristics

17 p3031 A69-33096

Astronomical Society of Australia - Conference, Sydney, December 1968

17 p3039 A69-33799

Orbital astronomy support facility research requirements analysis, discussing objectives and measurement needs, instrumentation, spacecraft and facilities, etc

18 p3206 A69-34369

Instruments for gamma ray astronomy including Ranger low energy detector, howitzer detector and cosmic spark chamber

18 p3138 A69-35135

Book on eclipse phenomena in astronomy covering moon, earth and other planets, occultation, planets transit over sun, influence in radio astronomy, etc

19 p3425 A69-36379

Digital computers standard programs for astronomical problems

20 p3596 A69-37317

Lunar spherical astronomy, discussing coordinate transformations, precessional and nutational motions, etc

21 p3798 A69-38605

Intensity interferometer applications comparison with Michelson interferometer, discussing sensitivities, radio and optical wavelength astronomy, space plane waves, etc

21 p3722 A69-38794

Collection of papers on astronomy and astrophysics, Volume 7, covering galactic radiation, nebulae, stellar composition, solar activity, etc

21 p3810 A69-39501

Book on high energy astrophysics covering violent stellar phenomena, radio galaxies, quasars, pulsars, cosmic rays origin, mystery neutron stars, etc

22 p4008 A69-39900

ASTROPHYSICS

Introduction to planetary physics, Terrestrial planets, covering solid interior constituents, solar system dynamics and origin and evolution

01 p0154 A69-10920

Liouville and Poisson equations solutions for locally ellipsoid stellar velocity distributions with constant coefficients

02 p0310 A69-11455

Solar wind directional fluctuation derived from wavy structure of comet Morehouse ionic tail rays, noting solar wind bulk velocity

02 p0311 A69-11459

Book on cosmic radiation origin and expansion of universe, covering astrophysical reasons for electric charging of galaxies in range of galactic and metagalactic dimensions

02 p0315 A69-11713

Plasma astrophysics - Conference, Varenna, Italy, July 1966

02 p0328 A69-12780

Plasma instabilities covering astrophysical phenomena, Rayleigh-Taylor instability, anisotropic and LF MHD, electrostatic and electromagnetics, warm plasmas, etc

02 p0293 A69-12783

Radio galaxies and quasars, discussing radio structure, observation methods, polarization, time variation, etc

02 p0329 A69-12791

Radiation due to collective effects in plasma physical aspects of astrophysics, discussing synchrotron radiation and bremsstrahlung

02 p0310 A69-12792

Iris satellite experiments in astrophysics including nuclear and solar induced electromagnetic radiation

03 p0427 A69-12849

Extensive air showers due to interaction of high energy particles with atmosphere, discussing astrophysics, cosmology and fundamental particle physics

03 p0498 A69-12938

F values for Ti II, Cr II and Fe II by empirical astrophysical line strength analysis, discussing f value determination from stellar growth curve

03 p0508 A69-13175

Time scale of cooling/heating process compared with gaseous clouds contraction/expansion for one solar mass protostar evolution in transparent stage

04 p0651 A69-14366

Advances in astronomy and astrophysics, Volume 6, covering periodic orbits, binary stellar systems, interstellar molecules and lunar luminescence

04 p0652 A69-14610

Homogeneous main sequence star models with convective cores, considering core chemical composition, size and energy generation ratio mechanism

05 p0829 A69-16777

Simulation experiments using artificial plasma for astrophysical rocket exploration, discussing experiments leading to barium-copper oxide mixture choice for plasma cloud

06 p0999 A69-16973

Cosmic rays, elementary particle physics and astrophysics - Conference, Aligarh, India, December 1967

06 p0986 A69-17268

Astrophysical aspects of primary energy spectrum deduced from shower size spectra and high energy interactions of extensive air showers

06 p0990 A69-17298

X ray astronomy use for probing hot regions of outer space and high energy electrons

06 p0991 A69-17307

Primary electrons implications on cosmic ray confinement in Galaxy, astrophysical aspects and problems of energy spectrum

06 p0991 A69-17308

Amount of flux carried by convection in late type stars, reevaluating drag role in mixing length theory

06 p1003 A69-17321

Solar type stellar activity, considering solar activity origin and correlation with stellar distances

06 p0996 A69-17447

Plasma instability role in radiant energy release from astronomical objects, noting plasma instabilities in solar system, cosmic rays, galactic and extragalactic objects

06 p1009 A69-17967

Cosmic X rays, gamma rays and electron production under astrophysical conditions, noting potential use in supernova and quasar research

07 p1204 A69-18391

Cosmic ray astrophysics, discussing chemical composition, energy spectrum and galactic sources

07 p1205 A69-18909

Soviet book on relativistic astrophysics covering evolution and structure of universe with reference to galaxies, stars, quasars, relativity theory, gravitation theory, etc

07 p1216 A69-18960

Satellite components of lines formed in stellar type differentially rotating disk

07 p1219 A69-19336

Atomic collision processes in astrophysics noting stellar continuum spectra, Ca ion and He lines, solar corona, heat balance in H I regions and planetary nebulae

07 p1224 A69-19653

M82 galaxy as Seyfert-like galaxy seen edge-on, using radio and optical data showing H alpha emission collisionally excited, discussing circular polarization

08 p1383 A69-20051

Astrophysics, solid state physics, plasma physics and lasers - Conference, Bologna, October 1967

08 p1387 A69-20216

Relativistic astrophysics, discussing quasar phenomenology, red shift cosmology and relationship with galaxies

08 p1388 A69-20222

Nucleosynthesis in stars and early stage expanding universe, considering related nuclear reactions, helium abundances and kinematics of stars in Galaxy

08 p1357 A69-20893

Nucleosynthesis in dynamics of massive star cores, noting element synthesis by neutron capture in supernova explosions

08 p1401 A69-20898

Variable gravitational number kappa, discussing effects on cosmology

09 p1603 A69-22270

Laboratory astrophysics - Conference, Luntenen, Netherlands, September 1968

10 p1780 A69-23670

Magnetic field and magnetic energy evolution in infinitely conducting homogeneous isotropic turbulent medium, applying results to galactic magnetic field model

10 p1783 A69-23793

Book on stellar atmospheres covering radiation theories, thermal equilibrium, measurement techniques, spectral analysis, etc, emphasizing sun
11 p1961 A69-25084

Stellar physics, Volume 1, covering stellar structure, evolution, physical processes, statistical physics, quantum theory, classical mechanics, etc
12 p2152 A69-25785

Pulsars discovery, emission, regularity, narrow frequency band and pulse changes, physical nature and aspects of Crab Nebula source
12 p2160 A69-26895

Book on astrophysics and stellar astronomy covering stellar radiation, binary and variable stars, positions, magnitudes, galaxies, cosmologies, etc
13 p2337 A69-27463

Atomic and molecular spins dynamic orientation in anisotropic radiation field, examining medium properties and astrophysical consequences
13 p2350 A69-27861

IR astrophysics, discussing detection, instrumentation, IR stars and stellar evolution
14 p2516 A69-28868

Book on New Cosmos covering classical astronomy concepts, stellar astrophysics and galaxies
14 p2522 A69-29684

Soviet papers on astrophysics covering solar flares, degenerate gas explosion, nonadiabatic shock waves, chromospheric H line excitation, prominences, stellar rotation, etc
15 p2682 A69-30505

Unsteady nonadiabatic shock waves in stellar gas dynamics, analyzing energy losses due to ionization at shock fronts by extended Chiznell-Wisem method
15 p2682 A69-30508

Possible existence in universe of large number of difficult-to-observe particles with zero rest mass left over from superdense phase
16 p2814 A69-31801

BetaCrB atmospheric microturbulence velocity, ionization and excitation temperatures, electron pressure and abundances determined by spectrophotometer
16 p2864 A69-32592

Soviet book on cosmos and hypotheses covering origin and physical characteristics of earth, moon, Venus and Mars
20 p3596 A69-37234

Threshold photoneutron cross section for Mg 26, discussing resonances as primary production mechanism for stellar neutrons
21 p3788 A69-38599

Collection of papers on astronomy and astrophysics, Volume 7, covering galactic radiation, nebulae, stellar composition, solar activity, etc
21 p3810 A69-39501

Physics of massive starlike objects, discussing high entropy requirement, eventual nonrelativistic collapse and gravitational fields produced by low entropy equilibrium
21 p3811 A69-39516

NGC 7023 nebula physical characteristics observation based on flux and brightness measurement, noting spectral energy distribution and causes
21 p3816 A69-39724

Book on high energy astrophysics covering violent stellar phenomena, radio galaxies, quasars, pulsars, cosmic rays origin, mystery neutron stars, etc
22 p4008 A69-39900

Astrophysical ions acceleration model based on magnetic field annihilation theory
22 p3987 A69-41002

Book on stellar structure, Volume 1, Physical principles, covering interier conditions, thermodynamic and radiation theories, stellar temperature, energy and opacity, etc
23 p4211 A69-41377

Complex phenomena in theoretical astronomy including neutrino pair emission in stellar interiors, molecular H in interstellar gas, neutron stars, etc
23 p4217 A69-42316

Galactic magnetic field existence arguments, discussing general and optical evidences, radio emissions, Faraday rotation from extragalactic sources and from pulsars, etc
23 p4217 A69-42321

Observational cosmology developments with radio and X ray astronomy emphasizing existence, origin, effects and anisotropy of excess microwave background
23 p4219 A69-42327

Plasma instabilities in astrophysics - Conference, Monterey, October 1968
24 p4377 A69-42681

Nonthermal phenomena of astrophysics in relation to plasma physics, considering planetary and stellar regions, supernova envelopes, interstellar medium, cosmic rays, radio galaxies, etc
24 p4377 A69-42682

Explosions mechanism in radio galaxies and quasars mechanism based on observed phenomena, emphasizing galactic flares
24 p4378 A69-42698

Stellar structures and evolution stressing composition and processes of stellar interiors
24 p4379 A69-42782

Book on physics and evolution of galaxies covering properties, stellar content, interstellar matter, high energy particles and radio galaxies
24 p4384 A69-43167

ASYMMETRY

Asymmetry causes on cosmogonic scale in view of symmetry in small space-time regions /microworlds/ determinable within framework of Einstein theory
14 p2516 A69-28866

Reentry cones with mass and configuration asymmetries, studying nonlinear aerodynamic characteristics by wind tunnel and full scale flight tests [AIAA PAPER 69-867]
21 p3823 A69-39393

Asymmetry method for precision alignment of rectilinear systems, using laser light diffraction behind misaligned target
21 p3742 A69-39781

Solar magnetic field measurements for fine structure of magnetic asymmetry at different heights and within sunspots, discussing asymmetry for corona and interplanetary space
22 p4010 A69-39990

Solar wind north-south component sector dependent asymmetry implied from tangential discontinuities orientations as observed by Mariner 4
22 p4004 A69-40303

Solar protons delayed access into polar regions during 2 November 1967 solar particle event, discussing north-south asymmetry
24 p4368 A69-43183

Asymmetric metal flanges effect on beam tilt of aperture antennas
24 p4288 A69-43765

ASYMPTOTES

Asymptotic behavior of probabilities of large deviations of sums of independent random variables with moments of any order
01 p0104 A69-10264

Matrix procedures for stability of nonlinear control with nonlinearities, discussing system with three actuating elements
01 p0050 A69-10355

Asymptotic forms of Navier-Stokes equations for laminar motions of incompressible viscous fluid, discussing validity and applications [ONERA-TP-651]
01 p0059 A69-10383

Asymptotic behavior of curvature and conformal curvature tensors on asymptotically flat space-time
01 p0116 A69-10393

Asymptotic stability conditions for delayed quasi-linear nonautonomous systems periodic solutions derived by Shimanov method
02 p0280 A69-11705

Zero solution asymptotic stability for linear differential equations with continuous functions
03 p0465 A69-13129

Asymptotic behavior of periodic solution of neutral type equation with small delay
03 p0455 A69-13258

Asymptotic solutions for prolate spheroidal wave functions satisfying given differential equation, producing asymptotic expansions in terms of confluent hypergeometric functions
04 p0623 A69-14892

Asymptotic solution to problem of finding time optimal transformation for controlled plant with motion in phase space described by matrix differential equation
10 p1666 A69-23883

Asymptotic stability of discrete homogeneous linear minimum-variance estimation formulas
11 p1860 A69-25449

Asymptotic behavior of function in Cauchy problem solution for heat conduction, basing method on Laplace transform inversion formula
13 p2380 A69-28685

Asymptotic theory of Orr-Sommerfeld problem for symmetric channel flow stability
17 p2958 A69-34151

Asymptotic behavior of probabilities of large deviations of sums of independent random variables with moments of any order
19 p3360 A69-36199

N-th order differential systems using first approximation, finding conditions for bounded solutions, solutions asymptotic to zero and stability
23 p4181 A69-41722

ASYMPTOTIC METHODS

Asymptotic solution of Orr-Sommerfeld equation by multiple scales method for linear and general velocity profile
01 p0059 A69-10332

Automatic phase control effective bandwidth determined by asymptotic method, presenting computer calculated dependence on circuit parameters
01 p0030 A69-10590

Asymptotic method for analyzing small long wave perturbations in plasma, showing instability with respect to perturbations propagating at angles to ion-acoustic wave
01 p0131 A69-10788

Asymptotic integration of three dimensional elasticity equations for thin anisotropic shells and plates, deriving variability exponent of stress under given load
01 p0170 A69-10878

Radiant heat transfer in optically thick gray gas situated between parallel black diffusively emitting walls, using matched asymptotic expansion method
01 p0178 A69-11411

Electromagnetic wave propagation problems, using asymptotic solutions of differential and integral equations in domains containing transition points
02 p0208 A69-12130

Asymptotic constitutive approximations for rapid finite deformation of general viscoelastic materials, noting isotropic solids and fluids
03 p0523 A69-13020

Asymptotic decay of coupling for infinite phased arrays proved valid for infinite parallel linear plate array immersed in magnetized cold plasma
04 p0571 A69-14314

Asymptotic estimates of radiation patterns of nonequidistant antenna array represented in integral form
04 p0576 A69-14772

Slender wing theory extension to not-so-slender wings approached as singular perturbation problem, using matched asymptotic expansions method
04 p0544 A69-14891

Doubly infinite sets of simultaneous linear equations used in electromagnetic boundary value problems solved by Asymptotic Anticipation Method
04 p0560 A69-15214

Reflection and transmission of radiation from very thick and semiinfinite homogeneous atmospheres with arbitrary phase function, using asymptotic fitting method
04 p0595 A69-15285

Asymptotic solutions of restricted three body problem for one parameter periodic orbits in earth-moon synodic system, determining motion near moon
04 p0663 A69-15382

Asymptotic computation and graphical display of imaginary mu-zeros of combinations of cross product Bessel functions
05 p0836 A69-15874

Asymptotic formulas for field diffracted by conducting wedge illuminated by line source usable for self consistent field analyses
05 p0720 A69-16344

Nonsteady expansion of gas into vacuum in analysis of asymptotic solutions of Sedov
05 p0751 A69-16676

Asymptotic solutions for nonlinear differential equations with gradually varying coefficients of great resistivity
06 p0947 A69-17392

Asymptotic theory concerning nonsimilar structure of blast wave with expanding interface applied to hypersonic perfect gas flow
06 p0860 A69-17636

Asymptotic wave equation application conditions in describing field behavior near caustic surface, using Airy functions
07 p1076 A69-18520

Matched asymptotic expansions method applied to magnetic field induction in thin toroidal wire and flow past circular cylinder at small Reynolds number
07 p1180 A69-18811

Homogeneous linear systems conditions for asymptotic growth of solutions of nonhomogeneous linear differential equations system
08 p1342 A69-20348

Time response of second order nonlinear overdamped systems calculated by Krylov-Bogoliubov method of variation of parameters

08 p1297 A69-20356

Hankel functions and vibration equations solutions, discussing asymptotic behavior and monotonic properties in neighborhood of ellipses

08 p1416 A69-20714

Numerical studies of initial value problems by boundary value techniques for cases having available asymptotic estimates or periodicity of solutions

09 p1532 A69-21610

Matched asymptotic expansions method applied to problem of hypervelocity atmospheric entry, noting solution division into outer Keplerian region and inner expansion region

09 p1430 A69-21964

Asymptotic behavior of frequency function of fluctuations for generalized ensemble parameters, noting characteristic function convergence to Gaussian at thermodynamic limit

09 p1623 A69-22395

Book on special functions and approximations covering differential and integral equations and attendant theories arising in mathematical physics analysis

10 p1717 A69-22801

Automatic phase control effective bandwidth determined by asymptotic method, presenting computer calculated dependence on circuit parameters

10 p1653 A69-23105

Asymptotic method for analyzing small long wave perturbations in plasma, showing instability with respect to perturbations propagating at angles to ion-acoustic wave

10 p1653 A69-23107

Asymptotic boundary curves for two dimensional and axisymmetric incompressible irrotational flows into throat of convergent duct

10 p1680 A69-23893

Asymptotic methods for integral equations of plane mixed problems of elasticity theory for nonclassical regions

11 p1971 A69-24647

Stress concentration analysis of interactions between stress raisers and cross section changes, considering asymptotic expansion method

11 p1972 A69-24650

Asymptotic solutions for transverse oscillations of wedge and cone by virtual displacements principle, considering nonlinear law of elasticity and energy dissipation

11 p1975 A69-24762

Asymptotic method for single and multifrequency oscillations of quasi-linear control systems with distributed parameters and delayed time coordinate

11 p1916 A69-24766

Shell theory foundations and basic equations, discussing classical shell equations asymptotic nature and errors

11 p1978 A69-24808

Asymptotic methods for three dimensional equations in thin and thick elastic shell theory for determining two dimensional systems

11 p1978 A69-24810

Asymptotic series solutions for initial value problem involving nonlinear ordinary differential equation with small parameter epsilon

11 p1908 A69-24881

Asymptotic theory for obtaining nearly free molecular flow solutions uniformly valid throughout flow field based on linearized Boltzmann equation

11 p1818 A69-25283

Initial conditions estimation problem for nonlinear system asymptotic stability and satisfaction of output constraints on state variables

11 p1909 A69-25290

Mathematical model for initial conditions of asymptotically stable nonlinear control system to estimate region of acceptable motions

11 p1861 A69-25453

Nonstiffness of nonshallow spherical dome using asymptotic method, applying nonlinear Reissner equations to finite symmetric deformation of thin shells of revolution

11 p1996 A69-25733

Axisymmetric problem of stress in elastic space weakened by plane annular slit solved by asymptotic method in terms of equations for parameter lambda

11 p1996 A69-25735

Asymptotic controllability of linear system, giving stabilization procedures based on solutions to limiting differential equations

12 p2053 A69-26515

Asymptotic stability inferred by examining higher order derivatives of Liapunov function, noting application to learning and adaptive control

12 p2122 A69-26522

Enclosures for large eigenvalues of ordinary second and fourth order differential equations based on asymptotic solutions of linear homogeneous second order differential equations

12 p2124 A69-26892

Matched asymptotic expansions to obtain slider bearing load carrying capacity [ASME PAPER 68-LUBS-18]

13 p2266 A69-27270

Free and forced vibrations of elastic layer, using iteration procedure based on asymptotic integration of linear theory of elasticity dynamic equations

13 p2363 A69-28126

Autonomous and nonautonomous transient processes in conservative and nonconservative nonlinear systems, deriving equations describing perturbations under loads, solving by asymptotic method

13 p2300 A69-28529

Homogeneous finite automaton asymptotic analysis, calculating series terms for matrix transition probability function

13 p2239 A69-28535

Asymptotic control theory for two point boundary value problems, considering Euler equation

14 p2425 A69-28904

Statistical synthesis of optimal control for quasi-harmonic systems by extending asymptotic method to include unremovable measurement error in output value

14 p2426 A69-29420

Asymptotic power series solutions of viscous solar wind equations

14 p2515 A69-29969

Sufficient conditions for asymptotic stability of motion in finite and whole of nonlinear systems by Liapunov second method

15 p2652 A69-30660

Asymptotically almost periodic solutions of almost autonomous differential equation

15 p2645 A69-31096

Asymptotic Krylov-Bogoliubov methods application to solving boundary value problems for hyperbolic quasi-linear equations with distributed parameters and retardation

15 p2653 A69-31192

Asymptotic solutions of optimum control for systems with constraints as linear differential equations and quadratic type functional

15 p2583 A69-31234

Asymptotic Liapunov stability of perturbed solutions to weakly coupled multifrequency systems

15 p2654 A69-31258

Stability and asymptotic stability theorems related to Liapunov second method, considering linear differential equations zero solution

15 p2654 A69-31259

Numerical analysis of asymptotic solution for earth-moon particle trajectories in idealized restricted three body problem

16 p2857 A69-32155

Asymptotic solutions to second order differential equations with slowly varying parameters and large resistance applied to mathematical pendulum damped swinging motion

16 p2804 A69-32253

Isolated symmetric doubly asymptotic solutions existence in neighborhood of symmetric periodic solutions of nonautonomous canonical system with one degree of freedom near resonance

17 p2996 A69-33619

Asymptotic solutions for vector fields and propagation constants of axial modes in circular cylindrical waveguides, noting changes in dielectric constant

17 p2921 A69-33673

Asymptotic series expansion for solutions of differential equations containing parameter

18 p3163 A69-34328

Parametric variations of nonlinear system moving in medium with nonlinear drag, using Bogoliubov-Krylov asymptotic method

18 p3171 A69-34564

Asymptotic form of axisymmetric solution with Dirichlet integral for Navier-Stokes equations applied to flow past bodies of revolution with smooth surfaces

19 p3298 A69-36143

Space transitions identified with asymptotic solutions at system field equations transition points

19 p3445 A69-36811

Asymptotic evaluation of complex frequency integrals in theory of radiation from transient sources in

dispersive media, interpreting results in terms of space-time rays

20 p3494 A69-37841

Asymptotic method for analyzing small long wave perturbations in plasma, showing instability with respect to perturbations propagating at angles to ion-acoustic wave

20 p3582 A69-38005

Asymptotic integration method of nonlinear elasticity equations for first approximation theory of anisotropic plates moderately large deflections

20 p3630 A69-38129

Asymptotic solution, existence and uniqueness of integral equations occurring in elasticity theory and mathematical physics

21 p3772 A69-39618

Geomagnetic field and aerodynamic perturbation effects on satellite motion about center of mass, using asymptotic methods of nonlinear oscillation theory

21 p3830 A69-39835

Oscillations of highly viscous incompressible fluid in partially filled cavity of body moving about fixed point, solving Navier-Stokes equations by asymptotic method

22 p3929 A69-40111

Asymptotic methods for differential equations containing parameter, discussing reduction to integral equations system

22 p3976 A69-41124

Analog problem solution for semiinfinite medium with Newtonian cooling at boundary, noting first term of asymptotic expansion in heat conduction equation

22 p4052 A69-41126

Motion equations of quasi-linear nonautonomous systems with many degrees of freedom, obtaining periodic solutions by asymptotic integration

23 p4183 A69-42477

ASYMPTOTIC SERIES

Three dimensional flow at large distance and in front of shock wave for three dimensional body traveling at sonic velocity

01 p0005 A69-10159

Asymptotic and approximate waves constructed for system of nonlinear partial differential equations for phases corresponding to multiple characteristics

02 p0271 A69-12034

Uniform asymptotic expansion series for saddle point integrals applied to probability distribution in noise interference problems

03 p0398 A69-13832

Asymptotic expansion for transonic flow of viscous fluid at great distance from plane obstacle

04 p0544 A69-15057

Asymptotic expansion of solution to linear singular perturbation problem of elliptic type in bounded strictly convex domain

05 p0786 A69-15928

Space-time diffraction for asymptotic solution of Klein-Gordon equation, studying one dimensional dispersive medium

05 p0802 A69-15930

Matched asymptotic expansions for establishing relationship between inner and outer expansions of unknown function, discussing classes of singular perturbation

07 p1180 A69-18809

Uniform matched asymptotic approximations derived for various functions, with application to boundary value problem for ordinary differential equation with turning point

07 p1180 A69-18810

Asymptotic expansions of solutions to non-homogeneous differential equation with perturbation

14 p2471 A69-29680

Asymptotic series expansion for solutions of differential equations containing parameter

18 p3163 A69-34328

Asymptotic behavior of solution to parabolic equation for t approaching infinity, proposing asymptotic formula to Cauchy problem for heat conduction

18 p3231 A69-35310

Boundary layer development on body accelerating in viscous incompressible fluid, using straight lines approximation and asymptotic expansions

22 p3929 A69-40110

Free viscous layers structure at large Reynolds numbers, using matched asymptotic expansions for two dimensional compressible flow

22 p3932 A69-40927

Asymptotic approximation formulas to compute on-axis Fresnel region fields for coupling between two large aperture antennas

23 p4136 A69-41582

ATELECTASIS

Atelectatic and direct toxic effects of oxygen on human subjects
22 p3873 A69-40208

ATHLETES

Hypokinesia effect on dynamics of metabolic processes in athletes muscular system by comparison of diuresis, creatinine excretion and cutaneous fat layer indices
10 p1646 A69-23582

ATHODYDS

U RAMJET ENGINES

ATLANTIC OCEAN

Aeromagnetic profiles across Reykjanes ridge southwest of Iceland, noting magnetic anomalies symmetry and ocean floor spreading since Mesozoic
04 p0592 A69-14660

Potential gradient, small ion density and space charge density measurements for atmosphere on Atlantic Ocean during 1965
04 p0594 A69-15159

Aircraft reports of clear air turbulence over North Atlantic, discussing jet stream proximity and large amplitude ridge associated with occlusion point
08 p1345 A69-19885

Navigation accuracy and telecommunications system capacity interrelationships in economical improvement of air traffic control system over North Atlantic
10 p1723 A69-23704

Satellite networks for air traffic control and aircraft communications in North Atlantic
13 p2296 A69-27831

North Atlantic aircraft navigation and traffic control system using satellites
16 p2809 A69-32054

Long range weather forecasts attempt from relation between northern Atlantic Ocean water temperature anomaly and monthly satellite cloud data changes
20 p3569 A69-36987

ATLAS CENTAUR LAUNCH VEHICLE

Atlas/Centaur/Surveyor flights guidance accuracy, discussing postflight analysis of injection errors due to hardware, software and propulsion system
[AIAA PAPER 68-842] 24 p4348 A69-43239

ATLAS SLV-3 LAUNCH VEHICLE

Mission analysis for 1972 Venus launch opportunity, discussing launch period selection and trajectory constraints for Atlas/Centaur vehicle
[AAS PAPER 68-135] 21 p3805 A69-39208

ATMOSPHERIC ATTENUATION
NT AURORAL ABSORPTION

Atmospheric temperature and airglow spectra from IR measurements noting OH bands, atmospheric structure between 10 and 200 km at midlatitude and atmospheric absorption
[UN PAPER 68-5471] 01 p0108 A69-10464

Signal absorption in negative ionospheric ions effect on maximal frequency for space radio communication
[UN PAPER 68-95272] 01 p0029 A69-10529

Radar reflectivity and refractive index spectra in clear atmosphere simultaneously measured and compared with theoretical calculations
01 p0032 A69-10969

Stellar brightness attenuation in atmosphere, determining extinction factor using computer calculations
01 p0157 A69-11192

Radio telescope measurements of total vertical atmospheric absorption to determine effective mean free path of oxygen and water vapor for absorption
02 p0206 A69-11450

Performance characteristics of 300 GHz Dicke type superheterodyne radiometer receiver for measuring atmospheric attenuation of electromagnetic waves
02 p0209 A69-12336

Radiometric measurement of attenuation, emission and noise fluctuations due to earth atmosphere in 4 cm to 8 mm range
02 p0210 A69-12432

Ionospheric absorption measurements using beacon satellite emission compared to Kazantsev results
02 p0246 A69-12742

Vertical atmospheric turbidity distributions of haze and water vapor, noting effect of variations on scattering and absorption determination
02 p0277 A69-12777

Digital transmission at 35 GHz, noting atmospheric and rainfall effect on terrestrial millimeter wave propagation
03 p0389 A69-13192

Atmospheric limitations for laser communications, discussing scattering and absorption effects
03 p0389 A69-13193

Absorption as factor influencing correlation between solar activity, sporadic E layer probability of occurrence and reflection stability
03 p0423 A69-13537

Telluric lines halfwidth and depth dependence on observation point altitude and intervening air mass, determining absorption line contours for isothermal atmosphere
03 p0512 A69-13695

Graphical data on atmospheric and rainfall attenuation of spacecraft earth signal, emphasizing transmission via satellites
03 p0397 A69-13727

Submillimeter wave observation of sun to study anomalous absorption region
03 p0513 A69-13774

Visible light extinction properties of continental and maritime air, probing urban, desert and oceanic atmospheres with stable photodiode radiometer
04 p0596 A69-14280

Absorption effect on fluctuation of signal level propagating in turbulent atmosphere taking into account absorption in water vapor
05 p0717 A69-15634

Frequency dependence of atmospheric noise intensity from 1 to 1000 kHz at low and medium latitudes
05 p0758 A69-16410

Atmospheric turbidity coefficient distribution in Northern Hemisphere from direct solar radiation measurements, noting application to IGY data
05 p0789 A69-16585

Atmospheric IR spectral transparency measurement, describing optical system, recording devices and data processing
05 p0759 A69-16639

Submillimeter wave absorption by dimeric water in atmosphere, using interferometer and maser
05 p0759 A69-16658

Atmospheric noise at 33.5 GHz observed most on days of cumulus clouds probably due to local convective activity
05 p0721 A69-16661

IR radiation attenuation in transparency windows of atmosphere, using searchlights as radiation sources
05 p0760 A69-16695

Radio astronomical methods for total atmospheric absorption of radio waves by atmospheric thermal radio emission measurements based on sky brightness temperature
05 p0723 A69-16779

Australian sounding rocket programs carried out in conjunction with U.S. satellite experiments
[UN PAPER 68-95214] 06 p1013 A69-17076

VHF space communication signals with radio fluctuations along propagation path through turbulent atmosphere, giving diversity reception effect when transmitting linearly polarized waves
06 p0889 A69-17653

Cosmic radio noise absorption in ionosphere, discussing diurnal, seasonal and longer variations of integral absorption
06 p1008 A69-17727

Radio emission and microwave absorption spectrum dependence on physical properties of clouds in millimeter and centimeter wavelength range
06 p0954 A69-17998

Radio wave absorption measurements in atmosphere at superhigh frequencies, considering earth radiation, antenna sidelobes anisotropy, instrument effects, etc
07 p1076 A69-18518

Atmospheric extinction coefficient and backscattering function determined by laser radar using differential equation
07 p1126 A69-18966

Qualitative criterion for observing atmospheric turbulence structure by shadowgraph based on medium statistical properties, using ray optics
07 p1183 A69-19650

Energy dissipation of solar particles in atmosphere for 3914 and 5577 Å bands, computing light emissions associated with PCA
08 p1378 A69-20186

Atmospheric turbidity and visibility measuring instrument /videograph/ using light backscattering, noting shipboard, coast guard service, large cities and weather stations applications
08 p1314 A69-20376

Light intensity dispersion logarithm calculated along axis of laser beam propagating in atmosphere
08 p1351 A69-20437

Atmospheric effects on laser beam attenuation, noting application to optical visibility measurement by ruby laser
08 p1327 A69-21089

Propagation and noise effects on frequency choice for communication satellite service to aircraft and ships, noting tropospheric and ionospheric attenuation considerations
09 p1451 A69-21288

Albedo over Antarctic, measuring solar radiation reflected by surface and atmosphere by Eppley radiometer
09 p1484 A69-21404

Spectral distribution of X ray atmospheric absorption used to determine high energy photoelectrons spectrum
09 p1577 A69-21774

Solar radiation absorption measurements by balloon for atmospheric water vapor distribution
09 p1536 A69-21864

Atmospheric propagation properties of laser light, discussing particle absorption, gaseous absorption and refractive index disturbance effects
09 p1518 A69-22129

Asymmetrical solar wind volume variations of magnetic inhomogeneities and cosmic ray absorption in earth atmosphere, including barometric coefficients of neutron component
10 p1760 A69-22844

VHF space communication signals with radio fluctuations along propagation path through turbulent atmosphere, giving diversity reception effect when transmitting linearly polarized waves
10 p1775 A69-23191

Vertical atmospheric absorption of radio waves by water vapor and oxygen molecules near rotational resonance based on radio emission measurements
10 p1658 A69-23944

Millimeter wave propagation over water, discussing fading characteristics and atmosphere absorption effects
11 p1836 A69-24989

Atmospheric interference effects on optical PCM signal, analyzing absorption, beam bending, scintillation and correlation with visibility and weather
11 p1888 A69-25308

Air movement component of winter anomaly effect on radio wave absorption in mesosphere directly detected by rocket sounding
11 p1913 A69-25436

Radiation attenuation in hazy lower atmosphere, calculating attenuation coefficients and using spherical model of haze particles and empirical formula for haze spectra
11 p1913 A69-25571

Laser radiation transmission in atmosphere examined for information transmission applications
11 p1841 A69-25638

Calculation method for electromagnetic wave supplementary attenuation due to auroral absorption for distances up to 4000 km
11 p1841 A69-25760

Fading velocity short period characteristics and duration and depth of field strength variations over transhorizon path compared with corresponding atmospheric parameters
12 p2028 A69-25897

Atmospheric boundary layer transparency to gas laser emissions in IR spectrum, determining attenuation factor dependence on humidity and visibility range
12 p2028 A69-25957

Molecular O and total number densities between 70 and 120 km determined with rocket measurements of atmospheric absorption of solar UV and X rays
12 p2065 A69-26106

IR absorptance data for atmospheres of ammonia and ammonia nitrogen mixtures at various wavelengths indicating absorption in strong line region for gas pressures used
12 p2132 A69-26247

Shapes of extreme wings of collision-broadened carbon dioxide lines, noting absorption deviation from Lorentz-shaped lines
12 p2132 A69-26248

Refractive index and attenuation factor of ionosphere
12 p2070 A69-26689

Atmosphere effects on solar IR spectra, discussing role of absorbing molecule distribution in transmittance calculations
13 p2341 A69-27589

Atmospheric attenuation of solar radiation, discussing submillimeter astronomy at low altitude observatories
13 p2327 A69-27590

Nuclear explosions electromagnetic effects on electronic systems, considering signals emitted from

fireball and signal attenuation by changed atmospheric propagation

13 p2234 A69-28344

F cosine i theorem validity for VLF radio wave absorption in ionosphere tested using exponential electron density models, noting Brewster angle influence on reflection coefficient

13 p2222 A69-28473

Troposphere effects on millimeter wave radio astronomy measurements, discussing solar noise fluctuations due to clouds and precipitation

13 p2223 A69-28607

Atmospheric LF and HF sound transmission anomalies, discussing Tyndall paradox for fog signals propagation over ocean

13 p2301 A69-28666

Atmospheric IR spectral transparency measurement, describing optical system, recording devices and data processing

14 p2433 A69-28795

Latitudinal cut-off of manmade VLF signals in short path through ionosphere to OGO 2 satellite, noting strong noise following signal cut-off

14 p2434 A69-28958

Nighttime molecular O densities between 100-130 km determined from Schumann-Runge absorption data for successive far UV spectra of hot star

14 p2435 A69-28959

Noon ionospheric absorption data for Freiburg on different frequencies for lunar variation of ionospheric absorption of radio waves

14 p2438 A69-29104

Functional relations expressing short wave radiation absorption and scattering in atmosphere

15 p2648 A69-30222

Remote polarized light source photometric observation on background of polarized light scattered horizontally, considering atmosphere optical state effect on laser communications

15 p2649 A69-30655

Submillimeter atmospheric absorption spectra, emphasizing absorption by isotopic and vibrationally excited forms of water molecules

15 p2568 A69-30699

Corpuscular radiation intensity during geomagnetic disturbances measured during rocket flights at 50-100 km, discussing effects on lower ionospheric radio absorption

15 p2677 A69-31327

Auroral absorption influence on ionospheric wave propagation calculated for distances over 4000 km

16 p2749 A69-31603

Atmospheric absorption calculations, noting direct D layer reflection effects on lower HF oblique propagation

16 p2752 A69-32389

Absorption effect on fluctuation of signal level propagating in turbulent atmosphere taking into account absorption in water vapor

16 p2754 A69-32492

Atmospheric extinction determined by monochromatic photometry in Chile in 3000 to 6000 A range, discussing components

17 p3031 A69-33100

Attenuation statistics due to rain measured on earth-space path at 16 and 30 GHz, using sun as signal source

17 p2920 A69-33398

Photoelectric spectra of pulsating auroras in visible and near UV range, considering atmospheric opacity

17 p2961 A69-33416

Cosmic ray heavy nucleus enders flux by nuclear emulsions for balloon flights at various atmospheric depths

17 p3025 A69-34219

Star magnitude variation caused by earth atmosphere related by equation to star altitude, station height, sensor response, spectral radiance, etc

18 p3168 A69-34814

High temperature air spectral absorption indices determined at different pressures and temperatures

18 p3231 A69-35122

Water vapor absorption at submillimeter wavelengths in atmospheric window regions related to foreign gas pressure, using HCN maser

18 p3152 A69-35241

Aircraft measurements of scintillation of ground based light source, calculating autocorrelation functions and intensity fluctuations spectra

19 p3279 A69-36881

A scope laser radar to measure atmospheric particles spatial distribution through echo pattern and beam attenuation

20 p3487 A69-37284

Maser submillimeter emission lines used to determine atmospheric and water vapor absorption, noting role of pressure

20 p3553 A69-37296

Mesosphere and lower thermosphere molecular O density from solar radiation atmospheric absorption, using satellite measurements

20 p3523 A69-37413

Residual nighttime radio wave absorption in ionosphere, noting absorption-magnetic activity relation existence

20 p3528 A69-37678

Atmospheric ozone detection by three-color photometer measurements of solar UV radiation attenuation in Hartley continuum

20 p3543 A69-37802

Space contamination due to manned vehicles and debris atmosphere effects on dim light source observations

21 p3793 A69-38341

Atmospheric transmission determined in submillimeter solar radiation spectra using Bouguer law, identifying absorption lines in nocturnal and diurnal spectra

21 p3796 A69-38472

Earth resources observation technology from satellites, reviewing sensors and methods, electromagnetic spectrum, atmospheric attenuation and windows, passive-active devices

21 p3720 A69-38624

Ozone measurement from satellite by direct beam and scattered light methods employing UV sunlight attenuation

21 p3721 A69-38625

Molecular O distribution in thermosphere from Ariel 3 observations of solar radiation attenuation, showing large and systematic variation with longitude

21 p3717 A69-39263

Daily simultaneous solar measurements of microwave atmospheric absorption and emission to determine frequency correlation between meteorological phenomena and atmospheric parameters

21 p3718 A69-39747

Atmospheric ionization rates due to attenuation of 1-100 A nonflare solar X rays, giving solar fluxes and absorption cross sections

22 p4004 A69-40447

Rocket UV spectra indicating Venus atmosphere weak absorption and low ozone abundance and possible Jupiter surface depressions

22 p4028 A69-40661

Planetary atmosphere effect on Fresnel diffraction of ultrashort radio waves determined from short wave approximation of damping function

22 p3901 A69-40948

Absorbed dose and dose equivalent radiation rates at various depths in atmosphere due to proton spectrum of energetic solar flare

23 p4204 A69-41337

Zenith atmospheric attenuation in 183-325 GHz region measured by wideband Ge bolometer detector and spectral convolution technique

23 p4115 A69-41586

Pure water vapor and water vapor-air mixture continuum absorption of carbon dioxide laser radiation measured to determine atmospheric attenuation

23 p4173 A69-41631

EHF earth-satellite link communication channel emphasizing down link, discussing weather models, atmospheric absorption and temperature, channel coherence bandwidth, etc

23 p4129 A69-42506

Absorption observation of solar radiation at sunset by nitric acid in three wavelength intervals on different balloon flights

24 p4308 A69-42969

Solar grazing ray absorption calculated by tracing through earth atmosphere, noting extinction for arbitrary ozone and aerosol profile

24 p4350 A69-43013

ATMOSPHERIC CHEMISTRY

Initial production of metallic gases associated with sporadic E layers by processes other than vaporization or photodissociation, discussing Na atom production mechanisms

01 p0071 A69-11167

Metal ionic reactions with weak chemical bond breaking and three body reactions forming molecular ions without bond breaking, discussing sporadic E deionization

01 p0071 A69-11168

Upper atmosphere structure, phenomena and composition, discussing interactions between photons, electrons, atoms and molecules

02 p0242 A69-11902

Photochemistry in dry atmosphere, discussing ozone density vertical distribution in upper atmosphere and influence of O and ozone reactions with H compounds

02 p0245 A69-12694

Atmospheric ozone photochemistry, studying time dependence on hydrogen compounds, equilibrium concentration effects on reaction rates, latitude and season

06 p0916 A69-17004

Evening twilight nitric oxide density profile in gamma bands deduced from rocket measurements

07 p1125 A69-18842

Chemical abundances in planetary atmospheres based on spectroscopic determinations, considering terrestrial and Jovian planets

08 p1406 A69-20934

Photochemical production of reduced organic compounds of C and N in primitive earth atmosphere

09 p1444 A69-21465

IR day and night airglow of upper atmosphere utilized for atmospheric energy content and reactions analysis

13 p2252 A69-27585

Ion chemistry of D and E regions to be studied during years of solar maximum in framework of IQSY/IUCSTP

14 p2439 A69-29111

Corrosive wear due to atmospheric O in sliding metal systems, noting oxidation rate relation to wear rate and activation energy

15 p2622 A69-30605

Molecular oxygen rate of dissociation resulting from absorption in Schumann-Runge bands, calculating effects on chemistry of lower thermosphere and upper mesosphere

20 p3534 A69-38089

ATMOSPHERIC CIRCULATION

CRT method of processing contoured data from hemispheric and global numerical models simulating general atmospheric circulation

01 p0109 A69-10539

Objective layer of maximum wind /LRMW/ analysis technique for Northern Hemisphere jet stream, noting generation of initial guess fields

01 p0110 A69-10689

Wind profile harmonic analysis based on meteor trail observations, noting wind power spectra and propagating waves in atmosphere

01 p0072 A69-11170

Midlatitude ionospheric wind profiles noting seasonal and time differences in circulation patterns, speed, shear, wavelength, energy content and dissipation

01 p0072 A69-11171

Solitary mesoscale waves from air mass motion in troposphere, neglecting Coriolis force and turbulence

02 p0274 A69-11445

Wind perturbations characteristics near large convective cloud banks as function of ascending current, wind shear and turbulence

02 p0274 A69-11446

Atmospheric circulation influence on earth rotation velocity, discussing estimation methods

02 p0236 A69-11641

Free atmospheric turbulence theory extended to include ionosphere, deriving equations for horizontal ionospheric wind together with turbulence coefficient

02 p0274 A69-11678

Atmospheric circulation on rotating and nonrotating planets with shallow atmospheres applied to Mars and Venus atmospheres

02 p0320 A69-12110

Taylor column existence in compressible atmosphere, discussing baroclinicity and stratification effects in earth and Jupiter atmospheres

02 p0326 A69-12697

Zonal temperature and spectral characteristics of stratospheric circulation, noting westward rotation of second harmonic

02 p0246 A69-12759

Air movements in lower stratosphere analyzed on basis of ozone measurements, showing correlation with north-south gradient of total ozone amount

02 p0246 A69-12762

Factors producing wind deviations from geostrophic pattern under various atmospheric conditions

03 p0458 A69-13267

Planetary long waves behavior in atmospheric models, explaining unsteady components by means of filtered equations

03 p0459 A69-13274

Mean meridional circulation models in tropics based on vorticity equation

03 p0460 A69-13334

Planetary Rossby waves vertical propagation through weak westerly wind wave guides, using adiabatic linear model

03 p0460 A69-13335

Thermal convection in rotating fluid annulus, discussing suppression of frictional constraint on lateral boundary

03 p0460 A69-13339

Quasi-biennial oscillation in tropical stratosphere as result of long period gravity waves interaction with zonal wind

03 p0461 A69-13342

Large scale disturbances in summertime stratosphere observed from high level balloon, discussing diurnal wind patterns and planetary traveling waves

03 p0461 A69-13343

Ekman-Okkerblom problem for electrically conducting atmosphere located in external magnetic field, obtaining altitude distribution for wind velocity components

03 p0461 A69-13510

Diurnal upward and downward flows of atmospheric matter following upper atmosphere temperature nighttime minimum and daytime maximum

03 p0423 A69-13533

Long period variations in zonally symmetric circulations of tropical stratosphere, using zonally averaged momentum, continuity and heat and heat energy equations for numerical model

03 p0461 A69-13681

Thermal forcing role in diurnal oscillation of planetary boundary layer wind above sloping terrain

03 p0462 A69-13682

Sufficient conditions for stability of compressible atmospheric flows for rigid lid types of upper boundary condition

03 p0417 A69-13796

Hydrodynamic model of atmospheric circulation in equatorial region, using group invariant method

03 p0462 A69-13931

Lateral transport of constituents in planetary exospheres, considering planetary rotation

03 p0515 A69-14010

Gravity wave contribution to atmospheric wind motion at 100 km

03 p0426 A69-14031

Covariances of temperature and meridional wind component and relation to northward flux of sensible heat due to transient eddies in stratosphere

04 p0627 A69-15084

Mean meridional pressure profiles and atmospheric mass readjustment time dependence for initially at rest atmosphere with mean baroclinity, using frozen gradient model

04 p0627 A69-15086

Digital computers for global atmospheric circulation, describing circulation models and computer produced color movies utilization

04 p0628 A69-15363

Rocket and radiosondes data from measurements over Northern Hemisphere used to study stratospheric and mesospheric circulation during three midwinter periods

05 p0753 A69-15800

F region seasonal and magnetic storm behavior from region daily behavior showing global upper atmospheric circulation

05 p0757 A69-16404

General atmospheric circulation characteristics estimation for earth, Mars, Venus and Mercury based on thermodynamic and hydrodynamic laws

05 p0828 A69-16635

Energy integral of equations used in studying atmospheric motions in quasi-geostrophic approximation

05 p0759 A69-16641

Satellites role in observing and forecasting global atmospheric behavior, discussing World Weather Watch and Global Atmospheric Research Program

06 p0916 A69-16854

Wind data from Arctic upper mesosphere showing easterly winds increasing with height, resolving diurnal and semidiurnal oscillations

06 p0949 A69-17005

Curvilinear plasma motions in ionosphere same as cyclones and anticyclones in troposphere, solving ionospheric unstable wind as function of pressure gradients

06 p0919 A69-17722

Time dependent model of photochemical, advective and turbulent effects on meridional ozone distribution

07 p1122 A69-18253

Mars polar cap ice cap and dry ice theories, discussing dark wave and cloud distribution meteorological observations

07 p1212 A69-18603

A-130

Jupiter Red Spot vorticity at perimeter indicated by interaction with dark spots circulating along south equatorial belt

07 p1213 A69-18606

Dynamics of large scale processes in atmosphere extended to two week predictions using nine level hemispheric moist general circulation model

07 p1175 A69-18895

Atmospheric circulation intensity measurement, using potential energy conversion to kinetic or kinetic energy dissipation by friction

07 p1175 A69-18947

Constant level sounding balloon systems providing global data on atmospheric circulation, discussing icing problems and average life improvement

07 p1053 A69-18955

Similarity of mean flow patterns of natural local wind to model wind in wind tunnel

07 p1176 A69-18964

Large scale tropical eddies using two layer dry atmospheric model containing nongeostrophic effects and parameterized dissipation

07 p1176 A69-19035

Planetary wave-zonal flow interaction interpretation in terms of potential vorticity eddy transport, deriving zonal wind change and temperature field

07 p1126 A69-19037

Response of stably stratified atmosphere to differential heating across coastlines

07 p1126 A69-19038

Wave motion onset and waveforms in rotating annulus with sinusoidally varying temperature differences

07 p1126 A69-19039

Coupling and other factors affecting large scale motions in tropics

07 p1176 A69-19045

Eole satellite and meteorological balloons telecommunications. used to study wind distribution in Southern Hemisphere and other atmospheric parameters

07 p1084 A69-19134

Interhemispheric transfer of atmospheric angular momentum, noting hemispheric angular momentum contents and annual variations

07 p1127 A69-19258

Two level quasi-geostrophic model to probe atmospheric general circulation, noting functional dependence of zonal momentum meridional flux

08 p1346 A69-20314

Mean and eddy terms contribution to momentum and heat balance of troposphere and lower stratosphere at solstices, describing zonal wind equations

08 p1308 A69-20318

Unsteady atmospheric motions on planetary scale using Legendre polynomials

08 p1311 A69-21158

Power spectral analysis of upper wind data of equatorial lower stratosphere noting quasi-biennial oscillation

09 p1537 A69-22297

Zonal momentum vertical transport due to large scale moving disturbances in westerlies of equatorial lower stratosphere

09 p1537 A69-22299

Ionospheric movements from sampling radio diffraction pattern at 89 points and conversion into visible pattern

09 p1492 A69-22756

Long and ultralong waves in baroclinic zonal current, investigating current stability and wave perturbation characteristics by applying linearized perturbation equations to multilayer model

10 p1682 A69-23325

Venus atmosphere radial mass velocities measured spectrographically with Fabry-Perot interferometer, noting retrograde rotation

10 p1778 A69-23409

Particulate radioactivity for study of stratospheric motions, demonstrating negligible long time particle settling with comparative measurements of particulate Sr 90 and gaseous C 14

10 p1682 A69-23410

Thomson scatter bistatic sounder data on ionization transports in F region, describing diurnal variations by hourly values of velocities

10 p1685 A69-23830

Atmospheric circulation contribution to velocity variations in earth rotation calculated by force moment method

11 p1952 A69-24258

Pacific atmospheric circulation and Pacific equatorial sea temperature winter anomalies, noting Hadley circulations, northeast westerlies, trade winds and Walker circulation

11 p1911 A69-24322

Mean and eddy motions in atmosphere described by mathematical expressions for total and mean kinetic energies

11 p1911 A69-24323

Meteorological rocket probes in Spain for wind and temperature measurements, including stratospheric circulation data

11 p1877 A69-24519

Stability of barotropic perturbations superimposed on wind velocity profile of basic currents in geostrophic multilayer models

11 p1911 A69-24586

Air movement component of winter anomaly effect on radio wave absorption in mesosphere directly detected by rocket sounding

11 p1913 A69-25436

Jet flows instabilities with vertical and horizontal velocity drifts from numerical integration of atmospheric motion equations linearized with respect to small perturbations

12 p2125 A69-25950

Zonal and meridional wind components monthly global cross sections for stratosphere and mesosphere from sounding and radar data

12 p2070 A69-26577

Neutral gas motions causing plasma motions in F region, obtaining vertical plasma velocity component pronounced diurnal variations

12 p2070 A69-26684

Oscillation cycle of atmospheric circulation, analyzing solar activity effects on lunar and solar semidiurnal tides and transition from zonal to meridional circulation

12 p2070 A69-26692

Wind structure in atmosphere meteor region from persistent meteor trail radio echoes amplitude fluctuations, noting horizontal wind velocity profiles

12 p2074 A69-26962

Air mass displacements and diurnal variations in potential temperature at tropopause level

13 p2252 A69-27608

Blocking processes synchronous development involving atmospheric circulation disturbances in Northern and Southern Hemispheres, noting localization in Pacific and Atlantic oceans

13 p2292 A69-27840

Wind shifts and mean gustiness calculation from short range weather forecasts, using dynamic model for wind motion in atmospheric boundary layer

13 p2293 A69-27844

Atmospheric pressure and wind data at equatorial latitudes, determining relation between rms meridional and zonal wind and pressure gradient

13 p2293 A69-27845

Hydrodynamics of large scale atmospheric circulation, analyzing interactions between different scales and between atmosphere and underlying surface

13 p2253 A69-27849

Latitudinal and vertical variations in six-month zonal wind cycles in equatorial and tropical stratosphere and lower mesosphere, utilizing rocket observations

13 p2294 A69-27854

Mesopause wind measurements at high latitude locations by sounding rockets noting relation to noctilucent clouds

13 p2294 A69-28466

Mean seasonal atmospheric and synoptic circulation types examined by criterion for identifying analog types

13 p2295 A69-28652

Free atmospheric turbulence theory extended to include ionosphere, deriving equations for horizontal ionospheric wind and turbulence coefficient

13 p2295 A69-28709

Planetary long waves behavior in atmospheric models, explaining unsteady components by means of filtered equations

14 p2472 A69-28782

General atmospheric circulation characteristics estimation for earth, Mars, Venus and Mercury based on thermodynamic and hydrodynamic laws

14 p2516 A69-28791

Energy integral of equations used in studying atmospheric motions in quasi-geostrophic approximation

14 p2433 A69-28797

Three dimensional model of atmospheric drift currents in equatorial region of world ocean system based on nonlinear differential equations

14 p2472 A69-29405

Collection of Soviet papers on planetary atmospheric circulation covering tropospheric and stratospheric temperature distribution, cloud patterns, wind fluctuations, etc

14 p2472 A69-29723

Equatorial stratospheric wind fluctuations from pressure fluctuation data, relating southern fluctuations,

stratospheric fluctuations and seasonal hemispheric air exchange

14 p2442 A69-29726

Soviet collection of articles on aviation forecasting of cloud cover, high altitude wind and turbulence

14 p2473 A69-29734

Soviet collection of papers on general circulation of atmosphere

14 p2475 A69-29818

Hydrodynamic theory of climate and atmospheric circulation, emphasizing numerical experiments role in studying large scale processes

14 p2476 A69-29819

General atmospheric circulation instability factors for statistical weather forecasting, considering atmosphere as nonlinear oscillating system, analyzing relaxation time

14 p2476 A69-29820

Spatial correlation function of Northern Hemisphere geopotential, using model based on random distribution of potential vortex fluctuations for atmospheric circulation

14 p2476 A69-29822

Atmospheric circulation integral characteristics, calculating kinetic energy in Northern Hemisphere

14 p2476 A69-29824

Atmospheric circulation by energy concepts, giving quantitative analysis of interaction between upper and lower atmosphere

14 p2477 A69-29825

Radiation in atmospheric circulation, considering radiative equilibrium, cloudiness and surface interactions, surface temperature and heat input

14 p2477 A69-29826

Zonal and meridional components of air circulation in troposphere and lower stratosphere for Northern Hemisphere

14 p2477 A69-29829

Ozone concentration changes in polar regions and tropical zone due to meridional atmospheric circulation

14 p2442 A69-29830

Jet streams as indicators of atmospheric circulation, considering all altitude observance and dynamics-energetics aspects

14 p2477 A69-29831

Troposphere behavior and stratosphere structure over Southern Hemisphere based on rocket measurements, comparing hemispheric atmospheric circulation intensities

14 p2477 A69-29832

Two year cyclic monsoon type variations in zonal wind distribution in tropical stratosphere and mesosphere obtained by rocket measurements

14 p2478 A69-29834

Earth orography influence on climatological distribution of wind and geopotential fields, stressing central asiatic mountains role in atmospheric circulation

14 p2478 A69-29835

Secular fluctuations of atmospheric circulation over Northern Hemisphere analyzed using isobaric and composite-kinematic surface maps, discussing analogies with Southern Hemisphere

14 p2478 A69-29836

Epochs in atmospheric circulation development over Northern Hemisphere, emphasizing solar activity roles in epochs appearances

14 p2478 A69-29837

Atmospheric heat exchange and circulation simulated by rotating containers, reproducing temperature field and dynamic structure above large area

14 p2478 A69-29840

Atmospheric dynamics parameters of Mercury, Venus, Mars and Jupiter, discussing generalized circulation theory

14 p2526 A69-29841

Atmospheric motions equations in mesometeorology prognostic problems taking into account free atmosphere and boundary layer interactions

15 p2646 A69-30107

Large scale atmospheric wave motions analyzed by spherical harmonic representation of height fields over earth, detailing wave components and quasi-stationary fluctuations

15 p2647 A69-30216

Kinetic energy balance equation of mean zonal flow in symmetrical polar cap derived from basic concepts of mechanics, discussing relative coordinate system rotation

15 p2595 A69-30219

Energetics relations of limited atmospheric region to global energy budget, discussing interaction, potential energy, generation, boundary flux and conversion terms

15 p2648 A69-30220

Energy budget equations applicable to limited atmospheric region using available potential energy concept, discussing relation to global energy

15 p2648 A69-30221

Atmospheric motions on Jupiter, considering highly symmetric flow, baroclinic waves and red spot

15 p2694 A69-30856

Upper atmosphere winds and temperature measurements from rocket grenade, discussing TMA experiments

15 p2598 A69-31317

Average angular velocity of upper atmosphere from changes in orbital inclinations of satellites, discussing wind speeds

15 p2600 A69-31352

Seasonal and latitudinal models of atmospheric wind and temperature structure between 30 and 120 km altitude

15 p2600 A69-31367

Regional distribution of relative angular momentum transport over equator, noting advective and turbulent transfer

16 p2773 A69-31793

Pressure gradients and moving ions driven neutral-air winds in F region, using asymmetric pressure model

16 p2779 A69-32302

Combined midlatitude neutral air wind and equatorial electrodynamic drift effect on F 2 layer diurnal variations

16 p2781 A69-32316

Subsonic thermal convection or internal gravity waves from formal scale analysis of equations of motion in plane parallel atmosphere

17 p2960 A69-33155

Atmospheric stability influence on vertical spectra of refractive index and air velocity deduced from beam swinging experiments and compared with radiosondes data

17 p2960 A69-33157

Zonal flow intensity, velocity and kinetic energy of standing and traveling waves compared for Northern and Southern Hemispheres

17 p2997 A69-33392

Adiabatic and diabatic processes contributions to vertical atmospheric motions profile and IR cooling components comparison

17 p2962 A69-33689

Papers on experimental and theoretical research on atmospheric circulations, jetstream and cyclonic disturbances

17 p2999 A69-33757

Planetary jetstream and general circulation energy transformations, applying circulation model results to specific weather situations

17 p3000 A69-33758

Rocket and radiosondes data from measurements over Northern Hemisphere used to study stratospheric and mesospheric circulation during three midwinter periods

17 p2962 A69-33779

Space diversity reception and diurnal variations of F region ionospheric motions, comparing IQSY program

17 p2969 A69-33999

Tropical circulation long term mean values of wind and temperature fields, momentum and heat fluxes from weather stations data, noting consistent pattern and energy source

18 p3165 A69-34418

Air motion and precipitation patterns in travelling wave depression, considering Doppler radar data, rainfall rates, orographic influences, etc

18 p3166 A69-34419

Earth atmospheric large scale motion simulated in laboratory and by numerical technique

18 p3127 A69-34668

Atmospheric flow with respect to mesoscale disturbances, examining conditions for hydrodynamic stability

18 p3167 A69-35343

Numerical weather prediction using four level primitive atmospheric model for studying frontogenetic processes in deepening cyclone

19 p3303 A69-36408

Atmospheric horizontal mixing caused by quasi two dimensional macroturbulent motions, describing micro and mesoscale processes using numerical model

19 p3363 A69-36500

Numerical integrations for modified model incorporating ozone production equation and heating from ozone radiation absorption and long wave cooling for upper atmospheric circulation

19 p3363 A69-36502

Large atmospheric motions analyzed by elliptic partial differential equation and hydrostatic and quasi-geostrophic approximations

19 p3364 A69-36504

Numerical integration of atmospheric motion equations in global domain using hexagonal grid, including sphericity corrections and Coriolis term

19 p3364 A69-36509

Vertical atmospheric motions, considering wind velocity measurements associated with synoptic processes

19 p3366 A69-36673

Meridional circulations in kinetic energy budget of Northern Hemisphere troposphere based on winter and summer climatic mean data, noting Hadley circulation

20 p3523 A69-37505

Small scale inhomogeneities motions in E and sporadic E layers, processing data with method of full correlation analysis and statistical method

20 p3528 A69-37683

Radar observations of convective pattern types in clear atmosphere consisting of thermal- and Benard-like convection cells

20 p3573 A69-38059

Radial diffusion coefficient calculation in presence of magnetic shell splitting in magnetosphere

20 p3534 A69-38094

Circulation near turbopause effect on lower thermosphere composition changes, noting heat source for warmth over winter polar region

21 p3704 A69-38366

Upper atmosphere horizontal unsteady wind with pressure gradient time dependence, solving heat conduction type equation by integral representations

21 p3758 A69-38411

Midlatitude thermosphere vertical air motions to balance divergence and convergence caused by large scale horizontal wind systems

21 p3714 A69-38553

Venus, Mars and Jupiter lower atmospheric motions, considering atmospheres thermal and chemical composition

21 p3811 A69-39511

Martian atmosphere circulation compared to terrestrial, considering absence of oceans, radiative coupling and planetary scale motions

21 p3814 A69-39569

Circulation and temperature fields indices used for studying tropospheric-stratospheric interactions during stratospheric warming at constant pressure levels

22 p3977 A69-39929

Convective cells and periodic variations in vertical gradient of electroatmospheric field

22 p3934 A69-39939

Linear equations of motions of inviscid ideal gas atmospheres, describing climatology of propagation parameters for point impulse sources

22 p3938 A69-40446

Earth rotation rate variations connected to longitude variations of continentals time services, noting atmospheric circulation and inertial forces role

22 p4024 A69-40609

Long term computer produced multiple image satellite photomosaics for Southern Hemisphere, analyzing circulation, meridional bands, polar ice, cloud cover variations, etc

22 p3977 A69-40733

Radial velocity data monitored during Venera 4 descent used for determining vertical and horizontal atmospheric flows velocities

22 p4034 A69-41099

Atmospheric zonal circulation compatible with meridional obtained from model based on dynamic and heat flux equations and Williams and Davis hypothesis

23 p4183 A69-41522

Qualitative model of atmospheric mass circulation constructed from radar meteor trail drifts observations, considering solar thermal radiation and zonal wind direction

23 p4214 A69-41862

Cloud cover forms in circulatory-climatic zones of earth based on Zond 5 picture analysis, discussing air-mass exchanges and motions direction

23 p4184 A69-42486

Radiation contribution to large scale atmospheric mass circulation simulation, considering short wave radiation, temperature variations, exponential and aerosol attenuation

23 p4184 A69-42487

Atmospheric variability at proposed flight levels, analyzing meteorological requirements of SST operations, discussing annual cycles in stratospheric circulation

24 p4251 A69-42711

Mesospheric circulation related to noctilucent cloud data, discussing seasonal variations

24 p4307 A69-42965

Absolute atmospheric kinetic energy, comparing equations deduced from Euler equations with equa-

tions deduced from equations of motion for inertial system

24 p4345 A69-43151

Hadley and equatorial cell models for mean meridional circulation in terms of vorticity equation

24 p4345 A69-43152

Atmospheric model consisting of varied mass liquids in water tank for studying circulation conditions, discussing earth zone and layer partitioning and Prandtl analysis

24 p4346 A69-43153

ATMOSPHERIC COMPOSITION

NT IONOSPHERIC COMPOSITION

Optical radar for studying atmospheric water vapor, density, temperature and aerosols

01 p0090 A69-10540

Electron density and temperature, ion density, composition and temperature and plasma space potential relative to space vehicle potential measured by spherical probe assembly

01 p0065 A69-10549

Cosmic rays extensive air showers from interaction of particles with nuclei of elements in atmosphere

01 p0144 A69-10752

Chemical composition of upper atmosphere and interplanetary space measured by Soviet sounding balloons and rockets, discussing flask sampling techniques

01 p0025 A69-10940

Sporadic E structure and composition measured above White Sands by rocket-borne planar ion trap and two RF ion mass spectrometers

01 p0071 A69-11166

Initial production of metallic gases associated with sporadic E layers by processes other than vaporization or photodissociation, discussing Na atom production mechanisms

01 p0071 A69-11167

Light polarization properties in atmosphere noting aerosols effect

01 p0075 A69-11189

Twilight sky brightness measurements at 5200 angstroms for estimating upper atmospheric dust component, discussing error rates

01 p0075 A69-11191

Lower thermosphere neutral composition diurnal variations, noting molecular N and O, Ar, He and atomic O

01 p0076 A69-11231

Metal corrosion in atmosphere - ASTM Conference, Boston, June 1967

01 p0100 A69-11350

Titanium-base alloys resistance to atmospheric corrosion based on weight change measurements and tensile tests after multiyear exposures

01 p0100 A69-11351

Atmospheric stress corrosion tests of aluminum alloys in various environments, comparing aging results with accelerated laboratory tests

01 p0100 A69-11352

Long term atmospheric corrosion test program for aluminum and magnesium base alloys, comparing tensile strength of exposed and control specimens

01 p0100 A69-11353

Weathering tests on wrought aluminum alloys exposed at U.S. sites compared to British industrial atmospheric exposure results

01 p0101 A69-11354

Planetary atmosphere composition determination using mass spectrometry for neutral components, ion spectrometry for ionic components and data system optimization

[AAS PAPER 68-183] 02 p0247 A69-11468

Mariner 5 Venus Lyman alpha emission observations, noting atomic hydrogen and oxygen resonance radiation measurements and apparent presence of molecular hydrogen or deuterium

[AAS PAPER 68-220] 02 p0313 A69-11486

High sensitivity mercury vapor analysis automated to provide continuous monitoring of Hg in atmosphere, discussing winter and summer concentrations

02 p0244 A69-12019

Mars lower atmospheric pressure, temperature and composition, noting consistency between photometric, spectroscopic and occultation techniques

02 p0319 A69-12104

Photoelectron energy loss mechanisms in planetary atmospheres, considering possible constituents in Mars and Venus upper atmospheres

02 p0321 A69-12118

Venus atmospheric structure from surface to 20,000 km radial distance from Mariner 5 radio experiments, noting large mass-2 hydrogen component in upper atmosphere

02 p0330 A69-12802

Stellar image and spectrum distortions during occultation observed from satellite, discussing recovery of atmospheric composition data from stellar spectra

03 p0421 A69-13346

Electron temperature and concentration and solar UV absorption data from sounding rockets, estimating ion exchange rate, recombination coefficient and heat flux

03 p0422 A69-13508

Satellite drag data to determine upper atmospheric composition according to density distribution with height

03 p0423 A69-13532

Atmospheric gas composition effects on shock layer radiative heat transfer and heat shield response in Venus entry simulated by earth reentry

[AIAA PAPER 68-1148] 03 p0412 A69-13672

Lower thermosphere composition over New Mexico, discussing rocket flight mass spectrometer measurements during summer 1967

03 p0425 A69-14009

Lateral transport of constituents in planetary exospheres, considering planetary rotation

03 p0515 A69-14010

Solar emission line absorption by oxygen and nitrogen atomic lines, discussing effect on upper atmosphere composition measurements

03 p0425 A69-14019

Stationary vertical distribution of weightless radioactive substance in surface air layer, accepting two layer exponent law for vertical turbulent diffusion coefficient

04 p0593 A69-15091

Atmospheric fine structure studied by amplitude distribution and autocorrelation functions for different heights of scatter volume in microwave range

04 p0628 A69-15306

Lithium abundance in sunspots and undisturbed solar atmosphere from measurements of solar atmosphere and spot spectra

05 p0821 A69-15850

Venus and Mars atmosphere structure, comparing Venus atmosphere model with Mariner 5 observations

05 p0824 A69-16248

Solar hydrogen Lyman alpha line profile measurement by rocket-borne spectrophotograph, obtaining flux available for scattering by atomic hydrogen in geocorona

05 p0815 A69-16254

Rocket measured profiles of electron density and ion abundances in E region, discussing role of minor atmospheric constituents

05 p0757 A69-16408

Dynamic properties of upper atmosphere, discussing variations in temperature, density and composition

[UN PAPER 68-05755] 06 p0917 A69-17042

Upper atmosphere physics, atmospheric composition and separation of gases, nature of air flow, water vapor content and lower ionosphere structure determinations by rocket

[UN PAPER 68-95693] 06 p0949 A69-17058

Atmospheric droplets diameter, number density and scattering cross sections determined from laser radar return equation and Mie theory

06 p0888 A69-17483

Twilight resonance emissions due to atmospheric sodium, lithium and potassium, noting similarity of annual sodium and lithium twilight abundance variations

[AFCLR-69-0097] 06 p0918 A69-17494

Beryllium abundance in solar atmosphere from spectra observed at Oslo Solar Observatory

06 p1010 A69-17971

Atmospheric influence on friction endurance of solid powdered lubricants at constant layer thickness

[IME PAPER 3] 07 p1138 A69-18563

Mars lower ionosphere ionization from spectroscopic and Mariner 4 occultation data, discussing various ionization sources

07 p1213 A69-18607

Ion composition and charged particle temperatures at 300-600 km from sounding rocket and topside sounder Alouette 2 measurements

07 p1124 A69-18839

Atmospheric helium nonthermal escape mechanisms, noting ion loss from polar ionosphere

07 p1125 A69-18946

Atmospheric and alloying elements effects on casehardening by gas carburization of structural steels, noting carbon potential

07 p1167 A69-19344

Hydrogen concentration above earth surface during minimum-solar activity from ionospheric rocket and satellite measurements

07 p1129 A69-19612

Ozone distribution in Venus atmosphere measured by Soviet space probe Venera 4

08 p1382 A69-19887

Monte Carlo method for calculating atomic hydrogen escape rate from carbon dioxide atmosphere, considering Mars and Venus atmospheres

08 p1386 A69-20076

Seasonal maximum ozone concentration variations, discussing vertical ozone distribution

08 p1307 A69-20260

Horizontal ozone distribution at high cyclones and anticyclones in middle stratosphere

08 p1308 A69-20261

Atmospheric structure and energy distribution of planetary nebulae central stars

08 p1393 A69-20570

Mars and Venus atmospheric properties, noting influence of biosphere and human activity on earth atmosphere

08 p1408 A69-21160

Ozone and carbon dioxide stratospheric and tropospheric horizontal distribution from weather data collected on polar flight

09 p1484 A69-21403

Atmospheric sodium measured at night by tuned laser radar, giving average column number density

09 p1484 A69-21464

Deuterium escape in Venus upper atmosphere to explain anomalous Lyman-alpha glow observed by Mariner 5

[SRCC-91] 09 p1594 A69-21696

Quadrupole mass filter for rocket-borne measurements of thermospheric helium content, discussing turbopause level and winter helium bulge

09 p1489 A69-21712

Carbon dioxide abundance in Mars atmosphere measured with three etalon Fabry-Perot spectrometer

09 p1607 A69-22427

Stellar atmosphere parameters analyzed over pulsation cycle by high dispersion spectra of cepheid variable RT Aurigae

10 p1778 A69-23605

Lunar atmosphere molecule and atom concentration from isotropic and uniform surface evaporation due to micrometeorite impact

10 p1783 A69-23921

Venus atmosphere observations compared with Venera 4 measurements of temperature, pressure and carbon dioxide content

10 p1791 A69-24200

Computerized autocorrelation function analysis of radioactivity distributions in atmosphere at different altitudes, showing no correlation between values

11 p1945 A69-24320

Carbon dioxide concentration in upper troposphere and lower stratosphere recorded during commercial aircraft flights over polar route

11 p1879 A69-25254

Balloon-borne IR spectrometry to study atmospheric nitric acid vapor compared with absorption by ozone and methane

11 p1879 A69-25407

Atmospheric optics by spacecraft and high altitude probes concerning ozone and aerosol distributions, scattering indicatrix polarization and dust cloud inhomogeneities

12 p2055 A69-25815

Molecular O and total number densities between 70 and 120 km determined with rocket measurements of atmospheric absorption of solar UV and X rays

12 p2065 A69-26106

Spectrum analysis of Jupiter atmospheric composition, obtaining abundances of minor constituents

12 p2155 A69-26205

Atmospheric element contents of F stars of Cyg, Her and Boo, using Planckian gradients and computer calculations for growth curves of atmospheric models

12 p2157 A69-26335

Meteoritic dust particles collections prediction in atmosphere for low and high entry fluxes

12 p2158 A69-26342

Atmospheric ozone vertical distribution and total amount determined by radiative transfer and perturbation theory, presenting error analysis

13 p2255 A69-28493

He 3 production and loss in atmosphere, discussing precipitation of energetic magnetospheric particles, thermal escape, nonthermal processes, etc

14 p2435 A69-28965

Time and altitude induced variations in daytime NO and molecular and atomic oxygen ions

14 p2435 A69-29050

Atomic hydrogen vertical profiles with increased high-low altitude ratio for interpreting observations of thermospheric and exospheric hydrogen abundance
14 p2440 A69-29130

Comet atmosphere dust component, relating physical properties to brightness characteristics in stellar magnitudes
15 p2685 A69-30528

Vertical ozone profiles computed from known total ozone data based on profiles taken by Umkehr method
15 p2597 A69-30896

Polar exosphere near solar maximum investigation by Explorer 19 and Explorer 24 drag satellites, considering density and atomic oxygen concentration measurements
15 p2600 A69-31351

Upper atmosphere structure and variations including density and composition in lower thermosphere, diurnal variations, variations with solar activity, etc
15 p2600 A69-31355

RF mass spectrometric measurements of diurnal variation of thermosphere and ionospheric E and F regions composition, noting oxygen concentration
15 p2601 A69-31371

Rocket and satellite measurements of density, temperature and composition in lower thermosphere, considering altitude dependence
15 p2602 A69-31383

Ion whistlers recorded by Alouette 2 VLF receiver providing information on ion composition of terrestrial ionosphere, showing variation with latitude and relationship to solar cycle
15 p2604 A69-31410

Venus microwave spectrum analyzed by comparing various thermal and nonthermal emission models, discussing surface temperature and atmospheric composition
16 p2853 A69-31597

Venus atmosphere carbon dioxide content origin from interior degassing during molten phase, using atmospheric model
16 p2857 A69-32098

Atmospheric ozone production by silent discharges near ground level during first stage of storm cell development
16 p2785 A69-32623

Atmospheric ozone distribution in meridional plane including time effects of photochemistry, advection and turbulence assuming zonal symmetry
16 p2785 A69-32624

Ozone vertical distribution variations over India observed by Brewer electrochemical ozonesonde, noting effects of dry and monsoon seasons
16 p2786 A69-32627

Horizontal and vertical ozone distributions synoptic study, comparing soundings made on both sides of Atlantic
16 p2786 A69-32628

Weather forecasting correlation between atmospheric ozone vertical profiles and postsounding ground meteorological situation, describing computer data processing
16 p2786 A69-32629

Ozone concentration photochemistry between 30-35 km, determining parameters in Hampson theory/hydrogen-oxygen atmosphere/
16 p2787 A69-32636

Ozone soundings in upper stratosphere, discussing vertical temperature profiles relationship to vertical ozone profiles
16 p2787 A69-32640

Variations in difference between integrated ozone amount by soundings and total ozone by Dobson spectrophotometers
16 p2792 A69-32642

Atmospheric ozone distribution as function of photochemical reactions, advection and vertical motions
16 p2787 A69-32643

Photosynthesis and respiration rate in vegetables in controlled temperature, humidity, illumination levels, carbon dioxide and oxygen contents
17 p2912 A69-32933

Atmospheric extinction determined by monochromatic photometry in Chile in 3000 to 6000 Å range, discussing components
17 p3031 A69-33100

Emission intensity ratio change as function of polar auroral height compared to variation in atmospheric concentration ratio of oxygen to nitrogen
17 p2963 A69-33956

Composition and temperature of daytime and nighttime neutral tropic lower thermosphere, obtaining atomic and molecular oxygen ratios
18 p3128 A69-34936

Atmospheric aerosols influence on ion density profile in stratosphere obtained from numerical solution of equilibrium ionization equation
18 p3129 A69-34962

Venus atmosphere physical properties and chemical composition, considering Venera 4 and Mariner 5 data
18 p3201 A69-35164

Vertical distribution of concentration, microstructure and chemical composition of solid aerosol in troposphere and stratosphere from high altitude balloon measurements
18 p3132 A69-35340

Earth satellite sweeping mass spectrometer for measuring atmospheric neutral particle and positive ion concentration
19 p3314 A69-36681

Dynamic properties of upper atmosphere, discussing variations in temperature, density and composition
20 p3519 A69-36983

Rare gas distribution in earth atmosphere explained as outgassing from primordial solid particles, discussing stony meteorites composition
20 p3600 A69-37489

Cations of sulphates photosensitizing role in photolysis of amino acids and peptides in various atmospheres
20 p3477 A69-37626

Resolving power and field of view relations of holographic device for images recording through inhomogeneous atmosphere
20 p3540 A69-37728

Primitive earth upper atmosphere thermal models, considering roles of exospheric temperature and free hydrogen availability in methane dominated environment
20 p3608 A69-38056

Methane abundance and rotational temperature of Jupiter, considering effects of line saturation
20 p3613 A69-38174

Structure, composition and temperature of Venus atmosphere from spacecraft measurements and ground based observations
20 p3614 A69-38256

Circulation near turbopause effect on lower thermosphere composition changes, noting heat source for warmth over winter polar region
21 p3704 A69-38366

Neutral components of arctic thermosphere measured with rocket-borne RF mass spectrometers, discussing origin of atomic hydrogen and water lines
21 p3704 A69-38367

Upper atmosphere particles, luminosity and electron concentration measurements documented in input, storage and energy radiation classes, determining recombination coefficients
21 p3707 A69-38491

Spectra and intensities of rocket releases for upper atmosphere composition, temperature and reaction kinetics, noting chemiluminescence and atomic and molecular emissions
21 p3712 A69-38522

Intensity changes of OI nightglow emission at 100 km by transport associated with tides, gravity waves and turbulent mixing
21 p3713 A69-38526

Planetary atmosphere structure and mean molecular weight determination from onboard measurements tested at high altitude in earth atmosphere, based on NASA Program
21 p3715 A69-39023

Stellar lithium and beryllium, discussing production and destruction processes in stellar atmospheres and abundance in various stars
21 p3810 A69-39505

Flashlamp-pumped dye laser for resonance scattering studies of upper atmospheric composition, describing laser construction and tuning
22 p3962 A69-40440

Helium-carbon star BD plus 10 degrees 2179 re-analyzed by grid of constant flux models containing right amount of C
22 p4026 A69-40652

Jupiter spectrum observations in 2.8-14 micron range, describing absorption strength and brightness temperature, basing analysis on ammonia, methane and hydrogen absorption
22 p4028 A69-40662

Troposphere fine scale properties, comparing simultaneous results of five experimental methods
22 p3941 A69-40914

DC beam experiment for determining molecule sticking coefficients of gas beams incident on Ti, Ba and Sr gettering surfaces at cryogenic temperature
23 p4151 A69-41544

Spaceborne planetary UV spectroscopic search for atoms and molecules basic to life, specifically molecular N and water vapor photodissociation products
23 p4113 A69-41616

Mars atmospheric features from measurements during entry and after landing, discussing atmospheric state properties, diurnal variability, clouds and winds
23 p4212 A69-41617

Nitric acid vapor in atmosphere as function of altitude from spectrograph, predicting downward diffusion
23 p4155 A69-41634

Biochemical evolution role in porphyrin synthesis forming hemoproteids base, discussing assimilation of carbon dioxide in early earth atmosphere
23 p4088 A69-41814

Carbon monoxide presence in Martian atmosphere from Mars line spectra, giving content, surface pressure and concentration
23 p4220 A69-42379

Atmospheric gas composition effects on shock layer radiative heat transfer and heat shield response in Venus entry simulated by earth reentry
24 p4394 A69-43248

Electrical and optical properties correlation of air in fog, discussing droplets distribution with regard to dimensions
24 p4347 A69-43506

Atmospheric gases emission spectra excited by electron beam as function of pressure
24 p4353 A69-43698

ATMOSPHERIC CONDITIONS U METEOROLOGY

ATMOSPHERIC CONDUCTIVITY NT IONOSPHERIC CONDUCTIVITY

Free atmospheric turbulence theory extended to include ionosphere, deriving equations for horizontal ionospheric wind together with turbulence coefficient
02 p0274 A69-11678

Ekman-Okkerblom problem for electrically conducting atmosphere located in external magnetic field, obtaining altitude distribution for wind velocity components
03 p0461 A69-13510

Stationary and nonstationary weak discontinuity surfaces propagation for ideal and viscous compressible conductive atmosphere with regard to heat flux, using Hadamard method
03 p0422 A69-13511

Laboratory atmospheric electrical conductivity meter, discussing structural elements
04 p0600 A69-15106

Electric fields and conductivity in thunderclouds by parachuting rotating differential electric field mills
08 p1345 A69-19813

Electric field profile and turbulence ratio relationship in free atmosphere as function of vertical current density, conductivity, potential gradient and charge density
13 p2295 A69-28523

Free atmospheric turbulence theory extended to include ionosphere, deriving equations for horizontal ionospheric wind and turbulence coefficient
13 p2295 A69-28709

N wave propagation across nonuniform medium described by cloud or front layer, using geometrical optics
16 p2812 A69-31924

Earth bow shock electrical conductivity estimation from macroscopic equations without knowing microscopic dissipation processes
18 p3131 A69-35191

Steady state vertical distribution of small ions in ground layer assuming atmospheric dynamic and thermal sublayers, calculating air resistance and electric field potential
21 p3715 A69-38836

ATMOSPHERIC DENSITY

Photographic image degradation resulting from wave front distortion due to atmospheric refractive density gradients over long oblique optical path
01 p0107 A69-10223

Seasonal variation of evening-morning difference in maximum density heights of twilight sodium layer
01 p0063 A69-10275

Upper atmosphere physical properties, discussing density and temperature
01 p0066 A69-10942

Thermodynamics of nonadiabatic vertical ascent of overheated individual air volumes in stably stratified atmosphere
02 p0274 A69-11441

ATMOSPHERIC DENSITY

Meteor masses and atmospheric density calculation inaccuracy by use of effective stellar magnitudes of meteors

02 p0314 A69-11695

Mariner 4 ionospheric densities to deduce Martian atmospheric modes, discussing validity of using ionospheric properties to discriminate between models

02 p0320 A69-12114

Accelerometric measurement of atmospheric drag with satellite 1968-59B, obtaining upper atmosphere density profile at 130-160 km

02 p0245 A69-12728

Earth atmosphere air density and temperature profiles from drag acceleration measurements in falling sphere experiment

02 p0251 A69-12809

Synoptic density maps for postreentry altitudes derived from constant pressure charts and horizontal gradients

04 p0626 A69-14909

Electromagnetic phase measurement for determining integrated air density near earth surface

04 p0598 A69-14910

Neptune atmosphere height scale and density from photometric observation of star occultation

04 p0660 A69-15061

Delay between solar activity and density changes in upper atmosphere using Harris-Priester model

04 p0594 A69-15121

Atmospheric density variation measurements by density gages on Explorer 32 satellite confirm wave propagation in neutral thermosphere as free internal gravity waves

05 p0754 A69-16261

Midlatitude neutral thermosphere density and temperature measurements, noting effect of atomic oxygen adsorption by instruments

05 p0755 A69-16268

Neutral interstellar matter particle fluxes and densities for earth, noting effects on upper atmosphere gas densities

05 p0828 A69-16653

Atmospheric vertical density and pressure profiles determined from satellite measurements of light beam phase shift and refraction angle

05 p0760 A69-16694

Dynamic properties of upper atmosphere, discussing variations in temperature, density and composition [UN PAPER 68-05755]

06 p0917 A69-17042

Upper atmosphere semiannual density variations, using satellite drag analysis

06 p0918 A69-17380

Semiannual variations in exospheric density near 1100 km derived from Echo 2 orbit, noting phases during solar cycle

06 p0918 A69-17385

Rocket-borne Rayleigh scattering instrumentation to measure atmospheric density, discussing instrumentation and flight results

06 p0927 A69-17698

Temperature variability data for 120-km altitude from observations of grenade glow clouds, calculating molecular diffusion coefficients and atmospheric temperature and density

07 p1127 A69-19277

Upper atmosphere density variations and multiplicative factor necessary for adjustment of density variations of reference models

08 p1397 A69-20761

Upper atmospheric density relation to AE indices sum and solar radio flux during geomagnetic disturbances

09 p1488 A69-21657

Air density at 470 km from orbit of satellite 1966-118 A, confirming large semiannual variation

09 p1488 A69-21659

Gamma ray scattering gauge design optimum parameters to measure Mars atmospheric density

09 p1495 A69-21842

Atmospheric density profile from satellite measurements of light wave phase and refraction angles, discussing ionospheric, water vapor and diffraction effects on errors

09 p1490 A69-21862

Laser radar atmospheric applications, noting particulate matter mapping, backscatter density profiles and use of lidar

09 p1521 A69-22795

Atmospheric density analyzed on basis of photographic observations of meteors, comparing vertical profile with CIRA profile

10 p1688 A69-23936

Semiannual density variations in thermosphere and exosphere as function of mixopause height variations

12 p2064 A69-26012

Nightglow intensity variations at sunspot minimum from measurements in South West Africa, considering relationship to ionospheric vertical movements and density variations

12 p2066 A69-26133

Satellite 1968-5A orbit analyzed for atmospheric density at 140-180 km, noting semiannual variation

12 p2066 A69-26229

Autocorrelation and cross correlation analysis of rapid density variations in F region determined from satellite deceleration and geomagnetic data

12 p2069 A69-26436

Upper atmosphere density variations investigation using Eurobs system, correlating density to geomagnetic activity and 10.7 cm solar radio emission

12 p2069 A69-26437

Kinetic equation solved for radiation propagation in atmosphere, considering neutron density variations and spatial distribution

12 p2149 A69-26683

Lunar surface environmental factors including molecular gas behavior under weak gravity and low atmospheric density, radiation and temperature effects, meteorite bombardment, etc

13 p2352 A69-27904

Meteor masses and atmospheric density calculation inaccuracy by use of effective stellar magnitudes of meteors

13 p2355 A69-28726

Thomson scatter probes for diurnal variations of daytime atmospheric density at 100 km altitude

14 p2440 A69-29125

Worldwide observation of atmosphere with occultation satellites, correcting orbit perturbations to obtain air pressure

14 p2447 A69-29517

Nonlinear internal gravity waves in stratified atmosphere of unbounded inviscid incompressible fluid, noting wave amplitude inverse proportion to atmospheric density

14 p2441 A69-29574

Atmospheric density measurement above 50 km by aerodynamic and atmosphere excitation probes, emphasizing beta ray, bremsstrahlung and molecular fluorescence densitometers

15 p2615 A69-31284

Diurnal variations of wind velocity, temperature and density at high altitude measured by Skylark rockets

15 p2598 A69-31319

Atmospheric density and temperature variations between 200-600 km from Cosmos satellite data, noting solar activity effect

15 p2599 A69-31343

Air density at various heights determined from analysis of satellite low perigee orbits, discussing periodic density variations and correlation with daily geomagnetic index

15 p2599 A69-31348

Air densities from satellite obtained orbital data, comparing accuracy of values and methods of analysis

15 p2600 A69-31349

Upper atmospheric density effects on satellite orbits, discussing variations due to solar activity, day-night and semiannual changes and atmospheric rotation

15 p2600 A69-31350

Polar exosphere near solar maximum investigation by Explorer 19 and Explorer 24 drag satellites, considering density and atomic oxygen concentration measurements

15 p2600 A69-31351

Upper atmosphere structure and variations including density and composition in lower thermosphere, diurnal variations, variations with solar activity, etc

15 p2600 A69-31355

Wintertime short term density variability in upper atmosphere obtained from rocket measurements

15 p2601 A69-31374

Satellites orbits analysis for semiannual variation of air density in upper atmosphere

15 p2601 A69-31378

Longitudinal variations of density, temperature and pressure distributions in stratosphere and mesosphere based on rocket observations, emphasizing arctic and subarctic regions

15 p2602 A69-31379

Rocket and satellite measurements of density, temperature and composition in lower thermosphere, considering altitude dependence

15 p2602 A69-31383

Atmospheric density measurements by triaxial accelerometer system, ionization gauges and orbital decay of OV1-15 satellite

15 p2602 A69-31384

Low altitude atmospheric density satellite OV1-16 measurements, showing agreement between onboard accelerometer and orbital drag data

15 p2602 A69-31385

Atmospheric density determination based on long period variations of drag coefficients from satellite Proton 2, considering satellite orientation

15 p2602 A69-31392

Diurnal thermospheric density, temperature and wind variations due to direct solar EUV heat input and tidal wave from lower atmosphere

15 p2605 A69-31439

Atmospheric density dependence on solar and geomagnetic activity at low latitudes, discussing atmospheric expansion

15 p2605 A69-31441

Drag measuring requirements and comparison of accelerometer or drag-free satellite control systems usage for atmospheric density determination

16 p2788 A69-31722

Kinetic theory and gas-surface interactions for upper atmospheric density measurements by mass spectrometers, pressure gages and satellite drag, detailing adsorption effect

16 p2776 A69-32089

Atmospheric density at 130-160 km measured from satellite 1968-59B orbit, noting agreement with CIRA 1965

16 p2776 A69-32095

Atmospheric gas constituents number densities determined as function of altitude by correlating laser beam scattering and absorption data

16 p2781 A69-32387

Atmospheric optical density vertical distribution curves in near UV from spectrophotometer data of Echo type satellites entry into earth shadow

16 p2788 A69-32638

Atmospheric density semiannual variation in thermosphere base, suggesting origin at lower heights in mesosphere or stratosphere

17 p2958 A69-32863

Air density measurement at high altitudes by falling instrumented sphere ejected by missile in upper atmosphere

17 p2971 A69-32898

Clear air turbulence uninfluenced by mesoscale disturbances or terrain, discussing relationship between density profile curvature and heat and momentum transfer

17 p2998 A69-33733

Vertical structure concepts for air density, wind and sound velocity profiles in rocket climatology, discussing vertical relationship of wind shear statistics

17 p3000 A69-33794

Dynamic properties of upper atmosphere, discussing variations in temperature, density and composition

20 p3519 A69-36983

Explorer 32 atmospheric density measurements revealing neutral thermosphere latitudinal variations during geomagnetically undisturbed times

20 p3535 A69-38100

F region atmospheric density measurements obtained from aerodynamic drag on San Marco 2 satellite in equatorial orbit, comparing data with San Marco 1

21 p3704 A69-38369

Earth atmospheric density measurement by microwave radio occultation techniques, transmitting coherent radio signal to repeater spacecraft from master station

21 p3705 A69-38375

Flight vehicle motion in high density medium reacting with static, vortex and dynamic forces analyzed for optimal regime via Lagrange-Euler equation

21 p3768 A69-39824

Air density height distribution determined from satellite orbit decay analysis, noting semiannual density variations

22 p3935 A69-39971

Neutral exosphere model for nonrotating planet permitting barosphere uniform rotation at certain angular velocity, determining velocity distribution and density

22 p4023 A69-40524

Equatorial stratosphere and mesosphere wind, temperature and density data from rocket and balloon sounding, noting seasonal variations and possible stratosphere-ionosphere coupling

23 p4159 A69-42423

Leak detection techniques efficiency determined for airtight atmospheric air sampling devices used at low pressure and concentration

24 p4296 A69-42656

Air density determination using transit time method involving microwave phase measurements

24 p4313 A69-42898

- Clear air turbulence in upper atmosphere and in mountain waves, discussing density variations
24 p4343 A69-42913
- Atmospheric density above 158 km altitude measured near equator with cold cathode magnetron pressure gage on satellite OV1-15
24 p4310 A69-43179
- Lower ionosphere atmospheric density, temperature and pressure profiles diurnal variations from data of radio meteor echoes
24 p4311 A69-43504
- ATMOSPHERIC DIFFUSION**
- Atmospheric diffusion measurement based on analysis of thoron emitted continuously from point source, permitting study of diffusion in atmospheric boundary layer
01 p0144 A69-10043
- Dispersion relation of internal acoustic gravity wave motion in compressible nonviscous and nonheatconducting atmosphere
02 p0242 A69-11868
- Eddy diffusivity in planetary boundary layer determined by vertical velocity spectrum
03 p0460 A69-13338
- Geostrophic trajectories of horizontal diffusivity estimated in midlatitude troposphere and lower stratosphere
08 p1308 A69-20310
- F2 layer diffusion and sporadic E layer characteristics from equatorial ionosphere soundings on Zaria schooner
09 p1486 A69-21548
- Venusian upper atmosphere dissociation and ionization, considering photochemical and dynamic processes and molecular, eddy and ambipolar diffusions
13 p2344 A69-27643
- Diffusion of ozone distribution tracers in stratosphere, based on photochemistry in oxygen- only and oxygen-hydrogen atmospheres
13 p2294 A69-28492
- Light polarization diffusely reflected by earth atmosphere measured from balloon, using gain compensated photoelectric polarimeter
16 p2781 A69-32320
- F 2 layer diffusion and sporadic E layer characteristics from equatorial ionosphere soundings on Zaria schooner
16 p2784 A69-32543
- Trapped protons acceleration through bimodal diffusion in magnetosphere, noting spatial patterns and temporal behavior of proton and electron belts
16 p2851 A69-32618
- Vertical turbulent diffusion and altitude distribution of radioactivity from short lived radon decay products in atmosphere
20 p3533 A69-38076
- Pluto positions /1930-1965/ from photographic observations, ascribing declination errors to atmospheric dispersions
22 p4025 A69-40612
- Nitric acid vapor in atmosphere as function of altitude from spectrograph, predicting downward diffusion
23 p4155 A69-41634
- ATMOSPHERIC ELECTRICITY**
- NT AURORAL ELECTROJETS
NT EQUATORIAL ELECTROJET
NT IONOSPHERIC CURRENTS
- Soviet collection of papers on atmospheric electricity
04 p0593 A69-15101
- Laboratory atmospheric electrical conductivity meter, discussing structural elements
04 p0600 A69-15106
- Aircraft instrumentation for measuring aircraft electrostatic charge, atmospheric electric field intensity and currents of aircraft
04 p0549 A69-15107
- Potential gradient, small ion density and space charge density measurements for atmosphere on Atlantic Ocean during 1965
04 p0594 A69-15159
- Small scale filament structure of current systems in earth magnetosphere, noting coherence of magnetic disturbances in conjugate regions
05 p0753 A69-16049
- Air-earth current and conductivity measurements, noting greater conduction current at one mile altitude
05 p0758 A69-16419
- Solar flare influence on potential gradient and air-earth current properties at high mountain stations
05 p0759 A69-16634
- Fast Ba ion filament cloud injection into ionosphere using explosive shaped charge technique, noting application to ionospheric electric field measurement
09 p1539 A69-21752
- Air-earth current density variations with universal time, noting hemispherical dependence of storm activity effects
10 p1682 A69-23415
- Monograph on method and results of measurements of mobilities spectrum ion density and conductivity in upper troposphere and stratosphere
11 p1877 A69-24636
- Magnetospheric substorm as discharge process of associated electric current system, discussing relaxation processes, explosive release of energy, etc
11 p1879 A69-25249
- Atmospheric electricity and space charges ionization and equilibrium in earth atmosphere, discussing electric fields in lower atmosphere, ionosphere and magnetosphere
12 p2076 A69-27105
- Electric field profile and turbulence ratio relationship in free atmosphere as function of vertical current density, conductivity, potential gradient and charge density
13 p2295 A69-28523
- Point discharge measuring based on pulsed nature of discharge current, outlining field experiment results
15 p2610 A69-30698
- Physical process providing EMF for maintaining electrical structure of stratosphere and mesosphere shown to center in lower ionospheric thermally driven tidal motions
18 p3130 A69-35103
- Magnetic field variation rates characteristics during magnetic storms investigated for longitudinal dependence and influence of equatorial electric current
20 p3520 A69-37037
- Small scale filament structure of current systems in earth magnetosphere, noting coherence of magnetic disturbances in conjugate regions
20 p3532 A69-37958
- Electrostatic charge formations in atmosphere, discussing atmospheric electricity during precipitation and thunderstorms
21 p3758 A69-38785
- Convective cells and periodic variations in vertical gradient of electroatmospheric field
22 p3934 A69-39939
- Ball lightning as positively charged region of electroluminescent air maintained in dynamic structure and molecular composition by atmospheric electric field
22 p3940 A69-40536
- ATMOSPHERIC EMISSION**
U AIRGLOW
- ATMOSPHERIC ENTRY**
- NT HYPERBOLIC REENTRY
NT HYPERSONIC REENTRY
NT MANNED REENTRY
NT REENTRY
NT SPACECRAFT REENTRY
- Sustained high deceleration load effects on quartz crystals during atmospheric entry studied by centrifuge test program on oscillator circuits
01 p0042 A69-10417
- Tungusk meteorite preceding and succeeding atmospheric events, explosion and origin
01 p0159 A69-11378
- Direct planetary atmosphere measurement by vehicles entering atmosphere, using Mars and Venus model atmospheres for accuracy expectation
02 p0311 A69-11472
- Active control system augmentation of inherent aerodynamic damping assuring acceptable limits on oscillatory rotational motion during hypersonic Martian atmospheric entry
02 p0333 A69-11742
- Mars planetary entry and landing model tests, demonstrating technological feasibility of mission
02 p0333 A69-11746
- Ablative heat shield materials for Mars and Venus atmospheric entries
02 p0333 A69-11750
- Radiation heating characteristics of shock layer gases surrounding Venus entry vehicle, noting domination of carbon monoxide band and UV spectrum
02 p0351 A69-11751
- Downstream radiation flux distribution calculated for blunt entry bodies, considering self absorption effects
02 p0354 A69-12547
- Two dimensional representation of Venus entry probe target data for determining probe capability to provide real time data transmission to earth
02 p0331 A69-12820
- Mission requirements influence on aerothermodynamic environment for vehicle entering Venus atmosphere, considering different entry modes
02 p0332 A69-12823
- Entry phase flight data of Missions AS-202, Apollo 4 and 6 compared with wind tunnel aerodynamics data
03 p0519 A69-13556
- Aerothermal-structural reentry safety evaluation for SNAP-27 radioisotope Graphite Lunar Module Fuel Cask at orbital and superorbital velocities
03 p0465 A69-13561
- Blunt and conical body optimum heat shield shapes for Jupiter atmospheric entry, noting shallow flight path
03 p0520 A69-13565
- Aeroshell structural development for Mars flyby and entry landing mission compatible with Atlas/Centaur launch vehicle
03 p0521 A69-13667
- Entry and terminal deceleration systems for unmanned Martian landers, discussing parachute landing and lifting entry vehicles
03 p0521 A69-13670
- Design of interface between Mariner Mars spacecraft and Mars planetary entry/landing capsule
03 p0521 A69-13671
- Atmospheric gas composition effects on shock layer radiative heat transfer and heat shield response in Venus entry simulated by earth reentry
03 p0412 A69-13672
- Entry corridor thermal entry limits for Apollo spacecraft defined for design of thermal protection system
03 p0521 A69-13673
- Monograph on radiation gas dynamics, thermal radiation, applied spectroscopy and ablation and applications in high speed atmospheric entry
04 p0685 A69-14597
- Correlations of stagnation point radiative heat transfer for earth reentry, noting use of nongray absorption coefficient models
04 p0685 A69-14736
- Structural design options for decelerative aeroshell configurations for atmospheric entry on unmanned planetary explorations
04 p0683 A69-15507
- Spacecraft trajectory during atmospheric reentry determined from projections of longitudinal acceleration onto coordinate axes connected with spacecraft
06 p1014 A69-17581
- Thermal radiative reflectance characteristics of low density charring ablators subjected to planetary entry environment simulation
06 p0947 A69-18148
- Atmospheric entry testing in terms of velocity-altitude duplication, suggesting multistage rocket propelled aeroballistic range type testing
06 p0907 A69-18189
- Three dimensional atmospheric entry trajectories equations for satellite with aerodynamic lift, examining aerodynamic factors and bank angle effects
07 p1230 A69-19608
- Coordination technique for pressure, density and temperature measurements by probes during parachute reentry into planetary atmospheres, taking into account reentry dynamics
09 p1609 A69-21775
- Matched asymptotic expansions method applied to problem of hypervelocity atmospheric entry, noting solution division into outer Keplerian region and inner expansion region
09 p1430 A69-21964
- Aerothermoelasticity problems for Mars entry vehicles, discussing deceleration loads, separated hot gas flow, shield thermal gradients and oscillatory body motion
09 p1610 A69-21991
- Book on reentry and planetary entry physics and technology covering entry dynamics, thermodynamics, radiation, ablation and heat transfer
11 p1967 A69-25573
- Reentry and planetary entry physics and technology, II, Advanced concepts, experiments, guidance-control and technology
11 p1967 A69-25718
- Configuration, trajectory planning, instrumentation, calorimetry and aerodynamic heating for planetary atmosphere entry
11 p1968 A69-25719

Lifting entry concepts for return from earth orbit, discussing deceleration, heating and heat protection
11 p1968 A69-25720

Environmental problems of entry vehicle returning from lunar or planetary mission, discussing heat protection system efficiency
11 p1968 A69-25721

Venus and Mars atmospheric braking entry and associated equipment, discussing potential cost savings
11 p1968 A69-25722

Entry propulsion and lower systems technology for planetary entry and atmospheric reentry vehicles
11 p1945 A69-25723

Guidance and control concepts and hardware for atmospheric entry of Mercury, Gemini and Apollo spacecraft
11 p1914 A69-25724

Program definition and government-industry relationships in entry research and development program management
11 p2005 A69-25726

Stony meteoric particles size and velocity during passage through atmosphere
12 p2157 A69-26341

Apollo spacecraft command module aerodynamic characteristics during entry compared with wind tunnel test predictions
[AIAA PAPER 68-1008] 12 p2012 A69-26789

Spacecraft longitudinal control during reentry of lunar orbiter into atmosphere, analyzing final range prediction, trajectory tracking and accelerometers performance
13 p2355 A69-27681

Spacecraft range control algorithm during reentry at parabolic velocity into atmosphere with varying parameter distributions
13 p2355 A69-27682

Optimal control algorithm for spacecraft descent in atmosphere based on nominal trajectory and acceleration measurements
13 p2355 A69-27683

Spacecraft sterilization by destructive heating with thermite or high velocity entry friction before entering planet atmosphere
15 p2560 A69-31472

Convective plus radiative shock tube model stagnation point heating rate measurements for planetary entry heating rate in air and Venus gas
[AIAA PAPER 69-635] 17 p2890 A69-33272

Shock layer properties, radiative and convective heat transfer about two hypersonic blunt bodies at zero angle of attack in assumed Martian atmosphere
[AIAA PAPER 69-634] 17 p2891 A69-33281

Collection of papers on thermal design principles of spacecraft and entry bodies
18 p3227 A69-34372

Maximum trajectory for glider entering earth atmosphere at supercircular velocity, subject to maximum altitude constraint
19 p3399 A69-35667

Mars autonomous entry navigation, discussing flight path angle control with onboard sensors using realistic sun, Canopus and planet line of sight tracker accuracies
19 p3368 A69-35790

Approach navigation accuracy for planetary atmosphere braking to orbit about Mars and Venus
[AAS PAPER 68-122] 19 p3402 A69-35937

Drop test method to obtain subsonic terminal velocity and base pressure data for planetary entry probe configurations
19 p3238 A69-35959

Environment effect on scientific and telecommunication equipment mounted on exploratory probe during Venus atmosphere entry for acceleration loading in design
19 p3431 A69-36037

Saint-Severin amphoteric geometrically reconstructed from fragments in form prior to atmospheric breakup, noting agreement with track densities of iron ions
19 p3416 A69-36128

Shock histories of hexahedrites and Ga-Ge group III octahedrites based on metallographic and X ray diffraction analysis, noting meteorites shocked preterrestrially
19 p3418 A69-36136

Distance of spacecraft descending on parachute through planetary atmosphere measured from center of planetary mass using onboard instrument data
19 p3432 A69-36633

Adaptive control for Mars entry based on sensitivity analysis
[AIAA PAPER 68-8355] 20 p3573 A69-37193

Atmospheric entry-capsule dynamics, considering angle of attack motion under gravity forces influence and aerodynamic normal force stability relations
20 p3617 A69-37197

Soviet book on shock waves propagated by meteorite intrusion into earth atmosphere, covering interaction with earth surface, Tungusk meteorite, etc
20 p3613 A69-38205

Planar tumbling in atmospheric entry, describing arrest by approximating Painleve equation
21 p3819 A69-39033

Reentry Vehicle Altitude-Velocity Sensor for continuously measuring hypersonic vehicles free stream density and velocity in atmosphere at low angle of attack
[AIAA PAPER 69-866] 21 p3725 A69-39392

Spacecraft descent trajectory optimization during atmospheric reentry, proposing algorithm for continuous trajectory determination
21 p3766 A69-39647

Spacecraft atmospheric entry descent trajectory optimization by stochastic procedure, requiring onboard digital computer to realize optimal algorithms
21 p3767 A69-39648

Aerodynamic deceleration systems for space missions, considering deployment of subsonic parachute and inflatable configuration following atmospheric entry
[AIAA PAPER 68-1081] 22 p4036 A69-40542

Aerothermal-structural reentry safety evaluation for SNAP-27 radioisotope Graphite Lunar Module Fuel Cask at orbital and superorbital velocities
[AIAA PAPER 68-1166] 22 p3979 A69-40551

Atmospheric gas composition effects on shock layer radiative heat transfer and heat shield response in Venus entry simulated by earth reentry
[AIAA PAPER 68-1148] 24 p4394 A69-43248

ATMOSPHERIC ENTRY SIMULATION

Upgrading wave superheater for evaluation of reentry materials
01 p0054 A69-10917

Ground simulation of reentry observables with ablation, studying ablation products interaction with flow-field of wave superheater hypersonic tunnel
02 p0229 A69-12502

Planetary atmosphere determination error analysis using Kalman filter, noting results of simulated Martian atmosphere entry
02 p0331 A69-12806

Atmospheric gas composition effects on shock layer radiative heat transfer and heat shield response in Venus entry simulated by earth reentry
[AIAA PAPER 68-1148] 03 p0412 A69-13672

Reentry plasma sheath simulation in wind tunnel by injection of nitrogen plasma from model vehicle nose
03 p0412 A69-13679

Closed system toroidal electrogasdynamic facility proposed for reentry simulation, discussing velocity generation
04 p0585 A69-15323

Shock tube measurements of radiation from simulated Jupiter atmosphere related to thermodynamic conditions encountered by entry probe
[AIAA PAPER 69-184] 06 p0908 A69-18207

Aerodynamic measurements on Apollo CM model at hypersonic flow simulating earth orbital reentry trajectory
12 p2012 A69-26800

Hypervelocity reentry simulation problems for slender and blunt bodies, defining significant parameters
15 p2681 A69-30376

Martian entry test facility for real size entry systems, discussing design, fabrication and operation
15 p2587 A69-30390

Thermal control of Mars entry capsule with fiberglass honeycomb sandwich shell analyzed with and without aft thermal curtain, emphasizing cruise-flight phase
[AIAA PAPER 68-1082] 19 p3429 A69-35949

Atmospheric gas composition effects on shock layer radiative heat transfer and heat shield response in Venus entry simulated by earth reentry
[AIAA PAPER 68-1148] 24 p4394 A69-43248

Vector matrix second order sensitivity equation application to Mars entry guidance, performing numerical simulation of second order sensitivity guidance and tabulating results
24 p4388 A69-43690

Image intensifier coupling to electron scanning image-converter to increase time-resolving spectrograph sensitivity in simulated reentry studies
24 p4317 A69-43759

ATMOSPHERIC HEAT BUDGET

Near mesopause atmospheric layer energy balance, noting atomic oxygen diffusion role in redistributing absorbed solar energy among atmospheric layers
03 p0422 A69-13408

Sensible and latent heat meridional transport associated with standing eddies computed from climatic mean data
04 p0627 A69-15085

Carbon dioxide absorption and emission in mesosphere, discussing vibrational relaxation time and radiative heating rate
08 p1308 A69-20308

IR radiative temperature changes as function of latitude, season and height in region 30-110 km
12 p2064 A69-26008

Atmospheric energy budget of latent and sensible heat and potential energy between equator and 60 degree N
12 p2066 A69-26132

Atmospheric heat exchange and circulation simulated by rotating containers, reproducing temperature field and dynamic structure above large area
14 p2478 A69-29840

Atmospheric radiative balance measurement on board Cosmos 149, describing design and operation of device
15 p2597 A69-30652

Adiabatic and diabatic processes contributions to vertical atmospheric motions profile and IR cooling components comparison
17 p2962 A69-33689

Earth albedo in lower latitudes measured by satellites and surface stations, comparing solar energy absorption by oceans and atmosphere
20 p3591 A69-38058

ATMOSPHERIC HEATING

Upper atmosphere oxygen emission and heating during geomagnetic disturbances
02 p0235 A69-11421

Vertical wind velocity structure and turbulent heat flux temperature measurements over steppe and sea, noting underlying surface influence
03 p0458 A69-13270

Atmospheric rotation speed dependence on specific heat, thermal conductivity, air absorption coefficient and lower boundary pressure, discussing diurnal variation of thermosphere
[AFRL-69-0363] 04 p0649 A69-15130

Rocket and radiosondes data from measurements over Northern Hemisphere used to study stratospheric and mesospheric circulation during three midwinter periods
05 p0753 A69-15800

Atmospheric heat sources and heat sinks distribution based on Cosmos satellite data
06 p0949 A69-17048

Response of stably stratified atmosphere to differential heating across coastlines
07 p1126 A69-19038

Midwinter warmings in upper stratosphere for differences between various stratospheric and mesospheric levels, noting need for additional upper air data
08 p1345 A69-20134

Magnetospheric plasma heating by magnetosheath generated electromagnetic waves
11 p1950 A69-25149

Upper atmosphere response to time dependent heating based on approximate analytic solutions of heat conduction equation
11 p1878 A69-25151

Empirical determination of heating efficiency of extreme solar UV radiation interacting with carbon dioxide atmosphere of Mars and Venus
12 p2155 A69-26019

Solar chromosphere and corona heat intensity above 1000 km attributed to tongues of turbulence, considering convective zone exciting MHD waves mechanism
13 p2337 A69-27549

Vertical wind velocity structure and turbulent heat flux temperature measurements over steppe and sea, noting underlying surface influence
14 p2471 A69-28778

Gravity waves in thermospheric heating during magnetic storm, discussing electron density and temperature and ion velocity variations
15 p2605 A69-31435

Rocket and radiosondes data from measurements over Northern Hemisphere used to study stratospheric and mesospheric circulation during three midwinter periods
17 p2962 A69-33779

Steady state solution of quasi-geostrophic perturbation equations for atmospheric forced response to parameterized heating as global monsoon theory
19 p3362 A69-36405

Partial differential equation representing influence of radiative and turbulent transfers of atmospheric heat, based on absorption coefficients for terrestrial radiation
19 p3363 A69-36498

Ionospheric electron density and collision frequency profiles examined for changes during December 1967 to January 1968 stratospheric warming
21 p3714 A69-38556

Upper stratosphere warming and associated structure of mesosphere from rocket sounding, discussing high winds related to pressure gradient, upward vertical motion, etc
22 p3977 A69-39928

Chromospheric heating above sunspots by analyzing MHD wave generation and propagation in sunspots and solar atmosphere
22 p4010 A69-39992

Heat conduction equation applied to thermospheric heating in auroral zone to account for local temperature and density variations, introducing horizontal transport mechanisms
22 p3941 A69-40717

Ionospheric absorption relationship to major stratospheric sudden warmings, considering regional coincidence and interaction mechanism
24 p4306 A69-42680

ATMOSPHERIC IMPURITIES **U AIR POLLUTION**

ATMOSPHERIC IONIZATION **NT AURORAL IONIZATION**

D region composition at and shortly after sunrise, noting negative ion factor changes, ionization source and quasi-equilibrium conditions
01 p0066 A69-10597

Ionization, neutralization and charge exchange processes in ionosphere, detailing dependence of photodissociation and collision detachment of negative ions
01 p0066 A69-10598

Ionospheric negative ion coefficient variations, analyzing formation microprocesses
01 p0066 A69-10599

Nuclear radiation dose rate and atmospheric ionization from radioactive fallout and natural sources, discussing fallout effect on population
01 p0145 A69-10982

Martian upper atmospheric ionization process analogous to cometary material ionization in solar wind
02 p0320 A69-12117

Nocturnal electron concentrations and temperature at Manitoba measured by rocket-borne Langmuir probe, compared with F1 region
03 p0502 A69-14008

F2 layer formation and fast neutral particles ionization source due to charge exchange between solar wind protons and moving interstellar hydrogen
04 p0592 A69-15009

Photoelectric absorption studies on molecular nitrogen indicate predissociation contributing to atomic nitrogen production in upper atmosphere
05 p0756 A69-16282

Rocket measured profiles of electron density and ion abundances in E region, discussing role of minor atmospheric constituents
05 p0757 A69-16408

Electron formation in lower ionosphere due to cosmic ray-atmosphere interaction, analyzing ionization of subrelativistic and relativistic solar and galactic cosmic rays
06 p0920 A69-17726

Vertically moving ionized formations relation to solar and magnetic activity
06 p0920 A69-17730

Formation dynamics of thin sporadic layers of E region, determining maximum ionization and electron concentration and electron-neutral atoms collision frequency
06 p0922 A69-17751

Mars lower ionosphere ionization from spectroscopic and Mariner 4 occultation data, discussing various ionization sources
07 p1213 A69-18607

Computational techniques for determining magnetic field geometry for backscatter reflections
07 p1125 A69-18850

Ion-molecule reactions constants studied directly in ionosphere, using air injection from geophysical probe and airborne RF mass spectrometer
08 p1311 A69-21159

Maximum ionization altitude, thickness, electron density profile and temperature mean variations in summer of IGY and IQSY at Moscow station
09 p1486 A69-21544

Aeronomics parameters effect on ionospheric effect of SC magnetic storm, calculating maximum ionization levels, F layer ionization and vertical ionization profile parameters
09 p1486 A69-21546

Solar quiet day variations studied by annual amplitude dependence on number of sunspots, considering E layer ionization
09 p1575 A69-21550

Corpuscular radiation contributions to D layer ionization determined from intensity measurements
09 p1577 A69-21770

Nonequilibrium three dimensional boundary layer over slightly yawed cone analyzed for air dissociation and ionization parameters, noting binary scaling application
09 p1430 A69-21965

Space electric fields research by artificial clouds of vaporized barium launched by rockets, noting neutral atmosphere and ionospheric results
09 p1492 A69-22800

Ionization in lower ionosphere over polar cap under solar corpuscular fluxes measured by radio wave absorption
10 p1759 A69-22838

Thomson scatter bistatic sounder data on ionization transports in F region, describing diurnal variations by hourly values of velocities
10 p1685 A69-23830

Nonlinear charge exchange and dissociative recombination effects on night F region decay compared with linear theory
10 p1685 A69-23832

Nitrogen dioxide molecular ions formation in air, discussing absence at lower pressures and early afterglow dominance in air ionized and dissociated by microwave pulses
11 p1879 A69-25158

Overlay technique for analysis of F region transition into F1 and F2, noting ionization and recombination
12 p2065 A69-26102

Production source of ionization due to low energy electron influx and inclusion in ionospheric continuity equation, noting quiet ionosphere
12 p2066 A69-26112

Mean annual characteristics of F2 layer ionization state, using results of worldwide observation station system
12 p2071 A69-26701

Atmospheric electricity and space charges ionization and equilibrium in earth atmosphere, discussing electric fields in lower atmosphere, ionosphere and magnetosphere
12 p2076 A69-27105

Venusian upper atmosphere dissociation and ionization, considering photochemical and dynamic processes and molecular, eddy and ambipolar diffusions
13 p2344 A69-27643

Neutral gas ionization in lower ionosphere, discussing physicochemical reactions, recombination coefficients, equilibrium processes, etc
13 p2255 A69-28540

Galactic and relativistic and subrelativistic solar cosmic rays effect on electron production rate in ionosphere, detailing low energy SCR-atmosphere interactions
13 p2333 A69-28544

Minimum height of monochromatic radiation ionization in atmosphere assuming spherical earth for space science applications
13 p2256 A69-28653

High latitude ionization spikes observed by POGO spacecraft, noting frequency correlation with magnetic disturbances and development by high energy electron injections
14 p2511 A69-28950

Zonal drift influence on morning ionization anomaly in F region, noting shifts to West with increasing height and electron production rate
14 p2442 A69-29732

Interstellar particle penetration into solar system, discussing impact ionization of earth ionosphere by interstellar neutral hydrogen and helium
15 p2699 A69-31390

Shock wave propagation in isothermal atmosphere, discussing radiation and ionization effects on thermal jump
16 p2858 A69-32207

Meteoritic elements ionization and loss mechanisms in E region, discussing roles of atomic oxygen and metal ions chemical reactions
16 p2780 A69-32313

Maximum ionization altitude, thickness, electron density profile and temperature mean variations in summer of IGY and IQSY at Moscow station
16 p2783 A69-32539

Aeronomics parameter effect on ionospheric effect of SC magnetic storm, calculating maximum ionization levels, F layer ionization and vertical ionization profile parameters
16 p2783 A69-32541

Solar quiet day variations studied by annual amplitude dependence on number of sunspots, considering E layer ionization
16 p2851 A69-32545

Atmospheric aerosols influence on electric field in ground layer to account for ionization, demonstrating number and turbulent exchange coefficient relationship
17 p2996 A69-33036

Nonequilibrium multicomponent ionization calculations for stagnation merged shock layer of hypersonic blunt body by successive accelerated replacement [AIAA PAPER 69-655]
17 p2892 A69-33469

Effective rate coefficients of ion-molecular processes, dissipative recombination and ion production in F2 layer at midlatitudes
17 p2966 A69-33979

F1 layer observation at 80-87 degree solar zenith angles explained by additional ionospheric maximum development in presence of temperature gradients
17 p2967 A69-33985

Reflection and ionization heights diurnal variations in F region, obtaining data for sporadic E formation
17 p2968 A69-33995

Radio meteor ionization profiles, discussing electron line density measurements by backscatter system
19 p3283 A69-35992

Meteor radio electronics principles, methods and equipment, discussing ionized meteor trail formation, radar tracking and utilization of trails for communications
19 p3277 A69-36591

Ion production rates vertical distribution and temporal changes at midlatitudes during solar activity minimum and maximum above F2 layer
20 p3525 A69-37656

Corpuscular radiation indicated as ionization source in lower ionosphere from rocket sounding data, noting role in D region formation
21 p3787 A69-38352

Atmospheric ionization rates due to attenuation of 1-100 A nonflare solar X rays, giving solar fluxes and absorption cross sections
22 p4004 A69-40447

Air afterglows electron loss mechanisms, measuring electron densities decay rates after microwave ionization
22 p4006 A69-40527

Atmospheric small gaseous ions nature and properties, discussing solid elastic and composite interaction, complex, cluster, intermediate and Langevin ions, etc
22 p3940 A69-40538

Air ionization and beta and gamma dose rates measurements for natural radiation from cosmic rays compared to nuclear weapons tests fallout, considering biological effects
22 p4007 A69-40915

Blunt body stagnation point air ionization by chemical nonequilibrium thin viscous shock layer analysis, predicting electron density
23 p4060 A69-41917

Ionization irregularities in equatorial E region observed in various scale sized by rocket-borne Langmuir and plasma-noise probes
23 p4160 A69-42430

Ionized meteor trails reflection zone altitudes determination by interferometric measurements of phase differences
24 p4311 A69-43508

ATMOSPHERIC MODELS **NT REFERENCE ATMOSPHERES**

Weather forecasting, discussing atmospheric models and computer operations for long range forecasting based on hydrodynamic theory and statistics
01 p0108 A69-10398

Atmospheric model development relating temperature, density, moisture and energy measurements from satellite observations for long term weather forecasting [UN PAPER 68-95397]
01 p0108 A69-10463

Cirrus IR radiance model for explaining measured cloud radiance characteristics, considering thermal emission and irradiance scattering
01 p0111 A69-10848

Hydrogen line profiles in various early stars compared with profiles predicted from model atmosphere calculations for rotating and nonrotating early stars
01 p0154 A69-10876

Microturbulent velocity parameter correlation to iron-to-hydrogen ratio for G dwarfs, using model atmosphere abundance analyses
01 p0154 A69-10877

Low altitude atmospheric turbulence model evaluated from analysis of A-6A aircraft gust load data, comparing model estimates with aircraft response characteristics
01 p0056 A69-11053

Cross field plasma instability resulting in charge density irregularities shown to meet requirements for ionospheric irregularities model
01 p0073 A69-11178

Six level model for numerical geopotential forecast allowing for quasi-static and quasi-geostrophic approximations
02 p0273 A69-11434

Boundary layer effect on large scale atmospheric processes from analyzing two layer free atmosphere model, plotting weather forecast charts
02 p0273 A69-11435

Axisymmetric model of unsteady convective cumulus cloud produced by time dependent heat source in unsteady atmosphere
02 p0274 A69-11436

Thermodynamics in homogeneous steady state fog over rough terrain representing absolutely absorbing surface
02 p0274 A69-11442

Direct planetary atmosphere measurement by vehicles entering atmosphere, using Mars and Venus model atmospheres for accuracy expectation
[AAS PAPER 68-187] 02 p0311 A69-11472

Perturbed geomagnetic field structure during magnetic storm recovery phase calculated by magnetosphere magnetic field model, accounting for various external field sources
02 p0237 A69-11666

Stratospheric dust effect on twilight sky color, evaluating scattered radiation chromaticity for atmospheric models containing ozone
02 p0243 A69-12014

Romanova method for solution of scalar equation of radiative transfer in plane parallel atmosphere
02 p0319 A69-12106

Model spectra applied to carbon dioxide bands in Venus spectrophotometric measurements
02 p0319 A69-12107

Venus microwave phase effect analyzed assuming dry massive Venus atmospheric model, discussing heat transfer processes
02 p0319 A69-12108

Venus exospheric temperature for various composition models, discussing carbon dioxide concentration effects
02 p0319 A69-12109

Martian upper atmosphere and ionosphere, considering Mariner 4 occultation results and various atmospheric models
02 p0320 A69-12112

Mariner 4 ionospheric densities to deduce Martian atmospheric modes, discussing validity of using ionospheric properties to discriminate between models
02 p0320 A69-12114

Radio amplitude and phase measurements during Mariner-Mars encounter, providing evidence for Martian atmospheric models
02 p0320 A69-12116

Global cloud models construction techniques, discussing vertically pointing radars, airborne panoramic cameras, radiometry, meteorological satellites and light detection and ranging
02 p0275 A69-12381

Thermal tidal oscillations in earth atmosphere using circulation model attributed to solar radiation absorption by atmospheric vapor and ozone
02 p0457 A69-13030

Planetary long waves behavior in atmospheric models, explaining unsteady components by means of filtered equations
03 p0459 A69-13274

ELF radio wave propagation characteristics using two layered ionospheric model, noting deeper penetration than VLF
03 p0421 A69-13326

Mean meridional circulation models in tropics based on vorticity equation
03 p0460 A69-13334

Long period variations in zonally symmetric circulations of tropical stratosphere, using zonally averaged momentum, continuity and heat and heat energy equations for numerical model
03 p0461 A69-13681

Photosphere models comparison based on theoretical rotational temperatures of various diatomic molecular free radicals, using faint lines method
03 p0512 A69-13694

Hydrodynamic model of atmospheric circulation in equatorial region, using group invariant method
03 p0462 A69-13931

Nonstationary model of mesoscale atmospheric vortex with vertical axis based on atmospheric thermohydrodynamics
03 p0462 A69-13932

Mean meridional pressure profiles and atmospheric mass readjustment time dependence for initially at rest atmosphere with mean baroclinity, using frozen gradient model
04 p0627 A69-15086

Bearing deviation in model HF transionospheric propagation with three dimensional electron density variation and no magnetic field
04 p0559 A69-15209

Digital computers for global atmospheric circulation, describing circulation models and computer produced color movies utilization
04 p0628 A69-15363

Antarctic spread F irregularities, examining models and performing ray tracing
04 p0595 A69-15439

Venus and Mars atmosphere structure, comparing Venus atmosphere model with Mariner 5 observations
05 p0824 A69-16248

Ionospheric models for studying nature of difference in relationships between HF radio waves Doppler shifts and changing ionosphere
05 p0755 A69-16269

Inhomogeneous dielectric filling to simulate curvature in model earth-ionosphere waveguide
05 p0732 A69-16346

Multiple light scattering in spherical planetary atmosphere based on geometrical model, calculating twilight glow brightness
05 p0828 A69-16632

Multilevel numerical weather forecast scheme with stable initial data
05 p0789 A69-16636

Model for Evershed effect postulating unipolar symmetrical sunspot surrounded by magnetic knots of opposite polarity
06 p0999 A69-16977

Terminal velocities of dust particles for two Venus atmospheric models from Mariner 5 and Venera 4 data, obtaining vertical wind velocity requirements
06 p1001 A69-17172

Mercury atmospheric models for preliminary environmental criteria to be used in spacecraft design and engineering trade-off studies
[AIAA PAPER 69-54] 06 p1010 A69-18042

Upper atmospheric models, considering satellite orbital and solar panel torques, prediction, atmospheric density and composition measurements, etc
[AIAA PAPER 69-50] 06 p1011 A69-18085

Venusian atmosphere model developed from satellite and earth based radar data for environmental criteria in spacecraft design and mission planning
[AIAA PAPER 69-51] 06 p1011 A69-18096

Double scattering effects of sky radiation and outgoing radiation balance in disturbed atmosphere, using homogeneous plane parallel atmospheric model
07 p1175 A69-18270

Terrestrial and Cytherean atmospheres evolution based on gray atmosphere model, surface energy budget and partition of water and carbon dioxide
07 p1213 A69-18608

Radiative transfer problems in inhomogeneous anisotropically scattering plane parallel planetary atmospheres with internal source distributions solved by recursive method
07 p1213 A69-18610

ELF radio waves reflection coefficients calculated from two layer ionospheric model, noting ion collision frequency effect in Schumann resonance frequency band
07 p1124 A69-18820

Dynamics of large scale processes in atmosphere extended to two week predictions using nine level hemispheric moist general circulation model
07 p1175 A69-18895

Long wave radiative water vapor cooling in troposphere determined by numerical prediction model, including vertical distribution of cloud and moisture effects
07 p1175 A69-18896

Similarity of mean flow patterns of natural local wind to model wind in wind tunnel
07 p1176 A69-18964

Large scale tropical eddies using two layer dry atmospheric model containing nongeostrophic effects and parametrized dissipation
07 p1176 A69-19035

Wave motion onset and waveforms in rotating annulus with sinusoidally varying temperature differences
07 p1126 A69-19039

Mathematical frame for cloud models, discussing condensation, collection and advection processes and freezing and electrical effects
07 p1176 A69-19041

Solar photosphere model with two stream columnar representation of granulation for predicting continuous radiation field
07 p1217 A69-19238

Quiescent solar prominences horizontal oscillations, explaining periods, damping times and prominence shape changes by model of freely oscillating prominence in corona
07 p1205 A69-19245

Truncation error reducing scheme for balanced forecast models
07 p1176 A69-19629

Clear atmosphere model based on path of sight equilibrium radiance and nonabsorption permitting integration of equation of transfer
07 p1130 A69-19643

Collisional processes relevant to daytime and nighttime models of upper atmosphere neutral density and temperature
07 p1130 A69-19654

Diffuse reflection and transmission of parallel rays by homogeneous two layer slab, solving simultaneous integral equations governing auxiliary functions
08 p1350 A69-19799

Emission line formation in homogeneous chromosphere for noncoherent scattering, considering various chromosphere models
08 p1381 A69-19800

Linearized model for vertical propagation of Rossby waves through atmosphere with Newtonian cooling, discussing atmospheric wind effects
08 p1344 A69-19812

Synthesis of oblique incidence ionograms for quasi-linear ionospheric model with spherical earth-ionosphere geometry neglecting geomagnetic field
08 p1274 A69-20044

Collisional excitation and ionization rates comparison in statistical equilibrium model atmosphere calculations
08 p1385 A69-20065

Preliminary model atmospheres for cepheid variable eta Aquilae, discussing mass loss processes
08 p1386 A69-20089

Weather forecasting using statistical technique and Subsynchronous Advection Model of Weather Bureau, discussing mathematical background for various early morning predictions
08 p1345 A69-20298

Two level quasi-geostrophic model to probe atmospheric general circulation, noting functional dependence of zonal momentum meridional flux
08 p1346 A69-20314

Atmospheric haze effect on Umkehr measurements, considering computation from direct sounding of vertical ozone distribution and from model atmospheres
08 p1308 A69-20316

Upper atmosphere density variations and multiplicative factor necessary for adjustment of density variations of reference models
08 p1397 A69-20761

Chemical composition of stellar atmospheres by model atmospheres, considering atomic transition, line broadening and thermodynamic equilibrium
08 p1402 A69-20904

Aurigae star HD 35620 with respect to epsilon Virginis using model atmosphere and high dispersion spectra
08 p1403 A69-20913

Nighttime Venus ionosphere models compared with Mariner 5 observations, discussing implications with regard to He and H abundance consequences and nightglow
09 p1594 A69-21695

Model of auroral backscatter from E region including ionospheric refraction, comparing computations to

experimental HF auroral backscatter data for aspect sensitivity

09 p1488 A69-21700

Density inversion in convective zone of stellar photospheres occurring in Eridani atmospheric model under certain conditions

09 p1595 A69-21843

Atmospheric models for metal deficient stars of K and G spectral type, studying reduced metal abundance effect on atmospheric structure

09 p1596 A69-22055

Large scale heat sources influence on formation and dynamics of ultralong waves in atmosphere, using linear time dependent quasi-geostrophic model

09 p1491 A69-22164

Subdwarf HD 25329 studied with model atmosphere approach, using H alpha, Na I and Mg I profiles for effective temperature

09 p1600 A69-22199

Optically thick planetary atmospheres in radiative-convective equilibrium investigated by models with adiabatic temperature gradient in troposphere, discussing gray stratospheric solution

09 p1600 A69-22200

Dipole magnetosphere model with cylindrical or spherical forbidden band for studying plasma motion in quasi-hydrodynamic approximation

10 p1769 A69-23901

Conductivity and permittivity for ion and electron resonance region of ionospheric plasma model calculated in quasi-hydrodynamic approximation

10 p1686 A69-23908

Radio astronomical observations of Venus atmosphere interpreted noting agreement with model based on Venera 4 data

10 p1791 A69-24202

Nongray models of atmospheres of early stars, giving Avrett-Krook method of correcting temperature distribution

11 p1954 A69-24361

Growth rates for convective disturbances propagation in atmosphere with linear entropy variation, noting WKB approximation

11 p1957 A69-24422

Model for radiative transfer in atmosphere-ocean system by Monte Carlo method, considering Rayleigh and Mie scattering

11 p1877 A69-24851

Model for shock propagation from point energy source into cold atmosphere with exponential density variation

11 p1871 A69-25123

D/H ratio in Venus exosphere, discussing isotopic fractionation mechanisms and Lyman alpha data from Mariner 5

11 p1962 A69-25145

Full wave calculation of gravity waves for thermospheric model, describing wave type reflection, transmission, conversion and coupling by scattering matrix elements

11 p1878 A69-25150

Model ion-exosphere for nonrotating planet with static dipole magnetic field generalized by permitting density and temperature variations over baropause

11 p1879 A69-25284

Radiation attenuation in hazy lower atmosphere, calculating attenuation coefficients and using spherical model of haze particles and empirical formula for haze spectra

11 p1913 A69-25571

Venus brightness temperatures vs phase angle to define spectra of day and night face at short wavelengths, using model atmosphere

12 p2153 A69-25806

Linearized atmosphere model above flat earth, applying variational principle to energy between geostrophic equilibrium and reestablished states

12 p2125 A69-25954

Density stratified model of troposphere and constant gravity field for ground level pressure perturbations in mesoscale region

12 p2126 A69-26016

Theories for universal time controlled polar F region reevaluated in light of satellite low energy charged particle observations

12 p2065 A69-26103

Atmospheric element contents of F stars of Cyg, Her and Boo, using Planckian gradients and computer calculations for growth curves of atmospheric models

12 p2157 A69-26335

Atmospheric models for electromagnetic scattering of monochromatic IR and microwave radiation by natural suspensions as hazes clouds and precipitation

12 p2030 A69-26467

Quantitative magnetic field models of magnetosphere for analyzing field configuration variations and adiabatic particle motion

12 p2072 A69-26738

Satellite observations of geomagnetic tail in magnetosphere near midnight meridian plane, discussing formation, shape, plasma sheet and models

12 p2072 A69-26739

Auroras and polar magnetic substorm observations limited comparison due to magnetospheric models inability to interpret daytime precipitation zones and particle energy spectra

12 p2072 A69-26740

Internal guiding of microwaves by elevated tropospheric layer noting refractive index, radius of curvature and attenuation

12 p2032 A69-26856

Spectral model used for analysis of atmospheric turbulence as related to loads on gliders

12 p2127 A69-26931

Nonuniform two dimensional hydromagnetic waves incident on idealized lower ionosphere, discussing validity of various models

12 p2074 A69-26960

Magnetospheric field configuration in midnight meridian, considering cavity boundary surface and trapping region currents and tail sheet current

13 p2252 A69-27532

Steady state model envelopes of Be stars, determining excitation and ionization states for hydrogen atoms

13 p2338 A69-27559

Stellar atmosphere models of pure hydrogen in hydrostatic, radiative and statistical equilibrium, including Lyman-alpha and continua, discussing nonLTE deviations

13 p2338 A69-27560

RR Lyrae gap stellar model atmospheres including radiation spectra, temperature radiation and convection, etc

13 p2338 A69-27561

White dwarf atmospheric structure, analyzing masses and radii for DA stars and surface parameters of Eri B, based on grid of line blanketed models

13 p2339 A69-27563

Model atmosphere source function, mean intensity and flux by matrix methods

13 p2288 A69-27564

Solar atmosphere five minute oscillations observed by Frazer divided into two harmonic atmospheric model for studying oscillation region height and mean temperature

13 p2343 A69-27627

Numerical methods for time integrating first order differential equations, emphasizing atmospheric oscillations in baroclinic model, evaluating errors

13 p2290 A69-27636

Two temperature lapse rate and single moisture lapse rate troposphere model for calculating temperature and moisture from satellite radiometry

13 p2252 A69-27638

Venusian atmospheric model based on Venera 4 measurements, calculating probe distance travel, temperature, density and pressure profiles

13 p2345 A69-27688

Venus atmosphere optical properties on basis of Venera 4 data, proposing models for measured rotational temperature and subcloud atmosphere radiative equilibrium

13 p2345 A69-27691

Magnetospheric ring current model from ground stations data to interpret observed magnetic field disturbances

13 p2253 A69-27699

Wind shifts and mean gustiness calculation from short range weather forecasts, using dynamic model for wind motion in atmospheric boundary layer

13 p2293 A69-27844

Meteorological problems in Italy analyzed by digital computer program through numerical integration of atmospheric models to provide weather forecasts

13 p2295 A69-28651

Perturbed geomagnetic field structure during magnetic storm recovery phase calculated by magnetospheric magnetic field model, accounting for various external field sources

13 p2257 A69-28697

Planetary long waves behavior in atmospheric models, explaining unsteady components by means of filtered equations

14 p2472 A69-28782

Multilevel numerical weather forecast scheme with stable initial data

14 p2472 A69-28792

Ionograms in vertical depletion duct in horizontally stratified isotropically refractive plasma, considering vertical propagation and ray paths traces dependence on electron concentration

14 p2434 A69-28945

He 3 production and loss in atmosphere, discussing precipitation of energetic magnetospheric particles, thermal escape, nonthermal processes, etc

14 p2435 A69-28965

Low energy charged particle motion parallel with magnetic force lines analyzed in magnetosphere model with constant electric field

14 p2512 A69-29040

Magnetic field intensity, plasma pressure and energy density relations for macroscopic plasma motion inside neutral sheet from two dimensional model

14 p2440 A69-29119

Thermally excited diurnal wind oscillations in lower mesosphere using model atmosphere in CIRA 1965, discussing daytime ozone density profiles

14 p2441 A69-29379

Three dimensional model of atmospheric drift currents in equatorial region of world ocean system based on nonlinear differential equations

14 p2472 A69-29405

Microwave brightness temperatures for downward viewing over open seas from above atmosphere, using tropospheric model containing homogeneous layer clouds

14 p2415 A69-29515

General atmospheric circulation instability factors for statistical weather forecasting, considering atmosphere as nonlinear oscillating system, analyzing relaxation time

14 p2476 A69-29820

Climate studies with allowance for radiative heat inputs, constructing nonadiabatic motions model for improving prognosis

14 p2477 A69-29827

Water-air interface models unreliability in calculating atmospheric heat and humidity turbulent flow over ocean

14 p2443 A69-29839

Atmospheric heat exchange and circulation simulated by rotating containers, reproducing temperature field and dynamic structure above large area

14 p2478 A69-29840

Atmospheric dynamics parameters of Mercury, Venus, Mars and Jupiter, discussing generalized circulation theory

14 p2526 A69-29841

Ionospheric models for motion of slightly ionized homogeneous cold plasma influenced by electrostatic field and neutral particles flow, considering geomagnetic effects

14 p2499 A69-29863

Ionospheric inhomogeneity model for motion of infinite elliptical cylinder of cold plasma in neutral particle flow and ambient electrostatic and magnetostatic fields

14 p2500 A69-29864

Ionospheric inhomogeneities models for plasma motions, considering electron-ion collisions

14 p2443 A69-29865

Supergiant HD-33579 in Magellanic cloud by model atmospheres, discussing abundances

14 p2529 A69-29979

Outer convection zone of cool white dwarf by atmospheric models, using mixing length theory and abundances

14 p2529 A69-29982

Hydrogen Lyman alpha nightglow models, discussing solar photon scattering in geocorona and hydrogen vertical distribution

15 p2595 A69-30191

Nonlinear limb darkening corresponding to nongray stellar atmosphere model applied to light curve for compact eclipsing binary systems

15 p2689 A69-30563

Pure hydrogen stellar atmosphere nonLTE models, calculating surface temperature rise due to H alpha line effect on continuum energy balance

15 p2693 A69-30777

Surface gravity and temperature model atmospheres for O-type stars with UV line blanketing

15 p2693 A69-30778

Solar cycle effect on high latitude magnetic activity, discussing annual variations and Lassen auroral zone model confirmation

15 p2598 A69-31207

Seasonal and latitudinal models of atmospheric wind and temperature structure between 30 and 120 km altitude

15 p2600 A69-31367

Atmospheric models for pressure variation and neutral air winds in thermosphere, discussing wind velocity vector relation to satellites orbital inclination
15 p2603 A69-31403

Plasmasphere hydrogen and He ion concentration models, using diffusive equilibrium theory for plasmasphere parameters
15 p2677 A69-31447

Jet stream blocking process simulation using geostrophic system of equations, considering effects of orography and contrast heating due to land-sea distribution
16 p2809 A69-32602

Horizontal shear effect on structure of growing baroclinic waves by two layer model, assuming small radius of deformation, compared to planetary scale
17 p2960 A69-33150

Flow over uniformly rough surface in planetary boundary layer from mixing length wind spiral model, using surface shear stress and wind direction data
17 p2997 A69-33153

Mixing length model to relate turbulent shear stress to mean velocity field within planetary boundary layer above surface roughness change
17 p2997 A69-33154

Temperature correction procedures for line-blanketed model atmospheres modified, noting effect on convergence to flux constancy
17 p3039 A69-33730

Lateral mixing of air masses in jet stream by water fluid model experiments, discussing steady and non-steady state turbulent momentum exchange
17 p3000 A69-33759

Cyclonic vortices production by horizontal convergence in rotating water bowl as function of bottom surface inclination, modeling cyclogenesis in jet stream entropy field
17 p3000 A69-33760

Ionospheric absorption and virtual heights relationships for electron density distribution in lower ionosphere, computing model profiles
18 p3125 A69-34248

Earth atmospheric large scale motion simulated in laboratory and by numerical technique
18 p3127 A69-34668

Anisotropic ionospheric model for VLF TM and TE modes excitation, noting nighttime phase velocity variations
18 p3101 A69-34797

Stochastic meteorological models based upon presence of weather regimes, illustrating association with statistical inference problems
18 p3166 A69-34822

Acoustic gravity waves generated in isothermal atmosphere by ground energy source calculated using stationary phase method and kinematic theory
18 p3129 A69-34953

Secor data reduction to correct tropospheric refractive effects of radio ranging on earth satellites using tropospheric model
18 p3104 A69-35200

Fourier transform laboratory spectroscopy for absorption near earth atmosphere millimeter wave spectrum, discussing integrated absorption strength and dimeric effect
18 p3177 A69-35240

Error sources in forecasts for heights of isobaric surfaces obtained by numerical integration of prognostic equations of equivalent barotropic models
19 p3361 A69-35770

Monte Carlo relaxation method for physically self consistent model stellar atmospheres, discussing stability, accuracy and convergence of solution
19 p3425 A69-36337

Atmospheric models for specified effective temperatures, hydrogen-to-metal ratios and surface gravities in studying metal deficiency effect on stellar atmosphere
19 p3425 A69-36338

Numerical weather prediction using four level primitive atmospheric model for studying frontogenetic processes in deepening cyclone
19 p3303 A69-36408

Partial differential equation representing influence of radiative and turbulent transfers of atmospheric heat, based on absorption coefficients for terrestrial radiation
19 p3363 A69-36498

Atmospheric horizontal mixing caused by quasi two dimensional macro turbulent motions, describing micro and mesoscale processes using numerical model
19 p3363 A69-36500

Numerical integrations for modified model incorporating ozone production equation and heating from

ozone radiation absorption and long wave cooling for upper atmospheric circulation
19 p3363 A69-36502

Operational circulation model numerical experiment suggesting elimination of spurious divergence-on-divergence interactions from implied vorticity equations in primitive equations
19 p3363 A69-36503

Optimum aerological network design, discussing atmospheric model, numerical analysis, data acquisition, weather forecasts, rms measurement error, etc
19 p3364 A69-36505

Plasma flow structure near frontal point in earth magnetosphere, using quasi-hydrodynamic two dimensional model to obtain power series solution
20 p3594 A69-37019

Plasma concentration in nondipole magnetosphere model from pc 5 pulsations periods for high geomagnetic latitudes, noting solar winds effect
20 p3521 A69-37043

ELF radio wave propagation characteristics analyzed by two layer ionosphere model
20 p3488 A69-37285

Wind velocity below 100 meters from Laikhtman atmospheric boundary layer model, solving equations for horizontally homogeneous, stationary and nonadvective air flow
20 p3571 A69-37695

Primitive earth upper atmosphere thermal models, considering roles of exospheric temperature and free hydrogen availability in methane dominated environment
20 p3608 A69-38056

Thermosphere temperature shape parameters from probe flights, showing dependence on hour angle
20 p3534 A69-38088

Nongray greenhouse model of Venus atmosphere possessing IR opacity due to carbon dioxide, water and diatomic N compatible with Mariner 5 and Venera 4 results
20 p3615 A69-38259

Auroral electric current system model to explain magnetic disturbances associated with auroral breakups
21 p3710 A69-38505

Dungey reconnection model of magnetosphere with dayside current sheet and pseudotrapping region compared with dayside observations of precipitation regions
21 p3711 A69-38511

Ionosphere characteristics in terms of airglow, describing daytime F/D layers formation model provided by photoionization, loss processes and ambipolar diffusion
21 p3712 A69-38517

Airglow and vertical eddy transport photochemical models, analyzing O green line and OH emission distribution
21 p3713 A69-38523

Sharply bounded homogeneous ionospheric model to solve modal equation, discussing lower ionospheric conductivity from VLF transmission sudden enhancements of strength (SES)
21 p3714 A69-38554

Daytime electron and ion composition model for height range from 150 to 1500 km at moderate latitudes and minimum solar activity
21 p3714 A69-38555

LTE departure calculated for He I in hot star model atmospheres for effects on populations of singlet and triplet states
21 p3801 A69-38761

Layer model of random discrete inhomogeneities used to derive harmonic wave one dimensional scattering field and mean square of field
21 p3673 A69-38993

Geopotential field forecast for 500 mb surface, comparing results from quasi-solenoidal and quasi-geostrophic models
21 p3758 A69-39110

Tropospheric refractivity height profile model, computing corrections to satellite Doppler or range data
21 p3678 A69-39748

Vertical heat exchange flux model using heat conduction equation compensating for tropospheric and stratospheric radiation divergence, calculating diffusion coefficient
22 p3936 A69-40137

Spectrophotometric observations of delta Scuti short period variable stars compared with model atmospheres
22 p4015 A69-40150

Nongray models representing atmospheres of F and G supergiants computed and tabulated for 5400-6600 K and various surface gravities
22 p4015 A69-40152

Type 3 solar radio bursts observed during April-October 1967 for two alternative models of active region streamers in outer corona
22 p4003 A69-40300

Neutral exosphere model for nonrotating planet permitting barosphere uniform rotation at certain angular velocity, determining velocity distribution and density
22 p4023 A69-40524

Helium-carbon star BD plus 10 degrees 2179 re-analyzed by grid of constant flux models containing right amount of C
22 p4026 A69-40652

Model atmospheres of late type stars with solar abundances, effective temperatures between 2000-4000 K and gravities corresponding to dwarf, giant and supergiant stars
22 p4027 A69-40654

Exact solution of macroscopic line transfer equation including electron scattering terms for Milne-Eddington model atmosphere, discussing electron scattering effect on growth curves
22 p4007 A69-40903

WE and SN wind components models from 60 to 130 km for different months and latitudes, discussing meridional and interhemispheric circulations
23 p4154 A69-41306

Atmospheric zonal circulation compatible with meridional obtained from model based on dynamic and heat flux equations and Williams and Davis hypothesis
23 p4183 A69-41522

Uniform random field model development by taking moments in linear transformation form of certain initial field
23 p4183 A69-41523

Acoustical ray tracing in horizontally layered and vertically sectioned atmosphere on digital computer using shifting Cartesian coordinate system
23 p4154 A69-41532

F region dynamic model, including variations in temperature, electron and molecular ion concentrations, etc
23 p4156 A69-41843

Qualitative model of atmospheric mass circulation constructed from radar meteor trail drifts observations, considering solar thermal radiation and zonal wind direction
23 p4214 A69-41862

LF hydromagnetic waves propagation along geomagnetic field lines in gyrotronic ionosphere model taking Hall effect into account
23 p4157 A69-41864

Numerical weather forecasting at high and middle latitudes, discussing geostrophic forecasting equations and barotropic models
23 p4183 A69-42024

Density model for free oscillations of earth, noting dependence on core radius and S wave velocity at top and bottom of D layer
23 p4158 A69-42117

Noncyclic daily solar quiet variation in mean hourly geomagnetic field by including noncyclic variation term in regression model
23 p4158 A69-42170

Distribution function for thermalization distances derived for infinite atmosphere with plane source in incoherent light scattering
23 p4192 A69-42403

Atmospheric model for calculating wind velocity profile and turbulence of stable atmospheric boundary layer with given temperature stratification and pressure gradient distribution
23 p4184 A69-42489

Model atmosphere analysis of line identifications and equivalent width data for relatively cool Ap star HD 204411, discussing atmospheric composition
24 p4376 A69-42664

Radiative cooling models for various midlatitude synoptic features, including stationary front and cyclones
24 p4343 A69-43064

Angular grid spacing resolution near poles effect tests in global prediction model for geophysical fluid dynamics, investigating forecast height and wind fields
24 p4344 A69-43066

Model for ozone formation, distribution and decomposition at 15-45 km assuming zonal symmetry, including time effects of photochemistry, advection and turbulence
24 p4309 A69-43147

- Hadley and equatorial cell models for mean meridional circulation in terms of vorticity equation
24 p4345 A69-43152
- Atmospheric model consisting of varied mass liquids in water tank for studying circulation conditions, discussing earth zone and layer partitioning and Prandtl analysis
24 p4346 A69-43153
- Polar cap ionospheric response to solar cosmic ray events observed by Mariners 2 and 4 solar proton measurements used to test magnetosphere models
24 p4373 A69-43621

ATMOSPHERIC MOISTURE

- Total atmospheric moisture content by measuring radio wave absorption at water vapor molecule rotational spectrum absorption line
02 p0274 A69-11438
- Atmospheric water vapor content from summer-fall 1966 measurements of atmospheric radio wave absorption of thermal radio emission, describing experimental apparatus
02 p0274 A69-11439
- Vertical atmospheric turbidity distributions of haze and water vapor, noting effect of variations on scattering and absorption determination
02 p0277 A69-12777
- Atmospheric temperature and water vapor variations and seasonal environmental changes effects on cosmic ray neutron and meson monitor counting rates
03 p0498 A69-12936
- Environmental temperature and water vapor increases associated with ascending thermals estimated by penetrative convection
03 p0460 A69-13340
- Northern California humidity to 32 km utilizing alpha radiation hygrometer and associated balloon sounding equipment
03 p0461 A69-13345
- Atmospheric water vapor content determination from microwave radiation measurements and satellite aircraft
06 p0953 A69-17996
- Atmospheric microwave radiation and sensitivity of airborne radiometric sounding in water and moisture contents determination
06 p0954 A69-18001
- Imagery degradation by moisture condensation on thermal IR scanners optics during aircraft descent from higher to lower altitude
08 p1311 A69-19821
- Aircraft structural aluminum alloy fatigue life, considering atmospheric relative and absolute humidity
09 p1521 A69-21390
- Atmospheric humidity effect on efficiency of geomagnetic field scales with taut-strip suspension and temperature fluctuation
09 p1494 A69-21518
- Solar radiation absorption measurements by balloon for atmospheric water vapor distribution
09 p1536 A69-21864
- Condensation kinetics in clouds, determining cloud spectrum evolution taking stochastic processes into account
10 p1722 A69-23972
- Statistical analysis of convective layer thickness and moisture content effect on convective cloud configurations, using satellite TV pictures
11 p1912 A69-24827
- Mean vertical moisture profile for summer and winter midlatitude stratosphere from Soviet radiosonde data
12 p2070 A69-26582
- Tenuous cirrus cloud influence on 6.4-6.9 micron Nimbus 2 water observations, discussing equivalent black body temperatures correspondence to cloud and clear areas
12 p2075 A69-27003
- Two temperature lapse rate and single moisture lapse rate troposphere model for calculating temperature and moisture from satellite radiometry
13 p2252 A69-27638
- Venusian water vapor spectroscopic data indicating longitudinal and time dependent variations in abundance
13 p2345 A69-27650
- Satellite and rocket probe measurements of water vapor in mesosphere
13 p2253 A69-27694
- Incoming IR flux measurements at high altitude, noting flux increase due to water vapor condensation in troposphere
13 p2256 A69-28647

- Temperature of underlying surface and moisture content of atmosphere from satellite thermal radio emission measurements
15 p2648 A69-30641
- Harmonic analysis for computing diffusing matter with periodically varying surface concentration applied to electrical insulants degradation by atmospheric moisture
15 p2592 A69-31057
- Virtual temperature change with respect to height of saturated air rising during water vapor condensation, discussing actual temperature and precipitation factor
16 p2808 A69-32454
- Latent heat of condensation related to atmospheric dynamics in cloud formation processes with allowance for moisture exchange
17 p2997 A69-33188
- Vertical tropospheric humidity distribution estimation from IR spectra obtained by TIROS satellites
18 p3126 A69-34284
- Atmospheric temperature and moisture fields obtained by linear equations and objectively analyzed, considering underlying sea surface energy and cumulus cloud distribution
20 p3523 A69-37351
- Satellite onboard transmission measurements determining atmospheric water vapor influence on integrated refractivity at specific absorption line resonant frequency
20 p3545 A69-38097
- Condensation kinetics in clouds, determining cloud spectrum evolution taking stochastic processes into account
21 p3760 A69-39658
- Water vapor abundance in Mars atmosphere determined from spectrograms, noting restricted existence on surface
22 p4018 A69-40268
- Subjective feeling of dampness correlation with relative humidity of air at zero and below zero C temperatures
23 p4109 A69-41870
- Mean absolute relative humidity variations above earth surface over various time intervals during cloudless nights, obtaining spatial humidity differences and corresponding extinction coefficients
24 p4346 A69-43158
- ATMOSPHERIC NEUTRON FLUX DENSITY**
U NEUTRON FLUX DENSITY
- ATMOSPHERIC NOISE**
U ATMOSPHERICS
- ATMOSPHERIC PHYSICS**
NT CLOUD PHYSICS
- Optical radar for studying atmospheric water vapor, density, temperature and aerosols
01 p0090 A69-10540
- Atmospheric optical data recorded by instrumented aircraft near Crater Lake, discussing surface spectral irradiance data
01 p0111 A69-10846
- Energy transport in atmosphere studied by considering sphere in isotropic fluid in infinite field without gravity, using first law of thermodynamics
01 p0067 A69-11032
- Tropical 6300 angstrom red oxygen nightglow enhancements related to variations in height of nighttime F 2 layer, noting implications for layer structure and physics
01 p0068 A69-11113
- Linearized perturbation treatment developed for photochemical and dynamical effects in gravity wave production of E-region ionospheric irregularities, including ion convergence
01 p0073 A69-11175
- Atmospheric optical properties stability determination for various optical densities, assuming horizontally homogeneous medium with properties constant during observation
01 p0074 A69-11186
- Automatic spectrophotometer for measuring sky spectral brightness at 6910-4040 angstroms, determining point of minimum brightness
01 p0074 A69-11187
- Boundary layer effect on large scale atmospheric processes from analyzing two layer free atmosphere model, plotting weather forecast charts
02 p0273 A69-11435
- Charts summarizing daily solar phenomena, cosmic rays, geomagnetic variation, ionosphere, radiowave propagation and airglow observations in Japan
02 p0315 A69-11732
- Surface radiation balance measurements in India during IQSY, discussing diurnal, seasonal and spatial variations of net radiation
02 p0307 A69-11820

- Tropical night F layer maintenance mechanism, noting airglow enhancement and ionization source association with plasma drifts
02 p0242 A69-11825
- Upper atmosphere structure, phenomena and composition, discussing interactions between photons, electrons, atoms and molecules
02 p0242 A69-11902
- Mars and Venus atmospheres, Martian atmosphere dynamics, Mars ionosphere and use of space probes
02 p0318 A69-12102
- Relationships derived by dimensional arguments connecting vertical heat fluxes and horizontal momentum in constant flux layer with other relevant variables
02 p0275 A69-12692
- Taylor column existence in compressible atmosphere, discussing baroclinicity and stratification effects in earth and Jupiter atmospheres
02 p0326 A69-12697
- Probabilistic model for scattering function to solve radiative transfer problems in externally illuminated spherical shell atmosphere with perfectly absorbing core
02 p0328 A69-12751
- Weighting functions for finite optically thick atmospheres, discussing emission line formation
02 p0328 A69-12755
- Barotropic instability analyses by method of jet stream like fields and energy transport from zonal current to wave disturbances based on vorticity equation
02 p0276 A69-12758
- Sunrise effects in lower D region by solar eclipse, discussing anomaly in ionospheric absorption due to negative ion factor or recombination coefficient
02 p0246 A69-12767
- Horizontal drifts at E region level measured in India by spaced phase path technique
03 p0421 A69-13330
- Air mass cumulus cloud growth stimulation by means of vertical updrafts capable of perforation of retaining layers
03 p0461 A69-13409
- Structure and mean molecular weight measurement of unknown atmosphere assessed from high altitude tests in earth atmosphere
[AIAA PAPER 68-1054] 03 p0512 A69-13699
- Nonstationary model of mesoscale atmospheric vortex with vertical axis based on atmospheric thermohydrodynamics
03 p0462 A69-13932
- Airborne radiometric /8 to 14 micron/ temperature measurements, determining emissivities of ocean, stratus clouds, desert and snow
04 p0592 A69-14653
- East-West aligned fast auroral waves, suggesting origin in hydromagnetic processes occurring near equatorial plane
04 p0594 A69-15123
- Far IR observations of atmospheric molecular lines, using high altitude aircraft platforms
04 p0628 A69-15146
- Ionosphere structure, properties and research techniques
04 p0594 A69-15166
- Long distance propagation of acoustic gravity waves ducted in thermosphere, noting effect of seasonal variations in polar region
04 p0595 A69-15437
- International cooperation results in field of optical tracking of satellites for solving problems of atmospheric physics, geophysics and geodesy
06 p1042 A69-17050
- Upper atmosphere physics, atmospheric composition and separation of gases, nature of air flow, water vapor content and lower ionosphere structure determinations by rocket
[UN PAPER 68-95693] 06 p0949 A69-17058
- Interamerican Experimental Network of Meteorological Investigation with Rockets /EXAMET- NET/, discussing atmospheric parameters measurement at high altitude
[UN PAPER 68-95903] 06 p0950 A69-17062
- Regularization methods in inverse problems of atmospheric optics, analyzing atmospheric thermal sounding and interpretation of radiation measurements
06 p0919 A69-17616
- Mathematical techniques for treating satellite based atmospheric data involving radiative transfer equation inversion, noting scattering and temperature measurement problems
06 p0957 A69-17618
- Inert gas discontinuous injection into nonequilibrium laminar boundary layer
06 p0860 A69-17635

Relation between satellite data concerning thermal microwave radiation and meteorological conditions in lower atmosphere for possible use in weather forecasting

06 p0953 A69-17995

Microwave absorption and scattering by atmospheric precipitation as function of temperature and water droplet size

06 p0954 A69-17997

High altitude plastic balloon platforms for atmospheric research noting increased capacities in altitude, payload and flight duration
[AIAA PAPER 69-156]

06 p1010 A69-18067

Atmospheric measurements and experiments using aircraft as platforms, noting aircraft operation in severe weather, electrical supply problem and aircraft wake problem
[AIAA PAPER 69-157]

06 p0869 A69-18153

Receiving system of CENFAM multistation radar project for meteoric and upper atmosphere studies composed of antennas connected to form product-interferometer pairs

07 p1077 A69-18674

Dynamics of large scale processes in atmosphere extended to two week predictions using nine level hemispheric moist general circulation model

07 p1175 A69-18895

Tropospheric energy cycle interannual variability and quasi-biennial oscillation from geostrophic computations of eddy kinetic energy, energy transfer and internal redistribution

07 p1129 A69-19628

Radiative transfer by doubling very thin layers in problem of diffuse reflection from plane-parallel atmosphere eliminates numerically solving transfer equation

08 p1420 A69-20064

Ionospheric plasma flute instability considered as possible cause of occurrence of elongated small scale inhomogeneities in F2 layer

08 p1309 A69-20425

Recombination rate of nitrogen atoms using NO titration method, tabulating reactions and emissions during various stages of titration

08 p1309 A69-20454

Mars and Venus atmospheric properties, noting influence of biosphere and human activity on earth atmosphere

08 p1408 A69-21160

Spin stabilized spherical satellite in high elliptical orbit for lower thermosphere measurements during entire solar cycle

09 p1610 A69-22009

Radiation field at optical depths within plane parallel Rayleigh scattering atmosphere subjected to generalized free surface boundary conditions

09 p1606 A69-22423

Atmospheric extinction function in Chile by using photoelectric spectrum scans, observing neutral component, Rayleigh scattering and ozone absorption variations

10 p1777 A69-23386

Silicon carbide particle growth and motion in carbon star atmospheres

10 p1781 A69-23678

Atmospheric influence on plane oscillations of space vehicle moving at 100-150 km heights

10 p1792 A69-24208

Mean and eddy motions in atmosphere described by mathematical expressions for total and mean kinetic energies

11 p1911 A69-24323

Stability of barotropic perturbations superimposed on wind velocity profile of basic currents in geostrophic multilayer models

11 p1911 A69-24586

Jet flows instabilities with vertical and horizontal velocity drifts from numerical integration of atmospheric motion equations linearized with respect to small perturbations

12 p1215 A69-25950

Linearized atmosphere model above flat earth, applying variational principle to energy between geostrophic equilibrium and reestablished states

12 p1215 A69-25954

Airborne Q switched ruby laser for studying upper atmosphere meteoric formations optical characteristics and kinetics against background of underlying surface

12 p1215 A69-25955

Semiannual density variations in thermosphere and exosphere as function of mixtopause height variations

12 p2064 A69-26012

Overlay technique for analysis of F region transition into F1 and F2, noting ionization and recombination

12 p2065 A69-26102

Linearized steady state equations of motion solved for boundary conditions of fluid lying between horizontal planes with temperature varying horizontally

12 p2066 A69-26134

Atmospheric turbulent energy spectra in boundary surface layer, considering homogeneous axisymmetric model in presence of temperature and velocity gradients

12 p2067 A69-26355

Optimum coordination between homogeneous isotropic geopotential field and derivatives, estimating efficiency of geopotential and wind fields simultaneous analysis

12 p2126 A69-26580

Physics of magnetosphere - Conference, Washington, D.C., September 1968

12 p2071 A69-26734

Dynamics of magnetosphere, discussing auroral oval position, ring currents, plasma density and magnetic field variations in near polar region

12 p2072 A69-26741

Earth radiation belts formation as function of particle injection into trapped radiation zones or proton and electron leakage

12 p2150 A69-26742

Ballistically effective atmospheric parameters for rocket vehicle design manuals involving application of climatological concepts of meteorology

12 p2175 A69-26874

Kelvin waves relation to quasi-biennial oscillation, using zonal wind and temperature variance data taken at Canton Island

13 p2290 A69-27391

Integral particle flux of protons and electrons in upper atmosphere, discussing energy and angular distribution

13 p2328 A69-27757

Heat convection mechanism in two phase autooscillatory system generalized to convective heat transfer in cloudy atmosphere

13 p2292 A69-27798

Electron flux-atmosphere interaction solved by numerical integration on computer, discussing auroral ionosphere

14 p2513 A69-29069

Daytime ionospheric screening effect on low latitude geomagnetic micropulsations estimated using ionosphere model

14 p2441 A69-29380

Algorithm for solving Dirichlet problem of nonlinear elliptical differential equations representing atmospheric dynamics balance equation

14 p2470 A69-29401

Line of sight atmospheric path measurements for atmospheric inhomogeneities, using phase quadrature, microwave and near IR techniques

14 p2415 A69-29516

Atmospheric multifrequency probing accuracy limitation imposed by irregularities based on scatter theory

14 p2449 A69-29535

Hydrodynamic theory of climate and atmospheric circulation, emphasizing numerical experiments role in studying large scale processes

14 p2476 A69-29819

Dynamic meteorology quasi-stable problems solved using sequential approximations solution for barotropic model of Euler equations

14 p2476 A69-29821

Time spectra of wind velocity, temperature, pressure and turbulent heat transfer and momentum in synoptic region

14 p2476 A69-29823

Climate studies with allowance for radiative heat inputs, constructing nonadiabatic motions model for improving prognosis

14 p2477 A69-29827

Ocean and atmospheric interactions analyzed by using hydrodynamic equations for boundary layers

14 p2442 A69-29838

Atmospheric motions equations in mesometeorology prognostic problems taking into account free atmosphere and boundary layer interactions

15 p2646 A69-30107

Self maintenance of absolute angular momentum in atmosphere as explanation of subtropical jet stream origin

15 p2647 A69-30192

Atmospherics observations in Japan during last 40 years, discussing relation to meteorology, statistical

characteristics, whistlers, noise phenomena, periodic variations, solar effects and ray theory

15 p2595 A69-30418

External wind shear influence on isolated cumulus cloud evolution based on hydrodynamic and thermodynamic equations numerical integration

15 p2648 A69-30644

Solar wind and solar breeze theories distinguished, discussing applications to geocoronal hydrogen emission and solar corona expansion

15 p2676 A69-30858

Magnetic field effect on thermal convection onset in compressible polytropic atmosphere compared with results from thin layer approximation

16 p2855 A69-31658

Shock wave growth or decay in atmospheres with density and temperature variation using singular surface theory

16 p2768 A69-31663

Electron cooling rates due to vibrational excitation of molecular oxygen calculated as function of electron temperature in E region

16 p2774 A69-31982

Horizontal magnetic variation peak at eight degree dip latitude, noting F region contribution to magnetic tubes of force integrated transverse conductance

16 p2778 A69-32189

Atomic oxygen density role in ionospheric E and F region magnetic stability, noting heat loss effect of atomic excitation

16 p2780 A69-32314

Friction and wind relationships expressing actual and geostrophic wind as complex numbers or by corresponding vectors in Gauss-Argand diagram

16 p2808 A69-32455

Latent heat of condensation related to atmospheric dynamics in cloud formation processes with allowance for moisture exchange

17 p2997 A69-33188

Suspected phase anomaly and Mercury atmosphere

17 p3034 A69-33414

Vertical structure concepts for air density, wind and sound velocity profiles in rocket climatology, discussing vertical relationship of wind shear statistics

17 p3000 A69-33794

Soviet book on ionospheric processes summarizing published studies covering neutral atmosphere structure, ionizing solar radiation component composition and intensity, etc

18 p3126 A69-34358

Classification of synoptic processes, discussing condensation of parameters characterizing state of atmosphere

18 p3166 A69-34815

Relation between atmospheric processes in troposphere and upper stratosphere in cold half year

18 p3166 A69-34817

Solitary waves in stratified polytropic atmosphere allowing for convection and disregarding viscosity and turbulence

18 p3167 A69-35338

Cumulative shock waves in vaporized products of electrical explosion of conical copper wire configuration, discussing atmospheric ionized vortical configuration formation

19 p3372 A69-35823

Atmospheric slant path molecular absorption and emission from band model methods, discussing computer program prediction capabilities

19 p3375 A69-36052

Steady state solution of quasi-geostrophic perturbation equations for atmospheric forced response to parameterized heating as global monsoon theory

19 p3362 A69-36405

Wind and temperature profiles in Ekman boundary layer, using numerical integrations of dynamic equations including time derivative terms

19 p3363 A69-36501

Vertical profiles of pressure, temperature and density variations due to upper troposphere pressure changes with and without zero layer effect

19 p3365 A69-36580

Microwave application in determining atmosphere meteorological characteristics compared with visual and IR wavelength measurements

20 p3569 A69-36984

Atmospheric temperature and moisture fields obtained by linear equations and objectively analyzed, considering underlying sea surface energy and cumulus cloud distribution

20 p3523 A69-37351

Solar activity effect on short term meteorological processes and dynamic state of mesosphere and ionosphere

sphere, emphasizing relationship to entire atmosphere dynamics
20 p3590 A69-37684

Soviet collection of papers on physics of atmospheric boundary layer covering wind profile, turbulent energy balance, etc
20 p3571 A69-37694

Atmospheric turbulence statistical distribution mass measurements using velocity, gravity and weight recordings based on calibration of aircraft as turbulence measuring instrument [ONERA-TP-699]
20 p3541 A69-37754

Topside ionospheric structure from Alouette 2 data, discussing thermopause temperature, plasma temperature, electron density profiles, satellite plasma frequency, etc
20 p3532 A69-37895

Atmospheric predictability as revealed by naturally occurring analogs, noting superposed error
20 p3573 A69-38057

Atmospheric structure, greenhouse effect and convective instability in window gray and nongray planetary atmospheres
20 p3615 A69-38257

Venus atmosphere structure determined from Mariner 5 flyby S band radio occultation measurements of ionosphere and atmosphere at illuminated and dark sides
21 p3794 A69-38380

Twilight airglow excitations governed by solar radiation, indicating presence of alkali metals, positive calcium ions and H lines, positive sodium ion bands, etc
21 p3711 A69-38515

Planetary boundary layer top formation, considering particle velocity, earth surface roughness role, geostrophic wind, etc
21 p3715 A69-38566

Dispersion and correlation function for atmospheric transparency due to water vapor from statistical model of absorption bands and effective mass
21 p3759 A69-39113

Nonograms for spectral transparency of atmosphere at 2.8-5.6 microns
21 p3759 A69-39117

Soviet book on earth atmosphere fluctuations covering propagation of acoustic, gravity and gyroscopic waves using linearized equations of hydrodynamics
21 p3717 A69-39528

Cosmic ray neutron studies of atmospheric nucleon component equilibrium and flux fluctuations at atmosphere top
22 p4002 A69-40092

Dayglow O I lambda 1304 and 1356 A radiations photoelectron excitation rates theoretical calculation and experimental data on altitude dependence characteristics
22 p3939 A69-40517

Retarding potential analyzers determining ionospheric structure, noting linearization of analysis
22 p3940 A69-40523

Lidar technology application to atmospheric and meteorological problems in clouds and cloud structures, air motion and inhomogeneity in clear air
22 p3977 A69-40535

Incident proton flux atmospheric altitude profile during PCA period, comparing balloon observations with preliminary satellite data
23 p4204 A69-41485

Ground antenna array for ionospheric physics experiments, consisting of wire dipoles connected to receive circular or linear polarization
24 p4286 A69-42607

Satellite-based meteorological observation system for global atmospheric research program, discussing wind measurement, IR and microwave sounding possibilities, etc [AAS PAPER 69-120]
24 p4307 A69-42817

Initialization technique for primitive forecast equations balancing Coriolis and pressure forces effects on atmospheric observations
24 p4344 A69-43065

Energetics of planetary boundary layer /Prandtl layer/ from system of hydrodynamic equations, discussing flux divergence term importance in free-windless convection transition region
24 p4309 A69-43148

Magnetic dipole field variations effects on planetary atmosphere erosion by solar wind, discussing Mars and Venus atmospheres above ionosphere
24 p4385 A69-43224

Midlatitude sporadic E model, discussing overdense ionization layers spatial distribution, wind shear effects, periodic variations, etc
24 p4311 A69-43743

ATMOSPHERIC PRESSURE

Blood volume in rats exposed to high altitude and deacclimated at ambient pressure, noting changes and control level restoration
01 p0015 A69-10922

Gases emissivity at high temperatures calculated for different gas layer thicknesses and atmospheric pressures, giving results in tabular form
02 p0285 A69-11567

Venus lower atmosphere noting graphically wide variation of surface pressure estimates
02 p0319 A69-12103

Mars lower atmospheric pressure, temperature and composition, noting consistency between photometric, spectroscopic and occultation techniques
02 p0319 A69-12104

Integral spectral emissivity of gas arc plasmas at high temperatures and atmospheric pressure
02 p0291 A69-12484

Venus atmosphere from Mariner 5 and Venera 4 data, discussing surface temperatures and pressures, cloud top region, McElroy model and maximum wind velocities
02 p0330 A69-12803

Human auditory function during exposure to prolonged low barometric pressure unaffected with normal oxygen partial pressure
03 p0378 A69-14206

Atmospheric exposure chamber design for small animals, discussing dynamic and recirculating operations and gas scrubbing system
04 p0584 A69-14678

Air density fluctuation effects on aircraft dynamic stability around center of gravity during climbing and diving maneuvers, discussing atmospheric pressure and flight path angle
04 p0548 A69-14825

Meteorological PTU /pressure, temperature, humidity/ probe for lower atmospheric layers, discussing detectors and assembly qualities
04 p0601 A69-15229

Turbulence characteristics and wind velocity in atmospheric boundary layer determined from pressure and temperature fields
05 p0788 A69-16453

Atmospheric vertical density and pressure profiles determined from satellite measurements of light beam phase shift and refraction angle
05 p0760 A69-16694

Meteorological satellite TV data of earth cloud cover for determining atmosphere pressure field [UN PAPER 68-95654]
06 p0949 A69-17052

Lower atmosphere pressure field determination based on meteorological satellite observations of amount and types of clouds and upper boundary altitude
06 p0952 A69-17987

Supersonic molecular beam sampling system for coupling mass spectrometer to alkali metal-air reacting flow system in kinetics study, noting gas dynamic effects [AIAA PAPER 69-94]
06 p0930 A69-18099

Pressure-altitude transducers for atmospheric pressure measurements on balloon flights including diaphragm, thermoconductivity, radioactive density and hypsometer gauges
07 p1132 A69-18873

Physicochemical synthesis of monosaccharides from human waste products at atmospheric and elevated pressures, considering methane oxidation by nitrogen oxides and ozone
07 p1071 A69-18971

Double diurnal oscillation of atmospheric pressure and vertical gradient of electromagnetic field, noting agreement between diagrams and role of atmospheric tides
08 p1306 A69-19866

Mars and Earth atmospheric carbon dioxide simulation and spectroscopic measurement for developing planetary surface pressure estimating procedures from IR transmission measurements
08 p1354 A69-20151

Venus atmosphere observations compared with Venera 4 measurements of temperature, pressure and carbon dioxide content
10 p1791 A69-24200

Nitrogen plasma total radiation intensity under pressure and at high temperatures calculated from radiation spectrum
11 p1922 A69-24231

Nitrogen dioxide molecular ions formation in air, discussing absence at lower pressures and early afterglow dominance in air ionized and dissociated by microwave pulses
11 p1879 A69-25158

Jet stream winds direction correlated with direction of LF pressure disturbances crossing microbarograph array
12 p2125 A69-26015

Density stratified model of troposphere and constant gravity field for ground level pressure perturbations in mesoscale region
12 p2126 A69-26016

Venus atmosphere chemical composition, surface temperature and pressure obtained by Venera 4 and Mariner 5
12 p2155 A69-26129

Height and temperature vertical variability in mid and upper stratosphere determined from constant pressure charts /1964-1966/
13 p2290 A69-27637

Venusian atmospheric pressure and temperature measurements by Venera 4 probe, noting agreement with Mariner 5 observations
13 p2345 A69-27689

Atmospheric pressure and wind data at equatorial latitudes, determining relation between rms meridional and zonal wind and pressure gradient
13 p2293 A69-27845

Atmospheric pressure variation coefficients computation based on harmonic analysis of wave behavior
13 p2295 A69-28648

Time dependent evolution of probability pressure distribution maximum obtained from Liouville equation
14 p2472 A69-29406

Worldwide observation of atmosphere with occultation satellites, correcting orbit perturbations to obtain air pressure
14 p2447 A69-29517

Atmospheric transmission functions dependences on absorbing material, pressure and temperature in 15 micron band of carbon dioxide, introducing corrections
15 p2597 A69-30653

Monograph on large scale cloud distribution in extratropical low pressure regions, using classical meteorological observations and Tiros weather satellite data
15 p2650 A69-31212

Longitudinal variations of density, temperature and pressure distributions in stratosphere and mesosphere based on rocket observations, emphasizing arctic and subarctic regions
15 p2602 A69-31379

Combustion of pure crystalline boron single particles injected into hot oxidizing gases streams at atmospheric pressure [AIAA PAPER 69-562]
16 p2880 A69-32741

Vertical atmospheric pressure distribution measured directly with Pirani-Israel gauge in Skylark rocket, transforming dynamic pressure data into static pressures on ground
17 p2971 A69-33037

Objective analysis of pressure trend fields and surface pressure retaining field with scale of 100 km, using filtering procedure
18 p3166 A69-34816

Venusian atmospheric features obtained from Venus 5 and 6 and Mariner 5 observations, indicating extremely high temperatures and pressures
19 p3401 A69-35840

Colpoda maupais resistance to Martian atmospheric pressure and oxygen partial pressure noting adaptation, reproduction and existence
20 p3478 A69-37627

Numerical prediction experiment for dynamical structure of tropical atmosphere in equatorial latitudes, constructing pressure, temperature and vertical motion distributions from wind field
20 p3573 A69-37910

Physicochemical synthesis of monosaccharides from human waste products at atmospheric and elevated pressures, considering methane oxidation by nitrogen oxides and ozone
20 p3483 A69-38219

Friction and orography effects on vertical currents in planetary boundary layer and numerical forecasting of baric field
21 p3758 A69-38837

Gravitational fields and atmospheric pressure effects on soils subjected to static and dynamic loading, using aircraft parabolic gravity simulation [AIAA PAPER 69-1009]
22 p3921 A69-40382

Errors due to neutron counter radioactivity in cosmic rays nucleon measurements analyzed in reducing readings to barometric pressure
23 p4206 A69-41855

Surface pressure field forecast by meteorological fields expansion into orthogonal components, estimating number of predictors in regression equation
23 p4184 A69-42491

Amplitude and phase maps for annual global variations in atmospheric pressure based on harmonic data analysis, suggesting standing wave type distributions
23 p4185 A69-42493

Leak detection techniques efficiency determined for airtight atmospheric air sampling devices used at low pressure and concentration
24 p4296 A69-42656

Northern Hemisphere 500-mb height pattern series expansion, using optimal sets of orthonormal functions, obtaining rms error
24 p4346 A69-43157

Barometric pressure affecting convective heat transfer from human body in air, deriving empirical formula as function of air density, speed and temperature
24 p4267 A69-43384

Lower ionosphere atmospheric density, temperature and pressure profiles diurnal variations from data of radio meteor echoes
24 p4311 A69-43504

Isobaric inhomogeneous atmosphere effect on sonic boom determined, using analytic equation relating transmitted wave intensity to local free stream Mach number
24 p4254 A69-43728

ATMOSPHERIC RADIATION

NT AIRGLOW
NT AURORAL ARCS
NT AURORAS
NT DAWN CHORUS
NT DAYGLOW
NT GEOCORONAL EMISSIONS
NT IONOSPHERIC NOISE
NT NIGHTGLOW
NT RADIO AURORAS
NT RED ARCS
NT SKY RADIATION
NT STRATOSPHERE RADIATION
NT TWILIGHT GLOW
NT WHISTLERS

Scattered solar Lyman alpha radiation measurement by Vertical Space Probe station in upper atmosphere including UV radiation
01 p0152 A69-10577

Jet stream cirrus radiative characteristics from airborne IR measurements, noting cirrus cloud emission and transmission and cirrus height and temperature estimates
01 p0110 A69-10694

Ionospheric and stratospheric UV radiation effects on survival of microorganisms
01 p0018 A69-11088

Hydromagnetic emissions observed at Antarctic auroral zone, discussing relation to sudden storm commencement
02 p0241 A69-11726

X ray airglow in daytime sky, suggesting origin in atmospheric N and O K alpha lines due to fluorescent excitation by solar X rays
02 p0307 A69-12022

Radiometric measurement of attenuation, emission and noise fluctuations due to earth atmosphere in 4 cm to 8 mm range
02 p0210 A69-12432

Mean atmospheric downward radiation fluxes for large territories, using simple model atmospheres in derivation of computational formulas
03 p0422 A69-13410

Temperature determination of subjacent surface from airborne measurements of outgoing radiation in earth atmosphere in 10 to 12 micron interval
03 p0424 A69-13933

Meteorological rocket measurement of corpuscular radiation intensity in upper atmosphere at various latitudes
05 p0814 A69-16052

IR radiation in upper atmosphere, indicating sources of error in data
05 p0753 A69-16058

Radio astronomical methods for total atmospheric absorption of radio waves by atmospheric thermal radio emission measurements based on sky brightness temperature
05 p0723 A69-16779

Airborne polarimeter to measure Stokes parameters of linearly polarized visible atmospheric radiation in four narrow spectral regions
06 p0923 A69-16924

Regularization methods in inverse problems of atmospheric optics, analyzing atmospheric thermal sounding and interpretation of radiation measurements
06 p0919 A69-17616

Inverse problems in radiative transfer applied to remote measurements of IR radiation from planetary atmospheres, noting temperature and water vapor inversions
06 p0919 A69-17617

Collection of Soviet papers on microwave radiation transport in atmosphere covering radiation field, water vapor content determination, absorption and scattering by precipitation, etc
06 p0953 A69-17994

Atmospheric microwave radiation and sensitivity of airborne radiometric sounding in water and moisture contents determination
06 p0954 A69-18001

Shock tube measurements of radiation from simulated Jupiter atmosphere related to thermodynamic conditions encountered by entry probe
[AIAA PAPER 69-184] 06 p0908 A69-18207

Neutron counter for measurements of atmospheric and earth leakage flux of secondary cosmic ray neutrons, discussing design and calibration
07 p1209 A69-19454

Radiative transfer equation solution for spectral line formed in two dimensionally varying atmosphere extended to continuum radiation in inhomogeneous atmospheres
08 p1386 A69-20077

Aircraft measurements of earth atmosphere radiance in 8-14 micron window compared to calculated values as functions of altitude
08 p1311 A69-21094

Local enthalpy measurements in atmospheric argon arc plasma jet at various arc currents, comparing calorimetric and spectrometric methods
09 p1547 A69-21602

Bismuth bolometer as sensor recording IR radiation for thermal radiation fluctuations in atmosphere caused by temperature inhomogeneities
09 p1490 A69-21868

Flux and energy spectrum of secondary electrons at balloon altitude in atmosphere, correcting Beedle and Webber plotting error
09 p1490 A69-21914

Large scale heat sources influence on formation and dynamics of ultralong waves in atmosphere, using linear time dependent quasi-geostrophic model
09 p1491 A69-22164

Slow atmospheric neutron energy spectrum determined by resonance detectors and l/v detectors, measuring cadmium ratio dependence on longitude and latitude
10 p1758 A69-22831

Relative band intensities of atmospheric and IR atmospheric systems of molecular oxygen compared with Franck-Condon factor calculations
10 p1681 A69-23163

Two dimensional autocorrelation functions of outgoing radiation fields usable as quantitative characteristics of cloud distribution structures
11 p1913 A69-24832

Atmospheric thermal radio emission fluctuations effects on radio telescope sensitivity, evaluating dispersion at low angles to horizon
12 p2031 A69-26643

Monograph on atmospheric radiation transfer including absorption, scattering, direct, diffuse, global, thermal and net radiation
12 p2073 A69-26918

Corrections for atmosphere thickness needed for satellite measurements of underlying surface temperature
13 p2293 A69-27850

Atmospheric IR emission measured at high altitudes by interferometer spectrometers behind nitrogen cooled chopper
13 p2254 A69-28261

High energy electron photon cascades event recorded with X ray photography, discussing origin in related atmospheric cosmic ray showers component subgroups
13 p2331 A69-28398

Radio emission of atmospheric cosmic ray showers observed with multiple wideband half wave dipole antenna system, obtaining radiation spatial distribution
13 p2332 A69-28407

Radiation in atmospheric circulation, considering radiative equilibrium, cloudiness and surface interactions, surface temperature and heat input
14 p2477 A69-29826

Electromagnetic noise radiation structure during lightning flash by measuring time duration distribution between pulses
14 p2445 A69-29885

Earth thermal emission intensity measured by two beam radiometer onboard Cosmos 149, noting discrepancy between empirical and theoretical transfer functions of atmosphere
15 p2596 A69-30651

Atmospheric radiative balance measurement on board Cosmos 149, describing design and operation of device
15 p2597 A69-30652

Scattered solar Lyman alpha radiation measurement by Vertical Space Probe station in upper atmosphere including UV radiation
15 p2691 A69-30747

IR horizon of earth from ionospheric IR emission spectra obtained by sounding capsule, discussing earth geometric horizon and particular spectral bands [ONERA-TP-709]
15 p2601 A69-31370

Atmospheric IR spectra determination from transmission functions overlapping effects of atmospheric gases
16 p2814 A69-31792

Hydroxyl band contamination of emission and background radiation from night sky
16 p2774 A69-31987

Ozone and temperature profiles influence on atmospheric radiation intensities measurement by satellite in five spectral regions, noting pressure broadening effect
16 p2786 A69-32633

Radio wave trajectories for waves emitted at 15, 20 and 25 kHz within spherically stratified ionosphere below F 2 maximum
17 p2969 A69-34001

Spectral density of outgoing radiation in 0.6-0.8 micron frequency range, noting reflected radiation and cloud fields correlation functions
19 p3366 A69-36672

Radiating gas flows during hypersonic planetary reentry, discussing atmospheric composition, shock layer characteristics, nonequilibrium flows, etc
20 p3513 A69-36982

Meteorological rocket measurement of corpuscular radiation intensity in upper atmosphere at various latitudes
20 p3591 A69-37962

IR radiation in upper atmosphere, indicating sources of error in data
20 p3533 A69-37968

Effective thinness approximation for spectral line formation from photon degradation processes and random walk of scattered photons, discussing optical thickness
20 p3612 A69-38159

Particle albedos and extinction cross sections computed by Mie theory showing dependence on refractivity, considering thermal radiation from cloudy planetary atmospheres
20 p3614 A69-38255

Atmospheric emissions - NATO Conference, Norway, July-August 1968
21 p3705 A69-38482

Magnetospheric electromagnetic phenomena explained by equations of motion for particle acceleration, forbidden regions and MHD processes
21 p3707 A69-38485

Charged particles beam penetration effects produced in atmosphere, determining particle diffusion and trajectory using Spencer moments and Monte Carlo methods
21 p3709 A69-38502

OH emission rise after sunset and decay at sunrise attributed to strong solar dissociation of ozone
21 p3712 A69-38520

Long wave radiation influx toward atmospheric layers generated naturally by clouds, discussing radiation cooling of atmosphere in cloudy and clear weather
21 p3758 A69-39112

Satellite determination of underlying surface temperature by IR spectroscopy, measuring emitted radiation in atmospheric windows
21 p3759 A69-39114

Daily simultaneous solar measurements of microwave atmospheric absorption and emission to determine frequency correlation between meteorological phenomena and atmospheric parameters
21 p3718 A69-39747

IR molecular radiation spectra of upper atmosphere in 3-8 micron range investigated by rockets and satellites, discussing radiation energy density during magnetic storms
21 p3792 A69-39772

Anomalous X ray signals from Explorer 30 satellite showing saturation in ionization chamber possibly due to enhanced solar and atmospheric X rays
21 p3792 A69-39808

Vertical heat exchange flux model using heat conduction equation compensating for tropospheric and stratospheric radiation divergence, calculating diffusion coefficient
22 p3936 A69-40137

Auroral UV and 3914 A radiation during charged particle precipitation measured by satellite
22 p3939 A69-40507

Fredholm integral equation for source function of Greenhouse effect and finite atmospheres solved by computational algorithm
23 p4239 A69-41607

Radiative transfer theory applied to layer cloud with normal liquid moisture content, discussing volume extinction, scattering and absorption coefficients, etc
23 p4184 A69-42177

Atmospheric gases emission spectra excited by electron beam as function of pressure
24 p4353 A69-43698

ATMOSPHERIC REFRACTION
NT RADIO WAVE REFRACTION

Photographic image degradation resulting from wave front distortion due to atmospheric refractive density gradients over long oblique optical path
01 p0107 A69-10223

Atmospheric influence on ground visibility reduction of airborne objects, using radiative transfer equation to calculate contrast transmission function
01 p0111 A69-11100

Solar limb image vibrations caused by turbulent pulsations in refractive index of lowest atmospheric layers
01 p0156 A69-11183

Refractive index structure constant for different atmospheric turbulence conditions, discussing possibility of improved capabilities for imaging systems
02 p0275 A69-11930

Mean square amplitude and phase fluctuations for propagation of light beam with Gaussian amplitude distribution through medium with randomly varying refractivity
02 p0208 A69-12308

Refractivity distribution at ground level and at one km over India, correlating surface refractivity with difference, noting seasonal and diurnal variations
03 p0393 A69-13304

Atmospheric refractive index for IR radiation in one to six micron region
04 p0591 A69-14300

Reflection and transmission of radiation from very thick and semiinfinite homogeneous atmospheres with arbitrary phase function, using asymptotic fitting method
04 p0595 A69-15285

Electromagnetic wave refraction angles in earth atmosphere, noting effect of stratified discontinuities on angle magnitude
06 p0887 A69-17450

Light waves refractive index distribution from balloon sounding data found to decrease with height in winter regardless of time of day
09 p1536 A69-21917

Atmospheric propagation properties of laser light, discussing particle absorption, gaseous absorption and refractive index disturbance effects
09 p1518 A69-22129

Conical refraction of magnetosonic waves occurring when Alfvén waves propagate at speed of sound in conducting fluid in presence of constant uniform magnetic field
10 p1727 A69-23091

Disturbed index of refraction scattering cross sections and aircraft acceleration increments for clear air turbulence, deriving correlation for measurements
10 p1656 A69-23651

Calculated UV spectra of solar radiation reflected from atmosphere compared with satellites photometric measurements, attributing radiation intensity distribution asymmetries to seasonal dependence of ozone content
12 p2064 A69-25952

Optimum emission wavelengths in atmospheric refractive index determination in optical range finder/refractometer system, noting laser applicability
13 p2260 A69-27826

Vertical refraction effect on gas laser beam propagation near earth surface under various meteorological conditions, comparing index for diffuse light
13 p2220 A69-27827

Refraction error in measurements with simple and radar interferometers, considering atmospheric effect
13 p2221 A69-27961

Large scale ionospheric inhomogeneities anisotropy, dimensions and drift velocities from simultaneously measured irregular refraction
14 p2436 A69-29053

Remote sensing of lower atmosphere refractive structure, using Rake tropospheric scatter channel-sounding technique
14 p2448 A69-29525

Data tabulation and calculation for atmospheric refraction between 5-40 km based on GOST standard atmosphere
15 p2646 A69-30160

Measured atmospheric refraction of bright astronomical objects less than calculated data for large zenith distances
15 p2679 A69-30161

Hydromagnetic fast shock strength and direction in inhomogeneous gravitational atmosphere with uniform magnetic field, discussing heating in solar corona
15 p2680 A69-30202

Plane electromagnetic wave refraction and scattering in solar corona during eclipsed observations of cosmic sources, calculating angular distribution of radiation intensity
15 p2688 A69-30555

UHF propagation in spherically stratified super-refractive troposphere with trapping surface layer, discussing distant field strength dependence on refractivity profile
16 p2752 A69-32388

Air refractivity variations across horizontal and vertical boundary planes between two air masses of slightly different temperatures
17 p3028 A69-32880

Optical distance measurement using laser and atmospheric dispersion method through average refractive index determination over path
18 p3152 A69-35198

Secor data reduction to correct tropospheric refractive effects of radio ranging on earth satellites using tropospheric model
18 p3104 A69-35200

Monochromatic undulating light vertical refraction path curvature radii calculation based on refractive index
18 p3174 A69-35201

Geodetic satellite measurements employing curve fitting approach using least squares analysis to resolve atmospheric refraction and shimmer problem
18 p3104 A69-35202

Light refraction in Venusian atmosphere from Venera 4 probe measured data, noting horizontal rays traversing planet along circumference at 8.3 km height
19 p3427 A69-36625

Electromagnetic wave refraction angles in earth atmosphere, noting effect of stratified discontinuities on angle magnitude
20 p3496 A69-37935

Microwave refraction method for satellite horizontal probing of earth atmosphere, discussing phase delay data inversion, air density and intersatellite relative velocity
21 p3671 A69-38376

Trajectory of light ray propagating through atmosphere based on known refractive index defined by function of special Cartesian coordinates
21 p3675 A69-39245

Atmospheric natural turbulence effect of degradation of laser signal phase and amplitude characteristics, noting refractive index inhomogeneities effect on optical tracking system
21 p3675 A69-39397

Tropospheric refractivity height profile model, computing corrections to satellite Doppler or range data
21 p3678 A69-39748

Laser application to distance measurement in air for determining atmospheric influence, using two wavelengths
22 p3959 A69-39901

Coherent light propagation through turbulent atmosphere observed by applying He-Ne lasers to simultaneous measurements of scintillation effects over homogeneous optical paths
24 p4344 A69-43114

ATMOSPHERIC SCATTERING
NT TROPOSPHERIC SCATTERING

Scattered solar Lyman alpha radiation measurement by Vertical Space Probe station in upper atmosphere including UV radiation
01 p0152 A69-10577

Light polarization properties in atmosphere noting aerosols effect
01 p0075 A69-11189

Partially polarized light and polarization degree measured by photoelectric polarimeter, obtaining scattering indicatrices and polarization degree dependences
01 p0075 A69-11190

Aerosol scattering indicatrix of atmospheric ground layer theoretical estimation to make up for lack of experimental values
02 p0274 A69-11443

Aerosol size distribution and variation with humidity effects on visual range, comparing computations with transmissometer and scattering recorder measurements
02 p0276 A69-12760

Vertical atmospheric turbidity distributions of haze and water vapor, noting effect of variations on scattering and absorption determination
02 p0277 A69-12777

Atmospheric limitations for laser communications, discussing scattering and absorption effects
03 p0389 A69-13193

Directional intensity of radiation emerging from top and bottom of Rayleigh scattering atmosphere
03 p0426 A69-14026

Correlation of received signals with diversified angles of arrival due to scattering by turbulently excited ionosphere
03 p0399 A69-14129

Laser scatter measurements in mesosphere and above for optical radar system parameters
05 p0758 A69-16414

Multiple light scattering in spherical planetary atmosphere based on geometrical model, calculating twilight glow brightness
05 p0828 A69-16632

Vertical ozone distribution in upper atmosphere from satellite measurements of UV solar radiation scattering by solving integral Laplace equation
06 p0996 A69-17733

Double scattering effects of sky radiation and outgoing radiation balance in disturbed atmosphere, using homogeneous plane parallel atmospheric model
07 p1175 A69-18270

Visible radiation scattering around Venus spherical atmosphere computed on basis of Venus 4 and Mariner 5 data
07 p1213 A69-18609

Diffuse reflection and transmission of parallel rays by homogeneous two layer slab, solving simultaneous integral equations governing auxiliary functions
08 p1350 A69-19799

Atmospheric haze effect on Umkehr measurements, considering computation from direct sounding of vertical ozone distribution and from model atmospheres
08 p1308 A69-20316

Rotational Raman scattering in planetary atmospheres, analyzing spectra of deep solar Fraunhofer lines
09 p1601 A69-22207

Limits in applicability of earth equivalent radius to measuring microwave diffraction field in atmosphere
09 p1456 A69-22284

Radiation field at optical depths within plane parallel Rayleigh scattering atmosphere subjected to generalized free surface boundary conditions
09 p1606 A69-22423

Scattered light mean intensity determination in twilight aerosol atmosphere from satellite observations, formulating boundary value problem
10 p1689 A69-23970

Laser radiation backscatter along oblique paths in atmosphere, calculating transmission over horizontal and oblique paths
10 p1659 A69-24220

Multiple scattering of solar radiation in turbid atmosphere, considering equations of sky radiation and radiative transfer
11 p1911 A69-24587

Atmospheric scattering behavior under reduced visibility conditions for laser wavelengths of 0.69 and 1.06 micron
11 p1837 A69-25040

Atmospheric effects on laser beam width, using Born approximation and Gaussian model to obtain TEM mode scattered power expressions
12 p2111 A69-27166

Radar echoes observed from clear atmosphere, discussing scattering mechanisms of thin stable inversions, convective thermals, Benard convection cells, breaking gravity waves, etc
14 p2415 A69-29518

Acoustic sounding of atmospheric structure, utilizing energy backscattered from temperature fluctuations in turbulent regions
14 p2448 A69-29527

Errors in magnitude equation and atmospheric dispersion calculated for 400 mm astrograph, emphasizing constant errors due to objective
15 p2646 A69-30162

Functional relations expressing short wave radiation absorption and scattering in atmosphere
15 p2648 A69-30222

Scattered solar Lyman alpha radiation measurement by Vertical Space Probe station in upper atmosphere including UV radiation
15 p2691 A69-30747

Cauchy system for reflection and transmission functions of finite isotropically scattering atmospheres with specular reflectors, noting use for ozone and cloud heights measurements
15 p2597 A69-31152

Wavelength dependence of polarization of sunlight scattered by Venus atmosphere, including Rayleigh and Mie scattering mechanisms
16 p2860 A69-32237

Multiple light scattering solutions accuracy by diffraction peak omission from cloud and haze analytic phase functions compared for optically thick and thin planetary atmospheres
17 p3032 A69-33159

Cloud scattering corrections added to synthetic spectrum analysis of carbon dioxide bands and water vapor line in Venus spectrum
17 p3032 A69-33161

Earth-reflected solar energy /albedo energy/ distribution model, assuming isotropic scattering by homogeneous atmosphere
[AIAA PAPER 69-591]
17 p2961 A69-33292

Far IR angular scattering observations as diagnostic tool to examine microstructure of high altitude cirrus clouds
18 p3126 A69-34281

Star magnitude variation caused by earth atmosphere related by equation to star altitude, station height, sensor response, spectral radiance, etc
18 p3168 A69-34814

Cloud layer multiple scattering in Jovian atmosphere, discussing influence on Lorentzian contour of planetary absorption lines
18 p3203 A69-35332

Scattered light mean intensity determination in twilight aerosol atmosphere from satellite observations, formulating boundary value problem
21 p3717 A69-39656

Flashlamp-pumped dye laser for resonance scattering studies of upper atmospheric composition, describing laser construction and tuning
22 p3962 A69-40440

Radio wave scattering cross section in wake of body moving in ionosphere, using simplified procedure with asymptotic expressions
22 p3901 A69-41094

Radiation scattering by thick planetary atmosphere according to Rayleigh law, considering luminance variation and absorption ray polarization
23 p4213 A69-41698

Low energy electrons energy loss by inelastic collisions in moving through atmosphere, estimating cross sections and loss rates
24 p4351 A69-42763

Scattered light meter accuracy as function of aerosol particles atmospheric distribution according to size, analyzing measurement errors
24 p4343 A69-42966

ATMOSPHERIC STRATIFICATION

Sonic bang intensities in stratified atmosphere obtained by geometrical acoustics and linear theory modifications to take account of nonlinear effects
01 p0008 A69-10056

Seasonal variation of evening-morning difference in maximum density heights of twilight sodium layer
01 p0063 A69-10275

Soviet rocket and satellite night, twilight, airglow and auroral studies, discussing day sky brightness, night airglow and atmospheric stratification
01 p0066 A69-10941

Tropospheric inhomogeneities properties and wind conditions in relation to lunar limb image deformations
01 p0156 A69-11182

Solar limb image vibrations caused by turbulent pulsations in refractive index of lowest atmospheric layers
01 p0156 A69-11183

Spikes on sonic boom pressure waveforms due to simultaneous focusing and diffraction of planar N wave by inhomogeneous atmosphere layer
01 p0011 A69-11280

Thermodynamics of nonadiabatic vertical ascent of overheated individual air volumes in stably stratified atmosphere
02 p0274 A69-11441

Aerosol scattering indicatrix of atmospheric ground layer theoretical estimation to make up for lack of experimental values
02 p0274 A69-11443

Unusual stratification of F region during solar activities, noting role of traveling inhomogeneities
02 p0237 A69-11663

Similarity theory results for turbulent diffusion in atmospheric surface layer compared with concentration measurements from Project Prairie Grass
02 p0276 A69-12695

Radiative heat loss effect on atmospheric cellular convection, analyzing critical Rayleigh number and width to height ratio of cells
02 p0276 A69-12776

Air mass cumulus cloud growth stimulation by means of vertical updrafts capable of perforation of retaining layers
03 p0461 A69-13409

Ionospheric perturbations involving stratifications at various heights move toward LF and HF sections of ionograms
03 p0423 A69-13538

Frequency distribution of wind velocity as function of height, averaging time and thermal stratification
04 p0628 A69-15088

Electromagnetic wave refraction angles in earth atmosphere, noting effect of stratified discontinuities on angle magnitude
06 p0887 A69-17450

Formation dynamics of thin sporadic layers of E region, determining maximum ionization and electron concentration and electron-neutral atoms collision frequency
06 p0922 A69-17751

Convective clouds effect on large scale stratification, showing cumulus and cumulonimbus self amplifying convection as factor in tropical cyclogenesis
09 p1536 A69-22165

Air layer between target and instrument effect on earth surface temperature conducted with airborne radiometers
09 p1536 A69-22166

Relation between Rayleigh and dynamic Richardson numbers in atmospheric boundary layer in presence of cellular convection
09 p1491 A69-22709

Electron density profile from oblique ionogram calculated by iteration, assuming concentric spherically stratified ionosphere
10 p1684 A69-23826

Stratified atmosphere mean vertical flux due to ground disturbances, obtaining results for various wind and temperature profiles
10 p1685 A69-23856

Characteristic plane harmonic free internal neutral atmospheric wave oblique propagation through horizontally stratified quiet atmosphere for various thermospheric parameters
12 p2065 A69-26101

Forced convection in atmospheric boundary layer above nonuniformly heated earth surface, noting roles of wind and stratification parameters
12 p2126 A69-26579

Thermal stratification effect on wind structure in Ekman layer, assuming turbulent transfer and height dependence
13 p2290 A69-27390

Cellular convection in horizontal gas layer analyzed for causes of vertical air circulation and effect of vertical temperature profile
13 p2291 A69-27725

Temperature vertical profiles rms deviations calculated from temperature measurements during unstable atmospheric stratification
13 p2293 A69-27847

Corrections for atmosphere thickness needed for satellite measurements of underlying surface temperature
13 p2293 A69-27850

Geopotential and wind prediction by integration of prognostic equations of single level atmosphere
13 p2294 A69-27852

E layer fine scale structure, F 1 reactions and F 2 reflected signals analysis during 20 May 1966 solar eclipse
13 p2255 A69-28541

Unusual stratification of F region during solar activities, noting role of traveling inhomogeneities
13 p2256 A69-28694

Turbulence and temperature fluctuations spectral characteristics in thermally stratified atmosphere characterized for various wave numbers, using energy and mass transfer functions
14 p2472 A69-29402

Nonlinear internal gravity waves in stratified atmosphere of unbounded inviscid incompressible fluid, noting wave amplitude inverse proportion to atmospheric density
14 p2441 A69-29574

Turbulent heat and momentum fluxes spectra measured in atmospheric ground layer, describing changes as function of height and stratification conditions
15 p2649 A69-30648

Time variation of altitude distribution of cosmic dust layer in upper atmosphere by Pandora II collector using inflight shadowing technique
15 p2698 A69-31353

Discrete layers criterion for multilayer approximation to real atmosphere in acoustic gravity wave propagation
16 p2774 A69-31980

Numerical method based on thin film optics to determine ionospheric electromagnetic transmission and reflection coefficients for vertical incidence
16 p2752 A69-32392

Relation between Rayleigh and dynamic Richardson numbers in atmospheric boundary layer in presence of cellular convection
16 p2808 A69-32488

F region stratification during solar minimum and maximum, discussing regularities of plasma frequencies and diurnal variations
17 p2959 A69-33005

Horizontal shear effect on structure of growing baroclinic waves by two layer model, assuming small radius of deformation, compared to planetary scale
17 p2960 A69-33150

Turbulence origin and structure in stably stratified media for finite disturbance instability in sloping flows experimentally observed with visualization techniques
17 p2999 A69-33735

Centrifugation effects on body composition and growth of mice
17 p2910 A69-33746

Horizontally stratified ionosphere radio wave reflection and transmission properties, calculating full wave by differential equations
17 p2927 A69-33862

Reflection and transmission coefficient matrices for stratified magnetoionic medium determined by thin film optical technique and iteration procedure
17 p2927 A69-33863

Solitary waves in stratified polytropic atmosphere allowing for convection and disregarding viscosity and turbulence
18 p3167 A69-35338

Turbulence energy spectra in free atmosphere with convective layer surmounted by inversion layer, noting power law followed by velocity components
19 p3362 A69-36406

Large scale cloud layers vertical boundaries approximate determination using atmospheric temperature and moisture data from aircraft sounding
20 p3569 A69-36986

Electromagnetic wave refraction angles in earth atmosphere, noting effect of stratified discontinuities on angle magnitude
20 p3496 A69-37935

Layer model of random discrete inhomogeneities used to derive harmonic wave one dimensional scattering field and mean square of field
21 p3673 A69-38993

Thermal structure of middle atmosphere, discussing heat sources and sinks, photochemical theories of ozone distribution, IR radiative transfer, etc
22 p3940 A69-40537

Acoustical ray tracing in horizontally layered and vertically sectioned atmosphere on digital computer using shifting Cartesian coordinate system
23 p4154 A69-41532

ATMOSPHERIC TEMPERATURE

NT IONOSPHERIC TEMPERATURE

Reversed thermal conditions in mesopause, examining atomic oxygen IR radiation effect
01 p0062 A69-10129

Atmospheric temperature and airglow spectra from IR measurements noting OH bands, atmospheric structure between 10 and 200 km at midlatitude and atmospheric absorption
[UN PAPER 68-95471]
01 p0108 A69-10464

Selective chopper radiometer for remote atmospheric temperature sounding, discussing satellite versions for Nimbus D and Nimbus E
[UN PAPER 68-95797]
01 p0080 A69-10531

Jet stream cirrus radiative characteristics from airborne IR measurements, noting cirrus cloud emission and transmission and cirrus height and temperature estimates
01 p0110 A69-10694

Atmospheric temperature corrections for measurements by rocketsonde and balloonsonde with thermistor, noting dissipation factors and thermal time constants
01 p0081 A69-10697

Jovian atmospheric rotational temperature from rotational lines in methane band
01 p0153 A69-10856

Upper atmosphere physical properties, discussing density and temperature
01 p0066 A69-10942

Turbulence characteristics from light wave fluctuation measurements, discussing applications to small scale inhomogeneities in atmospheric temperature distribution
02 p0274 A69-11437

Atmospheric temperature profiles by regularizing algorithm, discussing influence of random errors in measured radiation and kernel of integral equation on interpretation accuracy
02 p0274 A69-11448

Effective temperature values of ozone used to determine onset time and disturbance height in ionosphere
02 p0238 A69-11670

Mars lower atmospheric pressure, temperature and composition, noting consistency between photometric, spectroscopic and occultation techniques
02 p0319 A69-12104

Venus exospheric temperature for various composition models, discussing carbon dioxide concentration effects
02 p0319 A69-12109

Zonal temperature and spectral characteristics of stratospheric circulation, noting westward rotation of second harmonic
02 p0246 A69-12759

Radiative heat loss effect on atmospheric cellular convection, analyzing critical Rayleigh number and width to height ratio of cells
02 p0276 A69-12776

Atmospheric temperature and water vapor variations and seasonal environmental changes effects on cosmic ray neutron and meson monitor counting rates
03 p0498 A69-12936

Acoustical thermometer-interferometer to measure air temperature between 20 and 50 km
03 p0429 A69-13269

Environmental temperature and water vapor increases associated with ascending thermals estimated by penetrative convection
03 p0460 A69-13340

Middle stratospheric diurnal temperature variation based on model eliminating radiation error of rawinsonde
03 p0461 A69-13344

Diurnal upward and downward flows of atmospheric matter following upper atmosphere temperature nighttime minimum and daytime maximum
03 p0423 A69-13533

Temperature change and fog forecasting diagram modified by Swinbank relation in place of Brunt formula
03 p0462 A69-13965

Mathematical model derivation for observed atmospheric tide phenomena, taking into account thermal and other effects
03 p0426 A69-14098

Electron, ion and neutral particle temperatures of upper atmosphere
04 p0592 A69-14975

Covariances of temperature and meridional wind component and relation to northward flux of sensible heat due to transient eddies in stratosphere
04 p0627 A69-15084

Meteorological PTU /pressure, temperature, humidity/ probe for lower atmospheric layers, discussing detectors and assembly qualities
04 p0601 A69-15229

COSPAR manual on stratospheric temperature and wind measurements, discussing synoptic and time variation study by Arcas and Loki-Judi meteorological sounding rocket systems
05 p0752 A69-15706

Synthesis of simulated aircraft cabin pure fluidic temperature control system
[ASME PAPER 68-WA/FE-30]
05 p0705 A69-16103

Midlatitude neutral thermosphere density and temperature measurements, noting effect of atomic oxygen adsorption by instruments
05 p0755 A69-16268

Turbulence characteristics and wind velocity in atmospheric boundary layer determined from pressure and temperature fields
05 p0788 A69-16453

Stratospheric temperature, wind and ozone concentration measurement during solar eclipse by sounding rocket system
06 p0916 A69-17008

Dynamic properties of upper atmosphere, discussing variations in temperature, density and composition
[UN PAPER 68-05755]
06 p0917 A69-17042

Microwave radiometer for measuring mesosphere and stratosphere temperature as function of altitude using atmospheric oxygen line
06 p0924 A69-17247

IR spectrometer for Nimbus meteorological satellite for terrestrial spectral radiance data for atmospheric temperature profiles
06 p0926 A69-17621

Relaxation method for inversion of full radiative transfer equation, determining temperature profile in atmosphere from outgoing radiance
[JPL-TR-32-1351]
06 p0922 A69-17805

Nightglow intensities correlated with atmospheric ozone concentration and stratospheric temperatures
07 p1123 A69-18675

Optical device for measurement of temperature changes with height in upper atmosphere by rockets or satellites
07 p1132 A69-18676

Annual temperature variation in lower tropical stratosphere, noting effect of equatorial upward motion
07 p1126 A69-19043

Temperature variability data for 120-km altitude from observations of grenade glow clouds, calculating molecular diffusion coefficients and atmospheric temperature and density
07 p1127 A69-19277

Rawin systems for upper air measurements of wind and thermodynamic parameters, using balloon-borne radiosonde
07 p1057 A69-19581

Continuous variate duration estimates by Markov process, giving example of surface air temperature conditional probability distribution
08 p1346 A69-20731

Temperature advection dependence on local temperature changes, discussing variation with atmospheric layer thickness
09 p1534 A69-21509

Automatic measuring device for short term air temperature and wind velocity fluctuations leading to air mixtures propagation
09 p1535 A69-21515

Upper atmosphere temperature distribution estimation on basis of twilight zenith sky intensity measurements, discussing influence of various parameters on accuracy
09 p1487 A69-21653

Emission spectra of BaO during barium release compared with computed spectra for upper atmosphere temperatures evaluation
09 p1488 A69-21664

Atmospheric molecular oxygen temperatures from photoelectric recordings of absorption bands, analyzing relaxation process and photoeffects in oxygen molecules
09 p1490 A69-21863

Atmospheric thermal sounding by measuring outgoing thermal radiation with infinite resolution device, describing regularization method
09 p1491 A69-22707

Stratified atmosphere mean vertical flux due to ground disturbances, obtaining results for various wind and temperature profiles
10 p1685 A69-23856

Venus atmosphere observations compared with Venera 4 measurements of temperature, pressure and carbon dioxide content
10 p1791 A69-24200

Solar chromospheric flares effect on temperature of upper atmosphere observed by satellite at perigee altitude
12 p2149 A69-26447

Kelvin waves relation to quasi-biennial oscillation, using zonal wind and temperature variance data taken at Canton Island
13 p2290 A69-27391

IR day and night airglow of upper atmosphere utilized for atmospheric energy content and reactions analysis
13 p2252 A69-27585

Air mass displacements and diurnal variations in potential temperature at tropopause level
13 p2252 A69-27608

Two temperature lapse rate and single moisture lapse rate troposphere model for calculating temperature and moisture from satellite radiometry
13 p2252 A69-27638

Venusian atmospheric pressure and temperature measurements by Venera 4 probe, noting agreement with Mariner 5 observations
13 p2345 A69-27689

Wind velocity, geopotential and atmospheric layer temperature fields constructed from Tiros 9 satellite cloud data using least squares method and trigonometric polynomials
13 p2292 A69-27733

Temperature vertical profiles rms deviations calculated from temperature measurements during unstable atmospheric stratification
13 p2293 A69-27847

Corrections for atmosphere thickness needed for satellite measurements of underlying surface temperature
13 p2293 A69-27850

Probable sign-invariant periods of air temperature anomalies based on random Gaussian processes
13 p2294 A69-27855

Soviet book on temperature regime of free atmosphere above Northern Hemisphere covering aerological data processing, statistical estimates, latitudinal and seasonal variations
13 p2294 A69-27934

Rocket grenade measurements of earth atmosphere, finding lowest temperature in Alaska
13 p2255 A69-28637

Effective temperature values of ozone used to determine onset time and disturbance height in ionosphere
13 p2294 A69-28701

Acoustical thermometer-interferometer to measure air temperature between 20 and 50 km
14 p2445 A69-28777

Turbulence and temperature fluctuations spectral characteristics in thermally stratified atmosphere determined for various wave numbers, using energy and mass transfer functions
14 p2472 A69-29402

Turbulent heat exchange coefficient radiation absorption and diurnal vertical variations effects on temperature field in surface layer of sea and atmospheric boundary layer
14 p2472 A69-29462

Temperatures and geopotentials of isobaric surfaces in Northern and Southern Hemispheres compared for summer and winter seasons
14 p2473 A69-29724

Tropospheric and stratospheric temperature distribution in 1965 summer and winter from radiosonde and rocket data
14 p2442 A69-29725

Water-air interface models unreliability in calculating atmospheric heat and humidity turbulent flow over ocean
14 p2443 A69-29839

Solar telescope imaging quality measured as function of atmospheric turbulence and temperature above land level
14 p2453 A69-29973

Atmospheric transmission functions dependences on absorbing material, pressure and temperature in 15 micron band of carbon dioxide, introducing corrections
15 p2597 A69-30653

Statistical correlation of temperature and tail-wind data for London-New York route at 50 mb for SST operation
15 p2651 A69-30690

Surface gravity and temperature model atmospheres for O-type stars with UV line blanketing
15 p2693 A69-30778

Upper atmosphere winds and temperature measurements from rocket grenade, discussing TMA experiments
15 p2598 A69-31317

Diurnal variations of wind velocity, temperature and density at high altitude measured by Skylark rockets
15 p2598 A69-31319

Atmospheric density and temperature variations between 200-600 km from Cosmos satellite data, noting solar activity effect
15 p2599 A69-31343

Seasonal and latitudinal models of atmospheric wind and temperature structure between 30 and 120 km altitude
15 p2600 A69-31367

Internal gravity waves suggested as possible cause for anomalous mesospheric temperatures
15 p2601 A69-31376

Longitudinal variations of density, temperature and pressure distributions in stratosphere and mesosphere based on rocket observations, emphasizing arctic and subarctic regions
15 p2602 A69-31379

Rocket and satellite measurements of density, temperature and composition in lower thermosphere, considering altitude dependence
15 p2602 A69-31383

Atmospheric temperature and vertical gradient in E region based on measured instantaneous wind profiles
15 p2603 A69-31399

Exospheric temperature variations by Thomson scattering related to solar and geomagnetic activity, discussing seasonal effect on thermospheric variables
15 p2604 A69-31409

Diurnal thermospheric density, temperature and wind variations due to direct solar EUV heat input and tidal wave from lower atmosphere
15 p2605 A69-31439

Temperature measurements of neutral polar atmosphere at 120-170 km using artificial Na clouds
15 p2606 A69-31448

Spectroscopic observations of Venus atmosphere rotational temperature based on carbon dioxide band at 7883 Å
16 p2852 A69-31563

Virtual temperature change with respect to height of saturated air rising during water vapor condensation, discussing actual temperature and precipitation factor
16 p2808 A69-32454

Atmospheric thermal sounding by measuring outgoing thermal radiation with infinite resolution device, describing regularization method
16 p2782 A69-32487

Spectroscopic study of P Cygni showing ionization temperature, Balmer decrement agreement with calculated value and chemical composition
16 p2864 A69-32595

Sonic anemometers for atmospheric turbulence, discussing variance spectra of vertical wind component and temperature in atmospheric surface layer
16 p2808 A69-32600

Ozone soundings in upper stratosphere, discussing vertical temperature profiles relationship to vertical ozone profiles
16 p2787 A69-32640

Semidiurnal oscillation in thermalgeostrophic atmosphere examined using atmospheric model for tidal oscillations response study
17 p2959 A69-33148

Nonlinear least squares optimization program applied to atmospheric temperature sounding, solving for temperatures at various altitudes from simulated carbon dioxide intensity measurements
17 p2960 A69-33156

IR radiometer to measure Jupiter atmospheric temperature by calculating certain constituents heat radiation levels through Planck formula assuming black body properties
17 p2974 A69-33425

Temperature correction procedures for line-blanketed model atmospheres modified, noting effect on convergence to flux constancy
17 p3039 A69-33730

F1 layer observation at 80-87 degree solar zenith angles explained by additional ionization maximum development in presence of temperature gradients
17 p2967 A69-33985

Composition and temperature of daytime and nighttime neutral tropic lower thermosphere, obtaining atomic and molecular oxygen ratios
18 p3128 A69-34936

Statistical regularization for determining vertical atmospheric temperature profile from measurements of earth radiation in 15 micron carbon dioxide band
18 p3167 A69-35339

Atmosphere radio brightness temperature dependence on discrepancies between real and standard altitude profiles of thermodynamic temperature
19 p3275 A69-36339

Orthogonal functions for determining atmospheric vertical temperature profile from satellite measurement of earth outgoing radiation in carbon dioxide absorption band
19 p3303 A69-36409

Dynamic properties of upper atmosphere, discussing variations in temperature, density and composition
20 p3519 A69-36983

UV solar radiation variation effects on Mars and Venus upper atmosphere temperatures
20 p3595 A69-37136

Atmospheric temperature and moisture fields obtained by linear equations and objectively analyzed, considering underlying sea surface energy and cumulus cloud distribution
20 p3523 A69-37351

Japanese meteorological sounding rocket for atmospheric temperature and wind from 60 km down to balloon observation level, discussing principles and payload separation
20 p3543 A69-37795

Ambient atmospheric temperature and molecular nitrogen density measured simultaneously by rocket-borne electron beam luminescence method
20 p3543 A69-37799

Numerical prediction experiment for dynamical structure of tropical atmosphere in equatorial latitudes, constructing pressure, temperature and vertical motion distributions from wind field
20 p3573 A69-37910

Structure, composition and temperature of Venus atmosphere from spacecraft measurements and ground based observations
20 p3614 A69-38256

Temperature structure of nongray planetary atmospheres, discussing scattering and absorption of solar energy by gas molecules, cloud aerosols and ground
20 p3615 A69-38258

Upper atmospheric temperature by spectroscopy, considering rotational, OH nightglow, nitrogen cation dayglow and twilight temperatures
21 p3712 A69-38516

Spectra and intensities of rocket releases for upper atmosphere composition, temperature and reaction kinetics, noting chemiluminescence and atomic and molecular emissions
21 p3712 A69-38522

Ionospheric electron density and collision frequency profiles examined for changes during December 1967 to January 1968 stratospheric warming
21 p3714 A69-38556

Circulation and temperature fields indices used for studying tropospheric-stratospheric interactions during stratospheric warming at constant pressure levels
22 p3977 A69-39929

Thermal structure of middle atmosphere, discussing heat sources and sinks, photochemical theories of ozone distribution, IR radiative transfer, etc
22 p3940 A69-40537

Model atmospheres of late type stars with solar abundances, effective temperatures between 2000-4000 K and gravities corresponding to dwarf, giant and supergiant stars
22 p4027 A69-40654

Methane rotational temperature in Jovian atmosphere deduced from equivalent widths of lines at 1.1 micron band
22 p4028 A69-40663

Steady state distribution of visible and IR radiation in planetary atmosphere illuminated from outside, calculating atmospheric temperature profile
22 p4031 A69-40910

F region dynamic model, including variations in temperature, electron and molecular ion concentrations, etc
23 p4156 A69-41843

Subjective feeling of dampness correlation with relative humidity of air at zero and below zero C temperatures
23 p4109 A69-41870

Minimum air temperature forecast by terrestrial thermal or long wave radiation balance measurement, using radiometer data
23 p4184 A69-42211

Equatorial stratosphere and mesosphere wind, temperature and density data from rocket and balloon sounding, noting seasonal variations and possible stratosphere-ionosphere coupling
23 p4159 A69-42423

EHF earth-satellite link communication channel emphasizing down link, discussing weather models, atmospheric absorption and temperature, channel coherence bandwidth, etc
23 p4129 A69-42506

Lower atmospheric temperature continuous radio measurement as function of altitude, calculating temperature gradient
24 p4342 A69-42677

Equator-to-pole temperature gradient relation with planetary pressure belts, comparing observational data with theoretical circulation criterion
24 p4345 A69-43149

Lower ionosphere atmospheric density, temperature and pressure profiles diurnal variations from data of radio meteor echoes
24 p4311 A69-43504

Isobaric inhomogeneous atmosphere effect on sonic boom determined, using analytic equation relating transmitted wave intensity to local free stream Mach number
24 p4254 A69-43728

ATMOSPHERIC TIDES

Thermal tidal oscillations in earth atmosphere using circulation model attributed to solar radiation absorption by atmospheric vapor and ozone
03 p0457 A69-13030

Mathematical model derivation for observed atmospheric tide phenomena, taking into account thermal and other effects
03 p0426 A69-14098

Double diurnal oscillation of atmospheric pressure and vertical gradient of electromagnetic field, noting agreement between diagrams and role of atmospheric tides
08 p1306 A69-19866

Zonal westerlies variations associated with tidal cycles, discussing principal component analysis, zonal index, bandpass filtering, aliasing, prediction and stepwise regression
09 p1537 A69-22242

Luni-solar tide interpretation in F2 critical frequency based on sum and difference frequencies production by nonlinear atmospheric response to forces
10 p1685 A69-23829

Data requirements and acquisition for detection and description of tides and gravity waves in upper atmosphere
10 p1685 A69-23833

Reversible ion heating by atmospheric tides, noting radar Thomson scatter observations of E region ion temperature height profiles
11 p1879 A69-25159

Diurnal thermospheric density, temperature and wind variations due to direct solar EUV heat input and tidal wave from lower atmosphere
15 p2605 A69-31439

Wind effects on ionospheric electric currents, using equivalent circuits to study tidal modes and current patterns
16 p2775 A69-32087

Equatorial and polar semidiurnal oscillations in earth atmospheric tides related to inertial oscillations originating in autobarotropic field
17 p2996 A69-32862

Diurnal wind variations below 30 km plotted on constant pressure charts, showing topographical influence on tidal fluctuations
18 p3166 A69-34828

Physical process providing EMF for maintaining electrical structure of stratosphere and mesosphere shown to center in lower ionospheric thermally driven tidal motions
18 p3130 A69-35103

Meteor winds analysis method used on tidal period wind measurement data obtained by chemical release from rocket in 95-135 km region
20 p3574 A69-38092

Lunar semimonthly variations in noon values of D region absorption at Singapore, noting opposite phases of lunar tides in D and F regions
22 p4035 A69-41211

Thermotidal energy transfer from lower neutral atmosphere to and above lower ionosphere, considering tidal wave transmission mechanism
23 p4155 A69-41561

Diurnal and solar cycle variations of thermosphere density and temperature generated by solar EUV input and tidal wave, using two dimensional model
24 p4367 A69-43003

ATMOSPHERIC TURBULENCE

NT CLEAR AIR TURBULENCE

NT GUSTS

NT LOW LEVEL TURBULENCE

Turbulence characteristics up to 150 m above ground, noting surface roughness length directional dependence, longitudinal turbulence spectra and turbulent energy budget
01 p0110 A69-10695

Laser beam phase fluctuations for propagation through turbulent atmosphere, noting interferometer for simultaneous measurements for pairs of rays
01 p0091 A69-10845

Microturbulent velocity parameter correlation to iron-to-hydrogen ratio for G dwarfs, using model atmosphere abundance analyses
01 p0154 A69-10877

Amplitude scintillations of satellite radio signals during sunrise due to ionospheric turbulence induced electron content variations
01 p0067 A69-10980

Atmospheric turbulence power spectra for design criteria of future low altitude aircraft from LO-LOCAT program, analyzing turbulence scale lengths [AIAA PAPER 68-216]
01 p0011 A69-11023

- Light aircraft all-weather flight feasibility, discussing storm and clear air turbulence detection and icing prevention
01 p0111 A69-11049
- Blob existence in temperate latitude sporadic E from ionosonde and VHF oblique incidence measurements
01 p0070 A69-11162
- Spikes on sonic boom pressure waveforms due to simultaneous focusing and diffraction of planar N wave by inhomogeneous atmosphere layer
01 p0011 A69-11280
- Turbulence characteristics from light wave fluctuation measurements, discussing applications to small scale inhomogeneities in atmospheric temperature distribution
02 p0274 A69-11437
- Wind perturbations characteristics near large convective cloud banks as function of ascending current, wind shear and turbulence
02 p0274 A69-11446
- Turbulence conditions in atmospheric boundary layer within similarity theory, including wind velocity and temperature profile
02 p0274 A69-11447
- Free atmospheric turbulence theory extended to include ionosphere, deriving equations for horizontal ionospheric wind together with turbulence coefficient
02 p0274 A69-11678
- Refractive index structure constant for different atmospheric turbulence conditions, discussing possibility of improved capabilities for imaging systems
02 p0275 A69-11930
- Stress and heat flux spectra estimation using Busch-Panofsky observations
02 p0276 A69-12698
- Vertical wind velocity structure and turbulent heat flux temperature measurements over steppe and sea, noting underlying surface influence
03 p0458 A69-13270
- Turbulent parameter and turbulent diffusion vertical profile diurnal variations determination based on measurements of Rn 220 and thorium-B concentrations near ground
03 p0459 A69-13273
- Radar method to estimate turbulent motions in clouds
03 p0459 A69-13289
- Planetary boundary layer response to time varying pressure gradient force
03 p0460 A69-13337
- Nonstationary model of mesoscale atmospheric vortex with vertical axis based on atmospheric thermohydrodynamics
03 p0462 A69-13932
- Standard deviation of wind direction fluctuations by simultaneous measurements of wind vane displacements and number of wind direction reversals
04 p0626 A69-14911
- Tetron flight observations of eddy velocities in planetary boundary layer, noting effects of height and seasonal variations
04 p0626 A69-14912
- Turbulent transport of energy in atmospheric boundary layer near earth surface resulting from forced convection
04 p0627 A69-15087
- Wind turbulence measurement by shock wave tracking using Doppler radar, stressing relative location of antenna and sound source
04 p0628 A69-15149
- Absorption effect on fluctuation of signal level propagating in turbulent atmosphere taking into account absorption in water vapor
05 p0717 A69-15634
- Turbulence characteristics and wind velocity in atmospheric boundary layer determined from pressure and temperature fields
05 p0788 A69-16453
- Submillimeter plane monochromatic wave amplitude and phase fluctuations during propagation in turbulent atmosphere surface layer, considering absorption by water vapor
05 p0722 A69-16778
- Solar flares acceleration processes related to solar atmospheric currents
06 p0995 A69-17442
- Atmospheric wind velocity in Northern and Southern Hemisphere, noting increase with height
06 p0921 A69-17747
- Image averaging time effects on modulation transfer function (MTF) of system comprising telescope objective and horizontal propagation path in turbulent atmosphere
06 p0890 A69-17806
- Wing penetration into zone of sharply localized gust, deriving equations for forces and moments acting on wing
07 p1050 A69-18742
- Lifting rotor blades flapping response to atmospheric turbulence, discussing time averaging and perturbation schemes
[AIAA PAPER 69-206] 07 p1057 A69-19577
- Qualitative criterion for observing atmospheric turbulence structure by shadowgraph based on medium statistical properties, using ray optics
07 p1183 A69-19650
- Spherical wave generalization for plane light wave propagating in turbulent medium, describing circular objective averaging effect on intensity fluctuations
08 p1351 A69-20438
- Automatic measuring device for short term air temperature and wind velocity fluctuations leading to air mixtures propagation
09 p1535 A69-21515
- Cross-spectral density of pressure induced on lifting surface by isotropic atmospheric turbulence, solving integral equation
[ONERA-TP-681] 09 p1613 A69-21689
- Mean and turbulent energies and energy spectra of large scale wind velocity pulsations, analyzing annual variation for fixed wave numbers
09 p1536 A69-21861
- Laser beam optical scintillation under atmospheric turbulence conditions, showing log amplitude variance saturation and decrease
09 p1517 A69-22079
- Acoustic waves pressure field micropulsations in turbulent fluid, analyzing space-time spectrum
09 p1492 A69-22710
- Solar outburst and storm accompanying 9 June 1968 flare, noting radio evidence for coronal instability before flare
09 p1582 A69-22747
- Statistical characteristics of transverse shifts of ray directions in turbulent atmosphere for arbitrary wave parameter values
10 p1657 A69-23942
- Atmospheric turbulence effect on linear antenna gain in direction of radiation pattern maximum determined together with antenna dimensions
11 p1844 A69-24435
- He-Ne laser light coherence distortion by atmospheric turbulence
11 p1894 A69-24452
- Coherent optical target recognition through randomly turbulent medium for imaging system offsetting image degradation due to turbulence
11 p1894 A69-24470
- Atmospheric turbulence effects on aircraft flight noting causes of turbulence
11 p1911 A69-24527
- Holographic techniques application to optical systems for high resolution images of distant objects by overcoming atmospheric turbulence and light diffraction limitations
11 p1883 A69-24688
- Turbulence induced depolarization of linearly polarized He-Ne laser beam at 6328 Å traversing atmosphere near ground level
11 p1896 A69-24842
- Aircraft dynamic response to three dimensional turbulence, establishing unique correspondence between spatial symmetry properties of ambient fields of turbulence and aircraft
11 p1823 A69-25503
- Statistical turbulence theory applied to turbulent flow transport properties in lower atmosphere
12 p2125 A69-25894
- Linearized atmosphere model above flat earth, applying variational principle to energy between geostrophic equilibrium and reestablished states
12 p2125 A69-25954
- Turbulent boundary layer in lower atmosphere downward of abrupt change of surface roughness, determining surface shear stress and roughness height
12 p2125 A69-26014
- Jet stream winds direction correlated with direction of LF pressure disturbances crossing microbarograph array
12 p2125 A69-26015
- Spherical wave propagation in homogeneous turbulent medium, discussing nonstationary statistics as applied to vertical propagation in atmosphere
12 p2029 A69-26251
- Atmospheric turbulence effects on detection and resolution of incoherent objects, discussing error probabilities of threshold and maximum-likelihood systems
12 p2029 A69-26252
- Atmospheric turbulent energy spectra in boundary surface layer, considering homogeneous axisymmetric model in presence of temperature and velocity gradients
12 p2067 A69-26355
- Variable solar activity effect on earth upper atmosphere rotation at altitudes from 200 to 300 km
12 p2069 A69-26442
- Satellite position errors due to atmospheric instability, discussing altitude-temperature relation and stellar scintillation synchronism for stars at small angular distances
12 p2158 A69-26445
- Horizontal wind velocity energy spectra, attributing free atmosphere meso and microscale turbulence to meso and micrometeorological processes
12 p2070 A69-26575
- Atmospheric boundary layer mean turbulence and vertical velocity calculations, tabulating layer characteristics for various turbulent heat flux and geostrophic wind velocity values
12 p2126 A69-26578
- Spectral model used for analysis of atmospheric turbulence as related to loads on gliders
12 p2127 A69-26931
- Solar atmosphere five minute oscillations observed by Frazer divided into two harmonic atmospheric model for studying oscillation region height and mean temperature
13 p2343 A69-27627
- Numerical methods for time integrating first order differential equations, emphasizing atmospheric oscillations in baroclinic model, evaluating errors
13 p2290 A69-27636
- Radiation fields and large scale atmospheric disturbances analyzed, using radiation maps from Cosmos satellites
13 p2291 A69-27727
- Blocking processes synchronous development involving atmospheric circulation disturbances in Northern and Southern Hemispheres, noting localization in Pacific and Atlantic oceans
13 p2292 A69-27840
- Vortices interaction effect on vertical turbulent heat flow in atmosphere boundary layer, determining dependence of vortex mean vertical temperature gradient
13 p2293 A69-27841
- Electric field profile and turbulence ratio relationship in free atmosphere as function of vertical current density, conductivity, potential gradient and charge density
13 p2295 A69-28523
- Free atmospheric turbulence theory extended to include ionosphere, deriving equations for horizontal ionospheric wind and turbulence coefficient
13 p2295 A69-28709
- Vertical wind velocity structure and turbulent heat flux temperature measurements over steppe and sea, noting underlying surface influence
14 p2471 A69-28778
- Turbulent parameter and turbulent diffusion vertical profile diurnal variations determination based on measurements of Rn 220 and thorium-B concentrations near ground
14 p2472 A69-28781
- Turbulence and temperature fluctuations spectral characteristics in thermally stratified atmosphere determined for various wave numbers, using energy and mass transfer functions
14 p2472 A69-29402
- Electro-optical automatic gain control system to reduce atmospheric turbulence produced fluctuations in received optical signal strength
14 p2459 A69-29491
- Focused beam wave applied to atmospheric turbulence probing for spectral density of index of refraction, structure constant and wind velocity
14 p2414 A69-29512
- Log amplitude fluctuations of laser beam in turbulent atmosphere, obtaining asymptotic expressions for near field of transmitter aperture
14 p2460 A69-29638
- Solar telescope imaging quality measured as function of atmospheric turbulence and temperature above land level
14 p2453 A69-29973
- Turbulence coefficient in layers between main isobaric surfaces based on wind and temperature fields analysis
15 p2648 A69-30646
- Air masses transformation, solving nonlinear simultaneous system of equations of motion, heat influx and turbulent energy balance
15 p2649 A69-30647

Turbulent heat and momentum fluxes spectra measured in atmospheric ground layer, describing changes as function of height and stratification conditions

15 p2649 A69-30648

Photoelectric index of main sequence stars in F5 to G2 spectral range as indicator of atmospheric microturbulent velocities

15 p2695 A69-30999

Interferometer for measuring electric fields spatial correlation function at camera aperture, describing laser light coherence measurements after propagation through turbulent atmosphere

15 p2653 A69-31164

Rocket ejected vapor trails structure in lower thermosphere showing no evidence of atmospheric turbulence

15 p2602 A69-31393

Optical communications experiments for quantitative data at 6328 Å on system fading due to scintillation and atmospheric turbulence effects on coherent propagation at 10.6 micron

16 p2748 A69-31564

Piloting errors due to false instrument readings during turbulent atmosphere flight

16 p2734 A69-32007

Horizontal wind pulsations in precipitations obtained from pulsed Doppler radar data, including degree of turbulent flow anisotropy

16 p2807 A69-32271

Vertical wind velocity pulsations in precipitation and passage through subfrontal clouds measured by pulse radar

16 p2807 A69-32272

Turbulence dissipation rate in clouds and precipitations determined from rms width of vertical sounding radar signal fluctuation spectra, distinguishing gravity and turbulence effects

16 p2807 A69-32273

Turbulence and SST, discussing subsonic accidents, probability of encountering gust induced accelerations, turbulence at cruise altitudes, radar storm return and mountain waves

16 p2808 A69-32368

Acoustic waves pressure field micropulsations in turbulent fluid, analyzing space-time spectrum

16 p2782 A69-32489

Absorption effect on fluctuation of signal level propagating in turbulent atmosphere taking into account absorption in water vapor

16 p2754 A69-32492

Sonic anemometers for atmospheric turbulence, discussing variance spectra of vertical wind component and temperature in atmospheric surface layer

16 p2808 A69-32600

Mixing length model to relate turbulent shear stress to mean velocity field within planetary boundary layer above surface roughness change

17 p2997 A69-33154

Analog correction method to suppress pilot maneuver effects during analysis of aircraft accelerations induced by atmospheric turbulence

[ICAS PAPER 68-39] 17 p2901 A69-33590

Turbulence origin and structure in stably stratified media for finite disturbance instability in sloping flows experimentally observed with visualization techniques

17 p2999 A69-33735

Meteorological analysis of stratospheric clear air turbulence flights, discussing vertical temperature structure in terms of wave motion and turbulence intensity

17 p2999 A69-33736

Phase fluctuation measurements of laser beam propagating through turbulent atmosphere

17 p2927 A69-33855

Laser beam propagation through turbulent medium, investigating statistical distribution of phase shift fluctuations

17 p2976 A69-33857

Radial velocities differences as indicator of stellar atmospheric turbulence, applying method to sun

17 p3044 A69-34177

Artificial horizon indicator design modifications to facilitate maintaining horizontal aircraft position, discussing automatic pilot advantages in turbulence and flight simulators

17 p2903 A69-34214

Soviet monograph on turbulence in free atmosphere covering measurement and statistical techniques, tropospheric and stratospheric disturbances, wind pulsations, effects on aircraft flights, etc

18 p3165 A69-34351

Correlation between disturbances in troposphere and in geomagnetic field observed after widespread high winds and magnetic storms, using superposed epoch method

18 p3127 A69-34648

Climatological patterns of atmospheric kinetic energy dissipation in free atmosphere derived from upper wind statistics of Northern Hemisphere, using Kolmogoroff functions

18 p3166 A69-34825

Solitary waves in stratified polytropic atmosphere allowing for convection and disregarding viscosity and turbulence

18 p3167 A69-35338

Atmospheric flow with respect to mesoscale disturbances, examining conditions for hydrodynamic stability

18 p3167 A69-35343

Operational flight tests of IR atmospheric turbulence detection system

[AIAA PAPER 69-799] 19 p3367 A69-35631

Light rigid civil aircraft response to continuous atmospheric turbulence estimated using two rigid body degrees of freedom method for vertical and lateral gusts

[AIAA PAPER 69-766] 19 p3433 A69-35657

Turbulence energy spectra in free atmosphere with convective layer surmounted by inversion layer, noting power law followed by velocity components

19 p3362 A69-36406

Diurnal and seasonal phase-difference fluctuation measurement of radio waves propagating along ground layer caused by atmospheric turbulence

20 p3485 A69-36971

High altitude aircraft range requirements for airborne turbulence detector, taking into account passenger comfort, turbulence geometry, maneuverability and pilot decision making

20 p3537 A69-37164

Atmospheric turbulence and impurities diffusion considered as stochastic processes, deriving equations and covariance functions for flow characteristics

20 p3570 A69-37426

Thermal stability and radioelectric turbulence parameter derivative relationship for dry adiabatic stratification of lower troposphere and for inversions

20 p3571 A69-37509

Atmospheric phenomena effects on terrain imaging radar systems performance, discussing tropospheric turbulence and ionospheric irregularities

20 p3490 A69-37647

Components of turbulent energy balance at 1 and 4 meter heights, discussing average motion energy transformation into turbulent energy

20 p3571 A69-37696

Atmospheric turbulence statistical distribution mass measurements using velocity, gravity and weight recordings based on calibration of aircraft as turbulence measuring instrument

[ONERA-TP-699] 20 p3541 A69-37754

Received electromagnetic fields fluctuations due to transhorizon propagation, emphasizing fading, tropospheric turbulence correlation and rapid fluctuations due to small scale index variations

20 p3494 A69-37810

Doppler radar observations of precipitation induced mesoscale wind oscillations near melting layer produced by pressure perturbations due to horizontal variations in cooling

20 p3572 A69-37909

Electrohydraulic servosystem to counteract atmospheric turbulence effects on B-52 global bombers, noting reduction in aircraft fatigue and structural damage

20 p3467 A69-38184

Diurnal entrainment deviations and atmospheric turbulence effects on flash photographs from Geos 1

21 p3793 A69-38339

Wind motion and turbulence in upper atmosphere from Rehbar 15 and 16 rocket observations

21 p3703 A69-38362

Turbulent field structure between 90-120 km estimated from sodium clouds diameters variation ejected from rockets

21 p3713 A69-38524

Scattering equations for sonic boom waveform spike perturbations produced by atmospheric turbulence, discussing supersonic aircraft pressure signatures

21 p3646 A69-38689

Atmospheric natural turbulence effect of degradation of laser signal phase and amplitude characteristics, noting refractive index inhomogeneities effect on optical tracking system

[AIAA PAPER 69-871] 21 p3675 A69-39397

Optical communication through random atmospheric turbulence via heterodyne and video detection, estimating performance from optical wave propagation analysis

23 p4125 A69-42186

Three dimensional structure of large scale disturbances in lower stratosphere and upper troposphere in equatorial Pacific, using power spectral and synoptic analysis

23 p4159 A69-42345

Atmospheric model for calculating wind velocity profile and turbulence of stable atmospheric boundary layer with given temperature stratification and pressure gradient distribution

23 p4184 A69-42489

Terrain surface irregularities influencing electromagnetic wave propagation in inhomogeneous atmosphere, using perturbation calculation

24 p4281 A69-42611

Log amplitude mean value for Gaussian or laser-like optical beam propagating horizontally in turbulent atmosphere

24 p4282 A69-42970

Coherent light propagation through turbulent atmosphere observed by applying He-Ne lasers to simultaneous measurements of scintillation effects over homogeneous optical paths

24 p4344 A69-43114

Energy density distribution in power spectra of turbulence in long wave region in free atmosphere

24 p4346 A69-43155

Thunderstorm turbulence relationship to weather radar echoes from storm penetrations in Oklahoma by instrumented aircraft

24 p4347 A69-43720

ATMOSPHERICS

NT DAWN CHORUS

NT HISS

NT IONOSPHERICS

NT SUDDEN ENHANCEMENT OF ATMOSPHERICS

NT WHISTLERS

Atmospheric noise at millimeter wavelengths, discussing solar radiation and antenna near and far field patterns

01 p0028 A69-10420

Spectral parameters of VLF radio noise given as functions of azimuth from atmospherics analyzer observations

01 p0033 A69-10971

Soviet collection of papers on atmospheric electricity

04 p0593 A69-15101

Histograms construction for azimuthal distribution of atmospherics from visual and photographic data obtained by CRT display goniometer

04 p0593 A69-15102

Observation data on source distribution of atmospherics with respect to distance from observation point

04 p0593 A69-15103

CRT direction finder with linear scanning to determine statistical data for azimuthal distribution of atmospherics

04 p0600 A69-15104

Near earth atmospherics spectrum characteristics determined by analytical expressions for elementary signals in 2-30 kHz range

04 p0593 A69-15105

Frequency dependence of atmospheric noise intensity from 1 to 1000 kHz at low and medium latitudes

05 p0758 A69-16410

Atmospheric noise at 33.5 GHz observed most on days of cumulus clouds probably due to local convective activity

05 p0721 A69-16661

Ground based radio telescope sensitivity to radio emission from earth atmosphere and galactic sources

07 p1099 A69-18515

Magnetospheric ELF noise, discussingOGO 3 spectrum analysis

07 p1124 A69-18834

Atmospheric radio noise at 27 kc measured at European stations, showing field strength variations, latitude dependence and amplitude distribution

09 p1491 A69-22163

Coherent FSK LF/VLF radio communication modem with large predetection bandwidth for improvement of reception in atmospheric noise

09 p1458 A69-22473

VLF polar chorus emission and geomagnetic variations caused by compressions or expansions of magnetosphere

10 p1681 A69-22803

Artificial magnetospheric VLF noise triggering by Morse code dots at 14.7 kHz from NAA verified at Antarctica

11 p1878 A69-25155

Electromagnetic energy spectra of lightning expressed as function of electric field spectral density of atmospheric
14 p2437 A69-29076

Atmospherics observations in Japan during last 40 years, discussing relation to meteorology, statistical characteristics, whistlers, noise phenomena, periodic variations, solar effects and ray theory
15 p2595 A69-30418

Earth ionosphere cavity model for atmospheric waveform shape, considering ELF pulse distortion after propagation through antipode
16 p2750 A69-31978

Modified pulse height analyzer /PHA/ for sample amplitude height occurrence frequency measurements obtaining amplitude probability distribution/APD/ and three moments of atmospheric noise
18 p3102 A69-34960

Atmospheric sources automatic location by direction finding network based on triangulation network principle
18 p3102 A69-34961

Antarctic VLF emissions observations at 12 kHz, showing dependence on geomagnetic disturbances, auroras and radio absorption in ionosphere
18 p3102 A69-34964

Atmosphere radio brightness temperature dependence on discrepancies between real and standard altitude profiles of thermodynamic temperature
19 p3275 A69-36339

Terrestrial radio noise source aspects including atmospheric, propagation influence, lightning-generated noise and whistlers, radio interference, etc
19 p3276 A69-36434

Terrestrial radio noise from lightning discharges measured by Ariel 3 satellite to deduce sources distribution
21 p3759 A69-39259

Nighttime atmospheric shape analysis created by lightning and propagating in earth lower ionosphere waveguide
22 p3941 A69-40961

ELF atmospheric propagation, determining slow-tail atmospheric group velocity, relating characteristics to spectral characteristics of lightning
23 p4114 A69-41362

ELF atmospheric excitation, discussing cloud to ground and intracloud lightning discharges Fourier integration and current moment spectrum
23 p4115 A69-41562

Earth sphericity and earth-ionosphere waveguide effects on terrestrial atmospheric, deriving form by computer
23 p4157 A69-41860

Peak field strengths of atmospheric radio noise bursts from lightning flashes at VHF and flash distance estimates at tropical latitudes
23 p4126 A69-42355

Wideband vertical electric field noise reduction in ELF/VLF atmospheric receiving systems using bucking, delayed feedback and frequency rejection units
23 p4128 A69-42504

ATOM CONCENTRATION

Field ion microscope study of imaging solute atoms of dilute Pt-based W, Pd, Co, Ni and Au alloys
01 p0092 A69-10055

Nondegenerate dense plasma thermodynamic stability by nonclassical methods, discussing atomic concentration dependence on ionic concentration
05 p0802 A69-15892

Interaction between point defects and magnesium atoms in aluminum irradiated by neutrons, analyzing magnesium concentration effect on recovery
05 p0781 A69-16613

Noncoherent scattering of atoms with Maxwellian distribution in moving atmosphere, discussing Doppler broadening expansion in Legendre polynomials
07 p1219 A69-19286

He concentration measurement in transient He-air mixture by spectroscopic analysis of fluorescence excited by high energy electron beam
08 p1312 A69-19860

Photometric methods for determination of H atom and hydroxyl radical concentrations in hot gases in convergent-divergent nozzles, noting Li/ lithium hydroxide absorption
09 p1496 A69-21952

Pd-D resistivity variation with D concentration at room and liquid He temperatures, discussing structural resistivity
10 p1745 A69-23357

Fast electron energy distribution function and atom concentration in first excited level in weakly ionized plasma, considering transitions between excited levels
10 p1739 A69-23628

Atomic hydrogen vertical profiles with increased high-low altitude ratio for interpreting observations of thermospheric and exospheric hydrogen abundance
14 p2440 A69-29130

Number and mass of sodium atoms in comet Ikeya-Seki 1965f head calculated from spectral observations, ascribing D lines to resonance scattering of photospheric radiation
15 p2685 A69-30526

Rb 87 vapor laser output power and spectral line width dependence on optical pumping intensity and atom density in resonator
19 p3336 A69-36343

Radiative recombination in GaAs p-n structures having region with concentrations of Ge atoms
21 p3780 A69-39044

ATOMIC BATTERIES
U RADIOISOTOPE BATTERIES

ATOMIC BEAMS

Molecular and atomic beam focusing in electric and magnetic fields with helical symmetry of specified type
06 p0959 A69-16917

Total ionization cross section for symmetric collisions measured as function of energy by using neutral atomic beams of neon and krypton
08 p1356 A69-20740

Ionization within intersecting alkali atomic and slow electron beams, observing ionization cross sections increment near ionization threshold
15 p2655 A69-30726

Atomic beam for H maser operation prepared by using nonadiabatically changing magnetic field in transition region
15 p2635 A69-31103

Single hyperfine-state atomic beam selector effect on hydrogen maser stability, discussing DC magnetic field variation
18 p3153 A69-35306

Reactive scattering from solid surfaces, discussing atom beam reaction of O with heated Ge and Si single crystals
19 p3377 A69-36178

Ar-Kr integral collision cross sections based on density measurements of Ar beam passed through liquid nitrogen cooled Kr filled scattering chamber
19 p3378 A69-36185

Ion production in K/diatomic Br system by high energy K beam, obtaining total ionization cross section as function of energy
19 p3378 A69-36187

Spherical aberration effect on atomic beam focusing in six pole magnetic system
19 p3380 A69-36602

Metastable atom detection system for ground state atom beams, measuring Ar beam density five orders lower than background gas density
22 p3950 A69-41230

DC beam experiment for determining molecule sticking coefficients of gas beams incident on Ti, Ba and Sr gettering surfaces at cryogenic temperature
23 p4151 A69-41544

ATOMIC CLOCKS

Ephemeris Time and Atomic Clock Time roles in astronomy, discussing errors in daylength determination for mechanical, Shortt and atomic clocks, UT and Ephemeris Time
01 p0156 A69-10989

Laboratory equipment for atomic and astronomical time and frequency measurement
05 p0827 A69-16582

Atomic clocks frequency standards, discussing masers, atomic beam resonators and gas cells and various applications
09 p1501 A69-22598

Earth rotation velocities nonuniformity according to astronomical observation data obtained from Universal Time and atomic time scales comparison
11 p1957 A69-24407

Atomic clock with sequential optical pumping using resonance frequency of hyperfine transition of ground state Rb 87
12 p2090 A69-26291

Atomic and astronomical time and frequency measurement via Loran C and VLF/Omega phase tracking receivers
15 p2615 A69-31285

Airborne clock used to synchronize atomic clocks at different locations, discussing equipment and error sources
17 p2975 A69-33593

National Physical Laboratory atomic clock improvements, describing use of cesium 133 as second of time standard and phase shift effects on precision
21 p3720 A69-38548

Earth rotation velocities nonuniformity according to astronomical observation data obtained from Universal Time and atomic time scales comparison
24 p4391 A69-43797

ATOMIC COLLISIONS

Analytical mechanics of chemical reactions, discussing natural collision coordinates for three dimensional reactions and exchange collisions for molecule and atom
01 p0123 A69-10681

Soviet book on atomic collisions and elementary processes in plasma covering atomic interactions, elastic and inelastic collisions, negative ions, autoionization, ion mobility and recombination
01 p0132 A69-11200

Diatomic dissociating gas free atoms virial coefficient used to study thermodynamic properties and transport coefficients of gases
02 p0283 A69-11574

Polarized orbital method for calculating electron-atom scattering amplitudes, noting discontinuous wave function, nonvariational technique and strong dependence on parameter
02 p0284 A69-12702

Saturation effect theory in gas system, taking into account Doppler expansion and collisions based on density matrix
03 p0437 A69-13042

Ionizing shock front structure in monatomic gas, considering atom-atom and electron-atom collisional ionization rates
03 p0414 A69-13138

Energy distribution among products of reactive collision of atomic H with Br molecule yielding HBr and Br atom, using perturbed Morse oscillator approximation
03 p0472 A69-13316

Interatomic collisions effect on multimode He-Ne lasers output power and spectral composition
04 p0610 A69-14383

Effect of dipole/dipole resonance interaction between excited and nonexcited atoms on gas thermodynamic properties, showing unstable quasi-molecules formation
04 p0632 A69-14551

Distribution functions for fast electrons near anode calculated by kinetic theory, assuming weakly ionized plasma with smaller Debye length than collision mean free path
04 p0635 A69-14764

Separation of center of mass and rotational coordinates from N electron diatomic Schroedinger equation
04 p0554 A69-14861

Interaction of gas atoms with solid surface, giving mathematical model assumptions
04 p0632 A69-15008

Continuous radiation production in positive plasma column of inert gas considered as manifestation of plasma electrons bremsstrahlung from interaction with gas atoms
05 p0800 A69-15741

Three atom interaction contribution to nonideal dissociating gas state equation, determining quantum correction for third virial coefficient
05 p0796 A69-15893

Atomic hydrogen-bromine linear collision reaction intermediate formation and reactive scattering cross sections quantum mechanical calculation, using perturbed Morse oscillator approximation
05 p0796 A69-15911

Noble gas atom simultaneous ionization and excitation by removal of metastable electron in fast collision
06 p0961 A69-17137

Ratios of gas kinetic electron-atom collision integrals of Ramsauer for Ar
06 p0963 A69-17822

Linear approximation of ionization instability in disk channel of nonequilibrium MHD generator, calculating interatomic collisions frequency as function of temperature
06 p0871 A69-17911

Rotational inelastic transitions in atom-diatomic collisions, discussing restricted distorted-wave approximation, transition probabilities, impact parameters, inelastic and glory quenching, etc
07 p1185 A69-19302

Physics of electronic and atomic collisions - Conference, Leningrad, July 1967
07 p1186 A69-19651

Cross sections for inelastic interactions of electrons with atoms and heavy impurity ions and processes of atomic excitation

07 p1195 A69-19652

Atomic collision processes in astrophysics noting stellar continuum spectra, Ca ion and He lines, solar corona, heat balance in H I regions and planetary nebulae

07 p1224 A69-19653

Collisional processes relevant to daytime and nighttime models of upper atmosphere neutral density and temperature

07 p1130 A69-19654

Electron collisional excitation cross section calculations for atoms and ions using modified Born approximation taking into account three physical effects

07 p1187 A69-19658

Atomic excitation and ionization involving inner shell electrons during collisions between atoms and ions, examining photoabsorption by inner shell electrons

07 p1187 A69-19659

Cross section calculations for elastic and inelastic electron collisions with atoms, ions and molecules and ionization of atomic systems by electrons and photons

07 p1187 A69-19660

Atomic collision theory, discussing cross section calculations by Gryzinski classical method, variational methods and Fadeev equations for three particles

07 p1187 A69-19661

Atomic and electronic collisions experimental study techniques, noting three data logging systems

07 p1187 A69-19662

Electron collision excitation of positive ions, calculating collision cross sections for transitions between levels of P term

07 p1187 A69-19714

Forward scattering of metastable and ground state argon atoms after argon ion-atom charge transferring collisions, discussing excitation resonances

08 p1354 A69-19809

Interaction between atom and plane monochromatic traveling wave taking into account pressure effect occurring in strong collision model

08 p1354 A69-19954

Polarization of Lyman alpha radiation in hydrogen rare gas collisions calculated in Born and distortion approximations including rotational coupling

08 p1355 A69-20207

Collision cross sections between monatomic gas impurities and metastable atoms in He-Ne laser from output curve and impurity partial pressure

08 p1325 A69-20278

Total ionization cross section for symmetric collisions measured as function of energy by using neutral atomic beams of neon and krypton

08 p1356 A69-20740

Channel coupling effects in elastic electron-atom collisions involving electric dipole transitions, noting phase shifts and differential cross section

09 p1542 A69-21623

Complex trajectory method for describing tunnel effect during atom ionization in strong light wave field, using quasi-classical approximation

09 p1543 A69-22658

Linear dependence of saturation parameter on active medium density of He-Ne laser explained by considering exchange collisions of neon atoms

09 p1521 A69-22687

Thermodynamic potential of rarefied plasma from Coulomb interactions of atoms with electrons and ions

10 p1728 A69-23134

Direct Coulomb interaction matrix elements between hydrogen atoms in ground states calculated, presenting interaction potential

11 p1921 A69-24416

Translational-vibrational energy transfer value between atom and diatomic molecule determined using steric factor with repulsive interaction potential

12 p2134 A69-25988

Charged state variations during protons and inert gas atoms interactions analyzed by coincidence method

12 p2133 A69-26543

Negative charge production by H atoms collisions with rare gases and hydrogen, noting smooth rise of cross section with energy for rare gases

13 p2302 A69-27459

Oscillations and decomposition of diatomic gas molecules at high temperatures during atom/molecule collisions, deriving kinetic equations for energy level changes

13 p2302 A69-27797

Inelastic interaction cross sections of nuclear active cosmic ray particles with atomic Fe and Pb in 100 to 1000 gev range

13 p2330 A69-28384

Spatial distribution patterns of gaseous argon atoms scattered from solid argon surface

13 p2300 A69-28658

Interatomic collisions effect on multimode He-Ne lasers output power and spectral composition

14 p2456 A69-28756

Elastic collision effect on gas laser atoms velocity distribution and gain factor determined for strong collision model

14 p2459 A69-29388

Coupled equations for heavy particle motion expressed by introducing generalized matrix operator for effective momentum in atomic collision problems

14 p2489 A69-29997

Partial wave description for calculating cross sections of fine structure transitions of Na in collision with He, discussing shape resonances

15 p2655 A69-30198

Electron ion recombination role in atomic collision process in rare gases ionization path, considering scintillation mechanism

15 p2655 A69-30961

Resonances in elastic cross section for electron/hydrogen atom scattering noting wide structure

15 p2657 A69-31265

Interstellar particle penetration into solar system, discussing impact ionization of earth ionosphere by interstellar neutral hydrogen and helium

15 p2699 A69-31390

Initial ionization processes in strong shock wave in hydrogen, determining ionization relaxation length and cross section of atom-atom excitation collisions

16 p2815 A69-31590

Stripping and low-energy collisions of H atoms on O and N molecules, showing target ionization to projectile stripping ratio dependence on ionization potential

16 p2814 A69-31773

Diatomic heavy particle collisions with emphasis on epithermal energy range, discussing elastic scattering and inelastic processes

16 p2815 A69-32259

Interatomic potential between alkali ions and rare gas atoms, using model accounting for repulsive and attractive exchange forces

16 p2815 A69-32464

Cross sections threshold behavior for Cs II resonance lines excitation due to Cs ion-He collision

17 p3008 A69-33388

Long lived highly excited atoms production in electron collisions with CO, O and N molecules

18 p3177 A69-35125

Atom-atom scattering potential from phase shifts, using WKB formula and Jeffreys-Born approximation

19 p3378 A69-36189

Spectral lines due to magnetic dipole transitions in fine structure levels in collisionally excited neutral H clouds, discussing theoretical difficulties in interpretation

19 p3379 A69-36225

Atom-atom collisional excitation cross sections obtained from ionization cross sections, noting Thomson classical theory

20 p3580 A69-37500

Optical pumping and selective population applications, considering double magneto-optic resonance and inelastic interatomic collisions

21 p3735 A69-38454

Diatomic-monatomic oxygen collision cross section determined from rotational line width in diatomic oxygen Schumann-Runge emission spectra

22 p3983 A69-40099

Impact parameter versions of two state and Born approximations to calculate single excitation cross sections of H atoms ground state collisions

22 p3987 A69-41006

Hydrogen-hydrogen excitation collisions by impact parameter treatment, investigating rotation coupling influence in four state cross sections approximation

22 p3987 A69-41007

Antimatter motion in solar system and earth atmosphere, discussing vaporization and annihilation energy in collisions with interplanetary gas atoms

22 p4034 A69-41100

Collisional radiative recombination and ionization coefficients for weakly ionized H plasmas using rate equations

22 p3988 A69-41154

Atoms and ions collision strengths and photoionization cross sections for nitrogen, oxygen and neon fitted

to interpolation formulas for temperature and frequency effects

22 p3988 A69-41244

Atomic spectrophotometry to monitor O atom formation rate behind shock waves in oxygen-argon mixtures, noting dissociation over 2850-5550 K temperature range

23 p4194 A69-42209

Atomic nitrogen collisional ionization and recombination rates under assumed quasi-steady nonequilibrium distribution of electron state populations

24 p4353 A69-43700

ATOMIC ENERGY LEVELS

Pionic 2p-1s X ray transition energy and natural linewidth and muonic 2p-1s X ray transition energy measurements for Na 23

01 p0122 A69-10035

Partial maser effect in recombination lines of hydrogen atoms in nebular plasma due to overpopulation of energy levels at thermodynamic equilibrium

01 p0148 A69-10042

Statistical equilibrium equations solution for thermodynamic equilibrium variations of populations of very high energy levels in hydrogen and complex atoms

01 p0150 A69-10395

Spectral lines source functions for formation in multilevel atom and radiative transfer in atmosphere of three level Na atoms and four level O atoms

01 p0124 A69-10962

Radiation, Stark and van der Waals level broadening constants for Mg I and Si I calculated to interpret solar and stellar spectral line widths

02 p0310 A69-11454

Multiphoton ionization cross section of atom via perturbed Green function, considering light wave electromagnetic field perturbing effects on atomic levels

02 p0283 A69-11539

Metastability of 1D state of negative N ion, instability of 3P state and energies of both states

02 p0284 A69-12598

Atomic transition probabilities, discussing improvement attributed to wider interest in space science, astrophysics, plasma physics and research technique developments

03 p0471 A69-13169

Electron impact ionization cross sections for second quantum level of atomic H, using Born exchange approximation and Vainshtein approximation

06 p0961 A69-17138

C III 2p super 2 presuper 1 D level mean life measurement using beam-foil technique, noting corresponding Einstein A coefficient

07 p1184 A69-18643

Enhanced two photon emission between 6S and 4S levels of K, discussing stimulated three photon Raman scattering and four photon parametric coupling processes

[IEEE PAPER S-8] 07 p1154 A69-19080

Level crossing effect in stimulated emission and application to determination of hyperfine splitting in Xe 129 excited electronic state during laser transition

07 p1156 A69-19398

Hydrogenic approximation validity in evaluation of atomic energy levels and radiative absorption cross sections for computation of stellar opacity

07 p1223 A69-19626

Mutual influence of two laser modes, showing reduced transition rates due to perturbation of lower level

08 p1325 A69-20283

Molecular beam gas laser operating at transitions between ground state and resonance excited state of inert gas atom, obtaining population inversion

08 p1325 A69-20325

Mean square radii for assigned terms of Fe I energy diagram from Van der Waals line broadening

08 p1392 A69-20559

Population inversion in ground state sublevels of ruby laser, deriving required conditions

11 p1900 A69-25572

Double focalization in atomic hydrogen maser by hexapolar magnets selecting hyperfine energy transitions

12 p2105 A69-26050

Distortionless propagation of light through optical two level atoms medium, considering relation to Poynting theorem, hyperbolic secant solution and pendulum analogy

12 p2130 A69-26313

Spectral line formation in nonlinear multilevel atom line transfer problems, considering radiation transfer through plane parallel atmospheres of H and Mg atoms

12 p2133 A69-26967

Shift of certain Hg spectral line by high power pulse from Nd laser through perturbation of atomic energy levels
13 p2270 A69-27202

Forbidden NI transitions in nighttime upper atmosphere observed with Fabry-Perot spectrometer
14 p2440 A69-29120

Nuclear level density and mass shell correlations relationship for deformed and undeformed nuclei
14 p2488 A69-29337

Solar Mg b and Na D line spectra, computing profiles for Doppler cores of lines for multilevel model atoms and selected chromospheric parameter ranges
15 p2693 A69-30779

Radiation diffusion in plane-parallel isothermal gas layer of two and three level atoms, considering stimulated emission and frequency redistribution
16 p2864 A69-32587

Polychromatic scattering of light in medium with three energy level atoms
16 p2813 A69-32589

Molecular beam gas laser operating at transitions between ground state and resonance excited state of inert gas atom, obtaining population inversion
17 p2981 A69-33315

Mean lives of 1s super 2 2p super 2 super 1D level in F VI and O V measured by beam foil technique
17 p3009 A69-34188

Shock tube application to transition probability measurements with emphasis on thermodynamic state of radiating gas, noting temperature dependence of level population
18 p3176 A69-34446

Electronic levels excitation in S I and II by beam foil method
18 p3177 A69-35015

Upper bounds for electromagnetic transition rates for Ne 20 determined using Hartree-Fock wave functions
18 p3177 A69-35166

Quantum transitions between molecular or atomic energy levels noting microwave spectroscopy utilization
18 p3099 A69-35405

Resonance effects between H levels by induced electric dipole transitions, using spatially periodic potential barriers
18 p3179 A69-35488

Two photon decay of metastable levels of hydrogenic and He-like ions in solar corona, depopulating via proton collisional excitation to 2p level
19 p3396 A69-36218

Unquantized field calculations extended to include atomic field effect on atom, predicting spontaneous decay rate from excited state and light frequency time dependence
21 p3769 A69-38578

Thermally insensitive technique for atomic transition probability measurement
22 p3983 A69-40100

Solar Zeeman triplet for excited atomic state comparable to or shorter than Larmor precession period, discussing polarization
22 p4019 A69-40287

Solar Zeeman triplet pseudo-pi-component at 5250 Å /Fe I/, using Unno theory to calculate visibility, contrast and displacement
22 p4019 A69-40289

Ionic excited states statistical equilibrium populations calculated for various electron densities and temperatures including effects of dielectronic, radiative and three body recombinations
22 p3985 A69-40666

Self consistent field molecular orbital method in LCAO /linear combination of atomic orbitals/ approximation applied to LiH ground state for potential energy curve
22 p3985 A69-40721

Argon laser lower operating level decay probabilities, using spectrum analysis to study role of radiative decay
22 p3965 A69-40965

ATOMIC EXCITATIONS

Multiphonon orbit-lattice relaxation of excited states of rare earth ions in crystals, measuring fluorescence lifetimes, quantum efficiencies and transition rates
01 p0134 A69-10011

Nonradiative transfer of excitation energy between mixed trinuclear complexes of Tb and Eu ions with lactose in aqueous solution
01 p0023 A69-10288

Radiative lifetimes for four N II excited states emitting UV during transition to lower level
02 p0280 A69-11928

Electron impact excitation of Lyman alpha emission from 2p state of atomic H, noting discrepancy below 50 Mev
02 p0283 A69-12466

Excited atomic H state radiative mean life measurements using beam-foil excitation method
03 p0469 A69-12920

Emitted light and excited state populations resulting from two electron collisional radiative recombination related to free electron density
03 p0469 A69-12923

Spectroscopy of fast atoms resulting from fast ion impact with gas targets and electron capture into excited state
03 p0471 A69-13162

EUV emission line radiative lifetime measurement by foil-excitation technique, noting correction for cascading, He II and transition probabilities for N II and O III
03 p0471 A69-13165

Free excited H atom Lyman alpha radiation intensity study using beam-foil excitation method
03 p0471 A69-13167

Radial profile measurement technique for individual emission line intensities in plasma applied to populations of excited atomic and ionic Ar in capillary discharges
04 p0634 A69-14441

Effect of dipole/dipole resonance interaction between excited and nonexcited atoms on gas thermodynamic properties, showing unstable quasi-molecules formation
04 p0632 A69-14551

Time dependence of laser output in C and N atoms following dissociative excitation transfer explained in terms of measured populations of excited states
05 p0795 A69-15663

Multiphonon orbit lattice relaxation of excited states of rare earth ions in crystals, using results to design quantum electronic devices
05 p0774 A69-16318

First Born approximation cross sections for He excitation from ground state by proton impact calculated, using wave functions
06 p0960 A69-17027

Noble gas atom simultaneous ionization and excitation by removal of metastable electron in fast collision
06 p0961 A69-17137

Electron impact ionization cross sections for second quantum level of atomic H, using Born exchange approximation and Vainshtein approximation
06 p0961 A69-17138

Polarization of diatomic molecular line radiation excited by electron impact
06 p0961 A69-17140

Optical excitation process of energy states by light pulses of short duration compared to relaxation time, predicting Raman echoes
07 p1152 A69-19062

Fluorescent light polarization of neon atoms subjected to gas discharge, static magnetic field and laser beam
07 p1155 A69-19084

Level crossing effect in stimulated emission and application to determination of hyperfine splitting in Xe 129 excited electronic state during laser transition
07 p1156 A69-19398

Cross sections for inelastic interactions of electrons with atoms and heavy impurity ions and processes of atomic excitation
07 p1195 A69-19652

Electron collisional excitation cross sections for upper states in Ar ion lasers
07 p1157 A69-19656

Electron collisional excitation cross section calculations for atoms and ions using modified Born approximation taking into account three physical effects
07 p1187 A69-19658

Atomic excitation and ionization involving inner shell electrons during collisions between atoms and ions, examining photoabsorption by inner shell electrons
07 p1187 A69-19659

He concentration measurement in transient He-air mixture by spectroscopic analysis of fluorescence excited by high energy electron beam
08 p1312 A69-19860

Wavelike photodissociation of gas molecules under quasi-monochromatic pulsed radiation, investigating associated supersonic disturbances
08 p1354 A69-19950

Atomic and molecular excitation mechanisms in nonequilibrium gases up to 20000 K
08 p1354 A69-20146

Cross sections computed for excitation and ionization of atoms and ions by electrons, using peaking approximation to evaluate Coulomb-Born matrix approximation
08 p1355 A69-20206

Absolute excitation cross sections for emission of second positive bands of nitrogen under electron impact
08 p1355 A69-20208

Mutual influence of two laser modes, showing reduced transition rates due to perturbation of lower level
08 p1325 A69-20283

Excitation cross sections of Fe XIV lines in solar coronal spectra, comparing computations with Coulomb-Born approximation
08 p1392 A69-20563

Channel coupling effects in elastic electron-atom collisions involving electric dipole transitions, noting phase shifts and differential cross section
09 p1542 A69-21623

Rotational excitation and scattering cross sections for rigid diatomic molecules reduced to yield distorted wave approximation, resulting in inelastic transition probabilities
10 p1726 A69-23524

Fast electron energy distribution function and atom concentration in first excited level in weakly ionized plasma, considering transitions between excited levels
10 p1739 A69-23628

Simultaneous photoexcitation and photoionization of He near threshold at 186 Å, measuring probability
11 p1921 A69-24926

Cross section for ionization of atoms by positive ion bombardment near threshold
11 p1922 A69-25322

Nonlinear algebraic equation system describing populations of excited atoms of low pressure nonequilibrium cesium plasma, determining ionization coefficient and molecular ion concentration
11 p1934 A69-25567

Negative pion from 600 MeV synchrocyclotron stopped in thin Li 6 target in search for excited states of triton
12 p2132 A69-26297

Metastable molecules and fragments produced by electron excitation of nitrogen, hydrogen, carbon dioxide and nitrous oxide, noting excitation functions, kinetic energy, etc
13 p2301 A69-27362

Nonequilibrium radiation from first negative band of molecular nitrogen ion excited by shock wave electron impact
13 p2245 A69-27380

Excited levels in Li I produced by Li 7 ion passage through carbon foil, measuring excitation mean lives by beam foil technique
13 p2301 A69-27454

Steady state model envelopes of Be stars, determining excitation and ionization states for hydrogen atoms
13 p2338 A69-27559

Twilight helium emission observed by Fabry-Perot spectrometer, noting consistency with triplet He atom excitation by photoelectron collision with ground state atoms
14 p2440 A69-29124

CdS crystals emission spectrum during two photon excitation by ruby laser, noting dependence on pump power
14 p2458 A69-29167

Electron energy distribution functions and energy transfer rates to inelastic levels of carbon dioxide and nitrogen in laser
14 p2460 A69-29603

Fe and Ti line growth in 12 July 1961 solar flare spectrum, finding ionized titanium, neutral and ionized iron excitation temperatures
14 p2514 A69-29720

Oxygen K-shell X ray production cross section and stopping power of aluminum oxide thin films for 20-100 keV protons
14 p2489 A69-29994

Mode competition of 5861 and 6470 Å lines in ionized Kr laser attributed to electronic level excitation processes
15 p2635 A69-31106

Atomic coherence and inhomogeneous broadening effects on laser amplifier ultrashort electromagnetic high peak power pulses
15 p2635 A69-31239

Photoinduced shock processes involving metastable hydrogen atoms and molecules, discussing vibrational and rotational levels
16 p2813 A69-31754

Atomic oxygen density role in ionospheric E and F region magnetic stability, noting heat loss effect of atomic excitation
16 p2780 A69-32314

He II excitation spectrum for interparticle potential using pair Hamiltonian with repulsive core and attractive well
17 p3008 A69-33118

Atomic excitation and ionization by thermal electrons, using Monte Carlo trajectories to determine adiabatic collisions effects on energy transfer near dissociation limit
18 p3176 A69-34790

Long lived highly excited atoms production in electron collisions with CO, O and N molecules
18 p3177 A69-35125

Forbidden lines in solar corona, discussing ionization equilibrium and excitation of levels in highly ionized atoms
19 p3422 A69-36216

Collisional excitation of forbidden lines in planetary nebulae from 5537/5517 intensity ratio measurements, noting density and intensity relationship
19 p3422 A69-36221

Laser action from atomic bromine produced by flash photolysis of gaseous iodine monobromide, discussing pulsed output, optical gain, chemical reversibility and atomic excitation
19 p3337 A69-36444

Atom-atom collisional excitation cross sections obtained from ionization cross sections, noting Thomson classical theory
20 p3580 A69-37500

Atomic sources local multipolar field in anisotropic dielectrics determined from magnetic dipole radiation spatial distribution measurements
21 p3779 A69-38531

Invalidity of Pagel method for intrinsic and interstellar reddening for peculiar objects, discussing excitation mechanism for forbidden lines of ionized Fe for Eta Carinae
21 p3815 A69-39616

Absorption spectrum of CS atoms excited by electrical discharge and irradiated by monochromatic light and ionized by electron collisions
22 p3984 A69-40418

Dayglow O I lambda 1304 and 1356 A radiations photoelectron excitation rates theoretical calculation and experimental data on altitude dependence characteristics
22 p3939 A69-40517

Off-diagonal matrix elements of Breit interaction between singlet-triplet transitions for helium isoelectronic sequences
22 p3986 A69-40783

Nonlinear theory of optically excited semiconductor laser for conditions of self excitation, steady state lasing amplitude and lasing frequency shift
23 p4174 A69-41733

ATOMIC EXPLOSIONS

U NUCLEAR EXPLOSIONS

ATOMIC GASES

U MONATOMIC GASES

ATOMIC PHYSICS

Plasma radiation, including atomic processes and radiation by variation of constituent kinetic energy
03 p0483 A69-14237

Atomic physics of lasers and active materials, noting multiplet spectra of atoms, molecular spectroscopy, energy level population distribution and amplification
06 p0937 A69-18004

Atomic and electronic collisions experimental study techniques, noting three data logging systems
07 p1187 A69-19662

Self consistent field calculations of effective quantum numbers for nd, nf and ng electrons for atomic configurations from 2-126 Z
08 p1355 A69-20734

Time dependent statistical equilibrium equations solutions for describing time development of atomic populations by means of ergodic Markov chain
09 p1542 A69-22218

Plasma oscillations of electrons of atomic system, using simple hydrodynamic model
20 p3580 A69-37818

ATOMIC RECOMBINATION

NT OXYGEN RECOMBINATION

Chemical nonequilibrium, mass transfer and viscous interaction effects on spherically blunted cones at hypersonic conditions, emphasizing stagnation point [AIAA PAPER 69-168]
06 p0862 A69-18047

Heat and mass transfer interaction at wall for laminar boundary layer on flat plate, considering catalytic effect of wall in atomic nitrogen recombination
15 p2716 A69-30415

Radiative recombination of atomic oxygen ions in nighttime F region UV radiation detected by polar-orbitingOGO 4 satellite
18 p3129 A69-34957

Resonance theory of thermolecular atomic recombination kinetics based on transition complexes identification as quasi-bound states or orbiting resonances
20 p3579 A69-37345

ATOMIC SPECTRA

Spectroscopic quantitative analytical method for measuring atomic absorption in flame based on determining integral absorption magnitude during evaporation
20 p3539 A69-37605

Absorption spectroscopy using resonance broadened atomic lines for two phase mixtures study
21 p3774 A69-39239

Mars upper atmosphere ionized carbon dioxide and CO emission spectra in 1900-4300 A region measured by Mariner 6, observing atomic hydrogen and oxygen lines
22 p4023 A69-40568

ATOMIC STRUCTURE

Martensite transformation by simple shear in equiatomic Ni-Ti alloy, using transmission electron microscopy
02 p0265 A69-12024

Dipole shielding factor in coupled Hartree-Fock approximation for atomic S state
02 p0281 A69-12179

Molybdenum interband transitions noting low energy optical property anomalies and origin of two absorption bands
03 p0442 A69-12986

Beam-foil spectroscopy above 5.5 Mev for multiply ionized atoms, noting use of Tandem accelerator, spectral resolution, beam intensity and Doppler effect
03 p0471 A69-13163

Components relationships in binary phase diagrams of III a and VI a transition metals on basis of electronic structure
08 p1331 A69-20191

Self consistent field calculations of effective quantum numbers for nd, nf and ng electrons for atomic configurations from 2-126 Z
08 p1355 A69-20734

Line blanketing for two level atom with spectral line formed in pure absorption and noncoherent scattering, studying wavelength and depth dependence
09 p1606 A69-22424

Surface atomic structure effects on polar faces in InSb semiconductor crystal established from measurements of contact potential difference by dynamic capacitor
10 p1747 A69-23965

Soviet collection of articles on atomic ordering effects on alloy properties
11 p1936 A69-24701

Order-disorder in alloys with several phase transition temperatures, discussing crystal lattices, interstitial alloys, atomic and magnetic ordering
11 p1936 A69-24702

Superstructures in multicomponent alloys, transition mode and temperature, ordered state and atomic interactions
11 p1937 A69-24703

Pressure effects on hcp crystalline lattice alloys order-disorder transformations
11 p1937 A69-24704

Young modulus temperature dependence and order-disorder transformations in ternary nickel alloys
11 p1904 A69-24705

Order-disorder transformations in nickel alloys under loading operations
11 p1904 A69-24706

Electronegativity and work function relationship from thermodynamic and quantum mechanics standpoint, describing electrons structure by spin orbitals localized around lattice sites
14 p2505 A69-29263

Atomic size and outer electron effect on Fe, Co and Mn polymorphism, noting change in crystal lattices
15 p2638 A69-30321

Monograph on vanadium selenides and tellurides with NiAs structure covering existence regions, superstructures and equiatomic compounds from viewpoint of thermodynamics
15 p2667 A69-30602

Solid solutions atomic ordering effect on friction and wear in vacuum, using CuAu and FeCo systems
18 p3149 A69-35183

Emissivity of high melting point compounds measured, considering electronic structure and atomic weight
18 p3158 A69-35260

Two point tensor function symmetries of nonlocal cohesive finite elastic materials determined from atomic lattice theory, obtaining Green function
19 p3444 A69-36798

Photoelastic behavior in amorphous solids, proposing microstructural mechanism for deformation birefringence
22 p3972 A69-40081

Hartree-Fock calculations for wavelengths of K alpha X ray transitions, tabulating configuration and term energies, dipole integrals and relative multiplet strengths
22 p3984 A69-40156

Inelastic proton scattering cross sections for target nuclei in 2s-1d shell calculated in distorted wave Born approximation with projected Hartree-Fock wave functions
22 p3988 A69-41045

Spontaneous polarization onset in perovskite ferroelectrics, analyzing influence of Curie point, Jahn-Teller effect and atomic structure
22 p3995 A69-41159

ATOMIC THEORY

NT HEISENBERG THEORY

Thomas-Fermi approximation applied to calculation of equations of state and thermodynamic functions at high pressure from differential equations of statistical atom model
22 p3984 A69-40186

Laser quantum theory compared to stationary atoms semiclassical theory, emphasizing role of cavity mode spatial structure
24 p4327 A69-42789

ATOMIZERS

Flame burnout of atomized hydrocarbon fuel in gas turbine combustion chambers as function of ratio of time to total burnout time
08 p1420 A69-19999

ATOMS

NT METASTABLE ATOMS

Metal atom production by bombarding metal with positive ions from microwave discharge, obtaining isolation in inert gas matrix and UV spectra
06 p0957 A69-17113

Kinetics of combustion promotion of hydrogen-hydrocarbon mixtures by active particles, free atoms and free radicals using differential equations
17 p3069 A69-33139

Gaseous and solid phase properties of atomic and molecular systems, treating statistical energy distribution, kinetics, excited states and relaxation
18 p3178 A69-35406

ATP

U ADENOSINE TRIPHOSPHATE [ATP]

ATROPHY

Musculoskeletal system and weightlessness state, concerning muscular disuse atrophy possibility during prolonged space flights
06 p0873 A69-17018

Physiological response of human skeleton to hypogravity and hypodynamics studied by bed rest experiments, suggesting disuse atrophy of bone
06 p0873 A69-17019

Mineral dynamics during hibernation and disuse atrophy in connection with organismal homeostasis and chronic-term manned space flight, noting skeletal effect of immobility
21 p3660 A69-39175

Brain atrophy clinical diagnosis aided by biochemical analyses, including age frequencies and symptoms to control incidence among aviation personnel
23 p4089 A69-41816

ATS [SATELLITES]

U APPLICATIONS TECHNOLOGY SATELLITES

ATTACHMENT

Bistable fluid device utilizing Coanda effect along convex surface for wall attachment [ASME PAPER 68-WA/FE-27]
05 p0749 A69-16101

Vibratory acceleration limiting equipment attachment for resonance conditions, utilizing attachment stiffness reduction above predetermined value [ASME PAPER 69-VIBR-23]
10 p1806 A69-24170

Attachment coefficients for negative oxygen ion formation in low energy electron swarms over various voltage/pressure ratios
21 p3774 A69-39238

ATTACHMENTS
U ACCESSORIES

ATTACK AIRCRAFT
NT A-1 AIRCRAFT
NT A-6 AIRCRAFT
NT A-7 AIRCRAFT
NT B-52 AIRCRAFT
NT B-70 AIRCRAFT
NT BOMBER AIRCRAFT
NT BUCCANEER AIRCRAFT
NT F-2 AIRCRAFT
NT F-4 AIRCRAFT
NT F-5 AIRCRAFT
NT F-104 AIRCRAFT
NT F-106 AIRCRAFT
NT F-111 AIRCRAFT
NT FIGHTER AIRCRAFT
NT G-91 AIRCRAFT
NT JAGUAR AIRCRAFT
NT OV-10 AIRCRAFT
NT P-117 AIRCRAFT
NT SAAB 37 AIRCRAFT

Operational research in RAF, discussing weapons tactics and research, strike aircraft speed and height effect on target-finding, VTOL and STOL dispersion value, etc
01 p0180 A69-10863

Navigation and tactical data with correlative map information provided on single CRT display in aircraft, storing map data on video tape
03 p0464 A69-13246

Jaguar combat trainer/tactical support aircraft to meet France and UK military requirement, noting supersonic performance and honeycomb construction
04 p0549 A69-15062

Jaguar aircraft equipment conformity to maximum standardization with equipment for other programs
04 p0550 A69-15063

Engine air intake for operational Harrier V/STOL strike/reconnaissance fighter, describing intake instrumentation ring, temperature and pressure probe development and pressure recording
05 p0767 A69-16773

Characteristics, employment and tactics of Huey Cobra attack helicopter in Vietnam, discussing three primary weapon configurations
06 p0867 A69-17661

First flight test phase of multipurpose Viggan aircraft designed as basic platform for attack, trainer, reconnaissance and fighter versions
06 p0867 A69-17662

Concorde supersonic transport and Jaguar Military Strike/Trainer programs, discussing management and international cooperation
06 p1043 A69-17831

Flying qualities considerations in design and development of Huey Cobra for helicopter attack mission, describing stability and control augmentation systems
[AHS PAPER 217] 07 p1053 A69-18871

Time division telemetry technique resolving data and control flow to and from remote locations/tactical aircraft/, noting application to environmental pollution control
07 p1081 A69-19100

Avionics systems with integration and federation applied to integrated light attack avionics system/ILAA5/ design to provide navigation, weapon delivery and flight control
17 p2976 A69-34057

Cost comparison of single and twin engine layouts for tactical strike/close support aircraft
19 p3248 A69-36855

Automated design system producing wire format data for cabling avionics subsystems of light attack aircraft
[AIAA PAPER 69-976] 22 p3912 A69-40356

ATTACKING [ASSAULTING]
Kormoran airborne missile weapon system for attacking sea-going targets, discussing navigation guidance, radar tracking and homing system
17 p3050 A69-33697

ATTENTION
Attention shifts in maintained discrimination, discussing combined responses of varying and constant visual and auditory stimuli in pigeons
24 p4275 A69-43198

ATTENUATION
U ACOUSTIC ATTENUATION
U ATMOSPHERIC ATTENUATION
U AURORAL ABSORPTION
U MANDELSTAM REPRESENTATION

U RADAR ATTENUATION
U RADIO ATTENUATION
U SHOCK WAVE ATTENUATION
U SIDELOBE REDUCTION
U WAVE ATTENUATION

ATTENUATION COEFFICIENTS
Raindrop size distribution law effect on radio wave attenuation coefficient and differential effective backscattering cross section of rain
02 p0208 A69-12259

Visible light extinction properties of continental and maritime air, probing urban, desert and oceanic atmospheres with stable photodiode radiometer
04 p0596 A69-14280

Standing wave methods for measuring permittivities of liquids having attenuation coefficients over considerable range
04 p0599 A69-15015

Attenuation calibration of optical resonator using transparent plate coated by thin metal layer
04 p0613 A69-15415

Initial equations for plane wave diffraction at grids of squared beams, calculating transmission and reflection coefficients by reflection method and computer
07 p1084 A69-19149

Open resonator reflection coefficient resonance curve compared with transmission coefficient, noting low Q waves excitation role
07 p1106 A69-19152

Laser beam propagation in scattering media, noting attenuation coefficients for coherent and incoherent radiation
08 p1328 A69-21092

Transfer function of low pass filters with Chebyshev attenuation characteristic in stopband and predetermined phase or delay time realized by ladder network
08 p1300 A69-21171

Radiation attenuation in hazy lower atmosphere, calculating attenuation coefficients and using spherical model of haze particles and empirical formula for haze spectra
11 p1913 A69-25571

Calculation method for electromagnetic wave supplementary attenuation due to auroral absorption for distances up to 4000 km
11 p1841 A69-25760

Stratospheric aerosol attenuation factor vertical distribution statistical structure, tabulating normalized correlation matrices, eigenvectors and eigenvalues
12 p2125 A69-25956

Atmospheric boundary layer transparency to gas laser emissions in IR spectrum, determining attenuation factor dependence on humidity and visibility range
12 p2028 A69-25957

Refractive index and attenuation factor of ionosphere
12 p2070 A69-26689

Elliptical waveguide design dimensions for minimum attenuation in fundamental mode, giving formulas for attenuation constant and minor-major axis ratio
12 p2044 A69-27070

Short laser pulses reflection from artificial fog and smoke, showing dependence on reflecting medium attenuation coefficient
15 p2562 A69-30077

Numerical method based on thin film optics to determine ionospheric electromagnetic transmission and reflection coefficients for vertical incidence
16 p2752 A69-32392

Reflection and transmission coefficient matrices for stratified magnetoionic medium determined by thin film optical technique and iteration procedure
17 p2927 A69-33863

He-Ne laser emission attenuation coefficient relation to water content of artificial fogs for 0.63, 1.15 and 3.39 microns
21 p3738 A69-39118

Aerosol attenuation coefficients vs altitude in troposphere and stratosphere, noting seasonally dependent surface convective dust layer and temperature dependent aerosol maximum altitude
21 p3718 A69-39773

ATTENUATORS
NT RESISTORS
NT THERMISTORS

Disturbing TM mode generation effect on attenuation measurement accuracy in TE mode attenuators
08 p1283 A69-20126

Power gain in TWT attenuators with linear tapered ends, considering conversion loss due to tapering
12 p2044 A69-27102

Near constant phase variable attenuator for RF signal containing Doppler information, centering design around p-i-n diode as control element
21 p3681 A69-38410

ATTITUDE [INCLINATION]
NT PITCH [INCLINATION]
NT ROLL
NT SATELLITE ORIENTATION
NT YAW

Vestibular analyzer role in spatial orientation under weightlessness conditions during aircraft flights, discussing underestimations of rotation angle of Barany chair
08 p1262 A69-19840

Galaxies classification using rectified images, noting pitch and inclination angles
08 p1408 A69-21135

Jet fighter pilot spatial disorientation during flight and on ground, emphasizing vestibular neunititis diagnosis
10 p1649 A69-23382

Stress effect on laser damage crack orientation in transparent organic dielectrics, estimating gas pressure in cracks
10 p1703 A69-23621

Geomagnetic storm induced temporary radiation zones located by determining Explorer 30 attitude and spin axis orientation
14 p2514 A69-29384

ASTRID high altitude sounding rockets orientation system aligning payload cones to target outside earth atmosphere, discussing software simulation with analog and digital computers, etc
17 p3001 A69-33424

Lifting rotors with thrust or tilting moment feedback control, deriving blade equations of motion
[AHS PAPER 340] 17 p2899 A69-33510

Three dimensional coupled flexural and attitude dynamics of libration-damped cruciform gravity gradient satellite, discussing effects of orbital eccentricity, solar radiation pressure, etc
[AAS PAPER 68-126] 21 p3819 A69-39211

ATTITUDE CONTROL
NT DIRECTIONAL CONTROL
NT LATERAL CONTROL
NT LONGITUDINAL CONTROL
NT SATELLITE ATTITUDE CONTROL
NT THRUST VECTOR CONTROL

Advance indication based on extrapolation for aiding manual attitude control of VTOL aircraft in hovering flight, noting results on flight simulator
03 p0366 A69-13645

Minimum fuel attitude control of spacecraft by Pontryagin principle and extended steepest descent method
03 p0522 A69-14100

Multiframe platform stabilization, analyzing dynamic coupling due to possible avoidance of adjusting moment and effect of coupling on attitude control
04 p0629 A69-14830

Electrohydraulic attitude servomechanism for controlling movements of pilot training cabin, describing hydraulic system and electric control circuit
06 p0906 A69-16966

Attitude control system for maintaining orientation of experimental package relative to space stabilized platform, noting transient response and steady state accuracy
06 p0955 A69-17587

Attitude stabilization for astronomical satellites
06 p1015 A69-17588

Three axis attitude servomechanism design to adjust attitude and angular velocity of spacecraft
06 p0955 A69-17589

Translational forces on Mariner 5 stemming from attitude control system studied to determine trajectory for scientific and operational purposes
[AIAA PAPER 69-114] 06 p1018 A69-18108

Rocket propulsion with gaseous bipropellant systems and attitude control
08 p1376 A69-20870

Diffraction limited telescope fine guidance experiment to improve pointing stability in space, noting attitude control system and nonmechanical suspension
08 p1317 A69-21072

Single rotation for reorienting rigid body from initial to arbitrary final attitude together with corresponding control torques
09 p1610 A69-21998

Attitude control system effect on roll resonance in rocket boosted projectile
09 p1610 A69-22001

Electrolytic bubble level during wind tunnel tests for aircraft model attitude
10 p1672 A69-23268

Fluid rotor angular accelerometer design for stabilization and control, noting applications to centrifuge speed and thruster gas consumption
10 p1633 A69-23273

Magnetic attitude detection and control system for Radio Astronomy Explorer satellite
[AIAA PAPER 68-855] 12 p2174 A69-26779

Optimal stochastic controller synthesis theory applied to stabilizing and controlling orientation of rotating bodies in central gravitational fields
13 p2300 A69-28326

Control system design for Black Arrow satellite launch vehicle based on Black Knight test vehicle system
14 p2530 A69-29630

Earth sensor for spin stabilized spacecraft to maintain specific orientation with earth, discussing use of blue and red filters
15 p2609 A69-30593

Stochastic saturating systems optimal control computation, considering attitude control and tracking system design by elliptical differential equation of dynamic programming
15 p2582 A69-30601

Europa 1 first stage attitude control system adaptation to Europa 2 requirements, discussing design modifications and improvements and inertial guidance system introduction
16 p2866 A69-31726

Reaction forces for jet lift VTOL attitude control during hover and transition, considering hot gas and pitch ducting applications
[AIAA PAPER 69-545] 16 p2735 A69-32756

Contaminants formation during pulse mode operation of liquid bipropellant attitude control rocket engine, discussing exhaust plume effects
[AIAA PAPER 69-574] 16 p2870 A69-32774

Tacite rocket probe to study space IR radiation, using passive stellar sensor for recording reference stars positions to recalibrate gyroscope kinetic motion for attitude restoration
[ONERA-TP-731] 17 p3001 A69-33220

Fluidic attitude control systems performance prediction from conventional control analysis emphasizing steady state positioning accuracy
17 p2904 A69-34069

Manned space telescope attitude stabilization using counter-rotational triaxial gyro system
18 p3206 A69-34371

Attitude control system for Apollo Telescope Mount, discussing selection features based on manned orbital space platform requirements
18 p3168 A69-34683

Attitude and heading reference devices for aircraft navigation, describing instruments, gyroscopes and gravity sensors
18 p3169 A69-34853

Parameter optimization of launch vehicle attitude control system of fixed structure for various computation techniques
18 p3210 A69-35092

Optimal asymptotic stabilization of gyrostair relative equilibrium, determining norm constraints for application to global gyrostair attitude control
18 p3210 A69-35145

Attitude control rocket exhaust plume impingement effect on electrical performance and mechanical damage of commercial silica covered silicon solar cells
19 p3252 A69-35700

Active attitude control method with energy increases and decreases induced to modify attitude motions for particles and rigid bodies
19 p3429 A69-35958

Titan 3 transtage attitude control system hydrazine rocket engine design and performance, emphasizing problems associated with monopropellant
[AIAA PAPER 69-422] 19 p3394 A69-36300

Cassiopee device for spacecraft or sounding rocket attitude control, describing gyroscopic control unit, sensor element and jet control devices
[ONERA-TP-707] 19 p3432 A69-36686

Equations of motion for optimal attitude of suborbital aircraft regarding time and distance range
21 p3795 A69-38440

Attitude control system for launch vehicles, providing commanded thrust vector angle proportional to desired angular displacement of acceleration vector
21 p3819 A69-39032

Spacecraft control systems with computer command redundant jets for linear and angular pulses, relating configuration design to level-of-redundancy and task dimension
[AIAA PAPER 69-845] 21 p3822 A69-39375

Frequency domain and Liapunov instability criteria for attitude control system design of large booster, noting nonlinear feedback
[AIAA PAPER 69-853] 21 p3687 A69-39381

Controllers design for reaction jet controlled aerospace vehicles, studying second order pitch-plane representation with actuator modeled as pure delay
[AIAA PAPER 69-854] 21 p3822 A69-39382

Precision autocollimating solar sensor design for attitude alignment changes, including detector calibration and sounding rocket flight test results
[AIAA PAPER 69-858] 21 p3762 A69-39386

Analytical and graphical methods for characteristics of optima produced by quadratic performance index for VTOL prefilter model reference attitude control system
[AIAA PAPER 69-884] 21 p3764 A69-39411

Manual attitude control for Lunar Module employing directional stability, coordinated turn and attitude command
[AIAA PAPER 69-892] 21 p3824 A69-39417

Gyro test package, dynamic test facility and real time attitude algorithm to investigate operational capabilities of strapdown inertial attitude package
[AIAA PAPER 69-849] 21 p3765 A69-39424

Dornier ASTRID attitude stabilization system design for spinning rocket nose cone with instrument payload, using first stage biaxial inertial platform and second stage star tracker
21 p3826 A69-39639

Nonlinear adaptive reaction jet attitude control for long life space vehicles, providing optimal performance over bias acceleration disturbances
[AIAA PAPER 69-945] 22 p4036 A69-40328

Representative data of actual forces and moments applicable to large spacecraft attitude control system for typical crew activities obtained through simulation programs
[AIAA PAPER 69-1006] 22 p3921 A69-40380

Three axis motion simulator for in-orbit spacecraft attitude control evaluation using earth, sun and star sensor references
[AIAA PAPER 69-1029] 22 p3924 A69-40398

Two degrees of freedom control moment gyro for astronaut attitude control during EVA, discussing muscle-controlled shoe-mounted stilts and precessional feedback forces
[AAS PAPER 69-472] 24 p4272 A69-42846

Translational forces on Mariner 5 stemming from attitude control system, determining trajectory for scientific and operational purposes
[AIAA PAPER 69-114] 24 p4394 A69-43256

Attitude control system with rate of change limiter to minimize launch vehicle drift during first stage ascent through atmosphere
24 p4394 A69-43277

Parallel wire array fluidic sun sensor for solar pointing fluidic attitude control, discussing design and breadboard test
24 p4348 A69-43297

ATTITUDE GYROS

Fluidic pulse time modulated angular position sensor for two axis hydrostatically supported gyroscope
02 p0249 A69-12087

Long life gravity gradient stabilization system using Vee configured control moment gyros to semipassively damp vehicle librations
07 p1228 A69-18345

Resistojet control system combined with control moment gyro payload capability for long duration manned orbital spacecraft missions
[AIAA PAPER 69-255] 09 p1561 A69-21220

Electric outside-in attitude gyro display system prototype tested and compared with contemporary inside-out display
[SAE PAPER 69-0326] 11 p1890 A69-24507

Space station attitude control through resistojets and control moment gyros /CMG/, discussing propulsion, safety features, weight factors, etc
11 p1965 A69-24531

Control moment gyro /CMG/ and use in space vehicle attitude control system, emphasizing control laws
[AIAA PAPER 67-589] 12 p2129 A69-26777

Tacite rocket probe to study space IR radiation, using passive stellar sensor for recording reference stars positions to recalibrate gyroscope kinetic motion for attitude restoration
[ONERA-TP-731] 17 p3001 A69-33220

Manned space telescope attitude stabilization using counter-rotational triaxial gyro system
18 p3206 A69-34371

Attitude and heading reference devices for aircraft navigation, describing instruments, gyroscopes and gravity sensors
18 p3169 A69-34853

Cassiopee device for spacecraft or sounding rocket attitude control, describing gyroscopic control unit, sensor element and jet control devices
[ONERA-TP-707] 19 p3432 A69-36686

Two degrees of freedom control moment gyro for astronaut attitude control during EVA, discussing muscle-controlled shoe-mounted stilts and precessional feedback forces
[AAS PAPER 69-472] 24 p4272 A69-42846

ATTITUDE INDICATORS

Spacecraft attitude ion sensor using charged thermal ions of earth atmosphere as reference, stressing reliability, economy and response
01 p0079 A69-10293

Rocket released probe orientation determination from polarization measurements on telemetry signal
02 p0207 A69-11813

Fluidic pulse time modulated angular position sensor for two axis hydrostatically supported gyroscope
02 p0249 A69-12087

Radar attitude sensing system for determining vehicle roll, pitch, yaw, altitude and velocity of earth and lunar orbital vehicles
03 p0388 A69-13183

Attitude determination and hydrogen peroxide control system for spacecraft orientation in Syncom, Early Bird and ATS
[AIAA PAPER 67-532] 09 p1610 A69-21988

Dual pendulum with tilt sensitivity at wide passband frequencies and damping due to horizontal oscillations
14 p2450 A69-29570

Space vehicle electronic attitude measurement method for reference coordinate and fixed coordinate systems based on rectangular coordinates of RF wave propagation directions
20 p3574 A69-37703

Precision autocollimating solar sensor design for attitude alignment changes, including detector calibration and sounding rocket flight test results
[AIAA PAPER 69-858] 21 p3762 A69-39386

ATTITUDE STABILITY

NT DIRECTIONAL STABILITY
NT GYROSCOPIC STABILITY
NT LATERAL STABILITY
NT LONGITUDINAL STABILITY

Energy dissipation effects on attitude stability of dual-spin satellites with damping mechanism on rotating sections
04 p0665 A69-14703

Optimal flight stabilization of VTOL aircraft in hovering mode based on linear rotation dampers system
05 p0702 A69-16024

Attitude stabilized balloon telescope for measuring interplanetary scattered light and nightglow
06 p0999 A69-16972

Soviet achievements in space research, comparing satellites with U.S. counterparts
06 p1005 A69-17561

Department of Defense Gravity Experiment /DODGE/ attitude stabilization simulation with time-lag magnetic damping
06 p1014 A69-17584

Damping boom flutter and magnetic dipoles effects on attitude stability of gravity gradient satellites with three axis stabilization
07 p1227 A69-18332

Semiactive gravity gradient stabilization system /SAGS/ for active pitch control and semipassively roll/yaw control
07 p1228 A69-18342

Long life gravity gradient stabilization system using Vee configured control moment gyros to semipassively damp vehicle librations
07 p1228 A69-18345

GEOS 2 attitude stabilization by means of gravity gradient principle and passive energy dissipator, noting effects of orbit eccentricity, thermal distortion, radiation, etc
07 p1229 A69-18349

Fluidic control systems for angular rate and attitude stabilization flight-tested, noting good impact and acceleration resistance
[AGARDGRAPH-118] 08 p1257 A69-20955

Space vehicle attitude stabilization based on rotating flywheel resistance to changes in rotation axis attitude, noting grease lubricated hydrodynamic bearing system
12 p175 A69-26893

Spacecraft attitude control and stabilization by three degree of freedom control moment gyro with controllable gyro spin angular velocity
13 p2355 A69-27445

Equations of motion computerized simulation for attitude stabilization of orbiting telescope coupled to crew compartment
13 p2261 A69-27952

Magnetometers role in Aurorae satellite attitude stabilization, discussing operation principle, characteristics and performances
15 p2611 A69-31087

- Passive attitude stabilization of interplanetary probe, using conically shaped sails elastically connected to payload
17 p3047 A69-33225
- Numerical integration of Eole satellite attitude equations compared with results obtained by analog simulation or hybrid computation
17 p3048 A69-33232
- Manned space telescope attitude stabilization using counter-rotational triaxial gyro system
18 p3206 A69-34371
- Floating body attitude and stability analysis based on system potential energy balance, considering Archimedes principle, torques, equilibrium conditions, body shape, etc
[SAWE PAPER 773]
18 p3172 A69-34874
- Gravity torque influence on axisymmetric dual spin satellites in fixed attitudes, using attitude stability studies of spinning single rigid bodies
19 p3429 A69-35917
- Spring restrained, momentum-wheel inertial orientation and stabilization system for exoatmospheric vehicles, noting mission constraints and hardware parameter variations allowances
21 p3819 A69-39214
- Aerodynamic and gravitational torque effects on orbiting satellites attitude stability, applying Liapunov direct method in case of conservative aerodynamic torque
[AIAA PAPER 69-832]
21 p3821 A69-39363
- Spacecraft attitude acquisition/reorientation and stabilization controller design implemented by control moment gyro, proposing control algorithm using control actuator nonlinearity
21 p3826 A69-39641
- Black Arrow third stage velocity increment vector accuracy, considering attitude errors due to spin-up and spring separation systems, separated stages interactions, light-up impulses, etc
23 p4209 A69-41301
- ATTRITION [MATERIALS]**
U COMMUNITION
- AUDIO EQUIPMENT**
Jumbo jet audio entertainment and service systems, describing digital pulse multiplexing technique
19 p3285 A69-35806
- AUDIO FREQUENCIES**
Time compression system with ultrasonic diffraction cell allows coherent light optical spectrum analyzer to function at audiofrequencies
01 p0035 A69-11283
- MOST devices characteristics at cryogenic temperatures, studying variation in gain over audio frequency range
03 p0405 A69-13642
- Continuous and triggered audio frequency noise bands associated with ionospheric lower hybrid resonance frequency observed on OGO 2
05 p0754 A69-16257
- Audio frequency noise in p channel MOST at cryogenic temperatures, noting trap contribution
06 p0979 A69-17151
- Soft magnetic materials, ferrites and magnetic particle composites as two layer laminates for shielding in audio and microwave frequencies
09 p1500 A69-22310
- Audio frequencies internal friction measurement of austenitic stainless steels subjected to heat treatment and corrosion, discussing time dependence and carbide precipitates morphology
10 p1713 A69-23819
- Data distortion elimination by improved superimposing of sinusoidal audio frequency signal on DC voltage of automatic Langmuir probe second derivative ploters
17 p2970 A69-32855
- Self rhythms of low audio frequencies in motor nerves under electric pulses influence at VLF related to viscosity changes of nerve substance
23 p4092 A69-42057
- AUDIOLOGY**
Retarded voice tests apparatus using graphical recording to determine intensity of deformations by autoaudition, considering application to recruitment investigation
24 p4270 A69-42604
- AUDIOMETRY**
Pure tone threshold determination based on pulse tone technique with modified audiometer
06 p0882 A69-17836
- Auditory analyzer functional changes due to prolonged slow rotation
20 p3470 A69-37251
- Surrounding noise effects on quick check audiometry test reliability, discussing pathological effects
21 p3725 A69-39286
- Flight personnel hearing tests per ICAO recommendations and flight safety requirements, using tonal audiogram and vocal audiometric test
24 p4277 A69-43377
- AUDITORY DEFECTS**
Hearing adaptation measurements after aircraft noise stresses for estimation of induced noise damage
23 p4110 A69-42051
- AUDITORY PERCEPTION**
Probability density distributions for monaural detection of tonal signal in continuous background of Gaussian noise as modified noncentral chi distribution
02 p1201 A69-11821
- Human auditory function during exposure to prolonged low barometric pressure unaffected with normal oxygen partial pressure
03 p0378 A69-14206
- Stereoscopy effects on pattern recognition in visual noise
06 p0880 A69-17214
- Pure tone threshold determination based on pulse tone technique with modified audiometer
06 p0882 A69-17836
- Cepstrum /Fourier transform of log-spectrum of signal/ as model for prediction of perception of pitches in harmonic residue /ambiguity of pitch/
11 p1834 A69-24571
- Auditory temporal masking of tonal signal by narrow band noise and perception of temporal order noting effects of intensity, frequency and time
11 p1830 A69-24795
- Noise level perception and subjective judgments for broadband noise with single, modulated and multiple tones, considering tone correction procedures
11 p1830 A69-24796
- Prolonged visual deprivation effect on pressure sensitivity of finger, forearm, neck and leg, noting effects after restoration of normal visual stimulation
13 p2210 A69-28313
- Noise duration and spectral complexity effect on subjective rating of disturbance level
14 p2408 A69-29152
- Ear-hand coordination adaptability tested by exposure to auditory rearrangement entailing 30 degree rotation of interaural axis produced by electronic pseudophones
21 p3663 A69-38899
- Speech interference aspects of noise measured as function of level and spectrum of speech and noise at listener ear, using simplifying nomogram
23 p4101 A69-41495
- Whispered vowels pitch perception test using listen-and-compare method to determine formants for comparison with complex analysis procedure
23 p4190 A69-41575
- Efferent innervation influence of one ear to another in feline auditory system, based on afferent neurons responses to contralateral and binaural stimulation
23 p4094 A69-42073
- Combined eye and ear identification of bimodally presented signals in noise over oscilloscope and earphones, noting significance of independent observers model
23 p4111 A69-42168
- Flight personnel hearing tests per ICAO recommendations and flight safety requirements, using tonal audiogram and vocal audiometric test
24 p4277 A69-43377
- AUDITORY SIGNALS**
Mathematical model of spike activity of auditory neurons constructed from functional point of view
07 p1070 A69-18384
- Noise level perception and subjective judgments for broadband noise with single, modulated and multiple tones, considering tone correction procedures
11 p1830 A69-24796
- Auditory evoked response /AER/ as measure of narcosis induced at depth in diving personnel, discussing hyperbaric nitrogen and oxygen effects
14 p2407 A69-29302
- Bisensory auditory and visual signals characteristics effects on human reaction time, noting different results for unilateral and bilateral signal pairs
23 p4083 A69-41454
- AUDITORY STIMULI**
Acoustical vestibular stimulation in guinea pig, showing activation of receptors
03 p0376 A69-14076
- Attenuation of visual vigilance decrement through visual stimulation combined with various sound conditions
06 p0880 A69-17213
- Auditory startle stimuli effect on human performance, noting decrease in mental and sensorimotor activity
07 p1066 A69-19421
- Cortical auditory-evoked response during eye movement in cats, discussing relation to central mechanism
17 p2911 A69-34171
- Vestibular neurons activity in decerebrated cats under ipsilateral and contralateral labyrinth polarization combined with acoustic and caloric stimulation
20 p3471 A69-37254
- Cats vestibular neurons reactions to labyrinths mon- and binaural polarization and caloric stimulation
20 p3471 A69-37255
- EEG patterns evoked from left and right cerebral hemisphere by visual and verbal stimuli, showing asymmetrical role of hemispheres in governing cognitive behavior
21 p3656 A69-38976
- Brain weight and cholinesterase activity in rats after exposures to acoustic and light stimuli
21 p3662 A69-39627
- Unit activities in cerebellar cortex by auditory stimulation in cats, discussing response patterns obtained by histograms
22 p3876 A69-40264
- Topography of potentials induced by acoustic clicks in auditory cortex of dogs, including ectosylvian gyrus distribution
22 p3888 A69-41269
- Cortical biopotentials in cats induced by strychnine under acoustic click stimuli of increasing intensity
22 p3888 A69-41270
- Dependence of cochlear microphonics and summating potential on endocochlear potential
23 p4085 A69-41574
- Klaxon hooter sudden sound used as auditory startle stimulus to determine hand sensorimotor activity and standing stability in pilot error causes
23 p4088 A69-41808
- Efferent innervation influence of one ear to another in feline auditory system, based on afferent neurons responses to contralateral and binaural stimulation
23 p4094 A69-42073
- Stimulus correlated with neuronal discharge periodicities in colliculus inferior, deriving structure models, discussing acoustic channel below geniculate medialis
23 p4096 A69-42089
- Sound evoked DC changes on intact skull of adult humans using data from AgCl electrodes, investigating intensity function, analyzing data by computer
23 p4098 A69-42101
- Attention shifts in maintained discrimination, discussing combined responses of varying and constant visual and auditory stimuli in pigeons
24 p4275 A69-43198
- Circadian periodicity of human reaction times tested during normal diurnal cycles and 24 hour wakefulness, noting acoustic and visual stimuli effects on learning
24 p4267 A69-43387
- AUDITORY TASKS**
Human information processing rates during one and two axis compensatory tracking tasks with secondary auditory task
10 p1650 A69-23880
- Continuous and intermittent noise effects on audiovisual checking task performing subjects, considering omission errors
17 p2911 A69-34009
- AUGER EFFECT**
Auger and photoelectron spectroscopy for chemical analysis, noting effects of sample thickness, sample potential, surface contamination and X ray incident angle
07 p1075 A69-19775
- Surface structures, work function changes, Auger electron and surface plasma losses for Cs on clean W surface
19 p3392 A69-36733
- AUGMENTATION**
U THRUST AUGMENTATION
- AURIGA CONSTELLATION**
Auriga star HD 35620 with respect to epsilon Virginis using model atmosphere and high dispersion spectra
08 p1403 A69-20913

Stellar atmosphere parameters analyzed over pulsation cycle by high dispersion spectra of cepheid variable RT Aurigae

10 p1778 A69-23605

AURORAL ABSORPTION

Electron and positive ion density measurements during nighttime auroral absorption event

03 p0421 A69-13327

Polar auroral region cosmic radio noise absorption bays diurnal variations attributed to drift of electrons captured in magnetosphere

03 p0423 A69-13520

Auroral absorption position and height deduced from VLF phase measurements, discussing diurnal fluctuations in reflection layer

05 p0758 A69-16415

Seasonal variations in auroral absorption zone position interpreted as consequence of asymmetric shape of magnetosphere

06 p0920 A69-17728

Calculation method for electromagnetic wave supplementary attenuation due to auroral absorption for distances up to 4000 km

11 p1841 A69-25760

Auroral cosmic noise absorption relationship to auroral geomagnetic disturbances, investigating absorption diurnal distribution

12 p2071 A69-26706

Auroral absorption influence on ionospheric wave propagation calculated for distances over 4000 km

16 p2749 A69-31603

Auroral absorption occurrence patterns mappable onto magnetotail developed as function of magnetic activity, discussing magnetotail neutral sheet source width changes

16 p2848 A69-31968

Green line suppression in type B auroral based on negative ion-electron chemistry below O transition region

16 p2778 A69-32191

Auroral absorption bays from 1963 to 1964, noting effect of ionization agent intensity changes on absorption diurnal variations

17 p2965 A69-33965

Auroral absorption distribution from arctic riometric observations mapped for evaluating radio communications reliability

17 p2967 A69-33990

Auroral absorption maximum frequency correlation with years of solar activity reduction and magnetic activity from riometric data long term variations

17 p2968 A69-33991

Ionospheric auroral anomalous radio wave absorption frequency dependence index determined from cosmic radio emission intensity data

20 p3587 A69-37033

Auroral absorption longitudinal motion from riometer recordings, showing movement from midnight meridian simultaneously eastward and westward along auroral zone

20 p3520 A69-37034

Auroral absorption relation to visual aurora and measured particle fluxes

21 p3707 A69-38488

Spatial gradient and amount of auroral radio absorption measured by riometers at magnetically conjugate and closely spaced stations

22 p3934 A69-39966

HF radio waves auroral absorption in ionosphere reviewed for first decade of riometry

22 p3902 A69-41218

Geomagnetic ring current effect on position of auroral absorption zone in northern polar region, noting storm time part of disturbance

23 p4157 A69-41859

AURORAL ACTIVITY

U AURORAS

AURORAL ARCS

NT RED ARCS

Auroral electron energy spectrum observed by sounding rocket reveals smooth continuum with peak to produce auroral arcs

05 p0756 A69-16274

Monochromatic midlatitude auroral arc /M arc/ observation on 28-29 September 1967 at Moscow, Idaho

12 p2065 A69-26105

Auroral arcs drift as function of polar storm initial phase, noting agreement with satellite data on plasma motion in magnetosphere

12 p2071 A69-26694

Gustafsson pattern for variations in position of quiet homogeneous arcs, noting diurnal variations from visual observations at antarctic station

12 p2073 A69-26951

Visual ashen light observation on Venus possibly attributable to solar particle bombardment from dark side emission detection by spectroscopic and photometric studies

16 p2861 A69-32300

Auroral arcs orientation curves for IQSY evaluated from all sky camera data, comparing results with IGY curves

24 p4308 A69-43009

AURORAL ECHOES

Model of auroral backscatter from E region including ionospheric refraction, comparing computations to experimental HF auroral backscatter data for aspect sensitivity

09 p1488 A69-21700

Correlation function of auroral reflection radio signals with allowance for polar ionospheric scattering and pulse signal transmission and reception

14 p2436 A69-29055

Periodic fading in 42 MHz auroral backscatter by high speed polarization measurements, discussing scatter bursts and pulsating primary electron flux relationship

18 p3102 A69-34950

AURORAL ELECTROJETS

Equatorial and auroral electrojets, discussing origin theories and ionospheric irregularities

02 p0236 A69-11433

Characteristics of electrovortices and auroral electrojets of polar disturbance field, discussing dynamics during geomagnetic storms

02 p0240 A69-11723

Auroral electrojet precursors and geomagnetic variations before onset of bays, noting satellite observations

10 p1681 A69-22804

Toroidal magnetic fields in ionosphere associated with solar quiet daily variations producing electric current and equatorial auroral electrojets

10 p1681 A69-22805

Joule heating role in generating internal gravity wave energy in auroral electrojet region, using linear model

12 p2064 A69-26010

Auroral zone X ray pulsations during great geomagnetic disturbance and auroral electrojet development to maximum phase, noting atmospheric feedback modulation

12 p2065 A69-26109

High latitude capture region boundary for electrons in upper radiation belt determined relative to current electrojets in ionosphere from satellite observations

13 p2327 A69-27700

Auroral electrojet index in relation to magnetic storm sudden commencements, ring current main phase and energetic solar protons

14 p2511 A69-28954

Infrasonic waves identified with supersonic auroral electrojets crossing zenith from northwest during substorm activity

16 p2780 A69-32303

Westward traveling auroral surge associated with electron flux during absence of H beta emission

18 p3130 A69-35189

Auroral electric current system model to explain magnetic disturbances associated with auroral breakups

21 p3710 A69-38505

Artificial ion plasma cloud experiment for studying auroral electric fields

21 p3710 A69-38507

Auroral zone Birkeland currents in magnetosphere, analyzing particle trajectories for plasma sheet energy distribution and Alfvén layer position

21 p3792 A69-39567

Sounding rocket measurements of electric and magnetic fields near auroral electrojet

24 p4310 A69-43188

AURORAL EMISSION

U AURORAS

U LIGHT EMISSION

AURORAL IONIZATION

Horizontal electric fields relations to charged particle fluxes in polar auroral ionosphere

14 p2437 A69-29070

Lower auroral ionosphere rocket measurements of electrons, positive ions and energy particles, deriving height variation of ion pair production and ion-ion recombination

16 p2778 A69-32187

Ionization, recombination and charge transfer in upper atmosphere during aurora, considering quasi-equilibrium ion-electron concentrations

17 p2961 A69-33417

Retarding potential analyzers to measure rocket vehicle potentials and ambient electric fields in active auroras

20 p3542 A69-37793

Ionization and light emission cross sections for collisions of protons and hydrogen atoms with atmospheric nitrogen used to analyze auroral events

24 p4368 A69-43177

AURORAL IRRADIATION

Winter polar mesosphere atomic-oxygen distribution by analyzing data concerning intensity and energy of corpuscular fluxes in auroras

12 p2070 A69-26690

Quiet aurora atomic O red and green lines intensity ratio measured from rocket

18 p3201 A69-35192

AURORAL SPECTROSCOPY

Intensity ratio of first negative nitrogen band and oxygen line varies in auroral displays

02 p0235 A69-11425

Transition probability measurement of 5577 Å auroral green line of oxygen used to investigate quadrupole nature of transition

03 p0424 A69-13936

Polar aurora incident energetic particles spectroscopic analysis, showing system of lines and bands intensity dependence on particle energy spectrum and magnetic activity

05 p0752 A69-15799

Auroral spectrum observations for absolute brightness of nitrogen Meinel and ING systems, considering background night airglow and atmospheric extinction

10 p1681 A69-23161

Polar aurora spectroscopic studies, discussing main spectral features, influence of observation time and location, analysis methods, etc

14 p2518 A69-29100

Aurora electron and proton excitation patterns determined spectroscopically, discussing ground based observations of emission geomagnetic latitude-time distribution

15 p2593 A69-30017

Photoelectric spectra of pulsating auroras in visible and near UV range, considering atmospheric opacity

17 p2961 A69-33416

Polar ionosphere investigation based on vertical sounding and riometric observations, earth electromagnetic field and polar auroras spectrum intensity variations

17 p2963 A69-33950

Proton and electron auroral ovals, deriving H alpha intensity and frequency distributions as function of geomagnetic latitude and time from patrol spectrographs in Canada

19 p3302 A69-35993

Auroral spectroscopy for high resolution coverage at maximum wavelength range, discussing plane diffraction grating

21 p3707 A69-38486

N I nebular doublet and auroral and nebular lines of O I obtained with multiplier scanning photometer in France, Norway and at magnetic equator

21 p3712 A69-38519

Accelerating electric field model to interpret energy and angular distribution of auroral particles, noting electric potential limitations

22 p3938 A69-40445

AURORAL ZONES

Radio wave abnormal absorption in auroral zone of ionosphere, investigating index of frequency dependence in absorption vs frequency relation

01 p0063 A69-10425

Latitudinal variations in auroral and subauroral region F layer diurnal and magnetic storm pattern shown by scintillation measurements

01 p0069 A69-11127

Electrostatic plasma wave instabilities in ionosphere along auroral field lines, noting critical electron flux and subsequent acceleration of electrons

01 p0075 A69-11222

Anomalous radio wave absorption in polar aurora region ionosphere, discussing disturbance characteristics

02 p0207 A69-11688

Hydromagnetic emissions observed at Antarctic auroral zone, discussing relation to sudden storm commencement

02 p0241 A69-11726

Magnetosphere studies in France noting magnetospheric characteristics, wave propagation, charged particles, particle precipitation mechanisms in auroral zones and polar caps

02 p0242 A69-11904

- Electron concentration profile change in ionospheric F region in auroral zone during negative magnetic bay disturbances
03 p0423 A69-13530
- Energetic electron fluxes measured at 2000 km over auroral and polar regions and at 17 earth radii in magnetotail plasma sheet
03 p0503 A69-14013
- Auroral zone X ray measurements obtained by simultaneous balloon flights over Northern Scandinavia
05 p0813 A69-15822
- Bounce resonant scattering of auroral zone electrons, noting contribution to microbursts and mirror point diffusion
05 p0754 A69-16260
- Field aligned Birkeland currents generation at auroral latitudes
05 p0755 A69-16266
- Electron cooling rates in midlatitude and auroral zone thermosphere measured by probe rockets
05 p0755 A69-16267
- High resolution electron and proton energy measurements by sounding rockets indicating plasma sheet as source of energetic auroral electrons
05 p0756 A69-16273
- Seasonal variations in auroral absorption zone position interpreted as consequence of asymmetric shape of magnetosphere
06 p0920 A69-17728
- Radio noise generation in topside ionosphere, noting Cerenkov radiation from intense soft fluxes of auroral electrons
07 p1127 A69-19257
- Auroral zone X ray measurements emphasizing temporal intensity variations, energy spectra changes and source region movements during magnetospheric substorms
08 p1379 A69-20534
- Polar auroral far UV spectra using Ebert-Fastie monochromator flanked by photometers with same visual field
08 p1311 A69-21026
- Auroral oval boundary and median line variations with increasing magnetic storm time intensity; noting ring current effect on polar aurora location
09 p1485 A69-21532
- Auroral electron flux from particle fluxes measured with shielded Geiger-Muller telescopes mounted in rocket launched into diffuse aurora
09 p1576 A69-21663
- Irregular pulsations in morning sky brightness using all-sky photographic airborne auroral observations along auroral oval
09 p1594 A69-21666
- Electrical phenomena in upper atmosphere and solar wind may control geomagnetic disturbances and aurora
10 p1686 A69-23903
- Auroral infrasonic waves morphology related to temporal and spatial distributions of supersonic auroral motions during polar magnetic storms
11 p1878 A69-25152
- Auroral zone X ray pulsations during great geomagnetic disturbance and auroral electrojet development to maximum phase, noting atmospheric feedback modulation
12 p2065 A69-26109
- Auroral and polar zone ionosphere effects on propagation in HF through low VHF spectrum, considering nongreat circle mode, sporadic E ionization, etc
12 p2032 A69-26859
- RF synchrotron radiation emitted by electrons trapped in geomagnetic fields above auroral zones, discussing electron flux and cosmic background
12 p2151 A69-26949
- ESRO I/Aurora project for ionospheric phenomena connected with incoming protons and electrons, describing orbit and alignment with geomagnetic field
13 p2356 A69-27747
- Auroral phenomena investigation by ESRO I satellite, measuring particle flux arriving at auroral height
13 p2381 A69-27748
- Medium energy trapped and dumped protons at high latitudes and auroral zone, using semiconductor radiation detectors on ESRO I satellite
13 p2328 A69-27756
- Anomalous radio wave absorption in polar aurora region ionosphere, discussing disturbance characteristics
13 p2224 A69-28719
- Polar auroral region displacement ascribed to distant magnetic field disturbances, proposing calculation method
14 p2436 A69-29059
- Rocket measured electron densities of nighttime auroral E region over Canada at different magnetic activity levels, noting frequency and plasma density relations
14 p2439 A69-29117
- Auroral substorms concept extended to include associated effects at all local times throughout magnetosphere, considering particle precipitation influence on substorms in midnight sector
15 p2593 A69-30008
- Solar cycle effect on high latitude magnetic activity, discussing annual variations and Lassen auroral zone model confirmation
15 p2598 A69-31207
- Faraday rotation measurements of signals from Explorer 22 analyzed to determine scintillation boundary in auroral ionosphere
15 p2605 A69-31443
- Radio wave emission bursts at 28 MHz at onset of nighttime absorption dip and close to auroral zone from riometer recordings, noting relation to geomagnetic storms
16 p2775 A69-32085
- Auroral oval boundary and median line variations with increasing magnetic storm time intensity, noting ring current effect on polar aurora location
16 p2783 A69-32527
- Polar auroral zone boundaries from C-180 camera photographs related to magnetic disturbance level, noting evening-morning asymmetry
17 p2963 A69-33951
- Daytime magnetospheric disturbances in auroral zone, discussing time lag of perturbations for absorption and geomagnetic field bays
17 p2964 A69-33962
- Vertical distribution of ionospheric drift velocity in auroral zone, evaluating role and intensity of electric field formed in dynamo region
17 p2964 A69-33964
- Electric field variations in vicinity of auroral forms from motions of Ba vapor clouds released from Nike-Tomahawk rockets
18 p3128 A69-34935
- Waves in auroral ionosphere due to particle precipitation, indicating ionospheric plasma instabilities
18 p3130 A69-35187
- Proton and electron auroral ovals, deriving H alpha intensity and frequency distributions as function of geomagnetic latitude and time from patrol spectrographs in Canada
19 p3302 A69-35993
- Auroral absorption longitudinal motion from riometer recordings, showing movement from midnight meridian simultaneously eastward and westward along auroral zone
20 p3520 A69-37034
- Frequency spectra of Pi2 geomagnetic field pulsations, noting effects of auroral zone location, configuration and structure
20 p3520 A69-37038
- Altitude asymmetry of instantaneous auroral oval plotted for geomagnetic pole and earth surface
20 p3522 A69-37056
- F 2 region critical frequencies obtained during winter at Northern and Southern Hemisphere stations located in auroral and polar zones, correlating changes with ionization
20 p3526 A69-37665
- VLF electric and magnetic fields observed in auroral zone with Javelin 8.46 sounding rocket, noting HF electrostatic noise bursts
20 p3533 A69-38080
- Simultaneous observations of 5 to 15 second period modulated energetic electron fluxes at synchronous altitude and auroral zone
20 p3592 A69-38082
- Flux magnitude and pitch angle distribution relationship for postsubstorm auroral electrons, noting particle precipitation and acceleration models
20 p3592 A69-38083
- Energy spectrum, spatial characteristics and displacements of auroral zone X rays from X ray spectrometry
21 p3787 A69-38359
- Lower thermosphere ion and neutral minor constituent concentrations in nighttime auroral zone, considering ionization due to electron precipitation and bremsstrahlung
21 p3704 A69-38365
- Auroral phenomena observations at magnetically conjugate regions including luminous aurora, riometry of auroral radio absorption, balloon-measured X rays and magnetic disturbances
21 p3708 A69-38493
- VLF and LF emission characteristic features and origin mechanism in auroral regions of ionosphere, discussing satellite observation of noise spectrum in space
21 p3708 A69-38495
- Auroral zone geomagnetic pulsations on nightside and dayside of earth related to magnetospheric substorm and particle precipitation
21 p3708 A69-38497
- Auroral electron and proton fluxes precipitation measurements by satellite, studying data in terms of spatial, energy and angular distributions
21 p3709 A69-38500
- Optical data supporting satellite observations of soft electron precipitation on poleward side of normal auroral zone
21 p3709 A69-38501
- Particle precipitation into auroral zone and plasma-energetic particle relationship in geomagnetic tail, discussing plasma sheet extent, energetic electron fluxes, etc
21 p3711 A69-38510
- Auroral zone X rays measurement counting rate vs time patterns from balloon flights at Kiruna
21 p3791 A69-39252
- Electron energy loss spectrum of nitrogen, suggesting atmospheric auroral nitrogen emissions compatibility with low energy electron impact excitation mechanisms
22 p3935 A69-39970
- Spectral characteristics of structured areas of luminosity in polar cap region, reporting spatial and time variations plotted from NASA airborne survey
22 p3940 A69-40522
- Heat conduction equation applied to thermospheric heating in auroral zone to account for local temperature and density variations, introducing horizontal transport mechanisms
22 p3941 A69-40717
- Auroral VLF emission bursts simultaneous with sharp ionospheric absorption dip and SC deflections in geomagnetic H, noting corpuscular ionization
24 p4308 A69-43001
- AURORAS**
NT AURORAL ARCS
NT RADIO AURORAS
NT RED ARCS
- Enhanced 6300 angstrom emission from F region auroral latitudes in terms of reaction between oxygen ions and atoms
01 p0062 A69-10137
- Auroral emission rates and heating effects as function of altitudes
02 p0235 A69-11426
- Plasma waves and particle interaction in nonuniform magnetosphere, considering propagation across sheets of steep density gradient and auroral precipitation
02 p0235 A69-11429
- Polar aurora fine scale structure interpretation based on plasma instabilities characteristics
02 p0239 A69-11693
- Geophysical effects observed in Northern Hemisphere during low solar activity, discussing polar auroral intensities and positions
02 p0239 A69-11694
- Canadian program of scientific rocket sounding of auroral phenomena, outlining systems approach, engineering and scientific cooperation requirements, etc.
02 p0335 A69-12689
- Auroral observations from constant local time westward flights of jet plane
02 p0245 A69-12738
- Simultaneous VLF hiss, auroral light and X rays observed during Norwegian balloon study
02 p0309 A69-12744
- Aurora displays distribution over earth, analyzing magnetosphere dependence on astronomical orientation of geomagnetic field in relation to solar wind
02 p0247 A69-12772
- Diurnal, magnetic and solar cycle dependences of auroral emission variations and auroral occurrence
03 p0420 A69-13325
- Cone instability role in auroral electron and proton dynamics, discussing plasma instability control of maximum captured particle densities in various magnetosphere regions
03 p0501 A69-13526
- Satellite-borne auroral particle spectrometer calibration to minimize uncertainty in measuring absolute particle flux of electrons and protons
04 p0599 A69-15022
- East-West aligned fast auroral waves, suggesting origin in hydromagnetic processes occurring near equatorial plane
04 p0594 A69-15123

Ohz intensity variation in bright homogeneous auroras prior to and during breakup observed visually and with image orthicon TV systems 04 p0594 A69-15129

Spatial and temporal conjugacy of visual auroras during magnetically quiet periods 05 p0753 A69-16247

Latitudinal distribution of auroral and airglow emissions in Northern Hemisphere photometrically surveyed by jet aircraft 05 p0754 A69-16258

Ratio of volume emission rate of 5577 Å photons to volume emission rate of one band of positive nitrogen molecule first negative system in aurora 05 p0756 A69-16360

Flaming auroras observations with auroral image orthicon TV systems, calculating electron release points on field line of station 05 p0758 A69-16413

Image intensifier-vidicon closed circuit TV network for auroral cinematography at low light levels 06 p0925 A69-17382

Correspondence between HF radar backscatter, optical aurora and electron precipitation, noting application to gross tracking of auroral oval 06 p0918 A69-17383

Soviet and French coordinated geophysical studies at magnetically conjugate points in northern U.S.S.R. and Indian Ocean 06 p0918 A69-17391

Jovian limb H alpha line due to auroral emission obtained from high dispersion spectra with long light path through upper atmosphere 07 p1214 A69-18614

Universal instability theory relevance to pulsating optical auroras and fast quasi-periodic variations of auroral X ray fluxes 07 p1125 A69-18852

Auroral electron penetration into atmosphere analyzed on basis of independent electron particle motion, using auroral electron angular distributions and energy spectra above atmosphere 07 p1128 A69-19368

Geomagnetic storms, substorms and auroral displays as functions of processes in solar wind and upper atmosphere 08 p1307 A69-20188

Nocturnal auroral electron showers configuration and displacement determined from sounding balloon measurement of X rays due to showers braking in upper atmosphere 08 p1308 A69-20281

Ion number densities time dependence in pink afterglow of N measured with quadrupole mass spectrometer 08 p1308 A69-20292

Auroral oval boundary and median line variations with increasing magnetic storm time intensity, noting ring current effect on polar aurora location 09 p1485 A69-21532

Geomagnetic field irregular pulsations relationship with polar aurora and ULF radiation pulsations, stressing choruses appearance 09 p1485 A69-21536

Auroral French rocket probe in Norway, studying low energy particles, relations between electron showers and high altitude electric fields, etc 09 p1498 A69-22160

Ratio of volume emission rates of 5577 Å and band of positive N molecular ion first negative system for use in auroral observations 09 p1491 A69-22607

Auroral H beta intensities determined from photographs by image intensifier, describing equipment and data reduction method 10 p1684 A69-23824

Auroral electron energy diurnal variation, noting ground observations of polar auroras, riometric absorption, vertical changes in ionization layer maximum position, etc 10 p1687 A69-23915

Nitrogen, oxygen and air luminescence spectra excited by fast electrons at low gas pressures in IR spectral region compared with polar auroral spectra 10 p1687 A69-23916

Auroral oval and ring current in magnetosphere, analyzing boundaries of lines of force on night side of earth 10 p1689 A69-24203

Space radiation phenomena, discussing auroral precipitations and characteristics and solar flare particle ejection 11 p1948 A69-24859

Low light level slow scan Owl TV camera system with secondary electron conduction camera tube for satellite-borne observation of auroral light emission 12 p2079 A69-25904

Auroral electrons intensity modulation by source at L equals 6 magnetic shell on geomagnetic equator, noting dispersion effects 12 p2065 A69-26108

Nighttime distribution of nitrogen ion and lambda 3755 emission in ionosphere with incidence of aurora 12 p2066 A69-26110

Auroras and polar magnetic substorm observations limited comparison due to magnetospheric models inability to interpret daytime precipitation zones and particle energy spectra 12 p2072 A69-26740

Dynamics of magnetosphere, discussing auroral oval position, ring currents, plasma density and magnetic field variations in near polar region 12 p2072 A69-26741

Solar wind induced magnetospheric convection for interpretation of geomagnetic storms, aurora and trapped particle belts, noting electric fields 12 p2073 A69-26749

Solar-terrestrial environment, discussing mathematical development of solar wind, satellite measurement, magnetic storms, aurora and cosmic rays 12 p2161 A69-26941

Auroral luminosity determination by two photometers on ESRO I satellite 13 p2253 A69-27752

Diurnal hemisphere auroras assuming origins in magnetosphere tail with pressure responsible for tail formation, discussing tentative model and implications 13 p2256 A69-28654

Coding of morphological evolution in time of auroral displays as generalization of existing IUGG code 13 p2256 A69-28655

Polar aurorae fine scale structure interpretation based on plasma instabilities characteristics 13 p2258 A69-28724

Geophysical effects observed in Northern Hemisphere during low solar activity, discussing polar auroral intensities and positions 13 p2258 A69-28725

Polar aurora rays mean length diurnal variations determined from photographic and visual observations in Tiksi bay 14 p2437 A69-29077

Radio noise of auroral origin analyzed from Northern and Southern Hemisphere reports indicating correlation with auroras, magnetic activity, sunspot cycles and synchrotron radiation 14 p2411 A69-29108

H alpha line emission preceding auroral breakup by data analysis of Antarctica Meinel-type patrol spectrograph, noting magnetic activity role 14 p2441 A69-29386

Polar auroras temporal and spatial variations and relation to solar activity 14 p2442 A69-29719

Low energy electron and proton precipitation, discussing acceleration mechanisms and periodicity in relation to auroras and airglows 15 p2594 A69-30018

Auroral substorm westward traveling surge and poleward, eastward and equatorward motion analyzed from all sky photographs 15 p2595 A69-30214

Auroral displays observed in combined field of view of polar all sky camera networks, considering simultaneous geomagnetic disturbances over Alaska 15 p2595 A69-30215

ESRO I/Aurorae scientific satellite for ionospheric phenomena observation, discussing management structure and development process 15 p2702 A69-31080

ESRO I/Aurorae satellite for Arctic ionosphere and aurorae observation, discussing electrons and protons measurements and auroral photometry 15 p2702 A69-31081

Photometric rocket measurements in hydrogen auroras, finding vertical H beta emission profile estimate of proton energy spectrum for H beta production cross section 15 p2595 A69-31307

Numerical analysis of charged particles radial distribution in radiation belts extended to geomagnetic tail for low energy auroral electrons 16 p2850 A69-32102

Pulsating and flaming auroral patches recorded by image intensifier vidicon camera, calculating upward field aligned speeds for luminosity enhancement 16 p2780 A69-32305

He I/1.083 mu/ and O I/5577 Å/ absolute brightness measured in sunlit aurora for various shadow heights of solar radiation, considering primary electron precipitation 16 p2780 A69-32311

Auroral oval boundary and median line variations with increasing magnetic storm time intensity, noting ring current effect on polar aurora location 16 p2783 A69-32527

Geomagnetic field irregular pulsations relationship with polar aurora and ULF radiation pulsations, stressing choruses appearance 16 p2783 A69-32531

Auroral electrons measurement by rocket, discussing difficulties due to secondary electrons and method permitting primary electrons detection threshold determination as function of rocket position 16 p2785 A69-32617

Rocket instrumentation for electron and proton spectra measurement in aurora borealis 17 p2972 A69-33038

Soviet collection of papers on polar auroras 17 p2962 A69-33949

U shaped polar auroras development, examining relation with magnetic activity and current system configuration in lower ionosphere 17 p2963 A69-33952

Magnetic activity influence on polar auroras height 17 p2963 A69-33953

Polar auroras pulsation attributed to background brightness fluctuations, discussing intensity diurnal variation 17 p2963 A69-33954

Polar auroras appearance at solar activity maximum /IGY/ and minimum /QSY/ at oval zone latitudes 17 p2963 A69-33955

Emission intensity ratio change as function of polar auroral height compared to variation in atmospheric concentration ratio of oxygen to nitrogen 17 p2963 A69-33956

Ionospheric processes associated with changes in polar aurora height, noting glow in E layer and soft electron emission into earth atmosphere 17 p2964 A69-33957

Midday aurora oval and polar cap region airborne observation, noting relation to sporadic E layer 18 p3126 A69-34258

Artificial aurora generated at 100 km altitude by electron beam fired downward from aerobee 350 rocket above 230 km along earth magnetic field lines 18 p3127 A69-34365

Precipitated low energy protons and electrons measurements during breakup aurora, discussing fluxes and poleward boundaries 18 p3187 A69-34946

Electron temperature, density and magnetic disturbances measurements at 1000 km compared with visual observations during 25-26 May 1967 magnetic storm and aurora 18 p3129 A69-34954

Antarctic VLF emissions observations at 12 kHz, showing dependence on geomagnetic disturbances, auroras and radio absorption in ionosphere 18 p3102 A69-34964

Plasma density in magnetosphere by measuring geomagnetic pi 2 micropulsations in direction related to polar aurora oval southern boundary, determining period of pi 2 oscillations 19 p3303 A69-36205

H alpha auroral activity on Jupiter isolated by using Fabry-Perot etalons, showing photograph reproductions 20 p3598 A69-37414

Auroral sounding rocket research and instrumentation in Scandinavia, discussing auroral particles, optical measurements, probe experiments and scientific objectives 20 p3542 A69-37794

Auroral displays photographed by all-sky cameras at magnetically conjugate stations, morphological similarities and electron precipitation role 20 p3535 A69-38187

Auroral parameters coordinated measurements at varying rocket pitch angles during penetration of diffuse aurora breakup phase 21 p3703 A69-38361

Auroral science from 1600 to IGY/1965/ including Gilbert earth magnet theory, Birkeland auroras proposal, spectroscopy, geomagnetic and solar particle data, etc 21 p3706 A69-38483

Image intensifiers and orthicons, plumbicons, vidicons as photoelectric devices in TV auroral observation from ground stations and jet aircraft 21 p3706 A69-38484

Morphology of discrete polar cap and polar glow auroras, noting diurnal variations correlation with magnetic activity changes at low latitude

21 p3707 A69-38487

Rocket measurement data of auroral particle precipitation classified in substorm phases of quiet and breakup period, breakup and postbreakup events and morning events

21 p3707 A69-38489

Rocket measurements of primary auroral particles energy spectra indicating spectral structure acceleration peaks associated with electrostatic fields

21 p3707 A69-38490

Optical pulsations in aurora, studying relations to pulsations in geomagnetism, telluric currents, X rays from aurora and variations in primary particles flux

21 p3708 A69-38492

Auroral phenomena observations at magnetically conjugate regions including luminous aurora, riometry of auroral radio absorption, balloon-measured X rays and magnetic disturbances

21 p3708 A69-38493

Auroras and VLF emissions observations at ground stations to correlate emissions with auroral displays, noting low ionospheric absorption role

21 p3708 A69-38494

Rocket measurements indicating auroral electrons modulation near equatorial plane, noting intensity changes as function of rocket flight time and altitude

21 p3709 A69-38499

Field-aligned currents effect on ionosphere and precipitation of auroral primary particles, analyzing with mathematical model of ionospheric density height distribution

21 p3710 A69-38506

Ionospheric currents geophysical DC electric fields measurement from sounding rockets, indicating anticorrelation with auroral luminosity

21 p3710 A69-38508

Helium in atmosphere, aurora and solar wind, discussing geophysical problems, interplanetary neutral H, etc

21 p3710 A69-38509

Semiempirical electron impact cross sections and energy loss functions applied to dayglow and auroral intensities calculation, discussing atomic and aeronomic implications

21 p3713 A69-38527

Quantitative criteria imposed on balloon measurements of auroral emissions from Kiruna, considering times of sunrise and sunset at different altitudes

21 p3716 A69-39250

Satellite observations of auroral particle precipitations indicating latitude dependence of auroral electrons averaged pitch angle and energy spectral distributions

22 p3938 A69-40502

Auroral UV and 3914 A radiation during charged particle precipitation measured by satellite

22 p3939 A69-40507

Spectral characteristics of structured areas of luminosity in polar cap region, reporting spatial and time variations plotted from NASA airborne survey

22 p3940 A69-40522

Balloon-borne instrument for auroral X ray measurements at Antarctic station, discussing design requirements, circuit characteristics and improvement recommendations

23 p4166 A69-42011

Rocket measurements of plasma densities and temperatures in visual aurora using electrostatic onboard and ejected Langmuir probes, observing hyperthermal electron

23 p4167 A69-42334

Pulsating aurora diurnal variations and dependence on latitude and magnetic activity, photometric observations

24 p4308 A69-43004

N II 4176 A emission line occurrence in connection with type B auroras, studying secondary electrons energy spectra

24 p4309 A69-43012

H beta production in hydrogen aurora measured during rocket flight, obtaining proton energy spectrum

24 p4309 A69-43170

Auroral short period pulsations in 6300 A O I, discussing percentage modulation, quenching rate, etc

24 p4309 A69-43171

Auroral activity and lunar phases correlation from IMP-1 measurements of lunar magnetic field

24 p4311 A69-43502

AUSFORMING

Consumable electrode vacuum melted steels, discussing ausforming and stress corrosion cracking

04 p0604 A69-14528

AUSTENITE

Structural transformations of quenched Fe-Ni-Nb austenitic alloy from X ray diffraction microstructure examination and hardness measurements

01 p0095 A69-10603

Composition dependence of carbon activity and carbon diffusivity in austenite

13 p2279 A69-27763

Phase shape deformation and austenite stabilization in Fe-Ni and Fe-Ni-Ti alloys following secondary alpha phase of reversed martensite-austenite transformation

18 p3159 A69-35448

AUSTENITIC STAINLESS STEELS

High pressure hydrogen environment on tensile properties of stainless steel with and without strain induced martensite

01 p0093 A69-10062

Precipitation hardening of gamma phase in austenitic stainless steels studied for phase transformations by dilatometry after aging and quenching

01 p0096 A69-10613

Structural stability of manganese austenitic steels at high temperatures, discussing phase transformations and carbide precipitation changes

01 p0100 A69-11294

Light austenitic grain boundaries in heat treated Cr-Mo-W-V alloy steels

01 p0100 A69-11295

Ferrite and sigma phase formation in austenitic stainless steels with nickel and chromium content

02 p0269 A69-12764

Lattice parameters of austenitic Fe-Ni-Ti alloys as function of titanium content, using Debye-Scherrer camera

03 p0443 A69-13123

Corrosion rates and stress corrosion cracking sensitivity of explosively shocked austenitic stainless steels

03 p0444 A69-13308

Ferrite-austenitic stainless steels with Ti analyzed during aging at 450-600 C for excess phase nature

04 p0615 A69-14641

Plastic deformation effect on structure, yield point and tensile strength of aged austenitic alloy containing Ni, Cr and Ti

04 p0618 A69-15177

Fully austenitic stainless steel welding electrodes for welds in cryogenic or high temperature applications, noting creep rupture test results

04 p0607 A69-15220

Pitting corrosion resistance improvement in austenitic stainless steels with added molybdenum through electroslog resmelting

05 p0781 A69-16499

Austenitic Fe-Ti alloys sulfur solubility and internal sulfidation rate computed, noting stronger Ti-S interaction with temperature decrease and sulfur diffusion role

06 p0942 A69-17226

Localized microstructural changes and fatigue crack propagation in cantilever type notched specimens of austenitic stainless steel under cyclic bending at constant load

06 p0943 A69-17237

Retained austenite content control, strain aging and ausforming to improve toughness of high strength martensitic stainless steel without strength loss

08 p1330 A69-20010

Crystallographic fracture path of stress corrosion cracks in austenitic stainless steels using scanning electron microscopy

09 p1522 A69-21486

Negative creep in austenitic steel samples explained as possible redistribution of elements inside austenite grains at high temperatures

10 p1708 A69-22999

Chemical composition of chromium steels for optimum heat resistance properties, noting effects of nickel, nitrogen and ferrite and austenite-forming elements

10 p1708 A69-23000

Austenite to martensite strain induced transformation effect on energy absorption during crack propagation

10 p1709 A69-23074

Surface temperature rise of solution treated austenitic steel measured during double repeated rotating bending fatigue tests at room and elevated temperatures

10 p1711 A69-23393

Audio frequencies internal friction measurement of austenitic stainless steels subjected to heat treatment and corrosion, discussing time dependence and carbide precipitates morphology

10 p1713 A69-23819

Monograph on effect of boron, zirconium and titanium on austenite transformation of CrMo steels bainite and martensite covering carbides, nitrides, mechanical properties, etc

11 p1903 A69-24634

W, Mo and heat treatment effects on phase composition and heat resistance of ferrite and austenitic steels

13 p2283 A69-28487

Short time creep rupture behavior of austenitic stainless steel at high temperature ranges, noting rupture times various stresses and data correlation [ASME PAPER 68-WA/MET-2]

14 p2464 A69-29439

Precipitation processes and effect on properties of Cr-Ni-W-Ti heat resistant austenitic steel, using electron diffraction and transmission electron microscopy

17 p2984 A69-32833

Austenitic alloy structure and stress rupture after boron addition

17 p2985 A69-32908

Microfractographic observations of Al, Al alloy, Nimonic 90 and austenitic steel 18/10 after creep rupture

17 p2986 A69-32910

Mechanical properties and weldability of austenitic steel for cryogenic applications

18 p3158 A69-35417

Sigma phase and temperature effects on toughness of austenitic stainless steel weldments

18 p3150 A69-35429

Electron beam welds orientation effects on tensile and deformation properties of strengthened and welded austenitic stainless steels

18 p3151 A69-35432

Austenitic stainless steels nonreproducible passivating tendencies, determining electrochemical and corrosion characteristics, discussing critical anodic current density role

20 p3562 A69-37750

Precipitation hardening stainless steels applications in aerospace industry, discussing steel selection and heat treatment

20 p3563 A69-37931

Mechanical and thermal properties of vanadium alloys and austenitic stainless steels compared to determine applicability in high temperature reactor fuel jackets

22 p3971 A69-40973

High strength austenitic Cr-Mn-N-Ni steel applicability to welded pressure vessels for cryogenic fluid storage, discussing operating temperature stability, weldability, etc

23 p4175 A69-41475

AUSTRALIA

Satellite telecommunications, discussing Australian experience, ground stations location, national network and international cooperation [UN PAPER 68-95286]

06 p0886 A69-17066

Solar radio astronomy in Australia including solar atmosphere, bursts, instruments, etc

10 p1777 A69-23383

Radiophysics Laboratory/Sidney/, discussing radio astronomy, radioheliographs, radio telescopes, cloud physics and research

10 p1784 A69-23988

Australian space research including space flight programs in cooperation with NASA

15 p2724 A69-31450

Australia spatial triangulation and trilateration using geometric satellite geodesy, including station position accuracy tests

18 p3132 A69-35499

Multichannel spectral line receiver for 210 ft Australian radio telescope with front ends covering wide frequency range

24 p4283 A69-43115

AUSTRALITES

Australites from Port Campbell and Princetown region of Western Australia

03 p0507 A69-13096

Australasian microtektite physical and chemical properties, comparing refractive indices, specific gravities, composition trends, etc

08 p1305 A69-19815

Correction of thermally lowered fission track ages of australites

15 p2696 A69-31140

K-Ar dates on cores and excess radiogenic Ar in flanges of australites for age determination

23 p4209 A69-41343

AUSTRIA

Austrian space research covering satellite observation, receiving and evaluating picture transmissions, theoretical investigations, etc

15 p2724 A69-31432

AUTOCOLLIMATORS

U COLLIMATORS

AUTOCORRELATION

Sunspots autocorrelation functions in sunspot area on solar disk, tabulating extremal values

02 p0314 A69-11677

Diversity antenna continuous short wave radio signal envelope distribution, autocorrelation functions, damping rate and cross correlation coefficients

03 p0394 A69-13522

Spatial autocorrelation functions of amplitude and phase fluctuations in plane parallel to wavefront of incident wave for conditions of multiple scatter

03 p0468 A69-13807

Atmospheric fine structure studied by amplitude distribution and autocorrelation functions for different heights of scatter volume in microwave range

04 p0628 A69-15306

Viscosity coefficient tensor in terms of autocorrelation functions, using linear reaction theory of mechanical disturbances

05 p0794 A69-15785

Autocorrelation function distortion determined for Barker signal passing through linear system and RC filter, noting passband influence on function shape

05 p0720 A69-16443

Root mean square time delay error with respect to playback time and autocorrelation function of tape recorded sine wave for studying jitter spectra

07 p1132 A69-18827

Computerized objective analysis of meteorological variables based on weight determination involving autocovariances

08 p1345 A69-20309

Power spectrum of nonstationary processes with periodicity in two dimensional autocorrelation function based on Fourier transform

09 p1455 A69-21847

Computerized autocorrelation function analysis of radioactivity distributions in atmosphere at different altitudes, showing no correlation between values

11 p1945 A69-24320

Two dimensional autocorrelation functions of outgoing radiation fields usable as quantitative characteristics of cloud distribution structures

11 p1913 A69-24832

Holograms reconstructing images of points with diameters approximated by width of autocorrelation functions

11 p1886 A69-25058

Thinned arrays design based on array excitation autocorrelation function, considering element spacing

11 p1856 A69-25661

Autocorrelation and cross correlation analysis of rapid density variations in F region determined from satellite deceleration and geomagnetic data

12 p2069 A69-26436

Sunspots autocorrelation functions in sunspot area on solar disk, tabulating extremal values

13 p2355 A69-28708

False alarm stabilization circuits efficiencies compared in unsteady Gaussian noise, considering phase autocorrelator performance

15 p2567 A69-30342

General autocorrelation function for input signal composed of two amplitude modulated noise waves and background noise from detecting system composed of half wave element

15 p2569 A69-30805

Fluctuation spectra of monatomic gases, using two time probability distributions for distribution function autocorrelations

16 p2817 A69-31669

Error analysis of one bit autocorrelation method of spectral estimation, noting decrease in spectral variance with increased sampling rate

16 p2752 A69-32390

Autocorrelation function distortion determined for Barker signal passing through linear system and RC filter, noting passband influence on function shape

16 p2753 A69-32475

Jodrell Bank RF digital autocorrelation spectrometer based on time delay related to signal power spectrum through Fourier transform

17 p2970 A69-32856

Viscosity coefficient tensor in terms of autocorrelation functions, using linear reaction theory of mechanical disturbances

18 p3173 A69-35037

Autocorrelation function for unsteady temperature and stress fields in bar located in gas stream leaving combustion chamber

19 p3440 A69-36685

Aircraft measurements of scintillation of ground based light source, calculating autocorrelation functions and intensity fluctuations spectra

19 p3279 A69-36881

Quadrupole self and cross correlations of directional jet noise patterns, including frequency spectra and corrections

22 p3931 A69-40891

Optimum signals for high resolution radar and communication systems, using transmitter waveform design of autocorrelation and cross correlation functions

23 p4132 A69-42545

AUTODYNES

Autodyne frequency converters minimum noise and conversion factor calculation and optimal mode determination

09 p1469 A69-22631

Amplitude-frequency characteristic and noise bandwidth of electron tube reflex autodyne operating in over or under voltage mode and including IR feedback

16 p2761 A69-32477

AUTOGYROS

VFW H3 Sprinter autogyro maintenance, reliability and operating costs

16 p2735 A69-32056

AUTOIONIZATION

Autoionizing states effects on absorption cross sections for ejection of outer subshell electron from atomic oxygen

04 p0633 A69-15127

Red autoionizing lines relative gf values for calcium measured by shock tube experiment

09 p1601 A69-22208

Autoionization lines effect on stellar structure by computing contributions to Rosseland mean opacity

20 p3612 A69-38165

AUTOKINESIS

Visual long term storage capability demonstration, describing negative aftereffect of motion perceived after fixation of moving spiral pattern

21 p3661 A69-39332

After image measuring method of eccentric fixation during autokinetic light tracking

22 p3878 A69-40837

AUTOMATA THEORY

Mathematically stylized simple systems representing systems with functional law varying as function of acquired experience

01 p0050 A69-10377

Self reproducing automata, noting description of cellular system and applications to systems science

05 p0723 A69-15826

Algorithm for calculating Moore automaton or connected network channel capacity and source of input symbols for full capacity utilization

07 p1088 A69-19707

Mathematically stylized simple systems representing systems with functional law varying as function of acquired experience

12 p2054 A69-26670

Human operator as servo system element of subassemblies in tracking and equilibrium tasks, stressing results of electromyographic analysis

12 p2025 A69-27081

Synthesizable automata with sequential homogeneous structure formed by standard fixed units combination

13 p2224 A69-27249

Reliability functions and cycles number before breakdown of finite automaton with account of randomness of malfunctions, structure and input signal distribution

13 p2224 A69-27250

Finite state probabilistic automata reduction problems

13 p2239 A69-28534

Homogeneous finite automaton asymptotic analysis, calculating series terms for matrix transition probability function

13 p2239 A69-28535

Finite automaton malfunctions, discussing input sequences construction and output sequences analysis for malfunction subsets recognition

13 p2239 A69-28536

Group code decoding, discussing equivalent transformations of reference matrix and reduction of equipment losses

13 p2225 A69-28537

Finite automaton used to construct minimum automaton with periodic structure, discussing representability of regular events

13 p2239 A69-28553

Lower bound determination of automaton memory elements, describing coding procedure and algorithm for machine states

13 p2239 A69-28554

Probabilistic automata stochastic matrices algebraic properties of definite, quasi-definite, periodic and quasi-periodic sets

15 p2645 A69-31141

Checking automation languages defined as one way stack languages subfamily forming full AFL closed under substitution

16 p2755 A69-32078

AUTOMATIC CONTROL

NT ADAPTIVE CONTROL

NT CASCADE CONTROL

NT DYNAMIC CONTROL

NT FEEDBACK CONTROL

NT LEARNING MACHINES

NT NUMERICAL CONTROL

NT OFF-ON CONTROL

NT OPTIMAL CONTROL

NT PROPORTIONAL CONTROL

NT SELF ADAPTIVE CONTROL SYSTEMS

NT SELF ALIGNMENT

NT SEQUENTIAL CONTROL

NT TIME OPTIMAL CONTROL

Multivariable PFM control system stability analysis using Liapunov function as Hermitian quadratic form

01 p0050 A69-10207

Root-mean-square error determination in automatic control system by digital computer for realizing control function, investigating harmonic and random input effects

01 p0050 A69-10208

Respiratory system control processes hypotheses experimental verification

01 p0019 A69-10209

Automatic phase control effective bandwidth determined by asymptotic method, presenting computer calculated dependence on circuit parameters

01 p0030 A69-10590

Monte Carlo method accuracy improvement for calculating probability characteristics of nonlinear ordinary differential equations, describing nonlinear automatic control

01 p1015 A69-10730

Soviet collection of articles on analysis and synthesis of automatic control systems

01 p0051 A69-10793

Forced processes in continuous extremal control systems, proposing algorithm for designing dynamic model

01 p0052 A69-10798

Variational law of control elements for automatic control systems with parameters subject to random changes

01 p0052 A69-10800

Automatic control systems correction by compensating for nonlinear statistical dynamic characteristics with aid of nonlinear devices

01 p0053 A69-10801

Stability of two coordinate automatic angular tracking systems

01 p0053 A69-10803

Hydrocarbon-air fuel cell producing electric power automatically for five days

01 p0013 A69-10965

Soviet book on design of multidimensional automatic control systems, covering structural circuit synthesis and individual element characteristics

01 p0053 A69-10995

Soviet book on automatic control and telemechanics in hydrometeorological measurements covering sensors, transducers, amplifiers, etc

01 p0111 A69-10997

Autonomous solution to orbital navigation problem yielding direct measure of orbital parameters

01 p0114 A69-11005

Automatic life support system tried on leeches for space applications

01 p0021 A69-11080

Solid body automatic orientation, discussing data units for angular error and angular velocity

01 p0122 A69-11302

Expanded describing functions used in studying nonlinear control systems with multiplication points, considering systems with/without integral response

01 p0054 A69-11359

Two parameter dynamic system of fourth order optimization based on gradient method modified for discrete optimization

02 p0224 A69-11594

- Automatic devices to count bacterial colonies Petri dishes consisting of culture plate scanner and data processor
02 p1201 A69-11773
- Liquid fluidic amplifiers combined into controller for modulating coolant temperature to control flight suit temperature automatically
02 p0202 A69-11923
- Proportional navigation guidance systems for interceptor missiles optimized by adding biased term to guidance equation
02 p0278 A69-11973
- Pulsed ruby laser power supply incorporating facilities for variable output, automatic cutout for fully charged capacitors and automatic/manual triggering
02 p0256 A69-12095
- Mercury ion thrusters and facilities automatic controls durability testing, discussing vacuum chamber systems, unattended operation and control [AIAA PAPER 68-576]
02 p0229 A69-12385
- Pneumatic elements, discussing development from process control via modules systems to logic elements and fluid sensors
02 p0197 A69-12795
- Automated real time monoradar surveillance system based on azimuthal monotonicity of radar plots and flexible tracking strategies
03 p0383 A69-12872
- Soviet book on electronic countermeasures and intelligence covering jamming methods for automatic systems
03 p0385 A69-12927
- Linear pulse control systems monotone stabilization, estimating required number of controls
03 p0409 A69-12975
- Approximation of correlation or transfer function obtained through exponential polynomial to determine stochastic process spectral density
03 p0409 A69-12976
- Tracking breakdown probability during unsteady operation of nonlinear automatic control system analyzed by statistical linearization techniques and Fokker-Planck equation
03 p0409 A69-13070
- Statistical linearization coefficients for arbitrary nonlinearities in automatic control systems via techniques applying characteristic functions
03 p0409 A69-13071
- Undetected defects and false alarm probabilities for automatic test equipment, emphasizing quality and confidence limits
03 p0428 A69-13187
- Synthesis of statistically optimal self adaptive system for dynamic characteristics stabilization of automatic control system main loop
03 p0410 A69-13256
- Automatic checkout of space systems, discussing cost effectiveness tradeoffs, ground and onboard equipment utilization, vehicle design and mission success risk
03 p0411 A69-13392
- Topological principles of gate and contact self correcting circuits not using self correcting codes
03 p0410 A69-13421
- Automatic recording device for cosmic ray bursts utilizing information time delay to allow detailed initial period study
03 p0430 A69-13545
- Multivariable automatic control systems stability, discussing applicability of Nyquist theorem and alternate frequency criterion
04 p0581 A69-14601
- Stochastic problems in control - Conference, Ann Arbor, June 1968
04 p0581 A69-14693
- Motion control for nonlinear system with small initial perturbation
04 p0583 A69-15096
- Global and nonglobal stability of continuous systems with multiplicative feedback
04 p0583 A69-15112
- Computer controlled photometric telescope, describing star setting, photometric measurements and data processing
04 p0602 A69-15380
- Digital radar systems, discussing control computers, beam steering computers, signal processors, mode control, displays and chirp networks
05 p0718 A69-15748
- Time domain synthesis of multivariable automatic control with predetermined output signal shape, allowing for internal cross coupling effects
05 p0737 A69-15887
- Identification of nonlinear control systems, determining nonlinearities in differential equation by curve fit or iteration method [ASME PAPER 68-WA/AUT-19]
05 p0738 A69-16173
- Continuous parameter identification methods for parameter optimization in automatic control system analysis and synthesis, using modified steepest descent optimization
05 p0725 A69-16474
- Automatic phase control and transient processes in resonant amplifier in presence of phase discontinuities of input signal
05 p0721 A69-16533
- Book on electric elements and circuits for automatic control, discussing electric machines as control loop elements, stability criteria and synthesis, electric drives, etc
05 p0739 A69-16545
- Articles on automatic control systems stability, discussing relation between method of Lure and Popov criteria
05 p0740 A69-16667
- Simulation in design of automated flight test data system
05 p0743 A69-16759
- Integrated automatic data processing system/NEC-TAR/performance and operation
05 p0726 A69-16765
- Electronic system checkout in SAAB 37 Viggen, using computer controlled test equipment
05 p0726 A69-16767
- Manual and automatic spacecraft rendezvous and docking, discussing docking of Cosmos 186 and 188 in 1967 [UN PAPER 68-95764]
06 p1013 A69-17057
- Integrated circuit interconnection patterns computerized design, discussing automatic laser mask-making control
06 p0931 A69-17199
- Learning control system design, using a priori information in subgoal selection, control situation grid extensions and controller initialization
06 p0900 A69-17355
- Automatic compensation of unwanted signal level fluctuation in measuring setups including microwave generators and detectors
06 p0903 A69-17489
- Clearing and blocking control over frequently overadjusted automatic equipment in precision machine and device construction
06 p0931 A69-17692
- Automatic control textbook covering theoretical and practical principles of control engineering, analysis, design, servomechanisms and instrumentation
06 p0904 A69-17856
- Automatic air traffic control systems design, development and application to civil and military aviation
06 p0955 A69-17858
- Digital computer algorithm for automatic processing of IR weather data transmitted by Cosmos 122 and 144 meteorological satellites
06 p0929 A69-17981
- Flexible vehicle control, using cybernetic model for system design and response [AIAA PAPER 69-115]
06 p1018 A69-18088
- Automatic test set for measuring dopant concentration profiles in epitaxial films
07 p1130 A69-18245
- Transistor HF noise factor measurement by semiautomatic device with saturated diode comparison noise source heater current automatically controlled
07 p1090 A69-18292
- Automatic laser tracker system for close-up photographic coverage of rocket test [SMPTE PREPRINT 101-91]
07 p1116 A69-18949
- Aircraft separation standards, considering separate space for VTOL in automated high density airways system [AIAA PAPER 69-210]
07 p1178 A69-19579
- Computer aided automatic drawing of printed circuits, including design and manufacture of films for engraving
08 p1296 A69-19979
- Differential method with invariance principle used to analyze nonlinear invariant systems, determining physical realizability conditions
08 p1296 A69-20234
- Function generator for approximating function of many variables without recourse to multiplication, providing continuous functions representation
08 p1278 A69-20235
- Nonlinear controller design by dynamic programming method, discussing block diagram
08 p1296 A69-20236
- Automation and instrumentation - Conference, Milan, November 1968, Volume 1
08 p1296 A69-20301
- Fluidic power control switch for supersonic fluid amplifier, presenting performance data and possible industrial applications
08 p1256 A69-20304
- Stability region of second order nonlinear autonomous system determined by numerical computational method
08 p1297 A69-20358
- Identification method for cyclic plants operating in mode characterized by recurrence of initial conditions, giving numerical results and error assessment
08 p1298 A69-20421
- Cybernetic theory application to automatic spacecraft, discussing control problems in Mariner 4 and Surveyor 7 missions and attitude stabilization system
08 p1409 A69-20583
- Automatic transistor reliability testing system based on measured data and reliability research
08 p1294 A69-21119
- Nonlinear control theory for constant temperature hot-wire anemometers with large velocity fluctuations, noting second harmonic generation
09 p1493 A69-21421
- Optimum gathering of information for linear automatic control system with distributed parameters in presence of random input disturbance
09 p1471 A69-21437
- Stability of systems with periodic parameters, relation to automatic control systems and frequency characteristics role
09 p1473 A69-21855
- Probability approach to control system optimization problem for plant with incomplete information
09 p1473 A69-21856
- DC/AC collectorless step electric motors operation and commutation circuits
09 p1442 A69-21860
- Future launch vehicle programs for automated space missions, discussing higher launch velocities and economics [AIAA PAPER 68-447]
09 p1610 A69-21983
- Automatic level measuring system, consisting of decade control oscillator, digital level generator and selective level meter for 200Hz-2MHz range
09 p1501 A69-22577
- Nonlinear control plants model with pure delay effect identified by harmonic balance method
09 p1475 A69-22669
- Electrooculographic method to study eye movements control system for fixation on stationary point or following discretely or continuously moving target
09 p1447 A69-22675
- Stability and dissipativity conditions for nonlinear controlled systems subjected to parametric and continuously acting disturbances
09 p1476 A69-22717
- Automatic phase control effective bandwidth determined by asymptotic method, presenting computer calculated dependence on circuit parameters
10 p1653 A69-23105
- Rocket engine test facilities automation noting cost reduction and improved capabilities
10 p1671 A69-23258
- Test facility automation, discussing pretest preparations, test operations, data reduction and system planning
10 p1671 A69-23260
- Real time computer controlled telemetry system readiness testing and validation, describing automatic closed loop checkout methods and remote display controller
10 p1660 A69-23270
- Root sensitivity of characteristic equation of linear automatic control system to system parameter changes applied to aircraft angular stabilization
10 p1666 A69-23610
- Luna 9 automatic station flight control complex, detailing communication, orientation and stabilization systems operation after separation from acceleration module
10 p1792 A69-24197
- Flight control system for automatic interplanetary stations /AIS/, comparing Venera series orientation and correction system to Mariner systems
10 p1792 A69-24198
- Automatic ground traffic control of aircraft on airport taxiway without visual detection, noting induction

loop detection in surface traffic control system /STRACS/

11 p1913 A69-24267

Conjugated gradient components of optimization criterion in automatic control determined by applying sensitivity method to computation

11 p1857 A69-24367

Parametric damping of oscillations in second order automatic control systems, taking into account control function constraints

11 p1857 A69-24556

Periodic solutions of strongly nonlinear differential equations for behavior of automatic control systems with delayed argument, noting autonomous and nonautonomous systems

11 p1916 A69-24765

Steady state and dynamic characteristics of linear plant with constant lag element based on correlation function moments

11 p1859 A69-24965

Automatic support systems for advanced maintainability - IEEE Conference, St. Louis, November 1968

11 p1863 A69-25059

High speed automatic test sets and rapid repair procedures under adverse conditions for individuals of relatively low technical skill

11 p1851 A69-25063

Abbreviated Test Language for Avionics Systems /ATLAS/ as standard compiler input language for commercial airline automatic test equipment /ATE/

11 p1842 A69-25064

Universal test equipment compiler /UTEC/ built for use with languages designed to control automatic test equipment

11 p1842 A69-25066

Modular designed automatic test system consisting of central computer controlled system with multiplexed remote test stations for depot level maintenance

11 p1864 A69-25067

Single purpose, multipurpose and multistation automatic test systems for production and maintenance

11 p1864 A69-25068

Multipurpose test system analysis emphasizing support section containing self test elements, power monitoring and control, interconnection techniques and packaging

11 p1864 A69-25069

Compatibility effects of automatic test equipment on avionics hardware design

11 p1865 A69-25070

Hardware-software interface defined for design of computer controlled test system, discussing criteria for designing economical systems

11 p1842 A69-25071

Mathematical model for prediction of automatic test equipment utilization and determination of time for performance of intended test function

11 p1865 A69-25074

Optimized automated system for direct support maintenance of AH-56A subsystem equipment

11 p1865 A69-25075

Semiautomatic and automatic off-line module testing machines, comparing costs for different test populations

11 p1865 A69-25076

Real time/process computer interface with electric power systems, discussing compatibility, reliability, etc., problems in connection with management and engineering personnel

11 p2004 A69-25302

Extremal controlled plants identification by Chebyshev orthogonal polynomials, comparing results with regression analysis

11 p1861 A69-25713

Lock-on characteristics of automatic tracking systems evaluated for case of variable vector signal, calculating transient response

11 p1861 A69-25716

In-circuit diodes testing by semiautomatic low current regulated voltage test set

12 p2035 A69-25835

Canonical transformations of unsteady control system motion equations, simplifying control process study and controller simulation on analog computer

12 p2045 A69-25960

Feedback design for monotonically stabilized linear sampled data control system

12 p2045 A69-25961

Linear automatic control system floating response to harmonic effects achieved by coinciding open loop system transfer function poles with disturbance pattern poles

12 p2045 A69-25967

Computer controlled network analyzer performing automatic microwave measurements of passive and active networks, based on signal splitting and detecting

12 p2037 A69-26048

Multivariable control systems - Conference, Duesseldorf, October 1968, Volume 2

12 p2045 A69-26058

Synthesis of multivariable control systems at minimal integral square quality functional

12 p2046 A69-26061

Recursive estimation of noisy nonlinear multivariable systems in white noise by Kalman, second order nonlinear and iteration filters

12 p2046 A69-26062

Digital computer analysis of multivariable control system in frequency domain, using operational array technique programming method

12 p2046 A69-26064

Multivariable control systems - Conference, Duesseldorf, October 1968, Volume 1

12 p2046 A69-26069

Minimal representation in state variables for multivariable control system, discussing algorithms, identification methods and flow graph techniques

12 p2047 A69-26070

Group theory application to multidimensional symmetrical linear dynamic control systems optimization, considering natural vibrations of three material points

12 p2129 A69-26071

Matrix transfer functions factorization to obtain irreducible representations of multivariable control systems used for studying invariant linear multidimensional processes

12 p2047 A69-26072

Multivariable control system decoupling by appropriate choice of decoupling network structure and location in system

12 p2048 A69-26074

Canonical forms for observable and controllable linear time invariant systems by simultaneous transformations of system state and input and output vectors

12 p2048 A69-26075

Multivariable automatic control system consisting of similar local subsystems studied by transforming system equations into equivalent diagonal form

12 p2048 A69-26076

Nonlinear multivariable control systems synthesis, considering synthesis expressibility in known linear formulation

12 p2048 A69-26077

Uncontrollable modes effect on transient/steady behavior and limit cycles characteristics of nonlinear multivariable control system

12 p2048 A69-26078

Stability conditions for control systems consisting of linear multivariable stationary neutral plant and multivariable pulse frequency modulator, using Liapunov direct method

12 p2049 A69-26080

Self and forced oscillations in multivariable relay control system, considering relays with hysteresis and dead band and stability of periodic states

12 p2049 A69-26084

Multivariable control systems - Conference, Duesseldorf, October 1968, Supplement

12 p2051 A69-26092

Dynamic properties and reliability of linear time invariant multivariable control systems

12 p2051 A69-26093

Canonical representation of multivariable control system in state space using matrix of differential operators acting on vectors of input-output quantities

12 p2051 A69-26094

Steady modes of operation analysis for optimal single channel differential relay system with inertial controlled plant, assuming constant rate varying plant input

12 p2052 A69-26278

Operational Q factor of optimal differential relay system with inertial plant during tracking process, noting cadence pulses high repetition rate influence

12 p2052 A69-26279

Equivalent subsystems for designing multivariable linear automatic control system

12 p2052 A69-26280

Electro-optical scanning device and electro-optical matrix for mechanization of difference measurements in automatic photointerpretation of surveillance maps

12 p2090 A69-26302

Concorde SST equipment and systems noting microelectronics, automatic control, inertial navigation, head-up displays, linear instruments and hydraulic systems

12 p2091 A69-26360

Furnace for automatic high temperature cycling in controlled oxidizing environment

12 p2093 A69-26483

Approximate solution of boundary value problems for Fokker-Planck equation to determine probability of exceeding limits in nonlinear automatic control systems

12 p2054 A69-26653

Differential equations of probability theory for studying control systems and processes involving random variables

12 p2124 A69-27142

Nonlinear control systems error signals convergence to steady states in frequency domain, applying step or ramp functions to single feedback system

13 p2237 A69-27188

Nonlinear control systems analysis by successive approximations, separating dominant component in transfer function of linear part

13 p2237 A69-27252

Discrete automatic control systems determination by adjustable model, considering quasi-steady state conditions

13 p2238 A69-27253

Designs and capabilities of digital processing systems for automatic air traffic control radar information stressing future use of display for computerized control

13 p2295 A69-27332

Stabilization of nonlinear control systems steady motions for two pairs of imaginary roots

13 p2298 A69-27745

Statistical analysis of radiation temperature structure for automatic recognition of meteorological situations from actinometric satellite observations

13 p2293 A69-27842

Regional boundaries in control-parameter space constructed by computer algorithm, involving parameter vibration direction changes in parameter plane

13 p2225 A69-27967

Perturbations stabilization in electrically conducting fluid by distributed automatic control system, determining feedback operators via boundary value problem

13 p2311 A69-28105

Book on control theory covering automatic and remote position control, diagrams, transfer functions, operators, Laplace transform use with differential equations

13 p2238 A69-28345

Linear automatic control optimization by modified Newton method for determining real function zero value of real argument

13 p2239 A69-28436

Set of states for control system described by linear differential equation with constant coefficients and brought to zero phase coordinates

13 p2239 A69-28437

Automatic device for impedances and complex transmission factors measurement at meter and decimeter wavelengths, noting reflection factor

13 p2235 A69-28520

Multivariable PFM control system stability analysis using Liapunov function as Hermitian quadratic form

14 p2424 A69-28743

Root-mean-square error determination in automatic control system by digital computer for realizing control function, investigating harmonic and random input effects

14 p2424 A69-28744

Respiratory system control processes hypotheses experimental verification

14 p2408 A69-28745

Tracking breakdown probability during unsteady operation of nonlinear automatic control system analyzed by statistical linearization techniques and Fokker-Planck equation

14 p2424 A69-28752

Statistical linearization coefficients for arbitrary nonlinearities in automatic control systems via techniques applying characteristic functions

14 p2424 A69-28753

Linear control design to synthesize system with prescribed spectrum, deriving formula yielding control coefficients as function of eigenvalues

14 p2425 A69-28821

Automatic search-free optimization by sensitivity functions, deriving algorithms by Q factor and discrepancy extrapolation

14 p2425 A69-28823

Fluidic systems for automatic control of fuel supply to ramjet engine combustor, coolant rationing and distribution to engine structure and performance efficiency maintenance

14 p2508 A69-28875

Automatic control circuit zero drift compensation during external disturbance, using algorithm for com-

puter minimizing of losses caused by control and response inaccuracy
14 p2425 A69-29140

Input signal piecewise linear approximation for investigating response of dynamic automatic control systems to nonstandard input signal
14 p2426 A69-29143

Identification method for cyclic plants operating in mode characterized by recurrence of initial conditions, giving numerical results and error assessment
14 p2427 A69-29659

Signal phase measurement accuracy by discrete phase technique ensured by using wideband signals and automatic control of input SNR
15 p2574 A69-30130

Automatic recording inverted dilatometer employing fused quartz vertical pedestal and yoke type pushrod
15 p2607 A69-30153

Large telescope dome movements automatic control, considering central and eccentric telescope mounting
15 p2588 A69-30441

Automatic hybrid apparatus for solving linear equations, using Gauss-Seidel iterative method and stressing control arrangement, communication circuits, etc
15 p2572 A69-31089

Automatic multichannel system for turbine blades static tests, discussing operation principles, component sections, programmed tape and vibration modes
15 p2672 A69-31209

Fluidic digital position sensor consisting of fluidic monostable amplifier, analyzing operation by characteristics method
15 p2554 A69-31301

Nonlinear discrete on-off system phase plane system analysis by motion separation method
16 p2763 A69-31628

Automatic quantitative checkout equipment for telemetry circuit of Diamant satellite booster before launching
16 p2750 A69-31727

Automatic nonrepairable control elements reliability evaluated statistically with differentiable lifetime distribution function
16 p2764 A69-32199

Stability determination for nonlinear automatic control systems, describing mathematical methods based on Liapunov functions
16 p2804 A69-32242

Automatic meteorological radar data processing system incorporating MRL-1 radar and low speed digital computer
16 p2791 A69-32279

Automatic phase control and transient processes in resonant amplifier in presence of phase discontinuities of input signal
16 p2753 A69-32474

Stability and dissipativity conditions for nonlinear controlled systems subjected to parametric and continuously acting disturbances
16 p2765 A69-32550

Automated patching system design for analog and hybrid computers to reduce number of switches required
16 p2756 A69-32551

Equipment- and program-type methods for solving automatic digital control systems synthesis problems, evaluating efficiency based on accuracy
17 p2933 A69-33120

Pulsed control systems sensitivity relationship to discreteness period described via differential equations
17 p2994 A69-33143

Automatically controlled dynamic systems reliability estimation in terms of failure probability illustrated with autopilot-aircraft case
17 p3001 A69-33144

Brake system components automatic testing for pneumatic or hydraulic integrity essential to safe system performance
17 p2978 A69-33377

Digital computer for aircraft engine control covering in-flight health monitoring, automatic flight checkout, diagnostic failure routines, etc
17 p3022 A69-33603

Automatic device for logarithmic damping decrement measurement from vibrograms, showing structural arrangement and electrical circuitry
17 p2976 A69-33931

Automated analog scaling for in hybrid computer systems imposing magnitude and frequency constraints, using equations for amplifier input factors
18 p3105 A69-34617

Automatic ultrasonic instrument monitoring on-line welding conditions of RF longitudinally seamwelded tubes
18 p3136 A69-34778

Automated handling of mass properties data, describing data stored, central bank, report outputs, system logic, etc
[SAWE PAPER 811] 18 p3221 A69-34899

Automatic ultrasonic inspection device search head, servomechanism and electronic system used for detecting weld defects and cracks
18 p3137 A69-35111

Controlled vehicle disturbed trajectory multiple correction, considering constrained control or limited accessible coordinates for observations
18 p3174 A69-35316

Automatic control system transient response oscillatory and aperiodic components calculation using open loop system transfer function
18 p3112 A69-35458

Automatic ultrasonic method for determining dissolved gases content in liquid sample, using increasing acoustic oscillations amplitude for bubble development
19 p3308 A69-35822

Automatic systems for complex plant control, discussing synthesis of complex control systems
19 p3286 A69-35889

Automatic control systems for plants with distributed parameters, discussing stabilizing resonance shell with space-time dispersion of controlled processes
19 p3372 A69-35893

Feasibility of automatic stationkeeping for synchronous satellites by using solar sailing techniques and low thrust systems
[AAS PAPER 68-151] 19 p3429 A69-35950

Evaluation method for strapdown spacecraft guidance systems on automated interplanetary missions, using cost and system performance efficiency probability model
[AIAA PAPER 68-828] 19 p3370 A69-35953

Digital computer controlled antenna positioning system computing spacecraft tracking trajectory from given parameter input set
19 p3267 A69-35997

Precompression automatic wild point rejection from sampled telemetry data for data compressors evaluated by digital computer simulation
19 p3273 A69-36263

Eurocontrol Experimental Data Processor for automation in air traffic control, discussing system size configuration and environment
19 p3280 A69-36654

Observation space transformed from statistical synthesis of nonlinear closed systems to multiple control system subjected to statistically assigned perturbations
19 p3287 A69-36662

Newton gravitational constant determination from measured acceleration and known magnitude of masses, describing control system
20 p3537 A69-37140

Control system concept for axisymmetric supersonic inlet operation in mixed compression mode noting test results
[AIAA PAPER 68-581] 20 p3585 A69-37151

Automation application to rocketry, discussing process control in installations including control circuits and electronic direct digital control system
20 p3617 A69-37340

Spacecraft discrete automatic control system computerized simulation, discussing logic elements, applications to design, etc
20 p3502 A69-37393

Hydraulic power pack for automatically raising or lowering landing gear in small aircraft
20 p3467 A69-38183

Automatic planetary electrophotometer designed for earth atmosphere and lunar photometry, noting operational data
20 p3547 A69-38310

Contactless correcting devices based on magnetic moments for automatic control
21 p3685 A69-38453

Automatic electropolisher for copper disks
21 p3720 A69-38597

Gyroscopic platforms automatic stability relative to inertial reference system, considering functional equations and error computation
21 p3760 A69-38734

Admissible controls set for discontinuous stochastic automatic control systems, deriving mean optimal averaging of controls
21 p3770 A69-38855

Computer programming procedures in automatic control of hole boring processes for aircraft components
21 p3731 A69-38881

Automatic stationkeeping /geosynchronization/ for maintaining satellite in circular synchronous orbit at all geocentric longitudes for prolonged time with low fuel consumption
21 p3805 A69-39213

Automatic instrument for star detection and azimuth derivation, scanning nighttime zenith star field
[AIAA PAPER 69-861] 21 p3762 A69-39389

Orbital results for Automatic Orbit Control System of Lincoln Experimental Satellite LES 6, using pulsed plasma microthrusters and self contained orbit measurement and control methods
[AIAA PAPER 69-934] 21 p3824 A69-39428

Computer controlled automatic radar for survey through 360 degrees in azimuth and zero to 60 degrees in elevation
21 p3677 A69-39566

High temperature electronic tensile testing device utilizing SCR to study strain rate effect on metals properties
21 p3727 A69-39811

Scattered light photoelasticity dual observation method, describing automatic data collecting and interpreting system
22 p3945 A69-40079

Dynamic characteristics of temperature control systems using crystal oscillators determined by nonlinear automatic control theory
22 p3869 A69-40254

Self testing and repairing /STAR/ aerospace computer for automatic maintenance of unmanned interplanetary spacecraft
[AIAA PAPER 69-966] 22 p3906 A69-40347

Low visibility VSTOL instrument landing system and associated electronic structures, discussing instrument to visual flight transition
22 p3979 A69-40675

Carrier frequency monitoring amplifier with automatic bridge tuning for coupling to passive sensors including strain gages, inductive transmitters, etc
22 p3915 A69-40937

Automatic phase control system stability range determination in piecewise linear approximation and in presence of proportional integrating filter
22 p3918 A69-40956

Automation of single pass electric spark machining of high alloy steels and hard alloys, including anodic-mechanical profiling, cutting and drilling
23 p4168 A69-41308

Automated air photo identification of crop types, utilizing stereo height as discriminating variable
23 p4155 A69-41721

Digital computer systems for automating machine parts design main metal cutting operations, emphasizing optimal instrument usage, reliability, digital algorithm language and economics
23 p4169 A69-41952

Invariance theory in automatic dynamic systems
23 p4145 A69-42368

Combined automatic control systems stability having principal coordinates related by loading equation
23 p4145 A69-42370

Man-machine /semiautomatic/ control for optimal decision making, discussing automatic control disadvantages and limitations, multilevel system hierarchical structures, three level models, etc
23 p4112 A69-42443

Recursive estimation of noisy nonlinear multivariable systems in white noise by Kalman, second order nonlinear and iteration filters
23 p4146 A69-42447

Computer selection for given automatic control system, considering efficiency criterion and operational constraints satisfaction
24 p4285 A69-42952

Automatic system failure sequence statistical analysis, considering randomly time variable external effects
24 p4289 A69-42953

Automatic control - Conference, Boulder, August 1969
24 p4289 A69-43267

AUTOMATIC CONTROL VALVES
NT PRESSURE REGULATORS
NT RELIEF VALVES

Vortex valve characteristics, noting Reynolds number and geometry effects on flow and turndown ratio
02 p0195 A69-12079

Pneumatic stepping motor actuation system with pure fluid valves and signal processing and minimum

- number of moving mechanical parts for high g and temperature environments 02 p0196 A69-12086
- Fluidic vortex valve warm gas flow control for rocket application [AIAA PAPER 69-118] 06 p0872 A69-18147
- Hydraulic control valves for guidance of rockets by secondary liquid injection into nozzle skirt, discussing structure, single nozzle missile and mass gain 07 p1230 A69-19293
- Dynamic behavior of electrohydraulic servomechanisms over wide range of loads using differential equations of motion 08 p1256 A69-20718
- Gas servo design utilizing floating flapper disk switching valves and pulse-length modulated pressure waves to actuate on-off switch [AGARDOGRAPH-118] 08 p1257 A69-20950
- Flapper valves in high pressure hydraulic aircraft systems, with hydrodynamic equations and charts for design and performance characteristics 09 p1435 A69-21296
- Flow control valve for hydraulic motor speed regulation operated by remote pressure signal 11 p1827 A69-25646
- Servovalves with fluidic and electrical inputs compared for gas servovalves performance, considering use as sensors in closed-loop hydraulic circuit 19 p3255 A69-36711
- C-5A transport modular valve design for improved maintenance and high reliability due to manifold-cartridge arrangement 20 p3466 A69-38178
- Stability criteria for electrical interconnection in parallel operating valve controlled hydraulic servomotors applied to gimbaled system 24 p4256 A69-43310
- AUTOMATIC DATA PROCESSING**
U DATA PROCESSING
- AUTOMATIC FLIGHT CONTROL**
- Soviet book on inertial control of ballistic rockets covering rocket flight deviations measured by onboard sensors and computer 01 p0113 A69-10994
- Missile control during propulsion period, emphasizing vane deflection required for lateral wind compensation 01 p0163 A69-11297
- Test equipment for rapid automatic checkout and evaluation of automatic flight control systems on commercial and jet transport aircraft 05 p0742 A69-15883
- Self contained electrically servoed transducers for flight control, noting angle of attack transducer and force 05 p0766 A69-16750
- Airborne area navigational capability achieved by course line computer processing VOR information 07 p1178 A69-19763
- Automatic flight control system /AOOSY/ for German Azur satellite 09 p1459 A69-22563
- Secondary radar for air traffic control automation in France, discussing onboard equipment 10 p1723 A69-23705
- Multiple drone aircraft automatic control system, discussing preprogrammed mission path and controls of altitude, plan position and velocity 14 p2392 A69-29495
- Automatic navigation and sighting system for French specified Jaguar combat aircraft development 16 p2809 A69-31760
- Flight command computer for V/STOL aircraft, discussing design concepts, operating modes, displays, etc [AHS PAPER 313] 17 p3001 A69-33543
- Self monitored subsystems in automatic flight control of Concorde, describing operation mode and landing display 17 p3003 A69-34196
- Air traffic control/electronics automation developments and controllers responsibilities in Great Britain and Netherlands 18 p3168 A69-34805
- Air traffic control ground equipment developments including radio direction finders, surveillance radar, interconsole marking, etc 18 p3168 A69-34806
- Automatic flight control, discussing equipment, components and relationship between autopilot and navigation system 18 p3170 A69-34856
- TAPIR automatic pilot, describing components and automatic landing 19 p3371 A69-36704
- Flight control system providing variable stability in pitch axis of NF-8D Crusader, discussing flight evaluation of power approach short period configurations [AIAA PAPER 69-896] 21 p3648 A69-39420
- Linear flight control system synthesis by using optimal control theory associated with quadratic performance index 22 p3864 A69-40588
- Triple redundant actuator for fly-by-wire control system, noting electrohydraulic servomechanisms in side-by-side arrangement 22 p3870 A69-41242
- Digital computers effect on aircraft automatic power unit controls, discussing safety, reliability, self monitoring and redundant computer systems 24 p4253 A69-43113
- AUTOMATIC FREQUENCY CONTROL**
- Millimeter wave oscillator AFC system utilizing inherent stability of molecular rotational transition applied to reflex klystron stabilization 01 p0044 A69-10628
- Reduction of ATR switch pulse peak in automatic frequency control system of radar station 01 p0047 A69-10784
- Stabilization system for klystron automatic frequency control, noting use in voice communication microwave generators and resonance spectroscopy 02 p0216 A69-12096
- Automatic device for charging storage capacitors in plasma devices provides voltage and operational frequency control 04 p0580 A69-14493
- Nonlinear phase locked automatic frequency control system dynamics, noting asymptotic stability of equilibrium state in whole 04 p0559 A69-15137
- Phase locked automatic frequency control system with additional frequency control loop and nonlinear filter in phase control loop, analyzing dynamics 04 p0559 A69-15140
- Balanced diode shunt bridges with electronically tunable carrier selection high-Q N-path filter from 0 to 200 kHz, using single integrated module 07 p1089 A69-18249
- Tuning design optimization of single circuit LF automatic control systems, using transfer functions and phase amplitude graphs 08 p1297 A69-20418
- Reduction of ATR switch pulse peak in automatic frequency control system of radar station 10 p1661 A69-23113
- Noise stability of FM receiver with automatic control of IF amplifier resonance frequency in presence of weak noise 15 p2564 A69-30144
- Automatic frequency control of laser and regenerative amplifier, considering frequency stability 15 p2633 A69-30238
- Automatic tuning of superconducting cavity resonant frequency using optical feedback, discussing phase error processing and frequency deviation 17 p2937 A69-33781
- Lock-on band of phase locked AFC system calculated by asymptotic method, considering frequency integrating filters with nonlinear capacitances 19 p3277 A69-36569
- Frequency stabilization in He-Ne three mode laser by stabilizing LF oscillations via automatic adjustment of laser resonator length 21 p3738 A69-39078
- Automatic frequency control circuit for stabilizing beat emissions of coupled multifrequency gas lasers 21 p3738 A69-39079
- Balloon-borne transmitter consisting of oscillator, driver and final output and connectable automatic frequency control circuit 21 p3682 A69-39251
- Frequency locking of HCN laser transition at 890 GHz to harmonic of crystal controlled oscillator 22 p3963 A69-40567
- AUTOMATIC GAIN CONTROL**
- Optimum gain control for diversity receivers used for radar and digital data transmission through fading media 03 p0410 A69-13833
- SNR analysis at amplifier output with AGC, noting increase with signal strength 05 p0729 A69-16085
- Optimized gain control configuration using field effect transistor with broadband control to maintain high signal to noise ratio with low distortion 07 p1115 A69-18889
- Channel output SNR optimization in AM/FM telemetry system by using automatic gain control, discussing AGC time response and general characteristics 09 p1454 A69-21799
- Current driven AGC effectiveness in selective amplifiers, including conductance variation effect on pass-band instability and frequency response 12 p2043 A69-26887
- Electro-optical automatic gain control system to reduce atmospheric turbulence produced fluctuations in received optical signal strength 14 p2459 A69-29491
- Baseband automatic gain control in AM/FM systems, determining time constant and steady state and tracking error 19 p3274 A69-36276
- AUTOMATIC LANDING CONTROL**
- Laser gyro in future inertial navigation systems for Category 1 landing without position updating 03 p0463 A69-13210
- Automatic all-weather landing system for scheduled civil passenger aircraft, discussing safety, display devices, Category 2 and 3 conditions 03 p0465 A69-13697
- Airline safety programs focused on developing reliable automatic landing system, realistic pilot training and airborne monitoring/recording system 06 p1041 A69-16840
- Soviet lunar probe Zond 6 achievements in controlled Earth landing and lunar surface photography 13 p2355 A69-27342
- Trident category 3 automatic landing, discussing triplex pitch and roll control, duplex rudder, autothrottle and azimuth paravision display 13 p2296 A69-27976
- Boeing 747 problems including noise and automatic landings in CAT-II conditions 16 p2734 A69-31631
- L-1011 fail operative automatic landing system design, operational characteristics and test programs [SAE PAPER 690407] 23 p4185 A69-41657
- Localizer acquisition system quasi-optimization technique based on time optimal control theory, with application to SST ILS problem 24 p4348 A69-43312
- AUTOMATIC PATTERN RECOGNITION**
U PATTERN RECOGNITION
- AUTOMATIC PICTURE TRANSMISSION**
- Cloud pictures from weather satellites reception according to automatic picture transmission /APT/ system, discussing design and field strength measurements [UN PAPER 68-95451] 01 p0108 A69-10458
- Satellite automatic picture transmission application to meteorological and hydrological problems including wind estimates, atmospheric stability and cloud distributions [UN PAPER 68-95300] 01 p0108 A69-10462
- Automatic picture transmission station equipment including antenna, cavity filters, tape recorder, oscilloscope, facsimile system and kincscope [UN PAPER 68-95450] 01 p0054 A69-10522
- Computer programming of satellite orbit tracking angles for automatic picture transmission receiving stations 04 p0558 A69-14917
- French space meteorology, discussing reception of automatic picture transmission from Tiro, Essa and Nimbus satellites [UN PAPER 68-95838] 06 p0950 A69-17081
- Satellite picture signal reception from ESSA, Nimbus and ATS to ascertain instrument requirements 06 p0888 A69-17651
- Budapest University satellite radio observation APT station design, equipment and methods 12 p2059 A69-26449
- Israel research on space data for meteorological purposes, describing automatic picture transmission data and errors in surface temperature determination by satellite radiometry 15 p2650 A69-31422
- Antenna array construction for reception of weather satellite transmissions, noting automatic picture transmission systems /APT/ 17 p2946 A69-33767
- Daily European weather surveys based on meteorological satellite pictures transmitted during third quarter 1967 17 p3000 A69-33769

- Computer program for satellite APT geographical grid production, discussing latitude-longitude intersections transformation to Cartesian coordinates
21 p3718 A69-39749
- Gridding technique for satellite APT pictures taken with camera axis perpendicular to earth surface
24 p4314 A69-42992
- AUTOMATIC PILOTS**
- Operational reliability of manual and automatic flight control systems and components and current safety standards
08 p1255 A69-20720
- Motion equations for dynamics of aircraft control surface controlled by autopilot with rigid feedback
16 p2809 A69-32134
- Automatically controlled dynamic systems reliability estimation in terms of failure probability illustrated with autopilot-aircraft case
17 p3001 A69-33144
- Artificial horizon indicator design modifications to facilitate maintaining horizontal aircraft position, discussing automatic pilot advantages in turbulence and flight simulators
17 p2903 A69-34214
- Automatic flight control, discussing equipment, components and relationship between autopilot and navigation system
18 p3170 A69-34856
- Autopilot for flight simulation of stability and control of pilot-airframe combined performance on reentry missions, using airborne analog computer for vehicle response
18 p3208 A69-35000
- TAPIR automatic pilot, describing components and automatic landing
19 p3371 A69-36704
- C-5 aircraft stability augmentation and autopilot development with consideration for unusual design required by takeoff weight, inertia and low approach speed
20 p3461 A69-36927
- Digital autopilots for Apollo CSM and CSM/LM vehicles thrust vector control, describing modifications of onboard computers and programs
[AIAA PAPER 69-847] 21 p3762 A69-39377
- Computerized optimization of flexible booster autopilot design, considering criteria for stability margins, closed loop roots and structural load relief
[AIAA PAPER 69-875] 21 p3823 A69-39401
- Head-Up Display /HUD/ incorporated with autopilot for human participation in flight control for all-weather operation
23 p4109 A69-41871
- AUTOMATIC ROCKET IMPACT PREDICTORS**
- U COMPUTERIZED SIMULATION
U IMPACT PREDICTION
- AUTOMATION**
- Automatic equipment for sampling and preparing gases by dual column gas chromatography for subsequent mass spectral analysis of carbon isotopes during methane metabolism
02 p0205 A69-12603
- Automatic test equipment applicability to testing problems created by increasing complexity of communications equipment
03 p0410 A69-13189
- Automatic support systems development and capabilities with recommendations for future R and D developments
03 p0411 A69-13190
- Automatic preventive maintenance program for hybrid computer system by checking individual units
04 p0568 A69-15359
- Air traffic control /ATC/ automation, discussing display, data acquisition, automated radar terminal systems /ARTS/, etc
05 p0790 A69-16719
- Book on optimal control of systems governed by partial differential equations, noting systems of automation, existence theorems and numerical analysis
09 p1471 A69-21580
- Test facility automation, discussing pretest preparations, test operations, data reduction and system planning
10 p1671 A69-23260
- Directional properties of electro-optical goniometric system based on known design parameters
14 p2420 A69-29332
- Automation application to rocketry, discussing process control in installations including control circuits and electronic direct digital control system
20 p3617 A69-37340

AUTOMOBILE ACCIDENTS

- Occupant restraint systems for automobiles, aircraft and manned space vehicles, discussing cost, practicability, ease of use, acceptability and possible improvements
03 p0380 A69-13459
- Alcohol and drug intake effects on drivers control of motor vehicles, describing postrotatory nystagmus test for toxicity measurement
21 p3652 A69-38791

AUTOMOBILE ENGINES

- Transistorized tachometer for rotational speed measurement and overspeed protection of automotive internal combustion engines
12 p2090 A69-26240

AUTOMOBILES**NT AMBULANCES**

- Telemetric control of urban transportation systems and law enforcement, considering automobiles as prime vehicle
19 p3272 A69-36256
- Intercity air transportation compared with automobile and train travel, attributing air travel dead time to ground route and airspace congestion
24 p4416 A69-42561
- Linear viscoelastic model parameters optimization for designing automobile lap seat belts, assuming abrupt impact stop
[ASME PAPER 69-APMW-25] 24 p4275 A69-43094

AUTONOMIC NERVOUS SYSTEM**NT SYMPATHETIC NERVOUS SYSTEM**

- Pharmacological tools in autonomic nervous system research, discussing norepinephrine biosynthesis, storage, release and inactivation in mammals
02 p0200 A69-12722
- Autonomic nervous system in control of heart rate in acceleratively stressed monkeys, discussing sympathetic, parasympathetic and bradycardiac influence
06 p0875 A69-17844
- Neurological changes in men due to hypokinesia, analyzing tremor data, EEG recordings and stabilography fluctuations
10 p1647 A69-23585
- Autonomic nervous system role in controlling body functions after rapid decompression, increasing tolerance to pressure gradients by physical training
13 p2212 A69-28622

AUTONOMY

- Autonomous system steady motion with rotating phase and deviating argument solved by successive approximation over infinite time interval
18 p3175 A69-35323

AUTOPILOTS**U AUTOMATIC PILOTS****AUTORADIOGRAPHY**

- Radioactivity induced in solid materials for components microautoradiography and radiograph information quantitative evaluation
13 p2297 A69-28157
- Electron microautoradiograph preparation determining trace element amount and distribution by utilizing radioactive isotopes and high resolution of electron micrographs
13 p2263 A69-28168
- Autoradiographic methods for diffusion and phase transformation in Fe-Cr alloys by application of photographic emulsion with tracer element on metal surface
20 p3561 A69-37416
- Autoradiographic technique for spatial distribution in solid of B at ppm concentration, using electron microscope
20 p3567 A69-38263

AUTOROTATION

- Future development in rotorcraft, discussing augyros, helicopters, tilt rotor and wing aircraft
05 p0702 A69-16392
- Autrotation characteristics of various shapes in subsonic and hypersonic flows for mechanics of free flight reentry to earth impact
[AIAA PAPER 69-132] 06 p0863 A69-18062
- Increasing rotation of axisymmetric body about velocity vector ascribed to asymmetry in mass distribution, defining conditions for occurrence
09 p1431 A69-22077
- Increasing rotation of axisymmetric body about velocity vector ascribed to asymmetry in mass distribution, defining conditions for occurrence
23 p4060 A69-41968

AUTOTROPHS**NT HYDROGENOMONAS**

- Ribulose diphosphate carboxylase and phosphoribulokinase activity in chemosynthetic autotrophs *Thiobacillus thioautotrophicus* and *Thiobacillus neapolitanus*, noting sedimentation and gel filtration characteristics
02 p0199 A69-11866

AUXILIARY EQUIPMENT [COMPUTERS]**U PLOTTERS****AUXILIARY POWER SOURCES****NT CHEMICAL AUXILIARY POWER UNITS****NT NUCLEAR AUXILIARY POWER UNITS****NT SNAP 8****NT SNAP 10A****NT SNAP 13****NT SNAP 21****NT SNAP 27****NT SOLAR AUXILIARY POWER UNITS****NT SPACE POWER UNIT REACTORS**

- Pneumatics for aircraft systems integration, proposing engine bleed air use for high power short term duties, heat recovery from cabin air conditioning, etc
01 p0012 A69-10594

- Solid propellant cartridges, discussing uses for starting large engines and providing auxiliary power in missiles or actuating devices
02 p0302 A69-11524

- Onboard electric power systems of transport aircraft, analyzing constant frequency systems for supersonic aircraft
02 p0196 A69-12166

- Electric space propulsion systems and auxiliary power sources development in West Germany, noting solar cells, isotope generators and reactors with conversion systems
03 p0496 A69-13996

- Onboard gas turbine auxiliary power units for executive jet transport aircraft
[SAE PAPER 690332] 11 p1824 A69-24501

- Out-of-core thermionic systems with heat pipes usable in space applications, meeting advanced auxiliary power and nuclear propulsion requirements
14 p2480 A69-29188

- Business aircraft electrical power sources, discussing electromechanical constant speed drive /EMCSD/ and comparison with DC/inverter and hydraulic CSD
[SAE PAPER 690346] 15 p2552 A69-30091

- Storage batteries for satellite electrical power sources emphasizing operation in overcharged state
16 p2735 A69-31729

- Electrochemical generators for space applications - Conference, Paris, December 1967
16 p2736 A69-32405

- Electrochemical generators space applications, discussing nuclear, solar and rechargeable cells
16 p2737 A69-32407

- Civil transport aircraft power plant and auxiliary systems as sources of delays, presenting critical path analysis
17 p2898 A69-33213

- Aircraft auxiliary power system influence on power plant installation and aerodynamic design
17 p3017 A69-33216

- Aircraft auxiliary power systems, discussing weight and power requirements, component design, driving methods and influence on power plant design
17 p3018 A69-33217

- Aircraft secondary power sources reliability dependence on electric loads, charge control and maintenance, discussing hermetically sealed batteries features
17 p2905 A69-34113

- Secondary power sources for space applications in solar arrays, static and dynamic thermal systems, high power batteries and fuel cells, discussing NASA machinery procurement
19 p3255 A69-36323

AVAILABILITY

- Steady state availability of system with limited repairable spares for online units, considering statistical dependence among similar units
18 p3144 A69-34493

- Availability measure defined in terms of maintenance demand rate and mean downtime for cost prediction involving various parameters
19 p3327 A69-36036

AVALANCHE DIODES

- Transient nonlinear mode partially responsible for anomalous operation of IMPATT diodes below transit time cut-off frequency
01 p0043 A69-10559

- Zener diode function generators used in analog computers for solution of complex problems involving nonlinear relationship
02 p0214 A69-11595

Transit time and anomalous modes of oscillation in high pulsed power punch-through Si avalanche diode microwave oscillators

02 p0216 A69-12145

Miniaturized X band IMPATT microstrip power sources based on Si avalanche transit time diodes integrated with microstrip oscillator circuits

02 p0216 A69-12146

Amplitude noise spectra of X band microwave oscillators with Si avalanche diodes, noting various contributions and dependence on circuit and operating parameters

02 p0221 A69-12456

Microwave energy generation with solid state equipment, noting Gunn effect diodes, avalanche diodes and limited space charge accumulation /LSA/ devices

03 p0402 A69-12971

Temperature and current distribution in avalanching silicon p-n junctions

03 p0487 A69-13637

Multiplication effects on noise in Si avalanche diodes, noting high resolution apparatus for measurement of spatial variations

04 p0573 A69-14332

Single punch through silicon avalanche diode structure and two distinct modes of oscillation making possible pulsed generation of microwaves

04 p0573 A69-14334

High efficiency microwave oscillations in Si p-n and p-n-n positive avalanche diodes under pulsed conditions

04 p0580 A69-15491

Large signal model for analysis of RF output and efficiency of IMPATT diode oscillator, noting frequency tuning

05 p0733 A69-16555

P-n planar avalanche photodiode without guard ring noting electrical properties, uniform multiplication and fabrication

05 p0733 A69-16559

Si IMPATT diode oscillator and amplifier for CW operation at 50 GHz noting fabrication, performance and phase locking properties

05 p0733 A69-16560

Nearly abrupt X band Si avalanche IMPATT diodes irradiated by fast neutrons, noting effects on DC and microwave characteristics

06 p0976 A69-16874

Large signal impedance measurements and dynamic characteristics explain Si avalanche diodes efficiency degradation at higher frequencies

06 p0893 A69-16938

Noise generation mechanism of Read microwave avalanche diode under large signal conditions

06 p0895 A69-17472

Avalanche diode oscillators efficiency of continuous wave operation in transit time mode and high current multiresonant modes

07 p1098 A69-18456

High efficiency punch-through avalanche transit time diode for generating microwaves over three octaves

07 p1098 A69-18457

Large signal avalanche diode oscillators parameter effect on operating characteristics at any transit angle

07 p1098 A69-18458

Frequency variation during oscillation pulse in avalanche transit time diodes, discussing related thermally dependent diode voltage rise

07 p1098 A69-18459

IMPATT diode microwave oscillator, discussing large signal characterization and model for efficiency dependence on load conductance and admittance plane characteristics

07 p1101 A69-18650

Relaxation oscillations in Si p-i-n junction diode reverse-biased into avalanche calculated by computer program

07 p1101 A69-18651

Epitaxial GaAs IMPATT diodes for generating CW X band power, noting high efficiencies and low noise characteristics

07 p1102 A69-18660

Frequency modulation of CW mm-wave IMPATT diode oscillator with wide band tunability and related harmonic generation effects

07 p1106 A69-19146

Microwave oscillator design employing avalanche transit time diodes

07 p1107 A69-19155

Noise generator design employing diffused Ge avalanche transit time diode

07 p1107 A69-19156

Microwave amplification using silicon diodes in avalanche resonance pumped modes

08 p1279 A69-19909

High field domains in Gunn effect diode in transit time mode of operation probed with stroboscopic electron beam in scanning electron microscope

08 p1283 A69-20162

Epitaxially grown guard rings for GaAs p-n junction and Schottky barrier avalanche diodes

08 p1284 A69-20368

Passivated metal semiconductor IMPATT diode for microwave CW oscillation

08 p1286 A69-20862

Cascaded avalanche diodes in negative resistance amplifying mode for increased output power and extended dynamic range

09 p1462 A69-21408

Large signal analysis of IMPATT oscillators with carrier velocity saturation, discussing two frequency mode of operation

09 p1463 A69-21846

Anomalous mode avalanche diodes for pulse power generation noting output, efficiency, mode of operation, microwave oscillations and IMPATT diodes

09 p1466 A69-22455

Thermal effects on modulation sensitivity and inherent AM percentage as functions of modulation frequency in IMPATT oscillators

09 p1468 A69-22588

Pulse generator switch consisting of avalanche transistors in series, describing voltage production and transmission, trigger pulse jitter and pulse amplitude

09 p1468 A69-22589

Microwave avalanche diode oscillators performance estimates, discussing operation modes and transit time

10 p1665 A69-23873

Frequency retuning characteristics of oscillator employing avalanche transit-time diode with complementary varactor subject to current or voltage variation

11 p1844 A69-24449

Si IMPATT diode current and voltage waveforms of oscillation, noting small signal theory inapplicability

12 p2036 A69-25914

High current density filaments formation in silicon p-n-n avalanche diodes caused by incremental negative resistance in static current-voltage characteristics

12 p2036 A69-25916

Avalanche Schottky barrier photodiodes fabricated by plating GaAs with thin Pt layer and forming proton radiation guard ring, discussing gain bandwidth and SNR

13 p2226 A69-27195

High efficiency LF oscillations in avalanche diodes, noting evidence for parametric generation and condition for high efficiency

13 p2227 A69-27239

Electrical breakdown mechanism in semiconductors determined by measuring Zener current in avalanche breakdown

13 p2317 A69-27660

Ultrahigh speed microwave diode switch used as transmitter-modulator in PCM systems, utilizing varactor diode avalanche breakdown

13 p2229 A69-27671

Avalanche diodes as high power pulsed microwave sources, noting power yields and efficiencies

14 p2418 A69-28890

Noise reduction techniques using injection phase locking and high-Q cavities for HF oscillator high order multiplier and avalanche diode oscillator microwave sources

14 p2420 A69-29458

Avalanche diode oscillators stacked in series for combined power output

14 p2421 A69-29543

Neutron irradiation effect on efficiency and other parameters of IMPATT diode

14 p2423 A69-29761

Waveguide below cut-off resonators for active microwave circuits, describing experiments with avalanche and Gunn diodes

15 p2577 A69-30613

Computer model for avalanche transit time diode oscillator with single and double resonant circuit

15 p2577 A69-30615

X band avalanche diode oscillator operated as super-regenerative amplifier, noting frequency response characteristics ascribed to diode susceptance modulation

16 p2757 A69-31585

Zinc diffused GaAs avalanche diode high CW power and efficiency in normal mode

16 p2760 A69-32015

Soviet book on avalanche transit time diodes and applications in microwave technology, describing p-n junction model, negative resistance, dynamic characteristics, synchronized oscillators, etc

16 p2761 A69-32109

Si planar IMPATT diodes anomalous mode continuous wave UHF oscillations, noting DC density and DC/RF power conversion efficiency

17 p2934 A69-32846

GaAs IMPATT diodes breakdown voltage, impurity density and outer layer thickness compared with Si IMPATT diodes

20 p3504 A69-36914

AVALANCHES

NT ELECTRON AVALANCHE

Charge multiplication in crystals, analyzing ionization rate, avalanche breakdown in p-n junctions, pair production and impact of impurities

04 p0641 A69-14503

AVERAGE

NT MEAN

Time averaged products and squares of fluid turbulence signals at LF, using Hall effect multiplier device and integrating voltmeter

04 p0601 A69-15116

Analog-hybrid computer configurations for average and rms values of signals with respect to time

06 p0891 A69-17220

Averaging procedures to represent highly time variable actual hydrometeorological fields by less variable equivalent fields

06 p0952 A69-17989

Time average holography for analysis of vibrations, overcoming fringe peak decrease with large amplitude and loss of phase information

09 p1495 A69-21749

Accuracy improvement of method of averages applied to equations of small motions and disturbances of two rotor gyrocompass on ship performing circular maneuvers

18 p3139 A69-35378

Averaging methods applied to nonlinear equations in mechanics, discussing solution convergence estimation

20 p3576 A69-37440

Bogoliubov method of partial averaging for nonlinear integral equations, noting application to automatic gain control theory

23 p4181 A69-41731

AVIATION

U AERONAUTICS

AVIATORS

U AIRCRAFT PILOTS

AVIONICS

Avionics in forest resource inventories management, noting design of radar altimeter for low level aerial photography

01 p0080 A69-10352

Avionics technology and systems for future SST aircraft noting improved air traffic control systems

02 p0279 A69-12364

Avionics, discussing use of electronics in control of aerospace vehicles

03 p0431 A69-14085

NASA civil aviation electronics research program, discussing feasibility of V/STOL aircraft all-weather operations

05 p0850 A69-16718

F-111 interdiction capability, discussing avionics subsystems for low level penetration flying and Vietnam performance

07 p1052 A69-18550

Avionic systems development, discussing criteria for realization of operational requirement and engineering product satisfying requirement

[AGARDOGRAPH-114] 08 p1317 A69-20982

Microelectronic equipment for aerospace application and integrated circuit production in UK

[AGARDOGRAPH-114] 08 p1292 A69-20992

Airborne digital computers for optimization of aircraft control and monitoring functions, discussing avionics and circuit technology

08 p1349 A69-21194

Deterministic model for cost effectiveness of avionics support programs based on subsystems support ability, test philosophy and test equipment design and manufacture

[AIAA PAPER 69-305] 09 p1478 A69-22377

Large scale integration applications to avionics including self testing, self repair, cost factors, etc

11 p1845 A69-24530

Computer controlled flight line tester performing automatic real time testing of aircraft avionics systems on flight line or hanger

11 p1864 A69-25060

Computer controlled testing of commercial aircraft avionic systems for automatic, semiautomatic and manual operation to perform repair and calibration tasks
11 p1864 A69-25061

Compatibility effects of automatic test equipment on avionic hardware design
11 p1865 A69-25070

Airborne computer controlled data acquisition system for real time fault detection and isolation in avionics
11 p1843 A69-25082

Automatic system self test technique known as central integrated test subsystem /CITS/ for logically testing avionics systems
11 p1866 A69-25083

Comparative evaluation of avionic installations in design stage, detailing parameters for civil aeronautical use
11 p1887 A69-25212

Monograph on physicochemical principles of takeoff monitoring systems for large aircraft covering taxiing, safety control systems design, analog simulation, etc
12 p2128 A69-26119

A-New avionics system for carrier based VSX aircraft used in U.S. Navy aerial submarine hunting, discussing TV, lasers, sonobuoy system, radar, etc
14 p2392 A69-29430

Solid state programmable avionics converter for signal processing, information conversion and aircraft control
14 p2405 A69-29687

Markov chain applications to avionics weapons system reliability specifications starting with mission profile, failure rates, success probabilities, etc
15 p2581 A69-31136

Avionics clean room workshops, discussing turbulent and laminar flow rooms and contamination monitoring of controlled environment facility
16 p2767 A69-32369

High intensity light adaptation effects on visibility of raster scan, TV type and avionic displays for symbol luminance needs
16 p2746 A69-32788

AH-56A Cheyenne integrated avionics, armament and fire control system for precise weapons delivery and navigation
[AHS PAPER 312] 17 p2903 A69-33542

Avionics systems with integration and federation applied to integrated light attack avionics system /ILAAS/ design to provide navigation, weapon delivery and flight control
17 p2976 A69-34057

Electronic computers for avionics system design in terms of technology, performance and cost, discussing reliability prediction and failure rate data
17 p2976 A69-34058

TC-2 general purpose digital avionics computer in A-7D/E avionics system performing tasks in weapon delivery, navigation and guidance, display updating, self testing, etc
17 p2933 A69-34059

Tactical fighter aircraft avionics technical risk and integration, considering initial and operating costs, combat sequence and weapon control
17 p2902 A69-34128

Avionic subsystems warranty costs estimates, considering reliability prediction and hardware recycling
18 p3232 A69-34506

Avionics of Naval E-2C airborne sentry and command and control system, discussing digital computer, search radar, etc
18 p3108 A69-34811

Collection of articles on avionics navigation systems covering navigation equations, airborne digital and analog computers, radio, Doppler and inertial navigation, etc
18 p3168 A69-34843

Airborne digital computers techniques in avionics stressing memory design, packaging, reliability and maintainability
18 p3106 A69-34846

Aerospace technology application to commercial avionic system for cost effectiveness in functions expansion, phase-over, installation, maintenance and operation, discussing added information functions
18 p3108 A69-35069

Aircraft avionics subsystems and weapon system functional integration reflecting aircraft mission, operational, natural and enemy environments
18 p3109 A69-35140

Lockheed C-5 Galaxy aircraft avionics systems with Doppler inertial navigation equipment to operate with precision without ground based aids
18 p3104 A69-35465

Avionics and electronic countermeasures equipment design, development, installation and application problems for high performance military aircraft to meet hostile electronic environment
[AIAA PAPER 69-822] 19 p3243 A69-35599

Time/frequency technology using time-ordered reporting digital data for air traffic control to avoid airborne collision
[AIAA PAPER 69-795] 19 p3367 A69-35635

Closed-loop system for test, failure analysis and corrective action in avionics reliability growth, showing cost effectiveness relationship to test program
19 p3282 A69-35784

Avionics system analysis, engineering, design, fabrication and testing problems
20 p3545 A69-37929

Northrop F-5-21 fighter design, avionics, performance and operational existence
21 p3646 A69-38732

Environmentally scaled connector for avionics packaging with die-cast Al alloy shell meeting specification ARINC 404 requirements
22 p3910 A69-39946

Automated design system producing wire format data for cabling avionics subsystems of light attack aircraft
[AIAA PAPER 69-976] 22 p3912 A69-40356

Aircraft digital control hardware and applications including airborne computer proper, distributed systems, loop control, system integrity, etc
[RAES PAPER 4] 22 p3908 A69-40485

Systems approach to avionics optimization, discussing instruments, devices, display and automation techniques
[RAES PAPER 6] 22 p3946 A69-40487

Heat pipes design for avionic applications, using wicking bench tests
23 p4075 A69-42305

Flammability control for aerospace avionics systems safety, considering risk, test method, acceptability criteria, confidence level and ignition source
24 p4336 A69-43422

F-111D computer complex to provide selective functional redundancy and flexibility to accommodate mechanization changes
[AIAA PAPER 68-837] 24 p4285 A69-43719

AVOIDANCE
U COLLISION AVOIDANCE

AXES [COORDINATES]
U COORDINATES

AXES [REFERENCE LINES]
Radome axis error due to phase /dielectrics/ and metallic obstacles
07 p1112 A69-19542

AXES OF ROTATION
Multibody dual spin spacecraft spin axis motion with active internal devices, using digital simulation
02 p0332 A69-11739

Rotation deviation of rigid body around axis, discussing three point body measurement and applicability
04 p0599 A69-15017

Selenographic and celestial selenocentric coordinate systems, noting precession and nutation of lunar rotation axis
04 p0662 A69-15250

Self balancing single degree of freedom free fall space environment simulator, discussing coincidence of mass and rotation centers
04 p0586 A69-15468

Ellipticity of trajectory of free motions of pole of revolution of earth, using harmonic analysis of motion amplitudes and phases
06 p0919 A69-17536

Azimuthal drift of rotor axis of directional gyroscope mounted on sloping base, showing vertical component responsibility via truncated equations of motion
09 p1502 A69-22702

Gyrator center axial displacements due to axial load, noting equal load distribution between bearings with resilient cover plates
09 p1502 A69-22703

Optical sensing devices for angle measurement between celestial body and satellite axes
12 p2078 A69-25871

Mass distribution for bodies fallen on planets during formation estimated from present inclination of planetary axes of rotation, using limit theorems of probability theory
13 p2345 A69-27652

Dynamic balance for rotating aerospace vehicles, discussing error in principal axis location between rotor on machine and free body in space
[SAWE PAPER 740] 18 p3137 A69-34887

AXIAL COMPRESSION LOADS

Earth polar wanderings attributed to rotation axis angular displacements generated by density redistribution on geologic time scale
20 p3535 A69-38192

Ariel 3 satellite attitude determination, using solar aspect sensors to define conical surface containing spin axis
21 p3820 A69-39260

Ariel 3 satellite spin axis direction determination by optical means from analyzing sunlight glints reflected from surfaces
21 p3820 A69-39261

Three axis motion simulator for in-orbit spacecraft attitude control evaluation using earth, sun and star sensor references
[AIAA PAPER 69-1029] 22 p3924 A69-40398

Multifunction lightweight antenna system package for spin stabilized near synchronous satellite having axis normal to orbital plane
22 p3913 A69-40694

Astatic gyro motion with horizontal rotor axis, defining suspension error with allowance for external force moments
24 p4317 A69-43707

AXIAL COMPRESSION LOADS
Variable thickness circular annular disk bending in centrifugal force field, establishing dependence between angular velocity and axial pressure intensity
01 p0168 A69-10401

Dynamic behavior of elastoplastic beam column model with one degree of freedom subjected to axial compressive force
02 p0337 A69-11717

Fiberglass reinforced plastic laminates failure under biaxial compression due to layer separation with strain energy as endurance criterion
02 p0270 A69-12142

Orthotropic stiffened multilayer circular cylindrical shells buckling under axial compression, lateral pressure, etc
02 p0346 A69-12510

Unreinforced circular cutouts effects on buckling behavior of circular cylindrical shells under axial compression, using photoelastic plastic shells
03 p0523 A69-12988

Creep buckling of circular cylindrical shells under axial compression and bending, using Al alloy test specimens
03 p0523 A69-12995

Initial deviations or imperfections effects on load capacity of infinite and finite length thin circular cylindrical shells under axial compression
[ASME PAPER 68-WA/APM-22] 04 p0669 A69-14398

Circular cylindrical shell creep behavior and buckling under axial compression and internal pressure, using multimembrane model
[AIAA PAPER 68-108] 04 p0676 A69-14706

Smooth cylindrical shell stability under axial compression noting effects of scale factor, initial defects, initial stresses and deflections in welded seam, etc
04 p0680 A69-14929

Uniaxial compression load effect on activation energy in p-type GaSb single crystals
04 p0644 A69-15269

Axial buckling load for thin walled circular cylindrical shell, noting design of internal mandrel for control of boundary expansion conditions
05 p0831 A69-15581

Annular stress in rib reinforced cylindrical shells under axial compression load and internal pressure, using successive approximation
05 p0841 A69-16208

Initially imperfect axially compressed cylindrical shells strength using variational principle, shell theory and deformation theory of plasticity
[AIAA PAPER 69-91] 06 p1028 A69-18181

Initial geometric imperfections effect on buckling and postbuckling behavior of laminated composite cylindrical shells under axial compression, considering reinforcing fiber orientations
[AIAA PAPER 69-93] 06 p1029 A69-18194

Buckling of long cylinders with homogeneous random axisymmetric geometric imperfections under axial compression, using truncated hierarchy technique
07 p1236 A69-19473

Simply supported isotropic cylindrical panel stability under axial compression, obtaining asymptotic series expansion for upper critical stress
08 p1419 A69-21182

Multilayer orthotropic cylindrical shells stability under distributed external load and off-center compression, analyzing subcritical deformation on critical load
09 p1613 A69-21685

Buckling of eccentrically stiffened thin circular cylindrical shell under uniform combined axial compression and torsion loads with lateral pressure
09 p1616 A69-21955

Buckling capabilities of inflation rigidized wire film and shell film cylinders in axial compression and bending
09 p1617 A69-21997

Axisymmetric free edge buckling of semiinfinite heterogeneous orthotropic cylindrical shells in axial compression, noting stability condition
10 p1802 A69-23889

Stiffener geometry and spacing effects on buckling of axially compressed cylindrical and conical shells
11 p1979 A69-24815

Thin walled circular cylinders postbuckling behavior and stability under axial compression calculated for design loads
11 p1979 A69-24816

Critical axial compressive load for cylindrical shells reinforced with longitudinal ribs, noting internal pressure and rib spacing effects
11 p1985 A69-25177

Buckling and postbuckling equilibrium behavior of fiber reinforced cylindrical shell under uniform axial compression
12 p2187 A69-26843

Imperfection surface effect on buckling load of circular cylindrical shell under axial compression, locating limit points of postbuckled states
13 p2362 A69-28122

Experimental and predicted shock axial pressure variations for semiinfinite metallic targets during high velocity impact, using Al alloys and Cu
[AIAA PAPER 69-361] 13 p2366 A69-28294

Uniaxial compressive stability of rectangular boron-epoxy laminated plates clamped on loaded edges, determining buckling loads by Southwell plots
13 p2287 A69-28669

Orthotropic cylindrical shell stability under uniform axial compression and internal pressure, taking into account subcritical state duration
14 p2532 A69-28981

Geometric discrepancies influence on stability modes and loads for thin shells up to point of collapse
14 p2533 A69-29022

Heterogeneous orthotropic circular cylindrical shell stability during axial critical compression
14 p2533 A69-29024

Buckling of ring stiffened cylinders subject to axial compression, considering prebuckling lateral wall displacements
14 p2534 A69-29030

Machine for measuring creep deformation of polytetrafluoroethylene under uniaxial compressive loads, discussing stress-strain relationship
14 p2469 A69-29412

Bound excitons spectra in Cu doped gallium arsenide crystals, analyzing line oscillation structure and uniaxial compression effect
16 p2824 A69-31571

Heated cylindrical shell with braces subjected to given compression and internal pressure, having elastic beams along edges, analyzing local deformations effect on shell strength and stability
16 p2873 A69-32131

Prestressed beams, columns and plates nonlinear response, statistical behavior and transverse cracking under axial compression, describing strength and stiffness
17 p3060 A69-33568

Cylindrical shell stability under axial compression, studying buckling process and wave formation
18 p3217 A69-34597

Stress and displacement waves propagation in thin walled elastic cylindrical shell under compressive axisymmetric force based on momentless theory
18 p3218 A69-34600

Stress-strain state of elastoplastic material subjected to quasi-static uniaxial tension and compression, considering Bauschinger type effects by scalar parameters
18 p3222 A69-34909

Displacement patterns for buckled shapes of axially compressed thin walled circular, cylindrical and conical shells
19 p3443 A69-36793

Thin curved panels postbuckling behavior under axial compression, basing study on thin shell finite deformation theory and Galerkin method
20 p3629 A69-38112

Noncircular curved shell stability under axial compression, using strain energy method to determine upper and lower critical stresses
21 p3834 A69-38715

Prebuckling deformation influence on compressive buckling load for orthotropic cylindrical shells with elasticity principal axes in axial and circumferential directions
22 p4047 A69-41182

Cylindrical shell load carrying capacity under axial compression, considering middle surface initial distortions influence
23 p4228 A69-41989

Circular cylindrical thin walled shells creep buckling under uniform axial compression
23 p4234 A69-42413

Circular cylindrical photoelastic shells buckling modes under axial compression using high speed isoclinic photography, discussing shallow shell equations applicability to early stages
24 p4404 A69-43652

Computer program determination of barreling effect on strength of ring and stringer stiffened shells designed to support axial compression loads
24 p4405 A69-43671

AXIAL COMPRESSORS

U TURBOCOMPRESSORS

AXIAL FLOW

Acoustic resonance excitation in axial flow compressor annulus by wake shedding from blades
01 p0142 A69-10058

Tangential velocity profile growth in laminar axial flow through concentric annulus with rotating inner cylinder, using Navier-Stokes equations for prediction
01 p0058 A69-10143

Circumferential inhomogeneity of flow through impeller blades of axial flow compressor
03 p0361 A69-12954

Cylindrical wave approximation modified to include axial effects, discussing time histories of deflection and applicability range
04 p0671 A69-14410

Flat decelerating cascades boundary layer in compressible flow during change in axial flow-density ratio and upstream turbulence
11 p1818 A69-24639

Flexible cylinder vibration in nominally axial flow, discussing length, mass, flexural rigidity and diameter variation effects on vibration amplitude
11 p1984 A69-25166

Velocity and static pressure redistribution in distorted flow field upstream of axial flow compressors
[AIAA PAPER 69-485] 16 p2842 A69-32694

Vortex breakdown in rotating fluids associated with wave motion along axis of rotation, considering effects of nonzero wave amplitude
[AIAA PAPER 69-645] 17 p2892 A69-33478

Turbocompressors, reviewing axial and radial compressors
19 p3395 A69-36749

Axial flow fan blade row noise generation, discussing equation linearization, acoustic energy prediction and effects of flowing medium
[ASME PAPER 69-FE-12] 20 p3460 A69-37989

Forced flow against infinite rotating disk, showing von Karman similarity equations solution for axial flow at large distances toward disk
24 p4244 A69-42718

Mixing length theory including eddies axial motion, discussing turbulent field of temperature or concentration
24 p4407 A69-42917

AXIAL FLOW COMPRESSORS

U TURBOCOMPRESSORS

AXIAL FLOW PUMPS

U TURBINE PUMPS

AXIAL FLOW TURBINES

Axial flow turbine blade cascade in transonic flow
03 p0365 A69-14103

Tip turbine driven flush thin profile wing or platform lift fan design and operating considerations
05 p0696 A69-15554

Wall friction influence on three dimensional flow in axial flow turbomachines, introducing shear stresses between flow planes
08 p1252 A69-20724

Aerodynamic and thermal considerations in axial flow turbine blade design, discussing internal air cooling
[IME PAPER 2] 12 p2146 A69-25788

Reynolds number, incident flow turbulence and interblade channels roughness effects on friction losses in axial flow turbines
15 p2547 A69-30074

Axial gas turbine efficiency and work functions, discussing turbine using isothermal high velocity combustor
16 p2837 A69-32064

Optimum efficiency of turbines with small volumetric flow rate, determining height of air-gas flow, partial admittance and flow angle in clearance
18 p3184 A69-34983

Potential flow interaction effects between blade rows in axial flow compressor stage, emphasizing inlet guide vane-rotor interaction
21 p3643 A69-38439

Spanwise velocity profiles through cascades and axial flow turbomachines, analyzing loading, secondary losses and inlet conditions interacting on downstream profile
23 p4061 A69-42110

AXIAL LOADS

Elastoplastic stress-strain behavior of concentric composite cylinders under uniaxial tension using analytical model, predicting transverse stresses during axial loading
01 p0171 A69-11263

Instability of struts subjected to axial force and radiant heat, considering elastic and thermal deformation
02 p0337 A69-11716

Dynamical strength of solid cylinder under axial loads increasing in time at given rate, using constitutive equations of thermodynamic theory
02 p0342 A69-12278

Stresses around two reinforced circular openings in thin elastic plate of isotropic material under biaxial loads
02 p0349 A69-12799

Stress diffusion from axially loaded stiffeners into cylindrical elastic shells
03 p0530 A69-14065

Stress concentration around centrally placed circular bolt in axially loaded bar, using theory of infinite systems of linear equations
04 p0681 A69-15195

Uniaxial loading effect determination by change of harmonics amplitude of inductive pickup signal
05 p0763 A69-15995

Elastoplastic element structural growth induced by thermal cycling analyzed as function of temperature and sustained axial load
[ASME PAPER 68-WA/MET-14] 05 p0837 A69-16067

Axisymmetric form of stability loss of cylindrical shell under effect of axial load suddenly applied along generatrix, considering inertia forces and obtaining differential equations
06 p1021 A69-17181

Circular bar elastoplastic behavior under combined axial force and torque in strain hardening range, noting elastic compressibility effects
06 p1023 A69-17371

Exponential decay of stresses in circular elastic cylinders subject to axisymmetric self equilibrated end loads
06 p1023 A69-17507

Axial loading of unidirectional composite with hexagonal array of isotropic circular filaments generalized for filament anisotropy, discussing matrix elastic modulus and Poisson ratio
07 p1170 A69-18724

Stress-strain relationship of composite bars consisting of single glass fiber with thin metal coating layer and under axial load
07 p1235 A69-19385

Axially loaded viscoelastic constrained bar instability for large deformation
07 p1235 A69-19440

Stability of cylindrical shell reinforced by circular ribs under combined action of external pressure and axial forces, using characteristic equation
07 p1238 A69-19687

Dynamic stress intensity factor for axisymmetric loading of circular crack in infinite isotropic elastic medium
08 p1413 A69-20412

Strength hypothesis for structures under multiaxial vibration load, taking into account plane stress state
09 p1620 A69-22575

Gyrator center axial displacements due to axial load, noting equal load distribution between bearings with resilient cover plates
09 p1502 A69-22703

Strength of laminated glass filament reinforced plastic material in biaxial loading, discussing strength theories
10 p1794 A69-22943

Yield points compared for axial and biaxial tensile loading of aluminum alloy sheets
10 p1801 A69-23849

Pressure vessels burst tests for investigating alloys, fabrication processes and biaxial loading effects, noting vessel configurations and test temperatures
10 p1714 A69-23974

Axial torque effect on critical speeds of continuous rotor with motion described by partial differential equations
[ASME PAPER 69-VIBR-52]

10 p1804 A69-24152

Free vibrations in axisymmetrically loaded orthotropic circular conical shells with longitudinal and circumferential stiffening based on linearized theory, considering shear deformation and inertia

11 p1969 A69-24327

Static and dynamic stability of flexible shallow spherical shell under axisymmetric load and elastically hinged along contours

11 p1976 A69-24763

Semiinfinite circular cylindrical shell buckling under axial load, computing forces, moments and displacements by thin shell equation

11 p1979 A69-24818

Nonlinear free vibration of beams with clamped and supported ends subjected to axial load, considering symmetric and antisymmetric modes

11 p1983 A69-25024

Optimal parameters selection for rib-reinforced cylindrical shells determined with respect to axial critical loading magnitude

11 p1985 A69-25173

Frequency characteristics of flexible compensated manifolds for aircraft engines, considering axial force

11 p1826 A69-25332

Dynamic plastic response of finite bar subject to axial impact load noting reflected waves, stress-strain histories and residual strain

11 p1991 A69-25512

Support system for McDonald 107 inch telescope mirror, adopting Couder design using tily pad single lever supports for axial thrust

12 p2058 A69-26417

Accelerated structural tests under creep conditions, noting isothermal structures subjected to uniaxial and complex stress loads

12 p2186 A69-26838

Elastic buckling and initial postbuckling behavior of clamped shallow spherical shells under axisymmetric load

12 p2187 A69-26842

Local failure of axially loaded plastic foam core sandwich panels, using face wrinkling analysis procedures

13 p2357 A69-27207

Stress and displacement fields for uniaxially loaded infinite elastic continua with doubly periodic array of holes and inclusions, using finite element method

13 p2363 A69-28133

Stress-strain state of circular annular plate with varying thickness subjected to concentrated axisymmetric load and shearing force applied to internal perimeter

13 p2369 A69-28563

Linear elastic columns dynamic stability under time dependent axial load, investigating almost-sure asymptotic stability

16 p2872 A69-31911

Local stability of viscoelastic shells of revolution under axisymmetric loads, discussing asymmetric snaphthrough of dome

18 p3216 A69-34573

Bending of rigid freely supported plastic plates under local axisymmetric dynamic load, discussing rectangular pulse effects and velocity fields

18 p3217 A69-34593

Thin walled cylindrical shells deflections under axial impact load, assuming deformations resembling cylindrical surface bending

18 p3217 A69-34599

Dynamic instability regions of parametric resonance of cylindrical shells with curved generating lines under axial and radial pressure

18 p3223 A69-34979

Limiting equilibrium of variable thickness shallow spherical and conical shells of revolution under axisymmetric loads, assuming rigid plastic shell material

18 p3225 A69-35370

Elastic oscillations of inhomogeneous orthotropic ring under time-variable axisymmetrical load analyzed by Fourier method

19 p3434 A69-35828

Axial load fatigue crack propagation tests on Al alloy sheets for stress ratio effects

19 p3346 A69-36435

Shells of revolution bearing capacity under axisymmetric loads determined by linear programming and finite difference method

20 p3622 A69-37326

Ronay effect in reversed cyclic torsion or tension in thin cylindrical viscoelastic tube showing creep under sustained load

20 p3625 A69-37596

Stress and displacement in thin circular plates of ductile materials under axisymmetric loading predicted by nonlinear analysis

20 p3628 A69-37787

Axial forces effects on dynamic load factors of beams under transverse impulsive loads, considering various end conditions

20 p3629 A69-38113

Vacuum apparatus for measuring uniaxially loaded metal surfaces interfacial adhesion, showing surface oxide removal effectiveness influence in adhesion strength

21 p3689 A69-38594

Momentless orthotropic spherical shell of variable thickness stress analyzed, assuming large deformations under uniform axisymmetric load distribution

22 p4039 A69-39916

Closed circular cylindrical shell stability and oscillations under ring-shaped axial load, defining stress-strain state by radial displacements and force function

22 p4049 A69-41280

Vector properties of isotropic strain hardenable materials in stress vector space applied to tubular brass subject to biaxial tension and complex loading

23 p4227 A69-41714

Creep stress analysis of circular cylindrical shells under axisymmetric loading, plotting stresses and deformations for various parameters

23 p4233 A69-42352

AXIAL STRAIN

Linear cumulative damage theory defining low cycle fatigue region of classic S-N curve, providing biaxial strain mode by centrifugally loading rotors
[ASME PAPER 68-WA/MET-8]

05 p0838 A69-16151

Computer program for axisymmetrically deformed shells of revolution and combinations of such shells

06 p1026 A69-18019

Existence and uniqueness theorems for boundary value problems of axisymmetric deformation of circular membrane at normal pressure, using membrane theory and shooting method

07 p1233 A69-19299

Stress distribution around equal size holes at ends of crack for normal uniaxial tension, based on photoelastic and brittle lacquer technique

08 p1412 A69-20257

Foil type strain gage for measurement of tangential strains along circumference of hole in plate under uniaxial and equibiaxial tension

08 p1314 A69-20258

Axisymmetric states of stress determined by photoelasticity, analyzing meridional slice under normal and oblique incidence

08 p1412 A69-20259

Static axisymmetric deformation of elastic paraboloid of revolution, using integration of equilibrium equation in Lamé displacement

09 p1613 A69-21631

Axisymmetric vibration modes of cylindrical-hemispherical membrane tank partly filled with liquid
[AIAA PAPER 67-75]

09 p1482 A69-21940

Polyurethane foam high velocity deformation properties, discussing results of dynamic uniaxial stress tension and compression tests

11 p1907 A69-25648

Hollow circular viscoelastic cylinder axisymmetric plain strain problem, considering displacement, traction and mixed boundary conditions, noting applicability to rocket solid fuel core

12 p2181 A69-26396

Axial support systems for large astronomical mirrors, considering gas support system for flat mirror submerged and floating in isostatic liquid

12 p2057 A69-26412

Axisymmetric deformation of thin orthotropic laminar spherical shells under internal loads calculated on computer using Legendre polynomials

12 p2181 A69-26611

Axisymmetric elastic stresses in ring stiffened segmented shells of revolution, noting finite difference method for nonlinear analysis and computer program

12 p2185 A69-26818

Polyfluoroethylene resin breakdown under uniaxial tension, considering continuity disruption

13 p2286 A69-28321

Linear cumulative damage theory defining low cycle fatigue region of classic S-N curve, providing biaxial strain mode by centrifugally loading rotors
[ASME PAPER 68-WA/MET-8]

14 p2535 A69-29438

Thick walled pressurized cylinder fatigue test results compared with axial tension and rotating beam tests on same material

15 p2709 A69-30676

Uniaxial stress effect in Schottky barrier diodes measured by beam balance noting higher sensitivity

16 p2758 A69-31619

Transient wave processes of deformation in spherical shell under load abruptly applied to geometrical pole

16 p2875 A69-32288

Plastic energy dissipation rate during stable crack growth in sheet under uniaxial tension

18 p3212 A69-34345

Differential equations of shells of revolution theory assuming rotationally symmetric stress and strain in thin elastic shells

18 p3215 A69-34549

Axisymmetric deformation of cylindrical wound fiberglass reinforced plastic shell analyzed by methods of rigid normals and nonlinearly elastic fiber system

18 p3222 A69-34974

Nonlinear axisymmetric oscillations and motion stability of cylindrical wound elastic glassfiber shell under time dependent uniform internal pressure

18 p3222 A69-34975

Equations of motion for axisymmetric elastic deformation of inhomogeneous body of revolution subjected to torsion and steady oscillations

19 p3436 A69-35845

Generalized Love functions in axisymmetric micropolar elasticity, deriving stress functions expressing all state components

19 p3440 A69-36585

Nonlinear theory based on Euler-Bernoulli hypothesis for axisymmetric deformations of heterogeneous orthotropic shells of revolution under rotationally symmetric mechanical and thermal loads

20 p3625 A69-37592

Rigid thermoplastic cylindrical shell creep under axisymmetrical loads, giving computer algorithm and time dependent criterion for rupture strength

22 p4045 A69-40750

High speed radially resistant ball bearing, analyzing effect of lubrication film on axial rigidity

23 p4169 A69-41555

Statics of axisymmetric deformation of cylindrical and conical shells of revolution of moderate thickness under uniformly and nonuniformly distributed loads

23 p4226 A69-41705

Stress analysis in elastic bodies induced by axisymmetric strains in presence of mass forces and temperature gradients, obtaining equilibrium equation

23 p4229 A69-41997

Permanent deformation of axial rod subjected to blast load predicted using partial differential equation in conjunction with stress-strain relationship

24 p4406 A69-43699

AXIAL STRESS

Mechanical properties of AZ5G-Zr-Cr alloy welded sheet subjected to biaxial stress at low temperature

01 p0088 A69-11152

Successive approximations utilizing analytic stress functions used to obtain solution for infinite plate with arbitrary holes under biaxial stresses
[ASME PAPER 68-PVP-1]

03 p0523 A69-12998

Anisotropic plasticity in sheet metals under uniaxial and balanced biaxial tension

05 p0837 A69-16030

Axially symmetric torsion of finite elastic cylindrical rod partially bonded to elastic half space, discussing coupling between dual Dini series and integral equations

07 p1236 A69-19474

Minimum weight analysis of Michell trusses transmitting given load to bars within allowable range of axial stress

08 p1410 A69-19893

Elastic cone stresses due to axial force at point on axis, solving problem in terms of convergent integrals

08 p1415 A69-20689

Failure criteria for predicting filamentary composite strength under uniaxial and combined stresses from properties and fabrication process considerations

09 p1611 A69-21479

Radial and tangential stresses in double glass fiber assuming different Poisson coefficients, determining conditions for axial stress redistribution prevention

09 p1614 A69-21741

Axial vibration effects on frictional losses in gear systems under dry friction or boundary lubrication conditions
[ASME PAPER 69-VIBR-15]

10 p1701 A69-24169

Biaxial stress effect on creep properties of thin walled tubes of polymethyl methacrylate at controlled temperature and humidity

10 p1717 A69-24216

Three dimensional theory of elasticity for finite hollow cylinder under axisymmetric deformation, considering stress and pressure distribution over surface
11 p1983 A69-25022

Stress concentration around square hole in celluloid plate subjected to creep under biaxial tension analyzed by photocreep method
12 p2178 A69-26000

Nonlinear theory for whirling of heavy string under constant axial tension, considering orbitally stable modes for eigenvalues of rotation
13 p2359 A69-27264

Membrane and bending stresses around elliptic hole in thin circular cylindrical shell, considering axial tension
[NAL-TN-13]
13 p2362 A69-28123

Stainless steel biaxial residual surface stresses from grinding and finish machining determined by dissection technique
[ASME PAPER 68-WA/MET-9]
14 p2455 A69-29437

Isothermal deformations in linear viscoelastic material under uniaxial stress, determining optimum strain rate history for maximum work lower bound
15 p2707 A69-30637

Clamped circular plates impulse load tests with sheet explosives, showing finite difference program for computing large deflection dynamic response
15 p2709 A69-30675

Fracture strength of Al alloy in biaxial stress field, considering strain rate influence on material toughness
17 p2986 A69-32985

Differential equations of shells of revolution theory assuming rotationally symmetric stress and strain in thin elastic shells
18 p3215 A69-34549

Stability loss of shells of revolution under axial tension and radial pressure, considering shells of Gaussian curvature, calculating critical force
18 p3222 A69-34976

Fiberglass reinforced plastics short and long term strength anisotropy, correlating stress and logarithm of time to rupture under tension along different directions
18 p3162 A69-35352

Fredholm integral equation solution of circularly axisymmetric stress state for bodies of revolution
18 p3226 A69-35375

Multiaxial stress effect at room temperature on fracture strength of silicon carbide tubular specimens
20 p3565 A69-36939

Linear limit uniaxial stresses for stress-strain and stress-birefringence in photoelastic and mechanical model materials
20 p3628 A69-37777

Radial and tangential stresses in double glass fiber assuming different Poisson coefficients, determining conditions for axial stress redistribution prevention
20 p3630 A69-38217

Creep measurements in Al alloy during uniaxial tensile stresses between 200-350 C, determining deformation dependence on time and stress
21 p3744 A69-38871

Plastic deformation by uniaxial tension during transition from dynamic to static loading from microscopic and macroscopic standpoint, noting slip lines
22 p4047 A69-41081

AXISYMMETRIC BODIES

Sonic flow at large distance and behind shock wave for axisymmetric body of revolution of finite dimensions in inviscid fluid
01 p0058 A69-10160

Ablation rate optical measurement near stagnation point of Teflon cylinder models, noting effect of nose curvature and temperature at supersonic speed
01 p0006 A69-10758

Axially symmetric bodies shape for static pressure at location independent of Mach number
04 p0542 A69-14738

Lift and drag parameters of axisymmetric bodies in Newtonian flow at random incidence by summation of appropriate portions
04 p0542 A69-14745

Optimum stabilization of uniformly rotating axisymmetric satellite, using Liapunov theorem on asymptotic stability
04 p0666 A69-14921

Sting diameter and cylindrical protuberance length effects on base pressure of axisymmetric body in turbulent supersonic flow
05 p0697 A69-15712

Lagrange multipliers of variational problem of point motion and isochronal derivatives in field of attraction of axisymmetric planet
05 p0823 A69-16015

Rotation wave propagation in elastic homogeneous isotropic centrosymmetric body in asymmetric elasticity theory
05 p0843 A69-16645

Approximate solution for determining satellite motion around axisymmetric planet
06 p1005 A69-17563

Viscous interaction solution obtained for near wake of axisymmetric bodies by integral moment method and axisymmetric incompressible similar wake solutions
06 p0860 A69-17633

Turbulent density fluctuations in near wake of hypersonic axisymmetric slender body measured photometrically with near UV absorption of sulfur dioxide in flow
[AIAA PAPER 69-70]
06 p0864 A69-18158

Laminar boundary layer on axisymmetric blunt body in dissociated air taking into account nonequilibrium homogeneous chemical reactions
07 p1050 A69-18734

Symmetrical body rotational motion with asymmetrical mass distribution about center of mass, determining minimum initial value of angular velocity
09 p1595 A69-21762

Increasing rotation of axisymmetric body about velocity vector ascribed to asymmetry in mass distribution, defining conditions for occurrence
09 p1431 A69-22077

Small angle precessional motion of axisymmetric spin stabilized bodies subject to disturbing moments
10 p1724 A69-22932

Axisymmetric bodies longitudinal contours for hypersonic flow minimum drag, considering Newtonian pressure distribution and skin friction
10 p1632 A69-23886

Boundary value problem for gravity induced wake motion of ideal fluid in axisymmetric vessel with annular ribs, noting application to bodies of revolution
11 p1868 A69-24769

Supersonic gas flow past plane and axisymmetric bodies with broken generatrix, determining tangential discontinuities and shock waves shape and position
11 p1820 A69-25470

Large deflection elastic-plastic analysis of axisymmetric shells of revolution indicating role of plastic yielding in buckling pressure reduction
12 p2186 A69-26839

Elastoplastic deformations of thin axisymmetric shells of revolution with variable thickness, exemplifying shell with piecewise constant thickness
14 p2533 A69-28982

Shock waves from accelerated, decelerated and stationary axisymmetric bodies flying at supersonic velocities in stratified isothermal atmosphere
15 p2551 A69-31171

Godunov finite difference method modified for steady or unsteady flowfields about planar axisymmetric blunt bodies, presenting body pressures and shock shapes
16 p2732 A69-31886

Trajectory calculation of axisymmetrical body during ballistic and vertical flight, assuming air drag proportional to square of velocity
17 p2889 A69-32950

Base flow component of total drag for axisymmetric supersonic afterbody with single exhaust jet, considering turbulent mixing
[AIAA PAPER 69-650]
17 p2956 A69-33485

Nonuniform gas flow past axisymmetric body from supersonic source simulating jet discharging into vacuum, using power series of stream function
19 p3238 A69-35851

Nonequilibrium laminar boundary layer of dissociating air on axisymmetric body determined using concentration profiles of oxygen and nitrogen components
19 p3239 A69-36395

Finite element method in stress analysis for axisymmetric rotors design, describing computer program and applications
19 p3445 A69-36826

Plastic tension of axisymmetric sample involving necking and small inhomogeneity, assuming Tresca yield condition and associated flow law
19 p3446 A69-36847

Generalized series solutions of boundary layer flows over pointed and blunt nosed axisymmetric bodies, noting general potential flow extending Mangler transformation usefulness
20 p3514 A69-37211

Cone-conical-frustum configurations meeting center of gravity requirements for higher hypersonic lift-drag ratios in axisymmetric manned spacecraft
21 p3644 A69-39237

Stress analysis of thin axisymmetric shells by plane frame analysis program, noting stiffness matrix for conical shell element
21 p3843 A69-39312

Closed form solution to stability of coupled libration motion of slender axisymmetric satellite in circular orbit limited to small amplitude vibrations
22 p4008 A69-39936

Radiative transfer effects in low Reynolds number or merged layer regime of hypersonic flow about axisymmetric blunt bodies, including thin shock layer theory
23 p4059 A69-41885

Inviscid transonic flow past circular arc bodies of revolution, applying Hosokawa technique to pressure distribution solution
23 p4059 A69-41899

Increasing rotation of axisymmetric body about velocity vector ascribed to asymmetry in mass distribution, defining conditions for occurrence
23 p4060 A69-41968

Free vertical shear layers structure solutions singularities in rotating fluids, considering motion by rising or spinning axisymmetric body
23 p4153 A69-42356

Nonlifting blunt axisymmetric hypersonic shape determination to maximize pressure drag for given convective heat transfer, diameter and free-stream conditions
24 p4244 A69-42960

AXISYMMETRIC DEFORMATION

U AXIAL STRAIN

AXISYMMETRIC FLOW

NT ANNULAR FLOW

Axisymmetric MHD flow in turbulence chamber at large Hartmann numbers studied for flow boundary layer effects
01 p0130 A69-10772

Two dimensional Navier-Stokes equations of axisymmetric motion of viscous incompressible fluid, giving integral and solutions for stream function
02 p0231 A69-12135

Exact solutions for Navier-Stokes equations for nonsteady incompressible viscous flow near two dimensional or axisymmetrical stagnation point
02 p0233 A69-12527

Combustion and flame stabilization in axisymmetric laminar or turbulent H flows, noting combustion rates and flame breakdown conditions
02 p0355 A69-12673

Turbulent front structure of axisymmetric compressible wake at supersonic speeds, measuring intermittency factor distribution
03 p0419 A69-13949

Numerical solution of axisymmetric incompressible viscous fluid flows about rotating cylinder, Taylor vortex between cylinders and through labyrinth seal
03 p0419 A69-13990

Stokes-like region around yawed needle in hypersonic strong interaction regime, discussing asymptotic analysis under Stewartson conditions
04 p0542 A69-14732

Stability of nondissipative stratified rotating flows with constant density to axisymmetric disturbances
04 p0588 A69-14740

Ekman boundary layer problem of steady axisymmetric viscous incompressible flow between infinite coaxial rotating disk, studying laminar range of Taylor number R
05 p0744 A69-15665

Axisymmetric hypersonic flow of model gas over slender bodies with strong viscous interaction and shock wave extended to power law viscosity variation
05 p0749 A69-15720

Source and sink method application to direct axisymmetric problems of hydrodynamics
05 p0747 A69-16039

Stream function approximation for plane axisymmetric vortex free transonic inviscid gas flow
06 p0910 A69-17336

Viscous interaction solution obtained for near wake of axisymmetric bodies by integral moment method and axisymmetric incompressible similar wake solutions
06 p0860 A69-17633

Axisymmetric hypersonic near wake with base injection, discussing zero injection case, jet-plume interaction and mixing region
[AIAA PAPER 69-66]
06 p0914 A69-18115

Stability theory application to laminar boundary layer transition prediction on two dimensional and axisymmetric flows having pressure distributions in incompressible flow
[AIAA PAPER 69-10]
06 p0914 A69-18127

Axisymmetric liquid nitrogen turbulent jet propagating under supercritical pressure in gaseous nitrogen medium

07 p1049 A69-18398

NonNewtonian effects in axisymmetric rotational flows of elastico-viscous liquids

07 p1180 A69-18815

Axisymmetric jet impingement against solid plane from tube at finite distance, using nonlinear partial differential equation in finite difference form [AICHE PAPER 31F]

08 p1302 A69-19847

Green function in closed form for energy transport equation solution in axisymmetric Oseen flow

08 p1305 A69-20850

Finite difference numerical solutions to free streamline axisymmetric potential fluid flow, noting independent and dependent variables consideration in boundary value problem

09 p1481 A69-21920

Closed form solution for boundary shape of underexpanded axisymmetric jet in still air

09 p1482 A69-21968

Time dependent procedure for axisymmetric transonic nozzle flows, programming governing equations for high speed computer

09 p1431 A69-21974

Steady axisymmetric gas flow from galactic center, determining supersonic to subsonic transition by equations of motion

09 p1599 A69-22189

Finite difference method computer programs for calculation of velocities and streamlines on blade to blade surface of revolution of turbomachine [ASME PAPER 69-GT-48]

09 p1432 A69-22495

Axisymmetric flow theory for turbomachine of non-free vortex design in distributed equilibrium state, considering boundary conditions and blade leading edges [ASME PAPER 69-GT-10]

09 p1432 A69-22504

Incompressible axisymmetric flow in turbomachines, analyzing flow field and velocity distribution

10 p1631 A69-22910

Circle theorem for iterated equation of generalized axisymmetric potential theory, noting Stokes flow of viscous liquid

10 p1680 A69-23718

Axisymmetric turbulent supersonic incompressible fluid jet, calculating momentum flow distribution and excess heat flow densities in basic segment

11 p1818 A69-25346

Self similar axisymmetric and plane laminar viscous gas channel flows noting exponential or hyperbolic law of decrease in static pressure along channel

11 p1875 A69-25482

Axisymmetric detached flow past slender solid of revolution by ideal incompressible fluid at zero angle of attack and with small cavitation numbers

11 p1877 A69-25741

Flow stability of axisymmetric jet with parabolic velocity profile in fluid at rest, calculating critical Reynolds numbers

13 p2244 A69-27300

Chemically reacting flow field and solid surfaces, formulating nonequilibrium laminar boundary layer equations for two dimensional and axisymmetric flows

13 p2377 A69-28147

Reduction of noise from underexpanded axisymmetric jet flows using radial jet flow impingement [AIAA PAPER 68-81]

13 p2248 A69-28212

Near wake in axisymmetric supersonic flow past slender body with/without base injection, obtaining pressure, temperature, Mach number, velocity and concentration distributions

14 p2389 A69-29017

Velocity distribution effect on electric field at walls for axisymmetric flow of electrolyte in circular channel in magnetic field of E shaped inductor

14 p2501 A69-29915

Numerical estimates of momentum integral error in applying locally similar solutions to nonsimilar problems, assuming two dimensional or axisymmetric flow

16 p2772 A69-32174

Combustion effects on mixing of axisymmetric supersonic and turbulent free jets to obtain species concentrations, pitot pressures and temperatures [AIAA PAPER 69-538]

16 p2843 A69-32705

Axisymmetric supersonic gas flow with attached shock wave past cone, calculating flow parameters between body and shock wave

17 p2890 A69-33123

Wave equations governing evolution of long nonlinear axially symmetric wave motion in inviscid rotating fluids

18 p3120 A69-34441

Three dimensional supersonic flow past pointed nonaxisymmetrical bodies characterized by great local surface curvature changes, using new approximation

18 p3086 A69-34705

Quantitative density data from schlieren measurements by photomultiplier technique for axisymmetric flow outside diffraction bands

19 p3306 A69-35741

Asymptotic form of axisymmetric solution with Dirichlet integral for Navier-Stokes equations applied to flow past bodies of revolution with smooth surfaces

19 p3298 A69-36143

Flow separation and reattachment points and line of zero velocity jet mixing determined by injecting smoke [ASME PAPER 69-FE-29]

20 p3517 A69-37994

Axisymmetric solutions of magnetohydrostatic equations for large conductivity media satisfying second order partial differential equation containing two arbitrary functions

21 p3778 A69-39498

Axisymmetric and two dimensional flows over blunt bodies at high Mach numbers by integral relations method

21 p3645 A69-39790

Semianalytic solution for axisymmetrical supersonic inviscid flow near stagnation region of spherically blunted body with detached shock waves

22 p3861 A69-41178

Axisymmetric supersonic flow around spherically blunted body at small angles of attack, deriving equations for shock deformation perturbations and surface pressure

22 p3861 A69-41179

Axisymmetric separated flow in Chapman model shown nonexistent by flow visualization technique

23 p4060 A69-41905

Transition from axisymmetric to nonaxisymmetric flow in rotating annulus, using two layer quasi-geostrophic model

24 p4345 A69-43150

Heat exchange at stagnation point during interaction between underexpanded axisymmetric supersonic jet and flat obstruction, using method of characteristics

24 p4246 A69-43493

Gas dynamic functions of axisymmetric supersonic gas flows determined using flow density distribution optical measurements

24 p4247 A69-43496

Hypersonic viscous interaction, studying axisymmetric flow over slender sharp nose cones at zero angle of attack and three dimensional flow over sharp flat plate

24 p4248 A69-43579

AXISYMMETRY U SYMMETRY

AXLES

U SHAFTS [MACHINE ELEMENTS]

AXONS

Visual field meridians in circumstriate visual cortex of monkey determined by tracing degenerating axons stained by Nauta method

22 p3881 A69-40858

AZIDES [INORGANIC] NT SODIUM AZIDES

Compatibility of inorganic azides with organic explosives from elevated temperature interactions using trinitrobenzene as model

02 p0304 A69-12499

AZIDES [ORGANIC] NT SODIUM AZIDES

Neat alpha styryl azide transformation into 2-phenylazirine, 3,6-diphenylpyridazine and 2,5-diphenylpyrrole after one month at room temperature in brown glass bottle

10 p1651 A69-23307

AZIMUTH

Spectral parameters of VLF radio noise given as functions of azimuth from atmospheric analyzer observations

01 p0033 A69-10971

Error reduction in initial azimuth alignment and azimuth and level axis gyro drifts in long range air transport gyro accelerometer inertial systems

02 p0278 A69-12361

Primary cosmic ray intensity variation with cut-off energy of particular secondary component, using ground based monitors

06 p0925 A69-17295

Azimuthal drift of rotor axis of directional gyroscope mounted on sloping base, showing vertical component responsibility via truncated equations of motion

09 p1502 A69-22702

Coupling coefficients for integral charged component of cosmic rays determined from measuring

azimuthal geomagnetic effect on rays observed in crossed telescopes

10 p1770 A69-23925

Binary-quantized signal packet center for target azimuth determination, discussing antenna radiation pattern role

15 p2566 A69-30332

Direction finding accuracy of pulsed radar with binary-quantized detector signals, discussing azimuth minimum variance and quantization threshold optimization

15 p2566 A69-30333

Reflecting or reradiating obstacle proximity as cause of siting errors in azimuth radio measurements, discussing omnidirectional obstacles effect

15 p2651 A69-31090

Azimuthal particle distribution expressions for analyzing cosmic ray jets

16 p2849 A69-32045

Instrument azimuth determination, discussing observations and theory

16 p2791 A69-32227

Azimuth error from observations of circumpolar stars at greatest elongation using transit instrument

17 p3028 A69-32878

Azimuth angle distribution of secondary particles forming cosmic ray diffused cone with high energy, showing asymmetry and deducing particle transverse momentum upper limit

17 p3024 A69-33763

Graphic representation of time dependence of sub-satellite points and orbital azimuths for relating satellite photographs to locality

18 p3128 A69-34818

Precision azimuth reference accuracy standards with confidence limits for gyrocompass evaluation, emphasizing astro and transfer angle repeatability [AIAA PAPER 69-859]

21 p3725 A69-39387

AZINES

Polymeric Schiff bases synthesis, thermal stability and nature of pyrolytic decomposition of polyazines and derived polystilbenes

07 p1074 A69-18628

Aminazine and adrenaline effects on adrenocortical function in patients with diencephalic syndrome

22 p3888 A69-41272

Rotational spectra of methylchlorodiazirine at room and dry ice temperature, using K band and Stark effect spectrometers

23 p4194 A69-42207

AZO COMPOUNDS

NT RDX

Deuterated diazomethane prepared by base catalyzed reaction of hydrazine with chloroform

06 p0885 A69-17885

Nitrosoazomethine derivatives deoxygenation for generation of azomethine nitrenes, discussing preparation by oxidation and dehydrogenation of secondary amidoximes

10 p1651 A69-23305

Block tractable azomethine copolymers prepared by reaction of insoluble oligomers with monomers or of two different fusible oligomers, noting high thermal stability

13 p2217 A69-28317

Curing agents for carboxy and hydroxy functional prepolymers synthesis and evaluation including sulfonyl, acyl and ureido aziridines [AIAA PAPER 69-436]

16 p2747 A69-32777

Monograph on thermally stable polymeric azomethines synthesis by polycondensation reactions

23 p4113 A69-42019

AZOLES

NT INDOLES

NT PYRROLES

NT TRYPTOPHAN

Aminotetrazole preparation to obtain tetrazole derivatives and explosive salts

10 p1651 A69-23013

Photolytic cleavage of vic-triazole ring when unsubstituted at N, finding phenylacetoneitrile production mechanism

19 p3264 A69-35971

X ray radiation damage to white mice blood serum proteins disappearing following intraperitoneal administration of imidazole or benzimidazole

23 p4077 A69-41300

AZOTOBACTER

Poly A-poly U synthesized by Azotobacter Vinelandi RNA polymerase in unprimed reaction containing ATP and UTP, following short lag period

10 p1647 A69-24185

A2F AIRCRAFT

U A-6 AIRCRAFT

B

B STARS

Far UV spectra of O and B stars in Orion photographed from Aerobee rocket, describing wavelength measurements and line identifications
02 p0327 A69-12712

Hydrogen alpha line strength in 951 O, B and early A stars from narrow band photoelectric measurements for stellar luminosity
03 p0511 A69-13435

Photometric investigation in UBV and H alpha of early B stars in Scorpio-Centaurus association, computing intrinsic colors and magnitudes corrected for interstellar absorption
06 p1001 A69-17195

Rapid differential rotation effect on massive main sequence O and B stars, discussing bolometric magnitude deficiencies and shifted position in Hertzsprung-Russell diagram
07 p1220 A69-19390

Expanding atmospheres in OB supergiants from radial velocity measurements, proposing tentative temperature and velocity fields
08 p1387 A69-20091

Abundance analysis of B3 V star in Orion association, noting titanium and strontium overabundance and oxygen underabundance
08 p1407 A69-21133

Hydrogen beta emission profiles for pole-on type Be stars, measuring stellar rotational velocity by Huang-Struve method
09 p1596 A69-22052

Spectrum analysis for early B type star Barnard 29 in M13 globular cluster
09 p1599 A69-22193

Spectral type and rotational velocity estimation for 83 stars near double cluster in Perseus, emphasizing Be stars
09 p1599 A69-22195

Effects of opacity arising from silicon bound-free transition on emergent fluxes and hydrogen line profiles for A and late B stellar atmospheres
09 p1604 A69-22403

A and B stars near North Galactic Pole and with magnitudes from 5 to 14.5, noting photoelectric UBV and four color photometric measurements
10 p1773 A69-22963

Interstellar medium density distribution as function of stellar action spherical coordinates applied to determining stellar motion forces and B stars brightness difference
11 p1955 A69-24386

B star HD 191980 spectral variations from B-3 to B-8 noting helium to carbon line intensity ratio, interstellar D line strength and radial velocity measurements
11 p1958 A69-24594

Physical parameters and chemical composition of DD Lac atmosphere from spectral analysis
12 p2156 A69-26219

Spectrum of abnormal B-type star HR 3817, noting Balmer line profiles and instrumentation
12 p2172 A69-27160

Rocket spectrographic observations of Alpha Virginis noting hydrogen Lyman absorption lines
13 p2338 A69-27555

Steady state model envelopes of Be stars, determining excitation and ionization states for hydrogen atoms
13 p2338 A69-27559

Fe III line profiles and equivalent widths from spectrograms of zeta Cas and gamma Peg for Fe abundance, using model atmospheres
13 p2347 A69-27715

Short period variability of B, A, and F stars observed in photometry of New Delta Scuti stars
13 p2348 A69-27803

OB stars absolute magnitude and intrinsic colors in Cleveland system related to MK system
13 p2348 A69-27806

Positions, spectral types and B magnitudes for possible field horizontal-branch stars at high galactic latitudes, selected from faint A star list
13 p2348 A69-27807

Balmer jumps for B star temperature scale, discussing relation between observed Balmer jumps and observed U-B color indices
14 p2518 A69-29132

Sco-Cen B stars radial velocities, determining spectroscopic binaries
14 p2519 A69-29136

Lacerta OB 1 B spectroscopic binaries periods and orbital elements, noting limits for secular variation
14 p2519 A69-29137

Radial velocities of southern OB stars and supergiants noting tabulation of information
14 p2519 A69-29368

Surface convection zone in atmospheres of global cluster and halo B stars determined to study He depletion efficiency
14 p2529 A69-29976

B-type stellar spectra, discussing atmospheres and local thermal equilibrium from considerations of He I and P II lines relative strength
15 p2679 A69-30046

Spectral classifications and UBV photometry for southern association Sco OB 1 containing cluster NGC 6231
15 p2692 A69-30771

Spectral characteristics of B stars group, reviewing causes of spectral line profile deformation
16 p2855 A69-31828

Radial velocity and spectral line variations of HD 124224, suggesting main sequence star of B6 to B9 spectral type
16 p2859 A69-32223

Polarimetric observations of Be stars, noting dependence and self absorption by hydrogen of polarization produced by electron scattering
16 p2863 A69-32397

Depolarization of extragalactic radio sources at low Galactic latitudes attributed to ionized hydrogen produced by B2 star tunneling through interstellar hydrogen cloud
18 p3194 A69-34425

UBV photoelectric observation of OB and open cluster Tr 16 stars in Carina-Centaurus, suggesting no limit in depth distribution
18 p3200 A69-35133

Galactic rotation in Cassiopeia region, studying O, B and A stars circular velocities as function of distance from galactic center
18 p3201 A69-35142

HD 217050 spectroscopic study, determining Balmer envelope temperature from comparison of homologous Balmer and Paschen lines intensities
18 p3201 A69-35144

Balmer line spectrum formation in extended atmospheres of Be and shell stars, noting influence of angle of inclination to observer
18 p3204 A69-35349

MK spectral types for bright southern O and B stars
20 p3612 A69-38161

Omicron Andromedae radial velocity measurements /1961-1966/ during normal B star periods
22 p4028 A69-40755

MK system spectral types determination for B, A and F type stars from slit spectrograms near NGC 2264
23 p4211 A69-41487

Faint OB stars data tabulation between Carina and Centaurus, noting open clusters and MK classification
23 p4211 A69-41488

Radial velocities for O and B stars in Milky Way field in Scorpius determined from prism spectrograms with specific dispersion at H gamma line
23 p4211 A69-41489

Tabulated spectroscopic observations of Be stars included in Merrill and Burwell catalog
23 p4213 A69-41720

OB stars near emission nebula RCW 103, describing galactic structure in Norma
23 p4220 A69-42384

Atomic hydrogen departures from LTE computed for models of B star atmospheres, assuming detailed balance in hydrogen lines
24 p4376 A69-42665

Interstellar medium density distribution as function of stellar action spherical coordinates applied to determining stellar motion forces and B stars brightness difference
24 p4390 A69-43776

B- 52 AIRCRAFT

Efficient allocation of maintenance resources in USAF, analyzing B-52 costs and substitution of capital for labor
13 p2382 A69-28041

Stability augmentation system for B-52, noting flight test performance evaluation for structural vibrations and rigid body motions of aircraft
20 p3461 A69-37157

Electrohydraulic servosystem to counteract atmospheric turbulence effects on B-52 global bombers, noting reduction in aircraft fatigue and structural damage
20 p3467 A69-38184

B- 70 AIRCRAFT

Propulsion performance of XB-70A aircraft calculated by gas generator method
20 p3461 A69-37152

XB-70 aircraft test data as applied to SST safety, describing aircraft design, flight characteristics, instrumentation, takeoff and landing, etc
22 p3868 A69-41143

B-103 AIRCRAFT

U BUCCANEER AIRCRAFT

BABBITT METAL

U BEARING ALLOYS

BABOONS

Cardiovascular responses of baboons and dogs subjected to anoxic near vacuum environment by rapid decompression
06 p0875 A69-17846

Neurological impairment in baboons exposed to prolonged decompression simulating high altitude aircraft cabin structural failure, noting neuropathological examination results
07 p1067 A69-19426

Bigemini pattern in baboon social behavior, noting diurnal rhythm independence from social deprivation, light cycling and food supply
24 p4260 A69-42705

BAC AIRCRAFT

NT VC-10 AIRCRAFT

BAC Three-Eleven 220 seat airliner for short and middle distance routes, discussing operating costs, thrust and range
02 p0193 A69-12067

BAC 111 AIRCRAFT

TU-134 jet passenger aircraft performance characteristics noting similarity to BAC 111
13 p2202 A69-27931

BACILLUS

Ribulose diphosphate carboxylase and phosphoribulokinase activity in chemosynthetic autotrophs Thiobacillus thioautotrophicus and Thiobacillus neapolitanus, noting sedimentation and gel filtration characteristics
02 p0199 A69-11866

Defective bacteriophage PBSH in Bacillus subtilis after mitomycin C treatment, showing DNA synthesis and marker frequency change
15 p2555 A69-30446

B Coli commune cultivated on various substrates, studying oxygen consumption under aerobic/ anaerobic conditions
18 p3097 A69-35302

Adenosine triphosphate /ATP/ production in normal cells and sporulation mutants of bacillus subtilis, discussing applications of ATP synthesis response to C sources
22 p3886 A69-41076

BACK INJURIES

Vertebral column fracture resulting from aircraft ejection, studying ejection seat geometry and personal equipment design influence on spinal curvature relation to catapult thrust
23 p4102 A69-41681

BACKFIRE

Short backfire antenna radiation fields calculation by approximate method
02 p0219 A69-12339

Backfire antenna radiation characteristics and physical dimensions for tracking and telemetry applications, including five element array model
19 p3271 A69-36251

BACKGROUND NOISE

Optimal calculator of detection of Gaussian random signal against Gaussian noise background by reducing input signal to white noise
02 p0206 A69-11606

Optimal detection of random signals on background of noise of unknown intensity and persistent false alarm probability
02 p0208 A69-12264

Noise emitted by gas filled cavity perturbed by strong coherent signal computed by Nyquist equation
02 p0211 A69-12448

Signal detection by four terminal receiver network optimal for background Gaussian noise
04 p0557 A69-14776

Optimal detection of deterministic signals with random initial phase on background of unknown intensity noise under condition of constant false alarm probability
04 p0557 A69-14788

Cosmic ray electron energy spectrum compared with galactic radio noise for estimating galactic magnetic field

06 p0992 A69-17377

Signal resolution during space diversity reception with nondirective or weakly directive antennas and noncorrelated receiver background noise, discussing signal processing

06 p0890 A69-17800

Tape flutter and additive noise time base errors in coherent demodulation of suppressed carrier AM multiplex

07 p1082 A69-19119

Discrete signal detection providing optimum SNR for frequency and time domain differences between signal and noise

07 p1088 A69-19676

Extraterrestrial cosmic emissions responsible for background noise of communications engineering, discussing factors affecting frequency sharing with other services

09 p1586 A69-21294

Optimal detection of determinate signal and signal with random amplitude and phase, estimating probability of false and correct detection

09 p1456 A69-22286

Optimal calculator of detection of Gaussian random signal against Gaussian noise background by reducing input signal to white noise

11 p1835 A69-24713

Real time correlator in periodic signal extraction from noise background, discussing multichannel sampler as special case of cross correlation extraction

11 p1837 A69-25094

Bayes theory and nonclassical variation method to solve optimal energy distribution available for identifying weak signals in background noise

14 p2410 A69-28817

Computerized calculation of likelihood coefficients for identifying steady random processes against background noise, minimizing mean risk of erroneous solution

14 p2410 A69-28818

Algorithms for optimal detection of signals on background of normal noise with time varying intensity

15 p2563 A69-30133

Differential equations for optimum reception to synthesized detectors of deterministic signals against nonGaussian background noise using Markov process

15 p2567 A69-30340

Spectral correlation characteristics of amplitude modulated signal with background noise at envelope detector output

15 p2576 A69-30348

General autocorrelation function for input signal composed of two amplitude modulated noise waves and background noise from detecting system composed of half wave element

15 p2569 A69-30805

Logic circuits abstract synthesis for detecting signals against noise background using known conditional quantized signal distributions

16 p2749 A69-31627

Probabilistic analysis of code message distortion due to pulse noise in modulation systems and comparison between linear and quadratic detections

17 p2919 A69-33145

VHF band surface incidental radio noise levels over metropolitan areas compared with airborne data

17 p2921 A69-33672

NaI/Tl/ and CsI/Tl/ scintillation counters effectiveness in recording low energy protons against counter noise background

18 p3138 A69-35255

Target discrimination from background, discussing spatial, spectral, temporal and polarization effects

19 p3373 A69-36054

M-ary detection for optical communication investigated for maximum likelihood detection of one of M Poisson processes in background noise

19 p3276 A69-36486

Representation theory of signal detection in non-Gaussian noise environments applied for improved near optimum system performance [IEEE PAPER 69-TP-10-COM]

19 p3277 A69-36488

Temporal position of pulse signal on noise background determined by measuring signal passage time through linear filter zero point

19 p3278 A69-36596

Discrete signal detection providing optimum SNR for frequency and time domain differences between signal and noise

20 p3488 A69-37458

Phase error in monopulse antenna system attributed to far field background noise sources during passive or active objects tracking

20 p3492 A69-37707

Ionospheric background noise levels and sources determined from Alouette data

20 p3495 A69-37874

Surrounding noise effects on quick check audiometry test reliability, discussing pathological effects

21 p3725 A69-39286

Electronic stethoscopes for use in high background noise environments for patients on air evacuation flights

21 p3667 A69-39444

Radio emission data from 20 May 1966 partial solar eclipse, giving radio noise and brightness distribution data

22 p4010 A69-39986

Error probability of Gaussian signal detector in Gaussian noise background determined from quadratic form of probability distribution density

22 p3901 A69-40955

Point images reference groups identification by human operator with limited visual perception in background noise, comparing results with automatic system using selection algorithms

23 p4109 A69-41955

BACKGROUND RADIATION

French radio astronomy, presenting sky background radiation and solar emission results from Rubis 02 and 04 rockets

02 p0316 A69-11908

Far IR background due to superposition of IR galaxies, noting galaxies contribution to extragalactic radio background

02 p0308 A69-12128

Cosmic microwave background radiation measurement, discussing measurement techniques for antenna temperature at microwave frequencies

02 p0210 A69-12431

Normal galaxies radio emission and brightness of metagalactic radio background

02 p0325 A69-12564

Cosmic ray origins, considering hard protons, X rays, gamma rays, very soft protons, background radiation, charged particles and neutrinos

03 p0497 A69-12932

Earth velocity through 3 K cosmic background radiation, measuring velocity by determining anisotropy of radiation

03 p0511 A69-13475

Extraterrestrial background gamma radiation /0.3-2 Mev/ observations used to derive upper limits for cosmic ray protons and CNO nuclei in interstellar space

03 p0501 A69-13934

Moving isotropic black body radiation, discussing effect on energy flux and earth velocity measurement through 3K cosmic background radiation

04 p0649 A69-15150

Cosmic X ray background production mechanisms

05 p0814 A69-15848

Photomultipliers response to energetic particles in terms of background current using data from OGO experiments

06 p0923 A69-16932

X ray and gamma astronomy, discussing galactic gamma radiation source and diffuse X ray background radiation

06 p0998 A69-16969

Isotropic background cosmic X ray flux measurements using low latitude balloon to minimize atmospheric background, obtaining hard solar X ray flux upper limits

06 p0992 A69-17311

Nonlinear coupling between background illumination and illumination signal producing lateral electrical fields in p-n junction, noting effect on sensitivity of position sensor

07 p1101 A69-18654

Discrete extragalactic X ray sources model for explanation of diffuse X ray background, noting evolutionary aspects

07 p1206 A69-19255

Luminosity distance, distance by apparent size, number counts, background radiation and apparent angular motion of sources in homogeneous anisotropic model universe

07 p1218 A69-19282

Background radiation intensity upper limits for mm and submillimeter wavelengths in interstellar medium, noting intense flux in far IR

07 p1221 A69-19404

Sky background light automatic compensation in stellar photography, using single or double channel photometer

08 p1313 A69-20247

Sky background of soft X ray emission in spectral band explained by emission lines from galaxies

08 p1380 A69-20769

Cosmic microwave background variations produced by nonthermal gravitational radiation, imposing limits on equivalent mass density

08 p1398 A69-20773

Astronomical data on background radiation examined for existence of galactic radio halo

09 p1590 A69-21395

Galactic and intergalactic ionic fine structure transitions effect on background microwave radiation intensity

09 p1590 A69-21445

Cosmological implications of diffuse X ray background, noting Compton black body process effect on isotropic cosmic X rays

09 p1578 A69-22152

Inverse Compton scattering of far IR background radiation proposed as explanation of high energy gamma ray flux

09 p1580 A69-22296

Diffuse cosmic X ray background measured during balloon flight with actively shielded and collimated detector

09 p1584 A69-22767

Universe rotation from observations of microwave background and using closed universe model

10 p1771 A69-22851

Solid hydrogen condensation on graphite grains for microwave background, discussing hydrogen grain promotion of galactic and stellar formation

10 p1776 A69-23216

Diffuse X radiation spectrum below 4 kev measured with beryllium window proportional counter at rocket altitudes

10 p1770 A69-24094

Supplemented data to analyze intergalactic gas diffuse X ray background radiation

10 p1792 A69-24209

Nonthermal intergalactic bremsstrahlung model as isotropic X ray background due to subatomic electron interactions with thermal ionized gas in expanding universe

11 p1947 A69-24595

Polarization of continuum background of planetary nebulae in window in visible spectrum from scattering of nucleus star radiation by electron gas

13 p2339 A69-27567

Cosmic X ray background measurements and Crab Nebula observation during sounding rocket flight

13 p2326 A69-27570

Microwave background radiation by intense sources studied by homogeneous and isotropic Friedmann and steady state models

13 p2339 A69-27574

Night sky background observation by near IR radiation flux, using rocket-borne telescope and ground based equipment

13 p2342 A69-27600

Spotted scattered background contrast relation to scattering system geometry during laser scattering by suspended Lycopodium spores

13 p2273 A69-28550

Ideal quantum receiver to detect coherent narrow band optical signal in presence of thermal background radiation, noting error probability

14 p2414 A69-29502

Extragalactic background radiation intensity in isotropic world models as function of universe thermal history

14 p2514 A69-29769

X ray energy spectrum from Crab Nebula and diffuse background on celestial sphere near galactic anticenter, noting spectral index

15 p2675 A69-30759

Relative motion of 3 K cosmic background radiation with covariant photon equilibrium distribution

15 p2657 A69-31494

Hydroxyl band contamination of emission and background radiation from night sky

16 p2774 A69-31987

High energy cosmic ray proton, electron and photon propagation through cosmic microwave background, discussing mean free paths

16 p2852 A69-32819

Earth motion relation to cosmic background radiation excess determined from radiometer study of galactic radiation

17 p3022 A69-32864

Low pressure and background radiation conditions via cryogenically cooled surfaces, citing data on cryopumping under vacuum conditions for space simulation chambers

17 p3006 A69-33683

Metagalactic light measurements by lunar based night sky photography

18 p3189 A69-34242

Microwave background anisotropy induced by gravitational effects interpreted using spatially flat Friedmann model for substratum

18 p3190 A69-34286

Milky Way continuum radiation at 4170 MHz using parabolic antenna, mapping discrete sources concentration at galactic equator

18 p3200 A69-34996

Radio interferometry for suppressing background variance between microwave radiometer antenna and random terrestrial background

20 p3506 A69-37712

Unresolved background radiation at 2695 MHz surveyed for galactic wing extent determination

20 p3606 A69-37830

Cosmic X ray background spectral measurement from rocket flight near geomagnetic pole

21 p3787 A69-38351

Soft x ray extragalactic background flux measurements, considering correction for absorption by interstellar medium

21 p3788 A69-38541

X rays and gamma rays extragalactic components, calculating background component intensity for given model of universe

21 p3789 A69-38818

Radio background radiation produced by Galaxy, considering energy, isotropy of radiation and black body character

21 p3790 A69-38821

Ariel 3 satellite attempted background radiation measurement between 2-4 MHz to show absorption onset in Galaxy

21 p3806 A69-39258

Temperature fluctuations in microwave background radiation from primeval perturbations compared with perturbations from discrete radio sources

21 p3815 A69-39611

Critique of Shivanandan suggestion of background radiation spectrum distortions

21 p3815 A69-39612

Microwave background radiation in steady state cosmological model, attempting interpretation as discrete extragalactic radio sources population

22 p4029 A69-40765

High energy astronomical diffuse radiation component properties tabulated, discussing power law and thermal X ray background, gamma rays, etc

23 p4207 A69-42319

Observational cosmology developments with radio and X ray astronomy emphasizing existence, origin, effects and anisotropy of excess microwave background

23 p4219 A69-42327

Cosmic radio background noise spectrum near north galactic pole based on Radio Astronomy Explorer satellite experiments

23 p4219 A69-42375

Fluctuations in 3K radiation, considering scattering effect on gravitational fields of galactic clusters and large coherence or wavelength scattering by gravitational radiation

23 p4222 A69-42401

Homogeneous axisymmetric anisotropic cosmological models, analyzing magnetic fields and initial anisotropies effect on 3K radiation and primordial He production

23 p4222 A69-42402

Soft cosmic X ray background flux from rocket observations on 21 September 1968 from White Sands, discussing flux origins

24 p4368 A69-43220

BACKINGS

U BACKUPS

BACKLOBES

Multiplicative feed system for monopulse angle tracking antennas, discussing influence of sidelobe and backlobe responses on control function slope determining antenna bearing angle

20 p3510 A69-37704

BACKSCATTERING

Forward and backward scattered modes over frequency range in multimode nonuniform waveguide, transforming coupled modes telegraphist equations into Volterra equations

01 p0043 A69-10621

Backscattering diagram of Venus at 40 cm determined from Doppler spectrum and reflected signals range energy distribution

02 p0314 A69-11639

Fluctuating radar echoes from cloud targets with vibrating drops, noting amplitude modulation effect of changing cross section on backscattered signals

02 p0208 A69-12021

Raindrop size distribution law effect on radio wave attenuation coefficient and differential effective backscattering cross section of rain

02 p0208 A69-12259

Mode theory of backscattered radar cross section of elongated dielectric bodies capable of sustaining traveling wave

03 p0384 A69-12907

Radar return signal generation for computer simulations of airborne radar systems, using digital computer program for time varying radar backscatter

03 p0429 A69-13199

Polarization of laser radiation scattered forward and back in artificial fog and smoke

03 p0393 A69-13275

Reflections from input and output ducts influence on gain of TWT strophotron amplifier with/without allowance for back radiation

03 p0407 A69-13980

Mie total and differential backscattering cross sections at laser wavelengths for Junge size distribution aerosol models

04 p0609 A69-14290

Electron backscattering from cathode to cathode due to collisions with molecules, assuming isotropy of scattering

05 p0800 A69-15738

Directly backscattered light /echoes/ from dielectric plane surface with roughness and volume scattering, comparing indicatrices with moon echo

06 p0887 A69-17173

Correspondence between HF radar backscatter, optical aurora and electron precipitation, noting application to gross tracking of auroral oval

06 p0918 A69-17383

Backscattering due to collisions for electrons from emitter accelerated through positive ion sheath into plasma in thermionic diodes

06 p0898 A69-17773

Radar backscattering from turbulent rocket exhaust plumes [AIAA PAPER 69-71]

06 p0891 A69-18071

Computational techniques for determining magnetic field geometry for backscatter reflections

07 p1125 A69-18850

Partial reflections from ionosphere, analyzing electron number densities, noting relation between D region ionization increases and small solar proton events

07 p1205 A69-18956

Atmospheric extinction coefficient and backscattering function determined by laser radar using differential equation

07 p1126 A69-18966

Small amplitude surface irregularities effect on backscattering properties of radar calibration metal sphere, using full wave boundary perturbation method

08 p1273 A69-20027

Forward and backscattering of radio waves at electron concentration discontinuity near reflecting ionospheric layer with vertical nonuniformity

09 p1453 A69-21525

HF ionospheric radar ground scatter map showing separated land-sea backscattered radio waves by Doppler technique

09 p1454 A69-21681

Model of auroral backscatter from E region including ionospheric refraction, comparing computations to experimental HF auroral backscatter data for aspect sensitivity

09 p1488 A69-21700

Sporadic E region HF backscatter observed during IQSY, using PPI display

09 p1489 A69-21701

Laser radar atmospheric applications, noting particulate matter mapping, backscatter density profiles and use of lidar

09 p1521 A69-22795

Combination backscattering on ionic sound waves assumed responsible for unexpected features of radio signals reflected from sun

10 p1776 A69-23219

Laser radiation backscatter along oblique paths in atmosphere, calculating transmission over horizontal and oblique paths

10 p1659 A69-24220

Radar backscatter and rocket profiles of ionospheric electron temperature, noting agreement in daytime flight measurements

11 p1951 A69-25162

Polar cap sporadic E investigation with backscatter at 28 MHz, noting geographic distribution, annual and diurnal variations

12 p2069 A69-26464

Optical radar studies of lower atmosphere, giving Mie theory calculations of clear atmosphere volume backscattering cross sections for four laser wavelengths

12 p2033 A69-27001

Optical wavelength backscattering functions for nebulae in Pleiades cluster, noting color differences and surface brightness

13 p2340 A69-27577

Polarization of laser radiation scattered forward and back in artificial fog and smoke

14 p2410 A69-28783

Forward and backscatter soundings compared to verify focusing mechanism of HF sky waves

14 p2435 A69-28967

Multiple scattering of electromagnetic waves in underdense plasma, deriving transport equation for radar backscatter

14 p2412 A69-29453

Radar backscatter analysis for Arctic ice identification, deriving ice surface roughness factors from Kirchhoff-Huygens principle

14 p2416 A69-29530

Spectral density function derivation for energy scattered from underdense turbulent wake

16 p2732 A69-31893

Fluorescence noise in Q switched ruby laser atmospheric backscattering experiments, noting relation to optical radar spurious and enhanced returns

16 p2777 A69-32183

Angle nature from backscattering patterns at radar station with one transmitting and two receiving antennas

16 p2779 A69-32275

Forward and backscattering of radio waves at electron concentration discontinuity near reflecting ionospheric layer with vertical nonuniformity

16 p2754 A69-32520

Backscattered impulse response waveforms of conducting circular cylinder for broadside incidence utilizing Fourier synthesis

17 p2917 A69-32918

Continental and maritime hygroscopic particles associated with increasing relative humidity, determining effect on backscattered power from laser beam using Mie scattering equations

17 p2981 A69-33160

Periodic fading in 42 MHz auroral backscatter by high speed polarization measurements, discussing scatter bursts and pulsating primary electron flux relationship

18 p3102 A69-34950

Wavelength dependence of total and depolarized backscatter laser light cross section for rough metallic surfaces

18 p3172 A69-35011

Radio meteor ionization profiles, discussing electron line density measurements by backscatter system

19 p3283 A69-35992

Backscattering intensity measurements by optical elements at 180 degrees to beam propagation direction, using CW He-Ne laser as radiation source

20 p3554 A69-37609

Terrain radar returns emphasizing surface roughness influence in man-made target backscattering, determining radar cross section with radar range equation

20 p3490 A69-37646

Sporadic E layer large scale irregularities direction and velocity determined by inclined backscatter method, using plan position indicator

20 p3528 A69-37682

HF backscattering characteristics of infinite conducting cylinder with radially inhomogeneous plasma sheath, using Bessel functions, geometrical optics and graphs

20 p3494 A69-37843

Modified geometrical diffraction theory applied to determination of vertically polarized radar backscattering from rear of cylinders and frustums

20 p3495 A69-37851

Lunar surface scattering properties at 2.5 cm wavelength determined using computerized backscattering diagram and equations for obtaining scattering data

20 p3606 A69-37971

Ground backscatter elevation angle recorded by phase comparison method, postulating ionospheric tilts to interpret data

20 p3535 A69-38188

Bistatic auroral backscatter communications conducted by recording CW transmissions from beacon transmitters to study radio aurora

21 p3709 A69-38498

Simulation and display for radar ground-backscatter signatures by computer ray tracing, using model ionosphere containing realistic traveling disturbances

21 p3717 A69-39280

Chemical analysis of lunar surface by devices exploiting alpha particle backscattering and proton production by alphas placed by Surveyor 5, 6 and 7

22 p4012 A69-40088

Electromagnetic backscattering by perfectly conducting prolate spheroid, predicting echo signal in resonance region

23 p4115 A69-41584

HF backscatter, long delay signals and round-the-world echoes as radio wave propagation modes

23 p4116 A69-41602

BACKUPS

Fiber glass reinforced plastic backing phase of composite armor, noting test method for evaluation of performance

09 p1507 A69-22319

Multiwall meteoroid protection design in Apollo program, discussing bumper, backup sheet and honeycomb cells insulation [AIAA PAPER 69-372]

13 p2367 A69-28304

BACKWARD WAVE TUBES

NT CARCINOTRONS
NT HELITRONS

Frequency and power stable backward wave oscillators as energy pumps for molecular and wideband parametric amplifiers used in satellite receivers

07 p1095 A69-18430

X band internal cavity voltage tunable magnetron operating in theta mode, solving output loading, interaction limitations and cavity dimensions

07 p1102 A69-18670

High performance silicon carbide backward diode, discussing device design and operational characteristics

09 p1470 A69-22787

Synchronized backward wave oscillator transmitting tube for space communication stations

13 p2232 A69-28058

Magnetically shielded O type backward wave oscillators for military and commercial applications

13 p2232 A69-28059

Crossed field backward wave tubes gain with stepwise varying interaction space found greater than with constant height interaction space

13 p2237 A69-28583

BACKWARD WAVES

Equations for self oscillating mode of operation for O-type backward wave generator with electrostatically focused electron beam and finite values of amplification parameter

03 p0407 A69-13986

Backward plasma waves in region of anomalous dispersion indicated by opposite directions of RF wave phase and group velocities

11 p1927 A69-25116

BACTERIA

NT AZOTOBACTER
NT BACILLUS
NT ESCHERICHIA
NT HYDROGENOMONAS
NT NITROBACTER
NT PSEUDOMONAS
NT STEAROTHERMOPHILUS

Rats on casein, soybean and Chlorella diets for protein source noting soybean diet produced no appreciable changes in intestinal flora

02 p0197 A69-11490

Electron transport of Halobacterium cutirubrum, discussing spectrophotometric identification of cytochromes

07 p1068 A69-19481

Energy deposits from decay of tritium incorporated into bacteria, using computer simulation for radiation dose distribution

07 p1068 A69-19490

Amber suppressors conversion to ochre suppressors in RNA of bacterium or bacteriophage using uracil mutagen

07 p1068 A69-19493

Ionizing radiation-initiated degradation of deoxyribonucleic acid in bacteria, noting role of defective prophage

07 p1068 A69-19494

Escherichia coli WWU multiauxotrophic revertants with nonsense suppression, noting role in aberrant morphology and in catabolizing thymidine for energy and carbon

07 p1069 A69-19503

Degree of organization in bacterial cell, discussing pool size and DNA synthesis

07 p1069 A69-19505

High vacuum effects on oxidative processes in bacteria and physiological activities of enzymes

15 p2557 A69-31354

Salts and organic solvents effect on halophilic Halobacterium cutirubrum catalase, noting enzyme activity inhibition by cation and anion

18 p3096 A69-35291

BACTERICIDES

Antimicrobial spacecraft materials, discussing feasibility of impregnation or chemical combination of materials with bactericides

05 p0713 A69-15944

Activated carbons and ion exchange resins bactericidal action as function of silver coating techniques

13 p2216 A69-28621

BACTERIOLOGY

Automatic devices to count bacterial colonies Petri dishes consisting of culture plate scanner and data processor

02 p1201 A69-11773

Escherichia coli detection and differentiation from other bacteria by direct gas chromatographic analysis of culture media

03 p0382 A69-13550

Hydrogenomonas eutropha as means of protein food source independent of conventional agriculture for animal feed supplement

10 p1644 A69-23306

Oxygen physiological and biochemical effects on Pseudomonas saccharophila, discussing sucrose uptake, lipid synthesis and polysaccharide formation

15 p2556 A69-31045

B Coli commune cultivated on various substrates, studying oxygen consumption under aerobic/ anaerobic conditions

18 p3097 A69-35302

Ferredoxin from thermophilic and mesophilic Clostridia, noting difference in heat stability due to iron and sulfide environments

22 p3897 A69-41068

BACTERIOPHAGES

Lethal effect of solar UV radiations on dried Coliphage T-1 exposed to space at sounding rocket altitudes

01 p0017 A69-11086

Inactivation of T4 bacteriophage by tritium decay incorporated into DNA and phage protein

07 p1068 A69-19491

Amber suppressors conversion to ochre suppressors in RNA of bacterium or bacteriophage using uracil mutagen

07 p1068 A69-19493

Inhibition of gamma ray induced DNA degradation by infection with bacteriophage

07 p1069 A69-19709

Defective bacteriophage PBSh in Bacillus subtilis after mitomycin C treatment, showing DNA synthesis and marker frequency change

15 p2555 A69-30446

Bacteriophage desoxyribonucleic acid /DNA/ degradation by gamma irradiation in vitro by Co 60, discussing breaks, cross links and molecular weight

23 p4079 A69-41402

Thin films of infectious DNA of bacteriophage bombarded by slow protons, determining differential inactivation cross sections

23 p4081 A69-41431

BAFFLES

Activation energies in baffle stabilized flame deduced from reaction zone using gas chromatography

06 p1035 A69-17930

Hydraulic analog for determining acoustic behavior of baffle cell used in liquid rocket engines, comparing ring and spoke type baffles

09 p1570 A69-22004

Temperature influence of homogeneous kerosene-air mixture on flame stabilization by mechanical and gas dynamic baffle systems

21 p3850 A69-38859

Circular baffle mounted above flat-bottomed cylindrical tank outlet, discussing effect on remaining tank fluid volume and flow behavior under low gravity conditions

21 p3696 A69-39232

BAGS

Small hovercraft simple and bag skirts design characteristics, considering materials

13 p2202 A69-27545

BAILOUT

Ocular injuries during bailout from Vampire aircraft, noting hemorrhages

10 p1649 A69-23380

BAINITE

Bainite beta to alpha transformation in titanium-oxygen system, using high temperature metallography techniques

04 p0613 A69-14559

BAINITIC STEEL

Monograph on effect of boron, zirconium and titanium on austenite transformation of CrMo steels bainite and martensite covering carbides, nitrides, mechanical properties, etc

11 p1903 A69-24634

BAKEOUT

U DEGLASSING

BAKER-NUNN CAMERA

Baker-Nunn photometry from Apollo tracking utilizing photographs for brightness, dynamics and duration of rocket exhausts and venting clouds

15 p2571 A69-31338

BALANCE

Unbalance effects on rigid naval turborotor on oil film bearings in flexibly mounted housings investigated at varying critical speeds and housing stiffness [ASME PAPER 69-DE-9]

14 p2453 A69-28839

Aerospace balancing system with hydrostatic spindle, describing component construction and functions [SAWE PAPER 737]

18 p3118 A69-34890

Skin friction balance for shear stress measurements in presence of ablation, describing balance construction, calibration, flexure range, etc

19 p3292 A69-35735

Pressure loads and balancing force determination in kinematic pairs of link gear of landing mechanism

23 p4062 A69-41415

BALANCED AMPLIFIERS

U PUSH-PULL AMPLIFIERS

BALANCING

Balancing criteria for rotors of rotating machines, discussing acceptable residual specific unbalance, center of gravity displacement and machine vibration tolerance [ASME PAPER 69-VIBR-60]

10 p1804 A69-24149

Dynamic balancing mechanics covering graphical representation, mass asymmetries corrections or adjustment calculations and ballasting equations [SAWE PAPER 736]

18 p3220 A69-34891

BALL BEARINGS

Ball bearings lubrication and wear in cryogenic hydrogen turbopumps by transfer films provided from self lubricating cage

01 p0084 A69-10109

Fatigue life, kinematics, dynamics, etc, of thrust loaded ball bearings, considering inertial effects of hollow balls

01 p0087 A69-10908

Ball bearing test apparatus for evaluation of greases and solid lubricants at high temperatures [ASLE PREPRINT 68AM 7C-2]

01 p0087 A69-10912

Axial rigidity effect of centrifugal force acting on balls of rapidly rotating radial thrust bearing

04 p0605 A69-14606

Sodium nitrite and sodium stearate as grease additives for lubrication of ball bearings running in helium [IME PAPER 1]

07 p1137 A69-18559

Rolling elements for high temperatures, discussing solid film lubricants, unlubricated rolling contact and materials and surface treatment [IME PAPER 2]

07 p1138 A69-18566

Solid lubricant compacts for ball bearing separator materials, describing fabrication, design and friction and wear properties in air and vacuum [ASLE PAPER 68-LC-16]

07 p1139 A69-18626

Cooling requirements for high speed polytetrafluorethylene lubricated ball bearings operating in cold hydrogen gas, developing minimum gas flow rate equation [ASLE PAPER 68-LC-2]

07 p1141 A69-19310

Contact conformity effects on spinning torque and friction coefficient in angular contact ball bearings from lubricated and unlubricated tests [ASME PAPER 68-LUB-10]

15 p2628 A69-30901

High speed ball bearing skidding, proposing analytic model as design tool, discussing effects of thrust load, speed, oil temperature and flow rate
[ASME PAPER 69-LUBS-20]

18 p3140 A69-34377

Steel ball bearing high temperature fatigue life tested with synthetic paraffinic oil, fluorocarbon and polyphenyl ether
[ASME PAPER 69-LUBS-18]

18 p3140 A69-34378

Ball bearing lubrication simulation by rolling disk apparatus, emphasizing surface slip and related thermal effects alterable by geometric expansion
[ASME PAPER 69-LUBS-16]

18 p3140 A69-34380

Elastohydrodynamic solution for ball torque spinning without rolling in nonconforming groove, showing increase in torque with stress and spinning and decreasing conformity
[ASME PAPER 69-LUBS-11]

18 p3140 A69-34381

Polyphenyl ether lubricants and self lubricating materials compared for antifriction ball bearings in thrust reversing actuator gear box
[SAWE PAPER 68-LC-1]

18 p3148 A69-35003

Oxygen concentration effects on oxidation of synthetic paraffinic and type II ester lubricants determined from ball bearing tests at 400 and 450 degrees F

18 p3149 A69-35177

Hydrostatic bearings analysis for high pressure cryogenic rocket engine turbopumps to predict steady state and time dependent performance, noting turbulence, inertia and compressibility

22 p3955 A69-40408

High speed radially resistant ball bearing, analyzing effect of lubrication film on axial rigidity

23 p4169 A69-41555

BALLISTIC CAMERAS

Ballistics room of Royal Belgian Observatory for observation of geodetic satellites

08 p1272 A69-19993

Multiple frame camera with image compensation as ballistic phototeodolite

12 p2084 A69-26153

Schlieren high speed photography systems for ballistic projectile studies, discussing use of gas lasers as nanosecond light sources

12 p2088 A69-26182

High speed photography for hypervelocity aeroballistic ranges, using giant pulse ruby laser for front lighting

19 p3306 A69-35732

BALLISTIC MISSILE EARLY WARNING SYSTEM

Paper-honeycomb sandwich radome structure for protecting monopulse UHF radar antennas used in BMEWS

07 p1111 A69-19537

BALLISTIC MISSILES

NT INTERCONTINENTAL BALLISTIC MISSILES
NT MINUTEMAN ICBM
NT POLARIS MISSILES
NT V-2 MISSILE

Soviet book on inertial control of ballistic rockets covering rocket flight deviations measured by onboard sensors and computer

01 p0113 A69-10994

Psychomotor reactions to zero gravity during ballistic rocket flights, analyzing electrical activity of cortex in animals

06 p0874 A69-17649

Ballistic missile and aircraft operational effectiveness, discussing data collection, reliability, availability and capability surveillance by computer

18 p3145 A69-34500

Reliability assessment of ballistic missile inertial guidance system, discussing objectives and requisites

22 p3953 A69-40028

BALLISTIC RANGES

High enthalpy, Mach and Reynolds number flight studies on ballistic ranges, describing launchers, flight simulation, measuring and recording techniques

06 p0860 A69-17632

Ballistic range tests to study ablation effects on aerodynamic characteristics of ablating and nonablating slender cones
[AIAA PAPER 69-179]

06 p1036 A69-18083

Atmospheric entry testing in terms of velocity-altitude duplication, suggesting multistage rocket propelled aeroballistic range type testing
[AIAA PAPER 69-166]

06 p0907 A69-18189

Electrostatic probes in nonequilibrium collision dominated ionized gas flow ballistic ranges

19 p3291 A69-35716

Electrostatic probes calibration and use for hypersonic wakes behind projectiles in ballistic range

19 p3291 A69-35717

Nanosecond pulse coherent Doppler radar for monostatic measurements of turbulent wakes in shock tunnels and ballistic ranges

19 p3293 A69-35743

BALLISTIC TRAJECTORIES

Monkey psychomotor reactions during ballistic flight, noting alertness reduction during weightlessness

01 p0017 A69-11082

Relative weight of fuel required for flight along prescribed flight trajectory

03 p0519 A69-12964

Approximate method for calculating vertical velocity distribution in atmospheric braking of bodies along ballistic trajectories

04 p0541 A69-14485

Ballistic reentry trajectories, considering point mass motion in central force field under tangential thrust action and spherical atmospheric density distribution

06 p1006 A69-17564

Ablative and insulative performance of reference heat shield materials under transient heating simulating ballistic vehicle reentry trajectory, using plasma jet facility

06 p0907 A69-18110

Ballistic reentry vehicle roll-pitch coupling, showing influence of nose asymmetries

06 p1018 A69-18156

Anomalous roll behavior of spinning ballistic reentry vehicles with compound aerodynamic asymmetry consisting of lateral offset combined with trim angle of attack

06 p1019 A69-18168

Longitudinal stability of unsteady motion of flight vehicle along ballistic trajectory, using linear differential equations

07 p1230 A69-19701

Differential equation for droplet motion along ballistic trajectory in gas flow, noting applicability to solid bodies via computer programming

09 p1483 A69-22222

Psychomotor reaction time and motions, myogenic tonus at rest and precision of monkeys during rocket flights along ballistic curve, noting weightlessness effect

10 p1646 A69-23575

Differential coefficients applied to Izsak-Borchers ballistic trajectory and errors produced by perturbations of initial vectors, applying results to data capsule recovery

16 p2857 A69-32156

Trajectory calculation of axisymmetrical body during ballistic and vertical flight, assuming air drag proportional to square of velocity

17 p2889 A69-32950

Halley Comet rendezvous mission, comparing low thrust mode with ballistic Jupiter or Saturn swingby mode

21 p3809 A69-39360

Laser shadowgraph technique for visual observation of projectiles surface flying at hypersonic velocity along ballistic trajectory

22 p3963 A69-40601

Ballistic equations for mass center movement in vertical plane defined by projectile initial velocity

23 p4183 A69-42482

BALLISTIC VEHICLES

Rolling ballistic vehicles mass and aerodynamic characteristics determined from dynamic motion data by performing Fourier analysis on roll axis equation of motion

06 p0862 A69-18039

Intermittent flow facilities for ballistic and lifting reentry flight simulation including shock tubes, ballistic ranges and shock and gun tunnels

11 p1863 A69-25016

Aerodynamic characteristics of ballistic reentry vehicles from flight test dynamic measurements, illustrating results

18 p3085 A69-34670

BALLISTICS

NT INTERIOR BALLISTICS

NT TERMINAL BALLISTICS

Ballistic deviations of gyropendulum vertical damped by astatic gyroscope

06 p0927 A69-17687

Pyrotechnical devices for two stage solid propellant ballistic rocket, discussing self priming electric cells and auxiliary power and gas generators

10 p1752 A69-23024

Ballistically effective atmospheric parameters for rocket vehicle design manuals involving application of climatological concepts of meteorology

12 p2175 A69-26874

Mathematical models for ballistic limit of single and double wall structures, yielding equations for relation to projectile and target characteristics
[AIAA PAPER 69-370]

13 p2367 A69-28302

Hypervelocity projectile size and density effect on ballistic limit of dual sheet spacecraft meteoroid protection structures, considering penetration of low and high density particles
[AIAA PAPER 69-376]

13 p2367 A69-28306

Ballistic wake structure and jump conditions for plane plasma shock waves with electrostatic turbulence

15 p2660 A69-30914

Stability conditions determination for spinning projectile based on ballistic equations, discussing role of Magnus effect

21 p3772 A69-39294

BALLISTOCARDIOGRAPHY

Amplitude variations in ULF ballistocardiograms of young normal airline stewardesses and applicants, discussing cardiovascular reactivity

09 p1444 A69-22544

Flow rate in ascending aorta, stroke volume and cardiac output determination by ballistocardiography, calculations based on Hagen-Poiseuille theory

17 p2915 A69-33772

BALLOON FLIGHT

Energetic X ray intensities from large and small Magellanic clouds investigated by balloon flight sky survey, noting energy flux upper limits

01 p0150 A69-10370

French balloon types, manufacture, behavior at ceiling, CNES launching center and satellite interrogation

02 p0193 A69-11915

Balloon flown High Altitude Particle Physics Experiments /HAPPE/ for research on high energy cosmic rays and particle interactions

03 p0499 A69-12943

Rigidity spectra of total primary cosmic radiation by ascending or descending balloon-borne detectors in atmosphere, with changing mean response energy

06 p0989 A69-17279

Transistorized multichannel pulse height analyzer and recording system for balloon-borne cosmic ray payloads, discussing performance capacity

06 p0924 A69-17284

Spark chambers for primary cosmic ray study in balloon flights, detailing construction and performance

06 p0924 A69-17285

X ray sources intensity and spectrum variation with time, describing proposed balloon experiments with equatorial launching for performing measurements

06 p0992 A69-17312

Pressure-altitude transducers for atmospheric pressure measurements on balloon flights including diaphragm, thermoconductivity, radioactive density and hypsometer gauges

07 p1132 A69-18873

Northern sky scan for discrete sources of gamma rays in 240 to 1000 kev energy region by telescope on balloon flight

11 p1946 A69-24593

Balloon-borne instrumentation for detection of far IR extended emission regions and bright point sources, describing results of initial flights

13 p2342 A69-27599

Mixed balloon systems for long duration stratospheric flights with open balloon to carry payload and overpressure balloon as stabilizer or aerial buoy

15 p2551 A69-30703

GHOST Balloon Project, emphasizing launch and ascent control and location and life expectancy of superpressure balloons in tropical stratosphere

15 p2551 A69-31361

Zonal winds in temperate latitude analyzed as function of latitude and month from GHOST balloon flights in Southern Hemisphere at 200 mb

17 p2997 A69-33163

Stabilization system design for stratospheric balloon gondolas, discussing optimal system with flywheel and weight combination

17 p2898 A69-33242

Stratospheric balloon vertical oscillations and gondola attitude during long flights

19 p3248 A69-36689

Balloon-borne gondola azimuth stabilization using lunar tracker

20 p3538 A69-37300

EOLE constant level balloon flights in troposphere, discussing short lifetime due to overloading with ice in dense cirrus cloud

21 p3646 A69-38373

Balloon location by low orbit meteorological satellites, discussing balloon movement due to wind and geometric and nongeometric effects on errors

21 p3760 A69-38618

Auroral zone X rays measurement counting rate vs time patterns from balloon flights at Kiruna

21 p3791 A69-39252

Cosmic radiation altitude profiles, giving tabulation of counting rates obtained by SPARMO flights at different locations

21 p3791 A69-39253

Splash and return albedo electrons in cosmic ray electron spectrum between 12 Mev-1 Gev measured by high altitude balloon flight

22 p4005 A69-40510

Earth observations from balloons - Conference, Washington, D.C., February 1969

22 p3864 A69-40803

Wind information obtained for design and operation of tethered or hovering free floating balloon systems

22 p3864 A69-40804

Balloon flights for testing remote sensor systems prior to space flight, considering return beam vidicon and tracking telescope suitability for experimentation

22 p3865 A69-40806

Balloon flights with space available for secondary experiments, discussing launching agencies and experiment design restrictions

22 p3865 A69-40807

Microwave power transmission to high or low altitude balloon systems for stationkeeping, describing flexible diode array rectifier antenna

22 p3870 A69-40809

Hot air balloon observational platform capabilities and advantages compared with helicopters, fixed wing aircraft and He balloons

22 p3865 A69-40810

Acrostatic and aerodynamic characteristics of Dart Vee tethered balloon system

22 p3865 A69-40813

High altitude balloon stationkeeping system combining battery powered propeller and drag chute

22 p3866 A69-40941

BALLOON SOUNDING

Balloon, rocket probe and satellite payloads, noting French contributions and CNES role

02 p0333 A69-11914

Northern California humidity to 32 km utilizing alpha radiation hygrometer and associated balloon sounding equipment

03 p0461 A69-13345

Stratospheric balloons for space research, emphasizing stabilization equipment suitability

03 p0366 A69-13589

Cosmic ray intensity after solar flare shown greater than during quiet periods from balloon data at Murmansk and Mirnyi

04 p0648 A69-14375

Balloon observations of solar far IR spectrum and brightness temperature

04 p0652 A69-14419

Auroral zone X ray measurements obtained by simultaneous balloon flights over Northern Scandinavia

05 p0813 A69-15822

Balloon-borne instrumentation X ray measurements, discussing detector electronics, telemetry, pressure transducer, power supply, environmental tests, energy limit and calibration

05 p0762 A69-15824

Time coding system for recording balloon measurements on magnetic tape

05 p0762 A69-15825

Attitude stabilized balloon telescope for measuring interplanetary scattered light and nightglow

06 p0999 A69-16972

Radiation bursts in subpolar stratosphere recorded by gas discharge counters on board sounding balloons

06 p0921 A69-17744

Upper wind observation and computation accuracy, comparing radar and slide rule instrument errors

06 p0950 A69-17788

Constant level sounding balloon systems providing global data on atmospheric circulation, discussing icing problems and average life improvement

07 p1053 A69-18955

Gamma ray telescope development for balloon-borne astronomy in search for discrete gamma sources and supernova explosions

07 p1134 A69-19192

Nocturnal auroral electron showers configuration and displacement determined from sounding balloon measurement of X rays due to showers braking in upper atmosphere

08 p1308 A69-20281

Ion exchange fuel cells for emitter-receiver on atmospheric constant ceiling balloon, stressing pressure effect on operation and fuel storage

08 p1260 A69-21042

Pilot balloon and radiosonde measurements for p as function of wind direction, velocity and stability, discussing variation with air layers

09 p1535 A69-21516

Centaurus constellation search for gamma rays using balloons, discussing radio and X ray luminosity

09 p1580 A69-22269

Weak X ray sources at 20-100 Kev photon energies observed during balloon flight, finding hard rays from Ara XR-1 and Nor XR-1

09 p1583 A69-22763

High energy X ray observational data for Sagittarius sources scanned by active telescope during February 1968 balloon flight

09 p1583 A69-22764

Spectrum of high energy X ray flux from Sco XR- 1 during balloon flight using active collimator detector and graded shield detector

09 p1584 A69-22766

Statistical distributions of refractive index parameters in tropospheric radio propagation from psychrometer soundings, discussing lapse rate

13 p2254 A69-28428

Proton and alpha particle fluxes above specified vertical geomagnetic cut-off rigidity measured by balloon-borne Cerenkov scintillation counter telescope

14 p2511 A69-28951

Mixed balloon systems for long duration stratospheric flights with open balloon to carry payload and overpressure balloon as stabilizer or aerial buoy

15 p2551 A69-30703

Systematic error pattern in raw data obtained during tracking ROSE balloons by two radar systems, estimating range resolver error

15 p2649 A69-30897

Cadmium sulfides thin film solar cells for supplying power to instrumentation and data telemetry on longer lived balloons

15 p2553 A69-31287

Balloon for in situ measurements of atmospheric optical parameters using two axis sun pointer, spectropolarimeter and airborne telemetry

15 p2615 A69-31288

Balloon-borne UV polarimetry of stars and planets, studying linear polarization between 2000 and 3000 A

15 p2616 A69-31380

Stratospheric balloons launching and nacelles for measurement of cosmic rays, atmosphere high altitude characteristics, discussing French launching center

16 p2734 A69-31759

Hydrogen-oxygen ion exchange membrane fuel cells for sounding balloons, discussing flight duration and power requirements, gas supply pressure effects, etc

16 p2738 A69-32413

Fast atmospheric neutrons flux and spectrum measurement during two balloon flights, tabulating results and evaluating albedo flux during quiet sun period

16 p2851 A69-32616

Vertical distribution of concentration, microstructure and chemical composition of solid aerosol in troposphere and stratosphere from high altitude balloon measurements

18 p3132 A69-35340

M-87 X ray luminosity from balloon-borne detectors, considering background counting rate relation to azimuth

20 p3588 A69-37488

Solar protons intensity increase observed by balloon-borne instruments over Antarctica, describing decay phases

20 p3589 A69-37556

Pilot balloon observation errors due to inaccurate balloon height determination, relating error determination to wind speed and direction errors

20 p3572 A69-37699

Electronic computer for processing observational data from pilot balloons, utilizing algorithms of values in programming for accuracy and time saving

20 p3572 A69-37700

Balloon-borne transmitter consisting of oscillator, driver and final output and connectable automatic frequency control circuit

21 p3682 A69-39251

Buoyant Venus Station balloon for deployment and inflation during parachute descent into Venus atmosphere tested with scale model balloons in wind tunnels

[AIAA PAPER 69-1017]

22 p3922 A69-40389

Diurnal variations of electron flux based on balloon observations near polar cap consistent with geomagnetic cut-off variations of magnetospheric models

22 p4005 A69-40511

Earth observations from balloons - Conference, Washington, D.C., February 1969

22 p3864 A69-40803

Agricultural and forestry applications of tethered balloons, discussing observation angle effect on spectral signature response and signal preprocessing

22 p4053 A69-40805

Hot air balloon observational platform capabilities and advantages compared with helicopters, fixed wing aircraft and He balloons

22 p3865 A69-40810

Photographic platform applications of tethered balloons, discussing powered systems for low and high altitudes and free balloons

22 p3865 A69-40811

Balloon-borne instrument for auroral X ray measurements at Antarctic station, discussing design requirements, circuit characteristics and improvement recommendations

23 p4166 A69-42011

High energy gamma rays point source in Sagittarius indicated from evidence obtained by high altitude balloon flights

24 p4365 A69-42606

Isotropic cosmic X rays measured by balloon-borne scintillation telescope, discussing agreement with electron energy spectral distribution

24 p4368 A69-43185

Solar high energy gamma ray flux abrupt increase detected by neutral particle plastic scintillators at balloon altitude

24 p4371 A69-43612

BALLOONS

NT HIGH ALTITUDE BALLOONS

NT METEOROLOGICAL BALLOONS

NT TETHERED BALLOONS

French balloon types, manufacture, behavior at ceiling, CNES launching center and satellite interrogation

02 p0193 A69-11915

Balloon satellite orbital time and eccentricity correlated, investigating earth shadow and solar radiation effects

19 p3427 A69-36628

Hot air balloon observational platform capabilities and advantages compared with helicopters, fixed wing aircraft and He balloons

22 p3865 A69-40810

Scientific balloon vehicle design and development approaches for altitude, flight duration and payload capacity extension, discussing plastic balloons

22 p3865 A69-40812

BALMER SERIES

IR and violet sulfur lines for Seyfert galaxies, noting substantial reddening in nuclei

02 p0325 A69-12593

Electron temperatures and optical depths for planetary nebulae outer regions derived using radio spectra and Balmer line isophotes

06 p1009 A69-17962

Stark broadening of Balmer H alpha, H beta, H gamma and H delta lines in plasma region in strong magnetic fields

09 p1542 A69-22248

Solar Lyman alpha, Lyman beta and Balmer alpha lines of He 2 for electron temperature and density and optical thickness of emitting layer

10 p1772 A69-22859

Hydrogen balmer lines broadening by Stark and Doppler effects, finding prominences and chromosphere electron concentrations

11 p1955 A69-24389

Photometric and colorimetric characteristics of hot gas optically thin in continuous spectrum with optical thickness of several units in Balmer series lines

12 p2159 A69-26667

Spectrum of abnormal B-type star HR 3817, noting Balmer line profiles and instrumentation

12 p2172 A69-27160

Hydrogen content in Ia supergiant spectra of type B, noting lack of Stark wings of Balmer lines

13 p2348 A69-27722

Ultimate resolvable line dependence of Balmer series on electron density, considering line broadened by Stark and Doppler effects

13 p2351 A69-27865

- Magnetic A star HD 152107 anomalous intensification of Balmer series H lines observed by spectrograms 13 p2352 A69-27873
- Excited hydrogen RF spectral lines from nebula NGC 6618, calculating frequency for transitions by Balmer formula 13 p2353 A69-28433
- Balmer jumps for B star temperature scale, discussing relation between observed Balmer jumps and observed U-B color indices 14 p2518 A69-29132
- Balmer alpha emission for abundance and distribution of hydrogen around earth, relating temporal variations to azimuth 15 p2700 A69-31437
- Balmer line H alpha emission and absorption coefficients measured with hydrogen plasma generated in high current low voltage free burning arc 16 p2822 A69-32040
- Nonocculted areas of Algol during eclipse using Balmer discontinuity spectrophotometric method, determining apparent stellar diameters 16 p2858 A69-32216
- Spectroscopic study of P Cygni showing ionization temperature, Balmer decrement agreement with calculated value and chemical composition 16 p2864 A69-32595
- HD 217050 spectroscopic study, determining Balmer envelope temperature from comparison of homologous Balmer and Paschen lines intensities 18 p3201 A69-35144
- Balmer line spectrum formation in extended atmospheres of Be and shell stars, noting influence of angle of inclination to observer 18 p3204 A69-35349
- Balmer and Ca II/K line profiles computed by program based on model atmospheres, comparing computed and observed data for F stars 19 p3426 A69-36578
- O stars absolute magnitudes scales, discussing use of Balmer discontinuity in magnitude calculations 23 p4213 A69-41699
- Hydrogen balmer lines broadening by Stark and Doppler effects, finding prominences and chromosphere electron concentrations 24 p4390 A69-43779
- BALSA**
- Balsa wood laminates as aircraft structural material noting thermal properties, fire and fatigue resistance, weight savings, etc 01 p0101 A69-10595
- BANACH SPACE**
- Soviet book on linear differential equations in Banach space covering equations with unrestricted operators, continuous semigroups, partial differential equations and asymptotic methods 01 p0106 A69-10996
- Volterra equation generalization by method involving operator for mapping of topological space into Banach space 02 p0270 A69-11534
- Nonlinear A/x/ operators in reflexive Banach space Y characterized by weak closure of values, defining solvability conditions for equations having such operator 10 p1720 A69-23563
- Successive approximation techniques for problems in optimum control theory, considering maximum principle and Banach space 11 p1908 A69-24771
- Boundedness criteria for second order hyperbolic equation boundary value problem solution in Banach space 12 p2122 A69-26573
- Closed linear operators in topological vector space generalized for Banach space case 13 p2288 A69-27734
- Zlmal theorems refinements by means of Banach theorem of fixed points for Liénard differential equation 13 p2289 A69-27925
- Liapunov first stability theorem generalized for differential equations in Banach space 19 p3360 A69-35860
- Fixed point existence in study nonlinear mapping determined on semiordeed Banach space, noting results applicability to integral equations and boundary value problems 19 p3361 A69-36640
- Monotonic minimization algorithm for nonsmooth extremal problems of mathematical programming, game theory, approximations and optimal control in arbitrary Banach space 23 p4181 A69-41524

BAND STRUCTURE OF SOLIDS

- GaAs photoemissive yield spectrum analysis, discussing transition energies and energy band structure models 01 p0140 A69-11254
- Heterojunction band model and carrier transport mechanisms emphasizing applications to heterophotodiodes, solar cells and hetero field effect transistors 02 p0294 A69-11598
- Gray tin band structure, noting Shubnikov-de Haas oscillations, transport properties, piezo-Hall effect, magnetoreflection and free carrier absorption 02 p0295 A69-11783
- Electroreflectance spectra of Ge-Si alloys, noting concentration dependence and band structure of Si and Ge 02 p0295 A69-11784
- Electron band structure of copper-nickel alloys, discussing thermoelectric properties, energy ranges and effect of alloying additions 02 p0301 A69-12765
- Impurity profiles and energy band diagram for cuprous sulfide-CdS heterojunction based on capacitance, Hall and electron microprobe measurements 03 p0368 A69-13075
- Gunn effect and resulting electron transfer mechanism in semiconductor devices 03 p0486 A69-13610
- Bound excitons spectra in CdS, semiconductor band structure and tabulating positions of lines identified with excitons 03 p0488 A69-13784
- Energy structure parameters for ZnTe-CdTe and ZnSe-ZnTe crystals, obtaining forbidden bandwidth dependence on composition 03 p0492 A69-14173
- ZnTe electronic structure from photoemission study, noting emitted electron energy distribution 03 p0493 A69-14239
- Superconductivity and band structure from pseudopotential for zinc and cadmium, analyzing values of electron phonon mass enhancement 04 p0642 A69-14965
- Electron beam modulation of germanium reflectance 05 p0807 A69-15816
- Gallium arsenide injection lasers properties, analyzing band structure, optical transitions, recombination lifetimes, conduction band states, optical gain, etc 05 p0772 A69-16228
- Design theory of esaki diodes relation to internal parameters of degenerate semiconductors, discussing Fermi level position and maximum state density in purity band 05 p0732 A69-16298
- Nonlinear optical coefficients in group IV and III-V semiconductors, calculating contribution from conduction and core electrons [IEEE PAPER V-7] 05 p0776 A69-16329
- BiTeBr semiconductor band structure determined from electrical and optical properties 05 p0810 A69-16609
- GaAs IR emitters efficiency due to semiconductor material band structure 06 p0894 A69-17248
- Impurities effect on electron energy spectrum in semiconductors at zone boundary and arbitrary doping levels, using Green function 09 p1554 A69-21467
- Alkali halide single crystals disintegration by laser radiation differs as function of crystal physicochemical properties and band structure 10 p1745 A69-23322
- Band structure and reflection spectra of vanadium dioxide and pentoxide single crystals, noting changes in metal-semiconductor phase transition 12 p2145 A69-26724
- Solid state physics applications to fracture problems and structure of solids, considering crystallography, lattice vibrations, defects, electron bands, alloys and surface physics 13 p2316 A69-27221
- GaS, GaSe and InSe crystals band structure from analyzing reflection spectra, noting sensitivity to visible, IR and hard radiation 13 p2317 A69-27883
- Conduction band structure in GaSb noting temperature dependence 13 p2319 A69-27899
- Burstein-Moss effect observed in studying n-GaAs crystals electrical reflection spectra with large free carrier concentration at two temperatures and low energy levels 15 p2666 A69-30060
- X pocket Fermi surface of ferromagnetic Ni, considering magnetic breakdown effects 15 p2668 A69-30687
- Impurities effect on electron energy spectrum in semiconductors at zone boundary and arbitrary doping levels, using Green function 15 p2669 A69-30712
- Impurity levels in semiconductors with multiconduction bands, noting impurities influence on photoluminescence, laser action and Gunn effect 19 p3385 A69-36514
- Band structure and optical constants of InSb, InAs and GaSb, calculating linear momentum matrix elements and state density with spin-orbit effects included 19 p3385 A69-36515
- Band structure for narrow energy gaps of GeTe and SnTe by perturbation model, noting constant free path and relaxation time 19 p3385 A69-36516
- Combined resonance transition in n-type InSb by IR radiation, plotting intensity against magnetic field for different carrier concentrations to infer band structure 19 p3385 A69-36520
- Narrow band gap alloys and ferromagnetic semiconductors, using transport properties for characterization 19 p3385 A69-36541
- Low temperature energy band gap in n-type single semiconductor crystals of In-Sb-Bi alloys analyzed by measuring Hall constant and optical absorption coefficient 19 p3390 A69-36552
- Band structure and reflection spectra of vanadium dioxide and pentoxide single crystals, noting changes in metal-semiconductor phase transition 21 p3781 A69-39137
- Thermal EMF in cadmium arsenide specimens with various electron concentrations determined to verify parabolic subband structure of conduction band 22 p3993 A69-40607
- BANDPASS FILTERS**
- NT CRYSTAL FILTERS
- NT TRACKING FILTERS
- Multistub filter for microstripline using shorted and open stubs 01 p0041 A69-10200
- Filter uncertainty for time or frequency resolution in analysis of waveform, decomposing characteristic functions and determining least uncertain realizable filter 02 p0226 A69-12306
- Conventional TWT theory modified to include interaction between beam and two spatial harmonics, investigating TWT stability near edges of pass band 03 p0407 A69-13976
- Tunable ferrimagnetic bandpass filter using magic T configuration to permit low magnetic field strength and retain nonstacked configuration advantages 04 p0573 A69-14343
- Narrow bandpass filters based on ripple adjustment in response of low or high pass prototype 04 p0574 A69-14345
- Recirculator with sign variable feedback coefficient for delay line passband increase 04 p0575 A69-14464
- Active RC low pass filters sensitivity to component changes, discussing effect of below minimum limit value 04 p0578 A69-15070
- Digital filter design with complex coefficients for analytic signals and complex envelopes 04 p0579 A69-15460
- Instrument profile of birefringent Lyot filter for H alpha line determined from photographic spectra with grating spectrograph 04 p0664 A69-15524
- Diagrams for power transfer parameters between double tuned bandpass filters with arbitrary coupling 05 p0729 A69-15964
- Five layer thin film band elimination filters amplitude and phase frequency characteristics 05 p0729 A69-16088
- Waveform distortions of trapezoidal wave passing through Gaussian filter in pulse transmission, discussing ideal filter effects on degradation 05 p0719 A69-16296
- Broadband LC filters having prescribed amplitude response and constant group delay, emphasizing IF filters for radio relays 05 p0732 A69-16343

Harmonic ion cyclotron waves shown to possess stop and passband characteristics, supporting quasi-static ion cyclotron mode theory

06 p0970 A69-17953

Frequency modulated signal envelope passage through bandpass filter of inductively coupled circuits described by differential equation

07 p1100 A69-18555

Statistical analysis of cascade of bandpass limiter, ideal phase detector and video filter for mathematical modeling of coherent communication systems

07 p1084 A69-19147

Frequency transformation allowing comb-line filters of narrow and wide bandwidth, using resonance type filters with lumped elements

07 p1108 A69-19487

Pseudoexact Chebyshev response curves for bandpass filter design, discussing phase response and time delay characteristics

08 p1283 A69-20227

Chebyshev filter with flat group delay obtaining transfer function, noting cascade synthesis and extended bisection theorem

08 p1299 A69-21169

Equal element elliptic function filters, noting lower dissipation loss when applied to bandpass and bandstop filters

08 p1300 A69-21175

Cut-off coupled microwave bandpass filters for use in dielectric filled waveguide systems

09 p1466 A69-22447

Pseudoexact bandpass filter response curves and electrical characteristics based on ripple Chebyshev responses

09 p1470 A69-22794

Digital sampled data spectra conditioning, deriving linear functions for low pass, bandpass and band rejection numerical filters and spectrum shaping

10 p1654 A69-23292

Chebyshev filter design problems including minimum highest dissipation loss, bandwidth, resonators, etc

10 p1665 A69-23875

Wideband RF amplifier manufacturing problems, comparing operation of vacuum triodes and pentodes in passband circuits

11 p1849 A69-24958

Transmission characteristics of narrow band microwave bandpass filters with power cascade and Chebyshev behavior

11 p1857 A69-25677

Electronic switching circuits controlled by binary counter triggers for variable passband filters

12 p2040 A69-26489

Coupling coefficients for common-base/common-base circuits of bandpass filters in two circuit selective transistor amplifier

13 p2226 A69-27219

Chebyshev polynomial of even order used in synthesis of equally terminated low pass lumped and distributed filters of even order

13 p2233 A69-28068

Multiband frequency conversion in filters or correcting circuits with four terminal networks, noting prototypes

13 p2235 A69-28519

FM measurements of angle distortion introduced by single pole bandpass filters compared to theoretical distortion

14 p2416 A69-29552

Negative resistance amplifier with stabilizing resistor in compensating circuit for operation in microwave duct mismatched beyond amplifier passband range

15 p2573 A69-30118

Wideband multiplexers design with directional filters, discussing operational characteristics

15 p2581 A69-31524

Pseudoexact bandpass filter design, presenting graphs for passband loss, voltage standing wave ratio and time delay as function of frequency

15 p2581 A69-31526

Stepped digital narrow band bandpass microwave elliptic function filters design and construction

16 p2759 A69-31939

Microwave bandpass linear phase filters design and synthesis for simultaneous flat amplitude and delay response

16 p2759 A69-31941

Holographic method of a posteriori restoration of images formed by coherent and incoherent light by spatial frequency retrieval

19 p3304 A69-35603

Transient phenomenon analysis and filtering based on stage separation tests in vacuum chamber, with emphasis on selective integration method [ONERA-TP-684]

19 p3293 A69-35747

Coherent phase locked loop receiver as carrier and modulation loops combination with parallel bandpass filter for ranging signal reception and FM demodulation

19 p3274 A69-36277

Multiple filter technique for seismic multimode dispersed signals, checking time and frequency resolution by diagnostic diagram

22 p3934 A69-39872

Microwave bandpass step filters, listing structural dimensions and design parameters

23 p4139 A69-41947

Q multiplier UHF device as preselection filter for closely spaced channel signals, discussing channel interference reduction

23 p4141 A69-42220

Noise elimination by filtering in high power microwave transmitters, noting practical design tradeoffs

23 p4142 A69-42235

BANDWIDTH

NT BROADBAND

NT SPECTRAL LINE WIDTH

Automatic phase control effective bandwidth determined by asymptotic method, presenting computer calculated dependence on circuit parameters

01 p0030 A69-10590

Piecewise analysis of large structures, showing incompatibility of minimum computer storage and minimum number of multiplication requirements through bandwidth schemes

01 p0169 A69-10637

Delay line bandwidth reduction for video or digital information, noting radar tracking application

03 p0392 A69-13251

Impulse bandwidth measurement error determination by trapezoidal numerical integration

03 p0398 A69-13902

Conventional TWT theory modified to include interaction between beam and two spatial harmonics, investigating TWT stability near edges of pass band

03 p0407 A69-13976

Bandwidth effect on wave recordings cross spectra interpretation from spatially separated sites, deriving relationship between propagation velocity and velocity bandwidth

05 p0756 A69-16272

Log-periodic circuits for application to microwave amplifiers in antenna design, noting bandwidth

05 p0739 A69-16554

CW laser mode steady excitation and narrow bandwidth obtainable by highly stable pumping and stable temperature of active element

06 p0934 A69-17681

Harmonic ion cyclotron waves shown to possess stop and passband characteristics, supporting quasi-static ion cyclotron mode theory

06 p0970 A69-17953

Laser small signal step response measured, deducing medium bandwidth [IEEE PAPER G-9]

07 p1151 A69-19056

Bit probability of PCM/FM for receiver with IF bandwidth equal to or greater than data rate, limiter-discriminator detection and postdetection filter

07 p1082 A69-19106

Finite IF filter bandwidth degradation of SNR of receiver for biphasic modulated signals using integrate and dump filter

08 p1270 A69-19851

Center feed system for broadening frequency bandwidth in X-band edge slotted waveguide array antenna

08 p1286 A69-20836

Minimum bandwidth of M real equal energy signals with specified code or correlation matrix, noting optimum waveforms

09 p1452 A69-21313

Noniterative wideband amplifiers having single pole transfer functions overall gain bandwidth product optimization, deriving rigorous conditions for maximum

09 p1469 A69-22606

Automatic phase control effective bandwidth determined by asymptotic method, presenting computer calculated dependence on circuit parameters

10 p1653 A69-23105

Simultaneous transmission of information signals and pseudonoise synchronization waveforms in common bandwidth [IEEE PAPER 67-TP-1173-COM]

10 p1655 A69-23532

Intracavity acoustooptic devices based on isotropic and anisotropic acoustic Bragg diffraction, discussing efficiency, bandwidth and acoustic column width

10 p1697 A69-23871

Chebyshev filter design problems including minimum highest dissipation loss, bandwidth, resonators, etc

10 p1665 A69-23875

Mechanical damping and electrical matching effects on bandwidth of piezotransducer in ultrasonic flaw detection equipment

10 p1697 A69-24073

Upper bounds for increment of band limited signal in sampling interval by increasing integral expressions of increment

11 p1834 A69-24551

Tunnel diode self excited SHF oscillators synchronization, deriving single frequency generation conditions

11 p1849 A69-24955

Bandwidth potential increase of parametric amplifier obtained by adding active filter elements to signal circuit, noting satellite communication band

12 p2039 A69-26380

Two idler parametric amplifiers bandwidth properties investigated using equivalent circuit, noting role of idler circuit design

13 p2233 A69-28066

Wave propagation and bandwidth characteristics of rectangular waveguide loaded with H plane lossless dielectric slab

13 p2222 A69-28075

Microwave cavity bandwidth determined from reflection coefficient measurements, considering reflection magnitude and phase

13 p2223 A69-28606

Linear mean square estimator for restoration of images degraded by system with bandlimited spread function

15 p2611 A69-31032

Stepped digital narrow band bandpass microwave elliptic function filters design and construction

16 p2759 A69-31939

Bandwidth requirement of single channel monopulse limiter, discussing signals conversion to IF

16 p2761 A69-32471

Energy criteria inconsistency in evaluating frequency band changes attributed to simultaneous narrowing and broadening of different signal power bands

19 p3278 A69-36716

Recording devices for storing bandwidth data in time sequence, studying design parameters using light beam recorder implemented with CRT for read-in process

20 p3540 A69-37640

Discrete delay line measuring FM noise, discussing special case of narrow band cavity resonator method

23 p4137 A69-41606

M-ary noncoherent signal structures requiring less transmission bandwidth than conventional FSK, deriving SNR

23 p4122 A69-41773

Hologram electronic transmission, obtaining required bandwidth reduction by differential recording of image and scene diffraction pattern

24 p4317 A69-43761

BANG-BANG CONTROL

U OFF-ON CONTROL

BANKING FLIGHT

U TURNING FLIGHT

BARANY CHAIR

Vestibular analyzer role in spatial orientation under weightlessness conditions during aircraft flights, discussing underestimations of rotation angle of Barany chair

08 p1262 A69-19840

BARDEEN APPROXIMATION

U BARRIER LAYERS

U ELECTRICAL PROPERTIES

U SURFACE PROPERTIES

BARDEEN-COOPER-SCHRIEFFER THEORY

U BCS THEORY

BARIUM

Lanthanum isotopes beta decay, analyzing excitation of near spherical daughter nuclei of barium isotopes

01 p0122 A69-10100

Artificial visible plasma clouds in space interacting with electric and magnetic fields around earth

01 p0151 A69-10533

Absorption oscillator strengths of Ba 2 lines in UV and visible spectral regions, using cascade arc in argon with barium vapor

02 p0242 A69-11872

Barium plasma density measurements by Langmuir, microwave probes and resonance fluorescence scattering compared in Q device
02 p0288 A69-12172

Barium, oxygen and BaO adsorption influence on Mo and Ti thin films conductivity and work functions
06 p0978 A69-16900

Continental diabases and oceanic tholeiites in light of rare earth and barium abundances and partition coefficients indicating fusion process
08 p1310 A69-20945

Fast Ba ion filament cloud injection into ionosphere using explosive shaped charge technique, noting application to ionospheric electric field measurement
09 p1539 A69-21752

Space electric fields research by artificial clouds of vaporized barium launched by rockets, noting neutral atmosphere and ionospheric results
09 p1492 A69-22800

Barium vapor effect on converter materials, examining metals-ceramics compatibility at high temperatures
14 p2467 A69-29215

Thermal emission converter, using Cs-Ba mixture in low voltage arc mode, detailing construction
14 p2403 A69-29247

Electric field variations in vicinity of auroral forms from motions of Ba vapor clouds released from Nike-Tomahawk rockets
18 p3128 A69-34935

Ca-rich achondrites genesis implied from rare earth and Ba absolute and relative concentrations
19 p3409 A69-36091

Stony meteorite barium isotopes and iron meteorite and terrestrial silicate inclusions analyzed using double spike method for laboratory fractionation correction
19 p3425 A69-36422

Density, ion temperature, electron temperature and ion drifts in Ba or Ba doped plasmas determined by resonance fluorescence and optical pumping
22 p3962 A69-40532

BIARIUM COMPOUNDS

Nonlinear optical properties of barium sodium niobate in ferroelectric tetragonal phase above room temperature, noting spontaneous parametric emission
09 p1515 A69-21354

Ground and metastable state photoionization cross sections of BaI to explain artificial Ba clouds, using many channel quantum defect method
18 p3177 A69-35238

BIARIUM OXIDES

Emission spectra of BaO during barium release compared with computed spectra for upper atmosphere temperatures evaluation
09 p1488 A69-21664

Oxide coated thermionic cathodes, noting semiconductor properties of alkaline earth oxides, particularly barium oxide and adsorption and optical properties
09 p1470 A69-22700

BIARIUM TITANATES

Dielectric constants of barium titanate single crystals as function of electric field intensity at different frequencies
01 p0139 A69-10889

Ferroelectric transition of barium titanates doped in OH or oxygen vacancies, using pyroelectric method
03 p0491 A69-14059

Nonadjustable Fabry-Perot scanning interferometer for gas laser spectra analysis, using barium titanate piezoceramic elements
04 p0598 A69-14854

Repolarization processes in barium titanate single crystals by variable sinusoidal voltage pulses
05 p0808 A69-16215

Domain structure of barium titanate single crystals during polarization reversal by sinusoidal AC field
06 p0981 A69-17893

Microwave oscillation and amplification in long bulk GaAs with barium titanate sheets on surface due to differential negative resistance across terminals
07 p1197 A69-18452

Observation of photocurrents generated in Schottky barrier diodes on barium titanate, suggesting practical utility of photon-to-electron conversion efficiencies
07 p1104 A69-18905

Microwave absorption by free carriers in c domain barium titanate crystals inserted in waveguide during polarization reversal
08 p1374 A69-21189

Nonadjustable Fabry-Perot scanning interferometer for gas laser spectra analysis, using barium titanate piezoceramic elements
15 p2608 A69-30246

Dielectric constants of barium titanate single crystals as function of electric field intensity at different frequencies
18 p3182 A69-34720

Microwave absorption by free carriers in c domain barium titanate crystals inserted in waveguide during polarization reversal
18 p3183 A69-35158

Repolarization processes in barium titanate single crystals by variable sinusoidal voltage pulses
20 p3584 A69-37785

Impurities effect on domain structure of barium titanate single crystals grown from solution in KF melt determined by inner stresses
21 p3783 A69-39559

Piezoelectric characteristics of surface layers of Ba titanate single crystals, using static and dynamic electromechanical methods
22 p3995 A69-41156

Dielectric constant and IR spectra of Ba titanate single crystals doped with hydroxyl, showing dependence on temperature and crystal thickness
22 p3995 A69-41157

Waveguide-resonance investigation of temperature dependence of dielectric constant and paraelectric dispersion of Ba and Sr titanate single crystals at millimeter wavelengths
22 p3995 A69-41158

Defect structure of ceramic Ba titanate doped with Cr ions, evaluating visible, IR and EPR spectra
22 p3996 A69-41160

Ba titanate modifiers, classifying cations replacing Ti and Ba ions
22 p3996 A69-41161

Temperature dependence of heat capacity of Ba and Sr titanate solid solutions in ferroelectric phase transition region
22 p3996 A69-41162

Dielectric polarization of barium titanate and barium strontium titanate in pulsed fields in paraelectric phase, analyzing coefficient B in free energy function and equilibrium state
22 p3996 A69-41165

Electric properties and domain structure changes of polycrystalline Ba titanate and other ferroelectrics characterized by high dielectric nonlinearity
22 p3996 A69-41166

BIARIUM ZIRCONATES

Electron emitters tested for gas laser operations, discussing nonreactive and reactive gases cases, matrix structures containing BaSrO and barium zirconate cathodes
23 p4172 A69-41394

BAROCLINIC WAVES

Symmetric baroclinic instability role in Jupiter equatorial acceleration
03 p0508 A69-13347

Long and ultralong waves in baroclinic zonal current, investigating current stability and wave perturbation characteristics by applying linearized perturbation equations to multilayer model
10 p1682 A69-23325

Atmospheric motions on Jupiter, considering highly symmetric flow, baroclinic waves and red spot
15 p2694 A69-30856

Horizontal shear effect on structure of growing baroclinic waves by two layer model, assuming small radius of deformation, compared to planetary scale
17 p2960 A69-33150

Instability theory of baroclinic vortices in incompressible and inviscid fluid, investigating symmetric meridional motions time evolution by numerical integration of hydrodynamic equations
23 p4153 A69-42346

BAROCLINITY

Weather forecasting, discussing atmospheric models and computer operations for long range forecasting based on hydrodynamic theory and statistics
01 p0108 A69-10398

Taylor column existence in compressible atmosphere, discussing baroclinicity and stratification effects in earth and Jupiter atmospheres
02 p0326 A69-12697

Unsteady baroclinic planetary atmosphere boundary layer turbulent states with various pressure and temperature gradient distributions, using boundary layer model
10 p1722 A69-23973

Unsteady baroclinic planetary atmosphere boundary layer turbulent states with various pressure and temperature gradient distributions, using boundary layer model
21 p3760 A69-39659

Steady state baroclinic boundary layer over two dimensional terrain in f plane, noting layer thickness dependence on stability and terrain slope
24 p4347 A69-43356

BAROMETRIC PRESSURE U ATMOSPHERIC PRESSURE

BAROTRAUMA

Gangrene and caisson disease due to diving accidents, discussing emergency treatment with hyperbaric oxygen
17 p2911 A69-33775

Barotrauma during hyperbaric oxygenation at flight descent or reentry into caisson, including ear trauma symptoms and use of paracetamol
17 p2911 A69-33776

BAROTROPIC FLOW

Barotropic instability analyses by method of jet stream like fields and energy transport from zonal current to wave disturbances based on vorticity equation
02 p0276 A69-12758

Planetary Rossby waves vertical propagation through weak westerly wind wave guides, using adiabatic linear model
03 p0460 A69-13335

Asymptotic similarity in neutral barotropic planetary boundary layers, solving Ekman flow by singular perturbation methods
03 p0460 A69-13336

Large scale disturbances in summertime stratosphere observed from high level balloon, discussing diurnal wind patterns and planetary traveling waves
03 p0461 A69-13343

Validity of finite difference approximations for barotropic instability of zonal currents
09 p1537 A69-22298

Characteristics method for solution of differential equations representing time changes of wind and pressure fields in divergent barotropic channel flow
11 p1911 A69-24585

Stability of barotropic perturbations superimposed on wind velocity profile of basic currents in geostrophic multilayer models
11 p1911 A69-24586

Potential triple traveling space waves in barotropic gas with arbitrary equation of state, analyzing adjacent and three dimensional self similar flows
12 p2061 A69-25889

Stability theorems for barotropic vorticity equation integrated within limited region for flow through boundary without existing physical boundary conditions
13 p2294 A69-28494

Air mass analysis, discussing homogeneity, quasi-barotropic fluids, noise elimination to arrive at smooth flow pattern, etc
15 p2647 A69-30193

Horizontal shear flow effect on linear geostrophic adjustment in unbounded barotropic fluid, discussing gravity waves, vorticity equations, available energy, etc
15 p2648 A69-30217

Finite difference schemes for barotropic fluid free surface model primitive equations tested for numerical integration stability and accuracy
17 p2997 A69-33691

Model calculations for movement of barotropic and initially symmetric vortices in rotating fluids with Coriolis parameter or fluid depth varying horizontally
17 p3000 A69-33761

Linear dynamic modeling of barotropic fluid in rigid circular tube, presenting axial velocity profile by confluent hypergeometric function with complex arguments
[ASME PAPER 69-FLCS-18]

20 p3516 A69-37982

BAROTROPISM

Dynamic meteorology quasi-stable problems solved using sequential approximations solution for barotropic model of Euler equations
14 p2476 A69-29821

Error sources in forecasts for heights of isobaric surfaces obtained by numerical integration of prognostic equations of equivalent barotropic models
19 p3361 A69-35770

BARRICADES

U BARRIERS

BARRIER LAYERS

Electrical properties of gold-gallium arsenide n-type junctions investigated for influence of crystallographic orientation of surface and charge carrier density
01 p0138 A69-10432

Beam-lead fabrication on dual Schottky barrier diodes for low noise integrated microwave mixers
02 p0222 A69-12474

Potential distribution approximations for junction semiconductor devices, noting application to barrier layers and electron tunneling

03 p0408 A69-14107

Electron emission into vacuum from forward biased Schottky barrier consisting of cesiated thin layer of Pt on n-type ZnS

03 p0493 A69-14186

Shot noise in Si Schottky barrier diodes for frequencies between 100 Hz and 50 kHz

05 p0734 A69-16564

Potential barrier curvature influence in aluminum trioxide tunnel junctions, noting ionic space-charge effect on shape

07 p1196 A69-18243

Barrier capacitance of semiconductor diodes for exact temperature measurement, discussing application to temperature to frequency converters

07 p1100 A69-18556

Gunn effect for cathode contacts with interface resistance, developing control characteristic boundary condition concept for explaining cathode fall and other phenomena

07 p1199 A69-18649

Epitaxially grown guard rings for GaAs p-n junction and Schottky barrier avalanche diodes

08 p1284 A69-20368

Magnetoelectric characteristics of inversion layers below gate region in transistors, noting Hall mobility

08 p1372 A69-20460

Destructive breakdown in Schottky barrier diodes by evaporating contact metal through mask onto silicon, showing local heating by thin wax layer

08 p1286 A69-20860

Field effect transistors with Schottky-barrier gates using epitaxial layers of silicon on substrates and gallium arsenide on seminsulating substrates

08 p1286 A69-20863

Forward volt-ampere characteristics and differential resistance peak of Schottky barrier diode on doped Si

09 p1557 A69-21744

Trapping state effect on tunneling probability in Schottky barriers, discussing current-voltage characteristics

09 p1557 A69-21748

Schottky barriers on n-type GaAs, measuring forward current characteristics for various electron concentrations and temperatures

10 p1745 A69-23358

Gallium phosphide Schottky barrier diodes, discussing construction and metals used, barrier height relationships to impurity concentration and temperature, rectifying characteristics and internal quantum efficiency

16 p2757 A69-31613

Tunnel junctions with low background currents made by reacting active gas layer adsorbed on Nb film surface with Pt upper film to form barrier

17 p3016 A69-33788

BARRIERS

Stopping barriers for jet aircraft landing design and operation

11 p1862 A69-24354

Reflecting or reradiating obstacle proximity as cause of siting errors in azimuth radio measurements, discussing omnidirectional obstacles effect

15 p2651 A69-31090

Capillary barriers to provide propellant positioning, expulsion capability and slosh dampening for spacecraft propulsion systems during rotational maneuvers

[AIAA PAPER 69-529]- 16 p2868 A69-32713

Knife-edge obstacle diffraction of nonisotropic transmitter analyzed via isotropic source model propagation path noting accuracy

17 p2917 A69-32847

BARS

NT ELASTIC BARS
NT PRISMATIC BARS

Nichrome bars production dispersion hardened by alumina and zirconia inclusions, noting extrusion temperature influence

01 p0085 A69-10397

Torsion of variable cross sectional thin walled bars using shell theory equations

02 p0337 A69-11559

Stress-strain relationship of composite bars consisting of single glass fiber with thin metal coating layer and under axial load

07 p1235 A69-19385

Axially loaded viscoelastic constrained bar instability for large deformation

07 p1235 A69-19440

Stress intensity magnification factors in surface flawed tension plates and notched round tension bars, evaluating fracture toughness

10 p1797 A69-23080

Thickness and drilled holes effects on notch toughness of Charpy V notch bars over wide temperature range

10 p1798 A69-23087

Flat bar optimal cross section under tensile stress applied to minimize stress in large structural components using elasticity theory

11 p1986 A69-25203

Dynamic plastic response of finite bar subject to axial impact load noting reflected waves, stress-strain time histories and residual strain

11 p1991 A69-25512

Acrodynamic energy dissipation during vibrations of bars in airstreams characterized by energy loss per cycle and logarithmic decrement

17 p3066 A69-33948

Autocorrelation function for unsteady temperature and stress fields in bar located in gas stream leaving combustion chamber

19 p3440 A69-36685

Natural torsional-flexural vibrations of bars with single symmetry, using matrix equations of equilibrium, displacements and natural coupled vibrations

22 p4043 A69-40456

BARYCENTER

U CENTER OF GRAVITY

BARYONS

NT COLD NEUTRONS
NT FAST NEUTRONS
NT HYPERONS
NT K-MESONS
NT MESON RESONANCES
NT MESONS
NT MUONS
NT NEUTRONS
NT PHOTONEUTRONS
NT PIONS
NT PROTONS
NT SOLAR PROTONS
NT THERMAL NEUTRONS

Cosmic ray penetrating component properties identical to muon component at mountain level, indicating baryon passive nuclear state nonexistence

13 p2331 A69-28400

Baryon passive nuclear state nonexistence indicated by above and below ground calorimetric telescope method of nuclear cascade observation

13 p2331 A69-28401

Quarkian core substance in superstars of great masses, discussing existence as primordial state forming baryon and nuclei and origin in stellar gravitational contraction

19 p3401 A69-35912

Harrison primordial inhomogeneity postulate concerning baryon numbers distribution in universe, precluding possibility of considering cosmic rays bulk as universal

21 p3810 A69-39469

BASALT

Surveyor 6 magnet experiment following lunar landing, noting presence of magnetic material in Sinus Medii indicating basaltic composition

02 p0317 A69-12015

Magnetic paleointensity studies in basalts from Flagstaff, Arizona, noting oxidation effect on magnetic strength after heating

02 p0244 A69-12018

Excess radiogenic argon in deep sea basalts from crest of East Pacific Rise, noting relation to glass content

02 p0244 A69-12568

Friction resistance between steel and ground basalt in ultrahigh vacuum, showing increase by adhesion

13 p2298 A69-28014

Chemical composition of basaltic achondrites /eucrites and howardites/, indicating dominant role of physical process over magmatic differentiation

24 p4382 A69-42928

BASE FLOW

Plane supersonic base flows studied using integral analysis of turbulent reattachment, noting prediction of wall pressure distribution

03 p0361 A69-12990

Axisymmetric hypersonic near wake with base injection, discussing zero injection case, jet-plume interaction and mixing region

[AIAA PAPER 69-66] 06 p0914 A69-18115

Thermal and pressure environments analysis in Saturn S-1C stage base during flight tests, noting base gas flowfield and heating

[AIAA PAPER 69-318] 09 p1611 A69-22383

Turbulent base flowfields in multinozzle configurations, considering adiabatic flow and determining base pressure distribution from reverse jet impingement

[AIAA PAPER 69-570] 16 p2733 A69-32751

Separated flow patterns in base flow at body recesses, emphasizing shock wave boundary layer interaction, laminar flow and flow in front of recess

17 p2949 A69-33124

Base flow component of total drag for axisymmetric supersonic afterbody with single exhaust jet, considering turbulent mixing

[AIAA PAPER 69-650] 17 p2956 A69-33485

BASE HEATING

Telemetry technique utilizing thermocouple sensors for base heating determinations on free flight blunt cone in shock tunnels, noting electrical noise reduction

[AIAA PAPER 68-407] 04 p0604 A69-15514

Short duration tube wind tunnel supersonic testing, noting Saturn S-1C base heating and solid propellant rocket base burning tests

[AIAA PAPER 69-335] 13 p2242 A69-28271

BASE PRESSURE

Cylindrical afterbodies at free stream Mach 2 with hot argon gas ejection, discussing flow rate influence on base pressure

02 p0190 A69-12533

Sting diameter and cylindrical protuberance length effects on base pressure of axisymmetric body in turbulent supersonic flow

05 p0697 A69-15712

Stagnation pressure losses of adiabatic flow of compressible fluids through abrupt area expansion and contraction in subsonic range, discussing base pressure

[ASME PAPER 68-WA/FE-46] 05 p0750 A69-16113

Turbulence hypothesis for velocity of laminar fluid flow at dividing line, considering base pressure and adiabatic mixing zones

06 p0910 A69-17330

Base pressure calculation in initial turbulent boundary layer of supersonic flow about two dimensional backward facing step, using mass conservation conditions

07 p1119 A69-18747

Hypersonic missile interceptor vibration characteristics in lower atmosphere, noting role of base pressure excitation

09 p1614 A69-21890

Base pressure fluctuations behind cone in supersonic gas flow, noting complicated superposition of harmonics associated with various factors

09 p1431 A69-22327

Turbulent base flowfields in multinozzle configurations, considering adiabatic flow and determining base pressure distribution from reverse jet impingement

[AIAA PAPER 69-570] 16 p2733 A69-32751

Multichannel pressure telemetry system for base pressure measurements on small wind tunnel models, considering proximity effects on transducer-telemetry units

19 p3305 A69-35727

Drop test method to obtain subsonic terminal velocity and base pressure data for planetary entry probe configurations

19 p3238 A69-35959

Transition in near wake, from study of base pressure on circular cylinders in incompressible flow

19 p3242 A69-36809

Free flight telemetered base pressure test data correlation for high Mach numbers, noting facilities and instrumentation

20 p3458 A69-37196

Base pressure of peripheral jet ground effect machines in heaving motion, discussing flow patterns

22 p3866 A69-40817

Free flight telemetry base pressure measurements on slender cones and domed afterbodies in hypersonic laminar flow, using shock tunnel test facility

[AIAA PAPER 68-698] 24 p4249 A69-43675

BASES [CHEMICAL]

Polymeric Schiff bases synthesis, thermal stability and nature of pyrolytic decomposition of polyazines and derived polystylenes

07 p1074 A69-18628

Cross-linked polymers obtained by direct reaction of aryl polycarbonyls with aryl polyamines, studying char yields effect

08 p1269 A69-21059

Cross-links effect on char yields of azomethine polymers produced by aryl diamines with aryl diketones

08 p1269 A69-21060

- Schiff base cross-links effect on synthesis of polymeric azomethines produced by bis exchange reactions, carbonyl and amine
08 p1269 A69-21061
- Pyrimidine and purine bases analysis by time of flight mass spectrometry and paper chromatography
11 p1832 A69-24738

BASES [FOUNDATIONS]

U FOUNDATIONS

BATCH PROCESSING

- Network analysis for systems application program /NASAP/ in FORTRAN for batch and on-line analysis of electronic circuits
21 p3856 A69-39662

BATHS

U SALT BATHS

BATHYMETERS

- Airborne pulsed lasers for near shore bathymetric measurements, discussing feasibility results
15 p2609 A69-30459

BATHYMETRY

U BATHYMETERS

BATTERIES

U ELECTRIC BATTERIES

BAUSCHINGER EFFECT

- Energy dissipation and fatigue in metals under cyclic static loads, determining logarithmic decrements of vibrations and Bauschinger effect
12 p2181 A69-26612

- Stress-strain state of elastoplastic material subjected to quasi-static uniaxial tension and compression, considering Bauschinger type effects by scalar parameters
18 p3222 A69-34909

- Metals plastic behavior including strain hardening and Bauschinger effect
21 p3832 A69-38466

BAYARD-ALPERT IONIZATION GAGES

- Bayard-Alpert type ionization gage for low pressures with and without modulation, discussing role of electron oscillations
20 p3464 A69-37407

- Bent beam ionization gage linearity from calibrated nude Modulated Bayard-Alpert /MBA/ gage, discussing buried collector and tabulated magnetron gages
22 p3950 A69-41216

BAYES THEOREM

- Bayesian method for optimizing controlled plant characteristics using self adaptive model
02 p0223 A69-11566

- Bayes estimator in decision directed adaptive detection problem, noting allowance for decision errors
05 p0740 A69-16583

- Bayesian reliability growth model with random variable parameters, discussing multimode failures
09 p1504 A69-21912

- Algorithm for calculating Bayes estimates for unsteady Gaussian signals separation in presence of unsteady Gaussian noise by least squares method
11 p1833 A69-24443

- Bayes theory and nonclassical variation method to solve optimal energy distribution available for identifying weak signals in background noise
14 p2410 A69-28817

- Bayesian theory to determine maximum a posteriori estimation algorithms for optimum bit synchronization in digital communication systems
14 p2413 A69-29496

- Probability diagnosis and prognosis for buffeting zones based on Bayes formula, determining clear air turbulence zones
15 p2648 A69-30645

- Algorithm for calculating recognition error by applying pattern vectors having two multivariate Gaussian distribution to optimum Bayes classifier
15 p2572 A69-31113

- Gas turbine components life prediction, using Weibull distribution and Bayes theorem to estimate probability of crack initiation
19 p3394 A69-36004

- Bayesian reliability demonstration tests for predetermining sample size producer and consumer risks for equipment with exponential and binomial failure distributions
19 p3327 A69-36039

- Sequential Bayes procedure demonstrating mean time to failure exceeding acceptable value with given confidence coefficient
19 p3327 A69-36040

- Bayesian confidence limits for systems reliability, considering exponential and unspecified life distribution subsystems
19 p3328 A69-36041

- Bayesian estimate of individual truck maintenance costs based on optimum replacement maintenance age
23 p4241 A69-41577

- Adaptive multicategory pattern classification system, using independent samples to form mean-square approximations to Bayes discriminant functions
24 p4285 A69-43134

BAYESIAN STATISTICS

U BAYES THEOREM

BBGKY HIERARCHY

- Modified truncation for BBGKY hierarchy for plasma, obtaining kinetic equation identical with Balescu-Lenard equation
08 p1360 A69-19990

BCC LATTICES

U BODY CENTERED CUBIC LATTICES

BCS THEORY

- BCS theory application to metallic modification of hydrogen for obtaining high temperature superconductor
04 p0642 A69-14680

- White dwarfs transfer to superconducting state, using BCS theory for superconducting transition temperature dependence on electron density
08 p1391 A69-20546

BE B

U EXPLORER 22 SATELLITE

BEACON EXPLORER B

U EXPLORER 22 SATELLITE

BEACON SATELLITES

NT EXPLORER 22 SATELLITE

- Ionospheric absorption measurements using beacon satellite emission compared to Kazantsev results
02 p0246 A69-12742

- Radio waves behavior along paths between satellites and earth, studying preferred frequency bands for spacecraft transmitters used as beacons
09 p1451 A69-21293

- Acoustic waves in ionosphere relation to electron content fluctuations detected from beacon satellite BE-B signals
12 p2065 A69-26104

- Radio waves behavior along paths between satellites and earth, studying preferred frequency bands for spacecraft transmitters used as beacons
15 p2570 A69-31227

- Electrooptical/photomultiplier/ detection of satellite beacon flashes, establishing time of flash and measuring pulse shape and energy received
17 p2919 A69-33083

BEACONS

NT RADAR BEACONS

NT RADIO BEACONS

- Multiple beam electronically steerable retrodirective antenna array with automatic inertialess compensation for altitude or beacon location
02 p0212 A69-12816

BEADS

- Free stream dispersion without permeation using nonporous glass beads and solutes, examining flow rate, particle size distribution, solute diffusivity, etc
22 p3894 A69-39873

BEAM COLUMNS

U BEAMS [SUPPORTS]

U COLUMNS [SUPPORTS]

BEAM CURRENTS

- High voltage mercury electron bombardment ion thruster power efficiency
[ECS PAPER 170D]
05 p0812 A69-16233

- Beam transmission in electron guns having single apertured control grid, studying ratio of target current to cathode current
05 p0734 A69-16566

- Plasma electron beam for welding, deriving beam current from secondary emission by ion bombardment, discussing gas pressure, equipment and applications
19 p3320 A69-35555

BEAM PLASMA AMPLIFIERS

- Interaction between surface waves propagating along plane plasma boundary and parallel low density electron beam, noting wave amplification and excitation
03 p0480 A69-14135

- Coupling electromagnetic power to beam plasma amplifiers without use of helices and cavities, discussing modes of interaction, gap coupling and Cerenkov coupling
09 p1463 A69-21805

- Parametric amplification in beam plasma system, analyzing amplification of electron current component dependent on second order terms of velocity and charge density
10 p1740 A69-23791

- Beam-plasma interactions by nonlinear Vlasov equation, describing amplification of longitudinal waves
14 p2493 A69-29692

BEAM SPLITTERS

- Glan-Thompson and Rochon prisms modified by replacing one of two calcite halves of cemented oriented birefringent crystals with glass
02 p0280 A69-11924

- Static beam deflection in beam foil spectroscopy for determining parent ionization stage of emitting ions
04 p0595 A69-14279

- Holograms volume depth increased by reference beam splitting or by photographing holograms on same plate in sequence
05 p0761 A69-15651

- Picosecond structure of low power laser signals using calcite beam splitter and potassium diphosphate second harmonic generator
09 p1516 A69-21742

- Holograms on photochrome films by split beam He-Ne laser using special mirror system
11 p1881 A69-24631

- Equal inclination interference fringes effects on laser beam reflection from plane parallel glass plates, evaluating angular distance between adjacent fringes
11 p1896 A69-24840

- Photodetector requirements for autocollimators with beam splitters, considering spectral characteristics, photoresponse, time constant, positioning, etc
14 p2447 A69-29326

- Holograms volume depth increased by reference beam splitting or by photographing holograms on same plate in sequence
16 p2791 A69-32508

- Multiple index high contrast holographic contouring technique compared with analogous multiple frequency system
23 p4164 A69-41628

BEAM SWITCHING

- Phase, frequency and amplitude scanning, noting array design and applications
01 p0049 A69-11348

- Phased array radar antennas emphasizing beam steering of transmitting linear array with number of phase shifters
01 p0049 A69-11390

- Electronic multibeam switching X band antenna system design with separate transmitting and receiving antennas for use on continuous wave surveillance radar
08 p1289 A69-20967

- Feed shift beam switch for radiometric measurements of astronomical objects emission at millimeter wavelengths
11 p1836 A69-24996

- Laser beam discrete deflection method using Wollaston prism and electro-optical switch for changing polarization plane
14 p2459 A69-29391

BEAM WAVEGUIDES

- Multiple beam waveguide and optical delay line capacity increase by transmitting Gaussian beams clearly resolved at receiver
04 p0579 A69-15446

- Characteristic waves in gas-dielectric beamguides, calculating attenuation dependence on frequency
05 p0736 A69-16783

- Diffractional crosstalk in optical beam waveguide during simultaneous multibeam transmission arising from beam coupling by aperture diffraction
07 p1100 A69-18648

- Brewster angle lenses for low cost low loss laser beam transmission system
07 p1148 A69-18863

- Beam wave scattering by small sphere, discussing dielectric constant and difference from plane wave
08 p1273 A69-20028

- Fabry-Perot resonator and beam waveguide systems for laser beams, noting mode coupling and separation in laser optical systems
09 p1518 A69-22125

- Light waves transmission and beam guidance, analyzing solid lens type guide and automatic light path stabilizer
09 p1518 A69-22130

- Algorithm for mean energy transmission coefficient of fundamental mode in beam guide with given inhomogeneities, discussing mode conversions
09 p1469 A69-22629

- Mean losses in quasi-optical communication lines due to random irregularities in performance of waveguide phase correctors connected in series, noting random phase aberrations effect
10 p1658 A69-23954

Radio wave field distortions by dielectric prisms in lens waveguides, discussing beam transformation, noting both geometrical optics effects and diffraction role
11 p1833 A69-24436

Limiting frequencies of inhomogeneously filled lossless rectangular waveguides and field states, using Maxwell equations
11 p1855 A69-25620

Focusing power of hyperbolic gas lens for light beam waveguides, noting temperature distribution measurements and pole separation
12 p2107 A69-26392

Electromagnetic field in idealized medium of uniformly curved gas lens for light beam waveguide, describing lens radius effects on incident beam spot
13 p2270 A69-27181

Low pass quasi-optical waveguide filters, using metal strips in dielectric material to obtain broad stopband and low dissipation loss
13 p2229 A69-27675

Iris beam waveguide transmission loss as function of irises alignment, iris frame width and guide axis curvature
13 p2233 A69-28070

Wave propagation in open periodic two dimensional iris waveguide and beam reconstruction by diffraction, considering existence and character of modal fields
16 p2753 A69-32394

Multibeam transmission in optical beam waveguides by simulation, discussing intensity profiles phase fronts and cross scattering
17 p2974 A69-33400

Space charge wave propagation induced by electron beam moving in annular waveguide, considering radiated field and current redistribution
23 p4124 A69-42034

BEAMS

Stability loss of beams analyzed under compression allowing for various creep conditions in loading and unloading regions, calculating time to failure
22 p4039 A69-39917

BEAMS [RADIATION]

NT ATOMIC BEAMS
NT ELECTRON BEAMS
NT GAMMA RAY BEAMS
NT ION BEAMS
NT LIGHT BEAMS
NT MOLECULAR BEAMS
NT NEUTRAL BEAMS
NT PARTICLE BEAMS
NT PHONON BEAMS
NT PHOTON BEAMS
NT PION BEAMS
NT PROTON BEAMS
NT RADAR BEAMS

Beam laser as frequency standard, considering wavelength and molecular transfer constraints imposed by technology limitations and frequency stability requirements
03 p0440 A69-13715

Current distribution in scanning rectangular array with all-directional constant sidelobe and narrowest beamwidth
04 p0570 A69-14302

Directivity and beamwidth determination of large scanning Dolph-Chebyshev arrays
04 p0570 A69-14303

Butler matrix-fed circular array for continuous 360 degree beam scanning
04 p0573 A69-14329

Lossless multiple beam forming device operational principles, noting parallel plate radial transmission line network construction
04 p0576 A69-14768

Parabolic antenna beam scanning by defocusing, calculating relationship between reflector and beam tilt angles
07 p1089 A69-18248

Capture of parametrically coupled waves by pulses and beams of pumping radiation in case of different group velocities directions
10 p1705 A69-23956

Fluctuations of beam wave propagating through locally homogeneous medium, considering amplitude and phase correlation and structure functions
12 p2032 A69-26855

Laser beam light pressure bending of incompressible liquid surface leading to beam self focusing in linear medium
14 p2461 A69-29674

Theory of field distribution in antenna aperture extended to scanning with desired shape beam
15 p2578 A69-30634

Electromagnetic beam propagation in anisotropic media, discussing quasi-optical beam divergence
17 p2925 A69-33845

Beam shape loss /BSL/ for electronically steerable array in search mode, determining optimum search beam locations from BSL computations
20 p3506 A69-37717

Transverse wave-beam interaction propagation in fast wave structure in finite homogeneous magneto-static field, deriving wave-beam equation for non-relativistic beams
21 p3672 A69-38435

Charged particles beam penetration effects produced in atmosphere, determining particle diffusion and trajectory using Spencer moments and Monte Carlo methods
21 p3709 A69-38502

Circular antenna arrays radiation pattern synthesis in moving medium relative to main beam, noting medium motion influence on pattern changes
22 p3915 A69-40706

Beam wave propagation in conducting hollow circular cylinder applied to shielding cylinders design for aperture antenna transmission
24 p4282 A69-42987

BEAMS [SUPPORTS]

NT BOX BEAMS
NT CANTILEVER BEAMS
NT CURVED BEAMS
NT I BEAMS
NT RECTANGULAR BEAMS

Structural analysis by direct moment distribution, Volume 1, covering statistically indeterminate structures formed of prismatic members
01 p0165 A69-10156

Interlayer slip in layered wood beams with nail joints analyzed in terms of small deflection theory
01 p0169 A69-10638

Discrete model for investigating beam vibration under various end conditions, determining natural frequency dependence on degrees of freedom
02 p0336 A69-11462

Dynamic behavior of elastoplastic beam column model with one degree of freedom subjected to axial compressive force
02 p0337 A69-11717

Optimal thin walled cross section of hollow beam for pure bending, taking into account stability requirements
02 p0340 A69-12054

Upper and lower bounds for eigenvalues of differential problem connected with transverse vibrations of wedge shaped simply supported beam
02 p0272 A69-12193

Timoshenko beam theory accuracy, defining deflection and rotation in terms of average values over cross section
04 p0675 A69-14593

Beam vibration problems with mixed response-excitation input information solved by recasting equations of motion
04 p0676 A69-14711

Rayleigh-Ritz finite element method for approximate solution of nonlinear energy functional describing large deflection bending behavior of uniform beam under point loads
05 p0833 A69-15711

Equation governing transverse vibration of beams with exponentially varying properties, expressing solution in terms of Bessel functions
05 p0835 A69-15873

Plastic moments calculation of continuous steel beams under various loading patterns
05 p0837 A69-16035

Resonant beam tuned vibration damping device, noting weight saving potential
[ASME PAPER 68-WA/GT-2]
05 p0837 A69-16138

Generation of crack propagation data on notched rotating beam specimens by interrupted stressing techniques
[ASME PAPER 68-WA/MET-3]
05 p0838 A69-16148

Impulse loaded elastic-plastic beam response approximate solutions based on uniqueness proof
[ASME PAPER 68-WA/APM-23]
05 p0840 A69-16188

Free vibrations of plates and beams of pyrolytic graphite type materials, analyzing transverse shear deformation and rotary inertia
[AIAA PAPER 69-55]
06 p1027 A69-18070

Transverse motion of embedded or free semiinfinite beam with given initial displacement and velocity, using potentials leading to integral equations
[ONERA-TP-653]
07 p1230 A69-18264

Linearized simple beams and columns theory for anisotropic materials, discussing flexural and extensional effects coupling in tension test
07 p1171 A69-18727

Thin walled symmetrical angle section beam stability under bending moment by section deformation or torsional buckling
08 p1410 A69-19892

Nonhomogeneity effect on transverse vibrational frequency of uniform beams
08 p1413 A69-20413

Transverse vibration of beam rigidly fastened at one end, using series expansion in terms of set of eigenfunctions
08 p1414 A69-20445

Conformal mapping method for flexure function determination, discussing shear coefficients for arbitrary cross section beams in Timoshenko beam theory
09 p1612 A69-21611

Uniform gravity load effect on buckling of beam continuously supported by soft foundation and subjected to uniform lateral load
09 p1615 A69-21927

Stress formulation of thermoelasticity in simply connected body, noting uniform temperature change influence on stress components
09 p1617 A69-22007

Forced vibrations of elastic beam covered by viscoelastic layer subjected to transverse harmonic excitation
10 p1800 A69-23241

Experimental evidence of validity of shear coefficient in Timoshenko beam theory
10 p1801 A69-23538

Transverse reinforcing straps effects on torsional stiffness and bending behavior of open cross section profile thin walled prismatic beams
10 p1802 A69-23890

Frequency response dynamics of beam type periodic structures on elastic supports typical in flight vehicle designs
[ASME PAPER 69-VIBR-17]
10 p1804 A69-24150

Damped steady state response of elastic foundation beam subjected to cyclic moving loads to determine load movement frequencies for natural frequency excitation
[ASME PAPER 69-VIBR-13]
10 p1806 A69-24166

Nonlinear large amplitude vibrations of flexible beam with pinned ends supported simply on rigid base noting frequencies, modes, waveforms and stress distribution
[ASME PAPER 69-VIBR-43]
10 p1807 A69-24181

Validity limits of formulas for critical buckling load for oscillating continuous beams found to be elastic buckling
11 p1969 A69-24349

Transverse beam natural vibration frequency evaluation method from Timoshenko theory
11 p1970 A69-25481

Vibration problem of supported beam elastically restrained against rotation at both ends solved by Hermitian and linear differential operators
11 p1976 A69-24794

Nonlinear free vibration of beams with clamped and supported ends subjected to axial load, considering symmetric and antisymmetric modes
11 p1983 A69-25024

Dynamic stability of elastic beam type structures, using electronic simulation based on finite element approach
11 p1986 A69-25344

Electric analogy technique for torsion and flexure functions of uniform beams with terminal loads, considering Neumann boundary value problem
11 p1995 A69-25649

Bending of weightless thin elastic beams clamped to circular template by external force
12 p2181 A69-26572

Dynamic stability of flexural free transverse vibrations of supported thin walled elastic beam with initial velocity distribution and parametric excitation
13 p2369 A69-28353

Orthonormal aspect on vibration modes for nonuniform beams, evaluating normalization for end conditions by using Rayleigh technique
14 p2534 A69-29319

Beam deflection equations having different rigidity moduli on each half span
15 p2705 A69-30417

Natural frequencies and modes of complex structures composed of beam elements, considering hysteretic damping for response and transmissibility
15 p2706 A69-30431

Deformation functions for finite beam analysis allowing continuity at nodes and accurate eigenvalues
15 p2710 A69-30869

Elastoplastic strains in thin walled beams subjected to oblique bending by mobile loads of coupled concentrated forces, calculating deflections and plastic region distribution
15 p2711 A69-30971

Oscillating beams lateral buckling allowing for torsional stress in determining critical load
15 p2712 A69-31015

Power spectral density response of uniform beams to random pressures, evaluating joint acceptance of systems with pressure field
[ASA PAPER SVT2]
15 p2713 A69-31143

Krylov functions determined by distribution theory and operational calculus, discussing deformations and statics of straight beams
15 p2715 A69-31475

Stress and deformation in cross section of beam during complex loading using steepest-descent method
16 p2873 A69-32132

Bending oscillations of semiinfinite beam with periodically changing length
16 p2876 A69-32298

Prestressed beams, columns and plates nonlinear response, statistical behavior and transverse cracking under axial compression, describing strength and stiffness
17 p3060 A69-33568

Equations in series form to describe composite beams behavior under nonuniform torsion
18 p3211 A69-34343

Sandwich beams optimal design determined for case of constraint on elastic deflection and for load factor at plastic collapse
18 p3218 A69-34623

Beam torsion nodal line displacement dependence on flexural and torsional bending frequency
18 p3223 A69-34998

Tension, bending and buckling torsion in thin walled beams described by extended beam model considered as one dimensional continuum
18 p3224 A69-35296

Vibration response approximation of three layer sandwich beam with nonlinear viscoelastic material core during flexural vibrations
20 p3619 A69-36910

Monograph on beam impact force and bending stresses during transverse impact, noting Bernoulli and Hertz theories application
20 p3628 A69-37922

Axial forces effects on dynamic load factors of beams under transverse impulsive loads, considering various end conditions
20 p3629 A69-38113

Natural oscillations of end-hinged solid beam with variable parameters and concentrated masses, determining natural frequencies
21 p3833 A69-38575

Natural frequency equations for torsional vibration of fixed/fixed and fixed/simply supported uniform thin walled beams of open section based on energy method
22 p4040 A69-39935

Sandwich beams interlaminar shear stress calculations, considering roles of moduli of elasticity and layers thickness relative to beam
22 p4041 A69-40080

Variational method using Hamilton principle and calculus of variations to determine elastic curve and internal forces in static or dynamic loaded beam
22 p4043 A69-40459

Elastic curve shape effects on volume of minimum weight uniformly strong beam under combined longitudinal and transverse bending
23 p4225 A69-41421

Minimum weight and optimal cross sections design for statically determinate and indeterminate shell and H beams, using variational method
23 p4225 A69-41421

Prismatic beam stress-strain state under steady temperature field, deriving stresses, displacements and elastic curve equations
23 p4227 A69-41708

Field transfer matrices for simultaneous treatment of free and forced vibrations and buckling through axially loaded Timoshenko beam
23 p4234 A69-42400

Central transverse impacts of sphere on free-free beams, investigating maximum strains variation with impact velocity by narrow band tuned circuit filter
23 p4235 A69-42455

Adhesive joints design with uniform shear stress for prestressing wood beams
24 p4323 A69-43425

BEAMSHAPING U COLLIMATION

BEARING [DIRECTION]

Bearing deviation in model HF transionospheric propagation with three dimensional electron density variation and no magnetic field
04 p0559 A69-15209

Expression derived for correlation function and power spectrum of bearing of set of point radiators, taking into account receiver internal noise
05 p0719 A69-16219

Earth dipole magnetic field effect on bearing deviation in HF transionospheric propagation analyzed by computer ray tracing
07 p1086 A69-19224

Ionospheric electron content gradients from Faraday rotation observations of radio beacon satellites for direction finding of HF radio waves
11 p1837 A69-25004

Spatial direction determination from simultaneous photographs of Echo 2 at Nikolaev and Helwan stations, using circle of simultaneity
12 p2068 A69-26427

Optimal direction finding systems based on bearing angle representation in multidimensional Markov process, considering white and interference noise
13 p2219 A69-27254

Bearing errors reduction in vertical loop HF direction finders for ionospherically propagated signals in dual channel system
14 p2413 A69-29493

Position determination from radio bearings using complex numbers, noting application to reconnaissance flight path
14 p2479 A69-29499

Bearing errors from radio beacons with rotating or multilobe radiation patterns
15 p2567 A69-30343

Geometric conditions selection in directions determination in satellite and rocket aided triangulation, deriving formulas for chords directions of earth ellipsoid
15 p2689 A69-30572

Space direction by compensation method of cosmic triangulation network, using laser and optical observations of artificial satellites
15 p2699 A69-31377

Direction defining radio beacons performance, discussing signal amplitude and phase comparison systems and Doppler techniques
17 p2918 A69-33028

Scale determination in spatial direction networks, using polygonal transverse measured along continental surfaces and Secor method over water surfaces
18 p3131 A69-35196

Cramer-Rao and split-beam tracker techniques compared for optimum bearing error attainable with linear passive sonar array in spatially incoherent noise environment
20 p3576 A69-37322

BEARING ALLOYS
Erosion damage of bearing alloy lining in thin lubricating oil film, considering Cu-Pb alloy and tin base white metal
01 p0094 A69-10313

Plain and rolling metal bearings manufacture and use, discussing materials structure and properties, operating conditions, lubrication, etc
11 p1903 A69-24517

BEARINGS
NT ANTIFRICTION BEARINGS
NT BALL BEARINGS
NT FOIL BEARINGS
NT GAS BEARINGS
NT JOURNAL BEARINGS
NT ROLLER BEARINGS
NT THRUST BEARINGS

Hollow rolling elements for reducing centrifugal load on high performance bearings, discussing production, fatigue life, etc
01 p0085 A69-10294

Forced oscillations of unbalanced rotor on elastic bearings with nonlinear characteristics investigated for resultant forces and amplitude using motion equations
01 p0170 A69-10824

Idealized slider bearings with Maxwell liquid as lubricant, analyzing elasticity effects on pressure, load capacity and friction
02 p0253 A69-12413

Amplitude-frequency characteristics of rotor mounted on hydrostatic bearings calculated by equations of dynamic compliance method
03 p0432 A69-12961

Hydrostatic bearings, hydraulic drive system and hydraulic braking system for radio telescope with 2550 tons moving weight
[ASME PAPER 68-WA/PEM-2]
05 p0743 A69-16147

Three dimensional reinforcement composites for gear and bearing applications with improved interlaminar shear strength, thermal and wear properties
08 p1340 A69-25059

Hypersonic slipper bearing problem in rocket boosted sleds, discussing flow model consisting of laminar stagnation region and boundary layers
[AIAA PAPER 68-736]
09 p1477 A69-22003

Operational errors of floating gyroscopes with hydrostatic unloading of bearings, establishing eccentricity tolerances, axes misalignment and temperature field nonuniformity
09 p1497 A69-22103

Centering force and initial rigidity of magnetically suspended bearings of integrating floating gyroscope with allowance for mutual inductance of exciting coils
09 p1497 A69-22104

Rational shape selection for magnetoconductors of centering elements of magnetically suspended bearings, studying effects on initial rigidity
09 p1497 A69-22105

Bearing deposition test for evaluating degradation characteristics of aircraft gas turbine engine lubricants
10 p1700 A69-24070

Hydropendulum bearing linear horizontal vibration effect on vertex vibration, analyzing zero initial phase using precession theory
10 p1697 A69-24086

Radial hydrostatic bearing parameters calculated by pressure distribution diagram in bipolar coordinates, obtaining equations of motion
11 p1892 A69-25341

Friction and wear characteristics of ceramics and cermets as bearing materials, with tabulation of room temperature hardness and maximum service temperatures
13 p2284 A69-27232

Asymptotic analysis for stability and vibration response of spherical squeeze-film hybrid bearing, obtaining perturbation solutions
[ASME PAPER 68-LUBS-37]
13 p2267 A69-27281

Critical rotation rates of homogeneous shaft with two bearings under tension, considering shaft mass, stretching force magnitude and console disk gyroscopical effect
13 p2269 A69-28323

Magnetic suspension device replacing mechanical bearings of inertial guidance systems gyro rotors, evaluating device strength and stability
14 p2479 A69-29492

Face seals for jet engine mainshaft bearing compartments, emphasizing oil film and gas film seals
[ASLE FICFS PREPRINT 28]
15 p2620 A69-30487

Analytical method for designing pressure circular bearings verified by experiments concerning loading capacity
16 p2792 A69-31560

Multipad externally pressurized spherical bearing fed with incompressible fluid for satellite attitude control systems tests
16 p2793 A69-31728

MHD pivoted slider bearing with convex pad surface under azimuthal magnetic field
21 p3733 A69-39744

Rigid shaft dynamics in hinged and elastic bearings, eliminating inaccuracy by limiting analysis to forced vibration
23 p4171 A69-42483

BEAT
U SYNCHRONISM
BEAT FREQUENCIES

Negative Faraday effect and Doppler line width measurements for He-Ne IR gas laser tube by producing beat frequencies in ring laser system
01 p0088 A69-10028

Laser longitudinal oscillation modes beat frequencies measurement by grouping photocurrent velocities by HF field containing photomultiplier cathode
03 p0440 A69-13265

Output and beat frequency of carbon dioxide laser with various resonator configurations realizing single mode operation
07 p1156 A69-19157

Helium-Ne laser beat frequencies between neighboring axial modes shifting linearly with inserted cavity loss
07 p1156 A69-19412

Carbon dioxide rotational constants from CW beat measurement in bulk GaAs mixer between carbon dioxide vibrational-rotational laser lines
12 p2105 A69-26311

Laser output power amplitude fluctuations effect on beat frequency stability for traveling waves in annular laser with broadened Doppler emission line
12 p2107 A69-26541

Submillimeter wave generated in ZnTe by difference frequency mixing of Q switched ruby laser, discussing beat power
[IEEE PAPER B-4] 14 p2457 A69-28927

Gas laser secondary modes emission and beat frequency spectrum widths, using results of Lamb lasers theory
15 p2633 A69-30121

Fluid flow velocity measurements by Doppler shift of laser light scattered from moving fluid, determining beat frequencies
15 p2616 A69-31291

Beat frequency measurements in far IR due to harmonic mixing of klystrons, discussing noise role
17 p3006 A69-33674

Automatic frequency control circuit for stabilizing beat emissions of coupled multifrequency gas lasers
21 p3738 A69-39079

Human response to visual beat phenomena by combining intermittent stimuli, considering brightness estimation
22 p3884 A69-40889

BED REST

Basal metabolism in humans restricted to prolonged bed rest, noting decreased oxygen consumption rates
02 p0197 A69-11497

Prolonged bed rest effect on brain bioelectrical activity from EEG reactions of subjects to acoustic signals followed by light signals
05 p0710 A69-16520

Physiological response of human skeleton to hypogravity and hypodynamics studied by bed rest experiments, suggesting disuse atrophy of bone
06 p0873 A69-17019

Human organism reaction to prolonged limitation of muscular activity during weightlessness simulated by bed rest, noting hypokinetic component of weightlessness
08 p1262 A69-19837

Prolonged bed rest effect on human myogenic tonus and proprioceptive reflexes, comparing test subjects with and without physical exercises
10 p1646 A69-23583

Combined effect of prolonged bed rest and acceleration exposure on human blood circulation, noting increased heart rate and arterial blood pressure
10 p1646 A69-23584

Neurological changes in men due to hypokinesia, analyzing tremor data, EEG recordings and stabilography fluctuations
10 p1647 A69-23585

Bed rest effect on orthostatic tolerance of patients with acute myocardial infarction and without heart failure
10 p1648 A69-24189

Motion coordination capacity of persons subjected to 40 days bed rest studied by dynamographic technique, discussing nature of slackening
17 p2906 A69-32937

Prolonged hypokinesia effect on human resistance to physical stress, noting prophylactic influence of physical exercises
17 p2907 A69-32939

Bedrest as analog of weightlessness, evaluating role of extravascular dehydration in postrecumbency orthostatism
17 p2909 A69-33179

Prolonged bed rest effect on brain bioelectrical activity from EEG reactions of subjects to acoustic signals followed by light signals
18 p3096 A69-34739

BEDS

Viscous liquid layer flow down inclined plane under boundary conditions, taking into account drag and penetration at porous bed surface
02 p0234 A69-12774

BEDS (PROCESS ENGINEERING)

Digital computer program for heat and mass transfer characteristics of spacecraft carbon dioxide adsorption beds, discussing surface pressure of adsorbent material
[AICHE PAPER 19C] 09 p1446 A69-21931

BEER LAW

Transfer equation and Bouguer-Lambert-Beer equation application to multiple light scattering in plane medium
14 p2487 A69-29663

BETTERES

Flour beetle under irradiation and weightlessness during space flight, analyzing effects on somatic wing development, germ cells and pupal period
06 p0876 A69-18177

Circadian rhythm in dermestid beetles *Trogoderma glabrum* Herbst as response to compulsory constant light and temperature conditions
15 p2557 A69-31469

X irradiation and temperature effects on flour beetle *Tribolium confusum* pupae, noting wing abnormalities and pupal stage duration
17 p2910 A69-33748

Physiological and somatic effects on insects of radiation source onboard biosatellite 2, discussing wing abnormalities in flour beetle
20 p3476 A69-37619

BEHAVIOR

NT DECONDITIONING

NT HUMAN BEHAVIOR

Hypothalamic motivational systems and stimulation, discussing behavior patterns and plasticity
09 p1444 A69-21310

Monkey behavior in high atmosphere under weightless conditions, discussing problems connected with biological measurements, logic systems and vibration protection
09 p1447 A69-22722

Squirrel monkeys escape behavior under centrifuge simulated gravity in excess of earth gravity
21 p3665 A69-39174

Abnormal biologic rhythm in rhesus monkeys associated with behavioral stress, noting brain temperature periodicities sensed with implanted extradural thermistor
24 p4261 A69-42708

Behavioral patterns and physiological parameters of medical leech *Hirudo medicinalis* determined in natural environment prior to biological experiment in space
24 p4268 A69-43402

BELGIUM

Secondary radar system chosen by EUROCONTROL Agency for civil air traffic control at Shannon and Brussels airports
15 p2571 A69-31501

BELL AIRCRAFT

U UH-1 HELICOPTER

U X-22A AIRCRAFT

BELL MILITARY AIRCRAFT

U MILITARY AIRCRAFT

BELLMAN THEORY

Differential pursuit games solved by integrating Bellman equation for value function and determining set of possible positions in game with prescribed duration
05 p0788 A69-16536

Cauchy problem for Bellman dynamic programming equation in automatic control time minimization
14 p2426 A69-29478

BELLOWS

Bel lows sealed valve for measurement of fluorine thermodynamic properties at moderately high pressures
09 p1493 A69-21428

Longitudinal vibrations induced by internal flow in metal bellows resembling vortex shedding excitations of elastically restrained cylinders, discussing spring mass mechanical model
[ASME PAPER 69-VIBR-5] 10 p1805 A69-24163

Syphon geometry influence on rigidity and strength determined using integrating Meissner type differential equations with finite difference schemes
19 p3358 A69-35849

BENARD CELLS

Relation between Rayleigh and dynamic Richardson numbers in atmospheric boundary layer in presence of cellular convection
09 p1491 A69-22709

Benard convective flow as function of Rayleigh and Taylor numbers in thin variable rotating silicone oil layer determined by flow photographs
13 p2377 A69-28172

Relation between Rayleigh and dynamic Richardson numbers in atmospheric boundary layer in presence of cellular convection
16 p2808 A69-32488

Benard convection cells analyzed by Boussinesq approximation and Schmidt-Liapunov method, obtaining boundary value problem branching solution
19 p3301 A69-36791

Radar observations of convective pattern types in clear atmosphere consisting of thermal- and Benard-like convection cells
20 p3573 A69-38059

BENCHES

U SEATS

BENDING

NT ELASTIC BENDING

Boundary value bending problem for anisotropic shells of revolution under asymmetrical loading solved by finite difference technique
01 p0165 A69-10088

Bending of micropolar plates using differential equations, considering transverse displacement and microrotation vector
01 p0167 A69-10324

Orthotropic plates bending and thermal stress, analyzing basic equations
01 p0168 A69-10416

Optimal thin walled cross section of hollow beam for pure bending, taking into account stability requirements
02 p0340 A69-12054

Elastic springback and residual stress distribution in sheet metal formed by bending determined as function of radius sheet thickness and stress-strain characteristics
08 p1319 A69-20005

Transverse reinforcing straps effects on torsional stiffness and bending behavior of open cross section profile thin walled prismatic beams
10 p1802 A69-23890

Elastic-plastic bending of rectangular plates with asymmetrically inhomogeneous material in plastic range, using modified Ritz method
14 p2533 A69-28984

Bending problem of anisotropic /nonorthotropic/ plates solved by method of small parameter
16 p2875 A69-32294

Buckling stresses in thin walled box girder under bending determined using stationary potential energy criterion
18 p3224 A69-35344

Keyway stresses in shafts under tension, bending and torsion, using frozen stress photoelastic technique
19 p3445 A69-36827

Rectangular plates bending boundary value problems, deriving formulas for plates with free edges
20 p3630 A69-38291

BENDING FATIGUE

Low cycle fatigue life of aluminum alloy in reversed biaxial bending
01 p0093 A69-10116

Stress peak distribution effects on random load fatigue investigated for one and two degree of freedom systems
01 p0172 A69-11355

Plastic fatigue life of steel under rotary bending, proposing fracture criterion based on strain amplitude for low cycle stress levels
02 p0346 A69-12421

Fracture toughness of Ni maraging steel weldments, using bending tests
[AIAA PAPER 68-507] 03 p0450 A69-13910

Fatigue strength reduction of structural steels fatigued in rotating bending after tensile deformation
03 p0450 A69-13916

Localized microstructural changes and fatigue crack propagation in cantilever type notched specimens of austenitic stainless steel under cyclic bending at constant load
06 p0943 A69-17237

Flexural fatigue of glass-reinforced thermoplastics as function of various parameters, discussing test for autogenous dissipative heating
08 p1337 A69-20481

Aluminum plates bending fatigue tests, discussing mechanical properties, structural failure, grain size, strain hardening, stress-strain-time relations, heat treatment, etc
10 p1711 A69-23356

Surface temperature rise of solution treated austenitic steel measured during double repeated rotating bending fatigue tests at room and elevated temperatures
10 p1711 A69-23393

Device for elastic-plastic circular bending with constant bending moment and angular strain for low cycle fatigue testing
15 p2583 A69-30207

Rotating bending fatigue tests on aluminum alloys based on statistical analysis for material strength
17 p3052 A69-32979

Analytical-statistical weight prediction to derive and apply correlation expression, illustrated with bending stress equation applied to aircraft wing group
[SAWE PAPER 810] 18 p3221 A69-34900

- Fatigue life testing apparatus with computerized simulation of random load maxima and minima, describing rotating bend test application
19 p3434 A69-35777
- Plane strain fracture toughness of high strength steels and Ti alloy from precracked notched bend test method
19 p3346 A69-36436
- Bending creep tests on fabricated Al alloy box beams under constant load and temperature using continuous deflection and strain measurement
21 p3842 A69-39309
- Rotational bending fatigue strength of plain and notched conventional and maraging steels, evaluating gas nitriding effects
24 p4335 A69-43802
- ### BENDING MOMENTS
- Thin curved circular tube under in-plane bending [ASME PAPER 68-PVP-12]
03 p0523 A69-12999
- Calculation method for surface aircraft structures by treating normal forces and bending moments as unknown values
04 p0677 A69-14839
- Pointwise limitation of field dislocation and bending moments in elastic plates
05 p0831 A69-15599
- Stress-strain state of shell having one end clamped and other under concentrated bending moments and concentrated force acting along generatrix solved by integral equation
05 p0843 A69-16681
- Post-wrinkling nonlinear behavior of conical shell of revolution subjected to bending loads [AIAA PAPER 69-90]
06 p1027 A69-18074
- Heat resistance of Ti-Al-Mo-Zr alloys analyzed by bend tests, discussing phase diagrams
07 p1163 A69-18779
- Thin walled symmetrical angle section beam stability under bending moment by section deformation or torsional buckling
08 p1410 A69-19892
- Plastic crack propagation in nonstrain hardening doubly grooved bending specimens with two surface slip, discussing crack angles, crack ductilities and fatigue striations
10 p1797 A69-23077
- Bending creep vacuum testing device for brittle materials at high temperatures, noting load variation capability
10 p1696 A69-23851
- Moment stresses effect on stress concentration in plates with common type hole, considering uniaxial and triaxial bending and torsion
11 p1971 A69-24646
- Elastic bending moments and shear forces uniformly loaded flat plate structures with rectangular symmetry, using collocation technique and complex variable methods
11 p1986 A69-25241
- Stress concentration near circular hole in plate during bending, showing dependence on material constant
12 p2178 A69-25999
- Clamped edge anisotropic elliptical plate bending under varying loads, assuming torsional rigidity bearing constant ratio to geometric mean of bending rigidities
12 p2180 A69-26269
- Lateral bending and two dimensional thermal stress in rectangular orthotropic plates, considering alternating direction implicit method
12 p2188 A69-27100
- Infinite cylindrical shell stability under circular load solved by linearization about bending moment stress state and Galerkin method
14 p2531 A69-28808
- Cylindrical shell bending subjected to internal pressure and force uniformly distributed on round section solved by numerical integration of differential equations
15 p2653 A69-31195
- Analogy between Timoshenko plate theory and moment theory of elasticity achieved by reducing Timoshenko equations to biharmonic and Helmholtz equation
15 p2715 A69-31205
- Strains in elastoplastic curved beam under bending obtained from approximating stress-strain diagram by parabola
17 p3056 A69-33192
- Buckling loads of homogeneous anisotropic plates of composite materials with simply supported boundary conditions, noting Kirchhoff-Love nondeformable normal hypothesis
20 p3628 A69-37776
- Plastic bending of thin walled pipes taking into account cross section flattening
21 p3835 A69-38868
- Photoclastic technique of stress-freezing and slicing to determine bending stresses in transversely loaded plate supported at corners
22 p4045 A69-40900
- Hinged circular cylindrical shells reinforcing ribs effect on deflection and bending moments, assuming external pressure application
23 p4229 A69-42001
- ### BENDING THEORY
- Equations of linear theory of anisotropic elastic plates including Reissner-Green bending equations
01 p0168 A69-10387
- Variable thickness circular annular disk bending in centrifugal force field, establishing dependence between angular velocity and axial pressure intensity
01 p0168 A69-10401
- Sheba family of shell elements for matrix displacement method applied to problems of thin shells under membrane and bending action
01 p0170 A69-10865
- Deflection of orthotropic sandwich plates with unequal facing thickness with edges subjected to uniform and concentrated loading
01 p0172 A69-11270
- Predeformations of thin walled elastic isotropic spherical shells analyzed using Vlasov shell bending theory
02 p0336 A69-11555
- Bending of freely supported plates of polygonal planforms under transverse load with aid of R functions
02 p0341 A69-12140
- Creep buckling of circular cylindrical shells under axial compression and bending, using Al alloy test specimens
03 p0523 A69-12995
- Thin curved circular tube under in-plane bending [ASME PAPER 68-PVP-12]
03 p0523 A69-12999
- Elastoplastic bending of plates with nonlinear stress-strain diagram
04 p0667 A69-14269
- Thermal stress determination in two dimensional problem of theory of elasticity, using stress simulation by thin plate bending
04 p0668 A69-14272
- Thin cantilevered plate theory extended to large inextensional deflections to account for geometry changes in bending moments [ASME PAPER 68-APM/BB]
04 p0670 A69-14401
- Conically bent plate cross section distortion analysis employing von Karman large deflection theory, noting effect of tapering [ASME PAPER 68-APM/Y]
04 p0670 A69-14402
- Timoshenko beam theory accuracy, defining deflection and rotation in terms of average values over cross section
04 p0675 A69-14593
- Plate thickness effect on bending of elastic plate with crack, investigating stress distribution
04 p0678 A69-14890
- Plate bending in presence of unsteady creep and with zero stress-strain state in middle surface solved by variational method
04 p0679 A69-14923
- Bending of rectangular plate with partial clamping, obtaining solution by superposition method
04 p0681 A69-15289
- Symmetrical bending of laterally loaded circular micropolar plates
04 p0682 A69-15291
- Bending theory for sandwich plates with layers having different elastic properties using asymptotic integration of three dimensional equations
04 p0684 A69-15534
- Rayleigh-Ritz finite element method for approximate solution of nonlinear energy functional describing large deflection bending behavior of uniform beam under point loads
05 p0833 A69-15711
- Bending equations for shallow elastic three layer asymmetric shell with different isotropic layers and transversely isotropic rigid filler at various temperatures
05 p0840 A69-16197
- Large displacement bending of rods for constant deformation cross section, negligible shearing forces and exponential stress-strain relation
05 p0843 A69-16682
- Stability of rectangular transversely isotropic plate hinged at three sides under uniform pressure applied to two opposite hinged sides
06 p1021 A69-17178
- Bending general instability of stiffened shallow orthotropic cylindrical shells, noting buckling stress and application to shell design for various loadings
06 p1022 A69-17369
- Power law taperings for minimizing peak to trough deflection of cross section of strip bent longitudinally into cylindrical surface
06 p1023 A69-17374
- Small bending stiffness effect on inflated torus and cylindrical shells under radial load for determining large space structure stiffness
06 p1024 A69-17607
- Antisymmetric cross ply and angle ply laminated plates deflection under transverse loading with coupling between bending and middle-plane extension
07 p1231 A69-18711
- Fundamental problems of plane elastostatics with stress couples reduced to solution of integral equations, noting uniqueness theorem in plate bending theory
07 p1233 A69-19328
- Stability and bending of flexible plates and shallow shells obeying hereditary relations solved by singular kernel functions
08 p1413 A69-20335
- Plane and three dimensional stress concentration studies involving asymmetrical stress tensors, noting contributions to moment theory of elasticity
08 p1419 A69-21177
- Axisymmetric elastoplastic bending theory for cylindrical shell by applying Saint Venant plasticity conditions, determining stress distribution
08 p1419 A69-21179
- Governing equations for bending of fixed isotropic circular sandwich plate subjected to eccentric concentrated load
09 p1615 A69-21926
- Two point boundary value problems solution for parameter dependent nonlinear differential equations, noting application to hinged rod bending
10 p1718 A69-22846
- Linear viscoelastic bending of anisotropic plates based on equation for Voigt plate, considering elliptic and rectangular plates
10 p1793 A69-22881
- Crack propagation in plates and shells subjected to bending and direct loading, noting plate analysis modification for crack touching on compression side
10 p1795 A69-23061
- Infinitesimal bending oscillations and/or responses of thin rotating disks applied to thin disk galaxies, discussing Magellanic Cloud passage near galactic center
10 p1786 A69-24110
- Three dimensional bending problem for thick isotropic plate with curvilinear hole and normal and tangential stress applied to edge of hole
11 p1973 A69-24657
- Two dimensional elasticity and plate bending theories for calculating elastic isotropic panels and thin reinforced plates
11 p1974 A69-24664
- Stress concentrations in bending of thin perforated plates, considering potential and vortex stresses due to edge effect
11 p1976 A69-24784
- Semiinfinite circular cylindrical shell buckling under axial load, computing forces, moments and displacements by thin shell equation
11 p1979 A69-24818
- Bending theory for truncated multilayer anisotropic conical shells, defining relations between displacements and external forces
11 p1984 A69-25141
- Bent plates elastoplastic stress-strain state determination by elastic solution and finite differences, considering linear strengthening under uniform distribution of load
11 p1985 A69-25175
- Maximum stress under bending for thin walled circular cylindrical shell stiffened with uniform stringers
11 p1987 A69-25380
- Bending of half strip rigidly fastened along short edge, constructing integral equation for normal stress at clamping, investigating corners singularities
11 p1996 A69-25734
- Bending of weightless thin elastic beams clamped to circular template by external force
12 p2181 A69-26572
- Mathematical bending theory for three layer elastic plates containing light or rigid fillers
12 p2182 A69-26678

Buckling loads for anisotropic fiber reinforced composite plates with strong bending membrane coupling terms
12 p2186 A69-26840

Bending state of shells of revolution due to edge effects using nonlinear stress strain relation
13 p2362 A69-27921

Theory, function generator routine and testing for six node 18 degree of freedom triangular element for plate bending
15 p2706 A69-30430

Stiffness matrix for refined triangular plate bending finite element, considering Kirchhoff theory
15 p2706 A69-30434

Stress concentration near circular nonreinforced hole at bending of transversely isotropic rectangular plate analyzed in terms of transverse shear theory
15 p2707 A69-30580

Bending theory of orthotropic plates with variable elastic modulus under transverse loads, utilizing stress-strain relations and Kirchhoff-Love hypothesis
15 p2708 A69-30661

Boundary layer solution in three dimensional bending for plate with curvilinear hole to study stress-strain state at hole and over entire plate
15 p2708 A69-30662

Equations for bending of elastic cantilever plate with parallelogram shape in oblique angle coordinate system, constructing functions satisfying Poisson conditions at contour
15 p2710 A69-30861

Stiffness matrix of polygonal finite plate bending element derived using assumed stress distribution
15 p2710 A69-30867

Linear bending theory of elastic anisotropic sandwich plates with strong and weak cores
15 p2713 A69-31025

Bending surface of shells under crosswise load analyzed by moiré method, considering rotating cylindrical surfaces
15 p2713 A69-31056

Bending theory for two layer plate made of isotropic material under sinusoidal load obtained by elasticity and classical theory based methods
15 p2714 A69-31198

Analogy between Timoshenko plate theory and moment theory of elasticity achieved by reducing Timoshenko equations to biharmonic and Helmholtz equation
15 p2715 A69-31205

Bending method for unfolded honeycomb cores shaping for curvilinear sandwich structures
16 p2794 A69-32006

Parabolic and cardioid plates bending under uniform load by using point matching technique
16 p2874 A69-32166

Transverse bending of asymmetric sandwich plates with rigid filler taking into account stresses and strains in filler
17 p3055 A69-33129

Fatigue crack propagation in thin aluminum alloy plates under plane bending using microscopic surface observation and electron fractography, noting role of aging conditions
17 p3061 A69-33677

Error estimation in thin elastic plate bending problem approximate solution by equal deflection lines method, constructing two sided bound for boundary value problems
17 p3062 A69-33713

Side force problem for shallow helicoidal shell, shown as static geometric analogy of pure bending problem, solved by applying analogy
[ASME PAPER 69-APM-11]
18 p3213 A69-34387

Uniform thickness rectangular plates bending with rigidly clamped or freely hinged edges solved by refined version on digital computer
18 p3215 A69-34535

Bending of rigid freely supported plastic plates under local axisymmetric dynamic load, discussing rectangular pulse effects and velocity fields
18 p3217 A69-34593

Pure plastic bending of wide strip, determining stress strain state and plastic strain energy during constrained bending, noting application to corrugated panels
19 p3324 A69-35833

Plate material Poisson ratio determined by application of holographic interferometry to plate pure bending deformation contour lines
19 p3312 A69-36206

Bending of normally loaded simply supported rectangular plates in large deflection range solved by nonlinear differential equations and minimum potential energy principle
19 p3445 A69-36828

Rectangular plate bending element corresponding to finite difference method use, deriving stiffness matrix from strain energy approximation
20 p3619 A69-36949

Clamped uniformly loaded rectangular plate large deflection elastic behavior approximate analysis, using perturbation method
20 p3620 A69-36998

Flat rectangular plates large deflection due to uniform lateral pressure and compressive edge loading analyzed through partial differential equations, difference equations and computer program
20 p3620 A69-37000

Acoustic and internal dampings in freely supported uniform beams of circular and rectangular section, showing frequency dependence and vacuum effect
20 p3620 A69-37062

Swept cantilever thin elastic plates bending analyzed by power series representing deflection in oblique coordinate system
20 p3621 A69-37207

Composite laminates in cylindrical bending, discussing classical laminated plate theory limitations by comparing boundary value problems to corresponding theory of elasticity solutions
20 p3626 A69-37760

Unbalanced cross-ply elliptic laminated plates with bending membrane coupling, analyzing membrane boundary conditions with clamping assumed
20 p3626 A69-37762

Transverse shear deformation effect on bending of laminated rectangular plates, obtaining solutions for bending deflections, flexural vibration frequencies and buckling loads
20 p3627 A69-37770

Monograph on beam impact force and bending stresses during transverse impact, noting Bernoulli and Hertz theories application
20 p3628 A69-37922

Soviet book on thin plates and shells bending and stability during creep covering analytical and numerical solutions for various structural elements
20 p3630 A69-38207

Plate bending theory modified for applying successive linear conjugates method to partially clamped isotropic plate and plate with circular hole
21 p3834 A69-38721

Multiple support wing deformations, obtaining bending equations solutions by matrix methods
21 p3835 A69-38872

Bending of circular plate into shell, using stress-strain relation in finite strain, solving differential equations and boundary conditions
21 p3836 A69-39005

Strain distribution on surface of adhesive bonded box beam in simple bending, using water based brittle coating and self adhesive strain gages
21 p3844 A69-39325

Natural frequency of thin plate subject to cylindrical bending, analyzing panel flutter by three mode approximation for large buckling deflection
22 p4045 A69-40821

Cylindrical shells bending by finite element /cylindrical strips/ method, considering shells of arbitrary shape and variable thickness
22 p4046 A69-40968

Curved rectangular elements stiffness matrices derived for finite element analysis of cylindrical shells bending
22 p4046 A69-40969

Ambartsumian deflection theory applied to axisymmetric bending problem for transversely isotropic circular plates
22 p4049 A69-41278

Vlasov thin shell theory extended for undamped bending, transforming partial differential equations and stress function into integral equation solvable by successive approximations
23 p4225 A69-41407

Warping of doubly supported submerged wings, calculating stress and strains due to bending and constrained torsion
23 p4225 A69-41423

Inflation effect on circular cylindrical cantilever beam subsequent response to bending loads, using theory of small deformations superimposed on large deformations
23 p4227 A69-41881

Green formula and fundamental solution for determining displacements and stresses in contour integral form for plate bending problems
23 p4230 A69-42002

Three layer plate transverse bending in linear presentation, reducing problem to two displacement functions determination
24 p4395 A69-42594

Circular plates axisymmetric nonlinear bending, using variational method to derive equilibrium equations and boundary conditions
24 p4399 A69-42989

Triangular plate bending element using Herrmann variational method, deriving matrices for finite elements
24 p4404 A69-43591

Single series solution for rectangular plate deflection under arbitrarily located concentrated load, considering monolithic slab beam connection case
24 p4404 A69-43593

BENDING VIBRATION

Forced flexural vibrations of elastic truss systems with allowance for hysteresis friction
03 p0432 A69-12953

Damping properties of glass fiber reinforced plastics measured by flexural vibrations
03 p0454 A69-13824

Natural frequencies and mode shapes of coupled bending vibrations of pretwisted rectangular cross section beams determined by Rayleigh-Ritz energy method
03 p0529 A69-13989

Bending-torsion mode of rotating tapered twisted turbomachine blade, analyzing coupled flexural and torsional vibrations effect on natural frequency
[ASME PAPER 68-WA/GT-6]
05 p0838 A69-16141

Resonant frequencies for beam type bending oscillations of thin walled rib-reinforced circular cylindrical shell freely supported at outermost ribs
05 p0841 A69-16204

Longitudinal structural vibration and lateral bending response mass and spring coupling in Saturn AS-502 during boost with longitudinal excitation by pogo effect
[AIAA PAPER 69-58]
06 p1019 A69-18204

Anomalous spacecraft OGO-D motion explained by open section boom thermally induced oscillations, discussing corrective measures
07 p1231 A69-18331

Hingeless fiberglass rotary wings dynamics, discussing effects of in-plane bending to flapping frequency ratio
[AIAA PAPER 69-204]
07 p1054 A69-19548

Rotatory inertia and shear deformation effects on natural frequency and bending mode shape in equations of motion of rotating turbomachine blade
[ASME PAPER 69-VIBR-50]
10 p1804 A69-24148

Supersonic flutter solutions using finite elements, analyzing rectangular plate bending elements, square simply supported and clamped panels, low aspect ratio configurations, etc
11 p1991 A69-25516

Sine series solution for flexural vibration of rectangular isotropic plates applied to free vibration of orthotropic plates
13 p2363 A69-28128

Dynamic characteristics of Clough-Tocher triangle for natural frequency of simply supported plate, noting bending elements
13 p2365 A69-28246

Flexural vibrations of unstiffened doubly symmetric cylindrical tubes, obtaining natural frequencies of simply supported rectangular tube
15 p2703 A69-30210

Calculation of natural twisting and bending vibrations of beam with characteristics varying along length
16 p2873 A69-32130

Bending vibratory motion instability of rotor on elastic shaft with uniform mass distribution along axis, using variational methods
16 p2875 A69-32249

Bending oscillations of semiinfinite beam with periodically changing length
16 p2876 A69-32298

Axisymmetric bending oscillations of thin circular plates of constant thickness with allowance for energy dissipation in material, analyzing resonance and phase amplitude characteristics
17 p3064 A69-33919

Stationary liquid under pressure effect on energy dissipation of rectilinear pipelines under pure bending
17 p2904 A69-33930

Damping properties of turbine blade materials subjected to transverse bending vibrations in vacuum and at high temperatures, including Ti alloys
17 p2990 A69-33932

Damping properties of multilayer coatings for aircraft structures analyzed on duralumin samples subjected to bending at room, elevated and low temperatures
17 p2993 A69-33941

Beam torsion nodal line displacement dependence on flexural and torsional bending frequency

18 p3223 A69-34998

Crack analysis in stiffened vibrating plate based on dynamic stress distribution, showing high bending stresses at intersection

18 p3223 A69-35168

General system of equations derived for nonaxisymmetric oscillations of elastic spherical shells, obtaining expressions for oscillations from torsion, tension and bending

21 p3839 A69-39199

Differential equations of motion and associated boundary condition for axisymmetric flexural vibration of cylindrically anisotropic circular plate, using variational calculus

23 p4228 A69-41911

Flexural vibrations of simply supported lipped I section of cylindrical tubes, considering free-edge boundary conditions

23 p4233 A69-42350

Iterative weighted least squares method for reconstructing time history of coupled rotation and flexural oscillations of Radio Astronomy Explorer satellite

24 p4394 A69-43291

Flexural vibrations of rectangular cross sectioned rings, solving characteristic value problem for finite circular cylindrical shell

24 p4404 A69-43629

BENDS [PHYSIOLOGY]

U DECOMPRESSION SICKNESS

BENZENE

Benzene quadrupole moment estimates from second virial coefficient data with polarizability in intermolecular potential function and from molecular susceptibility anisotropy

01 p0124 A69-10687

Benzene anion radical in solid solution ESR spectrum, noting removal of orbital degeneracy at 4.2 degrees K

03 p0382 A69-13379

Molecular benzene emission spectra excited by electron beams in RF modulated source, tabulating lifetime measurements

15 p2562 A69-30468

Cyclohexane and benzene anodic oxidation at fuel cell electrodes, noting cathodic desorption products as function of potential and reactant [ECS PAPER 330]

15 p2562 A69-31540

BERENICE ROCKET VEHICLE

Hypersonic flight test data of Berenice missile compared to wind tunnel test data, discussing in-flight flow separation, Mach-Reynolds torque, etc

10 p1632 A69-23842

BERGMAN OPERATOR

Bergman integral operator to solve second order differential equations with two independent variables

03 p0527 A69-13742

BERNOULLI THEOREM

Plasma equation of motion in external electromagnetic field analyzed as generalization of Bernoulli equation in relativistic MHD

03 p0476 A69-13385

BERNSTEIN ENERGY PRINCIPLE

Upper bounds for Bernstein-Kolmogoroff multidimensional inequalities, analyzing independent random vectors

11 p1910 A69-25698

Stability analysis of Kippenhahn-Schluter model of solar corona filaments against arbitrary perturbations treated in MHD approximation using Bernstein energy principle

20 p3588 A69-37544

BERYL

Cosmic radiation and hibernation physiopathology of human organism, noting beryl as radiation resisting agent in spacecraft design

06 p0874 A69-17645

BERYLLIUM

Hydrostatic pressure effects on mechanical properties of hot pressed, extruded and rolled polycrystalline beryllium sheet

01 p0092 A69-10059

Chemical vapor deposition of beryllium metal coatings noting thickness, purity and processing effects on surface properties

01 p0097 A69-10644

Beryllium propellants for space applications, considering composite solid propellant with powdered Be as fuel

02 p0303 A69-11763

Electron beam welding of beryllium, discussing procedures, weld quality and tensile strength efficiencies

02 p0252 A69-11863

Friction induced plastic deformation of Be-Co-Zn single crystals with HCP structure

02 p0254 A69-12627

Beryllium reflector distortion in Plum Brook Reactor due to neutron embrittlement and gas formation, noting material surveillance, replacement, etc

03 p0465 A69-13131

Beryllium assemblies for aerospace and nuclear requirements, emphasizing braze joining structural components and effective manufacturing methods [SAE PAPER 680651]

03 p0433 A69-13454

Beryllium chemical and mechanical machining in quantity production, examining salvage and safety precautions

[SAE PAPER 680649]

03 p0434 A69-13455

Beryllium aerospace applications, considering advantages vs disadvantages in systems engineering [SAE PAPER 680648]

03 p0444 A69-13456

Beryllium nondestructive tests, discussing eddy current inspection, ultrasonics, film radiography and scintillation

[SAE PAPER 680652]

03 p0444 A69-13456

Beryllium properties, metallurgy, alloys, fabrication and applications in guidance components, aerospace structures and nuclear reactors

04 p0614 A69-14586

Deformation and fracture of Be bicrystals grown by seeding and floating zone melting method from Be single crystal

06 p0942 A69-17225

Beryllium abundance in solar atmosphere from spectra observed at Oslo Solar Observatory

06 p1010 A69-17971

Polycrystalline beryllium specimens fabricated from powders, discussing initial powder particle size and distribution effects on microyield strength

07 p1168 A69-19598

Chemical conversion coatings and low temperature enamels preventing corrosive attack on beryllium parts in environments containing moisture, chloride ions and/or high temperature oxidizers

07 p1169 A69-19762

Solution annealing and aging time and temperature effects on precipitation in quenched and aged beryllium

08 p1330 A69-20008

Grain-size refinement of beryllium castings and extrusions after compression in pressure chamber, determining effect on ductility

08 p1330 A69-20013

Strong p-type conductivity of silicon doped with beryllium by thermal diffusion, giving electrical and optical measurements

09 p1556 A69-21652

Forging techniques for forming Be into cylinders, rings, shafts and disks, investigating controlled texture forging for turbine engine components

09 p1504 A69-22073

Electron fractographic study of fatigue cracks in wrought beryllium sheet, noting transgranular and intergranular modes on fracture surface

09 p1500 A69-22324

Specific heat dependence of beryllium at low temperatures on sample impurities, considering Debye temperature

09 p1527 A69-22399

Cepheid variable and F and G stars observed for neutral lithium line, searching for resonance lines of ionized beryllium in similar stars

09 p1604 A69-22402

Metal composites of Ni or Mo fibers in Be matrix, discussing chemical compatibility in terms of reactions, solid solubility and diffusion at various temperatures

10 p1707 A69-22991

Model explaining intergranular crack initiation parallel to pulling axis in samples of spun beryllium broken under pressure

10 p1708 A69-22996

Electronic properties of beryllium doped silicon studied with IR absorption spectroscopy and electrical measurements, describing Be thermal diffusion

10 p1747 A69-23989

Early F stars Li/Be abundance ratios estimation from change in solar Be abundance, discussing stellar Li isotopes ratios

10 p1785 A69-24099

Beryllium properties and processing including magnesian reduction, powder purity, oxygen content, grain size and temperature effects on mechanical properties

11 p1904 A69-24897

Refractory cone models made of copper and Co coated Be for force tests in high enthalpy hypersonic arc tunnels at high simulated attitudes

12 p2059 A69-26796

Beryllium single crystals c axis compression behavior at three purity levels under hydrostatic pressures

13 p2279 A69-27760

Book on oxidation and shielding of beryllium in gas media for nuclear and aircraft technology

13 p2280 A69-27927

Adsorption of N, H, O and CO on thick vapor deposited Be films at room temperature

13 p2322 A69-28017

Rolled sheets from beryllium scrap converted into vacuum cast ingots, discussing preparation techniques

13 p2281 A69-28160

Electrolytic and mechanical polishing techniques for metallographic specimens of beryllium

13 p2281 A69-28161

High purity beryllium dynamic tests, determining Hugoniot equation of state, shock profile and spall threshold/onset of microcracking/for elastic pulses [AIAA PAPER 69-360]

13 p2283 A69-28293

Be billets fabrication from powders by cold hydrostatic pressing and pressureless sintering, noting hardness, density and grain size dependence on temperature

14 p2465 A69-29681

Plasma electron temperature determination by line intensity ratio of beryllium-like ions, noting excitation functions

14 p2496 A69-29789

Corrosion prevention in beryllium, testing conversion coatings and low fired porcelain enamels under various humidity and temperature conditions

14 p2466 A69-29939

Beryllium brake disks use on C-5A aircraft, comparing size, weight and peak temperature with steel structure

15 p2639 A69-30591

Beryllium production, properties and technology, discussing ductility, welding and soldering problems, temperature effects, etc

16 p2793 A69-31788

Combustion of pulse heated single Al and Be particles in various oxidizers [WSCI PAPER 69-2]

16 p2830 A69-32343

Creep tests on polycrystalline Be and Be alloy at various temperatures and stresses

17 p2986 A69-32912

Book on high purity beryllium metallurgy for nuclear reactor applications covering physical properties, crystallography, thermodynamics, production methods, etc

17 p2986 A69-32952

Full circle Be brake disks in C-5 aircraft, discussing properties at elevated temperature and fastening of friction lining

18 p3095 A69-35424

Beryllium wire reinforced Al composites, discussing layup techniques and coated filament advantages

19 p3340 A69-35508

Beryllium bonding, evaluating various surface preparations and adhesives

19 p3320 A69-35561

Be and BeAl alloy stress corrosion behavior in aqueous NaCl solution, discussing metallography and electron fractography

19 p3341 A69-35572

Be diffusion during vapor phase saturation of W, Mo, Nb and Ta, noting time and temperature dependence of layer thickness

20 p3549 A69-37364

Neutron activation analysis for oxygen determination in Be by gamma emission intensity from nitrogen 16, noting bound oxygen

20 p3544 A69-37811

Galvanostatic anodic and cathodic currents effect on stress corrosion of Be sheet in aerated synthetic sea water at 72 F

21 p3747 A69-39436

Forged corrosion in aqueous salt environment at various temperatures in unstressed and stressed conditions, considering Be usability in turbomachinery

21 p3749 A69-39493

Stellar lithium and beryllium, discussing production and destruction processes in stellar atmospheres and abundance in various stars

21 p3810 A69-39505

Plane strain fracture toughness of S-200 grade Be for 77-533 K temperature range, noting effects of loading, heat treatment and neutron irradiation

23 p4178 A69-42450

Surface chemistry effect on physical properties of pressure sintered Be metal, suggesting surface alloying approach by powder metallurgical techniques
24 p4332 A69-42963

Beryllium R and D emphasizing brittleness and fracture toughness for safe working stress levels of structurally loaded components
24 p4332 A69-43208

BERYLLIUM 7

Beryllium diffusion coefficients in Zr and Ti bcc phases, using radioactive beryllium 7 at high temperatures
18 p3157 A69-35251

Be 7 stability in galactic cosmic radiation, noting lifetime dependence on electron density around nucleus
18 p3189 A69-35482

BERYLLIUM 10

Cosmic ray produced Be 10 in iron meteorites for terrestrial age determination, considering Cl 36 and rare gas analysis
19 p3412 A69-36104

BERYLLIUM ALLOYS

Metallographic and radiographic analysis of zirconium corner in Zr-Be-Nb system, discussing phase transformation during quenching
02 p0262 A69-11843

Beryllium properties, metallurgy, alloys, fabrication and applications in guidance components, aerospace structures and nuclear reactors
04 p0614 A69-14586

VTOL aircraft materials for improved lightness, durability and cost, noting Be alloys, filamentary composite materials and future problems
05 p0702 A69-15962

Beryllium base cermets corrosion resistance increased in moist carbon dioxide at 700 C
10 p1711 A69-23338

Lightly loaded truss structures fabricated from Be, Be-Al alloy and uniaxial B filament reinforced epoxy tubing for unmanned spacecraft applications
19 p3340 A69-35504

Be/Al cast duplex alloy with Be embedded as discrete particles in Al matrix, detailing fabrication techniques and mechanical properties
19 p3340 A69-35524

Be and BeAl alloy stress corrosion behavior in aqueous NaCl solution, discussing metallography and electron fractography
19 p3341 A69-35572

Structural aerospace materials development with emphasis on Be and Ti alloys, discussing material combinations and composites
19 p3345 A69-36319

BERYLLIUM COMPOUNDS

NT BERYL

Beryllium cermet compositions, discussing beryllium oxide content, mechanical strength and elastic and shear moduli
10 p1711 A69-23334

BERYLLIUM FLUORIDES

Beryllium fluoride heat of formation from heat of combustion of Be-polytetrafluoroethylene mixture in fluorine
21 p3853 A69-39703

BERYLLIUM HYDRIDES

Linear combination of atomic orbitals-molecular orbitals self consistent fields calculation on beryllium dihydride, using Gaussian basis functions
05 p0811 A69-15910

BERYLLIUM ISOTOPES

Be I and Be II lines in solar spectra show no evidence for Be 7 and Be 10 in solar atmosphere
04 p0655 A69-14666

Formation cross sections of Li, Be and B isotopes produced from oxygen 16 spallation via high energy protons related to astrophysics and cosmic ray physics
14 p2512 A69-28968

Nonresonant and resonant cross sections for gamma ray transitions involving isobaric-spin mixed states in Be 8
22 p3987 A69-41043

BERYLLIUM OXIDES

Optical absorption index for molten beryllium oxide based on measurements of small beryllium/ solid propellant rocket motor exhaust plumes
08 p1351 A69-20149

Tensile deformation properties of copper single crystals strengthened by fine dispersions of BeO particles
08 p1334 A69-20575

Beryllium base cermets corrosion resistance increased in moist carbon dioxide at 700 C
10 p1711 A69-23338

Thermal conductivity of polycrystalline beryllium oxide as function of temperature and pressure in argon or helium atmosphere, discussing heat transfer mechanism
11 p1906 A69-25225

Beryllium oxide semiconductor thermistor for temperatures to 2500 K, discussing construction materials and test results
12 p2092 A69-26478

Polycrystalline BeO sound velocities determined as function of pressure and temperature using pulse superposition method
16 p2802 A69-32338

BESSEL FUNCTIONS

NT HANKEL FUNCTIONS

Tearing mode instability in Bessel function model preliminary to study of tearing mode in diffuse pinches
05 p0799 A69-15615

Equation governing transverse vibration of beams with exponentially varying properties, expressing solution in terms of Bessel functions
05 p0835 A69-15873

Asymptotic computation and graphical display of imaginary mu-zeros of combinations of cross product Bessel functions
05 p0836 A69-15874

Analytic integration of Langmuir equation for spherical space charge flow obtained in terms of Airy equation or Bessel functions solution
07 p1115 A69-18864

Stokes phenomenon, considering continuity solution of differential equations across Stokes lines
07 p1174 A69-19220

Horizontally moving body wake scattering cross section calculated with allowance for sphericity of incident and scattered radio waves, using Bessel functions
12 p2031 A69-26699

Electromagnetic step-function plane waves propagation in ionosphere using Fourier transform and Bessel functions
12 p2034 A69-27132

Book on Bessel functions with physical applications covering solution of Bessel and associated equations, integral representations, Fourier-Bessel series, Hankel transforms, etc
15 p2643 A69-30037

Neumann-Lommel formula generalization for obtaining Bessel functions product sums illustrated with FM wave distortion calculation in multichannel system
18 p3101 A69-34625

Bessel functions new addition theorem suggested from mathematical investigation of ideal discriminator output voltage
19 p3266 A69-35767

Bessel function applied to unsteady axisymmetric problem of heat conduction in thermally controlled coaxial cylinders with different physical properties
19 p3448 A69-35981

Stochastic motion in linear lattice of coupled harmonic oscillators analyzed by Schroedinger coordinates and Bessel functions for time behavior, energy flow and impurity effect
19 p3374 A69-36752

Approximation of linear unsteady dynamic systems at finite time interval expressed in Bessel or degenerate hypergeometric functions
22 p3917 A69-40616

BETA PARTICLES

Magnetic field effect on neutron beta decay rate, considering calculations applicability to elementary particle production
15 p2690 A69-30694

Low level beta, X and gamma radiation detector incorporating Geiger, proportional and scintillation counting features in various modes suiting radionuclide decay scheme
17 p2975 A69-33747

Silicon junction radiation detectors applications in cryogenics, measuring junction response to beta particles at low temperatures
20 p3546 A69-38275

Air ionization and beta and gamma dose rate measurements for natural radiation from cosmic rays compared to nuclear weapons tests fallout, considering biological effects
22 p4007 A69-40915

BETATRONS

Betatrions for nondestructive quality control for materials and products under special conditions
18 p3136 A69-34779

BIAS

NT RESPONSE BIAS

Red, blue and no bias light effects on spectral response of copper sulfide-cadmium sulfide cell, using model incorporating photoconductive layer
05 p0808 A69-16358

Substrate bias influence on AC characteristics of MOS transistors used in variable resistor region
07 p1102 A69-18860

Self biasing influence on tunnel diode amplifiers dynamic range, determining limiting conditions for amplitude characteristics
09 p1469 A69-22633

Bias elimination in intensity pattern of incoherent holograms by introducing narrow band time modulation of light
11 p1885 A69-24846

Bias circuit LF oscillations in short Gunn devices, analyzing sinusoidal and relaxation oscillations and stable bias in terms of terminal I-V characteristics
12 p2041 A69-26628

Ring laser bias in angular rotation measurement using optical phase shifters
21 p3735 A69-38651

Thermistor radiation detectors bias condition defined from equations and optimized in terms of responsivity, time constant and noise
21 p3727 A69-39782

Minimum bias criteria for selecting data fitting curves, allowing for unknown true equation in improving data predictability
22 p3975 A69-40332

[AIAA PAPER 69-950]

BIBLIOGRAPHIES

Optimal structural design since 1962
01 p0170 A69-10814

IR reflection and transmission properties of various semiconductor compounds, rubidium halides, strontium titanate, BN and Te
01 p0139 A69-10840

Satellite geodetic literature in U.S.S.R., discussing space triangulation geometric method and dynamic method for earth parameters and gravitational field
01 p0067 A69-10951

Bibliography of interstellar travel and communication
03 p0510 A69-13397

Bibliography on applications satellites covering communication satellites, technology, astronautical science, photography, etc
03 p0535 A69-13429

Stability derivative estimation at subsonic speeds for preliminary design engineer
05 p0700 A69-15545

Subject classification bibliography for thermal contact resistance
[ASME PAPER 68-WA/HT-18]
05 p0847 A69-16122

Bibliography on Gunn effect theory, experimental results and applications
05 p0810 A69-16565

Book on fluidics applications analyzing world literature dealing with fluidic devices
06 p0869 A69-17171

Heat transfer bibliography covering boundary layer, phase flow, conduction, liquid metals, low density, measurement techniques, natural convection, radiation, thermodynamic and transport properties, etc
06 p1033 A69-17558

Bibliography of astronomical literature, Volume 67
09 p1602 A69-22223

Supplementary bibliography of papers on metal insulator semiconductor theory and technology
10 p1743 A69-23169

Heat and humidity endurance limits in man
10 p1645 A69-23494

Alphabetical listing of references and abstracts of papers on acoustical holography
10 p1696 A69-23552

Bibliography of reports and papers on space sciences and research activities of national institutions of COSPAR members/1966-1967/
10 p1784 A69-24001

World literature on boundary lubrication for machine design, giving 2711 abstracts and extensive bibliographies
11 p1891 A69-24925

Bibliography of books and periodicals concerning heat transfer classified under applications, boundary layer, channel flow, conduction, liquid metals, MHD, etc
13 p2379 A69-28341

Bibliographies for aeronautics and astronautics /AIAA/ technical disciplines
14 p2542 A69-29510

Bibliography on laser applications in plasma physics covering plasma diagnostics and production
14 p2498 A69-29842

Bibliography of Soviet books and articles on heat and mass transfer covering thermodynamics, heat conduction, convection and radiation, etc
14 p2540 A69-29900

Dynamic seals literature review covering contact, mechanical, fixed clearance, film riding and elastomeric seals, systems and materials
[ASLE FICFS PREPRINT 29]
15 p2620 A69-30490

Lubrication and lubrication systems literature including compressible and incompressible fluid films, automotive, bearing, gear, friction, wear and boundary lubrication, seals and sealing systems
15 p2628 A69-30900

Soviet bibliography of heat and mass transfer covering thermodynamics, aerohydrodynamics, MHD, transfer processes in various media, etc
16 p2878 A69-31960

Laser induced gas breakdown covering breakdown mechanism and plasma expansion and decay, with bibliography
17 p2980 A69-33026

BICARBONATES U CARBONATES

BICRYSTALS

Slip band continuity across grain boundaries in aluminum bicrystals reexamined for geometrical criteria
01 p0095 A69-10607

Deformation and fracture of Be bicrystals grown by seeding and floating zone melting method from Be single crystal
06 p0942 A69-17225

Creep behavior of oriented Al bicrystals, emphasizing intergranular creep types and crystal orientation
17 p2985 A69-32906

Aluminum oxide relative grain boundary energy and surface diffusion coefficient, considering thermal grooving of bicrystals with symmetrical tilt boundaries
17 p2993 A69-34191

BIHARMONIC EQUATIONS

Digital computer method for Navier-Stokes equation in prototype cavity flow problems, noting applications to biharmonic problems
08 p1305 A69-20831

Partial derivatives of harmonic and biharmonic functions at surface of cylinder for three dimensional problem in elasticity theory, considering displacement vector
11 p1976 A69-24777

Stress in elastic cylinder under thermal expansion with one end clamped expressed by series expansion of biharmonic function using least squares method
14 p2534 A69-29284

Infinite strip plane elastic problem reduced to Hilbert problem by employing multiply connected region and biharmonic solutions
15 p2707 A69-30625

BILLETS

Be billets fabrication from powders by cold hydrostatic pressing and pressureless sintering, noting hardness, density and grain size dependence on temperature
14 p2465 A69-29681

BIMETALS

Temperature distributions and thermal stresses in bimetallic I-beam structures with dissimilar materials for skins and webs and with kinetic heating inputs
06 p1024 A69-17610

Compressor inlet temperature /CIT/ sensors, describing bimetal strip and liquid expansion aspirated types
[ASME PAPER 69-GT-18]
09 p1571 A69-22499

Screw dislocation interaction with partially bonded bimetallic interface, using isotropic elastic continuum approximation
10 p1802 A69-24027

Arc welding aluminum to steel using bimetal transition insert piece
11 p1891 A69-24929

Transition zone structure and phase composition in Ti/stainless steel bimetal as function of rolling conditions and heat treatment
13 p2283 A69-28490

Solid rocket motor ignition system based on exothermic alloying of bimetallic wire constituents
[AIAA PAPER 69-425]
16 p2832 A69-32653

Molten iron plane melt flow duration and mass in bimetallic castings production determined using nomogram
18 p3149 A69-35289

Annealing effect on transition zone cohesion strength in two layer steel-titanium sheet, investigating role of TiC formation
18 p3159 A69-35450

Fatigue resistance of bimetallic sheets of steel and Al alloys by fatigue resonant machine, analyzing lifetime distribution and failure probability
21 p3835 A69-38773

BINARY ALLOYS

Field ion microscope study of imaging solute atoms of dilute Pt-based W, Pd, Co, Ni and Au alloys
01 p0092 A69-10055

Thermoelectric properties of Ge-Te-GaTe system, analyzing phase diagrams, solid solution formation, substitutions and zone structure influence
01 p0138 A69-10404

Metastable phases of binary zirconium-niobium system, defining decomposition of solid solution in cooling
05 p0781 A69-16614

Ion nitrided binary iron alloys and steels electron microscopic studies reveal particle formation during hardenings
06 p0942 A69-17224

Austenitic Fe-Ti alloys sulfur solubility and internal sulfidation rate computed, noting stronger Ti-S interaction with temperature decrease and sulfur diffusion role
06 p0942 A69-17226

Transmission electron microscopy used to study phase transformations in Ti-Mo and Ti-V alloys, determining crystal structures
06 p0943 A69-17230

Corrosion resistance and mechanical properties of Ti-Mo alloy, developing processing methods for forgings, bars and sheets
07 p1163 A69-18781

Components relationships in binary phase diagrams of III a and VI a transition metals on basis of electronic structure
08 p1331 A69-20191

Binary vanadium alloys property change regularities using alloying elements
08 p1333 A69-20439

Carbidothemic production of metals and binary and ternary alloys, discussing eutectic properties
09 p1514 A69-22731

Omega phase transformation in binary and ternary Zr alloys after water quenching from within /alpha plus beta/ phase region
10 p1707 A69-22988

Transgranular stress corrosion crack propagation in thin sheet single phase magnesium-aluminum alloy
10 p1710 A69-23086

Silicon particle sizes in Al-Si system investigated for interactions with dislocations as function of strain and for effect in dispersion hardening
10 p1714 A69-23980

Vacuum deposition of Cr-Al film on Ni-Mo alloys, describing operating pressure, temperature and film thickness
10 p1715 A69-24013

Solid solution decomposition effect on binary Mg alloys recrystallization temperature containing Al and Nd, using X ray and microstructural analysis
11 p1902 A69-24272

Wetting and sessile drop contact angles between liquid binary Al alloys and solid Be, boron carbide and graphite under vacuum and in He
[ACS PAPER 15-C-68F]
12 p2114 A69-26301

Alloying effect on surface oxides determined from photoelectric polarization measurements for Ti- Nb and Ti-Ni
13 p2275 A69-27292

Martensite transformation in Ti-Cr binary alloys by thin foil electron microscopy, noting crystallographic theory
13 p2276 A69-27369

Gamma prime phase coherent equilibrium solubilities in Ni alloys of Al, Si and Ti from magnetic studies of particle coarsening and electron metallographic observations
13 p2276 A69-27370

Cleavage plane in stress corrosion cracking of alpha phase Ti-Al alloys
13 p2283 A69-28189

Homogeneous NbC and TiC specimens physical properties, discussing current carrier density and mobility dependence on composition
14 p2462 A69-28976

Monograph on mechanical behavior of crystalline solids at elevated temperatures, discussing creep properties of metals, solid solutions and two phase alloys
14 p2465 A69-29749

Co base high temperature binary alloys microstructure, investigating diffusion coefficients, stacking faults, vacancies, etc
14 p2465 A69-29890

Mu phase lattice constants and cell volume in Nb-Zn system
15 p2636 A69-30086

Crystal structures of intermediate phases in La-Co and Nd-Co systems by powder X ray diffraction technique
15 p2667 A69-30087

Chromium-cerium phase diagram determined by differential thermal, metallographic and X ray structural analysis
15 p2640 A69-30666

CR-B binary system phase diagram including lattice parameters, temperature of peritectic decomposition and characteristics of alloys
15 p2641 A69-31185

Electrical conductivity and thermoelectromotive force of bismuth telluride and bismuth telluride-bismuth selenide alloys obtained by sintering, hot pressing and annealing
15 p2670 A69-31248

Orientation relationships between phases in Co- TaC pseudobinary eutectic alloy, discussing Co fcc-hcp allotropic transformation
[ONERA-TP-714]
17 p2988 A69-33395

Thermionic emission parameters for faces of W- Re, Mo-Re and Ta-Mo single crystals determined by Richardson method of straight lines
17 p3015 A69-33630

Be/Al cast duplex alloy with Be embedded as discrete particles in Al matrix, detailing fabrication techniques and mechanical properties
19 p3340 A69-35524

Heat treatment effects on mechanical properties of Ti-Fe and Ti-Fe-Al alloys
19 p3344 A69-36151

Glassy semiconductors from metallic alloy binary and ternary systems of sulfide, selenide and telluride noting properties
19 p3392 A69-36641

Elements substitution for Al in gamma prime of Ni-Al alloy to change aged hardness by gamma prime mismatch and coherency strains
20 p3558 A69-36963

Autoradiographic methods for diffusion and phase transformation in Fe-Cr alloys by application of photographic emulsion with tracer element on metal surface
20 p3561 A69-37416

Crystallographic relations between mother gamma phase and bulk martensitic structure of Fe-Ni alloys with less than 20 percent Ni, using radioisotopes
20 p3562 A69-37781

WC-Co alloys microstructure and microproperties, considering individual phase behavior and grain-solid solution interactions
20 p3564 A69-38246

Ti emission and absorption K spectra in Ti-Al intermetallics, suggesting hypothesis concerning long wave and fundamental subbands origin
21 p3749 A69-39787

V systems applications and phase diagrams, discussing binary metallic systems, Kurnakov law, alloy properties dependence on composition, superconductivity, melting point, etc
22 p3968 A69-39887

Recovery process observation in pure binary Al-Cu alloy and commercial Al-Cu-Mg-Pb alloy, noting electron microscope applicability
22 p3968 A69-40062

Ellipsometer measurements for oxidation rates of binary Ti-Al alloys in vacuum and in pure and premixed gases, using in situ test cell
24 p4316 A69-43322

BINARY CODES

Serial BCD binary coder design, using Karnaugh diagrams to minimize synchronous and asynchronous counter stages
09 p1467 A69-22579

Decoding procedure for error locating binary code indicating location of single subblock containing errors in code word, employing feedback shift registers
11 p1857 A69-24549

Compression capabilities of combined frequency and phase shift keying in radar and sonar pulse modulation using binary noise codes
15 p2568 A69-30628

Algorithm for assigning binary codes to inputs, internal states and outputs for sequential machines by threshold logic
18 p3105 A69-34618

Optimum receiver design for binary coded data detection in two channel space communication system,
18 p3105 A69-34618

discussing phase error distribution and optimum decision function

19 p3275 A69-36286

BINARY DATA

Regenerative digital transmission system error, representing memory of binary regenerative channel with Markov model

01 p0027 A69-10249

Reliability of binary message in Gaussian noise impaired by amplitude limiting in case of evaluation by integration

01 p0031 A69-10736

Noncoherent binary communication detector for slow selective fading channel with additive quasi-stationary noise based on mathematical procedure of nonparametric classification

03 p0390 A69-13215

Shift and add property for majority combined binary composite codes with linear maximal sequences

03 p0391 A69-13229

Upper and lower bounds on mean reduced error of pulse code telemetering systems operating by binary code

03 p0396 A69-13687

Optimum conditions for signal analysis determined for symmetrical binary communications channel with unknown signal phase

04 p0556 A69-14492

Phase locked loop demodulator with quadrature channel modified for decision feedback to detect binary phase shift keyed signals

08 p1270 A69-19859

Electronic switching circuits controlled by binary counter triggers for variable passband filters

12 p2040 A69-26489

Fourier analysis of pseudorandom binary sequences, noting relation of sequence sampling properties to interchange of phase angles of sequence harmonic components

13 p2287 A69-27245

Deep space telemetry bit errors increased by reference signal phase noises and partial RF signal suppression, calculating equivalent signal to noise ratio degradation

13 p2223 A69-28609

Binary error investigation in noncoherent FSK communication link with nonselective fading, noting Doppler shift

14 p2414 A69-29498

Digital receiver of radar signals for performing binary quantization of input data with subsequent processing by digital computer

15 p2563 A69-30136

Algorithm for processing binary-quantized echo signal packets, obtaining useful and noise signals relation

15 p2571 A69-30331

Binary-quantized signal packet center for target azimuth determination, discussing antenna radiation pattern role

15 p2566 A69-30332

Direction finding accuracy of pulsed radar with binary-quantized detector signals, discussing azimuth minimum variance and quantization threshold optimization

15 p2566 A69-30333

Robust detection of binary signal in additive noise, using extreme value theory /EVT/ to estimate probability density function and system error and threshold

17 p2944 A69-33624

Optimum receiver design for binary coded data detection in two channel space communication system, discussing phase error distribution and optimum decision function

19 p3275 A69-36286

Binary storage system operation during binary quantization of signal, applying results to storage efficiency improvement

19 p3278 A69-36597

Optical information rates for photocount detection systems based on coherent field model, considering binary channels with or without Gaussian noise

20 p3485 A69-36923

Optimum and suboptimum synchronizers for extracting bit synchronization from binary data, showing performance dependence on pertinent system parameters

21 p3673 A69-38923

Partially coherent PSK-modulated binary detection, deriving noisy phase reference by narrow band tracking filter, analyzing bit output error as function of SNR

23 p4122 A69-41772

Error probability bounds for self synchronized binary PSK communication systems, simulating decision feedback, phase doubling and maximum likelihood systems

23 p4128 A69-42501

BINARY DIGITS

Primitive trinomials of high degree for use in pseudorandom sequence generation of zeros and ones

03 p0455 A69-13373

Trigonometric and arithmetic functions for reducing size of MOS read-only memories to reduce required bit count, discussing cost, structure and applications

07 p1089 A69-19778

Nonlinear filter theory applied to digital telemetry binary processes, using continuous time stochastic process

19 p3274 A69-36281

BINARY FLUIDS

Volatile liquid pressurization, discussing pressurants, heat sources and system design

02 p0232 A69-12382

Laminar flow of isotropic binary gas mixture in circular cylindrical tube with porous walls, determining concentration field variation with wall suction Reynolds number

05 p0744 A69-15618

Binary gas flow past curved body for stationary problem studied by solving Boltzmann equations in form of matched asymptotic expansions

11 p1867 A69-24753

Thermomechanical theory for nonreacting binary fluid mixtures, discussing free energy function, entropy flux vector, equations of motion, constraints, etc

12 p2191 A69-26927

Heat and mass transfer coefficients in binary laminar boundary layer during natural convection, taking into account enthalpy and thermal diffusion effects

13 p2378 A69-28312

Two temperature gasdynamics for binary gas mixtures of differing molecular weight components, analyzing ultrasound and shock wave propagation

13 p2250 A69-28447

BINARY INTEGRATION

Binary block codes for correction of substitution and synchronization errors

09 p1452 A69-21316

BINARY MIXTURES

NT EUTECTIC ALLOYS

NT EUTECTICS

Thermistor assembly apparatus for measuring coefficient of thermal conductivity of pure and binary mixture of gases

05 p0845 A69-15616

Two stage thermal treatment inhibiting influence on swelling and porosity linked to Kirkendall effect during sintering of Fe-Ni powder mixtures

05 p0782 A69-16616

Gas mixture separation in supersonic jet, noting results for hydrogen-nitrogen mixture and diffusion flux

06 p0911 A69-17553

Ignition of binary mixtures of hydrocarbons at high and minimum ignition temperatures of components

06 p1035 A69-17935

Monograph on shock wave structure in binary gas mixtures covering gas kinetics and shock tube measurements of heavy component density distribution

08 p1304 A69-20711

Two fluid kinetic model for analyzing shock wave structure in binary mixtures of monatomic inert gases, noting no overshoot in velocity profiles

08 p1304 A69-20813

Variational calculation of coefficients of viscosity, thermal conductivity, thermal diffusivity and diffusion in binary mixture

11 p1997 A69-24285

Transport coefficients for almost Lorentzian mixture, computed as perturbation to coefficients for true Lorentzian mixture, compared to Chapman-Enskog method results

11 p1997 A69-24286

Gravitational effects on thermodynamic variable equilibrium composition of liquid-vapor binary mixtures near critical point, discussing changes in phase with altitude

11 p1999 A69-24914

Air-hydrogen supersonic mixing and combustion, characterizing hot hydrogen jet discharging into supersonic concentric air stream at atmospheric pressure

13 p2378 A69-28275

Convective heat and mass transfer in binary turbulent vertical boundary layer

13 p2378 A69-28311

Thermal ignition of methane-oxygen mixture, observing flame propagation

13 p2380 A69-28459

Dielectric constant of liquid hydrogen and hydrogen-helium mixtures measured with resonance method

14 p2487 A69-29668

Two component heat pipe operating characteristics on basis of thermodynamic phase equilibrium for binary mixtures

[AIAA PAPER 69-631] 17 p3071 A69-33268

Energy balance equation for two phase liquid-gas mixture ignition process, deriving formula for speed of combustion zone movement

18 p3231 A69-35123

Heat loss from cylinders at low Reynolds numbers in N-He and N-Ne binary mixtures

21 p3848 A69-38706

Nitrogen and water vapor effects on hydrogen-oxygen system recombination, using shock tubes for design of exhaust nozzles for hypersonic flow vehicles

21 p3669 A69-38801

Numerical analysis of plane Couette flow of rarefied binary gas mixture using relaxation type kinetic model equations, discussing slip velocity, friction coefficient, etc

22 p3931 A69-40778

Binary gas mixtures transport coefficients approximated by self consistent matrix procedure based on Chapman-Cowling expressions

24 p4352 A69-43135

BINARY STARS

NT ECLIPSING BINARY STARS

Pulsars features explained by model based on binary system of neutron stars, discussing associated stellar plasmas as directional HF radio wave source

01 p0156 A69-10981

Position of binary stars in photometric diagrams at Geneva observatory, discussing sequence profile of HR diagram

03 p0517 A69-14094

Light and radial velocity changes in close binary systems, including limb and gravity darkening of distorted stars in analysis of spectroscopic effects

04 p0653 A69-14612

Mass exchange and evolution of close binaries /Main Sequence stars/

04 p0653 A69-14614

Photographic plates based parallax determinations of nearby stars weights, relative and absolute values, probable error and observation interval

04 p0663 A69-15381

Spectra of close binary systems, analyzing abundance anomalies, noting metallicity results

05 p0822 A69-15854

Evolution of close spectroscopic binaries and Am stars

05 p0822 A69-15855

Origin of binaries from angular momentum vectors orientation and separation distribution

05 p0822 A69-15856

Spectroscopic binary 16 Piscium, showing unusual period of 47.25 days

07 p1214 A69-18662

Photometric effects of UVB color indices ineffective in detecting double stars in Galaxy

07 p1216 A69-18854

Stars of higher multiplicity, discussing numerical membership and gravitational binding of star clusters and binary stars

07 p1219 A69-19295

Lines displacement in binary star spectrum due to blending, presenting graphs displaying magnitude of effect under various conditions

07 p1223 A69-19624

Frequency and radial velocity for various cepheid binaries, discussing hot companions detection through photometry

07 p1223 A69-19627

UV emission spectrum of double star Boss 1985, excitation potential effect on Fe II lines and table identifying emission lines

08 p1385 A69-20060

Orbital elements of visual double star and O-C residuals, noting dynamical parallax and ephemerides

08 p1393 A69-20568

Binary stars systems with same total mass calculated for evolution from main sequence stage through mass exchange to white dwarfs

08 p1393 A69-20569

Close binaries evolution and Algol type systems origin, discussing hydrogen exhaustion in center

08 p1395 A69-20633

Nonisotropic mass ejection from components of close binary system effects on orbital elements for small initial eccentricity case

08 p1395 A69-20634

Gas flows in close binary systems of dwarf stars

08 p1396 A69-20648

Stars closer than five parsecs including binary systems, luminosity, spectral type and mass
08 p1407 A69-21130

Pulsar NP 0532 identified with Baade south preceding star in Crab Nebula, noting pulsed optical radiation
09 p1592 A69-21458

Radial velocities of stars near cluster NGC 7380, discussing discovered stars, double lined spectroscopic binaries and photometric information
09 p1597 A69-22060

Low mass close binary systems evolution, describing components inside critical Roche lobe in initial detached phases
10 p1777 A69-23310

Delta Cepheid blue companion /delta Cep C/ rapid radial velocity variations, noting spectral proximity between delta Cep A and C
11 p1957 A69-24405

Evolutionary stages of visual binary components based on magnitudes and color indices
11 p1962 A69-25111

Dynamical effects of mass exchange in close binary systems ejection modes from point of view of orbital elements evolution
11 p1962 A69-25113

Optical flashes recorded from Crab Nebula M1 close to central double star with periodicity equal to radio pulses discovered earlier
11 p1962 A69-25250

Least squares iterative program, deriving orbits for O binaries HD 93403 and HD 135240
11 p1963 A69-25257

Micrometric and photometric measurements of coude spectra of magnetic variable HD 125248, showing spectroscopic binary nature and computing orbital elements
11 p1963 A69-25264

Close binaries evolution and mass exchange for stars of 5 solar masses with very short periods, using modified Henyey method
11 p1964 A69-25414

Statistical data for visual binary systems with known spectral classes or colors and one component near main sequence
12 p2159 A69-26666

Spectroscopic and eclipsing binaries in zodiac tabulated for photometric studies at lunar occultations
12 p2171 A69-27152

Book on astrophysics and stellar astronomy covering stellar radiation, binary and variable stars, positions, magnitudes, galaxies, cosmologies, etc
13 p2337 A69-27463

Parallax and mass ratio of visual type K6 dwarf binary system, ADS 1865, BD plus 30339
13 p2349 A69-27811

Parallax and orbital motion of spectroscopic binary Tau Persei determined from Sproul refractor photographs
13 p2349 A69-27812

Relative parallax, fractional mass and luminosity of visual binary 1785 determined from photographs taken with Sproul refractor
13 p2349 A69-27814

Visual binary star parallax, motions and mass ratio determined using photographic data
13 p2349 A69-27815

Shock heated gas radiation frequency dependence and UB and B-V color indices determination, studying role in close binary systems luminescence
13 p2350 A69-27860

Sec-Cen B stars radial velocities, determining spectroscopic binaries
14 p2519 A69-29136

Lacerta OB 1 B spectroscopic binaries periods and orbital elements, noting limits for secular variation
14 p2519 A69-29137

Metallic line /Am/ stars Zeeman observations, showing 16 Ori as spectroscopic binary, dubious binary nature of 15 Vul and doubtful presence of magnetic fields
15 p2692 A69-30775

Spectral Pt II lines in Ap stars of Hg class observed during analysis of double lined spectroscopic binary HR 4072
15 p2695 A69-30891

Close binary system components approximated by two nonsimilar ellipsoids, obtaining interpretation of light curves
15 p2695 A69-30957

Close visual binaries separations for checking large aperture telescope resolution, listing binaries, orbits and ephemeris
16 p2855 A69-31662

Photoelectric visible radiation observations of binary star AH Vir
16 p2858 A69-32215

DQ Herculis photometric measurements synchronized with white dwarf component pulsation, discussing equipment, eclipse curve and binary period dependence on time
16 p2862 A69-32373

Motion of two rigid spheroids with mutual gravitational attraction based on Hamilton-Jacobi theory applicable to binary stars
16 p2863 A69-32402

Planetary systems interrelationship with binaries and rotating stars, emphasizing occurrence frequency study based on stellar angular momentum orientation
17 p3032 A69-33105

Light changes caused by distortion of binary components, computing theoretical brightness variations by numerical integration of emerging atmospheric intensities over visible surface
17 p3044 A69-34179

Mean rotational velocity of finite width gaseous ring in close binary system from rotational velocity measured on spectrograms
17 p3044 A69-34180

Physical nature of HZ 22 short period hot subdwarf binary, noting arguments against normal B type binary hypothesis
17 p3044 A69-34181

Curve of growth analysis for close binary HR 5317 indicating Mg, Mn, Ca and Sr overabundance respecting standard star 110 Her
18 p3191 A69-34297

Masses of visual binaries above main sequence with published orbits determined as function of position in H-R diagram, using spectroscopic parallaxes
18 p3195 A69-34429

HD 30353 He binary star invisible component suggested as KO type supergiant from IR photometric data
18 p3203 A69-35348

Geometric determination of visual binary orbits, noting inadequacy of graphical method based on apparent orbit eclipse properties
19 p3403 A69-35968

Forbidden emission transition probabilities in high excitation symbiotic stars, novae, Cygni stars and peculiar binaries
19 p3423 A69-36227

Visual binary star ADS 12447 orbit elements calculated using Zwiers method
20 p3598 A69-37466

Orbital elements of visual binaries Don 91 and ADS 9756 derived graphically, tabulating observations with ephemerides
20 p3600 A69-37480

Right ascension and flux density of source in Crab Nebula measured at meter wavelengths, evaluating spectrum and relative position to binary star center
20 p3607 A69-38040

Book on white dwarf formation through mass exchange covering binary star system, primary star mass losses and evolution into white dwarf
22 p4021 A69-40421

VV Cephei type binaries cool and hot primary stars light variations, discussing duration, orbital cycle correlation, mass loss, etc
24 p4386 A69-43346

Temperature distribution on surfaces of close binary stars as basis for predicting variation of monochromatic reflection effect
24 p4387 A69-43350

Blue component of HD 237006 and VV Cephei spectra, suggesting greater luminosity of blue star in late type supergiant
24 p4387 A69-43353

Delta Cepheid blue companion /delta Cep C/ rapid radial velocity variations, noting spectral proximity between delta Cep A and C
24 p4391 A69-43795

BINARY SUMMATORS

U ADDING CIRCUITS

BINARY SYSTEMS [DIGITAL]

U DIGITAL SYSTEMS

BINARY SYSTEMS [MATERIALS]

NT EUTECTIC ALLOYS

NT EUTECTICS

High temperature research on systems formed by zirconium dioxide with samarium and gadolinium sesquioxides near melting point
01 p0101 A69-10044

Time dependent viscoelastic stress distribution in two phase composite material, using plane stress model for approximation
02 p0348 A69-12540

Nonlinear constitutive equations for mixture of two elastic solids linearized, assuming small displacements and subsequent temperature changes
03 p0529 A69-14063

Bainite beta to alpha transformation in titanium-oxygen system, using high temperature metallography techniques
04 p0613 A69-14559

Solid solutions of O in Ti and Zr, noting superstructure formation and physical properties
04 p0618 A69-15078

Vanadium-carbon and niobium-carbon binary systems revised phase diagrams, noting effect of sublattice order transformations
05 p0779 A69-15988

Binary mixture condensation on cooled vertical plate, formulating predictive theory based on conservation laws and other physical principles
[ASME PAPER 68-WA/HT-21]
05 p0847 A69-16124

Two phase self lubricating composite materials for high temperature, detailing impact strength, friction and wear tests
[IME PAPER 12]
07 p1137 A69-18560

Thermodynamic properties of binary and ternary liquid metal systems, noting electromotive force and vapor pressure measurements
07 p1165 A69-18939

Ductile fracture behavior of two phase stainless steel examined by straining smoothed and notched tensile and Charpy impact specimens
08 p1333 A69-20574

Correlation between interfacial tension in binary and ternary systems and reciprocal solubility of bulk phases, assuming concentration as function of thickness
09 p1448 A69-21909

Concentration changes in binary metal-gas solutions during simultaneous degassing kinetics and metal evaporation
09 p1528 A69-22732

Pd-D resistivity variation with D concentration at room and liquid He temperatures, discussing structural resistivity
10 p1745 A69-23357

X ray investigation of niobium, aluminum and niobium-aluminum systems to obtain K-spectra and L-spectra
14 p2508 A69-29664

Binary Nb-Hf system phase diagram below solidus line noting lattice parameters and oxygen and nitrogen effects on phase equilibrium boundaries
18 p3157 A69-35247

InSb-InAs, InSb-GaSb, InP-GaAs and InP-GaP quasi-binary systems solid solutions optical and electrical properties, determining energy gap change as function of composition
19 p3390 A69-36554

Phase analysis of systems Mn-S, Mn-Sc and MnS-MnSc by X ray diffraction techniques, revealing homogeneity ranges
20 p3485 A69-38286

Diffusion layers and elasticity-dependent interdiffusion coefficients of Ti binary systems, using X rays
21 p3745 A69-38954

Soviet book on liquid binary systems covering physicochemical analysis and quantitative methods
21 p3670 A69-39529

BINDERS [ADHESIVES]

U ADHESIVES

BINDERS [MATERIALS]

NT PROPELLANT BINDERS

NT SOLID ROCKET BINDERS

Tungsten replacement by chromium or molybdenum in heavy metals shown possible for binding material of group 6A metals
05 p0780 A69-15991

Unidirectional fibrous materials stability, finding characteristic equation in form of infinite determinant by solving three dimensional stability of reinforcing fibers in binder
11 p1985 A69-25172

Shrinkage and heat release of polyglycol maleinate binder during gamma radiation consolidation compared with thermochemical consolidation
12 p2117 A69-25991

Microfibrous boehmite as binder for molybdenum disulfide in formation of ductile water resistant dry lubricant films
[ASLE PAPER 68-LC-14]
15 p2642 A69-30606

Silico-organic liquid water repellent coatings for increasing binder adhesion to glass fiber in glass fiber reinforced plastic materials of aircraft components
21 p3752 A69-38876

Cement materials to attach thermocouple to stainless steel tubing in nuclear rocket engine nozzle, considering thermal conductivity, bond and tensile and compressive strengths
21 p3753 A69-39699

BINDING
Binding of lysine-rich proteinoids to organismic or thermally synthesized polynucleotides, noting polyanhydroamino acid interactions with polynucleotides
07 p1074 A69-18635

BINOCULAR VISION
Depth distortions in binocular visual fields from misleading size cues
21 p3653 A69-38900
Holographic photogrammetry compared with conventional holography in monocular and binocular parallax reconstruction and stationary stability of objects
22 p3944 A69-40044
Eye movement control mechanisms during binocular fixation used to determine corrective roles of flicks and drifts
22 p3883 A69-40876

BINOMIAL COEFFICIENTS
Lunar gravitational potential and lunar surface radius vector binomial series coefficients determination from Luna 10 data used for lunar surface shape calculations
20 p3596 A69-37308

BIOACOUSTICS
Interspecific synthetic signals research for effective bioacoustic bird scaring techniques including optical signals
17 p2914 A69-33364

BIOASSAY
Analytical techniques for in-flight monitoring of aerospace water supplies for potability, emphasizing rapidity, sensitivity and reproducibility
01 p0019 A69-11339
Biological monitoring during assembly of Technological Feasibility Spacecraft /Mars lander/ to evaluate thermal control techniques and microbiological burden prior to sterilization
02 p1201 A69-11774
Technology Feasibility Spacecraft /TFS/ sterilization and bioassay program during assembly, analyzing sampling and cleaning procedures
09 p1446 A69-22358
Sterilization assembly development laboratory /SADL/ quality assurance program for microbiological monitoring according to NASA planetary quarantine requirements
15 p2559 A69-31123
Pre and postflight leukocyte chromosome aberration analyses of Gemini astronauts
17 p2908 A69-33173
Lignin presence in New Zealand moss gametophytes observed for characteristic color reaction and UV spectra, noting contrast with north temperate species
17 p2912 A69-34176
Biocrystallography of organic form and structure emphasizing liquid crystals, polymers, epitaxy, inclusion compounds, electrical properties, prelife compounds, etc
21 p3656 A69-38922

BIOASTRONAUTICS
Automatic life support system tried on leeches for space applications
01 p0021 A69-11080
Analytical techniques for in-flight monitoring of aerospace water supplies for potability, emphasizing rapidity, sensitivity and reproducibility
01 p0019 A69-11339
Automatic bioprobe life support system for long duration interplanetary space flight, discussing blood leech as suitable research animal
02 p0199 A69-11828
Membrane vapor diffusion for water reclamation from urine and wash water on space missions
03 p0379 A69-12992
Weightlessness effect on blood circulation system of human beings and animals during suborbital/ orbital space flight
03 p0376 A69-14194
Flour beetle under irradiation and weightlessness during space flight, analyzing effects on somatic wing development, germ cells and pupal period
06 p0876 A69-18177
Reactions of respiratory and cardiovascular system of dogs in biocompartment of ballistic missiles, discussing biopotential of myocardium, arterial pressure, etc
07 p1060 A69-18576

Oculomotor activity of cosmonauts during orbital flight, analyzing electrooculograms taken during vestibular tests
07 p1063 A69-18594
Plants growth from seeds exposed to space environment onboard Cosmos 110 biological satellite compared with control plants
07 p1064 A69-18972
Enzymes in simulated Martian environment exhibit higher resistance than in earth atmosphere at 4 C
07 p1065 A69-18974
Permissible irradiation doses established for spacecraft crews making short and long flights, considering roles of life span, somatic effects, leukemia and genetics
07 p1069 A69-19618
Clinical report on Apollo 7 and 8 mission medical data, discussing preflight preventive medical activities, inflight treatment, radiation levels, etc
09 p1446 A69-22542
Automatic computer processing of physiological data during space flights, discussing choice of computers and computer programs
10 p1649 A69-23509
Space travel and lunar exploration medical problems
13 p2210 A69-27909
Weightlessness, increased gravitational fields and radiation effects on biological systems at organismal, cellular and subcellular levels, discussing biosatellite experiments
14 p2406 A69-29097
Aerospace biomedical technology transfer analysis, discussing spinoff, popular interest, transfer barriers, etc
18 p3236 A69-35104
Plants growth from seeds exposed to space environment onboard Cosmos 110 biological satellite compared with control plants
20 p3479 A69-38220
Enzymes in simulated Martian environment exhibit higher resistance than in earth atmosphere at 4 C
20 p3479 A69-38222
NASA Lunar Receiving Laboratory functional areas and physical, chemical, biological and quarantine activities for crew and lunar samples
21 p3690 A69-38896
S-4 human blood experiment during Gemini 2 flight, studying spaceflight ionizing radiation interaction effects on single and multiple break chromosome aberrations
23 p4085 A69-41600
Space physiology, describing laboratory and onboard experiments
23 p4086 A69-41686
Behavioral patterns and physiological parameters of medical leech *Hirudo medicinalis* determined in natural environment prior to biological experiment in space
24 p4268 A69-43402

BIOCHEMISTRY
NT BACTERIOLOGY
NT ENZYMOLOGY
NT PHYSIOCHEMISTRY
Space technology contributions to medical problems, discussing organization and achievements of biochemical application program of NASA [UN PAPER 68-95417]
01 p0020 A69-10471
Molecular mechanisms leading to mineralization of organic tissues, noting role of protein and glycoprotein matrices
04 p0555 A69-14888
Psychochemical research theory and methodology, relating biochemical phenomena to human brain function
04 p0553 A69-14976
Bioadhesive investigation in echinoderms extended to class Holothuroidea, using electron microscope with correlative light microscopy for tube feet of sea cucumbers
05 p0708 A69-15984
Binding of lysine-rich proteinoids to organismic or thermally synthesized polynucleotides, noting polyanhydroamino acid interactions with polynucleotides
07 p1074 A69-18635
Inhibition of gamma ray induced DNA degradation by infection with bacteriophage
07 p1069 A69-19709
Hypothermia induced alterations in biochemical processes studied with isolated rat liver perfused at low temperature
10 p1642 A69-23119
Preferential shifts in consumption of metabolic fuels following exposure to hydrazine or monomethylhydrazine, considering biochemical and physiological responses
14 p2407 A69-29303

Electrokinetic converter of biochemical parameters for diagnosis and control of organism behavior, noting biomechanical utility
14 p2409 A69-29471
Dynamic differential thermal analysis with He flow performed on biological specimens, proteins and starches, showing discrete decomposition peaks monitoring pyrolysis process
16 p2747 A69-31807
Cell-like structures containing biochemicals as inevitable event under various hypothetical primitive earth conditions
23 p4085 A69-41479
O-hemoglobin dissociation curve shape effect on O affinity of hemoglobin
23 p4095 A69-42086
Psychological, psychophysiological and biochemical effects of prolonged sleep deprivation in human males, noting transient ego disruption
23 p4099 A69-42195

BIOCLIMATOLOGY
Circadian rhythm effect between individuals of separate twin pairs, noting application to physiological research in medical genetics and human biometeorology
04 p0553 A69-15152

BIOCONTROL SYSTEMS
Biological systems optimal control theory, considering various control structures and energetic and informational bases of optimization
22 p3893 A69-40786

BIODYNAMICS
X ray study of biomechanics of respiratory act under long term acceleration stresses
05 p0710 A69-16522
Viscoelastic rod model of human spine subjected to accelerations
07 p1072 A69-19725
Electrokinetic converter of biochemical parameters for diagnosis and control of organism behavior, noting biomechanical utility
14 p2409 A69-29471
Human locomotion analysis, measuring metabolic expenditure and mechanical energy levels of principal body segments during walking
15 p2558 A69-30587
X ray study of biomechanics of respiratory act under long term acceleration stresses
18 p3096 A69-34741
Change in weight, plasma volume, urine flow and hematocrit in man before and after immersion up to chin in thermally neutral bath
23 p4096 A69-42087

BIOELECTRIC POTENTIAL
Flexible printed circuitry electrode arrays fabrication for surface cortical potentials recording in animals
02 p0204 A69-12601
Prolonged bed rest effect on brain bioelectrical activity from EEG reactions of subjects to acoustic signals followed by light signals
05 p0710 A69-16520
Prolonged bed rest effect on brain bioelectrical activity from EEG reactions of subjects to acoustic signals followed by light signals
18 p3096 A69-34739
Mapping of biological potentials evoked in primary somatosensory fields by electrical signals on dorso-lateral surface of brain cortex of cats
22 p3886 A69-41121
Topography of potentials induced by acoustic clicks in auditory cortex of dogs, including ectosylvian gyrus distribution
22 p3888 A69-41269
Cortical biopotentials in cats induced by strychnine under acoustic click stimuli of increasing intensity
22 p3888 A69-41270
Oscillatory electric field disturbances monitored near human body concurrent with heart beat and respiration, showing signals unrelated to blood flow or streaming potentials
23 p4101 A69-41449
Dependence of cochlear microphonics and summating potential on endocochlear potential
23 p4085 A69-41574
Electroretinogram and visually evoked cortical potential as response potentials in human visual system
24 p4271 A69-42644

BIOELECTRICITY
Decrease in bioelectric activity of skeletal muscles in animals and man during intermittent acceleration and weightlessness
07 p1062 A69-18591

Synaptic configurations in neuropil of planarian *Dugesia dorotocephala* brain, discussing neurotransmitters at phyletic level
16 p2741 A69-31555

Miniaturized FM telemeter for transmitting electrical activity of single nerve cells in brain of awake and unrestrained animal
19 p3261 A69-36270

Neuron activity simulation applied to vestibular neurons electrical activity analysis, discussing feedback circuitry and cathodic depression
20 p3471 A69-37256

Stimulus correlated with neuronal discharge periodicities in colliculus inferior, deriving structure models, discussing acoustic channel below geniculatum mediale
23 p4096 A69-42089

Radioisotopic determination of haemodynamic and bioelectric disturbances of rat striated muscles subjected to acceleration and hypokinesia
24 p4268 A69-43409

BIOENGINEERING

NT BALLISTOCARDIOGRAPHY

NT BIOINSTRUMENTATION

NT BIOMETRICS

NT BIOTELEMETRY

NT BODY MEASUREMENT [BIOLOGY]

NT CARDIOGRAPHY

NT ELECTROCARDIOGRAPHY

NT ELECTROENCEPHALOGRAPHY

NT ELECTROMYOGRAPHY

NT ELECTROPLETHYSMOGRAPHY

NT ELECTRORETINOGRAPHY

NT PLETHYSMOGRAPHY

Biological problems in prolonged space voyages including oxygen replacement, water supply and food regeneration
01 p0020 A69-11075

Allelopathy, discussing application to gas liberating activity of edible plants as ingredients of space flight life support systems
02 p0198 A69-11509

Hard space suit for use on planetary surfaces and extravehicular activity, discussing design, fabrication and mobility
03 p0379 A69-12993

Data sampling and statistical verification in large scale sterilization procedures, discussing biological indicator /*Bacillus stearothermophilus*/ and incubation time
05 p0714 A69-15952

Standardization requirement for laboratory and field research into vibration effects on humans, stressing subjective rating and performance measurements
13 p2213 A69-28091

Internal and external heat transfer instrumentation and equipment bioengineering, listing thermal conductivity and diffusivity of biological materials
13 p2213 A69-28150

Flow mechanics applications to medicine, discussing vascular and technical systems and measuring equipment adaptation to human organisms
17 p2915 A69-33771

Life support system sterilization maintenance problem for biosatellite experiment over one year
20 p3477 A69-37624

Bicycle ergometer combined with induction clutch, investigating effect of eccentric dynamic work with arms and legs
21 p3663 A69-38902

Collection of papers on biomedical engineering and medical physics covering cardiac pumps, neural models, control theory, telemetry and laser applications, etc
22 p3893 A69-40784

BIOGENESIS

U BIOLOGICAL EVOLUTION

BIOGENY

Optical activity measurement for exobiology applications, considering polarimetry, gas-liquid chromatography, mass spectrometry and radioactivity detection
23 p4213 A69-41622

BIOINSTRUMENTATION

NT BIOTELEMETRY

Man as main component of future spacecraft or planetary station closed ecological system, discussing spacecrew physiological monitoring for biological cycles optimization
01 p0020 A69-11076

Respiratory pressure recording with tracheal cannulae applied on cats to obtain pneumograms and oscillograms of respiratory neurons
07 p1131 A69-18538

Internal and external heat transfer instrumentation and equipment bioengineering, listing thermal conductivity and diffusivity of biological materials
13 p2213 A69-28150

Pyroelectric conductor sensors permitting continuous measuring and recording of air inhaled during chosen time intervals
15 p2559 A69-31230

Peak amplitude selector for electrophysiological phenomena analysis, describing memory schemes, threshold crossing detectors and display, input and output circuits, timing, etc
15 p2612 A69-31266

Aeromedical developments by NASA biomedical applications program applied to general medical equipment including cardiac sensors, surgical sterilization, ballistocardiograph, etc
16 p2882 A69-32430

Diathermy instrument using solid state circuits to provide square wave pulses, discussing operating parameters for bipolar coagulation and advantages over spark gap instruments
18 p3134 A69-34537

Rapid component of nystagmus using photostagnography, noting dependence on afferent pulse of ampullar apparatus
20 p3481 A69-37272

Electronystagmographic method of eye movement recording, noting applications to vestibular and visual analysis and study of oculomotor nuclei- vegetative centers relations
20 p3481 A69-37273

Equipment with minimum semicircular canals stimulation for vestibular analyzer studies
20 p3481 A69-37274

Biological material flow phenomena, discussing rheological approach, microcirculation, macrocirculation, instrumentation and mathematical model for quantitative observation
20 p3473 A69-37602

Biomedical electrical signals analysis by optical data processing, discussing conversion, SNR and filtering techniques
21 p3666 A69-39440

Low noise physiological recording with dry electrodes, discussing material, construction, preamplifier design and experimental data in electrocardiography
21 p3666 A69-39441

Flash lamp for biological applications, discussing control unit circuitry, pulse duration, frequency and color, flash-dark ratio, etc
23 p4110 A69-42054

Electric potential measuring device for frog isolated skeletal muscle fiber mounted on micromanipulator
23 p4111 A69-42058

Central nervous, cardiovascular and metabolic data of *Macaca nemestrina* during simulated Biosatellite flight, testing data acquisitions systems
24 p4260 A69-42703

Pressure wave transmission in liquid filled tubes, determining attenuation and phase shift for hemodynamics applications
24 p4279 A69-43798

BIOLOGICAL ACTIVITY

U ACTIVITY [BIOLOGY]

BIOLOGICAL ANALYSIS

U BIOASSAY

BIOLOGICAL CELLS

U CELLS [BIOLOGY]

BIOLOGICAL EFFECTS

NT RELATIVE BIOLOGICAL EFFECTIVENESS [RBE]

Surface dose rate and depth dose distribution for materials used for space vehicle and biological tissue protection from cosmic and internal radiation [UN PAPER 68-95260]
01 p0144 A69-10477

UV and visible light interaction effect on biological activity of *Paramecia unicellular infusoria*, noting cell division rates and cell deaths
01 p0017 A69-11085

Lethal effect of solar UV radiations on dried *Coliphage* T-1 exposed to space at sounding rocket altitudes
01 p0017 A69-11086

Pituitary-adrenocortical axis and neuro-endocrine functions in animals maintained in oxygen atmosphere, discussing norepinephrine and epinephrine excretion values, etc
01 p0019 A69-11343

Chronic gamma radiation biological damage in rats exposed to maximum nonlethal to minimum lethal doses for various periods
02 p0197 A69-11494

Deuteron microbeam for simulating biological effects of ionization by heavy cosmic ray particles
03 p0373 A69-13493

Biological effects of proton irradiation of monkeys investigated to provide improved protective shield design data with minimum weight penalty
03 p0373 A69-13496

Acute somatic effects in monkeys irradiated with protons of various discrete energies representing significant portions of space proton spectrum
03 p0374 A69-13497

Biological effects on rhesus monkeys of high energy protons compared to effects of cobalt 60 gamma radiation
03 p0374 A69-13498

Biological effects in man due to heavy particles emission during major solar cosmic ray events, noting protective effect of human body
03 p0374 A69-13500

In vivo hyperbaric hyperoxia effect on erythrocytes unsaturated fatty acid composition alterations of tocopherol deficient mice
03 p0375 A69-14070

Weightlessness effect on blood circulation system of human beings and animals during suborbital/ orbital space flight
03 p0376 A69-14194

Cardiovascular system, respiratory system and metabolism of cosmonauts on three man flight of Vostok, noting physiological and biochemical studies
03 p0377 A69-14195

Circadian rhythms disruption during long distance flights, discussing adverse effects on pilot and passenger performance
03 p0378 A69-14260

Asthmatic attacks in military air crews, discussing flight stress factors including altitude, ventilation and insecurity as possible causes
05 p0710 A69-16624

Cerebral circulation under longitudinal acceleration, discussing rheoplethysmographic measurements of heart rate
05 p0710 A69-16625

Biological effects of VHF electromagnetic radiation from radar antennas
05 p0715 A69-16701

Biological systems response to inertial environment, escape from earth gravity, planetary gravity and artificial gravity
06 p0872 A69-17011

Soviet monograph on UV radiation of sun and sky emphasizing biological effects
07 p1221 A69-19506

Biological effects of laser radiation on mammalian retina, noting thermal injury [AGARDOGRAPH-111]
08 p1266 A69-20676

Soviet book on space radiobiology, discussing somatic effects, influence of flight factors, relative biological effectiveness of various radiations and radiation safety
11 p1827 A69-24263

Biological effects of cosmic ionizing radiation in supersonic commercial aircraft at high altitudes, showing spatial distribution based on balloon experiments
11 p1830 A69-24865

Biological radiation doses and protection from galactic, solar particle and trapped radiation in space, noting secondary radiation and bremsstrahlung in absorber
11 p1831 A69-24866

Space biological tests performed on lower animals and vegetables relating to higher organisms reactions during prolonged manned space flights, reviewing Nasa experiments
12 p2019 A69-26494

Earth contamination by returned lunar or Martian material, discussing extraterrestrial biota survival on earth
13 p2210 A69-28467

Biological effects of low magnetic field environments studied by physiological, visual and psychological tests on animal, plant and human subjects
13 p2211 A69-28596

Shield facility and Helmholtz coil system used to investigate chronic effects on man of zero magnetic field regulated to cancel geomagnetic field variations
15 p2586 A69-30382

Weightlessness and vibration effects on soft red winter wheat seedlings
15 p2557 A69-31368

White rats diet containing alcohol-soluble fraction of *Chlorella* and *Scenedesmus* biomass, noting changes in adrenal cortex and renal glomerus
17 p2906 A69-32930

Drug action on decompression sickness in rats compared with action on nitrogen narcosis and oxygen toxicity
17 p2913 A69-33172

Biological effects of radioactivity and X rays irradiation of whole body and cells, considering DNA degradation
19 p3257 A69-35978

Noble gases effect at low pressures on O consumption by mammalian tissue, noting Xe, Kr, N and nitrous oxides effect on rat liver
19 p3258 A69-36454

Vestibular stimulation effect on human blood composition during rocking test indicating blood eosinophile content as function of hypophysis and adrenal cortex reactions
20 p3473 A69-37268

Biological effects of cosmic radiation on crewmen and protection measures, noting ground radiobiological and medical hygienic investigations
20 p3478 A69-37628

Muscular strength dynamometric measurements in subjects during prolonged inactivity with restricted caloric and protein intake, showing decrease in strength
21 p3653 A69-38901

Biological responses to weightlessness prediction, considering gravity perception mechanisms, cellular metabolism, etc
21 p3656 A69-38921

Photographic and photometric study of absorption and reflection of ruby laser light incident on biological objects
21 p3665 A69-39060

Somatic radiation effects on human organism related to manned space flights
21 p3660 A69-39172

Manned relativistic space flight limitations dependence on biomagnetic levitation of human body in inhomogeneous magnetic field to compensate inertial forces during acceleration
22 p3889 A69-39906

Nutritive value of mycelium of *Cantharellus cibarius* mushroom on rats compared with eggs and fresh and sour milk
22 p3892 A69-40273

Diffusion in biological systems by random walks with emphasis on gaseous diffusion in lung, noting probabilistic tree model
22 p3885 A69-40978

D-amphetamine effect on single tectal neurons activity of cat optimum recorded by steel microelectrodes before and after intravenous injection
23 p4084 A69-41466

Biological effects by cosmic ray heavy ions and solar flares, using direct correlation between damages caused and trajectories
23 p4089 A69-41831

Insect gametes response to space flight and radiation in reduced gravity including plants and microorganisms
23 p4091 A69-42050

Spinal cord temperature effect on stretch responses of muscle spindles of triceps surae, anterior tibialis and extensor digitorum longus in anesthetized cats
23 p4093 A69-42067

Radio and microwaves biological effects, discussing differences between U.S. and Soviet assessments of radiation hazards
23 p4099 A69-42516

Microwave radiation effects on biological systems, discussing categories according to radiation protection guide /RPG/ numbers, tissue properties and interactions
24 p4270 A69-42579

Biological and physiopathological effects of UHF electromagnetic radiation of radar antennas, reviewing localized effects
24 p4273 A69-42996

Hyperventilation effect on flight personnel, discussing oxygen and carbon dioxide partial pressures, symptoms and clinical signs
24 p4269 A69-43410

BIOLOGICAL EVOLUTION
NT ABIOTIC GENESIS

Space environment barriers to man due to biological evolution and transition from land to space in single generation, noting orientation problems
03 p0380 A69-14067

Molecular mechanisms leading to mineralization of organic tissues, noting role of protein and glycoprotein matrices
04 p0555 A69-14888

Experimental research concerned with origin of life, studying synthesis of precursor polymers and self assembly into protocells
10 p1641 A69-23035

Axiomatic explanation of complete self reproduction, noting logical mathematical biological reasoning and evolution theories
10 p1645 A69-23385

Simulated weightlessness used in determining ontogenesis of otolith organ in tadpoles and eggs as function of acceleration forces
10 p1647 A69-24021

Protein and nucleic acid building blocks sequence differences influence on evolutionary relationship of living organisms, comparing fish and mammal globins
11 p1828 A69-25456

Abiogenic synthesis of prebiological membranes under assumed primitive earth conditions by UV radiation of alkanes on phosphate and Mg ions aqueous solutions
11 p1828 A69-25462

Origin of life data, discussing self ordered polymers, propagative cell-like systems, protenoids, cellular evolution, etc
12 p2018 A69-25781

Book on genesis and evolutionary development of life covering carbon compounds, protobionts and evolutionary biochemical investigations of present living organisms
12 p2019 A69-26300

Life origin and organic-inorganic systems, emphasizing protein colloids-mineral salts interactions at protocell stage
14 p2408 A69-29632

Life detection for space missions based on detecting optical asymmetry in biogenic molecules by gas chromatography involving diastereomeric esters synthesis
15 p2556 A69-31315

Soviet book on theories of origin, nature and evolution of life from viewpoint of dialectic materialism, covering evolution trends, cell differentiation, etc
19 p3259 A69-36746

Sediments and crude oils analyzed for fatty acids, considering abiological or bacterial origin of acids
20 p3523 A69-37538

Probability of biological development leading to human life on another planet
21 p3652 A69-38786

NonDarwinian evolution of protein and DNA, comparing expectations of evolution models for protein and amino acid changes
22 p3871 A69-40060

Cell-like structures containing biochemicals as inevitable event under various hypothetical primitive earth conditions
23 p4085 A69-41479

Biochemical evolution role in porphyrin synthesis forming hemoproteins base, discussing assimilation of carbon dioxide in early earth atmosphere
23 p4088 A69-41814

BIOLOGICAL MODELS
U BIONICS

BIOLOGICAL RHYTHM
U RHYTHM [BIOLOGY]

BIOLOGY

Respiratory system control processes hypotheses experimental verification
01 p0019 A69-10209

Respiratory system control processes hypotheses experimental verification
14 p2408 A69-28745

BIOLUMINESCENCE

Biochemiluminescent luminol-peroxide reaction to detect iron porphyrin proteins in microorganisms for extraterrestrial life search, discussing reaction kinetics
15 p2556 A69-31325

Adenosine triphosphate /ATP/ content of terrestrial soils, based on firefly bioluminescent reaction, for Mars soil problems
20 p3473 A69-37567

BIOMECHANICS
U BIODYNAMICS

BIOMETEOROLOGY
U BIOCLIMATOLOGY

BIOMETRICS

NT BALLISTOCARDIOGRAPHY

NT BODY MEASUREMENT [BIOLOGY]

NT CARDIOGRAPHY

NT ELECTROCARDIOGRAPHY

NT ELECTROENCEPHALOGRAPHY

NT ELECTROMYOGRAPHY

NT ELECTROPLETHYSMOGRAPHY

NT ELECTRORETINOGRAPHY

NT PHONOCARDIOGRAPHY

NT PLETHYSMOGRAPHY

Physiological measurements onboard Soviet bioprobes and biosatellites including electrocardiography, phonocardiography, sphygmography, seismocardiography and pneumography
01 p0015 A69-10947

Neural buoyancy microelectrode for prolonged recording from single nerve units
02 p0202 A69-11865

Mechanical model of human body used to study response to vibration, impact, blast and decompression loads
04 p0552 A69-14470

Bloodless heart flow measurement methods, noting simultaneous external recording of carotid and femoral pulses and impedance plethysmography
09 p1448 A69-22730

Neurological changes in men due to hypokinesia, analyzing tremor data, EEG recordings and stabilography fluctuations
10 p1647 A69-23585

Arterial tone and human muscular activity limitations, analyzing hypodynamic effects on aorta, arm and leg vessels constriction
10 p1647 A69-23586

Graphical method for plotting electrophysiological observations, showing hodographs application in biopotential studies of cortical reactions
11 p1829 A69-24540

Digital computer program for physiological measurements, outlining interpolation of mathematical functions describing signals time variations
17 p2912 A69-32941

Brain weight and cholinesterase activity in rats after exposures to acoustic and light stimuli
21 p3662 A69-39627

BIONICS

Cardiovascular system simulation using computer models transport and perturbation methods
03 p0380 A69-13855

Simulation of regulatory function of cardiovascular system during weightlessness
03 p0376 A69-14193

Learning model of brain stem reticular formation based on nonlinear probabilistic hybrid computer concepts
05 p0711 A69-15802

Cybernetic problems in bionics - Conference, Dayton, May 1966
07 p1069 A69-18380

Analytical model for frog retinal bug detector cell to make possible signal measurement in frog optic fibers
07 p1070 A69-18383

Mathematical model of spike activity of auditory neurons constructed from functional point of view
07 p1070 A69-18384

Cybernetic structural model for learning and mentation comprehending symbol systems, languages, homeostatic mechanisms, etc
07 p1070 A69-18385

Computer simulations, comparing self adaptive /neurotron/ control of spacecraft energy allocation subsystem to programmed control
07 p1058 A69-18389

Analog computer modeling of human systemic arterial tree, based on lump parameter circuit approximation
07 p1072 A69-19727

Mathematical model of closed biological cycle regenerating part of life support products, incorporating astronaut, storage and regenerating waste disposal units
10 p1649 A69-23580

Analytic model resembling thick walled ellipsoid of revolution incorporating three dimensional shape of human left ventricle and ventricular wall thickness effects
12 p2022 A69-26235

Linear passive electrical analog model of human systemic arterial tree, discussing artery segment modeling, vessels input impedance, wave travel, etc
17 p2908 A69-33007

Digital simulation of biological model for visual images classification derived from human visual system aspects
17 p2911 A69-34094

Human ear frequency discrimination, discussing nonlinear functional modeling systems
18 p3097 A69-35440

Book on simulation in biology and medicine covering mathematical models, blood circulation, pulmonary ventilation, etc
19 p3260 A69-35894

Transfer function in pulmonary ventilation and O tension in arterial blood analyzed by automatic control
19 p3260 A69-35897

Book on neurocybernetics and neurobionics covering mathematical and physiological models, artificial neurons, image recognition theories, biological control systems, etc
19 p3263 A69-36747

Two body mechanical system operating within dynamics laws simulating backward and forward bending motions of falling cat
19 p3259 A69-36832

Cerebral circulation arterial system pulsatile flow flexible vessel digital simulation models distribution
19 p3264 A69-36867

Multilevel mathematical model of oculomotor apparatus using neuron networks and complex activators, including computer analysis
20 p3470 A69-37245

Neuron activity simulation applied to vestibular neurons electrical activity analysis, discussing feedback circuitry and cathodic depression
20 p3471 A69-37256

Biological clocks, discussing circadian rhythms of organisms using animal experiments and physical oscillator model
21 p3653 A69-38895

Model for lateral inhibitory interaction in human retina, providing systematic account of simultaneous brightness contrast
21 p3653 A69-38898

Multiple cues in paired comparisons, discussing mathematical model of psychological process in information extraction and combination
21 p3664 A69-38970

Cardiac and arterial change frequency among young people, describing hydraulic model for morphological variations of carotidogram appearing with age, arterial hypertension and arteriosclerosis
21 p3661 A69-39272

NonDarwinian evolution of protein and DNA, comparing expectations of evolution models for protein and amino acid changes
22 p3871 A69-40060

Biological model describing spacecraft operator sensorimotor activity in response to various spacecraft control stimuli, outlining computer algorithm
22 p3892 A69-40281

Sensory and logic behavior model of sequence selection based on received information, considering perception, sense, desire, concept and criteria levels
23 p4109 A69-41976

Learning model of motor behavior in brain cortex of higher animals and man, discussing M automaton, information reception, correlation, memory, emotions, desires and actions
23 p4109 A69-41977

Nerve and muscle tissues subthreshold reactions on analog model, discussing transient characteristics under various excitations
23 p4109 A69-41980

Model of nerve elements, discussing subthreshold processes parameter system and analog investigation of transient processes for various stimuli at model input
23 p4110 A69-41981

Mathematical model for information processing of biological memory as cybernetic system
23 p4110 A69-41982

Cybernetic approach to memory, proposing model characterized by hierarchical structural order and sequence to study physiological rhythms
23 p4110 A69-41983

Mathematical model construction to simulate light adaptation in human vision based on Maxwell disk experimental results
23 p4110 A69-41985

Model for human hemoglobin dissociation into subunits taking into account molecular explanation of oxygen dissociation curves
23 p4097 A69-42096

Paradoxical inhibition negative feedback principle in oscillatory systems, using mathematical model of nerve membrane
23 p4112 A69-42444

Brain and machine model of pattern recognition, pattern synthesis, memory, learning and speech, using concept of similarity, context and signal analysis
24 p4273 A69-42909

S-RETIC vertebrate command model, discussing computer simulation of reticular formation Golgi anatomy capable of habituation, conditioning, extinction, generalization and error discrimination
24 p4273 A69-42910

Steady state model for human respiratory system analysis, discussing controlled and controlling parts
24 p4276 A69-43272

Adaptive model of human operator control strategy in response to sudden changes in plant dynamics and transient disturbances
24 p4276 A69-43325

BIOPHYSICS

Extraterrestrial vestibular research, discussing human otolithic apparatus regulation subjected to change from geocentric to heliocentric orientation [UN PAPER 68-95389]
01 p0014 A69-10508

Objective evaluation of metabolic reactivity of organism based on biophysical model compared with experimental individual
06 p0874 A69-17595

Blood vessel model in form of cylindrical shell filled with liquid for studying cardiovascular system dynamic and static problems
12 p2018 A69-25989

Consecutive reaction equations for idealized soil column solved for nitrifying metabolite concentrations as functions of time and depth
19 p3264 A69-35606

Book on simulation in biology and medicine covering mathematical models, blood circulation, pulmonary ventilation, etc
19 p3260 A69-35894

Collection of papers on biomedical engineering and medical physics covering cardiac pumps, neural models, control theory, telemetry and laser applications, etc
22 p3893 A69-40784

BIOREGENERATION

U REGENERATION [PHYSIOLOGY]

BIOSATELLITE 2

Radiobiology of Tradescantia clone orbited in Biosatellite 2, analyzing space effects on spontaneous and radiation induced mutation and cytological changes
15 p2556 A69-31321

Radiation effects on microorganisms and plants during space flight on Biosatellite 2 and Gemini 11 missions
20 p3476 A69-37617

Physiological and somatic effects on insects of radiation source onboard biosatellite 2, discussing wing abnormalities in flour beetle
20 p3476 A69-37619

BIOSATELLITES

NT BIOSATELLITE 2

Physiological measurements onboard Soviet biosatellites and biosatellites including electrocardiography, phonocardiography, sphygmography, seismocardiography and pneumography
01 p0015 A69-10947

Phonocardiograms, EKGs, sphygmograms, heart and respiration rates, body temperature and motor activity recorded/transmitted by TV during canine confinement in Soviet biological capsules
07 p1061 A69-18578

Plants growth from seeds exposed to space environment onboard Cosmos 110 biological satellite compared with control plants
07 p1064 A69-18972

Biomedical experiment onboard Cosmos 110 concerning nonpathological changes
08 p1261 A69-19827

Weightlessness, increased gravitational fields and radiation effects on biological systems at organismal, cellular and subcellular levels, discussing biosatellite experiments
14 p2406 A69-29097

Biosatellite attitude control systems design development and flight test results for payload perturbing effects, discussing simulation activity
18 p3210 A69-35094

Geotropic response reciprocity in oat seedlings grown in two axis clinostat compared with acceleration constraints of biosatellites, considering imposition of centrifugal force
20 p3477 A69-37620

Life support system sterilization maintenance problem for biosatellite experiment over one year
20 p3477 A69-37624

Plants growth from seeds exposed to space environment onboard Cosmos 110 biological satellite compared with control plants
20 p3479 A69-38220

BIOSENSORS

U BIOINSTRUMENTATION

BIOSIMULATION

U BIONICS

BIOSPHERE

U EARTH HYDROSPHERE

U LOWER ATMOSPHERE

BIOSYNTHESIS

Hypoxia exposure effect on RNA synthesis in rat anterior pituitary cultured in vitro
01 p0015 A69-10923

Pharmacological tools in autonomic nervous system research, discussing norepinephrine biosynthesis, storage, release and inactivation in mammals
02 p0200 A69-12722

Amino acid biosynthesis control in microorganisms by end product/feedback/inhibition of enzyme action
06 p0876 A69-18238

Uptake, metabolism and enzymatic synthesis of adrenaline in mammalian brain
07 p1066 A69-19260

Degree of organization in bacterial cell, discussing pool size and DNA synthesis
07 p1069 A69-19505

Hypokinesia effects on rats noting body and organ weights, liver glycogen and N content and tissue proteolysis of skeletal muscles
08 p1262 A69-19928

Origin of life in terms of polymers synthesis under thermodynamic and geological conditions
12 p2017 A69-25764

Defective bacteriophage PBSh in *Bacillus subtilis* after mitomycin C treatment, showing DNA synthesis and marker frequency change
15 p2555 A69-30446

BIOT METHOD

Biot variational principle applied to combined conduction and radiation heat transfer
04 p0685 A69-14734

Completeness of Biot solution in theory of thermoelectricity, discussing Mindlin theorem and Boussinesq-Papcovich solution
07 p1236 A69-19470

Transient one dimensional temperature distribution determined for bodies with internal heat generation and nonlinear boundary condition, using Biot variational method [ASME PAPER 68-HT-6]
13 p2374 A69-27775

Algorithm using Biot-Savart law for determining induced velocity of curved vortex lines in aerodynamics, noting required line integration method
20 p3458 A69-37169

BIOTECHNOLOGY

Chlorella and *Scenedesmus* unicellular algae mixture tested for biological protein value in humans for possible food source
01 p0021 A69-11079

Automatic devices to count bacterial colonies Petri dishes consisting of culture plate scanner and data processor
02 p1201 A69-11773

Biological aspects of space exploration, analyzing human response to artificial environment in prolonged space missions [UN PAPER 68-95715]
06 p0873 A69-17035

Thermal problems in biotechnology - ASME Conference, New York, December 1968
06 p0879 A69-17084

Transient method for measuring thermal properties of biological materials, concerning thermal conductivity, inertia and blood flow rate
06 p0879 A69-17086

Ergonomics and aviation medicine, discussing biotechnological aspects of information in man machine systems and observation tasks
17 p2915 A69-33770

He speech processor for aerospace applications, discussing He speech distortion nature
17 p2911 A69-34095

Biotelemetry system as candidate prototype of generalized system for clinical applications
19 p3262 A69-36272

Device producing step-like output representing amplitude of ECG R-wave on beat by beat basis
21 p3667 A69-39443

Flight indicators monitoring by pilots, describing physiological and psychotechnical criteria for dials and clocks arrangement to improve efficiency
23 p4108 A69-41827

Ergonomic study of experimental tests design for comparing equipments efficiency with man
24 p4275 A69-43023

BIOTELEMETRY

Telemetric system for in-flight measurements of jet pilot heart and circulatory system to determine flight stresses leading to pilot failure
05 p0715 A69-16707

Space and immersion suits physiological evaluation by pulse duration multiplexing telemetry, using commercial FM receiver
06 p0883 A69-17845

Tape recorder for simultaneous double channel recording of physiological experiments, describing circuit modifications and additional circuits
07 p1131 A69-18640

Telemetering aortic blood pressure and heart rate from dogs under various physical activities and emotional stress
07 p1071 A69-19133

Miniaturized transmitter for single channel biotelemetric system to transmit electromyograms incorporating thin film components
08 p1265 A69-19836

Psychic stress effect on physiological parameters of helicopter pilots during critical flight situations, considering biotelemetric examination of heart and circulatory systems
11 p1829 A69-24347

Biotelemetry of human physiological processes in space for assuring physiopsychological control and immediate intervention for emergencies, discussing application in Mercury and Gemini projects
12 p2023 A69-26491

EEG monitor helmet for aircraft or flight simulator programs, discussing sensing and transmitting system
12 p2023 A69-26553

Multichannel telemetry system for chronic implantation in animals to monitor physiological parameters
15 p2559 A69-31044

Telemetry techniques, based on pulse rate measurements, permitting continuous examination of humans under natural working conditions
15 p2559 A69-31228

Blood pressure telemetry of pilot during flight including determination of psychophysical relations
15 p2559 A69-31229

Lightweight sensor for telemetering oxygen partial pressure in respiration air
15 p2559 A69-31231

Computer analysis of EEG recording, presenting model studies under rest and performance conditions
15 p2560 A69-31232

EEG and pilots flight performance relations, discussing in-flight telemetric measurements from ground station
15 p2560 A69-31233

Oscillator without reactive components for integrated circuit biotelemeter, noting transmission in AM broadcast band
19 p3261 A69-36244

EEG monitoring during decompression illness /bends/ treatment by hyperbaric procedure using small multichannel telemetry pack
19 p3261 A69-36268

Wireless telemetry system design for physiological signals in human diagnosis, discouraging casual use of wireless transmission
19 p3261 A69-36269

Miniaturized FM telemeter for transmitting electrical activity of single nerve cells in brain of awake and unrestrained animal
19 p3261 A69-36270

EKG signal transmission to hospital during cardiac patient transportation by emergency vehicle, noting prototype system construction and tests
19 p3262 A69-36271

Biotelemetry system as candidate prototype of generalized system for clinical applications
19 p3262 A69-36272

Automated computer network analyzing electrocardiograms, using telephone lines for bidirectional communications between cardiac data acquisition stations and computer center
19 p3262 A69-36273

EEG with combined multichannel radiotelemetry and telephone for onward data transmission
21 p3664 A69-38978

Low noise physiological recording with dry electrodes, discussing material, construction, preamplifier design and experimental data in electrocardiography
21 p3666 A69-39441

Real time metabolic rate analysis of suited astronaut using heart rate and O methods during thermal vacuum and extravehicular mobility tests
22 p3893 A69-40371

Telemetry in medicine and biology, describing applications and operation of various systems
22 p3893 A69-40787

Single channel pressure telemetry unit with magnetic latching or RF switch for chronic implantation
23 p4100 A69-41295

Heart rate measurements in ski jumpers with radio telemetric system revealing tachycardia during climbing and emotional stress
23 p4078 A69-41313

Telemetered heart rate response to progressively increased distance swimming competition compared with equidistance running events for change patterns, magnitude and recovery
23 p4100 A69-41444

Oscillatory electric field disturbances monitored near human body concurrent with heart beat and respiration, showing signals unrelated to blood flow or streaming potentials
23 p4101 A69-41449

EKG data telemetry from personnel to receiver located within same closed metallic chamber, discussing FM/AM and FM/FM systems
23 p4103 A69-41766

Orbital biomedical laboratory for in-flight measurement to assure human safety and optimize astronauts performance in extended space mission
23 p4223 A69-41801

Equal bandwidth multichannel FM/FM EEG telemeter system using subcarrier frequencies and HF modulation via varactor diodes
23 p4106 A69-41802

Jet pilot blood pressure response during positive acceleration in actual flight measured by telemetry compared with centrifuge test
23 p4089 A69-41822

BIPLANES
Soviet book on practical aerodynamics of An-2 aircraft covering aerodynamic characteristics, equilibrium, stability and control for various flight conditions, including icing
18 p3090 A69-34340

BIPROPELLANTS
U LIQUID ROCKET PROPELLANTS

BIRDS
NT CHICKENS
NT HOMEOTHERMS
NT PIGEONS

Aircraft safety hazards due to birds, discussing radar role in plotting bird migrations
11 p1837 A69-25247

Radar application to meteorology, entomology and ornithology, discussing clear air turbulence detection and flight tracking of birds and insects
12 p2034 A69-27004

Birds as pests - Conference, London, September 1967
17 p2898 A69-33362

Aircraft designers and operators problems with danger and damage caused by bird strikes, considering warning devices and protective windshield panels
17 p2899 A69-33363

Interspecific synthetic signals research for effective bioacoustic bird scaring techniques including optical signals
17 p2914 A69-33364

Airfield bird scaring methods including Very pistol shell cracker firing and broadcast calls on civilian and military airfields
17 p2915 A69-33365

Radar cross section of bird represented as unit density dielectric spheroid for bird hazard monitoring, discussing meteorological, insect and bird echoes
17 p2919 A69-33366

Bird warning and forecast systems based on radar data covering 50 mile radius from airport
17 p2899 A69-33367

Habitat modification for airport bird population control, discussing draining of wet areas, waste control, etc
17 p2915 A69-33368

Bird impact resistance of polyurethane foam filled tailplane
17 p2901 A69-33648

Bird hazard in aviation, discussing aircraft/bird collisions in France, protective measures and airport environment control against nesting and breeding
18 p3090 A69-34695

BIREFRINGENCE
Quantum theory of electrical birefringence of noninteracting diamagnetic molecules /Kerr effect/ subjected to static electric field and polarized plane wave
02 p0279 A69-11538

Glan-Thompson and Rochon prisms modified by replacing one of two calcite halves of cemented oriented birefringent crystals with glass
02 p0280 A69-11924

Rayleigh scattering from circularly birefringent media generalized for medium with no preferred internal axes
04 p0609 A69-14291

Instrument profile of birefringent Lyot filter for H alpha line determined from photographic spectra with grating spectrograph
04 p0664 A69-15524

Wideband multichannel optical signals nonlinear distortions during transmission by electrooptical modulators using Pockels effect
05 p0718 A69-15655

Optical investigation of defects in crystal lattices on stress induced birefringence basis, describing stress visualization results for Si and glass
11 p1887 A69-25199

Electromagnetic wave propagation in rectangular waveguide containing uniaxial anisotropic birefringent medium, deriving field equations
11 p1853 A69-25350

Polymers stress-strain behavior and corresponding birefringence within limited temperature range and strain rates
15 p2642 A69-30678

Wideband multichannel optical signals nonlinear distortions during transmission by electro-optical modulators using Pockels effect
16 p2754 A69-32512

Nonlinear analog of conical refraction in biaxial crystals, considering birefringence in piezoelectric uniaxial crystals and laser beam propagation
19 p3330 A69-35604

Linear limit uniaxial stresses for stress-strain and stress-birefringence in photoelastic and mechanical model materials
20 p3628 A69-37777

Poincare sphere properties representing birefringent behavior of materials and qualitative measurement technique for elliptically polarized light
21 p3844 A69-39318

Lummer-Gehrcke plate type polarizer made of birefringent material for Nd glass laser, discussing reflection coefficients in quartz crystals
21 p3739 A69-39541

Thermostatic electronic control device of birefringent filter in Wroclaw Observatory coronagraph during prominence observations
22 p3943 A69-40000

Photoelastic behavior in amorphous solids, proposing microstructural mechanism for deformation birefringence
22 p3972 A69-40081

Birefringent element within Fabry-Perot cavity for identification of direction of electron density change in z-pinch discharge
22 p3946 A69-40438

Babinet compensator with birefringent wedges made of stress frozen photoelastic material rather than quartz
22 p4042 A69-40442

BIREFRINGENT COATINGS
Birefringent coatings application to plane stress in orthotropic glass-fiber reinforced plastic materials noting stress-strain relations
11 p1995 A69-25647

Stress concentration on circular holes and notches in anisotropic oriented glass fiber reinforced plastics determined by using photoelastic birefringent coatings
15 p2713 A69-31053

BIRTH
Stillbirth and neonatal death in stressed rats exposed to mild and acute gravitational loads in automobile ride and aircraft flight
24 p4266 A69-43381

BISMUTH
Electrical properties of vacuum deposited Bi, noting association of negative temperature coefficient of resistance in Bi thin films with grain-boundary effects
02 p0296 A69-11878

Thermoelectric and thermomagnetic properties of bismuth at low temperatures, assuming thermal EMF due to phonon capture of carriers
03 p0488 A69-13885

Electrical conductivity and Hall effect in thin evaporated bismuth films under vacuum using three point method in variable temperature cryostat
09 p1557 A69-21692

Thermoelectric and thermomagnetic properties of bismuth at low temperatures, assuming thermal EMF due to phonon capture of carriers
11 p1938 A69-25686

Low resistance Bi thin film complex electrical impedance in IR range, stating methods and equivalent circuits for determining impedance
13 p2322 A69-28011

Electrode surface bismuth coating selected for reducing electrostatic analyzers photocurrents
14 p2446 A69-29048

BISMUTH ALLOYS

Low temperature energy band gap in n-type single semiconductor crystals of In-Sb-Bi alloys analyzed by measuring Hall constant and optical absorption coefficient

19 p3390 A69-36552

BISMUTH COMPOUNDS

Phase diagram, dielectric and magnetic properties of Bi manganate/Pb titanate solid solutions of perovskite structure, showing dependence on composition and temperature

22 p3996 A69-41163

BISMUTH OXIDES

Bismuth oxide introduction into Y and Y-Al garnets, noting effect on formation and properties

13 p2320 A69-27998

BISMUTH TELLURIDES

Phase diagram of BiTeI degenerate semiconductor crystals synthesized by heat treatment, discussing crystallization methods and physical properties

02 p0294 A69-11540

Bismuth selenide inhomogeneous distribution effect on thermoelectric properties of bismuth telluride alloy

04 p0644 A69-15265

Electrical conductivity and thermoelectromotive force of bismuth telluride and bismuth telluride-bismuth selenide alloys obtained by sintering, hot pressing and annealing

15 p2670 A69-31248

BISTABLE AMPLIFIERS

U FLIP-FLOPS

BISTABLE CIRCUITS

Optically bistable operation of continuous wave GaAs p-n junction laser at 20 K

01 p0090 A69-10565

Bistable zones in series oscillator circuit consisting of inductor and nonlinear p-n junction capacitance subjected to DC and AC voltage sources

04 p0575 A69-14463

Bistable fluid device utilizing Coanda effect along convex surface for wall attachment [ASME PAPER 68-WA/FE-27]

05 p0749 A69-16101

Mathematical model for voltage step-down DC to DC converter with hysteretic bistable trigger circuit regulating output voltage

06 p0904 A69-17941

Bistable zones in series oscillator circuit consisting of inductor and nonlinear p-n junction capacitance subjected to DC and AC voltage sources

14 p2418 A69-28834

BISTATIC REFLECTIVITY

Bistatic radar cross sections of simple shapes calculated based on optics and resonance region, noting forward, nonforward and Rayleigh scattering

03 p0384 A69-12906

Hologram form of forward scatter bistatic radar or sonar

07 p1078 A69-18866

Inverse scattering technique for electromagnetic bistatic scattering by expressing field produced by incident plane wave as sum of incident field and Fourier transform

16 p2754 A69-32569

Bistatic radar scattering cross sections for reentry vehicle with ionized wake

23 p4116 A69-41593

BIT SYNCHRONIZATION

Maximum likelihood bit synchronizer for baseband PCM signals in Gaussian noise, stressing system noise performance analysis and measurements

07 p1105 A69-19093

PCM bit synchronizer/signal conditioners performance characteristics and specification

07 p1106 A69-19120

Bit error probability estimation of NRZ PCM synchronizer and detector operating in presence of fluctuating data frequency source

07 p1083 A69-19121

Binary block codes for correction of substitution and synchronization errors

09 p1452 A69-21316

Optimum timing extraction/bit synchronization/pulse code transmission, analyzing probabilistic structure by statistical parameter estimation and deriving system

09 p1455 A69-22115

Bayesian theory to determine maximum a posteriori estimation algorithms for optimum bit synchronization in digital communication systems

14 p2413 A69-29496

Nonlinear filter theory application to PCM bit synchronization, relating bit error rates to SNR and timing jitter

19 p3270 A69-36245

Absolute value type of early-late gate bit synchronizer phase noise performance determined by Fokker-Planck method, comparing results with different circuits performance

19 p3270 A69-36246

High bit rate signal conditioning, bit and group synchronization of NRZ PCM, considering gain and power bandwidth limitations and delays

19 p3271 A69-36247

PCM bit synchronizer signal to noise ratio measurement by input video signal zero crossings counting

19 p3271 A69-36248

PCM bit synchronizer models, discussing phase errors gate and differentiating devices

19 p3271 A69-36249

Optimum and suboptimum synchronizers for extracting bit synchronization from binary data, showing performance dependence on pertinent system parameters

21 p3673 A69-38923

Digital transition tracking symbol synchronizer for low SNR coded telemetry systems, discussing phase locked loop analysis and phase detector simulation by Monte Carlo method

23 p4130 A69-42513

BITERNARY CODE

Bandwidth restriction effect on performance of linear codes for digital communication with space vehicles, noting bit and word error probabilities

08 p1276 A69-20597

BITS

Bit reduction in digital transfer functions with LF poles in sampled data systems using zero order hold function

04 p0584 A69-15464

Computer simulation of unbiased digital recording composed of sequential computations intended for various bit densities [IEEE PAPER 3.3]

09 p1461 A69-22562

High speed ten-bit analog to digital converter with medium scale integration (MSI) elements, considering conversion accuracy and time

11 p1845 A69-24520

BITUMENS

Construction practice for hot-mix bituminous pavements covering production, composition, application and quality control

01 p0057 A69-11276

BLACK BODY RADIATION

Two element interferometer observing Saturn, Uranus and Neptune at 3.12 cm, determining equivalent black body disk temperature

01 p0148 A69-10052

Aerial radiation temperature measurement, damping factor of atmosphere and determination of ground and water surface temperatures by radiometry

01 p0110 A69-10693

Far IR rocket observations of night sky background radiation

01 p0121 A69-11249

Solid body surface roughness influence on radiative properties, deriving expressions relating radiative properties to surface roughness parameters

02 p0350 A69-11575

Radiative heat transfer through transmission layers sandwiched between black bodies with variable blackness spectra

02 p0350 A69-11578

Metagalaxy temperature brightness explained from radio sources combined radiation with inversion spectra

02 p0313 A69-11632

Thermal noise from passive linear multiports, noting influence of temperature and absorption coefficients

02 p0211 A69-12443

Threshold conditions for laser pumping with emission of perfect black body

03 p0442 A69-14220

Moving isotropic black body radiation, discussing effect on energy flux and earth velocity measurement through 3K cosmic background radiation

04 p0649 A69-15150

Intergalactic continuum study showing universe behavior like black body with 2.7 K radiation temperature, noting cosmological and cosmogonic importance

05 p0827 A69-16593

Black body radiation coherence properties characterization by stochastic Gaussian scalar potential correlation function

05 p0795 A69-16819

Black body cavity radiation distribution as seen by observer in arbitrary uniform motion with respect to radiation mass center

08 p1380 A69-19784

Inverse Compton effect and universal black body radiation from less energetic radio photons of galactic and metagalactic origin

08 p1381 A69-19786

Early evolution of universe related to present upper bound of primordial black body gravitational radiation temperature

09 p1601 A69-22210

Sco X-1 optical spectrum magnitude and color changes, proposing variable black body model

09 p1601 A69-22213

Small microwave antenna calibration by method of two black bodies exposed to different temperatures, reducing influence of cloudiness and humidity

11 p1844 A69-24450

Relativistic coherence theory of black body radiation in transparent medium, deriving expressions for second order correlation tensors by phenomenological quantum electrodynamics

11 p1920 A69-25563

Specularly vs diffusely reflecting cylinders for cavity type sources of approximately black body radiant energy, noting ray tracing of cones

12 p2130 A69-26245

Isotropic 3 K black body radiation implications for hot cosmological model, formation of galaxies, existence of superdense bodies and density nonuniformity during prestellar stage

12 p2167 A69-27047

Two channel IR radiometer for 1969 Mariner mission measuring equivalent black body surface temperature

17 p2972 A69-33085

Thermal emission and spectral degree of blackness of W derived from electron motion equation

18 p3156 A69-34715

Threshold power, gain, output power and radiation energy during optical pumping of Q switched molecular laser by black body radiation

20 p3554 A69-37722

Force fields to establish nature and position of remotely located conditions, discussing radiated power, electromagnetic waves, black body radiation, etc

20 p3494 A69-37747

Radio background radiation produced by Galaxy, considering energy, isotropy of radiation and black body character

21 p3790 A69-38821

Radiative transfer in interior of two concentric spheres in motion assuming low density of residual gas

22 p4031 A69-40907

Planck law for black body radiation spectrum theoretically derived on basis of classical Lorentz-invariant electromagnetic radiation at absolute zero temperature without quantum assumption

22 p3982 A69-41001

Black body radiation at very high temperatures, discussing pion-nucleon interaction in pion gas in thermal equilibrium

23 p4238 A69-41358

Diffuse cosmic X rays from Compton collisions between galactic leakage electrons and extragalactic background photons to verify microwave blackbody radiation properties

24 p4368 A69-43202

Transmission functions probabilistic model for solving radiative transfer problems in spherical shell medium surrounding emitting black core or point source, using integrodifferential equations

24 p4415 A69-43637

BLACK BRANT 2 SOUNDING ROCKET

High altitude observations of luminous wake behind Black Brant 2 rockets by mounted dual wavelength spatially scanning photometer

06 p0918 A69-17511

Aerodynamic failure investigation of Black Brant 2 single stage sounding rockets

15 p2703 A69-31545

BLACK KNIGHT ROCKET VEHICLE

Gamma type 2 rocket engine for second stage of Black Arrow satellite launcher

01 p0143 A69-10834

Black Arrow space vehicle uprating, considering engines burning kerosene with HTP and turbopumping systems

01 p0143 A69-10835

Increased payload in orbit capability for future versions of Black Arrow vehicle, discussing propellant

02 p0335 A69-12681

Facilities at High Down Test Site for testing Black Arrow launch vehicles, discussing mechanical and electrical equipment test procedures 04 p0585 A69-15041

Black arrow rocket vehicle flight path computer programming, discussing geographical restrictions on design 09 p1593 A69-21616

Structure, equipment and weight breakdown of Black Arrow X3 spacecraft 13 p2357 A69-28478

Propellant pressurization system for British Black Arrow composite vehicle, describing valve design and performance 14 p2509 A69-29629

Control system design for Black Knight test vehicle system 14 p2530 A69-29630

Black Arrow third stage velocity increment vector accuracy, considering attitude errors due to spin-up and spring separation systems, separated stages interactions, light-up impulses, etc 23 p4209 A69-41301

BLACKBURN B-103 AIRCRAFT
U BUCCANEER AIRCRAFT

BLACKOUT [PROPAGATION]
NT ATMOSPHERICS
NT COSMIC NOISE
NT DAWN CHORUS
NT ELECTROMAGNETIC NOISE
NT HISS
NT IONOSPHERIC CROSS MODULATION
NT IONOSPHERIC NOISE
NT IONOSPHERICS
NT POLAR RADIO BLACKOUT
NT SHOT NOISE
NT SUDDEN ENHANCEMENT OF ATMOSPHERICS
NT THERMAL NOISE
NT WHISTLERS

Radio frequency signal transmission between orbiting spacecraft and vehicle entering VM-10 model atmosphere, examining near wake approximations and plasma-electromagnetic interaction 09 p1455 A69-22002

Amplitude modulation of electromagnetic waves by modulated magnetic fields for communications through rocket exhausts and reentry plasma sheaths during blackout 14 p2417 A69-29591

Mars entry capsule ionized wake producing circularly polarized antenna radiation null region, noting effect on communication blackout time 22 p3914 A69-40701

BLADDER
Pressure garments weight reduction methods, comparing partial pressure systems equipped with bladder, capstan, airpipe or foam rubber 06 p0884 A69-18037

BLADE TIPS
Self excited rotor blade oscillation at high subsonic Mach numbers during flight tests of Sikorsky NH-3A compound helicopter 07 p1053 A69-18870

Rotor dynamics of stowed rotor aircraft, analyzing blade stiffness in wind tunnel [AIAA PAPER 69-207] 07 p1057 A69-19578

BLADES
Potential flow past plane array of thin blades, analyzing perturbed dynamic behavior 21 p3696 A69-39243

BLANKING [CUTTING]
Ti alloy blanks production technology and quality control, noting rolling of sectional profiles 07 p1161 A69-18765

Electromagnetic shaping of metallic parts using equations describing magnetic and electric field intensity as function of blank profile and cylindrical blank wall thickness 18 p3151 A69-35456

BLASIUS EQUATION
Blasius-Chaplygin formula for generalizing Kutta-Joukowski theorem concerning jet profiles, calculating resultant of hydrodynamic forces 11 p1867 A69-24355

Compressible laminar boundary layer behind shock or thin expansion wave past moving flat plate solved by transforming governing equations into Blasius equation 24 p4305 A69-43596

BLASIUS FLOW
MHD boundary layer equations in Blasius problem reduced to differential equations and solved by Laplace transform 01 p0127 A69-10337

Inviscid hypersonic flow of uniform equilibrium gas past axisymmetric blunt body 04 p0542 A69-14723

Boundary layer over impulsively started flat plate, describing flow transition from unsteady /Rayleigh/ to steady /Blasius/ state by iterative methods 16 p2769 A69-31812

BLAST LOADS
Mechanical model of human body used to study response to vibration, impact, blast and decompression loads 04 p0552 A69-14470

Structures response to explosive blast, discussing damage criterion in terms of blast wave impulse and critical time 04 p0671 A69-14476

Effective slip systems in hexagonal close packed magnesium alloy under static and hydroexplosive loading, examining flow mechanism for fine structure formation 04 p0615 A69-14639

Finite inelastic deformations under transverse impulsive loading of clamped thin rectangular planform shells idealized as membranes, using incremental plasticity theory 09 p1616 A69-21939

Compression waves observed ahead of luminous discharge plasma below Mach 12-15 in electric shock tube, describing shock structure by blast wave theory 16 p2768 A69-31664

Blast response of model structures fabricated from material differing from prototype structures, testing in dynamic, impulsive and quasi-static loading realms 16 p2874 A69-32164

Hot dense plasma used as driver gas producing plane stable current-free high Mach number shock fronts resembling plane blast waves 24 p4359 A69-43647

Permanent deformation of axial rod subjected to blast load predicted using partial differential equation in conjunction with stress-strain relationship 24 p4406 A69-43699

BLASTOFF
U ROCKET LAUNCHING

BLEACHING
Bleaching of absorption hologram diffraction gratings for improved light efficiency, discussing bleaching materials results 04 p0596 A69-14284

BLEED-OFF
U PRESSURE REDUCTION

BLEEDING
Bleed air environmental system utilizing air to air jet pumps as flow multipliers for cabin pressurization air supply in commercial turboprop aircraft [SAE PAPER 690331] 11 p1941 A69-24494

BLENDS
U MIXTURES

BLIND LANDING
Jumbo jet instrument landing difficulties, suggesting specific improvements in aircraft and airport equipment 15 p2549 A69-30189

Monograph on low visibility landing in civil aviation, considering visibility determination methods and equipment and IR sighting devices 20 p3574 A69-38064

All-weather landing in civil air operations, discussing ground/air systems in tracking, visual reference and aircraft performance required for safe landing capability 20 p3574 A69-38119

Kalman filter simulation for estimating aircraft position and velocity from airborne digital computer data in zero-zero landing system [AIAA PAPER 69-944] 22 p3978 A69-40327

BLINDNESS
NT FLASH BLINDNESS

Retinal burn resulting from prolonged viewing of sun, laser or thermonuclear explosion, noting effects on choroid, receptors and pigment cells 08 p1267 A69-20680

Visual systems of hamster brain, discussing relative visual localization and discrimination blindness produced by ablation of cortical or tectal areas 08 p1265 A69-20685

Human visual response to moving spatially periodic patterns, analyzing critical frequencies, dependence on stimulus area and period, phase blindness and pattern reversal 22 p3880 A69-40850

BLISTERS [PROTUBERANCES]
U PROTUBERANCES

BLOCH BAND
Two band model for determining linear and non-linear electromagnetic responses of small band gap semiconductors in magnetic field 03 p0487 A69-13753

Electron states at deep levels in InSb by deriving equations for Bloch wave functions of conduction and valence bands 09 p1556 A69-21508

BLOCKING
Thermal protection by ablation calculated, emphasizing blocking phenomenon and effectiveness of laminated and reinforced resins 02 p0351 A69-11890

Blocking processes synchronous development involving atmospheric circulation disturbances in Northern and Southern Hemispheres, noting localization in Pacific and Atlantic oceans 13 p2292 A69-27840

Jet stream blocking process simulation using geostrophic system of equations, considering effects of orography and contrast heating due to land-sea distribution 16 p2809 A69-32602

Blockage effects of flat plates and solid bluff bodies in closed wind tunnels compared concerning drag coefficient values 17 p2890 A69-33245

Sotalol and propranolol cardiovascular effects, comparing toxicity and blocking action against circulatory and cardiac effects of catecholamines 23 p4080 A69-41403

BLOOD
NT EOSINOPHILS
NT ERYTHROCYTES
NT LEUKOCYTES
NT LYMPHOCYTES
NT RETICULOCYTES

Insignificant or recoverable changes observed in blood acetylcholine content and cholinesterase activity of rabbits subjected to 8 g acceleration 02 p0197 A69-11491

Diffusion coefficients for oxygen transport in whole blood, discussing effects of intact red cell concentration 02 p0200 A69-12479

Biochemical indicators of pilot reactions to flights complicated by unexpected autopilot failures, using postflight chemical analysis of blood and urine 05 p0710 A69-16525

Regional uptake of melatonin from blood or cerebrospinal fluid by rat brain 09 p1444 A69-21466

Decreased antidiuretic activity measured in blood of chronically centrifuged rats, noting role of antidiuretic hormone /ADH/ 14 p2407 A69-29301

Glucose disappearance rate from dogs blood at simulated 27,000 ft altitude compared with tolerance at ground level, discussing chlorpromazine administration effect 14 p2408 A69-29305

Biochemical indicators of pilot reactions to flights complicated by unexpected autopilot failures, using postflight chemical analysis of blood and urine 18 p3096 A69-34744

Pathological effects of single 120 Mev proton doses on rats blood in rotating cylinder, discussing leukopenia and benign and malignant tumors development 21 p3658 A69-39058

Blood oxygen content measured by oxygen tension after release by carbon monoxide without lysing cells 22 p3873 A69-40203

Yield stress of normal human blood related to endogenous fibrinogen concentration as function of total protein concentration, proposing fibrinogen adsorption and coupling model 22 p3874 A69-40223

Digital computer program for determining avascular and capillary blood gas compositions corresponding to ventilation-perfusion values, considering dissolved oxygen and inert gas exchange 22 p3875 A69-40230

Oxygen supersaturation in unstirred blood under temperature effects, noting tension loss during stirring 23 p4077 A69-41296

S-4 human blood experiment during Gemini 2 flight, studying spaceflight ionizing radiation interaction effects on single and multiple break chromosome aberrations 23 p4085 A69-41600

Human blood viscosity measurement over wide range of shear rates, obtaining rheological data, suggesting osmotic red cell crenation role
23 p4095 A69-42078

BLOOD CIRCULATION

NT BRAIN CIRCULATION

NT CORONARY CIRCULATION

NT PULMONARY CIRCULATION

Hypokinesia and transverse accelerations combined effect on human cardiovascular system and regional blood circulation
02 p0197 A69-11495

Cardiovascular system simulation using computer models transport and perturbation methods
03 p0380 A69-13855

Weightlessness effect on blood circulation system of human beings and animals during suborbital/ orbital space flight
03 p0376 A69-14194

Changes in blood circulation, external respiration and gas exchange rates in humans during prolonged hypodynamia
03 p0377 A69-14204

Combined effect of prolonged bed rest and acceleration exposure on human blood circulation, noting increased heart rate and arterial blood pressure
10 p1646 A69-23584

Blood oxygen metabolism, analyzing content and volume circulation in dogs under oxygen partial pressure decrease in inhaled air
12 p2019 A69-26346

Compensative adaptational reactions to weightlessness, discussing blood supply to thorax area, external respiration, gas exchange and energy loss during parabolic and orbital flights
17 p2909 A69-33384

Ultrasonic detection of gas bubbles in blood, discussing device with bubble chamber attached to circulating liquid and receiver crystal harmonics
18 p3098 A69-34821

Statistical relations between minute blood circulation volume, O capacity and consumption rate in tissues of men and dogs
19 p3260 A69-35896

Linearized wave propagation digital simulation models to predict arterial blood flow characteristics and impedance, comparing phase velocity and transmission per wavelength
19 p3264 A69-36868

Biological material flow phenomena, discussing rheological approach, microcirculation, macrocirculation, instrumentation and mathematical model for quantitative observation
20 p3473 A69-37602

Bubble size and blood perfusion effect on gas bubbles absorption in tissues, noting decompression sickness
21 p3651 A69-38389

Rheography of blood circulation of forearm after tightening with pneumatic cuff, analyzing amplitude increase and information about vascular system
21 p3653 A69-38838

Left ventricular function in intact anesthetized dogs analyzed during graded hypovolemia produced by lower body negative pressure
22 p3874 A69-40225

Whole body LF mechanical vibration effects on anesthetized dogs peripheral circulation and vascular smooth muscle
22 p3875 A69-40228

Arterial and deep venous blood from human forearm analyzed following rest and rhythmic exercise on ergometer in hyperbaric oxygen chamber
22 p3878 A69-40834

Heart beat rate, arterial pressure, blood volume and peripheral blood pressure increase observed in dogs running 7 min at 10 km/hr
22 p3885 A69-40966

Flow profile effect on signal of Doppler ultrasonic flowmeter, noting limited application to quantitative blood circulation measurements
23 p4166 A69-42085

Venous tone, peripheral venous pressure, skin and muscle blood flow, alterations of heart rate and respiration in men during leg exercise
23 p4096 A69-42090

Receptor and adrenergic blockade effects on blood loss, tolerated period and metabolic sequels of hypotension in dogs
23 p4098 A69-42102

Blood flow, volume and venous pressure measurements in right hand at low and high altitudes in residents and newcomers
23 p4098 A69-42106

Central circulatory responses of humans to rapid skin temperature changes during continuous exercises
24 p4258 A69-42633

Blood viscosity as possible key factor in physiology and pathology of circulation, suggesting causes of myocardial infarction and coronary occlusion
24 p4261 A69-42725

BLOOD COAGULATION

Dogs blood coagulation system functional state after 22 day space flight onboard Cosmos 110
08 p1262 A69-19830

Blood coagulation in animals under acute hypoxia at exposures to pressure corresponding to 5000 m altitude, noting blood morphology
12 p2019 A69-26348

Hypokinesia and nutrition deficiency effect on blood coagulation, noting combination with accelerations may lead to hypocoagulation
13 p2212 A69-28625

Arterial occlusion effects on retinal structure in cats, describing degrees of cell degeneration
22 p3884 A69-40883

BLOOD FLOW

Blood volume in rats exposed to high altitude and deacclimated at ambient pressure, noting changes and control level restoration
01 p0015 A69-10922

High energy X ray irradiation of head of *Macaca mulatta*, determining effect on cerebral blood flow and blood pressure
03 p0376 A69-14075

Transient method for measuring thermal properties of biological materials, concerning thermal conductivity, inertia and blood flow rate
06 p0879 A69-17086

Oxygen saturation in outflowing and inflowing renal blood in dogs under normal and hypoxic conditions, assessing cannula technique
14 p2406 A69-28916

Cardiac output determined simultaneously in adult male humans by thoracic impedance changes and radioisotope dilution
14 p2408 A69-29304

Gastric perfusion rate in restrained animals determined by Rb 86 clearance technique
17 p2908 A69-33170

Flow rate in ascending aorta, stroke volume and cardiac output determination by ballistocardiography, calculations based on Hagen-Poiseuille theory
17 p2915 A69-33772

Sheet geometry of lung blood vessel system, discussing histological evidence and fluid dynamic consequences of sheet flow
19 p3263 A69-36656

O conductance nonlinear equation solution applied to O uptake at sea level and at altitude, noting blood transport problems
21 p3654 A69-38906

Decompression gas emboli detection while moving in flow streams of arteries and veins using ultrasonic Doppler shift principle and square-wave electromagnetic flowmeter
21 p3663 A69-38914

Critical closing phenomenon in dog gracilis muscle, using pressure flow measurements and tissue staining techniques, detecting sudden vessel closure in microcirculation
22 p3873 A69-40202

Blood sheet flow velocity distribution and pressure gradients in pulmonary alveolar septa determined, allowing for system elasticity
22 p3874 A69-40216

Unilateral hypoventilation effect during bronchspirometry on human pulmonary blood flow
22 p3875 A69-40229

Pulsatile blood flow physical characteristics in short vascular segments
22 p3878 A69-40785

Carbon dioxide washout during square wave hyper-ventilation in man, postulating blood flow factor
22 p3885 A69-40975

Gilson cuvette densitometer used for blood flow measurement in canine forelimb and human forearm and hand during constant intrabrachial arterial dye infusion
23 p4077 A69-41294

Stratified blood flow distribution in lung lobule from analyzing breath-holding changes on expired Ar and nitrous oxide tension plateaus during rest and exercise
23 p4078 A69-41315

Pulmonary capillary blood flow, stroke volume and heart rate measured in tilted and supine subjects during

respiration, discussing tourniquets and intravenous atropine effects
23 p4082 A69-41445

Pump system to obtain indocyanine green dye dilution curves without blood loss in small animals and infants
23 p4101 A69-41450

Coronary vessel lumen changes under oligemic hypotension resulting from circulating blood volume decrease in anesthetized cats, discussing constrictory coronary vessel responses
23 p4084 A69-41470

Acceleration effect on greyhound cardiac output and regional blood flow from Saprirstein radioisotope uptake technique, studying blood, skin, skeletal muscle, etc
23 p4089 A69-41823

Forearm skin capacity vessels tonus as function of intrapulmonary pressure during positive and negative pressure breathing
23 p4093 A69-42068

Microrheological property of blood measured with microglass fiber viscosimeter, noting sensitivity to intercellular friction of erythrocytes
23 p4098 A69-42100

Pulsatile flow in coronary arteries simplified model compared with experiment in anesthetized dogs
23 p4098 A69-42103

Sinus outflow relationship to oxygen content in anterior cardiac vein blood and right ventricle systolic pressure
23 p4098 A69-42105

Hemolysis rates in various blood flows, considering effects on energy dissipation
23 p4100 A69-42533

Alaska sled dogs cardiovascular performance and flow distribution during cross country runs
24 p4256 A69-42624

Pulmonary capillary blood flow pulse of healthy men in supine position recorded by nitrous oxide/plethysmograph and phonocardiogram
24 p4259 A69-42638

Stewart-Hamilton formula for cardiac output measurements and regional blood flow determination
24 p4271 A69-42784

BLOOD PLASMA

P32 distribution in protein of blood serum, liver and brains of rats bombarded with high energy protons
02 p0198 A69-11507

Sonic boom effect on corticosteroid level in human blood, noting no changes
03 p0378 A69-14209

Identity between growth hormone degrading activity of pituitary gland and plasmin
06 p0873 A69-17105

Sympathetic neurohormones measurement in plasma of race car drivers
07 p1067 A69-19424

Acetate carbon 14 utilization in centrifurats rats, analyzing metabolism by measuring plasma glucose, FFA and lipids synthesis
07 p1067 A69-19429

Microwave radiation effects on body weight and peripheral blood hemograms of mice, discussing maximum safe exposure related to generator output
08 p1266 A69-20678

Monomethylhydrazine /MMH/ toxic effects on cornea and blood aqueous barrier studied in vivo on dogs
09 p1447 A69-22547

Repeated blood sampling effect on plasma cholinesterase, acid phosphatase, alkaline phosphatase and hematocrit ratios in domestic chickens
10 p1644 A69-23158

High altitude acclimatization effects on cardiovascular system, external respiration, blood composition, optical and vestibular analyzers in human subjected to various stresses
13 p2212 A69-28623

X ray radiation damage to white mice blood serum proteins disappearing following intraperitoneal administration of imidazole or benzimidazole
23 p4077 A69-41300

Physical and psychic stress effects on phosphatidyl glycerol and related phospholipids concentration in human and rat blood plasma
23 p4088 A69-41815

Change in weight, plasma volume, urine flow and hematocrit in man before and after immersion up to chin in thermally neutral bath
23 p4096 A69-42087

Respiratory effects of body temperature changes separation from blood osmolarity changes in dehydrated man
23 p4097 A69-42094

Stewart-Hamilton theorems for total input-output analysis of body cholesterol in man
24 p4259 A69-42639

BLOOD PRESSURE
NT HYPERTENSION
NT HYPOTENSION
NT SYSTOLIC PRESSURE

Human systolic and diastolic blood pressure measuring apparatus and method
01 p0079 A69-10296

Cardiac output during space flight based on rebreathing method for estimation of gas tension in mixed venous blood and Fick equation [UN PAPER 68-95746]
01 p0151 A69-10527

Ocular motor failures in pilots due to convergent and divergent strabismus, discussing low pressure chamber tests and blood pressure effects on cranial nerve
03 p0370 A69-13470

High energy X ray irradiation of head of Macaca mulatta, determining effect on cerebral blood flow and blood pressure
03 p0376 A69-14075

Astronauts increased heart beat, respiration rates and higher blood pressure subsides during repeated weightlessness tests
07 p1061 A69-18582

Telemetering aortic blood pressure and heart rate from dogs under various physical activities and emotional stress
07 p1071 A69-19133

Blood pressure fluctuations in multiple extra systoles during tilt table studies for flying fitness of pilot
10 p1645 A69-23379

Dogs orthostatic tolerance and resistance to transverse acceleration after 14-day hypodynamia, studying tachycardia and arterial pressure
10 p1645 A69-23499

Bed rest effect on orthostatic tolerance of patients with acute myocardial infarction and without heart failure
10 p1648 A69-24189

Single channel pressure telemetry unit for chronic implantation into cardiac chambers or major blood vessels in unrestrained animals for measuring ventricular pressure
11 p1831 A69-25642

Acceleration component in pelvis to head direction found influencing hyperemia of brain at various g forces
13 p2212 A69-28626

Blood pressure telemetry of pilot during flight including determination of psychophysical relations
15 p2559 A69-31229

Intravascular pressure and sound measured in anesthetized dogs and humans using fiberoptic pressure catheter
17 p2917 A69-34172

Vestibular analyzer function relation to arterial pressure during otolith stimulation experiments on subjects susceptible and nonsusceptible to motion sickness
20 p3472 A69-37264

Pulmonary arterial pressure for perfusion of excised dog lungs after inflation not due to shunt channels through atelectasis areas
21 p3651 A69-38386

Heart beat rate, arterial pressure, blood volume and peripheral blood pressure increase observed in dogs running 7 min at 10 km/hr
22 p3885 A69-40966

Static pressure-diameter measurements on small pulmonary blood vessels of frogs, analyzing capillary septal area as function of intravascular pressures noting high compliance
22 p3885 A69-40974

Cardiovascular effects of hypoxia in conscious and anesthetized dogs in environmental chamber, discussing artery pressure, tachycardia, stroke volume and cardiac output
23 p4078 A69-41314

Arterial pressure and heart rate responses to increased intrapulmonary pressure in anesthetized dogs via simulated Valsalva tests
23 p4078 A69-41365

Mathematical formulation for relative values of cardiac output and peripheral resistance as two contributing factors to arterial pressure change
23 p4085 A69-41473

Physiological response to steady state hypoxia from exposure to 12 percent oxygen atmosphere, noting minimal heart rate and blood pressure changes
23 p4085 A69-41673

Jet pilot blood pressure response during positive acceleration in actual flight measured by telemetry compared with centrifuge test
23 p4089 A69-41822

Aortic pressure effect on left ventricular function, emphasizing effect of heart rate hematocrit and oxygen consumption
23 p4092 A69-42061

Sinusoidal pressure electric stimuli frequency effects in isolated carotid sinus on canine peripheral blood pressure, determining dynamic characteristics from observation data
23 p4092 A69-42062

Diurnal rhythms of heart rate and blood pressure reactions to posture changes on tilt table, finding orthostatic lability maxima
23 p4094 A69-42072

Portal blood pressure decrease effects on diuresis in unanesthetized rats, discussing osmotic diuresis
23 p4094 A69-42074

Human arterial pressure reflex regulation during sleep, assessing baroreflex sensitivity
24 p4257 A69-42626

Gravitational stress effect on heart and venous system, discussing digital computer model simulating pressure changes under head-up and down tilt
24 p4271 A69-42783

BLOOD VESSELS
NT AORTA
NT ARTERIES
NT CAPILLARIES [ANATOMY]
NT VEINS

HF pressure waves dispersion in blood vessels ascribed to viscoelastic behavior of walls
02 p0204 A69-12602

Thermal radiation effects on cutaneous vasomotor and sudomotor control of human organism [AGARDOGRAPH-111]
08 p1265 A69-20672

Small eye movements measurement and retinal image stabilization based on tracking edge of blood vessel in optic disk
09 p1446 A69-21908

Arterial tone and human muscular activity limitations, analyzing hypodynamic effects on aorta, arm and leg vessels constriction
10 p1647 A69-23586

Sheet geometry of lung blood vessel system, discussing histological evidence and fluid dynamic consequences of sheet flow
19 p3263 A69-36656

Ultrasonic Doppler flowmeter for detection of circulating gas emboli of animal blood vessels during decompression
21 p3663 A69-38915

Critical closing phenomenon in dog gracilis muscle, using pressure flow measurements and tissue staining techniques, detecting sudden vessel closure in microcirculation
22 p3873 A69-40202

Alveolar and mixed venous carbon dioxide pressure during absence of gas exchange across mammalian lung
22 p3885 A69-40976

Coronary vessel lumen changes under oligemic hypotension resulting from circulating blood volume decrease in anesthetized cats, discussing constrictory coronary vessel responses
23 p4084 A69-41470

BLOWDOWN WIND TUNNELS
NT LOW DENSITY RESEARCH

Blow-down facility for hypersonic testing of air breathing engines, describing test cell, air heating system, exhausters and data system
02 p0227 A69-11756

Blowdown wind tunnel designed for studying closed cycle MHD converters, describing subsystems
10 p1673 A69-23474

Toshiba blowdown MHD test facility experiments on nonequilibrium ionization, using K seeded He for working gas
10 p1673 A69-23477

Error analysis for pressure measurements in blowdown supersonic tunnel
19 p3292 A69-35728

Supersonic blowdown wind tunnel operating at Mach numbers obtained by fixed nozzles for aerodynamic optimization of wings and bodies
20 p3510 A69-37422

Panel flutter testing in supersonic blowdown wind tunnels, analyzing model and test chamber layout
21 p3847 A69-39859

BLOWING

Determining influence of blowing various gases into boundary layer on friction and heat and mass transfer when external flow velocity varies according to power law
02 p0234 A69-12581

Hypersonic boundary layer on flat plate with strong hypersonic viscous interaction and uniform surface blowing distribution
04 p0588 A69-14722

Lift augmentation by lateral blowing over lifting surface, discussing wind tunnel pressure tests on wings, flaps and stabilizers [AIAA PAPER 69-193]
07 p1051 A69-19554

Laminar boundary layer control by combined blowing and suction, analyzing surface roughness influence concerned with underwater vehicle skin friction reduction [AIAA PAPER 69-387]
15 p2591 A69-30477

Supersonic flow past cone in presence of blowing normal to cone surface, calculating flow field parameters behind conical shock wave
15 p2548 A69-31175

Laminar boundary layer control on two dimensional body by combined blowing and suction in presence of roughness, noting skin friction reduction [AIAA PAPER 68-641]
17 p2957 A69-34015

Circulation control by blowing and application to stopped rotor aircraft, discussing data from model scale blade experiments
19 p3248 A69-36767

Blowing effect on surface friction coefficient and heat transfer in turbulent boundary layer in compressible fluid with pressure gradient
21 p3643 A69-38636

Steady constant density two dimensional flow in laminar boundary layer over permeable curved surfaces, showing effects of suction or blowing
23 p4153 A69-42399

Mass injection by strong blowing across Couette-Poiseuille shear flow
24 p4301 A69-43554

Similarity solutions to massive blowing problem, discussing inviscid flow model compatible with no-slip condition
24 p4305 A69-43658

BLUE GREEN ALGAE

Fatty acids in blue-green algae related to phylogenetic position
05 p0707 A69-15751

Gas vacuoles development in blue green algae by cell transfer from defined medium to distilled water
10 p1644 A69-23184

Microstructure of Proterozoic nanofossils bracketed by dated granitic events compared with living Eucapsis of blue green Chroococcaceae algal family
22 p3936 A69-40059

Blue green alga Anabaena flos-aquae A-37 growth limitation by absence of K or Na from culture medium
23 p4079 A69-41386

BLUFF BODIES

Model for asymptotic separated flow in wake behind broadside of bluff body, discussing separation point, interaction, reattachment, base flow and near wake
02 p0188 A69-11986

Equivalent cross section theory relating air resistance of randomly tumbling bluff objects to resistance of equivalent spheres
09 p1431 A69-22000

Nitrogen dilution low pressure simulation technique for subsonic flow flame stabilization of bluff bodies
09 p1624 A69-22614

Two dimensional stratified flow over obstacle in finite height channel, noting lee waves and drag increase with decreasing speed
11 p1869 A69-24892

Turbulent jet theory, thermal ignition theory and flameout characteristics of bluff body flame stabilizers
16 p2879 A69-32141

Blockage effects of flat plates and solid bluff bodies in closed wind tunnels compared concerning drag coefficient values
17 p2890 A69-33245

Laminar separation in incompressible fluid flowing past bluff body at high Reynolds number, investigating shock wave interaction with laminar boundary layers
18 p3122 A69-34918

Spanwise velocity correlations of turbulent vortices shed by two dimensional bluff body of D section with different aspect ratios, noting end plates effect
23 p4234 A69-42397

Turbulence characteristics of flow influence on critical flameout conditions of disk shaped flame stabilizer, circulation zone length and combustion efficiency by bluff body
24 p4408 A69-43078

BLUFFS [LANDFORMS]
U CLIFFS

BLUNT BODIES

Supersonic air flow around blunt body studied near critical line with allowance for viscosity, thermal conductivity and radiant energy transfer, assuming thermodynamic equilibrium

01 p0006 A69-10378

Ablation rate optical measurement near stagnation point of Teflon cylinder models, noting effect of nose curvature and temperature at supersonic speed

01 p0006 A69-10758

Hypersonic gas flow past blunt body problem solved by integral correlation method, taking into account radiation effects and gas dynamic parameter distribution in shock wave layer

02 p0188 A69-11651

Rarefied merged stagnation shock layer of hypersonic body, considering chemical reactions of nonequilibrium dissociative relaxation of air

02 p0189 A69-12521

Downstream radiation flux distribution calculated for blunt entry bodies, considering self absorption effects

02 p0354 A69-12547

Supersonic flow past blunt body with convex corner calculated to establish sonic point on body

03 p0362 A69-13406

Nosetip cooling system based on discrete subsonic forward liquid injection through ablative nosetip opening of blunted reentry vehicle

[AIAA PAPER 68-1141] 03 p0532 A69-13559

Reentry shock layer radiative heat transfer to surface of blunt superorbital vehicle

[AIAA PAPER 68-1151] 03 p0532 A69-13560

Blunt and conical body optimum heat shield shapes for Jupiter atmospheric entry, noting shallow flight path

[AIAA PAPER 68-1150] 03 p0520 A69-13565

Scaling laws for nose bluntness effects on hypersonic aerodynamics of bodies of revolution

[AIAA PAPER 68-1158] 03 p0362 A69-13566

Soviet book on hypersonic flow past truncated cones at various angles of attack with allowance for physicochemical equilibrium transformations

03 p0362 A69-13633

Problem of viscous supersonic flow past blunt bodies based on Navier-Stokes equations formulated and solved numerically with explicit difference scheme

03 p0363 A69-13653

Supersonic flow region about blunt body calculated on basis of gasdynamic equations for steady flow of inviscid nonheat conducting gas

03 p0363 A69-13658

Ideal gas flow near stagnation line for blunt bodies, applying van Dyke series truncation method to numerical solution

03 p0364 A69-13660

Heat input influence on hypersonic flows past sphere and circular cylinder

[DVL-844] 03 p0364 A69-13663

Numerical algorithm for supersonic gas flow past blunt bodies with shock wave separation, using Dorodnitsyn method of integral correlation

04 p0587 A69-14621

Cone tip blunting effect on cone local laminar heat transfer rate noting cone configuration, semivertex cone angle and Mach number

04 p0542 A69-14721

Inviscid hypersonic flow of uniform equilibrium gas past axisymmetric blunt body

04 p0542 A69-14723

Blunt cone hypersonic roll damping derivative, using Mach number distribution and graphical integration

04 p0542 A69-14739

Telemetry technique utilizing thermocouple sensors for base heating determinations on free flight blunt cone in shock tunnels, noting electrical noise reduction

[AIAA PAPER 68-407] 04 p0604 A69-15514

Hypersonic laminar and transitional heat transfer rate distribution on spherically blunted cones

05 p0696 A69-15707

Blockage correction for blunt based bodies of revolution in wind tunnels at low Mach numbers

05 p0699 A69-16395

Nonequilibrium supersonic flow calculation of detonating mixture past blunt bodies applied to flow of hydrogen-oxygen mixture past sphere

06 p0859 A69-17343

Aircraft aerodynamic characteristics determination from numerical computer solution of supersonic gas flow past blunt body with broken generatrix

06 p0859 A69-17582

Dynamic behavior of shock layer of supersonic rarefied gas flow past disk and sphere

06 p0861 A69-17812

Laminar near wake flow field of two dimensional adiabatic circular cylinder with surface mass transfer

[AIAA PAPER 69-67] 06 p0862 A69-18044

Chemical nonequilibrium, mass transfer and viscous interaction effects on spherically blunted cones at hypersonic conditions, emphasizing stagnation point

[AIAA PAPER 69-168] 06 p0862 A69-18047

Electron density shock layer profiles measured by Langmuir probe in hypersonic tunnel on blunt body for air flows and gas densities

[AIAA PAPER 69-81] 06 p0863 A69-18101

Time dependent technique for inviscid blunt body flows to analyze viscous rarefied shock layer regime, using Navier-Stokes equations

[AIAA PAPER 69-139] 06 p0865 A69-18173

Effects of multidimensional flow through porous matrices in mass transfer cooling, analyzing one dimensional model for blunt axisymmetric surfaces

[AIAA PAPER 69-149] 06 p1038 A69-18179

Dynamic stability derivatives of large angle blunted conical spacecraft near transonic speed in simulated Mars environment for various angles of attack

[AIAA PAPER 69-104] 06 p1019 A69-18210

Laminar boundary layer on axisymmetric blunt body in dissociated air taking into account nonequilibrium homogeneous chemical reactions

07 p1050 A69-18734

Hypersonic flow past blunt body near stagnation point, noting surface layer characterized by increased density and decreased entropy of gas

07 p1050 A69-18755

Solar wind flow past earth and magnetosphere correspondence to external aerodynamics of round nosed bodies in supersonic stream

07 p1128 A69-19360

Partially ionized argon plasma stagnation flow past blunt body using multifluid theory, obtaining flow profiles

08 p1369 A69-20817

One strip method of integral relations applied to inviscid supersonic blunt body problem

09 p1430 A69-21972

Fluid injection into flowfield from porous forward portion of blunt body in stagnation region flow, determining reservoir pressure and mass flow rate

09 p1430 A69-21973

Hypersonic drag and shock wave characteristics of blunt bodies including cones, spherical nose and concave nose bodies

09 p1433 A69-22568

Spherically blunted 15 degree semivertex angle cone flow field parameters at Mach 8.6, measuring pitot pressure and shock shape

11 p1818 A69-25143

Supersonic air flow past blunt body of revolution in presence of nonequilibrium chemical reactions, ionization and molecular excitation

11 p1820 A69-25474

Supersonic and hypersonic flow of rarefied gas around blunted cylinders at various angles of attack, noting pressure distribution on model surface

11 p1821 A69-25478

Supersonic air flow around blunt body studied near critical line with allowance for viscosity, thermal conductivity and radiant energy transfer, assuming thermodynamic equilibrium

12 p2012 A69-26669

Flow field instability over concave bodies in supersonic free stream computed by integration of gasdynamic equations, noting application to supersonic parachutes

[AIAA PAPER 68-946] 13 p2199 A69-28228

Angle of attack and blunting effect on aerodynamic lift and drag coefficients of flat plates in hypersonic flow at low Reynolds number

13 p2200 A69-28358

Supersonic wake recirculation flow over rearward facing two dimensional steps and blunt bases

14 p2389 A69-29031

Shock wave and blunt faced cylinder interaction in supersonic gas flow in two chamber shock tube observed with high speed photography

14 p2390 A69-29467

Supersonic gas flows in shock layer past blunt bodies taking into account selective radiation and radiative transfer in continuum, applying method of characteristics

14 p2390 A69-29477

Heat transfer at gas flow stagnation point past blunt body under radiation from air layer in shock wave wake, using gray gas model

14 p2390 A69-29614

Spatial supersonic ideal gas flows past blunt bodies analyzed by numerical finite difference methods, discussing flow fields and entropy

14 p2390 A69-29616

Laminar and turbulent hypersonic wakes trailing blunt bodies studied by finite difference method, taking into account pressure gradients and nonequilibrium chemical reactions effects

14 p2391 A69-29618

Boundary layer physical and chemical processes effect on dynamic parameters of high temperature hypersonic gas flow past blunt bodies

14 p2391 A69-29620

Hypervelocity reentry simulation problems for slender and blunt bodies, defining significant parameters

15 p2681 A69-30376

Godunov finite difference method modified for steady or unsteady flowfields about planar axisymmetric blunt bodies, presenting body pressures and shock shapes

16 p2732 A69-31886

Aerodynamic characteristics of cone/cylinder and cone/cylinder/cone configurations with blunted cones in hypersonic flows at small angles of attack

17 p2889 A69-33122

Mach number, cone angle, bluntness and wall to recovery temperature ratio effects on slender cones boundary layer transition measurements at hypersonic speeds

17 p2890 A69-33250

Nongray equilibrium radiative heat transfer in viscous radiating shock layer around blunt body entering high temperature nonisothermal carbon dioxide-nitrogen atmosphere

[AIAA PAPER 69-636] 17 p3070 A69-33258

Shock layer properties, radiative and convective heat transfer about two hypersonic blunt bodies at zero angle of attack in assumed Martian atmosphere

[AIAA PAPER 69-634] 17 p2891 A69-33281

Nongray absorption and radiation cooling on smooth symmetric blunt bodies included in modified Maslen flow field method for radiation and large blowing

[AIAA PAPER 69-637] 17 p2891 A69-33290

Hypersonic boundary layer transition on blunt slender cones at M equal 10 obtained independent Reynolds number

[AIAA PAPER 69-705] 17 p2954 A69-33455

Surface pressure and heat transfer over blunt conical body in hypersonic flow with uniform mass addition of various gases

[AIAA PAPER 69-716] 17 p2891 A69-33463

Nonequilibrium multicomponent ionization calculations for stagnation merged shock layer of hypersonic blunt body by successive accelerated replacement

[AIAA PAPER 69-655] 17 p2892 A69-33469

Electrical characteristics of equilibrium plasma sheaths at stagnation point of blunt body in high speed air, considering current collection regimes

[AIAA PAPER 69-702] 17 p3011 A69-33473

Cone boundary layer transition location and Reynolds number as function of nose bluntness combined effect with Ar, air and He mass injection

[AIAA PAPER 67-706] 17 p2955 A69-33476

Precursor plasma electron number densities calculations for blunt reentry vehicles, analyzing extreme UV radiation emanating from bow shock

[AIAA PAPER 69-718] 17 p2893 A69-33487

MGD hypersonic shock layer at spherically blunted body analyzed by utilizing induction equation including Hall effect

[AIAA PAPER 69-722] 17 p3012 A69-33494

Flow field study of merging between bow shock and viscous layer upstream of highly cooled axisymmetric blunt body in rarefied hypersonic stream

[AIAA PAPER 69-656] 17 p2893 A69-33498

Flow measurements about high Mach number low Reynolds number laminar wake behind spherically blunted cones, including surface and wake flow field data, radial wake profiles, etc

[AIAA PAPER 69-714] 17 p2894 A69-33500

Three dimensional incompressible wake behind blunt obstacle at leading edge of flat plate compared with mathematical model by Oseen linearization

18 p3083 A69-34403

Flow structure in wake of blunt bodies placed perpendicular in parallel airstream determined from hot-wire anemometry

[AIAA PAPER 69-746] 18 p3084 A69-34409

Radiative energy emission by blunt vehicle shock layer under severe entry conditions, discussing flow properties and radiative transfer coupling

[AIAA PAPER 69-719] 18 p3084 A69-34416

Aerodynamic characteristics of sphere and blunt cone in highly rarefied gas flow, noting molecular collision effect

18 p3086 A69-34708

Rarefied gas dynamics for continuous medium and discrete molecules assemblage, discussing flow over blunt model and free jet flow from sonic orifice
18 p3122 A69-34812

Transport processes effect in shock wave on hypersonic flow past blunt body in neighborhood of stagnation point, noting heat transfer
18 p3086 A69-34910

Rarified gas dynamics of blunt and sharp-pointed slender bodies in supersonic stream and free jet sonic expansion into high vacuum
18 p3123 A69-34924

Integral relation method analysis of supersonic gas flow past blunt body of revolution
18 p3086 A69-35051

Heat exchange in stagnation point region of blunt body, using shock test simulation of high speed flight
18 p3086 A69-35118

Systematic mathematical ordering of knowledge concerning three dimensional flow patterns around blunt bodies, emphasizing high speed computers role
18 p3089 A69-35269

Drag measurements for sharp and blunt-nosed bodies shot into wind tunnel supersonic gas counterflows, discussing shock waves for different configurations
19 p3239 A69-36401

Nose bluntness effect on hypersonic flow for slender blunt bodies with arbitrarily shaped lateral surfaces at small attack angle
19 p3239 A69-36402

Supersonic flow past segmented and blunt bodies, investigating flow characteristics
19 p3242 A69-36783

Stagnation point heating in hypersonic gas flow past blunt bodies, considering radiative transfer effects on shock wave temperature and density distribution, wave separation, etc
20 p3457 A69-36981

Hypersonic gas flow past blunt bodies valid for any optical thickness of gas, allowing for absorption coefficients dependence on temperature, pressure and frequency
20 p3457 A69-36993

Electron density distribution in laminar air boundary layer on sharp wedges and cones predicted by reducing chemical kinetic model to ordinary differential equations [AIAA PAPER 68-733]
20 p3458 A69-37181

Generalized series solutions of boundary layer flows over pointed and blunt nosed axisymmetric bodies, noting general potential flow extending Mangler transformation usefulness
20 p3514 A69-37211

Gaseous injection effect on laminar boundary layer hypersonic flow around transpiration-cooled blunt bodies analyzed by integral method and Newtonian model
21 p3644 A69-39014

Radiation self absorption effects on heating loads of blunt body during hyperbolic entry
21 p3644 A69-39040

Axisymmetric and two dimensional flows over blunt bodies at high Mach numbers by integral relations method
21 p3645 A69-39790

Dynamic stability derivatives of large angle blunted conical spacecraft near transonic speed in simulated Mars environment for various angles of attack
22 p4036 A69-40550

Piston motion influence on gaseous motion set up by constant energy explosion, applying to steady high Mach number flow past blunt nosed object
22 p3931 A69-40892

Transient flow resulting from plane shock diffraction by analytic blunt body, basing analysis on Taylor series expansions in space and time variables
22 p3860 A69-40895

Semianalytic solution for axisymmetrical supersonic inviscid flow near stagnation region of spherically blunted body with detached shock waves
22 p3861 A69-41178

Axisymmetric supersonic flow around spherically blunted body at small angles of attack, deriving equations for shock deformation perturbations and surface pressure
22 p3861 A69-41179

Radiative transfer effects in low Reynolds number or merged layer regime of hypersonic flow about axisymmetric blunt bodies, including thin shock layer theory
23 p4059 A69-41885

Blunt body stagnation point air ionization by chemical nonequilibrium thin viscous shock layer analysis, predicting electron density
23 p4060 A69-41917

Detachment in incompressible turbulent flows around thick body analyzed to predict base pressure, vortex volume, etc
24 p4299 A69-42674

Nonlifting blunt axisymmetric hypersonic shape determination to maximize pressure drag for given convective heat transfer, diameter and free-stream conditions
24 p4244 A69-42960

Supersonic flows past blunt bodies, formulating approximate similarity law for shock layers in subsonic regions
24 p4246 A69-43495

Reentry shock layer radiative heat transfer to surface of blunt superorbital vehicle [AIAA PAPER 68-1151]
24 p4414 A69-43567

Mass injection effects on viscous hypersonic low Reynolds number shock layer downstream and at stagnation point in blunt forebody region analyzed for non-reacting gas
24 p4249 A69-43663

Pressure distribution correlation over blunted slender cone at various angles of attack by tangent cone method, describing hypersonic wind tunnel tests
24 p4249 A69-43681

BLUNTNESS
U ELLIPTICITY

BLURRING
Image deblurring and aperture synthesis using a posteriori processing by Fourier transform holographic spatial filtering
21 p3722 A69-38793

Motion-distorted photograph deblurring method using extended range holographic Fourier transform division
22 p3944 A69-40020

BMEWS
U BALLISTIC MISSILE EARLY WARNING SYSTEM

BO-105 HELICOPTER
BO-105 helicopter design, testing and characteristics noting four bladed rigid rotor [AHS PAPER 200]
07 p1052 A69-18869

BODIES
Distribution of steady state solutions for equations of helical motion of body in infinite fluid, noting coaxial control surfaces
11 p1868 A69-24782

Kinematic equations of motion of body about fixed point, considering Steklov solution
11 p1918 A69-24791

BODIES OF REVOLUTION
NT CELESTIAL SPHERE
NT CONICAL BODIES
NT CYLINDRICAL BODIES
NT PARABOLIC BODIES
NT POINCARÉ SPHERES
NT ROTATING CYLINDERS
NT ROTATING SPHERES
NT SLENDER CONES
NT SPHERES
NT TORUSES

Boundary value bending problem for anisotropic shells of revolution under asymmetrical loading solved by finite difference technique
01 p0165 A69-10088

Sonic flow at large distance and behind shock wave for axisymmetric body of revolution of finite dimensions in inviscid fluid
01 p0058 A69-10160

Exact solution of shallow shells of revolution equations governing linear deformation compared with asymptotic integration procedure
01 p0166 A69-10234

Galerkin method for solving dimensionless Reissner equation for symmetrically loaded thin nonshallow shells of revolution
01 p0168 A69-10380

Critical internal pressure induced plastic instability in membrane shells of revolution determined by graphical numerical method
02 p0338 A69-11719

Complex revolution vessels and multilobed structures analyzed by electronic computers, considering doubly stressed state of shells and bending moments from external forces
02 p0339 A69-11894

Geometric optics inverse scattering method for smooth conducting convex bodies of revolution, demonstrating bounds on size and shape
02 p0280 A69-11929

Matrix displacement method for nonlinear elastic analysis of shells of revolution under symmetrical and asymmetrical loadings
02 p0346 A69-12511

Minimum drag configurations with low heat transfer for hypersonic bodies of revolution, noting performance at supersonic speeds
02 p0191 A69-12578

Photographic flow patterns of separated flows with vortex formation obtained in wind tunnel for different aerodynamic configurations of revolution
02 p0191 A69-12586

Finite difference schemes for axisymmetric oscillations of shells of revolution filled with liquid
03 p0523 A69-12951

Supersonic flow past blunt body with convex corner calculated to establish sonic point on body
03 p0362 A69-13406

Scaling laws for nose bluntness effects on hypersonic aerodynamics of bodies of revolution [AIAA PAPER 68-1158]
03 p0362 A69-13566

Computer method calculating stressed state of elliptical bottom of cylindrical pressure vessel based on differential bending equations for shell of revolution
04 p0668 A69-14275

Aerodynamics of bodies of revolution in nonplanar motion using nonlinear functional analysis of moments for motion about center of gravity [AIAA PAPER 68-20]
04 p0542 A69-14714

Stability of circular cylindrical viscoelastic and elastic shells with local effects due to radial load on circumference or thermally induced tangential stress
04 p0680 A69-14928

Point matching method for analysis of stress in incompressible solids of revolution, noting application to solid propellant rocket charges
04 p0683 A69-15518

Reissner nonlinear equations for nonshallow symmetrically loaded shells of revolution
04 p0684 A69-15538

Exact geometrical equations and internal equilibrium for elastoplastic deflections of orthotropic shells of revolution using thin shell theory
05 p0831 A69-15680

Stress-strain state of thin elliptical shell of revolution under rapidly varying cyclic edge loads
05 p0832 A69-15686

Ductile creep rupture of thin walled membrane shell of revolution subjected to time dependent internal pressure and strain hardening [ASME PAPER 68-WA/MET-15]
05 p0838 A69-16153

Asymmetrically loaded systems composed of shells of revolution, developing digital computer algorithm for solution of statics problems
05 p0840 A69-16201

Blockage correction for blunt based bodies of revolution in wind tunnels at low Mach numbers
05 p0699 A69-16395

Finite elastic-plastic deflections of orthotropic shells of revolution, deriving exact geometrical relations and equilibrium equations
05 p0842 A69-16642

Stress calculation for internal pressure in moment-less shell of revolution
05 p0843 A69-16690

Stability loss of shells of revolution under effect of axial compression and radial pressure with no restrictions on generatrix curvature, using strain energy method
06 p1021 A69-17179

Wall temperature and Mach number effect on heat flux distribution at spreading line of flow for supersonic gas on ellipsoid of revolution
06 p0858 A69-17331

Automatic data processing method for analyzing multiply connected elastoplastic shells of revolution
06 p1025 A69-17614

Ellipsoids of revolution in viscous flow at very low Reynolds number, determining optimum shapes and minimum resistance values
06 p0911 A69-17780

Computer program for axisymmetrically deformed shells of revolution and combinations of such shells
06 p1026 A69-18019

Post-wrinkling nonlinear behavior of conical shell of revolution subjected to bending loads [AIAA PAPER 69-90]
06 p1027 A69-18074

Geometrically exact finite element for thin shells of revolution, using approximation to predict boundary layer stress distribution during vibration [AIAA PAPER 69-56]
06 p1029 A69-18193

Boundary layer approximation for steady laminar flow of viscous incompressible fluid past paraboloid of revolution, obtaining vorticity distribution
07 p1120 A69-18812

Steady rotation of insulating body of revolution in unbounded electrically conducting fluid permeated by applied axial magnetic field

07 p1190 A69-18814

Rotating incompressible liquid drop held together by surface tension noting spheroidal and toroidal shapes, energies and case of surrounding denser medium

07 p1120 A69-19267

Rupture times in analysis of creep tensile instability in uniformly pressurized thin walled membrane shells of revolution, comparing two criteria

07 p1234 A69-19378

Local stability of thin walled elastic shells of revolution subjected to external pressure

07 p1237 A69-19686

Approximate equations for transonic viscous heat conducting gas flow past finite body of revolution

08 p1251 A69-20322

Transformation of laminar stationary incompressible boundary layer equations for body of revolution in incident flow, using difference method

08 p1252 A69-20703

Static axisymmetric deformation of elastic paraboloid of revolution, using integration of equilibrium equation in Lamé displacement

09 p1613 A69-21631

Symmetrical body rotational motion with asymmetrical mass distribution about center of mass, determining minimum initial value of angular velocity

09 p1595 A69-21762

Finite difference method computer programs for calculation of velocities and streamlines on blade to blade surface of revolution of turbomachine

09 p1432 A69-22495

Pressure coefficients determination on slender body surface to estimate effects of quadratic terms, considering body of revolution with thin cruciform lifting surfaces

10 p1632 A69-22911

Book on statics of thin walled shells of revolution covering stress-strain analysis for geometrical shapes

10 p1800 A69-23197

Bodies of revolution in sonic flow of ideal gas, showing same perturbational effect of source and dipole on flow before shock front

10 p1632 A69-23364

Strength analysis of revolving shallow shell with jumpwise thickness variations under axisymmetric distributed load, considering rigidity and plastic deformation

11 p1968 A69-24318

Scattering of spherical electromagnetic wave emitted by electric and magnetic dipoles with equal moments at truncated infinitely thin ideally conducting paraboloid of revolution

11 p1846 A69-24614

Second approximation of asymptotic damping of disturbances in viscous heat conducting gas supersonic flow about solid of revolution at critical velocity

11 p1817 A69-24627

Boundary value problem for gravity induced wave motion of ideal fluid in axisymmetric vessel with annular ribs, noting application to bodies of revolution

11 p1868 A69-24769

Finite deformation equations for flat annular membranes deduced from equations for thin shells of revolution, discussing displacement equations and fixed edge forces

11 p1979 A69-24813

Symmetrically loaded weak moment shells of revolution made of materials with different moduli of elasticity

11 p1980 A69-24819

Elastic two cavity revolving hyperboloid deformation by arbitrary forces solved by spherical functions

11 p1984 A69-25169

Aerodynamic forces causing deformation and breakup of liquid droplet with ellipsoid of revolution form in constant velocity gas flow

11 p1875 A69-25466

Supersonic air flow past blunt body of revolution in presence of nonequilibrium chemical reactions, ionization and molecular excitation

11 p1820 A69-25474

Interference between bodies of revolution and wings in supersonic flow, using Volterra method for calculation

11 p1820 A69-25476

Bending and membrane stresses determination in shallow thin shells of revolution under large axisymmetric deflections, using normal and radial displacements relationship

11 p1995 A69-25651

Theorem for integral expansion applied to boundary value problems of mathematical physics and elasticity theory for single sheet hyperboloids of revolution

11 p1910 A69-25731

Nonstiffness of nonshallow spherical dome using asymptotic method, applying nonlinear Reissner equations to finite symmetric deformation of thin shells of revolution

11 p1996 A69-25733

Axisymmetric detached flow past slender solid of revolution by ideal incompressible fluid at zero angle of attack and with small cavitation numbers

11 p1877 A69-25741

Analytic model resembling thick walled ellipsoid of revolution incorporating three dimensional shape of human left ventricle and ventricular wall thickness effects

12 p2022 A69-26235

Conformal transformation reducing transverse thermal resistance of cylinder of revolution to thermal resistance of semiinfinite medium

12 p2190 A69-26292

Galerkin method for solving dimensionless Reissner equation for symmetrically loaded thin nonshallow shells of revolution

12 p2182 A69-26679

Nose bluntness effect on hypersonic unsteady aerodynamics of flared and conical bodies of revolution

[AIAA PAPER 68-889]

12 p2012 A69-26794

Complex two layered shell of revolution under static and dynamic axisymmetric loads analyzed using SABOR/DRASTIC computer codes

12 p2184 A69-26811

Axisymmetric elastic stresses in ring stiffened segmented shells of revolution, noting finite difference method for nonlinear analysis and computer program

12 p2185 A69-26818

Large deflection elastic-plastic analysis of axisymmetric shells of revolution indicating role of plastic yielding in buckling pressure reduction

12 p2186 A69-26839

Bending state of shells of revolution due to edge effects using nonlinear stress strain relation

13 p2362 A69-27921

Motion of slender axisymmetric bodies in rotating fluid, relating Long hypotheses to flow reversal and dipole distribution effects on lee waves

13 p2248 A69-28170

Residual field in inner airspace of magnetostatic shielding thin walled stretched ellipsoids of revolution

13 p2237 A69-28610

Elastoplastic deformations of thin axisymmetric shells of revolution with variable thickness, exemplifying shell with piecewise constant thickness

14 p2533 A69-28982

Integral representation of p -analytic functions of complex variable, applying axisymmetric boundary value problems of elasticity theory for cylindrical surfaces and paraboloid of revolution

15 p2714 A69-31191

Exact solution for motion of conducting solid of revolution rotating in infinite conducting viscous fluid, describing magnetic field

16 p2817 A69-31666

Torsional stability of shallow shells of revolution, solving eigenvalue problem obtained from perturbation of nonlinear equations by finite differences

16 p2871 A69-31879

Eigenvalues of truncated orthotropic shells of revolution with degenerate poles and various rigidities and geometries

16 p2873 A69-32133

Elastic spheroidal shell of revolution under external pressure described by buckling and postbuckling theory

16 p2874 A69-32162

Stress-strain rate of glass fiber reinforced plastic pressure vessels under internal pressure, determining optimal fiber pattern

17 p3057 A69-33195

Approximate equations for transonic viscous heat conducting gas flow past finite body of revolution

17 p2891 A69-33312

Strain displacement and compatibility equations of finite symmetrical deflections of thin shells of revolution

[ASME PAPER 69-APM-14]

18 p3214 A69-34391

Differential equations of shells of revolution theory assuming rotationally symmetric stress and strain in thin elastic shells

18 p3215 A69-34549

Local stability of viscoelastic shells of revolution under axisymmetric loads, discussing asymmetric snaphthrough of dome

18 p3216 A69-34573

Stability loss of shells of revolution under axial tension and radial pressure, considering shells of Gaussian curvature, calculating critical force

18 p3222 A69-34976

Integral relation method analysis of supersonic gas flow past blunt body of revolution

18 p3086 A69-35051

Limiting equilibrium of variable thickness shallow spherical and conical shells of revolution under axisymmetric loads, assuming rigid plastic shell material

18 p3225 A69-35370

Fredholm integral equation solution of circularly axisymmetric stress state for bodies of revolution

18 p3226 A69-35375

Equations of motion for axisymmetric elastic deformation of inhomogeneous body of revolution subjected to torsion and steady oscillations

19 p3436 A69-35845

Asymptotic form of axisymmetric solution with Dirichlet integral for Navier-Stokes equations applied to flow past bodies of revolution with smooth surfaces

19 p3298 A69-36143

Three dimensional laminar boundary layer on conical body of revolution in low Reynolds number compressible fluid flow

19 p3241 A69-36762

Shells of revolution bearing capacity under axisymmetric loads determined by linear programming and finite difference method

20 p3622 A69-37326

Nonlinear theory based on Euler-Bernoulli hypotheses for axisymmetric deformations of heterogeneous orthotropic shells of revolution under rotationally symmetric mechanical and thermal loads

20 p3625 A69-37592

Perturbed motion of solid body containing axisymmetric cavities partially filled with ideal incompressible fluid, solving boundary value problems of fluid oscillations

20 p3518 A69-38296

Coordinate transformation of Euler equations governing precession and nutation of self gravitating bodies of viscous fluid in inertial coordinates

21 p3797 A69-38539

Inertial motion of body produced by revolving uniformly deformed configuration, showing constant semiaxes without kinetic energy losses

21 p3772 A69-39620

Electromagnetic radiation and scattering from conducting bodies of revolution, obtaining formulation in integrodifferential equation from potential integrals and boundary conditions

22 p3899 A69-40014

Nonlinear shallow shell theory of stress and strain formulated via shell of revolution problem

22 p4048 A69-41198

Inviscid transonic flow past circular arc bodies of revolution, applying Hosokawa technique to pressure distribution solution

23 p4059 A69-41899

Aerodynamic characteristics of moving and rotating bodies of revolution in free molecular rarefied gas flow, assuming Maxwellian thermal velocity distribution and diffuse specular interaction

24 p4243 A69-42583

Subsonic wind tunnel balance and holders investigated for effects on lift, drag and stability of models of body of revolution

24 p4297 A69-43084

BODY CENTERED CUBIC LATTICES

Point defects in body centered cubic transition metals, discussing thermal equilibrium, irradiation cold work, high and low temperature recovery, etc

03 p0447 A69-13817

Localized umklapp scattering effect on galvanomagnetic properties of nearly free electron bcc metal with spherical Fermi surface

03 p0493 A69-14240

Heterodiffusion of metallic impurities in body centered phases of doped zirconium and titanium, determining diffusion coefficients via radioactive isotopes

04 p0613 A69-14557

X ray diffraction studies of deformation effects on bcc niobium alloys in terms of particle size, strain, faulting probability and dislocation density

04 p0618 A69-15202

Dislocation distributions in cold worked fcc, bcc and hcp metals, discussing dislocation structures in deformed single crystals and work hardening theories

05 p0778 A69-15754

Vacancy relaxations in bcc crystals using energy dependence on radial displacements from defect of nearest neighbor sets, discussing crystal size and shape
05 p0809 A69-16529

Slip geometry in bcc metals, discussing slip-line observations by light and electron microscopy techniques
05 p0781 A69-16537

High pressure high temperature synthesis and superconducting properties of yttrium sesquicarbide, noting effect of ambient pressure annealing
07 p1201 A69-19600

Structure and properties of high heat resistant alloys based on high melting point metals with bcc lattice explained by electron theory
09 p1525 A69-22139

Beryllium diffusion coefficients in Zr and Ti bcc phases, using radioactive beryllium 7 at high temperatures
18 p3157 A69-35251

Creep behavior of dispersion strengthened Nb base bcc alloy, studying temperature and stress effects on steady state creep rate
19 p3343 A69-35924

Alloy softening in bcc Fe-N and Fe-Ni, discussing causes of thermal stress component reduction in interstitial and substitutional alloys
22 p3969 A69-40164

Solid solution softening in bcc alloys, discussing alloy atoms intervention in low temperature deformation process
22 p3969 A69-40165

Bcc metals strengthening and alloy softening mechanisms, studying temperature and additives effects
22 p3970 A69-40166

Single crystal Ta and Ta base bcc solid solution strengthening and weakening as function of temperature and strain rate
23 p4178 A69-42358

BODY COMPOSITION [BIOLOGY]

Transensor implantation, sham implantation, no implantation and lighting effects on rat body composition, noting fat and water content
12 p2020 A69-26557

Body composition of USAF flying personnel, evaluating obesity by using radioactive potassium /K-40/ method
14 p2409 A69-29295

Centrifugation effects on body composition and growth of mice
17 p2910 A69-33746

BODY FLUIDS

NT BLOOD

NT CEREBROSPINAL FLUID

NT EOSINOPHILS

NT ERYTHROCYTES

NT LEUKOCYTES

NT LYMPH

NT LYMPHOCYTES

NT SWEAT

NT URINE

Changes in organism during sudden decompression, analyzing pressure equalization, dissolved gases transformation and body fluids vaporization
01 p0020 A69-10753

Renal excretion response to blood fluid volume shift resulting from altered orientation within gravity or from absence of gravity
06 p0873 A69-17015

Heart rate and bodily fluid changes in aestivating desert anurans, discussing weight loss and metabolism reduction
11 p1827 A69-24923

Respiratory effects of body temperature changes separation from blood osmolarity changes in dehydrated man
23 p4097 A69-42094

BODY KINEMATICS

Hypokinesia and transverse accelerations combined effect on human cardiovascular system and regional blood circulation
02 p0197 A69-11495

Human nervous system and vestibular and auditory analyzers functional changes under combined hypokinesia and radial accelerations effects
02 p0197 A69-11496

Physiological, cytochemical and histological effects on muscular activity, nervous system, adrenal and thyroid glands and liver of mice during 30 day hypokinesia
02 p0198 A69-11502

Hypokinesia and acceleration effects on human organism immunity and resistance to inflammatory diseases in 62 day test
02 p0198 A69-11513

Data acquisition program for Apollo crew motion disturbances experiment consisting of ground simulations and orbital experiment establishing mathematical model of human body
02 p0201 A69-11759

Changes in blood circulation, external respiration and gas exchange rates in humans during prolonged hypodynamia
03 p0377 A69-14204

Human motor activity under hypodynamia and increased carbon dioxide, discussing positive effects of prescribed physical exercises
03 p0377 A69-14205

Vectorometric EKG analysis of cardiac activity during hypokinesia with and without exercise and medication
05 p0710 A69-16519

Collection of papers on hypodynamia and hypogravics, physiology of inactivity and weightlessness
06 p0872 A69-17010

Subjects sensory reactions to weightlessness during parabolic flight, studying coordination of writing, eating and drinking motions
07 p1060 A69-18575

Arbitrary human motions coordination in reorganization phases determined during weightlessness for cyclographic analysis of adjustment time
07 p1065 A69-18979

Damping flywheel to stabilize permanent rotation of weightless solid body moving by inertia, obtaining differential equations of motion
07 p1183 A69-19678

Human organism reaction to prolonged limitation of muscular activity during weightlessness simulated by bed rest, noting hypokinetic component of weightlessness
08 p1262 A69-19837

Hypokinesia muscular activity deficit in males confined to bed rest compensated for by physical exercise, noting orthostatic resistance, acceleration endurance, immunity, etc
08 p1263 A69-19932

Dogs orthostatic tolerance and resistance to transverse acceleration after 14-day hypodynamia, studying tachycardia and arterial pressure
10 p1645 A69-23499

Hypokinesia effects on human neurology on extended space flights simulated by 72-day bed rest
10 p1646 A69-23506

Space flight hypokinesia simulation experiments to study oxygen balance in man
10 p1646 A69-23507

Hypokinesia effect on dynamics of metabolic processes in athletes muscular system by comparison of diuresis, creatinine excretion and cutaneous fat layer indices
10 p1646 A69-23582

Thin deformable body motion in disturbed potential flow of ideal incompressible fluid
11 p1876 A69-25488

Motion of heavy body with gyroscope, using coordinate system to reduce problem to linear second order differential equation
11 p1920 A69-25746

Equations of motion of body with fixed point, deriving solutions representable as segments of trigonometric series in variable related to time differentially
11 p1920 A69-25748

Solid body motions containing cavity filled with viscous fluid under influence of gravity, formulating motion equations for fluid and body
12 p2061 A69-25884

Hypokinesia effects on transversostriated muscle fibers of mice, noting changes in myofibrillar apparatus, mitochondria and sarcoplasm
13 p2212 A69-28616

Calcium isotopes tracer migration in caged rats in metabolism study
13 p2212 A69-28618

Three dimensional thermal laminar boundary layer around body moving with constant acceleration in incompressible fluid, considering wall temperature and Prandtl number
13 p2380 A69-28631

Quasi-steady state supersonic gas flow past two closely spaced coaxial separating bodies at different velocities, showing dependence on separation rates
14 p2391 A69-29617

Soviet book on partially liquid filled solid body dynamics from viewpoint of space and aircraft applications
14 p2530 A69-29815

Integrable cases of equations of motion of solid body around fixed point located in potential field of elastic supports
15 p2653 A69-31194

Motion coordination capacity of persons subjected to 40 days bed rest studied by dynamographic technique, discussing nature of slackening
17 p2906 A69-32937

Stable motions determination of solid bodies with liquid filled cavities and satellites motions stability in central Newtonian force field
17 p3005 A69-33228

Dynamic model of bodies with microstructure and nondissipative energy motion, discussing action steadiness, invariance conditions and Galilean relativity
17 p3067 A69-34149

Fixed point reaction force in mobile system of solids coupled kinematically, examining zero dynamic components
18 p3172 A69-34590

Vectorometric EKG analysis of cardiac activity during hypokinesia with and without exercise and medication
18 p3096 A69-34738

Two body mechanical system operating within dynamics laws simulating backward and forward bending motions of falling cat
19 p3259 A69-36832

Arbitrary human motions coordination in reorganization phases determined during weightlessness for cyclographic analysis of adjustment time
20 p3479 A69-38227

Real time servo driven simulator of human body in zero-g activity used to study self induced rotation and astronaut mobility under thruster forces
21 p3664 A69-39034

Rodrigues formula derivation procedure and summation formula derivation for finite rotations of solid body, noting simplifications from kinematic considerations
21 p3772 A69-39183

Time-similar and isotropic geodetic curves simulating paths of test bodies in Riemann space corresponding to gravitational field
21 p3772 A69-39621

Motion of body with cavity completely filled with viscous fluid about center of mass in potential mass-force field, applying small parameter method
22 p3980 A69-40109

Boundary layer development on body accelerating in viscous incompressible fluid, using straight lines approximation and asymptotic expansions
22 p3929 A69-40110

Saint Venant principle of elastic equivalence of kinematically equivalent displacement systems at small surface area of elastic body
22 p4048 A69-41276

Sphere set in motion at constant velocity by impulsive force submerged in incompressible fluid in half space
24 p4298 A69-42585

Inertial motions, equipotential surfaces and Coriolis forces on earth ellipsoid, discussing pendulum-like oscillations
24 p4346 A69-43156

BODY MEASUREMENT [BIOLOGY]

NT ELECTROPLETHYSMOGRAPHY

Nomogram for estimating body fat and specific gravity from height and weight, considering two component model of body composition and lean body weight
07 p1067 A69-19428

Acceleration injury noting water immersion effect on cat lung due to intense body vibration, suggesting restraint as practical solution
17 p2913 A69-33009

Centrifugation effects on body composition and growth of mice
17 p2910 A69-33746

Physical exercise effect on adolescent males, comparing oxygen uptake, heart volume and height in training and nontraining groups
23 p4077 A69-41312

BODY SIZE [BIOLOGY]

Nomogram for estimating body fat and specific gravity from height and weight, considering two component model of body composition and lean body weight
07 p1067 A69-19428

White mice gastrocnemius muscle wet mass, dry mass and noncollagen-nitrogen /NCN/ content, noting /NCN/ content dependence on body mass
23 p4080 A69-41406

BODY SWAY TEST

Human perception in space as function of nervous relationships involving optic, kinesthetic, vestibular and other analysors
08 p1263 A69-19938

BODY TEMPERATURE

Critical body temperature for intracranial self stimulation in white rats
03 p0375 A69-13897

Conduction equations for conduction cooling of human body solved by finite difference method
06 p0880 A69-17088

Oxygen intake and body temperature of basal and sleeping Andean natives at high altitude
06 p0874 A69-17835

Human body cold tolerance and relation to BMR seasonal variation
06 p0876 A69-18024

Thermoregulatory reactions of human body to sharp increase of ambient radiant temperature [AGARDOGRAPH-111]
08 p1264 A69-20670

Skin and subcutaneous temperature during exposure to intense thermal radiation, discussing estimation of subcutaneous temperature from skin temperature data [AGARDOGRAPH-111]
08 p1264 A69-20671

Human body heat loss control during water immersion, discussing insulative garments and technologies of energy conversion systems [AGARDOGRAPH-111]
08 p1267 A69-20681

Learned behavior performance failure in hypothermia as temperature dependent phenomenon using rat, guinea pig, chinchilla, mouse, gerbil and hamster
10 p1643 A69-23124

Human body temperature regulating factors in low temperature environment, studying metabolism, lung ventilation and onset of shuddering
10 p1648 A69-23298

Hamsters responses to helium-oxygen and nitrogen-oxygen at ambient temperatures, comparing respiration rates, weights and body temperatures
10 p1646 A69-23564

Altitude effects on body chilling rate in rats noting hypoxia role in inducing hypothermia
13 p2210 A69-28532

Combined hypoxic hypoxia and high ambient temperature found relieving strain on humans by increasing heat release by evaporation
13 p2212 A69-28628

Light effects on circadian rhythms in monkeys, describing changes in deep body temperature and locomotor activity phase relationships
15 p2556 A69-31336

Diurnal pressure cycles found as zeitgeber to entrain body temperature endogenous circadian rhythm in pocket mice under constant environmental temperature and light
16 p2745 A69-32447

Oxygen consumption and rectal temperature in male mice confined in nitrogen and helium diluted hyperoxic atmosphere at specific temperature and humidity ranges
17 p2906 A69-32932

Vestibular reactions in rats under hypothermal conditions by measuring postrotatory nystagmus beats number and duration, respiration rates and rectal temperature
17 p2906 A69-32934

Desynchronization and resynchronization of human circadian rhythms of activity, body temperature and urine excretion during isolation in underground bunker in various conditions
21 p3660 A69-39173

Circadian variations in human temperature regulation, measuring peripheral and rectal temperatures and peripheral heat and arterial blood flows in clothed resting males
22 p3872 A69-40201

Thermoregulatory responses to cooling in spinal man, discussing deep temperature sensitive structures and relationship between skin and central regulatory structures
22 p3873 A69-40209

Rat survival rate after prolonged gradually decreased body temperature without motion restraint or kept in fixed position
22 p3877 A69-40278

Hyperventilation induced hemolysis in dogs measured as function of exposure time, body temperature and blood pH
22 p3887 A69-41192

Severe heat stress effects on respiratory frequency, rectal temperature, blood gases and pH of conscious dog
23 p4081 A69-41432

Human thermal regulatory mechanism using analog simulation compared with experimental results of resting subjects responses to climatic chamber
23 p4111 A69-42079

Respiratory effects of body temperature changes separation from blood osmolality changes in dehydrated man
23 p4097 A69-42094

Spinal cord temperature influence on stretch response of tonic and phasic alpha-motoneurons by filament recordings from ventral roots in anesthetized cats
23 p4098 A69-42099

Calorimetry-thermometry discrepancy during prolonged exercise in hot dry environment, measuring rectal temperature with increasing exposure time
23 p4098 A69-42104

Circadian rhythm phase relationships between photoperiodism and heart rate, locomotor activity and deep body temperature/DBT/ in unrestrained monkeys
24 p4260 A69-42706

Barometric pressure affecting convective heat transfer from human body in air, deriving empirical formula as function of air density, speed and temperature
24 p4267 A69-43384

BODY TEMPERATURE REGULATION
U THERMOREGULATION

BODY VOLUME [BIOLOGY]

Leg volume changes in response to lower body negative pressure due to blood redistribution
17 p2908 A69-33171

Volume prediction of human body exposed to vacuum based on animal skin elasticity and anatomical features
19 p3258 A69-36456

BODY WEIGHT

Vertical vibration stimulation of growth of onion bulbs and mice body weights
01 p0014 A69-10584

Nomogram for estimating body fat and specific gravity from height and weight, considering two component model of body composition and lean body weight
07 p1067 A69-19428

Hypokinesia effects on rats noting body and organ weights, liver glycogen and N content and tissue proteolysis of skeletal muscles
08 p1262 A69-19928

Microwave radiation effects on body weight and peripheral blood hemograms of mice, discussing maximum safe exposure related to generator output
08 p1266 A69-20678

Hamsters responses to helium-oxygen and nitrogen-oxygen at ambient temperatures, comparing respiration rates, weights and body temperatures
10 p1646 A69-23564

Vertical vibration stimulation of growth of onion bulbs and mice body weights
15 p2555 A69-30754

Caucasian and Bantu males oxygen consumption at different work rates, gross body weight accounted for 70 percent of differences between individuals
21 p3655 A69-38911

Effects of oxygen saturation variations of blood on rates of weight gain in isolated perfused canine lung, noting pulmonary edemogenesis
22 p3887 A69-41189

Astronaut weight loss during space flight related to mission duration, noting dehydration and catabolism roles
23 p4100 A69-41303

White mice gastrocnemius muscle wet mass, dry mass and noncollagen-nitrogen/NCN/ content, noting /NCN/ content dependence on body mass
23 p4080 A69-41406

Body weight and organ sizes in hibernating cold and warmth adapted golden hamsters, discussing lungs, heart, kidney, pancreas and liver weight increases
23 p4084 A69-41462

Change in weight, plasma volume, urine flow and hematocrit in man before and after immersion up to chin in thermally neutral bath
23 p4096 A69-42087

Oxygen consumption, ventilation and cardiac frequency relationship to body weight during submaximal exercise in normal human beings
23 p4099 A69-42169

BODY-WING AND TAIL CONFIGURATIONS

Wing-body combinations analysis and design at supersonic and subsonic speeds by aerodynamic influence coefficients method [AIAA PAPER 68-55]
01 p0006 A69-11016

Unsteady aerodynamic forces on coplanar lifting surfaces in subsonic flow induced by wing/ horizontal tail interference
04 p0543 A69-14819

Tandem airfoils wing-tail interaction flutter analysis, using three dimensional vortex lattice aerodynamic theory [AIAA PAPER 69-57]
06 p1028 A69-18105

Critical flutter behavior of variable geometry aircraft with wing of 70 degree leading edge sweep, noting wing-tail interference
11 p1991 A69-25517

High order conical motions past cruciform wing-body and tail-body systems, reducing problem to flow past cruciform wing
15 p2548 A69-31023

Supersonic inviscid flow past wing-body configuration, determining pressure distribution
20 p3458 A69-37099

Modified tailed delta configuration selection for U.S. SST, discussing power plant installation choice [RAES PAPER 17]
22 p3863 A69-40496

BOEING AIRCRAFT

NT B- 52 AIRCRAFT

NT CH- 46 HELICOPTER

NT CH- 47 HELICOPTER

NT VZ- 2 AIRCRAFT

Boeing SST designs, discussing performance, flying qualities and operational characteristics of configurations
06 p0868 A69-17830

Concorde and Boeing supersonic transport overland sonic booms, discussing social, political and legal reactions
06 p0868 A69-17899

Helicopter design, discussing blade deicers, landing gear, vibration absorbers, cargo capacity, etc
13 p2202 A69-27836

BOEING MILITARY AIRCRAFT
U MILITARY AIRCRAFT

BOEING 2707 AIRCRAFT

Boeing 2707-300 Mach 2.7 supersonic transport, discussing flight controls, hydraulic system, environmental controls, operational characteristics, flight deck and instrumentation
07 p1052 A69-18271

BOEING 707 AIRCRAFT

All-weather landing flight director systems and fault warning display simulator studies of Boeing 707-720B aircraft in Category 3-C environment
01 p0010 A69-10455

Air Transport Total In-Flight Simulator-707 /AT/TIFS-707/ concept for pilot training, stressing airframe and major flight systems [SAWE PAPER 747]
18 p3118 A69-34884

BOEING 747 AIRCRAFT

Boeing 747 characteristics for passenger and cargo service noting economic gain, operational performance, control cabin, engine, etc [AIAA PAPER 67-397]
01 p0010 A69-10636

Boeing 747 performance, propulsion, structural and circuit characteristics, mass production and airport passenger installations
01 p0011 A69-11067

Forming and processing facility for producing one million titanium alloy parts per month for Boeing 747 aircraft
09 p1504 A69-22063

Giant landing gear steel parts fabrication for Boeing 747 aircraft, discussing material and processing problems including Cr and Cd-Ti coatings application
09 p1434 A69-22064

High recovery inlet design for Boeing 747 high bypass ratio fan engine, considering throat Mach number, lip losses and auxiliary passage losses [ASME PAPER 69-GT-41]
09 p1570 A69-22482

Cost-profit sharing agreement with aerospace manufacturing companies involved in Boeing 747 construction, detailing final assembly building
09 p1514 A69-22713

Boeing 747 aircraft, discussing weight and cost reduction, flap design, structural philosophy, powerplants, fuel system, flying controls, power systems, etc
09 p1435 A69-22714

Fueling procedures for Boeing 747 aircraft, discussing design and operation of large capacity fuel trucks
10 p1674 A69-23631

Fueling procedures for Boeing 747 aircraft, discussing design of high rate mobile fuel dispensers
10 p1674 A69-23633

Boeing 747 operational and economic considerations including capacity, airport constraints, noise factors, landing gear, compatibility, etc
13 p2201 A69-27340

Weight and cost control program for Boeing 747 aircraft through combined value and weight engineering methods
13 p2383 A69-28096

Boeing 747 problems including noise and automatic landings in CAT-II conditions
16 p2734 A69-31631

Large subsonic transport aircraft effect on economics of air operations with emphasis on airport facilities for Boeing 747
17 p3077 A69-34205

Aircraft structural weight optimization based on design consideration of grouped related elements, noting application to Boeing 747 trailing edge flap drive [SAWE PAPER 757]
18 p3220 A69-34881

Boeing 747 design and development, discussing aircraft characteristics, performance, inertial navigation system, production costs, etc [SAWE PAPER 746]
18 p3091 A69-34907

Boeing 747 design, fitting to operation, airline planning for flight training, airport facilities, ground equipment, service functions, etc [RAES PAPER 12]
22 p3864 A69-40621

B-747 safety assurance program, discussing organization, management, hazard sources, accident statistics, night visual approach and maintainability
22 p3867 A69-41135

Boeing 747 safety engineering program, discussing organization, design review, system safety, systems design-analysis and tests
22 p4054 A69-41136

Boeing 747 exhaust reverser design and control, discussing stopping distance, cascades, materials, etc [SAE PAPER 690409]
23 p4200 A69-41637

JT9D engine fuel and vane control systems for Boeing 747, noting computing system positioning of throttle valve for fuel flow control [SAE PAPER 690405]
23 p4201 A69-41658

BOGOLIUBOV THEORY

Bogoliubov transformations effect on quasi-free translationally invariant states of fermion fields, using Clifford algebra based on Hilbert space
03 p0455 A69-13364

Finite formulation of field theory applied to quantum electrodynamics, assuming Bogoliubov causality and TCP invariance of S operator
07 p1181 A69-18957

Parametric variations of nonlinear system moving in medium with nonlinear drag, using Bogoliubov-Krylov asymptotic method
18 p3171 A69-34564

Bogoliubov averaging method of perturbation in wave mechanics for radiation and matter interaction, considering monochromatic and broad spectral incident wave for resonance study
18 p3175 A69-35483

Bogoliubov method of partial averaging for nonlinear integral equations, noting application to automatic gain control theory
23 p4181 A69-41731

BOHR MAGNETON

Penfield-Haus solution to magnetodynamic effect problem as inertial effect of orbital angular momentum, deriving Bohr magneton formula from Einstein equivalence principle
11 p1919 A69-25098

BOILERS

Fatigue strength tests of steels simulating boiler installation operating conditions, reproducing corrosion characteristics of water
19 p3347 A69-36741

Freon boiler designed for Rankine cycle heater fired on hydrocarbons with over 2000 F flame front temperature, considering radiant/convective heat transfer
23 p4068 A69-42239

BOILING

NT FILM BOILING
NT LEIDENFROST PHENOMENON
NT NUCLEATE BOILING

Heat transfer procedure and equipment during boiling under short term weightlessness
01 p0177 A69-11313

Pressure induced variations in stability constant characterizing bubble structure in two phase boundary layer of several liquids during boiling with natural convection
03 p0534 A69-14149

Experimental apparatus for measuring heat transfer coefficients into boiling K in tubes, investigating vapor-liquid mixtures hydrodynamic and electrical properties
03 p0534 A69-14150

Safety problems associated with transient boiling of liquid metals in fast nuclear reactors, emphasizing behavioral differences between liquid metals and water
08 p1420 A69-20101

Heat pipe boil-off control system for reducing cryogenic boil-off during long term space storage
12 p2191 A69-26793

Oxygen boiling point studied via calibration of capsule type platinum resistance thermometers
14 p2540 A69-29888

Graph analytical method for calculating heat transfer in diathermic exchangers during boiling together with critical thermal loads
24 p4408 A69-43080

BOLIDES

Bolide fireball radiation maximum efficiency from observed spectra, using monochromatic radiation efficiency data for rarefied atoms and ions in meteor comas
03 p0512 A69-13692

Vilna meteorite bolide observation with all-sky camera noting seismic and analytic records
13 p2334 A69-27189

Eyewitness data concerning bright bolide observed over Dzhaus/Uzbek SSR, tabulating estimations for occurrence time, light duration, color, sound and trajectory azimuths
18 p3196 A69-34536

Spectral and orbital evidence of connection among fireballs with orbit inclination, comets and carbonaceous meteorites
23 p4208 A69-41285

BOLKOW AIRCRAFT
U BO-105 HELICOPTER

BOLKOW BO-105 HELICOPTER
U BO-105 HELICOPTER

BOLOGRAMS
U BOLOMETERS

BOLOMETERS

DC biased microwave bolometer/barretter/detector, describing small signal dynamic equivalent circuit for output voltage
01 p0044 A69-10626

Very far IR techniques applications in molecular and solid state spectroscopy and relationship with impurity band conduction
02 p0296 A69-11791

High responsivity high speed performance Ge bolometer detector for very far IR region, discussing performance theory and noise equivalent power
08 p1313 A69-20132

Bismuth bolometer as sensor recording IR radiation for thermal radiation fluctuations in atmosphere caused by temperature inhomogeneities
09 p1490 A69-21868

Bolometric luminosity-red shift relations of Friedmann dust universes corrected for inhomogeneities, using locally inhomogeneous Swiss cheese models
09 p1605 A69-22411

Output impedance measurements for accurate calibration in UHF region, using mobile discontinuity and bolometer for linear or nonlinear systems
14 p2422 A69-29583

Broadband thermal radiometer containing InSb electronic bolometer under magnetic field, discussing astronomical applications
17 p2969 A69-32823

Zenith atmospheric attenuation in 183-325 GHz region measured by wideband Ge bolometer detector and spectral convolution technique
23 p4115 A69-41586

Thin film bolometer for monitoring RF radiation of arbitrary polarization and direction of propagation
24 p4311 A69-42572

BOLTS

Bolt materials selection criteria in design of high strength lightweight joints, showing fatigue curves and temperature effects
13 p2268 A69-27758

Large diameter bolts in aircraft structures resisting hydrogen embrittlement and stress corrosion, noting fatigue properties
22 p3957 A69-40827

Strain gage and mechanical types of load-determining bolts selected on basis of application requirements and installation costs
22 p3957 A69-40829

External load distribution in bracket between bolts and joint, verifying Reshetov mounting bolt formulas
23 p4168 A69-41417

Traction stresses distribution over contact surfaces using photoelastic frozen stress model
23 p4235 A69-42461

BOLTZMANN DISTRIBUTION

Electron distribution function for homogeneous weakly ionized gas in presence of alternating electric field, discussing solution of Boltzmann equations
05 p0797 A69-16604

Nonisotropic relaxation of Boltzmann gas in homogeneous space, expressing collision integral moments in terms of distribution function moments for any molecule
06 p0910 A69-17347

Time derivatives of Boltzmann H function with respect to dilute gas
07 p1121 A69-19407

Inertia limited flow transition to mobility limited flow in gas diodes by taking velocity moments of Boltzmann equation for electron velocity distribution function
09 p1462 A69-21325

Boltzmann H function for moderately dense gas of identical particles with discrete velocity distribution in cases of nonisotropic binary and ternary collisions
10 p1725 A69-23790

Shock wave structure in single component monatomic gas by expanding Boltzmann equation distribution function in terms of Hermite polynomial
18 p3124 A69-35170

BOLTZMANN TRANSPORT EQUATION

Chapman-Enskog method applied to Boltzmann equations for transport coefficients for low density polyatomic gases
01 p0123 A69-10388

Continuum eigenfunction problem for hard sphere gas in spherically symmetric state, applying theory of singular integral equations
01 p0061 A69-10813

Partial differential equation for distribution function in transport of charged particles in earth magnetosphere
01 p0147 A69-11320

Transport equation for electromagnetic waves multiple scattering by turbulent plasma
03 p0478 A69-13959

Second approximation to Boltzmann equation solved for rigid sphere gas by reducing integral equation to differential equation
04 p0633 A69-15434

Boltzmann equation for weakly ionized gas electron component, solved by transformation to integral equation, applied to Lorentz gas in alternating electric field
05 p0795 A69-15619

Kinetic model construction of maximum number of Boltzmann collision integral properties
05 p0797 A69-16679

Monte Carlo solution of linearized Boltzmann equation in rarefied gas dynamics, noting Knudsen layer and Couette flow applications
06 p0910 A69-17345

Kinetic theory of sharp leading edge parallel to supersonic flow using Boltzmann equation, determining flow field
06 p0861 A69-17637

Width of strong shock wave front and transition layers estimated, using Boltzmann kinetic equation and H-theorem
07 p1118 A69-18702

Green function applied to isotropic scattering of radiation in three dimensional homogeneous space
07 p1241 A69-18808

Variational solution of linearized molecular chemical-kinetic Boltzmann equation, discussing perturbation of Maxwell distribution, nonequilibrium correction to reaction rate and activation energy
07 p1185 A69-19301

Gas kinetics application to various flow problems by solving Boltzmann equation for monoatomic single component gas
08 p1351 A69-20708

Kinetic equations for polyatomic gases obtained by extending 13 moment approximation to solve inelastic Boltzmann equation, resulting in 17 moment approximation
08 p1357 A69-20784

Time harmonic, spherical harmonic and power series expansion of Boltzmann equation
08 p1353 A69-20793

HF breakdown of air using Boltzmann equation to determine net ionization frequency relation with electric field strength
08 p1357 A69-20810

Kinetic coefficients of carrier motion in semiconductor obtained by Boltzmann equation, considering impacts between carriers
09 p1554 A69-21468

Normal solutions of linearized Boltzmann equation for initial and boundary conditions in hydrodynamics solved by approximation 09 p1480 A69-21667

Enskog method for Boltzmann equation, analyzing asymptotic nature of integral kinetic equation for molecular mean free paths and Laplace probabilities 09 p1481 A69-21889

Boltzmann equation with BGK model as governing equation for sharp leading edge problem in supersonic flow 11 p1817 A69-24288

Boltzmann equation for system of equations governing evolution of gas of identical particles with discrete velocity distribution, applying Chapman-Enskog method 11 p1921 A69-24325

Binary gas flow past curved body for stationary problem studied by solving Boltzmann equations in form of matched asymptotic expansions [ONERA-TP-694] 11 p1867 A69-24753

Kinetic theory for examining transition regime of rarefied gas dynamics, discussing Boltzmann equations and models with related boundary value problems 11 p1870 A69-25005

Angular distribution of electrons leaving plasma at electrode boundary, using kinetic Boltzmann equation with scattering function and specular reflection 11 p1933 A69-25546

Wave damping in plasma, developing Boltzmann analysis of electron mode dispersion relations involving momentum transfer and relaxations of electron-ion temperature and anisotropy 13 p2305 A69-27377

Transport equation numerical solution for unsteady radiation field by straight lines method, allowing for scattering indicatrix forms with passage of time 13 p2350 A69-27858

Collisions effect on wave propagation in homogeneous plasma, calculating permittivity tensor and electron equilibrium current using Boltzmann kinetic equation 13 p2311 A69-28104

Gasdynamic and Boltzmann equations relations in rarefied gas kinetics, applying physical and mathematical boundedness concept to setting boundary conditions for moment equations 13 p2250 A69-28320

Gain and loss collision integrals in Boltzmann equation for rigid sphere gas evaluated for distribution expressed as linear combination of Maxwellians 14 p2431 A69-29578

Minimum error criteria for shock wave structure determined by applying Mott-Smith distribution to Boltzmann equations for rigid sphere gas 14 p2431 A69-29579

Particle drift velocity distribution of fully ionized plasma in magnetic field calculated by integration of Boltzmann equation 15 p2659 A69-30707

Kinetic coefficients of carrier motion in semiconductor obtained by Boltzmann equation, considering impacts between carriers 15 p2669 A69-30713

Book on mathematical methods in kinetic theory covering boundary value problems associated with Boltzmann equation, model equations, rarefied gas dynamics, etc 16 p2811 A69-31721

Linearized Boltzmann equation in kinetic theory for weakly ionized plasma electrons under alternating electric and circularly polarized magnetic field, noting higher harmonics generation 16 p2820 A69-31752

Boltzmann kinetic equation describing rarefied neutral or weakly ionized gas state evolution, showing solution existence, uniqueness and successive approximation convergence 16 p2814 A69-31958

Fixed mass of monatomic gas unsteady spherically symmetric expansion into vacuum by asymptotic Boltzmann equation expansion 16 p2772 A69-32168

Nonlinear theoretical derivation of creep equations for three dimensional processes in polymers, based on Boltzmann-Volterra creep heredity concept using stress-strain summation 16 p2803 A69-32290

Boltzmann equation for Lorentzian plasma in elliptic magnetic field solved by expanding distribution function in Legendre polynomials 17 p3009 A69-32827

Supersonic leading edge problem using nonlinear Boltzmann equation with ellipsoidal model, calculating molecular distribution functions for flow field [AIAA PAPER 69-652] 17 p2892 A69-33464

Rarefied gas flow between parallel plates using linearized Boltzmann transport equation, deriving integral equation for mass flow velocity 19 p3296 A69-35621

Spatially homogeneous Boltzmann equation containing initial distribution functions expandable into Hermitean polynomials analyzed via ordinary differential equations 19 p3373 A69-36202

Electron momentum transfer cross sections by numerically solving electron energy distribution function from Boltzmann equation in Lorentz approximation 21 p3773 A69-38396

Thermal conductivity coefficient of gas mixtures at low temperatures obtained using quantum diffusion model and Chapman-Enskog method for Boltzmann equation 21 p3848 A69-38638

Nonlinear transport equations solution methodology covering transformations, invariants, boundary value problems, numerical methods, etc 21 p3697 A69-39729

Boltzmann equation analysis used to study near surface electron temperature for weakly ionized plasmas, showing nonequilibrium absorption layer governing electron temperature profile 22 p3989 A69-40528

Time dependent diffusion of light particles of Lorentz fluid approximated by Boltzmann equation leading to microscopic telegrapher equation 22 p3984 A69-40530

Molecular transport equations of dilute gases, considering relaxation time spectrum, obtaining kinetic equations and correlation function expressions for transport coefficients 23 p4193 A69-41512

Hydrodynamic equations derived from Boltzmann equation, obtaining molecular expressions for transport coefficients 23 p4151 A69-41513

Fokker-Planck plasma collision equation derived from Boltzmann equation, Markov process and Liouville equation 23 p4195 A69-41516

Book on flow equations for composite gases derived from Boltzmann equation, BGK approximation application, etc 24 p4299 A69-42766

Monte Carlo method applied to heat transfer in rarefied gas flow between parallel plates involving temperature jump in Knudsen layer 24 p4246 A69-43490

Rarefied gas one dimensional transverse motions consistent with Boltzmann kinetic equation, solving integrodifferential equations for shock wave structure 24 p4351 A69-43491

BOLTZMANN-VLASOV EQUATION

Longitudinal excitations, discussing plasma equilibrium distributions 08 p1362 A69-20286

Generalized Riemann function obtained as solution of transformed Boltzmann-Vlasov equation, discussing one dimensional and multidimensional cases 10 p1724 A69-22908

Perturbation theory for nonlinear oscillations in ionized plasma, treating electron-neutral collisions effect by Boltzmann-Vlasov equation relaxation term, noting distribution function 16 p2820 A69-31702

Boltzmann equation for electron distribution function of Lorentzian plasma traversed by transverse traveling wave, showing existence and uniqueness of solution 24 p4354 A69-42675

BOLZA PROBLEMS

Bolza problem of calculus of variations extended to trajectory optimization problems with several subarcs 17 p3026 A69-32837

BOMBER AIRCRAFT

NT A-6 AIRCRAFT
NT B-52 AIRCRAFT
NT B-70 AIRCRAFT
NT BUCCANEER AIRCRAFT

U.S.S.R. manned bomber role in air strategy, discussing mutual effects of U.S.-U.S.S.R. military posture developments and ICBM 14 p2392 A69-29431

BOMBS [PRESSURE GAGES]

U PRESSURE GAGES

BOMBS [SAMPLERS]

U SAMPLERS

BONDING

NT CERAMIC BONDING
NT EXPLOSIVE WELDING
NT METAL BONDING

NT METAL-METAL BONDING

NT RESIN BONDING

Book on adhesive bonding techniques covering chemical types, mechanical and handling characteristics, application and mixing, joint design, non-destructive testing, documentation tooling, etc 01 p0084 A69-10130

Stress concentrations around elliptical perforations in shrunk plates with bonded boundaries based on photoelastic models 02 p0345 A69-12391

Microelectronic components joining technique by compliant bonding, utilizing deformable medium between tool and beam leads to eliminate intricate tool shapes and alignments 02 p0254 A69-12473

Fokker bond tester and structural details of different types of sandwich structure, giving attention to adhesive bonding of panels, adhesive application, etc 03 p0434 A69-13791

Fiber geometry and partial debonding effects on bond stress distributions around single rigid fiber in infinite elastic plate subject to tensile stress 07 p1170 A69-18717

Bond shear effects on dynamic behavior of two layered cylindrical shell, identifying bond stiffness parameters [AIAA PAPER 68-354] 09 p1616 A69-21941

Controlled expansion of captive silicone rubber used to achieve pressure control for adhesive bonding interface 09 p1512 A69-22367

RF measurement techniques and interpretation of bonding impedance characteristics through VHF region 12 p2040 A69-26472

Mathematical model of yielding of adhesive bonds in form of viscous threads between elastic bodies, obtaining solution to two dimensional problem 18 p3215 A69-34569

Bonded solderless solar cell panel prototype withstanding high annealing temperature and thermal shock without electrical or mechanical degradation 19 p3251 A69-35688

Technical and metrological characteristics of short base strain gages and bonding to specimen, investigating sensitivity and creep 20 p3544 A69-37817

Wire, flip-chip and beam-lead bonding processes effects on hybrid microcircuits reliability 22 p3911 A69-39956

Anaerobic adhesives for aircraft bonding tested for mechanical properties, noting advantages over epoxy adhesives 24 p4338 A69-43464

BONE MARROW

Bone marrow distribution in dogs as basis for study of compensatory reactions of hemopoietic organs in response to radiation damage 08 p1262 A69-19835

Radioprotective effects of 5-azacytidine on bone marrow and blood leukocytes of X ray irradiated AKR mice 23 p4080 A69-41429

Radiation effects on population kinetics of granulocyte system forming bone marrow, discussing radiosensitivity and radiation-induced granulocytopenia 23 p4090 A69-41965

BONES

NT CARTILAGE
NT CEREBRUM
NT CRANIUM
NT MARROW
NT SCIATIC REGION
NT SKULL

Mineral dynamics during hibernation and disuse atrophy in connection with organismal homeostasis and chronic-term manned space flight, noting skeletal effect of immobility 21 p3660 A69-39175

Laser pulse effects on bones of rats, observing metabolic deviations in Ca 45 uptake 23 p4101 A69-41464

BOOLEAN ALGEBRA

Book on error detecting logic for digital computers covering error detection codes, logic circuits, checkers in data paths, etc 02 p0212 A69-11453

Logic networks of Boolean analogs analyzed by algebraic signal flow theory, introducing variational derivative for test detection in combinational and sequential networks [AAS PAPER 69-236] 24 p4288 A69-42811

BOOLEAN FUNCTIONS

Minimization algorithm for complex and switching functions using unique identifiers on Karnaugh map 16 p2764 A69-31710

BOOM

Equations of motion of rapidly rotating spacecraft, considering deformations of long elastic booms 18 p3207 A69-34582

BOOMS [EQUIPMENT]

Boom flutter effects on attitude dynamics of OV1-10 satellite, noting introduction of angular momentum by tip mass elliptical vibration 04 p0666 A69-15520

RAE satellite boom deployment to achieve gravity gradient capture 07 p1228 A69-18346

Wire screen deployable boom concept for avoiding thermal bending of slender tubes problem in application to gravity gradient stabilization and antennas of spacecraft 07 p1229 A69-18350

Thermally induced oscillatory instabilities in spacecraft booms, rederiving thermal torque equation to predict finite twist response 11 p1994 A69-25531

Erectable metal booms and meshes structural analysis, design and mounting and deployment techniques for space applications 19 p3433 A69-35544

Radio Astronomy Explorer satellite boom deployment method resulting in gravity gradient capture, emphasizing role of predeployment attitude and antenna Vee angle [AIAA PAPER 69-920] 21 p3821 A69-39350

Reaction boom attitude control systems for improving stabilization and maneuvering capability of earth pointing satellites, describing configurations [AIAA PAPER 69-834] 21 p3822 A69-39365

Spacecraft booms thermally induced vibration and flutter, considering damping and solar exposure effects 22 p4043 A69-40545

Motion stability of rapidly spinning satellite, discussing elastic booms effect 22 p4037 A69-41091

BOOST

U ACCELERATION [PHYSICS]

BOOSTER ROCKET ENGINES

NT M-1 ENGINE

Soviet rocketry origin, technology, launch vehicles, boosters and orbital assembly concept 01 p0162 A69-11066

Turquoise satellite booster, using stages of SSBS and MSBS ballistic missiles 02 p0334 A69-12232

Vacuum engineering problems during booster rocket engine ground tests, simulating flight environment [TR-781-O] 09 p1570 A69-22300

Supersonic ramjet propelled air breathing booster for speeds up to Mach 12, discussing flight mechanics, aerodynamics, propulsion, heating and air intake design 09 p1573 A69-22608

Deformations of thick walled cylinder with internal surface subjected to uniform pressure and externally connected to rigid chamber, calculating solid rocket booster charge 11 p1942 A69-25347

Aerodynamic heating of ELDO-A booster rocket, calculating flow field, heat transfer and conduction by method of characteristics and thermal models 11 p1966 A69-25433

Boosters and space vehicles including earth satellites, lunar probes and interplanetary spacecraft 13 p2356 A69-27914

Saturn 5 S-1C stage propulsion performance, using engine parameters from telemetry rather than accelerometer data, analyzed by iterative techniques and computer program [AIAA PAPER 69-733] 16 p2839 A69-32672

Large booster nozzle reuse, discussing design, refurbishment, performance, costs and test evaluation [AIAA PAPER 68-657] 19 p3394 A69-35944

Frequency domain and Liapunov instability criteria for attitude control system design of large booster, noting nonlinear feedback [AIAA PAPER 69-853] 21 p3687 A69-39381

Computerized optimization of flexible booster autopilot design, considering criteria for stability margins, closed loop roots and structural load relief [AIAA PAPER 69-875] 21 p3823 A69-39401

Booster digital guidance and control system, discussing communication device providing data

transfer between airborne digital computer and control device

[AIAA PAPER 69-988] 22 p3978 A69-40368

Booster engines for thrust augmentation of commercial transports, considering tradeoffs in takeoff distance, payload, range, safety and noise patterns [SAE PAPER 690381] 23 p4201 A69-41667

BOOSTER ROCKETS

Destructible low cost meteorological sounding rocket Dart for global observation of upper atmosphere [UN PAPER 68-95467] 01 p0161 A69-10510

Fracture mechanics concepts for cost effective booster pressure vessel design and fabrication from commercial steels using boiler plate techniques and minimal NDT quality control 21 p3837 A69-39028

BOOSTERS

Optimal control for minimum trajectory sensitivity of booster using algorithm and Ricatti equation 13 p2261 A69-27943

BORANES

NT CARBORANE

Vibration and absorption bands in IR spectra of diborene hydrazine stabilized by boiling in benzene 12 p2027 A69-26917

Borane carbonyl pyrolysis in low pressure tubular flow reactor measured by mass spectrometry, noting wall collision role in diborane bond dissociation 14 p2410 A69-29282

BOREL SETS

Integral operators on space of Borel measurable functions bounded considering weight function, giving condition for infinite complex matrices, mapping analytic sequence spaces 01 p0107 A69-11244

Spacecraft return probabilities with time constraints and redundant access, using Borel set concept for counting and summing coverage belts 21 p3819 A69-39017

BORES

U CAVITIES

BORESIGHTS

Closed loop and electronically calibrated radome measurement systems for beam deflection, boresight shift and transmission loss measurements 07 p1109 A69-19517

Boresight error in missile radome-antenna combination due to reflection and surface wave effects 07 p1111 A69-19536

Apollo LM and CSM tracking systems boresight shift reducible by decreasing modulation indices or scaling factor alpha 10 p1672 A69-23277

Electronic boresight shift in space-borne monopulse radar system, expressing antenna and signal parameters in terms of equivalent branch and channel asymmetries 14 p2411 A69-28895

Lockheed C-5 Galaxy aircraft avionics systems with Doppler inertial navigation equipment to operate with precision without ground based aids 18 p3104 A69-35465

BORIC ACIDS

Aged boric acid coated silica reaction vessels, showing reduced surface effects and high reproducibility in oxidation reactions 02 p0205 A69-12322

BORIDES

NT CHROMIUM BORIDES

NT TITANIUM BORIDES

Composites reinforcement with single crystal flakes of aluminum diboride 05 p0785 A69-16581

Lanthanum hexaboride single crystal field emitters for vacuum devices, describing construction and performance 09 p1468 A69-22601

Characteristic temperature, Young modulus and rms atomic displacement in metal borides of various porosities, using dynamic method based on ultrasonic oscillations measurement 12 p2115 A69-26615

Polycrystalline diborides fabrication technology, discussing additives, thermal, physical and mechanical properties, specific applications, etc 19 p3355 A69-35526

BORING MACHINES

Ruby laser boring and welding apparatus cooled by evaporated nitrogen gas, suitable for diamond boring 03 p0434 A69-13720

Cutting loads measured as function of cutting rate and cutting tool geometry during boring of Cr-Ni steel pipe blanks 21 p3731 A69-38878

Computer programming procedures in automatic control of hole boring processes for aircraft components 21 p3731 A69-38881

BORN APPROXIMATION

Ionized plasma radiation near plasma frequency, deriving formula for bremsstrahlung coefficient from Born approximation 02 p0286 A69-11589

Born approximation for calculating low temperature plasma transport properties from quantum mechanical scattering cross sections on Debye potential 02 p0291 A69-12486

First Born approximation cross sections for He excitation from ground state by proton impact calculated, using wave functions 06 p0960 A69-17027

Low pressure measurement by electron scattering using Born approximation 07 p1181 A69-19218

Polarization of Lyman alpha radiation in hydrogen rare gas collisions calculated in Born and distortion approximations including rotational coupling 08 p1355 A69-20207

Born-Mayer parameters simplifying computation of interatomic potential, tabulating numerical values for 104 mononuclear pairs of neutral ground state atoms 13 p2301 A69-27453

Plane wave scattering by semiinfinite turbulent dielectric slab, using Born approximation to develop asymptotic series for stochastic components of forward scattered field [OSA PAPER WH-16] 18 p3174 A69-35245

Atom-atom scattering potential from phase shifts, using WKB formula and Jeffreys-Born approximation 19 p3378 A69-36189

Impact parameter versions of two state and Born approximations to calculate single excitation cross sections of H atoms ground state collisions 22 p3987 A69-41006

Boron filaments reinforced epoxy aircraft landing gear structure prototype, discussing development, fabrication, and testing

09 p1508 A69-22340

Bonded Al-B metal matrix composite materials hot press fabrication and design, discussing temperature pressure time cycles and honeycomb sandwich structures

09 p1510 A69-22351

Fabrication, machining and contouring of boron-epoxy composite for sandwich type aircraft structure, noting F-5 supersonic fighter main landing gear strut door

12 p2103 A69-26826

Boron filament wound composite structures fabrication noting physical properties

14 p2455 A69-29413

Aluminum-boron metal matrix composite joining methods including electron beam, resistance spot, plasma arc and fusion welding [ASM PAPER W9-23.4]

14 p2455 A69-29449

Boron combustion for air augmented rocket applications, discussing single boron particle ignition and combustion characteristics

16 p2828 A69-31737

Combustion of pure crystalline boron single particles injected into hot oxidizing gases streams at atmospheric pressure

[AIAA PAPER 69-562]

16 p2880 A69-32741

Molded composites application to engine components, discussing turboprop reduction gear case design using polymer matrix boron composite [AIAA PAPER 69-466]

16 p2795 A69-32763

Austenitic alloy structure and stress rupture after boron addition

17 p2985 A69-32908

Macrostructural differences between filaments of B and SiC vapor deposited onto small diameter W wire, discussing radial cracks due to dilatation

18 p3160 A69-34266

Composite material applications in space vehicle structures, noting strength and stiffness of boron fibers in plastic or metal matrices

19 p3340 A69-35502

Lightly loaded truss structures fabricated from Be, Be-Al alloy and uniaxial B filament reinforced epoxy tubing for unmanned spacecraft applications

19 p3340 A69-35504

B-epoxy and B-Al composites compared for strength/weight and modulus/weight ratios, moisture absorption, corrosion resistance, projected costs, etc.

19 p3340 A69-35506

Forming, machining and joining characteristics of B-Al composite sheet metal material for space structures

19 p3318 A69-35507

Silicon carbide coated boron fibers in aluminum alloy matrix, discussing tensile and structural properties of braze bonded specimens

19 p3340 A69-35509

Mechanical properties and thermal aging of laminated specimens of collimated B monofilament reinforced composites preimpregnated with polyimide resin

19 p3354 A69-35514

Glass overlaid B filament laminates interleaved with C and silica fabrics, evaluating ablative properties in solid rocket motor tests

19 p3354 A69-35515

Boron epoxy strut prototype for support system of advanced nuclear flight stage with nonintegral cryogenic tankage configuration, achieving weight reduction

19 p3354 A69-35516

Silicon carbide coated boron fiber reinforced /Bor- sic/ Al composites tensile strength and elastic properties

19 p3344 A69-35926

Boron, Li and Cl contents in iron and stone meteorites by fluorometric, thermal-neutron activation and pyrohydrolytic separation methods, tabulating results

19 p3408 A69-36085

Boron thermal diffusion effects on plastic properties of pure Mo subjected to recrystallization

19 p3328 A69-36160

Titanium monocoque fuselage reinforced by composite boron filaments in polyimide resin matrix tested for SST applications, noting weight savings over all titanium structure [AIAA PAPER 69-763]

19 p3329 A69-36298

Boron fiber reinforced Al matrix composite material for high performance aircraft gas turbine engine compressor blading [AIAA PAPER 68-1037]

20 p3586 A69-37153

Boron fiber reinforced Al alloys spall failure and shock induced filament damage, using flyer plate technique

20 p3562 A69-37772

Composite materials application in aerospace industry, discussing boron and carbon filament properties, epoxy resins, etc

20 p3563 A69-37930

Diffusion bonding of Al and boron filament layers into continuous structural material, studying process variables including heat treatment and cross rolling effects

[AIME PAPER S69-6]

20 p3564 A69-38197

Authoradiographic technique for spatial distribution in solid of B at ppm concentration, using electron microscope

20 p3567 A69-38263

Al-B composite aircraft structure fabrication, discussing wingspan segment, resistance spot welding, hot forming of joggles, etc

[AIME PAPER S69-1]

21 p3732 A69-39471

B composite materials in helicopter development, including B and C filament production and B filament applications

22 p3971 A69-40899

Boron fiber reinforced composite materials in aircraft structures, comparing rigidity with glass fiber plastics and weight gains

23 p4179 A69-42155

Redesigned Al wing structure using B-epoxy composite applied to pressurized fuel carrying section, including material, fabrication and test data

24 p4323 A69-43418

Aircraft structure fabrication combining unidirectional strength and stiffness of B composite with metal, including test and weight/ cost data

24 p4323 A69-43419

Tensile strength improvement in Al-B composites by heat treatment to T6 condition and subsequent cold rolling

24 p4334 A69-43449

Boron epoxy composites evaluation for use in aircraft dynamic components, considering fatigue failure mechanism identification

24 p4337 A69-43450

Al-B composites fracture toughness obtained by comparing notched tensile data with unnotched specimens

24 p4335 A69-43451

BORON ALLOYS

Supersaturation of dissolved B in splat quenched Fe-Ni-B alloys, noting interstitial and substitutional B in martensitic and austenitic phases

10 p1707 A69-22987

CR-B binary system phase diagram including lattice parameters, temperature of peritectic decomposition and characteristics of alloys

15 p2641 A69-31185

Boron effect on sintered porous Ni friction at high sliding velocities and temperatures, analyzing oxide film destruction restraint by decreased Ni plasticity

15 p2641 A69-31187

Phase equilibria in ternary systems Nb-Fe-B and Nb-Co-B, determining structural types and lattice constants by using X ray and microstructural analysis

15 p2641 A69-31246

BORON CARBIDES

Boron carbide continuous filaments preparation and properties, discussing use in resin and metal composites [ECS PAPER 210]

05 p0783 A69-16236

Boron carbide body armor fabrication by hot pressing in graphite molds

08 p1320 A69-20411

Boron carbide filaments as reinforcements for metal structures, noting vapor deposition use of silica

09 p1529 A69-22070

Silicon and boron carbides wettability with liquid metals during contact reactions at various temperatures, discussing wetting mechanism

18 p3156 A69-35153

BORON CHLORIDES

Boron diffusion in silicon, using nitrogen carrier and boron trichloride diffusant at high temperature for determination of critical oxygen flow rate

02 p0297 A69-11994

Carbon dioxide laser radiation frequency controlled by varying boron trichloride pressure in cell inserted in resonator

08 p1323 A69-19804

BORON COMPOUNDS

NT BORANES

NT BORIC ACIDS

NT BORIDES

NT CARBORANE

NT CHROMIUM BORIDES

NT DIBORANE

NT TITANIUM BORIDES

Magnetic and semiconducting properties of samarium boride, noting effect of decreasing temperature

07 p1200 A69-19403

BORON FLUORIDES

Boron 10 absorption cross sections from counting ratios measurements of boron trifluoride proportional counter used to monitor neutron fluxes

17 p3008 A69-33753

Boron 11 nuclear quadrupole coupling constants in solid boron halides, finding fine structure on nuclear magnetic resonance in boron fluoride

20 p3483 A69-36935

BORON HYDRIDES

U BORANES

U CARBORANE

BORON ISOTOPES

Formation cross sections of Li, Be and B isotopes produced from oxygen 16 spallation via high energy protons related to astrophysics and cosmic ray physics

14 p2512 A69-28968

Boron 11 nuclear quadrupole coupling constants in solid boron halides, finding fine structure on nuclear magnetic resonance in boron fluoride

20 p3483 A69-36935

BORON NITRIDES

Hot pressed boron nitride properties and fabrication, noting low moisture absorptivity and aerospace applications

02 p0270 A69-11802

High temperature capacitor consisting of thin wafers of pyrolytic boron nitride noting fabrication, dissipation factor and capacitance

04 p0551 A69-15299

Boron nitride coated boron reinforced metal matrix composites, discussing continuous liquid infiltration, fiber-matrix reactions and heat treatment

13 p2283 A69-28671

Refractory materials based on BN and silicon nitride, studying effect of sintering conditions and chemical composition on mechanical properties

15 p2643 A69-31244

Boron nitride synthesis by gas phase reaction of boron chloride or diborane with ammonia, determining purity from equilibrium gas mixture components

17 p2992 A69-33432

Boron nitride and boron nitride composite under high temperatures in air and vacuum for various time periods, discussing thermal shock and oxidation resistance

19 p3359 A69-36208

BORON 10

Boron 10 absorption cross sections from counting ratios measurements of boron trifluoride proportional counter used to monitor neutron fluxes

17 p3008 A69-33753

BOROSILICATE GLASS

Composite materials consisting of brittle inorganic glass matrix with metallic or inorganic crystal microspheres, noting strength and elasticity

12 p2115 A69-26830

Thermal accommodation coefficient and critical supersaturation for nucleation of mercury vapor on pyrex glass

13 p2321 A69-28005

BOSE-EINSTEIN STATISTICS

U QUANTUM STATISTICS

BOSON FIELDS

Zero point energy, evolutionary cosmology, negative kinematic pressure and space curvature, assuming physical vacuum as ground state of Bose field

10 p1780 A69-23649

BOSONS

NT ALPHA PARTICLES

NT KAONS

NT LIGHT BEAMS

NT MESON RESONANCES

NT PHOTON BEAMS

NT PHOTONS

Superfluidity and superconductivity under cosmic conditions, discussing Bose-Einstein condensation, Fermi particles, boson systems, neutron stars, etc

16 p2853 A69-31595

He II excitation spectrum for interparticle potential using par Hamiltonian with repulsive core and attractive well

17 p3008 A69-33118

Proton-antiproton high energy elastic scattering by bosons exchange, introducing vertex functions for non-local Lagrangian

21 p3775 A69-39467

BOUGUER LAW

- Transfer equation and Bouguer-Lambert-Beer equation application to multiple light scattering in plane medium 14 p2487 A69-29663
- Atmospheric transmission determined in submillimeter solar radiation spectra using Bouguer law, identifying absorption lines in nocturnal and diurnal spectra 21 p3796 A69-38472

BOUNDARIES

- NT FLUID BOUNDARIES
- NT FREE BOUNDARIES
- NT GAS-SOLID INTERFACES
- NT GRAIN BOUNDARIES
- NT JET BOUNDARIES
- NT LIQUID-LIQUID INTERFACES
- NT LIQUID-SOLID INTERFACES
- NT LIQUID-VAPOR INTERFACES
- Moving and stationary interphase boundaries segregation during phase transformation, discussing embrittlement 03 p0450 A69-13883
- Magnetosphere boundary configuration calculated with allowance for geomagnetic dipole inclination to geographic axis and nondipole section of geomagnetic field 10 p1686 A69-23902
- Regional boundaries in control-parameter space constructed by computer algorithm, involving parameter vibration direction changes in parameter plane 13 p2225 A69-27967
- Turbojet engine open and closed loop boundary control systems performance during maximum penetration of prohibited operating area induced by HF external disturbances [AIAA PAPER 69-543] 16 p2841 A69-32681
- Elastoplastic boundaries of wave propagation of combined longitudinal and torsional stresses at tube end [ASME PAPER 69-APM-13] 18 p3213 A69-34389
- Exponential boundedness of system motion for Lure type forced systems, using quadratic Liapunov functions 18 p3164 A69-34674
- Maneuverability domains optimization with semilinear boundaries, noting application to orbital transfer 19 p3399 A69-35668

BOUNDARY LAYER COMBUSTION

- Self excited vibrating laminar diffusion flames, discussing coupling, jet spacing radial heat transfer and boundary layer interaction 16 p2876 A69-31711
- Flame acceleration data applied to unburnt gas boundary layer analysis, discussing velocity and temperature profiles, layer thickness variation and expansion phase backflow 19 p3450 A69-36359

BOUNDARY LAYER CONTROL

- NT POROUS BOUNDARY LAYER CONTROL
- Soviet monograph on laminar boundary layer in presence of suction covering incompressible flow through porous surface, drag reduction and optimal suction at high velocities 01 p0060 A69-10615
- Determining influence of blowing various gases into boundary layer on friction and heat and mass transfer when external flow velocity varies according to power law 02 p0234 A69-12581
- Blowing boundary layer control /BLC/ system designed for STOL seaplanes 05 p0695 A69-15546
- Acrodynamic technology applied to takeoff and landing, discussing STOL airplanes in descent and boundary layer control /BLC/ flap system 05 p0696 A69-15569
- Decreasing secondary flows in spatial boundary layer on porous plate by boundary layer control /BLC/ through suction or blowing, using Prandtl partial differential equations 06 p0909 A69-17185
- Radiative-convective heat transfer in gray gas plane layer blown into turbulent flow past permeable plate 07 p1242 A69-18991
- Tangential air jet for separation control of two dimensional incompressible flow along circular cylindrical wall 09 p1431 A69-22277
- Three dimensional laminar boundary layer of incompressible flow controlled by suction or injection, considering similarity flow solutions and role in satellite design 10 p1678 A69-22936

Monograph on optimal design of free-running drag turbines for boundary layer suction in aircraft, emphasizing gliders performance 12 p2011 A69-26117

- Laminar boundary layer control by combined blowing and suction, analyzing surface roughness influence concerned with underwater vehicle skin friction reduction [AIAA PAPER 69-387] 15 p2591 A69-30477
- Laminar boundary layer control on two dimensional body by combined blowing and suction in presence of roughness, noting skin friction reduction [AIAA PAPER 68-641] 17 p2957 A69-34015
- Optimal boundary layer control ensuring minimum heat transfer to porous plate from incompressible flow of hot gas of cooling system 21 p3849 A69-38846
- Integral relations method applied to air jet flow along cylinder with boundary layer control by suction or blowing 21 p3698 A69-39845
- STOL seaplane bottom pressure distribution from tests on scale model of PX-S seaplane, discussing boundary layer control effects 22 p3864 A69-40586

BOUNDARY LAYER FLOW

- NT REATTACHED FLOW
- NT SECONDARY FLOW
- NT SEPARATED FLOW
- Boundary layer of MHD flow past semifinite plate, using Navier-Stokes equations 01 p0130 A69-10771
- Axisymmetric MHD flow in turbulence chamber at large Hartmann numbers studied for flow boundary layer effects 01 p0130 A69-10772
- Time history of unsteady heat transfer in laminar boundary layer over semiinfinite flat plate due to step change in wall temperature or wall flow 01 p0177 A69-11401
- Unsteady laminar boundary layer flow at curved surfaces, analyzing frequency and curvature parameter influence on basis of small disturbances method [DVL-863] 02 p0231 A69-12053
- Plate temperature oscillation effects on forced convection laminar viscous incompressible MHD boundary layer flow from semiinfinite flat plate 02 p0288 A69-12143
- Compressible and incompressible laminar boundary layer with constant wall shear stress, using initial profiles 02 p0233 A69-12535
- Unsteady incompressible boundary layer flow over leading edge boundary layer calculated by three dimensional time dependent equations 02 p0233 A69-12543
- Viscous liquid layer flow down inclined plane under boundary conditions, taking into account drag and penetration at porous bed surface 02 p0234 A69-12774
- Planetary boundary layer response to time varying pressure gradient force 03 p0460 A69-13337
- Eddy diffusivity in planetary boundary layer determined by vertical velocity spectrum 03 p0460 A69-13338
- Thermal convection in rotating fluid annulus, discussing suppression of frictional constraint on lateral boundary 03 p0460 A69-13339
- Finite difference schemes to solve fundamental equations in boundary layer flow theory 03 p0416 A69-13655
- Implicit finite difference scheme to integrate unsteady boundary layer equations for compressible gas 03 p0416 A69-13656
- Heat transfer covering heat conduction, channel flow, boundary layer flow, separated flow, etc 04 p0684 A69-14354
- Unsteady compressible laminar boundary layer flow over insulated or isothermal flat plate moving with arbitrary time variant velocity in viscous fluid 04 p0588 A69-14715
- Boundary layer flow of viscous incompressible liquid past wedge embedded circular cylinder 04 p0590 A69-15276
- Entry region flow and convective heat transfer prediction in cooled vertical pipe open at both ends, considering wall temperature 05 p0845 A69-15717
- Wall jet type fluidic elements subjected to hydroaerodynamic effects, discussing use of boundary layer flow properties 05 p0705 A69-16016

Suction effect on incompressible flow through step expansion in circular pipe through sudden enlargement, considering inlet flow with thin boundary layer [ASME PAPER 68-FE-11] 05 p0748 A69-16074

- Laminar flow stability along flexible boundary, using broken linear velocity profile instead of boundary layer profile 06 p0909 A69-17207
- Universal equations for three dimensional laminar boundary layer of incompressible fluid on walls of axisymmetric channel with vortical external flow 06 p0909 A69-17328
- Approximate solution of equations for boundary layer flow of conducting medium on insulating and electrode walls of MHD generator channel 06 p0871 A69-17914
- Nonsimilar laminar boundary layer solutions with negative pressure gradient compared to experimental boundary layer velocity profiles, momentum and displacement thicknesses [AIAA PAPER 69-35] 06 p0913 A69-18094
- Analytical model developed from turbulent shear flow study, discussing Reynolds number effect [AIAA PAPER 69-163] 06 p0914 A69-18139
- Differential equations governing free convection boundary layer flow past isothermal semiinfinite vertical flat plate solved for large Prandtl numbers by matched asymptotic expansions 07 p1239 A69-18266
- Dirichlet and Neumann problems solvability using potential theory methods, limiting study to three dimensional domains 07 p1173 A69-18496
- Transformation of laminar stationary incompressible boundary layer equations for body of revolution in incident flow, using difference method 08 p1252 A69-20703
- Constant property turbulent boundary layer flow, developing finite difference solution for prediction of velocity profiles and skin friction coefficient 09 p1482 A69-21950
- Steady laminar boundary layer flow calculations extended to temperature boundary layer for given heat flow or temperature distribution at wall 10 p1808 A69-22915
- Existence and uniqueness to boundary layer continuation problem based on flow equation for steady gas flow 10 p1679 A69-23569
- Turbulent boundary layers on flat wall of supersonic wind tunnel, determining velocity profiles, thicknesses and skin friction coefficients 10 p1680 A69-23643
- Laminar boundary steady two dimensional constant velocity flow over curved surface equation derived from Navier-Stokes equation 11 p1867 A69-24375
- Turbulent boundary layer velocity distributions in uniform/accelerated compressible flow over flat plate, using change of variables based on mixing length formula [ONERA-TP-693] 11 p1867 A69-24752
- Shock induced boundary layer flow establishment on semiinfinite flat plate, measuring heat transfer rates and transition to turbulence 11 p1869 A69-24890
- Second order effects on two dimensional laminar boundary layer flow of incompressible fluid 11 p1872 A69-25127
- Reverse transition in two dimensional accelerated incompressible turbulent boundary layer flow, noting skin friction coefficient and turbulent intensity profiles 11 p1872 A69-25129
- Heat transfer and skin friction in convective and stagnation flow laminar film boiling in boundary layer flows with appreciable radiation 11 p1873 A69-25242
- Free convection boundary layer flow past vertical flat plate analyzed for nonlinear wall temperature distributions using series solutions 11 p2002 A69-25243
- Buoyancy effect on boundary layer flow over semiinfinite vertical plate heated to constant temperature in uniform free stream 11 p1874 A69-25352
- Wing geometry and wing lower surface boundary layer effects on rolled-up tip vortices geometry and strength 11 p1819 A69-25372
- Thin spherical layer flow stability with respect to small disturbances, showing unsteady motion above critical Reynolds numbers and secondary flow features 11 p1875 A69-25486

Similarity solutions for incompressible, steady hydrodynamic and thermal boundary layers on longitudinally curved walls, allowing for displacement and curvature effects

12 p2060 A69-25761

Wall pressure fluctuations due to turbulent boundary layer flow, calculating statistical properties [AIAA PAPER 68-642]

13 p2244 A69-27246

Conducting liquid boundary layer flow and heat flux on electrodes of MHD generator, including one dimensional flow outside boundary layer

13 p2309 A69-28028

Boundary layer physical and chemical processes effect on dynamic parameters of high temperature hypersonic gas flow past blunt bodies

14 p2391 A69-29620

Boundary value problem in three dimensional boundary layer theory for incompressible flow near stagnation point

14 p2432 A69-29677

Flow phenomena associated with electrically conducting boundary layer jet injection through slot into uniform slipstream in presence of transverse magnetic field

14 p2501 A69-29917

Power law fluids boundary layer near flat plate studied by series expansion and steepest descent methods, determining velocity gradient and skin friction coefficient

15 p2589 A69-30002

Flow and temperature boundary layers on longitudinally curved walls, giving higher approximation exact solutions

15 p2591 A69-30933

Eigenvalue bounds for amplification rates, wave speeds and linear stability conditions for Orr-Sommerfeld equation governing parallel flow in boundary layer and round pipes

16 p2768 A69-31591

Boundary layer over impulsively started flat plate, describing flow transition from unsteady /Rayleigh/ to steady /Blasius/ state by iterative methods

16 p2769 A69-31812

Ion and electron distributions in chemical nonequilibrium boundary layer flow over hypersonic reentry vehicle, discussing plasma sheath and boundary layer thickness relations

16 p2769 A69-31874

Laminar boundary layer on rotating blades and yawed infinite wings, solving partial differential equations numerically by implicit finite difference scheme on computer

16 p2732 A69-31885

Systematic formalism specialization of group theory techniques for similarity analysis applied to three dimensional incompressible boundary layer flows

16 p2773 A69-32379

Pressure and temperature surveys of Mach 27-47 nozzle boundary layer at Ames M-50 He tunnel, determining velocity profiles, wall friction coefficient, etc [AIAA PAPER 69-686]

17 p2953 A69-33441

Three dimensional hypersonic laminar boundary layer subdivided into inner and outer regions, obtaining flow description by matching inner and outer solutions [AIAA PAPER 69-710]

17 p2955 A69-33467

Turbulent boundary layer on disk rotating in free air, using circumferential and radial momentum integral equations and entrainment equation

17 p2957 A69-33601

Boundary layer equation for steady incompressible flow past flat plate with parabolic leading edge, obtaining series solution in inverse powers of Reynolds number

18 p3124 A69-35270

Hydrodynamic stability of incompressible fluid boundary layer flow during blowing or suction through porous surface, determining Reynolds number lower bounds

18 p3124 A69-35381

Rough wall turbulent boundary layer development in pipe flow determined for different roughness geometries in zero and adverse pressure gradients

18 p3125 A69-35387

Rayleigh criteria extension for boundary layers of rotationally symmetrical bodies with curved meridian, utilizing orthogonal coordinate system

19 p3298 A69-36309

Tangential and radial velocities in vortex boundary layer flow, relating diminishing amplitudes to increasing height using iterative method

19 p3363 A69-36499

Generalized series solutions of boundary layer flows over pointed and blunt nosed axisymmetric bodies, noting general potential flow extending Mangler transformation usefulness

20 p3514 A69-37211

Rice-Ramsperger-Kassel kinetic theory applied to sulfur hexafluoride injection into boundary layer of high speed reentry vehicle

20 p3514 A69-37226

External natural convection flows, studying laminar instability, transition and turbulence in boundary layer flow

20 p3633 A69-37718

Boundary layer velocity distribution in turbulent swirling pipe flow produced by twisted tape inserts [ASME PAPER 69-FE-14]

20 p3516 A69-37990

Three dimensional laminar boundary layer hypersonic flow about slender conical vehicles, analyzing transverse surface curvature effect, studying Reynolds number, cone angle, etc [ASME PAPER 69-FE-23]

20 p3460 A69-37992

Unsteady laminar incompressible time dependent boundary layer flows with cylindrical symmetry, transverse boundaries and no swirl [ASME PAPER 69-FE-47]

20 p3517 A69-37997

Unsteady boundary layer flows of compressible fluid over semiinfinite flat plate, discussing heat transfer rate

20 p3518 A69-38318

Boundary layer flow past permeable surface, generalizing integral equations for case with suction

21 p3691 A69-38573

Boundary layer equations solved for MHD version of Falkner-Skan problem, using Laplace transform and steepest descent technique

21 p3693 A69-38750

Free convection boundary layer singular character at low Prandtl numbers, deriving expression for Nusselt-Grashof relation

21 p3849 A69-38772

Skin friction results from free stream velocity boundary layers with varying injection and suction wall conditions, describing flow characteristics

21 p3696 A69-39431

Flow stability regions at surface of flight vehicle, considering boundary layer flow of incompressible fluid

21 p3645 A69-39827

Interaction between boundary layer and external vortex flows and stability transitions of heated rotating fluid annulus

21 p3698 A69-39869

Numerical calculations for boundary layer flows allowing similar solutions, using iterative numerical integration of integral equation

22 p3929 A69-39925

Velocity profile and skin friction in boundary layer on flat plate with periodic vorticity near leading edge

22 p3929 A69-40015

Velocity and temperature boundary layers on plane wall developed by ideal shock tube flow for weak shock and expansion waves

22 p3932 A69-40894

Friction, heat transfer and mass transfer theory of flow represented by two dimensional parabolic boundary layer equations

22 p3933 A69-40940

Nonequilibrium boundary layer of dissociated diatomic gas over catalytic flat plate in hot hypersonic uniform flow

22 p3934 A69-41181

Asymptotic description of laminar hypersonic boundary layer acceleration approaching sharp corner, assuming small interaction with outer inviscid flow [AIAA PAPER 68-67]

23 p4059 A69-41883

Boundary layer method for calculation of viscous damping coefficients for small amplitude progressive waves propagating in nonhomogeneous fluid

23 p4153 A69-42408

Shock wave/boundary layer interaction calculation methods circumventing simultaneous large longitudinal and transverse pressure gradients and viscous effects

24 p4243 A69-42582

Parallel magnetic field effect on free boundary layer type flows stability of low Reynolds number between parallel streams of viscous incompressible conducting fluid

24 p4298 A69-42596

Turbulent boundary layer at inlet section of gas blown tube based on solutions of energy and momentum equations, deriving relations for inlet section length

24 p4300 A69-43079

Boundary layer equations with heat transfer for laminar and turbulent incompressible flows about two dimensional and axisymmetric flows, using finite difference method [ASME PAPER 69-HT-7]

24 p4304 A69-43561

Uniform flow and wall boundary layer growth measurement in conical nozzle of reflected shock tunnel operating at high enthalpy conditions

24 p4247 A69-43575

Superimposed free vortex swirl effect on flow and heat transfer in three dimensional axisymmetric laminar boundary layer

24 p4304 A69-43584

Physical flows characteristics with self similar laminar boundary layers, performing inverse transformation of Falkner-Skan equation

24 p4304 A69-43586

BOUNDARY LAYER NOISE U AERODYNAMIC NOISE

BOUNDARY LAYER SEPARATION

Flow in square to rectangular constant area transition piece having straight walls with outlet aspect ratio of 5 fitted with exit duct

02 p0189 A69-12412

Hypersonic flow distribution and separation types over highly swept delta wings with trailing edge flaps at Mach 6 [AIAA PAPER 68-97]

02 p0189 A69-12522

Incompressible turbulent boundary layer with near zero wall friction at circular cylinder situated longitudinally in flow

03 p0416 A69-13664

Modified Karman-Pohlhausen pulse integral equation for calculating boundary layers is more accurate when seeking flow separation point

04 p0591 A69-15408

Laminar boundary layer separation and reattachment near concave corner on cooled reentry body in supersonic flow

06 p0911 A69-17592

Three dimensional boundary layer problems analyzed by exact numerical method [AIAA PAPER 69-138]

06 p0911 A69-18041

Incompressible laminar Falkner-Skan boundary layer suffering sudden acceleration by moving belt, noting boundary layer separation [AIAA PAPER 69-40]

06 p0912 A69-18049

Separation of subcritical and supercritical compressible turbulent boundary layers under strong pressure gradients using method based on integral equations [AIAA PAPER 69-34]

06 p0912 A69-18077

Isoenergetic two dimensional supersonic turbulent base flow, noting boundary layer separation properties upstream and downstream [AIAA PAPER 69-68]

06 p0864 A69-18137

Nonsimilar MHD channels boundary layers on insulating walls noting influence of loading factor, wall temperature and Hall effect on separation [AIAA PAPER 69-46]

06 p0972 A69-18192

Hypersonic laminar boundary layers on compression corner model, studying flap lengths effects and mass transfer [AIAA PAPER 69-36]

06 p0866 A69-18214

Three dimensional boundary layer separation assuming zero friction

07 p1050 A69-18736

Boundary layer discontinuity on helicopter rotor blade in hovering using flow visualization [AIAA PAPER 69-197]

07 p1051 A69-19561

Mixed three dimensional separation of boundary layer on ellipsoid of revolution at ten degree angle of attack, ignoring heat flux

08 p1251 A69-19876

Laminar boundary layer behavior in neighborhood of separation, discussing regressive influence beyond separation in Prandtl equations [ONERA-TP-677]

08 p1303 A69-19878

Boundary layer separation and vortex street buildup conditions of gas flow in circular cylinder wake

08 p1252 A69-20713

Heat flux effect on laminar boundary layer separation in supersonic flow stressing free interaction zone

09 p1429 A69-21690

Equilibrium theory of parametric pump using cyclic flow of binary mixture through column with heated and cooled bed of solid absorbent

09 p1481 A69-21910

Laminar boundary layer separation and heat transfer on zero incidence cone at hypersonic speed, noting wall temperature and Reynolds number effects

09 p1433 A69-22609

Semiactuator disk method for boundary layers and velocity of stall flutter cascade blades vibrating in transient mode, considering nonstall flutter

11 p1818 A69-25028

LF spectral analysis of flowing water pressure pulsations behind single bulge on hydrodynamic channel smooth wall at low disturbance level

13 p2246 A69-27535

Demixed layer at wall in shear flow of nonsedimenting suspensions with different geometries due to viscous and inertia effect superposition

13 p2251 A69-28498

Flow structure in conical shock wave-sharp flat plate interaction zone in supersonic flow, noting turbulent boundary layer before separation
14 p2428 A69-28897

Turbulent boundary layers behavior near flow separation, obtaining equations for equilibrium layers
15 p2591 A69-30638

Trailing shock wave position in air breathing jet engine channels, determining supersonic-subsonic boundary, noting Mach number effects on pressure ratio
16 p2768 A69-31743

Supersonic laminar boundary layer separation calculated by integral method using free parameters for velocity and enthalpy profiles, considering boundary layer-external flow interaction
16 p2731 A69-31834

Critical review of paper on suction effect on hypersonic laminar boundary layer separation
16 p2771 A69-31928

Distributed boundary layer suction effectiveness for controlling supersonic transitional flow separation
16 p2772 A69-32149

Two dimensional model for analyzing turbulent separation and reattachment at blade trailing edge at supersonic speed
[ONERA-TP-678]
16 p2733 A69-32258

Normal and negative Magnus force experienced by rotating cylinder in air flow, discussing wind tunnel tests, laminar and turbulent boundary layers separation, pressure distribution, etc
17 p2958 A69-34213

Laminar separation in incompressible fluid flowing past bluff body at high Reynolds number, investigating shock wave interaction with laminar boundary layers
18 p3122 A69-34918

Wing tunnel and theoretical studies of hypersonic wall flow on cone, considering static pressure and convection heat flux density effects
19 p3241 A69-36759

Supersonic flow past antisymmetrical thin delta wing by flow separation from subsonic leading edges, noting wing surface pressures
19 p3241 A69-36779

LF spectral analysis of flowing water pressure pulsations behind single bulge on hydrodynamic channel smooth wall at low disturbance level
20 p3518 A69-38202

Prandtl boundary layer theory problems, considering solution uniqueness and stability, unsteady flow, boundary layer separation, existence conditions, etc
21 p3697 A69-39698

Secondary losses in flat large scale turbine lattice attributed to LF pulsating flow separation on back of blade
21 p3645 A69-39717

Hypersonic turbulent boundary layer separation over cone-cylinder flare configuration at zero angle of attack and high Reynolds number
22 p2930 A69-40557

Initial pressure rise and consequent laminar boundary layer separation during interaction with shock wave
23 p4151 A69-41691

Boundary layer separation and free mixing phenomena between streams behind thin flat plate by finite difference methods and Prandtl exchange coefficient
23 p4060 A69-41912

Boundary layer separating collisionless plasma from one dimensional magnetic field for anisotropic particle velocity distribution functions, preserving charge neutrality in boundary layer
23 p4197 A69-42415

Boundary layer separation zones in laminar, transition and turbulent fluid flows past conical bodies with widening skirts
24 p4245 A69-43481

Laminar boundary layer separation in supersonic flow, constructing method for flow distribution functions, perturbed flow region dimensions and pressure perturbation amplitude
24 p4246 A69-43482

Separation flows in flat channel with step recess, analyzing dynamic characteristics in mixing region, in wake of rarefaction waves and in attachment zone
24 p4247 A69-43498

BOUNDARY LAYER STABILITY

Hydromagnetic stability of free boundary layer between two uniform streams in presence of aligned uniform magnetic field at large Reynolds number
02 p0287 A69-11832

Natural convection boundary layer stability on heated isothermal vertical plane wall, discussing Grashof number as laminar to turbulent flow transition criterion
02 p0188 A69-12038

Unsteady laminar boundary layer flow at curved surfaces, analyzing frequency and curvature parameter influence on basis of small disturbances method
[DVL-863]
02 p0231 A69-12053

Stability of laminar flow along flexible boundary using broken linear velocity profile
02 p0232 A69-12353

Numerical solution of chemically reacting boundary layer equations, noting loss of accuracy due to numerical cancellations
04 p0588 A69-14737

Irregular Sturm-Liouville first and higher order perturbation problem in boundary layer theory providing analytical approximations to complete orthogonal set of characteristic functions
04 p0590 A69-15001

Stability of laminar natural convection boundary layer flow, discussing thermal capacity coupling between fluid and wall and Prandtl number
05 p0744 A69-15719

Stability theory application to laminar boundary layer transition prediction on two dimensional and axisymmetric flows having pressure distributions in incompressible flow
[AIAA PAPER 69-10]
06 p0914 A69-18127

Geometrically exact finite element for thin shells of revolution, using approximation to predict boundary layer stress distribution during vibration
[AIAA PAPER 69-56]
06 p1029 A69-18193

Equilibrium stability of horizontal layer of fluid in field of modulated temperature gradient having layer thickness greater than penetration depth of heat waves
07 p1241 A69-18696

Velocity profiles in unsteady laminar incompressible boundary layer over flat plate in shock tube by two parameter integral method
11 p1871 A69-25026

Vortices interaction effect on vertical turbulent heat flow in atmosphere boundary layer, determining dependence of vortex mean vertical temperature gradient
13 p2293 A69-27841

Turbulence constant for flows near walls, analyzing viscosity dependence on wall distance by utilizing maximum stability principle
15 p2590 A69-30048

Wall curvature effect on hydrodynamic stability of laminar incompressible boundary layer with respect to perturbing Tollmien-Schlichting waves
19 p3299 A69-36587

Dimensionless radial and transverse velocity profiles for unsteady incompressible boundary layer on rotating disk in rotating fluid
19 p3300 A69-36720

Unsteady boundary layer with distributed injection or suction on porous plate, determining acceleration and flow parameter functions from velocity profiles
21 p3692 A69-38609

Lower boundary approximation for theory of thermal laminar steady state boundary layer on isothermal immersed plate
23 p4150 A69-41334

Unsteady periodic boundary layer stability on flat plate, presenting model for disturbance wave packet propagation streamwise pressure gradients effects in transition flow
23 p4152 A69-41888

Atmospheric model for calculating wind velocity profile and turbulence of stable atmospheric boundary layer with given temperature stratification and pressure gradient distribution
23 p4184 A69-42489

Steady state baroclinic boundary layer over two dimensional terrain in f plane, noting layer thickness dependence on stability and terrain slope
24 p4347 A69-43356

BOUNDARY LAYER TRANSITION

Turbulent to laminar boundary layer reversal by applying negative pressure gradient
01 p0058 A69-10066

Turbulent boundary layer reversion to laminar state associated with departures from inner law velocity distribution in presence of favorable pressure gradients
03 p0414 A69-13016

Axial magnetic field effect on steady linear Ekman boundary layer
03 p0474 A69-13141

Asymptotic similarity in neutral barotropic planetary boundary layers, solving Ekman flow by singular perturbation methods
03 p0460 A69-13336

Boundary layer transition measurements on flight tests of experimental 22 degree conical reentry vehicle with Be heat shield and graphite nose
[AIAA PAPER 68-1152]
03 p0362 A69-13648

Boundary layer transition to turbulence shown to have influence on magnitude of lifting reentry body heating rate
[AIAA PAPER 68-1155]
03 p0416 A69-13674

Stokes and Rayleigh layer formation during solid body rotation of semiinfinite fluid and infinite disk
03 p0417 A69-13797

Hypersonic turbulent boundary layer in adverse pressure gradients studied for transition, measuring static/pitot pressure, stagnation temperature and heat transfer rates
[AIAA PAPER 68-44]
04 p0588 A69-14716

Ekman boundary layer problem of steady axisymmetric viscous incompressible flow between infinite coaxial rotating disk, studying laminar range of Taylor number R
05 p0744 A69-15665

Hypersonic laminar and transitional heat transfer rate distribution on spherically blunted cones
05 p0696 A69-15707

Boundary layer transition detection at supersonic speeds, using thin film gages to infer local laminar and turbulent supersonic skin friction
[AIAA PAPER 69-9]
06 p0912 A69-18075

Dynamic stability loss on ablating vehicles ascribed to boundary layer transition effect from turbulent aft body heating
[AIAA PAPER 69-106]
06 p1037 A69-18087

Spatial distribution of three dimensional laminar boundary layer transition zone on sharp half angle cone from hypersonic wind tunnel tests
[AIAA PAPER 69-12]
06 p0863 A69-18112

Stability theory application to laminar boundary layer transition prediction on two dimensional and axisymmetric flows having pressure distributions in incompressible flow
[AIAA PAPER 69-10]
06 p0914 A69-18127

Width of strong shock wave front and transition layers estimated, using Boltzmann kinetic equation and H-theorem
07 p1118 A69-18702

Transition boundary layer on flat plate in subsonic wind tunnel measured by hot-wire method, obtaining velocity fluctuation distribution and turbulence intensity
07 p1121 A69-19329

Computer study of analytical model of boundary layer transition from laminar to turbulent flow
[AIAA PAPER 68-38]
09 p1482 A69-21945

Tolerable surface roughness for transition stability in incompressible laminar boundary layer, including analysis of two and three dimensional roughness shape effects
12 p2063 A69-26774

Boundary layer between cold plasma and vacuum magnetic field, considering transverse velocity component perpendicular to field
12 p2139 A69-26944

Thermal stratification effect on wind structure in Ekman layer, assuming turbulent transfer and height dependence
13 p2290 A69-27390

Radiated aerodynamic noise effects on boundary layer transition on sharp leading edge hollow cylinders in wind tunnels, noting Reynolds numbers correlation
[AIAA PAPER 68-375]
13 p2241 A69-28211

Roughness effects on boundary layer transition up to Mach 16 in hotshot wind tunnel
[AIAA PAPER 68-377]
13 p2242 A69-28213

Supersonic boundary layer acoustic characteristics measured in wind tunnel on cylindrical model with several forebody configurations
[AIAA PAPER 69-344]
13 p2249 A69-28279

Temperature factor effect on transition from laminar to turbulent flow in boundary layer of plate
13 p2251 A69-28558

Gas compressibility influence on laminar to turbulent boundary layer transition determined using Taylor hydrodynamic finite perturbation model
14 p2389 A69-28974

Subliming ablation effects on boundary layer transition for cones in hypersonic flow, discussing Reynolds numbers measured in wind tunnel tests
[AIAA PAPER 68-40]
16 p2732 A69-31881

Laminar-turbulent transition in boundary layer on thermally decomposing surface, discussing gasification rate, Reynolds number effects, heat transfer and turbulence onset mechanism
16 p2878 A69-31951

Boundary layer trip geometry, size and location effects on position of transition at hypersonic speeds
17 p2950 A69-33249

Mach number, cone angle, bluntness and wall to recovery temperature ratio effects on slender cones

boundary layer transition measurements at hypersonic speeds

17 p2890 A69-33250

Amplified boundary layer oscillations and transition at swept flat nosed wing attachment line with/without boundary layer suction analyzed by wind tunnel tests

17 p2890 A69-33251

Free stream disturbances influence on hypersonic boundary layer transition Reynolds number in heated and unheated flows

[AIAA PAPER 69-704] 17 p2953 A69-33453

Hypersonic boundary layer transition on blunt slender cones at M equal 10 obtained independent Reynolds number

[AIAA PAPER 69-705] 17 p2954 A69-33455

Cone boundary layer transition location and Reynolds number as function of nose bluntness combined effect with A_r , air and He mass injection

[AIAA PAPER 67-706] 17 p2955 A69-33476

Nonuniform heating rates during laminar boundary layer transition on slender cone at hypersonic speeds

18 p3085 A69-34435

Boundary layer transition from laminar to turbulent flow on flat plate, considering supersonic and hypersonic flow, pressure gradients, surface curvature and roughness, etc

18 p3123 A69-34920

Atmospheric horizontal mixing caused by quasi two dimensional macroturbulent motions, describing micro and mesoscale processes using numerical model

19 p3363 A69-36500

Wind and temperature profiles in Ekman boundary layer, using numerical integrations of dynamic equations including time derivative terms

19 p3363 A69-36501

Stability theory formulation for evaluation of boundary layer transition from laminar to turbulent states

[AIAA PAPER 68-669] 20 p3514 A69-37184

Turbulent boundary layer growth predicted for adverse pressure gradients, using entrainment theory for two dimensional and axisymmetric flows

[ASME PAPER 69-FE-16] 20 p3517 A69-37991

Boundary layer development on body accelerating in viscous incompressible fluid, using straight lines approximation and asymptotic expansions

22 p3929 A69-40110

Electromagnetic cascade showers transition effect in various materials, measuring energy deposition as function of position

22 p3987 A69-41003

Unsteady periodic boundary layer stability on flat plate, presenting model for disturbance wave packet propagation streamwise pressure gradients effects in transition flow

23 p4152 A69-41888

Boundary layer transition to turbulence shown to have influence on magnitude of lifting reentry body heating rate

[CIIA PAPER 68-1155] 24 p4300 A69-43251

Boundary layer separation zones in laminar, transition and turbulent fluid flows past conical bodies with widening skirts

24 p4245 A69-43481

Boundary layer and heat transfer measurements for turbulent boundary layer laminarizing in conical nozzle flow with wall cooling

[ASME PAPER 69-HT-56] 24 p4303 A69-43538

Luminescent turbulent boundary layer prediction using mixing length model modified for viscous sublayer structural changes near wall compared with heat transfer data

[ASME PAPER 69-HT-13] 24 p4303 A69-43556

Air flow laminarizing turbulent boundary layer, determining velocity, turbulence intensity, temperature profiles and local heat transfer coefficients

[ASME PAPER 69-HT-10] 24 p4413 A69-43558

High enthalpy shock tube and nozzle gas flows for incident shock Mach numbers analyzed for laminar boundary layers and boundary layer transitions

24 p4305 A69-43664

BOUNDARY LAYERS

NT COMPRESSIBLE BOUNDARY LAYER

NT HYPERSONIC BOUNDARY LAYER

NT LAMINAR BOUNDARY LAYER

NT THERMAL BOUNDARY LAYER

NT THREE DIMENSIONAL BOUNDARY LAYER

NT TURBULENT BOUNDARY LAYER

Atmospheric diffusion measurement based on analysis of thoron emitted continuously from point source, permitting study of diffusion in atmospheric boundary layer

01 p0144 A69-10043

MHD boundary layer equations in Blasius problem reduced to differential equations and solved by Laplace transform

01 p0127 A69-10337

Transverse pressure gradient and streamwise derivatives effect on free convection laminar heat transfer on isothermal vertical plate at low Prandtl numbers

01 p0177 A69-11409

Transverse plasma velocity component effect on boundary layer structure between cold plasma and confined magnetic field

02 p0235 A69-11424

Boundary layer effect on large scale atmospheric processes from analyzing two layer free atmosphere model, plotting weather forecast charts

02 p0273 A69-11435

Turbulence conditions in atmospheric boundary layer within similarity theory, including wind velocity and temperature profile

02 p0274 A69-11447

Infinite system of first order integral equations derived from Prandtl boundary layer equation and continuity equation

02 p0231 A69-12059

Boundary layer local densities in high temperature gas flows obtained by measuring monochromatic soft X rays attenuation in layer

02 p0233 A69-12489

Long wave radiative heat flux in boundary layers of cloud during solid overcast, discussing dependence on various cloud and atmospheric parameters

03 p0458 A69-13271

Thermal forcing role in diurnal oscillation of planetary boundary layer wind above sloping terrain

03 p0462 A69-13682

Boundary layer effects on shadow deformation, emphasizing two dimensional flow with image projected by parallel light beams perpendicular to flow plane

03 p0364 A69-13787

Laminar flow of viscous fluid along wall with fixed leading edge and moving surface, discussing conditions of boundary layer formation and dynamic similarity

03 p0417 A69-13792

Boundary layer equations for uniform motion of semiinfinite flat plate through incompressible conducting fluid at rest and in magnetic field, using numerical method

03 p0477 A69-13794

Sufficient conditions for stability of compressible atmospheric flows for rigid lid types of upper boundary condition

03 p0417 A69-13796

Instability and disturbance amplification in external laminar natural convection boundary layer over vertical flat surface with uniform heat flux

03 p0533 A69-13951

Laminar accelerating flow of thin film falling along vertical wall, emphasizing growth and decrease of boundary layer and film thickness

[ASME PAPER 68-APM/Z] 04 p0586 A69-14388

Cylindrical sound pulse propagation in homogeneous layer under inhomogeneous half space

04 p0630 A69-14531

Difference approximation with second order accuracy of numerical solution for parabolic type equations

04 p0622 A69-14618

Numerical solution of nonlinear two point boundary value problems of boundary layer type, noting shock wave formation in supersonic nozzle

04 p0544 A69-14889

Tetron flight observations of eddy velocities in planetary boundary layer, noting effects of height and seasonal variations

04 p0626 A69-14912

Conventional fuselage and streamline body shapes effect on drag at subsonic speeds, noting boundary layer development

05 p0697 A69-15827

Turbulence characteristics and wind velocity in atmospheric boundary layer determined from pressure and temperature fields

05 p0788 A69-16453

Solution to system of equations in boundary layer theory of steady incompressible fluid flow

05 p0751 A69-16454

Turbomachinery research, discussing two and three dimensional incompressible flow in cascades near end wall and in rotating machines

05 p0751 A69-16534

Nonscattered, singly and multiply scattered light of beam from point source analyzed at boundary layer of turbid medium

05 p0789 A69-16640

Integral method for backward boundary layers, developing third order polynomials for two dimensional potential flow toward opening

05 p0752 A69-16737

Boundary layer on flat plate with homogeneous suction, discussing dimensionless displacement/ momentum thickness and wall shearing stress

05 p0752 A69-16744

Viscous MGD channel flow in boundary layer approximation with heat conduction, transforming resultant partial differential equations set to system of ordinary differential equations

06 p0966 A69-17523

Electromagnetic wave transmission and reflection at boundary of relativistic collisionless plasma, using Laplace transformation

06 p0968 A69-17783

Maximum downwind and crosswind vertical wind shear in boundary layer, noting effect on swept wing jet aircraft landing

06 p0951 A69-17790

Transient development of reacting boundary layer near stagnation point of vaporizing drop in gas stream

[AIAA PAPER 69-174] 06 p0912 A69-18056

Shock wave-boundary layer interaction configurations for hypersonic propulsion device inlets under transitional and turbulent conditions, noting heat transfer rate

[AIAA PAPER 69-8] 06 p0915 A69-18172

Nonequilibrium electron temperature, concentration and reflection in reentry boundary layers, discussing heat transfer and ionization energy diffusion

[AIAA PAPER 69-82] 06 p0915 A69-18190

Cross hatching on various body surfaces due to periodic surface pressure fluctuations, discussing origin from counterrotating longitudinal vortices in boundary layer

[AIAA PAPER 69-11] 06 p0915 A69-18213

Modified schlieren interferometer for quantitative investigation of free convection boundary layer temperature profiles

07 p1130 A69-18263

Approximate solution for hollow circular cylinder with fixed ends under axial displacement and cylindrical surfaces free from traction, using boundary layer technique

07 p1230 A69-18265

Underexpanded nozzle ejected supersonic turbulent jet off-design behavior, discussing static pressure distribution, boundary layer and Mach number effect

07 p1049 A69-18397

Boundary layer approximation for steady laminar flow of viscous incompressible fluid past paraboloid of revolution, obtaining vorticity distribution

07 p1120 A69-18812

Discontinuity effect on Ekman layer development at leading edge of flat plate

07 p1120 A69-19044

Boundary layer effect on flow coefficient of fluid amplifier feed nozzle, noting flow uniformity, incompressibility, velocity and velocity distribution assumptions

07 p1059 A69-19320

Jet flow and wakes in external stream and tailored pressure gradients, deriving similarity solutions for boundary layer equations

08 p1252 A69-20782

Power series solutions of MHD boundary layer equations for flat plate with transverse magnetic field and arbitrary pressure gradient, discussing skin friction

09 p1545 A69-21396

Turbulent diffusion from point source in boundary layer, discussing horizontal and vertical effects

09 p1535 A69-21513

Boundary layer at tube wall behind shock wave propagating in gas-vapor mixture, analyzing condensation rate

09 p1480 A69-21591

Modified first order theory of magnetosphere boundary shape incorporating effects of neutral sheet currents of extended geomagnetic tail

09 p1488 A69-21661

Boundary layer suction sound emission, analyzing turbulent flow past elastic plate with reinforced slots performing flexural and torsional vibrations

09 p1483 A69-22638

Relation between Rayleigh and dynamic Richardson numbers in atmospheric boundary layer in presence of cellular convection

09 p1491 A69-22709

Numerical solution of MHD equations for boundary layer electrically conducting gas flow near flat plate when velocity distribution of external flow obeys power law

10 p1727 A69-23093

Low temperature optically thick boundary layers influence on spectroscopic temperature measurements in plasma MHD channels
10 p1731 A69-23434

MHD boundary layer nonlinear instability, treating laminar to turbulent flow transition as reversible process
10 p1734 A69-23452

Similar boundary layers in Prandtl approximation determining similarity conditions for second order effects due to curvatures and outer vorticity
10 p1632 A69-23700

Boundary layers influence on external electrical characteristics of MHD generator
11 p1824 A69-24221

Flat decelerating cascades boundary layer in compressible flow during change in axial flow- density ratio and upstream turbulence
11 p1818 A69-24639

Viscous effects of wall boundary layer behind primary shock wave on flow in shock tube, noting pressure and temperature changes
11 p1870 A69-25010

Criteria for reversion of turbulent to laminar flow /r-verse transition/ as special cases of Reynolds number criterion, noting boundary layer properties role
11 p1873 A69-25134

Plasmapause position measurements by ion mass spectrometers and broadband VLF receivers on OGO 1 and OGO 3 and by broadband recordings at Antarctica
11 p1878 A69-25153

Turbulent viscosity and thermal conductivity coefficients for entire cross section of fluid flow including wall boundary layers
11 p1873 A69-25228

Porous cermet electrodes thermochemical protection by blowing neutral gas into electrode boundary layer, examining effect on volt-ampere characteristics
11 p1826 A69-25232

MHD free convection from horizontal isothermal plate in vertical uniform magnetic field, considering boundary layer thickness
11 p1930 A69-25277

Hypersonic viscous gas flow past thin bodies, deriving equations for interactions between boundary layer and external flow
11 p1820 A69-25472

Boundary layer calculation during laminar MHD channel flow under crossed magnetic and electric fields using successive approximation method
11 p1932 A69-25491

Atmospheric boundary layer transparency to gas laser emissions in IR spectrum, determining attenuation factor dependence on humidity and visibility range
12 p2028 A69-25957

Surface waves effect on electromagnetic waves incoherent reflection from plasma-vacuum boundary, describing polarization and angular and spectral distributions
12 p2031 A69-26530

Rarefied Ar plasma flow current-voltage characteristics in discharge tube, noting plasma boundary layer thickness influence on saturation current
12 p2137 A69-26532

Atmospheric boundary layer mean turbulence and vertical velocity calculations, tabulating layer characteristics for various turbulent heat flux and geostrophic wind velocity values
12 p2126 A69-26578

Forced convection in atmospheric boundary layer above nonuniformly heated earth surface, noting roles of wind and stratification parameters
12 p2126 A69-26579

Boundary layer parameters behind shock wave front in ionized gas calculated with allowance for charged particle diffusion
12 p2139 A69-26713

Boundary layer theory covering viscous fluid motion laws, laminar and turbulent boundary layers, transition, etc
12 p2063 A69-26869

Wind shifts and mean gustiness calculation from short range weather forecasts, using dynamic model for wind motion in atmospheric boundary layer
13 p2293 A69-27844

Convective heat transfer, discussing coordinate transformation, similarity analysis similitude and Mcksyn integration of boundary layer equations
13 p2376 A69-28139

Boundary layer characteristics of incompressible flow in wind tunnel with asymmetric two dimensional contraction, discussing flow profiles
13 p2249 A69-28235

Boundary layer equations describing momentum, energy and mass concentration conservation in axisymmetrical turbulent jet flame solved for Lewis number unity in von Mises plane
13 p2379 A69-28455

Wall flows and wake laws validity analyzed by wall balance technique, considering boundary layers under perturbation and core flow restrictions
13 p2251 A69-28633

Long wave radiative heat flux in boundary layers of cloud during solid overcast, discussing dependence on various cloud and atmospheric parameters
14 p2471 A69-28779

Nonscattered, singly and multiply scattered light of beam from point source analyzed at boundary layer of turbid medium
14 p2482 A69-28796

Boundary layer equation of viscous incompressible fluid with moment stresses, noting flow around thin plate and submerged jet problems
14 p2428 A69-28815

Ocean and atmospheric interactions analyzed by using hydrodynamic equations for boundary layers
14 p2442 A69-29838

Atmospheric motions equations in mesometeorology prognostic problems taking into account free atmosphere and boundary layer interactions
15 p2646 A69-30107

Shock tube hot flow duration, contact surface configuration and boundary layer thickness
15 p2590 A69-30297

Boundary layers coalescence on plane convergent channel walls investigated with analytic formulas for velocity distribution, shear stress, layer thickness, etc
15 p2592 A69-31009

Pressure distribution in wake produced by obstacle with secondary fluids injection into boundary layer, obtaining coefficient governing resistance of obstacle to forward motion
16 p2768 A69-31604

Thick gas model for monochromatic one dimensional radiant flux near diffusely emitting and reflecting boundaries, discussing gray gas and exponential kernel approximations
16 p2769 A69-31871

Flow field around sharp slender cones with surface mass transfer at zero angle of attack in low density supersonic and hypersonic flow
16 p2732 A69-31887

Ablation injectants effect on supersonic stream pressure distribution inside cavity and upstream boundary layer velocity profiles
16 p2770 A69-31902

Relation between Rayleigh and dynamic Richardson numbers in atmospheric boundary layer in presence of cellular convection
16 p2808 A69-32488

Near field flow noise generated in boundary layer of water vehicle measured for rotating cylinder, ship and buoyant unit using hydrophone
17 p3004 A69-32953

Separated flow patterns in base flow at body recesses, emphasizing shock wave boundary layer interaction, laminar flow and flow in front of recess
17 p2949 A69-33124

Flow over uniformly rough surface in planetary boundary layer from mixing length wind spiral model, using surface shear stress and wind direction data
17 p2997 A69-33153

Mixing length model to relate turbulent shear stress to mean velocity field within planetary boundary layer above surface roughness change
17 p2997 A69-33154

Conducting fluid incompressible flow in entrance of MHD channel by momentum integral method, permitting edge stress existence at boundary layer free stream interface
17 p2952 A69-33436

Accelerated boundary layers classified in terms of integral balance of pressure, inertia, wall friction forces and entrainment momenta
17 p2955 A69-33462

Reflected shock and boundary layer interaction in shock tube, discussing bifurcation effect on flow and turbulence transition
18 p3116 A69-34448

Boundary layer theory application to dynamics of gyroscope in gimbal suspension, defining nutational and precessional motion
18 p3135 A69-34559

Higher order boundary layer theory development from Prandtl simplification of Navier-Stokes equations to successive approximations for incompressible and compressible flows
18 p3123 A69-34923

Difference method for parabolic differential equations solution for Rayleigh boundary layer in dissociating gas, using integral estimates to determine stability
18 p3124 A69-35295

NonNewtonian power law fluids flow behavior in circular pipe entry region, taking into account energy loss due to viscous dissipation in boundary layer
19 p3240 A69-36472

Boundary layer formed in miniature nozzle studied for effect on jet spreading discharged into space at high Mach numbers
19 p3395 A69-36760

Electron density distribution in laminar air boundary layer on sharp wedges and cones predicted by reducing chemical kinetic model to ordinary differential equations [AIAA PAPER 68-733]
20 p3458 A69-37181

Singular perturbations and boundary layer theory for approximating solutions to simple ordinary differential equations
20 p3515 A69-37583

Wind velocity below 100 meters from Laikhtman atmospheric boundary layer model, solving equations for horizontally homogeneous, stationary and nonadvective air flow
20 p3571 A69-37695

Heat conduction in thin layer near boundary surface of solid by approximating one dimensional conduction in half space with allowance for curvature
20 p3633 A69-38213

Planetary boundary layer top formation, considering particle velocity, earth surface roughness role, geostrophic wind, etc
21 p3715 A69-38566

Heat transfer coefficients, boundary layer thicknesses and temperature and velocity distributions in free convection boundary layer in closed axisymmetric volumes
21 p3848 A69-38634

Instantaneous frozen layer thickness and temperature profile in solidified layer obtained by iteration technique
21 p3852 A69-39433

Prandtl boundary layer theory problems, considering solution uniqueness and stability, unsteady flow, boundary layer separation, existence conditions, etc
21 p3697 A69-39698

Shock tube boundary layers dependence on shock strength determined using vorticity transport to define boundary layer coordinate
22 p3930 A69-40531

Free viscous layers structure at large Reynolds numbers, using matched asymptotic expansions for two dimensional compressible flow
22 p3932 A69-40927

Boundary layer calculation in incompressible turbulent flow with closed streamlines, avoiding von Mises equation
22 p3932 A69-40931

Finite-difference grid procedure for predicting friction heat and mass transfer in two dimensional boundary layers
22 p3932 A69-40939

Interaction between two temperature plasma flux and electrodes in MHD channel with crossed electric and magnetic fields, studying boundary layer dynamics
22 p3991 A69-41022

Mean flow properties of incompressible turbulent three dimensional jets and wakes, treating flow within boundary layer theory context
23 p4060 A69-41908

Boundary layer effects in turbulent spiral vortex flow of compressible fluid in supersonic centrifugal compressor, discussing flow geometry, using momentum integral method
23 p4152 A69-42109

Energetics of planetary boundary layer /Prandtl layer/ from system of hydrodynamic equations, discussing flux divergence term importance in free-windless convection transition region
24 p4309 A69-43148

Taylor Goertler vortex formation effect on heat transfer through boundary layer on concave wall [ASME PAPER 69-HT-3]
24 p4414 A69-43563

BOUNDARY LUBRICATION

Surface preparation effects on Ni-Cr-Fe alloy boundary friction studied by repeated sliding of cylinders on hard Pd-Pt-Au alloy cylinder [ASLE PREPRINT 68AM 6D-4]
07 p1139 A69-18625

World literature on boundary lubrication for machine design, giving 2711 abstracts and extensive bibliographies
11 p1891 A69-24925

BOUNDARY VALUE PROBLEMS
NT NEUMANN PROBLEM

Initial value method applied to Fredholm integral equation for radiative transfer, neutron transport and multiple scattering, verifying invariant imbedding method

01 p0103 A69-10002

Dynamic programming methods to avoid dimensionality problem arising in solution of boundary value problems by digital computer

01 p0103 A69-10006

Boundary value bending problem for anisotropic shells of revolution under asymmetrical loading solved by finite difference technique

01 p0165 A69-10088

Boundary value problems for steady, three dimensional MHD flow of viscous incompressible conducting fluid past various bodies, proving existence of solutions

01 p0126 A69-10164

Vector potential used to express equations of incompressible fluid motion in form suitable for digital solution, discussing boundary conditions

01 p0058 A69-10228

Axisymmetric transient thermoelastic problem for transversely anisotropic hollow cylinder, examining boundary value problems

01 p0166 A69-10302

Second order systems of linear differential equations eliminating all nonessential difficulties associated with initial value problem

01 p0104 A69-10316

Mixed boundary value problem of elastostatics for isotropic elastic cylinder containing strip crack opened by internal pressure, using auxiliary functions

01 p0167 A69-10317

Upper and lower bounds for static or geometric field in two and three dimensional elasticity theory, using Green functions

01 p0167 A69-10328

Orthotropic plates bending and thermal stress, analyzing basic equations

01 p0168 A69-10416

Symmetrically truncated right angle E-plane corner, placing electric and magnetic walls in symmetry plane, solving resulting boundary value problems

01 p0044 A69-10624

Finite difference method for boundary value problem for second order differential equation, demonstrating convergence

01 p0105 A69-10721

Boundary value problems in thin shallow shells of arbitrary planform analyzed by partial differential equations

01 p0171 A69-11071

Idealized delta wing free-free oscillations determination by deriving equations of motion for flexibility and rigidity and formulating boundary value problems

01 p0172 A69-11358

Contact problem of pair of nonhomogeneous semicircular regions solved by singular integral equations solution method

02 p0336 A69-11553

Thermoviscoelasticity equation solution for class of dynamic problems, giving problem solution for half space with arbitrary temperature field boundary condition

02 p0336 A69-11554

Boundary value technique for initial boundary value problems for linear and mildly nonlinear wave equations

02 p0271 A69-11733

Boundary value problem solution for arbitrary nonshallow cylindrical shells by small parameter method, assuming arbitrary geometry and hinged rectilinear edges

02 p0339 A69-11960

Nonlinear boundary value problem, discussing existence and uniqueness of solutions

02 p0272 A69-12131

Nonlinear boundary value problems direct generalized solutions based on linearization of Bubnov-Galerkin and Ritz method

02 p0272 A69-12136

Errors arising from inaccurate insertion of initial conditions in autonomous determination of coordinates of object moving along surface of spherical earth

02 p0281 A69-12137

Monograph of lectures on numerical solutions of linear, singular and nonlinear differential equations for boundary value problems using finite differences

02 p0272 A69-12157

Normal derivative of solutions to Dirichlet problem for elliptic quasi-linear equation and construction of given mean curvature hyperspace in curved space

02 p0272 A69-12221

First boundary value problem for linear second order parabolic equation with unbounded lowest order discontinuous coefficients and free terms, discussing solvability

02 p0272 A69-12222

Mixed boundary value problem for system of Navier-Stokes equations for viscous incompressible fluid in stationary motion in vessel, noting rotating fluid

02 p0272 A69-12223

Nonlinear integrodifferential equations of parabolic type with delayed argument, discussing boundary value problems with caloric and hereditary operators

02 p0273 A69-12249

Uniqueness and existence theorem concerning stability of solutions of mixed nonlinear boundary value problem, discussing generalized heat transfer phenomena

02 p0352 A69-12255

Method of particular solutions for use with quasi-linearization in solving nonlinear boundary value problems

02 p0273 A69-12550

Soviet book on linear and quasi-linear second order elliptic equations, emphasizing boundary value problems in various functional spaces

02 p0273 A69-12566

Optimal control of open loop aperiodically modulated discrete time systems, discussing solution of associated two point boundary problem

02 p0226 A69-12732

Convergence of Rayleigh-Ritz approximations to solution of elliptic boundary value problem applied to subsonic airfoil problem for 2D steady isentropic irrotational flow

03 p0361 A69-12846

Three dimensional unsteady heat conduction and temperature distributions in finite hollow circular cylinder under time dependent boundary conditions of second kind

03 p0530 A69-12861

Iterative transfer of boundary values to fictitious contour in numerical solution of partial differential equations [ONERA-TP-646]

03 p0454 A69-12874

Bounded solutions for systems of ordinary second order differential equations

03 p0455 A69-13257

Cauchy problem and mixed boundary value problem for parabolic system solved with thermal potential theory

03 p0455 A69-13259

Dirichlet problem for elliptical system, showing solvability of inhomogeneous system with uniform boundary values for half plane and circle cases

03 p0456 A69-13602

Second order elliptical operator for m-dimensional Euclidean space with open region bounded by closed surface

03 p0456 A69-13604

Critique of paper on theory of gradient instability in semiconductor currents, questioning boundary value problems solution validity

03 p0487 A69-13728

Numerical technique using transfer matrices to solve boundary value problems in structural analysis

03 p0526 A69-13736

Planar phased array of circular waveguides arranged in equilateral triangular grid, solving boundary value problem

03 p0406 A69-13829

Elastodynamic boundary value problem solution for stability in linear elasticity

03 p0530 A69-14066

Variational theorems on eigenvalues of Laplace finite difference operator with first order boundary conditions

03 p0457 A69-14230

Two point boundary value problems for determining buckling behavior of two hinged circular arches [ASME PAPER 68-WA/APM-18]

04 p0669 A69-14399

Plates yield point loads limit determination formulated as mathematical programming problem, using finite element representations for velocity and moment fields [ASME PAPER 68-WA/APM-21]

04 p0670 A69-14405

Ordinary nonlinear differential equations with linear boundary conditions, discussing formulation and proof of lemma and theorems to demonstrate existence

04 p0621 A69-14416

Ricmann boundary value problems for n pairs of functions, noting relation to validity of Noether theory

04 p0622 A69-14513

Book on nonlinear boundary value problems for ordinary second order differential equations, illustrating difference between linear and nonlinear problems concerning existence and uniqueness

04 p0622 A69-14600

Algorithm for numerical solution of variational problems for functions of two independent variables and boundary value problems using local variations method

04 p0622 A69-14616

Boundary value problem of hyperbolic equation with discontinuous boundary conditions

04 p0622 A69-14617

Nonlinear boundary value problem of elastokinetics solved by step-by-step integration to study thin walled shells stability under axial impact [DVL-853]

04 p0677 A69-14836

Numerical solution of nonlinear two point boundary value problems of boundary layer type, noting shock wave formation in supersonic nozzle

04 p0544 A69-14889

Variational theorems for stress function formulation of boundary value problems in linear theory of thin elastic shells

04 p0678 A69-14894

Differential-difference equations and nonlinear initial boundary value problems for linear hyperbolic partial differential equations, noting procedure based on method of characteristics

04 p0623 A69-14949

Existence theorem for periodic solutions of parabolic boundary value problem for infinite space time cylinder

04 p0624 A69-15004

Green matrix of periodic boundary value problem for system of linear differential equations

04 p0624 A69-15098

Periodic solutions for linear and weakly nonlinear heat conduction equations, obtaining omega-periodic solutions for initial boundary value problems

04 p0625 A69-15109

Method of lines for parabolic differential equations, transforming boundary value problems into initial value problem for system of ordinary differential equations

04 p0625 A69-15132

Numerical solution of elliptic equations by iteration result in convergence prevention and solution of Laplace and Poisson equations with singular Laplace operator

04 p0625 A69-15133

Doubly infinite sets of simultaneous linear equations used in electromagnetic boundary value problems solved by Asymptotic Anticipation Method

04 p0560 A69-15214

Book on linear boundary value problems of mathematical physics based on Green function covering Hilbert spaces, integral equations and spectral theory of differential operators

04 p0625 A69-15232

Book on boundary value problems of mathematical physics emphasizing solutions, Green functions, transforms and variational methods

04 p0625 A69-15233

Boundary condition description effect on numerical accuracy of series solution to boundary value problem by direct method

04 p0681 A69-15283

Numerical integration of elliptic mixed boundary value problem in region with curved boundary programmed in FORTRAN for general linear second order partial differential equation

04 p0625 A69-15287

Hybrid assumed mode solution of nonlinear partial differential equations/initial value problems/ in time-like independent variable

04 p0566 A69-15345

Point matching method for analysis of stress in incompressible solids of revolution, noting application to solid propellant rocket charges

04 p0683 A69-15518

Boundary conditions in oblique reaction waves in supersonic flow, adding or subtracting heat by chemical reaction

05 p0697 A69-15828

First order linear differential equations having complementary solutions of exponential type to determine effective initial and boundary conditions

05 p0786 A69-15926

Existence and uniqueness of solution to Cauchy problem for class of second order nonlinear differential equations, applying results to mixed boundary value problem

05 p0786 A69-16061

Boundary value problems for second order degenerate elliptic equations, formulating and proving theorems for existence of generalized solutions
05 p0786 A69-16422

Boundary value problems for unstable quasi-linear elliptic differential operator class, proving theorems on properties of quasi-linear elliptic-parabolic equations in bounded space
05 p0787 A69-16424

Functions satisfying mixed boundary conditions derived for boundary value problems involving regions of complex form
05 p0787 A69-16455

Invariant imbedding and multipoint boundary value problems in control theory and identification of systems
05 p0787 A69-16478

Approximate methods for integration of equations of plane isentropic motion of gas at supersonic velocities
05 p0699 A69-16674

Uniqueness theorem validity for boundary value problem in linear elastostatics for homogeneous media
05 p0844 A69-16739

Korn constant for boundary value problem of linear elastostatics applied to circular ring domain
05 p0844 A69-16740

Kinetic boundary value problem of gas flow over plane wall with constant mass-velocity gradient
06 p0910 A69-17346

Exponential decay of stresses in circular elastic cylinders subject to axisymmetric self-equilibrated end loads
06 p1023 A69-17507

Two point boundary value problems of optimal trajectories solved by offset vector method
06 p0903 A69-17577

Fiberglass reinforced plastic bottoms design for integration with cylindrical shells, discussing design, shapes and boundary value problems
06 p1025 A69-17685

Variational solutions of one dimensional nonlinear Poisson-Boltzmann boundary value problems in theory of colloids and plasmas
06 p0968 A69-17784

Shock wave in two dimensional mixed transonic airfoil flows, discussing initial value problem for flow downstream of shock
[AIAA PAPER 69-43] 06 p0915 A69-18180

Soviet collection of papers on boundary value problems and integral equations
07 p1172 A69-18495

Solvability of third boundary value problem for Laplace operator in three dimensional domains bounded by irregular surfaces
07 p1173 A69-18497

Elliptic equation solution of Dirichlet problem with zero boundary condition, examining dependence of modulus of continuity of solution on boundary properties
07 p1173 A69-18498

Cosserat functions for homogeneous isotropic elastic body filling finite domain with sufficiently smooth boundaries, noting eigenfunctions for first and second boundary value problems
07 p1173 A69-18499

Quasi-static theory of antenna in magnetoactive plasma subjected to resonance, solving boundary value problem
07 p1099 A69-18522

Gunn effect for cathode contacts with interface resistance, developing control characteristic boundary condition concept for explaining cathode fall and other phenomena
07 p1199 A69-18649

Methods to obtain uniqueness for partial differential /elliptic/ equations boundary problem extended to parabolic conditions, analyzing necessary conditions for existence
07 p1173 A69-18728

Linear differential system with boundary conditions, obtaining equivalent Fredholm integral equation and perturbation theorem
07 p1173 A69-18729

Boundary value problems for second order differential equation with continuous f satisfying local Lipschitz condition
07 p1173 A69-18730

Complex variable theory usefulness in investigating existence and uniqueness of solutions for boundary values in partial differential equation
07 p1173 A69-18731

Matched asymptotic expansions for establishing relationship between inner and outer expansions of unknown function, discussing classes of singular perturbation
07 p1180 A69-18809

Uniform matched asymptotic approximations derived for various functions, with application to boundary value problem for ordinary differential equation with turning point
07 p1180 A69-18810

Boundary value problem of temperature field and heat conduction in transparent media heated by laser radiation producing thermoelastic stresses leading to breakdown
07 p1149 A69-18925

Existence and uniqueness theorems for boundary value problems of axisymmetric deformation of circular membrane at normal pressure, using membrane theory and shooting method
07 p1233 A69-19299

Boundary value problem solved for free air geoid, developing expressions for height anomaly from free air anomalies
07 p1129 A69-19396

Shallow spherical shells equilibrium under uniformly distributed internal pressure, analyzing nonlinear boundary value problems by algorithm
07 p1237 A69-19685

Accelerating convergence of one step methods for numerical solution of ordinary differential equations, discussing various initial value problems
07 p1174 A69-19724

Boundary conditions for reflection and transmission properties of absorbing shell of arbitrary shape
08 p1273 A69-20025

Longitudinal excitations, discussing plasma equilibrium distributions
08 p1362 A69-20286

Sensitivity coefficients to solve two point boundary value problem arising from Pontryagin principle, with application to time optimal control studies
08 p1296 A69-20297

Mixed initial boundary problem for hyperbolic equations with given boundary outgoing variables, determining incoming data
08 p1342 A69-20347

Stieltjes transform relating initial boundary value problems for partial differential equations of various classifications
08 p1342 A69-20352

Error bounds and variational methods for nonlinear boundary value problems for ordinary differential equations
08 p1343 A69-20536

Soviet book on theory of heat conductivity covering physical principles of transfer and boundary value problems
08 p1421 A69-20647

Approximation method applied to closed viscous streamline flow in rectangular cavity, discussing constant shear stress boundary condition
08 p1304 A69-20811

Capacitance and lowest eigenvalue bounds for two dimensional anisotropic media as exemplified by transverse vibrations of stretched membrane
08 p1418 A69-20848

Two dimensional boundary value problem for symmetrical entry of wedge into incompressible nonviscous fluid using complex variable theory
08 p1305 A69-20995

Boundary value problem for linearized system of Navier-Stokes equations in three dimensional space, determining velocity vector and pressure
08 p1344 A69-21156

Sobolev type boundary value problems for elliptic operators using manifold theory
08 p1344 A69-21157

Cauchy problem of invariant imbedding satisfying nonlinear boundary value problem, discussing optimal control and radiative transfer applications
09 p1531 A69-21413

Particular solutions in nonlinear two point boundary value problems, showing convergence for uncontrolled and controlled systems
09 p1531 A69-21416

Numerical studies of initial value problems by boundary value techniques for cases having available asymptotic estimates or periodicity of solutions
09 p1532 A69-21610

Stabilization rate of boundary value problem for parabolic equation in n dimensional space
09 p1532 A69-21627

Normal solutions of linearized Boltzmann equation for initial and boundary conditions in hydrodynamics solved by approximation
09 p1480 A69-21667

Incompressible jets bounded by infinite auxiliary thin jets, discussing straight wall jets and establishing existence and uniqueness of boundary value problem solution
09 p1480 A69-21734

Irrrotational plane subsonic flow of compressible fluid about obstacle, reducing problem to integration of linear partial differential equation with boundary conditions
09 p1480 A69-21735

Difference schemes for approximating boundary value problems of elliptic equation free of mixed derivatives in rectangular region
09 p1532 A69-21788

Nonlinear boundary value problem algorithm in shell theory, showing aid of numerical technique
09 p1614 A69-21887

Perturbation theory for analyzing nonlinear boundary value problems
09 p1540 A69-21894

Single and double transformed Fourier series reduced to forms satisfying certain definite conditions, even with finite number of terms series
09 p1533 A69-22258

Solutions boundedness in autonomous nonlinear systems with single nonlinearity, using Lure type Liapunov functions to prove theorems
09 p1533 A69-22449

Electromagnetic wave diffraction on conducting sphere in inhomogeneous medium with given refractive index variation law, using asymptotic solution for boundary value problem
09 p1459 A69-22628

Fundamental solutions of initial value problems related to Euler-Poisson-Darboux equation generalized for radially symmetric case, developing convolution integrals
09 p1533 A69-22796

Higher order Rayleigh-Ritz approximations to eigenvalues and eigenfunctions of elliptic boundary value problem
09 p1534 A69-22798

Boundary value problems solutions for quasi-linear elliptic and parabolic equations of arbitrary order applied to nonlinear differential equations
10 p1717 A69-22809

Two point boundary value problems solution for parameter dependent nonlinear differential equations, noting application to hinged rod bending
10 p1718 A69-22846

Minimal distance of image boundary from origin and second coefficient of univalent function in unit disk
10 p1718 A69-22860

Five parameter class of linear iterative methods for solution of linear equations systems in application to elliptic boundary value problems
10 p1718 A69-22878

Numerical analysis for stresses in finite or infinite plate with arbitrary holes, considering boundary value problems
10 p1793 A69-22882

Navier-Stokes boundary value problem bifurcation solution analysis, determining stability ranges
10 p1677 A69-22901

Pointwise bounding of eigenfunctions in vibration and stability problems in elasticity theory
10 p1794 A69-22925

Generalized solutions of elliptic boundary value problems by applying Green functions
10 p1718 A69-23207

Finite difference schemes of high order of accuracy for Strum-Liouville and boundary value problems with regular singularity
10 p1719 A69-23365

Scheme for choosing approximating system of difference equations for degenerate linear and nonlinear elliptic boundary value problems
10 p1719 A69-23515

Boundary value problem for elliptic-parabolic partial differential equations in theory of random processes, obtaining analytical solution in terms of hypergeometric functions
10 p1719 A69-23516

Factorization procedure for iterative solution of systems of algebraic equations from discretization of elliptic boundary value problems
10 p1719 A69-23520

Stable difference expressions for initial and mixed boundary value problems
10 p1720 A69-23594

Singular perturbations for Cauchy and boundary value problems, considering differential operators and Hilbert space
10 p1720 A69-23635

Existence and oscillation of initial and boundary value problems solutions for real scalar second order differential equations
10 p1720 A69-23637

Existence and uniqueness for nonlinear boundary value problems satisfying Lipschitz condition
10 p1721 A69-23640

Equation for one dimensional heat conduction with nonlinear heat generation transformed from boundary to initial value problem

10 p1809 A69-23689

Existence and uniqueness of solution to Cauchy problem for class of second order nonlinear differential equations, applying results to mixed boundary value problem

10 p1721 A69-23885

Equivalence of initial boundary value problem and integral equations obtained by regularization using potential theory

10 p1721 A69-23959

Scattered light mean intensity determination in twilight aerosol atmosphere from satellite observations, formulating boundary value problem

10 p1689 A69-23970

Uniqueness and nonuniqueness of solutions of initial value problems for second order semilinear parabolic equations

10 p1722 A69-24069

Linear two and three dimensional boundary value problems in mechanics of continua for multiply connected regions

11 p1972 A69-24651

Two dimensional contained plastic deformation in asymmetrical elasticity theory based on Cosserat medium, examining boundary value problems, stress concentration and elastic wave propagation at holes

11 p1973 A69-24659

Conformal mappings for solving boundary value problems in elasticity and plasticity theories for regions having singular points

11 p1973 A69-24662

Mixed boundary value problem concerning expanding elastic space weakened by cracks located at same plane solved by integral transforms and Fredholm equations

11 p1973 A69-24663

Random periodic forces effect on single frequency oscillations of nonlinear nonautonomous system with distributed parameters, discussing perturbed boundary value problem

11 p1916 A69-24761

Boundary value problem for gravity induced wave motion of ideal fluid in axisymmetric vessel with annular ribs, noting application to bodies of revolution

11 p1868 A69-24769

Numerical method for coupled moments of inertia and integral equations of boundary value problems for fluid in moving cavities

11 p1868 A69-24774

Mixed boundary value problem in theory of axisymmetric potential of three dimensional boundary layer reduced to solution of linear integral equation

11 p1918 A69-24787

Boundary value problems numerical solutions accuracy assessed as function of grid spacing size

11 p1908 A69-24789

Asymptotic series solutions for initial value problem involving nonlinear ordinary differential equation with small parameter epsilon

11 p1908 A69-24881

Solution existence of nonlinear two point boundary value problems from uniqueness

11 p1909 A69-24883

Existence and completeness of eigenfunctions for boundary value problem arising in theory of small amplitude motions of stratified polytropic gas

11 p1868 A69-24884

Slip flow problem for general specular-diffuse boundary condition in kinetic theory of gases, noting molecular distribution function

11 p1869 A69-24893

Steady heat flow in cylindrical bodies with curvilinear rectangular cross sections, solving equation in form of Fourier series according to trigonometric functions

11 p2000 A69-24974

Kinetic theory for examining transition regime of rarefied gas dynamics, discussing Boltzmann equations and models with related boundary value problems

11 p1870 A69-25005

Stress-strain state of shells with opposite edges hinged and rigidly clamped solved by numerical method after reduction to boundary value problem

11 p1985 A69-25174

Initial conditions estimation problem for nonlinear system asymptotic stability and satisfaction of output constraints on state variables

11 p1909 A69-25290

Dynamic programming approach to numerical solution of elliptic boundary value problems, using Laplace equations

11 p1910 A69-25411

Optimal design of structures with constraints on strength and natural frequency, developing steepest descent boundary value method

11 p1989 A69-25496

Integral transforms in composite one dimensional space and application to boundary value problems of physics

11 p1910 A69-25574

Wave reflections due to rotationally symmetrical jump in circular waveguide cross section, using orthogonal expansion to solve resulting boundary value problem

11 p1855 A69-25622

Boundary conditions for time dependent temperature variations of calorimeter operating in regular thermal regime

11 p2003 A69-25702

Flow in linear MHD channel with two permeable electrodes, solving Riemann boundary value problem for electric field in channel

11 p1934 A69-25727

Theorem for integral expansion applied to boundary value problems of mathematical physics and elasticity theory for single sheet hyperboloids of revolution

11 p1910 A69-25731

Polynomial coefficients multiplication by weighted damping factors for increased conformal mapping and boundary value problems solutions accuracy for doubly connected regions

12 p2178 A69-25998

Nonoscillatory solutions of second order nonlinear differential equations

12 p2120 A69-26033

Optimization problem with bounded state variable, noting conditions on trajectories and relations for co-state vector at connecting or branching point

12 p2050 A69-26087

Elliptic boundary value problem for differential equation and pseudodifferential boundary conditions, obtaining Green formula from formulated conjugate problem

12 p2121 A69-26200

Periodic solution to boundary value problem for quasi-linear parabolic equation with nonlinear boundary conditions obtainable by Rothe method

12 p2121 A69-26282

Boundedness criteria for second order hyperbolic equation boundary value problem solution in Banach space

12 p2122 A69-26573

Approximate solution of boundary value problems for Fokker-Planck equation to determine probability of exceeding limits in nonlinear automatic control systems

12 p2054 A69-26653

Volterra operator algebra for boundary value problems involving linear viscoelasticity with continuous relaxation time and delay time spectra

12 p2182 A69-26677

Boundary value problems of thermoelasticity, discussing existence and uniqueness theorems, ellipticity, thermoelastopotentials, Liapunov-Tauber theorem, Fredholm theorems, etc

12 p2182 A69-26726

Boundary value problems for hyperbolic and mixed equations using model of wave, Lavrentiev-Bitsadze and Tricomi equations

12 p2123 A69-26727

Dirichlet problem for elliptic second order differential equations with constant coefficients in region of Euclidean space of two real variables bounded by ellipse

12 p2123 A69-26728

Cylinder buckling and other boundary value problems, applying inverse differential operators to solution of integrodifferential equations

12 p2186 A69-26841

Laser active media polarization in strong electromagnetic fields, solving boundary value problems

12 p2110 A69-26907

Existence theorems for partial differential equations theory for traction boundary value problem of linearized elastostatics

12 p2188 A69-26928

Dirichlet problem for second order linear hyperbolic partial differential equations in cylindrical domain, deriving necessary and sufficient condition for solution uniqueness

12 p2124 A69-26932

Smooth solutions to Navier-Stokes equation obtained by imposing bound on associated pressure pertaining to weak solution

12 p2124 A69-26971

Earth gravitational field representation by separating geopotential into normal and disturbing potential for

solving geodetic boundary value problem for satellite geodesy

12 p2076 A69-27089

Homeomorphism theorem of Petrovskii and homogeneous elliptic systems applied to boundary value problems and Green formula

13 p2287 A69-27515

Partially characteristic boundary value problem for partial differential equations

13 p2288 A69-27527

MHD generator analysis, formulating boundary value problem for ion diffusion and Fourier series solution for end effect of electrodes pair

13 p2208 A69-27613

Solar atmosphere surface radiation intensity determined by initial value theory including source function and resolvent

13 p2350 A69-27859

Second order differential equations eigenvalues with Sturm boundary conditions analyzed by difference method

13 p2288 A69-27922

Monograph on gravity covering gravimetric boundary value problem, iterative solutions, error analysis, gravity reduction, integral equations, etc

13 p2254 A69-27929

Boundary value problem for one dimensional unsteady equations for inviscid conducting gas during transition processes in MHD duct

13 p2309 A69-28027

Current distribution in MHD duct with permeable electrodes with tensor conductivity, obtaining Riemann-Hilbert heterogeneous boundary value problem solution by finding electric field

13 p2310 A69-28030

Perturbations stabilization in electrically conducting fluid by distributed automatic control system, determining feedback operators via boundary value problem

13 p2311 A69-28105

Stationary radial source flow of liquid particles into vacuum, discussing boundary value problem equations, parameters effects on flow structure and flow field characteristics

13 p2248 A69-28210

Variational difference method application to second order elliptic equations with inhomogeneous boundary conditions, applying results to boundary value problems in elasticity theory

13 p2289 A69-28318

Pointwise estimate for gradient of solution of first boundary value problem /Dirichlet problem/ for second order elliptic equation

13 p2289 A69-28319

Gasdynamic and Boltzmann equations relations in rarefied gas kinetics, applying physical and mathematical boundedness concept to setting boundary conditions for moment equations

13 p2250 A69-28320

Stability theorems for barotropic vorticity equation integrated within limited region for flow through boundary without existing physical boundary conditions

13 p2294 A69-28494

Steady state problems of elastic orthotropic cylinder solutions applicable to boundary value problems of laminar orthotropic elliptical cylinders

13 p2369 A69-28528

Green function for boundary value problems of heat conduction equation constructed by heat potentials method

13 p2380 A69-28548

Viscous incompressible fluid self similar mixing problems, performing group analysis for complete boundary value problem

14 p2428 A69-28803

Stress-strain problem of piecewise-homogeneous plane with cut normal to interface line reduced to Wiener Hopf equation, obtaining solution for arbitrary boundary conditions

14 p2531 A69-28805

Plane mixed boundary value problem in elasticity theory for infinite wedge

14 p2531 A69-28809

Asymptotic control theory for two point boundary value problems, considering Euler equation

14 p2425 A69-28904

Boundary value problem for nonlinear functional differential equations, discussing matrix and general operators

14 p2470 A69-28906

Liquid sloshing in vessel of complex geometry reduced to boundary value problem

14 p2428 A69-28969

Integral equations for classical elasticity boundary value problems, stressing analogous Stokes flow hydrodynamic equations

14 p2535 A69-29361

Two point boundary value problem converted into Cauchy problem, deriving power series solution method and algorithms for nonlinear problems

14 p2430 A69-29362

Difference schemes for elasticity theory plane dynamic problem with mixed boundary conditions, establishing scheme absolute stability

14 p2536 A69-29474

Boundary value problem in three dimensional boundary layer theory for incompressible flow near stagnation point

14 p2432 A69-29677

Computational accuracy of point matching solution for uniform nonsymmetric waveguides

14 p2423 A69-29758

Boundary problems solution for electromagnetic field two dimensional distributions in MHD channels at arbitrary magnetic Reynolds numbers, considering longitudinal terminal effects

14 p2500 A69-29906

Necessary and sufficient conditions for solution existence to second order boundary value problems, considering second order differential equation involving function of three variables

14 p2471 A69-29951

Variational principle for solving boundary value problems and reciprocal formula for error estimation, discussing applicability to general transport phenomena problems

15 p2716 A69-30022

Necessary and sufficient conditions for boundary point regularity in Dirichlet problem for heat conduction equation assuming Holder condition

15 p2716 A69-30047

Boundary value problem for quasi-linear equation of unsteady transonic gas flows, including linear model and operators for group of transformations

15 p2590 A69-30049

Green function construction for boundary value problems of heat conduction on rectilinear segment with dynamic boundaries, using integral equations

15 p2716 A69-30075

Finite difference treatment of mixed boundary value problems in two dimensional elastostatics, using first derivatives of displacement components at grid points

15 p2706 A69-30432

Averaging procedure for solving Cauchy problem applied to two point boundary value problem for nonlinear differential equations

15 p2644 A69-30449

Integral equation for diffraction from infinitely extended grating as mixed boundary problem of electromagnetic field, discussing single anomaly

15 p2568 A69-30795

High order plasma wave echoes formulation and relation to initial perturbations based on Landau solution of initial value problem for Vlasov equation

15 p2661 A69-30926

Monograph on stress fields in plane plastic flow as solutions to boundary value problems

15 p2711 A69-30932

Nonlinear boundary value problems for isotropic plasma with known magnetic field, examining electromagnetic waves scattering at magnetic fluctuations

15 p2569 A69-30938

Stress calculation for thermoelastic mixed boundary value problem in infinite isotropic plate with cylindrical stress free cavity

15 p2712 A69-31013

Heat propagation in rod of two sections with different properties, formulating relevant boundary value problem, solving with Duhamel principle

15 p2718 A69-31066

Attenuation of small perturbations in shape of plane shock wave propagating into uniform medium in presence of rigid or interfacial boundaries

15 p2592 A69-31145

Integral representation of p-analytic functions of complex variable, applying axisymmetric boundary value problems of elasticity theory for cylindrical surfaces and paraboloid of revolution

15 p2714 A69-31191

Asymptotic Krylov-Bogoliubov methods application to solving boundary value problems for hyperbolic quasi-linear equations with distributed parameters and retardation

15 p2653 A69-31192

Boundary value problem for linearized system of Navier-Stokes equations in three dimensional space, determining velocity vector and pressure

15 p2645 A69-31249

Sobolev type boundary value problems for elliptic operators using manifold theory

15 p2645 A69-31250

Book on mathematical methods in kinetic theory covering boundary value problems associated with Boltzmann equation, model equations, rarefied gas dynamics, etc

16 p2811 A69-31721

Langrangian equations resulting from restricted variational principles corresponding to heat conduction problem derived for boundary condition inclusion

16 p2877 A69-31872

Mixed boundary problem for elliptic equations with variable coefficients reduced to finite system of algebraic equations

16 p2804 A69-32062

Viscoelastic half space properties effect on self excited vibration boundaries determination

16 p2873 A69-32063

Plate bending problems, comparing various approximate analytical methods including point matching, Galerkin, Ritz, Kantorovich and least squares techniques [AIAA PAPER 68-296]

16 p2874 A69-32160

Unsteady heat conduction equations for elliptic cylinder with convection solved by point matching

16 p2879 A69-32171

Variational problem formulated for boundary value problem of steady heat conduction with general boundary conditions

16 p2880 A69-32378

Quasi-linearization algorithm for solution of boundary value problems for ordinary differential equations, formulating representation and convergence theorems

17 p2994 A69-32835

Algebra of quasi-homogeneous pseudodifferential operators applied to lateral boundary values of solutions of parabolic differential equations, discussing function spaces

17 p2994 A69-32842

Plane oscillations of liquid in rectangular elastic vessel determined to obtain frequencies and mode shapes of natural oscillations from velocity potential boundary conditions

17 p2950 A69-33200

Frequency and mode shapes of conical shell free oscillations related to shell parameters and boundary conditions

17 p3058 A69-33201

Initial thermostructural stresses in homogeneous quasi-isotropic two component medium, solving statistical boundary value problem thermoelastically

17 p3058 A69-33316

Wave diffraction problem solution method based on Rayleigh hypothesis equivalent to extended boundary condition method

17 p2920 A69-33422

Error estimation in thin elastic plate bending problem approximate solution by equal deflection lines method, constructing two sided bound for boundary value problems

17 p3062 A69-33713

Adaptive random search algorithm utilizing boundary cost-function hypersurfaces measurement to implement Pontryagin maximum principle, discussing hybrid computer use, iterative solution and convergence properties

17 p2933 A69-33745

Electromagnetic waves radiation in general time invariant linear media with general boundary conditions, using Green function

17 p2924 A69-33834

Numerical solution of boundary value problems, discussing spectral domain and scattering matrix formalisms

17 p2929 A69-33882

Forced harmonic oscillations of one dimensional mechanical girder systems allowing for nonlinear resisting forces calculated by boundary value problem reduction to Cauchy problem

17 p3064 A69-33917

Transformation of two dimensional boundary value equations for laminar power law nonNewtonian fluid flow to yield similar solutions

17 p2957 A69-34016

Orthogonal polynomials for solving plane elasticity theory boundary value problems without constructing mapping functions, noting applications

17 p3067 A69-34144

Green functions theory for finite integral Lebedev-Kantorovich transforms derivation, with application to elastostatics boundary value problems

17 p3067 A69-34148

Taylor vortices calculated as branching solutions of nonlinear Navier-Stokes boundary value problem

17 p2958 A69-34152

Alternating direction iteration method for nonlinear systems of equations applied to steady state heat conduction problem with nonlinear boundary conditions

18 p3163 A69-34329

Computer implementation of Bergman solution to initial value problem for partial differential equation of compressible fluid flow

18 p3164 A69-34614

Equations of motion for plate vibration derived by complementary variational principle, including boundary conditions and thin plate transverse vibrations

18 p3218 A69-34626

State space procedure for mixed boundary value problems applied to structural analysis, fluid mechanics and eigenvalues for deformable bodies

18 p3164 A69-34685

Parabolic differential equations solved by variational methods, constructing numerical representations for solutions of initial boundary value problems

18 p3164 A69-34841

Boundary conditions of orthotropic shell stability under external pressure and axial tension, analyzing critical pressure by strain energy method

18 p3222 A69-34977

Linear boundary value problem solution using iterative method

18 p3165 A69-35050

Periodic solution of boundary value problem involving motion equation of viscous fluid

18 p3123 A69-35053

MHD flow, deriving equation system and boundary conditions for gas dynamic process

18 p3181 A69-35054

Regular integral equations solvability for boundary value problems in shallow shell theory, using method of potential representations and Green matrices

18 p3224 A69-35309

Classical solution existence to mixed boundary value problems for second order hyperbolic operators obtained by Laplace transforms

18 p3165 A69-35313

Law for time variations of modulus-restricted control action at trajectory end, two point boundary value problem solution and use of Pontryagin principle

18 p3175 A69-35324

Plate dynamics generalized equations independent of plate theory hypotheses, discussing algorithm and initial and boundary conditions

18 p3226 A69-35376

Iterative algorithm applied to shell theory boundary value problem of stress concentrations at shallow shell holes

19 p3436 A69-35847

Two dimensional thermoelasticity problem for nonlinear media, obtaining solutions for thermal stress concentration and boundary value problems

19 p3436 A69-35848

Convergence rate estimates for singular perturbations solutions of linear elliptic boundary value problems

19 p3360 A69-35899

Function theoretic solution of dual integral equations applied to boundary value problem of supersonic flow over infinite span thin wing

19 p3239 A69-36311

Existence and uniqueness theorems for operator equation in differential equations theory for application to boundary value problem

19 p3360 A69-36373

Boundary conditions of incompressible fluid viscous flow on semiinfinite plate edge defined using difference methods for Navier-Stokes equations

19 p3299 A69-36394

Least squares method application to boundary value problem approximate solution for plane, axisymmetric, creeping and incompressible irrotational flows

19 p3299 A69-36475

Boundary conditions for shells with reinforced nonsymptotic boundaries, assuming coincident beam axis deformation with shell boundary deformation

19 p3443 A69-36781

Thermodynamic equilibrium stability general theory extended to arbitrary boundary conditions using properties of entropy balance equation

19 p3452 A69-36789

Benard convection cells analyzed by Boussinesq approximation and Schmidt-Liapunov method, obtaining boundary value problem branching solution

19 p3301 A69-36791

Number of forms of stability of plates and shells derived from eigenvalues of nonlinear boundary value problem containing generalized von Karman equations

19 p3445 A69-36816

Heat transfer problem involving temperature determination of body and ambient medium, deriving ex-

istence and uniqueness theorems for boundary value problems in curvilinear regions

20 p3631 A69-36991

Boundary value problem of wave propagation in three dimensional region of waveguide bounded by surface solved by variational method

20 p3487 A69-37078

Modified residue-calculus technique combined with scattering matrix multiple reflection techniques for boundary value problems in waveguide phased arrays, diffraction gratings, etc

20 p3505 A69-37298

Boundary conditions for differential approximation to radiative transfer, noting optically thick slip conditions

20 p3633 A69-37524

Particular solutions and quasi-linearization combined to solve nonlinear two point boundary value problems, illustrating method with Falkner-Skan equation

20 p3515 A69-37532

Plane membranes finite deformation, deriving energy theorems for potential U bounds estimation

20 p3624 A69-37588

Composite laminates in cylindrical bending, discussing classical laminated plate theory limitations by comparing boundary value problems to corresponding theory of elasticity solutions

20 p3626 A69-37760

Unbalanced cross-ply elliptic laminated plates with bending membrane coupling, analyzing membrane boundary conditions with clamping assumed

20 p3626 A69-37762

Buckling loads of homogeneous anisotropic plates of composite materials with simply supported boundary conditions, noting Kirchhoff-Love nondeformable normal hypothesis

20 p3628 A69-37776

Difference method for initial value problems in quasi-linear hyperbolic first order approximations extended to wider quasi-linear problems, assessing convergence

20 p3568 A69-37833

Rectangular plates bending boundary value problems, deriving formulas for plates with free edges

20 p3630 A69-38291

Perturbed motion of solid body containing axisymmetric cavities partially filled with ideal incompressible fluid, solving boundary value problems of fluid oscillations

20 p3518 A69-38296

Nonlinearly elastic plates with reinforced edges, deriving differential equations for boundary conditions

21 p3833 A69-38574

Jet efflux from two dimensional symmetric nozzles of arbitrary shape determined using conformal mapping and Riemann-Hilbert solution to mixed boundary value problem

21 p3692 A69-38686

Reduction of boundary value problems to initial value problems through variables transformation, considering application to eigenvalue problems

21 p3754 A69-38747

Shooting method difficulties in boundary value problem numerical solutions using computer programs to integrate differential equations

21 p3755 A69-38753

Combined analytical and numerical method for thermoelastic boundary problem of unidirectional infinite strip

21 p3836 A69-38927

Error function for boundary methods

21 p3755 A69-39008

Electromagnetic wave diffraction in three dimensional space divided by dielectric orthogonal half planes/wedges/, using contact boundary value problem

21 p3673 A69-39012

Partial differential equation initial value problems analyzed by ordinary differential equations via functional approximation method

21 p3756 A69-39132

Generalized solutions of elliptic boundary value problems by applying Green functions

21 p3756 A69-39148

Equivalence of initial boundary value problem and integral equations obtained by regularization using potential theory

21 p3756 A69-39150

Small parameter method applied to axisymmetric problems of elastoplastic nearly spherical bodies undergoing exponential hardening process, deriving linearized expressions for boundary conditions

21 p3839 A69-39198

Molodenskii boundary value problem exact solution by successive approximations for determination of earth figure, noting quasi-geoid surface

21 p3716 A69-39248

Approximate boundary conditions in electrodynamics of stratified tensor media estimated for ferrite layers

21 p3675 A69-39282

Closed form solution for minimum fuel constant thrust trajectories for vehicle transfer in vacuum between arbitrary boundary conditions

21 p3806 A69-39337

Nonlinear electromagnetic wave propagation by perturbation method previously employed to treat nonlinear boundary value problems involving partial differential equations

21 p3677 A69-39465

Relativistic solution by Landau procedure of initial value problem for one dimensional electron plasma wave coexisting with charged immobile background

21 p3778 A69-39579

Scattered light mean intensity determination in twilight aerosol atmosphere from satellite observations, formulating boundary value problem

21 p3717 A69-39656

Galerkin method application to solve differential equation and boundary value conditions for elastic stability of bars, showing linear relation between critical loads

21 p3845 A69-39678

Nonlinear differential equations for flow of viscous liquid thin sheet on horizontal plane, solving initial value problems for zero slope bed

21 p3697 A69-39680

Flight dynamics boundary value problem for spacecraft trajectories optimization, using variational method

21 p3817 A69-39817

Temperature field in system of coaxial cylinders by solving heat equation with corresponding initial and boundary conditions

21 p3855 A69-39855

Electromagnetic radiation and scattering from conducting bodies of revolution, obtaining formulation in integrodifferential equation from potential integrals and boundary conditions

22 p3899 A69-40014

Variational principles equivalent to mixed problems for parabolic equations with initial boundary conditions, noting heat conduction theory

22 p3974 A69-40231

Minimization of unconstrained function of several variables by gradient dependent techniques, discussing applications to boundary value problems in optimal control

22 p3975 A69-40333

Nonresonant Green functions of auxiliary boundary value problems for deriving integral equations for Dirichlet and Neumann diffractions at open screens

22 p3901 A69-40949

Elasticity boundary value problems solution based on equilibrating method and differential equation

22 p4046 A69-40967

Straight line method for boundary problems solutions with errors for partial differential equations

22 p3976 A69-41110

Analog problem solution for semiinfinite medium with Newtonian cooling at boundary, noting first term of asymptotic expansion in heat conduction equation

22 p4052 A69-41126

Lower boundary approximation for theory of thermal laminar steady state boundary layer on isothermal immersed plate

23 p4150 A69-41334

Boundary problem for differential equation of mixed type reduced to singular boundary problem for hyperbolic partial differential equations

23 p4181 A69-41409

Successive approximations method applied to boundary problem for quasi-linear parabolic equation in n dimensional Euclidean space

23 p4181 A69-41411

Boundary value problem solution for inviscid fluid flow past compliant body with analytical behavior of flow discontinued at points

23 p4151 A69-41525

Boundary effects on time dependent transport theory based on star product, noting application to transmission line theory and radiative and neutron transfer

23 p4190 A69-41571

N-th order differential systems using first approximation, finding conditions for bounded solutions, solutions asymptotic to zero and stability

23 p4181 A69-41722

Bernstein modes initial value-boundary value problem for half space of plasma bounded by wall and parallel unperturbed magnetic field

23 p4196 A69-41875

Differential equations of motion and associated boundary condition for axisymmetric flexural vibration of cylindrically anisotropic circular plate, using variational calculus

23 p4228 A69-41911

Boundary value problem of hydrodynamic equations discontinuous solution stability under random perturbations, analyzing combustion and detonation models

23 p4239 A69-41961

Normal derivative of solutions to Dirichlet problem for elliptic quasi-linear equation and construction of given mean curvature hyperspace in curved space

23 p4182 A69-41972

First boundary value problem for linear second order parabolic equation with unbounded lowest order discontinuous coefficients and free terms, discussing solvability

23 p4182 A69-41973

Mixed boundary value problem for system of Navier-Stokes equations for viscous incompressible fluid in stationary motion in vessel, noting rotating fluid

23 p4183 A69-41974

Complex configuration shells described by single analytical expression using R-conjunctive and R-disjunctive functions yielding boundary equations

23 p4229 A69-41991

Three dimensional mixed boundary value problem in elasticity by dominant states method, examining generalized Fourier series feature in Legendre polynomials

23 p4229 A69-41998

Differential operators representing potential energy of thin shell, discussing self conjugacy of boundary value problems

23 p4229 A69-41999

Rectangular waveguide with inhomogeneity represented by half space dielectric filling with boundary causing polarization, obtaining reflection elimination or minimization reflection

23 p4125 A69-42047

Numerical method for calculating unsteady two dimensional boundary layers in laminar incompressible flow

23 p4152 A69-42108

Stress concentration in shallow spherical perforated shell under loads, reducing boundary value problem to infinite algebraic equations solution

23 p4233 A69-42342

Uncoupled torsional vibrations of simply supported open cylindrical tubes analyzed by approximation equations, considering free edge boundary conditions

23 p4233 A69-42347

Flexural vibrations of simply supported lipped I section of cylindrical tubes, considering free-edge boundary conditions

23 p4233 A69-42350

Rigid/plastic solids subjected partly to uniform fluid pressure and partly to general boundary conditions, analyzing uniqueness and stability criteria

23 p4235 A69-42460

Wave propagation in dynamical theory of thermoelasticity, considering half space subject to step time strain, temperature and stress distributed over free surface

23 p4235 A69-42464

Kalman-Bucy filtering technique for estimation of initial conditions and smoothing in linear dynamic systems, noting rectilinear motion of randomly accelerated spacecraft

23 p4132 A69-42546

Elastoplastic boundary dynamic behavior in strip with crack determined by solving boundary value problem in elliptic integrals form

24 p4395 A69-42591

Buckling of truncated conical shells under torsion with various boundary conditions, applying Galerkin method to estimate critical load and wave number

24 p4395 A69-42715

Perturbation velocity potential of unsteady potential flow of barotropic gas past cascade of thin blades oscillating harmonically

24 p4244 A69-42716

Continuous dependence of boundary value problems of linear elastic body in smooth three dimensional region on force, elasticity and initial data

24 p4397 A69-42750

Boundary conditions for Tricomi equation in symmetric positive form, showing analytical and finite difference solutions

24 p4339 A69-42792

Initial deflection and internal pressure effects on supersonic panel flutter boundary of simply supported rectangular plates under diverse middle- surface stress conditions
24 p4400 A69-43056

Iterative finite difference method for initial value problems applied to hyperbolic system representing one dimensional time dependent flow of compressible polytropic gas
24 p4340 A69-43226

Wrong boundary conditions influence decay in over-determined difference approximations to hyperbolic partial differential equation
24 p4340 A69-43227

Optimization problems solution applied to separable but bounded state variable problem, providing control over commercial errors
24 p4292 A69-43286

Surface wave terms found in long wavelength limit during solution of initial value problem for semiinfinite hot plasma
24 p4356 A69-43364

Chaplygin equation applied to eddy flow past semicylindrical surface, discussing stagnation points and boundary value problems
24 p4245 A69-43477

Numerical solutions for time dependent boundary value problems governed by heat equation applied to transient heat conduction in irregularly shaped two dimensional regions
[ASME PAPER 69-HT-50] 24 p4410 A69-43521

Finite deformation of circular elastic membrane spinning with constant angular velocity, solving nonlinear differential equations by Runge-Kutta method for three boundary conditions
24 p4404 A69-43651

BOUSSINESQ APPROXIMATION

Boussinesq approximation for compressible fluids, discussing perturbation pressure and velocities and vertical scale motions
12 p2061 A69-26013

Viscous heat conducting compressible fluid response to abrupt change in circular cylinder angular velocity at stable temperature distribution, considering Boussinesq approximation
13 p2245 A69-27378

Optical refraction effects from refractive index gradients in stressed models as limitation on moire interferometry usefulness in Boussinesq problem and expanding pulse studies
14 p2531 A69-28883

Surface displacements at end of elastic semiinfinite circular cylinders due to annular axisymmetric loading, employing Boussinesq solution
15 p2711 A69-30872

Benard convection cells analyzed by Boussinesq approximation and Schmidt-Liapunov method, obtaining boundary value problem branching solution
19 p3301 A69-36791

BOW SHOCK WAVES

U SHOCK WAVES

BOW WAVES

Numerical calculations for oscillatory solutions of system of nonlinear differential equations, noting circularly polarized magnetic oscillations observed near earth bow shock front
02 p0241 A69-11729

Vela 3A and Explorer 33 elapsed time observations of earth bow shock
02 p0244 A69-12299

Quantitative determination of reentry shock precursor absorption level and effect on surface radiation heating, calculating radiative flux from shock layer enthalpy distribution
02 p0354 A69-12528

Solar wind interaction with moon, discussing core/surface layer conductivity and lunar limb shock wave formation
03 p0502 A69-14006

Detection of electric field turbulence in earth bow shock, noting wave amplitude correlation with magnetic field structure
04 p0592 A69-14681

Energetic electrons of terrestrial origin behind bow shock and upstream in solar wind
05 p0815 A69-16253

Plasma physics in space research, discussing solar wind, planetary atmosphere bow shock and convective motions of magnetosphere plasma
[ISAS-431] 06 p1000 A69-17026

Solar wind, bow shock and magnetosheath observations by charged particle analyzers on Vela satellites
07 p1208 A69-19361

Magnetopause, magnetosheath, bow shock and adjoining interplanetary domain study by IMP-1 satellite, discussing macroscopic plasma variables and fluid model for solar wind
07 p1129 A69-19374

Bow shock wave position and shape in rectilinear flight with constant acceleration
09 p1433 A69-21386

Reflected particle acceleration at magnetospheric bow shock front attributed to interplanetary electric field
09 p1577 A69-21714

Solar wind interaction with geomagnetic field, considering bow shock, field confinement in magnetosphere and stretching out of lines of force
12 p2072 A69-26735

Satellite observations of geomagnetic tail in magnetosphere near midnight meridian plane, discussing formation, shape, plasma sheet and models
12 p2072 A69-26739

Inviscid supersonic flow in right angle corner of varied angular intersecting wedges with bow waves remaining planar up to intersection line
13 p2200 A69-28251

Bow shock wave during rectilinear flight with varying acceleration, describing sonic boom loop mechanism
16 p2734 A69-32005

Transmission of Alfvén waves through earth bow shock based on hydromagnetic shocks theory, discussing amplitude amplification
16 p2777 A69-32099

Flow field study of merging between bow shock and viscous layer upstream of highly cooled axisymmetric blunt body in rarefied hypersonic stream
[AIAA PAPER 69-656] 17 p2893 A69-33498

Earth bow shock waves in far upstream interplanetary medium observed from magnetic data of Explorer 34 satellite
18 p3199 A69-34941

Earth bow shock electrical conductivity estimation from macroscopic equations without knowing microscopic dissipation processes
18 p3131 A69-35191

Shock wave interaction and bow shock wave establishment near sphere in presence of ionization relaxation, using time resolved schlieren photography
19 p3450 A69-36361

Magnetic fluctuations in various frequency ranges, associated with earth bow shock, detected with search coil magnetometer on OGO 3
22 p3938 A69-40501

MHD Rankine-Hugoniot equations for ion density, thermal pressure and convective velocity magnitude and orientation during Pioneer 6 traversal of earth bow shock
23 p4222 A69-42417

Fluctuating electric fields relations to MHD bow shock structure, using LF fluxgate magnetometer aboard OGO 5
24 p4306 A69-42693

Solar wind collisionless hydromagnetic flow interaction with planetary atmosphere, using mathematical model to determine bow shock position limits in atmosphere
24 p4368 A69-43178

BOX BEAMS

Box girders stress distribution analyzed by stress-freezing method compared with photoelastic measurement
15 p2705 A69-30419

Design laws of warping-free multicellular box beams under torsion or bending, using variational method
19 p3443 A69-36786

Bending creep tests on fabricated Al alloy box beams under constant load and temperature using continuous deflection and strain measurement
21 p3842 A69-39309

Strain distribution on surface of adhesive bonded box beam in simple bending, using water based brittle coating and self adhesive strain gages
21 p3844 A69-39325

Vibration properties of cantilever parallelogram box beam, using existing static deformation equations under large aspect ratio condition
21 p3846 A69-39803

BRACKETS

External load distribution in bracket between bolts and joint, verifying Reshetov mounting bolt formulas
23 p4168 A69-41417

BRADYCARDIA

Autonomic nervous system in control of heart rate in acceleratively stressed monkeys, discussing sympathetic, parasympathetic and bradycardia influence
06 p0875 A69-17844

Electrocardiographic T-wave changes related to bradycardia in healthy individuals, discussing T-wave inversion in people with vagotonia
09 p1445 A69-22557

BRAGG ANGLE

Bragg reflection of electrons by standing light waves of giant pulse laser
02 p0255 A69-11833

Phase grating formation in giant pulse laser Q switching liquid by reflecting light beam from Lippman plate at Bragg angle
05 p0771 A69-15811

Acoustical Bragg reflection and Debye-Sears effect with application to light and ultrasonics interaction
07 p1144 A69-18285

Far field of line source in medium with sinusoidally stratified dielectric constant, studying diffraction effects due to Bragg mechanism
17 p2925 A69-33842

Polarimeter using 45 degree Bragg angle reflection applied to rocket payload design for determining polarization of celestial sources X rays
23 p4207 A69-42382

BRAIN

NT CEREBELLUM

NT CEREBRAL CORTEX

NT CEREBRUM

NT HIPPOCAMPUS

Surgical radiolesion in human brain by high energy protons
03 p0374 A69-13501

Hypoxia effect on animal brain gamma-aminobutyric acid levels
04 p0552 A69-14482

One dimensional integral solution for cylindrical source generated transient temperature field and relation to thermal diffusivity of brain tissue
06 p0879 A69-17085

Uptake, metabolism and enzymatic synthesis of adrenaline in mammalian brain
07 p1066 A69-19260

Regional uptake of melatonin from blood or cerebrospinal fluid by rat brain
09 p1444 A69-21466

Computer analysis of cortical and subcortical activity in yellow bellied marmot during sleep, hibernation and hypothermia
10 p1643 A69-23122

Epinephrine forming enzyme phenylethanolamine-N-methyl transferase /PNMT/ in various brain regions of rats, cats, hens and turtles
10 p1644 A69-23303

Histochemical studies on nucleus basalis of Meynert of squirrel monkey
12 p2018 A69-25774

Penile erection electrically evoked from Macaca mulatta forebrain, measuring density and distribution of responding points
12 p2018 A69-25775

Measurement system for recording of small localized temperature changes in brain
15 p2606 A69-30152

Synaptic configurations in neuropil of planarian Dugesia dorotocephala brain, discussing neurotransmitters at phyletic level
16 p2741 A69-31555

Miniaturized FM telemeter for transmitting electrical activity of single nerve cells in brain of awake and unrestrained animal
19 p3261 A69-36270

Enzymes distribution in subfornical organ in squirrel monkey
20 p3478 A69-37934

Electrophysiological data for directionally sensitive units in optic tectum of mammals, indicating midbrain as site for rotating spiral motion aftereffects
20 p3480 A69-38264

Mammalian brain epinephrine metabolism data after isotonic saline perfusion into cranial vasculature
21 p3650 A69-38323

Control circuits in nature and sensory information data processing in human work, including servomechanism of brain-muscle system
21 p3652 A69-38784

Ultrasound-echo-encephalography in diagnosis of posttraumatic intercranial hemorrhage of skull and brain trauma, noting neuroanatomical techniques
21 p3652 A69-38790

EEG patterns evoked from left and right cerebral hemisphere by visual and verbal stimuli, showing asymmetrical role of hemispheres in governing cognitive behavior
21 p3656 A69-38976

Hyperbaric oxygen convulsions origin and site, studying pressure effect on brain electrical activity in rabbit by EEG

21 p3656 A69-38977

Brain weight and cholinesterase activity in rats after exposures to acoustic and light stimuli

21 p3662 A69-39627

Olfactory bulb removal effects on uptake decline of telencephalic norepinephrine, noting use for mapping adrenergic pathways

22 p3871 A69-40055

Mapping of biological potentials evoked in primary somatosensory fields by electrical signals on dorso-lateral surface of brain cortex of cats

22 p3886 A69-41121

D-amphetamine effect on single tectal neurons activity of cat opticum recorded by steel microelectrodes before and after intravenous injection

23 p4084 A69-41466

Brain and machine model of pattern recognition, pattern synthesis, memory, learning and speech, using concept of similarity, context and signal analysis

24 p4273 A69-42909

BRAIN CIRCULATION

Cerebral circulation under longitudinal acceleration, discussing rheoplethysmographic measurements of heart rate

05 p0710 A69-16625

Blood circulation in brain during acceleration analyzed by tensometric sensors and electroplethysmography, noting intracranial sensitivity to gravitational changes

06 p0874 A69-17646

Acceleration component in pelvis to head direction found influencing hyperemia of brain at various g forces

13 p2212 A69-28626

Cerebral circulation arterial system pulsatile flow flexible vessel digital simulation models distribution

19 p3264 A69-36867

Positive pressure breathing effects on cerebral arterial and venous blood pressure, hypothalamus and adrenal glands catecholamine content and cerebrum histological changes in dogs

24 p4265 A69-43371

Centrifugation for removal of bullet fragment floating freely in ventricular system of human brain to fixed safe position in left lateral ventricle wall

24 p4265 A69-43372

BRAIN DAMAGE

Head injury clinical and laboratory long term follow-up data, discussing conscious state alterations, focal neurological deficit, EEG abnormalities, etc

01 p0022 A69-11346

Cerebellar cortex function disorders of rats subjected to 10 g acceleration under weak anesthesia

02 p0198 A69-11504

Visual systems of hamster brain, discussing relative visual localization and discrimination blindness produced by ablation of cortical or tectal areas

08 p1265 A69-20685

Mechanical vibrations and noise effects on acetylcholine concentration, esterase activity and synthesis ability in rat brain

23 p4079 A69-41381

Civil pilots medical certification after head trauma, evaluating current methods efficiency

23 p4086 A69-41687

Brain atrophy clinical diagnosis aided by biochemical analyses, including age frequencies and symptoms to control incidence among aviation personnel

23 p4089 A69-41816

BRAIN STEM

Learning model of brain stem reticular formation based on nonlinear probabilistic hybrid computer concepts

05 p0711 A69-15802

Unisensory and multisensory signal processing in cortical and brain stem regions of albino rat by electronic averaging and time histogram techniques

23 p4092 A69-42055

BRAKES [FOR ARRESTING MOTION]

NT AERODYNAMIC BRAKES

NT AIRCRAFT BRAKES

NT DRAG CHUTES

NT LEADING EDGE SLATS

NT TRAILING-EDGE FLAPS

NT WING FLAPS

Brake system components automatic testing for pneumatic or hydraulic integrity essential to safe system performance

17 p2978 A69-33377

Pressure distribution over lining of brake shoe for brake drums design, discussing pressure compensation after wear

18 p3149 A69-35287

Descent device for emergency egress from jumbo jets based on centrifugal brake, including test data on C-5 fuselage section

19 p3255 A69-36146

BRAKING

Exterior arresting devices for commercial aircraft full scale tests

03 p0367 A69-14104

BRANCHING [PHYSICS]

Perturbation theory for branching analysis of perfect and imperfect discrete conservative structural systems

08 p1417 A69-20822

BRASSES

Material memory effect in plastically prestrained thin walled brass tubes analyzed on basis of kinematic strain hardening theory

02 p0336 A69-11551

Dry dynamic friction of brass disk against steel surface reduced using ultrasonic oscillations creating air gap

18 p3135 A69-34587

BRAYTON CYCLE

Thermodynamic comparison of MHD generators using Brayton and Rankine cycles, showing Rankine cycle conversion at higher channel Mach numbers for nonequilibrium ionization

03 p0369 A69-14154

Mathematical model, analog computer simulation and information comparison of closed Brayton cycle systems for power conversion [ASME PAPER 69-GT-50]

09 p1442 A69-22479

Small gas turbine Brayton cycle analysis treating component efficiencies as dependent variables in examining single stage radial compressor and turbine aerodynamic configuration [IME PAPER 5]

12 p2147 A69-25794

Turbomachinery buffer seals, buffer gas regulation and cleanup systems for operation of closed Brayton cycle power conversion system with gas cooled nuclear reactor

13 p2268 A69-27367

Nuclear energy conversion for long space missions, comparing dynamic Brayton, liquid metal MHD gas, dynamic Rankine and LMMHD Rankine cycles

16 p2810 A69-31748

Closed Brayton cycle power systems for space, lunar, terrestrial and undersea environmental conditions, discussing design and performance

23 p4071 A69-42277

Brayton-B generator for 2-10 kwe production, describing design, heat source/rejection, efficiencies and preliminary test data analysis

23 p4071 A69-42278

Argon turboalternator design and testing for Brayton cycle space power system, discussing inlet operating temperature and shaft bearings and rotation

23 p4071 A69-42279

Analog computer simulation of single shaft Brayton cycle system dynamics, including startup and shutdown transients

23 p4071 A69-42280

BRAZIL

Brazilian space activities covering launching sites, rocket experiments in meteorology, ionosphere and X ray astronomy, balloon experiments and ground observations

15 p2724 A69-31434

BRAZING

NT LOW TEMPERATURE BRAZING

Beryllium assemblies for aerospace and nuclear requirements, emphasizing braze joining structural components and effective manufacturing methods [SAE PAPER 680651]

03 p0433 A69-13454

Braze bonds of refractory electrical contacts using induction heating

04 p0607 A69-15218

Titanium alloy interaction porosity with fillers during diffusion brazing, discussing joint strength as function of time, temperature and pressure

06 p0945 A69-17896

Reliable fluid transmission systems by brazed joints, noting base and filler metals, fitting designs and various processes

09 p1507 A69-22333

Joining methods for fabricating thorium dispersion strengthened nickel and nickel chromium materials

09 p1509 A69-22342

Vacuum brazing technique for joining dissimilar metals without oxide and nitride film contamination

09 p1509 A69-22343

Radiographic, ultrasonic, thermographic and leak test quality control for brazed liquid propellant rocket engine components

10 p1699 A69-23054

Metal joints mechanisms in soldering, brazing and welding

14 p2455 A69-29344

Salt bath brazing for honeycomb structures, describing brazing techniques for thorium dispersed Ni and NiCr, Rene 41 and Ti honeycomb panels

19 p3320 A69-35557

Ti honeycomb sandwich panels, comparing properties of Ti and Al based brazing alloys

21 p3730 A69-38665

Bonding mechanisms in Mo-Mn-Ti metallizing and Cu brazing in metal to ceramic seals by strength test, microscopy and electron probe microanalysis

21 p3733 A69-39599

Step cathodic flux cleaning of furnace brazed Al assemblies used in combination with ultrasonic and chemical conversion coating techniques

24 p4319 A69-42938

Al brazed Ti honeycomb sandwich structures brazed in vacuum and Ar, analyzing mechanical properties and corrosion resistance as functions of temperature and pressure

24 p4324 A69-43435

BREADBOARD MODELS

Breadboard chip for use in computer aided design and analysis of integrated circuits, describing components and application to differential amplifiers

03 p0402 A69-13008

Electron beam meter application as lunar surface electric field detector, discussing breadboard model and performance characteristics

03 p0429 A69-13221

Breadboard technique and interconnection for fluidic circuits in large systems

05 p0705 A69-16009

Linear limit uniaxial stresses for stress-strain and stress-birefringence in photoelastic and mechanical model materials

20 p3628 A69-37777

BREAKAWAY

U BOUNDARY LAYER SEPARATION

BREAKDOWN

Gas breakdown in HF uniform electric field with/without steady transverse magnetic field

07 p1194 A69-19415

Dynamics of pulsed microwave breakdown in nonuniform field at waveguide fed mica aperture, noting electric field distribution change due to initial plasma configuration

07 p1107 A69-19448

Microwave breakdown dependence on elevated gas temperature in electric arc shock tube, considering air, nitrogen and argon

16 p2749 A69-31693

BREAKERS [ELECTRIC]

U CIRCUIT BREAKERS

BREATHING

Respiratory system control processes hypotheses experimental verification

01 p0019 A69-10209

Physiological effects of breathing cool dehumidified air in hot humid environment, tabulating tolerance time, heart rate, temperature changes and sweat loss

09 p1446 A69-22543

Respiratory system control processes hypotheses experimental verification

14 p2408 A69-28745

BREATHING APPARATUS

NT OXYGEN MASKS

High oxygen concentration breathing effect on foveal thresholds, using sea level tests on trained observers

02 p0203 A69-12216

BRECCIA

Amphoterite (LL) chondrites Rb-Sr age determination, noting high brecciation

21 p3814 A69-39583

Meteorite impact hypothesis supported by autotichonous and mixed breccias, shattercones and microscopic shock deformation evidence in central uplift rocks at La Malbaie structure

22 p4021 A69-40410

BREEDER REACTORS

Liquid metals as coolants in breeder and space vehicle reactors for stable two phase flows

05 p0803 A69-15998

BREMSSTRAHLUNG

Ionized plasma radiation near plasma frequency, deriving formula for bremsstrahlung coefficient from Born approximation

02 p0286 A69-11589

Solar radio emission slowly varying component theory, discussing main characteristics of cyclotron and bremsstrahlung radiations of thermal electrons

02 p0314 A69-11636

Dipole and quadrupole bremsstrahlung and damping of electron plasma oscillations, finding negative k-square collisional electron-ion contribution

03 p0475 A69-13149

Enhanced bremsstrahlung from supraluminous and subluminal waves in thermal isotropic homogeneous Maxwellian electron plasma, noting applicability to Crab Nebula

03 p0507 A69-13150

X ray emission from Seyfert galaxy nuclei, noting model with bremsstrahlung from hot source

04 p0649 A69-15387

Magnetobremstrahlung /synchrotron/ and Cerenkov radiation of ultrarelativistic particles, radiation reabsorption and magnetic field measurement

06 p0962 A69-17245

Solar X ray bursts decay curves and spectra in 10 to 150 keV range interpreted as hot coronal condensation during flare and electron bremsstrahlung

07 p1206 A69-19250

Sco XR 1 optical and X ray spectra simultaneous observations during rocket flights

07 p1220 A69-19391

Electron energy distribution function in plasma heated by electron-cyclotron resonance in adiabatic trap determined from bremsstrahlung spectrum

08 p1365 A69-20547

High temperature regions cooling as applied to solar flares, considering energy losses due to heat conduction, bremsstrahlung, line emission and recombination radiation

09 p1588 A69-21362

Hard X ray event spectrum representation by thermal bremsstrahlung spectrum emitted by energetic electrons, determining various physical parameters of source

09 p1579 A69-22180

Nonthermal intergalactic bremsstrahlung model as isotropic X ray background due to subcosmic electron interactions with thermal ionized gas in expanding universe

11 p1947 A69-24595

Poisson formula in double logarithmic approximation for photon emission cross section in analysis of bremsstrahlung involving high energy particles

11 p1922 A69-25758

X ray emission from radio galaxies as possible bremsstrahlung radiation of hot gas, noting Crab Nebula

12 p2166 A69-27037

Form factor of nucleus effect on high energy muons bremsstrahlung cross section

13 p2333 A69-28422

Plasma electron temperatures from electron bremsstrahlung spectra measurements in X ray region

14 p2496 A69-29783

Low energy neutral bremsstrahlung cross sections for Ne, Ar and Xe, using rapid scanning spectrometer

15 p2657 A69-31159

Radiative scattering cross sections of electrons from neutral O and atomic and molecular N using rapid scanning spectrometer for bremsstrahlung intensity

15 p2657 A69-31160

Near horizontal air showers relationship to direct muon production and heavy triplet particles of unit charge, discussing nuclear interactions and muon bremsstrahlung

15 p2678 A69-31499

Continuum radiation measurements for bremsstrahlung and recombination of neutral and ionized nitrogen

16 p2823 A69-32466

Origin of galactic gamma rays, discussing evidence in support of interstellar gas in galactic disk and production of neutral pions and bremsstrahlung

16 p2852 A69-32806

Center to limb variation of solar hard X ray bursts, suggesting inverse Compton effect and bremsstrahlung from anisotropic electrons

17 p3023 A69-33055

High temperature regions cooling as applied to solar flares, considering energy losses due to heat conduction, bremsstrahlung, line emission and recombination radiation

18 p3197 A69-34752

Neutrino-pair bremsstrahlung for hot degenerate electron gas during Coulomb scattering on imbedded nuclei in stellar regimes including lattice structure effects

18 p3176 A69-35004

Solar bremsstrahlung intensity dependence on heliographic longitude, noting maximum intensity shift toward electron beam direction

20 p3589 A69-37552

Cosmic X ray bremsstrahlung due to collisions of suprathermal protons with ambient electrons, giving clue about diffuse sky background of X rays

22 p4006 A69-40643

Stellar neutrino energy loss due to electron-electron neutrino bremsstrahlung in nondegenerate gas determined from transition probability for charged baryons or leptons interaction

24 p4351 A69-42794

Solar X ray bursts decay curves and spectra in 10 to 150 keV range interpreted as hot coronal condensation during flare and electron bremsstrahlung

24 p4372 A69-43613

BREWSTER ANGLE

Parallel and coplanar Brewster angle grinding of maser tube ends

03 p0440 A69-13302

Brewster angle window degradation of high power ionized argon gas lasers

[IEEE PAPER L-4] 05 p0775 A69-16322

Brewster angle lenses for low cost low loss laser beam transmission system

07 p1148 A69-18863

F cosine i theorem validity for VLF radio wave absorption in ionosphere tested using exponential electron density models, noting Brewster angle influence on reflection coefficient

13 p2222 A69-28473

BRIDGMAN METHOD

Temperature gradients effects on GaAs crystals grown by Bridgman method

23 p4199 A69-42469

BRIGHTNESS

NT SKY BRIGHTNESS

Metagalaxy temperature brightness explained from radio sources combined radiation with inversion spectra

02 p0313 A69-11632

Mercury radio emission phase dependence, discussing brightness temperature value approximation and surface layer properties

02 p0314 A69-11640

Solar continuum intensity determination in middle IR, obtaining solar disk center brightness temperature measurement by comparison with black body model

02 p0318 A69-12041

Mercury radio emission theory, calculating Mercurian brightness temperature as function of solar illumination and distance from sun

03 p0512 A69-13688

Photospheric brightness differences and structure of large scale intensity fluctuation, discussing association with solar supergranulation and chromospheric network

03 p0515 A69-14037

Venus brightness temperature between 0.75 and 1.65 cm from radio emission measurements, taking into account water vapor in Venus atmosphere

04 p0658 A69-14960

Spectral brightness of clouds and various terrains in visible and near IR regions measured from aircraft

06 p0953 A69-17991

Radio wave brightness temperatures and contrast characteristics in presence of clouds and precipitation

06 p0954 A69-17999

Lunar opposition effect theory applied to Mars opposition effect on brightness

07 p1214 A69-18616

Solar intensity measurements at 1.2 mm during partial solar eclipse, noting solar limb brightening and intense solar outburst near end of eclipse

07 p1217 A69-19243

Whipple and Douglas-Hamilton systematic corrections for periodic comets, considering constant coma brightness of P/Tempel 2 since 1874-1904 observations

08 p1408 A69-21137

Amplitudes and rates of brightness increase during supernova outbursts, calculating released energies

09 p1587 A69-21358

Brightness curves of eclipsing systems under monotonicity of unknown functions, using stable algorithm

09 p1588 A69-21363

Limb darkening nonlinearity effects on solutions for brightness curves of eclipsing binaries

09 p1588 A69-21364

Galactic dust layer spatial structure and relation to brightness of Milky Way based on analysis of photoelectric color excesses in Aql and Cyg stars

09 p1590 A69-21381

Auroral spectrum observations for absolute brightness of nitrogen Meinel and ING systems, considering background night airglow and atmospheric extinction

10 p1681 A69-23161

Sagittarius A occultation by moon, determining peak brightness and flux density of radio source

11 p1958 A69-24592

Atmospheric scintillation effect on planetary brightness distribution over disk from photometric measurements

11 p1960 A69-24729

Brightness coefficients for isotropic scattering of homogeneous plane layer in turbid medium, using Legendre polynomials

11 p1960 A69-24733

Brightness temperature distributions from intensity interferometric measurements reconstructed by computation

11 p1888 A69-25256

Photospheric magnetic fields, coronal emission and filaments distribution relationship with 1420 MHz radio emission, noting brightness and plasma density increase

11 p1964 A69-25417

Instability phenomena encountered in galaxies determined based on classification of galaxies according to mass and brightness

12 p2163 A69-27019

Model atmosphere source function, mean intensity and flux by matrix methods

13 p2288 A69-27564

Far IR and millimeter solar continuum, analyzing flatness of limb darkening curves and brightness temperature near minimum

13 p2341 A69-27591

Luminous spherical fog layer surrounding burning zirconium droplet during free fall through oxygen containing atmosphere, noting effect on mass and heat transfer processes

13 p2380 A69-28462

Shock wave radiation screening by thermodynamically unstable gas, discussing brightness and gas temperature relative to shock wave front position

14 p2493 A69-29673

Photographic photometry of comet Ikeya-Seki during passage near sun, plotting isophotes of coma and tail and brightness distribution diagrams

15 p2685 A69-30527

Photographic observations of comet Kilsten 1966b, estimating brightness, absolute magnitude and color index

15 p2685 A69-30529

Radio observation of 20 May 1966 solar eclipse at 9470 and 3300 MHz, discussing brightness distribution of S component sources

17 p3030 A69-33057

Angular velocity effects on meteors apparent brightness

17 p3045 A69-34222

Venus brightness temperature between 0.75 and 1.65 cm from radio emission measurements, taking into account water vapor in Venus atmosphere

18 p3197 A69-34723

Amplitudes and rates of brightness increase during supernova outbursts, calculating released energies

18 p3197 A69-34748

Brightness curves of eclipsing systems under monotonicity of unknown functions, using stable algorithm

18 p3197 A69-34753

Limb darkening nonlinearity effects on solutions for brightness curves of eclipsing binaries

18 p3197 A69-34754

Galactic dust layer spatial structure and relation to brightness of Milky Way based on analysis of photoelectric color excess in Aql and Cyg stars

18 p3198 A69-34769

Noctilucent cloud layer spectral brightness and transparency in E region determined from transhorizon rocket observations

18 p3130 A69-35148

White light solar corona brightness distribution observations /1964-1967/, considering solar flux relationship and equatorial electron densities

18 p3205 A69-35394

Brightness distribution over source, discussing regularization algorithms for radio astronomical data reduction from crossed telescope 20 p3606 A69-38033

Lunar photometric function near zero phase from Apollo 8 closeup photography, noting higher reflected brightness than at 1.5 degree phase angle 23 p4220 A69-42380

BRIGHTNESS DISCRIMINATION

Visual sonar target detectability probability function of retinal position and brightness contrast 02 p0203 A69-12218

Lunar thermal radiation measurements at 8.6 and 3.2 mm wavelengths, noting brightness temperature-time relationship in curves and as Fourier components 02 p0327 A69-12717

Observations of Venus at 15.4 GHz establishing upper limit for brightness variation with phase angle 08 p1382 A69-19818

Brightness in blue light and radial velocity variability of metallic line star 28 Andromedae 08 p1395 A69-20637

Celestial navigation system using photodetectors, comparing numbers and brightness of S4, S20 and silicon stars 10 p1775 A69-23190

Polarized brightness distributions of supernova remnants IC 443 and W44 at 6-cm wavelength from observations with 6 minute resolution 10 p1787 A69-24113

Star motion perturbations by invisible body, stressing bright bodies invisible by position near perturbed star 17 p0304 A69-33407

Brightness of fixated element in visual field as function of element luminance 22 p3880 A69-40853

Linear models with self excitation for brightness and contrast perception studies in human visual system 22 p3881 A69-40862

Hue shift and brightness enhancement of flickering light measured as function of illuminance, wavelength and target size 22 p3882 A69-40871

Human response to visual beat phenomena by combining intermittent stimuli, considering brightness estimation 22 p3884 A69-40889

Brightness discrimination judgments for gray chips by humans, using psychophysical limits method and white, noncoherent red and He-Ne laser light sources 24 p4276 A69-43323

BRILLOUIN EFFECT

Radiation damage in CdS irradiated by normal mode or Q-switched ruby laser, discussing stimulated Brillouin scattering 02 p0257 A69-12614

Ruby laser to study stimulated Mandelstam-Brillouin scattering in liquids and in various crystals in UV 03 p0438 A69-13053

Laser power increase noting influence of Mandelstam-Brillouin induced backscattering 04 p0612 A69-15414

Passive Q switching of solid state lasers based on stimulated Mandelstam-Brillouin light scattering 05 p0770 A69-15699

Laser beam scattering by acoustic waves of ionized crystal, reconsidering stimulated Brillouin emission theory for ultrasonic yield 05 p0777 A69-16610

Stimulated Mandelstam-Brillouin scattering in compressed N and H as function of pressure, using ruby laser pulses 09 p1516 A69-21562

Light polarization from stimulated Brillouin effect in compressed gaseous nitrogen, presenting depolarization variations as function of gas density and laser power 09 p1516 A69-21691

Stimulated Mandelstam-Brillouin scattering at second harmonic of ruby laser and neodymium glass laser 09 p1520 A69-22684

First Stokes component of stimulated Mandelstam-Brillouin scattering and line defects caused by self focusing of single pulse laser beam 09 p1521 A69-22686

Stimulated Brillouin scattering application to measurement of hypersonic velocities and absorption in gigahertz frequency range, laser frequency shifting and Q switching, etc 23 p4167 A69-42183

BRILLOUIN FLOW

Trajectory equations for outermost electron on beam in TWT operating in dynamic mode for Brillouin flux 03 p0406 A69-13974

Spontaneous reverse current due to Brillouin EMF observed in diode in thermal noise range 10 p1661 A69-22950

BRIQUETS

Molybdenum fiber sintering activation by adding nickel, noting decrease in impact viscosity 10 p1711 A69-23336

BRISTOL-SIDDELEY OLYMPUS 593 ENGINE

Low pressure fuel system and turbine rotor blade temperature measurement method for Concorde Olympus 593 engine [ASME PAPER 68-GT-63] 06 p0984 A69-17187

BRITISH AIRCRAFT CORP AIRCRAFT

U BAC AIRCRAFT

BRITTLENESS

Spin tests to determine brittle fracture under plane strain, using cyclic thermal stress or hydrostatic pressure to generate fatigue crack in rotor blank 03 p0524 A69-13060

Brittle surface films role in stress-corrosion phenomena in various environments 03 p0448 A69-13873

Theoretical buckling load for single edge notched struts, discussing brittleness effects 05 p0837 A69-16064

Griffith biaxial fracture criterion for porous brittle materials based on continuum model with random infinitely sharp cracks [ASME PAPER 68-WA/MET-12] 05 p0838 A69-16152

Hydrostatic tension test of brittle material using spherical specimen bonded into center of cube of matrix material 05 p0784 A69-16434

Griffith crack in brittle material, discussing validity for rock-like material with nonlinear stress-strain relationship 06 p1020 A69-17128

Ultrahigh strength steel susceptibility to brittle fracture, describing methods of testing rupture toughness and stress intensity factor 07 p1158 A69-18402

Crack front and zone in brittle elastic body under high pressure at wall inside body 07 p1231 A69-18699

Hydride, cold, irreversible and reversible hydrogen brittleness in titanium and titanium alloys 07 p1162 A69-18772

Brittle fracture models compared with experimental stress analysis results, noting plane strain and plane stress fracture toughness 07 p1234 A69-19379

Prandtl brittle fracture model modified for semi-finite crack in infinite body, discussing microscopic and macroscopic relation and crack propagation kinetics 07 p1237 A69-19682

Brittle crack theory analyzed to justify Irwin criterion at crack ends, dismissing Kristianovich-Barenblatt assumption and solutions for elastic problems 07 p1238 A69-19689

Stresses nature at ends of brittle cracks, discrediting finiteness under certain conditions 07 p1238 A69-19691

Brittleness and physical causes of cold shortness in Cr, discussing high purity metal formation and fine and superfine grain structures synthesis 09 p1526 A69-22147

Refractory ceramic materials use for advanced combustion chamber design, stressing brittleness effect and current fabrication techniques 09 p1531 A69-22624

Micromechanism of crack propagation in brittle fracture, considering kinematics for steady state crack in plane strain and energy dissipation 10 p1796 A69-23070

Bending creep vacuum testing device for brittle materials at high temperatures, noting load variation capability 10 p1696 A69-23851

Dissolved gases and carbon effect on transition temperature from plastic to brittle state of high melting metals including niobium and vanadium 10 p1715 A69-24011

Brittle fracture of steel analyzed using statistical model, attributing occurrence to coalescence of arrested cracks initiated at different points 10 p1803 A69-24033

Semibrittle material decompaction influence on stress distribution in infinite plate with edge loaded circular hole, noting stress-strain relation nonlinearities 11 p1972 A69-24656

Three dimensional problems in crack theory for unbounded brittle body, deriving critical loads from limiting equilibrium equation 12 p2178 A69-25997

Strain rate and pressurization effect on ductile-brittle transition temperature of polycrystalline sintered W, discussing yield stress 12 p2117 A69-27138

Metallographic aspects of fracture, analyzing very brittle solids, Griffith cracks, ductile solids and ductile to brittle transition 13 p2274 A69-27225

Structural modes of fracture, analyzing brittle, ductile, fatigue and stress corrosion fractures using fractography 13 p2274 A69-27226

Continuum mechanics for brittle fracture analysis in metal structures, discussing plastic limit loads 13 p2275 A69-27228

Stress waves analysis of brittle fractures, considering loading time role and cavitation of viscous fluids relation to fracture incipience 13 p2275 A69-27229

Sensitivity decrease of reversible temper brittleness of low alloy steels due to Mo inhibiting effect on phosphorus diffusion 13 p2283 A69-28491

Oxygen content and grain structure influence on TS5 Ti alloy mechanical properties, notch and crack growth sensitivity at low temperature 15 p2637 A69-30266

Brittle toughness determination method compared with Robertson and notch impact tests, evaluating steel susceptibility to brittle failure propagation 16 p2795 A69-32796

Dislocation and energy balance analysis of ductile and brittle metal cracks for determining metal fracture strength from plastic deformation 17 p3052 A69-32984

Ti-Al base alloys brittleness and stress corrosion cracking, discussing diffusion mechanism, hydrogen mobility, dislocations, etc 17 p2987 A69-33372

Alloying elements effects on low temperature metal fracture, considering changes in ductile-brittle transition flow due to solute 17 p2988 A69-33551

Fracture toughness of structural steels, discussing evaluation methods for brittle fracture resistance, toughness values and ratings correlation, etc 17 p2989 A69-33554

Reliable structural joints and attachments design for components fabricated from nonmetallic refractory brittle materials, discussing departures from conventional practices 17 p3061 A69-33569

Stressed state analysis in dynamic brittle breakdown wave front of compression waves propagating in brittle rod under longitudinal impact 18 p3217 A69-34592

Elastic bodies brittle stability weakened by cut, developing criterion for determining critical cut length 18 p3224 A69-35314

Limiting equilibrium of infinite brittle body weakened by internal plane elliptical crack, determining critical loads and stresses at crack 18 p3226 A69-35379

Limiting equilibrium stress state of unbounded brittle body with elliptical crack under monotonically increasing tensile or compression load, noting influence of crack curvature 19 p3441 A69-36745

Brittle failure models, discussing rheological properties, Griffith energy criterion properties, crack behavior in elastic and linear viscoelastic media, etc 21 p3839 A69-39194

Stability of unbounded homogeneous brittle body containing circular planform crack, determining elastic stresses and critical load by macrocrack propagation theory 21 p3839 A69-39195

Hot salt stress corrosion of Ti alloy, discussing hydrogen generation during elevated temperature exposure and embrittlement as manifestation of strain rate 21 p3747 A69-39434

Beryllium R and D emphasizing brittleness and fracture toughness for safe working stress levels of structurally loaded components 24 p4332 A69-43208

- Structural ceramics and testing of brittle materials - U.S. Army Conference, Chicago, March 1967
24 p4333 A69-43337
- Mechanical testing procedures for brittle materials, discussing test philosophy, tabular data, laboratory tests correlation, etc
24 p4333 A69-43340
- Parametric influence on strength of brittle materials, considering volume, surface, notch, strain rate, modulus variations and material variability effects
24 p4333 A69-43341
- Brittle materials mechanical properties test programs design based on nature of material, use of data and available techniques
24 p4333 A69-43342

BROADBAND

- Microwave transistor amplifier computerized design, discussing wide bandwidth and flat in-band gain response optimization on high dielectric substrates
01 p0040 A69-10194
- Wideband electronically scanned receiver, using varactor diode upper sideband parametric frequency upconverter for frequency mixing
01 p0048 A69-11036
- Noise performance of broadband traveling wave masers with longitudinal or transverse stagger tuned magnetic field
02 p0257 A69-12428
- Broadbanding of S-band three port stripline circulator, discussing effect of tuning and mode suppressor screws
03 p0404 A69-13472
- Error probability for discriminator detection of wideband PCM/FM, considering IF bandwidth/bit duration product and low pass filtering effect
08 p1271 A69-19864
- Wideband acceleration instrumentation for Rover ground test facility liquid hydrogen turbopumps to study structural and flow induced vibrations
10 p1692 A69-23250
- Broadband double balanced mixer/modulators compared with single balanced and unbalanced mixer/modulators
10 p1665 A69-23876
- Panchromatic illumination in radar systems for image quality, tracking and detection problems, suggesting application to polypanchromatic radar
14 p2416 A69-29529
- Broadband microwave double balanced mixer/modulators, discussing bandwidth, conversion loss, noise figure, intermodulation and power dissipation
15 p2580 A69-31077
- Broadband low VSWR transitions between rectangular waveguides and coaxial transmission lines, discussing asymmetrical probe and ridge types
16 p2757 A69-31584
- Broadband thermal radiometer containing InSb electronic bolometer under magnetic field, discussing astronomical applications
17 p2969 A69-32823

BROADBAND AMPLIFIERS

- Broadband parametric amplifier used as front amplifier in satellite communication systems ground station receiver, noting cryogenic operation capability
01 p0041 A69-10243
- Low noise front end wideband amplifier for 100-150 MHz broadband receivers, using distributed amplifier techniques
02 p0216 A69-12028
- Liquid helium cooled broadband parametric amplifier, discussing circuits and noise performance
02 p0221 A69-12458
- Low noise broadband parametric amplifier for communication satellite ground stations
03 p0406 A69-13733
- Frequency and power stable backward wave oscillators as energy pumps for molecular and wideband parametric amplifiers used in satellite receivers
07 p1095 A69-18430
- Helium cooled low noise high gain wideband parametric amplifier for spacecraft communication
07 p1099 A69-18462
- Monolithic planar process to fabricate DC coupled amplifiers having less than nanosecond risetime
07 p1103 A69-18878
- Noise power ratio at output of wideband amplifier with angle modulated multicarrier input, obtaining intermodulation products from Bessel functions expansion
08 p1285 A69-20595
- Noniterative wideband amplifiers having single pole transfer functions overall gain bandwidth product optimization, deriving rigorous conditions for maximum
09 p1469 A69-22606

- Wideband RF amplifier manufacturing problems, comparing operation of vacuum triodes and pentodes in passband circuits
11 p1849 A69-24958
- Ultrawideband DC transistor amplifier for pulsed switching circuits with subnanosecond risetimes, discussing multistages with feedback dipoles, transient response and drift problems
11 p1854 A69-25612
- Traveling wave tubes with broadband CW power, discussing energy dissipation
13 p2232 A69-28057
- High gain broadband amplifiers with triple tuned coaxial resonators and gridded power tubes, discussing phase stability
14 p2418 A69-28892
- Wideband transistorized amplifier frequency response analysis by simplified approximations, subdividing operational frequency range
15 p2573 A69-30113
- Wideband tunnel diode amplifier design, discussing implementation to out-of-band circulator characteristics and VSWR suppression
15 p2578 A69-30804
- Wideband selective amplifier design methods proposed by Martini and Schiaffino
16 p2761 A69-32442
- Wide tuning range S band low noise maser amplifier system, discussing bandwidth, gain and packaging for antenna mounting
17 p2979 A69-32914
- Solid state broadband RF power amplifier for airborne HF radio, eliminating total servosystem and all higher voltage components
17 p2942 A69-34114
- Parametric amplifier developed for unattended satellite communication ground stations, featuring low noise broadband characteristics
19 p3270 A69-36240
- One kw HF ground grid wideband untuned power amplifier in transformer coupled cascade stages
20 p3488 A69-37286
- BROADCASTING**
- Space broadcasting possibilities and problems, considering home reception and group participation at community centers
[UN PAPER 68-95287] 01 p0028 A69-10497
- Propagation tests of skywave field strength reduction by orthogonal transmission
03 p0395 A69-13597
- Sound and TV broadcasting from satellites, discussing systems for future individual user pickup
04 p0558 A69-15120
- Low noise room temperature satellite broadcast receiver for UHF, using room temperature parametric amplifiers
05 p0728 A69-15672
- Communication satellites applied to broadcasting, considering point to point satellite link and distribution systems
08 p1272 A69-19925
- Direct radio and TV broadcasting from satellite-borne radio transmitter to general public, giving visibility, gains, frequencies and bandwidths tables
09 p1586 A69-21286
- TV broadcasting from synchronous satellites direct to ordinary UHF receivers in 1980s
11 p1833 A69-24529
- Compatible single sideband /CSSB/ modulation suitability for broadcasting, analyzing signal spectrum, demodulation distortion and signal generation methods
23 p4125 A69-42111
- BROMIDES**
U CHROMIUM BROMIDES
U POTASSIUM BROMIDES
- BROMINE**
- Antimony bromine and mercury abundances in meteoritic materials determined by neutron activation analysis
08 p1404 A69-20919
- Br molecular dissociation rate in argon excess determined, considering visible emission intensity behind shock front
18 p3176 A69-34465
- Ion production in K/diatomic Br system by high energy K beam, obtaining total ionization cross section as function of energy
19 p3378 A69-36187
- Laser action from atomic bromine produced by flash photolysis of gaseous iodine monobromide, discussing pulsed output, optical gain, chemical reversibility and atomic excitation
19 p3337 A69-36444

- Cs ionization by bromine, measuring relative cross section velocity dependence by crossed molecular beam technique
23 p4194 A69-42208
- BROMINE COMPOUNDS**
NT CHROMIUM BROMIDES
NT POTASSIUM BROMIDES
- Bromine containing unsaturated polyesters for fire retardancy and physical strengths, noting use in reinforced plastics for laminates, molding and corrosion
08 p1340 A69-20504
- Fire retardant brominated epoxy systems for wet filament winding process, noting viscosity, pot life and NOL ring mechanical properties
08 p1340 A69-20507
- BRONCHIAL TUBE**
U TRACHEA
- BRONZES**
- Chromium bronze blanks compacted from granules for hardness and electrical conductivity, noting improved high strength characteristics over conventional production methods
02 p0266 A69-12127
- Electro-optic properties of tungsten-bronze niobate ferroelectric crystals
[IEEE PAPER F-7] 05 p0808 A69-16313
- BROWNIAN MOVEMENTS**
- High aspect ratio submicroscopic whiskers of beta-SiC, investigating rheological properties of suspensions in various fluids
01 p0102 A69-11260
- Fluids structural relaxation analyzed by nonequilibrium thermodynamics and molecular kinetic theory, considering Brownian motion
13 p2299 A69-28037
- BUBBLE CHAMBERS**
- Particle physics and discovery of K mesons and hyperons emphasizing track recording, cloud and bubble chamber techniques
24 p4352 A69-43039
- BUBBLES**
- Time dependent interaction of hot gas bubble with chemically reactive liquid stream, detailing thermal boundary layer theory
01 p0058 A69-10162
- Grain boundary gas bubbles growth in chemically vapor deposited tungsten as function of annealing time, temperature and fluorine content
01 p0097 A69-10646
- Dynamics of moving gas bubble injected in quiescent liquid, considering velocity, heat flow and mass transfer
[ASME PAPER 67-WA/HT-30] 02 p0351 A69-12201
- Bubble motion inside liquid in spherical cavity, allowing for bubble surface deformation
03 p0418 A69-13813
- Pressure induced variations in stability constant characterizing bubble structure in two phase boundary layer of several liquids during boiling with natural convection
03 p0534 A69-14149
- Ellipsoidal gas bubble dissolution in low viscosity fluid, discussing rate of steady motion, deformation degree and diffusion rate
07 p1120 A69-18990
- Rise velocity of large gas bubbles in liquid calculated, assuming velocity is determined by propagation of bubble produced wave disturbance
07 p1120 A69-18999
- Bubble leak testing of components to understand effects of gas and liquid viscosity, surface tension, pressure differential and temperature
09 p1503 A69-21391
- Bubble spiral path motion toward axis of rotation of liquid rotating at constant angular velocity
09 p1483 A69-22006
- Electrolytic bubble level during wind tunnel tests for aircraft model attitude
10 p1672 A69-23268
- Self similar solutions for collapse of empty cylindrical cavity in gas with given equation of state, describing gas motion past cavity
10 p1679 A69-23367
- Vibration characteristics of circular cylindrical shells containing water under axial excitation, investigating bubble formation and shell-fluid interaction
[ASME PAPER 69-VIBR-4] 10 p1805 A69-24162
- Hot inert gas bubble thermal stability in cool reactive liquid
11 p1998 A69-24475

Characteristic frequencies approximation formula for gas bubbles in liquids compared with exact solutions 11 p1915 A69-24582

Gas bubble formation in Ti welding associated with gas nuclei in metal, molten dwell time, gas diffusion coefficients, joint edge conditions, etc 11 p1892 A69-25669

Temperature measurement associated with bubbles leaving heat source in subcooled pool boiling carbon tetrachloride analyzed, using high speed motion pictures by schlieren optical system [ASME PAPER 68-HT-47] 13 p2374 A69-27779

Microlayer thickness in nucleate boiling, studying liquid-vapor interface motion of growing bubble near heated surface 13 p2375 A69-27789

Bubble boiling onset in forced fluid flow, deriving equations for calculating minimum temperature difference between wall and fluid, discussing applicability range 16 p2878 A69-31954

Bamberg zenith telescope investigation, noting level constant dependence on level tube bubble length 17 p2970 A69-32882

Ultrasonic detection of gas bubbles in blood, discussing device with bubble chamber attached to circulating liquid and receiver crystal harmonics 18 p3098 A69-34821

Surface tension gradients caused thermocapillary convection solved for spherical fluid film under weightlessness conditions 19 p3452 A69-36392

Bubble oscillations in water filled pressure chamber with alternating pressure generated by piston, measuring temporal development 19 p3302 A69-36871

Bubble size and blood perfusion effect on gas bubbles absorption in tissues, noting decompression sickness 21 p3651 A69-38389

Book on mathematical model for heat and material exchange in bubbles covering bubble formation, transition period and quasi-stationary bubble rise 21 p3847 A69-38448

Contact lenses hazards during high altitude aircraft piloting analyzed via bubble development 23 p4106 A69-41806

Air bubbles rise velocity and path in water based on time measurement of bubble traversing two light beams, describing electronic recording system 24 p4299 A69-42918

Decompression disease symptoms from standpoint of gas bubbles formation in blood vessels, examining factors preventing air metabolism 24 p4269 A69-43414

Dynamic behavior of gas bubble in ideal fluid plane flow, considering bubble shape, velocity field, gas pressure and stagnation point pressure determination 24 p4302 A69-43478

Unsteady axisymmetric potential flow of ideal incompressible fluid with free surfaces, deriving differential equations for gas bubble dynamics and surface geometry 24 p4302 A69-43500

Bubble flow evolution at various pressures up to critical value [ASME PAPER 69-HT-30] 24 p4411 A69-43529

Cylindrical bubbles stability in vertical pipes from photographs, describing wake, spacing, pressure pulsations and convection cells effects [ASME PAPER 69-HT-28] 24 p4411 A69-43540

BUCCANEER AIRCRAFT

Buccaneer aircraft development, considering structure, air bleed, aerodynamics, controls, electric systems, flight refueling, aircrew escape, armament and weapons delivery 09 p1435 A69-22775

BUCKLING

NT CREEP BUCKLING
NT ELASTIC BUCKLING
NT EULER BUCKLING
NT THERMAL BUCKLING

Shear buckling test data for shallow corrugated webs compared with theoretical analysis with web buckling as orthotropic plate or local mode 01 p0170 A69-10866

Nonlinear buckling analyzed by mathematical models and computational procedures using organized matrix approach to structural analysis based upon finite element 01 p0171 A69-10964

Critical loads in elastoplastic buckling of cylindrical shells analyzed using power series 02 p0340 A69-12058

Orthotropic stiffened multilayer circular cylindrical shells buckling under axial compression, lateral pressure, etc 02 p0346 A69-12510

Buckling of electroformed thin conical shells under hydrostatic pressure, proving theory for cones of large taper ratio 02 p0347 A69-12515

Recent advances in shell buckling, discussing imperfection sensitivity, boundary conditions and wall configuration [AIAA PAPER 68-103] 02 p0347 A69-12516

Mathematical programming in optimized truss design noting reduction of components under buckling 02 p0347 A69-12536

Unreinforced circular cutouts effects on buckling behavior of circular cylindrical shells under axial compression, using photoelastic plastic shells 03 p0523 A69-12988

Two point boundary value problems for determining buckling behavior of two hinged circular arches [ASME PAPER 68-WA/APM-18] 04 p0669 A69-14399

Impulse buckling threshold for elastic-plastic cylinder with elastic core after development of unstable motion 04 p0671 A69-14414

Schaefer theory of two parameter eigenvalue problems applied to stability of twisted bars, discussing quick estimate of critical loads 04 p0682 A69-15290

Iteration method for determination of critical buckling load for straight rods 05 p0832 A69-15689

Stability functions for local buckling of long thin flat walled structures loaded for longitudinal compression and shear 05 p0833 A69-15709

Stiffness matrices for buckling or vibration analysis of long thin flat plate structures connected at longitudinal edges 05 p0836 A69-16029

Theoretical buckling load for single edge notched struts, discussing brittleness effects 05 p0837 A69-16064

Circumferential buckling of ellipsoid of revolution due to internal pressure, assuming linear deflection and uniform thin shell [ASME PAPER 68-WA/PVP-12] 05 p0840 A69-16190

Buckling of long cylinders with homogeneous random axisymmetric geometric imperfections under axial compression, using truncated hierarchy technique 07 p1236 A69-19473

Dynamic stability of thin flat plates and applications in ship and aircraft deck construction, studying dynamic buckling for rectangular plate 08 p1415 A69-20665

Uniform gravity load effect on buckling of beam continuously supported by soft foundation and subjected to uniform lateral load 09 p1615 A69-21927

Buckling of eccentrically stiffened thin circular cylindrical shell under uniform combined axial compression and torsion loads with lateral pressure 09 p1616 A69-21955

Buckling capabilities of inflation rigidized wire film and shell film cylinders in axial compression and bending 09 p1617 A69-21997

Buckling deformation and stress fields around central slits in photoelastic models and metal sheets under tensile load 10 p1796 A69-23069

Axisymmetric free edge buckling of semiinfinite heterogeneous orthotropic cylindrical shells in axial compression, noting stability condition 10 p1802 A69-23889

Postbuckling behavior and subsequent imperfection sensitivity of thin walled cylinders subjected to torsion, considering perturbation 11 p1979 A69-24814

Stiffer geometry and spacing effects on buckling of axially compressed cylindrical and conical shells 11 p1979 A69-24815

Thin walled circular cylinders postbuckling behavior and stability under axial compression calculated for design loads 11 p1979 A69-24816

Nodal lines shape in individual flats for long plates in combined shear and compression with sinusoidal edge rotations in longitudinal direction 11 p1983 A69-25137

Buckling of long flat panel in combined compression and shear with sinusoidal edge moments and support on two edges and on point supports 11 p1984 A69-25138

Shear buckling of simply supported infinitely long plates orthogonally reinforced by stiffeners with flexural and torsional rigidity 11 p1984 A69-25142

Flutter design charts for isotropic panels stressed to verge of buckling for typical values of structural damping 11 p1992 A69-25524

Large deflection elastic-plastic analysis of axisymmetric shells of revolution indicating role of plastic yielding in buckling pressure reduction 12 p1886 A69-26839

Buckling loads for anisotropic fiber reinforced composite plates with strong bending membrane coupling terms 12 p1886 A69-26840

Cylinder buckling and other boundary value problems, applying inverse differential operators to solution of integrodifferential equations 12 p1886 A69-26841

Buckling and postbuckling equilibrium behavior of fiber reinforced cylindrical shell under uniform axial compression 12 p1887 A69-26843

Axisymmetric plastic buckling of complete spherical shells subjected to external hydrostatic pressure 13 p2361 A69-27439

Shear buckling of clamped rectangular linearly tapered plates, considering uniform shear stress and load 13 p2361 A69-27443

Imperfection surface effect on buckling load of circular cylindrical shell under axial compression, locating limit points of postbuckled states 13 p2362 A69-28122

Rectangular plate buckling analyzed by finite element method with deflection function 13 p2364 A69-28225

Uniaxial compressive stability of rectangular boron-epoxy laminated plates clamped on loaded edges, determining buckling loads by Southwell plots 13 p2287 A69-28669

Buckling of unsymmetric cross-ply rectangular plates under uniform shear, considering hinge-support boundary conditions 13 p2371 A69-28679

Postbuckling of rectangular plates with exponential variation in thickness, analyzing large deflection equations using dynamic relaxation method 15 p2704 A69-30291

Oscillating beams lateral buckling allowing for torsional stress in determining critical load 15 p2712 A69-31015

Buckling load of cylindrical shell with inclined stiffeners, using method for stability of thin walled cylinder under transverse end load at free end 16 p2872 A69-31912

Mixed plate element application to vibration and buckling eigenvalue problems based on Reissner variational principle, considering quadrilateral elements 16 p2874 A69-32176

Load carrying capacity of thin steel plates fatigued by cyclic shear buckling 17 p3052 A69-32980

Nonaxisymmetric stability loss /buckling/ of closed toroidal shell of circular cross section under uniformly distributed external pressure, considering Volmir linear theory 17 p3055 A69-33130

Critical buckling stress for cylinders wound with fiber reinforced plastics /FRP/, establishing stability criteria for fiber reinforced shells 17 p3058 A69-33430

Discrete element displacement method applied to buckling analysis of flat rectangular plates under arbitrary membrane loading, calculating critical load intensities 17 p3066 A69-34048

Structural members stability mathematical models using lumped bars and springs simulating postbuckling behavior 18 p3211 A69-34342

Buckling stresses in thin walled box girder under bending determined using stationary potential energy criterion 18 p3224 A69-35344

Nonlinear shell theory for thin elastic circular cylinders, obtaining equations for investigating equilibrium configurations of postbuckled states 19 p3440 A69-36636

Displacement patterns for buckled shapes of axially compressed thin walled circular, cylindrical and conical shells
19 p3443 A69-36793

Buckling and postbuckling of complete spherical shells with symmetric initial shape deviations and elastic deformations
19 p3446 A69-36834

Plastic deformation effect on dynamic buckling of elastic-plastic simple shallow truss subjected to step and impulsive loading
19 p3446 A69-36836

Deep circular arches undergoing large deflections and stability loss, determining buckling load variations
20 p3622 A69-37210

Critical buckling loads for uniform compression of clamped or simply supported parabolic and semielliptic plates
20 p3622 A69-37223

Matrix displacement method of structural analysis applied to dynamic buckling of clamped shallow spherical caps under step pressure loading
20 p3622 A69-37229

Torsional-flexural buckling of thin walled open sections under eccentric load, emphasizing singly symmetric sections loaded in plane of symmetry
20 p3625 A69-37653

Thin curved panels postbuckling behavior under axial compression, basing study on thin shell finite deformation theory and Galerkin method
20 p3629 A69-38112

Gas turbine compressor blade buckling during blade fabrication by hydraulic pellet jet technique eliminated by controlling working pressure of jet
21 p3731 A69-38879

Buckling stability of thin cylindrical shell under torsion, allowing for finite displacements due to shear in initial stress-strain state
21 p3838 A69-39187

Bifurcation and hardening rate of rigid-plastic bodies presented on buckling of rectangular plate with lateral restraint
21 p3840 A69-39299

Postbuckling of filled circular cylindrical shell using Ritz energy method for load deformation relation, discussing stabilizing effect of core
22 p4038 A69-39895

Buckling strength prediction for circular cylindrical shells reinforced by circumferential and longitudinal stiffeners, solving torsional buckling of orthotropic shells under internal pressure
22 p4042 A69-40171

Supersonic panel flutter boundary of buckled and unbuckled clamped rectangular plates, discussing in-plane stress effects
22 p3930 A69-40584

Discrete rib effect on buckling resistance of cylindrical shell under combined external and axial compression loads, using Laplace transforms
23 p4229 A69-41990

Buckling of truncated conical shells under torsion with various boundary conditions, applying Galerkin method to estimate critical load and wave number
24 p4395 A69-42715

Postbuckling analysis by equilibrium solutions of conservative system near critical point, considering stability failure in elastic structure under increasing load
24 p4396 A69-42730

Shearing force and shear buckling deformation influence on supersonic panel flutter boundary of simply supported rectangular plates, basing analysis on deflection approximation
24 p4400 A69-43055

Buckling of thick homogeneous rectangular plates subjected to constant normal stress, noting error for thin plate approximation
24 p4406 A69-43696

BUDGETING

Federal Government budgeting, discussing systems analysis, planning-programming, etc
10 p1811 A69-23351

Federal Government systems politics and budgeting, noting dichotomies, time dependence, taxonomy, etc
10 p1811 A69-23352

MACRO /methodology for allocating corporate resources to objectives/ for R and D, discussing program for optimal budget management
15 p2720 A69-30958

Expenditures for R and D effect upon U.S. economy
17 p3076 A69-34041

BUFFER STORAGE

Buffer storage for telemetry nonstationary video data compression, analyzing requirements, predictor algorithm and variable aperture control using simulation
19 p3272 A69-36260

Swedish satellite onboard computer for particle experiment, discussing functional design based on buffer unit for experimental data
20 p3501 A69-37386

BUFFERS [CHEMISTRY]

DNA denaturation without variance from pH 7.0 by adding NaOH observed with viscosity measurements, obtaining similar results with hydrochloric acid
24 p4263 A69-43225

BUFFETING

Buffeting tests of model wing in wind tunnel as function of angle of attack and Mach number
06 p0857 A69-17096

Probability diagnosis and prognosis for buffeting zones based on Bayes formula, determining clear air turbulence zones
15 p2648 A69-30645

Wind tunnel tests of swept wing fighter aircraft for transonic buffet onset lift coefficient resulting from camber and leading and trailing edge deflection [AIAA PAPER 69-793]
19 p3238 A69-36297

Acroelasticity of supersonic aircraft in flight, discussing buffeting, wing flutter and control surface flutter
22 p3862 A69-40003

BUILDING MATERIALS

U CONSTRUCTION MATERIALS

BULBS

Vertical vibration stimulation of growth of onion bulbs and mice body weights
01 p0014 A69-10584

Vertical vibration stimulation of growth of onion bulbs and mice body weights
15 p2555 A69-30754

BULGING

Sheet metals deformation behavior during punch stretching and hydraulic bulging, noting effects of lubrication, stress-strain relation, anisotropy and microcracks
20 p3551 A69-38115

BULK MODULUS

Isothermal secant and tangent bulk moduli of silicon fluids and correlation with pressure, volume and temperature
01 p0102 A69-10913

Adiabatic elastic constants of molybdenum-rich rhenium alloys, studying concentration effects on bulk modulus, Debye temperatures and interatomic forces
04 p0613 A69-14455

Bulk aerodynamic method for heat and water vapor fluxes from data obtained at Chiba /1966/, introducing modified integral diffusivity
07 p1176 A69-18965

BULKHEADS

Low profile bulkheads for launch vehicles and spacecraft compartments to obtain structural weight reduction
02 p0334 A69-12370

BUMPERS

Multiwall meteoroid protection design in Apollo program, discussing bumper, backup sheet and honeycomb cells insulation [AIAA PAPER 69-372]
13 p2367 A69-28304

Bumper materials effect on two component hypervelocity impact shields performance, noting material density influence [AIAA PAPER 69-379]
13 p2283 A69-28309

Two plate meteoroid shields effectiveness determined by analyzing debris cloud ejected behind front plate after hypervelocity impact [AIAA PAPER 69-380]
13 p2368 A69-28310

BUNCHING

NT ELECTRON BUNCHING

Bulk queuing with service time distribution assuming customer arrival in batches and service discontinuance
02 p0271 A69-12060

Photon bunching effect in spatially coherent noise field enhanced by superposing monochromatic coherent signal and/or shaping incident noise spectra
16 p2749 A69-31694

BUOYANCY

Buoyancy in turbulent shear flow, rotation or streamline curvature effects and meteorological parameters, drawing formal exact algebraic analogy
11 p1870 A69-24894

Buoyancy effect on boundary layer flow over semi-infinite vertical plate heated to constant temperature in uniform free stream
11 p1874 A69-25352

Buoyancy-driven system instability mechanism, showing Prandtl number increment effect and relation to Coriolis-driven instability of rotating fluids
11 p1876 A69-25559

Normal modes stability analysis of fluid layer adjacent to flat plate submerged in liquid, considering effects of interfacial surface tension and buoyant forces [AIAA PAPER 69-386]
15 p2590 A69-30476

Buoyant plumes and thermals defined as vertical motions produced under gravity by density or temperature contrast between incompressible source fluid and environment
18 p3122 A69-34917

Similarity solutions describing buoyancy effect on laminar and turbulent wakes of heated body in incompressible fluid vertically ascending flow
19 p3296 A69-35761

Neutral buoyancy simulation of astronaut performing module replacement and repair task in zero-g environment [AIAA PAPER 69-1005]
22 p3921 A69-40379

Plane Poiseuille flow with nonlinear temperature distribution, studying vortex type secondary flow onset due to buoyant forces [ASME PAPER 69-HT-37]
24 p4411 A69-43533

BUOYS

NOMAD buoy telemetry system for synoptic oceanographic and meteorological data, using digital processing and dual frequency transmissions
03 p0391 A69-13223

BUREAUS [ORGANIZATIONS]

Accident prevention program of Bureau of Aviation Safety, discussing probable cause analysis and function in feedback loop, hazard analysis and accident data center
22 p3867 A69-41140

BURGER EQUATION

Equation of characteristic functional for Burgers one dimensional model fluid turbulence using logarithmic expansion method, discussing change in time of energy spectrum
01 p0059 A69-10338

Burger condition for distortion field of dislocation lines in continuous medium, considering arbitrary shape in arbitrary motion
19 p3439 A69-36477

Hydrodynamic turbulence in statistical prediction for Burger equation, considering statistical inference problem for initial conditions and prediction criterion with estimable error
21 p3697 A69-39673

Solution stability and secondary solutions growth beyond critical points investigation for Burgers equations for laminar-turbulent transition
24 p4302 A69-43360

BURNERS

Flame stabilization on rectangular burners, discussing blow-off limits correlation by velocity gradients close to corners
02 p0353 A69-12320

BURNING

U COMBUSTION

BURNING PROCESS

U COMBUSTION

BURNING RATE

Diacytyle burning and spontaneous combustion regularities, determining reaction kinetics at moderate temperature
02 p0351 A69-11981

Spherical flames of spark-ignited dust clouds, discussing streak film photographs, flame propagation, particle burnout time and burning velocities
02 p0353 A69-12323

Combustion model for rapidly burning involatile condensed materials, obtaining combustion rates
02 p0355 A69-12672

Plateau effect in burning of platonized propellants due to lead compound additives
03 p0494 A69-12881

Ultrahigh pressure test vessel for determining pressure vs burning rate characteristics of propellants and explosives
04 p0645 A69-14472

Coal grain combustion rate and duration at finite air excess coefficient, solving combustion process equations under steady state assumption
04 p0687 A69-15168

Burning rate of composite propellant with gamma irradiated ammonium perchlorate, noting enhancement at atmospheric pressure

04 p0647 A69-15519

Burning rates of solid propellants by variable pressure method, taking into account environmental heat loss and gaseous condensation

06 p0982 A69-17505

Turbulent premixed flames stabilization, determining gas flow velocity, turbulence intensity, flame thickness and burning velocity relation to intensity

06 p1035 A69-17931

Solid propellant burning rate behavior during abrupt environmental pressure excursions, using transient combustion model

[AIAA PAPER 69-172] 06 p1036 A69-18046

Unstable combustion of ammonium perchlorate (AP), discussing correlation between propellant particle diameter and frequency in burning rate

[AIAA PAPER 69-177] 06 p1036 A69-18063

Photographic study of burning metalized composite propellant under acceleration, noting burning rate augmentation by heat transfer from alumina particles retained on propellant surface

[AIAA PAPER 69-173] 06 p0983 A69-18151

Solid propellant burning rates from condensed phase decomposition kinetics, discussing kinetic rates of thermal decomposition

[AIAA PAPER 69-145] 06 p1039 A69-18182

Strong electrostatic fields effects on burning rates of double base and composite propellants

[WSCIPAPER 68-24] 07 p1241 A69-18366

Tungsten delay powders combustion mechanism and intermediate stages of burning process, noting burning rate

[WSCIPAPER 68-19] 07 p1202 A69-18370

Catalytic effect of potassium bichromate and chromic oxide additives on burning of ammonium perchlorate and mixtures

08 p1375 A69-19997

Vanadium pentoxide addition effect on combustion rates of mixtures of ammonium perchlorate and metallic fuels in nitrogen atmosphere

08 p1375 A69-20342

Burning rate of solid grains of hybrid rocket engine, using calculated diagrams for quick computations of engine

08 p1376 A69-20590

Pure ammonium perchlorate single crystal self deflagration, determining energy transfer mechanisms from pressure effects, combustion characteristics and subsurface profile

[AIAA PAPER 69-142] 09 p1560 A69-21900

Burning rate catalysts mechanism and location in composite propellant combustion at high pressure

09 p1622 A69-21954

Nonmetalized composite propellant solid phase heterogeneities effect on oscillatory combustion, inducing coherent burning rate oscillations with external pressure oscillations

09 p1622 A69-22085

Hydrodynamic effects in flame spreading, ignitability and steady burning of liquid fuels, using analogy of films floating on water

11 p1999 A69-24484

Combustion rates of condensed systems under positive and negative accelerations at atmospheric pressure

11 p2001 A69-25195

Solid propellant rockets, discussing composite and double base propellants and use of polymers

11 p1941 A69-25588

Component ratio effect on pressure dependence of burning rate in ammonium and potassium perchlorate mixed with organic compounds, graphitic and tungsten

12 p2027 A69-26474

Polymethyl methacrylate burning rates in mixture with ammonium perchlorate or in hybrid systems when mixed with ammonium chloride

13 p2324 A69-28503

Compressed ammonium perchlorate combustion rate and pressure requirements established from initial temperature effects

14 p2508 A69-28914

Dipercchlorates different in organic part of structure and explosive transformation heats, showing strong dependence of combustion velocity on pressure

15 p2716 A69-30108

Solid rocket motor propellant burning rate increased by adding special fine ammonium perchlorate (SFAP) to optimize particle size distribution

[AIAA PAPER 69-519] 16 p2793 A69-31850

Thermal layer theory of composite propellant combustion leading to minimum steady state burning rate under ideal thermal conditions

[WSCIPAPER 69-5] 16 p2830 A69-32346

Composite solid propellant burning rate by solving energy equation, yielding heat release, flame thickness and standoff distance

[WSCIPAPER 69-7] 16 p2830 A69-32348

Burning velocity inhibitors effects on hydrocarbon-oxygen-nitrogen mixtures ignition temperature, reporting data on 20 additives at ambient temperature and pressure

[WSCIPAPER 69-14] 16 p2831 A69-32352

Point defect structure to control ammonium perchlorate burning rate, discussing thermal analysis data correlations, isothermal decomposition, etc

[WSCIPAPER 69-17] 16 p2831 A69-32355

Doped recrystallized ammonium perchlorate effects on composite propellant burning rates

[WSCIPAPER 69-18] 16 p2831 A69-32356

Pure monopropellant steady droplet burning rate for determining heat-up and convection transport rates in droplet combustion products of flat flame burner

[AIAA PAPER 69-563] 16 p2834 A69-32722

Flame front structure and combustion rates of gases as function of temperature dependence of thermal conductivity, diffusion coefficients, density and molecular weight

17 p3069 A69-33136

Mode transition characteristics of free burning argon electric arc with transpiration cooled anode, noting current blowing parameter

[AIAA PAPER 69-696] 17 p3011 A69-33451

Nonlinear periodic oscillations in liquid rocket combustion chambers for different chamber models and burning rate response formulations

19 p3449 A69-36352

Flame pressure tube and burning velocity related, discussing stream tube area expansion error

21 p3849 A69-38806

Ammonia addition effect on laminar flame speeds of propane-air mixtures

21 p3849 A69-38809

Acceleration effects on solid propellant rocket motors combustion characteristics

[AIAA PAPER 68-530] 21 p3786 A69-39217

Laminar burning rate of premixed propane-air flames at one atmospheric pressure in DC electric fields, using cooled porous plug burned method

21 p3852 A69-39596

Concentric or eccentric rotation effect on burning rate and geometry of small hybrid rocket motors using hydrogen peroxide-organic fuel

23 p4203 A69-41932

BURNING TIME

Mathematical analysis of oxygen diffusion to coal grains during coal dust combustion, evaluating kinetic constants by burning time

04 p0687 A69-15167

Flame burnout of atomized hydrocarbon fuel in gas turbine combustion chambers as function of ratio of time to total burnout time

08 p1420 A69-19999

BURNOUT

Nucleate boiling burnout heat flux data for ethane, ethylene and ethane-ethylene mixtures at various pressures, discussing applicability of Noyes equations

15 p2671 A69-31118

BURNS (INJURIES)

Retinal burns from intense light sources using rabbit eyes as function of irradiation rate, exposure time and image size

02 p0204 A69-12496

Protection against burn producing intense thermal exposures, noting double layer of fire resistant material

[AGARDOGRAPH-111] 08 p1266 A69-20674

Retinal burn resulting from prolonged viewing of sun, laser or thermonuclear explosion, noting effects on choroid, receptors and pigment cells

08 p1267 A69-20680

BURSTS

NT RADIO BURSTS
NT SOLAR RADIO BURSTS
NT TYPE 2 BURSTS
NT TYPE 3 BURSTS
NT TYPE 4 BURSTS
NT TYPE 5 BURSTS

Bursts of high speed rotor occurring at diametric cross section and around hub as function of hub size

01 p0142 A69-10306

BUTADIENE

Electron beam radiation curing of mercaptan terminated butadiene-acrylonitrile liquid copolymers at ambient temperatures in air

09 p1512 A69-22368

BUTANES

Chromatographic analysis of products formed during induction period of 2-methylbutane gaseous oxidation in flow system at low temperatures and long residence times

21 p3669 A69-38798

BUTT JOINTS

Butt weld fatigue properties improvement in maraging steels, using shot peening and prestretching

03 p0434 A69-13762

Filler metals for HY steels, discussing tensile and yield strength, elongation and area reduction of butt welds deposited

08 p1320 A69-20406

Continuous butt welding with CW carbon dioxide laser, noting heat affected area, remelt zone and weld efficiency

15 p2617 A69-30099

BUTYRIC ACID

Mice convulsions at varying hyperbaric oxygen pressures and carbon dioxide content correlated with decreasing brain alpha aminobutyric acid levels

19 p3257 A69-35972

BYPASSES

High bypass turbofan design, discussing JT9D engine combustion, materials and cooling

05 p0811 A69-15552

Shunted resonators on transmission line with asymmetrical response offering selectivity from resonance frequency standpoint

08 p1271 A69-19917

Pulsed ultrasonic flaw detectors resolving power enhancement by shunting semiconductor diodes across piezoelectric elements of scanning heads to shorten scan pulse duration

18 p3137 A69-35112

TF39 high bypass ratio engine design, development and tests, noting low smoke combustor

[RAES PAPER 21] 22 p4000 A69-40622

GABA shunt contribution to total metabolism of alpha ketoglutarate to succinate and high pressure O effect on system under in vitro conditions

22 p3877 A69-40776

C

C BAND

C band waveguide window for average power transmission featuring relatively small biconcave dielectric disk

07 p1096 A69-18435

C-5 AIRCRAFT

Systems analysis application to determination of C-5 effectiveness noting loading, productivity and effectiveness analysis computer programs

[SAE PAPER 680729] 03 p0379 A69-13440

C-5A transport flight test and progress report, discussing taxi runs, first flights and flight-flutter program

06 p0867 A69-17665

Technology of titanium for C-5A aircraft, discussing structural and functional components and machining, welding, forging, etc

[ASM PAPER D8-26.2] 07 p1143 A69-19672

Design, metallurgical and manufacturing problems of titanium application in superjet C5 and SST engines

09 p1570 A69-22062

C-5 engine inlet development, presenting two phase nacelle forebody and five phase model tests, scale corrections inlet/cowl optimization and prototype tests

[ASME PAPER 69-GT-52] 09 p1570 A69-22481

Flight test telemetry data processing system designed for C-5

10 p1660 A69-23269

Design of 126 channel PCM telemetry unit for C-5 aircraft flight test, discussing FET analog multiplexing

10 p1693 A69-23275

Flight testing and preflight simulated testing of Lockheed C-5 Galaxy transport aircraft

10 p1634 A69-23599

Galaxy C-5A aircraft Value Control Program stressing design organization, upper management authority, budgetary adjustments, etc

13 p2383 A69-28095

L500 cargo transport commonality with C-5 showing need for aggressive weight control program

[SAWE PAPER 745] 18 p3091 A69-34908

Lockheed L-500 aircraft weight consideration in structural design as all cargo lifter, describing engine

thrust, payload, options, etc
18 p3092 A69-35464

Lockheed C-5 Galaxy aircraft avionics systems with Doppler inertial navigation equipment to operate with precision without ground based aids
18 p3104 A69-35465

Real time terrain following computer for C-5A transport, discussing automatic throttle system and speed bleedoff utilization
[AIAA PAPER 69-797] 19 p3367 A69-35633

C-5A aircraft model high subsonic speed tests, correlating data from three transonic wind tunnels
[AIAA PAPER 69-794] 19 p3237 A69-35636

Product reliability program for C-5A to provide high delay/abort reliability during operational usage
19 p3247 A69-36011

Man machine interface problems in C-5 equipment and system design
19 p3261 A69-36024

Descent device for emergency egress from jumbo jets based on centrifugal brake, including test data on C-5 fuselage section
19 p3255 A69-36146

C-5 air force logistic transport, discussing structural design, configuration, payload, aerodynamics and flight testing
[AIAA PAPER 69-758] 19 p3248 A69-36295

C-5 aircraft stability augmentation and autopilot development with consideration for unusual design required by takeoff weight, inertia and low approach speed
20 p3461 A69-36927

C-5A transport aircraft airframes manufacture, discussing Lockheed profits, contract disputes and Cheyenne helicopter contract cancellation
20 p3640 A69-37355

C-5A Galaxy military transport hydraulic system, considering applications for industrial hydraulics
20 p3466 A69-38177

C-5A transport modular valve design for improved maintenance and high reliability due to manifold- cartridge arrangement
20 p3466 A69-38178

C-5A transport landing gear assembly design, illustrating air turbine kneeling-drive module
20 p3466 A69-38179

C-130 AIRCRAFT
Lockheed C-130 Hercules modified as STOL aircraft studied in laboratory by computerized simulation and graphics techniques for pilot view during landing
18 p3092 A69-35466

C-141 AIRCRAFT
C-141 Category IIIb all weather landing system, discussing system concept, components, operations and performance
14 p2479 A69-29701

C-141 aircraft reliability growth history, discussing fleet performance, aging trends and delivery vs production sequence
18 p3090 A69-34521

C-141 engine health monitoring program, applying results to maintenance costs reduction
[AIAA PAPER 69-775] 19 p3244 A69-35646

C-142 AIRCRAFT
U XC-142 AIRCRAFT

CABIN ATMOSPHERES
NT SPACECRAFT CABIN ATMOSPHERES

Pressurized Navajo aircraft environmental system, discussing ventilation, pressurization, heating and air cooling systems
[SAE PAPER 690330] 11 p1829 A69-24504

Urine excretion following water load in male subjects exposed to normal, hot/dry and comfortable/dry environment applied to airline crews
17 p2914 A69-33182

Closed compartment fire mathematical model to analyze combustion parameter effects, atmosphere pressure and temperature during fire
[AIAA PAPER 69-618] 17 p3074 A69-33704

Renal calculus incidence among aircrews of long and short haul airlines, considering effects of dry cabin environment and dehydration
23 p4108 A69-41826

Physical and physiological factors involved in determining aircraft passengers time of safe unconsciousness permissible after cabin decompression
24 p4278 A69-43398

CABLES
Design and tests of cable assemblies for F-111 aircraft
05 p0731 A69-16246

Flat conductor cable technology, discussing design, manufacture, specifications, etc
[ASME PAPER 69-DE-8] 14 p2393 A69-28855

CABLES [ROPES]

Parachute deployment load control by use of line ties from rocket sled tests
11 p1823 A69-25386

Carrying cables shape optimization for suspended structures under load, using minimum weight criterion
18 p3212 A69-34354

CADMIUM

Electrical properties of p-n junctions of diffused Cd or Zn in indium phosphide
02 p0294 A69-11628

Superconductivity and band structure from pseudopotential for zinc and cadmium, analyzing values of electron phonon mass enhancement
04 p0642 A69-14965

Cadmium ionization energy in InAs using heat treatment in hydrogen to eliminate anomalies
06 p0979 A69-16998

Diffusion method for fabricating negative resistance diodes consisting of Cd doped silicon, introducing Cd into n-type silicon plates in evacuated vials
09 p1462 A69-21477

Diffusion method for fabricating negative resistance diodes consisting of Cd doped silicon, introducing Cd into n-type silicon plates in evacuated vials
15 p2578 A69-30722

Maxwell coefficient change of Cd atoms /in molecular beam/ diffusely reflected from metal surfaces related to reflector temperature, material and fabrication method
20 p3580 A69-37814

Bright cadmium plating by electrolysis, describing processes during electrodeposition from sulfate electrolytes
22 p3959 A69-41266

CADMIUM ANTIMONIDES

Temperature dependence of electrical properties of In and Cu doped CdSb single crystals prepared by zone refining
04 p0643 A69-15264

Structural imperfections of CdSb single crystals undoped and doped with tellurium and indium noting etching techniques, grain boundaries and impurities
11 p1938 A69-25030

Phase diagram for physicochemical study of CdSb-Ge cross section of Cd-Sb-Ge ternary system, discussing exo-endothermal fusion effects, microstructure, etc
14 p2503 A69-28975

CADMIUM COMPOUNDS

Second harmonic generation in ternary semiconductor compounds
03 p0489 A69-13894

Electrical properties of n-type Cd tin arsenide single crystals with impurity concentrations at various temperatures
05 p0809 A69-16375

Second harmonic generation in ternary semiconductor compounds
11 p1939 A69-25695

Cadmium arsenide carriers effective mass under strong transverse magnetic field, noting restricted role of thermal EMF and Hall coefficients
13 p2318 A69-27897

Lattice component of heat conductivity in n-type cadmium arsenide at low temperatures by suppressing electron component of conductivity with strong transverse magnetic field
16 p2824 A69-31568

Electronic properties changes in amorphous CdGeAs caused by long range order loss studied by measuring optical and transport properties
19 p3390 A69-36557

Thermal EMF in cadmium arsenide specimens with various electron concentrations determined to verify parabolic subband structure of conduction band
22 p3993 A69-40607

CADMIUM ISOTOPES

High power output CW laser oscillation measured at 4416 Å laser transition in Cd 2 using single isotope of Cd 114
02 p0259 A69-12653

Isotope shifts in 4416 Å cadmium laser, showing change of double peaked to single peaked profile with doubled active tube length
10 p1705 A69-23812

CADMIUM NICKEL BATTERIES

U NICKEL CADMIUM BATTERIES

CADMIUM SELENIDES

CdSe single crystal dislocation loops and growth defects, using X ray topograms
02 p0298 A69-12048

Radiation absorption variations in KC-19 CdSe glass during ruby laser radiation, noting microcrystals and nonlinear effects role in determining optical properties
03 p0436 A69-13036

Two photon absorption and stimulated emission mechanism of CdS-CdSe mixed crystals investigated by ruby laser output
03 p0438 A69-13052

Perfect piezosemiconductor resonator /phasor/ with CdSe/CdS/ crystal, discussing vibration excitation in wurtzite type crystal in electric field of electron drift
03 p0431 A69-13930

CdSe single crystal films vacuum deposition for use of photocells base with p-n heterojunctions
07 p1198 A69-18512

Dark and photocurrent volt-ampere characteristics induced by capture of carriers injected into illuminated CdS single crystals
09 p1555 A69-21506

Slow recombination centers parameters in CdSe single crystals during heat treatment in vacuum or hydrogen atmosphere
09 p1560 A69-22664

Stimulated emission characteristics of CdS-CdSe mixed crystals subjected to two photon excitation, studying pulse energy at 77 K as function of pumping power
19 p3332 A69-35867

Gold/polycrystalline cadmium selenide film contact found ohmic in darkness and barrier in light, noting potential distribution, electron concentration and energy gap
19 p3384 A69-36480

Cadmium sulfide-selenide single crystals reflection coefficient polarimetric measurement, observing reflection peaks relationship to absorption spectral temperature dependence
19 p3391 A69-36607

CADMIUM SILVER BATTERIES
U SILVER CADMIUM BATTERIES

CADMIUM SULFIDES
Laser CRT with beam pumped aluminized CdS crystals, discussing single spot low duty operation
01 p0039 A69-10175

Thin film transistors prepared from spray deposited cadmium sulfide, discussing carrier mobility and low stability
02 p0214 A69-11596

Neutron and gamma irradiation effects on CdS crystals structure and properties, outlining electron energy level scheme
02 p0298 A69-12119

Radiation damage in CdS irradiated by normal mode or Q-switched ruby laser, discussing stimulated Brillouin scattering
02 p0257 A69-12614

Two photon absorption and stimulated emission mechanism of CdS-CdSe mixed crystals investigated by ruby laser output
03 p0438 A69-13052

Thermal cycling tests showing improvement in cadmium sulfide solar cell stability, noting effect of thermal cycling stresses
03 p0367 A69-13074

Impurity profiles and energy band diagram for cuprous sulfide-CdS heterojunction based on capacitance, Hall and electron microprobe measurements
03 p0368 A69-13075

Photovoltaic properties of CdS thin film solar cells and silicon cells at Jupiter temperature and solar intensity
03 p0368 A69-13076

Contact resistance of In or In-Ga on CdS single crystals
03 p0487 A69-13638

Photocurrent pinch-off effect in high resistivity thin CdS crystals for evaluating donors, acceptors and surface states
03 p0488 A69-13757

Bound excitons spectra in CdS, semiconductor band structure and tabulating positions of lines identified with excitons
03 p0488 A69-13784

Perfect piezosemiconductor resonator /phasor/ with CdSe/CdS/ crystal, discussing vibration excitation in wurtzite type crystal in electric field of electron drift
03 p0431 A69-13930

CdS Hall coefficient, Hall mobility and magnetoresistance coefficient dependence on electric field, magnetic field and scattering mechanisms
03 p0490 A69-13945

Modulated photocurrent in CdS crystal obtained by irradiation with intensity modulated electron beam, noting relaxation time and trap concentration
03 p0490 A69-13946

Hall mobility of photoelectrons in cadmium sulfide layers
03 p0491 A69-14055

Refractive index temperature dependence of cadmium sulfide single crystals grown from gas phase
04 p0644 A69-15268

Pulse radiation effect on dielectric constant of sintered CdS photoresistors, discussing capacitance dependence on intensity, type and frequency of light
05 p0806 A69-15694

Surface photovoltaic effect in copper electroplated single crystal CdS solar cells, discussing Fermi level and Hall effect
05 p0704 A69-15958

Surface recombination rate effect on lux-ampere characteristic of photomagnetic effect in CdS single crystals of low and high photosensitivity
05 p0809 A69-16377

Cadmium sulfide films with larger than bandgap photovoltages, analyzing photovoltage decay and temperature and light intensity effects
06 p0980 A69-17772

CdS single crystals excess conductivity observed at room temperature
08 p1374 A69-21083

Photocells with p-n heterojunctions from sintered CdS, describing spectral sensitivity and temperature dependence of no-load open EMF
08 p1374 A69-21084

Time dependent recoverable isothermal decrease of photocurrent in CdS crystals in vacuum, noting trap mechanism involving electron redistribution
08 p1374 A69-21187

IR radiation effects in cadmium sulfide crystals with green edge emission at low temperatures, discussing luminescence, photoconductivity and conductivity glow curves
10 p1746 A69-23565

Structure of epitaxial single crystal layers of CdS vacuum deposited on mica surface at various temperatures
11 p1939 A69-25709

Thermodynamic method for determination of conditions for CdS single crystal synthesis from gas phase, analyzing equilibrium between solid and gas phases
12 p2144 A69-26585

Standing waves and single mode room temperature laser emission from electron beam pumped cadmium sulfide thin crystal, discussing emission at 77 K
12 p2109 A69-26639

CdS acoustoelectric oscillator steady state oscillation frequency dependence on voltage and conductivity compared with linear acoustoelectric amplification theory
13 p2227 A69-27244

Carrier dragging in CdS single crystals under Q switched ruby laser light due to photon stream
13 p2271 A69-27661

Capture levels at photosensitive CdS crystals surface determined by studying field effect mobility dependence on electric field
13 p2318 A69-27884

Nonequilibrium conductivity and radiation of CdS, GaAs and PbS single crystals in waveguide cell under electron beam
13 p2318 A69-27886

CdS single crystals spectral dependence of photocurrent, photoconductivity quantum yield and photoelectromotive force in exciton absorption region
14 p2504 A69-28990

Ruby laser beam effects on CdS crystals optical properties, measuring absorption spectrum and light dispersion in crystal
14 p2457 A69-28999

CdS crystals emission spectrum during two photon excitation by ruby laser, noting dependence on pump power
14 p2458 A69-29167

Space environment simulation tests of cadmium sulfide thin film solar cells, noting output loss
14 p2405 A69-29538

Ceramic CdS photovoltaic solar cell properties and model, classifying junctions according to preparation method
14 p2508 A69-29886

CdS films vacuum deposited on optically polished single crystals used for converting microwave radio signals into hypersonic waves
15 p2575 A69-30236

Cadmium sulfides thin film solar cells for supplying power to instrumentation and data telemetry on longer lived balloons
15 p2553 A69-31287

IR quenching of photocurrent under field effect in CdS crystal
16 p2827 A69-32044

Superconducting cavities for resolving optically induced changes in dielectric constant of CdS at 4.2 K
17 p3016 A69-33782

Hall mobility of photoelectrons in cadmium sulfide layers
18 p3182 A69-35048

Time dependent recoverable isothermal decrease of photocurrent in CdS crystals in vacuum, noting trap mechanism involving electron redistribution
18 p3183 A69-35156

Copper sulfide-cadmium sulfide heterojunction model for photovoltaic effect, considering surface layer intrinsic absorption and CdS photoconductivity
19 p3250 A69-35683

Photovoltaic effect at copper sulfide-cadmium sulfide heterojunction, studying depletion layer width, diffusion lengths and spectral response
19 p3382 A69-35684

Resistivity, layer thickness, postbarrier heat treatment and impurity effects on cadmium sulfide-copper sulfide solar cell
19 p3250 A69-35685

Cadmium sulfide solar cells and Kapton coverslides under proton irradiation, noting annealing of damage in samples exposed to air
19 p3253 A69-35705

Integrated thin film solar cell array consisting of CdS cells deposited on Kapton single sheets connected in series and covered by Mylar single sheet
19 p3254 A69-35710

ZnS-CdS crystals luminescence during varied forbidden bandwidth, discussing two photon and ruby laser excitation and temperature dependence
19 p3331 A69-35866

Stimulated emission characteristics of CdS-CdSe mixed crystals subjected to two photon excitation, studying pulse energy at 77 K as function of pumping power
19 p3332 A69-35867

Cadmium sulfide-selenide single crystals reflection coefficient polarimetric measurement, observing reflection peaks relationship to absorption spectral temperature dependence
19 p3391 A69-36607

Optical and thermal attenuation of current induced by low energy electron bombardment in CdS crystal
19 p3392 A69-36727

Injection and excitation of charge carriers in CdS single crystals, analyzing current-voltage characteristics dependence on electrode separation, temperatures and electric field
21 p3779 A69-38423

Transient current change with minor change in voltage with double injection of electrons and holes in CdS single crystals, obtaining time dependence
21 p3780 A69-38833

Changes in CdS crystals spontaneous and coherent emissions caused by electron beam radiation damage, determining intensity and spectral composition dependence
21 p3780 A69-39047

Electromechanical effect dependence on CdS semiconductor surface state, noting relationship between microhardness and discharge current
21 p3781 A69-39072

Radioactive decay and conductivity changes with time in high and low resistivity CdS single crystals after irradiation with 14 Mev and reactor fast neutrons
22 p3993 A69-40728

Performance degradation in cadmium sulfide solar cells, discussing cause identification technique, I-V curve parameter changes, etc
23 p4070 A69-42271

Optimal CdS single crystals growth from gaseous phase achieved with 2 to 1 ratio between Cd and S concentration
23 p4199 A69-42468

CADMIUM TELLURIDES

Acceptor defect levels in cadmium telluride crystals prepared under various cadmium vapor pressures, demonstrating ionization energy variation by electrical measurements
02 p0294 A69-11546

HgTe-CdTe single crystals homogeneity and Cd distribution obtained by Bridgman and/or zone melting studied for carrier concentration and electron mobility
09 p1557 A69-21737

Electrical resistivity of epitaxial CdTe films produced by vacuum sublimation on hot orienting mica and single crystal substrates
10 p1742 A69-23001

Current voltage characteristics of p-n junctions in cadmium telluride, discussing spectral sensitivity bands
10 p1744 A69-23212

IR absorption spectrum of Br-doped n-CdTe specimen, considering donor level transfer mechanism
12 p2142 A69-25979

Temperature effects on photosensitivity spectra of cadmium telluride thin films
13 p2318 A69-27889

Cadmium telluride laser characteristics including emission wavelength and electron beam threshold current density
13 p2272 A69-27896

Photovoltaic effects in cadmium mercury tellurides, considering band-gap variations, effective masses, mobilities, majority carrier concentration and pair lifetime
19 p3381 A69-35680

Electroabsorption oscillations in CdTe films compared with results of interband transitions theory
19 p3386 A69-36523

Superradiance and recombination radiation from CdTe with high compensation, using model assuming narrowing from superradiance onset for analysis
19 p3389 A69-36550

Hot electrons effect on Fe-doped CdTe optical absorption by measuring optical transmission vs photon wavelength at liquid helium temperatures
19 p3389 A69-36551

HgTe-CdTe single crystals homogeneity and Cd distribution obtained by Bridgman and/or zone melting studied for carrier concentration and electron mobility
20 p3584 A69-38215

HgCdTe as IR satellite detector for terrestrial, atmospheric and ocean mapping, IR astronomy and optical communication
24 p4362 A69-43666

Donor and acceptor impurity effect on absorption and reflection spectra of CdTe single crystals, analyzing In, Ga, S and Se
24 p4362 A69-43735

CALCIFICATION

Parasitic calcifications of soft parts in flight personnel studied radiologically, noting filariasis, bilharziasis and worms
09 p1446 A69-22729

CALCINATION

U ROASTING

CALCITE

Calcite crystals stability anisotropy to ruby laser radiation, studying threshold power as function of beam polarization
11 p1900 A69-25553

Calcite IR absorption dependence on pressure, discussing calcite-aragonite transformation
12 p2141 A69-25783

CALCIUM

Ionized calcium lines in spectra of light bridges of sunspots, observed by diffraction spectroscopy, indicating similarity to chromospheric flares
01 p0154 A69-10894

Red autoionizing lines relative gf values for calcium measured by shock tube experiment
09 p1601 A69-22208

Vegetable diet including 210 g of dry Chlorella biomass decreases effect on calcium and magnesium assimilation to produce insignificant negative balance of K and Mn
10 p1647 A69-23590

Two component calcium plage associated with proton flare of July 1966, describing initial development in old region periphery and component merging
10 p1763 A69-23729

Chromospheric heating and polarization in late stars, considering association with Ca II K line emission cores
13 p2340 A69-27579

Fine structure of absorption lines of circumstellar Ca ejected from Nova Delphini 1967, determining ejection dates and photospheric radius
13 p2346 A69-27709

Solar activity indices based on Ca flocculi, emphasizing index representing emission excess over chromospheric emission
14 p2525 A69-29722

Ca II forbidden lines in photospheric spectrum identified with weak Fraunhofer line by photoelectric spectrometer scans
14 p2528 A69-29962

Ca XV spectrum in vacuum UV under laboratory conditions, discussing fine structure of ground level of Ca XV and coronal lines
15 p2688 A69-30553

Center limb observations of Ca II emission core interpretations, discussing chromospheric thickness effects on Doppler width
16 p2854 A69-31653

Solar Ca chromospheric plage decay curves obtained from area measurements, showing similarity and exponential mean curve
16 p2859 A69-32222

Ca 2 resonance line profiles in large disk flares and in surrounding plage, discussing H and K line behavior
17 p3023 A69-33054

Intensity ratios effect of forbidden Fe and Ca transitions in solar corona on Fe/Ca ratio, noting cascading configurations
19 p3422 A69-36219

Absorption spectra from excited metastable states in tunable dye laser pumped atomic Ca, using fast flashlamp continuum
21 p3775 A69-39740

Temperature dependence of action potential, isometric tension development and relaxation rate of mammalian myocardium at low temperature, considering Ca ions role
23 p4092 A69-42060

CALCIUM CARBONATES
NT CALCITE
Amino acid composition of organic matrix in modern and fossil calcareous oolites
04 p0553 A69-14978

CALCIUM COMPOUNDS
U CALCITE
U FLUORITE
U PEROVSKITES
CALCIUM FLUORIDES
Emission spectrum of laser employing electron-vibrational transitions in samarium doped calcium difluoride crystal, noting spectrum shift with increasing crystal temperature
08 p1326 A69-20544

Specific level role in emission of optical radiation by ruby laser stimulated calcium fluoride crystals doped with divalent Dy ions
11 p1894 A69-24618

Ultrasonic paramagnetic resonance investigations of Pr ions ground state energy levels in calcium fluoride
24 p4360 A69-42790

CALCIUM ISOTOPES
Calcium isotopes tracer migration in caged rats in metabolism study
13 p2212 A69-28618

CALCIUM METABOLISM
Calcium isotopes tracer migration in caged rats in metabolism study
13 p2212 A69-28618

Calcium mobilization control by adequate calcium intake and programmed exercise during space flight suggested from metabolic balance data
15 p2557 A69-31468

Laser pulse effects on bones of rats, observing metabolic deviations in Ca 45 uptake
23 p4101 A69-41464

CALCIUM OXIDES
CaO and MgO reflectance spectra measurements at high resolution and at low temperature including exciton spectra at 25 K, obtaining fine structure
18 p3181 A69-34274

CALCIUM TUNGSTATES
Paramagnetic resonance of Er ion in calcium tungstate single crystal, determining spin-Hamiltonian parameters
04 p0643 A69-15141

Output characteristics of slowly Q switched neodymium in calcium tungstate laser
04 p0612 A69-15206

Pulsed solid state Nd doped calcium tungstate fundamental longitudinal modes selection by insertion of Fabry-Perot interferometers, lenses and diaphragms into resonator
11 p1894 A69-24471

Stimulated emission cross section measurement of Nd ions in calcium tungstate using Edwards method
11 p1938 A69-25049

Negative dispersion of light in neodymium activated calcium tungstate single crystal using neodymium glass laser source, analyzing interference bands in spectral diagrams
15 p2632 A69-30051

CALCULATION
U COMPUTATION

CALCULATORS
Three probe impedance meter with graphic arithmetical element designed to cover frequency range from 50-1000 MHz
[ONERA-TP-605] 05 p0764 A69-16590

Mechanical calculators for solving spherical triangle problem of navigation
07 p1135 A69-19207

Calculator for obtaining moments of inertia data to determine control power for vehicle orientation and to avoid control systems over design
[SAWE PAPER 792] 18 p3118 A69-34865

CALCULI
Renal calculus incidence among aircrews of long and short haul airlines, considering effects of dry cabin environment and dehydration
23 p4108 A69-41826

CALCULUS
U ASYMPTOTIC SERIES
U COLLINEARITY
U CONTINUITY [MATHEMATICS]
U COPLANARITY
U CURL [VECTORS]
U DIFFERENTIAL CALCULUS
U FOURIER SERIES
U INTEGRAL CALCULUS
U LIMITS [MATHEMATICS]
U PADE APPROXIMATION
U POWER SERIES
U SERIES [MATHEMATICS]
U SINE SERIES
U TAYLOR SERIES
U VECTOR ANALYSIS
U VORTICITY

CALCULUS OF VARIATIONS
Microstrip-like transmission lines analyzed by method based on line capacitance variational calculation and charge density distribution
01 p0044 A69-10625

Variational law of control elements for automatic control systems with parameters subject to random changes
01 p0052 A69-10800

Book on variational methods in optimum control theory covering necessary and sufficient conditions for extremum and functional constraints
01 p0053 A69-11107

Discrete time optimal control problems solved by second order variational algorithm, developing recurrence relations for perturbation equations
01 p0054 A69-11416

Variation method for optimal solution of antenna synthesis problem for given radiation pattern
02 p0217 A69-12260

Elastic stability equations solved in geometrical linearization for thin anisotropic plates under transverse shear, using variational method
03 p0525 A69-13130

Variational theorems on eigenvalues of Laplace finite difference operator with first order boundary conditions
03 p0457 A69-14230

Algorithm for numerical solution of variational problems for functions of two independent variables and boundary value problems using local variations method
04 p0622 A69-14616

Variational method applied to maximization of electronic efficiency of O-type TWT
04 p0577 A69-14791

Book on calculus of variations methods and applications covering extremum problems, elasticity theory, strain and stress, Rayleigh-Ritz method, etc
04 p0623 A69-14847

Book on boundary value problems of mathematical physics emphasizing solutions, Green functions, transforms and variational methods
04 p0625 A69-15233

Variational methods for nonequilibrium thermodynamic processes noting fluctuation theory introduction
04 p0551 A69-15314

Gyrotropically filled waveguides propagation parameters calculation by variational method
05 p0718 A69-15648

Functions satisfying mixed boundary conditions derived for boundary value problems involving regions of complex form
05 p0787 A69-16455

Variational coefficients for vertical and inclined meson telescopes, deriving primary cosmic rays anisotropy parameters from daily variations
06 p0924 A69-17293

Stable stationary positions for spacecraft determined by formulating variational equations for perturbing effects of earth triaxiality
06 p1006 A69-17565

Channel parameters, magnetic field level, electrical potential and channel output pressure for optimal integral characteristic of MHD system selected by variational method
06 p0969 A69-17917

Current load distribution for optimizing MHD generator efficiency determined by variational method, noting dependence on relative length
07 p1058 A69-19012

High density plasma dynamic stability in magnetic containment using variational calculations
08 p1359 A69-19984

Variational techniques for unstable problems including input determination in system with known impulse response and measured output
08 p1342 A69-20350

Time response of second order nonlinear overdamped systems calculated by Krylov-Bogoliubov method of variation of parameters
08 p1297 A69-20356

Ultimate state periodic analysis of nonlinear electric systems by approximation methods in calculus of variations, discussing functional concept
09 p1474 A69-22448

Nonlinear second order elliptic difference equations in associated variational problems, considering differentiable solution of Dirichlet problem
10 p1718 A69-22879

Ordinary and inverse variational methods for stress-strain state of solid body, using Lagrange multipliers to reduce variational problem
10 p1793 A69-22885

Variational method for necessary and sufficient conditions of terminal state invariance of dynamic control system
10 p1718 A69-23206

Thermal stresses for mixed boundary conditions calculated from combined use of integral transforms and variational techniques, reducing computational labor
10 p1801 A69-23429

Variational calculation of coefficients of viscosity, thermal conductivity, thermal diffusivity and diffusion in binary mixture
11 p1997 A69-24285

Variational equations for rotation of heavy solid body with fixed point about horizontal axis, noting mass distribution
11 p1917 A69-24778

Variational method for weak second order resonant interactions among waves with position and time varying amplitudes and phase angles
13 p2297 A69-27634

Book on calculus of variations and optimal control theory, discussing functional analysis for use in space science
13 p2289 A69-28054

Finite difference Newton-Raphson algorithm extension to solve variational equations for simultaneous optimization of trajectories and associated parameters [AIAA PAPER 68-115]
13 p2353 A69-28203

Variational difference method application to second order elliptic equations with inhomogeneous boundary conditions, applying results to boundary value problems in elasticity theory
13 p2289 A69-28318

Variational method for time invariant states of collisionless plasma in oscillating electromagnetic field
13 p2314 A69-28365

Bayes theory and nonclassical variation method to solve optimal energy distribution available for identifying weak signals in background noise
14 p2410 A69-28817

Singular and sliding modes/unique extremals/ in calculus of variations for optimal control problems with nonlinear equations and linear control
16 p2764 A69-31629

Low thrust trajectories for minimum time rendezvous between continuous thrust interceptor and passive target vehicle, comparing calculus of variations and steepest ascent analyses
16 p2857 A69-32177

Gyrotropically filled waveguides propagation parameters calculation by variational method
16 p2754 A69-32505

Eigenvalue conversion of second variation test for algebraic and differential constraints to Jacobi accessory minimum problem by introducing norm in coordinate perturbation space
19 p3400 A69-35672

Kalman filter based on calculus of variations, evaluating object trajectory during vertical atmospheric descent

19 p3307 A69-35794

Design laws of warping-free multicellular box beams under torsion or bending, using variational method

19 p3443 A69-36786

Algorithm for Chernousko local variation method during application to solution of variational problems involving nonadditive functionals, assessing convergence

20 p3513 A69-36990

Boundary value problem of wave propagation in three dimensional region of waveguide bounded by surface solved by variational method

20 p3487 A69-37078

Perturbation matrix derivation in rectangular coordinates using Sitarsky two body variational equation for all motions

20 p3568 A69-37200

Optimization for processes expressed in differential equations, stressing use of calculus of variations and limitation

21 p3795 A69-38400

Optimum form for hypersonic profile with minimum drag for given bending strength solved by variational method

21 p3644 A69-39099

Variational method for necessary and sufficient conditions of terminal state invariance of dynamic control system

21 p3756 A69-39147

Ray theory of radio propagation by two variation techniques of phase paths

21 p3675 A69-39279

Book on optimal aerodynamic shapes by means of variational method, covering conventional and triangular thick wing lift systems in supersonic flow

21 p3644 A69-39667

Variational problem involving winged flight vehicles ascending and descending flight optimal program determination, considering necessary extremal conditions

21 p3767 A69-39823

Euler equation in variational problems for optimized process described by ordinary differential equations, deriving final extremal relationship

21 p3829 A69-39825

Variational method using Hamilton principle and calculus of variations to determine elastic curve and internal forces in static or dynamic loaded beam

22 p4043 A69-40459

Book on fundamentals of dynamics of deformable bodies of increasing dynamic complexity, using calculus of variations

23 p4226 A69-41474

Variational formulation of nonlinear differential equations, treating vector fields in Hilbert spaces, finding relations useful in quantum mechanics

23 p4181 A69-41723

Convergence of Rayleigh-Ritz approximations for variational problem, considering functionals of scalar valued function

24 p4339 A69-42793

Triangular plate bending element using Herrmann variational method, deriving matrices for finite elements

24 p4404 A69-43591

Optimum climb trajectories at constant lift coefficient, using variational methods with final altitude and final flight path angle as end point constraints

24 p4254 A69-43727

CALIBRATING

NT WIND TUNNEL CALIBRATION

Laser cone calorimeters calibration to determine heat capacity

01 p0079 A69-10220

Calibration of pressure transducers in liquid hydrogen to liquid helium temperature range using cryogenic test equipment

01 p0080 A69-10300

Electrical conductivity standards and eddy current measurements noting calibration facility

01 p0081 A69-10830

Rapid scan spectrometer design and calibration, noting application to diagnostics of high density transient Xe and H plasmas

01 p0082 A69-10838

Scaled and translated composite curve technique for reducing calibration data for spectrograph film system response characteristics

01 p0082 A69-10839

Microwave radiometer with two reference temperatures, discussing overall stability of design, sensitivity and airborne design for operation in X band [DVL-895]

02 p0220 A69-12435

Calibration of coaxial line noise sources in terms of rectangular waveguide standard, discussing use of adapter for comparison

02 p0210 A69-12436

Microwave thermal noise standards, discussing construction, calibration and errors for field operational liquid nitrogen cooled waveguide noise standard

02 p0210 A69-12438

X band radiometer to minimize errors in calibration of microwave noise sources

02 p0220 A69-12440

Mismatched errors associated with Y factor power ratio measurement effect on microwave noise-temperature calibrations [JPL-TR-32-1345]

02 p0211 A69-12442

Radar cross section data interpretation, discussing calibration, unwanted signals, averaging, scattering matrix and power spectra

03 p0385 A69-12913

Laser interferometer gauges for machine tool accuracy, discussing operation, application, manufacture, cost and closed loop numerical control systems

04 p0606 A69-14880

Decibel scaling advantages in vibration measurements

04 p0602 A69-15324

Attenuation calibration of optical resonator using transparent plate coated by thin metal layer

04 p0613 A69-15415

Thin foil heat flux sensor for radiative and convective heating rates over wide range and dynamic response, noting error mechanisms, calibration and accuracy

04 p0602 A69-15426

Solar and terrestrial thermal radiometer absolute calibration noting standards and methods

04 p0602 A69-15429

Calibration procedures for cameras and photographs in photogrammetry, noting least squares method and tolerance criteria

06 p0925 A69-17469

High accuracy microwave phase standard for calibration laboratories, discussing broadband differential phase shifter

06 p0896 A69-17487

Shipboard direction finder calibration accuracy, emphasizing radio operator training

06 p0897 A69-17533

Multichannel radiometers calibration and testing for spacecraft and solar simulation applications, noting exposure to sun onboard X-15 aircraft at high altitudes

06 p0926 A69-17620

Calibrating long wave actinometric instruments designed for Soviet meteorological satellites

06 p0929 A69-17978

Calibration curve for constant temperature hot-wire anemometer, taking into account high wire temperature and gas pressure effects

06 p0930 A69-18218

Sun as calibration signal source for L and S band telemetry, discussing receiving system noise temperature determination and antenna gains

07 p1082 A69-19113

Onboard calibration system for gamma ray spectrometers and X ray detector in earth satellites, describing fabrication and test results for radioactive sources [IEEE PAPER 3A-6]

07 p1134 A69-19193

ONERA vertical bench for dynamometric calibration to 20 tons used for engine and rocket thrust measurement

07 p1116 A69-19217

Simulated solar EUV laboratory spectrophotometry used in preparing optical space flight experiments, discussing instrumentation and calibration

08 p1267 A69-19888

Small amplitude surface irregularities effect on backscattering properties of radar calibration metal sphere, using full wave boundary perturbation method

08 p1273 A69-20027

Pointing calibration of Haystack parabolic antenna by using radiometric measurements of cosmic ray sources

08 p1281 A69-20032

Stellar absolute magnitudes recalibration for consistency with photometric distance moduli of clusters

08 p1408 A69-21139

Photometric standard based on calibration of Vega by Hayes compared with six color magnitudes

09 p1603 A69-22233

Calibration for instrument systems including strain gages, piezoelectric, thermoelectric and thermoresistive transducers

10 p1691 A69-23229

Optimum calibration interval program for determining test equipment calibration frequencies on basis of mean time between failures and acceptable reliability levels

10 p1699 A69-23288

Skin friction measurement with rectangular mouthed Preston tubes of constant thickness ratio, analyzing calibration curves and difference from circular tubes

11 p1880 A69-24376

Laser beam for determining instrumental profile of high resolution double pass solar spectrograph, noting influence of slits width

11 p1893 A69-24431

Small microwave antenna calibration by method of two black bodies exposed to different temperatures, reducing influence of cloudiness and humidity

11 p1844 A69-24450

Radio sources optical positions for independent calibration sources

11 p1958 A69-24465

AM-FM calibration modulator for microwave oscillator noise measurement

11 p1856 A69-25631

Photometric standardization and calibration of meteor spectrograms for real meteor masses determination using spectroscensitometer

12 p2154 A69-25820

Calibration and accuracy check of measuring instruments at National Center of Space Studies in France, emphasizing reference instruments

12 p2080 A69-26123

Comparative calibration characteristics determination, discussing absolute measurements method for thermal conductivity parameters

12 p2091 A69-26363

Gallium arsenide thermometer calibration in 1 to 100 K range using interpolation formula derived from p-n junction diode equation

12 p2093 A69-26484

Construction and calibration of combined temperature and pressure probe for compressible flow

13 p2242 A69-28226

Transistors scatter matrix parameters determined, describing measuring bench calibration system

14 p2420 A69-29393

Output impedance measurements for accurate calibration in UHF region, using mobile discontinuity and bolometer for linear or nonlinear systems

14 p2422 A69-29583

Oxygen boiling point studied via calibration of capsule type platinum resistance thermometers

14 p2540 A69-29888

Calibration of interference measuring instruments, stressing input impedance calibration of field intensity meters

15 p2577 A69-30375

Photometric calibration correction for /B-V/ and /U-B/ colors taking into account hydrogen line blocking

15 p2694 A69-30786

Reciprocity method for absolute calibration of piezoelectric accelerometer mounted on electrodynamic shaker table

15 p2615 A69-31283

Dual channel waveguide insertion loss test set for calibrations at 90 GHz in radio astronomy and communication systems, using sprayed thermistor mount

16 p2760 A69-31945

Scintillation index determination, discussing data reduction methods, standard test records, calibration at stations with modest equipment and simulation on digital computer

16 p2751 A69-32105

Maintaining of flow similarity in calibration of nozzle type water meters for study of working processes of pumps

16 p2772 A69-32145

Radar calibration and precipitation measurements equation taking Gaussian approximation for antenna radiation pattern

16 p2806 A69-32264

Hot-wire anemometers calibration technique providing accurate and direct velocity measurements in slow moving liquids

17 p2971 A69-32901

Piezoelectric shaker consisting of combination of damped resonant cylindrical elements for wide frequency calibration of vibration pickups

17 p2975 A69-33665

Shock tube calibration for aerodynamic loading, determining flow parameters by observing particle

trajectories with high speed photography of smoke tracers

18 p3085 A69-34469

Automated analog scaling for in hybrid computer systems imposing magnitude and frequency constraints, using equations for amplifier input factors

18 p3105 A69-34617

Solar cells volt-ampere characteristics calibrated at various solar incidence angles on LES-6 satellite in synchronous orbit

19 p3254 A69-35712

Electrostatic probes calibration and use for hypersonic wakes behind projectiles in ballistic range

19 p3291 A69-35717

Small continuum electrostatic probes calibration and operation in ionized plasma flow with sheath dimensions larger than boundary layer dimensions

19 p3304 A69-35719

Transient calibrations for Ge surface thermocouple heat flux sensors used in hypervelocity impulse tunnel

19 p3292 A69-35725

Calibration of inertial and surface temperature heat transfer transducers for hotshot and shock tube measurements developed and tested at ONERA [ONERA-TP-683]

19 p3305 A69-35726

Transducer with single crystal Ge for high heat flux measurement, noting calibration by direct conduction

19 p3307 A69-35748

Radiometric measurement, discussing characteristics and calibration of instruments for measuring radiant intensity or radiance

19 p3311 A69-36071

FM radioaltimeter for Concorde aircraft, describing autocorrelation and automonitoring device, signal characteristics, reliability, etc

19 p3315 A69-36699

Near-polar circular orbiting satellite for calibrating and evaluating ground-based radars observing space objects

20 p3617 A69-37714

Tape recorder premission calibration requiring standard and external test instruments

20 p3546 A69-38233

Cosmic ray muons for calibrating dE/dx counter used in particle identification by determining cosmic particles distribution as function of energy losses due to ionization

21 p3724 A69-39075

Digital computers used in error calculation in calibration curves of turboengines and other pneumatic devices

21 p3724 A69-39100

Radar calibration techniques for accurate real time tracking data, describing GEOS-B C-band experiment [AIAA PAPER 69-872]

21 p3675 A69-39398

Light sources with uniform variable luminance field designed for calibrating cameras used in space exploration

21 p3726 A69-39580

Space vehicle data system synthesizer /SVDS/ for dynamic calibration of automatic control and checkout systems during prelaunch and countdown operations

21 p3680 A69-39633

Standardizing strain gage with long time stability characteristics, analyzing statistically strain calibration results

22 p3945 A69-40078

Magnetic field inhomogeneities effect on line contours and magnetographic measurements, constructing two stream models using Unno solution of transfer equations

22 p4019 A69-40288

Mariner Mars 1969 TV system environmental test and calibration program

22 p3920 A69-40372

Clark oxygen electrode calibration by preparation of oxygen standard aqueous solutions, noting repair by ammonium hydroxide treatment

23 p4101 A69-41451

Vacuum gage calibration standards and methods

23 p4162 A69-41530

High intensity electromagnetic fields generation equipment for calibrating field intensity monitors, discussing anechoic chamber, transmitting antenna, etc

24 p4312 A69-42577

Flotation technique for laboratory calibration of low level accelerometers, noting accuracy dependence on flotation fluid density stability [AIAA PAPER 68-874]

24 p4315 A69-43242

Aerodynamic frequency response calibration measurements of wind anemometer by input velocity and output drag values under unsteady flow conditions

24 p4315 A69-43262

Hot-wire anemometer calibration technique for measuring velocity of very slowly moving liquids [ASME PAPER 69-HT-A]

24 p4316 A69-43527

CALIFORNIA

Prokaryotic and eucaryotic nanofossils localized in prePaleozoic microflora, noting radiometric age and association with stromatolites

22 p3935 A69-40052

CALORIC REQUIREMENTS

Human performance and adaptation to space flight effects under low calorie diet including optimal proportion of basic nutrients and amino acids

20 p3482 A69-37621

Muscular strength dynamometric measurements in subjects during prolonged inactivity with restricted caloric and protein intake, showing decrease in strength

21 p3653 A69-38901

CALORIC STIMULI

Threshold variations in caloric nystagmus in pigeons subjected to accelerations in head to tail direction in centrifuge at various temperatures

20 p3471 A69-37252

Vestibular neurons activity in decerebrized cats under ipsilateral and contralateral labyrinth polarization combined with acoustic and caloric stimulation

20 p3471 A69-37254

CALORIMETERS

Continuous wave laser absolute power measurement by calorimeter consisting of wire wound in shape of cone

01 p0078 A69-10029

Laser cone calorimeters calibration to determine heat capacity

01 p0079 A69-10220

Internal temperature distributions of present and proposed calorimeter geometries operating at high pressure and extreme heating rates compared, using one and two dimensional heat conduction programs

01 p0079 A69-10299

Microcalorimetric measurement of radiation flux of flames of condensed burning material, noting surface temperature distribution

02 p0355 A69-12671

Twin differential calorimeter for measuring heat dissipation by wire specimen under fatigue tests, using semiconductor thermopiles

04 p0618 A69-15205

Fast response thin skinned calorimeters for high heat flux profiles of arc jet flows

04 p0602 A69-15427

Plane reaction cell unit for use in differential flux calorimeters and devices for differential enthalpy analysis

05 p0764 A69-16607

Vanadium monoxides and oxycarbides heat capacity using adiabatic calorimeter, calculating entropy, enthalpy and characteristic temperatures

09 p1523 A69-21739

Pyrotechnic activated calorimeter for reentry package design of vehicles entering earth atmosphere at lunar return velocities

10 p1669 A69-23026

Calorimeter for IR carbon-dioxide laser output power measurement, noting range calibration and accuracy

11 p1885 A69-24903

Photoelectric, calorimetric and photon-momentum methods for measuring laser output energy and power emphasizing liquid, wire and pyroelectric calorimeters

11 p1899 A69-25196

Boundary conditions for time dependent temperature variations of calorimeter operating in regular thermal regime

11 p2003 A69-25702

Velocity, enthalpy and mass flux radial distributions in laminar boundary layer from calorimetry of argon subsonic flow [ASME PAPER 68-HT-16]

13 p2374 A69-27776

Cosmic ray postinteraction nuclear active particle energy spectrum measurements with ionization calorimeter, noting energy underrating

13 p2331 A69-28392

Ionization calorimeter energy measurement systematic errors

13 p2331 A69-28394

Cell current and calorimetric measurements of electrical power and heat generation with heat pipe-thermionic converter

14 p2402 A69-29238

Calorimeter for CW laser output power absolute measurement, discussing operation principles, structural features, circuit and accuracy

15 p2608 A69-30320

Acoustic flow calorimeter for evaluating power transducers under loaded conditions

16 p2790 A69-32079

Solid W enthalpy from 2800 K to melting point measured with drop calorimeter, tabulating heat capacity, entropy and free energy function

17 p2987 A69-33075

Heats of solution of Au and Cu in dilute Au-Cu-Sn alloys determined using liquid metal solution calorimeter, calculating self interaction coefficients

17 p2987 A69-33077

Guarded disk type emissometer for hemispherical emittance measurements of sample materials in 88 to 420 K range based on steady state calorimetry [AIAA PAPER 69-600]

17 p2973 A69-33280

Flat wire grid calorimeter used as radiation sensor in measuring pulsed ruby laser

19 p3339 A69-36755

Calorimeters for laser energy measurement, discussing radiation damage avoidance and modifications for various modes

22 p3961 A69-40243

CALORIMETRY

U HEAT MEASUREMENT

CALUTRONS

U CYCLOTRONS

CAMBER

NT WING CAMBER

Numerical solutions of thick cambered jet flap in ground effect for flat plate and diamond shaped airfoil [AIAA PAPER 69-738]

18 p3083 A69-34404

CAMBERED WINGS

Inverse transformation method for plane subsonic flow extended to flow past cambered profiles at angle of attack, obtaining velocity distribution

19 p3240 A69-36473

CAMEL AIRCRAFT

U TU-104 AIRCRAFT

CAMERA SHUTTERS

Shutter drive circuits for image converter camera noting focusing, deflection system, applications in plasma research, etc

12 p2082 A69-26138

Meshless shutter tube with nine images double deflection capability, using deflectron and semiconducting plates assembly

12 p2083 A69-26144

Diode type image shutter tube with proximity focusing for high speed photography

12 p2083 A69-26145

RLC integrated low inductance circuit for magnetooptical high speed camera shutters, Q switched ruby laser and short light pulses in spark gap

12 p2084 A69-26149

Multiple lens high speed camera with mechanical shutter for investigating AC arc in circuit breaker during zero current, noting framing rate and capacity

12 p2085 A69-26159

Lens shutters durability, analyzing break-in, cock-and-release cycles and cause of failures

12 p2094 A69-26600

Lens shutter design, discussing exposure process automation, shutter speed range extension and exposure accuracy

12 p2094 A69-26601

High speed plate holder and shutter mechanisms for observing 20 May 1966 annular solar eclipse

15 p2686 A69-30534

Superwide angle camera with aerial photogrammetric lens system, discussing light distribution, rotary disk shutter, etc

22 p3944 A69-40047

CAMERA TUBES

NT IMAGE DISSECTOR TUBES

NT IMAGE ORTHICONS

NT VIDICONS

Tv transmission of two dimensional transparency hologram with reduced resolution requirements on camera tube, eliminating zero order terms

17 p2974 A69-33401

CAMERAS

NT BAKER-NUNN CAMERA

NT BALLISTIC CAMERAS

NT FRAMING CAMERAS

NT HIGH SPEED CAMERAS

NT LALLEMAND CAMERAS

NT SCHMIDT CAMERAS

NT STROBOSCOPIC CAMERAS

NT TELEVISION CAMERAS

X ray spectrographic camera for nondestructive spectrum analysis of small samples

03 p0427 A69-13101

Calibration procedures for cameras and photographs in photogrammetry, noting least squares method and tolerance criteria
06 p0925 A69-17469

IR camera determining surface temperatures, discussing construction and space applications
08 p1315 A69-20455

Design and operation of Polaroid camera for use with telescope, noting six exposures per negative
08 p1316 A69-20617

Aerial panoramic camera with instantaneous exposure using combined Bouwers concentric lens system and between lens shutter
09 p1499 A69-22246

Multiple pinhole camera for X ray astronomy, suggesting cross correlation image recovery technique based on Fourier convolution theorem
09 p1502 A69-22768

Hologram obtained by recording interference pattern displayed by ultrasonic camera, discussing real time viewing
10 p1696 A69-23550

Time registration delays during photographic observations of satellites, describing NAFA type satellite camera and mechanical and electrical systems
11 p1880 A69-24365

Observatory camera for satellite observation, discussing objective focusing and diameter and manual/automatic operation
12 p2092 A69-26450

Wobble-spin technique for spacecraft inversion for earth photography using flywheel
12 p2174 A69-26780

Vibrating camera for photographic measurement of flow velocities and trajectories of bodies marked by light spots
13 p2261 A69-27913

Satellite tracking cameras developed in East Germany, discussing optical systems
13 p2262 A69-27958

Photodielectric tape camera with optical images stored on tape in form of charge pattern
16 p2792 A69-32558

Mosaic mirror and lens camera system for multiple image high resolution photography
17 p2972 A69-33089

Gemini program for geologic orbital photography, discussing equipment used
18 p3131 A69-35274

Aerial camera AFA-TES-10, discussing mean square aiming error, photogrammetric distortion and contrast
18 p3139 A69-35328

Adaptor for Debye-Scherrer powder camera to take high quality photographs even at liquid N temperature
19 p3313 A69-36493

Wide view angle holocamera to produce 360 degree hologram in strips for simultaneous image reconstruction from single laser beam
20 p3536 A69-36932

X ray heliography by Fresnel-Soret type zoneplate camera to obtain solar photographs from rockets
20 p3544 A69-37803

Cameras photogrammetric parameters determined from stellar photographs, considering distortion components, reference points, etc
20 p3545 A69-38054

Auroral displays photographed by all-sky cameras at magnetically conjugate stations, morphological similarities and electron precipitation role
20 p3535 A69-38187

Extended source Fourier transform holography for single image synthesis of multiple identical images produced by multiple pinhole camera in X ray astronomy
22 p3943 A69-40019

Tethered polyethylene balloon carrying radio controlled camera for time lapse photographs of wave generated near shore currents
22 p3865 A69-40808

Photogrammetric camera system developed from NASA requirements to document lunar surface environment during manned space flight exploration
22 p3948 A69-40989

CANADA

Canadian upper atmosphere and space research programs organization, management and results
[UN PAPER 68-95551] 06 p1042 A69-17034

Canadian domestic satellite system requirements to extend existing terrestrial communications systems to improve coverage, capacity, flexibility and cost factors
06 p1043 A69-17832

Aircraft accident investigation procedures in Canada for routine/major accidents and public inquiries, outlining organization
13 p2201 A69-27540

Air Canada flight safety system including company philosophy, safety activities, incident and accident handling and information schemes
13 p2201 A69-27541

Canadian air cushion vehicle industry, considering materials, design, production, tests, components and quality control
13 p2381 A69-27544

Report on Canadian space activities to COSPAR covering scientific satellite program, high altitude sounding rocket program, space radio communications, international cooperative programs, etc
15 p2723 A69-31429

CANADAIK AIRCRAFT

U CL-84 AIRCRAFT

CANADAIK CF-104 AIRCRAFT

U F-104 AIRCRAFT

CANADAIK CL-84 AIRCRAFT

U CL-84 AIRCRAFT

CANALS

Martian canals nature based on high contrast photographs obtained by Mariner 4 space probe
12 p2171 A69-27133

Martian diagonal and longitudinal-meridional canals mapped into grid systems, noting differences between Martian and lunar crusts tectonic activity
13 p2337 A69-27533

CANCER

Cosmic radiation interactions with living viruses, considering X ray effects and optimal radiation dosage for cancer cell destruction
01 p0013 A69-10157

CANNONS

U GUNS [ORDNANCE]

CANNULAE

Oxygen saturation in outflowing and inflowing renal blood in dogs under normal and hypoxic conditions, assessing cannula technique
14 p2406 A69-28916

CANONICAL FORMS

Mach principle in scalar-tensor gravitation theory, discussing self energy calculations in canonical formalism for solitary neutral and charged point particles
01 p0120 A69-10858

Canonical equations for Lagrangian form of gravitational field equations in empty space
04 p0658 A69-14899

Canonical correlations used to analyze relations between values of geopotential field
05 p0789 A69-16637

Relativistic systems and relativistic Hamiltonian systems defined by second order equation, discussing canonical transformations conserving vector field Hamiltonian character
07 p1182 A69-19331

Canonical forms for second order elliptic systems with constant coefficients, studying Dirichlet problem solvability for systems reduced to canonical forms
07 p1174 A69-19476

Clebsch transformation application to equations describing viscous fluid, deducing canonical equations equivalent to Navier-Stokes equations
08 p1303 A69-20125

Canonical equations of planet satellite intermediate orbits using harmonics of gravitational potential
09 p1589 A69-21374

Canonical invariance of Hamiltonians noting nature of solutions of differential equations, existence of periodic solutions and application to three body problem
10 p1721 A69-23987

Canonical transformations of unsteady control system motion equations, simplifying control process study and controller simulation on analog computer
12 p2045 A69-25960

Canonical forms for observable and controllable linear time invariant systems by simultaneous transformations of system state and input and output vectors
12 p2048 A69-26075

Canonical representation of multivariable control system in state space using matrix of differential operators acting on vectors of input-output quantities
12 p2051 A69-26094

Rational transfer function matrix realization into irreducible Jordan canonical form state equation by nonsingular transformations
12 p2122 A69-26511

Thermodynamic equivalence of limit theorems for canonical and grand canonical ensembles, discussing Massieu-Planck function analog relation by Legendre transformation
12 p2191 A69-27148

Microwave filters for canonical realization of non-minimum phase transfer functions, combining magic-T or hybrid junction with ladder structure network
13 p2228 A69-27668

Canonical transformation and Hamilton-Jacobi theories applied to space vehicle trajectory analysis, discussing elliptical coast arc and optimal low thrust problems
13 p2353 A69-28202

Canonical correlations used to analyze relations between values of geopotential field
14 p2472 A69-28793

Autonomous canonical system with two degrees of freedom, determining equilibrium position stability in resonance case, calculating earth satellite rotational stability
14 p2482 A69-28813

Isolated symmetric doubly asymptotic solutions existence in neighborhood of symmetric periodic solutions of nonautonomous canonical system with one degree of freedom near resonance
17 p2996 A69-33619

Quasi-periodic solutions for canonical systems of differential equations in plane n-body problem
17 p3035 A69-33620

Canonical equations of planet satellite intermediate orbits using harmonics of gravitational potential
18 p3198 A69-34762

Moment and discrete ordinate methods in radiative transfer problems in planar, radiating and nonscattering media, noting conical transformation of moment equations
18 p3174 A69-35237

Canonical transformations depending on small parameter, utilizing Lie series
19 p3397 A69-35608

Canonical forms for three dimensional diffraction problem of elastic harmonic waves propagating along circular cylinders infinite array
19 p3437 A69-36144

Algorithm for determining multidimensional random process from canonical representation of current state, noting minimum rms prediction error
19 p3287 A69-36663

Sedov canonic equations for supersonic gas flow solved by applying Chaplygin function to determination of Riemann function for potential and stream function equations
21 p3643 A69-38637

Thermodynamic properties of hydrogen atoms, protons and electrons, using canonical group analysis to determine bound and free states
21 p3850 A69-38964

Optimal explicit method for parameters estimation not restricted to linear Gaussian problem derived in canonical form
[AIAA PAPER 69-947] 22 p3975 A69-40330

CANOPIES

Light interaction with stacked leaves and plant canopy, determining reflectance and transmittance
12 p2097 A69-26985

Aircraft canopy scratches effects on pilot visual discrimination
13 p2214 A69-28533

Shock force calculation for parachute of arbitrary canopy design, illustrating simplification permitting differential equation solution in closed form
15 p2551 A69-31172

CANT

U SLOPES

CANTILEVER BEAMS

Stress distribution in composite cantilever beams of three layers with end loading solved by closed form elasticity method
01 p0172 A69-11266

Point load subjected deflections of cantilevers and circular rings found using electronic analog computers
03 p0522 A69-12865

Natural frequencies and mode shapes of coupled bending vibrations of pretwisted rectangular cross sec-

CAMS

Program to study interactive graphic display console systems use for solving mechanical design problems involving plate cam and follower mechanisms
05 p0724 A69-16384

Minimum radius of three dimensional cam gears calculated from driven element motion and pressure angle
23 p4168 A69-41413

tion beams determined by Rayleigh-Ritz energy method

03 p0529 A69-13989

Multidegree of freedom systems for modeling optimum design of cantilever and simply supported beams for sudden loading

04 p0674 A69-14590

Thermally induced vibration and flutter of flexible spacecraft boom, discussing stability by considering boom as cantilever beam
[AIAA PAPER 69-21]

06 p0869 A69-18144

Root fixture and grip load effects on cantilever beam damping, using bandwidth and logarithmic decrement measurement methods

10 p1800 A69-23244

Warping rigidity effect on stability of cantilever bar under eccentric follower end load, discussing bending torsional flutter and buckling

12 p2179 A69-26212

Cantilever beam profile optimization methods using iterative analog computation to achieve minimum deflection, showing application of Pontryagin maximum principle

15 p2709 A69-30671

Transient behavior of finite damped cantilever beam and circular plate analyzed by direct finite element method, noting applicability to dynamic problems

15 p2710 A69-30868

Transverse free vibration of slender cantilever subjected to compressive follower force

16 p2871 A69-31899

Stresses and displacements in elastoplastic cantilever beams and beams fastened at both ends calculated by stress-strain diagrams of material

17 p3056 A69-33191

Test facility to determine factors influencing aerodynamic energy dissipation of cantilever rods oscillating in airstream

17 p2947 A69-33928

Vibration modes and damping of rectangular cantilevered prismatic steel rods, showing effects of transverse vibration, material and stress on logarithmic decrement

17 p3065 A69-33936

Thin walled cantilevered fiberglass reinforced shafts damping characteristics dependence on natural vibration modes and fibers orientation

17 p3065 A69-33938

Transverse and torsional vibration characteristics of tapered cantilever beams and shafts analyzed by lumped inertia force method

17 p3066 A69-34052

Vibration properties of cantilever parallelogram box beam, using existing static deformation equations under large aspect ratio condition

21 p3846 A69-39803

Young modulus for wire or strip shaped specimens determined from unloaded cantilever vibration considerations

22 p4042 A69-40443

Inflation effect on circular cylindrical cantilever beam subsequent response to bending loads, using theory of small deformations superimposed on large deformations

23 p4227 A69-41881

CANTILEVER MEMBERS

Stress distribution and spring rates in cantilever cone ring combination
[ASME PAPER 68-WA/DE-3]

05 p0839 A69-16168

Cantilever blades tangential vibrations effect on damping characteristics measured by free vibration excitation and static hysteresis loop

17 p3065 A69-33935

Cantilever truncated conical shell stability under tensile stresses solved by strain energy technique

18 p3216 A69-34574

Stress-strain state calculations of ribs reinforcing cantilever shell under external pressure, using differential-difference equations

18 p3223 A69-34980

CANTILEVER PLATES

Rib positioning effect on mechanical behavior of cantilevered rectangular plate in gas flow, considering critical flow velocities and rigidity relationships

01 p0165 A69-10085

Thin cantilevered plate theory extended to large in-extensional deflections to account for geometry changes in bending moments
[ASME PAPER 68-APM/BB]

04 p0670 A69-14401

Rotating twisted blades vibrations, deriving equations and vibration tests with models

09 p1618 A69-22236

Equations for bending of elastic cantilever plate with parallelogram shape in oblique angle coordinate system, constructing functions satisfying Poisson conditions at contour

15 p2710 A69-30861

Acroelastic divergence and stability range for cantilevered and end supported structures computed as function of forward resistance and lift caused by wind

16 p2870 A69-31557

Moire reflection technique applied to study of stress-strain state of partially clamped rectangular cantilever plates under various loads

17 p3058 A69-33203

Swept cantilever thin elastic plates bending analyzed by power series representing deflection in oblique coordinate system

20 p3621 A69-37207

CANTILEVER WINGS

U WINGS

CAPACITANCE

Capacitance variation in junction varactors with linear graded, abrupt and hyperabrupt junctions, storage switching diodes and storage varactors

01 p0038 A69-10168

Microstrip-like transmission lines analyzed by method based on line capacitance variational calculation and charge density distribution

01 p0044 A69-10625

Capacitance-voltage relationships for PETN initiation by various diameter gold exploding bridgewires, noting optimum capacitance dependence on energy transfer efficiency

01 p0141 A69-10679

Germanium tunnel diode capacitance as function of bias voltage and HF signal magnitude, considering circuit design

02 p0214 A69-11614

Frequency conversion in sheath capacitance of glow discharge plasma contained within metallic coaxial cylinders

04 p0634 A69-14456

Stability limits of regenerative echo amplifier during simultaneous variation of network capacitance and negative resistance

04 p0577 A69-14778

Cathode ray curve tracer to record capacitance-voltage characteristics of p-n junctions

04 p0602 A69-15406

Diffusion capacitance of p-n junctions, short base semiconductor diodes and p-n-p transistor, discussing systematic error in quasi-steady state calculation

04 p0580 A69-15489

Pulse radiation effect on dielectric constant of sintered CdS photoresistors, discussing capacitance dependence on intensity, type and frequency of light

05 p0806 A69-15694

Equivalent capacitance derivation of space charge limited current from filamentary cathode

05 p0734 A69-16567

Voltage dependence of depletion layer width, maximum electric field and capacitance of Gaussian diffused plane, cylindrical and spherical p-n junctions

07 p1196 A69-18242

Barrier capacitance of semiconductor diodes for exact temperature measurement, discussing application to temperature to frequency converters

07 p1100 A69-18556

Differential capacity of Li doped zinc oxide single crystals between vapor deposited asymmetrical In electrode contacts

08 p1371 A69-19883

Capacitance and effective height for VLF umbrella antennas using multiple wire structural members to increase effective antenna surface area

08 p1282 A69-20041

High Q capacitance loaded coaxial cavity resonator for study of electric susceptibility of ionized gas

08 p1313 A69-20214

Capacitance and lowest eigenvalue bounds for two dimensional anisotropic media as exemplified by transverse vibrations of stretched membrane

08 p1418 A69-20848

Rechargeable nickel cadmium batteries state of charge determination by monitoring capacitance

09 p1435 A69-21425

Selenium diffusion in indium antimonide, determining concentration gradients in junction space charge region by capacitance method

09 p1554 A69-21469

Differential capacitance of n-n heterojunction calculated by metal semiconductor contact method

09 p1555 A69-21476

Capacitance methods for measuring adhesives mechanical properties in thin film bonded joints, noting results for tension, compression and shear loading

09 p1500 A69-22309

Germanium tunnel diode capacitance as function of bias voltage and HF signal magnitude, considering circuit design

11 p1847 A69-24722

Capacitance pressure transducer capable of detecting pressure changes equivalent to 0.2 mm water

11 p1885 A69-24902

Dynamometer based on electrical capacitance change in sensor element, discussing working range, circuit diagram and mechanical design

11 p1887 A69-25207

Differential capacitance, diffusion voltage and exponent alpha of hyperabrupt junction varactor

12 p2039 A69-26375

Barrier capacitance measurement in mm wavelength parametric and multiplication diodes eliminating socket capacitance influence, describing oscilloscope and indicator methods

12 p2043 A69-26885

Tunnel diode nonlinear p-n junction capacitance influence on characteristics of diode microwave self excited oscillator

12 p2043 A69-26889

Discontinuity capacitance of coaxial line terminated in circular waveguide calculated using Rayleigh-Ritz variational technique

14 p2423 A69-29754

Capacitive parametric modulator transient processes and second harmonic effect analysis, obtaining transient response and recovery time

15 p2574 A69-30125

Frequency response of MIS capacitance beyond inversion voltage, discussing recombination rate and generation-recombination current in space charge region

15 p2565 A69-30179

Selenium diffusion in indium antimonide, determining concentration gradients in junction space charge region by capacitance method

15 p2669 A69-30714

Differential capacitance of n-n heterojunction calculated by metal semiconductor contact method

15 p2669 A69-30721

High temperature capacitance strain gage development, discussing extensometer prototype systems

15 p2614 A69-31278

Controlled electric field capacitance probes for non-destructive testing, discussing field projection pattern and direction effective depth of field, applications, etc

15 p2616 A69-31503

Two donor levels and conduction properties of n-type semiconductors demonstrated by capacitance measurements of single crystal tungsten oxide in presence of electrolyte

16 p2825 A69-31609

Lock-on band of phase locked AFC system calculated by asymptotic method, considering frequency integrating filters with nonlinear capacitances

19 p3277 A69-36569

Metal insulator semiconductor volt-capacitance changes due to light flux, introducing surface recombination rate to improve model

20 p3585 A69-38273

GaAs-GaP heterojunctions, analyzing continuous conduction band, capacitance and current-voltage characteristics, photoresponse and modulation effect

21 p3779 A69-38424

Differential capacitance transducer measuring small displacements in heated transformer oil, air, castor oil or glycerin

22 p3946 A69-40439

Time varying resistance wire to arrest oscillations in pulsed capacitor discharge circuit, deriving over, under and critical damping conditions

22 p3917 A69-41228

Capacitance sensor of vertical with flexible mobile electrode, describing diagram and operation

23 p4163 A69-41550

Capacitive coupling vs DC coupling between data input and transmitter exciter in FM telemetry system, based on pulse series Fourier analysis

23 p4119 A69-41744

CAPACITANCE SWITCHES

RLC integrated low inductance circuit for magneto-optical high speed camera shutters, Q switched ruby laser and short light pulses in spark gap

12 p2084 A69-26149

Erosion of contacts under capacitive loads noting cable length, arc duration and battery voltage

13 p2269 A69-28608

Waveguide capacitive screw tuners effects on dissipative loss, discussing microwave measurements with copper screw tuners

16 p2757 A69-31586

CAPACITORS

Megagauss magnetic field generation methods, discussing high explosives, initial field, flux compression, capacitor discharges and applications

01 p0115 A69-10049

Electromagnetic forming principles and applications describing large capacitor bank facility design for multipurpose research
[ASTME PAPER MR68-418]

02 p0252 A69-11798

Active and reactive impedance components of plane capacitor immersed in plasma and at LF noting dependence on plasma conductivity

03 p0477 A69-13713

Space charge layer thickness determination in plasma filled capacitor by capacitance measurement, noting thickness dependence on plasma potential

03 p0477 A69-13714

Automatic device for charging storage capacitors in plasma devices provides voltage and operational frequency control

04 p0580 A69-14493

High temperature capacitor consisting of thin wafers of pyrolytic boron nitride noting fabrication, dissipation factor and capacitance

04 p0551 A69-15299

Fluctuation voltage mean square value at polar dielectric capacitor terminals determined by applying stochastic properties of Poisson point processes to statistical model

08 p1295 A69-21151

Accelerated reliability tests of electronic capacitors using voltage as main forcing factor, establishing correlations between lifetimes in accelerated and long term tests

09 p1464 A69-22244

Surface charge exchange in metal oxide silicon capacitors generated at low temperatures by surface state free carrier trapping

10 p1744 A69-23179

Type 2 ceramic capacitor manufacture, selection and control in Concerto space program

11 p1853 A69-25393

Microwave harmonic generation in plasma capacitor, considering power resonances dependence on electron temperature and density

12 p2037 A69-25939

Inhomogeneous and anisotropic cold plasma filled plane capacitor resonance in steady magnetic field applied to plasma diagnostics, using calculus of variations

13 p2304 A69-27240

Prebreakdown and breakdown electrical properties of thin film capacitors with certain oxides, fluorides and Teflon dielectrics

13 p2322 A69-28012

Solid electrolyte tantalum condensers reliability under repeated service voltage applications for calculating defective condenser probability

15 p2626 A69-30836

Ceramic condensers with very high reliability mass produced for Concerto program, describing component characteristics and production methods

15 p2627 A69-30844

Prebreakdown and breakdown electrical properties and light emission during destructive breakdown in thin film capacitors

16 p2761 A69-32323

Surface state density determination as function of surface potential in MIS capacitors, discussing MIS capacitance method theory and computer programs

16 p2827 A69-32556

Capacitor discharge stud welding on Ti alloys, discussing weld zone microstructure, arc and mechanical properties

18 p3151 A69-35431

Electric dose variometer principles, emphasizing differential pressure meter, differential capacitor and capacitor meter

24 p4315 A69-43143

CAPE KENNEDY LAUNCH COMPLEX

Apollo/Saturn 5 base at Kennedy Space Center and facilities and equipment supporting manned lunar mission, discussing site location choice and launch complex design concept

16 p2767 A69-32429

Thunderstorm probabilities at Cape Kennedy, giving data on frequency, duration, multiple occurrence, nonoccurrence, runs and conditional probabilities

18 p3167 A69-35100

Kennedy Space Center Vehicle Assembly Building construction, capacity and operation for manned spacecraft

19 p3288 A69-35500

Crawler-Transporter at Kennedy Space Center for moving ground support equipment, Apollo/Saturn space vehicle and mobile launcher, describing design and components

21 p3690 A69-38754

Cape Kennedy space research and national priorities, indicating performance and progress of future space operations

[AAS PAPER 69-110] 24 p4419 A69-42879

Cape Kennedy Space Center mobile launchers and auxiliary equipment for Saturn vehicles, discussing functions, design and systems

24 p4297 A69-43036

CAPILLARIES [ANATOMY]

Intrarenal capillary hydrostatic pressure effect on hemodynamically induced changes in sodium excretion

07 p1063 A69-18629

Pulmonary capillary gas exchange and venous admixture model and inclusion into respiratory system model, discussing pressure and concentration gradients, pathological effects, etc

07 p1068 A69-19482

Static pressure-diameter measurements on small pulmonary blood vessels of frogs, analyzing capillary septal area as function of intravascular pressures noting high compliance

22 p3885 A69-40974

Cerebral and retinal capillary permeability to ions in rats analyzed by electron microscope using Prussian blue reaction

23 p4081 A69-41433

CAPILLARY FLOW

Thermal diffusion coefficient and composition of gas mixtures by measuring gas flow rate in capillary tube as function of viscosity

04 p0688 A69-15410

Fluid support by capillary forces, fluid support by pressure with surface tension stabilization and capillary gas barriers for long life missions

[AIAA PAPER 68-465] 04 p0646 A69-15505

Theory of capillary flow for fluidic resistor design

05 p0705 A69-16011

Rarefied gases back diffusion between parallel plates used for studying diffusion in capillaries, deriving volume flow equation valid for any density

10 p1677 A69-22903

Load capacity, stiffness and flow requirement of capillary and orifice compensated oil lubricated externally pressurized rectangular thrust bearings

12 p2102 A69-26239

Limiting heat power transported by sodium heat pipes dependent on capillary network geometry, inclination angle and operating temperature

14 p2538 A69-29205

Liquid-vapor interaction in loop plates with different heat pipe capillary geometries using water as heat transporting medium

14 p2539 A69-29207

Capillary barriers to provide propellant positioning, expulsion capability and slosh dampening for spacecraft propulsion systems during rotational maneuvers

[AIAA PAPER 69-529] 16 p2868 A69-32713

Surface tension gradients caused thermocapillary convection solved for spherical fluid film under weightlessness conditions

19 p3452 A69-36392

Digital computer program for determining aveolar and capillary blood gas compositions corresponding to ventilation-perfusion values, considering dissolved oxygen and inert gas exchange

22 p3875 A69-40230

Alveolar and mixed venous carbon dioxide pressure during absence of gas exchange across mammalian lung

22 p3885 A69-40976

Pulmonary capillary blood flow pulse of healthy men in supine position recorded by nitrous oxide/plethysmograph and phonocardiogram

24 p4259 A69-42638

CAPILLARY TUBES

Capillary arc source spectroscopy, determining plasma temperature and pressure dependence on capillary geometry and discharge current

02 p0286 A69-11573

Transient electro-osmosis of water in capillary tubes for pumping and generation modes, analyzing response to step change in pressure or voltage change under external loading

04 p0555 A69-14862

Simulated solar radiation heating of cesium vapor thermionic converters with multicapillary transmitters

07 p1058 A69-18951

Argon discharges in metal capillary cathodes noting effects of electron density, flow velocity, electrode phenomena and gas temperature

10 p1733 A69-23450

Diffusion equation unsteady solution for flasks of equal volumes connected by capillary, considering end effect and transient processes

13 p2251 A69-28561

Dimensionless approach to maximum flow in heat pipes and optimization of capillary structure

14 p2539 A69-29206

CAPILLARY WAVES

U BAROCLINIC WAVES

U GRAVITY WAVES

CAPSULES

Explosive containment capsule for nuclear reactor irradiation

04 p0629 A69-14480

Aluminum capsule used in test reactor to irradiate explosive and propellant samples, determining radiation effects

17 p3004 A69-32945

CAPSULES [SPACECRAFT]

U SPACE CAPSULES

CAPTIVE TESTS

U STATIC FIRING

CAPTURE CROSS SECTIONS

U ABSORPTION CROSS SECTIONS

CAPTURE EFFECT

Phonon capture by electrons in semiconductors with high permittivity in external electric field

03 p0489 A69-13891

Gradual capture in p-n junctions and p-n-p transistors at AC voltage, noting diffusion capacitance and resistance

03 p0491 A69-14051

Capture of comets by large planets

03 p0517 A69-14128

Capture of electrically charged micrometeorites and corpuscles in magnetic field of gravitating dipole, noting necessary condition on particle motion

04 p0659 A69-14962

Dark and photocurrent volt-ampere characteristics induced by capture of carriers injected into illuminated CdS single crystals

09 p1555 A69-21506

Satellite altitude stabilization by gravity gradient capture in earth elliptical orbit, showing effect of increase in damping

10 p1791 A69-22926

Phonon capture by electrons in semiconductors with high permittivity in external electric field

11 p1939 A69-25692

Capture centers effect on current-voltage characteristic of p-i-n diodes during injection, noting negative resistance appearance

13 p2236 A69-28525

Minimum time single axis capture of satellite spinning about pitch axis by low thrust jets, considering gravity gradient phenomenon

17 p3048 A69-33237

Resonances and doublets observation by neutron radiative capture and transmission of W and Zr isotopes in kev region, noting partial wave strength functions

18 p3175 A69-34314

Capture of electrically charged micrometeorites and corpuscles in magnetic field of gravitating dipole, noting necessary condition on particle motion

18 p3197 A69-34725

Group cross section generating techniques to calculate neutron capture rates and spatial capture distribution in depleted thick U slab, using GAROL program

18 p3177 A69-35179

Solar neutrinos capture rate estimation by using Li 7 as detector

20 p3588 A69-37420

Moon possible origin, discussing spin off from earth, accretion from same dust cloud or formed elsewhere and captured

20 p3603 A69-37559

Direct flight and Jupiter swingby heliocentric trajectory modes of elliptic capture orbits compared for unmanned missions to outer planets

[AAS PAPER 68-105] 21 p3805 A69-39221

Capture and gravity gradient stabilization of LIDOS satellite in eccentric orbit

[AIAA PAPER 69-921] 21 p3821 A69-39351

- Lepton nonconservation implications for experiments involving solar neutrinos, showing effect on capture rate at earth for pep neutrinos
23 p4194 A69-41596
- Cross sections of charge carrier capture by ions in gamma irradiated P-Al-Si glass with metal oxides additions measured for evaluating radiation stability improvement
23 p4180 A69-42470
- Air electrical conductivity reduction in fog ascribed to small ions concentration, increase in droplets capture efficiency and particle concentration
24 p4347 A69-43509
- CAPTURED AIR BUBBLE VEHICLES**
French air cushion vehicle technology for water and land, outlining principles of lift, propulsion and control and specifications of several craft
08 p1254 A69-20198
- CARAVELLE AIRCRAFT**
U SE-210 AIRCRAFT
- CARBAMATES [TRADENAME]**
U URETHANES
- CARBIDES**
NT BORON CARBIDES
NT CHROMIUM CARBIDES
NT HAFNIUM CARBIDES
NT MOLYBDENUM CARBIDES
NT NIOBIUM CARBIDES
NT SILICON CARBIDES
NT TANTALUM CARBIDES
NT TITANIUM CARBIDES
NT TUNGSTEN CARBIDES
NT VANADIUM CARBIDES
NT ZIRCONIUM CARBIDES
- Vacuum carburization of surface layers of transition metals
04 p0614 A69-14572
- Chemical composition and phase identification in commercial grades of cemented carbides
05 p0780 A69-15989
- Microstructural changes during liquid phase sintering of alloys, considering temperature effect on carbide grain growth and activation energies
07 p1168 A69-19599
- High pressure high temperature synthesis and superconducting properties of yttrium sesquicarbide, noting effect of ambient pressure annealing
07 p1201 A69-19600
- Carbides and silicides temperature coefficient of electrical resistivity and Hall constant plotted as function of metal carbides solid solutions concentration
09 p1523 A69-21740
- Carbidothermic production of metals and binary and ternary alloys, discussing eutectic properties
09 p1514 A69-22731
- Carbide precipitation in stainless steels using metal foil and extraction replicas, discussing grain boundaries corrosion relation
10 p1713 A69-23820
- Free carbon content by weight in titanium, zirconium and hafnium carbides
10 p1714 A69-23846
- Molten high melting compounds obtained by arc furnace with consumable electrode and adjustable protecting atmosphere
12 p2055 A69-26264
- Oxide and carbide high-melting-point materials for MHD generator electrode walls
13 p2284 A69-27471
- Anodic stain etching technique for carbide precipitates of niobium-base alloy Cb 132, noting X ray diffraction
13 p2282 A69-28162
- Vacuum carburization of surface layers of transition metals
15 p2638 A69-30273
- Vaporization rates of Ti, Zr, Hf, Nb and Ta carbides at high temperatures measured by Langmuir method
15 p2640 A69-30983
- Carbidothermic process for high melting metals and alloys production stressing Ti alloys
16 p2800 A69-31777
- Carbide phase growth rate in Mo-TZC alloy with particle size distribution maintained over time-temperature spectrum, noting diffusion and interface controlled processes
18 p3155 A69-34632
- Carbide coatings formation on graphite in molten media, determining diffusion coefficient of carbon in molten Zr
20 p3566 A69-37372
- Carbides and silicides temperature coefficient of electrical resistivity and Hall constant plotted as function of metal carbides solid solutions concentration
20 p3585 A69-38216
- Enthalpy and heat capacity of high melting point homogeneous Ti, Zr and Nb carbides, analyzing influence of Me-Me bonds and carbon sublattice defects
21 p3742 A69-38614
- Destructive interaction of refractory carbides and graphite compositions with chemically active high temperature gas streams
21 p3751 A69-38640
- Compactibility dependence of Fe, Co and Ni powders with Zr, Nb and Mo carbide additives on pressure, carbide content and lubricant
22 p3970 A69-40634
- CARBOHYDRATE METABOLISM**
NT HYPERGLYCEMIA
NT HYPOGLYCEMIA
- Glucose, lactate, free fatty acids, hepatic glycogen and endocrine activity in fasting hibernating dormouse and rat in deep hypothermia
10 p1642 A69-23118
- Phagocytic activity and carbohydrate metabolism in peripheral blood neutrophils of men exposed to atmosphere with increased O content, noting neutrophil energy exchange disorder role
17 p2907 A69-32942
- CARBOHYDRATES**
NT ADENINES
NT CELLULOSE
NT CHOLINE
NT FATS
NT GLUCOSE
NT MONOSACCHARIDES
NT NUCLEOSIDES
NT STARCHES
NT SUCROSE
NT SUGARS
- Physicochemical method for converting human urine and feces into carbohydrates in closed ecological systems
03 p0381 A69-14199
- Sweet potatoes productivity and nutritive value as carbohydrates source in manned spaceflights
13 p2216 A69-28619
- Paleozoic plant fossils carbohydrate content
21 p3669 A69-39333
- Carbohydrate analyses of upper carboniferous plant fossils in England, noting monosaccharides separation
21 p3661 A69-39534
- CARBON**
Saturation solubility of carbon in cobalt and nickel with respect to graphite determined by vapor transport experiments over large temperature range
01 p0092 A69-10060
- Electron density in arc discharge between carbon electrodes and in discharge with Na vapor, noting relation to temperature and current
01 p0128 A69-10433
- Electropulsion by thruster using colloidal carbon particles charged by electron bombardment to provide thrust, noting specific impulse
03 p0495 A69-13396
- Thermodynamic and kinetic interactions of high melting point metal oxides reduction by carbon
03 p0445 A69-13568
- Metal oxide and carbon interaction during spatial separation of reagents, noting influence of reducing agent activity on metal vapors
03 p0445 A69-13569
- Carbon formation during production of high purity semiconductor Si, using C 14 tagged hydrogen impurities and methylated chlorine silanes contained in siliconchloroform
03 p0486 A69-13635
- NonHookian behavior of stiff strong carbon fibers under stress
03 p0454 A69-13937
- Manufacture and properties of carbonaceous materials for nuclear and aerospace technologies, discussing pyrolytic graphite, vitreous carbon and carbon fiber
05 p0786 A69-16657
- Carbon molecule photodissociation in cometary atmospheres, discussing intensity level distribution based on model
06 p1004 A69-17534
- Transmittance and absorption cross sections of carbon particles suspended in flowing stream of nitrogen gas
06 p1034 A69-17804
- Electron momentum density in diamond, graphite and carbon black from Compton profile measurement by X ray scattering vector
06 p0982 A69-18233
- High strength carbon fibers development and applications in reinforced composite materials and aerospace industry
06 p0947 A69-18236
- Carbon influence on cast Waspaloy, discussing chemical segregation, chemical gradients and tensile ductility
07 p1158 A69-18307
- C III 2p super 2 presuper 1 D level mean life measurement using beam-foil technique, noting corresponding Einstein A coefficient
07 p1184 A69-18643
- Electron impact induced fragmentation of ring D in steroids involving loss of carbon atoms analyzed by mass spectrometry
07 p1069 A69-19497
- High modulus and high strength carbon fibers and composites, discussing mechanical properties and interlaminar shear strength
08 p1338 A69-20488
- Laser beam diffraction method for measurement of apparent filament diameters, emphasizing high modulus carbon filaments
08 p1316 A69-20499
- Laminates and filament wound structures using carbon fibers with silicon carbide whiskerized surfaces, noting compositing and laminating techniques
08 p1339 A69-20501
- Shop-ready high modulus carbon and fiberglass composite reinforcement system, stressing effect of modulus fibers amount in laminate
08 p1340 A69-20508
- Mechanical properties of ceramic material consisting of pure silica matrix reinforced by carbon fibers
08 p1341 A69-20700
- Stigmatic profiles of solar C II doublet resonance lines obtained by rocket-borne echelle spectrograph
09 p1592 A69-21456
- Carbon rich star models with and without neutrinos, considering carbon burning, central stars of planetary nebulas and hot white dwarfs
09 p1606 A69-22419
- Stress graphitizing and boron codeposition effect on dynamic mechanical properties of pyrolytic carbon, noting increase in internal friction and dynamic modulus
10 p1716 A69-23036
- Differential energy losses of fission fragments in thin carbon films as function of mass and initial energy mapped by time of flight method
10 p1694 A69-23348
- Surface density of carbon foils measured accurately by determining trapped carbon dioxide pressure after burning in pure oxygen
10 p1746 A69-23663
- Free carbon content by weight in titanium, zirconium and hafnium carbides
10 p1714 A69-23846
- Diffusion coefficients of carbon in tantalum, niobium and vanadium by sectioning method, using carbon 14 as tracer
11 p1906 A69-25575
- Dynamic response of distended carbon materials to shock loading defined by measuring equation of state, unloading behavior and spallation strength
12 p2119 A69-26847
- Dielectronic recombination influence on radio recombination lines of carbon under typical nebular conditions
13 p2346 A69-27703
- Composition dependence of carbon activity and carbon diffusivity in austenite
13 p2279 A69-27763
- Wilson chamber and ionization calorimeter determination of cosmic ray particle-carbon nuclei interaction energy characteristics
13 p2330 A69-28379
- Nuclear interactions between high energy nuclear active particles and C nuclei, studying electron-photon component energy with nuclear photoemulsions
13 p2331 A69-28388
- Activated carbons and ion exchange resins bactericidal action as function of silver coating techniques
13 p2216 A69-28621
- Transition probabilities for radiative lifetime of Swan and Mulliken diatomic C bands calculated from lifetime data using Franck-Condon factors
15 p2694 A69-30789
- Carbon atoms presence in Venus upper atmosphere from Venus spectrum obtained by Aerobee rocket experiment
15 p2698 A69-31341
- Carbon fiber reinforced plastics properties improvement by applying organosilanes, discussing silanol bond formation
16 p2803 A69-31806

Carbon stars in south galactic pole region detected in objective prism survey, including variable R Scl and early R stars

16 p2860 A69-32232

Carbon fibers fine structure graphitized at high temperatures studied by X ray diffraction and electron microscopy

16 p2803 A69-32572

Carbon fiber reinforced plastics development for aerospace use, presenting criteria for resins selection

17 p2992 A69-33647

Fiber reinforced carbon and graphite with application to reentry and propulsion systems and high temperature gas turbines, noting three dimensional woven quartz

19 p3354 A69-35519

Hollow thin walled carbon spheres developed as filler material for resins in low weight high temperature applications

19 p3355 A69-35522

High temperature materials for aerospace and spacecraft applications, considering carbon/carbon composites, oxides, carbides, fibers and ablative systems

19 p3346 A69-36320

C and O atoms chemisorption on Mo surface demonstrated by surface striation

20 p3562 A69-37782

Composite materials application in aerospace industry, discussing boron and carbon filament properties, epoxy resins, etc

20 p3563 A69-37930

C content and microstructure effect on electrochemical parameters of Fe and steels in dilute sulfuric acid, discussing Tafel constants and current density

20 p3563 A69-38002

Elements nucleosynthesis during thermonuclear burning of carbon at series of temperatures and for several initial compositions

20 p3612 A69-38163

Carbon fiber reinforced plastics application to aircraft metal components for weight reduction, low cost and high mechanical properties

21 p3750 A69-38428

Carbon fiber reinforced materials applications in aerospace industry, discussing long term potential and applications in F-5 aircraft

21 p3732 A69-38989

B composite materials in helicopter development, including B and C filament production and B filament applications

22 p3971 A69-40899

High temperature pyrolysis of simple organic molecules in shock tube, considering diatomic C formation and decay rate

23 p4113 A69-41693

Carbon materials manufacture, properties and applications in space technology, discussing carbon fibers, textiles, graphite, pyrolytic carbon, composites and vitreous carbon

23 p4180 A69-42160

Gas concentration liberated during each revolution in atmospheres of short period comets to explain impulsive forces upon nuclei, noting diatomic carbon density

23 p4221 A69-42387

Carbon fiber reinforced plastic components aerospace applications, discussing honeycomb sandwich satellite structure for investigating lamination methods, shapes, bonding and machining

24 p4336 A69-43209

Carbon fibers and resin composites used as rocket motor systems ablative liners and structures, noting role in motor weight reduction

24 p4336 A69-43210

Teflon dielectric properties evaluated during fast laser beam heating, noting presence of C by microwave measurement

24 p4336 A69-43266

Composite-to-metal joints design and fabrication, using carbon yarn in epoxy matrix for missile interstage application

24 p4323 A69-43426

High modulus carbon filament composite structural elements for missile interstage application, showing weight savings

24 p4325 A69-43444

High performance void free carbon fiber laminates preparation using polyimide resins, describing flexural strengths, moduli and interlaminar shear strengths

24 p4325 A69-43445

CARBON ARCS

Excitation heating energy pumping mechanism for explaining dynamic equilibrium in C rich arc plasmas with high ion temperature/electron temperature ratio

01 p0126 A69-10276

Polyesters reaction with dimethyl p-phenylene diamine compared under UV exposure from carbon arc and natural sunlight

10 p1716 A69-23978

CARBON COMPOUNDS

NT BORON CARBIDES
NT CALCITE
NT CALCIUM CARBONATES
NT CARBIDES
NT CARBONATES
NT CHROMIUM CARBIDES
NT DOLOMITE (MINERAL)
NT HAFNIUM CARBIDES
NT MOLYBDENUM CARBIDES
NT NIOBIUM CARBIDES
NT POLYCARBONATES
NT SILICON CARBIDES
NT SODIUM CARBONATES
NT TANTALUM CARBIDES
NT TITANIUM CARBIDES
NT TUNGSTEN CARBIDES
NT VANADIUM CARBIDES
NT ZIRCONIUM CARBIDES

Book on genesis and evolutionary development of life covering carbon compounds, protobionts and evolutionary biochemical investigations of present living organisms

12 p2019 A69-26300

Carbon diffusion parameters in alloys of Nb with Ti, Zr, W and Mo, using radioactive carbon 14

18 p3157 A69-35250

Relative gas phase acidities of carbon acids determined using ion cyclotron resonance spectroscopy

19 p3265 A69-36291

Carbon trioxide formation during ozone photolysis in liquid carbon dioxide and sulfur hexafluoride, noting ozone disappearance quantum yield independence of oxygen/ozone ratio

23 p4112 A69-41338

CARBON DIOXIDE

Carbon dioxide laser stabilization using laser profile and three mirror system

01 p0089 A69-10183

Carbon dioxide laser pulsed mode for generating giant pulses, noting applications and electron impact role

01 p0090 A69-10787

Drilling and welding with sealed-off continuous carbon dioxide gas laser with outcoming beam collimated by Ge lens

01 p0086 A69-10821

Carbon dioxide spectral line broadening and self broadening coefficients, using carbon dioxide laser radiant energy

01 p0091 A69-10844

Spectral transmission for water vapor and carbon dioxide bands

02 p0236 A69-11451

Carbon dioxide ionization by Q switched laser beam, using proportional counter

02 p0255 A69-11702

Model spectra applied to carbon dioxide bands in Venus spectrophotometric measurements

02 p0319 A69-12107

Two dimensional diffuse shock waves in carbon dioxide, noting effect of shock curvature equivalence to thickness

02 p0233 A69-12534

Gas phase photolysis of carbon dioxide in far UV, searching for carbon trioxide

03 p0381 A69-13318

Dog adaptation to 60 or 90 mm Hg carbon dioxide in 260 mm Hg total pressure environment, noting arterial pH and bicarbonate level

03 p0375 A69-14071

Emission amplification coefficients of gas laser using pure carbon dioxide, carbon dioxide/air mixtures and carbon dioxide/air/helium mixtures

04 p0611 A69-14426

Electron radiation temperature measurement in carbon dioxide laser with N and He additions by microwave technique, noting average electron energy and optical gain

04 p0611 A69-14445

Carbon dioxide laser noting output for added gases, efficiency, energy levels, excitation mechanism and tuning to single line and mode

04 p0612 A69-15173

Natural convection heat transfer through enclosed horizontal layer of supercritical carbon dioxide, discussing flat plate configuration data

04 p0688 A69-15398

Water and carbon dioxide IR spectra compared with laboratory measurements

05 p0759 A69-16638

Vibrational excitation by electron impact in kinetic energy range 30-60 ev studied for water vapor and carbon dioxide, determining intensities relative to elastic scattering

06 p0960 A69-17108

Coupled cavity carbon dioxide laser interferometer with feedback for measurement of transient plasma density in theta pinch, noting sensitivity

06 p0935 A69-17706

Recombination mechanism between CO and O produced by photodissociation of carbon dioxide in upper atmosphere of Venus and Mars

07 p1214 A69-18615

Thermal disturbance radiative decay time in carbon dioxide at low pressures and for nonzero vibrational relaxation times

07 p1215 A69-18843

Competition effects between rotational levels of carbon dioxide rotation-vibration band in traveling and standing wave lasers

07 p1151 A69-19055

Nonsaturated gain of laser radiation in gas discharge in carbon dioxide with N and He

07 p1151 A69-19060

Gain enhancement effect of CO on carbon dioxide CW laser performance by accelerating relaxation of bending mode

07 p1155 A69-19088

Sealed carbon dioxide lasers life and power outputs with Xe and H additives

07 p1155 A69-19091

Sampled data regulator for maintenance of constant alveolar carbon dioxide during steady state and transient ventilatory responses to hypoxic stimulation

07 p1072 A69-19480

Depolarized Rayleigh line widths measured for carbon dioxide, nitrogen and hydrogen, using measurements to calculate reorientation cross sections

07 p1157 A69-19485

Population inversion mechanism based on electron collisional excitation cross sections for molecular vibrational levels in carbon dioxide lasers

07 p1157 A69-19655

Electron energy distribution measurements in carbon dioxide laser discharges noting similarity of distribution for nitrogen

08 p1323 A69-19801

Monte Carlo method for calculating atomic hydrogen escape rate from carbon dioxide atmosphere, considering Mars and Venus atmospheres

08 p1386 A69-20076

Mars and Earth atmospheric carbon dioxide simulation and spectroscopic measurement for developing planetary surface pressure estimating procedures from IR transmission measurements

08 p1354 A69-20151

Carbon dioxide absorption and emission in mesosphere, discussing vibrational relaxation time and radiative heating rate

08 p1308 A69-20308

Carbon dioxide bending mode deactivation by orthohydrogen, parahydrogen and deuterium through rotational transitions

08 p1358 A69-21010

Near resonant transfer of vibrational energy from carbon dioxide nu 3 mode to N 14 and N 15 molecules in collisions

08 p1358 A69-21011

Carbon dioxide laser with two gas absorption cells in cavity for emission wavelength control and HF pulsed mode of operation

08 p1327 A69-21088

Segmented anode, carbon dioxide-hydrogen performance and hollow cathode erosion tests on low power MPD arc thruster, noting current measurements

09 p1563 A69-21236

Gas lasers, discussing amplification, resonance, internal and external mirror lasers, outputs, and He-Ne, carbon dioxide and ion lasers

09 p1517 A69-22121

Nonadiabatic collision broadening theory for IR spectral lines applied to carbon dioxide-carbon dioxide and carbon dioxide-nitrogen collisions, estimating rotational line widths

09 p1543 A69-22250

Carbon dioxide laser upper level rotational relaxation rate constant measurement, observing CW gain

10 p1701 A69-22948

Amino alcohol regenerable absorbers of carbon dioxides toxicological characteristics, discussing absorbing ability in rats

10 p1646 A69-23502

Venus atmosphere observations compared with Venera 4 measurements of temperature, pressure and carbon dioxide content

10 p1791 A69-24200

High power CW carbon dioxide laser saturation and discharge conditions analyzed by rate equation

11 p1898 A69-25050

Carbon dioxide laser for production of high peak power pulse, discussing mw peak power design and oscillation problem in high gain amplifiers

11 p1899 A69-25053

Carbon dioxide-N-He laser amplifier, noting gain time dependence and thermal relaxation rate after gas heating

11 p1899 A69-25054

Gain decrease due to saturation during amplification of pulses from Q switched carbon dioxide laser oscillator, noting rotational sublevels relaxation rate

11 p1899 A69-25055

Vibrational relaxation frequency of asymmetric stretching mode of carbon dioxide determined by measuring rate of thermal emission in shock waves near 4.3 microns

11 p1922 A69-25128

Carbon dioxide temperature distribution, absorption and concentration as functions of molecular dissociation behind shock wave determined by measuring IR bands intensity

11 p1873 A69-25226

Shapes of extreme wings of collision-broadened carbon dioxide lines, noting absorption deviation from Lorentz-shaped lines

12 p2132 A69-26248

Carbon dioxide rotational constants from CW beat measurement in bulk GaAs mixer between carbon dioxide vibrational-rotational laser lines

12 p2105 A69-26311

Carbon dioxide dissociation in carbon dioxide laser gas discharge plasma for various flow rates, pressures, discharge current densities and tube diameters

12 p2107 A69-26540

Single frequency sealed off carbon dioxide amplifier, giving saturated gain

12 p2109 A69-26640

Carbon dioxide laser as light source in Michelson interferometer for plasma electron density measurement

12 p2100 A69-27177

Venus carbon dioxide spectral band analysis methods, discussing spectral lines and rotational temperatures obtained

13 p2344 A69-27649

Heat transfer coefficients for carbon dioxide near thermodynamic critical point for flow through electrically heated duct, noting turbulent forced convection as mechanism

[ASME PAPER 68-HT-32] 13 p2373 A69-27769

Lifetime of vibrational levels of carbon dioxide molecules as function of discharge current and power dissipation, noting gas heating

13 p2273 A69-28579

Energy level population of carbon dioxide molecules, noting intensity of spontaneous emission

13 p2274 A69-28580

Laser based on carbon dioxide molecules formed chemically in electrical discharge studied for designing special carbon electrode laser

13 p2274 A69-28585

Libroelastic wave propagation and dispersion characteristics /solid carbon dioxide/ evaluated by using Raman scattering measurements

13 p2286 A69-28668

Water and carbon dioxide IR spectra compared with laboratory measurements

14 p2433 A69-28794

Carbon dioxide band vibration-rotation transitions saturation characteristics, stressing role of collisions in molecular gas lasers

14 p2457 A69-28928

Blue continuum emission from hot carbon dioxide measured in shock tube, discussing applications to temperature measurement of gases containing carbon dioxide

14 p2427 A69-29014

Carbon dioxide dissociation by electron impact, determining reaction rate in positive column of DC glow discharge

14 p2488 A69-29095

NADH stimulation of ATP dependent carbon dioxide fixation in crude extracts of Hydrogenomonas facilis, considering allosteric regulation of phosphoribulokinase activity

15 p2554 A69-30036

Atmospheric transmission functions dependences on absorbing material, pressure and temperature in 15 micron band of carbon dioxide, introducing corrections

15 p2597 A69-30653

Pressure, temperature, density and enthalpy of carbon dioxide behind primary and reflected shock waves determined by method suitable for computer

15 p2592 A69-31054

Relative intensities of lines in vibration and rotation bands of isotopic carbon dioxide in planet Venus, tabulating partition functions

15 p2656 A69-31154

Monosaccharide production from carbon dioxide from respiration or human waste incineration, evaluating toxicological effects of synthetic monosaccharides

15 p2557 A69-31471

Spectroscopic observations of Venus atmosphere rotational temperature based on carbon dioxide band at 7883 A

16 p2852 A69-31563

Carbon dioxide dissociation relaxation times measured in shock tube at 1900-2400 K and 1.5-2.5 km/sec

16 p2766 A69-31910

Pressure dependence of trapped spontaneous decay of resonant radiation carbon dioxide

18 p3179 A69-35478

Acetate-2-C 14 conversion to C 14 carbon dioxide and C 14 fatty acids in rats with 2/3 of liver removed

19 p3257 A69-35976

Deactivation rate constants of carbon dioxide vibrationally excited by high temperature collision with carbon dioxide or nitrogen molecules, describing laser apparatus and reaction cells

20 p3578 A69-36937

Carbon dioxide laser pulsed mode for generating giant pulses, noting applications and electron impact role

20 p3555 A69-38004

Relaxation time for rotational transitions of linear polyatomic carbon dioxide calculated by using Brout theory for diatomic H rotational relaxation calculations

20 p3581 A69-38121

Carbon dioxide band in Venus spectrum by dispersion analysis, deriving rotational temperature

20 p3614 A69-38254

Heats of adsorption of carbon dioxide on silver /I/ oxide and copper /II/ oxide by gas chromatography

20 p3485 A69-38277

Equilibrium absorption and desorption rates of carbon dioxide-argon mixtures from silica gel measured as function of temperature using gas dynamics method

21 p3848 A69-38707

Vibration relaxation time and dissociation rate constant of carbon dioxide in high temperature shock waves, using IR emission

21 p3775 A69-39801

Age and carbon dioxide tension effects on EEG of adolescents and adults, discussing end-tidal carbon dioxide during routine hyperventilation

22 p3872 A69-40162

Peripheral chemoreceptor carbon dioxide sensitivity, measuring human respiratory response to large carbon dioxide breath in oxygen at sea level and high altitude

22 p3890 A69-40207

Carbon dioxide free jet expanding from conical nozzle into low density atmosphere, using freeze up method

22 p4000 A69-40594

Excited states lifetime of carbon dioxide and nitrous oxide ions deduced from spontaneous radiative deexcitation in vacuum after passage through gaseous target

22 p3985 A69-40715

Carbon trioxide formation during ozone photolysis in liquid carbon dioxide and sulfur hexafluoride, noting ozone disappearance quantum yield independence of oxygen/ozone ratio

23 p4112 A69-41338

Carbon dioxide inhalation and intravenous isoproterenol effects on hemorrhagic consolidation occurring after left pulmonary artery ligation in dogs

23 p4082 A69-41441

Biochemical evolution role in porphyrin synthesis forming hemoproteins base, discussing assimilation of carbon dioxide in early earth atmosphere

23 p4088 A69-41814

IR radiation transmission in pulsed carbon dioxide discharge as function of time, proposing pumping and relaxation mechanism model

23 p4174 A69-42196

Raman spectra analysis of solid carbon dioxide, nitrous oxide, nitrogen and CO, determining lattice mode intensities from oriented gas model

23 p4194 A69-42205

Dry ice ablating models for unheated supersonic and hypersonic wind tunnel tests, noting mass addition rate extension

24 p4297 A69-43255

CARBON DIOXIDE CONCENTRATION

Flight vehicle cabins ventilation for undesirable gas contaminants removal, discussing contaminant concentration calculation and automatic control

02 p0200 A69-11512

Venus exospheric temperature for various composition models, discussing carbon dioxide concentration effects

02 p0319 A69-12109

Electronic transition moment for C /Swan/ bands measured in shock tube in carbon dioxide and argon mixtures

02 p0285 A69-12833

Human motor activity under hypodynamia and increased carbon dioxide, discussing positive effects of prescribed physical exercises

03 p0377 A69-14205

Carbon dioxide pressure in earth atmosphere through geologic time determined by carbon input rate and transfer efficiency to crust

08 p1310 A69-20946

Ozone and carbon dioxide stratospheric and tropospheric horizontal distribution from weather data collected on polar flight

09 p1484 A69-21403

Carbon dioxide abundance in Mars atmosphere measured with three etalon Fabry-Perot spectrometer

09 p1607 A69-22427

EEG, EKG, respiratory motions and pulmonary ventilation recordings in study of carbon dioxide additions effect on human tolerance to hypoxic conditions

10 p1650 A69-23898

Carbon dioxide temperature distribution, absorption and concentration as functions of molecular dissociation behind shock wave determined by measuring IR bands intensity

11 p1873 A69-25226

Carbon dioxide concentration in upper troposphere and lower stratosphere recorded during commercial aircraft flights over polar route

11 p1879 A69-25254

Venus atmosphere carbon dioxide content origin from interior degassing during molten phase, using atmospheric model

16 p2857 A69-32098

Respiratory gas exchange in exercise during He-O breathing, analyzing effects on O consumption, carbon dioxide production and minute ventilation of human subjects

17 p2910 A69-33751

Mice convulsions at varying hyperbaric oxygen pressures and carbon dioxide content correlated with decreasing brain alpha aminobutyric acid levels

19 p3257 A69-35972

Carbon dioxide levels monitoring in spacesuit research including limits of physiological acceptability

21 p3665 A69-39170

Ventilatory response to hypoxia and hypercapnia in hypothermic anesthetized dogs, noting decreased sensitivity of central chemoreceptors to carbon dioxide

22 p3885 A69-40977

Oxygen exchange in Scenedesmus and Chlorella as function of carbon dioxide, compensation point, Hill activity and photorespiration, using mass spectrometry

23 p4099 A69-42528

CARBON DIOXIDE LASERS

Carbon dioxide laser inversion kinetics, combining pulse pumping with Q switching to observe rise, life and decay times

14 p2457 A69-28926

Pulsed lasers with pure carbon dioxide and mixture with N and He, discussing inversion mechanism, peak emission power and gas temperature effects in different modes

14 p2458 A69-29162

Continuous butt welding with CW carbon dioxide laser, noting heat affected area, remelt zone and weld efficiency

15 p2617 A69-30099

Gas laser cutting of thin carbon films on thick pyrex glass and ceramic substrates

15 p2635 A69-31037

Thin film carbon resistors cutting with carbon dioxide gas laser, considering cylindrical bodies and aging properties

15 p2635 A69-31038

Spontaneous self pulsing and cavity dumping in carbon dioxide laser Q switched by internal GaAs electro-optic cell without saturable absorber

16 p2797 A69-32014

Homodyne detection of IR radiation from carbon dioxide laser scattered from moving diffuse target, noting applicability to IR radar, heterodyne spectroscopy, etc

17 p2971 A69-32913

Optical heterodyne communication system with single mode and frequency carbon dioxide laser, noting coherent photon noise limit

17 p2919 A69-33086

Fog removal by high power carbon dioxide lasers, evaluating possibility of clearing airport runways [AIAA PAPER 69-670]

17 p2945 A69-33449

Carbon dioxide flowing gas laser pumped by thermally excited nitrogen, discussing power gain and absence of chemical and charged particle effects

18 p3151 A69-34264

Population inversion in carbon dioxide laser related to pumping frequency, discussing molecular dissociation effect in gas mixture

18 p3151 A69-34620

Intensity changes in visible sidelight emission from carbon dioxide laser switched on and off, calculating vibrational temperatures

18 p3153 A69-35243

Luminophors for carbon dioxide laser radiation visualization noting controlled sensitivity, quick response and resolution

18 p3153 A69-35259

Self mode locking of carbon dioxide laser with high order transverse mode oscillations in vibrational-rotational transitions of P branch

19 p3330 A69-35602

Rotational-vibrational relaxation and molecular diffusion effect on saturation parameter of carbon dioxide laser, measuring gain as function of input power

19 p3338 A69-36692

Rotating mirror Q switched carbon dioxide laser for high peak powers, analyzing pulse structure and duration dependence on collision induced relaxations

19 p3338 A69-36694

Carbon dioxide lasers near IR spontaneous emission spectra

19 p3339 A69-36697

Central tuning dip on rotation-vibration transitions of nitrous oxide and carbon dioxide laser with nitrogen, noting frequency discriminator generation

19 p3339 A69-36698

Primary excitation mechanism in pulsed carbon dioxide lasers found to be electron impact

20 p3556 A69-38122

Electrical excitation discharge effect on molecular composition of flowing carbon dioxide gas laser, noting dissociation characteristics

21 p3736 A69-38940

Carbon dioxide laser amplifiers gain saturation time dependence characteristics by theoretical model taking rotational relaxation into account

21 p3736 A69-38941

Normal frequencies, force constants and moment of inertia of carbon dioxide isotope molecules from spectroscopic data, calculating atmospheric transmission of carbon dioxide laser radiation

21 p3742 A69-39780

Carbon dioxide laser development, discussing gain, static amplifier and high pressure operations

22 p3962 A69-40474

Carbon dioxide and carbon dioxide mixture mirror Q switched laser peak power generation, using pulsed excitation

22 p3963 A69-40564

Q switched pulsed discharge carbon dioxide laser, determining peak power dependence on delay between pulse excitation and Q switching

22 p3963 A69-40566

Population and excitation rates of working levels of carbon dioxide laser calculated on basis of emission power, amplification coefficient and spontaneous emission intensity

22 p3964 A69-40795

Electron excitation and collisional energy transfer processes in laser level of pure carbon dioxide fill and carbon dioxide-water vapor mixture

23 p4171 A69-41390

Gaseous absorption cell variable attenuator for carbon dioxide laser radiation at specific wavelength, using forced convection to eliminate thermal defocusing effects

23 p4172 A69-41396

Carbon dioxide laser amplifier operation, showing photon-induced current changes dependence on amplifier gain

23 p4172 A69-41398

Nitrogen-carbon dioxide-helium lasers CW operation at various pressures and N flow rates

23 p4173 A69-41496

Closed cycle gas cooling techniques for self contained CW kilowatt carbon dioxide laser, relating output power to flow velocity and input power

23 p4173 A69-41497

Output power dependence of repetitively Q switched carbon dioxide laser on repetition time measured with thermopile, noting decrease in mirror system

23 p4173 A69-41566

Pure water vapor and water vapor-air mixture continuum absorption of carbon dioxide laser radiation measured to determine atmospheric attenuation

23 p4173 A69-41631

Electron energy measurement accuracy in carbon dioxide laser plasma by S band radiometer

24 p4327 A69-42613

N or He additions effects on carbon dioxide laser design and power output

24 p4327 A69-42640

Diffraction coupling of power from carbon dioxide laser, computing angular distribution of output light

24 p4329 A69-43753

CARBON DIOXIDE REMOVAL

Transient changes in oxygen consumption, carbon dioxide elimination and respiratory quotients during and after induced hypoxia to rabbits

06 p0876 A69-18026

Oxygen reclamation from carbon dioxide using solid oxide electrolyte, noting water vapor catalytic effect

07 p1071 A69-19423

Digital computer program for heat and mass transfer characteristics of spacecraft carbon dioxide adsorption beds, discussing surface pressure of absorbent material [AICHE PAPER 19C]

09 p1446 A69-21931

Experimental program to evaluate regenerable sorbents for carbon dioxide removal in space cabin environments

09 p1447 A69-22552

Lithium peroxide utilization feasibility for oxygen supply and carbon dioxide control in extravehicular portable life support systems [AIAA PAPER 69-620]

17 p2914 A69-33303

Regenerative life support systems, discussing water reclamation, carbon dioxide removal, onboard oxygen generation and radio isotope thermal energy sources

19 p3262 A69-36318

Oxygen supply and carbon dioxide absorption in long term life support systems, noting energy balances comparison of ecological systems

20 p3477 A69-37625

Carbon dioxide washout during square wave hyperventilation in man, postulating blood flow factor

22 p3885 A69-40975

Oxygen and carbon dioxide transfer in membrane oxygenators, considering liquid dispersion and membrane diffusion limitations

24 p4279 A69-43799

CARBON DIOXIDE TENSION

NT HYPERCAPNIA

Alveolar and mixed venous carbon dioxide pressure during absence of gas exchange across mammalian lung

22 p3885 A69-40976

CARBON ISOTOPES

Automatic equipment for sampling and preparing gases by dual column gas chromatography for subsequent mass spectral analysis of carbon isotopes during methane metabolism

02 p0205 A69-12603

Experimental measurement of He and C isotope composition of cosmic radiation

05 p0817 A69-16709

Carbon content and isotopic composition in light and dark portions of gas-rich chondrites Breitscheid and Pantar

19 p3408 A69-36081

Carbon isotopes compared in interstellar formaldehyde transition for galactic nucleosynthesis, discussing spectrum analysis of radio astronomical telescope observations

23 p4220 A69-42376

CARBON MONOXIDE

Carbon monoxide ion dynamics in envelopes of comets exhibiting fountain behavior, discussing electron-collisional ionization within envelopes as main plasma production mechanism

02 p0310 A69-11423

Gain enhancement effect of CO on carbon dioxide CW laser performance by accelerating relaxation of bending mode

07 p1155 A69-19088

IR absorbance of CO below room temperature, determining strength and half widths of lines in R branch of fundamental band

07 p1183 A69-19644

Flowing CO-N-He laser with power enhancement and high efficiency, noting role of gases

08 p1324 A69-20163

Electron impacts role on dissociation rates of CO molecules in upper layers of solar photosphere

09 p1590 A69-21376

IR spectrum of NML Cygnus star with Michelson interferometer, noting CO bands and IR excess

09 p1602 A69-22229

Fourth positive carbon monoxide system observed in absorption in vacuum UV region, discussing rotational and vibrational band structure

09 p1607 A69-22429

CO adsorption on tungsten, determining work function changes and Fowler-Nordheim preexponentials on field emitter single crystal faces

14 p2409 A69-29093

CO absorption lines in solar spectrum analyzed theoretically and experimentally indicating random distribution of molecules

15 p2688 A69-30552

Nitrous oxide-CO bimolecular reaction and O-CO recombination in single pulse shock tube

16 p2748 A69-32793

High positive g sub x acceleration effects on red cells destruction rate, measuring endogenous CO production of Gemini astronauts

17 p2908 A69-33176

Electron impacts role on dissociation rates of CO molecules in upper layers of solar photosphere

18 p3198 A69-34764

Carbon monoxide displacement rate of oxygen from combination with oxyhemoglobin solutions from human adult and fetal, horse, goat, dog, cat and rabbit

21 p3650 A69-38384

Oxygen replacement rate by CO from combination with oxyhemoglobin in cells at various temperatures

21 p3650 A69-38385

Spectral transmittance of mixture of carbon monoxide and nitrous oxide for overlapping absorption bands [AIAA PAPER 67-600]

21 p3819 A69-39013

Blood oxygen content measured by oxygen tension after release by carbon monoxide without lysing cells

22 p3873 A69-40203

Electron recombination and diffusion in afterglow following short pulsed DC discharge in CO, using microwave diagnostic techniques

22 p3984 A69-40478

Carbon monoxide dissociation at high temperatures observed spectroscopically, finding complex reaction chain with diatomic C as intermediate

23 p4113 A69-41692

Oxygen steady state transfer across thin layers of centrifuged erythrocytes at 37 degrees C before and after hemoglobin saturation with CO

23 p4093 A69-42064

Raman spectra analysis of solid carbon dioxide, nitrous oxide, nitrogen and CO, determining lattice mode intensities from oriented gas model

23 p4194 A69-42205

Carbon monoxide presence in Martian atmosphere from Mars line spectra, giving content, surface pressure and concentration

23 p4220 A69-42379

Isotopic exchange reaction rate between O 18 and CO in shock tube coupled to time of flight spectrometer, noting rate increase with time

24 p4353 A69-43807

CARBON MONOXIDE POISONING

General aviation accidents and hazards presented by drugs, ethyl alcohol, pesticides and carbon monoxide

07 p1068 A69-19435

Carbon monoxide effect on dog lung volume, mechanical properties and diffusing capacity

22 p3874 A69-40224

CARBON STEELS

Shot peening effect on fatigue properties of maraging and Al-Zn-Mg alloy steel welds, using repeated tensile tests

02 p0253 A69-12061

Stress variation cycles pattern effects on fatigue strength of materials, discussing results of low-carbon steel tests under sinusoidal loading

04 p0673 A69-14535

Free surface strain increment components on high carbon steel compression specimens to estimate tensile plastic instability onset, noting ductile fracture criterion

08 p1328 A69-19891

Eutectoid pearlite growth by pure iron-carbon specimen heat treatment

13 p2281 A69-28158

Quench rate effect on martensite start temperature and fine structure of Fe-C and Fe-C-Ni steel, using transmission electron microscopy
20 p3557 A69-36956

CARBON TETRACHLORIDE
Temperature measurement associated with bubbles leaving heat source in subcooled pool boiling carbon tetrachloride analyzed, using high speed motion pictures by schlieren optical system
[ASME PAPER 68-HT-47] 13 p2374 A69-27779

CARBON 12
Absorption cross section for 68 Mev positive pion absorption by 1p 3/2 neutron in C12 nucleus followed by single proton emission at 11 degrees
02 p0282 A69-11460
Radiation damage in yeast cells irradiated by high energy C 12 ions evaluated from survival rate study
14 p2406 A69-28915
Pure carbon 12 stellar models evolution studied to determine production mechanism of planetary nebulae, discussing shell burning and surface layers unbinding role
18 p3191 A69-34298
Normal frequencies, force constants and moment of inertia of carbon dioxide isotope molecules from spectroscopic data, calculating atmospheric transmission of carbon dioxide laser radiation
21 p3742 A69-39780

CARBON 13
Molecular ion C13H line found in zeta Oph at 4232.08 A, measuring equivalent width and finding C12/C13 ratio
09 p1603 A69-22266

CARBON 14
Acetate carbon 14 utilization in centrifuged rats, analyzing metabolism by measuring plasma glucose, FFA and lipids synthesis
07 p1067 A69-19429
Urease activity determined by using C 14 urea in stored, preserved /Permafrost/ and irradiated soils
18 p3095 A69-34543
Carbon diffusion parameters in alloys of Nb with Ti, Zr, W and Mo, using radioactive carbon 14
18 p3157 A69-35250
Acetate-2-C 14 conversion to C 14 carbon dioxide and C 14 fatty acids in rats with 2/3 of liver removed
19 p3257 A69-35976
C 14-tryptophan incorporation into C 14-protein in cultured rat pineals, noting norepinephrine stimulation
22 p3871 A69-40054
Radiocarbon natural production by cosmic ray neutrons, utilizing proportional counters filled with N atmospheres
22 p4003 A69-40095

CARBONACEOUS METEORITES
NT MURRAY METEORITE
NT ORGUEIL METEORITE
Carbonaceous, enstatite and stony meteorite classification on basis of siderophyllic, chalcophyllic and lithophyllic element proportions or isotope composition, discussing thermodynamic equilibrium
01 p0025 A69-11368
Boron determination in type 1 carbonaceous chondrites by nonaqueous colorimetry, comparing results with ordinary chondrites
04 p0661 A69-15147
Solar system elements abundance compilation based on carbonaceous chondrites and nucleosynthesis in stars
08 p1401 A69-20903
Ne and Xe in carbonaceous chondrites, noting large amounts of fission Xe and implications for galactic nucleosynthesis models
08 p1405 A69-20925
Magnetite morphological variations of type 1 carbonaceous meteorites, discussing isometric crystals, spheres, spherulites, platelets and filaments
08 p1406 A69-20932
Organic matter signals in carbonaceous meteorites, discussing possible relation to extraterrestrial life and origin
11 p1953 A69-24342
Freshly fallen meteorites from Portugal and Mexico, determining exposure age and classifying into iron meteorite and carbonaceous chondrite types
12 p2160 A69-26935
C3 and C4 carbonaceous chondrites origin, evolution and classification based on mineralogic and petrologic data
19 p3413 A69-36109
Lance chondrite C III, studying mineral composition of chondrules and heterogeneous crystalline fragments
19 p3413 A69-36110

Carbonaceous meteorites mineralogically identified by selected-area electron diffraction, suggesting formation from minerals mixtures
19 p3311 A69-36111
Carbonaceous meteorites specimen petrographic observations, noting genetic interrelations with ureilites regarding S-C and reduced Fe oxidized Fe ratios
19 p3413 A69-36112
Isoprenoids and isomeric alkanes identification in carbonaceous chondrites by gas-chromatographic mass-spectrometric analyses, including results from troilite nodules
19 p3414 A69-36113
Organic geochemical investigations of lunar rock samples based on analysis methods for carbonaceous meteorites and early Precambrian sedimentary rocks
20 p3476 A69-37616
Morphological, chemical and X ray analysis of ureilite meteorite, identifying diamonds with kamacite and troilite admixtures from carbonaceous material
21 p3816 A69-39626
Meteorites pigments identification as porphyrins for extraterrestrial life evidence, noting sample analyses of Orgueil, Murray, Cold Bokkeveld and Mokoia carbonaceous chondrites
22 p4008 A69-39889
Spectral and orbital evidence of connection among fireballs with orbit inclination, comets and carbonaceous meteorites
23 p4208 A69-41285
Chemical composition of carbonaceous chondrites /Orgueil, Nogoya and Ormans/ and LL group chondrite /Ngawi/, confirming Ca/Al ratio
24 p4382 A69-42927
Trapped Ne in carbonaceous chondrites and gas-rich meteorites, observing Ne 20/Ne 22 ratio variance
24 p4385 A69-43217
Allende carbonaceous meteorite age determination by thermoluminescence method, assuming internal radioactivity source
24 p4385 A69-43219
Fe abundance in sun and carbonaceous chondrites, noting agreement between solar and meteorite abundances of Ni, Mg, Si and Li
24 p4385 A69-43223

CARBONACEOUS ROCKS
U COAL

CARBONATES
NT CALCITE
NT CALCIUM CARBONATES
NT DOLOMITE [MINERAL]
NT POLYCARBONATES
NT SODIUM CARBONATES
Polydiethylene glycol-bis-allyl carbonate /PBAC/ Hugoniot equation of state, reporting shock data, discussing applications to propellant testing
16 p2879 A69-32179
Doped silver carbonate defect structure and doping effect on reaction kinetics by X rays and electron paramagnetic resonance, finding new crystal structure
22 p3993 A69-40720

CARBONIZATION
Cellular carbon castings fabrication by carbonization of polyurethane polyfurfuryl alcohol foam for high temperature applications, noting properties
17 p2992 A69-33373
Carbon fiber composites in construction of rocket motor cases, pressure vessels and support structures, including carbonization for ablation and insulation applications
23 p4180 A69-42158

CARBONYL COMPOUNDS
Cross-linked polymers obtained by direct reaction of aryl polycarbonyls with aryl polyamines, studying char yields effect
08 p1269 A69-21059
Borane carbonyl pyrolysis in low pressure tubular flow reactor measured by mass spectrometry, noting wall collision role in diborane bond dissociation
14 p2410 A69-29282
Thermal decomposition of molybdenum carbonyl, deriving general equations, noting agreement with experimental data
20 p3558 A69-37015
Negative electric potential effect on deposition rate of Mo from molybdenum carbonyl and on deposit chemical composition during pyrolysis
20 p3559 A69-37016
Emission band intensities of carbonyl fluoride in 2.0-6.0 micron region with scanning spectrometer, comparing results for room and shock temperature with theoretical data
21 p3669 A69-38759

CARBORANE
High pressure combustion of ortho-barenes /carboranes/, determining formation heat and amounts of boric acid and carbon dioxide
21 p3670 A69-39625

CARBOXYLIC ACIDS
U ACETIC ACID
U ALANINE
U DICARBOXYLIC ACIDS
U FORMIC ACID
U LACTIC ACID
U LYSINE
U TRYPTOPHAN

CARBURIZING
Thermodynamic study of carburization of liquid titanium and zirconium, examining effects of atmosphere, graphite porosity and alloying elements
03 p0446 A69-13572
Carburization structure on surface of Mo and Nb castings cast in graphite molds showing changes in plastic properties of metals
04 p0619 A69-15391
Atmospheric and alloying elements effects on casehardening by gas carburization of structural steels, noting carbon potential
07 p1167 A69-19344
Carburization structure on surface of Mo and Nb castings cast in graphite molds showing changes in plastic properties of metals
18 p3156 A69-35019
Pyrolyzed tetraethoxysilane for carburizing steels and Ti alloys at 850-1050 C
19 p3328 A69-36161
Carburizing spherical powders of Nb, Mo and W to obtain carbides, noting agreement between theoretical and experimental data
19 p3345 A69-36162

CARCINOMA
U CANCER

CARCINOTRONS
Capitron locked oscillator with wide electronic tuning range, describing CW operation characteristics and application to ground station microwave transmitters
23 p4135 A69-41302

CARDIAC AURICLES
Isolated pacemaker tissue from rabbit heart under dynamic and static stretching, discussing spontaneous frequency phenomena
23 p4096 A69-42092

CARDIAC VENTRICLES
Left ventricle rapid filling period measurement from rapid filling wave of apexcardiogram, noting possible influences of age and sex
03 p0376 A69-14081
Single channel pressure telemetry unit for chronic implantation into cardiac chambers or major blood vessels in unrestrained animals for measuring ventricular pressure
11 p1831 A69-25642
Left ventricular function in intact anesthetized dogs analyzed during graded hypovolemia produced by lower body negative pressure
22 p3874 A69-40225
Pulmonary capillary blood flow, stroke volume and heart rate measured in tilted and supine subjects during respiration, discussing tourniquets and intravenous atropine effects
23 p4082 A69-41445
Cerebrospinal fluid /CSF/ formation in male monkeys as function of fluid pressure at third ventricle level following temperature stress and feeding
23 p4084 A69-41469
Aortic pressure effect on left ventricular function, emphasizing effect of heart rate hematocrit and oxygen consumption
23 p4092 A69-42061
Cat hearts ventricular pressure curves dv/dt and dp/dt correlated with left heart ventricle mechanical performance
23 p4095 A69-42076
Myocardial muscle fibers transient inward current components during sheep ventricle voltage clamp analysis
23 p4095 A69-42080
Sinus outflow relationship to oxygen content in anterior cardiac vein blood and right ventricle systolic pressure
23 p4098 A69-42105
Refractory period adaptation to sudden heart rate changes in dogs
24 p4257 A69-42628
Supraventricular arrhythmias after acute myocardial infarction, noting benefit of early DC shock
24 p4262 A69-42729

Pneumatic driving system for heart assist or total replacement pumps, discussing design features and performance characteristics

24 p4273 A69-42983

CARDIOGRAPHY

NT BALLISTOCARDIOGRAPHY
NT ELECTROCARDIOGRAPHY
NT PHONOCARDIOGRAPHY

Cardiac output during space flight based on rebreathing method for estimation of gas tension in mixed venous blood and Fick equation
[UN PAPER 68-95746]

01 p0151 A69-10527

Coronary angiography for evaluating cardiac problems of aircrew, giving case histories and clinical and laboratory findings

19 p3263 A69-36461

Nonsurgical methods of cardiac output measurement in aerospace medicine, considering simultaneous recording of carotid and femoral pulses and impedance plethysmography

23 p4088 A69-41813

Errors in estimating cardiac function from aortic and peripheral pulses, using cadaver experiments

24 p4262 A69-42728

Stewart-Hamilton formula for cardiac output measurements and regional blood flow determination

24 p4271 A69-42784

CARDIOLOGY

Left ventricle rapid filling period measurement from rapid filling wave of apexcardiogram, noting possible influences of age and sex

03 p0376 A69-14081

Cosmonauts cardiac activity and respiration changes during physical exertion in orbital flight on Voshkod spacecraft

03 p0377 A69-14196

Cardiac function changes during orthostatic tests and problems in predicting reactions of cosmonauts in flight

03 p0381 A69-14229

Vectorometric EKG analysis of cardiac activity during hypokinesia with and without exercise and medication

05 p0710 A69-16519

Cardiac arrhythmias during positive G sub x acceleration, treadmill exercise and tilt table testing

06 p0874 A69-17834

Vectorometric EKG analysis of cardiac activity during hypokinesia with and without exercise and medication

18 p3096 A69-34738

Cardiac and arterial change frequency among young people, describing hydraulic model for morphological variations of carotidogram appearing with age, arterial hypertension and arteriosclerosis

21 p3661 A69-39272

Chronic congestive heart failure in dogs compared to pulmonary system, discussing effect on cardiac lymphatics

23 p4078 A69-41364

Cytoplasmic protein synthesis mechanism using rats heart-lung preparation with precise hemodynamic parameters control, noting variance with change in cardiac work level

23 p4083 A69-41456

CARDIOVASCULAR SYSTEM

NT AORTA
NT ARTERIES
NT BLOOD VESSELS
NT CAPILLARIES [ANATOMY]
NT CARDIAC AURICLES
NT CARDIAC VENTRICLES
NT DIASTOLE
NT EOSINOPHILS
NT ERYTHROCYTES
NT HEART
NT LEUKOCYTES
NT LYMPHOCYTES
NT MYOCARDIUM
NT OXYHEMOGLOBIN
NT RETICULOCYTES
NT SYSTOLE
NT VEINS

Cardiovascular changes in male students during tilt and negative pressure tests with bed rest studied from heart rate, blood pressure and leg volume measurements

01 p0021 A69-11334

Hypokinesia and transverse accelerations combined effect on human cardiovascular system and regional blood circulation

02 p0197 A69-11495

Control mechanisms of hemodynamic shifts from dogs subjected to acceleration under anesthesia

02 p0198 A69-11503

Long term restriction of muscular activity noting effects on dynamics of cardiac contraction

02 p0198 A69-11515

Cardiovascular system simulation using computer models transport and perturbation methods

03 p0380 A69-13855

Simulation of regulatory function of cardiovascular system during weightlessness

03 p0376 A69-14193

White rat physiological processes while maintained on hypothermic cardiopulmonary bypass with small membrane type heart-lung machines

05 p0708 A69-15971

G suit inflation acute and prolonged effects on cardiovascular dynamics in recumbent and passively tilted individuals

06 p0883 A69-17843

Cardiovascular responses of baboons and dogs subjected to anoxic near vacuum environment by rapid decompression

06 p0875 A69-17846

Cardiovascular disease incidence among airline flight deck personnel in relation to increase in average age of personnel

06 p0875 A69-17848

Reactions of respiratory and cardiovascular system of dogs in biocompartment of ballistic missiles, discussing biopotential of myocardium, arterial pressure, etc

07 p1060 A69-18576

Human and animal cardiovascular system reactions to weightlessness, noting vagus nerve role in adjusting organism

07 p1061 A69-18583

Statistical correlation between cardiovascular activity and respiration dynamics of cosmonauts during orbital flight, discussing heart beat and respiration rates

07 p1061 A69-18584

Cardiovascular system medical examinations for selection of aircraft and spacecraft crew members from healthy men with no apparent disorders or complaints

07 p1066 A69-18983

Axial waves in blood vessels, determining phase velocities and damping, noting anisotropic behavior of artery wall

[SESA PAPER 1350]

07 p1069 A69-19726

Dogs cardiovascular activity mathematical analysis from physiological indices during long space flight

08 p1261 A69-19828

Brief intense thermal stresses effects on cardiovascular system of man, noting criticality of effective blood volume for circulatory competence

08 p1264 A69-20668

Tilt-table and acceleration tolerance of athletes and inactive students, comparing cardiovascular responses, heart rate and blackout level

[DVL-834]

09 p1444 A69-21304

Amplitude variations in ULF ballistocardiograms of young normal airline stewardesses and applicants, discussing cardiovascular reactivity

09 p1444 A69-22544

Pathological changes in respiratory and cardiovascular systems of white rats due to various levels of hyperoxia

10 p1646 A69-23577

Long term hypokinesia effect on cardiovascular system of athletes indicating human orthostatic resistance increase due to physical exercises

10 p1646 A69-23581

Single channel pressure telemetry unit for chronic implantation into cardiac chambers or major blood vessels in unrestrained animals for measuring ventricular pressure

11 p1831 A69-25642

Blood vessel model in form of cylindrical shell filled with liquid for studying cardiovascular system dynamic and static problems

12 p2018 A69-25989

High altitude acclimatization effects on cardiovascular system, external respiration, blood composition, optical and vestibular analyzers in human subjected to various stresses

13 p2212 A69-28623

Cardiac output determined simultaneously in adult male humans by thoracic impedance changes and radioisotope dilution

14 p2408 A69-29304

Physiologic and psychologic aging in professional pilots analyzed on basis of cardiovascular, pulmonary, exercise tolerance and sense testing

14 p2408 A69-29309

Cardiovascular system, neuromuscular activity and mental fitness of subjects performing physical and men-

tal assignments with prescribed work-rest schedule during confinement

17 p2906 A69-32936

Gastric perfusion rate in restrained animals determined by Rb 86 clearance technique

17 p2908 A69-33170

Leg volume changes in response to lower body negative pressure due to blood redistribution

17 p2908 A69-33171

Beta adrenergic blockade in differential diagnosis of cardiovascular changes produced by stress induced catecholamine liberation and organic disease

17 p2909 A69-33184

Pubertal puppy and adult dog cardiovascular system during inhalation of various nitrogen-oxygen mixtures, comparing heart beat rates, minute blood volumes, etc

19 p3257 A69-36169

Cardiovascular system medical examinations for selection of aircraft and spacecraft crew members from healthy men with no apparent disorders or complaints

20 p3480 A69-38231

Cardiovascular illnesses incidence among airline flight personnel, discussing coronary insufficiency detection

21 p3661 A69-39271

Cardiac and arterial change frequency among young people, describing hydraulic model for morphological variations of carotidogram appearing with age, arterial hypertension and arteriosclerosis

21 p3661 A69-39272

Amyl nitrite inhalation effects on cardiovascular system, discussing tachycardia and carotidograms

21 p3661 A69-39278

Dogs cardiovascular responses to histamine liberator /compound 48/80/, describing shock and acidosis with elevated histamine levels

22 p3873 A69-40206

Hemodynamic characteristics of decortication in rabbits, noting upsets of compensatory and adaptive capabilities of cardiovascular system

22 p3888 A69-41271

Cardiovascular effects of hypoxia in conscious and anesthetized dogs in environmental chamber, discussing artery pressure, tachycardia, stroke volume and cardiac output

23 p4078 A69-41314

Sotalol and propranolol cardiovascular effects, comparing toxicity and blocking action against circulatory and cardiac effects of catecholamines

23 p4080 A69-41403

Cat papillary muscle length-tension curves before and after inotropic intervention, noting optimal length changes

23 p4084 A69-41461

Cardiovascular changes induced in animals by prolonged weightlessness, using implanting polyethylene cannulas in neck or head

23 p4108 A69-41824

Alaska sled dogs cardiovascular performance and flow distribution during cross country runs

24 p4256 A69-42624

Cardiovascular autonomic effects dynamic characteristics under severe arterial hypoxia in unanesthetized rabbit

24 p4258 A69-42632

Central circulatory responses of humans to rapid skin temperature changes during continuous exercises

24 p4258 A69-42633

Neural integration of cardiorespiratory responses and suprabulbar control during arterial hypoxemia in rhinencephalic thalamic pontine rabbits

24 p4258 A69-42635

M-1 Valsalva maneuver induced cardiovascular stresses effect on oculobulbar vergence of subjects observing Thorington scale, discussing probable physiological mechanisms

24 p4266 A69-43373

Circulatory reactions of humans under g forces in centrifuge for various periods, with or without anti-g suit

24 p4267 A69-43385

Cardiopulmonary bypass developed for studies of long term weightlessness on cardiovascular system of mice, white rats and squirrel monkeys

24 p4278 A69-43394

CARDS

Thematic apperception test /TAT/ cards for assessing attitudes in naval recruiting, respiratory responses during ejections and aviation psychology

23 p4112 A69-42365

CARET WINGS

Hypersonic wave riders lift and drag coefficients, lift drag ratio, shock profile and pressure distribution, discussing wind tunnel measurements of caret wings
21 p3645 A69-39802

Perturbation equations for oscillating wedges and caret wings with attached bow shock in hypersonic and supersonic flows
24 p4249 A69-43659

CARGO

NT AIR CARGO

Cargo handling systems for worldwide door to door service from marketing systems viewpoint
[RAES PAPER 1]
22 p4053 A69-40482

CARGO AIRCRAFT

NT C-5 AIRCRAFT

Air cargo traffic increase, discussing technical and economical prospects, use of intermodal containers and transportation automation tendency
01 p0008 A69-10030

Air cargo and world trade, discussing economics, cargo tariffs, customs procedures, cargo airports and convertible aircraft
03 p0536 A69-14088

Flow fields about upswept rear fuselages of rear loading cargo transport aircraft
06 p0859 A69-17492

Air cargo transportation in 1970s, discussing Boeing 747 and Lockheed 500 super airfreighters, terminals, rates, marketing, etc
13 p2381 A69-27336

Skyvan 3 light passenger/freight carrier design, detailing power plant, installation and power management
17 p2902 A69-34192

Flight compartment and cabin layout of Skyvan 3 designed as freighter with passenger capability
17 p2903 A69-34195

L500 cargo transport commonality with C-5 showing need for aggressive weight control program
[SAWE PAPER 745]
18 p3091 A69-34908

Lockheed L-500 aircraft weight consideration in structural design as all cargo lifter, describing engine thrust, payload, options, etc
18 p3092 A69-35464

Cargo aircraft future design regarding engine development, structural flexibility, airport compatibility, cargo handling, etc
18 p3092 A69-35467

Aircraft interior conversion for passenger or cargo service, discussing convertible aircraft and quick change concepts
[AIAA PAPER 69-784]
19 p3244 A69-35642

Civil cargo aircraft characteristics and development trends, discussing cargo and passenger traffic management, communications network, etc
22 p3863 A69-40427

CARGO SPACECRAFT

Low cost efficient shuttle system for personnel and cargo transport to earth orbit for NASA and DOD needs
21 p3827 A69-39695

CAROTID SINUS REFLEX

Sympathetic nerve activity inhibition due to afferent baroreceptor nerves reflexes, studying carotid sinus and aortic nerves as pathways to vasomotor center
20 p3479 A69-38073

Renal vascular circulation in carotid occlusion pressor reflex by vasoconstriction in absence of renal autoregulation
22 p3887 A69-41190

Sinusoidal pressure electric stimuli frequency effects in isolated carotid sinus on canine peripheral blood pressure, determining dynamic characteristics from observation data
23 p4092 A69-42062

Electrical stimulation effects of carotid sinus on sinus rate and atrioventricular conduction for vagi and sympathetic nerves interruption to heart in dogs
24 p4257 A69-42629

CARRIER FREQUENCIES

Chirp pulse generation by carbon dioxide laser, discussing carrier frequency sweep
04 p0609 A69-14333

Solid state precision frequency standard for L multiplex carrier equipment, using four precision quartz crystal oscillators
04 p0561 A69-15451

Carrier energy dispersal in communication satellite telephony and TV systems, noting attendant RF bandwidth increase as function of distortion
09 p1450 A69-21277

Carrier disappearance method for FM telemetry transmitter characteristics measurements including frequency deviation sensitivity, linearity and frequency response
14 p2411 A69-28881

Limiting incoherent or coherent interference signals at frequency of biphase or quadriphase digital signal
14 p2413 A69-29483

Ionospheric parameter recording accuracy by vertical sounding, discussing errors in frequency- height curve
17 p2969 A69-34002

Optimum power allocation for RF carrier phase error and synchronization error in two channel system
19 p3274 A69-36283

Pulse-to-pulse carrier frequency stability of microwave radar transmitter tube for fixed target suppression
20 p3485 A69-36943

Carrier frequency monitoring amplifier with automatic bridge tuning for coupling to passive sensors including strain gages, inductive transmitters, etc
22 p3915 A69-40937

Tradeoff between Doppler measurement capability and subcarrier demodulation in coherent digital communication system quantitatively presented for various SNR
23 p4122 A69-41771

CARRIER INJECTION

Electron-hole collisions effect on drift and electron and hole diffusion in semiconductors at high injection levels
01 p0137 A69-10257

Negative resistance behavior of InSb diodes at 77 K, extending double injection theory for insulators to extrinsic semiconductors
02 p0294 A69-11722

Punch-through microwave negative resistance diode explained and contrasted with similar Read and Shockley structures
02 p0215 A69-11938

Step voltage transient behavior of electron-hole plasma injected into Ge, noting current time dependence
02 p0301 A69-12651

Conduction mechanism in unstable range of Au doped double injection Ge diode at 77 K
02 p0222 A69-12686

Photon emission in germanium at high injection levels during uniaxial compression
04 p0643 A69-15255

Emitter base lateral diode carrier injection effect on current gain properties of small area double diffused planar transistors
05 p0728 A69-15808

Injection characteristics of n-aluminum gallium arsenides-p-GaAs heterojunctions from recombination radiation spectra
06 p0979 A69-16993

Ambipolar motion of light injected photocarriers in cadmium-mercury-telluride in terms of diffusion and drift in electric fields
06 p0979 A69-17154

Gallium arsenide double injection diode using vacuum deposited film electrode on single crystal substrate, noting current controlled negative resistance
06 p0893 A69-17156

Silicon double injection diode, discussing HF noise measurement, Nyquist noise equivalent circuit for double injection process and source of LF noise
06 p0898 A69-17762

Injection locking method for reducing FM noise in Gunn effect oscillators
07 p1102 A69-18862

GaAs lasers radiation power hysteresis manifested in generating starts and stops at different injection current levels
07 p1157 A69-19593

Dark and photocurrent volt-ampere characteristics induced by capture of carriers injected into illuminated CdS single crystals
09 p1555 A69-21506

Electron-hole collisions effect on drift and electron and hole diffusion in semiconductors at high injection levels
09 p1559 A69-22650

Electron injection into ZnO from aqueous solutions of stable substances, correlating injection with oxidation potential of substance
10 p1651 A69-22940

Injection locked oscillator FM demodulator, analyzing signal distortion, intermodulation noise, differential gain and differential phase
11 p1845 A69-24565

Minority carrier density in base region of uniform base transistor at arbitrary injection level, using two dimensional model
11 p1845 A69-24569

Negative resistance formation in impurity compensated semiconductor diodes ascribed to injected carrier drift path increment with increasing current, deriving I-V characteristics
13 p2230 A69-27877

Current-voltage characteristics for double injection processes in nonideal contact p-i-n semiconductors operating in ohmic relaxation mode
13 p2323 A69-28524

Capture centers effect on current-voltage characteristic of p-i-n diodes during injection, noting negative resistance appearance
13 p2236 A69-28525

Injection phase-locking characteristics of LSA /limited space charge accumulation/ mode transferred-electron diode oscillators, employing negative conductance and equivalent circuit
14 p2421 A69-29544

Charge flow injection into MOS substrate attributed to gate pulses, correlating charge magnitude with pulse frequency
15 p2573 A69-30033

Injection level effects on minority carrier lifetimes in lithium-doped devices and solar cells irradiated by electrons and reactor neutrons
19 p3252 A69-35698

Collector efficiency limitation of surface barrier-limited photoconductors attributed to photogenerated carrier diffusion into electrode
20 p3583 A69-37732

Injection and excitation of charge carriers in CdS single crystals, analyzing current-voltage characteristics dependence on electrode separation, temperatures and electric field
21 p3779 A69-38423

Transient current change with minor change in voltage with double injection of electrons and holes in CdS single crystals, obtaining time dependence
21 p3780 A69-38833

Electroluminescence in doped p-type GaAs single crystal diodes ascribed to double injection of nonequilibrium current carriers
24 p4288 A69-43739

CARRIER MOBILITY

NT ELECTRON MOBILITY

NT HOLE MOBILITY

Intense laser emission interaction with current carriers in semiconductors, analyzing dependence of thermoelectric field produced by light absorption on intensity, frequency and temperature
01 p0139 A69-10895

Carrier mobility variation with electric field related to structure of epitaxial field effect transistors
02 p0294 A69-11541

Thin film transistors prepared from spray deposited cadmium sulfide, discussing carrier mobility and low stability
02 p0214 A69-11596

Heterojunction band model and carrier transport mechanisms emphasizing applications to heterophotodiodes, solar cells and hetero field effect transistors
02 p0294 A69-11598

Current carrier mobility in GaTe and tin selenide semiconducting stratified lattices, noting injection of free carriers and polarized nonpolar phonons
02 p0295 A69-11777

P-n junction under arbitrary transient conditions, solving one dimensional, two carrier transport equations by numerical iterative method
03 p0487 A69-13639

CdS Hall coefficient, Hall mobility and magnetoresistance coefficient dependence on electric field, magnetic field and scattering mechanisms
03 p0490 A69-13945

Hall mobility of photoelectrons in cadmium sulfide layers
03 p0491 A69-14055

Resistivity and Hall mobility periodic change effect on probe measurements in semiconductors
04 p0642 A69-14534

Distribution of current carrier concentration and mobility in p-type silicon doped with phosphorus ions
04 p0643 A69-15254

Carrier scattering from defects in neutron irradiated semiconductors, noting mobility and relaxation time
06 p0974 A69-16864

Faraday effect at free carriers in indium antimonides and gallium arsenides, analyzing frequency dependence of rotation angle
06 p0979 A69-16996

- Interface states effects on characteristics of p-channel MOS transistors
06 p0979 A69-17117
- Digital method for quantitative study of carrier circulation phenomena in semiconductors, noting Algor program and continuously polarized p-n junction
08 p1280 A69-19973
- Magnetoelectric characteristics of inversion layers below gate region in transistors, noting Hall mobility
08 p1372 A69-20460
- Kinetic coefficients of carrier motion in semiconductor obtained by Boltzmann equation, considering impacts between carriers
09 p1554 A69-21468
- HgTe-CdTe single crystals homogeneity and Cd distribution obtained by Bridgman and/or zone melting studied for carrier concentration and electron mobility
09 p1557 A69-21737
- Electronic states and minority carrier transport in mixed semiconductors with graded composition, noting position dependent band gaps and effective masses
10 p1745 A69-23360
- Carrier dragging in CdS single crystals under Q switched ruby laser light due to photon stream
13 p2271 A69-27661
- MOS transistor Hall voltage, mobility and constant verified by magnetoelectric measurements of Si p-inversion layer
13 p2323 A69-28331
- Dislocations effect on carrier mobility and concentration in p-type and n-type InSb crystals
14 p2507 A69-29646
- Kinetic coefficients of carrier motion in semiconductor obtained by Boltzmann equation, considering impacts between carriers
15 p2669 A69-30713
- Book on semiconductor devices physics covering principles and operational characteristics, carrier distribution and transport properties, materials, junctions, thin films, etc
15 p2670 A69-31062
- Microwave power loss and semiconductor conductivity relationship measured for carrier lifetime and mobility, noting nonlinearity and accuracy
16 p2825 A69-31617
- Hall mobility of photoelectrons in cadmium sulfide layers
18 p3182 A69-35048
- HgTe-CdTe single crystals homogeneity and Cd distribution obtained by Bridgman and/or zone melting studied for carrier concentration and electron mobility
20 p3584 A69-38215
- CARRIER MODULATION**
U MODULATION
- CARRIER ROCKETS**
U LAUNCH VEHICLES
- CARRIER SYSTEMS**
U WIRELESS COMMUNICATIONS
- CARRIER WAVES**
- Amplitude modulation factors expressed as carrier and sideband power for sinusoid and square wave signals, considering negative clipping by modulator cut-off
01 p0028 A69-10419
- Transient signal propagation in lossless isotropic and homogeneous plasma for Gaussian pulse modulated carrier, discussing amplitude change and carrier phase distortion
02 p0290 A69-12351
- Analog FM subcarrier modulation selected for real time TV picture transmission via electro-optic space communication system
04 p0562 A69-15474
- Resonance effects during piezoelectric interaction between charged drift wave and flexural wave in semiconductors with one sign current carriers
08 p1371 A69-19806
- Frequency measurement of moving spacecraft RF carrier waves at low SNR by analog recording of noisy signal and HF trigger tone, noting data processing and signal fading rate
12 p2038 A69-26051
- Transmission system with baseband spectrum divided into subbands, cascade phase modulating carrier in multiplication chain
12 p2030 A69-26385
- Subcarrier phase modulated single sideband sinusoidal carrier synthesis, discussing signal power ratios, signal efficiency, design sensitivity, etc
14 p2413 A69-29489
- Electromagnetic waves as data carriers for earth resources and technology satellite sensors
15 p2607 A69-30231
- Maximum a posteriori estimate of modulation on carrier with noise, discussing iterative technique and FM test
17 p2994 A69-32917
- CARTESIAN COORDINATES**
- Numerical integration for continuously thrusting spacecraft optimal trajectory, considering rectangular Cartesian and polar cylindrical coordinates characteristics
[AIAA PAPER 69-903] 21 p3798 A69-38546
- Acoustical ray tracing in horizontally layered and vertically sectioned atmosphere on digital computer using shifting Cartesian coordinate system
23 p4154 A69-41532
- CARTILAGE**
- Invertebrate endoskeletal cartilage and cartilage-like tissues occurrence and nature, discussing cellular tissues and origin
15 p2555 A69-30412
- CARTOGRAPHY**
U MAPPING
- CARTRIDGE ACTUATED DEVICES**
U ACTUATORS
U EXPLOSIVE DEVICES
- CASCADE CONTROL**
- Divergent-convergent and convergent-divergent cascaded exponential lines, determining equivalent length of uniform transmission line
01 p0044 A69-10623
- Multiple loop feedback systems synthesis utilizing extended node introduction synthesis theory, considering filter response functions characteristics
10 p1667 A69-24037
- Filter network synthesis for realization of rational functions, discussing numerator polynomial inclusion by choice of divisor polynomial and branch introduction and parallel systems
10 p1667 A69-24038
- Storage varactors and frequency dependent diode input power for multiplier cascades control, discussing series connections and limitations by thermal noise
11 p1841 A69-25607
- Antenna switch for cascading and separating RF channels of high power wideband broadcasting systems
11 p1854 A69-25617
- Cascaded limiter and phase detector, analyzing SNR transfer characteristics for specific PM signals
23 p4131 A69-42525
- CASCADE FLOW**
- Heat transfer in cooled portion of air gas flow area of high temperature gas turbines
03 p0495 A69-12957
- Centrifugal force field influence on heat exchange between gas and blade cascade studied with noncooled blades at low temperatures
03 p0531 A69-12959
- Axial flow turbine blade cascade in transonic flow
03 p0365 A69-14103
- Cascade acceleration of plasma by two stage device noting plasma dispersion, plasma losses and highest final plasma velocity
03 p0482 A69-14215
- Blade oscillations in cascade flow of axial turbomachinery calculated as function of pitch ratio, stagger angle, angle of attack and camber
[ASME PAPER 68-FE-7] 05 p0837 A69-16069
- Heat transfer performance of porous nozzle blade cascade represented by two dimensional mathematical model
05 p0812 A69-16400
- Turbomachinery research, discussing two and three dimensional incompressible flow in cascades near end wall and in rotating machines
05 p0751 A69-16534
- Initial turbulence influence on wakes formed behind trailing edges of cascade blades
09 p1431 A69-22235
- Incompressible two dimensional potential flow analysis with compressibility effects for thick highly cambered multibodies in cascade, noting slotted compressor blade performance
[ASME PAPER 69-GT-6] 09 p1432 A69-22507
- Flat decelerating cascades boundary layer in compressible flow during change in axial flow-density ratio and upstream turbulence
11 p1818 A69-24639
- Semiautuator disk method for boundary layers and velocity of stall flutter cascade blades vibrating in transient mode, considering nonstall flutter
11 p1818 A69-25028
- Flow through turbine stage with inclined guide vanes at moderate Mach numbers, discussing exit blade angle formula for swept cascades
15 p2547 A69-30570
- Soviet book on theory and design of turbocompressors covering gas dynamic cascade theory, thermodynamics and aerodynamics, viscous gas flow, etc
20 p3459 A69-37238
- Soviet book on hydrodynamic cascade theory covering mathematical methods and numerical solutions for ideal fluid flow problems
21 p3696 A69-39527
- Compressor type cascade experiments to find closest possible traverse position to blade trailing edge
22 p3859 A69-40065
- Cascade thermoelectric heat pump reducing temperature gradient in legs of element near cold junction and reducing Joule heating in cold junction area
22 p3869 A69-40133
- Airfoils and cascades design for incompressible flow by numerical methods
23 p4058 A69-41610
- Spanwise velocity profiles through cascades and axial flow turbomachines, analyzing loading, secondary losses and inlet conditions interacting on downstream profile
23 p4061 A69-42110
- Perturbation velocity potential of unsteady potential flow of barotropic gas past cascade of thin blades oscillating harmonically
24 p4244 A69-42716
- Edge effects in efficiency of air cooled turbine blade cascades with cooling air ejection from blade trailing edges into gas flow
24 p4364 A69-43090
- CASCADE WIND TUNNELS**
- Cascade wind tunnels performance experiments, investigating effect of exit side walls lengths
19 p3241 A69-36753
- CASCADES**
- Cascaded avalanche diodes in negative resistance amplifying mode for increased output power and extended dynamic range
09 p1462 A69-21408
- CASCADES (FLUID DYNAMICS)**
U FLUID DYNAMICS
- CASE BONDED PROPELLANTS**
- Three dimensional thermal stress distribution in case bonded solid propellant determined by scattered light photoelastic technique coupled with transparent rocket motor model
[AIAA PAPER 68-512] 02 p0345 A69-12371
- CASES (CONTAINERS)**
U ROCKET ENGINE CASES
- CASSEGRAIN ANTENNAS**
- Critical parameters for optimum design of Cassegrain antenna used in space communications
[UN PAPER 68-95280] 01 p0043 A69-10481
- Aperture blockage by subreflector in Cassegrain antenna system, computing effects on far field radiation patterns
03 p0401 A69-12853
- Cassegrain two reflector antenna modification by discrete phased array, allowing for subunit redesign
04 p0572 A69-14326
- Contour pattern analysis of AN/FQP-6 monopulse radar Cassegrainian antenna, giving three dimensional drawings
04 p0576 A69-14769
- Low noise shaped beam Cassegrain antenna design for space communications earth station service, noting gain/noise temperature figure and antenna construction
05 p0728 A69-15669
- Galactic H 2 regions radio observation using Cassegrain antenna and Dicke radiometer
06 p1008 A69-17696
- Antenna gain increase, using matched pair of Cassegrain reflectors with one primary source
10 p1664 A69-23799
- RMS surface error compensation in radome-housed Cassegrain parabolic antenna including weight analysis
23 p4150 A69-42137
- Envelope characteristics of earth station Cassegrain antenna sidelobes, deriving formulas for central and spar blocking and forward feed spillover
23 p4143 A69-42517
- Space vehicle multibeam Cassegrain antenna system design meeting radiometric mapping requirements in microwave frequency range, discussing mounting, degrees of freedom, etc
[ONERA-TP-713] 23 p4143 A69-42527
- CASSEGRAIN OPTICS**
- Astronomical two mirror telescope with aplanatic secondary focus, describing prime and secondary focus field correctors
05 p0761 A69-15733

- Quasar and radio galaxy spectra obtained on Cassegrainian focusing diffraction spectroscopy
11 p1951 A69-24236
- Nova Delphini 1967 observational data and equipment including Cassegrain spectrograph, reflector telescope and photoelectric photometer
15 p2682 A69-30439
- Prismatic Cassegrainian-focus spectrograph of telescope at Shemakha Observatory, discussing camera inclination, instrumental contour for yellow neon line, astigmatism, optical temperature effects, etc
19 p3313 A69-36582
- Two channel TV Cassegrain telescope, describing color separation system for obtaining integral and monochromatic images of astronomical objects
20 p3547 A69-38309
- CASSIOPEIA A**
- Linear polarization measurements at 2.07 cm for 29 radio sources
02 p0326 A69-12705
- RF spectral lines due to OH molecule detected in interstellar space in absorption of RF radiation from Cassiopeia A source
09 p1586 A69-21295
- Preliminary observations of Tau-A, Cas-A and Cyg-A with multiple-element interferometer
10 p1777 A69-23397
- Magnetic fields in interstellar neutral hydrogen clouds in direction of radio source Cassiopeia A, noting field amplification
10 p1785 A69-24096
- Electron concentration fluctuation in inhomogeneousities estimated from Cassiopeia A radio emission
12 p2070 A69-26687
- Energetic gamma rays emission from radio source Cassiopeia A by high altitude balloon observations, using high resolution telescope
15 p2675 A69-30760
- RF spectral lines due to OH molecule detected in interstellar space in absorption of RF radiation from Cassiopeia A source
15 p2697 A69-31226
- Radio source Cassiopeia A flux density in terms of expanding radio source theory, noting frequency and time correlation with flux density changes
23 p4215 A69-42112
- Cassiopeia A luminous filaments motion study noting stellar remnant magnitude
24 p4389 A69-43746
- CASSIOPEIA CONSTELLATION**
- Galactic rotation constant calculated from radial velocities of O, B and A stars in Cassiopeia constellation, using Fehrenbach objective prism
07 p1214 A69-18664
- Statistical comparison of scintillation depths of Transit 4A satellite to radio star Cassiopeia A
07 p1215 A69-18821
- Galactic rotation in Cassiopeia region, studying O, B and A stars circular velocities as function of distance from galactic center
18 p3201 A69-35142
- Atomic and molecular absorption lines and width measurement in spectrum of WZ Cassiopeiae carbon star in visual and IR region
18 p3204 A69-35350
- Spectral energy distribution of gamma-Cas in 1967 based on observations in seven color photometric system
19 p3426 A69-36565
- Radio emission intensity of Cas-A and Cyg-A at 30-60 cm, giving spectral indices
19 p3428 A69-36876
- Eta Cassiopeiae orbit analysis with emphasis on multiple exposure photographic observations, noting companion mass
22 p4013 A69-40120
- Equal velocity contour diagrams for interstellar matter emission and absorption study in Cassiopeia-Perseus region
24 p4384 A69-43050
- CASTIGLIANO VARIATIONAL THEOREM**
- Variational principles of dynamic shell theory using Legendre transform for relations and boundary conditions of Timoshenko theory
01 p0166 A69-10262
- Castigliano variational principle applied to thermal stresses in rectangular plate by expanding stress function in double series of cosine binomials
08 p1419 A69-21178
- CASTING**
- NT INVESTMENT CASTING
NT PROPELLANT CASTING
NT SLIP CASTING
- Potential usage of titanium in cast parts for gas turbine engines, emphasizing alloys development [ASME PAPER 69-GT-24]
09 p1513 A69-22494
- Cast and forged steel mechanical properties noting starting materials and production methods roles in cast steel improvement
11 p1904 A69-24644
- Rolled sheets from beryllium scrap converted into vacuum cast ingots, discussing preparation techniques
13 p2281 A69-28160
- Induced stressing method for complex castings by controlled cooling during heat treatment applied to front frame of J-79 turbojet engine
13 p2269 A69-28184
- Casting variables of Co base superalloys, discussing variables effects on ultimate mechanical properties, investment casting, etc
14 p2456 A69-29893
- Filament reinforced metal matrix composites made by continuous casting process, discussing tensile tests results and production costs
19 p3318 A69-35511
- Low melting point material selected model melt simulating shrinking process in castings of melt with broad liquidus-solidus interval
21 p3733 A69-39720
- CASTING SOLVENTS**
U PLASTICIZERS
- CASTINGS**
NT INGOTS
NT PROPELLANT CASTING
- Carburization structure on surface of Mo and Nb castings cast in graphite molds showing changes in plastic properties of metals
04 p0619 A69-15391
- Metal castings around ceramic cores for economic manufacture of jet engines
09 p1503 A69-21907
- Titanium alloy castings fatigue behavior at room and elevated temperatures in annealed and heat treated conditions [ASME PAPER 69-GT-22]
09 p1619 A69-22497
- Cast high temperature alloys for gas turbine components, discussing production, temperature capability, composition, oxidation, hot corrosion and weldability [IME PAPER 10]
12 p2147 A69-25795
- Fatigue fracture surfaces in cast steel and Al alloys, studying fracture morphology, crack propagation rate and striation spacing with microfractographic methods
12 p2116 A69-26916
- Carburization structure on surface of Mo and Nb castings cast in graphite molds showing changes in plastic properties of metals
18 p3156 A69-35019
- Molten iron plane melt flow duration and mass in bimetallic castings production determined using nomogram
18 p3149 A69-35289
- Shrinkage cavity volume formulas for alloy castings with wide liquidus to solidus range, considering effects of diffused porosity and clustering for Mg alloy
20 p3548 A69-37329
- High quality castings unified standards for European aerospace industry
20 p3551 A69-38029
- Deformation rates effect on failure of cast aluminum alloys under various loading rates for tension and compression
21 p3746 A69-38958
- Large contoured nozzle fabrication using liquid epoxy as casting material, presenting molding process based on experimental data
24 p4318 A69-42643
- CASUALTIES**
- Hazards model for probabilistic prediction of casualties by exploding solid propellant rockets, deriving casualty expectation equation [AIAA PAPER 69-461]
16 p2869 A69-32749
- CATALASE**
- Optical Fourier transform applied to structural analysis of catalase crystalline media by gas laser
06 p0928 A69-17890
- Salts and organic solvents effect on halophilic Halobacterium cutriburum catalase, noting enzyme activity inhibition by cation and anion
18 p3096 A69-35291
- CATALOGS**
- Four color photometry data of late F type stars in general catalog tabulated with columns for HD and GC numbers, apparent visual magnitude, etc
18 p3195 A69-34430
- M 31 nebula radio continuum survey, describing discrete sources catalog and Andromeda nebula radiation distribution
20 p3601 A69-37493
- CATALOGS [PUBLICATIONS]**
- Catalog of meridian program star observations made in Brorfelde, determining position relative to FK 4 stars by using impersonal photographic micrometer
02 p0315 A69-11815
- Catalog of orbital elements for periodic comets during perihelion passage
10 p1777 A69-23396
- Pitch determination of micrometer screw by scalar star pairs derived from FK3 and Washington zenith catalog noting temperature and dampness effects
16 p2859 A69-32218
- Equinox and equator corrections of orientation elements of FK3 and FK4 catalogs based on meridian solar observations
17 p3027 A69-32871
- Bright and faint stars absolute declinations compared in vertical circle systems used in Goloseevo and Pulkov catalogs
17 p3027 A69-32872
- Parkes catalog of 1780 radio sources, noting inclusion of data concerning polarization, source structure, optical identifications, etc
17 p3045 A69-34199
- Radial velocity measurements with objective prisms and results in SA8
18 p3201 A69-35143
- Monte Carlo method for constructing catalogs of stellar positions, distances and velocities
20 p3605 A69-37829
- Radio source flux density values in revised 3C catalog determining spectrum, discussing effects of relativistic electron energy distribution, self absorption and spatial distribution
20 p3609 A69-38138
- CATALYSIS**
- Solvent effect in catalytic hydrogenation reaction of Schiff bases of alpha-keto acids with optically active alpha-alkylbenzylamine
12 p2026 A69-25779
- CATALYSTS**
NT ELECTROCATALYSTS
- Catalytic effect of potassium bichromate and chromic oxide additives on burning of ammonium perchlorate and mixtures
08 p1375 A69-19997
- Manganese catalyst photoreaction in photosynthetic oxygen evolution in Mn deficient alga Anacystis nidulans cells
13 p2210 A69-28257
- Double skeleton catalyst type VARTA fuel cell system for space power, using potassium hydroxide as electrolyte
16 p2739 A69-32418
- CATALYTIC ACTIVITY**
- Electroless deposition of various metals with emphasis on nickel, discussing mechanism, plating solutions, substrates, deposit properties and applications
01 p0099 A69-11060
- Metal oxides catalytic and inhibitory effects on photolysis of alanine by UV light
01 p0025 A69-11095
- Electron paramagnetic resonance study of interaction between adsorbed nitric oxide and NaY and decaionized Y zeolites surfaces, considering catalytic activity
02 p0205 A69-11900
- Heat and mass transfer by catalytic effect at wall, noting interaction of laminar boundary layer on flat plate
06 p1030 A69-17115
- Surface UV irradiated MgO powder catalytic activity for hydrogen-deuterium exchange reaction
07 p1073 A69-18374
- Burning rate catalysts mechanism and location in composite propellant combustion at high pressure
09 p1622 A69-21954
- Reaction kinetics between hydrazine and esters in benzene solution at 55 C, using amides as catalytic agents
14 p2409 A69-29033
- Heat and mass transfer interaction at wall for laminar boundary layer on flat plate, considering catalytic effect of wall in atomic nitrogen recombination
15 p2716 A69-30415
- Gas environment effect on catabolic activities and enzymatic reactions of trachoma and meningopneumonitis agents of genus Chlamydia
16 p2747 A69-31865

Solid fuel ignition with gaseous oxygen in presence of copper chromate and other catalysts

16 p2829 A69-31913

Packed bed catalytic reactors cooling capacity in promoting endothermic reactions of hydrocarbon fuels, using computerized temperature and composition profiles

[AIAA PAPER 69-588] 17 p3071 A69-33265

Catalytic activity enhancement of complex Co/III/ compounds on standing explained by hydrated Co/II/ ions appearance

17 p2988 A69-33433

Chemical species flux decay in turbulent boundary layer with catalytic wall, obtaining solution of conservation equation by using shear stress distribution

[AIAA PAPER 69-709] 17 p2955 A69-33480

Solar energy release by quark fusion catalysis of alpha reaction without production of neutrinos, noting temperature dependent reaction rate

18 p3186 A69-34643

Temperature and concentration measurements of H radical in hydrogen flames

21 p3669 A69-38807

Proton transfer mechanism of copper chromite catalyzed thermal decomposition of ammonium perchlorate, noting electron transfer

21 p3783 A69-38810

Catalyst poisoning and hydrazine material compatibility during hydrazine propulsion systems sterilization and decontamination

21 p3786 A69-39768

Catalytic, physical and chemical properties of enzyme lactate dehydrogenase isolated from lobster tail muscle

22 p3897 A69-41069

Properties, relative magnitudes and relationship of pyrophosphate exchange reactions catalyzed by DNA polymerase from *Escherichia coli*

22 p3898 A69-41072

Nonequilibrium boundary layer of dissociated diatomic gas over catalytic flat plate in hot hypersonic uniform flow

22 p3934 A69-41181

CATAPULTS

Aircraft steam catapult test facilities, noting construction and operational requirements

10 p1674 A69-24068

CATARACTS

Pulsed and CW microwave power effects on rabbit eyes, noting lens opacities produced

10 p1648 A69-23185

CATCHERS

Double gap catchers for klystron amplifiers and oscillators

07 p1095 A69-18432

CATECHOLAMINE

Epinephrine forming enzyme phenylethanolamine-N-methyl transferase (PNMT) in various brain regions of rats, cats, hens and turtles

10 p1644 A69-23303

Corticosteroid and catecholamine metabolism change in rabbits during sharp limitation of motor activity

12 p2021 A69-26973

Hypoxic hypoxia effect on catecholamine content and cytochemical changes in hypothalamus of cat exposed to simulated altitude, using Euler method

14 p2407 A69-29297

Beta adrenergic blockade in differential diagnosis of cardiovascular changes produced by stress induced catecholamine liberation and organic disease

17 p2909 A69-33184

Male patients urine tests during sinusoidal vibration, noting catecholamine excretion as criterion of emotional stress under various environmental conditions

21 p3654 A69-38909

Sotalol and propranolol cardiovascular effects, comparing toxicity and blocking action against circulatory and cardiac effects of catecholamines

23 p4080 A69-41403

Supersonic flying effect on urinary catecholamine excretion rates in pilots, noting emotional state

24 p4265 A69-43370

Positive pressure breathing effects on cerebral arterial and venous blood pressure, hypothalamus and adrenal glands catecholamine content and cerebrum histological changes in dogs

24 p4265 A69-43371

CATEGORIES

Information categories concept defined in relation to formulations of classical mechanics principles, considering theories of Newton, Gauss and Hertz

20 p3576 A69-37585

CATHETERIZATION

Electromagnetic catheter flowmeter with flexible sensor suitable for branch and artery application to minimize surgical intervention

22 p3889 A69-40058

CATHETOMETERS

Intravascular pressure and sound measured in anesthetized dogs and humans using fiberoptic pressure catheter

17 p2917 A69-34172

CATHODE RAY TUBES NT PICTURE TUBES

Laser CRT with beam pumped aluminized CdS crystals, discussing single spot low duty operation

01 p0039 A69-10175

CRT method of processing contoured data from hemispheric and global numerical models simulating general atmospheric circulation

01 p0109 A69-10539

Navigational and tactical data with correlative map information provided on single CRT display in aircraft, storing map data on video tape

03 p0464 A69-13246

Laser display technology, discussing experimental systems, light sources, modulation and scanning

03 p0431 A69-13850

Display techniques, discussing cold cathode luminous gas discharge /plasmas/ tube, electroluminescence and cathode ray tube

04 p0600 A69-15029

Histograms construction for azimuthal distribution of atmospheric data from visual and photographic data obtained by CRT display goniometer

04 p0593 A69-15102

CRT direction finder with linear scanning to determine statistical data for azimuthal distribution of atmospherics

04 p0600 A69-15104

Cathode ray curve tracer to record capacitance-voltage characteristics of p-n junctions

04 p0602 A69-15406

Plastic virtual infinity lens system for large aperture cathode ray tube direct view simulator displays

05 p0760 A69-15592

Photorecording techniques for command and control systems requirements, discussing association with large screen computer generated CRT projection display equipment

06 p0928 A69-17923

Dynamic cathode ray tube spot size measurement by two slit technique, noting relationship to beam current and luminance

21 p3719 A69-38329

CRT graphic display/plotter for small digital computers, describing device operation, control and applications

21 p3679 A69-39608

CRT display system coupling interface with magnetic storage determined from algorithms and time diagrams, describing character storage and system logic design

22 p3908 A69-40936

Automatic analysis and classification of images stored on 35-mm film using CRT flying spot scanner with computer control and memory

24 p4286 A69-42744

CATHODES

NT CELL CATHODES

NT COLD CATHODE TUBES

NT HOT CATHODES

NT PHOTOCATHODES

NT PHOTOMULTIPLIER TUBES

NT PHOTOTUBES

NT THERMIONIC CATHODES

NT TUBE CATHODES

Cathode emission site analysis by measuring prebreakdown current under ultrahigh vacuum conditions

05 p0800 A69-15740

Equivalent capacitance derivation of space charge limited current from filamentary cathode

05 p0734 A69-16567

Gunn effect for cathode contacts with interface resistance, developing control characteristic boundary condition concept for explaining cathode fall and other phenomena

07 p1199 A69-18649

Back bombardment of magnetron cathode as single surface multipactor, noting effects of cathode grooves and output loading

07 p1101 A69-18656

SERT 2 thruster hollow cathode durability tested in bell jar

[AIAA PAPER 69-304] 09 p1562 A69-21224

Hollow cathode mercury electron bombardment thruster design, emphasizing low specific impulse operation and discharge chamber improvements

[AIAA PAPER 69-300] 09 p1569 A69-21880

Gas laser materials, fabrication and performance, analyzing gas cleanup, cathode degradation, bore erosion and optical surface contamination effects

11 p1896 A69-24743

Heats of condensation and vaporization of W, Re and Mo cathodes of thermoelectric converter with Cs arc for various output powers and Cs vapor pressure

12 p2017 A69-26544

Incandescent cathode temperature effect on He-Ne laser output, ascertaining mixture parameters, cathode voltage and power dependence on discharge current

12 p2109 A69-26716

Tangential drag measurements at electrodes of arc in plasma accelerator, ion current partitioning at cathode and electrode damage

[AIAA PAPER 67-657] 13 p2312 A69-28219

Ionization manometer flange transducer with axial cathode and collector for high vacuum measurements, describing air resistant yttrium oxide coated cathode with Ir core

21 p3724 A69-39077

Cathode materials role in high temperature zirconia electrolyte fuel cell performance, discussing metals, collector-embedded and electronically conducting oxides properties

22 p3869 A69-40734

Electrochemical dimensional machining of metals and alloys with rotating cathode in parts manufacture from mechanically intractable materials

23 p4168 A69-41309

Electron emitters tested for gas laser operations, discussing nonreactive and reactive gases cases, matrix structures containing BaSrO and barium zirconate cathodes

23 p4172 A69-41394

Mush cathode fabrication and characteristics for high power klystrons, comparing efficiency to oxide cathodes

23 p4144 A69-42532

Step cathodic flux cleaning of furnace brazed Al assemblies used in combination with ultrasonic and chemical conversion coating techniques

24 p4319 A69-42938

CATIONS

NT METAL IONS

Rocket sounding for studying positive ions nighttime composition in E layer after magnetic storm at midlatitudes

02 p0239 A69-11686

Positive Ar ion energy distribution for beam extracted from nonmagnetic hot cathode gas discharge ion source under various source conditions

03 p0427 A69-13102

Electron and positive ion density measurements during nighttime auroral absorption event

03 p0421 A69-13327

Topside ionosphere composition data by energy spectrometer on satellite Ariel 1, discussing positive ions and diurnal, seasonal and secular variations

03 p0424 A69-13806

Cation concentration requirement of halophilic NADH dehydrogenase for stability and maximum activity

10 p1651 A69-23127

Sommerfeld type and Fermi type approximation analytical solutions of Thomas-Fermi differential equations for positive ions

10 p1726 A69-23525

Global coverage of positive ion composition and temperature, and electron density and temperature measurements during AURORAE mission of ESRO 1 satellite

13 p2253 A69-27753

Rocket sounding for studying positive ions nighttime composition in E layer after magnetic storm at midlatitudes

13 p2258 A69-28717

Binary encounter model for ionization by charged particle impact modified to evaluate cross section for ionization of positive ions by electron impact

14 p2489 A69-29996

Maximum likelihood methods applied to device performing ion swarm experiments, measuring positive ion mobility in hydrogen

16 p2788 A69-31670

Charge transfer cross section between mercury ion and Cs assessed, considering ion engine positive ion beam neutralization

16 p2835 A69-31895

Sporadic E ionization by rocket sounding, comparing positive ion density measurements with separate wind shear observations

16 p2780 A69-32310

Townsend discharge formation time determination, taking into account impact ionization in positive ion cloud moving from anode to cathode

19 p3381 A69-36603

Earth satellite sweeping mass spectrometer for measuring atmospheric neutral particle and positive ion concentration

19 p3314 A69-36681

Cations of sulphates photosensitizing role in photolysis of amino acids and peptides in various atmospheres

20 p3477 A69-37626

Drift velocity and lateral diffusion of positive hydronium, hydrogen and K ions in hydrogen with zero field mobilities

20 p3580 A69-38026

Effective Gaunt factors for threshold excitation of positive ions by electron collisions for 23 dipole transitions in 15 isoelectronic sequences

20 p3581 A69-38175

Cations desorption from O, H and N films adsorbed at graphite surface under electron bombardment, studying desorption cross sections discrepancies

22 p3972 A69-39957

Electron transport chain of monovalent and divalent cations and of polyamines, studying effects on menadione reductase activity to determine salt dependence

22 p3886 A69-41077

Ba titanate modifiers, classifying cations replacing Ti and Ba ions

22 p3996 A69-41161

Electrodialysis method for depleting positive Na, K, Ca and Mg ions from Anabaena flos-aquae A-37, noting algae survival rate

23 p4079 A69-41387

CATS

Respiratory pressure recording with tracheal cannulae applied on cats to obtain pneumograms and oscillograms of respiratory neurons

07 p1131 A69-18538

Ventral posterolateral potentials in anesthetized immobilized cats in response to electric stimulation of mesenteric nerves and mechanoreceptors, studying thalamus nucleus role

12 p2020 A69-26562

Immobilization effects on alpha rhythm, locomotor coordination and visual alimentary motor reflexes of cats

13 p2212 A69-28617

Hypoxic hypoxia effect on catecholamine content and cytochemical changes in hypothalamus of cat exposed to simulated altitude, using Euler method

14 p2407 A69-29297

Histological and histochemical studies of dephosphorylating enzyme distribution in muscle spindle capsule of guinea pig thigh muscles and cat calf muscles

15 p2554 A69-30406

Cortical auditory-evoked response during eye movement in cats, discussing relation to central mechanism

17 p2911 A69-34171

Two body mechanical system operating within dynamics laws simulating backward and forward bending motions of falling cat

19 p3259 A69-36832

Cats vestibular neurons reactions to labyrinths mon- and binaural polarization and caloric stimulation

20 p3471 A69-37255

Stimulation effects of reticular formation, hippocampus and septum on sensory responses of posterior hypothalamic neurones in cats

21 p3656 A69-38979

Cortical and thalamic evoked activities changes during sensory conditioning of freely moving cat

22 p3872 A69-40160

Unit activities in cerebellar cortex by auditory stimulation in cats, discussing response patterns obtained by histograms

22 p3876 A69-40264

Local electroretinogram responses produced in cats by light intensity incremental changes

22 p3878 A69-40835

Neuronal organization of initial afferent inflow in thalamic visual center /lateral geniculate body /LGB/ of unanesthetized cats/, noting unit activity

22 p3879 A69-40845

Psychopharmacological drug effects on retinal neuron activity in cats measured by microelectrodes, noting spontaneous activity decrease

22 p3879 A69-40846

Psychopharmacological drug effect on visually evoked responses in cats from recordings from visual cortex, noting latencies increase with dose

22 p3879 A69-40847

Cat intraretinal DC component and b-wave separation based on sensitivity to visual stimuli, discussing electroretinogram recorded with microelectrodes

22 p3883 A69-40881

High intensity flash effects on local electroretinogram, late receptor and slow potentials and ganglion cell activity in area centralis of cat retina

22 p3883 A69-40882

Arterial occlusion effects on retinal structure in cats, describing degrees of cell degeneration

22 p3884 A69-40883

Anesthetized cats with electrodes in visual cerebral cortex, investigating simulation of conditioned alimentary reflexes in response to light signals by electric signals

22 p3885 A69-41066

Functional relation between primary response individual phases and neurons activity in cats cerebral cortex

22 p3886 A69-41067

Electric responses of anterior and posterior gyrus cinguli to stimuli of sciatic nerve in cats

22 p3886 A69-41175

Cortical biopotentials in cats induced by strychnine under acoustic click stimuli of increasing intensity

22 p3888 A69-41270

Feline lung injury produced by vertical sinusoidal vibrations during upright water immersion attributed to chest wall impact

23 p4082 A69-41447

Positive phase shift relation to elastic modulus enhancement of smooth muscles of rabbit, cat and dog bladder, pulmonary artery and large veins

23 p4083 A69-41459

Reflex activity of single preganglionic sympathetic fibers during coronary occlusion in cats, discussing left third thoracic /T3/ ramus communicans

23 p4084 A69-41460

Cat papillary muscle length-tension curves before and after inotropic intervention, noting optimal length changes

23 p4084 A69-41461

D-amphetamine effect on single tectal neurons activity of cat opticum recorded by steel microelectrodes before and after intravenous injection

23 p4084 A69-41466

Temperature dependence of afferent and efferent spontaneous activity of spinal cord, using filament recordings from ventral and dorsal roots in anesthetized cats

23 p4093 A69-42066

Spinal cord temperature effect on stretch responses of muscle spindle endings of triceps surae, anterior tibialis and extensor digitorum longus in anesthetized cats

23 p4093 A69-42067

Efferent innervation influence of one ear to another in feline auditory system, based on afferent neurons responses to contralateral and binaural stimulation

23 p4094 A69-42073

Cat hearts ventricular pressure curves dv/dt and dp/dt correlated with left heart ventricle mechanical performance

23 p4095 A69-42076

Primary muscle spindle afferents from gastrocnemius muscle of cat before, during and after cold shivering, utilizing ramp stretches of same muscle

23 p4096 A69-42091

Spinal cord temperature influence on stretch response of tonic and phasic alpha-motoneurons by filament recordings from ventral roots in anesthetized cats

23 p4098 A69-42099

Isometric contraction tension after sudden isotonic to isometric contraction mode change in cat papillary muscle, discussing temperature effects, tension development changes, etc

24 p4258 A69-42631

CAUCHY PROBLEM

Difference methods in solution of incorrect Cauchy problem simulating ideal gas flow in nozzle

01 p0006 A69-10379

Cauchy problem correctness for one dimensional hyperbolic equation of arbitrary order with data on degeneracy line

01 p0104 A69-10699

Nonlinear interaction between longitudinal Langmuir waves and parallel wave vectors in heated plasma fluid, based on Cauchy problem of kinetic equation for electron distribution

02 p0285 A69-11461

Cauchy-Poisson problem for viscous liquid, calculating free liquid surface response to point impulse or initial displacement

03 p0414 A69-13015

Cauchy problem and mixed boundary value problem for parabolic system solved with thermal potential theory

03 p0455 A69-13259

Finite difference methods to solve Cauchy problem for three dimensional Laplace equation

03 p0424 A69-13661

Operator methods in engineering sciences, discussing integral transformations, Riesz method application to Cauchy problem, etc

03 p0457 A69-13744

Riemann boundary value problems for n pairs of functions, noting relation to validity of Noether theory

04 p0622 A69-14513

Computer solution of Cauchy problem of ordinary differential equations in form of Taylor series

04 p0622 A69-14624

Cauchy equation derived, giving rise to definite differential equation for materially uniform elastic bodies with inhomogeneities

05 p0834 A69-15730

Existence and uniqueness of solution to Cauchy problem for class of second order nonlinear differential equations, applying results to mixed boundary value problem

05 p0786 A69-16061

Approximate methods for integration of equations of plane isentropic motion of gas at supersonic velocities

05 p0699 A69-16674

Riemann problem in regions, showing integral operators become bounded if closed rectifiable Jordan curve without cusps becomes curve of bounded rotation

06 p0947 A69-16893

Three dimensional steady/unsteady flows of conducting inviscid gas in magnetic field, in absence of electric field, solving related Cauchy problem

06 p0966 A69-17541

Cauchy problem for nonstationary linearized Navier-Stokes equations for fixed container partially filled with liquid

06 p0959 A69-17888

Incorrect problem solving method applied to Cauchy problem solution for nonlinear partial differential equations, considering Ritz method applicability

07 p1174 A69-19005

Stability and perturbation theory of abstract Cauchy problem with difference scheme, showing application to parabolic differential equations

08 p1343 A69-20537

Cauchy problem of invariant imbedding satisfying nonlinear boundary value problem, discussing optimal control and radiative transfer applications

09 p1531 A69-21413

Singular perturbations for Cauchy and boundary value problems, considering differential operators and Hilbert space

10 p1720 A69-23635

Existence and uniqueness of solution to Cauchy problem for class of second order nonlinear differential equations, applying results to mixed boundary value problem

10 p1721 A69-23885

Existence theorems for hyperbolic genuinely nonlinear systems of conservation laws, studying Cauchy problem

11 p1909 A69-25163

Cauchy problem solution for linear/nonlinear differential equations with analytic right hand sought in form of power series

12 p2120 A69-26199

Difference methods in solution of incorrect Cauchy problem simulating ideal gas flow in nozzle

12 p2012 A69-26671

Pseudodifferential operators theory application to uniqueness of solutions of Cauchy problem

12 p2124 A69-26930

Cauchy problem for initial functionals, determining spherical limiting harmonic function for solution stabilization

13 p2375 A69-27795

Nonnegative solutions of second order linear divergence structure parabolic differential equations, discussing Cauchy problem solution, Green function, etc

13 p2290 A69-28539

Asymptotic behavior of function in Cauchy problem solution for heat conduction, basing method on Laplace transform inversion formula

13 p2380 A69-28685

Dynamic programming method applied to Cauchy problem of large deflections in compressed rods, using recurrent functional equations

14 p2533 A69-28988

Two point boundary value problem converted into Cauchy problem, deriving power series solution method and algorithms for nonlinear problems

14 p2430 A69-29362

Cauchy problem for Bellman dynamic programming equation in automatic control time minimization

14 p2426 A69-29478

Riemann problem with arbitrary jump data for extended hyperbolic systems of equations, showing conditions for unique solution

14 p2433 A69-29678

Functional analysis methods to solve Cauchy problem for linear nonhomogeneous differential equations with delayed argument

15 p2643 A69-30101

Averaging procedure for solving Cauchy problem applied to two point boundary value problem for nonlinear differential equations

15 p2644 A69-30449

Modified Chaplygin method for approximate integration of Cauchy problem for differential equations, estimating rate of convergence

15 p2644 A69-30656

Pseudo Runge-Kutta methods stability in numerically integrating two point Cauchy problems

15 p2646 A69-31261

Plane Cauchy problem solution for differential equations in heat and mass transfer theory, applying contour integral method in matrix construction

15 p2719 A69-31262

Forced harmonic oscillations of one dimensional mechanical girder systems allowing for nonlinear resisting forces calculated by boundary value problem reduction to Cauchy problem

17 p3064 A69-33917

Cauchy problem for homogeneous linear difference scheme with constant complex coefficients, giving stability lemmas

18 p3165 A69-35049

Multiple characteristics and Levi-Lax conditions for hyperbolicity to prove correctness of Cauchy problem

18 p3165 A69-35277

Asymptotic behavior of solution to parabolic equation for t approaching infinity, proposing asymptotic formula to Cauchy problem for heat conduction

18 p3231 A69-35310

Generalized Cauchy problem solution stabilization for ultraparabolic equation by integral representation of solution in positive initial functionals

18 p3165 A69-35312

Gas dynamics equations solution applied to Cauchy problem

19 p3297 A69-35861

Global properties of solution of inverse detached shock problem analyzed by characteristic coordinates at low Mach number

19 p3301 A69-36788

Homogeneous deformations of space and Cauchy problem for homogeneous free molecular motions, considering velocity fields and accelerations

19 p3444 A69-36803

Heat conduction in medium with phase transitions, solving one dimensional nonlinear problem by calculation of isotherms and reduction to Cauchy problem

19 p3453 A69-36838

Nonlinear partial differential equations numerical solution applied to solving Cauchy problem encountered in Goursat problem

20 p3569 A69-38293

Cauchy problem solution for first order nonlinear Volterra integrodifferential equation, using Runge-Kutta method

20 p3569 A69-38294

Nonlinear relativistic wave velocity distribution within spherical nucleus bounded by shock wave in superdense gas determined by Cauchy problem

22 p3861 A69-41114

Cauchy problem for partial differential equations linear parabolic system with coefficients depending on unknown functions

23 p4181 A69-41410

Absolute invariance conditions for closed isolated subsystem of nonlinear differential equations of Cauchy normal form

23 p4183 A69-42372

CAVES

Collapse theory of dimple craters, analogies with terrestrial sink holes and dimple craters as channels for gas escape from interior

05 p0818 A69-15589

CAVITATION CORROSION

Temperature and pressure effect on cobalt base alloy cavitation in liquid sodium, using vibratory apparatus and loss rate contour diagram

18 p3157 A69-35184

Hydraulic systems incipient failure detection, discussing destructive cavitation, component defects, human error, etc

19 p3255 A69-36018

CAVITATION FLOW

Inviscid cavity and wake flows behind submerged bodies, analyzing mathematical and theoretical models

04 p0587 A69-14608

Cavitation stream calculation methods for ideal incompressible fluid with free boundaries, noting cavitation generators and Riabouchinsky problems

04 p0589 A69-14994

Jet pump head rise deterioration parameter for prediction of cavitation

05 p0745 A69-15791

Laminar natural convection in enclosed rectangular cavity, discussing temperature gradient effects

06 p1033 A69-17556

Approximation method applied to closed viscous streamline flow in rectangular cavity, discussing constant shear stress boundary condition

08 p1304 A69-20811

Digital computer method for Navier-Stokes equation in prototype cavity flow problems, noting applications to biharmonic problems

08 p1305 A69-20831

Global characteristics and similarity of ventilated cavity flows by injecting air behind immersed profiles of symmetrical wedge at zero incidence

10 p1680 A69-23788

Stress waves analysis of brittle fractures, considering loading time role and cavitation of viscous fluids relation to fracture incipience

13 p2275 A69-27229

Radial liquid flow between flat annular rings /face seals/, discussing film cavitation

13 p2267 A69-27365

Heat transfer coefficients for supersonic open cavity flow recompression steps noting influence of step and flow shapes

13 p2375 A69-27786

Ablation injectants effect on supersonic stream pressure distribution inside cavity and upstream boundary layer velocity profiles

16 p2770 A69-31902

Convective heat transfer in centrifugal force field of cavity between two rotating disks in turbulent gas flow

16 p2837 A69-32139

Dielectric breakdown thresholds and cavitation in organic liquids observed during Q switched and pulsed ruby radiation

17 p2979 A69-32826

Noncavitating and cavitating performance of low area ratio water jet pumps, analyzing efficiency, area ratio, throat length, nozzle spacing and diffuser geometry

18 p3095 A69-35176

Water jets with greater than half sound speed created by shock wave impinging on cavity within liquid, discussing mechanism, maximum speed, shape, etc

19 p3301 A69-36815

Flow characteristics and wall heat transfer in separated flow region of annular cavity at free stream hypersonic speed and high gas temperature

[AIAA PAPER 68-672] 20 p3458 A69-37185

Desinent cavitation on hemispherical nosed bodies in water at various temperatures and velocities, considering isothermal case for surface nuclei

[ASME PAPER 69-FE-1] 20 p3516 A69-37986

Continuous cavitation model for incompressible fluid one dimensional unsteady motion

21 p3693 A69-38752

Cavitation flow of water and ethyl alcohol in venturi tube, noting effect of varying vapor concentration and thermodynamic properties

21 p3696 A69-39101

CAVITIES

NT PINHOLES

Rapid uniform expansion of spherical cavity in compressible elastic-plastic solid, obtaining similarity solution

03 p0528 A69-13798

Axisymmetric stress field around spheroidal inclusions and cavities in transversely isotropic material

[ASME PAPER 68-WA/APM-14] 04 p0669 A69-14400

Unsteady two dimensional flow in square cavity with fluid initially at rest and constant velocity upper surface of cavity, noting vortex center

[AICHE PAPER 25C] 04 p0587 A69-14510

Heat transfer and drag of cylinders with cavities at hypersonic speeds measured by platinum film thermometer and strain gauge balance in gun tunnel

[DVL-850] 04 p0543 A69-14822

Cavities elongation in automatic inert gas shielded welds in titanium alloys

05 p0767 A69-15972

Convection in conducting fluid filled cavities with variable wall temperature due to magnetic field, with results applicable to rheological systems

07 p1241 A69-18921

Thermal gradients in artificial satellites, considering heat exchange among various points of closed cavity surface by gray body diffuse radiation and reflection

08 p1421 A69-20157

Hollow turbine disks for provision of coolant to high performance aircraft gas turbine engines, fabricating disk in two axial halves

09 p1509 A69-22345

Plasma cavity shape formed by magnetic field effect due to several parallel line currents

[ISAS-433] 09 p1553 A69-22569

Self similar solutions for collapse of empty cylindrical cavity in gas with given equation of state, describing gas motion past cavity

10 p1679 A69-23367

Stress concentration at holes and cavities in thin elastic shells under static and dynamic loads, considering physical nonlinearities of material

11 p1974 A69-24665

Numerical method for coupled moments of inertia and integral equations of boundary value problems for fluid in moving cavities

11 p1868 A69-24774

Helical motions of body bounded by multiply connected surface immersed in infinite ideal incompressible fluid, discussing congruence

11 p1868 A69-24790

Cavity formation on water and wet cement surfaces by impingement of axisymmetric air jet noting cavity shape, depth and diameter

11 p1869 A69-24888

Optimum controller design for dynamic stability of ideal incompressible fluid in cavity of body constrained to horizontal rectilinear translational motions

11 p1966 A69-25330

Two and three dimensional quasi-static problems in coupled thermoelasticity, obtaining solutions for space containing cylindrical cavity and for solid cylinder

12 p2177 A69-25993

Shadow zone diffraction of plane step function compressional wave by circular cavity, using Friedlander wave front approximations

13 p2368 A69-28347

Membrane analogy for flexure of prismatical beams with square cross section and longitudinal cavities, employing Saint-Venant solution

15 p2704 A69-30288

Parametric interaction of electromagnetic field with spherical cavity having time variable radius, considering wave diffraction and TM oscillations

16 p2751 A69-32029

Creep experiments on Mg alloys, discussing dispersed phases influence on creep cavitation and grain boundaries mobility

17 p2985 A69-32907

Surface cavity profiles created by pulsed laser on Ti, Al, Cu, Pb and Zn, compared with isotherms computed from heat conduction models

20 p3552 A69-36917

Shrinkage cavity volume formulas for alloy castings with wide liquidus to solidus range, considering effects of diffused porosity and clustering for Mg alloy

20 p3548 A69-37329

Monograph on motion of solid body with cavities containing viscous liquid, covering kinetics involving completely or partly filled fluids

20 p3578 A69-38200

Differential equations for variable mass solid body motion about fixed point having cavities filled with ideal fluid

21 p3771 A69-39106

Natural convection in rectangular cavity with nonuniform lateral surfaces temperature, using finite difference scheme with numerical analysis

21 p3855 A69-39853

Anisotropic porous media model for fluid motion in rectangular fuel cell cavities, analyzing pressure, velocity, stream functions and purge time

23 p4075 A69-42300

Compressible gas flow into cavity of various volumes in presence of supercritical pressure gradients

24 p4298 A69-42587

CAVITY RESONATORS

Maximum power efficiency of pulsed injection laser with Fabry-Perot cavity expressed in terms of two dimensionless geometric variables

01 p0089 A69-10119

Optimum coupling for intracavity second harmonic generation in multilevel lasers

01 p0089 A69-10181

Microwave selective filter using resonant cavity with single coupling component in feedback circuit of amplifier traveling wave tube or klystron

01 p0042 A69-10384

Intracavity laser diffraction gratings for single wavelength output

01 p0092 A69-10897

Cavity excitation and support of limited space-charge accumulation mode oscillations in n-GaAs epitaxial diode

02 p0297 A69-11940

End to end cavity oscillators, folded line type cavity oscillators and reentrant cavity oscillators for use with disk seal tubes, pencil tubes and metal-ceramic tubes

02 p0216 A69-12029

Submillimeter wave oscillator/orotron/ involving open resonator with mirror having reflection grating period less than wavelength

02 p0250 A69-12248

Weak signal interaction between electron beam and microwave resonators, obtaining electron conductance, gain and transfer admittance

02 p0208 A69-12265

Cavity stabilization of microwave oscillator for noise reduction

02 p0220 A69-12451

Pumping beam width influence on optical range resonator excited coupled oscillations, deriving approximate equations

03 p0437 A69-13043

Parametric light generation in resonator with nonlinear medium, discussing continuous pumping with laser modes matched with pumping frequency

03 p0437 A69-13044

Parametric light generation employing KDP nonlinear crystals with mechanically tuned frequency

03 p0437 A69-13045

Nonlinear influence of resonator losses on stimulated emission of ruby laser, noting cut-off action

03 p0439 A69-13058

Geomagnetic field topology of nighttime magnetosphere, showing pi 2 pulsations excitation mechanism in terms of Alfvén waves resonance in external cavity

03 p0423 A69-13524

Single transverse electromagnetic mode power output for laser radar transmitter, using near hemispherical mirror resonator

04 p0609 A69-14287

Traveling waves interaction effects on emission modes of gas laser with circular resonator

04 p0611 A69-14545

258 GHz reflection amplifier with saturated gas resonance, analyzing amplification variation with gas pressure, pumping power, frequency, Q values and cavity tuning

04 p0557 A69-14754

Helium-neon gas laser cavity beam for automatic high speed particle sizing

04 p0611 A69-15023

Attenuation calibration of optical resonator using transparent plate coated by thin metal layer

04 p0613 A69-15415

Frequency vs power absorption characteristics of deactivated klystrons, noting resonance frequencies and perturbation effect of electron beam loading

05 p0729 A69-15978

Input admittance of confocal Fabry-Perot resonator, with waveguide coupled infinitely long conic-section cylindrical reflectors, taking into account diffraction and resistive losses

05 p0731 A69-16295

Two cavity large storage box atomic hydrogen maser, obtaining self excited oscillations coupled with high gain amplifier [IEEE PAPER C-8]

05 p0774 A69-16310

Composite equivalent circuits method for complex waveguide-resonator couplings based on variational principle for admittance matrices of electromagnetic volume couplings

05 p0736 A69-16785

Resonant frequencies and fields in circular cylindrical microwave cavity containing cold uniform magnetoplasma dielectric

06 p0968 A69-17763

Coupled cavity short slit delay lines in high power traveling wave tubes

07 p1095 A69-18428

Design of coupled cavity extended interaction output resonators for klystron amplifiers

07 p1095 A69-18431

Double gap catchers for klystron amplifiers and oscillators

07 p1095 A69-18432

Traveling wave microwave and optical resonators synthesis, determining design conditions for resonant frequencies

07 p1145 A69-18477

Sideband amplification via saturated gas resonance in 258 GHz reflection amplifier with hydrogen cyanide gas filled cylindrical cavity

07 p1145 A69-18479

X band internal cavity voltage tunable magnetron operating in theta mode, solving output loading, interaction limitations and cavity dimensions

07 p1102 A69-18670

Doped crystal and gas lasers, discussing resonant cavities, axial modes, relaxation oscillation, mode locking and Lamb theory

08 p1323 A69-19869

High Q capacitance loaded coaxial cavity resonator for study of electric susceptibility of ionized gas

08 p1313 A69-20214

Frequency shift and Q change of microwave cavity caused by lossy dielectrics and plasmas, examining perturbing volume requirements for conductor behavior

09 p1544 A69-21323

Fabry-Perot resonator and beam waveguide systems for laser beams, noting mode coupling and separation in laser optical systems

09 p1518 A69-22125

Cavity system for constructing paramagnetic masers with different active materials

09 p1519 A69-22288

Quasi-static modified field distributions in inhomogeneously filled cavities and waveguide tubes, comparing with homogeneously filled cavities and obtaining matrix eigenvalues

09 p1467 A69-22561

Laser resonator loss factor and axial mode frequencies calculation by interferometry

09 p1520 A69-22679

Two mirror resonators, discussing curvatures formation and stability conditions to derive natural frequencies

09 p1520 A69-22680

Gas laser output increase by nonconstricted discharge in aluminum tube cathode with mirror resonator

09 p1520 A69-22681

Linear ion accelerators noting particle motion, RF cavity design, RF power sources, injection and applications

09 p1553 A69-22697

High density plasma in resonant cavity obtained by frequency shifting power source

10 p1727 A69-22955

Resonator interferometry of pulsed submillimeter wave lasers, analyzing mode structure, pulse shapes and molecular mechanism of laser emission

10 p1705 A69-23810

Resonator field inhomogeneities effect on transient processes in quantum oscillator, considering two active crystals in cavity

10 p1705 A69-23948

Perturbation theory applied to emitting density matrix in nonlinear polarization of resonance media, considering gas laser in coaxial magnetic field

11 p1895 A69-24630

Ideal mode conversion and transmission by circular aperture of cylindrically symmetric cavity

11 p1899 A69-25056

Electromagnetic fields in cylindrically symmetrical microwave resonator filled with premagnetized ferrite along cylinder axis

11 p1855 A69-25625

Gallium arsenide junction laser resonant modes from theoretical model, calculating frequency separation

12 p2108 A69-26637

Inhomogeneous permittivity and boundary effects influence on electric fields of laser with open cavity containing inhomogeneous active medium

12 p2110 A69-26908

Frequency memory in cavity controlled Gunn oscillators, discussing loop gain and bandwidth dependence on oscillation mode and bias voltage

13 p2229 A69-27677

Microwave cavity bandwidth determined from reflection coefficient measurements, considering reflection magnitude and phase

13 p2223 A69-28606

Noncollinear single cavity optical parametric oscillation with specified energy conversion using ruby laser-pumped lithium niobate, discussing tuning

14 p2460 A69-29605

Waveguide below cut-off resonators for active microwave circuits, describing experiments with avalanche and Gunn diodes

15 p2577 A69-30613

Characteristics of neodymium-glass laser with unstable resonator noting transverse modes and radiation angular distribution

15 p2634 A69-30730

Laser cavity optimization for producing minimum short light pulse width in fast Q switching of optical maser

16 p2796 A69-31802

Electromagnetic fields in closed one dimensional resonators with oscillating boundary, analyzing amplitude buildup

16 p2751 A69-32030

Electromagnetic cavity resonances in rotationally induced gravitational field by relativistic approach

16 p2812 A69-32048

Nonlinear response of single Helmholtz resonator subjected to finite amplitude pressure oscillations, detailing entrance, orifice and cavitation flow [AIAA PAPER 69-481]

16 p2844 A69-32719

Multiple mode phase locking of He-Ne laser with fixed cavity length and laser tube fixed position in cavity, generating high speed optical pulses

17 p2980 A69-32957

Geomagnetic field effects on microwave noise spectrum in earth-ionosphere resonator, calculating field energy spectrum near resonance maximum, discussing excitation by lightning

17 p2918 A69-33034

Broadband intracavity SHF modulation of He-Ne laser emission in 10 cm band, showing agreement with calculations

17 p2981 A69-33112

Modified liquid fueled pulsating combustion chamber operating as Helmholtz cavity resonator, measuring chamber pressure as function of time

17 p3074 A69-33410

Automatic tuning of superconducting cavity resonant frequency using optical feedback, discussing phase error processing and frequency deviation

17 p2937 A69-33781

Superconducting cavities for resolving optically induced changes in dielectric constant of CdS at 4.2 K

17 p3016 A69-33782

Wave excitation in resonant dissipative and inhomogeneous structures, discussing resonator geometry, mode spectra, etc

17 p2926 A69-33849

Simultaneous integral equations numerical solution for open optical resonator mode analysis, using kernel function and Fresnel approximation

17 p2983 A69-33883

Diffraction of modal field by semimfinite waveguide, integral representation for Wiener Hopf kernel factorization and applications to open resonators

17 p2930 A69-33888

Transformed kinetic equation used to study relaxation of quantum oscillator to thermodynamic equilibrium state

18 p3152 A69-35126

Radiation emission by molecules in electromagnetic field, considering cavity resonators and waveguides excitation

18 p3178 A69-35404

Tunnel diode coupling with spheroidal resonant cavity, describing method of measuring elements for interpretation

19 p3283 A69-35998

Stable mode generation in ruby laser with ability for modulation, using convex resonator and uniform illumination

20 p3553 A69-37607

Simultaneous mode locking of Nd YAG laser and intracavity second harmonic generation in high temperature Li niobate or BaNa niobate

20 p3555 A69-37731

Holographic image range contouring produced by multifrequency emission from resonant output reflector in pulsed ruby laser cavity

20 p3540 A69-37733

Amplification saturation in spatially inhomogeneous laser field, relating power to active medium and resonator parameters

21 p3740 A69-39549

Annular gas laser cavity designs with additional mirrors for longitudinal oscillation mode selection, noting positive results for He-Ne laser

21 p3740 A69-39553

Eigenmodes of asymmetric cylindrical confocal laser resonator with single output coupling aperture, obtaining diffraction loss factors and mirror field distributions

21 p3741 A69-39564

Accuracy and frequency stability of H masers in terms of wall collision effect and cavity resonator tuning

21 p3741 A69-39685

Axial mode frequencies, loss coefficients and optimal parameters of three and four mirror resonators of gas lasers, including designs with maximum selectivity

22 p3964 A69-40796

Mirror mount for shock tube laser cavity with alignment capability, noting seal against internal pressures

22 p3951 A69-41233

Longitudinal modes locking and ultrashort light pulse generation in laser cavity resonator with nonlinear refractive index

23 p4171 A69-41389

Discrete delay line measuring FM noise, discussing special case of narrow band cavity resonator method

23 p4137 A69-41606

Time dependent natural oscillations of plane open resonators infinite periodic sequence, considering electromagnetic energy transfer into ambient medium

23 p4139 A69-42039

Laser quantum theory compared to stationary atoms semiclassical theory, emphasizing role of cavity mode spatial structure

24 p4327 A69-42789

Laser cavity modes phase equality demonstrated by oscilloscope trace in two photon fluorescent method

24 p4327 A69-42981

Polarization characteristics of He-Ne ring laser emission with circularly anisotropic resonator, analyzing ellipticity as function of half wave cavity plate

24 p4328 A69-43160

GaAs laser diodes differential external quantum efficiency and gain per unit length dependence on laser resonator length, taking into account optical losses

24 p4330 A69-43767

GaAs junction laser total stimulated light power dependence on resonator length taking into account optical losses

24 p4330 A69-43768

CEILOMETERS

U CLOUD HEIGHT INDICATORS

CELESTIAL BODIES

NT A STARS
NT ANDROMEDA GALAXIES
NT AREND-ROLAND COMET
NT ASTEROIDS
NT B STARS
NT BINARY STARS
NT BOLIDES
NT CASSIOPEIA A
NT CEPHEID VARIABLES
NT COMETS
NT CRAB NEBULA
NT DEIMOS
NT DWARF STARS
NT EARLY STARS
NT EARTH [PLANET]
NT ECLIPSING BINARY STARS
NT GALAXIES
NT GIANT STARS
NT HERCULES NOVA
NT HOT STARS
NT IAPETUS
NT ICARUS ASTEROID
NT JUPITER [PLANET]
NT LEONID METEORIODS
NT MAGNETIC STARS
NT MAIN SEQUENCE STARS
NT MARS [PLANET]
NT MERCURY [PLANET]
NT METEORITES
NT METEOROID SHOWERS
NT METEORIODS
NT MICROMETEORIODS
NT MILKY WAY GALAXY
NT MOON
NT MOREHOUSE COMET
NT MRKOS COMET
NT NATURAL SATELLITES
NT NEBULAE
NT NEPTUNE [PLANET]
NT NEUTRON STARS
NT NOVAE
NT O STARS
NT ORIONID METEORIODS
NT PERSEID METEORIODS
NT PHOBOS
NT PLANETARY NEBULAE
NT PLANETS

NT PLUTO [PLANET]
NT PROTOSTARS
NT PULSARS
NT QUASARS
NT RADIO GALAXIES
NT RADIO METEORS
NT RADIO SOURCES [ASTRONOMY]
NT RADIO STARS
NT SATURN [PLANET]
NT SCHWASSMANN-WACHMANN COMET
NT SOLAR SYSTEM
NT SPIRAL GALAXIES
NT SPORADIC METEORIODS
NT STAR CLUSTERS
NT STARS
NT SUN
NT SUPERGIANT STARS
NT SUPERNOVAE
NT T TAURI STARS
NT URANUS [PLANET]
NT VARIABLE STARS
NT VENUS [PLANET]
NT VIRGO STAR CLUSTER
NT WHITE DWARF STARS
NT ZETA AURIGAE STAR
NT ZODIACAL DUST

Self gravitating pulsating cylindrical and ring shaped cosmic masses from group theory standpoint compared with oscillating stars

01 p0148 A69-10124

Faraday angle of rotation of radio signals polarization plane from satellites and celestial bodies

01 p0030 A69-10574

Differential rotation of celestial body maintained in resonance state by locking photosphere oscillation onto rotational period

01 p0156 A69-11136

Astronomical alignment accuracy by rocket Cassiopeia system, discussing scientific payload rotation and orientation by celestial bodies

03 p0462 A69-12850

Pulsar characteristics absence in X ray sources, noting data for Scorpius XR-1

07 p1218 A69-19254

Bright celestial IR sources in Ursa Major detected in spectral region by rocket-borne telescope, discussing luminosities of quasi-stellar sources

09 p1603 A69-22230

Isophot system characterizing photometric structure of elongated celestial objects constructed by equidensitometric method based on Sabatier photographic phenomenon

11 p1952 A69-24255

Optical sensing devices for angle measurement between celestial body and satellite axes

12 p2078 A69-25871

Correlation coefficients, comparing galactic X ray sources distribution with classical cepheids, old novae, planetary nebulae and Wolf-Rayet stars

12 p2171 A69-27155

Resonant long-period orbits around Lagrange equilateral points for critical mass ratio of main bodies

13 p2346 A69-27706

Q switched ruby laser designed for lidar probing of cosmic bodies and earth atmosphere

14 p2460 A69-29660

Measured atmospheric refraction of bright astronomical objects less than calculated data for large zenith distances

15 p2679 A69-30161

Faraday angle of rotation of radio signals polarization plane from satellites and celestial bodies

15 p2568 A69-30744

Dim astronomical sources observability from sunlit spacecraft, considering coma of micron sized ice crystals influence on scattering by condensation model

16 p2861 A69-32301

Solar radiation pressure windmill effect in rotational bursting and elimination from solar system of small magnetic celestial bodies

21 p3814 A69-39584

IC 3258 emission line spectrum observations, discussing blueshift, extragalactic location, possible nature, etc

23 p4219 A69-42374

CELESTIAL MECHANICS

N-body problem in celestial mechanics, using differential equations, reduced to quadratures [UN PAPER 68-95268]

01 p0150 A69-10476

Perturbations on major axes of slow moving comets in nearly parabolic original orbits by fast moving stars, discussing statistics of stellar encounters

01 p0153 A69-10871

N body systems with/without external field, noting galactic field effect on system flattening

02 p0322 A69-12270

Collective stability of collisionless gravitating systems based on variational principles resembling energy principle

02 p0323 A69-12275

Coordinates interpretation in Schwarzschild problem, projecting space of events by light beams onto Galilean system at infinity

03 p0506 A69-13090

French atlas of planets covering ancient and modern planetary system and discoveries, physical nature and movement, etc

03 p0513 A69-13778

Capture of comets by large planets

03 p0517 A69-14128

Current state and research trends in celestial mechanics, discussing satellite orbit, planetary flight and other astrodynamical problems

03 p0517 A69-14223

Hill stability in unbounded three body problem, analyzing motion in baricentric coordinate system, deriving equations for curves defining conditions for stability

04 p0652 A69-14543

Stellar escapes from clusters and temporary captures in restricted three body problem with equal masses

05 p0827 A69-16595

Regularization of perturbed Keplerian motion in three dimensional space by means of Levi-Civita transformation generalized to three dimensions

05 p0827 A69-16602

Approximate solution of celestial mechanics differential equations by reducing to quadratures for n body problems

06 p1006 A69-17566

Soviet book on theoretical astronomy covering evolution from Ptolemy to Einstein, universal gravitation and principles of celestial mechanics

07 p1211 A69-18544

Stellar orbits in galactic plane represented as generalized Keplerian motion

08 p1381 A69-19792

Partially translatable one parameter continuous transformation group for complete system of integrals in celestial mechanics, discussing Wintner nonisolating integral and Poincare theorem

08 p1382 A69-19872

Space motions of bright F type stars from parallaxes obtained by photometry

08 p1386 A69-20074

Final motions of Hamiltonian conservative systems, analyzing Liouville type, homogeneous and similar systems

09 p1540 A69-21882

Particular solutions relative to system of invariant relationships in involution

09 p1596 A69-22049

General solution of Liouville equation for collisionless system of gravitationally interacting particles, with distribution function locally isotropic in momentum space

09 p1605 A69-22412

Intermediate orbits to construct motion theory of natural satellites of all planets

11 p1952 A69-24253

Stability of steady state motions of nonholonomic mechanical systems, noting Chetaev method for construction of Liapunov functions

11 p1920 A69-25742

Quasi-stochastic nonlinear one dimensional oscillations in periodically disturbed field applied to celestial mechanics of planetoids

12 p2130 A69-26373

Spiral galaxies rotation curve fluctuations attributed to kinematic properties of galactic matter and gas components

12 p2170 A69-27062

Hydromagnetic stability of spiral arm embedded in gravitating medium from analysis of instability of self gravitating incompressible cylinder

13 p2346 A69-27705

Restricted three body problem of conservative Hamiltonian systems with two degrees of freedom and mass ratio parameter, considering phase space around L sub 4

13 p2346 A69-27711

Messier 51 ionized hydrogen observations, discussing H II regions, radial velocities and galactic mass, rotation and noncircular nuclear motions

13 p2347 A69-27720

Comet Arend-Roland type-1 tail characteristics including accelerating disturbance, outward-moving waves, tail inclination, etc

13 p2349 A69-27816

Solar system light elements investigated assuming Li, Be and B abundance as nuclear reaction products of high energy particles accelerated in early sun formation
13 p2354 A69-28495

Coordinates interpretation in Schwarzschild problem, projecting space of events by light beams onto Galilean system at infinity
14 p2516 A69-28772

Fundamental principles of thermodynamics incorporation into general relativity and geometrodynamics, interpreting entropy growth in terms of space dynamics
14 p2538 A69-29019

Close galactic encounters in dense galactic clusters, discussing effects on internal motions dispersion and stellar dissipation
14 p2521 A69-29461

Celestial mechanics, Part 1, covering almost periodic functions, relation to classical astronomy and modern mathematics, implicit function theorem, three body problem, etc
18 p3199 A69-34928

Tabulated coherent S-band Doppler data from Pioneer 6 and 7 radio tracking, improving astronomical constants and ephemerides for earth-moon system [AAS PAPER 68-130]
20 p3595 A69-37179

Planet Mars opposition to earth, Jupiter and Saturn, including table showing Mars-Jupiter conjunctions
21 p3801 A69-38788

Dimensionless coupling constants predicted from causal relationship among strong, electromagnetic, weak and gravitational interactions in fluid region of universe
22 p3981 A69-40416

Periodic orbits obtained for special restricted three body problem in resonance using numerical integration
22 p4031 A69-40909

Grobner method of Lie series applied to numerical integration of spacecraft trajectories and n-body problems
23 p4223 A69-42476

CELESTIAL NAVIGATION
NT ASTRONAVIGATION

Celestial navigation, discussing position fixing on rotating earth, time input, navigation aids and sextant angle
03 p0463 A69-13207

Sight reduction tables for orbital plane determination checked out by sextant sightings onboard Gemini 7
07 p1177 A69-19206

Most probable position /MPP/ choosing methods accuracy, investigating relative effects of dead reckoning /DR/ and celestial lines of position /LOP/ errors
07 p1177 A69-19214

Polar flight navigation charts showing feasibility of three dimensional celestial positioning
09 p1538 A69-21406

Celestial navigation system using photodetectors, comparing numbers and brightness of S4, S20 and silicon stars
10 p1775 A69-23190

Simultaneous observations of altitudes of stars and moon for determination of longitude without time by navigators
14 p2479 A69-29855

Automatic celestial navigation, discussing star trackers design, mathematics of celestial fix and relationship to errors and physical and environmental constraints
18 p3169 A69-34852

Spacecraft-based navigation instruments for outer planet missions using celestial directions to outer planet natural satellites [AIAA PAPER 69-902]
21 p3761 A69-39348

Satellite attitude estimation from onboard telescope celestial sightings using iterative least squares method, considering measurement error noise and axes wobble
24 p4348 A69-43244

CELESTIAL OBSERVATION
U ASTRONOMY

CELESTIAL SPHERE

Magnetotelluric method for investigating earth vertical structure with allowance for sphericity
02 p0240 A69-11699

Great circle route determination based on celestial spherical triangulation
02 p0278 A69-12360

Schwarzschild perfect fluid spheres stability to radial perturbations, noting fluid adiabatic index relation to critical value
07 p1221 A69-19585

Magnetotelluric method for investigating earth vertical structure with allowance for sphericity
13 p2258 A69-28730

Celestial sphere scanning by passive method applicable to space missions requiring long lifetime and moderate pointing accuracies [AIAA PAPER 68-854]
21 p3767 A69-39764

CELL ANODES

Sealed nickel-cadmium cell design optimization, evaluating effects of various electrochemical treatments on energy density of nickel oxide positive electrode
10 p1639 A69-23992

Nonaqueous lithium anode high energy density electrochemical primary generators, considering energy factors and electrolytic couples
16 p2740 A69-32427

Irreversibility resulting from composition changes in operating fuel cell anode and cathode chambers and cell geometry influence
18 p3093 A69-34781

CELL CATHODES

Absolute short term current efficiency of aluminum electrolytic cell, stressing aluminum amount determination in cathode
06 p0869 A69-17233

Hydrogen-oxygen fuel cells with conducting and nonconducting hydrophobic electrode matrices
08 p1261 A69-21055

Metal fluoride compounds as cathodes for use with mixed fluoride electrolyte /LiF-NaF-KF eutectic/ in thermal batteries
10 p1640 A69-23997

Pseudosplitting/peroxide mechanism for O reduction at fuel cell cathodes, analyzing O molecule adsorption, H bonding and electron transfer at surface
16 p2748 A69-32809

Irreversibility resulting from composition changes in operating fuel cell anode and cathode chambers and cell geometry influence
18 p3093 A69-34781

CELL DIVISION

NT MITOSIS

Photoinhibition of cell division and growth in Euglenoid flagellates by fluorescent and incandescent visible light
01 p0014 A69-10903

Weightlessness effects on fertilized frog egg development on board Gemini 8 and 12 manned orbital flights, discussing cell division, differentiation and embryogenesis
01 p0017 A69-11084

UV and visible light interaction effect on biological activity of *Paramecia* unicellular infusoria, noting cell division rates and cell deaths
01 p0017 A69-11085

Mathematical models for *Chlorella* cell and biomass growth under illumination during space flight, noting ionizing radiation presence
02 p0198 A69-11508

Axial units with basal plates in spermatozoa of *Chlidia groenlandica* negatively stained with phosphotungstic acid, showing doublet microtubules
07 p1066 A69-19263

Postirradiation growth of cultured Chinese hamster cells exposed to UV light, including comparison with X irradiation
19 p3257 A69-35975

Local stress effect on immunocompetent cells differentiation in guinea pigs lymphatic ganglia, showing antibody producing cells number increase
22 p3877 A69-40277

CELLS (BIOLOGY)

NT AXONS

NT CHROMOSOMES

NT COLLAGENS

NT EOSINOPHILS

NT ERYTHROCYTES

NT GAMETOCYTES

NT HEMOCYTES

NT HEMOGLOBIN

NT LEUKOCYTES

NT LYMPHOCYTES

NT MITOCHONDRIA

NT NEURONS

NT OXYHEMOGLOBIN

NT RETICULOCYTES

Cell and tissue cultivation outside living organisms, discussing applications in space biology, space medicine and food protein sources
02 p0198 A69-11501

Mammalian cell survival, chromosome abnormalities and recovery from heavy ion and X ray irradiation
03 p0373 A69-13492

Cellular localization of acetyl-coenzyme A synthetase in yeast, noting enzyme distribution during aerobic growth on glucose
04 p0554 A69-15333

Magnetic fields role in neuropsychiatric and physiological experiments, noting effect on phagocyte activity
05 p0715 A69-16627

Cellular effects on weightlessness noting relation to size and cell complexity
06 p0872 A69-17013

Cultured Chinese hamster cells responses to UV light of different wavelengths indicating photon absorbing molecules inhibition of colony development
07 p1068 A69-19492

Degree of organization in bacterial cell, discussing pool size and DNA synthesis
07 p1069 A69-19505

Structural and functional changes in cells as result of freezing of muscular tissue or suspension of erythrocytes
10 p1642 A69-23117

Gas vacuoles development in blue green algae by cell transfer from defined medium to distilled water
10 p1644 A69-23184

Direct epoxy embedding of monolayer cells cultured on millipore filter and fixed, dehydrated and microscoped before immersion
10 p1649 A69-23404

Acceleration effects on cellular and subcellular structures enzyme activity in humans and animals, noting changes resulting from changed permeability of membranes
10 p1645 A69-23496

Origin of life data, discussing self ordered polymers, propagative cell-like systems, protozooids, cellular evolution, etc
12 p2018 A69-25781

Life origin and organic-inorganic systems, emphasizing protein colloids-mineral salts interactions at protocell stage
14 p2408 A69-29632

Invertebrate endoskeletal cartilage and cartilage-like tissues occurrence and nature, discussing cellular tissues and origin
15 p2555 A69-30412

Continuous culture device for controlled growth of *Euglena gracilis*
15 p2555 A69-30445

Escherichia coli B/r cells plasmolyzed in sucrose observed under phase contrast, noting plasmolysis reduction in ions presence
19 p3257 A69-35973

Biological effects of radioactivity and X rays irradiation of whole body and cells, considering DNA degradation
19 p3257 A69-35978

Cultured mammalian cell growth morphology studied in situ with scanning electron microscope, discussing surface morphology changes during mitotic cycle of Chang liver cells
20 p3467 A69-37100

Biological experiments on cells with/without suppressors, discussing RNA, DNA, enzymatic and UAA codon activities
20 p3480 A69-38265

Long microextensions on cultivated human liver cells, using scanning electron microscope
20 p3480 A69-38287

Heart muscle ultrastructure during general hypoxia in dogs, noting development of compensatory-adaptational and dystrophic changes in myocardial intracellular components
21 p3651 A69-38412

Organism growth physiology based on decisive enzymic reactions, considering synthesis of biological proteins from DNA and molecular life processes
21 p3652 A69-38787

Canine cerebellar Purkinje cells electron microscopy after rapid decompression to near vacuum
21 p3660 A69-39177

Scenedesmus algae cell wall structure degrading to increase digestibility of cell bound protein, describing mechanical, enzymatic and chemical methods
21 p3667 A69-39701

Cell interactions and motions correlation for animal locomotion
21 p3662 A69-39708

Erythroblasts fractionating method based on size, density and resistance of immature erythroblasts which change during maturation
22 p3877 A69-40761

Cell origin in self organizing natural polymers in terms of molecular evolutionary priority of polynucleotides and poly alpha amino acids
22 p3896 A69-40781

Adenosine triphosphate /ATP/ production in normal cells and sporulation mutants of *Bacillus subtilis*,

discussing applications of ATP synthesis response to C sources

22 p3886 A69-41076

Retarded immunological recovery in sublethally X-irradiated mice by additional thymic exposure reversal with injected marrow cells

22 p3887 A69-41194

Critical oxygen pressure dependence on buffer in diluted heart muscle sarcosome suspensions and effect of hemoglobin or myoglobin

23 p4080 A69-41427

DNA interaction with ribosomes enhancing amino acid incorporation into cell-free protein synthesizing system extracted from *Chlorella pyrenoidosa*

23 p4080 A69-41430

Cell-like structures containing biochemicals as inevitable event under various hypothetical primitive earth conditions

23 p4085 A69-41479

Steady state and time dependent concentration gradients in and around cells due to oxygen diffusion and depletion in radiobiology

23 p4090 A69-41966

Viruslike particles in fat body cells and oenocytes of *Drosophila melanogaster* imagoes, in glial cells of cephalic ganglionic center of flies and in gamma radiated cells

23 p4091 A69-42021

Inoculum dose effect on complement-fixing antigen production, heat lability and separation from BHK-21 cells infected with lymphocytic choriomeningitis virus

24 p4263 A69-43336

CELLULOSE

Threshold criteria of gas phase thermal ignition for cellulose materials, considering heating by radiant energy

11 p1940 A69-24474

CELLULOSE NITRATE

Heat production rate equivalence to heat removal rate during ignition of ballistite powder by incandescent wires

02 p0354 A69-12668

Cellulose nitrate sheets applicability in detecting cosmic ray relativistic heavy nuclei, considering etchable tracks

06 p0924 A69-17286

Tensile tests on time dependent Pb and cellulose nitrate, including stress-strain curve prediction from creep test data

19 p3445 A69-36829

CELSIUS TEMPERATURE SCALE

U TEMPERATURE SCALES

CEMENTATION

Conditions for obtaining concentrated Ti-containing melts free of Al and V chlorides by cementing with metallic Ti and Ti-containing materials

22 p3957 A69-40918

CEMENTS

Phosphate cements for bonding mica ceramic to titanium in jet engine equipment

05 p0786 A69-16799

Polymers and organic optical cements transparent in 1 to 13 micron IR region, noting organosilicon resin

08 p1336 A69-20387

Cement materials to attach thermocouple to stainless steel tubing in nuclear rocket engine nozzle, considering thermal conductivity, bond and tensile and compressive strengths

21 p3753 A69-39699

Error correction of strain gage/cement combination reading relaxation under prolonged steady loading at elevated temperature

22 p4042 A69-40313

CEMS SYSTEM

U CENTRAL ELECTRONIC MANAGEMENT SYSTEM

CENSORED DATA [MATHEMATICS]

Multiply censored data plotting on various type hazard papers for engineering information on time to failure distribution

20 p3567 A69-38288

CENTAUR LAUNCH VEHICLE

NT ATLAS CENTAUR LAUNCH VEHICLE

Liquid hydrogen and LOX boost pump design for Centaur missile and liquid hydrogen and LOX chill-down pump design for Saturn 4B missile

01 p0087 A69-11149

Nose cone ejecting system with pyrotechnic devices for two stage Centaur rockets /Sud-Aviation/ with RF mass spectrometer

10 p1635 A69-23034

Centaur computer assimilating Centaur vehicle hardware functions performed by digital computer, discussing modules, flight control system, cost reduction, etc

[AIAA PAPER 69-943] 22 p3904 A69-40326

CENTAURUS CONSTELLATION

Optical identification of X ray source Cen XR-2 as variable star WX Cen, discussing colors and similarity to Sco X-1

01 p0145 A69-10857

Photometric investigation in UVB and H alpha of early B stars in Scorpio-Centaurus association, computing intrinsic colors and magnitudes corrected for interstellar absorption

06 p1001 A69-17195

Spectral line profiles of 3 Centauri A during microdisturbance, showing turbulent velocity and metal element abundances

07 p1211 A69-18407

Polarization and intensity distribution of extended supernova remnant in Centaurus, discussing remnant effect on galactic magnetic field

09 p1598 A69-22184

Centaurus constellation search for gamma rays using balloons, discussing radio and X ray luminosity

09 p1580 A69-22269

X rays from galactic center and Centaurus regions, discussing Cen X-2 flux

09 p1583 A69-22765

Sco-Cen B stars radial velocities, determining spectroscopic binaries

14 p2519 A69-29136

Spatial distribution of stellar densities and velocity distributions in phase space, using Greenwich catalog of positions and proper motions of omega Centauri cluster stars

16 p2859 A69-32220

Low energy X ray flux existence in Cen X-2 observed by rocket flight

22 p4007 A69-40773

CENTER OF GRAVITY

Spacecraft periodic motion near center of mass determined by point transformation combined with bifurcation theory, studying stability and parametric dependence

01 p0161 A69-10205

Radio emission center of gravity from 3C 273 quasar determined by radio telescope together with A and B component fluxes

03 p0506 A69-13092

Satellite nonlinear spatial oscillations about center of mass during circular orbit, using perturbation theory and analog computer

04 p0665 A69-14270

Hill stability in unbounded three body problem, analyzing motion in baricentric coordinate system, deriving equations for curves defining conditions for stability

04 p0652 A69-14543

Air density fluctuation effects on aircraft dynamic stability around center of gravity during climbing and diving maneuvers, discussing atmospheric pressure and flight path angle

04 p0548 A69-14825

Center of gravity of two dimensional gravitating bodies by gravitational anomaly technique, based on conformal mapping of bilinear function

05 p0792 A69-15696

Helicopter instability on ground with propulsion system operating and inoperative, discussing overturning, restoring moments and pilot training

09 p1433 A69-21385

Symmetrical body rotational motion with asymmetrical mass distribution about center of mass, determining minimum initial value of angular velocity

09 p1595 A69-21762

Integration time reduction for equations of motion of vehicle center of mass during parabolic reentry, using Runge principle

09 p1532 A69-21763

Onboard aircraft weighing system /OBAS/ for accurate gross weight and CG measurements, describing axle shear deflection transducer system

10 p1693 A69-23276

Gyrostabilized satellite steady state motions in Newtonian force field having displaced satellite center of mass orbital plane relative to center of attraction

12 p2173 A69-25885

Earth center of mass determination from simultaneous satellite observations by photography or laser radar

12 p2068 A69-26425

Satellite motion relative to center of mass and resonances by approximate solutions to motion equations, applying asymptotic methods

13 p2357 A69-28502

Spacecraft periodic motion near center of mass determined by point transformation combined with bifurcation theory, studying stability and parametric dependence

14 p2530 A69-28741

Radio emission center of gravity from 3C 273 quasar determined by radio telescope together with A and B component fluxes

14 p2516 A69-28774

Vibration damping and elastic bond positioning in nonlinear systems with coincident centers of gravity and rigid damping

14 p2537 A69-29746

Pendulum motion about stationary axis of solid body containing damper, ascribing instability to center of gravity shift with respect to cavity

18 p3135 A69-34557

STAN integral weight and balance system providing aircrews with takeoff gross weight and CG data [SAWE PAPER 755]

18 p3136 A69-34882

Computer program for weight and center of gravity tolerance data for assembly aerospace vehicle [SAWE PAPER 734]

18 p3221 A69-34892

Economics evaluation for operation of commercial fixed wing aircraft at aft center of gravity position, noting fuel saving from drag reduction

18 p3091 A69-34902

Cone-conical-frustum configurations meeting center of gravity requirements for higher hypersonic lift-drag ratios in axisymmetric manned spacecraft

21 p3644 A69-39237

Geomagnetic field and aerodynamic perturbation effects on satellite motion about center of mass, using asymptotic methods of nonlinear oscillation theory

21 p3830 A69-39835

Spacecraft spherical motion about mass center under inertial force using Euler differential equations

21 p3830 A69-39838

Controlled motion of space vehicle about center of mass analyzed by equation expressing nutation angle invariance

21 p3830 A69-39839

Satellite orientation by determining rotation parameters about centers of mass with respect to certain coordinates

22 p4037 A69-41089

Proton 2 satellite orientation and motion about center of mass determined from telemetric data analysis under aerodynamic moment

22 p4037 A69-41090

Ballistic equations for mass center movement in vertical plane defined by projectile initial velocity

23 p4183 A69-42482

CENTIGRADE TEMPERATURE SCALE

U TEMPERATURE SCALES

CENTRAL AMERICA

Telecommunications network for air traffic in Central America to attain higher degree of reliability

03 p0399 A69-14182

CENTRAL ELECTRONIC MANAGEMENT SYSTEM

Automatic system self test technique known as central integrated test subsystem /CITS/ for logically testing avionics systems

11 p1866 A69-25083

CENTRAL NERVOUS SYSTEM

NT BRAIN

NT BRAIN STEM

NT CEREBELLUM

NT CEREBRAL CORTEX

NT CEREBRUM

NT HIPPOCAMPUS

NT SPINAL CORD

NT SPINE

NT THALAMUS

Psychochemical research theory and methodology, relating biochemical phenomena to human brain function

04 p0553 A69-14976

Rats sensitivity to accelerations found dependent on excitation-inhibition ratio in central nervous system and hypophyseal-adrenal system reactions during acoustic excitation

10 p1645 A69-23497

Transverse accelerations effect on dogs gastrointestinal tract secretory activity, noting central nervous system role

10 p1645 A69-23498

Tremographic studies of central nervous system during supersonic flight as engineering psychology application to man machine relations in aircraft-spacecraft industries

19 p3259 A69-35834

Averaged cortical evoked response characteristics relationship to performance in traditional threshold

procedures, discussing stimulus sensitivity and intensity control in central nervous system
21 p3653 A69-38897

Cerebral subcortical structures controlling effect on central and peripheral nervous systems, discussing motion coordination, space orientation, search reflexes and physiological sleep
22 p3889 A69-41275

Neural integration of cardiorespiratory responses and suprabulbar control during arterial hypoxemia in rhinencephalic thalamic pontine rabbits
24 p4258 A69-42635

S-RETIC vertebrate command model, discussing computer simulation of reticular formation Golgi anatomy capable of habituation, conditioning, extinction, generalization and error discrimination
24 p4273 A69-42910

CENTRAL NERVOUS SYSTEM DEPRESSANTS

Barbamyl effect with and without somatotropic hormone injection in mice during prolonged isolation and hypokinesia, noting sleep duration
10 p1646 A69-23576

CENTRIFUGAL COMPRESSORS

Shockload on axial intake fan leading edge of radial flow compressor, calculating flow field
08 p1251 A69-20604

Unsteady relative flow in centrifugal impeller passage running at part capacity and zero flow observed by hydrogen bubble flow visualization method [ASME PAPER 69-GT-35]
09 p1432 A69-22489

Gas turbine centrifugal compressor design considerations for impellers and diffusers, including blade loading and pressure gradients determination and aerodynamics [IME PAPER 1]
12 p2146 A69-25790

Unsteady aerodynamic processes in centrifugal compressor stage with impeller, vaneless diffuser and annular receiver chamber
15 p2547 A69-30073

Centrifugal compressor impeller disk design, considering stress analysis for shielding portion profile determination to satisfy equal strength condition
17 p3057 A69-33193

Diffuser for high performance centrifugal compressors based on discrete pipe drillings [ASME PAPER 68-GT-38]
19 p3240 A69-36420

Internal aerodynamics of centrifugal compressor impeller, discussing impeller channel airflow model, impeller exit flow, rotating channel flow, etc [RAES PAPER 19]
22 p3859 A69-40498

Discrepancy between theoretical and experimental coefficients of friction losses on blades of centrifugal compressor impeller wheels, using lattice theory
23 p4058 A69-41727

Boundary layer effects in turbulent spiral vortex flow of compressible fluid in supersonic centrifugal compressor, discussing flow geometry, using momentum integral method
23 p4152 A69-42109

CENTRIFUGAL FORCE

Hollow rolling elements for reducing centrifugal load on high performance bearings, discussing production, fatigue life, etc
01 p0085 A69-10294

Variable thickness circular annular disk bending in centrifugal force field, establishing dependence between angular velocity and axial pressure intensity
01 p0168 A69-10401

Centrifugal force field influence on heat exchange between gas and blade cascade studied with noncooled blades at low temperatures
03 p0531 A69-12959

Shape and stability of interface between liquids subjected to surface tension and mass force field in vessel
03 p0417 A69-13809

Axial rigidity effect of centrifugal force acting on balls of rapidly rotating radial thrust bearing
04 p0605 A69-14606

Centrifugal instability of plasma column generated by cyclotron absorption of microwave power in magnetic mirror field
11 p1931 A69-25366

Dynamics of deployable space structures stiffened by centrifugal forces due to spin, discussing LF radio telescope
11 p1994 A69-25530

Plasma rotation by Lorentz force in homopolar gas discharge device, considering centrifugal forces effect on flow pattern
13 p2315 A69-28556

Spiral disk galaxies stability analysis assuming centrifugal force balancing self gravitation, transforming

linearized equations of motion into eigenvalue equations
18 p3200 A69-35131

Geotropic response reciprocity in oat seedlings grown in two axis clinostat compared with acceleration constraints of biosatellites, considering imposition of centrifugal force
20 p3477 A69-37620

Squirrel monkeys exposed to centrifugally generated artificial gravity trained to respond for food reinforcement at selected gravity levels
23 p4081 A69-41434

Centrifugation for removal of bullet fragment floating freely in ventricular system of human brain to fixed safe position in left lateral ventricle wall
24 p4265 A69-43372

Rotating wickless hollow shaft heat pipe utilizing centrifugal acceleration for return pumping of condensate and transferring high heat fluxes [ASME PAPER 69-HT-19]
24 p4413 A69-43550

Centrifugal forces effect on stability of inviscid liquid film over rotating cylinder under from stagnation region, noting film thickness stabilization effect
24 p4305 A69-43597

CENTRIFUGAL PUMPS

Gas flow deflection at centrifugal pump wheel outlet for wheels having different inlet and outlet vane angles
15 p2547 A69-30571

CENTRIFUGES

NT HUMAN CENTRIFUGES

Space-station-centrifuge configuration dynamic stability exhibiting instabilities at lower and higher centrifuge rotational speeds [AIAA PAPER 68-142]
02 p0334 A69-12373

Space research centrifuge counteracting null gravity physiological deconditioning, discussing linear and angular accelerations sensitivity and deconditioning effect on reentry task performance
18 p3114 A69-34368

Centrifuge on board orbiting spacecraft as research tool for biological and physical experiments relevant to prolonged missions and spacecraft design
23 p4108 A69-41833

CENTRIFUGING

Selective g-force application as centrifugation treatment for retinal detachment, applying minimal load on circulation and optimal load on retina
24 p4268 A69-43405

CENTRIFUGING STRESS

Coriolis stimulus effect during centrifugal g load on spatial orientation and accompanying stick performance
06 p0876 A69-18023

Otolith and cupular apparatus interaction in human vestibular analyzer during gravitational changes
07 p1062 A69-18589

Acetate carbon 14 utilization in centrifuged rats, analyzing metabolism by measuring plasma glucose, FFA and lipids synthesis
07 p1067 A69-19429

Human operator manual control of spacecraft under accelerations up to 18 g, noting performance and efficiency of males
08 p1265 A69-19936

Gravity preference tests on rats subjected to simulated Aerobee 150 A rocket launching and flight in ground based spiral centrifuge
13 p2213 A69-28090

Decreased antidiuretic activity measured in blood of chronically centrifuged rats, noting role of antidiuretic hormone /ADH/
14 p2407 A69-29301

Central adrenergic mechanisms role in neurosecretory function of hypothalamo-hypophyseal system of rabbits under transverse accelerations in centrifuge
15 p2554 A69-30055

Centrifugation effects on body composition and growth of mice
17 p2910 A69-33746

Threshold variations in caloric nystagmus in pigeons subjected to accelerations in head to tail direction in centrifuge at various temperatures
20 p3471 A69-37252

Squirrel monkeys escape behavior under centrifuge simulated gravity in excess of earth gravity
21 p3665 A69-39174

Centrifuge on board orbiting spacecraft as research tool for biological and physical experiments relevant to prolonged missions and spacecraft design
23 p4108 A69-41833

Bonded strain gages for experimental stress analysis of high speed rotating machinery under high centrifugal loads
24 p4397 A69-42740

Urine osmolality of centrifuged rats compared with ad libitum or pair-fed control animals, indicating enhanced free water excretion and antidiuretic hormone involvement
24 p4262 A69-42904

CENTRIPETAL FORCE

Physiological studies of centripetal and Coriolis accelerations effects on vestibular function of humans in rotating chamber
02 p0197 A69-11498

CEPHEID VARIABLES

Frequency and radial velocity for various cepheid binaries, discussing hot companions detection through photometry
07 p1223 A69-19627

Preliminary model atmospheres for cepheid variable eta Aquilae, discussing mass loss processes
08 p1386 A69-20089

Period-age relations for delta Cephei stars based on stellar evolution theory and initial abundance of hydrogen
08 p1392 A69-20564

Color index and mean light curves constructed for Cepheid Variables
08 p1395 A69-20635

Polaris cepheid variable star system color index and absolute magnitude from photometric observations
08 p1408 A69-21138

Cepheid stars as distance indicators in extragalactic space, using periodicity-luminosity relation
08 p1408 A69-21147

Cepheid variable and F and G stars observed for neutral lithium line, searching for resonance lines of ionized beryllium in similar stars
09 p1604 A69-22402

Atomic line spectrum computation for F-K supergiant or cepheid, using observational data on standard star spectrum
10 p1771 A69-22854

Galactic structure and space distribution of known Classical Cepheids, noting interstellar absorption and variation of period with distance to galaxy center
10 p1773 A69-22962

Cepheid variable stars light curves analyzed to determine radii and absolute magnitudes
10 p1775 A69-23200

Hot companion presence for RW Camelopardalis confirmed from UVB photometry
10 p1775 A69-23201

Stellar atmosphere parameters analyzed over pulsation cycle by high dispersion spectra of cepheid variable RT Aurigae
10 p1778 A69-23605

Cepheids variations used to measure intergalactic distances, noting method of calibrating absolute Cepheid luminosity
10 p1780 A69-23646

Delta Cepheid blue companion /delta Cep C/ rapid radial velocity variations, noting spatial proximity between delta Cep A and C
11 p1957 A69-24405

Oort constant A and solar motion components in galactic plane determined from Classical Cepheids data
12 p2153 A69-25804

Cepheid variable I Carinae position in H-R diagram suggested from microturbulent velocity role in pulsational instability
14 p2522 A69-29590

Photoelectric /UBV/ photometry of Cepheids in Cygnus and Monoceros noting sequence stars near Nova Cyg 1948
15 p2692 A69-30772

BCD classification for cepheids, discussing /sigma/ surface definition, locus of normal stars of population I and interstellar reddening
17 p3038 A69-33725

Cepheid observation, nature and evolution
21 p3795 A69-38403

Cepheid variable stars distance estimated from UVB three color photoelectric photometry data
22 p4031 A69-40943

VV Cephei type binaries cool and hot primary stars light variations, discussing duration, orbital cycle correlation, mass loss, etc
24 p4386 A69-43346

Blue component of HD 237006 and VV Cephei spectra, suggesting greater luminosity of blue star in late type supergiant
24 p4387 A69-43353

Delta Cepheid blue companion /delta Cep C/ rapid radial velocity variations, noting spatial proximity between delta Cep A and C
24 p4391 A69-43795

CEPHEUS CONSTELLATION

Interstellar light absorption in Milky Way region of Cepheus analyzed by excess color technique
07 p1216 A69-18855

Distance of bright stars in Cepheus OB2 region by MK spectral classification and UVB photometry, noting early main sequence and supergiant stars
09 p1599 A69-22194

Cepheus light attenuation curve explained by applying polymodal particle size distribution, obtaining interstellar dust density
20 p3608 A69-38048

CERAMAL PROTECTIVE COATINGS

U CERMETS
U PROTECTIVE COATINGS

CERAMALS

U CERMETS

CERAMIC BONDING

Phosphate cements for bonding mica ceramic to titanium in jet engine equipment
05 p0786 A69-16799

Sintered metal powder process for metal-to-ceramic seals for thermionic converters, giving results for tensile strength, thermal cycling and cesium corrosion
14 p2454 A69-29211

Glass ceramic coated and bonded silicon semiconductor material in integrated circuits devices fabrication, noting matched thermal expansion
15 p2669 A69-31040

Bonding mechanisms in Mo-Mn-Ti metallizing and Cu brazing in metal to ceramic seals by strength test, microscopy and electron probe microanalysis
21 p3733 A69-39599

CERAMIC COATINGS

Arc driven shock tube with alumina ceramic liner to reduce driver gas contamination, noting shock speed and test time increase
[AIAA PAPER 68-366] 09 p1570 A69-21957

Refractory metal, precious metal and ceramic material compatibility tested by metallography and by microprobing for protective coatings possibilities
09 p1477 A69-22325

Density distribution vs thickness in sprayed ZrC, NbC and aluminum oxide coatings obtained by plasma jet
12 p2118 A69-26258

Metal insulating seals using preliminary metallization or direct brazing for applications in thermionic converter technology and irradiation capsules
14 p2455 A69-29212

Glass ceramic coated and bonded silicon semiconductor material in integrated circuits devices fabrication, noting matched thermal expansion
15 p2669 A69-31040

Test program simulating solar wind outside magnetosphere to evaluate high melting point high density ceramic oxides as white thermal control coating pigments
[AIAA PAPER 69-641] 17 p2993 A69-33762

Composite ceramic armor systems for airborne vehicles and personnel, air cushion vehicles and ground troops, discussing weight and contour forming advantages
19 p3355 A69-35525

Temperature fields and stresses in heat resistant ceramic coatings, illustrating alumina coating on Mo to calculate heating rate
20 p3565 A69-37359

Metal or ceramic layers application to substrate by flame spraying process
21 p3731 A69-38938

CERAMICS

NT CERAMIC BONDING
NT CERAMIC COATINGS
NT PORCELAIN
NT PYROCEAM [TRADEMARK]

Crack growth in ceramics from velocity measurements on glass and sapphire as function of applied force, temperature and moisture environment
01 p0101 A69-10767

Pre-cracked ceramic rocket nozzle throat inserts, discussing improved thermal displacement accommodation, load transmission, fracture tolerance, articulation capability, etc
02 p0334 A69-12369

Porous ceramic heat shields for lifting reentry vehicles, noting crack propagation resistance and load redistribution
[SAE PAPER 680643] 03 p0453 A69-13457

Special ceramics - Conference, Stoke-on-Trent, Staffs., England, July 1967
06 p0946 A69-17527

Metal fiber reinforced ceramic matrix composites, discussing model system, bond strength, loading and elastic properties
06 p0946 A69-17528

Ceramic radomes for hypervelocity aerospace vehicles, considering wide temperature environment effects on stability and properties
07 p1171 A69-19511

Radome design and manufacture, considering airborne requirements, antenna systems and electromagnetic energy, with emphasis on ceramic material melting, forming, grinding and finishing
07 p1142 A69-19526

Processing techniques for fabrication of ceramic radomes from alumina and silica
07 p1142 A69-19527

Ceramic radome materials resistance to rain erosion at high Mach numbers
07 p1171 A69-19532

X ray and photomicrographic study of metal layer-ceramic seal interface reaction products, discussing phase transformations, temperature effects and time dependence
08 p1320 A69-20375

Mechanical properties of ceramic material consisting of pure silica matrix reinforced by carbon fibers
08 p1341 A69-20700

Metal castings around ceramic cores for economic manufacture of jet engines
09 p1503 A69-21907

Oxide ceramics finishing processes, discussing leaching, machining, surface finishing, strengthening by compressive surface layers and joining
09 p1510 A69-22350

Ceramic whiskers and metallic matrix chemical reactions during composite formation, analyzing coated and uncoated SiC whiskers in titanium matrix
09 p1527 A69-22359

Silicated alumina attachment for high temperature radomes and leading surface heat shields, discussing stress concentration and load transfer
09 p1477 A69-22370

Refractory ceramic materials use for advanced combustion chamber design, stressing brittleness effect and current fabrication techniques
09 p1531 A69-22624

Ceramic substrate cutting with carbon dioxide laser by scribing perforation pattern,
10 p1699 A69-23302

Ceramics strength and fracture behavior in terms of modified Griffith equation, discussing effective surface energy and initial crack size
11 p1907 A69-25238

Type 2 ceramic capacitor manufacture, selection and control in Concerto space program
11 p1853 A69-25393

Fabricable materials with low plastic deformation for gas turbine components, noting strength vs temperature for alloys, fiber composites and ceramics
[IME PAPER 8] 12 p2147 A69-25791

Metallic and ceramic whiskers and fibers for material reinforcement, discussing properties and fabrication techniques
12 p2111 A69-25856

Book on ceramic fibers and fibrous composite materials as structural reinforcements covering dynamic testing of fine filaments and whiskers, material characterization, etc
12 p2118 A69-26340

Pressure calcining process in production of fine grained ceramics at low temperatures
12 p2119 A69-26832

Friction and wear characteristics of ceramics and cermets as bearing materials, with tabulation of room temperature hardness and maximum service temperatures
13 p2284 A69-27232

Chemical corrosion of zirconia-based refractories in MHD generators, considering thermal cycling and shock, seed migration and prevention
13 p2284 A69-27469

Refractory ceramic materials thermal stability in high temperature subsonic ionized gas flow products, emphasizing zirconia and magnesia
13 p2285 A69-27472

One inch ceramic vidicon with slow scan photoconductor, electrostatic focusing and magnetic deflection to withstand sterilization and environmental testing for space applications
13 p2234 A69-28262

Ceramic and cermet materials insulating, physical and mechanical properties for use in thermionic converters
14 p2467 A69-29214

Barium vapor effect on converter materials, examining metals-ceramics compatibility at high temperatures
14 p2467 A69-29215

Metallo-ceramic materials strength as function of porosity calculated for tension, shear, bending and torsion deformations
15 p2638 A69-30283

Erosion wear of graphitic and mica-ceramic materials used for sealing turbine compressors at high temperatures, including test installation
15 p2643 A69-31186

Ceramic heat transfer gage for supersonic wind tunnel investigation of blunt swept wing leading edges aerodynamic heating
15 p2613 A69-31272

Ceramic phase reinforcement of metals and alloys, discussing interfacial energies, binding forces and elastic stress fields
[ONERA-TP-661] 16 p2802 A69-32204

Sliding friction and wear properties of metal ceramic composites applied to aircraft brakes
17 p2987 A69-33375

Injection holding for ceramic parts from nonplastic materials, presenting time-temperature schedules for low temperature removal of molding material without damage
17 p2978 A69-33376

Transient effects of nuclear radiation bursts on dielectric properties of refractory low loss ceramics at L, S and X bands
20 p3584 A69-38065

Book on phase diagrams for ceramists, 1969 supplement
22 p3971 A69-40782

Parametric losses in nonlinear centrosymmetrical ferroelectric ceramic in strong microwave field at temperatures above Curie point
22 p3996 A69-41164

Mechanical properties of glass and glass-ceramics products improvement through prestressing
24 p4335 A69-43034

Silicon nitride ceramics fabrication technology and dimensional stability during nitridation, discussing applicability to aerospace precision or joined ceramic shapes
24 p4336 A69-43211

Structural ceramics and testing of brittle materials - U.S. Army Conference, Chicago, March 1967
24 p4333 A69-43337

Polycrystalline ceramics chemical and microstructural control through thermomechanical and thermochemical hot forming techniques, discussing pressure sintering, hot extrusion, strain annealing, etc
24 p4321 A69-43338

Structural analysis and statistical fracture approach to design and testing for polycrystalline ceramic materials, including combined stress testing and load redistribution models
24 p4333 A69-43339

CEREBELLUM

High energy X ray irradiation of head of Macaca mulatta, determining effect on cerebral blood flow and blood pressure
03 p0376 A69-14075

Lactate dehydrogenase and monoamine oxidase distribution in medulla oblongata and cerebellum of squirrel monkey
12 p2018 A69-25778

Nerve tissue oxidation processes relation to nervous system radiation sensitivity in dogs with cerebellum X rayed after enzyme poisons administration
21 p3658 A69-39053

Canine cerebellar Purkinje cells electron microscopy after rapid decompression to near vacuum
21 p3660 A69-39177

Spatiotemporal patterns learning among sensory and motor organs with linearly ordered components by nonlinear networks in terms of embedding fields theory
22 p3887 A69-41196

Information transfer capacity of afferent and efferent cell system and fiber tracts of human cerebellum numerically defined with regard to cybernetics
23 p4084 A69-41467

CEREBRAL CORTEX

Cerebellar cortex function disorders of rats subjected to 10 g acceleration under weak anesthesia
02 p0198 A69-11504

Phosphodiesterase activity of anterior pituitary, median eminence, heart and cerebral cortex of rat, studying effects of caffeine, theophylline and hydrocortisone
02 p0199 A69-11885

Flexible printed circuitry electrode arrays fabrication for surface cortical potentials recording in animals
02 p0204 A69-12601

Cerebral cortical neurons response to visual stimuli during stationary and rapid eye movement
03 p0369 A69-13360

High oxygen concentration influence at normal pressure on evoked potential of cortical optic zone and sub-cortical zones
05 p0709 A69-16515

Prolonged bed rest effect on brain bioelectrical activity from EEG reactions of subjects to acoustic signals followed by light signals
05 p0710 A69-16520

Psychomotor reactions to zero gravity during ballistic rocket flights, analyzing electrical activity of cortex in animals
06 p0874 A69-17649

Visual systems of hamster brain, discussing relative visual localization and discrimination blindness produced by ablation of cortical or tectal areas
08 p1265 A69-20685

Graphical method for plotting electrophysiological observations, showing hodographs application in biopotential studies of cortical reactions
11 p1829 A69-24540

Oxidative and dephosphorylating enzymes and esterases in rat and squirrel monkey cerebral cortexes, noting neuron activity
12 p2018 A69-25773

Soviet book on nervous mechanisms of vestibular reactions emphasizing mathematical description of operation, neuro rhythmic changes in cerebral cortex and oculomotor activity modeling
16 p2746 A69-32605

High oxygen concentration influence at normal pressure on evoked potential of cortical optic zone and sub-cortical zones
18 p3096 A69-34734

Prolonged bed rest effect on brain bioelectrical activity from EEG reactions of subjects to acoustic signals followed by light signals
18 p3096 A69-34739

Glutamic acid metabolism compartmentation in brain cortex demonstrated in vitro, using isotopic labeling
18 p3096 A69-35172

Electrical response of frog and human visual cortex neurons to thermal vestibular and light flash stimulation
20 p3469 A69-37242

Labyrinth polarization effect on stimulation and neuron activity in visual cortex of cats, using electroencephalograph
20 p3469 A69-37244

Visual and vestibular analysors interrelation in subjects receiving light pulses before and after rotation, noting role of cortical elements
20 p3470 A69-37249

Averaged cortical evoked response characteristics relationship to performance in traditional threshold procedures, discussing stimulus sensitivity and intensity control in central nervous system
21 p3653 A69-38897

Radiotelemetric EEG recording variation possibility, examining dynamic behavior of human cerebral rhythms
22 p3889 A69-40158

Cortical and thalamic evoked activities changes during sensory conditioning of freely moving cat
22 p3872 A69-40160

Spatial distribution of amplitude and onset of pre-mo-tion positivity, readiness and motor potential changes in human cerebral cortex preceding voluntary finger movements
22 p3875 A69-40261

Unit activities in cerebellar cortex by auditory stimulation in cats, discussing response patterns obtained by histograms
22 p3876 A69-40264

Cerebellar cortex reactions to sciatic nerve stimulation in rats under transverse accelerations in centrifuge
22 p3877 A69-40279

Responsiveness of cortex and visual pathway during transient hypotension induced by increased gravitational stress, discussing intraocular pressure of cat
22 p3878 A69-40779

Squirrel monkey retinas spectral stimulation, determining differential color responses reaching striate and prestriate cortex
22 p3879 A69-40844

Visual field meridians in circumstriate visual cortex of monkey determined by tracing degenerating axons stained by Nauta method
22 p3881 A69-40858

Nocturnal and diurnal monkeys spectral sensitivity functions determined from simultaneous recordings of light-evoked cortical and retinal responses
22 p3882 A69-40867

Topographic distribution of cortical potentials produced with tachistoscope and by stroboscopic stimulation, studying occipital and frontal differences
22 p3884 A69-40885

Anesthetized cats with electrodes in visual cerebral cortex, investigating simulation of conditioned alimentary reflexes in response to light signals by electric signals
22 p3885 A69-41066

Functional relation between primary response individual phases and neurons activity in cats cerebral cortex
22 p3886 A69-41067

Topography of potentials induced by acoustic clicks in auditory cortex of dogs, including ectosylvian gyrus distribution
22 p3888 A69-41269

Cortical biopotentials in cats induced by strychnine under acoustic click stimuli of increasing intensity
22 p3888 A69-41270

Cerebral subcortical structures controlling effect on central and peripheral nervous systems, discussing motion coordination, space orientation, search reflexes and physiological sleep
22 p3889 A69-41275

Structural differences effect of gyral and sulcal areas of acoustic projection cortex on primary induced acoustic responses
23 p4079 A69-41380

Learning model of motor behavior in brain cortex of higher animals and man, discussing M automaton, information reception, correlation, memory, emotions, desires and actions
23 p4109 A69-41977

Unisensory and multisensory signal processing in cortical and brain stem regions of albino rat by electronic averaging and time histogram techniques
23 p4092 A69-42055

Electroretinogram and visually evoked cortical potential as response potentials in human visual system
24 p4271 A69-42644

CEREBRAL VASCULAR ACCIDENTS

Airline pilots simulated incapacitation involving myocardial infarction or cerebrovascular accident, discussing effect on crew behavior during flight task performance
24 p4277 A69-43386

CEREBROSPINAL FLUID

Regional uptake of melatonin from blood or cerebrospinal fluid by rat brain
09 p1444 A69-21466

Cerebrospinal fluid /CSF/ formation in male monkeys as function of fluid pressure at third ventricle level following temperature stress and feeding
23 p4084 A69-41469

CEREBRUM

Vestibular neurons activity in decerebrized cats under ipsilateral and contralateral labyrinth polarization combined with acoustic and caloric stimulation
20 p3471 A69-37254

Protein rates and RNA synthesis in cerebra of rats analyzed as factor of high altitude hypoxia adaptation
22 p3886 A69-41122

Electric responses of anterior and posterior gyrus cinguli to stimuli of sciatic nerve in cats
22 p3886 A69-41175

Cerebral and retinal capillary permeability to ions in rats analyzed by electron microscope using Prussian blue reaction
23 p4081 A69-41433

CERENKOV COUNTERS

Pulsar CP 1133 high energy gamma ray emission, using atmospheric Cerenkov detection technique for high energy neutral cosmic rays
02 p0307 A69-11823

Primary cosmic radiation charge spectrum measurement during 1965 minimum solar activity, using balloon-borne Cerenkov scintillation counter
02 p0308 A69-12043

Splash albedo flux measurement, using Cerenkov counter telescope surrounded by anticoincidence shield
06 p0989 A69-17278

High energy muons Cerenkov radiation, using water filled counter as function of muon momentum, noting no intensity decrease
06 p0991 A69-17306

Fast charged particles measurements by Cerenkov counter in Cosmos 137 satellite, noting hard electron flux and cosmic ray radiation spectrum
13 p2327 A69-27693

Night sky Cerenkov light detectors observations of pulsars CP 1133, NP 0532 and NP 0527, noting instrumental limitation in detecting ultrashort light pulses
18 p3200 A69-34994

CERENKOV RADIATION

Gamma ray fluxes from pulsating radio sources, using detection of Cerenkov light generated by energetic particles in atmosphere
03 p0513 A69-13772

Magnetobremsstrahlung /synchrotron/ and Cerenkov radiation of ultrarelativistic particles, radiation reabsorption and magnetic field measurement
06 p0962 A69-17245

High energy muons Cerenkov radiation, using water filled counter as function of muon momentum, noting no intensity decrease
06 p0991 A69-17306

Magnetoacoustic waves generated by Cerenkov radiation from corpuscular fluxes due to star interaction with stellar wind, determining deceleration forces on star
11 p1955 A69-24385

Natural oscillations excitation in magnetoactive plasma by modulated electron beam ascribed to Doppler or Cerenkov effects
11 p1932 A69-25535

Cerenkov radiation from point charge uniformly moving along external magnetostatic field in warm anisotropic plasma, noting excitation modes and propagation frequencies
13 p2307 A69-27964

ISIS A satellite fixed and sweep frequency ionograms indicating electron density variations, ionospheric resonances and Cerenkov radiation
15 p2604 A69-31416

Analogy between Cerenkov and quasi-Cerenkov radiation in nonlinear crystal by intense laser light used to determine conditions for quasi-Cerenkov radiation
21 p3741 A69-39669

Magnetoacoustic waves generated by Cerenkov radiation from corpuscular fluxes due to star interaction with stellar wind, determining deceleration forces on star
24 p4390 A69-43775

CERIUM

Meteoritic materials investigated for Sc, Ce and Eu content and distribution in various phases, using neutron activation analysis
01 p0026 A69-11376

Ce activated garnet crystals optical properties, noting IR and near UV absorption spectra and room and low temperature fluorescence
07 p1201 A69-19647

Chromium-cerium phase diagram determined by differential thermal, metallographic and X ray structural analysis
15 p2640 A69-30666

Ce II line reversal from absorption to emission in solar spectrum, noting reversal position dependence on wavelength and line source function scattering term
20 p3613 A69-38168

CERIUM COMPOUNDS

IR spectral transmittance and physicochemical properties of tellurite glasses with vanadium and cerium oxides, showing polymer chains in structure
14 p2468 A69-29329

Stimulated emission of cerium trifluoride-positive trivalent Nd ion laser noting absorption, luminescence, excitation, emission spectra and metastable state lifetime
14 p2460 A69-29645

CERMETS

Beryllium cermet compositions, discussing beryllium oxide content, mechanical strength and elastic and shear moduli
10 p1711 A69-23334

Beryllium base cermets corrosion resistance increased in moist carbon dioxide at 700 C
10 p1711 A69-23338

Thermal stability of refractory and cermet materials, analyzing small samples subjected to cyclic high energy radiative heating and air-water cooling
12 p2118 A69-26262

Friction and wear characteristics of ceramics and cermets as bearing materials, with tabulation of room temperature hardness and maximum service temperatures
13 p2284 A69-27232

Chemical composition of cermet material for radial sealing of high temperature gas turbines, ensuring structural stability and oxidation resistance
13 p2275 A69-27344

CERTIFICATION

Thin film cermet resistors for integrated circuits produced by thermal vapor deposition in vacuum, cathodic sputtering and explosive vapor deposition
13 p2268 A69-27466

Ceramic and cermet materials insulating, physical and mechanical properties for use in thermionic converters
14 p2467 A69-29214

X ray diffractometer stress analysis of WC-Co cermets, discussing surface preparation and heat treatment
16 p2802 A69-32339

Co content influence on temperature stress in WC-Co cermets using one exposure and two exposure X ray diffraction
16 p2802 A69-32340

Facility for evaluating thermal stability of heat resistant materials and cermets in constant temperature gas flow
20 p3565 A69-36979

Heat resistance and strength properties of porous Ni-base cermet materials with mica additions under high temperature oxidation
21 p3751 A69-38615

Wear resistant Ti carbide based cermets with alloy steel binder, noting electrical and heat conductivity dependence on composition and temperature
22 p3971 A69-40919

CERTIFICATION

Civilian transport aircraft operation realities vs theoretical performance certification
14 p2392 A69-29698

Abnormalities of routine electrocardiograms in medical certification of pilots, indicating errors in screening
19 p3263 A69-36462

Airworthiness certification of civil aircraft, discussing international cooperation on inspection, accident investigation, etc
19 p3456 A69-36688

Engine powered lift civil aircraft certification factors taking into account traffic growth, accident rates, learning rate and acceptable safety level
22 p3862 A69-39962

Civil pilots medical certification after head trauma, evaluating current methods efficiency
23 p4086 A69-41687

CESIUM

Optical absorption of thin film cesium between 2300 and 11000 Å
03 p0491 A69-14060

Li and Cs electrical conductivity measured from 300-1200 K, obtaining interpolation formulas by least squares method
03 p0481 A69-14148

Varian cesium resonator as prime frequency testing standard with accuracy dependent on electronic system for quartz slaving
04 p0600 A69-15068

Work function and desorption energy measurements of alkali metals from metallic substrates with modulated molecular beam, noting surface contamination
09 p1558 A69-21808

Indium, Rb and Cs abundances obtained from sun-spot spectra by comparison with Zr and Ti lines
13 p2343 A69-27626

Positive ion concentration in subsonic high velocity laminar flames determined by interpreting kinetic and diffusion factors of adding cesium to flame
13 p2380 A69-28463

Nuclear type cylindrical thermionic converter with porous adsorbent structure and liquid cesium tank
14 p2397 A69-29174

Thermal emission converter, using Cs-Ba mixture in low voltage arc mode, detailing construction
14 p2403 A69-29247

Langmuir S curves for tungsten single crystals in presence of adsorbed cesium, discussing orientation, theoretical and experimental correlation and instrumentation
14 p2506 A69-29271

Surface structures, work function changes, Auger electron and surface plasma losses for Cs on clean W surface
19 p3392 A69-36733

Absorption spectrum of CS atoms excited by electrical discharge and irradiated by monochromatic light and ionized by electron collisions
22 p3984 A69-40418

CESIUM DIODES

Backscattering due to collisions for electrons from emitter accelerated through positive ion sheath into plasma in thermionic diodes
06 p0898 A69-17773

Predicting electrode geometry effect on saturation ion currents in diode exposed to ionizable vapor in equilibrium with liquid Ce
09 p1440 A69-21832

Electron transport phenomenon in high pressure cesium diodes, noting quasi-static assumption of particle distribution functions
14 p2401 A69-29229

Inverse current in ignited mode diode linearly related to spacing, noting emitter sheath
14 p2401 A69-29230

Voltage drop of ignited mode related to current density in cesium diode, noting plasma zones
14 p2401 A69-29232

Preignition volt-ampere curves for thermionic cesium diodes exhibiting nonsaturation characteristics under low temperature and electron-rich emission conditions
14 p2403 A69-29253

Spectral lines emitted from low voltage discharge in cesium filled diode with hot cathode, giving current-voltage characteristics as function of pressure and temperature
14 p2491 A69-29260

CESIUM ENGINES

Cesium electron bombardment microthruster system, discussing ion engine, feed, discharge neutralizer, power conditioning and control electronics [AIAA PAPER 69-293]
09 p1561 A69-21223

Cesium microthruster system using beam deflection for satellite control, describing ion engine subsystem and control logic/power conditioner subsystem [AIAA PAPER 69-292]
09 p1569 A69-21875

Cs contact ion microthruster system design, fabrication and flight qualification, noting control logic/power conditioning unit and electronic packaging [AIAA PAPER 68-552]
21 p3785 A69-39212

Cs contact ion engine with tubular W ionizer tested for performance and reliability in vacuum chamber
22 p4000 A69-40592

CESIUM IODIDES

Electrical conductivity of cesium iodide single crystals with anion and cation impurities noting temperature dependence
16 p2824 A69-31573

CESIUM ION

Effective cross section of resonant cesium ions charge exchange determined by retarding field method, considering dependence on ion velocity
06 p0959 A69-16908

Barkhausen oscillator for LF domain by substituting Cs and K positive ions for electrons, giving oscillation curves and spectral analysis
08 p1280 A69-19981

Cs and K ions drift velocity calculations in vapors of own atoms under various electric field strengths effect
11 p1922 A69-24226

Cesium ions decay time in thermionic converter operating in gas kinetic mode by pulse ionization, noting dependence on interelectrode potential distribution
14 p2403 A69-29252

Cross sections threshold behavior for Cs II resonance lines excitation due to Cs ion-He collision
17 p3008 A69-33388

Cs ionization by bromine, measuring relative cross section velocity dependence by crossed molecular beam technique
23 p4194 A69-42208

CESIUM OXIDES

Plasma anode technique for work functions measurements of polycrystalline W and Re wires in cesium vapor with cesium oxide additive
14 p2507 A69-29274

Ultrahigh vacuum cleaved GaAs-Cs and GaAs-cesium monoxide photoemission acceptor densities, noting crystal parameters role
23 p4198 A69-41548

CESIUM PLASMA

Alkali metal quadrupole spectral doublets used as diagnostic for determining alkali-metal plasma electron temperature
02 p0286 A69-11584

Plasma physics experiments and theoretical studies, discussing plasma heating by magnetic compression and irreversible expansion, Cs plasmas, plasma diagnostics, etc
02 p0289 A69-12200

Ionization and recombination in low temperature plasmas, noting fast electron distribution function deviation from Maxwellian form and calculation for Cs plasma
02 p0292 A69-12559

Probe and spectral techniques compared for investigation of low voltage arc of cesium plasma thermionic converter
03 p0478 A69-13836

Low voltage Knudsen arc in cesium argon mixture using tungsten electrodes, analyzing current voltage characteristics
06 p0963 A69-16920

Thermal metal-plasma thermodynamic equilibrium, using surface ionization of inner and outer potentials and work function, discussing ion and electron extraction
06 p0979 A69-17249

Cesium plasma produced inside hot cylindrical tantalum cavity at 1400 K by contact ionization at wall while obtaining electrons from internal filament
06 p0927 A69-17707

Recombination coefficients for dense weakly ionized cesium plasma, treating recombination process as diffusion generated by electron collisions
08 p1359 A69-19844

Dominant ionic species in cesium plasma through mass spectrometer analysis, measuring total ion and electron currents
09 p1544 A69-21335

Ionic species identification in argon-cesium discharges for thermionic converter design
09 p1440 A69-21830

Electrical conductivity, electron energy balance, ionization equilibrium time and channel parameters in pulse discharge nonequilibrium Cs plasma containing inert gas addition
10 p1731 A69-23439

Ionization relaxation in atmospheric pressure Ar-Cs plasma, considering two and three body recombination and O impurity effects
10 p1733 A69-23445

Plasma decay coefficient, charge recombination coefficient and electron scattering in cooling electron gas of quasi-steady cesium discharge plasma under high pressure
10 p1733 A69-23448

Mercury cesium plasma in crossed electric and magnetic fields as working fluid of MHD generators based on Rankine cycle
10 p1636 A69-23458

Cesium plasma confinement time improvement in symmetrically heated tungsten end plates of Q machine
11 p1925 A69-24314

Arc mode thermionic Cs converter nonlinear I-V characteristics explained by current-dependent temperature and potential fields in plasma
11 p1827 A69-25400

Positive column contraction in Ar and Ar-Cs mixtures, developing theory for nonisothermal local collision arc
11 p1932 A69-25539

Nonlinear algebraic equation system describing populations of excited atoms of low pressure nonequilibrium cesium plasma, determining ionization coefficient and molecular ion concentration
11 p1934 A69-25567

Back scattered electron inelastic LEED spectra of cesium plasma in W/100/-Cs system, noting strong loss peak
12 p2132 A69-26116

Decaying arc discharge Cs plasma luminosity anomalous behavior due to combined effect of intrinsic monotonic and complex nonmonotonic emissions
14 p2490 A69-28996

Low voltage arc in cesium thermionic converter, investigating current-voltage characteristics, electron temperature, electron density and plasma potentials in ignited mode
14 p2401 A69-29231

Unignited mode converter and emitter work function patches, calculating electron-cesium momentum transfer cross sections from saturation current measurements
14 p2490 A69-29240

Rasor phenomenological theory of space ionization in arc mode regime of Cs thermionic converter
14 p2402 A69-29242

Cesium plasma electron temperature in narrow electrode space of thermionic converter determined using electrode and changeable space diode
14 p2491 A69-29243

Low voltage Cs arc in thermionic converter with slotted cathode surface, determining electron concentration and temperature distribution
14 p2403 A69-29250

Electron temperature and density distributions across cesium converter interelectrode gap determined spectroscopically, noting maxima toward emitter
14 p2491 A69-29259

Work function measurements of polycrystalline W, Re and Ni disks in high pressure cesium plasma for low probe temperature range
14 p2506 A69-29266

Ionization and recombination in low temperature plasmas, noting fast electron distribution function deviation from Maxwellian form and calculation for Cs plasma
15 p2658 A69-30256

Electronic density of collisional cesium plasma, comparing measurements made by Langmuir and HF spherical probes
15 p2659 A69-30300

Shock wave propagation through collisionless magnetized plasma, using gun driven, laser and cesium plasma flow methods
19 p3379 A69-35759

Electron temperatures and densities in interelectrode plasma of close spaced high current cesium plasma diode
19 p3380 A69-36415

Electron energy distribution for Cs plasma in emitter region of ignited mode thermionic converter, noting nonequilibrium ionization effect
19 p3380 A69-36442

Measurement method for relative phase shift between density and potential oscillations in Cs plasma
24 p4354 A69-42676

Steady state interaction between collisionless plasma flow and immersed stationary magnetized or unmagnetized objects by inserting Cs ion accelerator into plasma wind tunnel
24 p4359 A69-43646

CESIUM VAPOR

Electron impact ionization cross section in cesium vapor measured with Tate-Smith apparatus
01 p0137 A69-10285

Plasma decay at high pressure in helium and argon with cesium vapor admixture and pure cesium vapor, using Saha equation
03 p0480 A69-14052

Doublet structure suppression in mixtures of cesium and foreign gases, discussing absorption observations
08 p1356 A69-20736

Charge exchange collisions in ground state and ionic hydrogen incident on cesium vapor, measuring beam components after passage through target
08 p1356 A69-20737

Saturation electron emission characteristics from incompletely outgassed Ta wire emitters immersed in Cs vapor using plasma anode technique, noting oxygen effects
09 p1437 A69-21812

Predicting electrode geometry effect on saturation ion currents in diode exposed to ionizable vapor in equilibrium with liquid Ce
09 p1440 A69-21832

Thermionic converters stability and safety maintainable at high Ce pressures
09 p1441 A69-21837

Adsorption process limits when used as Cs reserve in thermionic converter
09 p1441 A69-21839

Gas breakdown model for analyzing breakdown of Ce vapor filled crack in thermionic trilayer insulator
09 p1441 A69-21840

Momentum transfer cross sections, recombination coefficients and ionization coefficients of working gases for MHD energy converter
10 p1733 A69-23446

Heats of condensation and vaporization of W, Re and Mo cathodes of thermoelectric converter with Cs arc for various output powers and Cs vapor pressure
12 p2017 A69-26544

High pressure Cs thermionic converter with cold region, measuring Cs partial pressure distribution in Ar filled tube
14 p2397 A69-29176

Cesium sorption in materials for thermionic converters reservoirs, discussing dimensional stability of porous alumina, W and C samples
14 p2463 A69-29220

Low voltage arc discharge characteristics in cesium vapor, considering energy balance, electron temperature, energy losses, volt-ampere characteristics, ignition, cathode temperatures, etc
14 p2401 A69-29234

Thermionic converter stability as function of cesium pressure, heat input, reservoir temperature, load voltage or resistance
14 p2402 A69-29236

Cs mixture effects with Ba and I on cathode electron emission in thermionic converter
14 p2402 A69-29239

Thermionic converter current-voltage characteristics under various emitter temperatures and cesium vapor pressures, noting role of Schottky effect
14 p2402 A69-29241

Low voltage arc in thermionic cesium vapor diode with lengthy electrodes and temperature variations along emitter, discussing plasma and current density distributions
14 p2402 A69-29244

Knudsen arcs kinetic theory with cesium/inert gas mixtures in narrow gap between parallel plate electrodes, discussing fast particle beams and electron scattering
14 p2491 A69-29245

Current oscillations and electromagnetic radiation in low pressure cesium thermal emission converters using glass diode with plate geometry metal electrodes
14 p2402 A69-29246

Low voltage Knudsen arc in cesium-argon mixture for thermal emission converters
14 p2403 A69-29248

Experimental and theoretical data correlation on low voltage arc in thermionic converters using cesium vapor, describing discharge plasma by solving differential equation system
14 p2404 A69-29254

Ionization mechanisms in ignited mode cesium thermionic converter, discussing positive ions production for electron space charge neutralization and ion density calculations
14 p2404 A69-29258

Radiation effects on Cs thermionic converter, discussing radiation interaction with alkaline atoms to complete space charge neutralization by supplementary ion creation
14 p2404 A69-29261

Plasma anode technique for work functions measurements of polycrystalline W and Re wires in cesium vapor with cesium oxide additive
14 p2507 A69-29274

Electron work function profile determined for polycrystalline Mo and W single crystals with and without Cs vapors by emission microscope and photomultiplier
14 p2507 A69-29276

Mass transfer during Cs condensation from moving vapor mixture containing Ar in water-cooled tube
15 p2718 A69-30998

Plasma decay at high pressure in helium and argon with cesium vapor admixture and pure cesium vapor, using Saha equation
18 p3181 A69-35045

Cs jet device eliminating wall influence in nonlinear radiation-atom interaction phenomena
19 p3376 A69-36174

Longitudinal electric field, electron density and temperature in positive column of low pressure Cs-Ar DC arc discharge, discussing Cs vapor depletion
19 p3380 A69-36441

Flow and thermodynamic variables of Ar-Cs mixture behind normal shock in shock tube at various temperatures and pressures
23 p4150 A69-41335

Electron density in positive column of Cs vapor discharge related to current and gas pressure, discussing field strength effects on drift velocities
23 p4196 A69-42197

CESIUM 133

GaAs laser used as optical sweep generator for display of Cs 133 spectral line shape, studying fluorescence and radiation lifetime
19 p3339 A69-36696

National Physical Laboratory atomic clock improvements, describing use of cesium 133 as second of time standard and phase shift effects on precision
21 p3720 A69-38548

CESSNA AIRCRAFT

Military forward air control aircraft conversion from lightweight commercial tandem engine aircraft noting visibility, communication and navigation equipment [SAE PAPER 690313]
11 p1822 A69-24511

CESSNA MILITARY AIRCRAFT

U MILITARY AIRCRAFT

CF-104 AIRCRAFT

U F-104 AIRCRAFT

CH-34 HELICOPTER

Night vision requirements of Vietnam combat pilots investigated for relationship to Skyraider fatal crash during target strafing and H-34 helicopter crash landing
23 p4107 A69-41807

CH-46 HELICOPTER

CH-46 Sea-Knight and CH-47 Chinook transport helicopters experience in Vietnam war, discussing missions, payloads, speeds, operating ranges, etc
01 p0009 A69-10405

Flight recorder program determining combat operating environments of CH-46D helicopters analyzed and compared with aircraft design criteria [AHS PAPER 375]
17 p3059 A69-33513

CH-46 helicopter flight simulation program for pilot response to large perturbation maneuvers, using six degrees of freedom mathematical models [AHS PAPER 361]
17 p2946 A69-33521

CH-47 HELICOPTER

CH-46 Sea-Knight and CH-47 Chinook transport helicopters experience in Vietnam war, discussing missions, payloads, speeds, operating ranges, etc
01 p0009 A69-10405

CH-54 HELICOPTER

Combat fielded cargo-carrying CH-54A Flying Crane helicopter industry-government reliability/maintainability field test evaluation
19 p3247 A69-36017

CH-113 HELICOPTER

U CH-46 HELICOPTER

CHAFF

Mesospheric wind measurement by meteorological rockets based on radar determination of drift trajectories of chaff clouds
20 p3529 A69-37797

CHAIRS

U SEATS

CHALCOGENIDES

NT ALUMINUM OXIDES

NT ANATASE

NT BARIUM OXIDES

NT BERYLLIUM OXIDES

NT BISMUTH OXIDES

NT BISMUTH TELLURIDES

NT CADMIUM SELENIDES

NT CADMIUM SULFIDES

NT CADMIUM TELLURIDES

NT CALCIUM OXIDES

NT CARBON DIOXIDE

NT CARBON MONOXIDE

NT CESIUM OXIDES

NT CHROMITES

NT CHROMIUM OXIDES

NT COBALT OXIDES

NT COPPER OXIDES

NT COPPER SULFIDES

NT DISULFIDES

NT GALLIUM SELENIDES

NT GERMANIUM OXIDES

NT HEAVY WATER

NT HYDROGEN PEROXIDE

NT HYDROGEN SULFIDE

NT ILMENITE

NT INDIUM SULFIDES

NT INDIUM TELLURIDES

NT IRON OXIDES

NT LEAD OXIDES

NT LEAD SELENIDES

NT LEAD SULFIDES

NT LEAD TELLURIDES

NT LITHIUM OXIDES

NT MAGNESIUM OXIDES

NT MAGNETITE

NT MANGANESE OXIDES

NT MERCURY TELLURIDES

NT METAL OXIDES

NT MOLYBDENUM DISULFIDES

NT MOLYBDENUM OXIDES

NT MOLYBDENUM SULFIDES

NT NICKEL OXIDES

NT NIOBIUM OXIDES

NT NITRIC OXIDE

NT NITROGEN DIOXIDE

NT NITROGEN OXIDES

NT NITROGEN TETROXIDE

NT NITROUS OXIDES

NT OXIDES

NT PEROXIDES

NT PYROXENES

NT QUARTZ

NT RUTILE

NT SAPPHIRE

NT SELENIDES

NT SILICON DIOXIDE

NT SILICON OXIDES

NT SULFIDES

NT SULFUR OXIDES

NT TELLURIDES

NT THORIUM OXIDES

NT TIN OXIDES

NT TIN TELLURIDES

NT TITANIUM OXIDES

NT TROLITE

NT TUNGSTEN OXIDES

NT URANIUM OXIDES
NT VANADIUM OXIDES
NT WURTZITE
NT ZINC OXIDES
NT ZINC SELENIDES
NT ZINC SULFIDES
NT ZINC TELLURIDES
NT ZIRCONIUM OXIDES

Soviet book on semiconductor compounds, production and properties covering crystal structures, phase diagrams, etc

01 p0137 A69-10353

Current carrier mobility in GaTe and tin selenide semiconducting stratified lattices, noting interaction of free carriers and polarized nonpolar phonons

02 p0295 A69-11777

Dynamic current-voltage characteristics of thin film diodes on chalcogenide glass base

02 p0223 A69-12834

Diffusion anomaly of native acceptor defect in zinc selenium telluride p-n junctions, discussing applications in triple diffusion technique of preparing p-n junction diodes

05 p0808 A69-16286

Soviet book on methods of investigating semiconductors as applied to lead chalcogenides PbTe, PbSe and PbS covering physical and physicochemical properties

12 p2145 A69-26851

Monograph on vanadium selenides and tellurides with NiAs structure covering existence regions, superstructures and equiatomic compounds from viewpoint of thermodynamics

15 p2667 A69-30602

Chalcogenide semiconductor film switches time parameters, showing delay time decrement with thickness decrease and voltage increase

21 p3780 A69-39045

CHAMBERS

Optimum design of spherical and ellipsoidal pumping chambers for solid state lasers determined from numerical calculation of radiation transfer efficiency

24 p4327 A69-42986

CHANCE-VOUGHT MILITARY AIRCRAFT

U MILITARY AIRCRAFT

CHANNEL CAPACITY

Multichannel amplitude analyzer for space applications, noting use as gamma-spectrometer component in Lunik 10 and 4096 bit/channel traffic capacity

01 p0084 A69-11315

Multistage detection systems probability characteristics with parallel stage realization, taking into account signal losses

02 p0206 A69-11604

Frequency locked loop /FLL/ to optimize loop filter and quantization of amplitude channel

03 p0390 A69-13202

Channel identification coding for data compressors, deriving optimum code word length for bit compression ratio and overflow identification scheme

03 p0391 A69-13219

Gaussian channels capacity, studying supremum of information transmission rates with small error probability

04 p0558 A69-15006

Multiple beam waveguide and optical delay line capacity increase by transmitting Gaussian beams clearly resolved at receiver

04 p0579 A69-15446

Domestic satellite communication system model for greatest possible amount of traffic using Saturn 5 propulsion systems, multibeam antennas, synchronous repeater platforms, etc

04 p0561 A69-15447

Satellite communication channel number and distribution optimization, obtaining malfunction probability for telephone service communication system [UN PAPER 68-95772]

06 p0886 A69-17030

Transistorized multichannel pulse height analyzer and recording system for balloon-borne cosmic ray payloads, discussing performance capacity

06 p0924 A69-17284

Data compression techniques compared for use in communications systems to minimize required number of samples and bits per sample

07 p1077 A69-18758

Waveform distortion resulting from adjacent channel crosstalk and from amplitude and phase nonlinearity in channel filters in DSB/SC telemetry link

07 p1083 A69-19130

Optimum linear feedback code for additive noise systems with average power constraint on transmitter to increase channel capacity

07 p1085 A69-19181

Algorithm for calculating Moore automaton or connected network channel capacity and source of input symbols for full capacity utilization

07 p1088 A69-19707

Multichannel microwave amplifier at L band frequencies, using several amplifiers in parallel

09 p1466 A69-22446

Simultaneous transmission of information signals and pseudonoise synchronization waveforms in common bandwidth [IEEE PAPER 67-TP-1173-COM]

10 p1655 A69-23532

Navigation accuracy and telecommunications system capacity interrelationships in economical improvement of air traffic control system over North Atlantic

10 p1723 A69-23704

Multistage detection systems probability characteristics with parallel stage realization, taking into account signal losses

11 p1835 A69-24711

Noise rejection and carrying capacity of wideband and narrowband discrete systems transmitting complex signals in concentrated noise spectrum

13 p2218 A69-27213

Delay time of pulse signals in radio channel transmission described by standard deviation of channel properties

13 p2218 A69-27215

Optimum thermal and nonlinear noise intensities distributions in frequency division multiplex satellite communications systems, relating relay station power, frequency band and channels

14 p2412 A69-29426

Two beam short wave channel capacity with beam separation at receiving end, noting dependence on channel properties and fading correlations

15 p2562 A69-30115

Unknown channels classes epsilon capacity applied to estimating capacity of channels with additive noise, discussing models and upper and lower bounds

15 p2570 A69-31142

Channel dropping filter for millimeter wave in low loss circular waveguide for overland telecommunications in bandwidth over 10 GHz

17 p2936 A69-33032

Communication channel information capacity determination through particle ensembles entropy analysis

19 p3334 A69-35885

Tactical Satellite Communications /Tacsat/ cost reduction, discussing jamming avoidance and mitigation, communications security, capacity increase and spectrum conservation

20 p3497 A69-38315

Geostationary satellite orbit used for communication satellites, noting ultimate limit of channels as related to separation angles between satellites

21 p3673 A69-38757

Satellite communication system capacity for segment of geostationary orbit extended to models involving two angular dimensions

23 p4131 A69-42521

Data compression from standpoint of epsilon entropy theory, considering precise measure of channel capacity necessary to describe data source

23 p4134 A69-42526

N-dimensional theorem for evaluating time continuous channel capacity or rate distortion function of random process

24 p4284 A69-42721

CHANNEL FLOW

NT OPEN CHANNEL FLOW

Inertia effect of flow between eccentric cylinders with rotating outer cylinder, calculating pressure and shearing distribution and force on inner cylinder

01 p0059 A69-10307

Gravity waves train propagation in cylindrical channel, discussing derivation by three dimensional flow analysis method

01 p0059 A69-10382

Indeformable gravity waves in horizontal cylindrical channel, using first and second order approximations for nearly uniform flow equations solutions

01 p0060 A69-10392

Two dimensional ionized plasma flow in coaxial channels calculated using differential equations

01 p0130 A69-10723

Steady state circular motion of fluid with variable rheological characteristics between coaxial cylindrical surfaces, obtaining velocity distribution

01 p0061 A69-10733

Steady state three dimensional MHD flow in variable profile channels calculated by reducing problem to two dimensional approximation using curvilinear coordinate system

01 p0131 A69-10776

Electromagnetic fields effect on turbulent boundary layer characteristics of compressible fluid on insulating wall of MGD channel

01 p0131 A69-10777

Turbulent flow between parallel plates, discussing turbulence generation by energy addition

01 p0061 A69-10993

MHD flow through circular, elliptic and rectangular straight channels with external magnetic field transverse to flow direction

01 p0132 A69-11209

Fluid logic circuits miniaturization for flow in straight and curved channels of various cross sections

02 p0196 A69-12084

Heat transfer of steady laminar flow of incompressible, viscous and electrically conducting fluid between parallel porous plates

02 p0289 A69-12235

Algorithm for Orr-Sommerfeld equation applied to stability of laminar flow, noting profile resembling mean velocity profile of turbulent flow in flat tube

02 p0233 A69-12573

Velocity measurement and flow pattern determination of plane shock waves during passage through channel diaphragm

02 p0234 A69-12589

Elastoviscous flow in curved channels, analyzing nonNewtonian effects for case of circular and elliptic walls

02 p0234 A69-12608

Similarity law for channel wall influence in wind tunnels valid for all flow velocities

02 p0192 A69-12830

Transonic flow around profile in blocked plane channel and in free jet, noting channel wall and jet edge effects on flow along profile

03 p0361 A69-13018

Steady laminar flow in two dimensional channel with different permeability porous walls and large injection at both walls

03 p0417 A69-13795

Stationary, moving and pulsating electrohydrodynamic flow between parallel dielectric plates and Couette flow, noting reaction concentration near wall

03 p0419 A69-13919

Unperturbed tube flow theory extended to flow through short axisymmetric tube

03 p0419 A69-13969

Thermodynamic comparison of MHD generators using Brayton and Rankine cycles, showing Rankine cycle conversion at higher channel Mach numbers for nonequilibrium ionization

03 p0369 A69-14154

Heat transfer covering heat conduction, channel flow, boundary layer flow, separated flow, etc

04 p0684 A69-14354

Average energy dissipation in MHD duct flow of arbitrary cross sectional shape, evaluating bulk temperature, net wall heat flux and pressure gradient

04 p0635 A69-14724

MHD channel flow temperature distributions with Hall effect, using formulation for momentum and energy equations

04 p0635 A69-14746

Reynolds number similarity argument, establishing relation between mean velocity at pipe or channel center and shear stress at wall

04 p0589 A69-14895

Monochromatic flexural waves passage through elastic insert between plates, determining wave absorptivity dependence on wave frequency

04 p0679 A69-14906

Quasi-neutral, steady, inviscid and nonheat conducting flow of conducting gas with high magnetic Reynolds number in plane channel with transverse magnetic field

04 p0636 A69-14984

Magnetic field effects on heat transfer between Ar plasma flow and channel wall, noting effects of temperature and Reynolds number

04 p0636 A69-14989

Irrational almost uniform plane flow of two immiscible inviscid liquids on horizontal bottom in channel, noting permanent gravity waves

04 p0590 A69-15055

MHD flow in square cross sectional channel in transverse magnetic field with conducting walls parallel to magnetic field

05 p0799 A69-15697

Real liquid turbulent flow of two parallel eddy streams between two parallel walls with given periodic roughness

05 p0747 A69-16034

Incompressible turbulent boundary layers in channel flow using constant temperature hot-wire anemometer, emphasizing measurement in viscous sublayer [ASME PAPER 68-FE-26] 05 p0747 A69-16066

Pressure recovery of straight channel divergence diffusers at high inlet Mach numbers [ASME PAPER 68-WA/FE-19] 05 p0698 A69-16095

Mathematical problem of MHD thermal entrance regions for parallel plate channel solved by Galerkin method [ASME PAPER 68-WA/HT-10] 05 p0803 A69-16118

Approximate method for calculating subsonic gas flows in curvilinear channels for gas admission control in arc welding 06 p0908 A69-16828

Viscous MGD channel flow in boundary layer approximation with heat conduction, transforming resultant partial differential equations set to system of ordinary differential equations 06 p0966 A69-17523

Shock formation in supersonic plasma flow guided by magnetic channel up to magnetic barrier 06 p0966 A69-17524

Lorentz force sustained energy discharge, discussing cesium added argon flow across magnetic field in disk channel 06 p0969 A69-17910

Linear approximation of ionization instability in disk channel of nonequilibrium MHD generator, calculating interatomic collisions frequency as function of temperature 06 p0871 A69-17911

MHD flows in channels of MHD devices, emphasizing two and three dimensional problems 06 p0969 A69-17913

Approximate solution of equations for boundary layer flow of conducting medium on insulating and electrode walls of MHD generator channel 06 p0871 A69-17914

Nonsimilar MHD channels boundary layers on insulating walls noting influence of loading factor, wall temperature and Hall effect on separation [AIAA PAPER 69-46] 06 p0972 A69-18192

Steady flow circuit characteristics in square cross section channels of planar geometry fluid control elements in case of laminar flow 07 p1118 A69-18293

Natural frequency of fluid oscillations in complex pipelines 07 p1119 A69-18745

Numerical analysis of stabilization of one component conducting plasma in two dimensional coaxial duct 07 p1190 A69-18757

Conducting gas acceleration in strong unsteady electromagnetic field, discussing channel flow in relation to time and pressure gradient 07 p1191 A69-18988

Navier-Stokes equations solved for viscous incompressible fluid flow due to laminar jet flow into channel in presence of magnetic field 07 p1120 A69-18997

MHD flow in channels with abruptly widening sections and finned walls under transverse magnetic field, discussing effects on drag 07 p1192 A69-19016

Power losses in MHD channel due to longitudinal end effects related to finite dimensions of electrodes and terminal insulators 07 p1193 A69-19030

Weightlessness effect on critical heat flow during forced motion of water in different kinds of channels 07 p1243 A69-19616

Turbulent incompressible MHD flow between two parallel smooth plates in transverse magnetic field, determining magnetic Reynolds number 07 p1195 A69-19736

Semilogarithmic law of velocity and temperature for turbulent flow in circular channel, examining analogy between momentum and energy transfer 08 p1420 A69-19877

Free surface of electrically conducting liquid in gradually varied supercritical regime in horizontal rectangular channel 08 p1362 A69-20273

Discharge structure and stability of nonequilibrium plasma undergoing supersonic flow through linear MHD channel 08 p1366 A69-20788

Highly turbulent boundary layers on walls in channels using laser light sources 09 p1515 A69-21434

Convective MHD channel flow in vertical channel subjected to temperature and pressure gradients, discussing wall conductances effects on flow rate and heat transfer 09 p1545 A69-21441

Navier-Stokes equations solution applicable to source type low Reynolds number flow through conical nozzles 09 p1482 A69-21976

Subsonic channel flow of frictionless barotropic gas through oscillating grid, investigating perturbation velocity field and aerodynamic forces on airfoils 10 p1631 A69-22905

Incompressible Newtonian flow between two parallel plates, noting marginal stability condition, mean velocity profile and turbulence 10 p1678 A69-22909

Optimum operation modes of MHD converter 10 p1636 A69-23095

MHD flows in MHD generator channel under magnetic field, analyzing steady laminar flow during entry and Hall effect on conductivity temperature dependence 10 p1734 A69-23455

Quasi-neutral plasma formation in hydrodynamic channel flow, discussing ignition and breakdown processes in preionized gaseous flow 10 p1737 A69-23467

Two dimensional flow of unipolar medium in electrodynamic power generation channel, discussing stationary model, electric field and ion density distributions 10 p1638 A69-23486

Thin wall flow of circular jets in bounded transverse flow, showing hydrodynamical parameter of mixture effect on jets dimensionless path 10 p1679 A69-23567

Laminar elasticoviscous flow of liquid with short memory in two dimensional channel with porous walls 10 p1680 A69-23668

Magnetic field induced nonequilibrium argon plasma ionization relaxation processes obtained with allowance for flow parameters change in relaxation zone 11 p1922 A69-24225

Heat transfer in MHD parallel plate channel flow in entrance regions analyzed by Galerkin method, noting Hall current effect 11 p1923 A69-24290

Characteristics method for solution of differential equations representing time changes of wind and pressure fields in divergent barotropic channel flow 11 p1911 A69-24585

Two dimensional stratified flow over obstacle in finite height channel, noting lee waves and drag increase with decreasing speed 11 p1869 A69-24892

Self similar axisymmetric and plane laminar viscous gas channel flows noting exponential or hyperbolic law of decrease in static pressure along channel 11 p1875 A69-25482

Boundary layer calculation during laminar MHD channel flow under crossed magnetic and electric fields using successive approximation method 11 p1932 A69-25491

Viscous flow-induced vibrations of elastically restrained flat plates in narrow channel, considering one dimensional viscous flow theory 11 p1991 A69-25515

Flow in linear MHD channel with two permeable electrodes, solving Riemann boundary value problem for electric field in channel 11 p1934 A69-25727

Gas jets collision flowing from parallel wall channels, applying solution to calculating geometrical characteristics of fluid jet amplifiers 12 p2016 A69-25879

Navier-Stokes equations for compressible gas, generalizing viscous channel flow of heat conducting gas to slip flow of rarefied gas 12 p2061 A69-25887

Electrohydrodynamic channel flow using boundary problem and approximations corresponding to flow of unipolarly charged and polarized media 12 p2135 A69-26400

Monochromatic flexural waves passage through elastic insert between plates, determining wave absorptivity dependence on wave frequency 12 p2182 A69-26659

Incompressible elastic-plastic solid flow through rough converging conical channel analyzed using Mises yield condition and Prandtl-Reuss equations 12 p2063 A69-27114

One dimensional calculations of finite length MHD uniform traveling wave induction generator, discussing

magnetic field distribution, electrical impedance and conversion efficiency 13 p2206 A69-27494

MHD induction converters operational characteristics calculations with simultaneous considerations for finite length and channel width 13 p2207 A69-27496

Nonconducting vanes end effects on electrical characteristics of MHD channels, analyzing current density, Joule losses and finite length vanes 13 p2306 A69-27497

MHD channel mercury flow with hydraulic shock in transverse magnetic field, determining characteristic values distribution over range of principal parameters 13 p2307 A69-27499

Laminar-turbulent transition in MHD channel in transverse and longitudinal magnetic fields, discussing Reynolds equation for large Hartmann numbers 13 p2307 A69-27500

Velocity profiles of MHD flow through electrically insulated circular channel in transverse magnetic field 13 p2307 A69-27501

Optimal mean radius and half height of channel of liquid metal coaxial linear induction MHD generator with unilateral and bilateral excitation 13 p2207 A69-27507

Rayleigh-Taylor instability in synchronous liquid metal MHD generators, showing stabilization by channel positioning and threshold power rating 13 p2307 A69-27508

LF spectral analysis of flowing water pressure pulsations behind single bulge on hydrodynamic channel smooth wall at low disturbance level 13 p2246 A69-27535

Resonance tube excitation from energy depletion in central part of subsonic jet supplying tube 13 p2247 A69-27738

Turbulent flow in circular tube and parallel plate channel, considering molecular viscosity and duct shear stress variation 13 p2248 A69-28131

Combined free and forced convection flows in parallel channel systems and in single channels, discussing metastable flow regimes, single phase laminar flows, etc 13 p2377 A69-28152

Model to study viscous flow characteristics in channel with porous walls and constant suction, noting non-monotonic velocity profile 14 p2429 A69-29015

MHD channel flow calculations by quasi one dimensional approximation, considering potential drops at electrodes 14 p2500 A69-29904

Boundary problems solution for electromagnetic field two dimensional distributions in MHD channels at arbitrary magnetic Reynolds numbers, considering longitudinal terminal effects 14 p2500 A69-29906

Pressure drop fluctuations amplitude and frequency effect on channel resistance and magnetic field effect on fluctuations intensity in laminar conducting fluid flow 14 p2501 A69-29909

Shunting effect of conducting channel walls in induction MHD machines, discussing wall effects on pressures during pumping and generating operation modes 14 p2405 A69-29912

Velocity distribution effect on electric field at walls for axisymmetric flow of electrolyte in circular channel in magnetic field of E shaped inductor 14 p2501 A69-29915

Longitudinal pressure distribution in MHD channel with electrodes parallel to applied transverse magnetic field 14 p2501 A69-29918

Monograph on Prandtl number effect on heat transfer and pressure loss in artificially roughened channels 15 p2717 A69-30934

Radiative luminescence of gas discharge plasmas in channel with substantial radial heat transfer determined from energy balance measurement 15 p2662 A69-30978

Boundary layers coalescence on plane convergent channel walls investigated with analytic formulas for velocity distribution, shear stress, layer thickness, etc 15 p2592 A69-31009

Eigenfrequency spectrum and stability of perfectly conducting inviscid incompressible fluids in cylindrical channels and twisted magnetic fields, noting flowfields and critical wavelenghts 15 p2664 A69-31063

Heat and mass transfer in porous medium with bulk flow in thin adjacent channel, applying Green function analysis to hydrogen-oxygen fuel cell
15 p2552 A69-31115

Wind tunnel investigation of turbulent gas flow heat transfer and hydrodynamic drag in variable pressure gradient field of divergent-convergent channel
15 p2548 A69-31173

Nonequilibrium plasma boundary layer along channel insulator wall, noting different electron and heavy particle temperatures
[AIAA PAPER 68-134] 16 p2821 A69-31873

Diagonal conducting wall /DCW/ MHD generator channel flows in formulation including Hall effect, electrode drop and electrode wall angle
16 p2736 A69-32172

Linearized motion equations for conducting gas in magnetic and electric field solved for coaxial channel and free jet, assuming small Reynolds number and parallel flow
17 p3010 A69-33016

Conducting fluid and plasma rotation between concentric cylinders due to crossed fields, determining velocity distribution, induced magnetic field and kinetic energy
[AIAA PAPER 69-726] 17 p3011 A69-33472

Turbulent velocity distribution and wall friction calculated from eddy viscosity distribution for concentric annulus
17 p2956 A69-33575

Minimum Reynolds number and Malkus theory of turbulent channel flow, discussing stability, equilibrium flow, and stationary turbulence via variational theorem
17 p2957 A69-33764

Asymptotic theory of Orr-Sommerfeld problem for symmetric channel flow stability
17 p2958 A69-34151

Channel heat transfer determination based on thermal conductivity coefficients as functions of temperature gradients in channel wall materials
18 p3230 A69-34988

Flow viscosity and heat conduction effects on shock wave propagation in bent channel with weak Mach reflection
18 p3124 A69-35326

Fraunhofer holography for measurement of three dimensional flowfield velocity components, investigating rectangular channel flow
19 p3305 A69-35729

Combined free and forced convection hydromagnetic flow and heat transfer of electrically conducting fluid subjected to temperature variations in vertical channel
19 p3380 A69-36304

Interaction effects between mixing and pressure distribution of heterogeneous flow in channel, deriving criteria for predicting pressure variation sign
19 p3300 A69-36785

Laminar flow of compressible viscous gas in channels of variable cross section
20 p3457 A69-37089

Thesis on turbulent velocity distribution and wall friction in flow channels of various cross sections
20 p3515 A69-37925

Prandtl mixing length theory for flow in pipes and channels described by spatial exponential form, developing velocity profile and friction factor
[ASME PAPER 69-FE-48] 20 p3516 A69-37978

LF spectral analysis of flowing water pressure pulsations behind single bulge on hydrodynamic channel smooth wall at low disturbance level
20 p3518 A69-38202

Heat transfer in curved channel as function of inlet configurations, obtaining Nusselt number equations for thermal and mixed convection and laminar flow
21 p3850 A69-38866

Channel flows energy stability, discussing Couette and plane Poiseuille flows, velocity profiles, vorticity maxima, etc
21 p3697 A69-39675

Flow structure in wake behind cylinder in plane channel, discussing circulation zone variation and velocity and turbulence distribution at various channel cross sections
21 p3698 A69-39850

Viscoelastic fluid steady flow in porous walled channel, examining mass flow solution continuity
22 p3930 A69-40118

Laminar MHD flow in porous walled channel in transverse magnetic field, determining velocity distributions, induced fields and current over channel cross section
22 p3989 A69-40256

Internal aerodynamics of centrifugal compressor impeller, discussing impeller channel airflow model, impeller exit flow, rotating channel flow, etc
[RAES PAPER 19] 22 p3859 A69-40498

Skin friction and mean velocity profiles measured for fully developed 1000-10,000 Reynolds number flows in pipes and channels
22 p3932 A69-40897

Pulsed energy balance expressions for turbulent characteristics of incompressible circular flow in channel with inserted rotating cylinder
22 p3933 A69-41028

Linear stability criteria for two dimensional wave perturbations effects on nonNewtonian fluid flow between parallel plates
22 p3933 A69-41108

Momentum, heat and mass transfer in turbulent channel flow emphasizing phenomena close to wall, using boundary layer growth-breakdown model
24 p4407 A69-42914

Prandtl number influence on heat transfer and pressure drop characteristics of roughened channels, determining friction factor
24 p4407 A69-42915

Transition from axisymmetric to nonaxisymmetric flow in rotating annulus, using two layer quasi-geostrophic model
24 p4345 A69-43150

Separation flows in flat channel with step recess, analyzing dynamic characteristics in mixing region, in wake of rarefaction waves and in attachment zone
24 p4247 A69-43498

Secondary flow occurrence and geometry in viscous turbulent flow in square channel, using iterative solution
24 p4303 A69-43501

Local Nusselt number beyond abrupt circular channel expansion tested for Reynolds numbers with air as working fluid
[ASME PAPER 69-HT-35] 24 p4411 A69-43532

Gas phase self induced pressure field and laminar velocity distribution of working fluid within closed heat pipe channels analyzed by momentum integral method
[ASME PAPER 69-HT-22] 24 p4412 A69-43546

Gas velocity and pressure influence on electrical breakdown potential of Ar, N and He between parallel flat plate and concentric electrodes
24 p4359 A69-43693

CHANNELS

Single channel binary PSK communication systems performance influenced by degree of RF coherence between transmitter and receiver
07 p1082 A69-19109

Low temperature optically thick boundary layers influence on spectroscopic temperature measurements in plasma MHD channels
10 p1731 A69-23434

CHANNELS (DATA TRANSMISSION)

Cross correlation methods for determining systems time domain response adapted to communications channel evaluation, discussing computer simulation of on-line testing
16 p2750 A69-31757

Signal propagation in channel subject to static investigated using Fokker-Planck type equation in statistical mechanics methods
16 p2753 A69-32437

Automatic multichannel transient monitor for electrical transient detection and data processing, transmission and storage on aircraft
17 p2947 A69-34135

Meteor burst communication channel parameters for low data rate telemetry, considering signal amplitudes, decay, duty cycle, multipath, phase stability, trail location and variations
19 p3271 A69-36250

Optimum power allocation for RF carrier phase error and synchronization error in two channel system
19 p3274 A69-36283

Noiseless feedback schemes for digital and analog transmission over additive white Gaussian noise channels
21 p3671 A69-38405

Radio relay FM channel data transmission, evaluating cumulative thermal noise due to IF amplification at each station
21 p3672 A69-38653

EEG with combined multichannel radiotelemetry and telephone for onward data transmission
21 p3664 A69-38978

Single channel pressure telemetry unit with magnetic latching or RF switch for chronic implantation
23 p4100 A69-41295

Algebraic decoding techniques, discussing channel models, errors correction, hardware and software, etc
23 p4119 A69-41746

Linear filtering effects in channel with binary direct sequence antipodal biphase modulation in presence of white noise and sinusoidal interference, noting variance
23 p4122 A69-41774

EHF earth-satellite link communication channel emphasizing down link, discussing weather models, atmospheric absorption and temperature, channel coherence bandwidth, etc
23 p4129 A69-42506

CHAPLYGIN EQUATION

Self adaptive circuit parameters synthesis of systems using amplitude-frequency characteristic by Chaplygin theorem
03 p0410 A69-13685

Approximate methods for integration of equations of plane isentropic motion of gas at supersonic velocities
05 p0699 A69-16674

Hodograph for lifting airfoil with subsonic velocity at infinity, using Chaplygin compressibility law for computation
[ONERA-TP-631] 07 p1049 A69-18416

Approximation of Chaplygin plane motion equations of gas flow at high supersonic velocities
07 p1120 A69-18754

Blasius-Chaplygin formula for generalizing Kutta-Joukowski theorem concerning jet profiles, calculating resultant of hydrodynamic forces
11 p1867 A69-24355

Modified Chaplygin method for approximate integration of Cauchy problem for differential equations, estimating rate of convergence
15 p2644 A69-30656

CHAPMAN-ENSKOG THEORY

Chapman-Enskog method applied to Boltzmann equations for transport coefficients for low density polyatomic gases
01 p0123 A69-10388

Plasma kinetic equation obtained by method similar to Chapman-Enskog method
08 p1369 A69-20816

Electrical conductivity of partially ionized plasma, noting nonapplicability of Enskog-Chapman method and use of Lorentzian gas model
09 p1546 A69-21584

Enskog method for Boltzmann equation, analyzing asymptotic nature of integral kinetic equation for molecular mean free paths and Laplace probabilities
09 p1481 A69-21889

Transport coefficients for almost Lorentzian mixture, computed as perturbation to coefficients for true Lorentzian mixture, compared to Chapman-Enskog method results
11 p1997 A69-24286

Chapman-Enskog procedure extension for binary gas mixtures, obtaining diffusion equation from revised relaxation time of component velocities
11 p1921 A69-24308

Boltzmann equation for system of equations governing evolution of gas of identical particles with discrete velocity distribution, applying Chapman-Enskog method
11 p1921 A69-24325

Chapman-Enskog theory applied to observed stellar velocity distribution function, attributing deviation from Maxwellian function to negative K effect
15 p2687 A69-30549

Thermal conductivity coefficient of gas mixtures at low temperatures obtained using quantum diffusion model and Chapman-Enskog method for Boltzmann equation
21 p3848 A69-38638

CHAPMAN-FERRARO PROBLEM

Chapman-Ferraro approximation for magnetic interior field line configuration in plasma flow around two dimensional dipole, allowing for tail formation and neutral sheet
18 p3129 A69-34955

CHAPMAN-JOUGET FLAME

U CHEMICAL EQUILIBRIUM

U DETONATION

U FLAME PROPAGATION

CHAPMAN SHEAR LAYER

U SHEAR LAYERS

CHARACTER RECOGNITION

Image recognition algorithms estimated for effectiveness by formulas minimizing classification error probability
23 p4134 A69-41954

CHARACTERISTIC EQUATIONS

U EIGENVALUES

U EIGENVECTORS
CHARACTERISTIC FUNCTIONS
 U EIGENVALUES
 U EIGENVECTORS
CHARACTERISTIC METHOD
 U METHOD OF CHARACTERISTICS
CHARACTERS
 U SYMBOLS
CHARGE CARRIERS
 NT FREE ELECTRONS
 NT HOLES [ELECTRON DEFICIENCIES]
 NT MAJORITY CARRIERS
 NT MINORITY CARRIERS
 Recombination rate dependence on nonequilibrium charge carriers concentration at semiconducting surface 01 p0136 A69-10253
 Nonequilibrium carriers during semiconductor depolarization, noting microwave oscillation energy absorption in silicon and zinc sulfide crystals 01 p0138 A69-10434
 Recombination radiation from excitons and free carriers in epitaxial GaAs with impurities at liquid He temperatures 01 p0140 A69-11253
 Faraday effect of free carriers on n-type GaSb at 20 K, determining mass and mobility of electrons from Hall effect and conductivity 02 p0298 A69-12039
 Anisotropic pressure influence on silicon diodes parameters 02 p0223 A69-12839
 Carrier generation-recombination in space charge region of asymmetric p-n junction, noting experimental results for InSb diodes 03 p0487 A69-13641
 Carrier scattering mechanisms in n-type GaP, measuring IR radiation absorptivity in Te doped GaP 03 p0492 A69-14168
 N-type GaAs single crystal magnetoresistivity, noting charge carrier scattering mechanisms 03 p0492 A69-14177
 Quality control of semiconductor materials, analyzing homogeneity by statistical distribution of nonequilibrium carriers based on photoconductivity measurement 04 p0642 A69-14856
 Electric field strength and helix pitch in induced cholesteric-nematic phase transitions, noting activation energy for charge carrier production 04 p0555 A69-14964
 Distribution of current carrier concentration and mobility in p-type silicon doped with phosphorus ions 04 p0643 A69-15254
 Current carrier concentration temperature dependence in Te-doped silicon single crystals by analyzing photoconductivity spectra 04 p0644 A69-15267
 Charge carrier concentration determination by double probe in plasma with Druyvesteyn distribution of incident electron flow 05 p0800 A69-15737
 Impurity transfer in doped and undoped epitaxially grown GaAs films, studying substrate dopants effect on carrier concentration profiles 05 p0807 A69-15957
 Fresnel drag produced by relativistic addition of electron velocities in semiconductors measured by changes in refractive index 05 p0807 A69-16026
 High temperature effects on gallium arsenide crystals current carriers lifetime, discussing recombination characteristics and impurity photoconductivity 05 p0809 A69-16551
 Recovery of carrier concentration and lifetime in n- and p-type Si during annealing after irradiation by 10 Mev electrons, noting impurities effects 06 p0974 A69-16865
 Hall effect and resistivity of n-type gallium arsenide phosphides doped with Te and Se 06 p0978 A69-16988
 Charge carrier lifetime measured in intrinsic conductivity range of Cd doped InAs to define recombination mechanism, relating temperature dependence to surface impurities recombination 06 p0979 A69-16997
 Ambipolar motion of light injected photocarriers in cadmium-mercury-telluride in terms of diffusion and drift in electric fields 06 p0979 A69-17154
 Energy separation and electrons effective mass ratio of conduction bands of tellurium doped GaSb obtained by free carrier Faraday rotation measurements 07 p1201 A69-19464

Resonance effects during piezoelectric interaction between charged drift wave and flexural wave in semiconductors with one sign current carriers 08 p1371 A69-19806
 Time dependent velocity distribution functions for carriers calculated in weakly ionized plasma in external electric field 08 p1362 A69-20265
 Distribution and carrier type in germanium bar in electric field, relating distribution obtained by using Hall effect to avalanche phenomenon 08 p1372 A69-20277
 Semiconductor current fluctuations associated with generation, recombination and annihilation of random electron-hole pairs at ohmic contacts 08 p1372 A69-20545
 HgTe-CdTe single crystals homogeneity and Cd distribution obtained by Bridgman and/or zone melting studied for carrier concentration and electron mobility 09 p1557 A69-21737
 Inhomogeneity distribution of carrier concentration and electrovoltaic effect in GaAs devices analyzed by scanning electron microscope 09 p1557 A69-21746
 Static characteristics of transistors dependence on current carriers surface recombination in inactive base region, noting strong electric field influence 09 p1464 A69-22287
 Recombination rate dependence on nonequilibrium charge carriers concentration at semiconducting surface 09 p1559 A69-22646
 Radial distribution profiles of charge carriers in low temperature gas discharge plasma accounted for in terms of volume recombination 11 p1925 A69-24330
 Metallic impurities effect on Ge surface charge and recombination properties, noting fast and slow electron density changes by forbidden band penetration 11 p1939 A69-25703
 LF noise mechanism for forward biased semiconductor p-n junction, noting charge carrier capture in electron traps of carrier depleted region 11 p1857 A69-25705
 Current-voltage characteristics of p-n-p-n diodes, discussing collector voltage effect on current carrier concentration distribution in diode base 13 p2236 A69-28531
 Nondrifting n-p-n semiconductor current gain dependence on surface recombination rate 13 p2236 A69-28547
 Anisotropic scattering of current carriers in semiconductors, obtaining general expression for mobility tensor with variational principle 14 p2508 A69-29667
 Inhomogeneous distribution of nonequilibrium current carrier concentrations in semiconductors with electrons and holes of different lifetimes, noting instability 15 p2665 A69-30041
 LF electrostatic oscillations of inhomogeneous solid state plasma with small number of current carriers in parallel external electric and magnetic fields 15 p2665 A69-30042
 Finite scattering cross section in current carriers scattering on impurities in compensated semiconductors, assuming unscreened Coulomb potentials 15 p2666 A69-30063
 Quality control of semiconductor materials, analyzing homogeneity by statistical distribution of nonequilibrium carriers based on photoconductivity measurement 15 p2667 A69-30248
 Carrier lifetime in p-nu-n diodes, discussing error of forward pulsed diode method by Wilson and alternative model 16 p2757 A69-31615
 External magnetic force and internal Coulomb force influence on carriers in conduction or valence band of semiconductor, considering H atom spectra 16 p2826 A69-31824
 Multilayer multijunction solar cells with carrier generation within diffusion length of junction, discussing epitaxial techniques 19 p3251 A69-35690
 Fe-doped p-type gallium arsenide single crystal radiative recombination emission during current carriers transition from deep acceptor level into valence band 19 p3392 A69-36611
 HgTe-CdTe single crystals homogeneity and Cd distribution obtained by Bridgman and/or zone melting studied for carrier concentration and electron mobility 20 p3584 A69-38215

Injection and excitation of charge carriers in CdS single crystals, analyzing current-voltage characteristics dependence on electrode separation, temperatures and electric field 21 p3779 A69-38423
 Current carrier concentration and magnetic field as factors influencing laser frequency resonance mixing in semiconductors with narrow forbidden bands 21 p3737 A69-38998
 Electrical properties of semiconductors in HF electromagnetic field, showing Dember type EMF dependence on carrier response to field inhomogeneity 22 p3993 A69-40605
 Cross sections of charge carrier capture by ions in gamma irradiated P-Al-Si glass with metal oxides additions measured for evaluating radiation stability improvement 23 p4180 A69-42470
 Electroluminescence in doped p-type GaAs single crystal diodes ascribed to double injection of nonequilibrium current carriers 24 p4288 A69-43739
CHARGE DISTRIBUTION
 Microstrip-like transmission lines analyzed by method based on line capacitance variational calculation and charge density distribution 01 p0044 A69-10625
 Cross field plasma instability resulting in charge density irregularities shown to meet requirements for ionospheric irregularities model 01 p0073 A69-11178
 Charge image detector for reading information as extended spatial charge distribution on dielectric layer surface, using vibrating conducting probe scanner 02 p0248 A69-11822
 Step recovery switching silicon transistor combining planar and mesa technologies, discussing charge storage and fall times 02 p0215 A69-11937
 Charge and energy composition of particles in solar flare, discussing rigidity spectra of singly and multiply charged nuclei 06 p0989 A69-17280
 Cosmic ray magnetic spectrograph for measurement of momentum spectrum, charge ratio and specific ionization of muons, discussing magnetic and scattering displacement 06 p0925 A69-17302
 Long transmitting dipole antenna, studying current and charge distributions by Wiener-Hopf technique 08 p1281 A69-20019
 Distribution and carrier type in germanium bar in electric field, relating distribution obtained by using Hall effect to avalanche phenomenon 08 p1372 A69-20277
 Transient processes in conduction type MHD generators due to external circuits induction distribution 12 p2017 A69-26545
 Electrostatic charge distribution on ultrahigh vacuum cleaved silicates including instrumentation, UV irradiation, half life, Paschen relation, etc 13 p2322 A69-28018
 Electric field profile and turbulence ratio relationship in free atmosphere as function of vertical current density, conductivity, potential gradient and charge density 13 p2295 A69-28523
 Integral charge neutrality effect on local space charge density of MHD generator channel, examining electrode couple for Faraday generators 15 p2664 A69-31055
 Einstein field equations solutions generated via static spherically symmetric mass and charge distributions 16 p2812 A69-32053
 High energy cosmic ray muon charge ratios at large zenith angles measured as function of momentum by using spectrometer 17 p3023 A69-33321
 Biased electrostatic probes determining free stream charge density and ionization risetime in supersonic flows in arc heated pressure driven shock tube 19 p3291 A69-35715
 Computerized design parameters for realizable over-driven bimode varactor frequency doubler based on charge-voltage relationship at break point 20 p3505 A69-37299
 Dielectric response of semifinite metal surface to external point charge in linearized Fermi-Thomas approximation, discussing potential in metal and vacuum 20 p3583 A69-37498
 Negative charge distribution in thunderstorm clouds related to direction of storm movement, noting vertical column 20 p3572 A69-37908

Steady state sunlit lunar surface electrostatic charge and potential distributions, noting electrons photoemission and solar wind particles collection
20 p3609 A69-38077

Ionization formula linking nitrogen ion charge density ratio to plasma temperature
22 p3990 A69-40714

CHARGE EXCHANGE

Ionization, neutralization and charge exchange processes in ionosphere, detailing dependence of photodissociation and collision detachment of negative ions
01 p0066 A69-10598

Ion-molecule collisions of Ar-Co and N-No pairs, discussing charge exchange reaction rates and spiraling nature
05 p0797 A69-16428

Energy flux into earth thermosphere due to fast corpuscular neutrals arising from charge transfer collisions between solar protons and neutral interstellar H
05 p0817 A69-16654

Charge exchange cross sections in methane and ammonia, noting dissociative charge exchange role
06 p0884 A69-17114

Perturbation methods for exchange and Coulomb energy of hydrogen molecule, calculating Hamiltonian by wave function
07 p1186 A69-19446

Charge exchange collisions in ground state and ionic hydrogen incident on cesium vapor, measuring beam components after passage through target
08 p1356 A69-20737

Nonlinear charge exchange and dissociative recombination effects on night F region decay compared with linear theory
10 p1685 A69-23832

Slow charged products of charge exchange collisions by ions in molecular gases, comparing kinetic energies during various reactions
13 p2301 A69-27455

Sodium atoms and NO molecules role in atomic O 6300 and 5577 Å emissions in comet Mrkos 1957d due to charge exchanges and dissociative recombination
14 p2523 A69-29707

Elementary processes cross sections in charged states changes during proton-hydrogen molecule interactions
15 p2655 A69-30963

Charge transfer cross section between mercury ion and Cs assessed, considering ion engine positive ion beam neutralization
16 p2835 A69-31895

Ion momentum transfer through charge exchange in mixture of ion gases and parent neutral gases under thermal nonequilibrium, noting role of Boltzmann equation
16 p2822 A69-32108

Interatomic potential between alkali ions and rare gas atoms, using model accounting for repulsive and attractive exchange forces
16 p2815 A69-32464

Charge exchange cross sections and electron losses in hydrogen ion beam impacting on water vapor molecules
19 p3378 A69-36190

Afterglow decay rates of Zn II laser lines in spontaneous emission measured, indicating thermal energy charge exchange excitation and CW oscillation
21 p3735 A69-38598

Charge exchange of solar wind protons passing shock front, noting turbulent subsonic motion of randomized hot solar wind protons in shadow cone
22 p4008 A69-41208

CHARGE SEPARATION

U POLARIZATION [CHARGE SEPARATION]

CHARGE TRANSFER

Low collision energy charge transfer and dissociative charge transfer between rare gas ions and molecular nitrogen, measuring nitrogen ion kinetic energy distributions
05 p0796 A69-15909

Charge transfer cross sections for slow ion production in nitrogen molecular ion beams incident on hydrogen and deuterium
05 p0796 A69-15914

Effective cross section of resonant cesium ions charge exchange determined by retarding field method, considering dependence on ion velocity
06 p0959 A69-16908

Potassium ion resonant charge exchange, determining relation between effective cross section and ion velocity, using retarding field method
06 p0959 A69-16909

Two body rate coefficients for charge transfer reactions of nitrogen, oxygen and NO positive ions to Na atoms measured using flowing afterglow system
07 p1185 A69-19303

Forward scattering of metastable and ground state argon atoms after argon ion-atom charge transferring collisions, discussing excitation resonances
08 p1354 A69-19809

Diffusion coefficient, velocity distribution function and velocity averages for gaseous ions moving in strong electric fields, considering ion-gas molecule charge transfer collisions
08 p1355 A69-20209

Phase characteristics and magnetic mirrors effect on charge motion in spatially periodic magnetic field
09 p1551 A69-22036

Charge and traveling wave interaction in circular waveguide in resonance regime solved by Krylov-Bogoliubov asymptotic method
09 p1551 A69-22037

Surface charge exchange in metal oxide silicon capacitors generated at low temperatures by surface state free carrier trapping
10 p1744 A69-23179

Charge transport in high pressure RF glow discharge in air at atmospheric pressure based on model plasma
10 p1740 A69-23662

Organic semiconductors physical properties and intermolecular charge transfer between donor and acceptor
13 p2317 A69-27799

Charge transfer and vibrational excitations in hydrogen molecular ion-hydrogen gas collisions
13 p2302 A69-28196

Alkaline metal adsorption on high work function metals with charge transfer, measuring polycrystalline Mo photoelectric emission as function of Cs coverage
14 p2507 A69-29275

Charge flow injection into MOS substrate attributed to gate pulses, correlating charge magnitude with pulse frequency
15 p2573 A69-30033

Reaction rate constants of ion-molecule interchange reaction as function of temperature, flow velocity, activation energy and constant part of steric factor P
16 p2747 A69-32312

Ionization, recombination and charge transfer in upper atmosphere during aurora, considering quasi-equilibrium ion-electron concentrations
17 p2961 A69-33417

Charge transport in n and p type samples of beta phase semiconducting iron disilicide, noting effect of room temperature doping
19 p3390 A69-36556

CHARGED PARTICLES

NT ALPHA PARTICLES

NT ANIONS

NT ANTIPROTONS

NT ARGON PLASMA

NT ARTIFICIAL RADIATION BELTS

NT BETA PARTICLES

NT CATIONS

NT CESIUM PLASMA

NT COLD PLASMAS

NT COLLISIONLESS PLASMAS

NT CONDUCTION ELECTRONS

NT COSMIC PLASMA

NT DEUTERIUM PLASMA

NT DEUTERONS

NT ELECTRON PLASMA

NT ELECTRONS

NT FREE ELECTRONS

NT HELIUM PLASMA

NT HIGH ENERGY ELECTRONS

NT HIGH TEMPERATURE PLASMAS

NT HOT ELECTRONS

NT HYDROGEN PLASMA

NT INNER RADIATION BELT

NT MAGNETICALLY TRAPPED PARTICLES

NT METAL IONS

NT METALLIC PLASMAS

NT NEGATONS

NT NONEQUILIBRIUM PLASMAS

NT NONUNIFORM PLASMAS

NT OUTER RADIATION BELT

NT PHOTOELECTRONS

NT PI-ELECTRONS

NT PLASMA CLOUDS

NT PLASMA JETS

NT PLASMA LAYERS

NT PLASMA SHEATHS

NT PLASMA SLABS

NT PLASMAS [PHYSICS]

NT POLARONS

NT POSITRONS

NT PROTON BELTS

NT PROTONS

NT RADIATION BELTS

NT RAREFIED PLASMAS

NT RELATIVISTIC PLASMAS

NT ROTATING PLASMAS

NT SOLAR PROTONS

NT SOLAR WIND

NT STELLAR WINDS

NT THERMAL PLASMAS

NT TOROIDAL PLASMAS

Semiclassical wave emission and absorption theory applied to charged particles interaction with waves in magnetized plasmas
01 p0126 A69-10123

Soviet investigations of solar and cosmic electromagnetic and charged particle radiations by balloon, rocket and satellite measurements
01 p0145 A69-10945

Inner Van Allen belt proton dose rate and spectral charged particle environment profiles correlated, noting agreement with theoretical values
01 p0145 A69-11081

Partial differential equation for distribution function in transport of charged particles in earth magnetosphere
01 p0147 A69-11320

Leptonic quarks with various charges in cosmic rays, determining upper limit of flux in underground measurements
02 p0306 A69-11547

Electric discharge in gas flow with magnetic field, showing varying charged particle density as function of argon-cesium pressure
02 p0285 A69-11570

Coupling coefficients of global and vertical fluxes of charged cosmic ray component in stratosphere measured by radiosondes
02 p0306 A69-11659

Magnetosphere studies in France noting magnetosphere characteristics, wave propagation, charged particles, particle precipitation mechanisms in auroral zones and polar caps
02 p0242 A69-11904

Primary cosmic radiation charge spectrum measurement during 1965 minimum solar activity, using balloon-borne Cerenkov scintillation counter
02 p0308 A69-12043

Diffusion effect on particle buildup in deionizing steady plasma flux linked to plasma concentration in presence of electron temperature gradients
02 p0291 A69-12483

Etching techniques for revelation and viewing of fossil charged particle tracks in meteoritic and terrestrial minerals
02 p0245 A69-12569

Scattering of energetic charged particles in weakly unstable plasma for integrated spectrum of plasma electric field autocorrelation function
03 p0475 A69-13151

Electropropulsion by thruster using colloidal carbon particles charged by electron bombardment to provide thrust, noting specific impulse
03 p0495 A69-13396

Charged particle dynamics in spiral interplanetary magnetic field model, discussing electric drift velocity, point of origin and distribution
03 p0503 A69-14015

Acceleration of charged particles in strong DC magnetic field by electrostatic waves with spatially varying phase velocities integrated numerically on IBM 360/65
03 p0479 A69-14028

Stormer problem of charged particle motion in magnetic dipole field, discussing analytical method for high and low energy particles
03 p0504 A69-14127

Charged particle density of unsteady plasma from Stark broadening of Balmer H beta line, using time scanning image converter
03 p0481 A69-14145

Charged particle motion in time dependent external magnetic field
03 p0504 A69-14235

Charged particles motion in spatially modulated magnetic field solved using modification of Krylov-Bogoliubov asymptotic method
04 p0633 A69-14297

Asymptotic method for studying charged particle motion in spatially modulated magnetic field
04 p0634 A69-14298

Charge multiplication in crystals, analyzing ionization rate, avalanche breakdown in p-n junctions, pair production and impact of impurities
04 p0641 A69-14503

Ion and electron contaminating currents removal in vacuum evaporating devices, using biased field plates
04 p0577 A69-14875

Capture of electrically charged micrometeorites and corpuscles in magnetic field of gravitating dipole, noting necessary condition on particle motion
04 p0659 A69-14962

Total conserved momentum-energy of electromagnetic interaction of system of point charges in Wheeler-Feynman theory, noting mass defect of connected system
04 p0631 A69-15058

H resonator for charged particle beams combination at output of double beam linear accelerator
05 p0727 A69-15639

Multielectrode analyzers for measuring properties of ionospheric charged particles
05 p0761 A69-15702

Charged particle motion in constant direction magnetic field varying exponentially with time, discussing electric field effect on particle motion
05 p0801 A69-15744

Dynamic response of solids induced by charged particle interaction noting laser interferometric measurement of surface stresses
05 p0771 A69-15817

Spectroscopic charged particle concentration determination, discussing error and limits of applicability in low temperature plasma
05 p0762 A69-15899

Charged particles injection into captured radiation zone of Van Allen belts during main phase of magnetic storm indicated by proton data analysis
05 p0815 A69-16057

Diurnal variations of neutral and charged particle temperatures in equatorial F region
05 p0755 A69-16270

Electrogasdynamics /EGD/ engineering, discussing generators and compressors
05 p0804 A69-16586

Equation for charged particle motion in electromagnetic wave field propagated along magnetic field applied to nonlinear wave propagation in plasma near cyclotron resonance
06 p0963 A69-16905

Photomultipliers response to energetic particles in terms of background current using data from OGO experiments
06 p0923 A69-16932

Soviet satellite exploration of space magnetic fields and charged particles, noting Proton satellites and protons and carbon nuclei inelastic interactions [UN PAPER 68-95768]
06 p0986 A69-17031

Charged particle environment in synchronous orbit region, discussing electrons and protons under influence of geomagnetic field
07 p1204 A69-18340

Energy losses of clusters of charged particles moving through unbounded isotropic plasma manifesting non-linearity in interaction of particle generated fields
07 p1189 A69-18528

Simplification of equations for two temperature plasma composed of electrons, singly charged ions and neutral atoms, noting effect of viscosity and thermal force
07 p1190 A69-18693

Plasma diagnostics by spectroscopic techniques, measuring polarity dependences of temperature and charged particle concentration for flows with shock wave and periodic structure
07 p1190 A69-18695

Ion composition and charged particle temperatures at 300-600 km from sounding rocket and topside sounder Alouette 2 measurements
07 p1124 A69-18839

Charged particle motion in electromagnetic field from basic equation of motion for magnetosphere, discussing dipolar magnetic field, Stormer trapped particle theory, etc
07 p1208 A69-19355

Geomagnetic field line stretching outward due to energy entry in form of large number of charged particles or increase in particle temperature /inflation/
07 p1127 A69-19357

Low energy charged particles in earth magnetosphere observed by OGO satellite
07 p1208 A69-19358

Particle dynamics measured by ATS satellite synchronous orbit, discussing flux time variations during geomagnetic disturbances
07 p1209 A69-19371

Equation describing statistically trapped particle motion under influence of fields varying in time and space
07 p1209 A69-19375

Plasma flux measurements by charged particle traps in Venus vicinity by space vehicle Venus 4, discussing low concentration of charged particles
07 p1222 A69-19613

Solution of equations of motion of charged particles in constant magnetic field and variable electric field
08 p1361 A69-20213

Integrated charged particle energy spectra from gridded electrostatic analyzers, relating retarding potential curve to particle floating potential, kinetic temperature, etc
08 p1364 A69-20521

Cosmic ray Li, Be and B nuclei measurements, analyzing differential energy spectra, L-M ratio, atmospheric and solar modulation
08 p1380 A69-20638

Charged body moving at subsonic velocity normally through stratified elastic half space composed of film on homogeneous half space
08 p1417 A69-20753

Inertia of electrically charged spherical body calculated on basis of relativistic stress energy
08 p1352 A69-20756

Charged particles concentration change during vertical propagation of acoustic wave in F layer found transforming electric field into circularly polarized wave
09 p1484 A69-21528

Vertical transport rate of charged particles in F region, allowing for vertical velocity gradients
09 p1485 A69-21529

Charged particles equations of motion in earth magnetosphere in polar storms, considering auroral zone, diurnal variations and electron and proton velocities
09 p1485 A69-21535

Charged particle acceleration in interplanetary medium, discussing protons and plasma oscillations interactions
09 p1575 A69-21541

Quantum mechanical description of ionizing reactions of highly charged positive ions in solar corona, obtaining approximate sum and selection rules
09 p1596 A69-22054

Cosmic charged particle acceleration in electromagnetic field described by vector and scalar potentials, constituting plane electromagnetic wave propagating along z axis
10 p1756 A69-22816

Charged particles motion in geomagnetic field from analyzing spatial distribution within framework of two dipole magnetosphere model
10 p1756 A69-22818

Primary specific ionization in noble gases by charged particles
10 p1726 A69-23128

Book on thermodynamics of charged and polarized layers covering matter in electric fields, general framework theory, applications, etc
10 p1724 A69-23159

Solid state AC voltage circuitry for measuring and controlling charged particle detector signals
10 p1662 A69-23256

Nonequilibrium ionization in central regions of low temperature plasma, describing charged particle drift by using diffusion time concept
10 p1732 A69-23440

Coupling coefficients for integral charged component of cosmic rays determined from measuring azimuthal geomagnetic effect on rays observed in crossed telescopes
10 p1770 A69-23925

Density modulated charged particle beam interaction with plasma under paramagnetic resonance, analyzing longitudinal oscillations and parametric instability zone
10 p1741 A69-23947

Longitudinal electric field distribution and charged particle density in magnetic mirror under potential difference between magnetic equator and plane
10 p1689 A69-24204

Adiabatic theory of charged particle motion in electromagnetic field, applying asymptotic methods of nonlinear oscillations theory
11 p1948 A69-24857

Stable particle trapping zone in magnetosphere, discussing results of adiabatic theory application to charged particle motion in earth magnetic field
11 p1948 A69-24858

Solar cells degradation by charged particles in space, considering protection by filter, silicon properties and use of cadmium cells
11 p1825 A69-24870

Charged particle motion in periodic electromagnetic field, constructing dynamic variables describing motion
11 p1927 A69-25100

Charged particle concentration near electrodes in high current pulsed discharge with separated flames at atmospheric pressure determined by measuring quadratic Stark effect
11 p1927 A69-25219

Charged aerosols production for electrohydrodynamic processes by spraying liquids through capillary at high electric field strengths into high pressure air flows
12 p2138 A69-26631

Boundary layer parameters behind shock wave front in ionized gas calculated with allowance for charged particle diffusion
12 p2139 A69-26713

Charged particle population dynamics in outer radiation zone of magnetosphere, discussing ring current particles, protons, electrons, alpha particles and electric field
12 p2150 A69-26743

Charged particles influx from cusp shaped regions of stagnant plasma trapped in vicinity of two magnetic cusps on polar magnetopause
12 p2151 A69-26945

Charged primary cosmic rays responsible for relative intensities of muon-poor extensive air showers at mountain and sea levels
12 p2152 A69-27099

Electrohydrodynamic flows at large electric Reynolds numbers, obtaining Bernoulli and Cauchy-Lagrange integrals
13 p2305 A69-27379

Slow charged products of charge exchange collisions by ions in molecular gases, comparing kinetic energies during various reactions
13 p2301 A69-27455

Fast charged particles measurements by Cerenkov counter in Cosmos 137 satellite, noting hard electron flux and cosmic ray radiation spectrum
13 p2327 A69-27693

Comet interaction with solar wind, assuming field tail coupling of ionized comet material to solar wind ions
13 p2349 A69-27817

Cerenkov radiation from point charge uniformly moving along external magnetostatic field in warm anisotropic plasma, noting excitation modes and propagation frequencies
13 p2307 A69-27964

Charged particles generation by liquid subjected to high electric field for efficient bipolar microthruster [AIAA PAPER 67-728]
13 p2325 A69-28220

Stable particles heavier than nucleons in extensive cosmic ray showers detected by delayed coincidences relative to shower electron photon component
13 p2331 A69-28402

High energy ionization bursts in cosmic ray showers electron photon component, obtaining bursts power spectrum and component energy dependence
13 p2332 A69-28404

Cosmic ray particles with fractional charge at sea level searched by scintillation counters with spark chambers, estimating quark flux intensity
13 p2333 A69-28425

Coupling coefficients of global and vertical fluxes of charged cosmic ray component in stratosphere measured by radiosondes
13 p2334 A69-28690

Effective recombination coefficient in lower ionosphere determined from charged particle spectra obtained by rocket sounding in Canada
14 p2511 A69-28960

Electrostatic screening in isothermal symmetrically charged and quasi-neutral plasmas, noting confinement in electrostatic trap
14 p2490 A69-29035

Low energy charged particle motion parallel with magnetic force lines analyzed in magnetosphere model with constant electric field
14 p2512 A69-29040

Electric field determination from charged particle concentration in wake of body moving in rarefied plasma, noting hydrodynamics similarity
14 p2517 A69-29068

Horizontal electric fields relations to charged particle fluxes in polar auroral ionosphere
14 p2437 A69-29070

Geomagnetic cut-off influence on charged particle dynamics in geomagnetic field, applying charged particle motion theories to magnetosphere fields
14 p2513 A69-29099

Stark effect applicability to charged particle concentration in nonstationary plasma
14 p2497 A69-29790

Duoplasmatron charged particles energy spectra analyzed as function of discharge parameters
14 p2501 A69-29955

Charged particle motion in magnetic mirror trap, observing time dependence with respect to orbital magnetic moment conservation
15 p2659 A69-30724

Steady oscillations of active nonlinear system of nonisothermal plasma and charged particle flux, noting steady ion-acoustic waves

15 p2662 A69-30947

Spectroscopic measurements of charged particle concentrations in jet produced by pulsed plasma generator

15 p2663 A69-30991

Charged particle motion in superposed Heliotron and biconical cusp magnetic fields, considering particle confinement

16 p2817 A69-31643

Numerical analysis of charged particles radial distribution in radiation belts extended to geomagnetic tail for low energy auroral electrons

16 p2850 A69-32102

H resonator for charged particle beams combination at output of double beam linear accelerator

16 p2762 A69-32497

Charged particles concentration change during vertical propagation of acoustic wave in F layer found transforming electric field into circularly polarized wave

16 p2783 A69-32523

Vertical transport rate of charged particles in F region, allowing for vertical velocity gradients

16 p2783 A69-32524

Charged particles equations of motion in earth magnetosphere in polar storms, considering auroral zone diurnal variations and electron and proton velocities

16 p2783 A69-32530

Charged particle acceleration in interplanetary medium, discussing protons and plasma oscillations interactions

16 p2851 A69-32536

Charged colloids generation by electrostatic spraying for thruster concept, subjecting metal capillary needles to AC voltage [AIAA PAPER 69-495]

16 p2846 A69-32773

Ground state energy inequalities for N particle non-relativistic quantum mechanical system, showing non-saturating gravitational forces and increasing binding energy per particle

17 p3028 A69-32900

Atmospheric ion concentration increment by electrostatic lens to facilitate electrical properties measurements of charged particles in submicroscopic range

17 p2971 A69-32928

Cosmic ray shower axis mean distance from apparatus determined by measuring muon to charged particles densities ratio

17 p3024 A69-33580

Linear irreversible thermodynamics theory as applied with conservation principles and Maxwell relations to charged particle motion in electromagnetic field, noting Onsager coefficients role

17 p3075 A69-34142

Capture of electrically charged micrometeorites and corpuscles in magnetic field of gravitating dipole, noting necessary condition on particle motion

18 p3197 A69-34725

Positive ion concentration in D region, using spherical stationary electrostatic probe in weakly ionized collision dominated gas

18 p3128 A69-34804

Inhomogeneities time buildup in lower ionosphere weakly ionized plasma during charged particle concentration perturbations and source temperature variations

20 p3525 A69-37658

Charged particles injection into captured radiation zone of Van Allen belts during main phase of magnetic storm indicated by proton data analysis

20 p3591 A69-37967

Upper atmosphere particles, luminosity and electron concentration measurements documented in input, storage and energy radiation classes, determining recombination coefficients

21 p3707 A69-38491

Charged particles beam penetration effects produced in atmosphere, determining particle diffusion and trajectory using Spencer moments and Monte Carlo methods

21 p3709 A69-38502

Universal dependence of density fluctuations on specific entropy derived from equation describing material composed of neutral particles and equal number of charged and antiparticles

21 p3771 A69-38995

Reentrant albedo flux and singly charged particles directional asymmetry in upper atmosphere estimated from oriented telescope observations over Hyderabad

22 p4005 A69-40519

Infinites in statistical theory of radiative processes when applied to plasmas containing charged particles and radiation

22 p3991 A69-41055

Thermal conductivity relationship to heat transport coefficients for gases and liquids with charged or uncharged particles

23 p4237 A69-41324

Electron concentration vertical profile in ionosphere in presence of horizontal wind shifts determined using E layer charged particle redistribution approximation

23 p4155 A69-41840

Magnetospheric stable charged particle beams for pearl pulsations and discrete VLF radiation in geomagnetic field, attributing synchronization to space charge

23 p4206 A69-41851

Quark mass and charge interpretation during particle track photographic analysis of air shower cores by delayed expansion Wilson cloud chamber

24 p4383 A69-42945

CHARGING

Aerospace NiCd batteries charge control, discussing depth of discharge, limiting voltage and environmental temperature interrelationship

23 p4071 A69-42282

CHARPY IMPACT TEST

Natural aging effects on fracture characteristics of aluminum weldments, investigating precracked Charpy impact toughness

01 p0086 A69-10537

Fracture mechanics and data from instrumented Charpy impact test

05 p0780 A69-16431

Thickness and drilled holes effects on notch toughness of Charpy V notch bars over wide temperature range

10 p1798 A69-23087

Thin walled maraging steel tube toughness determined by Charpy precrack testing of transverse and longitudinal impact properties

13 p2269 A69-28183

Fracture toughness of AlZnMgCu alloys, employing sharp notch tension, tear and precracked Charpy impact tests

16 p2800 A69-31780

CHARRING

Charring phenolic nylon ablator material pyrolysis and surface recession for cyclic and constant combined convective and radiative heating [AIAA PAPER 69-151]

06 p1036 A69-18055

Charring ablator char zone nonequilibrium flow and chemical reaction kinetics as function of temperature, using thermal environment simulator

24 p4409 A69-43512

CHARTS

NT FLOW CHARTS

NT GRAPHS [CHARTS]

NT METEOROLOGICAL CHARTS

NT PATTERN MAP

Radar range height angle charts for plotting earth based radio or radar system vertical plane coverage diagrams

01 p0031 A69-10633

Secular variations distribution on earth surface, plotting isopor charts from mean annual values of magnetic elements /1960-1965/

10 p1687 A69-23920

Viscosity-temperature chart for hydrocarbons permitting linear extrapolations into low viscosity high temperature regions

10 p1753 A69-23975

Cartographic representation methods in climatological regional charts, discussing topographical elements, scale, screen patterns and area color

12 p1214 A69-25893

Eye chart determination and layout for digital transmission system by computer simulation

21 p3678 A69-38776

Illumination effect on air navigation chart reading during flight, using questionnaire data

24 p4271 A69-42605

CHEBYSHEV APPROXIMATION

Chebyshev polynomials maximum property, examining effect of roundoff errors in Horner scheme for floating point arithmetic

03 p0456 A69-13553

Single row riveted joints, representing rivet forces by Chebyshev functions in homogeneous arrangements and obtaining equations for continuous joints from limit procedure

04 p0682 A69-15292

Ascent algorithm for Chebyshev solution of inconsistent linear equations, noting use for linear programming

04 p0626 A69-15318

Pseudoexact Chebyshev response curves for band-pass filter design, discussing phase response and time delay characteristics

08 p1283 A69-20227

Error estimation technique for Chebyshev series solution to ordinary differential equations

08 p1344 A69-20828

All-pass transfer functions of new class type for design of quadrature filter networks, using Chebyshev approximation

08 p1277 A69-21167

Chebyshev error norms of polynomial approximations for ideal filter minimized by emphasizing role of transfer function even and odd parts

08 p1299 A69-21168

Chebyshev filter with flat group delay obtaining transfer function, noting cascade synthesis and extended bisection theorem

08 p1299 A69-21169

Iterative Chebyshev approximation for computerized network design by linearizing original nonlinear programming

08 p1299 A69-21170

Transfer function of low pass filters with Chebyshev attenuation characteristic in stopband and predetermined phase or delay time realized by ladder network

08 p1300 A69-21171

Theorem for necessary and sufficient condition for continuity of Chebyshev operator

10 p1718 A69-22875

Low pass filters synthesis based on Chebyshev polynomials properties noting requirements of critical frequency, frequency response decline rate and tolerance range

11 p1887 A69-25210

Extremal controlled plants identification by Chebyshev orthogonal polynomials, comparing results with regression analysis

11 p1861 A69-25713

Chebyshev polynomial of even order used in synthesis of equally terminated low pass lumped and distributed filters of even order

13 p2233 A69-28068

Polynomial approximations in perturbational navigation and guidance schemes including Chebyshev and least square approximations

19 p3368 A69-35664

Chebyshev series approximations for Bose-Einstein functions of orders one to ten, noting computability of Fermi-Dirac functions and polylogarithms

24 p4341 A69-43231

CHECKOUT

Data analysis methods for integrated data processing system for onboard in-flight checkout for launch vehicle evaluation [AIAA PAPER 67-911]

01 p0037 A69-11024

In-flight and flight line checkout techniques for foreign object damage to jet engines

01 p0056 A69-11055

Automatic preventive maintenance program for hybrid computer system by checking individual units

04 p0568 A69-15359

Dual processor checkout system providing isolation of malfunctioning unit from memory and ensuring decision making by operative unit

04 p0568 A69-15361

Interpretive Checkout Test Language /CCTL/ designed in near English form for aerospace checkout tasks

04 p0569 A69-15364

Electronic system checkout in SAAB 37 Viggen, using computer controlled test equipment

05 p0726 A69-16767

Real time computer controlled telemetry system readiness testing and validation, describing automatic closed loop checkout methods and remote display controller

10 p1660 A69-23270

Flexible control module for real time automated checkout requiring programming by personnel with strong software background

11 p1843 A69-25072

Automatic system self test technique known as central integrated test subsystem /CITS/ for logically testing avionics systems

11 p1866 A69-25083

Scientific satellite checkout system tests by manual, automatic and self test control

13 p2243 A69-28480

Automatic quantitative checkout equipment for telemetry circuit of Diamant satellite booster before launching
16 p2750 A69-31727

Mathematical model for operational readiness of dormant systems /periodically checked missiles/, discussing time distribution to failure detection, occurrence and between tests
18 p3142 A69-34477

Failure detection methods, discussing percent checkout, failure sensitivity, undetectable failures, etc
18 p3146 A69-34511

Signature analysis diagnostic methods for reliability tests involving final product checkout and early fault detection
19 p3322 A69-35574

CHECKOUT EQUIPMENT

U TEST EQUIPMENT

CHELATE COMPOUNDS

U CHELATES

CHELATES

Liquid lasers properties and composition including organic complex compounds, organic dyes, rare earth elements in polyphosphoric acid, etc
11 p1893 A69-24353

CHEMICAL ANALYSIS

NT ELECTROPHOTOMETRY

NT GAS ANALYSIS

NT GAS SPECTROSCOPY

NT MICROANALYSIS

NT NEPHANALYSIS

NT NEUTRON ACTIVATION ANALYSIS

NT OZONOMETRY

NT PAPER CHROMATOGRAPHY

NT QUALITATIVE ANALYSIS

NT QUANTITATIVE ANALYSIS

NT SPECTROSCOPIC ANALYSIS

NT URINALYSIS

NT VOLUMETRIC ANALYSIS

Meteoritic extraterrestrial materials sampling for chemical, petrographic and metallurgical analyses, discussing microstructure and optimum specimen weight for representative analysis
[UN PAPER 68-95381] 01 p0150 A69-10480

Analytical techniques for in-flight monitoring of aerospace water supplies for potability, emphasizing rapidity, sensitivity and reproducibility
01 p0019 A69-11339

Volcanic gas from lava lake, noting carbon and sulfur gases depletion during cooling and solidification
02 p0236 A69-11466

Lunar surface material chemical composition in lunar mare and on Tycho crater north rim, noting Surveyors 5, 6, and 7 alpha analyses
04 p0655 A69-14658

Microchemical analysis for diffusion measurement of laser produced lithium plasma in uniform magnetic field
05 p0762 A69-15960

Gas-liquid and thin layer chromatography and nuclear magnetic resonance techniques to steric analysis of diketopiperazines
07 p1075 A69-19498

Auger and photoelectron spectroscopy for chemical analysis, noting effects of sample thickness, sample potential, surface contamination and X ray incident angle
07 p1075 A69-19775

Priming explosives analysis suggesting physicochemical methods for high purity products for space applications
10 p1750 A69-23012

Chemical and mineralogical study of Kodaikanal meteorite silicate and metal phases, using optical, X ray and electron microprobe techniques
11 p1953 A69-24335

Chemical composition analysis of one mesosiderite and seven chondrites, with notes on mineralogy and chemical procedures
11 p1953 A69-24336

Bioorganic comparative analysis of desert soils, Precambrian shales and meteorites by automated pyrolysis-gas chromatography-mass spectrometry system for future Mars soil analysis
[JPL-TR-32-1368] 11 p1832 A69-25640

Aircraft accident toxicology, guidelines for collection, preservation, shipment and analysis of specimens and test result interpretation
12 p2022 A69-25842

Quantitative separation of elements in gamma prime from precipitation hardened high temperature nickel-base alloys by anodic dissolution
13 p2277 A69-27408

Organic analysis of Pueblito de Allende meteorite using thin layer chromatography or combined gas chromatography and mass spectrometry
13 p2337 A69-27520

Sugars identification as trifluoroethylacetyl polyol derivatives by gas-liquid chromatography
15 p2558 A69-31539

Sterile soil from Antarctica found to contain organic carbon, noting significance for biological exploration of Mars
16 p2746 A69-31552

Extraterrestrial life detection experiments integrated into single multipurpose space laboratory, including chemical analyses, metabolism identification, observation for molecular and/or cellular growth and replication
17 p2912 A69-32970

Free lysine and dinitrophenyl /DNP/ derivatives determined quantitatively by ion exchange chromatography
17 p2917 A69-33651

Chemical analysis and paragenesis of manganian ilmenite from Sierran adamellite using electron microprobe
19 p3302 A69-35977

Iron meteorites analysis for Ni, Co, P, C, S and Cu elements by milling technique, noting superiority degree based on Co-Ni correlation
19 p3417 A69-36130

Ti determination in presence of Nb or Ta by extraction-photometric method with diantipyrylmethane and thiocyanate
20 p3544 A69-37812

Colorimetric method to determine small amounts of Mn in metallic Ti by potassium periodate solution
20 p3544 A69-37813

Aircraft breathable LOX purity, water percentage and carbon dioxide and methane proportions, determining other contaminants after concentration by refrigeration
21 p3666 A69-39273

Chemical analysis of lunar surface by devices exploiting alpha particle backscattering and proton production by alphas placed by Surveyor 5, 6 and 7
22 p4012 A69-40088

Norwegian lichen species chemical investigation for aromatic compounds, hydroxy fatty acids, amino acids, soluble and bound sugars
23 p4080 A69-41428

CHEMICAL ATTACK

U INTERGRANULAR CORROSION

CHEMICAL AUXILIARY POWER UNITS

Secondary cells with liquid lithium anodes and immobilized fused salt electrolytes
04 p0552 A69-15330

CHEMICAL BONDS

NT HYDROGEN BONDS

Temperature dependent isomer shift and anharmonic binding of Sn 119 in niobium stannide, measuring Mossbauer recoil free fraction
01 p0134 A69-10009

Second order susceptibilities of III-V and II-VI compounds using Phillips model, discussing second optical harmonic in III-V compounds with tetrahedral bonds
01 p0138 A69-10365

Metal ionic reactions with weak chemical bond breaking and three body reactions forming molecular ions without bond breaking, discussing sporadic E deionization
01 p0071 A69-11168

Photoionization curves and threshold energies for fluorocarbon and trifluoromethyl halide molecules and ions, calculating ionic heats of formation and bond dissociation energies
02 p0205 A69-12464

Photolytic conversion of allene to cyclopropylidene, discussing cyclononadiene in vapor phase and resulting product
02 p0205 A69-12721

Liquid metal adsorption induced embrittlement, noting bond strength reduction and grain boundaries penetration
03 p0448 A69-13872

Hydrogen effect on interatomic bonds of Ti beta alloy and Young modulus, noting measurements at various temperatures
04 p0618 A69-15178

Activation energies of bimolecular multivalent transfer reactions of gaseous compounds, considering bond dissociation energy, length and order
[WSCI PAPER 68-48] 07 p1239 A69-18321

Enthalpies determination of adduct formation of sulfoxides, sulfanilamides and thionylamides with

trimethylalane, noting replacement effect on electron donating ability of oxygen
07 p1074 A69-18631

Chemical bond nature and properties in cyclic compounds of carbon and graphite, presenting bond energy computation method
07 p1171 A69-18932

Direct chemical bonding effect on flexural strength and flexural modulus of glass fiber reinforced plastics, noting degradation reactions
08 p1341 A69-20514

Rotational spectrum of ethylene episulfoxide to determine molecular structure, particularly orientation of C sub 2 S ring
08 p1268 A69-20535

Increased Ti heat resistance by forming solid solutions and compounds having various dispersions and bond strength
09 p1525 A69-22140

Mass spectral fragmentation of substituted aliphatic glycols and hydroxylated carbon-carbon bond
09 p1448 A69-22551

Covalence degree of activator-ligand chemical bonds effect on spectroscopic properties of transition metals
11 p1907 A69-25031

Ionic and biradical mechanisms in thermal and photo cis-trans isomerizations elucidated by planar and twisted configurations of polyenes
13 p2216 A69-27618

Glass finish and glass resin chemical bond adhesion roles in filament wound structures response, failure and filament strength
14 p2468 A69-29345

Carbon fiber reinforced plastics properties improvement by applying organosilanes, discussing silanol bond formation
16 p2803 A69-31806

Sulfur hexafluoride dissociation in argon at various temperatures and pressures, using shock tube techniques to determine unimolecular parameters
18 p3100 A69-35475

Active center chemical bond alteration influences on luminescence characteristics of phosphate glasses, noting quick energy transfer via ions
20 p3552 A69-37017

Molecular rearrangements of nitrene intermediates, suggesting role in bond formation and breaking at nitrogen
20 p3484 A69-37485

Chemical bond nature and properties in cyclic compounds of carbon and graphite, presenting bond energy computation method
21 p3752 A69-39153

Adenylates condensation in protein-associated amino acids as clue to peptide bond synthesis within protocellular structures
22 p3895 A69-40048

Deoxyribonucleoside triphosphate substrate binding to Escherichia coli DNA polymerase, conducting equilibrium dialysis
22 p3898 A69-41074

DNA and d/A-T/ oligomers enzyme binding to DNA polymerase by sucrose density gradient centrifugation
22 p3898 A69-41075

Dimer bond energies analysis in Mg and Ca dimer molecules, approximating characteristic temperatures and virial coefficients
23 p4195 A69-42210

Sequence preparation of protected peptide polymer bond with anion exchange resin using solid phase transesterification
24 p4279 A69-42713

Helix to coil transition for triple stranded macromolecule in solution, calculating ring weighting and partition functions and intact bonds
24 p4353 A69-43812

CHEMICAL CLEANING

Solution velocity and turbulence effects on solvent cleaning of corrosion resistant steel tubing, discussing fluidity forces and cleaning formulation
08 p1318 A69-19807

Substrates ultraclean surface preparation methods, examining crystal cleaving and crushing, heating, chemical cleaning, ion bombardment, etc
14 p2455 A69-29348

Step cathodic flux cleaning of furnace brazed Al assemblies used in combination with ultrasonic and chemical conversion coating techniques
24 p4319 A69-42938

Ti-Al alloy structure manufacturing technology covering forming, cleaning, chem-milling, machining, fastening and welding
24 p4324 A69-43431

Chemical treatment of Ti during processing, discussing protective coating, scale conditioning, surface contaminant removal and acid pickling
24 p4324 A69-43432

CHEMICAL COMPOSITION
NT CARBON DIOXIDE CONCENTRATION

Chemical composition effect on duraluminum supersaturated solid solution stability, presenting time vs temperature C curves of isothermal decomposition
01 p0094 A69-10396

Graphical and analytical interpolation methods for representing initial compositions in equilibrium thermodynamic systems
01 p0176 A69-10403

Venus cloud layer thickness and lower boundary estimation from data on chemical composition, temperature and pressure profiles of atmosphere
01 p0152 A69-10580

Microturbulent velocity parameter correlation to iron-to-hydrogen ratio for G dwarfs, using model atmosphere abundance analyses
01 p0154 A69-10877

Chemical composition of upper atmosphere and interplanetary space measured by Soviet sounding balloons and rockets, discussing flask sampling techniques
01 p0025 A69-10940

Chemical composition of various types of chondrites, determining quantitative proportions soluble and insoluble in acids
01 p0026 A69-11381

Stone meteorite chemical composition, analyzing chondrites Borodino, Lavrentevka, Alfianello and Nardoo II
01 p0026 A69-11382

Lunar composition analysis by measuring atomic and nuclear radiation emission from orbiter [AAS PAPER 68-197]
02 p0312 A69-11475

Capillary arc source spectroscopy, determining plasma temperature and pressure dependence on capillary geometry and discharge current
02 p0286 A69-11573

Tabular reduction of crystal structure chemical information for metals and semiconductors for material selection use
02 p0295 A69-11786

Numerical solution for ambipolar diffusion and kinetic decomposition of rotating body of complex chemical composition in ionized airstream
02 p0191 A69-12580

Sulfur-organic compounds association with aromatic hydrocarbons, noting oxidation inhibiting effect on petroleum oil
03 p0494 A69-13800

Combustion products temperature and composition in chamber or at nozzle exit calculated for fuels containing excess oxidizer ratios greater than unity
04 p0684 A69-14486

Lunar surface material chemical composition in lunar mare and on Tycho crater north rim, noting Surveyors 5, 6, and 7 alpha analyses
04 p0655 A69-14658

Amino acid composition of organic matrix in modern and fossil calcareous oolites
04 p0553 A69-14978

Chemical compositions and structural states of feldspar in recrystallized /Type 6/ chondrite meteorites, using electron microprobe analysis and X ray diffraction techniques
05 p0819 A69-15626

Chemical composition and phase identification in commercial grades of cemented carbides
05 p0780 A69-15989

Chemical composition of nuclear cosmic rays with Z greater than 22, noting etching techniques for utilizing meteoritic minerals as detectors
05 p0816 A69-16355

Stony meteorite Krahenberg, determining isotopic composition, rubidium and strontium age of dark and light portions by neutron activation analysis
05 p0826 A69-16439

Homogeneous main sequence star models with convective cores, considering core chemical composition, size and energy generation ratio mechanism
05 p0829 A69-16777

Elementary composition and origin of primary cosmic rays, discussing space techniques for observation of components
05 p0818 A69-16816

Chemical composition and morphological, structural, textural and mineralogical characteristics of chondrules and chondrites
07 p1212 A69-18548

Ti alloys chemical composition, fatigue life, stress rupture strength, crack susceptibility and nature of stress-strain rate
07 p1161 A69-18763

Ti alloy beta phase variations in quantity, composition and dispersion during quenching, thermomechanical treatment and aging
07 p1163 A69-18777

Chemical composition relationship to heat resistance of titanium alloys, using diagrams for establishing composition of new multicomponent alloys
07 p1163 A69-18780

Magnetic susceptibility of InP-GaAs solid solutions at various temperatures and for varying GaP content
07 p1200 A69-19013

Australasian microtektite physical and chemical properties, comparing refractive indices, specific gravities, composition trends, etc
08 p1305 A69-19815

Quantitative spectroscopy methods for determining data on chemical constitution of plasmas, treating optically thin LTE plasmas
08 p1363 A69-20465

Chemical composition of stellar atmospheres by model atmospheres, considering atomic transition, line broadening and thermodynamic equilibrium
08 p1402 A69-20904

Chemical composition and element abundance in solar atmosphere and photosphere, noting solar absorption and emission and energy spectrum data
08 p1402 A69-20905

Chemical composition of diffuse Orion Nebula and stars compared for lighter elements, considering solar system formation from interstellar medium
08 p1402 A69-20908

Chemical composition of atmospheres of oldest Galactic stars, considering element abundances, metal and helium content and nuclear activity of massive stars
08 p1402 A69-20909

Abundance determinations and spectrum intercomparisons in late type peculiar stars, discussing carbon and heavy metal star classes
08 p1403 A69-20910

Heat resistant nickel alloys for castings, tabulating chemical composition, mechanical properties, heat treatment, weldability, etc
09 p1522 A69-21608

Alloying elements effects on structure, mechanical properties, aging and composition of precipitation hardening intermetallic phases in Ni and Fe based alloys
09 p1525 A69-22143

Viscosity coefficients approximation for chemical compositions in chromosphere and coronal gas
09 p1602 A69-22217

Cepheid variable and F and G stars observed for neutral lithium line, searching for resonance lines of ionized beryllium in similar stars
09 p1604 A69-22402

Primordial solar system chemical composition for studies of origin and evolution, compiling solar composition data
09 p1608 A69-22745

Neutral atomic H content of small angular diameter galaxies, noting systematic radial velocities and total mass of galaxies
10 p1773 A69-22956

Chemical composition of chromium steels for optimum heat resistance properties, noting effects of nickel, nitrogen and ferrite and austenite-forming elements
10 p1708 A69-23000

Psychological, physiological and biochemical responses to controlled diets, determining regional and total body sweat composition of men working in temperate environment
10 p1644 A69-23314

Prolateness of Venus radius on basis of satellite microwave temperature measurements, chemical compositions and ice cap model
10 p1784 A69-23958

Chemical composition effect on glass fibers strength, discussing reasons for increased surface layer strength
10 p1717 A69-24045

Circumstellar grain compositions of stars with various O to C abundance ratios, calculating molecular equilibrium of condensates and gaseous compounds in stellar atmospheres
10 p1786 A69-24103

Nebular abundances allowing for temperature variations in nebula along line of sight, correcting changes in electron temperature along path of observation
10 p1787 A69-24116

Stellar evolution, computing sequences to establish solar model of primordial composition, comparing models with spectroscopic observations
10 p1788 A69-24126

Stellar models for chemical compositions to explain gap above main sequence in color-magnitude diagram of NGC 188
10 p1789 A69-24127

Chemical compositions and ages of M67 and NGC 188 determined from color-magnitude diagrams, noting stellar distribution near gap in diagram and He content
10 p1789 A69-24128

Lunar surface chemical composition using RF mass spectrometer
10 p1698 A69-24207

Chemical composition analysis of one mesosiderite and seven chondrites, with notes on mineralogy and chemical procedures
11 p1953 A69-24336

Liquid lasers properties and composition including organic complex compounds, organic dyes, rare earth elements in polyphosphoric acid, etc
11 p1893 A69-24353

Chemical composition of stony meteorites by analytical methods, discussing sample preparation and X ray fluorescence
11 p1953 A69-24358

Quality assessment of quantitative data on chemical composition of stony meteorites, considering precision and accuracy
11 p1953 A69-24359

Ethylene oxide and ethane low pressure fuel-rich flames mass spectrometry, analyzing composition and temperature profiles and OH radical role
11 p1831 A69-24478

Direct analysis of lunar surface chemical composition, considering soft landing probe and X ray isotope fluorescence method
11 p1832 A69-24629

Chemical composition of Venusian atmosphere by Mariner and Venus satellites, comparing upper atmospheres of Venus and earth
11 p1960 A69-24971

Equilibrium compositions of reaction products calculated by permutation over limiting equilibrium surface in reaction space, considering charged components and condensation products
11 p2001 A69-25224

Venus atmosphere chemical composition, surface temperature and pressure obtained by Venera 4 and Mariner 5
12 p2155 A69-26129

Physical parameters and chemical composition of DD Lac atmosphere from spectral analysis
12 p2156 A69-26219

Component ratio effect on pressure dependence of burning rate in ammonium and potassium perchlorate mixed with organic compounds, graphite and tungsten
12 p2027 A69-26474

Transensor implantation, sham implantation, no implantation and lighting effects on rat body composition, noting fat and water content
12 p2020 A69-26557

Temporal variation of metal content in galaxy, discussing stellar radiation pressure effects on heavy element abundance of interstellar gas
12 p2160 A69-26854

Quasar properties from cosmological nature, discussing red shift, luminosity, radiation intensity, absorption features, distribution, chemical composition, etc
12 p2168 A69-27049

Chemical composition of cermet material for radial sealing of high temperature gas turbines, ensuring structural stability and oxidation resistance
13 p2275 A69-27344

Chemical composition of nuclear active particle component of primary cosmic rays in extensive air showers
13 p2326 A69-27464

Hydrogen content in Ia supergiant spectra of type B, noting lack of Stark wings of Balmer lines
13 p2348 A69-27722

Composition dependence of carbon activity and carbon diffusivity in austenite
13 p2279 A69-27763

Solar wind quiet state thermal properties and chemical composition compared with coronal expansion hydrodynamic model predictions
14 p2513 A69-29098

Pressure sensitive adhesives composition, tapes tacking and peeling theory and tests including electrolytic corrosion and insulation evaluation
14 p2468 A69-29342

Stellar Si burning at constant temperature studied for various initial abundance compositions, noting convergence toward pure Si relaxation

14 p2529 A69-29983

Chemical composition effect on Cr-Ni-Mo-Ti stainless maraging steels mechanical properties

15 p2640 A69-30631

Chlorapatite and whitlockite compositions of phosphate minerals from chondrites determined by electron microprobe

15 p2690 A69-30706

Venus cloud layer thickness and lower boundary estimation from data on chemical composition, temperature and pressure profiles of atmosphere

15 p2691 A69-30750

Lower oxides of Si, studying chemical composition, formation conditions, stability and chemical and physical properties

15 p2643 A69-31245

Lattice components of heat conductivity and chemical composition relations of magnesium alloy solid solutions

16 p2824 A69-31567

Lower solar corona composition changes due to pressure and thermal gradients calculated with multicomponent diffusion equations

17 p3030 A69-33059

Gravimetric and IR absorption spectra analysis for determining heat resistance and chemical changes in organosilicon resins during heating

17 p2992 A69-33744

Curve of growth analysis for close binary HR 5317 indicating Mg, Mn, Ca and Sr overabundance respecting standard star 110 Her

18 p3191 A69-34297

Earth ecosystem chemical composition compared with Mars and Venus ecosystems to determine presence of life

18 p3193 A69-34361

Thermal coefficient of optical glasses refractive index determined by interferometry, noting relation to glass chemical composition

18 p3172 A69-35013

Sharps chondrite chemical, petrographic and mineralogical studies suggesting formation from complex and repetitious high temperature events and agglomeration processes

19 p3408 A69-36086

Reflectivity and chemical composition of metallic phase minerals in stone meteorites, showing optical characteristics sensitivity to composition

19 p3415 A69-36124

Mercury internal constitution and chemical composition, discussing models with iron cores and iron admixtures in mantle

20 p3597 A69-37331

Monograph on solid rocket propellants covering composition, combustion characteristics and energetic, mechanical and operational properties

20 p3585 A69-37441

Mare Tranquillitatis surface chemical composition data from Surveyor 5, comparing element abundances with meteorites and terrestrial rocks

20 p3601 A69-37517

Elements nucleosynthesis during thermonuclear burning of carbon at series of temperatures and for several initial compositions

20 p3612 A69-38163

Differential curve-of-growth analysis of late type giant stars yielding chemical compositions, discussing nature and size of uncertainties in estimates

21 p3800 A69-38700

Cosmic rays composition, origin, acceleration and propagation, describing two component models

21 p3789 A69-38814

Meteoritic compositions used to determine prehistoric cosmic rays composition and energy spectrum

21 p3789 A69-38815

Aluminum alloy laminates composed of two metallurgically bonded Al alloys of different composition

21 p3745 A69-38936

Electrical excitation discharge effect on molecular composition of flowing carbon dioxide gas laser, noting dissociation characteristics

21 p3736 A69-38940

Galactic cosmic rays, discussing chemical composition, isotopic separation, proton and alpha particles energy spectra, propagation, interactions, etc

21 p3791 A69-39502

Composition and thermal treatment effects on weldability of precipitation hardened Ni base alloy, analyzing heat affected zone cracking sensitivity

22 p3968 A69-39885

V systems applications and phase diagrams, discussing binary metallic systems, Kurnakov law, alloy properties dependence on composition, superconductivity, melting point, etc

22 p3968 A69-39887

Stony meteorite composition and structure studied for conditions of preplanetary stage of solar system

22 p4012 A69-40084

Chemical composition of galactic and solar cosmic rays, discussing differences from universal cosmic abundances, using Cerenkov counters, emulsions, etc

22 p4002 A69-40090

Fractionation mechanisms in early phases of planetary evolution sought to explain abundance problem in terrestrial planets

22 p4018 A69-40185

Preferential welding oxidation emphasized as element transfer mechanism in weld metal composition control

22 p3955 A69-40460

Weld porosity in Al alloys as function of composition variations, discussing water vapor contamination of welding arc

22 p3956 A69-40461

Meteorite chemical and mineralogical composition and classification

22 p4032 A69-40981

Joints structure, phase and chemical composition in kinetics of titanium diffusion brazing with copper

22 p3958 A69-41203

Tektites chemical composition showing minor concentration changes during melting used for parent material identification

23 p4210 A69-41346

Ivory Coast microtektites chemical composition from electron microprobe analysis

23 p4211 A69-41351

Component proportion and diffraction spectrum of macroblock thin films of indium telluride phase of In-Te system, using X ray and microanalysis

24 p4361 A69-42995

Gradually decreasing N concentration effects on composition, tissue production and oxygen yield of unicellular algae in continuous culture

24 p4263 A69-43201

CHEMICAL COMPOUNDS

Gas chromatography technique for separation and purification of chemical compounds for ionizing radiation detectors

02 p0249 A69-12011

CHEMICAL EFFECTS

Chemical treatment effects on mechanical properties of titanium alloy tubes

03 p0434 A69-13914

Adiabatic kinetic calculations of chemical additive effects on ignition delay of hydrogen-oxygen-argon gas mixtures

07 p1239 A69-18316

Chemical effects of solar wind and cosmic protons on solid bodies in space, discussing possible relation to origin of life

08 p1407 A69-20935

Chemical mechanism of two stage spontaneous ignition controlled by cool flames of alkane-air mixtures under engine conditions to avoid knocking

11 p1998 A69-24479

Porous cermet electrodes thermochemical protection by blowing neutral gas into electrode boundary layer, examining effect on volt-ampere characteristics

11 p1826 A69-25232

Reinforced plastics corrosion resistance, showing dependences on coupling agent and chemical compatibility between resin and fibers

14 p2467 A69-28853

Molybdenum disulfide dry film lubricant wear theory and test correlation problems, considering sintering self propagation due to chemical effect of environment

19 p3323 A69-35580

Potent chemical factors released from anterior hypothalamus of rhesus monkeys in response to thermal stress during thermoregulation

23 p4084 A69-41472

CHEMICAL ELEMENTS

NT ACTINIDE SERIES
NT ALKALI METALS
NT ALUMINUM
NT ALUMINUM 26
NT ANTIMONY
NT ARGON
NT ARGON ISOTOPES
NT ARSENIC
NT BARIUM
NT BERYLLIUM
NT BERYLLIUM 7
NT BERYLLIUM 10

NT BERYLLIUM ISOTOPES
NT BISMUTH
NT BORON
NT BORON ISOTOPES
NT BORON 10
NT BROMINE
NT CADMIUM
NT CADMIUM ISOTOPES
NT CALCIUM
NT CALCIUM ISOTOPES
NT CARBON
NT CARBON ISOTOPES
NT CARBON 12
NT CARBON 13
NT CARBON 14
NT CERIUM
NT CESIUM
NT CESIUM VAPOR
NT CESIUM 133
NT CHLORINE
NT CHROMIUM
NT CHROMIUM ISOTOPES
NT COBALT
NT COBALT ISOTOPES
NT COBALT 60
NT COPPER
NT DEUTERIUM
NT DYSPROSIUM
NT ERBIUM
NT EUROPIUM
NT FLUORINE
NT GADOLINIUM
NT GALLIUM
NT GERMANIUM
NT GOLD
NT HAFNIUM
NT HALOGENS
NT HELIUM
NT HELIUM ATOMS
NT HELIUM ISOTOPES
NT HYDROGEN
NT HYDROGEN ATOMS
NT HYDROGEN IONS
NT HYDROGEN ISOTOPES
NT HYDROGEN PLASMA
NT INDIUM
NT IODINE
NT IODINE ISOTOPES
NT IRIIDIUM
NT IRON
NT IRON ISOTOPES
NT ISOTOPES
NT KRYPTON
NT KRYPTON ISOTOPES
NT KRYPTON 85
NT LANTHANUM
NT LANTHANUM ISOTOPES
NT LEAD [METAL]
NT LEAD ISOTOPES
NT LIGHT ELEMENTS
NT LIQUID HELIUM
NT LIQUID HYDROGEN
NT LIQUID NITROGEN
NT LIQUID POTASSIUM
NT LIQUID SODIUM
NT LITHIUM
NT LITHIUM ISOTOPES
NT MAGNESIUM
NT MAGNESIUM ISOTOPES
NT MANGANESE
NT MANGANESE ISOTOPES
NT MERCURY [METAL]
NT MERCURY VAPOR
NT METALLOIDS
NT MOLYBDENUM
NT NEODYMIUM
NT NEON
NT NEON ISOTOPES
NT NICKEL
NT NIOBIUM
NT NITROGEN
NT NITROGEN ATOMS
NT NITROGEN IONS
NT NITROGEN 16
NT NUCLIDES
NT ORTHO HYDROGEN
NT OSMIUM
NT OXYGEN ISOTOPES
NT OXYGEN 18
NT PALLADIUM
NT PARA HYDROGEN
NT PHOSPHORUS 32
NT PLATINUM
NT PLUTONIUM ISOTOPES
NT PLUTONIUM 238
NT POLONIUM ISOTOPES
NT POTASSIUM
NT POTASSIUM ISOTOPES
NT POTASSIUM 40
NT POWDERED ALUMINUM
NT PRASEODYMIUM
NT RADIOACTIVE ISOTOPES
NT RADIUM 226
NT RADON

NT RARE EARTH ELEMENTS
 NT RARE GASES
 NT REFRACTORY METALS
 NT RHENIUM
 NT RHODIUM
 NT RUBIDIUM
 NT RUBIDIUM ISOTOPES
 NT RUBIDIUM 86
 NT RUTHENIUM
 NT SAMARIUM
 NT SCANDIUM
 NT SCANDIUM ISOTOPES
 NT SELENIUM
 NT SILICON
 NT SILVER
 NT SINTERED ALUMINUM POWDER
 NT SODIUM
 NT SODIUM ISOTOPES
 NT SODIUM VAPOR
 NT SODIUM 22
 NT STRONTIUM
 NT STRONTIUM ISOTOPES
 NT STRONTIUM 90
 NT SULFUR
 NT TANTALUM
 NT TELLURIUM
 NT TERBIUM
 NT THALLIUM
 NT THORIUM
 NT THORIUM ISOTOPES
 NT THULIUM ISOTOPES
 NT TIN
 NT TITANIUM
 NT TRACE ELEMENTS
 NT TRANSITION METALS
 NT TRITIUM
 NT TUNGSTEN
 NT URANIUM
 NT URANIUM ISOTOPES
 NT URANIUM 235
 NT VANADIUM
 NT XENON
 NT XENON ISOTOPES
 NT XENON 129
 NT XENON 133
 NT YTTRIUM
 NT ZINC
 NT ZIRCONIUM
 NT ZIRCONIUM ISOTOPES
 NT ZIRCONIUM 95

Origin and distribution of elements - Conference, Paris, May 1967
 08 p1398 A69-20892

S-process nucleosynthesis and temperature averaged neutron capture cross sections studied in relation to solar system, considering elemental and specific isotopic abundances
 08 p1357 A69-20896

Solar system elements abundance compilation based on carbonaceous chondrites and nucleosynthesis in stars
 08 p1401 A69-20903

Chemical composition of atmospheres of oldest Galactic stars, considering element abundances, metal and helium content and nuclear activity of massive stars
 08 p1402 A69-20909

Element abundances in magnetic stars, discussing Zeeman effect and anomalies in spectra
 08 p1403 A69-20911

Primitive elemental abundances in solar system, discussing composition of sun, meteorites and lunar maria
 08 p1403 A69-20914

Statistical distribution of chemical elements average abundances in earth crust and meteorites and nucleosynthesis of elements under specific astral conditions
 08 p1310 A69-20941

Element abundances of sharp lined field early A stars using model atmosphere
 09 p1600 A69-22198

Models for emission line region of 3C 273, considering ionization distributions for estimation of relative abundances
 10 p1790 A69-24137

Approximate ionization potentials for high ionization stages of elements with atomic numbers 31 to 92 obtained by binding energy calculations
 14 p2488 A69-29923

Solar system matter evolutionary beginning traced to chemical elements synthesis by considering radioactive decay irreversible processes
 19 p3406 A69-36076

Minor element influence on high temperature weldability of high Ni alloys and weld quality
 22 p3967 A69-39879

Mn, S and rare earth additions influence on Inconel alloy weld microfissuring including material, hot ductility and tensile strength data
 22 p3967 A69-39883

Ti, Al, S and P influence on Ni alloys weldability, discussing chemical composition, susceptibility to hot cracking and ductility temperatures
 22 p3967 A69-39884

Nuclear theory of elements origin, discussing nucleosynthesis to interpret abundances
 24 p4386 A69-43334

Elements origin and development in universe, discussing energy generation, structure and population of stars in Galaxy
 24 p4386 A69-43335

CHEMICAL ENERGY

NT ENERGY OF FORMATION

Convective instability by active stress, discussing composition dependent stress fields in continuous and mechanically isolated material and chemical to kinetic energy conversion
 14 p2540 A69-29634

Monograph on solid rocket propellants covering composition, combustion characteristics and energetic, mechanical and operational properties
 20 p3585 A69-37441

CHEMICAL ENGINEERING

Chemical processing for manufacture of solid propellant motors, discussing mixing, casting and curing of composite propellants
 16 p2829 A69-31992

Color chemistry concept producing high quality color negatives and prints in existing black and white processing systems
 22 p3948 A69-40990

CHEMICAL EQUILIBRIUM

NT ACID BASE EQUILIBRIUM

Complex chemical equilibrium calculation, analyzing thermodynamic principles and solution to nonlinear equations
 01 p0023 A69-10588

Chemical rockets theory for case of chemical equilibrium and frozen nozzle expansions
 03 p0495 A69-13004

Nonequilibrium dissociation effects on constant pressure laminar mixing for diatomic molecules and atoms, analyzing concentration and temperature of free shear layer
 04 p0588 A69-14733

Chemical nonequilibrium, mass transfer and viscous interaction effects on spherically blunted cones at hypersonic conditions, emphasizing stagnation point
 [AIAA PAPER 69-168] 06 p0862 A69-18047

Graphite ablation in air, N, Ar and He assuming chemical equilibrium, equal diffusion coefficients and steady state ablation
 [AIAA PAPER 69-148] 06 p0947 A69-18155

Laminar boundary layer on axisymmetric blunt body in dissociated air taking into account nonequilibrium homogeneous chemical reactions
 07 p1050 A69-18734

Equilibrium between H and OH radicals in turbulent H flames, noting component concentrations in H-O-N flames of different composition
 11 p1999 A69-24487

Equilibrium compositions of reaction products calculated by permutation over limiting equilibrium surface in reaction space, considering charged components and condensation products
 11 p2001 A69-25224

Electronic analog model for differential equations of equilibrium of gaseous combustion products based on asymptotic stability
 15 p2717 A69-30862

Electrical characteristics of equilibrium plasma sheaths at stagnation point of blunt body in high speed air, considering current collection regimes
 [AIAA PAPER 69-702] 17 p3011 A69-33473

Rocket motor combustion efficiency evaluated by chemical energy conversion to equilibrium, applicable to fuels, oxidizers and combustors at subsonic or supersonic velocity
 23 p4239 A69-41919

CHEMICAL EXPLOSIONS

NT GAS EXPLOSIONS

Powders and explosives - Conference, Brussels, September 1966
 02 p0301 A69-11519

Initiation of detonation by incident shock waves in hydrogen-oxygen-argon mixtures
 02 p0304 A69-12313

Explosion limits in hydrogen-oxygen reaction measured in diffusion regime, giving rate constant of branching step
 02 p0353 A69-12319

Detonation capacity of mixture of ammonium perchlorate base and polymethyl methacrylate and polystyrene, noting critical particle size dependence on composition
 02 p0305 A69-12674

Prevention of and protection against accidental explosion of munitions, fuels and other hazardous mixtures - Conference, New York, October 1966
 04 p0644 A69-14467

Mixing function vs time relationship for liquid propellant explosion hazards prediction, noting thermocouple grid for maximum information
 04 p0646 A69-14478

Liquid nitrogen inertant for continuous suppression of pressurized fuel tank explosion
 05 p0703 A69-16505

Chain reaction theory defining kinetic mechanism giving rise to explosion, noting conservation of free valences and formation and disappearance of radicals
 06 p1031 A69-17415

One dimensional lattice model for heterogeneous explosive detonation, discussing hot spots, grain burning ignition time, ignition site types and RDX detonation [WSCI PAPER 68-30]
 07 p1240 A69-18357

Gas dynamics, thermodynamics, chemical properties, energy and products of hydrocarbon-air detonations in tubes under standard atmospheric conditions [WSCI PAPER 68-26]
 07 p1241 A69-18369

Transverse wave spacing in self sustaining detonations in H-O mixtures, noting evidence against acoustic theory and for characteristic chemical dimension
 09 p1622 A69-21953

Piston motion influence on gaseous motion set up by constant energy explosion, applying to steady high Mach number flow past blunt nosed object
 22 p3931 A69-40892

CHEMICAL EXTINGUISHERS

U FIRE EXTINGUISHERS

CHEMICAL FUELS

NT AEROZINE
 NT AIRCRAFT FUELS
 NT HYDROCARBON FUELS
 NT HYDROGEN FUELS
 NT JET ENGINE FUELS
 NT JP-4 FUEL
 NT METAL FUELS

Transverse wave spacings for self sustaining detonations in oxygen and diluents mixtures with hydrogen, methane, acetylene or ethylene fuel, noting dilution
 13 p2378 A69-28217

CHEMICAL INDICATORS

Cladonia rangiferina resistance to stresses, considering suitable indices for stress response
 18 p3095 A69-34539

CHEMICAL KINETICS

U REACTION KINETICS

CHEMICAL LASERS

Chain and branched halogen-hydrogen reactions kinetic analysis for developing chemical laser with radiation energy weakly dependent on pumping energy
 02 p0259 A69-12645

Stimulated emission of cyanine dyes, discussing amplification coefficients
 04 p0612 A69-15373

Uranium hexafluoride-hydrogen hydrogen fluoride chemical laser, discussing conditions for negligible collisional deactivation and defined rotational temperature determination
 05 p0771 A69-15906

Laser emission of neodymium salt dissolved in polonium-chlorine, discussing fluorescence intensity
 06 p0936 A69-17778

Laser excited vibrational fluorescence for determining vibrational energy transfer rates in HCl-carbon dioxide, HCL-HI and HI-carbon dioxide
 07 p1144 A69-18289

Power output and radiation spectra of trivalent Nd doped liquid lasers based on phosphoryl chloride with tin and titanium chlorides
 11 p1894 A69-24620

Laser with molecular H and Cl mixture at HCl vibrational transitions
 14 p2461 A69-29672

Passive Q switching of chemical laser operating on vibrational-rotational line of vibrational transition of HCl
 16 p2796 A69-31840

Stimulated emission of cyanine dyes, discussing amplification coefficients
 16 p2797 A69-32120

Continuous explosion laser study of stationary detonation waves to determine conditions leading to partial population inversion and critical population density

19 p3336 A69-36360

Laser action from atomic bromine produced by flash photolysis of gaseous iodine monobromide, discussing pulsed output, optical gain, chemical reversibility and atomic excitation

19 p3337 A69-36444

Lasers based on organic dye solutions, discussing operation, structural formulas, absorption and luminescence spectra

20 p3555 A69-38011

Chemical high pressure laser action produced by stimulated phototransition of electrons at contact moment between pair of reacting nonexcited gas molecules

22 p3965 A69-41117

Hydrogen fluoride chemical laser emission spectrum, studying rotational-vibrational transition of molecules triggered optically or electrically

23 p4172 A69-41493

CHEMICAL MACHINING

NT ELECTROCHEMICAL MACHINING

Beryllium chemical and mechanical machining in quantity production, examining salvage and safety precautions [SAE PAPER 680649]

03 p0434 A69-13455

Fluosilicic acid in chemical milling of Ti and Ti alloys

21 p3669 A69-38966

Ti-Al alloy structure manufacturing technology covering forming, cleaning, chem-milling, machining, fastening and welding

24 p4324 A69-43431

CHEMICAL PROPERTIES

NT ACIDITY

NT HEAT OF COMBUSTION

NT HEAT OF FORMATION

NT HEAT OF SOLUTION

NT HEAT OF VAPORIZATION

NT THERMOCHEMICAL PROPERTIES

Polymeric film properties related to metal substrate interface corrosion, considering effects of stress concentration, surface cleanliness and adsorbed gases

02 p0265 A69-11896

Book on properties of liquid and solid helium 3 and 4 physical characteristics, phase behavior and experimental techniques

04 p0630 A69-14688

Ti metallochemistry investigations, noting atomic radius, electronegative valency effect, first atom ionization potential and production of special Ti alloys

07 p1161 A69-18764

Textural variation relation to mineralogical and chemical characteristics of chondrites from review of published data

08 p1391 A69-20516

Soviet book on fluid semiconductor properties at high temperatures during transition from solid to liquid state

10 p1744 A69-23316

Description and automated research of correlation /DARC/ for establishing quantitative relationships between topology and properties of chemical substance

12 p2026 A69-26361

Physicochemical and operational properties of trimethylol propane esters as lubricating oils under static and dynamic conditions

12 p2103 A69-27090

Polymer structure relationship to thermal, mechanical and chemical properties of electrical insulating materials

13 p2285 A69-27986

Physical and physicochemical properties of ferrites - Conference, Minsk, Belorussian SSR, 1967

13 p2319 A69-27991

Artificial aging effect on spinel structure and properties of ferrites using X ray analysis, neutron diffraction and electron microscopy

13 p2320 A69-27997

Polyvinyl acetate and polyvinyl alcohol thermoplastic adhesives, discussing gluing properties, chemical properties, preparation, polymerization methods

14 p2469 A69-29347

Lower oxides of Si, studying chemical composition, formation conditions, stability and chemical and physical properties

15 p2643 A69-31245

Hypersonic aircraft induced changes in chemical and thermodynamic properties of air influencing aerodynamic forces on vehicle

17 p2895 A69-33576

Lunar based physics and chemistry, discussing exploration of and survival in lunar environment

18 p3112 A69-34235

Lunar conditions differing from simulations in laboratories, examining surface, physicochemical properties and friction

18 p3113 A69-34241

Chemical modifications effects on Escherichia coli, DNA polymerase, including Hg atom addition to sulfhydryl group of enzyme

22 p3898 A69-41071

Soviet book on silicoorganic protective coatings preparation, physical, chemical and operational characteristics, with emphasis on silicates and metals

24 p4336 A69-43232

CHEMICAL PROPULSION

NT HYBRID PROPULSION

Chemical rockets theory for case of chemical equilibrium and frozen nozzle expansions

03 p0495 A69-13004

High performance chemical propulsion systems feasibility, discussing propellant combinations

06 p0983 A69-17627

Advanced electrical and nuclear propulsion systems for European launchers, comparing performances with chemical propulsion

06 p0984 A69-17628

Explosive and pyrotechnical elements for Grillo 1, Grillo 2 and Trigone 1 hot water rockets, detailing nozzle closure and chemical reaction activation

10 p1753 A69-23028

Electric and chemical rocket propulsion systems

13 p2325 A69-28255

Advanced liquid fuels and oxidizers development from rocket propulsion reaction principle

16 p2828 A69-31747

Interagency Chemical Rocket Propulsion Group method of treating measurement error for liquid rocket engine performance parameters, using uncertainty model

[AIAA PAPER 69-734] 16 p2846 A69-32781

Chemical relaxation, optimum propellant mixture ratio, combustion chamber pressure, gas jet impulse, mass flow and drive capacity of space propulsion systems

18 p3229 A69-34773

Book on chemical rockets and flame and explosives technology covering propulsion systems, combustion, propellant ingredients, etc

22 p3998 A69-40866

Manned flyby and stopover missions to Mars and Venus with chemical propulsion and Saturn 5 launch vehicles, noting short duration low energy missions [AAS PAPER 69-492]

24 p4380 A69-42839

CHEMICAL REACTION CONTROL

Hydrogen and basic electrolyte cold cells, studying control systems for reactants supply, current, reaction by-products, etc

16 p2738 A69-32410

CHEMICAL REACTIONS

NT ATOMIC RECOMBINATION

NT CARBONIZATION

NT DECARBOXYLATION

NT DEHYDROXYGENATION

NT DEIONIZATION

NT DEOXIDIZING

NT ELECTROCHEMICAL OXIDATION

NT ENDOTHERMIC REACTIONS

NT EXOTHERMIC REACTIONS

NT FLUORINATION

NT GLYCOLYSIS

NT HALOGENATION

NT HYDROGENATION

NT HYDROLYSIS

NT ION RECOMBINATION

NT NITRIDING

NT OXIDATION

NT OXYGEN RECOMBINATION

NT OXYGENATION

NT PHOSPHORYLATION

NT PHOTOCHEMICAL REACTIONS

NT PHOTOCROMISM

NT PHOTODECOMPOSITION

NT PHOTOLYSIS

NT PHOTOOXIDATION

NT PHOTOSYNTHESIS

NT PYROLYSIS

NT RADIOLYSIS

NT REDUCTION [CHEMISTRY]

NT SULFATION

NT THERMAL DISSOCIATION

Hydrocarbon formation mechanisms under conditions resulting from graphite filament explosions in hydrogen atmospheres, emphasizing stepwise radical formation and methane role

01 p0120 A69-10675

Chemical phenomena during explosions of wires in various gaseous atmospheres, using apparatus with electronic crowbar for current flow regulation

01 p0081 A69-10680

Analytical mechanics of chemical reactions, discussing natural collision coordinates for three dimensional reactions and exchange collisions for molecule and atom

01 p0123 A69-10681

HI and DI reaction into HD and 2I, noting need for rotational or vibrational excitation in addition to translational energy of collision

01 p0123 A69-10686

Very high temperature air flow laminar boundary layers on rotating bodies with unsteady chemical reactions, determining flow dynamic behavior

01 p0060 A69-10725

Ion reactions with neutral molecules, discussing analogies with conventional chemical systems

01 p0124 A69-10859

Vacuum distillation technique for isolation and recovery of alkali metal reaction products with Ta, Ni, V and oxygen

01 p0083 A69-10927

Reaction rate and mechanism for low temperature reaction between lithium hydride and liquid ammonia, noting chemisorbed ammonia dissociation at interface

01 p0025 A69-11285

Local mass transfer from wall with homogeneous or heterogeneous chemical reactions in uniform velocity flow, Couette flow and boundary layer flow

02 p0232 A69-12234

Rarefied merged stagnation shock layer of hypersonic body, considering chemical reactions of nonequilibrium dissociative relaxation of air

02 p0189 A69-12521

Chemical reaction fluctuations and oxygen electron attachment omission effects on density fluctuations in turbulent wakes, noting electron density fluctuation, bimodal model, etc

02 p0233 A69-12538

Chain and branched halogen-hydrogen reactions kinetic analysis for developing chemical laser with radiation energy weakly dependent on pumping energy

02 p0259 A69-12645

Chemical reaction scheme effect on hot zone structure of hydrogen-oxygen diffusion flame, considering influence of hydroxyl radical

03 p0531 A69-12895

Energy distribution among products of reactive collision of atomic H with Br molecule yielding HBr and Br atom, using perturbed Morse oscillator approximation

03 p0472 A69-13316

Metal oxide and carbon interaction during spatial separation of reagents, noting influence of reducing agent activity on metal vapors

03 p0445 A69-13569

Chemical nitrogen fixation methods for life support systems, discussing organometallic chlorides and bromides

03 p0382 A69-14198

Confined jet mixing region at entrance of tubular reactor, discussing mass and momentum transfer, chemical conversion and effect of Reynolds number [AIChE PAPER 25A]

04 p0586 A69-14508

Various reaction mechanisms proposed for interstellar medium, discussing formation and destruction of interstellar molecules

04 p0653 A69-14613

Numerical solution of chemically reacting boundary layer equations, noting loss of accuracy due to numerical cancellations

04 p0588 A69-14737

Angular distribution of reactive elastic scattering analyzed by opacity function /reaction probability/

04 p0554 A69-14859

Enhanced light emission rate in adiabatically expanded NO-O reaction ascribed to molecular clusters

04 p0555 A69-14864

Shock tube and samples of fluoroethylene, difluorodichloroethylene and fluoromethane in argon diluent used to prepare carbon difluoride, discussing electronic oscillator strengths

04 p0632 A69-14944

Thermal explosion in Poiseuille flow of reacting viscous fluid in infinite circular cylindrical channel or between two rotating infinite cylinders

04 p0686 A69-14986

Chemical compatibility estimation of lead and tin tellurides thermoelectric materials with metallic alloys

04 p0551 A69-15315

Boundary conditions in oblique reaction waves in supersonic flow, adding or subtracting heat by chemical reaction

05 p0697 A69-15828

Atomic hydrogen-bromine linear collision reaction intermediate formation and reactive scattering cross sections quantum mechanical calculation, using perturbed Morse oscillator approximation
05 p0796 A69-15911

Gas lasers involving gas-discharge collisions, selective pumping or chemical reactions to produce necessary inversion, giving theoretical analysis of excitation mechanisms
05 p0772 A69-16226

Ultrahigh molecular weight polyethylene terephthalate synthesis from commercial solid state materials, noting effects of several parameters
05 p0797 A69-16496

Fluorinated polyurethanes synthesis for liquid oxygen environments and cryogenic structural utility, noting structural effects on LOX compatibility
05 p0717 A69-16498

Compressible combustor turbulent shear flow analysis, discussing eddy diffusivity, density fluctuations, vorticity intensification and turbulent transport [WSCIPAPER 68-27]
06 p1034 A69-17793

Cholesteric liquid crystals application to trace contamination detection, describing color response measurement
06 p0885 A69-17842

Compressibility transformation theory extended for turbulent boundary layer, involving mass transfer with/without chemical reactions [AIAA PAPER 69-161]
06 p0912 A69-18045

Nonadiabatic reacting homogeneous system undergoing density changes, predicting chemical reaction rates and intermediate combustion products from chain reaction kinetics [AIAA PAPER 69-87]
06 p1036 A69-18054

Transient development of reacting boundary layer near stagnation point of vaporizing drop in gas stream [AIAA PAPER 69-174]
06 p0912 A69-18056

Supersonic molecular beam sampling system for coupling mass spectrometer to alkali metal-air reacting flow system in kinetics study, noting gas dynamic effects [AIAA PAPER 69-94]
06 p0930 A69-18099

Parasitic eigenvalue in integration of equations governing one dimensional flow of chemically reactive gas
07 p1118 A69-18317

Analog simulation of chemically reacting system applied to thermal decomposition of oxygen difluoride [WSCIPAPER 68-49]
07 p1073 A69-18318

Kinetics calculations in shock tube data interpretation, determining elementary rate constants and complex reaction mechanism [WSCIPAPER 68-50]
07 p1073 A69-18319

Activation energies of bimolecular multivalent transfer reactions of gaseous compounds, considering bond dissociation energy, length and order [WSCIPAPER 68-48]
07 p1239 A69-18321

Lewis acidity of alanes, discussing interactions of trimethylalane with amines, ethers and phosphines
07 p1074 A69-18630

Acidic, neutral and basic proteinoids thermal synthesis, discussing characterization and tendency to form microparticles
07 p1074 A69-18633

Chemical reactions in boundary layer on porous plate in oxygen stream, discussing similar solution of laminar boundary layer equations with flame front
07 p1119 A69-18735

Ti-Zr-Sn alloys phase equilibria and interaction between titanium nitride and solid solution of Ti and Zr
07 p1162 A69-18770

Synthesis and nucleophilic reactions of stable alpha-bromoorganolithium reagent
07 p1074 A69-19479

Chemical analysis, isotopic composition, structure and mineralogy of meteorites for classification into iron and stony, discussing time variation of temperature, pressure, etc
07 p1224 A69-19710

Chromium oxide additions effects on reaction rates decrease during ammonium perchlorate and nitrate combustion
08 p1375 A69-20340

Cross-linked polymers obtained by direct reaction of aryl polycarbonyls with aryl polyamines, studying char yields effect
08 p1269 A69-21059

Schiff base cross-links effect on synthesis of polymeric azomethines produced by bis exchange reactions, carbonyl and amine
08 p1269 A69-21061

Chemical processes in silicon carbide due to reactive deposition and chemical conversion, noting silicon growth mechanism involving outward diffusion
09 p1554 A69-21351

Oxygen depletion effect in chemical reactions between pyrolysis gases and air stream on surface recession of charring ablators [AIAA PAPER 68-302]
09 p1622 A69-21982

Electron microscopy for continuous observation and recording of dynamic reactions in high temperature materials
09 p1499 A69-22304

Mass spectrometric determination of pyrolysis products generated from heated polymer samples
09 p1448 A69-22314

Ceramic whiskers and metallic matrix chemical reactions during composite formation, analyzing coated and uncoated SiC whiskers in titanium matrix
09 p1527 A69-22359

Supersonic free jet with real gas effects and chemical reactions calculated by approximation
10 p1631 A69-22898

Metal composites of Ni or Mo fibers in Be matrix, discussing chemical compatibility in terms of reactions, solid solubility and diffusion at various temperatures
10 p1707 A69-22991

Venus atmosphere origin, discussing high temperature effects and chemical composition via space probe and terrestrial observations
10 p1775 A69-23183

Neat alpha styryl azide transformation into 2-phenylazirine, 3,6-diphenylpyridazine and 2,5-diphenylpyrrole after one month at room temperature in brown glass bottle
10 p1651 A69-23307

Polymerization of monomers considered for direct synthesis of iminobenzylidene
10 p1651 A69-23308

Polyesters reaction with dimethyl p-phenylene diamine compared under UV exposure from carbon arc and natural sunlight
10 p1716 A69-23978

Poly A-poly U synthesized by Azotobacter Vinelandi RNA polymerase in unprimed reaction containing ATP and UTP, following short lag period
10 p1647 A69-24185

Laminar flow stream containing periodic fluctuation of mass fraction of chemical species over flat plate with reactive surface
11 p1831 A69-24284

Critical conditions in spherical reacting mass, noting oscillatory nature of critical parameters in truncated Arrhenius rate on basis of nontruncated form
11 p1998 A69-24480

Explosive reactions between hydrogen and oxygen flashed in presence of nitrogen dioxide, chlorine or bromine as sensitizers, considering thermal contribution
11 p1832 A69-24878

Vibrationally excited nitrous oxide formation in reaction of N atoms with nitrogen dioxide, noting IR emission and vibrationally excited nitric oxide
11 p1832 A69-24880

Chemical species and reactions determined for propellants in calculating nonequilibrium rocket engine performance
11 p1940 A69-24905

Liquid rocket propellants chemical reactions identification during kinetic expansion [WSCIPAPER 68-7]
11 p1942 A69-24906

Chemical reaction rate data for propellant systems containing boron or aluminum and hydrogen, chlorine and fluorine, based on finite kinetics expansions [AIAA PAPER 69-182]
11 p1940 A69-24907

Planning, instrumentation and analysis of shock tube experiments in chemical kinetics, noting gas phase reaction rates at high temperatures
11 p1863 A69-25015

Combustion chemical reactions kinetics of gaseous phase systems, discussing temperature, reaction rates extrapolation, hydrogen and hydrocarbons
11 p2000 A69-25185

Ignition dynamics of solid materials with differing kinetic and thermophysical parameters, emphasizing temperature growth during chemical reaction leading to ignition
11 p2000 A69-25188

Ignition critical conditions based on reactions in condensed phase, discussing initiation from pulsed and continuous external heat sources, heat release by chemical reactions of ignition, etc
11 p2001 A69-25191

Composition and thermodynamic properties of gaseous system reacting at low temperatures with condensed phase formation, discussing iterative process convergence in approximation
11 p2001 A69-25223

Equilibrium compositions of reaction products calculated by permutation over limiting equilibrium surface in reaction space, considering charged components and condensation products
11 p2001 A69-25224

Supersonic air flow past blunt body of revolution in presence of nonequilibrium chemical reactions, ionization and molecular excitation
11 p1820 A69-25474

Inviscid reacting flow free of molecular transport analyzed locally near stagnation point, using Lighthill-Freeman gas model
11 p1876 A69-25560

Ductile metal powder chemical reactions during comminution in pure or oxygenated water
13 p2216 A69-27762

Electrochemical synthesis of chlorine pentafluoride formation from chlorine trifluoride-anhydrous hydrogen fluoride-sodium fluoride system
13 p2217 A69-28134

Chlorine pentafluoride formation from chlorine in anhydrous hydrogen fluoride in electrochemical cell, noting formation rate
13 p2217 A69-28135

Chemically reacting flow field and solid surfaces, formulating nonequilibrium laminar boundary layer equations for two dimensional and axisymmetric flows
13 p2377 A69-28147

Block tractable azomethine copolymers prepared by reaction of insoluble oligomers with monomers or of two different fusible oligomers, noting high thermal stability
13 p2217 A69-28317

HNO role in hydrogen-NO reaction rate data reexamined by numerical integration of governing differential equations
13 p2218 A69-28457

Coupled heat and mass transfer with zero order reactions in two phase systems consisting of drops, bubbles or solid particles
14 p2537 A69-29012

Borane carbonyl pyrolysis in low pressure tubular flow reactor measured by mass spectrometry, noting wall collision role in diborane bond dissociation
14 p2410 A69-29282

Chemical reaction-rate theory for creep tests, analyzing extrapolation equations for time-to-rupture dependence on temperature and stress
14 p2464 A69-29442

Laminar and turbulent hypersonic wakes trailing blunt bodies studied by finite difference method, taking into account pressure gradients and nonequilibrium chemical reactions effects
14 p2391 A69-29618

Perturbed molecular distribution in translational and internal degrees of freedom in dilute chemically reacting gases with low ion concentrations
14 p2410 A69-29988

Isothiocyanates and phenyl isocyanate reaction with hydrazinoethanol and hydrazinoethyl hydrogen sulfate
16 p2747 A69-31808

Chemical reaction between combustible solid fuel surface and oxidizer-containing gas in space capsule
16 p2877 A69-31896

Hybrid rockets combustion mechanism, discussing turbulent boundary layer with heat and mass transfer, chemical reactions, etc
16 p2879 A69-32002

Meteoritic elements ionization and loss mechanisms in E region, discussing roles of atomic oxygen and metal ions chemical reactions
16 p2780 A69-32313

Chemical reactions in compressible turbulent mixing flows, analyzing flow characteristics, rate equation and Reichardt theory [AIAA PAPER 69-537]
16 p2747 A69-32701

Boron nitride synthesis by gas phase reaction of boron chloride or diborane with ammonia, determining purity from equilibrium gas mixture components
17 p2952 A69-33432

Chemical species flux decay in turbulent boundary layer with catalytic wall, obtaining solution of conservation equation by using shear stress distribution [AIAA PAPER 69-709]
17 p2955 A69-33480

Chemical reactions activation energy at high temperature, noting cross section shape role for deducing activation energy from rate data
18 p3099 A69-34443

Velocity and angular distributions of KBr formed in reactive collisions between crossed molecular beams of K and thermal HBr/DBr/
18 p3178 A69-35476

Nuclear environment irradiation effects on materials, emphasizing radiation chemical processes affecting polyimide and copolymer of styrene and alpha-methylstyrene

19 p3356 A69-35530

Proton and deuteron energy used to study solid state chemical reactions effects on meteorites composition and properties, obtaining hydroxyl ions and hydrocarbons

19 p3414 A69-36114

Flame and pressure /or velocity/ oscillations interaction in unstable combustion regimes, considering tubes with propane-air mixtures

19 p3450 A69-36357

Computer program for numerical integration of chemical reaction rate equations behind steady state hydrogen-oxygen shock wave

19 p3451 A69-36366

Finite chemical reaction rate detonation wave interaction with rarefaction wave, noting mixture activation energy and heating power influence

19 p3298 A69-36384

Thermal conductivity calculation for chemically reacting multicomponent gas mixture, comparing results from Brokaw method and simplified formula

20 p3483 A69-36974

Nonequilibrium laminar heat transfer in viscous flow of chemically unstable gases past blunt body and plate

20 p3513 A69-37087

Physical state changes, chemical reactions, gaseous diffusion in solids and solid-gas interactions in vacuum, considering saturated vapor pressure, condensation, evaporation, etc

20 p3576 A69-37408

C-nitroso compounds chemistry covering various nitrosation reactions connected with reduction and deoxygenation

20 p3484 A69-37486

Gas phase ion-molecule chemistry of HCN by ion-cyclotron resonance spectroscopy identifying individual reactions by double resonance

20 p3485 A69-38262

H release, pressure and oxide layer formed by reaction during ball milling Cr in water

21 p3728 A69-38567

Destructive interaction of refractory carbides and graphite compositions with chemically active high temperature gas streams

21 p3751 A69-38640

Chemical processes responsible for transformation of vast gas and dust cloud into planetary system

21 p3804 A69-39200

Chemical and thermal behavior of materials corrosion in propellant exhaust gases with analysis of reactions involving hydrogen, nitrogen, water, carbon dioxide, etc

21 p3784 A69-39489

Volatile oxygen organic compounds subjected to RF electrodeless discharge, explaining product distribution in terms of reaction sequences

21 p3670 A69-39737

Solar proton bombardment of lunar surface, discussing luminescence and chemical effects

22 p4012 A69-40089

Book on rate constants of chemical reactions from flames covering flame propagation, mass spectroscopy, electron spin resonance, particles diffusion, combustion physics, etc

22 p3895 A69-40318

Chemical high pressure laser action produced by stimulated phototransition of electrons at contact moment between pair of reacting nonexcited gas molecules

22 p3965 A69-41117

Reaction zone following overdriven detonation wave propagating into mixtures of fluorine oxide and hydrogen molecules showing HF laser emission

22 p4052 A69-41188

Polypeptide synthesis as function of 5S ribosomal RNA dissociated from 50S ribosomal subunits by EDTA treatment

23 p4113 A69-41491

Chemical reaction kinetics in high temperature gases in terms of collision theory, discussing gaseous statistics and Boltzmann equation

23 p4113 A69-41518

Transesterification of amino acid peptide alkyl and fatty acid esters by treatment with anion-exchange resin

24 p4280 A69-43513

Prebiological chemical evolution, studying synthesis and degradation rates relationship at primitive environment energy levels

24 p4269 A69-43514

CHEMICAL REACTORS

Pilot chamber initiated thermal decomposition reactor concept for monopropellant thruster, discussing thrust levels and throttling ratios

[AIAA PAPER 69-420] 16 p2841 A69-32685

CHEMICAL RELAXATION U MOLECULAR RELAXATION

CHEMICAL STERILIZATION

Spacecraft sterilization techniques efficiency in terrestrial and extraterrestrial environments noting dry heat, radiation, ethylene oxide, isopropanol and formaldehyde in methanol

05 p0712 A69-15937

Ethylene oxide sterilization rate dependence on temperature, gas concentration, relative humidity and medium surrounding microorganisms

05 p0707 A69-15940

Spacecraft sterilization by hydrogen peroxide solutions mixed with selected anion active detergents

05 p0713 A69-15943

Antimicrobial spacecraft materials, discussing feasibility of impregnation or chemical combination of materials with bactericides

05 p0713 A69-15944

Formic acid catalytic action on sterilizing effectiveness of ethylene oxide

05 p0713 A69-15945

Sterilization without damage by mixing steam and formaldehyde at 80 C under subatmospheric pressure, noting thorough penetration

05 p0713 A69-15946

Thermal stabilization and ethylene oxide effect on spaceborne electronic component sterilization and decontamination

08 p1283 A69-20266

CHEMICAL TESTS

NT ELECTROPHOTOMETRY

NT GAS ANALYSIS

NT GAS SPECTROSCOPY

NT MICROANALYSIS

NT NEPHANALYSIS

NT NEUTRON ACTIVATION ANALYSIS

NT OZONOMETRY

NT PAPER CHROMATOGRAPHY

NT QUALITATIVE ANALYSIS

NT QUANTITATIVE ANALYSIS

NT SALT SPRAY TESTS

NT SPECTROSCOPIC ANALYSIS

NT URINALYSIS

NT VOLUMETRIC ANALYSIS

Lignin presence in New Zealand moss gametophytes observed for characteristic color reaction and UV spectra, noting contrast with north temperate species

17 p2912 A69-34176

CHEMILUMINESCENCE

Long lived low level chemiluminescence due to gaseous reactions at low concentrations induced by mercury lamp irradiation or Tesla coil discharge

01 p0024 A69-10618

Wake temperature turbulent fluctuation decay rates deduced from atomic oxygen recombination chemiluminescence

02 p0190 A69-12525

Enhanced light emission rate in adiabatically expanded NO-O reaction ascribed to molecular clusters

04 p0555 A69-14864

Chemiluminescence and chemionization in flames, considering electrically conducting properties and spectral analysis

06 p1032 A69-17423

Chemiluminescence in high temperature oxidation of methane studied in shock tube

06 p0885 A69-17937

Biochemiluminescent luminol-peroxide reaction to detect iron porphyrin proteins in microorganisms for extraterrestrial life search, discussing reaction kinetics

15 p2556 A69-31325

Rate coefficients for chemiluminescent reactions of excited Hc with N, O, carbon monoxide and dioxide determined from spatial dependence of visible emission

20 p3483 A69-36936

CHEMISORPTION

Adsorbed gas influence on X ray emission from exploding tungsten wires noting ungasged and degassed specimens in vacuum

01 p0118 A69-10668

Chemisorption of H onto Nb /110/ surface, measuring low energy electron diffraction and inelastic electron scattering from clean and H-covered surfaces

06 p0980 A69-17758

Chemisorbed oxygen effect on electrical conductivity of zinc doped polycrystalline tin oxides

07 p1201 A69-19478

Work function change of tungsten single crystal /100/ surface measured as time function during surface molecular gas adsorption

09 p1521 A69-21338

Experimental program to evaluate regenerable sorbents for carbon dioxide removal in space cabin environments

09 p1447 A69-22552

Platinum based metal binary catalysts as anodes for hydrogen/carbon monoxide fuel mixtures oxidation, discussing alloy surface chemisorption of CO

12 p2026 A69-25937

Desorption kinetics of atomic and oxide phases, analyzing composition of surface film formed from W and Mo single crystals interaction with oxygen

12 p2026 A69-26115

Alkaline metal adsorption on high work function metals with charge transfer, measuring polycrystalline Mo photoelectric emission as function of Cs coverage

14 p2507 A69-29275

Low energy electron diffraction oxygen adsorption kinetics on planes of tungsten at coverages below monolayer and work function measurements

18 p3183 A69-35106

Oxygen 18 adsorption on silicon activation analysis measurements used to obtain kinetic curve for chemisorption from monolayers

18 p3183 A69-35107

Surface structures, work function changes, Auger electron and surface plasma losses for Cs on clean W surface

19 p3392 A69-36733

Oxygen environment influence on Inconel X-750 surface deformation and cracking during fatigue related to chemisorption and oxidation

20 p3558 A69-36966

C and O atoms chemisorption on Mo surface demonstrated by surface striation

20 p3562 A69-37782

Field emission and field-ion microscopic adsorption studies, discerning major states in chemisorption for metal-crystal surfaces

22 p3895 A69-39898

Adsorption kinetics in ternary mixture of nitrogen, methane and hydrogen, using concentration-time /breakthrough/ curves measurement on activated coconut shell charcoal

[NAS-NRC PAPER H-4] 22 p3981 A69-40629

CHEMISTRY

Lunar physics and chemistry - IAA Conference, Belgrade, September 1967

18 p3112 A69-34234

CHEMONUCLEAR PROPULSION

U CHEMICAL PROPULSION

U NUCLEAR PROPULSION

CHEMORECEPTORS

Peripheral chemoreceptor carbon dioxide sensitivity, measuring human respiratory response to large carbon dioxide breath in oxygen at sea level and high altitude

22 p3890 A69-40207

CHEMOTHERAPY

Medicinal therapy and flight safety of pilots and astronauts, discussing drug use, self treatment, tolerance and environmental factors

01 p0014 A69-10583

Essential hypertension in selection and evaluation of airline pilots, discussing use of thiazide therapy

06 p0875 A69-17850

Therapeutic potential of dimethyl sulfoxide in aerospace medicine

06 p0883 A69-17851

Medicinal therapy and flight safety of pilots and astronauts, discussing drug use, self treatment, tolerance and environmental factors

15 p2555 A69-30753

Psychiatric morbidity as absenteeism cause among ground and flight personnel in civil aviation, recommending psychotherapy and chemotherapy

24 p4266 A69-43378

CHICKENS

Increased chronic acceleration physiological effects on chickens, comparing hematological observations with exercise capacity, survival and sexual development

10 p1641 A69-23041

Repeated blood sampling effect on plasma cholinesterase, acid phosphatase, alkaline phosphatase and hematocrit ratios in domestic chickens

10 p1644 A69-23158

Chronic acceleration effects on erythrocyte number, plasma volume, globulin fractions, erythrocyte size and plasma A/G ratio in chickens

11 p1828 A69-25458

CHILLING

Hypoxia tolerances in nitrogen dilution chamber of chickens at sea level and high altitudes, discussing role of hematocrit and heart mass

22 p3874 A69-40214

CHILLING

U COOLING

CHIMES

U AUDITORY SIGNALS

CHIMPANZEES

Constant illumination intensity effects fixed ratio lever pressing behavior for appetitive reinforcement with chimpanzee in temperature and humidity controlled environment

24 p4260 A69-42702

CHINA

U CHINESE PEOPLES REPUBLIC

CHINESE PEOPLES REPUBLIC

Communist China civil aviation, discussing major, local and international routes and agreements, aircraft types and national origin, total mileage, etc

16 p2882 A69-32337

CHINOOK HELICOPTER

U CH-47 HELICOPTER

CHIRP SIGNALS

Ultrasonic diffraction delay line operation interpretation as radar chirp signal correlator

01 p0026 A69-10072

Chirp pulse generation by carbon dioxide laser, discussing carrier frequency sweep

04 p0609 A69-14333

Chirp radar signal compression by proton spin echo phenomena, noting compression ratio and SNR

11 p1834 A69-24566

CHLORATES

Ammonium chlorate thermal decomposition by measuring formed noncondensable gas pressure and weight loss in solid state kinetic investigation

21 p3669 A69-38800

CHLORELLA

Mathematical models for Chlorella cell and biomass growth under illumination during space flight, noting ionizing radiation presence

02 p0198 A69-11508

Mineralized human wastes solutions utilization for Chlorella cultivation, noting growth rates

02 p0200 A69-11511

Organic compounds /metabolites/ extracting technique from nutrient media of Chlorella cultures indicate unsaturated amine and phenol composition

08 p1262 A69-19833

Mineral nutrition elements concentration stabilization by correcting solution additions during prolonged Chlorella cultivation with medium recycling

10 p1646 A69-23578

Vegetable diet including 210 g of dry Chlorella biomass decreases effect on calcium and magnesium assimilation to produce insignificant negative balance of K and Mn

10 p1647 A69-23590

Chlorella seaweed hybrid strains containing larger amounts of amino acids than original parent species

13 p2216 A69-28620

White rats diet containing alcohol-soluble fraction of Chlorella and Scenedesmus biomass, noting changes in adrenal cortex and renal glomerus

17 p2906 A69-32930

Microbial protein extraction from Chlorella algae and Torulla yeasts using urca soaking method

21 p3662 A69-39712

Survival rates of continuously cultivated Chlorella plants in air-carbon dioxide atmosphere after single exposure to gamma radiation, using microcolony counting technique

22 p3876 A69-40275

Restoration processes in Chlorella pyrenoidosa to distinguish intense and less intense gamma ray irradiations

22 p3878 A69-40792

DNA interaction with ribosomes enhancing amino acid incorporation into cell-free protein synthesizing system extracted from Chlorella pyrenoidosa

23 p4080 A69-41430

Oxygen exchange in Scenedesmus and Chlorella as function of carbon dioxide, compensation point, Hill activity and photorespiration, using mass spectrometry

23 p4099 A69-42528

Chlorella enzymes activity in reducing nitrate to nitrite and nitrite to ammonia

24 p4263 A69-43136

CHLORIDES

NT ALUMINUM CHLORIDES
NT AMMONIUM CHLORIDES
NT BORON CHLORIDES

NT CARBON TETRACHLORIDE

NT HYDROCHLORIC ACID

NT IRON CHLORIDES

NT MAGNESIUM CHLORIDES

NT POTASSIUM CHLORIDES

NT SODIUM CHLORIDES

NT TITANIUM CHLORIDES

Salt water stress corrosion cracks morphology in titanium alloy, discussing crack propagation, brittle nature and chloride contamination effect

[SAE PAPER 680642] 03 p0444 A69-13458

Magnon density of states of ferromagnetic gadolinium trichloride in magnetic field, using high resolution optical spectroscopy

03 p0494 A69-14257

Titanium tetrachloride reduction to titanium by magnesium, showing autocatalytic process

07 p1163 A69-18784

Motion sickness treatment with bethanechol chloride, noting negative results with 12 airskip student naval aviators

12 p2024 A69-26561

Niobium deposition on graphite from vapor-gas phase assuming heterogeneous process

15 p2629 A69-30992

Co 2 chloride aqueous and alcoholic solutions by X-ray diffraction to find potential ligands relative coordinating abilities

20 p3484 A69-37496

Conditions for obtaining concentrated Ti-containing melts free of Al and V chlorides by cementing with metallic Ti and Ti-containing materials

22 p3957 A69-40918

CHLORINE

Cl 35 nuclear quadrupole resonance spectra of 3,6-dichloropyridazine, tetrachloropyridazine, 2,6-dichloropyrazine and chloropyrazine

01 p0123 A69-10290

Chlorine as indicator of terrestrial contamination in iron meteorites, using neutron activation analysis and metallographic observation

08 p1405 A69-20923

Chlorine pentafluoride formation from chlorine in anhydrous hydrogen fluoride in electrochemical cell, noting formation rate

13 p2217 A69-28135

Additives effect on flame propagation velocity and stability in N diluted hydrogen-chlorine preflamants, noting entrained air role

[WSCI PAPER 69-13] 16 p2831 A69-32353

Boron, Li and Cl contents in iron and stone meteorites by fluorometric, thermal-neutron activation and pyrohydrolytic separation methods, tabulating results

19 p3408 A69-36085

Ar 39 and Cl 36 production rates and ratios in stone and stony-iron meteorites metal phases, discussing terrestrial age calculation

19 p3411 A69-36100

Solar He abundance limits and discrepancies of Cl 37 solar neutrino count experiment

20 p3592 A69-38068

CHLORINE COMPOUNDS

NT ALUMINUM CHLORIDES

NT AMMONIUM CHLORIDES

NT AMMONIUM PERCHLORATES

NT BORON CHLORIDES

NT CARBON TETRACHLORIDE

NT CHLORATES

NT CHLORIDES

NT CHLOROSILANES

NT DICHLORODIPHENYLTRICHLOROETHANE

NT HYDROCHLORIC ACID

NT HYDROXYLAMMONIUM PERCHLORATES

NT IRON CHLORIDES

NT MAGNESIUM CHLORIDES

NT MAGNESIUM PERCHLORATES

NT NITRONIUM PERCHLORATE

NT PERCHLORATES

NT POTASSIUM CHLORIDES

NT POTASSIUM PERCHLORATES

NT SODIUM CHLORIDES

NT TITANIUM CHLORIDES

Titanium aluminum alloys two stage direct production by aluminothermal reduction of titanium tetrachloride

07 p1159 A69-18536

Flame resistant chlorine containing polyester resins, discussing preparation, curing characteristics, physical properties and reinforced plastics application

08 p1340 A69-20505

Nb-gaseous Nb chlorides equilibrium from transpiration measurements at 800-1400 C, confirming importance of Nb pentachloride, Nb tetrachloride and Nb trichloride

23 p4112 A69-41339

CHLORINE FLUORIDES

Thermal dissociation of chlorine trifluoride behind incident shock waves at high temperature, discussing bimolecular reaction rate constant

[WSCI PAPER 68-40] 07 p1202 A69-18355

Electrochemical synthesis of chlorine pentafluoride formation from chlorine trifluoride-anhydrous hydrogen fluoride-sodium fluoride system

13 p2217 A69-28134

Chlorine pentafluoride formation from chlorine in anhydrous hydrogen fluoride in electrochemical cell, noting formation rate

13 p2217 A69-28135

Thermal dissociation of chlorine trifluoride behind incident shock waves as function of temperature using UV absorption spectroscopy

21 p3670 A69-39739

CHLOROAROMATICS

NT CHLOROBENZENES

Cl 35 nuclear quadrupole resonance spectra of 3,6-dichloropyridazine, tetrachloropyridazine, 2,6-dichloropyrazine and chloropyrazine

01 p0123 A69-10290

CHLOROBENZENES

Raman spectra and temperature dependent nuclear quadrupole resonance frequencies of p-dichlorobenzene and p-dichlorobenzene-D, calculating librational amplitudes

01 p0122 A69-10286

Ion cyclotron double resonance technique to identify collision-induced ion fragmentation pathways illustrated with p-chloroethylbenzene

19 p3265 A69-36292

CHLOROFORM

Crystal and molecular structure of mu-oxo-bis(chlorobis/2, 4-pentanedionato/titanium/IV/-chloroform solved by symbolic sign determination method and Patterson map interpretation

01 p0023 A69-10411

CHLOROFORMATE

Reagent menthyl chloroformate use in optical analysis of asymmetric amino and hydroxyl compounds by gas chromatography

07 p1075 A69-19499

CHLOROPHYLLS

Q switching of ruby lasers by natural chlorophyll a and derivatives pheophytin a and Cu chlorophyllin Na

11 p1900 A69-25581

Manganese deficiency effect on growth and chlorophyll content of algae with and without hydrogenase

15 p2558 A69-31551

CHLOROPLASTS

Interactions between intermediate fluorescence quenching trapping center and associated electron acceptor of oxygen evolving photosynthetic spinach chloroplast photosystem

01 p0024 A69-10928

Deoxyribonucleic acid conformations in spinach leaf chloroplasts by electron microscopy

20 p3479 A69-38001

CHLOROSILANES

Halocarbon solvent for application of chlorosilane finish to heat cleaned glass fabric for reinforcement of plastic, noting relative humidity effect

08 p1341 A69-20513

SiC part fabrication by chemical vapor deposition through pyrolysis of chlorosilanes from vapor state onto machined substrates of graphite and metals

09 p1509 A69-22344

CHLORPROMAZINE

Glucose disappearance rate from dogs blood at simulated 27,000 ft altitude compared with tolerance at ground level, discussing chlorpromazine administration effect

14 p2408 A69-29305

CHOCTAW HELICOPTER

U CH-34 HELICOPTER

CHOICE

U SELECTION

CHOKES (RESTRICTIONS)

Mixing regimes for flows with different stagnation enthalpies subject to mass flow limitation due to thermal choking

13 p2251 A69-28499

Swirl influence on choking constraint in transonic flow through nozzle throat

[AIAA PAPER 68-693] 23 p4151 A69-41887

CHOLESTEROL

Electric field strength and helix pitch in induced cholesteric-nematic phase transitions, noting activation energy for charge carrier production

04 p0555 A69-14964

Exercise effects on hepatic cholesterol of rats on diets high in saturated or unsaturated fats

21 p3653 A69-38903

Cholesterol-protein metabolism in muscles, liver and cerebrum of lethal X ray exposed guinea pigs compared with unexposed group

21 p3657 A69-39052

Brain weight and cholinesterase activity in rats after exposures to acoustic and light stimuli

21 p3662 A69-39627

Stewart-Hamilton theorems for total input-output analysis of body cholesterol in man

24 p4259 A69-42639

CHOLINE

1.5 g angular acceleration effects on acetylcholine metabolism in guinea pig brains and hearts

02 p0198 A69-11505

Mechanical vibrations and noise effects on acetylcholine concentration, esterase activity and synthesis ability in rat brain

23 p4079 A69-41381

Regression process in acetylcholine level in rats after mechanical vibrations and noise exposure

23 p4079 A69-41382

Optic nerve spikes elicited by acetylcholine application on isolated perfused retina of frog, varying response by prostigmine and atropine

23 p4084 A69-41465

CHOLINESTERASE

Insignificant or recoverable changes observed in blood acetylcholine content and cholinesterase activity of rabbits subjected to 8 g acceleration

02 p0197 A69-11491

CHONDRITES

NT CARBONACEOUS METEORITES

NT MURRAY METEORITE

NT ORGUEIL METEORITE

NT PANTAR CHONDRITES

Replicate neutron activation determinations of Ga, Ge, In and Ir in L group chondrites, proposing model which accounts for observations

01 p0155 A69-10976

Chondrules in Sharps /H-3/ chondrite show evidence of recrystallization and homogeneous olivines and pyroxenes

01 p0156 A69-10977

Chemical composition of various types of chondrites, determining quantitative proportions soluble and insoluble in acids

01 p0026 A69-11381

Stone meteorite chemical composition, analyzing chondrites Borodino, Lavrentevka, Alfanello and Nardoo II

01 p0026 A69-11382

Enstatite chondrites structure and mineral content and composition using microscopic and X ray analysis, grouping parameters in distinguishing types

02 p0317 A69-12016

Rubidium, Sr and Sr isotopic composition of normal gray hypersthene chondritic falls, noting Rb/Sr and Sr87/Sr86 ratio determination of Bath Furnace L chondrite isochron

02 p0317 A69-12020

Meteorite fragments fall and distribution at Bur-Gheluai, Somalia, discussing crust morphology, mineralogical composition and structure

03 p0507 A69-13095

Oxygen partial pressure, temperature and olivine composition related, determining distribution coefficient of Fe and Mg between olivine and pyroxene

03 p0516 A69-14082

Disordered chondritic pyroxenes, analyzing X ray patterns of meteoritic and synthetic crystals

03 p0516 A69-14083

Nepheline occurrence in unequilibrated chondrites, discussing crystallographic evidence from X ray powder patterns

04 p0659 A69-15010

Heavy xenon isotopic anomalies in carbonaceous chondrites, rejecting plutonium 244 spontaneous fission decay mechanism

05 p0819 A69-15625

Chemical compositions and structural states of feldspar in recrystallized /Type 6/ chondrite meteorites, using electron microprobe analysis and X ray diffraction techniques

05 p0819 A69-15626

Nitrogen abundances in chondritic meteorites determined by carrier gas fusion extraction

05 p0825 A69-16301

Electron microprobe analysis of vanadium in presence of titanium by compositional measurement of chromite in chondritic meteorites

07 p1073 A69-18419

Chemical composition and morphological, structural, textural and mineralogical characteristics of chondrules and chondrites

07 p1212 A69-18548

Textural variation relation to mineralogical and chemical characteristics of chondrites from review of published data

08 p1391 A69-20516

Chondrite meteorite fall /1969/ in Mexico, noting opaque and microcrystalline matrices and gamma rays from short lived isotopes

08 p1396 A69-20686

Fractionation of abundant lithophile element ratios in chondrites emphasizing Si-Mg ratio

08 p1403 A69-20915

Indium abundances in chondritic and achondritic meteorites and terrestrial rocks determined by radiochemical neutron activation analysis

08 p1404 A69-20917

Mercury concentration relation to thermal history of chondritic meteorites, using activation analysis

08 p1404 A69-20920

Trace element distribution in metal phase of chondrites and iron meteorites, using neutron activation analysis with radiochemical separation

08 p1404 A69-20921

Redistribution of potassium and argon in meteorites and rock samples, discussing thermal diffusion and grain size

08 p1405 A69-20926

Electron probe analysis of olivine and pyroxene in LL-group chondrites, discussing iron and fayalite composition and unequilibrated stones

08 p1406 A69-20931

Cosmic ray induced radioactivity in lunar surface and meteorites calculated together with cosmic ray intensity variations

10 p1756 A69-22817

Chemical composition analysis of one mesosiderite and seven chondrites, with notes on mineralogy and chemical procedures

11 p1953 A69-24336

Quality assessment of quantitative data on chemical composition of stony meteorites, considering precision and accuracy

11 p1953 A69-24359

Lithophile elements relationship in chondrites and basaltic achondrites, tabulating Ca-Al ratios and Ca, Al, Ti, Zr, Sr, Ba and Sc percentages

11 p1954 A69-24360

Chondritic meteorites arsenic, tin and antimony content determined by anion-exchange chromatography and neutron activation analysis

13 p2344 A69-27630

Rb 87-Sr 87 age of bronzite chondrites, analyzing olivine bronzite chondrite falls for K, Rb and Sr elemental concentrations

14 p2526 A69-29881

Geochemistry of fission Xe component in chondrites, suggesting Xe derivation from superheavy elements with Z 112 to 119

15 p2681 A69-30325

Chondritic Cr and Mn content studied by X ray fluorescence, noting positive correlation in H and L groups and negative correlation in carbonaceous chondrites

15 p2681 A69-30416

Volatiles percentage at 1000 C in nitrogen atmosphere for chondrites, considering cosmo-petrological significance of microchondrule coalescence

17 p3030 A69-33067

Cosmogenic Al 26 in achondrites and chondrites measured by nondestructive gamma-gamma coincidence counting

17 p3034 A69-33584

Bovedy Chondrite fall in Northern Ireland, describing fragments trajectory and metal, sulphide and silicate presence

18 p3200 A69-34993

Iron distribution inconsistency indicated in Group H and L chondrites through Ni and Co analysis of fractionated samples, plotting atomic ratios on Prior diagram

19 p3407 A69-36078

Mossbauer spectra of Fe minerals in unequilibrated ordinary chondrites, noting ratios of olivine to pyroxene iron

19 p3408 A69-36082

Sharps chondrite chemical, petrographic and mineralogical studies suggesting formation from complex and repetitious high temperature events and agglomeration processes

19 p3408 A69-36086

Fractionation of abundant lithophile element ratios of Si, Mg, Ca, Al and Ti in carbonaceous, common and enstatite chondrites

19 p3409 A69-36087

Tieschitz and Mezo-Madaras chondrites and chondrules formation from considerations of coexisting minerals and interstitial ground mass

19 p3409 A69-36089

Ar 39 content in chondrites interpreted for meteorite size, exposure age and orbital elements

19 p3411 A69-36101

Radiation ages of bronzite chondrites, amphoteric and hypersthene from cosmic ray activities

19 p3412 A69-36102

Lance chondrite C III, studying mineral composition of chondrules and heterogeneous crystalline fragments

19 p3413 A69-36110

Chondritic meteorites initial orbits evolution to earth impact calculated by Monte Carlo method, considering relationships to meteorite sources

19 p3415 A69-36118

Quantitative mineralogical characterization of chondrites by modal analysis using electron microprobe

19 p3416 A69-36125

Black chondrite inclusions in Cumberland Falls meteorite, discussing inclusion chemical, mineralogical and electron probe data

19 p3416 A69-36127

Kamacite analysis for P and Ni in chondrites, palasite and iron meteorites, considering cooling rate and rhadbit

19 p3417 A69-36131

Dynamically deformed structures in chondrites and hexahedrites observed to discriminate among theories about origin of chondrules and meteorites

19 p3418 A69-36135

K 40-Ar 40 age measurements in separated mineral phases of chondrites, including production rates of spallation isotopes

19 p3418 A69-36137

V 50/V 51 abundance ratios in chondrite, terrestrial diabase standard W-1 and reagent V

20 p3601 A69-37501

Petrology, mineralogy and phase composition of Siena chondrite, interpreting meteorite as ignimbritic rock or welded tuff

20 p3602 A69-37534

Amphoterite /LL/ chondrites Rb-Sr age determination, noting high brecciation

21 p3814 A69-39583

Meteorites pigments identification as porphyrins for extraterrestrial life evidence, noting sample analyses of Orgueil, Murray, Cold Bokkveid and Mokoia carbonaceous chondrites

22 p4008 A69-39889

Olivine-bronzite chondrite fragments found near Oshkosh, Wisconsin, in fall of 1961

22 p4021 A69-40413

Ilmenite composition in equilibrated ordinary chondrites, analyzing Fe, Mg, Ti and Cr content

24 p3382 A69-42890

Rb-Sr isotopic determinations for Olivenza olivine-hypersthene chondrite, noting isotopic ratio vs age

24 p4385 A69-43214

CHONDRULE

Chondrules in Sharps /H-3/ chondrite show evidence of recrystallization and homogeneous olivines and pyroxenes

01 p0156 A69-10977

Chemical composition and morphological, structural, textural and mineralogical characteristics of chondrules and chondrites

07 p1212 A69-18548

Rare earth elements and yttrium in meteoritic chondrules determined by radiochemical neutron activation analysis

08 p1403 A69-20916

Volatiles percentage at 1000 C in nitrogen atmosphere for chondrites, considering cosmo-petrological significance of microchondrule coalescence

17 p3030 A69-33067

Meteorite origin theory limitations from microscopic examination and microprobe analyses of chondrules in unequilibrated meteorites

17 p3034 A69-33585

Ramsdorf meteoritic chondrules and metal particles formation attributed to shock-induced partial melting and rapid cooling

19 p3409 A69-36088

Tieschitz and Mezo-Madaras chondrites and chondrules formation from considerations of coexisting minerals and interstitial ground mass

19 p3409 A69-36089

Bjurbole chondrules composition and density, discussing formation of homogeneous olivines and pyroxenes

19 p3409 A69-36090

Dynamically deformed structures in chondrites and hexahedrites observed to discriminate among theories about origin of chondrules and meteorites

19 p3418 A69-36135

Pyroxene crystallization in meteoritic chondrules, noting normal spherulite crystallization

22 p4033 A69-41065

CHOPPERS [ELECTRIC]

U ELECTRIC CHOPPERS

CHORDS [GEOMETRY]

Velocity, lifting force, pressure moment and circulation around linear array of thin foils with direction normal to profile chords calculated by Birnbaum-Glauret method

11 p1817 A69-24348

Geometric conditions selection in directions determination in satellite and rocket aided triangulation, deriving formulas for chords directions of earth ellipsoid

15 p2689 A69-30572

CHOROID MEMBRANES

Retinal burn resulting from prolonged viewing of sun, laser or thermonuclear explosion, noting effects on choroid, receptors and pigment cells

08 p1267 A69-20680

CHORUS [DAWN PHENOMENON]

U DAWN CHORUS

CHROMA PHENOMENON

U DAWN CHORUS

CHROMATES

NT POTASSIUM CHROMATES

Cleaning, deoxidizing and chromating process effects on chromate coated Al, using salt spray corrosion tests

19 p3321 A69-35570

CHROMATOGRAPHY

NT GAS CHROMATOGRAPHY

NT PAPER CHROMATOGRAPHY

NT THIN LAYER CHROMATOGRAPHY

Dispersion in gel permeation chromatograph, noting contributions of injection and detection systems to peak broadening and retention time

04 p0555 A69-14884

Dispersion in gel permeation chromatography, noting eddy diffusion in chromatographic columns

04 p0555 A69-14885

Gas-liquid chromatography of natural protein amino acids in biological substances, noting separation characteristics

13 p2217 A69-28258

Polychromator measurement of hydrogen plasma electron density produced by normal ionizing shock wave, using Stark broadening study of H beta line

14 p2494 A69-29767

Free lysine and dinitrophenyl (DNP) derivatives determined quantitatively by ion exchange chromatography

17 p2917 A69-33651

Gel permeation chromatography of nominally linear aliphatic polyesters, using tetrahydrofuran solvent at 37 degrees C

21 p3670 A69-39806

Aromatic and nonaromatic hydrocarbon fractions in terrestrial graphite, discussing classification and analysis by chromatography and mass spectrometry

22 p3934 A69-39890

CHROME

U CHROMIUM

CHROMITES

Thermal decomposition of ammonium perchlorate and ammonium perchlorate-copper chromite mixtures

02 p0304 A69-12312

Electron microprobe analysis of vanadium in presence of titanium by compositional measurement of chromite in chondritic meteorites

07 p1073 A69-18419

CHROMIUM

Irradiation influence on chromium transition temperature explained by defect clusters and embrittling impurity redistribution

01 p0095 A69-10604

Mechanical properties of thermally diffused layers obtained by vacuum chromizing of steel, establishing need to decarburize substrate material

03 p0450 A69-13913

Cr gas deposition on steel by means of chromium chloride salt, noting chromizing conditions effect on carbide growth and friction resistance

04 p0605 A69-14577

Cobalt concentration reduction in maraging steels by Cr replacement and increased Mo and Ti additions

04 p0616 A69-14649

Chemical vapor deposition of chromium metal on substrates, discussing influence of temperature, gas flow rate and chromium chloride concentration [ECS PAPER 223]

05 p0769 A69-16232

Brittleness and physical causes of cold shortness in Cr, discussing high purity metal formation and fine and superfine grain structures synthesis

09 p1526 A69-22147

Chromium concentrations induced line shift in ruby single crystals spectra, determining principal lines position

10 p1744 A69-23321

Chondritic Cr and Mn content studied by X ray fluorescence, noting positive correlation in H and L groups and negative correlation in carbonaceous chondrites

15 p2681 A69-30416

Annealed Cr structural changes during creep at 900 C in air, discussing crystalline disorientation X ray studies and stress

18 p3160 A69-35453

Tau-luminescence in thin gamma-colored and uncolored ruby crystals containing Cr ions measured, discussing ions absorption spectrum changes

19 p3335 A69-36166

Steels chromized by vacuum diffusion, studying depth, microstructure and properties of chromized layer

19 p3329 A69-36572

H release, pressure and oxide layer formed by reaction during ball milling Cr in water

21 p3728 A69-38567

Grain boundary grooving kinetics for Cr, W and Mb in Ar and vacuum, determining interface free energies and surface self diffusion coefficients

21 p3744 A69-38740

Bright chromium electrodeposition principles and properties of coatings

22 p3958 A69-41263

CHROMIUM ALLOYS

Deformation in aged Fe-Cr alloy studied for rate-controlling solid solution mechanism as function of stress

01 p0095 A69-10601

Cooling rate effect during aging on heat resistance of forged blanks of nickel based chromium alloy

02 p0266 A69-12125

Chromium bronze blanks compacted from granules for hardness and electrical conductivity, noting improved high strength characteristics over conventional production methods

02 p0266 A69-12127

Cr-Si diffusion layers on Ti, noting results of roentgenographic and metallographic studies

04 p0614 A69-14578

Nb and Cr additions effects on Hadfield type steel mechanical properties, noting improvement especially at low temperatures

04 p0614 A69-14579

Quasi-ternary titanium dichromide-V-Mo system composition at high temperatures, physical properties and phase diagrams

04 p0618 A69-15080

Be, Co, V and Ti additions effect on oxidizability of cast, forged and cold worked Nb-Cr-Mo alloys

04 p0618 A69-15081

Hot working temperature effects on Rene 63 mechanical properties and microstructures, using tensile and stress rupture tests, electron microscopy and X ray diffraction analysis

05 p0781 A69-16446

Long term creep behavior of nickel-chromium-molybdenum alloy, noting temperature effect on grain boundaries

05 p0781 A69-16500

Cobalt chromium high temperature oxidation and scale formation [ECS PAPER 413]

08 p1332 A69-20363

Cobalt chromium alloys high temperature oxidation kinetics, discussing thermographic study of oxidation rate and oxygen pressure role [ECS PAPER 413]

08 p1332 A69-20364

Joining methods for fabricating thoria dispersion strengthened nickel and nickel chromium materials

09 p1509 A69-22342

Spontaneous martensite phase transformation in Ti-Cr alloy thin foils formed electrolytically

10 p1708 A69-22994

Long range order formation in Ni-Cr alloys analyzed by direct neutron diffraction, considering disorder-order transition temperature and chemical composition

10 p1714 A69-23964

Vacuum deposition of Cr-Al film on Ni-Mo alloys, describing operating pressure, temperature and film thickness

10 p1715 A69-24013

Ductile metal clads and coatings of silicides, aluminides and noble metals to protect Cr alloys against nitrogen embrittlement and air oxidation

12 p2114 A69-26495

Thoria strengthened Ni-Cr alloys high temperature stability, noting thoria particle size influence

14 p2465 A69-29682

Cr-Si diffusion layers on Ti, noting results of roentgenographic and metallographic studies

15 p2638 A69-30279

Chromium-cerium phase diagram determined by differential thermal, metallographic and X ray structural analysis

15 p2640 A69-30666

CR-B binary system phase diagram including lattice parameters, temperature of peritectic decomposition and characteristics of alloys

15 p2641 A69-31185

Chromium ternary systems phase diagrams and crystallographic structures, using heat treatment and X ray analysis

18 p3158 A69-35262

Group 7A and group 8 elements alloying effect on Cr dislocation structure and mechanical properties, discussing ductile-brittle transition temperature and electronic theory

18 p3160 A69-35452

Ni-Cr alloy unidirectionally solidified, grain and eutectic structure and alloy strength

19 p3343 A69-35921

Abrasion and corrosion resistant Cr-Co-B cast alloys in aggressive media, concluding resistance is due to chromium boride and fine dendritic structure

19 p3347 A69-36742

Stress corrosion cracking of stainless steels and Incoloy and Inconel alloys in chloride, caustic, oxygenated and miscellaneous environments

19 p3349 A69-36890

Authoradiographic methods for diffusion and phase transformation in Fe-Cr alloys by application of photographic emulsion with tracer element on metal surface

20 p3561 A69-37416

Equilibrium vapor compositions and activities over Fe-Cr-Ni alloys at 1600 C determined by collecting effusate from thoria Knudsen cells

23 p4175 A69-41503

Chromium composites mechanical properties, studying effects of alloying with spinel and magnesium oxides

23 p4177 A69-41672

CHROMIUM BORIDES

Abrasion and corrosion resistant Cr-Co-B cast alloys in aggressive media, concluding resistance is due to chromium boride and fine dendritic structure

19 p3347 A69-36742

CHROMIUM BROMIDES

Faraday effect for magnetic properties of chromium tribromide along various isotherms near critical point, confirming scaling laws

15 p2668 A69-30686

CHROMIUM CARBIDES

Cobalt base high chromium carbide strengthened superalloy, evaluating physical and mechanical properties

11 p1901 A69-24259

Stainless steels stress corrosion susceptibility, detecting chromium carbide in martensitic matrix by galvanic nondestructive test method

14 p2466 A69-29935

Ni based superalloy mechanical properties, determining chromium carbide discontinuous precipitation effects at various temperatures

23 p4176 A69-41507

CHROMIUM COMPOUNDS

NT CHROMATES

NT CHROMITES

NT POTASSIUM CHROMATES

Dilatometric and X ray study of temperature dependence of linear expansion coefficients of lattice constants of chromium disilicon

04 p0619 A69-15392

Young modulus of sintered nonporous titanium, zirconium and chromium nitrides, computing characteristic temperature and root mean square atomic displacements in lattices

06 p0938 A69-16830

Dilatometric and X ray study of temperature dependence of linear expansion coefficients of lattice constants of chromium disilicon
18 p3156 A69-35020

Cr-S and Cr-Fe-S systems phase relations, using silica tube and collapsible tube experiments, correlating formation conditions of meteoritic sulfide assemblages
19 p3359 A69-36123

CHROMIUM ISOTOPES

Microsectioning technique applied to measurement of diffusion coefficients of Cr 51 in polycrystalline Nb at 1220-1766 K temperature range
11 p1903 A69-24577

CHROMIUM OXIDES
NT CHROMITES

Catalytic effect of potassium bichromate and chromic oxide additives on burning of ammonium perchlorate and mixtures
08 p1375 A69-19997

Chromium oxide additions effects on reaction rates decrease during ammonium perchlorate and nitrate combustion
08 p1375 A69-20340

CHROMIUM STEELS

Light austenitic grain boundaries in heat treated Cr-Mo-W-V alloy steels
01 p0100 A69-11295

Chromium steel /El961/ susceptibility to structural damage under cyclic loads by nondestructive inspection of magnetic hysteresis and eddy current losses
07 p1141 A69-19316

Chemical composition of chromium steels for optimum heat resistance properties, noting effects of nickel, nitrogen and ferrite and austenite-forming elements
10 p1708 A69-23000

Monograph on effect of nitrogen on precipitation behavior of austenitic chromium-nickel steel covering carbides, intermetallics, phase transportations, corrosion resistance, etc
11 p1902 A69-24369

Monograph on effect of boron, zirconium and titanium on austenite transformation of CrMo steels bainite and martensite covering carbides, nitrides, mechanical properties, etc
11 p1903 A69-24634

Aging effects on hardness and tensile strength of nickel-chromium steels at various high temperatures and time periods
11 p1906 A69-25439

Etching, spray etching and photo-resist methods for producing CrNi steel heating elements for propeller deicing
12 p2102 A69-26370

Dynamic strain aging of Fe-Cr-C and Fe-Mo-C steels, analyzing strength, ductility and secondary hardening by using microprobes, foils diffraction and extraction replicas
13 p2276 A69-27403

Double notch creep rupture tests of Cr-Mo steels, investigating changes in notch profile, dimensions and structure
[ASME PAPER 68-WA/MET-7]
14 p2464 A69-29441

Creep rates measurement errors at low stresses in intermediate temperature range, examining log creep rate vs log stress plot in Cr-Mo steel
15 p2639 A69-30599

Chemical composition effect on Cr-Ni-Mo-Ti stainless maraging steels mechanical properties
15 p2640 A69-30631

Damping, fatigue and optimal heat treatment of Cr-Ni steel for compressor blades operating at temperatures up to 500 K
17 p2990 A69-33933

Nondestructive eddy current testing of chromium steel for early stage fatigue damage of aircraft components
18 p3136 A69-34777

Cutting loads measured as function of cutting rate and cutting tool geometry during boring of Cr-Ni steel pipe blanks
21 p3731 A69-38878

Ce, Zr, Nb and B effect on heat resistance and structure of low alloy CrMoWV steels (type CSN 41 5335/
22 p3972 A69-41079

V contents influence on high temperature strength and fine structure interrelation in low alloy CrMoWV steels
22 p3972 A69-41083

High strength austenitic Cr-Mn-Ni steel applicability to welded pressure vessels for cryogenic fluid storage, discussing operating temperature stability, weldability, etc
23 p4175 A69-41475

CHROMOSOMES

Mammalian cell survival, chromosome abnormalities and recovery from heavy ion and X ray irradiation
03 p0373 A69-13492

Three dimensional Fourier synthesis at low resolution for calculating ribosome electron density distribution in chromatoid bodies
07 p1074 A69-19394

Corneal epithelium chromosome rearrangements in gamma irradiated white adult mice, noting radiation dosage and duration
17 p2907 A69-32944

Pre and postflight leukocyte chromosome aberration analyses of Gemini astronauts
17 p2908 A69-33173

S-4 human blood experiment during Gemini 2 flight, studying spaceflight ionizing radiation interaction effects on single and multiple break chromosome aberrations
23 p4085 A69-41600

CHROMOSPHERE

Chromospheric flares photometric measurements during near minimum solar activity, discussing characteristics
01 p0149 A69-10127

Ionized calcium lines in spectra of light bridges of sunspots, observed by diffraction spectroscopy, indicating similarity to chromospheric flares
01 p0154 A69-10894

Chromospheric and photospheric solar observations made in Belgium in 1967, noting heliographic sunspot latitudes
02 p0313 A69-11533

Ionized metals emission lines intensity in chromosphere observed with coronagraph, determining hydrogen concentration
02 p0314 A69-11635

French solar research program, emphasizing protosphere-chromosphere transition zone
02 p0316 A69-11905

Coronagraphic determination of hydrogen concentration in luminescence regions of ionized metals in lower chromosphere
03 p0420 A69-13086

Solar flares effect on ozonosphere, calculating time necessary for solar radiation to increase ozone concentration by 50 percent
03 p0424 A69-13542

Solar chromosphere dark mottles size, shape and evolution, using high resolution photography near solar disk center
03 p0515 A69-14038

Chromosphere fine structure in Lyman alpha intensity, compiling isophote map
03 p0515 A69-14039

Chromospheric flare development and motion with respect to magnetic field of sunspot clusters
04 p0648 A69-14371

Time variations of chromospheric network of bright points covering solar disk in spectrograms, noting contrast and interspaces variation with 11-year solar cycle
04 p0651 A69-14372

Solar flares and sunspots number decrease near central meridian
04 p0660 A69-15040

Bright streaks in H alpha disk chromosphere, noting predominantly horizontal loop structures
04 p0664 A69-15525

High resolution H alpha line photographs of solar chromosphere, showing superpenumbra-like dark fibrils around isolated sunspots
04 p0664 A69-15526

Chromospheric /optical/ flares caused by dense material falling from corona into chromosphere
06 p0993 A69-17430

Small scale mass motions in chromospheric structures surrounding solar flare indicating changes in magnetic field
06 p0993 A69-17431

Flare-like phenomena in chromosphere, discussing moustaches, dashes and spicules and relation to changes in magnetic field
06 p0994 A69-17433

Stellar chromosphere and flare spectra observations with image tube spectrograph using Hc 10803 line, noting possible contribution to X ray background
06 p1003 A69-17449

Solar radio emissions analysis using radio telescope measurements, observing quasi-periodic LF fluctuations caused by chromospheric processes
06 p1004 A69-17535

Chromospheric velocity field temporal characteristics in quiet region of sun, determining power spectra of Doppler shifts of H alpha spectra
07 p1217 A69-19240

Three dimensional information pictures of chromospheric alpha H line using special camera attached to solar telescope diffraction grating spectrograph
07 p1217 A69-19241

Solar flare initial development model assuming high temperature chromospheric point explosion, noting subsequent expansion and large density gradient effects
07 p1205 A69-19246

Emission line formation in homogeneous chromosphere for noncoherent scattering, considering various chromosphere models
08 p1381 A69-19800

Photoelectric measurement of chromospheric heights by method requiring neither high telescopic resolution nor best seeing, discussing trials during September 1967
08 p1385 A69-20070

Synoptic charts of chromosphere, giving position and magnitude of sunspots, faculae plages and prominences during synodic revolution of sun
08 p1379 A69-20378

Spectroscopic evidence for mass loss from CH Cygni based on observations of chromospheric lines of high dispersion spectrograms
08 p1396 A69-20651

Flares and chromospheric absorption features locations compared with H alpha magnetograms, noting double emission ribbons development
09 p1579 A69-22179

Viscosity coefficients approximation for chemical compositions in chromosphere and coronal gas
09 p1602 A69-22217

Solar magnetic fields compared in chromospheric and photospheric layers using magnetograph measurements, noting correlation with solar event
10 p1762 A69-23727

Solar spectra of Mg II doublet lines during September 22, 1968 eclipse, considering chromospheric activity effects on emission peaks
11 p1958 A69-24591

Solar activity complex development based on magnetic, photospheric, chromospheric and coronal observations
11 p1964 A69-25418

Chromospheric heating and polarization in late stars, considering association with Ca II K line emission cores
13 p2340 A69-27579

Coronagraphic determination of hydrogen concentration in luminescence regions of ionized metals in lower chromosphere
14 p2433 A69-28768

Solar activity indices based on Ca II H, emphasizing index representing emission excess over chromospheric emission
14 p2525 A69-29722

Excitation sources distribution in chromosphere from observed H alpha line contour, considering resonant scattering and internal excitation
15 p2683 A69-30509

Chromospheric spicules formation, density, pressure gradient, vertical motion, velocity fluctuations and luminosity
15 p2675 A69-30551

Short period pulsations in solar magnetic fields and chromosphere, determining optimum conditions for formation of standing oscillations
15 p2688 A69-30556

Solar Mg b and Na D line spectra, computing profiles for Doppler cores of lines for multilevel model atoms and selected chromospheric parameter ranges
15 p2693 A69-30779

Thermal conductivity coefficients in solar corona and chromosphere computed and tabulated for H plasma
15 p2694 A69-30788

Center limb observations of Ca II emission core interpretations, discussing chromospheric thickness effects on Doppler width
16 p2854 A69-31653

Solar chromosphere metal abundance determined taking into account local thermodynamic equilibrium departures
16 p2855 A69-31657

Solar Ca chromospheric plage decay curves obtained from area measurements, showing similarity and exponential mean curve
16 p2859 A69-32222

Chromospheric spectrum outside of eclipse, wave lengths 3040 to 9266 A, listing emission lines taken at McMath solar telescope
16 p2861 A69-32257

Nondivergent oscillations in solar atmosphere forming normal modes or free oscillations, assuming free surface of chromosphere coronal interface and large density in convective zone
17 p3029 A69-33048

- Fine structure of 9 June 1968 solar flare related to nonflare chromosphere in active regions
17 p3024 A69-33802
- Power spectral analysis of chromospheric inhomogeneities in July 1967 and June 1968, tabulating mean heights of formation in solar atmosphere
17 p3040 A69-33811
- Chromospheric inhomogeneities rapid changing properties observable in H and K lines above sunspot umbrae
18 p3204 A69-35389
- Umbral chromosphere flashes visual and photometric observations at 5 sec intervals on K line filtergrams using Halle filter
18 p3204 A69-35390
- Photospheric radiation field role in temperature inversion of stellar chromospheres with dominant H ion opacity, postulating mechanical energy dissipation
20 p3613 A69-38173
- Chromospheric heating above sunspots by analyzing MHD wave generation and propagation in sunspots and solar atmosphere
22 p4010 A69-39992
- Statistical analysis of chromospheric flares connections with sunspots, using frequency distributions of flares occurrences in sunspot groups
22 p4001 A69-39996
- Coronal jet resulting from chromospheric burst observed during 22 September 1968 total solar eclipse
22 p4028 A69-40716
- Solar flares associated optical phenomena including filaments enhancement, destabilization and distortion, high speed ejections, explosions and loop prominences
24 p4371 A69-43607
- Solar chromospheric spicules acceleration mechanism based on magnetic field structure on supergranulation boundaries
24 p4374 A69-43635
- CHRONIC CONDITIONS**
- Increased chronic acceleration physiological effects on chickens, comparing hematological observations with exercise capacity, survival and sexual development
10 p1641 A69-23041
- Chronic acceleration effects on erythrocyte number, plasma volume, globulin fractions, erythrocyte size and plasma A/G ratio in chickens
11 p1828 A69-25458
- Single channel pressure telemetry unit with magnetic latching or RF switch for chronic implantation
23 p4100 A69-41295
- CHRONOGRAPHS**
U CHRONOMETERS
- CHRONOLOGY**
NT RADIOACTIVE AGE DETERMINATION
- Late type stars, discussing main sequence for Population 1 and Population 2 stars and ages and chemical composition of old galactic clusters and globular clusters
01 p0158 A69-11325
- Uranium in meteorites, discussing U content and isotope composition, Pb isotope ratios, radiogenic Pb, origin of matter and meteorite ages
01 p0025 A69-11369
- Galactic halo chronology determination by positron component flux measurement in primary cosmic rays
08 p1386 A69-20084
- Open clusters age determination method to study giant star distribution as function of age
08 p1388 A69-20237
- Color magnitude distribution as function of age for giant stars of open clusters, discussing error sources
08 p1388 A69-20238
- Kodaikanal iron meteorite measurements for cosmogenic rare gases and K-Ar isotopes ages for glass inclusions
09 p1596 A69-22047
- Initial Sr isotopic composition at time of planetary objects formation in solar system and precision measurements for age determination of basaltic achondrites
11 p1953 A69-24357
- Rb-Sr and other radioactive isotopes cosmochronology in solar system, analyzing age of elements and r process
11 p1955 A69-24393
- Solar system age based on decay rate of natural radioactive elements
11 p1961 A69-24972
- Lunar craters circularity measurements relation to age, discussing fracture system and stress history associated with mare formation
13 p2344 A69-27645

- Pulsar dispersion-removing technique, discussing pulsar mean flux density decrease with age
14 p2517 A69-29091
- Gaunt lunar craters, discussing lunar age and defining surface steady state
16 p2863 A69-32404
- Photoelectric photometric stellar spectroscopy for calculating metal abundance from Fraunhofer absorption lines, relating results to star age
17 p3043 A69-34140
- Rb-Sr and other radioactive isotopes cosmochronology in solar system, analyzing age of elements and r process
24 p4390 A69-43783

CHRONOMETERS

- Remote control spectrophotochronograph to study radiation of high speed high temperature processes, giving construction data and diagrams
12 p2085 A69-26161
- High speed curtain type photographic shutters testing by chronograph with phosphorescent and photographic recording, determining movement rate including acceleration and braking
12 p2093 A69-26598

CHRONOPHOTOGRAPHY

- Aerial chronophotography of Southern Hemisphere conducted on around world polar flight analyzed for meteorological and geographical aspects and compared with satellite data
09 p1534 A69-21405
- Meteorological application of ATS observations in form of time lapse movies of weather in motion, describing camera and data flow [AIAA PAPER 68-1094]
12 p2174 A69-26804
- Variable time lapse videoscintiscopes in medical applications, discussing implementation of TV camera, signal tape recording and audio activation
18 p3134 A69-34541
- Umbral chromosphere flashes visual and photometric observations at 5 sec intervals on K line filtergrams using Halle filter
18 p3204 A69-35390
- Tethered polyethylene balloon carrying radio controlled camera for time lapse photographs of wave generated near shore currents
22 p3865 A69-40808

CHRONOTRONS

- U PULSE RATE
U TIME LAG

CHUGGING

- U COMBUSTION STABILITY

CINEFLUOROGRAPHY

- U MOTION PICTURES
U RADIOGRAPHY

CINEMATOGRAPHY

- Image intensifier-vidicon closed circuit TV network for auroral cinematography at low light levels
06 p0925 A69-17382
- Optical evidence for mass motions in solar flares /1937-1967/
06 p0993 A69-17428
- Cine-holographic apparatus consisting of ruby laser and semitransparent mirror, noting capability of photographing within 10-100 nsec intervals
12 p2087 A69-26172
- Cinematic holography as continuous motion uninterrupted viewing system compared with standard cinematography, noting flicker-free shutterless reproduction
12 p2087 A69-26173
- Shadowgraph cinematography technique for testing attenuating influence of symmetrical diaphragm system on shock wave
12 p2088 A69-26184
- Ultrahigh speed cinematographic materials, discussing mirror turbines, streak and synchronized framing cameras
12 p2090 A69-26197

CINERADIOGRAPHY

- U MOTION PICTURES
U RADIOGRAPHY

CINETHEODOLITES

- Multiple frame camera with image compensation as ballistic phototherodolite
12 p2084 A69-26153

CIRCADIAN RHYTHMS

- Weak alternating electric field effects on human circadian rhythms
01 p0013 A69-10167
- Daily sleep and wakefulness periodicity changes effect on heart rate, respiration and body temperature

- diurnal rhythms in human males under isolation conditions
03 p0377 A69-14203

- Circadian rhythms disruption during long distance flights, discussing adverse effects on pilot and passenger performance
03 p0378 A69-14260

- Circadian rhythm effect between individuals of separate twin pairs, noting application to physiological research in medical genetics and human biometeorology
04 p0553 A69-15152

- Brain norepinephrine effect on daily rhythmic changes in activity of tyrosine transaminase in livers of starved adrenalectomized rats
05 p0707 A69-15582

- Rapid global transportation effect on circadian rhythmic patterns in human body functions, discussing kidney excretion and pituitary adrenal cortical system
09 p1444 A69-22545

- Circadian rhythms characteristics in humans, animals and plants, noting possible effects of rhythm disturbances on astronauts
13 p2211 A69-28614

- Circadian rhythm of optic nerve impulses in isolated eye of sea hare *Aplysia californica* in total darkness
14 p2406 A69-28870

- Constant light/darkness effects on stress response rhythm of hypothalamic-pituitary-adrenocortical system in female rats
15 p2556 A69-31330

- Light effects on circadian rhythms in monkeys, describing changes in deep body temperature and locomotor activity phase relationships
15 p2556 A69-31336

- Latent desynchronization, discussing life system and distortion, body rhythms coordination, circadian rhythms and adaptation to new system of time
15 p2557 A69-31457

- Diurnal variations in radiation sensitivity of mice and rats to irradiation with median lethal doses, noting sine curve survival function
15 p2557 A69-31458

- Alternating electric field effects on circadian rhythms in men, discussing period shortening and internal desynchronization
15 p2557 A69-31461

- Circadian rhythm in dermestid beetles *Trogoderma glabrum* Herbst as response to compulsory constant light and temperature conditions
15 p2557 A69-31469

- Long distance air flights through different time zones, discussing circadian physiological cycles, light-dark ratio shifts effects and methods of lessening desynchronization effects
16 p2745 A69-32444

- Diurnal pressure cycles found as zeitgeber to entrain body temperature endogenous circadian rhythm in pocket mice under constant environmental temperature and light
16 p2745 A69-32447

- Diurnal periodicity of physiological functions of flight crews flying through several time zones found to correspond to time zone of permanent residence
17 p2906 A69-32935

- Urinalysis of crew members of first transatlantic helicopter flight indicating interindividual endocrine-metabolic variability and circadian trends modification
19 p3263 A69-36452

- Biological clocks, discussing circadian rhythms of organisms using animal experiments and physical oscillator model
21 p3653 A69-38895

- Desynchronization and resynchronization of human circadian rhythms of activity, body temperature and urine excretion during isolation in underground bunker in various conditions
21 p3660 A69-39173

- Circadian rhythm phase shifts during ontogenesis produced by hormone concentration changes resulting from light variations
22 p3872 A69-40198

- Circadian variations in human temperature regulation, measuring peripheral and rectal temperatures and peripheral heat and arterial blood flows in clothed resting males
22 p3872 A69-40201

- Circadian rhythms characteristics of healthy human beings as reference standards for comparing investigation data from different continents
23 p4083 A69-41457

- Subjects confined in caves for two to six months to note physiological rhythms time evolution and associated desynchronization and resynchronization
23 p4107 A69-41818

Circadian rhythm in man for artificial light-dark cycles including twilight transitions and temperature rhythm
23 p4094 A69-42070

Autonomous circadian rhythm in man under complete isolation and light-dark cycles and illumination intensity changes
23 p4094 A69-42071

Circadian rhythms in nonhuman primates - Conference, Atlanta, July 1968
24 p4259 A69-42701

Constant illumination intensity effects fixed ratio lever pressing behavior for appetitive reinforcement with chimpanzee in temperature and humidity controlled environment
24 p4260 A69-42702

Bigeminus pattern in baboon social behavior, noting diurnal rhythm independence from social deprivation, light cycling and food supply
24 p4260 A69-42705

Circadian rhythm phase relationships between photoperiodism and heart rate, locomotor activity and deep body temperature/DBT/ in unrestrained monkeys
24 p4260 A69-42706

Physiological circadian rhythms in isolated and nonisolated Macaca Nemestrinas living under varied light intensities, noting telemetered deep body temperature, urine volume and sodium, etc
24 p4261 A69-42707

Nonhuman primate circadian rhythms as functions of phase shift carried out in advance or delay
24 p4261 A69-42709

Urine sampling conditions for kidney function circadian rhythm during global flight, considering food and water intake, sampling intervals and body position
24 p4266 A69-43374

Circadian periodicity of human reaction times tested during normal diurnal cycles and 24 hour wakefulness, noting acoustic and visual stimuli effects on learning
24 p4267 A69-43387

Psychophysiological effects of fatigue and correlation with somatic parameters following circadian rhythm
24 p4268 A69-43407

CIRCLES (GEOMETRY)
NT GREAT CIRCLES

Surface temperature of flat plate cooled convectively and insulated by circular spot, determining effects of spot radius and Biot number
03 p0531 A69-12863

Volterra problem with given singularities for exterior of circle applied to fluid mechanics
24 p4339 A69-42679

CIRCUIT BOARDS

Printed circuit board wiring technique for strain gage rosettes application in extensive airframe static tests
02 p0250 A69-12231

Additive processing technique for fabrication of single sided, double sided and multilayer printed circuit boards
07 p1100 A69-18621

IR evaluation of multilayer etched circuit boards, discussing testing of circuit distributive properties and individual layers
07 p1117 A69-19698

Microsoldering techniques for thin and thick film hybrid circuits and microminiature printed circuit boards
09 p1510 A69-22349

Flexible-rigid hybrid polyimide-epoxy glass multilayer board to fill gap between all flexible and all rigid circuit boards
19 p3319 A69-35545

CIRCUIT BREAKERS

Exploding wire self healing fuse feasibility demonstrated with Hg, noting dynamics of conversion of electric to mechanical energy
01 p0120 A69-10677

Plasma physics of electric arc transition from conducting plasma to insulating gas in electric circuit interruption, noting interrupter interaction with power system
12 p2133 A69-25905

Cut-in and cut-out characteristics of fast acting composite transistor circuit, noting pulse duration
13 p2235 A69-28517

CIRCUIT DIAGRAMS

Digital computer circuit design book covering requirements of circuit for digital logic and memory functions and physical properties of components
06 p0892 A69-17869

Multistage amplifier design with frequency compensation by eliminating stages in HF region
07 p1103 A69-18877

Computer aided circuit design by singular imbedding, beginning with prespecified topology and undetermined elements
07 p1115 A69-19148

Operational principles and characteristics of pulse width modulator designed on basis of autooscillator amplifier, giving circuit diagrams
10 p1664 A69-23817

Plasma diagnostics facilities design, circuit diagrams and operation based on Q switched ruby laser and optical recording system
14 p2461 A69-29782

Photometer for simultaneous stellar photometry in UVB bands, purposes and performance characteristics and circuit diagrams
16 p2790 A69-32209

Ionosonde electric circuit modified to permit radio wave absorption measurements over wide frequency range, calculating electron collision frequencies in F region
17 p2968 A69-33994

Computer program for generation of test patterns for multiterminal devices and networks
21 p3679 A69-39604

X ray scintillation spectrometers temperature stabilizing circuit, describing amplitude- frequency conversion technique for position stability
21 p3727 A69-39856

CIRCUIT PROTECTION

Energy source specifications and control techniques evaluated for microwave amplifier arrays, discussing use of common power supply and energy storage bank
01 p0047 A69-10998

Malfunction elimination in asynchronous fluidic switching circuit by locating static hazards
02 p0195 A69-12080

Pulsed radar quantum paramagnetic amplifier protection from driving pulse leakage power by transient processes
05 p0728 A69-15644

Pulsed radar quantum paramagnetic amplifier protection from driving pulse leakage power by transient processes
16 p2762 A69-32501

Overload protection guidelines for power subsystems, discussing source and protective device characteristics emphasizing spacecraft requirements
17 p2904 A69-34088

Ignition hazards in electrical circuits contaminated by glycol fluids, describing hazard detection by RF methods, decontamination procedures, safety checks, etc
19 p3359 A69-36028

Spark gap protection of input transistors in radio receivers against antenna-collected static charge damage
21 p3681 A69-38395

Gunn oscillators protection from catastrophic breakdown phenomena, using carrier velocity saturation in n-type Ge
21 p3682 A69-38777

Laser beam circuitry miniaturization facilitating laser circuit assembly isolation from thermal, mechanical and ambient changes
24 p4328 A69-43327

CIRCUIT RELIABILITY

Schmitt trigger current-voltage characteristic for determining switching behavior and switching point temperature, examining formulas and equivalent circuits
01 p0039 A69-10171

Reliability system design, emphasizing circuit design analysis, failure drifts and component failure modes by use of computer programs /ECAP, CIRC and IMAG/
04 p0608 A69-15224

Controlled transient signal distortion by shock monitoring instrumentation circuits using piezoelectric accelerometers
04 p0603 A69-15430

Semiconductor device failure modes temperature dependence, discussing bonds, metallization and packaging
06 p0894 A69-17218

Error origin and control in high gain operational amplifier in time differentiation of voltage signal used for photoemission studies
06 p0897 A69-17700

Miniature microwave tuners with solid state reliability and reduced power consumption, using YIG, mixer circuits and integrated control circuitry
07 p1102 A69-18672

Alternative balancing technique utilizing linear combination of two equal and opposite drift characteristics to minimize drift in integrated differential amplifiers
07 p1102 A69-18874

Precision monolithic circuits fabrication techniques, describing differential amplifier design incorporating emitter feedback and direct DC errors compensation
07 p1102 A69-18875

IR evaluation of multilayer etched circuit boards, discussing testing of circuit distributive properties and individual layers
07 p1117 A69-19698

Flip-flops built with complementary symmetry MOS, discussing power, noise and load stability due to n and p channel series transistors
07 p1113 A69-19766

Microcircuit components and microelectronic systems reliability assessment including short term testing, noting digital systems, packaging, production controls, etc
08 p1291 A69-20984

Microcircuits, integrated circuits and other monolithic solid state circuits failure mechanisms examined and applied to reliability methodology [AGARDOGRAPH-114]
08 p1292 A69-20987

Catastrophic failures in logic circuit and system design, considering thermal effects, complexity, statistical methods and computer use
08 p1299 A69-21107

Conventional electronic and microelectronic circuits reliability, discussing external stress effects on improvement in avionics and rocket applications
08 p1293 A69-21112

Reliability distribution parameters for electronic components, determining time and tolerance dependence of reliability
08 p1293 A69-21114

Integrated semiconductor circuits reliability in electronics and microelectronics, discussing hybrid and monolithic circuits in thin/thick film design and on Si monocrystals
08 p1294 A69-21118

Nonlinear capacitive parallel frequency converter circuit stability, using filtered circuit method
08 p1299 A69-21148

Accelerated reliability tests of electronic capacitors using voltage as main forcing factor, establishing correlations between lifetimes in accelerated and long term tests
09 p1464 A69-22244

Ruggedized ballistic range telemetry system survivability and in-flight stability after gun launching, presenting temperature, strain and stagnation point pressure measurements
10 p1654 A69-23281

Reliability function for electronic device during initial period of operation, based on use of lower bound
10 p1662 A69-23318

State probabilities of finite stochastic queueing system for calculating equipment reliability parameters
10 p1664 A69-23693

Electronic systems and component reliability in space, considering electric parameter variation effects
11 p1848 A69-24867

In-circuit diodes testing by semiautomatic low current regulated voltage test set
12 p2035 A69-25835

Computer programs for linear systems fault isolation, discussing technique theory and limitations
12 p2040 A69-26568

Tactical air navigation system redesign with integrated circuits, obtaining weight reduction and improved performance and reliability
13 p2227 A69-27389

Electric relays reliability requirements, discussing specifications, minimum current, load and frequency effects, etc
13 p2231 A69-28045

Satellite circuit assembly reliability achievement by high reliability components, redundancy and optimal utilization
15 p2624 A69-30819

Integrated circuit failure analysis in military and space applications utilizing type-test programs
15 p2624 A69-30820

Management and scientific computer reliability difference, considering circuits, component assembly, software, maintenance, etc
15 p2624 A69-30821

Reliability of integrated circuits with emphasis on errors
15 p2626 A69-30831

Third generation computer reliability including preparation and test of integrated logic circuits
15 p2626 A69-30832

Transistors and IC reliability for memory control evaluated by Concerto subprograms
15 p2627 A69-30842

Reliability of high resolution accelerometer composed of semiconductor integrated circuits
15 p2627 A69-30843

Microelectronic technology for mass production of high reliability hybrid thin film circuits
15 p2628 A69-30845

Thin film tantalum nitride resistors technology and production, evaluating projected reliability of resistance circuits as function of operating and environmental conditions
15 p2628 A69-30846

Disturbances simulation in instrumentation utilizing digital integrated circuits for reliability computation in complex circuits
15 p2628 A69-30848

Computer aided design /CAD/ of component selection for circuit optimization applied to circuit performance and sensitivity calculations
15 p2628 A69-30849

Radiology and thermography in nondestructive reliability testing of electronic equipment
15 p2610 A69-30850

Complex systems reliability, describing uses of computer programs in analysis of circuit design, component failure modes and faults due to drifts
15 p2572 A69-31042

Microwave strip transmission line, discussing evolutionary improvements, computerized design, materials, semiconductors, packaging, reliability, etc
15 p2721 A69-31074

Quality control of high volume microelectronic circuit assembly of military computer emphasizing preventive action
15 p2580 A69-31129

Integrated circuits screens, developing sequence of life and environmental tests to remove units of potential reliability hazards
15 p2580 A69-31130

Integrated circuits failure analysis in space program applications, describing electrical analog for notification, fact gathering, part analysis and corrective action functions
15 p2580 A69-31132

Metal oxide semiconductor integrated circuits, showing failure rates and degradation causes
16 p2759 A69-31851

Large scale integrated circuits reliability with emphasis on multilayer metalization, designing test vehicles for failure mechanisms
17 p2935 A69-32887

Scanning electron mirror microscope advantages over electron mirror and scanning electron microscopes for examining integrated circuits
17 p2971 A69-32891

Al interconnections discontinuities at integrated circuit contact windows observed by scanning electron microscope, noting catastrophic failure and Si presence
17 p2936 A69-32893

Test structure model for studying semiconductor-insulator interface related failure mechanisms in large scale integrated circuitry
17 p2936 A69-32894

Fluidic thrust reversal control system for turbojet achieving cost and weight reduction, illustrating fluidic circuit and noting circuit reliability
17 p3018 A69-33329

Beam lead sealed junction transistor and integrated circuits reliability, describing test conditions and failure mechanisms
18 p3145 A69-34497

Epoxy encapsulated transistors reliability, data from long term maximum rated life and accelerated tests
18 p3145 A69-34498

Wave soldering reliability and cost saving potential in miniature circuits manufacture for aerospace applications, noting process control and machine design relationship
18 p3146 A69-34512

Computer program and component part models for nonlinear DC circuit simulation at various temperatures
18 p3108 A69-34525

Integrated circuits failure analysis techniques utilizing pin-to-pin curve tracer tests and thermal measurements
19 p3282 A69-35786

Failure mechanisms and analyses of large scale integrated circuits based on bipolar and MOS transistors, describing measurement and probing techniques
19 p3282 A69-35787

Intermediate level mathematical reliability model relating failure mechanism, part strength and interaction of application stresses to parts failure rates, with emphasis on microcircuits
19 p3283 A69-36019

Microelectronics and IC process and quality control check list including conductor screening, resistor abraiding and discrete part attachment
19 p3283 A69-36020

MOS arrays failure mechanisms, discussing oxide defects, contamination and metal migration due to mode of operation and fabrication techniques
21 p3684 A69-39605

Flexible circuitry for reliable spaceborne data processing equipment electronic packaging
22 p3903 A69-39951

Hybrid microelectronic circuit failure mechanisms for thick and thin film resistors, conductors and capacitors, noting packaging contributions
22 p3910 A69-39954

Failure analysis of corrosion products in hybrid thin film circuits, discussing detection technique, instrumentation and results
22 p3911 A69-39955

Wire, flip-chip and beam-lead bonding processes effects on hybrid microcircuits reliability
22 p3911 A69-39956

Stability boundaries of discrete circuits employing delay lines with forward and feedback links, deriving equations
22 p3918 A69-40957

Ultrasonic oscillations effects on magnetic permeability of ferrite circuit components
23 p4138 A69-41873

Electromagnetic compatibility /EMC/ filter design and test methods to achieve effectiveness and reliability, emphasizing transfer impedance characteristics
23 p4142 A69-42233

Phase-pulse multistable circuit reliability improvement by additional negative feedback increasing parametric variation tolerance, feeding voltages and temperature
23 p4143 A69-42338

Active Ni centers properties in Si with emphasis on increasing and reducing minority carrier lifetime in silicon integrated circuits, discussing energy levels
24 p4360 A69-42759

CIRCUITS

NT ADDING CIRCUITS
NT ANALOG CIRCUITS
NT AUTODYNES
NT BISTABLE CIRCUITS
NT CIRCULATORS [PHASE SHIFT CIRCUITS]
NT COINCIDENCE CIRCUITS
NT COUNTING CIRCUITS
NT COUPLING CIRCUITS
NT DELAY CIRCUITS
NT DIGITAL INTEGRATORS
NT DISCRIMINATORS
NT ECHO SUPPRESSORS
NT ELECTRIC BRIDGES
NT EQUIVALENT CIRCUITS
NT FEEDBACK CIRCUITS
NT FLIP-FLOPS
NT FLUID SWITCHING ELEMENTS
NT GATES [CIRCUITS]
NT INTEGRATED CIRCUITS
NT LC CIRCUITS
NT LIMITER CIRCUITS
NT LINEAR CIRCUITS
NT LOGIC CIRCUITS
NT MAGNETIC CIRCUITS
NT MATRICES [CIRCUITS]
NT MICROWAVE CIRCUITS
NT MIXING CIRCUITS
NT MONOSTABLE MULTIVIBRATORS
NT MULTIVIBRATORS
NT NEGATIVE RESISTANCE CIRCUITS
NT PHASE DETECTORS
NT PHASE SHIFT CIRCUITS
NT PNEUMATIC CIRCUITS
NT POWER SUPPLY CIRCUITS
NT PRINTED CIRCUITS
NT RC CIRCUITS
NT RLC CIRCUITS
NT SQUELCH CIRCUITS
NT SWITCHING CIRCUITS
NT THRESHOLD GATES
NT TRANSISTOR CIRCUITS
NT TRANSMISSION CIRCUITS
NT TRIGGER CIRCUITS
NT VARACTOR DIODE CIRCUITS
NT WHEATSTONE BRIDGES
NT WIRE BRIDGE CIRCUITS

Soviet collection of papers on electric circuits and electromagnetic systems
01 p0046 A69-10744

Active circuit analysis by state variable method, defining state vector as set of voltages between nodes and reference node
03 p0410 A69-13831

Electrical circuits time domain analysis, describing method for computer solution of circuit equations
05 p0737 A69-15766

Circuit and system theory - Conference, University of Illinois, October 1968
06 p0901 A69-17394

Shunted resonators on transmission line with asymmetrical response offering selectivity from resonance frequency standpoint
08 p1271 A69-19917

Sine wave oscillator circuits and performance prediction for NERO thrust measurement test stand
08 p1300 A69-20155

Pulsed ultrasonic flaw detectors resolving power enhancement by shunting semiconductor diodes across piezoelectric elements of scanning heads to shorten scan pulse duration
18 p3137 A69-35112

GABA shunt contribution to total metabolism of alpha ketoglutarate to succinate and high pressure O effect on system under in vitro conditions
22 p3877 A69-40776

CIRCULAR CONES

Mach number effects on pattern of vortex flow past delta wing and circular cones at various Reynolds numbers
06 p0858 A69-17339

Three dimensional laminar boundary layer near windward generator of cone subjected to uniform mass transfer by suction or injection
11 p1874 A69-25281

Supersonic combustible gas mixture flow around circular cone, discussing ignition by shock wave and flow modification by conical flame front
15 p2548 A69-31007

Flow measurements about high Mach number low Reynolds number laminar wake behind spherically blunted cones, including surface and wake flow field data, radial wake profiles, etc
17 p2894 A69-33500

HF radar scattering by finite circular cone as function of frequency and aspect angle using modified diffraction pattern theory
20 p3495 A69-37849

N strip algorithm of integral relations to analyze flow around circular cone at incidence in supersonic flow
20 p3460 A69-38128

Fluid mechanical structure of laminar hypersonic wake behind sharp circular cone, investigating flow field at zero angle of attack and adiabatic wall temperature
24 p4247 A69-43576

CIRCULAR CYLINDERS

Circular, cylindrical thin walled shell dynamic response to moving shock solved by Flugge equations in series form
01 p0164 A69-10057

Simultaneous partial integro-differential equations governing natural vibrations of arbitrary cross section cylindrical tubes, suggesting Fourier series solution
01 p0164 A69-10065

Unsteady heat flow in finite composite hollow circular cylinder using inverse method of eigenfunction expansion /method of finite integral transformation/
01 p0175 A69-10230

Convective heat transfer across fluid film limited by right sections of two parallel circular hollow steel cylinders
01 p0176 A69-11135

Transverse curvature effect on skin friction and heat transfer in laminar flows past slender circular cylinders
02 p0232 A69-12210

Diffraction of cylindrical and plane waves in system of two parallel circular cylinders, using equivalent circuit method
02 p0217 A69-12261

Plane inhomogeneous thermal stress in isotropic elastic circular infinitely long cylinder produced by plane unsteady temperature distribution
02 p0349 A69-12826

Three dimensional unsteady heat conduction and temperature distributions in finite hollow circular cylinder under time dependent boundary conditions of second kind
03 p0530 A69-12861

HF approximations, discussing plane wave diffraction by conducting circular cylinder using Watson transform
03 p0384 A69-12903

Stresses in circular cylindrical shell subjected to local heating
03 p0523 A69-12952

Unreinforced circular cutouts effects on buckling behavior of circular cylindrical shells under axial compression, using photoelastic plastic shells
03 p0523 A69-12988

Creep buckling of circular cylindrical shells under axial compression and bending, using Al alloy test specimens

03 p0523 A69-12995

Heat input influence on hypersonic flows past sphere and circular cylinder
[DVL-844]

03 p0364 A69-13663

Submerged rigid circular cylinder displacement under influence of plane acoustic pressure wave solved by operational method

04 p0667 A69-14261

Directional properties of electric vibrator positioned at reflecting circular cylinder, discussing radiation patterns and cylindrical wave diffraction

04 p0574 A69-14459

Kinematic and dynamic relations determined for vortex flow of ideal incompressible fluid past circular cylinder, noting use for calibrating cylindrical adapters

04 p0541 A69-14484

Flow field of impulsively started circular cylinder, noting drag due to nonlinear convection

04 p0544 A69-14897

Steady flows of incompressible viscous fluid exterior or interior to circular cylinder

04 p0589 A69-14898

Dielectric waveguide propagation, impedance and attenuation characteristics and insertion loss and launching efficiency of mode transducer

04 p0577 A69-14971

Steady longitudinal motion of insulating cylinder in conducting fluid, discussing analog between steady MHD and acoustic scattering

04 p0638 A69-15192

Boundary layer flow of viscous incompressible liquid past wedge embedded circular cylinder

04 p0590 A69-15276

Local pressure and skin friction distribution around circular cylinder in cross flow in large range of Reynolds numbers

05 p0744 A69-15716

Tangential stress distribution and heat transfer in circular cylinder with attached wall jet

05 p0746 A69-16022

Liquid rise in partially filled circular cylinder with free surface accelerated from rest to constant angular velocity

[ASME PAPER 68-FE-13]

05 p0747 A69-16065

Circular cylinder near wake in cross flow measured with hot-wire anemometry for various Reynolds numbers, noting data processing on digital computer

[ASME PAPER 68-FE-5]

05 p0747 A69-16068

Lift and drag coefficients for circular cylinder immersed in time dependent flow analyzed using potential flow model

[ASME PAPER 68-FE-15]

05 p0747 A69-16072

Unsteady potential flow and wake near oscillating circular cylinder noting velocity, pressure and correlation measurements

[ASME PAPER 68-WA/FE-23]

05 p0749 A69-16099

Unsteady supersonic flow around thin circular cylinder representing rocket stage, calculating flutter and response to random environment

[ONERA-TP-666]

06 p0857 A69-17098

Inviscid incompressible fluid flow stability against helical disturbances in circular cylinder

06 p0910 A69-17332

Laminar near wake flow field of two dimensional adiabatic circular cylinder with surface mass transfer

[AIAA PAPER 69-67]

06 p0862 A69-18044

Approximate solution for hollow circular cylinder with fixed ends under axial displacement and cylindrical surfaces free from traction, using boundary layer technique

07 p1230 A69-18265

Strouhal and Reynolds numbers relation from data on vortex streets of circular cylinder in two dimensional flow

07 p1119 A69-18749

Nonaxisymmetric temperature field of unbounded hollow cylinder with moving heating boundary, expanding surface temperature into Fourier series

07 p1241 A69-18924

Short cylinder of perfectly plastic Coulomb yield conditions compressed between rigid plates, discussing cylinder-plate interface frictions, angles of internal friction and cohesion

08 p1410 A69-19890

Boundary layer separation and vortex street buildup conditions of gas flow in circular cylinder wake

08 p1252 A69-20713

Steady motion through rarefied gas of circular cylinder due to surface temperature difference

08 p1305 A69-20888

Dynamic response of anisotropic circular cylinders to uniformly distributed pressure varying periodically with time analyzed using Laplace transformation

09 p1611 A69-21440

Three dimensional vibration analysis of circular homogeneous elastic cylinder, obtaining differential equations and zero stress conditions

09 p1612 A69-21601

Three dimensional analysis of torsional vibrations of circular elastic homogeneous cylinder, stressing new torsional vibrations

09 p1612 A69-21603

Plane thermal stress field in discontinuous temperature distribution within isotropic linear elastic circular cylinder of infinite length

10 p1793 A69-22884

Antiplane strain model for describing cracks and dislocation arrays within circular cylindrical inhomogeneity surrounded by elastic material

10 p1803 A69-24031

Numerical solutions for incompressible Newtonian flow around circular cylinder for various Reynolds numbers

11 p1867 A69-24279

Thin walled circular cylinders postbuckling behavior and stability under axial compression calculated for design loads

11 p1979 A69-24816

Radiation pattern of axial slot on circular conducting cylinder based on wedge diffraction and creeping wave theory

11 p1836 A69-24993

Maximum stress under bending for thin walled circular cylindrical shell stiffened with uniform stringers

11 p1987 A69-25380

Skin friction drag coefficient for right circular cylinder calculation coefficient on basis of Blasius solution for flow

11 p1819 A69-25384

Thermal stresses in hollow finite circular cylinder having smooth rigid insulating cover on curved surfaces and temperature distribution on plane ends

12 p2180 A69-26268

Torsion in composite inhomogeneous circular cylinder, obtaining solutions for elastic displacements and stresses

12 p2180 A69-26274

Hollow circular viscoelastic cylinder axisymmetric plain strain problem, considering displacement, traction and mixed boundary conditions, noting applicability to rocket solid fuel core

12 p2181 A69-26396

Monograph on shell calculations by linear three dimensional elasticity theory, relating displacements and stresses

12 p2188 A69-26902

Thermoelastic waves in stretched circular cylindrical bar, analyzing displacements, secondary pressure and temperature field by using Frobenius method

12 p2189 A69-27115

Minimum volume face sheet design of circular cylindrical sandwich shell obeying Mises yield criterion for loads transverse to lateral surface and axisymmetric

12 p2189 A69-27117

Dynamic response of imperfect circular cylinder to constant velocity load, noting applicability of Hoff nonlinear equation for dynamic buckling of columns

13 p2359 A69-27260

Viscous heat conducting compressible fluid response to abrupt change in circular cylinder angular velocity at stable temperature distribution, considering Boussinesq approximation

13 p2245 A69-27378

Self controlled vibration of elastically supported cylinder in fluid stream due to von Karman shedding, considering fluidelastic interaction, structural deformation and natural frequency

13 p2360 A69-27437

Guided waves in circular cylindrical radially inhomogeneous medium, using vector theory based on Maxwell equations

13 p2221 A69-28062

Stresses in infinite solid elastic circular cylinder due to rotating line source of heat

13 p2364 A69-28206

Loitsianski method of parametric approximation extended to include flat plate with constant surface suction and flow past circular cylinder

13 p2249 A69-28247

Directional properties of electric vibrator positioned at reflecting circular cylinder, discussing radiation patterns and cylindrical wave diffraction

14 p2418 A69-28830

Vibrations of thick walled shallow circular cylinder with thickness change in time, applying dynamic elasticity and Volterra equations

14 p2533 A69-28985

Axisymmetric impact of circular cylindrical plates, obtaining two dimensional dynamic stress distributions for materials of linear elastic compressibility and plastic behavior in shear

14 p2534 A69-29027

Creep strain rate and stress distribution of thick walled cylinders under internal pressure at elevated temperature, using variational principle

15 p2703 A69-30070

Periodic radial heat flux in infinite cylinder with varying heat sources, assuming time variable heat exchange on surface

15 p2717 A69-30575

Thick walled pressurized cylinder fatigue test results compared with axial tension and rotating beam tests on same material

15 p2709 A69-30676

Surface displacements at end of elastic semiinfinite circular cylinders due to annular axisymmetric loading, employing Boussinesq solution

15 p2711 A69-30872

Thermoelastic stresses in isotropic circular cylinder with surface locally heated by external Newtonian heat source, considering various heat transfer conditions

15 p2714 A69-31178

Thermal stresses in circular cylinder with regularly distributed cavities, establishing distribution laws for temperatures and stresses

15 p2714 A69-31196

Prebuckling deformations influence on circular cylindrical shell buckling under external pressure, applying Galerkin method to Donnell equations

16 p2872 A69-31905

Incompressible attached wall jet /Coanda flow/ over circular cylinder with finite incompressible injection normal to surface

16 p2772 A69-32148

Electromagnetic field eigenvalues along conductive circular cylinder in magnetoionic medium, assuming lossless medium and field frequency not equal to cyclotron frequency

16 p2754 A69-32568

Backscattered impulse response waveforms of conducting circular cylinder for broadside incidence utilizing Fourier synthesis

17 p2917 A69-32918

Two dimensional incompressible flow past circular cylinder at moderate Reynolds number, reducing partial differential equations of motion by series truncation for flow field

17 p2896 A69-33600

Asymptotic solutions for vector fields and propagation constants of axial modes in circular cylindrical waveguides, noting changes in dielectric constant

17 p2921 A69-33673

Stress level reduction in pressurized circular cylinder with circumferential ring stiffener and longitudinal crack, using shallow shell equations

18 p3212 A69-34347

Secondary vortex generation in near wake of circular cylinders under forced oscillation, analyzing motion dependent transition regimes using hydrogen bubbles flow visualization

[AIAA PAPER 69-755]

18 p3084 A69-34411

Vortex wakes behind circular cylinder subject to transverse sinusoidal oscillations in uniform water flow at specific Reynolds numbers, photographing varied frequency flow patterns

18 p3086 A69-35169

Fluctuating heat transfer and flow measurements for circular cylinder in crossflow with simultaneously imposed transverse standing sound field

18 p3124 A69-35384

Hypersonic rarefied gas flow past flat plate with sharp leading edge and past circular cylinder, noting wake structure similarity to viscous theory prediction

19 p3294 A69-35755

Plasma density and potential distributions along circular cylinder surface in weakly ionized high speed low pressure gas flow, noting boundary layer separation point

19 p3380 A69-35839

Canonical forms for three dimensional diffraction problem of elastic harmonic waves propagating along circular cylinders infinite array

19 p3437 A69-36144

Nonlinear shell theory for thin elastic circular cylinders, obtaining equations for investigating equilibrium configurations of postbuckled states

19 p3440 A69-36636

- Transition in near wake, from study of base pressure on circular cylinders in incompressible flow
19 p3242 A69-36809
- Mach reflection limiting parameters of conical shock wave in Plexiglas cylinders, showing head wave curvature radius linear relationship to cylinder diameter
19 p3302 A69-36845
- Stress distribution in finite and semifinite solid cylinders under end normal load, using Fourier-Bessel series
20 p3621 A69-37199
- Roshko correlation for estimating vortex shedding from circular cylinder in sheared flow with velocity in Strouhal and Reynolds numbers
20 p3515 A69-37228
- Load carrying capacity of orthotropic circular cylindrical shell under uniformly distributed normal load, considering edge support conditions
20 p3629 A69-38075
- Field patterns, propagation constants and losses determined for axially propagating modes guided by circular cylindrical inhomogeneous dielectric, using perturbation method
20 p3497 A69-38130
- Narrow band vortex shedding from circular cylinder in critical Reynolds number range, noting increase in Strouhal number
21 p3644 A69-38690
- One dimensional spectra of turbulent wakes behind circular cylinders, discussing isotropy, anisotropy and Reynolds number
21 p3693 A69-38705
- Circular cylindrical freely supported shell moment state stability, solving critical parameters by infinite matrix eigenvalues determination
21 p3835 A69-38724
- Deformation of circular cylindrical shell of varying thickness, obtaining differential equation solutions through multiple scales method
21 p3837 A69-39159
- Postbuckling of filled circular cylindrical shell using Ritz energy method for load deformation relation, discussing stabilizing effect of core
22 p4038 A69-39895
- Buckling strength prediction for circular cylindrical shells reinforced by circumferential and longitudinal stiffeners, solving torsional buckling of orthotropic shells under internal pressure
22 p4042 A69-40171
- Forced convection heat transfer coefficient for fully developed turbulent flow in circular tube with time-varying circumferential heat flux
22 p4051 A69-40921
- Closed circular cylindrical shell stability and oscillations under ring-shaped axial load, defining stress-strain state by radial displacements and force function
22 p4049 A69-41280
- Inflation effect on circular cylindrical cantilever beam subsequent response to bending loads, using theory of small deformations superimposed on large deformations
23 p4227 A69-41881
- Semiempirical stability boundary for flutter of simply supported cylinders for various length-radius and radius-thickness ratios
23 p4228 A69-41914
- Beam wave propagation in conducting hollow circular cylinder applied to shielding cylinders design for aperture antenna transmission
24 p4282 A69-42987
- Transverse acoustic wave excitation of elastic circular cylindrical sandwich shell submerged in infinite fluid medium, describing simultaneous equations development for modal response
[ASME PAPER 69-APMW-17]
24 p4401 A69-43100
- Vortex shedding from circular cylinders rotating normal to free stream velocity, studying roles of rotation rate and Reynolds number
24 p4248 A69-43601
- CIRCULAR ORBITS**
NT STATIONARY ORBITS
- Particle moving in circular orbit perpendicular to axis of cylindrically symmetric magnetic field
01 p0120 A69-10816
- Near circular satellite orbits evolution taking into account gravitational fields zonal harmonics effect on motion
01 p0157 A69-11304
- Optimal circular satellite orbits for planetary surface mapping mission minimizing overlap
03 p0518 A69-14247
- Satellite nonlinear spatial oscillations about center of mass during circular orbit, using perturbation theory and analog computer
04 p0665 A69-14270
- Minimum fuel rendezvous maneuver for two space vehicles in circular orbit, considering propelled tracking equipment nonlinear equations of motion
05 p0823 A69-16036
- Nonlinear equations of motion for rendezvous in circular orbits, pursuer using minimum fuel and pursued having no propulsion
06 p1014 A69-17571
- Braking and acceleration speeds and maximum magnitude during transfer from circular orbit having earth center as focus to elliptical orbit within circular orbit
06 p1007 A69-17578
- Perturbation method in rectangular coordinates based on motions of Galilean satellites of Jupiter applied to nearly circular orbits of quasi-resonant systems
08 p1390 A69-20275
- Circular satellite orbit calculation from incomplete observations of one orbital pass
09 p1589 A69-21373
- Optimal rendezvous between satellite and spacecraft, determining power and time optimal coplanar rendezvous in circular orbit
09 p1538 A69-21759
- Periodic motion of satellite with magnetic damper along circular orbit, assuming small value of damping coefficient
09 p1609 A69-21761
- Circumpolar satellite orbits under lunar and solar perturbations based on two fixed centers problem, considering large amplitude disturbances
10 p1780 A69-23616
- Optimal interorbital transfers between closely spaced nearly circular noncoplanar orbits, taking into account active section length for low power thrusts
10 p1783 A69-23712
- Numerical solution for changing satellite orientation within circular orbit plane by applying force of onboard flywheel
10 p1792 A69-24194
- Plane planetary orbits construction extended to nearly circular and quasi-plane orbits by generalizing perturbations method to problems in space
15 p2690 A69-30622
- Rendezvous maneuver with minimum fuel in circular orbit solved without restrictive conditions for accelerations due to approach thrust
16 p2852 A69-31558
- Stability of steady circular motions in systems with hidden variables analyzed by using Lejeune-Dirichlet theorem
16 p2804 A69-31621
- Electrically propelled TV satellite control maneuvers to reach target position in synchronous circular orbit from spiral ascent trajectory
16 p2868 A69-31935
- Flywheels desaturated by magnetic action for optimizing stabilization system of satellite in circular orbit [ONERA-TP-732]
17 p3049 A69-33241
- Steady motion stability of satellite gyroscope in Cardan suspension traveling along circular orbit in Newtonian central force field
18 p3135 A69-34585
- Minimum fuel guidance from hyperbolic into specified circular orbit
19 p3367 A69-35663
- Minimum impulse transfer between circular and nearby noncoplanar elliptic orbit, applying Pontryagin principle
19 p3400 A69-35675
- Vehicles optimal flights with controlled or boundary level thrust in circular orbit neighborhood, using linearized equations of motion
19 p3427 A69-36612
- Optimal landing of spacecraft on moon surface from low circular orbit, analyzing rocket thrust, altitude and landing site distance effect on spacecraft mass
19 p3431 A69-36616
- Stability of periodic orbits in elliptic restricted three body problem
[AAS PAPER 68-086]
20 p3595 A69-37172
- Near-polar circular orbiting satellite for calibrating and evaluating ground-based radars observing space objects
20 p3617 A69-37714
- Automatic stationkeeping/geosynchronization/for maintaining satellite in circular synchronous orbit at all geocentric longitudes for prolonged time with low fuel consumption
21 p3805 A69-39213
- Trajectory optimization of second state of rocket launched into earth circular orbit in gravitational field by stepwise fuel control, using Pontryagin maximum principle
21 p3829 A69-39818
- Closed form solution to stability of coupled libration motion of slender axisymmetric satellite in circular orbit limited to small amplitude vibrations
22 p4008 A69-39936
- Optimal pulsed orbital transfer between close nearly circular orbits in central field of gravity realized by geometrical solution
22 p4033 A69-41085
- Nonlinear longitudinal dynamics of lifting orbital vehicle in near circular orbit, considering translational motion components effecting orbital decay or dilatation
[AAS PAPER 69-244]
24 p4392 A69-42857
- CIRCULAR PLATES**
- Variable thickness circular annular disk bending in centrifugal force field, establishing dependence between angular velocity and axial pressure intensity
01 p0168 A69-10401
- Torsional oscillations of elastic half space set up by rigid circular disk examined by integral equation method
01 p0169 A69-10809
- Strain rate effect of large deflections of clamped circular viscoplastic plates subject to rigid mass impact
02 p0349 A69-12798
- Large finite deflections of clamped thin elastic circular plate subject to transverse concentrated load at center solved by power series
04 p0675 A69-14596
- Circular disk stress-strain state due to thermoelastic strain applied at disk sector edge
04 p0681 A69-15171
- Elastic strain and stress in ribbed circular plate bent skew-symmetrically, using orthotropic plates theory
04 p0681 A69-15172
- Symmetrical bending of laterally loaded circular micropolar plates
04 p0682 A69-15291
- Circular plate elastic stability under unidirectional compression, using Rayleigh-Ritz-Timoshenko method to determine buckling load
04 p0683 A69-15515
- Displacement, distortions and unit stresses in rotating circular disk under plane strain
05 p0835 A69-15807
- Geometry changes influence on rigid plastic circular plate behavior under two independent distributed pressures
06 p1023 A69-17508
- Governing equations for bending of fixed isotropic circular sandwich plate subjected to eccentric concentrated load
09 p1615 A69-21926
- Natural vibration frequency of circular orthotropic plate with variable rigidity
09 p1618 A69-22238
- Flexible circular plate on elastic support connected at free edge, noting stress independent of working load
09 p1618 A69-22239
- Limit loads for circular and annular plates of smoothly varying profile under uniformly distributed transverse loads
11 p1982 A69-24946
- Liapunov type analysis of linear structural dynamic system excited by stochastic parametric load, discussing radially loaded thin circular plates
11 p1990 A69-25507
- Rigid plastic circular and annular plates dynamics taking into account yield point dependence on strain rate
12 p2177 A69-25994
- Torsional flow of incompressible anisotropic fluid between parallel circular plates rotating with constant angular velocity, showing resemblance to shear flow
12 p2062 A69-26277
- Thermal shock temperature distribution and thermal stresses in finite circular disk subjected to instantaneous point heat source
13 p2363 A69-28130
- Stress-strain state of circular annular plate with varying thickness subjected to concentrated axisymmetric load and shearing force applied to internal perimeter
13 p2369 A69-28563
- Axisymmetric impact of circular cylindrical plates, obtaining two dimensional dynamic stress distributions for materials of linear elastic compressibility and plastic behavior in shear
14 p2534 A69-29027
- Incompressible viscous fluid steady motion caused by rotating ellipsoid, determining drag moments for circular disk and sphere
14 p2432 A69-29627

Finite integral transform determination for solving circular plates forced vibrations with time dependent conditions
15 p2704 A69-30306

Circular curved foil steady oscillations near screen in semiinfinite space filled with incompressible fluid transformed into equivalent linearized problem
15 p2547 A69-30576

Stress-strain state of circular disk with diametral cracks determined by approximating limiting equilibrium equation
15 p2708 A69-30663

Clamped circular plates impulse load tests with sheet explosives, showing finite difference program for computing large deflection dynamic response
15 p2709 A69-30675

Transient behavior of finite damped cantilever beam and circular plate analyzed by direct finite element method, noting applicability to dynamic problems
15 p2710 A69-30868

Thermal stresses and displacements in isotropic inhomogeneous rotating circular disk with axle hole under steady temperature field
15 p2712 A69-31016

Extensional vibration of thin inhomogeneous circular plate with variable modulus of elasticity and central hole, calculating periods of vibration
15 p2713 A69-31026

Load carrying capacity of circular plates under axisymmetric load
16 p2875 A69-32289

Temperature field, strains and stresses induced in thin circular disk by unsteady heat source, noting time effect and resonant vibrations
17 p3054 A69-33021

Stress-strain state determination for axisymmetric shells applied to design of circular/annular plates and rotating disks
17 p3057 A69-33194

Axisymmetric bending oscillations of thin circular plates of constant thickness with allowance for energy dissipation in material, analyzing resonance and phase amplitude characteristics
17 p3064 A69-33919

Von Karman equations in dimensionless and finite difference forms for deflections of elastic circular plate with central hole under load solved by iteration [ASME PAPER 69-APM-20]
18 p3214 A69-34395

Stress conditions of anisotropic plate with soldered in circular isotropic aluminum disk in presence of notches at seam, assuming elastic symmetry of plate
18 p3218 A69-34602

Free oscillations of rigidly clamped circular plate carrying concentrated masses, deriving frequency equation and value of lower roots
18 p3226 A69-35377

Safety disk strength under static lateral pressure from rupture studies of thin circular plates under static and pulsating lateral pressure
19 p3434 A69-35773

Force on circular plate near screen due to incident potential incompressible jet flow
19 p3297 A69-35816

Variational method for computer calculation of supercritical bending of thermoelastic uniformly loaded circular plates, determining Ritz parameter influence on accuracy
19 p3434 A69-35829

Residual deformation of elastoplastically bent thin circular plate after perfect unloading from large deflection, considering equilibrium and compatibility conditions
19 p3438 A69-36306

Vibrating circular plate standing wave lateral displacements visualization by photographically recorded moire patterns
20 p3537 A69-37067

Buckling of eccentrically stiffened thin circular elastic plate under circumferential uniform compression, obtaining equations and critical loads
20 p3622 A69-37221

Heat transfer coefficient and flow patterns of horizontal circular plate for various Rayleigh numbers, noting surface temperature
20 p3632 A69-37523

Stress and displacement in thin circular plates of ductile materials under axisymmetric loading predicted by nonlinear analysis
20 p3628 A69-37787

Axisymmetric vibrations of thin drums consisting of circular cylindrical shell and two circular end plates
20 p3629 A69-38114

Stress analysis of circular elastic plate buckling under radial compression, noting Kirchhoff hypothesis influence on critical value of thickness-to-radius ratio
21 p3834 A69-38722

Flexible circular plate in stationary temperature field calculated for stress-strain state using perturbations method
21 p3835 A69-38830

Bending of circular plate into shell, using stress-strain relation in finite strain, solving differential equations and boundary conditions
21 p3836 A69-39005

Deformation of uniformly thick elastic circular plates containing circular holes reinforced by thin rigid elastic rings
21 p3846 A69-39713

Dynamic stability of circular isotropic plate with central hole subjected to torsional moment uniformly distributed over both edges by equilibrium equation
22 p4043 A69-40455

Stress-strain state of circular disks with arbitrarily varying thickness along radius under antisymmetrical load calculated by integral equations method
22 p4047 A69-41168

Ambartsumian deflection theory applied to asymmetric bending problem for transversely isotropic circular plates
22 p4049 A69-41278

Stress concentrations in circular plate with square hole subject to triaxial tension
23 p4227 A69-41712

Differential equations of motion and associated boundary condition for axisymmetric flexural vibration of cylindrically aeolotropic circular plate, using variational calculus
23 p4228 A69-41911

Deflections of heated circular plates with or without concentric circular hole and with different boundary conditions and temperature distributions
23 p4234 A69-42412

Three layered circular plate under harmonic excitation, analyzing forced vibrational characteristics by variational principle and Ritz method
23 p4236 A69-42495

Forced symmetrical vibrations of circular elastic plate analyzed by applying Gaussian hypergeometric, Legendre functions and Jacobi polynomial
24 p4397 A69-42746

Circular plates axisymmetric nonlinear bending, using variational method to derive equilibrium equations and boundary conditions
24 p4399 A69-42989

Transverse shear influence on circular plates small displacement theory determined from coupled linear partial differential equations of plates
24 p4405 A69-43655

Large deflections of circular air mat plates consisting of inflatable structures of two membranes connected by inextensible cords network
24 p4405 A69-43688

CIRCULAR POLARIZATION

Nonlinear interaction of steady state circularly polarized electromagnetic wave with cold plasma in constant longitudinal magnetic field
03 p0476 A69-13381

Balanced symmetrical four arm conical equiangular spiral antenna providing omnidirectional circularly polarized radiation pattern in azimuthal plane
03 p0404 A69-13471

Rayleigh scattering from circularly birefringent media generalized for medium with no preferred internal axes
04 p0609 A69-14291

Reciprocal latching ferrite phase shifters application to lightweight scamed phased arrays, noting quasi-circularly polarized modes with lowest insertion loss
04 p0572 A69-14320

Polarization tensor variation due to Faraday effect and differential absorption of ordinary and extraordinary waves for radiation propagating in magnetoactive cosmic plasma
05 p0805 A69-16650

Circularly polarized waveguide mode simulation for multislot leaky waveguide harmonic content measurement
07 p1105 A69-19046

Focal antennas and receivers of Nancy radio telescope to measure flux density and incoming waves polarization, noting circular polarization in quasars
08 p1392 A69-20567

Gas laser frequency stabilization by coupled oppositely circularly polarized components of single cavity mode in axial magnetic field
08 p1327 A69-21090

Charged particles concentration change during vertical propagation of acoustic wave in F layer found transforming electric field into circularly polarized wave
09 p1484 A69-21528

Plasma ions turbulent heating during electron-acoustic instability in field of circularly polarized electromagnetic wave at ion cyclotron frequency
10 p1728 A69-23137

Transverse waves induced by disk oscillations about state of steady rotation in MHD, revealing circularly polarized waves with different phase velocities
10 p1728 A69-23239

Type 3 solar flare circular and linear polarization at 23.5 MHz frequency
11 p1945 A69-24244

Anisotropic plasma density measurement by launching circularly polarized plane electromagnetic wave at small angles to magnetic field direction
11 p1930 A69-25286

Circular polarization of solar microwave radio emission in Southern and Northern Hemispheres due to solar magnetic field
13 p2326 A69-27550

Relativistic electrons synchrotron radiation by calculating magnetoactive plasma permittivity tensor, determining normal waves polarization characteristics
13 p2315 A69-28451

Vela pulsar PSR 0833-45 optical observations and Crab pulsar NP 0532 linear and circular polarization measurements by telescope- photomultiplier
13 p2354 A69-28470

Charged particles concentration change during vertical propagation of acoustic wave in F layer found transforming electric field into circularly polarized wave
16 p2783 A69-32523

Circular polarization in moving type 4 burst compared to stationary type 4 burst and related to preceding type 2 sources
17 p3024 A69-33806

Complex refractive index profiles and wave polarizations calculated for electromagnetic waves transmission through ionosphere at micropulsation frequencies
17 p2927 A69-33864

Circular polarization measurements of compact radio sources at 1420 MHz, finding no detectable polarization
20 p3606 A69-37831

Solar Zeeman triplet for excited atomic state comparable to or shorter than Larmor precession period, discussing polarization
22 p4019 A69-40287

Circularly polarized VHF antenna systems for spin stabilized satellites, discussing design and performance test results
22 p3913 A69-40695

Circular or linear polarization diversity reception for VHF earth-station-satellite communications through turbulent ionosphere, assuming Rayleigh distribution fading
23 p4115 A69-41585

Simple antenna with good circular polarization over wide space sector, showing geometry, normalized orthogonal field distributions and beamwidth range, considering slot combinations
23 p4137 A69-41590

Parabolic antenna properties generated by dual band circularly polarized focused two channel monopulse feed system, discussing tracking data from helicopter, Apollo 8 and Cassiopeia A
23 p4120 A69-41752

Radar return from clutter target with circular polarization, finding probability density functions and cumulative distributions of power ratio
23 p4131 A69-42540

CIRCULAR SHELLS

Multilayered shells equivalence to single layer shells for stress analysis, vibrations and stability
02 p0346 A69-12509

Circular cylindrical isotropic shell deformation rate under dynamic axial load described by second order linear differential equation
04 p0673 A69-14499

Optimal design of circular cylindrical sandwich shells under pressure and shear loads, showing acceptability of small shear coefficient values
08 p1416 A69-20722

Large uniform torsion of thin walled open section of circular cross section, deriving tube radius contraction observed in experiments
10 p1794 A69-22930

Free vibrations in axisymmetrically loaded orthotropic circular conical shells with longitudinal and circumferential stiffening based on linearized theory, considering shear deformation and inertia
11 p1969 A69-24327

- Semiinfinite circular cylindrical shell buckling under axial load, computing forces, moments and displacements by thin shell equation
11 p1979 A69-24818
- Inplane and rotary inertia effects on free vibration frequencies of circular cylindrical shells eccentrically stiffened by orthogonal set of stringers and/or rings
11 p1992 A69-25520
- Imperfection surface effect on buckling load of circular cylindrical shell under axial compression, locating limit points of postbuckled states
13 p2362 A69-28122
- Stressed state of cylindrical circular shell clamped at edges and subjected to concentrated radial forces
13 p2368 A69-28322
- Free vibrations of thin truncated circular conical shell and reinforcing rings and stringers, determining resonant frequencies for stiffened and unstiffened configurations
17 p3051 A69-32955
- Axisymmetrical vibration characteristics of circular sandwich shell with viscoelastic core layer analyzed via differential equation to obtain frequency equation and composite loss factors
18 p3211 A69-34327
- Circular cylindrical shell nonlinear response to uniform radial impulsive pressure, noting inextensionality constraint and equations of motion roles [ASME PAPER 69-APM-26]
18 p3214 A69-34399
- Nonlinear equations for elastic strain of circular-toroidal membrane shell under uniform pressure, computing stress and displacement fields
18 p3216 A69-34575
- Free vibrational characteristics of thin walled circular cylindrical shells with layers of anisotropic elastic material laminated about middle surface
20 p3627 A69-37767
- Stability of free and clamped spherical and circular cylindrical shells subjected to uniform or nonuniform heating, discussing effects of temperature stresses
21 p3838 A69-39190
- Infinite systems of algebraic equations in periodic problems for spherical shells with circular holes approximated by reduction method
23 p4227 A69-41706
- Creep stress analysis of circular cylindrical shells under axisymmetric loading, plotting stresses and deformations for various parameters
23 p4233 A69-42352
- Flexural vibrations of rectangular cross sectioned rings, solving characteristic value problem for finite circular cylindrical shell
24 p4404 A69-43629
- CIRCULAR TUBES**
- Steady state temperature distribution in heat generating fluid in plug flow in circular tube with arbitrary inlet and wall temperature distribution
03 p0530 A69-12862
- Thin curved circular tube under in-plane bending [ASME PAPER 68-PVP-12]
03 p0523 A69-12999
- Small twist of elastic circular cylindrical tube with nonorthogonal laminar acoloptropy, noting zero and nonzero warping conditions effects
05 p0831 A69-15580
- Laminar flow heat transfer of viscous incompressible fluid in entrance region of circular tube, using nonlinear equations
10 p1809 A69-23195
- Three dimensional compressible potential flow in curved circular duct analyzed by perturbation method
11 p1867 A69-24607
- Finite difference method for heat transfer for developing laminar flow at inlet of circular uniformly heated and isothermal tube, determining Nusselt number
12 p2062 A69-26242
- Turbulent flow in circular tube and parallel plate channel, considering molecular viscosity and duct shear stress variation
13 p2248 A69-28131
- Oscillation in resonance tubes excited by subsonic jet, analyzing pressure and frequency for small Mach numbers by using wave diagram
13 p2370 A69-28630
- Displacement of liquid by insoluble liquid from horizontal circular tube during laminar flow, analyzing flow characteristics
14 p2431 A69-29607
- NonNewtonian power law fluids flow behavior in circular pipe entry region, taking into account energy loss due to viscous dissipation in boundary layer
19 p3240 A69-36472

- Isotherms location in simple nonconstant area/diverging/ tube configuration investigated for heat transfer
20 p3632 A69-37219
- Fluid velocity in starting flow in circular tube using Laplace transform
22 p3931 A69-40688
- Stress analysis of cylindrical tubes under torsional and transverse static loads based on vibrational theory, applied to rectangular cantilever tube
23 p4228 A69-41916
- Uncoupled torsional vibrations of simply supported open cylindrical tubes analyzed by approximation equations, considering free edge boundary conditions
23 p4233 A69-42347
- Flexural vibrations of simply supported lipped I section of cylindrical tubes, considering free- edge boundary conditions
23 p4233 A69-42350
- Peristaltic pumping in circular cylindrical tube, discussing viscous fluid flow induced by axisymmetric traveling sinusoidal wave imposed on flexible tube wall [ASME PAPER 69-APMW-3]
24 p4275 A69-43108

CIRCULATION

- U ATMOSPHERIC CIRCULATION
- U BLOOD CIRCULATION
- U BRAIN CIRCULATION
- U CONGESTION
- U CORONARY CIRCULATION
- U PERIPHERAL CIRCULATION
- U PULMONARY CIRCULATION

CIRCULATORS [PHASE SHIFT CIRCUITS]

- Voltage tunable magnetron used in conjunction with ferrite circulator as phase locked amplifier
01 p0045 A69-10632
- Circulator power splitting and isolating function in integrated microwave network
02 p0222 A69-12475
- Broadbanding of S-band three port stripline circulator, discussing effect of tuning and mode suppressor screws
03 p0404 A69-13472
- H plane waveguide Y circulators engineering design based on circulation equations
04 p0575 A69-14460
- Recirculator with sign variable feedback coefficient for delay line passband increase
04 p0575 A69-14464
- Ferrite Y junction E plane circulator for airborne high power X band radar
07 p1100 A69-18639
- Band three port Y junction stripline circulator with triangular ferrite
08 p1286 A69-20838
- Miniaturized E-Tee three port circulator with wide bandwidth, noting negligible effect of static field small variations on performance
08 p1291 A69-20980
- Y-circulators specified, measured and calculated values correlated as function of leakage matrix elements and terminating dipoles reflection
09 p1473 A69-22114
- Waveguide Y circulator electrodynamic parameters by design algorithm and computer programs
10 p1661 A69-23108
- Microstrip circulator size reduction attained by tight inductive ferrite coupling for incorporation with microwave integrated circuits
13 p2230 A69-27679
- H plane waveguide Y circulators engineering design based on circulation equations
14 p2418 A69-28831
- Mathematical relations for ring laser beams polarization conditions, using slanted isotropic plate and phase circulator to separate polarization plane
20 p3553 A69-37606
- Small losses measurement in circulators and reciprocal quadrupoles, using scattering matrix to eliminate mismatch errors
22 p3875 A69-40259
- Waveguide Y-circulator parameters thermal stability equation, considering temperature, magnetization level and magnetic field resonance effects on tuning frequency
23 p4123 A69-41951

CIRCULATORY SYSTEM

- NT AORTA
- NT ARTERIES
- NT BLOOD VESSELS
- NT CAPILLARIES [ANATOMY]
- NT VASCULAR SYSTEM
- NT VEINS

- Orthostatic intolerance, with assessment of circulatory problem of weightlessness in prolonged space flight
06 p0873 A69-17016
- Analog computer modeling of human systemic arterial tree, based on lump parameter circuit approximation
07 p1072 A69-19727
- Brief intense thermal stresses effects on cardiovascular system of man, noting criticality of effective blood volume for circulatory competence
08 p1264 A69-20668
- Psychic stress effect on physiological parameters of helicopter pilots during critical flight situations, considering biotelemetric examination of heart and circulatory systems
11 p1829 A69-24347
- Dynamic stability of two degrees of freedom circulatory systems with bilinear hysteresis damping
13 p2363 A69-28127
- Human circulatory reactions to cumulative flight vegetative stimuli evaluated by cumulative stress simulation method
24 p4266 A69-43375
- High intensity and short duration acceleration effects on human beings, discussing mechanical resistance of spinal column and circulatory aspects
24 p4266 A69-43380

CIRCUMLUNAR TRAJECTORIES

- Soviet probe Zond 5 circumlunar flight to recover space vehicles from interplanetary paths
06 p1003 A69-17389
- Reentry trajectories from lunar surface and orbit obtained by computer with allowance for initial data spread
09 p1594 A69-21756
- Earth-moon and moon-earth trajectory parameters related to lunar orbit conditions for synthesizing lunar orbit trajectory
18 p3196 A69-34704

CIRRUS CLOUDS

- Jet stream cirrus radiative characteristics from airborne IR measurements, noting cirrus cloud emission and transmission and cirrus height and temperature estimates
01 p0110 A69-10694
- Cirrus IR radiance model for explaining measured cloud radiance characteristics, considering thermal emission and irradiance scattering
01 p0111 A69-10848
- Aircraft high level cloud data to estimate vertical distribution of cirriform clouds and tropical tropopause levels on airline routes
03 p0458 A69-13032
- Wind vector in respect to orientation of large scale cirrus bands based on stereophotogrammetry and radar observations
08 p1346 A69-20442
- High altitude radiant emittance of cirrus clouds and cloudless sky for IR transmissivity based on aircraft measurements
09 p1536 A69-21641
- Tenuous cirrus cloud influence on 6.4-6.9 micron Nimbus 2 water observations, discussing equivalent black body temperatures correspondence to cloud and clear areas
12 p2075 A69-27003
- Far IR angular scattering observations as diagnostic tool to examine microstructure of high altitude cirrus clouds
18 p3126 A69-34281
- Cirrus clouds occurrence, position and wind velocities on jetstream axes based on statistical analysis of aerological data and satellite TV pictures
19 p3366 A69-36669
- Cirrus cloud height above sea level and shape correlation with lower section static stability determined by stereophotogrammetric measurements
20 p3570 A69-37349
- EOLE constant level balloon flights in troposphere, discussing short lifetime due to overloading with ice in dense cirrus cloud
21 p3646 A69-38373

CISLUNAR SPACE

- Secular change examination in cislunar geomagnetic tail field gradient during summers of 1966 and 1967, using Explorer 33 and 35 results
01 p0077 A69-11237
- Cumulative flux of interplanetary and cislunar space dust particles by Mariner 4 and OGO 3 spacecraft, noting particle impact rate
15 p2699 A69-31394

European highly eccentric orbit satellite /HEOS/ cislunar probe to explore interplanetary space for magnetic fields, cosmic radiation, solar wind and earth shock wave
17 p3050 A69-33397

CITIES

Remote sensing of urban environments for metropolitan information systems noting photographic, thermal IR, radar and microwave applications
12 p2193 A69-27012

Air transport development relationship to city regional planning, including analysis of Heathrow airport design
19 p3296 A69-36850

Metropolitan downtown airports for STOL and VTOL aircraft stressing Los Angeles Metroport [SAE PAPER 690402]
23 p4147 A69-41660

Intercity air transportation compared with automobile and train travel, attributing air travel dead time to ground route and airspace congestion
24 p4416 A69-42561

Intercity travel demands simulation by linear graph model applied to Windsor-Montreal corridor [AAS PAPER 69-382]
24 p4417 A69-42805

Public policy for urban transportation system, using calculus of variations to determine optimal introduction curve
24 p4417 A69-42809

Demand curves for VTOL intercity transportation, discussing conventional helicopters, compound helicopters, tilt rotor, tilt wing, stored rotor and fan or jet lift
24 p4254 A69-43721

CIVIL AVIATION

Airline crew training, requalification, recurrent, upgrading and aircraft transition training for crew and pilot
01 p0019 A69-10450

Space techniques for application to civil aviation, discussing air to ground communications, air traffic monitoring and navigation and weather forecasting by satellite
[UN PAPER 68-95349]
01 p0179 A69-10490

Satellites and ocean platforms for civil aviation operations over North Atlantic, noting cost justification dependence on supersonic traffic increase
[UN PAPER 68-95887]
01 p0113 A69-10521

Head-Up Display /HUD/ flight information applied to civil aviation, noting operational safety improvement and pilot work load reduction
01 p0020 A69-10635

Boeing 747 characteristics for passenger and cargo service noting economic gain, operational performance, control cabin, engine, etc
[AIAA PAPER 67-397]
01 p0010 A69-10636

Analytical reliability ratio to operational reliability for airborne equipment taking into account electrical and thermal aspects
01 p0011 A69-11069

Air traffic control at Los Angeles International Airport, discussing simultaneous parallel ILS approaches and departures and STOL problems
01 p0057 A69-11356

Interim radar improvement program for air route traffic control centers pending development of automated terminal radar programs
01 p0114 A69-11357

Inertial navigation for commercial aircraft, discussing Sagem-Ferranti and Litton systems
02 p0278 A69-12239

Exterior arresting devices for commercial aircraft full scale tests
03 p0367 A69-14104

Synchronous extractor for simultaneous extraction and association of primary and secondary radar videos in civil system, discussing automatic identification process
05 p0721 A69-16592

NASA civil aviation electronics research program, discussing feasibility of V/STOL aircraft all-weather operations
05 p0850 A69-16718

Accident prevention and investigation procedures of National Transportation Safety Board /NTSB/, discussing management patterns
06 p1041 A69-16842

International problems of air traffic control, discussing legal and political basis for organization and ATC liability
06 p1042 A69-16846

Air carrier legal responsibility for commercial air safety as compared to liability in other transportation modes
06 p1042 A69-16847

Aviation industry passenger liability, discussing negligence litigation, compensation standards and roles of government, manufacturers and courts
06 p1042 A69-16851

Automatic air traffic control systems design, development and application to civil and military aviation
06 p0955 A69-17858

Air navigation and economics, discussing air traffic control and traffic density effects on fuel consumption and engine life
07 p1052 A69-18661

Nondemographic model predicting market shares of V/STOL aircraft in competition with automobiles and conventional airliners for short haul intercity business travel markets
07 p1244 A69-18967

General aviation accidents and hazards presented by drugs, ethyl alcohol, pesticides and carbon monoxide
07 p1068 A69-19435

Future commercial VTOL transportation, considering technical, political and socio-economic problems [AIAA PAPER 69-198]
07 p1056 A69-19567

Nondestructive testing methods for civilian transport aircraft production, overhaul and maintenance
07 p1143 A69-19702

STOL and V/STOL role in eliminating air traffic congestion at U.S. and West European airports and in short haul and municipal routes
08 p1254 A69-20093

National tasks in civil aeronautical research and development noting technological and social factors
08 p1422 A69-20171

STOL aircraft intercity test flights emphasizing curved ILS approach, using onboard computer for altitude and distance data
08 p1347 A69-20602

Civil aviation statistical data and airport planning
10 p1634 A69-23601

Airport operation and administration, discussing supply, costs, tariffs, etc
10 p1811 A69-23602

V/STOL aircraft performance characteristics related to civil aviation operations and certification requirements [ICAS PAPER 68-05]
11 p1822 A69-24463

Anticing for all-weather operation of business jets, discussing atmospheric conditions, ice formations, prevention and removal systems [SAE PAPER 690333]
11 p1822 A69-24500

Comparative evaluation of avionic installations in design stage, detailing parameters for civil aeronautical use
11 p1887 A69-25212

Aircraft engines future specifications as affected by expanding market, noting speed requirements and thrusts
11 p1942 A69-25215

Air transport prediction for West Europe by 1980
11 p2004 A69-25216

Aeromedical investigation of civil aircraft accidents by National Transportation Safety Board, noting post-mortem legal aspects and need for human factors investigation
12 p2021 A69-25840

Civil aircraft accident investigation, discussing organization and procedures of Bureau of Aviation Safety of National Transportation Safety Board
12 p2191 A69-25844

Aircraft hijacking prevention through technical and legal means, discussing national and international air piracy laws
13 p2381 A69-27528

Aircraft accident investigation procedures in Canada for routine/major accidents and public inquiries, outlining organization
13 p2201 A69-27540

Civilian transport aircraft operation realities vs theoretical performance certification
14 p2392 A69-29698

Civil airports design standards development noting advisory circulars
15 p2588 A69-30408

Air transportation problems in connection with rapid aviation growth noting crisis in near future
15 p2720 A69-30588

Rescue locator beacons and airborne search equipment of VHF and UHF capabilities available to international civil aircraft operations
15 p2552 A69-30852

Secondary radar system chosen by EUROCONTROL Agency for civil air traffic control at Shannon and Brussels airports
15 p2571 A69-31501

Book on competition in North Atlantic commercial air transport covering passengers, freight and mail from supply, demand and market point of view
16 p2881 A69-31866

Ground facilities long term planning, considering factors to determine air transport growth and changing commercial aviation pattern
16 p2766 A69-32020

Civil aircraft requirements from 1975 onward, discussing classes, categories and R and D
16 p2882 A69-32022

Aerodynamic problems in future civil aircraft design, emphasizing Concorde development possibilities, discussing VTOL intercity transport, subsonic swept wing and hypersonic aircraft, all-wing airbus, etc
16 p2732 A69-32023

Civil aircraft projected development regarding materials and structures, discussing new components and fuel contribution to weight and metals and composites for replacing Al
16 p2872 A69-32024

Book on soviet An-24 aircraft-construction and exploitation covering fuselage, powerplant, controls, fire prevention, air conditioning, maintenance, etc
16 p2735 A69-32112

FAA jurisdictional procedures for law infringement, discussing civil codes, delegation of enforcement authority and routine violations including low flying, weather, etc
16 p2882 A69-32335

CAB decisions regarding subsidy reduction, carrier mergers, and dense route certification requiring improved clarity and timeliness
16 p2882 A69-32336

Communist China civil aviation, discussing major, local and international routes and agreements, aircraft types and national origin, total mileage, etc
16 p2882 A69-32337

Airworthiness objectives for civil powered lift aircraft, discussing safety, traffic growth and accident rates
17 p2897 A69-33211

Civil transport aircraft power plant and auxiliary systems as sources of delays, presenting critical path analysis
17 p2898 A69-33213

Flying offenses committed by private and professional pilots in Great Britain, discussing role of authorities involved
17 p3077 A69-34202

Edwards Inquiry Report into British Civil Air Transport based on cost effective economic study, involving airlines and regulatory system
18 p3231 A69-34311

Soviet efforts to market civil aviation equipment in West
18 p3232 A69-34538

Tupolev Tu-154 three jet transport featuring automatic flight control system with inertial and Doppler navigation inputs, low speed wing devices
18 p3092 A69-34933

Aerospace technology application to commercial avionic system for cost effectiveness in functions expansion, phase-over, installation, maintenance and operation, discussing added information functions
18 p3108 A69-35069

Flight and piloting influence on morbidity of civil aviation personnel, noting incidence of enteric, hemorrhoidal and respiratory diseases
18 p3098 A69-35303

Los Angeles International Airport development planning, discussing airfield improvement, tunnel reconstruction, terminal layouts, parking, roads and access, etc
[AIAA PAPER 69-806]
19 p3288 A69-35590

Civil aviation center for R and D in aviation personnel education and training [AIAA PAPER 69-785]
19 p3453 A69-35597

Air travel and population growth requiring larger structures for office buildings, airport passenger terminals and aircraft servicing facilities [AIAA PAPER 69-809]
19 p3289 A69-35622

Airport facilities planning for conventional jet, STOL and SST aircraft ground handling, stressing facilities economy and transportation subsystems [AIAA PAPER 69-808]
19 p3289 A69-35623

General aviation missions in national transportation system /1968, 1975, 1980/, considering fuel taxes, overall system economics, ground facilities, etc [AIAA PAPER 69-818]
19 p3453 A69-35624

Light rigid civil aircraft response to continuous atmospheric turbulence estimated using two rigid body degrees of freedom method for vertical and lateral gusts [AIAA PAPER 69-766]
19 p3433 A69-35657

Legal liability in civil aviation, proposing international treaty 19 p3454 A69-35980

Air cushion vehicle legal status and cargo and passenger liability 19 p3455 A69-36330

Airworthiness certification of civil aircraft, discussing international cooperation on inspection, accident investigation, etc 19 p3456 A69-36688

VSTOL and conventional transport aircraft compared for short haul air transport services 20 p3461 A69-37281

Subsonic civil air transport navigation systems, discussing flight routes redistribution across North Atlantic to meet increased traffic 20 p3574 A69-37417

Monograph on low visibility landing in civil aviation, considering visibility determination methods and equipment and IR sighting devices 20 p3574 A69-38064

Cabin personnel occupational strain in civil aviation, relating heart rate to aerobic power while working during flight 21 p3665 A69-39180

RB 202 self contained lift fan engine design for high speed interurban civil VTOL operations, considering weight, cost, noise and fuel consumption 22 p3862 A69-39933

Turbofan engine influence on civil transport aircraft design as function of thrust, discussing engine ratings, number of engines, APU and thrust engine 22 p3862 A69-39961

Accident prevention program of Bureau of Aviation Safety, discussing probable cause analysis and function in feedback loop, hazard analysis and accident data center 22 p3867 A69-41140

Book on law making in International Civil Aviation Organization covering membership problems, air navigation and transport safety, settling of disputes, etc 23 p4240 A69-41297

Airport terminal planning, considering expansion, automation, backup measures, layout problems and solutions, etc [SAE PAPER 690399] 23 p4147 A69-41661

Civil pilots medical certification after head trauma, evaluating current methods efficiency 23 p4086 A69-41687

Sud commercial aircraft /1970-1980/, discussing market trends, airport saturation, Airbus power plants and seating capacities 24 p4416 A69-42563

Operational and economical aspects of V/STOL air transportation reevaluated for civil aviation promotion [AHS PAPER 69-325] 24 p4418 A69-42870

Food-borne diseases prevention in civil aviation, reporting gastroenteritis cases during flight 24 p4278 A69-43392

CL- 84 AIRCRAFT

Technological evolution of turboprop propeller powered tilt wing V/STOL aircraft, discussing XC-142A, CL-84 and VZ-2 aircraft 05 p0701 A69-15564

CX-84 two propeller tilt wing deflected slipstream V/STOL Military Evaluation Program related to support of surface forces [AHS PAPER 351] 17 p2900 A69-33526

Canadair CL-84 two propeller V/STOL utility tilt wing vehicle development program and flight tests to assess military potential of aircraft 17 p3077 A69-34065

CL-595 HELICOPTER

U XH-51 HELICOPTER

CLADDING

Explosive welding application to dissimilar metals and tube to tube plate welding, noting influence of detonation and sound bulk velocity 04 p0608 A69-15481

Exposure tests of corrosion resistant claddings for high strength Al alloys protection, finding higher purity alloy cladding superiority 19 p3322 A69-35571

Stainless steel cladding of metals to combine desirable properties into composite, describing bonding, product types and treatment 21 p3745 A69-38937

CLAIMING

Sonic boom damage legal claims, discussing causal relationship validity and claims processing 14 p2541 A69-29155

CLAMPS

End constraints and length/width ratio influence on composites off axis tensile tests, considering rigid clamping with/without end rotation 13 p2286 A69-28667

Scale factor determination for energy dissipation at clamped ends, analyzing geometric parameter and clamping force effect on oscillation damping constant 17 p3065 A69-33927

Clamping and sealing fastener for single direction installation consisting of pin, collar and sealing collar with insert 22 p3957 A69-40831

CLARK Y AIRFOIL

U AIRFOIL PROFILES

CLASSICAL MECHANICS

NT ASTRODYNAMICS
NT CELESTIAL MECHANICS
NT KEPLER LAWS
NT ORBITAL MECHANICS
NT SPACE MECHANICS

Equations of motion for kinematics of complex mechanisms, noting methods and relations 01 p0115 A69-10165

Keplerian motion parameters second derivatives determined from initial conditions by deriving differential equations 01 p0107 A69-11305

Trouton-Noble experiment to detect motion of earth through ether by electromagnetic torque on charged suspended parallel plate capacitor, explaining null results 03 p0517 A69-14106

Bound motion for particle in point electric dipole field, noting features of motion common to spherical pendulum motion 03 p0473 A69-14109

Book on theory of kinetic equations covering classical mechanics, Liouville equation and distribution functions, kinetic equations relation to fluid dynamics, KBG equations, etc 07 p1180 A69-18411

Statistical theory of fluids in equilibrium based on correlation functions for pair interactions between constituent molecules, invoking superposition closure approximation 08 p1350 A69-19868

Coherence theory of electromagnetic field from classical/wave/ or quantum /particle/ standpoint, stressing information theory 11 p1915 A69-24455

Test particle classical dynamics in closed expanding universe, discussing Newtonian inertial mass decrease and canonical methods for determining momentum, velocity and energy 11 p1920 A69-25561

Monograph on gasdynamics and classical theory of shock waves covering viscosity, heat conduction, gas cloud expansion into vacuum, etc 13 p2246 A69-27639

Nonholonomic coupling effect on mechanical system stabilization characteristics in terms of generalized coordinates 14 p2482 A69-28814

Invariants method and applications in classical and relativistic physics emphasizing theory of relativity, physical and mathematical theories relations and group theory applications 14 p2484 A69-28860

Book on deformable bodies mechanics covering load resisting members of structures and machines 18 p3222 A69-34927

Celestial mechanics, Part 1, covering almost periodic functions, relation to classical astronomy and modern mathematics, implicit function theorem, three body problem, etc 18 p3199 A69-34928

Paradox of incoming photons detection at two antennas without interference pattern disturbance explained by classical and quantum physics 20 p3538 A69-37415

Information categories concept defined in relation to formulations of classical mechanics principles, considering theories of Newton, Gauss and Hertz 20 p3576 A69-37585

Cavity Q dependence of intensity of single mode He-Ne laser above threshold for quantum and semiclassical theories 22 p3961 A69-40415

Planck law for black body radiation spectrum theoretically derived on basis of classical Lorentz-invariant electromagnetic radiation at absolute zero temperature without quantum assumption 22 p3982 A69-41001

Thermal average derived with classical path treatment for line broadening theories of gases or plasmas 23 p4192 A69-41378

CLASSIFICATIONS

NT DICHOTOMIES
NT HIERARCHIES
NT INDEXES [DOCUMENTATION]

Subject classification bibliography for thermal contact resistance [ASME PAPER 68-WA/HT-18] 05 p0847 A69-16122

Sunspot group classifications made at Zurich and Catania during 19th solar cycle compared to determine seeing influence 05 p0826 A69-16388

Feature selection in pattern recognition, discussing techniques, crop classification problem and parametric multiclass pattern recognition 06 p0892 A69-17396

Stieltjes transform relating initial boundary value problems for partial differential equations of various classifications 08 p1342 A69-20352

Spontaneous decomposition of image space into compact sets /images or classes/ using adaptive dispersion method to reduce system learning time 11 p1859 A69-24964

Rocket propulsion devices classifications, discussing energy sources, propellants, performance, space vehicle applications, liquid propellant rockets, engines, selection criteria and cooling methods 11 p1943 A69-25587

Spectroscopy and star classification on basis of spectra 12 p2155 A69-26122

Cometary tails maximum lengths compared with orbit parameters and absolute magnitudes, proposing classification scheme 15 p2689 A69-30566

Two dimensional spectral classifications for bright A stars including magnitudes and colors 16 p2860 A69-32233

Giant galaxy classified in terms of stellar population, discussing Orion, intermediate amorphous and combination categories 16 p2862 A69-32395

BCD classification for cepheids, discussing /sigma/ surface definition, locus of normal stars of population I and interstellar reddening 17 p3038 A69-33725

Periodic motions in single mass impact vibration system by point transformations method, noting complexity characteristics 18 p3172 A69-34565

Classification of synoptic processes, discussing condensation of parameters characterizing state of atmosphere 18 p3166 A69-34815

Quantitative analysis and classification of stony meteorites, including carbonaceous chondrites, by Mossbauer characteristics, discussing Prior plot and weather influence role in finds and falls 19 p3408 A69-36083

C3 and C4 carbonaceous chondrites origin, evolution and classification based on mineralogic and petrologic data 19 p3413 A69-36109

Iron meteorites genetic classification based on parent body cooling rate and Ga-Ge trace element content 19 p3416 A69-36129

Chemical classification of iron meteorites with Ge concentrations between 80 and 200 ppm, reporting concentrations of Ge, Ni, Ga and Ir 20 p3602 A69-37537

Ba titanate modifiers, classifying cations replacing Ti and Ba ions 22 p3996 A69-41161

Personnel training and selection systems, applying information processing models to diagnostic testing in job classification for performance improvement 24 p4274 A69-43020

CLASSIFYING

Adaptive pattern recognition, discussing classification techniques and merging into other aspects of artificial intelligence research 07 p1088 A69-18381

Unitary sorting influence on reliability of planar transistors subjected to irradiation recovery cycles and scaled stresses 15 p2626 A69-30834

Nonparametric partitioning algorithm for pattern classification, discussing pattern recognition, classifiers structure, real data applications, etc 24 p4285 A69-43062

CLEAN ROOMS

Control and sampling in sterile rooms, noting worker introduction of contaminants

05 p0714 A69-15953

High bay clean room design with laminar air flow, discussing air filtration, sound attenuation, construction, illumination, etc

10 p1673 A69-23354

Avionics clean room workshops, discussing turbulent and laminar flow rooms and contamination monitoring of controlled environment facility

16 p2767 A69-32369

Electrostatic control for portable clean rooms, describing fabrication, assembly and checkout problems with Instrument Unit /IU/ control center for Saturn launch vehicles

19 p3428 A69-35550

CLEANERS

U AIR FILTERS

CLEANLINESS

Pollution control forecast, contamination control specialist and systems approach

08 p1265 A69-19808

Hydraulic fluid cleanliness measured using microscopy, automatic particle counters and gravimetrics, discussing silting index and evaluator used by aerospace industry

19 p3256 A69-36715

CLEAR AIR TURBULENCE

Correlation between CAT and thermal gradient increase at standard isobaric levels found to be potential forecasting tool

02 p0275 A69-11818

Wind gust simulation procedures, discussing high altitude clear air turbulence and simulation of air perturbations

03 p0461 A69-13647

Correlations at regional scale between clear air turbulence aircraft observation, Richardson number and wind intensity and direction at flight level

03 p0462 A69-13966

Stratospheric critical clear atmospheric turbulence at midlatitudes, noting applications to supersonic aircraft design

06 p0950 A69-17789

Aircraft reports of clear air turbulence over North Atlantic, discussing jet stream proximity and large amplitude ridge associated with occlusion point

08 p1345 A69-19885

Disturbed index of refraction scattering cross sections and aircraft acceleration increments for clear air turbulence, deriving correlation for measurements

10 p1656 A69-23651

Aircraft reports of high level turbulence on European and Atlantic routes, noting rapid changes in large scale flow pattern occurring locally

12 p2127 A69-26901

Airborne scanning spectrometer for IR detection of clear air turbulence, presenting flight records

12 p2098 A69-26999

Airborne IR spectrometer for remote clear air turbulence detection, noting necessity for mirror stabilization in pitch axis

12 p2098 A69-27000

Radar application to meteorology, entomology and ornithology, discussing clear air turbulence detection and flight tracking of birds and insects

12 p2034 A69-27004

Radar echoes observed from clear atmosphere, discussing scattering mechanisms of thin stable inversions, convective thermals, Benard convection cells, breaking gravity waves, etc

14 p2415 A69-29518

Qualitative analysis of CAT parameters from radio sounding data, noting mean bumpiness probability dependence on Richardson number and wind vector shift

14 p2474 A69-29735

Synoptic criteria combined with qualitative criteria for CAT diagnostics from analysis of turbulent zones responsible for bumpiness in upper troposphere

14 p2474 A69-29736

Stratospheric turbulence producing bumpiness up to 18 km developing at levels characterized by abrupt changes in vertical temperature gradients

14 p2474 A69-29737

Probability diagnosis and prognosis for buffeting zones based on Bayes formula, determining clear air turbulence zones

15 p2648 A69-30645

Wind velocity fluctuations calculation in CAT based on closed equations numerical solution for turbulent layers in upper troposphere

15 p2649 A69-30649

Atmospheric turbulence in cloudless region above thunderstorms and relation between turbulence and radar pictures of storms

15 p2649 A69-31211

Boeing 747 problems including noise and automatic landings in CAT-II conditions

16 p2734 A69-31631

Clear air turbulence and detection - Conference, Seattle, August 1968

17 p2998 A69-33732

Clear air turbulence uninfluenced by mesoscale disturbances or terrain, discussing relationship between density profile curvature and heat and momentum transfer

17 p2998 A69-33733

Meteorological analysis of stratospheric clear air turbulence flights, discussing vertical temperature structure in terms of wave motion and turbulence intensity

17 p2999 A69-33736

Gust probes in model of low altitude atmospheric turbulence during USAF research program LO-LOCAT, plotting relationship between peak count distribution curves

17 p2999 A69-33737

Lee waves and orographic wind phenomena in Rocky Mountains near Boulder, noting stratospheric standing gravity waves and turbulence sampled by HI-CAT U-2

17 p2999 A69-33738

Temperature profiles and associated wind profiles obtained with Jimsphere/FPS-16 radar system at Cape Kennedy, discussing remote CAT detector assessment

17 p2999 A69-33739

Centrifugation effects on body composition and growth of mice

17 p2910 A69-33746

Energy dissipation near tropopause determined from measured clear air turbulence spectra and probabilities

19 p3303 A69-36407

High altitude CAT regions length distribution determined from level flight path sampling data correlation

20 p3570 A69-37168

Vertical wind shears, structure functions, turbulence and power spectra for transverse velocity fluctuations in troposphere and stratosphere, noting clear air turbulence

20 p3570 A69-37506

Radar observations of convective pattern types in clear atmosphere consisting of thermal- and Benard-like convection cells

20 p3573 A69-38059

Clear air turbulence computerized analysis and forecast over U.S. using upper air rawinsondes measurements

22 p3976 A69-39927

Clear air turbulence /CAT/ causes effect on aircraft control, discussing monitoring device and aircraft position maintenance under CAT conditions

22 p3977 A69-40007

Air traffic safety enhanced through flight crew awareness of hazards, clear air turbulence detection and avoidance, collision avoidance, etc

22 p3868 A69-41151

Clear air turbulence detection in troposphere by multifrequency radiometric sensor, noting multibeam system for supersonic aircraft

23 p4144 A69-42536

Wavelike structure observed near tropopause with sensitive radar system, suggesting clear air turbulence as cause of breakdown of gravitational wave

24 p4342 A69-42893

Simultaneous lower atmosphere clear air turbulence analysis by multiwavelength radar, jet aircraft and special rawinsondes

24 p4342 A69-42894

Clear air turbulence in upper atmosphere and in mountain waves, discussing density variations

24 p4343 A69-42913

CLEARANCES

Radial clearance influence on self lubricating porous bearing friction coefficient and oil losses as function of operation duration

16 p2794 A69-32067

CLEAVAGE

Microscopic cleavage strength of high nitrogen steel notched bars determined from critical tensile stress criteria using elastoplastic analysis method

01 p0169 A69-10765

Electrostatic charge distribution on ultrahigh vacuum cleaved silicates including instrumentation, UV irradiation, half life, Paschen relation, etc

13 p2322 A69-28018

Cleavage plane in stress corrosion cracking of alpha phase Ti-Al alloys

13 p2283 A69-28189

High strength titanium alloys subcritical stress corrosion crack propagation, studying stress and environment effects on cleavage mode

19 p3343 A69-35922

Metallographic analysis of stress corrosion cracking of Ti alloys of Al and Sn in aqueous magnesium chloride solutions, noting cleavage process

19 p3352 A69-36903

CLIFFS

Relative heights on moon, tabulating lunar topography and comparing micrometrical measurements and map data

10 p1782 A69-23697

CLIMATE

Climatic factors affecting pilot vision and contributing to misjudgement during landing procedures, noting effect of downward slope in runway approach

06 p0884 A69-18036

European pilots accustomed to equatorial climate tested during regular flying missions, discussing heat effects on urinary steroids

12 p2024 A69-26560

CLIMATOLOGY

NT BIOCLIMATOLOGY

NT MICROCLIMATOLOGY

Daily insolation observations at Blue Hill, Massachusetts, correlated by month with observations of temperature, snow cover, winds, sunshine, sky cover, pressure and precipitation

01 p0066 A69-10862

Correlations at regional scale between clear air turbulence aircraft observation, Richardson number and wind intensity and direction at flight level

03 p0462 A69-13966

Soviet book on aeronautical climatology covering methodology of climatologic indices useful for airfields, pilots and flight routes evaluation

04 p0627 A69-14935

Sensible and latent heat meridional transport associated with standing eddies computed from climatic mean data

04 p0627 A69-15085

Eole program to further data acquisition for climatology and weather forecasting [UN PAPER 68-95831]

06 p0950 A69-17073

Meteorological data for flight path climatologies, analyzing annual frequency distribution of maximum wind velocities

09 p1535 A69-21519

One and two dimensional frequency distributions for probability estimates of climatological quantities, discussing temperature and interdiurnal changes

09 p1535 A69-21520

Cartographic representation methods in climatological regional charts, discussing topographical elements, scale, screen patterns and area color

12 p2124 A69-25893

Ocean circulation as climate regulator, discussing role in redistributing climate-changing energy input from solar radiation or lunar tidal friction into atmosphere

12 p2067 A69-26333

Ballistically effective atmospheric parameters for rocket vehicle design manuals involving application of climatological concepts of meteorology

12 p2175 A69-26874

Soviet collection of papers on aviation climatology covering cloud covers, tropopause characteristics, icing conditions, etc

12 p2127 A69-26898

Complex climatological cloud profiles structural characteristics along given air traffic routes prepared for practical aviation problems

12 p2127 A69-26899

Westerly air flow frequency decline resulting in lower seasonal temperatures, tabulating Lamb categories daily maximum and minimum temperatures

13 p2222 A69-28474

Climatic environments development for physiological studies, considering ambient temperature, radiated heat and air velocity and movement

13 p2215 A69-28594

Helicopter climatic testing, discussing component, systems and field tests and facilities

14 p2427 A69-29505

Hydrodynamic theory of climate and atmospheric circulation, emphasizing numerical experiments role in studying large scale processes

14 p2476 A69-29819

Time spectra of wind velocity, temperature, pressure and turbulent heat transfer and momentum in synoptic region
14 p2476 A69-29823

Climate studies with allowance for radiative heat inputs, constructing nonadiabatic motions model for improving prognosis
14 p2477 A69-29827

Earth orography influence on climatological distribution of wind and geopotential fields, stressing central asiatic mountains role in atmospheric circulation
14 p2478 A69-29835

Functional relations expressing short wave radiation absorption and scattering in atmosphere
15 p2648 A69-30222

Ozone soundings data obtained over Australia and Colorado to obtain vertical picture of synoptic climatology of ozone at midlatitudes
15 p2649 A69-30898

Statistical analysis of Brewer-Mast electrochemical soundings of vertical ozone distribution for developing computer programs of climatological behavior
16 p2786 A69-32632

Martian surface features and climate with emphasis on atmospheric surface layers, assessing Mariner 4 data
17 p3029 A69-33040

Zonal winds in temperate latitude analyzed as function of latitude and month from GHOST balloon flights in Southern Hemisphere at 200 mb
17 p2997 A69-33163

Climatological patterns of atmospheric kinetic energy dissipation in free atmosphere derived from upper wind statistics of Northern Hemisphere, using Kolmogoroff functions
18 p3166 A69-34825

Electronic data collection for climatological stations, describing acquisition and processing of various identification signals and meteorological parameters
20 p3538 A69-37428

Soviet book on synoptic climatological and heliogeophysical long term weather forecasts, discussing monthly and seasonal anomalies, sun-earth interrelations, solar corpuscular elements, etc
21 p3759 A69-39523

Linear equations of motions of inviscid ideal gas atmospheres, describing climatology of propagation parameters for point impulse sources
22 p3938 A69-40446

Cloud cover forms in circulatory-climatic zones of earth based on Zond 5 picture analysis, discussing air-mass exchanges and motions direction
23 p4184 A69-42486

CLIMBING FLIGHT

Air density fluctuation effects on aircraft dynamic stability around center of gravity during climbing and diving maneuvers, discussing atmospheric pressure and flight path angle
04 p0548 A69-14825

Aerodynamic technology applied to takeoff and landing, discussing STOL airplanes in descent and boundary layer control/BLC/flap system
05 p0696 A69-15569

Conjugate gradient methods for optimization problems with terminal constraints, noting minimum time paths for V/STOL aircraft climb phase
12 p2013 A69-26763

Optimum climb trajectories at constant lift coefficient, using variational methods with final altitude and final flight path angle as end point constraints
24 p4254 A69-43727

CLINICAL MEDICINE

NT OTOLOGY

Head injury clinical and laboratory long term follow-up data, discussing conscious state alterations, focal neurological deficit, EEG abnormalities, etc
01 p0022 A69-11346

Clinical problems during interplanetary flights, stressing need for diagnostic algorithms and automated medical equipment
02 p0202 A69-12121

Book on space clinical medicine covering hypoxia, ebullism, decompression, acrotitis, dehydration, hypothermia, cabin atmosphere contamination, urinary calculus, etc
05 p0711 A69-16801

Clinical analysis of combat and noncombat ejection experience of USAF
06 p0878 A69-16960

Clinical spectrum of postural hypotension, treating vasodepressor syncope, orthostatic arterial anemia and idiopathic orthostatic hypotension
06 p0873 A69-17017

Clinical report on Apollo 7 and 8 mission medical data, discussing preflight preventive medical activities, inflight treatment, radiation levels, etc
09 p1446 A69-22542

Motion sickness treatment with bethanechol chloride, noting negative results with 12 airsick student naval aviators
12 p2024 A69-26561

Biotelemetry system as candidate prototype of generalized system for clinical applications
19 p3262 A69-36272

Coronary angiography for evaluating cardiac problems of aircrew, giving case histories and clinical and laboratory findings
19 p3263 A69-36461

Clinical data on ambulant airmen with complete left bundle branch block discovered on electrocardiogram, finding majority with evidence of organic heart disease
19 p3263 A69-36463

Private one doctor one nurse clinic at Sydney airport, discussing history, operating conditions, medical record and statistics
23 p4105 A69-41786

Brain atrophy clinical diagnosis aided by biochemical analyses, including age frequencies and symptoms, to control incidence among aviation personnel
23 p4089 A69-41816

Frequency analysis of second heart sound splitting in patients with coronary artery disease assessed clinically and by phonocardiography
24 p4261 A69-42726

Abnormally slow ultrasound diastolic slope detected by mitral valve motion study in patients with clinically pure mitral insufficiency
24 p4261 A69-42727

CLOCK PARADOX

Theory of relativity and role of time intervals in prediction experiments for rate of clocks
03 p0467 A69-13599

Clock paradox of Einstein special theory of relativity, reviewing work of Prokhovnik, Schlegel and Arley
10 p1772 A69-22865

Einstein interpretation of time in special relativity theory disputed by Fok time dilatation theory
11 p1915 A69-24345

CLOCKS

NT ATOMIC CLOCKS
NT CHRONOMETERS
NT CLOCK PARADOX

Worldwide clock synchronization by geostationary satellite transponder relaying VHF signals from reference clock, noting accuracy of radio propagation delay prediction
12 p2080 A69-26053

CLOSE PACKED LATTICES

Pressure effects on hcp crystalline lattice alloys order-disorder transformations
11 p1937 A69-24704

Slip band extrusions in hexagonal close packed Cd, Mg and Ti subject to cyclic stresses, noting microstructure changes
12 p2116 A69-26912

CLOSED CIRCUIT TELEVISION

Image intensifier-vidicon closed circuit TV network for auroral cinematography at low light levels
06 p0925 A69-17382

CLOSED CYCLES

MHD generator and compressor Joule losses effect on thermoelectric energy conversion closed cycle efficiency with electrical conductivity maintained by nonequilibrium ionization
03 p0369 A69-14152

GaAs injection diode laser cooled by closed cycle gas refrigeration system, noting time required to reach laser operating temperature
05 p0777 A69-16793

Helium closed cycle cooled very low noise high gain parametric amplifier for investigating interstellar atomic hydrogen radiation
07 p1098 A69-18461

High speed stable system by combining hunting type control system without closed cycles designed for plant optimization with recycling type controller
07 p1116 A69-19759

Mathematical model, analog computer simulation and information comparison of closed Brayton cycle systems for power conversion [ASME PAPER 69-GT-50]
09 p1442 A69-22479

MHD electrical power generation - Conference, Warsaw, July 1968, Volume 1, Closed cycle MHD with gaseous working fluids
10 p1729 A69-23433

Equilibrium loss in closed cycle MHD generator using rare gases binary mixtures as working fluid
10 p1737 A69-23468

Closed cycle MPD experiments with applied electric and magnetic fields emphasizing current leakage, segmentation, relaxation and aerodynamic effects
10 p1738 A69-23479

Experimental arrangement consisting of closed cycle system, ionization duct and inductive MPD converter with traveling wave component, using Hg as working medium
10 p1638 A69-23490

Closed loop cycle converter, composed of MHD generator and compressor consuming thermal energy, exhibiting moderate cycle efficiency decreases
11 p1824 A69-24223

Turbomachinery buffer seals, buffer gas regulation and cleanup systems for operation of closed Brayton cycle power conversion system with gas cooled nuclear reactor
13 p2268 A69-27367

Mechanical work recoverable from stored energy and heat absorbed by taking material through closed cycle in strain and entropy space
20 p3575 A69-37074

Temperature and pressure relations in power plant with closed gas cycles with radiative heat transfer, noting radiation area reduction influence
20 p3464 A69-37603

Closed cycle MHD with gaseous working fluids and steady state nonequilibrium ionization
21 p3777 A69-39479

Closed cycle gas cooling techniques for self contained CW kilowatt carbon dioxide laser, relating output power to flow velocity and input power
23 p4173 A69-41497

Closed Brayton cycle power systems for space, lunar, terrestrial and undersea environmental conditions, discussing design and performance
23 p4071 A69-42277

CLOSED ECOLOGICAL SYSTEMS

Man as main component of future spacecraft or planetary station closed ecological system, discussing spacecrew physiological monitoring for biological cycles optimization
01 p0020 A69-11076

Biological life support system based on continuous algae seaweed cultivation as link of closed ecological system, discussing design and performance
01 p0020 A69-11077

Biological life support system for regenerating closed atmosphere by photosynthesis, using gas exchange between man and microalgae
01 p0021 A69-11078

Mathematical models of energy and mass transfer processes in closed loop multicomponent life support systems
01 p0021 A69-11316

Rodents exposure to neon enriched atmosphere for three weeks in sealed recycling system, discussing body weight pregnancies and litter
01 p0019 A69-11342

Membrane vapor diffusion for water reclamation from urine and wash water on space missions
03 p0379 A69-12992

Microbiology of water management subsystem for manned space flight, discussing sterilization by heat and tests inside Integrated Life Support System [ILSS] [SAE PAPER 680718]
03 p0379 A69-13441

Physicochemical method for converting human urine and feces into carbohydrates in closed ecological systems
03 p0381 A69-14199

Life in spacecraft - Conference, Belgrade, September 1967
06 p0881 A69-17642

Life support system energy efficiency, treating transfer equations of closed space regeneration systems
06 p0882 A69-17644

Human endurance during isolation in closed space with prescribed veloeometric exercises, noting impairment of functional capacity
08 p1263 A69-19933

Reactors technical characteristics for high temperature mineralization of closed life systems biological wastes, deriving equations to estimate energy balance
10 p1649 A69-23504

Mathematical model of closed biological cycle regenerating part of life support products, incorporating astronaut, storage and regenerating waste disposal units
10 p1649 A69-23580

Human ecology in space flight - USN-NASA Conference, Princeton, October 1965, Volume 3
13 p2213 A69-27266

Soviet space biology and medicine, discussing ecological physiology, closed system ecology, exobiology and medical tests on cosmonauts
13 p2209 A69-27356

Closed life support systems tests, describing effects of long term /one year/ confinement of three human subjects
13 p2216 A69-28612

Artificial life support systems for sealed environments with application to specific missions, noting cryogenics use
17 p2915 A69-33682

Fire hazard in closed chamber associated with intestinal hydrogen and methane formed by space diets, comparing Gemini-type and bland diets
20 p3482 A69-37622

Mathematical model of optimal partially closed life support system consisting of man, recycling unit, storage unit and waste disposal outlet
22 p3892 A69-40272

CLOSED LOOP SYSTEMS
U FEEDBACK CONTROL

CLOSURE LAW
Closure conditions for Vlasov turbulence, discussing infinite systems of equations for dynamics of statistical quantities
17 p2958 A69-34228

Vlasov turbulence exact solutions, considering closure conditions, correlation length, Lundgren hierarchy, homogeneous turbulence, etc
17 p2958 A69-34229

CLOTH
U FABRICS

CLOTHING
U FLIGHT CLOTHING
U GLOVES
U HELMETS
U PRESSURE SUITS
U PROTECTIVE CLOTHING
U SHOES
U SPACE SUITS

CLOUD CHAMBERS
Cloud chamber for measuring specific ionization in relativistic region by muons in gases, using drop counting method
06 p0925 A69-17303

Simultaneous parallel penetrating muons observed in multiple cloud chambers, obtaining information about sea level muons interactions and EAS
06 p0991 A69-17304

Automatic counter for concentration of cloud condensation nuclei in thermal diffusion chamber, measuring light scattering coefficient of cloud
09 p1494 A69-21640

Particle physics and discovery of K mesons and hyperons emphasizing track recording, cloud and bubble chamber techniques
24 p4352 A69-43039

CLOUD COVER
NT COVERINGS

Tiros Operational Satellite system for global weather analysis data acquisition and cloud cover photography, noting sensor development for numerical weather prediction
[UN PAPER 68-95823] 01 p0108 A69-10473

Venus cloud layer thickness and lower boundary estimation from data on chemical composition, temperature and pressure profiles of atmosphere
01 p0152 A69-10580

Automated layered-nephanalysis and numerical total cloud cover prediction program using moisture data from Tiros 7 photographs
01 p0110 A69-10691

Apollo landmark sighting by astronaut using Apollo onboard navigation system, simulating cloud cover effects with Monte Carlo technique
01 p0110 A69-10692

Wind perturbations characteristics near large convective cloud banks as function of ascending current, wind shear and turbulence
02 p0274 A69-11446

Long wave radiative heat flux in boundary layers of cloud during solid overcast, discussing dependence on various cloud and atmospheric parameters
03 p0458 A69-13271

Radar method to estimate turbulent motions in clouds
03 p0459 A69-13289

Quantitative estimations of cloud and precipitation by radar meteorology, assuming homogeneous reflectivity distribution of clouds
04 p0626 A69-14507

Atmospheric processes interpretation from cloud cover pictures televised by orbiting satellite, examining indirect weather forecasting
[UN PAPER 68-95713] 06 p0949 A69-17029

Meteorological satellite TV data of earth cloud cover for determining atmosphere pressure field
[UN PAPER 68-95654] 06 p0949 A69-17052

Actinometric and nephelometric data on outgoing short wave radiation obtained by Cosmos 122 satellite, tabulating cloud cover data, digital radiation data and brightness curves
06 p0952 A69-17983

Interpretation of IR cloud images transmitted by Nimbus 1 and Cosmos 122 satellites, using radiation temperature contrasts
06 p0952 A69-17984

Atmospheric measurements from satellites, discussing ATS-1 cloud images for definition of wind and use of WEFAX through ATS 2 satellites for data transmission
[AIAA PAPER 69-158] 06 p0954 A69-18038

Mars polar cap ice cap and dry ice theories, discussing dark wave and cloud distribution meteorological observations
07 p1212 A69-18603

Test of Velikovsky theory for dense hydrocarbon clouds and dusts surrounding Venus, using IR reflection spectra
09 p1608 A69-22566

Vertical air flow asymmetrical distribution ascribed to cyclone motion and thermal inhomogeneity by studying spiral cloud configurations in cyclone area
11 p1912 A69-24829

Two dimensional autocorrelation functions of outgoing radiation fields usable as quantitative characteristics of cloud distribution structures
11 p1913 A69-24832

Tenuous cirrus cloud influence on 6.4-6.9 micron Nimbus 2 water observations, discussing equivalent black body temperatures correspondence to cloud and clear areas
12 p2075 A69-27003

Regression coefficients obtained from satellite cloud observations applicability in constructing geopotential fields, tabulating coefficients obtained from ground stations
13 p2292 A69-27731

Long wave radiative heat flux in boundary layers of cloud during solid overcast, discussing dependence on various cloud and atmospheric parameters
14 p2471 A69-28779

Microwave brightness temperatures for downward viewing over open seas from above atmosphere, using tropospheric model containing homogeneous layer clouds
14 p2415 A69-29515

High and low latitude cellular cloud patterns observed by meteorological satellites, noting frequent occurrence over oceans
14 p2473 A69-29727

Cloud pattern characteristics in intertropical convergence zone above Indian and Pacific oceans from meteorological satellite photographs and cloud formation maps
14 p2473 A69-29728

Venus cloud layer thickness and lower boundary estimation from data on chemical composition, temperature and pressure profiles of atmosphere
15 p2691 A69-30750

Monograph on large scale cloud distribution in extratropical low pressure regions, using classical meteorological observations and Tiros weather satellites data
15 p2650 A69-31212

Cloud distribution effect on global coverage of remote radiometric sounding of atmosphere, considering Nimbus 1 and 2 data
15 p2650 A69-31335

Multiple light scattering solutions accuracy by diffraction peak omission from cloud and haze analytic phase functions compared for optically thick and thin planetary atmospheres
17 p3032 A69-33159

Earth albedo effect on ionospheric D layer determined from aircraft sounding of E layer echo amplitude above reflecting cloud cover
18 p3127 A69-34800

Venusian cloud layer radius, discussing error in determination of occultation level height of Regulus by Venus
18 p3203 A69-35331

Cloud layer multiple scattering in Jovian atmosphere, discussing influence on Lorentzian contour of planetary absorption lines
18 p3203 A69-35332

Cloud masses vertical thickness estimated from study of cloud shadows on satellite TV pictures
19 p3366 A69-36670

APQ-97 side-looking radar for topographic mapping of continually cloud covered areas, noting data reduction and compilation methods
20 p3519 A69-36928

Cloud bank structure formation physical mechanism relationship with airflow using differential equations
20 p3569 A69-36985

Large scale cloud layers vertical boundaries approximate determination using atmospheric temperature and moisture data from aircraft sounding
20 p3569 A69-36986

Worldwide cloud cover simulation procedure providing data for computer simulation of earth oriented space missions, describing computer program using Monte Carlo mission simulation
20 p3573 A69-38120

Computer controlled TV cloud recognition equipment on meteorological satellites, discussing multistep process of automatic perspective distortion corrections by onboard computer
22 p3977 A69-40004

Long term computer produced multiple image satellite photomosaics for Southern Hemisphere, analyzing circulation, meridional bands, polar ice, cloud cover variations, etc
22 p3977 A69-40733

Venus atmosphere and clouds exploration by entry probes, discussing ground temperature, greenhouse model, cloud layer, etc
23 p4216 A69-42201

Cloud cover forms in circulatory-climatic zones of earth based on Zond 5 picture analysis, discussing air-mass exchanges and motions direction
23 p4184 A69-42486

Solid cloud cover moisture content relation to outgoing thermal radiation, obtaining correlation coefficient and regression equations
23 p4184 A69-42488

Multiple exposure averaging technique summarizing satellite cloud photographs for various periods, presenting entire earth cloud cover atlas
24 p4343 A69-42897

CLOUD GLACIATION
Critique of paper on water crystal existence on Venus, presenting arguments against existence of clouds of micron sized ice crystals
01 p0157 A69-11292

CLOUD HEIGHT INDICATORS
Cauchy system for reflection and transmission functions of finite isotropically scattering atmospheres with specular reflectors, noting use for ozone and cloud heights measurements
15 p2597 A69-31152

Heights of cloud bases and convective cloud tops determined by stereoscopic photogrammetry of Apollo 6 mission
20 p3569 A69-36926

Cirrus cloud height above sea level and shape correlation with lower section static stability determined by stereophotogrammetric measurements
20 p3570 A69-37349

CLOUD PHOTOGRAPHS
Venus UV photographs and drawings shown in short interval sequences, noting left to right shift in cloud features
02 p0320 A69-12111

Processing TV cloud data monitored by Molniya 1 and Meteor meteorological satellites, discussing computer interpretation of TV photographs
[UN PAPER 68-95759] 06 p0950 A69-17060

European cyclonic system developmental phases determined from characteristic structural features of satellite cloud pictures
[UN PAPER 68-95711] 06 p0950 A69-17070

Statistical analysis of lee wave clouds from satellite TV pictures, determining lengths and air flow direction
11 p1912 A69-24828

Computer program for interpreting IR cloud pictures from Cosmos 122 satellite based on potential function method
11 p1884 A69-24833

Vertical air motions and cloud behavior relationship based on statistical analysis of TV cloud pictures from Cosmos 122 satellite
13 p2291 A69-27724

IR TV cloud pictures from meteorological satellites used for sky condition diagnostics and forecasting through automatic interpretation by image brightness quantization
13 p2291 A69-27728

Cartographic interpretation of TV cloud pictures transmitted by Molniia 1 satellite

13 p2292 A69-27730

Baker-Nunn photometry from Apollo tracking utilizing photographs for brightness, dynamics and duration of rocket exhausts and venting clouds

15 p2571 A69-31338

Digitized video cloud picture data from ESSA satellite, discussing mesoscale archive and computer products including time averages and composites

19 p3279 A69-35810

Precipitation zone-cloud mass correlation based on Tiros cloud photographs, synoptic charts and weather maps for European U.S.S.R.

19 p3366 A69-36671

Heights of cloud bases and convective cloud tops determined by stereoscopic photogrammetry of Apollo 6 mission

20 p3569 A69-36926

Long range weather forecasts attempt from relation between northern Atlantic Ocean water temperature anomaly and monthly satellite cloud data changes

20 p3569 A69-36987

Synoptic and mesoscale cloud patterns near low level jet from Tiros 7 and 8 photographs, noting stratus formation and dissipation

20 p3570 A69-37404

Cloud velocity computations from ATS 1 and 3 satellites spin-scan photographs for prediction of neph systems motion and thunderstorms

21 p3757 A69-38370

Wind and cloud velocities from ESSA 3 and 5 and ATS 1 pictures for typhoon and tropical vortices in intertropical convergence zone

21 p3758 A69-38371

Equatorial anticyclones over eastern Pacific caused by large scale cross-equatorial flows determined by ATS-1 photographs, noting frictional convergence factor

24 p4342 A69-42895

Multiple exposure averaging technique summarizing satellite cloud photographs for various periods, presenting entire earth cloud cover atlas

24 p4343 A69-42897

CLOUD PHOTOGRAPHY

Cloud pictures from weather satellites reception according to automatic picture transmission (APT) system, discussing design and field strength measurements

[UN PAPER 68-95451] 01 p0108 A69-10458

Tiros Operational Satellite system for global weather analysis data acquisition and cloud cover photography, noting sensor development for numerical weather prediction

[UN PAPER 68-95823] 01 p0108 A69-10473

Utility of satellite cloud pictures to meteorological work, discussing weather observation in Israel Meteorological Service

[UN PAPER 68-95571] 01 p0109 A69-10482

Spiral structure of cloudiness in occluded cyclones studied by mathematical model based on meteorological satellite photographs

[UN PAPER 68-95429] 01 p0109 A69-10505

Global cloud models construction techniques, discussing vertically pointing radars, airborne panoramic cameras, radiometry, meteorological satellites and light detection and ranging

02 p0275 A69-12381

Cloud features produced by European tropospheric low pressure areas observed by meteorological satellite photographs, noting cyclonic systems development

06 p0950 A69-17619

Air flow distribution and wind velocities in cyclones constructed from Cosmos 122 TV cloud images

11 p1912 A69-24825

TV IR cloud images interpretation transmitted by Cosmos 122, discussing specific features of cloud covers and underlying surfaces

11 p1912 A69-24826

Statistical analysis of convective layer thickness and moisture content effect on convective cloud configurations, using satellite TV pictures

11 p1912 A69-24827

Noctilucent clouds morphological and kinematic characteristics based on photographs

18 p3132 A69-35335

Cirrus cloud height above sea level and shape correlation with lower section static stability determined by stereophotogrammetric measurements

20 p3570 A69-37349

CLOUD PHYSICS

Aircraft instrumentation system for cloud nucleation studies measures and records ice nucleus and aerosol concentration/distribution, temperature, etc

01 p0080 A69-10542

Axisymmetric model of unsteady convective cumulus cloud produced by time dependent heat source in unsteady atmosphere

02 p0274 A69-11436

Collection of Soviet papers on cloud physics and modification covering radar techniques, radio echoes and turbulent motions

03 p0459 A69-13285

Radar method to estimate turbulent motions in clouds

03 p0459 A69-13289

Large convective clouds in superheated air generated by static tests of Saturn 5 first stage

03 p0462 A69-14125

Atmospheric noise at 33.5 GHz observed most on days of cumulus clouds probably due to local convective activity

05 p0721 A69-16661

Water droplet simulation by glass spheres used in study of light scattering at cloud particles

06 p0953 A69-17992

Photoelectric equipment for nephelometric simulation studies of light scattering by cloud particles

06 p0953 A69-17993

Radio emission and microwave absorption spectrum dependence on physical properties of clouds in millimeter and centimeter wavelength range

06 p0954 A69-17998

Radio wave brightness temperatures and contrast characteristics in presence of clouds and precipitation

06 p0954 A69-17999

Mathematical frame for cloud models, discussing condensation, collection and advection processes and freezing and electrical effects

07 p1176 A69-19041

Electric fields and conductivity in thunderclouds by parachuting rotating differential electric field mills

08 p1345 A69-19813

Radiation scattering changes due to droplet size distribution change during stratus cloud formation calculated, using development model and Mie theory

08 p1346 A69-21093

Automatic counter for concentration of cloud condensation nuclei in thermal diffusion chamber, measuring light scattering coefficient of cloud

09 p1494 A69-21640

Simultaneous measurements of cumulus cloud thermal structure and concentration of water particles larger than 18 micron diameters

09 p1536 A69-21866

Convective clouds effect on large scale stratification, showing cumulus and cumulonimbus self amplifying convection as factor in tropical cyclogenesis

09 p1536 A69-22165

Condensation kinetics in clouds, determining cloud spectrum evolution taking stochastic processes into account

10 p1722 A69-23972

Radiophysics Laboratory (Sidney), discussing radio astronomy, radioheliographs, radio telescopes, cloud physics and research

10 p1784 A69-23988

Virial theorem extended to investigate star condensations in large interstellar gas clouds

10 p1787 A69-24119

High velocity neutral hydrogen cloud formation by cold condensations in hot corona, ejection from galactic nucleus, extragalactic objects and supernova envelopes

11 p1954 A69-24364

Theoretical models corresponding to initial phases in thermal-gravitational collapse of spherical clouds from interstellar gas for stellar formation

11 p1963 A69-25261

Cloud and fog droplet spectra due to condensation of water vapor on nuclei solved by partial differential equation

12 p2126 A69-26017

Ion cloud ambipolar diffusion and motion dependence on initial configuration and close magnetic field alignment above 95 km, discussing observations of meteor trains

12 p2074 A69-26961

Vertical air motions and cloud behavior relationship based on statistical analysis of TV cloud pictures from Cosmos 122 satellite

13 p2291 A69-27724

Heat convection mechanism in two phase autooscillatory system generalized to convective heat transfer in cloudy atmosphere

13 p2292 A69-27798

Radar and satellite TV clouds observation in meso and macroscale cloud systems

13 p2294 A69-27853

Sporadic E layer cloud configuration study based on explorer 20 satellite observations, discussing W echoes

14 p2434 A69-28943

Night airglow variations observed during Cosmos 92 satellite orbits, determining atmospheric albedo wavelength dependence for solid and medium cloudiness and clear skies

14 p2435 A69-29042

Nocturnal development of air mass stratus clouds in Texas and mechanism of formation, discussing turbulent mixing theory

15 p2649 A69-30893

Statistical data concerning noctilucent clouds formation during IQSY, noting tendency to form along geographic longitudes and day and night existence

15 p2598 A69-31255

Latent heat of condensation related to atmospheric dynamics in cloud formation processes with allowance for moisture exchange

17 p2997 A69-33188

Numerical simulation of macrophysical and microphysical processes in convective cloud, including cloud geometry and equations describing dry and moist phases

19 p3362 A69-36497

Horizontal wind components over U.S.S.R., Western Europe and Northeast Atlantic obtained from satellite photographs of vortex cloud systems

19 p3365 A69-36668

Cirrus clouds occurrence, position and wind velocities on jetstream axes based on statistical analysis of aerological data and satellite TV pictures

19 p3366 A69-36669

Cloud bank structure formation physical mechanism relationship with airflow using differential equations

20 p3569 A69-36985

Large scale cloud layers vertical boundaries approximate determination using atmospheric temperature and moisture data from aircraft sounding

20 p3569 A69-36986

Cirrus cloud height above sea level and shape correlation with lower section static stability determined by stereophotogrammetric measurements

20 p3570 A69-37349

Cloud physics problems of precipitation release from interaction of air motions and microphysical events, discussing raindrop growth initiation, artificial cloud modification, etc

20 p3572 A69-37906

Cumulus and cumulonimbus clouds electrical and microphysical properties measured by instrumented aircraft

20 p3572 A69-37907

Long wave radiation influx toward atmospheric layers generated naturally by clouds, discussing radiation cooling of atmosphere in cloudy and clear weather

21 p3758 A69-39112

Stratified cloud transport and evolution, solving kinetic equations by numerical method

21 p3759 A69-39119

Condensation kinetics in clouds, determining cloud spectrum evolution taking stochastic processes into account

21 p3760 A69-39658

Radiative transfer theory applied to layer cloud with normal liquid moisture content, discussing volume extinction, scattering and absorption coefficients, etc

23 p4184 A69-42177

Precipitation physics, discussing cloud structure on mountains and in free atmosphere, precipitation measurement on ground, raindrop size distribution, etc

24 p4343 A69-43037

Varying ratio between mean free path and spherical particle radius at 0-10 km, discussing free molecular flow effects in cloud physics

24 p4345 A69-43145

CLOUD SEEDING

Visibility improvement in warm fog by seeding with micron size hygroscopic particles, noting results for NaCl

01 p0111 A69-10696

Cloud seeding effects due to inhomogeneous distribution of freezing nuclei, discussing silver iodide distributions by Gaussian plume diffusion model

09 p1535 A69-21639

Sulfur dioxide, nitrogen dioxide and Aitken nuclei washout by artificial rain of known intensity and droplet size distribution

24 p4345 A69-43146

CLOUDS

NT ARTIFICIAL CLOUDS

NT CIRRUS CLOUDS

NT CUMULONIMBUS CLOUDS

NT CUMULUS CLOUDS

NT ELECTRON CLOUDS

NT NOCTILUCENT CLOUDS
NT PLASMA CLOUDS
NT STRATUS CLOUDS
Nonexistence of Biota-Cloud recontamination hazard for planetary lander proved by analysis of interactions between small particles and physical fields around vehicle
02 p1201 A69-11771
Lunar libration clouds, discussing visual observation at small phase angles for estimation of dominant cloud particle size
05 p0827 A69-16527
Astronomical maps of integrated hydrogen density, dispersion and velocity of high galactic latitude neutral hydrogen concentration, discussing kinetic temperature
13 p2347 A69-27718
Neutral hydrogen cloud observed at high galactic latitude, discussing top intensity velocity, peak intensity dispersion, age, hydrogen mass and density
13 p2347 A69-27719
Radiative heat transfer in nonisothermal scattering media of plane, spherical and cylindrical geometries separated by particle cloud
16 p2878 A69-31925
Cloud scattering corrections added to synthetic spectrum analysis of carbon dioxide bands and water vapor line in Venus spectrum
17 p3032 A69-33161
IR reflection spectra agreement for frost particles and Venus clouds, noting ice as clouds constituent
18 p3190 A69-34282
Ice clouds near IR spectral reflectivity dependence on particle size, noting application to planetary atmospheres
18 p3126 A69-34283
Magellanic clouds positions, associated gases, evolution, etc
19 p3401 A69-35757
Interstellar hydroxyl molecular clouds as radio wave sources, using very long baseline interferometry, suggesting natural masers in space for OH emissions
19 p3427 A69-36659
CLOUDS [METEOROLOGY]
NT ARTIFICIAL CLOUDS
NT CIRRUS CLOUDS
NT CUMULONIMBUS CLOUDS
NT CUMULUS CLOUDS
NT NOCTILUCENT CLOUDS
NT STRATUS CLOUDS
Spiral structure of cloudiness in occluded cyclones studied by mathematical model based on meteorological satellite photographs
[UN PAPER 68-95429] 01 p0109 A69-10505
Global cloud models construction techniques, discussing vertically pointing radars, airborne panoramic cameras, radiometry, meteorological satellites and light detection and ranging
02 p0275 A69-12381
Radar method of spiral scanning clouds and precipitation at constant altitude
03 p0459 A69-13286
Numerical radar information charts, plotting radio echo reflection boundaries from cloud and precipitation observations by weather radars
03 p0459 A69-13287
Heated liquid mercury rotation rate and direction counter to rotating bunsen flame related to Venus cloud formations high velocities
04 p0664 A69-15466
Cloud features produced by European tropospheric low pressure areas observed by meteorological satellite photographs, noting cyclonic systems development
06 p0950 A69-17619
IR scanning systems of meteorological satellites for detection of clouds and various underlying surfaces, determining detection probability and errors
06 p0952 A69-17986
Spectral brightness of clouds and various terrains in visible and near IR regions measured from aircraft
06 p0953 A69-17991
Atmospheric models for electromagnetic scattering of monochromatic IR and microwave radiation by natural suspensions as hazes clouds and precipitation
12 p2030 A69-26467
Complex climatological cloud profiles structural characteristics along given air traffic routes prepared for practical aviation problems
12 p2127 A69-26899
Soviet meteorological and geophysical rockets, satellites and techniques in cloud studies and weather forecasting, noting Cosmos results
13 p2290 A69-27348
Wind velocity, geopotential and atmospheric layer temperature fields constructed from Tiros 9 satellite

cloud data using least squares method and trigonometric polynomials
13 p2292 A69-27733
Radiation in atmospheric circulation, considering radiative equilibrium, cloudiness and surface interactions, surface temperature and heat input
14 p2477 A69-29826
Bidirectional reflectance of solar radiation and IR temperature data from Nimbus 2 satellite to differentiate clouds above snow surfaces
15 p2596 A69-30455
Radio wave single scattering at particles randomly grouped in space, showing correlation function of water content fluctuations in scattered field in clouds
16 p2807 A69-32267
Dimensions, concentration and spectrum of large precipitation particles in clouds and cloud water content by measuring reflectivity and absorptivity at different wavelength
16 p2807 A69-32268
Vertical wind velocity pulsations in precipitation and passage through subfrontal clouds measured by pulse radar
16 p2807 A69-32272
Turbulence dissipation rate in clouds and precipitations determined from rms width of vertical sounding radar signal fluctuation spectra, distinguishing gravity and turbulence effects
16 p2807 A69-32273
MRL-1 meteorological radar station detection of cloud types under steady rain, showers and storm conditions, describing radar data analysis procedure
16 p2808 A69-32278
Survey of six year period of satellite observed tropical Pacific cloud mapping
17 p2996 A69-33001
Precipitation zone-cloud mass correlation based on Tiros cloud photographs, synoptic charts and weather maps for European U.S.S.R.
19 p3366 A69-36671
Negative charge distribution in thunderstorm clouds related to direction of storm movement, noting vertical column
20 p3572 A69-37908
Wind and cloud velocities from ESSA 3 and 5 and ATS 1 pictures for typhoon and tropical vortices in intertropical convergence zone
21 p3758 A69-38371
Bidirectional reflectance of earth atmosphere and cloud formation above equatorial Pacific observed by synchronous satellite as function of angular dependence
24 p4346 A69-43154
CLUTTER
Adaptive detection mode for surveillance radar, using detection threshold proportional to spatially sampled clutter level estimates for regulation of false alarm probability
01 p0026 A69-10178
Moving target indicator (MTI)/ performance degradation by limiting clutter analyzed for various pulse cancellers and verified by time-domain Monte Carlo simulation
03 p0390 A69-13198
Weighted pulse trains for clutter suppression during radar target detection
04 p0562 A69-15467
Statistical analysis of Radicord /radar digitizing and recording/ clutter and signal spectra and moving target detection by pulse radar
05 p0721 A69-16619
Clutter residues of coherent MTI radar receiver, emphasizing IF stages saturation nonlinearity affecting cancelling circuits performance
13 p2220 A69-27941
Optimal radar receivers and waveforms with limited dynamic range for detecting point target masked by thermal noise and clutter returns
17 p2921 A69-33625
Compound fading exponential /CFE/ clutter model for radar target detection, describing automatic detection applications
23 p4117 A69-41604
Radar return from clutter target with circular polarization, finding probability density functions and cumulative distributions of power ratio
23 p4131 A69-42540
COAGULATION
NT BLOOD COAGULATION
Nickel alloy high temperature tests, noting coagulation of precipitated gamma prime phase, vacancies and creep rate increase
09 p1528 A69-22733

Plasticizer mechanical properties and content in paste, considering effects on texture of coagulation structure during die extrusion of compacts
12 p2118 A69-26257
Diathermy instrument using solid state circuits to provide square wave pulses, discussing operating parameters for bipolar coagulation and advantages over spark gap instruments
18 p3134 A69-34537
COAL
Mathematical analysis of oxygen diffusion to coal grains during coal dust combustion, evaluating kinetic constants by burning time
04 p0687 A69-15167
Coal grain combustion rate and duration at finite air excess coefficient, solving combustion process equations under steady state assumption
04 p0687 A69-15168
COALESCENCE
U COALESCING
COALESCING
Boundary layers coalescence on plane convergent channel walls investigated with analytic formulas for velocity distribution, shear stress, layer thickness, etc
15 p2592 A69-31009
COANDA EFFECT
Variable time delay achievement in fluid logic circuits based on Coanda effect devices
02 p0196 A69-12085
Coanda nozzle entrainment and flow augmentation approximating numerical stability by finite differences
05 p0746 A69-16021
Bistable fluid device utilizing Coanda effect along convex surface for wall attachment
[ASME PAPER 68-WA/FE-27] 05 p0749 A69-16101
Wall attachment phenomenon /Coanda effect/ basis for jet elements in digital and/or pulse-mode systems
10 p1638 A69-23553
Attachment and separation of free jet from wall, discussing model equations for wall attachment fluid amplifier
14 p2428 A69-28877
Incompressible attached wall jet /Coanda flow/ over circular cylinder with finite incompressible injection normal to surface
16 p2772 A69-32148
Coanda effect of separated jets reattachment to wall at high Knudsen number in pneumatic fluidic devices, discussing Reynolds and Mach numbers effect
[ASME PAPER 69-FLCS-37] 21 p3692 A69-38602
LF switching in wall attachment type digital fluid amplifiers, studying visual and quantitative values for switch pressure and flow as function of geometric variables
[ASME PAPER 69-FLCS-31] 21 p3649 A69-38604
COASTING FLIGHT
Coasting arc determination in rocket trajectory problems by Lagrange multipliers
09 p1595 A69-21969
Variational equations uniform closed solution for optimal trajectories during coast without use of numerical integration
19 p3399 A69-35671
Vector integral extension to optimal trajectory coordinate multiplier systems with constant of motion demonstrated for coast-arc problem
[AIAA PAPER 69-907] 21 p3807 A69-39339
COASTS
Magnetic anomalies off Cape Hatteras explained as possible edge effect, discussing ocean and continental magnetic crusts and igneous and magnetic rocks
11 p1879 A69-25405
Tethered polyethylene balloon carrying radio controlled camera for time lapse photographs of wave generated near shore currents
22 p3865 A69-40808
COATING
NT ANODIZING
NT ELECTROPLATING
NT ENCAPSULATING
NT METALLIZING
Pool boiling heat transfer from stainless steel coated with Teflon to produce nonwetted surfaces
[ASME PAPER 68-WA/HT-12] 05 p0847 A69-16119
Chemical vapor deposition of chromium metal on substrates, discussing influence of temperature, gas flow rate and chromium chloride concentration
[ECS PAPER 223] 05 p0769 A69-16232
COATINGS
NT ALUMINUM COATINGS

NT ANODIC COATINGS
 NT BIREFRINGENT COATINGS
 NT CERAMIC COATINGS
 NT ELECTROPLATING
 NT ENCAPSULATING
 NT GLASS COATINGS
 NT GLAZES
 NT GOLD COATINGS
 NT INORGANIC COATINGS
 NT MAGNETIC FILMS
 NT METAL COATINGS
 NT METALLIZING
 NT PAINTS
 NT PLASTIC COATINGS
 NT PRIMERS [COATINGS]
 NT PROTECTIVE COATINGS
 NT RUBBER COATINGS
 NT SPRAYED COATINGS

Dielectric surface coatings effect on transmission and loss properties of silicon-microstrip microwave transmission lines

01 p0041 A69-10201

Aged boric acid coated silica reaction vessels, showing reduced surface effects and high reproducibility in oxidation reactions

02 p0205 A69-12322

Scattering from coated absorbing conducting bodies, considering flat plane and curved surfaces in Rayleigh region

03 p0384 A69-12908

Molybdenum disilicide allotropy influence on coating growth rate and morphology [ONERA-TP-642]

08 p1335 A69-19967

Thermographic phosphor coatings to obtain optical quantitative heat transfer distribution on wind tunnel models

12 p2099 A69-27150

Wear-resistant hard thin layers deposited on various base material surfaces analyzed by electron microprobe

13 p2282 A69-28164

Boron nitride coated boron reinforced metal matrix composites, discussing continuous liquid infiltration, fiber-matrix reactions and heat treatment

13 p2283 A69-28671

Bonding strength of plasma coatings with substrate, testing aluminum oxide on steel

15 p2630 A69-31189

Thermal control coatings for solar cells of solar probe Helios

16 p2867 A69-31741

Gas products evolved from selected thermal control coating materials during UV radiation in vacuum, noting permanent reflectance loss [AIAA PAPER 69-640]

17 p2992 A69-33289

Damping properties of multilayer coatings for aircraft structures analyzed on duralumin samples subjected to bending at room, elevated and low temperatures

17 p2993 A69-33941

Elastomeric and coating materials for aerospace systems, considering temperature, rain, sand erosion, propellant and radiation resistant properties

19 p3357 A69-35586

Solar cell integral covers optical losses in vacuum as function of degradation by UV exposure, noting accelerated testing for time-cost reduction

19 p3253 A69-35703

Multilayer lead oxide and cryolite dielectric coatings stability to ruby laser radiation, noting breakdown coherent radiation power densities

19 p3334 A69-35886

Thermal control coatings, windows and mirrors for 1973 Mars Viking Lander vehicles under simulated Martian surface conditions [AIAA PAPER 69-1023]

22 p3923 A69-40393

COAXIAL CABLES

Hybrid digital transmission systems, discussing joint optimization of analog and digital repeaters and information rate of coaxial cable systems

01 p0027 A69-10248

Green function for linear antennas in warm plasma fed by coaxial air filled transmission line, computing current distribution and input admittance

02 p0215 A69-11942

End correction for input admittance of electrically thick monopole antenna with arbitrary radius driven from coaxial line

02 p0219 A69-12346

Calibration of coaxial line noise sources in terms of rectangular waveguide standard, discussing use of adaptor for comparison

02 p0210 A69-12436

Precision coaxial connectors, giving IEEE standard mechanical, electrical and environmental specifications

for general precision connectors using coplanar butt joints

02 p0222 A69-12757

Temperature effect on phase stability and electrical length of braided coaxial cables, considering dielectric constant and mechanical length

08 p1283 A69-20225

Coaxial radiator as feed for low noise paraboloid antennas, presenting pattern synthesis

11 p1856 A69-25635

TEM-DUAL surface wave propagation in coaxial cable with stratified dielectric structure to reduce attenuation calculated by addition theorem to Bessel functions

11 p1856 A69-25659

Discontinuity capacitance of coaxial line terminated in circular waveguide calculated using Rayleigh-Ritz variational technique

14 p2423 A69-29754

Broadband low VSWR transitions between rectangular waveguides and coaxial transmission lines, discussing asymmetrical probe and ridge types

16 p2757 A69-31584

COAXIAL FLOW

Steady state circular motion of fluid with variable rheological characteristics between coaxial cylindrical surfaces, obtaining velocity distribution

01 p0061 A69-10733

Coaxial jet mixing regimes in jet engines, determining requirements for compatibility by applying aerodynamic theory of ejectors [ONERA-TP-599]

02 p0187 A69-11619

Coaxial flow jet chamber flow patterns dependence on inlet gas velocity, density and length/diameter ratio [AICHE PAPER 25B]

04 p0587 A69-14509

Ducted turbulent mixing and burning of coaxial streams, presenting experimental results for rocket-air mixing system [AIAA PAPER 69-85]

06 p0984 A69-18082

Jet mixing applications to aircraft engines, discussing one dimensional calculation of coaxial streams mixing inside conduit

09 p1429 A69-21305

Optimal mean radius and half height of channel of liquid metal coaxial linear induction MHD generator with unilateral and bilateral excitation

13 p2207 A69-27507

Alternating current plasma arc coaxial flow stabilization [AIAA PAPER 68-706]

13 p2313 A69-28232

Turbulent gas coaxial mixing theory, deriving eddy viscosity model and semiempirical expressions for velocity, temperature and density fluctuations [AIAA PAPER 69-682]

17 p2952 A69-33434

Transport properties of free turbulent mixing of subsonic coaxial streams by introducing environmental distributions in integrals of momentum, energy and species continuity equations [AIAA PAPER 69-681]

17 p2956 A69-33495

Cold subsonic coaxial jets observed for relationship between noise output and flow characteristics, showing effect of relative annular and central jet velocities

20 p3513 A69-37063

Coaxial turbulent compressible gas jets propagation, discussing mass buildup data in coaxial jets

21 p3645 A69-39847

COAXIAL PLASMA ACCELERATORS

Gas flow model of coaxial electromagnetic plasma gun front profiles and speeds for operation with positive central electrode

02 p0288 A69-12032

Coaxial plasma accelerator for generation of pure injection plasmas, noting stability of propagating current sheath

03 p0481 A69-14213

Coaxial Hall plasma accelerator, noting interaction between radial applied magnetic field and axial applied electric field

05 p0806 A69-16734

Electromagnetic thrust equations for coaxial MPD accelerator, noting role of externally applied magnetic field [AIAA PAPER 69-108]

06 p0972 A69-18197

Axial striograms of noncylindrical focusing discharge for plasma structure in front of interior electrode of coaxial gun

08 p1362 A69-20279

Current sheet velocity in coaxial plasma accelerator, noting drag due to insulator ablation and degassing [AIAA PAPER 69-265]

09 p1566 A69-21258

Conducting gas flow parameters in coaxial duct, considering magnetic nonuniformity, Hall currents and fields distortion near electrodes

19 p3381 A69-36772

Rotational arc motion in MPD accelerators with strong axial fields predicted by plasma physics equations

23 p4201 A69-41909

H plasmoid tail cut-off eliminating plasma impurities during injection across octupole magnetic field from coaxial source

24 p4358 A69-43474

COAXIAL TRANSMISSION U TRANSMISSION

COBALT

Saturation solubility of carbon in cobalt and nickel with respect to graphite determined by vapor transport experiments over large temperature range

01 p0092 A69-10060

Friction induced plastic deformation of Be-Co-Zn single crystals with HCP structure

02 p0254 A69-12627

Cobalt concentration reduction in maraging steels by Cr replacement and increased Mo and Ti additions

04 p0616 A69-14649

Maraging steel with reduced Co, establishing optimal temperature range for short aging

04 p0616 A69-14650

Total and spectral emittance of cobalt surfaces conditioned by evaporating some cobalt from surface at high temperature in vacuo

05 p0716 A69-16447

Cobalt-tungsten solid solutions thermodynamic properties calculated by Borelius method using phase diagram

07 p1165 A69-18941

Lattice defects in annealed and plastically deformed cobalt, showing increase with increasing martensite transformations

12 p2113 A69-26042

Volumetric and allotropic changes during heating in electrolytic cobalt multiple phase transformations

12 p2114 A69-26455

Cobalt and Co alloys oxidation, sulfidation and hot corrosion data, summarizing characteristics of films and scales formed

20 p3562 A69-37751

Nb supersaturated solid solution in Co precipitation mechanism analyzed by X rays and electron microscope, noting diffusive scattering effects

21 p3750 A69-39788

Bright cobalt plating electrolytic processes, examining brighteners and formation mechanism of deposits

22 p3959 A69-41265

COBALT ALLOYS

Cobalt base alloy for construction in high temperature corrosive environment, discussing mechanical properties, oxidation and corrosion resistance and phase stability

01 p0095 A69-10546

Nickel-cobalt fcc alloys rolling and recrystallization textures established with filtered Aco K-alpha radiation, considering stacking fault energy effects

04 p0615 A69-14643

Structural stability of cobalt base superalloy at high temperature prolonged exposure under stress

05 p0781 A69-16448

Grain size dependence of yield, flow and fracture stresses of Fe-Co-V alloy for 77-298 K

17 p1166 A69-19264

Controlled solidification in Co-Ta-C system to develop pseudobinary eutectic mixture containing TaC crystals aligned parallel to growth direction [ONERA-TP-673]

07 p1167 A69-19339

Cobalt chromium high temperature oxidation and scale formation [ECS PAPER 413]

08 p1332 A69-20363

Cobalt chromium alloys high temperature oxidation kinetics, discussing thermographic study of oxidation rate and oxygen pressure role [ECS PAPER 413]

08 p1332 A69-20364

Self diffusion coefficients measurements for cobalt in nickel-cobalt alloys, using cobalt radioisotope 60

08 p1334 A69-20577

Monograph on precipitation hardening and mechanical properties of various heat resistant alloys with Co contents to 35 percent

08 p1334 A69-20763

Substructural changes during fatigue due to stacking fault energy variations related to morphology of fracture surface in solid solution Ni-Co alloys

10 p1795 A69-23060

Cobalt base high chromium carbide strengthened superalloy, evaluating physical and mechanical properties

11 p1901 A69-24259

Gadolinium-cobalt system investigation by X ray diffraction thermoanalysis and metallography for inter-

metallic compounds, noting structure transformation and homogeneity 11 p1903 A69-24574

Electrical resistivity and magnetization saturation in cobalt alloys during formation of modulated structures 11 p1904 A69-24707

Book on hard alloy properties, discussing bending and compression properties, tensile, torsional and impact strength, wear resistance and thermal shock resistance 12 p2111 A69-25902

Precipitated phase composition and structure of Co-Ti solid solution during aging 12 p2112 A69-26037

Phase composition and Co content effect in WC-Co and WC-TiC-Co alloys on magnetic properties behavior 13 p2275 A69-27343

Room temperature WC-Co compacts oxidation resistance in air noting increase with preliminary sintering temperature 13 p2275 A69-27345

Stress and plastic deformation influence on allotropic transformation of cobalt-nickel single crystals studied by X ray diffraction 13 p2279 A69-27761

Co base high temperature binary alloys microstructure, investigating diffusion coefficients, stacking faults, vacancies, etc 14 p2465 A69-29890

High temperature properties relationship to microstructure of Co base superalloys and strengthening methods 14 p2465 A69-29891

Processing characteristics of wrought Co base alloys, discussing thermomechanical treatment effects, yield strength, ductility, etc 14 p2456 A69-29892

Casting variables of Co base superalloys, discussing variables effects on ultimate mechanical properties, investment casting, etc 14 p2456 A69-29893

Crystal structures of intermediate phases in La-Co and Nd-Co systems by powder X ray diffraction technique 15 p2667 A69-30087

Dispersoids and temperature effect on coercive force of 19 Co base and 10 Fe plus 27 percent Co base 15 p2669 A69-30689

Co content influence on temperature stress in WC-Co cermets using one exposure and two exposure X ray diffraction 16 p2802 A69-32340

Orientation relationships between phases in Co-TaC pseudobinary eutectic alloy, discussing Co fcc-hcp allotropic transformation [ONERA-TP-714] 17 p2988 A69-33395

Temperature and pressure effect on cobalt base alloy cavitation in liquid sodium, using vibratory apparatus and loss rate contour diagram 18 p3157 A69-35184

WC-Co alloys structural changes under loads near yield limit, noting formation of slip bands 18 p3158 A69-35261

Co base alloy for gas turbines, discussing microstructure, creep, oxidation resistance and hot corrosion properties 18 p3158 A69-35421

Directionally solidified Co-Nb eutectic alloys mechanical properties and magnetic performance for elevated temperature space applications 19 p3341 A69-35542

Cobalt and Co alloys oxidation, sulfidation and hot corrosion data, summarizing characteristics of films and scales formed 20 p3562 A69-37751

Commercial Co base superalloys oxidation and hot corrosion resistance under controlled environments, examining role of various alloying elements [ASM PAPER D8-21.5] 20 p3564 A69-38134

WC-Co alloys microstructure and microproperties, considering individual phase behavior and grain-solid solution interactions 20 p3564 A69-38246

Plastic deformation and dislocation damping of cemented WC-Co alloys studied by compressive testing at room temperature 21 p3744 A69-38736

Burner rig hot corrosion test facility for evaluating Ni-Co alloys used in gas turbine engines operating in marine environment 22 p3928 A69-40673

Al-Ni-Co alloys precipitation mechanism effect on magnetic properties, including heat treatment and Ti alloying effects 23 p4175 A69-41298

Metallurgy and properties of quenched and tempered high strength Ni-Co steels, discussing welding and aerospace applications 23 p4175 A69-41299

Ternary diffusion at high temperature in Fe-Co-Ni alloy system covering entire ternary phase diagram, including computed interdiffusion coefficients 23 p4176 A69-41505

Cobalt-base superalloys analysis for temperature stability, corrosion resistance, creep, fatigue and strength in aircraft structures and parts applications 24 p4334 A69-43427

COBALT COMPOUNDS
NT COHENITE

Synthetic ferrites and sulfides of Ni and Co sulfated in presence of molten sodium pyrosulfate and sodium bisulfate 16 p2747 A69-32567

Catalytic activity enhancement of complex Co/III/ compounds on standing explained by hydrated Co/II/ ions appearance 17 p2988 A69-33433

Semiconducting properties of lanthanum-cobalt oxide measured, using Seebeck coefficient for analysis as function of resistivity 21 p3780 A69-38612

COBALT ISOTOPES

Co 2 chloride aqueous and alcoholic solutions by X ray diffraction to find potential ligands relative coordinating abilities 20 p3484 A69-37496

COBALT OXIDES

Thin foil preparation technique for transmission electron microscopy and selected etch pitting technique for CoO single crystals 12 p2112 A69-25944

CoO complex defects indicated by negative enthalpy of formation, considering isobaric electrical conductivity measurements at various temperatures and oxygen pressures 14 p2508 A69-29925

COBALT 60

Self diffusion coefficients measurements for cobalt in nickel-cobalt alloys, using cobalt radioisotope 60 08 p1334 A69-20577

Co 60 kernel heat source for multikilowatt space power supplies, stressing design for maximum safety 23 p4187 A69-42257

COCHLEA

Analog signal processing concepts based on models simulating mechanical function of ear cochlea 17 p2911 A69-34092

Dependence of cochlear microphonics and summating potential on endocochlear potential 23 p4085 A69-41574

COCKPIT SIMULATORS

Motion cues simulation system with seat of six differentially inflatable sections, discussing DYNASEAT 17 p2947 A69-34007

Manned aircraft air to air combat capabilities evaluated by simulator using two cockpits, digital computer and collimated displays [AIAA PAPER 68-253] 20 p3510 A69-37159

COCKPITS

Aircraft traffic control with cockpit self sufficiency for accurate and reliable navigation capability, discussing radar vector navigation and communication 07 p1177 A69-19210

Personal cooling in inadequately air conditioned cockpits, considering dry air, air ventilated suits and liquid circulated tubes near skin [AGARDOGRAPH-111] 08 p1267 A69-20684

Navigation and guidance systems for low altitude aircraft flight safety noting position determination, cockpit environment and fail-safe operation 17 p3002 A69-34080

Flight compartment and cabin layout of Skyvan 3 designed as freighter with passenger capability 17 p2903 A69-34195

Computerized crewstation geometry evaluation and design optimization using 23-pin-joint man-model [AIAA PAPER 69-977] 22 p3892 A69-40357

Cockpit displays for transport aircraft noting digital techniques and flight control-navigation integration 22 p3946 A69-40486

Cockpit noise intensity during normal cruising operations at various altitudes for 15 different single engine general aviation light aircraft 23 p4102 A69-41676

Commercial aircraft peak cockpit noise level during cruise and high speed descent, discussing damage risk criteria and inter-pilot speech interference 23 p4102 A69-41682

Noise levels in twin engine general aviation light aircraft cockpits, discussing protection against possible hearing damage 24 p4252 A69-42902

F-5 cockpit fogging during low flights and dive bombing in South Vietnam attributed to hot humid weather, recommending cockpit temperature control and pilot diet 24 p4277 A69-43376

CODERS

Microwave carrier graycode analog to digital converter capable of 1200 megabits per second 01 p0044 A69-10627

Time coding system for recording balloon measurements on magnetic tape 05 p0762 A69-15825

Phantom disk encoder for arc second digital position transducers 05 p0766 A69-16748

Serial BCD binary coder design, using Karnaugh diagrams to minimize synchronous and asynchronous counter stages 09 p1467 A69-22579

PDM command coder meeting NASA Tone Digital Command Standard for German central ground station 16 p2755 A69-31859

Flexible format adaptive telemetry encoder design, discussing system design and implementation technique with modular units 23 p4119 A69-41748

CODING
NT DECODING
NT ERROR CORRECTING DEVICES
NT REDUNDANCY ENCODING
NT SIGNAL ENCODING

Book on probabilistic information theory-discrete and memoryless models covering information transmission, digitalized sources, generating functions, decoding error, systematic codes and sequential decoding 01 p0037 A69-11030

Book on communication systems covering signal design, video signals, communication satellites and threshold decoding techniques 03 p0383 A69-12867

Synchronization in coded communication systems, considering phase lock loop and square wave correlation function 03 p0383 A69-12871

Error correcting coding on DCSP satellite channels, discussing single access communication through wide-band SHF repeaters in synchronous earth orbit 03 p0387 A69-13177

Clutter rejection using coded burst waveform for airborne early warning /AEW/ and airborne attack type radars 03 p0388 A69-13185

Channel identification coding for data compressors, deriving optimum code word length for bit compression ratio and overflow identification scheme 03 p0391 A69-13219

Shift and add property for majority combined binary composite codes with linear maximal sequences 03 p0391 A69-13229

TAF /time and frequency/ code written in FORTRAN language for computing steady state, frequency and time response from nonlinear simultaneous differential equations 04 p0565 A69-15341

Incidental modulation effect on accuracy, signal loss and sensitivity of pseudorandom code systems 06 p0890 A69-17824

Mariner 1969 high rate telemetry system portions pertinent to combinatorial mathematicians, discussing coding and encoding 06 p0890 A69-17862

Block coding for transmitting across noisy binary symmetric channel accompanied by noiseless delayless feedback channel 06 p0891 A69-17864

Upper and lower bounds for feedback decoding and definite decoding minimum distances of binary convolutional codes 06 p0904 A69-17865

Topological codes and simplicial subclass information rates, minimum weights and word length 06 p0948 A69-17866

Majority logic decoding of Euclidean or projective geometry codes in two steps 06 p0891 A69-17867

Sequences with small correlation functions as error correcting codes in word separation, synchronization and pulse compression systems

06 p0948 A69-17868

Fourier transform algorithm introduction leading to image coding technique with image transformed by Hadamard matrix operator

07 p1078 A69-18859

Optimum linear feedback code for additive noise systems with average power constraint on transmitter to increase channel capacity

07 p1085 A69-19181

Digital telemetry from spacecraft, discussing on-board processing, data compression, coding, sequence detection and receivers

08 p1276 A69-20592

Minimum bandwidth of M real equal energy signals with specified code or correlation matrix, noting optimum waveforms

09 p1452 A69-21313

Soviet literature on coding theory and applications, stressing contributions to nonSoviet specialists

09 p1460 A69-21393

Coding schemes for memoryless Gaussian channels with feedback considering error probabilities

09 p1454 A69-21794

Error correction of digital data with cyclic codes and probability function set extended to Bose-Chaudhuri-Hocquenghem codes and P super M codes

10 p1655 A69-23529

Tandem interleaved cyclic codes for digital HF communication with improved error rate at reduced decay time

10 p1655 A69-23530

Cosmic ray observation data automatic recording, presenting coding system for reading into computer

13 p3227 A69-27609

Algebraic and sequential coding-decoding method for data communication rates up to capacity of discrete memoryless channel, discussing error probabilities

13 p2219 A69-27664

Lower bound determination of automaton memory elements, describing coding procedure and algorithm for machine states

13 p2239 A69-28554

Coding of morphological evolution in time of auroral displays as generalization of existing JUGG code

13 p2256 A69-28655

Largest scalar product of class and identification codes in diagnostic problems, discussing recognition

14 p2417 A69-29144

Optimum time for telemetry data transmission by system using feedback combined with error correcting codes

14 p2412 A69-29428

Color coding effect on alphabetic filing names, comparing first and second letter codes and no color code condition

17 p2916 A69-34004

Encoding and decoding in IR tracking system, analyzing chopping rotating FM reticle pattern

19 p3268 A69-36058

Binary increment and residual class notation techniques for onboard spacecraft computer arithmetic

20 p3499 A69-37378

Programming aspects of computer uses in civil engineering, stressing engineer-coder communication via flow diagrams

22 p3903 A69-40138

Coding aspects of computers use in civil engineering, discussing language selection, program partitioning and storage use

22 p3903 A69-40139

Digital telemetry link coding as English language analogy, developing block code scheme combining bit, word and block error detection and correction methods

23 p4119 A69-41745

Digital transition tracking symbol synchronizer for low SNR coded telemetry systems, discussing phase locked loop analysis and phase detector simulation by Monte Carlo method

23 p4130 A69-42513

Pioneer 9 deep space probe with telemetry link operated in coded mode with sequential decoding, discussing ground and flight test data

23 p4131 A69-42522

Tree codes for memoryless time discrete sources with bounded fidelity criterion

24 p4284 A69-42720

Pseudorandom code development and possibilities for radar applications, considering signal processing, antenna requirements, radar signal phase modulation, etc

24 p4281 A69-42741

COEFFICIENT OF FRICTION

Frictional and heat transfer characteristics of laminar flow in porous tubes, using numerical solutions to flow and energy equations

01 p0177 A69-11408

Vacuum effect on steel friction, noting changes in residual gases and heat transfer conditions

03 p0434 A69-13915

Coefficient of friction variations for MHD flow of electrically conducting liquid across porous medium under transverse magnetic field

03 p0480 A69-14112

Incompressible turbulent boundary layer properties with arbitrary pressure gradient calculated by integral method resulting in single equation for skin friction coefficient

[ASME PAPER 68-WA/FE-22]

05 p0749 A69-16098

Runways slipperiness and grooving, discussing influence of wetness, tire form and speed on friction coefficient

10 p1674 A69-23707

Wear and friction properties of nylon and polyethylene sliding over unlubricated steel, considering adhesion theory

11 p1892 A69-25021

Velocity distributions and skin friction coefficients in turbulent boundary layers over flat plate with injection or suction through porous wall

11 p1871 A69-25027

Skin friction coefficient relation to pressure distribution in turbulent flow and development of momentum thickness along flow

11 p1819 A69-25385

Friction coefficients for turbulent flow through smooth pipes, considering average and friction velocity relations, fluid velocity measurements and flow Reynolds number

11 p1874 A69-25429

Friction coefficient dependence on interfacial potential between solids

12 p2129 A69-25982

Load carrying capacity and friction calculated for pivoted pad journal bearings for machine design use

[ASME PAPER 68-LUBS-27]

13 p2266 A69-27275

Friction wear of solid bodies based on microscopic contact system model, deriving particle distribution law from physicochemical analysis

13 p2268 A69-28051

Incompressible viscous fluid steady motion caused by rotating ellipsoid, determining drag moments for circular disk and sphere

14 p2432 A69-29627

Solid lubricant films friction and wear life determined under various conditions of contact, temperature, load and atmosphere

[ASLE PREPRINT 69AM 6C-1]

15 p2619 A69-30471

Hot pressed molybdenum disulfide-nickel composite film friction and wear tests in air and face seal configuration

[ASLE FICFS PREPRINT 23]

15 p2620 A69-30491

Contact conformity effects on spinning torque and friction coefficient in angular contact ball bearings from lubricated and unlubricated tests

[ASME PAPER 68-LUB-10]

15 p2628 A69-30901

Injected gas flow nonisothermicity and transversity effects on friction, heat transfer and flow parameters at cylindrical tube inlet

15 p2592 A69-30986

Drag and friction coefficients for laminar pulsating incompressible fluid flow in circular tubes obtained from Navier-Stokes equation

15 p2592 A69-30988

Turbulent boundary layer laminarization in conical nozzle flow, measuring velocity profiles and friction coefficient

[JPL-TR-32-1407]

16 p2732 A69-31894

Radial clearance influence on self lubricating porous bearing friction coefficient and oil losses as function of operation duration

16 p2794 A69-32067

Soviet book on rocket aerodynamics covering configurations, lifting, stabilizing and control surfaces, friction and heat transfer characteristics

17 p2889 A69-32829

Skin friction drag formula for tapered and delta wings with allowance for coefficient variation and Reynolds number dependence on chord length

17 p2896 A69-34037

Micropolar liquid basic flows, considering case with coupling constant relating microstructure to macroscopic flow greater than viscosity coefficient

18 p3121 A69-34786

Friction coefficient increase caused by metal surface textures anisotropic effect on friction force

18 p3149 A69-35151

Friction coefficient and elastic deformation magnitudes relation in polyurethane during sliding friction in various liquids/lubricants/

18 p3149 A69-35362

Geometrical model for surface contact area, noting influence of nonlimitations on friction coefficient in elastic deformation

19 p3329 A69-36494

Nylon wear curves and friction coefficients for steel-on-nylon pairs determined as function of normal load

19 p3329 A69-36495

Graphical representation of friction stresses produced on mechanical parts surface layers, using mathematical model based on Poisson ratio and friction coefficient

19 p3329 A69-36723

Wear and friction of fiber-metal Mo bodies impregnated with molybdenum disulfide, noting coating-endurance life

20 p3547 A69-36953

Blowing effect on surface friction coefficient and heat transfer in turbulent boundary layer in compressible fluid with pressure gradient

21 p3643 A69-38636

Nonlinear model including rocket rotary and forward motion inside smoothbore launcher utilizing dynamic friction coefficient

22 p4037 A69-41038

Friction characteristics during diamond honing of different steel grades, determining lubricating and cooling liquids effect on friction coefficient

22 p3958 A69-41170

Surface films effect on friction coefficient of sodium chloride and Zn single crystals under normal pressure loads, noting film thickness role

23 p4170 A69-42343

COEFFICIENTS

NT ACCOMMODATION COEFFICIENT

NT AERODYNAMIC COEFFICIENTS

NT ATTENUATION COEFFICIENTS

NT BINOMIAL COEFFICIENTS

NT COEFFICIENT OF FRICTION

NT COHERENCE COEFFICIENT

NT CORRELATION COEFFICIENTS

NT COUPLING COEFFICIENTS

NT DIFFUSION COEFFICIENT

NT DISCHARGE COEFFICIENT

NT FLOW COEFFICIENTS

NT HEAT TRANSFER COEFFICIENTS

NT INFLUENCE COEFFICIENT

NT IONIZATION COEFFICIENTS

NT NOZZLE THRUST COEFFICIENTS

NT ONSAGER PHENOMENOLOGICAL COEFFICIENT

NT RECOMBINATION COEFFICIENT

NT REGRESSION COEFFICIENTS

NT SCATTERING COEFFICIENTS

NT STRUCTURAL INFLUENCE COEFFICIENTS

NT WIGNER COEFFICIENT

Characteristic coefficients in method of integral relations calculated by Lagrange interpolation, noting application to numerical solution of differential equations

06 p0857 A69-17102

Transfer coefficients for inhomogeneous systems characterized by constant density, mean free path and activation energy of carriers at each point

07 p1193 A69-19024

Partition coefficients between natural melts and plagioclase phenocrysts determined for rare earth elements and barium by mass spectrometry

08 p1310 A69-20944

Transport coefficient density expansions obtained from time correlation functions in moderately dense gas with short range repulsive intermolecular forces

14 p2540 A69-29469

Differential coefficients applied to Izsak-Borchers ballistic trajectory and errors produced by perturbations of initial vectors, applying results to data capsule recovery

16 p2857 A69-32156

Inequalities for coefficients of univalent functions

22 p3975 A69-40453

Parabolic equation and equation systems with relaxed assumptions involving coefficients of first derivatives and unknown function, demonstrating Pogorzelski fundamental solutions validity

23 p4180 A69-41408

Hydrodynamic equations derived from Boltzmann equation, obtaining molecular expressions for transport coefficients
23 p4151 A69-41513

Fourier series solution of finite range Wiener Hopf equation, determining coefficients from Wiener Hopf procedure
23 p4181 A69-41608

Coefficient quantization in digital continuous time process controllers, applying results to nominal transfer function approximation
24 p4292 A69-43283

COENZYMES

Cellular localization of acetyl-coenzyme A synthetase in yeast, noting enzyme distribution during aerobic growth on glucose
04 p0554 A69-15333

COERCIVITY

Isochronic annealing effect on coercive force of Mo Permalloy samples bombarded with neutrons in nuclear reactor
05 p0783 A69-16815

Dispersoids and temperature effect on coercive force of 19 Co base and 10 Fe plus 27 percent Co base
15 p2669 A69-30689

COGNITION

Models for cognitive behavior and psychomotor behavior for maintenance tasks
12 p2025 A69-27086

COHENITE

Morphologies and mechanical properties for identification of phosphides /schreibersite/ and carbides /cohenite/ in iron meteorites, noting nucleation and growth
19 p3417 A69-36133

COHERENCE

Electric field correlation to magnetic fields in quantum theory of coherence, deriving dynamical equations governing space-time development of correlation matrix
20 p3575 A69-37304

COHERENCE COEFFICIENT

Spatial coherence of He-Ne laser radiation diffused by turbid medium calculated by using diffraction and interference measurements
22 p3964 A69-40798

Plane electromagnetic waves coherence properties, considering linear and arbitrary degree of polarization
24 p4350 A69-42982

COHERENT ACOUSTIC RADIATION

Ultrasonic pulse velocity and attenuation measurement in presence of noise, using coherent detection and signal averaging
14 p2449 A69-29564

COHERENT ELECTROMAGNETIC RADIATION

Coherent frequencies method for irregular component of satellite signal phase lead due to ionospheric inhomogeneities between satellite and ground station
06 p0890 A69-17799

Pulsar model based on rapidly rotating neutron star with radiating attached plasma, discussing test of radiation mechanism by means of coherence of emission
06 p1012 A69-18226

Passive electromagnetic circuit elements for laser light control such as circulators, isolators and phase shifters, discussing coherent light and polarization
09 p1518 A69-22127

Coherence theory of electromagnetic field from classical /wave/ or quantum /particle/ standpoint, stressing information theory
11 p1915 A69-24455

Relativistic coherence theory of black body radiation in transparent medium, deriving expressions for second order correlation tensors by phenomenological quantum electrodynamics
11 p1920 A69-25563

Electron density profiles in outer ionosphere and integral of electron density measured with coherent radio waves emitted from Electron satellite
14 p2438 A69-29106

Double aperture problem with partially coherent incident field, noting application to microwave antenna-reflector combination
17 p2929 A69-33877

Natural and man-made radio noise measurements, including formula for calculating signal strength of coherent interference
23 p4126 A69-42217

COHERENT LIGHT

Ultrasonic holography applications in nondestructive testing, describing conversion of ultrasonic field into optical field
01 p0078 A69-10132

Transmission of coherent ruby laser radiation through traveling wave amplifier noting spatial field structure changes
02 p0255 A69-11608

Resonance light pulse propagation in one dimensional medium containing n and m quantum emitters located in Fabry-Perot resonator
03 p0437 A69-13039

Generation and amplification of ultrashort optical pulses [IEEE PAPER H-12]
05 p0774 A69-16317

Electric and magnetic fields of narrow coherent polarized light beam in free space, noting longitudinal field components due to beam narrowness
05 p0777 A69-16789

Fluctuation phenomena in electromagnetic field in optical spectral region and coherence characteristics of optical fields, analyzing quantum noise
06 p0937 A69-18011

Laser applications to situations requiring highly bunched high power density light beams
06 p0938 A69-18012

Statistical properties of intensity fluctuations of light fields consisting of incoherent Gaussian component heterodyned with single frequency coherent beam
07 p1182 A69-19416

High quality holography with illumination possessing low degree of spatial coherence by means of interferometric arrangement with amplitude division
08 p1312 A69-20081

Ultrashort optical pulses of coherent light, discussing propagation in inhomogeneously broadened medium of two level systems
08 p1324 A69-20083

Helium-neon gas laser as coherent light source for holograms of vaporizing fuel films and for Michelson interferometer
08 p1327 A69-20874

Coherent light fluxes detection, noting correlation characteristics of output signals of photomultiplier illuminated by multimode He-Ne laser
09 p1515 A69-21438

He-Ne laser light coherence distortion by atmospheric turbulence
11 p1894 A69-24452

Coherent optical target recognition through randomly turbulent medium for imaging system offsetting image degradation due to turbulence
11 p1894 A69-24470

Transmission of coherent ruby laser radiation through traveling wave amplifier noting spatial field structure changes
11 p1895 A69-24715

Polarization effects of scattered coherent light on laser imagery, determining surface roughness and angle of incidence effects photographically on basis of Fung theory
11 p1896 A69-24849

Statistical properties of electromagnetic field diffracted by illuminated plane aperture studied in Fresnel zone on basis of partial coherence theory
11 p1836 A69-24978

Single and cladged glass fibers radii and refractive indices measurements on basis of laser light scattering
11 p1918 A69-25044

Coherence phenomena for gas laser transitions coupled by common level, noting coherent superposition
11 p1898 A69-25045

Space-time characteristics of coherent light giant pulse development in laser with instantaneous Q switching, deriving equations to describe linear and nonlinear phases
12 p2110 A69-26909

Diffraction images of coherently illuminated objects in presence of aberrations stressing images of edges, disks and bars
13 p2297 A69-27451

Irradiance distribution in far field diffraction patterns of partially coherent light diffracted by annular aperture, using Fourier transformation relationship of Schell
14 p2460 A69-29640

Image enhancement by coherent optical system without spatial filter, noting improved defocused transparencies
14 p2450 A69-29641

Laser-nonlinear crystal dynamical interactions, studying saturation and coherence properties of second harmonic wave generated inside laser cavity
15 p2632 A69-30026

Interferometer for measuring electric fields spatial correlation function at camera aperture, describing laser light coherence measurements after propagation through turbulent atmosphere
15 p2653 A69-31164

Holographic recording of temporal coherence pattern of wave train from pulsed radiation source, investigating single mode ruby laser
17 p2973 A69-33114

Laser beam propagation through turbulent medium, investigating statistical distribution of phase shift fluctuations
17 p2976 A69-33857

Statistical model for coherent functions obtained from laser equation, showing amplitude and frequency coupling of radiation fluctuations
18 p3152 A69-34820

Coherent light scattering from rough surface, studying effects of target tilt, translation and rotation on speckle patterns produced
18 p3174 A69-35281

Stimulated reflection experiment for correlation between coherent photon beams from independent lasers
18 p3153 A69-35292

Optical imaging with partially coherent nonthermal light, discussing correlation function propagation, transfer functions, spatial Fourier analysis, weak visibility and matrix form
19 p3372 A69-35907

Optical imaging with partially coherent nonthermal light, discussing reconstruction of object from image and similarity between object and image, including detection
19 p3372 A69-35908

Coherent emission from injection electron-hole plasma in indium antimonide without magnetic field, noting roles of crystal thickness and pinch effects
19 p3387 A69-36532

Information processing with coherent light, discussing holographic interferometry, contour mapping, three dimensional pictures, holographic coding, etc
21 p3722 A69-38797

Focal plane observation of granulation phenomena on scattering surface illuminated by coherent light from gas laser
21 p3741 A69-39575

Spatial coherence of He-Ne laser beam studied in Young interference experiment, noting multimode light percentage attributed to weak transverse modes
22 p3960 A69-40018

Coherent light focusing by helicoidal guide- extension to particle focusing, discussing analogy between index distribution for classical optics and potential distribution for electronic optics
22 p3981 A69-40475

Quadratically nonlinear filtering systems analysis and synthesis by linear methods, discussing application to partially coherent transilluminated optical systems
24 p4350 A69-42971

Coherent light propagation through turbulent atmosphere observed by applying He-Ne lasers to simultaneous measurements of scintillation effects over homogeneous optical paths
24 p4344 A69-43114

COHERENT RADAR

Spectrum distortion of intermediate frequency signal in coherent Doppler navigation radar
01 p0034 A69-11013

Coherent moving target indicator radar receiver behavior as function of input situation, using improvement factor
04 p0556 A69-14338

Hologram form of forward scatter bistatic radar or sonar
07 p1078 A69-18866

Atmospheric extinction coefficient and backscattering function determined by laser radar using differential equation
07 p1126 A69-18966

Angel type radar echoes from coherent pulses in centimeter and decimeter wavelengths characterized by daytime convection and presence of inversion/ isothermal layers
09 p1491 A69-22706

Clutter residues of coherent MTI radar receiver, emphasizing IF stages saturation nonlinearity affecting cancelling circuits performance
13 p2220 A69-27941

SNR changes loss factor effect during passage through MTI coherent receiver followed by video integrator
16 p2753 A69-32438

Angel type radar echoes from coherent pulses in centimeter and decimeter wavelengths characterized by daytime convection and presence of inversion/ isothermal layers
16 p2753 A69-32486

- Doppler radar based on triple pulse transmission at coherent frequencies, comparing echo pulses for target cancellation and extraction
21 p3672 A69-38436
- Coherent pulsed radars using pseudorandom modulation, explaining pulse position modulation and radar receiving equipment
24 p4282 A69-42743
- ### COHERENT RADIATION
- Noise emitted by gas filled cavity perturbed by strong coherent signal computed by Nyquist equation
02 p0211 A69-12448
- Radiation intensity from system of monoenergetic relativistic electrons in plasma, discussing maser effect in coherent synchrotron radiation
03 p0500 A69-13407
- Coherent emission in epitaxial structures with heterojunctions in AlAs-GaAs system
03 p0489 A69-13896
- Black body radiation coherence properties characterization by stochastic Gaussian scalar potential correlation function
05 p0795 A69-16819
- Helium-neon laser radiation of given spectral compositions, noting relation between spatial coherence and controlled number of frequencies
07 p1148 A69-18803
- Organic lasers, discussing coherent laser light emission induced from organic dye molecules
07 p1149 A69-18908
- Numerical determination of Doppler effect and reduced Doppler frequency difference for two coherent radio waves emitted from earth satellite
07 p1087 A69-19610
- Optical systems with quasi-monochromatic partially coherent illumination, discussing energy distribution computation program
08 p1353 A69-21096
- Coherent emission from rare earth ions in electro-optic crystals, noting oscillations and electric field modulation occurrence
09 p1514 A69-21339
- Temporal and spatial coherence effects of optical fields and relationship to multipole coherence effect
09 p1540 A69-22083
- Perturbation solution for propagation of fourth order coherence function in random medium extended to larger field fluctuations, deriving integrodifferential equation
10 p1724 A69-23042
- Coherent detection spectroscopy with laser oscillator, emphasizing high resolution and applications in astronomical spectroscopy and IR
10 p1696 A69-23684
- Gas lasers coherence properties and availability for holography, discussing continuous power output of He-Nc, Ar and Kr ion lasers
11 p1895 A69-24680
- Coherent emission in epitaxial structures with heterojunctions in AlAs-GaAs system
11 p1939 A69-25697
- Coherent radio emission mechanism in quasars and supernova remnants, discussing magnetic effects
12 p2168 A69-27050
- Ideal quantum receiver to detect coherent narrow band optical signal in presence of thermal background radiation, noting error probability
14 p2414 A69-29502
- Coherence-polarization in remote sensing by microwave and laser means, analyzing scattering functions of rough surfaces
14 p2448 A69-29532
- Optical communications experiments for quantitative data at 6328 Å on system fading due to scintillation and atmospheric turbulence effects on coherent propagation at 10.6 micron
16 p2748 A69-31564
- Partially coherent radiation scattering determined using Heisenberg operator, noting radiation absorption dependence on interfrequency band coherence
16 p2797 A69-32050
- Coherent radiation generation using gas lasers, analyzing interaction between EM radiation and matter
19 p3335 A69-36067
- Coherent radiation detection using laser optical sine waves, considering detection by heterodyning, laser preamplifier and parametric amplification
19 p3335 A69-36070
- Magneto-optical constants and conduction band parameters of GaAs by coherent radiation at high temperatures, measuring Faraday rotation
19 p3386 A69-36522

- Coherent recombinational radiation of semiconductors excited by electron beam
19 p3387 A69-36539
- Ionospheric data of local and integral electron concentration obtained by measuring phase shift of satellite emitted coherent radio waves
20 p3519 A69-37022
- Coherent radiation short pulses from mode locked laser permitting schlieren photography of plasma growth
21 p3736 A69-38795
- Helium-neon laser radiation of given spectral compositions, noting relation between spatial coherence and controlled number of frequencies
21 p3736 A69-38948
- Coherent light emission by molecules excited by laser pulses having duration comparable to active medium polarization relaxation time
21 p3737 A69-38999
- Changes in CdS crystals spontaneous and coherent emissions caused by electron beam radiation damage, determining intensity and spectral composition dependence
21 p3780 A69-39047
- Scalar waves propagation in bounded randomly fluctuating media, emphasizing interface effects on coherent wave motion
21 p3675 A69-39283
- Partially coherent PSK-modulated binary detection, deriving noisy phase reference by narrow band tracking filter, analyzing bit output error as function of SNR
23 p4122 A69-41772
- Amplified radiation of laser used for coherent optical pumping in two level low pressure gas laser
24 p4327 A69-43067

COHERENT SCATTERING

- Plasma diagnostics using scattering of laser electromagnetic radiation by plasma density function, discussing plasma species collision effect on line profiles
07 p1131 A69-18485
- Stimulated Compton scattering for laser action, noting voltage tunability and gain at far IR wavelengths [IEEE PAPER 5-9]
07 p1154 A69-19081
- Electron concentration in polar ionosphere measured by coherent scattering method
12 p2071 A69-26703
- Light intensity during coherent scattering based on complex refraction index of medium, noting scattering by clouds and diffraction by semitransparent hole
15 p2635 A69-31108
- Coherent light scattering from rough surface, studying effects of target tilt, translation and rotation on speckle patterns produced
18 p3174 A69-35281

COHERENT SOUND
U SOUND WAVESCOHERENT SOURCES
U RADIATION SOURCES

COHESION

- Physicotechnical problems of weightlessness, considering cohesive forces, surface tension and mechanical behavior of fluids and weightlessness simulation techniques
07 p1070 A69-18568
- Short cylinder of perfectly plastic Coulomb yield conditions compressed between rigid plates, discussing cylinder-plate interface frictions, angles of internal friction and cohesion
08 p1410 A69-19890
- Plane contact problems in elasticity theory allowing for cohesive forces solved by integral and differential equations
15 p2706 A69-30578
- Annealing effect on transition zone cohesion strength in two layer steel-titanium sheet, investigating role of TiC formation
18 p3159 A69-35450
- Two point tensor function symmetries of nonlocal cohesive finite elastic materials determined from atomic lattice theory, obtaining Green function
19 p3444 A69-36798

COHOMOLOGY
U HOMOLOGYCOIN AIRCRAFT
U OV-10 AIRCRAFT

COINCIDENCE CIRCUITS

- Tunnel diode subnanosecond coincidence circuit stability and time resolution, noting influence of polarization and input-pulse currents
05 p0735 A69-16743

- Polarity coincidence correlation method due to random processes state characterization applied to man machine systems
12 p2022 A69-25931

- Stable particles heavier than nucleons in extensive cosmic ray showers detected by delayed coincidences relative to shower electron photon component
13 p2331 A69-28402
- Demultiplexing of high speed multichannel optical pulse code transmission systems, based on coincidence detection using locally generated reference pulses
19 p3279 A69-36764

COINING

- Stress coining methods for improving aircraft structure fatigue life by controlling material yielding inside holes and materials surrounding holes and slots [AIAA PAPER 69-761]
19 p3433 A69-35659

COKE AIRCRAFT
U AN-24 AIRCRAFT

COLD ACCLIMATIZATION

- Brown adipose tissue providing internal heating jacket and metabolic heater overlying systemic vasculature, noting cold survival role
23 p4091 A69-42013

COLD CATHODE TUBES

NT PHOTOMULTIPLIER TUBES
NT PHOTOTUBES

- Glass pleats and cold cathodes in laser discharging tube, discussing angular displacements
03 p0435 A69-12981
- Display techniques, discussing cold cathode luminous gas discharge /plasmas/ tube, electroluminescence and cathode ray tube
04 p0600 A69-15029

- Microwave tube development, discussing cold cathodes, ferrite and semiconductor integration into tubes, tube failure physics, etc
11 p1847 A69-24745

COLD DRAWING

- Cold drawing workability of Nb, Mo and Ta using dies with lubrication for metal sheets
03 p0452 A69-14124
- Mechanical anisotropy of polyethylene terephthalate and relation to molecular structure and cold drawing
05 p0785 A69-16489

COLD FLOW TESTS

- Cold subsonic coaxial jets observed for relationship between noise output and flow characteristics, showing effect of relative annular and central jet velocities
20 p3513 A69-37063

COLD GAS

- Cold neutral H cloud existence in Galaxy from measurements of 21 cm line spectra
22 p4025 A69-40644

COLD NEUTRONS

- Whirling liquid hydrogen layer thermal and hydrodynamical conditions, noting application to cold neutrons source in high flux beam reactor
05 p0849 A69-16818

COLD PLASMAS

- RF characteristics of electrodes immersed in magnetoplasma, discussing potential distribution around point charge and RF probe measurement of plasma parameters
01 p0029 A69-10550
- Transverse plasma velocity component effect on boundary layer structure between cold plasma and confined magnetic field
02 p0235 A69-11424
- Nonlinear large amplitude electrostatic and electromagnetic oscillations in cold plasma having one dimensional spatial variations and fixed neutralized ion background
02 p0288 A69-12171
- Shear instability in unbounded collisionless cold plasma in external uniform magnetic field in current free case, noting dispersion relations
02 p0289 A69-12177
- Dispersion relations of axisymmetric and dipolar surface modes propagation along inhomogeneous plasma columns on dispersion relations
02 p0289 A69-12242
- Born approximation for calculating low temperature plasma transport properties from quantum mechanical scattering cross sections on Debye potential
02 p0291 A69-12486
- Ionization and recombination in low temperature plasmas, noting fast electron distribution function deviation from Maxwellian form and calculation for Cs plasma
02 p0292 A69-12559

Diffraction of cylindrical waves at half plane in cold anisotropic plasma, using Fresnel integrals
02 p0293 A69-12842

Existence and stability of periodic waves in cold collisionless plasma in magnetic field
03 p0474 A69-13143

Nonlinear interaction of steady state circularly polarized electromagnetic wave with cold plasma in constant longitudinal magnetic field
03 p0476 A69-13381

Synchrotron radiation excitation in system of relativistic monoenergetic electrons rotating in cold magnetoactive plasma
03 p0476 A69-13383

Cold plasma motion caused by electromagnetic wave pressure propagating along uniform magnetic field
03 p0477 A69-13413

Probe and spectral techniques compared for investigation of low voltage arc of cesium plasma thermionic converter
03 p0478 A69-13836

Kinetic theory to determine wave increments propagating across magnetic field in system of relativistic electrons in cold plasma
04 p0635 A69-14555

Input admittance of cylindrical dipole antenna immersed in cold isotropic lossless plasma medium and insulated by ion sheath or unit permittivity dielectric
04 p0580 A69-15490

Laser light scattering by plasma using theory of ionospheric scattering of radar signals, determining scattered spectrum
05 p0798 A69-15586

Low temperature plasma electric arc source operation describing current voltage characteristics and potential distribution
05 p0802 A69-15902

Plasma instabilities produced by beam plasma discharge in mirror magnetic trap
05 p0803 A69-16212

Explorer 35 measurements of low energy plasma in lunar orbit made by planar multigrad sensor programmed as retarding potential analyzer
05 p0825 A69-16278

Wave dispersion analysis for amplification in cold plasma filled cylindrical waveguide penetrated by electron beam of same radius
05 p0736 A69-16790

Oscillating electric dipole in cold plasma with ideal conductivity along lines of force of external magnetic field
06 p0921 A69-17743

Trapped mode wave propagation for cold uniform magnetoplasma cylinder in free space, studying dipole modes and one-wave approximation
06 p0967 A69-17756

Power flow in cyclotron and plasma modes propagating in waveguide filled with cold collisionless axially magnetized plasma
06 p0897 A69-17760

Electrostatic waves in inhomogeneous plasma in finite magnetic field, noting dispersion relation for cold plasma and stabilization of instability
06 p0967 A69-17761

Resonant frequencies and fields in circular cylindrical microwave cavity containing cold uniform magnetoplasma dielectric
06 p0968 A69-17763

Dispersion equation for dipolar surface waves in uniform cold lossless infinitely long magnetoplasma column in free space, obtaining numerical and asymptotic solutions
06 p0968 A69-17774

Transport properties of partially ionized low temperature plasmas, considering viscosity, electrical and heat conductivity of argon and nitrogen at high temperatures
06 p0969 A69-17907

Thickness of resistivity controlled hydromagnetic shock wave, using classical one fluid equations and generalized Ohm law
06 p0970 A69-17956

Magnetoplasma waves in semiconductors, discussing cold plasma dispersion, helicons, carrier densities, lattice dielectric constant and acoustic domain propagation
07 p1197 A69-18465

Comparative models of magnetoplasma, discussing wave propagation in cold plasma, warm plasma and microscopic model
07 p1190 A69-18919

Radiation resistance of short dipole immersed in cold magnetoionic medium, using polarized wave modes
07 p1107 A69-19226

Collisionless shock waves in high beta plasmas and in cold plasmas
07 p1194 A69-19366

Cold plasma stability during traversing by electron beams in presence of external magnetic field, obtaining dispersion relations for longitudinal and transverse modes
07 p1195 A69-19465

Antenna impedances in cold plasma with perpendicular static magnetic field
08 p1281 A69-20029

Nonlinear behavior of two stream instability between cold electron and ion streams
08 p1367 A69-20800

Power radiated by oscillating magnetic and electric dipoles in cold streaming plasma calculated by Poynting vector method
09 p1544 A69-21329

Cylindrical electromagnetic waves diffraction at impedance wedge in anisotropic cold plasma, using Maxwell equation and double contour integral
09 p1545 A69-21505

Total radiation of dense low temperature argon arc discharge plasma measured by bolometer, showing increase with arc current and pressure
09 p1547 A69-21595

Cold plasma magnetoacoustic resonance, showing nonlinear exciting magnetic field dependence on polarity and energy
09 p1548 A69-21668

Nonthermal microwave emission from cold cathode PIG discharge plasma, noting wide spectrum of electron cyclotron frequency harmonics
09 p1549 A69-22018

Nonequilibrium distribution functions for neutral atoms excited states in optically thin low temperature singly ionized plasma containing ions, electrons and neutrals
10 p1731 A69-23437

Incoherent synchrotron radiation by relativistic electrons gyrating in cold magnetoactive plasma rederived, correcting errors
10 p1741 A69-23858

Ionization instability in low temperature magnetized plasma, analyzing electron concentration perturbation caused by Joule heating during electron-ion collisions
10 p1741 A69-23962

Radial distribution profiles of charge carriers in low temperature gas discharge plasma accounted for in terms of volume recombination
11 p1925 A69-24330

Transient signal propagation through cold inhomogeneous plasma with electron density decreasing exponentially in direction of propagation
11 p1836 A69-24990

Synchrotron radiation amplification by monoenergetic electron stream helically gyrating in static magnetic field of cold plasma, discussing amplification rate frequency dependence
11 p1931 A69-25361

Electron-ion recombination coefficient for triple collisions in dense low temperature plasma, deriving finite electron Fokker-Planck equation
11 p1933 A69-25541

Resonance radiation output effect on electron distribution according to energies and concentration in low temperature plasma, solving relevant kinetic equations
11 p1935 A69-25757

Soviet book on plasma thermionic energy conversion covering operation modes, transport processes, current-voltage characteristics, density, temperature, electric field distribution
12 p2017 A69-26850

Boundary layer between cold plasma and vacuum magnetic field, considering transverse velocity component perpendicular to field
12 p2139 A69-26944

Inhomogeneous and anisotropic cold plasma filled plane capacitor resonance in steady magnetic field applied to plasma diagnostics, using calculus of variations
13 p2304 A69-27240

Near electrode layer calculation in low temperature plasma, solving kinetic ion equation for quasi-neutral and Poisson equation for space charge regions
13 p2312 A69-28117

Collective scattering of light from ruby laser by cold dense deuterium plasma produced by electrical discharge, deducing density and electron temperature
13 p2273 A69-28366

Monochromatic plane waves propagation in anisotropic homogeneous cold plasmas, treating dispersion surface, reflection, refraction and waveguide applications
14 p2492 A69-29399

Ionospheric models for motion of slightly ionized homogeneous cold plasma influenced by electrostatic field and neutral particles flow, considering geomagnetic effects
14 p2499 A69-29863

Ionospheric inhomogeneity model for motion of infinite elliptical cylinder of cold plasma in neutral particle flow and ambient electrostatic and magnetostatic fields
14 p2500 A69-29864

Ionization and recombination in low temperature plasmas, noting fast electron distribution function deviation from Maxwellian form and calculation for Cs plasma
15 p2658 A69-30256

Energy absorption by cold nonuniform plasma from externally driven electric field, noting relation between plasma and driving frequencies
15 p2661 A69-30922

Low density cold plasma effect on stability of cylindrical layer of charged particles against electrostatic perturbations in uniform magnetic field
16 p2816 A69-31635

Macroscopic quasi-linear theory of HF radiation in cold electron-proton plasma allowing direct use of plasma and Maxwell equations
16 p2819 A69-31684

Weak nonlinear hydromagnetic waves in cold collisionless plasma, using nonlinear perturbation method
17 p3010 A69-32866

Trapped modes in cold magnetoplasma slabs and rods in free space analyzed by Maxwell equation, assuming DC magnetic field and homogeneous electrons distribution
17 p2926 A69-33850

Whistlers propagation in cold plasma in uniform magnetic field, considering amplitude dispersion effect
18 p3179 A69-34437

Cold plasma approximation of whistler excitation of lower hybrid resonance at wake of body moving through ionosphere, comparing results with Alouette satellite observations
20 p3519 A69-37025

Plasma instabilities produced by beam plasma discharge in mirror magnetic trap
20 p3581 A69-37784

Transient phenomena in bounded dispersive medium emphasizing surface wave propagation, discussing space and surface waves excitation in bounded cold magnetoplasma
20 p3494 A69-37842

Nonlinear oscillations of inhomogeneous cold plasma in hybrid resonance region
21 p3672 A69-38588

Nonlinear interaction between extraordinary waves propagating perpendicular to static magnetic field in cold homogeneous magnetoplasma
23 p4195 A69-41538

Thermal radiation diffraction of dielectric cylinder /cold plasma model/ containing N plus one layers with arbitrary temperatures and permittivities
23 p4123 A69-42028

Plasma resonances driven into nonlinear regime, using models of cold plasma driven by wave source and unmagnetized Vlasov plasma by two grid source
23 p4197 A69-42418

Hydromagnetic radiation characteristics of electric and magnetic dipoles in homogeneous anisotropic cold plasma, obtaining field components and wave propagation modes
24 p4307 A69-42905

Whistlers nonlinear interaction during cold magnetoplasma propagation, considering energy exchanges between waves
24 p4309 A69-43174

COLD PRESSING

Be billets fabrication from powders by cold hydrostatic pressing and pressureless sintering, noting hardness, density and grain size dependence on temperature
14 p2465 A69-29681

COLD ROLLING

Elastic anisotropy and polycrystalline orientations in cold rolled titanium sheets investigated by Fourier series method, discussing Young modulus values
01 p0094 A69-10431

Cold rolling and annealing effects on tensile strength, heat resistance and ductility of sintered Al powder sheets
03 p0452 A69-14121

Alloying elements and cold rolling deformation effects on formation of texture in Ti alloys, noting inhomogeneity
04 p0617 A69-15077

Subsequent yield surfaces in cross shaped brass plates determined after prestraining or cold rolling
04 p0682 A69-15302

- Beta Ti alloy initial state effect on mechanical properties and dislocation structure after cold deformation by rolling
14 p2463 A69-29313
- Depth dependent variations in texture in Nb due to inhomogeneous plastic deformation during cold rolling
21 p3744 A69-38737

COLD STRENGTH

- Low temperature predeformation and disorientation of mosaic blocks to strengthen aluminum
20 p3562 A69-37819

COLD TOLERANCE

- Life raft thermal protection against exposure of aircrews to cold, noting chemically fueled heaters and IR reflective liners
06 p0883 A69-17841
- Human body cold tolerance and relation to BMR seasonal variation
06 p0876 A69-18024
- Norepinephrine, dinitrophenol and dicumaryl effect on brown adipose tissue of cold exposed rats
19 p3258 A69-36294
- Primary muscle spindle afferents from gastrocnemius muscle of cat before, during and after cold shivering, utilizing ramp stretches of same muscle
23 p4096 A69-42091

COLD TRAPS

- Anisotropic plasma cyclotron instability in magnetic trap with cold ion background and isotropic Maxwellian velocity distribution
02 p0292 A69-12554
- Anisotropic plasma cyclotron instability in magnetic trap with cold ion background and isotropic Maxwellian velocity distribution
15 p2658 A69-30251

COLD WALLS

U WALLS

COLD WEATHER

- Subjective feeling of dampness correlation with relative humidity of air at zero and below zero C temperatures
23 p4109 A69-41870
- Temperature dependence of action potential, isometric tension development and relaxation rate of mammalian myocardium at low temperature, considering Ca ions role
23 p4092 A69-42060

COLD WORKING

NT EXPLOSIVE FORMING

- Aging and cold work hardening effect on deformability of aluminum-magnesium-silicon-copper alloy
02 p0254 A69-12677
- Tangential and normal stress distribution in deformed metals, discussing work hardening of metals and cold working without softening effect
03 p0435 A69-14118
- Cold working considered for decreasing fatigue crack propagation rate in thin duraluminum sheets with various plastic deformations
04 p0681 A69-15170
- Dislocation distributions in cold worked fcc, bcc and hcp metals, discussing dislocation structures in deformed single crystals and work hardening theories
05 p0778 A69-15754
- Roll planishing and thermal treatments effects on gas tungsten arc welded Ti-6Al-4V alloy on residual stresses, tensile, formability and fracture toughness properties
08 p1319 A69-19966
- Cold worked high purity Mo wire recovery after plastic deformation at room temperature, considering electrical resistivity decrease as function of annealing temperature
15 p2636 A69-30082
- Prestrained material plastic behavior experiments and deformation lines of influence analysis, noting importance in cold working
17 p3067 A69-34146
- Martensite transformation, C content and work hardening relations in stainless steels studied for magnetic detection of embrittlement during deformation
18 p3138 A69-35117
- Nickel solid solutions strengthening under cold deformation studied by X ray, noting screw and edge dislocations role
18 p3157 A69-35246
- Low temperature predeformation and disorientation of mosaic blocks to strengthen aluminum
20 p3562 A69-37819
- Cold working and aging effects on mechanical properties of TiAl-V including creep and temperature effects
[DGLR-69-002] 23 p4177 A69-42163

- Stored energy of cold work and electrical resistivity of Ag-Mg solid solution alloys measured as functions of strain, Mg concentration and initial state of order
24 p4332 A69-43029

COLLAGENS

- Corneal stroma collagen fibrils and ground substance refractive indices, discussing corneal transparency and clouding
22 p3884 A69-40886

COLLAPSE

- Collapse pressure of flush cylindrical nozzle axisymmetrically intersecting conical pressure vessel for rigid plastic shells
15 p2704 A69-30289
- Fatigue collapse probability of fail-safe structure compared to safety factor design
22 p4045 A69-40820

COLLECTORS

U ACCUMULATORS

COLLEGES

U UNIVERSITIES

COLLIMATION

- Collimation of row and column steered phased arrays
04 p0570 A69-14304
- Single two dimensional coherent matched filter optical processor for simultaneous synthetic radar antenna beam sharpening and pulse compression
04 p0562 A69-15475
- Collimator lens design for transforming axisymmetric primary field into prescribed secondary field
06 p0895 A69-17454
- Population inversion distribution and wave processes in optical amplifier, showing beam transformation of constant section and dependence on crystal characteristics
11 p1893 A69-24447
- Collimator lens design for transforming axisymmetric primary field into prescribed secondary field
20 p3508 A69-37939

COLLIMATORS

- Reflection measurements in IR, investigating effect of angle of incidence and collimated beam on reflection spectra
01 p0120 A69-10891
- Modulation collimators determining angular sizes and celestial positions of X ray sources Sco X-1 and Taurus XR-1
10 p1678 A69-23326
- Celestial X ray source positions from rotating modulation collimator, predicting performance of collimator
10 p1722 A69-23328
- Photodetector requirements for autocollimators with beam splitters, considering spectral characteristics, photoresponse, time constant, positioning, etc
14 p2447 A69-29326
- Mechanical collimator using random aperture arrays for celestial observation at extreme UV and X rays
19 p3313 A69-36489

COLLINEARITY

- Superposition of discrete number of collinear amplitude modulated harmonic oscillations
02 p0281 A69-12252
- Optimal control stationkeeping for maintaining space probe stability around collinear points in three body problem
[AIAA PAPER 69-906] 21 p3807 A69-39338

COLLISION AVOIDANCE

- Aircraft flight safety, discussing structural and aerodynamic concepts, maintenance and operations
03 p0365 A69-12886
- Listen-in feature, allowing general aviation aircraft equipment to receive airborne SSR reply signals, provides air to air proximity warning
03 p0464 A69-13247
- Project Icarus for reduction of threat of asteroid collision with earth by deflection or disintegration, noting guidance, control and communications for rocket
04 p0652 A69-14564
- Industry airborne collision avoidance systems /CAS/ development program, discussing cooperative devices in aircraft
05 p0790 A69-16725
- Pilot warning indicators to equip all aircraft at low cost, discussing Doppler system
05 p0790 A69-16726
- Monograph on mathematical model for aircraft separation in air traffic safety control, analyzing aircraft motions and collision avoidance
08 p1347 A69-20712

- Air traffic lateral separation assurance over North Atlantic for increased routes capacity without safety reduction
08 p1349 A69-21200

- Aircraft electronic proximity warning devices applications, discussing compatibility in ATA collision avoidance system
[SAE PAPER 690340] 11 p1914 A69-24496

- Airborne collision avoidance system /CAS/ performance and operational requirements
11 p1914 A69-25430

- Collision avoidance system for air traffic, discussing false signal discrimination via electronic measurement of light pulse duration from aircraft Xenon discharge beacon lamp
12 p2129 A69-26772

- Aircraft collision avoidance systems development, current status and future prospects, discussing basic requirements, criteria and prototypes
13 p2295 A69-27330

- AH-56A helicopter manual and automatic terrain following and manual terrain avoidance systems, discussing nap-of-earth flight, design and simulation
[AHS PAPER 311] 17 p3002 A69-33544

- Situation/command system displays and maneuvers for collision avoidance systems, discussing pilot preferences
17 p3002 A69-34096

- Low cost pilot proximity warning instrument, discussing design influences of Xe strobe lights, atmospheric radiation transmission characteristics and detection considerations
17 p2917 A69-34103

- Bird hazard in aviation, discussing aircraft/bird collisions in France, protective measures and airport environment control against nesting and breeding
18 p3090 A69-34695

- Time/frequency technology using time-ordered reporting digital data for air traffic control to avoid airborne collision
[AIAA PAPER 69-795] 19 p3367 A69-35635

- Airborne collision avoidance system based on time-frequency techniques for use within ground based control systems, showing air/ground synchronization and collision geometry
19 p3371 A69-36735

- Air traffic safety enhanced through flight crew awareness of hazards, clear air turbulence detection and avoidance, collision avoidance, etc
22 p3868 A69-41151

COLLISION PARAMETERS

- Elastic scattering of electrons from argon atoms in argon air plasmas by shock tube microwave reflection method, measuring power reflection coefficient
[AIAA PAPER 68-138] 04 p0632 A69-14701
- Rarefied flow past sphere, analyzing collisionless flowfield structure and development as density increases
04 p0542 A69-14731
- Partially ionized hydrogen transport coefficients, using expressions containing collision integrals for charged particles
04 p0637 A69-15051
- Moment equations for general gas mixture from Boltzmann-like equations, evaluating collision integrals
04 p0633 A69-15436
- Elastic bodies collisions in presence of thermoelastic effects, investigating local inertial and thermoelastic forces effect on compression region shape
05 p0841 A69-16207
- Ion-molecule collisions of Ar-Co and N-No pairs, discussing charge exchange reaction rates and spiraling nature
05 p0797 A69-16428
- Kinetic model construction of maximum number of Boltzmann collision integral properties
05 p0797 A69-16679
- Parametric or impact parameter treatment for describing ion-atom collision at low or high impact velocities, reexamining approximate treatments
05 p0797 A69-16697
- Kinetic model describing collisions in nonequilibrium multicomponent plasma, studying pair collisions effect on stability of plasma-beam system
07 p1189 A69-18539
- Diffusion coefficients of H atoms in mixtures of He and Ar with hydrogen by catalytic sink technique, discussing rigid sphere collision diameters
07 p1185 A69-19300
- Rotational inelastic transitions in atom-diatom collisions, discussing restricted distorted-wave approximation, transition probabilities, impact parameters, inelastic and glory quenching, etc
07 p1185 A69-19302

Bounds on scattering lengths, phase shifts and other scattering parameters determining cross sections, noting variational bounds for zero incident energy
07 p1186 A69-19657

Partially ionized plasma oscillations in crossed magnetic and electric fields, noting role of LF particle collisions
08 p1370 A69-21079

Temperature stability of slightly ionized gas for arbitrary collision cross sections, discussing electron temperature variation as function of electric field strength
09 p1551 A69-22039

Local potential method extended to study plasma oscillations inhomogeneous kinetic equations in presence of linear or nonlinear collision operators
11 p1925 A69-24316

Direct Coulomb interaction matrix elements between hydrogen atoms in ground states calculated, presenting interaction potential
11 p1921 A69-24416

Collision integral kernels of kinetic equation for single component gas density matrix derived by Bogoliubov-Gubov method
14 p2458 A69-29169

Gain and loss collision integrals in Boltzmann equation for rigid sphere gas evaluated for distribution expressed as linear combination of Maxwellians
14 p2431 A69-29578

Rare gases total excitation cross sections absolute values measured in collision chamber, noting energy distribution of exciting electron beam, fine structure, etc
14 p2493 A69-29693

Linearized kinetic equation for perturbed electron distribution function, detailing plasma oscillations along magnetic field by Landau collision term
16 p2818 A69-31674

Kinetic model describing collisions in nonequilibrium multicomponent plasma, studying pair collisions effect on stability of plasma-beam system
21 p3776 A69-38691

Impact pressures during two body collisions, correlating pressure with particle speed
21 p3836 A69-38943

COLLISION RATES

Krook kinetic relaxation equation generalized to include approximate kinetic equations with velocity independent collision frequency
02 p0234 A69-12582

Electromagnetic oscillations in ionized plasma, assuming higher oscillation frequency than collision frequency
02 p0292 A69-12643

Frictional forces and collision frequencies for ions moving in neutral gases
03 p0421 A69-13328

Effective collision frequency deduced from ratio of microwave conductivity to electron density in PIG discharge plasma
05 p0804 A69-16442

Maximum number of binary collisions for three particles with zero range forces in relativistic rescattering singularities studies
08 p1353 A69-19788

Plasma electron density and collision frequency determination, using CW maser interferometer
08 p1359 A69-19987

Collisional excitation and ionization rates comparison in statistical equilibrium model atmosphere calculations
08 p1385 A69-20065

Voltage dependence of mobility limited electron current density in gas filled diode for collision frequency proportional to electron speed
09 p1462 A69-21326

D region electron concentrations and collision frequencies obtained from high power wave interactions experiment, presenting average winter collision frequency model
09 p1489 A69-21702

Electron density and collision frequency of MHD plasma determined directly by measuring phase shift and attenuation of propagating laser microwave signal
10 p1731 A69-23436

Molecular reaction rates and ion/electron vertical profile and concentrations in equatorial ionosphere, applying computer simulation to numerical solution of continuity equations
10 p1688 A69-23929

Electron flux parameters determination from ionograms and reflected signal amplitudes between 120-130 km, considering electron collision frequencies
10 p1688 A69-23931

Asymptotic solution for Fokker-Planck equation at low collision frequency, studying electron-ion collisions effect on universal instability in inhomogeneous plasma
11 p1930 A69-25358

Plasma turbulence effect on magnetosonic wave attenuation, noting increased electron and ion collision frequency and appearance of anomalous resistance
16 p2820 A69-31794

Electronic collision frequency measurement at F layer peak near ground sunrise time
16 p2779 A69-32197

Faraday effect and permittivity of hydrogen plasma measured simultaneously, determining electron density and collision frequency
17 p2919 A69-33394

Lower ionospheric electron concentration and collision frequency measurements by Nike-Apache rockets, suggesting geomagnetic anomaly in D region
18 p3127 A69-34798

Ionospheric electron density and collision frequency profiles examined for changes during December 1967 to January 1968 stratospheric warming
21 p3714 A69-38556

Ionospheric nondeviative radio wave absorption, noting roles of collisional and working frequencies and solar zenith angle
23 p4127 A69-42425

Ionospheric heating and velocity dependence of collision cross sections on transversely propagated equatorial hydromagnetic waves, discussing ordinary and extraordinary modes
23 p4161 A69-42437

Thermal nonequilibrium state and effective collision frequency between protons and electrons in solar wind plasma, explaining abnormal dissipation
24 p4368 A69-43187

COLLISION WARNING DEVICES

U WARNING SYSTEMS

COLLISIONLESS PLASMAS

Absorption of linearly polarized light in reflecting surface layer of collisionless plasma, calculating layer lifetime for reflection of light
01 p0127 A69-10283

Nonlinear hydromagnetic solitary wave propagation at angle to magnetic field in fully ionized quasi-neutral collisionless warm plasma, noting isotropic pressure effect
01 p0127 A69-10336

One dimensional Vlasov plasma nonlinear response to external electric field varying in space and time
01 p0133 A69-11214

Shear instability in unbounded collisionless cold plasma in external uniform magnetic field in current free case, noting dispersion relations
02 p0289 A69-12177

Collisionless plasma heating by hydromagnetic waves in solar wind
02 p0309 A69-12714

Green tensor for collisionless plasma, emphasizing relations between outgoing and ingoing electric fields
02 p0293 A69-12745

Existence and stability of periodic waves in cold collisionless plasma in magnetic field
03 p0474 A69-13143

Magnetosonic wave propagation across magnetic field in warm collisionless Maxwellian multicomponent plasma studied for small electron cyclotron and ion cyclotron radii
03 p0479 A69-14020

Fluctuations in multipole confined plasmas explained by solving general integral equation, yielding hydromagnetic and frequency modes
05 p0804 A69-16385

Solar wind model for electrons and collisionless ions temperatures and anisotropies
06 p0986 A69-16983

Cross field energy transfer in collisionless plasma across earth magnetospheric boundary, using computer and one dimensional sheet model simulation [ISAS-429]
06 p0916 A69-17023

Electromagnetic wave transmission and reflection at boundary of relativistic collisionless plasma, using Laplace transformation
06 p0968 A69-17783

Mixture Mach number defined for collisionless plasma flow about solid body by extending cold-ion theory [AIAA PAPER 69-78]
06 p0971 A69-18128

Wave propagation and instabilities in rotating anisotropic collisionless plasma, analyzing plane and cylindrical perturbations
07 p1195 A69-19438

Landau damping of long wavelength ion acoustic waves in collision-free one dimensional plasma with gravity field
08 p1359 A69-19983

Collisionless shock waves in rarefied plasma, discussing dispersion effect and oscillatory shock wave structure
08 p1303 A69-19996

Viscous stress tensor for collisionless plasma with anisotropic pressure in magnetic field
08 p1365 A69-20522

Quasi-linear theory of hydromagnetic waves in non-relativistic collisionless plasma, noting resonant diffusion effect on plasma heating mode
08 p1367 A69-20797

Microwave scattering from longitudinal plasma waves propagating in collisionless plasma column
08 p1276 A69-20798

Ion Landau damping and finite Larmor radius effects on dispersion relation of Kelvin-Helmholtz instability due to shear in ion fluid velocity
08 p1367 A69-20799

Fluid equations for collisionless plasma including finite ion Larmor radius and finite beta effects
08 p1368 A69-20802

Particle-wave interactions in weakly turbulent collisionless plasma, discussing ensemble average distribution function, diffusion, nonlinear Landau damping and nonlinear instabilities
08 p1368 A69-20803

Heating of collisionless plasma in magnetic mirror by random electric field transverse to magnetic field
08 p1368 A69-20805

Double adiabatic MHD fluid equations for electrons and ions with pressure gradients for collisionless plasma in magnetic field
08 p1369 A69-20815

Particle free path estimates for axisymmetric high specific impulse plasma accelerators, discussing collisionless plasma simulated by computer [AIAA PAPER 69-278]
09 p1563 A69-21233

Inhomogeneous collisionless plasma drift-oscillation stability in magnetic field augmented by E wave HF field
09 p1546 A69-21564

Collisionless plasma heating by damping hydromagnetic waves applied to solar wind qualitative model, discussing magnetoacoustic wave energy
09 p1607 A69-22426

Dynamics, stability and approach to equilibrium of bounded one dimensional collisionless plasma representing minimum energy states with nonlinear Vlasov equation solutions
11 p1924 A69-24305

Analog simulation of cylinder wave potential for hypersonic motion in collisionless plasma
11 p1926 A69-24756

Unstable ion sound wave propagation across magnetic field in collisionless shock waves, noting drift instability
11 p1930 A69-25273

Steady linearized aligned fields flow of collisionless plasma past slender body, noting effect of tensor conductivity
11 p1930 A69-25278

Steady equilibrium collisionless plasma in oscillating electromagnetic field, describing formalism for linear relation between perturbation and charges and currents induced in plasma
12 p2135 A69-26284

Nonlinear periodic wave propagation at angle to magnetic field in collisionless plasma studied by two fluid plasma equations
13 p2304 A69-27297

Magnetic curvature effect on collisionless plasma density gradient drift instabilities, covering mean ion Larmor radius and Alfvén modes
13 p2305 A69-27375

Variational method for time invariant states of collisionless plasma in oscillating electromagnetic field
13 p2314 A69-28365

I-V characteristics of electron emitting satellite in ionosphere, analyzing spherical Langmuir probe in collisionless plasma in magnetic field
14 p2511 A69-28956

Potential distribution between point in interelectrode gap and thermionic converter cathode in collisionless mode under transverse magnetic field
14 p2401 A69-29235

High speed streak cameras applicability to low density theta pinch studies, describing image converters design, operation and block diagrams
14 p2496 A69-29787

Collisionless Ce and K plasmas measurements to determine steady state parameters and LF oscillations, noting noise relationship to drift instability
14 p2499 A69-29849

Collisionless plasma slab drift mode stabilization at uniform temperature by oscillating electromagnetic field
14 p2499 A69-29851

Detached MHD shock wave formation in front of magnetic field acting as piston moving collisionless plasma, discussing time dependence, Alfvén speed and plasma parameters
14 p2502 A69-29958

Self consistent solutions for collisionless plasma penetration across magnetic field, showing electrons ability to accompany ions across field
15 p2661 A69-30923

Transverse instabilities in collisionless electron plasma in absence of permanent magnetic field with spheroidal velocity distribution, noting application to shock theory
16 p2817 A69-31645

Quasi-linear theory of waves in collisionless plasma in absence of external fields, relating wave energy growth and decay to plasma stability
16 p2817 A69-31646

Analytic expressions for motion of collisionless plasma created with isotropic velocities within uniform magnetic field, assuming equal electron and ion masses
16 p2818 A69-31673

Electromagnetic echo generation in collisionless spatially homogeneous plasma dependence on velocity distribution and magnetic interaction
16 p2818 A69-31677

One dimensional free expansion of collisionless plasma tested as function of thermal equilibrium and confinement, using Vlasov equations and computer
16 p2819 A69-31685

Collisionless drift plasma wave instability growth rate calculation noting destabilization from resonant electrons
16 p2820 A69-31691

Weak nonlinear hydromagnetic waves in cold collisionless plasma, using nonlinear perturbation method
17 p3010 A69-32866

Collisionless cylindrical Langmuir probe response in turbulent plasma for mean and statistical properties [AIAA PAPER 69-698] 17 p3010 A69-33438

Collision free earth shock wave gross and fine structure deduced fromOGO 5 plasma diagnostics [AIAA PAPER 69-676] 17 p2961 A69-33452

Structure of solitary waves propagating in collisionless plasma perpendicular to magnetic field, considering soliton wavefronts charge separation and relativistic velocity
17 p2922 A69-33696

Collisionless shock wave front turbulence in diluted plasma, including thickness, electron and ion component measurements
17 p3012 A69-33818

Collisionless shock wave generation and structure in zeta and theta pinches
17 p3013 A69-33819

Energy dissipation in collisionless shock waves generated in plasmas with 1-500 trillion/cm electron density by theta pinch, measuring axial ionic energy spectrum
17 p3013 A69-33820

Collisionless shock wave structure in plasmas, noting plasma and shock wave generation mechanisms
17 p3013 A69-33822

Collisionless plasma heating mechanisms from current layer turbulence in theta pinch experiment and shock wave front structure as function of initial magnetic field
17 p3013 A69-33824

Collisionless shock waves in plasma and ion and electron turbulent heating in high voltage theta pinches, noting magnetic disturbance
17 p3013 A69-33825

Anomalous absorption of electromagnetic wave in collisionless dense cylindrical plasma beam in circular waveguide, noting electric field strength for energy transfer
18 p3101 A69-34621

Damping of plane sinusoidal wave in cold collisionless plasma, studying supercritical amplitude oscillatory process
18 p3180 A69-34703

Shock wave propagation through collisionless magnetized plasma, using gun driven, laser and cesium plasma flow methods
19 p3379 A69-35759

Plasma ion and electron concentration perturbations in wake of body moving at high velocity in collisionless plasma under steady magnetic field
20 p3459 A69-37659

Thermal effects of resonant coupling hydromagnetic oscillations in inhomogeneous finite-beta plasmas, obtaining equations for coupling modes between Alfvén and magnetosonic waves
21 p3776 A69-38710

Antenna noise spectrum in collisionless isotropic plasma, considering plasma fluctuation theory and reciprocity theorem
21 p3683 A69-39284

Successive approximations convergence analyzed in solving supersonic collisionless plasma flow past magnetic dipole
23 p4156 A69-41853

Boundary layer separating collisionless plasma from one dimensional magnetic field for anisotropic particle velocity distribution functions, preserving charge neutrality in boundary layer
23 p4197 A69-42415

Guiding center Vlasov equation derived dielectric tensor of collisionless plasma, obtaining dispersion relation of Alfvén waves in warm plasma
23 p4197 A69-42416

Two stream instabilities, considering uniform infinite collisionless plasma with stream of electrons passing through ion-electron medium
24 p4355 A69-42685

Theoretical models for collisionless plasma shock waves in terms of nonlinear, magnetosonic, constant profile waves, turbulent- and electrostatic-shock structures, etc
24 p4355 A69-42694

Steady state interaction between collisionless plasma flow and immersed stationary magnetized or unmagnetized objects by inserting Cs ion accelerator into plasma wind tunnel
24 p4359 A69-43646

Light scattering from ruby laser beam passing through collisionless shock produced by H plasma compression measured by photomultiplier
24 p4360 A69-43748

COLLISIONS

NT ATOMIC COLLISIONS
NT COULOMB COLLISIONS
NT ENCOUNTERS
NT INELASTIC COLLISIONS
NT IONIC COLLISIONS
NT METEORITE COLLISIONS
NT MOLECULAR COLLISIONS
NT PARTICLE COLLISIONS

Aircraft in-flight collision, discussing difficulties and procedures of medical board of inquiry
05 p0715 A69-16628

COLLOCATION

Convergence of Multhopp collocation method for numerical solution of linear singular integrodifferential equation, noting use in airfoil, propeller and elasticity theory
02 p0271 A69-12056

Collocation method applied to solving contact thermoelasticity problem for short thick walled hollow cylinder attached to thin elastic shell in axisymmetric temperature field
18 p3217 A69-34595

Nonlinear free motion of conservative oscillator with one degree of freedom calculated by collocation method
19 p3438 A69-36308

COLLOIDAL GENERATORS

Charged colloids generation by electrostatic spraying for thruster concept, subjecting metal capillary needles to AC voltage [AIAA PAPER 69-495] 16 p2846 A69-32773

COLLOIDAL PROPELLANTS

Specific acoustic admittance of solid propellant burning surface for determining burning instability under rocket motor conditions
02 p0302 A69-11521

COLLOIDS

NT AEROSOLS
NT COLLOIDAL PROPELLANTS
NT FOG

Electropropulsion by thruster using colloidal carbon particles charged by electron bombardment to provide thrust, noting specific impulse
03 p0495 A69-13396

Variational solutions of one dimensional nonlinear Poisson-Boltzmann boundary value problems in theory of colloids and plasmas
06 p0968 A69-17784

Simulator for testing colloid microthruster, discussing spacecraft interfaces and time of flight thrust data [AIAA PAPER 69-314] 09 p1478 A69-22380

Virtual power principles applied to solving force acting on fluid consisting of colloidal suspension of polarized particles in neutral vehicle
12 p2136 A69-26404

COLOR

Stratospheric dust effect on twilight sky color, evaluating scattered radiation chromaticity for atmospheric models containing ozone
02 p0243 A69-12014

Relation between color index over lunar surface and solar rays angle of incidence, noting supplementary emission attributed to surface luminescence
03 p0506 A69-13089

Empirical relation between (B-V) color and radiation temperature by observing eclipsing variables undergoing total eclipses
03 p0469 A69-13964

Aircraft instrument lighting color effects on posture, exposure, scotopic absolute and acuity threshold and legibility for reading of instruments
03 p0380 A69-14073

Color and appearance properties of paint films and relations to amounts and properties of colorants, noting translucent plastics and metallized paint films
04 p0620 A69-14886

Photometric effects of UVB color indices ineffective in detecting double stars in Galaxy
07 p1216 A69-18854

Interstellar light absorption in Milky Way region of Cepheus analyzed by excess color technique
07 p1216 A69-18855

Relation between color index over lunar surface and solar rays angle of incidence, noting supplementary emission attributed to surface luminescence
14 p2516 A69-28771

Micrographic reagent coloring grains of Mo in relation to crystalline orientation applied to refractory metal welding and diffusion studies
14 p2505 A69-29221

Color signal light gun for aircraft control at airport towers, noting pilot tests for familiarity with signal code
17 p2914 A69-33185

Spectral reflectivity differences /color differences/ on lunar surface in visible region, indicating compositional difference origins
17 p3037 A69-33653

Color coding effect on alphabetic filing names, comparing first and second letter codes and no color code condition
17 p2916 A69-34004

Variation influence of total absorption to color excess ratio on galactic spiral structures indicating ineffective application of variable-extinction method to Q spectra
18 p3199 A69-34914

Color coded area sensitivity maps of photomultiplier tubes by multicolor display technique, noting focus electrode voltage
19 p3305 A69-35724

Wavelength dependence of stellar scintillation, discussing apparatus to detect color effect in twinkling
19 p3401 A69-35809

Colors production on electroluminescent display using phosphors impressed-frequency/emission-color relationships together with chromatic biasing
24 p4286 A69-42900

COLOR CENTERS

Ruby laser output energy degradation due to pump light absorption by color centers of ruby rod
02 p0256 A69-12358

Laser holography using colored KBr crystals subjected to hard gamma radiation as photosensitive material
04 p0598 A69-14855

Laser holography using colored KBr crystals subjected to hard gamma radiation as photosensitive material
15 p2608 A69-30247

Ruby laser output energy degradation due to pump light absorption by color centers, discussing roles of defects and impurities in center formation
16 p2795 A69-31697

Second harmonic generation in media with center of inversion following deformation by laser beam or static pressure
19 p3332 A69-35872

F center formation and X ray and photostimulated F-band luminescence in europium ion-activated potassi-

um halides as function of temperature and X ray dosage
19 p3383 A69-36164

Electron spin memory in optical pumping cycle of potassium halides F centers, measuring relaxed excited state g factors and spin resonance line widths
23 p4198 A69-42419

COLOR PHOTOGRAPHY

Aerial color photography for terrain analysis noting development of cameras, filters, high speed emulsions and processing equipment
01 p0077 A69-10023

Photoelectric photometry of Mercury, Venus, Mars, Jupiter and Saturn /1963-1965/, determining phase curves and monochromatic albedos
04 p0663 A69-15383

Color and black and white negatives effectiveness for photointerpretation, noting color imagery advantages
08 p1311 A69-19820

Color excesses in Kapteyn Selected Area 4 using photovisual /yellow/ and photographic /blue/ magnitudes from catalog data
08 p1388 A69-20241

Photogrammetric color negative prints, slides, etc, improved by scanning beam modulation
09 p1494 A69-21634

Qualitative considerations of color indices grouping for Abell-1781 cluster of galaxies, table of data and identification charts
10 p1775 A69-23204

Six color stellar photometry of 159 field stars including subdwarfs, high velocity stars and 50 Hyades stars, tabulating color data
10 p1788 A69-24122

Large scale color and color IR aerial photography evaluation to determine interpretability for improving range resource inventories
11 p1880 A69-24265

Multicolor hologram recording and reconstruction gas lasers, discussing control of ghosts in three dimensional image
11 p1882 A69-24679

Magellanic Clouds color composite photographs prepared from negatives taken in blue and IR light
12 p2152 A69-25801

Flow field over plain or complex bodies with pressure density changes, using high speed schlieren apparatus with color strip filter
12 p2088 A69-26183

Electric fields effect on flame front propagation structure and velocity, obtaining color toepelograms by high speed photography
12 p2190 A69-26192

Color photograph of group of meteor trails with red glow beneath by automatic camera from balloon at 30.6 km
12 p2157 A69-26231

Green flash photographed at sunset by aircraft at 10.6 km over Pacific, noting correspondence with visual observation
12 p2066 A69-26232

Variable comparison star identified from photoelectric observations of RR Lyrae star BR Aqr, showing light and color curves
14 p2519 A69-29139

Image quality of color disks in aerial photographs using panchromatic, color positive, color negative and false color films, measuring reflected sunlight
14 p2450 A69-29600

Color IR film improvement for high altitude remote sensor, using auxiliary minus-visual filters
15 p2609 A69-30457

Response color curves of U, B, V photometric system compatible for stellar observation, including U revision
15 p2689 A69-30562

13 color narrow band photometry of 1000 bright stars in tubular form, discussing sample points, Balmer discontinuity, absolute energy calibration, etc
17 p3038 A69-33692

Spectral reflectances of objects and vegetative backgrounds to generate color photographic technique increasing detection sensitivity and rate
18 p3133 A69-34247

Four color photometry data of late F type stars in general catalog tabulated with columns for HD and GC numbers, apparent visual magnitude, etc
18 p3195 A69-34430

Environmental studies using orbital photography, discussing color, color IR, black and white applications from Gemini and Apollo programs
18 p3132 A69-35275

Photographic film properties, discussing base material, emulsion, photochemical process, sensitometry, densitometry, granularity and color film
20 p3541 A69-37746

Schmidt camera image quality examined with spot diagrams, emphasizing methods of color confusion reduction over wide wavelength range
20 p3546 A69-38272

Comparative photointerpretation from panchromatic, color and Ektachrome IR aerial photography
22 p3944 A69-40039

Photogrammetric contours plotting from aerial color films
22 p3944 A69-40045

Cepheid variable stars distance estimated from UVB three color photoelectric photometry data
22 p4031 A69-40943

Color aerial photography - Conference, New York, June 1969
22 p3948 A69-40985

Glass filter systems for aerial color photography developed from spectral studies of sunlight, skylight and airlight in Rayleigh atmosphere
22 p3948 A69-40986

Multispectral processing of Apollo 6 earth photograph, evaluating geologic, vegetative and cultural features from red, green and blue portions of visible spectrum
22 p3941 A69-40987

Color chemistry concept producing high quality color negatives and prints in existing black and white processing systems
22 p3948 A69-40990

Photographic properties of Cibachrome silver dye bleach materials for yielding color reflection prints directly from color transparencies, discussing applications to aerial photography
22 p3949 A69-40991

Aerial color film processing systems
22 p3949 A69-40992

Color and color IR aerial photography compared for estuarine and marshland research, considering detection of turbidity, pollution, salinity, etc
22 p3942 A69-40993

Optical engineering and quality control of photogrammetric instruments for aerial color photography, discussing lenses, filters, projectors, plotters, electro-optical rectifier, etc
22 p3949 A69-40996

Multispectral color aerial photography using broadband spectral filters for detecting and identifying small environmental features of earth surface
22 p3949 A69-40997

Camera lenses and techniques for aerial color photography, discussing atmospheric influences, filters, films and exposure times
22 p3950 A69-40999

Xenon plasma continuous illumination sources design and operation for night and color aerial photography covering photogrammetric resource surveys, ground traffic, flight paths, etc
22 p3950 A69-41000

COLOR TELEVISION

Laser display technology, discussing experimental systems, light sources, modulation and scanning
03 p0431 A69-13850

Laser color TV projection-display system using moving mirrors and dual polarization scanner
07 p1137 A69-19740

Color TV system for Earth Resources Observation Satellite /EROS/, discussing resolution in relation to spectral separation through data simulation study [SMPTE PAPER 105-79]
12 p2077 A69-25767

Apollo 10 field sequential color TV system, describing camera modifications, systems design and equipment compatibility problems
18 p3101 A69-34810

Effective color TV transmission via satellite using PCM/PSK modulation, noting dependence on available equipment, bandwidth, desired error rate and SNR
23 p4130 A69-42520

Communication satellites european development, discussing economic and technological problems, stressing color TV and SHF/FM transmission, compared to conventional ground station transmission
24 p4393 A69-43133

COLOR VISION

Tinted ophthalmic media effect on detection and recognition of red signal lights in daylight, noting allowable coloration for aviation use
01 p0022 A69-11341

Aircraft instrument panel lighting color and intensity preference by pilots for taxiing, takeoff, cruising flight and landing
05 p0715 A69-16622

Aircraft instrument panel lighting, comparing red and white colors for general and peripheral vision
05 p0715 A69-16623

Instrumental reward experiment using concept learning paradigm with word-color compounds as stimuli
07 p1064 A69-18636

Foveal luminances for chromatic and absolute thresholds for hue identification in case of small targets
07 p1183 A69-19649

Squirrel monkey retinas spectral stimulation, determining differential color responses reaching striate and prestriate cortex
22 p3879 A69-40844

Flicker characteristics of eye color receptive systems by measuring modulation thresholds for sinusoidal flicker of color superimposed on complementary color background
22 p3880 A69-40851

Tritanope and trichromat experiments for parafoveal visual response of tritanope, measuring spectral sensitivity and absolute threshold values
22 p3882 A69-40869

Hue shift and brightness enhancement of flickering light measured as function of illuminance, wavelength and target size
22 p3882 A69-40871

Blue cone mechanism contribution to mesopic function in producing Purkinje shift with luminance decrease, measuring sensitivity by flicker technique
22 p3883 A69-40880

COLORATION

U COLOR

COLORIMETRY

Optimized formula for MacAdam color differences with modification in weighting of chromaticity and lightness, discussing Fortran IV computer programs development
04 p0564 A69-14883

Boron determination in type 1 carbonaceous chondrites by nonaqueous colorimetry, comparing results with ordinary chondrites
04 p0661 A69-15147

Cholesteric liquid crystals application to trace contamination detection, describing color response measurement
06 p0885 A69-17842

Cluster star color indices determination by measuring intensities at nodes of extrafoveal star spectra
08 p1387 A69-20122

Colorimetric studies of galaxies exhibiting red shift with increasing radial distance from center
12 p2164 A69-27025

Colorimetric method to determine small amounts of Mn in metallic Ti by potassium periodate solution
20 p3544 A69-37813

COLUMBIUM

U NIOBIUM

COLUMNS [PROCESS ENGINEERING]

Column method of measuring thermal conductivity of CO and oxygen in 350-1500 degrees K temperature range, discussing error sources and data reliability [AIAA PAPER 69-603]
17 p3073 A69-33298

COLUMNS [SUPPORTS]

NT TAPERED COLUMNS

Linearized simple beams and columns theory for anisotropic materials, discussing flexural and extensional effects coupling in tension test
07 p1171 A69-18727

Thin walled channel columns section stability analyzed in terms of overall /Euler/ and local buckling
13 p2361 A69-27440

Linear elastic columns dynamic stability under time dependent axial load, investigating almost-sure asymptotic stability
16 p2872 A69-31911

Prestressed beams, columns and plates nonlinear response, statistical behavior and transverse cracking under axial compression, describing strength and stiffness
17 p3060 A69-33568

Buckling in process of loading idealized elastoplastic Shanley column, noting continuous increase possibility
18 p3217 A69-34596

Wrinkling of pressurized cylindrical and conical fixed free membrane column under lateral load, considering membrane sheets elastic properties
22 p4045 A69-40814

Creep buckling time of simply supported column under nonuniform temperature distribution over cross sections 24 p4400 A69-43053

COMA

Two phase flow in comas of dust comets, noting acceleration of gaseous and particle phases of continuous streams and particle vaporization 06 p1000 A69-16984

COMBAT

Clinical analysis of combat and noncombat ejection experience of USAF 06 p0878 A69-16960

A-7 Corsair 2 introduction to fleet and combat operations in Southeast Asia 06 p0867 A69-17660

Characteristics, employment and tactics of Huey Cobra attack helicopter in Vietnam, discussing three primary weapon configurations 06 p0867 A69-17661

Aviation combat performance criterion by analyzing questionnaires sent to combat deployed flight surgeons, noting possible value of peer rating 09 p1447 A69-22549

Computerized air combat simulation with comparison of analog and digital approaches, noting Air to Air Combat/Fort Worth [AIAA PAPER 69-811] 19 p3289 A69-35629

Night vision requirements of Vietnam combat pilots investigated for relationship to Skyraider fatal crash during target strafing and H-34 helicopter crash landing 23 p4107 A69-41807

COMBINATIONS [MATHEMATICS]

Mariner 1969 high rate telemetry system portions pertinent to combinatorial mathematicians, discussing coding and encoding 06 p0890 A69-17862

COMBINED STRESS

Elastic/viscoplastic wave propagation in thin tubes under combined stress of tension and torsion, using viscoplastic constitutive equations 02 p0344 A69-12293

Creep behavior of nonlinear rigid polyurethane foam under combined stress and applicability of multiple integral and modified superposition principle 04 p0680 A69-15155

Elastic stability of thin circular cylindrical shell with elastic core, longitudinal and transverse ribs and initial defects under combined pressure and thermal stress 05 p0832 A69-15692

Circular bar elastoplastic behavior under combined axial force and torque in strain hardening range, noting elastic compressibility effects 06 p1023 A69-17371

Stability of cylindrical shell reinforced by circular ribs under combined action of external pressure and axial forces, using characteristic equation 07 p1238 A69-19687

Nodal lines shape in individual flats for long plates in combined shear and compression with sinusoidal edge rotations in longitudinal direction 11 p1893 A69-25137

Buckling of long flat panel in combined compression and shear with sinusoidal edge moments and support on two edges and on point supports 11 p1984 A69-25138

Tresca shear stress fatigue failure criterion and experimental data for combined bending and torsion acting out of phase 11 p1984 A69-25140

COMBUSTIBILITY

U FLAMMABILITY

COMBUSTIBLE FLOW

Combustion and flame stabilization in axisymmetric laminar or turbulent H flows, noting combustion rates and flame breakdown conditions 02 p0355 A69-12673

Compressible combustor turbulent shear flow analysis, discussing eddy diffusivity, density fluctuations, vorticity intensification and turbulent transport [WSCIPAPER 68-27] 06 p1034 A69-17793

Combustion in compressible turbulent mixing flows, discussing mixing facility, experimental results and numerical analysis [WSCIPAPER 68-28] 06 p0969 A69-17794

Viscid-inviscid equations solution, describing flows with coupled mixing, combustion and lateral pressure gradients [AIAA PAPER 69-83] 06 p1037 A69-18109

Mixing and combustion of gaseous and particle laden jets in air stream, analyzing turbulent, coaxial and jet mixing flows [AIAA PAPER 69-33] 06 p1038 A69-18146

Nonequilibrium chemical reaction effect on decay in spontaneous explosion for reactive expelled gas and inert expelling gas 07 p1119 A69-18705

Turbulent diffusion and Rayleigh-Taylor instability in inhomogeneous flow of combustion gases circulating through magnetic field 13 p2310 A69-28032

Supersonic combustible gas mixture flow around circular cone, discussing ignition by shock wave and flow modification by conical flame front 15 p2548 A69-31007

Trails arising in wake of fan type jets in transverse gas flow during uniform fuel-air mixture combustion 16 p2879 A69-32140

Model for mixing and combustion of compressible particle laden ducted flows [AIAA PAPER 69-460] 16 p2880 A69-32650

Combustion effects on mixing of axisymmetric supersonic and turbulent free jets to obtain species concentrations, pitot pressures and temperatures [AIAA PAPER 69-538] 16 p2843 A69-32705

Combustible mixtures flow past bodies, discussing equation for shock polar for exothermal discontinuities at subsonic and supersonic velocities 19 p3241 A69-36780

Hydrogen-air combustion in supersonic flow past sphere determined with allowance for chemical reactions nonequilibrium rates at high pressure and temperature 24 p4408 A69-43488

COMBUSTION

NT AFTERBURNING

NT BOUNDARY LAYER COMBUSTION

NT DEFLAGRATION

NT FUEL COMBUSTION

NT HYDROCARBON COMBUSTION

NT HYPERSONIC COMBUSTION

NT METAL COMBUSTION

NT PROPELLANT COMBUSTION

NT SOLID PROPELLANT IGNITION

NT SPONTANEOUS COMBUSTION

NT SUPERSONIC COMBUSTION

Wet oxidation process for management of organic waste products in closed ecologies of long term multimanned space missions [SAE PAPER 680714] 03 p0380 A69-13443

French collection of papers on oxidation and combustion covering reaction characteristics, thermodynamics, chain reactions, flammable gas mixtures, etc 06 p1030 A69-17412

Phenomenological characteristics of oxidation reactions and combustion, noting nature and physical state of mixtures, localization of reaction and chain mechanisms 06 p1031 A69-17413

French collection of articles on oxidation and combustion, Volume 2 06 p1032 A69-17419

Reciprocal interaction of combustion wave and field of turbulence, discussing aerodynamic principles, turbulence effect on flame propagation speed and measuring methods 06 p1032 A69-17420

Combustion in heterogeneous systems, considering diffusion flames and fine droplets dispersed into gaseous oxidizer in fog form 06 p1032 A69-17421

COMBUSTION CHAMBERS

Combustion chamber equation for liquid fuel rocket engine, considering time varying ignition lag 01 p0142 A69-10090

Adiabatic stirred reactor, discussing steady state nonlinear equations of reactant gases combustion 02 p0352 A69-12316

Flame stabilization on rectangular burners, discussing blow-off limits correlation by velocity gradients close to corners 02 p0353 A69-12320

Electrically controlled heat transfer between flat parallel flow hydrocarbon diffusion flame and walls of combustion chamber 02 p0353 A69-12324

Glass fiber reinforced plastic /GFRP/ roving end grains in rocket combustion chambers, discussing design and structural parameters 02 p0305 A69-12748

High pressure rocket engine design, considering complete combustion, propellant feed system overall efficiency and thermodynamic gain 03 p0495 A69-12888

Diathermal regenerative cooling of combustion chambers and engine nozzles with supercritical heat transfer mode 03 p0495 A69-12970

Jet engine exhaust composition and methods for reducing smoke emission through burner design changes, noting primary zone fuel and airflow pattern [SAE PAPER 680348] 03 p0495 A69-13350

Temperature drop in combustion chamber of open cycle MHD power plant due to added potassium carbonate as function of various parameters 03 p0369 A69-14162

Thermodynamic computations for combustion product temperature and flow rate as function of pressure in burner and excess air ratio 04 p0684 A69-14487

Soviet book on gas dynamics of solid fuel rocket motors covering combustion chamber flow, nozzle and thrust characteristics, pressure relaxation and channel charge 04 p0647 A69-15493

Spherical deflagration and detonation waves in diluted stoichiometric hydrogen-oxygen mixtures in hemispherical combustion chamber 06 p1034 A69-17927

Shock tunnel simulation of scramjet combustion chamber performance [AIAA PAPER 69-84] 06 p0985 A69-18165

HF instability of steady combustion process with allowance for elastic strains in chamber walls 07 p1242 A69-18993

Fuel mixing mechanism in diffusion type supersonic combustion, noting influence of combustor configuration and fuel density [AIAA PAPER 69-32] 07 p1242 A69-19266

Flame burnout of atomized hydrocarbon fuel in gas turbine combustion chambers as function of ratio of time to total burnout time 08 p1420 A69-19999

Optimal length conditions of liquid rocket combustion chambers, considering propellants, injection conditions, etc, noting graphs and differential equations solutions 08 p1376 A69-20606

Combustion in high power jet engine combustion chamber in case of continuous and intermittent liquid fuel injection 08 p1421 A69-20762

Combustion chamber design for advanced gas turbines, noting influence of fuel air mixing and air flow distribution 09 p1573 A69-22612

Performance analysis of combustion chambers with continuous air admission along flame tube, deriving governing equation from reaction kinetics 09 p1624 A69-22618

Heat release in combustion chambers of propulsion and lift engines considering various parameters of materials and design problems 09 p1625 A69-22619

Gas turbine engines smoke emission, considering smoke measurement, flame structure, carbon production, pressure effects fuel-air ratio, etc 09 p1573 A69-22622

Refractory ceramic materials use for advanced combustion chamber design, stressing brittleness effect and current fabrication techniques 09 p1531 A69-22624

Injected propellant behavior during one dimensional passage through rocket combustion gas chamber, considering Reynolds number and propellant characteristics 11 p1941 A69-24329

Combustion instability problems in rocket motors, emphasizing strongly coupled pressure oscillations in combustion chambers 11 p2003 A69-25597

Gas turbine combustion chamber design factors including combustion volume, burning zone, dilution zone, pressure drop, fuel preparation, injection and ignition, exhaust smoke, etc [IME PAPER 3] 12 p2146 A69-25789

Tubular gas turbine combustion chamber design for optimum mixing performance using flow and mixing data of cold air injection into hot gas stream [IME PAPER 15] 12 p2147 A69-25793

Fiber reinforced space vehicle combustion chambers and cryogenic fuel tanks, discussing design and elastomechanical problems 12 p2176 A69-25860

Helmholtz resonance in rocket injectors as function of frequency response of interaction between chamber pressure and dissolved gas-fuel injection flow rate 12 p2148 A69-26806

Turbine and jet engines kerosene fuels tests in small and medium size laboratory combustion chambers 13 p2240 A69-27932

Shorter combustors for high temperature jet engines of high speed aircraft, considering lifetime, shroud scoops, overheating, warpage, etc

14 p2509 A69-29433

Rocket motors with combustion chambers of variable geometry for hybrid propellants, stressing toroidal chamber

15 p2671 A69-30600

Axial gas turbine efficiency and work functions, discussing turbine using isothermal high velocity combustor

16 p2837 A69-32064

Combustion bomb testing of propellants containing fluorocarbon binder and ammonium perchlorate, noting unique ignition, combustion and extinction properties

[WSCIPAPER 69-9] 16 p2831 A69-32349

Pilot chamber initiated thermal decomposition reactor concept for monopropellant thruster, discussing thrust levels and throttling ratios

[AIAA PAPER 69-420] 16 p2841 A69-32685

Flight performance prediction for throttling bipropellant rocket engine utilizing ablative combustion chamber throat, discussing lunar module descent engine

[AIAA PAPER 69-452] 16 p2841 A69-32690

Metal oxide particle growth processes in rocket chambers and nozzles, using generalized kinetic-coagulation equation

[AIAA PAPER 69-541] 16 p2844 A69-32724

Supersonic combustion for high Mach number high altitude flight, discussing laboratory simulation for actual flight condition and chamber design

[AIAA PAPER 69-458] 16 p2880 A69-32743

Nonequilibrium inlet conditions effect on combustor performance during H and vitiated air combustion, studying ignition delays

[AIAA PAPER 69-457] 16 p2881 A69-32767

Temperature and flow measurements in jet engine combustion chamber, discussing design and calibration of gasdynamic thermometer, double thermocouple and flow probe

17 p2945 A69-32947

Continuous mode operation in hypergolic bipropellant low thrust rocket motors, discussing high temperatures reached by combustion chamber walls and cooling solutions

17 p3019 A69-33335

Fiberglass reinforced plastics internal heat shielding for isopropyl nitrate rocket combustion chamber, considering lining resistance and safety during repeated firing /Ludion motor/

17 p3019 A69-33343

Modified liquid fueled pulsating combustion chamber operating as Helmholtz cavity resonator, measuring chamber pressure as function of time

17 p3074 A69-33410

LF oscillations in simple combustion chamber using gaseous propane fuel, discussing association with progressive flame necking

18 p3230 A69-34837

High temperature combustion chamber as high velocity gas generator, noting application to MHD power generator research

18 p3184 A69-34931

Kinetic model and steepest descent method to optimize one dimensional combustor

[AIAA PAPER 68-644] 19 p3448 A69-35943

Acoustic measurements at room temperature for determining losses in rocket chamber during combustion instability, using small scale model

19 p3394 A69-35946

Low smoke emission combustors for aircraft turbine engines, discussing effects on ignition and exit temperature distribution

[AIAA PAPER 69-493] 19 p3394 A69-36299

Nonlinear periodic oscillations in liquid rocket combustion chambers for different chamber models and burning rate response formulations

19 p3449 A69-36352

Film vaporization of fuel in combustion chambers of aircraft turbines, determining concentration and velocity distributions of fuel and air

20 p3633 A69-37921

Film vaporizing gas turbine combustor design including performance tests and combustion physics

21 p3784 A69-38607

Liquid propellant rocket injectors response to HF chamber pressure oscillations using one dimensional model

21 p3786 A69-39235

Monograph on electrically heated turbulent flames in cylindrical combustion chamber, investigating temperature distribution and stability

21 p3853 A69-39707

Supersonic flow stability with energy input applied to reaction kinetics of processes in aircraft and rocket combustion chambers

24 p4248 A69-43642

Intermediate hydrazine-RFNA reaction product formed on injector nozzle and combustion chamber surfaces after fuel injection without ignition analyzed by various methods

24 p4365 A69-43669

COMBUSTION CONTROL

Hydrogen bromide, HI and HCl effects on hydrogen-air mixtures flammability, discussing flame propagation inhibition efficiency

02 p0304 A69-12315

Aged boric acid coated silica reaction vessels, showing reduced surface effects and high reproducibility in oxidation reactions

02 p0205 A69-12322

Factor analysis applied to identifying extremal plants, presenting regression analysis based on least squares techniques to calculate mathematical model coefficients

05 p0737 A69-15888

Flame inhibition with electron attachment observed using halogenated hydrocarbons

06 p1034 A69-17926

Activation energies in baffled stabilized flame deduced from reaction zone using gas chromatography

06 p1035 A69-17930

Extinction by depressurization of AP composite solid propellants theory to predict rate of pressure decrease required to achieve flameout

[AIAA PAPER 69-176] 06 p0983 A69-18102

Hydrogen-air supersonic combustion at low densities, discussing laboratory computer simulation based on boundary layer concepts and finite rate chemistry

[WSCIPAPER 68-29] 07 p1240 A69-18358

Tungsten delay powders combustion mechanism and intermediate stages of burning process, noting burning rate

[WSCIPAPER 68-19] 07 p1202 A69-18370

Heat release in combustion chambers of propulsion and lift engines considering various parameters of materials and design problems

09 p1625 A69-22619

Gas turbine combustion control at high pressure, considering mixing, fuel evaporation, spray penetration and cone angle

09 p1625 A69-22620

Chemical mechanism of two stage spontaneous ignition controlled by cool flames of alkane-air mixtures under engine conditions to avoid knocking

11 p1998 A69-24479

Semiempirical correlation of characteristic velocity for Otto Fuel II during monopropellant combustion, assuming droplet vaporization as rate controlling process

[AIAA PAPER 69-419] 16 p2877 A69-31843

Point defect structure to control ammonium perchlorate burning rate, discussing thermal analysis data correlations, isothermal decomposition, etc

[WSCIPAPER 69-17] 16 p2831 A69-32355

Kinetics of combustion promotion of hydrogen-hydrocarbon mixtures by active particles, free atoms and free radicals using differential equations

17 p3069 A69-33139

COMBUSTION EFFICIENCY

Laminar heat transmission coefficients in combustion zone for particular oxygen and kerosene mixture

08 p1421 A69-20585

Combustion in high power jet engine combustion chamber in case of continuous and intermittent liquid fuel injection

08 p1421 A69-20762

Performance analysis of combustion chambers with continuous air admission along flame tube, deriving governing equation from reaction kinetics

09 p1624 A69-22618

Gas turbine combustion control at high pressure, considering mixing, fuel evaporation, spray penetration and cone angle

09 p1625 A69-22620

Ionizing radiation effects on combustion of ammonium perchlorate compacts with and without fuel addition, considering X ray, electron and plasma radiation

11 p1941 A69-25194

Semiempirical correlation of characteristic velocity for Otto Fuel II during monopropellant combustion, assuming droplet vaporization as rate controlling process

[AIAA PAPER 69-419] 16 p2877 A69-31843

Combustion performance evaluation program demonstrating high performance with space storable propellant combination of FLOX, methane and ethane

[AIAA PAPER 69-507] 16 p2829 A69-31848

Combustion and exhaust losses in gas turbines, recommending pulsating combustion for increased useful energy

17 p3021 A69-33360

Rocket motor combustion efficiency evaluated by chemical energy conversion to equilibrium, applicable to fuels, oxidizers and combustors at subsonic or supersonic velocity

23 p4239 A69-41919

Li-F-H tripropellant study, discussing injection method variations and thrust chamber configuration effects on characteristic velocity efficiency and heat flux measurement

24 p4362 A69-43128

COMBUSTION HEAT U HEAT OF COMBUSTION

COMBUSTION PHYSICS

Gas combustion hydrodynamic stability using feedback equation and theorems for variations in mass and momentum vector

01 p0173 A69-10087

Combustion response of hydrazine-nitrogen tetroxide hypergolic rocket propellants to transverse gas flows, noting coupled and uncoupled oscillations

01 p0175 A69-10112

Book on combustion covering aerodynamic and chemical aspects, combustion instability, detonation and rocket propellant combustion

01 p0176 A69-10906

Olefins combustion studies, considering influence on hexane combustion at different oxidation stages leading to ignition

02 p0352 A69-12309

Spherical flames of spark-ignited dust clouds, discussing streak film photographs, flame propagation, particle burnout time and burning velocities

02 p0353 A69-12323

Combustion model for rapidly burning involatile condensed materials, obtaining combustion rates

02 p0355 A69-12672

Rocket engine combustion mechanism of ammonium perchlorate composite propellants

03 p0532 A69-13002

Unsteady motions of diffusion flame sheet due to perturbations of reactant concentration, approximating species and energy conservation requirements

03 p0532 A69-13014

Mathematical analysis of oxygen diffusion to coal grains during coal dust combustion, evaluating kinetic constants by burning time

04 p0687 A69-15167

Coal grain combustion rate and duration at finite air excess coefficient, solving combustion process equations under steady state assumption

04 p0687 A69-15168

Explosive combustion of hydrogen at high pressures, showing attainment of constant value of hydrogen peroxide

05 p0849 A69-16615

Chain reaction theory defining kinetic mechanism giving rise to explosion, noting conservation of free valences and formation and disappearance of radicals

06 p1031 A69-17415

Flame establishment and propagation in gas phase taking into account aerodynamic and chemical kinetics

06 p1031 A69-17418

Combustion in compressible turbulent mixing flows, discussing mixing facility, experimental results and numerical analysis

[WSCIPAPER 68-28] 06 p0969 A69-17794

Solid propellant burning rate behavior during abrupt environmental pressure excursions, using transient combustion model

[AIAA PAPER 69-172] 06 p1036 A69-18046

Nonadiabatic reacting homogeneous system undergoing density changes, predicting chemical reaction rates and intermediate combustion products from chain reaction kinetics

[AIAA PAPER 69-87] 06 p1036 A69-18054

Transverse secondary gaseous injection penetration into confined supersonic flow

[AIAA PAPER 69-2] 06 p0913 A69-18080

Nonsteady combustion models for gases, liquid fuels and solid propellants, reviewing errors in physics and mathematics

[AIAA PAPER 69-178] 06 p1037 A69-18100

Quasi-steady combustion model of fuel droplet with convection, including pressure effect

[AIAA PAPER 69-147] 06 p1037 A69-18114

Sustained combustion initiation in subatmospheric gaseous fuel-oxidant mixtures by UV radiation at room temperature, measuring parameters as function of mixture pressure

[AIAA PAPER 69-88] 06 p0983 A69-18118

Adiabatic kinetic calculations of chemical additive effects on ignition delay of hydrogen-oxygen-argon gas mixtures
[WSCI PAPER 68-52] 07 p1239 A69-18316

Regression rate model for pressure sensitive hybrid combustion based on classical turbulent flame theory
[WSCI PAPER 68-22] 07 p1240 A69-18362

Chromium oxide additions effects on reaction rates decrease during ammonium perchlorate and nitrate combustion
08 p1375 A69-20340

Combustion in advanced gas turbine systems - Conference, Cranfield, Bedfordshire, England, April 1967
09 p1624 A69-22611

Turbofan engines augmentation, evaluating duct heater, bluff body stabilizers, piloted can combustors, flameholding techniques and afterburner tests
09 p1573 A69-22617

Film cooling injection slots number and position over flame tube and minimum cooling airflow in aircraft gas turbines
09 p1625 A69-22623

Thermal approach to pulsating combustion, determining temperature-time variation, frequency and pressure from mathematical model
09 p1625 A69-22694

Nozzle flow temperature patterns of relaxing combustion gases compared at different temperatures and pressures, using kinetic-chemical calculations
[DVL-896] 10 p1809 A69-23644

Steady flames transition into spherical detonation in various gas mixtures using high speed photography in sealed volumes
10 p1810 A69-23897

Leading edge conditions of obstacle exuding fuel into oxidizer stream, using Oseen equations in parabolic coordinate system
11 p1997 A69-24307

Critical conditions in spherical reacting mass, noting oscillatory nature of critical parameters in truncated Arrhenius rate on basis of nontruncated form
11 p1998 A69-24480

Combustion chemical reactions kinetics of gaseous phase systems, discussing temperature, reaction rates extrapolation, hydrogen and hydrocarbons
11 p2000 A69-25185

Hydrodynamic instability of normal flame and turbulent combustion of gas mixtures, considering surface and volume combustion models
11 p2000 A69-25186

Combustion mechanism of condensed inflammable systems such as gunpowder and other explosives, discussing combustion stability
11 p2000 A69-25187

Ignition dynamics of solid materials with differing kinetic and thermophysical parameters, emphasizing temperature growth during chemical reaction leading to ignition
11 p2000 A69-25188

Ignition of condensed homogeneous combustible materials in presence of phase transition in heated layer, discussing temperature distribution and ignition delay time in ammonium perchlorate
11 p2000 A69-25189

Ignition critical conditions based on reactions in condensed phase, discussing initiation from pulsed and continuous external heat sources, heat release by chemical reactions of ignition, etc
11 p2001 A69-25191

Unsteady heating of fuel mixture in vertical cylindrical container with Arrhenius heat source, discussing heat conduction equations and wall temperature effects
11 p2001 A69-25192

Hybrid chemical rocket theory and design noting radiation effects, regression and convective heat transfer
11 p1944 A69-25589

Spherical monopropellant droplet radially symmetric burning during adiabatic vaporization and direct decomposition, examining near-equilibrium limit by asymptotic analysis
12 p2190 A69-25948

Soviet book on combustion, detonation and explosive energy of condensed systems covering stable/unstable processes
12 p2190 A69-26757

Steel cylinder wall materials effects on flame propagation at constant volume of propane-air mixtures
13 p2379 A69-28363

Turbulent burning velocity definition for one dimensional turbulent flow and average flame orientation perpendicular to flow direction, discussing transient flames in turbulent environment
13 p2379 A69-28452

Stable homogeneous combustion of condensed substances /CS/, systematizing and analyzing elementary CS combustion models
13 p2379 A69-28454

Equations for steady state combustion of fuel drops in oxidizing atmosphere integrated numerically, obtaining ignition and extinction conditions
13 p2379 A69-28456

Luminous spherical fog layer surrounding burning zirconium droplet during free fall through oxygen containing atmosphere, noting effect on mass and heat transfer processes
13 p2380 A69-28462

Positive ion concentration in subsonic high velocity laminar flames determined by interpreting kinetic and diffusion factors of adding cesium to flame
13 p2380 A69-28463

Small disturbances distribution in flow parameters along two dimensional combustion zone of finite width using thermal diffusion theory
14 p2537 A69-28986

Spherical symmetric unsteady conservation equations describing transient burning of volatile fuel droplets, obtaining time dependent fuel and heat distribution in flow field
14 p2537 A69-29016

Liquid fuel droplets combustion under free and forced convection noting combustion rate
15 p2719 A69-31174

Chemical reaction between combustible solid fuel surface and oxidizer-containing gas in space capsule
16 p2877 A69-31896

Reacting gas ignition by sudden contact with heated noncatalytic surface, deriving heating time and transferred heat amount by Blasius perturbation method
16 p2878 A69-31955

Combustion instability characteristics of solid propellants, discussing small scale testing methods
16 p2829 A69-31996

Feed-system-coupled combustion instability linearized mathematical models for liquid fuel rocket engines, discussing nonrigid injector and method for instability elimination
16 p2836 A69-32001

Laser ignited combustion of 365 micron Zr droplets falling in ultrapure oxygen using spectroscopic and photographic techniques, discussing vapor phase transport phenomena
[WSCI PAPER 69-4] 16 p2830 A69-32345

Thermal layer theory of composite propellant combustion leading to minimum steady state burning rate under ideal thermal conditions
[WSCI PAPER 69-5] 16 p2830 A69-32346

Collection of articles on ramjets including reaction propulsion, hypersonic inlets, combustion problems, Griffon aircraft, storable liquid fuels, etc
16 p2837 A69-32608

Model for mixing and combustion of compressible particle laden ducted flows
[AIAA PAPER 69-460] 16 p2880 A69-32650

Spontaneous reignition predictions for solid restartable rocket motors with solid propellant combustion terminated by liquid quenching
[AIAA PAPER 69-444] 16 p2842 A69-32695

Gas phase ignition theory with feedback of homogeneous propellant exposed to stagnant gas after shock reflection
[AIAA PAPER 69-559] 16 p2880 A69-32740

Supersonic combustion for high Mach number high altitude flight, discussing laboratory simulation for actual flight condition and chamber design
[AIAA PAPER 69-458] 16 p2880 A69-32743

German monograph on turbulence in isothermal free jets and free jet flames covering local flow variations, Reynolds number effects, exchange processes, etc
17 p3068 A69-32991

Powdered oxidizer and infusible polymer binder combustion at various pressures, studying gaseous phase temperature field by optical color analysis
17 p3069 A69-33135

Normal flame speed during gas combustion in calorimetric bomb with constant combustion volume calculated by approximate equations
17 p3069 A69-33137

Computer calculation of kinetic characteristics of normal flame propagation during gas combustion, constructing physical model and differential equation system
17 p3069 A69-33138

Temperature and pressure effects on flame propagation rates, burning time and combustion zone length in turbulent flows of homogeneous gas mixtures
17 p3069 A69-33140

Flame propagation mechanism on plastic fuel in oxygen-nitrogen atmospheres with variable pressures and
17 p3074 A69-33662

at different initial fuel temperatures, discussing safety and ignition problems
17 p3074 A69-33662

Closed compartment fire mathematical model to analyze combustion parameter effects, atmosphere pressure and temperature during fire
[AIAA PAPER 69-618] 17 p3074 A69-33704

Energy balance equation for two phase liquid-gas mixture ignition process, deriving formula for speed of combustion zone movement
18 p3231 A69-35123

Monograph on solid rocket propellants covering composition, combustion characteristics and energetic, mechanical and operational properties
20 p3585 A69-37441

Film vaporizing gas turbine combustor design including performance tests and combustion physics
21 p3784 A69-38607

Laser applications in combustion research, discussing interferometric, schlieren and deflection mapping, holography, velocity measurement, scattering, laser spectroscopy, ignition by laser beams, etc
21 p3741 A69-39589

Computer routines for approximations of thermochemical properties of gas mixtures, using JANAF /Joint Army Navy Air Force/ tables of combustion systems
21 p3670 A69-39591

Perfluorocyclobutane-oxygen mixture combustion, measuring burning velocities and adiabatic equilibrium flame temperatures
21 p3852 A69-39594

Book on rate constants of chemical reactions from flames covering flame propagation, mass spectroscopy, electron spin resonance, particles diffusion, combustion physics, etc
22 p3895 A69-40318

Book on chemical rockets and flame and explosives technology covering propulsion systems, combustion, propellant ingredients, etc
22 p3998 A69-40866

Slow combustion laser spark at intensity below optical breakdown obtained by focusing radiation pulse of Nd glass laser in discharge gap
23 p4172 A69-41492

Boundary value problem of hydrodynamic equations discontinuous solution stability under random perturbations, analyzing combustion and detonation models
23 p4239 A69-41961

Reaction broadening in hydrogen-oxygen diffusion flame for slow hydrogen dissociation, using matched asymptotic expansions
24 p4408 A69-42920

Supercritical burning of liquid fuel droplets in stagnant environment, using flame sheet model to obtain heat and mass fields
24 p4415 A69-43600

Supersonic flow stability with energy input applied to reaction kinetics of processes in aircraft and rocket combustion chambers
24 p4248 A69-43642

COMBUSTION PRODUCTS

Oxygen addition to fuel stream effect on formation of soot and polycyclic aromatic hydrocarbons in ethane-air and ethylene-air diffusion flames
02 p0205 A69-12318

Reactions kinetics contribution to nonequilibrium recombination occurring in supersonic nozzle flow of combustion products of hydrogen in air
02 p0353 A69-12488

Mass velocity of detonation products of hydrogen-oxygen mixtures measured by simultaneously recording internal resistance and induced voltage in ionized medium
02 p0354 A69-12628

Combustion products temperature and composition in chamber or at nozzle exit calculated for fuels containing excess oxidizer ratios greater than unity
04 p0684 A69-14486

Thermodynamic computations for combustion product temperature and flow rate as function of pressure in burner and excess air ratio
04 p0684 A69-14487

Thermodynamics of combustion products and aerothermochemistry noting temperature calculation, heat, mass and momentum transfer in gases and deflagration wave propagation
06 p1031 A69-17414

Combustion mixture composition dependence on electrical conductivity of products with potassium additive, discussing hydrocarbon fuels
06 p0870 A69-17908

Tank collection and spectrophotometric tests in determining aluminum oxide particle size produced by small rocket engine

[AIAA PAPER 69-146] 06 p0984 A69-18117

Gas dynamics, thermodynamics, chemical properties, energy and products of hydrocarbon-air detonations in tubes under standard atmospheric conditions [WSCI PAPER 68-26] 07 p1241 A69-18369

Optical constants of soot applied to heat flux calculations, discussing soot particles concentration determination in hydrocarbon combustion products [ASME PAPER 68-HT-13] 13 p2374 A69-27777

Temperature measurement of plasma consisting of combustion products in MHD duct, measuring spectral line contours by Fabry-Perot interferometer for accuracies 13 p2309 A69-28023

Electronic analog model for differential equations of equilibrium of gaseous combustion products based on asymptotic stability 15 p2717 A69-30862

Heat release rate during gas combustion products recombination in supersonic nozzle, using graphic interpolation of flow parameters 15 p2717 A69-30987

Compressible turbulent accelerating boundary layer flow model for convective heat transfer from rocket combustion gases, noting heat flux 16 p2878 A69-32000

Pure monopropellant steady droplet burning rate theory for determining heat-up and convection transport rates in droplet combustion products of flat flame burner [AIAA PAPER 69-563] 16 p2834 A69-32722

Spectral absorption coefficients and emissivities of thermodynamic equilibrium mixture of various combustion products at high temperatures, based on graphs 19 p3266 A69-36840

High pressure combustion of ortho-barenes /carboranes/, determining formation heat and amounts of boric acid and carbon dioxide 21 p3670 A69-39625

COMBUSTION STABILITY NT FLAME STABILITY

Combustion chamber equation for liquid fuel rocket engine, considering time varying ignition lag 01 p0142 A69-10090

Gas combustion stability with respect to one dimensional perturbations, considering flow compressibility stabilizing effect 01 p0174 A69-10107

Book on combustion covering aerodynamic and chemical aspects, combustion instability, detonation and rocket propellant combustion 01 p0176 A69-10906

Specific acoustic admittance of solid propellant burning surface for determining burning instability under rocket motor conditions 02 p0302 A69-11521

Combustion instabilities in solid propellant rocket engines, emphasizing acoustic types for longitudinal and tangential modes 02 p0303 A69-11531

Solid propellant combustion instability models describing combustion zone dynamics applied to acoustic and nonacoustic instability in LF regime [WSCI PAPER 67-13] 02 p0352 A69-12311

Combustion oscillations in liquid and solid propellant engines, noting destructive effect of LF vibrations and acoustic instability 02 p0305 A69-12494

Pressure and velocity couplings effects on oscillatory and transient motions in solid propellant rocket motors, emphasizing unsteady burning calculations 02 p0305 A69-12501

Air jet high temperature and low pressure influence on combustion stability in ramjet engine 03 p0531 A69-12968

Acoustic absorbers for combustion stabilization, discussing analytical model based on temporal damping coefficient for oscillation modes and allowance for nonuniform distribution 03 p0532 A69-13133

Perturbation behavior of solid propellant combustion, discussing relevance of analytical models and use of qualitative models 04 p0685 A69-14726

Relaxation induced self oscillations during combustion of gunpowder in semiclosed volume, noting combustion instability 04 p0686 A69-14987

Unstable combustion of ammonium perchlorate /AP/, discussing correlation between propellant particle diameter and frequency in burning rate [AIAA PAPER 69-177] 06 p1036 A69-18063

Oxidizer particle size and binder type effects on nonacoustic combustion instability of solid propellants [AIAA PAPER 69-175] 06 p0983 A69-18152

HF instability of steady combustion process with allowance for elastic strains in chamber walls 07 p1242 A69-18993

Kerosene droplets combustion stability studied by motion pictures, discussing pressure, temperature and O concentrations effects in turbulent carbon dioxide flow 08 p1421 A69-20345

Nonmetalized composite propellant solid phase heterogeneities effect on oscillatory combustion, inducing coherent burning rate oscillations with external pressure oscillations 09 p1622 A69-22085

Solid propellant combustion, calculating burning, flame standoff distance, flame thickness, heat transfer, energy losses, and distributed and unsteady combustion 09 p1623 A69-22091

Fluorine light-off detector /FLOD/ for sensing and indicating minimum light-off or blow out conditions in turbojet engine afterburner [ASME PAPER 69-GT-36] 09 p1501 A69-22488

Thermal approach to pulsating combustion, determining temperature-time variation, frequency and pressure from mathematical model 09 p1625 A69-22694

Injected propellant behavior during one dimensional passage through rocket combustion gas chamber, considering Reynolds number and propellant characteristics 11 p1941 A69-24329

Combustion mechanism of condensed inflammable systems such as gunpowder and other explosives, discussing combustion stability 11 p2000 A69-25187

Steady propagation of flame front initiated by local ignitor /spark/ in gas mixture, discussing critical requirements, boundary conditions, etc 11 p2001 A69-25190

Combustion rates of condensed systems under positive and negative accelerations at atmospheric pressure 11 p2001 A69-25195

Combustion instability problems in rocket motors, emphasizing strongly coupled pressure oscillations in combustion chambers 11 p2003 A69-25597

Soviet book on combustion, detonation and explosive energy of condensed systems covering stable/unstable processes 12 p2190 A69-26757

Solid propellant rocket engine design for combustion stability, discussing length, pulse induced and acoustic instability types [AIAA PAPER 68-532] 12 p2191 A69-26788

Stable homogeneous combustion of condensed substances /CS/, systematizing and analyzing elementary CS combustion models 13 p2379 A69-28454

Compressed ammonium perchlorate combustion rate and pressure requirements established from initial temperature effects 14 p2508 A69-28914

Galerkin method applied to axial, transverse and three dimensional linear combustion instability problems in liquid propellant rocket motors 14 p2538 A69-29021

Fuel drop combustion under unsteady conditions at high pressure in unlimited and limited air volume 15 p2719 A69-31476

Combustion in liquid propellant rockets, discussing aerothermochemical steady state and nonsteady behavior analysis and experiments 16 p2835 A69-31732

Solid propellants steady state combustion with emphasis on heterogeneous propellants 16 p2829 A69-31995

Combustion instability characteristics of solid propellants, discussing small scale testing methods 16 p2829 A69-31996

Feed-system-coupled combustion instability linearized mathematical models for liquid fuel rocket engines, discussing nonrigid injector and method for instability elimination 16 p2836 A69-32001

Small disturbances and effect on processes of fast combustion of inflammable compressible mixture 16 p2837 A69-32137

Rocket stability monitoring by temporal radiometry, using exhaust radiance measurement to detect frequencies in thrust chamber combustion pressure [AIAA PAPER 69-580] 16 p2839 A69-32670

Droplet vaporization model representing combustion processes of longitudinal oscillations in liquid rocket combustor [AIAA PAPER 69-483] 16 p2841 A69-32689

Composite propellants high pressure burning stability with various binders and oxidizers, showing ammonium perchlorate oxidized formulations susceptibility to instability [AIAA PAPER 69-438] 16 p2834 A69-32704

Linear and nonlinear pressure coupled combustion instability of solid propellants [AIAA PAPER 69-479] 16 p2834 A69-32725

Compositional and oxidizer particle size effects on combustion instability of plastic propellant based on ammonium perchlorate and polyisobutene [AIAA PAPER 69-478] 16 p2834 A69-32734

Stability criteria for longitudinal combustion instability tested for generality using data from various solid propellant formulations [AIAA PAPER 69-480] 16 p2834 A69-32736

Interaction between two phase dynamical and combustion parameters in one dimensional gas-gas-metal combustion system [AIAA PAPER 69-540] 16 p2880 A69-32742

Modified liquid fueled pulsating combustion chamber operating as Helmholtz cavity resonator, measuring chamber pressure as function of time 17 p3074 A69-33410

Finite amplitude standing transverse resonant acoustic field effects upon flow behavior of viscous fluid in cylindrical enclosure to acoustically model combustion instability [AIAA PAPER 69-667] 17 p2954 A69-33457

LF oscillations in simple combustion chamber using gaseous propane fuel, discussing association with progressive flame necking 18 p3230 A69-34837

Hydrodynamic stability of solid fuel combustion in presence of acoustic disturbances in gas phase, considering material erosion and particle dispersion 18 p3231 A69-35150

Acoustic measurements at room temperature for determining losses in rocket chamber during combustion instability, using small scale model 19 p3394 A69-35946

Flame and pressure /or velocity/ oscillations interaction in unstable combustion regimes, considering tubes with propane-air mixtures 19 p3450 A69-36357

Nonsteady propellant burning theory for Al melting role in suppressing combustion instability in solid propellant rocket motors 19 p3393 A69-36814

Laboratory unsteady burning data applied to analysis of small amplitude combustion instability in solid propellant rockets 20 p3586 A69-37224

Combustion turbulence effect on flame propagation velocity taking into account flame-generated pulsation velocity as function of temperature and flame velocity 21 p3850 A69-38861

Discontinuity characteristics of trough-shaped flame stabilizers for combustion in wake of poorly streamlined body during period of ignition arrest 21 p3851 A69-39092

Nonstationary solid rocket fuel combustion scheme, using unsteady combustion model for quantitative analysis of rocket engine irregularities attributed to excessive fuel 22 p4050 A69-40457

Unsteady combustion wave passage through inert obstacle in gunpowder in N filled pressure vessel 22 p4051 A69-41119

Detonation wave instability and damping in gas containing liquid or solid inflammable aerosol, considering atomized propellants 23 p4240 A69-42339

COMBUSTION TEMPERATURE

Stabilized low temperature ignition of cyclohexane using vertical flow reactor 02 p0304 A69-12314

Temperature and pressure measurements in low temperature combustion of n pentane covering slow reaction and cool flame regions 02 p0353 A69-12321

Optical measurement method for burning surface temperature of condensed systems, realizing radiation from surface of combustion by light guide of monocrystalline aluminum oxide 13 p2379 A69-28453

Jet engine combustion temperature measurements by thermocouples or gas analysis noting errors involved 23 p4165 A69-41650

COMBUSTION VIBRATION

Combustion oscillations in liquid and solid propellant engines, noting destructive effect of LF vibrations and acoustic instability

02 p0305 A69-12494

Initiation of HF combustion oscillation in premixed gas rocket
[ISAS-430]

06 p1029 A69-17025

Nonmetalized composite propellant solid phase heterogeneities effect on oscillatory combustion, inducing coherent burning rate oscillations with external pressure oscillations

09 p1622 A69-22085

Acoustic frequency of longitudinal self oscillations during vibrational fuel combustion in afterburner, taking into account nonlinear properties of heat supply zone

11 p2002 A69-25339

Self excited vibrating laminar diffusion flames, discussing coupling, jet spacing radial heat transfer and boundary layer interaction

16 p2876 A69-31711

Fuel injector-induced mass flux and mixture ratio distributions effects on combustion performance, chamber volume and stability, discussing combustion oscillation avoidance

16 p2877 A69-31731

Nonlinear periodic oscillations in liquid rocket combustion chambers for different chamber models and burning rate response formulations

19 p3449 A69-36352

Rocket body elastic vibrations, liquid fuel supply oscillations and engine thrust vibrations effects on system stability

20 p3617 A69-37604

Cylindrical shell with supersonic nozzle end, describing axisymmetric oscillations forced by burning filler in gas stream

24 p4300 A69-43073

COMBUSTION WAVES

U FLAME PROPAGATION

COMBUSTORS

U COMBUSTION CHAMBERS

COMETS

NT AREND-ROLAND COMET

NT MOREHOUSE COMET

NT MRKOS COMET

NT SCHWASSMANN-WACHMANN COMET

Perturbations on major axes of slow moving comets in nearly parabolic original orbits by fast moving stars, discussing statistics of stellar encounters

01 p0153 A69-10871

Secular perturbations produced by comet belt beyond Neptune on orbits of periodic comets of large aphelion

01 p0158 A69-11327

Carbon monoxide ion dynamics in envelopes of comets exhibiting fountain behavior, discussing electron-collisional ionization within envelopes as main plasma production mechanism

02 p0310 A69-11423

Gaseous hydrates formation in comet nuclei, discussing stability at given temperatures and pressures and solar radiation shielding by dust sheath

03 p0515 A69-14032

Capture of comets by large planets

03 p0517 A69-14128

Orientation and motion of bands in tail of comet Ikeya-Seki, discussing synchronous formations

04 p0652 A69-14378

Meteor spectrum from 1966 Leonid shower considered to be closer to comet nucleus spectra than previous spectra

04 p0655 A69-14664

Mathematical analysis for mechanism of spherical comet nucleus division as effect of nonuniform surface heating during rotation

04 p0659 A69-14997

Nongravitational impulses on short period comets

04 p0660 A69-15037

Cometary origin of meteorites, discussing and rejecting origin from recent asteroidal collisions

05 p0818 A69-15588

Zodiacal light, cometary contribution and solar activity

05 p0826 A69-16391

Solar corona effects on tail of comet Ikeya-Seki, describing model for interaction between tail and corona

06 p1000 A69-16982

Two phase flow in comas of dust comets, noting acceleration of gaseous and particle phases of continuous streams and particle vaporization

06 p1000 A69-16984

Carbon molecule photodissociation in cometary atmospheres, discussing intensity level distribution based on model

06 p1004 A69-17534

Ice nucleus formation in developing comet, discussing dissociation and vaporization characteristics of parent molecules as participants in process

06 p1004 A69-17537

Visual and photographic comet observations, including perihelion passage of P/Perinne-Mrkos in 1968

07 p1216 A69-19205

Solar phenomena correlation with brightness variations of comet Alcock 1963b, noting sunspot maximum followed by maximum in absolute magnitude of comet

08 p1394 A69-20620

Asteroidal and cometary orbits and origin of meteorites, discussing eccentricities, exposure ages and mass yield

08 p1406 A69-20929

Cometary origin of meteors and element abundance in primitive solar nebula, discussing neutron capture products in chondrites

08 p1406 A69-20930

Whipple and Douglas-Hamilton systematic corrections for periodic comets, considering constant coma brightness of P/Tempel 2 since 1874-1904 observations

08 p1408 A69-21137

Photographic and reflector observations of comets including orbit determinations and recoveries

08 p1408 A69-21140

Cometary magnetic fields by measuring depolarization of molecular resonance fluorescence

09 p1603 A69-22234

Low thrust space probe mission to Halley comet, utilizing nuclear electric propulsion

10 p1772 A69-22864

Total planet interaction energy of comets passing through solar system, showing non-Gaussian shape of distribution

10 p1774 A69-22970

Catalog of orbital elements for periodic comets during perihelion passage

10 p1777 A69-23396

Size and velocity measurements of particles suspended in gas expanding from nozzle into vacuum simulating cometary two phase flow with evaporation

10 p1674 A69-23686

Cometary nucleus dynamic center noncoincidence with photometric center, using computer calculations of Arend-Roland comet

10 p1784 A69-24035

Comet Berbon and minor planet positions photographically recorded /1964-1967/

11 p1962 A69-25121

Cometary, lunar and solar effects on precipitation, considering joint influence of meteoric streams and moon

11 p1965 A69-25420

Recently discovered comets including Comet Thomas, discussing magnitudes and perihelions

12 p2172 A69-27161

Comet interaction with solar wind, assuming field tail coupling of ionized comet material to solar wind ions

13 p2349 A69-27817

Soviet collection of articles on cosmic physics, Number 3, Comets, sun and interplanetary space

14 p2522 A69-29703

Comet scintillations and tail characteristics studied to obtain information on interplanetary flux field, magnetic fields and planetary structures

14 p2523 A69-29704

Cometary tail diffusion model based on luminous particle number decrease with time and particle accelerated motion and diffusion in space

14 p2523 A69-29705

Comet Ikeya-Seki phenomena near perihelion interpreted from mean surface and ice nucleus internal layers temperatures

14 p2523 A69-29706

Comet Ikeya-Seki head and tail structure -noting cloud ribbons at angle to tail axis

14 p2524 A69-29708

Comet Ikeya-Seki 1965f photometric investigation during perihelion, determining tail type according to Bredikhin classification

14 p2524 A69-29709

Comet Ikeya-Seki 1965f primary nucleus splitting date and rate established from dynamic solutions

14 p2524 A69-29710

Halley comet abrupt daily motion variation ascribed to solid particles ejection from ice nucleus stimulated by gas outflow

14 p2524 A69-29712

Nongravitational force dynamic effect and model for rotating cometary nucleus, including changes in orbital elements

14 p2524 A69-29713

Critical analysis of Oort cometary cloud existence, discussing stellar encounters of sun, planetary explosions, etc

14 p2524 A69-29714

Visual, photographic and spectral observations of comets during IQSY, discussing comets Tomita-herber-Honda 1964c and Ikeya-Seki 1965f

14 p2525 A69-29716

Solar UV radiation effects on processes in comet head, interpreting surface brightness distribution of comet 1959k in terms of photodissociation

14 p2525 A69-29717

Comets considered as natural interplanetary space probes, stressing need for international cooperation on solar system studies

15 p2679 A69-30011

Solar flares associated with intensive sodium D lines emission observed photoelectrically with telescope in unperturbed region, analyzing possibilities of comets solar origin

15 p2674 A69-30506

Soviet collection of articles on physics of comets covering solar radiation, solar corona, comet nucleus, comet spectra, comet tails, etc

15 p2683 A69-30515

Secular decline in absolute brightness of comet Encke from photometric curves obtained during past and present century

15 p2684 A69-30518

Gasdynamic model of comet nucleus region, discussing molecular collisions, surface brightness distribution and dust particle motion

15 p2684 A69-30520

Expression relating gas density, radial velocity and temperature at comet nucleus surface to nucleus surface temperature, applying results to unsteady sublimation process

15 p2684 A69-30521

Photoelectric comet observation techniques, tabulating narrow and wideband filter combinations for determining parameter Q for various cometary spectral emissions

15 p2684 A69-30522

Unidentified cometary spectra line emission possible interpretations, examining atomic hydrogen abundance in cometary atmosphere and ionic hydrogen recombination

15 p2685 A69-30523

Comet Ikeya-Seki tail spectra from nebular spectrograph, tabulating energy distribution in comet tail, noting similarity to solar spectrum

15 p2685 A69-30524

Polarimetric and photometric observations of comet Ikeya-Seki 1965f, plotting isophotes of head and polarized light distribution in tail

15 p2685 A69-30525

Number and mass of sodium atoms in comet Ikeya-Seki 1965f head calculated from spectral observations, ascribing D lines to resonance scattering of photospheric radiation

15 p2685 A69-30526

Photographic photometry of comet Ikeya-Seki during passage near sun, plotting isophotes of coma and tail and brightness distribution diagrams

15 p2685 A69-30527

Comet atmosphere dust component, relating physical properties to brightness characteristics in stellar magnitudes

15 p2685 A69-30528

Photographic observations of comet Kilston 1966b, estimating brightness, absolute magnitude and color index

15 p2685 A69-30529

Cometary tails maximum lengths compared with orbit parameters and absolute magnitudes, proposing classification scheme

15 p2689 A69-30566

Hansen method of partial anomalies for cometary orbits applied to comet Encke perturbed by earth and compared with perturbations by numerical integration

16 p2863 A69-32400

Luminous particles volumetric concentration calculation based on limiting surface density to determine bulk density in cometary head

17 p3032 A69-33189

Relativistic effect in pericenter motion of comets and natural satellites from major semiaxes and eccentricities of natural bodies

17 p3044 A69-34174

Ephemeris of comet Grigg-Skjellerup for reappearance in 1971/72, based on equations of motion integration and perturbations
17 p3044 A69-34183

Selection effects on comets discovery, comparing effectiveness of photographic and visual observation techniques
17 p3045 A69-34221

Orbit determination for short and long period comets using equations of motion including terms for radial components of nongravitational force
18 p3195 A69-34432

Distributions of close planet-comet encounters for various orbital elements, calculating trajectory by conic matching
18 p3195 A69-34433

Comet-solar wind interaction model, determining contact discontinuity size and shape around comet nucleus and ion specular reflection
18 p3188 A69-35190

Comet observations and orbit determinations, noting eccentricity of comet Thomas
19 p3403 A69-35970

Comet heads gas dynamics, analyzing coma or head region as continuum source flow of dusty gas
19 p3428 A69-36807

Definitive orbit of comet 1943 I determined from photographic and visual observations
20 p3596 A69-37310

Initial and future orbits of comet 1959 IV Alcock determined considering Venus, Jupiter, Saturn, Uranus and Neptune perturbations, noting elliptical to hyperbolic orbit transition
20 p3597 A69-37319

Comet tails orientation determination for solar wind and interplanetary plasma investigation, considering geometrical difficulties and suggesting computation procedure
20 p3599 A69-37467

Photometric and spectroscopic observations analysis of Comet Honda 1968c
20 p3614 A69-38252

Halley Comet rendezvous mission, comparing low thrust mode with ballistic Jupiter or Saturn swingby mode
[AIAA PAPER 69-933] 21 p3809 A69-39360

Cometary nuclei composition as last samples of early solar system composition, discussing dirty snowball model and radical lifetime problem
22 p4013 A69-40097

Cometary and asteroidal orbital differences and similarities, emphasizing limiting cases to study orbital evolution of meteors
23 p4208 A69-41284

Spectral and orbital evidence of connection among fireballs with orbit inclination, comets and carbonaceous meteorites
23 p4208 A69-41285

Spatial region accessible to earth launched probes determined for mission planning for exploration of aperiodic comets, discussing orbit parameters
23 p4212 A69-41536

Daylight observations of Comet Ikeya-Seki 1965-f at perihelion passage, discussing resulting emission line spectra within comet head
23 p4221 A69-42386

Gas concentration liberated during each revolution in atmospheres of short period comets to explain impulsive forces upon nuclei, noting diatomic carbon density
23 p4221 A69-42387

Space mission opportunities selection from analysis of short period comet perihelia, discussing flyby and rendezvous mission payloads
[AAS PAPER 69-320] 24 p4381 A69-42866

COMMAND **U THERMAL COMFORT** **COMMAND AND CONTROL**

Real time performance, ground control and data processing of Surveyor spacecraft during maneuvers
[AIAA PAPER 67-644] 04 p0586 A69-15502

Photorecording techniques for command and control systems requirements, discussing association with large screen computer generated CRT projection display equipment
06 p0928 A69-17923

Single rotation for reorienting rigid body from initial to arbitrary final attitude together with corresponding control torques
09 p1610 A69-21998

ELDO satellite command decoder performance in presence of noise, evaluating PDM bit decoder bit error probability and false command probability
11 p1834 A69-24563

PDM command coder meeting NASA Tone Digital Command Standard for German central ground station
16 p2755 A69-31859

Post Attack Command and Control System - Airborne Data Automation /PACCS-ADA/, describing components, operation, etc
17 p2977 A69-34116

Avionics of Naval E-2C airborne sentry and command and control system, discussing digital computer, search radar, etc
18 p3108 A69-34811

Robot command and control by computer assembly, describing engineering analog of vertebrate nervous system
21 p3679 A69-39603

COMMAND-CONTROL **U COMMAND AND CONTROL** **COMMAND GUIDANCE**

Technical characteristics of spacecraft telemetering, tracking and telecommand systems, stressing links between earth stations and spacecraft
09 p1451 A69-21291

Tracking and data acquisition systems for spacecraft and ground link through command, telemetry and tracking, noting data relay satellites, etc
17 p2919 A69-33371

Apollo 11 guidance and navigation systems involved in lunar landing, describing command and service modules design
24 p4295 A69-42550

COMMAND MODULES

Radiation measurements inside Apollo 4 and 6 command modules during passage through trapped radiation belts
[AIAA PAPER 69-17] 06 p0884 A69-18202

Apollo mission simulation, discussing Command Module Simulator /CMS/, onboard computer system and dynamic visual presentation via infinity-optics display
[SMPT PAPER 105-74] 12 p2055 A69-25768

Apollo spacecraft command module aerodynamic characteristics during entry compared with wind tunnel test predictions
[AIAA PAPER 68-1008] 12 p2012 A69-26789

Aerodynamic measurements on Apollo CM model at hypersonic flow simulating earth orbital reentry trajectory
12 p2012 A69-26800

Apollo navigation, guidance and control systems in command module and lunar module, discussing inertial, optical and computer hardware operation
19 p3369 A69-35799

Apollo 11 guidance and navigation systems involved in lunar landing, describing command and service modules design
24 p4295 A69-42550

COMMAND SERVICE MODULES

Apollo LM and CSM tracking systems boresight shift reducible by decreasing modulation indices or scaling factor alpha
10 p1672 A69-23277

Ultrasonic inspection systems to determine and record bond quality on all adhesive bonded assemblies of Saturn S-2 booster and Apollo Command and Service Modules
15 p2632 A69-31515

COMMERCE

Commercial orbital space stations economics and potential markets, considering fisheries, ocean transportation, air traffic control, resources surveys, pollution reduction, etc
06 p1007 A69-17599

COMMERCIAL AIRCRAFT

NT A-300 AIRCRAFT

NT BOEING 2707 AIRCRAFT

NT BOEING 707 AIRCRAFT

NT BOEING 747 AIRCRAFT

NT CV-990 AIRCRAFT

NT DC 3 AIRCRAFT

NT DC 8 AIRCRAFT

NT DC 10 AIRCRAFT

NT DH 121 AIRCRAFT

NT L-1011 AIRCRAFT

NT SE-210 AIRCRAFT

NT SUPERSONIC COMMERCIAL AIR TRANSPORT

NT TU-104 AIRCRAFT

NT TU-134 AIRCRAFT

NT VC-10 AIRCRAFT

Boeing 747 characteristics for passenger and cargo service noting economic gain, operational performance, control cabin, engine, etc
[AIAA PAPER 67-397] 01 p0010 A69-10636

BAC Three-Eleven 220 seat airliner for short and middle distance routes, discussing operating costs, thrust and range
02 p0193 A69-12067

Navigation system for American SST noting use of Doppler radar and inertial navigation
02 p0278 A69-12238

Inertial navigation for commercial aircraft, discussing Sagem-Ferranti and Litton systems
02 p0278 A69-12239

Exterior arresting devices for commercial aircraft full scale tests
03 p0367 A69-14104

Test equipment for rapid automatic checkout and evaluation of automatic flight control systems on commercial and jet transport aircraft
05 p0742 A69-15883

Federal government legal liability for commercial air safety in aircraft accident suits
06 p1042 A69-16848

Aeronautics - Conference, Beverly Hills, September 1968
06 p0866 A69-17658

LR-1 prototype design criteria and flight testing, discussing Model 99 airliners for commuter airlines
06 p0867 A69-17668

Commercial jet safety, analyzing aircraft accidents and accident rates
06 p0868 A69-17829

Nondemographic model predicting market shares of V/STOL aircraft in competition with automobiles and conventional airliners for short haul intercity business travel markets
07 p1244 A69-18967

Baseline requirements for commercial aircraft propulsion systems, stressing engine installation in aircraft
[ASME PAPER 69-GT-57] 09 p1572 A69-22514

JT15D business aircraft turbofan engine, discussing low costs and fuel consumption, maintenance, reliability, installation, etc
[ASME PAPER 69-GT-119] 09 p1572 A69-22524

Soviet supersonic transport Tu 144, describing wing unit, fuselage, passenger accommodation, tail unit, landing gear, power unit engine nacelle and navigation
10 p1634 A69-23838

Modular hydraulic power source systems for general aviation aircraft, discussing design selection, phase in and customer acceptance problems
[SAE PAPER 690329] 11 p1825 A69-24505

Military forward air control aircraft conversion from lightweight commercial tandem engine aircraft noting visibility, communication and navigation equipment
[SAE PAPER 690313] 11 p1822 A69-24511

Computer controlled testing of commercial aircraft avionics systems for automatic, semiautomatic and manual operation to perform repair and calibration tasks
11 p1864 A69-25061

Douglas DC-10 medium range aircraft, discussing engine placement, passenger and cargo capacity, construction data, etc
11 p1823 A69-25211

V/STOL aircraft in commercial aviation, discussing costs, noise reduction, propulsion systems, projected routes, etc
13 p2203 A69-28039

FAA additional airworthiness standards for small aircraft in air taxi and commercial operations, noting safety levels
[SAE PAPER 690320] 15 p2549 A69-30090

Business aircraft electrical power sources, discussing electromechanical constant speed drive /EMCSD/ and comparison with DC/inverter and hydraulic CSD
[SAE PAPER 690346] 15 p2552 A69-30091

Low cost inertial measurement unit /IMU/ for commercial and private aircraft, evaluating components and system
[SAE PAPER 690337] 15 p2606 A69-30092

Dassault Mercure short haul jumbo jet, discussing production costs and market potential
15 p2550 A69-30317

Dassault Mercure high speed twin turbojet aircraft, discussing capacity, range, propulsion, profitability threshold, etc
15 p2550 A69-30318

German VFW 614 short haul commercial jet aircraft design, marketing, etc
16 p2734 A69-31805

Book on competition in North Atlantic commercial air transport covering passengers, freight and mail from supply, demand and market point of view
16 p2881 A69-31866

Aircraft role in future transport systems for passengers and goods, emphasizing shorter distances, intercity and interurban communication, etc
16 p2881 A69-31932

High bypass ratio engine influence on short range civil aircraft design, considering performance, noise, engine location, etc
17 p2897 A69-33212

STOL and V/STOL short haul intercity airliners emphasizing propulsion systems, operational aspects and economics
17 p2898 A69-33356

Technical problems in converting long service civil aircraft to obtain more volume, easier loading access or greater flexibility
20 p3461 A69-36919

Economic effectiveness determination methods for commercial transport aircraft design analyzed quantitatively, using four engine 100-seat turboprop aircraft
21 p3855 A69-38873

Economic effectiveness of design and fabrication changes in aircraft construction industry for profitable operation of commercial transport aircraft
21 p3855 A69-38874

Engine powered lift civil aircraft certification factors taking into account traffic growth, accident rates, learning rate and acceptable safety level
22 p3862 A69-39962

Commercial jet aircraft thrust reversers and noise suppressors developed by Rolls-Royce, discussing compatibility, reliability and applications
[SAE PAPER 690410] 23 p4200 A69-41638

Booster engines for thrust augmentation of commercial transports, considering tradeoffs in takeoff distance, payload, range, safety and noise patterns
[SAE PAPER 690381] 23 p4201 A69-41667

Commercial aircraft peak cockpit noise level during cruise and high speed descent, discussing damage risk criteria and inter-pilot speech interference
23 p4102 A69-41682

Commercial aircraft environmental compatibility planning, considering problems of airport traffic growth and restrictive air traffic control regulations
[AAS PAPER 69-326] 24 p4252 A69-42808

FAA power spectral gust methods for computing design limit loads on commercial aircraft, noting British investigation
24 p4253 A69-43111

COMMERCIAL AVIATION

U CIVIL AVIATION

COMMUNITION

NT GRINDING [COMMUNITION]

Ductile metal powder chemical reactions during comminution in pure or oxygenated water
13 p2216 A69-27762

COMMITTEE ON SPACE RESEARCH

Bibliography of reports and papers on space sciences and research activities of national institutions of COSPAR members /1966-1967/
10 p1784 A69-24001

COMMUNES

U MOUNTAIN INHABITANTS

COMMUNICATING

NT BROADCASTING

NT INTERSTELLAR COMMUNICATION

NT POINT TO POINT COMMUNICATIONS

NT TELEPHONY

NT VERBAL COMMUNICATION

Technical communication patterns in R and D laboratories, discussing effects of work structure, social relations, etc
20 p3640 A69-38019

Communication in large organizations, describing internal communication model
24 p4419 A69-42930

COMMUNICATION CABLES

NT BEAM WAVEGUIDES

NT COAXIAL CABLES

NT PLASMA GUIDES

NT WAVEGUIDES

Data transmission on common communication circuits, noting circuit characteristics, limitations on performance and future digital service
04 p0559 A69-15207

Monograph on discrete signals transmission by FM, considering secondary signal compression device and wire communication channels
12 p2033 A69-26866

COMMUNICATION EQUIPMENT

NT BIOTELEMETRY

NT CLOSED CIRCUIT TELEVISION

NT COLOR TELEVISION

NT EDUCATIONAL TELEVISION

NT PULSE FREQUENCY MODULATION

NT PULSE FREQUENCY MODULATION TELEMETRY

NT RADIO COMMUNICATION

NT RADIO RECEIVERS

NT RADIO RELAY SYSTEMS

NT RADIO TELEGRAPHY

NT RADIO TELEMETRY

NT SATELLITE TELEVISION

NT SPACECRAFT TELEVISION

NT SUPERHETERODYNE RECEIVERS

NT TELEMETRY

NT TELEPHONY

NT TELEPHOTOMETRY

NT TELEVISION SYSTEMS

NT TRANSMITTER RECEIVERS

NT WHISTLER RECORDERS

Automatic picture transmission station equipment including antenna, cavity filters, tape recorder, oscilloscope, facsimile system and kinescope
[UN PAPER 68-95450] 01 p0054 A69-10522

Spacecraft pencil beam parabolic antenna design and installation, discussing directivity factor variation with diameter and orientation accuracy effects
01 p0030 A69-10581

Linear integrated circuit communication systems based on subsystem approach, showing example of IF strip and audio AGC/squelch amplifier
01 p0035 A69-11389

Automatic test equipment applicability to testing problems created by increasing complexity of communications equipment
03 p0410 A69-13189

Optical receivers for deep space optical communications link assuming PCM scheme
03 p0389 A69-13194

Data transmission on common communication circuits, noting circuit characteristics, limitations on performance and future digital service
04 p0559 A69-15207

Traveling wave tubes for Symphonic Communication Satellite, discussing design, performance and efficiency
07 p1095 A69-18429

Data transition tracking in digital communication systems by decision directed phase tracking loops
07 p1082 A69-19108

Communications for Apollo Applications Program, considering extended duration manned missions in low earth orbit and Gemini, Saturn and Apollo hardware
07 p1083 A69-19124

Mariner 1969 multimission high rate deep space telemetry system design, hardware and application
07 p1083 A69-19125

Suboptimum decision feedback communications systems incorporating simple digital processing compared with optimum Wald scheme
10 p1656 A69-23534

Solid state synchro data interfaces for angular information, noting synchro to digital and digital to synchro conversion techniques and synchro repeaters
11 p1842 A69-24543

Digital data transmission techniques and complex instrumentation systems design noting control, identification, synchronism and error reduction
11 p1834 A69-24545

Electrical engineering, Volume 3, communications, covering special theories, systems components, telecommunication, electroacoustics, digital and analog computers and programming
15 p2568 A69-30619

Spacecraft pencil beam parabolic antenna design and installation, discussing directivity factor variation with diameter and orientation accuracy effects
15 p2568 A69-30751

Unidigit and multidigit communications systems performance and transmission characteristics, emphasizing SNR improvements
17 p2918 A69-33066

Communication equipment reliability improvement through testing and failure analysis
19 p3282 A69-35783

Satellite and terrestrial point-to-point communication circuit costs, considering multiple access and small antenna earth stations
19 p3456 A69-36822

Booster digital guidance and control system, discussing communication device providing data transfer between airborne digital computer and control device
[AIAA PAPER 69-988] 22 p3978 A69-40368

More earth station equipment and design for satellite communication in INTELSAT network including antenna, feed and tracking, interconnect system, etc
22 p3900 A69-40679

Periodic ladder type design delay equalizer for linear delay characteristics in millimeter waveguide systems
23 p4135 A69-41361

COMMUNICATION SATELLITES

NT EARLY BIRD SATELLITES

NT INTELSAT SATELLITES

NT MOLNIYA SATELLITES

NT SYNCOM SATELLITES

Broadband parametric amplifier used as front amplifier in satellite communication systems ground station receiver, noting cryogenic operation capability
01 p0041 A69-10243

Space applications program including communications and navigation meteorology, earth resources survey and geodesy
[UN PAPER 68-95437] 01 p0178 A69-10472

International experimentation with U.S. communications satellites, noting design variations with participants and restraintless information exchange
[UN PAPER 68-95421] 01 p0108 A69-10474

Small earth stations in future communication satellite systems, discussing applications, characteristics and equipment
[UN PAPER 68-95751] 01 p0028 A69-10492

Space broadcasting possibilities and problems, considering home reception and group participation at community centers
[UN PAPER 68-95287] 01 p0028 A69-10497

Satellite educational TV, considering program distribution, satellite characteristics, ground terminals design, reliability, quality, programming and costs
[UN PAPER 68-95827] 01 p0029 A69-10499

Japanese space research organizations, sounding rockets, meteorology, satellite communications, geodesy, etc
[UN PAPER 68-95563] 01 p0151 A69-10501

Marine requirements possible satisfaction by using space techniques to improve long range communications to achieve safety at sea and shipping operations efficiency
01 p0161 A69-10503

British contributions to communication satellite earth station technology covering antennas, low noise amplifiers, traveling wave tubes and threshold extension demodulators
[UN PAPER 68-95843] 01 p0054 A69-10507

Communication satellites development in U.S.S.R., discussing Molniya 1 satellite design and objectives and Echo 2 satellite transmission experiments
01 p0032 A69-10949

Performance characteristics of hard limited and linear repeaters for satellite communications systems
01 p0032 A69-10966

Ground-air-ground communications system using pseudonoise through satellite and central ground based control facility, discussing system advantages, SNR and modulation schemes
01 p0033 A69-11009

Satellite communications with emphasis on European programs, discussing synchronous satellites, Europa 2 rocket and Saros and Symphonic projects
02 p0207 A69-11910

Multijet electrothermal systems for attitude control and stationkeeping of synchronous communications satellite
[AIAA PAPER 67-723] 02 p0305 A69-12375

Maritime radio communications satellite service for ship safety, discussing stationary equatorial satellite systems
[AIAA PAPER 68-232] 02 p0356 A69-12383

Book on communication systems covering signal design, video signals, communication satellites and threshold decoding techniques
03 p0383 A69-12867

Communication satellites systems, discussing Intelsat satellite specifications and modulation methods for multiple access
03 p0383 A69-12870

Space age communication, use of satellites by mass media - UNESCO Conference, Paris, December 1965
03 p0534 A69-13132

Error correcting coding on DCSP satellite channels, discussing single access communication through wideband SHF repeaters in synchronous earth orbit
03 p0387 A69-13177

Time division multiple access system for INTELSAT satellite, analyzing burst preamble and selection of frame period
03 p0388 A69-13179

Communications system considerations for lunar libration point relay satellite to support Apollo lunar far side mission
03 p0388 A69-13180

Aeronautical satellite system to relay communications at VHF or L band frequencies from aircraft flying over oceanic routes
03 p0464 A69-13235

Transoceanic air traffic control system with independent surveillance of aircraft positions, decision making agency and undelayed communications, using satellites
03 p0464 A69-13236

International satellite system for commercial aircraft communications and air traffic control
03 p0464 A69-13238

Low altitude satellite relay system, discussing modulation, antennas, frequency plans, telemetry, tracking, command and earth terminals
03 p0391 A69-13241

Mutual RF interference between satellite and terrestrial telecommunications microwave relay system at shared frequencies
03 p0392 A69-13242

Economic importance of European communications satellite system development
03 p0535 A69-13583

European regional satellite communication systems, discussing EUROVISION TV program broadcasting and multiple access telephony
03 p0395 A69-13585

Cooperation between U.S. and Europe in communication satellite programs
03 p0535 A69-13591

Intelsat application satellites, considering economy and global telecommunication
03 p0535 A69-13592

Ghost project for gathering weather data by balloons and transmission of data to central data processing stations by satellite
03 p0520 A69-13621

Low noise broadband parametric amplifier for communication satellite ground stations
03 p0406 A69-13733

Low degree earth gravity harmonics effect on 12 and 24 hour orbits of high altitude communications satellites
04 p0592 A69-14661

European launch vehicle development program, discussing economic limitations and employment possibilities
04 p0665 A69-14808

Electronic counterrotating antennas, developing turning model of antenna group of telecommunications satellite
04 p0578 A69-15065

Aeronautical service satellites, considering communications, surveillance for navigation, traffic control, collision avoidance and search and rescue, weather and border control functions
04 p0666 A69-15295

Economic and technical advantages and disadvantages of satellite telecommunications, discussing Telstar intercontinental TV transmission and Soviet Molniya system
04 p0662 A69-15328

Domestic satellite communication system model for greatest possible amount of traffic using Saturn 5 propulsion systems, multibeam antennas, synchronous repeater platforms, etc
04 p0561 A69-15447

Optimum spacing of communication satellites on inclined circular synchronous orbits, applying figure 8 packing schemes
04 p0562 A69-15458

Aeronautical satellite communications, discussing results with NASA ATS-1 satellite
05 p0790 A69-16721

French and German cooperative program Project Symphonie to develop telecommunications satellite for radio and TV broadcasting
05 p0830 A69-16817

Earth orbiting communication satellites, discussing multiple access by stations and use of higher frequencies
06 p0885 A69-16856

Soviet Orbita communication satellite system network operation, design and technical and economic aspects
06 p0886 A69-17043

Molniya 1 communication satellite using elliptical orbit to provide radio, telephone and TV service [UN PAPER 68-95771]
06 p1013 A69-17044

Quality control for TV transmissions via communication satellites, considering transmission accuracy improvement and error measurement automation [UN PAPER 68-95773]
06 p0886 A69-17047

Satellite telecommunications, discussing Australian experience, ground stations location, national network and international cooperation [UN PAPER 68-95286]
06 p0886 A69-17066

Project Symphonie, discussing stationary communication satellite, coverage, frequencies and characteristics
06 p0886 A69-17072

Communication satellites application to domestic live TV, telephone and data communication and long distance telecommunication in Canada [UN PAPER 68-95501]
06 p0887 A69-17075

Satellite educational TV capabilities, applications and planning [UN PAPER 68-95355]
06 p0887 A69-17078

Adaptive control of reflective satellite communication system
06 p0887 A69-17356

Communication satellites in synchronous equatorial orbit for two types of educational TV, discussing picture quality, modulation, power, bandwidth and system costs
06 p1017 A69-17624

Canadian domestic satellite system requirements to extend existing terrestrial communications systems to improve coverage, capacity, flexibility and cost factors
06 p1043 A69-17832

Space communication, discussing global network of Intelsat satellites ground facilities, regional switching, RF channels, etc
06 p0890 A69-17860

Communication satellites attitude control and stabilization due to antenna beam pointing, with future systems forecast, discussing exchange, distribution and collection systems
07 p1228 A69-18339

Traveling wave tubes for Symphonie Communication Satellite, discussing design, performance and efficiency
07 p1095 A69-18429

Tunnel diode amplifiers for amplifying weak microwave signals, discussing low noise wideband preamplifier for communication satellites
07 p1099 A69-18464

Predictor determining future position of TDMA/Time Division Multiple Access/ synchronous satellite communications system satellite from previously received bursts
07 p1076 A69-18553

Sensitivity problems in receiving microwave signals from communications satellite at deep space distances, considering noise factors
07 p1077 A69-18669

Satellite TV broadcast application for communication and education, discussing costs and benefits in single and multimission combinations
07 p1244 A69-18678

World satellite telecommunications network, discussing recommendations with reference to signal transmission, acoustic echoes, etc
07 p1079 A69-18942

Communication satellite system design by use of baseband equation relating SNR after detection to CNR at detector input
07 p1085 A69-19180

Satellite communications history covering passive and active satellites and Communication Satellite Act impact
07 p1085 A69-19182

Lincoln experimental satellites, discussing transition to UHF bands and orbital launching
07 p1087 A69-19630

Transponders for communication satellites, discussing design constraints, reliability and transmission capacity increase
08 p1279 A69-19905

Intelsat 2 satellite structural design for Apollo communications
08 p1408 A69-19907

Communication satellites applied to broadcasting, considering point to point satellite link and distribution systems
08 p1272 A69-19925

Large aperture low noise aerial design for satellite communication earth stations, discussing expected performance of 85-ft antenna at 4 GHz
08 p1279 A69-19956

Satellite communication requirements for UK defense establishment, describing SKYNET system
08 p1272 A69-19957

Multiple access techniques in civil satellite communications systems, noting proposed digital time and frequency division methods
08 p1272 A69-19959

Communication satellite ground test programs, discussing structural, electrical integration, thermal control and antenna pattern models for simulation tests
08 p1409 A69-19962

Regulatory content of international agreements concerning communication satellites problems
08 p1422 A69-20584

Reliability effect on operating costs of satellite communications system ground stations, calculating annual cost of channel with continuous time carry-over
08 p1276 A69-20586

Self focusing linear array for communication satellites, evaluating radiated field taking into account mutual coupling between elements
08 p1289 A69-20970

Communication satellite systems role in world telecommunication network, discussing traffic type, volume and routing, earth stations location and capacities and orbit selection
09 p1449 A69-21271

Experimental communication satellites Score, Courier, Telstar, Relay, Syncom, Intelsat 1 and Molniya 1, discussing equipment, results, and ATS program
09 p1608 A69-21272

Signal interference criteria in considering frequency sharing between communication satellite systems and terrestrial radio services
09 p1449 A69-21273

Frequency modulation methods and multiple access for communication satellite systems, considering bandwidth for space station transponder
09 p1449 A69-21274

Preamplifier applications compared in active communication satellite systems for frequency division multiplex telephony and for TV
09 p1449 A69-21275

Multiple access in communication satellite systems for achieving maximum flexibility of interconnection between earth stations
09 p1450 A69-21276

Carrier energy dispersal in communication satellite telephony and TV systems, noting attendant RF bandwidth increase as function of distortion
09 p1450 A69-21277

Maximum horizontally radiated power of earth stations in any 4-kHz band for multichannel telephony and TV using satellites
09 p1450 A69-21278

Earth station antennas for communication satellite service, discussing design, fabrication, main lobe gain, side and back lobe suppression and noise performance
09 p1461 A69-21281

Earth station antenna radiation patterns for studying mutual interference effects between radio relay stations and communication satellite earth stations
09 p1461 A69-21282

Communication satellite system design for operation with frequency bands above 10 GHz, noting wideband communication
09 p1450 A69-21284

Structure of quasi-linear and wideband satellite transponders, discussing possible improvements
09 p1609 A69-21619

Communication satellite power utilization optimized by matching final amplifiers to solar cell array [AIAA PAPER 68-437]
09 p1442 A69-21990

Detectability parameter for measuring performance of multiple and random access satellite communication system using PN codes
09 p1457 A69-22460

Scintillation fading of VHF beacons on synchronous satellites, noting amplitude fluctuation depth and rate
09 p1457 A69-22461

INTELSAT for design, construction, launching and maintenance of global communication satellites, noting transponders
09 p1457 A69-22466

Domestic satellite system for carrying maximum traffic by full use of rocket technology including Saturn 5 type propulsion systems, antennas, frequencies, etc
09 p1458 A69-22467

Synchronous and near synchronous satellites for communication systems, discussing stationkeeping and low thrust propulsion
09 p1458 A69-22468

Commercial communication satellite earth station at Australia, noting antenna, autotracking capability, preamplifiers, and computer for control and monitor functions
09 p1458 A69-22469

Low noise wideband amplifier system for commercial satellite communication ground terminal receiver, noting cryogenically cooled parametric amplifier
09 p1458 A69-22470

Satellite technology for government and defense communications systems, noting effects of rainfall attenuation, weather and solar interference on performance and reliability
12 p2028 A69-25932

Technological feasibility of satellite based global data relay service for small users
12 p2028 A69-25949

Traveling wave tube for European communication satellite power amplifiers, showing nonlinear distortions dependence on RF input/output power and helix voltage
[AIAA PAPER 68-430] 12 p2041 A69-26786

Antenna circular array for synchronous communications satellites, discussing directional patterns, supergain ratio, element spacing, etc
13 p2225 A69-27184

Instructional broadcast satellites programming for time cost reduction, discussing frequency allocation, interference and ground station design
13 p2381 A69-27373

Earth TV pictures from Molniia 1 communication satellite, showing advantages of high orbit over low orbit photography for global weather analysis and forecasting
13 p2292 A69-27729

Satellite networks for air traffic control and aircraft communications in North Atlantic
13 p2296 A69-27831

Nonlinear distortions in TWT for communication satellites applications, discussing relationship with efficiency
13 p2232 A69-28060

Communication satellite frequency and time divisions multiple access problem, detailing microwave multiplexers design
14 p2417 A69-29688

Communications mission of Symphonie project and satellite communications subsystem design
15 p2562 A69-30084

COMSAT thermal vacuum chamber specification configurations, discussing chamber orientation, vacuum and roughing systems, pumping mechanism, wiring, installation, testing, etc
15 p2587 A69-30393

Dioscures project for worldwide telecommunications, air traffic control and navigation by satellites, discussing technical, operational and economic characteristics
16 p2749 A69-31601

Demand assigned frequency division multiple access-PCM system designed by COMSAT for satellite communication
16 p2749 A69-31602

Bipropellant propulsion systems using Aerozine 50 and nitrogen tetroxide for Symphonie telecommunications satellite
16 p2828 A69-31733

Project Symphonie German-French communication satellite mission and technical data
16 p2868 A69-32055

Electrophysiological /electrospinalchogram/ medical data transmission via satellite from France to U.S. for real time computer processing
16 p2746 A69-32070

Ammonia jet device to stabilize telecommunication satellites consisting of electric heating element, ejection nozzle and thermal screens
17 p3018 A69-33236

Time function multiplex system for simultaneous communication via satellite between number of stations, considering transmission capacity decrease due to hard limiting amplifier
17 p2919 A69-33320

Satellite system TDM techniques and prototype equipment capable of combining 12 unrelated start-stop and synchronous telegraph channels
17 p2920 A69-33420

Bearing system for mechanically despun antenna in spin stabilized communications satellite, offering greater directional stability, lower weight and power losses
17 p2978 A69-33431

Satellite systems for air traffic control, navigation, communications and telemetry in view of regulations of frequency allocations
18 p3103 A69-35089

Educational TV coverage extension via synchronous satellites to areas of limited coverage, emphasizing South American countries
19 p3268 A69-36163

Laser and quasi-laser pulse modulation technique for global satellites telemetry system
19 p3272 A69-36257

Communication satellites equipment and techniques, considering global network, satellite design, millimeter wave systems, etc
19 p3275 A69-36314

Commercial satellite communication ground station at Arvi, India, discussing system design, operation and international standards
19 p3275 A69-36412

Nationwide TV system using synchronous communication satellite proposed for India, discussing antenna, modulation, multiplexed channels and educational aspects
19 p3275 A69-36413

Research satellite, commercial satellite, lunar spacecraft and military satellite missions, discussing Intelsat, Comsat, Early Bird, MOL and ESRO space program
19 p3432 A69-36750

ITU space communication projects, discussing frequency registration, progress reports from member countries and committees, UN resolutions, communication satellites, etc
19 p3456 A69-36821

Satellite telecommunication systems coordination, discussing transformation feasibility of consortium or international organ into international organization
20 p3637 A69-37120

Juridical norms defined by Madrid, Belgrade and Washington conferences regulating exploration and utilization of extraterrestrial bodies and space, considering satellite communications networks
20 p3638 A69-37123

International cooperation regarding space telecommunication systems, discussing INTELSAT and INTERSPUTNIK roles in achieving international coordination and equality
20 p3638 A69-37125

Global communication satellite system with 12 to 16 hour period equatorial orbit, discussing satellite daily switchings, motions relative to earth, etc
20 p3497 A69-38189

Satellite Airborne Communications /STAIRCOM/ design constraints
20 p3497 A69-38314

Tactical Satellite Communications /Tacsat/ cost reduction, discussing jamming avoidance and mitigation, communications security, capacity increase and spectrum conservation
20 p3497 A69-38315

Geostationary satellite orbit used for communication satellites, noting ultimate limit of channels as related to separation angles between satellites
21 p3673 A69-38757

Frequency assignment methods for Intelsat 2 and 3 communication satellites
[AIAA PAPER 68-454] 21 p3674 A69-39226

Technical and economic factors of program to provide communications services via satellite facilities in continental U.S.
[AIAA PAPER 68-412] 21 p3678 A69-39762

Multiple access techniques of SSB-PM and PCM-PM frequency translation for satellite communication system, comparing performance characteristics
21 p3678 A69-39807

Communication satellites with regard to international arrangements for fruitful exploitation noting COSMAT, INTELSAT, European and international developments
22 p4052 A69-40276

Synchronous communications satellite launch constraints for fixed time or node, noting application to IDCSP/A mission and sun angle, occultation and transfer orbit
[AIAA PAPER 68-445] 22 p4036 A69-40543

Spacecraft phase array designed for use on synchronous communication satellite, discussing low structural weight packaging and unfurling problems and helix approach
22 p3915 A69-40705

German ground station radio communications via Intelsat satellites, discussing transmitting facilities, TV picture and sound signals, etc
22 p3902 A69-41249

Communication satellite technology application to overlay network linking nationwide data machines for business mail service with virtually instantaneous delivery at low cost
23 p4117 A69-41669

Monopulse, high power, three channel antenna feed system design for communication satellites, noting orthogonal polarization of transmit and receive functions
23 p4120 A69-41750

RFI effects of earth based emitters on operation of geosynchronous satellites for data relay from near earth orbiting satellites, noting frequency assignments
23 p4120 A69-41757

Communication satellite systems using hydrazine engine thrust for trajectory correction, discussing trajectory deviations causes and ERNO engine design
[DGLR-69-013] 23 p4203 A69-42152

TDMA/PCM system for communication tests via Applications Technology Satellites, discussing time synchronization and bit and frame coherency
23 p4129 A69-42510

Multichannel time division multiple access system for communication satellite networks, considering PSK modems, PCM codes and channel capacity
23 p4129 A69-42511

Communication subsystem design of Defense Communication Satellite Program /DCSP/ for background information, noting repeater with toroidal pattern antenna
23 p4131 A69-42537

UHF satellites for mobile, broadcast and low cost services, discussing bandwidth expansion, interference effects, ground linking, UHF partition, satellite antenna sizes, etc
[AAS PAPER 69-333] 24 p4282 A69-42872

Remote manipulator spacecraft system for refurbishing synchronous communication satellite, emphasizing compatibility with standard shroud Titan 3C launch vehicle
24 p4297 A69-43041

Communication satellites european development, discussing economic and technological problems, stressing color TV and SHF/FM transmission, compared to conventional ground station transmission
24 p4393 A69-43133

COMMUNICATION SYSTEMS U TELECOMMUNICATION

COMMUNICATION THEORY

Exponential distributions in Markov chain models for communication channels, considering error free runs of tropospheric systems
01 p0027 A69-10267

Linear random processes including law of large numbers, covariance estimation and linear to normal process relationship
01 p0029 A69-10555

Narrow band normal steady state random processes applied to signal dispersion by extended oscillating body, obtaining statistical characteristics
02 p0206 A69-11602

Book on communication systems covering signal design, video signals, communication satellites and threshold decoding techniques
03 p0383 A69-12867

Array radar technology development offering multifrequency operations from common aperture
03 p0388 A69-13182

Pseudonoise generator producing controllable repetitive random signal patterns used to evaluate instrumentation system
03 p0403 A69-13188

Multimode propagation communications system /MMPCS/ utilizing digital computer to implement intermittent system
03 p0389 A69-13191

Extension of results of one dimensional representation theory treating nonGaussian processes as perturbations of log normal process to higher dimensions
03 p0392 A69-13248

Wide signal and noise statistics range to determine noise rejection characteristics of communication system used for single path and diversity reception
03 p0394 A69-13376

Gain from communications operation at maximum usable frequency estimated on basis of long range ionospheric prediction technique adapted to computer
03 p0421 A69-13377

Symmetric M-ary signaling scheme, considering given calls signal vector transmission through communication channel
05 p0720 A69-16297

Book on introduction to random signals and communication theory covering signal analysis, analog and digital data transmission, information theory, etc
06 p0887 A69-17144

Energy fluxes statistical distribution produced by random and regular energy sources
07 p1076 A69-18510

Signal multiplexing within linear algebra framework permitting use of orthonormality in receiver construction without orthonormal functions generation in multiplexer
07 p1078 A69-18830

Satellite communication requirements for UK defense establishment, describing SKYNET system
08 p1272 A69-19957

Error probability for transmission of one of M orthogonal, equally likely, equal energy signals over generalized incoherent channel

09 p1452 A69-21314

Intermittent feedback channel for transmitter using orthogonal signals, noting smaller error probability and improved communication reliability

09 p1452 A69-21315

Round trip delay effect on probability of error in uncertainty feedback communication systems operating at channel capacity

09 p1453 A69-21322

Book on communication theory principles covering Fourier transformation, signal transmission, electromagnetic noise, amplitude, phase, frequency and pulse modulation, etc

09 p1454 A69-21801

Noise factor of two port in terms of various sets of noise parameters and source immittances, giving table for conversion formulas

09 p1455 A69-21897

Pattern recognition as part of statistical communication theory, using Karhunen-Loeve expansion to minimize root-mean-square errors, showing application to handwritten numerals

09 p1461 A69-22292

Error correction of digital data with cyclic codes and probability function set extended to Bose-Chaudhuri-Hocquenghem codes and P super M codes

10 p1655 A69-23529

Reliability behavior of information transmission between transmitter-receiver pair in network of erasure channels without decoding and recoding at nodes

10 p1657 A69-23865

Radio wave propagation in unstable inhomogeneous medium with space-time dispersion, showing adiabatic compression or expansion of wave packet spectrum

10 p1658 A69-23955

Narrow band normal steady state random processes applied to signal dispersion by extended oscillating body, obtaining statistical characteristics

11 p1835 A69-24709

Limitations of N-port concept in microwave technology, proposing definitions to avoid contradictions

11 p1841 A69-25624

Optimal communication by signal feedback link between transmitter and receiver based on optimum control and dynamic programming

12 p2046 A69-26060

Focusing factor in stratified medium with refractive index depending exponentially on height

12 p2029 A69-26100

Book on elements of detection and signal design covering transmitter optimization for coherent and noncoherent digital communication systems, statistical decision theory, radar detection, etc

12 p2033 A69-26867

Wide signal and noise statistics range to determine noise rejection characteristics of communication system used for single path and diversity reception

14 p2410 A69-28826

Gain from communications operation at maximum usable frequency estimated on basis of long range ionospheric prediction technique adapted to computer

14 p2433 A69-28827

Electrical engineering, Volume 3, communications, covering special theories, systems components, telecommunication, electroacoustics, digital and analog computers and programming

15 p2568 A69-30619

Lagrange expansion theorem for shielded surface waves, obtaining modal functions and power flows

16 p2750 A69-31947

Neumann-Lommel formula generalization for obtaining Bessel functions product sums illustrated with FM wave distortion calculation in multichannel system

18 p3101 A69-34625

Problem-oriented languages in man-computer intercommunication

18 p3106 A69-34658

Man-computer speech communication, discussing model and aspects of acoustics, phonetics, linguistics, language training, physiology, psychology, bionics, etc

18 p3107 A69-35099

Book on statistical communication and applications to radio and radar systems technology to provide guidelines for design decisions

19 p3267 A69-35900

Cross correlation and probability metric in coded sequential detection telemetry system, giving optimum parameters, overflow and error probabilities using computer simulations

19 p3273 A69-36266

High index frequency modulated waveform spectrum analysis including upper bound on approximation error to avoid fallacy of Woodward theorem [IEEE PAPER 68-TP-74-COM]

19 p3276 A69-36485

Representation theory of signal detection in non-Gaussian noise environments applied for improved near optimum system performance [IEEE PAPER 69-TP-10-COM]

19 p3277 A69-36488

Energy criteria inconsistency in evaluating frequency band changes attributed to simultaneous narrowing and broadening of different signal power bands

19 p3278 A69-36716

Optimum signals for high resolution radar and communication systems, using transmitter waveform design of autocorrelation and cross correlation functions

23 p4132 A69-42545

COMMUNITIES

NT MOUNTAIN INHABITANTS

Space broadcasting possibilities and problems, considering home reception and group participation at community centers

[UN PAPER 68-95287] 01 p0028 A69-10497

Urban noise control over transportation systems including aircraft and highway traffic operating beyond local noise ordinance purview

14 p2541 A69-29157

Airport noise control responsibility for airport and community planners using perceived noise level, noise and number index and community annoyance index as planning criteria

14 p2541 A69-29506

Aircraft noise abatement oriented toward compatibility between airports and adjacent metropolitan environments, analyzing results for theoretical and actual airports

[AIAA PAPER 69-800] 19 p3453 A69-35593

Joint noise effect on real estate value, discussing market survey, insulation and navigation easement costs and litigation damages

[AIAA PAPER 69-802] 19 p3288 A69-35594

Geostationary satellite TV broadcasting to small contiguous areas with separate programs, discussing communication distribution problems

22 p3902 A69-41252

COMMUTATION

Optical commutation to permit multifield monitoring and recording with one sensor by employing high resolution imaging fiber optics elements feeding common focusing lens

06 p0926 A69-17678

Feedback systems analysis, considering single phase and polyphase coupled and uncoupled commutation networks in forward loop and linear transfer function feedback loop

08 p1295 A69-19853

COMMUTATORS

NT DECOMMUTATORS

Miniature telemetry systems for gun launched projectile instrumentation and ejection payloads, noting voltage controlled oscillators, commutators and VHF FM transmitters

10 p1654 A69-23280

Rapid low level commutator for temperature measuring circuit with thermocouples, discussing construction and performance

11 p1884 A69-24758

Brushless DC motor with commutation control by magnetic position sensor scanned at HF

12 p2017 A69-26894

COMPACTING

Compaction kinetics in continuous quasi-viscous medium having plastic flow material under applied load, discussing hot pressing of nichrome powders

04 p0618 A69-15389

Properties of electrolytic and reduced titanium powders and sinterability of porous compacts

05 p0782 A69-16795

Mathematical analysis of compaction process for powder mixtures of different metals assuming known characteristics of components

15 p2641 A69-31182

Explosive compacting of aluminum powder, describing operational and experimental techniques, compacts hardness and density, mass production feasibility, etc

16 p2793 A69-31790

Compactability dependence of Fe, Co and Ni powders with Zr, Nb and Mo carbide additives on pressure, carbide content and lubricant

22 p3970 A69-40634

Optimal conditions for extrusion compacting of hard alloy mixtures plasticized with paraffin, determining

plasticizer content, upsetting, pressure and temperature

22 p3956 A69-40635

COMPACTNESS

U VOID RATIO

COMPARATORS

Wide range linear delay circuit with compensated bootstrap circuit generating linear ramp waveform and regenerative Schmitt trigger comparator

01 p0041 A69-10241

Gunn effect application in fast logic circuit devices including comparators, adder and shift register circuits

01 p0042 A69-10438

Multiinput sine comparators graphical analysis and design considerations, emphasizing semiconductor circuit providing quadrilateral polar characteristic on impedance plane

12 p2039 A69-26350

COMPARISON

Application of modern stability theory to solution of practical problems by means of comparison theorems, demonstrating effectiveness of method

03 p0467 A69-13747

Multiple cues in paired comparisons, discussing mathematical model of psychological process in information extraction and combination

21 p3664 A69-38970

COMPARTMENTATION

U COMPARTMENTS

COMPARTMENTS

NT AIR LOCKS

NT AIRCRAFT COMPARTMENTS

NT ANECHOIC CHAMBERS

NT COMMAND MODULES

NT PRESSURE CHAMBERS

NT PRESSURIZED CABINS

NT SPACECRAFT CABINS

NT TEST CHAMBERS

NT VACUUM CHAMBERS

Glutamic acid metabolism compartmentation in brain cortex demonstrated in vitro, using isotopic labeling

18 p3096 A69-35172

COMPASSES

U GYROCOMPASSES

U MAGNETIC COMPASSES

COMPATIBILITY

Plastic material requirements for semiconductor device encapsulation noting electrical compatibility, mechanical and environmental protection and costs

02 p0270 A69-12161

Large scale electronic systems configuration compatibility concept, discussing modular line replaceable units /LRU/ assigned set of numbers

08 p1322 A69-21154

Compatibility effects of automatic test equipment on avionic hardware design

11 p1865 A69-25070

High temperature compatibility of Mo, W, Nb and Ta as canning materials with high melting point and formation energy filling materials

14 p2463 A69-29219

Metal matrix compatibility of metal coated graphitized, silicon carbide and boron fibers, discussing fiber weakening processes

[ASM PAPER W9-20.1] 21 p3751 A69-38670

COMPENSATION

Stability contours for sampling and delay effects analysis in analog/digital hybrid simulation loops, considering compensation quality over simulated system natural modes

21 p3680 A69-39609

COMPENSATORS

Hologram chromatic aberration compensation by two lens system

01 p0080 A69-10430

Stationary Babinet compensator for measuring longitudinal solar magnetic fields by means of fringes introduced in spectroheliograms

11 p1880 A69-24433

Feedback controller compensator for invariant linear systems having unstable modes

12 p2054 A69-26517

Time delay errors compensation methods in analog-digital computation loops, finding digital scheme inferior to analog

15 p2572 A69-30618

Ellipsometric dimensions calculations with aid of laser radiation, stressing formulas for compensator and polarizer assemblies

15 p2636 A69-31474

- Moldable plastic shim material for structural airframe components, discussing application requirements
19 p3319 A69-35551
- Adaptive compensation to minimize human task in continuous manual control system using various models
20 p3482 A69-37721
- Programmable digital compensator for single high performance control loop servomechanisms
21 p3688 A69-39704
- Nonlinear compensator characteristics determination for modifying compensated system output signal under various disturbances with inputs subjected to white noise
21 p3688 A69-39862
- Babinet compensator with birefringent wedges made of stress frozen photoelastic material rather than quartz
22 p4042 A69-40442

COMPENSATORY TRACKING

- Roll-motion cues for man-vehicle control in compensatory tracking task with disturbance input
10 p1650 A69-23879
- Human information processing rates during one and two axis compensatory tracking tasks with secondary auditory task
10 p1650 A69-23880

COMPETITION

- Competition and aeronautical progress in aircraft industry, examining costs and effects of government limits on Boeing 707 and Douglas DC-8
03 p0536 A69-14110
- Competition and aeronautical progress in aircraft industry, examining costs and effects of government limits on Boeing 707 and Douglas DC-8
11 p2004 A69-24372
- Structure and scoring method for judging alternatives in contract selection
20 p3640 A69-38023

COMPILATION [COMPUTERS]

U COMPILERS

COMPILE PROGRAMS

U COMPILERS

COMPILERS

- Book on FORTRAN computer programming language
06 p0891 A69-17364
- Abbreviated Test Language for Avionics Systems /ATLAS/ as standard compiler input language for commercial airline automatic test equipment /ATE/
11 p1842 A69-25064
- Universal test equipment compiler /UTEC/ built for use with languages designed to control automatic test equipment
11 p1842 A69-25066

COMPLETENESS

- Completeness of Biot solution in theory of thermoelasticity, discussing Mindlin theorem and Boussinesq-Papcovich solution
07 p1236 A69-19470
- Completeness theorem for integrodifferential operator to establish Schwarzschild criterion for stability of gaseous masses
14 p2470 A69-28902

COMPLEX NUMBERS

- Dynamic polarizability at imaginary frequencies, deriving upper and lower variational bounds with functionals containing trial functions
01 p0122 A69-10284

COMPLEX VARIABLES

- NT AIRY FUNCTION
- NT ANALYTIC FUNCTIONS
- NT BESSEL FUNCTIONS
- NT CONFORMAL MAPPING
- NT CONJUGATES
- NT ELLIPTIC FUNCTIONS
- NT ENTIRE FUNCTIONS
- NT EXPONENTIAL FUNCTIONS
- NT GAMMA FUNCTION
- NT HANKEL FUNCTIONS
- NT HARMONIC FUNCTIONS
- NT HYPERBOLIC FUNCTIONS
- NT HYPERGEOMETRIC FUNCTIONS
- NT LEGENDRE FUNCTIONS
- NT LOGARITHMS
- NT MATHIEU FUNCTION
- NT NONHOLONOMIC EQUATIONS
- NT ORTHOGONAL FUNCTIONS
- NT RATIONAL FUNCTIONS
- NT SINGULARITY [MATHEMATICS]
- NT SPHERICAL HARMONICS

- Book on approximate representation of regular functions of complex variable, discussing Faber polynomials, best approximation theorems, etc
01 p0104 A69-10616

- Stresses in infinite elastic plate containing rigid rectangular inclusion subject to uniform stress field, using complex variable method and Schwartz-Christoffel conformal mapping
02 p0348 A69-12796

- Stress state of circular cylindrical shell subjected to uniform inward radial line load along generator solved by closed form particular integral, discussing convergence
02 p0349 A69-12797

- Eigenvector approximation of complex matrix by inverse iteration, giving Algol 60 program
03 p0455 A69-13371

- Dirichlet problem deviation from Bitsadze system with Noetherian properties, giving Hausdorff normal solvability conditions for inhomogeneous problem
03 p0456 A69-13603

- Levinson duality theorem for linear programs in complex space proved on basis of duality theorem for linear programming in real space
04 p0623 A69-14947

- Ground influence on Helmholtz flow in presence of plate perpendicular to stream, reducing problem to mixed Volterra problem in complex half plane
04 p0590 A69-15221

- Plane thermal stress distribution determined around holes under steady temperature distribution, using complex variable approach
05 p0836 A69-15877

- Electrical impedance of semiconductor supporting two waves contains entire complex transcendental function with complex parameter and infinity of zeros in left half z plane
07 p1196 A69-18268

- Complex variable theory usefulness in investigating existence and uniqueness of solutions for boundary values in partial differential equation
07 p1173 A69-18731

- Complex variable theory solution of eigenvalue problem governing elastic stability of thin elastic plate subjected to hydrostatic in-plane compression
09 p1615 A69-21921

- Linear thin shell theory in complex dependent variable form for determining fourth order partial differential equations, considering elastic shells with edge loads
11 p1978 A69-24811

- Integral representation for Wiener Hopf factorization of functions of complex variables for numerical processing of radiation problems
11 p1851 A69-24998

- Optimal control of multivariable complex systems through multilevel /hierarchical/ structure, discussing coordination problems
12 p2049 A69-26082

- Convergence of Bubnov-Galerkin method in complex separable Hilbert space, proving theorems for sufficient conditions
12 p2123 A69-26607

- Parametric variations method for solving nonlinear algebraic and transcendental equations, determining number of solutions in complex space
12 p2123 A69-26608

COMPLEXITY

U TASK COMPLEXITY

COMPLIANCE [ELASTICITY]

U MODULUS OF ELASTICITY

COMPONENT RELIABILITY

- Schmitt trigger current-voltage characteristic for determining switching behavior and switching point temperature, examining formulas and equivalent circuits
01 p0039 A69-10171

- IR optics for indicating dynamic mechanical component reliability via surface temperature variations
01 p0085 A69-10295

- Nondestructive testing of brazed liquid propellant rocket engine components and assemblies, describing radiographic, ultrasonic, thermographic, and leak test methods
01 p0085 A69-10534

- Mathematical model constructed for behavior of multicomponent system subject to cannibalization
01 p0086 A69-10651

- In-flight and flight line checkout techniques for foreign object damage to jet engines
01 p0056 A69-11055

- Steel selection for heat treated parts, discussing strength and hardness, service conditions, carbon content, quenching, cost, etc
01 p0101 A69-11397

- Guaranteed estimations of system reliability for systems with incomplete element reliability data
02 p0251 A69-11652

- Planar transistor reliability test results noting failure rate, stability and effect of temperature
03 p0402 A69-13006

- Book on laws of failures in technical equipment with emphasis on quantitative description and practicality of reliability theory, discussing redundancy problems
03 p0433 A69-13009

- Beryllium reflector distortion in Plum Brook Reactor due to neutron embrittlement and gas formation, noting material surveillance, replacement, etc
03 p0465 A69-13131

- Reliability system design, emphasizing circuit design analysis, failure drifts and component failure modes by use of computer programs /ECAP, CIRC and IMAG/
04 p0608 A69-15224

- Laws of wear and average life, noting application to electric connector reliability
04 p0579 A69-15320

- Reliable information storage in memories designed from unreliable components
04 p0569 A69-15455

- Reliable computation in computing systems designed from unreliable components, considering two models for component malfunctions
04 p0569 A69-15456

- Test equipment for rapid automatic checkout and evaluation of automatic flight control systems on commercial and jet transport aircraft
05 p0742 A69-15883

- Spacecraft terminal dry heat sterilization procedures for minimal time and temperature conditions, using simple geometric configuration of spacecraft for thermal analysis
05 p0712 A69-15942

- Recovery and long term reliability of Si p-n-p transistors subject to gamma radiation, using military specifications for failure
06 p0976 A69-16878

- Nondestructive technique to measure residual and working stresses in machine parts, using specially designed circuit
06 p0926 A69-17497

- Engineering designs and hardware required for low risk flight of long duration manned space stations
06 p1007 A69-17601

- Solder joint cracking in discrete component assemblies, discussing cracking mechanism and crack elimination methods
07 p1140 A69-19102

- Fiber reinforced plastic and metallic composites for longevity and endurance of materials at high temperatures and extreme loads, discussing alumina whiskers
07 p1167 A69-19290

- Wind tunnel rain erosion testing of components of aircraft or missiles flying at high speed
07 p1117 A69-19534

- Fail-safe goals, design criteria, analytical methods and test procedures to achieve reliable damage tolerant dynamic rotating parts for V/STOL and helicopter transports
07 p1237 A69-19569

- Transponders for communication satellites, discussing design constraints, reliability and transmission capacity increase
08 p1279 A69-19905

- Thermal stabilization and ethylene oxide effect on spaceborne electronic component sterilization and decontamination
08 p1283 A69-20266

- Components production process effect on reliability based on values and functional relations of internal parameters, noting influence on accelerated testing
08 p1319 A69-20346

- Operational reliability of manual and automatic flight control systems and components and current safety standards
08 p1255 A69-20720

- Microcircuit components and microelectronic systems reliability assessment including short term testing, noting digital systems, packaging, production controls, etc
08 p1291 A69-20984

- Postselection estimation of component reliability in multicomponent systems, considering cases of binomial and exponential distributions of random variables
08 p1322 A69-21099

- Computerized simulation of time dependent reliability of multicomponent system based on statistical model of component breakdown
08 p1277 A69-21100

- Computer programs for systems statistical reliability characteristics using reliability tests and time to failure data, giving optimal breakdown probability functions
08 p1322 A69-21101

Assessing cost effectiveness of reliability and quality of semiconductor products, using mathematical models
08 p1292 A69-21102

Reliability of individual components of multicomponent systems under variable loads, using asymptotic distribution of minimal values
08 p1322 A69-21103

Failure distribution functions based on Eyring component aging model, including failure probability density function for Weibull and gamma type distributions
08 p1322 A69-21104

Electronic components reliability tests, determining correlation between material quality and failure
08 p1293 A69-21109

Process control data in acceptance procedures for high reliability electronic components, discussing supplier and user cooperation
08 p1293 A69-21110

Reliability distribution parameters for electronic components, determining time and tolerance dependence of reliability
08 p1293 A69-21114

Failure mechanism in high-voltage semiconductor diodes explained by effect of reverse voltage pulses, considering design reliability
08 p1294 A69-21116

Reliability in microelectronics estimated from failures expected during lifetime, describing various test methods
08 p1294 A69-21121

Triodes reliability for space application, emphasizing RH 7 C used during Mariner 4 expedition
08 p1295 A69-21122

Stochastic model for calculating expected component failures in transient state from Weibull distribution failure data for first generation
09 p1504 A69-22149

Space guidance and control system components, noting control moment gyro, actuator, brushless DC motor, electrically supported gyro and laser gyro
09 p1500 A69-22434

Elastoplastic stress in notch as cause of decreased lifetime of aircraft components, analyzing stress reversal and displacement during takeoff and landing
09 p1620 A69-22576

Electroexplosive element design for safe reliable devices in liftoff and space environment, considering stray electric currents, RF fields and electrostatic discharges
10 p1752 A69-23022

Argas test loop as model for MHD power plant study, discussing component testing including channel preionization and relaxation experiments
10 p1673 A69-23478

State probabilities of finite stochastic queueing system for calculating equipment reliability parameters
10 p1664 A69-23693

Spacecraft electronic components design, environmental and reliability criteria including weight and power
11 p1843 A69-24340

Electronic systems and component reliability in space, considering electric parameter variation effects
11 p1848 A69-24867

Value engineering and component/products improvement incentive contract clauses role in defense product quality improvement
13 p2383 A69-28100

Electron fractography used in machine parts failure analysis to detect internal and surface cracks, forging defects, stress corrosion, fluid leakage sources, etc
13 p2269 A69-28182

Crack initiation prediction in high temperature components subjected to arbitrary thermal-mechanical cycling
13 p2365 A69-28252

Material selection criteria for low cycle fatigue resistance in components design determined from tensile test and incremental step test curves
[ASME PAPER 69-DE-59] 14 p2461 A69-28852

Thermionic converter components reliability under mechanical load and failure models, showing probabilistic nature of failures
14 p2400 A69-29227

Flight worthiness of mishandled electronic equipment, analyzing fragility and performance of shock exposed components and connections
15 p2576 A69-30362

Equipment testing, discussing collaboration between government agencies and independent environmental testing laboratories
15 p2720 A69-30398

Cost effectiveness of test selection when statistical distribution of load and strength are known, presenting

curves for equally dispersed normal parameters distribution
15 p2720 A69-30401

Viggen computer development, stressing reliability towards aircraft vibrations
15 p2577 A69-30620

Reliability of electronic components for space - Conference, Grenoble, November 1968
15 p2622 A69-30816

Space equipment reliability, discussing manufacturing defects, design faults, component failures, maintenance, overloads, accidents and operating errors
15 p2624 A69-30817

Spacecraft electronic component reliability policy based on preferential lists, selection programs and component management
15 p2624 A69-30818

Satellite circuit assembly reliability achievement by high reliability components, redundancy and optimal utilization
15 p2624 A69-30819

Management and scientific computer reliability difference, considering circuits, component assembly, software, maintenance, etc
15 p2624 A69-30821

Space electronic component reliability, considering suppliers and laboratory-workshop partnership
15 p2624 A69-30822

Short term plan of European electronic component selection for ESRO satellite without established guaranteed failure rate
15 p2624 A69-30823

Planar bipolar transistors degradation under thermal and ionizing radiation stresses, analyzing surface recombination currents of silica films and silica-silicon interfaces
15 p2625 A69-30826

Mass-produced silicon transistors reliability, presenting tables and curves of lifetime tests
15 p2626 A69-30833

Unitary sorting influence on reliability of planar transistors subjected to irradiation recovery cycles and scaled stresses
15 p2626 A69-30834

Electronic components reliability by failure rates and drift behavior, assuming probabilities product rule and exponential law of life distribution
15 p2626 A69-30835

Reliability control of 1/4-W resistors of tin oxide on glass substrate manufactured in quantity
15 p2627 A69-30837

Passive components reliability subjected to ionizing radiation for families, types, batches and individuals
15 p2627 A69-30838

Screening techniques for semiconductor devices, considering component classification with respect to population strength distribution
15 p2627 A69-30840

Production line requirements for MOS and IC, considering high reliability at minimum cost for space applications
15 p2627 A69-30841

Transistors and IC reliability for memory control evaluated by Concerto subprograms
15 p2627 A69-30842

Ceramic condensers with very high reliability mass produced for Concerto program, describing component characteristics and production methods
15 p2627 A69-30844

Metal film resistor reliability for conventional and space use, outlining guidelines for fabrication and quality control
15 p2628 A69-30847

Computer aided design /CAD/ of component selection for circuit optimization applied to circuit performance and sensitivity calculations
15 p2628 A69-30849

Complex systems reliability, describing uses of computer programs in analysis of circuit design, component failure modes and faults due to drifts
15 p2572 A69-31042

Failure analysis techniques in electronic component reliability laboratory, discussing electrical and physical tests to detect weaknesses in manufacturing and design
15 p2722 A69-31133

Long life repairable equipment reliability and mean time between failure with limited life components and material in normal life maintenance environment
15 p2581 A69-31134

Electronic component life test sampling plans based on lognormal distribution and instantaneous failure rate or hazard rate criterion
15 p2630 A69-31137

Space vehicle subcontracted components reliability attainment, discussing reliability process specifications, motivation, product reliability and feedback programs
15 p2723 A69-31139

High reliability space system electronic parts control program to assure success of unmanned space missions
16 p2793 A69-31714

Concorde propulsion and ejection systems reliability, testing reheating duct, primary nozzle, secondary assembly, etc
16 p2837 A69-32072

Automatic nonrepairable control elements reliability evaluated statistically with differentiable lifetime distribution function
16 p2764 A69-32199

Remote disassembly and inspection methods for evaluating NRX-AG reactor components performance [AIAA PAPER 69-511]
16 p2810 A69-32712

Engine and components reliability, discussing design stage and programming [AIAA PAPER 69-476]
16 p2795 A69-32771

Scanning electron microscopy to study device failure and performance, discussing limitations and progress
17 p2936 A69-32890

Aircraft turbines mechanical parts reliability tests, discussing examples of blade fatigue rupture and rotor disk fatigue
17 p3020 A69-33347

Data inaccuracy used for calculating forecasts of reliability analyzed by Monte Carlo simulation
17 p2937 A69-33389

Maximum helicopter level flight speed loads spectrum shape and severity related to rotor component fatigue design strength [AHS PAPER 372]
17 p3059 A69-33516

Helicopter flight loads spectra data compared on statistical basis to establish component service lives [AHS PAPER 301]
17 p2901 A69-33548

Reliable structural joints and attachments design for components fabricated from nonmetallic refractory brittle materials, discussing departures from conventional practices
17 p3061 A69-33569

Soviet book on reliability of semiconductor radio devices of flight vehicles covering failures through production errors, power source instability, environment induced changes, etc
18 p3108 A69-34350

Spacecraft and aircraft components failure analysis for ensuring high reliability of final products
18 p3143 A69-34483

Reliability tasks vs product reliability, discussing differences in effectiveness and management programming
18 p3143 A69-34484

Physics of Control program for electronic devices reliability, discussing qualified parts, chemical, physical and electrical properties, parameter ranges, specifications and corrective action
18 p3143 A69-34488

Semiconductor life potential evaluation based on electrical parameters measurements at various voltages over wide temperature range
18 p3144 A69-34489

Radiation resistant devices for minimizing neutron and gamma radiation effects on military electronic components, discussing selection features and sampling lot sizes
18 p3144 A69-34491

Mechanical failure technology, describing programs of government coordinated Mechanical Failure Working Group /MFWG/
18 p3144 A69-34492

Beam lead sealed junction transistor and integrated circuits reliability, describing test conditions and failure mechanisms
18 p3145 A69-34497

Epoxy encapsulated transistors reliability, data from long term maximum rated life and accelerated tests
18 p3145 A69-34498

Prefailure detection of unreliable electronics parts from random samples of received parts lots, noting cost reductions
18 p3146 A69-34508

OGO program failure rate analysis with respect to cost, schedule and performance tradeoffs, considering component and systems design and reliability, prelaunch feedback, etc
18 p3207 A69-34519

Lunar Orbiter Parts Program for selection and control of electronic and electrical parts, discussing reliability and flight failures
18 p3207 A69-34520

Computer program and component part models for nonlinear DC circuit simulation at various temperatures 18 p3108 A69-34525

Statistical testing techniques using small sample size at low component levels to predict product performance 18 p3117 A69-34528

Equipment maintainability demonstration technique, discussing simulation, repair time rates mathematical distribution, range and limits 18 p3117 A69-34530

Glass encased electronic components with conformal coatings, considering glass breakage at low temperature 19 p3281 A69-35547

Signature analysis diagnostic methods for reliability tests involving final product checkout and early fault detection 19 p3322 A69-35574

Holographic interferometry for nondestructive testing of aircraft materials, discussing applications to quality control 19 p3322 A69-35576

System reliability evaluation based on failure analysis illustrated with examples covering initial requirement through parts production monitoring and control 19 p3454 A69-35782

Microwave equipment reliability considered in terms of various subsystems and components, showing carefully formulated and executed test program as essential 19 p3282 A69-35785

Gas turbine components life prediction, using Weibull distribution and Bayes theorem to estimate probability of crack initiation 19 p3394 A69-36004

Environmental testing of space hardware, discussing failure detection by thermal vacuum tests and mechanical signature analysis 19 p3430 A69-36009

Reliability measurements based on maintenance records, considering human factor and life limiting and random chance design 19 p3327 A69-36013

Reliability study of launch support equipment, presenting failure data for mechanical and electromechanical components 19 p3295 A69-36023

Mechanical components life or cycles to failure probability distributions determined by Monte Carlo method, comparing theory with aircraft engine parts field data 19 p3327 A69-36031

Time-dependent failures of components subjected to fatigue loading analyzed for reliability prediction 19 p3437 A69-36032

Environment effect on scientific and telecommunication equipment mounted on exploratory probe during Venus atmosphere entry for acceleration loading in design 19 p3431 A69-36037

Bayesian reliability demonstration tests for predetermining sample size producer and consumer risks for equipment with exponential and binomial failure distributions 19 p3327 A69-36039

Computer program using system simulation and Monte Carlo techniques to assess turbojet engine compressor disk reliability, discussing maintenance policy and engine design effects 19 p3394 A69-36042

FM radioaltimeter for Concorde aircraft, describing autocorrelation and automonitoring device, signal characteristics, reliability, etc 19 p3315 A69-36699

Hazard and renewal rate and bathtub curves for electronic equipment reliability, noting single and multiple probability densities 20 p3504 A69-37070

Component hazard rate distribution functions from unit time and failure analysis, noting confidence statements and simulation studies 20 p3548 A69-37158

Onboard computer reliability, discussing missile computers and maintenance procedures 20 p3503 A69-37400

C-5A transport modular valve design for improved maintenance and high reliability due to manifold-cartridge arrangement 20 p3466 A69-38178

MIL-STD-781B reliability tests with standard based on exponential distribution for equipment exhibiting constant failure rate, noting sampling 20 p3551 A69-38289

Encapsulation effects on piece parts in high density package, considering unexpected part failures elimination in Lunar Module Signal Conditioning Electronic Assembly 22 p3910 A69-39953

Techniques to control, measure and assure reliability of electronics systems and equipment, emphasizing Thorndike chart and Molina tables 22 p3953 A69-40026

Reliability testing and parts screening of electronic systems for best parts selection 22 p3953 A69-40029

Safety and failure of components - Conference, Brighton, England, September 1969 24 p4397 A69-42767

Gas turbine engine problem causing component failures, considering alternative replacement strategies 24 p4318 A69-42774

Engineering components service failures involving fatigue crack propagation, analyzing causes 24 p4398 A69-42775

Component reliability effect on airline operation of VC 10 aircraft, investigating failure modes and maintenance 24 p4318 A69-42776

Management role in ensuring products and components quality and reliability, analyzing failure reasons 24 p4416 A69-42778

High reliability of solenoid and pressure regulating valves under long duration space missions, considering design, tests and controls [AAS PAPER 69-238] 24 p4319 A69-42854

Equipment reliability determination from relations for efficiency characteristics of stochastic queueing system with finite number of sources having Markov character 24 p4287 A69-43129

Microelectronics test program consisting of four reliability screening levels based on Mil-Std 883 24 p4287 A69-43205

COMPONENTS

Passive circuit components electrical properties at HF using equivalent circuit 08 p1283 A69-20135

Bubble leak testing of components to understand effects of gas and liquid viscosity, surface tension, pressure differential and temperature 09 p1503 A69-21391

Subcontractors documentation coordination system for Mississippi Test Facility, identifying end items for maintenance and spares provisioning 18 p3118 A69-35063

State variables with delta functions for electrical network with discontinuously variable components, discussing application to parametron 19 p3287 A69-36763

COMPOSITE MATERIALS

NT CERMETS

NT LAMINATES

NT METAL MATRIX COMPOSITES

NT REINFORCED PLASTICS

NT THREE DIMENSIONAL COMPOSITES

NT WHISKER COMPOSITES

Mass or energy transfer in reinforced media, discussing components characteristics and role of diffusion processes 01 p0173 A69-10079

High temperature magnetic analysis of metallurgical structure of high strength steels and composites, including phase transformation and matrix grain structure 01 p0093 A69-10111

Highly oriented graphite crystallites in pyrographites and composite materials, discussing preparation and anisotropy ratios in physical properties 01 p0102 A69-10978

Composite material mechanical failure due to detachment of microfiber ends from elastic matrix while under tension 01 p0171 A69-11259

Fiber-fiber interaction effect on stress distribution and tensile strength of discontinuous aligned fiber composites 01 p0171 A69-11261

Elastoplastic stress-strain behavior of concentric composite cylinders under uniaxial tension using analytical model, predicting transverse stresses during axial loading 01 p0171 A69-11263

Thermal stresses near spherical inclusion in elastic matrix with uniform heat flow 01 p0171 A69-11264

Ribbon reinforcements in composite materials noting stiffness properties 01 p0172 A69-11265

Quantitative determination of phenolic content in composite materials by pyrolysis gas chromatography method 01 p0025 A69-11267

Elastic properties of epoxy resins, deriving relation by considering different shear properties in tension and compression 01 p0103 A69-11268

Diffusion zones in filament reinforced metal matrix composites, using metallographic technique 01 p0103 A69-11269

Stress transfer from loaded matrix to single fiber in composite materials determined by series and step formulations 01 p0172 A69-11271

Critique of paper on thermal conductivity of composite materials by long wave method 01 p0172 A69-11272

Off-axis test for hard orthotropic composite materials, discussing fixture design to reduce shear coupling effect 01 p0103 A69-11273

Reinforcing glass fiber fillers in thermoplastic commercial products, noting applicability to high speed fabrication by injection molding processes 02 p0269 A69-11794

Fracture process in composite films of stressed tetrafluoroethylene and fluorinated ethylene propylene 02 p0270 A69-12368

Composite tensile-failure modes, discussing failure load prediction, experimental data and statistical analysis of stress concentration effects [AIAA PAPER 68-173] 02 p0347 A69-12514

Time dependent viscoelastic stress distribution in two phase composite material, using plane stress model for approximation 02 p0348 A69-12540

Metal composite materials, discussing strengthening mechanism for inclusion of high elastic coefficient and creep limit fibers in weak ductile matrices 02 p0268 A69-12750

Fabrication of Cu-W composites with discontinuous fibers based on sintering and rolling 03 p0444 A69-13349

Composite main rotor blade for Sud-Aviation SA-330 helicopter consisting of steel spar/epoxy-glass envelope [SAE PAPER 68-0693] 03 p0366 A69-13444

Fiber-matrix interfacial bond function and bond strength role in fiber composites mechanical behavior 03 p0450 A69-13881

Elastohereditary characteristics of composite materials with random inhomogeneities based on Volterra principle 04 p0667 A69-14263

Radiation processed wood-plastic materials produced by impregnating natural wood with liquid monomer followed by ionizing radiation induced polymerization 04 p0605 A69-14582

VTOL aircraft materials for improved lightness, durability and cost, noting Be alloys, filamentary composite materials and future problems 05 p0702 A69-15962

Mechanical and physical properties and cryogenic wear tests performed on composite materials, considering NERVA cryogenic turbopump bearing retainer development [ASME PAPER 68-WA/LUB-10] 05 p0768 A69-16133

Flow stress of iron wire reinforced aluminum alloy composites [ASME PAPER 68-WA/MET-10] 05 p0780 A69-16150

Statistical model for tensile fracture of parallel fiber composites based on stress criterion for crack propagation [ASME PAPER 68-WA/RP-7] 05 p0783 A69-16159

Boron carbide continuous filaments preparation and properties, discussing use in resin and metal composites [ECS PAPER 210] 05 p0783 A69-16236

Glass, boron and graphite filament wound resin composites and liners for cryogenic pressure vessels 05 p0785 A69-16488

Cryogenic mechanical properties of epoxy resins and glass/epoxy composites 05 p0785 A69-16491

Composites reinforcement with single crystal flakes of aluminum diboride 05 p0785 A69-16581

Metal matrix composites - ASTM Conference, Boston, June 1967
06 p0938 A69-16940

Metal matrix composites highest potential for future use and development of filament-matrix compatibility in relation to high temperatures
06 p0939 A69-16941

Lattice strains in matrix phase of aluminum-boron and copper-tungsten composites measured by X ray diffraction
06 p0939 A69-16944

Metal matrix composites compression microstrain behavior, analyzing continuous fiber composites of magnesium-boron and copper-tungsten
06 p0939 A69-16945

Diffusion bonded aluminum-boron composite material, discussing mechanical, metallographic and radiographic properties
06 p0939 A69-16946

Plastic yielding and strain distribution in Al reinforced with stainless steel wires determined by electron microscopy
06 p0940 A69-16947

Micromechanics of boron filament reinforced aluminum composites
06 p0940 A69-16948

Aluminum-silica fiber reinforced metal composite, discussing mechanical behavior and effect upon engineering applications
06 p0940 A69-16949

Aluminum-stainless steel wire reinforced metal matrix composites, analyzing strain hardening and plastic deformation
06 p0940 A69-16950

Fatigue performance of composites consisting of W or Mo helical coils embedded in Cu matrix, discussing evaluation from microstructural behavior
06 p0940 A69-16951

Delamination effects on strength degradation of filament wound composites
06 p0946 A69-17126

Controlled microstructures of eutectic aluminum-copper aluminides produced for mechanical properties studies
06 p0942 A69-17227

Metal fiber reinforced ceramic matrix composites, discussing model system, bond strength, loading and elastic properties
06 p0946 A69-17528

Fiberglass reinforced plastic bottoms design for integration with cylindrical shells, discussing design, shapes and boundary value problems
06 p1025 A69-17685

Statistical theory of material strength with application to composite materials reinforced with whiskers and continuous fibers
[AIAA PAPER 69-123] 06 p1028 A69-18142

Incremental complementary energy method of stress analysis of orthotropic nonlinear materials having different behavior in tension and compression
[AIAA PAPER 69-119] 06 p1028 A69-18159

Initial geometric imperfections effect on buckling and postbuckling behavior of laminated composite cylindrical shells under axial compression, considering reinforcing fiber orientations
[AIAA PAPER 69-93] 06 p1029 A69-18194

High strength carbon fibers development and applications in reinforced composite materials and aerospace industry
06 p0947 A69-18236

Two phase self lubricating composite materials for high temperature, detailing impact strength, friction and wear tests
[IME PAPER 12] 07 p1137 A69-18560

Compressive strength of boron fiber-epoxy matrix composite, noting matrix support of fibers against buckling
07 p1170 A69-18713

Critical axial load for elastic instability of unidirectional equally spaced fibers in plane of composite plate and buckling modes
07 p1232 A69-18714

Stress concentration factors for composite body of two isotropic elastic phases in plane strain in plane of composite parameters
07 p1170 A69-18716

Fiber geometry and partial debonding effects on bond stress distributions around single rigid fiber in infinite elastic plate subject to tensile stress
07 p1170 A69-18717

Cylindrically orthotropic hollow cylinder elastic properties determination using experimental test for production of stress and strain states and end effects
07 p1232 A69-18718

Plane anisotropic rectangular plates with various boundary conditions, analyzing stability, natural frequencies, mode shapes and displacement under lateral loads
07 p1232 A69-18719

Sign conventions definition and importance for shear stress and strain analysis in laminated anisotropic composite materials, noting role in studying response
07 p1170 A69-18720

Technique for compressive mechanical behavior of viscoplastic nonlinear composites, discussing rate dependence and one dimensional stress-strain time properties
07 p1159 A69-18721

Statistical computations of elastic moduli of macroscopically isotropic particulate composites, discussing porosity and elastic properties of materials made by sintering
07 p1159 A69-18722

Anodizing effect on flexural properties of Al-aluminum oxide sandwich composites, emphasizing properties of oxide coatings as function of thickness
07 p1159 A69-18723

Axial loading of unidirectional composite with hexagonal array of isotropic circular filaments generalized for filament anisotropy, discussing matrix elastic modulus and Poisson ratio
07 p1170 A69-18724

Directional solidification of multicomponent metal alloys for matrix in fiber reinforced composites, using monovariant eutectic reactions
07 p1166 A69-19145

Fiber reinforced plastic and metallic composites for longevity and endurance of materials at high temperatures and extreme loads, discussing alumina whiskers
07 p1167 A69-19290

Elastic constants of composite materials by dispersion relation of sound waves for long wavelength, assuming periodicity in three dimensional rectangular lattice
07 p1236 A69-19457

Fabrication and processing techniques, tooling concepts and quality control for composite materials used in large aircraft, discussing honeycomb and sandwich structures
[ASM PAPER D8-25.4] 07 p1172 A69-19670

Yielding of matrix material and cell size of substructure relationship to dry abrasion resistance of SAP type aluminum alloy at room temperature
08 p1319 A69-19995

Fiber-metal matrix composites fabrication, applications, mechanical properties and powder metallurgy
08 p1332 A69-20204

Development of materials in aerospace structures and propulsion systems, discussing superelastic alloys, graphite fibers, composites, refractory metals and processing techniques
08 p1332 A69-20306

Translunar cracks in laminated graphite filament composites, noting effect of thermal stresses due to cooling
08 p1337 A69-20483

Susceptibility of high modulus graphite and boron fiber epoxy composites to lightning damage, noting degradation by pulse current
08 p1338 A69-20486

High modulus and high strength carbon fibers and composites, discussing mechanical properties and interlaminar shear strength
08 p1338 A69-20488

Filament winding process variables effect on carbon or fiberglass reinforced composites, determining mechanical properties
08 p1338 A69-20489

Fracture energy of unidirectional laminated composites related to diameter, debonding energy and strength of reinforcing filaments
08 p1414 A69-20493

Tensile characteristics of discontinuous unidirectional fiber reinforced glass-epoxy composites and filament wound material, discussing alignment and interfacial bonding
08 p1339 A69-20496

Nondestructive testing methods application to fiber-bonded composites, noting X ray diffraction, radiography and ultrasonics
08 p1339 A69-20498

Thermoelastic properties of particulate, filamentary and layered composites, summarizing Soviet theoretical and experimental work
08 p1339 A69-20500

Matched metal molding of short graphite fiber composites
08 p1339 A69-20502

Plastic composite reinforcements with boron, silicon carbide, graphite, single crystal alumina and laminating resins, discussing properties and fabrication
08 p1340 A69-20503

Shop-ready high modulus carbon and fiberglass composite reinforcement system, stressing effect of modulus fibers amount in laminate
08 p1340 A69-20508

Mechanical properties of cast epoxy resins correlation with corresponding composites strength under static and dynamic fatigue stressing
08 p1340 A69-20510

Composite materials based on carbon and boron filaments, discussing application in turbine blades, propeller and helicopter rotor blades and airframe components
08 p1341 A69-20601

Mechanical properties of ceramic material consisting of pure silica matrix reinforced by carbon fibers
08 p1341 A69-20700

Cylindrically deformed fiber reinforced material, obtaining kinematics and constitutive equations
08 p1418 A69-21002

Thermal stress field under uniform heat flow due to elliptical elastic inclusion for anisotropic case
08 p1418 A69-21003

Failure criteria for predicting filamentary composite strength under uniaxial and combined stresses from properties and fabrication process considerations
09 p1611 A69-21479

Composite materials and alloys for jet turbine components in 1970s, discussing anticipated temperatures and material properties
09 p1523 A69-22061

Boron and graphite fibers role in composites cost feasibility in 1970s
09 p1524 A69-22067

Boron-epoxy composites applications and properties, comparing strength to weight and stiffness to weight ratios with aluminum, titanium and beryllium
09 p1529 A69-22068

Development and fabrication of fiber-resin and fiber-metal composites, discussing application to aerospace technology
09 p1524 A69-22069

Four point flexure, ring flexure and NOL ring tension tests for evaluation of composite material mechanical properties
09 p1499 A69-22308

Fatigue behavior of composite disk modified from previously evaluated boron epoxy reinforced titanium compressor disk
09 p1619 A69-22323

Prepreg based on S glass with HTS finish and B staged epoxy resin, discussing tensile strength and moisture exposure
09 p1530 A69-22327

Automatic fabrication process for boron reinforced composite structures, concerning orienting and laminating jet flap skins
09 p1507 A69-22329

Magnesium boron composite fabrication by diffusion bonding and liquid metal infiltration, obtaining minimized property variations and high strength to density ratios
09 p1507 A69-22332

Subscale aircraft fuselage section fabricated with lightweight graphite fiber/epoxy resin composite material
09 p1509 A69-22341

Bonded Al-B metal matrix composite materials hot press fabrication and design, discussing temperature pressure time cycles and honeycomb sandwich structures
09 p1510 A69-22351

Ferromagnetic composite materials for microwave absorption and shielding over frequency band 0.3 to 10.0 GHz
09 p1510 A69-22352

Whisker metal matrix composite fabrication, discussing aligned whisker distribution without degrading strength or fracturing and detailing extrusion process
09 p1511 A69-22361

Graphite fiber electroplating with nickel on continuous basis for ribbon like continuous flexible twist free yarn
09 p1512 A69-22362

Pyrolytic carbon felt composite development and properties, measuring and tabulating mechanical, thermal and ablation properties
09 p1530 A69-22364

Materials, processing and testing variables effects on mechanical properties determined for metal matrix composites

[ASME PAPER 69-GT-23] 09 p1527 A69-22496

Titanium-boron composites for gas turbines, mechanical properties and service life in high temperature environment

[ASME PAPER 69-GT-1] 09 p1527 A69-22510

Static and dynamic strength tests and modulus data for graphite fiber/epoxy composite yarn, noting ply winding and dimensions

[ASME PAPER 69-GT-114] 09 p1531 A69-22520

Unidirectionally solidified eutectic composite of Al and Cu-Al intermetallic, noting tensile properties at room and high temperatures

10 p1708 A69-22995

Polymeric composites mechanical energy dissipation dependence on dimensions of interfacial region between matrix and filler phases, considering particle size and strain magnification

10 p1794 A69-23037

Pulse echo ultrasonic nondestructive testing of C-5 adhesive bonded aluminum composites with multiple bond lines

10 p1698 A69-23047

Cosserat continuum and elasticity models of dynamics of composite materials, analyzing dispersive longitudinal waves

10 p1798 A69-23148

Torsional vibrations of composite elastic orthotropic cylinders, including cylindrical shells and isotropic composite cylinder

10 p1800 A69-23243

Superconducting magnets steady state stability improvement by using composite conductors

10 p1746 A69-23634

Rubber modified thermoplastics structure and mechanical properties, emphasizing stress concentration around composite particles and crazing role in creep and fracture

10 p1716 A69-23985

Electroplating solutions test for filament winding and electroforming process used in fabricating fiber reinforced metal composites

11 p1890 A69-24337

Elastic waves propagation in inhomogeneous composite media, considering coefficient of structural stress concentration

11 p1972 A69-24649

Reinforced metals properties and applications including fibers and lamination, notch sensitivity, brittle fracture, failure and heat resistance characteristics

11 p1904 A69-24898

Varying diameter anisotropic composite shafts torsion based on strain and stress functions

11 p1982 A69-24975

Unidirectional fibrous materials stability, finding characteristic equation in form of infinite determinant by solving three dimensional stability of reinforcing fibers in binder

11 p1985 A69-25172

Shim joints design for composite material structural members reinforcement in joint region, considering weight factor

[AIAA PAPER 68-341] 11 p1987 A69-25369

Graphite and B filament-epoxy resin composites application to aeroelastic scaled dynamic models, analyzing weight savings, fabrication and component stiffness

11 p1990 A69-25508

Fiber reinforced materials shear and tensile strength effect on stress-strain state of composite materials machine parts, considering design requirements

11 p1907 A69-25680

Fabricable materials with low plastic deformation for gas turbine components, noting strength vs temperature for alloys, fiber composites and ceramics

[IME PAPER 8] 12 p2147 A69-25791

Composite materials for aerospace applications, discussing high modulus filaments, structural and non-structural design considerations, nondestructive testing techniques, etc

12 p2111 A69-25852

Heat resistant composites, discussing composition, properties and high temperature behavior, plastic materials, reinforcement filaments, whiskers and test methods

12 p2117 A69-25855

Fiber reinforced space vehicle combustion chambers and cryogenic fuel tanks, discussing design and elastomechanical problems

12 p2176 A69-25860

Book on design procedures for modern fibrous composites emphasizing stiffness properties and calculations, covering laminates orthotropic lamina, etc

12 p2179 A69-26238

Stress distribution in elements of unidirectionally fiber reinforced composite materials analyzed as function of fiber content and fiber-matrix elastic properties

12 p2180 A69-26263

Book on ceramic fibers and fibrous composite materials as structural reinforcements covering dynamic testing of fine filaments and whiskers, material characterization, etc

12 p2118 A69-26340

Thin multiple layer superinsulation protection against reentry heat, discussing composite design considerations and refractory materials selection

12 p2060 A69-26817

Composite materials consisting of brittle inorganic glass matrix with metallic or inorganic crystal microspheres, noting strength and elasticity

12 p2115 A69-26830

Stress distribution in matrix of unidirectionally fiber reinforced composite subject to shrinkage and normal transverse load, using three dimensional photoelastic analysis

12 p2189 A69-27162

Elastic deformation of cord reinforced compressible thin sheet and rectangular cuboid solved using linear stress strain law and strain tensor nonlinear components

13 p2359 A69-27262

Effective tensors of elastic moduli and yielding of composite materials, considering multiparticle interactions and use of equilibrium and incompatibility equations

13 p2360 A69-27382

Fiber polymer composite flexible insulating materials properties and applications stressing synthetic organic fibers

13 p2286 A69-27989

Finite control volume approach to shock Hugoniot in unidirectional fiber reinforced composite, computing shear force along matrix-fiber interface

[AIAA PAPER 69-359] 13 p2366 A69-28292

End constraints and length/width ratio influence on composites off axis tensile tests, considering rigid clamping with/without end rotation

13 p2286 A69-28667

Short fiber composites flow orientation in system of high volume glass fibers in epoxy resin measured by glass rheometer

13 p2287 A69-28670

Boron nitride coated boron reinforced metal matrix composites, discussing continuous liquid infiltration, fiber-matrix reactions and heat treatment

13 p2283 A69-28671

Shrinkage stresses in two phase materials, analyzing stress distribution in epoxy inclusions in plasticized matrix during curing by photoelastic method

13 p2371 A69-28675

Dielectric constants of nonconducting composite suspensions of spheres and parallel cylinders in terms of filler particles, matrix and volume fraction

13 p2287 A69-28677

Oriented composites obtained from organic system under various directional solidification conditions

13 p2287 A69-28680

Theoretical compression strength of reinforced materials determined assuming material components differing elasticity moduli

14 p2532 A69-28973

Tungsten alloy fiber reinforced nickel base alloy composites stress-rupture strength, oxidation and impact resistance for high temperature turbojet engine buckets

14 p2462 A69-29010

Composite airframe structural joint design and weight considerations for boron and glass fiber reinforced plastic materials

[ASM PAPER W9-23.1] 14 p2535 A69-29448

Organic and inorganic fabric reinforcements effects on thermal properties of composites noting thermal conductivity, diffusivity, specific heat constants and temperature ranges

15 p2642 A69-30466

Hot pressed molybdenum disulfide-nickel composite film friction and wear tests in air and face seal configuration

[ASLE FICFS PREPRINT 23] 15 p2620 A69-30491

Torsion of composite prismatic rod consisting of three different isotropic materials with two interfaces converging on cross section contour corner point

15 p2707 A69-30579

Tissue-type fiberglass reinforced material properties as prototype of continuous anisotropic hereditary elastic media

15 p2642 A69-30584

Heat resistant fiber composites produced by oriented eutectic crystallization in Co and Ni quaternary alloys [ONERA-TP-710]

16 p2799 A69-31765

Optical measuring methods of cross sections and mechanical properties of heat resistant fiber reinforced materials

16 p2803 A69-31804

Biaxial stress strain properties of graphite base refractory composites noting fracture strength predictions [AIAA PAPER 68-337]

16 p2803 A69-32150

Ceramic phase reinforcement of metals and alloys, discussing interfacial energies, binding forces and elastic stress fields [ONERA-TP-661]

16 p2802 A69-32204

High strength fibers and composite materials for structural design, considering anisotropy and low ultimate tensile strain

16 p2802 A69-32380

JT8D turbofan engine composite fan blades design and fabrication methods using aluminum-Borsic fiber, noting direct and indirect weight reduction [AIAA PAPER 69-465]

16 p2842 A69-32698

Composition effect on tensile and flexural moduli of composites containing randomly distributed fibrous strands, establishing strength-composition relationships

17 p2991 A69-32960

Composite modified cast-double-base rocket propellants with large proportions of metallic fuel and oxidizer, discussing application rocket propulsion

17 p3017 A69-33349

Sliding friction and wear properties of metal ceramic composites applied to aircraft brakes

17 p2987 A69-33375

Nondestructive tests for glass filament wound composites void content, considering test methods and mechanical properties prediction role

17 p2979 A69-33656

Filamentary composites elastic constants calculation extended to hexagonal symmetry by long waves method

17 p3061 A69-33666

Composite materials behavior studies for structural applications, using macroscopic and microscopic phenomenological approach

18 p3154 A69-34607

Composite and structured material forms combination for obtaining high performance and low cost

18 p3161 A69-34608

Composite polymers thermophysical properties at thermal destruction temperatures, noting increased heating rate effect on kinetic curves

18 p3161 A69-34696

Metal alloys mechanical properties summary for cryogenic applications, considering fracture and thermal behavior, cryogenic structures fabrication and composites applicability

18 p3158 A69-35416

Composite material applications in space vehicle structures, noting strength and stiffness of boron fibers in plastic or metal matrices

19 p3340 A69-35502

Beryllium wire reinforced Al composites, discussing layup techniques and coated filament advantages

19 p3340 A69-35508

Mechanical properties and thermal aging of laminated specimens of collimated B monofilament reinforced composites preimpregnated with polyimide resin

19 p3354 A69-35514

High modulus graphite epoxy composite material laminates fabricated and tested, correlating filament strength variation effect with composite tensile strength

19 p3354 A69-35518

Fiber reinforced carbon and graphite with application to reentry and propulsion systems and high temperature gas turbines, noting three dimensional woven quartz

19 p3354 A69-35519

Composite ceramic armor systems for airborne vehicles and personnel, air cushion vehicles and ground troops, discussing weight and contour forming advantages

19 p3355 A69-35525

Thermal and mechanical properties UV of diazidophosphoridines, carbodiimides and phosphorus amide epoxies resins composites for use in environmental extremes

19 p3356 A69-35528

Pyrolytic graphite coated composite as nozzle throat material for high energy metalized solid propellant motors

19 p3357 A69-35539

Ultrasonic nondestructive testing technique for fatigue induced damage location and criticality in filament wound fiberglass cylinders, correlating damage to residual life

19 p3322 A69-35577

Boron nitride and boron nitride composite under high temperatures in air and vacuum for various time periods, discussing thermal shock and oxidation resistance

19 p3359 A69-36208

Structural aerospace materials development with emphasis on Be and Ti alloys, discussing material combinations and composites

19 p3345 A69-36319

High temperature materials for aerospace and spacecraft applications, considering carbon/carbon composites, oxides, carbides, fibers and ablative systems

19 p3346 A69-36320

Jet engine compressors and fans, combustors, turbines and composite materials in evaluating thrust-weight ratio, engine size, weight and life, etc

19 p3395 A69-36322

Photoelastic model methods for two and three dimensional investigations of microstresses in composite materials

20 p3565 A69-36940

Geometry effects on stresses in discontinuous composite materials, studying fiber spacing, failure and discontinuities size and nature

20 p3565 A69-36942

Composites for weight sensitive aerospace vehicles including reentry vehicles and V/STOL aircraft, considering costs, fracture toughness, corrosion resistance, etc

20 p3565 A69-37291

Transverse stiffness and strength of unidirectional fiber-reinforced composites determined as function of fiber volume content, using finite element method and stress functions

20 p3623 A69-37354

Strength characteristics of high performance fibers and application to reinforced composite materials noting whiskers, polycrystalline and vitreous fibers

20 p3567 A69-37748

Random arrays representing random filament packing of actual composite materials, discussing effects on transverse stiffness

20 p3626 A69-37758

Elastic constants of composite containing parallel cylindrical fibers, discussing disturbance in stress field

20 p3626 A69-37759

Composite laminates in cylindrical bending, discussing classical laminated plate theory limitations by comparing boundary value problems to corresponding theory of elasticity solutions

20 p3626 A69-37760

Reinforcement unbonding onset in composite materials determined by continuous dynamic moduli and damping measurements of tensile specimens

20 p3511 A69-37761

Superposition principle extended for wave propagation in composite materials /nonhomogeneous elastic media/

20 p3627 A69-37765

Hugoniot prediction for shock moving along longitudinal direction of unidirectional fiber reinforced composite

20 p3627 A69-37768

Nonlinear oscillations of rectangular plates of composite materials by Berger approach and Reissner variational principle, noting rotary inertial and transverse shear deformation

20 p3627 A69-37771

Buckling loads of homogeneous anisotropic plates of composite materials with simply supported boundary conditions, noting Kirchhoff-Love nondeformable normal hypothesis

20 p3628 A69-37776

Composite materials application in aerospace industry, discussing boron and carbon filament properties, epoxy resins, etc

20 p3563 A69-37930

Graphite fiber reinforced graphite composites fabrication, discussing spray forming and physical and mechanical properties [ASM PAPER W9-20.4]

21 p3730 A69-38671

Collection of papers on composite engineering laminates covering mechanics, fiber reinforced plastics, sandwich construction, metal-clad products and flame sprayed coatings

21 p3752 A69-38930

Composites elastic behavior, considering stress-strain in anisotropic lamina, composite plates and shells theory, thermal stresses and buckling for improving heterogeneous structures design

21 p3836 A69-38931

Stainless steel cladding of metals to combine desirable properties into composite, describing bonding, product types and treatment

21 p3745 A69-38937

Carbon fiber reinforced materials applications in aerospace industry, discussing long term potential and applications in F-5 aircraft

21 p3732 A69-38989

Model of isotropic polycrystal generalized to composite materials including mechanical mixtures, calculating macroscopic constants in heat conduction, diffusion and elasticity

21 p3752 A69-39193

Hypersonic parachute structural design using nylon ribbon, glass fiber heat shield and ablative coating construction [AIAA PAPER 68-963]

21 p3647 A69-39230

Polyurethane foam composites for low heating rate thermal protection, noting astroquartz fiber additive effect on performance

21 p3753 A69-39236

Filament wound composites for structures, discussing fabrication, properties and aerospace applications

21 p3753 A69-39496

Boron and carbon reinforced composite materials aerospace structural application, discussing weight savings, components structural design and connection and load input problems

22 p4038 A69-39908

Reinforcement effect on stress relaxation and creep in hereditary elastic materials, assuming integral shear modulus operator with exponential kernel

22 p4045 A69-40744

B composite materials in helicopter development, including B and C filament production and B filament applications

22 p3971 A69-40899

Loading rate effects on fracture characteristics of unidirectional fiber reinforced materials, discussing fiber-resin interface strength

22 p3974 A69-41212

Large elastic deformations of isotropic materials by deflection of composite parallelepiped composed of elastic incompressible materials, applying Rivlin solutions

22 p4048 A69-41277

Chromium composites mechanical properties, studying effects of alloying with spinel and magnesium oxides

23 p4177 A69-41672

Low density polybenzimidazole composites as ablative heat shields, discussing arc-heated wind tunnel tests of linear and crosslinked structures

23 p4179 A69-41715

Boron fiber reinforced composite materials in aircraft structures, comparing rigidity with glass fiber plastics and weight gains

23 p4179 A69-42155

Carbon fiber composites in construction of rocket motor cases, pressure vessels and support structures, including carbonization for ablation and insulation applications

23 p4180 A69-42158

Overall elastic moduli evaluation for solid composite materials comprising matrix of homogeneous elastic materials embedded with cylindrical shape inclusions

24 p4396 A69-42731

Residual stress measurement in steels and composite materials by X ray diffraction, discussing specimen preparation, diffractometer alignment, elastic modulus determination, etc

24 p4331 A69-42736

Photothermoelastic investigation of thermal stress concentrations around circular cavities and inclusions in two dimensional composite models

24 p4396 A69-42739

Law of mixture governing creep strength of composite materials reinforced unidirectionally by continuous filaments, taking into account fibers and matrix viscoelastic properties

24 p4400 A69-43054

Static mechanical strength of syntactic foam tested by generating failure conditions based on combined biaxial and triaxial stress [ASME PAPER 69-APMW-24]

24 p4336 A69-43095

Dispersive pulse propagation in laminated composites compared with theoretical predictions for timing and amplitude of oscillations [ASME PAPER 69-APMW-22]

24 p4401 A69-43097

Initially sharp plane pressure pulse propagation through linear elastic composite material, determining wave front shape change and stresses behind front [ASME PAPER 69-APMW-11]

24 p4401 A69-43103

Carbon fibers and resin composites used as rocket motor systems ablative liners and structures, noting role in motor weight reduction

24 p4336 A69-43210

Redesigned Al wing structure using B-epoxy composite applied to pressurized fuel carrying section, including material, fabrication and test data

24 p4323 A69-43418

Aircraft structure fabrication combining unidirectional strength and stiffness of B composite with metal, including test and weight/ cost data

24 p4323 A69-43419

Postcured low void content graphite fiber reinforced polyimide resin composites fabrication including shear, flexural and tensile strength data

24 p4337 A69-43446

Molded fiber composites in aerospace components applications, considering weight, stiffness, production and cost

24 p4326 A69-43448

Potting material reinforcing honeycomb structures for fastener installation prior to bonding face sheets to core, noting mechanical properties

24 p4326 A69-43466

Composite and metal tubes compared to determine properties for various loadings [AIAA PAPER 68-340]

24 p4405 A69-43653

Composite media elastic moduli upper and lower bounds determination using variational principles to characterize displacement and stress in time harmonic deformation

24 p4406 A69-43701

COMPOSITE PROPELLANTS

Beryllium propellants for space applications, considering composite solid propellant with powdered Be as fuel

02 p0303 A69-11763

Rocket engine combustion mechanism of ammonium perchlorate composite propellants

03 p0532 A69-13002

Strain dependent modulus and Poisson ratio behavior of CTPB propellant, performing stress relaxation tests

04 p0646 A69-15510

Burning rate of composite propellant with gamma irradiated ammonium perchlorate, noting enhancement at atmospheric pressure

04 p0647 A69-15519

Extinction by depressurization of AP composite solid propellants theory to predict rate of pressure decrease required to achieve flameout

06 p0983 A69-18102

Low pressure deflagration limit dependence on strand size in terms of cross section dimensions for composite ammonium chlorate propellant

06 p0983 A69-18162

One dimensional lattice model for heterogeneous explosive detonation, discussing hot spots, grain burning ignition time, ignition site types and RDX detonation [WSCIPAPER 68-30]

07 p1240 A69-18357

Strong electrostatic fields effects on burning rates of double base and composite propellants [WSCIPAPER 68-24]

07 p1241 A69-18366

Burning rate catalysts mechanism and location in composite propellant combustion at high pressure

09 p1622 A69-21954

Nonmetalized composite propellant solid phase heterogeneities effect on oscillatory combustion, inducing coherent burning rate oscillations with external pressure oscillations

09 p1622 A69-22085

Solid propellant rockets, discussing composite and double base propellants and use of polymers

11 p1941 A69-25588

Polyester/ammonium perchlorate combustion, determining degradation rate by loss in weight method at different intervals

13 p2324 A69-28234

Solid fuel ignition with gaseous oxygen in presence of copper chromate and other catalysts

16 p2829 A69-31913

Chemical processing for manufacture of solid propellant motors, discussing mixing, casting and curing of composite propellants

16 p2829 A69-31992

Solid propellants steady state combustion with emphasis on heterogeneous propellants

16 p2829 A69-31995

Thermal layer theory of composite propellant combustion leading to minimum steady state burning rate under ideal thermal conditions
[WSCI PAPER 69-5] 16 p2830 A69-32346

Composite solid propellant burning rate by solving energy equation, yielding heat release, flame thickness and standoff distance
[WSCI PAPER 69-7] 16 p2830 A69-32348

IR spectrometric analysis of flames of composite rocket propellants, maintaining diffusion flames between surfaces of decomposing ammonium perchlorate and fuel source
[WSCI PAPER 69-10] 16 p2831 A69-32350

Linear pyrolysis of thermoplastics during combustion of composite solid propellants and ammonium perchlorate solid propellant deflagration mechanism studied by loose granule analog
[WSCI PAPER 69-16] 16 p2831 A69-32354

Doped recrystallized ammonium perchlorate effects on composite propellant burning rates
[WSCI PAPER 69-18] 16 p2831 A69-32356

Composite solid propellant combustion using differential scanning calorimeter and mechanical model of steady state combustion
[AIAA PAPER 69-504] 16 p2833 A69-32679

Composite propellants high pressure burning stability with various binders and oxidizers, showing ammonium perchlorate oxidized formulations susceptibility to instability
[AIAA PAPER 69-438] 16 p2834 A69-32704

Composite modified cast-double-base rocket propellants with large proportions of metallic fuel and oxidizer, discussing application rocket propulsion
17 p3017 A69-33349

Li-F-H tripropellant study, discussing injection method variations and thrust chamber configuration effects on characteristic velocity efficiency and heat flux measurement
24 p4362 A69-43128

COMPOSITE STRUCTURES
NT LAMINATES

Unsteady heat flow in finite composite hollow circular cylinder using inverse method of eigenfunction expansion / method of finite integral transformation/
01 p0175 A69-10230

Elastomeric bearings for support of heavy loads and accommodation of oscillatory motions, considering molded type for helicopter tail rotor
01 p0085 A69-10406

Directional solidification and composite structures, discussing structure changes effect on mechanical properties
03 p0449 A69-13877

Statistical energy approach for analyzing steady state vibration distribution in composite structures in terms of energy balances
04 p0675 A69-14687

Dynamic shear stresses at interface of embedded thin elastic filament and elastic matrix after subjecting filament to concentrated longitudinal line load
05 p0831 A69-15577

Elastic stability of three dimensionally reinforced composite cylindrical shells
[AIAA PAPER 69-122] 06 p1029 A69-18216

Stress concentration factors for composite body of two isotropic elastic phases in plane strain in plane of composite parameters
07 p1170 A69-18716

Stress-strain relationship of composite bars consisting of single glass fiber with thin metal coating layer and under axial load
07 p1235 A69-19385

Mechanical properties of cast epoxy resins correlation with corresponding composites strength under static and dynamic fatigue stressing
08 p1340 A69-20510

Two layer cylindrical shells stability under external pressure, assuming nonuniform shell rigidity
08 p1419 A69-21180

Automatic fabrication process for boron reinforced composite structures, concerning orienting and laminating jet flap skins
09 p1507 A69-22329

Plane deformation in nonorthotropic body composed of various anisotropic cylinders with different elastic constants
10 p1799 A69-23156

Composite shell carrying capacity under general load, studying closing shape between laminate layers, transverse contraction, supporting layers thicknesses ratio, etc
12 p2176 A69-25851

Fabrication, machining and contouring of boron-epoxy composite for sandwich type aircraft structure,

noting F-5 supersonic fighter main landing gear strut door
12 p2103 A69-26826

Buckling loads for anisotropic fiber reinforced composite plates with strong bending membrane coupling terms
12 p2186 A69-26840

Buckling and postbuckling equilibrium behavior of fiber reinforced cylindrical shell under uniform axial compression
12 p2187 A69-26843

Boron filament wound composite structures fabrication noting physical properties
14 p2455 A69-29413

Approximate analytic solution to transient response of infinitely long cylindrical shell surrounded by viscoelastic medium, discussing composite and elastic shells
[AIAA PAPER 68-351] 16 p2871 A69-31877

Equations in series form to describe composite beams behavior under nonuniform torsion
18 p3211 A69-34343

Fiber distribution in oriented fiberglass reinforced plastics, noting statistically isotropical distribution and use for regular structure model
18 p3162 A69-35355

Optimal structure model of fiberglass reinforced materials with polymer matrix, obtaining strength utilization coefficient dependence on length/ diameter ratio
18 p3162 A69-35356

Military storage and environment effects on strength of filament wound glass reinforced epoxy structures, tested on plastic motor case and pressure vessels
19 p3321 A69-35567

Tape placement machines to fabricate composite high modulus filamentary tape reinforced aerospace structures, anticipating future generations evolution into automatic control
19 p3323 A69-35584

Titanium monocoque fuselage reinforced by composite boron filaments in polyimide resin matrix tested for SST applications, noting weight savings over all titanium structure
[AIAA PAPER 69-763] 19 p3329 A69-36298

Elastoplastic state of composite structures with applicability of elasticity law and yield conditions illustrated by reinforced plate under plane stress
19 p3444 A69-36808

Storage and loss moduli measurement for laminated glass fiber reinforced epoxy composite beams, discussing moduli prediction
20 p3627 A69-37763

Composites elastic behavior, considering stress-strain in anisotropic lamina, composite plates and shells theory, thermal stresses and buckling for improving heterogeneous structures design
21 p3836 A69-38931

Composite laminated glass structures employed to improve safety characteristics of glass or to achieve special optical properties
21 p3752 A69-38934

Composite or sandwich construction design based on employing all available materials and setting up requirements for mechanical and physical properties
21 p3836 A69-38935

Al-B composite aircraft structure fabrication, discussing wingspan segment, resistance spot welding, hot forming of joggles, etc
[AIME PAPER S69-1] 21 p3732 A69-39471

Filament wound composites for structures, discussing fabrication, properties and aerospace applications
21 p3753 A69-39496

Wave trains of incident pulse diffraction in thin composite rod determined by transmission and reflection coefficients of plane waves at plane interfaces
21 p3845 A69-39677

Transient temperature response of cylindrical composite energy storage devices with thermal conductivity, density and specific heat independent of temperature
22 p3868 A69-40132

Axisymmetric vibrations of semiinfinite cylindrical shell constructed of fiber reinforced composite layers, obtaining frequency equation from equations of motions
22 p4044 A69-40559

Interlaminar shear stresses in cross-ply three ply symmetric laminated composite plate, analyzing interlaminar stress distribution under simple tension
24 p4399 A69-43052

Geometric dispersion of transient stress waves in linearly elastic laminated composite based on sinusoidal modes
[ASME PAPER 69-APMW-20] 24 p4401 A69-43098

Composite-to-metal joints design and fabrication, using carbon yarn in epoxy matrix for missile interstage application
24 p4323 A69-43426

High modulus carbon filament composite structural elements for missile interstage application, showing weight savings
24 p4325 A69-43444

Adhesive bonded joints for glass resin composite sandwich helicopter structures, describing aircraft applications
24 p4403 A69-43462

COMPOSITE WRAPPING

Boron filaments reinforced epoxy aircraft landing gear structure prototype, discussing development, fabrication, and testing
09 p1508 A69-22340

Nondestructive tests for glass filament wound composites void content, considering test methods and mechanical properties prediction role
17 p2979 A69-33656

High modulus filament wound composites used for propellant and pressurization tanks, discussing overwrap and liner permeability, porosity, weight, etc
19 p3354 A69-35513

Tape placement machines to fabricate composite high modulus filamentary tape reinforced aerospace structures, anticipating future generations evolution into automatic control
19 p3323 A69-35584

COMPOSITES
U COMPOSITE MATERIALS
COMPOSITION [PROPERTY]

NT ATMOSPHERIC COMPOSITION
NT ATMOSPHERIC MOISTURE
NT ATOM CONCENTRATION
NT BODY COMPOSITION [BIOLOGY]
NT CARBON DIOXIDE CONCENTRATION
NT CHEMICAL COMPOSITION
NT CONCENTRATION [COMPOSITION]
NT GAS COMPOSITION
NT IONOSPHERIC COMPOSITION
NT LUNAR COMPOSITION
NT METEORITIC COMPOSITION
NT METEOROID CONCENTRATION
NT MOISTURE CONTENT
NT PLANETARY COMPOSITION
NT PLASMA COMPOSITION

Composition of continental crust based on material balance and rare earth estimates of shales, discussing ocean floor and mantle derived rocks
08 p1309 A69-20939

Energy band gap variation as function of composition in In-Ga-P semiconductor crystals
19 p3390 A69-36553

Porosity and composition effects on thermal conductivity of glass fiber reinforced plastics, noting tests of multilayer textolite sheets
22 p3973 A69-40747

COMPRESSED AIR

Compressed air in aircraft manufacture, discussing versatility in production and testing of Concorde 002
02 p0253 A69-12069

COMPRESSIBILITY

Nitrogen compressibility and thermodynamic functions up to 10,000 atm pressure and 400 C
01 p0175 A69-10366

Electron fluid compression coefficient from simultaneous measurement and correlation of absolute magnitudes of ion acoustic wave potential and accompanying plasma density perturbation
03 p0475 A69-13148

Space-time hypersurfaces representations of shock waves of relativistic MHD, discussing compressibility role in proving consistency with relativistic theory
11 p1928 A69-25246

Network method for stability of thin nonlinearly elastic compressible material plates, noting difference operators for rigidly clamped plates
23 p4230 A69-42003

COMPRESSIBILITY EFFECTS

Ti for high temperature use in supersonic aircraft, noting compressibility limit on maneuvering load factor and cooling by H
02 p0192 A69-11891

Rapid uniform expansion of spherical cavity in compressible elastic-plastic solid, obtaining similarity solution
03 p0528 A69-13798

- Inhomogeneous dielectric filling to simulate curvature in model earth-ionosphere waveguide
05 p0732 A69-16346
- Stability loss of shells of revolution under effect of axial compression and radial pressure with no restrictions on generatrix curvature, using strain energy method
06 p1021 A69-17179
- Numerical values for cylindrical antenna admittance in uniaxial plasma, considering plasma compressibility and vacuum sheath
06 p0965 A69-17513
- Compressibility parameters role in pressure distribution derived for radial laminar compressible fluid flow between two disks
07 p1121 A69-19321
- Book on fluid mechanics fundamentals and applications covering incompressibility and compressibility effects, viscosity, hydrostatics, aerostatics, one dimensional, potential, turbulent flow and boundary conditions
07 p1121 A69-19376
- Grain-size refinement of beryllium castings and extrusions after compression in pressure chamber, determining effect on ductility
08 p1330 A69-20013
- Two dimensional flat geometry for initial solar flare development stage, discussing tearing mode energy source for solar flares and plasma compressibility effects
09 p1583 A69-22757
- Turbulent flow problems, discussing hot-wire techniques, viscosity effect, compressibility surface curvature, turbulent boundary layers, heat transfer, etc
11 p1871 A69-25017
- Rotating mirror streak cameras in quantitative measurements of extreme compressions by shock waves, analyzing spatial and temporal resolving power
12 p2084 A69-26151
- Elastic deformation of cord reinforced compressible thin sheet and rectangular cuboid solved using linear stress strain law and strain tensor nonlinear components
13 p2359 A69-27262
- Lubricant compressibility effect on spiral groove gas bearing load carrying capacity [ASME PAPER 68-LUBS-33]
13 p2266 A69-27274
- Multirecompression heater for pure airflow tests of ballistic vehicles and hypersonic aircraft [AIAA PAPER 69-332]
13 p2242 A69-28268
- Gas compressibility influence on laminar to turbulent boundary layer transition determined using Taylor hydrodynamic finite perturbation model
14 p2389 A69-28974
- Dynamic programming method applied to Cauchy problem of large deflections in compressed rods, using recurrent functional equations
14 p2533 A69-28988
- Lifting surface theory for cascade of blades in subsonic shear flow, determining blade surface pressure distribution, distinguishing shear and uniform flow compressibility effects
16 p2731 A69-31592
- Inertia, compressibility and viscous friction effects on dynamic response of long fluid line, constructing models
16 p2771 A69-32066
- Compressibility of material in stability problems of elastoplastic plates and shells
16 p2875 A69-32292
- Three dimensional potential surface flow past rotor blade in hover, accounting for compressibility and blade element theory limitations [AHS PAPER 324]
17 p2895 A69-33537
- Computer calculation of adiabatic expansion of air, allowing for specific heat ratio and compressibility factor changes
24 p4244 A69-43088
- COMPRESSIBLE BOUNDARY LAYER**
- Compressible and incompressible laminar boundary layer with constant wall shear stress, using initial profiles
02 p0233 A69-12535
- Similar solutions of boundary layer equations for compressible model fluid adjacent to wall, discussing velocity overshoot dependence on wall temperature
03 p0413 A69-13013
- Laminar compressible viscous boundary layer with arbitrary external pressure distribution, using implicit multiplace difference method
04 p0591 A69-15294
- Compressibility transformation theory extended for turbulent boundary layer, involving mass transfer with/without chemical reactions [AIAA PAPER 69-161]
06 p0912 A69-18045
- Separation of subcritical and supercritical compressible turbulent boundary layers under strong pressure gradients using method based on integral equations [AIAA PAPER 69-34]
06 p0912 A69-18077
- Nonsimilar laminar boundary layer solutions with negative pressure gradient compared to experimental boundary layer velocity profiles, momentum and displacement thicknesses [AIAA PAPER 69-35]
06 p0913 A69-18094
- Analytical model for compressible MHD boundary layers formulated by transport equations for turbulent fluctuations of species mass density, velocity and temperature
08 p1366 A69-20786
- Von Karman flow changes due to unsteady heat transfer from rotating disks impulsively changing temperatures, particularly steady state and response time
08 p1422 A69-20996
- Similarity solutions for laminar compressible boundary layer with reverse flow, considering various wall/stagnation temperature ratios
15 p2591 A69-30907
- Analytical expressions validity for skin friction in compressible turbulent boundary layer over wide range of Reynolds numbers and heat transfer conditions
16 p2771 A69-31926
- Compressible laminar boundary layer equations solutions for nonunit Prandtl number by direct numerical integration
16 p2772 A69-32173
- Adiabatic compressible turbulent boundary layer equations for two dimensional and axisymmetric flows, discussing methods of solution based on eddy viscosity formulation [AIAA PAPER 69-687]
17 p2955 A69-33470
- Compressible hypersonic turbulent boundary layers solution by finite difference method, relating mixing length to velocity profile shape factor [AIAA PAPER 69-684]
17 p2955 A69-33474
- Adiabatic compressible turbulent equilibrium boundary layer integral method analysis extended to study nonequilibrium laminar flows, deriving dissipation integrals, presenting numerical solutions [AIAA PAPER 69-689]
17 p2955 A69-33481
- Magnetic field effects on rotating cone compressible boundary layer at zero angle of attack, describing changes in drag coefficient, torque and velocity profiles [AIAA PAPER 69-721]
17 p2892 A69-33484
- Favorable pressure gradient effect on compressible two dimensional supersonic turbulent boundary using temperature and pressure probes and shear balance [AIAA PAPER 69-685]
17 p2956 A69-33489
- Compressible laminar boundary layer behind shock or thin expansion wave past moving flat plate solved by transforming governing equations into Blasius equation
24 p4305 A69-43596
- Laminar sublayer thickness in compressible turbulent boundary layers with and without heat transfer
24 p4306 A69-43724
- COMPRESSIBLE FLOW**
- NT HYPERSONIC FLOW
- NT MAGNETOHYDRODYNAMIC FLOW
- NT SUBSONIC FLOW
- NT SUPERSONIC FLOW
- NT TRANSONIC FLOW
- Gas combustion stability with respect to one dimensional perturbations, considering flow compressibility stabilizing effect
01 p0174 A69-10107
- Kernel function applied to compressible fluid flow computation for linear procedure to determine subsonic flow patterns
01 p0058 A69-10225
- Compressible relativistic flow in subsonic, transonic and supersonic regimes, noting pressure coefficient variations
01 p0007 A69-11203
- Implicit finite difference scheme to integrate unsteady boundary layer equations for compressible gas
03 p0416 A69-13656
- Sufficient conditions for stability of compressible atmospheric flows for rigid lid types of upper boundary condition
03 p0417 A69-13796
- Turbulent front structure of axisymmetric compressible wake at supersonic speeds, measuring intermittency factor distribution
03 p0419 A69-13949
- Second order difference scheme for calculation of plane or rotational compressible flow, investigating stationary flow as asymptotic limit of unsteady flow [ONERA-TP-652]
03 p0419 A69-14111
- Series solutions for compressible and incompressible flows at low Reynolds number, including axisymmetric and MHD Stokes flow
04 p0587 A69-14609
- Unsteady compressible laminar boundary layer flow over insulated or isothermal flat plate moving with arbitrary time variant velocity in viscous fluid
04 p0588 A69-14715
- Dynamic behavior of series and parallel flow thrust-balance systems for compressible and incompressible flow, using analog computer simulation
04 p0647 A69-15521
- Three dimensional boundary layers, extending Prandtl independence principle to laminar compressible flow over convex body
05 p0743 A69-15556
- Similar solutions for laminar boundary layer formed by convective and compressible flows
05 p0751 A69-16643
- Hyperbolic double waves found in compressible flow problems, presenting method of plotting all waves and determining geometrical characteristics
05 p0751 A69-16646
- Combustion in compressible turbulent mixing flows, discussing mixing facility, experimental results and numerical analysis [WSCI PAPER 68-28]
06 p0969 A69-17794
- Unstationary characteristics method applied to numerical computation of steady compressible flow around airfoil [ONERA-TP-630]
07 p1049 A69-18413
- Steady conical compressed flows in nonaxisymmetric ring nozzles characterized by discontinuities
07 p1120 A69-18989
- Irrational plane subsonic flow of compressible fluid about obstacle, reducing problem to integration of linear partial differential equation with boundary conditions
09 p1480 A69-21735
- Compressible gas flow problem in point body gravitational field solved with reference to sun and interstellar gas
09 p1577 A69-21769
- Three dimensional compressible potential flow in curved circular duct analyzed by perturbation method
11 p1867 A69-24607
- Flat decelerating cascades boundary layer in compressible flow during change in axial flow-density ratio and upstream turbulence
11 p1818 A69-24639
- Turbulent boundary layer velocity distributions in uniform/accelerated compressible flow over flat plate, using change of variables based on mixing length formula [ONERA-TP-693]
11 p1867 A69-24752
- Laminar compressible subsonic boundary layer flow on symmetrical cylinder bounded by circular arcs noting zero/nonzero angle of attack
12 p2062 A69-26272
- Different pressure and deflection measurements coherence in vortex flows verified assuming radial equilibrium conditions
12 p2012 A69-26362
- Diffusion-stabilized difference schemes for inviscid compressible flow equations in conservation form for arbitrary number of space dimensions
12 p2062 A69-26624
- Internal flows of compressible fluids with heat transfer in accelerating nozzles and constant area ducts, simplifying equations by assuming one dimensional flow
12 p2012 A69-26790
- Influence coefficients for compressible flow processes involving area, friction and total temperature changes
12 p2063 A69-26799
- Construction and calibration of combined temperature and pressure probe for compressible flow
13 p2242 A69-28226
- Laminar to turbulence transition in submerged and bounded jets, using schlieren visualization for compressible flow and birefringent visualization for incompressible flow
14 p2428 A69-28876
- Stagnation region dimensionless pressure effect on flow pattern, boundary conditions and oscillation mechanism in compressible flow through nozzle in circular duct
15 p2549 A69-31220

Compressible shear flow linear theory applied to transonic flow past thin airfoil, determining pressure distribution, discussing compressibility effects of nonuniform Mach number

16 p2731 A69-31593

Compressible flow over finite porous plate in supersonic stream with massive injection over surface analyzed using inviscid vortical flow model

16 p2770 A69-31884

Steady inviscid compressible flow past wavy wall with simulated ablation, studying reflections effect on relationship between surface pressure and wall geometry

16 p2770 A69-31909

Chemical reactions in compressible turbulent mixing flows, analyzing flow characteristics, rate equation and Reichardt theory [AIAA PAPER 69-537]

16 p2747 A69-32701

Simple waves in compressible isentropic flows of inviscid nonheat-conducting gas free of shock waves

18 p3121 A69-34534

Higher order boundary layer theory development from Prandtl simplification of Navier-Stokes equations to successive approximations for incompressible and compressible flows

18 p3123 A69-34923

Three dimensional laminar boundary layer on conical body of revolution in low Reynolds number compressible fluid flow

19 p3241 A69-36762

Heat transfer to compressible laminar jet flowing along flat wall, obtaining distributions of temperature, wall shearing stress, heat transfer rates and jet thicknesses [ASME PAPER 69-FLCS-30]

20 p3516 A69-37979

Computer solutions for nonlinear partial differential equations governing compressible flow patterns with shocks, using Lagrange coordinates

20 p3569 A69-38212

Multistep axisymmetrical supersonic exit cones optimum geometry design diagram based on external oblique and normal compression shock

21 p3785 A69-39104

Coaxial turbulent compressible gas jets propagation, discussing mass buildup data in coaxial jets

21 p3645 A69-39847

Laminar boundary layer in steady compressible gas flow past plane wing profile, studying surface temperature and suction effects

23 p4058 A69-41709

Subsonic compressible flow at two dimensional inlets, analyzing field representation, boundaries, surface configuration and optimal wedge

23 p4060 A69-41915

Nonlinear finite-amplitude instability of two dimensional compressible laminar wake flows, using Fourier expansion and Landau equation

24 p4245 A69-43357

COMPRESSIBLE FLUIDS

Lifting wing profiles in uniform transonic compressible fluid flow calculated by analog method, noting hodograph method simplification

02 p0187 A69-11536

Plane shock wave interaction with elastic shallow spherical shell in compressible fluid, formulating equations of motion

02 p0339 A69-11977

Asymptotic laminar boundary layer in compressible gas in presence of normal and tangential velocity components at body surface

02 p0231 A69-12138

Taylor column existence in compressible atmosphere, discussing baroclinicity and stratification effects in earth and Jupiter atmospheres

02 p0326 A69-12697

Similar solutions of boundary layer equations for compressible model fluid adjacent to wall, discussing velocity overshoot dependence on wall temperature

03 p0413 A69-13013

Stagnation pressure losses of adiabatic flow of compressible fluids through abrupt area expansion and contraction in subsonic range, discussing base pressure [ASME PAPER 68-WA/FE-46]

05 p0750 A69-16113

Interaction between supersonic jet and counterflow of ideal compressible fluid

05 p0751 A69-16501

MHD aligned flow of compressible fluid past slender body in wind tunnel

06 p0861 A69-17719

Dense gas effects in free piston hypersonic wind tunnel, discussing Longshot facility, free piston cycle, reservoir conditions decay and hypersonic nozzle flow [AIAA PAPER 69-169]

06 p0907 A69-18188

Permissible nonthermal convection modes in planetary interiors derived from conservation equations for self gravitating homogeneous nonrotating compressible fluid spheres

07 p1213 A69-18611

Convection in planetary interiors produced by combined thermal and nonthermal mechanisms, noting self gravitating homogeneous nonrotating compressible fluid spheres

07 p1214 A69-18613

Stability of motion of spherically symmetric mass of compressible gas with constant space density in absence of gravitational field

07 p1215 A69-18706

Linearized unsteady nonequilibrium flows produced by unsteady motion of thin foil or circular cylindrical shell in compressible gas

07 p1119 A69-18738

Theory of unsteady one dimensional motion of ideal compressible fluid, discussing equation of state

07 p1119 A69-18750

Group analysis of MHD equations, determining group properties of motion equations of compressible fluid, obtaining invariant solutions

07 p1191 A69-18994

MHD flow of compressible conducting fluid around cylindrical body with quasi-aligned magnetic field and velocity

07 p1194 A69-19350

Coupled wave equation solution based on spectral resolution for longitudinal components of electric and magnetic fields when source currents are present in compressible anisotropic plasma

08 p1274 A69-20031

Plane electromagnetic wave reflection and transmission by semiinfinite moving compressible plasma fluid, noting interaction of transmitted H wave

08 p1360 A69-20097

Two dimensional steady flow of finitely conducting compressible fluid subjected to magnetic field with two zero components

08 p1369 A69-20843

Axisymmetric oscillations of two spherical shells with noncoinciding centers of curvature immersed in compressible or incompressible fluids

11 p1875 A69-25467

Hamilton principle for inviscid compressible fluid in Euler coordinates, analyzing shortcomings found in variational principles and model in Lagrangian coordinates

11 p1875 A69-25483

Invariant transformation of Euler equations of motion for plane steady flows of perfect compressible fluid

11 p1877 A69-25739

Navier-Stokes equations for compressible gas, generalizing viscous channel flow of heat conducting gas to slip flow of rarefied gas

12 p2061 A69-25887

Boussinesq approximation for compressible fluids, discussing perturbation pressure and velocities and vertical scale motions

12 p2061 A69-26013

Controllable motions of compressible homogeneous isotropic solids, anisotropic solids and fluids with memory under constant body force

12 p2189 A69-27118

Viscous heat conducting compressible fluid response to abrupt change in circular cylinder angular velocity at stable temperature distribution, considering Boussinesq approximation

13 p2245 A69-27378

Compression forces during interaction of colliding shock waves in compressible fluid medium, discussing linear and nonlinear problems

13 p2246 A69-27523

Computer program for compressible fluid flows with space and time dependent variables, discussing hyper-velocity impact [AIAA PAPER 69-353]

13 p2365 A69-28286

Equations of motion of compressible fluid with non-zero resistivity near thin foil, solving supersonic and subsonic flow by Fredholm integral equations

13 p2200 A69-28360

Ideal compressible fluid motion and heat transfer, noting convective heat transfer intensification with increased twisting velocity of flow

13 p2251 A69-28559

Rigid obstacle unsteady motion in compressible fluid with load applied to surface layer, deriving numerical solution of pressure expansion

14 p2430 A69-29480

Two dimensional adiabatic transverse normal modes of inviscid compressible uniformly rotating fluid, discussing harmonic wave propagation in opposite directions and rotation effects

14 p2431 A69-29581

Compressible gas MHD steady one dimensional flow in electric and magnetic fields

14 p2500 A69-29905

Plane shock wave interaction with elastic shallow shell in compressible fluid, formulating equations of motion

15 p2704 A69-30262

Flush electrostatic probe edge effect, considering Couette flow of weakly ionized compressible gas past discontinuous wall potential

15 p2653 A69-30912

Book on mechanics of deformable media covering fluid and solid mechanics and applications to irrotational flows of compressible and incompressible fluids

16 p2813 A69-32789

Vortex diffusion in viscous compressible fluid approximated by linear differential equations

17 p2957 A69-33714

Resonance effects in finite hollow cylinder immersed in ideal compressible fluid and exposed to compression wave

18 p3215 A69-34567

Computer implementation of Bergman solution to initial value problem for partial differential equation of compressible fluid flow

18 p3164 A69-34614

Linear oscillations of sphere in compressible viscous fluid with slip at surface, noting drag variation

19 p3297 A69-35836

Laminar flow of viscous compressible fluid with density dependent on temperature, calculating steady state Navier-Stokes equations using vector function

19 p3297 A69-35852

Compressible fluid two dimensional supersonic and one dimensional unsteady flows similarities shown graphically, discussing hodograph-speedgraph relationship

19 p3300 A69-36777

Statistical equations for compressible gas, discussing turbulent quantities separated into fluctuating and macroscopic parts

19 p3300 A69-36784

Laminar flow of compressible viscous gas in channels of variable cross section

20 p3457 A69-37089

Homogeneous compressible fluid sphere with axisymmetric magnetic field, analyzing oscillations and stability using variational principle

20 p3605 A69-37822

Computation method of hydrodynamic blade cascade for compressible fluid and variable channel width by stream function

20 p3460 A69-37972

Unsteady boundary layer flows of compressible fluid over semiinfinite flat plate, discussing heat transfer rate

20 p3518 A69-38318

Compressible fluid flow characteristics in turbomachine stage, discussing simplified radial equilibrium method as basis for design

21 p3643 A69-38457

Blowing effect on surface friction coefficient and heat transfer in turbulent boundary layer in compressible fluid with pressure gradient

21 p3643 A69-38636

Small amplitude acoustic waves propagating in compressible fluid with parallel shear flow and within constant gravitational field

21 p3772 A69-39241

One dimensional flow of perfect compressible relativistic fluids, obtaining expression showing wave velocity dependence on relativistic speed of sound

22 p3931 A69-40711

Boundary layer effects in turbulent spiral vortex flow of compressible fluid in supersonic centrifugal compressor, discussing flow geometry, using momentum integral method

23 p4152 A69-42109

Two dimensional diverging flow of ideal compressible fluid past slender profile, using Prandtl-Glauert rule and linearized equation

24 p4243 A69-42584

Compressible fluid unsteady flow past deformable surface, constructing metric for surface and obtaining metric tensor coefficients

24 p4243 A69-42586

Compressible gas flow into cavity of various volumes in presence of supercritical pressure gradients

24 p4298 A69-42587

Dynamic pressure response of viscous compressible fluids in rigid tubes with dead ended volume termination, testing Ibrall theorem as function of Stokes number

24 p4301 A69-43287

COMPRESSING

Megagauss magnetic field generation methods, discussing high explosives, initial field, flux compression, capacitor discharges and applications
01 p0115 A69-10049

Thermodynamic cycle and optimum conditions of electric power source of MHD generator in combination with thermocompressor
09 p1435 A69-21592

Rapid decompression and recompression in stapedectomized cat, noting fibrous tissue response in middle ear at reconstructions utilizing polyethylene struts on gelfoam
14 p2406 A69-29292

Compression molding of molecular salt-like intermediate Pyrrone powders by two pressure method, noting volatiles elimination
14 p2469 A69-29415

Thermocompression joints strength measured using friction test, centrifuging and microtensile tests
15 p2573 A69-30081

Attainable signal compression coefficient in recirculator and relation to recirculator ring parameters, noting feedback coefficient stability
17 p2931 A69-33907

Laminar recompression behavior downstream of stagnation point behind hypersonic slender body, obtaining finite difference numerical solutions for near wake flow field
[AIAA PAPER 69-713]
18 p3085 A69-34417

COMPRESSION BUCKLING

U BUCKLING

COMPRESSION LOADS

NT AXIAL COMPRESSION LOADS

NT IMPACT LOADS

Strength analysis of cylindrical shells with rib and ring reinforcement under compression loads using network method
01 p0164 A69-10083

Elastic properties of epoxy resins, deriving relation by considering different shear properties in tension and compression
01 p0103 A69-11268

Eccentric compression in elastic domain for rigid homogeneous structural elements, considering traction and stress
02 p0341 A69-12258

Compressed cylindrical shell stability analyzed on basis of axisymmetric equilibrium form, noting dependence on mechanical characteristics and geometry
04 p0667 A69-14265

Dead-end microcracks stress fields, studying positive /tensile/ and negative /compressive/ nature dependence on crack size
04 p0674 A69-14548

Elastic rod buckling under dynamic longitudinal compression load, determining critical load
04 p0679 A69-14926

Circular plate elastic stability under unidirectional compression, using Rayleigh-Ritz- Timoshenko method to determine buckling load
04 p0683 A69-15515

Fatigue crack growth in notched samples of aluminum alloy subjected to cyclic compressive loading, noting residual tensile strength at notch root
[ASME PAPER 68-WA/MET-16]
05 p0838 A69-16154

Metal matrix composites compression microstrain behavior, analyzing continuous fiber composites of magnesium-boron and copper-tungsten
06 p0939 A69-16945

Three dimensional compression problem for two elastic bodies in contact, determining contact pressure distribution by iteration procedure on computer
06 p1026 A69-18014

Thermal insulating characteristics of low conductance interstitial materials under compressive loads, noting carbon paper and wire screens
[AIAA PAPER 69-25]
06 p1036 A69-18072

Compressive strength of boron fiber-epoxy matrix composite, noting matrix support of fibers against buckling
07 p1170 A69-18713

Two layer cylindrical shells stability under external pressure, assuming nonuniform shell rigidity
08 p1419 A69-21180

Failure modes in fiberglass reinforced epoxy laminates subjected to compression loadings, discussing cracks formation and delamination at glass-resin interface
09 p1529 A69-22305

Histogram approximation of plastic deformation of metals, analyzing tube under internal load and sandwiched layer compression
10 p1793 A69-22850

Nodal lines shape in individual flats for long plates in combined shear and compression with sinusoidal edge rotations in longitudinal direction
11 p1983 A69-25137

Buckling of long flat panel in combined compression and shear with sinusoidal edge moments and support on two edges and on point supports
11 p1984 A69-25138

Rectangular aluminum alloy rods carrying capacity under compression loads applied eccentrically to rod ends
11 p1986 A69-25326

Plane stress state in plate with different glide moduli during tension and compression, considering axisymmetrical deformations
12 p2178 A69-26003

Sinusoidal tension and compression radial support system for large solid disk primary mirror, noting pivot design and pad bonding adhesive
12 p2057 A69-26413

Postcritical deformations of thin conical elastic shells hinged along edges under external pressure using Pogorelov method for cylindrical shells
12 p2181 A69-26609

Finite plane deformations theory extended to incompressible materials with logarithmic change of volume proportional to pressure
12 p2181 A69-26613

Compression forces during interaction of colliding shock waves in compressible fluid medium, discussing linear and nonlinear problems
13 p2246 A69-27523

Beryllium single crystals c axis compression behavior at three purity levels under hydrostatic pressures
13 p2279 A69-27760

Elastoplastic cylindrical shell instability determination under axial compression applied to inelastic solids
13 p2363 A69-28124

Stress and strain fields for circular rubber ring under diametrical compression between flat plates, using moire, large strain analysis and photoelastic verification
14 p2531 A69-28884

Materials and structural failures under short time compressive loadings, showing structural response to tensile stresses produced by rarefaction waves
15 p2639 A69-30364

Minimum vibration frequency and compressive force for freely supported rectangular, triangular and circular plates simulated on analog computer
15 p2708 A69-30665

Annealed aluminum rods dynamically compressive impact loading used to study longitudinal plastic waves propagation velocity
15 p2709 A69-30677

Reinforced cylindrical shell stability under external compression load by pressurized air, determining critical pressure
15 p2715 A69-31204

Transverse free vibration of slender cantilever subjected to compressive follower force
16 p2871 A69-31899

Elastic spheroidal shell of revolution under external pressure described by buckling and postbuckling theory
16 p2874 A69-32162

Machine for testing vibration stability of polymer samples subject to tension or compression, noting stability of plastic during vibration lower than during static loading
17 p2972 A69-33043

Machine for testing high temperature creep under variable tensile-compressive stress while maintaining specimen stability, noting discrepancy between creep strains in heat resistant alloy
17 p3054 A69-33044

Tension-torsion-compression load testing machine of technological possibilities and accuracy
[ONERA-TP-596]
17 p2945 A69-33065

Plane wave propagation due to combined compressive and shear stresses in half space, assuming elastoplastic material
[ASME PAPER 69-APM-12]
18 p3213 A69-34388

Critical stresses and crack development near holes in compressed elastic plate
18 p3218 A69-34603

Spherical shells axisymmetric equilibrium properties under uniformly distributed external compression
18 p3224 A69-35318

Initial deflection effect on elastic cylindrical shell stability under compression, finding critical load by determining limiting point in successive loading
18 p3224 A69-35319

Thin brittle plastic shells mechanical properties differing under tension and compression described by solving differential equations in successive approximation
18 p3224 A69-35327

Elastic stability of sandwich materials in microvolume under compressive force analyzed using three dimensional linearized equations for small subcritical strains
18 p3226 A69-35374

Flat rectangular plates large deflection due to uniform lateral pressure and compressive edge loading analyzed through partial differential equations, difference equations and computer program
20 p3620 A69-37000

Stress analysis of circular elastic plate buckling under radial compression, noting Kirchhoff hypothesis influence on critical value of thickness-to-radius ratio
21 p3834 A69-38722

Nonlinear stability of shallow elliptical paraboloidal dome under uniformly distributed compression, solving by Bubnov-Galerkin method on computer
21 p3838 A69-39186

Dynamic stress concentrations and rigid body response of cylinder imbedded in elastic medium subjected to compressional wave
21 p3840 A69-39300

Stability loss of beams analyzed under compression allowing for various creep conditions in loading and unloading regions, calculating time to failure
22 p4039 A69-39917

Compressed rectangular beam stability under different creep conditions, deriving relation between creep time and initial deflection
22 p4039 A69-39918

Contact stability of hollow cylinder compressed between parallel planes measured optically, compared to approximation of elasticity theory
23 p4162 A69-41416

Postbuckling analysis by equilibrium solutions of conservative system near critical point, considering stability failure in elastic structure under increasing load
24 p4396 A69-42730

Shallow spherical sandwich shells critical buckling loads using differential pressure method
24 p4396 A69-42734

COMPRESSION TESTS

Uniaxial strain static and gas gun compression tests result compared for syntactic foam
02 p0345 A69-12295

Orthotropic fiberglass/epoxy faced honeycomb aircraft type sandwich structure elastic properties by edgewise compression test
24 p4403 A69-43443

COMPRESSION WAVES

Granite compressional wave velocity and electrical resistivity variations with depth, explaining discrepancy between in situ and laboratory measurements on dry samples
02 p0241 A69-11806

High speed compression waves, rarefaction waves and gas interface regions position and velocity measurement in shock tube by sensing electrical impedance
03 p0428 A69-13104

Strain rate and temperature effect on flow stress of 7075 aluminum bars
03 p0443 A69-13120

Planetary long waves behavior in atmospheric models, explaining unsteady components by means of filtered equations
03 p0459 A69-13274

Detached lunar compression wave, noting positive evidence from solar wind flux and direction measurements near lunar wake
05 p0824 A69-16251

Compressional and shear wave velocities vs porosity for sintered perlitic bricks
06 p1000 A69-17009

Steady compression waves properties in relaxing gases found independent of thermodynamic behavior and relaxation process
10 p1631 A69-22893

Shadow zone diffraction of plane step function compressional wave by circular cavity, using Friedlander wave front approximations
13 p2368 A69-28347

Planetary long waves behavior in atmospheric models, explaining unsteady components by means of filtered equations
14 p2472 A69-28782

Compression waves observed ahead of luminous discharge plasma below Mach 12-15 in electric shock tube, describing shock structure by blast wave theory
16 p2768 A69-31664

Ion energy distribution function and density profile in strong implosion wave generated by theta pinch discharge, investigating compression wave in deuterium

17 p3013 A69-33821

Resonance effects in finite hollow cylinder immersed in ideal compressible fluid and exposed to compression wave

18 p3215 A69-34567

Rod buckling under impact load, discussing compression strain wave front propagation

18 p3217 A69-34580

Stressed state analysis in dynamic brittle breakdown wave front of compression waves propagating in brittle rod under longitudinal impact

18 p3217 A69-34592

Piston driven shock tube at Kyoto University with performance tests results, investigating compression processes, shock speed and flow duration time

22 p3928 A69-41046

COMPRESSIVE STRENGTH

Controlled microstructures of eutectic aluminum-copper aluminides produced for mechanical properties studies

06 p0942 A69-17227

Short cylinder of perfectly plastic Coulomb yield conditions compressed between rigid plates, discussing cylinder-plate interface frictions, angles of internal friction and cohesion

08 p1410 A69-19890

Failure criteria for predicting filamentary composite strength under uniaxial and combined stresses from properties and fabrication process considerations

09 p1611 A69-21479

Compressive behavior of uniaxial filament reinforced epoxy tubes for aerospace structures, using hand layup method with Teflon mandrel and sleeve

09 p1508 A69-22339

Compressive and tensile creep of metals, discussing compressive stress, void nucleation, barreling specimen shape and platen lubrication

12 p2175 A69-25836

Theoretical compression strength of reinforced materials determined assuming material components differing elasticity moduli

14 p2532 A69-28973

German monograph on yttrium addition effects on tension and compression behavior of Nb and Mo at high temperature in vacuum

17 p2990 A69-33570

Temperature and pressurization effects on tensile and compressive properties of polycrystalline arc-cast W

18 p3154 A69-34273

Stiffened integrally formed panel stability evaluation based on compression structural efficiency and manufacturing costs

[AIAA PAPER 69-760]

19 p3434 A69-35660

Creep buckling strength reduction of aircraft compression structure, discussing initial eccentricity and loading mode effects on supersonic aircraft operation mode

21 p3842 A69-39308

COMPRESSOR BLADES

Acoustic resonance excitation in axial flow compressor annulus by wake shedding from blades

01 p0142 A69-10058

Aircraft gas turbine compressor parts erosion tests

01 p0099 A69-11058

Blade natural frequency distribution around rotor and mechanical coupling between blades effects on flexing amplitudes under forced vibration

[ASME PAPER 68-WA/GT-3]

05 p0837 A69-16139

Holographic interferometry, determining mechanical vibration amplitudes of compressor and turbine blades and airframe panel

[SAE PAPER 690265]

07 p1130 A69-18313

Diffusion bonding parameters for producing hollow Ti-Al compressor blades, discussing surface preparation, postboud heat treatment quality control and mechanical properties

[ASME PAPER 69-GT-46]

09 p1513 A69-22484

Incompressible two dimensional potential flow analysis with compressibility effects for thick highly cambered multibodies in cascade, noting slotted compressor blade performance

[ASME PAPER 69-GT-6]

09 p1432 A69-22507

Semiacuator disk method for boundary layers and velocity of stall flutter cascade blades vibrating in transient mode, considering nonstall flutter

11 p1818 A69-25028

Gas turbine centrifugal compressor design considerations for impellers and diffusers, including blade

loading and pressure gradients determination and aerodynamics

[IME PAPER 1]

12 p2146 A69-25790

Lifting surface theory for cascade of blades in subsonic shear flow, determining blade surface pressure distribution, distinguishing shear and uniform flow compressibility effects

16 p2731 A69-31592

Radial blade tip clearance effect on isentropic efficiency and air delivery in axial flow compressor with allowance for casing deformations and rotor displacements

16 p2837 A69-32004

Supersonic compressor blade sections performance prediction near maximum pressure ratio and efficiency by analyzing flow processes

[AIAA PAPER 69-522]

16 p2843 A69-32711

Blade length effects on performance of flow straightener vanes influenced by secondary flow, noting high deflection and low aspect ratio

17 p2896 A69-33606

Near resonant oscillations of warped turbine or compressor blades, discussing stress-strain relations

17 p3064 A69-33918

Damping, fatigue and optimal heat treatment of Cr-Ni steel for compressor blades operating at temperatures up to 500 K

17 p2990 A69-33933

Static tensile stresses effect on energy dissipation in alloys used in compressor blades found dependent on composition and heat treatment

17 p2991 A69-33934

Cantilever blades tangential vibrations effect on damping characteristics measured by free vibration excitation and static hysteresis loop

17 p3065 A69-33935

Boron fiber reinforced Al matrix composite material for high performance aircraft gas turbine engine compressor blading

[AIAA PAPER 68-1037]

20 p3586 A69-37153

Potential flow interaction effects between blade rows in axial flow compressor stage, emphasizing inlet guide vane-rotor interaction

21 p3643 A69-38439

Gas turbine compressor blade buckling during blade fabrication by hydraulic pellet jet technique eliminated by controlling working pressure of jet

21 p3731 A69-38879

Precision of gas turbine compressor blade positioning devices during machining, analyzing causes of inaccuracies

21 p3731 A69-38880

Compressor type cascade experiments to find closest possible traverse position to blade trailing edge

22 p3859 A69-40065

Discrepancy between theoretical and experimental coefficients of friction losses on blades of centrifugal compressor impeller wheels, using lattice theory

23 p4058 A69-41727

COMPRESSOR EFFICIENCY

Radial blade tip clearance effect on isentropic efficiency and air delivery in axial flow compressor with allowance for casing deformations and rotor displacements

16 p2837 A69-32004

Compressor surge effect on mixed compression inlet flow from numerical solution of one dimensional unsteady inviscid flow equations in variable area duct

[AIAA PAPER 69-484]

16 p2841 A69-32682

Jet engine compressor stalls in-flight investigation up to Mach 2 on F-111A by pressure sensors, noting steady state distortion role

[AIAA PAPER 69-488]

16 p2843 A69-32706

Supersonic compressor blade sections performance prediction near maximum pressure ratio and efficiency by analyzing flow processes

[AIAA PAPER 69-522]

16 p2843 A69-32711

Diffuser for high performance centrifugal compressors based on discrete pipe drillings

[ASME PAPER 68-GT-38]

19 p3240 A69-36420

COMPRESSOR ROTORS

Radial blade tip clearance effect on isentropic efficiency and air delivery in axial flow compressor with allowance for casing deformations and rotor displacements

16 p2837 A69-32004

Centrifugal compressor impeller disk design, considering stress analysis for shielding portion profile determination to satisfy equal strength condition

17 p3057 A69-33193

COMPRESSORS

NT CENTRIFUGAL COMPRESSORS

NT SUPERCHARGERS

NT SUPERSONIC COMPRESSORS

NT TRANSONIC COMPRESSORS

NT TURBOCOMPRESSORS

Compressor to inlet distortion tolerance design techniques for gas turbine compressors, noting rotor matching, blade chord length, blade geometry, etc

[ASME PAPER 69-GT-115]

09 p1572 A69-22525

Fluidic compressor bleed control unit for TF-30 jet engine to prevent stall at low rpm operation

10 p1753 A69-23559

Isentropic compression tube with piston compressor for producing hypervelocity test flows, noting shock speeds

[AIAA PAPER 69-334]

13 p2249 A69-28270

Multiple function combination probe design for compressor and turbine air flow research

16 p2766 A69-31917

Hypersonic test equipment and programs at CEAT /France/, describing compressor, wind tunnels and several experiments

16 p2766 A69-32071

Jet and compressor noise, discussing noise suppression techniques and engineering applications

[AIAA PAPER 68-550]

17 p3022 A69-34019

Glass fiber filled polytetrafluoroethylene materials for piston seals in high pressure oil-free reciprocating air compressors, discussing manufacturing and non-destructive tests

19 p3323 A69-35579

Oil-free linear motor resonant piston gas compressor, hermetically sealable to handle radioactive and dangerous gases

[ASME PAPER 69-FE-36]

20 p3466 A69-37996

COMPTON EFFECT

Transformation of differential mean and current densities and anisotropy of cosmic ray particles and photons observed in frames of reference relative to each other with isotropic flux

05 p0817 A69-16651

Stimulated Compton effect for energy transfer between relativistic electrons and radio photons in quasi-stellar objects

05 p0828 A69-16652

Diffuse cosmic X radiation flux and intensity law, noting inverse Compton effect of electrons on 3K black body radiation

05 p0817 A69-16714

Electron momentum density in diamond, graphite and carbon black from Compton profile measurement by X ray scattering vector

06 p0982 A69-18233

Stimulated Compton scattering for laser action, noting voltage tunability and gain at far IR wavelengths

[IEEE PAPER S-9]

07 p1154 A69-19081

Inverse Compton effect and universal black body radiation from less energetic radio photons of galactic and metagalactic origin

08 p1381 A69-19786

Cosmic gamma ray generation by Compton scattering in discrete sources, applying formulas to M87, Crab Nebula, M82, Cen A, Ngc 1275, and Cas A

08 p1377 A69-20053

Cosmological implications of diffuse X ray background, noting Compton black body process effect on isotropic cosmic X rays

09 p1578 A69-22152

Inverse compton scattering of far IR background radiation proposed as explanation of high energy gamma ray flux

09 p1580 A69-22296

Electromagnetic wave buildup by induced Compton effect as possible radio emission source, considering data for quasars and pulsars

11 p1957 A69-24402

Cosmic ray showers electron, positron and photon energy distribution functions calculated, considering positron annihilation, Compton effect and relativistic electrons formation

13 p2303 A69-28413

Energy transfer during fast electrons and photons interactions, indicating Compton energy losses related to space X ray and gamma radiation sources

15 p2676 A69-30953

Thermodynamic Green function for Compton scatter cross section of photons by electrons in hot plasma

15 p2664 A69-31479

Metagalactic electrons inverse Compton effect on relict radiation to interpret cosmic isotropic X radiation entire energy spectrum

16 p2847 A69-31800

Center to limb variation of solar hard X ray bursts, suggesting inverse Compton effect and bremsstrahlung from anisotropic electrons

17 p3023 A69-33055

Induced Compton scattering of plasma and electromagnetic waves under astrophysical conditions, discussing HF radio emission spectra from cosmic objects and quasar
20 p3607 A69-38035

Compton profile from single crystal of LiH measured with X ray scattering, noting valence- electron momentum distribution role
22 p3993 A69-40730

Electromagnetic wave buildup by induced Compton effect as possible radio emission source, considering data for quasars and pulsars
24 p4391 A69-43792

COMPUTATION
NT ORBIT CALCULATION
Collection of papers on computational fluid dynamics
01 p0061 A69-10916

Matrix computation operations devoid of sense and relevancy arising in interdisciplinary problems
11 p1910 A69-25522

COMPUTER COMPONENTS
NT CONTROL UNITS [COMPUTERS]
Computer systems definition, terminology and functional description, discussing engineering problems, flow charts, programming and techniques
04 p0563 A69-14515

Superconductors, discussing properties and materials for magnets, power systems, radiation detectors, HF devices and computer elements
04 p0642 A69-14584

Dual processor checkout system providing isolation of malfunctioning unit from memory and ensuring decision making by operative unit
04 p0568 A69-15361

Error analysis methods for inherent errors in analog, digital and linkage equipment of typical hybrid computer configuration
05 p0725 A69-16472

Typewriter keyboard computer system with CRT display having closed circuit TV link contents of file to add, delete or change information
06 p0891 A69-17204

Digital computer circuit design book covering requirements of circuit for digital logic and memory functions and physical properties of components
06 p0892 A69-17869

Microelectronics for digital adaptive controls, discussing digital filter design and chips required in fabrication
09 p1474 A69-22453

Complex electronic systems optimum redundant element content determination for ensuring adequate supply
14 p2426 A69-29422

Linear analog computing elements realizing voltage transfer function with poles and zeros independently controlled, basing method on dummy variable technique
14 p2422 A69-29551

Management and scientific computer reliability difference, considering circuits, component assembly, software, maintenance, etc
15 p2624 A69-30821

Quality control of high volume microelectronic circuit assembly of military computer emphasizing preventive action
15 p2580 A69-31129

Fluid amplifier with sudden widening applied to various computer tasks, utilizing for detection and measurement of viscosity, temperature and sonic or rotational velocity
17 p2903 A69-33010

Gunn effect theory and applications, discussing field domains in semiconductors, excited oscillations measurement, oscillators design, computer elements, etc
18 p3183 A69-35160

Onboard spacecraft computer design, programming and operation based on dual bussing system
20 p3500 A69-37384

Integrated logic circuits assembly for digital computers, considering high density, mechanical environment, reliability, accessibility and costs
20 p3505 A69-37401

COMPUTER DESIGN
Semiautomatic computer for determining torsional oscillation natural frequency in multimass in-line systems
01 p0035 A69-10596

Book on error detecting logic for digital computers covering error detection codes, logic circuits, checkers in data paths, etc
02 p0212 A69-11453

Hybrid computers, discussing analog and digital devices combination and distinction between use of computer for general purpose computation and control purposes
02 p0212 A69-11997

Onboard SDP-3 computer data system core for IMP spacecraft, considering payload
03 p0400 A69-13243

Aerospace digital computer design, discussing influence of data trends and reliability techniques
03 p0401 A69-14181

Limited speech recognition system /LISPER/ simplifies recognition by computer designed as research vehicle and pattern recognition system
04 p0565 A69-15338

Graphics system using computer configuration connected by conventional voice lines, noting hardware and components
04 p0566 A69-15343

Design and implementation of executive system for hybrid simulation, discussing requirements placed upon digital computer and operating software
04 p0567 A69-15350

MOS GP computer suitable for navigation applications
04 p0568 A69-15357

Semiconductor memory units, considering bipolar, p channel MOS and complimentary MOS chip technologies
04 p0569 A69-15362

Chronological development and future trends in high speed logic and memory hardware technology and implementation
04 p0569 A69-15366

Reliable information storage in memories designed from unreliable components
04 p0569 A69-15455

Reliable computation in computing systems designed from unreliable components, considering two models for component malfunctions
04 p0569 A69-15456

Nonreplicative self repairing control, describing prototype computer construction for testing feasibility
04 p0569 A69-15457

Special purpose computer for implementing programmable digital filter used in sampled data control systems
04 p0569 A69-15462

Digital computer interface systems design for simulation, control, instrumentation and data processing, discussing hybrid computer linkages
05 p0723 A69-16195

General purpose satellite computer, discussing on-board processor /OBP/ design, memory, central unit, input/output and software
05 p0725 A69-16710

Integrated automatic data processing system /NEC-TAR/ performance and operation
05 p0726 A69-16765

Typewriter keyboard computer system with CRT display having closed circuit TV link contents of file to add, delete or change information
06 p0891 A69-17204

Digital computer circuit design book covering requirements of circuit for digital logic and memory functions and physical properties of components
06 p0892 A69-17869

Gunn effect diodes application to ultrafast pulse electronic circuitry for computer logic
07 p1089 A69-18244

Single purpose analog computer with analog and hybrid elements for calculating Nyquist diagrams for feedback circuits
08 p1278 A69-20397

Analog video processor in omnidirectional radar system for flight safety, discussing construction, transistorization and circuitry
08 p1276 A69-20605

Decision oriented automatic data processing systems design, noting quantity and quality of upward directed information to management
08 p1423 A69-20733

Collection of papers on applications of microelectronics to aerospace equipment, noting design and reliability of circuits and computers
[AGARDOGRAPH-114] 08 p1291 A69-20981

Electrical design of low cost, highly maintainable general purpose computer optimized with respect to product of power and speed
[AGARDOGRAPH-114] 08 p1278 A69-20988

Complex digital computers designed for Apollo spacecraft missions, discussing construction techniques
[AGARDOGRAPH-114] 08 p1279 A69-20990

OMNITRAC general purpose airborne digital computer with permanent memory of 4096 words of 23 bits, noting modular construction
10 p1659 A69-22845

Sample data reduction methods combined in special purpose computer for measuring ablation in reentry vehicle heat shields
10 p1660 A69-23290

Solid logic technology /SLT/ computer circuits, discussing IBM 360 computer reliability, failure analysis information retrieval, SLT module and failure rate
11 p1843 A69-24341

Computer design for booster/satellite control, discussing systems reliability, low power and tradeoffs
11 p1843 A69-25320

Computer reliability by development and methodical employment of self repair techniques
12 p2034 A69-25941

Digital computer redundancy, analyzing triple modular redundancy in Saturn vehicles and quad design in primary processor and data storage for OAO
12 p2034 A69-26567

Electrical engineering, Volume 3, communications, covering special theories, systems components, telecommunication, electroacoustics, digital and analog computers and programming
15 p2568 A69-30619

Viggen computer development, stressing reliability towards aircraft vibrations
15 p2577 A69-30620

Third generation computer reliability including preparation and test of integrated logic circuits
15 p2626 A69-30832

Collection of papers on RCA computer design
16 p2756 A69-32554

Flight command computer for V/STOL aircraft, discussing design concepts, operating modes, displays, etc
[AHS PAPER 313] 17 p3001 A69-33543

Electronic computers for avionics system design in terms of technology, performance and cost, discussing reliability prediction and failure rate data
17 p2976 A69-34058

NDC-1070 solid state computer design featuring TTL, MSI and hybrid circuits, offering memory capacity flexibility and rapid maintainability
17 p2933 A69-34060

Patch panel programmed DDA computer having MHz iteration rate and 35 bit usable word length, discussing system design and demonstration model
17 p2934 A69-34073

Electromagnetic compatibility /EMC/ hardware design, discussing NDC 1060 computer configuration, requirements and service environment
17 p2947 A69-34136

Fluidic pressure ratio computing device based on two free jets interaction principle, describing prototype system design and analysis, electronics and overall error
18 p3133 A69-34309

IMP-1 experiment, describing design and applications of SDP-3 computer
19 p3280 A69-36265

Vibration phenomena analysis by transfer function computer, discussing precision spectrum analyzers
20 p3498 A69-37003

Onboard satellite computer design and programming language criteria, considering cost, reliability, weight, volume and energy requirements
20 p3499 A69-37379

Missile-borne and satellite-borne computers analogies, comparing design, operational conditions and functional requirements
20 p3500 A69-37380

Onboard aircraft computer design criteria, considering adaptability, maintainability, reliability, cost, prototype delivery time, weight and volume
20 p3500 A69-37381

Spacecraft onboard processor for digital filtration and data compression, discussing prototype design, construction, sample memory, weight memory, arithmetic unit and programmer
20 p3500 A69-37383

Onboard spacecraft computer design, programming and operation based on dual bussing system
20 p3500 A69-37384

SDP-3-A general purpose stored program computer designed for small scientific spacecraft onboard data system, noting computerized simulation
20 p3500 A69-37385

Swedish satellite onboard computer for particle experiment, discussing functional design based on buffer unit for experimental data
20 p3501 A69-37386

Onboard data processor design for Swedish satellite to study spatial and temporal variations of auroral particles

20 p3501 A69-37387

Onboard satellite computer for project Roseau experiments for magnetosphere study, discussing program switches, monitors and data compilers

20 p3501 A69-37388

Roseau satellite onboard computer systems design, emphasizing simulator and assembly programs for real time operation verification

20 p3501 A69-37389

Data handling system design for large astronomical satellite /LAS/, discussing spacecraft configuration, basic aims, program functions, subsystems, signal flow, flight repair, etc

20 p3501 A69-37390

Microminiature Elliott MCS 920 M digital computer for inertial guidance of CECLES-ELDO launcher, discussing construction, code, interrupt, guidance system and functions

20 p3501 A69-37391

Microminaturized digital computers for missiles and aircraft, discussing characteristics, environmental conditions and transformation possibility for use in satellites

20 p3502 A69-37392

Computer organization design employing distributed processor to provide general purpose computing while taking advantage of large scale integration

21 p3856 A69-39133

Dual role core /Ducor/ memory system with unique core stack assembly feature to achieve cost reduction and structural integrity for severe environmental conditions

22 p3903 A69-39950

Interactive experimenter computer system software and hardware design considerations based on astronaut-machine/experimenter question-answer interactions

[AIAA PAPER 69-953] 22 p3904 A69-40335

Fail-soft operation in array processor with cellular redundancy, discussing cellular autonomy, long life and ultrareliability

[AIAA PAPER 69-965] 22 p3906 A69-40346

Self testing and repairing /STAR/ aerospace computer for automatic maintenance of unmanned interplanetary spacecraft

[AIAA PAPER 69-966] 22 p3906 A69-40347

Digital data systems fault detection and isolation, describing diagnostic programs and hardware

[AIAA PAPER 69-967] 22 p3906 A69-40348

Spaceborne stored program computer design for OAO-C, noting auxiliary command storage, spacecraft monitoring and malfunction reporting, etc

23 p4132 A69-41736

SDP-3 small serial computer for engineering experiment on IMP spacecraft, discussing design modifications to improve performance

23 p4133 A69-41737

Modular data acquisition and processing system, describing input unit, checkpoint selection scanner, analog-digital converter, limit indicator, etc

23 p4167 A69-42459

F-111D computer complex to provide selective functional redundancy and flexibility to accommodate mechanization changes

[AIAA PAPER 68-837] 24 p4285 A69-43719

COMPUTER GRAPHICS

NT DATA PROCESSING TERMINALS

NT DIGITAL COMPUTERS

NT ERROR DETECTION CODES

NT PLOTTERS

Computer graphics technique for reducing photographic data from optical device to replace time consuming visual methods

18 p3134 A69-34373

Computer graphics engineering applications in line drawing displays for industry, including design programs and color TV flight simulation

18 p3106 A69-34659

Micromation and micrographics, discussing nonimpact printing in computer avoiding output imbalance by high speed microfilm recorder

18 p3234 A69-35059

Lockheed C-130 Hercules modified as STOL aircraft studied in laboratory by computerized simulation and graphics techniques for pilot view during landing

18 p3092 A69-35466

CRT graphic display/plotter for small digital computers, describing device operation, control and applications

21 p3679 A69-39608

EEG patterns computerized spatio-temporal display technique using CRT and motion picture camera

21 p3668 A69-39864

Interactive graphics system for rocket vehicle trajectory simulation and performance analysis

[AIAA PAPER 69-954] 22 p3905 A69-40336

Man-computer interactive Terminal Interface System /TITS/ compatible for programming graphics, character scopes and typewriter using FORTRAN

[AIAA PAPER 69-955] 22 p3905 A69-40337

COMPUTER PROGRAMMING

NT ASSEMBLER ROUTINES

NT LANGUAGE PROGRAMMING

NT ON-LINE PROGRAMMING

NT SYMBOLIC PROGRAMMING

Dynamic programming methods to avoid dimensionality problem arising in solution of boundary value problems by digital computer

01 p0103 A69-10006

Piecewise analysis of large structures, showing incompatibility of minimum computer storage and minimum number of multiplication requirements through bandwidth schemes

01 p0169 A69-10637

Representation for computer storage of contour map data for searching problem involving determination of aircraft ground track

01 p0036 A69-10704

JFIP computer language /Jet Propulsion Laboratory FORTRAN language with Intervals Preprocessor/ for extending FORTRAN 4 to utilize subroutines performing interval arithmetic

01 p0036 A69-10710

Finite f function computation by d/r circuit, discussing computation time

01 p0105 A69-10734

FORTRAN Deductive System to find solutions to theorem proving problems, discussing computer implementation

01 p0037 A69-10806

Digital computer systems design optimization based on operational experience in development of Saturn S-IC stage Automatic Test and Checkout System

03 p0400 A69-13233

Collection of Soviet articles on computer methods and programming covering fluid flow by numerical methods

03 p0362 A69-13649

Survey of papers on computer calculation of two and three dimensional gas flows, emphasizing method of characteristics and finite difference techniques

03 p0363 A69-13657

Open and closed path orthogonal analysis for structural network

03 p0526 A69-13735

Nonlinear aerodynamic problems of plane and asymmetric flows solved by digital computer, using modified Monte Carlo method

03 p0364 A69-13921

CASSANDRE language in computer simulation

03 p0401 A69-14178

Book on dynamic programming basic theory and standard computational algorithm and applications to optimization in diverse fields

04 p0563 A69-14652

Optimized formula for MacAdam color differences with modification in weighting of chromaticity and lightness, discussing Fortran IV computer programs development

04 p0564 A69-14883

Computer programming of satellite orbit tracking angles for automatic picture transmission receiving stations

04 p0558 A69-14917

Two dimensional elementary transformation for obtaining eigenvalues, considering programming aspects for computing characteristic roots of matrix

04 p0624 A69-14967

Algorithm for calculating discrete Fourier transform by computer

04 p0565 A69-15336

Arbitrary factor technique to derive fast Fourier transform, evaluating recursive properties of trigonometric functions

04 p0565 A69-15337

SALEM programming system developed for digital simulation of systems described by partial differential equations

04 p0565 A69-15340

TAF /time and frequency/ code written in FORTRAN language for computing steady state, frequency and time response from nonlinear simultaneous differential equations

04 p0565 A69-15341

Iterative solution of continuous-time-discrete-space /CTDS/ equations as approach to hybrid computation of certain partial differential equations

04 p0567 A69-15348

Hybrid executive development based on digitally oriented software, explaining assembly language routines

04 p0567 A69-15351

Interpretive Checkout Test Language /CTL/ designed in near English form for aerospace checkout tasks

04 p0569 A69-15364

Electrical circuits time domain analysis, describing method for computer solution of circuit equations

05 p0737 A69-15766

Multilevel modeling structure for interactive computer graphic design, discussing conversational display manipulation program and interconnection with analysis program

05 p0724 A69-16381

Programming technique using quaternion parameters for error reduction in simulation of spinning rigid body

05 p0724 A69-16469

Computer-analyzer system for nuclear chemistry, noting advantage of on-line data acquisition and analysis coupled with time sharing economy

05 p0725 A69-16584

On-line ground flight test data processing system

05 p0725 A69-16757

Book on FORTRAN computer programming language

06 p0891 A69-17364

Automation of meteorological fields analysis using computer

07 p1175 A69-18677

Book on computer calculation of structures covering programming, computer language, mathematical aspects of structural analysis, matrix computation, etc

07 p1233 A69-19349

Energy deposits from decay of tritium incorporated into bacteria, using computer simulation for radiation dose distribution

07 p1068 A69-19490

Discrete ordinate difference equations of radiative transfer for slab using invariant method, noting storage and computing time advantages

07 p1183 A69-19623

Sparse matrix scheme for computer analysis of structures, introducing term searching factor as efficiency guide for matrix routines

07 p1089 A69-19723

Computer program reliability enhancement, discussing significance of underestimation

08 p1278 A69-19845

Stochastic model for real time on demand weather predictions using REEP /regression estimation of event probabilities/ equations in Markov chain

08 p1345 A69-20299

Trajectory calculation of unguided meteorological rocket by digital computers and by equations of motion, discussing wind influence on ceiling and horizontal ranges

08 p1409 A69-20457

Soviet literature on coding theory and applications, stressing contributions to nonSoviet specialists

09 p1460 A69-21393

Multistep integration formulas treated as transfer system to examine properties in frequency domain for selection in digital simulation programs

09 p1460 A69-21417

Black arrow rocket vehicle flight path computer programming, discussing geographical restrictions on design

09 p1593 A69-21616

Time dependent procedure for axisymmetric transonic nozzle flows, programming governing equations for high speed computer

09 p1431 A69-21974

Man in loop computer facility for programmers to check out flight programs in simulated space flight environment

[AIAA PAPER 69-324] 09 p1479 A69-22384

Computer aided circuit design programs combining technical engineering skills with building block programs

10 p1659 A69-23141

Electronic circuit analysis by computer programming including system and program commands, network data, output control, discussing steady state circuit programming

10 p1659 A69-23143

Computer generated holograms using binary transmittance for wave fronts and three dimensional images construction

10 p1697 A69-23869

Matrix Computer for solution of algebraic and integrodifferential equations in linear and nonlinear

statics and dynamics, considering mechanical vibration problems
[ASME PAPER 69-VIBR-12] 10 p1806 A69-24167

Pneumatic diode function generator for simulating nonlinear control systems, discussing operating characteristics and programming methods 11 p1858 A69-24580

Computer processed pictures including transformation of graphical material, picture generation from data or abstract rules, discussing procedures, instrumentation, color and applications 11 p1842 A69-24588

Thin conical elastic shell stress-strain state calculated by computer for arbitrary thicknesses and loading conditions, considering temperature and edge forces effects 11 p1981 A69-24943

Flexible control module for real time automated checkout requiring programming by personnel with strong software background 11 p1843 A69-25072

Free vibration of discretely stiffened cylindrical shells with arbitrary end conditions programmed for digital computer, considering flexure, extension, torsion and nonsymmetric stiffener cross section 11 p1992 A69-25521

Digital computer analysis of multivariable control system in frequency domain, using operational array technique programming method 12 p2046 A69-26064

Computer program in ALGOL for computing satellite ephemerides applicable to satellites with direct or retrograde motion observed in Northern or Southern Hemispheres 12 p2159 A69-26448

Linear programming algorithms for optimal structural weight design 12 p2181 A69-26566

Digital computer methods for weak pulsars search using radio noise picked by telescopes 12 p2172 A69-27169

Parallel processing in system of computers with identical output, including probability graph for algorithm 13 p2224 A69-27426

Solar eclipses phases and elements calculation by Fortran language computer, using least squares method 13 p2336 A69-27447

Cosmic ray observation data automatic recording, presenting coding system for reading into computer 13 p2327 A69-27609

Turbulence measurement, considering handling and storage of data 13 p2263 A69-28148

Subroutines for computing characteristics of electromagnetic radiation scattered by absorbing and homogeneous sphere employing logarithmic derivative method 14 p2412 A69-29283

Monograph on reduction of satellite data using fixed stars covering ALGOL programming for computing satellite direction from photographic model 14 p2446 A69-29286

Computer based data handling and display for relating remote sensor signals to ground truth information derived from aerial photographs 14 p2416 A69-29534

Economical computer techniques for numerically integrated finite elements, creating 96 element square matrix 15 p2711 A69-30873

Lidar data obtained at Hamilton AFB, Calif., computer analyzed for lidar operational utility, determining cloud ceiling and visibility for aircraft landing operations 15 p2651 A69-30895

Nondeformable closed contour spatial gear kinematics using matrix tensor method suitable for computer programming 15 p2713 A69-31020

Computer analysis of EEG recording, presenting model studies under rest and performance conditions 15 p2560 A69-31232

Book on three dimensional flow of ideal gases past smooth bodies, emphasizing utility of finite difference methods 16 p2771 A69-32003

Approximation of vector linear differential equations with slowly varying matrix coefficients on time sharing computers, noting modeling possibilities 17 p2996 A69-33879

Computational approaches in applied mechanics - ASME Conference, Chicago, June 1969 18 p3105 A69-34657

Problem-oriented languages in man-computer intercommunication 18 p3106 A69-34658

Extremum disturbance analysis and optimum performance and design problems for structural and mechanical dynamic systems, basing solutions on linear, nonlinear and dynamic programming 18 p3106 A69-34663

Electronic data processing facilitating engineering design development work, including computer programming 18 p3106 A69-34838

Operational missile flight program validation plan noting mission analysis, computer programming, program preparation and performance prediction 19 p3279 A69-35955

Block structures and indirect addressing, discussing SNOBOL modifications and naming constraints 19 p3280 A69-36207

Computer program for numerical integration of chemical reaction rate equations behind steady state hydrogen-oxygen shock wave 19 p3451 A69-36366

Onboard spacecraft computer design, programming and operation based on dual bussing system 20 p3500 A69-37384

Electronic computer for processing observational data from pilot balloons, utilizing algorithms of values in programming for accuracy and time saving 20 p3572 A69-37700

Computer programming procedures in automatic control of hole boring processes for aircraft components 21 p3731 A69-38881

Transfer matrix symmetry about secondary diagonal in vibration analysis useful for computer programming 22 p4040 A69-39938

Programming aspects of computer uses in civil engineering, stressing engineer-coder communication via flow diagrams 22 p3903 A69-40138

Coding aspects of computers use in civil engineering, discussing language selection, program partitioning and storage use 22 p3903 A69-40139

Man-computer interactive Terminal Interface System (ITIS/ compatible for programming graphics, character scopes and typewriter using FORTRAN [AIAA PAPER 69-955] 22 p3905 A69-40337

SIMUPOL /Simulation Procedure Oriented Language/ system for hardware description and architecture and interface requirements of digital processor [AIAA PAPER 69-960] 22 p3905 A69-40341

Programming and checkout of computer for Edo inertial guidance system, including flight simulation and autopilot tests [AIAA PAPER 69-961] 22 p3978 A69-40342

Airline economics long term trends requiring management tools for cost control, operations simulation and monitoring, computer use and information data processing [SAE PAPER 690414] 23 p4241 A69-41641

Programmable data handling and telemetry systems for scientific satellites, noting system checkout, spacecraft integration, software and ground data processing 23 p4132 A69-41735

Integrated civil engineering system (ICES/ and structural design language /STRUDL/ programming and operating characteristics, including computer run example 23 p4134 A69-42146

Formulas for discriminant and regressive weather analysis for computer calculations under operational weather forecasting conditions 23 p4184 A69-42490

Tree codes for memoryless time discrete sources with bounded fidelity criterion 24 p4284 A69-42720

Memory gradient algorithm for reducing computing time by minimizing quadratic function of unconstrained variables compared with Fletcher-Reeves algorithm 24 p4340 A69-42957

Basic task archetypes in man-computer problem solving including detection, planning, optimization, designing, etc 24 p4274 A69-43019

COMPUTER PROGRAMS

NT APPLICATIONS PROGRAMS [COMPUTERS]
NT ASSEMBLER ROUTINES
NT COMPILERS
NT SUBROUTINES

Spacecraft illumination by reflected solar radiation calculated by computer method 01 p0151 A69-10576

Book on advanced linear programming computing techniques covering algebraic theory and construction of computer programs 01 p0035 A69-10701

Three leveled computer program library compiled for numerical analysis 01 p0036 A69-10709

Engine inlet thermal anticing analysis, detailing computer programs to determine air flow velocity, water impingement and thermal requirements 01 p0055 A69-11045

Electromagnetic wave path emitted by artificial satellites across anisotropic ionosphere due to geomagnetic field determined by computer program 01 p0068 A69-11115

Stellar brightness attenuation in atmosphere, determining extinction factor using computer calculations 01 p0157 A69-11192

Computer program for calculating density distribution of deviation of F 2 layer critical frequency from median value 02 p0239 A69-11692

Soviet book on kinematics of inertial navigation systems covering systems classification, equations derivation and computer algorithms for error analyses 02 p0278 A69-11793

Computer solution of forced torsional oscillation equations for periodic coupled machine system with viscous dampers 02 p0338 A69-11893

Geophysical theory and computers - Conference, University of Trieste, September 1967 02 p0242 A69-12005

Satellite digital video data analyzed by two dimensional filter computer technique, discussing biomedical applications 02 p0213 A69-12155

Collisionless computer model performing gravitational experiments with two dimensional galaxy 02 p0322 A69-12271

Computer study of collisionless self gravitating system using two dimensional model, obtaining gravitational field by solving Poisson equation 02 p0322 A69-12272

Computer models of one dimensional stellar problems, discussing fast relaxation of unsteady state to Fermi-Dirac distribution and slow relaxation to thermal equilibrium 02 p0323 A69-12274

Radar cross sections for arbitrary bodies calculated with computerized ray optics method taking into account depolarization 02 p0209 A69-12332

Multiprocessing system simulation using GPSS /General Purpose Simulation System/ model 02 p0213 A69-12492

Missile radar cross section based on modeling from simple forms, noting computer program 03 p0384 A69-12910

Stored program control for polynomial data compression in telemetry application 03 p0400 A69-13220

Radiation sensor PCM data processing by computer to detect radiation level using data decorrelation, data normalization and threshold test 03 p0400 A69-13313

Parametric analysis of life support systems developing scaling laws adapted to computer solutions, discussing manned orbital missions [SAE PAPER 680746] 03 p0379 A69-13438

Systems analysis application to determination of C-5 effectiveness noting loading, productivity and effectiveness analysis computer programs [SAE PAPER 680729] 03 p0379 A69-13440

Dipole model of geomagnetic field in terms of spatial distribution of vertical component, discussing computer program for calculating rectangular components 03 p0424 A69-13544

Analog sampled data simulator using field effect transistors and single value of holding capacitor for covering sample frequency variation 03 p0405 A69-13600

Numerical computer results applied to supersonic flow of perfect gas past staggered cones 03 p0363 A69-13659

Applications of electronic computers in construction - Conference, Weimar, June-July 1967 03 p0525 A69-13734

Computerized solution of three dimensional problems of elasticity theory using Ritz method 03 p0527 A69-13743

Two dimensional problem of elasticity by numerical solution, outlining program for computer 03 p0527 A69-13750

Computer program for electromagnetic wave metal shielding evaluation 03 p0398 A69-13901

Computer method calculating stressed state of elliptical bottom of cylindrical pressure vessel based on differential bending equations for shell of revolution 04 p0668 A69-14275

Computer programs for engineering analysis, design and simulation, presenting point selection program for curve plotting 04 p0563 A69-14516

Digital computer program for gas bearing analysis, discussing Reynolds equation and numerical approximations 04 p0604 A69-14518

Computer solution of Cauchy problem of ordinary differential equations in form of Taylor series 04 p0622 A69-14624

Numerical integration of elliptic mixed boundary value problem in region with curved boundary programmed in FORTRAN for general linear second order partial differential equation 04 p0625 A69-15287

Space oriented programming languages and compilers for translating languages, discussing software generating tools under development for space missions 04 p0564 A69-15297

Algorithm for simultaneous nonlinear equations solution on computer, noting quadratic convergence for convex space 04 p0565 A69-15335

Computer controlled photometric telescope, describing star setting, photometric measurements and data processing 04 p0602 A69-15380

Special purpose computer for implementing programmable digital filter used in sampled data control systems 04 p0569 A69-15462

Stored program computer for small scientific spacecraft, noting program and data memory capacities 04 p0569 A69-15472

Partial differential equations solution using analog, digital and hybrid computers, discussing heat transfer in parallel flow exchanger 05 p0723 A69-15705

Digital computer solution of Laplace equation using dynamic relaxation method to introduce dynamic terms into basic equation 05 p0697 A69-15713

Book on computer evaluation of mathematical functions, discussing errors, square and cube root, Chebyshev polynomials, approximation, rational function, asymptotic expansions, etc 05 p0723 A69-15955

Computer programming language for three dimensional geometry at symbolic level, noting use for placement problems 05 p0724 A69-16382

Three dimensional computer graphic modeling program, discussing SIGHT and LEGER programs 05 p0724 A69-16383

Computer programs and analysis methods for digitalization of continuous feedback network in missile control systems 05 p0725 A69-16470

Flight test data reduction on time sharing general purpose computer, noting hardware link between airborne equipment and computer 05 p0726 A69-16758

Square loop magnetic core model for computer aided circuit transient analysis 06 p0899 A69-16888

Satellite actinometric data computerized reduction in U.S.S.R., examining computer program features [UN PAPER 68-95763] 06 p0916 A69-17038

Processing TV cloud data monitored by Molniya I and Meteor meteorological satellites, discussing computer interpretation of TV photographs [UN PAPER 68-95759] 06 p0950 A69-17060

Random search and multiple integral based Monte Carlo method for computer solution of nonlinear aerodynamic problems 06 p0858 A69-17334

Characteristic impedance of rectangular waveguide computation curve explained on basis of computer program for cascade of transmission line sections 06 p0897 A69-17490

Optimum control problems solved numerically on computer, noting multivalence of extremal solutions and application to orbital transfer in central gravitational field 06 p0903 A69-17539

Space vehicle trajectory optimization using computerized step by step steepest descent to minimum cost, considering cost gradient vs control 06 p1006 A69-17570

M-20 digital computer program designed for calculating statistical characteristics of signals from IR TV scanning system of Cosmos 122 meteorological satellite 06 p0929 A69-17980

Soviet collection of papers on dynamics and strength of machines 06 p1026 A69-18013

Optimal computer calculation procedure for medium thickness anisotropic laminar plates with shear applied to rectangular and hinged plates 06 p1026 A69-18015

Computer program for axisymmetrically deformed shells of revolution and combinations of such shells 06 p1026 A69-18019

Stress distribution in shallow spherical shell with smooth cornered rectangular hole or biperiodically arranged set of holes, using computer program 06 p1027 A69-18020

Computer solution of incompressible two dimensional time dependent Navier-Stokes equations for oscillating body with rectangular boundaries [AIAA PAPER 69-185] 06 p0914 A69-18135

Fluid flow longitudinal temperature profiles for inclusion in heat transfer computer program [AIAA PAPER 69-30] 06 p1038 A69-18174

Computer program for predicting temperature distribution and heat transfer through coated and uncoated window systems of aerospace vehicles [AIAA PAPER 69-28] 06 p1038 A69-18178

Specular reflection computer program utilizing virtual image technique to determine reflection characteristics of enclosed diffusely emitting surface [AIAA PAPER 69-65] 06 p1040 A69-18215

Finite kinetics calculations by computer programs to generate reactions among prescribed reactants [WSCI PAPER 68-54] 07 p1072 A69-18314

Ignition pressure transient for solid propellant rockets predicted by computer program [WSCI PAPER 68-35] 07 p1203 A69-18352

NERVA transfer functions evaluation by computer data processing, using Fourier algorithm [IEEE PAPER 2B-2] 07 p1179 A69-19187

Complex transmission and reflection coefficients of dielectric film with permittivity gradient computed by modified Runge-Kutta method, noting plasma diagnostics application 07 p1194 A69-19334

Heuristic Dendral program to mechanize inductive inference in organic chemistry to determine isomers in chemical compounds 07 p1075 A69-19484

Computer programmed momentum theory for induced flow field of helicopter rotor in forward flight [AIAA PAPER 69-224] 07 p1052 A69-19562

Computer aided design program for testing equivalent circuits of bipolar transistors in static regime under various polarization conditions 08 p1280 A69-19972

Digital method for quantitative study of carrier circulation phenomena in semiconductors, noting Algol program and continuously polarized p-n junction 08 p1280 A69-19973

Controlled charge models for computer calculation of electronic circuits, discussing tunnel diode static characteristics and equivalent transistor circuits 08 p1280 A69-19975

MOS transistor equivalent circuit for computer aided calculations with IMAG I program, noting versatility of model 08 p1280 A69-19978

Computer aided automatic drawing of printed circuits, including design and manufacture of films for engraving 08 p1296 A69-19979

Fortran 4 program for computation of equilibrium compositions of gas mixtures at high temperatures 08 p1278 A69-20154

OMEGA airborne navigational computers, discussing earth ellipticity and phase variations problems for signal conversion into latitude and longitude coordinates 08 p1347 A69-20778

Digital computer method for Navier-Stokes equation in prototype cavity flow problems, noting applications to biharmonic problems 08 p1305 A69-20831

Computer programs for systems statistical reliability characteristics using reliability tests and time to failure data, giving optimal breakdown probability functions 08 p1322 A69-21101

Low thrust mission analysis techniques and computer programs, discussing electric propulsion 09 p1585 A69-21208

Predesign and mission analysis software capability for sizing, design, fabrication and developmental testing of flight hardware for electrically propelled interplanetary spacecraft 09 p1585 A69-21210

Smoothing data stability by least squares method, noting applicability to computer processing at random sequences 09 p1532 A69-21754

Specialized mathematical machine for expanding matrix determinants and solving combinatorial problems, discussing symbolic circuit 09 p1460 A69-21782

Linearized radio circuits frequency characteristics calculations using digital computers, noting system nodes number influence on computer rate 09 p1472 A69-21783

Computer program for continuous attitude determination for spin stabilized OGO-C satellite after malfunction of attitude control system, calculating angle between high rate data periods 09 p1610 A69-21987

Spacecraft onboard checkout systems and design of ground support equipment and software, noting adaptive dynamic analysis and maintenance /ADAM/ concept [AIAA PAPER 69-307] 09 p1478 A69-22382

Finite difference method computer programs for calculation of velocities and streamlines on blade to blade surface of revolution of turbomachine [ASME PAPER 69-GT-48] 09 p1432 A69-22495

Digital computer programs for aerodynamics of subsonic gas turbine combustion systems applicable to incompressible flow with specified flow boundaries, noting vortices distribution 09 p1573 A69-22621

Structural reliability tests using photoelasticity and associated techniques, discussing computer methods, materials research, etc 09 p1479 A69-22734

ATS satellite distorted photographs conversion into normal and Mercator projections, using computer programs 10 p1689 A69-22945

Waveguide Y circulator electrodynamic parameters by design algorithm and computer programs 10 p1661 A69-23108

Book on RCA computer applications covering computer programming, differential equations and basic time sharing, circuit analysis, microwave solid state power sources, etc 10 p1659 A69-23140

SNODE /spectra numerical ordinary differential equations/ computer program for solving differential equations and integration with basic time sharing system 10 p1659 A69-23142

Computer implemented analysis of aeroelastic stability for elapsed data reduction time, discussing frequency modes and digital filters 10 p1634 A69-23274

Computer controlled data acquisition and control system /DACS/ for wind tunnel applications, describing system and programs 10 p1673 A69-23286

Computer program for onboard medical checkups of spacecraft crews during extended space flights, discussing tests and intervals 10 p1649 A69-23505

Integration routines performance used in dynamic systems simulation by digital programs, comparing speed, accuracy and convenience 10 p1661 A69-23854

Flux density of quasars 3C 270 and 3C 278 at 40 cm determined by digital computer with point source program 11 p1954 A69-24383

Real time electronically scanned radar control using digital computer with input and output conversion for information handling, noting interface equipment 11 p1834 A69-24544

Gaussian summation for ion implantation profile control in semiconductors, describing computer program selecting optimum energies to fit predetermined profiles 11 p1857 A69-24546

Computer program for analysis of linear microwave multipoint circuit by means scattering matrix equivalent 11 p1858 A69-24572

Computer program for processing actinometric data transmitted from Cosmos 122 satellite 11 p1913 A69-24831

Computer program for interpreting IR cloud pictures from Cosmos 122 satellite based on potential function method

11 p1884 A69-24833

Computer program for electron and proton fluxes impinging on spacecraft, performing computation for Van Allen belts and solar flares

11 p1949 A69-24863

Physical data representation by approximation formulas for computer processing, considering polynomials, rational and spline functions and error curves

11 p1842 A69-24904

Constraint theory for analysis of mathematical models to alleviate software problems associated with simulation of complex large scale systems

11 p1858 A69-24936

Computer controlled flight line tester performing automatic real time testing of aircraft avionics systems on flight line or hanger

11 p1864 A69-25060

Computer controlled testing of commercial aircraft avionics systems for automatic, semiautomatic and manual operation to perform repair and calibration tasks

11 p1864 A69-25061

Hardware and software as single entity in small scale programs, describing English language oriented program code of Controller /Programmer/ Evaluator

11 p1864 A69-25062

Electronic module testing with integrated hardware/software system, noting module test console and manual capabilities

11 p1864 A69-25065

Hardware-software interface defined for design of computer controlled test system, discussing criteria for designing economical systems

11 p1842 A69-25071

Airborne computer controlled data acquisition system for real time fault detection and isolation in avionics

11 p1843 A69-25082

Monograph on computer aided air traffic control systems design, discussing air navigation, man-machine relations, equipment requirements, programs, plan position color display, etc

11 p1914 A69-25085

Least squares iterative program, deriving orbits for O binaries HD 93403 and HD 135240

11 p1963 A69-25257

SNR measurement with time interval counter and computer, discussing accuracy

11 p1839 A69-25299

Carrier to interference ratio /CIR/ between desired path and every other path within predetermined range in microwave system calculated by computer

11 p1840 A69-25312

Computer techniques application to radio engineering functions related to system performance, layout engineering, frequency coordination and administration, discussing decision parameters interrelationship

11 p1840 A69-25313

Dynamic unified structural analysis method in computer program, calculating stiffness matrix to obtain natural frequencies and mode shapes

11 p1987 A69-25367

Complex structure least weight optimization for specific frequency by computerized modification of existing member cross sectional properties

11 p1989 A69-25494

Digital program containing Eulerian formalism for multiple interconnected rigid members applied to gravity gradient stabilized satellite with flexible booms

11 p1989 A69-25502

Integrated computerized reliability monitoring program for detecting aircraft systems and components performance trends and optimizing cost, utility and response

12 p2055 A69-25972

Digital computer-aided reliability engineering methods for electronic equipment design and analysis

12 p2037 A69-25973

Time optimal controls for multivariable linear systems by computer programming of iterative calculations /Neustadt and fast convergence methods/

12 p2050 A69-26090

Computer program for model stellar envelopes of red supergiants with extended atmospheres

12 p2156 A69-26218

Computer program solving for station coordinates and dynamical parameters at Smithsonian Astrophysical Observatory from optical data, laser range and range rate

12 p2068 A69-26428

Computer programs for linear systems fault isolation, discussing technique theory and limitations

12 p2040 A69-26568

Linear two dimensional partial differential equations solved by Laplace transforms on analog computer

12 p2123 A69-26717

Nonlinear structure undergoing arbitrary load history including temperature variations solved by computerized force and subordinated step procedure

12 p2185 A69-26823

Computer program for worldwide analysis of mean hourly values of field components into constituent fields and associated ionospheric current systems

12 p2074 A69-26958

Self adjusting digital computer method for two dimensional gravitational anomalies

12 p2076 A69-27088

Computer determination of symbolic state equations for nonlinear circuits using FORTRAN notation

12 p2055 A69-27097

Computer method for solution of Banachiewicz graph analytic equivalent for parabolic orbits determination, noting geocentric distances variation

13 p2336 A69-27448

Computer program for obtaining information from stationary time series using Chree method of superposed epochs for processing unlimited data and epochs

13 p2225 A69-27617

Soviet book on automated information retrieval systems covering computer languages, search in complex ordered codes, translation from Russian into computer language, etc

13 p2225 A69-27933

Regional boundaries in control-parameter space constructed by computer algorithm, involving parameter vibration direction changes in parameter plane

13 p2225 A69-27967

Laminar boundary layer studies by finite difference computer program for Mach numbers up to 15

13 p2248 A69-28173

Two dimensional flow through nonuniform gauze by computerized analysis based on linearized theory

13 p2248 A69-28174

Thermal behavior of space vehicle window systems predicted by mathematical analysis and computer methods for heat transfer through glass

13 p2378 A69-28215

Matrix eigenvalues for nonlinear simultaneous algebraic equations, discussing computer program for numerical integration

13 p2289 A69-28227

Computer program for compressible fluid flows with space and time dependent variables, discussing hypervelocity impact

13 p2365 A69-28286

Meteorological problems in Italy analyzed by digital computer program through numerical integration of atmospheric models to provide weather forecasts

13 p2295 A69-28651

Computer program for calculating density distribution of deviation of F 2 layer critical frequency from median value

13 p2258 A69-28723

Computerized calculation of likelihood coefficients for identifying steady random processes against background noise, minimizing mean risk of erroneous solution

14 p2410 A69-28818

Automatic search-free optimization by sensitivity functions, deriving algorithms by Q factor and discrepancy extrapolation

14 p2425 A69-28823

COHORT-II Monte Carlo computer program written in Fortran IV to model radiation shielding problems

14 p2417 A69-29004

Complex structures lumped weight and inertia parameters automatic computation based on finite weight element method, using SCOWL computer program

14 p2533 A69-29025

Computer program for STV-F9 satellite communication parameters, using ELDO forecasting values as input data

14 p2530 A69-29689

Quasi-uniform pseudorandom numbers program transmitter statistical characteristics suited for solving problems by Monte Carlo method

15 p2572 A69-30336

Computer codes describing nuclear weapons effects associated with X ray transport, neutron transport and X ray interactions with material, fireball, blast environments, etc

15 p2652 A69-30381

Polygonal approximation to functional equation solution by using search algorithms, listing FORTRAN IV programs

15 p2644 A69-30424

FORTRAN program for calculation of magnitude and phase of digital filter transfer functions and power spectra of periodic waveforms

15 p2567 A69-30612

Spacecraft illuminance by reflected solar radiation calculated by computer method

15 p2691 A69-30746

Nova outburst dynamics investigation by time dependent hydrodynamics computer program including energy transport by radiation and convection

15 p2692 A69-30769

Transistors and IC reliability for memory control evaluated by Concerto subprograms

15 p2627 A69-30842

Microslip between concentrated contacts and design charts for maximum pressure, closing-in of contacting bodies and optimized shapes, giving computer programs

15 p2629 A69-30903

Plasma instabilities due to anisotropic velocity distributions computer analyzed to study nonlinear phenomena and validity limits of linear theory

15 p2661 A69-30920

Complex systems reliability, describing uses of computer programs in analysis of circuit design, component failure modes and faults due to drifts

15 p2572 A69-31042

Fast Fourier transform algorithm for low storage capacity computer programs

15 p2572 A69-31092

Literal algebra /SPASM/ computer program critical verification of Kozai short period lunar perturbations, discussing errors

15 p2699 A69-31381

Computerized finite element waveguide analysis for determining propagating modes and cut-off frequencies

16 p2760 A69-31942

Aircraft noise assessment, discussing computer programmed formula, noise contours and duration calculation, with appendices presenting engine noise characteristics, air and ground attenuation, etc

16 p2735 A69-32021

Multistage rocket trajectories optimized by second order numerical technique and digital computer program, considering coasting, vacuum flight and transition times

16 p2857 A69-32154

Computer programs for space engineering analytical and scientific computation using digital computers

16 p2756 A69-32555

Surface state density determination as function of surface potential in MIS capacitors, discussing MIS capacitance method theory and computer programs

16 p2827 A69-32556

Prebreakdown currents measurement in H and N for deducing ionization coefficients via Townsend and Lucas equations respectively, noting validity by digital computer technique

16 p2815 A69-32574

Statistical analysis of Brewer-Mast electrochemical soundings of vertical ozone distribution for developing computer programs of climatological behavior

16 p2786 A69-32632

FORTRAN computer program for quality control and calculation of total ozone measurements and lamp tests for Dobson ozone spectrophotometer

16 p2787 A69-32644

Saturn 5 S-IC stage propulsion performance, using engine parameters from telemetry rather than accelerometer data, analyzed by iterative techniques and computer program

16 p2839 A69-32672

Turbulent heat and mass diffusion in catalytic reactors for hydrazine decomposition, developing computer program to calculate temperature and reactant concentration distributions

16 p2846 A69-32768

Digital computer program for physiological measurements, outlining interpolation of mathematical functions describing signals time variations

17 p2912 A69-32941

Equipment- and program-type methods for solving automatic digital control systems synthesis problems, evaluating efficiency based on accuracy

17 p2933 A69-33120

Computer calculation of kinetic characteristics of normal flame propagation during gas combustion, constructing physical model and differential equation system

17 p3069 A69-33138

Numerical integration of Eole satellite attitude equations compared with results obtained by analog simulation or hybrid computation

17 p3048 A69-33232

Transient thermal analysis of space radiators excluding finite difference equations, noting computer adaptability and time saving
[AIAA PAPER 69-615]

17 p3070 A69-33261

Thermal contact resistance measurement at various ambient pressures compared with theoretical predictions with each parameter analyzed over interface by computer program
[AIAA PAPER 69-629]

17 p3073 A69-33299

Flow field of two dimensional nozzle exhausting to vacuum, describing computer program based on BGK equation and plotting exhaust region density, temperature and velocity
[AIAA PAPER 69-658]

17 p2893 A69-33490

Life cycle maintenance costs reduction in aerospace industry by computers, describing on-line and off-line test systems

17 p2979 A69-33649

Direct lift controller design for aircraft approach and landing by computer program based on Kalman linear state regulator theory

17 p2902 A69-34027

Patch panel programmed DDA computer having MHz iteration rate and 35 bit usable word length, discussing system design and demonstration model

17 p2934 A69-34073

Software remechanization of conventional hyperbolic LORAN for two passive closed loop one way direct range measurements to individual LORAN transmitters

17 p3002 A69-34079

Pressurized cylindrical shell creep analysis by elastic procedure extension using computer program

17 p3067 A69-34211

Saturn software configuration accounting and reporting system for document change and information retrieval

18 p3105 A69-34269

Book on operational meteorological information processing by computers, discussing synoptic and aerological data, automatic data processing in operational numerical forecasting, etc

18 p3105 A69-34332

Reliability engineering methods for software programs with emphasis on real time computation, describing SSD Exhibit 61-47 documentation

18 p3105 A69-34524

Computer program and component part models for nonlinear DC circuit simulation at various temperatures

18 p3108 A69-34525

Computer graphics engineering applications in line drawing displays for industry, including design programs and color TV flight simulation

18 p3106 A69-34659

Quadratic programming method for equations of elastic perfectly plastic solid applied to stress distribution in plate torsion and bending

18 p3218 A69-34661

Finite element analysis of nonlinear elastoplastic material-geometric behavior problems, describing computer program and incremental stiffness matrices

18 p3219 A69-34664

Computer quadratic method of evaluating ray propagation data for estimating inhomogeneous media properties

18 p3172 A69-34667

Time sharing remote computer station allowing on-spot data processing and output answers, formulating best-fit equation representing statistical data
[SAWE PAPER 799]

18 p3107 A69-34860

Solid propellant rocket motor predictive design by correlating performance and weight statistics via computer program
[SAWE PAPER 775]

18 p3184 A69-34873

Computer program for weight and center of gravity tolerance data for assembly aerospace vehicle
[SAWE PAPER 734]

18 p3221 A69-34892

Computer aided design analysis program to provide weight and sizing data for entry spacecraft
[SAWE PAPER 797]

18 p3208 A69-34903

Computer programs determining gaseous properties and aerodynamic characteristics for missiles, reentry vehicles and spacecraft at angles of attack

18 p3107 A69-35068

Multistage systems high reliability design, describing branch and bound computer method for optimal resource allocation of redundant components

18 p3148 A69-35081

Man-computer speech communication, discussing model and aspects of acoustics, phonetics, linguistics, language training, physiology, psychology, bionics, etc
18 p3107 A69-35099

Computer program to predict spectra from electronic transitions of diatomic molecules and atoms, noting line intensity distribution by Voigt profile

18 p3177 A69-35239

Modified Newton-Raphson methods for preliminary orbit determination, showing fast convergence and short computation times

19 p3397 A69-35613

Takeoff and landing analysis digital computer program /TOLA/ developed by Air Force Flight Dynamics Laboratory for quantitative performance analysis
[AIAA PAPER 69-810]

19 p3289 A69-35630

Digitized video cloud picture data from ESSA satellite, discussing mesoscale archive and computer products including time averages and composites

19 p3279 A69-35810

Variational method for computer calculation of supercritical bending of thermoelastic uniformly loaded circular plates, determining Ritz parameter influence on accuracy

19 p3434 A69-35829

Rapid Targeting Procedures computer program for optimized orbital payload and associated launch vehicle targeting data with one submittal and minimum user intervention
[AAS PAPER 68-148]

19 p3402 A69-35951

Impulsive orbit transfer optimization using accelerated gradient program based on Newtonian algorithm for digital computer method

19 p3402 A69-35956

Computer program using system simulation and Monte Carlo techniques to assess turbojet engine compressor disk reliability, discussing maintenance policy and engine design effects

19 p3394 A69-36042

Atmospheric slant path molecular absorption and emission from band model methods, discussing computer program prediction capabilities

19 p3375 A69-36052

Computer program designing multiplex taper to minimize FM/FM telemetry system carrier threshold SNR, examining noise behavior of multiplex system stages for system performance

19 p3273 A69-36275

Balmer and Ca II /K/ line profiles computed by program based on model atmospheres, comparing computed and observed data for F stars

19 p3426 A69-36578

Finite element method in stress analysis for axisymmetric rotors design, describing computer program and applications

19 p3445 A69-36826

Computer iteration accelerator based on modified Aitken process, noting application to vectors

20 p3498 A69-36950

Digital computers standard programs for astronomical problems

20 p3596 A69-37317

Worldwide cloud cover simulation procedure providing data for computer simulation of earth oriented space missions, describing computer program using Monte Carlo mission simulation

20 p3573 A69-38120

Computer solutions for nonlinear partial differential equations governing compressible flow patterns with shocks, using Lagrange coordinates

20 p3569 A69-38212

Three dimensional X ray pictures of flaws shape and location in various materials

20 p3551 A69-38311

Mathematical models and solution techniques for calculating optimal elastoplastic structures by computer, discussing methods for displacements preceding plastic failure

21 p3831 A69-38414

Computer experiment on 9000 particle plasma to test temporal echo theoretical prediction

21 p3777 A69-38713

Shooting method difficulties in boundary value problem numerical solutions using computer programs to integrate differential equations

21 p3755 A69-38753

Digital computers used in error calculation in calibration curves of turboengines and other pneumatic devices

21 p3724 A69-39100

Numerical procedure for structural systems analysis, discussing computer application to hydrodynamic, electric, magnetic, thermodynamic, elastostatic and elastodynamic problems
[AIAA PAPER 67-955]

21 p3839 A69-39216

Computer programs for design data, examining program complexity, reliability and availability, design data sheets, etc

21 p3732 A69-39304

Computerized aircraft structural analysis system, adopting finite element technique /direct stiffness method/ based on COSMOS system

21 p3842 A69-39307

Stress analysis of thin axisymmetric shells by plane frame analysis program, noting stiffness matrix for conical shell element

21 p3843 A69-39312

Finite element relaxation method for computing stress distribution in thin walled structure, considering computer program, storage and solving time

21 p3843 A69-39313

Computer program for eccentric geocentric satellite orbits evolution, discussing atmospheric drag, earth oblateness and solar radiation effects
[AIAA PAPER 69-928]

21 p3808 A69-39357

Spacecraft control systems with computer command redundant jets for linear and angular pulses, relating configuration design to level-of-redundancy and task dimension
[AIAA PAPER 69-845]

21 p3822 A69-39375

Computer program /TACTICS/ for simulating three vehicles simultaneous motion in space, considering interceptor-target guidance and intercept trajectories
[AIAA PAPER 69-890]

21 p3678 A69-39415

Computer controlled automatic radar for survey through 360 degrees in azimuth and zero to 60 degrees in elevation

21 p3677 A69-39566

Computer routines for approximations of thermochemical properties of gas mixtures, using JANAF /Joined Army Navy Air Force/ tables of combustion systems

21 p3670 A69-39591

Computer program for generation of test patterns for multiterminal devices and networks

21 p3679 A69-39604

Network analysis for systems application program /NASAP/ in FORTRAN for batch and on-line analysis of electronic circuits

21 p3856 A69-39662

Computer program for satellite APT geographical grid production, discussing latitude-longitude intersections transformation to Cartesian coordinates

21 p3718 A69-39749

Documentation aspects of computer programs use in civil engineering, describing maintenance, users and operators manuals

22 p3904 A69-40140

Digital computer program for determining alveolar and capillary blood gas compositions corresponding to ventilation-perfusion values, considering dissolved oxygen and inert gas exchange

22 p3875 A69-40230

Mission analysis and trajectory simulation /MATTS/ program, discussing computer controls, modular design, integration evaluation
[AIAA PAPER 69-939]

22 p3904 A69-40322

Computerized algorithm facilitating automatic synthesis of time invariant linear compensation for highly complex multiloop control systems
[AIAA PAPER 69-941]

22 p3917 A69-40324

Automated programmed instruction /API/ for training backup interceptor control personnel to conduct air defense operations
[AIAA PAPER 69-956]

22 p3905 A69-40338

NASA computer language CLASP coordinated with evolution of SPL /Space Programming Language/ for aeronautics and space programming
[AIAA PAPER 69-957]

22 p3905 A69-40339

Machine independent telemetry oriented language /MITOL/ to develop computer programs for real time and postflight telemetry data processing

22 p3905 A69-40340

System safety in aerospace software including ground checkout software, command and control software and onboard programs
[AIAA PAPER 69-962]

22 p3905 A69-40343

Fail-soft operation in array processor with cellular redundancy, discussing cellular autonomy, long life and ultracellularity
[AIAA PAPER 69-965]

22 p3906 A69-40346

Self testing and repairing /STAR/ aerospace computer for automatic maintenance of unmanned interplanetary spacecraft
[AIAA PAPER 69-966]

22 p3906 A69-40347

Computerized simulation for performance evaluation of System/4 Pi-EP multiprocessor for use in aerospace vehicle

22 p3907 A69-40353

Software support package for aerospace digital computer emulation, consisting of symbolic assembly program and interpretive simulator program and subprogram [AIAA PAPER 69-974] 22 p3907 A69-40354

Computerized solid rocket motor nozzle design with computer program providing weight, envelope and performance values for vehicle optimization studies [AIAA PAPER 69-975] 22 p3999 A69-40355

Support software costs reduction for launch vehicle systems by implementing computer techniques to provide requisite data [AIAA PAPER 69-978] 22 p4052 A69-40358

Computer optimization of spacecraft optical coatings for temperature control, using finite element analysis and matrix inversion [AIAA PAPER 69-979] 22 p4050 A69-40359

Computer system functional requirements for autonomous Martian surface roving vehicle, emphasizing vehicle motion control system [AIAA PAPER 69-980] 22 p3907 A69-40360

Software/hardware interface testing of real time system, including possible improvements to computer program management flow 22 p3908 A69-40364

Digital computer system for navigation, landing, fire control, monitoring and checkout aboard Saab 37 Viggen aircraft handling attack, reconnaissance and fighter missions [AIAA PAPER 69-985] 22 p3908 A69-40365

Horizontal Situation Display /HSD/ map computer mechanization transforming earth location to X, Y coordinates for Lambert conformal projection [AIAA PAPER 69-987] 22 p3908 A69-40367

Spherical lunar coordinates for arbitrary moment of time calculated by digital computer using Brown lunar motion theory 22 p4024 A69-40611

Meteorological data real time processing for automatic weather analysis and prognosis, program used and computer output charts 22 p3977 A69-40732

Flight training using digital simulators, including maneuver analysis for TWA 707 program 22 p3928 A69-41137

Frequency response of control systems analyzed by digital computer using operational arrays, noting extensions to time response and root locus computation 22 p3909 A69-41255

Stored program decommutation techniques involving small core storage elements insertion into data path between decommutator equipment and computer 23 p4133 A69-41749

Digital computer program for determining flight vehicle telemetry antenna performance from ground test readings 23 p4133 A69-41754

Flexible format generator for manned spacecraft data management system designed with memory for data sampling formats, emphasizing software counters and power strobing 23 p4133 A69-41762

Computer program for natural oscillations of plates and shells, deriving differential equations of motion for thin elastic shell by variational method 23 p4230 A69-42004

NASA structural analysis /NASTRAN/ program applied to large radio telescopes, discussing static and dynamic analysis, problem formulation, finite element method, etc 23 p4232 A69-42145

DENDRAL program used to construct all possible acyclic structural isomers of C, H, N and O 23 p4114 A69-42214

Space power systems analysis, using computer program to correlate systems characteristics with mission parameters for automated satellite repair vehicle and space stations 23 p4068 A69-42240

Pu-238 isotope organic Rankine cycle system analyzed for one year manned space station, using modified H-521 Space Power computer program 23 p4188 A69-42264

Book on matrix-computer methods in engineering covering matrix algebra and calculus, computer programming, Fourier transforms, etc 23 p4234 A69-42421

N-terminal parent networks with symmetry constraints derived for nonredundant one port configurations through combinatorial functions test patterns, using computer algorithm 23 p4134 A69-42524

Automatic analysis and classification of images stored on 35-mm film using CRT flying spot scanner with computer control and memory 24 p4286 A69-42744

Adaptive cost equations in computer programs supporting launch vehicle long range planning, based on launch vehicle anticipated usage [AAS PAPER 69-164] 24 p4392 A69-42815

Optimal control computing method applied to minimal time flight profile optimization 24 p4383 A69-42954

Computerized spectral analysis of vibrational frequency due to elastic waves in isotropic hollow spherical shells [ASME PAPER 69-APMW-8] 24 p4402 A69-43106

General purpose computer program for synthesis of multivariable systems decoupled by state feedback 24 p4294 A69-43307

Rectangular dielectric waveguide propagation modes, describing computer analysis based on electromagnetic field expansion in circular harmonics series terms 24 p4288 A69-43330

Electronic scanning and correlation techniques for terrain sensing required in automatic stereoperception 24 p4316 A69-43566

Computer program determination of barreling effect on strength of ring and stringer stiffened shells designed to support axial compression loads 24 p4405 A69-43671

Flux density of quasars 3C 270 and 3C 278 at 40 cm determined by digital computer with point source program 24 p4389 A69-43773

**COMPUTER SIMULATION
U COMPUTERIZED SIMULATION**

COMPUTER STORAGE DEVICES

NT ACCUMULATORS [COMPUTERS]
NT CORE STORAGE
NT DELAY LINES [COMPUTER STORAGE]
NT SHIFT REGISTERS

MOSFET drivers for low current memory fabricated in 64 unit monolithic strips, discussing driver performance data 01 p0039 A69-10172

Piecewise analysis of large structures, showing incompatibility of minimum computer storage and minimum number of multiplication requirements through bandwidth schemes 01 p0169 A69-10637

Gradual memory system for noise reduction in adaptive control system 02 p0212 A69-12606

Statistical linearization of nonlinear memory type elements with stationary Gaussian input, applying Wiener method to one class of problems 03 p0409 A69-13005

Holographic laser type memory with bulk storage capacity and short readout time 03 p0428 A69-13116

Design and principles of operation of SHF electron-optical multiply stable storage elements with dynamic attributes of states 03 p0441 A69-13982

ASTRE programming language applicability to maximum memory information treatment in aerial navigation 03 p0401 A69-14180

Ferrite core temporary storage unit with 500 nsec cycle time 04 p0564 A69-15222

Large scale integration and batch-fabricated processing of logic and storage elements for fourth generation computer, discussing partitioning design 04 p0567 A69-15355

Semiconductor memory units, considering bipolar, p channel MOS and complementary MOS chip technologies 04 p0569 A69-15362

Chronological development and future trends in high speed logic and memory hardware technology and implementation 04 p0569 A69-15366

Reliable information storage in memories designed from unreliable components 04 p0569 A69-15455

Stored program computer for small scientific spacecraft, noting program and data memory capacities 04 p0569 A69-15472

Semiconductor standard memory circuits, discussing arrays and density 06 p0894 A69-17202

Metal oxide semiconductor random-access memories, discussing large scale integration and static and dynamic circuits chip size 06 p0894 A69-17203

Multichannel pulse height analyzer with memory, small size and low power consumption for application to satellites [IEEE PAPER 3C-6] 07 p1135 A69-19200

Flip-flops built with complementary symmetry MOS, discussing power, noise and load stability due to n and p channel series transistors 07 p1113 A69-19766

Trigonometric and arithmetic functions for reducing size of MOS read-only memories to reduce required bit count, discussing cost, structure and applications 07 p1089 A69-19778

Gunn effect memory loop in pulse diodes consisting of two Gunn diodes connected in series 08 p1279 A69-19912

Automatic plasma needle arc fusion welding for computer memory arrays and miniature electronic devices 09 p1511 A69-22355

Gunn diode operating to VHF range with coaxial line to generate rectangular waves and to function as memory element 09 p1467 A69-22587

FET memory element charge storage two layer model for thin film dielectrics noting charge/discharge times 10 p1742 A69-22947

Associative holographic memories, discussing recall systems, logic circuits, etc 10 p1697 A69-23868

Large capacity holographic memory design based on page organization concept, considering lens parameters and hologram size 11 p1886 A69-25041

Dynamic multistable analog integrator capable of prolonged retention of integration, giving differential equation of device 13 p2224 A69-27427

Square matrices decomposition into orthogonal and triangular matrices products for computer storage applications 13 p2290 A69-28485

Ferrite core storages characteristics with rectangular hysteresis loop for digital control units, discussing optimal selection method 14 p2418 A69-29145

Fast Fourier transform algorithm for low storage capacity computer programs 15 p2572 A69-31092

NDC-1070 solid state computer design featuring TTL, MSI and hybrid circuits, offering memory capacity flexibility and rapid maintainability 17 p2933 A69-34060

Integrated nonvolatile read-write memory with addressing using variable threshold field effect transistor including cell operation, channel shielding and circuit 17 p2942 A69-34120

Airborne digital computers techniques in avionics stressing memory design, packaging, reliability and maintainability 18 p3106 A69-34846

Memory matrices sensitivity to laser beams with various emission power densities, considering matrices of thin metal layers on transparent base 19 p3335 A69-36198

Analog device to compute running ten minute average and store latest ten minute peak of unipolar data input for wind speed sensors 19 p3312 A69-36278

Computer memory with digit wire magnetic circuit /torus/, discussing capacity, access and output 20 p3503 A69-37402

Wire type memory model for satellite onboard computers, discussing nondestructive readout, power requirements, marginal temperatures, material and volume 20 p3503 A69-37403

Computer memory reduction through Fortran higher level language, discussing tradeoff between costs saved and additional logic hardware [AIAA PAPER 69-963] 22 p3905 A69-40344

Photochromic film behavior under high power argon ion laser excitation studied for display and computer memory applications, using excitation model 23 p4173 A69-41629

Flexible format generator for manned spacecraft data management system designed with memory for data sampling formats, emphasizing software counters and power strobing 23 p4133 A69-41762

Memory gradient algorithm for reducing computing time by minimizing quadratic function of unconstrained variables compared with Fletcher-Reeves algorithm
24 p4340 A69-42957

COMPUTER SYSTEMS PROGRAMS

NT ASSEMBLER ROUTINES

NT INPUT/OUTPUT ROUTINES

NT OPERATING SYSTEMS [COMPUTERS]

Dynamic Automated Reporting Technique /DART/ system for on-line conversational information storage and retrieval for use in large programs management
18 p3107 A69-35095

Closed Loop Ionogram Processor /CLIP/ on-line computer processing system for ionospheric data [AIAA PAPER 69-952]
22 p3904 A69-40334

Mariner Mars 1969 spacecraft real time test support system and recorded data analysis including routing to printers, CRT displays and incremental plotters [AIAA PAPER 69-982]
22 p3907 A69-40362

Digital computer systems for automating machine parts design main metal cutting operations, emphasizing optimal instrument usage, reliability, digital algorithm language and economics
23 p4169 A69-41952

COMPUTERIZED DESIGN

Nonlinear programming for optimal circuits design, discussing search method of ACOP /Automatic Circuit Optimization Program/
01 p0035 A69-10067

Microwave transistor amplifier computerized design, discussing wide bandwidth and flat in-band gain response optimization on high dielectric substrates
01 p0040 A69-10194

Algorithms for linear system of first order differential equations, emphasizing equations associated with computer oriented circuit design
01 p0036 A69-10708

Computer analysis of linear active nontime varying circuits by two graph topological approach based on Binet-Cauchy theorem
01 p0037 A69-11349

Computer stress analysis may result in automated designs, emphasizing finite element technique
02 p0341 A69-12153

Exact expressions for rates of change of eigenvalues and eigenvectors to facilitate computerized design of complex structures
02 p0347 A69-12532

Breadboard chip for use in computer aided design and analysis of integrated circuits, describing components and application to differential amplifiers
03 p0402 A69-13008

Hypersonic lifting body optimization under single and combined constraints of volumetric efficiency, heating and skin friction, using numerical search routine [AIAA PAPER 68-1157]
03 p0362 A69-13557

Computer program for electromagnetic wave metal shielding evaluation
03 p0398 A69-13901

Damping factor automatic determination by use of second derivatives of residuals for damped least squares method of optical design
04 p0630 A69-14295

Collection of papers on engineering applications of digital computers, examining programming, numerical methods and design and simulation problems
04 p0563 A69-14514

Computer programs for engineering analysis, design and simulation, presenting point selection program for curve plotting
04 p0563 A69-14516

Boeing/Vertol Hybrid Facility for solving engineering problems in V/STOL design and research
04 p0567 A69-15352

Device and logic/system designers and design aids integration area using MOS arrays
04 p0568 A69-15356

Simulation design of multiprocessing system to provide air traffic control capabilities through use of real time operations
04 p0629 A69-15365

Multilevel modeling structure for interactive computer graphic design, discussing conversational display manipulation program and interconnection with analysis program
05 p0724 A69-16381

Three dimensional computer graphic modeling program, discussing SIGHT and LEGER programs
05 p0724 A69-16383

Program to study interactive graphic display console systems use for solving mechanical design problems involving plate cam and follower mechanisms
05 p0724 A69-16384

Integrated circuit interconnection patterns computerized design, discussing automatic laser mask-making control
06 p0931 A69-17199

Computer tape controlled pulsed externally excited gas laser mask making machine with micropositioning coordinate table for integrated circuit fabrication
06 p0931 A69-17200

Aircraft aerodynamic characteristics determination from numerical computer solution of supersonic gas flow past blunt body with broken generatrix
06 p0859 A69-17582

Control system analysis and synthesis by means of generalized root-locus method on digital computer
07 p1114 A69-18291

Remote terminal computer for rotary-wing vehicles design, discussing programming language, engineer-computer interface and applications
07 p1052 A69-18868

Computer aided circuit design by singular imbedding, beginning with prespecified topology and undetermined elements
07 p1115 A69-19148

Book on computer calculation of structures covering programming, computer language, mathematical aspects of structural analysis, matrix computation, etc
07 p1233 A69-19349

Computer graphics and manufacturing, discussing man computer system for transformation of blueprint to numerically controlled machine tape with no time delay
07 p1089 A69-19741

Finding and representing graphically intersections of double curvature surfaces with planes within scope of digital computer design
08 p1278 A69-19921

Computer aided design methods for electronics and logic systems, noting linear circuits and one dimensional transistors
08 p1278 A69-19970

Computer aided design methods for electronic and mechanical materials, discussing basic concepts and problems
08 p1278 A69-19971

Computer aided design program for testing equivalent circuits of bipolar transistors in static regime under various polarization conditions
08 p1280 A69-19972

Computer aided automatic drawing of printed circuits, including design and manufacture of films for engraving
08 p1296 A69-19979

Structural iterative design convergence to minimum weight proved by dual linear programming, discussing global convergence and convergence rate
08 p1413 A69-20351

Iterative Chebyshev approximation for computerized network design by linearizing original nonlinear programming
08 p1299 A69-21170

Filter design using transformed frequency variables suitable for computer programs
08 p1300 A69-21172

Equations adaptable to computer for RLC circuits containing linear and nonlinear n-terminal networks derived by nodal method
09 p1472 A69-21779

Computer aided circuit design programs combining technical engineering skills with building block programs
10 p1659 A69-23141

Pseudodynamic programming for optimizing design of correlator supersynthesis antenna arrays used for radio source tracking
10 p1663 A69-23420

Graphic electronic visualization equipment for computerized design
10 p1660 A69-23795

Digital design techniques for electronic equipment including measuring instruments, generators, synthesizers, etc
10 p1664 A69-23796

Computerized design techniques for microwave components using diodes, detailing X band parametric amplifier
10 p1661 A69-23874

Computer simulation application to electronic systems, discussing design, performance optimization, implementation and environmental effects
11 p1843 A69-25319

Computer aided design of linear multivariable control systems applied to VTOL aircraft stability augmentation
12 p2013 A69-26068

Computerized design of optimal direct lift controller for aircraft and aerodynamic surfaces, using Kalman linear state regulator theory
12 p2014 A69-26765

Computer aided design - Conference, University of Southampton, England, April 1969
12 p2034 A69-27095

Computer simulation program for design and evaluation of digital Doppler processor, analyzing performance limitation due to quantization and white noise
12 p2035 A69-27096

Computer driven graphical techniques for aerospace design and analysis [ASME PAPER 69-DE-27]
14 p2454 A69-28854

Computerized design of inhomogeneous transformers with cascaded quarter wave sections
14 p2423 A69-29762

Computer aided design /CAD/ of component selection for circuit optimization applied to circuit performance and sensitivity calculations
15 p2628 A69-30849

Microwave strip transmission line, discussing evolutionary improvements, computerized design, materials, semiconductors, packaging, reliability, etc
15 p2721 A69-31074

Analog computer for design of control systems used in nonnuclear testing of nuclear rocket engine components and subsystems
15 p2589 A69-31289

Automation of wiring diagrams and printed circuit conductor patterns by computerization
15 p2632 A69-31520

Optical computerized design procedure for Ritchey-Chretien corrector, combining ray deviation error function and third order aberration design techniques
17 p2972 A69-33087

Turbine blade cooling emphasizing economics, service life and computerized calculations
17 p3020 A69-33352

Direct lift controller design for aircraft approach and landing by computer program based on Kalman linear state regulator theory
17 p2902 A69-34027

Aircraft generator weight in relation to system performance requirements, using digital computer to study generator design
17 p2904 A69-34087

Computer aided design of machines with custom LSI arrays, describing error detection procedures and MOS logic circuits
17 p2942 A69-34121

Computerized Markov effectiveness models of repairable and nonrepairable complex aerospace systems
18 p3195 A69-34527

Computerized analysis and design of nonlinear servomechanisms, using describing functions technique
18 p3110 A69-34672

Algorithm for minimum weight structures automated design, coupling strain energy criteria with linear interpolation search technique to cover stress and displacement constraints [SAWE PAPER 798]
18 p3219 A69-34861

Computer-aided design application to mass property engineering, describing repetitive mathematics functions, design information retrieval and display, automated synthesis, etc [SAWE PAPER 795]
18 p3107 A69-34863

Computer aided design analysis program to provide weight and sizing data for entry spacecraft [SAWE PAPER 797]
18 p3208 A69-34903

Finite element techniques of structural analysis for missile and space structures, including Apollo computerized analysis and structural optimization
19 p3438 A69-36324

Information theory, circuit optimization and computer aided design in radio wave information transmission
19 p3286 A69-36432

Computer-algorithm elements required for engineering design and invention problems including design requirements, selection of spaces for variables using computerized heuristics, etc
19 p3280 A69-36666

Computerized optimization and testing of aerospace vehicle designs, describing simulation techniques, algorithm and computer selection, display devices, etc
20 p3498 A69-37292

Computerized design parameters for realizable over-driven bimode varactor frequency doubler based on charge-voltage relationship at break point
20 p3505 A69-37299

Aerodynamic optimal shaping by multivariable search technique, comparing results with variational solutions for airfoil profiles
20 p3459 A69-37527

Computer programs for design data, examining program complexity, reliability and availability, design data sheets, etc
21 p3732 A69-39304

Computerized optimization of flexible booster autopilot design, considering criteria for stability margins, closed loop roots and structural load relief
[AIAA PAPER 69-875] 21 p3823 A69-39401

Computer program for generation of test patterns for multiterminal devices and networks
21 p3679 A69-39604

Handbook of electronic packaging including rigid and flexible printed wiring, soldering and mechanical interconnections, bonding, computer and military applications, etc
22 p3911 A69-40046

Computerized solid rocket motor nozzle design with computer program providing weight, envelope and performance values for vehicle optimization studies
[AIAA PAPER 69-975] 22 p3999 A69-40355

Automated design system producing wire format data for cabling avionics subsystems of light attack aircraft
[AIAA PAPER 69-976] 22 p3912 A69-40356

Computerized crewstation geometry evaluation and design optimization using 23-pin-joint man-model
[AIAA PAPER 69-977] 22 p3892 A69-40357

Germanium microwave backward diodes optimum design and performance prediction through computer calculation for important parameters
22 p3916 A69-41224

Digital computer systems for automating machine parts design main metal cutting operations, emphasizing optimal instrument usage, reliability, digital algorithm language and economics
23 p4169 A69-41952

Computerized evaluation of elastic deformations of 100 m parabolic reflector designs for Max Planck Institute radio telescope, outlining supports and dish structure
23 p4148 A69-42122

Large paraboloidal reflector antenna computerized structural design, detailing framing, steering control, support structure, etc
23 p4231 A69-42135

Integrated civil engineering system /ICES/ and structural design language /STRUDL/ programming and operating characteristics, including computer run example
23 p4134 A69-42146

Computerized design of potassium vapor turbine with supersaturation effects compared with equilibrium flow turbine design
23 p4187 A69-42251

Minimization algorithm for switching systems synthesis, describing design of mass spectrometer curve function generator and autonomous shift register
23 p4146 A69-42535

COMPUTERIZED SIMULATION
NT ANALOG SIMULATION
NT DIGITAL SIMULATION

Gunn generator efficiency dependence on diode and regime parameters using computer model
01 p0042 A69-10319

Digital simulation models for continuous systems determined by direct search minimization
01 p0036 A69-10706

Monte Carlo simulation procedure synthesizing probability distributions of reliability parameters with individually exponential components
01 p0036 A69-10707

Areas of expectation for single radar automatic tracking of flying objects derived on basis of equation of circle in polar coordinates
01 p0035 A69-11296

Multieingine Martian soft lander guidance and control system design with single engine failure accommodation based on six degrees of freedom computer simulation
02 p0277 A69-11740

Computer solution of six degrees of freedom flight equations, discussing advantages of using flight path axes for translational equations of motion
02 p0212 A69-11998

Heat transfer in pyrolytic graphite analyzed by hybrid computer simulation
02 p0353 A69-12387

Multiprocessing system simulation using GPSS /General Purpose Simulation System/ model
02 p0213 A69-12492

Multichannel digital data compression simulation, discussing algorithms, buffer queue control, identification coding and system performance measurements
02 p0213 A69-12814

Radar return signal generation for computer simulations of airborne radar systems, using digital computer program for time varying radar backscatterer
03 p0429 A69-13199

VLF system simulation for evaluating digital communications systems operating in presence of additive atmospheric noise
03 p0390 A69-13205

Diurnal variation of variation coefficient of F 2 critical frequency for steady and unsteady primary ionizing fluxes simulated on computer
03 p0423 A69-13516

Cardiovascular system simulation using computer models transport and perturbation methods
03 p0380 A69-13855

CASSANDRE language in computer simulation
03 p0401 A69-14178

Computer simulations defining conditions to produce series operation of Gunn effect diodes
04 p0573 A69-14340

Collection of papers on engineering applications of digital computers, examining programming, numerical methods and design and simulation problems
04 p0563 A69-14514

Computer programs for engineering analysis, design and simulation, presenting point selection program for curve plotting
04 p0563 A69-14516

Digital computers in space flight simulation and vehicle performance optimization, examining mission analysis
04 p0652 A69-14519

Design and implementation of executive system for hybrid simulation, discussing requirements placed upon digital computer and operating software
04 p0567 A69-15350

NASA-Ames hybrid simulation software systems, subsystems and implementation
04 p0567 A69-15353

Colliding waves synchronization and stability in angular gas laser by electronic simulation
05 p0770 A69-15645

Digitally controlled flight systems simulators, noting design improvements over conventional trainers
05 p0742 A69-15884

Baird-Hitchcock iterative method analog computer simulation by steepest descent
05 p0723 A69-15933

Digital computer interface systems design for simulation, control, instrumentation and data processing, discussing hybrid computer linkages
05 p0723 A69-16195

Collection of papers on computerized simulation covering dynamic modeling of ideas and systems
05 p0724 A69-16467

Programming technique using quaternion parameters for error reduction in simulation of spinning rigid body
05 p0724 A69-16469

Simulation in design of automated flight test data system
05 p0743 A69-16759

Combined neutron degradation and gamma induced effects on closed loop system simulated by SECURE program
06 p0899 A69-16889

Runway development for increased airport capability, discussing computer simulation model of airport operations
06 p0906 A69-17166

Recursive formulas for numerical evaluation of real convolution integral for simulation of control systems and electrical networks on digital computer
06 p0947 A69-17250

Digital computer motion pictures generation for ground controlled intercept simulation
06 p0906 A69-17397

Department of Defense Gravity Experiment /DODGE/ attitude stabilization simulation with time-lag magnetic damping
06 p1014 A69-17584

Digital computer simulation of nonlinear redundant structure variables including thermal influence, creep and arbitrary loads
[AIAA PAPER 69-120] 06 p1028 A69-18166

Space radiator dynamic model for predicting outlet temperature transient response to environmental variations
[AIAA PAPER 69-29] 06 p1039 A69-18205

Digital computer methods and numerical techniques to evaluate temperature distributions in spacecraft structures, discussing thermal modeling
[SAE PAPER 690199] 07 p1239 A69-18301

Hybrid simulation study of satellite attitude control system to replace momentum wheels and gas jets by commandable gravity gradient boom
07 p1227 A69-18335

Hydrogen-air supersonic combustion at low densities, discussing laboratory computer simulation based on boundary layer concepts and finite rate chemistry
[WSCI PAPER 68-29] 07 p1240 A69-18358

Computer simulations, comparing self adaptive /neutron/ control of spacecraft energy allocation subsystem to programmed control
07 p1058 A69-18389

Computer model of Gunn diode, discussing operations under pulse bias voltage and in resonator
07 p1097 A69-18449

Metal fatigue simulation by Monte Carlo method, showing programmed fatigue tests in form of life distribution functions
07 p1233 A69-19314

Optimum approach and departure paths for VTOL aircraft simulated by hybrid computer under constraints
[AIAA PAPER 69-209] 07 p1178 A69-19570

Analog computer modeling of human systemic arterial tree, based on lump parameter circuit approximation
07 p1072 A69-19727

Computer simulation on engines dynamic behavior covering thrust transfer functions, time behavior and engine and fuel controller operation
08 p1301 A69-20167

Computerized objective analysis of meteorological variables based on weight determination involving autocorrelations
08 p1345 A69-20309

Computerized simulation of time dependent reliability of multicomponent system based on statistical model of component breakdown
08 p1277 A69-21100

Particle free path estimates for axisymmetric high specific impulse plasma accelerators, discussing collisionless plasma simulated by computer
[AIAA PAPER 69-278] 09 p1593 A69-21233

Digital computer simulation and analysis of control loops for ion thruster control
[AIAA PAPER 69-239] 09 p1564 A69-21240

Maintenance process simulation for engine and major components to provide routine material usage forecast and policies
09 p1503 A69-21802

Computer study of analytical model of boundary layer transition from laminar to turbulent flow
[AIAA PAPER 68-38] 09 p1482 A69-21945

Thermogravimetric plastics analysis data applied as constants to degradation kinetics equations used in charring-ablator digital computer programs
09 p1529 A69-22312

Apollo/Saturn V automatic checkout test verification and debug program using real time computer simulation with digital space vehicle system model
[AIAA PAPER 69-321] 09 p1478 A69-22378

Sunde model of troposcatter channel as transmission medium in computer simulation of adaptive digital communication scheme for selective fading channels
09 p1458 A69-22471

Computer simulation of unbiased digital recording composed of sequential computations intended for various bit densities
[IEEE PAPER 3.3] 09 p1461 A69-22562

Glass covered microwire technology to realize RC element, analyzing equivalent element errors by simulating irrational transfer functions
09 p1476 A69-22677

Gunn diode field distribution with distributed capacitance electrode analyzed with one dimensional computer simulation
09 p1470 A69-22789

Simulation to correlate integrated logistic support recommendations for dynamic analysis of planned logistic network
10 p1668 A69-22975

Mass and velocity distribution of interstellar clouds from Oort model simulated by Monte Carlo method on computer, predicting rogue cloud existence
10 p1779 A69-23608

Hybrid simulation of transport lag with variable time delay, noting dynamic range limitations due to digital computer processing and memory capacity
10 p1661 A69-23852

Constraint theory for analysis of mathematical models to alleviate software problems associated with simulation of complex large scale systems
11 p1858 A69-24936

Apollo Range Instrumented Aircraft (ARIA)/telemetry antenna system for trajectory tracking, discussing computer program for simulation of behavior
11 p1840 A69-25309

Computer simulation application to electronic systems, discussing design, performance optimization, implementation and environmental effects
11 p1843 A69-25319

Dynamic stability of elastic beam type structures, using electronic simulation based on finite element approach
11 p1886 A69-25344

Automated Structural Analysis Procedure employing Displacement Method of Matrix analysis applied to validation studies of various finite elements for wing structures
12 p2184 A69-26809

Computer simulation models for prediction of individual and crew performance in man machine environments
12 p2026 A69-27087

UHF transistor small signal internal behavior, using computer simulation for deriving current gain alpha locus, current gain and f sub T
13 p2227 A69-27241

NOL hypervelocity launcher heat transfer and erosion analysis by experiment and computer simulation [AIAA PAPER 69-336]
13 p2242 A69-28272

High energy inelastic particle collisions observed at high altitude station, using Monte Carlo computations for nucleon-nucleon collision model
13 p2330 A69-28374

NASA manned aerospace simulation techniques and equipment as used at Ames Research Center, noting applications to various types of manned vehicles [ASME PAPER 69-DE-56]
14 p2427 A69-28844

Time domain method for hybrid simulation to compute interchannel distortions due to linear transducers in FM systems
14 p2417 A69-29556

Direct simulation Monte Carlo method for hypersonic rarefied gas flow past solids, modeling on digital computer
14 p2390 A69-29580

Analog computer simulation of helicopter dynamics after main and tail rotor blades partial loss, showing banking and controllability
14 p2393 A69-29744

Noise fluctuations transport in convergent flow crossed field electron guns using Monte Carlo method for two dimensional computerized gun simulation
15 p2572 A69-30031

Computer model for avalanche transit time diode oscillator with single and double resonant circuit
15 p2577 A69-30615

Equipment life cycle costs computer simulation for design and changes evaluation, including maintenance analysis example
15 p2723 A69-31138

Time and space on-line simulation of analog, digital and hybrid block diagram systems
16 p2755 A69-31709

Cross correlation methods for determining systems time domain response adapted to communications channel evaluation, discussing computer simulation of on-line testing
16 p2750 A69-31757

Global satellite communication networks design by computer simulation, discussing politicoeconomic interface problems, ground stations, atmospheric factors, system optimization, etc
16 p2750 A69-31852

Scintillation index determination, discussing data reduction methods, standard test records, calibration at stations with modest equipment and simulation on digital computer
16 p2751 A69-32105

Colliding waves synchronization and stability in anular gas laser by electronic simulation
16 p2798 A69-32502

Helicopter engine dynamic analysis, discussing modeling techniques, rotor responses and turbine speed control simulations and transition from mathematical models to hardware components [AHS PAPER 332]
17 p2946 A69-33531

Helicopter fire control systems evaluation by computer model for hit probability and impact point sensitivity to various parameters [AHS PAPER 316]
17 p2933 A69-33540

Analog signal processing concepts based on models simulating mechanical function of ear cochlea
17 p2911 A69-34092

Computer simulation model for Saturn 5 prelaunch system reliability analysis, using Bayesian techniques
18 p3207 A69-34529

Computer simulation of numerical fluid dynamic problems for compressible and incompressible flows, noting Marker and Cell method
18 p3106 A69-34665

Physiological processes computer simulation with aorta modeling as example, noting difficulties and major problems
18 p3098 A69-34669

Air Transport Total In-Flight Simulator-707/AT/TIFS-707/ concept for pilot training, stressing airframe and major flight systems [SAWE PAPER 747]
18 p3118 A69-34884

Computerized prediction of RF instrumentation system signal margins for missile flight tests based on trajectory and range balance equation
18 p3103 A69-35097

Lockheed C-130 Hercules modified as STOL aircraft studied in laboratory by computerized simulation and graphics techniques for pilot view during landing
18 p3092 A69-35466

Aircraft Economic Design Evaluation (AEDE)/ computerized model to estimate aircraft design performance differences economic impact to carriers [AIAA PAPER 69-814]
19 p3289 A69-35626

Computerized air combat simulation with comparison of analog and digital approaches, noting Air to Air Combat/Fort Worth [AIAA PAPER 69-811]
19 p3289 A69-35629

Fatigue life testing apparatus with computerized simulation of random load maxima and minima, describing rotating bend test application
19 p3434 A69-35777

DC 10 aircraft reliability program, discussing passenger attractiveness, dispatch reliability, maintenance cost, flight safety and computer simulation for reliability engineering
19 p3248 A69-36027

Computerized system-safety fault trees, discussing drawing, configuration control and simulation program
19 p3280 A69-36029

Modified Monte Carlo model applied to computerized meteorite orbit evolution, simulating secular perturbations by imposing sinusoidal variation on orbital elements
19 p3414 A69-36117

Precompression automatic wild point rejection from sampled telemetry data for data compressors evaluated by digital computer simulation
19 p3273 A69-36263

Aircraft simulation, discussing flight simulation, real time computer assembly operation, computer- auxiliary interfaces, etc
19 p3296 A69-36707

Computerized optimization and testing of aerospace vehicle designs, describing simulation techniques, algorithm and computer selection, display devices, etc
20 p3498 A69-37292

Roseau satellite onboard computer systems design, emphasizing simulator and assembly programs for real time operation verification
20 p3501 A69-37389

Spacecraft discrete automatic control system computerized simulation, discussing logic elements, applications to design, etc
20 p3502 A69-37393

Onboard computer and environment simulation for real time programs development, discussing instructions analysis, variables extraction and values and peripheral components
20 p3502 A69-37395

Roseau onboard computer simulation by IBM 360, discussing use of assembly language and FORTRAN
20 p3502 A69-37396

Onboard navigation digital computer simulation to verify calculation principle and logic units during design and construction
20 p3502 A69-37398

Double binary PSK system digital computer simulation for satellite communications, investigating filter and limiting effects on performance in error probability terms
20 p3492 A69-37705

Worldwide cloud cover simulation procedure providing data for computer simulation of earth
20 p3492 A69-37705

oriented space missions, describing computer program using Monte Carlo mission simulation
20 p3573 A69-38120

Eye chart determination and layout for digital transmission system by computer simulation
21 p3678 A69-38776

Real time servo driven simulator of human body in zero-g activity used to study self induced rotation and astronaut mobility under thruster forces
21 p3664 A69-39034

Simulation and display for radar ground-backscatter signatures by computer ray tracing, using model ionosphere containing realistic traveling disturbances
21 p3717 A69-39280

Computer program (TACTICS) for simulating three vehicles simultaneous motion in space, considering interceptor-target guidance and intercept trajectories [AIAA PAPER 69-890]
21 p3678 A69-39415

Stability contours for sampling and delay effects analysis in analog/digital hybrid simulation loops, considering compensation quality over simulated system natural modes
21 p3680 A69-39609

Computer simulation of radiation scattering of spherical nebula with central isotropic star, discussing proposed program and parameters
21 p3816 A69-39723

Simulation of passively stabilized satellites using in-line hybrid computer [AIAA PAPER 68-853]
21 p3680 A69-39758

Real time network support simulation allowing network configuration for nominal or perturbed trajectory for Saturn vehicles, applicable to any flight azimuth
22 p4020 A69-40319

Multispacecraft simultaneous simulation on hybrid computer using Encke perturbation method for translational motion and Hamilton quaternion method for inertial transformations [AIAA PAPER 69-937]
22 p4036 A69-40320

Mission analysis and trajectory simulation (MATS)/ program, discussing computer controls, modular design, integration evaluation [AIAA PAPER 69-939]
22 p3904 A69-40322

Real time digital computer hardware simulation of Apollo Telescope Mount (ATM)/ mission [AIAA PAPER 69-940]
22 p3919 A69-40323

Computerized simulation for performance evaluation of System/4 Pi-EP multiprocessor for use in aerospace vehicle
22 p3907 A69-40353

Software support package for aerospace digital computer emulation, consisting of symbolic assembly program and interpretive simulator program and subprogram [AIAA PAPER 69-974]
22 p3907 A69-40354

Software/hardware interface testing of real time system, including possible improvements to computer program management flow
22 p3908 A69-40364

Analog and digital computer elements combined in hybrid technique for aeronautic simulation
23 p4146 A69-41603

Mathematical model for information processing of biological memory as cybernetic system
23 p4110 A69-41982

Computer simulation of satellite electric power systems concerning solar array, thermal, battery and charge models for end-of-mission-life orbits
23 p4068 A69-42241

Analog computer simulation of single shaft Brayton cycle system dynamics, including startup and shutdown transients
23 p4071 A69-42280

Gravitational stress effect on heart and venous system, discussing digital computer model simulating pressure changes under head-up and down tilt
24 p4271 A69-42783

S-RETIC vertebrate command model, discussing computer simulation of reticular formation Golgi anatomy capable of habituation, conditioning, extinction, generalization and error discrimination
24 p4273 A69-42910

Computer made movies and time history plots for ion-dipole collisions involving polar molecules (CO, HCL and acetonitrile)
24 p4352 A69-43124

Quasi-optimum control law for aircraft landing control system design based on Friedland technique, evaluating effectiveness by computer simulation
24 p4253 A69-43280

COMPUTERS

NT AIRBORNE/SPACEBORNE COMPUTERS
NT ANALOG COMPUTERS
NT DIGITAL COMPUTERS
NT HYBRID COMPUTERS

NT IBM 360 COMPUTER
NT SEQUENTIAL COMPUTERS
NT SITE DATA PROCESSORS
NT UNIVAC COMPUTERS

Computing machinery - Conference, Las Vegas, August 1968

01 p0035 A69-10703

Probabilistic Information Processing System using men and machines to perform diagnostic information processing and to guide decision making

01 p0037 A69-10954

Human factors evaluation of computer based information storage and retrieval system using questionnaire and interview techniques

02 p0204 A69-12220

Information processing - AFIPS Conference, San Francisco, December 1968

04 p0568 A69-15358

Gas turbine engine development data system based on test stands subsystems and central computer

10 p1660 A69-23284

Matrix Computer for solution of algebraic and integrodifferential equations in linear and nonlinear statics and dynamics, considering mechanical vibration problems
[ASME PAPER 69-VIBR-12]

10 p1806 A69-24167

Electronic module testing with integrated hardware/software system, noting module test console and manual capabilities

11 p1864 A69-25065

Real time/process computer interface with electric power systems, discussing compatibility, reliability, etc, problems in connection with management and engineering personnel

11 p2004 A69-25302

Computer uses for air traffic control in Germany including flight plans and weather report data processing

15 p2650 A69-30230

Construction applications of electronic computers - Conference, Weimar, June-July 1967, Volume 1

21 p3831 A69-38413

Computers - Conference, Boston, May 1969, Volume 34

21 p3679 A69-39601

Computer selection for given automatic control system, considering efficiency criterion and operational constraints satisfaction

24 p4285 A69-42952

Human sciences contribution to man-computer interaction based on review of relevant human factors literature

24 p4273 A69-43015

Man-computer interaction problems for human factors research, considering conversational languages development and evaluation, use patterns and interaction modeling

24 p4274 A69-43016

COMSAT PROGRAM

Satellite communications history covering passive and active satellites and Communication Satellite Act impact

07 p1085 A69-19182

CONCAVITY

Heat transfer characteristics of single lines of circular air jets impinging on concave cylindrical surfaces, discussing nozzle target spacing effect
[ASME PAPER 68-WA/GT-1]

05 p0848 A69-16137

CONCENTRATION [COMPOSITION]

NT ATMOSPHERIC MOISTURE
NT ATOM CONCENTRATION
NT CARBON DIOXIDE CONCENTRATION
NT METEOROID CONCENTRATION
NT MOISTURE CONTENT

Saturation solubility of carbon in cobalt and nickel with respect to graphite determined by vapor transport experiments over large temperature range

01 p0092 A69-10060

Impurity concentration measurement for alloyed region of tunnel diode by determining Fermi level position

02 p0301 A69-12685

Turbulent mixing of scalar fields such as temperature or concentration noting fine structure, number and distribution of zero gradient points and minimal gradient surfaces

03 p0414 A69-13134

Lead isotope composition and concentrations of U, Th, Ra, total Pb and Pb 210 in recent volcanic rocks, noting disequilibrium due to chemical fractionations

04 p0593 A69-15011

HF inductive analyzer of concentrations of electrically conducting solutions and nonconducting mixtures

05 p0763 A69-15994

Experimental measurement of He and C isotope composition of cosmic radiation

05 p0817 A69-16709

Gold and iridium concentrations in meteoritic and terrestrial materials by neutron activation, discussing chondrules, meteoritic troilite and metallic spherules

08 p1404 A69-20918

Mineralizing metabolic wastes by catalytic oxidation of pyrolysis products, noting nutritive value of ash solutions for Chlorella cultivation

10 p1649 A69-23579

Excited cyanide molecules concentration in arc discharge determined from spectral bands absolute intensities during electron transition

15 p2654 A69-30080

Rocket observations of ozone concentration above 50 km by absorption spectroscopy, noting altitude dependence

15 p2603 A69-31397

Halon 1301/bromotrifluoromethane/ concentration for inerting Aerazine-50 spills or extinguishing fires, noting joint use of carbon dioxide and water

18 p3094 A69-35090

Molecular concentration-optical depth curves for combinations of two photospheric and two facular models, noting lines contrast dependence on dissociation energy

18 p3204 A69-35391

Aerated fuel spray effect on smoke reduction from high pressure ratio aircraft gas turbines engines, including smoke measurement and visibility

19 p3395 A69-36770

Adsorption kinetics in ternary mixture of nitrogen, methane and hydrogen, using concentration-time/breakthrough/ curves measurement on activated coconut shell charcoal
[NAS-NRC PAPER H-4]

22 p3981 A69-40629

Mixing length theory including eddies axial motion, discussing turbulent field of temperature or concentration

24 p4407 A69-42917

CONCENTRATORS

Computation and optimization of energy distribution over randomly oriented elements of radiation receiving surface of hollow collector of concentrator type solar device

09 p1442 A69-22534

Equatorial mounted solar energy concentrator efficiency compared to unconcentrated sunlight and artificial UV-visible light source in reducing Pb tetraacetate solution in acetic acid

16 p2736 A69-31814

Solar power concentrator-absorber system, discussing flux distribution in focal plane and cavity heater optimization

17 p3022 A69-33795

CONCENTRIC CYLINDERS

Elastoplastic stress-strain behavior of concentric composite cylinders under uniaxial tension using analytical model, predicting transverse stresses during axial loading

01 p0171 A69-11263

Heat transfer between concentric cylinders at different temperatures measured for argon, neon and helium

01 p0177 A69-11403

Accommodation coefficient effect on linearized heat transfer in rarefied gas between parallel plates and concentric cylinders

01 p0177 A69-11405

Coaxial cylindrical shells oscillation frequencies with interspace filled with incompressible liquid determined as functions of liquid level and interspace width

09 p1612 A69-21483

Viscous incompressible conducting fluid flow through porous coaxial nonconducting cylinders under radial magnetic field with pressure gradients functions of time

12 p2062 A69-26275

Hydromagnetic flow of viscous conducting fluids through porous coaxial cylinders in radial magnetic field solved by Laplace transform

12 p2135 A69-26276

Wave scattering from infinite line source by long convex cylinder, noting field prediction by geometrical diffraction theory

13 p2299 A69-28194

Neutral gas pressure in positive column plasma between two coaxial insulated cylinders as function of cylinders radii

14 p2490 A69-29036

Numerical approximation of Taylor vortices in viscous incompressible fluid flow between concentric rotating cylinders, using truncated eigenexpansions

15 p2593 A69-31518

One dimensional viscous magnetofluidynamic flow in annulus formed by concentric cylindrical electrodes, reducing problem to linear partial differential equation set

[AIAA PAPER 69-725] 17 p3012 A69-33493

Bessel function applied to unsteady axisymmetric problem of heat conduction in thermally controlled coaxial cylinders with different physical properties

19 p3448 A69-35981

Viscous fluid secondary flow stability between coaxial rotating cylinders, using nonlinear differential equations derived from equations of motion

19 p3299 A69-36391

Unsteady laminar MHD flow of electrically conducting viscous fluid between porous coaxial circular cylinders under radial magnetic field

20 p3581 A69-36912

Parameters of DC discharge between concentric cylinders calculated for plasma probes by pressure theory, noting ion neutral collisions and magnetic field effects

21 p3776 A69-38712

Air pressure wave forces on missile from silo wall motion resulting from close nuclear blast, using acoustic wave equation for concentric cylinder flow

21 p3691 A69-39765

Temperature field in system of coaxial cylinders by solving heat equation with corresponding initial and boundary conditions

21 p3855 A69-39855

CONCENTRICITY

Near free molecule heat transfer and density distribution between concentric spheres using BGM grid equation and Knudsen iteration technique

16 p2877 A69-31921

CONCORDE AIRCRAFT

Engine air intake design and development for Concorde aircraft, discussing design constraints
[AIAA PAPER 67-752]

01 p0006 A69-11014

Vertical flight path navigation requirements for supersonic aircraft based on computer simulated flights of Mach 2 Concorde

02 p0277 A69-11590

Concorde structural tests, discussing ground test program for simulating flight temperature and stress conditions at 2.6/2.7 station of wing-fuselage section

02 p0193 A69-11892

Wind tunnel pressure tests of Concorde air intake mockups in presence of aircraft wing and nose for Mach numbers 2, 2.2 and 2.35

03 p0361 A69-12879

Low pressure fuel system and turbine rotor blade temperature measurement method for Concorde Olympus 593 engine
[ASME PAPER 68-GT-63]

06 p0984 A69-17187

Concorde supersonic transport and Jaguar Military Strike/Trainer programs, discussing management and international cooperation

06 p1043 A69-17831

Concorde and Boeing supersonic transport overland sonic booms, discussing social, political and legal reactions

06 p0868 A69-17899

Solar flare in-flight radiation detection and warning system for Concorde SST, noting radiation hazards due to solar cosmic rays

07 p1131 A69-18551

Concorde testing program, detailing materials, structure, systems, engine, wind tunnel and flight tests

07 p1054 A69-19294

Concorde fuel management, discussing trim, fuel as coolant and booster pumps

07 p1057 A69-19705

Concorde equipment, summary of British companies activities in supplying components

07 p1057 A69-19706

Al alloys application to Concorde project and other aircraft structures, noting mechanical properties

08 p1335 A69-21141

Concorde SST industrial project in international cooperation and stage in transport history including supersonic boom, weight, fuel consumption rates and aerodynamic heating

12 p2013 A69-26356

Concorde SST turbojet engine integrated assembly consisting of air inlet, gas generator, reheater and convergent-divergent nozzle

12 p2147 A69-26357

Concorde design problems due to kinetic heating, aerodynamic characteristics, structure, equipment, modified delta wing planform, etc

12 p2012 A69-26358

Concorde SST equipment and systems noting microelectronics, automatic control, inertial navigation, headup displays, linear instruments and hydraulic systems

12 p2091 A69-26360

Concorde jet engine silencer concept and characteristics [AIAA PAPER 67-391]

12 p2148 A69-26759

Concorde thermal fatigue resistance tested by alternate heating and cooling cycles simulating supersonic flight profile

13 p2241 A69-28102

Optimal navigation system for supersonic Concorde aircraft, discussing in-flight and terminal navigation methods

14 p2480 A69-29859

Concorde aircraft and engine materials selection factors including mechanical properties of metals and nonmetals, corrosion resistance, service life, sealants, weight analysis, etc

15 p2639 A69-30464

Concorde aircrew seats design for electric operated tracking and lift, vertical movement accommodation seat and back tilt

15 p2553 A69-31167

Aircraft construction materials, discussing aluminum alloys use in Concorde project based on temperature tests, creep and fatigue properties and joint requirements

16 p2801 A69-31791

Aerodynamic problems in future civil aircraft design, emphasizing Concorde development possibilities, discussing VTOL intercity transport, subsonic swept wing and hypersonic aircraft, all-wing airbus, etc

16 p2732 A69-32023

Concorde propulsion and ejection systems reliability, testing reheating duct, primary nozzle, secondary assembly, etc

16 p2837 A69-32072

Franco-British aeronautical cooperation and Concorde development agreement of 29 November 1962

17 p3075 A69-32840

Concorde design, discussing planform, wing twist and camber, hypersustentation, kinetic heating, aeroelasticity, R and D, tests, etc

17 p2899 A69-33380

Self monitored subsystems in automatic flight control of Concorde, describing operation mode and landing display

17 p3003 A69-34196

Concorde aerodynamic design compromise between high and low speed requirements, kinetic heat problems and materials selection [AIAA PAPER 69-759]

19 p3245 A69-35661

FM radioaltimeter for Concorde aircraft, describing autocalibration and automonitoring device, signal characteristics, reliability, etc

19 p3315 A69-36699

Concorde Olympus 593 engines electronic control and adjustment devices

19 p3395 A69-36706

Concorde SST fire protection equipment, discussing fire and overheat detectors, fire extinguisher, crash fire protection, explosion suppression equipment, etc

19 p3256 A69-36864

Design concepts and principles of systems for monitoring of Concorde flight control actuators, considering servo control, control interconnections and control input system

20 p3467 A69-38190

Design criteria for Concorde SST servoflight control system reliability and safety

21 p3650 A69-39697

Commercial supersonic and subsonic air traffic growth forecast

22 p3862 A69-39934

Concorde structural tests emphasizing problems associated with thermal cycle, including fatigue test setup on complete airframe [RAES PAPER 16]

22 p4043 A69-40495

Design of Concorde wing for Mach 2 cruising speed including fuselage/wing relations, wing planform and landing edge camber, etc [RAES PAPER 18]

22 p3859 A69-40497

SNECMA thrust reverser system design on Concorde prototype, discussing performance, safety, airworthiness, operational requirements, reliability and maintenance [SAE PAPER 690412]

23 p4200 A69-41640

Concorde elvons sandwich construction to meet sonic environment, discussing core, adhesive, design and fabrication

24 p4403 A69-43429

CONCRETES

Maintenance practices for rigid concrete pavement of runways including joint and crack sealing and patching, considering necessary surface preparation and equipment

01 p0057 A69-11277

Direct plotting of vibrating wire strain gauge data for concrete structures, giving diagrams for grid and backing sheet scaling

08 p1312 A69-20104

CONDENSATES

Binary mixture condensation on cooled vertical plate, formulating predictive theory based on conservation laws and other physical principles [ASME PAPER 68-WA/HT-21]

05 p0847 A69-16124

Condensation and probe interference in planar expansion deflection nozzle measurements [AIAA PAPER 69-170]

06 p0863 A69-18059

Propellant condensation on surfaces near electric rocket exhaust, calculating particle arrival rates, backflow and desorption energies [AIAA PAPER 69-270]

09 p1565 A69-21252

Circumstellar grain compositions of stars with various O to C abundance ratios, calculating molecular equilibrium of condensates and gaseous compounds in stellar atmospheres

10 p1786 A69-24103

Stable homogeneous combustion of condensed substances /CS/, systematizing and analyzing elementary CS combustion models

13 p2379 A69-28454

Gas and polydispersed condensate parameters of nonequilibrium two phase flow in Laval nozzle, considering particle collisions and coagulation, energy exchange and momentum exchange

14 p2391 A69-29621

Condensation and probe interference in planar expansion deflection nozzle measurements [AIAA PAPER 69-170]

21 p3645 A69-39769

Adenylates condensation in protein-associated amino acids as clue to peptide bond synthesis within protocellular structures

22 p3895 A69-40048

CONDENSATION

Condensation-enhanced vaporization rates in nonisothermal systems, noting fume nucleation augmentation of rates into cooler environments

03 p0532 A69-13122

Motion of condensations within tail of comet Morehouse 1908 III from photographs

08 p1382 A69-19870

Electrostatic rocket exhaust condensation on spacecraft solar electric panels cover glasses, noting deleterious effects [AIAA PAPER 69-271]

09 p1569 A69-21874

Mass transfer during Cs condensation from moving vapor mixture containing Ar in water-cooled tube

15 p2718 A69-30998

Water vapor recondensation effect on structure of liquid particle flow into vacuum

16 p2769 A69-31869

Star formation in interstellar solid hydrogen clouds originating from cellular pressure created by hydrogen condensation onto interstellar grains

16 p2862 A69-32375

CONDENSATION TRAILS

U CONTRAILS

CONDENSER RADIATORS

U CONDENSERS [LIQUIFIERS]

U HEAT RADIATORS

CONDENSERS [LIQUIFIERS]

NT JET CONDENSERS

Condensing injector cycles internal efficiency for high velocity liquid metal flows in closed cycle MHD power plants

02 p0194 A69-11582

CONDENSING

NT FILM CONDENSATION

Imagery degradation by moisture condensation on thermal IR scanners optics during aircraft descent from higher to lower altitude

08 p1311 A69-19821

Boundary layer at tube wall behind shock wave propagating in gas-vapor mixture, analyzing condensation rate

09 p1480 A69-21591

Condensation kinetics in clouds, determining cloud spectrum evolution taking stochastic processes into account

10 p1722 A69-23972

Hetero-epitaxial germanium films on GaAs by germanium condensation from molecular beams in vacuum, obtaining p-type conductivity

11 p1938 A69-25033

Cloud and fog droplet spectra due to condensation of water vapor on nuclei solved by partial differential equation

12 p2126 A69-26017

Heats of condensation and vaporization of W, Re and Mo cathodes of thermoelectric converter with Cs arc for various output powers and Cs vapor pressure

12 p2017 A69-26544

Steam-water convergent condensing injector with supersonic inlet vapor, discussing axial pressure profiles and discharge pressure

13 p2372 A69-27486

Dropwise condensation, analyzing nucleation sites, growth, vapor capture, heat transfer rates and surface texture

13 p2376 A69-28143

Condensation kinetics in clouds, determining cloud spectrum evolution taking stochastic processes into account

21 p3760 A69-39658

CONDITIONED RESPONSES

U CONDITIONING [LEARNING]

CONDITIONING [LEARNING]

Physiological causes and prevention of motion sickness during space flight, emphasizing conditioned reflex, different analysors interactions and vestibular-vegetative changes during weightlessness

02 p0200 A69-12122

Classical and differential eyelid conditioning for truth or falsity of visually presented verbal statements

07 p1064 A69-18632

Instrumental reward experiment using concept learning paradigm with word-color compounds as stimuli

07 p1064 A69-18636

Classical and differential conditioning of eyelid response with correctness of solutions of arithmetic problems as discriminandum

07 p1064 A69-18637

High oxygen concentration effect on conditioned reflex and associated EEG responses to light flash in rabbits occurs in well defined sequences

07 p1065 A69-18976

High oxygen concentration effect conditioned reflex and associated EEG responses to light flash in rabbits occurring in well defined sequences

20 p3479 A69-38224

Cortical and thalamic evoked activities changes during sensory conditioning of freely moving cat

22 p3872 A69-40160

Anesthetized cats with electrodes in visual cerebral cortex, investigating simulation of conditioned alimentary reflexes in response to light signals by electric signals

22 p3885 A69-41066

Squirrel monkeys exposed to centrifugally generated artificial gravity trained to respond for food reinforcement at selected gravity levels

23 p4081 A69-41434

Fixed interval human performance control under various histories of conditioning and response cost conditions, considering effects of postreinforcement pauses

23 p4100 A69-41437

Hypoxia reaction elimination in human beings by repeated exposure to hypoxia, discussing nitrogen inhalation experiments and adaptive behavior of respiratory system

23 p4214 A69-41789

Continuous noise level effects on stabilized escape conditioning in male albino rats

24 p4262 A69-42948

CONDITIONS

U CHRONIC CONDITIONS

CONDUCTING

U CONDUCTION

CONDUCTING FLUIDS

Viscous electrically conducting fluid with aligned magnetic field flowing past flat plate at nonzero angle of attack

01 p0126 A69-10163

Plane MHD jets with variable conductivity, showing effective mixing length as function of distance

01 p0130 A69-10773

Growth rate of wave instability in conducting liquid jet in perpendicular electric field and accelerating under gravity

01 p0062 A69-11207

Instabilities for two highly conducting finite length streams in relative motion and coupled by transverse electric or longitudinal magnetic fields

01 p0062 A69-11208

Resistive spherical plasma expansion into external magnetic field noting magnetic stream function

01 p0132 A69-11211

Heat transfer of steady laminar flow of incompressible, viscous and electrically conducting fluid between parallel porous plates

02 p0289 A69-12235

Longitudinal short wave stability in conducting quasi-one dimensional gas flow, considering regions of high thermal emission

02 p0233 A69-12487

Diffusion in conduction process in dielectric fluids, discussing space charge limited current-voltage characteristics

03 p0415 A69-13140

Flow development around impulsively rotating dipole magnetized sphere in viscous incompressible conducting fluid, noting diffusing Alfvén waves and induced field

03 p0477 A69-13793

Coefficient of friction variations for MHD flow of electrically conducting liquid across porous medium under transverse magnetic field

03 p0480 A69-14112

Quasi-neutral, steady, inviscid and nonheat conducting flow of conducting gas with high magnetic Reynolds number in plane channel with transverse magnetic field

04 p0636 A69-14984

Transverse magnetic field effect on three dimensional nonisothermal lubrication layer of conducting gas at small magnetic Reynolds number

04 p0607 A69-14990

Steady longitudinal motion of insulating cylinder in conducting fluid, discussing analog between steady MHD and acoustic scattering

04 p0638 A69-15192

Flow of two conducting immiscible liquids between parallel porous moving plates under transverse magnetic field

05 p0743 A69-15600

Unsteady motion of ideally conducting gas flow in transverse magnetic field with allowance for gravitational forces

05 p0802 A69-15789

HF inductive analyzer of concentrations of electrically conducting solutions and nonconducting mixtures

05 p0763 A69-15994

MHD shock wave decay in one dimensional unsteady flow of ideal inviscid perfectly conducting compressible fluid subjected to transverse magnetic field

05 p0806 A69-16736

Steady two dimensional MHD flow of perfectly conducting fluid past nonconducting wedge with magnetic field orthogonal to flow velocity

06 p0964 A69-17244

Parametric instability of horizontal surface of ideally conducting or very high dielectric constant liquid in varying perpendicular electric field

06 p0957 A69-17542

Laminar heat transfer in electrically conducting fluids flowing in parallel plate channels [JPL-TR-32-1335]

06 p1033 A69-17555

MHD aligned flow of compressible fluid past slender body in wind tunnel

06 p0861 A69-17719

Steady rotation of insulating body of revolution in unbounded electrically conducting fluid permeated by applied axial magnetic field

07 p1190 A69-18814

Convection in conducting fluid filled cavities with variable wall temperature due to magnetic field, with results applicable to rheological systems

07 p1241 A69-18921

One dimensional flow of conducting inviscid compressible fluid in channel in presence of transverse fields, discussing steady velocity flows

07 p1191 A69-19014

Two dimensional flow of conducting fluid in channels with longitudinal transverse magnetic field and Hall effect, discussing gas motion equations linearization

07 p1192 A69-19015

Unsteady conducting incompressible viscous fluid flow past plate in magnetic field, analyzing surface friction reduction

07 p1192 A69-19018

Axisymmetric turbulent conducting fluid jet propagation in longitudinal magnetic field without induction

07 p1192 A69-19019

Laminar conducting wall jet injected in transverse magnetic field, analyzing partial differential equations obtained

07 p1192 A69-19020

Pulsation energy balance of turbulent jet of conducting fluid expanding in longitudinal magnetic field

07 p1192 A69-19021

Laminar flow of viscous conducting fluid between parallel walls in traveling magnetic field, using Hartmann number expansion

07 p1192 A69-19023

MHD flow of compressible conducting fluid around cylindrical body with quasi-aligned magnetic field and velocity

07 p1194 A69-19350

Free surface of electrically conducting liquid in gradually varied supercritical regime in horizontal rectangular channel

08 p1362 A69-20273

Vorticity behind shock waves in conducting gases when magnetic field is tangential or normal to shock surface using momentum equation

08 p1367 A69-20789

Linear perturbation theory to predict instability threshold conditions caused by electric field in poorly conducting liquid subject to vertical temperature gradient

08 p1352 A69-20790

Two dimensional steady flow of finitely conducting compressible fluid subjected to magnetic field with two zero components

08 p1369 A69-20843

Turbulent heat transfer in conducting fluid flow through circular tube in longitudinal magnetic field and constant wall heat flux, using Lyon relation

09 p1621 A69-21590

Lagrangian evolution criterion for electromagnetic conducting fluid and MHD flow, defining generalized fluxes and forces

10 p1727 A69-22904

Pyrotechnic circuit closer using jet to achieve conduction between hollow charge lining and coaxial electrode

10 p1635 A69-23031

Conical refraction of magnetosonic waves occurring when Alfvén waves propagate at speed of sound in conducting fluid in presence of constant uniform magnetic field

10 p1727 A69-23091

Numerical solution of MHD equations for boundary layer electrically conducting gas flow near flat plate when velocity distribution of external flow obeys power law

10 p1727 A69-23093

MHD fluid flow in rectangular duct with allowance for finite wall conductivity

10 p1727 A69-23098

Rotating disk induced viscous conducting fluid motion in axial magnetic field

10 p1727 A69-23099

Busbar effect on interaction between conducting fluid flow and traveling wave magnetic field created by long line with concentrated inductance and capacitance, deriving line gain

10 p1727 A69-23101

Sun-like alternating field generators, discussing dynamo theory of stellar and planetary magnetic fields based on nonmirror symmetrical turbulent motion in conducting fluid

10 p1782 A69-23703

Heat transfer in single phase medium at near critical static parameters

11 p1997 A69-24230

Turbulence formation in conducting liquid at increasing Reynolds numbers, discussing cause of spontaneous magnetic field appearance

11 p1955 A69-24392

Dispersion relation for internal gravity wave propagation across exponentially decreasing magnetic field in conducting fluid, noting atmospheric wave propagation in ionosphere

11 p1877 A69-24564

Motion equations for conducting paramagnetic fluid in magnetic field derived, including MHD equations and equation determining magnetic moment variation rates

11 p1932 A69-25465

Viscous incompressible conducting fluid flow through porous coaxial nonconducting cylinders under radial magnetic field with pressure gradients functions of time

12 p2062 A69-26275

Hydromagnetic flow of viscous conducting fluids through porous coaxial cylinders in radial magnetic field solved by Laplace transform

12 p2135 A69-26276

Electrohydrodynamic instability of incompressible conducting cylindrical viscous jet in external magnetic field, noting viscosity role in oscillation modes and growth rate

12 p2136 A69-26403

Steady state flow of viscous conducting liquid in inlet of channel with or without transverse magnetic field, emphasizing approach to Hartmann-Poiseuille patterns downstream

12 p2138 A69-26626

Incompressible conducting fluid turbulent flow velocity distribution in transverse magnetic field at small magnetic Reynolds numbers and constant MHD interaction frequency

13 p2246 A69-27498

Boundary value problem for one dimensional unsteady equations for inviscid conducting gas during transition processes in MHD duct

13 p2309 A69-28027

Conducting liquid boundary layer flow and heat flux on electrodes of MHD generator, including one dimensional flow outside boundary layer

13 p2309 A69-28028

Perturbations stabilization in electrically conducting fluid by distributed automatic control system, determining feedback operators via boundary value problem

13 p2311 A69-28105

Hydromagnetic waves propagation in finitely conducting fluid mass immersed in nonuniform inelastic field, using curvilinear coordinates based on lines of force

14 p2491 A69-29336

Coupled magnetoacoustic waves in conducting paramagnetic fluid in resonance region due to mechanical and magnetic motions, considering dissipation

14 p2492 A69-29609

Laser beam light pressure bending of incompressible liquid surface leading to beam self focusing in linear medium

14 p2461 A69-29674

Pressure drop fluctuations amplitude and frequency effect on channel resistance and magnetic field effect on fluctuations intensity in laminar conducting fluid flow

14 p2501 A69-29909

Entrainment of viscous electrically conducting liquid in long duct with narrow rectangular cross section and movable walls in magnetic induction field

16 p2816 A69-31606

Exact solution for motion of conducting solid of revolution rotating in infinite conducting viscous fluid, describing magnetic field

16 p2817 A69-31666

Temperature, velocity and density perturbation propagation as heat convection wave in viscoelastic thermally compressible heat conducting fluid, analyzing damping and frequency spectra

16 p2878 A69-31952

Linearized motion equations for conducting gas in magnetic and electric field solved for coaxial channel and free jet, assuming small Reynolds number and parallel flow

17 p3010 A69-33016

Conducting fluid incompressible flow in entrance of MHD channel by momentum integral method, permitting edge stress existence at boundary layer free stream interface [AIAA PAPER 69-724]

17 p2952 A69-33436

Conducting fluid and plasma rotation between concentric cylinders due to crossed fields, determining velocity distribution, induced magnetic field and kinetic energy [AIAA PAPER 69-726]

17 p3011 A69-33472

Unsteady motion of ideally conducting gas flow in transverse magnetic field with allowance for gravitational forces

18 p3181 A69-35040

Viscous electrically conducting fluid flow around thin profiles for equal Reynolds and magnetic Reynolds numbers, using Oseen method to linearize equations

18 p3124 A69-35285

Conducting medium steady one dimensional motions determined by assuming space-charged electric field interaction, considering electrohydrodynamic behavior of medium

18 p3181 A69-35315

Combined free and forced convection hydromagnetic flow and heat transfer of electrically conducting fluid subjected to temperature variations in vertical channel

19 p3380 A69-36304

Gravitational stability of infinite conducting fluid cylinder in axial magnetic field and surrounded by fluid of different density

19 p3380 A69-36483

Transport properties of liquid semiconductors, using model for liquid mercury with minimum state density

19 p3391 A69-36560

Level signaling device for high temperature conducting fluids, describing sensor construction and circuitry

20 p3536 A69-36980

Turbulent boundary layer of conducting fluids on dielectric plate in transverse magnetic field in presence and absence of pressure gradient

20 p3513 A69-37092

Incompressible electrically conducting fluid in presence of magnetic field and Coriolis forces, analyzing Rayleigh-Taylor instability by variational principles

20 p3577 A69-38195

Homogeneous dynamo in cylindrically symmetric volume with symmetrically moving fluid and large magnetic Reynolds number, demonstrating first and second approximations using Braginskii method

22 p3989 A69-40192

Kinematic dynamo waves, discussing excitation and maintenance of magnetic field by assumed motion of uniformly conducting fluid using small parameter and numerical methods

22 p3989 A69-40195

Homogeneous, viscous and electrically conducting fluid bounded at one end by infinite plane surface of rigid body vibrating relative to fluid body

22 p3991 A69-41036

Conducting fluid flow in spherical container in rotating magnetic field, calculating induced field velocity and inside and outside components

23 p4196 A69-41609

Hydrodynamic stability of conducting fluid in external magnetic field subject to attraction of external spherically symmetric gravitational field

23 p4213 A69-41717

Unsteady MHD conducting fluid flow in arbitrary ducts under transverse magnetic field, studying effects of pressure gradient impulsive change

24 p4359 A69-43678

Turbulence formation in conducting liquid at increasing Reynolds numbers, discussing cause of spontaneous magnetic field appearance

24 p4390 A69-43782

CONDUCTING MEDIA

U CONDUCTORS

CONDUCTION

Radiative heat transfer, discussing electromagnetic theory, transfer between surfaces and simultaneous conduction, convection and radiation

13 p3376 A69-28140

CONDUCTION BANDS

Gray tin band structure, noting Shubnikov-de Haas oscillations, transport properties, piezo-Hall effect, magnetoreflection and free carrier absorption

02 p0295 A69-11783

Conduction band anisotropy in n-type cadmium tin arsenides, analyzing galvanomagnetic tensor and distribution of isoenergetic surfaces for electrons

03 p0488 A69-13888

Light absorption in semiconductors with electron hole pair formation noting conduction and valence band

06 p0978 A69-16901

InAs solid solutions reflection spectra with CdTe, CdS, CdSe and ZnTe compounds, determining conduction bands

07 p1198 A69-18511

Energy separation and electrons effective mass ratio of conduction bands of tellurium doped GaSb obtained by free carrier Faraday rotation measurements

07 p1201 A69-19464

Conduction band anisotropy in n-type cadmium tin arsenides, analyzing galvanomagnetic tensor and distribution of isoenergetic surfaces for electrons

11 p1939 A69-25689

Solution for kinetic energy equation for organic semiconductors with narrow conduction band situated in strong electric field

12 p2144 A69-26673

P-type GaAs-Ge lasing on band to band or conduction band to acceptor impurity transitions or on both transitions simultaneously

13 p2270 A69-27193

Photoelectric characteristics of thin film CdS-CdTe heterojunction diodes, considering I-V illumination, spectral characteristics and conduction band continuity

13 p2230 A69-27882

Conduction band structure in GaSb noting temperature dependence

13 p2319 A69-27899

Amorphous semiconducting alloys single band model characteristics

15 p2667 A69-30199

Two donor levels and conduction properties of n-type semiconductors demonstrated by capacitance measurements of single crystal tungsten oxide in presence of electrolyte

16 p2825 A69-31609

External magnetic force and internal Coulomb force influence on carriers in conduction or valence band of semiconductor, considering H atom spectra

16 p2826 A69-31824

Laser emission theory for indirect band-band transitions, considering light absorption by free carriers in semiconductors with polar and unpolar scattering

19 p3332 A69-35873

Impurity levels in semiconductors with multiconduction bands, noting impurities influence on photoluminescence, laser action and Gunn effect

19 p3385 A69-36514

Electroreflection study of inversion asymmetry and warping induced interband magneto-optical transitions in InSb, employing low temperature electric field modulation technique

19 p3386 A69-36521

Magneto-optical constants and conduction band parameters of GaAs by coherent radiation at high temperatures, measuring Faraday rotation

19 p3386 A69-36522

Electron effective mass, density and mobility in α -Fe-doped degenerate GaSb-InSb single crystals

19 p3390 A69-36555

GaAs-GaP heterojunctions, analyzing continuous conduction band, capacitance and current-voltage characteristics, photoresponse and modulation effect

21 p3779 A69-38424

Transverse thermomagnetic EMF and Nernst-Ettingshausen coefficient in GaSb semiconductor with double conduction band and strong degeneracy of current carriers

21 p3783 A69-39558

Thermal EMF in cadmium arsenide specimens with various electron concentrations determined to verify parabolic subband structure of conduction band

22 p3993 A69-40607

CONDUCTION ELECTRONS

Nonlinear optical coefficients in group IV and III-V semiconductors, calculating contribution from conduction and core electrons

05 p0776 A69-16329

Absorption and amplification of sound in many valley semiconductors in strong electric field, noting dependence on electron heating and relaxation times

07 p1199 A69-18681

Quantum oscillations of magnetization, undamped magnetoplasma waves development and sound amplification by electron drift in crossed fields observed in semimetals

09 p1556 A69-21615

Electrons conduction and switching in noncrystalline semiconductors, discussing localized states and thermally activated hopping

11 p1938 A69-25239

Electron magnon interaction in ferromagnetic and antiferromagnetic semiconductors, showing conduction band and electron effective mass and magnetic moment dependences on temperature and spin direction

14 p2504 A69-28991

Thermal conduction by electrons in stellar matter, presenting opacity tables for H, He, C and red giant cores and solar composition

22 p4014 A69-40147

CONDUCTIVE HEAT TRANSFER

Stability of compound superconducting cables under conditions of controlled heat transfer from cable surface to liquid He

01 p0176 A69-10718

Alternating direction implicit (ADI) methods for solving parabolic heat conduction equation with variable coefficients in two and three space dimensions

01 p0106 A69-10987

Heat conduction in viscous fluid flows with large concentration of suspended solid particles

02 p0351 A69-12052

Gray radiation and conductive heat transfer in Oseen-like free mixing flow, computing temperature distribution by inversion integral

02 p0354 A69-12504

Heat conduction with change of phase in three dimensional melting and solidification problem under isotherm conditions and balanced energy at interface

02 p0354 A69-12548

Three dimensional unsteady heat conduction and temperature distributions in finite hollow circular cylinder under time dependent boundary conditions of second kind

03 p0530 A69-12861

Difference schemes for heat conduction analog simulation on electric integrators

03 p0410 A69-13300

Thermal contact rectangle with single side heat capacity, applying Fourier transform and Abel convergence tests

03 p0533 A69-13863

Composite heat transfer by conduction and radiation in nongray medium, outlining electronic computer program for numerical solutions

03 p0533 A69-13884

Theory of heat conduction with finite wave speeds for materials with memory

03 p0533 A69-13956

Controllable states of elastic heat conductors, analyzing deformations and temperature fields

03 p0529 A69-13957

Heat removal in multilayer superconducting devices, determining optimum number of layers

03 p0493 A69-14225

Constant thickness disk temperature field for inhomogeneous boundary conditions, considering roots of characteristic equations determination

04 p0685 A69-14498

Biot variational principle applied to combined conduction and radiation heat transfer

04 p0685 A69-14734

Thermal explosion in Poiseuille flow of reacting viscous fluid in infinite circular cylindrical channel or between two rotating infinite cylinders

04 p0686 A69-14986

Periodic solutions for linear and weakly nonlinear heat conduction equations, obtaining omega-periodic solutions for initial boundary value problems

04 p0625 A69-15109

Heat diffusion in cylinder with heat sources creating axisymmetric temperature distribution, using Gauss hypergeometric function and Meijer G-function

04 p0687 A69-15188

Energy transfer from radiating sphere to medium with molecular heat conduction

05 p0845 A69-15782

Nucleate pool boiling heat transfer data extended to relate effect of heating surface characteristics

05 p0847 A69-16125

Semidiscrete approximate solution by analog computer of inverse problem of transient heat conduction

05 p0848 A69-16127

Time independent solar wind equations applied to spherical symmetry and radial magnetic field at solar surface, noting thermal conductivity anisotropy

05 p0817 A69-16703

Whirling liquid hydrogen layer thermal and hydrodynamical conditions, noting application to cold neutrons source in high flux beam reactor

05 p0849 A69-16818

Conduction equations for conduction cooling of human body solved by finite difference method

06 p0880 A69-17088

Thermal nonequilibrium of unsteady adiabatic gas flow in nonheat conducting tube with open ends

06 p0911 A69-17813

Combined radiation and conduction heat transfer equation applied to temperature profile around opaque hollow sphere and in solid condensed gas layer

07 p1239 A69-18303

Heat conduction equation for convective flow applied to gunpowder combustion under harmonic pressure variation

07 p1241 A69-18708

Solar wind model including effects of rotation, magnetic fields and anisotropic heat conduction

08 p1380 A69-20643

Soviet book on theory of heat conductivity covering physical principles of transfer and boundary value problems

08 p1421 A69-20647

High temperature regions cooling as applied to solar flares, considering energy losses due to heat conduction, bremsstrahlung, line emission and recombination radiation

09 p1588 A69-21362

Radiative-conductive heat transfer in plane layer of gray heat conducting medium, solving energy equation
09 p1621 A69-21433

Convective MHD channel flow in vertical channel subjected to temperature and pressure gradients, discussing wall conductances effects on flow rate and heat transfer
09 p1545 A69-21441

Energy transfer in gases transmitting heat by interaction of thermal conduction and IR radiation
09 p1621 A69-21442

Conductive heat transfer between aerodynamically heated skin and barrel of Aerobee 150 sounding rocket telescope, noting effect of residual gas pressure
09 p1610 A69-22005

Kutta-Merson algorithm for converting partial differential equation for two dimensional unsteady state heat conduction to simultaneous ordinary differential equations
09 p1623 A69-22280

Equation for one dimensional heat conduction with nonlinear heat generation transformed from boundary to initial value problem
10 p1809 A69-23689

Emissivity of screened tube in presence of heat conducting connecting pieces between tube and screen
11 p1997 A69-24229

Electron-ion temperature relaxation near interface of two semiinfinite nonmagnetized different temperature plasmas brought into thermal contact
11 p1923 A69-24296

Cryogenic conductive heat transfer in solids, low temperature insulation and liquid-vapor interfaces, discussing boiling heat transfer, injection cooling and frost formation
11 p1998 A69-24461

Upper atmosphere response to time dependent heating based on approximate analytic solutions of heat conduction equation
11 p1878 A69-25151

Unsteady heating of fuel mixture in vertical cylindrical container with Arrhenius heat source, discussing heat conduction equations and wall temperature effects
11 p2001 A69-25192

Heat flux toward electrodes measured under high current discharge, showing conductive heat transfer and erosion effect
11 p1928 A69-25227

Unsteady heat conduction of semiinfinite thin rod with mobile end face, ideally insulated lateral surface and convective heat transfer on uninsulated portion
11 p2002 A69-25229

Aerodynamic heating of ELDO-A booster rocket, calculating flow field, heat transfer and conduction by method of characteristics and thermal models
11 p1966 A69-25433

Mathematical model for melting of finite paraffin slab based on method on numerical computer solution of heat conduction equations for thermal control devices
12 p2190 A69-26785

Viscous heat conducting compressible fluid response to abrupt change in circular cylinder angular velocity at stable temperature distribution, considering Boussinesq approximation
13 p2245 A69-27378

Analytical expressions for nonlinear partial differential equation of heat conduction in solids, giving temperature as function of time and location
13 p2372 A69-27434

Heat transfer and temperature distribution in thin fins with stochastic root temperature due to excitation by stochastic and Markov processes
[ASME PAPER 68-HT-35] 13 p2374 A69-27780

Combined conduction and radiation transfer equations solutions for absorbing-emitting gas, obtaining slip coefficient for diffusion solution correct boundary condition
13 p2374 A69-27784

Thermionic converter matched with solar cells analyzed for parabolic mirrors, assuming heat conduction power supply to cathode and uniform temperature distribution
13 p2209 A69-27970

Green function for boundary value problems of heat conduction equation constructed by heat potentials method
13 p2380 A69-28548

Asymptotic behavior of function in Cauchy problem solution for heat conduction, basing method on Laplace transform inversion formula
13 p2380 A69-28685

Heat conduction and Navier equations solved for temperature distribution and displacements in elastic solids, considering time dependent boundary conditions, body forces and heat generation
14 p2535 A69-29364

Solution methods for differential heat conduction equations, discussing methods of variable separation, Green function, thermal potentials, etc
14 p2539 A69-29456

Conduction solution to generalized nonlinear Benard problem showing existence of bifurcation and analyticity of convective motion
14 p2540 A69-29679

Green function construction for boundary value problems of heat conduction on rectilinear segment with dynamic boundaries, using integral equations
15 p2716 A69-30075

Periodic radial heat flux in infinite cylinder with varying heat sources, assuming time variable heat exchange on surface
15 p2717 A69-30575

Unsteady three dimensional heating of finite solid rectangular parallelepiped, deducing expressions for rectangle and slab
15 p2717 A69-30790

Thermoelastic stress in semiinfinite elastic medium due to discontinuous temperature distribution over free surface, solving associated heat conduction problem
15 p2712 A69-31006

Heat propagation in rod of two sections with different properties, formulating relevant boundary value problem, solving with Duhamel principle
15 p2718 A69-31066

Evaporation of liquid droplets from heating wall observed cinematographically, noting heat transfer by violent film boiling and conduction through thin vapor layer
15 p2718 A69-31117

Weakly damped transverse and thermal waves development and propagation in viscous heat conducting incompressible fluid under temperature and gravitational fields
15 p2718 A69-31168

Langrangian equations resulting from restricted variational principles corresponding to heat conduction problem derived for boundary condition inclusion
16 p2877 A69-31872

Simultaneous solution of continuity and heat conduction equations for ionospheric plasma consisting of electrons, atomic O ions and neutral gas species, discussing varying solar flux effects
16 p2849 A69-32082

Simultaneous solution of continuity and heat conduction equations for ionospheric electrons, ions and neutral species for studying F region magnetic storm behavior
16 p2775 A69-32083

Unsteady heat conduction equations for elliptic cylinder with convection solved by point matching
16 p2879 A69-32171

Variational problem formulated for boundary value problem of steady heat conduction with general boundary conditions
16 p2880 A69-32378

Thermal silicone grease type filler materials for heat transfer across bolted or clamped sheet metal surfaces in electronic equipment for space applications
16 p2794 A69-32560

Heat transfer in evacuated multilayer insulation by radiation and conduction, considering optically thin media separating reflective layers
[AIAA PAPER 69-607] 17 p3073 A69-33300

Radiative and conductive heat transfer in heated finite gaseous body with emphasis on collisional and radiative relaxation, noting cooling as two stage process
[AIAA PAPER 69-638] 17 p3073 A69-33311

Radiative and conductive heat transport mechanisms at cryogenic temperature applicable to thermal energy transport minimizing technique in containment system
17 p3074 A69-33680

Alternating direction iteration method for nonlinear systems of equations applied to steady state heat conduction problem with nonlinear boundary conditions
18 p3163 A69-34329

Lunar temperature prediction with emphasis on variable property models, noting assumptions about physical properties appearing in heat conduction equations
18 p3194 A69-34374

Exact analytic solution for thermal conductance of two dimensional eccentric constriction in dimensionless numbers
18 p3228 A69-34375

Orthonormalization methods applied to heat conduction, convection and radiation problems, noting digital computer programs modifications
18 p3229 A69-34662

High temperature regions cooling as applied to solar flares, considering energy losses due to heat conduction, bremsstrahlung, line emission and recombination radiation
18 p3197 A69-34752

Numerical methods using analog computer in linear one dimensional transient heat conduction
18 p3229 A69-34835

Energy transfer from radiating sphere to medium with molecular heat conduction
18 p3230 A69-35034

Flow viscosity and heat conduction effects on shock wave propagation in bent channel with weak Mach reflection
18 p3124 A69-35326

Bessel function applied to unsteady axisymmetric problem of heat conduction in thermally controlled coaxial cylinders with different physical properties
19 p3448 A69-35981

Heat conduction orientation anisotropy in linear amorphous high polymers due to uniaxial stretching, noting molecular weight distribution and temperature effects
19 p3359 A69-36443

Heat conduction in medium with phase transitions, solving one dimensional nonlinear problem by calculation of isotherms and reduction to Cauchy problem
19 p3453 A69-36838

Surface cavity profiles created by pulsed laser on Ti, Al, Cu, Pb and Zn, compared with isotherms computed from heat conduction models
20 p3552 A69-36917

Combined heat transfer by radiation and conduction in disperse media /thermal insulation/ described by system of nonlinear integrodifferential equations
20 p3631 A69-37097

Finite element discretization technique extended to time dependent processes emphasizing dynamics and heat conduction, discussing applications to aircraft transient response
20 p3575 A69-37204

Heat transfer mechanisms between fluidized beds and wall surfaces by application of film penetration theory of mass transfer, noting bubbling bed model
20 p3632 A69-37519

Heat conduction in thin layer near boundary surface of solid by approximating one dimensional conduction in half space with allowance for curvature
20 p3633 A69-38213

Temperature distributions and heat transfer in thermal entrance region for Hartmann liquid flows under constant pressure gradient between parallel electrically conducting walls at rest
21 p3847 A69-38442

Fourier heat equations functional corrections for determining temperatures of plate and cylinder heated simultaneously by radiation and convection
21 p3848 A69-38641

Effective thermal conductivity parallel to laminations and total conductance for combined parallel and normal heat flow in multilayer insulation
[AIAA PAPER 68-765] 21 p3853 A69-39763

Steady state digital-analog integrator for solving nonlinear heat conduction type equations
21 p3680 A69-39852

Vertical heat exchange flux model using heat conduction equation compensating for tropospheric and stratospheric radiation divergence, calculating diffusion coefficient
22 p3936 A69-40137

Variational principles equivalent to mixed problems for parabolic equations with initial boundary conditions, noting heat conduction theory
22 p3974 A69-40231

Heat flow in belt-type heat transport device allowing for conductive and mass transport effects, deriving expression for heat transfer capability
22 p4050 A69-40554

Heat conduction equation applied to thermospheric heating in auroral zone to account for local temperature and density variations, introducing horizontal transport mechanisms
22 p3941 A69-40717

Combined heat transfer calculations, considering moving radiating media and simultaneous convection or conduction
23 p4237 A69-41328

Thermal inertia index of semiconductor thermistor with one dimensional temperature field taking into account conductive heat transfer
23 p4163 A69-41556

Numerical solutions for time dependent boundary value problems governed by heat equation applied to transient heat conduction in irregularly shaped two dimensional regions
[ASME PAPER 69-HT-50] 24 p4410 A69-43521

Film-nucleate boiling transition for liquid nitrogen in vertical forced flow in electrically heated tube, discussing conduction model and agreement with visual experiment
[ASME PAPER 69-HT-26] 24 p4412 A69-43542

One dimensional numerical solution for steady state thermal behavior of trapezoidal profile annular fins transferring heat by conduction and radiation
[ASME PAPER 69-HT-6] 24 p4413 A69-43553

Lateral heat conduction and radiation along two parallel long plates separated by nonabsorbing dielectric with refractive index of unity
24 p4415 A69-43594

Heat conduction problems associated with radiant exchange in shells under discontinuous solar flux, considering spacecraft structures, illumination theory and astrophysics
24 p4416 A69-43689

CONDUCTIVITY METERS

NT ELECTRICAL CONDUCTIVITY METERS

Conductivity probe design for tenuous plasmas and ionized gases, discussing experimental confirmation of theoretical behavior
[AIAA PAPER 68-170] 09 p1496 A69-21936

Radiophase mapping utilizing VLF radio signals to detect conductive sheets and surface impedance of earth
12 p2075 A69-26982

CONDUCTORS

NT AIRCRAFT ANTENNAS
NT CASSEGRAIN ANTENNAS
NT DIPOLE ANTENNAS
NT DIRECTIONAL ANTENNAS
NT ELECTRIC CONDUCTORS
NT ELECTRIC CONNECTORS
NT ELECTRIC WIRE
NT ELECTROLYTES
NT EXPLODING WIRES
NT HELICAL ANTENNAS
NT HORN ANTENNAS
NT INERTIALESS STEERABLE ANTENNAS
NT ION EXCHANGE MEMBRANE ELECTROLYTES
NT LENS ANTENNAS
NT LOG PERIODIC ANTENNAS
NT LOG SPIRAL ANTENNAS
NT LOOP ANTENNAS
NT MICROWAVE ANTENNAS
NT MISSILE ANTENNAS
NT MOLTEN SALT ELECTROLYTES
NT MONOPOLE ANTENNAS
NT MONOPULSE ANTENNAS
NT MULTIPLE BEAM INTERVAL SCANNERS
NT OMNIDIRECTIONAL ANTENNAS
NT PARABOLIC ANTENNAS
NT PHOTOCONDUCTORS
NT RADAR ANTENNAS
NT RADIO ANTENNAS
NT RHOMBIC ANTENNAS
NT SLOT ANTENNAS
NT SPIRAL ANTENNAS
NT STEERABLE ANTENNAS
NT SUBREFLECTORS
NT SUPERCONDUCTORS
NT TWO REFLECTOR ANTENNAS
NT WAVEGUIDE ANTENNAS
NT YAGI ANTENNAS

Ground wave excited by dipole in conducting half space, discussing lateral wave character and optimum radiation angle
02 p0209 A69-12347

Electrodynamics of turbulent conducting media based on nonrelativistic MHD
03 p0479 A69-13972

Approximate solution of equations for boundary layer flow of conducting medium on insulating and electrode walls of MHD generator channel
06 p0871 A69-17914

Unsteady flow of viscous incompressible conducting fluid in MHD generator channel, discussing external circuit inductance and flow velocity during start-up
06 p0969 A69-17915

Moving conducting media velocity measurement using Reynolds number and electrical conductivity values, based on magnetic field distortion
10 p1731 A69-23435

High speed photography of W strip fracture, considering electric current effects and electric circuit interruption by fracture
12 p2113 A69-26195

Flat conductor cable technology, discussing design, manufacture, specifications, etc
[ASME PAPER 69-DE-8] 14 p2393 A69-28855

Pyroelectric conductor sensors permitting continuous measuring and recording of air inhaled during chosen time intervals
15 p2559 A69-31230

Acceleration waves propagation in nonlinear conducting thermoelastic solid, treating homogeneously deformed and undeformed media
16 p2873 A69-32060

Electromagnetic wave scattering from conducting bodies of arbitrary shape and electromagnetic properties
17 p2918 A69-33002

Integral equation method for electromagnetic scattering by perfectly conducting obstacles modified for volume scattering regions involving disparities in dielectric constant, permeability or conductivity
17 p2930 A69-33890

Penumbra current distribution in plane electromagnetic waves diffraction by conducting cylinder, obtaining transient solution for impulsive excitation, discussing time harmonic problem
[AFRL-69-0038] 18 p3100 A69-34232

Electromagnetic induction in concentric thin shell-enclosed solid conducting sphere immersed in varying electromagnetic field
[AFRL-69-0082] 18 p3101 A69-34803

Conductor material thermal conductivity contribution to self similar explosion in strong magnetic field, determining critical field strength
22 p3982 A69-41019

Coil under alternating current interacting with laminated conducting structure, giving recurrence formula for calculating deflector voltage
24 p4296 A69-42653

CONES

NT ABLATIVE NOSE CONES
NT CIRCULAR CONES
NT CONICAL BODIES
NT NOSE CONES
NT ROCKET NOSE CONES
NT SLENDER CONES

Numerical computer results applied to supersonic flow of perfect gas past staggered cones
03 p0363 A69-13659

Stress distribution and spring rates in cantilever cone ring combination
[ASME PAPER 68-WA/DE-3] 05 p0839 A69-16168

Asymptotic solutions for transverse oscillations of wedge and cone by virtual displacements principle, considering nonlinear law of elasticity and energy dissipation
11 p1975 A69-24762

Refractory cone models made of copper and Co coated Be for force tests in high enthalpy hypersonic arc tunnels at high simulated attitudes
12 p2059 A69-26796

Supersonic flow past cone in presence of blowing normal to cone surface, calculating flow field parameters behind conical shock wave
15 p2548 A69-31175

Subliming ablation effects on boundary layer transition for cones in hypersonic flow, discussing Reynolds numbers measured in wind tunnel tests
[AIAA PAPER 68-40] 16 p2732 A69-31881

Monograph on forces exerted by air during yawing motion of sharp cones in supersonic and hypersonic flows by semilinear method
20 p3460 A69-37919

CONFERENCES

Human factors in aviation - Conference, Los Angeles, June 1968
01 p0010 A69-10448

Photochemistry and radiation chemistry - Conference, Natick, Massachusetts, April 1968
01 p0024 A69-10617

Chemical vapor deposition of refractory metals, alloys and compounds - Conference, Gatlinburg, Tennessee, September 1967
01 p0096 A69-10640

Exploding wire - Conference, Boston, October 1967
01 p0116 A69-10654

Computing machinery - Conference, Las Vegas, August 1968
01 p0035 A69-10703

Applied magnetism - IEEE Conference, Washington, D.C., April 1968
01 p0045 A69-10712

Environmental effects on aircraft and propulsion systems - Conference, Bordentown, New Jersey, October 1968
01 p0055 A69-11043

Life sciences and space research - COSPAR Conference, London, July 1967
01 p0016 A69-11073

Cryogenic engineering - Conference, Brighton, England, May 1968
01 p0056 A69-11144

Temperate latitude sporadic E origin and structure - Conference, Vail, Colorado, June 1968
01 p0069 A69-11156

Cause and structure of temperate latitude sporadic E - Conference, Vail, Colorado, June 1968, Volume 2
01 p0072 A69-11169

Atmospheric optics - Conference, Pulkovo, U.S.S.R., November-December 1965 and December 1966
01 p0073 A69-11181

Metal corrosion in atmosphere - ASTM Conference, Boston, June 1967
01 p0100 A69-11350

Powders and explosives - Conference, Brussels, September 1966
02 p0301 A69-11519

Space projections - Conference, Denver, July 1968, Volume 2
02 p0332 A69-11734

Space projections - AIAA-AAS Conference, Denver, July 1968, Volume 3
02 p0226 A69-11755

Maritime and aeronautical developments - Conference, Paris, April 1967
02 p0192 A69-11886

Applied mechanics - Conference, Laval University, Quebec, May 1967
02 p0339 A69-11984

Geophysical theory and computers - Conference, University of Trieste, September 1967
02 p0242 A69-12005

Fluidics - Conference, London, November 1968
02 p0194 A69-12070

Vacancies and interstitials in metals - Conference, Julich, West Germany, September 1968
02 p0267 A69-12185

N body gravitational problem - Conference, Paris, August 1967
02 p0322 A69-12267

Mechanical behavior of materials under dynamic loads - Conference, San Antonio, September 1967
02 p0342 A69-12277

Voyage to planets - Conference, Washington, D.C., March 1967
02 p0323 A69-12301

Plasma astrophysics - Conference, Varenna, Italy, July 1966
02 p0328 A69-12780

Space projections - Conference, Denver, July 1968, Volume 1
02 p0330 A69-12801

Propulsion - Conference, Paris, October 1967
03 p0494 A69-12887

Cosmic rays - Conference, Calgary, Canada, June 1967
03 p0497 A69-12928

Nonlinear optics - Conference, Novosibirsk, U.S.S.R., June 1966
03 p0435 A69-13034

Space age communication, use of satellites by mass media - UNESCO Conference, Paris, December 1965
03 p0534 A69-13132

Beam-foil spectroscopy - NASA Conference, University of Arizona, November 1968, Volume 1
03 p0470 A69-13160

Beam foil spectroscopy - NASA Conference, University of Tucson, November 1967, Volume 2
03 p0507 A69-13168

Electronics and aerospace systems - IEEE Conference, Washington, D.C., September 1968
03 p0385 A69-13176

Space systems use for planetary geology and geophysics - Conference, Boston, May 1967
03 p0509 A69-13390

Space radiation biology - NASA Conference, Berkeley, September 1965
03 p0370 A69-13476

Applications of electronic computers in construction - Conference, Weimar, June-July 1967
03 p0525 A69-13734

Glass fiber reinforced plastics - Conferences, Freudenstadt, West Germany, October 1968
03 p0453 A69-13819

Physical and mechanical properties of surfaces and interfaces - Conference, Raquette Lake, New York, August 1967
03 p0448 A69-13867

Prevention of and protection against accidental explosion of munitions, fuels and other hazardous mixtures - Conference, New York, October 1966
04 p0644 A69-14467

Dynamics of structured solids - ASME Conference, New York, December 1968
04 p0675 A69-14684

Stochastic problems in control - Conference, Ann Arbor, June 1968
04 p0581 A69-14693

Plastics in electronic packaging - Conference, Binghamton, New York, October 1968
04 p0620 A69-14953

Information processing - AFIPS Conference, San Francisco, December 1968
04 p0564 A69-15334

Information processing - AFIPS Conference, San Francisco, December 1968
04 p0568 A69-15358

Subsonic aeronautics - Conference, New York, April 1967
05 p0699 A69-15541

Spacecraft propulsion - ELDO Conference, Paris, October 1967
05 p0791 A69-15593

Work hardening - Conference, Chicago, November 1966
05 p0777 A69-15752

Nonlinear physics - Conference, Munich, June-July 1966
05 p0792 A69-15767

Systems science and cybernetics - IEEE Conference, San Francisco, October 1968
05 p0741 A69-15801

Astronomy - Conference, Prague, August 1967
05 p0820 A69-15834

Sterilization techniques for instruments and materials as applied to space research - COSPAR Conference, London, July 1967
05 p0711 A69-15934

Electrical insulation - IEEE Conference, Los Angeles, December 1968
05 p0730 A69-16240

Cryogenic properties of polymers - NASA/Case Conference, Cleveland, April 1967
05 p0784 A69-16485

Solid state physics - Conference, Alta Lake, British Columbia, August-September 1967
05 p0809 A69-16552

Aeronautic electronics - Conference, Washington, D.C., September 1968
05 p0789 A69-16716

Aerospace instrumentation - Conference, Cranfield, Beds., England, March 1968
05 p0765 A69-16747

Air safety - Conference, Dallas, April 1968
06 p1040 A69-16834

Space science and technology - Conference, London, February 1968
06 p0997 A69-16852

Nuclear and space radiation effects - IEEE Conference, University of Montana, July 1968
06 p0973 A69-16861

Metal matrix composites - ASTM Conference, Boston, June 1967
06 p0938 A69-16940

Survival and personal equipment - Conference, San Diego, October 1968
06 p0877 A69-16952

Astronomy - Conference, Nuremberg, September 1968
06 p0998 A69-16967

Thermal problems in biotechnology - ASME Conference, New York, December 1968
06 p0879 A69-17084

Materials research - Conference, Tokyo, September 1967
06 p0941 A69-17120

Cosmic rays, elementary particle physics and astrophysics - Conference, Aligarh, India, December 1967
06 p0986 A69-17268

Adaptive processes - IEEE Conference, University of California, Los Angeles, December 1968
06 p0899 A69-17350

Circuit and system theory - Conference, University of Illinois, October 1968
06 p0901 A69-17394

Mass motions in solar flares - Conference, Anacapri, Italy, June 1968
06 p0992 A69-17426

Special ceramics - Conference, Stoke-on-Trent, Staffs., England, July 1967
06 p0946 A69-17527

Astrodynamics, guidance and control - Conference, Belgrade, September 1967, Volume I
06 p1004 A69-17560

Spacecraft systems, education - Conference, Belgrade, September 1967
06 p1015 A69-17596

Propulsion and reentry - Conference, Belgrade, September 1967
06 p0859 A69-17625

Life in spacecraft - Conference, Belgrade, September 1967
06 p0881 A69-17642

Aeronautics - Conference, Beverly Hills, September 1968
06 p0866 A69-17658

Fiber optics - Conference, Baltimore, April 1968
06 p0958 A69-17674

Error correcting codes - Conference, University of Wisconsin, May 1968
06 p0890 A69-17861

Cybernetic problems in bionics - Conference, Dayton, May 1966
07 p1069 A69-18380

Microwave and optical generation and amplification - Conference, Hamburg, September 1968
07 p1090 A69-18420

Geochemistry and cosmology - Conference, Prague, August 1968
07 p1212 A69-18546

Refractory metal alloys metallurgy and technology - Conference, Washington, D.C., April 1968
07 p1164 A69-18790

Nondestructive testing of welds - Conference, Chicago, January-February 1967
07 p1139 A69-18794

Physical sciences - USAF Conference, Albuquerque, June 1967
07 p1181 A69-18927

Telemetering - Conference, Los Angeles, October 1968
07 p1079 A69-19092

Nuclear science - IEEE Conference, Montreal, October 1968
07 p1179 A69-19184

Magnetosphere - Conference, Boston College, June 1967
07 p1207 A69-19351

Electromagnetic windows - Conference, University of Paris, September 1967
07 p1108 A69-19507

Physics of electronic and atomic collisions - Conference, Leningrad, July 1967
07 p1186 A69-19651

Heat and mass transfer - Conference, Minsk, May 1968
07 p1243 A69-19732

Astrophysics, solid state physics, plasma physics and lasers - Conference, Bologna, October 1967
08 p1387 A69-20216

Automation and instrumentation - Conference, Milan, November 1968, Volume I
08 p1296 A69-20301

Air safety - Conference, Seattle, July 1968
08 p1315 A69-20449

Plastics - Conference, Washington, D.C., February 1969
08 p1336 A69-20478

Solar particles and radiation - Conference, Kiel, October 1968
08 p1379 A69-20531

Maritime and aeronautical engineering - Conference, Paris, May 1968
08 p1255 A69-20652

Origin and distribution of elements - Conference, Paris, May 1967
08 p1398 A69-20892

Signal processing arrays - Conference, Dusseldorf, July 1966
08 p1287 A69-20957

Electrochemical generators for space applications - Conference, Paris, December 1967
08 p1258 A69-21034

Reliability in electronics - Conference, Budapest, October 1968, Volume A
08 p1321 A69-21098

Reliability in electronics - Conference, Budapest, October 1968, Volume D
08 p1292 A69-21105

Reliability in electronics - Conference, Budapest, October 1968, Volume B
08 p1293 A69-21111

Space sciences - USAF Conference, Albuquerque, June 1968
08 p1423 A69-21123

Electric propulsion - AIAA Conference, William-sburg, March 1969
09 p1584 A69-21201

Space systems and radio astronomy - Conference, Geneva, September-October 1968
09 p1448 A69-21268

Space systems and radioastronomy - Conference, Geneva, September-October 1968, Part 2
09 p1450 A69-21285

Meteorology - Conference, Berlin, September 1968
09 p1534 A69-21512

Thermionic conversion - Conference, Framingham, Mass., October 1968
09 p1436 A69-21806

Aerospace material investigation and fabrication techniques - Conference, Cocoa Beach, November 1968
09 p1504 A69-22301

Spacecraft electronics - Conference, Chicago, December 1968
09 p1465 A69-22433

Fatigue strength research - Conference, Darmstadt, West Germany, May 1968
09 p1619 A69-22570

Combustion in advanced gas turbine systems - Conference, Cranfield, Bedfordshire, England, April 1967
09 p1624 A69-22611

Vortex fluidic devices - Conference, Philadelphia, January-February, 1967
09 p1443 A69-22736

Solar system plasmas and X ray astronomy - Conference, Adelaide, Australia, August 1968
09 p1581 A69-22742

Cosmic ray physics - Conference, Novosibirsk, U.S.S.R., August-September 1967
10 p1754 A69-22810

Applied mathematics and mechanics - Conference, Prague, April 1968
10 p1675 A69-22874

Technology and education - Conference, Los Angeles, September 1968
10 p1668 A69-22971

Pyrotechnic and explosive elements in space systems - Conference, Tarbes, France, July 1968
10 p1748 A69-23003

Depressed metabolism - Conference, Washington, August 1968
10 p1641 A69-23116

Mechanics of generalized continua - Conference, Freudenstadt and Stuttgart, August and September 1967
10 p1798 A69-23146

Fundamentals of aerospace instrumentation - ISA Conference, Boston, June 1968, Volume I
10 p1690 A69-23224

Instrumentation in the aerospace industry - Conference, Boston, June 1968, Volume 14
10 p1670 A69-23245

MHD electrical power generation - Conference, Warsaw, July 1968, Volume 1, Closed cycle MHD with gaseous working fluids
10 p1729 A69-23433

MHD electrical power generation - Conference, Warsaw, July 1968, Volume 2, Closed cycle MHD with gaseous working fluid
10 p1735 A69-23464

Acoustical holography - Conference, Huntington Beach, California, December 1967, Volume I
10 p1694 A69-23540

Laboratory astrophysics - Conference, Lunteren, Netherlands, September 1968
10 p1780 A69-23670

Physicochemical methods of corrosion testing - Conference, Frankfurt am Main, April 1968
10 p1712 A69-23818

Power sources - U.S. Army Conference, Atlantic City, May 1968
10 p1639 A69-23990

Cryogenic Technology - Conference, Chicago, June, 1967
10 p1810 A69-24014

Holography - Conference, San Francisco, May 1968
11 p1881 A69-24675

Tube techniques - IEEE Conference, New York, September 1968
11 p1847 A69-24740

Theory of thin shells - Conference, Copenhagen, September 1967
11 p1977 A69-24801

Calculation of radiation doses in space - Conference, Toulouse, France, February 1968
11 p1947 A69-24854

Automatic support systems for advanced maintainability - IEEE Conference, St. Louis, November 1968
11 p1863 A69-25059

Space electronics, telemetry, antennas, computers - IEEE Conference, Cocoa Beach, Florida, November 1968
11 p1837 A69-25288

Structures, structural dynamics, materials and aerelasticity - ASME-AIAA Conference, New Orleans, April 1969
11 p1988 A69-25492

Welding - ASME-AISI Conference, Detroit, October 1968
12 p2100 A69-25825

Medical investigation of aviation accidents - Conference, Washington, D.C., September 1966
12 p2021 A69-25837

Reliability-quality control - Conference, Buffalo, May 1968
12 p2100 A69-25845

Astronautics - Conference, Braunschweig, West Germany, October 1968, Volume 3, Strength, material, methods of construction
12 p2176 A69-25850

Astronautics - Conference, Braunschweig, West Germany, October 1968, Volume 2, Energy sources
12 p2014 A69-25862

Astronautics - Conference Braunschweig, West Germany, October 1968, Volume 1, Flight control and electronics
12 p2127 A69-25870

Reliability-quality control - Conference, Ontario, April 1969
12 p2101 A69-25969

Precision electromagnetic measurements - IEEE Conference, Boulder, June 1968
12 p2037 A69-26046

Multivariable control systems - Conference, Duesseldorf, October 1968, Volume 2
12 p2045 A69-26058

Multivariable control systems - Conference, Duesseldorf, October 1968, Volume 1
12 p2046 A69-26069

Multivariable control systems - Conference, Duesseldorf, October 1968, Supplement
12 p2051 A69-26092

High speed photography - Conference, Stockholm, June 1968
12 p2080 A69-26135

Electrohydrodynamics - Conference, Cambridge, Mass., March-April 1969
12 p2135 A69-26397

Large astronomical mirrors support and testing - Conference, Tucson, December 1966
12 p2055 A69-26406

Physics of metal films - Conference, Kiev, October 1966
12 p2143 A69-26456

Physics of magnetosphere - Conference, Washington, D.C., September 1968
12 p2071 A69-26734

Structures, structural dynamics and materials - AIAA-ASME Conference, New Orleans, April 1969
12 p2183 A69-26807

Metal fatigue mechanisms - Conference, Brno, Czechoslovakia, June 1968
12 p2116 A69-26911

Remote sensing of environment - Conference, University of Michigan, Ann Arbor, April 1968
12 p2094 A69-26974

Unsteady phenomena in galaxies - Conference, Biurakhan, Armenian SSR, May 1966
12 p2161 A69-27015

Human behavior simulation - NATO Conference, Paris, July 1967
12 p2024 A69-27079

Computer aided design - Conference, University of Southampton, England, April 1969
12 p2034 A69-27095

Evaluation of wear testing - ASTM Conference, San Francisco, June 1968
13 p2265 A69-27230

Human ecology in space flight - USN-NASA Conference, Princeton, October 1965, Volume 3
13 p2213 A69-27266

Electricity from MHD - Conference, Warsaw, July 1968, Volume 5, Open-cycle MHD
13 p2284 A69-27468

Electricity from MHD - Conference, Warsaw, July 1968, Volume 3, Closed cycle MHD with liquid-metal working fluids
13 p2203 A69-27474

Microwaves - IEEE Conference, Detroit, May 1968
13 p2228 A69-27667

Plastics for electrical insulation - Conference, New York, January 1967
13 p2285 A69-27982

Physical and physicochemical properties of ferrites - Conference, Minsk, Belorussian SSR, 1967
13 p2319 A69-27991

Vacuum and thin film - Conference, Pittsburgh, October-November 1968
13 p2298 A69-28003

Electricity from MHD - Conference, Warsaw, July 1968, Volume 4, Open cycle MHD
13 p2308 A69-28021

Relays - Conference, Oklahoma State University, April 1969
13 p2230 A69-28042

Vacuum - Conference, Manchester, England, April 1968, Part 1
13 p2240 A69-28076

Vacuum equipment and systems - Conference, Manchester, England, April 1968, Part 2 vacuum - Conference, Manchester, England, April 1968, Part 2
13 p2262 A69-28082

Society of American Value Engineers Conference, San Diego, April 1969
13 p2382 A69-28092

Metallography - Conference, Denver, November 1968
13 p2280 A69-28154

Cosmic ray physics - Conference, Novosibirsk, U.S.S.R., August-September 1967
13 p2328 A69-28367

Physics, mathematics, mechanics - Conference Moscow, December 1964
13 p2300 A69-28430

Environmental studies - Conference, Paris, March-April 1969
13 p2214 A69-28587

Geophysics - Conference, Naples, May 1967
13 p2255 A69-28646

Philosophical problems of Einstein theory of gravitation and relativistic cosmology - Conference, Kiev, June 1966
14 p2482 A69-28856

Aviation and astronautics - Conference, Tel-Aviv and Haifa, March 1969
14 p2429 A69-29011

Noise as public health hazard - Conference, Washington, D.C., June 1968
14 p2541 A69-29149

Thermionic electrical power generation - Conference, Stresa, Italy, May 1968
14 p2394 A69-29172

Plastics engineering - Conference, Chicago, May 1969
14 p2469 A69-29411

Electronics - Conference, Rome, March 1969
14 p2422 A69-29685

Corrosion - Conference, Cleveland, March 1968
14 p2465 A69-29929

Statistical mechanics - Conference, Kyoto, September 1968
14 p2487 A69-29986

Solar-terrestrial physics, Solar aspects - IQSY/COSPAR Conference, London, July 1967, Part 1
15 p2672 A69-30005

Temperature measurements - Conference, Hawthorne, California, April 1969
15 p2606 A69-30151

Fatigue design procedures - Conference Munich, June 1965
15 p2705 A69-30355

Man and environment - Conference, Anaheim, California, April 1969
15 p2584 A69-30356

Lubrication - Conference, Atlantic City, October 1968
15 p2622 A69-30604

Magnetism and magnetic materials - IEEE and AIP Conference, New York, November 1968
15 p2668 A69-30683

Reliability of electronic components for space - Conference, Grenoble, November 1968
15 p2622 A69-30816

Heat transfer - AIChE/ASME Conference, Philadelphia, August 1968
15 p2718 A69-31114

Quality control - ASQC Conference, Los Angeles, May 1969
15 p2721 A69-31119

Test measurement - Conference, New York, October 1968
15 p2612 A69-31267

Instrumentation - ISA Conference, New York, October 1968
15 p2615 A69-31286

Instrumentation - ISA Conference, New York, October 1968
15 p2553 A69-31293

Nondestructive testing - Conference, Montreal, May 1967
15 p2630 A69-31502

Cyclohexane and benzene anodic oxidation at fuel cell electrodes, noting cathodic desorption products as function of potential and reactant [ECS PAPER 330]
15 p2562 A69-31540

Light metals - Conference, Leoben, Austria, June 1968
16 p2799 A69-31774

Physics of solids in intense magnetic fields - Conference, Chania, Crete, July 1967
16 p2826 A69-31819

Tactical rocket propulsion - Conference, La Jolla, California, April 1965
16 p2836 A69-31991

Aerospace medical association - Conference, San Francisco, May 1969
16 p2742 A69-32008

Radar meteorology - Conference, Dolgo-Prudnaya, U.S.S.R., April 1966
16 p2805 A69-32263

Electrochemical generators for space applications - Conference, Paris, December 1967
16 p2736 A69-32405

Reliability physics - IEEE Conference, Washington, D.C., December 1968
17 p2935 A69-32886

Creep - Conference, Saclay, Essonne, France, June 1967
17 p2984 A69-32903

Exobiology, Search for extraterrestrial life - AAS-AAAS Conference, New York, December 1967
17 p2907 A69-32967

Dimensioning and strength calculations - Conference, Budapest, October-November 1968
17 p3051 A69-32975

Short range transport - Royal Aeronautical Society Conference, London, May 1969
17 p2897 A69-33206

Satellite attitude control and stabilization - Conference, Paris, October 1968
17 p3045 A69-33219

Viscous drag reduction - Conference, Dallas, September 1968
17 p2950 A69-33247

Birds as pests - Conference, London, September 1967
17 p2898 A69-33362

Cryogenic technology applications - Conference, Chicago, June 1968
17 p3006 A69-33679

Clear air turbulence and detection - Conference, Seattle, August 1968
17 p2998 A69-33732

Astronomical Society of Australia - Conference, Sydney, December 1968
17 p3039 A69-33799

Plasma physics and controlled nuclear fusion research - Conference, Novosibirsk, U.S.S.R., August 1968, Volume 1
17 p3012 A69-33817

Plasma physics and controlled nuclear fusion research - Conference, Novosibirsk, U.S.S.R., August 1968, Volume 2
17 p3014 A69-33826

Electromagnetic waves - Conference, Stresa, Italy, June 1968
17 p2922 A69-33832

Ionospheric studies - Conference, Alma-Ata, U.S.S.R., September 1965
17 p2965 A69-33977

Technology and social progress - ASS Conference, Washington, D.C., March 1968
17 p3076 A69-34039

Commercial utilization of space - Conference, Dallas, May 1967
17 p3041 A69-34043

Aerospace electronics - IEEE Conference, Dayton, May 1969
17 p2939 A69-34056

Lunar physics and chemistry - IAA Conference, Belgrade, September 1967
18 p3112 A69-34234

Photogrammetry - Conference, Washington, D.C., March 1969
18 p3133 A69-34334

Advanced space experiments - AAS Conference, Ann Arbor, September 1968
18 p3192 A69-34359

Space exploitation for experimental research - AAS Conference, Dedham, Mass., May 1968, Volume 24
18 p3193 A69-34367

High temperature and short duration flows - Conference, Freiburg University, West Germany, April 1967
18 p3114 A69-34444

Reliability - Conference, Chicago, January 1969
18 p3140 A69-34476

Computational approaches in applied mechanics - ASME Conference, Chicago, June 1969
18 p3105 A69-34657

Circuits and systems - Conference, Pacific Grove, California, October-November 1968
18 p3109 A69-34671

Space, technology and society - Conference, Cocoa Beach, Florida, March 1969, Volume 2
18 p3233 A69-35055

Space, technology and society - Conference, Cocoa Beach, Florida, March 1969, Volume 1
18 p3234 A69-35070

Figure of earth and refraction - Conference, Vienna, March 1967
18 p3131 A69-35194

Aerodynamics of rotary wing and V/STOL aircraft - Conference, Buffalo, June 1969
18 p3087 A69-35216

Aerodynamics of rotary wing and V/STOL aircraft - Conference, Buffalo, June 1969, Volume 2, Wind tunnel testing, New concepts in rotor control
18 p3088 A69-35226

Polymers in high performance applications - Conference, London, June 1969
18 p3150 A69-35420

Materials and processes for aerospace applications in 70s - Conference, Los Angeles, April-May 1969
19 p3315 A69-35501

Space flight optimization - Conference, Liege, Belgium, June 1967
19 p3398 A69-35662

Photovoltaics - IEEE Conference, Pasadena, November 1968
19 p3249 A69-35678

Instrumentation in aerospace simulation facilities - Conference, Farmingdale, New York, May 1969
19 p3289 A69-35714

Materials research - Conference, Kyoto, September 1968
19 p3342 A69-35771

Failure analysis - IEEE Conference, Philadelphia, May 1969
19 p3281 A69-35781

Space navigation - Conference, Houston, April 1969
19 p3368 A69-35789

Reliability and maintainability - Conference, Denver, July 1969
19 p3324 A69-35999

IR technology - Conference, Ann Arbor, June 1969
19 p3309 A69-36051

Meteorite research - Conference, Vienna, August 1968
19 p3403 A69-36072

High and medium energy molecular beams - Conference, Cannes, July 1969
19 p3375 A69-36171

Forbidden transitions in stellar spectra - Conference, Liege, Belgium, June 1968
19 p3420 A69-36211

Telemetry - IEEE Conference, Washington, D.C., April 1969
19 p3268 A69-36237

Gas dynamics of explosions - IAA Conference, Brussels, September 1967
19 p3448 A69-36351

Radio science - Conference, Ottawa, August 1969
19 p3276 A69-36425

Numerical weather prediction - Conference, Tokyo, November-December 1968
19 p3362 A69-36496

Physics of semiconductors - Conference, Moscow, July 1968, Volume 1
19 p3384 A69-36513

Semiconductor physics - Conference, Moscow, July 1968, Volume 2
19 p3387 A69-36540

Applied mechanics - Conference, Waterloo, Ontario, Canada, May 1969
19 p3374 A69-36655

Fluid power - Conference, London, September 1968
19 p3255 A69-36710

Stress corrosion cracking - Conference, Columbus, Ohio, September 1967
19 p3347 A69-36883

Space law - Conference, New York, October 1968
20 p3634 A69-37102

Heat resistant coatings - Conference, Leningrad, May 1966
20 p3559 A69-37357

Onboard computers on rockets and satellites - Conference, Paris, December 1968
20 p3498 A69-37377

Life sciences and space research on biological effects of radiation in space - COSPAR Conference, Tokyo, May 1968
20 p3474 A69-37612

Imaging radars - Conference, University of Michigan, July-August 1969
20 p3488 A69-37631

Fundamentals of remote sensing - Conference, University of Michigan, July 1969
20 p3493 A69-37734

Small rocket instrumentation techniques - COSPAR Conference, May 1968
20 p3541 A69-37790

Space research - COSPAR Conference, Tokyo, May 1968
21 p3698 A69-38334

Construction applications of electronic computers - Conference, Weimar, June-July 1967, Volume 1
21 p3831 A69-38413

Atmospheric emissions - NATO Conference, Norway, July-August 1968
21 p3705 A69-38482

Cosmic ray studies - Conference, Bombay, November 1968
21 p3788 A69-38811

Scientific results from Ariel 3 satellite - Conference, London, April 1968
21 p3716 A69-39254

Stress analysis - Conference, London, March 1968
21 p3840 A69-39301

IEEE Conference - San Antonio, April 1969
21 p3676 A69-39437

Electricity from MHD - Conference, Warsaw, July 1968, Volume 6
21 p3777 A69-39477

Acrospace and marine corrosion technology - Conference, Los Angeles, July 1968
21 p3747 A69-39484

Stellar mass loss - Conference, Trieste, September 1968
21 p3812 A69-39520

Computers - Conference, Boston, May 1969, Volume 34
21 p3679 A69-39601

Guidance and control in space - Conference, Warsaw, June 1969
21 p3825 A69-39628

Guidance and control in space - Conference, Warsaw, June 1969
21 p3825 A69-39635

Guidance and control in space - Conference, Warsaw, June 1969
21 p3766 A69-39644

Reducing cost of space transportation - AAS Conference, Washington, D.C., March 1969
21 p3856 A69-39686

General and applied physics - Conference, Alma-Ata, U.S.S.R., May 1967
21 p3853 A69-39841

Minor element effects on Ni alloy weldability - Conference, Houston, October 1967
22 p3966 A69-39878

Electronic packaging and production - Conference, Anaheim, February 1969 and Philadelphia, June 1969
22 p3909 A69-39941

Solar physics and hydromagnetics - Conference, Sopot, Poland, September 1966
22 p4009 A69-39982

Reliability testing - Conference, Anaheim, April 1969
22 p3952 A69-40021

Extraterrestrial matter - Conference, Argonne, Illinois, March 1968
22 p4011 A69-40083

Physics applications to earth and planetary interiors - NATO Conference, Newcastle-upon-Tyne, England, March-April 1967
22 p4015 A69-40172

Lasers and mechanical engineering - Conference, London, November 1968
22 p3960 A69-40234

World airport planning - Conference, London, September 1969
22 p3925 A69-40424

Earth observations from balloons - Conference, Washington, D.C., February 1969
22 p3864 A69-40803

Electronic measurement and control in industry - Conference, Budapest, 1969
22 p3915 A69-40934

Color aerial photography - Conference, New York, June 1969
22 p3948 A69-40985

Air safety - Conference, Anaheim, October 1968
22 p3866 A69-41127

Ferroelectricity - Conference, Riga, May 1968
22 p3994 A69-41155

Geochemistry of tektites - Conference, Corning, New York, April 1969
23 p4209 A69-41340

Aerodynamics of rotary wing and V/STOL aircraft - Conference, Buffalo, June 1969, Volume 3
23 p4057 A69-41369

Thermionic conversion - IEEE Conference, Framingham, Mass., October 1968
23 p4064 A69-41718

Telemetry - Conference, Washington, D.C., September 1969
23 p4117 A69-41734

Aviation and space medicine - Conference, Oslo, August 1968
23 p4103 A69-41783

Structural technology for large radio and radar telescope systems - Conference, Cambridge, Mass., October 1967
23 p4147 A69-42120

Electromagnetic compatibility - IEEE Conference, Asbury Park, New Jersey, June 1969
23 p4140 A69-42215

Energy conversion - Conference, Washington, D.C., September 1969
23 p4064 A69-42236

Physics - Conference, Trieste, June 1968, Volume 1, Condensed matter, plasma physics, turbulence, quantum optics, statistical mechanics, astrophysics, quasars, pulsars, gravitation theory and cosmology
23 p4216 A69-42310

Equatorial aeronomy - Conference, Ahmedabad, India, February 1969
23 p4159 A69-42422

Communications - IEEE Conference, Boulder, June 1969
23 p4127 A69-42500

Plasma instabilities in astrophysics - Conference, Monterey, October 1968
24 p4377 A69-42681

Circadian rhythms in nonhuman primates - Conference, Atlanta, July 1968
24 p4259 A69-42701

Safety and failure of components - Conference, Brighton, England, September 1969
24 p4397 A69-42767

Man machine systems - IEEE Conference, Cambridge, England, September 1969
24 p4273 A69-43014

Meteorology and geophysics - Conference, Hamburg, April 1968
24 p4344 A69-43144

Materials in space technology - Conference, Bristol, England, April 1969
24 p4332 A69-43206

Automatic control - Conference, Boulder, August 1969
24 p4289 A69-43267

Structural ceramics and testing of brittle materials - U.S. Army Conference, Chicago, March 1967
24 p4333 A69-43337

Aerospace medicine - Conference, Amsterdam, September 1969
24 p4263 A69-43369

Aircraft Structures and Materials Application - Conference, Seattle, September 1969
24 p4321 A69-43416

Solar flare and space research - COSPAR Conference, Tokyo, May 1968
24 p4369 A69-43603

CONFIDENCE LIMITS

Undetected defects and false alarm probabilities for automatic test equipment, emphasizing quality and confidence limits

03 p0428 A69-13187

Statistical relations for best value, standard deviation and confidence limits for engineering data, noting weighted least squares polynomial for fitting [ASME PAPER 68-WA/PTC-1]

05 p0768 A69-16192

Monte Carlo digital computer simulations, considering sample sizes and confidence intervals in multinomial output

10 p1661 A69-23853

Minimum test error probability test limits for known test equipment and signal tolerances, developing semi-graphically single equation for calculation

11 p1865 A69-25079

Confidence limits determined for damping parameter of complex stationary Gaussian Markov process

11 p1910 A69-25700

Weapon systems integrated testing, determining test quantities as function of subsystems utilizing Neyman-Pearson confidence levels

15 p2619 A69-30400

System estimation methods compared for rational boundaries of lower confidence limit, discussing variables/attributes error propagation

15 p2722 A69-31135

Partial prior information utilization via confidence intervals for mean time to failure of exponential reliability model

19 p3360 A69-36038

Sequential Bayes procedure demonstrating mean time to failure exceeding acceptable value with given confidence coefficient

19 p3327 A69-36040

Bayesian confidence limits for systems reliability, considering exponential and unspecified life distribution subsystems

19 p3328 A69-36041

Mean time between failures/MTBF for component, equipment or system subjected to total unit test hours at various confidence levels

21 p3684 A69-39700

CONFIGURATION MANAGEMENT

Configuration management, establishing uniform and mutually supporting methods of configuration identification, control and accounting for systems and equipment

12 p2192 A69-25849

Book on industrial control engineering covering mathematics, semiconductor devices, feedback amplifier theory, closed loop systems, frequency response diagrams

12 p2051 A69-26244

Configuration management for managing technical requirements defining systems, system equipment or individual equipment and changes, discussing implementation procedures

20 p3640 A69-38021

CONFIGURATIONS

Substructure optimization in structural synthesis, minimizing number of cells for configuration parameter [AIAA PAPER 69-121]

06 p1027 A69-18069

Large scale electronic systems configuration compatibility concept, discussing modular line replaceable units/LRU/assigned set of numbers

08 p1322 A69-21154

Coronal open helmet streamer configurations, noting minimum temperature requirement for constriction to true geometrical throat

09 p1598 A69-22177

Diffuse configuration factors between small plane and large sphere by unit sphere method, presenting limiting cases

24 p4351 A69-43683

CONFINEMENT

Human behavior during stressed underground confinement, discussing adaptation processes

01 p0020 A69-10757

Isolation effects on higher nervous activity, motor and vegetative reactions, muscular strength and emotional state

03 p0377 A69-14202

Microbiological influence on astronauts efficiency during and after long space flights, stressing simulated microclimates and confinement effects on flora

18 p3097 A69-35304

CONFLUENCE

U CONVERGENCE

CONFORMAL MAPPING

Plane subcritical flow past lifting aerofoil analyzed using conformal mapping and difference scheme on annular mesh inside circle

06 p0859 A69-17470

Conformal mapping of regions with corners and large curvatures of boundary curves onto unit circle with digital computer, considering airfoil

10 p1724 A69-22880

Conformal mappings for solving boundary value problems in elasticity and plasticity theories for regions having singular points

11 p1973 A69-24662

Polynomial coefficients multiplication by weighted damping factors for increased conformal mapping and boundary value problems solutions accuracy for doubly connected regions

12 p2178 A69-25998

Conformal transformation reducing transverse thermal resistance of cylinder of revolution to thermal resistance of semiinfinite medium

12 p2190 A69-26292

Plane problems of elasticity theory solved numerically using conformal mapping

18 p3219 A69-34709

Horizontal Situation Display/HSPD map computer mechanization transforming earth location to X, Y coordinates for Lambert conformal projection [AIAA PAPER 69-987]

22 p3908 A69-40367

CONGESTION

Chronic congestive heart failure in dogs compared to pulmonary system, discussing effect on cardiac lymphatics

23 p4078 A69-41364

CONGRUENCES

Nonholonomic congruences of trihedrons in metric theory of straight line complex

03 p0457 A69-13865

CONICAL BODIES

NT SLENDER CONES

Force law determining impact processes of pyramidal and conical body penetration into smooth surface of rigid plastic metals

02 p0337 A69-11615

Turbulent boundary layer growth, pressure distributions and surface shear stresses on yawed semiangle cone [AIAA PAPER 68-98]

02 p0190 A69-12526

Blunt and conical body optimum heat shield shapes for Jupiter atmospheric entry, noting shallow flight path [AIAA PAPER 68-1150]

03 p0520 A69-13565

Soviet book on hypersonic flow past truncated cones at various angles of attack with allowance for physicochemical equilibrium transformations

03 p0362 A69-13633

Boundary layer transition measurements on flight tests of experimental 22 degree conical reentry vehicle with Be heat shield and graphite nose [AIAA PAPER 68-1152]

03 p0362 A69-13648

Three dimensional boundary layers on cones at small angle of attack, presenting numerical solutions with heat transfer effects for wind tunnel model [ASME PAPER 68-WA/PTM-24]

04 p0541 A69-14389

Cone tip blunting effect on cone local laminar heat transfer rate noting cone configuration, semivertex cone angle and Mach number

04 p0542 A69-14721

Blunt cone hypersonic roll damping derivative, using Mach number distribution and graphical integration

04 p0542 A69-14739

Truncated solid cones plastic yielding under quasi-static and dynamic axial loads at various strain rates

04 p0682 A69-15301

Hypersonic laminar and transitional heat transfer rate distribution on spherically blunted cones

05 p0696 A69-15707

Ablation surface patterns and resulting roll torques and roll behavior of hypervelocity vehicles [AIAA PAPER 69-180]

06 p1036 A69-18051

Flow measurements in near wake of 7 degree half angle cone at free stream Mach number 4.3, noting pressure measurements [AIAA PAPER 69-186]

06 p0863 A69-18068

Experimental and numerical nonequilibrium shock layer around cones in hypersonic pure oxygen flows with simultaneous rotational, vibrational and dissociation relaxation [AIAA PAPER 69-136]

06 p0864 A69-18141

Three dimensional hypersonic steady flow around blunt and pointed cones at nonzero angles of attack calculated by method of characteristics [AIAA PAPER 69-187]

06 p0865 A69-18176

Dynamic stability derivatives of large angle blunted conical spacecraft near transonic speed in simulated Mars environment for various angles of attack [AIAA PAPER 69-104]

06 p1019 A69-18210

Quasi-plane stress in rotating disks of unconventional profile emphasizing conic shaped disk analysis in terms of hypergeometric series

07 p1235 A69-19444

Elastic cone stresses due to axial force at point on axis, solving problem in terms of convergent integrals

08 p1415 A69-20689

Transition of hypersonic boundary layers on conical body using shock tunnel, obtaining surface heat transfer distributions [AIAA PAPER 68-39]

09 p1482 A69-21943

Base pressure fluctuations behind cone in supersonic gas flow, noting complicated superposition of harmonics associated with various factors

09 p1431 A69-22237

Short multiconical TE sub 01 mode X band taper for connecting two different diameter circular waveguides

09 p1468 A69-22604

Laminar boundary layer separation and heat transfer on zero incidence cone at hypersonic speed, noting wall temperature and Reynolds number effects

09 p1433 A69-22609

Spherically blunted 15 degree semivertex angle cone flow field parameters at Mach 8.6, measuring pitot pressure and shock shape

11 p1818 A69-25143

Numerical integration of equations for three dimensional laminar boundary layer on sharp elliptical cones in supersonic flow of ideal gas, discussing heat exchange

11 p1821 A69-25477

Axissymmetric vibration modal properties/frequencies and mode shapes/ of thin conical shell frustums, considering dimensional and boundary condition influences

11 p1992 A69-25519

Radiation field from sources on conical surface using Green functions

13 p2223 A69-28569

Axissymmetric supersonic gas flow with attached shock wave past cone, calculating flow parameters between body and shock wave

17 p2890 A69-33123

Surface pressure and heat transfer over blunt conical body in hypersonic flow with uniform mass addition of various gases [AIAA PAPER 69-716]

17 p2891 A69-33463

Magnetic field effects on rotating cone compressible boundary layer at zero angle of attack, describing changes in drag coefficient, torque and velocity profiles [AIAA PAPER 69-721]

17 p2892 A69-33484

Supersonic aerodynamic characteristics of flared cones with various flare angles studied by schlieren photography, showing geometrical parameters influence on flow patterns

19 p3239 A69-36387

Three dimensional laminar boundary layer on conical body of revolution in low Reynolds number compressible fluid flow

19 p3241 A69-36762

Reentry cones with mass and configuration asymmetries, studying nonlinear aerodynamic characteristics by wind tunnel and full scale flight tests [AIAA PAPER 69-867]

21 p3823 A69-39393

Dynamic stability derivatives of large angle blunted conical spacecraft near transonic speed in simulated Mars environment for various angles of attack

22 p4036 A69-40550

Deployable cross log periodic dipole/LPD/ array on conducting cone as potential application to spacecraft or missile requiring frequency independence in VHF-UHF band

22 p3913 A69-40693

Frictionless supersonic and hypersonic flow of ideal gas of constant specific heat past cone with deformed axis at zero angle of attack

23 p4058 A69-41579

Edge diffracted fields by conical body frustums evaluated, including equivalent currents for caustic regions

23 p4136 A69-41583

Supersonic free stream flow past finite conical body with subsonic surface gas injection

23 p4059 A69-41884

Second order differential equations of supersonic flows past bodies at small angles of attack, showing linearized characteristics method applicability for conical nose

24 p4243 A69-42581

Boundary layer separation zones in laminar, transition and turbulent fluid flows past conical bodies with widening skirts

24 p4245 A69-43481

Intense heat exchange narrow zones on blunted semicone surfaces in hypersonic gas flows ascribed to large Reynolds numbers
24 p4246 A69-43494

CONICAL FLARE
U CONES

CONICAL FLOW
Self similar solutions uniqueness of three dimensional laminar boundary layer equations for conical flow determined by supplementary conditions derived from flow pattern
02 p0233 A69-12572

Time independent flow of highly rarefied neutral gas past finite cone at zero angle of attack with freestream, noting molecular distribution function
04 p0541 A69-14712

Test of similarity theory of leading edge vortices above slender wings in subsonic conical flow
04 p0543 A69-14820

Conical diffuser/exit duct performance and model for estimating energy losses, discussing inlet flow and Reynolds number
[ASME PAPER 68-WA/FE-45]
05 p0698 A69-16112

Lift drag ratio for conical sector with V-shaped wing at zero incidence
06 p0858 A69-17340

Three dimensional flow field of incompressible fluid with purely axial development in conical ducts and turbomachines
09 p1480 A69-21597

Numerical integration of equations of three dimensional laminar boundary layer in conical flow, using integral relation method
09 p1430 A69-21789

Angle of attack and Reynolds number effect on hypersonic flow past circular cone, obtaining shock wave shape
[ONERA-TP-692]
11 p1818 A69-24751

Heat transfer for incompressible inviscid fluid flow in cone, expressing solution in terms of dimensionless numbers
13 p2375 A69-27788

Conical flow past cruciform wing-body and tail-body systems, considering various positions of leading edges with respect to Mach cone
15 p2548 A69-31002

High order conical motions past cruciform wing-body and tail-body systems, reducing problem to flow past cruciform wing
15 p2548 A69-31023

Streamline flow of ideal stable gas with constant ratio of specific heats around conical body with arbitrary taper, determining flow velocity components
16 p2732 A69-32126

Aerodynamic characteristics of sphere and blunt cone in highly rarefied gas flow, noting molecular collision effect
18 p3086 A69-34708

Wing tunnel and theoretical studies of hypersonic wall flow on cone, considering static pressure and convection heat flux density effects
19 p3241 A69-36759

CONICAL NOZZLES
Navier-Stokes equations solution applicable to source type low Reynolds number flow through conical nozzles
09 p1482 A69-21976

High enthalpy air flow in hypersonic conical nozzle, calculating chemical and thermodynamic nonequilibrium effects with computer program
09 p1433 A69-22610

Turbulent boundary layer laminarization in conical nozzle flow, measuring velocity profiles and friction coefficient
[JPL-TR-32-1407]
16 p2732 A69-31894

Inlet thermal boundary layer thickness effect on conical nozzle heat transfer and boundary layer determined by operating nozzle with cooled/uncooled inlet
[AIAA PAPER 69-474]
16 p2881 A69-32780

Laminar boundary layers in low density supersonic and hypersonic conical and axisymmetric nozzles, treating displacement, transverse curvature, velocity slip and temperature jump
[AIAA PAPER 69-653]
17 p2954 A69-33458

Pulsating flow analysis in finite and infinite conical nozzles under sinusoidal pressure disturbances
[ASME PAPER 69-APM-16]
18 p3214 A69-34392

Convergent conical nozzles discharge coefficient calculated as function of operation mode and nozzle geometry
24 p4364 A69-43074

Boundary layer and heat transfer measurements for turbulent boundary layer laminarizing in conical nozzle flow with wall cooling
[ASME PAPER 69-HT-56]
24 p4303 A69-43538

Uniform flow and wall boundary layer growth measurement in conical nozzle of reflected shock tunnel operating at high enthalpy conditions
24 p4247 A69-43575

CONICAL SHELLS
Critical points separating stable and unstable branches of equilibrium curve of nonlinear elastic systems, discussing flexible shallow conical shell in temperature field
02 p0341 A69-12256

Buckling of electroformed thin conical shells under hydrostatic pressure, proving theory for cones of large taper ratio
02 p0347 A69-12515

Conically bent plate cross section distortion analysis employing von Karman large deflection theory, noting effect of tapering
[ASME PAPER 68-APM/Y]
04 p0670 A69-14402

Elastic noncircular orthotropic conical shell stress-strain state, obtaining differential equations reducible to integrodifferential equations solvable by iteration
04 p0673 A69-14494

Approximate expressions for displacement state of orthotropically reinforced conical thin walled shell, finding stiffness matrix by numerical integration
05 p0835 A69-15829

Critical axisymmetric loads for instability in orthotropic multilayer conical shells obeying Hooke law under axial compression or external pressure
05 p0840 A69-16198

Steady state frequency response of conical and cylindrical shells under lateral excitation
06 p1021 A69-17147

Yield point for simply supported conical shell loaded through central boss at vertex
06 p1023 A69-17375

Post-wrinkling nonlinear behavior of conical shell of revolution subjected to bending loads
[AIAA PAPER 69-90]
06 p1027 A69-18074

Variational method for safety limits of perfectly plastic simply supported conical sandwich shells subjected to uniform internal pressure and obeying Mises yield criterion
08 p1416 A69-20702

Stress-strain problem of geometrically nonlinear conical shell subjected to creep, giving method for complex deformation solution
09 p1612 A69-21497

Buckling of cylindrical and conical sandwich shells with fiberglass/epoxy facings and aluminum honeycomb cores
[AIAA PAPER 68-294]
09 p1616 A69-21942

Free vibrations in axisymmetrically loaded orthotropic circular conical shells with longitudinal and circumferential stiffening based on linearized theory, considering shear deformation and inertia
11 p1969 A69-24327

Stiffener geometry and spacing effects on buckling of axially compressed cylindrical and conical shells
11 p1979 A69-24815

Thin conical elastic shell stress-strain state calculated by computer for arbitrary thicknesses and loading conditions, considering temperature and edge forces effects
11 p1981 A69-24943

Thin elastic conical shells asymmetric deformation under stresses and strains, deriving asymptotic solution
11 p1983 A69-25090

Bending theory for truncated multilayer anisotropic conical shells, defining relations between displacements and external forces
11 p1984 A69-25141

Surface wave patterns of truncated conical shells with free edges attributed to mechanical properties
12 p2178 A69-26002

Postcritical deformations of thin conical elastic shells hinged along edges under external pressure using Pogorelov method for cylindrical shells
12 p2181 A69-26609

Creep stresses and displacements in conical membrane shells at small angle of attack to supersonic flow field, discussing temperature distributions
13 p2364 A69-28205

Collapse pressure of flush cylindrical nozzle axisymmetrically intersecting conical pressure vessel for rigid plastic shells
15 p2704 A69-30289

Eigenvalues of truncated orthotropic shells of revolution with degenerate poles and various rigidities and geometries
16 p2873 A69-32133

Anisotropic conical shells free vibrations analyzed by Galerkin and operator-matrix methods, neglecting transverse shear deformation and rotatory inertia effects
16 p2874 A69-32165

Free vibrations of thin truncated circular conical shell and reinforcing rings and stringers, determining resonant frequencies for stiffened and unstiffened configurations
17 p3051 A69-32955

Frequency and mode shapes of conical shell free oscillations related to shell parameters and boundary conditions
17 p3058 A69-33201

Test stand for free oscillations frequencies and mode shapes of truncated conical shells of revolution with clamped edges and one free edge
17 p3058 A69-33202

Cylindrical and conical panels dynamic responses to time varying load distributions, using trigonometric series coupled with finite difference methods
[ASME PAPER 69-APM-22]
18 p3214 A69-34396

Cantilever truncated conical shell stability under tensile stresses solved by strain energy technique
18 p3216 A69-34574

Limiting equilibrium of variable thickness shallow spherical and conical shells of revolution under axisymmetric loads, assuming rigid plastic shell material
18 p3225 A69-35370

Structural analysis of thin walled conical shell with variable external loading and Winkler-base elastic filler, using linear differential equation with variable coefficients
19 p3436 A69-35846

Elastic closed and truncated conical shell stability with initial deflections under dynamic critical loading
21 p3834 A69-38716

Lift coefficients of idealized tunnel type ram wing consisting of truncated semiconical shell computed by lifting surface theory
22 p3860 A69-40819

Statics of axisymmetric deformation of cylindrical and conical shells of revolution of moderate thickness under uniformly and nonuniformly distributed loads
23 p4226 A69-41705

Algorithm for stress analysis of structurally orthotropic conical and cylindrical shells, resolving first order differential equations
23 p4229 A69-42000

Truncated conical sandwich shell suspended in free-free condition measured and analyzed for vibrational characteristics
23 p4235 A69-42462

Collapse load of shallow conical shells clamped at base and loaded through finite rigid boss, using Tresca yield condition for sandwich shell
23 p4236 A69-42496

Buckling of truncated conical shells under torsion with various boundary conditions, applying Galerkin method to estimate critical load and wave number
24 p4395 A69-42715

Longitudinal elastic waves produced in truncated hollow Al cone due to steel spheres impact
[ASME PAPER 69-APMW-15]
24 p4401 A69-43101

CONICS
U ELLIPSES
U HYPERBOLAS
U PARABOLAS

CONJUGATES
Micropulsations at magnetoconjugate points in Arctic and Antarctic, noting diurnal and seasonal variations and latitude dependence
01 p0068 A69-11112

World maps highlighting differences in geomagnetic field at conjugate localities
02 p0245 A69-12737

Spatial and temporal conjugacy of visual auroras during magnetically quiet periods
05 p0753 A69-16247

Magnetic activity dependence of VLF emission properties at magnetically conjugate points
06 p0920 A69-17735

Conjugate gradient and Davidson-Fletcher-Powell methods applied to nonlinear optimization problems
09 p1474 A69-22442

Geomagnetic fluctuations positive and negative correlations at conjugate pair stations Syowa base and Reykjavik
10 p1681 A69-22806

Conjugated gradient components of optimization criterion in automatic control determined by applying sensitivity method to computation
11 p1857 A69-24367

Elliptic boundary value problem for differential equation and pseudodifferential boundary conditions, obtaining Green formula from formulated conjugate problem

12 p2121 A69-26200

Auroral phenomena observations at magnetically conjugate regions including luminous aurora, riometry of auroral radio absorption, balloon-measured X rays and magnetic disturbances

21 p3708 A69-38493

Spatial gradient and amount of auroral radio absorption measured by riometers at magnetically conjugate and closely spaced stations

22 p3934 A69-39966

Conjugate points along lightlike geodesics in general theory of relativity, deriving existence from vector field matrix properties and Ricci curvature

23 p4213 A69-41724

Differential games derived for conjugate-point necessary conditions and definitions for minimum and maximum problems

24 p4340 A69-42959

CONJUGATION

Conjugate echoes in Alouette 2 topside sounder ionograms explained by multiple reflections between conjugate points of field line, noting magnetospheric waveguides role

08 p1274 A69-20045

CONNECTIONS

U JOINTS [JUNCTIONS]

CONNECTIVE TISSUE

U CARTILAGE

U COLLAGENS

U MARROW

CONNECTORS

NT UMBILICAL CONNECTORS

Precision coaxial connectors, giving IEEE standard mechanical, electrical and environmental specifications for general precision connectors using coplanar butt joints

02 p0222 A69-12757

Foldable tubular connection application to expandable lattice structure, analyzing cross sectional distortions

06 p1024 A69-17608

Glass vacuum systems grease free assembly method using heat shrinkable polyolefin sleeve tubing connector for compression of O ring joints

08 p1320 A69-20529

Short multiconical TE sub 01 mode X band taper for connecting two different diameter circular waveguides

09 p1468 A69-22604

CONNECTORS [ELECTRIC]

U ELECTRIC CONNECTORS

CONOIDS

U CONICAL BODIES

CONSERVATION

U WATER RECLAMATION

CONSERVATION EQUATIONS

Conservation equations for steady incompressible flow in variable area duct with mass transfer at walls simplified by linearizing inertial and convective terms

03 p0413 A69-13011

Permissible nonthermal convection modes in planetary interiors derived from conservation equations for self gravitating homogeneous nonrotating compressible fluid spheres

07 p1213 A69-18611

Gas segregation in positive column of DC discharge due to axial ion motion analyzed using conservation equation

08 p1361 A69-20145

Conservative system /with two degrees of freedom/ motion in plane harmonic force field with potential satisfying Laplace equation, discussing graphic trajectory construction

11 p1920 A69-25745

Boundary layer equations describing momentum, energy and mass concentration conservation in axisymmetrical turbulent jet flame solved for Lewis number unity in von Mises plane

13 p2379 A69-28455

Spherical symmetric unsteady conservation equations describing transient burning of volatile fuel droplets, obtaining time dependent fuel and heat distribution in flow field

14 p2537 A69-29016

Mach disk and Riemann wave location, size and strength in underexpanded jet flows, proposing model for conservation equation satisfaction

[AIAA PAPER 69-665] 17 p2954 A69-33460

Plane light wave propagation in homogeneous isotropic medium with fluctuating dielectric constant

using perturbation theory and integrating energy conservation law

18 p3173 A69-35127

CONSERVATION LAWS

Energy transport in atmosphere studied by considering sphere in isotropic fluid in infinite field without gravity, using first law of thermodynamics

01 p0067 A69-11032

Conservation laws of energy and linear momentum in general relativity formulated, noting application to radiating gravitational systems

01 p0121 A69-11286

Total conserved momentum-energy of electromagnetic interaction of system of point charges in Wheeler-Feynman theory, noting mass defect of connected system

04 p0631 A69-15058

Interaction between point charges in Wheeler-Feynman electrodynamics, noting impossibility of deducing momentum and energy conservation from variational principle

04 p0631 A69-15059

Local creation of mass in steady state universe as source of static field energy propagating away at speed of light

09 p1601 A69-22212

Matrix formulation of electromagnetic field equations and nonlinear conservation laws for measurable quantities

10 p1725 A69-24049

Hydrodynamic equations and conservation laws for nonviscous fluid in postNewtonian approximation of Brans-Dicke theory applied to gaseous mass dynamic instability

10 p1789 A69-24130

Charge bunching approach for gravitational hydrodynamic instability of infinite uniform self gravitating system in translational motion, using conservation laws

11 p1961 A69-25105

Existence theorems for hyperbolic genuinely nonlinear systems of conservation laws, studying Cauchy problem

11 p1909 A69-25163

Isotropic and anisotropic dust cosmological models density perturbation growth, considering angular momentum conservation in expanding universe

13 p2343 A69-27619

Newman-Penrose formalism for conserved quantities in general relativity, giving group theoretic interpretation

14 p2486 A69-29450

Energy release efficiency in gravitational collapse, estimating rest energy fraction from energy conservation, neutron star stability and spherically symmetrical systems collapse considerations

16 p2853 A69-31594

Conservation laws in general relativity, discussing Noether theorem, Bianchi identities, superpotential, Einstein-Klein theorem, momentum method and outgoing radiation

16 p2813 A69-32362

Critical review of Deriugin theory of scattering from rough lamellar surfaces using separation of variables method, discussing energy conservation violation

17 p2930 A69-33885

Conservation theorems for energy and mean circulation in inviscid rotating fluid, noting inertial wave spectrum continuity

18 p3121 A69-34550

Conservation laws and Liapunov stability of free rotation of rigid body about principal axes derived from kinetic energy and angular momentum

19 p3397 A69-35612

Integro-interpolation difference schemes for gas dynamic equations system satisfying laws of mass, momentum, energy conservation and energy balance

23 p4151 A69-41527

CONSOLES

U REMOTE CONSOLES

CONSOLIDATION

Shrinkage and heat release of polyglycol malcinate binder during gamma radiation consolidation compared with thermochemical consolidation

12 p2117 A69-25991

CONSTANTS

NT BOHR MAGNETON

NT GRAVITATIONAL CONSTANT

NT GRUNEISEN CONSTANT

NT SOLAR CONSTANT

Conversion of Woolard theory coefficients of tidal irregularity of earth rotation to new system of constants

09 p1484 A69-21383

Maxwell theory basis of special theory of relativity, discussing universal length constant

11 p1920 A69-25562

Torkington progressive rigidity model with successive minimum requirements relation to diagonal matrix elements of molecular force constants

17 p3068 A69-34230

Conversion of Woolard theory coefficients of tidal irregularity of earth rotation to new system of constants

18 p3127 A69-34771

CONSTELLATIONS

NT ANDROMEDA CONSTELLATION

NT AURIGA CONSTELLATION

NT CASSIOPEIA CONSTELLATION

NT CENTAURUS CONSTELLATION

NT CEPHEUS CONSTELLATION

NT CYGNUS CONSTELLATION

NT LYRAE CONSTELLATION

NT ORION CONSTELLATION

NT SAGITTARIUS CONSTELLATION

NT SCORPIUS CONSTELLATION

NT SCUTUM CONSTELLATION

NT TAURUS CONSTELLATION

OH emission source in constellation Canis Major discovered with interferometer in October 1968, noting nearby IR object

09 p1591 A69-21448

Relative element abundances in Cyg, Her and Boo atmospheres, calculating curves of growth by Planck gradient method for stellar spectra

14 p2519 A69-29356

Star chains around Eta Carinae, discussing nonrandom real groupings and probability criteria using ADH red sensitive plate without filter

16 p2856 A69-31931

Photoelectric observations of W Ursae systems, including observed and computed times of minimum light and period change

16 p2863 A69-32399

BetaCrB atmospheric microturbulence velocity, ionization and excitation temperatures, electron pressure and abundances determined by spectrophotometer

16 p2864 A69-32592

MK system spectral types determination for B, A and F type stars from slit spectrograms near NGC 2264

23 p4211 A69-41487

Proper motions and spectroscopic data of bright members of II Per and I Lac associations analyzed to determine expansion age

23 p4221 A69-42385

CONSTITUTIONAL DIAGRAMS

U PHASE DIAGRAMS

CONSTRAINTS

Optimum control with respect to minimum fuel and power consumption involving constraints based on Kuhn-Tucker conditions and saddle point theorem

02 p0223 A69-11564

Nonlinear programming of optimization of parameters and control functions of dynamic systems

03 p0408 A69-12974

RLC two terminal bridge network synthesis, considering two reactances, three resistances and constraints

09 p1464 A69-22291

Weight minimizing of circular disk subjected to behavioral and side constraints, considering resonance frequency of vibration and tolerances

[ASME PAPER 69-VIBR-1]

10 p1700 A69-24159

Constraint theory for analysis of mathematical models to alleviate software problems associated with simulation of complex large scale systems

11 p1858 A69-24936

Panel flutter under loads along profile, evaluating constraints dynamic characteristics by Hamilton principle

15 p2712 A69-31001

Acceleration injury noting water immersion effect on cat lung due to intense body vibration, suggesting restraint as practical solution

17 p2913 A69-33009

Scientific satellites structural design problems, considering limitations imposed by weight, layout, environmental conditions, mission and manufacture

18 p3208 A69-34792

Aircraft performance optimization using computationally oriented strategy for handling state variable inequality constraints

[AIAA PAPER 69-812] 19 p3243 A69-35628

Motion equations of holonomic system of elastic bodies subjected to scleronomic, ideal and statically determinate constraints, using Green tensor

19 p3374 A69-36584

Constraint restoration in holonomic and non-holonomic problems involving system of algebraic or transcendental equations or first order differential equations
19 p3361 A69-36758

1967 Space Treaty peaceful activities definition, suggesting explicit provisions regarding treaty province, enforcement machinery and implementation
20 p3636 A69-37112

Satellite Airborne Communications /STAIRCOM/ design constraints
20 p3497 A69-38314

Normalized hodographic mapping for constrained trajectory families, discussing mapping concepts, information content and applications
[AIAA PAPER 69-924] 21 p3809 A69-39362

Synchronous communications satellite launch constraints for fixed time or node, noting application to IDCSP/A mission and sun angle, occultation and transfer orbit
[AIAA PAPER 68-445] 22 p4036 A69-40543

Extremal trajectory formulations for state variable inequality constrained optimization problems, forming augmented functional
23 p4182 A69-41907

Tiltable conventional radio telescopes possibilities of passing gravitational limit for diameter and shortest wavelength, discussing dead load
23 p4231 A69-42138

N-terminal parent networks with symmetry constraints derived for nonredundant one port configurations through combinatorial functions test patterns, using computer algorithm
23 p4134 A69-42524

Slack variable to transform optimal control problem with scalar inequality constraint on state variables into unconstrained problem of higher dimension
24 p4291 A69-43270

Ionization rate limiting processes behind strong shock waves in pure N, plotting electron density profile diagrams
24 p4302 A69-43367

CONSTRUCTIONS

Exact analytic solution for thermal conductance of two dimensional eccentric constriction in dimensionless numbers
18 p3228 A69-34375

Coronary vessel lumen changes under oligemic hypotension resulting from circulating blood volume decrease in anesthetized cats, discussing constrictory coronary vessel responses
23 p4084 A69-41470

CONSTRUCTION

Cobalt base alloy for construction in high temperature corrosive environment, discussing mechanical properties, oxidation and corrosion resistance and phase stability
01 p0095 A69-10546

Construction practice for hot-mix bituminous pavements covering production, composition, application and quality control
01 p0057 A69-11276

Construction of large parabolic antennas for radio astronomy and satellite communication, noting dimensional accuracy, directional precision and dynamical behavior
09 p1476 A69-21650

Construction techniques for lightweight mirrors for secondaries, considering optical finishing and thermal expansion
12 p2058 A69-26420

Construction applications of electronic computers - Conference, Weimar, June-July 1967, Volume I
21 p3831 A69-38413

CONSTRUCTION MATERIALS

Structural weight fraction factor analysis leading to improvements in materials and structures
[AIAA PAPER 68-331] 01 p0011 A69-11021

Constitutive equations for dynamic material behavior permit consideration of large deformations in direct manner
02 p0343 A69-12286

Engineering glass manufacturing, properties and applications in buildings, vehicles, lamp and electronic devices, etc
04 p0619 A69-14585

Handbook of techniques in high pressure research and engineering, discussing construction materials, design and construction methods, measuring techniques, etc
07 p1137 A69-18412

Dynamic stability of thin flat plates and applications in ship and aircraft deck construction, studying dynamic buckling for rectangular plate
08 p1415 A69-20665

Lunar soil as building material and extraction of water, oxygen and rocket propellants from lunar materials for lunar colony needs
13 p2352 A69-27907

Thermosetting adhesives properties and structural applications in aircraft, space and automotive use, discussing polymer systems, moisture, surface preparation, aging, etc
14 p2468 A69-29340

Heterocyclic-aromatic organic polymer adhesives used for high temperature structural purposes, discussing processing, testing, formulating and impact on basic research
14 p2469 A69-29346

Mg alloys applications to construction, discussing strength-to-weight ratio of cast and wrought alloys
16 p2801 A69-31787

Aircraft construction materials, discussing aluminum alloys use in Concorde project based on temperature tests, creep and fatigue properties and joint requirements
16 p2801 A69-31791

Civil aircraft projected development regarding materials and structures, discussing new components and fuel contribution to weight and metals and composites for replacing Al
16 p2872 A69-32024

Cellular carbon castings fabrication by carbonization of polyurethane polyfurfuryl alcohol foam for high temperature applications, noting properties
17 p2992 A69-33373

Prestrained material plastic behavior experiments and deformation lines of influence analysis, noting importance in cold working
17 p3067 A69-34146

Airport runway surface construction materials requirements, taking into account factors different from highway pavement
17 p2948 A69-34215

Metal alloys mechanical properties summary for cryogenic applications, considering fracture and thermal behavior, cryogenic structures fabrication and composites applicability
18 p3158 A69-35416

Static dynamic and damage tolerant strengths of advanced materials for VTOL aircraft with emphasis on Ti, cryoformed 301 stainless steels and filamentary composites
[AIAA PAPER 69-764] 19 p3433 A69-35658

Electron beam welding for fabrication of aircraft structures, discussing fatigue strength of Ti and Al alloys and marring and low alloy steels
[SBAC PAPER 12] 20 p3550 A69-37456

Conducting and insulating construction materials at high temperatures for MHD conversion nozzles, noting lifetimes
21 p3751 A69-38456

Loaded bipropellant liquid propulsion system sterilization studies on structural and nonmetallic materials suitability for use in oxidizer
[AIAA PAPER 68-631] 21 p3785 A69-39025

Mounting elements alloys relaxation characteristics at various temperatures, considering effects of scale factor and stress concentrations
23 p4169 A69-41419

Low temperature mechanical properties of structural materials for high energy propulsion systems, using low boiling point propellants as liquid hydrogen, fluorine and oxygen
23 p4177 A69-42159

Fuel cells construction materials selecting and optimizing techniques using diffusion block and differential corrosion concepts
23 p4075 A69-42299

Aircraft Structures and Materials Application - Conference, Seattle, September 1969
24 p4321 A69-43416

Fastener materials selection for high temperature aircraft structures, considering various physical properties influence
24 p4325 A69-43441

CONSULTING

1967 Space Treaty legal aspects of consultation, suggesting international permanent body setup for resolving technical and political matters
20 p3636 A69-37111

CONSUMPTION

U FUEL CONSUMPTION
U OXYGEN CONSUMPTION
U WATER CONSUMPTION

CONTACT LENSES

Contact lenses hazards during high altitude aircraft piloting analyzed via bubble development
23 p4106 A69-41806

CONTACT POTENTIALS

Electromagnetic waves parametric interactions during unsteady Josephson effect as function of wavelength ratio, magnetic field penetration and contact dimensions
02 p0293 A69-11464

Equations for pn junction behavior valid at impurity concentrations beyond nondegenerate range, noting contact potential and carrier density
11 p1938 A69-25306

Optimum metal contact stripe width for CW operation of GaAs junction lasers bonded on copper heat sink
16 p2796 A69-31698

Ion beam sputtering, evaporation and electrical degradation of Al contacted Si solar cells observed in high temperature cyclic tests
19 p3250 A69-35686

Electrochemically passivated Ti/Pd/Ag contacts for Si solar cells tested in humidity stress and temperature cycling
19 p3250 A69-35687

Geometrical model for surface contact area, noting influence of nonlimitations on friction coefficient in elastic deformation
19 p3329 A69-36494

CONTACT RESISTANCE

Contact resistance of In or In-Ga on CdS single crystals
03 p0487 A69-13638

Electrical conductivity of high resistance epitaxial semiconducting films measured by three probe method
04 p0597 A69-14538

Subject classification bibliography for thermal contact resistance
[ASME PAPER 68-WA/HT-18] 05 p0847 A69-16122

Elastic contact between two parallel cylinders with rough surfaces noting contact area, spots and stress distribution
06 p1023 A69-17373

Gunn effect for cathode contacts with interface resistance, developing contact characteristic boundary condition concept for explaining cathode fall and other phenomena
07 p1199 A69-18649

Presprayed metal films influence on visibility and contact resistance of GaAs prior to fusing in Sn, In and lead contacts
10 p1748 A69-24214

Thermoelectric power generators energy output efficiency, discussing thermal and electric contact resistances influence for optimizing parameters
12 p2016 A69-26364

Contact between cylindrical surfaces in thermionic converters, determining thermal resistance and pressure in contact area
14 p2400 A69-29216

Thermal contact resistance measurement at various ambient pressures compared with theoretical predictions with each parameter analyzed over interface by computer program
[AIAA PAPER 69-629] 17 p3073 A69-33299

Terminal characteristics of composite superconductor, taking into account heat transfer to coolant, interface thermal contact resistance and superconductor size
17 p3007 A69-33792

Gold/polycrystalline cadmium selenide film contact found ohmic in darkness and barrier in light, noting potential distribution, electron concentration and energy gap
19 p3384 A69-36480

Metal semiconductor contact resistance determination from measuring voltage drop in current passing through contact and second metallic contact
21 p3780 A69-39046

Electrical sliprings assembly development with low dynamic resistance and long lifetime for space simulation testing, noting wear rate of rings and brushes
[AIAA PAPER 69-1035] 22 p3925 A69-40402

Thermal isolation characteristics of low conductance interstitial materials determined, using test apparatus of axially loaded radiation shielded cylindrical column in vacuum
[AIAA PAPER 68-31] 23 p4239 A69-41889

Potentiometer transient contact resistance determined as function of contacts physical parameters
23 p4166 A69-41996

CONTACTORS

Contactors for helium in dilution refrigerator mixing chamber, discussing design and thermal resistance determination
09 p1493 A69-21429

CONTACTS [ELECTRIC]
U ELECTRIC CONTACTS
CONTAINERS

Containerized freight, discussing means of transport, methods of distribution, suitable aircraft for carriage, economic and social effects and combined air-water-land transport

02 p0228 A69-11887

Aged boric acid coated silica reaction vessels, showing reduced surface effects and high reproducibility in oxidation reactions

02 p0205 A69-12322

CONTAINMENT
U NUCLEAR REACTOR CONTROLCONTAMINANTS
NT RADIOACTIVE CONTAMINANTS
NT TRACE CONTAMINANTS

Chlorine as indicator of terrestrial contamination in iron meteorites, using neutron activation analysis and metallographic observation

08 p1405 A69-20923

Hydrogen laser operation time reduction attributed to hydrocarbon formation on inner surface of storage flask, promoting atomic hydrogen recombination

15 p2634 A69-30942

CONTAMINATION
NT FUEL CONTAMINATION
NT SPACECRAFT CONTAMINATION

Salt water stress corrosion cracks morphology in titanium alloy, discussing crack propagation, brittle nature and chloride contamination effect [SAE PAPER 680642]

03 p0444 A69-13458

Ultrahigh vacuum electron microscope using differential sputter ion pumps to obtain low contamination environment

04 p0599 A69-15016

Microorganism viability in rocket engine combustion environments used to determine probability of biological contamination of Mars by Voyager missions

05 p0714 A69-15949

Split-seam process for inserting sterile objects into isolated sterile environment without contamination as method for sterile spacecraft repair

05 p0714 A69-15950

Mars contamination with terrestrial microorganisms, considering possibility of waste materials ejection from manned orbital vehicles

05 p0714 A69-15951

Microbiological surface sampling methods, noting role in detecting contamination on eating utensils, blankets, sheets, etc

05 p0715 A69-15982

Pollution control forecast, contamination control specialist and systems approach

08 p1265 A69-19808

Tritium contamination reduction in small ion accelerators for neutron production, discussing pumping problems and vacuum systems

12 p2059 A69-26499

Barbados airborne dust collections showing metal fragments and black magnetic spherules contaminants from handling, discussing deep sea cosmic spherules and zodiacal cloud

12 p2075 A69-26964

Earth contamination by returned lunar or Martian material, discussing extraterrestrial biota survival on earth

13 p2210 A69-28467

Avionics clean room workshops, discussing turbulent and laminar flow rooms and contamination monitoring of controlled environment facility

16 p2767 A69-32369

Gas particle concentrations on moon due to solar wind, surface emissions and atmospheric contamination by lunar operations and rocket motor products

18 p3189 A69-34236

Microbial contamination release from impact-fractured solids, examining bacterial spores growth in fractured methyl methacrylate plastic for application to space exploration

20 p3475 A69-37614

Soviet book on fluid contamination influence on aircraft hydraulic systems operational reliability covering friction, particle size, filtration, etc

21 p3649 A69-39530

CONTINENTS
NT AFRICA
NT AUSTRALIA
NT EUROPE
NT NORTH AMERICA
NT SOUTH AMERICA

Economic and scientific reasons for using artificial satellites to establish continental geodetic network, noting continental displacements and terrestrial pole motion observations

[UN PAPER 68-07445] 06 p0917 A69-17069

Circadian rhythms characteristics of healthy human beings as reference standards for comparing investigation data from different continents

23 p4083 A69-41457

CONTINUITY [MATHEMATICS]

Upper semicontinuity of subsolutions of second order elliptic partial differential equations in divergence form with discontinuous coefficients

02 p0270 A69-11548

Integral prediction method for arbitrary continuous function on right hand side of nonhomogeneous linear differential equation with constant coefficients

03 p0455 A69-13022

Stokes phenomenon, considering continuity solution of differential equations across Stokes lines

07 p1174 A69-19220

Tricomi theorem extension concerning intermediate value property of continuous real valued functions of real variable

09 p1533 A69-22797

Theorem for necessary and sufficient condition for continuity of Chebyshev operator

10 p1718 A69-22875

Continuity of optimal control of nonlinear plant, noting search time

21 p3686 A69-38884

CONTINUITY EQUATION

Exponential approximation with piecewise linear error criteria for continuous function over interval

01 p0107 A69-11415

Infinite system of first order integral equations derived from Prandtl boundary layer equation and continuity equation

02 p0231 A69-12059

Algorithm for Navier-Stokes and continuity equations used to derive curvilinear coordinate system

04 p0564 A69-14858

Motion of vapor derived from solid material vaporization and subsequent heating by nonequilibrium continuum radiation, noting continuity equations and energy transfer

04 p0686 A69-14985

Continuity and momentum equations for cosmic ray gas particles in interplanetary region

06 p0992 A69-17379

Simultaneous solution of time-dependent momentum and continuity equations for ions and neutral air in midlatitude F 2 region conditions

07 p1123 A69-18818

Existence and uniqueness to boundary layer continuation problem based on flow equation for steady gas flow

10 p1679 A69-23569

Electron number density LF oscillations for ionized gas identified with periodic solutions to neutral and charged particle plasma continuity equations

11 p1925 A69-24315

Production source of ionization due to low energy electron influx and inclusion in ionospheric continuity equation, noting quiet ionosphere

12 p2066 A69-26112

Elliptic second order equation showing nonequivalent regularity conditions for Laplace and continuous coefficient equations

13 p2288 A69-27743

Simultaneous solution of continuity and heat conduction equations for ionospheric plasma consisting of electrons, atomic O ions and neutral gas species, discussing varying solar flux effects

16 p2849 A69-32082

Simultaneous solution of continuity and heat conduction equations for ionospheric electrons, ions and neutral species for studying F region magnetic storm behavior

16 p2775 A69-32083

Wind velocity and precipitation particle terminal fallspeeds component determination from continuity equation for data collected by Doppler radar

17 p2919 A69-33162

Transport properties of free turbulent mixing of subsonic coaxial streams by introducing environmental distributions in integrals of momentum, energy and species continuity equations [AIAA PAPER 69-681]

17 p2956 A69-33495

Canopy filling time for parachutes under infinite mass conditions, using continuum equation and parachute inflation concept [AIAA PAPER 68-12]

17 p2902 A69-34032

LF oscillations in electron number density of ionized deuterium, Ne and He identified from particle continuity equation

22 p3986 A69-40759

Midlatitude F region continuity equation solutions, including east-west electric field effects on electron density

22 p3941 A69-40917

CONTINUOUS NOISE

Continuous noise level effects on stabilized escape conditioning in male albino rats

24 p4262 A69-42948

CONTINUOUS RADIATION
NT MODULATED CONTINUOUS RADIATION

Continuous wave laser absolute power measurement by calorimeter consisting of wire wound in shape of cone

01 p0078 A69-10029

Continuous wave solid state lasers active elements temperature fields calculated by differential equations

01 p0089 A69-10105

Continuous nonresonant visible radiation from Ar ion laser by utilization of wide bore, wall stabilized gas discharges, noting long time frequency stability

01 p0091 A69-10815

Continuous laser beam power output meter based on wire resistance thermometry method

01 p0081 A69-10822

One dimensional expansion of laser beam, using pairs of prisms with continuous wave output

01 p0091 A69-10852

Free bounded continuum processes effect in nonequilibrium gases of finite continuous opacity, noting curves of growth for finite plane parallel layer emission lines

01 p0121 A69-10959

LF continuous wave rocket propagation in D region presented in terms of electron density profiles

01 p0076 A69-11232

Polarization of nightglow, line vs continuum

02 p0235 A69-11428

Continuous wave GaAs injection lasers operation at high temperatures shown possible by using available threshold current densities with suitable heat sink materials

02 p0255 A69-11710

Solar continuum intensity determination in middle IR, obtaining solar disk center brightness temperature measurement by comparison with black body model

02 p0318 A69-12041

Additive noise measurement in microwave power amplifiers under continuous wave and pulsed conditions

02 p0221 A69-12454

High power output CW laser oscillation measured at 4416 Å laser transition in Cd 2 using single isotope of Cd 114

02 p0259 A69-12653

Tunable optical parametric oscillator using argon laser CW output as pump and lithium niobate as nonlinear crystal

02 p0260 A69-12701

High power output from submillimeter continuous wave gas laser

04 p0609 A69-14289

Continuum radiation of quasars, adopting cosmological interpretation of red shift

04 p0648 A69-14565

Relaxation method for separation of continuous electron/ion recombination spectrum from electron spectrum in nonequilibrium gas discharge plasma

04 p0639 A69-15369

Emission continuum intensity of negative nitrogen ion in nitrogen and air plasmas

04 p0639 A69-15370

Continuous absorption of coefficient hydrogen-carbon plasma at 40,000 degrees K and 70 atm in 230-460 nm spectral range

04 p0639 A69-15371

Continuous radiation production in positive plasma column of inert gas considered as manifestation of plasma electrons bremsstrahlung from interaction with gas atoms

05 p0800 A69-15741

High power continuous and quasi-continuous wave UV generation by ADP and KDP crystals in argon-ion laser cavity [IEEE PAPER B-1]

05 p0773 A69-16308

Continuous UV noble gas ion lasers, noting small signal gain and power output limit at various current densities for strong lines [IEEE PAPER L-1]

05 p0775 A69-16321

Continuum position location and total line absorption in solar spectrum, using Houtgast high dispersion intensity measurements of UV region

05 p0828 A69-16611

Optical mean energy distribution of quasars, discussing red shift effects, significance of physical origin of optical continuum radiation and K-term magnitude determination

06 p0999 A69-16975

Radial electron concentration profile determination by spectroscopic examination of continuous plasma radiation of pulsed discharge in capillary

06 p0964 A69-17253

CW room temperature laser using lanthanum sodium molybdate crystals with positive trivalent Nd ion impurity

06 p0934 A69-17262

CW laser mode steady excitation and narrow bandwidth obtainable by highly stable pumping and stable temperature of active element

06 p0934 A69-17681

High power noble gas CW UV ion laser with W disk structure, showing continuous UV output limitation by optical degradation effects

06 p0936 A69-17900

Nonequilibrium low temperature plasma theory for ionization and particle distribution based on discrete and continuous spectra states, discussing electron distribution function

06 p0969 A69-17906

Radio source CP 1133 at 408 Mc, noting upper and lower limit to continuous emission between pulses

06 p1009 A69-17969

X band CW traveling wave tube developed for communications, ECM and plasma research, discussing design, performance and gain ripple diminution

07 p1094 A69-18425

Avalanche diode oscillators efficiency of continuous wave operation in transit time mode and high current multiresonant modes

07 p1098 A69-18456

Iodine IR laser, discussing CW emission obtained at various wavelengths and attributed to electronic transitions in atom

07 p1154 A69-19082

Gain enhancement effect of CO on carbon dioxide CW laser performance by accelerating relaxation of bending mode

07 p1155 A69-19088

Frequency modulation of CW mm-wave IMPATT diode oscillator with wide band tunability and related harmonic generation effects

07 p1106 A69-19146

Output and beat frequency of carbon dioxide laser with various resonator configurations realizing single mode operation

07 p1156 A69-19157

Solar photosphere model with two stream columnar representation of granulation for predicting continuous radiation field

07 p1217 A69-19238

Radiative opacity in stellar atmospheres, discussing effect of UV continuum on photospheric radiation field

07 p1221 A69-19393

Stimulated emission of water cooled CW Nd doped lanthanum fluoride at room temperature

08 p1323 A69-19945

Radiative capture of electrons by chlorine, bromine and iodine atoms in shock heated plasma seeded with sodium halides from absolute intensities in continuous emission

08 p1355 A69-20735

Passivated metal semiconductor IMPATT diode for microwave CW oscillation

08 p1286 A69-20862

CW helium-neon laser used to detect and measure vibration frequencies of uniform diffuse surfaces

09 p1515 A69-21430

Continuous signal over finite time intervals represented by impulse functions of linear channel

09 p1454 A69-21723

Continuous radiation spectrum of Taurus A in far IR using indium antimonide detector of Rollin type

09 p1597 A69-22156

Intensity distribution in principal mode of TEM oscillations at various gain amplification levels, plotting intensity distribution generated by argon ion CW laser

09 p1520 A69-22685

Pulsed and CW lasers glass crystals temperature fields determination, including tangential and axial thermal stresses

10 p1702 A69-23428

Self focusing of CW argon laser beam due to absorptive heating in crown glass, emphasizing time dependence of beam diameter as function of distance

10 p1706 A69-24009

Polarization observation of star BL Lac continuum by multichannel scanner, noting photoelectric UVB observations and identification with radio source

10 p1785 A69-24090

Dye lasers CW operation feasibility, showing sufficient quenching of rhodamine 6G triplet state by oxygen dissolved in methanol

11 p1893 A69-24344

Gas lasers coherence properties and availability for holography, discussing continuous power output of He-Ne, Ar and Kr ion lasers

11 p1895 A69-24680

High power CW carbon dioxide laser saturation and discharge conditions analyzed by rate equation

11 p1898 A69-25050

Far IR CW gas laser design for maximum output, discussing pulsed operation, wavelength measurement and radiation detection

11 p1898 A69-25051

High CW power K-band Gunn oscillators attained through control over doping level, profile and GaAs epitaxial layer thickness

12 p2036 A69-25907

Phase pulsations between normal frequencies and combination tones in CW gas laser output, analyzing observations by scanning interferometer

12 p2108 A69-26635

Pulsed or continuous radiation generated in laser having active element of neodymium glass fragments

12 p2109 A69-26715

Far IR and millimeter solar continuum, analyzing flatness of limb darkening curves and brightness temperature near minimum

13 p2341 A69-27591

Radio emission from high level transitions in hydrogen calculated by superposing emission lines on background continuum, using Gaunt factor for free-free emission

13 p2327 A69-27596

Quasi CW solid state doped lasers excited by pyrotechnic pump sources with potassium perchlorate oxidant and zirconium fuel, noting power to weight ratio

13 p2272 A69-28116

CW lasers based on composite yttrium fluoride type crystals, noting large number of intense emission bands

13 p2273 A69-28316

Contour maps of Milky Way continuum radiation at 1410 and 2650 MHz from low latitude survey, listing sources with estimates of flux density

14 p2526 A69-29772

Calorimeter for CW laser output power absolute measurement, discussing operation principles, structural features, circuit and accuracy

15 p2608 A69-30320

Activity in Crab Nebula from 200-inch continuum and polarization plates, discussing nature and motion of wisps

15 p2691 A69-30758

Optimum metal contact stripe width for CW operation of GaAs junction lasers bonded on copper heat sink

16 p2796 A69-31698

Zinc diffused GaAs avalanche diode high CW power and efficiency in normal mode

16 p2760 A69-32015

Relaxation method for separation of continuous electron/ion recombination spectrum from electron spectrum in nonequilibrium gas discharge plasma

16 p2822 A69-32116

Emission continuum intensity of negative nitrogen ion in nitrogen and air plasmas

16 p2822 A69-32117

Continuous absorption of coefficient hydrogen-carbon plasma at 40,000 degrees K and 70 atm in 230-460 mm spectral range

16 p2822 A69-32118

Si planar IMPATT diodes anomalous mode continuous wave UHF oscillations, noting DC density and DC/RF power conversion efficiency

17 p2934 A69-32846

Q switching of CW 337 mu maser, gain factor measurements for pulse discharges and data on saturation and time dependence

17 p2981 A69-33088

Information storage of multichannel analyzer of continuous and pulsed processes

17 p2939 A69-33900

Milky Way continuum radiation at 4170 MHz using parabolic antenna, mapping discrete sources concentration at galactic equator

18 p3200 A69-34996

Solid state CW laser frequency control during operation, discussing emission properties and laser applications

19 p3331 A69-35864

Mode coupling effects in CW gas ring lasers, considering excitation density pulsations, traveling waves dispersion, polarization, etc

19 p3334 A69-36046

Continuous IR radiation source using electrically heated Mo ribbon, comparing emission from V shape and flat portions

19 p3313 A69-36491

Markarian galaxies with strong UV continua, discussing emission spectra, red shift, absolute magnitudes, etc

19 p3426 A69-36577

Solar disk edge polarization rate determined by applying Feautrier method to transfer equations for polarized radiation

19 p3427 A69-36728

Gas mixtures CW gain characteristics at 337 mu as function of pressure, current, mixture and flow rate, considering HCN laser systems

20 p3552 A69-36995

Ionosphere absolute phase height measurement methods independent of virtual height, using fixed frequency CW emission and pulsed sounding

20 p3520 A69-37032

Continuous signal over finite time intervals represented by impulse functions of linear channel

20 p3488 A69-37459

Bistatic auroral backscatter communications conducted by recording CW transmissions from beacon transmitters to study radio aurora

21 p3709 A69-38498

Output power of CW lasers employing HCN and water vapor active medium

22 p3959 A69-39958

Type V continuum emissions from solar flares suggested as due to synchrotron radiation from protons spiraling in magnetic field, noting Type III emission

22 p4003 A69-40301

Xenon plasma continuous illumination sources design and operation for night and color aerial photography covering photogrammetric resource surveys, ground traffic, flight paths, etc

22 p3950 A69-41000

Carbitron locked oscillator with wide electronic tuning range, describing CW operation characteristics and application to ground station microwave transmitters

23 p4135 A69-41302

Xenon laser CW operation on unclassified spectral lines of high ionization states, using laser induced spectroscopy

23 p4172 A69-41399

Nitrogen-carbon dioxide-helium lasers CW operation at various pressures and N flow rates

23 p4173 A69-41496

Closed cycle gas cooling techniques for self contained CW kilowatt carbon dioxide laser, relating output power to flow velocity and input power

23 p4173 A69-41497

Intensity of optical pulses from CW GaAs injection lasers observed with fast sampling techniques

23 p4173 A69-41500

CONTINUOUS WAVE RADAR

Radar cross section laboratory, discussing experimental techniques, electromagnetic range and pulse, FM/CW and CW radars

03 p0385 A69-12912

Digital method to produce radar reflectivity from analog audio frequency Doppler data extracted from terrain echo signal of CW scatterometer radar

15 p2572 A69-31111

Aircraft electromagnetic position finding system based on Doppler shift of CW carriers

17 p3002 A69-34078

Millimeter wave pseudorandom coded CW meteorological radar for precipitation drop size spectrum analysis and cloud studies, discussing overall system design

23 p4115 A69-41531

CONTINUUM FLOW

Monte Carlo direct simulation for treating rarefied supersonic flows about bodies in transitional regime between continuum and free molecular flow

02 p0189 A69-12523

Argon flow characteristics in converging nozzle in continuum, slip and free molecular regimes

[ASME PAPER 68-WA/FE-9]

05 p0698 A69-16089

Basic frequencies of uniformly almost periodic solutions of differential equations extended, noting applications

05 p0698 A69-16089

- tion to orbit closures decomposition of almost periodic continuous flows
07 p1174 A69-18733
- Continuum flow boundary in freely expanding jet estimated from molecular mean free path and modulus of random motion mean velocity
10 p1679 A69-23425
- Boltzmann H theorem and related mathematical topics, noting applications to subsonic gas flow and continuum flow around and over body
11 p1870 A69-25008
- Argon flow characteristics in converging nozzle in continuum, slip and free molecular regimes [ASME PAPER 68-WA/FE-9]
14 p2390 A69-29445
- Gas visco seals performance analyzed for continuum flow regime, noting coefficient agreement with laminar flow analysis [ASLE FICFS PREPRINT 34]
15 p2621 A69-30494
- Hypersonic slender cone zero angle of attack drag in rarefied continuum and noncontinuum flow in shock tunnel, indicating body dimension influence in transition regime [AIAA PAPER 69-711]
17 p2891 A69-33445
- Strong shock wave structural model, considering near molecular beam, upstream hypersonic and downstream subsonic flows and beam-continuum conversion by collision
18 p3120 A69-34457
- Small continuum electrostatic probes calibration and operation in ionized plasma flow with sheath dimensions larger than boundary layer dimensions
19 p3304 A69-35719
- Gas dynamics in transition regime between continuum motion at high gas density and free particle motion at low density limit
19 p3300 A69-36658
- Comet heads gas dynamics, analyzing coma or head region as continuum source flow of dusty gas
19 p3428 A69-36807
- ### CONTINUUM MECHANICS
- Two dimensional structural model of micropolar continuum involving orientable points joined by extensible and flexible rods
01 p0169 A69-10810
- Linear stationary thermoelasticity equations for Cosserat continua, discussing static and kinematic conditions, anisotropy and centrosymmetric isotropy equations
02 p0336 A69-11557
- General theory of constitutive equations for rational mechanics of deformation and flow
02 p0341 A69-12251
- Thermodynamics of viscoplastic materials under dynamic loads within framework of continuum mechanics of materials with memory
02 p0343 A69-12281
- Viscoelastic materials thermomechanical behavior, discussing constitutive equation and derivation of stress tensor and entropy density from viscoelastic potential
02 p0344 A69-12294
- Thermodynamics of directed continuous media, discussing kinematics, equations of state, entropy inequality and material objectivity principle
02 p0354 A69-12611
- Nonlinear problems in mechanics of deformable media and qualitative analysis of properties of mathematical models of physical processes involved
03 p0467 A69-13749
- Stability margin difficulties in equilibrium application to continuum mechanics
03 p0418 A69-13816
- Thickness twist and face shear vibrations of laminated layer, determining frequencies from stress equations of motion, constitutive equations and boundary conditions [ASME PAPER 68-WA/APM-10]
04 p0668 A69-14392
- Book on continuum theory of inhomogeneities in simple bodies
05 p0833 A69-15727
- Mathematical theory for describing mechanical behavior of continuous media based on principle of determinism for stress
05 p0833 A69-15729
- Nonlinear field theories for continuum mechanics noting heat, kinematics, isotropic materials, viscometric flows, elastic bodies, thermodynamics and wave motion
05 p0792 A69-15768
- Models of continuous media with internal degrees of freedom based on Lagrangian variational principle
05 p0793 A69-15775
- Book on continuum mechanics covering elasticity, fluid mechanics, plasticity and viscoelasticity, emphasizing basic concepts
05 p0843 A69-16713
- Simple dipolar stresses, noting effect of antisymmetry on equations of motion and energy equation
06 p1022 A69-17239
- Unified methods based on dislocation theory for direct solution of problems pertaining to physical properties of metals
06 p0944 A69-17502
- Complementary variational principles for boundary value problems in continuum mechanics of solids, obtaining generalized Hamilton canonical formalism
07 p1232 A69-19173
- Thin rods and shells elastic analysis, using Cosserat continua for representing bodies in kinematics and balance and constitutive equations
07 p1234 A69-19382
- Minimum theorems in elastoplastic theory extended to continua for plastic strains governed by holonomic and nonholonomic stress-strain laws
07 p1235 A69-19442
- Linear analysis of strain in continua in terms of one-one correspondence, relative displacement and stretch dyadic
07 p1236 A69-19445
- Radiative transfer equation solution for spectral line formed in two dimensionally varying atmosphere extended to continuum radiation in inhomogeneous atmospheres
08 p1386 A69-20077
- Relativistic kinematics analog model for deformable continua, introducing deformation gradient and tensors
08 p1416 A69-20693
- Families of eigenfunctions concept for stress and strain tensors of proper motions in continuous isotropic medium, considering vortices and gradients
08 p1417 A69-20752
- Circle theorem extensions and applications to mechanics of continua, noting supersonic and subsonic compressible fluid flow
10 p1723 A69-22877
- Finite element concepts for continuum theory of shells, noting bilinear approximation for displacement and fundamental decomposition principle for large deflection
10 p1794 A69-22891
- Mechanics of generalized continua - Conference, Freudenstadt and Stuttgart, August and September 1967
10 p1798 A69-23146
- Cosserat continuum and elasticity models of dynamics of composite materials, analyzing dispersive longitudinal waves
10 p1798 A69-23148
- Stress concentration in Cosserat continua based on model of six elastic constants in linear isotropic and notch case
10 p1799 A69-23150
- Concentrated loads in elastic Cosserat continuum involving body moments and small deformations
10 p1799 A69-23151
- Dual continuum model of nonelastic processes in elasticity and dislocation theory, including incompatibility effects of interaction forces between structural elements
10 p1799 A69-23152
- Continuum theory of dislocations and internal stresses in generalized Cosserat continuum as theoretical model for crystals
10 p1799 A69-23153
- Continuum theory of dislocations and plasticity in crystals, analyzing stress fields in elastoplastic materials
10 p1799 A69-23154
- Modified Rayleigh-Ritz method for prediction of stress concentration in elastostatic problems for elastic continua, noting plate bending
11 p1969 A69-24413
- Damping properties of nonlinear viscoelastic solids with applications to vibrating continua, using Gauss principle of least constraints
11 p1970 A69-24605
- Linear two and three dimensional boundary value problems in mechanics of continua for multiply connected regions
11 p1972 A69-24651
- Continuum mechanics analysis of fractures and crack extension, discussing solids elasticity, plasticity, boundary value problems, etc
11 p1974 A69-24670
- Nonlinear theories of deformable surfaces as two dimensional generalized continua applied to elastic shells, emphasizing elastic Cosserat surface
11 p1978 A69-24805
- Continuum theory for thin elastic shells with local structural effects, emphasizing shell constituted by Cosserat material
11 p1978 A69-24809
- Analytical expressions for Gaussian constraint of continuum, using continuity conditions as equations of internal geometric couplings
11 p1984 A69-25170
- Transient dynamic response of linearly viscoelastic structures and continua, presenting finite element displacement formulation
11 p1993 A69-25528
- Plane surface finite area deformation tensors in continuum mechanics permitting separation of volume and shape changes in constitutive equations
11 p1994 A69-25603
- Computationally stable solution of finite element analysis of elastic-plastic response of nonlinear discrete structures loaded beyond yield load
12 p2185 A69-26819
- Crack growth and crack initiation in cylindrical specimens subject to low cycle strain controlled tension-compression induced fatigue, noting measurement techniques
12 p2188 A69-26914
- Relativistic kinematics of continuum motion by invariant derivatives of deformation measures, discussing rigid body motion in Born sense
12 p2189 A69-27116
- Continuum mechanics for brittle fracture analysis in metal structures, discussing plastic limit loads
13 p2275 A69-27228
- Laminar MGD electrode boundary layer of thermal nonequilibrium plasma from collisionless Langmuir sheath and continuum theories
13 p2310 A69-28031
- Elastic materials with particle interactions of finite range, establishing continuum field and constitutive equations from particle mechanics
13 p2371 A69-28674
- Linear elastic structural analysis for one, two and three dimensional continua [ASME PAPER 69-DE-13]
14 p2531 A69-28843
- Two fluid continuum theory of incoherent scattering extended to include unequal electron and ion temperatures, considering backscatter power dependency on collision frequencies
14 p2510 A69-28946
- Electromagnetic scatter from perturbed continuous medium, expressing problem in terms of periodic functions instead of conventional power series
14 p2414 A69-29513
- Variational principles of solid mechanics for finite element analysis of solid continua
15 p2705 A69-30429
- Couple-stresses effect on stress concentration of plate containing infinite row of holes, solving linear elastic problem in isotropic Cosserat continua for plate
15 p2708 A69-30640
- Book on continuum mechanics covering concepts of stress and strain, constitutive equations, field equations and boundary conditions in fluids and solids, elasticity, etc
17 p3005 A69-33323
- Mechanics and thermodynamics equations for two dimensional continua, discussing applications
17 p2994 A69-33391
- Quasi-static crack growth in viscous bodies analyzed by continuum mechanics, rheological models and energy equation, discussing fine structure
18 p3215 A69-34570
- Models of continuous media with internal degrees of freedom based on Lagrangian variational principle
18 p3173 A69-35028
- Dynamic reciprocity relationship for linear directed continuous viscoelastic media, using Stieltjes convolution
19 p3373 A69-36307
- Burger condition for distortion field of dislocation lines in continuous medium, considering arbitrary shape in arbitrary motion
19 p3439 A69-36477
- Book on continuum mechanics and hydrodynamics covering elasticity, plasticity, thermodynamics, solid and structural mechanics, aerodynamics and gas dynamics
19 p3441 A69-36771
- Solid and structural mechanics theories noting continuum mechanics role
19 p3443 A69-36776
- Body relations in continuum mechanics of solids, examining temperature influence varying in time and space
19 p3444 A69-36805

Analytic functions representation and application to theory of singular integral equations in continuum mechanics, noting Cauchy kernels and boundary value problems

19 p3361 A69-36813

Continuous particle media on basis of microstructure, discussing granular media deformation, elastic media dilatation, turbulent flow and dilute suspensions

19 p3446 A69-36833

Adjoint system for determining equilibrium stability of elastic continuum subjected to follower type surface tractions

19 p3446 A69-36835

Static theory of fibrous surface media based on continuum mechanics, neighboring fibers noninteraction principle and additivity of mechanical properties

19 p3447 A69-36858

Finite elements general theory applied to wave propagation, gas kinetics, nonlinear partial differential equations, continuum mechanics and fluid dynamics

20 p3567 A69-36948

Continuum mechanics of micropolar fluids and solids, discussing thermodynamical restrictions on elasticity and viscosity coefficients, deriving field equations and boundary conditions

20 p3624 A69-37582

Constitutive equations for homogeneous viscous fluid and Kelvin-Voigt viscoelastic solid in electromagnetic field, using linear irreversible thermodynamics and continuum mechanics

21 p3851 A69-39289

Internal interactions of continua and concept of thermal isolation, discussing second law of thermodynamics

22 p4050 A69-40450

Continuum fracture concept indicating essential surface energy interpretation difference in otherwise similar adhesive and cohesive failures

22 p3974 A69-40760

CONTINUUMS

Equations of state for continuous media, using variational principles within framework of relativity theory

12 p2131 A69-26972

Thin disk galactic models small oscillations, discussing frequency spectra and types of continua

18 p3196 A69-34551

Sunspot penumbra model in hydrostatic equilibrium accounting for continuum and Fraunhofer lines observations

22 p4019 A69-40290

Sunspot position in H alpha core relative to continuum, discussing height differences between H alpha core and continuum levels

22 p4019 A69-40291

CONTOURS

Iterative transfer of boundary values to fictitious contour in numerical solution of partial differential equations [ONERA-TP-646]

03 p0454 A69-12874

Titanium fuselage skin contouring to shallow compound curvature of supersonic aircraft by elastic draping, shot peen forming and cold stretching, discussing residual stresses

09 p1512 A69-22374

Maximum principle for infinitesimal deformations of convex surface with nonnegative Gaussian curvature, noting application to rotation and displacement diagrams

13 p2361 A69-27741

Holographic image range contouring produced by multifrequency emission from resonant output reflector in pulsed ruby laser cavity

20 p3540 A69-37733

Photogrammetric contours plotting from aerial color films

22 p3944 A69-40045

Automatic contour plotting for orthoprojector based on adjacent profiles and linear interpolation

22 p3951 A69-41248

Multiple index high contrast holographic contouring technique compared with analogous multiple frequency system

23 p4164 A69-41628

CONTRACT MANAGEMENT

Lithium-doped silicon solar cells development for radiation environments, discussing contractor functions, dopants, etc

19 p3251 A69-35692

C-5A transport aircraft airframes manufacture, discussing Lockheed profits, contract disputes and Cheyenne helicopter contract cancellation

20 p3640 A69-37355

Maintainability as design requirement in system specifications and contracts, noting MIL-STD-471 program of maintainability demonstration tests

20 p3551 A69-38268

CONTRACT NEGOTIATION

Human engineering program plans for Phase 3 of SST Development Program in accordance with airframe and engine contracts

01 p0019 A69-10451

Incentive contracts design covering cost estimates, technical performance, realistic programs and multiple incentive arrangements

09 p1626 A69-22776

Incentive provisions used by mutual agreement between purchaser and contractor for project management covering planning, control, financial, technical and personnel functions

09 p1626 A69-22777

Nuclear power plant licensing, discussing public safety considerations by AEC and applicant responsibility in assuring freedom from undue risk

10 p1723 A69-23398

Value engineering proposal costs sustained by maintenance and overhaul industry in government contract negotiations, discussing reimbursement and proposed central agency

13 p2383 A69-28099

Value engineering and component/products improvement incentive contract clauses role in defense product quality improvement

13 p2383 A69-28100

Systems engineering approach to aerospace product defects minimization, discussing scope, contract development, mainstream functions, component development, design data and subsystem integration

15 p2719 A69-30085

Procurement procedures in management planning, discussing document flow charts, contract negotiation, etc

15 p2719 A69-30314

Cost plus award fee contracting incentive system based on after fact evaluation of performance effectiveness

15 p2720 A69-30426

Avionic subsystems warranty costs estimates, considering reliability prediction and hardware recycling

18 p2322 A69-34506

Cost risk management procedure in defense industry contracting, including risk percent limits and identification in proposals, specifications relief, escalation clauses, etc

18 p2323 A69-34655

Optimized contracting for systems engineering management, discussing industry views, scope, application, depth, procurement and performance measurement

19 p3454 A69-36005

Structure and scoring method for judging alternatives in contract selection

20 p3640 A69-38023

CONTRACTORS

Construction practice for hot-mix bituminous pavements covering production, composition, application and quality control

01 p0057 A69-11276

Space vehicle subcontracted components reliability attainment, discussing reliability process specifications, motivation, product reliability and feedback programs

15 p2723 A69-31139

Aerospace programs cost analysis system, using contractors accounting records as data source [AAS PAPER 69-465]

24 p4416 A69-42801

CONTRACTS

Project management in complex research, discussing incentive contracting decision model and resources allocation

02 p0356 A69-12476

Federal government contracting, discussing legality of NASA service contracts

05 p0850 A69-15987

CONTRAILS

Rocket ejected vapor trails structure in lower atmosphere showing no evidence of atmospheric turbulence

15 p2602 A69-31393

CONTRAST

U IMAGE CONTRAST

CONTROL

Linear differential equations zero solution stabilization by control formed as linear combination of measured coordinates of object

03 p0408 A69-12972

Nonsteady coordinates of linear delay system determined from observable linear combination of phase coordinates

04 p0583 A69-15094

Matrix Riccati and matrix quadratic equations in problems of stochastic control and filtering

05 p0740 A69-16601

Control systems digital simulation based on coupling of prediction correction procedure with integration and differentiation procedure, discussing simulation errors

08 p1296 A69-20110

Space flight fuel consumption optimization as function of acceleration of nozzle control

10 p1666 A69-22919

Observability of phase state of nonlinear control system noting Liapunov function

13 p2238 A69-27742

Sensitivity function in time domain defined for control system design

13 p2238 A69-27936

Delta modulated control system model for determining oscillation modes at sampling instants

13 p2221 A69-27962

Asymptotic control theory for two point boundary value problems, considering Euler equation

14 p2425 A69-28904

Hamilton modified principle applied to nonlinear control problems including time delay, servosystem with ideal relay and liquid level control

15 p2583 A69-31304

Starting weight increments in aircraft designs having various structural features and dimensions

16 p2735 A69-32144

Soviet collection of papers on complex control systems covering discrete systems for random processes, self adaptive systems, linear system stability and stabilizing resonance shell

19 p3285 A69-35888

CONTROL BOARDS

Operator handedness effect on control display movement stereotypes

02 p0203 A69-12212

Aircraft instrument panel lighting color and intensity preference by pilots for taxiing, takeoff, cruising flight and landing

05 p0715 A69-16622

Aircraft instrument panel lighting, comparing red and white colors for general and peripheral vision

05 p0715 A69-16623

Design and performance of large vacuum system with central control desk to study plasma dynamics, discussing visual monitoring at desk

07 p1116 A69-18261

Control-display panels design for accurate response with electronic and mechanical equipment, showing display stimulus and control response correspondence in rectangular configuration arrangement

07 p1070 A69-18907

Displays and controls requirements in manned spacecraft to integrate man into vehicle system, noting man capability for task diversity

08 p1312 A69-19968

Control operation time found dependent on gloves, physical characteristics of control and type of required operation

10 p1648 A69-23180

Glove characteristics effects on manipulability, finding operation time differences between gloved and barehanded operation dependent on type of required control operation

10 p1648 A69-23181

Minimum dimensions of circular nondetent knobs mounted on concentric shafts in case of intolerable frequent inadvertent operation of adjacent coaxial knobs

17 p2916 A69-34005

Optimum knob crowding, measuring reach time, turning time, inadvertent touching and influence of knob spacing, diameter and configuration

17 p2916 A69-34006

CONTROL DATA (COMPUTERS)

Space vehicle data system synthesizer (SVDSS) for dynamic calibration of automatic control and checkout systems during prelaunch and countdown operations

21 p3680 A69-39633

CONTROL EQUIPMENT

NT CRYOSTATS

NT PRESSURE REGULATORS

NT SERVOAMPLIFIERS

NT SPEED REGULATORS

NT THERMOSTATS

Conditions for nonlinear control systems observability determined for use in identification procedure and in designing control unit

01 p0049 A69-10206

Soviet book on design of multidimensional automatic control systems, covering structural circuit synthesis and individual element characteristics

01 p0053 A69-10995

Modular three dimensional mockup technique for economizing and facilitating design of control and display equipment

02 p0202 A69-11953

Equalization of multiple electromagnetic shakers for environmental vibration testing, using analog computer [JPL-TR-32-1364]

02 p0229 A69-12374

Tracking conditions for observability of nonlinear controlled systems with smooth characteristics

03 p0409 A69-13069

Solid state power supplies for turbine control and instrumentation, discussing control system manufacturer requirements and reliability specifications

03 p0368 A69-13432

Self oscillating pulse relay control system investigated by approximate method for harmonic linearization of nonlinearities, noting external effects

03 p0410 A69-13684

Book on control systems theory and applications covering artificial intelligence, linear stochastic systems, trajectory decomposition, etc

04 p0581 A69-14567

Multivariable automatic control systems stability, discussing applicability of Nyquist theorem and alternate frequency criterion

04 p0581 A69-14601

Dynamics of single loop nonlinear sampled data systems with integrator, deriving equations of periodic motions and stability conditions by means of point transformations

04 p0583 A69-15135

Nonlinear phase locked automatic frequency control system dynamics, noting asymptotic stability of equilibrium state in whole

04 p0559 A69-15137

Steady state response of inertialess discrete multivariable extremal system with noise, noting stepwise search systems

04 p0583 A69-15139

Frequency controlled time delay network for broadband phased array antenna steering

04 p0580 A69-15469

Defect localization in complex plants applied to damage cause determination and economic criteria

05 p0767 A69-15765

Stabilization of steady motions of nonlinear controlled systems with two purely imaginary roots, using Liapunov stability theory

05 p0794 A69-15790

Fluidics research and development of control elements and components

05 p0704 A69-16003

Aircraft turbine engines operation and control, discussing technology, simulation and system developments

05 p0812 A69-16528

Book on electric elements and circuits for automatic control, discussing electric machines as control loop elements, stability criteria and synthesis, electric drives, etc

05 p0739 A69-16545

Pulsed control systems stability with frequency pulse modulation analyzed by Liapunov direct method

05 p0740 A69-16670

Thermal performance of pressure transducers, accelerometers, displacement transducers, resistance thermometers and control mechanisms for NERVA reactor

06 p0956 A69-16885

Clearing and blocking control over frequently overadjusted automatic equipment in precision machine and device construction

06 p0931 A69-17692

Self organizing trainable logical networks (TLN) as stable controllers in multiaxis vehicle control problem, reviewing TLN concepts and training theory

07 p1070 A69-18388

Control system utilizing digital and linear integrated circuits for low power testing of Pewee 1 reactor of Rover program [IEEE PAPER 28-6]

07 p1179 A69-19188

Book on feedback control theory for engineering and applied physics noting signal theory, servomechanisms, transfer functions, system stability and Nyquist diagrams

08 p1295 A69-19841

Operational reliability of manual and automatic flight control systems and components and current safety standards

08 p1255 A69-20720

Fluidic devices for closed loop control of gas turbines [AGARDOGRAPH-118]

08 p1258 A69-20956

Laser triggered spark gap and Pockels cells producing consistently repeatable controlled duration pulses

09 p1515 A69-21427

Space guidance and control system components, noting control moment gyro, actuator, brushless DC motor, electrically supported gyro and laser gyro

09 p1500 A69-22434

Nonlinear one element control system design based on correlation between responses of linear systems

09 p1475 A69-22537

Frequency domain stability criteria accuracy for application to fourth order nonlinear position control system

09 p1475 A69-22591

Vortex fluid devices in control systems, considering electrical, mechanical and hydraulic systems

09 p1443 A69-22740

Test stand final control element for fluid flow application, noting analog control valve with digital to analog conversion and digital actuator

10 p1671 A69-23259

Microelectronic data and remote control function transmission system for wind tunnel testing of aircraft dynamic response to gusts and turbulence

10 p1672 A69-23283

Computer controlled data acquisition and control system /DACs/ for wind tunnel applications, describing system and programs

10 p1673 A69-23286

Fluidic control technology compared to other control modes, describing fluidic functions and devices

10 p1636 A69-23402

High gain proportional and bistable fluidic amplifier design, noting high impedance role in pressure sensing and computer circuits in aircraft engine control

10 p1638 A69-23555

Human pilot adaptation in simulated multiloop VTOL hovering task with series loop closure model

10 p1650 A69-23878

Real time electronically scanned radar control using digital computer with input and output conversion for information handling, noting interface equipment

11 p1834 A69-24544

Digital data transmission techniques and complex instrumentation systems design noting control, identification, synchronism and error reduction

11 p1834 A69-24545

Parametric damping of oscillations in second order automatic control systems, taking into account control function constraints

11 p1857 A69-24556

Asymptotic method for single and multifrequency oscillations of quasi-linear control systems with distributed parameters and delayed time coordinate

11 p1916 A69-24766

Flexible control module for real time automated checkout requiring programming by personnel with strong software background

11 p1843 A69-25072

Initial conditions estimation problem for nonlinear system asymptotic stability and satisfaction of output constraints on state variables

11 p1909 A69-25290

Digitally controlled formant /spectral maximum/ generator for terminal analog speech synthesizer

11 p1852 A69-25292

Kozhevnikov optimality principle for optimum averaging of discontinuous stochastic control systems extended to include intensities of discontinuities

11 p1966 A69-25329

Parachute deployment load control by use of line ties from rocket sled tests

11 p1823 A69-25386

Spacecraft design for minimization of structure interaction with control system, noting susceptibility of extendible booms to solar environment

11 p1967 A69-25500

Tracking system for gain and time delay parameter measurements of compensatory control crossover model

12 p0222 A69-25930

Multivariable control systems - Conference, Duesseldorf, October 1968, Volume 2

12 p0245 A69-26058

Synthesis of multivariable control systems at minimal integral square quality functional

12 p0246 A69-26061

Digital computer analysis of multivariable control system in frequency domain, using operational array technique programming method

12 p0246 A69-26064

Computer aided design of linear multivariable control systems applied to VTOL aircraft stability augmentation

12 p0213 A69-26068

Multivariable control systems - Conference, Duesseldorf, October 1968, Volume 1

12 p0246 A69-26069

Liapunov functions applied to stability analysis of nonlinear multivariable direct and indirect control systems with time lags

12 p0248 A69-26079

Third order multivariable control systems calculation with linear differential equations describing plant for design and digital optimization

12 p0249 A69-26085

Multivariable control systems - Conference, Duesseldorf, October 1968, Supplement

12 p0251 A69-26092

Canonical representation of multivariable control system in state space using matrix of differential operators acting on vectors of input-output quantities

12 p0251 A69-26094

Digital differential analyzer as control element, analyzing performance limitations imposed by scaling constraints with canonical realization of transfer functions

12 p0253 A69-26509

Complete observability in linear time invariant systems decoupled via state-variable feedback, deriving sufficient conditions

12 p0253 A69-26514

Control signal correction in microwave ferrite modulators, eliminating losses due to screening effect of feeder

13 p2226 A69-27216

Relay control systems limit cycle calculations, comparing classical differential equation, Laplace transformation and state and phase space analysis methods

13 p2238 A69-27396

Control system for thin diffraction limited orbiting astronomical telescope mirror based on structural analysis of static deflections

13 p2261 A69-27951

Asynchronous finite state sequential nonlinear controller synthesis with few flip-flops for dynamic space vehicle systems

[AIAA PAPER 67-988]

13 p2225 A69-28201

Scientific satellite checkout system tests by manual, automatic and self test control

13 p2243 A69-28480

Conditions for nonlinear control systems observability determined for use in identification procedure and in designing control unit

14 p2424 A69-28742

Tracking conditions for observability of nonlinear controlled systems with smooth characteristics

14 p2424 A69-28751

In-core thermionic reactor space power plants stability and control criteria, comparing linear and nonlinear models

14 p2481 A69-29189

Analog computer for design of control systems used in nonnuclear testing of nuclear rocket engine components and subsystems

15 p2589 A69-31289

Test facility for qualification of satellite fairings jet-tisoning system, describing accelerating tower and recording and control instrumentation

16 p2765 A69-31739

Radar control system based on load waveform monitoring by coupled control and modulating circuits

16 p2753 A69-32439

Cost optimization of mixture ratio control systems for liquid propellant launch vehicles, considering open and closed loop systems

[AIAA PAPER 69-441]

16 p2870 A69-32775

Equipment- and program-type methods for solving automatic digital control systems synthesis problems, evaluating efficiency based on accuracy

17 p2933 A69-33120

Cooling system control system for astronaut thermal equilibrium and work output maximization during extravehicular space missions

[AIAA PAPER 69-617]

17 p2914 A69-33278

Fluidic system applications to turbojet propulsion control, thrust stabilization control, temperature sensing, normal shock sensing, pressure ratio sensing, supersonic air inlet control and flight control

17 p2904 A69-34070

- Learning control systems research and applications noting trainable controllers, reinforcement control, Bayesian estimation and stochastic approximation
18 p3112 A69-35093
- Apollo navigation, guidance and control systems in command module and lunar module, discussing inertial, optical and computer hardware operation
19 p3369 A69-35799
- Control circuits in nature and sensory information data processing in human work, including servomechanism of brain-muscle system
21 p3652 A69-38784
- Parameter optimization technique for aircraft control equipment design
22 p3919 A69-41051

CONTROL SIMULATION

- Hybrid computers, discussing analog and digital devices combination and distinction between use of computer for general purpose computation and control purposes
02 p0212 A69-11997
- Reciprocal variational formulation for optimal control, estimating difference between suboptimal system response and optimum
03 p0457 A69-13766
- Aircraft turbine engines operation and control, discussing technology, simulation and system developments
05 p0812 A69-16528
- M measurement optimal feedback control algorithm for stochastic discrete time systems, considering nonlinear plant, constrained controls, nonquadratic cost and simulations
06 p0902 A69-17402
- Digital computer simulation and analysis of control loops for ion thruster control
[AIAA PAPER 69-239] 09 p1564 A69-21240
- Pneumatic diode function generator for simulating nonlinear control systems, discussing operating characteristics and programming methods
11 p1858 A69-24580
- Hydraulic servo actuators load effect included in control loop actuator simulation
12 p2016 A69-26266
- Apollo Lunar Module Environmental Control System /LM/ECS/ steady state performance simulation techniques, discussing vacuum chamber data of LTA-8/LM-3
[AIAA PAPER 69-616] 17 p2903 A69-33307
- Thermal control system for AZUR research satellite, tabulating extreme flight temperatures and permissible temperature range from simulation test data
17 p2903 A69-33427
- Biosatellite attitude control systems design development and flight test results for payload perturbing effects, discussing simulation activity
18 p3210 A69-35094
- Fighter aircraft higher order control system dynamics effects on longitudinal handling qualities evaluated by in-flight simulator for role of pilot induced oscillations tendencies
[AIAA PAPER 69-768] 19 p3245 A69-35655
- Control system concept for axisymmetric supersonic inlet operation in mixed compression mode noting test results
[AIAA PAPER 68-581] 20 p3585 A69-37151
- Spacecraft discrete automatic control system computerized simulation, discussing logic elements, applications to design, etc
20 p3502 A69-37393
- Real time digital computer hardware simulation of Apollo Telescope Mount /ATM/ mission
[AIAA PAPER 69-940] 22 p3919 A69-40323

CONTROL STABILITY

- Multivariable PFM control system stability analysis using Liapunov function as Hermitian quadratic form
01 p0050 A69-10207
- Nonlinear negative definite feedback control systems governed by parabolic partial differential equation, deriving asymptotic stability
01 p0050 A69-10239
- Stochastic Luric type systems stability using Liapunov method
01 p0050 A69-10240
- Matrix procedures for stability of nonlinear control with nonlinearities, discussing system with three actuating elements
01 p0050 A69-10355
- Stability properties of discrete-continuous feedback control systems with signal dependent sampling
02 p0226 A69-12733

- Dynamic properties of electrohydraulic servomechanisms having variable structure analyzed by analog computer
03 p0368 A69-13686
- Multivariable self adaptive control system design using sensitivity methods, obtaining adaptation stability by Liapunov synthesis
06 p0900 A69-17352
- Absolute stability of dynamic control systems with single nonlinear element function of two feedback state variables, giving sufficient conditions
06 p0905 A69-17948
- Control systems stability under perturbations using time optimal control
07 p1115 A69-18514
- Control-display panels design for accurate response with electronic and mechanical equipment, showing display stimulus and control response correspondence in rectangular configuration arrangement
07 p1070 A69-18907
- Absolute stability of distributed control system with nonlinear elements of backlash type analyzed by distributed parameters method
07 p1115 A69-19758
- High speed stable system by combining hunting type control system without closed cycles designed for plant optimization with recycling type controller
07 p1116 A69-19759
- Laser control of French rocket head guidance system, discussing gyroscopic master, stellar or solar detectors, etc
09 p1518 A69-22162
- Root sensitivity of characteristic equation of linear automatic control system to system parameter changes applied to aircraft angular stabilization
10 p1666 A69-23610
- Parametric damping of oscillations in second order automatic control systems, taking into account control function constraints
11 p1857 A69-24556
- Control sets corresponding to desired stability behavior of controlled motion, giving theorem concerning differential inequality
11 p1910 A69-25412
- Mathematical model for initial conditions of asymptotically stable nonlinear control system to estimate region of acceptable motions
11 p1861 A69-25453
- Canonical transformations of unsteady control system motion equations, simplifying control process study and controller simulation on analog computer
12 p2045 A69-25960
- Perturbation theory of nonlinear control systems with periodic coefficients and small perturbation terms, exemplifying satellite attitude control
12 p2173 A69-26067
- Uncontrollable modes effect on transient/steady behavior and limit cycles characteristics of nonlinear multivariable control system
12 p2048 A69-26078
- Liapunov functions applied to stability analysis of nonlinear multivariable direct and indirect control systems with time lags
12 p2048 A69-26079
- Stability conditions for control systems consisting of linear multivariable stationary neutral plant and multivariable pulse frequency modulator, using Liapunov direct method
12 p2049 A69-26080
- Sampled data time optimal control of linear multivariable system based on determination of system state variables control time and minimum sampling intervals
12 p2050 A69-26088
- Stability of single output sinusoidal perturbation extremal control system with output lag, discussing stability boundary
12 p2052 A69-26384
- Feedback controller compensator for invariant linear systems having unstable modes
12 p2054 A69-26517
- Stability test for linear unit feedback control system with second order lag and dead time compensated by PIO controller
13 p2238 A69-27395
- Optimal controller design and transfer functions in linear stabilization systems subjected to unknown disturbances determined by variational calculus
13 p2259 A69-27425
- Stabilization of nonlinear control systems steady motions for two pairs of imaginary roots
13 p2298 A69-27745
- Multivariable PFM control system stability analysis using Liapunov function as Hermitian quadratic form
14 p2424 A69-28743

- Control systems synthesis for nonlinear plants with known Liapunov functions and constraints, considering stability
14 p2424 A69-28819
- Collection of soviet articles on vibrations and stability of devices, machines and control system elements
14 p2536 A69-29741
- PCM oscillator synchronization system stability, considering sampled model by digital nature of equipment
15 p2565 A69-30171
- Dynamic vibration effects on guidance and control systems performance determined from spectral densities, cross spectral densities and vibratory environment amplitude distributions
15 p2608 A69-30367
- Sinusoidal perturbation extremal control system stability, using harmonic balance principle to obtain periodic solutions of system differential equations
15 p2582 A69-30616
- Aircraft neutral stability empirical and mathematical aspects, considering control stabilization, damping and phugoid motion
15 p2551 A69-31012
- Gyro controlled rigid rotor dynamic stability studied for stoppable rotor operation, developing analytical expressions for determining stability boundary of constant and rotor speed gyros
[AHS PAPER 343] 17 p2899 A69-33508
- Multiple input and output nonlinear time invariant feedback system under almost constant inputs
17 p2944 A69-33743
- Solid state single unit digital control computer performing stability augmentation, pilot relief functions and generating minimum fuel flight paths for VTOL landing
17 p2934 A69-34075
- Autopilot for flight simulation of stability and control of pilot-airframe combined performance on reentry missions, using airborne analog computer for vehicle response
18 p3208 A69-35000
- Liapunov method applied to stability evaluation of multiparameter self adaptive nonsearch gradient servosystems
19 p3286 A69-35891
- Stability of interrelated linear dynamic control systems with distributed parameters evaluated by using differential equations
19 p3286 A69-35892
- Automatic control systems for plants with distributed parameters, discussing stabilizing resonance shell with space-time dispersion of controlled processes
19 p3372 A69-35893
- Gyrator stability and frequency behavior obtained by controlled sources selection
19 p3287 A69-36739
- Attitude control system for launch vehicles, providing commanded thrust vector angle proportional to desired angular displacement of acceleration vector
21 p3819 A69-39032
- Frequency domain and Liapunov instability criteria for attitude control system design of large booster, noting nonlinear feedback
[AIAA PAPER 69-853] 21 p3687 A69-39381
- Spacecraft wide angle attitude control system stability analysis, using air bearing table simulation
[AIAA PAPER 69-856] 21 p3823 A69-39384
- Clear air turbulence /CAT/ causes effect on aircraft control, discussing monitoring device and aircraft position maintenance under CAT conditions
22 p3977 A69-40007
- Existence theorem for linear stochastic systems optimal control described by differential equation with random coefficients, providing rms stabilization
22 p3917 A69-40116
- Automatic phase control system stability range determination in piecewise linear approximation and in presence of proportional integrating filter
22 p3918 A69-40956
- Book on systems stability with random parameters, considering linear and nonlinear control systems, with application to stochastic approximation
23 p4181 A69-41510
- Seam welding processes and power supply effects on control efficacy based on electrode displacement for Al-Mg alloys
24 p4319 A69-42919
- Optimum control synthesis for nonlinear plant subject to white noise perturbation, using integral estimates of phase coordinate functions
24 p4289 A69-42949
- Digital analysis of nonlinear control systems dynamic stability under small perturbations, using linearized differential equations
[IS-ERI-71] 24 p4285 A69-42984

Stability criteria for electrical interconnection in parallel operating valve controlled hydraulic servomotors applied to gimbaled system

24 p4256 A69-43310

Pulse modulated feedback system for satellite attitude control, analyzing relationship between physical parameters to ensure two pulse limit cycle oscillation stability

24 p4295 A69-43318

CONTROL SURFACES

NT AERIAL RUDDERS
NTAILERONS
NT ELEVATORS [CONTROL SURFACES]
NT ELEVONS
NT FLAPS [CONTROL SURFACES]
NT GUIDE VANES
NT HORIZONTAL TAIL SURFACES
NT JET FLAPS
NT JET VANES
NT LEADING EDGE SLATS
NT SPOILERS
NT TABS [CONTROL SURFACES]
NT TRAILING-EDGE FLAPS
NT WING FLAPS

In-flight measurement of shear, bending moment and torque on lifting or control surfaces and loads on nose and main landing gear

04 p0677 A69-14842

Aircraft gust alleviation system for minimizing weighted sum of normal acceleration and pitch rate response by limiting control surface deflections

09 p1434 A69-22279

Motion equations for dynamics of aircraft control surface controlled by autopilot with rigid feedback

16 p2809 A69-32134

Series 3 Skyvan design, describing controls, electric and electronics equipment, weather protection, environmental and fuel systems

17 p2906 A69-34194

Parametric approach for weight estimation of surface control systems of transonic and supersonic combat and subsonic transport aircraft [SAWE PAPER 812]

18 p3221 A69-34898

Duplex servomotor package sized for stabilator channel of F-4 aircraft providing compact integrated control surface positioning [AIAA PAPER 69-788]

19 p3249 A69-35640

Circulation control by blowing and application to stopped rotor aircraft, discussing data from model scale blade experiments

19 p3248 A69-36767

Simulated degrading environment effect on spacecraft thermal control surfaces subjected to plume heating during apogee firing and solar irradiation [AIAA PAPER 69-1024]

22 p3923 A69-40394

CONTROL UNITS [COMPUTERS]

Vibration/acoustics digitally controlled environmental testing, describing configuration and operation of control system and statistical requirements for noise generation

15 p2587 A69-30388

CONTROL VALVES

Vortex valve and angular rate sensor based on amplification of tangential velocity component of swirl achieved by control jet or rotation

05 p0746 A69-16006

Transistorized frequency detector for sensing system load changes affects speeds of control valves of prime movers

06 p0896 A69-17478

Large signal vortex amplifier analysis using load lines to evaluate series orifice and vortex flow control valve characteristics

10 p1639 A69-23558

Static and dynamic characteristics of pressure compensated oil-hydraulic flow control valves and relief valves with emphasis on linearized effects

19 p3256 A69-36713

Miniature hydraulic controls with emphasis on four-way directional control valve for space and cost problems

22 p3870 A69-41243

CONTROLLABILITY

Approximate boundary controllability for heat equation by considering temperature variation with time

01 p0173 A69-10008

Controllability of dynamic systems obtained by studying vector function increments along system trajectories

01 p0051 A69-10698

Hovercraft handling characteristics, seakeeping and maneuverability during English Channel operation

02 p0277 A69-11592

Rotary wing handling qualities, discussing analytical tools, design and IFR capabilities for high speed range

05 p0701 A69-15550

Lifting body entry vehicles in low speed flight test program for determining handling qualities, discussing M2-F2 glide flights

05 p0702 A69-15571

Invariant subspaces, controllability and observability of linear dynamic systems

05 p0740 A69-16597

Controllable gyration use in nonlinear network synthesis

05 p0735 A69-16620

Control system controllability under discontinuous control constraints, presenting optimal response rate linear system synthesis with continuous restriction on control function

09 p1475 A69-22670

Optimal control of time invariant uncontrollable linear systems, noting asymptotic stability

10 p1666 A69-23887

Canonical forms for observable and controllable linear time invariant systems by simultaneous transformations of system state and input and output vectors

12 p2048 A69-26075

Controllability of linear multivariable time invariant optimal systems with additive parameters using Kalman controllability definition, noting role of Pontryagin principle

12 p2050 A69-26086

Asymptotic controllability of linear system, giving stabilization procedures based on solutions to limiting differential equations

12 p2053 A69-26515

Controllability of stationary linear multivariable systems using frequency domain criterion with application to optimal control laws for minimum fuel and time control problems

12 p2054 A69-26519

Helicopter rotors with rigid blades performance from viewpoint of controllability and load distribution

13 p2201 A69-27295

Mission task performance oriented approach to winged helicopters flying and handling qualities, considering wings and horizontal stabilizers influence [AHS PAPER 360]

17 p2900 A69-33522

Performance capabilities and handling quality characteristics of aircraft equipped for in-flight thrust reversing [AIAA PAPER 68-880]

17 p2902 A69-34031

Handling-qualities rating data evaluation for low computation cost information, noting reliability estimation

21 p3664 A69-38968

Aircraft characteristics influence on longitudinal handling qualities during carrier approach from visual landings on moving base simulator [AIAA PAPER 69-894]

21 p3648 A69-39418

Controllability and linear closed-loop controls in linear periodic systems

22 p3917 A69-40572

Time-invariant multivariable linear systems, discussing structure theorem for controllable systems and application to decoupling problem

24 p4294 A69-43314

CONTROLLED ATMOSPHERES

NT CABIN ATMOSPHERES
NT INERT ATMOSPHERE
NT SPACECRAFT CABIN ATMOSPHERES

Rodents exposure to neon enriched atmosphere for three weeks in sealed recycling system, discussing body weight pregnancies and litter

01 p0019 A69-11342

Atmospheric exposure chamber design for small animals, discussing dynamic and recirculating operations and gas scrubbing system

04 p0584 A69-14678

Control and sampling in sterile rooms, noting worker introduction of contaminants

05 p0714 A69-15953

High bay clean room design with laminar air flow, discussing air filtration, sound attenuation, construction, illumination, etc

10 p1673 A69-23354

Hamsters responses to helium-oxygen and nitrogen-oxygen at ambient temperatures, comparing respiration rates, weights and body temperatures

10 p1646 A69-23564

Brittle fracture at high temperatures in titanium alloys using scanning electron beam microanalysis, noting reaction diffusion with atmosphere and grain boundaries destruction

10 p1713 A69-23823

EEG, EKG, respiratory motions and pulmonary ventilation recordings in study of carbon dioxide additions effect on human tolerance to hypoxic conditions

10 p1650 A69-23898

Molten high melting compounds obtained by arc furnace with consumable electrode and adjustable protecting atmosphere

12 p2055 A69-26264

Oxygen consumption and rectal temperature in male mice confined in nitrogen and helium diluted hyperoxic atmosphere at specific temperature and humidity ranges

17 p2906 A69-32932

Photosynthesis and respiration rate in vegetables in controlled temperature, humidity, illumination levels, carbon dioxide and oxygen contents

17 p2912 A69-32933

Forge to determine refractory metals formability and ductility at high temperature in protective pressure

17 p2945 A69-33419

EKG, EEG, pneumograms and X ray pictures showed no pathological effect after prolonged confinement in sealed chamber having artificial atmosphere with variable gas composition

22 p3892 A69-40284

CONTROLLED FUSION

Plasma physics and controlled nuclear fusion research - Conference, Novosibirsk, U.S.S.R., August 1968, Volume 1

17 p3012 A69-33817

CONTROLLED STABILITY

U CONTROL

U STABILITY

CONTROLLERS

NT SERVOMULTIPLIERS

NT SERVOMECHANISMS

NT SERVO MOTORS

Multilevel optimization techniques for dynamic systems control evaluated, developing second level Newton-Raphson controller

01 p0051 A69-10440

Sensitivity reduction in specific optimal control by use of dynamical controller

01 p0051 A69-10441

Algorithm minimaxing performance index and sensitivity of controller design with and without saddle point

02 p0224 A69-11966

Mathematical basis for designing controllers of time lag systems by approximately solving differential equations

03 p0408 A69-12973

Bit reduction in digital transfer functions with LF poles in sampled data systems using zero order hold function

04 p0584 A69-15464

Nonlinear operation of pulse control system by means of triple modulation

05 p0736 A69-15764

Human operator as optimal controller, proposing quadratic performance index used by operator in judgement of own performance in tracking task

06 p0903 A69-17407

Electronic controller with integrated circuits and inexpensive SCR as coupler or interface between card reader and frequency synthesizer designed for unattended operation

06 p0897 A69-17704

Optimization of control independent cost functions in multidimensional system with linear controllers

06 p0905 A69-17945

Control system analysis and synthesis by means of generalized root-locus method on digital computer

07 p1114 A69-18291

Semiautomatic gravity gradient stabilization system [SAGS] for active pitch control and semipassive roll/yaw control

07 p1228 A69-18342

Self organizing trainable logical networks [TLN/ as stable controllers in multiaxis vehicle control problem, reviewing TLN concepts and training theory

07 p1070 A69-18388

Fluidic component application to propellant tank pressurization and controller design [AIAA PAPER 68-629]

09 p1442 A69-21980

Adaptive control algorithm operating on-line to make discrete time adjustments in controller parameters of continuous time control system

09 p1474 A69-22441

Stationary controller design for linear time varying control systems with state variables not always accessible for feedback

09 p1474 A69-22443

Optimal controllers analytical design for closed loop systems with pure time delay in actuating mechanism using differential equations
12 p2045 A69-25959

Time optimal regulator problem with recoverability constraint as restriction on system state during control synthesis
12 p2052 A69-26504

Optimal stochastic controller synthesis theory applied to stabilizing and controlling orientation of rotating bodies in central gravitational fields
13 p2300 A69-28326

Optimal control theory applications for controllers not characterized by bang bang time responses using Pontryagin maximum principle
18 p3090 A69-34681

Algebraic equations for determination of controller parameters, noting a priori fixed roots of characteristic equation
21 p3723 A69-38887

Integrated sensor controllers for missile directional control, discussing test results for two different systems [AIAA PAPER 69-837]
21 p3761 A69-39368

Controllers design for reaction jet controlled aerospace vehicles, studying second order pitch- plane representation with actuator modeled as pure delay [AIAA PAPER 69-854]
21 p3822 A69-39382

On-off limit cycle controllers for reaction-jet controlled systems, investigating delay effects
24 p4291 A69-43271

Coefficient quantization in digital continuous time process controllers, applying results to nominal transfer function approximation
24 p4292 A69-43283

Stochastic fuel regulator problem investigated by optimal and self organizing techniques, emphasizing realizability of resulting controllers
24 p4292 A69-43284

CONVAIR MILITARY AIRCRAFT
U MILITARY AIRCRAFT

CONVAIR 990 AIRCRAFT
U CV-990 AIRCRAFT

CONVECTION
NT FORCED CONVECTION
NT FREE CONVECTION

Quasi-steady combustion model of fuel droplet with convection, including pressure effect [AIAA PAPER 69-147]
06 p1037 A69-18114

Solar supergranules and hydrogen convection zone analysis based on polytropic atmosphere convection physics
07 p1211 A69-18408

Magnetic fields of solar supergranulation convective cells based on electromagnetic induction equation, indicating bipolar sunspots occurrence
09 p1588 A69-21366

Solar neutrinos and convective core mixing on short time scale resulting in flux reduction
09 p1574 A69-21453

Dependence of convection in planetary interiors upon magnitude of Rayleigh number for rigid and free surfaces
12 p2155 A69-26208

Radiative heat transfer, discussing electromagnetic theory, transfer between surfaces and simultaneous conduction, convection and radiation
13 p2376 A69-28140

Convective instability by active stress, discussing composition dependent stress fields in continuous and mechanically isolated material and chemical to kinetic energy conversion
14 p2540 A69-29634

Optical depths of convection related to metal deficiency for main sequence and giant stars
14 p2527 A69-29946

Surface convection zone in atmospheres of global cluster and halo B stars determined to study He depletion efficiency
14 p2529 A69-29976

Stratified fluid flow past obstacle, considering steady inviscid flow with nonlinear convection and vertical acceleration
19 p3240 A69-36474

Numerical simulation of macrophysical and microphysical processes in convective cloud, including cloud geometry and equations describing dry and moist phases
19 p3362 A69-36497

CONVECTION CURRENTS
Radiative heat loss effect on atmospheric cellular convection, analyzing critical Rayleigh number and width to height ratio of cells
02 p0276 A69-12776

Convective clouds effect on large scale stratification, showing cumulus and cumulonimbus self amplifying convection as factor in tropical cyclogenesis
09 p1536 A69-22165

Relation between Rayleigh and dynamic Richardson numbers in atmospheric boundary layer in presence of cellular convection
09 p1491 A69-22709

Growth rates for convective disturbances propagation in atmosphere with linear entropy variation, noting WKB approximation
11 p1957 A69-24422

Cellular convection in horizontal gas layer analyzed for causes of vertical air circulation and effect of vertical temperature profile
13 p2291 A69-27725

Azimuthal electric currents generation by Coriolis forces in hot stars with intensive radial flows in convective zones
13 p2350 A69-27862

Convective-current instability in finite length plasma column, analyzing spectrum of unstable harmonics
13 p2314 A69-28441

Relation between Rayleigh and dynamic Richardson numbers in atmospheric boundary layer in presence of cellular convection
16 p2808 A69-32488

Physical model for IGY radio aurora data correlated with Brice magnetospheric convection model
18 p3125 A69-34231

Solitary waves in stratified polytropic atmosphere allowing for convection and disregarding viscosity and turbulence
18 p3167 A69-35338

Turbulence energy spectra in free atmosphere with convective layer surmounted by inversion layer, noting power law followed by velocity components
19 p3362 A69-36406

Benard convection cells analyzed by Boussinesq approximation and Schmidt-Liapunov method, obtaining bundary value problem branching solution
19 p3301 A69-36791

Convective momentum exchange in mesoscale gravity wave
20 p3522 A69-37350

Radar observations of convective pattern types in clear atmosphere consisting of thermal- and Benard-like convection cells
20 p3573 A69-38059

High latitude magnetospheric convection patterns determined from ionospheric current distribution using magnetic disturbance plots
21 p3709 A69-38503

Oscillatory convection, energy transport and structure of sunspots, suggesting fast changes in equilibrium conditions for magnetic reconstruction and solar flares origin
24 p4374 A69-43624

CONVECTIVE FLOW
Thin rigid radial wall effect on convective flow in heated rotating annulus
02 p0275 A69-12013

Plate temperature oscillation effects on forced convection laminar viscous incompressible MHD boundary layer flow from semiinfinite flat plate
02 p0288 A69-12143

Environmental temperature and water vapor increases associated with ascending thermals estimated by penetrative convection
03 p0460 A69-13340

Laminar flow of isotropic binary gas mixture in circular cylindrical tube with porous walls, determining concentration field variation with wall suction Reynolds number
05 p0744 A69-15618

Lunar history reexamination including added mantle convection and recent rocket data
05 p0825 A69-16303

Similar solutions for laminar boundary layer formed by convective and compressible flows
05 p0751 A69-16463

Simultaneous natural and forced convection flow around wall, analyzing perturbations of hydrodynamic elements due to obstacle
06 p1030 A69-17095

Mixing effect on solar neutrino fluxes, assuming solar convective core with rapid thorough mixing
06 p1001 A69-17192

Permissible nonthermal convection modes in planetary interiors derived from conservation equations for self gravitating homogeneous nonrotating compressible fluid spheres
07 p1213 A69-18611

Convection in planetary interiors produced by combined thermal and nonthermal mechanisms, noting self gravitating homogeneous nonrotating compressible fluid spheres
07 p1214 A69-18613

Heat conduction equation for convective flow applied to gunpowder combustion under harmonic pressure variation
07 p1241 A69-18708

Unsteady MHD convective flow with suction of viscous incompressible electrically conducting fluid above vertical porous wall, noting horizontal magnetic field effect
07 p1195 A69-19477

Stellar rotation braking due to mass loss from coronae through stellar wind based on calculation of acoustic energy generation from convective zone
08 p1396 A69-20644

Electroconvective instability produced by uniform electric field in poorly conducting fluid under stabilizing vertical temperature gradient, noting heat flow increase
08 p1352 A69-20791

Convective MHD channel flow in vertical channel subjected to temperature and pressure gradients, discussing wall conductances effects on flow rate and heat transfer
09 p1545 A69-21441

Momentum and energy transfers analogy in turbulent convection fluid flow emphasizing difficulties in case of liquid metals
09 p1480 A69-21687

Natural convective oscillatory three dimensional flow in cylindrical annuli, describing inception, amplitude, period and wavelength
09 p1481 A69-21902

Warm plasma addition to mirror confined hot plasma stabilizing convective loss cone mode
09 p1551 A69-22040

Temperature gradient in semiconvective region, examining molecular weight distribution in mixing due to overstability
09 p1596 A69-22057

Hydromagnetic laminar natural convection flow and heat transfer of nonNewtonian fluid between parallel electrically conducting walls
10 p1728 A69-23237

Statistical analysis of convective layer thickness and moisture content effect on convective cloud configurations, using satellite TV pictures
11 p1912 A69-24827

Physical structure of convective envelopes of population II main sequence stellar models by mixing length theory, emphasizing hydrogen molecule formation and pressure ionization
11 p1961 A69-25109

Convective drift and flute instabilities of plasma stabilized by exerting HF forces on electrons, determining required HF field amplitudes
11 p1932 A69-25538

Two dimensional convective flow stability for arbitrary Rayleigh numbers in horizontal layer, assuming large Prandtl number and free boundary conditions
11 p2003 A69-25657

Forced convection in atmospheric boundary layer above nonuniformly heated earth surface, noting roles of wind and stratification parameters
12 p2126 A69-26579

Solar wind induced magnetospheric convection for interpretation of geomagnetic storms, aurora and trapped particle belts, noting electric fields
12 p2073 A69-26749

Planetary mantles thermal and nonthermal convection model, solving sphere density variations and radial velocity components due to internal time-independent motions
13 p2344 A69-27644

Planetary interior convection analysis extended to include variable viscosity, heat source distribution, thermal expansion and diffusivity, etc
13 p2344 A69-27646

Cellular convection suppression by parallel vertical thermally conducting walls inserted into bottom-heated fluid, analyzing effect on critical Rayleigh number
13 p2374 A69-27782

Combined free and forced convection flows in parallel channel systems and in single channels, discussing metastable flow regimes, single phase laminar flows, etc
13 p2377 A69-28152

Benard convective flow as function of Rayleigh and Taylor numbers in thin variable rotating silicone oil layer determined by flow photographs
13 p2377 A69-28172

Temperature disturbance amplification in laminar natural convection boundary layer formed on vertical flat surface measured with hot-wire anemometers
14 p2430 A69-29575

Conduction solution to generalized nonlinear Benard problem showing existence of bifurcation and analyticity of convective motion
14 p2540 A69-29679

Convective and nonconvective two stream instability for hot plasmas, approximating equilibrium distribution function for given temperature by resonance functions
14 p2499 A69-29844

Protostars collapse and flare up computations, including radiative and convective energy flow terms in hydrodynamic equations of motion
15 p2680 A69-30206

Convective neutral stability in Schwarzschild- Harm model for evolution of stars with large masses
15 p2681 A69-30422

Stellar magnetic field generation by convective motions of surface layers of slowly rotating stars
15 p2688 A69-30559

Similar solution for free convective flow past vertical porous wall and unsteady flow past porous wall with dissipation term, using group transforms
15 p2592 A69-31010

Two dimensional laminar convection cells asymptotic behavior for high Rayleigh number, discussing Robinson and Pillow models for fluid between horizontal plates heated from below
16 p2767 A69-31588

Secondary flow consisting of longitudinal vortices superposed on convection flow on inclined plate, obtaining flow pattern through flow visualization
18 p3124 A69-35383

External natural convection flows, studying laminar instability, transition and turbulence in boundary layer flow
20 p3633 A69-37718

Heat transfer in curved channel as function of inlet configurations, obtaining Nusselt number equations for thermal and mixed convection and laminar flow
21 p3850 A69-38866

Membrane vibration problems for combined free and forced laminar convection through vertical ducts, obtaining expressions for velocity, temperature and Nusselt numbers
21 p3851 A69-38974

Solar oblateness observed by Dicke and Goldenberg as interaction between slow uniform rotation and turbulent convection
22 p4017 A69-40175

Semiconvection zone occurrence in massive stars determined by stability considerations
22 p4022 A69-40470

Forced convection liquid flow past heated flat plate with variable viscosity and thermal conductivity, analyzing velocity and temperature distribution in boundary layer
22 p4051 A69-40685

Plasma pause form in equatorial plane in presence of magnetospheric tail subsonic potential convective flow
22 p3942 A69-41103

Phenomenological sunspot model describing granules, supergranules, magnetic fields and photospheric convection
24 p4378 A69-42691

Natural convection flow, discussing initial instability of laminar flow, disturbance amplification and transition to turbulent flow
[ASME PAPER 69-HT-29] 24 p4411 A69-43531

Transition from turbulent to laminar regime as consequence of high heating rates for internal convective flow, noting roles of Nusselt numbers and friction factors
[ASME PAPER 69-HT-9] 24 p4304 A69-43559

Outer solar convection zone structure dependence on change of parameters in mixing length theory examined to construct model
24 p4387 A69-43634

Free convection flows about inclined infinite cylinders with isothermal surfaces
24 p4416 A69-43687

CONVECTIVE HEAT TRANSFER

Steady state problem of convective heat transfer in half space with boundary conditions of third kind
01 p0174 A69-10103

Convective heat transfer across fluid film limited by right sections of two parallel circular hollow steel cylinders
01 p0176 A69-11135

Heat transfer rates from high temperature spheres into subcooled liquid sodium during forced convection, noting surface vapor formation
[ASME PAPER 67-WA/HT-32]

02 p0351 A69-12202

Closed form solution of convective heat transfer to yawed concave hemisphere in free molecule flow
02 p0354 A69-12529

Large convective clouds in superheated air generated by static tests of Saturn 5 first stage
03 p0462 A69-14125

Free convective heat transfer in liquid filled spherical volume with constant thermal flux density at boundary
04 p0686 A69-14992

Forced convection heat transfer coefficient invariance to flow reversal in Stokes and potential streaming flows past isothermal particles of arbitrary shape
04 p0590 A69-15274

Natural convection heat transfer through enclosed horizontal layer of supercritical carbon dioxide, discussing flat plate configuration data
04 p0688 A69-15398

Thin foil heat flux sensor for radiative and convective heating rates over wide range and dynamic response, noting error mechanisms, calibration and accuracy
04 p0602 A69-15426

Free convective heat transfer of cylinder in rarefied gas yielding Nusselt number as function of Grashof, Prandtl and Knudsen numbers
05 p0846 A69-15904

Heat transfer through vertical plane layer for various Prandtl numbers, discussing velocity and temperature profiles and effects of aspect ratio, Grashof and Rayleigh numbers
[ASME PAPER 68-WA/HT-4] 05 p0846 A69-16115

Surface vibrations effect on forced convection heat transfer normal to cylinder, discussing convective coefficients dependence on Reynolds number
[ASME PAPER 68-WA/HT-5] 05 p0846 A69-16116

Counter rotating vertical vortices produced by corona discharge on heated flat plate under free convection conditions
[ASME PAPER WA/HT-9] 05 p0846 A69-16117

Small aircraft gas turbine regenerators employing heat pipes, noting excessive cost and weight
[ASME PAPER 68-WA/GT-7] 05 p0812 A69-16142

Natural convection heat transfer for incipient vapor formation in liquid H and N and for nucleate boiling of liquid H
[ASME PAPER 68-WA/PID-4] 05 p0848 A69-16165

Sensible heat exchange from Gemini and Apollo space suits determined in environmental test facilities, presenting data for heat flux distributions
06 p0880 A69-17089

Amount of flux carried by convection in late type stars, reevaluating drag role in mixing length theory
06 p1003 A69-17321

Impinging jet flames on furnace hearth, analyzing thermal boundary layer characteristics and convective heat transfer rates
06 p1035 A69-17933

Modified schlieren interferometer for quantitative investigation of free convection boundary layer temperature profiles
07 p1130 A69-18263

Equilibrium stability of horizontal layer of fluid in field of modulated temperature gradient having layer thickness greater than penetration depth of heat waves
07 p1241 A69-18696

Convection in conducting fluid filled cavities with variable wall temperature due to magnetic field, with results applicable to rheological systems
07 p1241 A69-18921

Radiative-convective heat transfer in gray gas plane layer blown into turbulent flow past permeable plate
07 p1242 A69-18991

Convection inhibition effects on premain sequence evolution of solar mass star, discussing largely radiative models
08 p1386 A69-20088

Convective heat exchange coefficients for human organism in aircraft surroundings under homogeneous temperature conditions, deriving acclimatization equations
[AGARDOGRAPH-111] 08 p1266 A69-20673

Transient free convection laminar boundary layer equations for heat transfer from vertical semiinfinite flat plate
08 p1305 A69-20842

Local heat transfer coefficients in oscillating turbulent boundary layer over flat plate
[ASME PAPER 69-GT-34] 09 p1623 A69-22490

Flow and heat transfer measurements for heated air in subsonic flow through contraction section connecting tube to conical section
[JPL-TR-32-1348] 10 p1809 A69-23194

Statistical theories of turbulence applied to thermal convection between infinite slippery plates at large Prandtl number
11 p1997 A69-24283

Convection heat transfer and flow in rotating bodies, discussing laminar, turbulent and mixed flow in cones and disks, spheres and cylinders
11 p1998 A69-24459

Forced heat convection in steady turbulent air flow in circular cross sectioned tubes, noting laminar sublayer in wall regions
11 p2000 A69-25096

Heat transfer and skin friction in convective and stagnation flow laminar film boiling in boundary layer flows with appreciable radiation
11 p1873 A69-25242

Model evolution of flow in fluid layer suddenly heated from below at Rayleigh number convection sufficient for turbulence
11 p1874 A69-25351

Wavelength of convective motions, discussing effects of lid heat conductivity on Rayleigh number
11 p2003 A69-25354

Voltage characteristics in MHD generator with water cooled segmented electrodes using potential probes, considering forced convection heat transfer
12 p2017 A69-27178

Heat transfer coefficients for carbon dioxide near thermodynamic critical point for flow through electrically heated duct, noting turbulent forced convection as mechanism
[ASME PAPER 68-HT-32] 13 p2373 A69-27769

Thermal radiation effects on laminar free convection boundary layer of vertical flat plate, studying absorbing and nonabsorbing gases
[ASME PAPER 68-HT-43] 13 p2373 A69-27772

Transient one dimensional temperature distribution determined for bodies with internal heat generation and nonlinear boundary condition, using Biot variational method
[ASME PAPER 68-HT-6] 13 p2374 A69-27775

Surface vibrations effect on forced convection heat transfer normal to cylinder, discussing convective coefficients dependence on Reynolds number
[ASME PAPER 68-WA/HT-5] 13 p2374 A69-27781

Triangular profile circular fins efficiency determined from differential equations solution governing temperature distribution
13 p2375 A69-27790

Free convection heat transfer from heated inclined flat plate in air, studying effects of angular positions
13 p2375 A69-27794

Heat convection mechanism in two phase autooscillatory system generalized to convective heat transfer in cloudy atmosphere
13 p2292 A69-27798

Convective heat transfer, discussing coordinate transformation, similarity analysis similitude and Meksyn integration of boundary layer equations
13 p2376 A69-28139

Benard convective flow as function of Rayleigh and Taylor numbers in thin variable rotating silicone oil layer determined by flow photographs
13 p2377 A69-28172

Thermal behavior of space vehicle window systems predicted by mathematical analysis and computer methods for heat transfer through glass
[AIAA PAPER 68-65] 13 p2378 A69-28215

Convective heat and mass transfer in binary turbulent vertical boundary layer
13 p2378 A69-28311

Heat and mass transfer coefficients in binary laminar boundary layer during natural convection, taking into account enthalpy and thermal diffusion effects
13 p2378 A69-28312

Analytical model for free convection heat transfer from vertical plates with nonhorizontal leading edges, discussing flow field
13 p2379 A69-28342

Ideal compressible fluid motion and heat transfer, noting convective heat transfer intensification with increased twisting velocity of flow
13 p2251 A69-28559

Outer convection zone of cool white dwarf by atmospheric models, using mixing length theory and abundances
14 p2529 A69-29982

Convective heat and mass transfer coupling in laminar hydrodynamic duct flow, obtaining values for

bulk and wall temperatures, transfer coefficients and rates, etc

15 p2716 A69-30004

Temperature, velocity and density perturbation propagation as heat convection wave in viscoelastic thermally compressible heat conducting fluid, analyzing damping and frequency spectra

16 p2878 A69-31952

Compressible turbulent accelerating boundary layer flow model for convective heat transfer from rocket combustion gases, noting heat flux

16 p2878 A69-32000

Convective heat transfer in centrifugal force field of cavity between two rotating disks in turbulent gas flow

16 p2837 A69-32139

Unsteady heat conduction equations for elliptic cylinder with convection solved by point matching

16 p2879 A69-32171

Ammonium perchlorate pyrolysis by convective surface heating, monitoring IR emission as measure of surface temperature

[WSCIPAPER 69-23] 16 p2832 A69-32361

Ammonium perchlorate linear pyrolysis by convective surface heating, discussing propellant deflagration models

[AIAA PAPER 69-501] 16 p2835 A69-32758

Temperature fluctuations in solar photosphere, noting transition from convective to radiative energy transport

17 p3040 A69-33810

Superposition method for predicting tube wall temperatures with gas property and heating rate axial variation, noting application to gas flow problems

18 p3227 A69-34315

Temperatures of radiantly heated sun and shade leaves of white oak measured in low speed wind tunnel, considering differences in convective heat dissipation

18 p3095 A69-34540

Orthonormalization methods applied to heat conduction, convection and radiation problems, noting digital computer programs modifications

18 p3229 A69-34662

Convective heat flux from nonisothermal surface by temperature superposition method with Spalding function as turbulent heat transfer coefficient, noting wall temperature

18 p3229 A69-34836

Asymptotic behavior of solution to parabolic equation for t approaching infinity, proposing asymptotic formula to Cauchy problem for heat conduction

18 p3231 A69-35310

Ablative materials thermal protection characteristics at low heating rates evaluated by convective heating tests, stressing polyurethane foam composite

19 p3357 A69-35536

Combined free and forced convection hydromagnetic flow and heat transfer of electrically conducting fluid subjected to temperature variations in vertical channel

19 p3380 A69-36304

Heat and mass transfer on vertical surface under combined free and forced convection, solving laminar boundary layer equations by stream function

19 p3453 A69-36844

Convection within moon as explanation of maria on near side, presence of mascons, etc

20 p3603 A69-37561

Thermal convection in horizontal fluid layer heated from below, with zero shear boundaries above and below, noting critical Rayleigh number measured value

20 p3518 A69-38234

Natural convective heat transfer to gas turbine rotor blade and thermal resistance of cooling system using centrifugal pump

21 p3785 A69-39103

Natural convection in rectangular cavity with nonuniform lateral surfaces temperature, using finite difference scheme with numerical analysis

21 p3855 A69-39853

Internally air cooled turbine blades and vanes emphasizing coolant aerodynamics, heat transfer and blade life, high temperature in jet engines, etc

[RAES PAPER 22] 22 p4000 A69-40500

Combined heat transfer calculations, considering moving radiating media and simultaneous convection or conduction

23 p4237 A69-41328

Mars atmosphere response to surface temperature changes by radiative and convective heating, noting strong solar control of mean wind distribution

23 p4212 A69-41614

Nonlifting blunt axisymmetric hypersonic shape determination to maximize pressure drag for given convective heat transfer, diameter and free-stream conditions

24 p4244 A69-42960

Barometric pressure affecting convective heat transfer from human body in air, deriving empirical formula as function of air density, speed and temperature

24 p4267 A69-43384

Convective thermal flux at stagnation point in multicomponent partially ionized gas injected flow past body, considering effective ambipolar diffusion coefficient

24 p4246 A69-43485

Rectangular fins arrangement on horizontal surfaces for optimum free convection heat transfer coefficient, considering fin weight, height and spacing effects

[ASME PAPER 69-HT-44] 24 p4409 A69-43517

Transverse curvature effect on laminar free convection heat transfer from vertical isothermal cylinders

[ASME PAPER 69-HT-G] 24 p4410 A69-43522

Heat transfer data for laminar, transition and turbulent natural convection boundary layers from water experiment on constant heat flux vertical plate

[ASME PAPER 69-HT-D] 24 p4410 A69-43525

Natural convection local heat transfer on constant heat flux inclined surfaces for water and air in laminar, transition and turbulent regimes

[ASME PAPER 69-HT-C] 24 p4410 A69-43526

Local Nusselt number beyond abrupt circular channel expansion tested for Reynolds numbers with air as working fluid

[ASME PAPER 69-HT-35] 24 p4411 A69-43532

Electric arc stabilization in crossed convective and magnetic fields, discussing column slanting relationship to widening near downstream electrode

[AIAA PAPER 68-709] 24 p4359 A69-43572

CONVERGENCE

Convergence theorems for perturbed Newton methods for solution of nonlinear equation systems, suggesting algorithm holding Jacobian matrix elements constant during iterations

01 p0106 A69-10988

Unstable minimization problem of functional, examining construction of sequences and stability

02 p0271 A69-11648

Convergence of Multhopp collocation method for numerical solution of linear singular integrodifferential equation, noting use in airfoil, propeller and elasticity theory

02 p0271 A69-12056

Discharge coefficients for Herschel type smooth venturimeters, analyzing influence of transport coefficients, convergence angles and contraction ratios

02 p0250 A69-12414

Convergence of Rayleigh-Ritz approximations to solution of elliptic boundary value problem applied to subsonic airfoil problem for 2D steady isentropic irrotational flow

03 p0361 A69-12846

Finite element method convergence introduced as general numerical technique related to Ritz method in structural analysis with digital computers

03 p0527 A69-13745

Convergence of optimal control for denumerable system of differential equations treated by functional-space decomposition

04 p0583 A69-15095

Difference iteration method for solving three dimensional Dirichlet problem presented as system of plane Dirichlet problems

05 p0787 A69-16457

Convergence of improper integral evaluated along solution of differential equation, noting use in asymptotic control theory

05 p0788 A69-16481

Convergence of Grammel and Galerkin methods allows use of modified Green function

06 p1020 A69-17132

Structural iterative design convergence to minimum weight proved by dual linear programming, discussing global convergence and convergence rate

08 p1413 A69-20351

Book on stochastic convergence covering infinite sequences of random variables, stochastic integrals and derivatives, characterization of normal distribution and Wiener process

08 p1343 A69-20443

Command inputs handling by linear optimal control theory, investigating Riccati matrix differential equation convergence

08 p1298 A69-20856

Converging solutions for imaginary admittance and current distribution in linear cylindrical antennas

08 p1295 A69-21165

Convergence extensions in quasi-linearization for optimal control, showing results for brachistochrone and reentry trajectory problems

09 p1590 A69-21414

Particular solutions in nonlinear two point boundary value problems, showing convergence for uncontrolled and controlled systems

09 p1531 A69-21416

Rate estimates of convergence of multidimensional central limit theorem for sequence of identically distributed independent random variables with third order finite moments

10 p1719 A69-23400

Finite difference approximation to degenerate Dirichlet problem, obtaining a priori estimate to prove convergence

10 p1719 A69-23517

Convergence of zeta function for flows and diffeomorphisms

10 p1720 A69-23639

Solution of confluence in three dimensional shock and detonation polars for spinning detonation

11 p2002 A69-25353

Convergence of Bubnov-Galerkin method in complex separable Hilbert space, proving theorems for sufficient conditions

12 p2123 A69-26607

Nonlinear control systems error signals convergence to steady states in frequency domain, applying step or ramp functions to single feedback system

13 p2237 A69-27188

Variational principle and convergence of finite element method based on stress distribution

13 p2368 A69-28349

Convergent solutions of inviscid solar wind equations in expansions form including dimensionless distance from sun

14 p2515 A69-29968

Localization and convergence of Fourier series for fundamental systems of functions of Laplace operator, including eigenfunctions and trigonometric systems

15 p2644 A69-30287

Rapid convergence algorithms as second variation methods for dynamic optimization problems

15 p2645 A69-31235

Optimum overestimate to obtain bound permitting use as convergence criterion for iterative process in orbital glider reentry trajectory optimization

[ONERA-TP-628] 16 p2805 A69-32332

Reflected shock waves behind tapered shock tube section indicated by shock wave detectors, microwave absorption and optical emission measurements

18 p3085 A69-34474

Convergence of discrete approximations of Navier-Stokes equations to solutions of corresponding differential equations

18 p3121 A69-34613

Convergence of methods of tangential parabolas and hyperbolas used in nonlinear equation solution with nondifferentiable operators

18 p3164 A69-34707

Convergence properties of finite difference approximations to solutions of Dirichlet problem for Poisson equation

18 p3164 A69-34840

Steepest ascent convergence improved in orbital glider reentry trajectories optimization problems, discussing bang-bang and cosine control-variable changes

19 p3398 A69-35666

Convergence rate estimates for singular perturbations solutions of linear elliptic boundary value problems

19 p3360 A69-35899

Algorithm for Chernousko local variation method during application to solution of variational problems involving nonadditive functionals, assessing convergence

20 p3513 A69-36990

Averaging methods applied to nonlinear equations in mechanics, discussing solution convergence estimation

20 p3576 A69-37440

Difference method for initial value problems in quasi-linear hyperbolic first order approximations extended to wider quasi-linear problems, assessing convergence

20 p3568 A69-37833

Discrete extremum problems solution convergence to optimal control continuous problem as functional optimal value and optimal control

21 p3684 A69-38430

Book on convergence in calculation of elastoplastically deformable aircraft structures and continua,

covering matrix displacement method and stepwise linearized computational technique

22 p4044 A69-40619

Visual stimuli initiating horizontal eye vergence movement in human subjects, noting cerebral conditions for convergence

22 p3881 A69-40859

Shock wave transient motion during passage through ducts in inviscid gas containing convergences, using characteristics method

23 p4153 A69-42398

CONVERGENT-DIVERGENT NOZZLES

Laval nozzle resistance as result of friction and under expansion of gas, noting flow and pressure recovery coefficients

03 p0361 A69-12967

Relaxation equations for oscillatory degrees of freedom of molecular supersonic binary gas flow in Laval nozzle, obtaining population inversion

07 p1118 A69-18540

Variable geometry intake and convergent-divergent nozzle design for supersonic aircraft, noting subsonic installations

08 p1253 A69-21164

Photometric methods for determination of H atom and hydroxyl radical concentrations in hot gases in convergent-divergent nozzles, noting Li/lithium hydroxide absorption

09 p1496 A69-21952

Pressure and temperature effects on electrical conductivity of dense plasma ejected from Laval nozzle

10 p1739 A69-23492

Thermodynamic atomization in MHD energy conversion through convergent-divergent nozzles, noting nozzle efficiency and droplet size

13 p2245 A69-27477

Air-water and steam-water flows in two phase Laval nozzles, measuring flow rates and temperature and pressure variation

13 p2245 A69-27481

Gas and polydispersed condensate parameters of nonequilibrium two phase flow in Laval nozzle, considering particle collisions and coagulation, energy exchange and momentum exchange

14 p2391 A69-29621

Continuous supersonic plasma wind tunnel obtained using magnetic Laval nozzle made by modification of Q device normal magnetic field configuration

15 p2589 A69-30909

Fluidic sensors for jet engine control, analyzing convergent divergent nozzles, vortex and acoustic oscillators for pressure and gas temperature measurements [AIAA PAPER 69-542]

16 p2843 A69-32699

Viscous convergent-divergent nozzle flow slender channel approximations, discussing roles of nozzle geometry, Reynolds number and wall temperature, calculating velocity, enthalpy, etc [AIAA PAPER 69-654]

17 p2894 A69-33502

Divergence losses of noncircular C-D nozzles based on approximation by spherical source flows

19 p3238 A69-35960

Hydrogen jet structure ejected into vacuum from Laval nozzle at supersonic velocity, considering separation point from diffuser wall

19 p3240 A69-36601

He and Ar arc-heated flows into reservoir and expansion in converging-diverging supersonic nozzles, considering flow equilibrium effect on heat transfer and enthalpy

20 p3631 A69-37198

Relaxation equations for oscillatory degrees of freedom of molecular supersonic binary gas flow in Laval nozzle, obtaining population inversion

21 p3693 A69-38692

Quasi-one dimensional analysis for nonequilibrium flow of dissociated diatomic gas through converging-diverging nozzle, discussing critical mass flow rate

22 p3927 A69-40583

Transonic expansion analysis applied to flow through convergent-divergent nozzles with small throat radius of curvature, noting coordinate system selection

23 p4060 A69-41906

CONVERGENT NOZZLES

Interactions between outer and inner jets behind maximum cross section of jet engine nozzle [ONERA-TP-600]

02 p0187 A69-11620

Nozzle geometry influence on argon plasma flow parameters in shock tube, discussing measurement data behind shock wave front

03 p0481 A69-14160

Argon flow characteristics in converging nozzle in continuum, slip and free molecular regimes [ASME PAPER 68-WA/FE-9]

05 p0698 A69-16089

Asymptotic boundary curves for two dimensional and axisymmetric incompressible irrotational flows into throat of convergent duct

10 p1680 A69-23893

Steam-water convergent condensing injector with supersonic inlet vapor, discussing axial pressure profiles and discharge pressure

13 p2372 A69-27486

Argon flow characteristics in converging nozzle in continuum, slip and free molecular regimes [ASME PAPER 68-WA/FE-9]

14 p2390 A69-29445

Boundary layers coalescence on plane convergent channel walls investigated with analytic formulas for velocity distribution, shear stress, layer thickness, etc

15 p2592 A69-31009

Velocity decay and heat transfer rates measurement in cylindrical wall jet formed by jet emerging through convergent nozzle

21 p3695 A69-38972

Liquid alumina particles agglomeration in convergent and throat region of nozzle leading to performance decrease by increasing velocity and temperature difference between phases

22 p4001 A69-40929

Convergent conical nozzles discharge coefficient calculated as function of operation mode and nozzle geometry

24 p4364 A69-43074

CONVERTAPLANES

U V/STOL AIRCRAFT

CONVERTERS

Equivalence and stability for negative impedance converter of bridge circuits by symmetrical amplifier design

09 p1467 A69-22559

Wave-mode converter with feed for omnidirectional antenna excitation, discussing H to E wave conversion, waveguides, emitter, etc

11 p1854 A69-25616

Resonance method determining spurious modes excitation in natural mode converter, discussing construction, application and mathematical correlation

11 p1856 A69-25630

Inductive converters accuracy calculation by statistical method based on probability theory

13 p2259 A69-27424

Tubes faults monitoring in three phase Graetz converter bridges by measuring voltage across DC smoothing inductor

15 p2575 A69-30180

Fluidic curved-wall electropneumatic converter optimization, presenting steady state, step and pulse mode responses for various positions and lengths of resistive heaters

15 p2553 A69-31298

Stabilized DC to DC converter advantages in output voltage, overall dimensions and efficiency for battery driven mobile equipment

16 p2765 A69-32443

MPD converters in pulsed and continuous modes, discussing inductive propulsion system

22 p3999 A69-39905

Modularized static AC and DC inverters and converters for aerospace electrical power conditioning systems, discussing circuit functions and performance tests

23 p4073 A69-42292

Three phase DC-AC inverter with low harmonic distortion, good efficiency and packaging capability, stabilizing frequency by crystal controlled clock oscillator

23 p4074 A69-42294

CONVOLUTION INTEGRALS

Proper digital filters devoid of transient response analyzed as extension of time invariant filters

02 p0213 A69-12815

Recursive formulas for numerical evaluation of real convolution integral for simulation of control systems and electrical networks on digital computer

06 p0947 A69-17250

Upper and lower bounds for feedback decoding and definite decoding minimum distances of binary convolutional codes

06 p0904 A69-17865

Fundamental solutions of initial value problems related to Euler-Poisson-Darboux equation generalized for radially symmetric case, developing convolution integrals

09 p1533 A69-22796

Unsteady surface and internal waves diffraction induced by source in ideal incompressible fluid, obtaining solutions in form of convolution and transfer functions

12 p2061 A69-25953

Convolution property of Hermitian transform for odd integral values of n

15 p2645 A69-30863

Algorithm for constructing random error correcting convolutional codes

24 p4284 A69-42723

Liapunov functionals for time delay systems by path integrals in state space, using convolution equations involving distributions with compact support

24 p4295 A69-43317

CONVOLUTIONS [MATHEMATICS]
U CONVOLUTION INTEGRALS

CONVULSIONS

Mice convulsions at varying hyperbaric oxygen pressures and carbon dioxide content correlated with decreasing brain alpha aminobutyric acid levels

19 p3257 A69-35972

Hyperbaric oxygen convulsions origin and site, studying pressure effect on brain electrical activity in rabbit by EEG

21 p3656 A69-38977

COOLANTS

NT ENGINE COOLANTS

NT ORGANIC COOLANTS

Concorde fuel management, discussing trim, fuel as coolant and booster pumps

07 p1057 A69-19705

COOLING

NT AIR COOLING

NT EVAPORATIVE COOLING

NT FILM COOLING

NT LIQUID COOLING

NT QUENCHING [COOLING]

NT RADIANT COOLING

NT REGENERATIVE COOLING

NT SUPERCOOLING

NT SURFACE COOLING

NT SWEAT COOLING

Transpiration and dissipation effects on heat eddy diffusivity over two dimensional plate in turbulent flow for various Prandtl numbers

01 p0178 A69-11410

Cooling rate effect during aging on heat resistance of forged blanks of nickel based chromium alloy

02 p0266 A69-12125

Electron emitter cooling and plasma heating of thermionic converters noting effects of plasma density, diode spacing, etc

03 p0368 A69-13127

Solid body surface temperature relation to heat flux during cooling by fluid flow solved on computer

07 p1241 A69-18923

Cooling requirements for high speed polytetrafluorethylene lubricated ball bearings operating in cold hydrogen gas, developing minimum gas flow rate equation

[ASLE PAPER 68-LC-2] 07 p1141 A69-19310

Weld mechanical properties of Ti-6Al-2Sn-4Zr-2Mo titanium alloy as function of cooling rate changes or transformation rate shifts resulting in wide range of hardnesses

08 p1318 A69-19965

High temperature regions cooling as applied to solar flares, considering energy losses due to heat conduction, bremsstrahlung, line emission and recombination radiation

09 p1588 A69-21362

Optimum cooling of homogeneous isotropic cylindrical body with constraints on magnitude of thermoelastic stresses

11 p1976 A69-24772

Induced stressing method for complex castings by controlled cooling during heat treatment applied to front frame of J-79 turbojet engine

13 p2269 A69-28184

Martensite transformation with fcc lattice in Ti alloys containing 5.9 percent Fe analyzed as function of cooling rate using X ray analysis

15 p2636 A69-30105

High temperature regions cooling as applied to solar flares, considering energy losses due to heat conduction, bremsstrahlung, line emission and recombination radiation

18 p3197 A69-34752

Ramsdorf meteorite chondrules and metal particles formation attributed to shock-induced partial melting and rapid cooling

19 p3409 A69-36088

Heat protection efficiency of plane surface in turbulent boundary layer behind tangential slots, comparing cooling effects of insulating gas films

20 p3631 A69-37095

Temperature and fluid distribution in porous solid subjected to large suction, convective heating and radiative cooling on one surface

20 p3514 A69-37225

Heated body cooling off study via temperature field isothermal lines visualization on TV screen
20 p3539 A69-37437

Orthopyroxenes cooling history, studying order-disorder transitions between ferrous iron and magnesium
20 p3523 A69-37518

Titanium strengthened high strength hot-rolled steels, discussing cooling rates leading to complete ferrite phase transformation
21 p3743 A69-38652

Melt cooling rates effect on supersaturated solid solutions in Al ternary systems
21 p3745 A69-38955

Mathematical modeling techniques applied to thermoelastic cooling for plate without clamping and mechanical loads, examining integrator schematic diagram
21 p3680 A69-39851

COOLING FINS

Heat transfer efficiency of triangular radiating fin in diathermal medium producing aerodynamic heating
02 p0354 A69-12490

Heat transfer and temperature distribution in thin fins with stochastic root temperature due to excitation by stochastic and Markov processes
[ASME PAPER 68-HT-35] 13 p2374 A69-27780

Triangular profile circular fins efficiency determined from differential equations solution governing temperature distribution
13 p2375 A69-27790

Seam welded U-type fin efficiency and effectiveness, studying effects of fin height, heat transfer coefficient and thermal resistance
19 p3452 A69-36371

Rectangular fins arrangement on horizontal surfaces for optimum free convection heat transfer coefficient, considering fin weight, height and spacing effects
[ASME PAPER 69-HT-44] 24 p4409 A69-43517

One dimensional numerical solution for steady state thermal behavior of trapezoidal profile annular fins transferring heat by conduction and radiation
[ASME PAPER 69-HT-6] 24 p4413 A69-43553

COOLING SYSTEMS

Nosetip cooling system based on discrete subsonic forward liquid injection through ablative nosetip opening of blunted reentry vehicle
[AIAA PAPER 68-1141] 03 p0532 A69-13559

Active cooling systems for high performance reentry vehicles in thermal and shear stress environments
[AIAA PAPER 68-1154] 03 p0533 A69-13669

Increasing vortex tubes energetic cooling efficiency for cooling aircraft components by using potential energy of gas emitted from tubes
04 p0684 A69-14488

Helium cryostat designed to operate under overload and vibrations and used for cooling onboard superconducting devices of Cosmos 140 satellite
04 p0585 A69-15407

Lithium metal spray structural cooling system for refractory materials
[AIAA PAPER 68-358] 04 p0688 A69-15509

Nuclear rocket engine exhaust gas cooling by injecting water jet eliminates need for secondary cooling
[AIAA PAPER 68-604] 04 p0591 A69-15516

GaAs injection diode laser cooled by closed cycle gas refrigeration system, noting time required to reach laser operating temperature
05 p0777 A69-16793

Conduction equations for conduction cooling of human body solved by finite difference method
06 p0880 A69-17088

Optimizing radiating system consisting of radially diverging conical heat removing projections attached to cooled isothermal sphere
06 p1033 A69-17603

High turbine inlet temperature technology using thermosiphon cooling for gas turbine, possibly doubling specific horsepower of aircraft
[SAE PAPER 690034] 07 p1203 A69-18311

Circulating liquid laser system using neodymium in selenium oxychloride, discussing cooling advantages and components
[IEEE PAPER M-70] 07 p1153 A69-19069

Liquid fuel rocket engine design for cooling by propellant counter flows
08 p1376 A69-20588

Personal cooling in inadequately air conditioned cockpits, considering dry air, air ventilated suits and liquid circulated tubes near skin
[AGARDGRAPH-111] 08 p1267 A69-20684

Radiation cooled MPD arc thruster design and performance, noting specific impulse relation to arc spoke rotation frequencies
[AIAA PAPER 69-245] 09 p1566 A69-21259

Turbine blade cooling research programs, discussing effects of increased trailing edge thickness and cooling air on turbine efficiency
[ASME PAPER 69-GT-15] 09 p1432 A69-22501

Cooled turbine performance evaluation methods, noting promise of analytical methods
[ASME PAPER 69-GT-63] 09 p1572 A69-22517

Ranque vortex tube as cooling device in MA-3 ventilating garment
09 p1447 A69-22550

Spray cooling techniques for thermal protection of aerospace structures including lithium spray cooling, vapor collection and condensation, etc
11 p1966 A69-24532

TWT heat pipe cooled depressed collector designed as compact heat transfer device and electrical insulator
11 p1847 A69-24746

High power TWT tube cooling in space vehicle, discussing thermal control system based on heat pipe radiator
11 p1847 A69-24747

Initial nonuniformity effect of temperature distribution in main stream on efficiency of cooling by air injection through slit or porous collar
11 p2002 A69-25338

Rocket propulsion devices classifications, discussing energy sources, propellants, performance, space vehicle applications, liquid propellant rockets, engines, selection criteria and cooling methods
11 p1943 A69-25587

Ablation cooling application to aerodynamic heat shielding, discussing various materials, sublimation, rocket probe ascents, satellites and experimental aircraft
12 p2011 A69-25854

Heat removal from laser ruby rod by Cu prism connected to cooling system, discussing limiting factors in heat transfer area size
12 p2108 A69-26592

Fluidic systems for automatic control of fuel supply to ramjet engine combustor, coolant rationing and distribution to engine structure and performance efficiency maintenance
14 p2508 A69-28875

Freons applications to radiation detector cooling, calculating specific volumes and compressibility factors for Freon 14
14 p2447 A69-29330

Spray oil cooling to reduce aircraft generator weight, enhance reliability and lengthen overhaul intervals
15 p2552 A69-30326

Solar simulator with 20 kw xenon lamps, discussing performance, versatility and problems with collectors, folding mirrors and cooling system
15 p2586 A69-30384

Water cooled split-flow probe measuring enthalpy of high temperature subsonic streams
15 p2614 A69-31275

NERVA engine cooldown system for emergency shutdowns using high pressure liquid H followed by gaseous H warmup and liquid N cooldown
[AIAA PAPER 69-512] 16 p2810 A69-31846

Heat pipes design for rocket engines cooling, discussing connections to space radiator and to heat rejection device and heat transfer capability
[AIAA PAPER 69-582] 16 p2839 A69-32668

Packed bed catalytic reactors cooling capacity in promoting endothermic reactions of hydrocarbon fuels, using computerized temperature and composition profiles
[AIAA PAPER 69-588] 17 p3071 A69-33265

Cooling system control system for astronaut thermal equilibrium and work output maximization during extravehicular space missions
[AIAA PAPER 69-617] 17 p2914 A69-33278

Turbine blades materials with emphasis on oriented solidification of eutectic alloys, discussing blades cooling by thermosiphons or ducts
17 p2978 A69-33334

Continuous mode operation in hypergolic bipropellant low thrust rocket motors, discussing high temperatures reached by combustion chamber walls and cooling solutions
17 p3019 A69-33335

Turbine blade cooling emphasizing economics, service life and computerized calculations
17 p3020 A69-33352

Technology trends in airbreathing propulsion, discussing noise control for subsonic jet transports, turbine blade cooling, etc
[AIAA PAPER 69-774] 19 p3244 A69-35648

Water injection cooling of exhaust gases during stage testing of NERVA engine, discussing exhaust duct con-

figuration and flow characteristics, spray nozzle geometry, etc
[AIAA PAPER 69-514] 19 p3372 A69-36301

Vortex flow air cooling system for lasers using vortex effect of gas separation, resulting in minimum weight and dimensions and high cooling efficiency
21 p3734 A69-38399

Active cooling systems for high performance reentry vehicles in thermal and shear stress environments
[AIAA PAPER 68-39016] 21 p3851 A69-39016

Electronic equipment environmental cooling by controlled airflow systems, reviewing systems designs, control problems, etc
22 p3954 A69-40035

Cooldown of vacuum insulated transfer lines using liquid N and H, discussing flow characteristics reproduction by digital computer program
[NAS-NRC PAPER I-1] 22 p4050 A69-40625

Heat pipe design for electron tubes cooling at various temperatures, including dielectric heat pipes and traveling wave tubes
[ASME PAPER 69-HT-25] 24 p4412 A69-43543

Heat pipe coupled to air cooled heat exchanger to cool high power airborne radio component by dissipating thermal load into ambient air
[ASME PAPER 69-HT-16] 24 p4413 A69-43552

Scramjet engine active cooling with regenerative system using superalloy heat exchangers and hydrogen fuel as coolant
[AIAA PAPER 68-1091] 24 p4365 A69-43725

COORDINATE SYSTEMS
U COORDINATES

COORDINATE TRANSFORMATIONS

Analytic photogrammetric determination of lunar control coordinates from Ranger photography
01 p0147 A69-10022

Equations of motion of satellite in rotating coordinate system, noting effects of precession and nutation on transformation of orbital elements
01 p0150 A69-10445

Algorithm for Navier-Stokes and continuity equations used to derive curvilinear coordinate system
04 p0564 A69-14858

Computer programming of satellite orbit tracking angles for automatic picture transmission receiving stations
04 p0558 A69-14917

Einstein equations solution in Gaussian coordinates describing particles gravitational fields including point particles
07 p1180 A69-18507

Coordinate transformations eliminating singularities in gravitational radius of Schwarzschild metric, noting local Lorentz transformations
08 p1351 A69-19952

Terminal optimal control problem for linear system having control criterion not dependent on all phase coordinates
12 p2045 A69-25965

Convective heat transfer, discussing coordinate transformation, similarity analysis similitude and Meksyn integration of boundary layer equations
13 p2376 A69-28139

Equations derived for radar image coordinate transition to geodetic coordinates in aerial surveying by side-looking airborne radar
15 p2596 A69-30574

Cosmic ray shower axis mean logarithmic distance from apparatus calculated by transforming shower recording frequency radial distribution to lin-log coordinate system
17 p3024 A69-33581

Coordinate transformation of Euler equations governing precession and nutation of self gravitating bodies of viscous fluid in inertial coordinates
21 p3797 A69-38539

Computer program for satellite APT geographical grid production, discussing latitude-longitude intersections transformation to Cartesian coordinates
21 p3718 A69-39749

Horizontal Situation Display /HSD/ map computer mechanization transforming earth location to X, Y coordinates for Lambert conformal projection
[AIAA PAPER 69-987] 22 p3908 A69-40367

COORDINATES
NT ASTRONOMICAL COORDINATES
NT CARTESIAN COORDINATES
NT GEOCENTRIC COORDINATES
NT GEODETIC COORDINATES
NT HYPERBOLIC COORDINATES
NT INERTIAL COORDINATES
NT INERTIAL REFERENCE SYSTEMS
NT LAGRANGE COORDINATES
NT PLANETOCENTRIC COORDINATES
NT POLAR COORDINATES

Analytical mechanics of chemical reactions, discussing natural collision coordinates for three dimensional reactions and exchange collisions for molecule and atom

01 p0123 A69-10681

Errors arising from inaccurate insertion of initial conditions in autonomous determination of coordinates of object moving along surface of spherical earth

02 p0281 A69-12137

Coordinates interpretation in Schwarzschild problem, projecting space of events by light beams onto Galilean system at infinity

03 p0506 A69-13090

Optimum addition of abscissas in quadrature formulas by expansion of abscissas equation in Legendre polynomials

03 p0455 A69-13372

Maximum probability technique for measuring angular coordinate with unknown signal and noise intensity

03 p0399 A69-14132

Local cross sections method for optimal control, considering control plant with variable control range and constraints on phase coordinates

07 p1115 A69-19003

Transient heat flow in isotropic solids by electrical analog modeling in orthogonal curvilinear coordinate system

09 p1477 A69-22241

B. L. coordinates for mapping geomagnetically trapped particles distribution computed by perturbation method, using perfect dipole as zero order approximation

11 p1949 A69-24861

Inertial navigation systems error analysis based on method of state variables

11 p1914 A69-25434

Motion of heavy body with gyroscope, using coordinate system to reduce problem to linear second order differential equation

11 p1920 A69-25746

Fundamental concepts of nonholonomic coupling and coordinates in nonholonomic mechanics

12 p2129 A69-25990

Coordinates interpretation in Schwarzschild problem, projecting space of events by light beams onto Galilean system at infinity

14 p2516 A69-28772

Transit forecast of terrestrial satellite moving through fixed coordinate line in assigned reference

16 p2859 A69-32221

Rayleigh criteria extension for boundary layers of rotationally symmetrical bodies with curved meridian, utilizing orthogonal coordinate system

19 p3298 A69-36309

Thomas wave equation in fluid mechanics, examining coordinates system with normal hyperbolic metric of universe tube having given signature

20 p3598 A69-37430

Space vehicle electronic attitude measurement method for reference coordinate and fixed coordinate systems based on rectangular coordinates of RF wave propagation directions

20 p3574 A69-37703

Mathematical formulation and error analysis of two rotor gyroorbit used in plotting orbital system of satellite coordinates

21 p3765 A69-39636

Spherical lunar coordinates for arbitrary moment of time calculated by digital computer using Brown lunar motion theory

22 p4024 A69-40611

Natural coordinates in finite element method, giving formulas for straight or curved element analysis and polynomial integration

23 p4182 A69-41901

Geographical position coordinates of radio operator determined by distance difference measurement using Loran and digital computer methods

23 p4186 A69-42027

Combined automatic control systems stability having principal coordinates related by loading equation

23 p4145 A69-42370

Optimal control parameters for gyroscopic devices with constrained phase coordinates obtained on analog computer by introducing equivalent phase coordinates system

24 p4317 A69-43708

COORDINATION

Component total task relationships, analyzing simple and sequential practice effects with aid of Melton Complex Coordinator

02 p0203 A69-12214

Arbitrary human motions coordination in reorganization phases determined during weightlessness for cyclographic analysis of adjustment time

07 p1065 A69-18979

Optimal control of multivariable complex systems through multilevel/hierarchical/ structure, discussing coordination problems

12 p2049 A69-26082

Motion coordination capacity of persons subjected to 40 days bed rest studied by dynamographic technique, discussing nature of slackening

17 p2906 A69-32937

Human motion coordination under acceleration followed by weightlessness during jet flights along Keplerian orbits, discussing initial disturbance and subsequent subsiding

17 p2907 A69-32938

Hand movements in water environment, weightlessness and normal gravity conditions, discussing inner coordinative structure and muscular efforts

17 p2915 A69-33385

Arbitrary human motions coordination in reorganization phases determined during weightlessness for cyclographic analysis of adjustment time

20 p3479 A69-38227

COPILOTS

U AIRCRAFT PILOTS

COPLANARITY

Theory of fatigue crack growth crystal in metals in terms of coplanar dislocation arrays extended to oblique slip planes, discussing orientation

01 p0168 A69-10344

Optimal transfer between coplanar orbits in Newtonian force field without intersecting circle boundaries

10 p1790 A69-24191

Coplanar impulsive transfers and second variation test, using maximum principle and Lagrangian multiplier technique for propellant expenditure minimization

19 p3400 A69-35676

COPOLYMERS

Permittivity and loss tangent of unsaturated styrene polyester copolymers at various temperatures and frequencies

[ONERA-TP-662]

04 p0621 A69-15114

Polymer structure effect on chemical resistance of reinforced plastics, sulfuric acid and sodium hydroxide corrosion of polyester resins and model copolymers

08 p1338 A69-20490

Electron beam radiation curing of mercaptan terminated butadiene-acrylonitrile liquid copolymers at ambient temperatures in air

09 p1512 A69-22368

Block tractable azomethine copolymers prepared by reaction of insoluble oligomers with monomers or of two different fusible oligomers, noting high thermal stability

13 p2217 A69-28317

Enzyme transitions in RNA polymerase state during unprimed synthesis of r/I-C/ copolymer, noting dimer-monomer pattern during lag phase

22 p3895 A69-40050

COPPER

Surface fatigue significance in sliding wear studied from damage on copper single crystal using electron microscope techniques

01 p0085 A69-10368

Liquid copper electrical conductivity temperature dependence at very high temperatures from magnetic diffusion and flux penetration measurements, noting exploding wires role

01 p0119 A69-10673

Specific heats of Cu, GaAs, GaSb, InAs and InSb measured over low temperature ranges

01 p0140 A69-11252

Solar copper abundance determined from measuring Cu 1 and 2 and resonance lines transition probabilities in electric arc emission under LTE conditions

02 p0204 A69-11456

Recombination effects in high resistivity Cu doped gallium arsenide single crystals determined by photoconductivity methods

02 p0294 A69-11627

Dynamic tensile stress-strain curves for annealed Al, Cu and Fe at constant strain rates, describing experimental method

03 p0524 A69-13065

Dislocations effect on decomposition rates of solid solutions of InAs and Au, Ag or Cu

03 p0484 A69-13283

Fatigue mechanism in fcc metals at ultrasonic frequencies, comparing microstructural changes in copper and alpha-brass

04 p0613 A69-14448

Pulse broadening in MHD copper vapor laser

07 p1149 A69-18904

Impurity atoms effects on Cu diffusion and solubility in GaAs, determining Hall coefficient temperature dependence and conductivity

07 p1199 A69-19009

Tensile deformation properties of copper single crystals strengthened by fine dispersions of BeO particles

08 p1334 A69-20575

Copper diffusion coefficient in undoped n-type gallium arsenide measured by ultrasonic method

09 p1555 A69-21471

Dislocation substructure near fatigue fracture surface during tensile mode crack growth in copper single crystals by transmission electron microscopy

10 p1797 A69-23079

Etch pits behavior during diffusion and rediffusion of copper in low dislocation crystals of gallium arsenide, demonstrating vacancy nature

11 p1937 A69-25029

Copper and aluminum fatigue in vacuum and ultrahigh vacuum, discussing effects of hydrogen, nitrogen and oxygen pressures

13 p2280 A69-28088

Copper diffusion coefficient in undoped n-type gallium arsenide measured by ultrasonic method

15 p2669 A69-30716

Lattice vibration theory of solid state diffusion for Cu including anharmonic effects formulated using equilibrium statistical mechanics, considering interacting phonon events

17 p3015 A69-32822

Heat transfer from cylindrical copper surface to liquid helium at 4 degrees K, discussing temperature fluctuations in nucleate boiling region

17 p3074 A69-33780

Materials integral hemispheric radiative capacity determination based on cooling rate of thin walled specimen in vacuum, considering stainless steel, Ni and Cu

18 p3156 A69-34698

Automatic electropolisher for copper disks

21 p3720 A69-38597

COPPER ALLOYS

NT BRASSES

NT BRONZES

NT MANGANIN [TRADEMARK]

Electron band structure of copper-nickel alloys, discussing thermoelectric properties, energy ranges and effect of alloying additions

02 p0301 A69-12765

Aluminum additive effects on copper-titanium alloy decomposition, discussing Guinier complexes, heterogeneous nucleation, plastic deformation and low temperature aging

11 p1905 A69-24922

Heat resistant Fe and Cu alloys creep index affected by temperature, testing time and specimen grain size

15 p2639 A69-30569

Sliding friction tests of Cu and Cu-Be alloy plates in contact with various alloy sliders in air and vacuum [ASLE PAPER 68-LC-5]

15 p2622 A69-30610

Friction effects on friction couples made of two different nonferrous alloys, discussing temperature regime difference effects on microgeometry and structure

15 p2629 A69-31027

Joints structure, phase and chemical composition in kinetics of titanium diffusion brazing with copper

22 p3958 A69-41203

COPPER COMPOUNDS

Thermal decomposition of ammonium perchlorate and ammonium perchlorate-copper chromite mixtures

02 p0304 A69-12312

Unidirectionally solidified eutectic composite of Al and Cu-Al intermetallic, noting tensile properties at room and high temperatures

10 p1708 A69-22995

Proton transfer mechanism of copper chromite catalyzed thermal decomposition of ammonium perchlorate, noting electron transfer

21 p3783 A69-38810

COPPER OXIDES

Temperature dependence of resistivity of zirconium oxide with copper oxide additions indicates suitability as heat sensitive resistor material in 300 to 1000 degree C range

16 p2827 A69-32482

COPPER SULFIDES

Impurity profiles and energy band diagram for cuprous sulfide-CdS heterojunction based on capacitance, Hall and electron microprobe measurements

03 p0368 A69-13075

- Copper sulfide-cadmium sulfide heterojunction model for photovoltaic effect, considering surface layer intrinsic absorption and CdS photoconductivity
19 p3250 A69-35683
- Photovoltaic effect at copper sulfide-cadmium sulfide heterojunction, studying depletion layer width, diffusion lengths and spectral response
19 p3382 A69-35684
- Resistivity, layer thickness, postbarrier heat treatment and impurity effects on cadmium sulfide-copper sulfide solar cell
19 p3250 A69-35685
- CORDIERITE**
Cordierite application to radomes for high velocity engines, discussing dielectric properties at microwave frequencies, mechanical properties, temperature control and fabrication
07 p1168 A69-19525
- CORDITE**
U COLLOIDAL PROPELLANTS
U DOUBLE BASE PROPELLANTS
- CORE FLOW**
Axisymmetric MHD flow in turbulence chamber at large Hartmann numbers studied for flow boundary layer effects
01 p0130 A69-10772
- Solar interior rotational angular velocity influence on solar oblateness, noting reduction by turbulent mixing
09 p1600 A69-22201
- Wall flows and wake laws validity analyzed by wall balance technique, considering boundary layers under perturbation and core flow restrictions
13 p2251 A69-28633
- Fluid dynamic simulation of gas core nuclear rocket chamber for separating light and heavy gas via centrifugal force produced by MHD-driven rotational flow [AIAA PAPER 69-727]
17 p3004 A69-33483
- Fluid velocities at earth core surface inferred from magnetic data, considering velocity constraints and diffusion contributions to secular change
18 p3129 A69-34951
- Diverging nozzle flow of gas mixtures containing solid or liquid particles analyzed by one dimensional approximation separately averaging boundary layer and flow core
19 p3298 A69-36389
- Operational characteristics of multiple arcjet wind tunnel for time varying mass flow rate programs, calculating isentropic core densities and velocities [AIAA PAPER 68-229]
22 p3927 A69-40541
- Axial and angular momentum flux, flow force and circulation to determine strength and structure of narrow rotating axisymmetric vortex and swirling core flows
24 p4298 A69-42598
- CORE STORAGE**
Ferrite core storages characteristics with rectangular hysteresis loop for digital control units, discussing optimal selection method
14 p2418 A69-29145
- Dual role core /Ducor/ memory system with unique core stack assembly feature to achieve cost reduction and structural integrity for severe environmental conditions
22 p3903 A69-39950
- CORES**
NT HONEYCOMB CORES
NT MAGNETIC CORES
NT REACTOR CORES
- Red giants limiting helium core mass dependence on total stellar mass and initial composition from stellar evolutionary models
02 p0327 A69-12710
- Lunar core electrical conductivity determination based on induced magnetic field arising from time varying interplanetary magnetic field associated with solar wind plasma
07 p1215 A69-18832
- Metal castings around ceramic cores for economic manufacture of jet engines
09 p1503 A69-21907
- Star counts in star cluster neighborhoods, obtaining ratios of corona radius to nucleus radius as function of cluster mass
11 p1951 A69-24246
- Postbuckling of filled circular cylindrical shell using Ritz energy method for load deformation relation, discussing stabilizing effect of core
22 p4038 A69-39895
- CORIOLIS EFFECT**
Universal vestibulometric chair for inducing irritation in tests involving vestibular analyzer interaction with other body functions
02 p0200 A69-11517
- Coriolis acceleration dosages applied in vestibulometric tests of male subjects inclined in rotating chair
05 p0710 A69-16521
- Coriolis stimulus effect during centrifugal g load on spatial orientation and accompanying stick performance
06 p0876 A69-18023
- Human vestibular and sensory reactions to rotation and rocking, Coriolis acceleration and vestibular reaction inhibition on ground test stand for effects of temporary weightlessness
07 p1062 A69-18586
- Vestibular-vegetative reactions during angular and Coriolis accelerations alternating with weightlessness, noting increased parasympathetic and sympathetic activity
07 p1062 A69-18587
- Overt motion sickness prevention by incremental exposure to Coriolis accelerations
07 p1067 A69-19425
- Coriolis acceleration in rotating environment, discussing origins and role in human existence in rotating space station
09 p1540 A69-21891
- Motion sickness studied with slow rotation room having controlled Coriolis accelerations, discussing oculogyral illusion, nystagmus, dizziness and neuromuscular incoordination
12 p2019 A69-26547
- Human nystagmic reaction variations due to simultaneous rotation of head and body, studying coriolis couple in horizontal semicircular canals
12 p2020 A69-26565
- Azimuthal electric currents generation by Coriolis forces in hot stars with intensive radial flows in convective zones
13 p2350 A69-27862
- Stratified rotating fluid time dependent motion characterized by stability frequency ratio and Coriolis parameter within quasi-geostrophic approximation
13 p2248 A69-28171
- Coriolis effect in rotating spacecraft simulation, discussing optokinetic reflex responses as function of head turning angle with spin axis
14 p2409 A69-29300
- Equations for gradually changing motion by differentiating momentum and energy equations with respect to abscissa noting wall resistance, viscosity, turbulence and Coriolis coefficients
15 p2593 A69-31489
- Coriolis acceleration dosages applied in vestibulometric tests of male subjects inclined in rotating chair
18 p3096 A69-34740
- Coriolis acceleration effect on vestibulo-vegetative and vestibulo-somatic reflexes of humans subjected to forward tilting, noting pulse and respiration rates
20 p3472 A69-37259
- Vestibular functions of humans subjected to Coriolis acceleration via prolonged rotation at different angular velocity rates
20 p3472 A69-37260
- Vestibular analyzer dynamic characteristics under Coriolis acceleration, measuring heart beat rate, arterial pressure, head bending aftereffects, etc
20 p3472 A69-37262
- Vestibulometric tests for flight surgeon appraisal of applicants in flying profession, comparing Coriolis forces cumulative load tests with conventional tests
20 p3481 A69-37278
- Incompressible electrically conducting fluid in presence of magnetic field and Coriolis forces, analyzing Rayleigh-Taylor instability by variational principles
20 p3577 A69-38195
- Human susceptibility to motion sickness under Coriolis acceleration during parabolic flight weightlessness
21 p3659 A69-39168
- Initialization technique for primitive forecast equations balancing Coriolis and pressure forces effects on atmospheric observations
24 p4344 A69-43065
- Inertial motions, equipotential surfaces and Coriolis forces on earth ellipsoid, discussing pendulum-like oscillations
24 p4346 A69-43156
- CORNEA**
Corneal greyish opaque arc as warning of atherosclerosis in flight crews
05 p0711 A69-16631
- Monomethylhydrazine /MMH/ toxic effects on cornea and blood aqueous barrier studied in vivo on dogs
09 p1447 A69-22547
- Rabbit corneal damage thresholds for Gaussian beams of carbon dioxide laser IR radiation at various exposure times
11 p1830 A69-24844
- Corneal epithelium chromosome rearrangements in gamma irradiated white adult mice, noting radiation dosage and duration
17 p2907 A69-32944
- Corneal stroma collagen fibrils and ground substance refractive indices, discussing corneal transparency and clouding
22 p3884 A69-40886
- CORNERS**
Downstream secondary circulation resulting from sharp bend in fully developed turbulent pipe flow, noting departure from twin circulatory flow
03 p0419 A69-13952
- Two dimensional supersonic rotational flow around convex corner solved using coordinate system consisting of left running characteristics and streamlines
05 p0697 A69-15722
- Network method for Dirichlet problem of Laplace equation in regions with rounded corners, noting polar and composite errors
12 p2123 A69-26730
- Diffraction and mirror analyses of right angle corner in overmoded waveguide for scattered modes, discussing transmission loss
13 p2234 A69-28426
- Turbulent boundary layer in corner, measuring velocities, wall shear and turbulent normal stresses by employing momentum integral and similarity analyses
14 p2431 A69-29576
- CORONA DISCHARGES**
U ELECTRIC CORONA
- CORONAGRAPHS**
Space observations of solar intermediate corona, discussing balloon and rocket experiments and limitation of ground based observations [AAS PAPER 68-217]
02 p0313 A69-11483
- Coronagraphic determination of hydrogen concentration in luminescence regions of ionized metals in lower chromosphere
03 p0420 A69-13086
- Coronagraphic determination of hydrogen concentration in luminescence regions of ionized metals in lower chromosphere
14 p2433 A69-28768
- Optical and mechanical systems of Wrocław Observatory Lyot type coronagraph for prominence observations in H alpha line
22 p3943 A69-39999
- Thermostatic electronic control device of birefringent filter in Wrocław Observatory coronagraph during prominence observations
22 p3943 A69-40000
- CORONARY CIRCULATION**
Coronary atherosclerosis in military pilot fatalities of aviation accidents, demonstrating irrelevance of amount of flying time and type of aircraft
03 p0376 A69-14080
- Reflex activity of single preganglionic sympathetic fibers during coronary occlusion in cats, discussing left third thoracic /T3/ ramus communicans
23 p4084 A69-41460
- Coronary vessel lumen changes under oligemic hypotension resulting from circulating blood volume decrease in anesthetized cats, discussing constrictory coronary vessel responses
23 p4084 A69-41470
- Noradrenalin release from hearts of open chest dogs given artificial respiration upon occlusion of left descending coronary artery
23 p4092 A69-42053
- Coronary circulation response to hyperoxia after vagotomy and combined alpha and beta adrenergic receptors blockade in anesthetized intact dog
23 p4096 A69-42088
- Pulsatile flow in coronary arteries simplified model compared with experiment in anesthetized dogs
23 p4098 A69-42103
- Sinus outflow relationship to oxygen content in anterior cardiac vein blood and right ventricle systolic pressure
23 p4098 A69-42105
- Frequency analysis of second heart sound splitting in patients with coronary artery disease assessed clinically and by phonocardiography
24 p4261 A69-42726
- Risk factors in coronary diseases modified to provide base for estimating achievable mortality magnitude reduction
24 p4262 A69-43059
- CORONAS**
NT ELECTRIC CORONA
NT SOLAR CORONA

Stellar rotation braking due to mass loss from coronae through stellar wind based on calculation of acoustic energy generation from convective zone
08 p1396 A69-20644

Acoustic energy generation for helium rich stars, discussing X ray radiation from helium star corona
08 p1380 A69-20645

Star counts in star cluster neighborhoods, obtaining ratios of corona radius to nucleus radius as function of cluster mass
11 p1951 A69-24246

Red dwarf star YZ CMi corona structure showing possible estimation of additional carried energy by shock waves after flare
17 p3043 A69-34166

Stellar atmospheres acoustic energy generation rate calculations, studying corona mass ejection effects on stellar rotation
21 p3813 A69-39521

Coronae around helium stars and X ray sources, calculating acoustic energy generation rates in convection zones
21 p3813 A69-39522

CORPUSCULAR RADIATION

NT ARTIFICIAL RADIATION BELTS

NT ATOMIC BEAMS

NT BETA PARTICLES

NT CYCLOTRON RADIATION

NT ELECTRON BEAMS

NT ELECTRON PRECIPITATION

NT ELECTRON RADIATION

NT INNER RADIATION BELT

NT ION BEAMS

NT ION CYCLOTRON RADIATION

NT NEUTRAL BEAMS

NT OUTER RADIATION BELT

NT PARTICLE BEAMS

NT PION BEAMS

NT PRIMARY COSMIC RAYS

NT PROTON BEAMS

NT PROTON BELTS

NT RADIATION BELTS

NT SOLAR CORPUSCULAR RADIATION

NT SOLAR COSMIC RAYS

NT SOLAR PROTONS

Space X ray background measurements, considering relativistic electrons Compton emission and metagalactic gas bremsstrahlung as possible sources
01 p0147 A69-11310

Radiation accidents involving sudden brief exposure to penetrating radiation
03 p0374 A69-13502

F layer disturbance showing pronounced difference in corpuscular flux effect on day and nighttime ionosphere
03 p0512 A69-13517

Meteorological rocket measurement of corpuscular radiation intensity in upper atmosphere at various latitudes
05 p0814 A69-16052

Energy flux into earth thermosphere due to fast corpuscular neutrals arising from charge transfer collisions between solar protons and neutral interstellar H
05 p0817 A69-16654

Angular intensity distribution of corpuscular radiation in time independent geomagnetic field characterized by particle velocity distribution
07 p1210 A69-19619

Electromagnetic waves and photons coexistence, discussing wave mechanics and guidance of particles, photon guidance and corpuscular magnitudes, etc
08 p1351 A69-20117

Corpuscular radiation contributions to D layer ionization determined from intensity measurements
09 p1577 A69-21770

Winter polar mesosphere atomic-oxygen distribution by analyzing data concerning intensity and energy of corpuscular fluxes in auroras
12 p2070 A69-26690

Magnetospheric corpuscular fluxes night ionization role in E and D region, considering precipitation from outside, trapped and dumped particles of radiation belts
13 p2254 A69-28333

Cosmic ray penetrating component properties identical to muon component at mountain level, indicating baryon passive nuclear state nonexistence
13 p2331 A69-28400

High energy mu-mesons component of atmospheric cosmic ray showers by particle impact penetration using multiple underground ionization chambers
13 p2332 A69-28409

Comet scintillations and tail characteristics studied to obtain information on interplanetary flux field, magnetic fields and planetary structures
14 p2523 A69-29704

Corpuscular radiation intensity during geomagnetic disturbances measured during rocket flights at 50-100 km, discussing effects on lower ionospheric radio absorption
15 p2677 A69-31327

Multiple muon showers penetrating deep underground, discussing radial extent and occurrence frequency against multiplicity spectrum
15 p2678 A69-31485

Corpuscular radiation distribution function with trapped particles maximum density fixed in equatorial plane and reflection points vicinity of magnetic force line
19 p3396 A69-36630

Meteorological rocket measurement of corpuscular radiation intensity in upper atmosphere at various latitudes
20 p3591 A69-37962

Interplanetary proton and alpha particle radial gradients determined from Mariner data, considering Forbush decrease, particle solar origin, galactic cosmic radiation, etc
20 p3592 A69-38096

Corpuscular radiation indicated as ionization source in lower ionosphere from rocket sounding data, noting role in D region formation
21 p3787 A69-38352

Neutron flux measurements on Cosmos 53, discussing equipment and calculation of secondary neutrons due to bombardment of satellite components
22 p4003 A69-40274

Corpuscular radiation intensity measurements in upper atmosphere at midlatitudes by meteorological probe during geomagnetic storm, noting radio wave absorption
22 p4008 A69-41104

CORRECTION

U OPTICAL CORRECTION PROCEDURE

CORRELATION

NT ANGULAR CORRELATION

NT AUTOCORRELATION

NT CROSS CORRELATION

NT DATA CORRELATION

NT SIGNAL ANALYSIS

NT STATISTICAL CORRELATION

Modified admittance yielding Kubo admittance at nonzero frequencies, discussing transformation of correlations of Ising model
01 p0115 A69-10019

Generalized pair of space correlation and wave number spectrum functions applied to plasma electron density fluctuations and velocity fluctuations of background fluid
01 p0127 A69-10339

Regular and noise signal scattering by uneven surface determined by correlation functions, assuming monochromatic components scattering obeys Kirchhoff approximation
01 p0032 A69-10886

Time correlation of photons emitted by krypton gas discharge tube and helium-neon multimode laser
02 p0255 A69-11611

Approximation of correlation or transfer function obtained through exponential polynomial to determine stochastic process spectral density
03 p0409 A69-12976

Correlation of received signals with diversified angles of arrival due to scattering by turbulently excited ionosphere
03 p0399 A69-14129

Noise correlation effect on noise stability of diversity reception receiver with weighted coherent summation of signals
04 p0557 A69-14789

Ornstein-Zernike relation for homogeneous fluid relating direct and indirect correlation functions
04 p0591 A69-15435

Real shape of time correlation function computed from partially averaged data
05 p0786 A69-15924

Smith correlation of turbine stage efficiency for relating achievable efficiency to stage loading and flow factors used for total pressure loss coefficient data [ASME PAPER 68-WA/GT-5]
05 p0812 A69-16140

Expression derived for correlation function and power spectrum of bearing of set of point radiators, taking into account receiver internal noise
05 p0719 A69-16219

Electromagnetic wave scattering in ferromagnetic crystals with anisotropy, discussing correlation functions of characteristics fluctuations and magnetoacoustic resonance
05 p0809 A69-16547

Canonical correlations used to analyze relations between values of geopotential field
05 p0789 A69-16637

Black body radiation coherence properties characterization by stochastic Gaussian scalar potential correlation function
05 p0795 A69-16819

Sequences with small correlation functions as error correcting codes in word separation, synchronization and pulse compression systems
06 p0948 A69-17868

Sixth order correlations of laser beam fluctuations near threshold from delayed coincidence measurements with three photodetectors, noting time constants
07 p1144 A69-18252

Signal correlation functions measurement errors due to randomly fluctuating delay, investigating additive and multiplicative noise with periodic and random signals
08 p1296 A69-19923

Antenna tolerances theory, discussing illumination correlation function analytical evaluation for uniform and tapered illuminations
08 p1284 A69-20294

Coherent light fluxes detection, noting correlation characteristics of output signals of photomultiplier illuminated by multimode He-Ne laser
09 p1515 A69-21438

Correlation between responses of linear systems for transient input as performance criterion for servomechanisms
09 p1475 A69-22536

Geomagnetic fluctuations positive and negative correlations at conjugate pair stations Syowa base and Reykjavik
10 p1681 A69-22806

Correlation produced magnetoplasma mode in potassium confirmed by measurement of real part of surface impedance
10 p1728 A69-23168

Time correlation of photons emitted by krypton gas discharge tube and helium-neon multimode laser
11 p1895 A69-24718

Steady state and dynamic characteristics of linear plant with constant lag element based on correlation function moments
11 p1859 A69-24965

Relativistic coherence theory of black body radiation in transparent medium, deriving expressions for second order correlation tensors by phenomenological quantum electrodynamics
11 p1920 A69-25563

Correlation functions and spectral density of current fluctuations in weakly ionized plasma flows
11 p1934 A69-25715

Polarity coincidence correlation method due to random processes state characterization applied to man machine systems
12 p2022 A69-25931

Regular and noise signal scattering by uneven surface determined by correlation functions, assuming monochromatic components scattering obeying Kirchhoff approximation
12 p2031 A69-26650

Correlation spectrometer for air pollution surveillance from airborne and spaceborne platforms, noting scanning satellite system for continuous global coverage
12 p2096 A69-26981

Time correlation functions for wind vectors and components at various altitudes over Moscow in winter and summer
13 p2294 A69-27856

Correlation functions of fluctuations in electrical characteristics of nonequilibrium electron gas during scattering, determining spectral densities and populations by kinetic equation Green function
13 p2314 A69-28445

Canonical correlations used to analyze relations between values of geopotential field
14 p2472 A69-28793

Microstresses and distortions in quasi-isotropic solid bodies under strain evaluated by correlation functions
14 p2531 A69-28806

Statistical description of geomagnetic field as random vector field, presenting correlation functions from empirical estimates from geomagnetic charts
14 p2437 A69-29062

Light emission intensity correlation functions associated with LF oscillations in beam plasma discharge
14 p2498 A69-29814

Interferometer for measuring electric fields spatial correlation function at camera aperture, describing

laser light coherence measurements after propagation through turbulent atmosphere
15 p2653 A69-31164

Book on correlation theory of statistically optimal systems covering linear continuous, discrete, nearly optimal, nonlinear, decision element and adaptive systems
16 p2764 A69-32114

Radio wave single scattering at particles randomly grouped in space, showing correlation function of water content fluctuations in scattered field in clouds
16 p2807 A69-32267

Amplitude distribution and correlation functions of signals reflected from precipitations at various polarizations of waves emitted and received
16 p2807 A69-32269

Optimal linear mean square filtering for piecewise linear correlation functions
17 p2933 A69-33621

Rarefied gases transfer coefficients stochastic process calculation models, comparing results with correlation functions derived from transport equation
18 p3121 A69-34710

Optical imaging with partially coherent nonthermal light, discussing correlation function propagation, transfer functions, spatial Fourier analysis, weak visibility and matrix form
19 p3372 A69-35907

Spectral density of outgoing radiation in 0.6-0.8 micron frequency range, noting reflected radiation and cloud fields correlation functions
19 p3366 A69-36672

Positive and negative correlations in F 2 layer perturbations observed by network of paired conjugate ionospheric stations at low latitude
20 p3521 A69-37050

Eulerian correlation functions representation of wind variations in analytic form by three parameter function, noting field diagram
20 p3571 A69-37507

Range-Doppler data processing of radar echoes from spread targets, considering quadratic filter theory, emphasizing received signal correlation functions
20 p3490 A69-37648

Normalized SNR of aperture antennas determined in terms of random signal and noise fields correlation functions
20 p3494 A69-37845

Dispersion and correlation function for atmospheric transparency due to water vapor from statistical model of absorption bands and effective mass
21 p3759 A69-39113

CORRELATION COEFFICIENTS

Light field inside deep layers of turbid medium illuminated by narrow beam, discussing beam deviations inside medium, deviation dispersions and correlation coefficient
02 p0274 A69-11449

Longitudinal correlation lengths in grid turbulence air flow transport subjected to planar deformation measured from energy spectra of velocity fluctuations
02 p0192 A69-12626

Multichannel communication received signals irregular components, discussing signal phase and amplitude fluctuations correlation coefficients
03 p0394 A69-13519

Diversity antenna continuous short wave radio signal envelope distribution, autocorrelation functions, damping rate and cross correlation coefficients
03 p0394 A69-13522

Correlation coefficient between frequency diversified signals amplitudes estimated by approximation for two beam short wave radio channels
04 p0560 A69-15401

Correlation coefficients, comparing galactic X ray sources distribution with classical cepheids, old novae, planetary nebulae and Wolf-Rayet stars
12 p2171 A69-27155

Distribution function of multiple correlation coefficient for various sampling volumes and various numbers of predictors calculated using Fisher formula
13 p2293 A69-27843

Correlation coefficient between changes in F 2 layer critical frequency and sporadic E layer maximum frequency
13 p2254 A69-28330

Correlation coefficients between radial components of interplanetary magnetic field and solar wind velocity from Mariner 5 data due to Alfvén waves
14 p2510 A69-28949

Error correction for correlation coefficient between satellite data of earth radiation intensity and satellite vision field shift
14 p2435 A69-29043

Correlation coefficient of light fluctuations measured in Ar plasma in positive column of glow discharge, noting ionization wave appearance at critical gas pressure
16 p2822 A69-32039

Strength margins for combined random stresses, discussing average crossing frequency of curve by Gaussian stationary random vector with correlation coefficients included
17 p3066 A69-34038

Jupiter red spot prominence correlation with Zurich sunspot number
17 p3045 A69-34185

Stimulated reflection experiment for correlation between coherent photon beams from independent lasers
18 p3153 A69-35292

Cross correlation coefficient for submillimeter monochromatic wave amplitude and phase fluctuations in turbulent atmospheric boundary layer
21 p3674 A69-39129

Correlation role in navigation satellite analysis noting reduction in ephemeris error effects
[AAS PAPER 68-145] 21 p3761 A69-39222

Quantum mechanical multitime correlation functions derivation and applications to laser theory
22 p3965 A69-41152

Solid cloud cover moisture content relation to outgoing thermal radiation, obtaining correlation coefficient and regression equations
23 p4184 A69-42488

CORRELATION DETECTION

Closed form solution for two input correlator processing gain with error function transfer characteristics and operating in Gaussian environment
03 p0403 A69-13253

Self adaptive systems stability analyzed using filter and correlation methods, considering higher harmonics at rectifier and synchronous detectors output
04 p0582 A69-14796

Group delay time for dispersive wave propagation velocity determined using correlation method
15 p2562 A69-30094

CORRELATORS

NT IMAGE CORRELATORS

Ultrasonic diffraction delay line operation interpretation as radar chirp signal correlator
01 p0026 A69-10072

Closed form solution for two input correlator processing gain with error function transfer characteristics and operating in Gaussian environment
03 p0403 A69-13253

Radar signal matched filters synthesis using linear digital filters and digital correlators noting role in radar detection
05 p0722 A69-16733

Space-frequency equivalence between monochromatic correlator interferometer using directional antennas and wideband correlator interferometer using isotropic antennas
07 p1132 A69-18917

Real time correlator in periodic signal extraction from noise background, discussing multichannel sampler as special case of cross correlation extraction
11 p1837 A69-25094

Optical correlator for radar signal processing based on filtering first order diffracted light and integration on photomultiplier
12 p2028 A69-25911

Analog correlator performance interpreted as output SNR dependence on input signals and integrating system characteristics, covering filters and finite time integrators
14 p2413 A69-29485

Correlation protected ILS implementing conventional ILS with no operational restrictions on air traffic control, taking into account changing terminal conditions
22 p3978 A69-39963

CORROSION

NT CAVITATION CORROSION

NT ELECTROCHEMICAL CORROSION

NT FRETTING CORROSION

NT FUEL CORROSION

NT INTERGRANULAR CORROSION

NT SCALE [CORROSION]

NT STRESS CORROSION

Metal corrosion in atmosphere - ASTM Conference, Boston, June 1967
01 p0100 A69-11350

Steel corrosion by iodine noting effects of water and oxygen
03 p0444 A69-13310

Aluminum corrosion by fungi isolated from jet fuel system with predominance of Cladosporium resinace, noting protective coatings
04 p0616 A69-14765

Aluminum corrosion by fungus culture isolated from jet fuel system
06 p0941 A69-17123

Sulfite ion influence on pitting corrosion of stainless steels in sodium chloride solution
07 p1167 A69-19343

Corrosion - Conference, Cleveland, March 1968
14 p2465 A69-29929

Corrosive wear due to atmospheric O in sliding metal systems, noting oxidation rate relation to wear rate and activation energy
[ASLE PAPER 68-LC-11] 15 p2622 A69-30605

Electrode potentials of pure metals, Ni-Cr and Ni base alloys in molten salts applied to corrosion studies
17 p2990 A69-33650

Electrode potential measurements for corrosion study of metals and alloys in aqueous solutions, molten salts and gaseous atmospheres
18 p3150 A69-35412

Hydrogen effect on embrittlement of Cr-Ni stainless steel from viewpoint of corrosion cracking, using reverse bending apparatus
19 p3358 A69-35774

Aerospace and marine corrosion technology - Conference, Los Angeles, July 1968
21 p3747 A69-39484

Hydrogen fluoride corrosive effects in cryogenic propellant, emphasizing contamination by particulate matter from corrosion products
21 p3783 A69-39486

Failure analysis of corrosion products in hybrid thin film circuits, discussing detection technique, instrumentation and results
22 p3911 A69-39955

Corrosion of Ni through porous Au plate in humid sulfur dioxide atmospheric environments, analyzing product deposits and contact properties
23 p4176 A69-41534

CORROSION PREVENTION

Corrosion control, discussing corrosive concentration cells, coatings and sacrificial systems of protection, deep corrosion, corrosion augmented stress, forgings and titanium corrosion testing
01 p0093 A69-10148

Corrosion problems associated with electromagnetic shielding gaskets noting galvanic corrosion, corrosion prevention and insulation of gasket from mating surface
05 p0779 A69-15979

Chemical conversion coatings and low temperature enamels preventing corrosive attack on beryllium parts in environments containing moisture, chloride ions and/or high temperature oxidizers
07 p1169 A69-19762

Aircraft design, fabrication and finish techniques taking into account aircraft integral fuel tank corrosion due to contaminants associated with microbiological debris
[NACE PAPER 49] 08 p1320 A69-20599

EMI-RFI knitted wire mesh gasket for corrosion prevention, noting use of moisture tight seal
09 p1523 A69-21895

Fretting fatigue prevention in Al alloys, noting strength reduction due to fretting
09 p1526 A69-22148

Refractory alloys electrodes used for surface coating Ti alloys by electric spark method, studying microhardness and wear resistance
10 p1711 A69-23339

Aircraft integral fuel tanks corrosion causes and prevention, discussing microorganisms, maintenance and cleaning procedures, anticorrosive additives, etc
12 p2013 A69-25946

Additions of dialkyl and diaryldithiophosphates of Ba, Ca, Zn, Pb and Ni as antioxidants and corrosion inhibitors for hydrocarbons
12 p2027 A69-27091

Chemical corrosion of zirconia-based refractories in MHD generators, considering thermal cycling and shock, seed migration and prevention
13 p2284 A69-27469

Book on oxidation and shielding of beryllium in gas media for nuclear and aircraft technology
13 p2280 A69-27927

Corrosion mechanism in high temperature Nb-Zr/Li and Ta/Li heat pipes and heat transfer measurements, noting oxygen content of wall material
14 p2462 A69-29203

- Aluminum corrosion in ethylene glycol-water systems, discussing protection mechanisms of adsorption-type inhibitors and additives effects on corrosion rate
14 p2466 A69-29932
- Stannate immersion process for reduction of magnesium-steel couples galvanic corrosion, discussing bath operating limits
14 p2466 A69-29933
- Stress corrosion preventative metal-pigmented paints for titanium alloys, discussing chemicals added to increase cathodic potential
14 p2469 A69-29936
- Stress corrosion cracking prevention by shot peening, considering aircraft industry applications
14 p2466 A69-29937
- Corrosion at polymeric film-metal substrate interfaces, noting roles of film properties, bond strengths and primer coats
14 p2466 A69-29938
- Corrosion prevention in beryllium, testing conversion coatings and low fired porcelain enamels under various humidity and temperature conditions
14 p2466 A69-29939
- Corrosive wear by atmospheric air and moisture under nonsufficing conditions, noting control by dry nitrogen blanketing and oil additives
[ASLE PAPER 68-LC-10] 15 p2622 A69-30608
- Protective coatings of oxygen-free high melting point Si compounds and silicate binder, noting chemical stability in corrosive media
20 p3566 A69-37371
- Austenitic stainless steels nonreproducible passivating tendencies, determining electrochemical and corrosion characteristics, discussing critical anodic current density role
20 p3562 A69-37750
- Fuselage corrosion effect on structure and skin of older aircraft with emphasis on pressurized aircraft
21 p3646 A69-38392
- High strength steel landing gear components corrosion protective finishes, discussing paint over bare steel, porous Cd plating and vacuum deposited Cd
21 p3743 A69-38730
- Stress corrosion cracking prevention by selection of material, stress relief, compressive stresses introduction, protective coatings and by simulated accelerated tests
21 p3748 A69-39490
- Galvanic corrosion prevention measures for airframe fasteners, discussing crevice sealants, primers, zinc chromate, cadmium and aluminum coatings
22 p3957 A69-40825
- Aircraft fastener corrosion control with emphasis on surrounding joint and structure, discussing test programs, Al coatings, etc
24 p4334 A69-43442
- CORROSION RESISTANCE**
NT OXIDATION RESISTANCE
- Corrosion of steel surfaces in contact with molybdenum disulphide noting influence of high humidity, milling and inhibitors
01 p0094 A69-10367
- Cobalt base alloy for construction in high temperature corrosive environment, discussing mechanical properties, oxidation and corrosion resistance and phase stability
01 p0095 A69-10546
- Permissible JP-5 fuel sulfur content effect on hot corrosion of protective coated Ni-base superalloys in marine environment, noting atmospheric sea salt role
01 p0141 A69-11059
- Titanium-base alloys resistance to atmospheric corrosion based on weight change measurements and tensile tests after multiyear exposures
01 p0100 A69-11351
- Zirconium corner of Zr-Al-Cr system phase diagram within concentration limits from 1350-700 C, considering corrosion resistance
02 p0262 A69-11842
- Fe, Ni and Cr influence on corrosion resistance and mechanical properties of Zr-Cu-Mo system alloys
02 p0263 A69-11853
- Aluminum alloy with lithium and magnesium noting mechanical properties and electrical and corrosion resistance
03 p0443 A69-13026
- Fatigue and corrosion fatigue properties of aluminum alloys, noting elastic modulus, cyclic loading strength, corrosion resistance, etc
03 p0443 A69-13027
- Corrosion rates and stress corrosion cracking sensitivity of explosively shocked austenitic stainless steels
03 p0444 A69-13308
- Gas turbine alloys composition role in high temperature corrosion resistance under high sulfur diesel fuel combustion
03 p0444 A69-13309
- Methods of protecting industrial steel against hydrogen corrosion at high temperatures and pressures including cladding, carbon additions, surface film coating, etc
04 p0613 A69-14432
- Heat treatment effects on stress corrosion cracking resistance of Al-Zn-Mg alloys, using cantilever loading in aqueous solution
04 p0617 A69-14933
- Pitting corrosion resistance improvement in austenitic stainless steels with added molybdenum through electroslog resmelting
05 p0781 A69-16499
- Titanium applications in metallurgy, galvanic technology and chemistry making use of corrosion resistant properties
07 p1161 A69-18767
- Corrosion resistance and mechanical properties of Ti-Mo alloy, developing processing methods for forgings, bars and sheets
07 p1163 A69-18781
- Czechoslovakian heat resistant iron-carbon-aluminum alloy Pyroferal, properties and applications
07 p1168 A69-19345
- Aluminum coatings compared with cadmium coatings for aerospace fasteners, discussing plating methods
[ASM PAPER D8-5.2] 07 p1142 A69-19663
- Polymer structure effect on chemical resistance of reinforced plastics, sulfuric acid and sodium hydroxide corrosion of polyester resins and model copolymers
08 p1338 A69-20490
- Sulfidation attack and structural stability of nickel-base superalloy
[SAE PAPER 690103] 09 p1522 A69-21556
- Beryllium base cermets corrosion resistance increased in moist carbon dioxide at 700 C
10 p1711 A69-23338
- Aluminum bonded structures corrosion resistance through adhesive primers and surface treatments
10 p1700 A69-24088
- Optimal processing parameters for producing ingots and semifinished products from corrosion resistant Ti alloys with added Mo
11 p1902 A69-24273
- Monograph on effect of nitrogen on precipitation behavior of austenitic chromium-nickel steel covering carbides, intermetallics, phase transportations, corrosion resistance, etc
11 p1902 A69-24369
- Corrosion resistance rate of duralumin sheet in aqueous superphosphate solutions dependence on concentration
12 p2113 A69-26124
- High strength steels, discussing ductility, austenite to martensite transformation for increased strain hardening rate and elongation and corrosion resistance
12 p2115 A69-26829
- Reinforced plastics corrosion resistance, showing dependences on coupling agent and chemical compatibility between resin and fibers
[ASME PAPER 69-DE-60] 14 p2467 A69-28853
- Titanium corrosion resistance data tabulated for various environments and chemicals including salt solutions, organic chemicals and ionizable fluoride compounds
14 p2466 A69-29931
- Concorde aircraft and engine materials selection factors including mechanical properties of metals and nonmetals, corrosion resistance, service life, sealants, weight analysis, etc
15 p2639 A69-30464
- Thermal stability of Hastelloy Alloy C-276 determined from time and temperature tests for corrosion and grain boundary precipitation
16 p2799 A69-31719
- Stress corrosion resistance of AlZnMgCu and AlZnMg alloys, discussing combinations of alloy composition, heat treatment and stable precipitation conditions
16 p2800 A69-31779
- Ti corrosion resistance improved in special environments by oxidizing agents heavy metal ions and alloying
16 p2802 A69-32436
- Metallurgy, properties and applications of Co-Ni-Mo-Cr ultrahigh strength alloy, discussing corrosion
18 p3154 A69-34307
- Polyurethane corrosion resistance in various liquids determined from changes in sample hardness, weight, volume and deformation
18 p3162 A69-35360
- Fuel resistant elastomers evaluated for seal compounds for low temperature capability, noting epichlorohydrin-ethylene oxide as promising sealant
19 p3356 A69-35534
- Exposure tests of corrosion resistant claddings for high strength Al alloys protection, finding higher purity alloy cladding superiority
19 p3322 A69-35571
- Abrasion and corrosion resistant Cr-Co-B cast alloys in aggressive media, concluding resistance is due to chromium boride and fine dendritic structure
19 p3347 A69-36742
- Singular factors affecting stress corrosion cracking resistance of Ti alloys in salt water and hot salt, finding immune single phase alloys
19 p3353 A69-36908
- Aluminum alloying additives effects on tungsten disilicide corrosion resistance, studying plasticity properties and oxidation rate
20 p3561 A69-37376
- Design and processing tradeoffs for preventing stress corrosion cracking in Al alloy aircraft structural forgings
[ASM PAPER W9-14.4] 21 p3729 A69-38657
- Fuel cells construction materials selecting and optimizing techniques using diffusion block and differential corrosion concepts
23 p4075 A69-42299
- Corrosion resistant bonding materials, discussing metal-to-metal adhesive primers, Al honeycomb core and foil finish
24 p4334 A69-43421
- RTV silicone rubber for corrosion control coatings, high strength adhesives and low density sealants in aircraft structures
24 p4338 A69-43457
- Protective coatings on Ni base superalloys for gas turbine engine blade and vane components for hot corrosion and oxidation resistance
[SAE PAPER 690480] 24 p4335 A69-43515
- CORROSION TESTS**
NT SALT SPRAY TESTS
- Corrosion control, discussing corrosive concentration cells, coatings and sacrificial systems of protection, deep corrosion, corrosion augmented stress, forgings and titanium corrosion testing
01 p0093 A69-10148
- Protective coatings for gas turbine engine components in marine environments, considering corrosion of diffuser, impeller, compressor case and turbine blades
01 p0099 A69-11057
- Corrosive characteristics of jet fuels near condensing water studied by weight loss method, using copper alloy plates
01 p0142 A69-11099
- Long term atmospheric corrosion test program for aluminum and magnesium base alloys, comparing tensile strength of exposed and control specimens
01 p0100 A69-11353
- Weathering tests on wrought aluminum alloys exposed at U.S. sites compared to British industrial atmospheric exposure results
01 p0101 A69-11354
- Aluminum corrosion and inhibition mechanisms in ethylene glycol/water solutions, using controlled powder immersion tests
02 p0265 A69-11895
- Polymeric film properties related to metal substrate interface corrosion, considering effects of stress concentration, surface cleanliness and adsorbed gases
02 p0265 A69-11896
- Aluminum corrosion characteristics immersed in ion-exchanged water with trace impurities, determining corrosion rates
04 p0617 A69-14932
- Galvanic corrosion couples of metals and alloys tested in liquid fluorine, determining corrosion rates for possible missile components application
06 p0944 A69-17854
- Aluminum coatings compared with cadmium coatings for aerospace fasteners, discussing plating methods
[ASM PAPER D8-5.2] 07 p1142 A69-19663
- Physicochemical methods of corrosion testing - Conference, Frankfurt am Main, April 1968
10 p1712 A69-23818
- Audio frequencies internal friction measurement of austenitic stainless steels subjected to heat treatment and corrosion, discussing time dependence and carbide precipitates morphology
10 p1713 A69-23819
- Carbide precipitation in stainless steels using metal foil and extraction replicas, discussing grain boundaries corrosion relation
10 p1713 A69-23820

Liquid sodium corrosive action on vanadium, niobium, titanium and zirconium involving oxygen exchange from liquid to solid metal phase and energy of formation
10 p1713 A69-23821

Potential testing methods for corrosion induced changes in materials, discussing mechanical properties, corrosion fatigue and cracking and creep
10 p1713 A69-23822

Oxygen effects in Type 316 stainless steel, Nb- Zr alloy liquid potassium system, discussing thermal convection and forced circulation loops and corrosion rates
12 p2112 A69-25943

Incipient stress corrosion damage detection in aluminum alloys, using Rayleigh wave attenuation
12 p2114 A69-26306

Nickel maraging steel polarization behavior in acidic solutions, noting corrosion potential dependence on pH
13 p2282 A69-28188

NOL hypervelocity launcher heat transfer and erosion analysis by experiment and computer simulation [AIAA PAPER 69-336]
13 p2242 A69-28272

Time and temperature effects on corrosion and structure of Hastelloy alloy C-276
14 p2466 A69-29930

Aluminum corrosion in ethylene glycol-water systems, discussing protection mechanisms of adsorption-type inhibitors and additives effects on corrosion rate
14 p2466 A69-29932

Failure mechanism for intergranular stress corrosion cracking of vacuum annealed unalloyed Ti in alcohol iodine solutions
16 p2798 A69-31717

Microbiological corrosion and degradation of aircraft metals and organic materials in fuel tanks
19 p3341 A69-35569

Cleaning, deoxidizing and chromating process effects on chromate coated Al, using salt spray corrosion tests
19 p3321 A69-35570

Exposure tests of corrosion resistant claddings for high strength Al alloys protection, finding higher purity alloy cladding superiority
19 p3322 A69-35571

Cyclic stress frequency on mild steel corrosion fatigue tests, showing strength dependence on potential and stress current
19 p3342 A69-35775

Fatigue strength tests of steels simulating boiler installation operating conditions, reproducing corrosion characteristics of water
19 p3347 A69-36741

Cobalt and Co alloys oxidation, sulfidation and hot corrosion data, summarizing characteristics of films and scales formed
20 p3562 A69-37751

Commercial Co base superalloys oxidation and hot corrosion resistance under controlled environments, examining role of various alloying elements [ASM PAPER D8-21.5]
20 p3564 A69-38134

Temperature, applied stress and pressurization effects on materials corrosion by liquid F and F containing oxidizers
21 p3748 A69-39485

Impurities effect on corrosion of fluorine containing propellant oxidizer systems, noting aqueous and anhydrous hydrogen fluoride corrosion
21 p3784 A69-39487

Impurities effect on corrosivity of nitrogen tetroxide with tank construction metals, Al, stainless steel and Ti-Al-V alloy, noting temperature aging and concentration
21 p3748 A69-39488

Chemical and thermal behavior of materials corrosion in propellant exhaust gases with analysis of reactions involving hydrogen, nitrogen, water, carbon dioxide, etc
21 p3784 A69-39489

Forged corrosion in aqueous salt environment at various temperatures in unstressed and stressed conditions, considering Be usability in turbomachinery
21 p3749 A69-39493

Corrosion kinetics in metals using electrochemistry, stressing polarization techniques
21 p3749 A69-39494

Nondestructive testing for aerospace corrosion, discussing light, penetrants, X rays, sound, ultrasounds, electrical conductivity, magnetic reaction and radiation backscatter methods
21 p3733 A69-39495

Burner rig hot corrosion test facility for evaluating Ni-Co alloys used in gas turbine engines operating in marine environment
22 p3928 A69-40673

Fuel cells construction materials selecting and optimizing techniques using diffusion block and differential corrosion concepts
23 p4075 A69-42299

Dynamic hot corrosion rig test for operating environment and alloy composition effect on sulfidation attack during gas turbine fuel combustion
23 p4150 A69-42448

Thermochemical analysis of hot corrosion during sulfidization-oxidation of superalloy gas turbine engine components using Pourbaix method
23 p4178 A69-42449

Notch effect on corrosion fatigue behavior of high strength Al alloy under bending and direct stresses
24 p4330 A69-42553

CORRUGATED PLATES

Plane wave scattering from modulated corrugated structures, obtaining reflection coefficients for multimode propagation
01 p0033 A69-10973

Characteristic equation for corrugated surface wave line loaded with uniformly spaced thin metallic disks excited in E mode, considering spacing and groove depth
12 p2028 A69-25899

Laminated critical rate dampers consisting of ring shaped thin corrugated steel plates inserted between bearing and rotor, showing dependence on static load
17 p3066 A69-33945

Pure plastic bending of wide strip, determining stress strain state and plastic strain energy during constrained bending, noting application to corrugated panels
19 p3324 A69-35833

CORRUGATED SHELLS

Propagation modes in corrugated cylindrical waveguides determined by imposing nonisotropic surface reactance boundary condition at corrugated walls
08 p1284 A69-20295

Corrugated cylindrical waveguides used as hybrid mode feeds for reflector antennas
15 p2575 A69-30175

Corrugated conical horn used as antenna feed, studying modes in horn and associated radiation patterns by spherical hybrid functions analysis
15 p2575 A69-30176

Plane wave scattering by multimode corrugated structure with H mode incidence, revealing theoretically scattering resonance as P type Wood anomalies
17 p2925 A69-33844

CORRUGATING

Corrugated impedance antennas synthesized, using model in impedance surface form
04 p0577 A69-14786

CORTICES

Cortical responses by transient sensory stimulation of fingers EEG recorded, obtaining isomorphism between psychological and neurophysiological events
22 p3876 A69-40262

Rhesus monkeys visual responses recorded before and after unilateral striate lesions, optic tract section and inferotemporal lesions
22 p3876 A69-40263

CORTI ORGAN

Cortical auditory-evoked response during eye movement in cats, discussing relation to central mechanism
17 p2911 A69-34171

Astronaut vestibular and motor analyzer functions during flight and simulation tests, discussing illusory space orientation and role of cortical dynamics
20 p3469 A69-37241

CORTICOSTEROIDS

NT ALDOSTERONE

NT CORTISONE

Sonic boom effect on corticosteroid level in human blood, noting no changes
03 p0378 A69-14209

Corticosteroid and catecholamine metabolism change in rabbits during sharp limitation of motor activity
12 p2021 A69-26973

CORTISONE

Aldosterone and hydrocortisone introduced into bladders of adrenalectomized dogs to restore sodium metabolism contributing to normal water-salt homeostasis
21 p3656 A69-38965

CORUNDUM

U ALUMINUM OXIDES

COSINE

U TRIGONOMETRIC FUNCTIONS

COSMIC DUST

NT INTERPLANETARY DUST

NT ZODIACAL DUST

Frequency occurrence of small particles in meteor showers, discussing fragmentation and cosmic erosion as primary effects in small particle development
01 p0154 A69-10872

Meteorite structure and origin, discussing cosmic dust analysis and collection, Tungusk silicate-magnetite spherules, asteroid collisions and meteorite ages
01 p0159 A69-11367

Meteoric dust composition of Tungusk meteorite noting angular and spherical particles
01 p0160 A69-11386

Rotation and orientation of cosmic dust particles due to collisions with interstellar gas particles
03 p0511 A69-13420

Accretion rate of cosmic dust estimation from cosmogenic aluminum-26
03 p0514 A69-13935

Optical method of sounding cosmic matter penetrating into upper atmosphere by analyzing twilight phenomena
04 p0594 A69-15246

Diamond dust as major component of interstellar dust to explain observed properties
05 p0828 A69-16662

Cosmic dust concentration in interplanetary space near earth, noting suitability of satellite observation
06 p0999 A69-16971

Galactic dust layer spatial structure and relation to brightness of Milky Way based on analysis of photoelectric color excesses in Aql and Cyg stars
09 p1590 A69-21381

Far IR source in galactic center detected at 100 microns, noting thermal emission of interstellar dust grains as possible mechanism
09 p1603 A69-22264

Radio telescopic survey for OH emission at 1667 MHz in interstellar dust clouds for catalog compilation, tabulating results
09 p1603 A69-22267

Interstellar reddening material distribution within 2500 parsecs of sun, noting concentration in galactic plane, spiral arms and cloud complexes
10 p1773 A69-22961

Interstellar dust alignment mechanisms investigated by Monte Carlo model, discussing grain velocity maintenance by radiation pressure and effects of magnetic constraint on charged grain trajectory
10 p1781 A69-23675

Interstellar dust distribution ideas to explain observed variability in starlight polarization and similar phenomena
10 p1785 A69-24050

Color excess and 21 cm line intensity of RR Lyrae stars at high latitudes, confirming correlation between dust and atomic hydrogen
12 p2063 A69-25808

Isotropic and anisotropic dust cosmological models density perturbation growth, considering angular momentum conservation in expanding universe
13 p2343 A69-27619

Cosmic dust role in determining structure and dimensions of Galaxy
14 p2527 A69-29897

Milky Way structure, discussing dust bridge and density of absorbing matter between spiral arms of Sagittarius and Carina Cygnus
15 p2683 A69-30514

Neutral hydrogen in dark dust clouds in 21 cm line, showing hydrogen excesses and deficiencies
15 p2691 A69-30763

Time variation of altitude distribution of cosmic dust layer in upper atmosphere by Pandora II collector using inflight shadowing technique
15 p2698 A69-31353

MHD of interstellar gas-dust medium, analyzing gas-dust flow and gas-dust shock waves in magnetic fields
16 p2823 A69-32590

Galactic dust layer spatial structure and relation to brightness of Milky Way based on analysis of photoelectric color excess in Aql and Cyg stars
18 p3198 A69-34769

Ion and electron fluxes and drag force dependence on electrostatic charge and velocity of interstellar dust particle
19 p3425 A69-36562

Comet heads gas dynamics, analyzing coma or head region as continuum source flow of dusty gas
19 p3428 A69-36807

- Translating Tolman problem of cosmic dust motion into centrally symmetrical reading system, showing relativistic and Newtonian motion laws coincidence
20 p3594 A69-37079
- Cepheus light attenuation curve explained by applying polymodal particle size distribution, obtaining interstellar dust density
20 p3608 A69-38048
- Spectra of peculiar S zero galaxy NGC 7625 with irregular dust distribution, discussing central spheroid rotation and mass
20 p3610 A69-38142
- Galaxy NGC 3593 with large amounts of interstellar dust, calculating galactic mass and central density
20 p3610 A69-38143
- Irregular galaxy NGC 3077 with interstellar dust, measuring velocity field by spectroscopy
20 p3610 A69-38144
- Excitation temperatures and OH microwave line optical depths measured for dust clouds, discussing optical absorption lines and LF radio absorption
20 p3611 A69-38147
- Fe-Ni unmelted and unablated micrometeorites number at earth surface calculated, using space density of interplanetary particles and micrometeoritic theory
20 p3614 A69-38251
- Satellite measurements of small particles near-earth space density compared with chemical estimates of terrestrial cosmic material, suggesting particles origin in meteoroid ablation
21 p3701 A69-38342
- Electrostatically accelerated iron spheres interaction with thin metal and nitrocellulose foils to develop detectors for cosmic dust collection and recording
21 p3719 A69-38344
- Piezoelectric microphone sensor flown on rocket for recording micrometeoritic impacts during noctilucent cloud display, determining cosmic dust particles flux
21 p3793 A69-38348
- Optical method for upper atmosphere cosmic dust detection, emphasizing twilight luminance origin from light scattering
21 p3702 A69-38349
- Spherically symmetrical T models of dust matter yielding method for obtaining maximum total mass effect in general relativity theory different from Friedman closed model
21 p3803 A69-38994
- Diffuse galactic radiation intensity and distribution from photoelectric measurements compared with radiative transfer calculations using various interstellar dust models
22 p4013 A69-40096
- Evolutionary dynamic model for H II region produced by massive stars within dense dust-laden clouds, discussing grain sputtering and time scales
22 p4025 A69-40646
- Radiation transfer in circumstellar dust envelopes, considering thin and opaque clouds
22 p4027 A69-40655
- Galactic mass model and interstellar dust scattering data used to examine high latitude nebulae illumination possibility by integrated galactic light
22 p4033 A69-41059
- Stellar and diffuse galactic radiation intensity observations to obtain albedo values of interstellar dust particles
22 p4034 A69-41112
- Strong IR millimeter wave emission from galactic center due to interstellar dust grains resembling semiconductor structure
23 p4215 A69-42115
- Seyfert galaxies IR radiation attributed to dust grains thermal emission of energy absorbed from galactic nucleus
24 p4374 A69-43741
- Hydrogen gas role in galaxy formation, estimating quantity needed to dissipate gas cloud contraction energy, discussing formation mechanics of molecular hydrogen
15 p2680 A69-30204
- Diatomic hydrogen abundance evolution in uniform medium, discussing photodissociation effects and galactic evolution
15 p2680 A69-30205
- Neutral hydrogen high velocity clouds as possible extragalactic objects in Local Group not contracted to galactic dimensions or densities
15 p2694 A69-30785
- Optimization techniques for stellar kinetic theory problems, discussing kinematics distribution function, cosmic gas dynamics, interstellar matter, etc
15 p2695 A69-31004
- Cosmic helium origin, discussing evidence for big bang, galactic synthesis and stellar thermonuclear burning theories
16 p2853 A69-31598
- Equilibrium and stability of axisymmetric gaseous polytropes in toroidal magnetic fields, calculating harmonic oscillations by virial tensor method
21 p3797 A69-38534
- Galactic hydrogen distribution, discussing velocity field, spiral structure, symmetry, layer shape, ionization, spectra, etc
21 p3810 A69-39503
- Thermal balance of intergalactic gas, discussing plasma energy losses due to He emission and reverse Compton electron scattering and rapid cooling effect
24 p4389 A69-43771
- ### COSMIC NOISE
- Sudden cosmic noise absorption in ionosphere confirms relationship with solar chromospheric flares
02 p0306 A69-11667
- Far IR background due to superposition of IR galaxies, noting galaxies contribution to extragalactic radio background
02 p0308 A69-12128
- Large amplitude Pc 1 events at College, Alaska, noting more ionospheric cosmic noise absorption accompanying large events
02 p0244 A69-12397
- Cosmic microwave background radiation measurement, discussing measurement techniques for antenna temperature at microwave frequencies
02 p0210 A69-12431
- Earth velocity through 3 K cosmic background radiation, measuring velocity by determining anisotropy of radiation
03 p0511 A69-13475
- Polar auroral region cosmic radio noise absorption bays diurnal variations attributed to drift of electrons captured in magnetosphere
03 p0423 A69-13520
- Ariel 3 receiver for measuring galactic noise spectrum, discussing loop antenna use with swept receiver, false terrestrial signals, etc
03 p0404 A69-13581
- Frequency time displays of geomagnetic pulsations at Kiruna revealing Pc 1 pulsations accompanied by cosmic noise absorption /CNA/ and X ray enhancements
03 p0425 A69-14024
- Meter and decimeter solar radio bursts and sudden cosmic noise observed at Ahmedabad, India
03 p0518 A69-14259
- Cosmic X ray background production mechanisms
05 p0814 A69-15848
- Cosmic radio noise absorption in ionosphere, discussing diurnal, seasonal and longer variations of integral absorption
06 p1008 A69-17727
- Cosmic radio noise brightness distribution in Southern Hemisphere at 10.02 MHz, noting spectra of sources observed
07 p1206 A69-19272
- Cosmic radio noise intensity measurements by ATS 2 satellite-borne radiometer
07 p1224 A69-19715
- Cosmic microwave background variations produced by nonthermal gravitational radiation, imposing limits on equivalent mass density
08 p1398 A69-20773
- Antenna noise temperature at earth station due to rain on radomes, solar and cosmic noise, noting SNR degradation
09 p1461 A69-21283
- Extraterrestrial cosmic emissions responsible for background noise of communications engineering, discussing factors affecting frequency sharing with other services
09 p1586 A69-21294
- Solar cosmic ray event of July 7 1966, noting sudden cosmic noise absorption reduction and particle absorption domination start at 0120 UT
10 p1768 A69-23771
- Sudden cosmic noise absorption /SCNA/ in polar cap during July 7, 1966 solar proton flare, estimating SCNA latitudinal distribution and protons magnetic cut-off boundary
10 p1770 A69-23907
- Nonthermal cosmic radio emission spectral index angular variations during scanning of sky by receiver antenna, analyzing dependence on galactic latitude
10 p1784 A69-23940
- Auroral cosmic noise absorption relationship to auroral geomagnetic disturbances, investigating absorption diurnal distribution
12 p2071 A69-26706
- IR astronomy and cosmology, considering cosmic microwave background and isotropic radiation significance in distant IR
13 p2342 A69-27601
- Sudden cosmic noise absorption in ionosphere confirming relationship with solar chromospheric flares
13 p2334 A69-28698
- CNA and geomagnetic pulsations observed by ground based instruments in southern auroral region occurring near geomagnetic noon, noting electron precipitation role
15 p2597 A69-30697
- Cosmic radio emission absorption during IQSY at 24.6 MHz, relating diurnal variation of absorption and geomagnetic index F scatter occurrence
17 p2968 A69-33992
- Lower ionospheric effective electron collision number from cosmic noise recordings and radio wave absorption data obtained by vertical sounding rocket
20 p3528 A69-37679
- Cosmic radio background noise spectrum near north galactic pole based on Radio Astronomy Explorer satellite experiments
23 p4219 A69-42375
- ### COSMIC PLASMA
- Partial maser effect in recombination lines of hydrogen atoms in nebular plasma due to overpopulation of energy levels at thermodynamic equilibrium
01 p0148 A69-10042
- Electromagnetic waves trajectory distortion in moving plasma due to additional time delay noting propagation of pearl pulsations, whistling atmospherics and proton whistlers
01 p0068 A69-11114
- Formation mechanism for heterogeneous structure of interplanetary plasma based on plasma instability from temperature anisotropy
02 p0314 A69-11638
- Two fluid MHD equations in form of nonlinear ion waves with magnetic vector
04 p0662 A69-15244
- Polarization tensor variation due to Faraday effect and differential absorption of ordinary and extraordinary waves for radiation propagating in magnetoactive cosmic plasma
05 p0805 A69-16650
- Interplanetary plasma flow simulation around earth magnetosphere and planets not considering initial conditions influence
09 p1577 A69-21768
- Radio astronomical investigations of small scale inhomogeneity motion and dimensions in interplanetary plasma, using observations of 3C 48 scintillations in 1967
10 p1782 A69-23711
- Interplanetary plasma subsequent to July 7, 1966 flare monitored by detectors on Pioneer 6 and Explorer 33
10 p1783 A69-23775
- Interplanetary plasma measurements by Luna, Mars 1, Zond 2 and Venera 3 probes, including solar plasma flux energy spectra diagram
13 p2336 A69-27354
- Plasma viscosity relation to stellar magnetic fields generation, taking into consideration angular momentum transfer
15 p2700 A69-31492
- Proton concentrations, magnetic field strength and temperatures distribution in interplanetary plasma flows as function of latitudinal distance from center of active region
20 p3594 A69-37020
- Laboratory experiments applicability to interplanetary plasma physics, describing simulations of solar wind interactions, magnetosphere, collisionless shock waves, etc
22 p4028 A69-40689
- ### COSMIC RADIO WAVES
- #### U EXTRATERRESTRIAL RADIO WAVES

COSMIC RAY ALBEDO

- Splash albedo flux measurement, using Cerenkov counter telescope surrounded by anticoincidence shield
06 p0989 A69-17278
- Splash and return albedo electrons in cosmic ray electron spectrum between 12 Mev-1 Gev measured by high altitude balloon flight
22 p4005 A69-40510
- Cosmic ray albedo neutron decay /CRAND/ source for trapped protons, showing disagreement with intensities in inner zone measured on OV1 2 spacecraft
22 p4005 A69-40512

COSMIC RAY SHOWERS

- Distance between measurement equipment and extensive air showers axis varied as function of particles number and number of hit
01 p0144 A69-10749
- Cosmic rays extensive air showers from interaction of particles with nuclei of elements in atmosphere
01 p0144 A69-10752
- Cosmic ray air shower distribution from Crab Nebula, M87, M82, quasars, X ray sources and recent supernovac
02 p0308 A69-12597
- Underground search for massive strongly interacting cosmic ray particles, using shower selecting extension array and interaction detecting telescope
02 p0310 A69-12831
- Extensive air showers at sea level, presenting experimental data for muon and electron numbers spectra
03 p0498 A69-12937
- Extensive air showers due to interaction of high energy particles with atmosphere, discussing astrophysics, cosmology and fundamental particle physics
03 p0498 A69-12938
- Muons in EAS, single unaccompanied muons, underground muons and experiments involving neutrinos
03 p0499 A69-12946
- Geiger-Muller counter telescopes in conjunction with core selectors for studying geomagnetic effect of extensive air showers
03 p0430 A69-13303
- Gamma ray fluxes from pulsating radio sources, using detection of Cerenkov light generated by energetic particles in atmosphere
03 p0513 A69-13772
- Extensive air shower radio pulse polarization, using log periodic EW- and NS-arm antennas
04 p0595 A69-15425
- Astrophysical aspects of primary energy spectrum deduced from shower size spectra and high energy interactions of extensive air showers
06 p0990 A69-17298
- Low energy muons and nuclear active particles measured with extensive air showers array composed of scintillation detectors, spectrometer and Geiger counters
06 p0990 A69-17299
- Extensive air shower high energy muons measurements noting energy spectrum, lateral spread and dependence on shower size
06 p0990 A69-17300
- Extensive air showers characteristics based on models of high energy interactions of nucleons and pions with air nuclei
06 p0990 A69-17301
- Simultaneous parallel penetrating muons observed in multiplate cloud chambers, obtaining information about sea level muons interactions and EAS
06 p0991 A69-17304
- High energy pure photon showers in cosmic ray emulsions in relation to production of magnetic pole-antipole pairs
06 p0996 A69-17883
- Muon component of extensive cosmic ray showers, discussing effect of multiplicity of secondary particles created by high energy nuclear interactions
07 p1207 A69-19325
- Arrival time distribution and energy content of extensive air shower at large core distances, discussing photon energy spectra and Monte Carlo calculation
07 p1186 A69-19410
- Cosmic ray composition and nuclear interactions at very high energies, comparing results of Monte Carlo simulations with various experimental data
12 p2149 A69-26475
- Charged primary cosmic rays responsible for relative intensities of muon-poor extensive air showers at mountain and sea levels
12 p2152 A69-27099
- Chemical composition of nuclear active particle component of primary cosmic rays in extensive air showers
13 p2326 A69-27464

- Angular distribution of penetrating shower particles produced in nuclear interaction of cosmic rays with C, Sn, Cu and Pb
13 p2330 A69-28381
- Nuclear active particles energy in extensive air showers measured with ionization calorimeter, noting discrepancy attributed to ionization bursts
13 p2331 A69-28387
- Asymmetrical showers in interaction of high energy nuclear active particles with atomic nuclei, estimating target particle mass
13 p2303 A69-28391
- Nuclear active cosmic ray component energy spectrum determined from calorimetric ionization burst measurements, discussing nuclear particle interactions absorption coefficients
13 p2331 A69-28393
- Primary particle energy and extensive air shower electron density relationship derived from vertical spectral profiles
13 p2331 A69-28396
- Proton initiated nuclear cascade in atmosphere calculated using Monte Carlo method, relating electron number to primary proton energy
13 p2331 A69-28397
- High energy electron photon cascades event recorded with X ray photography, discussing origin in related atmospheric cosmic ray showers component subgroups
13 p2331 A69-28398
- Baryon passive nuclear state nonexistence indicated by above and below ground calorimetric telescope method of nuclear cascade observation
13 p2331 A69-28401
- Stable particles heavier than nucleons in extensive cosmic ray showers detected by delayed coincidences relative to shower electron photon component
13 p2331 A69-28402
- High energy muons energy spectrum in extensive cosmic ray showers from spectrum study of ionization bursts due to penetrating component
13 p2332 A69-28403
- High energy ionization bursts in cosmic ray showers electron photon component, obtaining bursts power spectrum and component energy dependence
13 p2332 A69-28404
- Extensive cosmic ray showers structure at sea level, using multiple hodoscopic counters and control system
13 p2332 A69-28405
- Sea level fluctuations of electron-photon, muon and active nuclear components of extensive cosmic ray showers determined, obtaining shower parameters
13 p2332 A69-28406
- Radio emission of atmospheric cosmic ray showers observed with multiple wideband half wave dipole antenna system, obtaining radiation spatial distribution
13 p2332 A69-28407
- Half wave dipole antenna operational factors analyzed for RF radiation spatial power distribution from atmospheric cosmic ray showers
13 p2332 A69-28408
- High energy mu-mesons component of atmospheric cosmic ray showers by particle impact penetration using multiple underground ionization chambers
13 p2332 A69-28409
- Cosmic ray showers components relationships, analyzing superhigh energy nuclear cascade development, discussing components distribution function at constant proton energy
13 p2332 A69-28410
- Primary particles energy determined by probability distribution functions of cosmic ray showers characteristics, using Monte Carlo computerized calculation
13 p2332 A69-28411
- Cosmic ray chain reaction particles energy spectrum determination in heavy media, discussing cascade parameter application in showers development
13 p2303 A69-28412
- Cosmic ray showers electron, positron and photon energy distribution functions calculated, considering positron annihilation, Compton effect and relativistic electrons formation
13 p2303 A69-28413
- Electron photon cascades energy dependence on primary particle energy determined in lead by various instruments
13 p2304 A69-28418
- High energy electrons producing electromagnetic cascades in electron photon showers in lead measured by scintillation detectors
13 p2332 A69-28419
- HF emission spectra of radio pulses from cosmic ray showers confirming Dublin group observations
13 p2333 A69-28471

- Lateral density distribution of muon component in central region of extensive air showers, using Lodz analyzer
15 p2677 A69-31481
- Three dimensional Monte Carlo calculations for hadronic component of extensive air showers using semiempirical model high energy nuclear interactions
15 p2678 A69-31482
- Ground level muon density of extensive air showers related to threshold energy and zenith angle for primary particles
15 p2678 A69-31483
- Frequency of multiple muons from extensive air showers as function of zenith angle, noting mean transverse momentum and density spectrum
15 p2678 A69-31484
- Multiple muon showers penetrating deep underground, discussing radial extent and occurrence frequency against multiplicity spectrum
15 p2678 A69-31485
- Electromagnetic muon-nucleon interaction explanation for observed horizontal air showers, reexamining shower data in view of triplet particles
15 p2678 A69-31498
- Near horizontal air showers relationship to direct muon production and heavy triplet particles of unit charge, discussing nuclear interactions and muon bremsstrahlung
15 p2678 A69-31499
- Earth atmosphere effect on cosmic ray variations, considering relation between extensive air showers and cosmic ray spectrum
16 p2851 A69-32381
- Cosmic ray shower axis mean distance from apparatus determined by measuring muon to charged particles densities ratio
17 p3024 A69-33580
- Cosmic ray shower axis mean logarithmic distance from apparatus calculated by transforming shower recording frequency radial distribution to lin-log coordinate system
17 p3024 A69-33581
- UHF radio pulses from zenith associated with extensive air showers, estimating threshold energy of scintillation trigger system
21 p3792 A69-39613
- Radio pulse emission from ionized disk of cosmic ray extensive air showers, noting importance of charge separation in geomagnetic field and selective positron absorption
21 p3792 A69-39614
- Monte Carlo methods for electromagnetic showers simulation, noting electron track length distribution in Pb glass absorber
22 p4007 A69-41057
- Air showers muon threshold energies deep underground as function of zenith angle, discussing nucleon-air-nucleus collision parameters variation effect
23 p4207 A69-42497
- Integral energy loss spectrum of extensive air showers recorded by Haverah Park 50-m array
23 p4207 A69-42499
- Quark mass and charge interpretation during particle track photographic analysis of air shower cores by delayed expansion Wilson cloud chamber
24 p4383 A69-42945
- Galactic X ray flux from H I region low energy cosmic ray nuclei, studying electron capture effects on line intensities
24 p4367 A69-43048
- Cosmic ray pions and muons anomalous measurements above 1000 Gev explained by medium-strong contact interaction between protons
24 p4353 A69-43194

COSMIC RAYS

- NT PRIMARY COSMIC RAYS
- NT SECONDARY COSMIC RAYS
- NT SOLAR COSMIC RAYS
- Cosmic radiation interactions with living viruses, considering X ray effects and optimal radiation dosage for cancer cell destruction
01 p0013 A69-10157
- Electron production rate and density created by galactic and solar cosmic rays in lower D region, considering ionization for PCA
01 p0063 A69-10426
- Energetic cosmic radiation in deep mines, giving hypothesis of new particles more effective than muons
01 p0144 A69-10444
- Soviet investigations of solar and cosmic electromagnetic and charged particle radiations by balloon, rocket and satellite measurements
01 p0145 A69-10945

13-day cycle variation in cosmic radiation intensity confirmed by Vercelli method, giving values of amplitudes and correlation coefficients among variations
01 p0145 A69-11031

Cosmic ray neutron integrated flux measurements up to 350 km for energies to 15 Mev, determining neutron leakage flux
01 p0146 A69-11223

Cosmic radio emission at 1.68 MHz measured by Cosmos 142 satellite, discussing receiver, antenna and radiation temperature
01 p0158 A69-11322

Preatmospheric meteorite size determination from distribution of radioactive isotopes resulting from nuclear reactions produced by cosmic rays, discussing error sources
01 p0159 A69-11375

Second harmonic cosmic ray daily variation, discussing density gradient model with particle diffusion along field direction
02 p0305 A69-11422

Leptonic quarks with various charges in cosmic rays, determining upper limit of flux in underground measurements
02 p0306 A69-11547

Cosmic ray propagation in interplanetary space taking into account reverse effect on solar wind, deriving integrodifferential equation
02 p0306 A69-11657

Solar and galactic cosmic rays measurement data to investigate variation in time of relations between cosmic rays modulation amplitude and solar activity variations
02 p0306 A69-11658

Coupling coefficients of global and vertical fluxes of charged cosmic ray component in stratosphere measured by radiosondes
02 p0306 A69-11659

Book on cosmic radiation origin and expansion of universe, covering astrophysical reasons for electric charging of galaxies in range of galactic and metagalactic dimensions
02 p0315 A69-11713

Cosmic ray meson diurnal anisotropies direction calculated on basis of subtracted diurnal vectors
02 p0306 A69-11730

Charts summarizing daily solar phenomena, cosmic rays, geomagnetic variation, ionosphere, radiowave propagation and airglow observations in Japan
02 p0315 A69-11732

Pulsar CP 1133 high energy gamma ray emission, using atmospheric Cerenkov detection technique for high energy neutral cosmic rays
02 p0307 A69-11823

Elementary particles and cosmic radiation, discussing current state of knowledge and observational techniques
02 p0307 A69-11907

Radioactive decay of neutral pions generated in metagalactic cosmic ray interactions as source of high energy isotropic gamma rays observed by OSO-3
02 p0308 A69-12092

Cosmic rays properties and sources, considering origin in supernovae, galaxies, quasars and unknown sources
02 p0308 A69-12158

Galactic Jupiter Probes investigating Jupiter atmosphere and emissions and deep space cosmic radiation
02 p0324 A69-12303

Cosmic rays - Conference, Calgary, Canada, June 1967
03 p0497 A69-12928

Metagalactic cosmic rays, galactic halo and sources of cosmic rays in Galaxy, noting models, electron component of cosmic rays and evolutionary cosmology
03 p0497 A69-12929

Cosmic ray origins, considering hard protons, X rays, gamma rays, very soft protons, background radiation, charged particles and neutrinos
03 p0497 A69-12932

Galactic cosmic ray modulation by interplanetary magnetic fields, discussing compatibility of several models with experimental data
03 p0498 A69-12933

Atmospheric temperature and water vapor variations and seasonal environmental changes effects on cosmic ray neutron and meson monitor counting rates
03 p0498 A69-12936

High energy strong interaction theory in cosmic ray physics, discussing Regge model, fireball production and quark problem
03 p0469 A69-12940

High energy interactions used to estimate energy of individual cosmic rays
03 p0498 A69-12941

High energy cosmic ray research facility at mountain altitudes, noting nucleon-proton interactions, particle identification and momentum analysis
03 p0499 A69-12942

Balloon flown High Altitude Particle Physics Experiments /HAPPE/ for research on high energy cosmic rays and particle interactions
03 p0499 A69-12943

High energy cosmic ray particles observed with SEZ-14 instrument aboard Proton 1 and 2 satellites
03 p0499 A69-12944

Ultrahigh energy interactions working model, suggesting interpretation of cosmic ray experimental data on basis of Aleph plus Pionization model
03 p0499 A69-12945

Large area proportional counter for cosmic ray design, construction and specifications
03 p0427 A69-12979

Cosmic ray and solar wind properties, discussing solar wind measurements, interplanetary magnetic field and solar wind sounding by cosmic rays
03 p0500 A69-13355

Heavy cosmic ray particles effect in manned space flight, noting results of deuteron microbeam experiment
03 p0373 A69-13494

Cosmic rays intensity increase due to meteor showers noting maximum solar activity effects
03 p0500 A69-13509

Galactic cosmic rays energy modulation spectrum in interplanetary space, showing influence of solar wind velocity and diffusion coefficient dependence
03 p0501 A69-13527

Automatic recording device for cosmic ray bursts utilizing information time delay to allow detailed initial period study
03 p0430 A69-13545

Cosmic ray solar diurnal variations for nucleonic component, discussing differential response functions
03 p0501 A69-13751

Cosmic ray meson component solar diurnal variation calculations noting amplitude, average deflection angle and dependence on zenith angle of arrival
03 p0501 A69-13752

Cosmic X ray sources resolved against diffuse background radiation lying close to galactic plane
03 p0501 A69-13767

Extraterrestrial background gamma radiation /0.3-2 Mev/ observations used to derive upper limits for cosmic ray protons and CNO nuclei in interstellar space
03 p0501 A69-13934

Cosmic ray time variation and anisotropies near earth, discussing galactic and solar cosmic rays, trajectories in geomagnetic field, etc
03 p0504 A69-14236

Meter and decimeter solar radio bursts and sudden cosmic noise observed at Ahmedabad, India
03 p0518 A69-14259

Amplitude and phase of cosmic ray meson diurnal variation, noting less variation in neutron diurnal variation
04 p0648 A69-14374

Cosmic ray intensity after solar flare shown greater than during quiet periods from balloon data at Murmansk and Mirnyi
04 p0648 A69-14375

Atmospheric, geomagnetic and interplanetary effects on cosmic ray flow, noting anisotropy and diurnal variation phase and amplitude averages
04 p0649 A69-14683

Moving isotropic black body radiation, discussing effect on energy flux and earth velocity measurement through 3K cosmic background radiation
04 p0649 A69-15150

Cosmic ray intensity increase of January 28, 1967, noting pressure corrected hourly data and lack of association with visible solar flare
04 p0649 A69-15442

Cosmic X ray background production mechanisms
05 p0814 A69-15848

High energy proton and neutron fluxes and spectra from nuclear emulsion stacks on Cosmos satellites, calculating cosmic radiation doses
05 p0814 A69-16051

Solar modulating function form changes resulting in hysteresis near solar minimum
05 p0815 A69-16249

Cosmic ray electron flux and energy spectrum from balloon data obtained at Palestine, Texas, monitoring proton flux periodically
05 p0815 A69-16250

Cosmic ray propagation, discussing interstellar matter effect on composition and diffusion effect necessary to study radiation models
05 p0816 A69-16361

Galactic magnetic field estimation obtained from cosmic ray electron spectrum and radio data
05 p0828 A69-16612

Transformation of differential mean and current densities and anisotropy of cosmic ray particles and photons observed in frames of reference relative to each other with isotropic flux
05 p0817 A69-16651

Experimental measurement of He and C isotope composition of cosmic radiation
05 p0817 A69-16709

Gamma ray production and high energy electrons in cosmic radiation
05 p0817 A69-16712

Diffuse cosmic X radiation flux and intensity law, noting inverse Compton effect of electrons on 3K black body radiation
05 p0817 A69-16714

Celestial X ray sources astronomy, discussing emission mechanism in 2 to 100 keV range and balloon observations in Cygnus and Taurus constellations
05 p0817 A69-16715

Low energy diffuse cosmic X radiation, considering adequacy of single exponent power law spectrum [ISAS-428]
06 p0986 A69-17024

Upper limit estimated for anomalous interaction between cosmic muons with greater than 100 BeV energy
06 p0986 A69-17246

Cosmic rays, elementary particle physics and astrophysics - Conference, Aligarh, India, December 1967
06 p0986 A69-17268

Cosmic radiation propagation in interstellar space, discussing differential kinetic energy spectra of protons, He, C and O nuclei and Fe
06 p0988 A69-17269

Cosmic ray propagation model, considering determination of He interstellar spectrum and amount of matter traversed at low energies
06 p0988 A69-17270

Lithium, Be, B and fluorine nuclei in cosmic radiation, discussing nature of spectra
06 p0988 A69-17271

Spectra analysis of proton and He nuclei having different charge-to-mass ratios to obtain information on solar modulation and injection spectra
06 p0988 A69-17272

Interstellar flux of heavy and superheavy nuclei calculated, assuming nuclei injection with source spectrum similar to M nuclei
06 p0988 A69-17273

Permanent magnet and nuclear emulsion for measuring He nuclei momentum spectra up to 100 gy rigidity
06 p0989 A69-17277

Solar neutron production and propagation to earth, discussing particle detectors
06 p0989 A69-17281

Production rates of nuclides measured in stack of glass plates under proton irradiation for calculating cosmic ray production rates in stone meteorites
06 p0989 A69-17283

Transistorized multichannel pulse height analyzer and recording system for balloon-borne cosmic ray payloads, discussing performance capacity
06 p0924 A69-17284

Cellulose nitrate sheets applicability in detecting cosmic ray relativistic heavy nuclei, considering etchable tracks
06 p0924 A69-17286

Modulation of galactic cosmic rays due to electromagnetic conditions of interplanetary space, considering time variations and Parkers model
06 p0989 A69-17287

Galactic cosmic rays anisotropies due to density gradient perpendicular to ecliptic plane studied, using diurnal and semidiurnal component and intensity deficiency
06 p0990 A69-17289

Cosmic ray daily variations relationship to geomagnetic activity, sector structure of interplanetary magnetic field and sunspot activity
06 p0990 A69-17291

27-day cosmic ray intensity variations related to solar wind velocity nonuniformity due to longitudinal distribution of coronal active regions
06 p0990 A69-17292

Large area scintillation telescopes with cubic geometry, measuring cosmic rays intensity from vertical and slant directions

06 p0925 A69-17296

Multiplicity of secondary neutrons counted by IGY neutron monitor detecting cosmic radiation

06 p0925 A69-17297

Cosmic ray magnetic spectrograph for measurement of momentum spectrum, charge ratio and specific ionization of muons, discussing magnetic and scattering displacement

06 p0925 A69-17302

Isotropic background cosmic X ray flux measurements using low latitude balloon to minimize atmospheric background, obtaining hard solar X ray flux upper limits

06 p0992 A69-17311

Cosmic ray electron energy spectrum compared with galactic radio noise for estimating galactic magnetic field

06 p0992 A69-17377

Continuity and momentum equations for cosmic ray gas particles in interplanetary region

06 p0992 A69-17379

Cosmic radiation and hibernation physiopathology of human organism, noting beryl as radiation resisting agent in spacecraft design

06 p0874 A69-17645

Metastable helium abundance in interstellar and intergalactic space, inferring low energy cosmic ray concentration

06 p1010 A69-17973

Cosmic X rays, gamma rays and electron production under astrophysical conditions, noting potential use in supernova and quasar research

07 p1204 A69-18391

Cosmic ray astrophysics, discussing chemical composition, energy spectrum and galactic sources

07 p1205 A69-18909

Local interstellar electron spectrum limits from measurements of cosmic ray electrons, nonthermal galactic radio emission and solar modulation effects

07 p1206 A69-19269

Balloon observations of cosmic X ray sources in Cygnus and Crab Nebula, discussing data application to energy spectra analysis

07 p1210 A69-19716

Black body cavity radiation distribution as seen by observer in arbitrary uniform motion with respect to radiation mass center

08 p1380 A69-19784

Cosmic gamma radiation with energies above 100 Mev in southern sky, discussing results of balloon-borne spark chamber flight

08 p1377 A69-19787

Cosmic gamma ray generation by Compton scattering in discrete sources, applying formulas to M87, Crab Nebula, M82, Cen A, Ngc 1275, and Cas A

08 p1377 A69-20053

Cosmic ray deuteron and He 3 secondary origin and determination of cosmic ray path length and residual interplanetary field modulation

08 p1378 A69-20066

Earth internal magnetic field effects on cosmic ray measurements, dipole approximation and effect of external sources

08 p1378 A69-20219

Solar activity modulation of galactic cosmic rays with more than 1 Gev energy

08 p1378 A69-20224

Long term modulation of cosmic rays by solar activity explained by Parker solar wind model, noting confirmation by direct satellite measurements

08 p1379 A69-20533

Cosmic ray Li, Be and B nuclei measurements, analyzing differential energy spectra, L-M ratio, atmospheric and solar modulation

08 p1380 A69-20638

Discrete source hypothesis for interpreting high energy cosmic gamma ray measurements obtained by OSO-3 spacecraft

08 p1380 A69-20699

Cosmic ray negatron and positron spectra using balloon-borne magnetic spectrometer, obtaining absolute solar modulation of positron flux

08 p1380 A69-20728

Nuclear particle plastic dielectric track detectors to record distribution of fissionable and heavy elements in nature and cosmic radiation

08 p1401 A69-20899

Meteorites radiogenic and cosmic ray exposure ages, orbits and parent bodies, discussing H and L group chondrites

08 p1405 A69-20928

Chemical effects of solar wind and cosmic protons on solid bodies in space, discussing possible relation to origin of life

08 p1407 A69-20935

Fluorescer-photomultiplier mobile telescope for measurement of vertical cosmic ray intensity and equator points in atmosphere

09 p1493 A69-21420

Cosmic gamma ray spectra from metagalactic proton-antiproton annihilation

09 p1574 A69-21459

Approximate solution of nonlinear differential equation describing interaction between galactic cosmic rays and solar wind, obtaining four domains

09 p1575 A69-21524

Cosmic ray intensity temperature dependence in stratosphere and anisotropy in interplanetary space determined from measurements over Arctic and Antarctic regions

09 p1575 A69-21542

Cosmic ray particle behavior in interplanetary medium, solving model equation for cosmic ray diffusion in cloud of outgoing scattering centers

09 p1575 A69-21598

Cosmic ray intensity diurnal variations from super neutron monitor observations, discussing anisotropy resulting from reduced intensity in gardenhose direction in ecliptic plane

09 p1576 A69-21706

Lunar photon leakage spectrum due to photons from capture and inelastic scattering of neutrons by galactic cosmic rays

09 p1597 A69-22088

Cosmological implications of diffuse X ray background, noting Compton black body process effect on isotropic cosmic X rays

09 p1578 A69-22152

Solar extreme UV, soft and hard solar X rays, cosmic X rays and gamma rays, cosmic ray particles and near earth visible radiation observed by OSO-3

09 p1578 A69-22167

Solar and cosmic X rays observed by OSO-C, stressing galaxy M 87 upper limits and Lupus XR-1 power law spectral form

09 p1578 A69-22171

Hard solar and cosmic X rays measured with satellite-borne telescope, considering flux and time variations

09 p1579 A69-22173

Galactic cosmic ray scattering and energy loss through solar wind interaction

09 p1580 A69-22202

Radio recombination lines of galactic hydrogen as sensitive test for low energy cosmic ray existence in interstellar medium

09 p1580 A69-22273

Compton scattering of microwave radiation on cosmic ray electrons proposed as mechanism generating 100 Mcv cosmic gamma rays

09 p1580 A69-22295

Inverse compton scattering of far IR background radiation proposed as explanation of high energy gamma ray flux

09 p1580 A69-22296

Renormalizable weak interaction mechanism for generation of high energy muons from Tev cosmic rays in upper atmosphere

09 p1581 A69-22530

Solar modulation of galactic cosmic rays, discussing disagreements between convection diffusion theory and observation

09 p1581 A69-22744

Anomalous Forbush decrease observations in November 1960 demonstrating cosmic ray flux anisotropy near earth

09 p1582 A69-22753

Diffuse cosmic X ray background measured during balloon flight with actively shielded and collimated detector

09 p1584 A69-22767

Solar activity influence on cosmic ray intensity 11 year variation, taking into account heliolatitudinal movement of sunspot regions in solar cycle as evidence of density gradient

10 p1754 A69-22802

Daily observational results of solar phenomena, cosmic rays, geomagnetic variations, ionosphere, radio wave propagation and airglow arranged according to solar rotation number

10 p1771 A69-22808

Cosmic ray physics - Conference, Novosibirsk, U.S.S.R., August-September 1967

10 p1754 A69-22810

Cosmic ray variations as means of studying solar wind characteristics and interplanetary medium

10 p1755 A69-22811

Quasars and explosive processes in galaxies as cosmic ray sources in expanding universe, studying relation between galactic and metagalactic cosmic rays

10 p1756 A69-22815

Cosmic charged particle acceleration in electromagnetic field described by vector and scalar potentials, constituting plane electromagnetic wave propagating along z axis

10 p1756 A69-22816

Cosmic ray induced radioactivity in lunar surface and meteorites calculated together with cosmic ray intensity variations

10 p1756 A69-22817

Satellite data on galactic cosmic ray variations near magnetosphere and in interplanetary space, discussing Forbush decreases

10 p1756 A69-22819

Cosmic rays origin, measurements of energy spectrum and stellar diurnal variations

10 p1757 A69-22823

Interplanetary magnetic fields characteristics and magnetic inhomogeneities spectra from cosmic ray variation studies used to obtain scattering mean free path

10 p1757 A69-22824

Solar wind and galactic magnetic field buffer layer, analyzing cosmic rays effect and space-time distribution

10 p1757 A69-22825

Superhigh energy cosmic ray interaction with neutrinos in universe, shape of cosmic ray spectrum and universe development

10 p1757 A69-22826

Cosmic ray anisotropy and diurnal density variation, analyzing influence of interplanetary magnetic field and subsonic solar wind

10 p1757 A69-22828

Forbush decreases spectra in low energy region from satellite measurements of neutron and hard component of cosmic rays

10 p1758 A69-22829

Cosmic ray electrons and gamma quanta at lower atmosphere recorded with balloon equipment, plotting vertical profiles of electron energy spectra

10 p1758 A69-22830

Galactic cosmic ray modulation and solar activity analyzed on basis of cosmic ray measurement in stratosphere

10 p1758 A69-22832

Cosmic ray anisotropy relation to scattering and sectorial structure of interplanetary magnetic field using neutron monitor data

10 p1758 A69-22834

Cosmic ray intensity variations by spectrographic method, noting geomagnetic effects

10 p1759 A69-22836

Electron production rates variations in lower ionosphere cosmic ray related to meteorological, geomagnetic and cosmic conditions

10 p1759 A69-22839

Cosmic ray absorption and modulation in lower ionosphere at midlatitudes, considering 11 year variations, Forbush effects and solar radiation on electron concentration

10 p1759 A69-22840

Solar activity effect on interplanetary electromagnetic field according to cosmic ray modulation data, noting ineffective correlation and solar wind effects

10 p1759 A69-22841

Cosmic ray modulation by solar wind, discussing anisotropic diffusion during propagation through interstellar magnetic field

10 p1759 A69-22842

Solar activity and 19 to 24 day variations in cosmic ray intensity

10 p1759 A69-22843

Asymmetrical solar wind volume variations of magnetic inhomogeneities and cosmic ray absorption in earth atmosphere, including barometric coefficients of neutron component

10 p1760 A69-22844

Phase equilibrium and dynamics of gas volume heated by cosmic rays and cooled by radiation

10 p1760 A69-23136

High energy cosmic radiation using Conversi detectors, noting design and internal efficiency

10 p1693 A69-23296

Cosmic protons interaction with interplanetary plasma, analyzing beam energy loss due to excitation of longitudinal electrostatic oscillations

10 p1760 A69-23617

Low energy cosmic ray intensity increase on July 7, 1966 registered with high latitude neutron monitors
10 p1766 A69-23762

Time dependence, anisotropy and spectral composition of cosmic radiation generated during series of flares during July 5-20, 1966 by Pioneer 6 observations
10 p1768 A69-23769

Forbush decrease associated with July 7 1966 proton event from cosmic ray intensity variation measurements by neutron monitors
10 p1768 A69-23774

Low energy particles during solar proton flare and effects on magnetosphere, cosmic ray intensity, ionosphere and geomagnetic activity
10 p1768 A69-23786

Interplanetary magnetic field sectoral structure effect on diurnal cosmic ray intensity and geomagnetic field, noting field direction influence
10 p1769 A69-23905

Algorithm for determining readings dispersion during cosmic ray recording, considering cosmic rays variability, statistical nature and instrument errors
10 p1770 A69-23906

Coupling coefficients for integral charged component of cosmic rays determined from measuring azimuthal geomagnetic effect on rays observed in crossed telescopes
10 p1770 A69-23925

Interstellar gas model based on calculations of heating by low energy cosmic rays, noting gravitational compression to form clouds
10 p1770 A69-24095

Stochastic and ergodic aspects of magnetic lines of force, discussing cosmic ray diffusion in interplanetary magnetic field
10 p1770 A69-24111

Stochastic model of interstellar magnetic field to account for observed cosmic ray mean life
10 p1771 A69-24112

Low energy cosmic rays and plasma turbulence in heating and ionizing interstellar gas, discussing acceleration and galactic sources
11 p1945 A69-24380

Cosmic ray cut-off energy for synchronous satellites computed by trajectory tracing method using magnetospheric model
11 p1949 A69-24860

Biological effects of cosmic ionizing radiation in supersonic commercial aircraft at high altitudes, showing spatial distribution based on balloon experiments
11 p1830 A69-24865

Laboratory simulation methods for cosmic nuclear radiation, discussing dosimetry methods
11 p1862 A69-24875

Radiation dose and radioactive isotopes induced in astronaut body by cosmic rays of various energies
11 p1831 A69-25463

Cosmic radiation origin in terms of sudden injection of particles in time, momentum and space, considering statistical fluctuations role in observed spectrum
12 p2148 A69-26206

Radio emission of fast cosmic ions by plasma wave conversion to electromagnetic waves, using nonlinear mechanism in turbulent plasma
12 p2149 A69-26209

X ray polarization from Sco X-1, noting spurious instrumental polarization due to cosmic ray anisotropy using X ray polarimeter
12 p2149 A69-26315

Inelastic interactions between Tev cosmic particles and light element nuclei, describing design and operation of measuring apparatus and derivable data
12 p2093 A69-26583

Cosmic radiation recorder designed for use onboard satellite to measure intensity space-time distribution under geomagnetic effect
12 p2094 A69-26697

Solar-terrestrial environment, discussing mathematical development of solar wind, satellite measurement, magnetic storms, aurora and cosmic rays
12 p2161 A69-26941

Cosmic rays during 11-year solar cycle, short term variations and radial gradient based on Luna, Zond and Venera probes and Cosmos observations
13 p2326 A69-27351

Cosmic ray propagation theory for steady streaming along magnetic field and down cosmic ray density gradient, noting MHD wave generation by anisotropy
13 p2326 A69-27569

Cosmic X ray background measurements and Crab Nebula observation during sounding rocket flight
13 p2326 A69-27570

Cosmic ray observation data automatic recording, presenting coding system for reading into computer
13 p2327 A69-27609

Cosmic ray physics - Conference, Novosibirsk, U.S.S.R., August-September 1967
13 p2328 A69-28367

High energy particle collisions, calculating inelastic interactions between cosmic nuclei
13 p2330 A69-28370

Four dimensional momenta transfer during high energy cosmic ray particle collisions, comparing various collision models
13 p2330 A69-28375

Wilson chamber and ionization calorimeter determination of cosmic ray particle-carbon nuclei interaction energy characteristics
13 p2330 A69-28379

Pionization cross sections at 100 gev for interactions of cosmic ray neutrons and pions with C and Pb nuclei
13 p2330 A69-28382

Inelastic interaction cross sections of nuclear active cosmic ray particles with atomic Fe and Pb in 100 to 1000 gev range
13 p2330 A69-28384

Cosmic ray postinteraction nuclear active particle energy spectrum measurements with ionization calorimeter, noting energy underrating
13 p2331 A69-28392

Nuclear active cosmic ray component particle energy spectrum and nuclear cascade avalanches curves, using ionization calorimeter with Pb absorber
13 p2303 A69-28399

Cosmic ray penetrating component properties identical to muon component at mountain level, indicating baryon passive nuclear state nonexistence
13 p2331 A69-28400

Cosmic ray muons energy and angular distribution measurements, obtaining curve with respect to projection angles
13 p2332 A69-28420

Cosmic ray muons angular distribution measuring device for determining pion/kaon ratio
13 p2332 A69-28421

Cosmic ray particles with fractional charge at sea level searched by scintillation counters with spark chambers, estimating quark flux intensity
13 p2333 A69-28425

Cosmic rays suggested as origin of interstellar grain alignment, discussing galactic central radiation, gas collisions and isotropic bombardment
13 p2333 A69-28469

Cosmic ray propagation in interplanetary space taking into account reverse effect on solar wind, deriving integrodifferential equation
13 p2333 A69-28688

Solar and galactic cosmic rays measurement data used to investigate variation in time of relations between cosmic rays modulation amplitude and solar activity variations
13 p2333 A69-28689

Coupling coefficients of global and vertical fluxes of charged cosmic ray component in stratosphere measured by radiosondes
13 p2334 A69-28690

Cosmic ray equators from trajectory tracing procedure for computing vertical cut-off rigidities with two different geomagnetic field simulations compared to experimental equators
14 p2511 A69-28961

Muonic component diurnal wave trains at 70 mwe during cosmic ray decreases, discussing Forbush decay as result of shock front advance
14 p2511 A69-28962

Cosmic ray intensity preceding Forbush effects as function of chromospheric flares solar longitude and solar wind velocity
14 p2512 A69-29044

Relativistic solar proton propagation fluctuation effects in interplanetary magnetic field during cosmic ray intensity increase
14 p2512 A69-29045

Cosmic ray angular distribution spectrum and interplanetary magnetic field properties determined from semidiurnal cosmic ray variations data
14 p2512 A69-29046

Geomagnetic cut-off influence on charged particle dynamics in geomagnetic field, applying charged particle motion theories to magnetosphere fields
14 p2513 A69-29099

Rocket-borne scintillation spectrometer for cosmic photon radiation
14 p2449 A69-29566

Frequency distribution of sudden cosmic ray intensity increases, considering Forbush phenomenon
14 p2514 A69-29773

Annihilation gamma ray spectra from equilibrium spectra of secondary galactic positrons
14 p2514 A69-29948

Cosmic ray intensity during solar cycles, considering minima relationship to Bartel index maxima and solar wind modulation theory
14 p2515 A69-29967

Cosmic ray observations on synoptic scale, discussing equipment and programs of IQSY world array of monitor stations
15 p2673 A69-30012

Cosmic ray intensity underground measurements, discussing solar modulation processes, sidereal day variations and interplanetary magnetic field influence
15 p2673 A69-30013

IQSY low energy galactic and solar cosmic ray observations made by various satellites and space probes, including hydrogen and helium energy spectra
15 p2673 A69-30014

Cosmic ray variation theory, presenting data on coupling of solar activity with large scale characteristics of solar wind during 11-year cycle
15 p2673 A69-30015

Quark detection in cosmic rays at sea level using scintillation counter and streamer chamber system
15 p2674 A69-30308

Galactic cosmic rays and Alfvén waves interaction, considering gyration frequency resonance, wave growth, Fokker-Planck equation and diffusion model
15 p2675 A69-30761

Low energy positrons in cosmic radiation due to beta decay of carbon, nitrogen and oxygen isotopes, estimating positron fluxes and energy spectra
15 p2676 A69-30887

Interstellar hydromagnetic waves due to streaming cosmic rays indicated by pulsar scintillations studies
15 p2676 A69-30889

Relative motion of 3 K cosmic background radiation with covariant photon equilibrium distribution
15 p2657 A69-31494

Interstellar cloud models, considering gas pressure, cosmic ray flux, magnetic field values, etc.
16 p2853 A69-31599

Low velocity heavy mass particle detection in sea level cosmic radiation, assuming deuterons
16 p2846 A69-31600

Metagalactic electrons inverse Compton effect on relic radiation to interpret cosmic isotropic X radiation entire energy spectrum
16 p2847 A69-31800

Azimuthal particle distribution expressions for analyzing cosmic ray jets
16 p2849 A69-32045

Book on cosmic ray variations and solar activity during IQSY covering energy spectrum, outer space radiation, magnetosphere, etc.
16 p2849 A69-32052

Solar wind speed transverse variation effect on cosmic ray intensity at earth analyzed using mathematical model
16 p2849 A69-32088

Cosmic ray second harmonic daily variations explainable by symmetrical gradient rising away from solar equatorial plane
16 p2850 A69-32304

Approximate solution of nonlinear differential equation describing interaction between galactic cosmic rays and solar wind, obtaining four domains
16 p2851 A69-32519

Cosmic ray intensity temperature dependence in stratosphere and anisotropy in interplanetary space determined from measurements over Arctic and Antarctic regions
16 p2851 A69-32537

Cosmic ray electron spectrum data obtained by balloon flights, showing electron flux reduction above 500 Mev with increasing solar activity
16 p2851 A69-32566

Earth motion relation to cosmic background radiation excess determined from radiometer study of galactic radiation
17 p3022 A69-32864

Cosmic X rays diffused component absolute intensity measurement using rotating collimator borne on sounding rocket, noting flat spectrum and Sco X-1 intensity variation
17 p3023 A69-33068

High energy cosmic ray muon charge ratios at large zenith angles measured as function of momentum by using spectrometer
17 p3023 A69-33321

Cosmic ray particle Pb nucleus interaction energy transfer to electron photon cascade in first inelastic collision, noting dependence on particle energy
17 p3008 A69-33387

European highly eccentric orbit satellite /HEOS/ cislunar probe to explore interplanetary space for mag-

netic fields, cosmic radiation, solar wind and earth shock wave

17 p3050 A69-33397

Cosmic ionizing radiation effects on electronic elements operation based on radiation and matter interaction principles

17 p2937 A69-33583

Interstellar H I regions and clouds heating and ionization by low energy cosmic rays from quantitative models, noting pressure equilibrium role

17 p3038 A69-33726

Cosmic ray heavy nucleus ends flux by nuclear emulsions for balloon flights at various atmospheric depths

17 p3025 A69-34219

Cosmic X rays diffuse component possible origin, discussing galactic gamma ray flux and disagreement with measured isotropy

18 p3185 A69-34275

Cosmic ray propagation equilibrium model for rays origin and storage in galaxy, considering energy dependence of nuclei relative abundances

18 p3185 A69-34276

Cosmic ray intensity short term stochastic variations in solar system related to turbulent solar wind day-to-day variations

18 p3186 A69-34300

Hard cosmic radiation hypothesis for Newton gravitation law for neighboring bodies, obtaining gravitational energy quanta and propagation velocity relationship

18 p3172 A69-34627

Cosmic ray diurnal anisotropy variations, correlating component annual means with magnetic activity

18 p3186 A69-34934

Cosmic ray approach directions computation for high latitude stations, discussing results for low rigidity galactic cosmic rays and solar corpuscular events detection

18 p3187 A69-34940

Low energy cosmic ray density in Galaxy due to pulsar PSR 0833-45 caused by mass ejection

18 p3187 A69-34995

Source requirements for cosmic radiation origin model, noting fluctuations in momentum changing process

18 p3188 A69-35005

Photodisintegration of ultrahigh energy cosmic rays by universal radiation field, analyzing implications on origin and propagation time

18 p3188 A69-35006

Source position of cosmic ray diurnal anisotropy relative to ecliptic plane from neutron monitor data at Mawson and Churchill stations

18 p3189 A69-35441

Be 7 stability in galactic cosmic radiation, noting lifetime dependence on electron density around nucleus

18 p3189 A69-35482

Cosmic ray produced radionuclides and rare gas isotopes from Saint-Severin meteorite surface, showing relative Kr spallation mass yields dependence on cosmic ray energy spectra

19 p3410 A69-36093

Cosmic ray produced radionuclides P 32, Cl 36, Ar 37 and Ar 39 determined in separate mineral phases of meteorites, emphasizing ratios in metals

19 p3410 A69-36094

Radiation ages of bronzite chondrites, amphoterite and hypersthene from cosmic ray activities

19 p3412 A69-36102

Cosmic ray produced Be 10 in iron meteorites for terrestrial age determination, considering Cl 36 and rare gas analysis

19 p3412 A69-36104

Meteoritic cosmic ray exposure time from method based on spallogenic Ar 36/Ar 38 ratio, noting impracticality for exposures longer than 5 million years

19 p3418 A69-36138

Proton satellites measurements reconciliation with diurnal stellar variation data and cosmic rays origin models

19 p3396 A69-36621

OGO-F neutron monitor for measuring cosmic ray neutron flux near earth, locating sensor on boom to minimize spacecraft produced neutrons

19 p3314 A69-36678

Cosmic rays sudden intensity increases during proton flares of 28 January 1967 and 7 July and 2 September 1966, plotting proton density vs pressure

20 p3587 A69-37045

Pulsars cosmic ray mass and charge spectra analyzed for evidence of neutron star origin

20 p3588 A69-37487

Meteorite minerals as detectors for studying fossil record of cosmic ray nuclei, emphasizing feldspars and pyroxenes

20 p3590 A69-37568

Biological effects of cosmic radiation on crewmen and protection measures, noting ground radiobiological and medical hygienic investigations

20 p3478 A69-37628

Cosmic radio emission absorption in D, E region and in F 2 layer above and below electron concentration maximum from vertical ionospheric sounding 1959 over Moscow

20 p3590 A69-37676

High energy proton and neutron fluxes and spectra from nuclear emulsion stacks on Cosmos satellites, calculating cosmic radiation doses

20 p3591 A69-37961

Cosmic protons and high energy heavy nuclei interaction with radiation in expanding universe, including estimates of light radiation influence on cosmic ray spectra

20 p3591 A69-38034

Twenty year wave in diurnal anisotropy component of galactic cosmic rays arriving at earth from asymptotic direction east of sun interpreted as magnetic reconnection

20 p3592 A69-38098

Diurnal variations in cosmic ray intensity from observations by inclined meson telescopes scanning equatorial plane

20 p3593 A69-38109

Anisotropy of relativistic cosmic ray electrons, considering electron exposure time to synchrotron effects, energy loss from inverse Compton effect, etc

20 p3593 A69-38145

Cosmic X ray background spectral measurement from rocket flight near geomagnetic pole

21 p3787 A69-38351

Charged particle acceleration in interplanetary plasma from analysis of cosmic ray intensity increases accompanied by SC magnetic storms and Forbush effects

21 p3788 A69-38587

Cosmic ray studies - Conference, Bombay, November 1968

21 p3788 A69-38811

Cosmic rays composition, origin, acceleration and propagation, describing two component models

21 p3789 A69-38814

Meteoritic compositions used to determine prehistoric cosmic rays composition and energy spectrum

21 p3789 A69-38815

Cosmic ray propagation from experimental data on cosmic ray nuclei

21 p3789 A69-38816

Interstellar matter, considering objects size, solar wind structure, galactic parameters, magnetic fields and cosmic ray heating

21 p3802 A69-38819

Galactic radio emission and magnetic field strength and structure, using radio surveys to obtain information on cosmic rays

21 p3790 A69-38820

Cosmic ray electron role in energetics of solar flares, stellar flares and explosions, galactic eruptions and quasars

21 p3790 A69-38823

Galactic gaseous disk dynamics, considering interstellar gas behavior and cosmic ray-magnetic field instability

21 p3802 A69-38824

Diurnal variations of cosmic ray neutrons corrected for barometric and temperature effects by harmonic analysis

21 p3791 A69-38840

Cosmic ray electron recorder for measuring intensity, energy spectrum and angular distribution of electron fluxes within specific energy range

21 p3724 A69-39074

Cosmic ray muons for calibrating dE/dx counter used in particle identification by determining cosmic particles distribution as function of energy losses due to ionization

21 p3724 A69-39075

Cosmic radiation altitude profiles, giving tabulation of counting rates obtained by SPARMO flights at different locations

21 p3791 A69-39253

Harrison primordial inhomogeneity postulate concerning baryon numbers distribution in universe, precluding possibility of considering cosmic rays bulk as universal

21 p3810 A69-39469

Galactic cosmic rays, discussing chemical composition, isotopic separation, proton and alpha particles energy spectra, propagation, interactions, etc

21 p3791 A69-39502

Galactic nuclei as collapsed old quasars from dynamics of gas cloud collection in galactic nucleus, discussing cosmic radiation emission from synchrotron mechanism

21 p3815 A69-39610

Sayan Sun Observatory experimental equipment, discussing instruments for solar observation, earth currents measurement and cosmic ray neutron components recording

22 p3943 A69-39997

Chemical composition of galactic and solar cosmic rays, discussing differences from universal cosmic abundances, using Cerenkov counters, emulsions, etc

22 p4002 A69-40090

Cosmic ray electrons component measurements at balloon altitudes with electron spectrometers

22 p4002 A69-40091

Cosmic ray neutron studies of atmospheric nucleon component equilibrium and flux fluctuations at atmosphere top

22 p4002 A69-40092

Cosmic radiation exposure of passengers and crew in supersonic transport at high altitude

22 p4002 A69-40093

Radiocarbon natural production by cosmic ray neutrons, utilizing proportional counters filled with N atmospheres

22 p4003 A69-40095

Geomagnetic disturbances and cosmic ray storm of 25-26 May 1967 caused by McMath plage region 8818, noting Forbush decreases and ring current effect

22 p4004 A69-40307

Cosmic ray proton cut-off increase at high latitudes during magnetospheric substorms, using balloon time observations of nuclear gamma ray flux

22 p4005 A69-40509

Splash and return albedo electrons in cosmic ray electron spectrum between 12 Mev-1 Gev measured by high altitude balloon flight

22 p4005 A69-40510

Cosmic gamma rays spectrum from neutral pions production and decay in metagalactic cosmic ray p-p collisions, deriving models based on Einstein general relativity theory

22 p4006 A69-40641

Pitch angle distribution of cosmic ray electrons in decreasing magnetic field for waves in ionized plasma, noting anisotropy due to synchrotron radiation

22 p4006 A69-40642

Cosmic X ray bremsstrahlung due to collisions of suprathermal protons with ambient electrons, giving clue about diffuse sky background of X rays

22 p4006 A69-40643

Cosmic ray diurnal phase and amplitude variations determined using superimposed records of cosmic ray stations inside limited rigidity region

23 p4204 A69-41481

Cosmic ray anisotropy direction during periodic intervals determination, noting application to event of December 1957

23 p4204 A69-41482

Geomagnetic disturbances relations to cosmic ray diurnal variation phase and amplitude, including Forbush decreases

23 p4204 A69-41483

Day-to-day variability of daily variation of cosmic ray intensity during quiet solar activity period using high latitude neutron monitor data

23 p4204 A69-41484

Radiometer for measurement of cosmic rays at 200-400 km altitudes range by satellites, presenting block diagram of radiation detector units

23 p4165 A69-41732

Cosmic ray detectors design for medium, low and very low energy events on IMP-1 spacecraft, noting PCM format

23 p4118 A69-41738

Biological effects by cosmic ray heavy ions and solar flares, using direct correlation between damages caused and trajectories

23 p4089 A69-41831

Outer anisotropic galactic cosmic particle flux distortion in interplanetary space, analyzing scattering in solar wind by isotropic diffusion equations

23 p4205 A69-41837

Cosmic ray flux intensity increases, discussing effects of solar wind, corpuscular flux velocity and interplanetary magnetic field

23 p4205 A69-41838

- Cosmic radio emission anomalous absorption measurements during PCA following July, August, September 1966 proton flares 23 p4156 A69-41845
- Anomalies of isotropic cosmic ray secular variations at high latitudes based on supermonitor neutron data 23 p4206 A69-41854
- Errors due to neutron counter radioactivity in cosmic rays nucleon measurements analyzed in reducing readings to barometric pressure 23 p4206 A69-41855
- Day-to-day changes of cosmic ray diurnal variation measured on meson and neutron components, showing relationship with interplanetary magnetic field 23 p4206 A69-42012
- Low energy galactic cosmic ray spectrum determined from ionization rate per hydrogen atom, correlating peak intensity with stellar particle emission high energy portion 24 p4365 A69-42608
- Fire hose instability growth rate in relativistic plasma with anisotropic pressure, discussing importance to cosmic ray liberation and isotropization at galactic halo 24 p4376 A69-42660
- IMP 4 satellite measurements of cosmic ray electrons in interplanetary space compared to predictions of electron intensity from interstellar proton-electron collisions 24 p4365 A69-42667
- Cosmic rays properties and dynamical effects in Galaxy disk including origin, lifetime, magnetic field instability, etc 24 p4366 A69-42695
- Transient sources of cosmic rays, discussing possible time variable intensity and momentum spectrum of Galaxy 24 p4367 A69-43006
- Equations governing cosmic ray modulation and approximate equations valid at high and low energies 24 p4367 A69-43169
- Cosmic ray electron energy spectrum and intensity measurements indicating time variations attributed to solar modulation effects 24 p4367 A69-43175
- Isotropic cosmic X rays measured by balloon-borne scintillation telescope, discussing agreement with electron energy spectral distribution 24 p4368 A69-43185
- Diffuse cosmic X rays from Compton collisions between galactic leakage electrons and extragalactic background photons to verify microwave blackbody radiation properties 24 p4368 A69-43202
- Soft cosmic X ray background flux from rocket observations on 21 September 1968 from White Sands, discussing flux origins 24 p4368 A69-43220
- Low energy cosmic rays and plasma turbulence in heating and ionizing interstellar gas, discussing acceleration and galactic sources 24 p4375 A69-43770
- COSMOGONY**
U COSMOLOGY
COSMOLOGY
- Stellar evolution, discussing stellar structure, pre- and post-main sequence evolution, solar system origin, supernovae, white dwarfs, variable stars and close binaries 01 p0148 A69-10046
- Viscous effects of neutrinos in anisotropic cosmological models examined using Boltzmann equation with simple collision term 01 p0148 A69-10053
- Age and initial helium abundance of stars in M15 globular clusters estimated from stellar evolution lifetime ratio 01 p0149 A69-10135
- Cosmology and quantum electrodynamics, discussing zero point oscillations and predicted spontaneous emission rate 01 p0149 A69-10139
- Open cosmological model containing radiation and matter, noting matter density relationship to visible matter average 01 p0150 A69-10371
- Solar system origin and evolution by future space mission experiments, discussing theories and mission objectives [AAS PAPER 68-191] 01 p0153 A69-10823
- Late type stars, discussing main sequence for Population 1 and Population 2 stars and ages and chemical composition of old galactic clusters and globular clusters 01 p0158 A69-11325
- Uranium in meteorites, discussing U content and isotope composition, Pb isotope ratios, radiogenic Pb, origin of matter and meteorite ages 01 p0025 A69-11369
- Lunar surface early geologic evolution noting bearing on earth geologic history [AAS PAPER 68-202] 02 p0312 A69-11478
- Observable surface of part of Friedmann universe calculated using analytical continuation of Schwarzschild coordinate system, noting angular extent and angle of observation effect 02 p0314 A69-11644
- Book on cosmic radiation origin and expansion of universe, covering astrophysical reasons for electric charging of galaxies in range of galactic and metagalactic dimensions 02 p0315 A69-11713
- Godel type solution of Einstein-Maxwell equation for dust filled universe, using Rainich equations 02 p0280 A69-11814
- Topochrone and generalized Hubble law considered for singular origin of universe with big bang explosions 02 p0321 A69-12195
- General covariant quantization of gravitation and cosmology 02 p0326 A69-12640
- Extensive air showers due to interaction of high energy particles with atmosphere, discussing astrophysics, cosmology and fundamental particle physics 03 p0498 A69-12938
- Sun motion with respect to extragalactic universe, discussing local supercluster kinematics 03 p0513 A69-13769
- Atomic electron spontaneous transition in theory of direct particle interaction, considering electrodynamic field zero-point oscillations role 03 p0468 A69-13773
- Secularly stable figures of equilibrium of rotating heterogeneous fluids of planetary size, noting dependence on laws of inertia and gravitation 03 p0513 A69-13780
- Observable horizons in expanding universe, considering absorption of extragalactic radiation 04 p0648 A69-14566
- Cosmology, experiments on gravitation, space-time theory and model of universal history 04 p0661 A69-15157
- Nonquadrupole nature of cosmological radio emission intensity distribution demonstrated for anisotropic homogeneous cosmological models without flat space 04 p0662 A69-15238
- Cometary origin of meteorites, discussing and rejecting origin from recent asteroidal collisions 05 p0818 A69-15588
- Energy definition in relativity for steady state universes, particularly Schwarzschild universes 05 p0792 A69-15683
- Intergalactic continuum study showing universe behavior like black body with 2.7 K radiation temperature, noting cosmological and cosmogonic importance 05 p0827 A69-16593
- Elementary composition and origin of primary cosmic rays, discussing space techniques for observation of components 05 p0818 A69-16816
- Existence of cosmic time functions based on stable causality condition / absence of closed timelike or null curves in Lorentz metric/ 06 p0957 A69-17471
- Complex distribution of quasar red shift interpreted as due to two simple distributions of cosmological and gravitational red shift 06 p1009 A69-17968
- Cosmology, discussing big bang and steady state models, arrow of time, red shift/distance relation, background radiation, etc 07 p1210 A69-18390
- Cosmological model describing relation between red shift and magnitude of quasars 07 p1211 A69-18406
- Geochemistry and cosmology - Conference, Prague, August 1968 07 p1212 A69-18546
- Soviet book on relativistic astrophysics covering evolution and structure of universe with reference to galaxies, stars, quasars, relativity theory, gravitation theory, etc 07 p1216 A69-18960
- Red shifts and intrinsic powers of radio galaxies and quasars, discussing local luminosity distribution, function of sources and cosmology 07 p1206 A69-19270
- Origin of galaxies, discussing initial conditions of formation including density, kinematic and composition inhomogeneities, time effect, etc 07 p1218 A69-19280
- Cosmological models with antipole, determining models consistent with spatial distribution of quasars and radio galaxies 07 p1219 A69-19284
- Plane symmetric perfect fluid cosmological model derived from class I considerations, evaluating scalar invariants for line element 07 p1222 A69-19586
- Relativistic cosmological models with radiation and matter, analyzing conversion from radiation-like models to dust-like models 07 p1222 A69-19587
- Commensurability among pairs of mean motions of natural satellites of major planets and hypothesis of tidal evolution of satellite systems 07 p1223 A69-19638
- Commensurability among pairs of mean motions of satellites of major planets and power law relation for orbital periods of satellites 07 p1224 A69-19639
- Neutral hydrogen distribution and dynamics in galaxies, discussing observations by spectrographic transit telescope, data processing and profiles 07 p1224 A69-19711
- Critical density ratio concept introduced into cosmological models for matter concentration into galaxies in expanding universe 08 p1381 A69-19794
- Primordial magnetic field effects on spatially homogeneous cosmological models with anisotropic Euclidean metric 08 p1383 A69-20049
- Galactic angular momentum of rotation, applying rotation theory to gravitational instability model of galactic formation 08 p1383 A69-20050
- Isotropic Newtonian cosmological models symmetry shown to have velocity distribution obtainable from solution of Vlasov equation 08 p1386 A69-20073
- Relativistic astrophysics, discussing quasar phenomenology, red shift cosmology and relationship with galaxies 08 p1388 A69-20222
- Evolutionary cosmological models, relevant observational cosmology, quasar red shift, cosmic black body radiation, cosmic He abundance and universe temperature history 08 p1388 A69-20223
- Metagalaxy stationary model in terms of relativity theory, investigating radiation pressure balancing of gravitation as imaginary situation 08 p1389 A69-20263
- Two gravitational fields theory of gravitation in general relativity for flat universe, discussing gravitational wave propagation 08 p1390 A69-20276
- Quasars optical and electrical properties, distance, nature and role in cosmology 08 p1390 A69-20377
- Origin and distribution of elements - Conference, Paris, May 1967 08 p1398 A69-20892
- Nucleosynthesis in stars and early stage expanding universe, considering related nuclear reactions, helium abundances and kinematics of stars in Galaxy 08 p1357 A69-20893
- Galaxy formation from elements primeval abundance viewpoint stressing initial helium abundance 08 p1400 A69-20894
- Plutonium-244 existence in early solar system concluded from relative abundance ratios of excess meteoritic heavy Xe isotopes 08 p1401 A69-20900
- Rotation effect on homogeneous gravitating systems stability, noting lack of unity in approaches to cosmogony by various authors 09 p1589 A69-21372
- Poincare recurrence theorem applicable to collapsing gravitational system with particles velocity dispersion other than zero 09 p1593 A69-21567
- Lipshits-Khalatnikov law applicability to early stages anisotropy of cosmological expansion and relic emission 09 p1593 A69-21568
- Theoretical models describing quasi-stellar objects and radio galaxies, noting objects locality, semilocality and cosmological distances 09 p1594 A69-21693

Quasar red shifts due to cosmological and gravitational factors, assuming correlation of QSO intrinsic luminosity with gravitational red shift values
09 p1597 A69-22151

Cosmological implications of diffuse X ray background, noting Compton black body process effect on isotropic cosmic X rays
09 p1578 A69-22152

Globular cluster origin as gravitationally bound gas clouds before galaxy formation from primeval fireball model
09 p1599 A69-22192

Early evolution of universe related to present upper bound of primordial black body gravitational radiation temperature
09 p1601 A69-22210

Absorption red shifts in quasi-stellar source due to dead galaxies in cosmologically flat model of universe
09 p1602 A69-22228

Variable gravitational number kappa, discussing effects on cosmology
09 p1603 A69-22270

Galaxies and galactic clusters regarded as particles in kinetic theory of cosmology, discussing distribution function choice and red shift
09 p1605 A69-22410

Bolometric luminosity-red shift relations of Friedmann dust universes corrected for inhomogeneities, using locally inhomogeneous Swiss cheese models
09 p1605 A69-22411

Brans-Dicke gravitation theory effects on solar evolution and neutrino flux, discussing solar luminosity
09 p1605 A69-22415

Characteristic length constant in open cosmological model of large scale properties of real space-time, noting relation to other constants
09 p1608 A69-22528

Cosmology, reviewing Friedman and Lemaitre model, big bang model, primeval fireball hypothesis for residual black body radiation and galactic origin theories
09 p1608 A69-22715

Primordial solar system chemical composition for studies of origin and evolution, compiling solar composition data
09 p1608 A69-22745

Universe rotation from observations of microwave background and using closed universe model
10 p1771 A69-22851

Homogeneous anisotropic cosmological models of pancake and cigar forms, discussing quasars and emission time effects on red shift and luminosity distance
10 p1771 A69-22856

Rocket IR astronomy in support of big bang hypothesis, considering photoelectric detectors and instrument system
10 p1772 A69-22868

X ray universe, considering contribution of X ray astronomy to phenomena of big bang, supernovae, neutron stars, exploding galaxies, etc
10 p1760 A69-22869

Galactic discontinuity near longitude 140 degrees attributed to stars deficiency in anticenter quadrant or interstellar cloud obscuration
10 p1776 A69-23215

Solid hydrogen condensation on graphite grains for microwave background, discussing hydrogen grain promotion of galactic and stellar formation
10 p1776 A69-23216

Einstein cosmological field equations solved after subjecting electromagnetic null field metric tensor to Einstein gravitational field equations, noting coordinates significance
10 p1778 A69-23406

Zero point energy, evolutionary cosmology, negative kinematic pressure and space curvature, assuming physical vacuum as ground state of Bose field
10 p1780 A69-23649

Book on relativity and cosmos, space and time in physics, astronomy and cosmology covering theoretical and empirical research
10 p1784 A69-24019

Radio sources log N-log S diagram, red shifts and luminosity functions in zero cosmological constant and Lemaitre type Friedmann universes
10 p1789 A69-24134

Radiation probability of transmission through intervening galaxy and screening of quasar emission in universes with positive cosmological constant
10 p1790 A69-24135

Rb-Sr and other radioactive isotopes cosmochemistry in solar system, analyzing age of elements and r process
11 p1955 A69-24393

Red shift hypothesis postulated on perfect cosmological principle and uniqueness of electromagnetic wavelength measurements, showing agreement with astronomical data
11 p1961 A69-25108

Book on stellar, galactic and nucleosynthetic evolution covering nuclear, Fermi, electromagnetic and gravitational interactions roles
11 p1964 A69-25413

Test particle classical dynamics in closed expanding universe, discussing Newtonian inertial mass decrease and canonical methods for determining momentum, velocity and energy
11 p1920 A69-25561

Space flight research programs including stellar and biological evolutions and environmental control
12 p1255 A69-26005

Stellar evolution model for primeval He abundance in population II stars in globular clusters for big bang confirmation
12 p1256 A69-26228

Quasars and radio-quiet objects numbers and properties, discussing red shifts interpretation by cosmological, gravitational and Doppler theories
12 p1261 A69-26937

Cosmogonic nature of galactic nuclei activity, emphasizing streamers ejection and new formations in galaxies
12 p1263 A69-27016

Isotropic 3 K black body radiation implications for hot cosmological model, formation of galaxies, existence of superdense bodies and density nonuniformity during prestellar stage
12 p1267 A69-27047

Galactic formation by massive matter cloud passage through antimatter cloud, discussing radio sources genesis
12 p1270 A69-27064

Statistical tests for cosmological hypothesis for origin of absorption lines in spectra of quasars, considering red shifts
13 p2334 A69-27307

Book on astrophysics and stellar astronomy covering stellar radiation, binary and variable stars, positions, magnitudes, galaxies, cosmologies, etc
13 p2337 A69-27463

IR astronomy and cosmology, considering cosmic microwave background and isotropic radiation significance in distant IR
13 p2342 A69-27601

Einstein theory of space and time analyzed with emphasis on inertial systems
13 p2297 A69-27633

Philosophical problems of Einstein theory of gravitation and relativistic cosmology - Conference, Kiev, June 1966
14 p2482 A69-28856

Rigid space concept in gravitation theory, discussing reference systems with nonrigid and rigid background
14 p2484 A69-28863

Space-time interpretation of static Einstein universe model and Friedmann space with variable positive curvature
14 p2484 A69-28865

Asymmetry causes on cosmogonic scale in view of symmetry in small space-time regions /microworlds/ determinable within framework of Einstein theory
14 p2516 A69-28866

Unlimited extrapolation into infinity to determine ranges of applicability of theories in relativistic cosmology noting paradoxes
14 p2516 A69-28867

Galactic formation in Lemaitre universe from statistically probable density fluctuations, using perturbation theory and Newtonian cosmology
14 p2520 A69-29373

Book on New Cosmos covering classical astronomy concepts, stellar astrophysics and galaxies
14 p2522 A69-29684

Extragalactic background radiation intensity in isotropic world models as function of universe thermal history
14 p2514 A69-29769

Lunar origin theories, considering moon/earth mass ratio, earth-moon system angular momentum deficiency and differential volatilization in earth
14 p2527 A69-29882

Low density Friedmann universe models with non-zero cosmological constant and long ages, deducing galaxy evolution rates from magnitude-red shift relations
14 p2527 A69-29944

Closed space cosmological model, discussing complex singularity behavior
15 p2680 A69-30200

Extragalactic research to solve problems in cosmological and cosmogonic theory, including relativistic cosmology and observations
15 p2681 A69-30436

Einstein equations solution for empty space without singularities containing metric, with closed homogeneous space type hypersurfaces expanding anisotropically
15 p2690 A69-30732

Hydrogen recombination in hot universe model, discussing emission of energetic quanta
15 p2690 A69-30734

Expanding isotropic universe with cosmological constant, noting stability for rotational perturbations and gravitational and sound waves
15 p2690 A69-30735

Relativity theorems applied to collapsing stars and expanding universe noting limitations of general relativity from prediction of singularities
15 p2694 A69-30854

Galaxies formation from superstars ascribed to superstar instabilities
15 p2696 A69-31151

Newtonian invariant mechanics, giving inertial interpretation of gravitation and Hubble expansion of universe
15 p2654 A69-31214

Inertial systems in homogeneous isotropic expanding universe model, giving expression for line element accounting for Hubble effect
15 p2654 A69-31495

Mathematical solutions of Einstein cosmological equations for radiation universe, discussing model limitations for universes older than 5-6 billion years
15 p2700 A69-31496

Cosmic helium origin, discussing evidence for big bang, galactic synthesis and stellar thermonuclear burning theories
16 p2853 A69-31598

Possible existence in universe of large number of difficult-to-observe particles with zero rest mass left over from superdense phase
16 p2814 A69-31801

Monograph on creation and evolution of physico-theoretical concepts of space, time and matter
16 p2812 A69-32110

Stellar system stability for corresponding stable barotropic gaseous system, discussing Schroedinger operator role
16 p2862 A69-32374

Cosmology and geophysics relationships using initial and boundary conditions concept
16 p2864 A69-32451

Irregular dwarf galaxies as source of faint objects in close galactic groups
16 p2864 A69-32597

Water bag spherically symmetrical universe model, discussing system stability, distribution function representation and polytrope equivalency
16 p2866 A69-32813

Particle production by gravitational fields in universe via quantum field theory, considering cosmological models
17 p3008 A69-33003

Asteroidal jet streams from Hirayama family Flora, difficult to reconcile with exploded planet view
17 p3030 A69-33070

Meteorite origin theory limitations from microscopic examination and microprobe analyses of chondrules in unequilibrated meteorites
17 p3034 A69-33585

Corrections to previous papers on extragalactic gamma rays, discussing effects on various cosmological models
17 p3025 A69-34168

Aligned galaxies, discussing possible formation by consecutive explosive ejections of new galaxies from parent galaxy
17 p3044 A69-34175

Heavy nuclei origin based on empirical abundance distribution, discussing stellar, galactic and cosmic events for nuclear genesis
17 p3009 A69-34190

Lunar origin, geological composition and water existence controversies from data gathered by various lunar probes
18 p3196 A69-34631

Rotation effect on homogeneous gravitating systems stability, noting lack of unity in approaches to cosmogony by various authors
18 p3198 A69-34761

General relativity theory applicability to cosmology, Einstein principle of equivalence and contradicting arguments of relativistic cosmology
18 p3200 A69-34997

Fluctuations evolution in density perturbations analyzed to obtain free fall and free expansion universe models, showing no difference between expanding and static Newtonian universes

18 p3203 A69-35347

Planetary cosmogony problems involving protoplanetary cloud origin, matter condensation, planets formation and moon origin, noting iron content in chondrites

18 p3205 A69-35437

Hydrogen atom excess charge creating universe repulsive force in analyzing cosmological gravitational contraction in terms of Newtonian mechanics

18 p3206 A69-35469

Cosmological model based on inertia and relativity principles, considering scalar gravitational and electrostatic potential, light velocity, gravitational interaction and observed galactic red shift

18 p3206 A69-35470

Primitive solar nebula physical model considered under angular momentum conservation in collapsing fragment

19 p3406 A69-36074

Meteorite data in planetary cosmogony, discussing iron meteorite ages, Xe retention in chondrites and synchronism of sun and protoplanetary cloud forming

19 p3406 A69-36075

Solar system matter evolutionary beginning traced to chemical elements synthesis by considering radioactive decay irreversible processes

19 p3406 A69-36076

Heat generation in meteorites by radioactive isotopes generated by early solar proton irradiation prior to solar system solidification

19 p3411 A69-36098

Boundary conditions for theory of solar system origin, discussing planetary atmospheres, surfaces, magnetic fields, composition and early solar wind

19 p3419 A69-36209

Physical characteristics of young planetary nebulae and nuclei, discussing classification of objects II 4997, M 3-27 and M 1-2

19 p3423 A69-36226

Spiral galaxy linear diameter relation to luminosity applied to Virgo galactic clusters, noting effect on distance modulus and Hubble constant

19 p3427 A69-36652

Soviet book on cosmos and hypotheses covering origin and physical characteristics of earth, moon, Venus and Mars

20 p3596 A69-37234

Thomas wave equation in fluid mechanics, examining coordinates system with normal hyperbolic metric of universe tube having given signature

20 p3598 A69-37430

Cosmic matter density and velocity in expanding universe with negative curvature within Einstein-Friedman theory

20 p3599 A69-37472

Cosmological constant and elementary particle theory

20 p3606 A69-38013

Universal hydrogen distribution, discussing atomic hydrogen needed to close universe

20 p3610 A69-38140

Gas in H II regions and associated stars radial velocities correlation and systematic difference suggesting relationship between nebulae and stars

20 p3611 A69-38150

Quasars observations interpretation, discussing red shift origin, gravitational collapse, lifetime, distribution, cosmological aspects, etc

21 p3802 A69-38825

Radio source counts from cosmological standpoint, discussing terrestrial location relative to quasars

21 p3802 A69-38828

Harrison primordial inhomogeneity postulate concerning baryon numbers distribution in universe, precluding possibility of considering cosmic rays bulk as universal

21 p3810 A69-39469

Quasi-stellar objects identification, distribution, emission lines interpretation, energy distribution, absorption spectra, radio properties, etc

21 p3811 A69-39515

Soviet book on cosmogony, discussing nonstationary objects in universe, superdense bodies, solar system, explosion processes in universe, stellar evolution, etc

21 p3813 A69-39525

Soviet collection of papers on universe covering history and development of astronomy, solar system, minor planets, comets, shooting stars, extraterrestrial civilizations, etc

21 p3814 A69-39531

Density fluctuations in universe during early stages, using hot big bang cosmological model

21 p3814 A69-39571

Book on high energy astrophysics covering violent stellar phenomena, radio galaxies, quasars, pulsars, cosmic rays origin, mystery neutron stars, etc

22 p4008 A69-39900

Gravitational constant secular change from considering relativistic cosmology and galactic structure, deriving equations of Newtonian cosmology

22 p4017 A69-40173

Variable gravitational constant hypothesis, theories of gravity and gravity laws for earth interior, solar motion, cosmological problem and earth orbit

22 p4017 A69-40174

Dirac cosmological principle of nuclear decay compared to Rutherford theory with respect to radioactive ages of terrestrial rocks and meteorites

22 p4017 A69-40176

Fractionation mechanisms in early phases of planetary evolution sought to explain abundance problem in terrestrial planets

22 p4018 A69-40185

Strategy for exploration of inner solar system leading to origin and history, detailing lunar exploration program

22 p4022 A69-40449

Time symmetric electrodynamics for various cosmological models, discussing position and negative space curvature

22 p4022 A69-40469

Nonexistence of second order clustering of galaxies and relationship to gravitational cut-off, relativistic cosmologies and red shifted light by exponential decay of photon energy

22 p4024 A69-40579

Free-free intergalactic absorption at LF as function of red shift for uniform zero pressure cosmological models

22 p4025 A69-40640

Universe expansion model, integrating Einstein gravitation equations with cosmological constant lambda to interpret Hubble effect

22 p4029 A69-40756

Cosmological constant closed relativistic universe, showing constant-observational data inconsistency

22 p4029 A69-40757

Extraterrestrial objects composition in defining cosmic abundance curve, including solar and meteoritic data

22 p4032 A69-40982

Primordial He 3 and deuterium production from magnetic effects during nucleosynthesis epoch of big bang cosmologies

22 p4035 A69-41210

Steady state cosmology for classical and quantum electrodynamics in local vicinity, deriving Lorentz-Dirac equation from variational principle

23 p4215 A69-42116

Radio galaxies and quasars number-flux density relations role in cosmology, discussing object identification, population, angular sizes, etc

23 p4218 A69-42324

Observational cosmology developments with radio and X ray astronomy emphasizing existence, origin, effects and anisotropy of excess microwave background

23 p4219 A69-42327

Observational cosmology in terms of relation between red shift and apparent luminosity of galaxies /Hubble relation/

23 p4219 A69-42328

Stellar evolutionary ages and gravitational theory relations based on initial abundance ratio U 235/U 238 and present interstellar medium heavy element content

23 p4219 A69-42329

Deceleration parameter lower and upper limits for zero pressure big bang cosmological Friedmann models imposed by density parameter, Hubble constant and universe age

23 p4219 A69-42373

Density fluctuations during later stages of formation of universe, emphasizing problems of galactic cluster formation

23 p4221 A69-42390

Universe behavior in time, discussing expansion observed by red shift, closed universe with future contraction phase and unlimited expansion open model

23 p4221 A69-42391

Homogeneous axisymmetric anisotropic cosmological models, analyzing magnetic fields and initial anisotropies effect on 3K radiation and primordial He production

23 p4222 A69-42402

Absorption lines in stellar spectra and significance in cosmogony, discussing ionized Ca K line detection during delta Orionis study, K and H lines components, etc

24 p4383 A69-42999

Book on physics and evolution of galaxies covering properties, stellar content, interstellar matter, high energy particles and radio galaxies

24 p4384 A69-43167

Particle creation and quantized fields in expanding universe using covariant generalization of special relativistic free field equations, studying zero- and arbitrary-spin particles

24 p4352 A69-43193

Rb-Sr and other radioactive isotopes cosmochronology in solar system, analyzing age of elements and r process

24 p4390 A69-43783

COSMONAUTS

Professional activity of cosmonauts, considering training, mental and physical qualities and engineering background

[UN PAPER 68-95716] 06 p0879 A69-17036

Statistical correlation between cardiovascular activity and respiration dynamics of cosmonauts during orbital flight, discussing heart beat and respiration rates

07 p1061 A69-18584

Astronaut selection and training in U.S. and U.S.S.R.

13 p2216 A69-28636

COSMOS SATELLITES

Satellite meteorological research in U.S.S.R., discussing Cosmos satellites instrumentation, earth thermal radiation distribution, IR and UV spectra and cloud photography

01 p0111 A69-10950

Analytical model of geomagnetic field constructed from Cosmos 49 data using spherical analysis

02 p0240 A69-11698

Cosmos 253 rocket reentry and fragmentation over England

05 p0830 A69-16656

Onset and development of typhoons observed by Cosmos satellites using TV type IR apparatus

[UN PAPER 68-95774] 06 p0949 A69-17039

U.S.S.R. system Meteor consisting of four Cosmos satellites in polar orbits to observe cloud distribution, snow and ice field boundaries, etc

06 p1013 A69-17053

Narrow and wide angle actinometric instruments on-board Cosmos 122, 144 and 156, describing optical and data acquisition systems

06 p0929 A69-17977

M-20 digital computer program designed for calculating statistical characteristics of signals from IR TV scanning system of Cosmos 122 meteorological satellite

06 p0929 A69-17980

Digital computer algorithm for automatic processing of IR weather data transmitted by Cosmos 122 and 144 meteorological satellites

06 p0929 A69-17981

Draconic period changes of satellite 1965-11-D /Cosmos 54 rocket/ during visual observations with Interob

12 p2174 A69-26444

Fast charged particles measurements by Cerenkov counter in Cosmos 137 satellite, noting hard electron flux and cosmic ray radiation spectrum

13 p2327 A69-27693

Radiation measurements by Cosmos 122 satellite over various regions, determining radiation temperature, long wave heat flux and albedo

13 p2291 A69-27726

Radiation fields and large scale atmospheric disturbances analyzed, using radiation maps from Cosmos satellites

13 p2291 A69-27727

Analytical model of geomagnetic field constructed from Cosmos 49 data using spherical analysis

13 p2258 A69-28729

Scientific equipment on Cosmos 237 satellite for recording extraterrestrial radiation data, discussing specifications, operation and mission purpose

14 p2446 A69-29047

Global mean monthly charts for IR radiation temperature, based on Cosmos 144 satellite data

15 p2596 A69-30643

Atmospheric density and temperature variations between 200-600 km from Cosmos satellite data, noting solar activity effect

15 p2599 A69-31343

Neutron flux measurements on Cosmos 53, discussing equipment and calculation of secondary neutrons due to bombardment of satellite components

22 p4003 A69-40274

COSMOS 5 SATELLITE

Molecular ion concentrations determined using flat probe collector trap on Cosmos 5 satellite at 200-300 km

20 p3519 A69-37021

COSMOS 6 SATELLITE

Radioactive debris distribution in space from 9 July 1962 thermonuclear explosion over Johnston island recorded by Cosmos 6 satellite

23 p4205 A69-41836

COSMOS 137 SATELLITE

Cosmos 137 proton spectra data obtained in inner radiation belt agreeing with Relay 1 data

22 p4007 A69-41093

COSMOS 149 SATELLITE

Cosmos 149 meteorological satellite telephotometer, radiometer and other electronic equipment for measuring atmosphere and underlying surfaces physical parameters

14 p2447 A69-29403

Cosmos 149 meteorological satellite telephotometers for measuring reflected solar radiation from earth

14 p2447 A69-29404

Earth thermal emission intensity measured by two beam radiometer onboard Cosmos 149, noting discrepancy between empirical and theoretical transfer functions of atmosphere

15 p2596 A69-30651

Atmospheric radiative balance measurement on board Cosmos 149, describing design and operation of device

15 p2597 A69-30652

Cosmos 149 satellite stabilization system, discussing three axis orientation and pitch, yaw and roll stabilizations by aerodynamic and/or gyroscopic moments

17 p3047 A69-33226

COSPAR [COMMITTEE]

U COMMITTEE ON SPACE RESEARCH

COST ANALYSIS

General aviation missions in national transportation system /1968, 1975, 1980/, considering fuel taxes, overall system economics, ground facilities, etc

[AIAA PAPER 69-818] 19 p3453 A69-35624

Large area Si solar cell arrays design, considering environment, cell layout, thermal expansion, coverslides fabrication, costs, etc

19 p3253 A69-35708

Optimal plastic design of circular sandwich ring assuming symmetric loading, minimum plastic resistance and cost justification of stronger cross section

20 p3625 A69-37590

Remote sensing systems costs, benefits and economic evaluation

20 p3493 A69-37742

Economic effectiveness determination methods for commercial transport aircraft design analyzed quantitatively, using four engine 100-seat turboprop aircraft

21 p3855 A69-38873

Economic effectiveness of design and fabrication changes in aircraft construction industry for profitable operation of commercial transport aircraft

21 p3855 A69-38874

Fracture mechanics concepts for cost effective booster pressure vessel design and fabrication from commercial steels using boiler plate techniques and minimal NDT quality control

21 p3837 A69-39028

Space transportation cost factors, discussing payload characteristics, carrier utilization, program duration, government participation and control, carrier design, hardware costs, launch costs, etc

21 p3857 A69-39687

Reusable Crew Module, Reusable Orbital System and Reusable All Systems options for low cost space transportation system

21 p3827 A69-39693

Vehicle designs and cost analyses for launch vehicle selection to minimize costs of 40,000- 150,000 pound payload placement into orbit

21 p3827 A69-39694

Aerial surveys flight functions cost plotted against degree of performance, allowing for obtainable accuracies

22 p3863 A69-40041

Computer memory reduction through Fortran higher level language, discussing tradeoff between costs saved and additional logic hardware

[AIAA PAPER 69-963] 22 p3905 A69-40344

Aerospace programs cost analysis system, using contractors accounting records as data source

[AAS PAPER 69-465] 24 p4416 A69-42801

Adaptive cost equations in computer programs supporting launch vehicle long range planning, based on launch vehicle development usage

[AAS PAPER 69-164] 24 p4392 A69-42815

Algorithm minimizing personnel number and training costs to meet uncertain skill requirements, applying to army aviation contingency force training composition

[AAS PAPER 69-116] 24 p4271 A69-42818

Military aircraft service life problems solved by alternative replacement policies comparative present value analysis

24 p4253 A69-43058

Cost analysis in low cost launch vehicle studies emphasizing sustaining engineering and plant economics

24 p4393 A69-43120

COST ESTIMATES

Microwave applications of monolithic and hybrid semiconductor circuit technologies, considering cost and performance

01 p0039 A69-10188

Cost prediction equations used in perturbed environment of learning curves subjected to design change in industry

01 p0180 A69-10652

Structural testing in aircraft design, discussing costs, environmental conditions, test rigs and apparatus

01 p0170 A69-10864

Phased array radar cost improvement based on solid state devices and microwave integrated circuits application

01 p0048 A69-11039

Electron tubes in phased array radar systems, discussing replacement limits by solid state devices, reliability and cost reduction

01 p0048 A69-11040

Transistors vs electron tubes as microwave power sources in UHF phased array radars, noting transistor cost competitive limit

01 p0048 A69-11041

Systematic approach to standard launch vehicle based on governmental expenditure minimization while attaining mission goals

01 p0162 A69-11096

Survival of PERT/Cost technique without government impetus noting advantages for planning, monitoring and controlling technical performance objectives

01 p0180 A69-11251

Performance cost functions for reaction jet controlled system during on-off limit cycle for stable and unstable plant

02 p0278 A69-11965

Cost factors in choosing single or twin-engine layout for tactical aircraft

02 p0193 A69-12066

Aluminum plastic sandwich products production costs compatibility with conventional materials

02 p0348 A69-12749

Systems analysis application to determination of C-5 effectiveness noting loading, productivity and effectiveness analysis computer programs

[SAE PAPER 680729] 03 p0379 A69-13440

Cost analysis techniques for aircraft design and development, considering passenger capacity, flight distances and flight frequencies for various aircraft types

03 p0366 A69-13646

Airline operators economic oriented airframe maintenance problems, discussing cost accounting improvement

03 p0434 A69-13698

Maintainability and reliability affect utilization and operating costs of commercial aircraft

04 p0547 A69-14806

Cost dependent utility characteristics in mathematical model for optimum research and development resource allocation, computing optimum fund distribution with Lagrange multipliers

04 p0689 A69-14807

European launch vehicle development program, discussing economic limitations and employment possibilities

04 p0665 A69-14808

Equipment for minimum cost laboratory for thin and thick film hybrid circuits

04 p0559 A69-15198

Estimate accuracy and project selection models in industrial research, examining company data for miscellaneous, technical and commercial failure

05 p0849 A69-15981

Project management decision making, noting decision nature, cost effectiveness concepts and incentives

[ASME PAPER 68-WA/MGT-2] 05 p0850 A69-16145

Cost and schedule planning and control /CSPC/ project progress reporting technique

05 p0850 A69-16300

Teichmann cost analysis extended to include frequency dependent and diversity dependent rain losses for satellite communication, using Bayes strategy

05 p0721 A69-16580

Space vehicle trajectory optimization using computerized step by step steepest descent to minimum cost, considering cost gradient vs control

06 p1006 A69-17570

Computing optimum flight profiles by Balakrishnan epsilon method, including equations of motion constraint in cost function to be minimized

[AIAA PAPER 69-75] 06 p0868 A69-18058

Rocket transportation for upper atmospheric measurements, discussing sensors and cost effectiveness

[AIAA PAPER 69-139] 06 p1018 A69-18066

Manned orbital space stations design, purposes and applications, balancing costs against benefits

06 p1019 A69-18237

Cost estimating relationships for vertiports and airports, comparing terminal costs per passenger for each facility

[AIAA PAPER 69-208] 07 p1245 A69-19564

Reliability effect on operating costs of satellite communications system ground stations, calculating annual cost of channel with continuous time carry-over

08 p1276 A69-20586

Defense project management and discrepancies between estimates and final costs

08 p1423 A69-20628

Cost control for project management based on detailed programming

08 p1423 A69-20629

Project control cycle, cost monitoring and reporting to management

08 p1423 A69-20630

Microelectronics technology and economics, discussing semiconductor integrated, discrete component and thin film hybrid circuits and MOSFET devices

[AGARDOGRAPH-114] 08 p1291 A69-20983

Assessing cost effectiveness of reliability and quality of semiconductor products, using mathematical models

08 p1292 A69-21102

Deterministic model for cost effectiveness of avionics support programs based on subsystems support ability, test philosophy and test equipment design and manufacture

[AIAA PAPER 69-305] 09 p1478 A69-22377

Effective cost improvement of product and profit planning activity in jet engines production stressing J47 and J79 engines

[ASME PAPER 69-GT-61] 09 p1513 A69-22516

Cost-profit sharing agreement with aerospace manufacturing companies involved in Boeing 747 construction, detailing final assembly building

09 p1514 A69-22713

Incentive contracts design covering cost estimates, technical performance, realistic programs and multiple incentive arrangements

09 p1626 A69-22776

Spacecraft propulsion systems comparison and evaluation, discussing quality, schedules and costs in relation to mission requirements

11 p1965 A69-25600

Methodology for technical feasibility and economic analysis of remote sensing applications

12 p2193 A69-27013

Instructional broadcast satellites programming for time cost reduction, discussing frequency allocation, interference and ground station design

13 p2381 A69-27373

ESRO 1 project management and organization, discussing cost control, time saving, program evaluation and review system /PERT/, etc

13 p2382 A69-27750

Aircraft design cost control emphasizing engineering performance direct inclusion in design costs including tooling, testing, etc

13 p2382 A69-28094

Systems design value analysis including alternate solutions to cost effectiveness for design development and production phases

13 p2383 A69-28097

Value engineering proposal costs sustained by maintenance and overhaul industry in government contract negotiations, discussing reimbursement and proposed central agency

13 p2383 A69-28099

Deterministic economic mathematical models for optimum airline networks, considering transportation cost

14 p2540 A69-29141

Cost estimates of R and D, considering planned profit and loss following products introduction to market

14 p2541 A69-29280

Capital budgeting for R and D, discussing control of rising costs

14 p2541 A69-29281

Space flight cost analysis, relative costs of various types of transportation and need for reusable single stage to orbit vehicles

15 p2719 A69-30186

Air cushion vehicles tests for public transportation facilities noting operation costs

15 p2550 A69-30409

Cost plus award fee contracting incentive system based on after fact evaluation of performance effectiveness

15 p2720 A69-30426

Mathematical model for money expenditure on product oriented research programs, based on accumulated profits

15 p2721 A69-31068

Program stretchout in aerospace procurement, discussing costs effect in relation to incentive contracts

15 p2721 A69-31071

Cost effectiveness of DOD/military systems, discussing principles and analytical model with case study

15 p2722 A69-31125

Integrated Logistics Support (ILS) cost effectiveness, discussing management of systems elements in addition to prime equipment including computer programs, training, maintenance, etc

15 p2722 A69-31126

Equipment life cycle costs computer simulation for design and changes evaluation, including maintenance analysis example

15 p2723 A69-31138

Economics of airport use, congestion and safety, discussing differentiated pricing systems

15 p2723 A69-31241

Cost effective pressure vessel design using fracture mechanics, discussing fabrication costs, service life requirements, etc

16 p2870 A69-31740

VFW H3 Sprinter autogyro maintenance, reliability and operating costs

16 p2735 A69-32056

Proposed projects selection for independent R and D development program in business entity, measuring merits in terms of future financial returns

17 p3077 A69-34129

Edwards Inquiry Report into British Civil Air Transport based on cost effective economic study, involving airlines and regulatory system

18 p3231 A69-34311

Development, manufacturing and logistic costs of reliability improvement in electronic equipment design

18 p3231 A69-34485

Avionic subsystems warranty costs estimates, considering reliability prediction and hardware recycling

18 p3232 A69-34506

Cost risk management procedure in defense industry contracting, including risk percent limits and identification in proposals, specifications relief, escalation clauses, etc

18 p3233 A69-34655

Market analysis program to evaluate relationship between launch vehicle jettison weight and total cost based on all projected missions

[SAWE PAPER 776]

18 p3208 A69-34872

Airframe cost element prediction and application to cost control, considering government specifications

[SAWE PAPER 731]

18 p3221 A69-34894

Closed-loop system for test, failure analysis and corrective action in avionics reliability growth, showing cost effectiveness relationship to test program

19 p3282 A69-35784

Cost model to trade off competing systems designs for space communications, navigation, operational availability and ballistic missile defense

19 p3454 A69-36007

System engineering to select hydraulics subsystem for advanced fighter aircraft by cost effectiveness analysis, noting maintainability and reliability

19 p3254 A69-36012

Structural design optimization based on reliability analysis stressing proof-load test and weight savings consideration under cost constraint

19 p3437 A69-36033

Availability measure defined in terms of maintenance demand rate and mean downtime for cost prediction involving various parameters

19 p3327 A69-36036

Cost and maintenance calculations for inertial navigation system (INS) based on three systems per aircraft, assuming 4000 hr/year aircraft utilization

19 p3371 A69-36734

Cost comparison of single and twin engine layouts for tactical strike/close support aircraft

19 p3248 A69-36855

Stochastic model for estimating manufacturing costs, discussing Mellin and Laplace transforms and Gram-Charlier series approximations

20 p3633 A69-36924

Valving concepts and functional approaches for inert gas attitude control thruster systems providing redundancy safeguards at minimum weight, volume and power costs

[AIAA PAPER 69-843]

21 p3786 A69-39373

Reliability incentive programs, considering linear and nonlinear curves for mean time before failure /MTBF/ vs incentive dollars and negative MTBF vs penalty dollars

22 p3952 A69-40024

Human factors methods importance in nonmilitary flight simulation training, discussing cost factors and skills evaluation

22 p3894 A69-41138

Bayesian estimate of individual truck maintenance costs based on optimum replacement maintenance age

23 p4241 A69-41577

Numerical control as manufacturing tool, with application to aircraft engine precision components

24 p4318 A69-42710

Fiscal requirements forecasting for space systems involving data analysis

[AAS PAPER 69-166A]

24 p4417 A69-42814

Operational and economical aspects of V/STOL air transportation reevaluated for civil aviation promotion

[AAS PAPER 69-325]

24 p4418 A69-42870

COST REDUCTION

Broadband steerable arrays design, describing Wulvenberger array with doublet aeriels yielding good radiation patterns and low cost construction

08 p1288 A69-20963

Boron and graphite fibers role in composites cost feasibility in 1970s

09 p1524 A69-22067

Flexible printed circuits manufactured by offset rotogravure printing, noting production cost economies

09 p1511 A69-22357

Electronic systems partitioning in preparation for MOS large scale integration for system performance and cost improvement

09 p1466 A69-22451

Boeing 747 aircraft, discussing weight and cost reduction, flap design, structural philosophy, powerplants, fuel system, flying controls, power systems, etc

09 p1435 A69-22714

Maintenance van loading technique for number of spares and test equipment in Minuteman weapon system for uncommissioned launch facilities at minimum cost

10 p1669 A69-22980

Howell engine hot section analyzer (HSA) developed to improve maintenance, flight safety and costs of jet aircraft engines

10 p1671 A69-23263

Semiautomatic and automatic off-line module testing machines, comparing costs for different test populations

11 p1865 A69-25076

Venus and Mars atmospheric braking entry and associated equipment, discussing potential cost savings

11 p1968 A69-25722

Reliability improvement influence on life cycle costs of high volume piece of military/commercial equipment

12 p2101 A69-25848

Materials rating method in pressure vessel applications, considering impact on design of minimum cost space launch vehicle

12 p2175 A69-26844

Efficient allocation of maintenance resources in USAF, analyzing B-52 costs and substitution of capital for labor

13 p2382 A69-28041

Galaxy C-5A aircraft Value Control Program stressing design organization, upper management authority, budgetary adjustments, etc

13 p2383 A69-28095

Weight and cost control program for Boeing 747 aircraft through combined value and weight engineering methods

13 p2383 A69-28096

U.S. Navy Numerical Value Rating System computing method of selecting lowest cost design approach to accomplish specific function

13 p2383 A69-28098

Military aircraft operating in various environments with low support costs emphasizing improved design, development and manufacturing standards

14 p2392 A69-29503

Cost effectiveness of test selection when statistical distribution of load and strength are known, presenting curves for equally dispersed normal parameters distribution

15 p2720 A69-30401

Production line requirements for MOS and IC, considering high reliability at minimum cost for space applications

15 p2627 A69-30841

Design philosophy for cost reductions on future space transportation systems, exemplifying application to booster system for earth orbital logistics

[AIAA PAPER 69-439]

16 p2882 A69-32654

Cost reduction criteria for rocket propulsion systems and components, discussing literature searches, engineering criteria, total program cost vs mission accomplished, etc

[AIAA PAPER 69-440]

16 p2883 A69-32748

Cost optimization of mixture ratio control systems for liquid propellant launch vehicles, considering open and closed loop systems

[AIAA PAPER 69-441]

16 p2870 A69-32775

Fluidic thrust reversal control system for turbojet achieving cost and weight reduction, illustrating fluidic circuit and noting circuit reliability

17 p3018 A69-33329

Life cycle maintenance costs reduction in aerospace industry by computers, describing on-line and off-line test systems

17 p2979 A69-33649

Commercial utilization of space technology, discussing cost reduction and role of NASA Apollo Program

17 p3043 A69-34044

Cost optimization in converting brush type to brushless aircraft AC power systems, using analog computer to determine modifications

17 p2905 A69-34109

Lunar orbital mission plans intended to optimize spacecraft procurement, flight schedules, science objectives and available funds

18 p3193 A69-34362

Composite and structured material forms combination for obtaining high performance and low cost

18 p3161 A69-34608

Cost and weight optimization for solid rocket motors using various steel casings

[SAWE PAPER 777]

18 p3208 A69-34871

Economics evaluation for operation of commercial fixed wing aircraft at aft center of gravity position, noting fuel saving from drag reduction

[SAWE PAPER 806]

18 p3091 A69-34902

Aerospace technology application to commercial avionic system for cost effectiveness in functions expansion, phase-over, installation, maintenance and operation, discussing added information functions

18 p3108 A69-35069

Rocket launch system cost role in space operations, discussing low cost expendable drop tank and Triamese reusable launch vehicle/spacecraft concepts

18 p3210 A69-35087

Ablative materials for solid rocket nozzles, discussing static firing tests, rating system, equipment design and cost reduction

19 p3357 A69-35537

Minimum cost design (MCD) of space launch vehicle, discussing material and process selection based on fracture-safe conditions

19 p3433 A69-35587

C-141 engine health monitoring program, applying results to maintenance costs reduction

[AIAA PAPER 69-775]

19 p3244 A69-35646

Low noise microwave devices performance and price, discussing transistor and tunnel diode amplifiers, traveling wave tubes and price reductions via manufacturing methods

20 p3504 A69-36913

Book on systems cost effectiveness covering methodology, system cost models, economics, etc

20 p3640 A69-37533

Low cost rate transportation as mandatory goal for future space program, discussing recovery and reuse, launch system costs, hardware development, etc

20 p3618 A69-38117

Tactical Satellite Communications /Tacsat/ cost reduction, discussing jamming avoidance and mitiga-

tion, communications security, capacity increase and spectrum conservation

20 p3497 A69-38315

Carbon fiber reinforced plastics application to aircraft metal components for weight reduction, low cost and high mechanical properties

21 p3750 A69-38428

Reducing cost of space transportation - AAS Conference, Washington, D.C., March 1969

21 p3856 A69-39686

Launch vehicle cost reduction by minimizing software, fabricating in commercial shops and avoiding sophistication, parts and acts of man

21 p3857 A69-39688

Cost reduction steps in reusable launch vehicle design, discussing aircraft design and development experience application

21 p3826 A69-39689

Space transportation cost saving options including booster systems, spacecraft/payload systems and support systems, discussing recovery and launching operations

21 p3857 A69-39690

Crew and passenger transportation to and from space station orbits, discussing cost reduction possibilities with current or future technology

21 p3827 A69-39691

Launch systems evolution, cost reduction breakthrough approach and application to future space transportation

21 p3857 A69-39692

Dual role core /Ducor/ memory system with unique core stack assembly feature to achieve cost reduction and structural integrity for severe environmental conditions

22 p3903 A69-39950

Support software costs reduction for launch vehicle systems by implementing computer techniques to provide requisite data

[AIAA PAPER 69-978] 22 p4052 A69-40358

Design and economic concepts of Lockheed L-1011 wide body trijets, discussing airport and airways congestion alleviation, passenger appeal, etc

[RAES PAPER 15] 22 p3863 A69-40494

General aviation airport application as freight consolidation terminals to reduce ground handling costs, circumvent air and ground traffic problems, etc

24 p4419 A69-43047

Cost analysis in low cost launch vehicle studies emphasizing sustaining engineering and plant economics

24 p4393 A69-43120

Aerospace fastening system requirements to lower in-place costs, extend service life and reduce weight of aircraft

24 p4325 A69-43440

COSTS

NT FREIGHT COSTS

Phase ionosonde cost, possibilities and errors

01 p0071 A69-11163

Permissible expenditures for decreasing aircraft structural weight

11 p2005 A69-25349

Relay reliability cost vs failure cost in spacecraft applications

13 p2231 A69-28044

Weighting factors relation in optimal systems integral squared error /ISE/ cost functional, characteristic coefficients and time response performance measures

14 p2534 A69-29317

Explosive welding principles, applications, materials limitations and advantages, stressing safeness and low cost

18 p3151 A69-35479

Satellite and terrestrial point-to-point communication circuit costs, considering multiple access and small antenna earth stations

19 p3456 A69-36822

COUETTE FLOW

Couette flow stability in axial magnetic field, considering time bounded perturbation energy during increasing angular velocity in radial direction

01 p0059 A69-10233

Plane Couette flow stability in heated nonlinear viscous fluid flowing between horizontal plates heated to different temperatures

02 p0235 A69-12828

Heat transfer in crossed field MHD Couette flow for incompressible fluid, assuming linear wall temperature in flow direction

03 p0476 A69-13306

Stationary, moving and pulsating electrohydrodynamic flow between parallel dielectric plates and Couette flow, noting reaction concentration near wall

03 p0419 A69-13919

Heat transfer, suction and injection in plane Couette flow analyzed for Rivlin-Ericksen fluid, using perturbation method

04 p0589 A69-14970

Secular equation for Couette flow stability in incompressible viscoelastic fluid

06 p0909 A69-17240

Monte Carlo solution of linearized Boltzmann equation in rarefied gas dynamics, noting Knudsen layer and Couette flow applications

06 p0910 A69-17345

Suction effect on temperature distribution and heat transfer in plane Couette flow and laminar flow in circular pipe

08 p1303 A69-20371

Bounds on mass and momentum transport by turbulent flow between parallel plates derived for Couette and Poiseuille flows

08 p1305 A69-20840

Transient heat transfer in formation of steady crossed fields MHD plane Couette flow for walls, giving momentum, induction and energy equations

13 p2375 A69-27791

Kolmogorov-Prandtl turbulence energy hypothesis extended from turbulent region of one dimensional flow to laminar sublayer, obtaining numerical solutions for Couette flow

13 p2250 A69-28339

Two dimensional Couette flow analysis showing stability at Reynolds number tending to infinity

14 p2428 A69-28802

Flush electrostatic probe edge effect, considering Couette flow of weakly ionized compressible gas past discontinuous wall potential

15 p2653 A69-30912

Heat transfer in rarefied gas plane Couette flow determined by BGK model and moments method of half range distribution functions

16 p2876 A69-31688

Hydrodynamic parameters of annular Couette flow in longitudinal magnetic field for variable Reynolds and Mach numbers

16 p2821 A69-31953

Equilibrium Couette flow of ionized multicomponent ideal gas between moving catalytic plates, obtaining thermal flow formulas and thermal conductivity coefficient

19 p3240 A69-36403

Channel flows energy stability, discussing Couette and plane Poiseuille flows, velocity profiles, vorticity maxima, etc

21 p3697 A69-39675

Numerical analysis of plane Couette flow of rarefied binary gas mixture using relaxation type kinetic model equations, discussing slip velocity, friction coefficient, etc

22 p3931 A69-40778

Mass injection by strong blowing across Couette-Poiseuille shear flow

24 p4301 A69-43354

COULOMB COLLISIONS

Ionized plasma radiation near plasma frequency, deriving formula for bremsstrahlung coefficient from Born approximation

02 p0286 A69-11589

Second virial coefficient of plasma at arbitrary temperature, noting small Coulomb interaction

02 p0292 A69-12639

Coulomb collision and microturbulence effect on plasma wave echo, noting echo dependence on perturbations in particle distribution

03 p0474 A69-13144

Cross sections computed for excitation and ionization of atoms and ions by electrons, using peaking approximation to evaluate Coulomb-Born matrix approximation

08 p1355 A69-20206

Loss rate of plasma from stellarator due to binary Coulomb collisions scattering particles in loss region, discussing diffusion coefficients

08 p1364 A69-20520

Thermodynamic potential of rarefied plasma from Coulomb interactions of atoms with electrons and ions

10 p1728 A69-23134

Multiple Coulomb scattering and range straggling effects in shielding against solar flare protons and trapped protons in Van Allen belt

10 p1723 A69-23164

Direct Coulomb interaction matrix elements between hydrogen atoms in ground states calculated, presenting interaction potential

11 p1921 A69-24416

Ionic diffusion in topside ionosphere analyzed using multipole gas mixture diffusion formula, noting Coulomb ionic collision role

14 p2441 A69-29381

Neutrino-pair bremsstrahlung for hot degenerate electron gas during Coulomb scattering on imbedded nuclei in stellar regimes including lattice structure effects

18 p3176 A69-35004

Lower ionospheric effective electron collision number from cosmic noise recordings and radio wave absorption data obtained by vertical sounding rocket

20 p3528 A69-37679

Effective Gaunt factors for threshold excitation of positive ions by electron collisions for 23 dipole transitions in 15 isoelectronic sequences

20 p3581 A69-38175

COULOMB POTENTIAL

Coulomb approximation for dipole and quadrupole transitions, calculating tables for radial matrix elements

01 p0124 A69-10901

Holtzmark plasma microfield, discussing neglect of term comparable to dipole moment during Fourier transform development for long range Coulomb field

02 p0287 A69-11871

Perturbation methods for exchange and Coulomb energy of hydrogen molecule, calculating Hamiltonian by wave function

07 p1186 A69-19446

Separable expansion for off shell two body t matrix with Coulomb potential to solve nonrelativistic three body problem with two body interactions

08 p1354 A69-20205

Cut-off Coulomb potential transport cross sections compared with exponentially screened potential for various cut-off radii

11 p1924 A69-24309

Two center Coulomb integrals expressed in terms of center separation, noting applications to molecular calculations

14 p2471 A69-29926

Integral formulation of scattering theory extended to Coulomb interactions by expanding Green function and treating kernel singularities

14 p2489 A69-29995

Finite scattering cross section in current carriers scattering on impurities in compensated semiconductors, assuming unscreened Coulomb potentials

15 p2666 A69-30063

External magnetic force and internal Coulomb force influence on carriers in conduction or valence band of semiconductor, considering H atom spectra

16 p2826 A69-31824

Coulomb interference corrections in pion-He scattering, discussing three specific formalisms

18 p3176 A69-35008

COULOMETRY

Analytical determination of traces of metals caused by wear in aircraft liquid fuels, hydraulic fluids and lubricants, noting polarography and coulometry

03 p0435 A69-14101

COUNTDOWN

ESRO 2/IRIS satellite launching checkout, countdown and breakdown of operations

01 p0163 A69-11104

Probability of completing countdown in single malfunction encounters, considering development of industry and government guidelines

10 p1792 A69-22979

Successful launch probability analyzed as function of launch strategy from past countdown hold data

19 p3430 A69-36034

Space vehicle data system synthesizer /SVDSS/ for dynamic calibration of automatic control and checkout systems during prelaunch and countdown operations

21 p3680 A69-39633

COUNTERFLOW

Interaction between supersonic jet and counterflow of ideal compressible fluid

05 p0751 A69-16501

COUNTERMEASURES

U CHAFF

U ELECTRONIC COUNTERMEASURES

U JAMMING

COUNTERS

NT CERENKOV COUNTERS

NT ELECTRON COUNTERS

NT GEIGER COUNTERS

NT NEUTRON COUNTERS

NT PARTICLE TELESCOPES

NT PROPORTIONAL COUNTERS
 NT QUANTUM COUNTERS
 NT RADIATION COUNTERS
 NT SCINTILLATION COUNTERS
 NT SPARK CHAMBERS

Large area X ray collector, matrix detector for ionizing radiation and inflatable gas counter, considering application to X ray optics and astronomy
 05 p0794 A69-16587

Counter/discounter assembly with slow resolution time for random fine pulses, using grouped tunnel diodes
 05 p0735 A69-16702

Phase measurement using phase lock loop, voltage controlled oscillator and synchronous counter
 05 p0722 A69-16766

Count rate meter for statistical frequency of signals applied to input of trigger with Poisson distribution of pulse intervals
 11 p1884 A69-24734

Semiconductor materials and fabrication methods for surface barrier junction n-type and p-type silicon counters used in hydrogen ion flux recording
 14 p2452 A69-29810

Counter for decimal counting and numeric display applications using integrated fluid logic elements
 15 p2616 A69-31295

COUNTING

Number count formula in zero pressure model universe for extragalactic radio sources with arbitrary luminosity and evolution functions, discussing red shifts
 08 p1390 A69-20388

COUNTING CIRCUITS

Diode pump type circuit without diodes in signal path providing accurate transfer function analysis considered for spacecraft use
 [IEEE PAPER 3A-3] 07 p1134 A69-19191

Transient processes in counting circuits with tunnel diode chains, discussing operating point position for various conditions
 14 p2419 A69-28921

PCM bit synchronizer signal to noise ratio measurement by input video signal zero crossings counting
 19 p3271 A69-36248

COUPLED MODES

Instabilities for two highly conducting finite length streams in relative motion and coupled by transverse electric or longitudinal magnetic fields
 01 p0062 A69-11208

Stroboscopic holography for repetitive scenes, using mode locked laser as source
 02 p0250 A69-12411

Nonlinear mode interactions in spatially inhomogeneous laser, analyzing suppression, phase locking and linear coupling among cavity modes
 02 p0258 A69-12632

Two photon fluorescence technique for display of picosecond laser pulses, discussing mode locking and ruby laser contrast ratios
 02 p0259 A69-12654

Mode locking and ultrashort pulses in giant pulses in giant pulse ruby laser with heated nitrobenzene or alpha-chloronaphthalene in resonator
 02 p0259 A69-12655

Dynamic mode locking of CW He-Ne laser by external regenerative feedback using RF beats between axial modes
 02 p0260 A69-12657

Simultaneous phase locking of longitudinal and transverse laser modes in He-Ne laser
 03 p0441 A69-14188

Hybrid Gunn domain and LSA mode operation in oversized bulk and epitaxially grown GaAs, noting large signal impedance data
 04 p0639 A69-14339

Bending-torsion mode of rotating tapered twisted turbomachine blade, analyzing coupled flexural and torsional vibrations effect on natural frequency
 [ASME PAPER 68-WA/GT-6] 05 p0838 A69-16141

Spacecraft control system and flexible structures interactions, discussing transient phenomena, limit-cycle oscillations and instabilities
 [AIAA PAPER 69-116] 06 p1019 A69-18187

Unified theory of normal mode analysis of RLC networks based on Tellegen theorem of Kirchhoff law, discussing coupled networks
 07 p1115 A69-18858

Single mode output power from 6328 Å He-Ne laser through mode coupling induced by added absorption cell containing excited Ne
 07 p1149 A69-18901

Lamb theory of mode self locking in gas lasers approximated to provide criteria for self locking
 07 p1156 A69-19413

Gas laser modes strong coupling and single mode induced by saturable absorbing medium within cavity resonator
 08 p1324 A69-20166

Gas laser frequency stabilization by coupled oppositely circularly polarized components of single cavity mode in axial magnetic field
 08 p1327 A69-21090

Frequency fluctuations in mode coupled gas laser used to determine natural emission line width
 09 p1516 A69-21670

Mode locked He-Ne laser pulses compression by multiple reflections from interferometer after application of linear electro-optic frequency sweep
 09 p1516 A69-21745

Coupling electromagnetic power to beam plasma amplifiers without use of helices and cavities, discussing modes of interaction, gap coupling and Cerenkov coupling
 09 p1463 A69-21805

Microwave resonator characteristics, deriving expressions for Q for pure or coupled electric or magnetic modes
 09 p1464 A69-22096

Mode locked laser operation, noting output and applications to optical communication, high speed photography, nonlinear optics and frequency standards
 09 p1518 A69-22123

Cut-off coupled microwave bandpass filters for use in dielectric filled waveguide systems
 09 p1466 A69-22447

Quasi-periodic coupling for broadband mode coupling application, describing normalized transferred power fluctuation along entire coupling region at various frequencies
 09 p1467 A69-22586

Longitudinal and transverse wave propagation in compressible isotropic turbulent plasma, noting mode coupling effect
 [AFRL-69-0289] 10 p1729 A69-23424

Dynamics of external loss modulation and Q switching methods of generating ultrashort pulses in mode locked laser
 10 p1703 A69-23624

Capture of parametrically coupled waves by pulses and beams of pumping radiation in case of different group velocities directions
 10 p1705 A69-23956

Radiating collinear open ended waveguides and near field coupling analyzed using simultaneous integral equations and Fourier series expansion of aperture field
 11 p1850 A69-24984

Coherence phenomena for gas laser transitions coupled by common level, noting coherent superposition
 11 p1898 A69-25045

Landau dispersion relation solutions, noting higher order Landau poles and coupling of spatial Landau modes and least damped wave
 11 p1929 A69-25265

Modal coupling in thermally stressed plates, obtaining solution for frequencies and stiffness
 11 p1990 A69-25509

Two transverse modes locking with multiple longitudinal modes in He-Ne laser, noting separate locking and alternate quenching
 12 p2104 A69-25923

Short circuit and variable frequency technique for measurement of coupling efficiency between dielectric loaded rectangular and trough waveguides, noting propagation modes
 12 p2039 A69-26374

Alternating electric field parametric effects on inhomogeneous plasma in magnetic field, obtaining electrostatic wave coupling dispersion relation by density gradients considerations
 13 p2304 A69-27298

Variational method used to determine accuracy of approximation technique for dielectric slab on sidewall of rectangular waveguide
 13 p2233 A69-28072

Instantaneous rotational impulse imparting steady motion of disk determined for coupled gyroscope
 13 p2264 A69-28527

Temperature behavior of resonant and antiresonant frequencies as function of electromechanical coupling and overtone order in piezoelectric resonators
 14 p2421 A69-29542

Coupled mode theory for surface wave propagation along tapered cylindrical dielectric rod, considering radiation field effects
 14 p2422 A69-29557

Convective heat and mass transfer coupling in laminar hydrodynamic duct flow, obtaining values for bulk and wall temperatures, transfer coefficients and rates, etc
 15 p2716 A69-30004

Power coupling among modes in semiconductor lasers in presence of spontaneous or forced microwave modulation of population inversion
 15 p2634 A69-30875

Mode-mode coupling calculation for finite amplitude collisional drift waves demonstrating inherently nonlinear phenomena
 15 p2660 A69-30916

Steady state solutions for parametric excitations in various limits in plasmas, allowing for higher order mode coupling
 15 p2661 A69-30919

Normal modes of electrons-electromagnetic field coupled system for many valley semiconductors, calculating dielectric constant for electron gas for ellipsoidal energy surfaces
 16 p2826 A69-31821

Waveguide bends fields expressed in coupled local annular modes derived by evaluating differential scattering coefficients
 16 p2760 A69-31943

Thin film optical method generalization accounting for intermode coupling and oblique incidence in plane stratified magnetoionic medium applied to ionospheric LF and hydromagnetic propagation
 16 p2753 A69-32393

Raman scattering by coupled plasmon-cyclotron-harmonic modes in semiconducting plasmas in homogeneous static magnetic field
 16 p2824 A69-32604

Linear array composed of dual mode elements radiating into parallel plate region, obtaining scan angle compensation of element impedance
 17 p2929 A69-33875

Mode coupling effects in CW gas ring lasers, considering excitation density pulsations, traveling waves dispersion, polarization, etc
 19 p3334 A69-36046

Mathematical model of CW ring laser mode coupling in limits of low excitation
 19 p3334 A69-36047

Coupled dilatational and equivoluminal modes of free vibration for elastic prisms and polygonal plates, using Poisson ratio and wave path construction
 19 p3444 A69-36801

Thermal effects of resonant coupling hydromagnetic oscillations in inhomogeneous finite-beta plasmas, obtaining equations for coupling modes between Alfvén and magnetosonic waves
 21 p3776 A69-38710

Hydrogen-hydrogen excitation collisions by impact parameter treatment, investigating rotation coupling influence in four state cross sections approximation
 22 p3987 A69-41007

Scanning Fabry-Perot interferometer interaction with laser source, calculating laser intensity and oscillation frequency changes for weak mode coupling
 24 p4329 A69-43756

COUPLERS

NT ANTENNA COUPLERS
 NT COUPLING CIRCUITS

Directional coupler for TEM waves composed of two waveguides and having locally dependent coupling function
 11 p1855 A69-25629

Mismatch correction in microwave power measurements based on directional coupler techniques
 12 p2038 A69-26055

Stripline microwave integrated circuits in terms of building blocks and components, discussing hybrids, backward wave coupler, balanced modulators and mixers, etc
 15 p2579 A69-31075

Equal ripple nonuniform tapered line coupler design and computed performance by evaluating cascade matrix as function of frequency
 16 p2760 A69-31944

Broadband continuously variable phase shifter with microstrip construction, describing phase rotation via stripline connected directional couplers
 16 p2763 A69-32582

COUPLES

Uniqueness formulation of concentrated load problem in linear theory of couple-stress elasticity
 02 p0338 A69-11720

COUPLING

NT COUPLES
 NT CROSS COUPLING
 NT GYROSCOPIC COUPLING
 NT MICROWAVE COUPLING
 NT OPTICAL COUPLING

NT SPIN-SPIN COUPLING
NT THERMODYNAMIC COUPLING

Exact solution for coupling effects between two waves with complex coupling function, defining region of validity for earlier perturbation theory
 01 p0027 A69-10252

Oppositely moving waves interaction during nonlinear transient process of oscillations buildup in annular solid state laser found dependent on coupling via scattering
 02 p0259 A69-12648

Multiframe platform stabilization, analyzing dynamic coupling due to possible avoidance of adjusting moment and effect of coupling on attitude control
 04 p0629 A69-14830

Composite equivalent circuits method for complex waveguide-resonator couplings based on variational principle for admittance matrices of electromagnetic volume couplings
 05 p0736 A69-16785

Vertistat H gravity gradient configuration prevents elastic deformation, permitting high pointing accuracy at synchronous altitudes
 07 p1229 A69-18351

Plasma wave coupling in absence of magnetic field in revolving system containing dielectrics and circular waveguide
 08 p1371 A69-21150

Coupling constants of fast space charge waves in three frequency parametric TWT amplifier and of stress waves in slow wave structure, using graphical methods
 11 p1844 A69-24446

Subregions method in coupled thermoelasticity, discussing numerical values for thin steel circular disk
 11 p1970 A69-24606

Fundamental concepts of nonholonomic coupling and coordinates in nonholonomic mechanics
 12 p2129 A69-25990

Pulses and sine waves coupling between parallel transmission lines obtained using Oliver elementary coupling theory
 19 p3266 A69-35768

Tunnel diode coupling with spheroidal resonant cavity, describing method of measuring elements for interpretation
 19 p3283 A69-35998

Junction lasers current-voltage characteristics, discussing coherence-pinch effect as explanation of threshold behavior
 19 p3337 A69-36531

Coupling conditions by distinct equations for two laminar flow regions, studying near wake and considering Euler, Navier-Stokes and Prandtl correlations [ONERA-TP-738]
 19 p3299 A69-36649

Negative energy waves presence, showing qualitative difference on theoretically derived parametric amplification in plasmas
 20 p3582 A69-38244

Aerodynamic pitch-roll coupling in spinning vehicles, showing unsteady components complicating data reduction
 21 p3647 A69-39038

Approximate expression derived for loose coupling in turbulence theory, suggesting possible explanation for inadmissibility of Kraichnan conclusion
 21 p3696 A69-39086

Rigid and flexible coupling devices for spacecraft rendezvous, describing general operating conditions
 22 p4036 A69-40008

Capacitive coupling vs DC coupling between data input and transmitter exciter in FM telemetry system, based on pulse series Fourier analysis
 23 p4119 A69-41744

Rectangular waveguides coupled by oblique subresonant slots in common face, discussing slot orientation and geometry roles
 23 p4123 A69-41941

COUPLING CIRCUITS

Direct couplings of autonomous noisy quadrupoles used for noise matching
 01 p0043 A69-10591

Circuits with magnetic coupling, describing digital computer algorithms for assembly of loop current equations
 01 p0036 A69-10745

Low noise high power transistor oscillator using directional coupler, noting isolated port for injection phase locking
 02 p0220 A69-12452

Equivalent circuit for parallel conductor array based on array capacitance matrix
 04 p0576 A69-14756

Transistor scattering matrix parameters determination, emphasizing directional coupler errors and impedance mismatches
 04 p0582 A69-15067

Small signal coupled mode analysis including relativistic effects for studying spiraling electron beam interaction with fast wave circuits
 07 p1114 A69-18436

Frequency modulated signal envelope passage through bandpass filter of inductively coupled circuits described by differential equation
 07 p1100 A69-18555

Series operation of Gunn devices with differing threshold currents at SHF
 09 p1463 A69-21684

Quasi-periodic coupling for broadband mode coupling application, describing normalized transferred power fluctuation along entire coupling region at various frequencies
 09 p1467 A69-22586

Multiaperture waveguide directional couplers analyzed by four port equivalent circuits, discussing synthesis method for optimizing coupling directivity
 13 p2228 A69-27669

Dispersion and coupling impedance of logarithmic spiral resting on anisotropic magnetodielectric layer for microwave devices design
 13 p2235 A69-28512

Hybrid coupled low power digital microwave phase shifters design, discussing lumped element L-C and variable C shifter theories, power limitations and construction techniques
 15 p2580 A69-31076

Radar control system based on load waveform monitoring by coupled control and modulating circuits
 16 p2753 A69-32439

Lumped element circuit producing directional coupling by electric and magnetic coupling of reactance quadrupoles, discussing insufficient coverage of calculated frequency range
 16 p2763 A69-32581

Directional couplers design considerations for use in microwave power meters, analyzing directivity and mismatch effect on system error
 19 p3282 A69-35826

CRT display system coupling interface with magnetic storage determined from algorithms and time diagrams, describing character storage and system logic design
 22 p3908 A69-40936

Dispersion and coupling impedance calculation for symmetrical or helical slow wave structures employed in traveling and backward wave tubes
 22 p3916 A69-40958

STAR /Stud and Rocker Panel/ four couple section improved by incorporating bonded tungsten electrical contacts for PbTe thermoelectric elements
 23 p4188 A69-42261

COUPLING COEFFICIENTS

Vortices coupling between superposed superconducting tin films as function of perpendicular magnetic field, primary current and temperature
 01 p0135 A69-10014

Coupling coefficients of global and vertical fluxes of charged cosmic ray component in stratosphere measured by radiosondes
 02 p0306 A69-11659

Magnetoelastic coupling constant b measured by propagating microwave signals in pure and substituted YIG
 02 p0299 A69-12243

Eigenvectors utilized in flutter computation for couplings [ONERA-TP-650]
 03 p0522 A69-12878

Coupling coefficients between primary and secondary ionizing cosmic ray variations, using stratospheric observations in Siberia during IQSY
 03 p0504 A69-14224

Mutual coupling and element efficiency for infinite linear arrays of dipoles
 04 p0571 A69-14317

Reflection coefficients of edge and center elements of large periodic two dimensional antenna array, noting TEM mode parallel plate horn arrays
 04 p0572 A69-14322

Quasi-periodic coupling for broadband mode coupling application, describing normalized transferred power fluctuation along entire coupling region at various frequencies
 09 p1467 A69-22586

Low momentum muon directional coupling coefficients based on latitude survey of directional meson intensity
 09 p1583 A69-22759

Coupling coefficients for integral charged component of cosmic rays determined from measuring azimuthal geomagnetic effect on rays observed in crossed telescopes
 10 p1770 A69-23925

Coupling coefficient and impedance for excitation of isotropic plasma column by ring of magnetic current outside plasma, noting surface wave resonance effect
 10 p1659 A69-24064

Coupling coefficients for common-base/common-base circuits of bandpass filters in two circuit selective transistor amplifier
 13 p2226 A69-27219

Numerical integration for coupling between two modes of propagation /electron and proton whistlers/
 13 p2254 A69-27981

Coupling coefficients of global and vertical fluxes of charged cosmic ray component in stratosphere measured by radiosondes
 13 p2334 A69-28690

Aerodynamic control surface/trim tab coupling coefficients in subsonic two dimensional unsteady flow using matrix method valid for motion involving harmonic oscillations
 17 p2895 A69-33597

Micropolar liquid basic flows, considering case with coupling constant relating microstructure to macroscopic flow greater than viscosity coefficient
 18 p3121 A69-34786

Dimensionless coupling constants predicted from causal relationship among strong, electromagnetic, weak and gravitational interactions in fluid region of universe
 22 p3981 A69-40416

Coupling coefficients and excitation increments determined for nonlinear interactions of surface waves in nonisothermal semibounded plasma
 22 p3990 A69-40790

COUPLINGS

Couple stresses effect on thin plate stress distribution due to pressure of rivet on one side of circular hole
 08 p1319 A69-20201

Jet fluidic differential amplifier transfer function determination, describing interconnection dynamics
 11 p1824 A69-24350

Transverse impact along flexible couplings, deriving motion equations in presence of elastoplastic deformation
 12 p2178 A69-26034

Equations of motion computerized simulation for attitude stabilization of orbiting telescope coupled to crew compartment
 13 p2261 A69-27952

Nonholonomic coupling effect on mechanical system stabilization characteristics in terms of generalized coordinates
 14 p2482 A69-28814

Gravity gradient stabilized satellite achieving best theoretical performance through Foucault current and magnetic hysteresis articulations
 17 p3048 A69-33234

COVALENT BONDS

Melting points of tetrahedral phases with stoichiometric vacancies found proportional to covalent bonds number in semiconductors
 02 p0297 A69-11881

Covalence degree of activator-ligand chemical bonds effect on spectroscopic properties of transition metals
 11 p1907 A69-25031

Dislocation mobility temperature dependence in n-type indium antimonide, noting role of covalent interatomic bonds
 12 p2143 A69-26453

Melting points of tetrahedral phases with stoichiometric vacancies found proportional to covalent bonds number in semiconductors
 18 p3182 A69-35041

COVARIANCE

Covariant statistical mechanics for equilibrium thermodynamics
 03 p0533 A69-13758

Tensor partial differential equations having spherical symmetry, examining covariant differentiation and contraction of tensors
 07 p1123 A69-18807

Computerized objective analysis of meteorological variables based on weight determination involving autocorrelations
 08 p1345 A69-20309

Error bounds for estimation error covariance matrix of fixed point smoothing and fixed interval smoothing algorithms for optimum linear estimation
 09 p1533 A69-22436

Nonsingular matrices inversion method by group partitioning applied to noise covariance matrix used in optimal prediction and control

12 p2123 A69-26754

Error bounds for covariance matrix used in optimum filtering and smoothing algorithms for control and communications systems operation

14 p2416 A69-29549

Bilinear covariant of linear differential form involving 2n independent variables used for grouping to achieve symplectic and contact transformations

16 p2804 A69-31623

Linear computer-controlled closed loop systems sensitivity analysis, deriving estimation error incremental covariance to demonstrate quality deterioration under perturbed initial conditions, parameters, etc

17 p2944 A69-33742

Relation between smoothed and filtered linear least squares estimates of signal process in white noise from deriving resolvent identity of covariance function

21 p3754 A69-38432

COVERINGS

Optimum solar cell cover glass systems selected by studying interplanetary space environment effects of proton impact, temperature and concurrent illumination on radiation damage

19 p3253 A69-35702

Large area Si solar cell arrays design, considering environment, cell layout, thermal expansion, coverslides fabrication, costs, etc

19 p3253 A69-35708

Solar cell degradation experiments on LES 4 and 5 satellites, discussing decay values and times for Si and CdTe cells with different cover thicknesses

19 p3254 A69-35713

COWELL METHOD

U NUMERICAL INTEGRATION

CRAB NEBULA

Pulsating radio sources near Crab Nebula noting possible coincidence with nebula, pulse dispersion and interstellar electron density

04 p0659 A69-14977

Crab Nebula and Cygnus XR-1 X ray spectra shown to have differential number power law spectra and same intensity

05 p0813 A69-15846

Book on supernovae covering galactic supernovae, type II supernovae remnants, Crab Nebula, primary cosmic radiation, etc

07 p1210 A69-18379

Crab Nebula pulsar NPO527 position measurement with split beam antenna, noting proximity and similar dispersion with NPO532

07 p1221 A69-19405

Balloon observations of cosmic X ray sources in Cygnus and Crab Nebula, discussing data application to energy spectra analysis

07 p1210 A69-19716

Strong light flashes detected from fast pulsar NP 0532 in Crab Nebula, discussing time-averaged optical flux

08 p1394 A69-20622

Strong light flashes from pulsar NP 0532 in Crab Nebula, noting UVB photometric analysis of nebular brightness

08 p1394 A69-20623

Pulsar NP 0532 identified with Baade south preceding star in Crab Nebula, noting pulsed optical radiation

09 p1592 A69-21458

Crab Nebula pulsar properties including pulse shape, dispersion and strong pulse emission

09 p1592 A69-21462

Condensed supernova remnants in Crab Nebula, considering various hypotheses for radio source

09 p1592 A69-21485

Modulation collimators determining angular sizes and celestial positions of X ray sources Sco X-1 and Taurus XR-1

10 p1678 A69-23326

Crab Nebula radio emission spectrum in decimeter wavelength range indicating emission spectral index decrease from Taurus A

10 p1784 A69-23941

Optical flashes recorded from Crab Nebula M1 close to central double star with periodicity equal to radio pulses discovered earlier

11 p1962 A69-25250

Crab Nebula pulsar detection by TV camera with image intensifier at focus of astronomical telescope, detailing instrumentation and observations

11 p1962 A69-25251

Pulsed radio source near Crab Nebula studied to estimate age of longer period pulsars and frequency of pulsar-producing events in galactic history

11 p1963 A69-25252

Crab Nebula X ray pulse detection attempt during balloon flight of telescope

12 p2149 A69-26226

Crab Nebula pulsar observations confirming wavelength independence of light velocity in space

12 p2157 A69-26233

Light curve shape as function of color, changing period and polarization angle of Crab Nebula optical pulsar

12 p2172 A69-27170

Crab Nebula pulsar NP 0532 photoelectric spectrophotometry results, noting main pulse and interpulse spectral energy distributions similarity to extended synchrotron radiation

13 p2335 A69-27317

Cosmic X ray background measurements and Crab Nebula observation during sounding rocket flight

13 p2326 A69-27570

Activity center in Crab Nebula, noting symmetrical configuration

13 p2343 A69-27621

X ray pulsations in Crab Nebula at frequency closely matching radio and optical pulsations, noting energy distribution

13 p2354 A69-28465

Vela pulsar PSR 0833-45 optical observations and Crab pulsar NP 0532 linear and circular polarization measurements by telescope-photomultiplier

13 p2354 A69-28470

Crab Nebula pulsar NP 0532 simultaneous optical and radio observations, noting influence of interstellar dispersion value uncertainty

15 p2680 A69-30233

Crab Nebula lunar occultation observed by Cassegrain array of deep space communication facility, finding radio brightness distribution similar to optical

15 p2687 A69-30539

Activity in Crab Nebula from 200-inch continuum and polarization plates, discussing nature and motion of wisps

15 p2691 A69-30758

X ray energy spectrum from Crab Nebula and diffuse background on celestial sphere near galactic anticenter, noting spectral index

15 p2675 A69-30759

Pulsar NP 0532 in Crab Nebula observed by rocket and telescope showing strong pulsed X ray signal

15 p2679 A69-31529

Nanosecond optical pulses from Crab pulsar NP 0532 detection indicating negative observations

16 p2865 A69-32801

Pulsar emission and magnetic field in Crab Nebula, discussing magnetic flux amplification, gravitational to magnetic energy conversion and pulsars as pulsed signals

17 p3026 A69-32859

Pulsed hard X radiation from NP 0532, discussing slow down rate and luminous intensity

18 p3186 A69-34316

NP 0532 slow down rate, using quadratic least squares method

18 p3191 A69-34317

IR and optical measurement of Crab pulsar NP 0532, analyzing energy density per pulse and smoothness of visual data

18 p3191 A69-34318

Faraday rotation in NP 0527 and CP 0328, measuring angular velocity and mean longitudinal magnetic fields

18 p3192 A69-34319

Ultrarelativistic electron acceleration in Crab Nebula maintaining synchrotron spectrum, obtaining power from compressional motion damping, gyrorelaxation effect and pitch angle anisotropy removal

19 p3424 A69-36336

Crab Nebula radio brightness at 2.16 and 8.2 mm measured and compared to Jupiter flux density

19 p3428 A69-36875

Gamma ray flux from processes associated with high energy electrons from pulsar NP 0532, noting light polarization

20 p3588 A69-37410

Radiation emission mechanism for NP 0532 associated with Crab Nebula, discussing shock-neutral sheet interaction

20 p3604 A69-37572

Pulsed X ray emission associated with pulsar NP 0532 in Crab Nebula measured by six element detector on Aerobee 150 rocket

20 p3590 A69-37574

Right ascension and flux density of source in Crab Nebula measured at meter wavelengths, evaluating spectrum and relative position to binary star center

20 p3607 A69-38040

Crab Nebula pulsar NP 0532 linear and circular optical polarization measurements

21 p3798 A69-38542

Galactic field augmentation by dynamo action from highly condensed objects, considering Crab Nebula field production by central body

22 p4035 A69-41207

Pulsars dispersion measure and distance relationship, particularly for Crab Nebula pulsars

23 p4220 A69-42381

Crab Nebula pulsars radio properties, possible neutron star origin, interstellar gas and magnetic fields, etc

24 p4375 A69-42556

Continuous electron acceleration in astrophysics, discussing Crab Nebula X ray flux and galactic and extragalactic radio source power law spectra

24 p4355 A69-42696

CRABS

Fiddler crab absorption of DDT residues from organic detritus in estuaries, discussing DDT residue entrance into diverse food chains

14 p2406 A69-28872

CRACK INITIATION

Crack initiation and propagation in Ti alloys during thermal cyclic heating, noting influence of gas saturation

01 p0094 A69-10215

Mixed boundary value problem of elastostatics for isotropic elastic cylinder containing strip crack opened by internal pressure, using auxiliary functions

01 p0167 A69-10317

Strain distribution for fracture initiation and steady state crack propagation in plane strain tension of plastic materials

01 p0169 A69-10764

Welding procedure for avoiding hydrogen cracking in high strength steels, stressing hydrogen escape from weld deposits

01 p0088 A69-11398

Kinetic theory of fracture initiation, discussing changes in relative orientation distribution of network chains

02 p0345 A69-12401

Ferroelectric domain structure to explain microcracks nucleated at twinband intersections in mechanically deformed lithium niobate

03 p0486 A69-13618

Plane strain yielding, stresses and fracture about notches and cracks in terms of flow and fracture stresses and crack tip radii

03 p0528 A69-13876

Crack propagation near arbitrary curvilinear hole, discussing hole exterior mapping and critical loads for crack initiation

04 p0674 A69-14562

Heat treatment effects on stress corrosion cracking resistance of Al-Zn-Mg alloys, using cantilever loading in aqueous solution

04 p0617 A69-14933

Crack nucleation in high strain fatigue based on plastic instability model

05 p0780 A69-16430

Spot weld strength of tungsten inert gas spot welding on Al-Mg-Si sheets greater than resistance welding, noting crack formation during inert gas welding

05 p0769 A69-16538

Crack formation and propagation in metallic materials under dynamic fatigue loading, noting dislocation during work hardening

05 p0781 A69-16542

Stress corrosion crack initiation in aluminum alloy observed by optical microscopy

06 p0944 A69-17855

Ultrahigh strength steel susceptibility to brittle fracture, describing methods of testing rupture toughness and stress intensity factor

07 p1158 A69-18402

Solder joint cracking in discrete component assemblies, discussing cracking mechanism and crack elimination methods

07 p1140 A69-19102

Surface environment effects on mode of microcrack formation during fatigue of Al single crystals, noting surface void formation mechanism

07 p1235 A69-19387

Brittle fracture criterion for small steel specimens based on interaction between stress concentration of initial crack and nearby slip band

07 p1238 A69-19694

Stress distribution around equal size holes at ends of crack for normal uniaxial tension, based on photoelastic and brittle lacquer technique
08 p1412 A69-20257

Displacements and stress intensity as function of crack length for compact tension specimen, considering load line and crack edge
09 p1503 A69-21392

Wrought superalloys fusion welding behavior, discussing hot cracking, hot microfissuring and strain age cracking
[SAE PAPER 690102]
09 p1503 A69-21558

Mechanical properties of welds of niobium and Ni based heat resistant alloys and susceptibility to crack formation at high temperatures
09 p1504 A69-22146

Model explaining intergranular crack initiation parallel to pulling axis in samples of spun beryllium broken under pressure
10 p1708 A69-22996

Liquid crystal coatings for determining fracture initiation flaws in material structures, considering stress concentration and hysteresis heating
10 p1699 A69-23053

Debonding mechanism role in fatigue crack development in notched aluminum alloy samples using optical and electron microscopy
10 p1710 A69-23076

Fatigue behavior of plastics classified noting temperature rises, crack initiation, etc
10 p1716 A69-23394

Brittle fracture of steel analyzed using statistical model, attributing occurrence to coalescence of arrested cracks initiated at different points
10 p1803 A69-24033

Macroscopic states of stress criteria for plastic flow initial yielding, plastic flow and brittle fracture of ductile and brittle metals
11 p1975 A69-24671

Dynamic and fatigue crack propagation theories for brittle and quasi-brittle solids and plates
11 p1975 A69-24672

Inclination effect of fatigue cracks on plane strain fracture toughness of 7075-T651 Al alloy, discussing cantilever bending
12 p2177 A69-25958

Fracture mechanics of polymers and fiberglass reinforced plastics, indicating microcracking under static and cyclic loading due to resin phase brittleness and low strength
12 p2120 A69-26849

Crack growth and crack initiation in cylindrical specimens subject to low cycle strain controlled tension-compression induced fatigue, noting measurement techniques
12 p2188 A69-26914

Fatigue crack initiation and propagation correlation with substructure formation by static and alternating stresses in Al
12 p2188 A69-26915

Fracture and equilibrium position of dislocations in discrete and continuously distributed dislocations arrays including stress due to crack, energy considerations and crack initiation
13 p2358 A69-27222

High strength alloys stress corrosion cracks, analyzing tensile ligament instability from plastic flow tests of bulk /compression/ specimens
13 p2277 A69-27404

Low cycle fatigue crack initiation in Ti-6Al-4V at room and high temperatures and in aqueous salt environment
13 p2278 A69-27413

Stress corrosion crack initiation and propagation in titanium alloy
13 p2282 A69-28165

Crack initiation prediction in high temperature components subjected to arbitrary thermal-mechanical cycling
13 p2365 A69-28252

Steady natural oscillations of unbounded brittle plane with cut under edge load, showing decreased critical load in presence of inertial effect
15 p2703 A69-30050

Crack initiation and propagation in Ti alloys during thermal cyclic heating noting influence of gas saturation
15 p2637 A69-30271

Longitudinal internal cracks in deformed Al alloys initiated by elastic stress concentration in areas of highest flow rate gradient
15 p2638 A69-30277

Plastic strains at crack tips in thin plate under concentrated forces, analyzing slip bands during initial deformation
15 p2708 A69-30659

Fatigue cracks initiation and propagation studied by surface plastic replication method, noting metallographical and continuum mechanical factors influence on low carbon steel
17 p3052 A69-32981

Dislocation and energy balance analysis of ductile and brittle metal cracks for determining metal fracture strength from plastic deformation
17 p3052 A69-32984

Heat treatment effect on stress corrosion cracking of ternary Al-Zn-Mg alloys noting aging strength, solution temperature, quenching rate and alloy content
17 p2990 A69-33676

Elastic bodies brittle stability weakened by cut, developing criterion for determining critical cut length
18 p3224 A69-35314

Nickel base superalloy high temperature fatigue properties, comparing crack initiation and propagation in directionally solidified and conventionally cast forms
19 p3342 A69-35919

Gas turbine components life prediction, using Weibull distribution and Bayes theorem to estimate probability of crack initiation
19 p3394 A69-36004

Stress corrosion cracking in stainless steel foils correlated with stacking fault energy and ordering, emphasizing environmental forming tendencies
19 p3350 A69-36892

Oxygen environment influence on Inconel X-750 surface deformation and cracking during fatigue related to chemisorption and oxidation
20 p3558 A69-36966

Fatigue crack initiation in relation to contact stresses due to fretting, studying causes of strength reduction and crack inclination to surface
20 p3563 A69-38110

Mean stresses effects on fatigue crack initiation and propagation under controlled fretting slip amplitude
20 p3563 A69-38111

Minor elements effect on cracking sensitivity of weld heat affected zone in Hastelloy alloy X, noting hot tearing and midrange cracking
22 p3967 A69-39881

Minor elements effect on weld-metal cracking resistance of wrought Ni-base heat resistant alloy by Circular Patch Test
22 p3967 A69-39882

Weldability of alloy Ni-Cr-Fe base-filler alloy combinations, noting threaded mold test and surface fissures
22 p3968 A69-39886

Metal fatigue crack nucleation at stresses below static fracture strength, determining local plastic strain under cyclic loading
22 p4041 A69-40053

Crack development in solid body, considering condition at crack tip not derivable from equation of motion and strain equation
22 p4047 A69-41123

Fatigue tests with cylindrical samples for observation of macrocrack formation and propagation at bottom of notches, discussing kinetics of fatigue failure
23 p4225 A69-41425

Structural changes in subsurface layer and surface microgeometry factors of metal fatigue failure, explaining crack formation and propagation
24 p4395 A69-42559

Flaw determinations accuracy from measuring ultrasonic shear wave reflection peak intensities
24 p4397 A69-42756

Fatigue crack initiation mechanism as used in design to prevent fatigue failures in service
24 p4397 A69-42770

Relative slip effect on fretting fatigue strength, deriving stress initiating fatigue cracks
24 p4404 A69-43628

CRACK PROPAGATION

Ultrasonic detection and measurement of fatigue cracks in notched cylinders subjected to reversed axial cyclic loading
01 p0078 A69-10113

Crack initiation and propagation in Ti alloys during thermal cyclic heating, noting influence of gas saturation
01 p0094 A69-10215

Theory of fatigue crack growth crystal in metals in terms of coplanar dislocation arrays extended to oblique slip planes, discussing orientation
01 p0168 A69-10344

Pressure and temperature dependence of slow crack growth in hardened steel in gaseous hydrogen environment
01 p0096 A69-10612

Plastic zone generation by slots cut in tensile test specimens before and during loading, discussing redistribution
01 p0098 A69-10762

Microfacets of metal surface cracks studied for plastic deformation and atomic separation mechanisms by electron diffraction
01 p0098 A69-10763

Strain distribution for fracture initiation and steady state crack propagation in plane strain tension of plastic materials
01 p0169 A69-10764

Moisture effects on crack propagation in high strength aluminum alloys studied by fatigue tests
01 p0098 A69-10766

Crack growth in ceramics from velocity measurements on glass and sapphire as function of applied force, temperature and moisture environment
01 p0101 A69-10767

Stress-strain behavior of crazes in glassy polymers, discussing crack propagation, craze formation and failure and molecular weight effects
01 p0102 A69-10915

Substructures around fatigue cracks in fcc metals and alloys, noting relation between structural formation and crack propagation
02 p0260 A69-11826

Metal fatigue crack propagation mechanism, deriving basic laws for failure in high and low stress regions, determining material parameters
02 p0340 A69-12025

Ductile crack propagation speed relation to dynamic flow properties of metals analyzed using Dugdale crack model
02 p0343 A69-12283

Spin tests to determine brittle fracture under plane strain, using cyclic thermal stress or hydrostatic pressure to generate fatigue crack in rotor blank
03 p0524 A69-13060

Corrosion rates and stress corrosion cracking sensitivity of explosively shocked austenitic stainless steels
03 p0444 A69-13308

Porous ceramic heat shields for lifting reentry vehicles, noting crack propagation resistance and load redistribution
[SAE PAPER 680643]
03 p0453 A69-13457

Subcritical crack growth kinetics in high strength materials, suggesting growth rate control by reaction rate or diffusion
03 p0449 A69-13874

Crack propagation near arbitrary curvilinear hole, discussing hole exterior mapping and critical loads for crack initiation
04 p0674 A69-14562

Brittle fracture resistance of low carbon maraging and martensitic steels with cracks established by crack growth measurements during tensile and impact tests
04 p0615 A69-14647

Torsional elastic wave scattering from penny shaped crack, determining local dynamic stress field
04 p0678 A69-14872

Cold working considered for decreasing fatigue crack propagation rate in thin duraluminum sheets with various plastic deformations
04 p0681 A69-15170

Generation of crack propagation data on notched rotating beam specimens by interrupted stressing techniques
[ASME PAPER 68-WA/MET-3]
05 p0838 A69-16148

Griffith biaxial fracture criterion for porous brittle materials based on continuum model with random infinitely sharp cracks
[ASME PAPER 68-WA/MET-12]
05 p0838 A69-16152

Fatigue crack growth in notched samples of aluminum alloy subjected to cyclic compressive loading, noting residual tensile strength at notch root
[ASME PAPER 68-WA/MET-16]
05 p0838 A69-16154

Statistical model for tensile fracture of parallel fiber composites based on stress criterion for crack propagation
[ASME PAPER 68-WA/RP-7]
05 p0783 A69-16159

Fracture propagation in organic glasses, considering density of hyperbolic markings in polymethyl methacrylate and Dugdale model
05 p0784 A69-16429

Circular inclusion effect on stresses around line crack in sheet under tension based on elasticity theory
05 p0841 A69-16432

Elastic displacements for edge cracked plate specimens used as crack extension indicator in plane strain fracture toughness measurements
05 p0841 A69-16433

Photoelastic study of interaction between overlapping parallel cracks in tensile stress field
05 p0842 A69-16435

Plastic yield on inclined slip planes at tip of crack deformed in antiplane strain
05 p0842 A69-16436

Crack tip displacements and strains in plastically yielded region measured with replica technique
05 p0780 A69-16437

Crack formation and propagation in metallic materials under dynamic fatigue loading, noting dislocation during work hardening
05 p0781 A69-16542

Fatigue crack propagation in machine parts under cyclic loading
05 p0842 A69-16543

Device based on stroboscopic effect for observing crack propagation on rotating specimens during fatigue tests
05 p0843 A69-16665

Strain distribution at crack base measured by Fabry-Perot interferometer and photoelastic coating
06 p1020 A69-17127

Strain near fatigue crack tip in notched steel plates measured by copper electroplating method
06 p1022 A69-17198

Localized microstructural changes and fatigue crack propagation in cantilever type notched specimens of austenitic stainless steel under cyclic bending at constant load
06 p0943 A69-17237

Crack front and zone in brittle elastic body under high pressure at wall inside body
07 p1231 A69-18699

Fracture mechanics for predicting crack propagation rate in rotor spars
07 p1053 A69-18872

Crack growth during cyclic loading in elastoplastic bodies
07 p1232 A69-18992

Brittle fracture models compared with experimental stress analysis results, noting plane strain and plane stress fracture toughness
07 p1234 A69-19379

Strain concentration design factors for notch effect in low cycle fatigue and crack propagation conditions
07 p1235 A69-19383

Forging and heat treatment parameters effect on Ti-Al-V alloy low cycle fatigue properties, relating crack initiation and propagation rates to microstructures [ASM PAPER D8-24.4]
07 p1169 A69-19669

Prandtl brittle fracture model modified for semi-infinite crack in infinite body, discussing microscopic and macroscopic relation and crack propagation kinetics
07 p1237 A69-19682

Stresses nature at ends of brittle cracks, discrediting finiteness under certain conditions
07 p1238 A69-19691

Mathematical models of crack propagation in solids noting similarity for equilibrium crack length
07 p1238 A69-19692

Heat generation effects by plastic deformations at tip of propagating crack in quasi-brittle materials, considering elastic stress field and crack velocity
08 p1412 A69-20144

Electrochemical kinetic and mass transport model for studying stress corrosion crack propagation in Ti [ECS PAPER I47]
08 p1332 A69-20359

Vibration characteristics of rectangular plate with fatigue crack and subject to tensile load, applying results to crack propagation in fuselage panels
08 p1413 A69-20399

Translunar cracks in laminated graphite filament composites, noting effect of thermal stresses due to cooling
08 p1337 A69-20483

Crack propagation in crosslinked glassy polymers, noting effects of added elastomers molecular weight
08 p1338 A69-20492

Grain morphology and preferred orientation effects on direction and propagation of stress corrosion cracking of aluminum alloy plate
09 p1521 A69-21399

Methanol-water-chloride solutions effect on titanium alloys failure time, noting effect of changing water volume on cracking
09 p1521 A69-21400

Crystallographic fracture path of stress corrosion cracks in austenitic stainless steels using scanning electron microscopy
09 p1522 A69-21486

Polymethyl methacrylate rupture time under stress determined from short and long time strength tests, noting relation to crack propagation time
09 p1528 A69-21853

Crack propagation properties of polymethyl methacrylate during bending and tension, noting temperature and loading time effect on crack size
09 p1529 A69-21854

Quasi-brittle fracture of plastic materials based on Griffith theory and crack propagation, analyzing real surface energy and work of plastic strain
09 p1614 A69-21883

Part-through and through-thickness fatigue crack growth observations in glassy plastics, using linear elastic fracture mechanics [SESA PAPER I348]
09 p1617 A69-22013

Ruby laser emission absorption in transparent dielectrics, noting crack formation and propagation producing opacity
09 p1520 A69-22655

Crack stability under mechanical and thermal stresses, noting critical tensile stress and thermal insulating character of crack
10 p1794 A69-22890

Model explaining intergranular crack initiation parallel to pulling axis in samples of spun beryllium broken under pressure
10 p1708 A69-22996

Aluminum alloy thin sheets with central transverse fatigue cracks subjected to increasing static loads to fracture, investigating crack tip deformation
10 p1709 A69-23056

Crack propagation velocity in titanium alloys over varying stress intensities under adverse environment
10 p1709 A69-23058

Strain fatigue mechanism of crack propagation in ductile metals, considering distribution of plastic cohesive stresses at crack tip
10 p1795 A69-23059

Crack propagation in plates and shells subjected to bending and direct loading, noting plate analysis modification for crack touching on compression side
10 p1795 A69-23061

Geometry at tip of growing fatigue crack, measuring crack propagation rate and fitting data to nucleation theory
10 p1795 A69-23062

Nonwork hardening elastic plastic material fracture criteria for antiplane strain, noting plastic zone shape effect on zone size and crack opening
10 p1795 A69-23064

Electron fractography of aluminum alloy fatigue for intermetallic particles and inclusions effects on crack growth
10 p1795 A69-23065

Fatigue crack propagation in cylindrical shells under fluctuating internal pressure, considering stress intensity factor
10 p1795 A69-23066

Micromechanism of crack propagation in brittle fracture, considering kinematics for steady state crack in plane strain and energy dissipation
10 p1796 A69-23070

Aluminum alloy crack propagation and fracture patterns as function of temperature under high strain amplitude and low strain rate
10 p1709 A69-23071

Mechanical model for investigating macrobehavior of cyclic fatigue crack propagation in plates of several metal alloys
10 p1796 A69-23072

Austenite to martensite strain induced transformation effect on energy absorption during crack propagation
10 p1709 A69-23074

Plastic crack propagation in nonstrain hardening doubly grooved bending specimens with two surface slip, discussing crack angles, crack ductilities and fatigue striations
10 p1797 A69-23077

Fatigue crack propagation and crack tip stresses measurements in tensioned cracked panels subjected to acoustic loading
10 p1797 A69-23078

Dislocation substructure near fatigue fracture surface during tensile mode crack growth in copper single crystals by transmission electron microscopy
10 p1797 A69-23079

Low cycle fatigue fracture behavior at high temperatures, noting fatigue crack behavior and crack density concept
10 p1797 A69-23081

Mechanical model for fatigue crack propagation assuming propagation as function of material strain cycling at crack tip
10 p1797 A69-23082

Environment influence on fatigue crack propagation mechanisms in aluminum alloys in vacuum, ambient air and distilled and sea water
10 p1710 A69-23084

Transgranular stress corrosion crack propagation in thin sheet single phase magnesium-aluminum alloy
10 p1710 A69-23086

Stress effect on laser damage crack orientation in transparent organic dielectrics, estimating gas pressure in cracks
10 p1703 A69-23621

Fatigue growth of disk shaped crack in infinite body, noting dependence on fourth power of stress intensity factor
10 p1802 A69-24028

Crack propagation through layer of viscous fibers joining orthotropic elastic half planes
10 p1803 A69-24029

Antiplane strain model for describing cracks and dislocation arrays within circular cylindrical inhomogeneity surrounded by elastic material
10 p1803 A69-24031

Mathematical theory of equilibrium cracks in stressed bodies with minimum loading for crack extension, analyzing crack tip zone and force transmission
11 p1974 A69-24668

Continuum mechanics analysis of fractures and crack extension, discussing solids elasticity, plasticity, boundary value problems, etc
11 p1974 A69-24670

Dynamic and fatigue crack propagation theories for brittle and quasi-brittle solids and plates
11 p1975 A69-24672

Three dimensional problems in crack theory for unbounded brittle body, deriving critical loads from limiting equilibrium equation
12 p2178 A69-25997

Fracture surfaces of thermally toughened glass plates using Cranz-Schardin spark camera, confirming internal front lead over front in surface layers
12 p2118 A69-26194

High speed photography of W strip fracture, considering electric current effects and electric circuit interruption by fracture
12 p2113 A69-26195

Fatigue crack propagation and fail-safe design for stiffened large Al alloy panels with crack stoppers, using residual strength analysis method
12 p2186 A69-26835

Fatigue crack propagation laws determined by material yielding at crack tips, stress intensity and exponential crack growth law
12 p2187 A69-26846

Crack growth and crack initiation in cylindrical specimens subject to low cycle strain controlled tension-compression induced fatigue, noting measurement techniques
12 p2188 A69-26914

Fatigue crack initiation and propagation correlation with substructure formation by static and alternating stresses in Al
12 p2188 A69-26915

Fatigue fracture surfaces in cast steel and Al alloys, studying fracture morphology, crack propagation rate and striation spacing with microfractographic methods
12 p2116 A69-26916

Macroscopic crack extension force, critical flaw size and minimum fracture strength calculated from microscopic quantities
13 p2275 A69-27227

Variational principle for admissible functions particular solution in elasticity theory involving solid bodies with cracks
13 p2359 A69-27290

Metal fatigue in Al alloys subjected to stress cycles, determining macrocracks propagation stages
13 p2359 A69-27291

Ambient air pressure effects on fatigue crack growth rate in strain hardened aluminum
13 p2276 A69-27393

Fatigue crack propagation in aged aluminum alloy sheets, studying specimen geometry and stress level variations effects
13 p2280 A69-27835

Stress corrosion crack initiation and propagation in titanium alloy
13 p2282 A69-28165

Fracture mechanics based on linear elasticity for evaluating crack propagation resistance, presenting plane strain fracture toughness test results for high strength alloys [ASME PAPER 69-DE-10]
14 p2461 A69-28842

Ultrasonic detection and measurement of fatigue cracks in notched cylinders subjected to reversed axial cyclic loading

14 p2445 A69-28882

Oxygen content and grain structure influence on TS5 Ti alloy mechanical properties, notch and crack growth sensitivity at low temperature

15 p2637 A69-30266

Crack initiation and propagation in Ti alloys during thermal cyclic heating noting influence of gas saturation

15 p2637 A69-30271

Three dimensional problem in crack theory for brittle body, determining stress concentration and critical loads

15 p2708 A69-30658

Fatigue cracks growth rate under combined static and cyclic stresses

15 p2709 A69-30808

Fatigue crack propagation caused by cumulative damage due to strain cycling at crack tip, relating resistance to cyclic ductility

15 p2710 A69-30812

Room temperature fatigue crack propagation rates for high strength aluminum alloy in heavy water environment compared with argon and distilled water

15 p2640 A69-30815

Crack growth monitoring and recording techniques during fracture testing, using foil gauge, potential flow and acoustic pickup methods

15 p2713 A69-31109

Equilibrium cracks propagation in linear hereditary elastic media using Volterra principle

15 p2715 A69-31201

Fatigue life gage on operational aircraft providing in situ monitoring of fatigue damage prior to and during propagation of running fatigue cracks

15 p2613 A69-31271

Brittle toughness determination method compared with Robertson and notch impact tests, evaluating steel susceptibility to brittle failure propagation

16 p2795 A69-32796

Fatigue cracks initiation and propagation studied by surface plastic replication method, noting metallographical and continuum mechanical factors influence on low carbon steel

17 p3052 A69-32981

Fatigue crack growth rates in stainless steel at elevated temperature measured as function of oxygen pressure in resonant fatigue machine

17 p2987 A69-33074

Arrest mechanisms to halt crack before gross failure, involving material toughness exploitation and subduing stress by structural configuration

17 p3060 A69-33560

Fatigue crack propagation in thin aluminum alloy plates under plane bending using microscopic surface observation and electron fractography, noting role of aging conditions

17 p3061 A69-33677

Plastic energy dissipation rate during stable crack growth in sheet under uniaxial tension

18 p3212 A69-34345

Longitudinal crack in cylindrical shell under internal pressure, calculating normal and bending stress singularity strengths against curvature/ cracklength parameter

18 p3212 A69-34346

Quasi-static crack growth in viscous bodies analyzed by continuum mechanics, rheological models and energy equation, discussing fine structure

18 p3215 A69-34570

Critical stresses and crack development near holes in compressed elastic plate

18 p3218 A69-34603

Crack analysis in stiffened vibrating plate based on dynamic stress distribution, showing high bending stresses at intersection

18 p3223 A69-35168

Fracture kinetics of biaxial oriented polymethyl methacrylate, discussing crack development and propagation as compared to unoriented polymer

18 p3162 A69-35354

High speed brittle fracture of polycarbonate resin subjected to static bending in liquid nitrogen determined from crack propagation speed of surface coating

19 p3358 A69-35776

Nickel base superalloy high temperature fatigue properties, comparing crack initiation and propagation in directionally solidified and conventionally cast forms

19 p3342 A69-35919

High strength titanium alloys subcritical stress corrosion crack propagation, studying stress and environment effects on cleavage mode

19 p3343 A69-35922

Axial load fatigue crack propagation tests on Al alloy sheets for stress ratio effects

19 p3346 A69-36435

Homogeneous heat flux effect on limit load of isotropic plate with rectilinear through crack, noting conditions for crack propagation

19 p3441 A69-36744

Linear-elastic fracture mechanics applied to environment enhanced crack growth /stress corrosion cracking/

19 p3349 A69-36888

Crack growth in steel tested in hydrogenated condition, distilled water and in combination by acoustic emission, relating time intervals to hydrogen diffusion

19 p3350 A69-36893

Hydrogen embrittlement mechanism in steel based on modified pressure theory, discussing crack propagation mechanisms and stress corrosion cracking

19 p3350 A69-36894

Aluminum 7 percent Mg alloys stress corrosion cracking, presenting aging kinetics and depletion zone dislocations at grain boundaries

19 p3350 A69-36896

Titanium alloys stress corrosion cracking in presence of chloride, bromide and iodide under potentiostatic conditions, postulating electrochemical kinetic and mass transport model

19 p3351 A69-36901

Ti alloy stress corrosion susceptibility in salt water, alcohols and alkanes, comparing stress intensity for crack propagation in dry air

19 p3353 A69-36907

Computed and experimental displacement distribution curves compared for anisotropic material concerning creep rate enhancement by small cracks

20 p3620 A69-36965

Mean stresses effects on fatigue crack initiation and propagation under controlled fretting slip amplitude

20 p3563 A69-38111

Crack growth measured and recorded by ultrasonic monitor, describing transducer position and movement

20 p3547 A69-38312

Axial through-cracks extension criteria in cylindrical pressure vessels, considering fracture toughness and plastic flow stress

[ASM PAPER W9-13.3] 21 p3833 A69-38658

Stability of unbounded homogeneous brittle body containing circular planform crack, determining elastic stresses and critical load by macrocrack propagation theory

21 p3839 A69-39195

Wave scattering in elastic medium by discontinuity line or finite crack, noting dynamic stress intensity dependence on incident wavelength and Poisson ratio

21 p3840 A69-39293

Alpha-beta Ti-Al-V-Mo-Zr alloy with high strength, fracture toughness and crack propagation resistance, low density and adequate ductility, discussing test results

[AIME PAPER S69-3] 21 p3747 A69-39472

Stress history and corrosive environment effects on fatigue crack propagation under constant and varying stress amplitude

21 p3750 A69-39814

Photographic study of epoxy resin breakdown kinetics under pulsed laser beams, showing crack area as function of time

22 p3973 A69-40743

Axial through-cracks extension criteria in cylindrical pressure vessels, considering fracture toughness and plastic flow stress

22 p4046 A69-41040

Energy equilibrium for crack growth in elastoplastic media, analyzing crack behavior during plastic deformation concentrated at edge of propagating crack

22 p4046 A69-41060

Fatigue tests with cylindrical samples for observation of macrocrack formation and propagation at bottom of notches, discussing kinetics of fatigue failure

23 p4225 A69-41425

Fracture toughness and crack propagation in annealed aircraft titanium alloys tested per ASTM procedure, comparing results with high strength steels and aluminum alloys

23 p4177 A69-42165

Stress corrosion cracks propagation from fatigue precrack in Al alloy exposed to organic liquid environments

23 p4178 A69-42452

Elastoplastic boundary dynamic behavior in strip with crack determined by solving boundary value problem in elliptic integrals form

24 p4395 A69-42591

Plane problem of infinite strip weakened by crack, determining crack form under uniformly distributed tensile loads applied to edges

24 p4395 A69-42592

Semiinverse method involving plane wave expansions to solve elliptical crack expansion and self similar phase transformation in anisotropic solid

24 p4397 A69-42749

Engineering components service failures involving fatigue crack propagation, analyzing causes

24 p4398 A69-42775

Model for estimating creep life of material containing wedge crack growth

24 p4399 A69-43032

Crack propagation in plate with stiffening ribs /riveted stringers/ under concentrated and tensile loads, determining rivet points displacements

24 p4406 A69-43709

CRACKING [FRACTURING]

Dynamic mechanical behavior of metal at tip of plain strain crack, discussing fracture strength relation to triaxial plastic stability

02 p0343 A69-12284

Precracked ceramic rocket nozzle throat inserts, discussing improved thermal displacement accommodation, load transmission, fracture tolerance, articulation capability, etc

02 p0334 A69-12369

Surface preparation effect on stress corrosion cracking of type 310 stainless steel wires in boiling aqueous magnesium chloride solutions

03 p0444 A69-13311

Salt water stress corrosion cracks morphology in titanium alloy, discussing crack propagation, brittle nature and chloride contamination effect

[SAE PAPER 680642] 03 p0444 A69-13458

Knee in stress-strain diagram and crack formation in glass fiber reinforced plastics, discussing effect on construction load capacity

03 p0453 A69-13820

Consumable electrode vacuum melted steels, discussing ausforming and stress corrosion cracking

04 p0604 A69-14528

High temperature eddy current crack detection technique for atomic reactor components under high thermal gradients

04 p0607 A69-14972

General linear theory of isotropic cumulative failure involving phenomenological consideration of fatigue damage accumulation

[ASME PAPER 68-WA/MET-6] 05 p0838 A69-16149

Green function for computation of stress intensity factors for edge cracks in rectangular plates with arbitrary loadings

[ASME PAPER 68-WA/MET-18] 05 p0839 A69-16156

Green function for stress intensity factors of rectangular plate edge cracks, noting application to thermal stresses

[ASME PAPER 68-WA/MET-19] 05 p0839 A69-16157

Simulated crack experiment illustrating Griffith energy balance fracture criterion

05 p0842 A69-16438

Stresses and displacement around crack under various conditions using two dimensional elasticity theory, deriving complex potentials for various loading types

07 p1231 A69-18269

Brittle crack theory analyzed to justify Irwin criterion at crack ends, dismissing Kristianovich-Barenblatt assumption and solutions for elastic problems

07 p1238 A69-19689

Critical analysis of Sedov contention of infinite stress development at ends of brittle cracks

07 p1238 A69-19690

Electron fractographic study of fatigue cracks in wrought beryllium sheet, noting transgranular and intergranular modes on fracture surface

09 p1500 A69-22324

Fracture surfaces of Ti and Ti-Sn alloys for stress corrosion cracking in methanol with HCl and in aqueous chloride solutions

10 p1710 A69-23085

Plastic energy dissipation and crack surface displacement of penny shaped crack in elastoplastic material

10 p1803 A69-24030

Stress corrosion cracking of Ti-6Al-4V alloy tensile tested in anhydrous methanol by electron fractography and diffraction, noting hydrogen embrittlement

11 p1903 A69-24576

Hydrostatic pressure-cycling technique for controlled fatigue precracking of spin burst fracture toughness specimens, noting ultrasonic flaw detection 11 p1995 A69-25650

Electron fractography used in machine parts failure analysis to detect internal and surface cracks, forging defects, stress corrosion, fluid leakage sources, etc 13 p2269 A69-28182

Cleavage plane in stress corrosion cracking of alpha phase Ti-Al alloys 13 p2283 A69-28189

Crack behavior and toughness of aluminum alloy parent metal and weldments, noting temperature effect 14 p2462 A69-29003

General linear theory of isotropic cumulative failure involving phenomenological consideration of fatigue damage accumulation [ASME PAPER 68-WA/MET-6] 14 p2535 A69-29436

Stress corrosion cracking prevention by shot peening, considering aircraft industry applications 14 p2466 A69-29937

Maraging steel weldability, discussing residual stresses, hydrogen cold cracking, age hardening and hot cracking 15 p2617 A69-30098

W single crystals cleavage cracks by spark discharge, showing effective surface energy dependence on crack initiation and propagation temperatures 15 p2637 A69-30226

Stress-strain state of circular disk with diametral cracks determined by approximating limiting equilibrium equation 15 p2708 A69-30663

Initial comparisons between theory and experiment of strain fields in cracked copper plate 15 p2640 A69-30810

Plane strain and stress compared for elastoplastic cracked plate in work hardening tension 15 p2710 A69-30811

Automated IR fatigue crack detection in sonic test facility capable of subjecting large aircraft or missile structures to intense sound fields 15 p2631 A69-31505

Stress corrosion cracks investigation by shear wave technique 16 p2876 A69-32334

Ti-Al base alloys brittleness and stress corrosion cracking, discussing diffusion mechanism, hydrogen mobility, dislocations, etc 17 p2987 A69-33372

Arrest mechanisms to halt crack before gross failure, involving material toughness exploitation and subduing stress by structural configuration 17 p3060 A69-33560

Fracture design for aircraft vehicles, discussing crack strength requirements and method for serviceability prediction 17 p3060 A69-33563

Prestressed beams, columns and plates nonlinear response, statistical behavior and transverse cracking under axial compression, describing strength and stiffness 17 p3060 A69-33568

Macrostructural differences between filaments of B and SiC vapor deposited onto small diameter W wire, discussing radial cracks due to dilatation 18 p3160 A69-34266

Hydrogen effect on embrittlement of Cr-Ni stainless steel from viewpoint of corrosion cracking, using reverse bending apparatus 19 p3358 A69-35774

Ti-Al alloys yield and fracture characteristics as function of high exposure temperatures, studying causes of embrittlement 19 p3344 A69-35927

Stress corrosion cracking - Conference, Columbus, Ohio, September 1967 19 p3347 A69-36883

Stress corrosion cracking research, history, engineering and education, incorporating stress corrosion data in mechanical design, terminology and nomenclature 19 p3348 A69-36884

Stress corrosion cracking of metals related to surface phenomena involving surface reaction layer ruptures or selective electrochemical dissolution along defects 19 p3349 A69-36885

Stress corrosion cracking mechanisms in liquid-solid metal combinations and solvent exposed plastics, discussing adsorption processes and cathodic polarization inhibition 19 p3349 A69-36887

Stress corrosion cracking of stainless steels and Incoloy and Inconel alloys in chloride, caustic, oxygenated and miscellaneous environments 19 p3349 A69-36890

Fracture surfaces of stress corrosion cracks in Fe-Cr-Ni alloys studied by electron microfractography, noting cleavage fracture 19 p3350 A69-36891

Stress corrosion cracking mechanism in Al alloys, discussing requisites for stress corrosion cracking 19 p3350 A69-36895

Stress corrosion cracking model for 7075 Al, correlating macroscopic yield stress and corrosion time to failure 19 p3351 A69-36897

Precipitation hardening, microstructure and dislocation influence on intergranular stress corrosion cracking /SCC/ of high strength Al alloys examined by transmission electron microscopy 19 p3351 A69-36898

Electrochemical analysis of stress corrosion cracking in Al-Zn-Mg alloy, noting oxide film growth at grain boundary 19 p3351 A69-36899

Ti and Ti alloys stress corrosion cracking, discussing metallurgical and environmental factors 19 p3351 A69-36900

Titanium alloys stress corrosion cracking /SCC/ from metallurgical-mechanical viewpoint, discussing phase transformations, dislocation arrangements, crack propagation, etc 19 p3352 A69-36902

Metallographic analysis of stress corrosion cracking of Ti alloys of Al and Sn in aqueous magnesium chloride solutions, noting cleavage process 19 p3352 A69-36903

Moisture and hydrogen role in hot chloride salt stress corrosion cracking of Ti alloys by radiotracer technique and mass spectrography 19 p3352 A69-36904

Titanium alloys hot salt stress corrosion cracking, studying effects of chlorides and surface oxides 19 p3352 A69-36905

Stress corrosion cracking of alpha Ti in liquid nitrogen tetroxide and various methanol environments, considering failure mechanisms 19 p3352 A69-36906

Singular factors affecting stress corrosion cracking resistance of Ti alloys in salt water and hot salt, finding immune single phase alloys 19 p3353 A69-36908

Alpha and alpha plus beta Ti alloys analyzed to relate phase composition and microstructure to stress corrosion cracking in NaCl solution 20 p3557 A69-36961

Crack density effects on stress-dependent creep rate in isotropic and anisotropic materials undergoing high temperature creep deformation 20 p3619 A69-36964

Design and processing tradeoffs for preventing stress corrosion cracking in Al alloy aircraft structural forgings [ASM PAPER W9-14.4] 21 p3729 A69-38657

Stress corrosion cracking of alpha and alpha-beta Ti alloys in aqueous environment at ambient temperature, noting Al content and microconstituents 21 p3743 A69-38663

Al alloys sheet, plate and weldments crack behavior and fracture toughness at cryogenic temperatures, using notched and surface flawed plane strain specimens [ASM PAPER W9-19.3] 21 p3743 A69-38669

Brittle failure models, discussing rheological properties, Griffith energy criterion properties, crack behavior in elastic and linear viscoelastic media, etc 21 p3839 A69-39194

Stress corrosion cracking prevention by selection of material, stress relief, compressive stresses introduction, protective coatings and by simulated accelerated tests 21 p3748 A69-39490

Stress corrosion cracking in aerospace situations, discussing corrective measures emphasizing fracture toughness criteria 21 p3748 A69-39491

Stress corrosion cracking of welded Al alloys in sea water solution, showing combined action of sustained stress, corrosive environment and heat treatment 21 p3748 A69-39492

C and B influence on heat affected zone hot cracking and postweld heat treatment on Ni base superalloys 22 p3967 A69-39880

Ti, Al, S and P influence on Ni alloys weldability, discussing chemical composition, susceptibility to hot cracking and ductility temperatures 22 p3967 A69-39884

Composition and thermal treatment effects on weldability of precipitation hardened Ni base alloy, analyzing heat affected zone cracking sensitivity 22 p3968 A69-39885

Nondestructive testing for fatigue cracks, considering X ray, magnetic particle, penetrant, ultrasonic and eddy current inspection techniques 23 p4234 A69-42451

Eigenfunction expansion technique to analyze three dimensional crack and wedge problems, emphasizing stress field near straight edged crack 24 p4395 A69-42641

CRACKS

NT MICROCRACKS NT SURFACE CRACKS

Plate thickness effect on bending of elastic plate with crack, investigating stress distribution 04 p0678 A69-14890

Steady state thermal stress distributions near external crack in solid, treating temperature distributions with respect to plane of crack 07 p1232 A69-19172

Fredholm equations from dual integral equations for studying penny shaped crack response to incident harmonic shear wave in elastic medium 07 p1233 A69-19175

Acoustic emission from welds in stainless steel plates used for detecting defects in single and multiple pass machine welds 08 p1318 A69-19963

Dynamic stress intensity factor for axisymmetric loading of circular crack in infinite isotropic elastic medium 08 p1413 A69-20412

Couple stresses effect on distribution of stresses in elastic solid due to crack analyzed on basis of Cosserat theory 10 p1800 A69-23242

Potential functions for three dimensional problems of elliptical crack in elastic solid 10 p1802 A69-24026

Dynamic IR inspection to detect fatigue cracks in aircraft and missile structure from distance 11 p1861 A69-24262

Mixed boundary value problem concerning expanding elastic space weakened by cracks located at same plane solved by integral transforms and Fredholm equations 11 p1973 A69-24663

Thermal stress and displacement fields in elastic solid weakened by crack outside of circular region, noting plastic zone size and energy dissipation 12 p2179 A69-26216

Symmetrical stressed state of shallow shell with crack edge loading solved in Cartesian coordinates 12 p2181 A69-26614

Elastic wave reflection and refraction around cracks, considering plane harmonic compressional and vertically-horizontally polarized shear waves 17 p3053 A69-32986

Stress level reduction in pressurized circular cylinder with circumferential ring stiffener and longitudinal crack, using shallow shell equations 18 p3212 A69-34347

Limiting equilibrium of infinite brittle body weakened by internal plane elliptical crack, determining critical loads and stresses at crack 18 p3226 A69-35379

Two dimensional stress analyzed near crack in infinite elastic sheet, considering crack shape and Young modulus 19 p3440 A69-36638

Limiting equilibrium stress state of unbounded brittle body with elliptical crack under monotonically increasing tensile or compression load, noting influence of crack curvature 19 p3441 A69-36745

Alpha Ti fatigue properties, studying internal precracking effects in alloys of various tensile strength 23 p4178 A69-42360

Time and plasticity effects on fracture determining solids strength as function of crack dimension 23 p4236 A69-42530

Orthotropic stiffness layer models for buckling of eccentrically stiffened shells of revolution with two unbonded orthotropic layers uncracked and circumferentially cracked 24 p4405 A69-43657

CRACK U VEHICLES

CRAMPS

U CONVULSIONS

CRANIUM

Single flash and rhythmic light stimuli effect on nystagmus of patients with tumoral posterior cranial fossa, recorded electroencephalographically
20 p3470 A69-37250

CRASH INJURIES

Occupant restraint systems for automobiles, aircraft and manned space vehicles, discussing cost, practicality, ease of use, acceptability and possible improvements
03 p0380 A69-13459

Impact/injury data used to estimate human tolerance to instantaneous accelerations
04 p0552 A69-14469

Business aircraft injury protection and impact survival design considerations, stressing upper torso restraint installations
[SAE PAPER 690335]
11 p1829 A69-24493

CRASH LANDING

NT DITCHING [LANDING]

Human survivability in severe light plane slow speed accidents due to stalling, turning, takeoff or approach, discussing crash load vectors and magnitude
[SAE PAPER 690336]
11 p1822 A69-24492

Large and small fixed wing airplane crashworthiness requirements, noting occupant protection in survivable crash environment and rapid safe evacuation
[SAE PAPER 690321]
11 p2004 A69-24509

Night vision requirements of Vietnam combat pilots investigated for relationship to Skyraider fatal crash during target strafing and H-34 helicopter crash landing
23 p4107 A69-41807

CRASHES

NT CRASH LANDING

NT DITCHING [LANDING]

Fragments and markings produced on aircraft aluminum by explosion as means of detecting sabotage in crashes
06 p0868 A69-17833

CRATERING

NT PROJECTILE CRATERING

Asymptotic estimate derived for size distribution function of fragments resulting from brittle impact destruction of rigid object applied to meteorites and lunar craters
03 p0512 A69-13691

Lunar crater formation studied to explain distortion in large craters or maria, discussing mass concentrations indicated by positive residuals of gravimetric map
04 p0654 A69-14632

Collapse theory of dimple craters, analogies with terrestrial sink holes and dimple craters as channels for gas escape from interior
05 p0818 A69-15589

Crater formation by gas erosion in vent of 4.3 kiloton nuclear explosion detonated at 280 ft depth in layered trachytic volcanic rocks
22 p3937 A69-40409

CRATERS

NT LUNAR CRATERS

NT METEORITE CRATERS

NT TYCHO CRATER

Martian crater density determined by comparison of statistical counts from Mariner 4 photographs
12 p2157 A69-26309

Mariner 6 TV pictures with description of craters and south polar cap, noting moon-like crater abundance, form, arrangement and crater sizes
21 p3803 A69-38981

CRAWLER TRACTORS

Crawler-Transporter at Kennedy Space Center for moving ground support equipment, Apollo/Saturn space vehicle and mobile launcher, describing design and components
21 p3690 A69-38754

CRAZING

U SURFACE CRACKS

CREEP ANALYSIS

Elastic analogue in creep stress analysis under time dependent boundary conditions and strain hardening theory
02 p0345 A69-12418

Model of creep in solids based on Markov process, discussing dislocation movement by means of thermal activation
03 p0529 A69-13942

Book on thermal time independent plastic and time dependent creep strains in structures through analogy permitting inelastic structures analysis
04 p0681 A69-15200

Long term creep behavior of nickel-chromium-molybdenum alloy, noting temperature effect on grain boundaries
05 p0781 A69-16500

Creep properties of EP-376 steel under slowly varying loads
05 p0782 A69-16692

Calculation of thin shell or beam structures with plasticity and isothermal creep based on linearization and local kinematic behavior
[ONERA-TP-667]
06 p1020 A69-17099

Buckling of rod with initial deflection as sinusoidal half wave, using Bubnov-Galerkin method and Laplace transform, calculating stresses of rod when subjected to nonsteady creep
06 p1021 A69-17182

Deformation and stresses in biaxially loaded stretched thin plate with central small hole during stress redistribution caused by creep
06 p1022 A69-17368

Digital computer simulation of nonlinear redundant structure variables including thermal influence, creep and arbitrary loads
[AIAA PAPER 69-120]
06 p1028 A69-18166

Anisotropic stress analysis of creep in theory of linear viscoelasticity
07 p1234 A69-19381

Hyperbolic sine creep law, discussing limiting stresses for approximation by linear or exponential relationship
07 p1235 A69-19384

Stress relaxation in structural elements, analyzing unsteady creep in case of strain hardening following power law
07 p1237 A69-19683

Dislocation climb theory of steady state creep, noting necessity of self diffusion mechanism in any high temperature creep theory
08 p1329 A69-20000

Single degree of freedom mechanical system under random excitation studied for creep effect on vibrations by harmonic analysis
09 p1617 A69-22095

Creep of high purity Nb-Mo alloys in 800-1300 C range and at 1500-13000 lb/square inch stresses, giving activation energy for creep
10 p1711 A69-23375

Stress concentration around square hole in celluloid plate subjected to creep under biaxial tension analyzed by photocreep method
12 p2178 A69-26000

Creep behavior of aluminum-alumina alloys analyzed using rupture time to determine deformation speed influence on elongation and crack formation
12 p2120 A69-26938

Creep strain rate and stress distribution of thick walled cylinders under internal pressure at elevated temperature, using variational principle
15 p2703 A69-30070

Heat resistant Fe and Cu alloys creep index affected by temperature, testing time and specimen grain size
15 p2639 A69-30569

Creep rates measurement errors at low stresses in intermediate temperature range, examining log creep rate vs log stress plot in Cr-Mo steel
15 p2639 A69-30599

Nonlinear theoretical derivation of creep equations for three dimensional processes in polymers, based on Boltzmann-Volterra creep heredity concept using stress-strain summation
16 p2803 A69-32290

Creep - Conference, Saclay, Essonne, France, June 1967
17 p2984 A69-32903

Pressurized cylindrical shell creep analysis by elastic procedure extension using computer program
17 p3067 A69-34211

Creep calculation with temperature considerations for multilayer cylinder under nonisothermal load, comparing stress-strain state of viscoelastic and elastic cylinders
18 p3225 A69-35358

Phenomenological creep theory for woven fiberglass reinforced plastic under moderate loads
18 p3226 A69-35373

Stoichiometric NiAl slip line and dislocation structures during creep at high temperatures, considering possible creep mechanisms
19 p3343 A69-35923

Thermal effects on viscoelastic structure response to applied loads, using equations for thermomechanics, linear and nonlinear thermoviscoelasticity and nonisothermal creep theorem
19 p3440 A69-36657

Primary and tertiary uniaxial creep strain rate changes based on internal stress redistribution described with mathematical model
20 p3619 A69-36941

Crack density effects on stress-dependent creep rate in isotropic and anisotropic materials undergoing high temperature creep deformation
20 p3619 A69-36964

Creep theory with anisotropic hardening during early creep stages based on analogy with plastic flow theory
21 p3839 A69-39196

Fatigue endurance determined from thermal stresses by balancing elastic strain rates, creep relaxation and mechanical cyclic loading with triangular waveform, discussing nonsteady creep
21 p3843 A69-39310

Creep long term deformation characteristics of plate and tube lead alloy model material predicted from short term room temperature creep deformation
21 p3844 A69-39320

Creep accumulation under time varying stress of Al alloy sheet, using creep recovery analysis to determine anelastic strain growth
21 p3747 A69-39323

Approximate generalized stress-strain rate relations for stationary creep analysis of thin shells compared with corresponding exact relations
22 p4041 A69-40013

Creep at 400 degree C in Ti alloy sheets in short period plastic deformation due to work hardening by stepwise drawing in extensometric device
22 p3971 A69-41032

Strain induced creep equation for hardened materials for fixed temperature and stresses range, noting application to steel and Al alloys
22 p3971 A69-41033

Dislocation structure of Al, Ni, Cu and Ag during creep, noting dependence of creep rate on stacking-fault energy
22 p3972 A69-41080

Partial differential equation for creep process in plane stressed metals, interrelating strain, rate, stress tensors, temperature and time
22 p4048 A69-41268

Model for estimating creep life of material containing wedge crack growth
24 p4399 A69-43032

CREEP BUCKLING

Elastic-plastic and creep deformation calculations of cylindrical shell, providing better estimate of critical time at higher stress levels by including plasticity
02 p0348 A69-12539

Creep buckling of circular cylindrical shells under axial compression and bending, using Al alloy test specimens
03 p0523 A69-12995

Circular cylindrical shell creep behavior and buckling under axial compression and internal pressure, using multimebrane model
[AIAA PAPER 68-108]
04 p0676 A69-14706

Creep buckling of shallow geometrically nonlinear spherical shell of linear viscoelastic material under constant external load
05 p0831 A69-15679

Creep buckling stability of shells, with emphasis on stress and strain states and critical time, considering circular cylindrical shell
08 p1411 A69-20143

Time scales for creep stress redistribution in structures subject to step loading
11 p1980 A69-24879

Buckling time of oval ring under unsteady creep based on strain hardening theory
17 p3062 A69-33716

Cylindrical shell stability under axial compression, studying buckling process and wave formation
18 p3217 A69-34597

Flanges flexural rigidity effect on load carrying capacity, failure mechanism and postbuckling behavior of webs in shear, noting permissible load
18 p3227 A69-35492

Creep buckling strength reduction of aircraft compression structure, discussing initial eccentricity and loading mode effects on supersonic aircraft operation mode
21 p3842 A69-39308

Stability loss of beams analyzed under compression allowing for various creep conditions in loading and unloading regions, calculating time to failure
22 p4039 A69-39917

Compressed rectangular beam stability under different creep conditions, deriving relation between creep time and initial deflection
22 p4039 A69-39918

Circular cylindrical thin walled shells creep buckling under uniform axial compression 23 p4234 A69-42413

Creep buckling time of simply supported column under nonuniform temperature distribution over cross sections 24 p4400 A69-43053

CREEP DIAGRAMS

High temperature creep, discussing creep curves and activation energy 17 p2986 A69-32911

Temperature influence on mechanical properties and creep curves of fiberglass reinforced textolites compared with data from elasticity theory 23 p4179 A69-41993

CREEP PROPERTIES

NT STEADY STATE CREEP
NT TENSILE CREEP

Creep behavior of chemical vapor deposited tungsten at high temperatures by creep-rupture tests compared with powder metallurgy tungsten 01 p0097 A69-10647

Creep relaxation and kinking of aluminum-nickel whiskers at elevated temperature, noting permanent plastic deformation after heat treatment 03 p0443 A69-13119

Second phase hardened materials recovery creep rate model, showing dependence on stress level 03 p0447 A69-13615

Grain boundary sliding influence on gross mechanical behavior and stress distributions, emphasizing creep behavior 03 p0450 A69-13882

Creep stress concentration at circular hole in thin sheets under loads in own plane, discussing infinite thin plates [AIAA PAPER 68-175] 04 p0676 A69-14708

Plate bending in presence of unsteady creep and with zero stress-strain state in middle surface solved by variational method 04 p0679 A69-14923

Creep behavior of nonlinear rigid polyurethane foam under combined stress and applicability of multiple integral and modified superposition principle 04 p0680 A69-15155

Soviet handbook on elasticity, plasticity and creep theories, emphasizing stresses and strains in solid thin walled shells and plates under bending, tension and torsion 04 p0683 A69-15499

Tension stress and shearing strain vs time for simultaneous stress relaxation and creep in polyurethane [ASME PAPER 68-WA/APM-8] 05 p0839 A69-16186

Stress rupture, creep and thermal stability of AT-3 titanium alloy, discussing possible applications 07 p1163 A69-18782

Hyperbolic sine creep law, discussing limiting stresses for approximation by linear or exponential relationship 07 p1235 A69-19384

Long life creep rupture of Type 304 stainless steel for linear, Larson-Miller and Dorn parameter curves, discussing isothermal curves and creep rate [ASM PAPER D8-9.6] 07 p1169 A69-19664

Generalized approximate method for solving problems in linear viscoelasticity theory to cover arbitrary creep and relaxation centers 08 p1412 A69-20327

Tensile and creep behavior of nickel at 600 C after oxidation at 1200 C, correlating results with structural differences caused by oxidation 08 p1333 A69-20556

Stress-strain problem of geometrically nonlinear conical shell subjected to creep, giving method for complex deformation solution 09 p1612 A69-21497

Oxidation effects on creep and fatigue properties of metals noting time and temperature roles 10 p1708 A69-22998

Negative creep in austenitic steel samples explained as possible redistribution of elements inside austenite grains at high temperatures 10 p1708 A69-22999

Biaxial stress effect on creep properties of thin walled tubes of polymethyl methacrylate at controlled temperature and humidity 10 p1717 A69-24216

Moire patterns for photoelastic strain analysis noting applications to elasticity, plasticity and creep problems 11 p1982 A69-24944

Added metal oxides solid solutions effect on creep kinetics and strain rate of zirconia samples during sintering 12 p2118 A69-26260

Tension stress and shearing strain vs time for simultaneous stress relaxation and creep in polyurethane [ASME PAPER 68-WA/APM-8] 13 p2362 A69-28121

Creep stresses and displacements in conical membrane shells at small angle of attack to supersonic flow field, discussing temperature distributions 13 p2364 A69-28205

Monograph on mechanical behavior of crystalline solids at elevated temperatures, discussing creep properties of metals, solid solutions and two phase alloys 14 p2465 A69-29749

Creeping flow model of Leidenfrost boiling with moving surface, discussing vaporization time for equivalent drop film boiling on stationary surface [AICHE PAPER 20] 15 p2718 A69-31116

Aluminum alloys high temperature creep effects distinguished from effects of long period at high temperature, discussing tensile test data and deformation-time curves 16 p2800 A69-31781

Structural modifications of metals and alloys accompanying various stages of creep, interpreting equations describing time-deformation relation 17 p2985 A69-32904

Grain boundaries contribution to creep deformation, discussing ratio of grain boundary slip strain to total creep strain 17 p2985 A69-32905

Creep behavior of oriented Al bicrystals, emphasizing intergranular creep types and crystal orientation 17 p2985 A69-32906

Low temperature creep mechanisms, discussing thermal activation of dislocation slip in perfect crystals 17 p2985 A69-32909

High temperature creep, discussing creep curves and activation energy 17 p2986 A69-32911

Annealing time effects on creep properties of Ni at various temperatures after work hardening 18 p3159 A69-35445

Preliminary plastic deformations effect on dispersion hardened nimonic-80 alloy creep properties 18 p3159 A69-35446

Computed and experimental displacement distribution curves compared for anisotropic material concerning creep rate enhancement by small cracks 20 p3620 A69-36965

Analog method for determining structural creep displacement by setting up boundaries for linear elasticity and perfect plasticity 20 p3628 A69-37915

Soviet book on fundamentals of theory of plasticity and creep covering stress-strain state, bending, torsion, pressure, plane deformation, etc 20 p3630 A69-38206

Soviet book on thin plates and shells bending and stability during creep covering analytical and numerical solutions for various structural elements 20 p3630 A69-38207

Stress determination in materials with creep in presence of nonuniform temperature field 21 p3833 A69-38571

Snap through in thin shells with initial irregularities during creep, determining critical time to failure by analyzing undisturbed buckling process 21 p3838 A69-39188

Creep long term deformation characteristics of plate and tube lead alloy model material predicted from short term room temperature creep deformation 21 p3844 A69-39320

Thermal fatigue combined with mean stress, reversed mechanical stress, low cycle fatigue and static creep in stainless steel 21 p3847 A69-39813

Reinforcement effect on stress relaxation and creep in hereditary elastic materials, assuming integral shear modulus operator with exponential kernel 22 p4045 A69-40744

Rigid thermoplastic cylindrical shell creep under axisymmetrical loads, giving computer algorithm and time dependent criterion for rupture strength 22 p4045 A69-40750

Soft fiber reinforced plastics creep and recovery properties, discussing test equipment, rheological properties, polishing effects, etc 23 p4179 A69-42006

CREEP RUPTURE STRENGTH

Creep and stress rupture strength of unidirectional glass fiber reinforced plastics, using tensile tests 01 p0101 A69-10080

Creep behavior of chemical vapor deposited tungsten at high temperatures by creep-rupture tests compared with powder metallurgy tungsten 01 p0097 A69-10647

Delayed rupture strength of metals and welded joints at fixed stress level 04 p0674 A69-14541

Fully austenitic stainless steel welding electrodes for welds in cryogenic or high temperature applications, noting creep rupture test results 04 p0607 A69-15220

Ductile creep rupture of thin walled membrane shell of revolution subjected to time dependent internal pressure and strain hardening [ASME PAPER 68-WA/MET-15] 05 p0838 A69-16153

Stress rupture, creep and thermal stability of AT-3 titanium alloy, discussing possible applications 07 p1163 A69-18782

Long life creep rupture of Type 304 stainless steel for linear, Larson-Miller and Dorn parameter curves, discussing isothermal curves and creep rate [ASM PAPER D8-9.6] 07 p1169 A69-19664

Parameters interrelating time and temperature used to present creep-rupture data for Al alloys, providing direct readings of stresses [ASM PAPER D8-9.7] 07 p1169 A69-19665

Gas turbine blade materials after long term service, analyzing tensile, impact and stress rupture properties and microstructure [ASME PAPER 69-GT-12] 09 p1527 A69-22503

Hydrogen effect on temperature dependence of tensile strength and stress rupture strength of Ti alloys, considering annealing, quenching and aging 11 p1905 A69-24962

Book on stress rupture parameters including least squares approach to Larson-Miller, Dorn, Manson-Haferd, Graham-Walles, Murry, Brozzo and Chitty-Duval 13 p2360 A69-27372

Microstructural stability Fe-Ni base heat resistant alloy Pyromet 860 during long time creep-rupture testing 13 p2279 A69-27764

Short time creep rupture behavior of austenitic stainless steel at high temperature ranges, noting rupture times various stresses and data correlation [ASME PAPER 68-WA/MET-2] 14 p2464 A69-29439

Double notch creep rupture tests of Cr-Mo steels, investigating changes in notch profile, dimensions and structure [ASME PAPER 68-WA/MET-7] 14 p2464 A69-29441

Chemical reaction-rate theory for creep tests, analyzing extrapolation equations for time-to-rupture dependence on temperature and stress 14 p2464 A69-29442

Austenitic alloy structure and stress rupture after boron addition 17 p2985 A69-32908

Microfractographic observations of Al, Al alloy, Nimonic 90 and austenitic steel 18/10 after creep rupture 17 p2986 A69-32910

In-process annealing and warm working temperature effects on long time creep rupture properties of Mo alloys tested in vacuum furnace 17 p2987 A69-33076

Long term creep rupture data based on short term tests in form of Larson-Miller time-temperature curves 18 p3150 A69-35422

Tensile and stress rupture strengths of diffusion bonded Ni superalloys, using spin tests of simulated hollow turbine disks 19 p3320 A69-35559

Nonlinear rotational viscoelastic membranes creep rupture and failure found dependent on function of accumulated energy and power dissipation during deformation 19 p3444 A69-36806

Multicomponent Nb alloy creep and rupture strength under loads after heat treatment, determining creep rates dependence on temperature 22 p3969 A69-40073

Creep strength as function of oxygen pressure for Ni at 510 and 600 C, dropping creep rupture life to plateau of nearly constant life 23 p4176 A69-41504

CREEP STRENGTH

Zr-Be-Nb alloys mechanical tensile properties above room temperature for low concentrations of Be and Nb 02 p0262 A69-11845

Metal composite materials, discussing strengthening mechanism for inclusion of high elastic coefficient and creep limit fibers in weak ductile matrices 02 p0268 A69-12750

Columbium alloys properties, discussing creep strength, oxidation resistance, costs, production, etc 07 p1164 A69-18791

Microstructure relationship to tensile strength and creep resistance in Zn-Ni-Ti alloy extrusions, discussing role of finely dispersed intermetallic particles
08 p1329 A69-20002

Nickel base superalloys for aircraft gas turbines, considering strengthening mechanisms for creep resistance [ASME PAPER 69-GT-7]
09 p1527 A69-22506

Beta parameter in exponential stress dependences of high temperature steady state creep rate and time to rupture of creep resistant alloys
10 p1712 A69-23719

Creep and hot working strain-rates relationships, showing work hardening and dynamic recovery relative levels dependence on plot used
13 p2278 A69-27417

Creep rate and temperature effect on creep resistance shown in direct correlation with Al-Mg alloys strength by long term high temperature tests
16 p2801 A69-31782

Preprogrammed deformation temperature influence on Ni creep strength, emphasizing smoothly changing loads effects
18 p3160 A69-35455

Creep strength of fiberglass reinforced polyester resins measured on structural components in long term tests under torsion
19 p3358 A69-35830

Creep resistance increase of Ni refractory alloy by thermovibrational treatment under stress relaxation conditions
21 p3744 A69-38869

Law of mixture governing creep strength of composite materials reinforced unidirectionally by continuous filaments, taking into account fibers and matrix viscoelastic properties
24 p4400 A69-43054

CREEP TESTS

Long term creep characteristics of metal structures from short duration relaxation tests, summarizing data on rheologically stable materials [ONERA-TP-639]
02 p0337 A69-11626

Machine for simultaneous creep and long term strength evaluation of multiple metallic specimens
04 p0584 A69-14537

Deformation dependence on strain hardening and recovery rate during transient and steady state creep
06 p0943 A69-17236

Four specimen vacuum device for simultaneous tensile creep tests at 1200 C, discussing linear and thermal expansion
07 p1116 A69-19318

Ductility as principal cause of postweld heat treated stress relaxation cracking in nickel based Waspaloy and alloy 718
08 p1318 A69-19964

Heat resistant nickel alloys static and dynamic properties at high temperature, creep- fatigue interaction, etc
09 p1523 A69-21609

Nickel alloy high temperature tests, noting coagulation of precipitated gamma prime phase, vacancies and creep rate increase
09 p1528 A69-22733

Bending creep vacuum testing device for brittle materials at high temperatures, noting load variation capability
10 p1696 A69-23851

Compressive and tensile creep of metals, discussing compressive stress, void nucleation, barreling specimen shape and platen lubrication
12 p2175 A69-25836

Accelerated structural tests under creep conditions, noting isothermal structures subjected to uniaxial and complex stress loads
12 p2186 A69-26838

Machine for measuring creep deformation of polytetrafluoroethylene under uniaxial compressive loads, discussing stress-strain relationship
14 p2469 A69-29412

Chemical reaction-rate theory for creep tests, analyzing extrapolation equations for time-to-rupture dependence on temperature and stress
14 p2464 A69-29442

Creep experiments on Mg alloys, discussing dispersed phases influence on creep cavitation and grain boundaries mobility
17 p2985 A69-32907

Creep tests on polycrystalline Be and Be alloy at various temperatures and stresses
17 p2986 A69-32912

Machine for testing high temperature creep under variable tensile-compressive stress while maintaining specimen stability, noting discrepancy between creep strains in heat resistant alloy
17 p3054 A69-33044

Tensile and creep deformation of fiber reinforced composites consisting of Mg-Li alloy matrix with high strength precipitation hardening stainless steel wire
17 p2986 A69-33073

Creep rate-stress-temperature relations for powder metallurgy rhodium, discussing activation energy
17 p2991 A69-34186

Dislocation structure of pure polycrystalline nickel subjected to high temperature creep, using electron microscopy following cold working and room temperature annealing
18 p3157 A69-35254

Longitudinal modulus of interlaminar slip during creep of fiberglass reinforced plastic determined by bending tests of beams under concentrated force
18 p3163 A69-35365

Annealed Cr structural changes during creep at 900 C in air, discussing crystalline disorientation X ray studies and stress
18 p3160 A69-35453

Tensile tests on time dependent Pb and cellulose nitrate, including stress-strain curve prediction from creep test data
19 p3445 A69-36829

Supersonic aircraft and power plant structural members operating under cyclic stress at elevated temperatures tested by various methods for interaction between creep and fatigue
20 p3620 A69-37001

Creep strain rate measurement at high temperatures by inductance strain gage to determine deformations from 0.2 microns
20 p3544 A69-37815

Creep measurements in Al alloy during uniaxial tensile stresses between 200-350 C, determining deformation dependence on time and stress
21 p3744 A69-38871

Bending creep tests on fabricated Al alloy box beams under constant load and temperature using continuous deflection and strain measurement
21 p3842 A69-39309

Short period creep and relaxation in various heat resistant alloys under heat treatments and loads, determining temperature dependence of cyclic thermal instability
22 p3969 A69-40071

Creep stress analysis of circular cylindrical shells under axisymmetric loading, plotting stresses and deformations for various parameters
23 p4233 A69-42352

CRESTATRONS

U TRAVELING WAVE TUBES

CRESTS

U WAVES

CREVICES

U CRACKS

CREWS

U FLIGHT CREWS

U SPACECREWS

CRIMPING

U FOLDING

CRITERIA

Criterion for magnetic plasma stability near magnetic axis, noting parameters for deriving criterion integrand
15 p2658 A69-30265

CRITICAL FLICKER FUSION

Physiological effects of intermittent light stimulation during helicopter flight, discussing visual and electric cortical functions at critical frequency threshold of subjective fusion
13 p2211 A69-28595

CRITICAL FLOW

Boron diffusion in silicon, using nitrogen carrier and boron trichloride diffusant at high temperature for determination of critical oxygen flow rate
02 p0297 A69-11994

Weightlessness effect on critical heat flow during forced motion of water in different kinds of channels
07 p1243 A69-19616

Thin spherical layer flow stability with respect to small disturbances, showing unsteady motion above critical Reynolds numbers and secondary flow features
11 p1875 A69-25486

Gas-liquid critical flows, considering compressibility, rate of momentum, mass and heat transfer, etc
13 p2376 A69-28144

CRITICAL FREQUENCIES

Lunar tidal effects on F 2 critical frequency and height maximum, evaluating variations with altitude
01 p0063 A69-10424

Sporadic E layer boundary frequencies disturbances at midlatitudes, noting solar activity effects, diurnal variations and effect of meteor fluxes
01 p0066 A69-10600

Numerical maps of sporadic E critical frequency for solar cycle maximum and minimum to estimate propagation
01 p0070 A69-11160

Tunnel diode oscillations in switching mode due to sinusoidal voltage excitation, discussing critical applied signal frequency separating switching and oscillation modes
02 p0213 A69-11535

Relation between north-south asymmetry of F 2 region critical frequencies and geomagnetic axis inclination angle, establishing increase in asymmetry during increased solar activity
02 p0237 A69-11662

11-year solar cycle influence on F 2 region critical frequency, investigating correlation coefficient between mean monthly values of F 2 variations and respective sunspot numbers
02 p0238 A69-11680

F 2 layer cut-off frequency predawn increase caused by sunrise, resulting in photoelectrons transfer along force lines at magnetically conjugate point
02 p0238 A69-11681

Ionospheric sporadic E layer reflection duration during solar activity cycle analyzed as function of critical frequency
02 p0207 A69-11684

Sporadic E layer critical frequencies seasonal and diurnal periodic variations, noting independence of solar activity cycle
02 p0239 A69-11685

Computer program for calculating density distribution of deviation of F 2 layer critical frequency from median value
02 p0239 A69-11692

F 2 layer critical frequencies variation coefficients, analyzing variation and root-mean-square deviations in terms of geomagnetic latitude and Wolf number
03 p0422 A69-13514

Diurnal variation of variation coefficient of F 2 critical frequency for steady and unsteady primary ionizing fluxes simulated on computer
03 p0423 A69-13516

Nighttime E layer mean variations noting critical frequencies, electron density and seasonal and solar activity effects at sunset, midnight and sunrise
03 p0398 A69-13899

Ionospheric electron content and slab thickness changes during magnetic storm in June 1965 using Faraday rotation and critical frequencies
05 p0759 A69-16420

Synoptic observations of F 2 layer in magnetically conjugate regions, comparing critical frequencies
06 p0919 A69-17723

Optimum length of Fourier time series approximating diurnal F 2 critical frequency variation on planetary scale
06 p0921 A69-17746

Variation in critical E layer frequencies at large solar zenith angles
06 p0921 A69-17748

Solar eclipse variations of E layer critical frequency explained by quasi-equilibrium between electron density and ionizing soft X ray radiation
07 p1204 A69-18823

Space-time variations for approximating sporadic E layer critical frequencies of geographic and time distribution curves
09 p1486 A69-21547

Numerical decile value maps of sporadic E layer ionization critical frequency for each month of solar cycle minimum and maximum year
10 p1682 A69-23418

Luni-solar tide interpretation in F2 critical frequency based on sum and difference frequencies production by nonlinear atmospheric response to forces
10 p1685 A69-23829

F 2 layer state prediction as function of solar activity by series expansion for describing space-time variations of monthly F 2 medians critical frequencies
10 p1687 A69-23927

Correlation coefficient between changes in F 2 layer critical frequency and sporadic E layer maximum frequency
13 p2254 A69-28330

Relation between north-south asymmetry of F 2 region critical frequencies and geomagnetic axis inclination angle, establishing increase in asymmetry during increased solar activity
13 p2256 A69-28693

11-year solar cycle influence on F 2 region critical frequency, investigating correlation coefficient between mean monthly values of F 2 variations and respective sunspot numbers

13 p2257 A69-28711

F 2 layer cut-off frequency predawn increase caused by sunrise, resulting in photoelectrons transfer along force lines magnetically conjugate point

13 p2257 A69-28712

Ionspheric sporadic E layer reflection duration during solar activity cycle analyzed as function of critical frequency

13 p2224 A69-28715

Sporadic E layer critical frequencies seasonal and diurnal periodic variations, noting independence of solar activity cycle

13 p2258 A69-28716

Computer program for calculating density distribution of deviation of F 2 layer critical frequency from median value

13 p2258 A69-28723

Solar X rays intensity and spectrum effects on E layer critical frequency and D region ionospheric absorption

15 p2677 A69-31346

F 2 critical frequency data at Hawaii for clarifying total electron content data obtained by geostationary satellite measurement of Faraday signal rotation

16 p2779 A69-32196

Space-time variations for approximating sporadic E layer critical frequencies of geographic and time distribution curves

16 p2784 A69-32542

Synoptic observations of F 2 region in magnetically conjugate regions of Kerguelen and Archangel, comparing critical frequencies during magnetic and ionospheric disturbances

16 p2784 A69-32612

Lunar tidal oscillations in F 2 layer critical frequency and F region minimum virtual height at Huancayo during IGY/IGC to study solar cycle effects

16 p2784 A69-32613

Latitude variations of day and night ionospheric critical frequencies, inhomogeneity and ionization, discussing generation of r type sporadic E layer in auroral zone

17 p2964 A69-33963

Magnetic declination effect on F 2 layer critical frequency diurnal variations attributed to vertical ionospheric drift due to neutral air winds

18 p3126 A69-34256

Global distribution of F 2 layer critical frequencies by expanding empirical function of diurnal variations into natural orthogonal components

20 p3521 A69-37051

Predawn F 2 layer critical frequency enhancement at Johannesburg, discussing electron density hump from corpuscular ionization increase

20 p3523 A69-37576

F 2 critical frequency meridional cross sections latitude profiles based on global network ionospheric stations observations, confirming daytime Northern Hemisphere ionization maximum

20 p3526 A69-37661

F 2 region critical frequencies obtained during winter at Northern and Southern Hemisphere stations located in auroral and polar zones, correlating changes with ionization

20 p3526 A69-37665

Seasonal anomaly of F 2 layer critical frequency in Northern and Southern Hemispheres during high and low solar activity, discussing geomagnetic effect

20 p3526 A69-37667

Alouette topside ionograms of ionospheric storms at midlatitudes indicating critical frequencies difference between F 1 and F 2 layers

20 p3532 A69-37894

Critical frequency variations of F 2 layer and M3000/F 2 with sunspot number for 19th solar cycle, noting dependence on geomagnetic latitude

21 p3715 A69-38560

Supercritical frequencies horizontal gradient ducting effects on backscatter sounding of F region magnetic field aligned irregularities

22 p3941 A69-40913

Rectangular waveguide with periodic array of infinitely thin metallic strips, studying intrinsic oscillations critical frequencies and amplitude spectrum

23 p4124 A69-42036

Diurnal variation of Pc type geomagnetic pulsations correlation with F 2 layers critical frequency diurnal variations

23 p4161 A69-42441

CRITICAL LOADING

Paradoxes associated with elastic-plastic limit load analysis of material satisfying Drucker stability postulates

02 p0337 A69-11562

Mechanical properties of free rolling contact surfaces subject to high loads, discussing effect of oil film separation and fatigue crack initiation

02 p0339 A69-11989

Critical loads in elastoplastic buckling of cylindrical shells analyzed using power series

02 p0340 A69-12058

Optimum critical impulse for snap-through of nonlinear dissipative dynamical system of one degree of freedom

[AIAA PAPER 68-143] 02 p0346 A69-12508

Direct matrix method for evaluation of critical loads and buckling modes for nonuniform flexural rigid plates having end and side constraints

03 p0522 A69-12866

Initial deviations or imperfections effects on load capacity of infinite and finite length thin circular cylindrical shells under axial compression

[ASME PAPER 68-WA/APM-22] 04 p0669 A69-14398

Elastic-plastic thin walled cylindrical shell axisymmetric behavior under radial pressure difference, noting load for collapse

[ASME PAPER 68-APM/AA] 04 p0670 A69-14404

Crack propagation near arbitrary curvilinear hole, discussing hole exterior mapping and critical loads for crack initiation

04 p0674 A69-14562

Load carrying capacity of V notched bars under axially symmetric tensile load, verifying influence of distance between two equal notches

04 p0680 A69-15169

Schaefer theory of two parameter eigenvalue problems applied to stability of twisted bars, discussing quick estimate of critical loads

04 p0682 A69-15290

NeoHookean /incompressible solid/ rectangular parallelepiped compressed between lubricated rigid plates, comparing stability bounds with predicted critical loads

04 p0682 A69-15303

Axial buckling load for thin walled circular cylindrical shell, noting design of internal mandrel for control of boundary expansion conditions

05 p0831 A69-15581

Iteration method for determination of critical buckling load for straight rods

05 p0832 A69-15689

Theoretical buckling load for single edge notched struts, discussing brittleness effects

05 p0837 A69-16064

Critical axisymmetric loads for instability in orthotropic multilayer conical shells obeying Hooke law under axial compression or external pressure

05 p0840 A69-16198

Yield point for simply supported conical shell loaded through central boss at vertex

06 p1023 A69-17375

Stress-strain response up to ultimate failure and ultimate strength of laminated composite with nonlinear orthotropic lamina

07 p1170 A69-18710

Compressive strength of boron fiber-epoxy matrix composite, noting matrix support of fibers against buckling

07 p1170 A69-18713

Low speed four-ball lubricating oil testing machine eliminating thermal effects associated with frictional heating for load carrying capacities of thin lubricant films

07 p1140 A69-18968

Large deflection behavior of shallow circular arch subjected to vertical point load by nonlinear Rayleigh-Ritz finite element method, discussing deformation path

08 p1411 A69-20140

Variational method for safety limits of perfectly plastic simply supported conical sandwich shells subjected to uniform internal pressure and obeying Mises yield criterion

08 p1416 A69-20702

Multilayer orthotropic cylindrical shells stability under distributed external load and off-center compression, analyzing subcritical deformation on critical load

09 p1613 A69-21685

Axisymmetric dynamic snap through critical load analysis for elastic clamped shallow spherical shells, considering impulsive and step loads

09 p1616 A69-21977

Multilayer pressure vessel load carrying capacity calculated, using Huber-Mises yield condition to estimate axial force influence

09 p1618 A69-22257

Validity limits of formulas for critical buckling load for oscillating continuous beams found to be elastic buckling

11 p1969 A69-24349

Statistical parameters of critical load distribution in buckling of imperfection sensitive elastic structures, noting probability of failure

11 p1969 A69-24415

Slender elastic rod stability under spatial finite deflection, analyzing critical load by using Kirchhoff analogy and gyroscope motion

11 p1970 A69-24609

Optimal parameters selection for rib-reinforced cylindrical shells determined with respect to axial critical loading magnitude

11 p1985 A69-25173

Critical axial compressive load for cylindrical shells reinforced with longitudinal ribs, noting internal pressure and rib spacing effects

11 p1985 A69-25177

Rectangular aluminum alloy rods carrying capacity under compression loads applied eccentrically to rod ends

11 p1986 A69-25326

Composite shell carrying capacity under general load, studying closing shape between laminate layers, transverse contraction, supporting layers thicknesses ratio, etc

12 p2176 A69-25851

Tensile strength and failure loading evaluation for structure, discussing stresses in neighborhood of crack, crack toughness measurement and fracture mechanics

12 p2176 A69-25861

Three dimensional problems in crack theory for unbounded brittle body, deriving critical loads from limiting equilibrium equation

12 p2178 A69-25997

Dynamic programming method for upper bound on collapse load of rotationally symmetric thin cylindrical shell under ring loading

12 p2179 A69-26214

Load capacity, stiffness and flow requirement of capillary and orifice compensated oil lubricated externally pressurized rectangular thrust bearings

12 p2102 A69-26239

Critical load for anisotropic right-angled isosceles triangular plate stability with large deflections obtained from differential equation

12 p2180 A69-26270

Postcritical deformations of thin conical elastic shells hinged along edges under external pressure using Pogorelov method for cylindrical shells

12 p2181 A69-26609

Equilibrium paths in initial postbuckling of elastic structural systems, discussing stability boundaries and relationships between imperfections and critical loads

13 p2359 A69-27261

Radial and polar load support of squeeze film gas bearing in form of sphere pulsating radially or moving along polar axis

[ASME PAPER 68-LUBS-3] 13 p2266 A69-27279

Orthotropic cylindrical shell stability under uniform axial compression and internal pressure, taking into account subcritical state duration

14 p2532 A69-28981

Rigid supporting ribs effect on annular plate critical loading, stability loss and buckling

14 p2533 A69-28983

Heterogeneous orthotropic circular cylindrical shell stability during axial critical compression

14 p2533 A69-29024

Steady natural oscillations of unbounded brittle plane with cut under edge load, showing decreased critical load in presence of inertial effect

15 p2703 A69-30050

Three dimensional problem in crack theory for brittle body, determining stress concentration and critical loads

15 p2708 A69-30658

Oscillating beams lateral buckling allowing for torsional stress in determining critical load

15 p2712 A69-31015

Load carrying capacity of circular plates under axisymmetric load

16 p2875 A69-32289

Critical loads and stability loss forms of annular plates flexibly clamped at edges in uniform stress field
17 p3057 A69-33197

Discrete element displacement method applied to buckling analysis of flat rectangular plates under arbitrary membrane loading, calculating critical load intensities
17 p3066 A69-34048

Critical stresses and crack development near holes in compressed elastic plate
18 p3218 A69-34603

Stability loss of shells of revolution under axial tension and radial pressure, considering shells of Gaussian curvature, calculating critical force
18 p3222 A69-34976

Initial deflection effect on elastic cylindrical shell stability under compression, finding critical load by determining limiting point in successive loading
18 p3224 A69-35319

Long term stability of orthotropic cylindrical shells under transverse shear stresses, calculating critical stress using Kirchhoff-Love model
18 p3225 A69-35357

Isotropic plate critical strength measurements, evaluating role of material shear modulus
18 p3225 A69-35361

Limiting equilibrium of infinite brittle body weakened by internal plane elliptical crack, determining critical loads and stresses at crack
18 p3226 A69-35379

Variational method for computer calculation of supercritical bending of thermoelastic uniformly loaded circular plates, determining Ritz parameter influence on accuracy
19 p3434 A69-35829

Homogeneous heat flux effect on limit load of isotropic plate with rectilinear through crack, noting conditions for crack propagation
19 p3441 A69-36744

Critical buckling loads for uniform compression of clamped or simply supported parabolic and semielliptic plates
20 p3622 A69-37223

Laminated composites ultimate strength prediction based on consecutive yield procedure with step-wise reduction of strength or load-carrying capacity used as design criterion
20 p3627 A69-37773

Automated device for load carrying ability of structural elements like gas turbine blades under thermal and mechanical cyclic loads
20 p3544 A69-37816

Curved beams ultimate strength using angular velocity considerations for collapse load
20 p3629 A69-38031

Load carrying capacity of orthotropic circular cylindrical shell under uniformly distributed normal load, considering edge support conditions
20 p3629 A69-38075

Noncircular curved shell stability under axial compression, using strain energy method to determine upper and lower critical stresses
21 p3834 A69-38715

Elastic closed and truncated conical shell stability with initial deflections under dynamic critical loading
21 p3834 A69-38716

Stability of unbounded homogeneous brittle body containing circular planform crack, determining elastic stresses and critical load by macrocrack propagation theory
21 p3839 A69-39195

Galerkin method application to solve differential equation and boundary value conditions for elastic stability of bars, showing linear relation between critical loads
21 p3845 A69-39678

Serrated yielding at high temperatures from dislocation theory viewpoint, considering critical strain relation to temperature and strain rate
21 p3749 A69-39710

Cylindrical shell load carrying capacity under axial compression, considering middle surface initial distortions influence
23 p4228 A69-41899

Space frame radome model elastic buckling tests for load deflection and maximum load predictions, considering individual beam failure and complex instability
23 p4232 A69-42143

Collapse load of shallow conical shells clamped at base and loaded through finite rigid boss, using Tresca yield condition for sandwich shell
23 p4236 A69-42496

Shallow spherical sandwich shells critical buckling loads using differential pressure method
24 p4396 A69-42734

Limiting load of square plate subjected to shear and reinforced by vertical stiffener, computing membrane and bending stresses as function of flexural rigidity
24 p4399 A69-42967

FAA power spectral gust methods for computing design limit loads on commercial aircraft, noting British investigation
24 p4253 A69-43111

CRITICAL MACH NUMBER
U MACH NUMBER

CRITICAL MASS
Critical density ratio concept introduced into cosmological models for matter concentration into galaxies in expanding universe
08 p1381 A69-19794

Resonant long-period orbits around Lagrange equilateral points for critical mass ratio of main bodies
13 p2346 A69-27706

Fast neutron spectrum for subcritical section of homogeneous U 235-polyethylene thermionic critical assembly measured by pulsed source time-of-flight method
18 p3170 A69-34313

CRITICAL PATH METHOD
Civil transport aircraft power plant and auxiliary systems as sources of delays, presenting critical path analysis
17 p2898 A69-33213

CRITICAL POINT
Critical state model of type 2 superconductor taking account of critical current on magnetic field and surface sheath currents, evaluating flux penetration, hysteresis, AC losses, etc
02 p0298 A69-12030

Critical points separating stable and unstable branches of equilibrium curve of nonlinear elastic systems, discussing flexible shallow conical shell in temperature field
02 p0341 A69-12256

Velocity of 1 MHz sound waves in He 4 along isotherms just above critical temperature, noting specific heat ratio for 4.5 and 5 K isotherms
06 p0957 A69-17142

Critical conditions in spherical reacting mass, noting oscillatory nature of critical parameters in truncated Arrhenius rate on basis of nontruncated form
11 p1998 A69-24480

Critical diameter of ammonium perchlorate stable detonation as function of initial temperature, water content, density and particle size
11 p1940 A69-24553

Gravitational effects on thermodynamic variable equilibrium composition of liquid-vapor binary mixtures near critical point, discussing changes in phase with altitude
11 p1999 A69-24914

Specific isochoric heat capacity of pure fluids, considering thermal equation of state, vapor pressure and boundary conditions at critical point
11 p2001 A69-25201

Thermodynamic properties of materials in critical region, discussing inhomogeneity
11 p2003 A69-25440

Heat transfer coefficients for carbon dioxide near thermodynamic critical point for flow through electrically heated duct, noting turbulent forced convection as mechanism
[ASME PAPER 68-HT-32] 13 p2373 A69-27769

Double light scattering near critical point, examining angular distribution
14 p2482 A69-28738

Light scattering in single component systems near critical point analyzed by critical phenomena classical theory and Rayleigh theory
14 p2485 A69-28995

Faraday effect for magnetic properties of chromium tribromide along various isotherms near critical point, confirming scaling laws
15 p2668 A69-30686

Self ignition of solid/fluid particles suspended in gas flow, discussing heat transfer coefficient, critical temperatures, etc
17 p3070 A69-33142

Existence conditions of critical points for autonomous differential equations in bounded flows
22 p3975 A69-40571

Laser produced Sb and Te vaporization near critical point, using time of flight mass spectrometer
22 p3993 A69-40719

Critical transition temperature of vanadium oxide semiconductors as function of doping element content and lattice constant, using X ray diffraction
23 p4198 A69-41564

Postbuckling analysis by equilibrium solutions of conservative system near critical point, considering stability failure in elastic structure under increasing load
24 p4396 A69-42730

Solution stability and secondary solutions growth beyond critical points investigation for Burgers equations for laminar-turbulent transition
24 p4302 A69-43360

CRITICAL PRESSURE

Critical internal pressure induced plastic instability in membrane shells of revolution determined by graphical numerical method
02 p0338 A69-11719

Hydromagnetic plasma stability in infinite electrical conductivity approximation applied to smooth closed systems, discussing ballooning instability mode
06 p0965 A69-17519

Reinforced cylindrical shell stability under external compression load by pressurized air, determining critical pressure
15 p2715 A69-31204

Correlation coefficient of light fluctuations measured in Ar plasma in positive column of glow discharge, noting ionization wave appearance at critical gas pressure
16 p2822 A69-32039

Stability of thin walled eccentrically reinforced cylindrical shell, determining eccentricity influence and critical pressure formula from considerations of Poisson ratio, reinforcement parameters, etc
18 p3216 A69-34576

Boundary conditions of orthotropic shell stability under external pressure and axial tension, analyzing critical pressure by strain energy method
18 p3222 A69-34977

Thin cylindrical pressure vessels with circular cutouts and radial branches, observing limit pressures during plastic deformation
20 p3629 A69-38027

Cylindrical shell stability during loading by uniform external pressure represented by Fourier series, determining critical pressure by solving nonlinear equations
21 p3846 A69-39715

Vapor pressure measurements on liquid fluorine from triple to critical point at one degree K intervals [NAS-NRC PAPER H-2]
22 p3998 A69-40624

Critical oxygen pressure dependence on buffer in diluted heart muscle sarcosine suspensions and effect of hemoglobin or myoglobin
23 p4080 A69-41427

Bubble flow evolution at various pressures up to critical value [ASME PAPER 69-HT-30]
24 p4411 A69-43529

CRITICAL REYNOLDS NUMBER
U REYNOLDS NUMBER

CRITICAL TEMPERATURE
Vanadium-gallide alloys critical temperature of transition into superconducting state determined by measuring cast alloy samples magnetic permeability
03 p0483 A69-13023

Critical body temperature for intracranial self stimulation in white rats
03 p0375 A69-13897

Velocity of 1 MHz sound waves in He 4 along isotherms just above critical temperature, noting specific heat ratio for 4.5 and 5 K isotherms
06 p0957 A69-17142

Film and transition boiling as functions of critical temperature, discussing role of heat transfer and vapor production
11 p1997 A69-24458

Niobium aluminide-niobium germanide alloys superconductivity and heat treatment influence on critical temperature
13 p2316 A69-27659

Superconductive tunneling measurements on thin Al films, discussing enhanced transition temperatures, energy gap dependence on temperature, electron microscope observation of crystallites, etc
16 p2825 A69-31634

P-V-T surface of fluids in critical region by dielectric measurements, presenting saturation densities of oxygen [NAS-NRC PAPER H-5]
22 p4050 A69-40623

Time dependent differential equation for order parameter in superconductors near critical temperature derived from density matrix equations
22 p3994 A69-41053

Graph analytical method for calculating heat transfer in diathermic exchangers during boiling together with critical thermal loads
24 p4408 A69-43080

CRITICAL VELOCITY

Flutter vibration in subsonic flows, analyzing critical velocity for membrane and damping destabilizing effects in nonconservative system

02 p0192 A69-12825

Critical end-on impact velocities calculated for reentering solid and granular radioisotopic fuel rods with solid and granular earth materials

04 p0630 A69-14800

Critical electron drift velocity threshold in surface wave amplification in semiconductor in magnetic field, noting partial effect of diffusion

05 p0810 A69-16648

Gyrostatic moments effects on critical angular velocities of varying and constant cross section rigidly and elastically supported hinged rotors

09 p1567 A69-21384

Angular inertia of lubricant in MHD hydrostatic thrust bearings, obtaining critical angular speed of rotor

09 p1503 A69-21443

Axial torque effect on critical speeds of continuous rotor with motion described by partial differential equations

[ASME PAPER 69-VIBR-52]

10 p1804 A69-24152

Critical speeds of multiple disk rotors with multiple supports, discussing continuous shaft sections including gyroscopic and transverse shear and rotary inertia effects

[ASME PAPER 69-VIBR-51]

10 p1804 A69-24153

Rotor shaft mounted on number of bearings and carrying masses and inertia angular precession and critical speeds, considering gyroscopic moments, rotary inertia and shear deformation

[ASME PAPER 69-VIBR-54]

10 p1805 A69-24154

Undamped rigid rotor critical speed analysis for firm and flexible foundations, discussing effect of center of gravity and rotor shapes

[ASME PAPER 69-VIBR-49]

10 p1808 A69-24184

Second approximation of asymptotic damping of disturbances in viscous heat conducting gas supersonic flow about solid of revolution at critical velocity

11 p1817 A69-24627

Rotor angular velocity and flexural strain interdependence at critical velocity

11 p1987 A69-25390

Critical rotation rates of homogeneous shaft with two bearings under tension, considering shaft mass, stretching force magnitude and console disk gyroscopic effect

13 p2269 A69-28323

Unbalance effects on rigid naval turborotor on oil film bearings in flexibly mounted housings investigated at varying critical speeds and housing stiffness

[ASME PAPER 69-DE-9]

14 p2453 A69-28839

Critical speeds of high speed turbine rotors running in friction bearings determined by varying natural frequencies of rotor and supports

18 p3147 A69-34545

Turbine disks stress-strain state, using wire strain gauge to determine residual strains, radial and tangential stresses as function of disks rpm

19 p3436 A69-35850

Nadai and Zyczkowski stress analysis for Tresca yield condition reexamined for determination of critical angular velocity of solid elastic perfectly plastic disk

23 p4235 A69-42480

CROCCO METHOD

Equations governing steady diabatic gas flows in Crocco velocity vector field, discussing changes in total pressure

21 p3695 A69-39007

CROSS CORRELATION

Doppler signal envelope cross correlation coefficient in two channel system, determining mutual density distribution for envelopes

01 p0032 A69-10887

Closed form solution for two input correlator processing gain with error function transfer characteristics and operating in Gaussian environment

03 p0403 A69-13253

Diversity antenna continuous short wave radio signal envelope distribution, autocorrelation functions, damping rate and cross correlation coefficients

03 p0394 A69-13522

Cross correlation function for two sequences of pulses arbitrarily distributed in time, noting noise stability of diversity reception systems

04 p0557 A69-14790

Multichannel HF resolution spectral analyzer of pulses reflected from ionosphere applied to dependence of cross correlation coefficient on frequency separation

06 p0897 A69-17740

Radar signal cross correlation function calculation with reference function, applying acousto-optical modulator

10 p1694 A69-23539

Drift elimination in linear system identification using binary m-sequences by crosscorrelating over two periods of output

11 p1834 A69-24547

Real time correlator in periodic signal extraction from noise background, discussing multichannel sampler as special case of cross correlation extraction

11 p1837 A69-25094

Laser emission noise and voltage noise cross correlation coefficient for CW GaAs laser diodes at 77 K, noting strong dependence on bias current

12 p2038 A69-26328

Autocorrelation and cross correlation analysis of rapid density variations in F region determined from satellite deceleration and geomagnetic data

12 p2069 A69-26436

Doppler signal envelope cross correlation coefficient in two channel system, determining mutual density distribution for envelopes

12 p2031 A69-26651

Drift correction schemes for periodic cross correlation comparison unification and extension

15 p2564 A69-30169

Universal transfer function computer based on synchronous spectrum analyzer having outputs combined in cross spectrum correlation computer to yield plot in Code form

15 p2615 A69-31282

Cross correlation methods for determining systems time domain response adapted to communications channel evaluation, discussing computer simulation of on-line testing

16 p2750 A69-31757

Remote sensing cross-beam cross correlation methods of determining spatially resolved average thermodynamic properties

16 p2789 A69-31868

Radio sources interplanetary scintillations and cross correlation coefficient real time determination

17 p3038 A69-33727

Cross correlation and probability metric in coded sequential detection telemetry system, giving optimum parameters, overflow and error probabilities using computer simulations

19 p3273 A69-36266

Quadrupole self and cross correlations of directional jet noise patterns, including frequency spectra and corrections

22 p3931 A69-40891

CROSS COUPLING

Strapdown gyros in back to back connection for reduction of component cross coupling errors

04 p0603 A69-15473

Time domain synthesis of multivariable automatic control with predetermined output signal shape, allowing for internal cross coupling effects

05 p0737 A69-15887

Multimode direction tracking with polarization tracker used simultaneously, analyzing cross coupling and conical horn/reflector antenna

06 p0888 A69-17652

Longitudinal structural vibration and lateral bending response mass and spring coupling in Saturn AS-502 during boost with longitudinal excitation by pogo effect

06 p1019 A69-18204

Trajectories of roots of two channel systems with antisymmetric cross couplings using geometrical and analytical methods, noting hodograph

21 p3686 A69-38886

CROSS RELAXATION

Finite cross relaxation rate effect on spectral distribution in CW laser oscillator output with inhomogeneous broadening, noting population inversion distribution

05 p0776 A69-16327

Cross relaxation and spin-lattice relaxation probabilities determination in ruby crystal based on inversion coefficients

06 p0980 A69-17458

Trivalent iron doped andalusite crystals dielectric and maser properties, investigating spin-lattice relaxation, cross relaxation times and inversion ratio

07 p1150 A69-19049

Cross relaxation and spin-lattice relaxation probabilities determination in ruby crystal based on inversion coefficients

20 p3584 A69-37941

CROSS SECTIONS

Torsion of variable cross sectional thin walled bars using shell theory equations

02 p0337 A69-11559

Effective cross section of resonant cesium ions charge exchange determined by retarding field method, considering dependence on ion velocity

06 p0959 A69-16908

Potassium ion resonant charge exchange, determining relation between effective cross section and ion velocity, using retarding field method

06 p0959 A69-16909

Charge exchange cross sections in methane and ammonia, noting dissociative charge exchange role

06 p0884 A69-17114

Rereflected shock waves behind tapered shock tube section indicated by shock wave detectors, microwave absorption and optical emission measurements

18 p3085 A69-34474

Stellar nuclear reactions at low energies studied to provide predictions of cross sections in carbon burning

20 p3612 A69-38164

Macroscopic rate coefficient relation to microscopic chemical reaction cross section, discussing microscopic reversibility and balance

23 p4113 A69-41519

CROSSED FIELD AMPLIFIERS

Permanent magnets used in conjunction with magnetrons, crossed-field amplifiers, klystrons, traveling wave tubes and microwave ferrite devices

01 p0045 A69-10713

Crossed field backward wave tubes gain with stepwise varying interaction space found greater than with constant height interaction space

13 p2237 A69-28583

Reflex klystron with closed electron flux in crossed electric and magnetic fields permitting interless frequency returning

21 p3682 A69-39128

CROSSED FIELD GUNS

Ionization and current growth in discharge in rotating plasma device with mirror shaped magnetic field

09 p1552 A69-22042

Noise fluctuations transport in convergent flow crossed field electron guns using Monte Carlo method for two dimensional computerized gun simulation

15 p2572 A69-30031

CROSSED FIELDS

Signal to cross modulation noise ratio in TWT tube during amplification of sinusoidal signals

01 p0031 A69-10780

Cross field plasma instability resulting in charge density irregularities shown to meet requirements for ionospheric irregularities model

01 p0073 A69-11178

Overheated semiconductor plasma instability in crossed electric and magnetic fields, deriving condition for occurrence

02 p0298 A69-12099

Tunnel diodes current voltage characteristics in crossed electric and magnetic fields, observing tunnel current decrease in GaSb

02 p0300 A69-12634

Transport phenomena in crossed electric and strong magnetic fields, developing semiclassical and quantum treatments

03 p0473 A69-12926

Heat transfer in crossed field MHD Couette flow for incompressible fluid, assuming linear wall temperature in flow direction

03 p0476 A69-13306

Dispersion equation for electron-ion and electron-hole plasma linear oscillations in crossed electric and magnetic fields

03 p0480 A69-14134

Cross field energy transfer in collisionless plasma across earth magnetospheric boundary, using computer and one dimensional sheet model simulation

06 p0916 A69-17023

Time rates for growth and damping of resistive instability in gaseous plasma in crossed electric and magnetic fields

08 p1369 A69-20886

Partially ionized plasma oscillations in crossed magnetic and electric fields, noting role of LF particle collisions

08 p1370 A69-21079

Scattering and transformation of electromagnetic waves in plasma in crossed electric and magnetic fields showing radiation spectrum maxima due to ion-acoustic oscillations propagation

08 p1277 A69-21080

Plasma conductivity tensor components in crossed fields calculated by Boltzmann kinetic equation, noting influence of magnetic field presence
09 p1546 A69-21565

Quantum oscillations of magnetization, undamped magnetoplasma waves development and sound amplification by electron drift in crossed fields observed in semimetals
09 p1556 A69-21615

Signal to cross modulation noise ratio in TWT tube during amplification of sinusoidal signals
10 p1653 A69-23109

Ionization front propagation rate in crossed electric and magnetic fields in Ar-Cs, Hg-Cs and Ne-Xe discharge plasmas
10 p1733 A69-23447

Instabilities in K seeded Ar plasma in crossed electric and magnetic fields and with nonequilibrium ionization, noting effects on MHD generator characteristics
10 p1734 A69-23457

Mercury cesium plasma in crossed electric and magnetic fields as working fluid of MHD generators based on Rankine cycle
10 p1636 A69-23458

Weakly ionized gas in crossed electromagnetic fields, formulating Ohm law from Ginzburg equations
11 p1925 A69-24319

Boundary layer calculation during laminar MHD channel flow under crossed magnetic and electric fields using successive approximation method
11 p1932 A69-25491

Chain mechanism of arc discharge development in crossed electric and magnetic fields explained by direct ionization of neutral particles by ions
11 p1932 A69-25540

Two beam electron flux instability in crossed magnetic and inhomogeneous electric fields using linearized hydrodynamic and Lagrangian formalism approximation
12 p2133 A69-26714

High speed photographic study of plasma luminescence front and charged particle concentration front counter to electrodynamic force in crossed electric and magnetic fields
12 p2141 A69-27130

Transient heat transfer in formation of steady crossed fields MHD plane Couette flow for walls, giving momentum, induction and energy equations
13 p2375 A69-27791

Linear approximation of electron temperature increment and electron mobility in nondegenerate polar semiconductor in crossed fields
14 p2508 A69-29662

Current distribution and Hall voltage in crossed fields discharge with split electrodes in nonequilibrium Ar and Cs plasmas
15 p2663 A69-30980

Nonlinear theory of $E \times B$ instability for weakly ionized plasma in presence of density gradient and parallel electric field perpendicular to magnetic field
16 p2819 A69-31682

Linearized Boltzmann equation in kinetic theory for weakly ionized plasma electrons under alternating electric and circularly polarized magnetic field, noting higher harmonics generation
16 p2820 A69-31752

Electron distribution function for weakly ionized plasma under alternating electric and circularly polarized rotating magnetic field, noting cyclotron resonance
16 p2820 A69-31753

Charge density irregularities of midlatitude ionospheric E region related to cross field plasma instability noting turbulence
16 p2773 A69-31972

Polarization operator and Green function of photon for propagation of plane electromagnetic waves in constant crossed field, noting refractive indices
18 p3103 A69-35128

Interaction between two temperature plasma flux and electrodes in MHD channel with crossed electric and magnetic fields, studying boundary layer dynamics
22 p3991 A69-41022

Crossed inhomogeneous electric and magnetic fields effect on H plasma fluxes dynamic behavior, deriving plasma motion formula
24 p4358 A69-43475

Electric arc stabilization in crossed convective and magnetic fields, discussing column slanting relationship to widening near downstream electrode
[AIAA PAPER 68-709] 24 p4359 A69-43572

CROSSLINKING
NT VULCANIZING

Low density polybenzimidazole composites as ablative heat shields, discussing arc-heated wind tunnel tests of linear and crosslinked structures
23 p4179 A69-41715

CROSSOVERS
Correlation of overshoot with gain crossover frequency, phase crossover frequency, phase margin and velocity error constant for linear feedback control systems
02 p0225 A69-12026

Tracking system for gain and time delay parameter measurements of compensatory control crossover model
12 p2022 A69-25930

CROSSTALK
NT IONOSPHERIC CROSS MODULATION
Diffractional crosstalk in optical beam waveguide during simultaneous multibeam transmission arising from beam coupling by aperture diffraction
07 p1100 A69-18648

Compatibility requirements and considerations of range telemetry tape crossplay operations, discussing major classes
07 p1133 A69-19117

Waveform distortion resulting from adjacent channel crosstalk and from amplitude and phase nonlinearity in channel filters in DSB/SC telemetry link
07 p1083 A69-19130

Critical signal assignments optimization in electrical/electronic connectors, considering bent pins, signal cross talk, adjacency requirements and corona
19 p3284 A69-36030

CROWDING
Environmental crowding effect on individual and group behavior in rat colony, using implanted passive resonant circuits for identification and passage information
19 p3257 A69-36243

CRUCIFORM WINGS
Pressure coefficients determination on slender body surface to estimate effects of quadratic terms, considering body of revolution with thin cruciform lifting surfaces
10 p1632 A69-22911

Conical flow past cruciform wing-body and tail-body systems, considering various positions of leading edges with respect to Mach cone
15 p2548 A69-31002

High order conical motions past cruciform wing-body and tail-body systems, reducing problem to flow past cruciform wing
15 p2548 A69-31023

CRUDE OIL
Petroleum sulfides advantageous effect on oxygen consumption during combustion
07 p1202 A69-19456

Viscosity-temperature chart for hydrocarbons permitting linear extrapolations into low viscosity high temperature regions
10 p1753 A69-23975

Sediments and crude oils analyzed for fatty acids, considering abiological or bacterial origin of acids
20 p3523 A69-37538

CRUISING FLIGHT
Aircraft and engine parameters for maximum theoretical range of turbojet for given cruising speed
03 p0366 A69-12950

Optimum cruise altitude, block time and fuel relations for Convair 600/640 aircraft for various temperatures, segment distances and weight
08 p1255 A69-21007

Supersonic flight altitude stability, studying effects of velocity, lift-drag ratio, thrust law, wind direction, engine unstarts, etc
[AIAA PAPER 69-813] 19 p3366 A69-35627

Thermal control of Mars entry capsule with fiberglass honeycomb sandwich shell analyzed with and without aft thermal curtain, emphasizing cruise-flight phase
[AIAA PAPER 68-1082] 19 p3429 A69-35949

Mariner attitude control system limit cycle operation during cruise, noting variation from ideal case to single side operation
[AIAA PAPER 69-844] 21 p3822 A69-39374

In-flight test to determine variation effects in bank angle control parameters on cruise flight handling qualities, considering spiral stability
[AIAA PAPER 69-893] 21 p3648 A69-39425

Sonic boom signatures produced by diverse SST configurations during cruise, indicating aircraft length as overpressure limit factor
24 p4253 A69-43661

CRUSTS
U EARTH CRUST

U LUNAR CRUST
CRYODEPOSITS

Test model thermal balance in space simulator, measuring effects of solar simulator irradiance reflected from carbon dioxide cryopanel deposits
[AIAA PAPER 69-1012] 22 p3922 A69-40385

CRYOGENIC EQUIPMENT
Calibration of pressure transducers in liquid hydrogen to liquid helium temperature range using cryogenic test equipment
01 p0080 A69-10300

High pressure transfer system to deliver liquid hydrogen to testing equipment and liquid hydrogen/liquid oxygen engines
01 p0013 A69-11145

Cryogenic plants for space simulation chambers, examining processes for cooling shroud below 100 K at given temperature differences
01 p0057 A69-11154

Cryopump design suitable for attachment as replacement for diffusion or ion pumps
01 p0088 A69-11155

Resonant interaction of radiation from liquid nitrogen cooled ruby laser with ruby crystal in temperature range 4.2-100 K
04 p0611 A69-14439

Soviet papers on apparatus and machines of oxygen and cryogenic installations covering film boiling, gas vessel, thermal design, etc
04 p0686 A69-15160

Helium cryostat designed to operate under overload and vibrations and used for cooling onboard superconducting devices of Cosmos 140 satellite
04 p0585 A69-15407

He refrigerators, noting 4 K design for large scale fixed installations and 20 K small scale design for airborne applications
05 p0704 A69-15671

Thermal losses in thermal regenerators used in cryogenic refrigerators
[ASME PAPER 68-WA/PID-2] 05 p0706 A69-16163

Low temperature thermometer based on temperature dependence of frequency of F-19 nuclear magnetic resonance in antiferromagnetic manganese difluoride
06 p0927 A69-17703

InAs thin film sensors using Hall effect to measure magnetic fields at cryogenic temperatures
10 p1696 A69-23717

Cryogenic applications including maser amplification, IR detection and superconductivity, discussing systems optimization and cost reduction
10 p1665 A69-24017

Gallium arsenide thermometer calibration in 1 to 100 K range using interpolation formula derived from p-n junction diode equation
12 p2093 A69-26484

Problem areas within cryogenic chemical and nuclear propulsion systems for space missions, noting available technology and limitations
[AIAA PAPER 67-454] 12 p2174 A69-26782

Thermal losses in thermal regenerators used in cryogenic refrigerators
[ASME PAPER 68-WA/PID-2] 13 p2203 A69-27421

Cryogenic heat exchanger design and application including vaporizers, recuperators, regenerators, reversing exchangers, nonsteady state flow and thermoelectric techniques
17 p3074 A69-33681

Forming and heat treatment process for stainless steel pressure containers using liquid N, discussing austenite-martensite transformation role
18 p3161 A69-34605

Possibility of combining individual yttrium ferrite single crystals to obtain noninteracting element for quantum paramagnetic traveling-wave amplifier operating at liquid nitrogen temperature
19 p3334 A69-35883

Adaptor for Debye-Scherrer powder camera to take high quality photographs even at liquid N temperature
19 p3313 A69-36493

Silicon junction radiation detectors applications in cryogenics, measuring junction response to beta particles at low temperatures
20 p3546 A69-38275

CRYOGENIC FLUID STORAGE
NASA LOX and liquid hydrogen barges, discussing storage tank design, acceptance testing and operating conditions
01 p0056 A69-11150

- Mass spectrometer helium leak testing of cryogenic storage vessels, noting procedures and insulation and evacuation of jacket space 02 p0252 A69-11811
- Safety planning for use of reactive cryogenics in large volume, noting FLOX and liquid fluorine 04 p0645 A69-14468
- Thermal design and test for liquefied gas vessels under unsteady insulation cooling conditions 04 p0687 A69-15162
- Electric field influence on fluid oscillation modes for Kortweg-Helmholtz force density on incompressible dielectric liquid immersed in electric field 04 p0591 A69-15504
- Cryogenic flexibility of thin polymeric film plies for use as spacecraft positive expulsion bladders 05 p0769 A69-16486
- Glass, boron and graphite filament wound resin composites and liners for cryogenic pressure vessels 05 p0785 A69-16488
- Thermal protection system optimization for storage of cryogenic propellants in space, noting vented systems [AIAA PAPER 69-27] 06 p1039 A69-18211
- Cryostat design, discussing vapor and radiation shielding, construction and insulation materials, safety features, cost considerations, etc 10 p1810 A69-24015
- Liquid helium vented and nonvented storage container design and handling techniques 10 p1810 A69-24016
- Thermal insulation for cryogenic storage in space, discussing Apollo service module conversion to cryogenic service module 12 p2175 A69-26827
- Refrigeration system for space flight use of cryogenic gas storage, suggesting mission time increase 15 p2587 A69-30395
- Back pressure control system for heat leak evaluation tests of cryogenic containers, discussing component selection and error analysis 15 p2702 A69-30397
- Aluminum nonheat-treatable alloys cryogenic vessels welding, considering TIG, pulsed arc and MIG processes with respect to plate thickness, joint and accessibility 15 p2630 A69-31210
- Physical and physiological hazards of cryogenic liquids, emphasizing fire and explosion problems associated with storage and handling 17 p3017 A69-33684
- High strength austenitic Cr-Mn-Ni steel applicability to welded pressure vessels for cryogenic fluid storage, discussing operating temperature stability, weldability, etc 23 p4175 A69-41475
- Optimal design and materials for cryogenic storage of O and H on lunar surface [AAS PAPER 69-051] 24 p4296 A69-42882
- Sprayable polyurethane foam external insulation for liquid hydrogen and oxygen storage aboard Saturn S-2 booster 24 p4337 A69-43453
- CRYOGENIC FLUIDS**
- NT FLOX
- NT LIQUID HYDROGEN
- NT LIQUID OXYGEN
- NT SOLIDIFIED GASES
- Ball bearings lubrication and wear in cryogenic hydrogen turbopumps by transfer films provided from self lubricating cage 01 p0084 A69-10109
- Cryogenic expansion to pressures below triple point and resulting formation of solid-vapor mixtures, discussing flow and heat transfer characteristics in heated tubes 01 p0176 A69-11146
- Bearing lubrication at low temperature, examining safety limits, working fluid in liquid or gaseous state [IME PAPER 9] 07 p1138 A69-18565
- Heat exchangers in cryogenic fluids in free and forced convection, discussing measurements in liquid H, D, Ne and N 08 p1420 A69-19914
- Heat and mass transfer between cryogenic fluid and superheated wall, analyzing experimental data 11 p1996 A69-24228
- Cryogenic liquid level temperature transducer with radiantly heated thermocouple sensitive element 17 p2975 A69-33670
- Phase equilibrium apparatus for measurement of thermodynamic properties of cryogenic fluid mixtures, including argon-methane data [NAS-NRC PAPER H-3] 22 p3947 A69-40630

- Dielectrophoretic zero gravity cryogenic liquid expulsion using lightweight high voltage ribbon electrode conduits and electrohydrodynamic bang-bang field effect 24 p4300 A69-43237
- CRYOGENIC MAGNETS**
- Cryogenic solenoids with pure Al conductor for production of strong magnetic fields, discussing softness and strain resistivity problems 12 p2016 A69-26497
- Variable voltage DC power supplies for energizing cryogenically cooled and superconductive electromagnets 12 p2017 A69-26498
- Manufacturing ultrahigh purity aluminum strip for cryogenic magnets, discussing ingot preparation, rolling, chemical milling and cleaning, arc welding, annealing and sampling 19 p3318 A69-35541
- CRYOGENIC ROCKET PROPELLANTS**
- Safety planning for use of reactive cryogenics in large volume, noting FLOX and liquid fluorine 04 p0645 A69-14468
- Radioisotopic propulsion stage design with liquid hydrogen working fluid, stressing tank insulation and hydrostatic flight behavior 05 p0811 A69-15595
- Inflatable solar shields for thermal protection of space vehicles utilizing cryogen propellants 06 p1017 A69-17609
- Thermal protection system optimization for storage of cryogenic propellants in space, noting vented systems [AIAA PAPER 69-27] 06 p1039 A69-18211
- Film cooling design criteria for small rocket engines [AIAA PAPER 68-617] 09 p1570 A69-21978
- Impingement pressure analysis associated with two phase cryogenic propellant venting to space environment [AIAA PAPER 69-571] 16 p2869 A69-32753
- Slush hydrogen for spacecraft propulsion, discussing fabrication, conservation and storage 17 p3017 A69-33339
- Liquid oxygen and hydrogen rocket engine HM4 design and operation, discussing fuel, low temperatures and heat exchange 17 p3020 A69-33345
- Hydrogen fluoride corrosive effects in cryogenic propellant, emphasizing contamination by particulate matter from corrosion products 21 p3783 A69-39486
- Cryogenic core concept for flexible and economical delivery system [AIAA PAPER 68-812] 21 p3827 A69-39753
- Hydrostatic bearings analysis for high pressure cryogenic rocket engine turbopumps to predict steady state and time dependent performance, noting turbulence, inertia and compressibility 22 p3955 A69-40408
- CRYOGENIC STORAGE**
- Model describing outflow of cryogenic propellant tank pressurized by pressurizing gas, predicting pressurant mass, gas and wall temperature distribution, inlet flow rate, etc 01 p0163 A69-11147
- Spacecraft single wall cryogenic storage system, discussing cost, pressure vessel and components, thermal and performance characteristics 24 p4393 A69-43045
- CRYOGENICS**
- NT CRYOGENIC MAGNETS
- Cryogenic engineering - Conference, Brighton, England, May 1968 01 p0056 A69-11144
- Low temperature microwave thermal noise standard, discussing waveguide termination, cryogenic cooling and temperature and pressure controls 02 p0211 A69-12446
- Freeze-out characteristics of MOS varactor, noting impurity effects and compensation 05 p0806 A69-15809
- Cryogenic properties of polymers - NASA/Case Conference, Cleveland, April 1967 05 p0784 A69-16485
- Thermal expansion of polymers at cryogenic temperatures 07 p1172 A69-19730
- Silicon dioxide glass thermal conductivity at very low temperature 09 p1493 A69-21426
- Surface charge exchange in metal oxide silicon capacitors generated at low temperatures by surface state free carrier trapping 10 p1744 A69-23179

- Cryogenic Technology - Conference, Chicago, June, 1967 10 p1810 A69-24014
- Cryogenic conductive heat transfer in solids, low temperature insulation and liquid-vapor interfaces, discussing boiling heat transfer, injection cooling and frost formation 11 p1998 A69-24461
- Specific heat of electron gas at temperatures approaching absolute zero, using method of displacements and collective variables 11 p1927 A69-24918
- Heat pipe boil-off control system for reducing cryogenic boil-off during long term space storage 12 p2191 A69-26793
- Temperature effects on fracture of various alloys, presenting strength and toughness values tested at cryogenic temperatures 17 p2990 A69-33567
- Cryogenic technology applications - Conference, Chicago, June 1968 17 p3006 A69-33679
- Radiative and conductive heat transport mechanisms at cryogenic temperature applicable to thermal energy transport minimizing technique in containment system 17 p3074 A69-33680
- Low pressure and background radiation conditions via cryogenically cooled surfaces, citing data on cryopumping under vacuum conditions for space simulation chambers 17 p3006 A69-33683
- Cryogenic applications to low noise reception development in radio astronomy, planetary radar and communication with deep space probes 17 p2921 A69-33685
- Temperature control below 5.2 K based on servoing He pressure above bath 18 p3136 A69-34641
- Metal alloys mechanical properties summary for cryogenic applications, considering fracture and thermal behavior, cryogenic structures fabrication and composites applicability 18 p3158 A69-35416
- Mechanical properties and weldability of austenitic steel for cryogenic applications 18 p3158 A69-35417
- Al cryogenic quenching using liquid N for slow and uniform heat removal to eliminate distortion 18 p3150 A69-35419
- Stimulated emission characteristics of CdS-CdSe mixed crystals subjected to two photon excitation, studying pulse energy at 77 K as function of pumping power 19 p3332 A69-35867
- Mechanical properties of welded joints in Kh 18N9T steel at very low temperatures using austenitic-ferritic and austenitic welds 22 p3958 A69-41204
- Superconducting leads with small electrical resistance and low thermal conductance for cryogenic applications, noting manganin wires coated with Pb-Sn alloy 22 p3997 A69-41236
- DC beam experiment for determining molecule sticking coefficients of gas beams incident on Ti, Ba and Sr gettering surfaces at cryogenic temperature 23 p4151 A69-41544
- Low temperature mechanical properties of structural materials for high energy propulsion systems, using low boiling point propellants as liquid hydrogen, fluorine and oxygen 23 p4177 A69-42159
- CRYOLITE**
- Multilayer lead oxide and cryolite dielectric coatings stability to ruby laser radiation, noting breakdown coherent radiation power densities 19 p3334 A69-35886
- CRYOPUMPING**
- Liquid hydrogen circulation pump design emphasizing heat leaks 01 p0087 A69-11148
- Liquid hydrogen and LOX boost pump design for Centaur missile and liquid hydrogen and LOX chill-down pump design for Saturn 4B missile 01 p0087 A69-11149
- Molecular flow in space simulation chambers with cryowalls, noting nonuniform flux density distribution 01 p0057 A69-11153
- Cryopump design suitable for attachment as replacement for diffusion or ion pumps 01 p0088 A69-11155
- Book on vacuum system design covering getter ion pumping, cryogenic pumping, liquid nitrogen handling, residual gas analyzers, etc 07 p1180 A69-18549

Vacuum pumping methods for large space simulation chambers, discussing cryopumping, economic and operational considerations
13 p2241 A69-28078

Hydrogen oxygen rocket engine two phase liquid hydrogen pump capability and hydrodynamic design, analyzing constant-quality flow, acoustic effects, compressible flow and cavitation
[AIAA PAPER 69-549]
16 p2845 A69-32759

Low pressure and background radiation conditions via cryogenically cooled surfaces, citing data on cryopumping under vacuum conditions for space simulation chambers
17 p3006 A69-33683

CRYOSORPTION
U **SORPTION**
CRYOSTATS

Helium cryostat designed to operate under overload and vibrations and used for cooling onboard superconducting devices of Cosmos 140 satellite
04 p0585 A69-15407

Onboard solid state neon cryostat for IR detector, noting resistance to missile vibration, acceleration and shock tests
06 p0906 A69-17103

Cryostat design, discussing vapor and radiation shielding, construction and insulation materials, safety features, cost considerations, etc
10 p1810 A69-24015

Gas bath cryostat to study volumetric properties of gaseous mixtures at low temperature and high pressure
17 p2975 A69-33669

Tensile cryostat for low temperature strain measurement, discussing design, insulation and vacuum sealed environment for heat leak reduction
[NAS-NRC PAPER J-3]
22 p3947 A69-40627

CRYOTRONS

Cryogenic applications including maser amplification, IR detection and superconductivity, discussing systems optimization and cost reduction
10 p1665 A69-24017

CRYSTAL DEFECTS
NT **EDGE DISLOCATIONS**
NT **FRENKEL DEFECTS**
NT **POINT DEFECTS**
NT **SCREW DISLOCATIONS**
NT **VACANCIES [CRYSTAL DEFECTS]**

Mechanical properties of lithium fluoride single crystals, taking into account equilibrium lattice defect structures
01 p0138 A69-10602

Ruby laser crystals optical inhomogeneity and residual mechanical stresses effects on laser beam angle of divergence
01 p0139 A69-10831

Electron irradiation induced damage in undoped GaSb single crystals at 77 K, noting dependence on energy and orientation
01 p0141 A69-11256

Acceptor defect levels in cadmium telluride crystals prepared under various cadmium vapor pressures, demonstrating ionization energy variation by electrical measurements
02 p0294 A69-11546

Stacking faults in Ge epitaxial layers revealed by etching reagents and X ray diffraction with photographic recording
02 p0297 A69-11880

CdSe single crystal dislocation loops and growth defects, using X ray topograms
02 p0298 A69-12048

Localized vibration modes of defects and IR absorption bands in compensated Si doped GaAs
02 p0299 A69-12402

Scanning electron beam display of space charge of defects and junction behavior of edge dislocation array in Ge and Si monocrystals
02 p0301 A69-12661

Temperature dependence of internal friction in molybdenum wire in moderate and high temperatures
03 p0446 A69-13576

Tellurium-doped gallium arsenides stacking-faults transmission electron microscopic study
03 p0486 A69-13614

Disordered chondritic pyroxenes, analyzing X ray patterns of meteoritic and synthetic crystals
03 p0516 A69-14083

Electrical properties of crystals relation to variations of electron or hole distributions, discussing inhomogeneities
04 p0641 A69-14506

Diffusion anomaly of native acceptor defect in zinc selenium telluride p-n junctions, discussing applica-

tions in triple diffusion technique of preparing p-n junction diodes
05 p0808 A69-16286

Vacancy relaxations in bcc crystals using energy dependence on radial displacements from defect of nearest neighbor sets, discussing crystal size and shape
05 p0809 A69-16529

Radiation defects stability in semiconductors, noting low temperature electron irradiation of Ge and effects of annealing
06 p0974 A69-16863

Carrier scattering from defects in neutron irradiated semiconductors, noting mobility and relaxation time
06 p0974 A69-16864

Disordered regions in electron irradiated silicon noting defect clusters concentration effect on electrical properties
06 p0974 A69-16866

Neutron irradiated Si transistors radiation and annealing characteristics determined for inverse configuration
06 p0975 A69-16872

Electron irradiation annealing and modification of 35 and 65 K defects in n-type Ge induced by 1 Mev electrons at low temperature
06 p0980 A69-17757

Hole concentration at deep energy levels in p-type indium antimonide single crystals containing structural defects
07 p1199 A69-18687

Lattice location of dopant elements implanted into Ge determined by carbon ion backscattering, noting substitutional concentrations above thermal equilibrium solubilities
07 p1199 A69-18903

Transient heat evolution response to reapplied stress of alloys plastically predeformed at 4.2 K attributed to thermally softened defect structures
07 p1165 A69-18906

Structural defects in annealed niobium crystals observed by optical microscopy, discussing etch pits
07 p1169 A69-19603

Failure mechanisms in semiconductors, discussing imperfections, fabrication errors and electrical, thermal and mechanical stresses
08 p1294 A69-21117

Li atoms and O interactions with electron radiation produced defects in Si studied by IR spectroscopy
09 p1554 A69-21337

Microimpurities in aluminum-yttrium garnets determined spectrographically by using gallium oxide as carrier and Teflon powder for fluorinator
10 p1747 A69-23843

Ruby laser crystals optical inhomogeneity and residual mechanical stresses effects on laser beam angle of divergence
11 p1936 A69-24698

Structural imperfections of CdSb single crystals undoped and doped with tellurium and indium noting etching techniques, grain boundaries and impurities
11 p1938 A69-25030

Optical investigation of defects in crystal lattices on stress induced birefringence basis, describing stress visualization results for Si and glass
11 p1887 A69-25199

Plasticity increase of molybdenum alloys during precipitation of second phase at high temperatures due to lattice defects redistribution and plastic deformation
11 p1906 A69-25685

Lattice defects in development of recombination centers on Ge semiconductor surfaces, discussing photoconductivity and field effect
12 p2142 A69-25978

Lattice defects in annealed and plastically deformed cobalt, showing increase with increasing martensite transformations
12 p2113 A69-26042

Collection of papers on crystal structure imperfections covering dislocation mobility, kinetic recrystallization and volume changes during phase transformation
12 p2142 A69-26452

Solid state physics applications to fracture problems and structure of solids, considering crystallography, lattice vibrations, defects, electron bands, alloys and surface physics
13 p2316 A69-27221

CoO complex defects indicated by negative enthalpy of formation, considering isobaric electrical conductivity measurements at various temperatures and oxygen pressures
14 p2508 A69-29925

Finite scattering cross section in current carriers scattering on impurities in compensated semiconductors, assuming unscreened Coulomb potentials
15 p2666 A69-30063

Bound excitons spectra in Cu doped gallium arsenide crystals, analyzing line oscillation structure and uniaxial compression effect
16 p2824 A69-31571

Flux grown magnetic garnet crystal internal defects analyzed by etching and Lang X ray transmission topography, revealing tubular structural deviations
16 p2825 A69-31692

Heat treatment effects on Te-doped GaAs, using photoluminescence and carrier concentration measurements to study defects formed
16 p2825 A69-31708

Neutron bombardment and ionizing radiation resistance of aluminum oxide MOS devices using gate insulator fabricated by plasma anodization
17 p2935 A69-32888

Activation energy of annealing of lattice defects in Au films deposited under irradiation with Au ions
18 p3182 A69-34349

Collection of papers on defects and properties of crystalline lattice
18 p3159 A69-35447

Imperfection photoconductivity in electron irradiated Li-doped Si annealed at room temperature, noting level rearrangement in O rich material
19 p3382 A69-35696

Ti and V sesquioxides and TiO-VO solid solutions crystallography and defect chemistry over entire range of compositions
20 p3484 A69-37526

Primitive low energy Fe-group nuclei irradiation of meteoritic crystals from studies of pyroxene and feldspar from meteorites, discussing astrophysical implications
20 p3590 A69-37569

Impurities effect on domain structure of barium titanate single crystals grown from solution in KF melt determined by inner stresses
21 p3783 A69-39559

Structural defects of neutron irradiated W wire noting microstress relaxation using autoionico microscope
21 p3749 A69-39623

Doped silver carbonate defect structure and doping effect on reaction kinetics by X rays and electron paramagnetic resonance, finding new crystal structure
22 p3993 A69-40720

Seizing characteristics of metals using electrical resistance as measure of lattice imperfection density due to friction
22 p3957 A69-41111

Defect structure of ceramic Ba titanate doped with Cr ions, evaluating visible, IR and EPR spectra
22 p3996 A69-41160

IR inspection system for detecting interstitially caused alpha segregation in Ti alloy disks
24 p4318 A69-42757

Donor and acceptor impurity effect on absorption and reflection spectra of CdTe single crystals, analyzing In, Ga, S and Se
24 p4362 A69-43735

CRYSTAL DISLOCATIONS
NT **EDGE DISLOCATIONS**
NT **SCREW DISLOCATIONS**

Shear accommodation kinking at second order twin bands in critically deformed magnesium investigated for dislocation mechanism
01 p0093 A69-10063

Yield condition of polycrystalline hcp metal, considering slip characteristics of hcp crystals
01 p0094 A69-10304

Theory of fatigue crack growth crystal in metals in terms of coplanar dislocation arrays extended to oblique slip planes, discussing orientation
01 p0168 A69-10344

Elastic anisotropy and polycrystalline orientations in cold rolled titanium sheets investigated by Fourier series method, discussing Young modulus values
01 p0094 A69-10431

Motion, field momentum and field kinetic energy equations of concentrated dislocations based on Zorski field theory of defects
02 p0336 A69-11556

Diffusion process in dislocation-free doped and undoped GaAs single crystals
02 p0296 A69-11792

Lattice deformation relationship to dislocation density in vanadium carbide powders
02 p0265 A69-12001

CdSe single crystal dislocation loops and growth defects, using X ray topograms

02 p0298 A69-12048

Crystal dislocation motion in viscous media, discussing velocity stress behavior and measurements by etching and ultrasonic attenuation methods

02 p0343 A69-12285

Strain rate effect on dislocation substructure in deformed niobium single crystals, investigating relationship between mechanical properties and dislocation substructure

02 p0268 A69-12287

Dislocations effect on decomposition rates of solid solutions of InAs and Au, Ag or Cu

03 p0484 A69-13283

Electrical properties of edge and screw type dislocations in germanium, using bilateral microscopy

03 p0488 A69-13761

Model of creep in solids based on Markov process, discussing dislocation movement by means of thermal activation

03 p0529 A69-13942

Dislocation effects on intensity jumps near K edge of absorption, using interferential transmission of X rays in Ge

03 p0490 A69-13944

Impurity-dislocation interaction in Al alloy by vacancy mechanism and repeated yielding phenomenon, establishing activation energy

04 p0613 A69-14440

Internal friction temperature effects on amplitude dependence in niobium and molybdenum

04 p0614 A69-14635

Nimonic alloys high temperature annealing effect on dislocation structure stability created by thermochemical treatment, using transmission microscopy

04 p0615 A69-14636

Dislocation distributions in cold worked fcc, bcc and hcp metals, discussing dislocation structures in deformed single crystals and work hardening theories

05 p0778 A69-15754

Stress-strain rate relation under combined stress fields derived from Gilman relation between dislocation velocity and force for single dislocation

05 p0834 A69-15756

Course slip during cyclic deformation of copper single crystals, discussing strain bursts dependence on stress amplitude rate, unidirectional prestrain and orientation

05 p0779 A69-15905

Book on plastic deformation of metals in terms of dislocation theory covering single crystals, alloying solid solutions, aggregates, annealing, etc

05 p0841 A69-16369

Slip geometry in bcc metals, discussing slip-line observations by light and electron microscopy techniques

05 p0781 A69-16537

Metals study using field ion microscope for detecting dislocations, crystal boundaries and growth surfaces and surface diffusion energies

06 p0943 A69-17376

Unified methods based on dislocation theory for direct solution of problems pertaining to physical properties of metals

06 p0944 A69-17502

Growth induced dislocation effect on lifetime of minority charge carriers in silicon single crystals

06 p0980 A69-17551

Selective etching technique in study of dislocations in epitaxial layers of gallium arsenide

06 p0981 A69-17891

Dislocation redistribution during annealing and shock deformation in liquid nitrogen of chromium, molybdenum and tungsten single crystals

07 p1159 A69-18534

Grain boundaries structure in tungsten wire using auto ion microscope, showing misorientation corresponds to high density coincidence site lattices

08 p1329 A69-19943

Subgrain diameter relation to misorientation in melt-grown aluminum single crystals from etch pitting and X ray techniques, discussing critical shear stress

08 p1330 A69-20011

Thermally activated processes influence on dislocation interaction and on temperature dependence of flow stress in niobium single crystals

08 p1333 A69-20446

Dislocations effect on intermediate body centered tetragonal phase precipitation in Fe-Ni-Cr-Be alloy using transmission electron microscopy

08 p1333 A69-20447

Dislocation model of strength of elastically inhomogeneous crystalline materials based on elastic interactions between dislocations and periodic fluctuations of shear modulus

08 p1333 A69-20557

Dislocation damping measurements made on Fe-18Cr-Ni alloys, noting damping relation to nickel content and stacking fault

08 p1334 A69-20576

Dislocation channeling process in polycrystalline Nb subject to tensile deformation after neutron irradiation

09 p1521 A69-21345

Heat resistance preservation in heat resistant alloys by inhibiting dislocation motion during operation at high temperatures

09 p1525 A69-22141

Dislocations effect on magnetization process in YIG crystals, using polarization optical method

09 p1559 A69-22532

Relaxation method for configurations and energies of atoms and stress induced crack opening displacements in crystalline solids

10 p1796 A69-23067

Dislocation substructure near fatigue fracture surface during tensile mode crack growth in copper single crystals by transmission electron microscopy

10 p1797 A69-23079

Impurities effect on plastic flow stress and activation, volume as functions of strain, strain rate and temperature in molybdenum crystals

10 p1710 A69-23089

Continuum theory of dislocations and internal stresses in generalized Cosserat continuum as theoretical model for crystals

10 p1799 A69-23153

Continuum theory of dislocations and plasticity in crystals, analyzing stress fields in elastoplastic materials

10 p1799 A69-23154

Alkali halide single crystals disintegration by laser radiation differs as function of crystal physicochemical properties and band structure

10 p1745 A69-23322

Electron bombardment produced clustered displacements, paired vacancies and interstitial atoms in Si, discussing possible mechanism for developing defects

10 p1747 A69-23713

Dislocations velocity in high purity aluminum single crystals determined as function of applied stress at 74 and 83 K

10 p1713 A69-23840

Alloying additions effect on plastic deformation anisotropy in GaAs single crystals, determining dislocation activation energies from creep tests

11 p1936 A69-24537

Etch pits behavior during diffusion and rediffusion of copper in low dislocation crystals of gallium arsenide, demonstrating vacancy nature

11 p1937 A69-25029

Dislocation structure and surface deformation markings correlation analyzed on fatigued Al electron microscope foils

11 p1905 A69-25184

Ni-Ti alloy intergranular deformation at constant tension within wide temperature range

12 p2113 A69-26044

Dislocation mobility temperature dependence in n-type indium antimonide, noting role of covalent interatomic bonds

12 p2143 A69-26453

Dislocations observations in fracture study of crystals, considering etching, decoration technique, X ray topography and diffraction electron microscopy

13 p2316 A69-27223

Molybdenum dislocation velocity and macrodeformation, noting thermal double kink mechanism inconsistencies and strain role in strain-rate relationship

13 p2276 A69-27392

Aluminum alloys ductile fatigue striations, considering dependence on grains crystallographic orientation and vacuum effect

13 p2278 A69-27415

Beryllium single crystals c axis compression behavior at three purity levels under hydrostatic pressures

13 p2279 A69-27760

N-type InSb single crystals with high dislocation density, investigating anisotropy of mobility, Hall effect and transverse and longitudinal magnetoresistance

14 p2503 A69-28734

Book on defects and radiation damage in metals covering collision cascades, point defects clustering and impurities behavior

14 p2503 A69-28889

Dislocation pattern in thin Mo foils deformed by hydroextrusion observed by transmission electron microscope

14 p2463 A69-29311

Beta Ti alloy initial state effect on mechanical properties and dislocation structure after cold deformation by rolling

14 p2463 A69-29313

Dislocations effect on carrier mobility and concentration in p-type and n-type InSb crystals

14 p2507 A69-29646

Diffuse Zn layers structure in GaAs single crystals, showing dislocations formation by anomalous Zn diffusion

15 p2670 A69-31048

X ray detectable preferred disorder in solids by shock loading studied in Ainsworth meteorite and in hexagonal alpha silicon dioxide

15 p2671 A69-31538

Polyethylene stainless steel lap joints and polyethylene samples yield strengths measurements at high temperature, suggesting yield mechanism based on dislocation loops

16 p2794 A69-32573

Low temperature creep mechanisms, discussing thermal activation of dislocation slip in perfect crystals

17 p2985 A69-32909

Shear stress theory of fatigue failure of ductile materials based on crystallographic orientation and probability of slip of neighboring crystals

18 p3211 A69-34344

Dislocation structure of pure polycrystalline nickel subjected to high temperature creep, using electron microscopy following cold working and room temperature annealing

18 p3157 A69-35254

Group 7A and group 8 elements alloying effect on Cr dislocation structure and mechanical properties, discussing ductile-brittle transition temperature and electronic theory

18 p3160 A69-35452

Annealed Cr structural changes during creep at 900 C in air, discussing crystalline disorientation X ray studies and stress

18 p3160 A69-35453

Stoichiometric NiAl slip line and dislocation structures during creep at high temperatures, considering possible creep mechanisms

19 p3343 A69-35923

Fe crystals dislocations dynamic behavior during plastic flow development, describing stress and temperature effects on dislocations propagation and interactions

21 p3833 A69-38569

Energy levels of multicharge acceptor centers and level splitting in InSb and GaAs deformed crystals, using multizone approximation

21 p3781 A69-39067

Dislocations multiplication and rearrangement structure in thermal fatigue of Mo single crystals produced by electron beam zone melting

21 p3746 A69-39162

Dislocation structures in Nb-Ti alloys formed after annealing

21 p3747 A69-39163

Single crystals dislocation dynamics and plasticity theory, discussing current tensor, conservation equation, slip systems, etc

21 p3845 A69-39676

Al discontinuous deformation noting role of intergranular boundary surface at low temperatures

21 p3750 A69-39789

Dislocation structure of Al, Ni, Cu and Ag during creep, noting dependence of creep rate on stacking-fault energy

22 p3972 A69-41080

Hafnium microstructure and impurity concentrations before and after electron beam melting

23 p4178 A69-42361

Mechanical properties and dislocation configurations and densities of Nb single crystals measured at various strain rates

24 p4332 A69-43030

CRYSTAL FILTERS

Narrow band LC 70 MHz IF filter design method

12 p2036 A69-25915

Elastic microwaves propagation attenuation along lithium niobate crystals trigonal axis at various temperatures

15 p2665 A69-30040

CRYSTAL GROWTH

NT CZOCHRALSKI METHOD

NT EPITAXY

NT HYDROTHERMAL CRYSTAL GROWTH

Electric field control of growth rates of insulating organic crystals from vapor phase

01 p0135 A69-10140

Acceptor defect levels in cadmium telluride crystals prepared under various cadmium vapor pressures, demonstrating ionization energy variation by electrical measurements

02 p0294 A69-11546

Injection laser emission from gallium arsenide base films grown epitaxially from gas phase in moist hydrogen atmosphere

02 p0255 A69-11879

Stacking faults in Ge epitaxial layers revealed by etching reagents and X ray diffraction with photographic recording

02 p0297 A69-11880

Thallium whisker growth /compression or squeeze/ method

04 p0641 A69-14457

Molybdenum oxide crystals growth and microstructure, using X ray and electron diffraction analyses

05 p0779 A69-15831

Metals study using field ion microscope for detecting dislocations, crystal boundaries and growth surfaces and surface diffusion energies

06 p0943 A69-17376

Growth induced dislocation effect on lifetime of minority charge carriers in silicon single crystals

06 p0980 A69-17551

Anomalous size effects in galvanomagnetic properties of zinc crystal samples caused by compensation

06 p0981 A69-18232

Polycrystalline W steady state creep rate at high temperatures noting effects of stress, grain size and subgrain size

07 p1158 A69-18241

Solution regrowth method to prepare epitaxial GaAs for Gunn effect devices

07 p1197 A69-18451

Controlled solidification in Co-Ta-C system to develop pseudobinary eutectic mixture containing TaC crystals aligned parallel to growth direction [ONERA-TP-673]

07 p1167 A69-19339

Crystal growth and deformation induced recrystallization in pure aluminum

[ONERA-TP-671] 07 p1167 A69-19340

Epitaxially grown guard rings for GaAs p-n junction and Schottky barrier avalanche diodes

08 p1284 A69-20368

Whiskerizing technique for growing small beta SiC single crystals on graphite filament surfaces, noting changes in interface geometry and chemistry

08 p1341 A69-20511

Chemical processes in silicon carbide due to reactive deposition and chemical conversion, noting silicon growth mechanism involving outward diffusion

09 p1554 A69-21351

HgTe-CdTe single crystals homogeneity and Cd distribution obtained by Bridgman and/or zone melting studied for carrier concentration and electron mobility

09 p1557 A69-21737

Surface characterization on chemical vapor deposited tungsten, evaluating grain size effect

09 p1558 A69-21810

Lead sulfide single crystals and polycrystalline films grown studied by electron microscopy during vacuum deposition on NaCl and other substrates

10 p1743 A69-23002

PbTe single crystal films growth on KCl studied by electron microscope, observing vapor crystal mechanism without coalescence of contacting crystals

10 p1745 A69-23323

Single crystal growth by controlled diffusion in silica gel using metathetical and decomplexation reactions

10 p1652 A69-23371

Acicular crystals growth and dendrites orientation in Mo ingots prepared by electron beam and arc melting analyzed by X rays

11 p1903 A69-24538

Surface-active additives effect on crystallization kinetics of silicate glasses, discussing surface tension

11 p1907 A69-25032

Thermodynamic method for determination of conditions for CdS single crystal synthesis from gas phase, analyzing equilibrium between solid and gas phases

12 p2144 A69-26585

GaAs crystallization for various deviations of melt from stoichiometric state, noting concentration supercooling at phase boundary layer

12 p2144 A69-26586

Yttrium garnet ferrite crystals grown by Czochralski method from inductor crucible exhibiting orthoferrite, iron garnet and eutectic phases along height

13 p2321 A69-28001

Ga phosphide p-n junctions formation from GaP- Ga solution, discussing electrical and luminescence properties

13 p2323 A69-28642

Tungsten emitting surfaces work functions, discussing dense crystalline planes electrolytic or pyrolytic deposit growth and surface chemical or electrolytic attack

14 p2506 A69-29268

Growth kinetics, lattice constant changes and hardness during aging of nimonic alloy from X ray diffraction diagrams

14 p2463 A69-29310

Nonuniform electrical resistivity distribution in InSb single crystals as function of growth direction

15 p2670 A69-31049

Flux grown magnetic garnet crystal internal defects analyzed by etching and Lang X ray transmission topography, revealing tubular structural deviations

16 p2825 A69-31692

Alpha alumina whiskers grown by vapor reaction examined by X ray microtopography and etching

16 p2802 A69-32341

Ta single crystal growth condition by zone melting, discussing orientation and purity relationship

16 p2803 A69-32490

Manufacturing in space based on nongravity and hard vacuum environment, considering crystal growth and refinement, perfectly shaped bodies, refractory metals ultrapurification, etc

18 p3234 A69-35066

Recrystallization limit effects on coarse grain growth in aluminum alloys extruded sections, studying roles of additives, extruding temperature and heat treatment duration

18 p3160 A69-35472

HgTe-CdTe single crystals homogeneity and Cd distribution obtained by Bridgman and/or zone melting studied for carrier concentration and electron mobility

20 p3584 A69-38215

Abnormal grain growth during secondary recrystallization of hydraulically extruded molybdenum as function of annealing

21 p3745 A69-38953

Fe whiskers formation and cross section determination by Fe dichloride reduction

22 p3919 A69-40233

Pyroxene crystallization in meteoritic chondrules, noting normal spherulite crystallization

22 p4033 A69-41065

Selenium distribution along GaSb single crystals during oriented crystallization determined by radiometry

23 p4198 A69-41725

Optimal CdS single crystals growth from gaseous phase achieved with 2 to 1 ratio between Cd and S concentration

23 p4199 A69-42468

Temperature gradients effects on GaAs crystals grown by Bridgman method

23 p4199 A69-42469

InTe phase recrystallization in thin films composed of two InTe phase mixtures, showing random concentrations and distribution of centers growing as spherulites

24 p4361 A69-42993

CRYSTAL LATTICES

NT BODY CENTERED CUBIC LATTICES

NT CLOSE PACKED LATTICES

NT CUBIC LATTICES

NT FACE CENTERED CUBIC LATTICES

Hydrogen content effect on relaxation spectrum of alpha titanium, using nondestructive tests

01 p0096 A69-10614

Two dimensional structural model of micropolar continuum involving orientable points joined by extensible and flexible rods

01 p0169 A69-10810

Energy function invariants for cubic and hexagonal systems of anisotropic media with coupled stresses

01 p0169 A69-10811

Resonance energy transfer mechanism in Forster-Dexter theory of electron energy transfer by resonance interaction in condensed media, using many particle treatment

01 p0121 A69-11257

Current carrier mobility in GaTe and tin selenide semiconducting stratified lattices, noting interaction of free carriers and polarized nonpolar phonons

02 p0295 A69-11777

Temperature dependence of A and C periods of Y crystal lattice at 77 to 300 K, discussing preparation of Y films and anomalous thermal expansion

02 p0298 A69-12047

Elastic constants of point defects for bcc and fcc crystals with vacancies and interstitials calculated by Born-Huang method for nonprimitive lattices

02 p0267 A69-12186

Acoustic wave fluctuations in semiconductors in external electromagnetic field, applying conduction electron and lattice elasticity kinetic equations

03 p0491 A69-14054

Displacement correlations and frequency spectra for mass disordered lattices, deriving cluster expansion for phonon Green function

03 p0493 A69-14241

Spectral study of crystal lattice of gallium phosphides for influence of vacancies and impurities on band formation

04 p0643 A69-15258

Dilatometric and X ray study of temperature dependence of linear expansion coefficients of lattice constants of chromium disilicon

04 p0619 A69-15392

Multiphonon orbit lattice relaxation of excited states of rare earth ions in crystals, using results to design quantum electronic devices [IEEE PAPER I-9]

05 p0774 A69-16318

P-n junctions and device structures formed by ion implantation, using Hall effect and channelling techniques to evaluate implanted layer nature

06 p0974 A69-16862

Mechanical equilibrium and stability conditions for system of interacting atoms in crystal structure

06 p0944 A69-17504

Plastic deformation in bcc, fcc and hcp metals as function of initial impact load energy, noting strain hardening effects

07 p1166 A69-19144

Ionic and nonionic mineral oxide powder fillers influence on stereopolymers lattices formed from phenolformaldehyde oligomers, discussing mechanical properties

08 p1335 A69-20331

Boron crystalline modification during transit through induction coupled Ar plasma producing better crystallized spheroids

08 p1372 A69-20687

Crystal lattice and orientation of precipitate responsible for hardening water quenched Ni-Cr-Nb alloy

08 p1334 A69-20852

Insertion-loss synthesis of narrow band crystal band-elimination filters, using narrow band approximation and pseudoreactance theory

08 p1300 A69-21173

Magnetic sublattices interactions in gadolinium ferrite garnet, estimating magnetization level temperature dependence

08 p1374 A69-21186

Ductile to brittle transition shown in tensile stress-strain curves of polycrystalline body centered cubic and hexagonal close packed materials

10 p1795 A69-23063

Relaxation method for configurations and energies of atoms and stress induced crack opening displacements in crystalline solids

10 p1796 A69-23067

Surface atomic structure effects on polar faces in InSb semiconductor crystal established from measurements of contact potential difference by dynamic capacitor

10 p1747 A69-23965

Diffusion constant of Ni in Ti alloys with Al, Mo and Nb, considering beta phase

11 p1902 A69-24274

Gadolinium-cobalt system investigation by X ray diffraction thermoanalysis and metallography for intermetallic compounds, noting structure transformation and homogeneity

11 p1903 A69-24574

Order-disorder in alloys with several phase transition temperatures, discussing crystal lattices, interstitial alloys, atomic and magnetic ordering

11 p1936 A69-24702

Young modulus temperature dependence and order-disorder transformations in ternary nickel alloys

11 p1904 A69-24705

Order-disorder transformations in nickel alloys under loading operations

11 p1904 A69-24706

Optical investigation of defects in crystal lattices on stress induced birefringence basis, describing stress visualization results for Si and glass

11 p1887 A69-25199

Silicon resistance strain gage sensitivity dependence on crystallographic orientation following cut-off from single crystal

11 p1887 A69-25209

- Quenched titanium-niobium alloy structure effect on superconductivity properties, using electron microscope and X rays
12 p2112 A69-26040
- Book on defects and radiation damage in metals covering collision cascades, point defects clustering and impurities behavior
14 p2503 A69-28889
- Gas-surface interaction for trapping and energy exchange, comparing continuum and discrete lattice models for solids
14 p2409 A69-29092
- Electronegativity and work function relationship from thermodynamic and quantum mechanics standpoint, describing electrons structure by spin orbitals localized around lattice sites
14 p2505 A69-29263
- Growth kinetics, lattice constant changes and hardness during aging of nimonic alloy from X ray diffraction diagrams
14 p2463 A69-29310
- Crystal structures of Ni-rich rare earth/Ni phases, including high temperature forms
15 p2637 A69-30213
- Atomic size and outer electron effect on Fe, Co and Mn polymorphism, noting change in crystal lattices
15 p2638 A69-30321
- Monograph on vanadium selenides and tellurides with NiAs structure covering existence regions, superstructures and equiatomic compounds from viewpoint of thermodynamics
15 p2667 A69-30602
- Structural formula of slowly cooled Mg and Al-Mg microwave ferrites, noting ion mobility during cooling
15 p2670 A69-31184
- CR-B binary system phase diagram including lattice parameters, temperature of peritectic decomposition and characteristics of alloys
15 p2641 A69-31185
- Lattice components of heat conductivity and chemical composition relations of magnesium alloy solid solutions
16 p2824 A69-31567
- Lattice component of heat conductivity in n-type cadmium arsenide at low temperatures by suppressing electron component of conductivity with strong transverse magnetic field
16 p2824 A69-31568
- Dilatometric and X ray study of temperature dependence of linear expansion coefficients of lattice constants of chromium disilicon
18 p3156 A69-35020
- Acoustic wave fluctuations in semiconductors in external electromagnetic field, applying conduction electron and lattice elasticity kinetic equations
18 p3182 A69-35047
- Magnetic sublattices interactions in gadolinium ferrite garnet, estimating magnetization level temperature dependence
18 p3183 A69-35155
- Binary Nb-Hf system phase diagram below solidus line noting lattice parameters and oxygen and nitrogen effects on phase equilibrium boundaries
18 p3157 A69-35247
- Chromium ternary systems phase diagrams and crystallographic structures, using heat treatment and X ray analysis
18 p3158 A69-35262
- Collection of papers on defects and properties of crystalline lattice
18 p3159 A69-35447
- ### CRYSTAL OPTICS
- Frequency mixing of IR signals with visible laser light in nonlinear crystals to detect IR signals
01 p0089 A69-10180
- Electric field induced IR absorption and Raman scattering by optical phonons in centrosymmetric crystals, discussing tensor coefficients
02 p0295 A69-11779
- Polarized low temperature laser excited Raman spectra of thulium gallium garnet
02 p0256 A69-11925
- Q switched neodymium-glass laser output conversion into second optical harmonic by passing beam through double Galilean telescope with adjustable focus
03 p0438 A69-13048
- Direct amplification of ultra and hypersonic surface waves in semiconducting crystals of wurtzite group, taking into account drift effects and boundary conditions
03 p0490 A69-13925
- Resonant interaction of radiation from liquid nitrogen cooled ruby laser with ruby crystal in temperature range 4.2-100 K
04 p0611 A69-14439
- Second harmonic generation in laser crystals by Gaussian beams of finite aperture
07 p1158 A69-19756
- Specific level role in emission of optical radiation by ruby laser stimulated calcium fluoride crystals doped with divalent Dy ions
11 p1894 A69-24618
- Nondestructive thermal tests using liquid crystals thermal sensitivity for measurement of temperature changes and visualization of temperature gradients
11 p1892 A69-25293
- Ruby crystal optical homogeneity and relation to main laser emission characteristics, discussing optical and structural surface properties
12 p2106 A69-26322 [IEEE PAPER U-7]
- Laser-nonlinear crystal dynamical interactions, studying saturation and coherence properties of second harmonic wave generated inside laser cavity
15 p2632 A69-30026
- Electrical conductivity and optical spectra changes of strontium titanate single crystals under constant electric field action
15 p2666 A69-30043
- Parametric conversion kinetics of monochromatic light waves in nonlinear crystals, using quantized electromagnetic field to study amplification and generation
19 p3332 A69-35870
- Tau-luminescence in thin gamma-colored and uncolored ruby crystals containing Cr ions measured, discussing ions absorption spectrum changes
19 p3335 A69-36166
- ### CRYSTAL OSCILLATORS
- Dynamic characteristics of temperature control systems using crystal oscillators determined by nonlinear automatic control theory
22 p3869 A69-40254
- Space simulation tests of satellite-borne quartz crystal oscillators for tracking based on Doppler effect
22 p3927 A69-40590
- ### CRYSTAL RECTIFIERS
- Current voltage characteristics in silicon carbide diodes having negative differential resistance
10 p1663 A69-23571
- Optical rectification in crystals by excitation of nonlinear /time constant and space variable/ polarization
23 p4174 A69-41874
- ### CRYSTAL STRUCTURE
- #### NT WIDMANSTATTEN STRUCTURE
- High temperature magnetic analysis of metallurgical structure of high strength steels and composites, including phase transformation and matrix grain structure
01 p0093 A69-10111
- Cycle dependent fatigue hardening and softening of metals in terms of crystal structure and stress amplitude
01 p0165 A69-10133
- Soviet book on semiconductor compounds, production and properties covering crystal structures, phase diagrams, etc
01 p0137 A69-10353
- Crystal and molecular structure of mu-oxo-bis(chlorobis(2, 4-pentanedionato)/titanium(IV)/-chloroform solved by symbolic sign determination method and Patterson map interpretation
01 p0023 A69-10411
- Highly oriented graphite crystallites in pyrographites and composite materials, discussing preparation and anisotropy ratios in physical properties
01 p0102 A69-10978
- Soviet book on structure of thin metal films covering electron microscopic and electronographic studies, crystallization and heat treatment effects
01 p0140 A69-11106
- Tabular reduction of crystal structure chemical information for metals and semiconductors for material selection use
02 p0295 A69-11786
- Electronographic determination of ternary alloys of germanium antimony tellurides noting hexagonal laminary with cell periods
02 p0298 A69-12046
- Neutron and gamma irradiation effects on CdS crystals structure and properties, outlining electron energy level scheme
02 p0298 A69-12119
- Crystal structure of boron filaments vapor deposited on tungsten wire substrate, using X ray diffraction and transmission-electron microscopy
02 p0268 A69-12405
- Crystals and molecules diffraction in superconductive molecular jets
02 p0284 A69-12629
- Structure of /111/ single crystal Si surface after chemical-mechanical polishing and ultrahigh vacuum annealing, noting presence of Fe impurity
02 p0301 A69-12660
- Vanadium-gallide alloys critical temperature of transition into superconducting state determined by measuring cast alloy samples magnetic permeability
03 p0483 A69-13023
- Ferroelectric domain structure to explain microcracks nucleated at twinband intersections in mechanically deformed lithium niobate
03 p0486 A69-13618
- Thermodynamic analysis of refractory compounds vapor transport conditions, illustrating integral free energy diagrams
03 p0453 A69-13619
- Transitional hexagonal omega phase of Ti-Fe alloys quenched in water and tempered
03 p0451 A69-13999
- Molybdenum oxide crystals growth and microstructure, using X ray and electron diffraction analyses
05 p0779 A69-15831
- Room temperature lattice spacings of PdIn, PtIn and PtSn alloys including magnetic susceptibility
05 p0779 A69-15832
- Electron microscopy of titanium alloys noting preparation, heat treatment of samples, crystallographic structure, etc
05 p0782 A69-16807
- Structural characteristics of Ni-Mo alloys analyzed using electron microscopy and X ray diffusion scattering
05 p0782 A69-16808
- Transmission electron microscopy used to study phase transformations in Ti-Mo and Ti-V alloys, determining crystal structures
06 p0943 A69-17230
- Mechanical equilibrium and stability conditions for system of interacting atoms in crystal structure
06 p0944 A69-17504
- Optical Fourier transform applied to structural analysis of catalase crystalline media by gas laser
06 p0928 A69-17890
- Structural and electrical properties of indium antimonide and arsenide films, noting dependence of electron concentration and mobility on thickness
06 p0981 A69-17892
- Dependence of microwave emission from n-InSb on crystalline orientations, noting anisotropy in case of rotation in perpendicular plane
07 p1198 A69-18647
- Trivalent iron doped andalusite crystals dielectric and mass properties, investigating spin-lattice relaxation, cross relaxation times and inversion ratio [IEEE PAPER C-2]
07 p1150 A69-19049
- Breakdown regularity of metals having different crystal structure, considering metal lifetime dependence on stress magnitude and test temperature
08 p1328 A69-19793
- Magnesium silicate crystal structure, discussing transformations under high pressure, crystallochemistry and implications for physics of earth mantle
08 p1267 A69-19904
- Nodal precipitation and cellular solidification substructure in commercial purity nickel, discussing supercooling, NiO and eutectic composition
08 p1332 A69-20289
- Vapor deposited tellurium thin films orientation, noting effect of characteristic spiral chain structure along c-axis
08 p1373 A69-20891
- Structural and optical properties of vacuum deposited GaP films at below 240-850 C
09 p1554 A69-21332
- Partial pole figures in vapor deposited and wrought cylindrical tungsten specimens, noting random surface produced by orientation
09 0 A69-21811
- Metals structure and mechanical properties after hydroexplosive forming analyzed by X ray diffraction
09 p1503 A69-21851
- Face effect in p- and n-type gallium antimonide single crystals doped with zinc and tellurium
09 p1558 A69-21870
- Primary silicon crystals content and grain size effect on wear of high silicon aluminum alloys
09 p1526 A69-22281
- Amorphous semiconductors, emphasizing structure and theory of liquid and amorphous states, electron energy spectra and scattering, impurities, Hall effect, etc
10 p1747 A69-23807

Carbide precipitation in stainless steels using metal foil and extraction replicas, discussing grain boundaries corrosion relation
10 p1713 A69-23820

Diamond-like glassy semiconductor compound of cadmium germanium arsenide, determining optical lattice vibrations from IR reflection spectra
10 p1747 A69-23963

Long range order formation in Ni-Cr alloys analyzed by direct neutron diffraction, considering disorder-order transition temperature and chemical composition
10 p1714 A69-23964

Structural inhomogeneity of Ti alloys cause increased susceptibility to production of sheets, forgings and drop forgings
11 p1902 A69-24276

Thin polycrystalline film structure and formation, using electron beam instrument
11 p1936 A69-24601

Surface-active additives effect on crystallization kinetics of sital type glasses, discussing surface tension
11 p1907 A69-25032

Structure of epitaxial single crystal layers of CdS vacuum deposited on mica surface at various temperatures
11 p1939 A69-25709

Vapor phase epitaxial production of indium arsenic phosphide crystalline layers, discussing electron mobilities, electrical resistivities and doping
12 p2142 A69-25934

Ti-Nb alloy structure in heat treatment states analyzed by diffuse scattering of X ray lines and by electron microscope
12 p2112 A69-26036

Heat treatment effects on molybdenum-rhenium alloy field emission and surface structure in alpha and sigma phase regions
12 p2113 A69-26041

Collection of papers on crystal structure imperfections covering dislocation mobility, kinetic recrystallization and volume changes during phase transformation
12 p2142 A69-26452

Magnetic domain structure in supercritical ferromagnetic films with perpendicular anisotropy
12 p2143 A69-26458

Soviet monograph on nuclear radiation effect on structure and properties of metals and alloys covering electron, gamma and neutron radiation
12 p2114 A69-26469

Mixed state of type 2 superconductors, stressing alloying elements effects in solid solution and structural inhomogeneities
12 p2145 A69-27119

Crystal microstructure and mechanical properties of unidirectionally solidified Ni-Ni-Nb intermetallic eutectic alloy at high temperature, examining deformation and fracture modes
13 p2276 A69-27402

Composition, gamma structure and mechanical properties of three unidirectionally solidified eutectics within Ni-Al-Cb, Ni-Al-Zr and Ni-Al-Ti systems
13 p2277 A69-27407

Precipitation influence on martensite formation kinetics and structure of Fe-Ni-Ti alloys
13 p2279 A69-27765

Grain size effect on room temperature tensile strength of alpha-titanium analyzed by tensile testing and electron transmission
13 p2280 A69-27766

Artificial aging effect on spinel structure and properties of ferrites using X ray analysis, neutron diffraction and electron microscopy
13 p2320 A69-27997

Transition zone structure and phase composition in Ti/stainless steel bimetal as function of rolling conditions and heat treatment
13 p2283 A69-28490

Magnetic properties of ferrites with garnet structure, discussing temperature effect on magnetic states of Gd, Li, Y and Lu sublattices
13 p2323 A69-28564

Microstresses and distortions in quasi-isotropic solid bodies under strain evaluated by correlation functions
14 p2531 A69-28806

Graphites wear rates and structural changes in machine parts under dynamic stresses in air or vacuum, noting pressure role
14 p2467 A69-28912

Micrographic reagent coloring grains of Mo in relation to crystalline orientation applied to refractory metal welding and diffusion studies
14 p2505 A69-29221

Monograph on mechanical behavior of crystalline solids at elevated temperatures, discussing creep properties of metals, solid solutions and two phase alloys
14 p2465 A69-29749

Crystal structures of intermediate phases in La-Co and Nd-Co systems by powder X ray diffraction technique
15 p2667 A69-30087

Temperature effects on magnetomechanical damping in Fe, Ni and mumetal, noting behavior difference due to domain structures
15 p2639 A69-30586

Ta single crystal growth condition by zone melting, discussing orientation and purity relationship
16 p2803 A69-32490

Carbon fibers fine structure graphitized at high temperatures studied by X ray diffraction and electron microscopy
16 p2803 A69-32572

Andalusite crystals as active media in paramagnetic quantum amplifiers, discussing design and performance
19 p3333 A69-35881

Fourth rank tensors analysis describing nonlinear optical effects for 32 classes of crystalline substances
19 p3334 A69-35882

Fast neutron irradiation effect in Ge crystals, using X ray diffraction and volumetric measurements
20 p3584 A69-38125

In-Te-Se system alloys structure and semiconductor properties analyzed by X rays
21 p3779 A69-38579

Impurities effect on domain structure of barium titanate single crystals grown from solution in KF melt determined by inner stresses
21 p3783 A69-39559

Structural changes in Mo single crystal under action of laser radiation of various power densities
21 p3750 A69-39842

Lamellar solids abrasiveness, effects of particle share in graphite and molybdenite samples
22 p3966 A69-39877

Photovoltaic cells electrical characteristics, discussing Cd sulfide, single crystal Si and dendritic type Si cells for spacecraft power
22 p3868 A69-40130

Doped silver carbonate defect structure and doping effect on reaction kinetics by X rays and electron paramagnetic resonance, finding new crystal structure
22 p3993 A69-40720

Aqueous hydrazine solution effect on Ti disulfide crystalline structure
23 p4112 A69-41426

Ingot dendrite arm spacing and thermomechanical treatment effects on fracture behavior and mechanical properties of Al alloy, finding ultimate and yield strengths
23 p4176 A69-41506

Ni-Nb alloys precipitates tetragonal structure as function of time and temperature using electron and X ray diffraction
24 p4331 A69-42903

Structural features and electrical resistivity of siliconated pyrolytic graphite, analyzing dependence on preparation conditions using X ray diffraction measurements
24 p4335 A69-42926

CRYSTAL SURFACES

Structure of /111/ single crystal Si surface after chemical-mechanical polishing and ultrahigh vacuum annealing, noting presence of Fe impurity
02 p0301 A69-12660

Photocurrent pinch-off effect in high resistivity thin CdS crystals for evaluating donors, acceptors and surface states
03 p0488 A69-13757

Orientation dependence of pitting and blistering in proton irradiated Al polycrystal surfaces
04 p0640 A69-14451

Grain strain measurements use in studies of high temperature creep
06 p0943 A69-17231

Chemisorption of H onto Nb /110/ surface, measuring low energy electron diffraction and inelastic electron scattering from clean and H-covered surfaces
06 p0980 A69-17758

Thermal faceting of tungsten single crystal surfaces in oxygen, using vibrating-capacitor work function probe with low energy electron diffraction
08 p1330 A69-20137

Interaction of nitrogen oxides and carbon dioxide on nickel crystal surface using low energy electron diffraction and mass spectrometer, discussing work function
08 p1268 A69-20138

Relative free energies of crystal zones of tungsten using field electron microscope, determining surface energy anisotropy from Wulff construction
08 p1330 A69-20139

Work function change of tungsten single crystal /100/ surface measured as time function during surface molecular gas adsorption
09 p1521 A69-21338

Temperature effect on work function minimum of cesiated tungsten single and polycrystal surfaces, using vibrating capacitor technique
09 p1558 A69-21809

Sr and La ionization on crystal surfaces of W and polycrystalline W, discussing temperature effect on oxidation and work function
12 p2142 A69-26113

Substructural patterns of epitaxial PbTe films obtained by condensation of vaporized PbTe on NaCl crystal surfaces, discussing formation kinetics and morphology
12 p2144 A69-26675

Electrooptical ADP modulator design for use with helium-neon laser, considering temperature stability and crystal faces parallelism
13 p2272 A69-28191

Substrates ultraclean surface preparation methods, examining crystal cleaving and crushing, heating, chemical cleaning, ion bombardment, etc
14 p2455 A69-29348

Field emission and field-ion microscopic adsorption studies, discerning major states in chemisorption for metal-crystal surfaces
22 p3895 A69-39898

CRYSTALLINITY

Amorphous semiconductors, emphasizing structure and theory of liquid and amorphous states, electron energy spectra and scattering, impurities, Hall effect, etc
10 p1747 A69-23807

Electrons conduction and switching in noncrystalline semiconductors, discussing localized states and thermally activated hopping
11 p1933 A69-25239

Heat conduction orientation anisotropy in linear amorphous high polymers due to uniaxial stretching, noting molecular weight distribution and temperature effects
19 p3359 A69-36443

Energy spectrum and transport mechanism for current carriers in amorphous-crystalline semiconductors, measuring thermostimulated conductivity, induced photoconductivity, optical quenching, etc
19 p3391 A69-36558

Amorphous semiconductors based on noncrystalline materials compared to crystalline materials, noting radiation damage resistance
19 p3392 A69-36660

CRYSTALLITES

U SPHERULITES

CRYSTALLIZATION

NT RECRYSTALLIZATION

Phase diagram of BiTel degenerate semiconductor crystals synthesized by heat treatment, discussing crystallization methods and physical properties
02 p0294 A69-11540

InAs-InP phase diagram taking into account equilibrium pressure of vapor over melts in preparing single crystals by controlled crystallization
03 p0483 A69-13024

Al/Zn/Mg alloys preprecipitation, discussing Guinier-Preston and critical zone sizes and reversible vacancy trap
03 p0447 A69-13613

Monograph on crystallization during polymerization, discussing categories, monomers capable of step reaction, chain reaction, nucleation crystal growth and perfection
05 p0783 A69-15967

Boron crystalline modification during transit through induction coupled Ar plasma producing better crystallized spheroids
08 p1372 A69-20687

GaAs crystallization for various deviations of melt from stoichiometric state, noting concentration supercooling at phase boundary layer
12 p2144 A69-26586

Macrostructure of steel, zinc and aluminum ingots using electromagnetic vibrations during crystallization, for stress relieving of welded structures
14 p2456 A69-29916

Monograph on GaAs injection laser electrical and optical properties during crystallization out of solution covering principle, p-n junction fabrication, I-V characteristics, doping effect, etc
17 p2982 A69-33571

Superdense stars torsional oscillations and crystallization among nuclei from comparison with melting temperature and transverse shear wave velocities of dense conventional matter

17 p3037 A69-33643

Barringerite as Fe-Ni phosphide occurring in meteorite Ollague pallasite, indicating troilite and schreibersite crystallization at high temperatures

18 p3205 A69-35433

Crystallization front topography and stratified structure of melt extracted n-type GaAs single crystals from anodic etching method

20 p3582 A69-37013

Selenium distribution along GaSb single crystals during oriented crystallization determined by radiometry

23 p4198 A69-41725

CRYSTALLOGRAPHY

Microfactors of metal surface cracks studied for plastic deformation and atomic separation mechanisms by electron diffraction

01 p0098 A69-10763

Highly oriented graphite crystallites in pyrographites and composite materials, discussing preparation and anisotropy ratios in physical properties

01 p0102 A69-10978

Elastic constants of point defects for bcc and fcc crystals with vacancies and interstitials calculated by Born-Huang method for nonprimitive lattices

02 p0267 A69-12186

Electromagnetic wave dispersion and damping in mixed molecular crystal, relating refractivity, wave absorption and concentration shift of bottom of excitation band to other parameters

03 p0484 A69-13279

Heavy titanium carbide precipitation on fatigue slip zones of stainless steel, noting rupture produced crystallographic facets

03 p0447 A69-13605

Metals study using field ion microscope for detecting dislocations, crystal boundaries and growth surfaces and surface diffusion energies

06 p0943 A69-17376

Widmanstätten angles relation to orientation of plane of section in iron meteorites

07 p1217 A69-19235

Grain morphology and preferred orientation effects on direction and propagation of stress corrosion cracking of aluminum alloy plate

09 p1521 A69-21399

Polarized light microscope for application to metallic crystallographic studies noting grain orientation, hcp grain basal pole orientation and etched fcc metals

09 p1499 A69-22302

Microstructure and crystallography of lamellar eutectic alloy of Ni and intermetallic Ni-Ti compound

10 p1707 A69-22986

Acicular crystals growth and dendrites orientation in Mo ingots prepared by electron beam and arc melting analyzed by X rays

11 p1903 A69-24538

Magnetic crystallographic anisotropy of Li-Ga ferrite single crystals at temperature range measured by ferromagnetic resonance techniques

12 p2144 A69-26721

Martensite transformation in Ti-Cr binary alloys by thin foil electron microscopy, noting crystallographic theory

13 p2276 A69-27369

Strain hardening experiments on single crystals of AlZn and AlAg alloys noting plastic behavior

16 p2800 A69-31776

Book on high purity beryllium metallurgy for nuclear reactor applications covering physical properties, crystallography, thermodynamics, production methods, etc

17 p2986 A69-32952

Titanium alloy martensites crystallography by electron microscope, discussing lattice parameters and spontaneous transformation

18 p3154 A69-34245

Fracture kinetics of biaxial oriented polymethyl methacrylate, discussing crack development and propagation as compared to unoriented polymer

18 p3162 A69-35354

Ti and V sesquioxides and TiO-VO solid solutions crystallography and defect chemistry over entire range of compositions

20 p3484 A69-37526

Crystallographic relations between mother gamma phase and bulk martensitic structure of Fe-Ni alloys with less than 20 percent Ni, using radioisotopes

20 p3562 A69-37781

Biocrystallography of organic form and structure emphasizing liquid crystals, polymers, epitaxy, inclu-

sion compounds, electrical properties, prelife compounds, etc

21 p3656 A69-38922

Magnetic crystallographic anisotropy of Li-Ga ferrite single crystals measured by ferromagnetic resonance techniques

21 p3781 A69-39134

High temperature single crystal X ray studies of natural Fe-rich orthopyroxene, detecting high-low clinopyroxene inversions

24 p4311 A69-43218

CRYSTALS

NT BICRYSTALS

NT CRYSTAL OSCILLATORS

NT DENDRITIC CRYSTALS

NT IONIC CRYSTALS

NT LIQUID CRYSTALS

NT METAL CRYSTALS

NT PIEZOELECTRIC CRYSTALS

NT POLYCRYSTALS

NT SINGLE CRYSTALS

NT SPHERULITES

NT WHISKERS [SINGLE CRYSTALS]

Sustained high deceleration load effects on quartz crystals during atmospheric entry studied by centrifuge test program on oscillator circuits

01 p0042 A69-10417

Voltage controlled oscillator with fixed frequency crystal oscillator, noting double mixing scheme and rejection of all discrete sidebands

01 p0042 A69-10418

Laser radiation influence on effectiveness of frequency doubling in KDP crystal

04 p0612 A69-15375

Laser radiation influence on effectiveness of frequency doubling in KDP crystal

16 p2797 A69-32122

Analogy between Cerenkov and quasi-Cerenkov radiation in nonlinear crystal by intense laser light used to determine conditions for quasi-Cerenkov radiation

21 p3741 A69-39669

CSM

U COMMAND SERVICE MODULES

CUBIC EQUATIONS

Ultrasonic phase approximation in nonlinear symmetric free oscillations applied to systems with hardening and softening cubic nonlinearities

01 p0107 A69-11418

Resonant oscillations amplitude of nonlinearly elastic hinged cylindrical shell determined with cubic equation taking into account Hooke law, linear stresses, shell theory displacements, etc

19 p3435 A69-35843

CUBIC LATTICES

NT BODY CENTERED CUBIC LATTICES

NT FACE CENTERED CUBIC LATTICES

Energy function invariants for cubic and hexagonal systems of anisotropic media with coupled stresses

01 p0169 A69-10811

Cubic β /silicon carbide films deposition by volatilization in presence of acetylene

09 p1554 A69-21350

Optical pumping in pure Si at 77 K, noting dichroism conditions for dipolar electric transitions in cubic crystal

19 p3389 A69-36548

CULTIVATION

Cultured Chinese hamster cells responses to UV light of different wavelengths indicating photon absorbing molecules inhibition of colony development

07 p1068 A69-19492

CULTURE TECHNIQUES

Biological life support system based on continuous algae seaweed cultivation as link of closed ecological system, discussing design and performance

01 p0020 A69-11077

Cell and tissue cultivation outside living organisms, discussing applications in space biology, space medicine and food protein sources

02 p0198 A69-11501

Mineralized human wastes solutions utilization for Chlorella cultivation, noting growth rates

02 p0200 A69-11511

Escherichia coli detection and differentiation from other bacteria by direct gas chromatographic analysis of culture media

03 p0382 A69-13550

Microbial contaminants on space hardware, discussing detection and enumeration techniques

05 p0714 A69-15954

Microbiological surface sampling methods, noting role in detecting contamination on eating utensils, blankets, sheets, etc

05 p0715 A69-15982

Direct epoxy embedding of monolayer cells cultured on millipore filter and fixed, dehydrated and microscopied before immersion

10 p1649 A69-23404

Mineral nutrition elements concentration stabilization by correcting solution additions during prolonged Chlorella cultivation with medium recycling

10 p1646 A69-23578

Continuous culture device for controlled growth of Euglena gracilis

15 p2555 A69-30445

Postirradiation growth of cultured Chinese hamster cells exposed to UV light, including comparison with X irradiation

19 p3257 A69-35975

Cultured mammalian cell growth morphology studied in situ with scanning electron microscope, discussing surface morphology changes during mitotic cycle of Chang liver cells

20 p3467 A69-37100

Blue green alga Anabaena flos-aquae A-37 growth limitation by absence of K or Na from culture medium

23 p4079 A69-41386

Gradually decreasing N concentration effects on composition, tissue production and oxygen yield of unicellular algae in continuous culture

24 p4263 A69-43201

CUMULONIMBUS CLOUDS

Lightning strikes to aircraft, discussing corona discharge, electric fields and meteorological measurements during thunderstorm in cumulonimbus clouds

03 p0458 A69-13031

Charts of horizontal cross sections of radio echo foci for radio echo reflections from cumulonimbus clouds

03 p0459 A69-13288

Electric fields and conductivity in thunderclouds by parachuting rotating differential electric field mills

08 p1345 A69-19813

Convective clouds effect on large scale stratification, showing cumulus and cumulonimbus self amplifying convection as factor in tropical cyclogenesis

09 p1536 A69-22165

Cumulonimbus clouds phase structure and spatial distribution based on radar signal polarization analysis, showing high nonuniformity and variability

16 p2806 A69-32266

Cumulus and cumulonimbus clouds electrical and microphysical properties measured by instrumented aircraft

20 p3572 A69-37907

CUMULUS CLOUDS

Axisymmetric model of unsteady convective cumulus cloud produced by time dependent heat source in unsteady atmosphere

02 p0274 A69-11436

Air mass cumulus cloud growth stimulation by means of vertical updrafts capable of perforation of retaining layers

03 p0461 A69-13409

Simultaneous measurements of cumulus cloud thermal structure and concentration of water particles larger than 18 micron diameters

09 p1536 A69-21866

Convective clouds effect on large scale stratification, showing cumulus and cumulonimbus self amplifying convection as factor in tropical cyclogenesis

09 p1536 A69-22165

External wind shear influence on isolated cumulus cloud evolution based on hydrodynamic and thermodynamic equations numerical integration

15 p2648 A69-30644

Radio emission and absorption of cumulus and stratus clouds at millimeter and centimeter wavelengths, giving maximum SNR defined by brightness temperature

16 p2807 A69-32270

Atmospheric temperature and moisture fields obtained by linear equations and objectively analyzed, considering underlying sea surface energy and cumulus cloud distribution

20 p3523 A69-37351

Cumulus and cumulonimbus clouds electrical and microphysical properties measured by instrumented aircraft

20 p3572 A69-37907

CURARE

Maximum voluntary isometric muscle strength relation to endurance time in static work during partial curarization

22 p3890 A69-40213

CURIE TEMPERATURE

Posistors heat capacity investigated as temperature function, showing maximum heat balance corresponds to Curie temperature

01 p0038 A69-10098

Electro-optical device using KDP crystal for laser beam deflection at temperatures near Curie point
03 p0435 A69-12984

Magnetic reversible phase holograms on thin film Mn-Bi by Curie-point writing technique
10 p1706 A69-24007

Spontaneous polarization onset in perovskite ferroelectrics, analyzing influence of Curie point, Jahn-Teller effect and atomic structure
22 p3995 A69-41159

Parametric losses in nonlinear centrosymmetrical ferroelectric ceramic in strong microwave field at temperatures above Curie point
22 p3996 A69-41164

CURING

Flame resistant chlorine containing polyester resins, discussing preparation, curing characteristics, physical properties and reinforced plastics application
08 p1340 A69-20505

Thermosetting resin curing behavior characterized by differential thermal analysis performed above atmospheric pressure to prevent volatilization
09 p1500 A69-22311

Electron beam radiation curing of mercaptan terminated butadiene-acrylonitrile liquid copolymers at ambient temperatures in air
09 p1512 A69-22368

Shrinkage stresses in two phase materials, analyzing stress distribution in epoxy inclusions in plasticized matrix during curing by photoelastic method
13 p2371 A69-28675

Epoxy adhesives physical chemistry, curing processes, formulation, surface application methods, testing and health hazards
14 p2468 A69-29339

Curing agents for carboxy and hydroxy functional prepolymers synthesis and evaluation including sulfonyl, acyl and ureido aziridines
[AIAA PAPER 69-436] 16 p2747 A69-32777

Polyimide resin system for glass reinforced laminates, noting processing characteristics and curing
19 p3353 A69-35505

Adhesive bonding of Al sheets for honeycomb sandwich material, using electrical conductivity to measure sheets age hardening progress during high temperature curing
19 p3321 A69-35565

CURL [VECTORS]
NT VORTICITY

Analysis of solution of Navier-Stokes equations describing two dimensional flow of viscous incompressible fluid by finite difference techniques and introduction of curl
03 p0416 A69-13652

CURRENT AMPLIFIERS
NT PHOTOMULTIPLIER TUBES

Integrated operational amplifiers for control systems, noting high stability and linearity through negative feedback
01 p0039 A69-10169

Small signal characteristics and frequency response of diode-stabilized integrated linear circuits, discussing feedback, impedance, bias- diode, etc
01 p0041 A69-10204

Transient behavior of DC measuring amplifiers with time variable feedback, using matrix method and Laplace transform
09 p1467 A69-22560

Maximum voltage and power gain of modulator-demodulator type nonresonant parametric amplifiers
11 p1849 A69-24956

Transistorized LF-HF RC filters and current amplifiers design, exhibiting polynomial type characteristics
12 p2040 A69-26488

Transistorized DC amplifier circuit with reversible and controllable transfer constant based on voltage conversion principle
13 p2235 A69-28511

CURRENT DENSITY

P-n junction cut-off current density and ohmic losses effect on injection laser efficiency determined by using quality parameter
01 p0091 A69-10883

GaAs injection lasers noting spectral function, I-V characteristics and relations among lasing wavelength, threshold current density and impurity concentration
02 p0256 A69-11993

Critical state model of type 2 superconductor taking account of critical current on magnetic field and surface sheath currents, evaluating flux penetration, hysteresis, AC losses, etc
02 p0298 A69-12030

Temperature dependence of electron beam pumped GaAs laser threshold current density and emission spectra, noting doping effects
02 p0260 A69-12683

GaAs injection laser transmission losses and threshold current density under influence of external optical coupling with spherical mirror
02 p0260 A69-12687

Minority carriers lifetime measurement in degenerate GaAs, showing dependence on current density and operating temperature
03 p0483 A69-12917

Xe gas discharge plasma resistivity dependence on current density measured in large tubular flash lamps
03 p0478 A69-13846

Substrate terminal current anomalous enhancement observed in n-channel Si MOS transistors beyond pinch-off
04 p0574 A69-14348

Argon-K plasma electrical conductivity as function of electric current density at 1400-2400 K
05 p0798 A69-15614

Transformation of differential mean and current densities and anisotropy of cosmic ray particles and photons observed in frames of reference relative to each other with isotropic flux
05 p0817 A69-16651

Relationship between microhardness of niobium and other variables characterizing superconductivity
05 p0810 A69-16805

Two section model of saturation drain conductance of MOS transistors
06 p0893 A69-17155

Passive current maxima during anodic polarization of stainless steel in sulfuric acid, using electrochemical and electron microprobes
06 p0944 A69-17853

Magnetic field generation in nonuniformly rotating plasma by current density from electron drift relative to positive ion gases due to viscous forces
06 p1009 A69-17966

Convergent high-perveance electron gun design for use in microwave tubes, reducing anode aperture effect on current density
07 p1101 A69-18658

GaAs lasers radiation power hysteresis manifested in generating starts and stops at different injection current levels
07 p1157 A69-19593

Plasma sheath-boundary interactions, analyzing emission, reflection and surface ionization effects on current densities and heat fluxes for cesium and argon
08 p1369 A69-20818

Oxidizer reducing and fuel oxidizing catalysts role in large current densities production at electrodes of low temperature carbon fuel cells
08 p1259 A69-21037

Voltage dependence of mobility limited electron current density in gas filled diode for collision frequency proportional to electron speed
09 p1462 A69-21326

Steady state currents effect on hydrodynamic waves propagated normal to magnetic field
09 p1547 A69-21662

Electric current spoke in MPD operation, using segmented anode and image converter methods with argon and helium propellant gases
09 p1548 A69-21962

Optimal working parameters and operational characteristics of laboratory electron gun, examining beam shape, convergence and current density distribution
09 p1464 A69-22243

Diffusion and minority carriers drift effect on current-voltage characteristics of p-n-p-n structure in high density current
10 p1742 A69-22997

Air-earth current density variations with universal time, noting hemispherical dependence of storm activity effects
10 p1682 A69-23415

Electrical conductivity, electron density and population temperature as functions of current density in Cs-Hc thermal plasma studied with non-equilibrium ionization model
10 p1732 A69-23443

Electron temperature distributions in Ar-K plasma of simulated Faraday type MHD generator for current distributions, determining current density distribution experimentally
10 p1734 A69-23453

Boundary conditions for nonlinear equations of MHD for vicinity of zero magnetic field line, considering plasma pinch and current density
10 p1739 A69-23626

Current-voltage characteristics and ionization equilibrium of low voltage arc plasma in narrow gap of thermionic converter at high current density
11 p1933 A69-25554

Emitter current density dependence on distance from center of drift transistor circular emitter, obtaining distributed base resistance in presence of arbitrary base current
11 p1853 A69-25565

High current density filaments formation in silicon p-n-n avalanche diodes caused by incremental negative resistance in static current-voltage characteristics
12 p2036 A69-25916

P-n junction cut-off current density and ohmic losses effect on injection laser efficiency determined by using quality parameter
12 p2109 A69-26647

Photon loss coefficients in electron beam pumped GaAs laser showing dependence on doping type and impurity concentration, noting threshold current density measurement
13 p2271 A69-27467

Nonconducting vanes end effects on electrical characteristics of MHD channels, analyzing current density, Joule losses and finite length vanes
13 p2306 A69-27497

Voltage drop of ignited mode related to current density in cesium diode, noting plasma zones
14 p2401 A69-29232

Nonlinear generation of sum and difference frequencies in ionized plasma current densities by nonuniform microwave fields noting electron scattering
14 p2507 A69-29350

Anisotropic scattering of current carriers in semiconductors, obtaining general expression for mobility tensor with variational principle
14 p2508 A69-29667

Josephson current density distribution in thin film superconductors, determining relation between tunneling density and magnetic field for films with/without current
15 p2667 A69-30196

Nonlinear wave scattering at plasma particles and weak plasma inhomogeneity effects on plasma current instability
15 p2662 A69-30965

Double diffused transistor with Gaussian impurity distribution analyzed by power series for carrier density distribution and frequency response
16 p2758 A69-31616

Wide argon plasma column by axial current density measurements, confirming existence of instability and determining critical magnetic field
16 p2819 A69-31680

Microwave field-plasma slab nonlinear interaction in rectangular waveguide, analyzing current and electron density and second harmonic TE and TM power
16 p2749 A69-31703

Nonlinear generation of sum and difference frequency components in magnetoplasma current density due to alternating electric fields, electron density and temperature gradients
16 p2821 A69-32036

Optimization of electrolytic extraction process of water from H-O fuel cells through choice of current density as function of electrolyte concentration
16 p2738 A69-32414

GaAs dual diode laser structure used to give electrical control of laser threshold and permit study of optical flux and current density role
17 p2980 A69-32959

Electromagnetic wave propagation in unbounded compressible plasma under drift velocity and magnetic field, obtaining dispersion equation for current density
18 p3179 A69-34261

Injection lasers threshold characteristics, studying temperature and doping level effects on current density and radiation energy
19 p3337 A69-36527

Electromagnetic radiation in moving uniaxially anisotropic medium, obtaining time dependent solutions for oriented magnetic dipole current distribution density
20 p3576 A69-37578

Porous hydrophilic oxygen electrodes behavior, showing electrochemical reaction influence on shape of current density vs voltage curves
20 p3484 A69-38071

High power density spacecraft hydrogen/oxygen fuel cells with open cycle heat and product-water removal subsystems and reactant tankage
23 p4076 A69-42309

Optimum thickness of dynamically stable composite superconducting tapes determined for substrate thickness as function of current density
24 p4361 A69-43121

CURRENT DISTRIBUTION

Planar arrays of linear antennas above stratified medium, showing antenna impedance and current distribution expressed in terms of free space environment
01 p0042 A69-10343

Current sheath surrounding exploding copper wire in vacuum, plotting current distribution as function of time and radius
01 p0119 A69-10669

Minority carrier density and diode current obtained as Laplace transforms from analyzing differential equations, describing charge carriers in semiconductor
01 p0049 A69-11361

Fourier transformation method for current distribution and driving point admittance of coupled antennas in dissipative medium
02 p0215 A69-11946

Dipole antenna current distribution, deriving simple, accurate formula for infinite, semiinfinite and finite cases
02 p0218 A69-12330

Temperature and current distribution in avalanching silicon p-n junctions
03 p0487 A69-13637

Anisotropically conducting spiral cone current phase distribution applied to frequency independent antennas analysis, discussing spiral motion and field azimuthal dependence effects
03 p0408 A69-14133

Current distribution in scanning rectangular array with all-directional constant sidelobe and narrowest beamwidth
04 p0570 A69-14302

Current nature on infinite cylindrical antenna in compressible anisotropic lossy plasma medium, noting characteristic waves on infinite cylinder
04 p0578 A69-15215

Distribution of current carrier concentration and mobility in p-type silicon doped with phosphorus ions
04 p0643 A69-15254

Beam transmission in electron guns having single apertured control grid, studying ratio of target current to cathode current
05 p0734 A69-16566

Absolute short term current efficiency of aluminum electrolytic cell, stressing aluminum amount determination in cathode
06 p0869 A69-17233

Statistical theory of traveling wave antennas for random phase-amplitude distribution of current, discussing phase errors
06 p0898 A69-17797

Current sheet pattern and gas flow stabilization in pulsed plasma accelerators
[AIAA PAPER 69-112] 06 p0971 A69-18140

Electromagnetic thrust equations for coaxial MPD accelerator, noting role of externally applied magnetic field
[AIAA PAPER 69-108] 06 p0972 A69-18197

Minority carrier distribution in doped semiconductors space-charge layer assuming relation between diffusion and Debye length
07 p1198 A69-18506

Diffusion current detection method applied to reverse biased volt-ampere characteristics of Ge diodes, noting surface leakage role
07 p1105 A69-19007

Surface recombination rate and retardation field effects on diffusion current in mesa diodes with low level injection
07 p1105 A69-19008

Current load distribution for optimizing MHD generator efficiency determined by variational method, noting dependence on relative length
07 p1058 A69-19012

Current and voltage distribution in electromagnetic compressor channel with solid electrodes of finite resistance, noting error analysis
07 p1059 A69-19029

Cylindrical antenna in uniaxial resonant plasmas, calculating current distribution and input admittance on basis of Wiener-Hopf technique
07 p1107 A69-19227

Long transmitting dipole antenna, studying current and charge distributions by Wiener-Hopf technique
08 p1281 A69-20019

Current distribution of long thin cylindrical antenna driven at arbitrary point along length
08 p1282 A69-20043

Magnetic field distribution and resistance of homogeneous type 2 superconductor cylinder at transition under effect of axial current
08 p1371 A69-20202

Radiation field patterns of linear antennas immersed in weakly ionized plasma evaluated for propagation constants of current distribution
08 p1285 A69-20551

Converging solutions for imaginary admittance and current distribution in linear cylindrical antennas
08 p1295 A69-21165

Electron drainage currents from dilute streaming plasmas to positively biased silicon and cadmium sulfide solar cell arrays
[AIAA PAPER 69-262] 09 p1436 A69-21726

Inhomogeneity distribution of carrier concentration and electrovoltaic effect in GaAs devices analyzed by scanning electron microscope
09 p1557 A69-21746

Ionization and current growth in discharge in rotating plasma device with mirror shaped magnetic field
09 p1552 A69-22042

Formation and acceleration of luminescent current layer in Z pinch discharge, noting density and electron mean free path in cold gas
09 p1552 A69-22397

Horizontal VLF cylindrical transmission antenna current distribution calculated with allowance for ground reaction, showing exponential decrease with distance
09 p1467 A69-22581

O shaped magnetic systems using unsaturated steel magnetic circuit to produce strong uniform magnetic fields for MHD machines
10 p1636 A69-23102

Current distribution and impedance of insulated cylindrical antenna embedded in dielectric cylinder immersed in compressible electron plasma
10 p1663 A69-23423

Two dimensional radiation from apertures in conducting cylinders of arbitrary cross section, solving current distribution, admittances and radiation patterns
11 p1836 A69-24985

Electric field vertical and radial components for time harmonic electric line sources with piecewise sinusoidal current distribution
11 p1836 A69-24995

Forward and reverse current-voltage characteristics and reverse biased capacitance for nZnSe-pGe emitter base diodes of heterojunction transistors
11 p1851 A69-25114

Current distribution on elements of circular arrays of tangential dipoles, discussing large odd component in zeroth order approximation
11 p1853 A69-25318

Current and voltage distribution around normal shock in MHD duct using conformal transformation, considering continuous and segmented electrode boundary conditions
11 p1931 A69-25359

Faraday type MHD energy converters in nonequilibrium conduction mode, analyzing two dimensional current and potential distributions in plane normal to magnetic field
11 p1826 A69-25397

Dielectric coated finite cylindrical antennas, using numerical and Wiener-Hopf methods to obtain input admittance and current distribution
12 p2041 A69-26604

Solar quiet currents in three dimensional ionosphere, considering ionospheric conductivity and horizontal layer equations
12 p2074 A69-26955

Fluctuations in electric field induced by plasma flow in constant magnetic field, performing spectral analysis of voltage and current fluctuations in plasma
13 p2310 A69-28029

Current distribution in MHD duct with permeable electrodes with tensor conductivity, obtaining Riemann-Hilbert heterogeneous boundary value problem solution by finding electric field
13 p2310 A69-28030

Current distribution along linear antenna array taking into account interaction between neighboring elements and effect on antenna radiation characteristics
13 p2236 A69-28572

Thermionic converters with matrix circuit connections, considering current flow patterns in matrices to evaluate electrical failure spreading
14 p2400 A69-29225

Current oscillations and electromagnetic radiation in low pressure cesium thermal emission converters using glass diode with plate geometry metal electrodes
14 p2402 A69-29246

Inhomogeneous distribution of nonequilibrium current carrier concentrations in semiconductors with electrons and holes of different lifetimes, noting instability
15 p2665 A69-30041

Current distribution and Hall voltage in crossed fields discharge with split electrodes in nonequilibrium Ar and Cs plasmas
15 p2663 A69-30980

Wind effects on ionospheric electric currents, using equivalent circuits to study tidal modes and current patterns
16 p2775 A69-32087

Current distribution and scattering cross section of missile with plume/ionized trail/ of tapered conductivity due to plane wave electromagnetic excitation
17 p2921 A69-33671

Steady state performance of multistrand superconducting compound conductors in current sharing state, using heat measurement from metal surface to He bath
17 p3016 A69-33786

Penumbra current distribution in plane electromagnetic waves diffraction by conducting cylinder, obtaining transient solution for impulsive excitation, discussing time harmonic problem
18 p3100 A69-34232

Equatorial electrojet current distribution determined using equivalent circuit method and magnetic force model, noting electron density profile influence on current density
18 p3130 A69-35186

Current distribution and input impedance of cylindrical antenna enclosed in uniaxial crystal and oriented along optical axis from thin antenna theory
19 p3285 A69-36878

High latitude magnetospheric convection patterns determined from ionospheric current distribution using magnetic disturbance plots
21 p3709 A69-38503

Scalar conductivity as governing parameter in determining current sheet diffusion and energy dissipation in MHD shock producing devices
21 p3776 A69-38708

Transient current change with minor change in voltage with double injection of electrons and holes in CdS single crystals, obtaining time dependence
21 p3780 A69-38833

MHD energy converters electric fields and current distributions, analyzing MHD flow problems
21 p3777 A69-39480

Direction finding characteristics of nonlinear antenna, including current determination and optimal angle for sidelobe level
21 p3684 A69-39619

Two dimensional analysis of junction transistor electrical behavior, analyzing DC and AC crowding effects, conduction and impedance of base and collector
22 p3911 A69-40011

Random function output current obtained in phototube and scintillation detector including amplitude distribution, time measurements and pulse shape discrimination
22 p3947 A69-40670

ELF atmospheric excitation, discussing cloud to ground and intracloud lightning discharges Fourier integration and current moment spectrum
23 p4115 A69-41562

CURRENT REGULATORS

Chemical phenomena during explosions of wires in various gaseous atmospheres, using apparatus with electronic crowbar for current flow regulation
01 p0081 A69-10680

Hydrogen and basic electrolyte cold cells, studying control systems for reactants supply, current, reaction by-products, etc
16 p2738 A69-32410

CURRENT SHEETS

Steady one dimensional motion of current sheets in plasma accelerators, noting condition of zero initial conductivity
01 p0133 A69-11220

Energy transfer from pulse network to mass associated with propagating current sheet in linear pinch discharge, discussing pulsed plasma accelerator efficiency
[AIAA PAPER 69-113] 06 p0971 A69-18123

Current sheet pattern and gas flow stabilization in pulsed plasma accelerators
[AIAA PAPER 69-112] 06 p0971 A69-18140

Pressure distribution in propagating current sheet structure in dynamic Z pinch discharge in argon, evaluating particle density, velocity and temperature profiles
[AIAA PAPER 69-264] 09 p1564 A69-21243

Current sheet velocity in coaxial plasma accelerator, noting drag due to insulator ablation and degassing [AIAA PAPER 69-265] 09 p1566 A69-21258

Modified first order theory of magnetosphere boundary shape incorporating effects of neutral sheet currents of extended geomagnetic tail 09 p1488 A69-21661

Electron and ion density distributions in propagating current sheet in Z pinch discharge in argon obtained by microwave reflection interferometer 16 p2816 A69-31639

Electromagnetic noise in current sheet in geomagnetic tail, discussing effects on distribution function [AFRL-69-0395] 16 p2781 A69-32317

Wave damping in current sheet in geomagnetic tail by radiating energy from sheet sides by electrostatic waves [AFRL-69-0396] 16 p2781 A69-32318

Shock and current sheet separation in magnetic shock tubes, determining electron temperature behind shock and within current layer 20 p3511 A69-38241

Dungey reconnection model of magnetosphere with dayside current sheet and pseudotrapping region compared with dayside observations of precipitation regions 21 p3711 A69-38511

Scalar conductivity as governing parameter in determining current sheet diffusion and energy dissipation in MHD shock producing devices 21 p3776 A69-38708

Collisional shocks in inverse pinch MHD shock producing device, discussing position in current sheet and effect on conductivity and diffusion 21 p3776 A69-38709

CURTISS-WRIGHT MILITARY AIRCRAFT
U MILITARY AIRCRAFT

CURVATURE

Asymptotic behavior of curvature and conformal curvature tensors on asymptotically flat space-time 01 p0116 A69-10393

Transverse curvature effect on skin friction and heat transfer in laminar flows past slender circular cylinders 02 p0232 A69-12210

Normal derivative of solutions to Dirichlet problem for elliptic quasi-linear equation and construction of given mean curvature hyperspace in curved space 02 p0272 A69-12221

Curved bodies substitution in unsteady hypersonic flow past slender sharp nosed bodies within framework of plane sections 02 p0191 A69-12576

Yaw parameter and curvature effects on accuracy of hot-wire anemometer, noting King law 03 p0426 A69-12845

Magnetic lines curvature behind pseudostationary hydromagnetic shock determined, assuming parallel magnetic field and velocity vectors 04 p0638 A69-15092

Two dimensional incompressible laminar boundary layer on curved wall for potential velocity inversely proportional to distance along origin [ASME PAPER 68-WA/FE-20] 05 p0749 A69-16096

Power law taperings for minimizing peak to trough deflection of cross section of strip bent longitudinally into cylindrical surface 06 p1023 A69-17374

Potential barrier curvature influence in aluminum trioxide tunnel junctions, noting ionic space-charge effect on shape 07 p1196 A69-18243

Reflected radio wave amplitude distributions related to distributions of curvature at reflector 07 p1086 A69-19225

Transverse magnetic field and shock strength effects on curvature ratio of attached shock waves and wedge 10 p1728 A69-23238

Buoyancy in turbulent shear flow, rotation or streamline curvature effects and meteorological parameters, drawing formal exact algebraic analogy 11 p1870 A69-24894

Electromagnetic field in idealized medium of uniformly curved gas lens for light beam waveguide, describing lens radius effects on incident beam spot 13 p2270 A69-27181

Flow and temperature boundary layers on longitudinally curved walls, giving higher approximation exact solutions 15 p2591 A69-30933

Triangular shell element SHEBA for arbitrary curvature variation as means of performing large displacement

matrix analyses, discussing local subelement, natural modes, cross sectional resultants, etc 16 p2872 A69-32025

Wall curvature effect on hydrodynamic stability of laminar incompressible boundary layer with respect to perturbing Tollmien-Schlichting waves 19 p3299 A69-36587

Normal derivative of solutions to Dirichlet problem for elliptic quasi-linear equation and construction of given mean curvature hyperspace in curved space 23 p4182 A69-41972

Transverse curvature effect on laminar free convection heat transfer from vertical isothermal cylinders [ASME PAPER 69-HT-G] 24 p4410 A69-43522

CURVE FITTING

Waveforms analyzer for mixtures of exponentially damped sine waves, noting application to interferometer curves in plasma wave propagation 17 p2970 A69-32852

Least squares method of smoothing curves or surfaces involving orthogonal base functions, discussing matrices conditioning and structure eigenmodes 18 p3218 A69-34642

Geodetic satellite measurements employing curve fitting approach using least squares analysis to resolve atmospheric refraction and shimmer problem 18 p3104 A69-35202

Minimum bias criteria for selecting data fitting curves, allowing for unknown true equation in improving data predictability [AIAA PAPER 69-950] 22 p3975 A69-40332

CURVED BEAMS

Elastoplastic stress-strain state of asymmetric profile thin walled beam under mobile load 05 p0841 A69-16205

Natural mode structural analysis matrix methods for small displacements, discussing curved local subbeam in space and circular arch 11 p1969 A69-24374

Strains in elastoplastic curved beam under bending obtained from approximating stress-strain diagram by parabola 17 p3056 A69-33192

Acoustic and internal dampings in freely supported uniform beams of circular and rectangular section, showing frequency dependence and vacuum effect 20 p3620 A69-37062

Curved beams ultimate strength using angular velocity considerations for collapse load 20 p3629 A69-38031

Torsion analysis of curvilinear rectangular prismatic beam reinforced by off-center circular rod, using conformal mapping 22 p4049 A69-41279

Elastic curve shape effects on volume of minimum weight uniformly strong beam under combined longitudinal and transverse bending 23 p4225 A69-41421

CURVED PANELS

Shot impact shaping of parts made of monolithic panels, relating curvature of profile to parameters of process 03 p0433 A69-12963

Natural vibrations of cylindrical panels analyzed on basis of Lamé parameters, shell equations and energy method 04 p0674 A69-14592

Simply supported isotropic cylindrical panel stability under axial compression, obtaining asymptotic series expansion for upper critical stress 08 p1419 A69-21182

Linear theory of cylindrical panel buckling and circumferential restraint along straight edges under lateral pressure, using Donnell equations 09 p1621 A69-22782

Stiffness matrix for doubly curved shallow shell element with rectangular plane projection applied to circular cantilevered cylinder and barrel vault 10 p1802 A69-23892

Laminar boundary steady two dimensional constant velocity flow over curved surface equation derived from Navier-Stokes equation 11 p1867 A69-24375

Similarity solutions for incompressible, steady hydrodynamic and thermal boundary layers on longitudinally curved walls, allowing for displacement and curvature effects 12 p2060 A69-25761

Pressure and heating rate correlations for rocket exhausts impinging on flat plates and curved panels, generating axisymmetric real gas exhaust plumes 12 p2190 A69-26781

Elastic directed curves dynamic theory, considering Hamilton principle, mass conservation and behavior of action density function under rigid body variations 13 p2360 A69-27321

Nonlinear Galerkin analysis of curved plate flutter, using shallow shell/von Karman equations and quasi-steady aerodynamic theory 13 p2364 A69-28207

Aerodynamic characteristics of plane inviscid fluid jets expanding over curvilinear surface, deriving force equations for surfaces in jet and rocket engines 19 p3296 A69-35815

Thin curved panels postbuckling behavior under axial compression, basing study on thin shell finite deformation theory and Galerkin method 20 p3629 A69-38112

Stiffness matrix for curved membrane shell, outlining discrete element representation of cylinders with widely spaced circumferential stiffeners 21 p3842 A69-39305

Curved shell elements in shell and plate analysis, discussing quadratic and cubic elements for space structures design 21 p3845 A69-39329

Curvature and temperature distribution in nonrotating long solid cylinders under solar radiation in interplanetary space 22 p4043 A69-40546

Curved rectangular elements stiffness matrices derived for finite element analysis of cylindrical shells bending 22 p4046 A69-40969

CURVED SURFACES
U CONTOURS
U SHAPES
U SURFACES

CURVES [GEOMETRY]
NT CYCLOIDS
NT S CURVES

Incompressible fluid steady motion in curved tube investigated by Fourier series, solving coupled nonlinear equations numerically 01 p0058 A69-10142

Numerical evaluation of curvilinear integrals and areas, using digital computer 01 p0106 A69-10867

Color index and mean light curves constructed for Cepheid Variables 08 p1395 A69-20635

Iterative method for least square polynomial curve fitting with abscissas and ordinates subject to error 08 p1343 A69-20827

Curve fitting for optimum redundancy reduction on sampled data, describing polygonal and approximate-polygonal techniques 09 p1533 A69-22458

Conformal mapping of regions with corners and large curvatures of boundary curves onto unit circle with digital computer, considering airfoil 10 p1724 A69-22880

CUSPS [MATHEMATICS]
NT DOUBLE CUSPS

Plasma stability criterion for universal mode, discussing cusp curvature stability 01 p0127 A69-10279

Optimum magnetic field axial component and plasma gun discharge voltage for high velocity plasma injection into symmetrical cusp field 05 p0805 A69-16655

Cusp magnetic field stabilizing superimposition on toroidal plasma discharge in polytron machine, noting role of Hall acceleration mechanism 06 p0965 A69-17514

Plasma lifetime in spherical multipole magnetic field trap compared to cusp trap 08 p1360 A69-20082

Electron and ion mobility in multiple cusp magnetic fields related to Polytron experiment 14 p2499 A69-29852

CUT-OFF

Cut-off frequency relation to geometry for dielectric ridge waveguide 05 p0777 A69-16579

Silicon resistance strain gage sensitivity dependence on crystallographic orientation following cut-off from single crystal 11 p1887 A69-25209

Taylor instability nonlinear oscillations, obtaining uniform solutions for wavenumbers near and larger than cut-off 21 p3693 A69-38703

CUT-OUTS
U OPENINGS

CUTTERS

CUTTERS

Screw-nut feeder and adjuster systems with compensation for clearance and wear of cutting tools, determining efficiency for conversion of rotary to translational motion

23 p4168 A69-41414

CUTTING

NT METAL CUTTING
NT MILLING [MACHINING]
NT SHEARING
NT SPARK MACHINING

Machine cutting tool for cutting and splicing endless magnetic tape 30 microns thick, noting film safety feature and nonmagnetic steel scissors

08 p1321 A69-20876

Ceramic substrate cutting with carbon dioxide laser by scribing perforation pattern,

10 p1699 A69-23302

Gas laser cutting of thin carbon films on thick pyrex glass and ceramic substrates

15 p2635 A69-31037

Thin film carbon resistors cutting with carbon dioxide gas laser, considering cylindrical bodies and aging properties

15 p2635 A69-31038

CV-990 AIRCRAFT

Radar cross section of missile and aircraft configurations, comparing theoretical and experimental results for Convair 990 static test model

03 p0384 A69-12911

Life raft thermal protection against exposure of aircrews to cold, noting chemically fueled heaters and IR reflective liners

06 p0883 A69-17841

CW RADAR

U CONTINUOUS WAVE RADAR

CYANIDES

NT CYANOGEN
NT HYDROGEN CYANIDES

Excited cyanide molecules concentration in arc discharge determined from spectral bands absolute intensities during electron transition

15 p2654 A69-30080

Polycrystalline ammonium cyanide IR absorption spectrum as function of temperature, discussing ammonium ion hydrogen bonding to C or N atoms

24 p4280 A69-43809

CYANO COMPOUNDS

NT ISOCYANATES

Methyl 2-cyanoacrylate adhesive bonding characteristics, noting importance of film thickness

09 p1529 A69-22316

Reflection and transmission measurements on as grown surfaces of tetracyanoquinodimethane, obtaining optical constants by Kramer-Kronig method

18 p3183 A69-35477

CYANOGEN

Cyanogen band absorption in nuclei of elliptical and spiral galaxies derived from photoelectric measurements indicating rich metal content in central cores

12 p2153 A69-25803

Cyanogen molecules increase attributed to nova shell compression from analyzing absorption spectrum of DQ Herculis 1934 after brightness maximum

15 p2688 A69-30558

Coupled equations for determining cross sections for rotational transitions in CN induced by low energy electron impact

21 p3773 A69-38476

CYANOPHYTA

U BLUE GREEN ALGAE

CYBERNETICS

Book on applications of information theory to dynamical systems with random initial conditions and cybernetic systems consisting of communication systems with feedback

04 p0580 A69-14520

Systems science and cybernetics - IEEE Conference, San Francisco, October 1968

05 p0741 A69-15801

Flexible vehicle control, using cybernetic model for system design and response [AIAA PAPER 69-115]

06 p1018 A69-18088

Cybernetic problems in bionics - Conference, Dayton, May 1966

07 p1069 A69-18380

Cybernetic structural model for learning and mentation comprehending symbol systems, languages, homeostatic mechanisms, etc

07 p1070 A69-18385

Adaptation process of management systems from point of view of control system philosophy [AIAA PAPER 68-807]

08 p1422 A69-20197

Cybernetic theory application to automatic spacecraft, discussing control problems in Mariner 4 and Surveyor 7 missions and attitude stabilization system

08 p1409 A69-20583

Book on neurocybernetics and neurobionics covering mathematical and physiological models, artificial neurons, image recognition theories, biological control systems, etc

19 p3263 A69-36747

Mathematical model for information processing of biological memory as cybernetic system

23 p4110 A69-41982

Cybernetic approach to memory, proposing model characterized by hierarchical structural order and sequence to study physiological rhythms

23 p4110 A69-41983

CYCLES

NT ACTIVITY CYCLES [BIOLOGY]

NT BRAYTON CYCLE

NT RANKINE CYCLE

NT SOLAR CYCLES

NT STIRLING CYCLE

NT STRESS CYCLES

NT SUNSPOT CYCLE

NT THERMODYNAMIC CYCLES

NT WORK-REST CYCLE

Periodic cycles in linear closed loop integral pulse FM systems, discussing existence conditions, periodic formulae and stability criterion

05 p0737 A69-15865

Oscillation cycle of atmospheric circulation, analyzing solar activity effects on lunar and solar semidiurnal tides and transition from zonal to meridional circulation

12 p2070 A69-26692

CYCLIC ACCELERATORS

U BETATRONS

U SYNCHROCYCLOTRONS

U SYNCHROTRONS

CYCLIC HYDROCARBONS

Oxygen addition to fuel stream effect on formation of soot and polycyclic aromatic hydrocarbons in ethane-air and ethylene-air diffusion flames

02 p0205 A69-12318

Photolytic conversion of allene to cyclopropylidene, discussing cyclononadiene in vapor phase and resulting product

02 p0205 A69-12721

Chemical bond nature and properties in cyclic compounds of carbon and graphite, presenting bond energy computation method

07 p1171 A69-18932

Ion pairing effects of cyclooctatetraene anion radical, studying electron spin resonance spectra temperature dependence

10 p1651 A69-22938

Interstellar extinction models of classical Mie particles and quantum mechanical polycyclic aromatic molecules

10 p1781 A69-23679

Analytical, IR absorption and polarographic analysis of cyclic niobium V/ and tantalum V/ esters

11 p1832 A69-24575

Gas chromatographic and mass spectrometric analyses of alicyclic hydrocarbons from Carboniferous organic materials, noting alkane distribution and evolutionary histories

17 p2917 A69-34184

Mono and bicyclic hydrocarbons effect on jet fuels combustion properties, considering burnup factor, deposit and smoke production levels

18 p3184 A69-35382

Chemical bond nature and properties in cyclic compounds of carbon and graphite, presenting bond energy computation method

21 p3752 A69-39153

CYCLIC LOADS

Ultrasonic detection and measurement of fatigue cracks in notched cylinders subjected to reversed axial cyclic loading

01 p0078 A69-10113

Low cycle fatigue life of aluminum alloy in reversed biaxial bending

01 p0093 A69-10116

Yield curve softening in hard Al subject to cyclic torsional loading, noting deformation resistance, surface hardness and yield strength

04 p0671 A69-14411

Inelastic strain measurement in metals during cyclic loads by impact tester

04 p0674 A69-14539

Glued metal joints under cyclic loading evaluated by change in short term strength as function of time at stress levels

04 p0605 A69-14540

Repeated loading influence on microstrain region, noting decrease in size with each cycle

05 p0836 A69-15876

Coupled heat equation to calculate transient and steady state temperature distributions in viscoelastic solids under cyclic deformations

05 p0836 A69-15878

Linear cumulative damage theory defining low cycle fatigue region of classic S-N curve, providing biaxial strain mode by centrifugally loading rotors [ASME PAPER 68-WA/MET-8]

05 p0838 A69-16151

Fatigue crack propagation in machine parts under cyclic loading

05 p0842 A69-16543

Polycarbonate surface stiffness increase associated with fatigue induced by repetition of loads

06 p0946 A69-17206

Fatigue life in nonstationary cyclic loading above endurance limit, describing methods of shortened fatigue tests for fatigue life

07 p1231 A69-18403

Static endurance of aircraft structural elements under single and multiple loading, based on real alloys and crystalline materials theories

07 p1231 A69-18554

Crack growth during cyclic loading in elastoplastic bodies

07 p1232 A69-18992

Chromium steel /E1961/ susceptibility to structural damage under cyclic loads by nondestructive inspection of magnetic hysteresis and eddy current losses

07 p1141 A69-19316

Impact cyclic loading fatigue tests of smooth and notched duralumin, discussing increased impact strength resulting from initial underloading

07 p1167 A69-19317

Strain concentration design factors for notch effect in low cycle fatigue and crack propagation conditions

07 p1235 A69-19383

Aircraft reliability under cyclic loads in flight taking into account stress fluctuations

08 p1322 A69-21106

Heat resistant nickel alloys static and dynamic properties at high temperature, creep-fatigue interaction, etc

09 p1523 A69-21609

Governing equations for bending of fixed isotropic circular sandwich plate subjected to eccentric concentrated load

09 p1615 A69-21926

Low cycle fatigue fracture behavior at high temperatures, noting fatigue crack behavior and crack density concept

10 p1797 A69-23081

Progressive accelerated fatigue testing for reliability in determining fatigue limits

10 p1800 A69-23349

Metal fatigue at elevated temperatures concerning viscosity, energy loss and stress, strain and temperature cycling

10 p1803 A69-24043

Damped steady state response of elastic foundation beam subjected to cyclic moving loads to determine load movement frequencies for natural frequency excitation [ASME PAPER 69-VIBR-13]

10 p1806 A69-24166

Incremental collapse of shells under cyclic loadings in terms of generalized variables, finding interaction surfaces of load multipliers

11 p1980 A69-24820

Fcc metals cyclic deformation and fatigue dependence on cross slip of screw dislocations, considering strain hardening and crack propagation

11 p1906 A69-25389

Zero Gaussian curvature rib reinforced shells free oscillations reduced to nonreinforced shell forced oscillations under cyclic loads

12 p2177 A69-25996

Energy dissipation and fatigue in metals under cyclic static loads, determining logarithmic decrements of vibrations and Bauschinger effect

12 p2181 A69-26612

Slip band extrusions in hexagonal close packed Cd, Mg and Ti subject to cyclic stresses, noting microstructural changes

12 p2116 A69-26912

Tension-compression fatigued alpha Ti twin formation contribution to fatigue damage during cyclic loading

12 p2116 A69-26913

Crack growth and crack initiation in cylindrical specimens subject to low cycle strain controlled ten-

sion-compression induced fatigue, noting measurement techniques
12 p2188 A69-26914

Low cycle fatigue crack initiation in Ti-6Al-4V at room and high temperatures and in aqueous salt environment
13 p2278 A69-27413

Ultrasonic detection and measurement of fatigue cracks in notched cylinders subjected to reversed axial cyclic loading
14 p2445 A69-28882

Linear cumulative damage theory defining low cycle fatigue region of classic S-N curve, providing biaxial strain mode by centrifugally loading rotors [ASME PAPER 68-WA/MET-8]
14 p2535 A69-29438

Repeated static stress limit of internal pressure vessels, emphasizing effect of redistribution of stresses and strains
15 p2712 A69-30973

Load carrying capacity of thin steel plates fatigued by cyclic shear buckling
17 p3052 A69-32980

Fatigue fracture due to heat generation in polycarbonate subjected to pulsating tensile load, presenting temperature change per unit stress increase
18 p3163 A69-35498

Ronay effect in reversed cyclic torsion or tension in thin cylindrical viscoelastic tube showing creep under sustained load
20 p3625 A69-37596

Automated device for load carrying ability of structural elements like gas turbine blades under thermal and mechanical cyclic loads
20 p3544 A69-37816

Fatigue endurance determined from thermal stresses by balancing elastic strain rates, creep relaxation and mechanical cyclic loading with triangular waveform, discussing nonsteady creep
21 p3843 A69-39310

Nonmetallic inclusions effect on steels cyclic strength dependence on inclusion composition and metallic matrix properties, derived from fatigue tests
22 p4047 A69-41064

Static and cyclic tensile fatigue of alumina by ring test method, measuring time to failure
24 p4334 A69-43343

CYCLING
U CYCLES

CYCLOHEXANE
Stabilized low temperature ignition of cyclohexane using vertical flow reactor
02 p0304 A69-12314

Cyclohexane and benzene anodic oxidation at fuel cell electrodes, noting cathodic desorption products as function of potential and reactant [ECS PAPER 330]
15 p2562 A69-31540

CYCLOIDS
Spherical trajectories control by star height maintenance, analyzing resulting cycloid and cartographic representations
23 p4186 A69-42023

CYCLONES
NT HURRICANES
NT TYPHOONS

Spiral structure of cloudiness in occluded cyclones studied by mathematical model based on meteorological satellite photographs [UN PAPER 68-95429]
01 p0109 A69-10505

European cyclonic system developmental phases determined from characteristic structural features of satellite cloud pictures [UN PAPER 68-95711]
06 p0950 A69-17070

Horizontal ozone distribution at high cyclones and anticyclones in middle stratosphere
08 p1308 A69-20261

Air flow distribution and wind velocities in cyclones constructed from Cosmos 122 TV cloud images
11 p1912 A69-24825

Vertical air flow asymmetrical distribution ascribed to cyclone motion and thermal inhomogeneity by studying spiral cloud configurations in cyclone area
11 p1912 A69-24829

Papers on experimental and theoretical research on atmospheric circulations, jetstream and cyclonic disturbances
17 p2999 A69-33757

Cyclonic vortices production by horizontal convergence in rotating water bowl as function of bottom surface inclination, modeling cyclogenesis in jet stream entropy field
17 p3000 A69-33760

Numerical weather prediction using four level primitive atmospheric model for studying frontogenetic processes in deepening cyclone
19 p3303 A69-36408

CYCLOTETRAMETHYLENE TETRANITRAMINE
U HMX

CYCLOTETRAMETHYLENE TRINITRAMINE
U RDX

CYCLOTRON FREQUENCY
Cyclotron drift instabilities of low pressure plasma containing charged impurities
03 p0478 A69-13834

Power flow in cyclotron and plasma modes propagating in waveguide filled with cold collisionless axially magnetized plasma
06 p0897 A69-17760

Epithermal microwave radiation from plasma produced by PIG Reflex in magnetic field with mirror geometry, discussing radiation at harmonics of electron cyclotron frequency
08 p1370 A69-21019

Increased energy losses and microwave emission at cyclotron frequency harmonics during plasma electron heating at cut-off plasma concentrations in magnetic trap
10 p1728 A69-23130

Electromagnetic wave transmission through anisotropic plasma, discussing incident wave field strength effects near cyclotron frequency
10 p1728 A69-23167

Cyclotron harmonic waves /CHW/ nonlinear decay instability and parametric amplification, considering applicability to practical amplifiers
12 p2135 A69-26314

Spatial harmonics of harmonic frequency instabilities of cyclotron half frequency in system of two symmetrical electron beams confined by magnetic field
13 p2314 A69-28364

Electromagnetic field eigenvalues along conductive circular cylinder in magnetoionic medium, assuming lossless medium and field frequency not equal to cyclotron frequency
16 p2754 A69-32568

Time resolved beam distribution functions resulting from cyclotron instability and harmonics in electron injection machine during beam-plasma experiment
17 p3014 A69-33829

PPi bursts interpreted as proton beams cyclotron instability in geomagnetic field
20 p3521 A69-37039

Pearl type geomagnetic micropulsation development by studying Alfvén waves cyclotron instability in plasma with hot protons anisotropic distribution
23 p4206 A69-41850

RF impedance probe used for ionospheric composition measurements, describing antenna operation in ion-electron cyclotron frequency range
24 p4308 A69-43008

CYCLOTRON RADIATION
Electron cyclotron harmonic waves in magnetoplasma irradiated by external microwaves
01 p0127 A69-10335

Solar radio emission slowly varying component theory, discussing main characteristics of cyclotron and bremsstrahlung radiations of thermal electrons
02 p0314 A69-11636

Electron cyclotron instability and HF ionization in beam-plasma experiment using electron beam guided by magnetic field through He gas
05 p0798 A69-15612

Nonlinear interaction between cyclotron harmonic waves, demonstrating synchronism conditions for traveling wave parametric amplification and passive mode conversion
07 p1189 A69-18439

Solar type 4 bursts characteristics accounted for by cyclotron mechanism, assuming models of spot magnetic field configuration and electron density distribution
07 p1205 A69-18959

Electromagnetic wave attenuation propagating along external magnetic field ascribed to cyclotron wave energy absorption by resonant plasma particles
08 p1277 A69-21077

Cyclotron waves interaction when propagating in solid state plasma in magnetic field, determining amplification zones and factors
08 p1374 A69-21078

Jupiter model /cyclotron/ of pulsar radiation generation
09 p1608 A69-22761

Plasma-cyclotron interaction wave coupling mechanism in symmetrical double beam system in uniform magnetic field leading to unstable wave excitation along beam
17 p3015 A69-33831

Electromagnetic and cyclotron waves interaction across opaque boundary in moving plasma in one dimensional approximation
18 p3181 A69-35027

Pulsar CP 0328 radiation mechanism, considering relativistic effects of rapid rotation
22 p4035 A69-41206

Proton cyclotron echoes on ionograms obtained from topside ionosphere by Alouette 2 satellite
24 p4310 A69-43189

CYCLOTRON RESONANCE
Anisotropic plasma cyclotron instability in magnetic trap with cold ion background and isotropic Maxwellian velocity distribution
02 p0292 A69-12554

Region of plasma electron capture during cyclotron electron resonance in magnetic trap with mirrors
03 p0478 A69-13849

Packet of finite amplitude VLF whistler waves, examining cyclotron resonance interaction with high energy electrons and development in magnetosphere
06 p0917 A69-17378

Cyclotron instability of outer radiation belt protons, taking into account data on spatial distribution and ion composition of exospheric plasma
06 p0919 A69-17721

Cyclotron resonance measurements of quantum effects in Ge valence bands by CW molecular gas laser, developing tunable submillimeter maser [IEEE PAPER C-6]
07 p1150 A69-19051

Cyclotron- and bounce-resonance scattering of electrons trapped in geomagnetic field for pitch-angle scattering, noting whistler mode disturbances
07 p1208 A69-19367

Ion cyclotron resonance acceleration and higher harmonic acceleration in axially nonuniformly magnetized plasma under influence of RF electric field
08 p1360 A69-20079

Nonadiabatic and stochastic mechanisms for cyclotron resonance trapping and heating in magnetic mirror geometries
08 p1364 A69-20518

Electron cyclotron resonance absorption of injected radiation magnetic mirror, noting effect of RF heating on plasma electron distribution
08 p1364 A69-20519

Resonant interaction between traveling charge with superimposed magnetic field and Alfvén wave in plasma cylinder, showing cyclotron orbit variations
09 p1551 A69-22035

Small signal and saturation characteristics for X band cyclotron resonance oscillator, discussing device design and configuration
09 p1470 A69-22786

Electron cyclotron resonance measurement in n-type indium antimonide using far IR emission from HCN and water vapor lasers, noting magnetic field strength effects
13 p2270 A69-27200

Electric field frequency effect on cyclotron resonance during gas discharge, establishing causes of discrepancy between theory and experiments
13 p2315 A69-28577

Cyclotron resonance of minority carriers measured in p-type InSb, giving temperature dependences of absorption derivative and field ratio to line half width
15 p2667 A69-30068

Anisotropic plasma cyclotron instability in magnetic trap with cold ion background and isotropic Maxwellian velocity distribution
15 p2658 A69-30251

Electron distribution function for weakly ionized plasma under alternating electric and circularly polarized rotating magnetic field, noting cyclotron resonance
16 p2820 A69-31753

Ion structure of keto and enol and McLafferty rearrangements determined by ion cyclotron resonance spectroscopy
19 p3265 A69-36288

Acetonitrile ion-molecule chemistry using ion cyclotron resonance, discussing reaction of vibrationally excited methyl ions from electron impact
19 p3265 A69-36290

Relative gas phase acidities of carbon acids determined using ion cyclotron resonance spectroscopy
19 p3265 A69-36291

Ion cyclotron double resonance technique to identify collision-induced ion fragmentation pathways illustrated with p-chloroethylbenzene
19 p3265 A69-36292

Ion-molecule reaction rate constants measurement by ion cyclotron resonance, assuming no ion and neutral gas molecules collisions

20 p3579 A69-37495

Frequency shifts observed in Alouette 2 cyclotron harmonic plasma resonances, noting antenna length and direction

20 p3496 A69-37892

CYCLOTRONS

NT MICROTURNS

NT SYNCHROCYCLOTRONS

Magnetoquantum-electric effect, analyzing center motion of cyclotron orbit during photon and phonon absorption and current quantity

16 p2826 A69-31823

CYGNUS CONSTELLATION

IR radiation of NML Cygnus with O/C ratio close to unity ascribed to circumstellar shell of graphite particles

03 p0513 A69-13775

Crab Nebula and Cygnus XR-1 X ray spectra shown to have differential number power law spectra and same intensity

05 p0813 A69-15846

Celestial X ray sources astronomy, discussing emission mechanism in 2 to 100 kev range and balloon observations in Cygnus and Taurus constellations

05 p0817 A69-16715

Identification of emission lines from 3200 to 7000 Å in Eta Carinae spectrum, noting P Cygni-like absorption lines

06 p1002 A69-17263

Radio spectra of supernova remnants Cygnus Loop and IC443, noting possible radiation from shell source

06 p1003 A69-17322

Balloon observations of cosmic X ray sources in Cygnus and Crab Nebula, discussing data application to energy spectra analysis

07 p1210 A69-19716

Radio observations of gamma Cygni source in Cygnus X complex showing nonthermal nature of source, noting weak but significant polarization

08 p1387 A69-20090

Galactic neutral hydrogen structure in region of Cygnus observed with parabolic antenna and frequency-switched radiometer

08 p1388 A69-20243

Spectroscopic evidence for mass loss from CH Cygni based on observations of chromospheric lines of high dispersion spectrograms

08 p1396 A69-20651

Narrow band photometry of variable stars and X ray source Cyg X-2, considering continuum variations with time

09 p1591 A69-21451

Hydrogen alpha emission nebulae catalog in western half of Cygnus X region, obtaining interstellar absorption from nebular distances determination

09 p1596 A69-22053

IR spectrum of NML Cygnus star with Michelson interferometer, noting CO bands and IR excess

09 p1602 A69-22229

Spectrographic observations indicating temperature range within individual filaments of Cygnus Loop, noting agreement with stratified models

09 p1607 A69-22430

Preliminary observations of Tau-A, Cas-A and Cyg-A with multiple-element interferometer

10 p1777 A69-23397

Spectroscopic observations of optical object identified with X ray source Cygnus X-2 noting radial velocity in absorption and emission lines

10 p1785 A69-24097

Spectrum of IR object NML Cygnus, discussing model based on circumstellar IR emission

10 p1785 A69-24101

Hydroxyl microwave emission sources in Cygnus not connected with continuum emission

11 p1964 A69-25403

UBV observations of stars P and 36 Cygni including short period variations and secular changes in brightness

12 p2172 A69-27159

Photoelectric scanning of CH Cygni spectrum calibrated and compared with 45 Arctis, discussing high dispersion, excess blue and UV continua, H beta emission, etc

13 p2338 A69-27557

Spectrophotometry of variable star SS Cyg, analyzing energy distribution in continuum, UV gradient and Balmer jump

13 p2351 A69-27868

P Cyg star HD 190603 atmospheric parameters from spectrograms analyzed by curve of growth method, in-

cluding ionization and excitation temperatures and electron density

14 p2519 A69-29357

Milky Way structure, discussing dust bridge and density of absorbing matter between spiral arms of Sagittarius and Carina Cygnus

15 p2683 A69-30514

Photoelectric /UBV/ photometry of Cepheids in Cygnus and Monoceros noting sequence stars near Nova Cyg 1948

15 p2692 A69-30772

Energetic gamma ray emission from Cygnus A and X-1, describing high altitude balloon telescope observation and gamma ray emulsion process

15 p2676 A69-30888

RF spectral line detection from ortho hydrogen ions in Omega Nebula and NML Cygnus

16 p2864 A69-32571

Spectroscopic study of P Cygni showing ionization temperature, Balmer decrement agreement with calculated value and chemical composition

16 p2864 A69-32595

Spectrophotometry of F stars 42 Cyg and nu Her atmospheres, analyzing microturbulence, excitation and ionization temperatures, electron pressures and abundances

16 p2864 A69-32596

Radio emission from Cygnus X-2 reporting on observations at 4.5 cm wavelength

16 p2865 A69-32804

MH alpha 328116 /Cygnus/ spectrum noting three Fe IV lines

16 p2866 A69-32815

Day sky brightness at altitude above 100 km obtained during rocket flight compared to night sky viewed from ground

17 p3037 A69-33664

NbO presence uncertainty in S type stars due to close coincidences with ZrO bandheads, noting 6484 and 6591 lines in R Cygni spectrogram

19 p3403 A69-35964

Forbidden emission transition probabilities in high excitation symbiotic stars, novae, Cygni stars and peculiar binaries

19 p3423 A69-36227

Radio emission intensity of Cas-A and Cyg-A at 30-60 cm, giving spectral indices

19 p3428 A69-36876

Balloon-borne proportional counters to measure X rays intensity and spectral distribution from Taurus X-1 and Cygnus X-1

20 p3593 A69-38153

IR spectrum of NML Cygnus star using rapid scanning Michelson interferometer, estimating temperature from CO bands

21 p3800 A69-38678

Photoelectric observation of EM Cygni eclipsing binary and old nova

22 p4015 A69-40151

P Cygni spectroscopy indicating existence and atmospheric structure of accelerating envelope about star, computing line profiles

22 p4023 A69-40471

Photoelectric observations of eclipsing binary 32 Cygni during 1968 eclipse using standard UVB color filters, tabulating results of UVB photometry

22 p4032 A69-40946

Absorption features of 21 cm neutral hydrogen line in part of Cygnus X and of W 49, showing equal velocity contour diagrams from right ascension scans

22 p4034 A69-41200

Photometric data for variable stars in Lyra and Cygnus including eclipsing variables

23 p4215 A69-42009

Photometric data for long period variable stars in Cygnus obtained from plates of various observatories

23 p4215 A69-42010

P Cygni characteristics and spectrum analysis, describing absorption lines, line widths, atmospheric composition, light variations, etc

24 p4391 A69-43803

CYLINDERS

Stress fields in Hertzian contact of parallel cylinders composed of anisotropic materials and transversely isotropic spherical bodies

08 p1414 A69-20524

Conformal transformation reducing transverse thermal resistance of cylinder of revolution to thermal resistance of semiinfinite medium

12 p2190 A69-26292

Shock detachment distance for flow around cylinders and spheres determined by microphotometric

tracing of negatives of photographs of forward stagnation streamlines

17 p2949 A69-32962

Forces on stationary cylinder under sinusoidal flow, considering symmetrically located vortex pairs and flowfield

[ASME PAPER 69-FE-13] 21 p3643 A69-38601

Heat loss from cylinders at low Reynolds numbers in N-He and N-Ne binary mixtures

21 p3848 A69-38706

Temperature potentials in cylinder of known radius, investigating optimal heating regime and thermal kinetic factor effect on maximum potential magnitude

21 p3837 A69-39089

Thermal stresses and displacements in long isotropic hollow cylinder heated on part of outer curved surface, analyzing temperature distribution

21 p3838 A69-39166

Flow structure in wake behind cylinder in plane channel, discussing circulation zone variation and velocity and turbulence distribution at various channel cross sections

21 p3698 A69-39850

CYLINDRICAL AFTERBODIES

U AFTERBODIES

CYLINDRICAL ANTENNAS

Fourier transform solution for cylindrical antennas of arbitrary length, discussing simplification and applications to solid antennas and antenna in conducting media

03 p0405 A69-13624

Current nature on infinite cylindrical antenna in compressible anisotropic lossy plasma medium, noting characteristic waves on infinite cylinder

04 p0578 A69-15215

Input admittance of cylindrical dipole antenna immersed in cold isotropic lossless plasma medium and insulated by ion sheath or unit permittivity dielectric

04 p0580 A69-15490

Numerical values for cylindrical antenna admittance in uniaxial plasma, considering plasma compressibility and vacuum sheath

06 p0965 A69-17513

Cylindrical antenna in uniaxial resonant plasmas, calculating current distribution and input admittance on basis of Wiener-Hopf technique

07 p1107 A69-19227

Current distribution of long thin cylindrical antenna driven at arbitrary point along length

08 p1282 A69-20043

Cylindrical antenna input impedance in isotropic plasma, assuming weak three dimensional plasma diffusion

08 p1285 A69-20428

Converging solutions for imaginary admittance and current distribution in linear cylindrical antennas

08 p1295 A69-21165

Current distribution and impedance of insulated cylindrical antenna embedded in dielectric cylinder immersed in compressible electron plasma

10 p1663 A69-23423

Radiation fields induced by constant current in elliptic ring, discussing analysis results applicability to elliptic capacitive antennas and annular slot

11 p1850 A69-24981

Two dimensional radiation from apertures in conducting cylinders of arbitrary cross section, solving current distribution, admittances and radiation patterns

11 p1836 A69-24985

Radiation pattern of axial slot on circular conducting cylinder based on wedge diffraction and creeping wave theory

11 p1836 A69-24993

Directional solar thermal field /sunlight/ effect on coupled nonplanar transverse and torsional vibrations of satellite cylindrical antennas in orbit

11 p1994 A69-25534

Electric field penetration into homogeneous plasma at frequencies near Langmuir frequency and current at surface of thin cylindrical antenna in plasma

11 p1853 A69-25551

Radiation pattern of circular cylindrical dielectric rod antenna excited in mixed magnetic and electric modes, discussing mode transducer

12 p2035 A69-25900

Dielectric coated finite cylindrical antennas, using numerical and Wiener-Hopf methods to obtain input admittance and current distribution

12 p2041 A69-26604

Subtraction procedure for feedpoint singularity in current on axially symmetric antenna with slice generator

12 p2041 A69-26864

Field patterns for wave radiation from electric dipole immersed in anisotropic plasma column excited by longitudinal DC magnetic field

12 p2034 A69-27103

Admittance of radiating elements in circular array with longitudinal slots on conducting cylinder, taking into account element interactions

13 p2234 A69-28505

Current distribution and input impedance of cylindrical antenna enclosed in uniaxial crystal and oriented along optical axis from thin antenna theory

19 p3285 A69-36878

Admittance of infinite cylindrical antennas driven from coaxial line

20 p3507 A69-37846

VHF cavity backed cylindrical gap antenna input tuning impedance and equatorial radiation patterns controlled by cavity adjustments

22 p3914 A69-40698

Equatorial radiation pattern of parallel plate TEM mode axial slot on elliptical conducting cylinders, using wedge diffraction and creeping wave theory

22 p3914 A69-40703

Synthesis of antenna arrays of longitudinal passive slot radiators on metallic cylinder excited by single active slot, including experimental patterns

23 p4138 A69-41936

Solid cylindrical antenna current and admittance calculation, considering reflection coefficient and multiple reflection phenomena at antenna ends

23 p4142 A69-42336

CYLINDRICAL BODIES

NT ROTATING CYLINDERS

Self gravitating pulsating cylindrical and ring shaped cosmic masses from group theory standpoint compared with oscillating stars

01 p0148 A69-10124

Axisymmetric transient thermoelastic problem for transversely anisotropic hollow cylinder, examining boundary value problems

01 p0166 A69-10302

Luminous flow in front of sphere and behind cylinder under high temperature and low density conditions, discussing profiles of shock waves

02 p0189 A69-12182

Reflection of plane electromagnetic wave from impedance cylinder in vacuum, using ray expansion method

02 p0217 A69-12262

Cylindrical afterbodies at free stream Mach 2 with hot argon gas ejection, discussing flow rate influence on base pressure

02 p0190 A69-12533

Permittivity measurements by measuring impedance on thin cylinders in rectangular waveguide or in cavity formed by coaxial transmission line

02 p0222 A69-12756

Scattering from thin conducting sheet obstacle on cylindrical surface

03 p0399 A69-14253

Heat transfer and drag of cylinders with cavities at hypersonic speeds measured by platinum film thermometer and strain gauge balance in gun tunnel [DVL-850]

04 p0543 A69-14822

Heat diffusion in cylinder with heat sources creating axisymmetric temperature distribution, using Gauss hypergeometric function and Meijer G-function

04 p0687 A69-15188

Secondary steady flow /Taylor vortices/ between rotating cylinders, discussing development due to stability loss of Couette flow

05 p0745 A69-15780

Quantitative analysis of nonsteady temperature field in long cylinder for sudden heating of semiinfinite axisymmetric lateral surface

05 p0845 A69-15797

Free convective heat transfer of cylinder in rarefied gas yielding Nusselt number as function of Grashof, Prandtl and Knudsen numbers

05 p0846 A69-15904

MHD flow of compressible conducting fluid around cylindrical body with quasi-aligned magnetic field and velocity

07 p1194 A69-19350

Scattering and diffraction of plane electromagnetic wave incident on conducting cylinder coated with moving anisotropic medium

07 p1086 A69-19469

Wake deformation for horizontal and vertical cylinders present in wake of hovering rotor, using flow visualization technique [AIAA PAPER 69-228]

07 p1051 A69-19551

Natural convective oscillatory three dimensional flow in cylindrical annuli, describing inception, amplitude, period and wavelength

09 p1481 A69-21902

Diffraction problem on cylindrical bodies of arbitrary shape reduced to integral equations by using Green functions for free spaces

09 p1459 A69-22634

Heat transfer coefficients for free convection from single horizontal cylinder to fluids computed from empirical correlation

09 p1625 A69-22693

Solid cylindrical body entrainment by viscous incompressible fluid flow in tube under constant pressure gradients and absence of gravitational force

10 p1678 A69-23366

Surface currents, scattered field and scattering cross section for perfectly conducting cylinder found by reducing two dimensional problem to solving coupled differential equations

10 p1657 A69-23860

Axisymmetric problems in thermoviscous plasticity, discussing stress-strain state of annular disks and thick walled cylinders made of rate sensitive materials

10 p1802 A69-24025

Analog simulation of cylinder wake potential for hypersonic motion in collisionless plasma

11 p1926 A69-24756

Optimum cooling of homogeneous isotropic cylindrical body with constraints on magnitude of thermoelastic stresses

11 p1976 A69-24772

Steady heat flow in cylindrical bodies with curvilinear rectangular cross sections, solving equation in form of Fourier series according to trigonometric functions

11 p2000 A69-24974

Sandwich electrode for direction and magnitude measurement of velocity gradients at wall for flow around cylinder at high Reynolds numbers

11 p1872 A69-25132

Finite difference solutions for time dependent equations of motion for steady flow around cylinder at large Reynolds numbers

11 p1872 A69-25133

Flexible cylinder vibration in nominally axial flow, discussing length, mass, flexural rigidity and diameter variation effects on vibration amplitude

11 p1984 A69-25166

Skin friction drag coefficient for right circular cylinder calculation coefficient on basis of Blasius solution for flow

11 p1819 A69-25384

Supersonic and hypersonic flow of rarefied gas around blunt cylinders at various angles of attack, noting pressure distribution on model surface

11 p1821 A69-25478

Channel wall effect on gain of apparent mass of cylindrical and elliptical bodies floating in channel and subject to vertical impact

11 p1875 A69-25487

Elastic waves propagation in micropolar cylinder, treating longitudinal and torsional monochromatic waves in Cosserat medium

11 p1995 A69-25606

Two and three dimensional quasi-static problems in coupled thermoelasticity, obtaining solutions for space containing cylindrical cavity and for solid cylinder

12 p2177 A69-25993

Large plastic deformation of two metallic cylindrical flat ended missiles in mutual longitudinal impact

12 p2179 A69-26217

Specularly vs diffusely reflecting cylinders for cavity type sources of approximately black body radiant energy, noting ray tracing of cones

12 p2130 A69-26245

Laminar compressible subsonic boundary layer flow on symmetrical cylinder bounded by circular arcs noting zero/nonzero angle of attack

12 p2062 A69-26272

Longitudinal and transverse frequencies of cylindrical metallic rod with spherical tip for sliding motion with dry friction

12 p2102 A69-26290

Cylindrical satellite drag rotating about transverse axis in earth magnetic field, including aerodynamic and magnetic moments

12 p2174 A69-26443

Resonance line radiation transfer in finite homogeneous cylinders of various shapes and optical thicknesses using Monte Carlo method

12 p2191 A69-26970

Couple stresses effect on dynamic stress concentrations, considering elastic compressional wave diffraction by cylindrical discontinuity

13 p2369 A69-28351

High temperature thermal resistance stability of multilayer cylindrical elements for thermionic converters determined by layer strain rate

14 p2539 A69-29218

Coupled mode theory for surface wave propagation along tapered cylindrical dielectric rod, considering radiation field effects

14 p2422 A69-29557

Electromagnetic field TM and TE modes uncoupling during oblique incidence scattering from radially inhomogeneous cylinders

15 p2565 A69-30170

Injected gas flow nonisothermicity and transversity effects on friction, heat transfer and flow parameters at cylindrical tube inlet

15 p2592 A69-30986

Thin film carbon resistors cutting with carbon dioxide gas laser, considering cylindrical bodies and aging properties

15 p2635 A69-31038

Integral representation of p-analytic functions of complex variable, applying axisymmetric boundary value problems of elasticity theory for cylindrical surfaces and paraboloid of revolution

15 p2714 A69-31191

Scattering of line focused electromagnetic waves by infinite cylinders obtained by modification of plane wave theory

15 p2664 A69-31478

Scattering of time harmonic linearly polarized plane electromagnetic wave by uniformly axially moving cylinder, analyzing first order velocity effects

16 p2748 A69-31579

Two term expansion for Nusselt number for laminar natural convection about isothermal horizontal cylinder in fluid with vanishingly small Prandtl number

17 p3068 A69-33014

Kinetic inductance measurements in linear circular and rectangular cylindrical superconductors, giving inductance temperature dependence for wires and both thick and thin films

17 p3016 A69-33783

Plane shock wave propagation around cylinders of various radii recorded with shadowgrams and Mach-Zehnder interferograms, discussing wave diffraction mechanics

18 p3120 A69-34472

Collocation method applied to solving contact thermoelasticity problem for short thick walled hollow cylinder attached to thin elastic shell in axisymmetric temperature field

18 p3217 A69-34595

Secondary steady flow /Taylor vortices/ between rotating cylinders, discussing development due to stability loss of Couette flow

18 p3123 A69-35032

Self excited vibration of flowing medium and infinite cylindrical duct wall in primary magnetic field, discussing vibration stability and critical speeds

18 p3226 A69-35462

Axial stagnation point flow in shock wave reflected from sphere or circular cylinder, determining velocity time variation, enthalpy pressure and reflection

19 p3298 A69-36385

Gravitational stability of infinite conducting fluid cylinder in axial magnetic field and surrounded by fluid of different density

19 p3380 A69-36483

Combustible mixtures flow past bodies, discussing equation for shock polar for exothermal discontinuities at subsonic and supersonic velocities

19 p3241 A69-36780

HF backscattering characteristics of infinite conducting cylinder with radially inhomogeneous plasma sheath, using Bessel functions, geometrical optics and graphs

20 p3494 A69-37843

Fourier heat equations functional corrections for determining temperatures of plate and cylinder heated simultaneously by radiation and convection

21 p3848 A69-38641

Karman vortex street formation indicated by smoke visualization method study of laminar wake behind single cylinder

21 p3644 A69-38687

Simultaneous equations for natural convection from horizontal cylinder at moderate Grashof numbers, using iteration digital computer method for boundary values

21 p3851 A69-38975

Cylindrically shaped projectiles low velocity impact upon horizontal surface of dry commercial Ottawa sand mass, estimating penetration for soft landing
21 p3839 A69-39231

Dynamic stress concentrations and rigid body response of cylinder imbedded in elastic medium subjected to compressional wave
21 p3840 A69-39300

Fracture strength of glass fiber-reinforced cylinders made by unidirectional filament winding predicted by analyzing three dimensional stress distributions
21 p3846 A69-39795

Transient temperature response of cylindrical composite energy storage devices with thermal conductivity, density and specific heat independent of temperature
22 p3868 A69-40132

Curvature and temperature distribution in nonrotating long solid cylinders under solar radiation in interplanetary space
22 p4043 A69-40546

Satellite aerodynamic characteristics, considering orbital position and attitude of cylindrical body and separate plate
22 p4037 A69-41102

Unsteady thermal conductivity calculated by approximate analytical method in simple shape bodies/infinite plate, long cylinder, sphere/ cooled or heated by thermal radiation
23 p4238 A69-41333

Contact stability of hollow cylinder compressed between parallel planes measured optically, compared to approximation of elasticity theory
23 p4162 A69-41416

Uncoupled torsional vibrations of simply supported open cylindrical tubes analyzed by approximation equations, considering free edge boundary conditions
23 p4233 A69-42347

Chaplygin equation applied to eddy flow past semicylindrical surface, discussing stagnation points and boundary value problems
24 p4245 A69-43477

Transverse curvature effect on laminar free convection heat transfer from vertical isothermal cylinders [ASME PAPER 69-HT-G]
24 p4410 A69-43522

Cylindrical models in hypersonic rarefied flow, determining drag data by free flight technique
24 p4249 A69-43677

Free convection flows about inclined infinite cylinders with isothermal surfaces
24 p4416 A69-43687

CYLINDRICAL CHAMBERS

Thermal conduction of chambers for selective and nonselective film detectors at low obturation frequencies
03 p0432 A69-14216

Vortex incompressible flow in thin cylindrical chamber, analyzing outer and inner region and interface tangential velocity, shear and static pressures
10 p1679 A69-23557

Elliptic cylindrical chambers optimum design for optical pumping of solid state lasers, discussing transfer efficiency and approximation by circular cylindrical chambers
10 p1706 A69-24010

Ideal mode conversion and transmission by circular aperture of cylindrically symmetric cavity
11 p1899 A69-25056

Deformations of thick walled cylinder with internal surface subjected to uniform pressure and externally connected to rigid chamber, calculating solid rocket booster charge
11 p1942 A69-25347

Linear inductive MHD converters, reducing effects of losses due to finite length of converter by cylindrical construction
13 p2207 A69-27505

Turbulent jets of gases in general stream of air spreading in cylindrical chamber, discussing distributions of gas dynamic parameters
13 p2200 A69-28501

CYLINDRICAL SHELLS

Circular, cylindrical thin walled shell dynamic response to moving shock solved by Flugge equations in series form
01 p0164 A69-10057

Strength analysis of cylindrical shells with rib and ring reinforcement under compression loads using network method
01 p0164 A69-10083

Flexible finite cylindrical shell undergoing arbitrary temporal and spatial motion, determining fluid/aerodynamic/forces acting on shell
01 p0005 A69-10229

Thin cylindrical shell deformation and stress under concentrated radial loading, analyzing singularity at load point
01 p0166 A69-10301

Hollow finite cylinder stress-strain analysis under normal loads on end faces solved by four partial differential equations
01 p0168 A69-10359

Detonation wave structure in solid cylindrical shell explosive, noting attainment of steady state structure
02 p0349 A69-11526

Three dimensional elastic theory using parametric expansion method developed for cylindrical translation shell profiles
02 p0338 A69-11718

Complex revolution vessels and multilobed structures analyzed by electronic computers, considering doubly stressed state of shells and bending moments from external forces
02 p0339 A69-11894

Boundary value problem solution for arbitrary nonshallow cylindrical shells by small parameter method, assuming arbitrary geometry and hinged rectilinear edges
02 p0339 A69-11960

Critical loads in elastoplastic buckling of cylindrical shells analyzed using power series
02 p0340 A69-12058

Plane strain plastic stress waves radial propagation from center of hollow cylinder subject to dynamic pressure load
02 p0344 A69-12292

Orthotropic stiffened multilayer circular cylindrical shells buckling under axial compression, lateral pressure, etc
02 p0346 A69-12510

Finite length cylindrical shell dynamic response to uniform radial impulse, noting simple harmonic motion and flexural mode excitation instability [AIAA PAPER 68-144]
02 p0347 A69-12517

Elastic-plastic and creep deformation calculations of cylindrical shell, providing better estimate of critical time at higher stress levels by including plasticity
02 p0348 A69-12539

Imperfection sensitivity of axially compressed stringer stiffened cylinder analysis via shell equations formulation using finite differences
02 p0348 A69-12542

Stress state of circular cylindrical shell subjected to uniform inward radial line load along generator solved by closed form particular integral, discussing convergence
02 p0349 A69-12797

Stresses in circular cylindrical shell subjected to local heating
03 p0523 A69-12952

Helicoidally symmetrical stress in cylindrical thin shells
03 p0529 A69-14056

Stress diffusion from axially loaded stiffeners into cylindrical elastic shells
03 p0530 A69-14065

Compressed cylindrical shell stability analyzed on basis of axisymmetric equilibrium form, noting dependence on mechanical characteristics and geometry
04 p0667 A69-14265

Initial deviations or imperfections effects on load capacity of infinite and finite length thin cylindrical shells under axial compression [ASME PAPER 68-WA/APM-22]
04 p0669 A69-14398

Elastic-plastic thin walled cylindrical shell axisymmetric behavior under radial pressure difference, noting load for collapse [ASME PAPER 68-APM/AA]
04 p0670 A69-14404

Impulse buckling threshold for elastic-plastic cylinder with elastic core after development of unstable motion
04 p0671 A69-14414

Circular cylindrical isotropic shell deformation rate under dynamic axial load described by second order linear differential equation
04 p0673 A69-14499

Natural vibrations of cylindrical panels analyzed on basis of Lamé parameters, shell equations and energy method
04 p0674 A69-14592

Temperature distributions, thermal stresses and natural frequencies of radial vibrations in thin circular cylindrical shells
04 p0675 A69-14704

Circular cylindrical shell creep behavior and buckling under axial compression and internal pressure, using multimembrane model [AIAA PAPER 68-108]
04 p0676 A69-14706

Buckling equations for orthotropic cylindrical shells with eccentric spiral stiffeners derived through variation method of total potential
04 p0676 A69-14710

Nonlinear boundary value problem of elastokinetics solved by step-by-step integration to study thin walled shells stability under axial impact [DVL-853]
04 p0677 A69-14836

Postbuckling equilibrium calculation for pressure loaded thin walled cylinders of finite length, using Donnell nonlinear shell theory
04 p0677 A69-14837

Stability of circular cylindrical viscoelastic and elastic shells with local effects due to radial load on circumference or thermally induced tangential stress
04 p0680 A69-14928

Smooth cylindrical shell stability under axial compression noting effects of scale factor, initial defects, initial stresses and deflections in welded seam, etc
04 p0680 A69-14929

Temperature distribution and thermal stresses in liquid filled cylindrical shell
04 p0682 A69-15413

Axial buckling load for thin walled circular cylindrical shell, noting design of internal mandrel for control of boundary expansion conditions
05 p0831 A69-15581

Elastic stability of thin circular cylindrical shell with elastic core, longitudinal and transverse reinforcement ribs, initial defects and under large strains
05 p0832 A69-15691

Elastic stability of thin circular cylindrical shell with elastic core, longitudinal and transverse ribs and initial defects under combined pressure and thermal stress
05 p0832 A69-15692

Stresses in cylindrical shell with elastic core loaded on curved surface solved, using elasticity theory for core and membrane solutions for shell
05 p0835 A69-15871

Stability of thin cylindrical shells of medium length with one or both ends rigidly clamped
05 p0840 A69-16199

Resonant frequencies for beam type bending oscillations of thin walled rib-reinforced circular cylindrical shell freely supported at outermost ribs
05 p0841 A69-16204

Annular stress in rib reinforced cylindrical shells under axial compression load and internal pressure, using successive approximation
05 p0841 A69-16208

Stress-strain state of shell having one end clamped and other under concentrated bending moments and concentrated force acting along generatrix solved by integral equation
05 p0843 A69-16681

Stability of three layer cylindrical shell in gas stream, analyzing oscillation mode and critical flutter dependence on filler resistance to transverse shear
05 p0843 A69-16683

Free vibration of thin laminated orthotropic cylindrical shells
06 p1020 A69-17145

Steady state frequency response of conical and cylindrical shells under lateral excitation
06 p1021 A69-17147

Dynamic response of semiinfinite cylindrical shells to traveling load
06 p1021 A69-17148

Stress concentration at circular hole in orthotropic cylindrical shell, using coordinates system and Bubnov-Galerkin method
06 p1021 A69-17180

Axisymmetric form of stability loss of cylindrical shell under effect of axial load suddenly applied along generatrix, considering inertia forces and obtaining differential equations
06 p1021 A69-17181

Oscillations of cylindrical orthotropic three layer shell having ideal fluid flow at variable rate, establishing parametric resonance and determining limits of shell motion instability regions
06 p1022 A69-17186

Bending general instability of stiffened shallow orthotropic cylindrical shells, noting buckling stress and application to shell design for various loadings
06 p1022 A69-17369

Thin circular cylindrical shells steady creep behavior under combined lateral and axial pressures, using Tresca criterion and associated flow rule
06 p1023 A69-17506

Small bending stiffness effect on inflated torus and cylindrical shells under radial load for determining large space structure stiffness
06 p1024 A69-17607

Fiberglass reinforced plastic bottoms design for integration with cylindrical shells, discussing design, shapes and boundary value problems
06 p1025 A69-17685

Buckling of elastic cylinders with rectangular cut-outs and reinforcements under axial or lateral loading, using modified Newton method [AIAA PAPER 69-92]
06 p1027 A69-18060

Radial vibrations of thin cylindrical shells subjected to thermal loadings, discussing temperature distributions, thermal stresses and natural frequencies [AIAA PAPER 69-59]
06 p1028 A69-18143

Initially imperfect axially compressed cylindrical shells strength using variational principle, shell theory and deformation theory of plasticity [AIAA PAPER 69-91]
06 p1028 A69-18181

Initial geometric imperfections effect on buckling and postbuckling behavior of laminated composite cylindrical shells under axial compression, considering reinforcing fiber orientations [AIAA PAPER 69-93]
06 p1029 A69-18194

Elastic stability of three dimensionally reinforced composite cylindrical shells [AIAA PAPER 69-122]
06 p1029 A69-18216

Cylindrically orthotropic hollow cylinder elastic properties determination using experimental test for production of stress and strain states and end effects
07 p1232 A69-18718

Linearized unsteady nonequilibrium flows produced by unsteady motion of thin foil or circular cylindrical shell in compressible gas
07 p1119 A69-18738

Circular cylindrical spinning shells vibrations by gyroscopically induced inertia loads, formulating equations of motion based on shallow shell theory
07 p1236 A69-19459

Buckling of long cylinders with homogeneous random axisymmetric geometric imperfections under axial compression, using truncated hierarchy technique
07 p1236 A69-19473

Stability of cylindrical shell reinforced by circular ribs under combined action of external pressure and axial forces, using characteristic equation
07 p1238 A69-19687

Stability of cylindrical shells under concentrated annular loads using finite difference method, discussing critical loads, moments and errors
07 p1238 A69-19688

Stability of finitely deformed thin cylindrical shell of rubberlike material, showing bending resistance and thickness effects
08 p1413 A69-20414

Optimal design of circular cylindrical sandwich shells under pressure and shear loads, showing acceptability of small shear coefficient values
08 p1416 A69-20722

Cylindrically deformed fiber reinforced material, obtaining kinematics and constitutive equations
08 p1418 A69-21002

Axisymmetric elastoplastic bending theory for cylindrical shell by applying Saint Venant plasticity conditions, determining stress distribution
08 p1419 A69-21179

Two layer cylindrical shells stability under external pressure, assuming nonuniform shell rigidity
08 p1419 A69-21180

Fragmentation behavior of small thin walled metal cylinders during explosions as function of expansion velocity and material parameters
09 p1611 A69-21352

Coaxial cylindrical shells oscillation frequencies with interspace filled with incompressible liquid determined as functions of liquid level and interspace width
09 p1612 A69-21483

Elastoplastic response of intersecting hemispheric/cylindrical shell structures compared with plastic deformation predictions
09 p1615 A69-21922

Accuracy of approximations using shell equations for predicting dynamic behavior of thin cylindrical shells, with exact solutions from Flugge shell equation [AIAA PAPER 69-447]
09 p1616 A69-21938

Bond shear effects on dynamic behavior of two layered cylindrical shell, identifying bond stiffness parameters [AIAA PAPER 68-354]
09 p1616 A69-21941

Buckling of cylindrical and conical sandwich shells with fiberglass/epoxy facings and aluminum honeycomb cores [AIAA PAPER 68-294]
09 p1616 A69-21942

Buckling of eccentrically stiffened thin circular cylindrical shell under uniform combined axial compression and torsion loads with lateral pressure
09 p1616 A69-21955

Buckling capabilities of inflation rigidized wire film and shell film cylinders in axial compression and bending
09 p1617 A69-21997

Pressure on unsteadily oscillating cylindrical shell in external or internal supersonic flow derived from asymptotic theory
09 p1618 A69-22256

Vibration natural frequencies and mode shapes in cylindrical shells clamped at both ends, using fundamental differential equation under dynamic surface loading
09 p1618 A69-22274

Thermal shock stresses in flat plates, solids and hollow cylinders, noting geometry, wall thickness, heat transfer characteristics and material properties effects [ASME PAPER 69-GT-107]
09 p1619 A69-22523

Torsional vibrations of unstiffened cylindrical tubes analysis by differential equations and applications to free-free rectangular cross section
09 p1620 A69-22769

Crack propagation in plates and shells subjected to bending and direct loading, noting plate analysis modification for crack touching on compression side
10 p1795 A69-23061

Fatigue crack propagation in cylindrical shells under fluctuating internal pressure, considering stress intensity factor
10 p1795 A69-23066

Proton flux density at axial point of thin cylindrical and slab shell shields bombarded by isotropic inverse power law spectrum of protons in space
10 p1723 A69-23165

Torsional vibrations of composite elastic orthotropic cylinders, including cylindrical shells and isotropic composite cylinder
10 p1800 A69-23243

Axisymmetric free edge buckling of semiinfinite heterogenous orthotropic cylindrical shells in axial compression, noting stability condition
10 p1802 A69-23889

Vibration characteristics of circular cylindrical shells containing water under axial excitation, investigating bubble formation and shell-fluid interaction [ASME PAPER 69-VIBR-4]
10 p1805 A69-24162

Thin plastic shell theory based on static and geometrical relations for shallow and circular cylindrical shells
11 p1978 A69-24807

Postbuckling behavior and subsequent imperfection sensitivity of thin walled cylinders subjected to torsion, considering perturbation
11 p1979 A69-24814

Stiffener geometry and spacing effects on buckling of axially compressed cylindrical and conical shells
11 p1979 A69-24815

Semiinfinite circular cylindrical shell buckling under axial load, computing forces, moments and displacements by thin shell equation
11 p1979 A69-24818

Thermal stresses in longitudinally reinforced cylindrical shell, combining moment and semimomentless shell theories to obtain numerical results
11 p1981 A69-24942

Stress analysis of reinforced cylindrical shells under external loading, using Vlasov semimomentless theory
11 p1982 A69-24949

Three dimensional theory of elasticity for finite hollow cylinder under axisymmetric deformation, considering stress and pressure distribution over surface
11 p1983 A69-25022

Heat generation in thin viscoelastic cylindrical shell with relaxation and resonance dispersion during torsional vibration
11 p2000 A69-25168

Stress concentration around curvilinear holes in three layer spherical and cylindrical isotropic shells with hard and soft fillers under external loads
11 p1984 A69-25171

Optimal parameters selection for rib-reinforced cylindrical shells determined with respect to axial critical loading magnitude
11 p1985 A69-25173

Critical axial compressive load for cylindrical shells reinforced with longitudinal ribs, noting internal pressure and rib spacing effects
11 p1985 A69-25177

Maximum stress under bending for thin walled circular cylindrical shell stiffened with uniform stringers
11 p1987 A69-25380

Cylindrical propellant tanks dynamic stability and parametric resonance, analyzing axial preload, liquid depth, top impedance and ullage pressure by Donnell theory
11 p1989 A69-25499

Cylindrical shells spectral response to random acoustic pressure excitation, noting natural modes and inner air column effects
11 p1990 A69-25506

Two dimensional elastic stress wave propagation in thick multilayered cylindrical shells for nonuniform external pressure distribution
11 p1991 A69-25511

Inplane and rotary inertia effects on free vibration frequencies of circular cylindrical shells eccentrically stiffened by orthogonal set of stringers and/or rings
11 p1992 A69-25520

Free vibration of discretely stiffened cylindrical shells with arbitrary end conditions programmed for digital computer, considering flexure, extension, torsion and nonsymmetric stiffener cross section
11 p1992 A69-25521

Nonlinear equations solvability for elastic cylindrical shells found existing for arbitrary load and clamping conditions
12 p2177 A69-25881

Method for preparation of vitreous materials in hollow cylindrical form, considering chemical homogeneity, porosity and geometrical shape
12 p2101 A69-25936

Dynamic programming method for upper bound on collapse load of rotationally symmetric thin cylindrical shell under ring loading
12 p2179 A69-26214

Thermal stresses in hollow finite circular cylinder having smooth rigid insulating cover on curved surfaces and temperature distribution on plane ends
12 p2180 A69-26268

Hollow circular viscoelastic cylinder axisymmetric plain strain problem, considering displacement, traction and mixed boundary conditions, noting applicability to rocket solid fuel core
12 p2181 A69-26396

Natural frequencies of ring-stiffened thin walled cylindrical shell determined by partial differential equations of motion, allowing for eccentricity
12 p2184 A69-26810

Finite deflection discrete element analysis of sandwich plates and cylindrical shells with unbalanced laminated faces
12 p2185 A69-26821

Cylinder buckling and other boundary value problems, applying inverse differential operators to solution of integrodifferential equations
12 p2186 A69-26841

Buckling and postbuckling equilibrium behavior of fiber reinforced cylindrical shell under uniform axial compression
12 p2187 A69-26843

Monograph on shell calculations by linear three dimensional elasticity theory, relating displacements and stresses
12 p2188 A69-26902

Minimum volume face sheet design of circular cylindrical sandwich shell obeying Mises yield criterion for loads transverse to lateral surface and axisymmetric
12 p2189 A69-27117

Stress distributions in two normally intersecting cylindrical shells subjected to internal pressure, using Donnell and Flugge equations
13 p2359 A69-27255

Thin cylindrical shell vibration with three supports analyzed by minimizing Lagrangian of vibration, obtaining frequencies and modes
13 p2359 A69-27257

Dynamic response of imperfect circular cylinder to constant velocity load, noting applicability of Hoff nonlinear equation for dynamic buckling of columns
13 p2359 A69-27260

Finite element displacement method extension to include geometric nonlinearity applied to arbitrary plate element, shallow cylindrical shell and shallow hyperbolic paraboloid
13 p2361 A69-27441

Torsional oscillation of cylindrical shell of non-homogeneous material under periodic shearing force
13 p2361 A69-27462

Imperfection surface effect on buckling load of circular cylindrical shell under axial compression, locating limit points of postbuckled states
13 p2362 A69-28122

Membrane and bending stresses around elliptic hole in thin circular cylindrical shell, considering axial tension [NAL-TN-13]
13 p2362 A69-28123

Elastoplastic cylindrical shell instability determination under axial compression applied to inelastic solids 13 p2363 A69-28124

Donnell small displacement equations for arbitrary open noncircular cylindrical shells under arbitrary normal pressure loadings 13 p2365 A69-28248

Stressed state of cylindrical circular shell clamped at edges and subjected to concentrated radial forces 13 p2368 A69-28322

Infinite cylindrical shell stability under circular load solved by linearization about bending moment stress state and Galerkin method 14 p2531 A69-28808

Stress concentration around holes in thin shells, including analysis of stress-strain state in cylindrical and spherical shells 14 p2532 A69-28977

Axisymmetric thermoelastic vibrations of infinite and finite cylindrical shells, determining natural frequencies and stress wave propagation 14 p2532 A69-28979

Thermoelastic stress-strain state of infinite circular cylindrical shell with elasticity modulus temperature dependence expressed by exponential function 14 p2532 A69-28980

Orthotropic cylindrical shell stability under uniform axial compression and internal pressure, taking into account subcritical state duration 14 p2532 A69-28981

Heterogeneous orthotropic circular cylindrical shell stability during axial critical compression 14 p2533 A69-29024

Buckling of ring stiffened cylinders subject to axial compression, considering prebuckling lateral wall displacements 14 p2534 A69-29030

Zero-moment cylindrical meshed shell equilibrium equations, discussing solution methods and difference analog 14 p2536 A69-29473

Flexural vibrations of unstiffened doubly symmetric cylindrical tubes, obtaining natural frequencies of simply supported rectangular tube 15 p2703 A69-30210

Oscillations of freely supported cylindrical shell of arbitrary cross section with breaks along generatrix, determining eigenvalue of infinite matrix with normal determinant 15 p2707 A69-30581

Plane monochromatic and pulsed electromagnetic waves penetration into metal cylindrical shells, deriving equations for electromagnetic field in interior 15 p2569 A69-30950

Bending surface of shells under crosswise load analyzed by moire method, considering rotating cylindrical surfaces 15 p2713 A69-31056

Cylindrical shell bending subjected to internal pressure and force uniformly distributed on round section solved by numerical integration of differential equations 15 p2653 A69-31195

Laminar thin orthotropic cylindrical shells natural and forced oscillations and dynamic deflection coefficient 15 p2715 A69-31202

Reinforced cylindrical shell stability under external compression load by pressurized air, determining critical pressure 15 p2715 A69-31204

Rotatory cylindrical shells supported at corners under symmetric load, determining deformation in arbitrary locations by moire method 15 p2715 A69-31546

Approximate analytic solution to transient response of infinitely long cylindrical shell surrounded by viscoelastic medium, discussing composite and elastic shells [AIAA PAPER 68-351] 16 p2871 A69-31877

Prebuckling deformations influence on circular cylindrical shell buckling under external pressure, applying Galerkin method to Donnell equations 16 p2872 A69-31905

Buckling load of cylindrical shell with inclined stiffeners, using method for stability of thin walled cylinder under transverse end load at free end 16 p2872 A69-31912

Heated cylindrical shell with braces subjected to given compression and internal pressure, having elastic beams along edges, analyzing local deformations effect on shell strength and stability 16 p2873 A69-32131

Potential and kinetic energy of cylindrical thin shell with cutout approximated by two dimensional finite difference methods, obtaining eigenvalue problem [AIAA PAPER 68-318] 16 p2874 A69-32158

Cylindrical shell aeroelastic dynamic stability subjected to supersonic flow field, considering geometric imperfections, edge constraint and prestability deformation [AIAA PAPER 68-285] 16 p2874 A69-32159

Oscillations and stability of cylindrical shell in gas flow taking into account inertia forces 16 p2875 A69-32287

Stresses in perforated ribbed cylindrical shell subjected to internal pressure using brittle coating, electrical strain gages, photoelasticity and micrometers 16 p2876 A69-32784

Reradiation and multiple reflection effects on radiant flux density distribution in cylindrical receivers of solar power installations 16 p2741 A69-32799

Supersonic flutter in square panels and cylindrical shells, measuring critical dynamic pressure 17 p3051 A69-32923

Damped vibrations of elastic open cylindrical shell under arbitrary loading, obtaining mean square of bending from correlation theory 17 p3054 A69-33094

Stress distribution in variable rigidity reinforcing frame of circular cylindrical shell using strain energy method 17 p3055 A69-33131

Nonlinear flexural vibrations excitation in cylindrical shell by longitudinal harmonic load, discussing solution of partial differential equations of motion 17 p3064 A69-33920

Cylindrical aluminum shell dynamic stability, analyzing steady state parametric oscillations, mode shape, frequency, amplitude and damping 17 p3065 A69-33929

Pressurized cylindrical shell creep analysis by elastic procedure extension using computer program 17 p3067 A69-34211

Longitudinal crack in cylindrical shell under internal pressure, calculating normal and bending stress singularity strengths against curvature/cracklength parameter 18 p3212 A69-34346

Cylindrical and conical panels dynamic responses to time varying load distributions, using trigonometric series coupled with finite difference methods [ASME PAPER 69-APM-22] 18 p3214 A69-34396

Circular cylindrical shell nonlinear response to uniform radial impulsive pressure, noting inextensibility constraint and equations of motion roles [ASME PAPER 69-APM-26] 18 p3214 A69-34399

Resonance effects in finite hollow cylinder immersed in ideal compressible fluid and exposed to compression wave 18 p3215 A69-34567

Cylindrical shell stability under axial compression, studying buckling process and wave formation 18 p3217 A69-34597

Thin walled cylindrical shells deflections under axial impact load, assuming deformations resembling cylindrical surface bending 18 p3217 A69-34599

Stress and displacement waves propagation in thin walled elastic cylindrical shell under compressive axisymmetric force based on momentless theory 18 p3218 A69-34600

Plastic cylindrical shell buckling under axial impact, predicting velocity required to cause flexural waves 18 p3218 A69-34624

Axisymmetric deformation of cylindrical wound fiberglass reinforced plastic shell analyzed by methods of rigid normals and nonlinearly elastic fiber system 18 p3222 A69-34974

Nonlinear axisymmetric oscillations and motion stability of cylindrical wound elastic glassfiber shell under time dependent uniform internal pressure 18 p3222 A69-34975

Boundary conditions of orthotropic shell stability under external pressure and axial tension, analyzing critical pressure by strain energy method 18 p3222 A69-34977

Constrained elastoplastic torsion of closed thin walled cylindrical shells, analyzing tangential and normal stress by using equilibrium equations 18 p3222 A69-34978

Dynamic instability regions of parametric resonance of cylindrical shells with curved generating lines under axial and radial pressure 18 p3223 A69-34979

Initial deflection effect on elastic cylindrical shell stability under compression, finding critical load by determining limiting point in successive loading 18 p3224 A69-35319

Long term stability of orthotropic cylindrical shells under transverse shear stresses, calculating critical stress using Kirchhoff-Love model 18 p3225 A69-35357

Microstresses in hollow-fiber reinforced cylindrical shell under longitudinal shear stress, determining modulus of elasticity and optimum component ratios 18 p3225 A69-35369

Cylindrical reinforced steel shells stability under external pressure 18 p3225 A69-35371

Stress-strain state of open cylindrical shells with arbitrary cross section determined for clamped-clamped, clamped-free and free-free supported shells 18 p3225 A69-35372

Plane LF oscillations of eccentric cylinder under harmonic pressure applied to lateral surfaces, noting natural oscillations 18 p3226 A69-35380

Asymptotic solution of supersonic linearized nonisentropic flow of viscous and heat conducting gas with internal heat sources past cylindrical shell, deriving surface pressure 18 p3089 A69-35460

Asymptotic theory of pressure on cylindrical shell subjected to unsteady oscillations in external and internal linearized supersonic flow using Laplace and Fourier transforms 18 p3089 A69-35461

Resonant oscillations amplitude of nonlinearly elastic hinged cylindrical shell determined with cubic equation taking into account Hooke law, linear stresses, shell theory displacements, etc 19 p3435 A69-35843

Natural frequencies and mode shapes of vibration of cylindrical shells orthogonally stiffened with rings and stringers [AIAA PAPER 68-349] 19 p3437 A69-35948

Natural oscillations and flutter of three layer cylindrical shell in supersonic gas flow analyzed by semimomentless theory, discussing boundary value problems, damping effects, etc 19 p3437 A69-36201

Closed form solutions for rigid viscoplastic cylindrical shell under dynamic loading based on constitutive equations for rate sensitive plastic material 19 p3439 A69-36478

Equilibrium equations for longitudinally hinged nonshallow cylindrical shells transformed into coupled equations with constant coefficients 19 p3439 A69-36581

Stress analysis of cylindrical shell-end closure junction for optimum pressure vessel configuration prediction for nuclear reactor applications 19 p3447 A69-36861

Elastic interactions between cylindrical shell and added band reinforcement turns, analyzing stress relaxation magnitude and effect on pressure vessel design 20 p3621 A69-37064

Thin circular cylindrical shells elastic equilibrium under loads producing deflection, elongation or contraction described by integrating equilibrium equations with constant coefficient 20 p3621 A69-37076

Thermal stress concentration near elliptical hole in thin walled liquid filled cylindrical shell in presence of temperature gradient across shell cross section 20 p3622 A69-37325

Free vibrational characteristics of thin walled circular cylindrical shells with layers of anisotropic elastic material laminated about middle surface 20 p3627 A69-37767

Axisymmetric vibrations of thin drums consisting of circular cylindrical shell and two circular end plates 20 p3629 A69-38114

Axial through-cracks extension criteria in cylindrical pressure vessels, considering fracture toughness and plastic flow stress [ASM PAPER W9-13.3] 21 p3833 A69-38658

Steady state temperature fields and thermal stresses determined in finite cylindrical shell by optimal parameters of reinforcing circular rib 21 p3834 A69-38714

Asymmetrical oscillations of cylindrical shell with elastic bottom containing liquid, discussing liquid level influence on natural oscillation frequencies 21 p3834 A69-38718

Linear hydrodynamic equations describing inviscid fluid flow past thin elastic cylindrical shells in circle with motions described by shallow shell equations 21 p3834 A69-38719

Natural oscillations of free surface liquid and elastic bottom of cylindrical cavity determined by integrodifferential equations based on liquid level
21 p3693 A69-38720

Stability loss for hinged circular cylindrical elastic shells reinforced by thin walled closed profile ribs, proposing minimum weight design method
21 p3835 A69-38723

Circular cylindrical freely supported shell moment state stability, solving critical parameters by infinite matrix eigenvalues determination
21 p3835 A69-38724

Optimal control of vibrations of liquid in cylindrical container with vertical generatrix and flat bottom, using dynamic programming
21 p3694 A69-38849

Free vibration of thin cylindrical shells with thickness discontinuity, considering natural frequencies and mode shapes dependence on thick/thin ratio
21 p3836 A69-38984

Stability of cylindrical shell of average length with elastic filler under uniform external radial pressure
21 p3837 A69-39088

Dynamic behavior of infinitely long cylindrical shells of ideally rigid plastic materials strengthened with ring ribs, determining distribution of moments and displacements
21 p3837 A69-39156

Buckling stability of thin cylindrical shell under torsion, allowing for finite displacements due to shear in initial stress-strain state
21 p3838 A69-39187

Stability of free and clamped spherical and circular cylindrical shells subjected to uniform or nonuniform heating, discussing effects of temperature stresses
21 p3838 A69-39190

Stiffness matrix for curved membrane shell, outlining discrete element representation of cylinders with widely spaced circumferential stiffeners
21 p3842 A69-39305

Computer program for stress analysis of cylindrical pressure vessel with flat-end closures by thin shell theory
21 p3842 A69-39306

Cylindrical shell stability during loading by uniform external pressure represented by Fourier series, determining critical pressure by solving nonlinear equations
21 p3846 A69-39715

Cylindrical shells vibrations using Lagrangian based on Flügge system of stress-strain relations
22 p4039 A69-39924

Intersection plane stresses in internally pressurized cylindrical shells joined over elliptic face
22 p4040 A69-39978

Buckling strength prediction for circular cylindrical shells reinforced by circumferential and longitudinal stiffeners, solving torsional buckling of orthotropic shells under internal pressure
22 p4042 A69-40171

Nonlinear stability for closed thin walled orthotropic cylindrical shell subjected to uniform external pressure, using Bubnov-Galerkin method for approximate solution
22 p4042 A69-40454

Axisymmetric vibrations of semiinfinite cylindrical shell constructed of fiber reinforced composite layers, obtaining frequency equation from equations of motions
22 p4044 A69-40559

Rigid thermoplastic cylindrical shell creep under axisymmetrical loads, giving computer algorithm and time dependent criterion for rupture strength
22 p4045 A69-40750

Cylindrical shells bending by finite element/cylindrical strips/ method, considering shells of arbitrary shape and variable thickness
22 p4046 A69-40968

Curved rectangular elements stiffness matrices derived for finite element analysis of cylindrical shells bending
22 p4046 A69-40969

Axial through-cracks extension criteria in cylindrical pressure vessels, considering fracture toughness and plastic flow stress
22 p4046 A69-41040

Meridional crack problem for cylindrical and spherical shells solved for uniform membrane load and bending moment, obtaining stress intensity components
22 p4046 A69-41041

Prebuckling deformation influence on compressive buckling load for orthotropic cylindrical shells with elasticity principal axes in axial and circumferential directions
22 p4047 A69-41182

Closed circular cylindrical shell stability and oscillations under ring-shaped axial load, defining stress-strain state by radial displacements and force function
22 p4049 A69-41280

Nonlinear differential equations for large deflections of multisandwich shells of arbitrary shape built of stiff and weak elastic layers, considering cylindrical shells
23 p4226 A69-41572

Statics of axisymmetric deformation of cylindrical and conical shells of revolution of moderate thickness under uniformly and nonuniformly distributed loads
23 p4226 A69-41705

Rib cross sections distribution for cylindrical shell under concentrated longitudinal forces obtainable by designing for minimum strain energy
23 p4228 A69-41988

Cylindrical shell load carrying capacity under axial compression, considering middle surface initial distortions influence
23 p4228 A69-41989

Discrete rib effect on buckling resistance of cylindrical shell under combined external and axial compression loads, using Laplace transforms
23 p4229 A69-41990

Stability of orthotropic cylindrical shells reinforced at edges by elastic ribs, analyzing axisymmetric buckling, natural oscillations and rigidity characteristics
23 p4229 A69-41992

Algorithm for stress analysis of structurally orthotropic conical and cylindrical shells, resolving first order differential equations
23 p4229 A69-42000

Hinged circular cylindrical shells reinforcing ribs effect on deflection and bending moments, assuming external pressure application
23 p4229 A69-42001

Creep stress analysis of circular cylindrical shells under axisymmetric loading, plotting stresses and deformations for various parameters
23 p4233 A69-42352

Circular cylindrical thin walled shells creep buckling under uniform axial compression
23 p4234 A69-42413

Dynamic response of anisotropic elastic cylindrical and spherical shells determined by application of Hankel transforms, considering time dependence of loads
23 p4235 A69-42481

Hot gas flow through multilayer cylindrical shells, calculating temperature fields in walls
24 p4407 A69-42588

Local stress distribution in cylindrical shells at concentrated load area solved by shallow shell theory
24 p4395 A69-42593

Cylindrical shell with supersonic nozzle end, describing axisymmetric oscillations forced by burning filler in gas stream
24 p4300 A69-43073

Transverse acoustic wave excitation of elastic circular cylindrical sandwich shell submerged in infinite fluid medium, describing simultaneous equations development for modal response
[ASME PAPER 69-APMW-17]
24 p4401 A69-43100

Flexural vibrations of rectangular cross sectioned rings, solving characteristic value problem for finite circular cylindrical shell
24 p4404 A69-43629

Circular cylindrical photoelastic shells buckling modes under axial compression using high speed isoclinic photography, discussing shallow shell equations applicability to early stages
24 p4404 A69-43652

Plastic inhomogeneity effects on yield stress of isotropic spherical shell and long cylindrical tube under internal pressure
24 p4405 A69-43672

CYLINDRICAL TANKS

Unsteady transient flow of viscous fluid in suddenly rotating open pot, taking into account effect of bottom in determination of velocity profile
03 p0414 A69-13019

Axisymmetric vibration modes of cylindrical-hemispherical membrane tank partly filled with liquid
[AIAA PAPER 67-75]
09 p1482 A69-21940

Rigid top mass effect on longitudinal response of model vehicle propellant tank, determining natural frequencies and forced asymmetric response
09 p1616 A69-21979

Planar ribbon winding for buildup control of material near polar openings of filament wound vessels, discussing ribbon width and density
09 p1507 A69-22328

Natural frequencies and mode shapes for longitudinal oscillations of liquid filled elastic circular cylindrical tank with flexible inverted conical bulkhead
[ASME PAPER 69-VIBR-11]
10 p1806 A69-24165

Unsteady heating of fuel mixture in vertical cylindrical container with Arrhenius heat source, discussing heat conduction equations and wall temperature effects
11 p2001 A69-25192

Liquid draining motion from transversely moving cylindrical tank in time varying gravity field with outlet pipe at bottom, discussing flow rate and free surface
[AIAA PAPER 69-679]
17 p2953 A69-33440

Fracture mechanics applied to cylindrical pressure vessels containing longitudinal defects for fracture behavior prediction from fracture toughness or stress intensity factor
19 p3439 A69-36439

Thin cylindrical pressure vessels with circular cutouts and radial branches, observing limit pressures during plastic deformation
20 p3629 A69-38027

Circular baffle mounted above flat-bottomed cylindrical tank outlet, discussing effect on remaining tank fluid volume and flow behavior under low gravity conditions
21 p3696 A69-39232

Simulated low gravity propellant sloshing in spherical, ellipsoidal and cylindrical tanks, discussing Bond number simulation and tank geometry effects
[AIAA PAPER 69-1004]
22 p3921 A69-40378

CYLINDRICAL WAVES

Diffraction of cylindrical and plane waves in system of two parallel circular cylinders, using equivalent circuit method
02 p0217 A69-12261

Diffraction of cylindrical waves at half plane in cold anisotropic plasma, using Fresnel integrals
02 p0293 A69-12842

Propagation of longitudinal transverse loading and unloading waves /with cylindrical symmetry/ in non-homogeneous elastic/viscoplastic medium, accounting for plastic dilatational strains
03 p0528 A69-13929

Cylindrical wave approximation modified to include axial effects, discussing time histories of deflection and applicability range
04 p0671 A69-14410

Directional properties of electric vibrator positioned at reflecting circular cylinder, discussing radiation patterns and cylindrical wave diffraction
04 p0574 A69-14459

Cylindrical and spherical waves propagation in weakly inhomogeneous plasma treated by geometrical optics, noting caustic surfaces
07 p1195 A69-19747

Cylindrical electromagnetic waves diffraction at impedance wedge in anisotropic cold plasma, using Maxwell equation and double contour integral
09 p1545 A69-21505

Analytical method for perturbations by spherical and cylindrical shock waves flowing toward common center
10 p1677 A69-22899

Converging cylindrical shock waves produced by discharging condenser bank into single turn coil surrounding gas container /theta pinch discharge/
10 p1678 A69-22933

Propagation of extensional cylindrical waves in elastic plates with free boundaries, considering plane stress and Lamb dispersion
11 p1969 A69-24414

Diffraction theory of schlieren photometric slot and wire methods for cylindrical light wave of even order, discussing Fresnel diffraction for spherical wave
12 p2088 A69-26180

Directional properties of electric vibrator positioned at reflecting circular cylinder, discussing radiation patterns and cylindrical wave diffraction
14 p2418 A69-28830

Cylindrical wave propagation in thermoelastic incompressible isotropic solids, considering cases of zero and nonzero coefficient of thermic dilation
15 p2707 A69-30626

Uniform approximation mathematical theory applied to wave propagation problems, considering cylindrical waves and rainbows and glory scattering
15 p2653 A69-31165

Scattering by cylindrical post of complex permittivity /plasma/ in rectangular waveguide, calculating reflection, transmission and absorption coefficients by computer
16 p2756 A69-31578

Fluid-shell interactions, using piston theory and cylindrical-wave approximations

18 p3223 A69-35174

Gas motion behind cylindrical shock wave created by piston motion in gravitating medium

19 p3298 A69-36386

Perturbation solution in power and asymptotic series for initial collapse phases of impulsively generated converging cylindrical and spherical shock waves in perfect gas

21 p3692 A69-38688

CYLINDROIDS

U CYLINDRICAL BODIES

CYSTEAMINE

Transverse acceleration overstrain effect on mice sensitivity to cystamine

17 p2909 A69-33386

Positive effect of shielding and cystamin administration on tonic and evacuator functions of rats gastrointestinal tract after gamma irradiation

22 p3877 A69-40285

CYSTEINE

Chlorella seaweed hybrid strains containing larger amounts of amino acids than original parent species

13 p2216 A69-28620

CYTOCHROMES

Electron transport of Halobacterium cutirubrum, discussing spectrophotometric identification of cytochromes

07 p1068 A69-19481

Flavoprotein/cytochrome b/559/ role as branch of Halobacterium electron transport in DPNH oxidase determined by salt dependence of reduced DPNH

20 p3484 A69-37101

CYTOGENESIS

Survival rates of continuously cultivated Chlorella plants in air-carbon dioxide atmosphere after single exposure to gamma radiation, using microcolony counting technique

22 p3876 A69-40275

CYTOLOGY

Cosmic radiation genetic, cytological and histological changes, particularly of pathological nature, on ecological systems employed in long duration Soviet manned flights

01 p0016 A69-10948

Cytological analysis of Tradescantia paludosa microspores for space flight influence onboard Cosmos 110

01 p0018 A69-11317

Physiological, cytochemical and histological effects on muscular activity, nervous system, adrenal and thyroid glands and liver of mice during 30 day hypokinesia

02 p0198 A69-11502

Axial units with basal plates in spermatozoa of Chlorella greenlandica negatively stained with phosphotungstic acid, showing doublet microtubules

07 p1066 A69-19263

Hypoxic hypoxia effect on catecholamine content and cytochemical changes in hypothalamus of cat exposed to simulated altitude, using Euler method

14 p2407 A69-29297

Oxygen physiological and biochemical effects on Pseudomonas saccharophila, discussing sucrose uptake, lipid synthesis and polysaccharide formation

15 p2556 A69-31045

Phagocytic activity and carbohydrate metabolism in peripheral blood neutrophils of men exposed to atmosphere with increased O content, noting neutrophil energy exchange disorder role

17 p2907 A69-32942

Mitochondrion-endoplasmic reticulum connection in hepatocytes, discussing possible protein molecule transfer

23 p4083 A69-41455

CYTOPLASM

Bioadhesive investigation in echinoderms extended to class Holothuroidea, using electron microscope with correlative light microscopy for tube feet of sea cucumbers

05 p0708 A69-15984

Cytoplasmic and ciliary connections between inner and outer segments of mammalian visual receptors

22 p3881 A69-40857

Cytoplasmic protein synthesis mechanism using rats heart-lung preparation with precise hemodynamic parameters control, noting variance with change in cardiac work level

23 p4083 A69-41456

CZECHOSLOVAKIA

Petrology of Czechoslovak moldavites, tabulating properties, mapping locations and distribution

23 p4210 A69-41350

Aero L-39 low wing cantilever monoplane jet trainer developed in Czechoslovakia

24 p4251 A69-42797

Czechoslovak L-400 high wing short range STOL transport aircraft powered turboprop engines, discussing passenger and cargo version

24 p4251 A69-42799

CZOCZRALSKI METHOD

Yttrium garnet ferrite crystals grown by Czochralski method from inductor crucible exhibiting orthoferrite, iron garnet and eutectic phases along height

13 p3231 A69-28001

D

D LINES

Automatic remotely operated sodium D line reversal temperature measuring apparatus, analyzing systematic errors

06 p1035 A69-17932

H alpha, H beta and D sub 3 /helium/ emission photographs of active prominence of July 9, 1966 using monochromatic filters for characteristic emissions from hydrogen and helium

10 p1764 A69-23738

Solar flares associated with intensive sodium D lines emission observed photoelectrically with telescope in unperturbed region, analyzing possibilities of comets solar origin

15 p2674 A69-30506

Number and mass of sodium atoms in comet Ikeya-Seki 1965f head calculated from spectral observations, ascribing D lines to resonance scattering of photospheric radiation

15 p2685 A69-30526

Solar Mg b and Na D line spectra, computing profiles for Doppler cores of lines for multilevel model atoms and selected chromospheric parameter ranges

15 p2693 A69-30779

H alpha/D3 intensity ratio variations in peripheral regions of prominences may be due to dynamic conditions of material emitting radiations

17 p3029 A69-33051

Interferometric photoelectric scans of interstellar Na D-lines in stellar spectra using Pepsios spectrometer

20 p3611 A69-38148

Sodium D line profiles in interstellar clouds, determining absorbers velocity distributions

20 p3611 A69-38149

Solar Na D lines analysis by direct inversion of line source function, finding Doppler core dependence on frequency

21 p3796 A69-38479

Total solar eclipse of 5 February 1962 observed for spectrophotometry of flash spectrum, finding abnormal intensity gradients of H alpha and D3 lines

24 p4388 A69-43636

D REGION

Electron production rate and density created by galactic and solar cosmic rays in lower D region, considering ionization for PCA

01 p0063 A69-10426

D region composition at and shortly after sunrise, noting negative ion factor changes, ionization source and quasi-equilibrium conditions

01 p0066 A69-10597

LF continuous wave rocket propagation in D region presented in terms of electron density profiles

01 p0076 A69-11232

Sunrise effects in lower D region by solar eclipse, discussing anomaly in ionospheric absorption due to negative ion factor or recombination coefficient

02 p0246 A69-12767

Narrowing of ionospheric absorption anomaly in D region during solar eclipses in long and medium wave ranges due to recombination equation variability

02 p0246 A69-12770

Solar X ray control of D layer based on Explorer 33 data, computing electron production rates due to typical X ray flux

03 p0500 A69-13224

Polarization diversity analysis to avoid fading in microwave scatter links in D and E layers

03 p0394 A69-13378

Solar X ray source identification using D layer ionization behavior during eclipse

04 p0650 A69-15533

Simultaneous rocket measurements of D region temperatures and electron densities on anomalous winter

day

05 p0758 A69-16411

Ionospheric D layer electron concentration profile from radio wave absorption frequency dependence

06 p0920 A69-17729

Irregularities producing partial radio wave reflection from midlatitude D region attributed to insufficient distribution

07 p1078 A69-18914

D region electron density vertical profiles measured using partially reflected echoes from lower ionosphere

08 p1307 A69-20189

D region electron concentrations and collision frequencies obtained from high power wave interactions experiment, presenting average winter collision frequency model

09 p1489 A69-21702

Diurnal variation of D region electron production rates, discussing Lyman alpha ionization of nitric oxide

09 p1577 A69-21717

Corpuscular radiation contributions to D layer ionization determined from intensity measurements

09 p1577 A69-21770

Rocket sounding data on ionospheric currents at mid and low latitudes, showing absence in D and above E region

10 p1686 A69-23909

Long wave propagation at 164 kHz in India during 1966 and 1967, determining D region recombination coefficient and long wave absorption diurnal variation

10 p1659 A69-24065

Iono-index about hard emission of solar active regions, analyzing field fluctuations and SID in D region under daytime conditions

12 p2148 A69-26107

Polarization diversity analysis to avoid fading in microwave scatter links in D and E layers

14 p2410 A69-28829

Vapor phase reaction sequence to explain water cluster ions in D region

14 p2434 A69-28940

Ion chemistry of D and E regions to be studied during years of solar maximum in framework of IQSY/IUCSTP

14 p2439 A69-29111

British and Soviet D region electron density distributions from same VLF and LF propagation data

14 p2439 A69-29112

Semimonthly lunar variation in D region absorption, discussing phase reversal of lunar tides between equatorial and high latitudes

14 p2439 A69-29113

Rocket sounding measurements of ionospheric D region electron density profile during 20 May 1966 solar eclipse, discussing D region ionization source

14 p2439 A69-29116

D region ionizable constituent density /presumably nitric oxide/ measured, using blunt probe to detect changes in conductivity produced by Lyman alpha ionizing radiation

15 p2598 A69-31316

Solar X rays intensity and spectrum effects on e layer critical frequency and D region ionospheric absorption

15 p2677 A69-31346

Ground based partial reflection and cross modulation or wave interaction techniques compared for studying D region electron densities

15 p2606 A69-31537

Lower auroral ionosphere rocket measurements of electrons, positive ions and energy particles, deriving height variation of ion pair production and ion-ion recombination

16 p2778 A69-32187

LF ground based absorption results compared with rocket measured D region electron density profiles

16 p2778 A69-32188

Ionosphere D region low field conductivity in presence of high field disturbing signal, assuming inelastic electron-neutral particle collisions

16 p2850 A69-32190

Atmospheric absorption calculations, noting direct D layer reflection effects on lower HF oblique propagation

16 p2752 A69-32389

D-1 SATELLITE

French satellites structure, power and communications systems, stabilization and detector groups

02 p0333 A69-11917

D1A satellite Doppler observations, noting effect of observation grouping on ground stations mutual position

21 p3701 A69-38336

Nocturnal D region conductivity enhancement relation to X radiation from Scorpius XR-1 and other sources, calculating ion production rate
17 p3024 A69-33378

Lower ionospheric electron concentration and collision frequency measurements by Nike-Apache rockets, suggesting geomagnetic anomaly in D region
18 p3127 A69-34798

D region electron densities from multifrequency absorption measurements by proton spectra analysis, noting cubic approximation
18 p3127 A69-34799

Earth albedo effect on ionospheric D layer determined from aircraft sounding of E layer echo amplitude above reflecting cloud cover
18 p3127 A69-34800

Positive ion concentration in D region, using spherical stationary electrostatic probe in weakly ionized collision dominated gas
18 p3128 A69-34804

Ionospheric radio propagation, considering D and F region theory and ionospheric disturbances
19 p3303 A69-36428

Ionosphere characteristics in terms of airglow, describing daytime F/D layers formation model provided by photoionization, loss processes and ambipolar diffusion
21 p3712 A69-38517

Phase amplitude recording of radio waves reflected from D and F regions of ionosphere, reversing smoothing process by Fourier methods
21 p3672 A69-38558

Identification, position and temperature of solar X ray sources derived from D layer ionization radio absorption behavior during eclipses and lunar reflection
22 p4004 A69-40308

Lunar semimonthly variations in noon values of D region absorption at Singapore, noting opposite phases of lunar tides in D and F regions
22 p4035 A69-41211

Density model for free oscillations of earth, noting dependence on core radius and S wave velocity at top and bottom of D layer
23 p4158 A69-42117

DACRON [TRADEMARK]
Mission sequential environment effects on Dacron parachute material mechanical properties
[AIAA PAPER 69-1018] 22 p3923 A69-40390

DAEMO [DATA ANALYSIS]
U DATA PROCESSING
U DATA REDUCTION
U DATA TRANSMISSION

DAMAGE
NT IMPACT DAMAGE
NT METEORITIC DAMAGE
NT PROTON DAMAGE
NT RADIATION DAMAGE
NT RAIN IMPACT DAMAGE
Cumulative damage theories application to fatigue data for high strength materials, discussing stress levels
04 p0668 A69-14379

Aircraft accident prevention and damage control
06 p0878 A69-16961

Sonic boom damage legal claims, discussing causal relationship validity and claims processing
14 p2541 A69-29155

Sonic boom damage to structures from supersonic aircraft overflights using inductive and deductive approaches
15 p2585 A69-30370

Legal, social and physical effects of supersonic flight, discussing damage claims validity and recovery resulting from breaking of sound barrier
17 p3075 A69-32841

DAMPERS
Pendulum motion about stationary axis of solid body containing damper, ascribing instability to center of gravity shift with respect to cavity
18 p3135 A69-34557

DAMPING
NT ELASTIC DAMPING
NT LANDAU DAMPING
NT VIBRATION DAMPING
NT VISCOUS DAMPING
Damping factor automatic determination by use of second derivatives of residuals for damped least squares method of optical design
04 p0630 A69-14295

Circular plate elastic stability under unidirectional compression, using Rayleigh-Ritz- Timoshenko method to determine buckling load
04 p0683 A69-15515

Shock wave damping at large distances from body situated in ideal gas three dimensional flow
04 p0591 A69-15535

Stability of Al-Mg alloy spherical shells under uniform external pressure beyond elastic limit
05 p0843 A69-16693

Ballistic deviations of gyropendulum vertical damped by astatic gyroscope
06 p0927 A69-17687

Eddy current damping systems for gravity gradient stabilized satellites, discussing electromagnetic torque and various parametric relationships
07 p1228 A69-18341

Periodic motion of satellite with magnetic damper along circular orbit, assuming small value of damping coefficient
09 p1609 A69-21761

Complex variable theory solution of eigenvalue problem governing elastic stability of thin elastic plate subjected to hydrostatic in-plane compression
09 p1615 A69-21921

Laminar hypersonic roll damping derivatives for 10 degree half angle cone at zero angle of attack for environmental flow conditions of hypersonic wind tunnel
09 p1430 A69-21958

Mathieu equation with square law damping effect on first order instability range
10 p1724 A69-22920

Piezoelectric transducer theory, discussing acoustically matched sandwich type damper and calculating frequency characteristics
10 p1697 A69-24074

Damping of solid state laser relaxation oscillations in power output due to diffusion of excitation
10 p1706 A69-24079

Response and stability of self sustained two degrees of freedom system with nonlinear damping, noting harmonic oscillations
[ASME PAPER 69-VIBR-24] 10 p1806 A69-24171

Bilinear hysteretic system undergoing random vibration, substantiating linearization analysis with analog computer simulation and comparing lifetime to linear system
[ASME PAPER 69-VIBR-25] 10 p1806 A69-24173

Structural damping coefficient of metals determined from complex Young modulus with transmissibility, using mass loaded cantilever beam experiment
[ASME PAPER 69-VIBR-36] 10 p1807 A69-24175

Damping accuracy sensitivity to circuit element tolerances in polynomial filters
11 p1850 A69-24970

Confidence limits determined for damping parameter of complex stationary Gaussian Markov process
11 p1910 A69-25700

Pi 2 micropulsations at African low latitude stations, considering damping effect on ionospheric micropulsation transmission signal dispersion and SNR
12 p2074 A69-26959

Temperature effects on magnetomechanical damping in Fe, Ni and mumetal, noting behavior difference due to domain structures
15 p2639 A69-30586

Transient behavior of finite damped cantilever beam and circular plate analyzed by direct finite element method, noting applicability to dynamic problems
15 p2710 A69-30868

Aircraft neutral stability empirical and mathematical aspects, considering control stabilization, damping and phugoid motion
15 p2551 A69-31012

Weakly damped transverse and thermal waves development and propagation in viscous heat conducting incompressible fluid under temperature and gravitational fields
15 p2718 A69-31168

Electronic-ultrasonic amplifiers with external electron stream and longitudinal or surface wave studied for damping influence, deriving dispersion equation
16 p2761 A69-32061

Liapunov functions applications in motion stability theory problems, considering dynamic systems, periodic orbits, optimum damping and control
16 p2804 A69-32248

Asymptotic solutions to second order differential equations with slowly varying parameters and large resistance applied to mathematical pendulum damped swinging motion
16 p2804 A69-32253

Hydrostatic stability and damping characteristics of perforated plates and screens for passive propellant control schemes from drop tower tests
[AIAA PAPER 69-531] 16 p2833 A69-32691

Elastic stability of warped rods, using small oscillations method for varying end conditions and torsional-moment vector behavior
17 p3057 A69-33196

Damping of gravity gradient stabilized satellites by hysteresis of materials, friction of viscous fluids, magnetic hysteresis and Foucault currents
17 p3047 A69-33230

Gravity gradient satellite stabilization and magnetic hysteresis damping systems, outlining energy dissipation device involving torques
17 p3047 A69-33231

Damping properties of multilayer coatings for aircraft structures analyzed on duralumin samples subjected to bending at room, elevated and low temperatures
17 p2993 A69-33941

Inertial characteristics determination error influence of solid body on damping system parameters
18 p3171 A69-34562

Adjoint system for determining equilibrium stability of elastic continuum subjected to follower type surface tractions
19 p3446 A69-36835

Damped linear system asymptotic stability inferred from dynamical equation structure, considering matrix eigenvalues and Thomson-Tait-Chetaev stability theorem
20 p3623 A69-37531

Damping effects on elastic systems stability under nonconservative forces, correlating stability and quasi-stability regions
22 p4040 A69-39981

Real shear modulus and mechanical damping characteristics of cured adhesives measured for temperature effect, using torsion pendulum apparatus
24 p4338 A69-43460

DAMPING IN PITCH

U PITCH [INCLINATION]

DAMPING IN ROLL

U ROLL

DAMPING IN YAW

U YAW

DAMPING TESTS

Spadocyte slide rule for damping determination from vibration decay traces, noting use in flight flutter tests
01 p0087 A69-11029

Damping properties of glass fiber reinforced plastics measured by flexural vibrations
03 p0454 A69-13824

Magnetic sample-and-hold damping using geomagnetic field for libration damping of gravity gradient stabilized satellite in near synchronous equatorial orbit
07 p1227 A69-18337

Friction damping properties of deployed structures vibrating in weightless state compared to damping in space for true determination
12 p2183 A69-26792

Vibrations attenuation by viscoelastic sandwich shear damping, discussing examples of aircraft equipment racks, gyro and airborne circuit board mountings
15 p2622 A69-30705

Damping constant of sandwich samples with foam plastic filler subjected to torsional and flexural vibrations determined for aircraft design applications
17 p2993 A69-33942

Acoustic and internal dampings in freely supported uniform beams of circular and rectangular section, showing frequency dependence and vacuum effect
20 p3620 A69-37062

DAMPNESS

U MOISTURE CONTENT

DANGER

U HAZARDS

DARK ADAPTATION

Detection time to light point source noting response to dark, star field and glare source backgrounds
06 p0881 A69-17215

Dark adaptation mechanisms studied from light intensity recovery after experimental flash, using electroretinography methods
10 p1647 A69-23588

Darkness adaptation, observing relationship between left and right eye
16 p2745 A69-32448

Subjective and objective thresholds of darkness adaptation in human subjects grouped from infancy to adulthood, using same variable intensity light source equipment
22 p3881 A69-40861

DARKENING

Photographic layers darkening process, using widely spaced or single giant pulses of ruby laser
13 p2260 A69-27612

- Limb darkening on earth night side observed by Aerobee rocket, with explanation based on atmospheric opacity in water vapor and carbon dioxide bands
17 p2960 A69-33167
- Martian seasonal darkening attributed to windblown dust
24 p4389 A69-43742

DART TURBOPROP ENGINES

U TURBOPROP ENGINES

DASSAULT AIRCRAFT

- Dassault Mercure short haul jumbo jet, discussing production costs and market potential
15 p2550 A69-30317
- Dassault Mercure high speed twin turbojet aircraft, discussing capacity, range, propulsion, profitability threshold, etc
15 p2550 A69-30318
- Short haul transport aircraft development, discussing twin jet Mercure aircraft with low operation cost and Category III weather conditions landing
24 p4250 A69-42565

DATA

NT CONTROL DATA [COMPUTERS]

- Atmospheric turbulence flight tests random data analysis to stimulate power spectra and transfer functions
05 p0767 A69-16756

DATA ACQUISITION

- Satellite automatic picture transmission application to meteorological and hydrological problems including wind estimates, atmospheric stability and cloud distributions
[UN PAPER 68-95300] 01 p0108 A69-10462
- Passive and active transmitters and receivers of electromagnetic radiation in earth orbital satellites to collect pictorial or numerical data to study hydrology
[UN PAPER 68-95333] 01 p0064 A69-10487
- Orbiting satellite global all-weather oceanographic data acquisition to complement higher resolution data from ships, buoys and aircraft remote sensors
[UN PAPER 68-95878] 01 p0064 A69-10491
- Aerospace research applications in agriculture and forestry, discussing information acquisition for worldwide coverage
[UN PAPER 68-95393] 01 p0065 A69-10504
- Meteorite particles recording by piezoelectric transducers, comparing data collected by Soviet and American scientists
01 p0152 A69-10587
- Ministriations in frequency graphs as evidence of standing waves in electrically exploded iron wires
01 p0118 A69-10661
- Sporadic E layer structure observed by rocket borne probes relation to ground based radio techniques, showing agreement between plasma and blanketing frequencies
01 p0070 A69-11161
- Directional antennas gain loss on ground sections calculated on basis of difference-phase measurements data
02 p0214 A69-11612
- Selenodetic data results and calculations of moon visible physical surface do not agree
02 p0314 A69-11643
- Solar and galactic cosmic rays measurement data to investigate variation in time of relations between cosmic rays modulation amplitude and solar activity variations
02 p0306 A69-11658
- Data acquisition program for Apollo crew motion disturbances experiment consisting of ground simulations and orbital experiment establishing mathematical model of human body
02 p0201 A69-11759
- Meteorological satellites for atmospheric data collection applicable to weather forecasting and synoptic analysis
02 p0277 A69-12778
- Aircraft high level cloud data to estimate vertical distribution of cirriform clouds and tropical tropopause levels on airline routes
03 p0458 A69-13032
- Agricultural remote sensing information system composed of data acquisition, processing and information extraction and interpretation phases, providing knowledge of earth resources
03 p0400 A69-13195
- Preliminary orbit determination, based on data collected during single pass by sensor, permitting preliminary orbital elements and data variance estimation
03 p0518 A69-14249
- Explosive detonated in external electric field to obtain data on gas state behind shock wave
04 p0634 A69-14430

- Observation data on source distribution of atmospheric with respect to distance from observation point
04 p0593 A69-15103
- Analog to digital converter parameters, considering selection of conversion technique
05 p0726 A69-16760
- Aircraft gas turbine component pressure data storage and scanning
05 p0726 A69-16768
- International 28-station global instrumentation ground support network for space tracking and data acquisition
[UN PAPER 68-95912] 06 p1043 A69-17059
- Eole program to further data acquisition for climatology and weather forecasting
[UN PAPER 68-95831] 06 p0950 A69-17073
- Anna 1-B geodetic satellite design, instruments and data acquisition
[UN PAPER 68-96195] 06 p0917 A69-17082
- Narrow and wide angle actinometric instruments on-board Cosmos 122, 144 and 156, describing optical and data acquisition systems
06 p0929 A69-17977
- Ground, aircraft and spacecraft actinometric data compared for clear sky
06 p0951 A69-17982
- Composite solid propellants ignition response measured by imbedded hot wires indicating distributed reaction
[WSCI PAPER 68-36] 07 p1201 A69-18354
- Constant level sounding balloon systems providing global data on atmospheric circulation, discussing icing problems and average life improvement
07 p1053 A69-18955
- Multifunction Receiver System rationale, concepts, background requirements and technical justifications for tracking, telemetry and ranging data acquisition by Goddard Center
07 p1081 A69-19101
- High reliability magnetic tape recorders for satellite, aircraft and drone applications
07 p1133 A69-19104
- Telemetry aortic blood pressure and heart rate from dogs under various physical activities and emotional stress
07 p1071 A69-19133
- Sensor data acquisition and processing and required levels of navigation integration for increasing air space capacity
07 p1177 A69-19211
- Secondary acquisition systems analysis by semiMarkov process model, defining minimum average acquisition time
08 p1270 A69-19852
- Meridional flow, angular momentum and energy flux in atmosphere calculated from IGY data
08 p1346 A69-20312
- Spacecraft applications of Langmuir probes, obtaining data from current-voltage characteristics for electron/ion concentrations, ion mass spectra and charged particle energy distribution
08 p1316 A69-20474
- Project control cycle, cost monitoring and reporting to management
08 p1423 A69-20630
- Optimum gathering of information for linear automatic control system with distributed parameters in presence of random input disturbance
09 p1471 A69-21437
- Pilot balloon and radiosonde measurements for p as function of wind direction, velocity and stability, discussing variation with air layers
09 p1535 A69-21516
- Scientific data acquisition and interpretation effects on electric spacecraft plasmas and field directions, noting electron interchange reactions effect
[AIAA PAPER 69-276] 09 p1568 A69-21727
- Asynchronous on-line digital data acquisition system with immediate access to on-site numerical real time printout for rocket engine performance tests
[AIAA PAPER 69-323] 09 p1478 A69-22381
- Clinical report on Apollo 7 and 8 mission medical data, discussing preflight preventive medical activities, inflight treatment, radiation levels, etc
09 p1446 A69-22542
- Symptom pattern observation technique for flight data analysis, discussing in-flight symptoms and SPOT chart in aircraft maintenance
10 p1669 A69-22982
- Airborne integrated data acquisition and analysis systems to determine aircraft technical performance
10 p1660 A69-23264

- Computer controlled data acquisition and control system /DACS/ for wind tunnel applications, describing system and programs
10 p1673 A69-23286
- Mississippi Test Facility /MTF/ hardware data acquisition system error analysis from extensive simulated static firing tests
10 p1673 A69-23287
- Data requirements and acquisition for detection and description of tides and gravity waves in upper atmosphere
10 p1685 A69-23833
- Solar flares theories, discussing data acquisition by space research and solar radio astronomy
11 p1946 A69-24516
- Directional antennas gain loss on ground sections calculated on basis of difference-phase measurements data
11 p1847 A69-24719
- Radiation measurements quality by wide angle receivers of Cosmos 122 satellite analyzed, showing agreement with data by other methods
11 p1912 A69-24830
- Airborne computer controlled data acquisition system for real time fault detection and isolation in avionics
11 p1843 A69-25082
- Integrated management information system /IMIS/, discussing logistics, reliability and quality assurance disciplines
11 p2005 A69-25304
- Dynamic stall data for helicopter rotor blade analyses obtained by oscillatory tests in pitch and in vertical translation at full scale Reynolds number
11 p1819 A69-25374
- Meteoritic dust particles collections prediction in atmosphere for low and high entry fluxes
12 p2158 A69-26342
- EEG monitor helmet for aircraft or flight simulator programs, discussing sensing and transmitting system
12 p2023 A69-26553
- Variational statistics applied to hourly meteorological data for predicting airport runways icing conditions time and duration
12 p2127 A69-26900
- Geographic and cartographic mapping applications of remote sensor data from orbital heights, discussing hardware, instrumentation, NASA role in data selection, etc
12 p2192 A69-26984
- Information collection by remote sensing and related economic principles, presenting mathematical formulation of linear programming model
12 p2193 A69-26988
- Radar remote sensing for terrain data acquisition
12 p2098 A69-27005
- Remote sensing of urban environments for metropolitan information systems noting photographic, thermal IR, radar and microwave applications
12 p2193 A69-27012
- Methodology for technical feasibility and economic analysis of remote sensing applications
12 p2193 A69-27013
- Computer program for obtaining information from stationary time series using Chree method of superposed epochs for processing unlimited data and epochs
13 p2225 A69-27617
- Lunar surface light scattering data cataloged for various phase angles from photometric observations of lunar features brightness
13 p2344 A69-27648
- Turbulence measurement, considering handling and storage of data
13 p2263 A69-28148
- Polishing-etching cell permitting continuous sample surface observation for use with inverted stage microscopes
13 p2281 A69-28156
- Solar and galactic cosmic rays measurement data used to investigate variation in time of relations between cosmic rays modulation amplitude and solar activity variations
13 p2333 A69-28689
- Solar radio emission data during IGY covering solar terrestrial disturbances, broadband bursts, solar indices, etc
14 p2513 A69-29321
- Pressure, temperature, vibrations and structural stresses data acquisition system for aeronautical applications
14 p2450 A69-29686
- Comet scintillations and tail characteristics studied to obtain information on interplanetary flux field, magnetic fields and planetary structures
14 p2523 A69-29704

Airglow research, discussing emission features, observation methods and instruments, ground station network, etc
15 p2594 A69-30020

Aerospace structures modal vibration tests data acquisition including multishake excitation methods
15 p2585 A69-30358

Meteorite particles recording by piezoelectric transducers, comparing data collected by Soviet and American scientists
15 p2691 A69-30757

Thermal conductivity coefficients in solar corona and chromosphere computed and tabulated for H plasma
15 p2694 A69-30788

Systematic error pattern in raw data obtained during tracking ROSE balloons by two radar systems, estimating range resolver error
15 p2649 A69-30897

Doppler tracking data from Lunar Orbiter missions for studying lunar gravity anomalies, plotting acceleration on lunar surface Mercator projection
15 p2697 A69-31313

Electronic equipment for data acquisition in extraterrestrial experiments including low noise charge amplifiers, discriminator, pulse lengthener, linear gate and logarithmic amplifier
16 p2759 A69-31857

F 2 critical frequency data at Hawaii for clarifying total electron content data obtained by geostationary satellite measurement of Faraday signal rotation
16 p2779 A69-32196

Ozone probe network data by Brewer-Mast electrochemical instruments, discussing vertical ozone distribution near Zurich
16 p2787 A69-32635

Neutron and photon transport properties in liquid hydrogen obtained from measuring radiation environment in propellant tank mockup suspended above NERVA reactor
[AIAA PAPER 69-475] 16 p2810 A69-32716

Satellite Proton 2 orientation from onboard measurement data, discussing general statistical method and data processing results
17 p3001 A69-33221

Tracking and data acquisition systems for spacecraft and ground link through command, telemetry and tracking, noting data relay satellites, etc
17 p2919 A69-33371

Ionospheric data acquisition and utilization for improved radio communications, considering contact between engineers and physicists, ionosondes, data reliability for prediction, etc
17 p2961 A69-33402

Ground simulations data of jet lift V/STOL compared with visual flight results, studying hover, lateral quick start and stop maneuver
[AHS PAPER 362] 17 p2946 A69-33519

Ballistic missile and aircraft operational effectiveness, discussing data collection, reliability, availability and capability surveillance by computer
18 p3145 A69-34500

Flight failure analysis, discussing methods and restrictions due to hardware unavailability, minimum data, urgency and publicity
18 p3145 A69-34502

Eyewitness data concerning bright bolide observed over Dzhaus /Uzbek SSR/, tabulating estimations for occurrence time, light duration, color, sound and trajectory azimuths
18 p3196 A69-34536

Ground data operations system for large astronomical satellite comprising UHF telemetry, PCM telecommand and processing and display equipment
18 p3117 A69-34794

Calculator for obtaining moments of inertia data to determine control power for vehicle orientation and to avoid control systems over design
[SAWE PAPER 792] 18 p3118 A69-34865

STAN integral weight and balance system providing aircrews with takeoff gross weight and CG data
[SAWE PAPER 755] 18 p3136 A69-34882

Oceanographic sensing satellite systems, discussing applications, data requirements, sensors, booster and earth coverage capabilities
18 p3210 A69-35091

Long term creep rupture data based on short term tests in form of Larson-Miller time-temperature curves
18 p3150 A69-35422

Wind profile data measured by AN/FPS-16 radar/superpressure balloon system, noting error sources
18 p3139 A69-35428

Digital data acquisition system with ultrahigh sampling rate for Ames electric arc shock tunnel, describing

ing analog to digital conversion, data storage, system performance, etc
19 p3293 A69-35744

High speed analog to digital multiple channel wide-band data acquisition system designed for short pulse Doppler radar and probe measurements
19 p3307 A69-35745

PCM data handling system for NASA Space Tracking and Data Acquisition Network with explanation for output capabilities, noting BIOSAT project
19 p3270 A69-36242

Stored program data processor used as PCM telemetry data acquisition system for postApollo applications, considering format and bit rate changes
19 p3274 A69-36280

Onboard data processing and acquisition for aircraft and spacecraft problems based on integrated data management approach, discussing readout and display
19 p3280 A69-36315

Optimum aerological network design, discussing atmospheric model, numerical analysis, data acquisition, weather forecasts, rms measurement error, etc
19 p3364 A69-36505

Optimal information selection for determining spacecraft trajectory, considering atmosphere, light speed and series expansion coefficients of planetary gravitational potentials
19 p3427 A69-36627

Ionospheric data of local and integral electron concentration obtained by measuring phase shift of satellite emitted coherent radio waves
20 p3519 A69-37022

Geomagnetic storms data compilation /1957-1964/, showing solar activity effect on solar corpuscular stream velocity
20 p3587 A69-37036

Pulsars pulse profiles data collected and interpreted with attempt to infer origin
20 p3597 A69-37335

Electronic data collection for climatological stations, describing acquisition and processing of various identification signals and meteorological parameters
20 p3538 A69-37428

Data acquisition amount estimation technique for vertical panoramic sounding of ionosphere
20 p3492 A69-37692

Data acquisition and processing ionograms from Alouette satellites telemetered sweep frequency top-side sounding data
20 p3503 A69-37860

Numerical and analog data acquisition system /CARINA/ for processing rocket, balloon and satellite data, describing distributor characteristics, control console, etc
20 p3511 A69-37914

Cosmic ray propagation from experimental data on cosmic ray nuclei
21 p3789 A69-38816

Satellite synoptic meteorological data collection systems, discussing configurations, global location requirements and digital code platforms position determination
[AIAA PAPER 68-1095] 21 p3819 A69-39029

Ariel 3 satellite management structure, responsibilities and orbit, stabilization, launch window, data acquisition and processing
21 p3856 A69-39255

Quasi-stellar objects identification, distribution, emission lines interpretation, energy distribution, absorption spectra, radio properties, etc
21 p3811 A69-39515

Residuals from earth based coherent two way radio Doppler data from Lunar Orbiter three orders of magnitude larger than observations from spacecraft
[AAS PAPER 68-131] 21 p3828 A69-39766

Heart electrical activity time sequence estimation based on multiple dipole binary model, deriving algorithm
21 p3668 A69-39865

Instruments for obtaining auxiliary data in aerial triangulation, describing stratoscope, profile recorder, radar altimeter, horizon camera, etc
22 p3944 A69-40042

Scattered light photoelasticity dual observation method, describing automatic data collecting and interpreting system
22 p3945 A69-40079

Support software costs reduction for launch vehicle systems by implementing computer techniques to provide requisite data
[AIAA PAPER 69-978] 22 p4052 A69-40358

Handbook on geochemistry, Volume 2/1, covering geophysics, cosmochemistry, etc
22 p3897 A69-40890

Aerial remote sensing data for earth resources program including agricultural, geothermal/ geological tests, hydrological, water pollution and soil and flood water control observations
22 p3949 A69-40994

Data acquisition techniques and devices in electronic data processing
22 p3908 A69-41251

Tracking and Data Relay Satellite System with synchronous orbit satellites to relay data between low altitude earth orbital spacecraft and mission control centers
23 p4120 A69-41755

Magnetic activity effect on electron density in topside ionospheres determined from Alouette 1 data statistical analysis
23 p4156 A69-41856

Rosman I reflector antenna for collecting data from earth orbiting satellites, discussing dynamic analysis of structural response to natural frequencies
23 p4231 A69-42133

Modular data acquisition and processing system, describing input unit, checkpoint selection scanner, analog-digital converter, limit indicator, etc
23 p4167 A69-42459

Central nervous, cardiovascular and metabolic data of Macaca nemestrina during simulated Biosatellite flight, testing data acquisitions systems
24 p4260 A69-42703

Aerospace programs cost analysis system, using contractors accounting records as data source
[AAS PAPER 69-465] 24 p4416 A69-42801

Radiation hard device specifications, comparing data with environmental considerations
24 p4287 A69-43204

DATA CONVERTERS
NT ANALOG TO DIGITAL CONVERTERS
NT DIGITAL TO ANALOG CONVERTERS

Computer oriented telemetry data processing systems designed to condition raw telemetry data for further processing by other systems
05 p0727 A69-16770

Solid state synchro data interfaces for angular information, noting synchro to digital and digital to synchro conversion techniques and synchro repeaters
11 p1842 A69-24543

Solid state programmable avionics converter for signal processing, information conversion and aircraft control
14 p2405 A69-29687

Automatic conversion receiver of meteorological radar data, examining reception amplitude sensitivity and frequency characteristics
16 p2791 A69-32280

Computer aided data interpretation system converting ionograms to vertical electron density profiles
20 p3504 A69-37866

Real time FM-to-digital converter for measuring periods of demodulated FM/FM data, discussing systems design
22 p3903 A69-39923

Nonlinear encoding for picture transmission using nonlinear analog to digital converter
23 p4119 A69-41747

DATA CORRELATION
NT SIGNAL ANALYSIS

Daily insolation observations at Blue Hill, Massachusetts, correlated by month with observations of temperature, snow cover, winds, sunshine, sky cover, pressure and precipitation
01 p0066 A69-10862

Entry phase flight data of Missions AS-202, Apollo 4 and 6 compared with wind tunnel aerodynamics data
[AIAA PAPER 68-1143] 03 p0519 A69-13556

Gas turbine exhaust silencer performance correlated in laboratory and in service
[ASME PAPER 68-WA/GT-9] 05 p0812 A69-16144

Laboratory measurement data of low light level TV performance converted to anticipated real world performance data
07 p1132 A69-18948

Spacecraft motion parameters and physical characteristics of space determined from statistical analysis of measurement data
09 p1495 A69-21764

Two dimensional signal analog correlation in noise background using optical spatial filtering Fraunhofer hologram and input as functions
09 p1499 A69-22276

Statistical method for determining accuracy of airfield weather reports on takeoff and landing conditions, visibility and cloud ceiling, correlating forecasts and actual conditions
11 p1913 A69-25205

Mars photographic and radar data correlation indicating smoothness of dark areas and roughness of desert areas

11 p1964 A69-25406

Description and automated research of correlation /DARC/ for establishing quantitative relationships between topology and properties of chemical substance

12 p2026 A69-26361

Mass transfer cooling data correlation for estimating mass injection effect on slender cone drag

13 p2199 A69-28224

Vaporizer temperature and collision efficiency correlation data for magnesium oxide-argon dilute diffusion flames studied for determining inverse temperature dependence

13 p2380 A69-28461

Error correction for correlation coefficient between satellite data of earth radiation intensity and satellite vision field shift

14 p2435 A69-29043

Experimental and theoretical data correlation on low voltage arc in thermionic converters using cesium vapor, describing discharge plasma by solving differential equation system

14 p2404 A69-29254

Fast folding algorithm for detection and correlation of digital data with weak noisy pulse trains of differing periods

14 p2416 A69-29548

Calculated and experimental surface wear damage data correlated for materials under friction conditions

15 p2618 A69-30106

Stellar scintillation spectra for different zenith distances, correlating data with meteorological conditions at time of observation

15 p2647 A69-30165

Subtractor performance for processing correlated random signals with different spectral widths in signal delay time indicator, discussing errors

15 p2572 A69-30346

Air densities from satellite obtained orbital data, comparing accuracy of values and methods of analysis

15 p2600 A69-31349

Synoptic observations of F 2 region in magnetically conjugate regions of Kerguelen and Archangel, comparing critical frequencies during magnetic and ionospheric disturbances

16 p2784 A69-32612

Fracture toughness of structural steels, discussing evaluation methods for brittle fracture resistance, toughness values and ratings correlation, etc

17 p2989 A69-33554

Initial phases of ionospheric and magnetic storms compared from data, noting good correlation due to ionospheric fields influence

17 p2967 A69-33988

Constant pressure adiabatic turbulent boundary layer characteristics measurements correlated in incompressible reference frame, using modified Mager compressibility transformation

17 p2958 A69-34051

Meteor dynamical and photometrical analyses compared quantitatively, determining mass loss value from fragmentation model

17 p3045 A69-34223

Physical model for IGY radio aurora data correlated with Brice magnetospheric convection model

18 p3125 A69-34231

Correlation between disturbances in troposphere and in geomagnetic field observed after widespread high winds and magnetic storms, using superposed epoch method

18 p3127 A69-34648

Satellite observation data association, estimating consistency of radar object with orbiting prediction, using computer program including Monte Carlo run

18 p3103 A69-35098

Molybdenum disulfide dry film lubricant wear theory and test correlation problems, considering sintering self propagation due to chemical effect of environment

19 p3323 A69-35580

C-5A aircraft model high subsonic speed tests, correlating data from three transonic wind tunnels [AIAA PAPER 69-794]

19 p3237 A69-35636

Supersonic transport aviation fuel thermal stability measurement data correlated with data deduced from heat transfer measurements

19 p3393 A69-36210

Balloon satellite orbital time and eccentricity correlated, investigating earth shadow and solar radiation effects

19 p3427 A69-36628

High altitude CAT regions length distribution determined from level flight path sampling data correlation

20 p3570 A69-37168

Free flight telemetered base pressure test data correlation for high Mach numbers, noting facilities and instrumentation

20 p3458 A69-37196

Correlation analysis accuracy using Fischer transformation in processing recorded data of small scale ionospheric inhomogeneities

20 p3503 A69-37688

Correlating IR lunar nighttime temperature and bearing strength of lunar materials, using expressions of thermal conductivity and bearing strength of porous media in vacuo

20 p3613 A69-38248

Model compounds and polymers solubility parameters correlated with refractive index data

21 p3751 A69-38552

Ionosphere drift measurements in LF range, noting relationship between correlation and similar-fade analyses for velocity data

21 p3714 A69-38557

VOR/DME information augmentation by air data /airspeed/ for positional accuracy improvement, describing error sources, optimum data filter and system sensitivity and performance [AIAA PAPER 69-841]

21 p3762 A69-39372

Daily simultaneous solar measurements of microwave atmospheric absorption and emission to determine frequency correlation between meteorological phenomena and atmospheric parameters

21 p3718 A69-39747

Meaningful comparisons between single stimulus EEG records and average evoked potential

22 p3890 A69-40163

Cosmos 137 proton spectra data obtained in inner radiation belt agreeing with Relay 1 data

22 p4007 A69-41093

Rotor aerodynamics research in terms of theoretical and experimental data comparison, rotor blade flow visualization and blade section camber

23 p4057 A69-41372

Disagreement between Mariner 2 and IMP 1 data concerning interrelation between solar wind velocity and geomagnetism ascribed to instrumental errors and changes in magnetospheric properties

23 p4205 A69-41848

Digital analysis of surface wave observations, discussing moving window, multiple filter, multicomponent recording, time variable filtration and cross correlation techniques

23 p4157 A69-42018

Ionospheric F region equatorial anomaly in electron density showing high correlation with equatorial electrojet range and poor correlation with Fugene range

23 p4160 A69-42432

Random signal behavior in hybrid correlator with analog and sampling channels, noting SNR expression and weak signal detection

24 p4283 A69-43139

Electrical and optical properties correlation of air in fog, discussing droplets distribution with regard to dimensions

24 p4347 A69-43506

Single frequency microwave solar bursts correlation with flares and associated active regions based on spectral grouping

24 p4372 A69-43616

Solar activity long term forecasts determined from comparison between Mount Wilson magnetic field synoptic chart latitude zones and sunspot groups

24 p4374 A69-43625

Pressure distribution correlation over blunted slender cone at various angles of attack by tangent cone method, describing hypersonic wind tunnel tests

24 p4249 A69-43681

DATA LINKS

Path length and path length rate variations in synchronous satellite communications link

04 p0561 A69-15448

Measurement methods at IF and baseband sections of microwave links, calculating noise superimposed on each swept measurement curve

05 p0722 A69-16728

Bit error probability for noncoherent binary FSK link involving Rician interfering signal

07 p1080 A69-19095

Technical characteristics of spacecraft telemetering, tracking and telecommand systems, stressing links between earth stations and spacecraft

09 p1451 A69-21291

Radio frequency signal transmission between orbiting spacecraft and vehicle entering VM-10 model atmosphere, examining near wake approximations and plasma-electromagnetic interaction

09 p1455 A69-22002

Power requirements for tracking, telecommand and telemetry of spacecraft over interplanetary distances, considering transmission problems, equipment weight and reliability

10 p1652 A69-22984

Telemetry data channel gain and phase correction with frequency response calibration technique using digital filtering

10 p1654 A69-23291

Data relay satellite concept, discussing orbits, communications between widely separated earth stations, and satellite tracking, telemetry and commanding

11 p1839 A69-25295

Data relay satellite systems for support of NASA R and D missions, discussing communications between satellites and to mission control

11 p1839 A69-25296

Technological feasibility of satellite based global data relay service for small users

12 p2028 A69-25949

Optimal communication by signal feedback link between transmitter and receiver based on optimum control and dynamic programming

12 p2046 A69-26060

Space Ground Link Subsystem as S-band communication link within Air Force Satellite Control Facility including unified telemetry, tracking and command systems

14 p2427 A69-28879

Optical carrier single channel telemetry system providing complete electrical isolation between shock tube data acquisition and data recording instrumentation

14 p2449 A69-29561

Wideband PM communication system with synchronous reception and automatic control of reception bandwidth, providing improvement in noise stability

15 p2564 A69-30147

Libration point relay satellites for continuous communication link between earth and lunar far side, discussing trajectories and halo orbit stationkeeping

15 p2680 A69-30188

Telemetry transmitter-receiver RF links quality determination, emphasizing nonlinear effects measurement by notch noise tests

19 p3270 A69-36239

Ground data handling equipment characteristics for PCM telemetry link utilizing convolutional coding

19 p3273 A69-36267

Representation theory of signal detection in non-Gaussian noise environments applied for improved near optimum system performance [IEEE PAPER 69-TP-10-COM]

19 p3277 A69-36488

Digital telemetry link coding as English language analogy, developing block code scheme combining bit, word and block error detection and correction methods

23 p4119 A69-41745

S band antenna systems for missiles, designed in various types to obtain RF telemetry links reliability by sharing effort between airborne and ground station equipment

23 p4137 A69-41753

Real time telemetry, tracking and command links by synchronous satellite relay, describing ATS-Nimbus E S-band experiment

23 p4121 A69-41759

HF data transmission system unaffected by high energy electromagnetic fields using GaAs IR emitting diode, glass fiber optic light guide and photomultiplier tube

23 p4121 A69-41768

EHF earth-satellite link communication channel emphasizing down link, discussing weather models, atmospheric absorption and temperature, channel coherence bandwidth, etc

23 p4129 A69-42506

Pioneer 9 deep space probe with telemetry link operated in coded mode with sequential decoding, discussing ground and flight test data

23 p4131 A69-42522

DATA PROCESSING

NT BATCH PROCESSING

NT CENSORED DATA [MATHEMATICS]

NT CENTRAL ELECTRONIC MANAGEMENT SYSTEM

NT COMPUTER GRAPHICS

NT KARHUNEN-LOEVE EXPANSION

NT SIGNAL ANALYSIS

NT SIGNAL PROCESSING

NT VOICE DATA PROCESSING

Digital computer system for storing, processing and displaying TV pictures

01 p0077 A69-10024

CRT method of processing contoured data from hemispheric and global numerical models simulating general atmospheric circulation

01 p0109 A69-10539

Spacecraft motion parameters determination under controlled acceleration using information from inertial sensors

01 p0161 A69-10569

Automatic heteroatomic plotting of high resolution mass spectral data, presenting relative intensity vs elemental composition in bar form

01 p0024 A69-10905

Probabilistic Information Processing System using men and machines to perform diagnostic information processing and to guide decision making

01 p0037 A69-10954

Data analysis methods for integrated data processing system for onboard in-flight checkout for launch vehicle evaluation [AIAA PAPER 67-911]

01 p0037 A69-11024

Structure oriented parallel algorithms for matrix operations, noting applicability to real time calculations for discrete Kalman filter and control problems

02 p0224 A69-11743

Satellite digital video data analyzed by two dimensional filter computer technique, discussing biomedical applications

02 p0213 A69-12155

Adaptive multiplex telemetry use in scientific satellite data management

02 p0212 A69-12817

Agricultural remote sensing information system composed of data acquisition, processing and information extraction and interpretation phases, providing knowledge of earth resources

03 p0400 A69-13195

Radiation sensor PCM data processing by computer to detect radiation level using data decorrelation, data normalization and threshold test

03 p0400 A69-13313

Visual observations data on noctilucent clouds /1963-1967/

04 p0595 A69-15307

Information processing - AFIPS Conference, San Francisco, December 1968

04 p0564 A69-15334

Lockheed hybrid computer system, describing features implemented by modifying and augmenting digital batch processing system

04 p0567 A69-15349

Real time performance, ground control and data processing of Surveyor spacecraft during maneuvers [AIAA PAPER 67-644]

04 p0586 A69-15502

Statistical relations for best value, standard deviation and confidence limits for engineering data, noting weighted least squares polynomial for fitting [ASME PAPER 68-WA/PTC-1]

05 p0768 A69-16192

Computer use evaluation, discussing standards for automatic data processing /ADP/ investment and operations

05 p0850 A69-16299

Program to study interactive graphic display console systems use for solving mechanical design problems involving plate cam and follower mechanisms

05 p0724 A69-16384

Automatic processing of electrocardiograms recorded during space flight by computer

05 p0715 A69-16524

Synchronous extractor for simultaneous extraction and association of primary and secondary radar videos in civil system, discussing automatic identification process

05 p0721 A69-16592

Atmospheric turbulence flight tests random data analysis to stimulate power spectra and transfer functions

05 p0767 A69-16756

Integrated automatic data processing system /NEC-TAR/ performance and operation

05 p0726 A69-16765

Computer oriented telemetry data processing systems designed to condition raw telemetry data for further processing by other systems

05 p0727 A69-16770

Data handling during ESRO satellite testing and launching, describing checkout equipment and programming of satellite computers

05 p0727 A69-16771

Air Force Eastern Test Range data processing systems perform real time operations during in-flight phases of ballistic missiles and orbiting vehicles

05 p0727 A69-16772

Data on muons indicating temperature effect diurnal maximum and pressure corrected daily variation

06 p0924 A69-17294

Radio spectrum and cosmic ray electron data evaluated concerning conditions in Galaxy, deducing mean magnetic fields

06 p0991 A69-17309

Automatic data processing method for analyzing multiply connected elastoplastic shells of revolution

06 p1025 A69-17614

Digital computer algorithm for automatic processing of IR weather data transmitted by Cosmos 122 and 144 meteorological satellites

06 p0929 A69-17981

Automation of meteorological fields analysis using computer

07 p1175 A69-18677

Data transition tracking in digital communication systems by decision directed phase tracking loops

07 p1082 A69-19108

High speed sampling for dynamic data analysis, considering random and transient vibrations

07 p1232 A69-19139

NERVA transfer functions evaluation by computer data processing, using Fourier algorithm [IEEE PAPER 2B-2]

07 p1179 A69-19187

Sensor data acquisition and processing and required levels of navigation integration for increasing air space capacity

07 p1177 A69-19211

Atomic and electronic collisions experimental study techniques, noting three data logging systems

07 p1187 A69-19662

Object restoration, discussing data processing method for single variable functions with small signal to noise ratios

07 p1137 A69-19721

Optical processing of planetary radar data for range Doppler image generation

08 p1270 A69-19816

Decision oriented automatic data processing systems design, noting quantity and quality of upward directed information to management

08 p1423 A69-20733

Delta modulation for analog to PCM encoding due to tapped binary shift register and up-down counter

09 p1455 A69-21844

Rapidly varying phase error effect on system performance in data detection process due to RF carrier tracking loop

09 p1456 A69-22459

Automatic flight control system /AOOSY/ for German Azur satellite

09 p1459 A69-22563

Airborne integrated in-flight data system to record and evaluate various engine parameters of operating jet engines

10 p1660 A69-23262

Airborne integrated data acquisition and analysis systems to determine aircraft technical performance

10 p1660 A69-23264

Flight test telemetry data processing system designed for C-5

10 p1660 A69-23269

Ground station integrated flight test data system with interactive data input terminals, on-line assembly and responsive program development

10 p1633 A69-23271

Automatic computer processing of physiological data during space flights, discussing choice of computers and computer programs

10 p1649 A69-23509

Suboptimum decision feedback communications systems incorporating simple digital processing compared with optimum Wald scheme

10 p1656 A69-23534

Civil aviation statistical data and airport planning

10 p1634 A69-23601

Human information processing rates during one and two axis compensatory tracking tasks with secondary auditory task

10 p1650 A69-23880

Processing of data obtained in continuous tracking of space objects using computer algorithms

10 p1791 A69-24193

Interplanetary magnetic field near Venus, analyzing data by magnetometer onboard Venera 4

10 p1791 A69-24199

Computer processed pictures including transformation of graphical material, picture generation from data or abstract rules, discussing procedures, instrumentation, color and applications

11 p1842 A69-24588

Soviet collection of articles on satellite data interpretation and use for meteorological services

11 p1911 A69-24824

Computer program for processing actinometric data transmitted from Cosmos 122 satellite

11 p1913 A69-24831

Physical data representation by approximation formulas for computer processing, considering polynomials, rational and spline functions and error curves

11 p1842 A69-24904

Polyharmonic predictive and self tunable filters synthesis based on signal periodic components detection, noting role in information transmission and processing systems

11 p1849 A69-24966

Data compression, redundancy reduction and applications to space flight technology

12 p0207 A69-25876

Optical data processing techniques and phase contrast method variations for statistics of surface roughness

12 p0209 A69-25910

Human operators instrument-monitoring behavior noting optimal control, information processing, physical limitations, etc

12 p0202 A69-25929

Parallel processing in system of computers with identical output, including probability graph for algorithm

13 p2224 A69-27426

Cosmic ray observation data automatic recording, presenting coding system for reading into computer

13 p2327 A69-27609

Automatic recording and data processing for ionospheric radiosonde observations from ground stations, giving block diagrams and subsystems

13 p2225 A69-27610

Computer program for obtaining information from stationary time series using Chree method of superposed epochs for processing unlimited data and epochs

13 p2225 A69-27617

Algebraic and sequential coding-decoding method for data communication rates up to capacity of discrete memoryless channel, discussing error probabilities

13 p2219 A69-27664

Satellite and aerological ground station data combined to determine geopotential fields and wind velocity fields for inadequately serviced areas

13 p2292 A69-27732

Ground station network and facilities for control of and acquisition and processing data from ESRO 1 satellite

13 p2220 A69-27751

Automatic processing and error analysis of horizontal, vertical, static and geostrophic wind data by U.S.S.R. Hydrometeorological Service

13 p2292 A69-27839

Turbulence measurement, considering handling and storage of data

13 p2263 A69-28148

Riometric data processing method for radio wave absorption measurement, considering nighttime cosmic radio emission intensity

14 p2436 A69-29056

Monograph on reduction of satellite data using fixed stars covering ALGOL programming for computing satellite direction from photographic model

14 p2446 A69-29286

H alpha line emission preceding auroral breakup by data analysis of Antarctica Meinel-type patrol spectrograph, noting magnetic activity role

14 p2441 A69-29386

Computer based data handling and display for relating remote sensor signals to ground truth information derived from aerial photographs

14 p2416 A69-29534

Computer uses for air traffic control in Germany including flight plans and weather report data processing

15 p2650 A69-30230

Automated shear difference analysis of three dimensional photoelastic model stress distribution by stress-freezing and slicing technique

15 p2609 A69-30680

Spacecraft motion parameters determination under controlled acceleration using information from inertial sensors

15 p2702 A69-30739

Statistical data concerning noctilucent clouds formation during IQSY, noting tendency to form along geographic longitudes and day and night existence

15 p2598 A69-31255

Doppler measurements in semidiurnal geodesy, processing data from Transit satellites collected at various Mediterranean ground stations

15 p2602 A69-31382

Airborne digital computer and display devices role in navigation management, discussing data processing and hybrid navigation systems

16 p2809 A69-32260

Data processing methods and equipment at Niemeck Observatory used for astronomical yearbook computations and geomagnetic requirements

16 p2767 A69-32463

Mascons implications in selenodetic data analysis conducted at U.S. space centers

17 p3028 A69-32922

On-line central data processing system connected to time shared computer for recording data from test facilities, discussing hardware configuration, software considerations and advantages

17 p2932 A69-33106

Satellite Proton 2 orientation from onboard measurement data, discussing general statistical method and data processing results

17 p3001 A69-33221

Data inaccuracy used for calculating forecasts of reliability analyzed by Monte Carlo simulation

17 p2937 A69-33389

Flight recorder program determining combat operating environments of CH-46D helicopters analyzed and compared with aircraft design criteria [AHS PAPER 375]

17 p3059 A69-33513

E layer inhomogeneities analysis concerning drift, chaotic processes, statistical parameters and reliability of data processing

17 p2962 A69-33896

Associative processor applied to interceptor radar system, noting processing time independence from target number and compatibility with real time systems

17 p2931 A69-34071

Beam control of optically fed two axis airborne electronically scanned phased arrays by on-array and off-array processing

17 p2942 A69-34085

Post Attack Command and Control System - Airborne Data Automation /PACCS-ADA/, describing components, operation, etc

17 p2977 A69-34116

Saturn software configuration accounting and reporting system for document change and information retrieval

18 p3105 A69-34269

Book on operational meteorological information processing by computers, discussing synoptic and aerological data, automatic data processing in operational numerical forecasting, etc

18 p3105 A69-34332

Lunar gravimetric data reprocessed to present in usable and readable form, plotting acceleration on Mercator projection of lunar surface

18 p3194 A69-34413

Mass spectroscopic structural analysis of organic compounds, discussing computer application to data recording, processing and evaluation

18 p3099 A69-34553

Computer quadratic method of evaluating ray propagation data for estimating inhomogeneous media properties

18 p3172 A69-34667

Automatic processing of electrocardiography recorded during space flight by computer

18 p3098 A69-34743

Ground data operations system for large astronomical satellite comprising UHF telemetry, PCM telecommand and processing and display equipment

18 p3117 A69-34794

Time sharing remote computer station allowing on-spot data processing and output answers, formulating best-fit equation representing statistical data [SAWE PAPER 799]

18 p3107 A69-34860

Automated handling of mass properties data, describing data stored, central bank, report outputs, system logic, etc

[SAWE PAPER 811]

18 p3221 A69-34899

Space vehicle checkout, launch control and data monitoring by general purpose ground system providing flexible stimuli generation, measurement acquisition, computation and information display

18 p3118 A69-35064

V/STOL wind tunnel data at low forward speeds, discussing test limit dependence on model size, downwash angle and tunnel geometry

18 p3119 A69-35229

Time/frequency technology using time-ordered reporting digital data for air traffic control to avoid airborne collision

[AIAA PAPER 69-795]

19 p3367 A69-35635

Continuously powered deep space vehicle orbit determination, discussing state estimation accuracy and use of continuous data filtering [AAS PAPER 68-144]

19 p3402 A69-35939

Ground data handling equipment characteristics for PCM telemetry link utilizing convolutional coding

19 p3273 A69-36267

Automated computer network analyzing electrocardiograms, using telephone lines for bidirectional communications between cardiac data acquisition stations and computer center

19 p3262 A69-36273

Onboard data processing and acquisition for aircraft and spacecraft problems based on integrated data management approach, discussing readout and display

19 p3280 A69-36315

Optimal timing of measurements to minimize dispersion of navigational observation parameters by least squares method with application to Keplerian orbit elements

19 p3370 A69-36614

Italian cross radio telescope noting added phase shifters to N-S arm, transistorized receiving system and modified data processing

19 p3295 A69-36643

Two procedures for processing statistical data concerning Gaussian processes made exchangeable by manageable formula

19 p3361 A69-36646

Pulsars pulse profiles data collected and interpreted with attempt to infer origin

20 p3597 A69-37335

Data handling system design for large astronomical satellite /LAS/, discussing spacecraft configuration, basic aims, program functions, subsystems, signal flow, flight repair, etc

20 p3501 A69-37390

Electronic data collection for climatological stations, describing acquisition and processing of various identification signals and meteorological parameters

20 p3538 A69-37428

Astronomical data collection and evaluation, discussing digital distance measurement, photoelectric photometry, servocontrols and electronic computers suited for Schmidt telescope output

20 p3539 A69-37525

Radar data optical spatial-domain processor providing azimuth processing in range channels without range compression capability, reviewing coherent optical channels properties

20 p3489 A69-37636

Range-Doppler data processing of radar echoes from spread targets, considering quadratic filter theory, emphasizing received signal correlation functions

20 p3490 A69-37648

Small scale inhomogeneities motions in E and sporadic E layers, processing data with method of full correlation analysis and statistical method

20 p3528 A69-37683

Correlation analysis accuracy using Fischer transformation in processing recorded data of small scale ionospheric inhomogeneities

20 p3503 A69-37688

Ionogram processing procedure, discussing presence of vertically moving ionospheric disturbances

20 p3529 A69-37691

Electronic computer for processing observational data from pilot balloons, utilizing algorithms of values in programming for accuracy and time saving

20 p3572 A69-37700

Human optical system as remote sensor consisting of transducing, data transmission and processing subsystems, defining perception function and describing visual aids

20 p3483 A69-37745

Data acquisition and processing ionograms from Alouette satellites telemetered sweep frequency top-side sounding data

20 p3503 A69-37860

Alouette 2 ionograms secondary resonances data indicating day-night effect in relative frequency of occurrence

20 p3496 A69-37889

Radar digital processing and display system for air traffic control with IC central processor and discrete data transmission over telephone lines from remote sites

21 p3760 A69-38328

Automatic speech recognition and tracking techniques of moving objects, considering applicability to processing data from earth resources satellites

21 p3721 A69-38630

Information processing with coherent light, discussing holographic interferometry, contour

mapping, three dimensional pictures, holographic coding, etc

21 p3722 A69-38797

Handling-qualities rating data evaluation for low computation cost information, noting reliability estimation

21 p3664 A69-38968

Communications, instrumentation and data handling for manned planetary missions, discussing data rate limitations

21 p3674 A69-39018

Residual analysis prior to statistical tests on experimental data

21 p3755 A69-39120

Numerical procedure for structural systems analysis, discussing computer application to hydrodynamic, electric, magnetic, thermodynamic, elastostatic and elastodynamic problems [AIAA PAPER 67-955]

21 p3839 A69-39216

Computer programs for design data, examining program complexity, reliability and availability, design data sheets, etc

21 p3732 A69-39304

Digital data analysis systems role in experimentation and R and D

21 p3843 A69-39315

Photoelastic data analysis for stress separations, discussing shear slope and Tesar methods

21 p3843 A69-39316

Biomedical electrical signals analysis by optical data processing, discussing conversion, SNR and filtering techniques

21 p3666 A69-39440

Discrete filters for optimal processing of down-linked satellite data, considering inverse filter development by Kalman filtering techniques

21 p3677 A69-39462

NASA current awareness service SCAN /selected current aerospace notices/, promoting selectivity in information transfer to abstract journals, accession lists and bibliographies

21 p3856 A69-39581

Scattered light photoelasticity dual observation method, describing automatic data collecting and interpreting system

22 p3945 A69-40079

Digital systems for acoustical or vibrational measurements reception and evaluation

22 p3945 A69-40168

Programmatic constraints on onboard processing of data collected by payload sensors [AIAA PAPER 69-942]

22 p3904 A69-40325

Machine independent telemetry oriented language /MITOL/ to develop computer programs for real time and postflight telemetry data processing

22 p3905 A69-40340

Telemetry data processing, describing designation, tasks and possibilities of data reduction laboratory attached to NASA Goddard Space Flight Center

22 p3919 A69-40352

Meteorological data real time processing for automatic weather analysis and prognosis, program used and computer output charts

22 p3977 A69-40732

Adaptive control system synthesis for reducing computation labor for controlled inertialess plant, reproducing probability density function to describe unknown parameters

22 p3918 A69-40739

Data evaluation, measurement accuracy and statistical procedure, using silicates chemical analysis

22 p3897 A69-40984

Data acquisition techniques and devices in electronic data processing

22 p3908 A69-41251

Frequency response transient vibration testing of standing man, discussing data analysis procedure, test stand, and Welch correction for instrument dynamics

23 p4101 A69-41494

Airline economics long term trends requiring management tools for cost control, operations simulation and monitoring, computer use and information data processing [SAE PAPER 690414]

23 p4241 A69-41641

Geomagnetic field spherical analysis from angular data and extrapolated values of time variable field coefficient

23 p4157 A69-41866

PCM telemetry system for transferring information from many remote sources to single local processing point

24 p4281 A69-42620

Spacecraft central data system for deep space solar probe data management

24 p4284 A69-42621

Fiscal requirements forecasting for space systems involving data analysis
[AAS PAPER 69-166A] 24 p4417 A69-42814

Personnel training and selection systems, applying information processing models to diagnostic testing in job classification for performance improvement
24 p4274 A69-43020

Mathematical method of processing test data air-frame panels subjected to repeated static loads to obtain lifetime equations and statistical characteristics
24 p4400 A69-43086

Mariner 6 and 7 TV data, discussing implications for Mars present state, past history and biological status
24 p4384 A69-43195

Sensory information processing model for tactile perception using array of airjet and piezoelectric stimulators applicable to display design and nervous system investigation
24 p4276 A69-43273

DATA PROCESSING EQUIPMENT

NT AIRBORNE/SPACEBORNE COMPUTERS

NT ANALOG COMPUTERS

NT COMPUTERS

NT DIGITAL COMPUTERS

NT HYBRID COMPUTERS

NT IBM 360 COMPUTER

NT PRINTERS [DATA PROCESSING]

NT SEQUENTIAL COMPUTERS

NT SITE DATA PROCESSORS

NT UNIVAC COMPUTERS

Automatic devices to count bacterial colonies Petri dishes consisting of culture plate scanner and data processor
02 p1201 A69-11773

Digital data processing equipment for space flight PCM telemetry
03 p0393 A69-13290

On-line ground flight test data processing system
05 p0725 A69-16757

OMEGA 4 100-k Hz ground station telemetry system for acquiring and processing outputs up to 23 FM and two TDM signals applied simultaneously from instrumentation recorder
07 p1105 A69-19103

Telemetry monitor systems for high speed rotating equipment, discussing data recording, transmission, decoding, thin-thick film microtechniques, etc
10 p1692 A69-23249

Data processing system for satellite telemetry signals, describing hardware construction and operation, data readout, etc
11 p1840 A69-25426

Vignetting effect on impulse response of general coherent optical Fourier processor, noting time varying character and input position sensitivity
12 p2036 A69-25912

Optical surface wave propagation on thin dielectric film waveguides, noting applications to integrated optical data processors
13 p2229 A69-27676

Data processing for scientific rocket research, considering pulse counters, multiplexers, converters and programmers
16 p2755 A69-31858

Automatic meteorological radar data processing system incorporating MRL-1 radar and low speed digital computer
16 p2791 A69-32279

Automatic conversion receiver of meteorological radar data, examining reception amplitude sensitivity and frequency characteristics
16 p2791 A69-32280

Data processing methods and equipment at Niemegk Observatory used for astronomical yearbook computations and geomagnetic requirements
16 p2767 A69-32463

Sampled data system with built-in data processing for observation of fine grain characteristics of pulsed signals used in radar systems
17 p2934 A69-34076

Electronic data processing facilitating engineering design development work, including computer programming
18 p3106 A69-34838

DYDRA data logger for dynamic measurements of pressure distributions on harmonically excited wind tunnel models, noting use as general transfer function analyzer
19 p3293 A69-35746

Earth orbit estimation by manual stadimeter, space sextant and small data processor, discussing orbital parameter errors due to instrument and environment uncertainties
19 p3369 A69-35793

Eurocontrol Experimental Data Processor for automation in air traffic control, discussing system size configuration and environment
19 p3280 A69-36654

Secondary radar IFF/SIF /Identification Friend or Foe-Selective Identification Feature/ system, describing ground and onboard radar and data processing equipment
19 p3278 A69-36702

Onboard data processor design for Swedish satellite to study spatial and temporal variations of auroral particles
20 p3501 A69-37387

Numerical and analog data acquisition system /CARINA/ for processing rocket, balloon and satellite data, describing distributor characteristics, control console, etc
20 p3511 A69-37914

Flexible circuitry for reliable spaceborne data processing equipment electronic packaging
22 p3903 A69-39951

Closed Loop Ionogram Processor /CLIP/ on-line computer processing system for ionospheric data [AIAA PAPER 69-952] 22 p3904 A69-40334

Fail-soft operation in array processor with cellular redundancy, discussing cellular autonomy, long life and ultrareliability [AIAA PAPER 69-965] 22 p3906 A69-40346

Digital data systems fault detection and isolation, describing diagnostic programs and hardware [AIAA PAPER 69-967] 22 p3906 A69-40348

Modular data acquisition and processing system, describing input unit, checkpoint selection scanner, analog-digital converter, limit indicator, etc
23 p4167 A69-42459

Linear electrical analogs for two dimensional optical data processing systems, discussing diffraction field model, quadratic phase filters, thin lenses, photographic film applications, etc
24 p4286 A69-42619

DATA PROCESSING TERMINALS

Man-computer interactive Terminal Interface System /ITIS/ compatible for programming graphics, character scopes and typewriter using FORTRAN [AIAA PAPER 69-955] 22 p3905 A69-40337

IBM 360-50 computer with I/O terminals to process PCM and analog data from Modular Auroral Probe series of sounding rockets on real time basis
23 p4133 A69-41764

DATA READOUT SYSTEMS

U DISPLAY DEVICES

DATA RECORDERS

Digital adaptive recording system /DARS/ 12 channel flight recorder
05 p0766 A69-16754

Sonic boom simulation methods using shock tube, booth type simulators, ballistic ranges and explosives, discussing unmanned data recorder as monitoring device
15 p2585 A69-30371

DATA RECORDING

Multibeam recording technique producing speckle-free images in redundant holograms of transparencies

01 p0082 A69-10850

Shock and vibration data recording, discussing transducer selection, accelerometer mounting, conditioning electronics and recording devices

01 p0083 A69-11050

Microstructure analysis and relationship between microvariations and macroscopic events, using magnetic variations recordings of IGY network

01 p0069 A69-11126

Electron concentration in ionospheric outer regions determined from coherent frequencies recorded on-board OGO-A

01 p0147 A69-11323

Automatic recording of neutral atom temperature and free electron density of partially ionized gas by Fabry-Perot interferometer

03 p0428 A69-13111

Photorecording techniques for command and control systems requirements, discussing association with large screen computer generated CRT projection display equipment

06 p0928 A69-17923

Three dimensional information pictures of chromospheric alpha H line using special camera attached to solar telescope diffraction grating spectrograph

07 p1217 A69-19241

IR beam profiles of carbon dioxide laser permanently recorded on foamed polystyrene

07 p1156 A69-19305

Magnetic tape recording of ultrasonic test information with oscilloscope used for playback
07 p1117 A69-19697

Magnetic tape recorder/reproducer for FM analog test data
10 p1691 A69-23233

Flight data recorders history and regulations, discussing parameters and design of systems
10 p1691 A69-23247

Maintenance recording systems for aircraft fleet, discussing operations objectives and research, data collection and implementation using systems engineering
10 p1671 A69-23261

Airborne integrated in-flight data system to record and evaluate various engine parameters of operating jet engines
10 p1660 A69-23262

Cosmic ray observation data automatic recording, presenting coding system for reading into computer
13 p2327 A69-27609

Automatic recording and data processing for ionospheric radiosonde observations from ground stations, giving block diagrams and subsystems
13 p2225 A69-27610

Scientific equipment on Cosmos 237 satellite for recording extraterrestrial radiation data, discussing specifications, operation and mission purpose
14 p2446 A69-29047

Computer analysis of EEG recording, presenting model studies under rest and performance conditions
15 p2560 A69-31232

On-line central data processing system connected to time shared computer for recording data from test facilities, discussing hardware configuration, software considerations and advantages
17 p2932 A69-33106

Onboard flight data recorder as integrated system for investigating aircraft accidents, describing German LEADS 200 model
17 p2974 A69-33429

X ray data in 44-60, 8-16 and 1-8 A bands telemetered by Solrad 9 satellite
20 p3588 A69-37473

Rocket measurement data of auroral particle precipitation classified in substorm phases of quiet and breakup period, breakup and postbreakup events and morning events
21 p3707 A69-38489

DATA REDUCTION

Data compression methods noting block and circuit diagrams

01 p0031 A69-10735

Data analysis methods for integrated data processing system for onboard in-flight checkout for launch vehicle evaluation

[AIAA PAPER 67-911] 01 p0037 A69-11024

Tabular reduction of crystal structure chemical information for metals and semiconductors for material selection use

02 p0295 A69-11786

Multichannel digital data compression simulation, discussing algorithms, buffer queue control, identification coding and system performance measurements

02 p0213 A69-12814

Adaptive multiplex telemetry use in scientific satellite data management

02 p0212 A69-12817

Adaptive compression system for predicting and encoding video data for transmission in noiseless channel

03 p0427 A69-12869

Radar cross section data interpretation, discussing calibration, unwanted signals, averaging, scattering matrix and power spectra

03 p0385 A69-12913

Channel identification coding for data compressors, deriving optimum code word length for bit compression ratio and overflow identification scheme

03 p0391 A69-13219

Stored program control for polynomial data compression in telemetry application

03 p0400 A69-13220

Visual observations data on noctilucent clouds /1963-1967/

04 p0595 A69-15307

Statistical relations for best value, standard deviation and confidence limits for engineering data, noting weighted least squares polynomial for fitting [ASME PAPER 68-WA/PTC-1]

05 p0768 A69-16192

Pattern classification algorithms classified according to type of input information required

05 p0725 A69-16571

Flight test data reduction on time sharing general purpose computer, noting hardware link between airborne equipment and computer 05 p0726 A69-16758

Integrated automatic data processing system /NEC-TAR/ performance and operation 05 p0726 A69-16765

Meteorological satellites data for quantitative weather forecasts, discussing error effects due to data treatment in adiabatic approximation 06 p0949 A69-17032

Satellite actinometric data computerized reduction in U.S.S.R., examining computer program features [UN PAPER 68-95763] 06 p0916 A69-17038

Processing TV cloud data monitored by Molniya 1 and Meteor meteorological satellites, discussing computer interpretation of TV photographs [UN PAPER 68-95759] 06 p0950 A69-17060

Averaging procedures to represent highly time variable actual hydrometeorological fields by less variable equivalent fields 06 p0952 A69-17989

Pattern recognition method dependent on preselection of good variables, discussing SELFIC and relationship to Karhunen-Loeve expansion and factor analysis 07 p1088 A69-18386

Data compression techniques compared for use in communications systems to minimize required number of samples and bits per sample 07 p1077 A69-18758

Nonvertical propagation effects on high altitude topside ionosphere sounder data reduction, using ray tracing 07 p1124 A69-18838

High speed sampling for dynamic data analysis, considering random and transient vibrations 07 p1232 A69-19139

Digital telemetry from spacecraft, discussing on-board processing, data compression, coding, sequence detection and receivers 08 p1276 A69-20592

Curve fitting for optimum redundancy reduction on sampled data, describing polygonal and approximate polygonal techniques 09 p1533 A69-22458

Data interpretation, discussing correlation describing effectiveness of independent variable and table giving values directly from sample size, t , z , F and chi square values 10 p1669 A69-23040

Test facility automation, discussing pretest preparations, test operations, data reduction and system planning 10 p1671 A69-23260

Airborne integrated data acquisition and analysis systems to determine aircraft technical performance 10 p1660 A69-23264

Computer implemented analysis of aeroelastic stability for elapsed data reduction time, discussing frequency modes and digital filters 10 p1634 A69-23274

Sample data reduction methods combined in special purpose computer for measuring ablation in reentry vehicle heat shields 10 p1660 A69-23290

Antenna for lunar occultation observations at 81.5 MHz, detailing experimental procedure and data reduction 10 p1779 A69-23606

Pattern classification algorithms classified according to type of input information required 11 p1843 A69-25445

Data compression, redundancy reduction and applications to space flight technology 12 p2027 A69-25876

Extrapolation and interpolation for data compression including polynomial concept 12 p2027 A69-25877

Power spectral analysis feasibility for data reduction for medical interpretation of changes in pulmonary impedance pneumograph in remote monitoring 12 p2024 A69-26558

Data analysis techniques for discrimination and identification of terrain surfaces from radar scatterometry information 12 p2099 A69-27010

Venus carbon dioxide spectral band analysis methods, discussing spectral lines and rotational temperatures obtained 13 p2344 A69-27649

Design and efficiency for signal-time compressors of spectral analyzers using electron beam tubes with charge storage 15 p2576 A69-30351

Scintillation index determination, discussing data reduction methods, standard test records, calibration at stations with modest equipment and simulation on digital computer 16 p2751 A69-32105

Mascons implications in selenodetic data analysis conducted at U.S. space centers 17 p3028 A69-32922

Flight recorder program determining combat operating environments of CH-46D helicopters analyzed and compared with aircraft design criteria [AHS PAPER 375] 17 p3059 A69-33513

Relative control data incorporation into sequential or simultaneous analytical triangulation systems, considering extraterrestrial photographs reduction 18 p3133 A69-34335

NASA photogrammetric lunar activities, discussing imagery and control data by Lunar Orbiter and photogrammetric data reduction for preparing manned lunar landing 18 p3133 A69-34336

Computer graphics technique for reducing photographic data from optical device to replace time consuming visual methods 18 p3134 A69-34373

Mass spectroscopic structural analysis of organic compounds, discussing computer application to data recording, processing and evaluation 18 p3099 A69-34553

Lunar origin, geological composition and water existence controversies from data gathered by various lunar probes 18 p3196 A69-34631

Thermoelectrical leg product specification /TELPS/ apparatus and data reduction technique for determining temperature dependent thermoelectric properties of material 18 p3093 A69-34783

Data compression using orthogonal functions, design curves for given functions, signal characteristics and error avoidance 18 p3103 A69-35060

Secor data reduction to correct tropospheric refractive effects of radio ranging on earth satellites using tropospheric model 18 p3104 A69-35200

Holographic velocimetry data reduction applicable to flow field holograms, using singlet interference pattern for spherical and plane wave illumination 19 p3305 A69-35730

Quantitative density data from schlieren measurements by photomultiplier technique for axisymmetric flow outside diffraction bands 19 p3306 A69-35741

Buffer storage for telemetry nonstationary video data compression, analyzing requirements, predictor algorithm and variable aperture control using simulation 19 p3272 A69-36260

Digital data compression system transmission error statistical analysis, emphasizing addressing schemes effect on compression ratio 19 p3272 A69-36261

Huffman minimum redundancy coding extension to run-length information based on Poisson distribution, including optimization and data compression applications 19 p3272 A69-36262

Precompression automatic wild point rejection from sampled telemetry data for data compressors evaluated by digital computer simulation 19 p3273 A69-36263

Maximum rms error comparison of redundancy reduction techniques, emphasizing limiting slope technique and worst case interpolation error 19 p3273 A69-36264

Spacecraft onboard processor for digital filtration and data compression, discussing prototype design, construction, sample memory, weight memory, arithmetic unit and programmer 20 p3500 A69-37383

Topside ionogram reduction for ionospheric electron density determination, using geomagnetic strength at all heights, iteration and change of variables 20 p3529 A69-37864

Brightness distribution over source, discussing regularization algorithms for radio astronomical data reduction from crossed telescope 20 p3606 A69-38033

Mean importance variations of sunspot groups in various latitude intervals, reducing data statistically with dispersion analysis and autocorrelation method 20 p3616 A69-38303

Residual analysis prior to statistical tests on experimental data 21 p3755 A69-39120

Digital data analysis systems role in experimentation and R and D 21 p3843 A69-39315

Closed Loop Ionogram Processor /CLIP/ on-line computer processing system for ionospheric data [AIAA PAPER 69-952] 22 p3904 A69-40334

Data compression and transmission technique for real time system to monitor manned space missions, noting Apollo telemetry data [AIAA PAPER 69-970] 22 p3906 A69-40350

Data evaluation, measurement accuracy and statistical procedure, using silicates chemical analysis 22 p3897 A69-40984

Integrated adaptive data transmission system accepting analog inputs through information compressing sampler or digital inputs by sampling 23 p4121 A69-41760

IBM 360-50 computer with I/O terminals to process PCM and analog data from Modular Auroral Probe series of sounding rockets on real time basis 23 p4133 A69-41764

Sound evoked DC changes on intact skull of adult humans using data from AgCl electrodes, investigating intensity function, analyzing data by computer 23 p4098 A69-42101

Brayton-B generator for 2-10 kwe production, describing design, heat source/rejection, efficiencies and preliminary test data analysis 23 p4071 A69-42278

Data compression from standpoint of epsilon entropy theory, considering precise measure of channel capacity necessary to describe data source 23 p4134 A69-42526

Automatic analysis and classification of images stored on 35-mm film using CRT flying spot scanner with computer control and memory 24 p4286 A69-42744

Lunar gravitational field data from Lunar Orbiter spacecraft reprocessed, discussing mascon effects on moon structure and evolution theories 24 p4379 A69-42785

On-board digital filtering applied to spectral estimation and data compression, discussing theory, techniques, computerized implementation and prototype design [AIAA PAPER 69-969] 24 p4285 A69-43510

DATA RETRIEVAL

NASA scientific and technical information program for building technical data and literature repository for scientists, engineers and technical managers, describing IAA and STAR [UN PAPER 68-95317] 06 p1043 A69-17068

Random data detection method applicable to low voltage SNR cases using real time correlation of probability functions 09 p1459 A69-22593

Associative holographic memories, discussing recall systems, logic circuits, etc 10 p1697 A69-23868

DATA SAMPLING

Validation study of pilots visual sampling behavior, using queueing model based on instrument and eye movement data from Link trainer mission flights 02 p2002 A69-11954

Optimum control of fourth order digital control system 03 p0408 A69-12916

Sampled data delay-lock loop for synchronizing pulsed envelope RF signals, using digital circuitry 03 p0390 A69-13216

Iterative method of determining orthogonalized bases for representation of sampled data signals 03 p0391 A69-13231

Analog sampled data simulator using field effect transistors and single value of holding capacitor for covering sample frequency variation 03 p0405 A69-13600

Book on qualitative theory of sampled data systems 04 p0630 A69-14563

Dynamics of single loop nonlinear sampled data systems with integrator, deriving equations of periodic motions and stability conditions by means of point transformations 04 p0583 A69-15135

Digital filter transfer functions design by sampled data transformation, noting role of analog filters 04 p0584 A69-15461

Special purpose computer for implementing programmable digital filter used in sampled data control systems 04 p0569 A69-15462

Bit reduction in digital transfer functions with LF poles in sampled data systems using zero order hold function

04 p0584 A69-15464

Data sampling and statistical verification in large scale sterilization procedures, discussing biological indicator /bacillus stearothermophilus/ and incubation time

05 p0714 A69-15952

Minimum sensitivity deadbeat sampled data control system design by frequency domain technique, using two controllers [ASME PAPER 68-WA/AUT-15]

05 p0738 A69-16177

Monograph on nonlinear sampled data systems covering Liapunov method, discrete systems, finite difference, flow graphs, Laplace transformations, etc

05 p0739 A69-16544

Time averages for estimating probability distribution, density and moments of random functions applied to deterministic signals, considering sampling frequency dependence

05 p0722 A69-16729

Pulse amplitude measurements comparison by sampling signal at given time and pulse peak detection, considering SNR

05 p0722 A69-16730

Digital computer optimization of representation of sampled data signals on orthogonal basis, using iterative method

06 p0901 A69-17363

Data compression techniques compared for use in communications systems to minimize required number of samples and bits per sample

07 p1077 A69-18758

Signal multiplexing within linear algebra framework permitting use of orthonormality in receiver construction without orthonormal functions generation in multiplexer

07 p1078 A69-18830

Presampling filtering, discussing effects on rms interpolation error for sampled data systems

07 p1083 A69-19129

High speed sampling for dynamic data analysis, considering random and transient vibrations

07 p1232 A69-19139

Sampled data regulator for maintenance of constant alveolar carbon dioxide during steady state and transient ventilatory responses to hypoxic stimulation

07 p1072 A69-19480

Image degradation in holograms undersampled with respect to space-bandwidth product, noting signal to noise ratio and resolution

08 p1312 A69-20078

Multiloop control plant described by Jacobian transfer matrix to control spectral characteristics of random processes

08 p1296 A69-20233

Curve fitting for optimum redundancy reduction on sampled data, describing polygonal and approximate polygonal techniques

09 p1533 A69-22458

Analog to digital conversion for data sampling systems including scanning, distributors, multiplexing, automatic ranging, noise reduction and data storage techniques

10 p1660 A69-23232

Sample data reduction methods combined in special purpose computer for measuring ablation in reentry vehicle heat shields

10 p1660 A69-23290

Digital sampled data spectra conditioning, deriving linear functions for low pass, bandpass and band rejection numerical filters and spectrum shaping

10 p1654 A69-23292

Monte Carlo digital computer simulations, considering sample sizes and confidence intervals in multinomial output

10 p1661 A69-23853

Programmed search and gradient search methods for determination of sampling intervals in synthesis of sampled data models of human operators

10 p1650 A69-23881

Solid state sampling circuit for low pulse repetition frequencies to improve signal to noise ratio, noting ratio of holding to learning time

11 p1849 A69-24900

Adaptive optimal estimation of sampled stochastic process with finite state unknown parameters, using separation technique

11 p1858 A69-24935

Sampled data multichannel telemetry using pseudorandom sequences generated by linear shift registers

12 p0208 A69-25925

Feedback design for monotonically stabilized linear sampled data control system

12 p2045 A69-25961

Sampled data time optimal control of linear multivariable system based on determination of system state variables control time and minimum sampling intervals

12 p2050 A69-26088

Asymptotic sampling error in closed loop hybrid systems, noting dependence on sampling period and execution time

12 p2053 A69-26508

Remote sensing and forest survey sampling designs, discussing nonstereo stratification, conventional photography and IR or radar imagery

12 p2097 A69-26991

Passive adaptive sampled data control system with conditional feedback, discussing transfer function role and minimization of external disturbances and internal parameter variations effects

13 p2238 A69-27394

Lunar topography harmonic analysis, noting sample point density and evenness variations effects on estimated coefficients

13 p2344 A69-27647

Microwave measurement methods, discussing uses of digital computers and sampling techniques

13 p2223 A69-28605

Relay sampled data phase plane trajectories periodic motions increased with increase of system duty factor

14 p2425 A69-28898

PCM oscillator synchronization system stability, considering sampled model by digital nature of equipment

15 p2565 A69-30171

Error analysis of one bit autocorrelation method of spectral estimation, noting decrease in spectral variance with increased sampling rate

16 p2752 A69-32390

Sampled data system with built-in data processing for observation of fine grain characteristics of pulsed signals used in radar systems

17 p2934 A69-34076

Digital data acquisition system with ultrahigh sampling rate for Ames electric arc shock tunnel, describing analog to digital conversion, data storage, system performance, etc

19 p3293 A69-35744

Precompression automatic wild point rejection from sampled telemetry data for data compressors evaluated by digital computer simulation

19 p3273 A69-36263

Fast Fourier Transform connection with circulant and permutation matrices for case with discrete time sample number equal to discrete frequency samples

23 p4182 A69-41761

Flexible format generator for manned spacecraft data management system designed with memory for data sampling formats, emphasizing software counters and power strobing

23 p4133 A69-41762

Stochastic approximation applied to sampled data system parameters including sampling interval

24 p4295 A69-43319

DATA SMOOTHING

Error and sensitivity analysis of on-line algorithms for fixed point linear smoothing

01 p0050 A69-10238

Scaled and translated composite curve technique for reducing calibration data for spectrograph film system response characteristics

01 p0082 A69-10839

Algorithms for error analysis, optimum filtering sensitivity and fixed interval smoothing solutions to linear estimation problems

02 p0224 A69-11961

Maximum likelihood smoother using measurements containing correlated noise for application to continuous linear dynamic systems such as inertial navigation

06 p0956 A69-17938

Least squares local smoothing by polynomials of noisy data in n dimensions

08 p1344 A69-20830

Geomagnetic field mean hourly values continuous smoothing from recordings at drifting arctic stations for determining time variations

09 p1487 A69-21553

Smoothing data stability by least squares method, noting applicability to computer processing at random sequences

09 p1532 A69-21754

Error bounds for estimation error covariance matrix of fixed point smoothing and fixed interval smoothing algorithms for optimum linear estimation

09 p1533 A69-22436

Lumped linear system state estimation with optimal linear smoothing instead of filtering, noting smoothing lag and variance

12 p2122 A69-26524

Smoothing problem for linear discrete time system, converting problem to special case of standard linear filtering problem

12 p2122 A69-26525

Error bounds for covariance matrix used in optimum filtering and smoothing algorithms for control and communications systems operation

14 p2416 A69-29549

Artificial earth satellites positional observations by graphical smoothing on azimuth and altitude, discussing advantages for space geodesy

15 p2594 A69-30029

Geomagnetic field mean hourly values continuous smoothing from recordings at drifting arctic stations for determining time variations

16 p2784 A69-32548

Astronomical and geophysical observations, selecting degree of smoothing via Whittaker method for curve construction

17 p3028 A69-32877

Least squares method of smoothing curves or surfaces involving orthogonal base functions, discussing matrices conditioning and structure eigenmodes

18 p3218 A69-34642

Minimum bias criteria for selecting data fitting curves, allowing for unknown true equation in improving data predictability [AIAA PAPER 69-950]

22 p3975 A69-40332

Kalman-Bucy filtering technique for estimation of initial conditions and smoothing in linear dynamic systems, noting rectilinear motion of randomly accelerated spacecraft

23 p4132 A69-42546

DATA STORAGE

Digital computer system for storing, processing and displaying TV pictures

01 p0077 A69-10024

Output p-channel MOS transistor selection tree for display and information storage systems

01 p0039 A69-10173

Representation for computer storage of contour map data for searching problem involving determination of aircraft ground track

01 p0036 A69-10704

Human factors evaluation of computer based information storage and retrieval system using questionnaire and interview techniques

02 p0204 A69-12220

Lithium niobate single crystals for holographic storage, noting use for optical information storage, processing and display devices

03 p0432 A69-14184

Stored program computer for small scientific spacecraft, noting program and data memory capacities

04 p0569 A69-15472

Electrostatic storage display tube characteristics, construction, applications and reliability

07 p1101 A69-18655

Holography principles to design high capacity high speed storage devices, using photochrome recording medium

07 p1133 A69-19158

Statistical theory and dynamic programming to synthesize optimal pulsed control systems having restrictions on control device storage capacity

09 p1476 A69-22673

Large capacity holographic memory design based on page organization concept, considering lens parameters and hologram size

11 p1886 A69-25041

Multiple information storage in sampled hologram in space division multiplexing holography, constructing hologram with sound waves and reconstructing images with laser light

12 p2079 A69-25921

Holographic storage of three dimensional measurement information using model formed by stacking plates

13 p2260 A69-27739

Lower bound determination of automaton memory elements, describing coding procedure and algorithm for machine states

13 p2239 A69-28554

Microwave tunnel diode switch design noting applications to information storage

15 p2574 A69-30132

Information storage of multichannel analyzer of continuous and pulsed processes

17 p2939 A69-33900

- Dynamic Automated Reporting Technique /DART/ system for on-line conversational information storage and retrieval for use in large programs management 18 p3107 A69-35095
- Spacecraft data storage requirements, discussing use of servo-driven tape recorders in data processing systems 18 p3107 A69-35096
- Binary storage system operation during binary quantization of signal, applying results to storage efficiency improvement 19 p3278 A69-36597
- Recording devices for storing bandwidth data in time sequence, studying design parameters using light beam recorder implemented with CRT for read-in process 20 p3540 A69-37640
- Ariel 3 satellite shape and systems including heat balance, data storage and compatibility problems 21 p3820 A69-39256
- DATA SYSTEMS**
- Scientific and technical information flow sources, showing DOD user need within defense industry and importance of local work environment 02 p0204 A69-12219
- Onboard SDP-3 computer data system core for IMP spacecraft, considering payload 03 p0400 A69-13243
- Multimode digital radar control paths and operating communication, discussing radar data, triggers, real time data and error localization 05 p0718 A69-15750
- Simulation in design of automated flight test data system 05 p0743 A69-16759
- Data handling equipment for Ariel 3 and future satellites emphasizing manufacturing of PFM and PCM systems 05 p0726 A69-16769
- Data handling during ESRO satellite testing and launching, describing checkout equipment and programming of satellite computers 05 p0727 A69-16771
- Data handling by groups in perceptron type pattern recognition and decision making problems based on algorithm involving second degree polynomials 08 p1278 A69-20420
- Centralized control with variable step interrogation of control points 08 p1298 A69-20422
- Analog to digital conversion for data sampling systems including scanning, distributors, multiplexing, automatic ranging, noise reduction and data storage techniques 10 p1660 A69-23232
- Ground station integrated flight test data system with interactive data input terminals, on-line assembly and responsive program development 10 p1633 A69-23271
- Gas turbine engine development data system based on test stands subsystems and central computer 10 p1660 A69-23284
- Turbulence measurement, considering handling and storage of data 13 p2263 A69-28148
- Deep space data return, discussing system function, design, operational interfaces and interplanetary spacecraft data compression methods 14 p2517 A69-29096
- Data handling by groups in perceptron type pattern recognition and decision making problems based on algorithm involving second degree polynomials 14 p2418 A69-29658
- Air data system consisting of aerodynamic and thermodynamic sensors and computer calculating flight parameters for automatic flight control 18 p3169 A69-34854
- PCM data handling system for NASA Space Tracking and Data Acquisition Network with explanation for output capabilities, noting BIOSAT project 19 p3270 A69-36242
- Temperature program generation for test chambers, verifying temperature programmers and readout, verification and recording systems 22 p3954 A69-40038
- Programmable data handling and telemetry systems for scientific satellites, noting system checkout, spacecraft integration, software and ground data processing 23 p4132 A69-41735
- Spacecraft onboard data handling system with MSI complementary MOS arrays, describing various components 23 p4133 A69-41739

- Data systems coordinating standards developed from experience with STADAN, discussing operating environment and administrative decisions influence on implementation 23 p4133 A69-41769
- Spacecraft central data system for deep space solar probe data management 24 p4284 A69-42621
- Satellite data management systems design, considering user-designer cooperation aspects for space programs [AAS PAPER 69-366] 24 p4417 A69-42806
- Stochastic approximation applied to sampled data system parameters including sampling interval 24 p4295 A69-43319

DATA TRANSMISSION

- NT AUTOMATIC PICTURE TRANSMISSION
- NT CHANNELS [DATA TRANSMISSION]
- Transistorized feedback amplifier for data transmission over high voltage lines in conveyed wave systems 01 p0038 A69-10074
- Hybrid digital transmission systems, discussing joint optimization of analog and digital repeaters and information rate of coaxial cable systems 01 p0027 A69-10248
- Regenerative digital transmission system error, representing memory of binary regenerative channel with Markov model 01 p0027 A69-10249
- Quantizing noise effect on reconstructed analog signal at reception terminal of digital data transmission system 01 p0027 A69-10250
- Transversal filters for equalization of data channels with pulse amplitude modulation, discussing pulse equalizability and convergence criteria for iterative search routine 01 p0027 A69-10251
- Optimal rank algorithm construction for signal detection in noise investigated for use in information transmission systems 01 p0027 A69-10374
- International experimentation with U.S. communications satellites, noting design variations with participants and restraints information exchange [UN PAPER 68-95421] 01 p0108 A69-10474
- NASA Technology Utilization Program, discussing information dissemination [UN PAPER 68-95313] 01 p0179 A69-10512
- Data compression methods noting block and circuit diagrams 01 p0031 A69-10735
- Reliability of binary message in Gaussian noise impaired by amplitude limiting in case of evaluation by integration 01 p0031 A69-10736
- Radio systems for discrete information transmission, emphasizing phase difference modulation, wideband, universal and adaptive systems 01 p0031 A69-10778
- Book on probabilistic information theory-discrete and memoryless models covering information transmission, digitalized sources, generating functions, decoding error, systematic codes and sequential decoding 01 p0037 A69-11030
- Two dimensional representation of Venus entry probe target data for determining probe capability to provide real time data transmission to earth 02 p0331 A69-12820
- Synchronization in coded communication systems, considering phase lock loop and square wave correlation function 03 p0383 A69-12871
- Digital transmission at 35 GHz, noting atmospheric and rainfall effect on terrestrial millimeter wave propagation 03 p0389 A69-13192
- Noncoherent binary communication detector for slow selective fading channel with additive quasi-stationary noise based on mathematical procedure of non-parametric classification 03 p0390 A69-13215
- WEFAX /Weather Facsimile/ experiment to explore operational feasibility of direct meteorological data transmission via satellite relay from central station to remote stations 03 p0411 A69-13240
- Delay line bandwidth reduction for video or digital information, noting radar tracking application 03 p0392 A69-13251
- Noise reduction techniques in digital and analog data transmission over space program distances, emphasizing deep space missions 03 p0394 A69-13398

- Ghost project for gathering weather data by balloons and transmission of data to central data processing stations by satellite 03 p0520 A69-13621
- Point to point millimeter wave communication system design, discussing propagation and data transmission 03 p0405 A69-13723
- Optimum gain control for diversity receivers used for radar and digital data transmission through fading media 03 p0410 A69-13833
- Optimum conditions for signal analysis determined for symmetrical binary communications channel with unknown signal phase 04 p0556 A69-14492
- Book on information coding and transmission and error detection and correction 04 p0558 A69-15066
- Data transmission on common communication circuits, noting circuit characteristics, limitations on performance and future digital service 04 p0559 A69-15207
- Modems for high data transmission rates on available voice bandwidth channels, noting point to point and multipoint polled networks and signal to noise ratio 04 p0564 A69-15208
- Digital communications between aircraft and flow control computers on ground to avoid runway saturation and automating routing functions 05 p0721 A69-16722
- Satellite and space communications and data transmission systems, emphasizing improvements in amount and rate of information for future requirements 06 p0886 A69-17045
- Communication satellites application to domestic live TV, telephone and data communication and long distance telecommunication in Canada [UN PAPER 68-95501] 06 p0887 A69-17075
- Typewriter keyboard computer system with CRT display having closed circuit TV link contents of file to add, delete or change information 06 p0891 A69-17204
- Laser displays for information transfer to provide improved computer driven read-out techniques, noting real image and holographic displays 06 p0928 A69-17924
- Digital computer algorithm for automatic processing of IR weather data transmitted by Cosmos 122 and 144 meteorological satellites 06 p0929 A69-17981
- Sensitivity problems in receiving microwave signals from communications satellite at deep space distances, considering noise factors 07 p1077 A69-18669
- Block coding systems performance in digital PCM data transmission through N-ary discrete channels in white Gaussian noise presence, discussing SNR upper bounds 07 p1080 A69-19096
- Bit probability of PCM/FM for receiver with IF bandwidth equal to or greater than data rate, limiter-discriminator detection and postdetection filter 07 p1082 A69-19106
- High data rate coherent telemetry systems synthesis, discussing multiphase modulation and demodulation to achieve bandwidth requirements 07 p1083 A69-19123
- Diode pump type circuit without diodes in signal path providing accurate transfer function analysis considered for spacecraft use [IEEE PAPER 3A-3] 07 p1134 A69-19191
- Laser modulation at optical and near IR frequencies, discussing beam characteristics changes and information transmission 07 p1158 A69-19742
- Data transmission techniques for aerospace and industrial applications, discussing radio link 08 p1271 A69-19906
- Digital information transmission error characteristics determining error distribution over time and relation to distribution function of intervals between errors 09 p1454 A69-21795
- Orbiting Data Relay Network communications system provides continuous wideband communication between ground and earth orbiting spacecraft via synchronous satellite repeaters [AIAA PAPER 68-432] 09 p1455 A69-21989
- Rapidly varying phase error effect on system performance in data detection process due to RF carrier tracking loop 09 p1456 A69-22459

- Optimum time interval for constant data transmission rate during single pass of satellite over ground station
09 p1457 A69-22462
- Microelectronic data and remote control function transmission system for wind tunnel testing of aircraft dynamic response to gusts and turbulence
10 p1672 A69-23283
- Simultaneous transmission of information signals and pseudonoise synchronization waveforms in common bandwidth
[IEEE PAPER 67-TP-1173-COM]
10 p1655 A69-23532
- Reliability behavior of information transmission between transmitter-receiver pair in network of erasure channels without decoding and recoding at nodes
10 p1657 A69-23865
- Digital data transmission techniques and complex instrumentation systems design noting control, identification, synchronism and error reduction
11 p1834 A69-24545
- Statistical characteristics of photocurrent pulse amplitudes during cathode exposure to gas laser outputs
11 p1834 A69-24611
- Polyharmonic predictive and self tunable filters synthesis based on signal periodic components detection, noting role in information transmission and processing systems
11 p1849 A69-24966
- Atmospheric interference effects on optical PCM signal, analyzing absorption, beam bending, scintillation and correlation with visibility and weather
11 p1888 A69-25308
- Laser radiation transmission in atmosphere examined for information transmission applications
11 p1841 A69-25638
- Pure inertial navigation system support by supplying additional or redundant navigational information, considering space flight applications and earth related problems
12 p2128 A69-25873
- Extrapolation and interpolation for data compression including polynomial concept
12 p2027 A69-25877
- Shift registers with binary switching elements for shaping signal spectrum in data transmission systems without phase distortions
12 p2040 A69-26486
- Meteorological application of ATS observations in form of time lapse movies of weather in motion, describing camera and data flow
[AIAA PAPER 68-1094]
12 p2174 A69-26804
- Algebraic and sequential coding-decoding method for data communication rates up to capacity of discrete memoryless channel, discussing error probabilities
13 p2219 A69-27664
- Coherent signal addition in systems with multibeam channels and incomplete beam separation, deriving expressions for signal shape effect on noise rejection
13 p2223 A69-28551
- Deep space data return, discussing system function, design, operational interfaces and interplanetary spacecraft data compression methods
14 p2517 A69-29096
- Optimum time for telemetry data transmission by system using feedback combined with error correcting codes
14 p2412 A69-29428
- Electromagnetic waves as data carriers for earth resources and technology satellite sensors
15 p2607 A69-30231
- ESRO Aurorae satellite telecommunication system, detailing information nature, PCM telemetry and remote control system standard
15 p2702 A69-31084
- AZUR research satellite HF communications system, describing telemetry transmitter, command receiver and data transmission
16 p2759 A69-31854
- Electrophysiological /electrospnchnogram/ medical data transmission via satellite from France to U.S. for real time computer processing
16 p2746 A69-32070
- Tacan navigation system developments including data transmission, links to airborne computers and air traffic control transponders
17 p3003 A69-34101
- Data compression using orthogonal functions, design curves for given functions, signal characteristics and error avoidance
18 p3103 A69-35060
- Discrete information transmission synchronization in communication systems concerning optimal signal detection, HF, phase and coded synchronization, etc
18 p3104 A69-35264
- Time/frequency technology using time-ordered reporting digital data for air traffic control to avoid airborne collision
[AIAA PAPER 69-795]
19 p3367 A69-35635
- Buffer storage for telemetry nonstationary video data compression, analyzing requirements, predictor algorithm and variable aperture control using simulation
19 p3272 A69-36260
- Digital data compression system transmission error statistical analysis, emphasizing addressing schemes effect on compression ratio
19 p3272 A69-36261
- Automated computer network analyzing electrocardiograms, using telephone lines for bidirectional communications between cardiac data acquisition stations and computer center
19 p3262 A69-36273
- Digital data transmission by pulse code modulation considered for minimum mean square error
19 p3274 A69-36282
- Antenna high noise temperature reduction in single channel combined transmission and reception of tracking and communication data
19 p3275 A69-36328
- Radio wave information transmission, discussing propagation in various media, antenna arrays, diffraction, scattering, plasmas, guided waves and periodic structures
19 p3276 A69-36431
- Information theory, circuit optimization and computer aided design in radio wave information transmission
19 p3286 A69-36432
- TV picture and newspaper pages simultaneous transmission via earth satellite /Orbit/ system, measuring SNR and crosstalk
19 p3277 A69-36567
- Optical information rates for photocount detection systems based on coherent field model, considering binary channels with or without Gaussian noise
20 p3485 A69-36923
- Time division multiplexing of asynchronous digital signals from independent sources in continuous or bit stuffing mode, evaluating reliability and efficiencies
20 p3493 A69-37715
- Human optical system as remote sensor consisting of transducing, data transmission and processing subsystems, defining perception function and describing visual aids
20 p3483 A69-37745
- FM data transmission distortion noise and error rate compared with AM and phase step modulation, noting role of bandwidth
20 p3496 A69-37905
- Technical communication patterns in R and D laboratories, discussing effects of work structure, social relations, etc
20 p3640 A69-38019
- Noiseless feedback schemes for digital and analog transmission over additive white Gaussian noise channels
21 p3671 A69-38405
- Geostationary satellite orbit used for communication satellites, noting ultimate limit of channels as related to separation angles between satellites
21 p3673 A69-38757
- Data transmission of variables in deterministic networks
21 p3673 A69-38775
- Eye chart determination and layout for digital transmission system by computer simulation
21 p3678 A69-38776
- EEG with combined multichannel radiotelemetry and telephone for onward data transmission
21 p3664 A69-38978
- Data compression and transmission technique for real time system to monitor manned space missions, noting Apollo telemetry data
[AIAA PAPER 69-970]
22 p3906 A69-40350
- Booster digital guidance and control system, discussing communication device providing data transfer between airborne digital computer and control device
[AIAA PAPER 69-988]
22 p3978 A69-40368
- Monograph on laser communication system in IR for industrial environments
22 p3900 A69-40617
- Airline management service to cockpit team for safe operation providing safety information sources and transmission channels and undesirable trend detection and correction
22 p4054 A69-41149
- Information transfer capacity of afferent and efferent cell system and fiber tracts of human cerebellum numerically defined with regard to cybernetics
23 p4084 A69-41467
- Loran C system for master station time and frequency dissemination, discussing application, coverage, timing accuracy and restrictions
23 p4116 A69-41601
- Communication satellite technology application to overlay network linking nationwide data machines for business mail service with virtually instantaneous delivery at low cost
23 p4117 A69-41669
- Capacitive coupling vs DC coupling between data input and transmitter exciter in FM telemetry system, based on pulse series Fourier analysis
23 p4119 A69-41744
- Stored program decommutation techniques involving small core storage elements insertion into data path between decommutator equipment and computer
23 p4133 A69-41749
- Integrated adaptive data transmission system accepting analog inputs through information compressing sampler or digital inputs by sampling
23 p4121 A69-41760
- EKG data telemetry from personnel to receiver located within same closed metallic chamber, discussing FM/AM and FM/FM systems
23 p4103 A69-41766
- HF data transmission system unaffected by high energy electromagnetic fields using GaAs IR emitting diode, glass fiber optic light guide and photomultiplier tube
23 p4121 A69-41768
- M-ary noncoherent signal structures requiring less transmission bandwidth than conventional FSK, deriving SNR
23 p4122 A69-41773
- Deep space communication capability projection, considering data volume and rate, channel frequency, large apertures, data enhancement and system losses
23 p4129 A69-42507
- PCM telemetry system for transferring information from many remote sources to single local processing point
24 p4281 A69-42620
- Hybrid display for data visual display using electroluminescent and thermochromic technologies for wide range of ambient illumination
24 p4313 A69-42899
- Analog feedback system for digital data transmission, describing feedback channel, error rate and SNR effects
24 p4289 A69-42977
- On-board digital filtering applied to spectral estimation and data compression, discussing theory, techniques, computerized implementation and prototype design
[AIAA PAPER 69-969]
24 p4285 A69-43510
- Hologram electronic transmission, obtaining required bandwidth reduction by differential recording of image and scene diffraction pattern
24 p4317 A69-43761

DATING

U CHRONOLOGY
U TIME MEASUREMENT

DAWN CHORUS

Geomagnetic field irregular pulsations relationship with polar aurora and ULF radiation pulsations, stressing choruses appearance
09 p1485 A69-21536

Solar flare effect on polar chorus variation determined by comparing Antarctica VLF data with low latitude magnetograms
14 p2514 A69-29385

Banded chorus, VLF discrete emissions in magnetosphere in single variable frequency band with frequency depending on equatorial electron gyrofrequency
16 p2774 A69-31981

Geomagnetic field irregular pulsations relationship with polar aurora and ULF radiation pulsations, stressing choruses appearance
16 p2783 A69-32531

DAYGLOW

Rocket observations of visible and UV dayglow, using electron density and temperature measurements for emission rates of various excitation mechanisms
12 p2076 A69-27108

Weak emissions in near IR daytime airglow using rocket-borne spectrometers
16 p2776 A69-32094

Day sky brightness at altitude above 100 km obtained during rocket flight compared to night sky viewed from ground
17 p3037 A69-33664

Equilibrium velocity distributions of F region photoelectrons produced by solar ionizing radiation, discussing dayglow as impact result
20 p3591 A69-38061

Semiempirical electron impact cross sections and energy loss functions applied to dayglow and auroral intensities calculation, discussing atomic and aeronomic implications
21 p3713 A69-38527

Dayglow O I λ 1304 and 1356 A radiations photoelectron excitation rates theoretical calculation and experimental data on altitude dependence characteristics
22 p3939 A69-40517

Forbidden O I 5577 A dayglow emission equatorial measurements with rocket photometer, discussing altitude profiles and excitation mechanism
24 p4314 A69-43005

DAYTIME

Seasonal variations in thickness of ionospheric E-F interlayer region during daylight and maximum integral ionization values
02 p0239 A69-11682

X ray airglow in daytime sky, suggesting origin in atmospheric N and O K alpha lines due to fluorescent excitation by solar X rays
02 p0307 A69-12022

Dayglow determination from aerosol spectrum obtained through data of brightness and polarization of day sky
07 p1211 A69-18545

Atomic N and NO daytime upper atmosphere density profiles, discussing production and loss mechanisms
08 p1307 A69-20185

Daytime sky radiation measurements by high altitude vehicles with spectrophotometer noting spectral radiance, luminance, polarization, albedo and near IR
08 p1317 A69-21071

Quasi-trapped particle currents having discontinuities on daytime and nighttime sides of earth
09 p1577 A69-21767

Daytime clear sky light polarization in UV and visible spectral regions calculated with considerations for aerosol components polarization effect
09 p1491 A69-22708

Frequent periodic variations existence in daytime ozone content associated with solar activity
12 p2070 A69-26693

Seasonal variations in thickness of ionospheric E-F interlayer region during daylight and maximum integral ionization values
13 p2257 A69-28713

Electron temperature observation in daytime ionosphere, considering energy loss to ions and neutral particles
15 p2603 A69-31402

Daylight sky spectral radiance in ruby laser spectral range as functions of scattering angle, height over horizon of observed point and sun altitude
21 p3734 A69-38397

Altitude variation of mesospheric daytime sky brightness from earth based measurements of twilight sky brightness, noting inconsistency in calculations based on standard atmospheres
21 p3716 A69-39116

Ground to satellite laser ranging experiments for daylight satellite range measurements
23 p4174 A69-42193

Daylight observations of Comet Ikeya-Seki 1965-f at perihelion passage, discussing resulting emission line spectra within comet head
23 p4221 A69-42386

DC 3 AIRCRAFT

DC 3 tail wheeled single skin piston aircraft conversion into first class luxury passenger aircraft for short haul service
20 p3460 A69-36918

DC 8 AIRCRAFT

Flight evaluation of direct lift control on DC-8 super 63 jet transport
06 p0867 A69-17666

DC [CURRENT]

U DIRECT CURRENT

DC 10 AIRCRAFT

Douglas DC-10 medium range aircraft, discussing engine placement, passenger and cargo capacity, construction data, etc
11 p1823 A69-25211

DC 10 aircraft reliability program, discussing passenger attractiveness, dispatch reliability, maintenance cost, flight safety and computer simulation for reliability engineering
19 p3248 A69-36027

DC 10 wing design, wind tunnel models, structural and systems testing, production and marketing [AIAA PAPER 69-830]
19 p3248 A69-36296

Safety standards for DC 10 aircraft, considering cockpit design, hydraulic, electric power, autoland and

direct lift control systems, structural safety and crash worthiness
22 p3867 A69-41133

DC-10 aircraft CF6 engine thrust reverser and spoiler design features impacting operational characteristics, maintainability, noise reduction, structural concept, control and actuation system [SAE PAPER 690411]
23 p4200 A69-41639

Douglas DC-10 aircraft design programs and methods stressing power plant reliability, maintainability and costs [SAE PAPER 690391]
23 p4201 A69-41664

DDT

U DICHLORODIPHENYLTRICHLOROETHANE

DE HAVILLAND AIRCRAFT

U DH 121 AIRCRAFT

DE HAVILLAND DH 121 AIRCRAFT

U DH 121 AIRCRAFT

DE LAVAL NOZZLES

U CONVERGENT-DIVERGENT NOZZLES

DEACCLIMATIZATION

U ACCLIMATIZATION

DEACTIVATION

Slow proton irradiation of ribonuclease thin layers, determining differential inactivation cross section for various proton energies
03 p0371 A69-13482

Inactivation of T4 bacteriophage by tritium decay incorporated into DNA and phage protein
07 p1068 A69-19491

Carbon dioxide bending mode deactivation by orthohydrogen, parahydrogen and deuterium through rotational transitions
08 p1358 A69-21010

Deactivation rate constants of carbon dioxide vibrationally excited by high temperature collision with carbon dioxide or nitrogen molecules, describing laser apparatus and reaction cells
20 p3578 A69-36937

DEAD RECKONING

Most probable position /MPP/ choosing methods accuracy, investigating relative effects of dead reckoning /DR/ and celestial lines of position /LOP/ errors
07 p1177 A69-19214

Navigation equations, discussing earth geometry, coordinates, gravity, dead reckoning and radio computations with regard to LORAN
18 p3169 A69-34845

DEADWEIGHT

U STATIC LOADS

DEAFNESS

U AUDITORY DEFECTS

DEBRIS

U SPACE DEBRIS

DEBUGGING

U CHECKOUT

DEBYE-HUCKEL THEORY

Debye potential for effective interaction between electron and proton of hydrogen atom in partially ionized plasma
08 p1365 A69-20746

DEBYE LENGTH

Rarefied plasma flow interactions with conductors having cross sections equal to Debye radius, noting production of self consistent electrostatic potential
01 p0134 A69-11307

Gaussian type microfield formation in plasma by placing constraints on plasma particles displacements
02 p0285 A69-11568

Plasma transport properties derived from Boltzmann equation using Debye shielded Lande potential to represent collisions, noting viscosity and thermal conductivity
09 p1553 A69-22539

Late type stars with emission peak wavelength approximating graphite Debye frequency induced by graphite impurity atoms
14 p2521 A69-29586

DEBYE-SCHERER METHOD

Adaptor for Debye-Scherer powder camera to take high quality photographs even at liquid N temperature
19 p3313 A69-36493

Shocked Bamle enstatite transformed to disordered enstatite, noting Debye-Scherer patterns similarity
21 p3792 A69-38321

DEBYE TEMPERATURE

U SPECIFIC HEAT

DECAMETRIC WAVES

Decameter wideband directional antenna system for investigation of ionosphere by retrodiffusion method
03 p0402 A69-12860

Meter and decameter solar radio bursts and sudden cosmic noise observed at Ahmedabad, India
03 p0518 A69-14259

Non-Lo controlled fifth source of Jupiter decametric radiation from/near visible planetary disk
05 p0813 A69-15604

Europa control of decametric emission from Jupiter
05 p0813 A69-15605

Flux density spectral dependence disagreement with power law for synchronous radiation mechanism for radio sources in 12.6 to 25 MHz interval
06 p1004 A69-17538

Groups of drifting lanes of emission in fine structure of dynamic spectra of Jupiter decasecond decametric radiation bursts
06 p1008 A69-17958

Milky Way local spiral arm 10 MHz absorption, noting interstellar absorption effect and evidence for cool electron gas
08 p1383 A69-19900

Decametric radio spectra from 0053 to 0200 UT during July 7, 1966 solar proton flare, discussing Type 4 phase
10 p1765 A69-23751

Jupiter decametric radio emission periodicity attributed to undiscovered satellite in unstable orbit, discussing application to satellite discovery
13 p2343 A69-27622

Decametric radio astronomy at frequencies from 10 to 40 MHz on wideband telescopes, discussing spectral types of discrete radiation sources
15 p2682 A69-30501

Decameter waves Doppler shift shown inversely proportional to wave frequency from electron density variation caused by acoustic wave propagation in ionosphere
16 p2755 A69-32610

Jupiter decametric radio source analysis suggesting two component model of rotation at both constant and variable rotational periods
18 p3202 A69-35212

DECARBOXYLATION

Optically active alanine synthesis from oxaloacetic acid by hydrogenolytic asymmetric transamination, noting role of decarboxylation
12 p2026 A69-25780

DECARBURIZATION

Reducing decarburization of titanium carbide in argon plasma by carbon containing atmosphere, obtaining stable spheroidal particles
05 p0767 A69-15976

DECAY

NT BIOLUMINESCENCE

NT CHEMILUMINESCENCE

NT ELECTROLUMINESCENCE

NT ELECTRON EMISSION

NT EMISSION

NT FIELD EMISSION

NT FLUORESCENCE

NT HALF LIFE

NT ION EMISSION

NT LIGHT EMISSION

NT LUMINESCENCE

NT LUNAR LUMINESCENCE

NT NEUTRON DECAY

NT NEUTRON EMISSION

NT NUCLEAR FISSION

NT OPTICAL RESONANCE

NT PARTICLE EMISSION

NT PHOSPHORESCENCE

NT PHOTOELECTRIC EFFECT

NT PHOTOELECTRIC EMISSION

NT PHOTOIONIZATION

NT PHOTOLUMINESCENCE

NT PLASMA DECAY

NT RADIO BURSTS

NT RADIO EMISSION

NT RADIOACTIVE DECAY

NT SECONDARY EMISSION

NT SHOCK WAVE LUMINESCENCE

NT SOLAR RADIO BURSTS

NT SOLAR RADIO EMISSION

NT SPECTRAL EMISSION

NT STIMULATED EMISSION

NT THERMAL EMISSION

NT THERMIONIC EMISSION

NT THERMOLUMINESCENCE

NT TYPE 2 BURSTS

NT TYPE 3 BURSTS

NT TYPE 4 BURSTS

NT TYPE 5 BURSTS

NT X RAY FLUORESCENCE

Swirl decay of turbulent flow in tubes, showing decrease with increasing axial Reynolds number and independence of initial swirl angle
16 p2772 A69-32170

- DECAY RATES**
NT ELECTRON DECAY RATE
 Solar microwave type 4 bursts spectra and decay rate time variations 04 p0648 A69-14364
 Nonequilibrium chemical reaction effect on decay in spontaneous explosion for reactive expelled gas and inert expelling gas 07 p1119 A69-18705
 Thermal disturbance radiative decay time in carbon dioxide at low pressures and for nonzero vibrational relaxation times 07 p1215 A69-18843
 Plasma decay coefficient, charge recombination coefficient and electron scattering in cooling electron gas of quasi-steady cesium discharge plasma under high pressure 10 p1733 A69-23448
 Excess velocity and temperature decay laws in axisymmetric jet in transverse flow obtained via jet momentum and heat conservation equations 10 p1679 A69-23568
 Nonmesonic to mesonic decay ratio estimated for delta hydrogen hyperfragments 12 p2133 A69-26298
 Mode locked lasers for measuring fast radiative decay in fluorescent systems 12 p2105 A69-26310
 Beam-foil technique for measuring radiative lifetimes of excited electronic states in ionic species of O, including transition probabilities 13 p2301 A69-27452
 Cesium ions decay time in thermionic converter operating in gas kinetic mode by pulse ionization, noting dependence on interelectrode potential distribution 14 p2403 A69-29252
 Radiative decay of polyatomic molecules, applying Green function form for transition probability to decay of manifold of closely spaced coupled levels 14 p2488 A69-29924
 Magnetic field effect on neutron beta decay rate, considering calculations applicability to elementary particle production 15 p2690 A69-30694
 Carrier lifetime in p-n-n diodes, discussing error of forward pulsed diode method by Wilson and alternative model 16 p2757 A69-31615
 Solar Ca chromospheric plage decay curves obtained from area measurements, showing similarity and exponential mean curve 16 p2859 A69-32222
 Chemical species flux decay in turbulent boundary layer with catalytic wall, obtaining solution of conservation equation by using shear stress distribution [AIAA PAPER 69-709] 17 p2955 A69-33480
 Mean life of D energy level in N IV, discussing Be I isoelectronic sequence 17 p3009 A69-34187
 Mean lives of 1s super 2 2p super 2 super 1D level in F VI and O V measured by beam foil technique 17 p3009 A69-34188
 Shock waves attenuation through multiple reflections at ends and interactions with expansion wave in shock tube by pressure transducer, noting exponential decay 18 p3121 A69-34475
 Pressure dependence of trapped spontaneous decay of resonant radiation carbon dioxide 18 p3179 A69-35478
 Solar cell degradation experiments on LES 4 and 5 satellites, discussing decay values and times for Si and CdTe cells with different cover thicknesses 19 p3254 A69-35713
 Wind shear effects on radar echo decay constant for finite meteor trail, considering roles of trail length and electron density variations 19 p3276 A69-36482
 Unquantized field calculations extended to include atomic field effect on atom, predicting spontaneous decay rate from excited state and light frequency time dependence 21 p3769 A69-38578
 Afterglow decay rates of Zn II laser lines in spontaneous emission measured, indicating thermal energy charge exchange excitation and CW oscillation 21 p3735 A69-38598
 Exponential decay and mean lives of lowest P levels in N V measured with beam foil source, noting agreement with theories taking configuration interaction into account 21 p3774 A69-38760
 Upper and lower bounds for growth or decay rate of solutions of parabolic differential equations for indefinitely increasing time 21 p3757 A69-39565
 Final period of decay for viscoelastic fluid in homogeneous isotropic turbulence, deriving expressions for double correlation function and energy decay 22 p3928 A69-39891
 Radio wave reflection from irregularly ionized meteor trains, discussing decay time scatter and electron line density 22 p3899 A69-39969
 Argon laser lower operating level decay probabilities, using spectrum analysis to study role of radiative decay 22 p3965 A69-40965
DECCA NAVIGATION
 TV transmission antenna radiation patterns measured with helicopter flown equipment and Decca navigation equipment 08 p1274 A69-20130
DECELERATION
NT SPIN REDUCTION
 Sustained high deceleration load effects on quartz crystals during atmospheric entry studied by centrifuge test program on oscillator circuits 01 p0042 A69-10417
 Particles behavior after separation from meteor, considering deceleration for separation altitudes and initial velocities 02 p0314 A69-11645
 Deceleration control system for aerobraking and skipout to orbit at Mars [AIAA PAPER 68-1146] 03 p0520 A69-13564
 Entry and terminal deceleration systems for unmanned Martian landers, discussing parachute landing and lifting entry vehicles [AIAA PAPER 68-1147] 03 p0521 A69-13670
 Dynamic analysis and development of response histories and tradeoff study charts for spherical impact limiters for protecting hard landing planetary payloads 04 p0683 A69-15508
 Deceleration of conducting plasmoids moving in channels in nonuniform magnetic field 05 p0801 A69-15781
 Abrupt deceleration effects on monkey heart rate, noting occurrence of relative bradycardia 06 p0876 A69-18031
 Prolonged iterative accelerations and decelerations on vestibular apparatus, discussing nystagmus measurement attempt and centrifugation tests on guinea pigs 13 p2211 A69-28592
 Deceleration of conducting plasmoids moving in channels in nonuniform magnetic field 18 p3181 A69-35033
 Finite electrical conductivity effect on sun angular momentum loss due to solar wind 18 p3189 A69-35398
 NASA planetary entry parachute program for rocket launched and balloon deployment tests [AIAA PAPER 68-934] 19 p3247 A69-35952
 Impact limiter system design for Mars landing vehicle noting balsa wood or phenolic honeycomb construction [AIAA PAPER 68-161] 21 p3820 A69-39228
 Deceleration control system for aerobraking and skipout to orbit at Mars [AIAA PAPER 68-1146] 21 p3828 A69-39761
 Aerodynamic deceleration systems for space missions, considering deployment of subsonic parachute and inflatable configuration following atmospheric entry [AIAA PAPER 68-1081] 22 p4036 A69-40542
 Deceleration parameter lower and upper limits for zero pressure big bang cosmological Friedmann models imposed by density parameter, Hubble constant and universe age 23 p4219 A69-42373
DECELERATORS
U BRAKES [FOR ARRESTING MOTION]
DECIMALS
 Mechanical vibration effects on human operation of various decimal input devices 17 p2916 A69-34010
DECISION ELEMENTS
U LOGICAL ELEMENTS
DECISION MAKING
 Probabilistic Information Processing System using men and machines to perform diagnostic information processing and to guide decision making 01 p0037 A69-10954
 Cost factors in choosing single or twin-engine layout for tactical aircraft 02 p0193 A69-12066
 Dynamic programming application to synthesis of unequally spaced symmetrical antenna arrays 02 p0219 A69-12338
 Project management in complex research, discussing incentive contracting decision model and resources allocation 02 p0356 A69-12476
 Cost dependent utility characteristics in mathematical model for optimum research and development resource allocation, computing optimum fund distribution with Lagrange multipliers 04 p0689 A69-14807
 Performance, operational, economic and management selection criteria for choosing rocket engine for particular vehicle and mission, noting rocket engine propellants 04 p0647 A69-15296
 Estimate accuracy and project selection models in industrial research, examining company data for miscellaneous, technical and commercial failure 05 p0849 A69-15981
 Project management decision making, noting decision nature, cost effectiveness concepts and incentives [ASME PAPER 68-WA/MGT-2] 05 p0850 A69-16145
 Computer use evaluation, discussing standards for automatic data processing /ADP/ investment and operations 05 p0850 A69-16299
 Bayes estimator in decision directed adaptive detection problem, noting allowance for decision errors 05 p0740 A69-16583
 Data handling by groups in perception type pattern recognition and decision making problems based on algorithm involving second degree polynomials 08 p1278 A69-20420
 Decision oriented automatic data processing systems design, noting quantity and quality of upward directed information to management 08 p1423 A69-20733
 U.S. Army Materiel Command R and D planning structure and technical planning processes influence on decisions improvement 08 p1423 A69-21153
 Search theory application to planetary exploration overall strategy for improving landing site decisions 09 p1595 A69-21994
 Operational research applications to management problems, discussing specific airlines operations cases 11 p1822 A69-24377
 Probability matrix for n order transition independent of decision taking method, applying fundamental matrices to analysis of mean number of false targets 14 p2410 A69-28836
 Data handling by groups in perception type pattern recognition and decision making problems based on algorithm involving second degree polynomials 14 p2418 A69-29658
 CAB decisions regarding subsidy reduction, carrier mergers, and dense route certification requiring improved clarity and timeliness 16 p2882 A69-32336
 Ergonomy and aviation medicine, discussing biotechnological aspects of information in man machine systems and observation tasks 17 p2915 A69-33770
 Aerospace R and D marketing decisions, considering capability identification, business opportunities, strategies and independent program funding 17 p3077 A69-34127
 Proposed projects selection for independent R and D development program in business entity, measuring merits in terms of future financial returns 17 p3077 A69-34129
 Reliability management simulation exercise training technique for government personnel, discussing decision making in development, production, testing and field usage of systems 18 p3117 A69-34487
 Operations research methods applied to systems effectiveness study, using key decision models with optimized alternatives 18 p3145 A69-34503
 Mathematical index model based on weighted factor analysis to facilitate management and technical decisions concerning achievement of numerous tasks with fixed funds 18 p3232 A69-34504
 Mathematical basis for human operators purposeful behavior in complex systems control situation requiring decision reaching 19 p3260 A69-35895

STOL aircraft to serve traffic needs of northeast corridor, discussing decision making regarding size, type, cost, speed and strip-length
20 p3462 A69-37352

Human operator decision making in vehicle manual control, considering success likelihood and possible outcome costs based on signal detection model
20 p3482 A69-37720

Structure and scoring method for judging alternatives in contract selection
20 p3640 A69-38023

Multiple cues in paired comparisons, discussing mathematical model of psychological process in information extraction and combination
21 p3664 A69-38970

Book on law making in International Civil Aviation Organization covering membership problems, air navigation and transport safety, settling of disputes, etc
23 p4240 A69-41297

Data systems coordinating standards developed from experience with STADAN, discussing operating environment and administrative decisions influence on implementation
23 p4133 A69-41769

Man-machine /semiautomatic/ control for optimal decision making, discussing automatic control disadvantages and limitations, multilevel system hierarchical structures, three level models, etc
23 p4112 A69-42443

Lunar landing decision, analyzing American space policy making process with aid of Huntington model [AAS PAPER 69-500]
24 p4418 A69-42853

Decision process model for man-machine decision task structuring by system designers
24 p4274 A69-43018

Optimal rule for decision to stop or continue observation of random variables after observing sequence of variables with continuous distribution function
24 p4341 A69-43235

DECISION THEORY

NT STATISTICAL DECISION THEORY

Optimal distribution of search effort for moving target location, suggesting Markovian decision models
01 p0104 A69-10653

Planetary quarantine and biological search strategy, discussing Voyager-Mars mission configuration, sterilization, back contamination and decisions
01 p0021 A69-11090

Optimal design of vibration tests based on decision theory [SAE PAPER 680753]
03 p0525 A69-13436

Finite state finite-action-space Markovian decision process, discussing optimal policies set in discrete dynamic programming
04 p0624 A69-14951

Nonparametric ranking procedures /based on order statistics/ guaranteeing preassigned probability for selection from random samples populations as good as control
08 p1342 A69-20172

Analytical synthesis of dynamic plant model to insure desired output in response to cyclic action
11 p1861 A69-25714

Error bounds for orthogonal signals in additive white Gaussian noise channels for class of generalized decision strategies permitting variable-size list decoding
12 p2029 A69-26204

Risk taking under uncertainty in individual and group decisions, analyzing gambling and group discussion situations
23 p4091 A69-42016

Electromagnetic compatibility /EMC/ quantification in system effectiveness by decision analysis technique, constructing conceptual model
23 p4145 A69-42227

DECLINATION

Magnetic declination from moving objects measured by geomagnetic vector projection in solar direction
09 p1486 A69-21538

Bright fundamental stars right ascensions observed in Chile, discussing instruments, declination range, systematic errors, etc
10 p1777 A69-23388

Magnetic declination from moving objects measured by geomagnetic vector projection in solar direction
16 p2783 A69-32533

Bright and faint stars absolute declinations compared in vertical circle systems used in Golosevo and Pul'kovo catalogs
17 p3027 A69-32872

Declination measurements of sources in 4C Catalogue by Arcicco 1000 ft radio telescope
22 p4014 A69-40128

DECODERS

Fluidic display systems, discussing thermochromic modules and decoder with miniature components
01 p0078 A69-10155

Digital phase locked loops synthesis for fading and sequential phase estimation in decoder using digital computation
03 p0388 A69-13178

ELDO satellite command decoder performance in presence of noise, evaluating PDM bit decoder bit error probability and false command probability
11 p1834 A69-24563

Cross correlation and probability metric in coded sequential detection telemetry system, giving optimum parameters, overflow and error probabilities using computer simulations
19 p3273 A69-36266

Satellite communication system high speed sequential decoder design, discussing parameters, simulation and test results on satellite channels
23 p4131 A69-42523

Distribution system for TV driving signals proposed for single synchronized system for all TV centers, describing decoder circuits
24 p4282 A69-42745

DECODING

Trunk and tree searching properties of Fano sequential decoding algorithms
06 p0902 A69-17400

L-step orthogonalization of Bose-Chaudhuri-Hocquenghem codes
06 p0903 A69-17532

Mariner 1969 high rate telemetry system portions pertinent to combinatorial mathematicians, discussing coding and encoding
06 p0890 A69-17862

Upper and lower bounds for feedback decoding and definite decoding minimum distances of binary convolutional codes
06 p0904 A69-17865

Majority logic decoding of Euclidean or projective geometry codes in two steps
06 p0891 A69-17867

Linear shift register synthesis algorithm found to coincide with Berlekamp iterative algorithm for decoding BCH codes
09 p1470 A69-21317

Infinite tree code ensemble upper bound on moments derived for sequential decoding governed by Fano algorithm
09 p1471 A69-21318

Decoding procedure for error locating binary code indicating location of single subblock containing errors in code word, employing feedback shift registers
11 p1857 A69-24549

Algebraic and sequential coding-decoding method for data communication rates up to capacity of discrete memoryless channel, discussing error probabilities
13 p2219 A69-27664

Group code decoding, discussing equivalent transformations of reference matrix and reduction of equipment losses
13 p2225 A69-28537

Algebraic decoding techniques, discussing channel models, errors correction, hardware and software, etc
23 p4119 A69-41746

DECOMMUTATORS

Stored program decommutation techniques involving small core storage elements insertion into data path between decommutator equipment and computer
23 p4133 A69-41749

DECOMPOSITION

NT GLYCOLYSIS
NT PHOTODECOMPOSITION
NT PHOTODISSOCIATION
NT PHOTOLYSIS
NT PROPELLANT DECOMPOSITION
NT RADIIOLYSIS

Dislocations effect on decomposition rates of solid solutions of InAs and Au, Ag or Cu
03 p0484 A69-13283

Wet oxidation process for management of organic waste products in closed ecologies of long term multimanned space missions [SAE PAPER 680714]
03 p0380 A69-13443

Hydrazine decomposition in glow discharge, analyzing emission spectra and threshold level of decomposition by gas chromatography
04 p0646 A69-14860

Titanium vanadium martensite decomposition kinetics during heating, showing shearing process and dependence on temperature during quenching
07 p1163 A69-18778

Spinodal decomposition effect on Al-Zn alloy mechanical properties noting strengthening, brittleness and work hardening capacity
09 p1522 A69-21501

Structure of spinodal decomposition in Al-Zn alloys by X ray diffraction noting anisotropy, periodicity and stability
09 p1522 A69-21502

Microstructure for spinodal decomposition in Al-Zn alloys noting Zn precipitation, fracture mechanics, dislocations and transmission electron microscopy results
09 p1522 A69-21503

Aluminum additive effects on copper-titanium alloy decomposition, discussing Guinier complexes, heterogeneous nucleation, plastic deformation and low temperature aging
11 p1905 A69-24922

DECOMPRESSION

U PRESSURE REDUCTION

DECOMPRESSION SICKNESS

Changes in organism during sudden decompression, analyzing pressure equalization, dissolved gases transformation and body fluids vaporization
01 p0020 A69-10753

Neurological impairment in baboons exposed to prolonged decompression simulating high altitude aircraft cabin structural failure, noting neuropathological examination results
07 p1067 A69-19426

Autonomic nervous system role in controlling body functions after rapid decompression, increasing tolerance to pressure gradients by physical training
13 p2212 A69-28622

Drug action on decompression sickness in rats compared with action on nitrogen narcosis and oxygen toxicity
17 p2913 A69-33172

Gangrene and caisson disease due to diving accidents, discussing emergency treatment with hyperbaric oxygen
17 p2911 A69-33775

Barotrauma during hyperbaric oxygenation at flight descent or reentry into caisson, including ear trauma symptoms and use of paracetamol
17 p2911 A69-33776

EEG monitoring during decompression illness /bends/ treatment by hyperbaric procedure using small multichannel telemetry pack
19 p3261 A69-36268

Bubble size and blood perfusion effect on gas bubbles absorption in tissues, noting decompression sickness
21 p3651 A69-38389

Physiological and psychological measurements of high pressure effects on man and animals, discussing decompression sickness, respiratory embarrassment, inert gas narcosis, helium tremble, etc
21 p3655 A69-38912

Decompression research on inert gas transport in body, discussing solubility factors in decompression damage
21 p3655 A69-38913

Decompression gas emboli detection while moving in flow streams of arteries and veins using ultrasonic Doppler shift principle and square-wave electromagnetic flow meter
21 p3663 A69-38914

Ultrasonic Doppler flowmeter for detection of circulating gas emboli of animal blood vessels during decompression
21 p3663 A69-38915

Intravascular gas emboli literature critique covering early nonclinical decompression experiments, clinical use of intravenous gas emboli, etc
21 p3655 A69-38916

Decompression sickness prevention in guinea pigs by heparin and papaverine combination nebulized in carbogen, discussing nitrogen elimination enhancement
21 p3655 A69-38917

Platelet role in decompression sickness pathology from experiments upon rats subjected to decompression after injection of antiplatelet serum
21 p3655 A69-38918

Space cabin and suit pressures for decompression sickness avoidance and fire hazard alleviation
22 p3890 A69-40212

Decompression sickness in simulated zoom flights, discussing bubble formation probability and instantaneous surface tension effect on bends resistance
23 p4077 A69-41292

Altitude decompression sickness in aviation, discussing physiological mechanisms underlying syndrome and treatment of conditions
24 p4269 A69-43412

Decompression disease symptoms from standpoint of gas bubbles formation in blood vessels, examining factors preventing air metabolism
24 p4269 A69-43414

DECONDITIONING
Space research centrifuge counteracting null gravity physiological deconditioning, discussing linear and angular accelerations sensitivity and deconditioning effect on reentry task performance
18 p3114 A69-34368

DECONTAMINATION
U SPACECRAFT STERILIZATION

DECOUPLING
Decoupling techniques for antennas on aerospace vehicles, noting effects on far field radiation pattern and antenna gain
05 p0729 A69-15977
Decoupling by state variable feedback and determination of inverse extended to linear time varying multivariable system
09 p1472 A69-21680
Decoupling force exerted by magnetic forming Be coil assembly on metallic plate during forming
11 p1888 A69-25310
Exact solutions for two state potential curve crossing in subexcitation molecular collisions in terms of various decoupling schemes
12 p2131 A69-25983
Multivariable control system decoupling by appropriate choice of decoupling network structure and location in system
12 p2048 A69-26074
Complete observability in linear time invariant systems decoupled via state-variable feedback, deriving sufficient conditions
12 p2053 A69-26514
HF electromagnetic decoupling pressure gage, using transducer with solid state strain gages as sensing elements
15 p2611 A69-31029
Decoupling structures, deriving expressions for infinitely long grooves self and mutual impedance
23 p4138 A69-41938
General purpose computer program for synthesis of multivariable systems decoupled by state feedback
24 p4294 A69-43307
Time-invariant multivariable linear systems, discussing structure theorem for controllable systems and application to decoupling problem
24 p4294 A69-43314

DEDUCTION
FORTRAN Deductive System to find solutions to theorem proving problems, discussing computer implementation
01 p0037 A69-10806

DEEP SPACE
NT INTERPLANETARY SPACE
NT INTERSTELLAR SPACE
Galactic Jupiter Probes investigating Jupiter atmosphere and emissions and deep space cosmic radiation
02 p0324 A69-12303
Mars and Venus probes antenna problems in environments of near earth space, deep space and nonearth planetary atmospheres
02 p0223 A69-12811
Noise reduction techniques in digital and analog data transmission over space program distances, emphasizing deep space missions
03 p0394 A69-13398
Manned spacecraft systems design optimization for extended space missions replacement modules
05 p0830 A69-16380
Controllability of deep space electromagnetic wave propagation in nonvacuum by calculating optimum values of control parametric functions
06 p0888 A69-17622
Cepheid stars as distance indicators in extragalactic space, using periodicity-luminosity relation
08 p1408 A69-21147
Power requirements for tracking, telecommand and telemetry of spacecraft over interplanetary distances, considering transmission problems, equipment weight and reliability
10 p1652 A69-22984
Hardware limitations on communications, instrumentation and data handling for manned deep space missions
13 p2219 A69-27666
Relativistic electron confinement within geomagnetic tail neutral sheet measured by Pioneer 7 deep space probe, confirming kinetic energy observations of IMP 1 satellite
14 p2433 A69-28934

Deep space data return, discussing system function, design, operational interfaces and interplanetary spacecraft data compression methods
14 p2517 A69-29096
Earth sensor for spin stabilized spacecraft to maintain specific orientation with earth, discussing use of blue and red filters
15 p2609 A69-30593
Spacecraft-based navigation instruments for outer planet missions using celestial directions to outer planet natural satellites
[AIAA PAPER 69-902]
21 p3761 A69-39348
Deep space communication capability projection, considering data volume and rate, channel frequency, large apertures, data enhancement and system losses
23 p4129 A69-42507
Spacecraft central data system for deep space solar probe data management
24 p4284 A69-42621

DEEP SPACE INSTRUMENTATION FACILITY
Deep space tracking network development, discussing capabilities and operational quality assurance
07 p1078 A69-18831
Pioneer 6 S band telemetry carrier Faraday rotation during corona occultation measured by deep space tracking antenna
15 p2700 A69-31419
Cryogenic applications to low noise reception development in radio astronomy, planetary radar and communication with deep space probes
17 p2921 A69-33685

DEEP SPACE NETWORK
Deep space tracking network development, discussing capabilities and operational quality assurance
07 p1078 A69-18831
Deep space network system for radio navigation of Mariner mission in 1969, discussing objectives, spacecraft, tracking and data system, mission accuracy, etc
16 p2749 A69-31725
Continuously powered deep space vehicle orbit determination, discussing state estimation accuracy and use of continuous data filtering
[AAS PAPER 68-144]
19 p3402 A69-35939

DEFECTS
NT AUDITORY DEFECTS
NT CRYSTAL DEFECTS
NT CRYSTAL DISLOCATIONS
NT EDGE DISLOCATIONS
NT FRENKEL DEFECTS
NT INCLUSIONS
NT POINT DEFECTS
NT SCREW DISLOCATIONS
NT SPEECH DEFECTS
NT SURFACE DEFECTS
NT VACANCIES [CRYSTAL DEFECTS]
Defect localization in complex plants applied to damage cause determination and economic criteria
05 p0767 A69-15765
Weld-nugget formation in resistance spot welding, using high-speed photography on model section of spot weld
05 p0769 A69-16539
Weld defects, discussing criteria for rejection, harmful and harmless defects, welding process and procedures and weld vs base metal defects
07 p1143 A69-19696
Welding defects, processes, inspection and personnel training problems
10 p1700 A69-23372
Analytic investigation of spectrum of electrical signals induced by spherical defects in ferroprobe sensors
10 p1675 A69-24072
Flow detection inaccuracies in shadow method due to interference effects when using Babinet principle
10 p1675 A69-24075
Weld defects effects on static and fatigue properties of weldments prediction, including tests of titanium-aluminum-vanadium joints
11 p1892 A69-24932
Standard reference radiographs for weld defects on steel sheets and plates
18 p3150 A69-35425
Echo amplitude measurements in ultrasonic testing to estimate flaw sizes and difficulties from artificial reflecting targets
19 p3323 A69-35578
Weld defect data analysis in relation to aerospace structure performance, emphasizing effect on fatigue behavior and acceptance standard
[SBAC PAPER 17]
20 p3550 A69-37450

Three dimensional X ray pictures of flaws shape and location in various materials
20 p3551 A69-38311
Ultrasonic method for detecting strength defects in filament wound materials
21 p3733 A69-39798
Grains with high defect concentration in circumstellar and interstellar space from energetic particles and photons bombardment, discussing lifetime and optical properties
22 p4023 A69-40472
Nondestructive testing techniques for flaw and defect detection, discussing radiography, ultrasonics, penetrants, thermal and magnetic methods, etc
23 p4169 A69-41529
Stress analysis in design techniques taking into account failure of flawed structures, discussing fracture mechanics
24 p4398 A69-42773

DEFENSE COMMUNICATIONS SATELLITE SYSTEM
Communication subsystem design of Defense Communication Satellite Program /DCSP/ for background information, noting repeater with toroidal pattern antenna
23 p4131 A69-42537

DEFENSE COMMUNICATIONS SYSTEM [DCS]
Satellite communication requirements for UK defense establishment, describing SKYNET system
08 p1272 A69-19957

DEFENSE INDUSTRY
Scientific and technical information flow sources, showing DOD user need within defense industry and importance of local work environment
02 p0204 A69-12219
Internationalized defense marketing, suggesting formation of international consortia of industrial companies to design and produce defense systems
14 p2540 A69-28933
Defense integrated management engineering system at California Naval Air Rework Facility
15 p2588 A69-30427
Cost risk management procedure in defense industry contracting, including risk percent limits and identification in proposals, specifications relief, escalation clauses, etc
18 p3233 A69-34655

DEFLAGRATION
Slowly exploding wires for igniting self sustaining deflagrations in PETN, RDX, HMX and tetryl, comparing circuit parameters for detonation initiation
01 p0141 A69-10678
Inflammable gas mixtures and deflagrations noting self ignition temperature, flame propagation, flame front structure and flame stability
06 p1031 A69-17417
Deflagration of solid and hybrid propellants in steady state for missile and rocket propulsion applications
06 p0982 A69-17422
Spherical deflagration and detonation waves in diluted stoichiometric hydrogen-oxygen mixtures in hemispherical combustion chamber
06 p1034 A69-17927
Low pressure deflagration limit dependence on strand size in terms of cross section dimensions for composite ammonium chlorate propellant
[AIAA PAPER 69-144]
06 p0983 A69-18162
Pure ammonium perchlorate single crystal self deflagration, determining energy transfer mechanisms from pressure effects, combustion characteristics and subsurface profile
[AIAA PAPER 69-142]
09 p1560 A69-21900
Limiting pressure for deflagration related to initial solid temperature of single crystals and pressed pellets of ammonium perchlorate
13 p3234 A69-27364
Steady deflagration of homogeneous monopropellant in condensed phase, considering nonequilibrium surface condition for mass decomposition rate
[WSCI PAPER 69-6]
16 p2830 A69-32347
Construction of single headed spin detonation polar as confluence of shock and deflagration waves by two dimensional hodograph
19 p3451 A69-36368
Adiabatic model deflagration limits for steady linear monopropellant burning at Lewis number of unity and one step gas phase reaction
24 p4415 A69-43670

DEFLATING
U INFLATABLE STRUCTURES
U PRESSURE REDUCTION

DEFLECTION

- Interlayer slip in layered wood beams with nail joints analyzed in terms of small deflection theory
01 p0169 A69-10638
- Integral equation solution for plate with internal support
03 p0528 A69-13799
- Conically bent plate cross section distortion analysis employing von Karman large deflection theory, noting effect of tapering
[ASME PAPER 68-APM/Y] 04 p0670 A69-14402
- Large finite deflections of clamped thin elastic circular plate subject to transverse concentrated load at center solved by power series
04 p0675 A69-14596
- Circular cylindrical shell creep behavior and buckling under axial compression and internal pressure, using multimembrane model
[AIAA PAPER 68-108] 04 p0676 A69-14706
- Rectangular thin beam Saint Venant deflection in case of moment stresses based on elasticity and shell theory
05 p0834 A69-15783
- Finite elastic-plastic deflections of orthotropic shells of revolution, deriving exact geometrical relations and equilibrium equations
05 p0842 A69-16642
- Antisymmetric cross ply and angle ply laminated plates deflection under transverse loading with coupling between bending and middle-plane extension
07 p1231 A69-18711
- Large deflection behavior of shallow circular arch subjected to vertical point load by nonlinear Rayleigh-Ritz finite element method, discussing deformation path
08 p1411 A69-20140
- Finite element analysis of large deflections in thin elastic plates subjected to transverse loading, including nonlinear geometric effects
09 p1615 A69-21924
- Large deflections and associated moments in circular ring of linearly viscoelastic material subjected to small strains
09 p1615 A69-21925
- Holographic scanning technique for laser beam deflection, noting two and three dimensional raster scanning
11 p1885 A69-24847
- Shallow hyperbolic paraboloidal shell with large deflections, analyzing nonlinear behavior with numerical method based on integral equations
12 p1885 A69-26820
- Linear plate theory deficiency for large plate deflections, considering approximation of nonlinear behavior permitting changes in form without additional terms
12 p1885 A69-26822
- Rectangular plate buckling analyzed by finite element method with deflection function
13 p2364 A69-28225
- Dynamic programming method applied to Cauchy problem of large deflections in compressed rods, using recurrent functional equations
14 p2533 A69-28988
- Postbuckling of rectangular plates with exponential variation in thickness, analyzing large deflection equations using dynamic relaxation method
15 p2704 A69-30291
- Finite element and iteration method for large deflection of rectangular plate, considering stiffness matrix for bending
15 p2706 A69-30435
- Unsteady oscillations after rupture in thin homogeneous isotropic elastic plate, assuming deflection amplitude smaller than thickness
16 p2873 A69-32033
- Deflection effect on flow and mixing process in flames covering enclosed turbulent diffusion flames in combustion chamber
17 p3068 A69-32966
- Large deflections of thin nonlinearly elastic ring under external pressure, using two layer model
17 p3062 A69-33715
- Strain displacement and compatibility equations of finite symmetrical deflections of thin shells of revolution
[ASME PAPER 69-APM-14] 18 p3214 A69-34391
- Rectangular thin beam Saint Venant deflection in case of moment stresses based on elasticity and shell theory
18 p3223 A69-35035
- Von Karman equations for large deflection of simply supported square plates solved using dynamic relaxation method, recommending optimum mesh spacing
20 p3619 A69-36938

- Natural frequency of thin plate subject to cylindrical bending, analyzing panel flutter by three mode approximation for large buckling deflection
22 p4045 A69-40821
- Initial deflection and internal pressure effects on supersonic panel flutter boundary of simply supported rectangular plates under diverse middle- surface stress conditions
24 p4400 A69-43056
- Large deflections of circular air mat plates consisting of inflatable structures of two membranes connected by inextensible cords network
24 p4405 A69-43688

DEFLECTORS

- Analytical design of SH-3 helicopter engine inlet ice deflector shield interior surfaces, defining potential flow pattern and moisture droplet trajectories
01 p0011 A69-11064
- Electro-optical device using KDP crystal for laser beam deflection at temperatures near Curie point
03 p0435 A69-12984
- Laser pulse deflection by acoustooptical system consisting of ultrasonic cell and oscillator
11 p1840 A69-25423

DEFOCUSING

- Experimental equipment and procedure to investigate defocusing of electron beam directly in cavity beam hole of TWT amplifier
03 p0407 A69-13975
- Parabolic antenna beam scanning by defocusing, calculating relationship between reflector and beam tilt angles
07 p1089 A69-18248
- Traveling wave amplifiers beam defocusing by RF circuits and space charge fields under large signal operating conditions, discussing magnetic field strength
07 p1094 A69-18424
- Laser beam absorption induced index changes associated with thermal blooming observed in iodine doped carbon tetrachloride, using Mach-Zehnder interferometer
07 p1149 A69-18899
- Image enhancement by coherent optical system without spatial filter, noting improved defocused transparencies
14 p2450 A69-29641
- Focused Gaussian laser beam expansion due to thermal changes in refractive index of air, noting focused spot area increase with pulse energy
19 p3330 A69-35601

DEFORMATION

- NT AXIAL STRAIN
- NT ELASTIC BENDING
- NT ELASTIC BUCKLING
- NT ELASTIC DEFORMATION
- NT PLASTIC DEFORMATION
- NT STATIC DEFORMATION
- NT TENSILE DEFORMATION
- NT WAVE FRONT DEFORMATION
- Streak interferometry method for measuring transient deformation data on metallic solid surfaces
01 p0078 A69-10117
- Deformation temperature and reduction effects on structure and properties of cylindrical specimens of various titanium alloys
02 p0266 A69-12124
- General theory of constitutive equations for rational mechanics of deformation and flow
02 p0341 A69-12251
- Free flight impact tests showing deformation curve for aluminum and copper single crystals representable as 1/4 power law
02 p0344 A69-12288
- Stress concentration near arbitrary hole, assuming small deformations and physical nonlinearities
04 p0667 A69-14268
- X ray diffraction studies of deformation effects on bcc niobium alloys in terms of particle size, strain, faulting probability and dislocation density
04 p0618 A69-15202
- Shear strength of grossly deformed solids noting extrusion and opposed anvils techniques
04 p0631 A69-15465
- Deformation dependence on strain hardening and recovery rate during transient and steady state creep
06 p0943 A69-17236
- Power law taperings for minimizing peak to trough deflection of cross section of strip bent longitudinally into cylindrical surface
06 p1023 A69-17374
- Fatigue damage of metals under cyclic stressing, noting deformation modes dependence on stress amplitude and material type
07 p1166 A69-19215

- Axially loaded viscoelastic constrained bar instability for large deformation
07 p1235 A69-19440

- Ductile fracture behavior of two phase stainless steel examined by straining smoothed and notched tensile and Charpy impact specimens
08 p1333 A69-20574

- Second order tensor describing deformation of particles of continuum determined by functional, noting invariance restrictions
08 p1416 A69-20690

- Relativistic kinematics analog model for deformable continua, introducing deformation gradient and tensors
08 p1416 A69-20693

- Time and temperature dependence of Mo and W deformation structure variation and primary recrystallization from metallographic investigations using electron microscopy
08 p1334 A69-21058

- Nonlinear Lagrange equations and iterative solutions for studying strain state of mechanical structures on basis of very small displacements
10 p1793 A69-22888

- Deformation processes of geometrically nonlinear rotational membrane shells under internal pressure
11 p1980 A69-24821

- Deformations and stresses in pressure vessel with elliptical cross section under uniform internal pressure, noting radial deflection and membrane, bending and skin stress
11 p1983 A69-25023

- Back stress role in strain rate equation for high temperature deformation and study of structure and applied stress effects
11 p1987 A69-25388

- Thin deformable body motion in disturbed potential flow of ideal incompressible fluid
11 p1876 A69-25488

- Plane surface finite area deformation tensors in continuum mechanics permitting separation of volume and shape changes in constitutive equations
11 p1994 A69-25603

- Thin ring-strut structure resting on elastic foundation, analyzing deformation taking warping effects into account, noting applicability to engine design
12 p184 A69-26812

- Fiber axis distribution resulting from mechanical working deformation of matrix containing initially randomly oriented fibers
12 p188 A69-26933

- Relativistic kinematics of continuum motion by invariant derivatives of deformation measures, discussing rigid body motion in Born sense
12 p189 A69-27116

- Maximum principle for infinitesimal deformations of convex surface with nonnegative Gaussian curvature, noting application to rotation and displacement diagrams
13 p2361 A69-27741

- Deformation functions for finite beam analysis allowing continuity at nodes and accurate eigenvalues
15 p2710 A69-30869

- Book on mechanics of deformable media covering fluid and solid mechanics and applications to irrotational flows of compressible and incompressible fluids
16 p2813 A69-32789

- Grain boundaries contribution to creep deformation, discussing ratio of grain boundary slip strain to total creep strain
17 p2985 A69-32905

- Unstable metal deformation, discussing volume displacement in necking leading to fracture, homogeneous total deformation and torsion
17 p3053 A69-32987

- Bag type deformation of incompressible viscous convective and nonevaporating droplets immersed in Stokes or potential flow pressure distributions, including Weber number
[AIAA PAPER 69-669] 17 p2954 A69-33456

- Transverse shear deformation and rotatory inertia effects on large amplitude lateral free vibrations of transversely isotropic plates
[ASME PAPER 69-APM-10] 18 p3213 A69-34386

- Deformation studies of high melting point metals and alloys at high temperatures in vacuum, noting crack formation resistance and annealing time variations
18 p3155 A69-34651

- Deformation detection by stress wave analysis technique /SWAT/, noting pressure vessel applications
18 p3223 A69-35080

- Second harmonic generation in media with center of inversion following deformation by laser beam or static pressure
19 p3332 A69-35872

Dynamically deformed structures in chondrites and hexahedrites observed to discriminate among theories about origin of chondrules and meteorites
19 p3418 A69-36135

Dynamic recrystallization in Ni and Ni-Fe alloys during torsional high temperature deformation
19 p3344 A69-36147

Quenching temperature and deformation conditions for Ti alloy bars optimal mechanical properties, emphasizing effect of primary structure
19 p3328 A69-36152

Homogeneous deformations of space and Cauchy problem for homogeneous free molecular motions, considering velocity fields and accelerations
19 p3444 A69-36803

Equations of deformation for elastoviscoplastic bodies with different properties under loading and unloading conditions
19 p3445 A69-36812

Yield strength, deformation modes and fracture characteristics of Ti-Al alloys, examining strength and fracture characteristics as function of structure and chemical composition
20 p3557 A69-36959

Rheology application to description, explanation and measurement of materials properties during deformation
20 p3561 A69-37599

Transverse shear deformation effect on bending of laminated rectangular plates, obtaining solutions for bending deflections, flexural vibration frequencies and buckling loads
20 p3627 A69-37770

Sheet metals deformation behavior during punch stretching and hydraulic bulging, noting effects of lubrication, stress-strain relation, anisotropy and microcracks
20 p3551 A69-38115

Metal deformation dynamics at elevated temperatures, discussing closed loop electrohydraulic testing machine for stress relaxation and strain rate sensitivity
21 p3689 A69-38595

Convergence of axes of plane-parallel jets due to reciprocal ejection effect, analyzing deformation of jet, rarefaction coefficient for air between jets, etc
21 p3696 A69-39095

Deformation of circular cylindrical shell of varying thickness, obtaining differential equation solutions through multiple scales method
21 p3837 A69-39159

Inertial motion of body produced by revolving uniformly deformed configuration, showing constant semiaxes without kinetic energy losses
21 p3772 A69-39620

Deformation of thin walled spherical shell reinforced with equatorial hoop by concentric equal forces
21 p3846 A69-39714

Meteorite impact hypothesis supported by autotchthonous and mixed breccias, shattercones and microscopic shock deformation evidence in central uplift rocks at La Malbaie structure
22 p4021 A69-40410

Deflections of heated circular plates with or without concentric circular hole and with different boundary conditions and temperature distributions
23 p4234 A69-42412

Elastoplastic boundary dynamic behavior in strip with crack determined by solving boundary value problem in elliptic integrals form
24 p4395 A69-42591

Soviet book on resistance of materials to deformation and fracture in complex stress states covering elasticity, mechanical theories of limiting stress state, experimental verification, etc
24 p4402 A69-43233

Holo-diagram device for making and evaluating holograms for small deformations measurement in large machine tool parts
24 p4317 A69-43760

DEFORMETERS

Fatigue gauge for plastic deformation based on plastic strain rates, cycles, temperature, etc
07 p1135 A69-19216

DEGASSING

NT DEOXYGENATION

Current sheet velocity in coaxial plasma accelerator, noting drag due to insulator ablation and degassing [AIAA PAPER 69-265]
09 p1566 A69-21258

Venus atmosphere carbon dioxide content origin from interior degassing during molten phase, using atmospheric model
16 p2857 A69-32098

DEGENERATION

Dirichlet problem of linear degenerate second order differential elliptic systems with independent variables
12 p2123 A69-26729

Electron-plasmon interaction in degenerate semiconductors, using mathematical model for rectifying metal contacts tunneling characteristics
19 p3382 A69-36049

DEGENERATIVE FEEDBACK
U NEGATIVE FEEDBACK

DEGRADATION

NT THERMAL DEGRADATION

Aircraft flight testing for determining airframe, engine and pilot degradation, examining flutter, handling characteristics, water ballast, propulsion, etc
01 p0054 A69-10292

Brewster angle window degradation of high power ionized argon gas lasers [IEEE PAPER L-4]
05 p0775 A69-16322

Ionizing radiation-initiated degradation of deoxyribonucleic acid in bacteria, noting role of defective prophage
07 p1068 A69-19494

Continuous-channel electron multipliers degradation in spacecraft environment simulation laboratory equipment
14 p2449 A69-29565

Solar cell degradation experiments on LES 4 and 5 satellites, discussing decay values and times for Si and CdTe cells with different cover thicknesses
19 p3254 A69-35713

Solar cells arrays degradation in Intelsat spacecraft at synchronous altitude, noting shielding gaps and low energy proton influence
23 p4072 A69-42287

DEGREES OF FREEDOM

Computer solution of six degrees of freedom flight equations, discussing advantages of using flight path axes for translational equations of motion
02 p0212 A69-11998

Summed and differential types of higher order oscillations in vibratory systems with multiple degrees of freedom under parametric excitation
02 p0346 A69-12422

Optimum critical impulse for snap-through of nonlinear dissipative dynamical system of one degree of freedom [AIAA PAPER 68-143]
02 p0346 A69-12508

Equilibrium of rotational degrees of freedom in gases undergoing relaxation, noting excitation, relaxation time, kinetics, transfer effects and measurements for hydrogen
02 p0284 A69-12667

Single degree of freedom structural damping estimations from viscous and hysteretic energy dissipation data
03 p0523 A69-12947

Matrix-harmonic method of vibration study extended to include autonomous vibrations of single degree of freedom machines
03 p0468 A69-13861

Symmetric structure stability with first and second order imperfections, analyzing discrete system with n degrees of freedom
03 p0529 A69-14062

Multidegree of freedom systems for modeling optimum design of cantilever and simply supported beams for sudden loading
04 p0674 A69-14590

Compatible triangular plate elements for normal and in-plane displacements, discussing nine degree of freedom element, strain energy, simply supported and clamped plates
04 p0677 A69-14742

Linear mechanical systems idealized by single degree of freedom system with viscous damping subjected to combined deterministic and random excitation
04 p0680 A69-14968

Self balancing single degree of freedom free fall space environment simulator, discussing coincidence of mass and rotation centers
04 p0586 A69-15468

Perturbed nonlinear systems with many degrees of freedom, analyzing resonant oscillatory and rotary motions
04 p0631 A69-15536

Models of continuous media with internal degrees of freedom based on Lagrangian variational principle
05 p0793 A69-15775

Response of single and multidegree of freedom systems to nonstationary random excitation, analyzing spectral density function of pressure field close to jet engine
05 p0844 A69-16763

Dynamic stability of systems with distributed parameters subjected to parametric loading, considering parametrically excited systems with infinite degrees of freedom
07 p1231 A69-18502

Analytic autonomous Hamiltonian differential equations with two degrees of freedom admitting unstable equilibrium point
07 p1215 A69-18732

Structural damping coefficient for free vibrations of one degree freedom general systems motion
09 p1617 A69-22076

Multiparameter optimum damping for harmonically excited linear stable strictly dissipative n degrees of freedom system, locating multivariable saddle points [ASME PAPER 69-VIBR-42]
10 p1807 A69-24180

Entropy minimization in feature extraction by dimensionality reduction with linear transformation of pattern vectors, noting recognition time and storage space savings
11 p1909 A69-25291

Periodic solutions of quasi-linear self contained system with several degrees of freedom in case of commensurate frequencies, showing coordinates functions breakdown
11 p1920 A69-25749

Autonomous two degrees of freedom Hamiltonian system triangular libration points found stable for all mass ratios in circular restricted three body problem
12 p2155 A69-25883

Synthesis of multivariable control systems at minimal integral square quality functional
12 p2046 A69-26061

Digital computer analysis of multivariable control system in frequency domain, using operational array technique programming method
12 p2046 A69-26064

Digital computer simulation of multidimensional stationary or nonstationary Gauss-Markov random processes with specified autocorrelation function, discussing time step choice
12 p2122 A69-26523

Potential error source in VTOL aircraft dynamics analysis suggested by dual function of symbol used in perturbation equations of motion
12 p2014 A69-26776

Energy transfer mechanisms between translational, rotational, vibrational, chemical and electronic degrees of freedom in hypersonic shock wave in high temperature air
12 p2063 A69-26969

Spacecraft attitude control and stabilization by three degree of freedom control moment gyro with controllable gyro spin angular velocity
13 p2355 A69-27445

Dynamic stability of two degrees of freedom circulatory systems with bilinear hysteresis damping
13 p2363 A69-28127

Autonomous canonical system with two degrees of freedom, determining equilibrium position stability in resonance case, calculating earth satellite rotational stability
14 p2482 A69-28813

Perturbed molecular distribution in translational and internal degrees of freedom in dilute chemically reacting gases with low ion concentrations
14 p2410 A69-29988

Theory, function generator routine and testing for six node 18 degree of freedom triangular element for plate bending
15 p2706 A69-30430

Finite element analysis of flat rectangular orthotropic multilayer stiffened panels, proposing six degrees of freedom model
15 p2708 A69-30668

Oscillations analysis in quasi-linear autonomous system with two degrees of freedom, using point mapping for case of resonance
15 p2653 A69-31193

Nonlinear vibrations of mechanical two degrees of freedom system during resonance described using Krylov-Bogoliubov method to obtain differential equations solutions
16 p2875 A69-32255

Force resonance oscillations of one degree of freedom system with randomly time varying natural frequency
16 p2813 A69-32285

Amplitude maxima for nonstationary oscillations of dynamic system with multiple degrees of freedom
16 p2876 A69-32296

Isolated symmetric doubly asymptotic solutions existence in neighborhood of symmetric periodic solutions

tions of nonautonomous canonical system with one degree of freedom near resonance
17 p2996 A69-33619

Nonlinear differential equations describing one degree of freedom systems oscillations, allowing for dry friction and internal friction in elastic element
17 p3007 A69-33913

Oscillations of nonlinear dissipative mechanical system with two degrees of freedom, possessing structural damping at joints between moving masses and base
17 p3064 A69-33915

Single freedom vibratory system response to imposed displacement harmonic excitation, analyzing response in terms of constrained system modes
17 p3067 A69-34139

Random excitations effects on vibrating nonlinear single degree of freedom system, statistically estimating resonance mode probability
18 p3171 A69-34554

Models of continuous media with internal degrees of freedom based on Lagrangian variational principle
18 p3173 A69-35028

One degree of freedom systems nonlinear oscillations differential equations periodic solutions by successive approximations, obtaining proof for convergence
18 p3174 A69-35311

Light rigid civil aircraft response to continuous atmospheric turbulence estimated using two rigid body degrees of freedom method for vertical and lateral gusts
[AIAA PAPER 69-766] 19 p3433 A69-35657

Free oscillation period of nonlinear oscillators with one degree of freedom, discussing approximation method
19 p3373 A69-36310

Self rotary motions of nearly conservative systems with one degree of freedom, deriving periodic solution of equation for phase trajectories
19 p3374 A69-36466

Liquid filled rigid bodies motion stability defined and solved for system with infinite number of degrees of freedom
19 p3301 A69-36810

Relative displacement spectra analysis illustrating shock spectra errors, comparing real system response with simple single degree of freedom system response
20 p3548 A69-37301

Degrees of freedom requirements in hinge couplings of multibody satellites, examining main body attitude control
21 p3820 A69-39233

Single degree of freedom gyroscope design factors applicable to strapdown guidance system, discussing torque-to-balance loop, multiple pulse bursting and error sources
[AIAA PAPER 69-848] 21 p3762 A69-39378

Dynamic systems stability with two degrees of freedom, determining second order time dependent integrals valid near periodic orbit
22 p4013 A69-40123

Kinetic theory for macroscopic transport phenomena in N-component polyatomic gas mixtures with internal degrees of freedom under nonlocal thermodynamic equilibrium
23 p4238 A69-41435

Motion equations of quasi-linear nonautonomous systems with many degrees of freedom, obtaining periodic solutions by asymptotic integration
23 p4183 A69-42477

DEHUMIDIFICATION

Physiological effects of breathing cool dehumidified air in hot humid environment, tabulating tolerance time, heart rate, temperature changes and sweat loss
09 p1446 A69-22543

DEHYDRATION

Hypohydration effects on isometric muscular strength, noting decreasing trends in maximal strength
05 p0708 A69-15983

Vacuum, radiation and freeze drying effects on survival rate of microorganisms, noting influence of protective materials on extent of damage
07 p1064 A69-18943

Prolonged dehydrated food diet effect on metabolism of humans, noting complete adaptation after three or four months
13 p2212 A69-28624

Bedrest as analog of weightlessness, evaluating role of extravascular dehydration in postrecumbency orthostatism
17 p2909 A69-33179

Renal calculus incidence among aircrews of long and short haul airlines, considering effects of dry cabin environment and dehydration
23 p4108 A69-41826

DEHYDROGENATION

Lithium aluminum hydride thermal decomposition using isothermal kinetics and differential thermal and thermogravimetric analyses, noting decomposition in four stages
02 p0304 A69-11898

Anoxia effect on succinic dehydrogenase and lactic dehydrogenase activities in digestive glands and organs sensitive to oxygen tension changes
22 p3887 A69-41193

Amino acid sequence of dogfish lactic dehydrogenase, isolating acylated amino-terminal peptide and arginine residues, indicating four polypeptide chain composition
24 p4280 A69-43051

DEICERS

Icing of airframes, discussing ice formation, deicing methods and protection of aircraft
02 p0192 A69-11889

Etching, spray etching and photo-resist methods for producing CrNi steel heating elements for propeller deicing
12 p2102 A69-26370

DEICING

Anti-icing system for business jets, noting activation prior to encountering visible moisture
06 p0868 A69-17669

Anticing for all-weather operation of business jets, discussing atmospheric conditions, ice formations, prevention and removal systems
[SAE PAPER 690333] 11 p1822 A69-24500

DEICING SYSTEMS

U DEICERS

DEIMOS

Deimos and Phobos mutual secular perturbations from calculated masses and orbital elements, using canonical systems of equations
10 p1780 A69-23615

DEIONIZATION

Metal ionic reactions with weak chemical bond breaking and three body reactions forming molecular ions without bond breaking, discussing sporadic E deionization
01 p0071 A69-11168

Ion pair annihilation average rate by single aerosol particle action in lower ionosphere noctilucent clouds
14 p2434 A69-28941

DEKATRONS

U COUNTERS

DELAY

Single frequency oscillations in stochastic quasi-linear differential equations with delay
01 p0170 A69-10825

Uniqueness theorem and successive approximations for delay functional differential equations, noting scalar problems
24 p4341 A69-43236

DELAY CIRCUITS

Wide range linear delay circuit with compensated bootstrap circuit generating linear ramp waveform and regenerative Schmitt trigger comparator
01 p0041 A69-10241

Variable time delay achievement in fluid logic circuits based on Coanda effect devices
02 p0196 A69-12085

Miniaturized adding sample and hold device with adjustable delay applied to digital filters
04 p0574 A69-14350

Soviet book on impulse generators in transistors covering multivibrators and pulse generators with timer circuits, crystal controlled frequency and delayed feedback
04 p0578 A69-15053

FET sample and hold circuit using error corrective feedback
08 p1298 A69-20837

Ultrahigh speed systems and logic circuits specifications implementation into electrical design, discussing circuit selection, line propagation delays, noise margins and temperature effects
[AGARDOGRAPH-114] 08 p1298 A69-20985

Modified scheme for simulation of delay with transient period independent of amount of delay, considering polynomial input
12 p2120 A69-25922

Spatial harmonic spectrum and tangential field distributions in microwave devices showing separation of higher harmonics through delay structure
13 p2236 A69-28576

Microwave dispersion systems, using waveguide loaded with dielectric material to obtain group linear frequency delay characteristic
14 p2412 A69-29395

Periodic ladder type design delay equalizer for linear delay characteristics in millimeter waveguide systems
23 p4135 A69-41361

DELAY LINES

NT ACOUSTIC DELAY LINES

Ultrasonic diffraction delay line operation interpretation as radar chirp signal correlator
01 p0026 A69-10072

Transistor distributed amplifier theory, noting effect of collector line and base line delay difference on gain and transient responses
01 p0041 A69-10203

Synthesis of infinite and finite Wiener optimal networks or equalizers using delay lines with feedforward and/or feedback taps
01 p0029 A69-10554

Fourier synthesis procedure optimized to design of large time bandwidth product dispersive filters employing nondispersive tapped delay lines
03 p0403 A69-13217

Delay line bandwidth reduction for video or digital information, noting radar tracking application
03 p0392 A69-13251

Pulse compression by optical correlation techniques, discussing laser beam control by diffraction grating in ultrasonic delay line
03 p0397 A69-13732

Recirculator with sign variable feedback coefficient for delay line passband increase
04 p0575 A69-14464

Nonsteady coordinates of linear delay system determined from observable linear combination of phase coordinates
04 p0583 A69-15094

Multiple beam waveguide and optical delay line capacity increase by transmitting Gaussian beams clearly resolved at receiver
04 p0579 A69-15446

Adaptation in nonstationary environment formulated for tapped delay line filters with adjustable time varying gains
05 p0737 A69-15806

Coupled cavity short slit delay lines in high power traveling wave tubes
07 p1095 A69-18428

Transversal equalizer circuit consisting of delay line and variable sampler and reinsertion coupler for microwave frequencies
07 p1102 A69-18671

Anti-interference TV circuit using delay lines applied to radar systems, discussing false alarm probability and detection probabilities
08 p1271 A69-19919

Variable phase shifters and delay lines, discussing mechanical and electronic adjustments
08 p1290 A69-20978

Surface wave reflection from free ends of ideally conducting rods forming semiinfinite grid to study rod delay systems and wave-duct antennas
11 p1833 A69-24438

Stability boundaries of discrete circuits employing delay lines with forward and feedback links, deriving equations
22 p3918 A69-40957

Delay line MTI receivers performance calculation accuracy, discussing error for general and restricted number of pulses from single and double cancellation at IF
23 p4117 A69-41605

Discrete delay line measuring FM noise, discussing special case of narrow band cavity resonator method
23 p4137 A69-41606

On-off limit cycle controllers for reaction-jet controlled systems, investigating delay effects
24 p4291 A69-43271

DELAY LINES [COMPUTER STORAGE]

Failure test algorithm for sequential units with delay lines of control digital computers, detecting replacement of output terminals by sensitive paths
20 p3502 A69-37394

DELIVERY

Gliding cargo airdrop system including automatic homing and manual control
[AIAA PAPER 68-958] 24 p4254 A69-43723

DELTA DART AIRCRAFT

U F-106 AIRCRAFT

DELTA FUNCTION

Delta functions use in extending domain of Laplacian operator in quantum mechanics
07 p1174 A69-19495

Delta functions spectrum in reciprocal time domain for LC and RC structures due to impulse response in distributed parameters
09 p1471 A69-21327

Green function type solutions of shell equations by small parameter technique for case of free terms consisting of Dirac delta function
09 p1614 A69-21886

State variables with delta functions for electrical network with discontinuously variable components, discussing application to parametron
19 p3287 A69-36763

Stress analysis fundamental equation for variable thickness plate under concentrated load, using two dimensional Dirac delta function
22 p4041 A69-40144

DELTA MODULATION

Delta modulation for analog to PCM encoding due to tapped binary shift register and up-down counter
09 p1455 A69-21844

Delta modulated control system model for determining oscillation modes at sampling instants
13 p2221 A69-27962

Adaptive signal pattern dependent feedback delta modulation for improved signal/quantization-noise ratio
15 p2565 A69-30177

DELTA WINGS

Idealized delta wing free-free oscillations determination by deriving equations of motion for flexibility and rigidity and formulating boundary value problems
01 p0172 A69-11358

Hypersonic flow distribution and separation types over highly swept delta wings with trailing edge flaps at Mach 6
[AIAA PAPER 68-97] 02 p0189 A69-12522

Hypersonic flow past delta wings with attached shock wave, analysis leads to determination of closed flow pattern
02 p0191 A69-12577

Hypersonic perfect gas flow past delta wing with blunt edges at small angles of attack, noting constant drag coefficient
02 p0191 A69-12584

Aerodynamic characteristics of delta wings for supersonic flow at large angles of attack, showing sweep-back angle influence on drag coefficient
02 p0191 A69-12585

Vortex breakdown effect on aerodynamic coefficients of small aspect ratio delta wings during yawing
04 p0543 A69-14821

Thickness effects on flow past sweptback wings in supersonic flight noting influence of oscillatory motion
[ASME PAPER 68-FE-31] 05 p0698 A69-16078

Delta wing head wave at zero angle of attack in steady supersonic flow during transition from subsonic to supersonic leading edges
[DVL-871] 06 p0858 A69-17242

Mach number effects on pattern of vortex flow past delta wing and circular cones at various Reynolds numbers
06 p0858 A69-17339

Leeward side of delta wing with sharp leading edges at hypersonic speeds, noting Prandtl-Meyer expansion
[AIAA PAPER 68-675] 09 p1431 A69-21992

Delta wing in three dimensional supersonic flow analyzed by method of characteristics, discussing leading edge problems
11 p1820 A69-25425

Concorde design problems due to kinetic heating, aerodynamic characteristics, structure, equipment, modified delta wing planform, etc
12 p2012 A69-26358

Optimum surface for thick delta wing in hypersonic flow obtained by variational method, assuming closed leading and trailing edges
16 p2731 A69-31559

Wall pressure and heat flux distribution in hypersonic flow on delta wings at variable angle of attack for low Reynolds numbers
16 p2731 A69-31605

Leading edge flap angle and planform effects on low speed vortex patterns of flat plate double delta wings, measuring aerodynamic forces
17 p2890 A69-33246

Supersonic and hypersonic flow of inviscid ideal gas over conical delta wings using three dimensional method of characteristics
[AIAA PAPER 69-646] 17 p2893 A69-33486

Leading edge vortices and shock detachment flow over delta wings, discussing drag reduction due to lift
17 p2896 A69-34025

Skin friction drag formula for tapered and delta wings with allowance for coefficient variation and Reynolds number dependence on chord length
17 p2896 A69-34037

Vortex breakdown on slender sharp edged and modified delta wings with varying sweep angles investigated in wind tunnel using schlieren system for flow visualization
[AIAA PAPER 69-778] 19 p3237 A69-35644

Magnetic suspension system used as dynamic balance for wind tunnel models, discussing delta wing test results
19 p3292 A69-35738

Series expansion for exponent of singularity of Laplace equation for flow near apex of plane delta wing
19 p3240 A69-36590

Supersonic flow past antisymmetrical thin delta wing by flow separation from subsonic leading edges, noting wing surface pressures
19 p3241 A69-36779

Conical delta wings in supersonic-moderate hypersonic flow, studying yaw effects on pressure distribution behind shock wave
20 p3459 A69-37593

Gust absorber system configuration flight tests and analysis, emphasizing application to delta wing aircraft
[ONERA-TP-698] 20 p3462 A69-37753

Mach 8 flow field effects and forces on small delta tail surfaces mounted on body of revolution at various angles of attack
[AIAA PAPER 68-891] 22 p3859 A69-40539

DEMAGNETIZATION

Wall streaming, creeping and parade motion in Ni-Fe films excited by hard axis pulses
[IEEE PAPER 11.8] 01 p0138 A69-10717

Magnetic desaturation of inertia flywheels of satellite in equatorial or slightly inclined orbit, discussing satellite stabilization
13 p2357 A69-28476

DEMAND [ECONOMICS]

Elasticity of demand theory applied to fare changes effect on passenger volume, noting interdependence of aircraft size and fare formulation
04 p0689 A69-14805

Economic planning of satellite earth station equipment in relation to expected traffic demand, emphasizing specifications for communication via Intelsat 2 and 3 satellites
07 p1117 A69-19347

Intercity travel demands simulation by linear graph model applied to Windsor-Montreal corridor
[AAS PAPER 69-382] 24 p4417 A69-42805

Demand curves for VTOL intercity transportation, discussing conventional helicopters, compound helicopters, tilt rotor, tilt wing, stored rotor and fan or jet lift
24 p4254 A69-43721

DEMODULATION

Optimum demodulation of PAM-FM signal for case of minimum mean square error as performance criterion
03 p0392 A69-13250

Nonlinear demodulation of amplitude modulated wave propagating in plasma
04 p0559 A69-15210

Tape flutter and additive noise time base errors in coherent demodulation of suppressed carrier AM multiplex
07 p1082 A69-19119

High data rate coherent telemetry systems synthesis, discussing multiphase modulation and demodulation to achieve bandwidth requirements
07 p1083 A69-19123

Soviet book on statistical theory of discrete signal demodulation, covering demodulator analysis and synthesis methods
09 p1455 A69-21933

ELDO satellite command decoder performance in presence of noise, evaluating PDM bit decoder bit error probability and false command probability
11 p1834 A69-24563

Probabilistic analysis of code message distortion due to pulse noise in modulation systems and comparison between linear and quadratic detections
17 p2919 A69-33145

Tradeoff between Doppler measurement capability and subcarrier demodulation in coherent digital communication system quantitatively presented for various SNR
23 p4122 A69-41771

DEMODULATORS

NT FREQUENCY COMPRESSION DEMODULATORS
NT PHASE DEMODULATORS

NT PHASE LOCK DEMODULATORS

Dynamic tracking filter analysis and capabilities as low threshold demodulator in frequency modulated frequency division multiplexing satellite system
01 p0034 A69-11140

Frequency feedback receiver capabilities as low threshold demodulator in frequency modulated frequency division multiplexing satellite system
01 p0034 A69-11141

Phase locked loop demodulators for binary PSK signals compared with and without decision directed feedback in presence of CW interference
03 p0409 A69-13201

Digital detection of angle modulated signals including zero crossing detectors, digital phase locked loops, differentiation and arcsine demodulator
03 p0391 A69-13230

Modems for high data transmission rates on available voice bandwidth channels, noting point to point and multipoint polled networks and signal to noise ratio
04 p0564 A69-15208

Signal/noise performance of frequency locked loop FM threshold extension demodulator compared to phase locked loop demodulator and conventional FM discriminator
06 p0886 A69-16934

Expected number of spikes of phase locked loop demodulators, extending determination method to FM discriminator threshold and maximum likelihood estimator
07 p1082 A69-19107

Frequency feed forward open loop technique for lowering threshold and linearity of FM demodulators
07 p1106 A69-19128

Frequency modulation feedback demodulator design procedure for satellite communications, noting importance of nonideal implementation
09 p1457 A69-22464

Injection locked oscillator FM demodulator, analyzing signal distortion, intermodulation noise, differential gain and differential phase
11 p1845 A69-24565

Trigger demodulator theory, design and circuits
14 p2419 A69-28907

DENDRITIC CRYSTALS

Dendrite formation and solidification relationship in highly alloyed materials from quantitative determination of controlling factors for segregation
01 p0098 A69-10899

Directional solidification and composite structures, discussing structure changes effect on mechanical properties
03 p0449 A69-13877

Acicular crystals growth and dendrites orientation in Mo ingots prepared by electron beam and arc melting analyzed by X rays
11 p1903 A69-24538

Abrasion and corrosion resistant Cr-Co-B cast alloys in aggressive media, concluding resistance is due to chromium boride and fine dendritic structure
19 p3347 A69-36742

DENSIFICATION

Silica glass hardness relationship to pressure induced densification at low temperatures
03 p0453 A69-13616

DENSITOMETERS

Atmospheric density measurement above 50 km by aerodynamic and atmosphere excitation probes, emphasizing beta ray, bremsstrahlung and molecular fluorescence densitometers
15 p2615 A69-31284

Satellite-borne experiments of neutral molecular beam-solid surface interactions, describing Molskin chamber, densitometer, sphere and paddlewheel satellites
19 p3377 A69-36182

Gilson cuvette densitometer used for blood flow measurement in canine forelimb and human forearm and hand during constant intrabrachial arterial dye infusion
23 p4077 A69-41294

DENSITY [MASS/VOLUME]

NT ATMOSPHERIC DENSITY

NT GAS DENSITY

NT SPACE DENSITY

Anomalous gravitational geopotential as function of mass, discussing density anomalies in spherical shells for harmonics as obtained from satellite observations
02 p0244 A69-12178

Temperature dependence of viscosity and density in molten thallium sulfide, noting structural changes absence in short range order
04 p0643 A69-14998

- Hydrogen absorption coefficients, giving number densities in hydrogen gas or plasma for wide range of temperature and pressure
07 p1184 A69-19165
- Specific gravity data for olivine-pyroxene and enstatite chondrites, aerolites, siderites, amphoterites, pallasites and Butler meteorites
08 p1389 A69-20262
- Surface density of carbon foils measured accurately by determining trapped carbon dioxide pressure after burning in pure oxygen
10 p1746 A69-23663
- Denser material beneath lunar maria revealed by precise tracking of lunar orbiting spacecraft, discussing geology and evolution
11 p1953 A69-24339
- Planetary mantles thermal and nonthermal convection model, solving sphere density variations and radial velocity components due to internal time-independent motions
13 p2344 A69-27644
- Aircraft preliminary design weight and volume characteristics relation to aircraft density [SAWE PAPER 813]
18 p3221 A69-34897
- Diameter density and atmosphere of Neptune revised based on star eclipse, noting altitude and temperature
18 p3205 A69-35438
- Cosmic matter density and velocity in expanding universe with negative curvature within Einstein-Friedman theory
20 p3599 A69-37472
- DENSITY [NUMBER/VOLUME]**
- NT ELECTRON DENSITY [CONCENTRATION]
NT ELECTRON DENSITY PROFILES
NT ELECTRON DISTRIBUTION
NT ION DENSITY [CONCENTRATION]
NT IONOSPHERIC ELECTRON DENSITY
NT IONOSPHERIC ION DENSITY
NT MAGNETOSPHERIC ELECTRON DENSITY
NT MAGNETOSPHERIC PROTON DENSITY
NT METEOROID CONCENTRATION
NT PACKING DENSITY
NT PARTICLE DENSITY [CONCENTRATION]
NT PLASMA DENSITY
NT PROTON DENSITY [CONCENTRATION]
NT SPACE DENSITY
- Impurity concentration measurement for alloyed region of tunnel diode by determining Fermi level position
02 p0301 A69-12685
- Hole density/Zn concentration ratio in Zn doped solution grown p-type GaP, noting anomalous electrical properties
09 p1557 A69-21750
- Impurity concentrations in expansion tube flow, measuring radiation intensities [AIAA PAPER 68-371]
09 p1477 A69-21961
- Equilibrium state of matter at high temperatures and densities with respect to nuclear reactions, determining neutron-proton ratio
11 p1957 A69-24403
- Minority carrier density in base region of uniform base transistor at arbitrary injection level, using two dimensional model
11 p1845 A69-24569
- Density ratios of H ions to H atoms in ground state calculated as function of quasi-neutral plasma electron density
16 p2820 A69-31770
- Atmospheric gas constituents number densities determined as function of altitude by correlating laser beam scattering and absorption data
16 p2781 A69-32387
- Equilibrium state of matter at high temperatures and densities with respect to nuclear reactions, determining neutron-proton ratio
24 p4391 A69-43793
- DENSITY [RATE/AREA]**
U FLUX DENSITY
- DENSITY DISTRIBUTION**
- Density gradient measurement method for plasma column with propagation and electric field perpendicular to external magnetic field
01 p0128 A69-10390
- Radio waves incoherent scattering to measure electron concentration profiles at mean latitudes, allowing for collisions
01 p0065 A69-10575
- Doppler signal envelope cross correlation coefficient in two channel system, determining mutual density distribution for envelopes
01 p0032 A69-10887

- Ring current particle energy density distribution for symmetric portion of magnetic storm derived from current magnetic field profile measurements
01 p0147 A69-11227
- Magnetospheric plasma distribution determination based on analysis of structured elements in micropulsations
01 p0076 A69-11229
- Error probability distribution density at output of optimal Gaussian random signal detection, using approximate solution of integral equations
02 p0206 A69-11605
- Longitudinal distribution of cycle sunspots in initial phase of solar activity from Greenwich Observatory data
02 p0314 A69-11647
- Plasma column density profile measurement by means of two resonant cavity modes for low pressure discharge in small diameter tubes
02 p0290 A69-12403
- Critical values of laser formed solid angle determined in plasma diagnostics of scattering spectrum density distribution
02 p0251 A69-12416
- Chemical reaction fluctuations and oxygen electron attachment omission effects on density fluctuations in turbulent wakes, noting electron density fluctuation, bimodal model, etc
02 p0233 A69-12538
- Earth atmosphere air density and temperature profiles from drag acceleration measurements in falling sphere experiment
02 p0251 A69-12809
- Ideal gas spectra and density fluctuations correlations calculated during Markovian and nonMarkovian wandering of particles
03 p0477 A69-13414
- Nonlinear cross sectional space charge density distribution in electron beam of traveling wave tube
03 p0407 A69-13984
- Lunar gravitational anomalies from internal density variation viewpoint, discussing isostasy in maria
04 p0654 A69-14631
- Lunar surface formation, emphasizing density variations and mass concentrations
04 p0654 A69-14633
- Mathematical density-depth model proposed for lunar outermost layer compared to Matveev model, noting Surveyor estimates
04 p0655 A69-14659
- Lunar intermare crater density variations data tabulation, presenting quantitative and qualitative estimates
04 p0656 A69-14671
- Rarefied flow past sphere, analyzing collisionless flowfield structure and development as density increases
04 p0542 A69-14731
- Stability of nondissipative stratified rotating flows with constant density to axisymmetric disturbances
04 p0588 A69-14740
- Delay between solar activity and density changes in upper atmosphere using Harris-Priester model
04 p0594 A69-15121
- Probability density distribution of time shifts in binary signal fronts caused by fading, applying results to FM signal reception
05 p0719 A69-16087
- Nonsteady expansion of gas into vacuum in analysis of asymptotic solutions of Sedov
05 p0751 A69-16676
- Static problem of electric field intensity and space charge density distribution in semiconductor with hot electrons and holes
06 p0978 A69-16989
- Numerical calculation of density profiles of shock waves in expansion flows
06 p0908 A69-17021
- Performance of short supersonic nozzles producing expansion and density jumps in flow, noting efficiency in obtaining maximum driving effect
07 p1050 A69-18753
- Evening twilight nitric oxide density profile in gamma bands deduced from rocket measurements
07 p1125 A69-18842
- Shock waves internal structure in perfect monatomic gases, discussing density distribution in shock layer experimental measurement
07 p1120 A69-18930
- Atomic N and NO daytime upper atmosphere density profiles, discussing production and loss mechanisms
08 p1307 A69-20185
- Multibeam Fabry-Perot interferometers for aerodynamics measurements of rarefied gas flows,

- determining density distribution, shape, structure and detachment of shock waves
08 p1314 A69-20385
- Models for lunar density distribution consistent with available data on lunar physical properties
08 p1393 A69-20579
- Monograph on shock wave structure in binary gas mixtures covering gas kinetics and shock tube measurements of heavy component density distribution
08 p1304 A69-20711
- Upper atmosphere density variations and multiplicative factor necessary for adjustment of density variations of reference models
08 p1397 A69-20761
- Spatial density distribution in star clusters, determining relation between mean stellar mass and density range in subsystems
09 p1589 A69-21368
- Dispersion equation to describe spectrum of LF density perturbations by pumping plane electromagnetic wave in transparent homogeneous plasma or fluid media
09 p1453 A69-21570
- Density inversion in convective zone of stellar photospheres occurring in Eridani atmospheric model under certain conditions
09 p1595 A69-21843
- Optimal working parameters and operational characteristics of laboratory electron gun, examining beam shape, convergence and current density distribution
09 p1464 A69-22243
- Radiation fields of Lyman alpha to Lyman 10 calculated for model planetary nebulas with constant and exponential density distributions in spherical symmetry
09 p1604 A69-22407
- Relativistically corrected Vlasov equation solved as approximate solution of exact relativistic equations of motion for low density media
10 p1724 A69-22924
- Invariant finite amplitude spherical shock wave propagation in medium with inversely radial density
10 p1778 A69-23405
- Atmospheric density analyzed on basis of photographic observations of meteors, comparing vertical profile with CIRA profile
10 p1688 A69-23936
- Interstellar medium density distribution as function of stellar action spherical coordinates applied to determining stellar motion forces and B stars brightness difference
11 p1955 A69-24386
- Infinite diameter detonation velocity vs loading density curve for ammonium perchlorate, finding quadratic mean error
11 p1940 A69-24486
- Perturbation theory applied to emitting density matrix in nonlinear polarization of resonance media, considering gas laser in coaxial magnetic field
11 p1895 A69-24630
- Error probability distribution density at output of optimal Gaussian random signal detection, using approximate solution of integral equations
11 p1835 A69-24712
- Diffusive flow with isopycnic lateral boundaries in porous medium and density distribution of diffusive motion, noting exact solution equivalence to previous solution
11 p1869 A69-24887
- External modulated currents induced electromagnetic field effect on density distribution of bounded plasma, discussing fluctuations in various configurations
11 p1927 A69-24910
- Shock wave propagation in gravitational field with pressure and density gradients, considering nonlinear equations of fluid flow
11 p1961 A69-25106
- Molecular O and total number densities between 70 and 120 km determined with rocket measurements of atmospheric absorption of solar UV and X rays
12 p2065 A69-26106
- Pulsed laser holography used in conjunction with schlieren three dimensional system for observing gas density gradients at different test positions
12 p2088 A69-26179
- Optical methods in three dimensional gas flow research, noting role in density field determination and conjunctive use with gas dynamics equations
12 p2011 A69-26191
- Density distribution vs thickness in sprayed ZrC, NbC and aluminum oxide coatings obtained by plasma jet
12 p2118 A69-26258

Autocorrelation and cross correlation analysis of rapid density variations in F region determined from satellite deceleration and geomagnetic data
12 p2069 A69-26436

Doppler signal envelope cross correlation coefficient in two channel system, determining mutual density distribution for envelopes
12 p2031 A69-26651

Kinetic equation solved for radiation propagation in atmosphere, considering neutron density variations and spatial distribution
12 p2149 A69-26683

Isotropic 3 K black body radiation implications for hot cosmological model, formation of galaxies, existence of supdense bodies and density nonuniformity during prestellar stage
12 p2167 A69-27047

Bhatnagar-Gross-Krook model for plane shock structure, considering moment and least squares methods and shock density gradient error analysis
12 p2063 A69-27112

Magnetic curvature effect on collisionless plasma density gradient drift instabilities, covering mean ion larmor radius and Alfvén modes
13 p2305 A69-27375

Cosmic ray propagation theory for steady streaming along magnetic field and down cosmic ray density gradient, noting MHD wave generation by anisotropy
13 p2326 A69-27569

Isotropic and anisotropic dust cosmological models density perturbation growth, considering angular momentum conservation in expanding universe
13 p2343 A69-27619

Galactic force law from observed stellar velocity and space density distribution
13 p2348 A69-27802

Dissipative drift instability due to electron density gradient and dissipative mechanism /neutral-electron and ion-electron collisions/ in plasma in constant magnetic field
13 p2308 A69-27979

Flux, density and pressure variations with position in vacuum system /nonuniform gas distribution/, discussing causes and consequences
13 p2299 A69-28019

Spatial density distribution and local values of attenuation of pulsed reflex discharge plasma determined from measured attenuation of microwave beam
13 p2312 A69-28112

Bumper materials effect on two component hypervelocity impact shields performance, noting material density influence
[AIAA PAPER 69-379] 13 p2283 A69-28309

Electromagnetic wave phase characteristics after free space passage through statistical medium with wave disturbance producing density and ionization fluctuations
14 p2435 A69-29049

Ionospheric horizontal discontinuities of electron density distribution parameters effect on penetration frequency, skip distances and arrival angles
14 p2436 A69-29057

British and Soviet D region electron density distributions from same VLF and LF propagation data
14 p2439 A69-29112

Plasma potential and density distribution in near-electrode plasma sheath of thermionic converter
14 p2491 A69-29257

Density distribution in axisymmetrical gravitating systems with ellipsoidal velocity distribution function, using integral equation of state for effective radii of cylindrical configurations
14 p2486 A69-29465

Transport coefficient density expansions obtained from time correlation functions in moderately dense gas with short range repulsive intermolecular forces
14 p2540 A69-29469

Quasi-distribution function differential equation for laser field with nonMarkoffian character derived from density matrix master equation
14 p2486 A69-29633

Luminescent material density distribution in comet Arend-Roland 1956h head determined from observed brightness variation with distance
14 p2524 A69-29711

Density fluctuations effect on fully ionized plasma electrical conductivity in large or zero frequency external electric fields
14 p2502 A69-29990

Airborne Doppler radar, estimating velocity distribution and density of pulse signals reflected from air and ground targets
15 p2567 A69-30349

Spiral density waves formation in galaxy model with differentially rotating and nonrotating subsystems based on collective interactions
15 p2688 A69-30550

Radio waves incoherent scattering to measure electron concentration profiles at mean latitudes, allowing for collisions
15 p2597 A69-30745

Combined distribution density of elevations and slopes for illuminated areas of stable statistically homogeneous random surface exposed to parallel rays beam
15 p2569 A69-30948

Air density at various heights determined from analysis of satellite low perigee orbits, discussing periodic density variations and correlation with daily geomagnetic index
15 p2599 A69-31348

Lateral density distribution of muon component in central region of extensive air showers, using Lodz analyzer
15 p2677 A69-31481

Ground level muon density of extensive air showers related to threshold energy and zenith angle for primary particles
15 p2678 A69-31483

Frequency of multiple muons from extensive air showers as function of zenith angle, noting mean transverse momentum and density spectrum
15 p2678 A69-31484

Multiple muon showers penetrating deep underground, discussing radial extent and occurrence frequency against multiplicity spectrum
15 p2678 A69-31485

Double diffused transistor with Gaussian impurity distribution analyzed by power series for carrier density distribution and frequency response
16 p2758 A69-31616

Steady state density profile dependence on electron density dependence of net volume ionization rate by analyzing ambipolar diffusion in RF excited magnetized plasmas
16 p2818 A69-31672

Density and density fluctuations in hypersonic turbulent boundary layer on shock tunnel nozzle wall measured using electron beam probe
16 p2770 A69-31907

Density and velocity fluctuations in hypersonic turbulent boundary layer based on Wallace data
16 p2770 A69-31908

Near free molecule heat transfer and density distribution between concentric spheres using BGK model equation and Knudsen iteration technique
16 p2877 A69-31921

Cosmic ray second harmonic daily variations explainable by symmetrical gradient rising away from solar equatorial plane
16 p2850 A69-32304

Atomic nitrogen and nitric oxide density in upper atmosphere during nighttime calculated, allowing for atomic and molecular diffusion
16 p2785 A69-32622

Luminous particles volumetric concentration calculation based on limiting surface density to determine bulk density in cometary head
17 p3032 A69-33189

Turbulent kinetic energy equation for determining turbulent flow fields applied to free mixing problem of constant density streams
[AIAA PAPER 69-683] 17 p2956 A69-33492

Supdense stars torsional oscillations and crystallization among nuclei from comparison with melting temperature and transverse shear wave velocities of dense conventional matter
17 p3037 A69-33643

Neptune radius, density and atmosphere deduced from observations during occultation of BD minus 17 degrees 4388 by Neptune
17 p3041 A69-33816

Quasars and intergalactic hydrogen density, using Schmidt law of increase in number density of quasars to construct plausible models
18 p3190 A69-34288

Spatial density distribution in star clusters, determining relation between mean stellar mass and density range in subsystems
18 p3198 A69-34757

Buoyant plumes and thermals defined as vertical motions produced under gravity by density or temperature contrast between incompressible source fluid and environment
18 p3122 A69-34917

Fluctuations evolution in density perturbations analyzed to obtain free fall and free expansion universe

models, showing no difference between expanding and static Newtonian universes
18 p3203 A69-35347

Laminar flow of viscous compressible fluid with density dependent on temperature, calculating steady state Navier-Stokes equations using vector function
19 p3297 A69-35852

Density profiles in far field of reaction control system plumes in vacuum obtained by method eliminating difficulties encountered by continuum method
19 p3238 A69-35954

Inelastic collisions and radiation effects on transport properties and shock structure in high temperature gases, obtaining density and temperature profiles
19 p3448 A69-36149

Surface tension of simple liquids consisting of interacting spherical particles, considering density variation in liquid-vapor phase transition zone
19 p3452 A69-36725

Fluidic feedback oscillator performance from fluid density effects analysis including supply jet, feedback line dynamics and load and control port impedances [ASME PAPER 69-FLCS-39]
20 p3465 A69-37984

Galaxy NGC 3593 with large amounts of interstellar dust, calculating galactic mass and central density
20 p3610 A69-38143

Fe-Ni unmelted and unablated micrometeorites number at earth surface calculated, using space density of interplanetary particles and micrometeoritic theory
20 p3614 A69-38251

Ammonia inversion radiation in Sgr B2 region, observing distribution of density, velocity and rotational excitation
21 p3799 A69-38647

Universal dependence of density fluctuations on specific entropy derived from equation describing material composed of neutral particles and equal number of charged and antiparticles
21 p3771 A69-38995

Density field surrounding leaking circular hatch of spacecraft treated as free molecular flow from annulus, superposing far field of effusive orifice flow
21 p3695 A69-39035

Gaussian type densities estimated by representing unknown density in terms of convolution expansion of Gaussian probability density and arbitrary distribution, discussing convergence rates
21 p3756 A69-39499

Parallel shear flow equilibrium in inviscid nonheat-conducting incompressible fluid with density varying as function of vertical coordinate
21 p3697 A69-39743

Small particle holography technique extended for dynamic properties of particle fields, determining velocity and density field, size distribution, flow structure and diffusion rate
21 p3726 A69-39776

Coherent MHD waves propagation in presence of plasma density fluctuations, applying perturbation technique to solve stochastic wave equation
22 p3990 A69-40529

Projected surface density upper limit of neutral atomic H between M31 and M33 galaxies, noting brightness temperature between NGC 4631 and 4656
22 p4024 A69-40578

Heat conduction equation applied to thermospheric heating in auroral zone to account for local temperature and density variations, introducing horizontal transport mechanisms
22 p3941 A69-40717

Fluidic proportional level control and density control systems, discussing advantages of low initial and maintenance cost, long life and temperature, shock, radiation resistance, etc
22 p3870 A69-41241

Density model for free oscillations of earth, noting dependence on core radius and S wave velocity at top and bottom of D layer
23 p4158 A69-42117

Density fluctuations during later stages of formation of universe, emphasizing problems of galactic cluster formation
23 p4221 A69-42390

Energy density distribution in power spectra of turbulence in long wave region in free atmosphere
24 p4346 A69-43155

Thermal conductivities /K/ of rock forming minerals reveals K as linear function of density for constant mean atomic weight
24 p4310 A69-43216

Gas dynamic functions of axisymmetric supersonic gas flows determined using flow density distribution optical measurements
24 p4247 A69-43496

Interstellar medium density distribution as function of stellar action spherical coordinates applied to determining stellar motion forces and B stars brightness difference

24 p4390 A69-43776

DENSITY MEASUREMENT

NT X RAY DENSITY MEASUREMENT

Density gradient measurement method for plasma column with propagation and electric field perpendicular to external magnetic field

01 p0128 A69-10390

Dense plasmas produced by explosions of wires and mercury filaments, discussing plasma conductivities

01 p0128 A69-10391

End holes and glass tube effects in TM 010 mode measurements of average electron number density in cylindrical plasmas

01 p0131 A69-10812

Plasma column density profile measurement by means of two resonant cavity modes for low pressure discharge in small diameter tubes

02 p0290 A69-12403

Boundary layer local densities in high temperature gas flows obtained by measuring monochromatic soft X rays attenuation in layer

02 p0233 A69-12489

Impurity concentration measurement for alloyed region of tunnel diode by determining Fermi level position

02 p0301 A69-12685

Earth atmosphere air density and temperature profiles from drag acceleration measurements in falling sphere experiment

02 p0251 A69-12809

Average plasma electron density measurement by feedback oscillator to determine dielectric constant

03 p0473 A69-13103

Turbulent parameter and turbulent diffusion vertical profile diurnal variations determination based on measurements of Rn 220 and thorium-B concentrations near ground

03 p0459 A69-13273

Lunar surface layer density measured radiometrically with scattered gamma rays by Luna 13

03 p0430 A69-13425

Plasma density spatial distribution determined from HF electromagnetic wave phase shifts without assuming axisymmetry

03 p0480 A69-14138

Time resolved electron number density and electron temperature in decaying plasma using laser interferometer

03 p0432 A69-14187

Electromagnetic phase measurement for determining integrated air density near earth surface

04 p0598 A69-14910

Midlatitude neutral thermosphere density and temperature measurements, noting effect of atomic oxygen adsorption by instruments

05 p0755 A69-16268

Rocket-borne Rayleigh scattering instrumentation to measure atmospheric density, discussing instrumentation and flight results

06 p0927 A69-17698

Coupled cavity carbon dioxide laser interferometer with feedback for measurement of transient plasma density in theta pinch, noting sensitivity

06 p0935 A69-17706

Density measurements of particle tracks in nuclear emulsions utilizing digitized video scan, discussing operation and instrumentation [IEEE PAPER 2A-7]

07 p1133 A69-19185

Whistlers and VLF emissions from ground based and satellite measurements, applying results to electron density mapping and ion detection

07 p1127 A69-19354

He concentration measurement in transient He-air mixture by spectroscopic analysis of fluorescence excited by high energy electron beam

08 p1312 A69-19860

Atmospheric sodium measured at night by tuned laser radar, giving average column number density

09 p1484 A69-21464

Coordination technique for pressure, density and temperature measurements by probes during parachute reentry into planetary atmospheres, taking into account reentry dynamics

09 p1609 A69-21775

Atmospheric density profile from satellite measurements of light wave phase and refraction angles, discussing ionospheric, water vapor and diffraction effects on errors

09 p1490 A69-21862

A-430

Electron density fluctuations in turbulent wakes of hypersonic projectiles in ballistic ranges, discussing use of cylindrical Langmuir probe for direct measurement

09 p1496 A69-21934

Refraction errors in plasma density measurement by microwave interferometry

09 p1496 A69-22031

Laser radar atmospheric applications, noting particulate matter mapping, backscatter density profiles and use of lidar

09 p1521 A69-22795

Gage for measurement of density variation between expansion chamber and driver gas of valve driven shock tube

10 p1673 A69-23342

HI cloud densities near fronts of H II regions by gasdynamic calculations based on observational data for electron density, temperature and particle velocity

10 p1782 A69-23683

Flux densities and spectral indices of radio sources in 3C and 3 CR catalogs, noting measurements at 86 MHz frequency

11 p1951 A69-24237

Quantitative schlieren technique for one dimensional recording of light refraction in density gradients of high speed flow fields

12 p2088 A69-26181

Upper atmosphere density variations investigation using Eurobs system, correlating density to geomagnetic activity and 10.7 cm solar radio emission

12 p2069 A69-26437

Electron concentration in polar ionosphere measured by coherent scattering method

12 p2071 A69-26703

Carbon dioxide laser as light source in Michelson interferometer for plasma electron density measurement

12 p2100 A69-27177

Ionization sensors and detectors classification and dynamic calibration for pressure measurement

13 p2262 A69-28083

Multichannel optical interference fluid manometer, using laser light source for fringe pattern photographic record

13 p2263 A69-28190

Diagnostic measurements in nonequilibrium nozzle flows compared to finite rate expansion calculations, measuring pressure, temperature and density [AIAA PAPER 69-328]

13 p2200 A69-28263

Pulsed laser holographic interferometry of density field created by high speed projectile motion in air [AIAA PAPER 69-347]

13 p2263 A69-28282

Turbulent parameter and turbulent diffusion vertical profile diurnal variations determination based on measurements of Rn 220 and thorium-B concentrations near ground

14 p2472 A69-28781

Noon electron densities between 65-90 km from measurements of differential absorption of partial reflections, discussing seasonal variations at midlatitudes

14 p2439 A69-29110

Air densities from satellite obtained orbital data, comparing accuracy of values and methods of analysis

15 p2600 A69-31349

Wintertime short term density variability in upper atmosphere obtained from rocket measurements

15 p2601 A69-31374

Atmospheric density measurements by triaxial accelerometer system, ionization gauges and orbital decay of OV1-15 satellite

15 p2602 A69-31384

Low altitude atmospheric density satellite OV1-16 measurements, showing agreement between onboard accelerometer and orbital drag data

15 p2602 A69-31385

Kinetic theory and gas-surface interactions for upper atmospheric density measurements by mass spectrometers, pressure gages and satellite drag, detailing adsorption effect

16 p2776 A69-32089

Atmospheric density at 130-160 km measured from satellite 1968-59B orbit, noting agreement with CIRA 1965

16 p2776 A69-32095

Electron density measurement method in plasma or vacuum based on refraction index in optical frequency range using laser interferometer mismatch as criterion

16 p2798 A69-32583

Air density measurement at high altitudes by falling instrumented sphere ejected by missile in upper atmosphere

17 p2971 A69-32898

Nitrogen density measurements up to 4000 atm and 1000 C, examining possible error sources

17 p3073 A69-33393

Extragalactic radiation depolarization through Milky Way transit determined from linear polarization and flux density measurements of discrete radio sources at 21.2 cm

18 p3190 A69-34287

Lunar surface bulk density determined from laboratory and spacecraft measurements of static bearing capacity as functions of depth and solids percentage

18 p3193 A69-34366

Low density plasma electrical conductivity determined by temperature and electron density measurements, using Ohm law

18 p3181 A69-35072

High electron density in transient mercury vapor plasma determined using He-Ne laser interferometer measurements

18 p3153 A69-35307

Quantitative density data from schlieren measurements by photomultiplier technique for axisymmetric flow outside diffraction bands

19 p3306 A69-35741

Pluto mass and density accuracy, questioning values derived from Neptune observations

19 p3403 A69-35969

Ar-Kr integral collision cross sections based on density measurements of Ar beam passed through liquid nitrogen cooled Kr filled scattering chamber

19 p3378 A69-36185

Jet and Mach disk density measured by fluorescence electron beam technique, calculating Mach disk thickness from density profiles

19 p3239 A69-36396

Explorer 32 atmospheric density measurements revealing neutral thermosphere latitudinal variations during geomagnetically undisturbed times

20 p3535 A69-38100

Earth atmospheric density measurement by microwave radio occultation techniques, transmitting coherent radio signal to repeater spacecraft from master station

21 p3705 A69-38375

Chemical composition and lechatelierite size frequency influence on moldavites bulk density, using data to elucidate origin

23 p4210 A69-41348

Near wake electron density distribution for reentry configuration models in shock tunnel with minimum flow interference [AIAA PAPER 68-161]

24 p4248 A69-43643

DENTISTRY

Rat dental pulp hemorrhages following acute hypoxia from exposure to decompression chambers, atmospheric pressure variations or high acceleration

21 p3661 A69-39276

Fighter pilot teeth loss prevention and curative treatments, describing various suitable dentures

21 p3661 A69-39277

DEOXIDIZING

Sintered molybdenum deoxidation effect with C, B and Si, analyzing hardness, tensile strength and ductility

02 p0265 A69-12002

Spray cleaning and deoxidizing of Al surfaces for structural bonding using sulfuric acid-sodium dichromate deoxidizer, noting tests with proprietary solutions

19 p3321 A69-35564

Cleaning, deoxidizing and chromating process effects on chromate coated Al, using salt spray corrosion tests

19 p3321 A69-35570

Aluminothermic reduction of Ti and Ni oxides for obtaining Ti-Ni-Al system

22 p3969 A69-40070

DEOXYGENATION

Nitrosoazomethine derivatives deoxygenation for generation of azomethine nitrenes, discussing preparation by oxidation and dehydrogenation of secondary amidoximes

10 p1651 A69-23305

Nonmetallic inclusions formation mechanism after reducing iron by Al, Zr and Ti, noting oxygen/ reducing agent ratio role

22 p3969 A69-40069

DEOXYRIBONUCLEIC ACID

UV induced excited-state properties of DNA using optical emission and electron spin resonance methods

03 p0372 A69-13488

Radiation structural and transcription damage to deoxyribonucleic acid (DNA), noting postirradiation repair on molecular level

03 p0372 A69-13489

Inactivation of T4 bacteriophage by tritium decay incorporated into DNA and phage protein

07 p1068 A69-19491

Ionizing radiation-initiated degradation of deoxyribonucleic acid in bacteria, noting role of defective prophage
07 p1068 A69-19494

Degree of organization in bacterial cell, discussing pool size and DNA synthesis
07 p1069 A69-19505

Inhibition of gamma ray induced DNA degradation by infection with bacteriophage
07 p1069 A69-19709

DNA replication in vivo as function of temperature sensitive polynucleotide ligase mutant Th, tsA80 in strand synthesis
10 p1647 A69-24188

Defective bacteriophage PBSh in *Bacillus subtilis* after mitomycin C treatment, showing DNA synthesis and marker frequency change
15 p2555 A69-30446

Biological effects of radioactivity and X rays irradiation of whole body and cells, considering DNA degradation
19 p3257 A69-35978

Deoxyribonucleic acid conformations in spinach leaf chloroplasts by electron microscopy
20 p3479 A69-38001

Intraperitoneal high polymer DNA administration normalizing effect on DNA and RNA contents in liver, spleen and intestinal mucosa of white rats exposed to X rays
21 p3657 A69-39050

NonDarwinian evolution of protein and DNA, comparing expectations of evolution models for protein and amino acid changes
22 p3871 A69-40060

DNA polymerase from *Escherichia coli*, discussing physical and chemical properties of enzyme and polypeptide chain consistency
22 p3898 A69-41070

Chemical modifications effects on *Escherichia coli*, DNA polymerase, including Hg atom addition to sulfhydryl group of enzyme
22 p3898 A69-41071

Properties, relative magnitudes and relationship of pyrophosphate exchange reactions catalyzed by DNA polymerase from *Escherichia coli*
22 p3898 A69-41072

Exonuclease function of DNA polymerase from *Escherichia coli*, discussing hydrolysis of polydeoxyribonucleotides and resistancy of oligonucleotides
22 p3898 A69-41073

Deoxyribonucleoside triphosphate substrate binding to *Escherichia coli* DNA polymerase, conducting equilibrium dialysis
22 p3898 A69-41074

DNA and d(A-T) oligomers enzyme binding to DNA polymerase by sucrose density gradient centrifugation
22 p3898 A69-41075

Bacteriophage desoxyribonucleic acid (DNA) degradation by gamma irradiation in vitro by Co 60, discussing breaks, cross links and molecular weight
23 p4079 A69-41402

DNA interaction with ribosomes enhancing amino acid incorporation into cell-free protein synthesizing system extracted from *Chlorella pyrenoidosa*
23 p4080 A69-41430

Thin films of infectious DNA of bacteriophage bombarded by slow protons, determining differential inactivation cross sections
23 p4081 A69-41431

DNA denaturation without variance from pH 7.0 by adding NaOH observed with viscosity measurements, obtaining similar results with hydrochloric acid
24 p4263 A69-43225

DEPENDENCE
U SPATIAL DEPENDENCIES
U TIME DEPENDENCE

DEPENDENT VARIABLES
Finite element method for exact solution of more general problems with one independent variable and extension to many dependent variables
04 p0676 A69-14741

Iterated logarithm law proved for class of stationary series extended to systems of dependent random variables with complete couplings
11 p1910 A69-25699

DEPLETION
Voltage dependence of depletion layer width, maximum electric field and capacitance of Gaussian diffused plane, cylindrical and spherical p-n junctions
07 p1196 A69-18242

DEPLOYMENT
Deployable appendages of OGO attitude controlled spacecraft design
06 p1017 A69-17606

Flight tests of deployment of 20 ft diam ribbon parachute at high dynamic pressures and supersonic speeds
11 p1823 A69-25383

Parachute deployment load control by use of line ties from rocket sled tests
11 p1823 A69-25386

Radio Astronomy Explorer satellite boom deployment method resulting in gravity gradient capture, emphasizing role of predeployment attitude and antenna Vee angle
[AIAA PAPER 69-920] 21 p3821 A69-39350

DEPOLARIZATION
Nonequilibrium carriers during semiconductor depolarization, noting microwave oscillation energy absorption in silicon and zinc sulfide crystals
01 p0138 A69-10434

Spontaneous Raman band shapes and depolarization ratios in liquid nitrogen and oxygen measured and compared to gas, discussing time dependence of rotational motion
06 p0962 A69-17817

Cometary magnetic fields by measuring depolarization of molecular resonance fluorescence
09 p1603 A69-22234

Turbulence induced depolarization of linearly polarized He-Ne laser beam at 6328 A traversing atmosphere near ground level
11 p1896 A69-24842

Book on depolarization of electromagnetic waves covering interface reflection and diffraction, scattered waves, anisotropic media, random scattering, Fresnel coefficients, Brewster angle, etc
14 p2412 A69-29315

Depolarization degree of angel echo signals measured by radar station, indicating insects and other foreign particles in atmosphere as reflection sources
16 p2779 A69-32274

Extragalactic radiation depolarization through Milky Way transit determined from linear polarization and flux density measurements of discrete radio sources at 21.2 cm
18 p3190 A69-34287

Depolarization of extragalactic radio sources at low Galactic latitudes attributed to ionized hydrogen produced by B2 star tunneling through interstellar hydrogen cloud
18 p3194 A69-34425

Electromagnetic wave scattering and depolarization by horizontally weakly inhomogeneous medium, using small perturbation method
18 p3101 A69-34788

Wavelength dependence of total and depolarized backscatter laser light cross section for rough metallic surfaces
18 p3172 A69-35011

DEPOLARIZERS
U DEPOLARIZATION

DEPOSITION
NT ANODIZING
NT ELECTRODEPOSITION
NT ELECTROPLATING
NT VACUUM DEPOSITION
NT VAPOR DEPOSITION

Silicon carbide deposition from liquid organic compounds using film boiling applied on heated tungsten wire substrate
02 p0252 A69-11804

Deposit formation in empty wing tanks due to autoxidative degradation of hydrocarbon fuel, noting results of environment simulation tests
[SAE PAPER 680733] 03 p0366 A69-13439

Accretion rate of cosmic dust estimation from cosmogenic aluminum-26
03 p0514 A69-13935

Bulk weld filler metals, discussing granular compositions, electrodes and iron, nickel and cobalt base deposits
11 p1891 A69-24931

Tungsten emitting surfaces work functions, discussing dense crystalline planes electrolytic or pyrolytic deposit growth and surface chemical or electrolytic attack
14 p2506 A69-29268

Coating deposition theory on high temperature materials, discussing interfacial energy and wetting properties of molten metal drop on solid base material surface
20 p3560 A69-37358

Silicate glass impurity droplet formations on alumina single crystals polished surfaces analyzed by electron microprobe as function of high temperature
23 p4176 A69-41597

DEPOSITS
U CRYCULI
U CRYCODEPOSITS

DEPRESSANTS
U CENTRAL NERVOUS SYSTEM DEPRESSANTS

DEPRESSURIZATION
U PRESSURE REDUCTION

DEPRIVATION
U SENSORY DEPRIVATION
U SLEEP DEPRIVATION

DEPTH MEASUREMENT
Depth distortions in binocular visual fields from misleading size cues
21 p3653 A69-38900

DEPTH PERCEPTION
U SPACE PERCEPTION

DERIVATION CALCULUS
U DIFFERENTIAL CALCULUS

DESCENT
NT PARACHUTE DESCENT

Approximation formula for calculating descent speed and lift-drag ratio
10 p1633 A69-22873

Barotrauma during hyperbaric oxygenation at flight descent or reentry into caisson, including ear trauma symptoms and use of paracetesis
17 p2911 A69-33776

Mathematical model for ascent and descent of high altitude tethered balloon, developing computer program and deriving differential equations of motion
[AIAA PAPER 68-942] 24 p4254 A69-43722

DESCENT TRAJECTORIES
NT REENTRY TRAJECTORIES

Constant thrust deceleration formula for gravity turn soft landing maneuvers expressed in elementary and trigonometric functions of initial conditions for descent
02 p0335 A69-12531

Angle of attack effect on motion throughout entry of spinning descending vehicle, noting effects of transverse angular velocity and spin rate
04 p0666 A69-15522

Optimal control algorithm for spacecraft descent in atmosphere based on nominal trajectory and acceleration measurements
13 p2355 A69-27683

Kalman filter based on calculus of variations, evaluating object trajectory during vertical atmospheric descent
19 p3307 A69-35794

Apollo lunar module landing radar, discussing descent phases, operating modes, assemblies and Surveyor radar
19 p3267 A69-35797

Optimal landing of spacecraft on moon surface from low circular orbit, analyzing rocket thrust, altitude and landing site distance effect on spacecraft mass
19 p3431 A69-36616

Distance of spacecraft descending on parachute through planetary atmosphere measured from center of planetary mass using onboard instrument data
19 p3432 A69-36633

Spacecraft descent trajectory optimization during atmospheric reentry, proposing algorithm for continuous trajectory determination
21 p3766 A69-39647

Spacecraft atmospheric entry descent trajectory optimization by stochastic procedure, requiring onboard digital computer to realize optimal algorithms
21 p3767 A69-39648

Spacecraft trajectory control algorithm for hypersonic reentry, describing onboard equipment role and simulation results
21 p3767 A69-39649

LM descent engine behavior upon contact with lunar surface simulated, basing test condition on statistical trajectory analysis indicating fire until touchdown possibility
[AIAA PAPER 69-1020] 22 p3923 A69-40391

Steep descent landing systems developmental phases for VTOL aircraft, discussing noise abatement, approach angle and descent rates
22 p3978 A69-40674

DESENSITIZING
Receivers EMC, discussing single parameter to evaluate system susceptibility to desensitization, cross modulation and intermodulation
23 p4142 A69-42232

DESERT ADAPTATION
Soil, moisture and other requirements for microorganism survival in simulated Martian environment
01 p0018 A69-11091

Heart rate and bodily fluid changes in aestivating desert anurans, discussing weight loss and metabolism reduction
11 p1827 A69-24923

DESIGN

Part selection, source control and application program for reliability of equipment design, noting derating
22 p3953 A69-40031

DESIGN OF EXPERIMENTS
U EXPERIMENTAL DESIGN

DESORPTION

Work function and desorption energy measurements of alkali metals from metallic substrates with modulated molecular beam, noting surface contamination
09 p1558 A69-21808

Inelastic interactions cross sections of slow electrons with adsorbed particles on W surface as function of temperature in surface bond vibration region
12 p2132 A69-26114

Desorption kinetics of atomic and oxide phases, analyzing composition of surface film formed from W and Mo single crystals interaction with oxygen
12 p2026 A69-26115

Cyclohexane and benzene anodic oxidation at fuel cell electrodes, noting cathodic desorption products as function of potential and reactant
[ECS PAPER 330]
15 p2562 A69-31540

Yttrium desorption from W wire by strong electric field, noting electron work function or temperature increase effects on desorption field
17 p3015 A69-33631

Equilibrium absorption and desorption rates of carbon dioxide-argon mixtures from silica gel measured as function of temperature using gas dynamics method
21 p3848 A69-38707

Cations desorption from O, H and N films adsorbed at graphite surface under electron bombardment, studying desorption cross sections discrepancies
22 p3972 A69-39957

Desorption of hydrogen and methane from Al, Mg and Mb under room temperature tensile deformation in ultrahigh vacuum
23 p4176 A69-41541

DESPINNING

U SPIN REDUCTION

DESTRUCTION

Spacecraft sterilization by destructive heating with thermite or high velocity entry friction before entering planet atmosphere
15 p2560 A69-31472

DESTRUCTIVE TESTS

Pressure vessels burst tests for investigating alloys, fabrication processes and biaxial loading effects, noting vessel configurations and test temperatures
10 p1714 A69-23974

Composite polymers thermophysical properties at thermal destruction temperatures, noting increased heating rate effect on kinetic curves
18 p3161 A69-34696

Reliability testing as complex element of reliability engineering noting nondestructive, destructive and selective demonstration testing, stress-time correlations, risk levels optimization, etc
22 p3952 A69-40022

DESYNCHRONIZED SLEEP

U RAPID EYE MOVEMENT STATE

DETACHMENT

Detached lunar compression wave, noting positive evidence from solar wind flux and direction measurements near lunar wake
05 p0824 A69-16251

Electron detachment cross sections for negative atomic and molecular O ions with incident energies between 3 and 100 eV
09 p1542 A69-21625

Shock wave detachment distance in front of spheres and cylinders in hypersonic flow, using magnetic shock tubes and Mach 5 and 18 wind tunnels
22 p3931 A69-40710

DETECTION

U AIRCRAFT DETECTION
U CORRELATION DETECTION
U ERROR DETECTION CODES
U RADAR DETECTION
U SIGNAL DETECTION
U TARGET RECOGNITION

DETECTORS

Book on laser communication system design covering modulation and detection methods
08 p1277 A69-20884

Detection of metastable He, H, Ne, Ar, Kr, Xe and molecular nitrogen with continuous channel electron multipliers
22 p3917 A69-41235

DETERGENTS

Spacecraft sterilization by hydrogen peroxide solutions mixed with selected anion active detergents
05 p0713 A69-15943

DETERMINANTS

Specialized mathematical machine for expanding matrix determinants and solving combinatorial problems, discussing symbolic circuit
09 p1460 A69-21782

DETERMINATION

U MEASUREMENT

DETONABLE GAS MIXTURES

One dimensional unsteady flows of combustible gas mixture with finite chemical reaction rates, considering piston motion, igniting shock wave propagation and point explosion
06 p0909 A69-17325

Nonequilibrium supersonic flow calculation of detonating mixture past blunt bodies applied to flow of hydrogen-oxygen mixture past sphere
06 p0859 A69-17343

Inflammable gas mixtures and deflagrations noting self ignition temperature, flame propagation, flame front structure and flame stability
06 p1031 A69-17417

Detonations in gases and solids, discussing limits, speed, initiation by deflagration, chemical factors, dimensional effects, etc
06 p1032 A69-17424

Gas dynamics, thermodynamics, chemical properties, energy and products of hydrocarbon-air detonations in tubes under standard atmospheric conditions
[WSCI PAPER 68-26]
07 p1241 A69-18369

Nonequilibrium chemical reaction effect on decay in spontaneous explosion for reactive expelled gas and inert expelling gas
07 p1119 A69-18705

Detonation wave propagation in H-O mixtures in supersonic flow, noting detonation front structure and velocity
08 p1420 A69-19882

Flame front instability in air-propane mixtures established by motion picture study
08 p1421 A69-20344

Gas pressure variations behind autonomous stable detonation fronts in propane-O mixtures, noting effect of diameter tubes and initial pressures
08 p1421 A69-20757

Laser induced breakdown spark ignition of detonable and nondetonable chemically reactive gas mixtures, noting blast waves
[AIAA PAPER 68-146]
09 p1622 A69-21951

Transverse wave spacing in self sustaining detonations in H-O mixtures, noting evidence against acoustic theory and for characteristic chemical dimension
09 p1622 A69-21953

Steady flames transition into spherical detonation in various gas mixtures using high speed photography in sealed volumes
10 p1810 A69-23897

Plane, cylindrical and spherical point explosions in combustible gas mixtures for different gas motion models, formulating scaling law for detonation wave model
19 p3449 A69-36353

Coordinate perturbation and second order solution for early collapse phases of cylindrical or spherical detonation wave in equimolar acetylene-oxygen mixture
19 p3449 A69-36354

Detonation in unbounded gas mixture starting from spherical flame, discussing stability of gasdynamic discontinuities and cellular structure
19 p3450 A69-36358

Stored energy release in exploding wire circuit during divergent detonation wave ignition in propane-oxygen mixture in circular sector
19 p3451 A69-36365

Transverse and longitudinal velocity components of detonation waves in stoichiometric hydrogen-oxygen propagating in fundamental mode in square section tube
19 p3451 A69-36367

Combustible mixtures flow past bodies, discussing equation for shock polar for exothermal discontinuities at subsonic and supersonic velocities
19 p3241 A69-36780

Fire hazard in closed chamber associated with intestinal hydrogen and methane formed by space diets, comparing Gemini-type and bland diets
20 p3482 A69-37622

Schlieren framing photography used for studying shock wave hydrodynamic structure and ignition dynamics during expansion into detonable gas region
21 p3849 A69-38803

Perfluorocyclobutane-oxygen mixture combustion, measuring burning velocities and adiabatic equilibrium flame temperatures
21 p3852 A69-39594

Hydrogen-air combustion in supersonic flow past sphere determined with allowance for chemical reactions nonequilibrium rates at high pressure and temperature
24 p4408 A69-43488

DETONATION

Detonation generation in granular explosive subject to different shock wave intensities due to variable impact velocity
02 p0349 A69-11527

Initiation of detonation by incident shock waves in hydrogen-oxygen-argon mixtures
02 p0304 A69-12313

Mass velocity of detonation products of hydrogen-oxygen mixtures measured by simultaneously recording internal resistance and induced voltage in ionized medium
02 p0354 A69-12628

Detonation capacity of mixture of ammonium perchlorate base and polymethyl methacrylate and polystyrene, noting critical particle size dependence on composition
02 p0305 A69-12674

Prevention of and protection against accidental explosion of munitions, fuels and other hazardous mixtures - Conference, New York, October 1966
04 p0644 A69-14467

Deficiencies in two hazard classification system for detonating and fire producing materials from analysis of chemical industry accident fatality statistics
04 p0645 A69-14471

Wedge shaped charge technique for evaluation of detonation hazards of liquid explosives
04 p0646 A69-14479

Detonation characteristics of gaseous explosives using equations of state for real gases, noting compressibility effect in mixture of hydrocarbons, O and N
05 p0848 A69-16337

Detonations in gases and solids, discussing limits, speed, initiation by deflagration, chemical factors, dimensional effects, etc
06 p1032 A69-17424

One dimensional lattice model for heterogeneous explosive detonation, discussing hot spots, grain burning ignition time, ignition site types and RDX detonation
[WSCI PAPER 68-30]
07 p1240 A69-18357

Steady flames transition into spherical detonation in various gas mixtures using high speed photography in sealed volumes
10 p1810 A69-23897

Critical diameter of ammonium perchlorate stable detonation as function of initial temperature, water content, density and particle size
11 p1940 A69-24553

Unsteady gas dynamics of explosions and detonation theory, noting applications to rocket propulsion systems performance
11 p1876 A69-25595

Initiation distance and time of detonation with weak ignition sources related to temperature, tube diameter, mixture composition and pressure
19 p3451 A69-36364

Cylindrical concentric detonation front and stability mechanism space-time measurement
20 p3632 A69-37215

Shock front reaction and detonation initiation in low density ammonium perchlorate
21 p3784 A69-39590

DETONATION WAVES

Detonation wave structure in solid cylindrical shell explosive, noting attainment of steady state structure
02 p0349 A69-11526

Detonation wave initiation in gaseous media, noting transition process for flames accelerating to detonation and explosions behind reflected shock wave
02 p0350 A69-11530

Propagation of detonation wave in tube containing single stream of diethylcyclohexane droplets dispersed in gaseous oxygen
03 p0415 A69-13139

Boundary conditions in oblique reaction waves in supersonic flow, adding or subtracting heat by chemical reaction
05 p0697 A69-15828

Asymptotic theory concerning nonsimilar structure of blast wave with expanding interface applied to hypersonic perfect gas flow
06 p0860 A69-17636

Spherical deflagration and detonation waves in diluted stoichiometric hydrogen-oxygen mixtures in hemispherical combustion chamber
06 p1034 A69-17927

Electromagnetic field induced energy and momentum changes effects on pressure, temperature and particle velocity of flows behind propagating gaseous detonation waves
[AIAA PAPER 69-44] 06 p0970 A69-18084

Electric signals by shock and detonation waves, describing detection technique
[WSCIPAPER 68-44] 07 p1240 A69-18360

Nonequilibrium chemical reaction effect on decay in spontaneous explosion for reactive expelled gas and inert expelling gas
07 p1119 A69-18705

Detonation wave propagation in H-O mixtures in supersonic flow, noting detonation front structure and velocity
08 p1420 A69-19882

Gas pressure variations behind autonomous stable detonation fronts in propane-O mixtures, noting effect of diameter tubes and initial pressures
08 p1421 A69-20757

Unsteady flow parameters for reaction products behind spherical detonation wave in gas mixtures based on Taylor solution
08 p1421 A69-20765

High velocity gas stream induced shattering of liquid drops, disintegration rate and breakup time
[AIAA PAPER 68-83] 09 p1482 A69-21947

Infinite diameter detonation velocity vs loading density curve for ammonium perchlorate, finding quadratic mean error
11 p1940 A69-24486

Solution of confluence in three dimensional shock and detonation polars for spinning detonation
11 p2002 A69-25353

Gasdynamic stability of detonation shock wave in case of arbitrary heat evolution kinetics using detonation model
12 p2062 A69-26672

Transverse wave spacings for self sustaining detonations in oxygen and diluents mixtures with hydrogen, methane, acetylene or ethylene fuel, noting dilution
13 p2378 A69-28217

Digital computers for aircraft engines control, discussing economic assessment, advantages and basic control system
15 p2671 A69-30323

Compression waves observed ahead of luminous discharge plasma below Mach 12-15 in electric shock tube, describing shock structure by blast wave theory
16 p2768 A69-31664

Small disturbances and effect on processes of fast combustion of inflammable compressible mixture
16 p2837 A69-32137

Two phase detonations of fuel in liquid layer on shock tube wall with gaseous oxidizer, presenting one dimensional approximation for film detonation propagation
16 p2879 A69-32151

Wave motion nonsteadiness influence on detonation front thickness using quasi-steady kinetic model of induction process, discussing agreement with experimental observations
17 p2952 A69-33403

Gas and small particle diffusion in turbulent boundary layer of blast wave propagating over land or water, assuming logarithmic vertical velocity profile
[AIAA PAPER 69-672] 17 p2953 A69-33439

Shock tube with cylindrical explosive to implode glass wall and produce high velocity glass particle jet, studying jet velocity and behavior and test gas pressure effects
18 p3116 A69-34460

Plane, cylindrical and spherical point explosions in combustible gas mixtures for different gas motion models, formulating scaling law for detonation wave model
19 p3449 A69-36353

Coordinate perturbation and second order solution for early collapse phases of cylindrical or spherical detonation wave in equimolar acetylene- oxygen mixture
19 p3449 A69-36354

Detonation in unbounded gas mixture starting from spherical flame, discussing stability of gasdynamic discontinuities and cellular structure
19 p3450 A69-36358

Continuous explosion laser study of stationary detonation waves to determine conditions leading to partial population inversion and critical population density
19 p3336 A69-36360

Stored energy release in exploding wire circuit during divergent detonation wave ignition in propane-oxygen mixture in circular sector
19 p3451 A69-36365

Transverse and longitudinal velocity components of detonation waves in stoichiometric hydrogen-oxygen propagating in fundamental mode in square section tube
19 p3451 A69-36367

Construction of single headed spin detonation polar as confluence of shock and deflagration waves by two dimensional hodograph
19 p3451 A69-36368

Shock and detonation waves refraction due to small disturbances in medium, noting causes of wave cellular structure
19 p3451 A69-36369

Detonation wave in gaseous media, current theories on wave initiation, structure and propagation
19 p3452 A69-36370

Finite chemical reaction rate detonation wave interaction with rarefaction wave, noting mixture activation energy and heating power influence
19 p3298 A69-36384

Electromagnetic effects on pressure, temperature and particle velocity in flow behind propagating gaseous detonation waves based on one dimensional flow field model
20 p3514 A69-37190

Electromagnetic piston produced shock wave interaction with detonation wave, producing overdriven detonations
20 p3631 A69-37209

Shock wave effect on ionization of detonation waves in propane-O mixtures producing stable high velocity plasma, measured by double probe method
21 p3853 A69-39745

Plane double front detonation wave attenuation by pursuing rarefaction waves, analyzing oscillations, onset mechanism and stability during transition to Chapman-Jouguet mode
22 p3929 A69-40112

Detonation velocity variation in nitromethane with initial pressure, discussing relationships
22 p4051 A69-40713

Reaction zone following overdriven detonation wave propagating into mixtures of fluorine oxide and hydrogen molecules showing HF laser emission
22 p4052 A69-41188

Detonation driven shocks of high Mach number obtained in improved membrane shock tube by heating and compressing driver gas
23 p4198 A69-41545

Detonation wave instability and damping in gas containing liquid or solid inflammable aerosol, considering atomized propellants
23 p4240 A69-42339

DETONATORS

Exploding wire detonators noting dependence of threshold burst current on bridgwire length and diameter, explosive surface, density, etc
01 p0119 A69-10672

Exploding wire detonators without primary explosive, discussing high precision fabrication, safety aspects and firing circuit
01 p0120 A69-10676

Electrical devices for detonation initiation in pyrotechnic equipment for space applications, tabulating characteristics
10 p1749 A69-23006

Detonating fuses for separation of missile and rocket stages, noting separation ease, aftereffects, priming capability and fabrication
10 p1752 A69-23023

Detonation system for exploding missile warheads, discussing trigger detonation and safety release elements
17 p3050 A69-33698

DEUTERIUM

IR and Raman spectra of solid and matrix isolated methylamine and deuterium derivatives, locating a mine twisting vibration in solid phase IR spectra
01 p0023 A69-10287

Deuterium gas ionization over high pressure range under action of short pulse Q switched neodymium glass laser, noting breakdown wave existence
02 p0255 A69-11545

Intensity of visible and UV light from beam of positive deuterium molecular ions excited by passage through thin C foil
03 p0471 A69-13166

Molecular jets obtained by charge exchange of triatomic ion beams consisting of hydrogen, deuterium and nitrogen, noting formation, energy level, etc
05 p0797 A69-16339

Carbon dioxide bending mode deactivation by orthohydrogen, parahydrogen and deuterium through rotational transitions
08 p1358 A69-21010

Deuterium escape in Venus upper atmosphere to explain anomalous Lyman-alpha glow observed by Mariner 5
09 p1594 A69-21696

Pd-D resistivity variation with D concentration at room and liquid He temperatures, discussing structural resistivity
10 p1745 A69-23357

D/H ratio in Venus exosphere, discussing isotopic fractionation mechanisms and Lyman alpha data from Mariner 5
11 p1962 A69-25145

Thermal energy rate constants of ion-molecule reactions in gaseous hydrogen, deuterium and HD, using ion cyclotron resonance method
20 p3578 A69-36934

Primordial He 3 and deuterium production from magnetic effects during nucleosynthesis epoch of big bang cosmologies
22 p4035 A69-41210

DEUTERIUM COMPOUNDS

NT HEAVY WATER

HI and DI reaction into HD and 2I, noting need for rotational or vibrational excitation in addition to translational energy of collision
01 p0123 A69-10686

Deuterated diazomethane prepared by base catalyzed reaction of hydrazine with chloroform
06 p0885 A69-17885

IR and Raman spectra of gas and liquid phase methylhydrazine and deuterated methylhydrazines, discussing vibrational motions, H bonding and thermodynamic functions
10 p1752 A69-23528

Pulsed laser emission from carbon dioxide collisionally pumped by vibrationally excited DF produced by reacting fluorine oxide with deuterium
12 p2104 A69-25986

DEUTERIUM OXIDES

U HEAVY WATER

DEUTERIUM PLASMA

Target production device for deuterium plasma clouds in vacuum with Q switched neodymium laser
01 p0090 A69-10222

Deuterium plasma evolution and creation modes obtained by short pulse laser discharge in gases, discussing detonation and phase wave ionization mechanisms
02 p0288 A69-12040

Deuterium plasma heating by means of high power focused pulsed laser beam, noting initial energy of laser and pulse duration
05 p0769 A69-15583

Magnetic field confinement of plasma produced by focusing Q switched laser output on solid deuterium pellet
05 p0798 A69-15585

Ultrahigh speed holographic interferometry for studying plasmas produced by focused laser beam, noting electron density evolution in deuterium plasma
05 p0760 A69-15587

X rays detection from laser produced deuterium plasma through calibrated absorbers, presenting electron temperatures
06 p0964 A69-17479

Thermonuclear neutron emission from high temperature deuterium plasma produced by focusing high power laser radiation on lithium deuteride surface
[IEEE PAPER O-11] 07 p1153 A69-19072

Deuterium plasma jets passage through pulsed magnetic field by means of thermal and diamagnetic probes, noting magnetic field strength effect
13 p2311 A69-28107

Collective scattering of light from ruby laser by cold dense deuterium plasma produced by electrical discharge, deducing density and electron temperature
13 p2273 A69-28366

DEUTERON IRRADIATION

Deuteron microbeam for simulating biological effects of ionization by heavy cosmic ray particles
03 p0373 A69-13493

Heavy cosmic ray particles effect in manned space flight, noting results of deuteron microbeam experiment

03 p0373 A69-13494

Proton and deuteron energy used to study solid state chemical reactions effects on meteorites composition and properties, obtaining hydroxyl ions and hydrocarbons

19 p3414 A69-36114

DEUTERONS

Absolute cross sections for coincidence detection of deuteron breakup by 42 Mev alpha particles, showing He 5 and Li 5 final state interaction peaks

03 p0472 A69-13469

Cosmic ray deuteron and He 3 secondary origin and determination of cosmic ray path length and residual interplanetary field modulation

08 p1378 A69-20066

Low velocity heavy mass particle detection in sea level cosmic radiation, assuming deuterons

16 p2846 A69-31600

Elastic scattering cross sections of negative pions by deuterons compared with Glauber model calculations

17 p3007 A69-32885

DEVELOPERS [PHOTOGRAPHY]

U PHOTOGRAPHIC DEVELOPERS

DEVITRIFICATION

U CRYSTALLIZATION

DEW

Dew /or frost/ point determination method for low temperature humidity measurement

09 p1502 A69-22691

DEWAR SYSTEMS

U CRYOGENIC EQUIPMENT

DH 121 AIRCRAFT

Trident 2E aspect ratio, wing area, high lift devices, fuel capacity, range improvement, etc

13 p2202 A69-27971

Trident 2E and 3B structural design and fail-safe tests, noting difference in fuselage length

13 p2202 A69-27972

Trident 2E aircraft, discussing fuel system, electric power installation, hydraulic system, air conditioning, pressurization and flying controls

13 p2202 A69-27973

Spey 512 turbofan and RB.162 booster turbojet engines for Trident 2E and 3B power plant

13 p2325 A69-27975

Trident category 3 automatic landing, discussing triplex pitch and roll control, duplex rudder, autothrottle and azimuth paravision display

13 p2296 A69-27976

DIABATIC PROCESSES

U HEAT TRANSFER

DIADEME SATELLITE

Laser measurements for DIADEME satellites tracking to reconstruct actual trajectory in semidynamic geodesy

15 p2600 A69-31365

Doppler shift measurements at two coherent frequencies from Diademe satellites to determine ionospheric electron content, discussing accuracy and parameters defining satellite passage

16 p2785 A69-32615

Diademe satellites stabilization system to measure station-to-satellite distance by laser pulse, discussing reflector, magnet for attitude control, damping device, etc

17 p3046 A69-33224

French space geodesy since Space Age, detailing Diapason and Diademe satellites program, techniques and results

17 p2961 A69-33382

DIAGNOSIS

Clinical problems during interplanetary flights, stressing need for diagnostic algorithms and automated medical equipment

02 p0202 A69-12121

High temperature effects on physiological functions of man noting cardiovascular system and heart performance, body heat exchange and blood and urine composition

05 p0710 A69-16523

Beta adrenergic blockade in differential diagnosis of cardiovascular changes produced by stress induced catecholamine liberation and organic disease

17 p2909 A69-33184

High temperature effects on physiological functions of man noting cardiovascular system and heart performance, body heat exchange and blood and urine composition

18 p3096 A69-34742

Wireless telemetry system design for physiological signals in human diagnosis, discouraging casual use of wireless transmission

19 p3261 A69-36269

Ultrasound-echo-encephalography in diagnosis of posttraumatic intracranial hemorrhage of skull and brain trauma, noting neuroradiological techniques

21 p3652 A69-38790

Surface electromyography (EMG)/frequency analysis of normal and pathological muscle or nerve contraction as diagnostic tool for industrial physician

21 p3664 A69-38920

Arrhythmia diagnosis instruction aided by cardiac pacemaker digital simulation, discussing clinical electrocardiograms generation mechanisms

21 p3667 A69-39606

Brain atrophy clinical diagnosis aided by biochemical analyses, including age frequencies and symptoms to control incidence among aviation personnel

23 p4089 A69-41816

Frequency analysis of second heart sound splitting in patients with coronary artery disease assessed clinically and by phonocardiography

24 p4261 A69-42726

Heart murmurs frequency analysis on patients to improve detection of aortic insufficiency in presence of mitral stenosis

24 p4279 A69-43800

DIAGRAMS

NT CIRCUIT DIAGRAMS

NT CREEP DIAGRAMS

NT FEYNMAN DIAGRAMS

NT HERTZSPRUNG-RUSSELL DIAGRAM

NT NYQUIST DIAGRAM

NT PHASE DIAGRAMS

NT S-N DIAGRAMS

Serial BCD binary coder design, using Karnaugh diagrams to minimize synchronous and asynchronous counter stages

09 p1467 A69-22579

Skiagrams results of retinoscopic measurements of eye peripheral refraction of pilots, attempting correlation between skiagram type and central refraction

24 p4267 A69-43399

DIALYSIS

U ELECTRODIALYSIS

DIAMAGNETISM

Quantum theory of electrical birefringence of noninteracting diamagnetic molecules /Kerr effect/ subjected to static electric field and polarized plane wave

02 p0279 A69-11538

Orientation of diamagnetic ground state Pb 207 atoms with nonzero orbital angular momentum by means of optical pumping and determination of nuclear moment

07 p1156 A69-19399

Pfirsch-Schluter factor calculation for stationary toroidal plasma diffusion enhancement due to current along magnetic field over diffusion over that associated with diamagnetic current

11 p1925 A69-24312

Coulomb interaction during optical transitions between Landau subbands of Ge semiconductor valence and conduction bands in magnetic field, observing diamagnetic excitons

11 p1936 A69-24640

Boundary conditions for equilibrium diamagnetic plasma in magnetic dipole having constant and isotropic pressure in system

14 p2489 A69-28910

Electron temperature and concentration in plasma determined by measuring diamagnetic signal and IR radiation intensity, emphasizing usefulness in plasmoid head portion

14 p2496 A69-29785

Plasma cluster interaction with axially symmetric magnetic field, deriving plasma diamagnetic current, inductance and resistance from measured coil flux dependence on distance

16 p2823 A69-32365

Equilibrium state of diamagnetic plasma configuration in inhomogeneous magnetic fields with complex potential near neutral point, noting solar flares and magnetic traps

19 p3380 A69-36467

DIAMANT LAUNCH VEHICLE

Solid, liquid and advanced propulsion techniques in France, discussing Diamant program and Europa booster

02 p0334 A69-11919

Electrohydraulic guidance of second stage of Diamant rocket used for orbiting satellites employing thrust vector orientation

04 p0551 A69-15183

Automatic quantitative checkout equipment for telemetry circuit of Diamant satellite booster before launching

16 p2750 A69-31727

DIAMETERS

Neptune mean diameter determination by photometric observations of stellar occultation by planet

01 p0150 A69-10386

Venus diameter determination from optical measurements, noting cloud layer height and height of suspended particles in upper atmosphere

05 p0818 A69-15621

Elastic limit of lunar outer layer determined from analysis of lunar crater dimensions variations as functions of diameter

07 p1212 A69-18600

Laser beam diffraction method for measurement of apparent filament diameters, emphasizing high modulus carbon filaments

08 p1316 A69-20499

Half intensity angular diameter upper limit of Seyfert galaxy NGC 4151 nucleus, considering nonthermal continuum

09 p1602 A69-22227

Stellar diameter interferometric measurements, discussing double slit arrangement and illumination in focal plane

13 p2334 A69-27305

Pitot tubes diameter effect on pressure gradients during measurement through shock wave

16 p2771 A69-31927

Stellar diameters in galactic cluster stars determined using original and modified spectrophotometric method compared with spectral types BOV-FOV

16 p2858 A69-32210

Particles maximum diameter numerical values for melting during injection into plasma jet calculated for various metals and refractory dielectrics

17 p3009 A69-32825

Control knob optimum diameter for minimum operation time, noting frictional resistance

21 p3664 A69-38969

Tube diameter effects on shock front propagation, observing front formation process with schlieren method

24 p4297 A69-43630

DIAMINES

Synthesis of N-/trimethylsilylalkyl/ diamines and N-/trimethylsilylalkyl-/N-/2-mercaptoethyl/ diamines, determining structure by IR spectra

15 p2561 A69-30414

DIAMOND WINGS

U LOW ASPECT RATIO WINGS

U SWEPT WINGS

DIAMONDS

NT METEORITIC DIAMONDS

Diamond dust as major component of interstellar dust to explain observed properties

05 p0828 A69-16662

X ray emission from powdered graphite, diamond and titanium carbides

06 p0946 A69-17545

Electron momentum density in diamond, graphite and carbon black from Compton profile measurement by X ray scattering vector

06 p0982 A69-18233

Optical constants of bulk diamonds compared with interstellar extinction, calculating extinction curves for diamond particles from Mie theory

12 p2157 A69-26230

Photocurrents and recombination luminescence in n-type diamonds subjected to UV, Ti 204 and X ray irradiation indicating local electron centers formation

19 p3383 A69-36167

Friction characteristics during diamond honing of different steel grades, determining lubricating and cooling liquids effect on friction coefficient

22 p3958 A69-41170

DIAPHRAGMS

Incremental and corresponding total strain theories of plasticity used to analyze hydrostatic bulging of circular diaphragm

08 p1418 A69-20826

DIAPHRAGMS [MECHANICS]

Shadowgraph cinematography technique for testing attenuating influence of symmetrical diaphragm system on shock wave

12 p2088 A69-26184

Liquid driver shock tubes dynamic and thermodynamic properties as functions of diaphragm pressure ratio and initial conditions

19 p3295 A69-36471

Image converter camera and astronomical telescope arrangement for photographing metal diaphragm openings in shock tube
20 p3538 A69-37227

Pressure transducers using heterode strain sensors evaporated directly onto pressure diaphragm
22 p3950 A69-41222

DIASTOLE

Abnormally slow ultrasound diastolic slope detected by mitral valve motion study in patients with clinically pure mitral insufficiency
24 p4261 A69-42727

DIATOMIC GASES

Hypersonic flow of nonequilibrium diatomic gas on and near wedge, studying shock curvature variations
01 p0005 A69-10161

Vibrational relaxation of diatomic gases behind shock waves, with variable heat bath temperature extended to constant enthalpy and constant total enthalpy conditions
01 p0061 A69-11204

Diatomic dissociating gas free atoms virial coefficient used to study thermodynamic properties and transport coefficients of gases
02 p0283 A69-11574

Numerical solution for excitation of oscillations in diatomic molecules during atom-molecule collisions at high temperatures, determining intermolecular interaction forces
02 p0284 A69-12485

Radiation attenuation cross sections of monatomic and diatomic xenon gas from UV absorption measurements near resonance line
02 p0284 A69-12551

Parameter changes of diatomic gas behind direct shock wave with simultaneous oscillatory and dissociative relaxation
03 p0418 A69-13835

Mass spectrometric measurements to determine energy distributions of ions produced in dissociative photoionization of O molecules
06 p0960 A69-17110

Vibrational excitation in diatomic gas mixtures by translation to vibration energy conversion in simple collisions and by vibrational energy exchange between components
06 p0962 A69-17821

Sonic transmission of diatomic nitrogen during nozzle flow, presenting density dependence of natural oscillation energies and temperature
10 p1632 A69-22912

Oscillations and decomposition of diatomic gas molecules at high temperatures during atom/molecule collisions, deriving kinetic equations for energy level changes
13 p2302 A69-27797

Adsorption of N, H, O and CO on thick vapor deposited Be films at room temperature
13 p2322 A69-28017

Diatomic hydrogen abundance evolution in uniform medium, discussing photodissociation effects and galactic evolution
15 p2680 A69-30205

Dynamic behavior of dissociating homonuclear diatomic gas, deriving instability equations, proposing stability loss in transonic region
15 p2548 A69-31065

Half maximum temperature of diatomic gases determined by extending relation between specific heat and molecular dissociation to diatomic molecules [DVL-899]
15 p2656 A69-31102

Absorption spectrum of diatomic oxygen excited by AC silent discharge photographed with vacuum spectrograph, associating lines with Schumann-Runge band
20 p3581 A69-38276

Diatomic-monatomic oxygen collision cross section determined from rotational line width in diatomic oxygen Schumann-Runge emission spectra
22 p3983 A69-40099

Dissociational nonequilibrium transonic flow near nozzle throat analyzed for diatomic gas with equilibrium vibrational energy, using perturbation method
22 p3861 A69-41177

Nonequilibrium boundary layer of dissociated diatomic gas over catalytic flat plate in hot hypersonic uniform flow
22 p3934 A69-41181

DIATOMIC MOLECULES

Photosphere models comparison based on theoretical rotational temperatures of various diatomic molecular free radicals, using faint lines method
03 p0512 A69-13694

Potential energy functions based on electronegativities instead of spectroscopic parameters for Li and K molecules
03 p0472 A69-13805

Photodissociation and photoionization of diatomic molecules at high temperatures with calculation of absorption cross sections
03 p0473 A69-14147

Nonequilibrium dissociation effects on constant pressure laminar mixing for diatomic molecules and atoms, analyzing concentration and temperature of free shear layer
04 p0588 A69-14733

Separation of center of mass and rotational coordinates from N electron diatomic Schroedinger equation
04 p0554 A69-14861

Polarization of diatomic molecular line radiation excited by electron impact
06 p0961 A69-17140

SH above photosphere in solar atmosphere, discussing dissociation equilibrium of diatomic molecules and possible abundances
06 p1002 A69-17317

Rotational inelastic transitions in atom-diatom collisions, discussing restricted distorted-wave approximation, transition probabilities, impact parameters, inelastic and glory quenching, etc
07 p1185 A69-19302

Electron impact cross sections for diatomic molecule ionization and excitation from modified Gryzinski theory, discussing results from molecular models
09 p1542 A69-22249

Emission-absorption intensity ratio temperature measurements of diatomic molecules under thermal nonequilibrium conditions, considering rotational population distribution during vibration temperature measurement
09 p1623 A69-22255

Temperature effect on pulsed laser action on electron transitions in diatomic molecules for rotational relaxation, discussing excitation mechanisms
09 p1520 A69-22654

Rotational excitation and scattering cross sections for rigid diatomic molecules reduced to yield distorted wave approximation, resulting in inelastic transition probabilities
10 p1726 A69-23524

Direct nonresonance excitation of rotational and vibrational states of diatomic molecular ions by electrons in Born-Coulomb approximation
10 p1726 A69-23627

Interstellar molecular hydrogen and CH photodissociation, discussing molecular formation rates in interstellar medium
10 p1781 A69-23672

Electrons resonance scattering by diatomic molecules from elastic and inelastic channel measurements in transmission
11 p1921 A69-24418

Translational-vibrational energy transfer value between atom and diatomic molecule determined using steric factor with repulsive interaction potential
12 p2134 A69-25988

Vibrational energy exchange between diatomic molecules by IR emission of CO fundamental behind shock waves
13 p2301 A69-27361

Dissociation equilibrium of diatomic molecules in solar atmosphere, comparing concentration above photosphere to MgH
14 p2528 A69-29963

Franck-Condon factors for band systems of molecular hydrogen, computing wave functions for vibrational levels using potential energy function, Part II
15 p2656 A69-31157

Diatom heavy particle collisions with emphasis on epithermal energy range, discussing elastic scattering and inelastic processes
16 p2815 A69-32259

Computer program to predict spectra from electronic transitions of diatomic molecules and atoms, noting line intensity distribution by Voigt profile
18 p3177 A69-35239

Forbidden transitions in diatomic molecules with nonzero spin and zero orbital angular momentum, stressing application in outer planets and M stars hydrogen spectra
19 p3421 A69-36213

Photodissociation of diatomic hydrogen by solar radiation for Venus atmosphere investigation, considering H atoms production rate by Stecher-Williams process
20 p3609 A69-38102

Coupled equations for determining cross sections for rotational transitions in CN induced by low energy electron impact
21 p3773 A69-38476

Diatom molecules rotational excitation calculated from electron molecule elastic scattering parameters in fixed nuclei approximation
21 p3775 A69-39665

High temperature pyrolysis of simple organic molecules in shock tube, considering diatomic C formation and decay rate
23 p4113 A69-41693

Positively charged diatomic hydrogen molecules in interstellar extinction and photodissociation cross section in terms of formation mechanisms
24 p4375 A69-42610

DIBORANE

Borane carbonyl pyrolysis in low pressure tubular flow reactor measured by mass spectrometry, noting wall collision role in diborane bond dissociation
14 p2410 A69-29282

Specific impulse deliverable performance of space storable propellant combination fluorine-oxygen/methane and oxygen difluoride/diborane [AIAA PAPER 69-505]
16 p2845 A69-32762

DICARBOXYLIC ACIDS

Normal, isoprenoid, dicarboxylic, keto and various aromatic acids isolated from controlled stepwise degradation of Green River kerogen by successive chromic acid oxidations
15 p2606 A69-31533

DICHLORODIPHENYLTRICHLOROETHANE

Fiddler crab absorption of DDT residues from organic detritus in estuaries, discussing DDT residue entrance into diverse food chains
14 p2406 A69-28872

DICHOTOMIES

Federal Government systems politics and budgeting, noting dichotomies, time dependence, taxonomy, etc
10 p1811 A69-23352

Dichotomy of Venus in eastern and western elongations, determining time of occurrence by graphical method
18 p3203 A69-35336

DICHOISM

Optical pumping in pure Si at 77 K, noting dichroism conditions for dipolar electric transitions in cubic crystal
19 p3389 A69-36548

DICHROMATES
U CHROMATES

DICKE RADIOMETERS

Performance characteristics of 300 GHz Dicke type superheterodyne radiometer receiver for measuring atmospheric attenuation of electromagnetic waves
02 p0209 A69-12336

Galactic H 2 regions radio observation using Cassegrain antenna and Dicke radiometer
06 p1008 A69-17696

Brans-Dicke scalar-tensor theory, showing radiative Riemann tensor existence in absence of usual spin-2 gravitational waves
07 p1216 A69-18894

DICTIONARIES

Geophysics international dictionary, Volume 1 /A-J/ covering seismology, geomagnetism, aeronomy, oceanography, geodesy, gravity, marine geophysics, meteorology, earth origin and evolution
19 p3303 A69-36511

Geophysics international dictionary, Volume 2 /K-Z/ covering seismology, geomagnetism, aeronomy, oceanography, geodesy, gravity, marine geophysics, meteorology, earth origin and evolution
19 p3304 A69-36512

DIELECTRIC MATERIALS
U DIELECTRICS

DIELECTRIC PERMEABILITY

Exciton spectrum for limiting case of large radius leading to Wannier-Mott equation with static dielectric permeability
03 p0486 A69-13416

Relative dielectric constant and permeability of inhomogeneously filled rectangular waveguide filling medium expanded into trigonometric series to calculate cut-off frequencies and field patterns
15 p2577 A69-30627

Magnetoplasma with Maxwellian velocity distribution, investigating quantitatively longitudinal dielectric function
22 p3988 A69-40066

DIELECTRIC POLARIZATION

Semiconductor nonlinear electron polarizability, using model to obtain correct order of magnitudes

03 p0483 A69-13035

Transparent dielectrics destruction by laser radiation noting stress development in medium

08 p1324 A69-19947

Rectangular waveguide with inhomogeneity represented by half space dielectric filling with boundary causing polarization, obtaining reflection elimination or minimization reflection

23 p4125 A69-42047

DIELECTRIC PROPERTIES

Phase constant of rectangular waveguide containing longitudinal dielectric slab of arbitrary cross section calculated using orthonormal waveguide functions with separated curl and potential fields

01 p0042 A69-10437

Dielectric constants of barium titanate single crystals as function of electric field intensity at different frequencies

01 p0139 A69-10889

Reflection elimination for single dielectric film on solid laser material substrate, calculating reflectance as function of frequency

02 p0256 A69-11926

Permittivity measurements by measuring impedance on thin cylinders in rectangular waveguide or in cavity formed by coaxial transmission line

02 p0222 A69-12756

Electromagnetic wave propagation in nonlinear media with permittivity dependent on modulus of magnetic field

03 p0396 A69-13707

Stray fields and domain dynamics in Gunn effect semiconductors covered with dielectric sheets

03 p0491 A69-13988

Radio waves diffraction around earth with atmospheric dielectric constant having linearly quadratic height dependence

03 p0399 A69-14130

Second dielectric virial coefficient of rare gases derived by cluster method

04 p0632 A69-14865

Permittivity and loss tangent of unsaturated styrene polyester copolymers at various temperatures and frequencies

[ONERA-TP-662]

04 p0621 A69-15114

Pulse radiation effect on dielectric constant of sintered CdS photoresistors, discussing capacitance dependence on intensity, type and frequency of light

05 p0806 A69-15694

Nonlinear optics, discussing frequency mixing, induced changes in dielectric constant and parametric amplification in microwave region of spectrum

05 p0772 A69-16229

Surface waveguide composed of inhomogeneous dielectric thin film used as low loss transmission line

05 p0731 A69-16294

Inhomogeneous dielectric filling to simulate curvature in model earth-ionosphere waveguide

05 p0732 A69-16346

Ultrasound propagation amplification coefficient in high permittivity semiconductors with electric field based electron-phonon interaction

05 p0809 A69-16372

Cut-off frequency relation to geometry for dielectric ridge waveguide

05 p0777 A69-16579

Electron plasma interaction with transverse EM wave propagating along magnetic field, calculating permittivity, density, field strength and applied frequency

05 p0805 A69-16699

Approximate method for wave equation with dielectric variation in propagation direction

06 p1030 A69-17116

Dielectric constant of liquid metals emphasizing Green function techniques for Wick theorem, Feynman diagrams, Dyson equation and diagrams in impulse space

07 p1196 A69-18298

Trivalent iron doped andalusite crystals dielectric and maser properties, investigating spin-lattice relaxation, cross relaxation times and inversion ratio

[IEEE PAPER C-2]

07 p1150 A69-19049

Lunar depth profiles of conductivity, dielectric constant and magnetic permeability from radar, radiothermic and magnetic measurements, discussing lunar models

07 p1216 A69-19221

Radome materials with superior dielectric and temperature characteristics for constructing high tolerance microwave multiband radome

07 p1109 A69-19514

Radome performance dependence on dielectric permittivity determined by digital program and simple design criterion

07 p1110 A69-19519

Statistical radomes design, analyzing dielectric constant and wall thickness tolerances effects on amplitude and phase of transmitted wave

07 p1111 A69-19531

Radome materials design and performance for guided weapons systems, describing research conducted in UK

07 p1112 A69-19540

Dielectric constant and loss angles measurement in Ku band used for onboard radars

07 p1112 A69-19544

Resonance conditions in dielectric sheathed or plug loaded phase arrays of waveguides

08 p1281 A69-20034

Temperature effect on phase stability and electrical length of braided coaxial cables, considering dielectric constant and mechanical length

08 p1283 A69-20225

Electromagnetic fields and magnetic and dielectric constants in fiberglass reinforced polymers determined by treating polymers as ideal dielectrics

08 p1336 A69-20336

Thin films of niobium oxide vapor-deposited on silicon and quartz substrates, discussing optical and dielectric measurements, dispersion and absorption coefficient

[ECS PAPER 17]

08 p1372 A69-20365

Radiation spectrum in nonrelativistic fully ionized gas in thermal equilibrium, obtaining dispersion relation for transverse electromagnetic waves and dielectric constant

08 p1357 A69-20748

Kinetic theory of electromagnetic wave propagation in infinite laminated plasma with different dielectrics, determining attenuation

09 p1550 A69-22023

Dielectric relaxation for analysis of defect structure, microstructure, surface behavior, structural changes kinetics and environmental effects in insulators and semiconductors

09 p1559 A69-22307

Micromin alumina substrates design data, determining dielectric constant, impedance vs line width and wavelength vs frequency

09 p1460 A69-22792

Polarized electromagnetic waves phase shift during total reflection from stratified dielectric region found dependent on transition zone width in addition to permittivity

10 p1657 A69-23862

Conductivity and permittivity for ion and electron resonance region of ionospheric plasma model calculated in quasi-hydrodynamic approximation

10 p1686 A69-23908

Attenuation losses on curved dielectric waveguide in X band

11 p1856 A69-25633

Surface dielectric constant and microwave opacity of Venus atmosphere as function of wavelength determined by radar observations

12 p2153 A69-25805

Dielectric properties of high loss nonmagnetic microwave materials used for waveguide absorbers and anechoic chamber linings

12 p2079 A69-26047

Dielectric loss tangents measurements combining coherent optical resonator with microwave techniques, noting application at mm wavelengths

12 p2080 A69-26057

Spatial dispersion of HF dielectric constant in semiconductor based on electron-hole pair production

12 p2145 A69-26723

Inhomogeneous permittivity and boundary effects influence on electric fields of laser with open cavity containing inhomogeneous active medium

12 p2110 A69-26908

Microwave propagation in coupled pairs of microstrip transmission lines for integrated circuit design, discussing dielectric Green function

13 p2229 A69-27672

Interacting carriers acoustoelectric waves in semiconductors with high dielectric constant, analyzing dispersion equation

13 p2317 A69-27878

Dielectric constant, loss and breakdown of electrical insulation materials, discussing atomic and molecular models and effects of polarizations, environment and manufacturing procedures

13 p2230 A69-27983

Dielectric properties measurement of plastics for electrical insulation, stressing techniques for complex dielectric constants in various frequency ranges

13 p2285 A69-27984

Polymeric insulation materials, discussing intrinsic properties dependence on temperature and atmosphere, stressing effect on aging

13 p2285 A69-27985

Polymer structure relationship to thermal, mechanical and chemical properties of electrical insulating materials

13 p2285 A69-27986

Resistivity, capacitance and dielectric loss measurements for diode reactive sputtering grown AlN films and film sandwich structures of Ta, Au and Al films

13 p2322 A69-28013

Transmission type E saki diode amplifier with stabilizing dielectric loaded rectangular waveguide

13 p2233 A69-28067

Relativistic electrons synchrotron radiation by calculating magnetoactive plasma permittivity tensor, determining normal waves polarization characteristics

13 p2315 A69-28451

Dielectric constants of nonconducting composite suspensions of spheres and parallel cylinders in terms of filler particles, matrix and volume fraction

13 p2287 A69-28677

Dielectric constant of liquid hydrogen and hydrogen-helium mixtures measured with resonance method

14 p2487 A69-29668

Relative dielectric constant and permeability of inhomogeneously filled rectangular waveguide filling medium expanded into trigonometric series to calculate cut-off frequencies and field patterns

15 p2577 A69-30627

Lunar radio emission linear polarization radial dependence at 0.8-cm wavelength using radio telescope, determining dielectric constant of emitting layer

15 p2697 A69-31251

Equivalent dielectric tensor for warm drifting electron plasma using model

16 p2820 A69-31701

Normal modes of electrons-electromagnetic field coupled system for many valley semiconductors, calculating dielectric constant for electron gas for ellipsoidal energy surfaces

16 p2826 A69-31821

Photodielectric tape camera with optical images stored on tape in form of charge pattern

16 p2792 A69-32558

Dielectric breakdown thresholds and cavitation in organic liquids observed during Q switched and pulsed ruby radiation

17 p2979 A69-32826

Faraday effect and permittivity of hydrogen plasma measured simultaneously, determining electron density and collision frequency

17 p2919 A69-33394

Asymptotic solutions for vector fields and propagation constants of axial modes in circular cylindrical waveguides, noting changes in dielectric constant

17 p2921 A69-33673

Superconducting cavities for resolving optically induced changes in dielectric constant of CdS at 4.2 K

17 p3016 A69-33782

Thin metal antenna average current and effective impedance in randomly inhomogeneous medium, discussing cases of strong and weak permittivity fluctuations

17 p2927 A69-33858

Dielectric constants of barium titanate single crystals as function of electric field intensity at different frequencies

18 p3182 A69-34720

Plane light wave propagation in homogeneous isotropic medium with fluctuating dielectric constant using perturbation theory and integrating energy conservation law

18 p3173 A69-35127

Ablation heat shields, emphasizing dielectric low cost fabrication and application to entry vehicles

19 p3318 A69-35538

Dielectric response of semiinfinite metal surface to external point charge in linearized Fermi-Thomas approximation, discussing potential in metal and vacuum

20 p3583 A69-37498

Dielectric recombination in plasma, considering role in populating highly excited levels

20 p3580 A69-38016

Transient effects of nuclear radiation bursts on dielectric properties of refractory low loss ceramics at L, S and X bands

20 p3584 A69-38065

Free space to dielectric waveguide millimeter wavelength ratio as function of frequency, discussing equipment and procedure
21 p3674 A69-39130

Spatial dispersion of HF dielectric constant in semiconductor based on electron-hole pair production
21 p3781 A69-39136

Dispersion relations for surface plasma oscillations in normal metals for single and multiple films taking into account retardation effects, noting dielectric function
22 p3992 A69-40419

Airborne electromagnetic systems measuring complex dielectric constant in earth crust for mineral and water resources exploration
[RAES PAPER 8]
22 p3946 A69-40481

Electrical conductivity of uppermost lunar surface layers, indicating dry powdered rocks with frequency independent dielectric loss tangent
22 p4023 A69-40570

Saturated liquid oxygen dielectric constant measurements to calculate polarizability
[NAS-NRC PAPER D-3]
22 p3998 A69-40620

Natural frequencies of N open dielectric waveguides system, obtaining fields expressions and dispersion equation for propagation constants
22 p3901 A69-40954

Dielectric constant and IR spectra of Ba titanate single crystals doped with hydroxyl, showing dependence on temperature and crystal thickness
22 p3995 A69-41157

Waveguide-resonance investigation of temperature dependence of dielectric constant and paraelectric dispersion of Ba and Sr titanate single crystals at millimeter wavelengths
22 p3995 A69-41158

Phase diagram, dielectric and magnetic properties of Bi manganate/Pb titanate solid solutions of perovskite structure, showing dependence on composition and temperature
22 p3996 A69-41163

Dielectric polarization of barium titanate and barium strontium titanate in pulsed fields in paraelectric phase, analyzing coefficient B in free energy function and equilibrium state
22 p3996 A69-41165

Electric properties and domain structure changes of polycrystalline Ba titanate and other ferroelectrics characterized by high dielectric nonlinearity
22 p3996 A69-41166

Polycrystalline ferroelectrics dielectric dispersion region in decimeter-centimeter wavelength range using waveguide resonance method employing wideband strip line
22 p3997 A69-41167

Plasma dielectric constant and RF wave energy and power absorption in anomalous dispersion region, noting plasma permittivity inverse relation to absorption band frequency
23 p4195 A69-41385

Variational principle for analyzing dispersion properties of closed regular waveguide with traveling wave-modulated dielectric constant
23 p4123 A69-41943

Dielectric materials permittivity determined by measuring amplitude ratios of reflected and transmitted plane electromagnetic waves
23 p4123 A69-41950

Guiding center Vlasov equation derived dielectric tensor of collisionless plasma, obtaining dispersion relation of Alfvén waves in warm plasma
23 p4197 A69-42416

Teflon dielectric properties evaluated during fast laser beam heating, noting presence of C by microwave measurement
24 p4336 A69-43266

Measurement technique using dielectric waveguides for studying microwave fields influence on and energy imparted to body tissue
24 p4279 A69-43705

DIELECTRICS

NT RADOME MATERIALS

Dielectric surface coatings effect on transmission and loss properties of silicon-microstrip microwave transmission lines
01 p0041 A69-10201

First normal modes characteristics and lateral wave in weak dielectric layer applicable to microwave propagation
01 p0033 A69-10975

Thermodielectric radiometer for transient radiant flux short duration pulse measurement, using thermally induced depolarization of polymer film dielectric
[AIAA PAPER 68-403]
02 p0250 A69-12392

Silicon dioxide dielectric isolation for high speed low power circuits, noting saturation resistance and transient characteristics
02 p0221 A69-12470

Charge accumulation elimination on dielectric electrodynamic channel walls, comparing resistive wall channel to high internal impedance generator
02 p0291 A69-12506

Dielectric dispersion in inhomogeneous dielectrics and semiconductors, discussing three layered equivalent circuit
02 p0301 A69-12837

Mode theory of backscattered radar cross section of elongated dielectric bodies capable of sustaining traveling wave
03 p0384 A69-12907

Radar cross section enhancement effect of corner reflectors, multiple reflectors and dielectric lenses
03 p0384 A69-12909

Cathode sputtering and thermal evaporation in vacuum used for preparing thin dielectric coatings on mirrors of optical resonators containing nonlinear crystals
03 p0438 A69-13049

Diffusion in conduction process in dielectric fluids, discussing space charge limited current-voltage characteristics
03 p0415 A69-13140

Electric or magnetic dipole antenna radiated electromagnetic field for antenna orientation perpendicular to striations of periodically stratified dielectric medium
03 p0398 A69-13802

Strain effects on transverse electromagnetic modes of anisotropic dielectric waveguides at p-n junctions
03 p0406 A69-13830

Stationary, moving and pulsating electrohydrodynamic flow between parallel dielectric plates and Couette flow, noting reaction concentration near wall
03 p0419 A69-13919

Electrodynamic generator for direct conversion of moving dielectric medium potential or thermal energy to electric power
03 p0369 A69-14153

Circuit properties of microwave dielectric resonators, discussing mode identification, resonant frequencies, coupling control, loaded Q, frequency tuning and periodic arrays
04 p0575 A69-14750

Rear gain control of dielectric rod antenna in airborne Doppler system with choke at feed point
04 p0576 A69-14770

Dielectric waveguide propagation, impedance and attenuation characteristics and insertion loss and launching efficiency of mode transducer
04 p0577 A69-14971

Shock wave produced polarization effects in dielectrics, noting reflected shock waves and experimental results for polymethyl methacrylate and carbon tetrachloride
04 p0589 A69-14988

Surface wave stability for horizontal layer of incompressible dielectric fluid in electric field, noting viscosity effect
04 p0638 A69-15193

Dielectric sheath effect on far zone radiation characteristics of aperture bounded by perfectly conducting ground plane
04 p0579 A69-15450

Characteristic waves in gas-dielectric beamguides, calculating attenuation dependence on frequency
05 p0736 A69-16783

Glow discharge technique for dielectric layer deposition between metal interconnection patterns in multilayer integrated circuits, noting adhesion and feedthrough problems
06 p0931 A69-17201

Deviation of dispersion equations for all modes existing in E-plane slabs of dielectrically loaded rectangular waveguides
06 p0888 A69-17486

Homogeneous fused silica and quartz reinforced resins as dielectric materials for reentry vehicle antenna windows
07 p1090 A69-18400

C band waveguide window for average power transmission featuring relatively small biconcave dielectric disk
07 p1096 A69-18435

Dielectrics refill and decal air isolation for silicon integrated circuit components
07 p1100 A69-18618

Specialization of field equations and boundary conditions of elastic dielectric for special case of rigid dielectric, using Lagrange multipliers
07 p1200 A69-19174

Argon plasma characteristics calculated from 8 mm interferometer data, interpreting transmission coefficients of dielectric film with permittivity gradient
07 p1194 A69-19324

Complex transmission and reflection coefficients of dielectric film with permittivity gradient computed by modified Runga-Kutta method, noting plasma diagnostics application
07 p1194 A69-19334

Glass/resin laminates behavior at high temperature
07 p1136 A69-19515

Phase shift and losses in wave propagation in dielectric environment, defining power transmission coefficient and insertion phase shift
07 p1087 A69-19518

Aberration of dielectric patches and rings attached to radome surface described by insertion phase
07 p1111 A69-19530

Radome axis error due to phase /dielectrics/ and metallic obstacles
07 p1112 A69-19542

Dielectric surface loading on GaAs for suppressing traveling high field domain mode oscillations
08 p1371 A69-19911

Mode designation and propagation characteristics of dielectric tube waveguide, noting practicability at higher microwave frequencies
08 p1284 A69-20296

Population inversion in semiconductors obtained by applying electric field through dielectric sphere /field effect/
08 p1374 A69-21082

Fluctuation voltage mean square value at polar dielectric capacitor terminals determined by applying stochastic properties of Poisson point processes to statistical model
08 p1295 A69-21151

Frequency shift and Q change of microwave cavity caused by lossy dielectrics and plasmas, examining perturbing volume requirements for conductor behavior
09 p1544 A69-21323

Magnetic field plane radiation patterns for tapered dielectric rod antennas computed by Schelkunoff principle, noting taper angle effect on lobes
09 p1464 A69-22097

Cut-off coupled microwave bandpass filters for use in dielectric filled waveguide systems
09 p1466 A69-22447

Ruby laser emission absorption in transparent dielectrics, noting crack formation and propagation producing opacity
09 p1520 A69-22655

FET memory element charge storage two layer model for thin film dielectrics noting charge/discharge times
10 p1742 A69-22947

Long and short duration pulses interactions with nonlinear dielectric, calculating frequency variations and spectral transformations
10 p1658 A69-23953

Electromagnetic wave propagation along longitudinally magnetized plasma column surrounded by isotropic dielectric medium, without making quasi-static assumption
10 p1658 A69-24061

Radio wave field distortions by dielectric prisms in lens waveguides, discussing beam transformation, noting both geometrical optics effects and diffraction role
11 p1833 A69-24436

Air gap tolerances effect on admittance of TEM mode dielectric and plasma coated slot antennas determined by variational method
11 p1851 A69-24986

TEM-DUAL surface wave propagation in coaxial cable with stratified dielectric structure to reduce attenuation calculated by addition theorem to Bessel functions
11 p1856 A69-25659

Transformation of longitudinal plasma wave into electromagnetic wave during collision with dielectric in plasma
11 p1934 A69-25708

Radiation pattern of circular cylindrical dielectric rod antenna excited in mixed magnetic and electric modes, discussing mode transducer
12 p2035 A69-25900

Short circuit and variable frequency technique for measurement of coupling efficiency between dielectric loaded rectangular and trough waveguides, noting propagation modes
12 p2039 A69-26374

Perturbation analysis in dielectric loaded rectangular waveguides, considering scattered modes and phase progression 12 p2039 A69-26381

Dielectric coated finite cylindrical antennas, using numerical and Wiener-Hopf methods to obtain input admittance and current distribution 12 p2041 A69-26604

Aircraft engine spark plugs development, reviewing ceramic and mica insulated plugs and four pole electrode spark plugs 13 p2324 A69-27333

Velocity profiles of MHD flow through electrically insulated circular channel in transverse magnetic field 13 p2307 A69-27501

Optical surface wave propagation on thin dielectric film waveguides, noting applications to integrated optical data processors 13 p2229 A69-27676

Dielectric thin film electrical and mechanical properties and preparation for semiconductor devices, emphasizing Si compounds 13 p2286 A69-28004

Prebreakdown and breakdown electrical properties of thin film capacitors with certain oxides, fluorides and Teflon dielectrics 13 p2322 A69-28012

Wave propagation and bandwidth characteristics of rectangular waveguide loaded with H plane lossless dielectric slab 13 p2222 A69-28075

Dispersion and coupling impedance of logarithmic spiral resting on anisotropic magnetodielectric layer for microwave devices design 13 p2235 A69-28512

Gas laser design utilizing internal window mirrors deposited with dielectric coating outside resonator 14 p2457 A69-29160

Coupled mode theory for surface wave propagation along tapered cylindrical dielectric rod, considering radiation field effects 14 p2422 A69-29557

Adapter between dielectrically loaded waveguides with different cut-off frequencies and sizes for pulse compression systems 14 p2423 A69-29760

Plasma microwave measurement error allowance for multiple reflection of waves from vacuum chambers dielectric walls 14 p2498 A69-29806

Equivalent circuits of dielectric loaded and unloaded rectangular waveguide Esaki diode reflection amplifier 15 p2578 A69-30801

MIS devices with dielectric properties avoiding positive space charge formation, discussing radiation effect 15 p2625 A69-30829

Propagation modes attenuation and guidance on circular hollow dielectric waveguides dependent on dielectric loss tangent 16 p2757 A69-31587

Deformation of amplitude and frequency envelopes of plane modulated electromagnetic waves with dispersion in isotropic dielectric with cubic nonlinearity 17 p2928 A69-33869

Integral equation method for electromagnetic scattering by perfectly conducting obstacles modified for volume scattering regions involving disparities in dielectric constant, permeability or conductivity 17 p2930 A69-33890

Electromagnetic field formulation of eigenvalue problem for optical coaxial dielectric waveguide, using computer root searching method 17 p2930 A69-33892

Reflection coefficient of symmetric parallel plate waveguide operating in TEM mode illuminating lossless dielectric layer, using wedge diffraction and geometrical optics methods 18 p3108 A69-34802

Plane wave scattering by semiinfinite turbulent dielectric slab, using Born approximation to develop asymptotic series for stochastic components of forward scattered field [OSA PAPER WH-16] 18 p3174 A69-35245

Plane electromagnetic wave interaction with moving conductive dielectric medium to obtain reflection and transmission coefficients, noting energy transfer 18 p3105 A69-35486

Transfer molded epoxy dielectrics, comparing encapsulation rate, pressure and cure times to compression molding 19 p3281 A69-35548

Interference filter design for IR devices on Fresnel equation basis, analyzing plane electromagnetic wave propagation through stratified dielectric multilayer 19 p3373 A69-36053

Second harmonic radiation generation in nonlinear dielectric by broadband short pulse optical signals 19 p3278 A69-36693

Turbulent boundary layer of conducting fluids on dielectric plate in transverse magnetic field in presence and absence of pressure gradient 20 p3513 A69-37092

Field patterns, propagation constants and losses determined for axially propagating modes guided by circular cylindrical inhomogeneous dielectric, using perturbation method 20 p3497 A69-38130

Radiation field of tapered dielectric rod antenna by Schelkunoff equivalence principle, investigating input impedance variation with axial length and taper angle 21 p3681 A69-38444

Atomic sources local multipolar field in anisotropic dielectrics determined from magnetic dipole radiation spatial distribution measurements 21 p3779 A69-38531

Electromagnetic waves attenuation and field structure within gas filled dielectric waveguide tube, tube walls and waveguide surroundings 21 p3674 A69-39123

Multiquantum photoemissive effect in metals, semiconductors and dielectrics emphasizing laser application for studying electromagnetic field 22 p3964 A69-40690

Resonance frequency behavior of waveguide cavity with evanescent air gap symmetrically loaded with dielectric 22 p3900 A69-40925

Electromagnetic propagation in infinite rectangular waveguide surrounded by dielectric medium described by Green dyadic 23 p4115 A69-41570

Waveguide fed rectangular aperture antenna with dielectric plug load, describing admittance resonant perturbation due to excited TE mode 23 p4136 A69-41589

Dielectric materials permittivity determined by measuring amplitude ratios of reflected and transmitted plane electromagnetic waves 23 p4123 A69-41950

Thermal radiation diffraction of dielectric cylinder /cold plasma model/ containing N plus one layers with arbitrary temperatures and permittivities 23 p4123 A69-42028

Fiber optics interferometers, analyzing light propagation along dielectric light pipes and wave interference 24 p4315 A69-43162

Ruby laser second harmonic generation statistical characteristics with dielectric surface scatterer, showing variety of modes and high cross sectional stability 24 p4328 A69-43164

Transmission properties and directional coupler determined for optical circuit dielectric rectangular waveguide with surrounding dielectrics of smaller refractivity 24 p4287 A69-43328

Light transmission through curved dielectric rectangular rod, studying optical waveguides of various cross sectional dimensions and radii of curvature 24 p4287 A69-43329

Rectangular dielectric waveguide propagation modes, describing computer analysis based on electromagnetic field expansion in circular harmonics series terms 24 p4288 A69-43330

Dielectric and semiconductor films vacuum deposition by CW carbon dioxide laser, discussing optical properties 24 p4329 A69-43755

DIENCEPHALON

Aminazine and adrenaline effects on adrenocortical function in patients with diencephalic syndrome 22 p3888 A69-41272

DIENES

NT BUTADIENE

Vibration and absorption bands in IR spectra of diborene hydrazine stabilized by boiling in benzene 12 p2027 A69-26917

DIES

Large hydraulic press forgings for light metals, discussing 50,000 ton machine used for Al alloys, tooling and die considerations [ASM PAPER C7-5.1] 04 p0604 A69-14521

Closed die development for forging very large and complex parts to meet needs of high Mach aircraft 04 p0604 A69-14523

Extrusion processes used for aluminum, magnesium and titanium extrusions, presenting die configurations 04 p0604 A69-14526

Interface friction and adhesion of alloys workpieces and die materials under pressure and temperatures typical of plastic deformation 15 p2629 A69-30902

Ti structural components for forgings, noting problems facing die-forging industry and machining equipment 21 p3728 A69-38459

DIETS

Rats on casein, soybean and Chlorella diets for protein source noting soybean diet produced no appreciable changes in intestinal flora 02 p0197 A69-11490

Nutritive value of protein from discolored algae biomasses on groups of rats kept on algae biomass, casein and soybean diets 02 p0198 A69-11510

Protein contained purine free basal and yeast ribonucleic acid diets effect on plasma and urinary uric acid production in male subjects 05 p0708 A69-15968

Protein free diets effects on rat intestinal microflora, noting decrease in lactic acid bacteria and increase in spore forming bacteria 05 p0709 A69-16516

Algae diet more effective than soya-protein diet in recovering metabolic processes in protein deficient white rats 07 p1065 A69-18977

In vivo hemolytic susceptibility to hyperoxia in mice deficient in tocopherol 07 p1066 A69-19422

Psychological, physiological and biochemical responses to controlled diets, determining regional and total body sweat composition of men working in temperate environment 10 p1644 A69-23314

Vegetable diet including 210 g of dry Chlorella biomass decreases effect on calcium and magnesium assimilation to produce insignificant negative balance of K and Mn 10 p1647 A69-23590

Human intolerance to bacteria as food, considering response to Hydrogenomonas eutropha and Aerobacter aerogenes 13 p2213 A69-27265

Sweet potatoes productivity and nutritive value as carbohydrates source in manned spaceflights 13 p2216 A69-28619

Prolonged dehydrated food diet effect on metabolism of humans, noting complete adaptation after three or four months 13 p2212 A69-28624

Food intake changes of female rats in response to changes in energy balance, discussing steroids as physiological tracer 15 p2555 A69-30693

White rats diet containing alcohol-soluble fraction of Chlorella and Scenedesmus biomass, noting changes in adrenal cortex and renal glomerus 17 p2906 A69-32930

Protein free diets effects on rat intestinal microflora, noting decrease in lactic acid bacteria and increase in spore forming bacteria 18 p3096 A69-34735

Algae soil-protein diet more effective in recovering metabolic processes in protein deficient white rats 20 p3479 A69-38225

Exercise effects on hepatic cholesterol of rats on diets high in saturated or unsaturated fats 21 p3653 A69-38903

Glider pilots fatigue attributed to nutritional habits 23 p4106 A69-41796

DIFFERENCE EQUATIONS

Optimal control problems for Markov chains solved by iterative method, using nonlinear finite difference equations to approximate degenerate elliptic functions 02 p0224 A69-11963

Difference schemes for heat conduction analog simulation on electric integrators 03 p0410 A69-13300

Finite difference method for symmetric positive linear differential equations, discussing methods to solve finite difference equations generated 03 p0455 A69-13370

Difference schemes to solve Navier-Stokes equations for viscous incompressible fluid by substituting fourth order partial differential equation 03 p0415 A69-13650

Problem of viscous supersonic flow past blunt bodies based on Navier-Stokes equations formulated and solved numerically with explicit difference scheme 03 p0363 A69-13653

Eigenvalues for Orr-Sommerfeld equation by difference technique for Reynolds number range 5780-729000, determining Poiseuille flow stability in plane channel

03 p0416 A69-13654

Nonlinear oscillatory systems with constant delay under random forces action, noting use of stochastic difference-differential equations

03 p0468 A69-13866

Asymptotic solutions of linear difference equations, discussing applications to eigenvalue problems of free oscillations of model galaxies

04 p0623 A69-14946

Differential-difference equations and nonlinear initial boundary value problems for linear hyperbolic partial differential equations, noting procedure based on method of characteristics

04 p0623 A69-14949

Asymptotic oscillation results for solutions to first order nonlinear difference-difference equations, obtaining existence-uniqueness theorems

04 p0624 A69-14950

Difference equation for two dimensional elastic flow

04 p0681 A69-15286

Discrete ordinate difference equations of radiative transfer for slab using invariant method, noting storage and computing time advantages

07 p1183 A69-19623

Stability and perturbation theory of abstract Cauchy problem with difference scheme, showing application to parabolic differential equations

08 p1343 A69-20537

Difference schemes for approximating boundary value problems of elliptic equation free of mixed derivatives in rectangular region

09 p1532 A69-21788

Nonlinear second order elliptic difference equations in associated variational problems, considering differentiable solution of Dirichlet problem

10 p1718 A69-22879

Numerical solution for three dimensional boundary layers based on stability determinations for linearized difference equations

10 p1631 A69-22902

Scheme for choosing approximating system of difference equations for degenerate linear and nonlinear elliptic boundary value problems

10 p1719 A69-23515

Stable difference expressions for initial and mixed boundary value problems

10 p1720 A69-23594

Diffusion-stabilized difference schemes for inviscid compressible flow equations in conservation form for arbitrary number of space dimensions

12 p2062 A69-26624

Linear difference equations with exponential coefficients for numerical methods of integrating differential equations

13 p2288 A69-27526

Higher order difference method for equilibrium and eigenvalue problems of two dimensional structures using iterative solution

13 p2365 A69-28239

Variational difference method application to second order elliptic equations with inhomogeneous boundary conditions, applying results to boundary value problems in elasticity theory

13 p2289 A69-28318

Difference schemes for elasticity theory plane dynamic problem with mixed boundary conditions, establishing scheme absolute stability

14 p2536 A69-29474

Difference schemes for quasi-linear hyperbolic equations, with applications to three dimensional supersonic flow past bodies

14 p2430 A69-29475

Iterative solution for difference equations approximating displacement vector determination problem in theory of elasticity, investigating algorithm convergence

14 p2536 A69-29479

Modeling nonstationary random processes using linear time-invariant difference equation, with applications to Kalman filtering and gyro drift

14 p2479 A69-29486

Trajectory differential equations in state- variable form, presenting compatible difference equation adjoint scheme for trajectory integration

15 p2645 A69-31236

Iteration process by difference scheme for numerical solution to Dirichlet problem of two dimensional Poisson equation

18 p3164 A69-34701

Single parameter family of two layer difference schemes with decomposing operators for general linear second order parabolic equations with mixed derivatives and variable coefficients

18 p3164 A69-34702

Cauchy problem for homogeneous linear difference scheme with constant complex coefficients, giving stability lemmas

18 p3165 A69-35049

Difference method for parabolic differential equations solution for Rayleigh boundary layer in dissociating gas, using integral estimates to determine stability

18 p3124 A69-35295

Boundary conditions of incompressible fluid viscous flow on semiinfinite plate edge defined using difference methods for Navier-Stokes equations

19 p3299 A69-36394

Autonomous functional differential equations with finite time interval dependent derivatives, resulting in periodicity theorem applicable to difference equations

19 p3361 A69-36600

Approximation error involved in difference optimal control problem substitution for differential optimal control problem based on functional minimization

20 p3509 A69-36989

Difference method for initial value problems in quasi-linear hyperbolic first order approximations extended to wider quasi-linear problems, assessing convergence

20 p3568 A69-37833

Difference method for solving multidimensional differential equations of higher orders

20 p3568 A69-38074

Partial difference methods from parabolic, elliptic and hyperbolic equations solved by splittings of locally one dimensional nature

21 p3754 A69-38745

Thermal buckling of skew plates clamped along all edges under radiant heating, measuring various characteristics, solving differential equations by difference method

22 p4044 A69-40599

Integro-interpolation difference schemes for gas dynamic equations system satisfying laws of mass, momentum, energy conservation and energy balance

23 p4151 A69-41527

Wrong boundary conditions influence decay in overdetermined difference approximations to hyperbolic partial differential equation

24 p4340 A69-43227

DIFFERENTIAL ALGEBRA U MATRICES [MATHEMATICS]

DIFFERENTIAL AMPLIFIERS

Alternative balancing technique utilizing linear combination of two equal and opposite drift characteristics to minimize drift in integrated differential amplifiers

07 p1102 A69-18874

Signal conditioning amplifiers covering carrier and DC amplifiers, differential amplifiers, charge amplifiers and active filters

10 p1691 A69-23230

Magnetograph in Italian observatory for weak solar magnetic field longitudinal components avoiding differential amplifier by electronic compensation

10 p1693 A69-23311

Jet fluidic differential amplifier transfer function determination, describing interconnection dynamics

11 p1824 A69-24350

Circuit designs using differential amplifier devices or operational amplifier integrated circuits

11 p1857 A69-25664

DIFFERENTIAL ANALYZERS U ANALOG COMPUTERS

DIFFERENTIAL CALCULUS

Differentiability of fundamental solution to elliptic equations based on exact theorems of smoothness

01 p1016 A69-10955

Numerical differentiation formulas for coefficients of given characteristic function, using tabulated Stirling numbers

02 p0271 A69-11653

Infinite system of first order integral equations derived from Prandtl boundary layer equation and continuity equation

02 p0231 A69-12059

Bilinear covariant of linear differential form involving 2n independent variables used for grouping to achieve symplectic and contact transformations

16 p2804 A69-31623

DIFFERENTIAL EQUATIONS NT BIHARMONIC EQUATIONS

NT BLASIUS EQUATION

NT BURGER EQUATION

NT DUFFING DIFFERENTIAL EQUATION

ELLIPTIC DIFFERENTIAL EQUATIONS

NT FALKNER-SKAN EQUATION

NT FOKKER-PLANCK EQUATION

NT GAUSS EQUATION

NT HELMHOLTZ VORTICITY EQUATION

NT LAME WAVE EQUATIONS

NT LIOUVILLE EQUATIONS

NT PARABOLIC DIFFERENTIAL EQUATIONS

NT PARTIAL DIFFERENTIAL EQUATIONS

NT POISSON EQUATION

NT VLASOV EQUATIONS

NT VORTICITY EQUATIONS

Bounds from asymptotic behavior of solutions of nonlinear integrodifferential equation arising from nonlinear oscillators in acoustics

01 p1013 A69-10001

Sobolev first embedding theorem providing relationship between global and local properties of functions in theory of differential equations

01 p1013 A69-10005

LCL /Liapunov, Cetaev and LaSalle/ functions for autonomous systems of second order extended to more general differential equation systems

01 p1013 A69-10007

Continuous wave solid state lasers active elements temperature fields calculated by differential equations

01 p0089 A69-10105

Linear ordinary differential equations with exponential coefficients, giving solutions asymptotic behavior for large values of independent variable

01 p1013 A69-10231

Nonlinear time dependent parameters systems, analyzing governing differential equations in terms of elliptic functions

01 p0050 A69-10237

Injection locked oscillator FM receiver consisting of linear mixer and negative resistance oscillator in phase locked configuration, solving receiver output differential equation

01 p0042 A69-10247

Second order systems of linear differential equations eliminating all nonessential difficulties associated with initial value problem

01 p1014 A69-10316

Bending of micropolar plates using differential equations, considering transverse displacement and microrotation vector

01 p1017 A69-10324

N-body problem in celestial mechanics, using differential equations, reduced to quadratures [UN PAPER 68-95268]

01 p0150 A69-10476

Optimal control system sensitivity definitions, analysis methods and design techniques, discussing equations of motion of dynamical system satisfying vector differential equation

01 p0051 A69-10553

Wave scattering in nonuniform cross section waveguides with large flare angles using coupled differential equations

01 p0044 A69-10622

Cauchy problem correctness for one dimensional hyperbolic equation of arbitrary order with data on degeneracy line

01 p1014 A69-10699

Algorithms for linear system of first order differential equations, emphasizing equations associated with computer oriented circuit design

01 p0036 A69-10708

Finite difference method for boundary value problem for second order differential equation, demonstrating convergence

01 p1015 A69-10721

Two dimensional ionized plasma flow in coaxial channels calculated using differential equations

01 p0130 A69-10723

Monte Carlo method accuracy improvement for calculating probability characteristics of nonlinear ordinary differential equations, describing nonlinear automatic control

01 p1015 A69-10730

Comparative analysis of variable structure adaptive systems and time optimal system for control of plant described by differential equation

01 p0052 A69-10795

Dynamic system for self adaptive control of inertial plant described by differential equations, noting synthesis method eliminates distortion

01 p0052 A69-10797

Determination of plant differential equation from time characteristics

01 p0053 A69-10804

General predictor-corrector method for system of m ordinary first order differential equations proved stable if Hermitian forms with coefficients are positive definite

01 p1015 A69-10807

Theory of generalized multistep methods, using off-grid point extended to special second order differential equation, applied to unperturbed orbit trajectory
01 p0153 A69-10808

Single frequency oscillations in stochastic quasilinear differential equations with delay
01 p0170 A69-10825

Multidimensional nonlinear plants adaptive control by direct integration, identifying differential equations coefficients
01 p0053 A69-10875

Reduction principle for study of linear differential equations stability
01 p0106 A69-10956

Soviet book on linear differential equations in Banach space covering equations with unrestricted operators, continuous semigroups, partial differential equations and asymptotic methods
01 p0106 A69-10996

Necessary and sufficient stability conditions for differential equation systems with selfadjoint quasiperiodic coefficients
01 p0107 A69-11130

Differential equations for dynamical problems in plates obtained by symbolic approach involving power series substitution into linear elasticity dynamical equations
01 p0172 A69-11282

Keplerian motion parameters second derivatives determined from initial conditions by deriving differential equations
01 p0107 A69-11305

Stable high order implicit methods to solve numerically differential equation systems with matrix coefficients used for heat conduction equation
01 p0107 A69-11364

N dimensional extensions of finite difference scheme for solution of differential heat conduction equation, noting practical limit by truncation error considerations
01 p0107 A69-11365

Boundedness theorem for all solutions of class of nonlinear second order differential equations
02 p0271 A69-11549

Iterative process for determining periodic solutions of nonlinear nonautonomous periodic differential equations without weak nonlinearity hypothesis applied to nonlinear synchronization
02 p0271 A69-11550

Cosmic ray propagation in interplanetary space taking into account reverse effect on solar wind, deriving integrodifferential equation
02 p0306 A69-11657

Numerical calculations for oscillatory solutions of system of nonlinear differential equations, noting circularly polarized magnetic oscillations observed near earth bow shock front
02 p0241 A69-11729

Periodic cubic differential equation of motion solved with special reference to location of fixed points and stability of solutions
02 p0280 A69-11816

Linear integrodifferential motion equations for turbulent flow within Heisenberg statistical turbulence theory
02 p0230 A69-11869

Convergence of Multihopp collocation method for numerical solution of linear singular integrodifferential equation, noting use in airfoil, propeller and elasticity theory
02 p0271 A69-12056

Eigenvalue problem solutions for ordinary differential equations, discussing coefficient replacement, Ritz polynomial substitution and error limits
02 p0271 A69-12057

Existence theorems for solutions to second order ordinary differential equations
02 p0272 A69-12129

Electromagnetic wave propagation problems, using asymptotic solutions of differential and integral equations in domains containing transition points
02 p0208 A69-12130

Bifurcation of closed orbits from equilibrium points of autonomous differential system
02 p0281 A69-12133

Monograph of lectures on numerical solutions of linear, singular and nonlinear differential equations for boundary value problems using finite differences
02 p0272 A69-12157

Approximate solution of linear functional, singular integral and integrodifferential equations by general theory of approximate methods
02 p0272 A69-12163

Grobner formulas for numerical analysis of differential equations, discussing applications to orbit computations in celestial mechanics
02 p0322 A69-12250

Numerical integration stability of differential equations, noting limiting integration step size for unsteady distillation
02 p0273 A69-12478

Motion stability of two tethered unsymmetrical earth pointing bodies in circular orbit, presenting nine degrees of freedom differential equations of motions
02 p0324 A69-12507

Nonlinear first order equations solution by reduction method, using nonlinear transformation of dependent variable, noting two axis gyro drift
02 p0273 A69-12541

Stress state of circular cylindrical shell subjected to uniform inward radial line load along generator solved by closed form particular integral, discussing convergence
02 p0349 A69-12797

Lie algebra of second order linear differential equations
02 p0273 A69-12841

Statistical analysis of unsteady dynamic systems describable by unstable differential equations containing random parameters
03 p0408 A69-12948

Differential equations of motion for holonomic system of points with variable mass
03 p0465 A69-12965

Linear differential equations zero solution stabilization by control formed as linear combination of measured coordinates of object
03 p0408 A69-12972

Mathematical basis for designing controllers of time lag systems by approximately solving differential equations
03 p0408 A69-12973

Integral prediction method for arbitrary continuous function on right hand side of nonhomogeneous linear differential equation with constant coefficients
03 p0455 A69-13022

Zero solution asymptotic stability for linear differential equations with continuous functions
03 p0465 A69-13129

Bounded solutions for systems of ordinary second order differential equations
03 p0455 A69-13257

Finite difference method for symmetric positive linear differential equations, discussing methods to solve finite difference equations generated
03 p0455 A69-13370

Role of second order internal resonance in problem of stability of equilibrium of system neutral in linear approximation
03 p0466 A69-13404

Bergman integral operator to solve second order differential equations with two independent variables
03 p0527 A69-13742

Single and double resonance in system of coupled nonlinear differential equations describing vibration phenomena in mechanical and similar systems
03 p0527 A69-13748

Nonlinear oscillatory systems with constant delay under random forces action, noting use of stochastic difference-differential equations
03 p0468 A69-13866

Linear differential equation theory corresponding to metric theory of dynamic systems, proving theorems with results of qualitative theory of differential equations
04 p0621 A69-14358

Ordinary nonlinear differential equations with linear boundary conditions, discussing formulation and proof of lemma and theorems to demonstrate existence
04 p0621 A69-14416

Generalized Riemann-Liouville fractional integrodifferential operator and application to representation of analytic and harmonic functions inside circle
04 p0622 A69-14512

Book on qualitative theory of sampled data systems
04 p0630 A69-14563

Comparison and oscillation theory of linear differential equations, discussing zeros of solutions and Sturm type theorems
04 p0622 A69-14598

Book on nonlinear ordinary differential equations in transport processes, noting iterative and numerical methods for diffusion, conduction, fluid mechanics and chemical kinetics
04 p0622 A69-14599

Book on nonlinear boundary value problems for ordinary second order differential equations, illustrating

difference between linear and nonlinear problems concerning existence and uniqueness
04 p0622 A69-14600

First-kind operator equation solution by reduction to dual extremum problem, proving existence and convergence
04 p0622 A69-14622

One-dimensional self similar motion of relaxing gas, noting ODEs of process and gas dynamic parameters of flow field
04 p0588 A69-14623

Computer solution of Cauchy problem of ordinary differential equations in form of Taylor series
04 p0622 A69-14624

Differential-difference equations and nonlinear initial boundary value problems for linear hyperbolic partial differential equations, noting procedure based on method of characteristics
04 p0623 A69-14949

Asymptotic oscillation results for solutions to first order nonlinear differential-difference equations, obtaining existence-uniqueness theorems
04 p0624 A69-14950

Convergence of optimal control for denumerable system of differential equations treated by functional-space decomposition
04 p0583 A69-15095

Averaging error of system of nonlinear differential equations with time periodic right-hand sides
04 p0624 A69-15097

Green matrix of periodic boundary value problem for system of linear differential equations
04 p0624 A69-15098

Nonlinear Volterra integral equation, extending topological dynamics application of nonautonomous ordinary differential equations
04 p0626 A69-15288

Second approximation to Boltzmann equation solved for rigid sphere gas by reducing integral equation to differential equation
04 p0633 A69-15434

First order linear differential equations having complementary solutions of exponential type to determine effective initial and boundary conditions
05 p0786 A69-15926

Laminar boundary layer equations, discussing generalized similar solutions based on parametric approximation
05 p0746 A69-16019

Existence and uniqueness of solution to Cauchy problem for class of second order nonlinear differential equations, applying results to mixed boundary value problem
05 p0786 A69-16061

Nonlinear steady state vibration of single degree of freedom system, obtaining relationships between non-dimensional pi parameters of differential equation of motion
[ASME PAPER 68-WA/DE-7]
05 p0839 A69-16172

Identification of nonlinear control systems, determining nonlinearities in differential equation by curve fit or iteration method
[ASME PAPER 68-WA/AUT-19]
05 p0738 A69-16173

Phase error mean square value in phase lock loop determined from linear differential equations to determine output SNR and noise threshold
05 p0720 A69-16342

Motion stability analysis of system represented by differential equation having continuously differentiable functions as continuously acting disturbances
05 p0794 A69-16450

Conditions for solution existence for n differential equations and Liapunov functions
05 p0787 A69-16451

Solution to system of equations in boundary layer theory of steady incompressible fluid flow
05 p0751 A69-16454

Linear differential equations with sinusoidal coefficients analyzed with aid of trinomial recursions
05 p0787 A69-16464

Existence of minimal solutions of doubly infinite trinomial linear recursions of Poincaré-Perron type
05 p0787 A69-16465

Engineering solution for integrodifferential equations of physical systems with electronic circuits
05 p0724 A69-16468

Harmonic oscillations for systems of two differential equations, analyzing relative and global boundedness for solutions
05 p0788 A69-16479

Convergence of improper integral evaluated along solution of differential equation, noting use in asymptotic control theory

05 p0788 A69-16481

Explicit solubility of asymptotically periodic linear systems of differential equations

05 p0788 A69-16483

Stability of differential systems with random parameters, developing Liapunov function approach and application to Ito equation

05 p0788 A69-16484

Differential pursuit games solved by integrating Bellman equation for value function and determining set of possible positions in game with prescribed duration

05 p0788 A69-16536

Characteristic coefficients in method of integral relations calculated by Lagrange interpolation, noting application to numerical solution of differential equations

06 p0857 A69-17102

Differential equations of rotational motion of systems of rigid bodies in gravitational field derived with Lagrange equation

06 p0957 A69-17130

Axisymmetric form of stability loss of cylindrical shell under effect of axial load suddenly applied along generatrix, considering inertia forces and obtaining differential equations

06 p1021 A69-17181

Asymptotic solutions for nonlinear differential equations with gradually varying coefficients of great resistivity

06 p0947 A69-17392

Finite parametric family of solutions to differential equations systems with deviating argument

06 p0948 A69-17500

Integrodifferential equation for plasma oscillations solved for effect of ion Larmor radius size and intrinsic electric field on flute instability of axially symmetric plasma

06 p0966 A69-17520

Approximate solution of celestial mechanics differential equations by reducing to quadratures for n body problems

06 p1006 A69-17566

Quasi-random properties of dynamic system generated by solutions of second order differential equations

06 p0948 A69-17657

General two dimensional second order hyperbolic differential equation analyzed by substitution method

06 p0948 A69-17786

Differential equations for two phase flow in axisymmetric supersonic nozzle, discussing existing solutions

06 p0861 A69-17815

Gradient method solution for class of optimal control problems, minimizing root mean square value of finite state components of object in motion

06 p0904 A69-17886

Differential equations for minimum variance linear filter separating signals from additive correlated noise, using discrete time optimum formulas [AIAA PAPER 69-73]

06 p0905 A69-18121

Second order half linear differential equation solutions compared with linear equation, investigating differences

07 p1172 A69-18262

Differential equations governing free convection boundary layer flow past isothermal semiinfinite vertical flat plate solved for large Prandtl numbers by matched asymptotic expansions

07 p1239 A69-18266

Boundedness and stability of second order differential equation solutions

07 p1172 A69-18377

Zeros of solutions of second order differential equations, discussing disconjugacy concepts

07 p1172 A69-18378

Frequency modulated signal envelope passage through bandpass filter of inductively coupled circuits described by differential equation

07 p1100 A69-18555

Approximate solution to differential equations describing primary radiation defects transformation into secondary defects in semiconductors

07 p1199 A69-18679

Geometrical optics method for differential equations of fourth order in applications to LF plasma oscillations

07 p1190 A69-18697

Linear differential system with boundary conditions, obtaining equivalent Fredholm integral equation and perturbation theorem

07 p1173 A69-18729

Boundary value problems for second order differential equation with continuous f satisfying local Lipschitz condition

07 p1173 A69-18730

Analytic autonomous Hamiltonian differential equations with two degrees of freedom admitting unstable equilibrium point

07 p1215 A69-18732

Basic frequencies of uniformly almost periodic solutions of differential equations extended, noting application to orbit closures decomposition of almost periodic continuous flows

07 p1174 A69-18733

Uniform matched asymptotic approximations derived for various functions, with application to boundary value problem for ordinary differential equation with turning point

07 p1180 A69-18810

Analytic integration of Langmuir equation for spherical space charge flow obtained in terms of Airy equation or Bessel functions solution

07 p1115 A69-18864

Liapunov functions construction for linear and nonlinear differential equations, including n th degree systems with multiple nonlinearities

07 p1181 A69-19002

Differential equations with singular problem solutions analyzed by reducing problem to solution of integral equation

07 p1174 A69-19004

Stokes phenomenon, considering continuity solution of differential equations across Stokes lines

07 p1174 A69-19220

Accelerating convergence of one step methods for numerical solution of ordinary differential equations, discussing various initial value problems

07 p1174 A69-19724

Differential method with invariance principle used to analyze nonlinear invariant systems, determining physical realizability conditions

08 p1296 A69-20234

Homogeneous linear systems conditions for asymptotic growth of solutions of nonhomogeneous linear differential equations system

08 p1342 A69-20348

Multiplication of solutions of homogeneous linear differential systems

08 p1342 A69-20349

Error bounds and variational methods for nonlinear boundary value problems for ordinary differential equations

08 p1343 A69-20536

Differential equation reduction for vibrational motion of rectangular plates subjected to variable tangential forces, discussing dynamic stability

08 p1415 A69-20666

Monograph on implicit Runge-Kutta formulas for numerical integration of first order differential equations

08 p1343 A69-20706

Error estimation technique for Chebyshev series solution to ordinary differential equations

08 p1344 A69-20828

Stress-strain distribution in rotor wheel with radial side blades, giving differential equations system for circular disk strains

09 p1612 A69-21494

Heat transfer mechanism in solid body, deriving integrodifferential equation with classical equation and hyperbolic equation of heat propagation as special case

09 p1621 A69-21587

Three dimensional vibration analysis of circular homogeneous elastic cylinder, obtaining differential equations and zero stress conditions

09 p1612 A69-21601

Numerical studies of initial value problems by boundary value techniques for cases having available asymptotic estimates or periodicity of solutions

09 p1532 A69-21610

Bar flexure determination for Saint Venant torsional and transverse loading, solving differential equations by finite element methods

09 p1614 A69-21722

Soviet book on methods of optimal statistical solutions and problems of optimal control covering basic equations of random processes, stochastic differential equations, etc

09 p1473 A69-21932

Integrodifferential equations describing longitudinal oscillation properties in nonlinear region of electron Maxwellian plasma waves and two cold electron beams

09 p1550 A69-22026

Optimal stochastic control, discussing dynamic mathematical models described by differential equations

09 p1475 A69-22567

Torsional vibrations of unstiffened cylindrical tubes analysis by differential equations and applications to free-free rectangular cross section

09 p1620 A69-22769

Third order nonlinear ordinary differential equation solutions oscillatory and nonoscillatory behavior for conditions on variable coefficients

09 p1533 A69-22772

Book on special functions and approximations covering differential and integral equations and attendant theories arising in mathematical physics analysis

10 p1717 A69-22801

Two point boundary value problems solution for parameter dependent nonlinear differential equations, noting application to hinged rod bending

10 p1718 A69-22846

Static, kinematic and elastic basic equations of shell theory integrated into differential equation for minimal surface helical shells

10 p1793 A69-22886

Determining transfer matrix and comparing solution of homogeneous differential equation to Floquet theory results

10 p1666 A69-22928

Maximum principle in integral form for optimal control problems with delay differential system equations, using vector matrix notation

10 p1718 A69-23038

SNODE /spectra numerical ordinary differential equations/ computer program for solving differential equations and integration with basic time sharing system

10 p1659 A69-23142

Optimum control involving plants with intermediate position between lumped and distributed parameters

10 p1666 A69-23363

Finite difference schemes of high order of accuracy for Sturm-Liouville and boundary value problems with regular singularity

10 p1719 A69-23365

Impulse induction MHD generator with cylindrical channel, finding differential equations for velocity and current

10 p1638 A69-23484

Stability and error bounds in numerical integration of ordinary differential equations, determining highest possible degree of stable finite difference form

10 p1719 A69-23517

Sommerfeld type and Fermi type approximation analytical solutions of Thomas-Fermi differential equations for positive ions

10 p1726 A69-23525

Probable spectrum stability criterion and reducibility derived for linear differential equation having recursion or almost periodic coefficients

10 p1720 A69-23562

Dynamical systems technique for nonautonomous differential equations leading to recurrent motions

10 p1720 A69-23636

Existence and oscillation of initial and boundary value problems solutions for real scalar second order differential equations

10 p1720 A69-23637

Comparison theorem for nonlinear real vector ordinary differential equation

10 p1720 A69-23638

Convergence of zeta function for flows and diffeomorphisms

10 p1720 A69-23639

Nonsymmetric periodic solutions of second order nonlinear differential equations

10 p1721 A69-23641

Correction of linear functional differential equations with time delay showing error due to incorrect interchange of order of integration involving Stieltjes integral

10 p1721 A69-23642

Differential equation for laminar flow of nonNewtonian fluid in annulus with porous walls of nonuniform permeability, considering inelastic and suction Reynolds numbers

10 p1680 A69-23690

Asymptotic solution to problem of finding time optimal transformation for controlled plant with motion in phase space described by matrix differential equation

10 p1666 A69-23883

Existence and uniqueness of solution to Cauchy problem for class of second order nonlinear differential

equations, applying results to mixed boundary value problem

10 p1721 A69-23885

Instabilities of numerical integration of ordinary differential equations on digital computer, considering difference approximation containing extraneous solutions

10 p1721 A69-24042

Optimal controls for differential system nonlinear in state function and linear in control function

10 p1667 A69-24057

Criteria governing solution uniqueness to Volterra equations system

10 p1722 A69-24067

Similarity solution for flow of fluid-particle suspension over disk rotating at constant velocity, solving differential equations for flow velocity distributions

11 p1867 A69-24280

Liapunov functions generation for deterministic ordinary differential equations, discussing integral methods, quadratic forms, partial differential equations, canonical forms, etc

11 p1908 A69-24317

Second order dynamic systems stability, analyzing nonlinear and self excited oscillations by using two differential equations

11 p1915 A69-24535

Order of finite order linear continuous completely controllable completely observable system, using impulse response matrix and order of corresponding differential equations

11 p1858 A69-24567

Turbulent flow velocity field evolution in presence of random forces using equation of motion

11 p1867 A69-24628

Periodic solutions of strongly nonlinear differential equations for behavior of automatic control systems with delayed argument, noting autonomous and nonautonomous systems

11 p1916 A69-24765

Oscillatory properties of solutions to second order nonlinear differential equations with delayed arguments

11 p1908 A69-24767

Asymptotic series solutions for initial value problem involving nonlinear ordinary differential equation with small parameter epsilon

11 p1908 A69-24881

Linear differential equation solution for elastic systems stability problems, discussing applications to heated rectangular plates

11 p1982 A69-24950

Control sets corresponding to desired stability behavior of controlled motion, giving theorem concerning differential inequality

11 p1910 A69-25412

Optimal control theory for systems modeled by ordinary differential equations, considering delay in control action

11 p1860 A69-25447

Transition density function of randomly excited diffusion process and confinement probability at fixed spatial point satisfying integrodifferential equation involving functional derivatives

11 p1860 A69-25451

Synthesis for nonlinear second order differential equations with terms satisfying Lipschitz condition, using two person games optimal strategy

11 p1910 A69-25602

Green tensor construction for systems of linear differential equations with constant coefficients

11 p1996 A69-25730

Motion of heavy body with gyroscope, using coordinate system to reduce problem to linear second order differential equation

11 p1920 A69-25746

Observation process optimization in system described by linear differential equations of motion reducible to optimal control problem

12 p2027 A69-25882

Optimal controllers analytical design for closed loop systems with pure time delay in actuating mechanism using differential equations

12 p2045 A69-25959

Nonoscillatory solutions of second order nonlinear differential equations

12 p2120 A69-26033

Linear differential equations solutions boundedness and unboundedness criteria, determining quantitative relations

12 p2120 A69-26035

Third order multivariable control systems calculation with linear differential equations describing plant for design and digital optimization

12 p2049 A69-26085

Monograph on rapid rotations of aircraft with fixed controls, covering spin and roll movements differential equations

12 p2013 A69-26118

Cauchy problem solution for linear/nonlinear differential equations with analytic right hand sought in form of power series

12 p2120 A69-26199

Elliptic boundary value problem for differential equation and pseudodifferential boundary conditions, obtaining Green formula from formulated conjugate problem

12 p2121 A69-26200

Differential equations application to electrical circuit problems, solving voltage for series LCR networks and transforming Mathieu into Hill equation

12 p2052 A69-26351

Nondeterministic differential games with imperfect state information, emphasizing linear system with quadratic cost functional and additive white Gaussian noise

12 p2053 A69-26505

Liapunov function construction with numerical algorithm, considering systems described by dx/dt equals y and dy/dt equals $f(x,y)$

12 p2122 A69-26520

Dahlquist linear multistep methods of stability analysis for ordinary differential equations extended to Volterra integrodifferential equations

12 p2123 A69-26753

Cylinder buckling and other boundary value problems, applying inverse differential operators to solution of integrodifferential equations

12 p1886 A69-26841

Order determination for single step Runge-Kutta methods for solving general system of differential equations

12 p2124 A69-26891

Enclosures for large eigenvalues of ordinary second and fourth order differential equations based on asymptotic solutions of linear homogeneous second order differential equations

12 p2124 A69-26892

Eigenvalue approximation for first order systems by introducing artificial periodicity through successive impulse functions of alternate sign

12 p2287 A69-27242

Transient response in liquid-metal conduction MHD generators, analyzing constant magnetic field using differential equation

13 p2207 A69-27506

Differential approach game for unfavorable pursued motion, examining optimum control laws

13 p2288 A69-27525

Linear difference equations with exponential coefficients for numerical methods of integrating differential equations

13 p2288 A69-27526

Numerical methods for time integrating first order differential equations, emphasizing atmospheric oscillations in baroclinic model, evaluating errors

13 p2290 A69-27636

Internal solution of Einstein equations for steady axisymmetric gravitational fields by integrating differential equations with initial conditions

13 p2351 A69-27863

Second order differential equations eigenvalues with Sturm boundary conditions analyzed by difference method

13 p2288 A69-27922

Zlamal theorems refinements by means of Banach theorem of fixed points for Lienard differential equation

13 p2289 A69-27925

Differential equations of single loop parametric amplifier response, analyzing forced oscillations

13 p2234 A69-28329

Energy transfer by simultaneous conduction and radiation between two media in intimate contact, detailing numerical solution method for resulting coupled nonlinear integrodifferential equations

13 p2378 A69-28340

Set of states for control system described by linear differential equation with constant coefficients and brought to zero phase coordinates

13 p2239 A69-28437

HNO role in hydrogen-NO reaction rate data reexamined by numerical integration of governing differential equations

13 p2218 A69-28457

Quasi-L-analytic functions for ordinary linear operator L

13 p2290 A69-28484

Increases of Newtonian potential, gradient and second derivative on gravitating body, considering positive and negative masses

13 p2300 A69-28545

Differential equations for shallow circular spherical shell transformation to equation describing stress-strain state of plate on elastic base

13 p2369 A69-28565

Phase and amplitude changes of arbitrary-Q self excited oscillator under external disturbance, using differential equations

13 p2300 A69-28574

Analogy between differential equations for skew isotropic plates and rectangular anisotropic plates

13 p2371 A69-28678

Cosmic ray propagation in interplanetary space taking into account reverse effect on solar wind, deriving integrodifferential equation

13 p2333 A69-28688

Contact problem for half plane with elastic stiffener reduced to Prandtl integrodifferential equation, determining contact stresses

14 p2531 A69-28804

Differential equation with finite jump type discontinuities

14 p2424 A69-28811

Completeness theorem for integrodifferential operator to establish Schwarzschild criterion for stability of gaseous masses

14 p2470 A69-28902

Boundary value problem for nonlinear functional differential equations, discussing matrix and general operators

14 p2470 A69-28906

Orbital elements evolution of binary or planetary system with decreasing mass by nonlinear nonautonomous differential equations

14 p2519 A69-29138

Numerical solution of differential equations for two channel PFM with pulse element, applying Dirac pulse sequence to input

14 p2426 A69-29148

Differential equations for ignited mode theory, considering ion and electron transport and energy flux

14 p2490 A69-29233

Singularity-free global solutions to nonlinear differential equations associated with variational principles, deriving necessary condition for existence from dilatation invariance considerations

14 p2470 A69-29367

Optimal control conditions for systems described by differential equations with deviating neutral type argument formulated in maximum principle form

14 p2426 A69-29419

Wentzel-Kramers-Brillouin approximation validity determined by sufficiency conditions based on differential equations series solution

14 p2471 A69-29454

Solution methods for differential heat conduction equations, discussing methods of variable separation, Green function, thermal potentials, etc

14 p2539 A69-29456

Quasi-distribution function differential equation for laser field with nonMarkoffian character derived from density matrix master equation

14 p2486 A69-29633

Von Karman swirling flow problem differential equations solved by extending Serrin existence theorems

14 p2432 A69-29676

Conduction solution to generalized nonlinear Benard problem showing existence of bifurcation and analyticity of convective motion

14 p2540 A69-29679

Asymptotic expansions of solutions to nonhomogeneous differential equation with perturbation

14 p2471 A69-29680

Integrodifferential equation derived and solved for evolution of collisional model of asteroids and debris

14 p2526 A69-29879

Nonoscillatory solution to nonlinear differential equation, presenting theorem describing sufficient condition for nonoscillation

14 p2471 A69-29950

Necessary and sufficient conditions for solution existence to second order boundary value problems, considering second order differential equation involving function of three variables

14 p2471 A69-29951

Convergent solutions of inviscid solar wind equations in expansions form including dimensionless distance from sun

14 p2515 A69-29968

Asymptotic power series solutions of viscous solar wind equations

14 p2515 A69-29969

Book on Bessel functions with physical applications covering solution of Bessel and associated equations, integral representations, Fourier-Bessel series, Hankel transforms, etc

15 p2643 A69-30037

Functional analysis methods to solve Cauchy problem for linear nonhomogeneous differential equations with delayed argument

15 p2643 A69-30101

Riccati equation solution for inhomogeneous and homogeneous lines obtained by Lagrangian method for differential equations

15 p2582 A69-30124

Differential equations for elastic stress distribution in thin rotating shell with arbitrary profile, obtaining analytical dimensionless solutions for potential profiles

15 p2703 A69-30158

Differential equations for optimum reception to synthesize detectors of deterministic signals against nonGaussian background noise using Markov process

15 p2567 A69-30340

Averaging procedure for solving Cauchy problem applied to two point boundary value problem for non-linear differential equations

15 p2644 A69-30449

Plane contact problems in elasticity theory allowing for cohesive forces solved by integral and differential equations

15 p2706 A69-30578

Sinusoidal perturbation extremal control system stability, using harmonic balance principle to obtain periodic solutions of system differential equations

15 p2582 A69-30616

Modified Chaplygin method for approximate integration of Cauchy problem for differential equations, estimating rate of convergence

15 p2644 A69-30656

Chetaev /A, lambda/ estimates of approximate integrations of system of ordinary differential equations, analyzing stability with aid of Liapunov functions

15 p2644 A69-30664

Runge-Kutta type method truncation error estimation, discussing validity conditions, evaluation processes and numerical tests

15 p2644 A69-30672

Electronic analog model for differential equations of equilibrium of gaseous combustion products based on asymptotic stability

15 p2717 A69-30862

Book on solution of linear ordinary differential equations and simultaneous systems using bar statics-equivalent beam method

15 p2711 A69-30929

Pontryagin maximum principle applied to time optimal control of autonomous second order system with constant coefficients and differentiation in transfer function numerator

15 p2583 A69-31059

Asymptotically almost periodic solutions of almost autonomous differential equation

15 p2645 A69-31096

Shock force calculation for parachute of arbitrary canopy design, illustrating simplification permitting differential equation solution in closed form

15 p2551 A69-31172

Sloping helicoid median surface with given parameters, obtaining equilibrium equations, elasticity and formulas relating deformations to displacements

15 p2714 A69-31197

Asymptotic solutions of optimum control for systems with constraints as linear differential equations and quadratic type functional

15 p2583 A69-31234

Trajectory differential equations in state- variable form, presenting compatible difference equation adjoint scheme for trajectory integration

15 p2645 A69-31236

Differential games theory with nonzero sum for application to economic analysis, discussing Nash equilibrium, minimax and noninferior strategies set

15 p2645 A69-31237

Stability and asymptotic stability theorems related to Liapunov second method, considering linear differential equations zero solution

15 p2654 A69-31259

Differential equations of steady motion construction from integral manifold

15 p2654 A69-31260

Plane Cauchy problem solution for differential equations in heat and mass transfer theory, applying contour integral method in matrix construction

15 p2719 A69-31262

Numerical integration of subdominant solutions of systems of ordinary differential equations, using partial Wronskians

15 p2646 A69-31519

Boundedness in mean square of solutions derived for linear differential equations forced oscillations with nonwhite Gaussian random functions parameters

16 p2873 A69-32058

Differential coefficients applied to Izsak-Borchers ballistic trajectory and errors produced by perturbations of initial vectors, applying results to data capsule recovery

16 p2857 A69-32156

Simultaneous unbounded solutions existence to homogeneous linear differential equations with continuous positive elastic and dissipative coefficients

16 p2804 A69-32251

Asymptotic solutions to second order differential equations with slowly varying parameters and large resistance applied to mathematical pendulum damped swinging motion

16 p2804 A69-32253

Nonlinear vibrations of mechanical two degrees of freedom system during resonance described using Krylov-Bogoliubov method to obtain differential equations solutions

16 p2875 A69-32255

Quasi-linearization algorithm for solution of boundary value problems for ordinary differential equations, formulating representation and convergence theorems

17 p2994 A69-32835

Shocks in gases, giving differential equation set for ideal gas behavior

17 p2948 A69-32845

Fluid filled spherical shell axisymmetric nontorsional motion analysis via differential equations obtained by Hamilton principle

17 p3051 A69-32956

Mechanical systems differential equations of motion solution behavior, discussing program constraints

17 p3053 A69-33017

Pulsed control systems sensitivity relationship to discreteness period described via differential equations

17 p2994 A69-33143

Friedrich qualitative analysis of ordinary differential operators modified to obtain quantitative information regarding eigenvalues distribution

17 p2995 A69-33404

Stability conditions for time lag differential equation systems over finite interval employing Liapunov functions, noting similarity with systems having continuously acting disturbances

17 p2995 A69-33616

Quasi-periodic solutions for canonical systems of differential equations in plane n-body problem

17 p3035 A69-33620

Spectrum of ordinary second order differential operators, correlating spectral properties with analytic function-theoretic properties of differential equation solutions

17 p2996 A69-33793

Monograph on solar system space flight trajectory calculations covering solutions to differential equations, error analysis and gravitational effects

17 p3039 A69-33798

Differential equations as Hamiltonian function for signal path, travel time and frequency variation in anisotropic nonpermanent absorbing medium

17 p2924 A69-33836

Approximation of vector linear differential equations with slowly varying matrix coefficients on time sharing computers, noting modeling possibilities

17 p2996 A69-33879

Nonlinear differential equations describing one degree of freedom systems oscillations, allowing for dry friction and internal friction in elastic element

17 p3007 A69-33913

Nonlinear differential equations of mechanical systems with restoring forces approximated by odd power displacement functions and energy dissipation approximated by displacement and velocity functions

17 p3007 A69-33914

Asymptotic series expansion for solutions of differential equations containing parameter

18 p3163 A69-34328

Differential equations of shells of revolution theory assuming rotationally symmetric stress and strain in thin elastic shells

18 p3215 A69-34549

Nonlinear systems of differential equations to free oscillations about equilibrium, obtaining periodic solutions

18 p3172 A69-34591

Convergence of discrete approximations of Navier-Stokes equations to solutions of corresponding differential equations

18 p3121 A69-34613

Nonlinear differential equations for nonequilibrium gases with internal degrees of freedom, considering

spatially homogeneous gas and oscillatory relaxation in harmonic oscillators

18 p3122 A69-34911

Linear boundary value problem solution using iterative method

18 p3165 A69-35050

One degree of freedom systems nonlinear oscillations differential equations periodic solutions by successive approximations, obtaining proof for convergence

18 p3174 A69-35311

Thin walled shell temperature and strain fields described by integrodifferential equations based on Kirchhoff hypothesis and coupled thermoelasticity reciprocity equations

18 p3225 A69-35368

Quadratic Liapunov function existence for exponentially stable linear system with varying coefficients described by vector differential equations

19 p3359 A69-35617

Two player zero-sum differential games with emphasis on play with state determined by differential equations, noting optimal solutions

19 p3359 A69-35665

Krein solution method for linear integral equations of first kind and related differential equations

19 p3360 A69-35780

Ordinary differential equations integration method, presenting algorithm based on double constraint of maximum accuracy and stability

19 p3279 A69-35805

Structural analysis of thin walled conical shell with variable external loading and Winkler-base elastic filler, using linear differential equation with variable coefficients

19 p3436 A69-35846

Syphon geometry influence on rigidity and strength determined using integrating Meissner type differential equations with finite difference schemes

19 p3358 A69-35849

Liapunov first stability theorem generalized for differential equations in Banach space

19 p3360 A69-35860

Spatially homogeneous Boltzmann equation containing initial distribution functions expandable into Hermitian polynomials analyzed via ordinary differential equations

19 p3373 A69-36202

Existence and uniqueness theorems for operator equation in differential equations theory for application to boundary value problem

19 p3360 A69-36373

Finite difference analogs with increasing error terms applied to simple differential Laplace operator for accuracy determination

19 p3365 A69-36510

Ordinary differential equations in linear topological space extended from Fattorini investigation, emphasizing use of linear operator

19 p3360 A69-36599

Autonomous functional differential equations with finite time interval dependent derivatives, resulting in periodicity theorem applicable to difference equations

19 p3361 A69-36600

Constraint restoration in holonomic and non-holonomic problems involving system of algebraic or transcendental equations or first order differential equations

19 p3361 A69-36758

Similarity method applied to linear integrodifferential equations of neutron transport in homogeneous space

19 p3361 A69-36774

Elastic shell theory to regularize singular integrodifferential equation, investigating load transfer from reinforcing ribs to circular cylindrical shell and numerical solution correlation

19 p3443 A69-36792

Matrix formulation for discrete element method applied to linear static and eigenvalue problems of thin walled segments, using homogeneous differential equations

19 p3445 A69-36831

Approximation error involved in difference optimal control problem substitution for differential optimal control problem based on functional minimization

20 p3509 A69-36989

Theorem extending results of techniques for analytical solutions of nonlinear ordinary differential equations applied to terrestrial brachistochrone problem

20 p3575 A69-37205

Asymptotic stability of null solution of matrix differential equation, considering linearized equations of

rotational motion for hinged two body gravity gradient satellite orbit

20 p3575 A69-37212

Singular perturbations and boundary layer theory for approximating solutions to simple ordinary differential equations

20 p3515 A69-37583

Minimax error technique used with finite difference methods to estimate error in approximations to functions defined by nonlinear differential equations

20 p3568 A69-37832

Monograph on periodic solutions and locking-in regions for differential equations with switching points describing motion of self excited oscillatory physical structures

20 p3577 A69-37923

Difference method for solving multidimensional differential equations of higher orders

20 p3568 A69-38074

Nonlinear partial differential equations numerical solution applied to solving Cauchy problem encountered in Goursat problem

20 p3569 A69-38293

Cauchy problem solution for first order nonlinear Volterra integrodifferential equation, using Runge-Kutta method

20 p3569 A69-38294

Optimization for processes expressed in differential equations, stressing use of calculus of variations and limitation

21 p3795 A69-38400

Variational or optimal control for delayed systems, involving integrated maximum principle for problems with nonlinear functional differential systems

21 p3754 A69-38429

Continuous optimal control problems, proving direct solutions existence for case of differential equations system linearity in control and state variables

21 p3684 A69-38431

Existence and uniqueness of optimal feedback control proved for autonomous nonlinear differential equations, allowing any finite number of variables

21 p3685 A69-38433

Optimal control of dynamic system motion described by linear differential equation, selecting vector function ensuring predetermined trajectory

21 p3685 A69-38452

First order linear differential equations subject to linear constraints, discussing solution uniqueness dependence on matrix nonsingularity

21 p3754 A69-38744

Shooting method difficulties in boundary value problem numerical solutions using computer programs to integrate differential equations

21 p3755 A69-38753

Time optimal control for second order automatic system with motion described by differential equations

21 p3770 A69-38856

Algorithms testing characteristic polynomials and differential equation classical stability relations

21 p3755 A69-38925

Linear and nonlinear differential equations systems stability and instability problems, describing procedures and theorems for solutions

21 p3755 A69-38960

Periodic motions of mechanical oscillators with velocity discontinuities analyzed by differential equations

21 p3771 A69-39009

Asymptotic stability of differential equations solutions in linear normalized spaces via Liapunov theorems extension

21 p3755 A69-39105

Differential equations for variable mass solid body motion about fixed point having cavities filled with ideal fluid

21 p3771 A69-39106

Stability of two differential equations in critical case, obtaining Liapunov stability and instability

21 p3755 A69-39107

Critical case of stable motion for differential equations having two zero roots

21 p3771 A69-39108

Synthesis by differential equation technique for linear antenna arrays of identical radiators radiation patterns

21 p3682 A69-39125

Deformation of circular cylindrical shell of varying thickness, obtaining differential equation solutions through multiple scales method

21 p3837 A69-39159

Arbitrary form temperature rate wave growth and decay, determining differential equation governing wave amplitude

21 p3853 A69-39671

Quasi-linear ordinary differential equations solutions for steady two dimensional stagnation point flows of nonNewtonian power law fluids

21 p3697 A69-39674

Periodic solutions of differential equation as example of locking in of frequencies, developing mapping procedure for perturbation methods application

22 p3979 A69-39894

Criterion for class of differential equations ensuring absence of nontrivial periodic solutions

22 p3974 A69-39897

Thomas-Fermi approximation applied to calculation of equations of state and thermodynamic functions at high pressure from differential equations of statistical atom model

22 p3984 A69-40186

Existence conditions of critical points for autonomous differential equations in bounded flows

22 p3975 A69-40571

Two dimensional gas dynamics differential equations for simple waves, discussing invariant solutions and conditions for group solutions

22 p3933 A69-41030

Time dependent differential equation for order parameter in superconductors near critical temperature derived from density matrix equations

22 p3994 A69-41053

Random processes correlation functions determined by stochastic differential equations applied to lunar surface statistical characteristics determination

22 p4033 A69-41092

Asymptotic methods for differential equations containing parameter, discussing reduction to integral equations system

22 p3976 A69-41124

Coupled set of differential equations describing generalized Volterra problem of conflicting populations and application to plasma oscillations

22 p3976 A69-41260

N-th order differential systems using first approximation, finding conditions for bounded solutions, solutions asymptotic to zero and stability

23 p4181 A69-41722

Variational formulation of nonlinear differential equations, treating vector fields in Hilbert spaces, finding relations useful in quantum mechanics

23 p4181 A69-41723

Nonlinear differential equations of injection phase locking solved by Riccati equation, discussing initial frequency offset to loop gain ratios

23 p4119 A69-41742

Existence theorem for relation between solutions of systems of ordinary differential equations

23 p4182 A69-41959

Differential operators representing potential energy of thin shell, discussing self conjugacy of boundary value problems

23 p4229 A69-41999

Invariance conditions for steady and unsteady systems by differential method compared to variational approach

23 p4145 A69-42371

Absolute invariance conditions for closed isolated subsystem of nonlinear differential equations of Cauchy normal form

23 p4183 A69-42372

Nonlinear loaded integrodifferential equation analytical and formal solutions, noting role of characteristic number relation to unity

24 p4339 A69-42595

Sufficient conditions theorems for investigation of instability of numerical integration methods to solve differential equations

24 p4339 A69-42646

Bethenod pendulum behavior using coupled nonlinear differential equations, discussing synchronization methods

24 p4349 A69-42673

Newton method providing continuing solutions of nonlinear differential equations through limit or bifurcation points, discussing elastic stability applications [ASME PAPER 69-APMW-14]

24 p4401 A69-43102

Positive cyclic systems of linear differential equations, proving existence and projective uniqueness of solution having positive n components for all t

24 p4340 A69-43131

Bellman equation analyzed for higher derivatives, suggesting bounded partial derivatives of optimal feedback control function

24 p4341 A69-43234

Uniqueness theorem and successive approximations for delay functional differential equations, noting scalar problems

24 p4341 A69-43236

Quasi-steady laminar flat plate boundary layer in shock tube determined by reducing boundary layer equations to linear differential equations

24 p4305 A69-43632

Vector matrix second order sensitivity equation application to Mars entry guidance, performing numerical simulation of second order sensitivity guidance and tabulating results

24 p4388 A69-43690

Synthesis of second order nonlinear differential equations reducible to linear third order equations for application to vibrations field

24 p4342 A69-43702

DIFFERENTIAL GEOMETRY

NT LIE GROUPS

NT RIEMANN MANIFOLD

NT SPINOR GROUPS

NT TENSOR ANALYSIS

Quasi-linear parabolic partial differential equations, discussing solutions, regularity, differential geometric aspects and Dirichlet problem

02 p0273 A69-12779

Four dimensional space-time immersion in conformally flat six dimensional space or flat eight dimensional space, noting group of isometries of tangent spaces

10 p1774 A69-23162

Triangular shell element SHEBA for arbitrary curvature variation as means of performing large displacement matrix analyses, discussing local subelement, natural modes, cross sectional resultants, etc

16 p2872 A69-32025

DIFFERENTIAL INTERFEROMETRY

Quantitative analysis of differential interferometer photographs using Wollaston prism with beam separation, applying method to sphere in low density hypersonic flow

12 p2089 A69-26187

Streak photographs by differential interferometer to study head wave standoff in shock tubes as function of time

18 p3085 A69-34473

Multifrequency dispersion interferometers applicability in plasma diagnostics, considering integral electron concentration measurements

22 p3947 A69-40959

DIFFERENTIAL OPERATORS

U OPERATORS [MATHEMATICS]

DIFFERENTIAL PRESSURE

Venturi meter design, discussing effects of turbulent velocity fluctuations, hole size and internal geometry on differential pressure measurement

11 p1880 A69-24468

Electric dose variometer principles, emphasizing differential pressure meter, differential capacitor and capacitor meter

24 p4315 A69-43143

DIFFERENTIAL THERMAL ANALYSIS

Thermosetting resin curing behavior characterized by differential thermal analysis performed above atmospheric pressure to prevent volatilization

09 p1500 A69-22311

Dynamic differential thermal analysis of dried plant and animal specimens and related substances yielding discrete decomposition peaks of exothermic type

15 p2555 A69-31000

Dynamic differential thermal analysis with He flow performed on biological specimens, proteins and starches, showing discrete decomposition peaks monitoring pyrolysis process

16 p2747 A69-31807

Premature exothermic decomposition suppression in propellant grade ammonium perchlorate, using differential thermal analysis

16 p2833 A69-32688

La-Rh system study by powder X ray diffraction, metallographic and differential thermal analysis, constructing equilibrium diagram and determining crystal structure data

21 p3744 A69-38739

DIFFERENTIATION [BIOLOGY]

Classical and differential eyelid conditioning for truth or falsity of visually presented verbal statements

07 p1064 A69-18632

DIFFERENTIATORS

Error origin and control in high gain operational amplifier in time differentiation of voltage signal used for photoemission studies

06 p0897 A69-17700

Error and noise sources in analog differentiators, discussing signal distortion minimization techniques and augmentation with linear phase filter

06 p0897 A69-17702

Differentiating network with nonlinear resistance and capacitance elements, noting improvement in pulse shaping properties

08 p1295 A69-19910

Pulse frequency signal processing continuous and discrete differentiators, analyzing time delay, constant frequency, accuracy and codes

09 p1454 A69-21755

Alloying pairs of metal pellets to n and p type semi-insulating GaAs, discussing photo effects

17 p3015 A69-32824

DIFFRACTION

NT ELECTRON DIFFRACTION

NT FRESNEL DIFFRACTION

NT NEUTRON DIFFRACTION

NT PULSE DIFFRACTION

NT WAVE DIFFRACTION

NT X RAY DIFFRACTION

Intracavity laser diffraction gratings for single wavelength output

01 p0092 A69-10897

Algebraic formulation of electromagnetic diffraction, discussing propagation of positive and negative time frequency components by dual operators

18 p3172 A69-35010

HF radar scattering by finite circular cone as function of frequency and aspect angle using modified diffraction pattern theory

20 p3495 A69-37849

Modified geometrical diffraction theory applied to determination of vertically polarized radar backscattering from rear of cylinders and frustums

20 p3495 A69-37851

Eigenmodes of asymmetric cylindrical confocal laser resonator with single output coupling aperture, obtaining diffraction loss factors and mirror field distributions

21 p3741 A69-39564

Equatorial radiation pattern of parallel plate TEM mode axial slot on elliptical conducting cylinders, using wedge diffraction and creeping wave theory

22 p3914 A69-40703

DIFFRACTION GRATINGS

U GRATINGS [SPECTRA]

DIFFRACTION PATHS

One way measurement of dual inband frequency diversity improvement on HF ionospheric path with frequency division multiplexed FSK modulation

10 p1656 A69-23536

DIFFRACTION PATTERNS

Crystals and molecules diffraction in supersonic molecular jets

02 p0284 A69-12629

Moire fringe interpolation and multiplication by shifting master interference grating, noting increased measurement sensitivity

03 p0524 A69-13063

Laser beam diffraction method for measurement of apparent filament diameters, emphasizing high modulus carbon filaments

08 p1316 A69-20499

Fabry-Perot fringes maxima in frequency response of laser interferometer, describing passive technique using eight wave plate

09 p1517 A69-21915

Diffraction pattern recording technique and application to thin film measurements

09 p1499 A69-22303

Hologram obtained by recording interference pattern displayed by ultrasonic camera, discussing real time viewing

10 p1696 A69-23550

Diffraction theory of schlieren photometric slot and wire methods for cylindrical light wave of even order, discussing Fresnel diffraction for spherical wave

12 p2088 A69-26180

Contrast interference patterns obtained in Michelson interferometer at various path differences, using He-Ne laser as light source

12 p2108 A69-26593

Natural unbroken tektite surface examination by interferometry, discussing fringe patterns for pit shapes and sizes

12 p2173 A69-27175

Visual observation of surface vibration nodal patterns by incoherent light illumination of object, noting holography

12 p2099 A69-27176

Diffraction images of coherently illuminated objects in presence of aberrations stressing images of edges, disks and bars

13 p2297 A69-27451

Multichannel optical interference fluid manometer, using laser light source for fringe pattern photographic record

13 p2263 A69-28190

Structural stress under acceleration loading simulated by two dimensional photoelastic model noting improvement of fringe patterns quality

14 p2532 A69-28885

Irradiance distribution in far field diffraction patterns of partially coherent light diffracted by annular aperture, using Fourier transformation relationship of Schell

14 p2460 A69-29640

Optical image diffraction method for analyzing radiation patterns of horn antenna sounding beams used in microwave measurement of expanding plasmoids

14 p2497 A69-29793

Random motions velocity of ionospheric inhomogeneities by extreme lines delineation of diffraction pattern during amplitude recording of reflected signal

14 p2444 A69-29872

Asymmetrical waves diffraction field at wide slots in circular waveguides determined in Huygens-Kirchhoff approximation

15 p2570 A69-30955

Stresses in fixed two dimensional photoelastic models analyzed by hologram interferometry, displaying isochromatic and isopachic interference patterns

15 p2611 A69-31110

Vibration measurement by hologram interferometry, explaining interference fringes as linear combination of vibrating object classical modes

18 p3135 A69-34635

Holographic velocimetry data reduction applicable to flow field holograms, using singlet interference pattern for spherical and plane wave illumination

19 p3305 A69-35730

Microwave holograms generated by spinning dipole field perturbation technique, showing zone plates and moire fringe resolution

19 p3315 A69-36824

Cranz-Schardin camera for high speed recording in dynamic photoelastic fringe pattern studies, discussing framing rates, fringe gradients and design

20 p3541 A69-37778

Diffraction pattern of satellite signal field-aligned amplitude scintillation during quiet geomagnetic conditions

20 p3497 A69-38108

Fringe multiplication techniques for moire fringe arrays of inhomogeneous strain fields

21 p3845 A69-39328

Moire technique for gaging surface deformations or surface configuration differences by optical interference patterns

21 p3726 A69-39775

Wedge fringes visibility and localization in hologram interferometry during focusing on surface under examination for displacements

22 p3943 A69-40016

Photographic high speed recording system characteristics effects on dynamic photoelastic fringe patterns fidelity

22 p3945 A69-40077

Isoclinic angle errors effects on photoelastic fringe order measurements accuracy

22 p3945 A69-40082

Edge diffracted fields by conical body frustums evaluated, including equivalent currents for caustic regions

23 p4136 A69-41583

Radio echoes diffraction patterns determination from reflection coefficients of polarized radio waves reflected from ionized meteor trails

23 p4214 A69-41846

Principal stresses determination in optically active photoelastic models from fringe pattern while obtaining sum from Dirichlet problem solution by straight line method

23 p4228 A69-41987

Lateral waves used to explain diffraction effects by light incident upon interface at critical angle of total reflection, discussing quasi-optical properties

23 p4191 A69-42148

Isoclinics determination from fringe patterns, obtaining continuous principal stress direction data for photoelastic model in bonded polariscope

24 p4396 A69-42738

Index of refraction turbulent fluctuations effect on beam traversing optically active medium, discussing far field diffraction pattern and incoherent scattering [AIAA PAPER 68-683]

24 p4304 A69-43578

DIFFRACTION PROPAGATION

Wave propagation in open periodic two dimensional iris waveguide and beam reconstruction by diffraction, considering existence and character of modal fields

16 p2753 A69-32394

Knife-edge obstacle diffraction of nonisotropic transmitter analyzed via isotropic source model propagation path noting accuracy

17 p2917 A69-32847

Far field of line source in medium with sinusoidally stratified dielectric constant, studying diffraction effects due to Bragg mechanism

17 p2925 A69-33842

Diffraction of plane polarized electromagnetic wave incident on dielectric wedge formulated as singular integral equation, discussing electric field amplitude

22 p3903 A69-41258

Edge diffraction effects in TEM axially slotted finite ground plane on radiation pattern in waveguides of different geometries

23 p4116 A69-41588

Linear diffraction equations in electronics in self consistent formulation reduced to complex transcendental equations, using perturbation method

23 p4124 A69-42033

DIFFRACTION TELESCOPES

U SPECTROSCOPIC TELESCOPES

DIFFRACTOMETERS

Diffraction effects on periodic structures in millimeter wavelength range, discussing apparatus for measurements of Fraunhofer zone field, polarization and phase characteristics

04 p0598 A69-14852

Diffraction effects on periodic structures in millimeter wavelength measurements of Fraunhofer zone field, polarization and phase characteristics

15 p2607 A69-30244

DIFFUSE RADIATION

Multiple light scattering in planetary atmospheres, discussing diffuse reflection and transmission by atmosphere of particles with anisotropic scattering pattern

02 p0319 A69-12105

Diffusive scattering effects on planetary surface reflection coefficient determined by radar observations

04 p0662 A69-15245

Diffuse cosmic X radiation flux and intensity law, noting inverse Compton effect of electrons on 3K black body radiation

05 p0817 A69-16714

Low energy diffuse cosmic X radiation, considering adequacy of single exponent power law spectrum [ISAS-428]

06 p0986 A69-17024

Spectral reflection computer program utilizing virtual image technique to determine reflection characteristics of enclosed diffusely emitting surface [AIAA PAPER 69-65]

06 p1040 A69-18215

Diffuse reflection of electromagnetic waves by rough random surface using probabilistic method and statistical distributions

07 p1075 A69-18280

Diffuse cosmic X ray background measured during balloon flight with actively shielded and collimated detector

09 p1584 A69-22767

Interstellar diffuse absorption bands due to resonance lines of impurity atoms trapped in low temperature hydrocarbon matrices

10 p1781 A69-23677

Diffuse galactic radiation reinterpretation by solving same transfer problem exactly for properties of interstellar particles

10 p1782 A69-23680

Diffuse X radiation spectrum below 4 keV measured with beryllium window proportional counter at rocket altitudes

10 p1770 A69-24094

Supplemented data to analyze intergalactic gas diffuse X ray background radiation

10 p1792 A69-24209

Double focus lens holography for diffusely reflecting surface deformation recording, discussing gas lasers, Polaroid photographic materials, etc

11 p1880 A69-24467

Diffuse reflection of monochromatic radiation by semiinfinite plane layer in case of isotropic scattering, reducing problem to power series

11 p1960 A69-24732

Specularly vs diffusely reflecting cylinders for cavity type sources of approximately black body radiant energy, noting ray tracing of cones

12 p2130 A69-26245

Radiation diffusion in medium of finite optical thickness, computation of source function and tabulation of matrices

12 p2131 A69-26661

Monograph on atmospheric radiation transfer including absorption, scattering, direct, diffuse, global, thermal and net radiation

12 p2073 A69-26918

Southern radio auroral zone observation with rhombic antennas, noting diffuse and discrete zones associated with proton and electron precipitation

12 p2033 A69-26950

Cosmic X ray background measurements and Crab Nebula observation during sounding rocket flight

13 p2326 A69-27570

Vertical refraction effect on gas laser beam propagation near earth surface under various meteorological conditions, comparing index for diffuse light

13 p2220 A69-27827

Light diffusive reflection from rough surface measured as function of angle of incidence in presence of specular component by goniospectrophotometer

14 p2485 A69-29171

X ray energy spectrum from Crab Nebula and diffuse background on celestial sphere near galactic anticenter, noting spectral index

15 p2675 A69-30759

Light polarization diffusely reflected by earth at atmosphere measured from balloon, using gain compensated photoelectric polarimeter

16 p2781 A69-32320

Time dependent radiation diffusion in inhomogeneous stationary medium applied to diffuse reflection of light

16 p2813 A69-32591

Cosmic X rays diffused component absolute intensity measurement using rotating collimator borne on sounding rocket, noting flat spectrum and Sco X-1 intensity variation

17 p3023 A69-33068

Radiant heat transfer predictions between isothermal plates based on diffuse plus specular directional property model

[AIAA PAPER 69-624] 17 p3070 A69-33259

Time dependent diffuse reflections related to solar activity, showing diffusion intensity variations with sporadic E layer height and electron concentration

17 p2968 A69-33997

Cosmic X rays diffuse component possible origin, discussing galactic gamma ray flux and disagreement with measured isotropy

18 p3185 A69-34275

Search for diffuse galactic light component between 2100-2800 Å by rocket measurements of night sky brightness, showing low albedo of interstellar dust

18 p3202 A69-35210

Time dependent collimated light diffuse reflection and transmission by finite inhomogeneous atmosphere, using principle of invariance

18 p3132 A69-35345

Occurrence, development and disappearance of diffused reflections, relating dynamic behavior to ionospheric electron concentration

20 p3529 A69-37687

Diffuse reflection of UV radiation from rough metallic surfaces, noting irregularities

21 p3770 A69-38796

Milky Way galactic diffuse radiation photometric study using Schmidt camera, stressing Northern Coal-sack commencement region

21 p3817 A69-39725

Diffuse coronal emission observation during total eclipse of February 1961 near solar prominences and polar ray form investigation in northern part of corona

22 p4002 A69-40002

Diffuse galactic radiation intensity and distribution from photoelectric measurements compared with radiative transfer calculations using various interstellar dust models

22 p4013 A69-40096

Diffuse reflection of electromagnetic longitudinal wave from magnetoactive plasma in oblique incidence

22 p3990 A69-40788

Spatial coherence of He-Ne laser radiation diffused by turbid medium calculated by using diffraction and interference measurements

22 p3964 A69-40798

Aperture distortions and spectral line shapes of electromagnetic radiation diffused by plasma

22 p3982 A69-40799

Stellar and diffuse galactic radiation intensity observations to obtain albedo values of interstellar dust particles

22 p4034 A69-41112

High energy astronomical diffuse radiation component properties tabulated, discussing power law and thermal X ray background, gamma rays, etc

23 p4207 A69-42319

Meter and decimeter wavelength range short period fading under conditions excluding optical sights, correlating specular and diffuse reflection

24 p4281 A69-42612

Diffuse cosmic X rays from Compton collisions between galactic leakage electrons and extragalactic background photons to verify microwave blackbody radiation properties

24 p4368 A69-43202

DIFFUSERS

Swirl flow through single and multistage Carnot shock diffuser, analyzing relation of pressure rise and diffuser aspect ratio

02 p0230 A69-11616

Short cylindrical diffusers efficiency in supersonic wind tunnel with exchangeable nozzles with conical supersonic section

03 p0365 A69-14226

Pressure recovery of straight channel divergence diffusers at high inlet Mach numbers

[ASME PAPER 68-WA/FE-19] 05 p0698 A69-16095

Inlet velocity profiles distortion effects on flow regimes and performance in two dimensional diffusers with turbulent boundary layers

[ASME PAPER 68-WA/FE-25] 05 p0698 A69-16100

Inlet conditions influence on two annular diffusers performance, using low speed tests

[ASME PAPER 68-WA/FE-38] 05 p0698 A69-16110

Conical diffuser/exit duct performance and model for estimating energy losses, discussing inlet flow and Reynolds number

[ASME PAPER 68-WA/FE-45] 05 p0698 A69-16112

Venturi meter with separable diffuser and radial outward step at transition from throat to diffuser, noting effect of step on efficiency

[ASME PAPER 68-WA/FM-2] 05 p0763 A69-16135

Venturi meter with separable diffuser and radial outward step at transition from throat to diffuser, noting effect of step on efficiency

[ASME PAPER 68-WA/FM-2] 14 p2447 A69-29447

Diffuser inlet geometry, studying effects of straight section length on flow pattern and diffuser resistance

14 p2391 A69-29899

Subsonic diffuser design, discussing flow distortion and turbulence levels and pressure loss characteristics

[AIAA PAPER 69-449] 16 p2843 A69-32700

Jet flap as alternative to rigid diffuser for momentum propulsion, discussing thrust augmentation

[AIAA PAPER 69-777] 19 p3393 A69-35645

Diffuser for high performance centrifugal compressors based on discrete pipe drillings

[ASME PAPER 68-GT-38] 19 p3240 A69-36420

Tridimensional infrasonic diffuser geometry effects on operational efficiency, considering opening angle, outlet/inlet section fields ratio and diffuser length/hydraulic radius ratio

24 p4243 A69-42560

Inverse transition from turbulent to laminar flow in radial diffusers, noting nonagreement of transition point prediction methods

[ASME PAPER 69-HT-33] 24 p4247 A69-43530

DIFFUSION

NT AMBIPOLAR DIFFUSION

NT ATMOSPHERIC DIFFUSION

NT ELECTRON DIFFUSION

NT GASEOUS DIFFUSION

NT IONIC DIFFUSION

NT MAGNETIC DIFFUSION

NT MOLECULAR DIFFUSION

NT PARTICLE DIFFUSION

NT PLASMA DIFFUSION

NT SPECIES DIFFUSION

NT SURFACE DIFFUSION

NT THERMAL DIFFUSION

NT TURBULENT DIFFUSION

Diffusion zones in filament reinforced metal matrix composites, using metallographic technique

01 p0103 A69-11269

Diffusion in conduction process in dielectric fluids, discussing space charge limited current-voltage characteristics

03 p0415 A69-13140

Electron plasma oscillations diffusion due to scattering by large amplitude ion wave background, noting electron wave spectrum evolution

03 p0483 A69-14256

Diffusion in compounds of elements of groups III-V

04 p0641 A69-14502

Cr-Si diffusion layers on Ti, noting results of roentgenographic and metallographic studies

04 p0614 A69-14578

Diffusion anomaly of native acceptor defect in zinc selenium telluride p-n junctions, discussing applications in triple diffusion technique of preparing p-n junction diodes

05 p0808 A69-16286

Double diffused planar Ge n-p-n and p-n-p transistors with high switching speed, noting fabrication and performance

05 p0809 A69-16557

Double diffused Si transistors, discussing temperature dependence of gain, injection efficiency, emitter and base regions energy gaps and excess noise

05 p0733 A69-16558

Computer tape controlled pulsed externally excited gas laser mask making machine with micropositioning coordinate table for integrated circuit fabrication

06 p0931 A69-17200

Low temperature technique for preparing solid-diffusion sources for silicon device fabrication based on gaseous hydrides as reagents

07 p1198 A69-18619

Single crystal growth by controlled diffusion in silica gel using metathetical and decomplexation reactions

10 p1652 A69-23371

Brittle fracture at high temperatures in titanium alloys using scanning electron beam microanalysis, noting reaction diffusion with atmosphere and grain boundaries destruction

10 p1713 A69-23823

Soviet collection of papers on diffusion processes in metals covering welding, annealing, anisotropic crystals, metal condensation layer, cast iron decarburization, etc

11 p1890 A69-24798

Diffusion processes in metal welding noting role of recovery, polygonization, recrystallization, polymorphic transformations, etc

11 p1890 A69-24799

Diffusion processes during annealing of metals irradiated by electrons and neutrons, discussing crystal damage, recovery and recrystallization

11 p1891 A69-24800

Diffusive flow with isopycnic lateral boundaries in porous medium and density distribution of diffusive motion, noting exact solution equivalence to previous solution

11 p1869 A69-24887

Etch pits behavior during diffusion and rediffusion of copper in low dislocation crystals of gallium arsenide, demonstrating vacancy nature

11 p1937 A69-25029

Characteristics method for stress waves from hyper-velocity impact of circular cylinder on half space, discussing numerical diffusion effect on pressure and flow fields

[AIAA PAPER 69-355] 13 p2365 A69-28287

Cr-Si diffusion layers on Ti, noting results of roentgenographic and metallographic studies

15 p2638 A69-30279

Elastic and inelastic evolution of concentrated gravitational systems, discussing stellar diffusion, evaporation, halos and rotating systems

15 p2687 A69-30548

Diffuse Zn layers structure in GaAs single crystals, showing dislocations formation by anomalous Zn diffusion

15 p2670 A69-31048

Mass dependence of self diffusion in Fe by serial sectioning in alpha, gamma and delta phases, determining isotope effect with Fe radioactive isotopes

19 p3346 A69-36440

Spectral line scattering during propagation of radiation in turbulent plasma

19 p3396 A69-36573

Be diffusion during vapor phase saturation of W, Mo, Nb and Ta, noting time and temperature dependence of layer thickness

20 p3549 A69-37364

Ventilation-perfusion inequality increase effects on lung overall gas exchange, using digital model

21 p3662 A69-38388

DIFFUSION COEFFICIENT

Mass or energy transfer in reinforced media, discussing components characteristics and role of diffusion processes

01 p0173 A69-10079

Vacancy diffusion in Ge, relation to precipitation of Cu impurities from supersaturated solid solution and determination of monovacancy migration energy

02 p0295 A69-11780

Diffusion data in binary compound semiconductors, tabulating impurities, electrical behavior, temperature variations and diffusion coefficients

02 p0296 A69-11809

Diffusion coefficients for oxygen transport in whole blood, discussing effects of intact red cell concentration

02 p0200 A69-12479

Radial diffusion coefficient for trapped electrons moving across field lines, obtaining time dependent solutions of Fokker-Planck equation

03 p0502 A69-14002

Heterodiffusion of metallic impurities in body centered phases of doped zirconium and titanium, determining diffusion coefficients via radioactive isotopes

04 p0613 A69-14557

Stationary vertical distribution of weightless radioactive substance in surface air layer, accepting two layer exponential law for vertical turbulent diffusion coefficient

04 p0593 A69-15091

Si diffusion rate in single crystal and polycrystalline Mo, using various donor materials

05 p0780 A69-15990

Unique solution for radial diffusion coefficient applicable to equatorially trapped electrons in artificial radiation belt

05 p0816 A69-16279

Graphite ablation in air, N, Ar and He assuming chemical equilibrium, equal diffusion coefficients and steady state ablation

[AIAA PAPER 69-148] 06 p0947 A69-18155

Temperature variability data for 120-km altitude from observations of grenade glow clouds, calculating molecular diffusion coefficients and atmospheric temperature and density

07 p1127 A69-19277

Diffusion coefficients of H atoms in mixtures of He and Ar with hydrogen by catalytic sink technique, discussing rigid sphere collision diameters

07 p1185 A69-19300

Kinetic theory development of equations for multicomponent gaseous mixtures symmetric diffusion coefficients

07 p1186 A69-19395

Diffusion coefficient of interstitial oxygen atoms in tantalum by elastic energy dissipation measurements as temperature function, discussing relaxation effect

07 p1168 A69-19452

Diffusion coefficient, velocity distribution function and velocity averages for gaseous ions moving in strong electric fields, considering ion-gas molecule charge transfer collisions

08 p1355 A69-20209

Loss rate of plasma from stellarator due to binary Coulomb collisions scattering particles in loss region, discussing diffusion coefficients

08 p1364 A69-20520

Self diffusion coefficients measurements for cobalt in nickel-cobalt alloys, using cobalt radioisotope 60

08 p1334 A69-20577

Selenium diffusion in indium antimonide, determining concentration gradients in junction space charge region by capacitance method

09 p1554 A69-21469

Gold diffusion and solubility in indium phosphide, analyzing temperature and vapor pressure effects

09 p1555 A69-21470

Copper diffusion coefficient in undoped n-type gallium arsenide measured by ultrasonic method

09 p1555 A69-21471

Nitrogen diffusion coefficients in TiN and alpha-Ti determined by metallographic and roentgenographic analyses, establishing linear equations for temperature dependence

09 p1523 A69-21736

Multicomponent diffusion coefficients of dissociated air as function of pressure, temperature and concentration, based on simplified model of binary diffusion

09 p1623 A69-22098

Plasma diffusion in toroidal stellarator, calculating collisional diffusion and diffusion constants

09 p1552 A69-22294

Solar cosmic rays proton intensity time variations and diffusion coefficient obtained by satellites, balloons and ground stations observations

10 p1755 A69-22812

Diffusion coefficient and cosmic ray motion in solar system, using satellite data of interplanetary magnetic field

10 p1757 A69-22822

Temperature vs compactness relationship in NbC compacts having nonstoichiometric composition and approximately equal specific surface, determining self diffusion coefficients

10 p1711 A69-23337

Diffusion constant of Ni in Ti alloys with Al, Mo and Nb, considering beta phase

11 p1902 A69-24274

Variational calculation of coefficients of viscosity, thermal conductivity, thermal diffusivity and diffusion in binary mixture

11 p1997 A69-24285

Microsectioning technique applied to measurement of diffusion coefficients of Cr 51 in polycrystalline Nb at 1220-1766 K temperature range

11 p1903 A69-24577

Diffusion coefficients of carbon in tantalum, niobium and vanadium by sectioning method, using carbon 14 as tracer

11 p1906 A69-25575

Diffusion coefficients for laminar multicomponent dissociating boundary layer at surfaces of thermally decomposing protective coatings

12 p2190 A69-25890

InAs-InP solid solutions diffusion rate and lattice constant for various compositions

12 p2144 A69-26587

Diffusion-stabilized difference schemes for inviscid compressible flow equations in conservation form for arbitrary number of space dimensions

12 p2062 A69-26624

Ions and electrons in ionosphere diffusion tensor components and ambipolar diffusion coefficient expressions derived for nonisothermal plasma

12 p2071 A69-26700

Drift velocity and longitudinal and transverse diffusion coefficient for low energy N ions in N gas in mass spectrometer at room temperature

13 p2302 A69-27458

Selenium diffusion in indium antimonide, determining concentration gradients in junction space charge region by capacitance method

15 p2669 A69-30714

Gold diffusion and solubility in indium phosphide, analyzing temperature and vapor pressure effects

15 p2669 A69-30715

Copper diffusion coefficient in undoped n-type gallium arsenide measured by ultrasonic method

15 p2669 A69-30716

Thermal diffusion coefficient for fully ionized plasma containing mixture of arbitrary charge ions in topside ionosphere

16 p2775 A69-32084

Turbulent diffusion inside sun as explanation of solar spin-down, Li depletion at surface and neutrino discrepant, discussing diffusion coefficient and stellar evolution

16 p2866 A69-32814

Flame front structure and combustion rates of gases as function of temperature dependence of thermal conductivity, diffusion coefficients, density and molecular weight

17 p3069 A69-33136

Aluminum oxide relative grain boundary energy and surface diffusion coefficient, considering thermal grooving of bicrystals with symmetrical tilt boundaries

17 p2993 A69-34191

Gaseous diffusion coefficients during argon, krypton, oxygen and nitrogen diffusion into helium measured by gas chromatography

18 p3099 A69-34280

Carbon diffusion parameters in alloys of Nb with Ti, Zr, W and Mo, using radioactive carbon 14

18 p3157 A69-35250

Beryllium diffusion coefficients in Zr and Ti bcc phases, using radioactive beryllium 7 at high temperatures

18 p3157 A69-35251

Diffusion during high temperature exposure of protective coatings on Mo, noting compact layers and carbide forming elements effect on thermal stability

19 p3345 A69-36156

Hydromagnetic wave-charged particle resonant interaction described by diffusion equation in momentum space, deriving diffusion coefficients and time evolution ultrarelativistic particle energy spectrum

19 p3424 A69-36335

Carbide coatings formation on graphite in molten media, determining diffusion coefficient of carbon in molten Zr

20 p3566 A69-37372

Eddy diffusion coefficients due to instabilities in internal gravity waves near mesopause

20 p3534 A69-38090

Radial diffusion coefficient calculation in presence of magnetic shell splitting in magnetosphere

20 p3534 A69-38094

Nitrogen diffusion coefficients in TiN and alpha-Ti determined by metallographic and roentgenographic

analyses, establishing linear equations for temperature dependence

20 p3564 A69-38214

Diffusion layers and elasticity-dependent interdiffusion coefficients of Ti binary systems, using X rays

21 p3745 A69-38954

Vertical heat exchange flux model using heat conduction equation compensating for tropospheric and stratospheric radiation divergence, calculating diffusion coefficient

22 p3936 A69-40137

Ternary diffusion at high temperature in Fe-Co-Ni alloy system covering entire ternary phase diagram, including computed interdiffusion coefficients

23 p4176 A69-41505

DIFFUSION ELECTRODES

Refractory metal silicon device technology noting high temperature diffusion masking properties for possible use in MOSFET technology

06 p0930 A69-17152

Fuel cell system using double skeleton catalyst gas diffusion electrodes, discussing design, mode of operation and performance

08 p1261 A69-21047

Lateral diffusion gas electrodes for electrochemical generators compared with classical electrodes

16 p2739 A69-32415

DIFFUSION FLAMES

Oxygen addition to fuel stream effect on formation of soot and polycyclic aromatic hydrocarbons in ethane-air and ethylene-air diffusion flames

02 p0205 A69-12318

Electrically controlled heat transfer between flat parallel flow hydrocarbon diffusion flame and walls of combustion chamber

02 p0353 A69-12324

Chemical reaction scheme effect on hot zone structure of hydrogen-oxygen diffusion flame, considering influence of hydroxyl radical

03 p0531 A69-12895

Unsteady motions of diffusion flame sheet due to perturbations of reactant concentration, approximating species and energy conservation requirements

03 p0532 A69-13014

Combustion in heterogeneous systems, considering diffusion flames and fine droplets dispersed into gaseous oxidizer in fog form

06 p1032 A69-17421

Temperature distribution in low pressure magnesium vapor-oxygen diffusion flames, discussing environmental conditions and visible radiation

[WSCI PAPER 68-20] 07 p1241 A69-18367

Hydrogen diffusion flames stabilization by flame holders in supersonic flow at low stagnation temperature, measuring burning limits

[DVL-815] 09 p1624 A69-22615

Boundary layer equations describing momentum, energy and mass concentration conservation in axisymmetrical turbulent jet flame solved for Lewis number unity in von Mises plane

13 p2379 A69-28455

Vaporizer temperature and collision efficiency correlation data for magnesium oxide-argon dilute diffusion flames studied for determining inverse temperature dependence

13 p2380 A69-28461

Self excited vibrating laminar diffusion flames, discussing coupling, jet spacing radial heat transfer and boundary layer interaction

16 p2876 A69-31711

IR spectrometric analysis of flames of composite rocket propellants, maintaining diffusion flames between surfaces of decomposing ammonium perchlorate and fuel source

[WSCI PAPER 69-10] 16 p2831 A69-32350

Deflection effect on flow and mixing process in flames covering enclosed turbulent diffusion flames in combustion chamber

17 p3068 A69-32966

Diffusion flame stability at inlet of fuel stream into oxidizer, showing ignition coordinates dependence on fuel, oxidizer and ratio of burning/flow rate

19 p3448 A69-35855

Temperature measurement in and near opposed-jet diffusion flame subjected to electric field, discussing flame behavior at low mass flow rate

21 p3852 A69-39597

Reaction broadening in hydrogen-oxygen diffusion flame for slow hydrogen dissociation, using matched asymptotic expansions

24 p4408 A69-42920

Three dimensional shadowgraph-like images in single exposure holograms of diffusely illuminated flame explained as time average holographic interferograms

24 p4317 A69-43764

DIFFUSION THEORY

Inelastic collisions effect on electron energy distribution in low temperature diffusion dominated discharges
04 p0637 A69-15047

Helium flux in lower thermosphere, using diffusion theory for multicomponent gas mixture to determine equation for equilibrium distribution
07 p1125 A69-18848

Impurity atoms effects on Cu diffusion and solubility in GaAs, determining Hall coefficient temperature dependence and conductivity
07 p1199 A69-19009

Rays associated Fokker-Planck relation for isotropic turbulence diffusion equation, discussing logarithmic refractive index, moments and path length
08 p1272 A69-20021

Positive column in longitudinal magnetic field in helium and neon, noting agreement with collision diffusion theory and Kadomtsev perturbation theory
08 p1361 A69-20212

Cosmic ray modulation by solar wind, discussing anisotropic diffusion during propagation through interstellar magnetic field
10 p1759 A69-22842

Solar activity and 19 to 24 day variations in cosmic ray intensity
10 p1759 A69-22843

Neon discharge positive column at medium gas pressures, discussing calculated and experimental data concerning diffusion theory to interpret parameters
10 p1740 A69-23723

Chapman-Enskog procedure extension for binary gas mixtures, obtaining diffusion equation from revised relaxation time of component velocities
11 p1921 A69-24308

Beam-plasma dispersion relations, obtaining dispersion equation for plasma waves and dispersion curves for longitudinal waves
11 p1925 A69-24366

Emission and diffusion theories of metal-semiconductor contacts for describing current characteristics of abrupt isotype nGe-nGaAs heterojunction
11 p1938 A69-25115

Transition density function of randomly excited diffusion process and confinement probability at fixed spatial point satisfying integrodifferential equation involving functional derivatives
11 p1860 A69-25451

Pitch angle diffusion of trapped electrons in terrestrial radiation zones, discussing diffusion theory based on Fokker-Planck equation, atmospheric Coulomb scattering mechanism, etc
12 p2150 A69-26746

Combined conduction and radiation transfer equations solutions for absorbing-emitting gas, obtaining slip coefficient for diffusion solution correct boundary condition
13 p2374 A69-27784

Diffusion equation unsteady solution for flasks of equal volumes connected by capillary, considering end effect and transient processes
13 p2251 A69-28561

Time dependent convection electric fields as agents for diffusing trapped magnetospheric radiation inward toward earth, discussing one dimensional diffusion equation
14 p2510 A69-28936

Elastomeric adhesives diffusion theory, tack increasing methods, cast polymer films, properties and applications in shoe manufacturing and sealants
14 p2468 A69-29341

Cometary tail diffusion model based on luminous particle number decrease with time and particle accelerated motion and diffusion in space
14 p2523 A69-29705

Galactic cosmic rays and Alfvén waves interaction, considering gyration frequency resonance, wave growth, Fokker-Planck equation and diffusion model
15 p2675 A69-30761

Harmonic analysis for computing diffusing matter with periodically varying surface concentration applied to electrical insulants degradation by atmospheric moisture
15 p2592 A69-31057

Spatial and temporal dependence of trapped particle energy spectra on basis of bimodal diffusion
16 p2852 A69-32619

Lattice vibration theory of solid state diffusion for Cu including anharmonic effects formulated using equilibrium statistical mechanics, considering interacting phonon events
17 p3015 A69-32822

Lower solar corona composition changes due to pressure and thermal gradients calculated with multicomponent diffusion equations
17 p3030 A69-33059

Polarization effect on diffusion equations of radiative transfer, noting anisotropy in Rayleigh scattering
21 p3847 A69-38473

Monochromatic radiation diffusion in one dimensional bounded medium, deriving equations for probability density of quantum yield and intensity of light fluxes
21 p3769 A69-38586

Wiener-Hermite truncated stochastic expansion used for velocity and concentration fields in turbulent flow convecting passive scalar, determining diffusivity and spectrum function
24 p4302 A69-43359

DIFFUSION WAVES

Cosmological implications of diffuse X ray background, noting Compton black body process effect on isotropic cosmic X rays
09 p1578 A69-22152

DIFFUSION WELDING

Diffusion welding of AMS 4921 titanium, discussing premature pressure removal before completion of first joining stage
01 p0086 A69-10535

Diffusion bonding and forming of large and complex Ti structures, noting advantages in freedom of design and in economy
04 p0604 A69-14525

[ASM PAPER C7-2.3]

Diffusion bonding of whisker reinforced aluminum in closed steel die in argon atmosphere
06 p0943 A69-17238

Microstructure of diffusion zone during contact fusion in magnesium-nickel system at high temperatures
06 p0945 A69-17895

Titanium alloy interaction porosity with fillers during diffusion brazing, discussing joint strength as function of time, temperature and pressure
06 p0945 A69-17896

Doped silicon dioxide films as controlled reproducible diffusion sources for silicon devices fabrication
07 p1198 A69-18620

Roll diffusion bonding technique for permitting complex design of coldplates and radiators of spacecraft electronic equipment
09 p1504 A69-22066

Diffusion bonding parameters for producing hollow Ti-Al compressor blades, discussing surface preparation, postbond heat treatment quality control and mechanical properties
09 p1513 A69-22484

[ASME PAPER 69-GT-46]

Fusion and solid state welding of steels, considering electron beam, HF resistance, friction and explosive welding
12 p2100 A69-25830

Diffusion bonded Ti honeycomb sandwich, demonstrating structural integrity, efficiency, low weight and cost effectiveness
12 p2115 A69-26828

Diffusion bonding as solid state metal joining process for nuclear and aerospace hardware, discussing tooling and nondestructive tests
14 p2454 A69-28840

[ASME PAPER 69-DE-7]

Diffusion bonding for leaktight joints in connectors using intermediate metal system of Au-Cu-Au
15 p2617 A69-30100

Diffusion bonding of metals, discussing interface joining processes and application to fluoric devices, jet engine servovalves and porous woven structures
17 p2978 A69-33374

Diffusion bonded Ti honeycomb sandwich, discussing production, structural efficiency, high strength/weight ratio, etc
19 p3320 A69-35558

Tensile and stress rupture strengths of diffusion bonded Ni superalloys, using spin tests of simulated hollow turbine disks
19 p3320 A69-35559

Soviet book on diffusion welding in vacuum covering ferrous metals, homogeneous nonferrous metals, equipment, cermets, etc
19 p3329 A69-36748

Diffusion bonding of Al and boron filament layers into continuous structural material, studying process variables including heat treatment and cross rolling effects
20 p3564 A69-38197

[AIME PAPER S69-6]

Diffusion welding and soldering of metallic wire with graphite and graphitized viscose applied to chromel, copel, chromel-alumel, Mo, W and W-Re
21 p3728 A69-38617

Joints structure, phase and chemical composition in kinetics of titanium diffusion brazing with copper
22 p3958 A69-41203

Room temperature tensile tests determining failure modes and defect influence on diffusion welds of unalloyed Ti, using electron microscopy and fractography
24 p4331 A69-42939

Metallurgical and structural production of diffusion bonded titanium honeycomb sandwich panels for aerospace hardware weight saving
24 p4324 A69-43434

DIFFUSIVITY

Turbulent fluid transport properties predicted by simple model for fluid behavior, obtaining mass, momentum and energy diffusivities
01 p0177 A69-11402

Heat of solution and diffusivity of nitrogen in molybdenum analyzed by quenching technique and resistivity measurements at liquid helium temperature
02 p0267 A69-12188

Composition dependence of carbon activity and carbon diffusivity in austenite
13 p2279 A69-27763

DIFLUORIDES

U CALCIUM FLUORIDES

DIFLUORO COMPOUNDS

U POLYTETRAFLUOROETHYLENE

DIGESTING

Scenedesmus algae cell wall structure degrading to increase digestibility of cell bound protein, describing mechanical, enzymatic and chemical methods
21 p3667 A69-39701

DIGESTIVE SYSTEM

NT ESOPHAGUS
NT GASTROINTESTINAL SYSTEM
NT INTESTINES
NT RECTUM
NT STOMACH

Anoxia effect on succinic dehydrogenase and lactic dehydrogenase activities in digestive glands and organs sensitive to oxygen tension changes
22 p3887 A69-41193

DIGITAL COMMAND SYSTEMS

Ground station command transmission equipment for German AZUR satellite, describing components based on NASA Tone Digital Command System
16 p2759 A69-31856

Digital autopilots for Apollo CSM and CSM/LM vehicles thrust vector control, describing modifications of onboard computers and programs
21 p3762 A69-39377

DIGITAL COMMUNICATION

U PULSE COMMUNICATION

DIGITAL COMPUTERS

NT IBM 360 COMPUTER
NT SEQUENTIAL COMPUTERS

Digital computer system for storing, processing and displaying TV pictures
01 p0077 A69-10024

Root-mean-square error determination in automatic control system by digital computer for realizing control function, investigating harmonic and random input effects
01 p0050 A69-10208

Numerical digital computer determination of ultra subharmonic response for Duffing equation
01 p0104 A69-10235

Numerical evaluation of curvilinear integrals and areas, using digital computer
01 p0106 A69-10867

Hybrid computers, discussing analog and digital devices combination and distinction between use of computer for general purpose computation and control purposes
02 p0212 A69-11997

Proper digital filters devoid of transient response analyzed as extension of time invariant filters
02 p0213 A69-12815

Multipulse propagation communications system /MMPCS/ utilizing digital computer to implement intermittent system
03 p0389 A69-13191

Digital computer systems design optimization based on operational experience in development of Saturn S-1C stage Automatic Test and Checkout System
03 p0400 A69-13233

Interferometer at lambda 21 cm using fully steerable paraboloids for processing output signal with on-line digital computer
03 p0411 A69-13468

Nonlinear aerodynamic problems of plane and asymmetric flows solved by digital computer, using modified Monte Carlo method
03 p0364 A69-13921

Digital electronic computer technique for control of aircraft power plant, describing self adaptive control
03 p0496 A69-14091

Aerospace digital computer design, discussing influence of data trends and reliability techniques
03 p0401 A69-14181

Collection of papers on engineering applications of digital computers, examining programming, numerical methods and design and simulation problems
04 p0563 A69-14514

Computer systems definition, terminology and functional description, discussing engineering problems, flow charts, programming and techniques
04 p0563 A69-14515

Digital computers for global atmospheric circulation, describing circulation models and computer produced color movies utilization
04 p0628 A69-15363

Digital radar systems, discussing control computers, beam steering computers, signal processors, mode control, displays and chirp networks
05 p0718 A69-15748

Digital signal processing in radar, sonar and communication
05 p0718 A69-15749

Multimode digital radar control paths and operating communication, discussing radar data, triggers, real time data and error localization
05 p0718 A69-15750

Digitally controlled flight systems simulators, noting design improvements over conventional trainers
05 p0742 A69-15884

Digital computer interface systems design for simulation, control, instrumentation and data processing, discussing hybrid computer linkages
05 p0723 A69-16195

Computer use evaluation, discussing standards for automatic data processing [ADP/ investment and operations
05 p0850 A69-16299

Flight test data reduction on time sharing general purpose computer, noting hardware link between airborne equipment and computer
05 p0726 A69-16758

On-line analysis with digital computer, noting system designed for vibration and random vibration analysis
05 p0726 A69-16761

Computer oriented telemetry data processing systems designed to condition raw telemetry data for further processing by other systems
05 p0727 A69-16770

Ranger pictures improvement by computer, eliminating image distortion due to electronic imaging systems
06 p0924 A69-17164

Digital computer optimization of representation of sampled data signals on orthogonal basis, using iterative method
06 p0901 A69-17363

Book on FORTRAN computer programming language
06 p0891 A69-17364

Digital computer motion pictures generation for ground controlled intercept simulation
06 p0906 A69-17397

Digital computer circuit design book covering requirements of circuit for digital logic and memory functions and physical properties of components
06 p0892 A69-17869

Onboard digital computer evaluation of trigonometric functions for antenna pointing
07 p1089 A69-19745

Complex digital computers designed for Apollo spacecraft missions, discussing construction techniques [AGARDOGRAPH-114]
08 p1279 A69-20990

Airborne digital computers for optimization of aircraft control and monitoring functions, discussing avionics and circuit technology
08 p1349 A69-21194

OMNITRAC general purpose airborne digital computer with permanent memory of 4096 words of 23 bits, noting modular construction
10 p1659 A69-22845

Conformal mapping of regions with corners and large curvatures of boundary curves onto unit circle with digital computer, considering airfoil
10 p1724 A69-22880

Analog to digital conversion for data sampling systems including scanning, distributors, multiplexing, automatic ranging, noise reduction and data storage techniques
10 p1660 A69-23232

Computer controlled data acquisition and control system /DACS/ for wind tunnel applications, describing system and programs
10 p1673 A69-23286

Instabilities of numerical integration of ordinary differential equations on digital computer, considering difference approximation containing extraneous solutions
10 p1721 A69-24042

Real time electronically scanned radar control using digital computer with input and output conversion for information handling, noting interface equipment
11 p1834 A69-24544

Dynamic behavior of nonlinear continuous multivariable systems represented by equations derived from block diagram, stressing digital computer properties
12 p2049 A69-26081

Automatic plotting devices for graphic readouts in analog and digital computers
12 p2091 A69-26303

Digital differential analyzer as control element, analyzing performance limitations imposed by scaling constraints with canonical realization of transfer functions
12 p2053 A69-26509

Digital computer redundancy, analyzing triple modular redundancy in Saturn vehicles and quad design in primary processor and data storage for OAO
12 p2034 A69-26567

Self adjusting digital computer method for two dimensional gravitational anomalies
12 p2076 A69-27088

Man machine interactive structural analysis using digital computer with CRT display, detailing design
12 p2035 A69-27098

Designs and capabilities of digital processing systems for automatic air traffic control radar information stressing future use of display for computerized control
13 p2295 A69-27332

Microwave measurement methods, discussing uses of digital computers and sampling techniques
13 p2223 A69-28605

Root-mean-square error determination in automatic control system by digital computer for realizing control function, investigating harmonic and random input effects
14 p2424 A69-28744

Largest scalar product of class and identification codes in diagnostic problems, discussing recognition
14 p2417 A69-29144

Digital computers for aircraft engines control, discussing economic assessment, advantages and basic control system
15 p2671 A69-30323

Vibration/acoustics environmental testing, discussing advantages of digital computer control system and digital noise generation techniques
15 p2586 A69-30387

Time delay errors compensation methods in analog-digital computation loops, finding digital scheme inferior to analog
15 p2572 A69-30618

Automatic meteorological radar data processing system incorporating MRL-1 radar and low speed digital computer
16 p2791 A69-32279

Computer programs for space engineering analytical and scientific computation using digital computers
16 p2756 A69-32555

Digital computer program for physiological measurements, outlining interpolation of mathematical functions describing signals time variations
17 p2912 A69-32941

On-line central data processing system connected to time shared computer for recording data from test facilities, discussing hardware configuration, software considerations and advantages
17 p2932 A69-33106

Astronomical satellite direct digital attitude control using digital computer between sensor and actuator to achieve optimal filtering and stabilization
17 p3049 A69-33244

Digital computer for aircraft engine control covering in-flight health monitoring, automatic flight checkout, diagnostic failure routines, etc
17 p3022 A69-33603

Electronic computers for avionics system design in terms of technology, performance and cost, discussing reliability prediction and failure rate data
17 p2976 A69-34058

TC-2 general purpose digital avionics computer in A-7D/E avionics system performing tasks in weapon delivery, navigation and guidance, display updating, self testing, etc
17 p2933 A69-34059

AN/ASN-24/V/ general purpose digital computer deployed in large worldwide jet transport fleet
17 p2933 A69-34061

Patch panel programmed DDA computer having MHz iteration rate and 35 bit usable word length, discussing system design and demonstration model
17 p2934 A69-34073

Solid state single unit digital control computer performing stability augmentation, pilot relief functions and generating minimum fuel flight paths for VTOL landing
17 p2934 A69-34075

General purpose /GP/, differential digital analyzer /DDA/ and CORDIC /coordinate rotation digital computer/ computers for navigation system computations
17 p3003 A69-34100

Airborne digital computers techniques in avionics stressing memory design, packaging, reliability and maintainability
18 p3106 A69-34846

PDP8 digital computer and Trebel vertical balancing machine combined for real time presentation of trim weights and positions, noting noise in force components
18 p3220 A69-34888

Computerized air combat simulation with comparison of analog and digital approaches, noting Air to Air Combat/Fort Worth [AIAA PAPER 69-811]
19 p3289 A69-35629

Takeoff and landing analysis digital computer program /TOLA/ developed by Air Force Flight Dynamics Laboratory for quantitative performance analysis [AIAA PAPER 69-810]
19 p3289 A69-35630

Precompression automatic wild point rejection from sampled telemetry data for data compressors evaluated by digital computer simulation
19 p3273 A69-36263

Stored program data processor used as PCM telemetry data acquisition system for postApollo applications, considering format and bit rate changes
19 p3274 A69-36280

Space environmental simulation facilities, discussing digital computers and equipment for simulating oxygen atmosphere, vacuum, heating and cooling, etc
19 p3295 A69-36326

Digital computers standard programs for astronomical problems
20 p3596 A69-37317

Binary increment and residual class notation techniques for onboard spacecraft computer arithmetic
20 p3499 A69-37378

Failure test algorithm for sequential units with delay lines of control digital computers, detecting replacement of output terminals by sensitive paths
20 p3502 A69-37394

Integrated logic circuits assembly for digital computers, considering high density, mechanical environment, reliability, accessibility and costs
20 p3505 A69-37401

Digital computers used in error calculation in calibration curves of turboengines and other pneumatic devices
21 p3724 A69-39100

Computer organization design employing distributed processor to provide general purpose computing while taking advantage of large scale integration
21 p3856 A69-39133

CRT graphic display/plotter for small digital computers, describing device operation, control and applications
21 p3679 A69-39608

Centaur computer assimilating Centaur vehicle hardware functions performed by digital computer, discussing modules, flight control system, cost reduction, etc [AIAA PAPER 69-943]
22 p3904 A69-40326

Spacecraft onboard computer for prelaunch targeting constants verification through checksum equation and error detection scheme, using generated number sequences [AIAA PAPER 69-946]
22 p3974 A69-40329

SIMUPOL /Simulation Procedure Oriented Language/ system for hardware description and architecture and interface requirements of digital processor [AIAA PAPER 69-960]
22 p3905 A69-40341

Software support package for aerospace digital computer emulation, consisting of symbolic assembly program and interpretive simulator program and subprogram [AIAA PAPER 69-974]
22 p3907 A69-40354

Digital computer system for navigation, landing, fire control, monitoring and checkout aboard Saab 37 Viggen aircraft handling attack, reconnaissance and fighter missions [AIAA PAPER 69-985]
22 p3908 A69-40365

Hybrid and monolithic integrated microcircuits application to electronic digital computer structures
24 p4284 A69-42907

DIGITAL DATA

Satellite digital video data analyzed by two dimensional digital computer technique, discussing biomedical applications

02 p0213 A69-12155

Multichannel digital data compression simulation, discussing algorithms, buffer queue control, identification coding and system performance measurements

02 p0213 A69-12814

Ground based control system via cockpit PPI display on transponder equipped aircraft broadcast with digital coding

03 p0464 A69-13244

Fast Fourier-Hadamard transform for digitized signal representation, classification, discrimination and efficiency

03 p0392 A69-13249

Delay line bandwidth reduction for video or digital information, noting radar tracking application

03 p0392 A69-13251

Optimum gain control for diversity receivers used for radar and digital data transmission through fading media

03 p0410 A69-13833

Digital communications between aircraft and flow control computers on ground to avoid runway saturation and automating routing functions

05 p0721 A69-16722

Block coding systems performance in digital PCM data transmission through N-ary discrete channels in white Gaussian noise presence, discussing SNR upper bounds

07 p1080 A69-19096

Data transition tracking in digital communication systems by decision directed phase tracking loops

07 p1082 A69-19108

Asynchronous on-line digital data acquisition system with immediate access to on-site numerical real time printout for rocket engine performance tests [AIAA PAPER 69-323]

09 p1478 A69-22381

Computer simulation of unbiased digital recording composed of sequential computations intended for various bit densities [IEEE PAPER 3.3]

09 p1461 A69-22562

Digital sampled data spectra conditioning, deriving linear functions for low pass, bandpass and band rejection numerical filters and spectrum shaping

10 p1654 A69-23292

Error correction of digital data with cyclic codes and probability function set extended to Bose-Chaudhuri-Hocquenghem codes and P super M codes

10 p1655 A69-23529

Tandem interleaved cyclic codes for digital HF communication with improved error rate at reduced decay time

10 p1655 A69-23530

Digital data transmission techniques and complex instrumentation systems design noting control, identification, synchronism and error reduction

11 p1834 A69-24545

Angle-to-code converter designed on basis of quantum magnetometers frequency sensors, transforming vector sum of bias magnetic fields into pulse repetition rates

12 p2016 A69-25963

Fast folding algorithm for detection and correlation of digital data with weak noisy pulse trains of differing periods

14 p2416 A69-29548

Stochastic saturating systems optimal control computation, considering attitude control and tracking system design by elliptical differential equation of dynamic programming

15 p2582 A69-30601

Alphanumeric listing and digital data x-y plotting by high speed printer, describing equipment modifications and control software

17 p2932 A69-33108

Taylor series expansion used in correcting quantized digital coefficient errors in hybrid feedback control system

18 p3111 A69-34687

Digitized video cloud picture data from ESSA satellite, discussing mesoscale archive and computer products including time averages and composites

19 p3279 A69-35810

Digital data transmission by pulse code modulation considered for minimum mean square error

19 p3274 A69-36282

Numerical and analog data acquisition system /CARINA/ for processing rocket, balloon and satellite data, describing distributor characteristics, control console, etc

20 p3511 A69-37914

Noiseless feedback schemes for digital and analog transmission over additive white Gaussian noise channels

21 p3671 A69-38405

Digital data analysis systems role in experimentation and R and D

21 p3843 A69-39315

Real time FM-to-digital converter for measuring periods of demodulated FM/FM data, discussing systems design

22 p3903 A69-39923

Digital data transition tracking loop mean square phase noise computed as function of input SNR by Fokker-Planck technique

23 p4130 A69-42514

Analog feedback system for digital data transmission, describing feedback channel, error rate and SNR effects

24 p4289 A69-42977

DIGITAL FILTERS

Signal to noise ratio requirements for sharp cut-off biphasic digital communication channel

13 p2221 A69-27959

Optimum nonlinear digital filter synthesis for smoothing, predicting and differentiating measured quantity having uniform probability distribution over finite number of discrete values

14 p2426 A69-29421

Digital notch filters synthesis based on bilinear transformation method

15 p2575 A69-30182

FORTAN program for calculation of magnitude and phase of digital filter transfer functions and power spectra of periodic waveforms

15 p2567 A69-30612

Probability density functions of waveforms from summation of digits in n-stage shift register generating m-sequence

15 p2568 A69-30617

Stepped digital narrow band bandpass microwave elliptic function filters design and construction

16 p2759 A69-31939

Book on linear digital filtering and discrete spectrum analysis, emphasizing frequency domain description of signals and systems

20 p3487 A69-37146

Spacecraft onboard processor for digital filtration and data compression, discussing prototype design, construction, sample memory, weight memory, arithmetic unit and programmer

20 p3500 A69-37383

Filtering optimization prior to limiting digital signals in strong noise, detailing bandwidth choice of single pole low pass filter

21 p3676 A69-39450

DIGITAL INTEGRATORS

Steady state digital-analog integrator for solving nonlinear heat conduction type equations

21 p3680 A69-39852

DIGITAL NAVIGATION

PDM command coder meeting NASA Tone Digital Command Standard for German central ground station

16 p2755 A69-31859

Airborne digital computer and display devices role in navigation management, discussing data processing and hybrid navigation systems

16 p2809 A69-32260

Onboard navigation digital computer simulation to verify calculation principle and logic units during design and construction

20 p3502 A69-37398

DIGITAL SIMULATION

Digital phase locked loops synthesis for fading and sequential phase estimation in decoder using digital computation

03 p0388 A69-13178

Radar or ECM/ECCM system simulation by digital computer, using signal and jamming spectral inputs

03 p0400 A69-13200

Digital simulation of demodulator/tracking phase locked loop of navigation/traffic control satellite system in thermal noise diffuse multipath fading environment

03 p0390 A69-13204

Digital simulation based on guided missile experience, discussing numerical methods for ordinary differential equations, literature, choice of method and simulation languages

03 p0401 A69-13763

Continuous dynamic systems digital simulation, noting run-time program determined by numerical integration structure

04 p0565 A69-15339

SALEM programming system developed for digital simulation of systems described by partial differential equations

04 p0565 A69-15340

System/360 Continuous Modeling Program, detailing input language, user-defined functions and documentation

05 p0723 A69-16196

Digital simulation of vehicle motion and control for six degree of freedom simulations of Gemini reentry and aircraft, missile control, etc

05 p0725 A69-16477

Digital simulation design for linear dynamic systems, noting role of digital transfer function

06 p0906 A69-17491

Control systems digital simulation based on coupling of prediction correction procedure with integration and differentiation procedure, discussing simulation errors

08 p1296 A69-20110

Multistep integration formulas treated as transfer system to examine properties in frequency domain for selection in digital simulation programs

09 p1460 A69-21417

Digital computer simulation as maintainability design and prediction tools, discussing fault localization in complex electronics systems

10 p1668 A69-22974

Monte Carlo digital computer simulations, considering sample sizes and confidence intervals in multinomial output

10 p1661 A69-23853

Integration routines performance used in dynamic systems simulation by digital programs, comparing speed, accuracy and convenience

10 p1661 A69-23854

Rigid body rotational simultaneous equations of motion transformed into explicit form for digital simulation

10 p1661 A69-23855

Digital simulation of phase locked receiver in diffuse multipath fading environment with band limited thermal noise

11 p1839 A69-25298

Space vehicle docking dynamics and matrix equations of motion amenable to numerical solution on digital computer, using Hamilton principle and Lagrange multipliers

11 p1967 A69-25501

Digital program containing Eulerian formalism for multiple interconnected rigid members applied to gravity gradient stabilized satellite with flexible booms

11 p1989 A69-25502

Digital computer simulation of multidimensional stationary or nonstationary Gauss-Markov random processes with specified autocorrelation function, discussing time step choice

12 p2122 A69-26523

Computer simulation program for design and evaluation of digital Doppler processor, analyzing performance limitation due to quantization and white noise

12 p2035 A69-27096

Digital simulation for radio systems nonlinear elements, outlining procedures to obtain algorithms

15 p2582 A69-30111

Digital simulation optimizing parameters of digital equipment to measure target azimuths in pulsed surveillance radar system, establishing optimum echo pulse quantization threshold

15 p2563 A69-30138

Digital computerized analysis and characteristics of variable stability aircraft, examining digital control system

15 p2549 A69-30229

Digital simulation of transient solar still processes, using finite difference approach for heat flow to and from soil

16 p2765 A69-31816

Digital simulation computer stability analysis scheme premised on use of perturbed transient responses

17 p2944 A69-32899

Digital simulation of biological model for visual images classification derived from human visual system aspects

17 p2911 A69-34094

Saturn 5 system simulation showing feasibility, efficiency and economy of real time simulation using large mathematical model and general purpose digital computer

18 p3113 A69-34268

Cerebral circulation arterial system pulsatile flow flexible vessel digital simulation models distribution

19 p3264 A69-36867

Linearized wave propagation digital simulation models to predict arterial blood flow characteristics and impedance, comparing phase velocity and transmission per wavelength

19 p3264 A69-36868

Ventilation-perfusion inequality increase effects on lung overall gas exchange, using digital model

21 p3662 A69-38388

Arrhythmia diagnosis instruction aided by cardiac pacemaker digital simulation, discussing clinical electrocardiograms generation mechanisms

21 p3667 A69-39606

SIMUPOL /Simulation Procedure Oriented Language/ system for hardware description and architecture and interface requirements of digital processor [AIAA PAPER 69-960]

22 p3905 A69-40341

Flight training using digital simulators, including maneuver analysis for TWA 707 program

22 p3928 A69-41137

Digital simulation of oxygen pressure fields and supply conditions in biological tissues

23 p4097 A69-42098

DIGITAL SYSTEMS

Integrated circuit digital filters design characterized by weight coefficients containing Lanczos factor for application to processing of signal transmitted from space vehicles

01 p0038 A69-10071

Hybrid digital transmission systems, discussing joint optimization of analog and digital repeaters and information rate of coaxial cable systems

01 p0027 A69-10248

Regenerative digital transmission system error, representing memory of binary regenerative channel with Markov model

01 p0027 A69-10249

Quantizing noise effect on reconstructed analog signal at reception terminal of digital data transmission system

01 p0027 A69-10250

Fluidic system controlling inlet guide vanes to high pressure compressor of two spool jet engine, using digital elements to drive hydraulic servosystem

02 p0305 A69-12090

Optimum control of fourth order digital control system

03 p0408 A69-12916

Generalized digital low pass filter synthesis by recursion technique, noting coefficient sensitivity simplification

03 p0403 A69-13227

Digital data processing equipment for space flight PCM telemetry

03 p0393 A69-13290

Digital processing of Doppler radar signals using matched filter concept

03 p0393 A69-13291

Noise susceptibility of integrated circuits in digital systems, discussing sources and specifications

03 p0410 A69-13579

CASSANDRE programming language for digital systems, noting application to logic systems

03 p0401 A69-14179

Granularity of beam positions in digital phased arrays based on method of moments and phase distribution

04 p0570 A69-14306

Miniaturized adding sample and hold device with adjustable delay applied to digital filters

04 p0574 A69-14350

Instrument and rounding-off errors of aircraft computers as function of digital network dimensions

04 p0563 A69-14491

High speed modular multiplier and digital filter for LSI development

04 p0567 A69-15354

Digital nth order phase locked loop for FM demodulation

04 p0561 A69-15452

Digital filter design with complex coefficients for analytic signals and complex envelopes

04 p0579 A69-15460

Digital filter transfer functions design by sampled data transformation, noting role of analog filters

04 p0584 A69-15461

Special purpose computer for implementing programmable digital filter used in sampled data control systems

04 p0569 A69-15462

Digital filters for moving target indicator radars compared with analog filter systems

04 p0580 A69-15463

Bit reduction in digital transfer functions with LF poles in sampled data systems using zero order hold function

04 p0584 A69-15464

Fluid amplifiers, discussing digital and proportional jet-interaction devices and circuits

05 p0704 A69-16004

Fast digitalized scan laser using Nd-YAG as active medium and containing crossed array of lithium niobate electro-optic switches for mode selection [IEEE PAPER R-2]

05 p0775 A69-16326

Digital controller weighting function sectionalization to simplify logic in developing adaptive control system

05 p0739 A69-16386

Upper and lower bounds for feedback decoding and definite decoding minimum distances of binary convolutional codes

06 p0904 A69-17865

Sequence pulse stuffing technique for rate equalization of digital channels, discussing coding effect and capacity for word signaling

07 p1080 A69-19094

Single channel binary PSK communication systems performance influenced by degree of RF coherence between transmitter and receiver

07 p1082 A69-19109

Design and construction of linear digital filters for signal processing, discussing digital filtering of various signals for space research

08 p1297 A69-20303

Fluidics in UK, discussing digital control elements and systems and transmission lines in alternating flow hydraulics

[AGARDOGRAPH-118]

08 p1257 A69-20952

Power spectrum of nonstationary processes with periodicity in two dimensional autocorrelation function based on Fourier transform

09 p1455 A69-21847

Common mode rejection technique to determine phasing differences in digital systems by measuring pulse delay

09 p1463 A69-21896

Joint filter optimization in combination analog-digital hybrid multilevel transmission system

09 p1457 A69-22465

Minimum error probability and optimal system regime relationship to noise rejection in memoryless communication investigated for limited repeated transmissions

09 p1459 A69-22639

Probability analysis of distortions caused by pulse noise action on digital information

09 p1476 A69-22678

Test stand final control element for fluid flow application, noting analog control valve with digital to analog conversion and digital actuator

10 p1671 A69-23259

Wall attachment phenomenon /Coanda effect/ basis for jet elements in digital and/or pulse-mode systems

10 p1638 A69-23553

Large scale integrated circuit accumulator chip as control element for design of digital system by design automated techniques

12 p2037 A69-25942

Digital logic techniques for high speed satellite communications, noting general purpose logic cards

12 p2040 A69-26465

Error due to amplitude quantization and design of digital control systems in discrete time optimum control theory

12 p2053 A69-26507

Ferrite core storages characteristics with rectangular hysteresis loop for digital control units, discussing optimal selection method

14 p2418 A69-29145

Limiting incoherent or coherent interference signals at frequency of biphasic or quadriphase digital signal

14 p2413 A69-29483

Bayesian theory to determine maximum a posteriori estimation algorithms for optimum bit synchronization in digital communication systems

14 p2413 A69-29496

Digital receiver of radar signals for performing binary quantization of input data with subsequent processing by digital computer

15 p2563 A69-30136

Digital simulation optimizing parameters of digital equipment to measure target azimuths in pulsed surveillance radar system, establishing optimum echo pulse quantization threshold

15 p2563 A69-30138

Disturbances simulation in instrumentation utilizing digital integrated circuits for reliability computation in complex circuits

15 p2628 A69-30848

Dispersion characteristics of open interdigital line structure by treating structure as radiator, applying linear antenna theory

16 p2748 A69-31580

Equipment- and program-type methods for solving automatic digital control systems synthesis problems, evaluating efficiency based on accuracy

17 p2933 A69-33120

Pulsed control systems sensitivity relationship to discreteness period described via differential equations

17 p2994 A69-33143

Digital IC radiosonde system, discussing sampling, pulse width modulation, time multiplexing, follow-on subsystems, etc

17 p2937 A69-33675

Linear computer-controlled closed loop systems sensitivity analysis, deriving estimation error incremental covariance to demonstrate quality deterioration under perturbed initial conditions, parameters, etc

17 p2944 A69-33742

Digital data acquisition system with ultrahigh sampling rate for Ames electric arc shock tunnel, describing analog to digital conversion, data storage, system performance, etc

19 p3293 A69-35744

High speed analog to digital multiple channel wide-band data acquisition system designed for short pulse Doppler radar and probe measurements

19 p3307 A69-35745

Digital data compression system transmission error statistical analysis, emphasizing addressing schemes effect on compression ratio

19 p3272 A69-36261

Optimal structural parameters of radar digital ranging servosystems derived from reproduction error, including computer simulation data

19 p3278 A69-36593

Digital frequency synthesizer design parameter selection, giving expressions for output frequency and division coefficient variations

19 p3284 A69-36594

Gunn effect applied to digital electronics, discussing diode characteristics, microwave amplifier design, pattern recognition, analog- numerical conversion, etc

19 p3285 A69-36708

Book on digital magnetic logic, considering digital magnetic core circuits consisting of magnetic components and interconnecting conductors

20 p3498 A69-37144

Double binary PSK system digital computer simulation for satellite communications, investigating filter and limiting effects on performance in error probability terms

20 p3492 A69-37705

Eye chart determination and layout for digital transmission system by computer simulation

21 p3678 A69-38776

Digital data analysis systems role in experimentation and R and D

21 p3843 A69-39315

Titan 3C launch vehicle digital flight control system using flight equations time-shared with guidance equations

21 p3824 A69-39404

Parse-implement approach to digital systems design, combining systems level /conceptual/ and engineering environmental level /physical/ viewpoints

21 p3680 A69-39663

Programmable digital compensator for single high performance control loop servomechanisms

21 p3688 A69-39704

Digital systems for acoustical or vibrational measurements reception and evaluation

22 p3945 A69-40168

Digital data systems fault detection and isolation, describing diagnostic programs and hardware [AIAA PAPER 69-967]

22 p3906 A69-40348

Booster digital guidance and control system, discussing communication device providing data transfer between airborne digital computer and control device

22 p3978 A69-40368

Aircraft digital control hardware and applications including airborne computer proper, distributed systems, loop control, system integrity, etc [RAES PAPER 4]

22 p3908 A69-40485

Integrated adaptive data transmission system accepting analog inputs through information compressing sampler or digital inputs by sampling

23 p4121 A69-41760

Multiple access discrete address system /MADA/ for digital modulation communication systems for satellite networks, using time division techniques

23 p4130 A69-42512

Digital transition tracking symbol synchronizer for low SNR coded telemetry systems, discussing phase locked loop analysis and phase detector simulation by Monte Carlo method

23 p4130 A69-42513

Coefficient quantization in digital continuous time process controllers, applying results to nominal transfer function approximation

24 p4292 A69-43283

Tristable fluid amplifiers, analyzing J functions of staticized variable, ternary logical characteristics, input equations, flow stability and switching measurements

24 p4255 A69-43298

Correction coefficients for time response of hybrid control systems with digital feedback elements containing quantized coefficients

24 p4293 A69-43302

DIGITAL TECHNIQUES

Digital matched filtering technique for RF interferometer employing carrier modulated by pseudo-noise sequence, discussing applications to antenna arrays

01 p0048 A69-11003

Moving window analysis digital technique for complex seismic surface waves in presence of noise and multimode propagation

02 p0243 A69-12006

Digital detection of angle modulated signals including zero crossing detectors, digital phase locked loops, differentiation and arcsine demodulator

03 p0391 A69-13230

Digital electronic computer technique for control of aircraft power plant, describing self adaptive control

03 p0496 A69-14091

Fourier coding method for coding images for digital transmission, achieving bandwidth reduction for televised images

04 p0556 A69-14429

Continuous dynamic systems digital simulation, noting run-time program determined by numerical integration structure

04 p0565 A69-15339

Hybrid executive development based on digitally oriented software, explaining assembly language routing

04 p0567 A69-15351

Radar echoes signal amplitude and phase digital recording with Radicord /radar digitizing and recording device

05 p0721 A69-16618

Statistical analysis of Radicord /radar digitizing and recording / clutter and signal spectra and moving target detection by pulse radar

05 p0721 A69-16619

Radar signal matched filters synthesis using linear digital filters and digital correlators noting role in radar detection

05 p0722 A69-16733

Digital adaptive recording system /DARS/ 12 channel flight recorder

05 p0766 A69-16754

Digital spectra analysis by Fourier transform and comb filter for determination of voltage and power spectra

05 p0722 A69-16762

Book on FORTRAN computer programming language

06 p0891 A69-17364

Digital FM techniques, signal spectral properties, discrimination detection, phenomenological model, etc

07 p1081 A69-19105

High speed sampling for dynamic data analysis, considering random and transient vibrations

07 p1232 A69-19139

Radome performance dependence on dielectric permittivity determined by digital program and simple design criterion

07 p1110 A69-19519

Multiple access techniques in civil satellite communications systems, noting proposed digital time and frequency division methods

08 p1272 A69-19959

Digital method for quantitative study of carrier circulation phenomena in semiconductors, noting Algol program and continuously polarized p-n junction

08 p1280 A69-19973

Receiving systems for digital telemetry signals from spacecraft, analyzing receiver performance by statistical methods

08 p1276 A69-20591

Digital telemetry from spacecraft, discussing on-board processing, data compression, coding, sequence detection and receivers

08 p1276 A69-20592

Digital information transmission error characteristics determining error distribution over time and relation to distribution function of intervals between errors

09 p1454 A69-21795

Microelectronics for digital adaptive controls, discussing digital filter design and chips required in fabrication

09 p1474 A69-22453

Digital signal tracking module operation and stability, considering use of interconnecting modules to achieve adaptive tracking

09 p1459 A69-22477

Digital reconstruction of images from optical holograms for acoustical data, discussing image degradations

10 p1695 A69-23547

Digital design techniques for electronic equipment including measuring instruments, generators, synthesizers, etc

10 p1664 A69-23796

Digitally controlled formant /spectral maximum/ generator for terminal analog speech synthesizer

11 p1852 A69-25292

Digital logic techniques for high speed satellite communications, noting general purpose logic cards

12 p2040 A69-26465

Digital computer methods for weak pulsars search using radio noise picked by telescopes

12 p2172 A69-27169

Error analysis involved in calculating tangent functions defined by nonlinear differential equation solution, using digital differential analyzer

13 p2225 A69-27968

Algorithm for optimal digital processing of pulse signals during multilevel quantization in Markov noise, including error analysis

15 p2571 A69-30126

Digital computerized analysis and characteristics of variable stability aircraft, examining digital control system

15 p2549 A69-30229

Vibration/acoustics environmental testing, discussing advantages of digital computer control system and digital noise generation techniques

15 p2586 A69-30387

Vibration/acoustics digitally controlled environmental testing, describing configuration and operation of control system and statistical requirements for noise generation

15 p2587 A69-30388

Vibration/acoustics digitally controlled environmental testing, describing random test signal generation and random vibration tests

15 p2587 A69-30389

Hybrid coupled low power digital microwave phase shifters design, discussing lumped element L-C and variable C shifter theories, power limitations and construction techniques

15 p2580 A69-31076

Counter for decimal counting and numeric display applications using integrated fluid logic elements

15 p2616 A69-31295

Optimizing control system design using fluidic digital circuitry and FM type transducers

15 p2583 A69-31296

Surface wave study techniques, discussing digital moving window analysis of group and phase velocity and use of time variable filters

16 p2784 A69-32576

Seismic surface wave observations analyzed by applying moving window method to orthogonal detector recordings permitting lateral refraction measurement, wave separation, etc

16 p2784 A69-32577

Airborne digital computers techniques in avionics stressing memory design, packaging, reliability and maintainability

18 p3106 A69-34846

Book on digital electronics for scientists covering digital circuits and instruments for measurement, control or computation

18 p3112 A69-34915

Book on linear digital filtering and discrete spectrum analysis, emphasizing frequency domain description of signals and systems

20 p3487 A69-37146

Strapped down phased array radar tracker mechanization with digital loop closure electronics for homing missiles, noting cost advantages

[AIAA PAPER 69-873] 21 p3763 A69-39399

Temperature program generation for test chambers, describing temperature programmers and readout, verification and recording systems

22 p3954 A69-40038

Digital processing of rocket-borne mass spectrometers for measurements in upper atmosphere, discussing calibration

22 p3904 A69-40232

Digital signal processing electronic device for linearizing signals from sensors with nonlinear frequency output by modifying time signal frequency

22 p3915 A69-40935

Digital telemetry link coding as English language analogy, developing block code scheme combining bit, word and block error detection and correction methods

23 p4119 A69-41745

Digital analysis of surface wave observations discussing moving window, multiple filter, multicomponent recording, time variable filtration and cross correlation techniques

23 p4157 A69-42018

Digital analysis of nonlinear control systems dynamic stability under small perturbations, using linearized differential equations

24 p4285 A69-42984

On-board digital filtering applied to spectral estimation and data compression, discussing theory, techniques, computerized implementation and prototype design

[AIAA PAPER 69-969] 24 p4285 A69-43510

DIGITAL TO ANALOG CONVERTERS

Pneumatic analog to digital and digital to analog converters, noting diaphragm force balance capsules, converters using stepping motors and factors affecting accuracy

[ASME PAPER 68-WA/AUT-16] 05 p0706 A69-16176

MSI 12 bit digital to analog converter in integrated circuit form using MOS switching circuit

[AIAA PAPER 69-968] 22 p3906 A69-40349

DIGITAL TRANSDUCERS

Phantom disk encoder for arc second digital position transducers

05 p0766 A69-16748

Production method for fabricating HF surface wave interdigital electrode transducers, discussing pattern replication, etching, etc

14 p2455 A69-29571

Electrode interactions effects in interdigital surface wave transducers on piezoelectric materials, using Fourier analysis

24 p4312 A69-42615

DIGITIZERS

U ANALOG TO DIGITAL CONVERTERS

DIGITS

U BINARY DIGITS

DIHEDRAL ANGLE

Polytropic gas unsteady motion in dihedral piston wake by solving mixed boundary value and Goursat problems

22 p3861 A69-41025

DIHEDRAL EFFECT

U LATERAL STABILITY

DILATION

U STRETCHING

DILATOMETERS

U EXTENSOMETERS

DILATOMETRY

Precipitation hardening of gamma phase in austenitic stainless steels studied for phase transformations by dilatometry after aging and quenching

01 p0096 A69-10613

Dilatometer for measuring thermal expansion of solid bodies over temperature range at various gas media pressures

03 p0432 A69-14151

Automatic recording inverted dilatometer employing fused quartz vertical pedestal and yoke type pushrod

15 p2607 A69-30153

DIMENSIONAL ANALYSIS

Dynamic programming methods to avoid dimensionality problem arising in solution of boundary value problems by digital computer

01 p0103 A69-10006

Electric arc properties, investigating volt-ampere characteristics by approximate similitude and dimensional analysis

01 p0125 A69-10099

Space diversity reception as applied to radio astronomical investigation of large scale ionospheric inhomogeneities

02 p0237 A69-11665

Relationships derived by dimensional arguments connecting vertical heat fluxes and horizontal momentum in constant flux layer with other relevant variables

02 p0275 A69-12692

- Hydrostatic journal gas bearings calculations for carrying capacity, gas consumption and optimal dimensions for maximum lifting capacity
03 p0432 A69-12960
- Thermovortex effect, determining functional relations between interdependent parameters by means of dimensional analysis
03 p0531 A69-12966
- Independent nature of variables in dimensional analysis, discussing temperature in kinetic and dimensional analyses
13 p2289 A69-28362
- Space diversity reception as applied to radio astronomical investigation of large scale ionospheric inhomogeneities
13 p2257 A69-28696

DIMENSIONAL MEASUREMENT

- Moon figure from meridional measurements of visible diameters at different angles of libration, deriving equation for polar and equatorial compression of lunar ellipsoid
03 p0512 A69-13690
- Cepheid stars as distance indicators in extragalactic space, using periodicity-luminosity relation
08 p1408 A69-21147
- Holographic interference method for measuring film height in analyses of fluid film vaporization under blowing hot gas
12 p2088 A69-26178
- Gas laser-Doppler radar system for moving materials velocity and length measurements in industrial processes
22 p3955 A69-40237
- Laser interferometric length measurement by fringe counting, considering mechanical and optical systems limitations and design tolerances
22 p3960 A69-40238
- Nondestructive thermal method of measuring wall thickness and channel blockage in investment castings used in aircraft parts production
24 p4312 A69-42754

DIMENSIONAL STABILITY

- NT SHELL STABILITY
NT STRUCTURAL STABILITY
- Cesium sorption in materials for thermionic converters reservoirs, discussing dimensional stability of porous alumina, W and C samples
14 p2463 A69-29220
- Liquid drop in electric field numerically analyzed for disintegration dynamics and instability through cross section computation at time intervals
23 p4151 A69-41694

DIMENSIONLESS NUMBERS

- NT FROUDE NUMBER
NT GRASHOF NUMBER
NT LEWIS NUMBERS
NT MACH NUMBER
NT NUSSELT NUMBER
NT PRANDTL NUMBER
NT RAYLEIGH NUMBER
NT REYNOLDS NUMBER
NT RICHARDSON NUMBER
NT SCHMIDT NUMBER
NT SIMILARITY NUMBERS
NT STANTON NUMBER
NT STROUHAL NUMBER
- Fracture toughness measurements by means of dimensionless fracture toughness parameters, noting results for materials with very different elastic moduli
05 p0780 A69-16080
- Heat transfer for incompressible inviscid fluid flow in cone, expressing solution in terms of dimensionless numbers
13 p2375 A69-27788
- Dimensionless approach to maximum flow in heat pipes and optimization of capillary structure
14 p2539 A69-29206
- Similitude applied to dynamics of disperse media, discussing role of dimensionless numbers in mechanics of suspensions and two phase flows in porous media
19 p3300 A69-36775

DIMENSIONS

- NT DIAMETERS
NT FILM THICKNESS
NT HEIGHT
NT LENGTH
NT RADII
NT SCALE HEIGHT
NT TARGET THICKNESS
NT THICKNESS
- Dimensions, temperature and electron density of quiet solar corona from radio interferometer measurements, noting activity and temperature at solar maximum and minimum
08 p1393 A69-20573

- Dimensioning and strength calculations - Conference, Budapest, October-November 1968
17 p3051 A69-32975
- DIMERS**
- Spectral measurements for matrix isolated lithium fluoride extended into far IR to obtain evidence for linear lithium fluoride dimer
02 p0205 A69-12465
- Submillimeter wave absorption by dimeric water in atmosphere, using interferometer and maser
05 p0759 A69-16658
- Luminescence spectra of aromatic polymers, monomers and dimers under high energy electron excitation using molecular resonance model
16 p2828 A69-32792
- Dimer bond energies analysis in Mg and Ca dimer molecules, approximating characteristic temperatures and virial coefficients
23 p4195 A69-42210

DIODES

- NT AVALANCHE DIODES
NT CESIUM DIODES
NT CRYSTAL RECTIFIERS
NT GERMANIUM DIODES
NT JUNCTION DIODES
NT PARAMETRIC DIODES
NT PHOTODIODES
NT PLASMA DIODES
NT THERMIONIC DIODES
NT TUNNEL DIODES
NT VARACTOR DIODES
- Small signal impedance of subcritically doped gallium arsenide Gunn diodes, using drift velocity vs electric field relationship
01 p0038 A69-10121
- X band mixer with reactively terminated image, using gallium arsenide barrier diodes and microwave integrated circuit techniques
01 p0039 A69-10189
- Diode structure optimization for monolithic integrated circuit for Ku-band reflective phase shifter
01 p0040 A69-10195
- Semiconducting diode base Dember effect impedance studied for recombination rates approaching zero or infinity
01 p0137 A69-10260
- Gunn generator efficiency dependence on diode and regime parameters using computer model
01 p0042 A69-10319
- YIG single crystal resonator tuning of Gunn diode in coaxial line circuit
01 p0042 A69-10320
- Limited space-charge accumulation mode efficiency for gallium-arsenide diodes, taking into account electron-lattice relaxation processes
01 p0137 A69-10321
- Semiconductor switching diode, evaluating operation with nonlinear time delay equivalent circuit
01 p0046 A69-10747
- Output power of Gunn effect microwave diode using equal area analysis and Fourier transforms
01 p0049 A69-11195
- Efficiency curve for step recovery diode frequency multipliers, using analog computer simulation
02 p0215 A69-11947
- Fluid mechanics of one stage momentum flueric diode
02 p0195 A69-12071
- Dynamic current-voltage characteristics of thin film diodes on chalcogenide glass base
02 p0223 A69-12834
- Clamp type diode holders for obtaining CW coherent emission from gallium arsenide injection lasers
03 p0435 A69-12985
- Small silicon diodes to explore depth-dose distributions in water phantom of proton beams
03 p0430 A69-13481
- Thermal and shot noise in pumped resistive diode for frequency conversion, analyzing equivalent circuits
03 p0406 A69-13828
- Diode mixer power series coefficients for spurious response prediction in superheterodyne receiver
03 p0399 A69-13905
- Computer simulations defining conditions to produce series operation of Gunn effect diodes
04 p0573 A69-14340
- Schottky barrier mixer diodes and point contact diodes failure, discussing criterion for degradation of noise figure, 1/f noise and reverse breakdown voltage
04 p0574 A69-14352
- Gamma radiation effects on transistors and diodes, discussing dosage and thermal changes within operational temperature range of germanium devices
05 p0728 A69-15695

- Peripheral surface damage effects on epitaxial GaAs bulk diodes breakdown characteristics, noting measurements on mechanically and chemically prepared elements
05 p0733 A69-16561
- Shot noise in Si Schottky barrier diodes for frequencies between 100 Hz and 50 kHz
05 p0734 A69-16564
- Equivalent circuit for microwave point diode noting waveform calculations, frequency dependent elements and recovery phenomena
05 p0735 A69-16605
- Diffused Si and GaAs diodes electroluminescence and current-voltage characteristics
06 p0893 A69-16898
- Spectral response of fast GaAs point-contact diode in mm and submillimeter wavelength ranges
06 p0893 A69-16939
- Active region doping effect on laser diode threshold current, noting current dependence on loss coefficient in interband transition model without selection rule
06 p0933 A69-17257
- Q factors dependence of IMPATT diode oscillator FM noise, noting excess noise temperature correlation with diode current
06 p0899 A69-17826
- Gunn effect diodes application to ultrafast pulse electronic circuitry for computer logic
07 p1089 A69-18244
- Richardson constant and tunneling effective mass for thermionic and thermionic field emission in Schottky barrier diodes
07 p1089 A69-18247
- Surface recombination rate and retardation field effects on diffusion current in mesa diodes with low level injection
07 p1105 A69-19008
- Controlled charge models for computer calculation of electronic circuits, discussing tunnel diode static characteristics and equivalent transistor circuits
08 p1280 A69-19975
- Quenched multiple domain mode oscillations in GaAs microwave diodes noting relationships between efficiency, power output, negative resistance and bias voltage
08 p1282 A69-20107
- Semiconductor laser with isolated diodes in cavity, noting watt-ampere characteristics during nonuniform excitation and threshold curves
08 p1326 A69-20539
- Inertia limited flow transition to mobility limited flow in gas diodes by taking velocity moments of Boltzmann equation for electron velocity distribution function
09 p1462 A69-21325
- Voltage dependence of mobility limited electron current density in gas filled diode for collision frequency proportional to electron speed
09 p1462 A69-21326
- Diffusion method for fabricating negative resistance diodes consisting of Cd doped silicon, introducing Cd into n-type silicon plates in evacuated vials
09 p1462 A69-21477
- Forward volt-ampere characteristics and differential resistance peak of Schottky barrier diode on doped Si
09 p1557 A69-21744
- Isothermal diode as study basis for internal complex controlling thermionic energy conversion
09 p1439 A69-21827
- Silicon diode array camera tube modified to permit X ray images to be displayed on TV monitor
09 p1463 A69-21845
- Gunn effect domains propagation calculated for nonuniform diodes of annular geometry, obtaining frequency variation
09 p1464 A69-22159
- Semiconducting diode base Dember effect impedance studied for recombination rates approaching zero or infinity
09 p1559 A69-22653
- Discontinuous vortex power amplifier and diode design, noting supply regulator effects and load matching
09 p1443 A69-22737
- Spontaneous reverse current due to Brillouin EMF observed in diode in thermal noise range
10 p1661 A69-22950
- Transient characteristics of negative resistance zinc alloy diodes, investigating temperature effects
10 p1662 A69-23157
- Computerized design techniques for microwave components using diodes, detailing X band parametric amplifier
10 p1661 A69-23874

Passive structural units in fluidic circuits, discussing tesla diode and proportional amplifier
11 p1825 A69-24542

High temperature and power gas diodes and thyratrons for nuclear electrical space power systems
11 p1847 A69-24744

AC diode switching circuits employed as threshold elements in functional rectifiers for approximating non-linear functions
11 p1857 A69-25717

In-circuit diodes testing by semiautomatic low current regulated voltage test set
12 p2035 A69-25835

Diode type image shutter tube with proximity focusing for high speed photography
12 p2083 A69-26145

Computer analysis on ideal step recovery diode frequency multipliers for optimum efficiencies
12 p2039 A69-26378

LF negative resistance of X band Gunn diodes with lumped components, using coaxial circuit
12 p2039 A69-26387

Matched diodes in monolithic balanced mixer by diode array fabrication for noise suppression
13 p2233 A69-28071

Operation mode of modulator with p-i-n diode, determining modulus and phase of reflection factor
13 p2235 A69-28518

Injection phase-locking characteristics of LSA /limited space charge accumulation/ mode transferred-electron diode oscillators, employing negative conductance and equivalent circuit
14 p2421 A69-29544

Diffusion method for fabricating negative resistance diodes consisting of Cd doped silicon, introducing Cd into n-type silicon plates in evacuated vials
15 p2578 A69-30722

Diode burn-in dissipation measurement for reliability testing
15 p2579 A69-31043

Optical and electrical properties of electroluminescent diffused gallium arsenide phosphide diodes with low donor concentrations, analyzing spectral emission and fabrication effects
16 p2758 A69-31699

Single balanced modulators using square law resistors /space charge limited diodes/, discussing noise properties, conversion losses and terminating conductance
16 p2758 A69-31756

Electrical switching in thin film arsenic selenium telluride semiconducting glass diodes, observing formation of liquid phase and conducting filaments
16 p2760 A69-32017

GaAs dual diode laser structure used to give electrical control of laser threshold and permit study of optical flux and current density role
17 p2980 A69-32959

Pulsed ultrasonic flaw detectors resolving power enhancement by shunting semiconductor diodes across piezoelectric elements of scanning heads to shorten scan pulse duration
18 p3137 A69-35112

Magnetic field effect on Gunn diode vibrations and LF oscillations, noting increase in threshold field and decrease in threshold current
18 p3183 A69-35267

Light emitting diodes /LED/, discussing operating voltage vs color, diode materials and applications
20 p3505 A69-37702

Step recovery diode principle and operation mode as frequency multiplier explained by models
21 p3684 A69-39736

S-band pin-diode switch for high CW power satellite and deep space probe communication, using multiple quarter-wave transformers to stepdown diode impedance
23 p4143 A69-42518

DIOXIDES

- U CARBON DIOXIDE
- U ENSTATITE
- U HYDROGEN PEROXIDE
- U PYROCERAM [TRADEMARK]
- U PYROXENES
- U QUARTZ
- U SILICON DIOXIDE

DIPLO ANTENNAS

Dipole array antenna radiation pattern, gain and beamwidth as function of number of dipoles, noting case for main beam scanning
01 p0046 A69-10737

Radiation pattern, gain and polarization of omnidirectional antenna consisting of dipoles or monopoles arranged along circular cone
01 p0046 A69-10738

Dipole antenna current distribution, deriving simple, accurate formula for infinite, semiinfinite and finite cases
02 p0218 A69-12330

Helical log periodic and log periodic dipole arrays impedance and radiation patterns measurements have similar characteristics
02 p0219 A69-12337

Short backfire antenna radiation fields calculation by approximate method
02 p0219 A69-12339

Ground wave excited by dipole in conducting half space, discussing lateral wave character and optimum radiation angle
02 p0209 A69-12347

Electric or magnetic dipole antenna radiated electromagnetic field for antenna orientation perpendicular to striations of periodically stratified dielectric medium
03 p0398 A69-13802

Infinite phased dipole array, discussing integral equation, current distributions and active admittances
04 p0571 A69-14316

Mutual coupling and element efficiency for infinite linear arrays of dipoles
04 p0571 A69-14317

Book on cylindrical dipole arrays covering theory and programs for computational analysis and design with desired characteristics
04 p0574 A69-14353

Input admittance of cylindrical dipole antenna immersed in cold isotropic lossless plasma medium and insulated by ion sheath or unit permittivity dielectric
04 p0580 A69-15490

Emission of thin metallic antenna in randomly inhomogeneous medium, determining effective impedance
06 p0894 A69-17451

Circular antenna array consisting of identical center fed cylindrical dipoles placed tangential to and in plane of circle and with equal spacing
06 p0898 A69-17765

Shot noise in dipole antenna immersed in hot plasma related to antenna input resistance, using Maxwellian velocity distribution
07 p1079 A69-18920

Radiation resistance of short dipole immersed in cold magnetoionic medium, using polarized wave modes
07 p1107 A69-19226

Algebraic expression for field pattern of asymmetrically driven long antenna with multiple excitations, using Wiener-Hopf integral equation
08 p1281 A69-20016

Long transmitting dipole antenna, studying current and charge distributions by Wiener-Hopf technique
08 p1281 A69-20019

Coupling between array antennas shown to reduce reflecting properties of Van Atta reflector consisting of linear half wave dipoles
08 p1282 A69-20037

Y-circulators specified, measured and calculated values correlated as function of leakage matrix elements and terminating dipoles reflection
09 p1473 A69-22114

Horizontal VLF cylindrical transmission antenna current distribution calculated with allowance for ground reaction, showing exponential decrease with distance
09 p1467 A69-22581

Antenna for lunar occultation observations at 81.5 MHz, detailing experimental procedure and data reduction
10 p1779 A69-23606

Radiation field of log periodic dipole array calculated as function of observation point and dipole currents
10 p1664 A69-23802

Approximate method for calculating linear multidipole antennas parameters in terms of power requirement, considering equidistant/nonequidistant element antennas
11 p1849 A69-24969

Log periodic dipole array antennas simulated with simple RLC circuit loading uniform transmission line
11 p1850 A69-24977

Current distribution on elements of circular arrays of tangential dipoles, discussing large odd component in zeroth order approximation
11 p1853 A69-25318

Far field radiation pattern, radiation resistance, power gain, directivity and effective aperture for center fed dipole antenna with feed points displaced arbitrarily
12 p2039 A69-26352

Input impedance of quarter wavelength antenna in anisotropic plasma, discussing plasma parameters role and use of probe antenna in plasma diagnostics
12 p2044 A69-27071

Field patterns for wave radiation from electric dipole immersed in anisotropic plasma column excited by longitudinal DC magnetic field
12 p2034 A69-27103

Antenna cross dipole array for vehicle tracking in VHF band, obtaining effect of local rotation by electrical phase shifting
13 p2226 A69-27185

Gain optimization for dipole endfire array through orthogonalization of element directivity noting effects of element spacing, element gain and mutual coupling
13 p2226 A69-27186

Radio emission of atmospheric cosmic ray showers observed with multiple wideband half wave dipole antenna system, obtaining radiation spatial distribution
13 p2332 A69-28407

Half wave dipole antenna operational factors analyzed for RF radiation spatial power distribution from atmospheric cosmic ray showers
13 p2332 A69-28408

Radiation pattern of electric and magnetic dipole on flat semiinfinite impedance system edge found similar
13 p2236 A69-28546

Diffraction of electromagnetic waves produced by vertical dipole on impedance sphere of large radius in isotropic medium, using moment method
16 p2751 A69-32028

Coupling between electric dipoles in warm plasma, determining electron density and temperature from resonance peak of mutual impedance at electron plasma frequency
17 p2925 A69-33846

Thin metal antenna average current and effective impedance in randomly inhomogeneous medium, discussing cases of strong and weak permittivity fluctuations
17 p2927 A69-33858

Van Atta array reflector retrograde effect, studying influence of transmission line length, interelement spacing and line-dipole matching on incident reflected radiation phase correlation
17 p2929 A69-33878

Emission of thin metallic antenna in randomly inhomogeneous medium, determining effective impedance
20 p3508 A69-37936

Deployable cross log periodic dipole /LPD/ array on conducting cone as potential application to spacecraft or missile requiring frequency independence in VHF-UHF band
22 p3913 A69-40693

Kirchhoff equations for synthesis of passive dipole arrays, obtaining best approximation to radiation patterns
23 p4138 A69-41935

Radiation characteristics of dipole on wedge edge with sinusoidal current, discussing spatial phase and polarization calculations by computer
23 p4138 A69-41937

Ground antenna array for ionospheric physics experiments, consisting of wire dipoles connected to receive circular or linear polarization
24 p4286 A69-42607

DIPLO MOMENTS
NT ELECTRIC MOMENTS
NT MAGNETIC MOMENTS

Magnetotropometer for measuring torque /proportional to magnetic dipole moment/ exerted on object by earth magnetic field
02 p0248 A69-11768

Paraelectric resonance spectroscopy on KCl, using bistable dipole model
06 p0982 A69-18235

Rotational spectrum of ethylene episulfide to determine molecular structure, particularly orientation of C sub 2 S ring
08 p1268 A69-20535

Magnetic masses of differentiating or integrating floating gyroscope effect on gyro moment sensor performance, examining utilization of multiple permanent magnet
09 p1497 A69-22102

Scattering of spherical electromagnetic wave emitted by electric and magnetic dipoles with equal moments at truncated infinitely thin ideally conducting paraboloid of revolution
11 p1846 A69-24614

Computer made movies and time history plots for ion-dipole collisions involving polar molecules /CO, HCL and acetonitrile/
24 p4352 A69-43124

DIRAC EQUATION

Vector potentials for Dirac equation derived assuming time independent external magnetic field without scalar potential
04 p0638 A69-15273

Higher dimensional Dirac Hamiltonians from L-matrix hierarchy using dimensional eigenvector
04 p0625 A69-15275

Second rank Dirac spinors with invariant components relative to Lorentz group transformations
19 p3361 A69-36817

Dirac hypothesis on varying G constant considered in formulating earth expansion theory without resorting to Ramsey hypothesis
22 p4018 A69-40178

Dirac equation in external electromagnetic fields, deriving solution for constant orthogonal electric and magnetic fields encountered in plasma transport
23 p4190 A69-41357

Steady state cosmology for classical and quantum electrodynamics in local vicinity, deriving Lorentz-Dirac equation from variational principle
23 p4215 A69-42116

DIRECT CURRENT

Brushless DC torque motor using reluctance magnetic circuit and toroidally distributed coil winding
01 p0012 A69-10154

Storm-Shattuck and push-pull tunnel diode DC-to-DC converters suitable for spacecraft power supplies
01 p0013 A69-10750

Amplifying channel processes of DC amplifier, discussing relations to couple channel with HF channels of operational operators and to synthesize amplifier frequency characteristics
01 p0053 A69-10802

DC beta falloff in transistors at large collector currents measured, discussing relation to emitter crowding
04 p0574 A69-14347

Low DC current measurement on board satellite, noting absence of elaborate compensation
04 p0602 A69-15399

Regulated high voltage DC to DC converter with output voltage programmable numerically, noting application on board HEOS A satellite
04 p0602 A69-15400

DC servo system with torque feedback to ensure sensitivity to load variation and provide optimal performance
05 p0736 A69-15659

DC servo system with torque feedback, discussing bang-bang system comparison, analog simulation, damping and quasi-optimum behavior
07 p1059 A69-19229

Mutual influence of two different laser modes corresponding to two transitions with same ground level, using He-Ne DC laser
08 p1325 A69-20284

Final stage of three phase DC/AC converter, noting three phase control circuit for power stages with germanium transistors
08 p1285 A69-20381

Closed loop regulated flyback DC to DC converter using constant frequency generator for duty cycle control
09 p1442 A69-22454

DC to DC converters design using HF transistors to achieve high switching speeds while reducing size and weight
10 p1635 A69-22983

DC conversion amplifier commutation induced noise and signal ratio as function of shunt capacitance across vibrator load investigated for increased noise stability
11 p1845 A69-24555

Time-pulse function generator with piecewise parabolic approximation for converting value given by DC voltage or time interval into DC voltage for arbitrary functional relation
12 p2079 A69-25968

DC to RF energy conversion in ungridded klystron gaps, calculating efficiency and optimum load conductance as function of gap dimensions
12 p2041 A69-26629

Brushless DC motor with commutation control by magnetic position sensor scanned at HF
12 p2017 A69-26894

Signal processing and DC restoration in line scan devices used in land/water terrain analysis
12 p2096 A69-26980

Single phase bidirectional AC/DC power convertor based on back-to-back SCR hybrid bridge
13 p2209 A69-28178

Tubes faults monitoring in three phase Gratz converter bridges by measuring voltage across DC smoothing inductor
15 p2575 A69-30180

Operating conditions influence on thermal stability of DC plasmatron arc to obtain high temperature source
15 p2663 A69-30994

Stabilized DC to DC converter advantages in output voltage, overall dimensions and efficiency for battery driven mobile equipment
16 p2765 A69-32443

Two dimensional numerical solution for Faraday DC MHD generators with variable conductivity, velocity and magnetic field
21 p3649 A69-39027

Two dimensional analysis of junction transistor electrical behavior, analyzing DC and AC crowding effects, conduction and impedance of base and collector
22 p3911 A69-40011

Capacitive coupling vs DC coupling between data input and transmitter exciter in FM telemetry system, based on pulse series Fourier analysis
23 p4119 A69-41744

DIRECT POWER GENERATORS

NT ALKALINE BATTERIES

NT DRY CELLS

NT FUEL CELLS

NT HYDROGEN OXYGEN FUEL CELLS

NT MAGNETOHYDRODYNAMIC GENERATORS

NT PHOTOELECTRIC GENERATORS

NT RADIOISOTOPE BATTERIES

NT REGENERATIVE FUEL CELLS

NT SNAP 10A

NT SNAP 13

NT SNAP 21

NT SNAP 27

NT SOLAR CELLS

NT THERMAL BATTERIES

NT THERMIONIC CONVERTERS

NT THERMOELECTRIC GENERATORS

Satellite power generation and transmission system for solar energy conversion, noting estimates of surface area and weight of collectors
02 p0323 A69-12296

Electrogasdynamics generator for direct conversion of moving dielectric medium potential or thermal energy to electric power
03 p0369 A69-14153

Fuel cells utilizing direct electrochemical conversion of energy of radioactive elements
08 p1269 A69-21054

Closed loop regulated flyback DC to DC converter using constant frequency generator for duty cycle control
09 p1442 A69-22454

DC to DC converters design using HF transistors to achieve high switching speeds while reducing size and weight
10 p1635 A69-22983

Thermodynamics of sinusoidal steady state energy converters governed by Onsager reciprocal relation, determining maximum conversion efficiency
11 p1826 A69-25396

Variable voltage DC power supplies for energizing cryogenically cooled and superconductive electromagnets
12 p2017 A69-26498

MHD energy converters electric fields and current distributions, analyzing MHD flow problems
21 p3777 A69-39480

Performance, size, weight, operational characteristics and cost estimates of ZrH reactor-organic Rankine power systems
23 p4189 A69-42265

DIRECTION

Cosmic ray approach directions computation for high latitude stations, discussing results for low rigidity galactic cosmic rays and solar corpuscular events detection
18 p3187 A69-34940

DIRECTION FINDERS [RADIO]
U RADIO DIRECTION FINDERS

DIRECTIONAL ANTENNAS

NT DIPOLE ANTENNAS

NT HELICAL ANTENNAS

NT HORN ANTENNAS

NT INERTIALESS STEERABLE ANTENNAS

NT LENS ANTENNAS

NT LOG PERIODIC ANTENNAS

NT LOOP ANTENNAS

NT PARABOLIC ANTENNAS

NT RADAR ANTENNAS

NT RHOMBIC ANTENNAS

NT SLOT ANTENNAS

NT STEERABLE ANTENNAS

NT TWO REFLECTOR ANTENNAS

NT YAGI ANTENNAS

Directional antennas gain loss on ground sections calculated on basis of difference-phase measurements data
02 p0214 A69-11612

Retrodirective antenna array with switched Butler matrix feed
02 p0223 A69-12813

Decameter wideband directional antenna system for investigation of ionosphere by retrodiffusion method
03 p0402 A69-12860

Radiation pattern of linear phased antenna array calculated during commutated scanning
04 p0577 A69-14785

Electronic counterrotating antennas, developing turning model of antenna group of telecommunications satellite
04 p0578 A69-15065

Multielement antenna array radiators interaction taking into account edge effects
05 p0727 A69-15638

Directive gain optimization of antenna array during 90 degree radiation deflection
05 p0728 A69-15652

Directional mirror antenna parameters measurement by finite focusing of radiating element
06 p0895 A69-17453

Mechanically and electronically despun spacecraft antennas, comparing designs and projected performances for spin stabilized Intelsat 3 satellite
06 p0897 A69-17590

Signal resolution during space diversity reception with nondirective or weakly directive antennas and noncorrelated receiver background noise, discussing signal processing
06 p0890 A69-17800

Telemetry and tracking antenna feed system in EC-135N instrumented aircraft for Apollo moon project
07 p1105 A69-19110

Focusing effect on far field directional pattern shifting of array normal, noting electronic scanning properties
08 p1285 A69-20400

Electronic beam-rotation systems operation using matrix network to feed circular arrays, noting applicability to direction finding or radar systems
08 p1288 A69-20964

Broadband multibeam antenna array with frequency independent beam directions, noting aperture gain limitation
08 p1288 A69-20965

Counterrotating antenna for spin stabilized satellite, noting linear phase shift influence on radiation pattern
08 p1289 A69-20968

Superdirective aerial endfire array of four unequally spaced half wave dipoles and only one fed element, calculating and measuring maximum gain
09 p1468 A69-22603

Apollo LM and CSM tracking systems boresight shift reducible by decreasing modulation indices or scaling factor alpha
10 p1672 A69-23277

Shipborne self pointing antenna for reception of telemetry signals from maneuverable missile, discussing tracking and compensation for ship platform motion
10 p1664 A69-23803

Directional antennas gain loss on ground sections calculated on basis of difference-phase measurements data
11 p1847 A69-24719

Self steered retrodirective antenna arrays with phase synthesizer, combining signals from individual elements at LF levels
11 p1850 A69-24983

Antenna cross dipole array for vehicle tracking in VHF band, obtaining effect of local rotation by electrical phase shifting
13 p2226 A69-27185

Electroacoustic transducers interaction effects in multibeam acoustical reflector type receiving antennas
13 p2227 A69-27536

Quasi-optical oversize waveguide directional coupler with two prisms interface matched by Brewster angle effect
14 p2424 A69-29764

Multielement antenna array radiators interaction taking into account edge effects
16 p2762 A69-32496

Directive gain optimization of antenna array during 90 degree radiation deflection
16 p2762 A69-32509

Retrodirective antennas for spacecraft, discussing design, operations and applications
16 p2762 A69-32557

Doubly curved reflectors for rotating search radar directional antenna, noting assembly of elliptical strips constituting segments of parabolic dishes and sidelobe suppression

16 p2763 A69-32790

Bearing system for mechanically despin antenna in spin stabilized communications satellite, offering greater directional stability, lower weight and power losses

17 p2978 A69-33431

Automatic radar station for meteor observations, discussing separate transmitting and receiving antennas directive gain and radio echo power

17 p2939 A69-33902

Directional transmitting and receiving antenna arrays for short wave meteor studies in Kharkov

17 p2939 A69-33903

Minimum weight design of tiltable enclosed antenna structure as subject to deformation constraints

18 p3211 A69-34341

Mechanical drives effectiveness for large antenna tracking/communications systems evaluated in terms of reliability and availability

18 p3100 A69-34522

Digital computer controlled antenna positioning system computing spacecraft tracking trajectory from given parameter input set

19 p3267 A69-35997

Backfire antenna radiation characteristics and physical dimensions for tracking and telemetry applications, including five element array model

19 p3271 A69-36251

Antenna high noise temperature reduction in single channel combined transmission and reception of tracking and communication data

19 p3275 A69-36328

Multiplicative feed system for monopulse angle tracking antennas, discussing influence of sidelobe and backlobe responses on control function slope determining antenna bearing angle

20 p3510 A69-37704

Phase error in monopulse antenna system attributed to far field background noise sources during passive or active objects tracking

20 p3492 A69-37707

Directional mirror antenna parameters measurement by finite focusing of radiating element

20 p3508 A69-37938

Intelsat 3 communications satellite mechanically despin high gain directive antenna, discussing system, control electronics, design and performance

22 p3913 A69-40691

Redirection of time varying signal between specified points by arbitrarily spaced antenna array elements with condition involving time delays for validity of retrodirection

23 p4136 A69-41580

Directional couplers applied to excitation of non-protruding surface wave antennas, examining ridge slot system

23 p4139 A69-41946

Antenna pointing and tracking accuracy by identifying error sources in servo, structural, mechanical and alignment factors

23 p4125 A69-42126

Design criteria for antenna control equipment for earth tracking from landing site on Martian surface [AIAA PAPER 68-868]

24 p4348 A69-43246

DIRECTIONAL CONTROL

NT THRUST VECTOR CONTROL

Hybrid electropneumatic and electrohydraulic servosystem for actuation of gas jet nozzles of sounding rocket automatic pointing system

04 p0550 A69-15182

Direction changing of large solid propellant motors by changing jets angle or gas injection

07 p1230 A69-19291

Single loop directional stripline filters synthesis, including general expression for frequency characteristics based on wave matrices

19 p3284 A69-36570

Integrated sensor controllers for missile directional control, discussing test results for two different systems [AIAA PAPER 69-837]

21 p3761 A69-39368

Miniature hydraulic controls with emphasis on four-way directional control valve for space and cost problems

22 p3870 A69-41243

Electromagnetic waveguides direction-changing capability, deriving expressions for permitted bending radius with respect to mode conversion

24 p4288 A69-43331

DIRECTIONAL STABILITY

NT GYROSCOPIC STABILITY

Directional gyroscope accuracy increased by self adaptive systems, based on precession theory and drift amplitude dependence

11 p1881 A69-24559

Directional solar thermal field /sunlight/ effect on coupled nonplanar transverse and torsional vibrations of satellite cylindrical antennas in orbit

11 p1994 A69-25534

Directional properties of electro-optical goniometric system based on known design parameters

14 p2420 A69-29332

Aircraft constant altitude-pressure flight navigation attained using Bellamy formula and loxodromic route for drift compensation

15 p2651 A69-30294

Skyvan 2 aircraft aerodynamic design, describing modifications to increase fuel capacity, directional stability and range capability

17 p2896 A69-34193

Manual attitude control for Lunar Module employing directional stability, coordinated turn and attitude command [AIAA PAPER 69-892]

21 p3824 A69-39417

Aircraft directional stability in terms of ideal nonholonomic coupling on mechanical system, noting servosystem role

21 p3830 A69-39836

DIRECTIVITY

Directivity and beamwidth determination of large scanning Dolph-Chebyshev arrays

04 p0570 A69-14303

Directive gain optimization of antenna array during 90 degree radiation deflection

05 p0728 A69-15652

Solar wind directional fluctuations at middle heliographic latitude, comparing Vela satellite measurements with comet Morehouse tail beam undulations

06 p0985 A69-16981

Self dual graphs and diagraphs enumeration and properties

06 p0947 A69-17410

Electromagnetic wave propagation direction in vacuum for reflection from semiinfinite plasma, noting effects of nonlinear transverse wave excitation

09 p1459 A69-22529

Emission spectrum of ruby laser as function of relative orientation of resonator and active crystal axes, noting spectrum width

12 p2104 A69-26029

Directive gain optimization of antenna array during 90 degree radiation deflection

16 p2762 A69-32509

Center to limb variation of solar hard X ray bursts, suggesting inverse Compton effect and bremsstrahlung from anisotropic electrons

17 p3023 A69-33055

Directional couplers design considerations for use in microwave power meters, analyzing directivity and mismatch effect on system error

19 p3282 A69-35826

Thermal calculations of objects near lunar surface, considering IR emission directivity effects

24 p4385 A69-43254

DIRECTORIES

U INDEXES [DOCUMENTATION]

DIRECTORS [ANTENNA ELEMENTS]

Directional properties of electric vibrator positioned at reflecting circular cylinder, discussing radiation patterns and cylindrical wave diffraction

04 p0574 A69-14459

Multielement antenna array radiators interaction taking into account edge effects

05 p0727 A69-15638

Multielement antenna array radiators interaction taking into account edge effects

16 p2762 A69-32496

DIRICHLET PROBLEM

Approximate solution for Dirichlet problem for linear Karman differential equation used in thin plate deflections obtained by Bubnov-Galerkin method

01 p0105 A69-10700

Normal derivative of solutions to Dirichlet problem for elliptic quasi-linear equation and construction of given mean curvature hyperspace in curved space

02 p0272 A69-12221

Quasi-linear parabolic partial differential equations, discussing solutions, regularity, differential geometric aspects and Dirichlet problem

02 p0273 A69-12779

Dirichlet problem for degenerating elliptical equations with nonlinear low order terms

03 p0456 A69-13601

Dirichlet problem for elliptical system, showing solvability of inhomogeneous system with uniform boundary values for half plane and circle cases

03 p0456 A69-13602

Dirichlet problem deviation from Bitsadze system with Noetherian properties, giving Hausdorff normal solvability conditions for inhomogeneous problem

03 p0456 A69-13603

Discretization error of Dirichlet problem analyzed in plane region with corners, discussing error in numerical solution of elliptic differential equations

03 p0457 A69-13741

Difference iteration method for solving three dimensional Dirichlet problem presented as system of plane Dirichlet problems

05 p0787 A69-16457

Dirichlet and Neumann problems solvability using potential theory methods, limiting study to three dimensional domains

07 p1173 A69-18496

Elliptic equation solution of Dirichlet problem with zero boundary condition, examining dependence of modulus of continuity of solution on boundary properties

07 p1173 A69-18498

Dirichlet problem for nonuniformly second order elliptic quasi-linear equation for case of arbitrary coefficient growth

07 p1173 A69-18500

Canonical forms for second order elliptic systems with constant coefficients, studying Dirichlet problem solvability for systems reduced to canonical forms

07 p1174 A69-19476

Existence and uniqueness of Dirichlet problem solutions for elliptic type equations with measurable and bounded coefficients

08 p1343 A69-20659

Nonlinear second order elliptic difference equations in associated variational problems, considering differentiable solution of Dirichlet problem

10 p1718 A69-22879

Finite difference approximation to degenerate Dirichlet problem, obtaining a priori estimate to prove convergence

10 p1719 A69-23517

Dirichlet problem solution for Volterra elliptic integrodifferential equation, considering existence theorem hypotheses

12 p2121 A69-26468

Dirichlet problem for elliptic second order differential equations with constant coefficients in region of Euclidean space of two real variables bounded by ellipse

12 p2123 A69-26728

Dirichlet problem of linear degenerate second order differential elliptic systems with independent variables

12 p2123 A69-26729

Network method for Dirichlet problem of Laplace equation in regions with rounded corners, noting polar and composite errors

12 p2123 A69-26730

Dirichlet problem for second order linear hyperbolic partial differential equations in cylindrical domain, deriving necessary and sufficient condition for solution uniqueness

12 p2124 A69-26932

Simultaneous Wiener-Hopf equations for electromagnetic wave diffraction, giving cyclic matrix solutions for Dirichlet and Neumann mixed boundary value problems

13 p2287 A69-27299

Elliptic second order equation showing nonequivalent regularity conditions for Laplace and continuous coefficient equations

13 p2288 A69-27743

Pointwise estimate for gradient of solution of first boundary value problem /Dirichlet problem/ for second order elliptic equation

13 p2289 A69-28319

Algorithm for solving Dirichlet problem of nonlinear elliptical differential equations representing atmospheric dynamics balance equation

14 p2470 A69-29401

Monograph on Dirichlet problem for quasi-linear elliptic differential equations with many independent variables

14 p2471 A69-29599

Necessary and sufficient conditions for boundary point regularity in Dirichlet problem for heat conduction equation assuming Holder condition

15 p2716 A69-30047

Stability of steady circular motions in systems with hidden variables analyzed by using Lejeune-Dirichlet theorem

16 p2804 A69-31621

Iteration process by difference scheme for numerical solution to Dirichlet problem of two dimensional Poisson equation
18 p3164 A69-34701

Convergence properties of finite difference approximations to solutions of Dirichlet problem for Poisson equation
18 p3164 A69-34840

Dirichlet polynomials double sequences and double series with positive exponents, defining conditions for convergence in bicylinder
19 p3361 A69-36639

Normal derivative of solutions to Dirichlet problem for elliptic quasi-linear equation and construction of given mean curvature hyperspace in curved space
23 p4182 A69-41972

Principal stresses determination in optically active photoelastic models from fringe pattern while obtaining sum from Dirichlet problem solution by straight line method
23 p4228 A69-41987

DISCHARGE

Electrodynamic law between current elements consistent with Newtonian dynamics, noting consequences in discharge and plasma control
14 p2485 A69-29320

DISCHARGE COEFFICIENT

Discharge coefficient nondependence on Reynolds number demonstrated by measurement at orifices with sharp edges
01 p0006 A69-10362

Sonic nozzle optimal profile determination with and without cylindrical throats, noting sonic line curvature importance on discharge coefficient
02 p0188 A69-12037

Discharge coefficients for Herschel type smooth venturimeters, analyzing influence of transport coefficients, convergence angles and contraction ratios
02 p0250 A69-12414

Discharge rates of metabolic products in men confined in pressure chamber wearing airtight suits and gas masks
10 p1646 A69-23508

Discharge coefficient and opening time of pneumatic and hydraulic systems incorporating disks, nozzles and valves
18 p3094 A69-34981

Servovalve orifice characteristics described by discharge, flow or loss coefficients for laminar and turbulent flow, noting use of Mises model
19 p3256 A69-36712

Relaxation time influence on discharge coefficient of sonic nozzle of revolution, considering expanding polyatomic gas problem
19 p3241 A69-36721

DISCHARGE TUBES

U GAS DISCHARGE TUBES

DISCONTINUITY

NT SHOCK DISCONTINUITY

Optimal control problems with discontinuities, noting jump discontinuities in state variable derivative arising in bang-bang control problems
01 p0049 A69-10003

Stationary and nonstationary weak discontinuity surfaces propagation for ideal and viscous compressible conductive atmosphere with regard to heat flux, using Hadamard method
03 p0422 A69-13511

Reflection coefficient of double discontinuity consisting of two closely spaced inductive irises in rectangular waveguide
09 p1453 A69-21444

Dynamic programming computational approach to optimization with state variable discontinuities, treating problems as multistage optimization with continuous subarc stages
09 p1474 A69-22440

Steady three dimensional flow of gases with thermodynamic relaxation, noting flow field weak discontinuities and effect of discontinuities in wall curvature
10 p1677 A69-22894

Galactic discontinuity near longitude 140 degrees attributed to stars deficiency in anticenter quadrant or interstellar cloud obscuration
10 p1776 A69-23215

Forced discontinuous vibrations of liquid in conduit experimentally analyzed, discussing test devices and procedures
11 p1875 A69-25485

Differential equation with finite jump type discontinuities
14 p2424 A69-28811

Tangential solar wind discontinuity observed by Vela 2A satellite, producing ground magnetic disturbances

conjunctively with magnetospheric, ground and ionospheric currents
14 p2512 A69-29041

Ray optics method of far field scattering by discontinuity in parallel plane waveguide applied to strips, apertures, bifurcations, etc
14 p2423 A69-29753

Discontinuities in interplanetary magnetic field direction presented on mesoscale from Pioneer 6 observation, emphasizing distribution in time
14 p2528 A69-29970

AI interconnections discontinuities at integrated circuit contact windows observed by scanning electron microscope, noting catastrophic failure and Si presence
17 p2936 A69-32893

Traveling ionospheric disturbances in form of large scale electron concentration discontinuities created by propagating internal gravitational waves
17 p2966 A69-33980

Wave scattering in elastic medium by discontinuity line or finite crack, noting dynamic stress intensity dependence on incident wavelength and Poisson ratio
21 p3840 A69-39293

DISCRETE FUNCTIONS

Optimal adaptive control of discrete linear systems with unknown gain, considering Gaussian distribution functions and random disturbances
02 p0224 A69-11962

Optimal control of open loop aperiodically modulated discrete time systems, discussing solution of associated two point boundary problem
02 p0226 A69-12732

Stability properties of discrete-continuous feedback control systems with signal dependent sampling
02 p0226 A69-12733

Fast Fourier-Hadamard transform for digitized signal representation, classification, discrimination and efficiency
03 p0392 A69-13249

Approximation for discretization error of discrete analog of Bergman harmonic kernel, discussing discretization error in Dirichlet and Neumann problems for Laplace equation
03 p0456 A69-13555

Discretization error of Dirichlet problem analyzed in plane region with corners, discussing error in numerical solution of elliptic differential equations
03 p0457 A69-13741

Book on qualitative theory of sampled data systems
04 p0630 A69-14563

Discrete time positive real functions defined for analyzing system stability with memoryless feedback
05 p0739 A69-16349

Optimal controls for linear systems with matrix elements and vector components discrete functions of time
09 p1473 A69-21787

Discrete predicting filter optimal synthesis in terms of rms error by solving normal Gaussian equations
09 p1473 A69-21858

Discrete variable approximation for computation of flight path optimization, discussing constrained and unconstrained minimizations
09 p1538 A69-22090

Optimal control of discrete processes with bounded phase coordinates, proving optimality conditions
09 p1475 A69-22668

Optimal control of discrete time linear system with random parameters, noting case of additive noise in measurements
12 p2052 A69-26501

Error due to amplitude quantization and design of digital control systems in discrete time optimum control theory
12 p2053 A69-26507

Discrete automatic control systems determination by adjustable model, considering quasi-steady state conditions
13 p2238 A69-27253

High energy neutron transport calculated using one dimensional discrete ordinates code with anisotropic scattering, comparing results with nucleon transport code calculations
14 p2481 A69-29592

Recognition system for discrete decision function generation to select one out of two classes of objects, deriving solutions for selection probability
17 p2932 A69-33119

Pulsed control systems sensitivity relationship to discreteness period described via differential equations
17 p2994 A69-33143

Matrix formulation for discrete element method applied to linear static and eigenvalue problems of thin

walled segments, using homogeneous differential equations
19 p3445 A69-36831

DISCRIMINATION

U BRIGHTNESS DISCRIMINATION
U SENSORY DISCRIMINATION
U TACTILE DISCRIMINATION
U VISUAL DISCRIMINATION

DISCRIMINATORS

Reduction of ATR switch pulse peak in automatic frequency control system of radar station
01 p0047 A69-10784

Simultaneous passage of useful and noise signals through differential frequency discriminator, determining spectrum by phase detection and detuned circuits
04 p0556 A69-14462

Smooth limiter effect on output of SNR for unbalanced and balanced FM discriminators, noting role of error function
07 p1106 A69-19127

Error probability for discriminator detection of wideband PCM/FM, considering IF bandwidth/bit duration product and low pass filtering effect
08 p1271 A69-19864

Reduction of ATR switch pulse peak in automatic frequency control system of radar station
10 p1661 A69-23113

Simultaneous passage of useful and noise signals through differential frequency discriminator, determining spectrum by phase detection and detuned circuits
14 p2410 A69-28833

FM discriminator click widths probability distribution function, defining click widths duration from input noise considerations
14 p2422 A69-29553

Unsaturable frequency discriminator influence in semiconductor laser feedback loop on laser emission spectrum
15 p2635 A69-30967

Bessel functions new addition theorem suggested from mathematical investigation of ideal discriminator output voltage
19 p3266 A69-35767

Wideband FM telemetry transmitters for S band, using symmetrical discriminator
23 p4119 A69-41741

DISEASES

NT ARTERIOSCLEROSIS
NT ASTHMA
NT ATLECTASIS
NT CANCER
NT CARBON MONOXIDE POISONING
NT EDEMA
NT EMPHYSEMA
NT EPILEPSY
NT FIBROSIS
NT HEART DISEASES
NT INFARCTION
NT INFECTIOUS DISEASES
NT INFLUENZA
NT NEPHRITIS
NT PARASITIC DISEASES
NT PNEUMONIA
NT PULMONARY LESIONS
NT RADIATION SICKNESS
NT RESPIRATORY DISEASES
NT TACHYCARDIA
NT TOXIC DISEASES
NT TUMORS
NT UROLITHIASIS

Space biomedical research trends, noting gastroenterology and lack of research on disease processes during space travel and overemphasis on space physiology
03 p0369 A69-12859

Food-born diseases prevention in civil aviation, reporting gastroenteritis cases during flight
24 p4278 A69-43392

DISHES

U PARABOLIC REFLECTORS

DISILICIDES

Dilatometric and X ray study of temperature dependence of linear expansion coefficients of lattice constants of chromium disilicon
04 p0619 A69-15392

Molybdenum disilicide allotropy influence on coating growth rate and morphology [ONERA-TP-642]
08 p1335 A69-19967

Oxidation influence on molybdenum disilicide coatings emissivity, determining degree of blackness over thermal stability range
09 p1522 A69-21588

Tungsten disilicide coated Ta-W alloy oxidation mechanisms, comparing coatings protective properties at high temperatures
13 p2280 A69-28137

Dilatometric and X ray study of temperature dependence of linear expansion coefficients of lattice constants of chromium disilicon

18 p3156 A69-35020

Charge transport in n and p type samples of beta phase semiconducting iron disilicide, noting effect of room temperature doping

19 p3390 A69-36556

Aluminum alloying additives effects on tungsten disilicide corrosion resistance, studying plasticity properties and oxidation rate

20 p3561 A69-37376

Molybdenum disilicide oxidation kinetics at various temperatures by thermal conductivity method, determining oxidation rates and activation energy

20 p3567 A69-37780

Thermodynamic properties of exchange reaction of Ti, Nb, Mo and W disilicides with graphite and pyrographite systems

22 p3970 A69-40638

DISINTEGRATION

Absolute cross sections for coincidence detection of deuteron breakup by 42 Mev alpha particles, showing He 5 and Li 5 final state interaction peaks

03 p0472 A69-13469

DISKS

Electron bombardment ion source generated Ar plasma beam to study wakes of disks and spheres, considering plasma interaction with bodies [AIAA PAPER 69-79]

06 p0865 A69-18200

DISKS [SHAPES]

NT ROTATING DISKS

Torsional oscillations of elastic half space set up by rigid circular disk examined by integral equation method

01 p0169 A69-10809

Electroerosion effect on fabrication of small disks for direct examination by electron microscopy, using refined and heat treated aluminum

03 p0427 A69-12880

Constant thickness disk temperature field for inhomogeneous boundary conditions, considering roots of characteristic equations determination

04 p0685 A69-14498

Circular disk stress-strain state due to thermoelastic strain applied at disk sector edge

04 p0681 A69-15171

Natural frequencies controllability by induced thermal membrane stresses examined for thin disk

04 p0682 A69-15494

Phantom disk encoder for arc second digital position transducers

05 p0766 A69-16748

Compressibility parameters role in pressure distribution derived for radial laminar compressible fluid flow between two disks

07 p1121 A69-19321

Logarithmic decrement and period of disks performing torsional oscillations measured in viscous fluid, noting dependence on oscillation amplitude

08 p1417 A69-20781

Fatigue behavior of composite disk modified from previously evaluated boron epoxy reinforced titanium compressor disk

09 p1619 A69-22323

Weight minimizing of circular disk subjected to behavioral and side constraints, considering resonance frequency of vibration and tolerances [ASME PAPER 69-VIBR-1]

10 p1700 A69-24159

Characteristic equation for corrugated surface wave line loaded with uniformly spaced thin metallic disks excited in E mode, considering spacing and groove depth

12 p2028 A69-25899

Velocity potential function for flow over disk shaped wing near screen, noting aerodynamic lift and drag

13 p2199 A69-27524

Steady rectilinear translational motion of circular disk-shaped slightly bent wings near solid wall in incompressible fluid medium in absence of vortices and external forces

15 p2547 A69-30583

Stress-strain state of circular disk with diametral cracks determined by approximating limiting equilibrium equation

15 p2708 A69-30663

Equilibrium equations for elastic medium with stress couples, presenting first term of asymptotic expansion of solution for disk and simply connected region

16 p2871 A69-31830

Vortex ring production in liquid jet by vibration induced pressure pulses at orifice, discussing plates formed under high g vibration [AIAA PAPER 68-132]

16 p2770 A69-31880

Fuel cell oxygen electrode problems, noting oxygen ionization reaction and disk electrodes role

16 p2739 A69-32416

Subsonic and supersonic turbulent air jets expansion over perpendicularly positioned plane disk obstacle, deriving equations for pressure distribution and stagnation temperature

18 p3123 A69-34990

Flow breakdown in wind tunnel tests of high disk loading systems at low forward speeds, investigating downwash distribution effect using disk loading and airfoil models

18 p3119 A69-35230

Transient thermal stresses in heat treated elastic-perfectly plastic disks with temperature dependent yield stress, considering stress distribution sequence and residual stresses

20 p3629 A69-37974

Stress strain state in thin circular elastoplastic disks under axially symmetric transient temperature distribution, noting moving annular plastic deformation region

20 p3629 A69-38028

Automatic electropolisher for copper disks

21 p3720 A69-38597

Enlargement of circular hole in disk with kinematic hardening and Tresca yield function compared with isotropic hardening

21 p3840 A69-39297

Nadai and Zyczkowski stress analysis for Tresca yield condition reexamined for determination of critical angular velocity of solid elastic perfectly plastic disk

23 p4235 A69-42480

DISLOCATIONS [MATERIALS]

NT CRYSTAL DISLOCATIONS

NT EDGE DISLOCATIONS

NT SCREW DISLOCATIONS

Graphical representation of stress distributions and forces on dislocations

03 p0529 A69-13973

Structural changes and cold shortness of molybdenum in deformation

04 p0615 A69-14637

Pointwise limitation of field dislocation and bending moments in elastic plates

05 p0831 A69-15599

Mathematical theory for describing geometric structure of simple bodies, discussing dislocation distribution and exact field equations for elastic bodies motion

05 p0834 A69-15731

Dual continuum model of nonelastic processes in elasticity and dislocation theory, including incompatibility effects of interaction forces between structural elements

10 p1799 A69-23152

Plastic energy dissipation and crack surface displacement of penny shaped crack in elastoplastic material

10 p1803 A69-24030

Fracture and equilibrium position of dislocations in discrete and continuously distributed dislocations arrays including stress due to crack, energy considerations and crack initiation

13 p2358 A69-27222

Necked tension specimens profiles for rigid-plastic nonhardening materials determined from compatibility equation for displacements and unloading rate

15 p2704 A69-30292

Dislocation and energy balance analysis of ductile and brittle metal cracks for determining metal fracture strength from plastic deformation

17 p3052 A69-32984

Somigliana dislocations effects on displacement field in linear isotropic elastic medium represented by integral with respect to line delineating surface

17 p3053 A69-33020

Linear isotropic elastic continuum dislocations distribution, deriving transport equations by statistical methods, noting analogy between energy/momentum and MHD equations

18 p3212 A69-34352

Burger condition for distortion field of dislocation lines in continuous medium, considering arbitrary shape in arbitrary motion

19 p3439 A69-36477

Dislocation effects on stress corrosion of metals, discussing behavior of porous structure and metal/corrosion film interface under applied stress

19 p3349 A69-36886

Precipitation hardening, microstructure and dislocation influence on intergranular stress corrosion cracking /SCC/ of high strength Al alloys examined by transmission electron microscopy

19 p3351 A69-36898

Plastic deformation and dislocation damping of cemented WC-Co alloys studied by compressive testing at room temperature

21 p3744 A69-38736

Serrated yielding at high temperatures from dislocation theory viewpoint, considering critical strain relation to temperature and strain rate

21 p3749 A69-39710

Thermodynamics of elastoplastic materials with dislocation motion related to internal state variables, including case of rate independent plasticity

23 p4226 A69-41537

DISORDERS

Fast reversible switching between highly resistive and conductive states in various disordered semiconductors, using electric field

01 p0140 A69-11248

DISORIENTATION

NT DISORDERS

Spatial disorientation as factor in accidents in operational command, noting relatively high experience level of involved pilots

07 p1072 A69-19431

Man psychic activity interference resistance, discussing stress effects characterized by theta and delta rhythms

08 p1262 A69-19839

DISPENSERS

Truss framework for support of eight 100-lb satellites through Titan 3C launch and dispensing of satellites at predetermined times, discussing materials and fabrication

09 p1512 A69-22369

DISPERSING

Airport warm fog dispersal, discussing full scale aircraft seeding of polyelectrolyte materials, noting ground dispenser

01 p0054 A69-10149

Dispersion and average monthly numbers of whistlers for propagation trajectories during solar activity minimum, discussing electron concentrations in magnetosphere

09 p1485 A69-21531

Dispersion and average monthly numbers of whistlers for propagation trajectories during solar activity minimum, discussing electron concentrations in magnetosphere

16 p2783 A69-32526

DISPERSION

Difference schemes implementation through fractional time step and phase error methods reduce dispersion

04 p0591 A69-15282

Dispersion of paraffin cork after instantaneous shock heating, noting expansion at various isentropic indices

19 p3301 A69-36839

Dispersion and correlation function for atmospheric transparency due to water vapor from statistical model of absorption bands and effective mass

21 p3759 A69-39113

Electromagnetic wave propagation in semiconductor plate under constant electric field, studying nonstandard carrier energy dispersion law effects on refractive index

22 p3994 A69-40751

DISPERSION PRECIPITATION HARDENING

U PRECIPITATION HARDENING

DISPERSIONS

NT AEROSOLS

NT COLLOIDAL PROPELLANTS

NT COLLOIDS

NT EMULSIONS

NT FOG

NT LIQUID-GAS MIXTURES

NT NUCLEAR EMULSIONS

NT PHOTOGRAPHIC EMULSIONS

NT SMOKE

Scattering data for optical diagnostic measurements on two component suspensions or gases, using random distributions of spheres

04 p0555 A69-14282

Dispersion in gel permeation chromatography, noting eddy diffusion in chromatographic columns

04 p0555 A69-14885

Laser beam propagation in scattering media, noting attenuation coefficients for coherent and incoherent radiation

08 p1328 A69-21092

DISPLACEMENT

Generalized plane stress concept extended for mathematical model to study out of plane displacement restraint in thin plates

01 p0165 A69-10114

Reciprocal theorem for displacements of solid skeleton caused by fluid sources action in infinite consolidating space

05 p0835 A69-15869

Linear analysis of strain in continua in terms of one-one correspondence, relative displacement and stretch dyadic
07 p1236 A69-19445

Curved tetrahedral and triangular elements in matrix displacement method covering linear and non-linear cases
08 p1415 A69-20631

Reissner algorithms for displacements of bent plate represented in finite series form as solutions of Euler equations
10 p1793 A69-22883

Variational method of displacements for calculating positive Gaussian curvature shells with allowance for shear strain, considering shallow shell equations and symmetrical load
12 p2178 A69-26006

Displaced layer thickness dependence on air injection parameters measured in wind tunnel
13 p2245 A69-27385

Iterative solution for difference equations approximating displacement vector determination problem in theory of elasticity, investigating algorithm convergence
14 p2536 A69-29479

Finite element analysis of flat rectangular panels, developing equilibrium equations based on specified displacement modes
15 p2708 A69-30667

Surface displacements at end of elastic semiinfinite circular cylinders due to annular axisymmetric loading, employing Boussinesq solution
15 p2711 A69-30872

Thermal stresses and displacements in isotropic inhomogeneous rotating circular disk with axle hole under steady temperature field
15 p2712 A69-31016

Triangular shell element SHEBA for arbitrary curvature variation as means of performing large displacement matrix analyses, discussing local subelement, natural modes, cross sectional resultants, etc
16 p2872 A69-32025

Somigliana dislocations effects on displacement field in linear isotropic elastic medium represented by integral with respect to line delineating surface
17 p3053 A69-33020

Transposition formula for finite displacements of solid body having fixed point relative to fixed axes
18 p3172 A69-34589

Stress and displacement waves propagation in thin walled elastic cylindrical shell under compressive axisymmetric force based on momentless theory
18 p3218 A69-34600

Weak displacements of opaque objects and optical distortion in solid state lasers analyzed by holographic interferometry
19 p3308 A69-35909

Displacement patterns for buckled shapes of axially compressed thin walled circular, cylindrical and conical shells
19 p3443 A69-36793

Relative displacement spectra analysis illustrating shock spectra errors, comparing real system response with simple single degree of freedom system response
20 p3548 A69-37301

Vibrational displacement phase measurement by Michelson interferometer with laser source
20 p3538 A69-37320

Airframe stability of VAK 191 examined by displacement method, using matrix calculations within Automatic System of Kinematic Analysis
20 p3462 A69-37515

Reaction forces calculated for system of connected solid bodies of various composition during accomplishment of given motion
21 p3771 A69-39085

Saint Venant principle of elastic equivalence of kinematically equivalent displacement systems at small surface area of elastic body
22 p4048 A69-41276

DISPLACEMENT MEASUREMENT

Time dependent tube wall radial displacement during explosive welding as function of distance from initial explosion
02 p0254 A69-12675

Electro-optical tracking devices for displacement and/or dislocation measurement without physical contact
05 p0763 A69-15986

Glass fiber optical angular displacement noncontacting nonloading transducer suitable for measuring torsional vibrations
06 p0923 A69-16929

Linearization unit for compensating hyperbolic characteristic of capacitive displacement sensor used for contactless displacement measurement
08 p1317 A69-20879

Temperature and displacement fields in unbounded elastic space due to instantaneous point heat source action
09 p1621 A69-21495

Structural damping coefficient of metals determined from complex Young modulus with transmissibility, using mass loaded cantilever beam experiment [ASME PAPER 69-VIBR-36]
10 p1807 A69-24175

Natural mode structural analysis matrix methods for small displacements, discussing curved local subbeam in space and circular arch
11 p1969 A69-24374

Deformation measurement by laser pulse holographic method, discussing laser source choice criteria
12 p2087 A69-26175

Resistance type bonded strain gages for seven adverse environments, discussing installations and transducers
12 p2099 A69-27165

Interferometric displacement transducer for measuring linear displacements up to one and one-half inches
15 p2614 A69-31280

Displacement of rectangularly mouthed pitot tubes in turbulent tube flow, determining roles of wall and shear effects
17 p2976 A69-34049

Wedge fringes visibility and localization in hologram interferometry during focusing on surface under examination for displacements
22 p3943 A69-40016

Short range telemetering strain gage system with astable multivibrator transmitter for measuring intercoupling displacement and shaft torque
22 p3946 A69-40314

Differential capacitance transducer measuring small displacements in heated transformer oil, air, castor oil or glycerin
22 p3946 A69-40439

Plane-truss joints displacements determined by graph-analytic method, discussing representation of fictitious forces and moments
23 p4225 A69-41420

Green formula and fundamental solution for determining displacements and stresses in contour integral form for plate bending problems
23 p4230 A69-42002

Holographic interferometry for measuring small static displacements of diffusely reflecting surfaces
23 p4167 A69-42185

Wave generation in infinite micropolar elastic solid, determining displacement and rotation fields and strain state
24 p4406 A69-43731

DISPLAY DEVICES

NT ANEMOMETERS
NT APPROACH INDICATORS
NT FLOW DIRECTION INDICATORS
NT HOT-WIRE ANEMOMETERS
NT KINOFORM
NT PLAN POSITION INDICATORS
NT POSITION INDICATORS
NT RADARSCOPIES
NT SONIC ANEMOMETERS
NT SPACECRAFT POSITION INDICATORS
NT SPEED INDICATORS
NT TACHOMETERS
NT WIND VANES

Fluidic display systems, discussing thermochromic modules and decoder with miniature components
01 p0078 A69-10155

Man machine relationship in VSTOL control display, discussing inflight simulators, emphasizing NASA X-14 and CH-3C programs
01 p0010 A69-10452

Airline area navigation system functions for developing map type pictorial display system including digital computer, cockpit control unit and microfilm charts
01 p0112 A69-10453

All-weather landing flight director systems and fault warning display simulator studies of Boeing 707-720B aircraft in Category 3-C environment
01 p0010 A69-10455

Head-Up Display /HUD/ flight information applied to civil aviation, noting operational safety improvement and pilot work load reduction
01 p0020 A69-10635

Modular three dimensional mockup technique for economizing and facilitating design of control and display equipment
02 p0202 A69-11953

Large scale information displays for group sharing in air traffic control, military operations and organization management
02 p0250 A69-12159

Operator handedness effect on control display movement stereotypes
02 p0203 A69-12212

Aircraft cockpit displays design for flight control and navigation, discussing integration, pictorial realism, moving part, pursuit tracking, frequency separation and optimum scaling
02 p0203 A69-12213

Navigation techniques for emergency helicopter services in medical evacuation and air/sea rescue missions, discussing displays and search patterns
02 p0279 A69-12363

Manual optimal guidance schemes for space vehicles to minimize computational and display requirements for pilot task loading
02 p0279 A69-12365

Two photon fluorescence technique for display of picosecond laser pulses, discussing mode locking and ruby laser contrast ratios
02 p0259 A69-12654

Alpha numerical and symbolic information combined for head up display /HUD/ systems, providing pilot with takeoff director
03 p0379 A69-12885

Navigational and tactical data with correlative map information provided on single CRT display in aircraft, storing map data on video tape
03 p0464 A69-13246

Vertical contact analog display /VCAD/ design, emphasizing need for integrated and supplementary information to pilots in systematic way
03 p0379 A69-13361

Automatic all-weather landing system for scheduled civil passenger aircraft, discussing safety, display devices, Category 2 and 3 conditions
03 p0465 A69-13697

Laser display technology, discussing experimental systems, light sources, modulation and scanning
03 p0431 A69-13850

Scanned laser beam display techniques based on cathode ray tube technology, noting flying spot scanner and beam deflection
04 p0600 A69-15028

Display techniques, discussing cold cathode luminous gas discharge /plasmas/ tube, electroluminescence and cathode ray tube
04 p0600 A69-15029

Research center for investigating man/computer interaction, discussing display systems, computers, languages and data entities
04 p0566 A69-15342

Graphics system using computer configuration connected by conventional voice lines, noting hardware and components
04 p0566 A69-15343

Visual factors of laser displays providing human factors recommendation for several visual variables
05 p0760 A69-15591

Plastic virtual infinity lens system for large aperture cathode ray tube direct view simulator displays
05 p0760 A69-15592

Multilevel modeling structure for interactive computer graphic design, discussing conversational display manipulation program and interconnection with analysis program
05 p0724 A69-16381

Three dimensional computer graphic modeling program, discussing SIGHT and LEGER programs
05 p0724 A69-16383

Program to study interactive graphic display console systems use for solving mechanical design problems involving plate cam and follower mechanisms
05 p0724 A69-16384

Typewriter keyboard computer system with CRT display having closed circuit TV link contents of file to add, delete or change information
06 p0891 A69-17204

Filter effectiveness in improving air to ground target identification performance on TV display
06 p0887 A69-17210

Map information display methods comparison for tactical image interpreters
06 p0924 A69-17212

Holography for display devices, nondestructive testing, quality control, high speed, microscopy, acoustic testing, sonar, data storage, etc
06 p0928 A69-17873

Light valving techniques applied to large screen display of computer generated video information, noting electron beam control mechanism for transmitted light
06 p0928 A69-17922

Photorecording techniques for command and control systems requirements, discussing association with large screen computer generated CRT projection display equipment

06 p0928 A69-17923

Laser displays for information transfer to provide improved computer driven read-out techniques, noting real image and holographic displays

06 p0928 A69-17924

Predictive display technique for remote manual control of roving lunar and planetary surface vehicles

06 p0928 A69-17925

Reading and reliability efficiency comparison in round vs vertical aircraft displays

06 p0883 A69-18025

Electrostatic storage display tube characteristics, construction, applications and reliability

07 p1101 A69-18655

Control-display panels design for accurate response with electronic and mechanical equipment, showing display stimulus and control response correspondence in rectangular configuration arrangement

07 p1070 A69-18907

Laser color TV projection-display system using moving mirrors and dual polarization scanner

07 p1137 A69-19740

Displays and controls requirements in manned spacecraft to integrate man into vehicle system, noting man capability for task diversity

08 p1312 A69-19968

Aircraft head-up display systems emphasizing all-weather operations and equipment characteristics

08 p1315 A69-20451

All-weather head-up displays /HUD/, discussing operational usage, hardware availability and design philosophy

08 p1315 A69-20452

Control and recording device for parameters and information relating to takeoff and landing, using detection elements and cross wire on runway

08 p1347 A69-20780

Peripheral fluidic devices for sequencing and monitoring machinery in hazardous areas, describing circuits

[AGARDOGRAPH-118] 08 p1257 A69-20954

Holographic displays using ultrasonic vibrations or laser outputs as optical sources, discussing recording materials, responses and computer applications

09 p1492 A69-21394

UHF telemetry conversion program at Pacific Missile Range, describing antenna, receive-record and separation display systems

09 p1454 A69-21800

Flight test evaluation program for airborne multisensor electro-optical display systems performance in TV mode under variety of optical conditions

[AIAA PAPER 69-317] 09 p1500 A69-22387

Pulsed RF spectra analyzer displays, noting responses to CW and pulsed signals and Fourier and pulsed repetition rate lines

09 p1460 A69-22791

Graphic electronic visualization equipment for computerized design

10 p1660 A69-23795

Manual control displays for instrument landing approach of large subsonic jet transport, evaluating closed loop system performance and scanning workload

10 p1650 A69-23877

Device to simultaneously observe integral and differential field effect curves on oscillograph screen as function of continuously varying field

10 p1698 A69-24210

Electro-optical tracking device with pyramidal reflector for field of view dissection, determining dead zones and trajectories for pointing error correction

10 p1698 A69-24219

Aircraft engine instrument displays evaluated by human factors, noting vertical scale design

[SAE PAPER 690328] 11 p1829 A69-24488

Electric outside-in attitude gyro display system prototype tested and compared with contemporary inside-out display

[SAE PAPER 690326] 11 p1890 A69-24507

Soviet book on electroluminescent devices covering panels, indicator contrast levels, control, multicolor indicators, image conversion and storage and optoelectrical systems

11 p1850 A69-24976

Apollo mission simulation, discussing Command Module Simulator /CMS/, onboard computer system and dynamic visual presentation via infinity-optics display

[SMPT PAPER 105-74] 12 p2055 A69-25768

Fourth angle driving law for different four gimbal systems used for simulation display and inertial platform isolation

12 p2055 A69-26265

Automatic plotting devices for graphic readouts in analog and digital computers

12 p2091 A69-26303

Alignment/test rig for head-up displays using laser light pencils

12 p2091 A69-26304

Man machine interactive structural analysis using digital computer with CRT display, detailing design

12 p2035 A69-27098

Designs and capabilities of digital processing systems for automatic air traffic control radar information stressing future use of display for computerized control

13 p2295 A69-27332

Pictorial display techniques aiding air traffic and aircraft control, discussing projection and directly viewed display

13 p2296 A69-27335

Computer based data handling and display for relating remote sensor signals to ground truth information derived from aerial photographs

14 p2416 A69-29534

Thermistor instrument for remote sensing, magnetic synchronous recording and linear display of temperature

14 p2449 A69-29562

Navigational information display in aircraft, discussing moving map technique and mechanization

15 p2558 A69-30692

Flexible glass fiber optics, discussing total internal reflection, light and image transmission, digit display and waveguide for laser communication

16 p2789 A69-31933

Airborne digital computer and display devices role in navigation management, discussing data processing and hybrid navigation systems

16 p2809 A69-32260

High intensity light adaptation effects on visibility of raster scan, TV type and avionic displays for symbol luminance needs

16 p2746 A69-32788

Integrated trajectory error display /ITED/ for flight path control of helicopters and VTOL, describing principles governing display synthesis

[AHS PAPER 314] 17 p3001 A69-33541

Situation/command system displays and maneuvers for collision avoidance systems, discussing pilot preferences

17 p3002 A69-34096

Airborne electric power systems maintenance aids, describing design and operation of annunciator for establishment and display of system failure causes

17 p2905 A69-34112

Self monitored subsystems in automatic flight control of Concorde, describing operation mode and landing display

17 p3003 A69-34196

Computer graphics engineering applications in line drawing displays for industry, including design programs and color TV flight simulation

18 p3106 A69-34659

Situation displays and flight instrument development including head-up, vertical tape and map systems

18 p3170 A69-34858

Luminophors for carbon dioxide laser radiation visualization noting controlled sensitivity, quick response and resolution

18 p3153 A69-35259

Pictorial display area navigation system for air traffic control in terms of cockpit utilization, interface with ground navigation aids, parallel multiple routes, etc

[AIAA PAPER 69-798] 19 p3367 A69-35632

Controlled-variable prediction display based on Taylor series computation, describing acceleration system simulator and human operator performance

19 p3313 A69-36414

Heated body cooling off study via temperature field isothermal lines visualization on TV screen

20 p3539 A69-37437

Receiving and display telemetry system for obtaining direct ionospheric topside ionograms from Alouette 1 satellite, discussing video data tape recording cost

20 p3507 A69-37861

Radar digital processing and display system for air traffic control with IC central processor and discrete data transmission over telephone lines from remote sites

21 p3760 A69-38328

Psychology and physiology of vision in relation to large screen display design, discussing effects of symbol size and spacing, color usage, etc

21 p3662 A69-38330

Simulation and display for radar ground-backscatter signatures by computer ray tracing, using model ionosphere containing realistic traveling disturbances

21 p3717 A69-39280

HF direction finder for display of time varying multimode propagation phenomena, using analog computer and phase sensitive interferometer

21 p3677 A69-39456

CRT graphic display/plotter for small digital computers, describing device operation, control and applications

21 p3679 A69-39608

EEG patterns computerized spatio-temporal display technique using CRT and motion picture camera

21 p3668 A69-39864

Aircraft navigation system requiring computer and display for approach guidance to circular orbit over fixed ground area

[AIAA PAPER 69-986] 22 p3978 A69-40366

Horizontal Situation Display /HSD/ map computer mechanization transforming earth location to X, Y coordinates for Lambert conformal projection

[AIAA PAPER 69-987] 22 p3908 A69-40367

Cockpit displays for transport aircraft noting digital techniques and flight control-navigation integration

22 p3946 A69-40486

CRT display system coupling interface with magnetic storage determined from algorithms and time diagrams, describing character storage and system logic design

22 p3908 A69-40936

Reconstruction properties of image plane holography for producing bright white light displays, using reference beams

23 p4164 A69-41627

Photochromic film behavior under high power argon ion laser excitation studied for display and computer memory applications, using excitation model

23 p4173 A69-41629

Moving map pictorial display system for on board capability of area navigation, noting crew reaction

[SAE PAPER 690393] 23 p4186 A69-41663

Flight indicators monitoring by pilots, describing physiological and psychotechnical criteria for dials and clocks arrangement to improve efficiency

23 p4108 A69-41827

Senior commercial jet pilots ability to visualize flight instruments

23 p4089 A69-41829

Head-Up Display /HUD/ incorporated with autopilot for human participation in flight control for all-weather operation

23 p4109 A69-41871

Hybrid display for data visual display using electroluminescent and thermochromic technologies for wide range of ambient illumination

24 p4313 A69-42899

Colors production on electroluminescent display using phosphors impressed-frequency/emission-color relationships together with chromatic biasing

24 p4286 A69-42900

Display system design principles and procedures, discussing checklists, formal procedures and behavior theory

24 p4274 A69-43017

Sensory information processing model for tactile perception using array of airjet and piezoelectric stimulators applicable to display design and nervous system investigation

24 p4276 A69-43273

DISPOSAL

U WASTE DISPOSAL

DISSIPATION

Chebyshev filter design problems including minimum highest dissipation loss, bandwidth, resonators, etc

10 p1665 A69-23875

DISSIPATORS

U DISSIPATION

DISSOCIATION

NT AUTOIONIZATION
NT GAS DISSOCIATION
NT PHOTODISSOCIATION
NT THERMAL DISSOCIATION

Nonequilibrium dissociation effects on constant pressure laminar mixing for diatomic molecules and atoms, analyzing concentration and temperature of free shear layer

04 p0588 A69-14733

Dissociation energy and vibrational terms of ground state hydrogen

05 p0796 A69-15908

Hydrogen ions collision-induced dissociation cross section angular dependence measured, showing qualitative agreement with theoretical predictions

05 p0798 A69-16698

Dissociation of hydrogen on tantalum using modulated molecular beam mass spectrometry
06 p0960 A69-17107

Dissociation equilibrium of negative H ions in solar type stellar atmospheres, noting H molecule vibrational and rotational levels and continuous thermal radiation
07 p1223 A69-19635

Dissociation equilibrium of diatomic molecules in solar atmosphere, comparing concentration above photosphere to MgH
14 p2528 A69-29963

Half maximum temperature of diatomic gases determined by extending relation between specific heat and molecular dissociation to diatomic molecules [DVL-899]
15 p2656 A69-31102

Molecular concentration-optical depth curves for combinations of two photospheric and two facular models, noting lines contrast dependence on dissociation energy
18 p3204 A69-35391

Hydrogen molecular ion dissociation due to ion-molecule inelastic collisions, comparing measured and calculated velocity distributions of protons produced
19 p3375 A69-35985

Quantum-mechanical theory of unimolecular kinetics and predissociation developed from generalized Fano theory of resonant scattering
22 p3986 A69-40724

O-hemoglobin dissociation curve shape effect on O affinity of hemoglobin
23 p4095 A69-42086

Thermodynamic calculation of equilibrium constant and homolytic dissociation degree of tetrafluorohydrazine based on enthalpy and statistical entropy
24 p4280 A69-42788

DISSOLUTION

U DISSOLVING

DISSOLVING

Ellipsoidal gas bubble dissolution in low viscosity fluid, discussing rate of steady motion, deformation degree and diffusion rate
07 p1120 A69-18990

Lifetime of highly soluble isolated dense spherical solute particle in solvent, taking into account molecular diffusion, kinetic limitations, etc
10 p1651 A69-22939

DISSYMMETRY

U ASYMMETRY

DISTANCE

NT DEBYE LENGTH
NT MISS DISTANCE
NT MISSILE RANGES
NT RADAR RANGE
NT RADIO RANGE
NT RANGE AND RANGE RATE TRACKING
NT REENTRY RANGE

Neutral hydrogen content in directions of pulsars related to distance estimates
01 p0149 A69-10271

Hovercraft range operating at constant speed as function of design efficiency, power apportionment, fuel consumption and initial specific resistance
03 p0367 A69-13909

Pulsar distance estimates based on evaluation of galactic H absorption of 21 cm radiation
06 p1012 A69-18225

Pulsar distance estimates, discussing effect of interstellar electron and H densities and temperature dependence of H density-electron density ratio within disk
08 p1397 A69-20698

Short range passenger aircraft, considering payloads, weights and economical classification
13 p2201 A69-27294

Distance and mass-luminosity relation for Hyades stars relative to sun-Sirius type stars
13 p2339 A69-27565

Quasar red shifts distance dependence indicated by visually bright quasar faintness in radio range
13 p2344 A69-27635

Spiral galaxy linear diameter relation to luminosity applied to Virgo galactic clusters, noting effect on distance modulus and Hubble constant
19 p3427 A69-36652

Pulsar distance determined by electron content in line of sight to pulsar compared with neutral H amount integrated through galaxy in pulsar direction
20 p3597 A69-37409

Discreteness of distances to extragalactic objects, tabulating red shift values from Wilson formula for galaxy clusters
21 p3802 A69-38843

Pulsars dispersion measure and distance relationship, particularly for Crab Nebula pulsars
23 p4220 A69-42381

Flight range and fuel consumption formulas of power gliders used for transportation compared with automobiles
24 p4253 A69-43142

DISTANCE MEASURING EQUIPMENT

NT ALTIMETERS
NT OPTICAL RANGE FINDERS
NT RADIO ALTIMETERS
NT RANGE FINDERS

Electro-optical tracking devices for displacement and/or dislocation measurement without physical contact
05 p0763 A69-15986

Conversion of range telemetry systems /CORTS/ program noting installations and standardization
05 p0743 A69-16306

Distance measurement by distance relay circuit composed of intermediate current transformers and rectifier bridges
05 p0765 A69-16746

Photoelectric measurement of chromospheric heights by method requiring neither high telescopic resolution nor best seeing, discussing trials during September 1967
08 p1385 A69-20070

Radio location system based on measuring distance between object and two stationary satellites, noting application to air traffic over North Atlantic
09 p1537 A69-21269

Distance measurements of several hundred feet to resolution of three millionth of inch by applying He-Ne laser interferometer
09 p1519 A69-22475

Cepheids variations used to measure intergalactic distances, noting method of calibrating absolute Cepheid luminosity
10 p1780 A69-23646

VOR/DME ground facilities accuracy improvement by complementing navigation computation with signals from inertial navigation system [SAE PAPER 690338]
11 p1914 A69-24499

Distance vs time and velocity vs time measurements for high speed model missiles by means of laser interferometry and optical Doppler shift method
11 p1886 A69-25042

Communication systems in interplanetary space covering telemetry, remote control, Doppler and distance measurements, coherent PCM/PSK/PM, demodulation, deep space network, etc
12 p2027 A69-25875

Astronomical unit determined by measuring radial velocity of radio wavelength spectral line source
13 p2350 A69-27822

Space direction by compensation method of cosmic triangulation network, using laser and optical observations of artificial satellites
15 p2699 A69-31377

Auroral absorption influence on ionospheric wave propagation calculated for distances over 4000 km
16 p2749 A69-31603

Laser measurements of earth-moon distance applied to determinations of earth axis motion and lunar shape, relief, dimensions and motion
16 p2788 A69-31624

Stellar group Ba 6 distance measured using three color photometry in RGU system
16 p2854 A69-31650

Open galactic cluster NGC 2254 distance determined by three color photometry in RGU system
16 p2854 A69-31651

Pulsars distance determined using H II region data covering line of sight stars and Galaxy hydrogen distribution
17 p3026 A69-32858

Lunar rotation elements determined from distances between Moesting A and limb craters, using Iakovkin position angle method
17 p3028 A69-32876

Diademe satellites stabilization system to measure station-to-satellite distance by laser pulse, discussing reflector, magnet for attitude control, damping device, etc
17 p3046 A69-33224

Proper motions, color magnitude and distance modulus of stars in galactic cluster in direction of Large Magellanic Cloud using Cape wide angle photometry
17 p3034 A69-33411

Cosmic ray shower axis mean distance from apparatus determined by measuring muon to charged particles densities ratio
17 p3024 A69-33580

Cosmic ray shower axis mean logarithmic distance from apparatus calculated by transforming shower recording frequency radial distribution to lin-log coordinate system
17 p3024 A69-33581

Optical distance measurement using laser and atmospheric dispersion method through average refractive index determination over path
18 p3152 A69-35198

Electrooptical distance measurement based on laser pulse traveling time and phase measurements to determine satellite range
18 p3103 A69-35199

Radio distance meter design for accurate distance measurement, discussing transit time and advantages over optical meters
18 p3139 A69-35493

Distance of spacecraft descending on parachute through planetary atmosphere measured from center of planetary mass using onboard instrument data
19 p3432 A69-36633

VOR/DME information augmentation by air data /airspeed/ for positional accuracy improvement, describing error sources, optimum data filter and system sensitivity and performance [AIAA PAPER 69-841]
21 p3762 A69-39372

Distance measuring method limitations for modulated CW laser determined by laser transmitter receiver in conjunction with retroreflector target fixed position
21 p3739 A69-39457

Laser application to distance measurement in air for determining atmospheric influence, using two wavelengths
22 p3959 A69-39901

Astronomical unit determination, discussing dynamical and radar methods and Doppler shift of neutral hydrogen line spectra in radio astronomy method
22 p4022 A69-40464

Target distance and direction monocular estimates with stabilized and nonstabilized retinal images, finding eye movements not improving spatial judgment accuracy
22 p3878 A69-40838

Cepheid variable stars distance estimated from UVB three color photoelectric photometry data
22 p4031 A69-40943

Airline area navigation test programs involving use of VOR/DME signals and inertial navigation system within air traffic control system
23 p4185 A69-41662

Fixed-tuned telemetry receiver as miss distance indicator /MDI/ to provide information in missile performance program
23 p4138 A69-41781

Geographical position coordinates of radio operator determined by distance difference measurement using Loran and digital computer methods
23 p4186 A69-42027

DISTANCE PERCEPTION

U SPACE PERCEPTION

DISTILLATION

Numerical integration stability of differential equations, noting limiting integration step size for unsteady distillation
02 p0273 A69-12478

Vacuum distillation determination of O in Li, evaluating accuracy through O additions and recoveries, method blank and residue identification
22 p3897 A69-40932

DISTILLATION EQUIPMENT

Vacuum distillation technique for isolation and recovery of alkali metal reaction products with Ta, Ni, V and oxygen
01 p0083 A69-10927

DISTORTION

NT FLOW DISTORTION
NT SIGNAL DISTORTION
NT SURFACE DISTORTION

Visual distortion in discrimination of figure proportion
06 p0875 A69-18022

Compressor to inlet distortion tolerance design techniques for gas turbine compressors, noting rotor matching, blade chord length, blade geometry, etc [ASME PAPER 69-GT-115]
09 p1572 A69-22525

He-Ne laser light coherence distortion by atmospheric turbulence
11 p1894 A69-24452

Ray tracing application to evaluating aberrations produced by Fresnel holograms for optimizing design of aplanatic lens holography system
11 p1885 A69-24848

Nonlinear holograms distortions analyzed by five point method utilizing relation between irradiance and amplitude transmittance of photographic emulsion
12 p2090 A69-26255

Distortionless propagation of light through optical two level atoms medium, considering relation to Poynting theorem, hyperbolic secant solution and pendulum analogy
12 p2130 A69-26313

Burger condition for distortion field of dislocation lines in continuous medium, considering arbitrary shape in arbitrary motion
19 p3439 A69-36477

Holographic technique for reduction of image distortion during penetration through inhomogeneous medium
24 p4314 A69-42975

DISTRIBUTED AMPLIFIERS

Transient response of distributed gain amplifier employing m-derived filters and vacuum tubes
13 p2235 A69-28516

RF band multimode parametric pulsed oscillations in distributed system using one dimensional resonators
16 p2758 A69-31796

Multiloop feedback in active distributed RC networks for low parameter sensitivity with low amplifier gain compared to single loop circuits
18 p3111 A69-34679

DISTRIBUTION [PROPERTY]

NT ANGULAR DISTRIBUTION
NT ANTENNA RADIATION PATTERNS
NT BOLTZMANN DISTRIBUTION
NT CHARGE DISTRIBUTION
NT CURRENT DISTRIBUTION
NT DIFFRACTION PATTERNS
NT ELECTRON DENSITY PROFILES
NT ELECTRON DISTRIBUTION
NT ENERGY DISTRIBUTION
NT FLOW DISTRIBUTION
NT FORCE DISTRIBUTION
NT FREQUENCY DISTRIBUTION
NT HOLE DISTRIBUTION [ELECTRONICS]
NT HOLE DISTRIBUTION [MECHANICS]
NT INTERFERENCE LIFT
NT ION DISTRIBUTION
NT LOAD DISTRIBUTION [FORCES]
NT MASS DISTRIBUTION
NT MOMENT DISTRIBUTION
NT NEUTRON DISTRIBUTION
NT PRESSURE DISTRIBUTION
NT RADIAL DISTRIBUTION
NT RADIATION DISTRIBUTION
NT SIDELOBES
NT SPATIAL DISTRIBUTION
NT SPECTRAL ENERGY DISTRIBUTION
NT STAR DISTRIBUTION
NT STRESS CONCENTRATION
NT TEMPERATURE DISTRIBUTION
NT VELOCITY DISTRIBUTION
NT VERTICAL DISTRIBUTION

Redistribution of potassium and argon in meteorites and rock samples, discussing thermal diffusion and grain size
08 p1405 A69-20926

Three dimensional log amplitude and phase fluctuation distributions of collimated and focused Gaussian beams propagated through random inhomogeneous medium, evaluating mean-square values
12 p2130 A69-26393

Correlation coefficients, comparing galactic X ray sources distribution with classical cepheids, old novae, planetary nebulae and Wolf-Rayet stars
12 p2171 A69-27155

MHD channel mercury flow with hydraulic shock in transverse magnetic field, determining characteristic values distribution over range of principal parameters
13 p2307 A69-27499

Anomalous meteorological field distribution as observed by correlated stations, determining independent stations number observing same data
13 p2293 A69-27851

Far and near side lunar crater chains regularities in distribution and size
18 p3202 A69-35329

DISTRIBUTION FUNCTIONS

Reliability analysis of technological systems, determining characteristics as distribution function of time to specified number of failures
01 p0085 A69-10210

Electron-hole collisions effect on drift and electron and hole diffusion in semiconductors at high injection levels
01 p0137 A69-10257

Molecular velocity distribution function in nonequilibrium flows, detailing asymptotic expansions in different velocity domains for weak shock
01 p0059 A69-10330

Odd and even translational two sample test statistics uncorrelated when combined sample distribution function is equally symmetric
01 p0106 A69-10925

Landau damping in plasma, noting competing effects of nonlinearities and collisions on formation of plateau in spatially homogeneous distribution function
01 p0133 A69-11215

Partial differential equation for distribution function in transport of charged particles in earth magnetosphere
01 p0147 A69-11320

Electron distribution function of isotropic homogeneous Lorentzian plasma subjected to frequency modulated electric field calculated by successive approximation method
02 p0285 A69-11543

Envelope distribution of echo signal during reflection scattering by extended turbulent meteor trails
02 p0207 A69-11690

Trimodal solutions for strong shock structure in gas of spherocylindrical molecules
03 p0414 A69-13136

Linear processing effect on digital communications systems performance by channel impulse response and input-output relationship as distributional convolution equation
03 p0391 A69-13226

Extension of results of one dimensional representation theory treating nonGaussian processes as perturbations of log normal process to higher dimensions
03 p0392 A69-13248

Distribution functions for fast electrons near anode calculated by kinetic theory, assuming weakly ionized plasma with smaller Debye length than collision mean free path
04 p0635 A69-14764

Distribution free sequential probability ratio procedure for detecting signal in multiple resolution element radar
05 p0717 A69-15609

Mathematical theory for describing geometric structure of simple bodies, discussing dislocation distribution and exact field equations for elastic bodies motion
05 p0834 A69-15731

Electron distribution function effect on microwave emission and HF conductivity of weakly ionized discharge plasma
05 p0799 A69-15734

Electron distribution function for homogeneous weakly ionized gas in presence of alternating electric field, discussing solution of Boltzmann equations
05 p0797 A69-16604

Linear distributed parameter system identification by stochastic approximation, obtaining constant parameters sequentially
06 p0900 A69-17358

Electrostatic waves interaction to electrons in plasma characterized by bump-in-tail distribution function, deducing mechanism of wave particle interaction
06 p0966 A69-17521

Plasma diffusion in toroidal stellarator using integrals of drift equations for particle trajectories, determining distribution function
07 p1191 A69-18985

Kinetic description of inhomogeneous plasma in ring approximation, discussing Vlasov equation and velocity distribution function
07 p1193 A69-19034

Noncoherent scattering of atoms with Maxwellian distribution in moving atmosphere, discussing Doppler broadening expansion in Legendre polynomials
07 p1219 A69-19286

Metal fatigue simulation by Monte Carlo method, showing programmed fatigue tests in form of life distribution functions
07 p1233 A69-19314

Angular intensity distribution of corpuscular radiation in time independent geomagnetic field characterized by particle velocity distribution
07 p1210 A69-19619

Absolute stability of distributed control system with nonlinear elements of backlash type analyzed by distributed parameters method
07 p1115 A69-19758

Plasma instability with isotropic ion or electron velocity distribution function /nonMaxwellian/, discussing magnetic field and particle energy distribution functions
08 p1359 A69-19949

Time dependent velocity distribution functions for carriers calculated in weakly ionized plasma in external electric field
08 p1362 A69-20265

Electromagnetic waves attenuation and scattering by rainfalls calculated using droplet distribution function
08 p1275 A69-20430

Electron energy distribution function in plasma heated by electron-cyclotron resonance in adiabatic trap determined from bremsstrahlung spectrum
08 p1365 A69-20547

Slow distribution function of magnetoactive plasma, deriving kinetic equation in quasi-linear approximation for analyzing particle-HF electromagnetic wave interactions
08 p1365 A69-20550

Particle-wave interactions in weakly turbulent collisionless plasma, discussing ensemble average distribution function, diffusion, nonlinear Landau damping and nonlinear instabilities
08 p1368 A69-20803

One dimensional distribution law of random process with arbitrary correlation function, verifying normality hypotheses by integral criterion
08 p1299 A69-21069

Postselection estimation of component reliability in multicomponent systems, considering cases of binomial and exponential distributions of random variables
08 p1322 A69-21099

Planckian stellar velocity distribution function, moduli and projections on coordinate planes determined by ellipsoidal approximation
09 p1589 A69-21370

Digital information transmission error characteristics determining error distribution over time and relation to distribution function of intervals between errors
09 p1454 A69-21795

General solution of Liouville equation for collisionless system of gravitationally interacting particles, with distribution function locally isotropic in momentum space
09 p1605 A69-22412

Electron-hole collisions effect on drift and electron and hole diffusion in semiconductors at high injection levels
09 p1559 A69-22650

Quasi-linear relaxation of electron beam in magnetoactive plasma, noting instability of plateau in velocity distribution function
09 p1553 A69-22659

Rate estimates of convergence of multidimensional central limit theorem for sequence of identically distributed independent random variables with third order finite moments
10 p1719 A69-23400

Nonequilibrium distribution functions for neutral atoms excited states in optically thin low temperature singly ionized plasma containing ions, electrons and neutrals
10 p1731 A69-23437

Tracking filter steady state oscillation amplitude and phase distributions determined from Fokker-Planck equation for high and low noise levels
11 p1844 A69-24441

Pitch angle distribution function of thermal protons in magnetosphere taking into account earth gravitational field
12 p2067 A69-26354

Partial differential equation with stochastic characteristics reducible to parabolic equation by introducing additional variables
12 p2121 A69-26366

Distribution function of multiple correlation coefficient for various sampling volumes and various numbers of predictors calculated using Fisher formula
13 p2293 A69-27843

Electron velocity distribution function in gaseous plasma with known collective oscillations and frequency/wave number relationship
13 p2313 A69-28327

Monograph on velocity distribution function in turbulent boundary layer, discussing hot wire anemometer for mean velocity, turbulence intensity and higher order moments determination
13 p2250 A69-28336

Cosmic ray showers components relationships, analyzing superhigh energy nuclear cascade development, discussing components distribution function at constant proton energy
13 p2332 A69-28410

Envelope distribution of echo signal during reflection scattering by extended turbulent meteor trails
13 p2224 A69-28721

Reliability analysis of technological systems, determining characteristics as distribution function of time to specified number of failures
14 p2453 A69-28747

Extremal system of adaptive circuits adjusted by random search with varying random step distribution function
14 p2425 A69-28824

Mathematical model of mechanical wear in surface friction based on approximation of cross section profiles, using Fokker-Planck equation for distribution function
14 p2455 A69-29331

Orientation distribution of lineal and areal elements in space, expanding density function definition of two dimensional lineal array
14 p2470 A69-29363

Graphical method for plotting contours of Rice distribution function as rocket-borne radar reflection data, determining leakage factor
14 p2416 A69-29536

Minimum error criteria for shock wave structure determined by applying Mott-Smith distribution to Boltzmann equations for rigid sphere gas
14 p2431 A69-29579

Electron energy distribution functions and energy transfer rates to inelastic levels of carbon dioxide and nitrogen in laser
14 p2460 A69-29603

Quasi-distribution function differential equation for laser field with nonMarkoffian character derived from density matrix master equation
14 p2486 A69-29633

Relativistic corrections to particle distribution functions for high temperature plasma in thermodynamic equilibrium by integrating Gibbs distribution
14 p2499 A69-29847

Kinetic theory of fluctuations in turbulent plasmas based on construction of many particle distribution functions
14 p2502 A69-29989

Radial distribution functions for dense hydrogenous plasma near ionization temperature by solving Percus-Yevick equations
14 p2502 A69-29998

Distribution function of SNR from coherent optimal estimate of signal amplitude
15 p2564 A69-30149

Pressure fluctuation relaxation model to close turbulent distribution function equations at one point level, solving equation for rectilinear flows and periodic wake decay
15 p2591 A69-30906

Ionospheric VLF emission and particle measurements, discussing energy, distribution and flux of protons and electrons
15 p2605 A69-31425

Krylov functions determined by distribution theory and operational calculus, discussing deformations and statics of straight beams
15 p2715 A69-31475

Fluctuation spectra of monatomic gases, using two time probability distributions for distribution function autocorrelations
16 p2817 A69-31669

Heat transfer in rarefied gas plane Couette flow determined by BGK model and moments method of half range distribution functions
16 p2876 A69-31688

Electron distribution function for weakly ionized plasma under alternating electric and circularly polarized rotating magnetic field, noting cyclotron resonance
16 p2820 A69-31753

Automatic nonrepairable control elements reliability evaluated statistically with differentiable lifetime distribution function
16 p2764 A69-32199

Precipitation intensity measurements, obtaining distribution parameters from radar reflectivity at two wavelengths and microwave attenuation factor at third wavelength
16 p2806 A69-32265

Distribution function, harmonic and statistical linearization methods applied to study forced oscillations in nonlinear oscillatory system
16 p2813 A69-32284

Electromagnetic noise in current sheet in geomagnetic tail, discussing effects on distribution function [AFCLR-69-0395]
16 p2781 A69-32317

Lynden-Bell statistical mechanics of relaxation in collisionless one dimensional stellar system, discussing low energy particles distribution
16 p2862 A69-32376

One dimensional distribution law of random process with arbitrary correlation function, verifying normality hypotheses by integral criterion
16 p2765 A69-32484

Water bag spherically symmetrical universe model, discussing system stability, distribution function representation and polytrope equivalency
16 p2866 A69-32813

Boltzmann equation for Lorentzian plasma in elliptic magnetic field solved by expanding distribution function in Legendre polynomials
17 p3009 A69-32827

Constitutive equation variation effect on near wall flow pattern of dilute polymer solutions
17 p2951 A69-33257

Ion energy distribution function and density profile in strong implosion wave generated by theta pinch discharge, investigating compression wave in deuterium
17 p3013 A69-33821

Time resolved beam distribution functions resulting from cyclotron instability and harmonics in electron injection machine during beam-plasma experiment
17 p3014 A69-33829

Gas laser power dip in presence of elastic collisions, using equilibrium equations for particles velocity distribution function
17 p2983 A69-33972

Lorentz gas approximation to Boltzmann collision operator generalized for heavy molecule nonMaxwellian gas distribution function, obtaining equilibrium distribution applicable to ionized gas
18 p3179 A69-34438

Planckian velocity distribution function, moduli and projections on coordinate planes determined by ellipsoidal approximation
18 p3198 A69-34759

Shock wave structure in single component monatomic gas by expanding Boltzmann equation distribution function in terms of Hermite polynomial
18 p3124 A69-35170

Natural oscillations frequency spectrum of turbomachine impeller blades subjected to random variations determined with frequency distribution function obtained by moments method
19 p3436 A69-35844

Spatially homogeneous Boltzmann equation containing initial distribution functions expandable into Hermitian polynomials analyzed via ordinary differential equations
19 p3373 A69-36202

Corpuscular radiation distribution function with trapped particles maximum density fixed in equatorial plane and reflection points vicinity of magnetic force line
19 p3396 A69-36630

Solar wind temperature, using distribution function for solar wind ions in anisotropic Maxwell distribution form
19 p3396 A69-36631

Component hazard rate distribution functions from unit time and failure analysis, noting confidence statements and simulation studies
20 p3548 A69-37158

Electron momentum transfer cross sections by numerically solving electron energy distribution function from Boltzmann equation in Lorentz approximation
21 p3773 A69-38396

Quantum theory for single mode laser radiation, considering photon distribution function and mean field damping decrement by phase quantum fluctuations
21 p3737 A69-38996

Antenna array synthesis optimization for limited deviations of source distribution function from prescribed function
22 p3916 A69-40952

Distribution function for thermalization distances derived for infinite atmosphere with plane source in noncoherent light scattering
23 p4192 A69-42403

Optimal rule for decision to stop or continue observation of random variables after observing sequence of variables with continuous distribution function
24 p4341 A69-43235

DISTRIBUTION MOMENTS
NT MEAN
NT STANDARD DEVIATION
NT VARIANCE [STATISTICS]
Nonisotropic relaxation of Boltzmann gas in homogeneous space, expressing collision integral moments in terms of distribution function moments for any molecule
06 p0910 A69-17347
Shallow shells two dimensional theory including effects of transverse shear deformation and of moments turning about normal to middle surface
22 p4048 A69-41197

Optimal scheme of combining moment estimators set derived for computational simplicity and asymptotic efficiency
24 p4342 A69-43704

DISTURBANCE THEORY
U PERTURBATION THEORY
DISTURBING FUNCTIONS
Stability and dissipativity conditions for nonlinear controlled systems subjected to parametric and continuously acting disturbances
09 p1476 A69-22717
Optimal controller design and transfer functions in linear stabilization systems subjected to unknown disturbances determined by variational calculus
13 p2259 A69-27425
Stability and dissipativity conditions for nonlinear controlled systems subjected to parametric and continuously acting disturbances
16 p2765 A69-32550
Short term motion of lunar satellite, discussing third body disturbing functions and perturbation solution of nonsingular orbit elements
19 p3402 A69-35934

DISULFIDES
Disulfide effects on jet fuel operating characteristics and demercaptanization influence on thermal stability, corrosive action and sedimentation
01 p0142 A69-11098
Aqueous hydrazine solution effect on Ti disulfide crystalline structure
23 p4112 A69-41426

DITCHING [LANDING]
Passenger and crew members escape from aircraft following water accidents, discussing ditching, evacuation, survival and rescue facilities
08 p1254 A69-20453
Safety measures for aircraft ditching at sea, discussing low wing configuration advantages and life rafts
14 p2392 A69-29697

DITHIOLS
U THIOLS
DIURESIS
Short latency antidiuresis following initiation of food ingestion by food deprived rats, noting possible signaling factor
01 p0014 A69-10860
Physical factors affecting proximal and distal tubular sodium reabsorption in dogs undergoing water diuresis
13 p2210 A69-28482
Portal blood pressure decrease effects on diuresis in unanesthetized rats, discussing osmotic diuresis
23 p4094 A69-42074
Diuresis during total immersion in thermally neutral water, interpreting urine flow increase caused by intrathoracic blood volume expansion
23 p4094 A69-42075

DIURNAL RHYTHMS
U CIRCADIAN RHYTHMS
DIURNAL VARIATIONS
North-south ionospheric drift velocities near magnetic equator, noting marked seasonal characteristics and diurnal variations
01 p0062 A69-10138
Exosphere diurnal and latitudinal variations in electron and proton content, ion composition, and electron, proton and positive O ion densities
01 p0063 A69-10422
Night ionosphere electron content changes in Southern Hemisphere, discussing diffusion from exosphere and corpuscular radiation as sources of ionization
01 p0063 A69-10423
Ionospheric inhomogeneities vertical and latitudinal distributions and diurnal variations, measuring Explorer 22 signals Faraday fading with space diversity reception
01 p0064 A69-10446
Ionospheric negative ion coefficient variations, analyzing formation microprocesses
01 p0066 A69-10599
Whistler rate and dispersion daily and annual variations derived relative to propagation conditions and magnetospheric behavior over North Italy
01 p0067 A69-11033
Latitudinal variations in auroral and subauroral region F layer diurnal and magnetic storm pattern shown by scintillation measurements
01 p0069 A69-11127
Gross behavior patterns of intense sporadic E including seasonal, diurnal and geographic variations and latitudinal and longitudinal effects
01 p0070 A69-11157

Lower thermosphere neutral composition diurnal variations, noting molecular N and O, Ar, He and atomic O

01 p0076 A69-11231

Electron intensity diagram of diurnal trapped electron variation from Cosmos 5 satellite data, including harmonic analysis of data

01 p0147 A69-11321

Second harmonic cosmic ray daily variation, discussing density gradient model with particle diffusion along field direction

02 p0305 A69-11422

Sporadic E layer critical frequencies seasonal and diurnal periodic variations, noting independence of solar activity cycle

02 p0239 A69-11685

Cosmic ray meson diurnal anisotropies direction calculated on basis of subtracted diurnal vectors

02 p0306 A69-11730

Middle ionosphere temperature diurnal variations analyzed on basis of rocket experiments and electron density asymmetry

02 p0246 A69-12768

Diurnal variation in horizontal magnetic component of South American stations close to electrojet during IGY

02 p0246 A69-12771

Diurnal, magnetic and solar cycle dependences of auroral emission variations and auroral occurrence

03 p0420 A69-13325

Middle stratospheric diurnal temperature variation based on model eliminating radiation error of rawinsonde

03 p0461 A69-13344

Earth ionosphere resonator natural frequencies, considering diurnal variation and geomagnetic field eccentricity

03 p0422 A69-13512

Diurnal variation of variation coefficient of F 2 critical frequency for steady and unsteady primary ionizing fluxes simulated on computer

03 p0423 A69-13516

Polar auroral region cosmic radio noise absorption bays diurnal variations attributed to drift of electrons captured in magnetosphere

03 p0423 A69-13520

Diurnal upward and downward flows of atmospheric matter following upper atmosphere temperature nighttime minimum and daytime maximum

03 p0423 A69-13533

Geomagnetic field quiet day solar variations current system calculated, using 2000 LT as zero level basis

03 p0424 A69-13541

Thermal forcing role in diurnal oscillation of planetary boundary layer wind above sloping terrain

03 p0462 A69-13682

Cosmic ray solar diurnal variations for nucleonic component, discussing differential response functions

03 p0501 A69-13751

Cosmic ray meson component solar diurnal variation calculations noting amplitude, average deflection angle and dependence on zenith angle of arrival

03 p0501 A69-13752

Diurnal variations of low latitude VLF emissions observed at Hiraiso, Japan

03 p0398 A69-13900

Amplitude and phase of cosmic ray meson diurnal variation, noting less variation in neutron diurnal variation

04 p0648 A69-14374

Atmospheric, geomagnetic and interplanetary effects on cosmic ray flow, noting anisotropy and diurnal variation phase and amplitude averages

04 p0649 A69-14683

Daily solar indices monthly averages errors due to evaluation for days presenting favorable weather conditions

04 p0657 A69-14700

Diurnal variations of visual meteoric activity mean hourly rates compared with earlier observations

04 p0658 A69-14879

Frequency of cold front passages during year in French part of Switzerland and times of occurrence during day

04 p0628 A69-15089

Atmospheric rotation speed dependence on specific heat, thermal conductivity, air absorption coefficient and lower boundary pressure, discussing diurnal variation of thermosphere

[AFRL-69-0363]

04 p0649 A69-15130

VLF phase measurements for apparent and equivalent diurnal height variation for lower ionosphere waveguide

05 p0752 A69-15666

Electron cooling rates in midlatitude and auroral zone thermosphere measured by probe rockets

05 p0755 A69-16267

Diurnal variations of neutral and charged particle temperatures in equatorial F region

05 p0755 A69-16270

Lunar tide effect on height distribution and velocity of ionospheric electron density daily variations near magnetic equator

05 p0756 A69-16401

F region seasonal and magnetic storm behavior from region daily behavior showing global upper atmospheric circulation

05 p0757 A69-16404

Lower ionospheric diurnal variations in electron density observed by beacon satellite, noting effect on high power VHF forward scatter circuits

05 p0757 A69-16405

Ion temperature diurnal variations at 250-475 km obtained from Thomson scatter spectra

05 p0757 A69-16407

Wind data from Arctic upper mesosphere showing easterly winds increasing with height, resolving diurnal and semidiurnal oscillations

06 p0949 A69-17005

Galactic cosmic rays anisotropies due to density gradient perpendicular to ecliptic plane studied, using diurnal and semidiurnal component and intensity deficiency

06 p0990 A69-17289

Cosmic ray daily variations relationship to geomagnetic activity, sector structure of interplanetary magnetic field and sunspot activity

06 p0990 A69-17291

Variational coefficients for vertical and inclined meson telescopes, deriving primary cosmic rays anisotropy parameters from daily variations

06 p0924 A69-17293

Data on muons indicating temperature effect diurnal maximum and pressure corrected daily variation

06 p0924 A69-17294

Day and night reversals in NmF2 north-south asymmetry related to neutral wind direction

06 p0918 A69-17384

Diurnal field strength and phase variations of VLF transmissions over transequatorial path from Australia to Japan

06 p0889 A69-17654

Phase and amplitude record changes in sunrise and sunset transitions in VLF transmissions over long path

06 p0889 A69-17655

Global geomagnetic anomalies influence on longitudinal pattern of solar quiet day variations and in phases of second harmonics of components

06 p0920 A69-17734

Optimum length of Fourier time series approximating diurnal F 2 critical frequency variation on planetary scale

06 p0921 A69-17746

Magnetospheric ring current effect on main phase of geomagnetic storms, calculating diurnal storm-time portion of perturbation field

07 p1122 A69-18296

Lunar daily geomagnetic periodicities by periodogram or spectral analysis, comparing amplitudes obtained by spectral analysis to those by harmonic analysis

07 p1123 A69-18817

Equatorial hourly storm time part of disturbances field for 1958, discussing magnetic storm effects

07 p1124 A69-18822

Nighttime equatorial Pi 2 micropulsations, noting seasonal and diurnal distributions and dependence on three hour index of magnetic activity

07 p1125 A69-18841

VLF diurnal phase change observations, showing deviations from theoretical first mode and second mode dominance

07 p1078 A69-18912

Diurnal thermal wave form driven by harmonically oscillating ground temperature in nongray atmosphere, calculating results for terrestrial and Martian atmospheres

07 p1126 A69-19036

Soviet monograph on diurnal solar cosmic ray variations from maximum to minimum solar activity, discussing model based on anisotropic particle scattering theory

07 p1209 A69-19500

Double diurnal oscillation of atmospheric pressure and vertical gradient of electromagnetic field, noting agreement between diagrams and role of atmospheric tides

08 p1306 A69-19866

Equatorial counter-electrojet and inverse quiet day solar diurnal variation current layers, noting regular diurnal variation horizontal component and latitude effect

08 p1306 A69-19884

Flight test performance of airborne Omega radio navigation system capable of worldwide coverage, discussing diurnal variations effects in phase velocity

08 p1348 A69-21191

Solar quiet day variations studied by annual amplitude dependence on number of sunspots, considering E layer ionization

09 p1575 A69-21550

Zero reference field for quiet day solar variations, considering magnetic field levels and errors

09 p1575 A69-21551

Cosmic ray intensity diurnal variations from super neutron monitor observations, discussing anisotropy resulting from reduced intensity in gardenhose direction in ecliptic plane

09 p1576 A69-21706

Diurnal variation of D region electron production rates, discussing Lyman alpha ionization of nitric oxide

09 p1577 A69-21717

Diurnal nutation and periodic terms of local coordinates using OPL model of Danjon astrolabe, presenting harmonic and Fourier analysis

09 p1596 A69-22059

Atmospheric radio noise at 27 kc measured at European stations, showing field strength variations, latitude dependence and amplitude distribution

09 p1491 A69-22163

Geomagnetic activity correlation to cosmic ray solar daily variation underground, observing primary cosmic ray flux with meson telescopes

09 p1583 A69-22755

Cosmic rays origin, measurements of energy spectrum and stellar diurnal variations

10 p1757 A69-22823

Cosmic ray anisotropy relation to scattering and sectorial structure of interplanetary magnetic field using neutron monitor data

10 p1758 A69-22834

Solar diurnal variation amplitude and phase instability, considering anisotropic cosmic ray fluxes superposition

10 p1759 A69-22837

Air-earth current density variations with universal time, noting hemispherical dependence of storm activity effects

10 p1682 A69-23415

Thomson scatter bistatic sounder data on ionization transports in F region, describing diurnal variations by hourly values of velocities

10 p1685 A69-23830

Nighttime ionospheric recombination studies by model reference heights varying diurnally, seasonally and with solar flux and geographic location

10 p1685 A69-23834

Secondary corpuscular stream effect on diurnal variations in cosmic ray intensity obtained from statistical analysis

10 p1769 A69-23904

Interplanetary magnetic field sectorial structure effect on diurnal cosmic ray intensity and geomagnetic field, noting field direction influence

10 p1769 A69-23905

Auroral electron energy diurnal variation, noting ground observations of polar auroras, riometric absorption, vertical changes in ionization layer maximum position, etc

10 p1687 A69-23915

Lunar diurnal variation parameters at Irkutsk determined from IGY data concerning geomagnetic field components

10 p1687 A69-23918

Diurnal variations in sporadic E layer and wind in ionosphere during equinox and solstice periods, noting wind shear mechanism and ambient electron density

10 p1688 A69-23932

Nitrogen dioxide molecular ions formation in air, discussing absence at lower pressures and early afterglow dominance in air ionized and dissociated by microwave pulses

11 p1879 A69-25158

Neutral gas motions causing plasma motions in F region, obtaining vertical plasma velocity component pronounced diurnal variations

12 p2070 A69-26684

Diurnal and seasonal variations in drift velocity vector of small scale inhomogeneities in F 2 region

12 p2070 A69-26688

- Auroral cosmic noise absorption relationship to auroral geomagnetic disturbances, investigating absorption diurnal distribution
12 p2071 A69-26706
- Gustafsson pattern for variations in position of quiet homogeneous arcs, noting diurnal variations from visual observations at antarctic station
12 p2073 A69-26951
- Solar control of day-to-day variability in phase of solar diurnal variation of horizontal magnetic intensity on quiet days
12 p2073 A69-26954
- Solar quiet currents in three dimensional ionosphere, considering ionospheric conductivity and horizontal layer equations
12 p2074 A69-26955
- Sea tides and ionospheric effects on lunar variation of geomagnetic field vertical component
12 p2161 A69-26957
- Geomagnetic field daily variations, discussing observational techniques, observation analysis, S-field seasonal changes, equatorial electrojet, solar wind effects, dynamo theory, etc
12 p2077 A69-27143
- Air mass displacements and diurnal variations in potential temperature at tropopause level
13 p2252 A69-27608
- Stable geomagnetic pulsations related to plasma density shock position in magnetosphere and to magnitude of diurnal variations
13 p2253 A69-27692
- Probable sign-invariant periods of air temperature anomalies based on random Gaussian processes
13 p2294 A69-27855
- Sporadic E layer critical frequencies seasonal and diurnal periodic variations, noting independence of solar activity cycle
13 p2258 A69-28716
- Muonic component diurnal wave trains at 70 mwe during cosmic ray decreases, discussing Forbush decay as result of shock front advance
14 p2511 A69-28962
- Diurnal variation of cosmic ray muon intensity near geomagnetic equator and primary anisotropy monitored by cubical counter telescope
14 p2512 A69-28966
- Cosmic ray angular distribution spectrum and interplanetary magnetic field properties determined from semidiurnal cosmic ray variations data
14 p2512 A69-29046
- Time and altitude induced variations in daytime NO and molecular and atomic oxygen ions
14 p2435 A69-29050
- Polar aurora rays mean length diurnal variations determined from photographic and visual observations in Tiksi bay
14 p2437 A69-29077
- Thomson scatter probes for diurnal variations of daytime atmospheric density at 100 km altitude
14 p2440 A69-29125
- Polar cap absorption riometer recorded during 2-6 September 1966 event compared to satellite measurements of solar protons, discussing diurnal variations and oxygen role in associative detachment reactions
14 p2440 A69-29126
- Thermally excited diurnal wind oscillations in lower mesosphere using model atmosphere in CIRA 1965, discussing daytime ozone density profiles
14 p2441 A69-29379
- Daytime ionospheric screening effect on low latitude geomagnetic micropulsations estimated using ionosphere model
14 p2441 A69-29380
- Turbulent heat exchange coefficient radiation absorption and diurnal vertical variations effects on temperature field in surface layer of sea and atmospheric boundary layer
14 p2472 A69-29462
- Zonal drift influence on morning ionization anomaly in F region, noting shifts to West with increasing height and electron production rate
14 p2442 A69-29732
- F 2 region small scale inhomogeneities drift observations showing seasonal and diurnal velocity and direction changes
14 p2444 A69-29868
- Radio signals F region scattering related to electron density fluctuations in ionosphere
14 p2444 A69-29870
- Waveguide mode propagation theory for determining earth-ionosphere spherical waveguide upper boundary height diurnal variation for VLF waves
15 p2595 A69-30224
- Diurnal variations of wind velocity, temperature and density at high altitude measured by Skylark rockets
15 p2598 A69-31319
- Diurnal change in equatorial electrojet parameters observed by magnetometers on Nike Apache rockets
15 p2598 A69-31320
- Atmospheric density and temperature variations between 200-600 km from Cosmos satellite data, noting solar activity effect
15 p2599 A69-31343
- Upper atmosphere structure and variations including density and composition in lower thermosphere, diurnal variations, variations with solar activity, etc
15 p2600 A69-31355
- RF mass spectrometric measurements of diurnal variation of thermosphere and ionospheric E and F regions composition, noting oxygen concentration
15 p2601 A69-31371
- Diurnal variations of atmospheric ion composition at 100-200 km from rocket experiments
15 p2603 A69-31401
- Diurnal thermospheric density, temperature and wind variations due to direct solar EUV heat input and tidal wave from lower atmosphere
15 p2605 A69-31439
- Diurnal variations in radiation sensitivity of mice and rats to irradiation with median lethal doses, noting sine curve survival function
15 p2557 A69-31458
- Diurnal variations of IR atmospheric oxygen bands in airglow observed with filter photometer on balloon flights
16 p2776 A69-32091
- Cosmic ray second harmonic daily variations explainable by symmetrical gradient rising away from solar equatorial plane
16 p2850 A69-32304
- Direct wind measurement and momentum transport estimates obtained from cyclones and anticyclones daily displacements over Northern Hemisphere, applying results to planetary atmospheres
16 p2780 A69-32306
- Solar quiet day geomagnetic variations harmonic analysis with respect to time intervals centered around noon, defining parameters responsible for modulated Sq
16 p2781 A69-32452
- Equations of transformation for hourly data harmonic terms used in computation and representation of solar and lunar daily magnetic variations
16 p2782 A69-32457
- Lunar components in mean values of geomagnetic field daily variations, discussing lunar phase during selected quiet days
16 p2782 A69-32458
- Semiannual variation in amplitude of solar daily quiet geomagnetic variation, discussing sunspot dependence of seasonal secondary minimum and maxima
16 p2782 A69-32459
- Upper atmospheric winds to produce solar quiet day magnetic variations based on dynamo theory, illustrating solenoidal, irrotational and mixed winds
16 p2782 A69-32460
- Solar quiet day variations studied by annual amplitude dependence on number of sunspots, considering E layer ionization
16 p2851 A69-32545
- Zero reference field for quiet day solar variations, considering magnetic field levels and errors
16 p2851 A69-32546
- Vertical ozone distribution determination discrepancies between Brewer-Mast electrochemical sonde and Umkehr methods, discussing influence of seasonal and diurnal variations
16 p2786 A69-32630
- Nighttime latitude variations in Danjon astrolabe observations at Poltava, noting decrease from early evening to midnight
17 p2959 A69-32870
- Upper atmospheric gas density and temperature distribution diurnal and seasonal variations calculated from satellites orbiting time changes
17 p2959 A69-32924
- F region stratification during solar minimum and maximum, discussing regularities of plasma frequencies and diurnal variations
17 p2959 A69-33005
- Semidiurnal oscillation in thermalgeostrophic atmosphere examined using atmospheric model for tidal oscillations response study
17 p2959 A69-33148
- Scattered ionospheric reflection distribution at evening/morning periods showing deviation, using coherent method
17 p2927 A69-33860
- Meteor trail drift radar observations in Kharkov, giving wind velocity diurnal and seasonal variations
17 p3041 A69-33897
- Polar auroras pulsation attributed to background brightness fluctuations, discussing intensity diurnal variation
17 p2963 A69-33954
- High latitude geomagnetic field quiet solar diurnal variations during magnetically quiet IGY winter days, relating type and amplitude at low and midlatitudes
17 p2964 A69-33960
- Unsteady model taking into account photoionization, neutralization and diffusion, describing electron concentration diurnal and seasonal variations in ionosphere F 2 region at midlatitudes
17 p2966 A69-33978
- Postsunset apparent reflection height and electron density variability in equatorial F 2, discussing singularities of diurnal variation in November-January
17 p2967 A69-33984
- Reflection and ionization heights diurnal variations in F region, obtaining data for sporadic E formation
17 p2968 A69-33995
- Diurnal sporadic E layer height variations analyzed for singularities in height peak behavior as function of geography, season and magnetic activity
17 p2968 A69-33996
- Space diversity reception and diurnal variations of F region ionospheric motions, comparing IQSY program
17 p2969 A69-33999
- Reexamination of polar F region electron density diurnal variation data contradicting Krich-Kohl theory of rotating neutral winds role
18 p3125 A69-34255
- Magnetic declination effect on F 2 layer critical frequency diurnal variations attributed to vertical ionospheric drift due to neutral air winds
18 p3126 A69-34256
- Cosmic ray intensity short term stochastic variations in solar system related to turbulent solar wind day-to-day variations
18 p3186 A69-34300
- Diurnal wind variations below 30 km plotted on constant pressure charts, showing topographical influence on tidal fluctuations
18 p3166 A69-34828
- Cosmic ray diurnal anisotropy variations, correlating component annual means with magnetic activity
18 p3186 A69-34934
- Dawn-dusk electric field in outer radiation zone associated with magnetospheric plasma convection, comparing electron densities for magnetically quiet periods
18 p3128 A69-34942
- Whistlers occurrence and dispersion rate variations from data obtained at lower latitudes during magnetic storms
18 p3102 A69-34967
- Source position of cosmic ray diurnal anisotropy relative to ecliptic plane from neutron monitor data at Mawson and Churchill stations
18 p3189 A69-35441
- Vertical profiles of pressure, temperature and density variations due to upper troposphere pressure changes with and without zero layer effect
19 p3365 A69-36580
- Proton satellites measurements reconciliation with diurnal stellar variation data and cosmic rays origin models
19 p3396 A69-36621
- Diurnal and seasonal phase-differing fluctuation measurement of radio waves propagating along ground layer caused by atmospheric turbulence
20 p3485 A69-36971
- Global distribution of F 2 layer critical frequencies by expanding empirical function of diurnal variations into natural orthogonal components
20 p3521 A69-37051
- Diurnal, seasonal and cyclic altitude and maximum ionization median value variations of undisturbed ionosphere from vertical sounding data obtained at Yakutsk, Siberia
20 p3527 A69-37668
- Diurnal F 1 layer development over Irkutsk, Siberia, during minimum and maximum solar activity, using semiquantitative method
20 p3527 A69-37670
- Ionospheric radio wave absorption seasonal and diurnal variations over Tiflis from pulsed ionospheric sounding at 2.2 MHz
20 p3491 A69-37677
- Alouette 2 ionograms secondary resonances data indicating day-night effect in relative frequency of occurrence
20 p3496 A69-37889

Diurnal and seasonal variations of primary atmospheric ions in topside ionosphere correlated with solar zenith angle, using ion mass spectrometer on Explorer 32

20 p3534 A69-38087

Diurnal variations in cosmic ray intensity from observations by inclined meson telescopes scanning equatorial plane

20 p3593 A69-38109

Diurnal entrainment deviations and atmospheric turbulence effects on flash photographs from Geos 1

21 p3793 A69-38339

Morphology of discrete polar cap and polar glow auroras, noting diurnal variations correlation with magnetic activity changes at low latitude

21 p3707 A69-38487

Rocket measurement data of auroral particle precipitation classified in substorm phases of quiet and breakup period, breakup and postbreakup events and morning events

21 p3707 A69-38489

Equatorial plasma sheet role in magnetotail assessed from Vela satellite data, noting diurnal density variations

21 p3711 A69-38512

Spectrum, latitude dependence and diurnal variation of night airglow emission, noting space and time correlation and magnetic activity relationship to luminous intensity

21 p3711 A69-38514

Diurnal intensity variations in OI 5577 A line emission connected with vertical movements in 90 km level of atmosphere

21 p3713 A69-38525

Primary cosmic rays solar diurnal modulation, measuring relative amplitudes and phases over full cycle

21 p3788 A69-38547

Geomagnetic field horizontal component daily variations in relation to solar wind, noting effects of ambient field night side decrease

21 p3714 A69-38549

Diurnal variations of cosmic ray neutrons corrected for barometric and temperature effects by harmonic analysis

21 p3791 A69-38840

Daily simultaneous solar measurements of microwave atmospheric absorption and emission to determine frequency correlation between meteorological phenomena and atmospheric parameters

21 p3718 A69-39747

Venus and Mercury diurnal period commensurability associated with Venus spin-orbit resonance with earth orbit

22 p4018 A69-40270

Ionospheric electron temperature profiles for mid-day equinoctial conditions noting protonospheric and conjugate heating effects

22 p3939 A69-40506

Diurnal variations of electron flux based on balloon observations near polar cap consistent with geomagnetic cut-off variations of magnetospheric models

22 p4005 A69-40511

Daily variation of trajectory derived high latitude vertical cut-off rigidities in magnetospheric model consistent with proton and electron experiments

22 p4005 A69-40513

Rocket measurements of diurnal variations of F region concentrations and temperature of molecular N and O, showing disagreement with satellite drag data

22 p3939 A69-40515

Cosmic ray diurnal phase and amplitude variations determined using superimposed records of cosmic ray stations inside limited rigidity region

23 p4204 A69-41481

Geomagnetic disturbances relations to cosmic ray diurnal variation phase and amplitude, including Forbush decreases

23 p4204 A69-41483

Day-to-day variability of daily variation of cosmic ray intensity during quiet solar activity period using high latitude neutron monitor data

23 p4204 A69-41484

Day-to-day changes of cosmic ray diurnal variation measured on meson and neutron components, showing relationship with interplanetary magnetic field

23 p4206 A69-42012

Diurnal rhythms of heart rate and blood pressure reactions to posture changes on tilt table, finding orthostatic lability maxima

23 p4094 A69-42072

Noncyclic daily solar quiet variation in mean hourly geomagnetic field by including noncyclic variation term in regression model

23 p4158 A69-42170

Faraday rotation diurnal variation plotted by analyzing radio transmissions from Canary Bird geostationary satellite, considering ionospheric electron density peak

23 p4160 A69-42433

Diurnal variation of Pc type geomagnetic pulsations correlation with F 2 layers critical frequency diurnal variations

23 p4161 A69-42441

Geomagnetic activity hourly and daily variations during solar cycle at Huancayo

23 p4162 A69-42442

Diurnal variations in solar cosmic ray muon component near sea level, using scintillation counters assembled in muon telescope array

23 p4207 A69-42498

Bigeminus pattern in baboon social behavior, noting diurnal rhythm independence from social deprivation, light cycling and food supply

24 p4260 A69-42705

Solar wind kinetic energy density using geomagnetic field horizontal component daily variation, treating earth as plasma probe

24 p4308 A69-42968

Diurnal and solar cycle variations of thermosphere density and temperature generated by solar EUV input and tidal wave, using two dimensional model

24 p4367 A69-43003

Pulsating aurora diurnal variations and dependence on latitude and magnetic activity, photometric observations

24 p4308 A69-43004

Circadian periodicity of human reaction times tested during normal diurnal cycles and 24 hour wakefulness, noting acoustic and visual stimuli effects on learning

24 p4267 A69-43387

Lower ionosphere atmospheric density, temperature and pressure profiles diurnal variations from data of radio meteor echoes

24 p4311 A69-43504

DIVERGENCE

Measurement of helium-neon laser radiation divergence emitted in TEM sub nm modes

07 p1148 A69-18804

Emission intensity and beam divergence of p-n junction GaAs laser with nonlinear passive element in resonator

09 p1515 A69-21474

Adaptive filtering to prevent divergence observed in application of Kalman filter to orbit determination

12 p2045 A69-26059

Emission intensity and beam divergence of p-n junction GaAs laser with nonlinear passive element in resonator

15 p2633 A69-30719

Operational circulation model numerical experiment suggesting elimination of spurious divergence-on-divergence interactions from implied vorticity equations in primitive equations

19 p3363 A69-36503

Measurement of helium-neon laser radiation divergence emitted in TEM sub nm modes

21 p3736 A69-38949

Adaptive filtering to prevent divergence observed in application of Kalman filter to orbit determination

23 p4146 A69-42446

DIVERGENT NOZZLES

Interactions between outer and inner jets behind maximum cross section of jet engine nozzle [ONERA-TP-600]

02 p0187 A69-11620

Diverging nozzle flow of gas mixtures containing solid or liquid particles analyzed by one dimensional approximation separately averaging boundary layer and flow core

19 p3298 A69-36389

DIVERTERS

Trapping of plasmoids injected from two coaxial plasma sources through magnetic gaps of diverter, discussing alternate and simultaneous injection

12 p2133 A69-25976

Dynamic characteristics of plasma fluxes across magnetic field of diverter inside plasma cylinder formed during injection

12 p2134 A69-25977

DME-A SATELLITE

U EXPLORER 31 SATELLITE

DNA

U DEOXYRIBONUCLEIC ACID

DO- 31 AIRCRAFT

Dornier Do 31 VTOL jet aircraft noise alleviation in far field, discussing shielding, interference, ground attenuation and reflection

22 p3862 A69-39932

DOCKING

U SPACECRAFT DOCKING

DOCUMENT STORAGE

USAF accident information, reporting and retrieving, describing Directorate of Aerospace Safety structure and functioning

06 p1041 A69-16843

Holographic storage of three dimensional measurement information using model formed by stacking plates

13 p2260 A69-27739

DOCUMENTATION

Military systems trouble documentation and evaluation, emphasizing computerized monitoring of reliability and maintainability

15 p2722 A69-31121

Subcontractors documentation coordination system for Mississippi Test Facility, identifying end items for maintenance and spares provisioning

18 p3118 A69-35063

Documentation aspects of computer programs use in civil engineering, describing maintenance, users and operators manuals

22 p3904 A69-40140

DOCUMENTS

NT CATALOGS [PUBLICATIONS]

NT ENGINEERING DRAWINGS

NT HANDBOOKS

NT MANUALS

NT TEXTBOOKS

Diffusion data in binary compound semiconductors, tabulating impurities, electrical behavior, temperature variations and diffusion coefficients

02 p0296 A69-11809

DODGE SATELLITE

Department of Defense Gravity Experiment /DODGE/ attitude stabilization simulation with time-lag magnetic damping

06 p1014 A69-17584

Doppler tracking of near synchronous DODGE satellite from single frequency data, noting error sources [AAS PAPER 68-128]

21 p3674 A69-39202

DOGHOUSES

U PROTUBERANCES

DOGS

Prophylactic and therapeutic vitamin and organic compounds complexes in radiation damage reduction and death prevention for dogs exposed to X rays

02 p0197 A69-11493

Control mechanisms of hemodynamic shifts from dogs subjected to acceleration under anesthesia

02 p0198 A69-11503

Dog adaptation to 60 or 90 mm Hg carbon dioxide in 260 mm Hg total pressure environment, noting arterial pH and bicarbonate level

03 p0375 A69-14071

Cardiovascular responses of baboons and dogs subjected to anoxic near vacuum environment by rapid decompression

06 p0875 A69-17846

Reactions of respiratory and cardiovascular system of dogs in biocompartment of ballistic missiles, discussing biopotential of myocardium, arterial pressure, etc

07 p1060 A69-18576

Physiological reactions of dogs during acceleration and weightlessness in suborbital flights of ballistic rockets

07 p1061 A69-18577

Phonocardiograms, EKGs, sphygmograms, heart and respiration rates, body temperature and motor activity recorded/transmitted by TV during canine confinement in Soviet biological capsules

07 p1061 A69-18578

Human and animal cardiovascular system reactions to weightlessness, noting vagus nerve role in adjusting organism

07 p1061 A69-18583

Telemetry aortic blood pressure and heart rate from dogs under various physical activities and emotional stress

07 p1071 A69-19133

Dogs cardiovascular activity mathematical analysis from physiological indices during long space flight

08 p1261 A69-19828

Test dogs feeding through enteropancreatic fistula homogenized mixture containing juice excretion stimulating agents during long space flight

08 p1265 A69-19829

Dogs blood coagulation system functional state after 22 day space flight onboard Cosmos 110

08 p1262 A69-19830

Bone marrow distribution in dogs as basis for study of compensatory reactions of hemopoietic organs in response to radiation damage

08 p1262 A69-19835

Motion sickness inhibitive effect on stomach motor activity, measuring biopotential of stomach wall, pyloric sphincter and ganglions

08 p1263 A69-19935

Local shielding effectiveness of dogs against proton irradiation at minimum lethal dose, noting bone marrow role

08 p1263 A69-19939

Monomethylhydrazine /MMH/ toxic effects on cornea and blood aqueous barrier studied in vivo on dogs

09 p1447 A69-22547

X ray irradiated dogs subjected to heat stresses to determine thermoregulatory ability

09 p1445 A69-22548

Transverse accelerations effect on dogs gastrointestinal tract secretory activity, noting central nervous system role

10 p1645 A69-23498

Dogs orthostatic tolerance and resistance to transverse acceleration after 14-day hypodynamia, studying tachycardia and arterial pressure

10 p1645 A69-23499

Blood oxygen metabolism, analyzing content and volume circulation in dogs under oxygen partial pressure decrease in inhaled air

12 p2019 A69-26346

Oxygen saturation in outflowing and inflowing renal blood in dogs under normal and hypoxic conditions, assessing cannula technique

14 p2406 A69-28916

Glucose disappearance rate from dogs blood at simulated 27,000 ft altitude compared with tolerance at ground level, discussing chlorpromazine administration effect

14 p2408 A69-29305

Gastric perfusion rate in restrained animals determined by Rb 86 clearance technique

17 p2908 A69-33170

EKG during electrical defibrillation of heart in immobilized dogs

19 p3257 A69-36168

Pubertal puppy and adult dog cardiovascular system during inhalation of various nitrogen-oxygen mixtures, comparing heart beat rates, minute blood volumes, etc

19 p3257 A69-36169

Supralethal doses of pulsed mixed gamma-neutron radiations from TRIGA reactor administered to unshielded, head shielded and trunk shielded beagles

19 p3259 A69-36459

Pulmonary arterial pressure for perfusion of excised dog lungs after inflation not due to shunt channels through atelectasis areas

21 p3651 A69-38386

Heart muscle ultrastructure during general hypoxia in dogs, noting development of compensatory-adaptational and dystrophic changes in myocardial intracellular components

21 p3651 A69-38412

Aldosterone and hydrocortisone introduced into bladders of adrenalectomized dogs to restore sodium metabolism contributing to normal water-salt homeostasis

21 p3656 A69-38965

Nerve tissue oxidation processes relation to nervous system radiation sensitivity in dogs with cerebellum X rayed after enzyme poisons administration

21 p3658 A69-39053

Canine cerebellar Purkinje cells electron microscopy after rapid decompression to near vacuum

21 p3660 A69-39177

Critical closing phenomenon in dog gracilis muscle, using pressure flow measurements and tissue staining techniques, detecting sudden vessel closure in microcirculation

22 p3873 A69-40202

Dogs cardiovascular responses to histamine liberator /compound 48/80/, describing shock and acidosis with elevated histamine levels

22 p3873 A69-40206

Carbon monoxide effect on dog lung volume, mechanical properties and diffusing capacity

22 p3874 A69-40224

Left ventricular function in intact anesthetized dogs analyzed during graded hypovolemia produced by lower body negative pressure

22 p3874 A69-40225

Whole body LF mechanical vibration effects on anesthetized dogs peripheral circulation and vascular smooth muscle

22 p3875 A69-40228

Heart beat rate, arterial pressure, blood volume and peripheral blood pressure increase observed in dogs running 7 min at 10 km/hr

22 p3885 A69-40966

Ventilatory response to hypoxia and hypercapnia in hypothermic anesthetized dogs, noting decreased sensitivity of central chemoreceptors to carbon dioxide

22 p3885 A69-40977

Effects of oxygen saturation variations of blood on rates of weight gain in isolated perfused canine lung, noting pulmonary edemogenesis

22 p3887 A69-41189

Monomethylhydrazine absorption through canine skin noting metabolic aftereffects and methemoglobinemia

22 p3887 A69-41191

Hyperventilation induced hemolysis in dogs measured as function of exposure time, body temperature and blood pH

22 p3887 A69-41192

Topography of potentials induced by acoustic clicks in auditory cortex of dogs, including ectosylvian gyrus distribution

22 p3888 A69-41269

Cardiovascular effects of hypoxia in conscious and anesthetized dogs in environmental chamber, discussing artery pressure, tachycardia, stroke volume and cardiac output

23 p4078 A69-41314

Chronic congestive heart failure in dogs compared to pulmonary system, discussing effect on cardiac lymphatics

23 p4078 A69-41364

Arterial pressure and heart rate responses to increased intrapulmonary pressure in anesthetized dogs via simulated Valsalva tests

23 p4078 A69-41365

Severe heat stress effects on respiratory frequency, rectal temperature, blood gases and pH of conscious dog

23 p4081 A69-41432

Carbon dioxide inhalation and intravenous isoproterenol effects on hemorrhagic consolidation occurring after left pulmonary artery ligation in dogs

23 p4082 A69-41441

Positive phase shift relation to elastic modulus enhancement of smooth muscles of rabbit, cat and dog bladder, pulmonary artery and large veins

23 p4083 A69-41459

Acceleration effect on greyhound cardiac output and regional blood flow from Sapirstein radioisotope uptake technique, studying blood, skin, skeletal muscle, etc

23 p4089 A69-41823

Noradrenalin release from hearts of open chest dogs given artificial respiration upon occlusion of left descending coronary artery

23 p4092 A69-42053

Sinusoidal pressure electric stimuli frequency effects in isolated carotid sinus on canine peripheral blood pressure, determining dynamic characteristics from observation data

23 p4092 A69-42062

Energy cost of muscular exercise in gastrocnemius muscle of dogs anesthetized with morphine, chloralose and urethane

23 p4093 A69-42065

Coronary circulation response to hyperoxia after vagotomy and combined alpha and beta adrenergic receptors blockade in anesthetized intact dog

23 p4096 A69-42088

Sinus outflow relationship to oxygen content in anterior cardiac vein blood and right ventricle systolic pressure

23 p4098 A69-42105

Alaska sled dogs cardiovascular performance and flow distribution during cross country runs

24 p4256 A69-42624

Vascular interface histological and chemical responses to acute mechanical stress in dog aorta

24 p4257 A69-42625

Alveolar and pleural pressures affecting pulmonary interstitial pressure in anesthetized dogs, applying Starling law of transcapillary exchange

24 p4257 A69-42627

Refractory period adaptation to sudden heart rate changes in dogs

24 p4257 A69-42628

Electrical stimulation effects of carotid sinus on sinus rate and atrioventricular conduction for vagi and sympathetic nerves interruption to heart in dogs

24 p4257 A69-42629

Cardiac myosin characteristics obtained from dogs with naturally occurring heart failure, showing reduced

adenosinetriphosphatase activity as compared with normal dogs

24 p4258 A69-42630

Contraction frequency increment effects on myocardial oxygen consumption in dogs determined for various heart rate levels, using isovolumic left ventricular preparation

24 p4258 A69-42634

Experimental myocardial infarction in dogs, examining lysosomal enzymes activity changes in soluble and particle-bound fraction

24 p4259 A69-42636

Positive pressure breathing effects on cerebral arterial and venous blood pressure, hypothalamus and adrenal glands catecholamine content and cerebrum histological changes in dogs

24 p4265 A69-43371

DOLOMITE [MINERAL]

Thermoluminescence intensity of dolomite specimens from Kaali meteorite craters, discussing meteorite impact thermomechanical effect and crystal lattice defects

01 p0159 A69-11371

DOMAIN WALL

Intervalley scattering model for Gunn domain dynamics, noting effects comparable to diffusion

06 p0893 A69-16937

DOMAINS

NT MAGNETIC DOMAINS

Gunn domains reduction in sheet type GaAs oscillators by spreading of field lines out of active region

02 p0215 A69-11933

Domain operating point application to Gunn domain buildup including trajectory graphs

02 p0297 A69-11948

Traveling high electric field domains in bulk semiconductors use in high speed integrated electronics, noting domain properties of GaAs and CdS

02 p0216 A69-12144

Acoustoelectric domains in CdS, making time evolution visible by means of modified optical strain birefringence and stroboscopic illumination

02 p0258 A69-12618

Optical modulation near intrinsic edge in n-type bulk GaAs due to Franz-Keldysh effect, noting carrier production by photon initiated excitation

02 p0300 A69-12650

Small transverse dimensions effect and domain formation criterion for surface oriented Gunn diodes prepared on thin epitaxial GaAs layers

04 p0639 A69-14335

Semiinsulating GaAs mobile electric domains, determining electric field strength from electrooptical effect measurements

04 p0643 A69-15261

Acoustoelectric domain propagation in N-type GaAs, noting flux influence on peak acoustic density

05 p0806 A69-15815

Electrothermal domains in semiconductors, examining domain velocity of motion under external potential

06 p0981 A69-17880

Delta functions use in extending domain of Laplacian operator in quantum mechanics

07 p1174 A69-19495

High field domains in Gunn effect diode in transit time mode of operation probed with stroboscopic electron beam in scanning electron microscope

08 p1283 A69-20162

Gunn effect domains propagation calculated for nonuniform diodes of annular geometry, obtaining frequency variation

09 p1464 A69-22159

Torsion theory for modules over integral domain, giving definition of injective sums

13 p2287 A69-27339

Electrothermal domains in semiconductors, examining domain velocity of motion under external potential

14 p2503 A69-28789

Impurities effect on domain structure of barium titanate single crystals grown from solution in KF melt determined by inner stresses

21 p3783 A69-39559

Electric properties and domain structure changes of polycrystalline Ba titanate and other ferroelectrics characterized by high dielectric nonlinearity

22 p3996 A69-41166

DOMES [STRUCTURAL FORMS]

NT RADOMES

Large telescope dome movements automatic control, considering central and eccentric telescope mounting

15 p2588 A69-30441

Nonlinear stability of shallow elliptical paraboloidal dome under uniformly distributed compression, solving by Bubnov-Galerkin method on computer
21 p3838 A69-39186

DONNELL EQUATIONS

Linear theory of cylindrical panel buckling and circumferential restraint along straight edges under lateral pressure, using Donnell equations
09 p1621 A69-22782

Donnell small displacement equations for arbitrary open noncircular cylindrical shells under arbitrary normal pressure loadings
13 p2365 A69-28248

DONOR MATERIALS

Poole-Frenkel model for internal field assisted thermal emission with compensation for relative densities of donor and acceptor sites
04 p0640 A69-14450

Si diffusion rate in single crystal and polycrystalline Mo, using various donor materials
05 p0780 A69-15990

Gold donor level impurity photovoltaic effect in silicon, noting solar cell efficiency reduction due to minority carrier recombination
19 p3381 A69-35679

Donor and acceptor impurity effect on absorption and reflection spectra of CdTe single crystals, analyzing In, Ga, S and Se
24 p4362 A69-43735

DOPES

Lattice location of dopant elements implanted into Ge determined by carbon ion backscattering, noting substitutional concentrations above thermal equilibrium solubilities
07 p1199 A69-18903

Quenched one dimensional bulk GaAs oscillators with linearly increasing and decreasing concave and convex doping gradients, showing profiles
10 p1663 A69-23667

DOPING [ADDITIVES]

U ADDITIVES

DOPPLER EFFECT

Negative Faraday effect and Doppler line width measurements for He-Ne IR gas laser tube by producing beat frequencies in ring laser system
01 p0088 A69-10028

Laser Doppler velocity profile measurement at localized points in flow stream without disturbing flow
01 p0090 A69-10298

Laser beam spectra for modulation by electrooptic Doppler shift, considering sawtooth and triangular functions for applied electric field
01 p0091 A69-10843

Optical path variations and angle of emergence calculation in dynamic ionosphere
01 p0068 A69-11111

Pulsar frequency Doppler shift due to general relativistic corrections to optical path of photons in field of sun
02 p0315 A69-11836

Radar target amplitude, angle and Doppler scintillation from analysis of echo signal propagation in space
02 p0211 A69-12447

Goldberg-Unno method for determining Doppler width, microturbulence velocity and convection errors, considering photosphere as hot ascending and cold descending columns
02 p0328 A69-12752

Doppler effect in centimeter wave range demonstrated by radio interferometer, noting amplitude difference between reference wave and wave reflected from moving reflector
03 p0393 A69-13333

Complex Doppler effect for oscillating source moving in dispersive medium, analyzing time behavior of radiation field
03 p0396 A69-13630

Table of equivalent widths of isolated lines with combined Doppler and collision broadened profiles
05 p0796 A69-15747

Radio aurora radar measurement, determining echo and Doppler velocity distribution and dependence on aspect angle, magnetic latitude, height, azimuth and time
05 p0754 A69-16265

Ionospheric models for studying nature of difference in relationships between HF radio waves Doppler shifts and changing ionosphere
05 p0755 A69-16269

Laser Doppler meter model: interpreting output frequency in terms of particle crossing set of fringes
06 p0932 A69-16927

Quasars, stressing local Doppler and gravitational hypotheses for observed red shifts
06 p0998 A69-16968

Velocities of neutral and ionic species in MPD flow determined from Doppler shift of selected spectral lines
[AIAA PAPER 69-109] 06 p0971 A69-18116

Doppler shift measurements of axial and rotational velocities in MPD arc, using reference lines from iron arc
[AIAA PAPER 69-110] 06 p0972 A69-18171

Doppler shift in zodiacal light spectrum, noting variation of dust concentration and possible orbits
06 p1012 A69-18227

Chromospheric velocity field temporal characteristics in quiet region of sun, determining power spectra of Doppler shifts of H alpha spectra
07 p1217 A69-19240

Velocity measurement by combination of Doppler principle and schlieren method involving reflection, refraction or diffraction of laser beam
07 p1135 A69-19259

Noncoherent scattering of atoms with Maxwellian distribution in moving atmosphere, discussing Doppler broadening expansion in Legendre polynomials
07 p1219 A69-19286

Secondary maxima observed in pulses with binary phase shift keying for cases of large Doppler shifts
07 p1086 A69-19488

Astronomical unit determined by measuring Doppler shift of spectral features of galactic hydrogen
07 p1222 A69-19590

Numerical determination of Doppler effect and reduced Doppler frequency difference for two coherent radio waves emitted from earth satellite
07 p1087 A69-19610

Motion measurement using Doppler shift of scattered laser light, noting high resolution
09 p1492 A69-21398

Three dimensional laser Doppler velocity instrument for mean velocity and turbulence measurements in subsonic jet shear layer
[SAE PAPER 690266] 09 p1494 A69-21555

Doppler effect in ionospheric acoustic perturbations caused by strong ground explosion, noting accord with nonlinear acoustic wave propagation theory
09 p1488 A69-21694

Wideband signal Doppler distortion influence on parameter estimate accuracy
09 p1454 A69-21725

Laser induced line narrowing in coupled Doppler broadened transitions, noting mode crossing and spontaneous emission
09 p1519 A69-22282

Conventional and dual beam laser Doppler methods for velocity measurement of solids, liquids and gases
11 p1893 A69-24333

Hydrogen balmer lines broadening by Stark and Doppler effects, finding prominences and chromosphere electron concentrations
11 p1955 A69-24389

Distance vs time and velocity vs time measurements for high speed model missiles by means of laser interferometry and optical Doppler shift method
11 p1886 A69-25042

Optical modulation through Doppler frequency shift obtained by rotating radial diffraction grating
[AOLR-69-1] 11 p1889 A69-25394

Natural oscillations excitation in magnetoactive plasma by modulated electron beam ascribed to Doppler or Cerenkov effects
11 p1932 A69-25535

Natural oscillations excitation instabilities by modulated ion beams in magnetoactive plasma ascribed to anomalous Doppler effect
11 p1932 A69-25536

Communication systems in interplanetary space covering telemetry, remote control, Doppler and distance measurements, coherent PCM/PSK/PM, demodulation, deep space network, etc
12 p2027 A69-25875

Plasma velocity measurement by Doppler shifts of spectral lines with photoelectric recording, using Fabry-Perot interferometer
12 p2079 A69-26021

Laser Doppler flowmeter for heterodyne detection of laser light scattered from moving fluid applied to fluid velocity and velocity distribution measurements
12 p2093 A69-26546

Laser Doppler particle sensor to measure velocities in rocket exhausts, using He-Ne laser light source and Fabry-Perot interferometer frequency filter
[AIAA PAPER 68-723] 12 p2094 A69-26783

Statistical distribution of instantaneous frequency and power of signal associated with Doppler spectrum for exponentially distributed and determinate frequencies
12 p2032 A69-26863

Quasars and radio-quiet objects numbers and properties, discussing red shifts interpretation by cosmological, gravitational and Doppler theories
12 p2161 A69-26937

Laser Doppler method for measuring local particle velocities in two phase flows of liquid-metal MHD generators
13 p2260 A69-27476

Horizontal gradients below satellite orbit effect on reduced and minimum difference in Doppler frequency shifts of coherent radio waves from satellite in inhomogeneous ionosphere
13 p2219 A69-27701

Ultimate resolvable line dependence of Balmer series on electron density, considering line broadened by Stark and Doppler effects
13 p2351 A69-27865

Remote optical heterodyne measurement of Doppler shift as method for determining vector wind velocity, noting influence of air pollution
14 p2448 A69-29523

Magnetic mirrors, Doppler and relativistic effects, wave attenuation and radiation pressure during gyroresonant particle acceleration in nonuniform magnetostatic and HF fields
14 p2499 A69-29845

Inlet shape and Reynolds number effects on entrance flow development, using laser flowmeter based on Doppler effect to obtain laminar velocity profiles
15 p2589 A69-30001

Correlated noise effect on accuracy of suboptimal servosystem velocity measurements from recording Doppler frequencies
15 p2567 A69-30341

Radial velocities measuring tracking rate meter performance for Doppler frequencies, allowing for multiplicative noise
15 p2576 A69-30350

Laser Doppler heterodyning for monitoring motion noting solid surfaces vibration, liquid and solid surfaces linear velocity and turbulence in liquids and gases
15 p2614 A69-31276

Doppler geodetical measurements, emphasizing relative orientation between station and orbit influence on coordinates determination accuracy, presenting electromagnetic wave propagation theory
15 p2601 A69-31375

Doppler measurements in semidynamical geodesy, processing data from Transit satellites collected at various Mediterranean ground stations
15 p2602 A69-31382

Doppler effect significance in radio astronomy including galaxies relative motion and information concerning isolated hydrogen clouds between galaxies
16 p2853 A69-31565

Axial velocities in ammonia MPD thruster exhaust by measuring Doppler shifts of spectral lines emitted by plasma constituents
16 p2835 A69-31890

Asymptotic formulas for X and Y functions for resonance radiation scattering in layer, analyzing Doppler absorption and line profiles
16 p2813 A69-32588

Decameter waves Doppler shift shown inversely proportional to wave frequency from electron density variation caused by acoustic wave propagation in ionosphere
16 p2755 A69-32610

First order Doppler shift in ionosphere and horizontal gradients influence, discussing total electron content determination method made from geodetic satellites using two coherent frequencies
16 p2755 A69-32614

Doppler shift measurements at two coherent frequencies from Diadem satellites to determine ionospheric electron content, discussing accuracy and parameters defining satellite passage
16 p2785 A69-32615

FM detecting resolution using free running multimode uniphase Ar laser with Doppler broadened bandwidth
17 p2981 A69-33091

Lamb theory of Doppler broadened gas laser extended to arbitrary intensities for single mode operation, calculating detuning curves and inversion densities
19 p3335 A69-36048

Laser Doppler velocimeter /LDV/ for fluid velocity measurements, noting advantages
20 p3552 A69-37004

Ionospheric electron content and concentration variations analysis based on data of radio waves propagating from satellite, considering Doppler shift and Faraday effect
20 p3486 A69-37027

Wideband signal Doppler distortion influence on parameter estimate accuracy
20 p3488 A69-37461

Doppler technique for ionospheric electron density measurement by VLF ground based radio transmitter, noting HF method
20 p3542 A69-37792

H alpha line for emission nebulae analyzed by Fabry-Perot etalon, noting Doppler profile
20 p3607 A69-38039

Doppler broadened atomic O emission line measurement providing indication of exospheric temperature storm-time variations
20 p3546 A69-38099

Doppler observations of ionospheric motions associated with magnetic micropulsations, noting hydromagnetic and neutral gas waves
20 p3535 A69-38194

DIA satellite Doppler observations, noting effect of observation grouping on ground stations mutual position
21 p3701 A69-38336

Optimum wideband signal for minimum Doppler distortion, describing pulse compression by linear-period modulation
21 p3671 A69-38406

Alford and Gold light modulation effect expanded to include one frequency spectrum with Doppler shift, discussing applications to optical radar for range and velocity measurements
21 p3672 A69-38409

Intensity integral inversion for Doppler core of strong solar absorption lines to obtain line source function for solar atmosphere
21 p3796 A69-38478

Solar Na D lines analysis by direct inversion of line source function, finding Doppler core dependence on frequency
21 p3796 A69-38479

Ultrasonic Doppler flowmeter for detection of circulating gas emboli of animal blood vessels during decompression
21 p3663 A69-38915

Doppler tracking of near synchronous DODGE satellite from single frequency data, noting error sources [AAS PAPER 68-128]
21 p3674 A69-39202

Astronomical unit determination, discussing dynamical and radar methods and Doppler shift of neutral hydrogen line spectra in radio astronomy method
22 p4022 A69-40464

Space simulation tests of satellite-borne quartz crystal oscillators for tracking based on Doppler effect
22 p3927 A69-40590

Electromagnetic radiation characteristics from vibrating electrons or electric dipole moving in compressible isotropic plasma and from stationary dipole in moving medium, emphasizing Doppler effects
23 p4114 A69-41359

Tradeoff between Doppler measurement capability and subcarrier demodulation in coherent digital communication system quantitatively presented for various SNR
23 p4122 A69-41771

Flow profile effect on signal of Doppler ultrasonic flowmeter, noting limited application to quantitative blood circulation measurements
23 p4166 A69-42085

Relativistic Doppler shift effect observed from radio signal periodic variation of GEOS-1 satellite
23 p4126 A69-42389

Ionospheric electron content measurements at low latitudes close spaced frequency and differential Doppler shift technique, using BE-B and BE-C satellite transmission
23 p4161 A69-42435

Stellar radial velocity measurement accuracy dependence on dispersion, spectrum and line width
24 p4386 A69-43347

Hydrogen balmer lines broadening by Stark and Doppler effects, finding prominences and chromosphere electron concentrations
24 p4390 A69-43779

Rotating mirrors used for light signal Doppler frequency shifting
24 p4351 A69-43806

DOPPLER NAVIGATION

Navigation system for American SST noting use of Doppler radar and inertial navigation
02 p0278 A69-12238

Transatlantic aircraft cross-track air navigation error reducible by augmenting Doppler system with satellite ranging system
03 p0464 A69-13237

Optimum inertial/Doppler satellite navigation system, discussing position fixes application in resetting
08 p1349 A69-21199

Omega/VLF transmission range rate measurements for satellite Doppler navigation to provide velocity and location data, noting propagation error
14 p2479 A69-29857

Doppler and inertial self contained systems for long range navigation, considering air traffic control separation standards
15 p2651 A69-31544

Direction defining radio beacons performance, discussing signal amplitude and phase comparison systems and Doppler techniques
17 p2918 A69-33028

Aircraft electromagnetic position finding system based on Doppler shift of CW carriers
17 p3002 A69-34078

Doppler navigation, explaining radar beam mechanization, Doppler spectrum, scanning noise, spectral compression and tracking
18 p3169 A69-34849

Lockheed C-5 Galaxy aircraft avionics systems with Doppler inertial navigation equipment to operate with precision without ground based aids
18 p3104 A69-35465

DOPPLER RADAR

Doppler signal envelope cross correlation coefficient in two channel system, determining mutual density distribution for envelopes
01 p0032 A69-10887

Spectrum distortion of intermediate frequency signal in coherent Doppler navigation radar
01 p0034 A69-11013

Digital modified discrete Fourier transform Doppler radar processor for tactical aircraft
03 p0389 A69-13196

Digital processing of Doppler radar signals using matched filter concept
03 p0393 A69-13291

Wind shear and reflectivity gradient effects on Doppler radar spectra
03 p0461 A69-13341

Level crossing rate meter correction for boxcar-ed and receiver noise readings in incoherent weather radars
04 p0557 A69-14915

Wind turbulence measurement by shock wave tracking using Doppler radar, stressing relative location of antenna and sound source
04 p0628 A69-15149

Doppler radar inertial navigation, discussing developments in sensors and digital computers
06 p0956 A69-17859

Optical processing of planetary radar data for range Doppler image generation
08 p1270 A69-19816

Range-Doppler processing in pulsed radar applied to imaging of rigid rotating body with motion compensating resolution cells
08 p1270 A69-19861

Wind changes calculated from Doppler data and inertial system, noting role of heading and air speed
08 p1346 A69-20317

Doppler signal envelope cross correlation coefficient in two channel system, determining mutual density distribution for envelopes
12 p2031 A69-26651

Computer simulation program for design and evaluation of digital Doppler processor, analyzing performance limitation due to quantization and white noise
12 p2035 A69-27096

Pseudorandom FM waveforms for simultaneous range and Doppler shift radar measurements
13 p2221 A69-27944

Doppler radar clearance hole packaging method for ruggedized dual in-line integrated circuits with conventional etching, tooling and double-sided printed wiring techniques
14 p2419 A69-29102

Doppler echo from random rough surface, discussing average power return, frequencies, amplitudes, antenna beamwidth and radar data correlation
14 p2413 A69-29488

Airborne Doppler radar, estimating velocity distribution and density of pulse signals reflected from air and ground targets
15 p2567 A69-30349

Digital method to produce radar reflectivity from analog audio frequency Doppler data extracted from terrain echo signal of CW scatterometer radar
15 p2572 A69-31111

Wind velocity and precipitation particle terminal fallspeeds component determination from continuity equation for data collected by Doppler radar
17 p2919 A69-33162

Doppler inertial system with remote attitude capability, detailing sensor operation by airborne computers
17 p3002 A69-34097

Short term frequency stability measured for Doppler radar and space tracking communication applications, reviewing FM theory for spectral purity relationship
18 p3100 A69-34277

Meteorological Doppler radar information display for real time identification of hazardous winds and turbulence in storms
18 p3139 A69-35427

Navigational accuracy dependence on spacecraft geometry, determining information content and critical error sources of earth based Doppler radio tracking data
19 p3402 A69-35935

Imaging radar study based on optical imaging and electromagnetic wave processes, discussing Doppler signal processing, synthetic aperture radars and microwave holography
20 p3489 A69-37632

Ambiguity function interaction with target scattering function in range-Doppler radar, discussing matched filtering application
20 p3490 A69-37641

Moving target indication, discussing target motion effects dependence on Doppler imaging radar scan rate and compression ratio
20 p3490 A69-37644

Range-Doppler data processing of radar echoes from spread targets, considering quadratic filter theory, emphasizing received signal correlation functions
20 p3490 A69-37648

Doppler radar observations of precipitation induced mesoscale wind oscillations near melting layer produced by pressure perturbations due to horizontal variations in cooling
20 p3572 A69-37909

Navigational accuracy of two way Doppler tracking of interplanetary spacecraft during heliocentric and planetary encounter trajectory phases [AIAA PAPER 69-899]
21 p3761 A69-39334

Gas laser-Doppler radar system for moving materials velocity and length measurements in industrial processes
22 p3955 A69-40237

DORNIER AIRCRAFT

NT DO-31 AIRCRAFT
Dornier R and D, discussing single and twin engined aircraft, utility aircraft, helicopter, VTOL transport, safety, etc
22 p3862 A69-39931

DORNIER DO-31 AIRCRAFT

U DO-31 AIRCRAFT

DOSAGE

U RADIATION DOSAGE

DOSIMETERS

NT THRESHOLD DETECTORS [DOSIMETERS]
High energy interactions greater than 10 Gev from dosimetric point of view
03 p0371 A69-13477

Negative pion beams for therapy, radiobiology and dosimetry
03 p0371 A69-13478

Radiation accidents involving sudden brief exposure to penetrating radiation
03 p0374 A69-13502

Nuclear pulsed radiation dosimeter based on strain gage measurement of induced thermal expansion, noting separation of neutron and gamma ray components
06 p0922 A69-16892

Laboratory simulation methods for cosmic nuclear radiation, discussing dosimetry methods
11 p1862 A69-24875

Radiation dosimetry and shielding onboard Cosmos 110 artificial satellite, noting earth belt proton radiation
13 p2356 A69-27702

Psychopharmacological drug effects on retinal neuron activity in cats measured by microelectrodes, noting spontaneous activity decrease
22 p3879 A69-40846

Psychopharmacological drug effect on visually evoked responses in cats from recordings from visual cortex, noting latencies increase with dose
22 p3879 A69-40847

DOSIMETRY

U DOSIMETERS

DOUBLE BASE PROPELLANTS

Heat production rate equivalence to heat removal rate during ignition of ballistite powder by incandescent wires

02 p0354 A69-12668

DOUBLE BASE ROCKET PROPELLANTS

Strong electrostatic fields effects on burning rates of double base and composite propellants [WSCI PAPER 68-24]

07 p1241 A69-18366

Solid propellant rockets, discussing composite and double base propellants and use of polymers

11 p1941 A69-25588

Composite modified cast-double-base rocket propellants with large proportions of metallic fuel and oxidizer, discussing application rocket propulsion

17 p3017 A69-33349

DOUBLE CUSPS

Osculatory interpolation explicit method demonstration with error terms determination

24 p4341 A69-43230

DOUBLE SIDEBAND TRANSMISSION

Waveform distortion resulting from adjacent channel crosstalk and from amplitude and phase nonlinearity in channel filters in DSB/SC telemetry link

07 p1083 A69-19130

Frequency division multiplex telemetry technique with double sideband-quadrature carrier multiplexing system, discussing data signals, channels and distortion

07 p1084 A69-19131

Double sideband suppressed carrier FM telemetry system as airborne data recorder, discussing noise, environmental conditions, laboratory and flight tests

07 p1084 A69-19132

DOUGLAS AIRCRAFT

U A-1 AIRCRAFT

U DC 3 AIRCRAFT

U DC 8 AIRCRAFT

U DC 10 AIRCRAFT

DOUGLAS DC-3 AIRCRAFT

U DC 3 AIRCRAFT

DOUGLAS DC-8 AIRCRAFT

U DC 8 AIRCRAFT

DOUGLAS MILITARY AIRCRAFT

U MILITARY AIRCRAFT

DOVAP

U DOPPLER EFFECT

DOWN-CONVERTERS

Mathematical model for voltage step-down DC to DC converter with hysteretic bistable trigger circuit regulating output voltage

06 p0904 A69-17941

Signal conversion by multiple modulation in optical communication system, discussing electrooptic modulators and modulation spectrum

07 p1075 A69-18472

UHF down-converter design used in various Navy missiles UHF telemetry/miss-distance information system

23 p4137 A69-41778

DOWNWASH

Rotor downwash in ground effect in presence of step, using two dimensional analysis for flow field calculation

[AIAA PAPER 69-225]

08 p1253 A69-21032

Wing elastic strains effect on vertical velocity in downwash, noting wing tail combination

18 p3086 A69-34999

DRAFTING (DRAWING)

Printed circuits development based on use of grid without aid of draftsmen

02 p0216 A69-12051

DRAG

NT AERODYNAMIC DRAG

NT FRICTION DRAG

NT INTERFERENCE DRAG

NT MINIMUM DRAG

NT PRESSURE DRAG

NT SATELLITE DRAG

NT SUPERSONIC DRAG

NT VISCOUS DRAG

NT WAVE DRAG

Variational calculus applied to time optimal trajectories between two points in range altitude space, discussing aircraft thrust and drag laws

01 p0009 A69-10414

Wind tunnel measurement of rear parts drag of small scale aircraft models [ONERA-TP-633]

02 p0226 A69-11624

Approximate solution for turbulent jet expansion in opposing stream, discussing hydraulic drag coefficient formula derivation

07 p1118 A69-18396

Hydraulic drag coefficient in MHD fluid flows in traveling magnetic field from motion equations for turbulent flows, considering velocity profiles

07 p1192 A69-19017

Current sheet velocity in coaxial plasma accelerator, noting drag due to insulator ablation and degassing [AIAA PAPER 69-265]

09 p1566 A69-21258

Drag and friction coefficients for laminar pulsating incompressible fluid flow in circular tubes obtained from Navier-Stokes equation

15 p2592 A69-30988

Blockage effects of flat plates and solid bluff bodies in closed wind tunnels compared concerning drag coefficient values

17 p2890 A69-33245

Drag measurements for sharp and blunt-nosed bodies shot into wind tunnel supersonic gas counterflows, discussing shock waves for different configurations

19 p3239 A69-36401

Energy losses due to drag in unstable laminar fluid flow in tube

20 p3513 A69-36973

Drag effect on plasma motion in high current pulsed plasma accelerators of Marshall type, calculating current variations, voltage, particle velocity, efficiency and impulse

21 p3778 A69-39548

Hypersonic reentry spheres drag coefficients derived from radar measurements

23 p4059 A69-41898

Stagnation point Mach number gradient, sonic point location and drag coefficient of hemisphere at zero angle of incidence

23 p4060 A69-41910

DRAG BALANCE

U AERODYNAMIC BALANCE

U LIFT DRAG RATIO

DRAG CHUTES

High altitude balloon stationkeeping system combining battery powered propeller and drag chute

22 p3866 A69-40941

DRAG COEFFICIENT

U AERODYNAMIC COEFFICIENTS

DRAG DEVICES

NT AERODYNAMIC BRAKES

NT LEADING EDGE SLATS

NT SPOILERS

NT TRAILING-EDGE FLAPS

NT WING FLAPS

Stopping barriers for jet aircraft landing design and operation

11 p1862 A69-24354

Monograph on optimal design of free-running drag turbines for boundary layer suction in aircraft, emphasizing gliders performance

12 p2011 A69-26117

DRAG MEASUREMENT

Drag and spray effects due to slush and water on runways during aircraft takeoffs

01 p0011 A69-11048

Accelerometric measurement of atmospheric drag with satellite 1968-59B, obtaining upper atmosphere density profile at 130-160 km

02 p0245 A69-12728

Airplane drag prediction by wind tunnel tests

05 p0695 A69-15543

Drag force measurement in low density flows using modulation techniques

06 p0861 A69-17638

Drag coefficients for spheres and sharp cones in rarefied hypersonic air flow obtained in shock tunnel using free flight technique

[AIAA PAPER 69-140]

06 p0865 A69-18184

Hypersonic drag and shock wave characteristics of blunt bodies including cones, spherical nose and concave nose bodies

09 p1433 A69-22568

Pressure distribution measurement over sphere with cylindrical afterbody in magnetofluid dynamic flow, showing drag decrease at large magnetic field

11 p1873 A69-25136

Aircraft test setup design and techniques to simultaneously measure engine thrust and engine thrust minus drag, noting nozzle configurations variations effect

[AIAA PAPER 68-395]

12 p2059 A69-26769

Small body drag in wake of large satellite using two dimensional model noting methods for calculating distribution function moments in wake regions

12 p2012 A69-26798

Thrust balance for scale model of powered nacelle fan jet engine from drag analysis in wind tunnel, deriving fan nozzle velocity coefficient

13 p2199 A69-27446

Tangential drag measurements at electrodes of arc in plasma accelerator, ion current partitioning at cathode and electrode damage

[AIAA PAPER 67-657]

13 p2312 A69-28219

Free flight sharp cone drag measurements in rarefied hypersonic flow

13 p2199 A69-28244

Initial flow turbulence effects on drag coefficient for prismatic bodies in low velocity gas flow determined by wind tunnels

14 p2391 A69-29625

Wind tunnel investigation of turbulent gas flow heat transfer and hydrodynamic drag in variable pressure gradient field of divergent-convergent channel

15 p2548 A69-3117

Drag measuring requirements and comparison of accelerometer or drag-free satellite control systems usage for atmospheric density determination

16 p2788 A69-31722

Hypersonic slender cone zero angle of attack drag in rarefied continuum and noncontinuum flow in shock tunnel, indicating body dimension influence in transition regime [AIAA PAPER 69-711]

17 p2891 A69-33445

Lift and drag determination for moving rectangular coils over infinite plane sheet for magnetic suspension and guidance for rocket sleds

17 p2946 A69-33789

Cylindrical models in hypersonic rarefied flow, determining drag data by free flight technique

24 p4249 A69-43677

DRAG REDUCTION

Polyvinyl chloride coating for reducing aerodynamic skin friction drag, noting water saturation effect on polyurethane foam

[AIAA PAPER 69-165]

06 p0912 A69-18043

Turbulent skin friction on compliant skins stretched over damping fluid in shallow bath in flat plate

[AIAA PAPER 69-164]

06 p0914 A69-18163

Minimum drag wing flap profile design, discussing application for trailing edge flaps

08 p1251 A69-20441

Optimum aerodynamic shapes theory, considering linearized and nonlinearized supersonic flow, Newton-Busemann hypersonic flow, free molecular flow, mathematical models and variational problems

08 p1253 A69-21127

Three dimensional optimum hypersonic wings construction for wave drag minimization for given lift

[AIAA PAPER 68-158]

09 p1430 A69-21944

Axial and radial turbulence intensities for flow through smooth round tubes, measuring velocity profiles and drag coefficients

15 p2590 A69-30003

Viscous drag reduction - Conference, Dallas, September 1968

17 p2950 A69-33247

Turbulence measurements and roughness effects on viscous drag reduction with polymer solution in pipe flow, discussing friction factor, wall velocity profile, etc

17 p2951 A69-33252

Concentration, flow rate and tube diameter effects on viscous drag reduction in nonpolar soap solutions, using pressure drop measurements to observe turbulent flow behavior

17 p2951 A69-33253

Skin friction drag reducing high polymer solution injected into turbulent boundary layer to test effectiveness on marine vehicles

17 p2951 A69-33254

Normal stress effects in viscoelastic fluid theories applied to one dimensional Burgers model of weak turbulence predicting drag reduction

17 p2951 A69-33256

Constitutive equation variation effect on near wall flow pattern of dilute polymer solutions

17 p2951 A69-33257

Magnetic field effects on rotating cone compressible boundary layer at zero angle of attack, describing changes in drag coefficient, torque and velocity profiles [AIAA PAPER 69-721]

17 p2892 A69-33484

Drag minimization as extremization of products integrals powers, noting application to optimum wings and fuselages

19 p3242 A69-36800

Transonic flow around profiles with heat input, showing drag reduction in supersonic part of flow field

23 p4061 A69-42414

Newton formula and Ritz method to determine wing shape with blunt leading edge, considering minimum drag achievement at hypersonic velocities

24 p4247 A69-43497

Turbulent skin friction on compliant skins stretched over damping fluid in shallow bath in flat plate

[AIAA PAPER 69-164]

24 p4306 A69-43685

DRAGULATORS

U BRAKES [FOR ARRESTING MOTION]
U DRAG DEVICES

DRAINAGE

Liquid draining motion from transversely moving cylindrical tank in time varying gravity field with outlet pipe at bottom, discussing flow rate and free surface [AIAA PAPER 69-679] 17 p2953 A69-33440
Nonlinear free surface effects in low gravity tank draining, finding domains of validity for linearized and nonlinear analyses [AIAA PAPER 69-680] 17 p2953 A69-33450

DRAINING

U DRAINAGE

DRAWINGS

U ENGINEERING DRAWINGS

DRIFT

Electric drift instability in semiconductors with hot electrons, discussing diffusion, electron heat conduction, energy transfer, space charge density, etc 13 p2318 A69-27891
Drift correction schemes for periodic cross correlation comparison unification and extension 15 p2564 A69-30169

DRIFT [INSTRUMENTATION]

Rubidium self oscillating magnetometer long term stability, noting changes affecting accuracy and sensitivity 02 p0250 A69-12394
Traveling wave tube segmentation, analyzing effects of drift, grouping and selecting sections on efficiency and amplification 03 p0407 A69-13985
Ion and electron contaminating currents removal in vacuum evaporating devices, using biased field plates 04 p0577 A69-14875
Directional gyroscope accuracy increased by self adaptive systems, based on precession theory and drift amplitude dependence 11 p1881 A69-24559
Gyroscopes orientation influence on dynamic drift of triaxial power gyrostabilizer on rocking platform, noting optimum orientations 11 p1881 A69-24560
Dynamics of triaxial gyrostabilizer with additional rotor mounted on base, showing systematic drift 13 p2259 A69-27428
Automatic control circuit zero drift compensation during external disturbance, using algorithm for computer minimizing of losses caused by control and response inaccuracy 14 p2425 A69-29140
Electronic components reliability by failure rates and drift behavior, assuming probabilities product rule and exponential law of life distribution 15 p2626 A69-30835
Drift of two connected gyroscopes, discussing equations of motion assuming unperturbed rotation and weightlessness 18 p3135 A69-34561
Strapdown electrostatic aerospace navigator /SEAN/ using electrostatically suspended gyros /ESG/ for inertial reference, including drift and computer tests 19 p3369 A69-35802

DRIFT RATE

Temperature dependence of hot electron drift velocity in silicon at high electric fields, using space charge perturbation theory 01 p0135 A69-10120
North-south ionospheric drift velocities near magnetic equator, noting marked seasonal characteristics and diurnal variations 01 p0062 A69-10138
Electrostatic polarization field formation by acoustic wave propagation through ionosphere, calculating effect on ionization drift velocity 01 p0068 A69-11110
Electron drift velocity, diffusion coefficient and trapping time in GaAs, measuring variation with electric field 01 p0140 A69-11255
Mathematical modeling of gyro drift rate in inertial navigation based on stationary and nonstationary time series analysis 03 p0463 A69-13213
Horizontal drifts at E region level measured in India by spaced phase path technique 03 p0421 A69-13330
Cyclotron drift instabilities of low pressure plasma containing charged impurities 03 p0478 A69-13834

Charged particle dynamics in spiral interplanetary magnetic field model, discussing electric drift velocity, point of origin and distribution 03 p0503 A69-14015
Nighttime variations of F region electron density profiles at Puerto Rico, discussing seasonal and solar cycle variations in temperature and vertical drift velocity 03 p0503 A69-14017
Charged particle motion in time dependent external magnetic field 03 p0504 A69-14235
Drifting temperature fluctuations in semiconductors in presence of strong electric field 04 p0643 A69-15256
Drift and diffusion of electron pulse advancing through gas, providing physical basis for Townsend ionization coefficient 04 p0633 A69-15443
Oxygen ions motion in oxygen, measuring drift velocities in glow discharge 05 p0795 A69-15662
Threshold velocities of acoustoelectric current oscillations in elemental piezo- and nonpiezoelectric semiconductors, taking into account amplification and losses of phonons 05 p0807 A69-15956
Plasma confined in transverse magnetic field analyzed for drift rates, noting role of injection direction 06 p0963 A69-16907
Magnetic field generation in nonuniformly rotating plasma by current density from electron drift relative to positive ion gases due to viscous forces 06 p1009 A69-17966
Drift measurements of rate constants for charge transfer in ion-molecule processes 08 p1355 A69-20210
Trapped particles drift velocity in time dependent meridional magnetic and perpendicular electric field 08 p1368 A69-20809
Drift rate of gyroscopic devices in space based on kinematic theorem, stressing free gyroscope subjected to harmonically varying moment 09 p1498 A69-22111
Azimuthal drift of rotor axis of directional gyroscope mounted on sloping base, showing vertical component responsibility via truncated equations of motion 09 p1502 A69-22702
VHF radar observations of electron density irregularity in nighttime equatorial electrojet, comparing day and night time electron drift rates and directions 10 p1769 A69-23837
Ionospheric discontinuities drift velocities from diversity reception data indicating no dependence on solar activity 10 p1686 A69-23911
Cs and K ions drift velocity calculations in vapors of own atoms under various electric field strengths effect 11 p1922 A69-24226
Drift elimination in linear system identification using binary m-sequences by crosscorrelating over two periods of output 11 p1834 A69-24547
Drift velocity of earth magnetic field based on spherical harmonic analysis of geomagnetic secular variation 12 p2077 A69-27111
Triaxial gyrostabilizer systematic drifts during rocking at large platform displacement angles, analyzing drift direction and rate dependence 13 p2259 A69-27430
Drift velocity and longitudinal and transverse diffusion coefficient for low energy N ions in N gas in mass spectrometer at room temperature 13 p2302 A69-27458
Unstable weakly ionized HF magnetoplasma fluctuations with no axial drift, noting phase velocity parametric dependence 13 p2312 A69-28197
Large scale ionospheric inhomogeneities anisotropy, dimensions and drift velocities from simultaneously measured irregular refraction 14 p2436 A69-29053
Radio astronomical observations of shape and drift velocity of focusing ionospheric discontinuities 14 p2436 A69-29054
Three dimensional model of atmospheric drift currents in equatorial region of world ocean system based on nonlinear differential equations 14 p2472 A69-29405
Ionospheric inhomogeneity model for motion of infinite elliptical cylinder of cold plasma in neutral particle flow and ambient electrostatic and magnetostatic fields 14 p2500 A69-29864

F 2 region small scale inhomogeneities drift observations showing seasonal and diurnal velocity and direction changes 14 p2444 A69-29868
Radio equipment for studying ionospheric inhomogeneities using space diversity reception, presenting vertical component of drift velocities of small scale inhomogeneities 14 p2453 A69-29876
Aircraft constant altitude-pressure flight navigation attained using Bellamy formula and loxodromic route for drift compensation 15 p2651 A69-30294
Particle drift velocity distribution of fully ionized plasma in magnetic field calculated by integration of Boltzmann equation 15 p2659 A69-30707
Collisionless drift plasma wave instability growth rate calculation noting destabilization from resonant electrons 16 p2820 A69-31691
Geomagnetic field westward drift related to earth core rotation from calculating drift at earth surface and at core 16 p2774 A69-31983
Continuity conditions for drifting magnetoplasmas without ionic effects, discussing eigenvalue equation of refractive index and electromagnetic modes propagation 17 p2926 A69-33851
Meteor trail drift radar observations in Kharkov, giving wind velocity diurnal and seasonal variations 17 p3041 A69-33897
Radar unit for network component /wind patrol/ in statistical observations of wind drift conditions in meteor trails 17 p2939 A69-33901
Vertical distribution of ionospheric drift velocity in auroral zone, evaluating role and intensity of electric field formed in dynamo region 17 p2964 A69-33964
Electromagnetic wave propagation in unbounded compressible plasma under drift velocity and magnetic field, obtaining dispersion equation for current density 18 p3179 A69-34261
Mean drift rates of single and two rotor gyroscopic linear acceleration integrators mounted on irregularly rocking base 18 p3135 A69-34586
Mesospheric wind measurement by meteorological rockets based on radar determination of drift trajectories of chaff clouds 20 p3529 A69-37797
Drift velocity and lateral diffusion of positive hydronium, hydrogen and K ions in hydrogen with zero field mobilities 20 p3580 A69-38026
Electron density in positive column of Cs vapor discharge related to current and gas pressure, discussing field strength effects on drift velocities 23 p4196 A69-42197
Electron intensities and substorm drift effects in outer radiation belt using two satellite technique 24 p4309 A69-43172
Drift characteristics of hydrogen plasma partially captured by transverse magnetic field, finding drift rate dependence on magnetic field level 24 p4357 A69-43470

DRILLING

Drilling and welding with sealed-off continuous carbon dioxide gas laser with outgoing beam collimated by Ge lens 01 p0086 A69-10821
Pulsed ruby laser of small output for hole drilling, studying correlation of vaporization, hole diameter and depth with laser output 09 p1504 A69-22247

DRINKING

Electrode stimulated hypothalamic drinking in rats compared with drinking induced by water deprivation, noting difference in consumption 17 p2910 A69-33750

DRIVES

MOSFET drivers for low current memory fabricated in 64 unit monolithic strips, discussing driver performance data 01 p0039 A69-10172

DROUGE PARACHUTES

U DRAG CHUTES

DROGUES

U TOWED BODIES

DRONE AIRCRAFT

NT FIREBEE 2 TARGET DRONE AIRCRAFT
NT TARGET DRONE AIRCRAFT

Operational system effectiveness information for reconnaissance drone system including test flights, discussing application to reliability and maintainability in project management

18 p3232 A69-34505

DRONE HELICOPTERS

U HELICOPTERS

DRONE VEHICLES

U FIREBEE 2 TARGET DRONE AIRCRAFT

U TARGET DRONE AIRCRAFT

DROP SIZE

Atmospheric droplets diameter, number density and scattering cross sections determined from laser radar return equation and Mie theory

06 p0888 A69-17483

Electromagnetic waves attenuation and scattering by rainfalls calculated using droplet distribution function

08 p1275 A69-20430

Simultaneous measurements of cumulus cloud thermal structure and concentration of water particles larger than 18 micron diameters

09 p1536 A69-21866

Mean drop size generated in vapor pressure regime of liquid water jet, noting effect of water temperature and orifice diameter

09 p1483 A69-21995

Dropletwise condensation, analyzing nucleation sites, growth, vapor capture, heat transfer rates and surface texture

13 p2376 A69-28143

Quantitative analysis of interaction between spray and ambient atmosphere, discussing atomization of flat sheet and drop behavior relationship to operating conditions

15 p2717 A69-30465

Sulfur dioxide, nitrogen dioxide and Aitken nuclei washout by artificial rain of known intensity and droplet size distribution

24 p4345 A69-43146

Pitot probe measurements of Hg drop growth rates and diameters, allowing for thermal and diffusion effects

24 p4316 A69-43583

DROP TESTS

Drop-weight tear tests dependence on specimen thickness and metallurgical properties

09 p1503 A69-21389

Impact testing machine with dropping load, noting provision for sample fastening to reduce reflected tensile wave effect

15 p2583 A69-30286

Hydrostatic stability and damping characteristics of perforated plates and screens for passive propellant control schemes from drop tower tests

[AIAA PAPER 69-531] 16 p2833 A69-32691

Drop test method to obtain subsonic terminal velocity and base pressure data for planetary entry probe configurations

19 p3238 A69-35959

Rain erosion process on aircraft surface, using single impact test apparatus with photographic recording and photoelastic study

23 p4227 A69-41872

DROPS (LIQUIDS)

NT RAINDROPS

Fluctuating radar echoes from cloud targets with vibrating drops, noting amplitude modulation effect of changing cross section on backscattered signals

02 p0208 A69-12021

Flame zone development of monopropellant droplets during heat-up period

02 p0352 A69-12310

Supercooled water drop frozen and observed to undergo explosive shattering and ejection of ice splinters

02 p0275 A69-12693

Propagation of detonation wave in tube containing single stream of diethylcyclohexane droplets dispersed in gaseous oxygen

03 p0415 A69-13139

Temperature measurement of moving droplets, noting influence of thermocouple electrode stability

04 p0688 A69-15423

Aspiration psychrometric probe for measurements of relative humidity of gas-vapor phase of gas flow containing liquid droplets

06 p0927 A69-17689

Water droplet simulation by glass spheres used in study of light scattering at cloud particles

06 p0953 A69-17992

Transient development of reacting boundary layer near stagnation point of vaporizing drop in gas stream

[AIAA PAPER 69-174] 06 p0912 A69-18056

Quasi-steady combustion model of fuel droplet with convection, including pressure effect

[AIAA PAPER 69-147] 06 p1037 A69-18114

Rotating incompressible liquid drop held together by surface tension noting spheroidal and toroidal shapes, energies and case of surrounding denser medium

07 p1120 A69-19267

Stability of rotating liquid mass held together by surface tension

07 p1121 A69-19268

Kerosene droplets combustion stability studied by motion pictures, discussing pressure, temperature and O concentrations effects in turbulent carbon dioxide flow

08 p1421 A69-20345

Vaporization of mist of small droplets by intense light beam for droplet extinction rate proportional to absorbed radiant energy

09 p1539 A69-21346

High velocity gas stream induced shattering of liquid drops, disintegration rate and breakup time

[AIAA PAPER 68-83] 09 p1482 A69-21947

Spark ignition of liquid fuel droplets atomized in air analyzed by spark discharge visualization for two phase mixture

09 p1623 A69-22220

Heat transfer rates for water, acetone and alcohol droplets splattering from heated plate, noting effect of impact angle and velocity

10 p1809 A69-23196

Aerodynamic forces causing deformation and breakup of liquid droplet with ellipsoid of revolution form in constant velocity gas flow

11 p1875 A69-25466

Spherical monopropellant droplet radially symmetric burning during adiabatic vaporization and direct decomposition, examining near-equilibrium limit by asymptotic analysis

12 p2190 A69-25948

Freezing of water droplets in thermal equilibrium with gas mixtures, considering droplet shattering and gas volume

12 p2126 A69-26018

Shock tunnel hypersonic flow effect on critical Weber number for zinconium drop breakup in partially and fully molten states

12 p2063 A69-26802

Dropletwise condensation, analyzing nucleation sites, growth, vapor capture, heat transfer rates and surface texture

13 p2376 A69-28143

Extinction kinetics of monopropellant droplet burning in inert gas reservoir with atmospheric temperature lower than adiabatic combustion temperature

13 p2378 A69-28250

Equations for steady state combustion of fuel drops in oxidizing atmosphere integrated numerically, obtaining ignition and extinction conditions

13 p2379 A69-28456

Spherical symmetric unsteady conservation equations describing transient burning of volatile fuel droplets, obtaining time dependent fuel and heat distribution in flow field

14 p2537 A69-29016

Sessile drop contact angles of alkali liquid metals on Re, W, Mo, Ta and Nb substrates related to substrate surface bare work function

14 p2506 A69-29270

Evaporation of liquid droplets from heating wall observed cinematographically, noting heat transfer by violent film boiling and conduction through thin vapor layer

15 p2718 A69-31117

Liquid fuel droplets combustion under free and forced convection noting combustion rate

15 p2719 A69-31174

Fuel drop combustion under unsteady conditions at high pressure in unlimited and limited air volume

15 p2719 A69-31476

Solid materials erosion rate as function of cumulative damage generated by liquid droplets impingement

16 p2794 A69-31904

Laser ignited Zr droplet free fall combustion in oxygen, analyzing metal conservation and luminosity correlation assuming reflux action from fog layer

[WSCI PAPER 69-1] 16 p2830 A69-32342

Laser ignited combustion of 365 micron Zr droplets falling in ultrapur oxygen using spectroscopic and photographic techniques, discussing vapor phase transport phenomena

[WSCI PAPER 69-4] 16 p2830 A69-32345

Pure monopropellant steady droplet burning rate theory for determining heat-up and convection trans-

port rates in droplet combustion products of flat flame burner

[AIAA PAPER 69-563] 16 p2834 A69-32722

Bag type deformation of incompressible viscous convective and nonevaporating droplets immersed in Stokes or potential flow pressure distributions, including Weber number

[AIAA PAPER 69-669] 17 p2954 A69-33456

Fuel droplet evaporation and combustion in still air as unsteady diffusion controlling phenomenon, basing calculations on flame front model

20 p3632 A69-37520

Liquid drop in electric field numerically analyzed for disintegration dynamics and instability through cross section computation at time intervals

23 p4151 A69-41694

Pitot probe measurements of Hg drop growth rates and diameters, allowing for thermal and diffusion effects

24 p4316 A69-43583

Supercritical burning of liquid fuel droplets in stagnant environment, using flame sheet model to obtain heat and mass fields

24 p4415 A69-43600

DROPSONDES

Dropsonde for vertical wind profile or wind shear measurement without tracking noting low cost

10 p1692 A69-23254

DROSOPHILA

Recessive lethal mutations frequency in gametes of male and female Drosophila melanogasters onboard Vostok spacecraft

07 p1063 A69-18598

Mortality kinetics of Drosophila melanogaster, comparing effects of gamma radiation-induced life shortening and natural aging

15 p2555 A69-30444

Oxygen effect on X ray induced somatic crossing over frequency in Drosophila melanogaster, noting bristle spots number modification on abdominal tergites

23 p4099 A69-42118

DROWSINESS

U SLEEP

DRUG THERAPY

U CHEMOTHERAPY

DRUGS

NT ADRENERGICS

NT ANESTHETICS

NT ANTIDIURETICS

NT ANTIDOTES

NT ANTIINFECTIVES AND ANTIBACTERIALS

NT ANTIRADIATION DRUGS

NT CENTRAL NERVOUS SYSTEM DEPRESSANTS

NT CHLOROFORM

NT CORTISONE

NT CYSTEINE

NT EPINEPHRINE

NT HISTAMINES

NT MOTION SICKNESS DRUGS

NT NARCOTICS

NT NORADRENALINE

NT NOREPINEPHRINE

NT STIMULANT

Phosphodiesterase activity of anterior pituitary, median eminence, heart and cerebral cortex of rat, studying effects of caffeine, theophylline and hydrocortisone

02 p0199 A69-11885

Therapeutic potential of dimethyl sulfoxide in aerospace medicine

06 p0883 A69-17851

General aviation accidents and hazards presented by drugs, ethyl alcohol, pesticides and carbon monoxide

07 p1068 A69-19435

Drug action on decompression sickness in rats compared with action on nitrogen narcosis and oxygen toxicity

17 p2913 A69-33172

Alcohol and drug intake effects on drivers control of motor vehicles, describing postrotatory nystagmus test for toxicity measurement

21 p3652 A69-38791

Pilots and automobile drivers functional impairment due to alcohol and drugs

21 p3663 A69-38792

Decompression sickness prevention in guinea pigs by heparin and papaverine combination nebulized in carbogen, discussing nitrogen elimination enhancement

21 p3655 A69-38917

Psychopharmacological drug effects on retinal neuron activity in cats measured by microelectrodes, noting spontaneous activity decrease

22 p3879 A69-40846

Psychopharmacological drug effect on visually evoked responses in cats from recordings from visual cortex, noting latencies increase with dose
22 p3879 A69-40847

Radioprotective effects of 5-azacytidine on bone marrow and blood leukocytes of X ray irradiated AKR mice
23 p4080 A69-41429

Noise level effects on pharmacological effectiveness of centrally acting drugs in rats
24 p4262 A69-42947

Hypnotic compounds properties influencing REM /rapid eye movements/ stage, discussing insomnia problems with jet flight crew and passengers
24 p4277 A69-43389

DRUMS [CONTAINERS]

Axisymmetric vibrations of thin drums consisting of circular cylindrical shell and two circular end plates
20 p3629 A69-38114

DRY CELLS

Sealed nickel-cadmium cell design optimization, evaluating effects of various electrochemical treatments on energy density of nickel oxide positive electrode
10 p1639 A69-23992

Signal electrode charge control of sealed Ni-Cd batteries, discussing signal voltage for overcharge control
10 p1640 A69-23993

Maintenance free high rate sealed Ni-Cd battery power system compatible with existing aircraft electrical systems
10 p1640 A69-23994

DRY FRICTION

Dry friction stabilizing effect on motion of astatic gyroscope with quasi-elastic compensation
04 p0597 A69-14605

Dry sliding friction and wear in ultrahigh vacuum, emphasizing slip rings and brushes for space applications
[IME PAPER 7] 07 p1138 A69-18561

Yielding of matrix material and cell size of substructure relationship to dry abrasion resistance of SAP type aluminum alloy at room temperature
08 p1319 A69-19995

Single axis gyro-stabilizer stability analysis allowing for dry friction in precession axis, noting asymptotic tendency of motions toward steady rotation
09 p1502 A69-22701

Dry friction whip role in radial rubs dynamic stability in labyrinth seals and blade tips of turbomachinery
[ASME PAPER 69-VIBR-56] 10 p1804 A69-24146

Longitudinal and transverse frequencies of cylindrical metallic rod with spherical tip for sliding motion with dry friction
12 p2102 A69-26290

Dry friction effects on stability of single axis gyro-stabilizer
14 p2445 A69-28922

Dry lubricant films of soft metals, self lubricating plastics and crystalline powders, noting design and tests
15 p2642 A69-30328

Unlubricated wear characteristics of polyimide resin sliding against carbon steel in air, noting effects of surface temperature, bearing pressure and velocity
[ASLE PREPRINT 69AM 5C-2] 15 p2619 A69-30473

Lunar conditions differing from simulations in laboratories, examining surface, physicochemical properties and friction
18 p3113 A69-34241

Casing bearings dry friction force moment effect on double rotor gyrocompass sensor motion, showing diminished device accuracy at high latitudes
18 p3135 A69-34560

Quasi-plastic impact resulting from incomplete elastic collision of two material points in presence of dry Coulomb friction, noting engineering role in pneumatic equipment
18 p3215 A69-34568

Dry dynamic friction of brass disk against steel surface reduced using ultrasonic oscillations creating air gap
18 p3135 A69-34587

Molybdenum disulfide dry film lubricant wear theory and test correlation problems, considering sintering self propagation due to chemical effect of environment
19 p3323 A69-35580

Harmonic linearization for analyzing dry friction effect on gyroscope stability with free play in mechanical couplings, showing effective damping of natural oscillations
23 p4163 A69-41554

DRY HEAT

Spacecraft sterilization techniques efficiency in terrestrial and extraterrestrial environments noting dry heat, radiation, ethylene oxide, isopropanol and formaldehyde in methanol
05 p0712 A69-15937

Dry heat destruction of spores, discussing dependence on spore water content and effect of surrounding gas volume on escape of water from spore
05 p0712 A69-15938

Dry heat sterilization of spacecraft, microorganism water content and recommendations for fabrication conditions for spacecraft
05 p0712 A69-15939

Mathematical model for estimating microbial survival in heat sterilization of spacecraft, including environmental and time cumulative effects
05 p0707 A69-15941

Spacecraft terminal dry heat sterilization procedures for minimal time and temperature conditions, using simple geometric configuration of spacecraft for thermal analysis
05 p0712 A69-15942

Dry heat destruction rates for microorganisms encapsulated in and on spacecraft hardware, concluding temperature and water conditions in spore as major factors
15 p2560 A69-31444

Spacecraft sterilization by destructive heating with thermite or high velocity entry friction before entering planet atmosphere
15 p2560 A69-31472

DRYING

U DEHUMIDIFICATION
U DEHYDRATION

DSIF [INSTRUMENTATION FACILITY]

U DEEP SPACE INSTRUMENTATION FACILITY

DTA [ANALYSIS]

U DIFFERENTIAL THERMAL ANALYSIS

DTMB-111 GROUND EFFECT MACHINE

U GROUND EFFECT MACHINES

DTMB-430 GROUND EFFECT MACHINE

U GROUND EFFECT MACHINES

DUCTED FAN ENGINES

Monograph on exhaust gases mixing with cold airstream in ducted fanjet engine, noting thrust and efficiency increase
03 p0496 A69-14048

Ducted fan engine turbine air flow rate and frontal gas temperature determined from air temperature/pressure measurements behind compressor and engine fuel flow
18 p3086 A69-34986

DUCTED FANS

Design parameters for optimum heavily loaded single rotation ducted fan characterized by ultimate wake vortex system
[AIAA PAPER 69-222] 08 p1253 A69-21030

DUCTED FLOW

NT KNUDSEN FLOW

MHD flow through circular, elliptic and rectangular straight channels with external magnetic field transverse to flow direction
01 p0132 A69-11209

Static pressure field induced by steady subsonic flow of compressible inviscid fluid through two dimensional duct with statistically distributed wall roughness
01 p0062 A69-11279

Flow in square to rectangular constant area transition piece having straight walls with outlet aspect ratio of 5 fitted with exit duct
02 p0189 A69-12412

Conservation equations for steady incompressible flow in variable area duct with mass transfer at walls simplified by linearizing inertial and convective terms
03 p0413 A69-13011

Average energy dissipation in MHD duct flow of arbitrary cross sectional shape, evaluating bulk temperature, net wall heat flux and pressure gradient
04 p0635 A69-14724

Ducted turbulent mixing and burning of coaxial streams, presenting experimental results for rocket-air mixing system
[AIAA PAPER 69-85] 06 p0984 A69-18082

Uniqueness theorem for laminar MHD duct flows
07 p1190 A69-18813

Flow rates characteristic of trapezoidal geometries encountered after schematization of noncylindrical ducts involving irrotational flow, leakage, heat exchanges and electrical conduction phenomena
08 p1303 A69-20270

Laminar turbulent transition conditions in MHD channel flow
10 p1727 A69-23097

MHD fluid flow in rectangular duct with allowance for finite wall conductivity
10 p1727 A69-23098

Nonuniformity of magnetic field effect on steady flow of incompressible inviscid electrically conducting fluid in duct, considering Reynolds and Alfven numbers
[JPL-TR-32-1376] 11 p1923 A69-24291

Three dimensional compressible potential flow in curved circular duct analyzed by perturbation method
11 p1867 A69-24607

Duct entrance region flow, analyzing eigenvalue problem and nonlinear transformation simplification
11 p1874 A69-25285

Current and voltage distribution around normal shock in MHD duct using conformal transformation, considering continuous and segmented electrode boundary conditions
11 p1931 A69-25359

Internal flows of compressible fluids with heat transfer in accelerating nozzles and constant area ducts, simplifying equations by assuming one dimensional flow
12 p2012 A69-26790

Effective electrical conductivity of two phase vapor-potassium flow in flat duct at flow temperature 800 C, showing dependence on volumetric vapor content
13 p2306 A69-27480

Shear stress and velocity profile in MHD duct, examining turbulence damping by electromagnetic coupling
13 p2309 A69-28024

Tensor conductivity measured and analyzed for MHD generator duct with electric and magnetic fields
13 p2309 A69-28026

Boundary value problem for one dimensional unsteady equations for inviscid conducting gas during transition processes in MHD duct
13 p2309 A69-28027

Current distribution in MHD duct with permeable electrodes with tensor conductivity, obtaining Riemann-Hilbert heterogeneous boundary value problem solution by finding electric field
13 p2310 A69-28030

Convective heat and mass transfer coupling in laminar hydrodynamic duct flow, obtaining values for bulk and wall temperatures, transfer coefficients and rates, etc
15 p2716 A69-30004

Static pressure distribution induced by statistically roughened duct walls on supersonic stream
15 p2593 A69-31148

Stagnation region dimensionless pressure effect on flow pattern, boundary conditions and oscillation mechanism in compressible flow through nozzle in circular duct
15 p2549 A69-31220

Entrainment of viscous electrically conducting liquid in long duct with narrow rectangular cross section and movable walls in magnetic induction field
16 p2816 A69-31606

Gas ducted flow at subsonic inlet velocity and critical outlet Reynolds numbers, proposing surface friction relation to Mach number
16 p2771 A69-31956

Model for mixing and combustion of compressible particle laden ducted flows
[AIAA PAPER 69-460] 16 p2880 A69-32650

Taylor vorticity transport theory and von Karman similarity hypothesis extended to consider three dimensional fluctuating velocity field in analyzing turbulent swirling ducted flow
[ASME PAPER 69-APM-19] 18 p3120 A69-34394

Monte Carlo method application to neutron streaming in hemispherical air-filled ducts in water tank to determine leakage through nuclear reactor shields
18 p3171 A69-35178

Conducting gas flow parameters in coaxial duct, considering magnetic nonuniformity, Hall currents and fields distortion near electrodes
19 p3381 A69-36772

Reynolds number dependence of turbulent velocity profile in circular tube and parallel plate channel analyzed by von Karman similarity hypothesis
20 p3513 A69-37081

Membrane vibration problems for combined free and forced laminar convection through vertical ducts, obtaining expressions for velocity, temperature and Nusselt numbers
21 p3851 A69-38974

Shock wave transient motion during passage through ducts in inviscid gas containing convergences, using characteristics method
23 p4153 A69-42398

DUCTED PROPELLERS

Laminar flow swirling motion in circular duct, studying separation and reversal 24 p4301 A69-43355

Unsteady MHD conducting fluid flow in arbitrary ducts under transverse magnetic field, studying effects of pressure gradient impulsive change 24 p4359 A69-43678

DUCTED PROPELLERS

U SHROUDED PROPELLERS

DUCTILITY

Maraging steels ductile and strength characteristics with increased Co and Mo as function of Ni content, tempering method and aging 01 p0098 A69-10731

Stability of ductility and fatigue strength of stainless steel under longtime static loads in vacuum and in liquid lithium 03 p0450 A69-13912

Grain-size refinement of beryllium castings and extrusions after compression in pressure chamber, determining effect on ductility 08 p1330 A69-20013

High strength steels, discussing ductility, austenite to martensite transformation for increased strain hardening rate and elongation and corrosion resistance 12 p2115 A69-26829

Strain rate and pressurization effect on ductile-brittle transition temperature of polycrystalline sintered W, discussing yield stress 12 p2117 A69-27138

Metallographic aspects of fracture, analyzing very brittle solids, Griffith cracks, ductile solids and ductile to brittle transition 13 p2274 A69-27225

Structural modes of fracture, analyzing brittle, ductile, fatigue and stress corrosion fractures using fractography 13 p2274 A69-27226

Dynamic strain aging of Fe-Cr-C and Fe-Mo-C steels, analyzing strength, ductility and secondary hardening by using microprobes, foils diffraction and extraction replicas 13 p2276 A69-27403

Reversion and drawing techniques for ultrahigh strength ductile maraging steel wire without excessive deformation 13 p2278 A69-27412

Aluminum alloys ductile fatigue striations, considering dependence on grains crystallographic orientation and vacuum effect 13 p2278 A69-27415

Strain-rate sensitivity measurements to determine ductility of materials, noting relation to elongation 13 p2278 A69-27416

Ductile metal powder chemical reactions during comminution in pure or oxygenated water 13 p2216 A69-27762

Dislocation and energy balance analysis of ductile and brittle metal cracks for determining metal fracture strength from plastic deformation 17 p3052 A69-32984

Alloying elements effects on low temperature metal fracture, considering changes in ductile-brittle transition flow due to solute 17 p2988 A69-33551

Smooth and notched tensile properties of Fe-Ni alloys in liquid Hg, discussing ductility and toughness 20 p3563 A69-38025

Alpha-beta Ti-Al-V-Mo-Zr alloy with high strength, fracture toughness and crack propagation resistance, low density and adequate ductility, discussing test results [AIME PAPER S69-3] 21 p3747 A69-39472

Ti, Al, S and P influence on Ni alloys weldability, discussing chemical composition, susceptibility to hot cracking and ductility temperatures 22 p3967 A69-39884

DUCTS

NT AIR DUCTS

Conical diffuser/exit duct performance and model for estimating energy losses, discussing inlet flow and Reynolds number [ASME PAPER 68-WA/FE-45] 05 p0698 A69-16112

Connecting duct influence on slide wire vertical air-speed indicator operating on barometric principle during aerial gravimetric surveying 13 p2260 A69-27828

Negative resistance amplifier with stabilizing resistor in compensating circuit for operation in microwave duct mismatched beyond amplifier passband range 15 p2573 A69-30118

Self excited vibration of flowing medium and infinite cylindrical duct wall in primary magnetic field, discussing vibration stability and critical speeds 18 p3226 A69-35462

Supercritical frequencies horizontal gradient ducting effects on backscatter sounding of F region magnetic field aligned irregularities 22 p3941 A69-40913

DUFFING DIFFERENTIAL EQUATION

Numerical digital computer determination of ultra subharmonic response for Duffing equation 01 p1014 A69-10235

DUMMY LOADS

U IMPEDANCE

U LOADING

DUNGEYS WIND SHEAR MECHANISM

U WIND SHEAR

DUOPLASMATRONS

Bilateral plasma outflow plasmatron with variable electrode diameter, discussing efficiency, current-voltage characteristics and size 01 p1025 A69-10102

Duo-plasmatron charged particles energy spectra analyzed as function of discharge parameters 14 p2501 A69-29955

DUPLEX OPERATION

Slide methods for duplex parallel and switchover redundant mission availabilities based on cost, reliability and maintainability 18 p3147 A69-34531

DUPLEXERS

S band thyatron waveguide switch as pretriggered megawatt balanced duplexer 01 p0048 A69-11035

DUPLICATING

U REPRODUCTION [COPYING]

DURATION

U TIME

DUST

NT COSMIC DUST

NT INTERPLANETARY DUST

NT LUNAR DUST

NT TERRESTRIAL DUST BELT

NT ZODIACAL DUST

Dust particle separation from inlet flow with S-bend duct to minimize engine dust ingestion, determining particle trajectories [AHS PAPER 211] 01 p0006 A69-10409

Spherical flames of spark-ignited dust clouds, discussing streak film photographs, flame propagation, particle burnout time and burning velocities 02 p0353 A69-12323

Terminal velocities of dust particles for two Venus atmospheric models from Mariner 5 and Venera 4 data, obtaining vertical wind velocity requirements 06 p1001 A69-17172

Comet atmosphere dust component, relating physical properties to brightness characteristics in stellar magnitudes 15 p2685 A69-30528

Arend-Roland comet head luminescence intensity, considering radiation scattering by dust component 21 p3804 A69-39080

Aerosol attenuation coefficients vs altitude in troposphere and stratosphere, noting seasonally dependent surface convective dust layer and temperature dependent aerosol maximum altitude 21 p3718 A69-39773

Martian seasonal darkening attributed to windblown dust 24 p4389 A69-43742

DUST COLLECTORS

Meteoritic dust particles collections prediction in atmosphere for low and high entry fluxes 12 p2158 A69-26342

Barbados airborne dust collections showing metal fragments and black magnetic spherules contaminants from handling, discussing deep sea cosmic spherules and zodiacal cloud 12 p2075 A69-26964

Inflight shadowing device incorporated into dust particle collection devices borne in Aerobee rocket sampling noctilucent cloud display over Fort Churchill 15 p2602 A69-31386

DWARF STARS

NT WHITE DWARF STARS

Microturbulent velocity parameter correlation to iron-to-hydrogen ratio for G dwarfs, using model atmosphere abundance analyses 01 p0154 A69-10877

Sky areas search for stars with UV excesses listed in Luyten Two-Tenths Catalog of Proper Motions 08 p1392 A69-20560

Gas flows in close binary systems of dwarf stars

08 p1396 A69-20648

Subdwarf HD 25329 studied with model atmosphere approach, using H alpha, Na I and Mg I profiles for effective temperature 09 p1600 A69-22199

Lyman alpha wing opacity effect on temperature scale and helium content in F and G subdwarf atmospheres 09 p1607 A69-22431

Dwarf and subdwarf stars limb darkening tables for unblanketed nongray radiative model atmospheres 12 p2171 A69-27153

Parallax and mass ratio of visual type K6 dwarf binary system, ADS 1865, BD plus 30339 13 p2349 A69-27811

Red dwarf star /YZ Canis Minoris/ radio outbursts observation noting stellar atmospheric spectrum, electron density and temperature and total flare energy 17 p3043 A69-34164

YZ Canis Minoris red dwarf star flare event observation record, noting optical spectrum energy output and slow decay 17 p3043 A69-34165

Red dwarf star YZ CMi corona structure showing possible estimation of additional carried energy by shock waves after flare 17 p3043 A69-34166

Physical nature of HZ 22 short period hot subdwarf binary, noting arguments against normal B type binary hypothesis 17 p3044 A69-34181

DYADICS

Waves in inhomogeneous warm magnetoplasmas with static pressure gradients, applying dyadic to planar stratified plasma case 01 p0129 A69-10561

Linear analysis of strain in continua in terms of one-one correspondence, relative displacement and stretch dyadic 07 p1236 A69-19445

Dyadic Green function technique extended to problems of electromagnetic scattering in inhomogeneous media with spherical symmetry 17 p2924 A69-33837

Electromagnetic propagation in infinite rectangular waveguide surrounded by dielectric medium described by Green dyadic 23 p4115 A69-41570

Group interaction finite Markov chain model, analyzing changes in interpersonal relationships based on balanced dyadic states 23 p4110 A69-42017

DYES

Organic dye lasers energy characteristics excited by monochromatic radiation, investigating radiation absorption during transitions from lower to higher electron-vibrational levels 01 p0090 A69-10381

Spectral absorption curves of hematoxylin stains in stained tissue sections of rat thyroid 01 p0015 A69-10924

Frequency and time dependent gains of dye solution lasers for pumping by lasers and flashlamps 02 p0257 A69-12616

Organic dye laser frequency variation with temperature, noting absorption and fluorescence spectra 02 p0258 A69-12617

Dye solution laser wavelength shift and simultaneous oscillations at different wavelength ranges for pumping by another dye laser 02 p0258 A69-12620

Stimulated emission of cyanine dyes, discussing amplification coefficients 04 p0612 A69-15373

Critical population inversion for xanthene dye solution laser, analyzing optical loss due to triplet state concentration [IEEE PAPER A-2] 05 p0773 A69-16307

Lasing threshold and spectral characteristics of organic dye solutions, using excitation of second harmonic of monopulse ruby laser 06 p0933 A69-17255

Light generation by lasing organic dye liquid solution with negative absorption on activator molecules and induced combination scattering for solvent molecules 06 p0933 A69-17256

Organic lasers, discussing coherent laser light emission induced from organic dye molecules 07 p1149 A69-18908

Phase matched optical harmonic generation by anomalous dispersion in liquid media, using dye fuchsin red [IEEE PAPER V-9] 07 p1155 A69-19086

Saturable dye filters used with ruby lasers, discussing relaxation time, residual absorption source and transient spectral hole burning

07 p1155 A69-19089

Organic cyanine dye solution laser pumped by Q switched ruby and another dye laser, discussing spectral distribution and modes

11 p1900 A69-25580

Organic dye lasers energy characteristics excited by monochromatic radiation, investigating radiation absorption during transitions from lower to higher electron-vibrational levels

12 p2109 A69-26676

Stimulated emission of cyanine dyes, discussing amplification coefficients

16 p2797 A69-32120

Polymethine dyes in passive Q switches of neodymium lasers, noting effects of absorption band intensity, width and position on single pulse laser energy yield

17 p2983 A69-33968

Lasers based on organic dye solutions, discussing operation, structural formulas, absorption and luminescence spectra

20 p3555 A69-38011

Emission from polymethine dye solution during optical pumping with pulses from Q switched Nd glass laser, discussing emission spectral, temporal and energy characteristics

21 p3739 A69-39542

Mode locking of organic dye laser by pumping laser with mode locked pulse train from Nd-glass laser, obtaining spectral bandwidth

21 p3740 A69-39545

Pumping and excitation spectra of solid solutions of cryptocyanine in glycerine irradiated by ruby laser, discussing population inversion and scattering and vibrational transitions

21 p3740 A69-39546

Flashlamp-excited organic dye lasers capable of tunable emission throughout most of visible spectrum

22 p3966 A69-41219

Low energy ultrafast flashlamp systems as optical pumps for lasers using fast decaying fluorescent materials /organic dyes/

23 p4174 A69-42187

with structural properties and contact formation conditions

01 p0136 A69-10256

Dynamic polarizability at imaginary frequencies, deriving upper and lower variational bounds with functionals containing trial functions

01 p0122 A69-10284

Organic dye lasers energy characteristics excited by monochromatic radiation, investigating radiation absorption during transitions from lower to higher electron-vibrational levels

01 p0090 A69-10381

Multilevel optimization techniques for dynamic systems control evaluated, developing second level Newton-Raphson controller

01 p0051 A69-10440

Forced processes in continuous extremal control systems, proposing algorithm for designing dynamic model

01 p0052 A69-10798

Automatic control systems correction by compensating for nonlinear statistical dynamic characteristics with aid of nonlinear devices

01 p0053 A69-10801

Determination of plant differential equation from time characteristics

01 p0053 A69-10804

Amplification equations for calculating unsteady lasing in Q switched ruby laser, considering changes in populations and fields along cavity

01 p0092 A69-10888

Soviet book on dynamics of radiation belts of earth covering theories concerning magnetosphere, magnetic fields and plasma and electromagnetic pulsations

02 p0307 A69-11799

Vortex valve characteristics, noting Reynolds number and geometry effects on flow and turnaround ratio

02 p0195 A69-12079

Vortex controlled fluid amplifiers, discussing static and dynamic performance characteristics

02 p0195 A69-12081

Book on dynamics of linear and nonlinear systems covering mathematical methods for control system design

02 p0225 A69-12228

Nonlinear programming of optimization of parameters and control functions of dynamic systems

03 p0408 A69-12974

Synthesis of statistically optimal self adaptive system for dynamic characteristics stabilization of automatic control system main loop

03 p0410 A69-13256

Multilevel optimal control and decomposition of trajectories by studying static and dynamic systems

04 p0581 A69-14570

Multiframe platform stabilization, analyzing dynamic coupling due to possible avoidance of adjusting moment and effect of coupling on attitude control

04 p0629 A69-14830

Gunn effect theory, discussing dynamic characteristics and domain propagation for inhomogeneous transmission line profile

05 p0807 A69-15821

Static and dynamic performance of pancake vortex flow field and application to signal amplification

05 p0704 A69-16001

Beam deflection fluid amplifiers dynamic properties determined by random signal testing

05 p0705 A69-16010

UK hovercraft research covering internal/external dynamics, propulsion systems and full scale tests

05 p0702 A69-16393

Large signal impedance measurements and dynamic characteristics explain Si avalanche diodes efficiency degradation at higher frequencies

06 p0893 A69-16938

Temperature dependence of dynamic viscoelastic properties of plasticized epoxy resins

06 p0946 A69-17125

Dynamic measurements of modulus of elasticity for polycrystalline nickel-tungsten alloys at elevated temperatures

06 p0943 A69-17232

Multivibrator with two widely different zones of discontinuous oscillation

06 p0896 A69-17474

Quasi-random properties of dynamic system generated by solutions of second order differential equations

06 p0948 A69-17657

He-Ne laser with small spark gap optimum parameters dependent on active medium and resonator field structure

06 p0935 A69-17683

Dynamic behavior of shock layer of supersonic rarefied gas flow past disk and sphere

06 p0861 A69-17812

Root-locus curve characterization of dynamic behavior of nonlinear control system, considering effects of changes in perturbing variable or reference input

07 p1114 A69-18290

Standing waves effect on spectral and power characteristics of laser with plane mirrors, determining dependence on pumping power

07 p1148 A69-18800

Magnetosphere dynamical properties, discussing atmosphere, ionosphere, magnetopause, magnetosheath, bow shock, solar wind, collisionless plasmas, etc

07 p1127 A69-19352

Plasma heating dynamics by straight turbulent discharge current influenced by initial plasma parameters

07 p1195 A69-19592

Computer simulation on engines dynamic behavior covering thrust transfer functions, time behavior and engine and fuel controller operation

08 p1301 A69-20167

Synoptic meteorological predictions using statistical dynamic approach, considering probability distributions and nocturnal temperature decay

08 p1345 A69-20300

Dynamic behavior of electrohydraulic servactuators over wide range of loads using differential equations of motion

08 p1256 A69-20718

Earth equipotential surface shape determination from satellite orbit dynamics, obtaining triaxial ellipsoid

09 p1487 A69-21635

Stabilized gyroscope platform internal dynamics analysis, outlining optimal orientation for full compensation of cross couplings

09 p1499 A69-22240

Electron microscopy for continuous observation and recording of dynamic reactions in high temperature materials

09 p1499 A69-22304

Microwave instabilities in bulk GaAs under strong electric fields, considering characteristics connected with structural properties and contact formation conditions

09 p1559 A69-22649

Stress graphitizing and boron codoping effect on dynamic mechanical properties of pyrolytic carbon, noting increase in internal friction and dynamic modulus

10 p1716 A69-23036

Characteristics of dynamic mechanical systems including solid state and hydrodynamic analogs of ideal incompressible fluids, based on statistical theory of turbulence

10 p1678 A69-23209

Torsiograph systems analysis for rotors angular acceleration recording, discussing dynamic characteristics, system, environmental problems, etc

10 p1692 A69-23252

Elastic release wave and pressure drop measurement in 2024-T4 aluminum at 313 kb for dynamic yield strength, considering surface velocity and stress

10 p1712 A69-23665

Frequency response dynamics of beam type periodic structures on elastic supports typical in flight vehicle designs

[ASME PAPER 69-VIBR-17]

10 p1804 A69-24150

Differential equations for effect of sinusoidal force with slowly varying frequency on dynamic behavior of nonlinear vibrator, using phase surface technique

11 p1916 A69-24760

Steady state and dynamic characteristics of linear plant with constant lag element based on correlation function moments

11 p1859 A69-24965

Dynamical effects of mass exchange in close binary systems ejection modes from point of view of orbital elements evolution

11 p1962 A69-25113

Inertial servomechanisms actuators, discussing dynamic characteristics, power, vibration damping, matching, couplers, etc

11 p1826 A69-25119

Frequency characteristics of flexible compensated manifolds for aircraft engines, considering axial force

11 p1826 A69-25332

DYNAMIC CHARACTERISTICS

NT AERODYNAMIC DRAG
NT AERODYNAMIC STABILITY
NT AIRCRAFT STABILITY
NT ATTITUDE STABILITY
NT BOUNDARY LAYER STABILITY
NT COMBUSTION STABILITY
NT CONTROL STABILITY
NT DIRECTIONAL STABILITY
NT DRAG
NT FLAME STABILITY
NT FLOW CHARACTERISTICS
NT FLOW DISTRIBUTION
NT FLOW STABILITY
NT FLOW VELOCITY
NT FREQUENCY STABILITY
NT FRICTION DRAG
NT GYROSCOPIC STABILITY
NT HOVERING STABILITY
NT INTERFERENCE DRAG
NT INTERFERENCE LIFT
NT JET LIFT
NT LATERAL STABILITY
NT LIFT
NT LONGITUDINAL STABILITY
NT LOW SPEED STABILITY
NT MAGNETOHYDRODYNAMIC STABILITY
NT MINIMUM DRAG
NT MOTION STABILITY
NT PRESSURE DRAG
NT ROTARY STABILITY
NT ROTOR LIFT
NT SATELLITE DRAG
NT SPACECRAFT STABILITY
NT SUPERSONIC DRAG
NT TRANSIENT RESPONSE
NT VISCOUS DRAG
NT WAVE DRAG

Heisenberg ferromagnet dynamics at low temperatures, calculating spectral weight function and other properties with low density expansion

01 p0135 A69-10016

Reliability analysis of technological systems, determining characteristics as distribution function of time to specified number of failures

01 p0085 A69-10210

Darlington composite transistor hybrid parameters used to describe performance characteristics, noting load resistances and source

01 p0041 A69-10244

Microwave instabilities in bulk GaAs under strong electric fields, considering characteristics connected

Amplitudes of forced bending vibrations of frames with superfluous elastohysteretic couplings by dynamic compliances method

11 p1986 A69-25333

Structural optimization of designs with requirements including restrictions on structure dynamic response and characteristics

11 p1989 A69-25495

Magnetically selective microwave filters using magnetodynamic natural oscillations in premagnetized ferrite sphere at cavity center

11 p1855 A69-25626

Dynamic properties of supply sources in carbon dioxide shielded welding as function of short circuit current statistical parameters, noting metal spatter correlation

11 p1892 A69-25667

Dynamic behavior of nonlinear continuous multivariable systems represented by equations derived from block diagram, stressing digital computer properties

12 p2049 A69-26081

Lunar surface layer temperature field dynamics obtained from stable periodic solution to parabolic differential equation with nonlinear nonautonomous boundary conditions

12 p2157 A69-26281

Amplification equations for calculating unsteady lasing in Q switched ruby laser, considering changes in populations and fields along cavity

12 p2109 A69-26652

Organic dye lasers energy characteristics excited by monochromatic radiation, investigating radiation absorption during transitions from lower to higher electron-vibrational levels

12 p2109 A69-26676

AZUR German research satellite main structure dynamic characteristics, solar panels, yo-yo despin system, electronic ignition devices and magnetometer boom

12 p2175 A69-26875

AZUR satellite structural development static and dynamic considerations, discussing center of gravity, notching technique and test results

12 p2187 A69-26876

Herringbone grooved gas lubricated journal bearing static and dynamic characteristics analyzed approximately, noting pressure distribution and vibration amplitudes [ASME PAPER 68-LUBS-7]

13 p2265 A69-27269

Design optimization for gas lubricated spiral grooved spool bearing based on narrow groove theory, analyzing static and dynamic characteristics for motion in axial direction [ASME PAPER 68-LUBS-12]

13 p2266 A69-27276

Elastic directed curves dynamic theory, considering Hamilton principle, mass conservation and behavior of action density function under rigid body variations

13 p2360 A69-27321

Optimal parameters of hydraulic sensor of angular accelerations for given dynamic and geometrical requirements

13 p2259 A69-27432

MHD induction converters operational characteristics calculations with simultaneous considerations for finite length and channel width

13 p2207 A69-27496

Volterra integral equation with nondifference type singular kernel for stress-strain state in long hollow viscoelastic cylinder with moving inner boundary

13 p2361 A69-27744

Conditions governing application of reduced Nielsen equations to anholonomic systems dynamics, discussing kinetic energy function

13 p2288 A69-27924

Trajectory terminal state error analysis using adjoint-generated sensitivities in nonlinear time-varying systems

13 p2296 A69-27940

Parameter identification in linear dynamical systems with transport lags, discussing linear differential-difference equations and finite difference theory

13 p2289 A69-27945

Ferrites dynamic characteristics in alternating magnetization pulse with variable amplitude indicating linearity loss in strong fields

13 p2320 A69-27994

Ionization sensors and detectors classification and dynamic calibration for pressure measurement

13 p2262 A69-28083

Dynamic characteristics of Clough-Tocher triangle for natural frequency of simply supported plate, noting bending elements

13 p2365 A69-28246

Gas laser modulation steady state characteristics with KDP crystal in cavity, noting output power dependence on applied electric field

13 p2273 A69-28432

Reactive parameter scatter effect on amplitude frequency characteristics of regenerative reflection amplifiers based on equivalent circuit

13 p2235 A69-28515

Cut-in and cut-out characteristics of fast acting composite transistor circuit, noting pulse duration

13 p2235 A69-28517

Operation mode of modulator with p-n diode, determining modulus and phase of reflection factor

13 p2235 A69-28518

Random signals and real time analysis systems for environment testing and transient signals

13 p2264 A69-28603

Reliability analysis of technological systems, determining characteristics as distribution function of time to specified number of failures

14 p2453 A69-28747

Surface equilibrium configurations and bifurcation points for rotating homogeneous right fluid cylinder confined by surface tension forces

14 p2428 A69-28816

Dynamic process during rms deviation of nonlinear system from prescribed trajectory described by nonlinear differential equations

14 p2425 A69-28822

Radio waves propagation along polar auroras region, obtaining ionospheric parameters for magnetic disturbances based on penetration probability

14 p2436 A69-29058

Linearized perturbation for photochemical and dynamical effects in internal atmospheric gravity wave production of E region ionospheric irregularities

14 p2440 A69-29128

Ground testing method to evaluate inertial navigation systems dynamic errors by programmed platform drift rates, position output comparisons and error source identification

14 p2479 A69-29490

Comet Ikeya-Seki 1965f primary nucleus splitting date and rate established from dynamic solutions

14 p2524 A69-29710

Nongravitational force dynamic effect and model for rotating cometary nucleus, including changes in orbital elements

14 p2524 A69-29713

Logarithmic amplifiers amplitude characteristics accuracy obtained by gain variations or successive summation of voltages, plotting curves illustrating error variations vs gain

15 p2574 A69-30128

Nanosecond pulse generator for powering semiconductor lasers, examining circuit diagram and elements design

15 p2633 A69-30234

Bladed disk assemblies vibrational properties, discussing dynamic characteristics of system with pairs of close natural frequency modes under forced vibration

15 p2704 A69-30304

Dynamic characteristics of local slope winds, considering thermal and geometrical effects of underlying surfaces

15 p2648 A69-30577

Minimum vibration frequency and compressive force for freely supported rectangular, triangular and circular plates simulated on analog computer

15 p2708 A69-30665

Monograph on dynamic behavior of jet engines especially during perturbations based on linear theory

15 p2671 A69-30931

Panel flutter under loads along profile, evaluating constraints dynamic characteristics by Hamilton principle

15 p2712 A69-31001

Dynamic characteristics of model of spacecraft-astronaut-tether system during approach, deriving kinetic potential

15 p2696 A69-31064

Dynamics of spin stabilized satellite with long crossed dipoles or slender beams, including linearized equations of motion

15 p2703 A69-31332

Comparisons and combinations of geodetic parameters from dynamic and geometric satellite solutions and Mariner flights

15 p2600 A69-31362

Monograph on transmission characteristics of mechanical vibration transducers covering frequency response operators and analog computer simulation

16 p2789 A69-31842

Kerr magneto-optic camera for 10 nsec exposures of dynamic magnetization configuration in magnetic thin film during high speed flux reversal

17 p2970 A69-32853

Stationary galaxy dynamical theory, assuming constant velocity body of physically homogeneous star subsystems in space

17 p3031 A69-33102

Automatically controlled dynamic systems reliability estimation in terms of failure probability illustrated with autopilot-aircraft case

17 p3001 A69-33144

Aircraft and missile dynamic characteristics for heavy loads and large heat flux, noting small harmonic vibrations of heated structures in plastic domain [ICAS PAPER 68-38]

17 p3061 A69-33589

Laser pulse development dynamics taking into account phase relations between field and active medium polarization

17 p2983 A69-33695

Book on solid bodies collision theory covering elastic bodies with ruled surfaces, dynamic effects associated with Rayleigh surface waves, thermodynamic effects, etc

18 p3210 A69-34259

Soviet book on hydraulic servo drive covering design and performance, static and dynamic characteristics and stability problems

18 p3093 A69-34356

Plastics behavior under loading and performance prediction, considering engineering design applications

18 p3161 A69-34609

Parametric and forced oscillations analogy for analyzing dynamic behavior of oscillatory systems with time dependent parameters

18 p3175 A69-35322

Dynamic performance accuracy of astatic gyroscope with three degrees of freedom improved by inner gimbal mass increase

19 p3308 A69-35825

Dynamical effects in structure of H II equilibrium region left behind expanding ionization front, showing temperature as function of distance from star

19 p3403 A69-35966

Liquid driver shock tubes dynamic and thermodynamic properties as functions of diaphragm pressure ratio and initial conditions

19 p3295 A69-36471

Static and dynamic characteristics of pressure compensated oil-hydraulic flow control valves and relief valves with emphasis on linearized effects

19 p3256 A69-36713

Two body mechanical system operating within dynamics laws simulating backward and forward bending motions of falling cat

19 p3259 A69-36832

Mechanical loss factors calculated by approximation formula from resonance curves of Voigt-Kelvin and Maxwell models

20 p3623 A69-37435

Occurrence, development and disappearance of diffused reflections, relating dynamic behavior to ionospheric electron concentration

20 p3529 A69-37687

Dynamic stall characteristics of high speed symmetrical and cambered helicopter rotor blade airfoils from two dimensional wind tunnel determinations [AHS PAPER 206]

20 p3463 A69-37806

Dynamic cathode ray tube spot size measurement by two slit technique, noting relationship to beam current and luminance

21 p3719 A69-38329

Monograph on control dynamics of gas turbines with adjustable guide vanes, using methods of control theory and applied mathematics

21 p3784 A69-38449

Automated rebound resilience apparatus for polymer dynamic mechanical properties studies over wide temperature range, using photoelectric device

21 p3689 A69-38593

Coupled gyroscopic systems two parameter stabilization problem analyzed for steady state characteristics by iterative method

21 p3723 A69-38829

Gyroscopic system behavior analyzed for steady state operation following transient period

21 p3723 A69-38832

Standing waves effect on spectral and power characteristics of laser with plane mirrors, determining dependence on pumping power

21 p3736 A69-38945

Potential flow past plane array of thin blades, analyzing perturbed dynamic behavior

21 p3696 A69-39243

Test pad isolation characteristics mathematical model to predict pad dynamic behavior [AIAA PAPER 69-860] 21 p3690 A69-39388

Test stand for measurement of forces and moments from thrust vector controlled rocket, analyzing dynamic characteristics of hydrostatic supports 21 p3691 A69-39631

Dynamics of relay gas jet preliminary vibration damping system of gravity gradient stabilized satellite, allowing for sensor limitations and stabilizer flexural vibrations 21 p3826 A69-39638

Artificial damping of longitudinal winged reentry vehicle motions in earth atmosphere, discussing vibration damper dynamic characteristics 21 p3829 A69-39828

Weighting function of statistically optimal automatic dynamic system generating stochastic loads, using Fredholm equations 21 p3688 A69-39861

Nonlinear compensator characteristics determination for modifying compensated system output signal under various disturbances with inputs subjected to white noise 21 p3688 A69-39862

Dynamical analysis of Bernard star motion, yielding companions in co-revolving, approximately coplanar, circular orbits 22 p4013 A69-40119

Radiotelemetric EEG recording variation possibility, examining dynamic behavior of human cerebral rhythms 22 p3889 A69-40158

Device determining dynamic mechanical properties of tissues and various transducers, evaluating elastic properties of polyurethane, Hevea rubber and descending thoracic aorta 22 p3890 A69-40204

Dynamic parameters of full scale and equivalent structures of electromechanical transducer circuits determined experimentally 22 p3869 A69-40249

Dynamic characteristics of temperature control systems using crystal oscillators determined by nonlinear automatic control theory 22 p3869 A69-40254

Linear equations of motions of inviscid ideal gas atmospheres, describing climatology of propagation parameters for point impulse sources 22 p3938 A69-40446

Ball lightning as positively charged region of electroluminescent air maintained in dynamic structure and molecular composition by atmospheric electric field 22 p3940 A69-40536

Metric state-time dynamical polysystem with sequentially compact topological space, noting sliding state trajectories 22 p3975 A69-40573

Performance characteristics of multivariable model reference adaptive systems synthesized by Liapunov method analyzed using computer simulation 22 p3919 A69-41201

Quantum mechanical systems dynamics in diagonal coherent state representation, discussing applications 22 p3983 A69-41259

Book on fundamentals of dynamics of deformable bodies of increasing dynamic complexity, using calculus of variations 23 p4226 A69-41474

Dynamic characteristics of nonlinear discrete systems by motion division method, using discontinuous Liapunov function for stability criteria 23 p4144 A69-41956

Teleological systems behavior modeling based on input, output, goals, operation duration, etc 23 p4134 A69-42059

Analog computer simulation of single shaft Brayton cycle system dynamics, including startup and shutdown transients 23 p4071 A69-42280

Rigid shaft dynamics in hinged and elastic bearings, eliminating inaccuracy by limiting analysis to forced vibration 23 p4171 A69-42483

Cardiovascular autonomic effects dynamic characteristics under severe arterial hypoxia in unanesthetized rabbit 24 p4258 A69-42632

Cosmic rays properties and dynamical effects in Galaxy disk including origin, lifetime, magnetic field instability, etc 24 p4366 A69-42695

Proportional fluid amplifiers analysis in cascade and with feedback by extended lumped parameter method, discussing dynamic characteristics of analog amplifiers with air 24 p4255 A69-43268

Dynamic equilibrium of making and breaking adhesion bonds between polymer segments and dissimilar surfaces through water, allowing thermal stresses relaxation 24 p4326 A69-43458

Dynamic behavior of gas bubble in ideal fluid plane flow, considering bubble shape, velocity field, gas pressure and stagnation point pressure determination 24 p4302 A69-43478

Composite and metal tubes compared to determine properties for various loadings [AIAA PAPER 68-340] 24 p4405 A69-43653

Jet dynamic characteristics injected into supersonic air slipstream incident on flat body, calculating configuration, shock wave geometry and parameters distribution in flow field 24 p4250 A69-43710

DYNAMIC CONTROL

Optimal control of discrete and continuous stochastic linear dynamical systems, discussing algorithms for instantaneous weighted minimum mean square error performance 01 p0051 A69-10439

Sensitivity reduction in specific optimal control by use of dynamical controller 01 p0051 A69-10441

Two parameter dynamic system of fourth order optimization based on gradient method modified for discrete optimization 02 p0224 A69-11594

Frequency domain stability criterion for nonlinear feedback system consisting of nonlinear amplifier, linear dynamical system and transducer with backlash 02 p0225 A69-11968

Linear filter performance degradation due to modeling error in estimate of state vector of stochastic linear dynamic systems 02 p0225 A69-11971

Book on dynamics of linear and nonlinear systems covering mathematical methods for control system design 02 p0225 A69-12228

Book on applications of information theory to dynamical systems with random initial conditions and cybernetic systems consisting of communication systems with feedback 04 p0580 A69-14520

Linear regression and related procedures in identifying dynamic processes 06 p0901 A69-17360

Absolute stability of dynamic control systems with single nonlinear element function of two feedback state variables, giving sufficient conditions 06 p0905 A69-17948

Observability theory of dynamic objects application to composing measurements for space flights, solving parametric observability problem 07 p1087 A69-19605

Variational method for necessary and sufficient conditions of terminal state invariance of dynamic control system 10 p1718 A69-23206

Active broadband vibration isolation of human subjects from severe vertical dynamic excitations experienced in low level high speed flight [ASME PAPER 69-VIBR-65] 10 p1650 A69-24157

Mathematical model for initial conditions of asymptotically stable nonlinear control system to estimate region of acceptable motions 11 p1861 A69-25453

Asynchronous finite state sequential nonlinear controller synthesis with few flip-flops for dynamic space vehicle systems [AIAA PAPER 67-988] 13 p2225 A69-28201

Transistorized DC amplifier circuit with reversible and controllable transfer constant based on voltage conversion principle 13 p2235 A69-28511

Multidimensional discrete control systems for spectral characteristics of random processes in vibrational and fatigue strength testing of machines and equipment 19 p3286 A69-35890

Stability of interrelated linear dynamic control systems with distributed parameteres evaluated by using differential equations 19 p3286 A69-35892

Invertibility of linear time invariant dynamical control systems, discussing L-inverses, sequential circuits,

inherent integration, reproducibility, pointwise and functional inverses 20 p3509 A69-37138

Variational method for necessary and sufficient conditions of terminal state invariance of dynamic control system 21 p3756 A69-39147

Model performance index /PI/ providing criterion for approximating one dynamic flight control system by another based on geometrical representation of linear autonomous systems [AIAA PAPER 69-885] 21 p3764 A69-39410

Stochastic motion control problems formulations in rocket dynamics 21 p3767 A69-39650

Programmable digital compensator for single high performance control loop servomechanisms 21 p3688 A69-39704

Approximation of linear unsteady dynamic systems at finite time interval expressed in Bessel or degenerate hypergeometric functions 22 p3917 A69-40616

Heart rate respiratory control model with inclusion of pressoreceptor feedback, considering posture effect in transient envelope alteration 22 p3894 A69-41202

Invariance theory in automatic dynamic systems 23 p4145 A69-42368

Absolute invariance of perturbations affecting dynamic plant achievable by inertial measurement of highest derivatives 23 p4145 A69-42369

Optimal deterministic inputs derived for estimating dynamic control system parameters from white observation noise 24 p4293 A69-43294

Time-invariant multivariable linear systems, discussing structure theorem for controllable systems and application to decoupling problem 24 p4294 A69-43314

Adaptive model of human operator control strategy in response to sudden changes in plant dynamics and transient disturbances 24 p4276 A69-43325

DYNAMIC LOADS

NT AERODYNAMIC LOADS

NT BLAST LOADS

NT CYCLIC LOADS

NT GUST LOADS

NT IMPACT LOADS

NT ROLLING CONTACT LOADS

NT SHOCK LOADS

NT THRUST LOADS

NT TRANSIENT LOADS

NT VIBRATORY LOADS

NT WING LOADING

Fatigue life, kinematics, dynamics, etc, of thrust loaded ball bearings, considering inertial effects of hollow balls 01 p0087 A69-10908

Mechanical behavior of materials under dynamic loads - Conference, San Antonio, September 1967 02 p0342 A69-12277

Thermodynamics of viscoplastic materials under dynamic loads within framework of continuum mechanics of materials with memory 02 p0343 A69-12281

Ductile crack propagation speed relation to dynamic flow properties of metals analyzed using Dugdale crack model 02 p0343 A69-12283

Plane strain plastic stress waves radial propagation from center of hollow cylinder subject to dynamic pressure load 02 p0344 A69-12292

Elastic/viscoplastic wave propagation in thin tubes under combined stress of tension and torsion, using viscoplastic constitutive equations 02 p0344 A69-12293

Solid viscosities effects on dynamic load factors of ring and hollow sphere subject to uniformly distributed impulsive loads along inner and outer edges 03 p0530 A69-14089

Stability against snap-through and final states of shallow arches on elastic foundations and subject to time varying loads [ASME PAPER 68-WA/APM-26] 04 p0669 A69-14394

Circular cylindrical isotropic shell deformation rate under dynamic axial load described by second order linear differential equation 04 p0673 A69-14499

Elastic rod buckling under dynamic longitudinal compression load, determining critical load 04 p0679 A69-14926

Truncated solid cones plastic yielding under quasi-static and dynamic axial loads at various strain rates
04 p0682 A69-15301

Parallel damped dynamic vibration absorbers, modifying conventional absorber by adding subsidiary undamped absorber mass
[ASME PAPER 68-WA/DE-6]
05 p0839 A69-16171

Elastoplastic stress-strain state of asymmetric profile thin walled beam under mobile load
05 p0841 A69-16205

Dynamic response of semiinfinite circular cylindrical shells to traveling load
06 p1021 A69-17148

Axisymmetric vortex free motion of ideal fluid in conical container with spherical bottom under axial acceleration
06 p0910 A69-17335

Snapping and buckling of simple elastic structures under dynamic load, noting influence of structural geometry and load duration
[AIAA PAPER 69-22]
06 p1029 A69-18206

Dynamic stress intensity factor for axisymmetric loading of circular crack in infinite isotropic elastic medium
08 p1413 A69-20412

Dynamic response of anisotropic circular cylinders to uniformly distributed pressure varying periodically with time analyzed using Laplace transformation
09 p1611 A69-21440

Asymptotic two dimensional moment theory of elasticity, analyzing stress concentration at curvilinear holes and fluctuating boundary loads
09 p1614 A69-21884

Axisymmetric dynamic snap through critical load analysis for elastic clamped shallow spherical shells, considering impulsive and step loads
09 p1616 A69-21977

Fatigue strength and stress-time functions obtained by programmed fatigue tests under time variable loads
09 p1620 A69-22572

Fatigue life evaluation by programmed fatigue strength tests, using frequency distribution of load set amplitudes
09 p1620 A69-22573

Liquid filled elastic shells natural frequencies and oscillation modes, deriving eigenfunction system from liquid velocity potential boundary conditions to determine dynamic load
11 p1870 A69-24951

Elastic and elastoplastic strains in materials under various loadings, determining temperature variations by thermoelectric method and verifying by tensile tests
11 p1985 A69-25178

Polyurethane foam high velocity deformation properties, discussing results of dynamic uniaxial stress tension and compression tests
11 p1907 A69-25648

Viscoelastic models for solving longitudinal oscillations of one degree of freedom system under dynamic load, taking into account energy dissipation
12 p2177 A69-25995

Complex two layered shell of revolution under static and dynamic asymmetric loads analyzed using SABOR/DRASTIC computer codes
12 p2184 A69-26811

Stress waves analysis of brittle fractures, considering loading time role and cavitation of viscous fluids relation to fracture incipience
13 p2275 A69-27229

Parallel damped dynamic vibration absorbers, modifying conventional absorber by adding subsidiary undamped absorber mass
[ASME PAPER 68-WA/DE-6]
13 p2360 A69-27422

High purity beryllium dynamic tests, determining Hugoniot equation of state, shock profile and spall threshold /onset of microcracking/ for elastic pulses
[AIAA PAPER 69-360]
13 p2283 A69-28293

Minimum weight design of structures excited to harmonic vibrations by given single load, with intensity dependent on time
13 p2369 A69-28350

Graphites wear rates and structural changes in machine parts under dynamic stresses in air or vacuum, noting pressure role
14 p2467 A69-28912

Design and test criteria for dynamically loaded structures from various viewpoints, discussing statistical variations, load strength and limitations
15 p2618 A69-30368

Annealed aluminum rods dynamically compressive impact loading used to study longitudinal plastic waves propagation velocity
15 p2709 A69-30677

Elastoplastic strains in thin walled beams subjected to oblique bending by mobile loads of coupled concentrated forces, calculating deflections and plastic region distribution
15 p2711 A69-30971

Moving load at plane interface between two elastic media in space related to direct trirectangular trihedron with vertically descending Oz axis
16 p2870 A69-31829

Inhomogeneity effects on elastic waves generated by impulsive loading of surface using asymptotic method, discussing high stress intensification regions
16 p2873 A69-32157

Bending of rigid freely supported plastic plates under local axisymmetric dynamic load, discussing rectangular pulse effects and velocity fields
18 p3217 A69-34593

Extreme disturbance analysis and optimum performance and design problems for structural and mechanical dynamic systems, basing solutions on linear, nonlinear and dynamic programming
18 p3106 A69-34663

Transverse vibrations of thin linear viscoelastic rectangular plate of constant thickness resting on elastic medium
18 p3223 A69-35171

Closed form solutions for rigid viscoplastic cylindrical shell under dynamic loading based on constitutive equations for rate sensitive plastic material
19 p3439 A69-36478

Plastic deformation effect on dynamic buckling of elastic-plastic simple shallow truss subjected to step and impulsive loading
19 p3446 A69-36836

Axial forces effects on dynamic load factors of beams under transverse impulsive loads, considering various end conditions
20 p3629 A69-38113

Elastic closed and truncated conical shell stability with initial deflections under dynamic critical loading
21 p3834 A69-38716

Solid viscosities effects on dynamic load factors of hollow sphere subjected to uniformly distributed impulsive loads, using three element model
22 p4044 A69-40598

Plastic deformation by uniaxial tension during transition from dynamic to static loading from microscopic and macroscopic standpoint, noting slip lines
22 p4047 A69-41081

Solid solutions precipitation effect during deformation process on static and dynamic tensile tests of Al alloy by electric resistance measurement
22 p3972 A69-41082

Stress-strain state of circular disks with arbitrarily varying thickness along radius under antisymmetrical load calculated by integral equations method
22 p4047 A69-41168

Scale factor in designing uniform strength structures for dynamic load effects determined by recording fatigue limit and failure location, using variable cross section samples
23 p4225 A69-41422

Mechanical model for dynamic buckling of elastic imperfection-sensitive structures under step loading, using perturbation method
24 p4405 A69-43656

DYNAMIC MODELS

Repeated elastoplastic deformation of polycrystalline body analyzed by dynamic model
01 p0164 A69-10082

Dynamic system for self adaptive control of inertial plant described by differential equations, noting synthesis method eliminates distortion
01 p0052 A69-10797

Forced processes in continuous extremal control systems, proposing algorithm for designing dynamic model
01 p0052 A69-10798

Hydrodynamic model of laser produced solid particle plasma, giving distributions of pressure, density, temperature and velocity
01 p0132 A69-11210

Transformation laws for thermodynamic quantities confirming conventional formulation by mechanical model of heat
01 p0122 A69-11288

Instability of struts subjected to axial force and radiant heat, considering elastic and thermal deformation
02 p0337 A69-11716

Neuromuscular actuation system model, noting compatibility with human physiological and anatomical data in tracking tasks
02 p0202 A69-11952

Dynamic flight simulators fidelity assessment, discussing hybrid method based on pilot psychomotor responses
02 p0203 A69-12215

Dynamical strength of solid cylinder under axial loads increasing in time at given rate, using constitutive equations of thermodynamic theory
02 p0342 A69-12278

Optimization of control functions and parameters of dynamic systems with variable structure and discontinuous phase coordinates
04 p0582 A69-14795

Sensitivity models for adaptive and self adaptive systems design
04 p0582 A69-14797

Electronic counterrotating antennas, developing turning model of antenna group of telecommunications satellite
04 p0578 A69-15065

Continuous dynamic systems digital simulation, noting run-time program determined by numerical integration structure
04 p0565 A69-15339

Cross slip model for work hardening of nickel aluminum crystals, discussing temperature dependence
05 p0779 A69-15760

Nonlinear system identification by learning model, assuming discrete on-line operation and Hammerstein form
05 p0737 A69-15805

Adaptation in nonstationary environment formulated for tapped delay line filters with adjustable time varying gains
05 p0737 A69-15806

Collection of papers on computerized simulation covering dynamic modeling of ideas and systems
05 p0724 A69-16467

Space radiator dynamic model for predicting outlet temperature transient response to environmental variations
[AIAA PAPER 69-29]
06 p1039 A69-18205

Fluid and thermodynamic modeling for ground test simulation of nuclear rocket vehicle liquid hydrogen propellant behavior
[SAE PAPER 690201]
07 p1178 A69-18306

Regression rate model for pressure sensitive hybrid combustion based on classical turbulent flame theory
[WSCI PAPER 68-22]
07 p1240 A69-18362

Radio wave propagation over smooth cylindrical surface with specified boundary impedance, discussing diffraction loss and effect of surmounted obstacle
08 p1273 A69-20024

Adaptation process of management systems from point of view of control system philosophy
[AIAA PAPER 68-807]
08 p1422 A69-20197

Weather forecasting using statistical technique and Subsynchronous Advection Model of Weather Bureau, discussing mathematical background for various early morning predictions
08 p1345 A69-20298

Photon whirls and formation of protogalaxies, discussing density inhomogeneities in hot model of universe in terms of pregalactic structure dynamics
09 p1587 A69-21355

Kinetic theory model of plasma sheath transition applied to sheath structure in unignited mode of thermionic converter
09 p1440 A69-21828

Mathematical, physical and physiological modeling for analysis of functional changes during varying gravity conditions
09 p1444 A69-22541

Optimal stochastic control, discussing dynamic mathematical models described by differential equations
09 p1475 A69-22567

Cosserat continuum and elasticity models of dynamics of composite materials, analyzing dispersive longitudinal waves
10 p1798 A69-23148

FM/AM telemetry circuits with three axis piezoelectric accelerometer for measurements during impact tests of soft landing models
10 p1654 A69-23279

Antiplane strain model for describing cracks and dislocation arrays within circular cylindrical inhomogeneity surrounded by elastic material
10 p1803 A69-24031

Polymer fatigue model from low cycle analysis of dynamic and thermal properties in structural plastics
10 p1717 A69-24217

Viscosity and electrical conductivity effects on axisymmetric instabilities of current carrying annular cylinder of mercury
11 p1923 A69-24292

Computational method for quasi-optimal control with parameter sensitivity function, noting application to dynamical system model

11 p1859 A69-25165

Mechanical model for oscillatory motion of solid body in Newtonian central force field

11 p1919 A69-25179

Model evolution of flow in fluid layer suddenly heated from below at Rayleigh number convection sufficient for turbulence

11 p1874 A69-25351

Graphite and B filament-epoxy resin composites application to aeroelastic scaled dynamic models, analyzing weight savings, fabrication and component stiffness

11 p1990 A69-25508

Dynamic modeling for spin stability of satellites with flexible parts, noting torques induced by attitude control

11 p1994 A69-25533

Analytical synthesis of dynamic plant model to insure desired output in response to cyclic action

11 p1861 A69-25714

Water vapor laser, discussing water vapor molecular structure, population inversion mechanism, perturbation model, etc

12 p2106 A69-26325

Ablation wedge model design for testing in wave superheater under controlled pressure gradients and constant temperature

12 p2059 A69-26816

Flow models for externally pressurized gas bearings, discussing pressure distributions, load capacity and flow rate

[ASME PAPER 68-LUBS-2]

13 p2267 A69-27285

Venusian upper atmosphere dissociation and ionization, considering photochemical and dynamic processes and molecular, eddy and ambipolar diffusions

13 p2344 A69-27643

Periodic solution to equations describing nonlinear autonomous time lag system close to Liapunov systems

14 p2482 A69-28799

Optical refraction effects from refractive index gradients in stressed models as limitation on moire interferometry usefulness in Boussinesq problem and expanding pulse studies

14 p2531 A69-28883

Structural stress under acceleration loading simulated by two dimensional photoelastic model noting improvement of fringe patterns quality

14 p2532 A69-28885

Searchless gradient self adaptive system for adjusting servosystem parameters to reference model characteristics, using auxiliary operator method

14 p2426 A69-29146

Engineering models for wearout reliability prediction in dynamical systems subject to random loading, demonstrating practical and statistical methods

15 p2705 A69-30366

Aluminum models of single cell simply supported folded plates to study instability phenomena possibly occurring in actual structure

15 p2709 A69-30679

Nova outburst dynamics investigation by time dependent hydrodynamics computer program including energy transport by radiation and convection

15 p2692 A69-30769

Thick gas model for monochromatic one dimensional radiant flux near diffusely emitting and reflecting boundaries, discussing gray gas and exponential kernel approximations

16 p2769 A69-31871

Feed-system-coupled combustion instability linearized mathematical models for liquid fuel rocket engines, discussing nonrigid injector and method for instability elimination

16 p2836 A69-32001

Collisional equilibrium and nonuniform formation models for spatial gradient development of early afterglow of He plasma molecular excited state densities

16 p2782 A69-32465

Gas turbine engine compressor system dynamic representation by one dimensional mathematical model

16 p2842 A69-32697

Wave motion nonsteadiness influence on detonation front thickness using quasi-steady kinetic model of induction process, discussing agreement with experimental observations

17 p2952 A69-33403

Dynamically scaled model rotor tested in wind tunnel to evaluate blade aeroelastic limits constructed with realistic mass and stiffness distributions

17 p3059 A69-33506

[AHS PAPER 341]

Helicopter engine dynamic analysis, discussing modeling techniques, rotor responses and turbine speed control simulations and transition from mathematical models to hardware components

17 p2946 A69-33531

Monte Carlo inversion of seismic body waves for transposing uncertainties of observations to velocity models

17 p2962 A69-33654

Ejection seat cushion dynamic characteristics influence on incidence of spinal injury during ejection, considering MIL specification dynamic model of human body

17 p2917 A69-34033

Dynamic equations solution for interacting rigid or elastic body system models using Cosserat bodies elastic theory, considering engineering applications

17 p3067 A69-34143

Dynamic model of bodies with microstructure and nondissipative energy motion, discussing action steadiness, invariance conditions and Galilean relativity

17 p3067 A69-34149

Physical model for IGY radio aurora data correlated with Brice magnetospheric convection model

18 p3125 A69-34231

System state phase modeling as method for evaluating safety and reliability by analysis of system states in mission phases through logic diagram

18 p3142 A69-34480

Physiological processes computer simulation with aorta modeling as example, noting difficulties and major problems

18 p3098 A69-34669

Photon whirls and formation of protogalaxies, discussing density inhomogeneities in hot model of universe in terms of pregalactic structure dynamics

18 p3197 A69-34745

Jet injection into free circular cross section cross wind using curvilinear dynamic model, assuming negligible Archimedean forces effect

18 p3124 A69-35149

Human ear frequency discrimination, discussing nonlinear functional modeling systems

18 p3097 A69-35440

Flash X ray unit with special film transport devices to obtain sequenced dynamic radiographs of ablating models during reentry simulation tests

19 p3291 A69-35720

Lumped parameter simulation model, based on vector mechanics for flexible spinning bodies, to study spin stabilized spacecraft or turbine rotors

19 p3280 A69-35990

Plane, cylindrical and spherical point explosions in combustible gas mixtures for different gas motion models, formulating scaling law for detonation wave model

19 p3449 A69-36353

Two body mechanical system operating within dynamics laws simulating backward and forward bending motions of falling cat

19 p3259 A69-36832

Surface stresses in rotating asymmetric profiled disks and axial deflection effects computed theoretically and compared to measurements on photoelastic models

19 p3447 A69-36862

Stress corrosion cracking model for 7075 Al, correlating macroscopic yield stress and corrosion time to failure

19 p3351 A69-36897

Saturn ring dynamical structure theory supported by observations of knots or condensations

20 p3600 A69-37482

Linear dynamic modeling of barotropic fluid in rigid circular tube, presenting axial velocity profile by confluent hypergeometric function with complex arguments

[ASME PAPER 69-FLCS-18]

20 p3516 A69-37982

Analytical relations in phenomenological model theories for turbulent flow near wall

21 p3695 A69-39010

Magnetic hysteresis dynamic model suitable for digital computer simulation of near-earth satellite attitude motions damping compared with experimentally generated loops

[AIAA PAPER 69-833]

21 p3821 A69-39364

Herzenberg geomagnetic dynamo model extensions including rigid rotors calculus, laminated rotors, induction problem and fluid rotors in rigid conductor

22 p3989 A69-40193

Model for statistically isotropic homogeneous turbulence in incompressible fluid, representing turbulence as superposition of individual vortex sheets

22 p3930 A69-40525

Recirculation concept for air cushion vehicle air curtain evaluated by two dimensional and circular models, discussing optimum cushion area/jet exit area ratio

22 p3866 A69-40816

Astrophysical ions acceleration model based on magnetic field annihilation theory

22 p3987 A69-41002

Nonlinear model including rocket rotary and forward motion inside smoothbore launcher utilizing dynamic friction coefficient

22 p4037 A69-41038

F region dynamic model, including variations in temperature, electron and molecular ion concentrations, etc

23 p4156 A69-41843

Potential energy modeling method for optimal design of structural systems with diverse performance criteria, giving truss design example

23 p4228 A69-41923

Theoretical models for collisionless plasma shock waves in terms of nonlinear, magnetosonic, constant profile waves, turbulent- and electrostatic-shock structures, etc

24 p3355 A69-42694

Continuous potential fields modeling based on electrodynamical analogy extended to flows involving stream separation

24 p4300 A69-43089

Linear viscoelastic model parameters optimization for designing automobile lap seat belts, assuming abrupt impact stop

[ASME PAPER 69-APMW-25]

24 p4275 A69-43094

Dynamic model of ablation pitching moment derivative and time lag effect on spinning reentry vehicle applied to Black Knight flight results

24 p4245 A69-43249

Rocket exhaust plume models for signal attenuation predictions, considering inhomogeneous plasma medium with varying electron density and collision frequency

24 p4408 A69-43253

Dynamic models for viscous fluid transmission lines using distributed parameter for accuracy and rational approximate form to avoid computational difficulty

24 p4301 A69-43289

Actuator disk model for study of azimuthally nonuniform MPD arc plasma dynamics

[AIAA PAPER 68-714]

24 p4359 A69-43570

DYNAMIC MODULUS OF ELASTICITY

Bounds for real and imaginary parts of dynamic moduli of composite viscoelastic systems

08 p1417 A69-20824

Dynamic modulus of elasticity measured for nonporous refractory compounds obtained by diffusion saturation

09 p1529 A69-21871

Apparent dynamic modulus and damping under multilevel loading during fatigue cycling to estimate stainless steel specimens cumulation fatigue lives

20 p3620 A69-36997

DYNAMIC PRESSURE

Plane strain plastic stress waves radial propagation from center of hollow cylinder subject to dynamic pressure load

02 p0344 A69-12292

Dynamic pressure pulse over band on solid elastic cylinder surface, analyzing time stress distribution throughout elastic cylinder

04 p0670 A69-14408

Flight tests of deployment of 20 ft diam ribbon parachute at high dynamic pressures and supersonic speeds

11 p1823 A69-25383

Compression forces during interaction of colliding shock waves in compressible fluid medium, discussing linear and nonlinear problems

13 p2246 A69-27523

Characteristics method for stress waves from hypervelocity impact of circular cylinder on half space, discussing numerical diffusion effect on pressure and flow fields

[AIAA PAPER 69-355]

13 p2365 A69-28287

Spherical stress wave reflected from plane surface, discussing tensile stress in target

[AIAA PAPER 69-363]

13 p2366 A69-28295

Pulsating mechanisms in alternative gas and liquid blocks two phase flow, using stochastic process specified by dynamic pressure time dependent fluctuations

24 p4305 A69-43633

DYNAMIC PROGRAMMING

Dynamic programming methods to avoid dimensionality problem arising in solution of boundary value problems by digital computer

01 p0103 A69-10006

Low thrust spacecraft motion continuous correction by dynamic programming, assuming continuous information on system state including fuel consumption

01 p0113 A69-10572

Dynamic programming to demonstrate sufficient conditions of optimality in maximum principle when regular control synthesis is realized

02 p0225 A69-11975

Dynamic programming application to synthesis of unequally spaced symmetrical antenna arrays

02 p0219 A69-12338

Optimum structural design based on linear, non-linear and dynamic programming
[SAE PAPER 680752]

03 p0525 A69-13437

Dynamic optimization problem with several decision and state variables, examining methods of solution

03 p0456 A69-13737

Dynamic programming application to function generation, determining breakpoints for best linear approximation of one dimensional function

03 p0401 A69-13765

Optimal control theory applied to systems described by partial differential/integral equations

04 p0581 A69-14571

Book on dynamic programming basic theory and standard computational algorithm and applications to optimization in diverse fields

04 p0563 A69-14652

Optimal stochastic control of small dynamic systems described by random differential equations, noting selective bibliography on several subjects

04 p0582 A69-14697

Finite state finite-action-space Markovian decision process, discussing optimal policies set in discrete dynamic programming

04 p0624 A69-14951

Dynamic programming and indeterminate Lagrange multipliers to formulate optimal control for discrete systems

05 p0737 A69-15886

Existence and uniqueness theorem for functional equation of optimal control problems, noting stability of solution

06 p0949 A69-17889

Dynamic programming for nonlinear suboptimal control system with minimum Q factor, developing nonlinear functional with controller motion restraint

08 p1297 A69-20416

Differential dynamic programming algorithms of second and first order for optimal control, considering nonlinear unconstrained and constrained problems

09 p1531 A69-21415

Dynamic programming computational approach to optimization with state variable discontinuities, treating problems as multistage optimization with continuous subarc stages

09 p1474 A69-22440

Statistical theory and dynamic programming to synthesize optimal pulsed control systems having restrictions on control device storage capacity

09 p1476 A69-22673

Dynamic programming method to achieve optimal control of discrete systems with lagging control variables, considering structural properties

09 p1476 A69-22674

Pseudodynamic programming for optimizing design of correlator supersynthesis antenna arrays used for radio source tracking

10 p1663 A69-23420

Dynamic programming to demonstrate sufficient conditions of optimality in maximum principle when regular control synthesis is realized

10 p1666 A69-23884

Dynamic programming determining optimal feedback control policies for optimal trajectories based on invariant imbedding

11 p1910 A69-25410

Dynamic programming approach to numerical solution of elliptic boundary value problems, using Laplace equations

11 p1910 A69-25411

Nonlinear bang-bang optimal control problems solution based on differential dynamic programming, noting use of Pontryagin adjoint variables

11 p1860 A69-25444

Optimal communication by signal feedback link between transmitter and receiver based on optimum control and dynamic programming

12 p2046 A69-26060

Discrete linear optimal control system with quadratic performance index synthesized by dynamic programming method, obtaining matrix equations

12 p2050 A69-26091

Dynamic programming method for upper bound on collapse load of rotationally symmetric thin cylindrical shell under ring loading

12 p2179 A69-26214

Dynamic programming method applied to Cauchy problem of large deflections in compressed rods, using recurrent functional equations

14 p2533 A69-28988

Optimal control problems solved by dynamic programming algorithm based on successive approximations of elementary control operation in space of states

14 p2426 A69-29472

Cauchy problem for Bellman dynamic programming equation in automatic control time minimization

14 p2426 A69-29478

Low thrust spacecraft action continuous correction by dynamic programming, assuming continuous information on system state including fuel consumption

15 p2651 A69-30742

Optimization of control system described by linear parabolic integrodifferential equation, using dynamic programming approach

15 p2645 A69-31024

Electronic hardware optimum quality assurance selected by dynamic programming in terms of failure mechanism detection efficiency per source allocation

15 p2722 A69-31127

Stochastic differential game theory, discussing nonlinear partial differential equations for solution, dynamic programming validity conditions, finite difference scheme, etc

17 p2994 A69-32844

Book on elements of optimal control covering methods for deterministic problems including calculus of variations, Pontryagin principle, dynamic programming, feedback control, etc

18 p3109 A69-34532

Quasi-linearization to overcome dynamic programming dimensionality difficulties, reducing computer memory requirement and computation time

21 p3754 A69-38751

Point mapping in optimal control, describing maximum principle, dynamic programming and substitution of variables

21 p3688 A69-39860

Algorithm for optimal solution to secondary optimization problem in nonserial dynamic programming

22 p3976 A69-41037

Adaptive control systems analysis and application, noting off-line and on-line optimization, dynamic programming, linear systems, etc

24 p4289 A69-42946

DYNAMIC RESPONSE

NT TRANSIENT RESPONSE

Circular, cylindrical thin walled shell dynamic response to moving shock solved by Flugge equations in series form

01 p0164 A69-10057

Combustion response of hydrazine-nitrogen tetroxide hypergolic rocket propellants to transverse gas flows, noting coupled and uncoupled oscillations

01 p0175 A69-10112

Structural vibration problems of SA 330 helicopter from test flight data, discussing natural frequency displacement of blades and dynamic response improvement of structure

01 p0009 A69-10158

Uniform transmission line response to independent distributed sources using extraction integrals, analyzing traveling wave transistor

01 p0043 A69-10562

Multiple configuration analysis of structures systematically predicting static and dynamic response of structures of single configuration class

01 p0169 A69-10639

Acoustic probe for measuring pressure fluctuations on hypersonic reentry vehicle, discussing flow characteristics and heat shield ablation effects on frequency response

01 p0008 A69-11278

Human body dynamic response to vibration combined with linear acceleration, noting changes in body mechanical impedance and resonance

01 p0022 A69-11335

Dynamic behavior of elastoplastic beam column model with one degree of freedom subjected to axial compressive force

02 p0337 A69-11717

Flight vehicle dynamics, discussing classical mechanics, fluid dynamics, structural dynamics and thermodynamics

02 p0193 A69-11985

Book on stability criteria for linear mechanical engineering systems covering response characteristics, encirclement theorem, Routh and Hurwitz criterions, root loci, D partition, etc

02 p0281 A69-12276

Finite length cylindrical shell dynamic response to uniform radial impulse, noting simple harmonic motion and flexural mode excitation instability
[AIAA PAPER 68-144]

02 p0347 A69-12517

Gyroscopically induced vibrational response of rectangular plates and membranes, determining spin and precession effects on natural frequencies

02 p0347 A69-12519

Pyroelectric crystals transparent at laser output wavelength used for recording transmitted radiation, noting response of triglycine sulfate crystal

03 p0438 A69-13050

Universal solution for static and dynamic response of structural components by method of initial parameters

03 p0527 A69-13746

Thin film lubricant effect on machine dynamic performance, proposing inclusion with machine structure for reducing vibration effect

03 p0435 A69-13948

Solid viscosities effects on dynamic load factors of ring and hollow sphere subject to uniformly distributed impulsive loads along inner and outer edges

03 p0530 A69-14089

Twisted yarns composed of continuous viscoelastic filaments dynamic response under periodic strain effect on dynamic modulus

04 p0619 A69-14686

Beam vibration problems with mixed response-excitation input information solved by recasting equations of motion
[AIAA PAPER 68-319]

04 p0676 A69-14711

Dynamics of single loop nonlinear sampled data systems with integrator, deriving equations of periodic motions and stability conditions by means of point transformations

04 p0583 A69-15135

Steady state response of inertialess discrete multivariable extremal system with noise, noting stepwise search systems

04 p0583 A69-15139

Dynamic behavior of series and parallel flow thrust-balance systems for compressible and incompressible flow, using analog computer simulation

04 p0647 A69-15521

Dynamic shear stresses at interface of embedded thin elastic filament and elastic matrix after subjecting filament to concentrated longitudinal line load

05 p0831 A69-15577

Dynamic response of solids induced by charged particle interaction noting laser interferometric measurement of surface stresses

05 p0771 A69-15817

Liquid flow systems dynamic response to periodic disturbances of system structural supports

05 p0747 A69-16073

Impulse loaded elastic-plastic beam response approximate solutions based on uniqueness proof
[ASME PAPER 68-WA/APM-23]

05 p0840 A69-16188

Dynamics of laser response in IR detection by means of optical mixing in He-Ne laser, noting bandwidth

05 p0776 A69-16331

Resonant amplifier response having stages identical to radio pulse with exponential envelope

05 p0720 A69-16444

Response of single and multidegree of freedom systems to nonstationary random excitation, analyzing spectral density function of pressure field close to jet engine

05 p0844 A69-16763

Transfer function coefficients from frequency response data determined to obtain information about dynamic system characteristics

05 p0844 A69-16764

Dynamic response of semiinfinite circular cylindrical shells to traveling load

06 p1021 A69-17148

Linear closed loop control system poorly damped response to deterministic inputs improved by stability constraint for minimization of mean squared error

06 p0905 A69-17950

Longitudinal structural vibration and lateral bending response mass and spring coupling in Saturn AS-502 during boost with longitudinal excitation by pogo effect
[AIAA PAPER 69-58]

06 p1019 A69-18204

Two signal four quadrant multiplier design having subnanosecond response

07 p1103 A69-18879

Direct coupled monolithic IF amplifier with active gain control, analyzing large signal response, stability, available gain and noise behavior
07 p1104 A69-18885

MHD flow in channels with abruptly widening sections and finned walls under transverse magnetic field, discussing effects on drag
07 p1192 A69-19016

Axisymmetric turbulent conducting fluid jet propagation in longitudinal magnetic field without induction
07 p1192 A69-19019

Dynamic internal thermal shock in spherical shells of arbitrary thickness, considering uncoupled dynamic thermoelasticity problems with spherically symmetrical temperature fields
07 p1236 A69-19471

Flexible rotor blade dynamic response to radially moving force, emphasizing helicopter rotor vibration characteristics associated with tip-vortex impingement [AIAA PAPER 69-203]
07 p1054 A69-19546

Stress-strain-time relations in magnesium alloy and aluminum plate impact load tests, discussing stress measurement, Hugoniot equation of state, yield point and dynamic response
08 p1330 A69-20102

Control technique to make aircraft insensitive to parameter variations and to achieve desired response to control
08 p1255 A69-20719

Response time of semiconductor diode from dependence of equivalent capacitance on direct displacement current
08 p1287 A69-20889

Dynamic response of anisotropic circular cylinders to uniformly distributed pressure varying periodically with time analyzed using Laplace transformation
09 p1611 A69-21440

Optimal linear quick response problem solving by fast convergence iterative procedure
09 p1473 A69-21791

Bond shear effects on dynamic behavior of two layered cylindrical shell, identifying bond stiffness parameters [AIAA PAPER 68-354]
09 p1616 A69-21941

Generalized orthogonality principles and expansion schemes for forced response of partial differential equations, noting applicability to rodlike structures
09 p1533 A69-21975

Rigid top mass effect on longitudinal response of model vehicle propellant tank, determining natural frequencies and forced asymmetric response
09 p1616 A69-21979

Fast response microwave interferometers classification and construction principles
09 p1496 A69-22028

High sensitivity gyroscopic HF angular acceleration sensor using special differentiator, obtaining motion equations and dynamic response
09 p1498 A69-22109

Fiber glass reinforced plastic backing phase of composite armor, noting test method for evaluation of performance
09 p1507 A69-22319

Lift engine model compressor response to inlet pressure distortion to determine nature and extent of critical area of spooling for axial flow compressors [ASME PAPER 69-GT-29]
09 p1571 A69-22493

Time varying linear system with input-output relation described by differential equation calculated for impulse response using Taylor series
09 p1459 A69-22580

Self biasing influence on tunnel diode amplifiers dynamic range, determining limiting conditions for amplitude characteristics
09 p1469 A69-22633

Control system controllability under discontinuous control constraints, presenting optimal response rate linear system synthesis with continuous restriction on control function
09 p1475 A69-22670

Aircraft modal control systems synthesis to improve response characteristics by altering pairs of complex conjugate and real eigenvalues simultaneously
09 p1435 A69-22779

Pseudoelectrical bandpass filter response curves and electrical characteristics based on ripple Chebyshev responses
09 p1470 A69-22794

EEG, heart beat, respiration rates, body temperature, motor activity, physical and mental efficiency of man during anechoic chamber confinement
10 p1646 A69-23510

Disturbed index of refraction scattering cross sections and aircraft acceleration increments for clear air turbulence, deriving correlation for measurements
10 p1656 A69-23651

Axial torque effect on critical speeds of continuous rotor with motion described by partial differential equations [ASME PAPER 69-VIBR-52]
10 p1804 A69-24152

Damped steady state response of elastic foundation beam subjected to cyclic moving loads to determine load movement frequencies for natural frequency excitation [ASME PAPER 69-VIBR-13]
10 p1806 A69-24166

Response and stability of self sustained two degrees of freedom system with nonlinear damping, noting harmonic oscillations [ASME PAPER 69-VIBR-24]
10 p1806 A69-24171

Structural damping coefficient of metals determined from complex Young modulus with transmissibility, using mass loaded cantilever beam experiment [ASME PAPER 69-VIBR-36]
10 p1807 A69-24175

Structure dynamic response for motion through homogeneous frozen random load field with spacewise variations, applying analysis method to beam [ASME PAPER 69-VIBR-38]
10 p1807 A69-24176

Multiparameter optimum damping for harmonically excited linear stable strictly dissipative n degrees of freedom system, locating multivariable saddle points [ASME PAPER 69-VIBR-42]
10 p1807 A69-24180

Nonstationary vibrations of mechanical systems subjected to harmonic or external limited energy source excitations
11 p1975 A69-24739

Topologies introduced on state space for differential equations to obtain dynamical systems
11 p1909 A69-25409

Structural optimization of designs with requirements including restrictions on structure dynamic response and characteristics
11 p1989 A69-25495

Aircraft dynamic response to three dimensional turbulence, establishing unique correspondence between spatial symmetry properties of ambient fields of turbulence and aircraft
11 p1823 A69-25503

Gust load predictions for aircraft design by treating aircraft load history as linear response to stationary Gaussian process excitation
11 p1823 A69-25504

Cylindrical shells spectral response to random acoustic pressure excitation, noting natural modes and inner air column effects
11 p1990 A69-25506

Dynamic plastic response of finite bar subject to axial impact load noting reflected waves, stress-strain histories and residual strain
11 p1991 A69-25512

Dynamic analysis of axisymmetric ring stiffened shells with attached asymmetric elastic structures, noting vibration modes
11 p1993 A69-25525

Polyurethane foam high velocity deformation properties, discussing results of dynamic uniaxial stress tension and compression tests
11 p1907 A69-25648

Space vehicle dynamic structure response, discussing vibration problems, test methods and responses to periodic, stochastic and forced excitations
12 p2176 A69-25857

Linear automatic control system floating response to harmonic effects achieved by coinciding open loop system transfer function poles with disturbance pattern poles
12 p2045 A69-25967

Dynamic response of distended carbon materials to shock loading defined by measuring equation of state, unloading behavior and spallation strength
12 p2119 A69-26847

Dynamic response of imperfect circular cylinder to constant velocity load, noting applicability of Hoff nonlinear equation for dynamic buckling of columns
13 p2359 A69-27260

Asymptotic analysis for stability and vibration response of spherical squeeze-film hybrid bearing, obtaining perturbation solutions [ASME PAPER 68-LUBS-37]
13 p2267 A69-27281

Thermocouples dynamic response attached to thin skinned model under constant heating rate, considering error reduction in temperature measurement
13 p2375 A69-27785

Multiband frequency conversion in filters or correcting circuits with four terminal networks, noting prototypes
13 p2235 A69-28519

Materials surface thermal stress analysis by strain gauges, considering behavior during rapid temperature changes
13 p2264 A69-28599

Cavity mounted pressure transducers response in high speed pressure measurements
14 p2445 A69-28874

Input signal piecewise linear approximation for investigating response of dynamic automatic control systems to nonstandard input signal
14 p2426 A69-29143

Dual pendulum with tilt sensitivity at wide passband frequencies and damping due to horizontal oscillations
14 p2450 A69-29570

Dynamic instrumental errors of quasi-steady state mechanical meters approximated by graph analytical method
14 p2451 A69-29747

Microwave filter tailored for frequency response in L through S band regions for high range resolution radar receiver
14 p2423 A69-29759

SST fuselage response to reverberant and turbulent boundary layer noise calculated for computing equivalent reverberant acoustic fields
15 p2549 A69-30302

Real time shock response analysis advantages over sequential analysis, describing equipment
15 p2618 A69-30359

Time dependence of maximum structural response of single degree of freedom mechanical system under random loading
15 p2705 A69-30365

Dynamic vibration effects on guidance and control systems performance determined from spectral densities, cross spectral densities and vibratory environment amplitude distributions
15 p2608 A69-30367

Clamped circular plates impulse load tests with sheet explosives, showing finite difference program for computing large deflection dynamic response
15 p2709 A69-30675

Molecular beam behavior in constant electric and magnetic fields, applying laser frequency dependence on magnetic field orientation to resonator
15 p2655 A69-30943

Power spectral density response of uniform beams to random pressures, evaluating joint acceptance of systems with pressure field [ASA PAPER SVT2]
15 p2713 A69-31143

Lunar dynamic response to discontinuities in interplanetary magnetic field to determine electrical conductivity and internal temperature
15 p2700 A69-31442

Mathematical optimization to achieve near equal-ripple response in passband for coaxial low pass filters having unequal line lengths
16 p2757 A69-31583

X band avalanche diode oscillator operated as super-regenerative amplifier, noting frequency response characteristics ascribed to diode susceptance modulation
16 p2757 A69-31585

Liquid free surface response to mass force variation during space flight near zero-g, discussing effects on ignition
16 p2866 A69-31735

Stress waves analysis in laminates design, assuming one dimensional linear elastic response to plane stress pulse on flat laminated plate surface
16 p2872 A69-31923

Inertia, compressibility and viscous friction effects on dynamic response of long fluid line, constructing models
16 p2771 A69-32066

Blast response of model structures fabricated from material differing from prototype structures, testing in dynamic, impulsive and quasi-static loading realms
16 p2874 A69-32164

System kinetics synthesis for nonlinear multiple lumped parameter system having responses in boundary region of phase-time space
16 p2812 A69-32247

Resonant amplifier response having stages identical to radio pulse with exponential envelope
16 p2753 A69-32476

Single freedom vibratory system response to imposed displacement harmonic excitation, analyzing response in terms of constrained system modes
17 p3067 A69-34139

Equations in series form to describe composite beams behavior under nonuniform torsion
18 p3211 A69-34343

Linear analysis of damped flexibly mounted rolling element bearings influence on dynamic rotor unbalance response, including optimum support characteristics
[ASME PAPER 69-LUBS-21]
18 p3212 A69-34382

Cylindrical and conical panels dynamic responses to time varying load distributions, using trigonometric series coupled with finite difference methods
[ASME PAPER 69-APM-22]
18 p3214 A69-34396

Ionospheric electric current systems dynamics in polar latitude in relation to 1966 geomagnetic storms
18 p3130 A69-35188

Light rigid civil aircraft response to continuous atmospheric turbulence estimated using two rigid body degrees of freedom method for vertical and lateral gusts
[AIAA PAPER 69-766]
19 p3433 A69-35657

Thermal effects on viscoelastic structure response to applied loads, using equations for thermomechanics, linear and nonlinear thermoviscoelasticity and nonisothermal creep theorem
19 p3440 A69-36657

Electrohydraulic servomechanism harmonic response showing nonlinear behavior, including jump resonance, analyzed by mathematical model and analog simulation
20 p3464 A69-36999

Bloch wall motion along hard direction of Permalloy films due to fast rising hard-axis pulses
20 p3584 A69-38191

Optimal control of dynamic system motion described by linear differential equation, selecting vector function ensuring predetermined trajectory
21 p3685 A69-38452

Control function ensuring minimal response time of controlled plant with motion described by integral equations system, using method of distributed moments
21 p3685 A69-38847

Spring mass nonlinear systems under constant force excitation, studying step function responses of systems with various restoring force characteristics
21 p3836 A69-38985

Damped mass spring system response to sonic booms, considering effects of structural damping, total/positive phase duration ratio and N wave rise time
21 p3647 A69-38987

Acoustoelastic interaction effects of sonic bangs on natural frequencies response of large windows backed by closed cavity
21 p3836 A69-38988

Response of three level particles system with equidistant spectrum under resonant action of acoustic and electromagnetic pulses sequence with different frequencies
21 p3737 A69-39068

Liquid propellant rocket injectors response to HF chamber pressure oscillations using one dimensional model
21 p3786 A69-39235

Optimal control synthesis by determining conditions for absolute minimum in quick response having no regular constraints on phase coordinates
21 p3689 A69-39863

Reaction impulse during steel spheres impacts at lead surface in vacuum dependent on kinetic energy, velocity and spheres material
22 p4047 A69-41101

Burning solid propellant behavior under pressure fluctuations expressed in response function terms defining small mass flux change ratio to small pressure change
23 p4201 A69-41922

Dynamic reactions of mathematical model representing vision and hearing process adaptation
23 p4110 A69-41984

Rosman I reflector antenna for collecting data from earth orbiting satellites, discussing dynamic analysis of structural response to natural frequencies
23 p4231 A69-42133

Dynamic response of anisotropic elastic cylindrical and spherical shells determined by application of Hankel transforms, considering time dependence of loads
23 p4235 A69-42481

Elastoplastic boundary dynamic behavior in strip with crack determined by solving boundary value problem in elliptic integrals form
24 p4395 A69-42591

Asymmetric dynamic response to free and forced vibrations of thin membrane shells at given stress state due to previous loads
24 p4399 A69-42990

Thermosphere dynamic response to low altitude geomagnetic disturbances, showing time lag dependence on perturbation intensity
24 p4310 A69-43180

Dynamic pressure response of viscous compressible fluids in rigid tubes with dead ended volume termination, testing Ibrall theorem as function of Stokes number
24 p4301 A69-43287

DYNAMIC STABILITY

NT AERODYNAMIC STABILITY

NT AIRCRAFT STABILITY

NT ATTITUDE STABILITY

NT BOUNDARY LAYER STABILITY

NT COMBUSTION STABILITY

NT CONTROL STABILITY

NT DIRECTIONAL STABILITY

NT FLAME STABILITY

NT FLOW STABILITY

NT FREQUENCY STABILITY

NT GYROSCOPIC STABILITY

NT HOVERING STABILITY

NT LATERAL STABILITY

NT LONGITUDINAL STABILITY

NT LOW SPEED STABILITY

NT MAGNETOHYDRODYNAMIC STABILITY

NT MOTION STABILITY

NT ROTARY STABILITY

NT SPACECRAFT STABILITY

Necessary and sufficient stability conditions for differential equation systems with selfadjoint quasi-periodic coefficients
01 p0107 A69-11130

Expanded describing functions used in studying nonlinear control systems with multiplication points, considering systems with/without integral response
01 p0054 A69-11359

Absolute input-output stability of time varying nonlinear feedback system established by frequency domain test similar to Popov test
01 p0054 A69-11414

Asymptotic stability conditions for delayed quasi-linear nonautonomous systems periodic solutions derived by Shimanov method
02 p0280 A69-11705

Dynamic stability of structural system excited by random load, discussing effect of nonlinearities and dynamic snapping problems
02 p0339 A69-11988

Collective stability of collisionless gravitating systems based on variational principles resembling energy principle
02 p0323 A69-12275

Book on stability criteria for linear mechanical engineering systems covering response characteristics, encirclement theorem, Routh and Hurwitz criterions, root loci, D partition, etc
02 p0281 A69-12276

Space-station-centrifuge configuration dynamic stability exhibiting instabilities at lower and higher centrifuge rotational speeds
[AIAA PAPER 68-142]
02 p0334 A69-12373

Logarithmic variation criteria for stability of feedback systems with time varying gains
03 p0409 A69-13073

Synthesis of statistically optimal self adaptive system for dynamic characteristics stabilization of automatic control system main loop
03 p0410 A69-13256

Application of modern stability theory to solution of practical problems by means of comparison theorems, demonstrating effectiveness of method
03 p0467 A69-13747

Conventional TWT theory modified to include interaction between beam and two spatial harmonics, investigating TWT stability near edges of pass band
03 p0407 A69-13976

Aircraft stability during sideslip, discussing influence of fuselage/wing interference
04 p0548 A69-14824

Air density fluctuation effects on aircraft dynamic stability around center of gravity during climbing and diving maneuvers, discussing atmospheric pressure and flight path angle
04 p0548 A69-14825

Modified versions of standard definitions of finite time stability, presenting converse theorems for necessary and sufficient conditions
04 p0624 A69-15005

Stability functions for local buckling of long thin flat walled structures loaded for longitudinal compression and shear
05 p0833 A69-15709

Stability theorems for discrete linear circulatory systems with N degrees of freedom for static and dynamic loss of stability in presence of velocity dependent forces
05 p0836 A69-15875

Discrete time positive real functions defined for analyzing system stability with memoryless feedback
05 p0739 A69-16349

Roll dynamics of spinning axisymmetric satellite in elliptical orbit, discussing eccentricity and gravity gradient torque effect
05 p0830 A69-16397

Articles on automatic control systems stability, discussing relation between method of Lure and Popov criteria
05 p0740 A69-16667

Pulsed control systems stability with frequency pulse modulation analyzed by Liapunov direct method
05 p0740 A69-16670

Dynamic instability of solid bodies, using modal vibration method to establish criteria on basis of equivalent energy conditions
05 p0844 A69-16742

Stability and weak oscillations of systems with distributed parameters, using method based on representation of characteristic equation in power series
06 p0956 A69-16822

Synthesis of linear controlled systems with variable parameters, reducing parameter determination problem to Chebyshev approximation of relations between linear components
06 p0899 A69-16829

Dynamic stability tests of tilt winged V/STOL aircraft model in ultralow speed range, discussing apparatus for stability derivatives
06 p0866 A69-17091

Axisymmetric form of stability loss of cylindrical shell under effect of axial load suddenly applied along generatrix, considering inertia forces and obtaining differential equations
06 p0121 A69-17181

Stability of tangential velocity discontinuity between two media with different densities situated in acoustic field
06 p0910 A69-17344

Geometry changes influence on rigid plastic circular plate behavior under two independent distributed pressures
06 p1023 A69-17508

Dynamic behavior of three layer plates in supersonic gas flow
06 p1024 A69-17552

Linear state variable feedback to obtain asymptotic stabilization of linear dynamic systems
06 p0905 A69-17947

Free flight static, dynamic stability and drag data for 10 degree semiangle cone obtained at 8-16 Mach numbers
[AIAA PAPER 69-133]
06 p0862 A69-18050

Lifting reentry dynamic stability of flare stabilizers and flap controls
[AIAA PAPER 69-182]
06 p1017 A69-18053

Dynamic stability loss on ablating vehicles ascribed to boundary layer transition effect from turbulent aft body heating
[AIAA PAPER 69-106]
06 p1037 A69-18087

Spherical caps axisymmetric static and dynamic buckling under load, using axisymmetric nonlinear elastic shell theory approximation and finite difference equations
[AIAA PAPER 69-89]
06 p1028 A69-18133

Transonic dynamic stability of free flight half angle cones in wind tunnel for high drag planetary entry vehicles, discussing Mars entry trajectories
[AIAA PAPER 69-105]
06 p1019 A69-18209

Maximum index of exponential growth of solution of linear Hamiltonian equation with periodic operator coefficient encountered in dynamic stability of elastic systems
07 p1231 A69-18501

Dynamic stability of systems with distributed parameters subjected to parametric loading, considering parametrically excited systems with infinite degrees of freedom
07 p1231 A69-18502

Transient stability of AC generator analyzed by Liapunov direct method, considering effects of flux decay, speed governor and voltage regulator
07 p1058 A69-18644

Dynamical stability in premain sequence stars, discussing adiabatic models for pure hydrogen composition and collapse initiation by low opacity
07 p1220 A69-19388

Longitudinal stability of unsteady motion of flight vehicle along ballistic trajectory, using linear differential equations
07 p1230 A69-19701

Nonautonomous linear systems stability, with coefficient varying with bounded time function and bounded derivative
08 p1296 A69-19922

Line shape for dynamic Stark effect during optical resonance field irradiation calculated as function of relaxation constants and beam intensity
08 p1325 A69-20282

Dynamics and instability of multilayered systems models in field of gravity, noting isostatic adjustment of layered globe
08 p1309 A69-20578

Dynamic stability of thin flat plates and applications in ship and aircraft deck construction, studying dynamic buckling for rectangular plate
08 p1415 A69-20665

Differential equation reduction for vibrational motion of rectangular plates subjected to variable tangential forces, discussing dynamic stability
08 p1415 A69-20666

Command inputs handling by linear optimal control theory, investigating Riccati matrix differential equation convergence
08 p1298 A69-20856

Almost periodic systems stability criteria derived from differential inequalities and Liapunov function, considering existence and uniqueness
09 p1532 A69-21612

Thermionic converters stability and safety maintainable at high Ce pressures
09 p1441 A69-21837

Stability analysis including delayed collector and structure coefficients, showing thermionic reactor instability with all negative reactivity coefficients
09 p1442 A69-21841

Stabilized gyroscope platform internal dynamics analysis, outlining optimal orientation for full compensation of cross couplings
09 p1499 A69-22240

Validity of finite difference approximations for barotropic instability of zonal currents
09 p1537 A69-22298

Stability of thin rotating disks of stars with respect to axisymmetric disturbances, noting overstabilities dependence on epicycles sizes
09 p1605 A69-22413

Digital signal tracking module operation and stability, considering use of interconnecting modules to achieve adaptive tracking
09 p1459 A69-22477

Stability and local parametric synthesis conditions of programmed optimal control established for optimal control problem within fixed interval
09 p1475 A69-22666

Stability conditions for nonlinear pulse width and pulse time modulation systems, considering pulse element properties and system continuous part frequency characteristic
09 p1476 A69-22672

Stability and dissipativity conditions for nonlinear controlled systems subjected to parametric and continuously acting disturbances
09 p1476 A69-22717

Numerical solution for three dimensional boundary layers based on stability determinations for linearized difference equations
10 p1631 A69-22902

Mathieu equation with square law damping effect on first order instability range
10 p1724 A69-22920

Probable spectrum stability criterion and reducibility derived for linear differential equation having recursion or almost periodic coefficients
10 p1720 A69-23562

Time varying linear optimal control system sensitivity obtained by comparing closed loop with open loop sensitivity to parameter variations
10 p1667 A69-24058

Axisymmetric models for stable and unstable oscillations of rapidly rotating zero temperature white dwarfs, discussing kinetic and potential energy
10 p1789 A69-24129

Hydrodynamic equations and conservation laws for nonviscous fluid in postNewtonian approximation of Brans-Dicke theory applied to gaseous mass dynamic instability
10 p1789 A69-24130

Dry friction whip role in radial rubs dynamic stability in labyrinth seals and blade tips of turbomachinery [ASME PAPER 69-VIBR-56]
10 p1804 A69-24146

Differential equation for dynamic behavior of acrobatic flight navigation instruments in steep flight, considering vertical gyroscopes, gimbal platforms and time optimal control
11 p1880 A69-24328

Stability of spherically symmetrical nonrotating mass systems moving in self consistent gravitational Einstein field, considering quasar applicability
11 p1956 A69-24394

Second order dynamic systems stability, analyzing nonlinear and self excited oscillations by using two differential equations
11 p1915 A69-24535

Gyroscopes orientation influence on dynamic drift of triaxial power gyrostabilizer on rocking platform, noting optimum orientations
11 p1881 A69-24560

Stability of barotropic perturbations superimposed on wind velocity profile of basic currents in geostrophic multilayer models
11 p1911 A69-24586

Dynamic stability of double pendulum with vibrating point of suspension, obtaining differential equations of motion by Lagrange equations application in averaging method
11 p1884 A69-24768

Differential equations describing system stability with delay in functional space
11 p1919 A69-25093

Optimum controller design for dynamic stability of ideal incompressible fluid in cavity of body constrained to horizontal rectilinear translational motions
11 p1966 A69-25330

Dynamic stability of elastic beam type structures, using electronic simulation based on finite element approach
11 p1986 A69-25344

Asymptotic stability of discrete homogeneous linear minimum-variance estimation formulas
11 p1860 A69-25449

Stability of systems with sector nonlinearities determined by converting feedback equation into positive operators equation and by introducing appropriate multiplier
11 p1860 A69-25450

Stability of linear time-varying systems via examples, comparing various techniques
11 p1861 A69-25452

Cylindrical propellant tanks dynamic stability and parametric resonance, analyzing axial preload, liquid depth, top impedance and ullage pressure by Donnell theory
11 p1989 A69-25499

Liapunov type analysis of linear structural dynamic system excited by stochastic parametric load, discussing radially loaded thin circular plates
11 p1990 A69-25507

Dynamic systems stability with periodically varying parameters analyzed by Hill type infinite determinant, exemplifying helicopter rotor aeroelastic stability in forward flight
11 p1990 A69-25510

Optimal multivariable linear control system design, based on Pontryagin principle using Laplace transform method, providing good approximation to finite interval controllers
11 p1861 A69-25663

Blood vessel model in form of cylindrical shell filled with liquid for studying cardiovascular system dynamic and static problems
12 p2018 A69-25989

Dynamic properties and reliability of linear time invariant multivariable control systems
12 p2051 A69-26093

Vector equation for correction masses for dynamic balancing of rotor supported on n points derived from bearing structure vibrations amplitude and phase
12 p2180 A69-26243

Steady modes of operation analysis for optimal single channel differential relay system with inertial controlled plant, assuming constant rate varying plant input
12 p2052 A69-26278

Helicoidal precession stability in sense of Liapunov, Poincare and Lagrange
12 p2130 A69-26286

Gasdynamic stability of detonation shock wave in case of arbitrary heat evolution kinetics using detonation model
12 p2062 A69-26672

Soviet book on strength, stability and vibrations covering stability of rods, plates and shells subjected to plastic and elastic deformations, etc
12 p2182 A69-26755

Nose bluntness effect on hypersonic unsteady aerodynamics of flared and conical bodies of revolution [AIAA PAPER 68-889]
12 p2012 A69-26794

Monograph on nonlinear servosystems covering nonlinearity with/without inertia, self oscillations, linearization by forced oscillations, stability theorems and Liapunov function choice
12 p2054 A69-26966

Instability phenomena encountered in galaxies determined based on classification of galaxies according to mass and brightness
12 p2163 A69-27019

Interacting NGC 4485 and 4490 galaxies instability, establishing early stage of evolution from morphological and spectroscopic results of photographic observations
12 p2169 A69-27056

Photographic studies of unsteady features of galaxies, discussing spectra, color, spiral arm instability and extragalactic H II regions
12 p2170 A69-27063

Asymptotic analysis for stability and vibration response of spherical squeeze-film hybrid bearing, obtaining perturbation solutions [ASME PAPER 68-LUBS-37]
13 p2267 A69-27281

Gas lubricated hybrid journal bearings with external pressure, noting load capacity and stability in steady state and dynamic analyses [ASME PAPER 68-LUBS-21]
13 p2267 A69-27284

Dynamic multistable analog integrator capable of prolonged retention of integration, giving differential equation of device
13 p2224 A69-27427

Linear oscillation modes of premain sequence star model of pure hydrogen composition with variable specific heats ratio, discussing dynamic instability of polytropes
13 p2336 A69-27449

Local stability of rotating stars in toroidal and poloidal magnetic fields, using linear stability analysis
13 p2346 A69-27707

Dynamic stability of two degrees of freedom circulatory systems with bilinear hysteresis damping
13 p2363 A69-28127

Minimal interference thin metal strap support system for dynamic stability tests of high fineness ratio wind tunnel models [AIAA PAPER 69-350]
13 p2243 A69-28284

Dynamic stability of flexural free transverse vibrations of supported thin walled elastic beam with initial velocity distribution and parametric excitation
13 p2369 A69-28353

Noise stability of nonoptimal radar detection system for noise and FM signals, deriving expressions for optimal spectral width
13 p2222 A69-28508

High gain broadband amplifiers with triple tuned coaxial resonators and gridded power tubes, discussing phase stability
14 p2418 A69-28892

Relay sampled data phase plane trajectories periodic motions increased with increase of system duty factor
14 p2425 A69-28898

Stable operation of pulsed system with signal modulated pulse frequency described by nonlinear integral equation
14 p2425 A69-28909

Root locus method for nonlinear systems analysis, determining existence, stability and parameters of periodic solutions
14 p2445 A69-28919

In-core thermionic reactor space power plants stability and control criteria, comparing linear and nonlinear models
14 p2481 A69-29189

Linear dynamic stability of spinning satellite in elliptic orbit, applying perturbation method to determine Floquet solutions
14 p2534 A69-29318

Magnetic suspension device replacing mechanical bearings of inertial guidance systems gyro rotors, evaluating device strength and stability
14 p2479 A69-29492

Slow neutrons irradiation compensated high resistivity p-InSb current instability

15 p2666 A69-30058

Noise stability of receiver network during detection of finite duration noise signal on white noise background, considering various narrow band preselectors

15 p2563 A69-30142

Expanding isotropic universe with cosmological constant, noting stability for rotational perturbations and gravitational and sound waves

15 p2690 A69-30735

Dynamic stability of elastic bodies with motion described by partial differential equation

15 p2652 A69-30860

Linear elastic columns dynamic stability under time dependent axial load, investigating almost-sure asymptotic stability

16 p2872 A69-31911

Nonlinear nonconservative systems asymptotic stability analysis, emphasizing Zubov construction procedure for Liapunov functions

16 p2873 A69-32059

Cylindrical shell aeroelastic dynamic stability subjected to supersonic flow field, considering geometric imperfections, edge constraint and prestability deformation [AIAA PAPER 68-285]

16 p2874 A69-32159

Stellar system stability for corresponding stable barotropic gaseous system, discussing Schroedinger operator role

16 p2862 A69-32374

Stability and dissipativity conditions for nonlinear controlled systems subjected to parametric and continuously acting disturbances

16 p2765 A69-32550

Cylindrical viscous jet transition points from stable to unstable modes of oscillation found same as for inviscid jet

16 p2773 A69-32570

German monograph on instability of nonrevolving rotating stars covering secular rotational perturbations, radiative zone rotation, spherical Cowling model, etc

17 p3029 A69-32997

Machine for testing vibration stability of polymer samples subject to tension or compression, noting stability of plastic during vibration lower than during static loading

17 p2972 A69-33043

Planetary zonal flows hydrodynamic instability characteristics analysis, using quasi-geostrophic numerical model to study earth atmospheric cyclone wave role

17 p2960 A69-33149

Atmospheric stability influence on vertical spectra of refractive index and air velocity deduced from beam swinging experiments and compared with radiosondes data

17 p2960 A69-33157

Elastic stability of warped rods, using small oscillations method for varying end conditions and torsional-moment vector behavior

17 p3057 A69-33196

Thermal wind instability by numerical integration of equations of motion, noting convective cells tilt

17 p2998 A69-33734

Compressed signal spectral analyzer resolving power, discussing dynamic amplitude range influence and weighting functions role

17 p2939 A69-33906

Cylindrical aluminum shell dynamic stability, analyzing steady state parametric oscillations, mode shape, frequency, amplitude and damping

17 p3065 A69-33929

Elastic beam-plate vibration natural frequency and dynamic instability in transverse static or oscillating magnetic field [ASME PAPER 69-APM-B]

18 p3215 A69-34400

Vibrations damping coefficient for asymptotic stability of inertial navigation system platform, determining stabilization errors

18 p3134 A69-34555

Viscous friction damping effect on impact vibrator stability, analyzing boundary region of multiply periodic single impact motion by point mapping

18 p3172 A69-34588

Numerical procedure for testing absolute stability and positive realness of free dynamic systems based on Routh algorithm

18 p3112 A69-34689

Dynamic balancing mechanics covering graphical representation, mass asymmetries corrections or adjustment calculations and ballasting equations [SAWE PAPER 736]

18 p3220 A69-34891

Dynamic instability regions of parametric resonance of cylindrical shells with curved generating lines under axial and radial pressure

18 p3223 A69-34979

Viscoelastic shaft stability rotating at harmonically variable angular velocity, considering internal and external damping

18 p3224 A69-35300

Dynamic stability of dual wheel gears for aircraft applications, discussing shimmy, tire characteristics, velocity effects, etc [AIAA PAPER 69-769]

19 p3245 A69-35654

Static dynamic and damage tolerant strengths of advanced materials for VTOL aircraft with emphasis on Ti, cryoformed 301 stainless steels and filamentary composites [AIAA PAPER 69-764]

19 p3433 A69-35658

Stability of periodic orbits in elliptic restricted three body problem [AAS PAPER 68-086]

20 p3595 A69-37172

Asymptotic stability of null solution of matrix differential equation, considering linearized equations of rotational motion for hinged two body gravity gradient satellite orbit

20 p3575 A69-37212

Amplification stability region in overexcited regenerative traveling wave amplifier with respect to parasitic emission buildup

20 p3506 A69-37724

Photometry methods for spacecraft brightness in dynamical states of rapid spin and tumble

21 p3671 A69-38340

General relativity effects on isotropic stars evolution, discussing dynamic stability and white dwarfs

21 p3798 A69-38540

Dynamic system absolute stability and sensitivity to parameter variations in linear part of system calculated by graphical and analytical techniques

21 p3685 A69-38729

Dynamic stability of linear systems with periodic coefficients based on iterative formulas, evaluating transition matrix

21 p3685 A69-38779

Constraint torque elimination from vector equations canonical system for attitude dynamics of satellite consisting of arbitrarily interconnected rigid bodies [AIAA PAPER 69-923]

21 p3821 A69-39354

Coupled acoustic and spiral EM waves drift instabilities in bounded plasma of solid body found to be convective

21 p3782 A69-39556

Dynamic systems stability with two degrees of freedom, determining second order time dependent integrals valid near periodic orbit

22 p4013 A69-40123

Normal radial vibrations in Newtonian and general relativistic stellar objects and dynamic instability, determining modes and natural frequencies

22 p4014 A69-40142

Dynamic stability of circular isotropic plate with central hole subjected to torsional moment uniformly distributed over both edges by equilibrium equation

22 p4043 A69-40455

Variational principle for stability of galactic models, developing perturbation potential in terms of operator similar to Hartree-Fock exchange operator

22 p4022 A69-40468

Stability boundaries of discrete circuits employing delay lines with forward and feedback links, deriving equations

22 p3918 A69-40957

Dynamic simulation for gas turbine engine components design to assure stable operation and rapid response characteristics [SAE PAPER 69-0386]

23 p4200 A69-41655

Semiempirical stability boundary for flutter of simply supported cylinders for various length-radius and radius-thickness ratios

23 p4228 A69-41914

Sufficient conditions derived for absolute stability of dynamic systems containing nonlinear functions of several state variables

23 p4145 A69-42445

Digital analysis of nonlinear control systems dynamic stability under small perturbations, using linearized differential equations [IS-ERI-71]

24 p4285 A69-42984

Optimum thickness of dynamically stable composite superconducting tapes determined for substrate thickness as function of current density

24 p4361 A69-43121

Centrifugal forces effect on stability of inviscid liquid film over rotating cylinder away from stagnation region, noting film thickness stabilization effect

24 p4305 A69-43597

Contraststreaming self gravitating gas streams stability taking into account thermal conduction and radiation effects

24 p4388 A69-43638

Stability of spherically symmetrical nonrotating mass systems moving in self consistent gravitational Einstein field, considering quasar applicability

24 p4390 A69-43784

DYNAMIC STRUCTURAL ANALYSIS

Equations of linear theory of anisotropic elastic plates including Reissner-Green bending equations

01 p0168 A69-10387

Collection of Soviet papers on problems of dynamics and strength, Number 15

01 p0086 A69-10826

Nonlinear buckling analyzed by mathematical models and computational procedures using organized matrix approach to structural analysis based upon finite element

01 p0171 A69-10964

Differential equations for dynamical problems in plates obtained by symbolic approach involving power series substitution into linear elasticity dynamical equations

01 p0172 A69-11282

Motion, field momentum and field kinetic energy equations of concentrated dislocations based on Zorski field theory of defects

02 p0336 A69-11556

Paradoxes associated with elastic-plastic limit load analysis of material satisfying Drucker stability postulates

02 p0337 A69-11562

Modal substitution method for free vibration analysis of large discrete undamped dynamic systems

02 p0338 A69-11747

Ductile crack propagation speed relation to dynamic flow properties of metals analyzed using Dugdale crack model

02 p0343 A69-12283

Dynamic mechanical behavior of metal at tip of plain strain crack, discussing fracture strength relation to triaxial plastic stability

02 p0343 A69-12284

Crystal dislocation motion in viscous media, discussing velocity stress behavior and measurements by etching and ultrasonic attenuation methods

02 p0343 A69-12285

Constitutive equations for dynamic material behavior permit consideration of large deformations in direct manner

02 p0343 A69-12286

Structure of sources of noise storm enhancements and stationary type 4 bursts, discussing head and tail components

02 p0328 A69-12753

Postbuckling behavior of elastic spherical shells from pressure and volume-displacement instrumentation and photography

03 p0524 A69-13062

Thickness twist and face shear vibrations of laminated layer, determining frequencies from stress equations of motion, constitutive equations and boundary conditions [ASME PAPER 68-WA/APM-10]

04 p0668 A69-14392

Stability against snap-through and final states of shallow arches on elastic foundations and subject to time varying loads [ASME PAPER 68-WA/APM-26]

04 p0669 A69-14394

Stresses and displacements in anisotropic elastic solids under mechanical loading, determining general solution for treatment of time dependent boundary conditions

04 p0675 A69-14595

Dynamics of structured solids - ASME Conference, New York, December 1968

04 p0675 A69-14684

Equilibrium and compatibility equations for axisymmetric stress distribution in finite length anisotropic elastic cylinder reduced to single integrodifferential equation

04 p0676 A69-14709

Optimization of control functions and parameters of dynamic systems with variable structure and discontinuous phase coordinates

04 p0582 A69-14795

Saturn ring formation by satellite spiral into Roche limit and disintegration

04 p0660 A69-15128

Symmetrical bending of laterally loaded circular micropolar plates

04 p0682 A69-15291

General kinematic yield mechanism and associated kinematically adequate multiplier formulated for structural elements characterized by plane deformation state

05 p0831 A69-15684

Equation governing transverse vibration of beams with exponentially varying properties, expressing solution in terms of Bessel functions

05 p0835 A69-15873

Mathematical model simulation of structures using building block approach

05 p0842 A69-16471

Soviet collection of papers on dynamics and strength of machines

06 p1026 A69-18013

Spacecraft control system and flexible structures interactions, discussing transient phenomena, limit-cycle oscillations and instabilities [AIAA PAPER 69-116]

06 p1019 A69-18187

Stresses and displacement around crack under various conditions using two dimensional elasticity theory, deriving complex potentials for various loading types

07 p1231 A69-18269

Fatigue life in nonstationary cyclic loading above endurance limit, describing methods of shortened fatigue tests for fatigue life

07 p1231 A69-18403

Dynamic stability of systems with distributed parameters subjected to parametric loading, considering parametrically excited systems with infinite degrees of freedom

07 p1231 A69-18502

Explicit transverse bending stiffness and mass matrices for triangular finite plate element with linear thickness variation, using matrices for natural frequencies of vibration

08 p1414 A69-20526

Reaction vs time relations in accidental impact of large commercial aircraft against rigid surface, detailing stress analysis of nuclear power plants structures

09 p1613 A69-21677

Geometry at tip of growing fatigue crack, measuring crack propagation rate and fitting data to nucleation theory

10 p1795 A69-23062

Time dependence criterion in dynamic fracture determined by spall stress relation to stress pulse duration during plate impact

10 p1803 A69-24032

Natural frequencies and associated composite loss factor for laminated plate with alternate elastic and viscoelastic layers, deriving partial differential equations [ASME PAPER 69-VIBR-68]

10 p1805 A69-24158

Structural damping coefficient of metals determined from complex Young modulus with transmissibility, using mass loaded cantilever beam experiment [ASME PAPER 69-VIBR-36]

10 p1807 A69-24175

Structure dynamic response for motion through homogeneous frozen random load field with spacewise variations, applying analysis method to beam [ASME PAPER 69-VIBR-38]

10 p1807 A69-24176

Two dimensional wavefront shape induced in finitely strained elastic body by impulsive point body force

11 p1969 A69-24338

Elastic waves propagation in inhomogeneous composite media, considering coefficient of structural stress concentration

11 p1972 A69-24649

Stress concentration analysis of interactions between stress raisers and cross section changes, considering asymptotic expansion method

11 p1972 A69-24650

Dynamic unified structural analysis method in computer program, calculating stiffness matrix to obtain natural frequencies and mode shapes

11 p1987 A69-25367

Structures, structural dynamics, materials and aeroelasticity - ASME-AIAA Conference, New Orleans, April 1969

11 p1988 A69-25492

Digital program containing Eulerian formalism for multiple interconnected rigid members applied to gravity gradient stabilized satellite with flexible booms

11 p1989 A69-25502

Classification of second order quasi-linear partial differential equations with two independent variables in structural dynamics with emphasis on elastic structures

11 p1991 A69-25513

Dynamic analysis of axisymmetric ring stiffened shells with attached asymmetric elastic structures, noting vibration modes

11 p1993 A69-25525

Transient dynamic response of linearly viscoelastic structures and continua, presenting finite element displacement formulation

11 p1993 A69-25528

Dynamics of deployable space structures stiffened by centrifugal forces due to spin, discussing LF radio telescope

11 p1994 A69-25530

Elastic free-free body deformation during motion based on equations of motion valid for rigid body, noting dynamic Green tensor

11 p1994 A69-25604

Space vehicle dynamic structure response, discussing vibration problems, test methods and responses to periodic, stochastic and forced excitations

12 p2176 A69-25857

Rigid plastic circular and annular plates dynamics taking into account yield point dependence on strain rate

12 p2177 A69-25994

Large plastic deformation of two metallic cylindrical flat ended missiles in mutual longitudinal impact

12 p2179 A69-26217

Vector equation for correction masses for dynamic balancing of rotor supported on n points derived from bearing structure vibrations amplitude and phase

12 p2180 A69-26243

Transverse symmetrical vibrations of thin elastic plates under Jacobi pressure distribution, giving displacement and velocity plots

12 p2180 A69-26271

Dynamic analysis methods for airframe flight control design noting equations of motion, system criteria and analysis and synthesis methods [AIAA PAPER 68-832]

12 p2174 A69-26758

Structures, structural dynamics and materials - AIAA-ASME Conference, New Orleans, April 1969

12 p2183 A69-26807

Simply supported laminated anisotropic rectangular plate with coupling occurring between bending and in-plane extension, discussing stiffness analysis by Fourier series method

12 p2184 A69-26808

Thermostructural simulation of lifting vehicle panel design, considering safety and trajectory shaping of flying laboratory

12 p2060 A69-26836

Accelerated structural tests under creep conditions, noting isothermal structures subjected to uniaxial and complex stress loads

12 p2186 A69-26838

Dynamic relaxation method for elastic deformation in mirrors, using tensor equations of elasticity in nonorthogonal curvilinear coordinates

12 p2187 A69-26890

Representation formula for response function of elastic materials having given isotropy group

12 p2188 A69-26926

Local failure of axially loaded plastic foam core sandwich panels, using face wrinkling analysis procedures

13 p2357 A69-27207

Load deflection equation solution based on row operations, involving three passes of coefficient matrix, using wavefront processing and modified Gauss algorithm

13 p2358 A69-27208

Natural vibration modes of linearly tapered rectangular plates, approximating plate characteristic shapes with series of products of beam characteristic shapes

13 p2358 A69-27211

Collection of papers on aerodynamic flutter covering airfoils, flow theory, aircraft structures, etc

13 p2358 A69-27234

Thin cylindrical shell vibration with three supports analyzed by minimizing Lagrangian of vibration, obtaining frequencies and modes

13 p2359 A69-27257

Plane stress theory for large elastic deformations of isotropic thin sheets, outlining successive substitutions method for neoHookean materials static and dynamic problems

13 p2359 A69-27320

Vibration modes in four lowest natural frequencies of clamped rectangular plates with linear thickness variation, using Ritz method

13 p2361 A69-27442

Plane problem for inhomogeneous elastic media based on assumption of elastic coefficients as functions

of two variables defined in domain occupied by medium

13 p2362 A69-27977

Stresses in elastic half plane with bonded disk of same elastic properties, describing stress production by expansion of disk

13 p2363 A69-28132

Inelastic structural system stresses, strains and displacements analyzed by differential stress-strain relationships, using finite element method [AIAA PAPER 68-291]

13 p2364 A69-28208

Dynamic stresses in case bonded cylinder due to transient angular accelerations, presenting numerical results for incompressible elastic cylinder

13 p2364 A69-28209

Projectile impacts into laminated targets consisting of plastic layers backed by Al substrates using SHAPE code with hydrodynamic elastoplastic distortional model [AIAA PAPER 69-356]

13 p2366 A69-28289

Experimental and predicted shock axial pressure variations for semiinfinite metallic targets during high velocity impact, using Al alloys and Cu [AIAA PAPER 69-361]

13 p2366 A69-28294

Couple stresses effect on dynamic stress concentrations, considering elastic compressional wave diffraction by cylindrical discontinuity

13 p2369 A69-28351

Dynamic stability of flexural free transverse vibrations of supported thin walled elastic beam with initial velocity distribution and parametric excitation

13 p2369 A69-28353

Complex structures lumped weight and inertia parameters automatic computation based on finite weight element method, using SCOWL computer program

14 p2533 A69-29025

Flexural vibrations of unstiffened doubly symmetric cylindrical tubes, obtaining natural frequencies of simply supported rectangular tube

15 p2703 A69-30210

Integrated structural and dynamic testing plans for proposed large interplanetary spacecraft, discussing acoustic testing, testing environments and flight environment transformation into laboratory

15 p2588 A69-30399

Uncoupled dynamic thermal stresses and displacements by heat generation in infinite flat plates, using classical thermoelasticity theory for infinitesimal displacements

15 p2709 A69-30669

Transient behavior of finite damped cantilever beam and circular plate analyzed by direct finite element method, noting applicability to dynamic problems

15 p2710 A69-30868

Deformation functions for finite beam analysis allowing continuity at nodes and accurate eigenvalues

15 p2710 A69-30869

Matrix eigenvalue problems with statistical properties, applying to dynamic structural systems and verifying solutions by Monte Carlo simulation

16 p2871 A69-31878

Blast response of model structures fabricated from material differing from prototype structures, testing in dynamic, impulsive and quasi-static loading realms

16 p2874 A69-32164

Aerodynamic aspects of tail rotor design and structural dynamics of stiff inplane configurations, discussing blade natural frequencies [AHS PAPER 342]

17 p3059 A69-33504

Network synthesis technique applied to structural dynamics design, using topological formulas to express systems response transfer functions

17 p2933 A69-33709

Numerical Fourier transform and inversion in random vibration performed on computer, noting use for stochastic structural dynamic analysis of complex structures

17 p2996 A69-33710

Blade vibration damper consisting of springs attached to blade, analyzing resonance stresses on basis of dynamic rigidities

17 p3066 A69-33944

Aircraft landing gear cylinder reinforcement rings design for minimum weight, using optimization iteration method for planar frames with elastic supports [AIAA PAPER 68-328]

17 p3066 A69-34030

Dynamic equations solution for interacting rigid or elastic body system models using Cosserat bodies elastic theory, considering engineering applications

17 p3067 A69-34143

Transient vibration linear analysis using Duhamel integral and Fourier and Laplace transformations, deriving receptances and application to aeroelastic systems

18 p3211 A69-34326

DYNAMIC TESTS

Axisymmetrical vibration characteristics of circular sandwich shell with viscoelastic core layer analyzed via differential equation to obtain frequency equation and composite loss factors
18 p3211 A69-34327

Book on deformable bodies mechanics covering load resisting members of structures and machines
18 p3222 A69-34927

Plate dynamics generalized equations independent of plate theory hypotheses, discussing algorithm and initial and boundary conditions
18 p3226 A69-35376

Soviet papers on dynamics and strength of machines covering oscillations of shells and impeller blades, stress concentration at shallow shell holes, thermoelasticity, etc
19 p3435 A69-35841

Von Karman equations for large deflection of simply supported square plates solved using dynamic relaxation method, recommending optimum mesh spacing
20 p3619 A69-36938

Vibration absorber incorporating polymer spring/damping elements for attachment to complex main system, noting butyl rubber as effective and convenient damper material
20 p3620 A69-36996

Flexible circular plate in stationary temperature field calculated for stress-strain state using perturbations method
21 p3835 A69-38830

Dynamic behavior of infinitely long cylindrical shells of ideally rigid plastic materials strengthened with ring ribs, determining distribution of moments and displacements
21 p3837 A69-39156

Numerical procedure for structural systems analysis, discussing computer application to hydrodynamic, electric, magnetic, thermodynamic, elastostatic and elastodynamic problems
[AIAA PAPER 67-955] 21 p3839 A69-39216

Field transfer matrices for simultaneous treatment of free and forced vibrations and buckling through axially loaded Timoshenko beam
23 p4234 A69-42400

Dynamic uniaxial tensile stress-strain data obtained at high rates by measuring kinematics of symmetrically expanding thin ring specimens
24 p4330 A69-42735

DYNAMIC TESTS

Rotary derivatives of aerodynamic forces and moments in subsonic and supersonic flow, emphasizing kinematic and dynamic oscillations
21 p3647 A69-38733

Bicycle ergometer combined with induction clutch, investigating effect of eccentric dynamic work with arms and legs
21 p3663 A69-38902

Gyro test package, dynamic test facility and real time attitude algorithm to investigate operational capabilities of strapdown inertial attitude package
[AIAA PAPER 69-849] 21 p3765 A69-39424

DYNAMICS

Variational principles of dynamic shell theory using Legendre transform for relations and boundary conditions of Timoshenko theory
01 p0166 A69-10262

Dynamic systems with impact interactions and nonlinear oscillation theory
16 p2875 A69-32295

Amplitude maxima for nonstationary oscillations of dynamic system with multiple degrees of freedom
16 p2876 A69-32296

Finite element discretization technique extended to time dependent processes emphasizing dynamics and heat conduction, discussing applications to aircraft transient response
20 p3575 A69-37204

Soviet collection of papers on static and dynamic problems in elasticity and plasticity theory covering plates, shells, beams, etc
22 p4038 A69-39911

DYNAMO THEORY

Earth magnetic field variations, discussing source of field, dynamo theory and paleomagnetic evidence for polarity reversals
03 p0420 A69-12935

Exact solutions with helical symmetry for hydromagnetic dynamo problem steady state equations
03 p0476 A69-13380

Reversals of earth magnetic field, discussing lavas, deep sea sediments, ocean floor magnetic pattern and dynamo theory
04 p0593 A69-15075

Magnetic field generation by dynamo action of liquid planetary cores, discussing evidence against magnetism around Mercury, Venus, Mars and Jupiter
07 p1210 A69-18371

F 2 layer drift relation to current systems of dynamo confirmed at middle and high latitudes
10 p1682 A69-23611

Sun-like alternating field generators, discussing dynamo theory of stellar and planetary magnetic fields based on nonmirror symmetrical turbulent motion in conducting fluid
10 p1782 A69-23703

Dynamo action produced magnetospheric currents in ionosphere computable without knowing real horizontal ionospheric current system
10 p1685 A69-23836

Geomagnetic field daily variations, discussing observational techniques, observation analysis, S-field seasonal changes, equatorial electrojet, solar wind effects, dynamo theory, etc
12 p0277 A69-27143

Upper atmospheric winds to produce solar quiet day magnetic variations based on dynamo theory, illustrating solenoidal, irrotational and mixed winds
16 p2782 A69-32460

Dynamo action origin of stellar and planetary magnetic fields, considering turbulent helical motions of H convection zone of sun
22 p4011 A69-39998

Homogeneous dynamo in cylindrically symmetric volume with symmetrically moving fluid and large magnetic Reynolds number, demonstrating first and second approximations using Braginskii method
22 p3989 A69-40192

Herzenberg geomagnetic dynamo model extensions including rigid rotors calculus, laminated rotors, induction problem and fluid rotors in rigid conductor
22 p3989 A69-40193

Bullard-Gellman dynamo, discussing magnetic field developed as series expansion, truncation levels and convergence
22 p4018 A69-40194

Kinematic dynamo waves, discussing excitation and maintenance of magnetic field by assumed motion of uniformly conducting fluid using small parameter and numerical methods
22 p3989 A69-40195

MHD dynamo construction with emphasis on fluid motion effect on magnetic field, considering spatially periodic dynamo derivation from kinematic considerations
22 p3989 A69-40196

Horizontally flowing eddies or Rossby waves in solar convection zone and photosphere, giving mathematical models showing hydromagnetic dynamo effects inducing reversing magnetic fields
22 p4019 A69-40294

Galactic field augmentation by dynamo action from highly condensed objects, considering Crab Nebula field production by central body
22 p4035 A69-41207

Solar quiet and lunar electric current systems deduced from geomagnetic data, discussing electrical conductivities and wind models in dynamo region
23 p4160 A69-42427

DYNAMOMETERS

ONERA vertical bench for dynamometric calibration to 20 tons used for engine and rocket thrust measurement
07 p1116 A69-19217

High temperature vacuum tensile test device for continuously direct recording various stress-strain diagram rates by interchangeable dynamometer scale
07 p1117 A69-19319

Dynamometer based on electrical capacitance change in sensor element, discussing working range, circuit diagram and mechanical design
11 p1887 A69-25207

DYNODES

Collection efficiency of continuous dynode electron multiplier arrays, discussing incident electron current
06 p0897 A69-17699

Temperature effect on amplification factor of box type dynode system of photoelectron multipliers made of alloy AMGK, using single electron method
11 p1846 A69-24626

DYSPROSIUM

Magnetic ordering in dysprosium phosphate observed by high resolution spectral line intensity measurements, finding Neel temperature
21 p3773 A69-38331

E

E REGION

NT E-2 LAYER
NT SPORADIC E LAYER

Vertical wind profiles and electron density profiles in E region, determining time dependence and ionization drift velocity
01 p0072 A69-11172

Linearized perturbation treatment developed for photochemical and dynamical effects in gravity wave production of E-region ionospheric irregularities, including ion convergence
01 p0073 A69-11175

Seasonal variations in thickness of ionospheric E-F interlayer region during daylight and maximum integral ionization values
02 p0239 A69-11682

E region electron concentration measurements during large solar zenith angles, noting anomalous behavior during low solar activity periods
02 p0239 A69-11683

Rocket sounding for studying positive ions nighttime composition in E layer after magnetic storm at midlatitudes
02 p0239 A69-11686

Algorithm for N/h ionospheric profiles calculations using both x and o magnetoeionic components, taking into account interlayer and underlying ionization influence
02 p0239 A69-11687

Phase path variations at three closely spaced points, measuring horizontal drifts at E region level, investigating time shift variability in spaced fading records
03 p0421 A69-13329

Horizontal drifts at E region level measured in India by spaced phase path technique
03 p0421 A69-13330

Polarization diversity analysis to avoid fading in microwave scatter links in D and E layers
03 p0394 A69-13378

Nighttime E layer mean variations noting critical frequencies, electron density and seasonal and solar activity effects at sunset, midnight and sunrise
03 p0398 A69-13899

Rocket measured profiles of electron density and ion abundances in E region, discussing role of minor atmospheric constituents
05 p0757 A69-16408

Variation in critical E layer frequencies at large solar zenith angles
06 p0921 A69-17748

Formation dynamics of thin sporadic layers of E region, determining maximum ionization and electron concentration and electron-neutral atoms collision frequency
06 p0922 A69-17751

Approximation formulas of Appleton-Hartree equations for nighttime medium wave frequency absorption in E region of ionosphere, discussing electron density
07 p1122 A69-18295

Solar eclipse variations of E layer critical frequency explained by quasi-equilibrium between electron density and ionizing soft X ray radiation
07 p1204 A69-18823

Model of auroral backscatter from E region including ionospheric refraction, comparing computations to experimental HF auroral backscatter data for aspect sensitivity
09 p1488 A69-21700

Heat sources in E region from electron temperature data analysis recorded by rockets during eclipses in July 1963
09 p1490 A69-21771

Electron gas heating at E region altitudes as function of ionization of atmospheric gases, noting rocket experiments during solar eclipse
09 p1490 A69-21772

Rocket sounding data on ionospheric currents at mid and low latitudes, showing absence in D and above E region
10 p1686 A69-23909

Reversible ion heating by atmospheric tides, noting radar Thomson scatter observations of E region ion temperature height profiles
11 p1879 A69-25159

Solar flare X ray and extreme UV radiation contribution to E and F1 region ionospheric effects observed by sudden frequency deviations
11 p1950 A69-25160

Pulsed radio waves for measuring phase height in E

- region, showing short period fluctuations
12 p2066 A69-26111
- E region radio waves triple splitting observed in probe ionograms, analyzing diurnal and seasonal variations in Z component reflections occurrence
12 p2031 A69-26686
- Magnetospheric corpuscular fluxes night ionization role in E and D region, considering precipitation from outside, trapped and dumped particles of radiation belts
13 p2254 A69-28333
- E layer fine scale structure, F1 reactions and F2 reflected signals analysis during 20 May 1966 solar eclipse
13 p2255 A69-28541
- Seasonal variations in thickness of ionospheric E-F interlayer region during daylight and maximum integral ionization values
13 p2257 A69-28713
- E region electron concentration measurements during large solar zenith angles, noting anomalous behavior during low solar activity periods
13 p2258 A69-28714
- Rocket sounding for studying positive ions nighttime composition in E layer after magnetic storm at midlatitudes
13 p2258 A69-28717
- Algorithm for N/h ionospheric profiles calculations using both x and o magnetoionic components, taking into account interlayer and underlying ionization influence
13 p2258 A69-28718
- Polarization diversity analysis to avoid fading in microwave scatter links in D and E layers
14 p2410 A69-28829
- Ion chemistry of D and E regions to be studied during years of solar maximum in framework of IQSY/IUCSTP
14 p2439 A69-29111
- Rocket measured electron densities of nighttime auroral E region over Canada at different magnetic activity levels, noting frequency and plasma density relations
14 p2439 A69-29117
- Linearized perturbation for photochemical and dynamical effects in internal atmospheric gravity wave production of E region ionospheric irregularities
14 p2440 A69-29128
- Solar X rays intensity and spectrum effects on e layer critical frequency and D region ionospheric absorption
15 p2677 A69-31346
- RF mass spectrometric measurements of diurnal variation of thermosphere and ionospheric E and F regions composition, noting oxygen concentration
15 p2601 A69-31371
- E region ionization redistribution by neutral winds, comparing calculated vertical drift velocities to observed electron density profiles
15 p2677 A69-31395
- Atmospheric temperature and vertical gradient in E region based on measured instantaneous wind profiles
15 p2603 A69-31399
- Electron cooling rates due to vibrational excitation of molecular oxygen calculated as function of electron temperature in E region
16 p2774 A69-31982
- Correlation between F region electrons vertical motion velocity variations and E region electrons horizontal motions in equatorial ionosphere
16 p2779 A69-32193
- Meteoritic elements ionization and loss mechanisms in E region, discussing roles of atomic oxygen and metal ions chemical reactions
16 p2780 A69-32313
- Atomic oxygen density role in ionospheric E and F region magnetic stability, noting heat loss effect of atomic excitation
16 p2780 A69-32314
- E region horizontal drift measurements at Ahmedabad from 1956 to 1966, noting solar activity and seasonal influences
17 p2962 A69-33678
- E layer inhomogeneities analysis concerning drift, chaotic processes, statistical parameters and reliability of data processing
17 p2962 A69-33896
- Ionospheric processes associated with changes in polar aurora height, noting glow in E layer and soft electron emission into earth atmosphere
17 p2964 A69-33957
- Kinesonde radio sounding system for three dimensional ground observations of E region microstructure and vertical motion of neutral air and ions
18 p3125 A69-34250
- Earth albedo effect on ionospheric D layer determined from aircraft sounding of E layer echo amplitude above reflecting cloud cover
18 p3127 A69-34800
- Noctilucent cloud layer spectral brightness and transparency in E region determined from transhorizon rocket observations
18 p3130 A69-35148
- Reactions determining ion composition in E region, discussing neutral composition variations from day to night and during solar activity cycles
20 p3520 A69-37031
- Small scale inhomogeneities motions in E and sporadic E layers, processing data with method of full correlation analysis and statistical method
20 p3528 A69-37683
- Vertically moving disturbances relationship to behavior of E and F layers over Tiflis, noting sporadic E layers formation
20 p3528 A69-37685
- Rocket observations of ionospheric E layer winds using Na release method
20 p3529 A69-37796
- Lower E region field-aligned plasma instability arising from neutral wind driving ionization across magnetic field
20 p3534 A69-38091
- Vertical neutral wind measurements in lower E region with wavelike spatial structure, noting vertical shear role in ionosphere dynamics
21 p3703 A69-38363
- Phase amplitude recording of radio waves reflected from D and F regions of ionosphere, reversing smoothing process by Fourier methods
21 p3672 A69-38558
- Magnetic activity effects on horizontal drifts, anisotropy and random change characteristics of E region ionization irregularities
21 p3715 A69-38561
- Magnetic dip equator position at E layer and gradient with time and altitude, using geomagnetic field models
23 p4160 A69-42428
- Ionization irregularities in equatorial E region observed in various scale sized by rocket-borne Langmuir and plasma-noise probes
23 p4160 A69-42430
- E-2 LAYER**
Ionization index, electron formation and effective recombination coefficient in E2 layer, noting solar activity effect
06 p0920 A69-17725
- Time-space variations in occurrence probability of ionospheric E-2 layer during solar activity maximum and minimum
20 p3527 A69-37672
- E-2 AIRCRAFT**
Avionics of Naval E-2C airborne sentry and command and control system, discussing digital computer, search radar, etc
18 p3108 A69-34811
- EAR**
NT COCHLEA
NT CORTI ORGAN
NT LABYRINTH
NT MIDDLE EAR
NT SEMICIRCULAR CANALS
NT VESTIBULES
Barotrauma during hyperbaric oxygenation at flight descent or reentry into caisson, including ear trauma symptoms and use of paracetesis
17 p2911 A69-33776
- Human ear frequency discrimination, discussing nonlinear functional modeling systems
18 p3097 A69-35440
- Distortion processes in ear, discussing sound pressure level/SPL measurements in rigid-walled couplers
23 p4085 A69-41573
- Stimulus correlated with neuronal discharge periodicities in colliculus inferior, deriving structure models, discussing acoustic channel below geniculatum mediale
23 p4096 A69-42089
- EAR PRESSURE TEST**
Rapid decompression and recompression in stapelotomized cat, noting fibrous tissue response in middle ear at reconstructions utilizing polyethylene struts on gelfoam
14 p2406 A69-29292
- EARLY BIRD SATELLITES**
Fucino earth station operation with Early Bird and Intelsat 2-F3 satellites receiving equipment and transmission system
[UN PAPER 68-95455] 01 p0028 A69-10493
- Attitude determination and hydrogen peroxide control system for spacecraft orientation in Syncom, Early Bird and ATS
[AIAA PAPER 67-532] 09 p1610 A69-21988
- EARLY STARS**
NT PROTOSTARS
NT T TAURI STARS
Relative proper motion of blue star in field of pulsar CP 1919 determined from photographic data analysis
01 p0149 A69-10270
- Hydrogen line profiles in various early stars compared with profiles predicted from model atmosphere calculations for rotating and nonrotating early stars
01 p0154 A69-10876
- Radio signals from hydroxyl radicals by maser action in early stars, noting emission magnitude and intensity spectrum dissimilarity at different frequencies
02 p3234 A69-12493
- Hydrogen alpha line strength in 951 O, B and early A stars from narrow band photoelectric measurements for stellar luminosity
03 p0511 A69-13435
- Rotational velocity correlation to space velocity for early stars, suggesting attainment of spin momentum and space velocity during close encounter in small cluster
06 p1010 A69-17972
- Three color photoelectric observations of stars near Orion Nebula, discussing gravitational contraction stars and color magnitude diagram
08 p1384 A69-20055
- Chemical composition of atmospheres of oldest Galactic stars, considering element abundances, metal and helium content and nuclear activity of massive stars
08 p1402 A69-20909
- Spectrum analysis for early B type star Barnard 29 in M13 globular cluster
09 p1599 A69-22193
- Distance of bright stars in Cepheus OB2 region by MK spectral classification and UVB photometry, noting early main sequence and supergiant stars
09 p1599 A69-22194
- Element abundances of sharp lined field early A stars using model atmosphere
09 p1600 A69-22198
- Early type stars spectrophotometric parameters, discussing hydrogen beta, gamma and delta line widths, magnitude, etc
10 p1777 A69-23387
- Early F stars Li/Be abundance ratios estimation from change in solar Be abundance, discussing stellar Li isotopes ratios
10 p1785 A69-24099
- Nongray models of atmospheres of early stars, giving Avrett-Krook method of correcting temperature distribution
11 p1954 A69-24361
- Correlation of stellar surface density distribution of young stars and neutral hydrogen gas in Small Magellanic Cloud
12 p2152 A69-25802
- Spinning rockets UV spectrophotometry of early type stars, discussing instrumentation, calibration, data recording and stellar spectra
12 p2153 A69-25812
- Spheroidal galaxies with early type spectra distinguished by UV continuum, discussing telescopic spectral and color observations
12 p2159 A69-26663
- Surface gravities and detection of metallic line early A stars from spectral classification using equivalent line widths
12 p2171 A69-27151
- High dispersion classification of early K2-M6 giants of high and low velocity, using titanium oxide band strengths criteria tested by atomic lines estimation
13 p2338 A69-27556
- Interstellar absorption and spatial distribution in northern Aquila with absence of early O-B2 stars, including luminosity function
15 p2683 A69-30513
- Carbon stars in south galactic pole region detected in objective prism survey, including variable R Scl and early R stars
16 p2860 A69-32322
- Photodestruction rate of H molecules by absorption of Lyman or Weber band radiation in interstellar space calculated at various distances from early stars
18 p3204 A69-35351
- Stars of spectral class F2 and earlier, brighter than magnitude 11.5, found in four regions of intermediate galactic latitude
20 p3612 A69-38162

EARLY WARNING SYSTEMS

- Finding list of spectral type A7 stars and earlier in region at south galactic pole compiled from prism survey data 22 p4021 A69-40436
- Rocket measurement of far UV spectral intensity of theta Orionis for far UV interstellar extinction law in Orion nebula region 22 p4030 A69-40770

EARLY WARNING SYSTEMS NT BALLISTIC MISSILE EARLY WARNING SYSTEM

- Clutter rejection using coded burst waveform for airborne early warning /AEW/ and airborne attack type radars 03 p0388 A69-13185
- Mechanical, electromagnetic and chemical signatures monitoring and analysis during system operation 06 p0932 A69-17875

EARTH [PLANET]

- Mass functions of real earth derived from satellite orbital perturbations [UN PAPER 68-95385] 01 p0064 A69-10460
- Soviet book on dynamics of radiation belts of earth covering theories concerning magnetosphere, magnetic fields and plasma and electromagnetic pulsations 02 p0307 A69-11799
- World maps highlighting differences in geomagnetic field at conjugate localities 02 p0245 A69-12737
- Kepler third law application to radar determinations of astronomical unit of length in general relativity 04 p0657 A69-14698
- Earth and planets shallow seas tidal dissipation reflected in Q values, noting larger planet pressure effect 08 p1393 A69-20581
- Chemical abundances in planetary atmospheres based on spectroscopic determinations, considering terrestrial and Jovian planets 08 p1406 A69-20934
- Rare earths relative and absolute terrestrial abundances in shales, basalts, rhyolites and granites 08 p1310 A69-20942
- Earth ellipsoid fundamental parameters for calculation of earth flattening and normal acceleration due to gravity 09 p1487 A69-21633
- Two fixed centers with force function approximating earth gravitational potential, deducing formula for gravity distribution at level surface 11 p1952 A69-24254
- Monograph on world of planets covering solar planetary system, atmospheres, water, seasons, organic life, etc 11 p1958 A69-24666
- Meteorology and space vehicle capabilities noting earth, outer space and earth atmosphere observations and measurements, relaying telecommunication signals, etc 12 p2126 A69-26126
- Earth center of mass determination from simultaneous satellite observations by photography or laser radar 12 p2068 A69-26425
- Earth contamination by returned lunar or Martian material, discussing extraterrestrial biota survival on earth 13 p2210 A69-28467
- Diurnal hemisphere auroras assuming origins in magnetosphere tail with pressure responsible for tail formation, discussing tentative model and implications 13 p2256 A69-28654
- Magnetovariational sounding procedure for determining vertical distribution of earth mean electrical conductivity using geomagnetic field spatial derivatives for spherical earth 14 p2438 A69-29081
- Catastrophic and noncatastrophic alternatives for earth capture of moon, discussing tidal action and spin-orbit resonance 18 p3198 A69-34823
- Earth bow shock waves in far upstream interplanetary medium observed from magnetic data of Explorer 34 satellite 18 p3199 A69-34941
- Earth bow shock electrical conductivity estimation from macroscopic equations without knowing microscopic dissipation processes 18 p3131 A69-35191
- Book on wave propagation around earth covering intermedia passage, terrain influence, diffraction zones, ground waves, roles of atmosphere, troposphere and ionosphere, etc 19 p3275 A69-36382

Mercury and Venus thermal histories based on analogy to earth models 20 p3597 A69-37333

Moon possible origin, discussing spin off from earth, accretion from same dust cloud or formed elsewhere and captured 20 p3603 A69-37559

Paleontological evidence to verify varying G constant hypothesis for expanding earth theory, discussing uncertainties of geological dating 22 p4017 A69-40177

Dirac hypothesis on varying G constant considered in formulating earth expansion theory without resorting to Ramsey hypothesis 22 p4018 A69-40178

Observations indicating slow earth expansion 22 p4018 A69-40179

Earth gravitational potential energy changes in examining expanding earth theory 22 p3936 A69-40180

Paleogeographical evolution in support of earth expansion, discussing polar wandering, global continental drift and final complete disruption 22 p3936 A69-40181

Venus and Mercury diurnal period commensurability associated with Venus spin-orbit resonance with earth orbit 22 p4018 A69-40270

Recurrent Lagrange multipliers for optimal low thrust earth-Jupiter transfers, using three dimensional solar system model 23 p4215 A69-41896

Density model for free oscillations of earth, noting dependence on core radius and S wave velocity at top and bottom of D layer 23 p4158 A69-42117

Design criteria for antenna control equipment for earth tracking from landing site on Martian surface [AIAA PAPER 68-868] 24 p4348 A69-43246

EARTH ALBEDO

- Surface radiation balance measurements in India during IQSY, discussing diurnal, seasonal and spatial variations of net radiation 02 p0307 A69-11820
- Aircraft measurements of stratus cloud absorption and albedo and earth surface albedo 04 p0627 A69-14914
- Meteorological satellites observation of energy exchange between earth and space, discussing planetary albedo, energy absorption and source and sink regions 07 p1127 A69-19261
- Albedo over Antarctic, measuring solar radiation reflected by surface and atmosphere by Eppley radiometer 09 p1484 A69-21404
- Satellite mounted radiometers for determining albedo variations, using Fredholm equation with allowance for instrument errors 10 p1689 A69-23969
- Night airglow variations observed during Cosmos 92 satellite orbits, determining atmospheric albedo wavelength dependence for solid and medium cloudiness and clear skies 14 p2435 A69-29042
- Earth reflected solar radiation spatial, angular and spectral distributions measured by telephotometers on-board Cosmos 149 15 p2596 A69-30650
- Earth albedo instrument on OSO 3 spacecraft to measure solar reflectance of earth at various wavelengths 15 p2614 A69-31279
- Earth reflected radiation pressure and perturbing effect on satellites 15 p2599 A69-31324
- Earth-reflected solar energy /albedo energy/ distribution model, assuming isotropic scattering by homogeneous atmosphere [AIAA PAPER 69-591] 17 p2961 A69-33292
- Earth albedo effect on ionospheric D layer determined from aircraft sounding of E layer echo amplitude above reflecting cloud cover 18 p3127 A69-34800
- Earth albedo in lower latitudes measured by satellites and surface stations, comparing solar energy absorption by oceans and atmosphere 20 p3591 A69-38058
- Satellite mounted radiometers for determining albedo variations, using Fredholm equation with allowance for instrument errors 21 p3717 A69-39655

Reentrant albedo flux and singly charged particles directional asymmetry in upper atmosphere estimated from oriented telescope observations over Hyderabad 22 p4005 A69-40519

EARTH ATMOSPHERE

- ARTIFICIAL RADIATION BELTS
NT D REGION
NT E-2 LAYER
NT E REGION
NT EXOSPHERE
NT F REGION
NT F 1 REGION
NT F 2 REGION
NT FREE ATMOSPHERE
NT INNER RADIATION BELT
NT IONOSPHERE
NT LOWER ATMOSPHERE
NT LOWER IONOSPHERE
NT MAGNETOPAUSE
NT MAGNETOSPHERE
NT MESOPAUSE
NT MESOSPHERE
NT MIDLATITUDE ATMOSPHERE
NT OUTER RADIATION BELT
NT OZONOSPHERE
NT PROTON BELTS
NT RADIATION BELTS
NT SPORADIC E LAYER
NT STRATOSPHERE
NT THERMOSPHERE
NT TROPOPAUSE
NT TROPOSPHERE
NT UPPER ATMOSPHERE
NT UPPER IONOSPHERE

Meteorological rocket soundings and global synoptic observations, noting influence of atmospheric middle region [UN PAPER 68-95405] 01 p0109 A69-10484

Atmospheric optics - Conference, Pulkovo, U.S.S.R., November-December 1965 and December 1966 01 p0073 A69-11181

Earth atmosphere transmission coefficients determination by relation between transparency and daytime sky brightness, noting limits of applicability 01 p0074 A69-11185

Atmospheric transmission factor and optical stability determination by photometer, estimating error due to solar aureole 01 p0075 A69-11193

Helium isotopes escape mechanism from earth atmosphere related to polar wind ionospheric plasma flow from earth 01 p0077 A69-11240

Earth atmosphere air density and temperature profiles from drag acceleration measurements in falling sphere experiment 02 p0251 A69-12809

Radio waves diffraction around earth with atmospheric dielectric constant having linearly quadratic height dependence 03 p0399 A69-14130

Atmospheric, geomagnetic and interplanetary effects on cosmic ray flow, noting anisotropy and diurnal variation phase and amplitude averages 04 p0649 A69-14683

Atmospheric density variation measurements by density gages on Explorer 32 satellite confirm wave propagation in neutral thermosphere as free internal gravity waves 05 p0754 A69-16261

General atmospheric circulation characteristics estimation for earth, Mars, Venus and Mercury based on thermodynamic and hydrodynamic laws 05 p0828 A69-16635

Meteorological satellite TV data of earth cloud cover for determining atmosphere pressure field [UN PAPER 68-95654] 06 p0949 A69-17052

Solar neutron production and propagation to earth, discussing particle detectors 06 p0989 A69-17281

Electromagnetic wave refraction angles in earth atmosphere, noting effect of stratified discontinuities on angle magnitude 06 p0887 A69-17450

Inverse problems in radiative transfer applied to remote measurements of IR radiation from planetary atmospheres, noting temperature and water vapor inversions 06 p0919 A69-17617

Terrestrial and Martian aerosols estimation based on carbon dioxide spectral and Mariner 4 RF occultation measurements [AIAA PAPER 69-52] 06 p1011 A69-18199

Terrestrial and Cytherean atmospheres evolution based on gray atmosphere model, surface energy budget and partition of water and carbon dioxide 07 p1213 A69-18608

Meteorological satellites observation of energy exchange between earth and space, discussing planetary albedo, energy absorption and source and sink regions

07 p1127 A69-19261

Mars and Earth atmospheric carbon dioxide simulation and spectroscopic measurement for developing planetary surface pressure estimating procedures from IR transmission measurements

08 p1354 A69-20151

Carbon dioxide pressure in earth atmosphere through geologic time determined by carbon input rate and transfer efficiency to crust

08 p1310 A69-20946

Aircraft measurements of earth atmosphere radiance in 8-14 micron window compared to calculated values as functions of altitude

08 p1311 A69-21094

Mars and Venus atmospheric properties, noting influence of biosphere and human activity on earth atmosphere

08 p1408 A69-21160

Photochemical production of reduced organic compounds of C and N in primitive earth atmosphere

09 p1444 A69-21465

Spin stabilized spherical satellite in high elliptical orbit for lower thermosphere measurements during entire solar cycle

09 p1610 A69-22009

Chemical composition of Venusian atmosphere by Mariner and Venera satellites, comparing upper atmospheres of Venus and earth

11 p1960 A69-24971

Meteorology and space vehicle capabilities noting earth, outer space and earth atmosphere observations and measurements, relaying telecommunication signals, etc

12 p2126 A69-26126

External perturbation effects of near earth environment on dynamics and attitude of slowly spinning multibody satellite

[AIAA PAPER 68-856]

12 p2174 A69-26795

Book on earth atmosphere and outer space influence on human physiology for life support systems design

12 p2024 A69-27074

Atmospheric electricity and space charges ionization and equilibrium in earth atmosphere, discussing electric fields in lower atmosphere, ionosphere and magnetosphere

12 p2076 A69-27105

Rocket grenade measurements of earth atmosphere, finding lowest temperature in Alaska

13 p2255 A69-28637

General atmospheric circulation characteristics estimation for earth, Mars, Venus and Mercury based on thermodynamic and hydrodynamic laws

14 p2516 A69-28791

Surface impedance of spherical earth isolated by nonconducting atmosphere from ionospheric currents producing alternating electromagnetic field

14 p2438 A69-29082

Q switched ruby laser designed for lidar probing of cosmic bodies and earth atmosphere

14 p2460 A69-29660

Soviet collection of articles on atmospheric optics

15 p2646 A69-30159

Synoptic meteorological conditions effect on stellar images vibration and on relationship between vibration and zenith distance

15 p2647 A69-30164

Atmospheric hydrogen and helium atoms emission in geomagnetic poles and winter hemisphere, comparing thermal dissipation and migration of light atoms

15 p2599 A69-31322

Cloud distribution effect on global coverage of remote radiometric sounding of atmosphere, considering Nimbus 1 and 2 data

15 p2650 A69-31335

Balmer alpha emission for abundance and distribution of hydrogen around earth, relating temporal variations to azimuth

15 p2700 A69-31437

Transmission of Alfvén waves through earth bow shock based on hydromagnetic shocks theory, discussing amplitude amplification

16 p2777 A69-32099

Direct wind measurement and momentum transport estimates obtained from cyclones and anticyclones daily displacements over Northern Hemisphere, applying results to planetary atmospheres

16 p2780 A69-32306

Light polarization diffusely reflected by earth atmosphere measured from balloon, using gain compensated photoelectric polarimeter

16 p2781 A69-32320

Earth atmosphere effect on cosmic ray variations, considering relation between extensive air showers and cosmic ray spectrum

16 p2851 A69-32381

Equatorial and polar semidiurnal oscillations in earth atmospheric tides related to inertial oscillations originating in autobarotropic field

17 p2996 A69-32862

Planetary zonal flows hydrodynamic instability characteristics analysis, using quasi-geostrophic numerical model to study earth atmospheric cyclone wave role

17 p2960 A69-33149

Limb darkening on earth night side observed by Aerobee rocket, with explanation based on atmospheric opacity in water vapor and carbon dioxide bands

17 p2960 A69-33167

Planetary atmospheres origin, discussing earth formation by planetesimals accumulation and similarity to Mars and Venus, volatiles in outer planets, etc

17 p3033 A69-33369

Earth ecosystem chemical composition compared with Mars and Venus ecosystems to determine presence of life

18 p3193 A69-34361

Earth atmospheric large scale motion simulated in laboratory and by numerical technique

18 p3127 A69-34668

Fourier transform laboratory spectroscopy for absorption near earth atmosphere millimeter wave spectrum, discussing integrated absorption strength and dimeric effect

18 p3177 A69-35240

Predictability of deterministic fluid systems with many scales of motion using vorticity equation for two dimensional incompressible flow, noting application to earth atmosphere

19 p3303 A69-36404

Shock wave parameters from meteoric body moving at high supersonic speeds through atmosphere, calculating specific heat ratio

19 p3428 A69-36841

Rare gas distribution in earth atmosphere explained as outgassing from primordial solid particles, discussing stony meteorites composition

20 p3600 A69-37489

Electromagnetic wave refraction angles in earth atmosphere, noting effect of stratified discontinuities on angle magnitude

20 p3496 A69-37935

Soviet book on shock waves propagated by meteorite intrusion into earth atmosphere, covering interaction with earth surface, Tungusk meteorite, etc

20 p3613 A69-38205

Automatic planetary electrophotometer designed for earth atmosphere and lunar photometry, noting operational data

20 p3547 A69-38310

Angular dependence of ocean surface-cloudless atmosphere reflectance for solar radiation studied with digitized camera signals from ATS 1 satellite

21 p3704 A69-38372

Earth atmospheric density measurement by microwave radio occultation techniques, transmitting coherent radio signal to repeater spacecraft from master station

21 p3705 A69-38375

Microwave refraction method for satellite horizontal probing of earth atmosphere, discussing phase delay data inversion, air density and intersatellite relative velocity

21 p3671 A69-38376

Helium in atmosphere, aurora and solar wind, discussing geophysical problems, interplanetary neutral H, etc

21 p3710 A69-38509

Atmospheric and hydrospheric evolution on primitive earth from geological point of view

21 p3806 A69-39290

Horizon definition for Apollo space navigation references from examining earth atmosphere visible and far IR spectrum

[AIAA PAPER 69-869]

21 p3763 A69-39395

Soviet book on earth atmosphere fluctuations covering propagation of acoustic, gravity and gyroscopic waves using linearized equations of hydrodynamics

21 p3717 A69-39528

Martian atmosphere circulation compared to terrestrial, considering absence of oceans, radiative coupling and planetary scale motions

21 p3814 A69-39569

Antimatter motion in solar system and earth atmosphere, discussing vaporization and annihilation energy in collisions with interplanetary gas atoms

22 p4034 A69-41100

Acoustic gravity waves propagation over spherical earth with isothermal windless atmosphere, determining pressure perturbations

23 p4158 A69-42175

Orographic inhomogeneities of underlying surfaces for radiating atmospheric waves formation, deriving formulas for plane stable atmosphere

23 p4185 A69-42492

Bidirectional reflectance of earth atmosphere and cloud formation above equatorial Pacific observed by synchronous satellite as function of angular dependence

24 p4346 A69-43154

EARTH CORE

Electromagnetic induction theory for spherical earth model involving conducting core with radial conductivity variation and concentric nonconducting mantle

03 p0423 A69-13523

Ponderomotoric forces and irregularities in earth rotation, considering core and lower mantle as closed system with respect to periodic electromagnetic and mechanical effects

09 p1487 A69-21636

Earth mantle and core friction interaction suggested as cause of secular change in orbital motion obliquity

13 p2253 A69-27821

Geomagnetic field secular variations relation to variations of magnetic field of optimum dipoles, noting earth core role

14 p2436 A69-29061

Geomagnetic field westward drift related to earth core rotation from calculating drift at earth surface and at core

16 p2774 A69-31983

Silicon in iron meteorites and earth core determined by activation analysis on octahedrites, hexahedrites and ataxites

16 p2865 A69-32807

Earth core conductivity effects on ionospheric shielding against geomagnetic changes from external sources, noting earth-ionosphere coupling

17 p2959 A69-32925

Fluid velocities at earth core surface inferred from magnetic data, considering velocity constraints and diffusion contributions to secular change

18 p3129 A69-34951

Ponderomotoric forces and sudden irregularities in earth rotation, discussing core-mantle electromagnetic coupling and toroidal field induction effects

19 p3302 A69-35769

Earth early thermal history with core formation before emplacement of earliest known rock possessing remanent magnetism

22 p3936 A69-40136

Book on geomagnetic quadrupole field temporal changes and effects on earth rotation, covering physical parameters in earth interior and earth conductivity model correlations

22 p3937 A69-40423

MHD disturbances in earth core produced by sudden introduction of magnetic dipole with axis positioned perpendicular to earth mantle and toroidal excitation fields

23 p4158 A69-42176

EARTH CRUST

Possible evolution of earth continents and ocean basin, considering ultrabasic, basic, and intermediate to acidic lunar highlands chemical composition

06 p1000 A69-17006

Gold and iridium concentrations in meteoritic and terrestrial materials by neutron activation, discussing chondrules, meteoritic troilite and metallic spherules

08 p1404 A69-20918

Composition of continental crust based on material balance and rare earth estimates of shales, discussing ocean floor and mantle derived rocks

08 p1309 A69-20939

Statistical distribution of chemical elements average abundances in earth crust and meteorites and nucleosynthesis of elements under specific astral conditions

08 p1310 A69-20941

Earth crust transition elements distribution and abundance compared to rare earths

08 p1310 A69-20943

Anomalous magnetic field energy spectrum obtained from aeromagnetic survey and approximation valid for earth crust and upper mantle

09 p1487 A69-21554

Magnetic anomalies off Cape Hatteras explained as possible edge effect, discussing ocean and continental magnetic crusts and igneous and magnetic rocks

11 p1879 A69-25405

EARTH CURRENTS

- Anomalous magnetic field energy spectrum obtained from aeromagnetic survey and approximation valid for earth crust and upper mantle 16 p2784 A69-32549
- Collection of papers on earth crust and upper mantle covering thermal history, oceanic heat flow, mass anomalies, gravitational variations, etc 21 p3717 A69-39731
- Variations in gravity, plotting results for U.S., with tables for Alaska, Mexico, India, Africa, etc 21 p3718 A69-39735
- Precambrian crustal geotectonic evidence of earth radius expansion based on dated orogenic fold belts distribution 22 p3936 A69-40182
- Airborne electromagnetic systems measuring complex dielectric constant in earth crust for mineral and water resources exploration [RAES PAPER 8] 22 p3946 A69-40481
- ## EARTH CURRENTS
- ### U TELLURIC CURRENTS
- ## EARTH FIGURE
- ### U GEODESY
- ## EARTH HYDROSPHERE
- Epochs in atmospheric circulation development over Northern Hemisphere, emphasizing solar activity roles in epochs appearances 14 p2478 A69-29837
- Ocean and atmospheric interactions analyzed by using hydrodynamic equations for boundary layers 14 p2442 A69-29838
- Atmospheric and hydrospheric evolution on primitive earth from geological point of view 21 p3806 A69-39290
- ## EARTH MANTLE
- Electromagnetic induction theory for spherical earth model involving conducting core with radial conductivity variation and concentric nonconducting mantle 03 p0423 A69-13523
- Velocity distribution in lower mantle, showing second major discontinuity in P wave travel time curve at 24 degrees 07 p1129 A69-19502
- Electrical conductivity in interior of earth stressing electromagnetic induction method, discussing mantle conductivity distribution value 08 p1306 A69-19825
- Magnesium silicate crystal structure, discussing transformations under high pressure, crystallochemistry and implications for physics of earth mantle 08 p1267 A69-19904
- Composition of continental crust based on material balance and rare earth estimates of shales, discussing ocean floor and mantle derived rocks 08 p1309 A69-20939
- Anomalous magnetic field energy spectrum obtained from aeromagnetic survey and approximation valid for earth crust and upper mantle 09 p1487 A69-21554
- Ponderomotive forces and irregularities in earth rotation, considering core and lower mantle as closed system with respect to periodic electromagnetic and mechanical effects 09 p1487 A69-21636
- Earth upper mantle wave velocity structure based on surface wave dispersion, noting low velocity layers thickness 09 p1491 A69-22153
- Thermal convection in earth mantle with temperature and pressure dependent viscosity, considering mechanisms for fluid-like mantle 10 p1682 A69-23412
- Model for perturbations in earth rotation and geomagnetic core-mantle coupling, discussing electromagnetic restoring torque 12 p2077 A69-27110
- Planetary mantles thermal and nonthermal convection model, solving sphere density variations and radial velocity components due to internal time-independent motions 13 p2344 A69-27644
- Earth mantle and core friction interaction suggested as cause of secular change in orbital motion obliquity 13 p2253 A69-27821
- Anomalous magnetic field energy spectrum obtained from aeromagnetic survey and approximation valid for earth crust and upper mantle 16 p2784 A69-32549
- Eclogite fractionation role in creation and spreading of suboceanic lithospheric plate, discussing density determination at 100 km depth 18 p3132 A69-35434

- Ponderomotive forces and sudden irregularities in earth rotation, discussing core-mantle electromagnetic coupling and toroidal field induction effects 19 p3302 A69-35769
- Collection of papers on earth crust and upper mantle covering thermal history, oceanic heat flow, mass anomalies, gravitational variations, etc 21 p3717 A69-39731
- Dynamic processes in upper earth mantle, discussing thermal convection currents and stress propagation 22 p3937 A69-40184
- Equation of state measurements of earth materials by shock wave techniques, applying to olivine for earth mantle constitution problem 22 p3937 A69-40188
- ## EARTH-MARS TRAJECTORIES
- Third phase dynamics of planetary approach of earth-Mars journey, computing approach trajectory on two body spacecraft-Mars assumption 11 p1968 A69-25725
- Planetary navigation using spacecraft measurements and Doppler data from earth-based radio tracking, determining accuracy for earth-Mars trajectory 19 p3368 A69-35791
- Abort capability mission selection criterion, evaluating energy requirements, Mars flyby and velocity contours [AAS PAPER 68-139] 21 p3805 A69-39209
- ## EARTH-MOON SYSTEM
- Synodic month length variations since late Cambrian, noting paleontological evidence in mollusks and stromatolites and associated geological changes 02 p0241 A69-11807
- Zodiacal light isophotes and near-earth component from relationship between brightness at various geomagnetic latitudes and position of moon 03 p0512 A69-13693
- Moon effect on intensity and angular distribution of energetic electron and proton shadowing as observed by Explorer satellites 05 p0824 A69-16252
- Lunar laser ranging for testing Einstein and Brans-Dicke gravitational theories, discussing pulse transit time and dominant nonNewtonian correction 05 p0825 A69-16362
- Lunar libration clouds, discussing visual observation at small phase angles for estimation of dominant cloud particle size 05 p0827 A69-16527
- Photographic investigation of gegenschein and cloud satellites at L sub 5 earth-moon libration point, noting gegenschein intensity peak 07 p1212 A69-18602
- Perturbing body influence on motion near triangular Lagrangian solutions of restricted elliptical three body problem applied to earth-moon system under solar perturbations 10 p1779 A69-23612
- Lunar origin theories, considering moon/earth mass ratio, earth-moon system angular momentum deficiency and differential volatilization in earth 14 p2527 A69-29882
- Laser measurements of earth-moon distance applied to determinations of earth axis motion and lunar shape, relief, dimensions and motion 16 p2788 A69-31624
- Apollo 11 moon reflector-laser beam experiment, discussing range changes produced by axial rotation and orbital motion and use for earth-moon dynamics 19 p3339 A69-36766
- Tabulated coherent S-band Doppler data from Pioneer 6 and 7 radio tracking, improving astronomical constants and ephemerides for earth-moon system [AAS PAPER 68-130] 20 p3595 A69-37179
- Hypothetical planet captured by earth, becoming earth satellite /moon/, discussing Mercury orbits peculiarities 20 p3603 A69-37562
- Laser range measurement from earth to lunar retroreflector to study earth tipping and gravitational constant secular decrease 22 p3960 A69-40190

EARTH-MOON TRAJECTORIES

- Asymptotic solutions of restricted three body problem for one parameter periodic orbits in earth-moon synodic system, determining motion near moon 04 p0663 A69-15382
- Libration point relay satellites for continuous communication link between earth and lunar far side, discussing trajectories and halo orbit stationkeeping 15 p2680 A69-30188

- Numerical analysis of asymptotic solution for earth-moon particle trajectories in idealized restricted three body problem 16 p2857 A69-32155
- Earth-moon and moon-earth trajectory parameters related to lunar orbit conditions for synthesizing lunar orbit trajectory 18 p3196 A69-34704

EARTH MOTION

- Earth velocity through 3 K cosmic background radiation, measuring velocity by determining anisotropy of radiation 03 p0511 A69-13475
- Ellipticity of trajectory of free motions of pole of revolution of earth, using harmonic analysis of motion amplitudes and phases 06 p0919 A69-17536
- Earth motion relation to cosmic background radiation excess determined from radiometer study of galactic radiation 17 p3022 A69-32864
- Magnetic fluctuations in various frequency ranges, associated with earth bow shock, detected with search coil magnetometer on OGO 3 22 p3938 A69-40501
- North Pole trajectories and geomagnetic fields assuming motion of earth mantle and interior 22 p3942 A69-41120

EARTH MOVEMENTS

- Spectral peaks for torsional oscillations of earth, estimating free periods from observations at six stations around earth 02 p0243 A69-12007
- Earth pole coordinates calculated from latitude variations at Pulkovo, Greenwich and Washington, giving components of earth motion 03 p0420 A69-13094
- Thermal convection in earth mantle with temperature and pressure dependent viscosity, considering mechanisms for fluid-like mantle 10 p1682 A69-23412
- Earth pole coordinates calculated from latitude variations at Pulkovo, Greenwich and Washington, giving components of earth motion 14 p2433 A69-28776
- Earth polar wanderings attributed to rotation axis angular displacements generated by density redistribution on geologic time scale 20 p3535 A69-38192
- Observations indicating slow earth expansion 22 p4018 A69-40179
- Paleogeographical evolution in support of earth expansion, discussing polar wandering, global continental drift and final complete disruption 22 p3936 A69-40181
- Dynamic processes in upper earth mantle, discussing thermal convection currents and stress propagation 22 p3937 A69-40184

EARTH ORBITS

- Errors arising from inaccurate insertion of initial conditions in autonomous determination of coordinates of object moving along surface of spherical earth 02 p0281 A69-12137
- Electric propulsion for payload transfer from low to synchronous orbit of ELDO launch vehicles 03 p0496 A69-13994
- Communications for Apollo Applications Program, considering extended duration manned missions in low earth orbit and Gemini, Saturn and Apollo hardware 07 p1083 A69-19124
- Satellite altitude stabilization by gravity gradient capture in earth elliptical orbit, showing effect of increase in damping 10 p1791 A69-22926
- Reliability and maintainability analysis of two year spacecraft mission combining earth orbits and Mars program, using computerized mathematical model [AIAA PAPER 68-1059] 12 p2174 A69-26797
- Earth TV pictures from Molniya I communication satellite, showing advantages of high orbit over low orbit photography for global weather analysis and forecasting 13 p2292 A69-27729
- Earth mantle and core friction interaction suggested as cause of secular change in orbital motion obliquity 13 p2253 A69-27821
- Earth orbital entry vehicles weight prediction, noting vehicle geometry as function of vehicle shape, hypersonic lift drag ratio and crew size [SAWE PAPER 770] 18 p3208 A69-34876

Earth ellipsoid determination by satellite observations, noting accuracy of polar flattening measurement on basis of perturbation or perigee argument
18 p3131 A69-35195

Geocentric orbital elements determination of lunar particles expelled into space by meteorite impact, using spheres of influence method
18 p3202 A69-35330

Future combined environment space simulation tests duplicating environment interaction encountered during earth orbits, deep space probes and manned flights
19 p3288 A69-35531

Earth orbit estimation by manual stadimeter, space sextant and small data processor, discussing orbital parameter errors due to instrument and environment uncertainties
19 p3369 A69-35793

Earth orbital space program mission effectiveness increased through utilization of standby launch vehicles, spacecraft and space station systems
19 p3430 A69-36010

Technology flow for future manned earth orbit and lunar operations and planetary exploration
[AAS PAPER 69-494] 24 p4380 A69-42840

EARTH PLANETARY STRUCTURE

Lunar surface early geologic evolution noting bearing on earth geologic history
[AAS PAPER 68-202] 02 p0312 A69-11478

Magnetotelluric method for investigating earth vertical structure with allowance for sphericity
02 p0240 A69-11699

Vertical and horizontal components of geomagnetic storm main phase magnetic variations applied to vertical electromagnetic soundings of earth
02 p0240 A69-11700

Earth structure model based on million random trials using eigenfrequencies, travel times of shear and compressional waves, mass and moments of inertia
02 p0243 A69-12009

Reversals of earth magnetic field, discussing lavas, deep sea sediments, ocean floor magnetic pattern and dynamo theory
04 p0593 A69-15075

Earth upper mantle wave velocity structure based on surface wave dispersion, noting low velocity layers thickness
09 p1491 A69-22153

Magnetotelluric method for investigating earth vertical structure with allowance for sphericity
13 p2258 A69-28730

Vertical and horizontal components of geomagnetic storm main phase magnetic variations applied to vertical electromagnetic soundings of earth
13 p2258 A69-28731

Comet scintillations and tail characteristics studied to obtain information on interplanetary flux field, magnetic fields and planetary structures
14 p2523 A69-29704

Chemical composition of earth, Venus, Mars, Mercury and moon calculated from mathematical models, constructing approximate equations of state at high pressure
14 p2526 A69-29878

Love wave amplitude data satisfying earth model with intrinsic internal friction at depths assumed due to single thermally activated relaxation
15 p2596 A69-30624

Planetary systems interrelationship with binaries and rotating stars, emphasizing occurrence frequency study based on stellar angular momentum orientation
17 p3032 A69-33105

Mars internal structure and composition modeling, considering core, mantle and temperature via earth analogy and Mariner 4 data
17 p3037 A69-33652

Monte Carlo inversion of seismic body waves for transposing uncertainties of observations to velocity models
17 p2962 A69-33654

Eclogite fractionation role in creation and spreading of suboceanic lithospheric plate, discussing density determination at 100 km depth
18 p3132 A69-35434

Book on thermal processes of earth and moon covering heat generation and transfer, internal temperatures, gravitational energy, etc
19 p3401 A69-35887

Stony meteorite barium isotopes and iron meteorite and terrestrial silicate inclusions analyzed using double spike method for laboratory fractionation correction
19 p3425 A69-36422

Satellite representations of earth gravity field portraying consistent pattern of mass anomalies due to density differences in layers
20 p3523 A69-37566

Planetary interiors from geophysical viewpoint emphasizing earth data
21 p3811 A69-39508

Earth temperature distribution using various models, noting excess of total heat production in interior vs heat flow during planet history
21 p3718 A69-39732

Earth early thermal history with core formation before emplacement of earliest known rock possessing remanent magnetism
22 p3936 A69-40136

Ancient and present earth radii ratios determined by triangulation using paleomagnetic sites situated on different paleomericidians
22 p3937 A69-40183

Geophysical aspects of earth chemical composition, structure and energy balance
22 p4032 A69-40983

North Pole trajectories and geomagnetic fields assuming motion of earth mantle and interior
22 p3942 A69-41120

Terrestrial type planetary evolution from early history and present internal configuration of earth, discussing gravitational energy associated with earth formation
23 p4212 A69-41613

Impedance of inhomogeneous earth from magnetic and electric fields and geomagnetic potential measurements
23 p4157 A69-41867

Model for accumulation of earth and planets from primitive solar nebula, implying inhomogeneous chemical composition of bodies in solar system
24 p4385 A69-43215

EARTH RADIATION

U TERRESTRIAL RADIATION

EARTH RESOURCES

NT COAL
NT CRUDE OIL
NT FARM CROPS
NT FORESTS
NT GRAINS [FOOD]
NT GRANITE
NT LAVA
NT RIVERS
NT ROCKS
NT SANDSTONES
NT SHALES
NT VEGETATION

Integrated landscape analysis with radar imagery for earth resources
15 p2608 A69-30454

Aerospace images information suppressing and enhancing methods to aid interpreter in making more accurate recognition and measurement of earth resources subjects
18 p3133 A69-34338

Satellite IR hyperaltitude imagery for earth resources application, obtaining geological, meteorological and hydrological information
20 p3536 A69-36930

Domestic and international law compared in connection with space program, considering legal aspects of using satellites in discovering and exploiting earth resources
20 p3639 A69-37132

Spacecraft and boosters for earth resources surveys, discussing design, payloads, orbits, etc
21 p3799 A69-38629

Airborne electromagnetic systems measuring complex dielectric constant in earth crust for mineral and water resources exploration
[RAES PAPER 8] 22 p3946 A69-40481

Systems analysis method for determining spacecraft remote sensors earth resources survey effectiveness by integrating specifications, mapping requirements and orbital characteristics
23 p4163 A69-41567

Orbiting vehicles remote sensing of earth resources, discussing instrumentation and accuracy requirements, data management and analysis and effectiveness criteria
24 p4315 A69-43199

EARTH RESOURCES PROGRAM

Earth orbital satellites for geologic applications, discussing Gemini photograph qualities and influence on Earth Resources Observational Satellite program
[UN PAPER 68-95441] 01 p0065 A69-10509

Remote sensors utilization in earth orbital space for discovery, inventory, evaluation, development and conservation of earth natural resources, noting satellite design
[UN PAPER 68-10464] 01 p0065 A69-10532

Book on Demeter-earth resources satellite system covering design, instrumentation, cost estimates, economic benefits and political considerations
01 p0163 A69-11333

European space programs requirements for satellite launch autonomy/independence from U.S. and U.S.S.R., discussing satellite applications for resource surveys, weather forecasting, etc
02 p0335 A69-12682

Agricultural remote sensing information system composed of data acquisition, processing and information extraction and interpretation phases, providing knowledge of earth resources
03 p0400 A69-13195

Application satellites for air traffic control, meteorology and earth resources, considering European participation
03 p0520 A69-13587

Technological base for planning space flight missions to obtain data on earth resources, detailing earth resources technology satellites /ERTS/
05 p0830 A69-15921

Earth resource information from spacecraft including landmapping, geological photographs, hydrological and oceanographic data, etc
06 p0916 A69-16855

TV system producing images with 5000 line resolution, proposing application in Earth Resources Observation Satellite
07 p1131 A69-18552

Color TV system for Earth Resources Observation Satellite /EROS/, discussing resolution in relation to spectral separation through data simulation study
[SMPT PAPER 105-79] 12 p0277 A69-25767

Space photography for natural resource inventory, describing Gemini photographs role in assessing vegetation, geological, metal and soil resources in Western Hemisphere
12 p2097 A69-26987

Remote sensing technology application to improving range resource inventories, discussing aerial photography, optical, IR and radar scanning, etc
12 p2098 A69-26992

European earth resource satellite systems technology, applications and costs
13 p2356 A69-27833

Earth Resources Technology Satellites design for complete spectrum of frequencies
14 p2453 A69-29952

Satellite and aircraft use compared for earth resource surveys, discussing proposed aircraft data collection system
16 p2881 A69-31632

Manned spacecraft earth resource sensing, discussing advantages and applications in agriculture, forestry, geography, hydrology, oceanography and geology
18 p3208 A69-35058

NASA Earth Resources Survey Aircraft Program, describing aircraft and remote sensors characteristics
19 p3312 A69-36259

International organizations and planning for earth observation satellite program involving exploitation in communications, meteorology and aircraft
21 p3855 A69-38622

Orbital images for earth resources satellite mission planning using Mercury, Gemini and Apollo synoptic terrain photographs
21 p3721 A69-38632

Aerial remote sensing data for earth resources program including agricultural, geothermal/ geological tests, hydrological, water pollution and soil and flood water control observations
22 p3949 A69-40994

Earth orbital remote sensing applications to forest and range resources management, discussing conventional aerial photography
[AAS PAPER 69-059] 24 p4307 A69-42823

Earth resources surveys by space flights and plans for future satellites, describing results of EROS and ERTS programs
[AAS PAPER 69-058] 24 p4307 A69-42824

EARTH RESOURCES TECHNOLOGY SATELLITES

Earth resources remote sensing from spacecraft noting meteorology, oceanography, forestry, agriculture and IR detection of plant diseases and pollution
12 p2192 A69-26978

Electromagnetic waves as data carriers for earth resources and technology satellite sensors
15 p2607 A69-30231

Satellite and aircraft use compared for earth resource surveys, discussing proposed aircraft data collection system
16 p2881 A69-31632

Earth resource satellites, discussing mapping, land evaluation, geological observation, agricultural and hydrological applications, electromagnetic spectrum information, sensors and photographs
16 p2881 A69-31763

Earth resources satellite /ERS/ TV camera configurations, return beam vidicon camera characteristics and devices for TV picture reproduction on film
21 p3720 A69-38619

Tiros M requirements for earth resources sensor systems, discussing spacecraft structure, dynamics, power, command and communications subsystems
21 p3818 A69-38621

Earth resources technology satellite global survey system carrying multispectral sensors in long life space platform
21 p3720 A69-38623

Earth resources observation technology from satellites, reviewing sensors and methods, electromagnetic spectrum, atmospheric attenuation and windows, passive-active devices
21 p3720 A69-38624

Multispectral radiometric analysis of ERTS images, discussing image registration, SNR and atmospheric and diffraction effects
21 p3721 A69-38627

Earth resources technology satellite /ERTS/ choice regarding local time of ascending node based on cloud cover and IR measurement considerations
21 p3798 A69-38628

Automatic speech recognition and tracking techniques of moving objects, considering applicability to processing data from earth resources satellites
21 p3721 A69-38630

Surveying earth resources from space, covering orbital height photography in cartographic programs, hydrologic engineering, pollution control and geology
22 p3936 A69-40170

Earth resources surveys by space flights and plans for future satellites, describing results of EROS and ERTS programs
[AAS PAPER 69-058] 24 p4307 A69-42824

EARTH ROTATION

Atmospheric circulation influence on earth rotation velocity, discussing estimation methods
02 p0236 A69-11641

Synodic month length variations since late Cambrian, noting paleontological evidence in mollusks and stromatolites and associated geological changes
02 p0241 A69-11807

Viscous damping of internal waves on rotating earth, analyzing spatial propagation attenuation in two layer system
02 p0247 A69-12775

Mean tropospheric wind vectors periods compared to annual variations of earth rotation and pole latitude
08 p1309 A69-20854

Conversion of Woollard theory coefficients of tidal irregularity of earth rotation to new system of constants
09 p1484 A69-21383

Ponderomotoric forces and irregularities in earth rotation, considering core and lower mantle as closed system with respect to periodic electromagnetic and mechanical effects
09 p1487 A69-21636

Upper atmosphere rotation perturbation effect on satellite orbit when scale height varies with height, showing inclination reduction
09 p1594 A69-21660

Earth rotation and aircraft speed effects on vertical gyroscopes during banking, obtaining formulas for gyro errors
09 p1498 A69-22107

Atmospheric circulation contribution to velocity variations in earth rotation calculated by force moment method
11 p1952 A69-24258

Earth rotation velocities nonuniformity according to astronomical observation data obtained from Universal Time and atomic time scales comparison
11 p1957 A69-24407

Variable solar activity effect on earth upper atmosphere rotation at altitudes from 200 to 300 km
12 p2069 A69-26442

Model for perturbations in earth rotation and geomagnetic core-mantle coupling, discussing electromagnetic restoring torque
12 p2077 A69-27110

Earth polar coordinates determined from latitude observations, discussing weighting functions for determining polar motion
17 p2959 A69-32869

Conversion of Woollard theory coefficients of tidal irregularity of earth rotation to new system of constants
18 p3127 A69-34771

Ponderomotoric forces and sudden irregularities in earth rotation, discussing core-mantle electromagnetic coupling and toroidal field induction effects
19 p3302 A69-35769

Earth-pole wobble /1951-1966/ by spectral analysis using least square fit method
21 p3716 A69-39244

Book on geomagnetic quadrupole field temporal changes and effects on earth rotation, covering physical parameters in earth interior and earth conductivity model correlations
22 p3937 A69-40423

Earth rotation rate variations connected to longitude variations of continentals time services, noting atmospheric circulation and inertial forces role
22 p4024 A69-40609

Earth rotation velocities nonuniformity according to astronomical observation data obtained from Universal Time and atomic time scales comparison
24 p4391 A69-43797

EARTH SATELLITES

NT ACTIVE SATELLITES
NT ALOUETTE SATELLITES
NT ALOUETTE 1 SATELLITE
NT ALOUETTE 2 SATELLITE
NT ANNA SATELLITES
NT APPLICATIONS TECHNOLOGY SATELLITES

NT ARIEL 3 SATELLITE
NT BEACON SATELLITES
NT BIOSATELLITE 2
NT BIOSATELLITES
NT COMMUNICATION SATELLITES
NT COSMOS SATELLITES
NT COSMOS 5 SATELLITE
NT COSMOS 6 SATELLITE
NT COSMOS 149 SATELLITE

NT D-1 SATELLITE
NT DIADEME SATELLITE
NT DODGE SATELLITE
NT EARLY BIRD SATELLITES
NT ECHO SATELLITES
NT ECHO 1 SATELLITE
NT ELEKTRON SATELLITES
NT ELEKTRON 4 SATELLITE
NT ESRO 1 SATELLITE
NT ESRO 2 SATELLITE
NT ESRO SATELLITES

NT ESSA SATELLITES
NT EUROPEAN 1 SPACECRAFT
NT EXPLORER SATELLITES
NT EXPLORER 1 SATELLITE
NT EXPLORER 16 SATELLITE
NT EXPLORER 18 SATELLITE
NT EXPLORER 20 SATELLITE
NT EXPLORER 22 SATELLITE
NT EXPLORER 26 SATELLITE
NT EXPLORER 29 SATELLITE
NT EXPLORER 30 SATELLITE
NT EXPLORER 31 SATELLITE
NT EXPLORER 33 SATELLITE
NT EXPLORER 35 SATELLITE
NT EXPLORER 38 SATELLITE
NT EXPLORER 40 SATELLITE

NT GEODETIC SATELLITES
NT GEOPHYSICAL SATELLITES
NT GEOS 2 SATELLITE
NT HEOS 1 SATELLITE
NT HEOS SATELLITES
NT IMP
NT INJUN SATELLITES
NT INTELSAT SATELLITES
NT ISIS-A
NT LINCOLN EXPERIMENTAL SATELLITES
NT METEOROLOGICAL SATELLITES
NT MICROMETEOROID EXPLORER SATELLITES

NT MOLNIYA SATELLITES
NT MOON
NT NAVIGATION SATELLITES
NT NIMBUS SATELLITES
NT NIMBUS 3 SATELLITE
NT OAO
NT OGO
NT OGO-D
NT OGO-E
NT OGO-F
NT ORBIS CAL SATELLITE
NT PROTON SATELLITES
NT PROTON 2 SATELLITE
NT RADIO ASTRONOMY EXPLORER SATELLITE

NT RELAY SATELLITES
NT SAN MARCO SATELLITE
NT SAN MARCO 2 SATELLITE
NT SYNCHRONOUS METEOROLOGICAL SATELLITE
NT SYNCOM SATELLITES
NT TIROS SATELLITES
NT TIROS 9 SATELLITE
NT TRANSIT 4A SATELLITE
NT TRANSIT SATELLITES

NT VELA SATELLITES
NT VENERA SATELLITES
NT VENERA 4 SATELLITE
NT ZODIACAL DUST

Ship navigation by altitude and azimuth measurements of artificial earth satellite, discussing position and reference errors and synchronous satellite advantages
[UN PAPER 68-95247] 01 p0112 A69-10461

First approximation stability of single rotation of artificial earth satellite about center of mass in Newtonian gravitational force field
01 p0161 A69-10585

Soviet artificial earth satellites, discussing Sputnik, Polet, Elektron, Cosmos, Molniya and Vostok series
01 p0162 A69-10937

Earth and lunar magnetic field studies in U.S.S.R., discussing Soviet earth satellite and lunar probe data
01 p0066 A69-10943

French satellites structure, power and communications systems, stabilization and detector groups
02 p0333 A69-11917

Geopotential resonant orbital perturbations of existing satellites, noting high inclination role
03 p0521 A69-13777

Earth resource satellites, discussing world ground station network for data reception and information dissemination and training and research center
[UN PAPER 68-95529] 06 p0917 A69-17067

Solar flare proton radiation effects on earth satellites and solar probes, considering sunspot cycle 20, earth magnetic field shielding and Van Allen radiation belts
12 p2151 A69-26873

Lunar surface and earth early satellite system, discussing maria distribution, satellite impacts and close passage collisions
13 p2345 A69-27654

Artificial earth satellites positional observations by graphical smoothing on azimuth and altitude, discussing advantages for space geodesy
15 p2594 A69-30029

First approximation stability of single rotation of artificial earth satellite about center of mass in Newtonian gravitational force field
15 p2702 A69-30755

Transit forecast of terrestrial satellite moving through fixed coordinate line in assigned reference
16 p2859 A69-32221

Attitude control system for 625 A-1 research earth satellite, detailing operation and test program
17 p3050 A69-33426

Ground traces of artificial earth satellites with respect to perturbations due to atmospheric drag, earth oblateness and moon and sun as third body
19 p3398 A69-35614

Attitude stabilization of symmetrical nonrotating earth satellite using earth-pointing rotor as gravitational anchor
19 p3429 A69-35914

Relative motion of two bodies linked by flexible weightless tether in artificial earth satellite orbit, simulating extravehicular walk
19 p3427 A69-36618

Instantaneous and integral solar irradiance of earth oriented satellite surface, noting solar illumination nomogram representation
19 p3432 A69-36629

Earth satellite sweeping mass spectrometer for measuring atmospheric neutral particle and positive ion concentration
19 p3314 A69-36681

Short radio wave damping of earth satellite transmitter due to ionospheric diffraction resulting from increasing satellite-ground station distance
20 p3491 A69-37689

Orbital parameters of short-lived low altitude earth satellites assuming no atmospheric drag, no orbital precession and flat earth condition
21 p3798 A69-38626

Linear multichannel spatial motion control systems for vehicles orbiting in earth atmosphere at supersonic velocities
21 p3766 A69-39645

Optimal control system for earth satellite orbital transfer, using wandering ellipse technique to develop trajectory correction algorithm
21 p3767 A69-39652

Algorithms for close earth satellite orbit calculation developed by numerical integration methods, discussing solution efficiency
[AIAA PAPER 69-948] 22 p4021 A69-40331

Integral electron concentration in column of space between earth satellite and ground determined by integral equation, assessing errors minimization methods
23 p4157 A69-41858

EARTH SHAPE
U GEODESY
EARTH SURFACE

Earth surface shape determinations by geodetic networks connecting ground observation points and satellite positions
[UN PAPER 68-95377] 01 p0065 A69-10528

Terradynamic research program for studying instrumented projectile penetration of terrestrial materials
02 p0228 A69-11767

Earth ionosphere resonator natural frequencies, considering diurnal variation and geomagnetic field eccentricity
03 p0422 A69-13512

Accretion rate of cosmic dust estimation from cosmogenic aluminum-26
03 p0514 A69-13935

Earth surface temperature change quantitative determination due to Milankovitch insolation variations
03 p0426 A69-14232

Lunar craters compared with underground explosion craters on earth, determining criteria for identifying explosion craters on moon
04 p0656 A69-14670

Electromagnetic phase measurement for determining integrated air density near earth surface
04 p0598 A69-14910

Aircraft measurements of stratus cloud absorption and albedo and earth surface albedo
04 p0627 A69-14914

Turbulent transport of energy in atmospheric boundary layer near earth surface resulting from forced convection
04 p0627 A69-15087

Radio wave diffraction by knife edge obstacle on conducting earth surface noting effect on radio propagation
[AFCRL-68-0375] 04 p0560 A69-15216

Earth space image interpretation in various spectral regions, discussing effectiveness of photography, spectrophotometry, radar and microwave observations
05 p0763 A69-16054

IR scanning systems of meteorological satellites for detection of clouds and various underlying surfaces, determining detection probability and errors
06 p0952 A69-17986

Radio profilograph designed for integrating aircraft excess altitudes and measured distances between aircraft and earth, discussing block diagram
07 p1132 A69-19006

Exchange coefficient of energy balance of earth surface for propagation studies of entrained atmospheric contaminants
09 p1535 A69-21514

Stereophotogrammetric measurements of smoke columns for wind soundings
09 p1535 A69-21517

Air layer between target and instrument effect on earth surface temperature conducted with airborne radiometers
09 p1536 A69-22166

Secular variations distribution on earth surface, plotting isopor charts from mean annual values of magnetic elements/1960-1965/
10 p1687 A69-23920

Forced convection in atmospheric boundary layer above nonuniformly heated earth surface, noting roles of wind and stratification parameters
12 p2126 A69-26579

Extensive cosmic ray showers structure at sea level, using multiple hodoscopic counters and control system
13 p2332 A69-28405

Sea level fluctuations of electron-photon, muon and active nuclear components of extensive cosmic ray showers determined, obtaining shower parameters
13 p2332 A69-28406

Surface impedance of spherical earth isolated by nonconducting atmosphere from ionospheric currents producing alternating electromagnetic field
14 p2438 A69-29082

Earth radar studies, relating echo behavior to rocket altitude and surface electrical characteristics
14 p2416 A69-29531

Stellar image vibration dependence on zenith distances and terrain relief determined from stellar traces by 200 mm telescope
15 p2647 A69-30163

Signal reflection elimination from underlying surface during aircraft flights by using two antenna array with identical radiation patterns
15 p2567 A69-30345

Dynamic characteristics of local slope winds, considering thermal and geometrical effects of underlying surfaces
15 p2648 A69-30577

Geomagnetic field westward drift related to earth core rotation from calculating drift at earth surface and at core
16 p2774 A69-31983

VLF radio wave propagation in waveguide channel formed by earth and inhomogeneous anisotropic ionosphere
16 p2751 A69-32032

Earth surface heat flow pattern measurement and distribution techniques, considering relation to surface features and tectonic movements of crust
[AIAA PAPER 69-589] 17 p2961 A69-33284

Topographic mapping by high altitude jet aircraft photography
18 p3134 A69-34339

Navigation equations, discussing earth geometry, coordinates, gravity, dead reckoning and orbit computations with regard to LORAN
18 p3169 A69-34845

Near and antipodal fields in earth-ionosphere waveguide using mode theory, ray theory, zonal harmonics series and method of images to derive field representations
19 p3283 A69-35931

Altitude asymmetry of instantaneous auroral oval plotted for geomagnetic pole and earth surface
20 p3522 A69-37056

Photogrammetric instruments applied to determination of spatial position of tectonic surfaces by aerial photography
20 p3539 A69-37511

Earth space image interpretation in various spectral regions, discussing effectiveness of photography, spectrophotometry, radar and microwave observations
20 p3545 A69-37964

Fe-Ni unmelted and unablated micrometeorites number at earth surface calculated, using space density of interplanetary particles and micrometeoritic theory
20 p3614 A69-38251

Planetary boundary layer top formation, considering particle velocity, earth surface roughness role, geostrophic wind, etc
21 p3715 A69-38566

Molodenskii boundary value problem exact solution by successive approximations for determination of earth figure, noting quasi-geoid surface
21 p3716 A69-39248

Nighttime atmospheric shape analysis created by lightning and propagating in earth lower ionosphere waveguide
22 p3941 A69-40961

Multispectral color aerial photography using broadband spectral filters for detecting and identifying small environmental features of earth surface
22 p3949 A69-40997

Spheroidal disturbances theoretical seismograms on surface of gravitating elastic sphere with homogeneous mantle and liquid core, considering gravity and polar radial stress effects
23 p4158 A69-42020

Mean absolute relative humidity variations above earth surface over various time intervals during cloudless nights, obtaining spatial humidity differences and corresponding extinction coefficients
24 p3436 A69-43158

EATING

Lateral hypothalamic stimulation bound eating motivation in animals, comparing electrical stimulation and hunger elicited eating
17 p2910 A69-33752

EBULLITION
U BOILING

ECCENTRIC ORBITS

Rotational locks for arbitrary eccentricity orbit satellites
19 p3397 A69-35609

Comet observations and orbit determinations, noting eccentricity of comet Thomas
19 p3403 A69-35970

First approximation stability of triangular Lagrange solutions of restricted elliptical three body problem, formulating power series for orbital eccentricity
20 p3575 A69-37318

Recurrence formulas for calculating Fourier expansions in elliptic motion in terms of eccentric and mean anomaly
21 p3807 A69-39342

Capture and gravity gradient stabilization of LIDOS satellite in eccentric orbit
[AIAA PAPER 69-921] 21 p3821 A69-39351

Practical stability of highly eccentric orbits quasi-normal to ecliptic, discussing parameters influence on orbital lifetime with reference to approximate stability criteria
[AIAA PAPER 69-926] 21 p3808 A69-39355

Computer program for eccentric geocentric satellite orbits evolution, discussing atmospheric drag, earth oblateness and solar radiation effects
[AIAA PAPER 69-928] 21 p3808 A69-39357

Errors in determining controlled satellite rotation periods, proposing scheme for corrected trajectory calculation of small eccentricity orbits
22 p4033 A69-41086

ECCENTRICITY

Inertia effect of flow between eccentric cylinders with rotating outer cylinder, calculating pressure and shearing distribution and force on inner cylinder
01 p0059 A69-10307

Orbits with small eccentricities and inclinations in generalized problem of two fixed centers, showing osculating elements relationship to intermediate orbit elements
10 p1779 A69-23613

Misalignment and eccentricity effect on face seal, discussing leakage dependence on phase angle
[ASLE FICFS PREPRINT 15A] 15 p2620 A69-30483

Eccentric face seal with tangentially varying film thickness, analyzing leakage flow proportional to eccentricity and surface waviness
[ASLE FICFS PREPRINT 15B] 15 p2620 A69-30484

Exact analytic solution for thermal conductance of two dimensional eccentric constriction in dimensionless numbers
18 p3228 A69-34375

Stability of thin walled eccentrically reinforced cylindrical shell, determining eccentricity influence and critical pressure formula from considerations of Poisson ratio, reinforcement parameters, etc
18 p3216 A69-34576

ECHO PROJECT

Communication satellites development in U.S.S.R., discussing Molniya 1 satellite design and objectives and Echo 2 satellite transmission experiments
01 p0032 A69-10949

ECHO SATELLITES

Solar UV radiation reflected from Echo satellites measured and compared with UV fluxes from Lyrae
14 p2447 A69-29408

ECHO SUPPRESSORS

Line filter compression and positioning of bipolar video pulse trains for conjunctive use with moving target indicator in echo elimination
04 p0558 A69-15071

ECHO 1 SATELLITE

Echo 1 aluminized plastic balloon satellite, discussing radio linkup by reflections, use in geodesy and atmospheric and radiation pressure effects on lifetime
10 p1792 A69-23804

ECHOES

NT ANGELS
NT AURORAL ECHOES
NT CLUTTER
NT LUNAR ECHOES
NT LUNAR RADAR ECHOES
NT RADAR ECHOES
NT RADIO ECHOES
NT SIGNAL REFLECTION
NT SOLAR RADAR ECHOES
NT VENUS RADAR ECHOES

Coulomb collision and microturbulence effect on plasma wave echo, noting echo dependence on perturbations in particle distribution
03 p0474 A69-13144

High order plasma wave echoes formulation and relation to initial perturbations based on Landau solution of initial value problem for Vlasov equation
15 p2661 A69-30926

Photography of laser echoes on satellites, tabulating results
15 p2570 A69-31311

Spatial ion wave echoes emphasizing echo line shape analysis and effects of ion-neutral and ion-ion collisions
16 p2818 A69-31676

Electromagnetic echo generation in collisionless spatially homogeneous plasma dependence on velocity distribution and magnetic interaction
16 p2818 A69-31677

Plasma wave echoes concept extended to transverse electromagnetic wave excitation propagating parallel to external magnetic field
16 p2823 A69-32467

- Earth albedo effect on ionospheric D layer determined from aircraft sounding of E layer echo amplitude above reflecting cloud cover
18 p3127 A69-34800
- Gas molecule collision influence on photon echo intensity produced by two linearly polarized laser pulses incident on sulfur hexafluoride
21 p3774 A69-38589
- Computer experiment on 9000 particle plasma to test temporal echo theoretical prediction
21 p3777 A69-38713
- Electromagnetic backscattering by perfectly conducting prolate spheroid, predicting echo signal in resonance region
23 p4115 A69-41584

ECLIPSES

NT LUNAR ECLIPSES

NT SOLAR ECLIPSES

- Book on eclipse phenomena in astronomy covering moon, earth and other planets, occultation, planets transit over sun, influence in radio astronomy, etc
19 p3425 A69-36379

ECLIPSING BINARY STARS

- Empirical relation between B-V color and radiation temperature by observing eclipsing variables undergoing total eclipses
03 p0469 A69-13964
- Photoelectric observations of Aurigae during 1963-1964 eclipse, noting reliability of equipment and effect on observation series
08 p1388 A69-20242
- Radial velocity curve, orbital elements and masses and radii of components of eclipsing binary system 9 Chamaeleontis/BV 430/
08 p1391 A69-20395
- Photoelectric light diagrams for eclipsing binary star
08 p1392 A69-20565
- Spectroscopic residual intensities variation of metallic and hydrogen lines of eclipsing system R Canis Majoris with phase, discussing surrounding gaseous matter
08 p1396 A69-20646
- Russell method application to combined data of both minima of eclipsing binary using electronic computers
08 p1408 A69-21136
- Brightness curves of eclipsing systems under monotonicity of unknown functions, using stable algorithm
09 p1588 A69-21363
- Limb darkening nonlinearity effects on solutions for brightness curves of eclipsing binaries
09 p1588 A69-21364
- Dimensions of 19 variable eclipsing binaries from published photometric and spectral orbital elements
09 p1590 A69-21378
- Eclipsing binary AU Puppis studied photoelectrically in yellow and blue light, noting period decrease by 1.3 sec in last 40 years
10 p1774 A69-22968
- Yellow and blue photoelectric observations of eclipsing binary CO Lac
10 p1775 A69-23202
- Photometric over dynamical ellipticity excess attributed to gravitational darkening in eclipsing binaries of W Ursae Maioris type
10 p1776 A69-23217
- Photometric consequences of reflection effect in close binaries, tabulating light curves
10 p1776 A69-23218
- Binary eclipsing visual star systems angular momentum, discussing evolution
10 p1777 A69-23313
- Absolute dimensions of 34 eclipsing variables having both components near main sequence, comparing mass luminosity and mass spectrum to homogeneous model stars
11 p1952 A69-24248
- UBV photometry observations of eclipsing binary AG Persei at Mount Palomar with 51 cm reflector
12 p2156 A69-26220
- Photoelectric and visual minima tabulated for eclipsing binaries, calculating light elements
12 p2160 A69-26853
- Two channel polarimeter capable of eliminating atmospheric scintillation effects used for observation of magnetic stars and eclipsing binary u Herculis
13 p2347 A69-27713
- Eclipsing close binary stars orbital planes spatial position determined from stellar emission polarization
15 p2688 A69-30560
- Nonlinear limb darkening corresponding to nongray stellar atmosphere model applied to light curve for compact eclipsing binary systems
15 p2689 A69-30563

- Spectrographic and photoelectric analyses of F type sharp line eclipsing binary HR 7484, tabulating masses, radii, color indices and absolute magnitudes
15 p2693 A69-30776

- Photoelectric observations program at Astronomical Observatory of Bucharest to determine smallest moments of several eclipsing stars
15 p2696 A69-31224

- Photoelectric observations in B and V colors of binary system S Equ
16 p2858 A69-32212

- Nonocculted areas of Algol during eclipse using Balmer discontinuity spectrophotometric method, determining apparent stellar diameters
16 p2858 A69-32216

- Eclipsing binary CQ Cephei envelope variability determined from photoelectric light curve, using astronomical telescope
16 p2864 A69-32593

- Brightness curves of eclipsing systems under monotonicity of unknown functions, using stable algorithm
18 p3197 A69-34753

- Limb darkening nonlinearity effects on solutions for brightness curves of eclipsing binaries
18 p3197 A69-34754

- Dimensions of 19 variable eclipsing binaries from published photometric and spectral orbital elements
18 p3198 A69-34766

- WY Gem star spectroscopic observation showing peculiarity about forbidden and absorption spectra superposition
20 p3598 A69-37464

- Fluxes and luminous efficiencies tabulated for main sequence and subgiant stars within reflection effect problem in eclipsing binaries and Chandrasekhar nongray atmospheric models
20 p3600 A69-37479

- Spectroscopic orbital elements of eclipsing binary IZ Per determined from 22 spectra using Wilsing and Russell method
21 p3795 A69-38469

- Photoelectric observation of EM Cygni eclipsing binary and old nova
22 p4015 A69-40151

- Photoelectric observations of eclipsing binary 32 Cygni during 1968 eclipse using standard UVB color filters, tabulating results of UVB photometry
22 p4032 A69-40946

- Eclipsing binaries spectroscopic and photometric data compared to Iben and Horn models of main sequence stars, noting stellar mass effects
23 p4208 A69-41287

- Photometric data for variable stars in Lyra and Cygnus including eclipsing variables
23 p4215 A69-42009

ECLIPTIC

- Source position of cosmic ray diurnal anisotropy relative to ecliptic plane from neutron monitor data at Mawson and Churchill stations
18 p3189 A69-35441

- Practical stability of highly eccentric orbits quasi-normal to ecliptic, discussing parameters influence on orbital lifetime with reference to approximate stability criteria [AIAA PAPER 69-926]
21 p3808 A69-39355

ECLOGITE

- Eclogite fractionation role in creation and spreading of suboceanic lithospheric plate, discussing density determination at 100 km depth
18 p3132 A69-35434

ECOLOGICAL SYSTEMS

U ECOLOGY

ECOLOGY

- Soviet space biology and medicine, discussing ecological physiology, closed system ecology, exobiology and medical tests on cosmonauts
13 p2209 A69-27356

- Earth contamination by returned lunar or Martian material, discussing extraterrestrial biota survival on earth
13 p2210 A69-28467

- Circadian rhythm in dermestid beetles *Trogoderma glabrum* Herbst as response to compulsory constant light and temperature conditions
15 p2557 A69-31469

- Earth ecosystem chemical composition compared with Mars and Venus ecosystems to determine presence of life
18 p3193 A69-34361

- Color and color IR aerial photography compared for estuarine and marshland research, considering detection of turbidity, pollution, salinity, etc
22 p3942 A69-40993

- Aerial photography for near-shore ecology, noting biological cover on ocean floor, submarine biological communities and human activities on submarine life
22 p3894 A69-40995

- Ecological foundations of Haley metalaw and implications of interstellar golden rule, discussing social interaction with alien life forms
23 p4240 A69-41304

ECONOMICS

NT DEMAND [ECONOMICS]

- Aerospace technology role in economic and social benefits [UN PAPER 68-95321]
01 p0178 A69-10467

- Book on Demeter-earth resources satellite system covering design, instrumentation, cost estimates, economic benefits and political considerations
01 p0163 A69-11333

- Economic importance of European communications satellite system development
03 p0535 A69-13583

- Passenger aircraft design to cope with air traffic volume increase in 1970s, discussing economic aspects of high capacity aircraft
04 p0546 A69-14804

- European launch vehicle development program, discussing economic limitations and employment possibilities
04 p0665 A69-14808

- Economic and technical advantages and disadvantages of satellite telecommunications, discussing Telstar intercontinental TV transmission and Soviet Molniya system
04 p0662 A69-15328

- Economic and scientific reasons for using artificial satellites to establish continental geodetic network, noting continental displacements and terrestrial pole motion observations [UN PAPER 68-07445]
06 p0917 A69-17069

- Commercial orbital space stations economics and potential markets, considering fisheries, ocean transportation, air traffic control, resources surveys, pollution reduction, etc
06 p1007 A69-17599

- Air navigation and economics, discussing air traffic control and traffic density effects on fuel consumption and engine life
07 p1052 A69-18661

- Nondemographic model predicting market shares of V/STOL aircraft in competition with automobiles and conventional airliners for short haul intercity business travel markets
07 p1244 A69-18967

- Reliability in aeronautics and astronautics, discussing safety, economic cost of technical delays and effect on public, air transport, design, development, testing, utilization, etc
07 p1053 A69-19287

- Future launch vehicle programs for automated space missions, discussing higher launch velocities and economics [AIAA PAPER 68-447]
09 p1610 A69-21983

- Airport evolution in London, discussing transportation, safety, international trade, economics, aircraft types and noise spectra
09 p1479 A69-22582

- Laser applications to production line metal working, discussing economics, welding, drilling, automation, thermal and atmospheric effects, etc
10 p1698 A69-22985

- V/STOL aircraft future, discussing Federal Government policies, economics, airport planning, engineering problems, etc
10 p1811 A69-23221

- Statistical, economic and psychological aspects of aeronautical and astronautical profitable reliability in relation to operation, using mathematical model
10 p1700 A69-23839

- Boeing 747 operational and economic considerations including capacity, airport constraints, noise factors, landing gear, compatibility, etc
13 p2201 A69-27340

- Application satellites effects on European economy
13 p2382 A69-27834

- Flexible skirt design for air cushion vehicle consisting of semicylindrical elements and permitting horse power and cost reductions
13 p2203 A69-28179

- Book on subdivision of aircraft structural design covering technology, economics, working conditions, performance, etc
14 p2456 A69-29860

- Digital computers for aircraft engines control, discussing economic assessment, advantages and basic control system
15 p2671 A69-30323

Turbulent process employing product constituents dilute suspensions in inert carrier /Quickmix/ to obtain solid propellant mixtures, discussing plant design and analysis, economics, etc
[AIAA PAPER 69-517] 17 p2978 A69-33033

Air transport systems aspects including efficiency, performance and economics interplay for subsonic and supersonic aircraft
17 p3018 A69-33218

Expenditures for R and D effect upon U.S. economy
17 p3076 A69-34041

R and D for economic growth, discussing interaction between management, planning, engineering, marketing, production, customers and competitors
17 p3077 A69-34126

Semiconductor reliability evaluation program for economical experimental design, noting stress tests
18 p3232 A69-34496

Jumbo aircraft production technology causing economic setback, recommending added emphasis on passenger/cargo requirements and operating environments for greater profitability
18 p3232 A69-34542

Crane helicopters for heavy lift transport mission, noting weight and size effect on productivity
[SAWE PAPER 782] 18 p3091 A69-34905

Cargo aircraft future design regarding engine development, structural flexibility, airport compatibility, cargo handling, etc
18 p3092 A69-35467

Jet noise effect on real estate value, discussing market survey, insulation and navigation easement costs and litigation damages
[AIAA PAPER 69-802] 19 p3288 A69-35594

Aircraft Economic Design Evaluation /AEDE/ computerized model to estimate aircraft design performance differences economic impact to carriers
[AIAA PAPER 69-814] 19 p3289 A69-35626

Space age metals supply and demand relationships, discussing system engineering criteria for maximum efficiency
19 p3346 A69-36635

Book on systems cost effectiveness covering methodology, system cost models, economics, etc
20 p3640 A69-37533

Space rendezvous methods from developmental environment to operational method
21 p3824 A69-39474

Airline economics long term trends requiring management tools for cost control, operations simulation and monitoring, computer use and information data processing
[SAE PAPER 690414] 23 p4241 A69-41641

Scaled Ni-Cd battery with bipolar construction to reduce internal resistance and increase power bursts capacity, emphasizing electrical characteristics and economic considerations
23 p4072 A69-42283

Management activities related to economics of failure in aerospace industry
24 p4416 A69-42777

SST contribution to commercial aircraft transportation, discussing economic and operational aspects, decision making process leading to fixed wing design, etc
[AAS PAPER 69-323] 24 p4252 A69-42869

Economic aspects of future space activities noting systems analysis, operations research, manned and unmanned space capabilities, etc
[AAS PAPER 69-113] 24 p4418 A69-42878

Communication satellites european development, discussing economic and technological problems, stressing color TV and SHF/FM transmission, compared to conventional ground station transmission
24 p4393 A69-43133

ECONOMY

Air traffic prediction based on mathematical econometric methods
03 p0536 A69-14105

Turbine blade cooling emphasizing economics, service life and computerized calculations
17 p3020 A69-33352

EDDIES

U VORTICES

EDDINGTON APPROXIMATION

Eddington approximation to solve radiative transfer equation
02 p0282 A69-12703

Eddington approximation to radiative transfer equation extended to time dependent multifrequency problems
09 p1541 A69-22254

EDDY CURRENTS

Electrical conductivity standards and eddy current measurements noting calibration facility
01 p0081 A69-10830

Beryllium nondestructive tests, discussing eddy current inspection, ultrasonics, film radiography and scintillation
[SAE PAPER 680652] 03 p0444 A69-13546

High temperature eddy current crack detection technique for atomic reactor components under high thermal gradients
04 p0607 A69-14972

Eddy current damping systems for gravity gradient stabilized satellites, discussing electromagnetic torque and various parametric relationships
07 p1228 A69-18341

Eddy current nondestructive tests of nonmagnetic thin metallic sheets and plates from single surface
10 p1698 A69-23046

Metal surface distribution of electromagnetic field from striding transducer in eddy current flow detection, calculating magnetic field component
10 p1697 A69-24071

Steady helical discharges /skin effect/ in air and Ar under high pressure without gas injection, discussing discharge stability factors
12 p2140 A69-27122

Electrical conductivity, hardness, ultimate tensile strength and yield strength correlations of age hardenable Al alloys by eddy current methods
15 p2641 A69-31513

Eddy current and ultrasonic applications to aircraft engine inspection, discussing electric and magnetic methods for quality control during fabrication
15 p2632 A69-31516

Nondestructive eddy current testing of chromium steel for early stage fatigue damage of aircraft components
18 p3136 A69-34777

Eddy current machine /nondestructive testing device/ for aircraft structures surface cracks detection
21 p3719 A69-38391

Eddy current plasmoids formation in potential magnetokinematic plasma flux found economical in terms of energy requirements
23 p4214 A69-41834

Mechanical stress measurement in cylindrical steel subjected to loads inside coaxial transducer, using transducer signal in contactless eddy current method
24 p4296 A69-42654

Structural detection in steel welded joints using higher harmonics from eddy current sensing element
24 p4319 A69-42886

EDDY DIFFUSION

U TURBULENT DIFFUSION

EDDY VISCOSITY

Incompressible turbulent boundary layer analysis by two region characterization for eddy viscosity, using Spalding generalized function and Prandtl free shear flow model
17 p2951 A69-33255

Adiabatic compressible turbulent boundary layer equations for two dimensional and axisymmetric flows, discussing methods of solution based on eddy viscosity formulation
[AIAA PAPER 69-687] 17 p2955 A69-33470

Turbulent velocity distribution and wall friction calculated from eddy viscosity distribution for concentric annulus
17 p2956 A69-33575

Turbulent Schmidt number as function of ratio between turbulent and molecular kinematic viscosities for He, carbon dioxide and normal octane eddy diffusivities
21 p3852 A69-39432

EDEMA

Effects of oxygen saturation variations of blood on rates of weight gain in isolated perfused canine lung, noting pulmonary edemogenesis
22 p3887 A69-41189

EDGE DISLOCATIONS

Slip band continuity across grain boundaries in aluminum bicrystals reexamined for geometrical criteria
01 p0095 A69-10607

Scanning electron beam display of space charge of defects and junction behavior of edge dislocation array in Ge and Si monocrystals
02 p0301 A69-12661

Effective slip systems in hexagonal close packed magnesium alloy under static and hydroexplosive loading, examining flow mechanism for fine structure formation
04 p0615 A69-14639

Plastic yield on inclined slip planes at tip of crack deformed in antiplane strain
05 p0842 A69-16436

Brittle fracture criterion for small steel specimens based on interaction between stress concentration of initial crack and nearby slip band
07 p1238 A69-19694

Edge dislocations effect in perpendicular slip planes on work hardening and strain aging, calculating dilatation centers absorbed
07 p1238 A69-19695

Slip band extrusions in hexagonal close packed Cd, Mg and Ti subject to cyclic stresses, noting microstructure changes
12 p2116 A69-26912

Plastic strains at crack tips in thin plate under concentrated forces, analyzing slip bands during initial deformation
15 p2708 A69-30659

Plastic flow anisotropy and texture shifting by rolling in Ti-Mo-V alloy, analyzing slip rotation, grain boundary shear and deformation mode
17 p2987 A69-33078

Nickel solid solutions strengthening under cold deformation studied by X ray, noting screw and edge dislocations role
18 p3157 A69-35246

Molybdenum single crystals deformation in direct shear, determining stress temperature dependence and critical regions for various slip systems
19 p3342 A69-35811

EDGE LOADING

Stress distribution in composite cantilever beams of three layers with end loading solved by closed form elasticity method
01 p0172 A69-11266

Deflection of orthotropic sandwich plates with unequal facing thickness with edges subjected to uniform and concentrated loading
01 p0172 A69-11270

Direct matrix method for evaluation of critical loads and buckling modes for nonuniform flexural rigid plates having end and side constraints
03 p0522 A69-12866

Stress-strain state of thin elliptical shell of revolution under rapidly varying cyclic edge loads
05 p0832 A69-15686

Green function for stress intensity factors of rectangular plate edge cracks, noting application to thermal stresses
[ASME PAPER 68-WA/MET-19] 05 p0839 A69-16157

Stress-strain state of shell having one end clamped and other under concentrated bending moments and concentrated force acting along generatrix solved by integral equation
05 p0843 A69-16681

Plate deflection in own plane under moments applied to ends using elasticity theory, deriving relation between stress tensor and stress function
06 p1021 A69-17177

Exponential decay of stresses in circular elastic cylinders subject to axisymmetric self equilibrated end loads
06 p1023 A69-17507

Semibrittle material compaction influence on stress distribution in infinite plate with edge loaded circular hole, noting stress-strain relation nonlinearities
11 p1972 A69-24656

Warping rigidity effect on stability of cantilever bar under eccentric follower end load, discussing bending torsional flutter and buckling
12 p2179 A69-26212

Symmetrical stressed state of shallow shell with crack edge loading solved in Cartesian coordinates
12 p2181 A69-26614

Bending state of shells of revolution due to edge effects using nonlinear stress strain relation
13 p2362 A69-27921

Stressed state of cylindrical circular shell clamped at edges and subjected to concentrated radial forces
13 p2368 A69-28322

Thin elastic plates buckling under small normal load and external edge force
14 p2531 A69-28810

Steady natural oscillations of unbounded brittle plane with cut under edge load, showing decreased critical load in presence of inertial effect
15 p2703 A69-30050

Strains determination for laterally edge loaded rectangular plate and sagittas determination of perpendicularly loaded plate proved analogous
15 p2704 A69-30295

EDGES

Flat rectangular plates large deflection due to uniform lateral pressure and compressive edge loading analyzed through partial differential equations, difference equations and computer program
20 p3620 A69-37000

Stress concentration in elastic plate reinforced at edge by straight rib analyzed in finite form by Cauchy integrals and Fourier transforms
22 p4041 A69-40114

Dynamic stability of circular isotropic plate with central hole subjected to torsional moment uniformly distributed over both edges by equilibrium equation
22 p4043 A69-40455

Elastically symmetric thin plate stress-strain state under uniformly distributed load applied to edges
22 p4046 A69-41061

Flat square plates loaded along two opposite straight edges, analyzing postbuckling behavior and geometric imperfections effects
23 p4234 A69-42395

Plane problem of infinite strip weakened by crack, determining crack form under uniformly distributed tensile loads applied to edges
24 p4395 A69-42592

Orthotropic fiberglass/epoxy faced honeycomb aircraft type sandwich structure elastic properties by edgewise compression test
24 p4403 A69-43443

EDGES

- U LEADING EDGES
- U SHARP LEADING EDGES
- U TRAILING EDGES

EDUCATION

- NT ASTRONAUT TRAINING
- NT FLIGHT TRAINING
- NT PILOT TRAINING
- NT SPACE FLIGHT TRAINING

Geostationary satellite transmissions for educational purposes
[UN PAPER 68-95533] 01 p0028 A69-10494

Space program effects in education, science and engineering, noting impact of first satellite on U.S. research and technology
01 p0179 A69-10500

Science education and training, discussing student motivation
[UN PAPER 68-95809] 01 p0179 A69-10515

NASA programs impact on U.S. education
[UN PAPER 68-95291] 01 p0180 A69-10519

Spacecraft systems, education - Conference, Belgrade, September 1967
06 p1015 A69-17596

Technology and education - Conference, Los Angeles, September 1968
10 p1668 A69-22971

On job training of logistic publications engineers, emphasizing technical publications and system engineering and development for Minuteman program
10 p1811 A69-22977

Management training goals and methods for executive development, comparing effective and ineffective programs
11 p2005 A69-25305

Combined cueing and knowledge of results for transfer of training in visual monitoring
13 p2213 A69-28256

Nondestructive testing education, current programs available and future needs
18 p2322 A69-34518

Space exploration influence on science education, showing NASA instructional materials for teachers in biology, chemistry, physics, mathematics, industrial arts, etc
18 p2325 A69-35077

NASA Pilot Program in instructional monographs to provide up-to-date material from current research for engineering education
18 p2326 A69-35078

Civil aviation center for R and D in aviation personnel education and training
[AIAA PAPER 69-785] 19 p3453 A69-35597

Universities and public service education noting NASA requirements and programs
20 p3641 A69-38282

Aerospace medical educational programs for MD, post-MD and practicing physicians at medical faculties in U.S. and at Ohio State University
23 p4106 A69-41799

EDUCATIONAL TELEVISION

Satellite educational TV, considering program distribution, satellite characteristics, ground terminals design, reliability, quality, programming and costs
[UN PAPER 68-95827] 01 p0029 A69-10499

Educational TV satellites, considering stationary ASCEND system with high power transmitters
02 p0335 A69-12747

Satellite educational TV capabilities, applications and planning
[UN PAPER 68-95355] 06 p0887 A69-17078

Communication satellites in synchronous equatorial orbit for two types of educational TV, discussing picture quality, modulation, power, bandwidth and system costs
06 p1017 A69-17624

Satellite TV broadcast application for communication and education, discussing costs and benefits in single and multimission combinations
07 p1244 A69-18678

Instructional broadcast satellites programming for time cost reduction, discussing frequency allocation, interference and ground station design
13 p2381 A69-27373

Educational TV satellite system design for U.S. in 1970s
18 p3235 A69-35076

Educational TV coverage extension via synchronous satellites to areas of limited coverage, emphasizing South American countries
19 p3268 A69-36163

Nationwide TV system using synchronous communication satellite proposed for India, discussing antenna, modulation, multiplexed channels and educational aspects
19 p3275 A69-36413

EEG [ELECTROENCEPHALOGRAMS]

- U ELECTROENCEPHALOGRAPHY

EFFECTORS

- U CONTROL EQUIPMENT

EFFERENT NERVOUS SYSTEMS

Physiological, cytochemical and histological effects on muscular activity, nervous system, adrenal and thyroid glands and liver of mice during 30 day hypokinesia
02 p0198 A69-11502

Human motor activity under hypodynamia and increased carbon dioxide, discussing positive effects of prescribed physical exercises
03 p0377 A69-14205

Motion sickness inhibitive effect on stomach motor activity, measuring biopotential of stomach wall, pyloric sphincter and ganglions
08 p1263 A69-19935

Corticosteroid and catecholamine metabolism change in rabbits during sharp limitation of motor activity
12 p2021 A69-26973

Astronauts physical training for space flight requirements
13 p2215 A69-28611

Immobilization effects on alpha rhythm, locomotor coordination and visual alimentary motor reflexes of cats
13 p2212 A69-28617

Astronaut vestibular and motor analyzer functions during flight and simulation tests, discussing illusory space orientation and role of cortical dynamics
20 p3469 A69-37241

Motor and tonic reactions in animals during weightlessness, discussing interaction between gravity receptors and visual analyzer
20 p3470 A69-37247

Information transfer capacity of afferent and efferent cell system and fiber tracts of human cerebellum numerically defined with regard to cybernetics
23 p4084 A69-41467

Learning model of motor behavior in brain cortex of higher animals and man, discussing M automaton, information reception, correlation, memory, emotions, desires and actions
23 p4109 A69-41977

Self rhythms of low audio frequencies in motor nerves under electric pulses influence at VLF related to viscosity changes of nerve substance
23 p4092 A69-42057

Temperature dependence of afferent and efferent spontaneous activity of spinal cord, using filament recordings from ventral and dorsal roots in anesthetized cats
23 p4093 A69-42066

Efferent innervation influence of one ear to another in feline auditory system, based on afferent neurons responses to contralateral and binaural stimulation
23 p4094 A69-42073

EFFICIENCY

- NT COMBUSTION EFFICIENCY
- NT COMPRESSOR EFFICIENCY
- NT ENERGY CONVERSION EFFICIENCY
- NT NOZZLE EFFICIENCY
- NT POWER EFFICIENCY

- NT PROPELLER EFFICIENCY
- NT PROPULSIVE EFFICIENCY
- NT THERMODYNAMIC EFFICIENCY
- NT TRANSMISSION EFFICIENCY

Efficiency curve for step recovery diode frequency multipliers, using analog computer simulation
02 p0215 A69-11947

Intracavity acoustooptic devices based on isotropic and anisotropic acoustic Bragg diffraction, discussing efficiency, bandwidth and acoustic column width
10 p1697 A69-23871

EGGS

Weightlessness effects on fertilized frog egg development on board Gemini 8 and 12 manned orbital flights, discussing cell division, differentiation and embryogenesis
01 p0017 A69-11084

Simulated weightlessness used in determining ontogenesis of otolith organ in tadpoles and eggs as function of acceleration forces
[DVL-855] 10 p1647 A69-24021

EGRESS

Psychophysiologic factors in USAF aircraft mishaps involving ground egress
06 p0878 A69-16959

Psychophysiologic factors in USAF aircraft mishaps involving ground egress
15 p2558 A69-30462

EIGENFUNCTIONS

- U EIGENVECTORS

EIGENSTATES

- U EIGENVECTORS

EIGENVALUES

Continuum eigenfunction problem for hard sphere gas in spherically symmetric state, applying theory of singular integral equations
01 p0061 A69-10813

Eigenvalue problem for Laplace operator for two dimensional region with boundary composed of piecewise-analytical simple closed curves solved by finite difference method
02 p0271 A69-11650

Numerical differentiation formulas for coefficients of given characteristic function, using tabulated Stirling numbers
02 p0271 A69-11653

Eigenvalue problem solutions for ordinary differential equations, discussing coefficient replacement, Ritz polynomial substitution and error limits
02 p0271 A69-12057

Upper and lower bounds for eigenvalues of differential problem connected with transverse vibrations of wedge shaped simply supported beam
02 p0272 A69-12193

Exact expressions for rates of change of eigenvalues and eigenvector to facilitate computerized design of complex structures
02 p0347 A69-12532

Generalization of characteristic relations for steady supersonic 3D motion of polytropic gas, obtaining complex screw motions
03 p0412 A69-12847

Necessary conditions for stability of trivial solutions of parabolic systems of partial differential equations
03 p0456 A69-13405

Eigenvalues for Orr-Sommerfeld equation by difference technique for Reynolds number range 5780-729000, determining Poiseuille flow stability in plane channel
03 p0416 A69-13654

Variational theorems on eigenvalues of Laplace finite difference operator with first order boundary conditions
03 p0457 A69-14230

Asymptotic solutions of linear difference equations, discussing applications to eigenvalue problems of free oscillations of model galaxies
04 p0623 A69-14946

Two dimensional elementary transformation for obtaining eigenvalues, considering programming aspects for computing characteristic roots of matrix
04 p0624 A69-14967

Irregular Sturm-Liouville first and higher order perturbation problem in boundary layer theory providing analytical approximations to complete orthogonal set of characteristic functions
04 p0590 A69-15001

Schaefer theory of two parameter eigenvalue problems applied to stability of twisted bars, discussing quick estimate of critical loads
04 p0682 A69-15290

Characteristic waves in gas-dielectric beamguides, calculating attenuation dependence on frequency
05 p0736 A69-16783

Lehmann-Maehly procedure for lower and upper bounds to eigenvalues of Hermitian operators in Hilbert space

06 p1020 A69-17131

Numerical methods for VLF electromagnetic wave propagation in earth-ionosphere waveguide, discussing boundary conditions assignment effect at ionosphere on eigenvalues

06 p0920 A69-17732

Capacitance and lowest eigenvalue bounds for two dimensional anisotropic media as exemplified by transverse vibrations of stretched membrane

08 p1418 A69-20848

Complex variable theory solution of eigenvalue problem governing elastic stability of thin elastic plate subjected to hydrostatic in-plane compression

09 p1615 A69-21921

Asymptotic behavior of frequency function of fluctuations for generalized ensemble parameters, noting characteristic function convergence to Gaussian at thermodynamic limit

09 p1623 A69-22395

Waveguides and resonators design by solving scalar problem for eigenvalues of elliptic operator

09 p1469 A69-22626

Duct entrance region flow, analyzing eigenvalue problem and nonlinear transformation simplification

11 p1874 A69-25285

Vibration eigenfrequencies of helicopter blades, discussing equation integration problems

11 p1995 A69-25673

Characteristic plane harmonic free internal neutral atmospheric wave oblique propagation through horizontally stratified quiet atmosphere for various thermospheric parameters

12 p2065 A69-26101

Inverse iteration method insensitive to small eigenvalue errors for finding eigenvectors

12 p2121 A69-26510

Enclosures for large eigenvalues of ordinary second and fourth order differential equations based on asymptotic solutions of linear homogeneous second order differential equations

12 p2124 A69-26892

Eigenvalue approximation for first order systems by introducing artificial periodicity through successive impulse functions of alternate sign

13 p2287 A69-27242

Second order differential equations eigenvalues with Sturm boundary conditions analyzed by difference method

13 p2288 A69-27922

Matrix eigenvalues for nonlinear simultaneous algebraic equations, discussing computer program for numerical integration

13 p2289 A69-28227

Higher order difference method for equilibrium and eigenvalue problems of two dimensional structures using iterative solution

13 p2365 A69-28239

End loaded two layer laminated elastic strip stress concentration and self equilibrating traction distribution analyzed by eigenvalue equation

13 p2370 A69-28672

Linear control design to synthesize system with prescribed spectrum, deriving formula yielding control coefficients as function of eigenvalues

14 p2425 A69-28821

Semifree elastic membranes standing waves fundamental frequency, developing variational principle for first eigenvalue

14 p2535 A69-29365

Impedance eigenvalues for eigenmodes of multiconductor transmission lines, discussing transverse field distributions along conical line

14 p2423 A69-29756

Perturbation analysis for error estimates in algebraic eigenvalues and eigenvectors problems for solving skewed membrane vibrations

15 p2703 A69-30211

Deformation functions for finite beam analysis allowing continuity at nodes and accurate eigenvalues

15 p2710 A69-30869

Eigenvalue bounds for amplification rates, wave speeds and linear stability conditions for Orr-Sommerfeld equation governing parallel flow in boundary layer and round pipes

16 p2768 A69-31591

Eigenvalues for class of nonself adjoint differential equations system treated as small perturbation of norm epsilon, assuming perturbation expansion

16 p2812 A69-31811

Matrix eigenvalue problems with statistical properties, applying to dynamic structural systems and verifying solutions by Monte Carlo simulation

16 p2871 A69-31878

Gradient iterative methods for finite element eigenvalue problem associated with stability and vibrations of elastic systems based on Rayleigh quotient

16 p2871 A69-31898

Regression rate of solid fuel in hybrid combustion determined as eigenvalue by Rayleigh flow model with evaporating boundary

16 p2879 A69-32013

Eigenvalues of truncated orthotropic shells of revolution with degenerate poles and various rigidities and geometries

16 p2873 A69-32133

Potential and kinetic energy of cylindrical thin shell with cutout approximated by two dimensional finite difference methods, obtaining eigenvalue problem [AIAA PAPER 68-318]

16 p2874 A69-32158

Mixed plate element application to vibration and buckling eigenvalue problems based on Reissner variational principle, considering quadrilateral elements

16 p2874 A69-32176

Electromagnetic field eigenvalues along conductive circular cylinder in magnetoionic medium, assuming lossless medium and field frequency not equal to cyclotron frequency

16 p2754 A69-32568

Eigenvalue problems in partial differential equations solved by extended Kantorovich method, considering vibration of rectangular membrane and stability of elastic rectangular plate

16 p2876 A69-32783

Friedrich qualitative analysis of ordinary differential operators modified to obtain quantitative information regarding eigenvalues distribution

17 p2995 A69-33404

Continuity conditions for drifting magnetoplasmas without ionic effects, discussing eigenvalue equation of refractive index and electromagnetic modes propagation

17 p2926 A69-33851

Electromagnetic field formulation of eigenvalue problem for optical coaxial dielectric waveguide, using computer root searching method

17 p2930 A69-33892

Laser eigenmodes determined iteratively from eigenvalue equation including spatial inversion inhomogeneities, atomic density and local loss

17 p2984 A69-34046

Least squares method of smoothing curves or surfaces involving orthogonal base functions, discussing matrices conditioning and structure eigenmodes

18 p3218 A69-34642

State space procedure for mixed boundary value problems applied to structural analysis, fluid mechanics and eigenvalues for deformable bodies

18 p3164 A69-34685

Eigenvalue conversion of second variation test for algebraic and differential constraints to Jacobi accessory minimum problem by introducing norm in coordinate perturbation space

19 p3400 A69-35672

Matrix formulation for discrete element method applied to linear static and eigenvalue problems of thin walled segments, using homogeneous differential equations

19 p3445 A69-36831

Ensembles of random Hermitian cyclic matrices in statistical theory of complex systems energy level spectra, noting Gaussian density function of eigenvalues

20 p3567 A69-36988

Naimark theorem extended to class of nonself-adjoint eigenvalue problems in hydrodynamic stability, considering Orr-Sommerfeld equation and Taylor stability problem

21 p3754 A69-38426

Reduction of boundary value problems to initial value problems through variables transformation, considering application to eigenvalue problems

21 p3754 A69-38747

Motion stability in nonresonant case of four pairs of imaginary roots in characteristic equation

21 p3770 A69-38883

Approximate boundary conditions in electrodynamics of stratified tensor media estimated for ferrite layers

21 p3675 A69-39282

Eigenmodes of asymmetric cylindrical confocal laser resonator with single output coupling aperture, obtaining diffraction loss factors and mirror field distributions

21 p3741 A69-39564

EIGENVECTORS

Unsteady heat flow in finite composite hollow circular cylinder using inverse method of eigenfunction expansion /method of finite integral transformation/

01 p0175 A69-10230

Continuum eigenfunction problem for hard sphere gas in spherically symmetric state, applying theory of singular integral equations

01 p0061 A69-10813

Numerical differentiation formulas for coefficients of given characteristic function, using tabulated Stirling numbers

02 p0271 A69-11653

Exact expressions for rates of change of eigenvalues and eigenvector to facilitate computerized design of complex structures

02 p0347 A69-12532

Generalization of characteristic relations for steady supersonic 3D motion of polytropic gas, obtaining complex screw motions

03 p0412 A69-12847

Eigenvectors utilized in flutter computation for couplings [ONERA-TP-650]

03 p0522 A69-12878

Eigenvector approximation of complex matrix by inverse iteration, giving Algol 60 program

03 p0455 A69-13371

Two dimensional elementary transformation for obtaining eigenvalues, considering programming aspects for computing characteristic roots of matrix

04 p0624 A69-14967

Irregular Sturm-Liouville first and higher order perturbation problem in boundary layer theory providing analytical approximations to complete orthogonal set of characteristic functions

04 p0590 A69-15001

Characteristic waves in gas-dielectric beamguides, calculating attenuation dependence on frequency

05 p0736 A69-16783

Field diffraction at finite metallic surface represented in eigenfunctions of discrete spectrum, considering forced oscillations of open circuit

07 p1084 A69-19151

Vector equation of transfer for planetary atmosphere describing light scattering by anisotropic particles and analysis of resonance line scattering

08 p1385 A69-20063

Families of eigenfunctions concept for stress and strain tensors of proper motions in continuous isotropic medium, considering vortices and gradients

08 p1417 A69-20752

Asymptotic behavior of frequency function of fluctuations for generalized ensemble parameters, noting characteristic function convergence to Gaussian at thermodynamic limit

09 p1623 A69-22395

Pointwise bounding of eigenfunctions in vibration and stability problems in elasticity theory

10 p1794 A69-22925

Existence and completeness of eigenfunctions for boundary value problem arising in theory of small amplitude motions of stratified polytropic gas

11 p1868 A69-24884

Liquid filled elastic shells natural frequencies and oscillation modes, deriving eigenfunction system from liquid velocity potential boundary conditions to determine dynamic load

11 p1870 A69-24951

Stresses and displacements in half plane with edge crack given as eigenfunction expansions using Wiener-Hopf technique

11 p1987 A69-25438

Characteristic plane harmonic free internal neutral atmospheric wave oblique propagation through horizontally stratified quiet atmosphere for various thermospheric parameters

12 p2065 A69-26101

Inverse iteration method insensitive to small eigenvalue errors for finding eigenvectors

12 p2121 A69-26510

Eigenvalues of finite matrix Hamiltonian, considering convergence radius of perturbation series, limits and renormalization

14 p2470 A69-29451

Perturbation analysis for error estimates in algebraic eigenvalues and eigenvectors problems for solving skewed membrane vibrations

15 p2703 A69-30211

Localization and convergence of Fourier series for fundamental systems of functions of Laplace operator, including eigenfunctions and trigonometric systems

15 p2644 A69-30287

Motion stability in nonresonant case of four pairs of imaginary roots in characteristic equation

21 p3770 A69-38883

Eigenmodes of asymmetric cylindrical confocal laser resonator with single output coupling aperture, obtaining diffraction loss factors and mirror field distributions
21 p3741 A69-39564

Eigenfunction expansion technique to analyze three dimensional crack and wedge problems, emphasizing stress field near straight edge crack
24 p4395 A69-42641

EINSTEIN EQUATIONS

Einstein-Maxwell equations corresponding to superposed electric and magnetic fields stationary solutions, noting singularities in metric tensor
01 p0115 A69-10020

Approximate integrals of Einstein equations for dipole and quadrupole electromagnetic radiation
01 p0115 A69-10263

Equatorial geodesic motion of rotating source in gravitational field, using exact empty space solutions of Einstein equations
01 p0157 A69-11289

Gravitational fields in Hamiltonian formulation of relativistic theory of gravitation, noting geometrical aspects and equivalence to Einstein theory
02 p0280 A69-11715

Godel type solution of Einstein-Maxwell equation for dust filled universe, using Rainich equations
02 p0280 A69-11814

Einstein equations obtained for axisymmetric distribution of masses in approximation of square of stellar rotation angular velocity in empty space
02 p0317 A69-11956

Lorentz invariant theories of gravitation compared with Einstein general relativity tests with respect to one body motion observations
02 p0318 A69-12094

Plane front gravitational waves analyzed on basis of gravitational radiation theory, discussing Einstein equations
02 p0332 A69-12836

Static locally flat solutions of Einstein vacuum field equation with line singularities and global space curvature, noting analogy to electromagnetic fields
03 p0466 A69-13389

Kerr family of solutions of Einstein and Einstein-Maxwell equations for gravitational field of rotating body, noting global structure and causality
03 p0466 A69-13473

Conformal change and connection relations in Einstein unified field theory, noting tensor applications
03 p0467 A69-13756

Factorizability of Einstein field equations in two dimensional spinor formulation
03 p0468 A69-13759

General relativity confirmation, discussing mass equivalence and classical and new experiments such as gravitational shift, rotation effect on perihelion and precession test
04 p0661 A69-15165

Necessary and sufficient conditions for Einstein spaces of second embedding class
06 p0957 A69-17547

Einstein equations solution in Gaussian coordinates describing particles gravitational fields including point particles
07 p1180 A69-18507

Axially symmetric static solutions of Einstein equations with singularities on z axis allowing for higher multipole moments in general relativity
08 p1350 A69-19783

Einstein space time concepts for unified formalism of matter interactions from elementary particles to astronomical bodies, discussing relativity theory
08 p1352 A69-20730

Gravitational wave solution of Einstein field equations, deriving Ricci and Riemann tensors for Einstein space
08 p1352 A69-20755

General theory of relativity and tensor field equations relating space time characteristics to local properties of matter and vacuum, using Palatini Lagrangian method
09 p1593 A69-21572

Clock paradox of Einstein special theory of relativity, reviewing work of Prokhovnik, Schlegel and Arley
10 p1772 A69-22865

Einstein cosmological field equations solved after subjecting electromagnetic null field metric tensor to Einstein gravitational field equations, noting coordinates significance
10 p1778 A69-23406

Generalized gravitational field equations derived on basis of principle of least action, noting vector potential of electromagnetic field
10 p1725 A69-23714

Stability of spherically symmetrical nonrotating mass systems moving in self consistent gravitational Einstein field, considering quasar applicability
11 p1956 A69-24394

Penfield-Haus solution to magnetodynamic effect problem as inertial effect of orbital angular momentum, deriving Bohr magneton formula from Einstein equivalence principle
11 p1919 A69-25098

Einstein field equations solutions for homogeneous cosmological models, assuming perfect fluid gravitation source and existence of simply transitive surface motions
11 p1919 A69-25245

Singularity of Schwarzschild spherically symmetrical solution to Einstein equations of general relativity theory, exemplifying Lemaitre coordinate system
12 p2129 A69-25974

Gravitational recoil due to gravitational emission of source analyzed in terms of Einstein equations
12 p2130 A69-26338

Conformally plane solutions to Einstein equations derived with energy momentum tensor characteristic of pulverized material representing gravitational fields
13 p2298 A69-27796

Internal solution of Einstein equations for steady axisymmetric gravitational fields by integrating differential equations with initial conditions
13 p2351 A69-27863

Einstein general theory of relativity, discussing evolution and disunity among physicists and philosophers on universal relativity of mechanical motion
14 p2483 A69-28857

General relativity theory philosophical substance and meaning, discussing Einstein formulations and bases of classical, relativistic and quantum physics
14 p2483 A69-28859

Gravitational recoil, showing integration of Einstein equations in axisymmetric case reduced to integration of equations for Fourier coefficients
14 p2485 A69-29358

Angular momentum-gravitational field coupling in collapsing star, applying rotational perturbation to spherically symmetric time dependent interior solution of Einstein field equation
14 p2520 A69-29374

Energy momentum tensor in Einstein field equations derived from covariant field equations for vector meson
14 p2486 A69-29452

First order approximation to spherically symmetric solution of Einstein equations, noting gravitational and cosmical lambda force potentials
14 p2521 A69-29455

Classical and relativistic gravitation theories using harmonic coordinate system, interpreting Einstein equations for insular distribution of masses and applications in geodesy
15 p2596 A69-30573

Einstein equations solution for empty space without singularities containing metric, with closed homogeneous space type hypersurfaces expanding anisotropically
15 p2690 A69-30732

Exact static exterior and interior solution of Einstein equations for thick plane plate, discussing surface energy-momentum tensor
15 p2654 A69-31477

Mathematical solutions of Einstein cosmological equations for radiation universe, discussing model limitations for universes older than 5-6 billion years
15 p2700 A69-31496

Gravitational effect of electromagnetic radiation evaluated on test particle using Einstein field equations
16 p2812 A69-32049

Einstein field equations solutions generated via static spherically symmetric mass and charge distributions
16 p2812 A69-32053

Einstein equations for empty space applied to degenerate gravitational fields with twisting rays, admitting shear-free twisting congruence of null geodesics
17 p3004 A69-32832

General relativity theory applicability to cosmology, Einstein principle of equivalence and contradicting arguments of relativistic cosmology
18 p3200 A69-34997

Einstein gravitational field equations series expansion in powers of gravity constant by Bondi method for gravitational waves
18 p3173 A69-35146

Five dimensional theory applied to Einstein generalized gravity equations for spherically symmetrical

gravitational waves, yielding gravity constant variation from Newton approximation
21 p3802 A69-38842

Einstein general theory of relativity and apparatus for gravitational radiation detection, discussing Dicke experiments and Riemann tensor measurement
23 p4192 A69-42331

Gravitational field quantization according to Einstein theory using classical Hamiltonian dynamics and quantum rules for constraints
23 p4192 A69-42332

Planck-Einstein equation derivation in special theory of relativity, discussing relativistic measurement of thermodynamic values in terms of Lorentz transformations
24 p4349 A69-42748

Stability of spherically symmetrical nonrotating mass systems moving in self consistent gravitational Einstein field, considering quasar applicability
24 p4390 A69-43784

EJECTION

NT STELLAR MASS EJECTION

Release windows for auxiliary body ejection from satellite in eccentric orbit, discussing visibility, celestial body interference, etc
03 p0505 A69-13003

Survival of aircrew after successful ejection over water and boarding life raft
06 p0878 A69-16958

Clinical analysis of combat and noncombat ejection experience of USAF
06 p0878 A69-16960

Photographic measurement of parachute exit velocity during ejection from chute, describing electronic recording and unit operation with block diagram
08 p1317 A69-20875

Nose cone ejecting system with pyrotechnic devices for two stage Centaur rockets /Sud-Aviation/ with RF mass spectrometer
10 p1635 A69-23034

Problems connected with rescue of crew members ejected over water
15 p2551 A69-30866

Concorde propulsion and ejection systems reliability, testing reheating duct, primary nozzle, secondary assembly, etc
16 p2837 A69-32072

Convergence of axes of plane-parallel jets due to reciprocal ejection effect, analyzing deformation of jet, rarefaction coefficient for air between jets, etc
21 p3696 A69-39095

EJECTION INJURIES

Psychological aspects of crew members resistance to eject from aircraft in trouble
06 p0877 A69-16956

Ocular injuries during bailout from Vampire aircraft, noting hemorrhages
10 p1649 A69-23380

Human resistance to short duration high accelerations applied to aircraft ejection studies, noting bone damage, consciousness retention, etc
13 p2215 A69-28591

Ejection seat cushion dynamic characteristics influence on incidence of spinal injury during ejection, considering MIL specification dynamic model of human body
17 p2917 A69-34033

Vertebral column fracture resulting from aircraft ejection, studying ejection seat geometry and personal equipment design influence on spinal curvature relation to catapult thrust
23 p4102 A69-41681

Thematic apperception test /TAT/ cards for assessing attitudes in naval recruiting, respiratory responses during ejections and aviation psychology
23 p4112 A69-42365

Radiology diagnosis of military jet pilots injuries during ejection and touchdown, discussing fractures, spine injuries and ejection seat spine position
24 p4266 A69-43379

EJECTION SEATS

Small column insulated delay /SCID/ aircraft seat ejection systems, illustrating weight saving
06 p0877 A69-16957

Ejection seat cushion dynamic characteristics influence on incidence of spinal injury during ejection, considering MIL specification dynamic model of human body
17 p2917 A69-34033

Vertebral column fracture resulting from aircraft ejection, studying ejection seat geometry and personal equipment design influence on spinal curvature relation to catapult thrust
23 p4102 A69-41681

EJECTORS

- Induced flow determination in pulsejet ejector, solving momentum and continuity equations by method of characteristics and mathematical model
[ASME PAPER 68-WA/FE-33] 05 p0812 A69-16106
- Ejector-diffuser performance improvement by reduction of backflow with orifice plate installed at inlet of straight diffuser duct 11 p1819 A69-25382
- Ejector driven wind tunnel for turbulent flow generation with arbitrary velocity profile, using jet arrays [AIAA PAPER 69-743] 18 p3114 A69-34408
- Supersonic air to air ejectors performance for low secondary-to-primary mass flow ratios, deriving correction factor for Fabry-Paulon theory 21 p3644 A69-38654

EKMANN LAYER

U BOUNDARY LAYER TRANSITION

ELASTIC ANISOTROPY

- Elastic stresses in rotating anisotropic disks with constant thickness, discussing solid, circular rigid shaft mounted and center drilled disks 17 p3067 A69-34138
- Reissner variational principle applied to incompressible and nearly incompressible anisotropic thermoelasticity 22 p4040 A69-39980

ELASTIC BARS

- Load diffusion from transverse tension bar into semiinfinite elastic sheet, considering line and area contact methods of stringer attachment [ASME PAPER 68-WA/APM-15] 04 p0669 A69-14396
- Longitudinal stress pulse propagation in finite length free-free bar with variable cross section, noting stresses in projectile impacting plane target 04 p0671 A69-14412
- Higher modes of longitudinal wave propagation in dispersive thin elastic rod, noting response to laser pulse 04 p0678 A69-14869
- Stability of elastoplastic clamped free rod, noting compressive force for production of new equilibrium state and occurrence of transition to state 04 p0679 A69-14925
- Elastic rod buckling under dynamic longitudinal compression load, determining critical load 04 p0679 A69-14926
- Stress concentration around centrally placed circular bolt in axially loaded bar, using theory of infinite systems of linear equations 04 p0681 A69-15195
- Torsional or longitudinal vibrations of nonuniform bar with elastic end constraints, developing frequency and mode form equations suitable for computer 04 p0681 A69-15196
- Elastic rods shape for maximum stability defined by solution of variational problem, assuming noninfinite compressive stresses 05 p0832 A69-15688
- Numerical method for stress function of elastic-plastic torsion of hollow bars during quasi-static monotonic twist compared with relaxation method solution 06 p1023 A69-17370

- Circular bar elastoplastic behavior under combined axial force and torque in strain hardening range, noting elastic compressibility effects 06 p1023 A69-17371
- Forced vibrations in semibounded elastic bar with various moduli of elasticity, discussing reversing longitudinal force and elastic waves propagation 10 p1799 A69-23155
- Asymptotic solution of two dimensional problem of elastic impact of bars, showing longitudinal and surface waves decay with time 11 p1996 A69-25737
- Thermoelastic waves in stretched circular cylindrical bar, analyzing displacements, secondary pressure and temperature field by using Frobenius method 12 p2189 A69-27115
- Galerkin method application to solve differential equation and boundary value conditions for elastic stability of bars, showing linear relation between critical loads 21 p3845 A69-39678
- Large deflection of three dimensional bar structures stability analyzed by potential energy minimization method, considering radome design 23 p4232 A69-42141

ELASTIC BENDING

- Point load subjected deflections of cantilevers and circular rings found using electronic analog computers 03 p0522 A69-12865

Reissner algorithms for displacements of bent plate represented in finite series form as solutions of Euler equations 10 p1793 A69-22883

Elastic bending moments and shear forces uniformly loaded flat plate structures with rectangular symmetry, using collocation technique and complex variable methods 11 p1986 A69-25241

Amplitudes of forced bending vibrations of frames with superfluous elastohysteretic couplings by dynamic compliances method 11 p1986 A69-25333

Bending of elastic triangular plates with free and supported corners under uniformly distributed transverse load determined using Ritz method 14 p2535 A69-29410

Beam deflection equations having different rigidity moduli on each half span 15 p2705 A69-30417

Elastoplastic strains in thin walled beams subjected to oblique bending by mobile loads of coupled concentrated forces, calculating deflections and plastic region distribution 15 p2711 A69-30971

Plate bending problems, comparing various approximate analytical methods including point matching, Galerkin, Ritz, Kantorovich and least squares techniques [AIAA PAPER 68-296] 16 p2874 A69-32160

Anisotropic elastic plate deflection weakened by circular hole with thin elastic ring reinforcement, assuming no load on ring and uniform stress-strain state of plate 17 p3055 A69-33128

Uniform thickness rectangular plates bending with rigidly clamped or freely hinged edges solved by refined version on digital computer 18 p3215 A69-34535

Tension, bending and buckling torsion in thin walled beams described by extended beam model considered as one dimensional continuum 18 p3224 A69-35296

Variational method for computer calculation of supercritical bending of thermoelastic uniformly loaded circular plates, determining Ritz parameter influence on accuracy 19 p3434 A69-35829

Residual deformation of elastoplastically bent thin circular plate after perfect unloading from large deflection, considering equilibrium and compatibility conditions 19 p3438 A69-36306

Curvilinear planform plates natural oscillations, assuming small elastic bending strain obeying Hooke's law 22 p4038 A69-39912

Elastic curve shape effects on volume of minimum weight uniformly strong beam under combined longitudinal and transverse bending 23 p4225 A69-41421

ELASTIC BODIES

- Natural vibration properties of elastic free-free body obeying Hooke law analysis from equilibrium and motion equations, determining Green tensor 01 p0167 A69-10323
- Elastic wind tunnel models used for testing at full scale dynamic pressures, discussing scaling laws and manufacturing and testing problems [AIAA PAPER 68-56] 01 p0011 A69-11018
- Nonlinear viscoelastic bodies arising in 3d rheological models with hidden parameters behaving according to law compatible with objectivity and 2nd thermodynamics principles 01 p0171 A69-11131
- Three dimensional stress concentration around cylindrical hole in semiinfinite elastic body loaded at infinity, using Fredholm integral equation 01 p0172 A69-11332
- Stress analysis of multiply connected bodies under large elastic strains, deriving second order potentials for plate with elliptical holes 02 p0340 A69-12139
- Menabrea theorem for anisotropic elastic body with internal incompressibility constraint, discussing validity during thermoelastic transformation 02 p0341 A69-12194
- Menabrea theorem for nonisothermal transformations of anisotropic elastic body with internal incompressibility constraint and initial stress 02 p0341 A69-12197
- Trajectories of elastic bodies analyzed by Hertz theory of impact 02 p0349 A69-12829

Equilibrium stability of elastic circular arch constrained in rigid cavity and subjected to uniformly distributed parallel loading 03 p0524 A69-13066

Kinematic parameters for elastic slender body aid in description of motion of body 04 p0668 A69-14271

Vertical, horizontal and rocking vibrations of body on surface of otherwise unloaded elastic half plane, estimating stiffness for coupled vibrations [ASME PAPER 68-WA/APM-12] 04 p0668 A69-14393

Elastic ring subject to uniform hydraulic pressure on inner boundary and with two opposite slipless quarter-arcs on outer boundary, noting stress and deformation [ASME PAPER 68-WA/APM-17] 04 p0669 A69-14395

Stresses and displacements in anisotropic elastic solids under mechanical loading, determining general solution for treatment of time dependent boundary conditions 04 p0675 A69-14595

Book on continuum theory of inhomogeneities in simple bodies 05 p0833 A69-15727

Cauchy equation derived, giving rise to definite differential equation for materially uniform elastic bodies with inhomogeneities 05 p0834 A69-15730

Mathematical theory for describing geometric structure of simple bodies, discussing dislocation distribution and exact field equations for elastic bodies motion 05 p0834 A69-15731

Static stability of three dimensional elastic bodies under subcritical strains, noting application to stability of cylindrical shells and rods 05 p0834 A69-15784

Elastic bodies collisions in presence of thermoelastic effects, investigating local inertial and thermoelastic forces effect on compression region shape 05 p0841 A69-16207

Rotation wave propagation in elastic homogeneous isotropic centrosymmetric body in asymmetric elasticity theory 05 p0843 A69-16645

Dynamic instability of solid bodies, using modal vibration method to establish criteria on basis of equivalent energy conditions 05 p0844 A69-16742

Three dimensional compression problem for two elastic bodies in contact, determining contact pressure distribution by iteration procedure on computer 06 p1026 A69-18014

Cosserat functions for homogeneous isotropic elastic body filling finite domain with sufficiently smooth boundaries, noting eigenfunctions for first and second boundary value problems 07 p1173 A69-18499

Crack front and zone in brittle elastic body under high pressure at wall inside body 07 p1231 A69-18699

Stress concentration factors for composite body of two isotropic elastic phases in plane strain in plane of composite parameters 07 p1170 A69-18716

Thin rods and shells elastic analysis, using Cosserat continua for representing bodies in kinematics and balance and constitutive equations 07 p1234 A69-19382

Mathematical theory generalization for smooth materially uniform simple bodies, discussing elastic body structure, material tangent bundle and index bundle, motion equations, etc 08 p1410 A69-19822

Uniqueness theorem for equations of dynamics of viscoelastic bodies, using energy and hereditary elasticity considerations 08 p1415 A69-20658

Elastic cone stresses due to axial force at point on axis, solving problem in terms of convergent integrals 08 p1415 A69-20689

Hertz impact theory application to aircraft tire in operation, considering imperfectly elastic body with impact expressible by Newton recovery factor of about one 10 p1633 A69-22887

Couple-stresses and singular stress concentrations in elastic solids with locally unbounded deformations and stress reduction around hole 10 p1798 A69-23149

Concentrated loads in elastic Cosserat continuum involving body moments and small deformations 10 p1799 A69-23151

Forced vibrations of elastic beam covered by viscoelastic layer subjected to transverse harmonic excitation
10 p1800 A69-23241

Potential functions for three dimensional problems of elliptical crack in elastic solid
10 p1802 A69-24026

Active feedback control of distributed parameter systems including elastic airplane and missile structures, noting feedback loop coupling problem [ASME PAPER 69-VIBR-61]
10 p1668 A69-24145

Two dimensional wavefront shape induced in finitely strained elastic body by impulsive point body force
11 p1969 A69-24338

Reduced modulus of elasticity dependence on form of plane stressed state, assuming initially anisotropic body with transversely isotropic elastic properties
11 p1986 A69-25182

Elastic free-free body deformation during motion based on equations of motion valid for rigid body, noting dynamic Green tensor
11 p1994 A69-25604

Thermal stress and displacement fields in elastic solid weakened by crack outside of circular region, noting plastic zone size and energy dissipation
12 p2179 A69-26216

Elastic stress created by perpetual motion of isotropic elastic solid in static space-time
12 p2130 A69-26283

Elastic mirror flexure and distortion patterns, considering periodic nature of load in polar coordinates, second flexure mode avoidance and friction elimination
12 p2056 A69-26407

Elastic deformation of cord reinforced compressible thin sheet and rectangular cuboid solved using linear stress strain law and strain tensor nonlinear components
13 p2359 A69-27262

Dynamic stability of flexural free transverse vibrations of supported thin walled elastic beam with initial velocity distribution and parametric excitation
13 p2369 A69-28353

Three dimensional equations of elasticity reduced to two dimensional equations of shell theory, discussing stressed states of thin elastic bodies
14 p2531 A69-28807

Heat conduction and Navier equations solved for temperature distribution and displacements in elastic solids, considering time dependent boundary conditions, body forces and heat generation
14 p2535 A69-29364

Elastic and elastoplastic bodies, showing vector field for surface condition as sufficient condition for stability
15 p2707 A69-30621

Dynamic stability of elastic bodies with motion described by partial differential equation
15 p2652 A69-30860

Perturbation formula for frequencies as function of Poisson coefficient, considering vibration modes of elastic body subject to boundary conditions
15 p2713 A69-31097

Stresses due to nucleus of thermoelastic strain in infinite elastic solid with two rigid circular inserts
16 p2872 A69-31906

Linear elastic columns dynamic stability under time dependent axial load, investigating almost-sure asymptotic stability
16 p2872 A69-31911

Wave generation in infinite micropolar elastic solid body analyzed by linearized equations of motion
17 p3053 A69-33018

Wave generation in infinite micropolar elastic body, studying axially symmetric displacement and rotation fields
17 p3053 A69-33019

Energy dissipation in elastic systems as function of limiting damping characteristics of oscillations
17 p3065 A69-33923

Dynamic equations solution for interacting rigid or elastic body system models using Cosserat bodies elastic theory, considering engineering applications
17 p3067 A69-34143

Book on solid bodies collision theory covering elastic bodies with ruled surfaces, dynamic effects associated with Rayleigh surface waves, thermodynamic effects, etc
18 p3210 A69-34259

Modified Bubnov-Galerkin-Ritz method for determining approximation coefficients in stress and displacement analysis, using mixed variational principle of elasticity theory
18 p3215 A69-34566

Load analysis for elastoplastic bodies by Prandtl-Reuss theory and Mises yield condition, considering avoidance of difficulties associated with nonlinear partial differential equation solution
18 p3216 A69-34571

Longitudinal oscillations of homogeneous elastic rod under nonconservative force at one end, deriving equations of motion and stability conditions
18 p3216 A69-34578

Static stability of three dimensional elastic bodies under subcritical strains, noting application to stability of cylindrical shells and rods
18 p3223 A69-35036

Elastic bodies brittle stability weakened by cut, developing criterion for determining critical cut length
18 p3224 A69-35314

Green functions for displacement and rotation fields of infinite homogeneous isotropic centrosymmetric micropolar elastic body subjected to time dependent mass forces and momenta
18 p3226 A69-35459

Motion equations of holonomic system of elastic bodies subjected to scleronomic, ideal and statically determinate constraints, using Green tensor
19 p3374 A69-36584

Thermoelastic deformation and mean rotation divergence formulas for elastic simply connected micropolar body
19 p3440 A69-36586

Plastic deformation effect on dynamic buckling of elastic-plastic simple shallow truss subjected to step and impulsive loading
19 p3446 A69-36836

Mooney and Rivlin theories compared for strain energy function W of ideal superelastic material
20 p3624 A69-37586

Transient thermal stresses in heat treated elastic-perfectly plastic disks with temperature dependent yield stress, considering stress distribution sequence and residual stresses
20 p3629 A69-37974

Optimal control of flight vehicle consisting of long thin elastic body under torsional deformations, solving by method of successive approximations
21 p3760 A69-38852

Steady motion of frictionless indenters along surface of elastic layer in plane strain, using Fourier transform and Fredholm equations for numerical solution
21 p3837 A69-39155

Stress-strain state of homogeneous anisotropic elastic body under action of internal forces, deriving equations to generalize state
21 p3838 A69-39184

Sequential design for economic description of potentially redundant elastic structures, noting redesign sequence
21 p3842 A69-39302

Equations of motion of elastic dumbbell satellite and two-mass spring-connected satellite in orbit, using energy and Floquet theory to investigate spinning motion stability
21 p3817 A69-39759

Protoelastic materials defined in terms of protopotential function, discussing stress tensor dependency on displacement gradients within body
22 p4042 A69-40452

Saint Venant principle of elastic equivalence of kinematically equivalent displacement systems at small surface area of elastic body
22 p4048 A69-41276

Book on fundamentals of dynamics of deformable bodies of increasing dynamic complexity, using calculus of variations
23 p4226 A69-41474

Boundary value problem solution for inviscid fluid flow past compliant body with analytical behavior of flow discontinued at points
23 p4151 A69-41525

Laplace-Carson integral transforms for analyzing surface waves generated by central impact of two elastic bodies
23 p4226 A69-41702

Stress analysis in elastic bodies induced by axisymmetric strains in presence of mass forces and temperature gradients, obtaining equilibrium equation
23 p4229 A69-41997

Continuous dependence of boundary value problems of linear elastic body in smooth three dimensional region on force, elasticity and initial data
24 p4397 A69-42750

Contact stress distribution between two two-dimensional finite nearly rectangular elastic bodies with general surface configurations for surface load expressed in trigonometric series [ASME PAPER 69-APMW-9]
24 p4397 A69-42750

24 p4402 A69-43104

Axisymmetric Lamb wave propagation in semi-infinite micropolar elastic solid, considering time varying load on half space boundary
24 p4406 A69-43730

Wave generation in infinite micropolar elastic solid, determining displacement and rotation fields and strain state
24 p4406 A69-43731

ELASTIC BUCKLING

Plate theories derived via strain energy potential integration through thickness, noting constitutive equations applicability to elastic buckling and postbuckling
02 p0340 A69-12055

Direct matrix method for evaluation of critical loads and buckling modes for nonuniform flexural rigid plates having end and side constraints
03 p0522 A69-12866

Postbuckling behavior of elastic spherical shells from pressure and volume-displacement instrumentation and photography
03 p0524 A69-13062

Initial deviations or imperfections effects on load capacity of infinite and finite length thin circular cylindrical shells under axial compression [ASME PAPER 68-WA/APM-22]
04 p0669 A69-14398

Buckling equations for orthotropic cylindrical shells with eccentric spiral stiffeners derived through variation method of total potential
04 p0676 A69-14710

Elastic rod buckling under dynamic longitudinal compression load, determining critical load
04 p0679 A69-14926

Circular plate elastic stability under unidirectional compression, using Rayleigh-Ritz-Timoshenko method to determine buckling load
04 p0683 A69-15515

Axial buckling load for thin walled circular cylindrical shell, noting design of internal mandrel for control of boundary expansion conditions
05 p0831 A69-15581

Three dimensional deformation and buckling of circular ring, discussing in-plane and out of plane deformations and loads [ASME PAPER 68-WA/DE-4]
05 p0839 A69-16169

Buckling of rod with initial deflection as sinusoidal half wave, using Bubnov-Galerkin method and Laplace transform, calculating stresses of rod when subjected to nonsteady creep
06 p1021 A69-17182

Buckling of elastic cylinders with rectangular cut-outs and reinforcements under axial or lateral loading, using modified Newton method [AIAA PAPER 69-92]
06 p1027 A69-18060

Initial geometric imperfections effect on buckling and postbuckling behavior of laminated composite cylindrical shells under axial compression, considering reinforcing fiber orientations [AIAA PAPER 69-93]
06 p1029 A69-18194

Snapping and buckling of simple elastic structures under dynamic load, noting influence of structural geometry and load duration [AIAA PAPER 69-22]
06 p1029 A69-18206

Thin walled symmetrical angle section beam stability under bending moment by section deformation or torsional buckling
08 p1410 A69-19892

Axisymmetric dynamic snap through critical load analysis for elastic clamped shallow spherical shells, considering impulsive and step loads
09 p1616 A69-21977

Linear theory of cylindrical panel buckling and circumferential restraint along straight edges under lateral pressure, using Donnell equations
09 p1621 A69-22782

Validity limits of formulas for critical buckling load for oscillating continuous beams found to be elastic buckling
11 p1969 A69-24349

Statistical parameters of critical load distribution in buckling of imperfection sensitive elastic structures, noting probability of failure
11 p1969 A69-24415

General perturbation theory for branching analysis of discrete structural systems, considering elastic postbuckling
12 p2179 A69-26213

Elastic buckling and initial postbuckling behavior of clamped shallow spherical shells under axisymmetric load
12 p2187 A69-26842

Equilibrium paths in initial postbuckling of elastic structural systems, discussing stability boundaries and relationships between imperfections and critical loads
13 p2359 A69-27261

Three dimensional deformation and buckling of circular ring, discussing in-plane and out of plane deformations and loads
[ASME PAPER 68-WA/DE-4]
13 p2360 A69-27420

Thin elastic plates buckling under small normal load and external edge force
14 p2531 A69-28810

Buckling of ring stiffened cylinders subject to axial compression, considering prebuckling lateral wall displacements
14 p2534 A69-29030

Linear static deformation and buckling of shallow spherical shells under asymmetric load by solving two dimensional finite difference equations
16 p2871 A69-31897

Prebuckling deformations influence on circular cylindrical shell buckling under external pressure, applying Galerkin method to Donnell equations
16 p2872 A69-31905

Elastic spheroidal shell of revolution under external pressure described by buckling and postbuckling theory
16 p2874 A69-32162

Local buckling of infinite continuous plane elastic membrane under longitudinal load in form of concentrated forces
16 p2875 A69-32293

Linear theory of elastic stability of structures, discussing deformation kinematics, perturbed and neutral equilibriums and solutions for buckling of beams, plate, shells, etc
17 p3054 A69-33042

Thin circular ring stability under uniform external transverse loading at various angles, discussing transverse shear deformation effects and buckling
17 p3061 A69-33707

Rod buckling under impact load, discussing compression strain wave front propagation
18 p3217 A69-34580

Buckling in process of loading idealized elastoplastic Shanley column, noting continuous increase possibility
18 p3217 A69-34596

Growth rate of stability loss intrinsic modes in elastic shells under severe load, discussing stress distribution during buckling
18 p3217 A69-34598

Plastic cylindrical shell buckling under axial impact, predicting velocity required to cause flexural waves
18 p3218 A69-34624

Tension, bending and buckling torsion in thin walled beams described by extended beam model considered as one dimensional continuum
18 p3224 A69-35296

Buckling behavior of idealized Shenley rod consisting of linearly reinforced elastoplastic materials under compression, formulating constraints for stability
19 p3446 A69-36846

Simply supported rectangular plates experiments showing prediction on buckling load
19 p3447 A69-36854

Buckling of eccentrically stiffened thin circular elastic plate under circumferential uniform compression, obtaining equations and critical loads
20 p3622 A69-37221

Stress analysis of circular elastic plate buckling under radial compression, noting Kirchhoff hypothesis influence on critical value of thickness-to-radius ratio
21 p3834 A69-38722

Buckled rectangular plates with constrained edges, analyzing natural frequencies as basis for supersonic panel flutter analysis
22 p4046 A69-41049

Prebuckling deformation influence on compressive buckling load for orthotropic cylindrical shells with elasticity principal axes in axial and circumferential directions
22 p4047 A69-41182

Space frame radome model elastic buckling tests for load deflection and maximum load predictions, considering individual beam failure and complex instability
23 p4232 A69-42143

Flat square plates loaded along two opposite straight edges, analyzing postbuckling behavior and geometric imperfections effects
23 p4234 A69-42395

Circular cylindrical photoelastic shells buckling modes under axial compression using high speed isoclinic photography, discussing shallow shell equations applicability to early stages
24 p4404 A69-43652

Mechanical model for dynamic buckling of elastic imperfection-sensitive structures under step loading, using perturbation method
24 p4405 A69-43656

Orthotropic stiffness layer models for buckling of eccentrically stiffened shells of revolution with two unbonded orthotropic layers uncracked and circumferentially cracked
24 p4405 A69-43657

ELASTIC CYLINDERS

Mixed boundary value problem of elastostatics for isotropic elastic cylinder containing strip crack opened by internal pressure, using auxiliary functions
01 p0167 A69-10317

Dynamical strength of solid cylinder under axial loads increasing in time at given rate, using constitutive equations of thermodynamic theory
02 p0342 A69-12278

Dynamic pressure pulse over band on solid elastic cylinder surface, analyzing time stress distribution throughout elastic cylinder
04 p0670 A69-14408

Equilibrium and compatibility equations for axisymmetric stress distribution in finite length anisotropic elastic cylinder reduced to single integrodifferential equation
04 p0676 A69-14709

Small twist of elastic circular cylindrical tube with nonorthogonal cylindrical aeolotropy, noting zero and nonzero warping conditions effects
05 p0831 A69-15580

Elastic contact between two parallel cylinders with rough surfaces noting contact area, spots and stress distribution
06 p1023 A69-17373

Exponential decay of stresses in circular elastic cylinders subject to axisymmetric self equilibrated end loads
06 p1023 A69-17507

Cylindrically orthotropic hollow cylinder elastic properties determination using experimental test for production of stress and strain states and end effects
07 p1232 A69-18718

Thermal stress concentrations in vicinity of cylindrical elastic inclusions embedded in elastic matrix, using displacement functions and photothermoelasticity
07 p1171 A69-18726

Axially symmetric torsion of finite elastic cylindrical rod partially bonded to elastic half space, discussing coupling between dual Dini series and integral equations
07 p1236 A69-19474

Two dimensional problems in classical theory of elasticity concerning zero normal stress and zero tangential stresses, noting formulas for right cylinder
08 p1415 A69-20660

Cylindrical elastic membranes with finite axisymmetric deformation, discussing exact solution by strain energy method
08 p1418 A69-21001

Three dimensional vibration analysis of circular homogeneous elastic cylinder, obtaining differential equations and zero stress conditions
09 p1612 A69-21601

Three dimensional analysis of torsional vibrations of circular elastic homogeneous cylinder, stressing new torsional vibrations
09 p1612 A69-21603

Plane thermal stress field in discontinuous temperature distribution within isotropic linear elastic circular cylinder of infinite length
10 p1793 A69-22884

Plane deformation in nonorthotropic body composed of various anisotropic cylinders with different elastic constants
10 p1799 A69-23156

Torsional vibrations of composite elastic orthotropic cylinders, including cylindrical shells and isotropic composite cylinder
10 p1800 A69-23243

Partial derivatives of harmonic and biharmonic functions at surface of cylinder for three dimensional problem in elasticity theory, considering displacement vector
11 p1976 A69-24777

Stresses in infinite solid elastic circular cylinder due to rotating line source of heat
13 p2364 A69-28206

Dynamic stresses in case bonded cylinder due to transient angular accelerations, presenting numerical results for incompressible elastic cylinder
13 p2364 A69-28209

Steady state problems of elastic orthotropic cylinder solutions applicable to boundary value problems of laminar orthotropic elliptical cylinders
13 p2369 A69-28528

Contact problem between elastic cylinder and rigid punch analyzed using integral equation, singularity isolation and series expansion
14 p2532 A69-28972

Stress in elastic cylinder under thermal expansion with one end clamped expressed by series expansion of biharmonic function using least squares method
14 p2534 A69-29284

Surface displacements at end of elastic semiinfinite circular cylinders due to annular axisymmetric loading, employing Boussinesq solution
15 p2711 A69-30872

Creep calculation with temperature considerations for multilayer cylinder under nonisothermal load, comparing stress-strain state of viscoelastic and elastic cylinders
18 p3225 A69-35358

Hollow cylinder plane stress-strain state analyzed for effect of variable modulus of elasticity of cylinder material
19 p3436 A69-35858

Nonlinear shell theory for thin elastic circular cylinders, obtaining equations for investigating equilibrium configurations of postbuckled states
19 p3440 A69-36636

Elastohydrodynamic lubrication of cylindrical rubber surface sliding over glass plate, using optical interference technique
23 p4171 A69-42531

ELASTIC DAMPING

Longitudinal elastic wave damping, excitation and propagation in lithium niobate crystals at frequencies from 200 to 2000 MHz
03 p0487 A69-13729

Supercritical damping of nonlinear mass elastic system with damping force function dependent on fractional powers of velocity, noting impact deceleration
04 p0671 A69-14413

Constrained layer damping and conventional techniques combination for vibration and noise control
04 p0606 A69-14691

Frictional losses in straight tubing and effect of system on ball type valve, using polyurethane foam damped flexible silastic tube
04 p0608 A69-15331

Damped steady state response of elastic foundation beam subjected to cyclic moving loads to determine load movement frequencies for natural frequency excitation
[ASME PAPER 69-VIBR-13]
10 p1806 A69-24166

Polynomial coefficients multiplication by weighted damping factors for increased conformal mapping and boundary value problems solutions accuracy for doubly connected regions
12 p2178 A69-25998

Vibration control by alternate layers of high damping viscoelastic material, discussing damping and loss factors, beams design and attachment
15 p2622 A69-30704

Vibrations attenuation by viscoelastic sandwich shear damping, discussing examples of aircraft equipment racks, gyro and airborne circuit board mountings
15 p2622 A69-30705

Damping techniques using viscoelastic materials, discussing mechanical hysteresis
17 p2992 A69-33660

Structural damping effects on semiinfinite panel boundary aeroelastic limit by Galerkin variational method
19 p3437 A69-36148

Apparent dynamic modulus and damping under multilevel loading during fatigue cycling to estimate stainless steel specimens cumulation fatigue lives
20 p3620 A69-36997

Tail plane shape for optimal damping of rotational motion and elastic torsional deformations of aircraft body around longitudinal axis using calculus of variations
21 p3647 A69-38845

Numerical method for solution of nonlinear systems applied to damped and undamped motion with symmetrical and asymmetrical elasticity under harmonic excitation
22 p4040 A69-39937

ELASTIC DEFORMATION

Repeated elastoplastic deformation of polycrystalline body analyzed by dynamic model
01 p0164 A69-10082

Exact solution of shallow shells of revolution equations governing linear deformation compared with asymptotic integration procedure
01 p0166 A69-10234

Asymptotic integration of three dimensional elasticity equations for thin anisotropic shells and plates, deriving variability exponent of stress under given load
01 p0170 A69-10878

Predeformations of thin walled elastic isotropic spherical shells analyzed using Vlasov shell bending theory
02 p0336 A69-11555

Deformation thermodynamics, discussing mechanics and thermokinetics of continuous media and wave propagation problem
02 p0339 A69-11990

Menabrea theorem for anisotropic elastic body with internal incompressibility constraint, discussing validity during thermoelastic transformation
02 p0341 A69-12194

Finite difference numerical integration technique for large elastoplastic deformation transient and permanent deflection responses of thin shells
02 p0347 A69-12518

Elastic-plastic and creep deformation calculations of cylindrical shell, providing better estimate of critical time at higher stress levels by including plasticity
02 p0348 A69-12539

Asymptotic constitutive approximations for rapid finite deformation of general viscoelastic materials, noting isotropic solids and fluids
03 p0523 A69-13020

Thermodynamics of materials with elastic range
03 p0529 A69-13955

Elastic ring subject to uniform hydraulic pressure on inner boundary and with two opposite slipless quarter-arcs on outer boundary, noting stress and deformation [ASME PAPER 68-WA/APM-17]
04 p0669 A69-14395

Resistance wire strain gages for measuring elastoplastic deformations in zones with high stress concentrations of strained machine elements
04 p0671 A69-14433

Difference equation for two dimensional elastic flow
04 p0681 A69-15286

Exact geometrical equations and internal equilibrium for elastoplastic deflections of orthotropic shells of revolution using thin shell theory
05 p0831 A69-15680

Displacement, distortions and unit stresses in rotating circular disk under plane strain
05 p0835 A69-15807

Constitutive equation for viscoelastic materials generalized, assuming instantaneous part of deformation to be nonlinear function of time dependent stress state
05 p0835 A69-15868

Coupled heat equation to calculate transient and steady state temperature distributions in viscoelastic solids under cyclic deformations
05 p0836 A69-15878

Three dimensional deformation and buckling of circular ring, discussing in-plane and out of plane deformations and loads [ASME PAPER 68-WA/DE-4]
05 p0839 A69-16169

Elastic-plastic analysis of flat plates in membrane stretching and flexure, using method of initial strains [ASME PAPER 68-WA/PVP-10]
05 p0840 A69-16191

Elastic displacements for edge cracked plate specimens used as crack extension indicator in plane strain fracture toughness measurements
05 p0841 A69-16433

Finite elastic-plastic deflections of orthotropic shells of revolution, deriving exact geometrical relations and equilibrium equations
05 p0842 A69-16642

Flow theories of fluids with elastic deformation of substructure, treating suspensions of irregularly shaped deformable particles
05 p0752 A69-16738

Plate deflection in own plane under moments applied to ends using elasticity theory, deriving relation between stress tensor and stress function
06 p1021 A69-17177

Three dimensional compression problem for two elastic bodies in contact, determining contact pressure distribution by iteration procedure on computer
06 p1026 A69-18014

Vertistat H gravity gradient configuration prevents elastic deformation, permitting high pointing accuracy at synchronous altitudes
07 p1229 A69-18351

Supercritical elastic states of closed spherical shell
07 p1232 A69-18934

Existence and uniqueness theorems for boundary value problems of axisymmetric deformation of circu-

lar membrane at normal pressure, using membrane theory and shooting method
07 p1233 A69-19299

Thin rods and shells elastic analysis, using Cosserat continua for representing bodies in kinematics and balance and constitutive equations
07 p1234 A69-19382

Stability of finitely deformed thin cylindrical shell of rubberlike material, showing bending resistance and thickness effects
08 p1413 A69-20414

Polar elastic media pure torsion solved, noting couple-stresses influence on Poynting effect
08 p1414 A69-20527

Cylindrical elastic membranes with finite axisymmetric deformation, discussing exact solution by strain energy method
08 p1418 A69-21001

Static axisymmetric deformation of elastic paraboloid of revolution, using integration of equilibrium equation in Lamé displacement
09 p1613 A69-21631

Supercritical elastic states in convex shells produced by load in presence of thermal flux, noting no flux effect on states
09 p1617 A69-22078

Elastic Cosserat plate and shell theory, considering constitutive equations imitating transversely isotropic material and elastic deformations
10 p1798 A69-23147

Couple-stresses and singular stress concentrations in elastic solids with locally unbounded deformations and stress reduction around hole
10 p1798 A69-23149

Concentrated loads in elastic Cosserat continuum involving body moments and small deformations
10 p1799 A69-23151

Plane deformation in nonorthotropic body composed of various anisotropic cylinders with different elastic constants
10 p1799 A69-23156

Long rectangular rods stability and vibrations under elastic deformations using bending theory
10 p1802 A69-24024

Slender elastic rod stability under spatial finite deflection, analyzing critical load by using Kirchhoff analogy and gyroscope motion
11 p1970 A69-24609

Stress distribution around holes in thin shells and plates during large elastic displacements, considering hole size, loading and shallow spherical shells
11 p1972 A69-24654

Stress-strain relation in crystalline media for pure tension and elongation epsilon several times conventional elastic limit, verifying by testing Al alloy [ONERA-TP-695]
11 p1975 A69-24754

Direct measurement device for metallic material response to mechanical stresses from stress force and global displacement /including material deformation/
11 p1884 A69-24757

Finite deformation equations for flat annular membranes deduced from equations for thin shells of revolution, discussing displacement equations and fixed edge forces
11 p1979 A69-24813

Nonlinear shell theory, determining elastic deformation as function of stress under external loads using Lagrange variational principle
11 p1979 A69-24817

Three dimensional theory of elasticity for finite hollow cylinder under axisymmetric deformation, considering stress and pressure distribution over surface
11 p1983 A69-25022

Thin elastic conical shells asymmetric deformation under stresses and strains, deriving asymptotic solution
11 p1983 A69-25090

Elastic two cavity revolving hyperboloid deformation by arbitrary forces solved by spherical functions
11 p1984 A69-25169

Hysteresis loop contour equation derivation based on energy dissipation dependence on stress amplitude in cyclically deformed vibrating system
11 p1985 A69-25176

Deformations of thick walled cylinder with internal surface subjected to uniform pressure and externally connected to rigid chamber, calculating solid rocket booster charge
11 p1942 A69-25347

Elastic free-free body deformation during motion based on equations of motion valid for rigid body, noting dynamic Green tensor
11 p1994 A69-25604

Plane stress state in plate with different glide moduli during tension and compression, considering axisymmetrical deformations
12 p2178 A69-26003

Transverse impact along flexible couplings, deriving motion equations in presence of elastoplastic deformation
12 p2178 A69-26034

Torsion in composite inhomogeneous circular cylinder, obtaining solutions for elastic displacements and stresses
12 p2180 A69-26274

Elastic mirror flexure and distortion patterns, considering periodic nature of load in polar coordinates second flexure mode avoidance and friction elimination
12 p2056 A69-26407

Antiflexure cylinder for large astronomical mirror, noting support by astatic counterpoint levers and simple flanges
12 p2056 A69-26409

Finite plane deformations theory extended to incompressible materials with logarithmic change of volume proportional to pressure
12 p2181 A69-26613

Dynamic relaxation method for elastic deformation in mirrors, using tensor equations of elasticity in nonorthogonal curvilinear coordinates
12 p2187 A69-26890

Elastic deformation of cord reinforced compressible thin sheet and rectangular cuboid solved using linear stress strain law and strain tensor nonlinear components
13 p2359 A69-27262

Perturbation theory of antiplane elastoplastic deformations based on plasticity theory, considering circular hole in body under uniform shear
13 p2359 A69-27263

Plane stress theory for large elastic deformations of isotropic thin sheets, outlining successive substitutions method for neoHookean materials static and dynamic problems
13 p2359 A69-27320

Inverse deformation in elastic materials, using variational principle to obtain equilibrium equations properties
13 p2360 A69-27324

Three dimensional deformation and buckling of circular ring, discussing in-plane and out of plane deformations and loads [ASME PAPER 68-WA/DE-4]
13 p2360 A69-27420

Elastoplastic deformations of thin axisymmetric shells of revolution with variable thickness, exemplifying shell with piecewise constant thickness
14 p2533 A69-28982

Constitutive equations for living soft tissues freely deforming under negligible stresses with Hooke law as limit
14 p2535 A69-29366

Elastic deformations of spherical sandwich shell of rigidly connected isotropic homogeneous layers, describing shell symmetrical expansion and inversion under stresses
15 p2707 A69-30582

Isothermal deformations in linear viscoelastic material under uniaxial stress, determining optimum strain rate history for maximum work lower bound
15 p2707 A69-30637

Sailplanes design, discussing structural flexibility, deformations, aeroelastic effects and plastics and man-made fibers
15 p2551 A69-30899

Coaxial deviator theory of nonlinear elasticity, applying deformation theory variant to shell theory
15 p2592 A69-31058

Sloping helicoid median surface with given parameters, obtaining equilibrium equations, elasticity and formulas relating deformations to displacements
15 p2714 A69-31197

Rotatory cylindrical shells supported at corners under symmetric load, determining deformation in arbitrary locations by moire method
15 p2715 A69-31546

Linear static deformation and buckling of shallow spherical shells under asymmetric load by solving two dimensional finite difference equations
16 p2871 A69-31897

Prebuckling deformations influence on circular cylindrical shell buckling under external pressure, applying Galerkin method to Donnell equations
16 p2872 A69-31905

Heated cylindrical shell with braces subjected to given compression and internal pressure, having elastic

beams along edges, analyzing local deformations effect on shell strength and stability
16 p2873 A69-32131

Stress and deformation in cross section of beam during complex loading using steepest-descent method
16 p2873 A69-32132

Cylindrical shell aeroelastic dynamic stability subjected to supersonic flow field, considering geometric imperfections, edge constraint and prestability deformation
[AIAA PAPER 68-285]
16 p2874 A69-32159

Linear theory of elastic stability of structures, discussing deformation kinematics, perturbed and neutral equilibria and solutions for buckling of beams, plate, shells, etc
17 p3054 A69-33042

Attitude and simple stability of deformable earth pointing satellite
17 p3047 A69-33229

Static implications of strong ellipticity condition in linearized elasticity theory, exemplifying homogeneous deformations
17 p3058 A69-33415

Large deflections of thin nonlinearly elastic ring under external pressure, using two layer model
17 p3062 A69-33715

Elastohydrodynamic theory of spherical bodies in normal approach contact, discussing lubrication and elasticity equations
[ASME PAPER 69-LUBS-3]
18 p3213 A69-34384

Nonlinear equations for elastic strain of circular-to-ridal membrane shell under uniform pressure, computing stress and displacement fields
18 p3216 A69-34575

Equations of motion of rapidly rotating spacecraft, considering deformations of long elastic booms
18 p3207 A69-34582

Thin walled cylindrical shells deflections under axial impact load, assuming deformations resembling cylindrical surface bending
18 p3217 A69-34599

Stress and displacement waves propagation in thin walled elastic cylindrical shell under compressive axisymmetric force based on momentless theory
18 p3218 A69-34600

Sandwich beams optimal design determined for case of constraint on elastic deflection and for load factor at plastic collapse
18 p3218 A69-34623

Two dimensional theory for anisotropic plates motion derived, using asymptotic integration of three dimensional elasticity equations
18 p3224 A69-35297

Friction coefficient and elastic deformation magnitudes relation in polyurethane during sliding friction in various liquids /lubricants/
18 p3149 A69-35362

Green functions for displacement and rotation fields of infinite homogeneous isotropic centrosymmetric micropolar elastic body subjected to time dependent mass forces and momenta
18 p3226 A69-35459

Elastic oscillations of inhomogeneous orthotropic ring under time-variable axisymmetrical load analyzed by Fourier method
19 p3434 A69-35828

Equations of motion for axisymmetric elastic deformation of inhomogeneous body of revolution subjected to torsion and steady oscillations
19 p3436 A69-35845

Residual deformation of elastoplastically bent thin circular plate after perfect unloading from large deflection, considering equilibrium and compatibility conditions
19 p3438 A69-36306

Geometrical model for surface contact area, noting influence of nonlimitations on friction coefficient in elastic deformation
19 p3329 A69-36494

Thermoelastic deformation and mean rotation divergence formulas for elastic simply connected micropolar body
19 p3440 A69-36586

Longitudinal and transverse wave propagation in homogeneously deformed isotropic elastic solids, considering Hadamard and Green materials
19 p3440 A69-36588

Plane elastic deformation in isotropic homogeneous medium using displacement vector, discussing finite difference equations and application to rectangular boundary
19 p3441 A69-36719

Boundary conditions for shells with reinforced nonasymptotic boundaries, assuming coincident beam axis deformation with shell boundary deformation
19 p3443 A69-36781

Reducibility conditions of flow theory for smooth and piecewise smooth yield surfaces to relations of small elastoplastic deformations
19 p3443 A69-36794

Buckling and postbuckling of complete spherical shells with symmetric initial shape deviations and elastic deformations
19 p3446 A69-36834

Stress and strain concentration factors under initial stages of elastoplastic deformation for circular hole in infinite medium, using method of successive approximation
19 p3447 A69-36860

Clamped uniformly loaded rectangular plate large deflection elastic behavior approximate analysis, using perturbation method
20 p3620 A69-36998

Flat rectangular plates large deflection due to uniform lateral pressure and compressive edge loading analyzed through partial differential equations, difference equations and computer program
20 p3620 A69-37000

Elastic interactions between cylindrical shell and added band reinforcement turns, analyzing stress relaxation magnitude and effect on pressure vessel design
20 p3621 A69-37064

Nonlinear theory based on Euler-Bernoulli hypothesis for axisymmetric deformations of heterogeneous orthotropic shells of revolution under rotationally symmetric mechanical and thermal loads
20 p3625 A69-37592

Asymptotic integration method of nonlinear elasticity equations for first approximation theory of anisotropic plates moderately large deflections
20 p3630 A69-38129

Rotation of antenna pattern of radio telescope parabolic mirror subjected to thermoelastic deformations due to asymmetric solar heating
20 p3497 A69-38307

Tail plane shape for optimal damping of rotational motion and elastic torsional deformations of aircraft body around longitudinal axis using calculus of variations
21 p3647 A69-38845

Optimal control of flight vehicle consisting of long thin elastic body under torsional deformations, solving by method of successive approximations
21 p3760 A69-38852

Multiple support wing deformations, obtaining bending equations solutions by matrix methods
21 p3835 A69-38872

Optimal control of rotational and transversal motions of elastic flight vehicles, considering torsional and flexural deformations
21 p3760 A69-38890

Stability of cylindrical shell of average length with elastic filler under uniform external radial pressure
21 p3837 A69-39088

Constitutive equation for nonlinear viscoelastic materials, noting validity for short times, slow motions or small deformations
21 p3840 A69-39288

Deformation of uniformly thick elastic circular plates containing circular holes reinforced by thin rigid elastic rings
21 p3846 A69-39713

Photoelastic behavior in amorphous solids, proposing microstructural mechanism for deformation birefringence
22 p3972 A69-40081

Protoelastic materials defined in terms of protopotential function, discussing stress tensor dependency on displacement gradients within body
22 p4042 A69-40452

Prebuckling deformation influence on compressive buckling load for orthotropic cylindrical shells with elasticity principal axes in axial and circumferential directions
22 p4047 A69-41182

Saint Venant principle of elastic equivalence of kinematically equivalent displacement systems at small surface area of elastic body
22 p4048 A69-41276

Large elastic deformations of isotropic materials by deflection of composite parallelepiped composed of elastic incompressible materials, applying Rivlin solutions
22 p4048 A69-41277

Book on fundamentals of dynamics of deformable bodies of increasing dynamic complexity, using calculus of variations
23 p4226 A69-41474

Deformation tractions in undeformed and curved cuboid flexure and inverse flexure determined by stress-strain relations for homogeneous isotropic compressible materials
23 p4226 A69-41521

Deformation of orthotropic layered elastic shells based on linear elasticity theory, assuming surface and stress constraints
23 p4226 A69-41535

Nonlinear differential equations for large deflections of multisandwich shells of arbitrary shape built of stiff and weak elastic layers, considering cylindrical shells
23 p4226 A69-41572

Thermoelastic stresses in rotating cylinders and disks with radial temperature distribution, deriving plane deformation approximate solutions
23 p4227 A69-41707

Supercritical elastic states in convex shells produced by load in presence of thermal flux, noting no flux effect on statics
23 p4228 A69-41970

Supercritical elastic states of closed spherical shell
23 p4228 A69-41971

Computerized evaluation of elastic deformations of 100 m parabolic reflector designs for Max Planck Institute radio telescope, outlining supports and dish structure
23 p4148 A69-42122

Large deflection of three dimensional bar structures stability analyzed by potential energy minimization method, considering radome design
23 p4232 A69-42141

Finite deformation of circular elastic membrane spinning with constant angular velocity, solving nonlinear differential equations by Runge-Kutta method for three boundary conditions
24 p4404 A69-43651

ELASTIC MEDIA

Temperature field and stress state in elastic plane with temperature insulated arc shaped crack
01 p0164 A69-10078

Stress-strain state of isotropic elastic medium using equations with stress tensor, noting role of curvilinear hole
01 p0164 A69-10081

Torsional oscillations of elastic half space set up by rigid circular disk examined by integral equation method
01 p0169 A69-10809

Electromagnetic field interaction with polarizable elastic medium in gravitation theory resolves definition of electromagnetic energy in matter
02 p0279 A69-11537

Equilibrium problem of elastic medium with stress couples in linearized elasticity theory, representing biharmonic function with aid of analytical functions
02 p0340 A69-12035

Viscoelastic materials thermomechanical behavior, discussing constitutive equation and derivation of stress tensor and entropy density from viscoelastic potential
02 p0344 A69-12294

Velocity field generated by vibrations propagating at finite velocity over elastic wing surface
02 p0190 A69-12571

Spherical wave reflection from nondeformable plane in elastic viscoplastic medium
03 p0528 A69-13926

Propagation of longitudinal transverse loading and unloading waves /with cylindrical symmetry/ in non-homogeneous elastic/viscoplastic medium, accounting for plastic dilatational strains
03 p0528 A69-13929

Controllable states of elastic heat conductors, analyzing deformations and temperature fields
03 p0529 A69-13957

Nonlinear constitutive equations for mixture of two elastic solids linearized, assuming small displacements and subsequent temperature changes
03 p0529 A69-14063

Stability against snap-through and final states of shallow arches on elastic foundations and subject to time varying loads
[ASME PAPER 68-WA/APM-26]
04 p0669 A69-14394

Torsional elastic wave scattering from penny shaped crack, determining local dynamic stress field
04 p0678 A69-14872

Acceleration wave propagation and growth in elastic materials, discussing thermodynamic influences
05 p0836 A69-15931

Stress concentration at thermally insulated holes in elastic material created by disturbance of uniform heat flow at holes

06 p1021 A69-17184

Specialization of field equations and boundary conditions of elastic dielectric for special case of rigid dielectric, using Lagrange multipliers

07 p1200 A69-19174

Fredholm equations from dual integral equations for studying penny shaped crack response to incident harmonic shear wave in elastic medium

07 p1233 A69-19175

Large amplitude longitudinal wave propagation in elastic rod solved by method of characteristics, prescribing end velocity as step function of time

07 p1233 A69-19176

Constitutive equations for propagation of plane waves of finite amplitude in nonsimple elastic solids, discussing holohedral isotropic solids and transverse harmonic circularly polarized waves

08 p1411 A69-20141

Dynamic stress intensity factor for axisymmetric loading of circular crack in infinite isotropic elastic medium

08 p1413 A69-20412

Polar elastic media pure torsion solved, noting couple-stresses influence on Poynting effect

08 p1414 A69-20527

Charged body moving at subsonic velocity normally through stratified elastic half space composed of film on homogeneous half space

08 p1417 A69-20753

Thermodynamics of nonsimple elastic materials with two temperatures, showing temperature and stress difference proportional to heat supply

08 p1422 A69-20847

Plane and three dimensional stress concentration studies involving asymmetrical stress tensors, noting contributions to moment theory of elasticity

08 p1419 A69-21177

Temperature and displacement fields in unbounded elastic space due to instantaneous point heat source action

09 p1621 A69-21495

Transversely isotropic elastic solid approximation for oriented fibers of polyethylene, nylon, polyethylene terephthalate and polypropylene, measuring elastic compliances

09 p1528 A69-21504

Finite elastic locking medium, discussing equation of state for thermodynamic variables and applications to thermoelasticity [IS-ERI-70]

09 p1612 A69-21561

Thermally generated stress wave propagation in dispersive elastic rod investigated experimentally and analytically, using ruby laser and differential equation

09 p1617 A69-22010

Reciprocity theorems of coupled and uncoupled thermoelasticity for macroisotropic and microisotropic simple homogeneous solids with microstructure

09 p1618 A69-22259

Micropolar elasticity using Green functions to solve wave equations in unbounded medium, noting effects of concentrated force and body couples

09 p1618 A69-22261

Micropolar thermoelasticity using Green functions to solve wave equations in unbounded medium and study displacement, rotation and temperature fields

09 p1618 A69-22262

Couple stresses effect on distribution of stresses in elastic solid due to crack analyzed on basis of Cosserat theory

10 p1800 A69-23242

Crack propagation through layer of viscous fibers joining orthotropic elastic half planes

10 p1803 A69-24029

Dynamics of conducting fluid stream coupled to elastic medium by transverse electric or parallel magnetic field, considering stability of system

11 p1923 A69-24289

Energy theorem for time dependent materials, deriving convexity conditions for minimum work and maximum complementary work functions

11 p1969 A69-24412

Elastic isotropic half plane weakened by circular hole with concentrated force applied along hole contour, considering stress distribution

11 p1972 A69-24653

Mixed boundary value problem concerning expanding elastic space weakened by cracks located at same plane solved by integral transforms and Fredholm equations

11 p1973 A69-24663

Stress concentrations in physically nonlinear multiply connected elastic media, discussing rods, thin plates and bodies with cavities

11 p1976 A69-24783

Two dimensional elastic reinforcements effects on stress, strain and elasticity of quasi-homogeneous anisotropic elastic medium

11 p1981 A69-24941

Thermodynamics of strain rate sensitive elastoviscoplastic solids, considering kinematic description of plastic deformation and choice of state variables

11 p1994 A69-25601

Axisymmetric problem of stress in elastic space weakened by plane annular slit solved by asymptotic method in terms of equations for parameter lambda

11 p1996 A69-25735

Representation formula for response function of elastic materials having given isotropy group

12 p2188 A69-26926

Plane problem for inhomogeneous elastic media based on assumption of elastic coefficients as functions of two variables defined in domain occupied by medium

13 p2362 A69-27977

Free and forced vibrations of elastic layer, using iteration procedure based on asymptotic integration of linear theory of elasticity dynamic equations

13 p2363 A69-28126

Stress and displacement fields for uniaxially loaded infinite elastic continua with doubly periodic array of holes and inclusions, using finite element method

13 p2363 A69-28133

Acoustic power transferred to plane homogeneous elastic structures and cylindrical shells by neighboring sound sources

13 p2363 A69-28186

Elastic medium properties recovered from reflected or transmitted plane waves at normal incidence, obtaining computational procedures and analytical solution from Schroedinger equation

13 p2300 A69-28664

Libroelastic wave propagation and dispersion characteristics /solid carbon dioxide/ evaluated by using Raman scattering measurements

13 p2286 A69-28668

Elastic materials with particle interactions of finite range, establishing continuum field and constitutive equations from particle mechanics

13 p2371 A69-28674

Linear elastic structural analysis for one, two and three dimensional continua [ASME PAPER 69-DE-13]

14 p2531 A69-28843

Tissue-type fiberglass reinforced material properties as prototype of continuous anisotropic hereditary elastic media

15 p2642 A69-30584

Thermoelastic stress in semiinfinite elastic medium due to discontinuous temperature distribution over free surface, solving associated heat conduction problem

15 p2712 A69-31006

Reflection of plane waves from stress free flat surface of micropolar elastic half space, presenting reflection laws and amplitude ratios

15 p2714 A69-31147

Equilibrium cracks propagation in linear hereditary elastic media using Volterra principle

15 p2715 A69-31201

Moving load at plane interface between two elastic media in space related to direct trirectangular trihedron with vertically descending Oz axis

16 p2870 A69-31829

Equilibrium equations for elastic medium with stress couples, presenting first term of asymptotic expansion of solution for disk and simply connected region

16 p2871 A69-31830

Acceleration waves propagation in nonlinear conducting thermoelastic solid, treating homogeneously deformed and undeformed media

16 p2873 A69-32060

Somigliana dislocations effects on displacement field in linear isotropic elastic medium represented by integral with respect to line delineating surface

17 p3053 A69-33020

Energy dissipation influence on elastic elements random vibrations, obtaining relations between displacements rms value and random disturbance intensity

17 p3064 A69-33921

Linear isotropic elastic continuum dislocations distribution, deriving transport equations by statistical methods, noting analogy between energy/ momentum and MHD equations

18 p3212 A69-34352

Shock wave propagation induced by nonuniform instantaneous internal heating of nonlinear elastic strain hardening solid material [SAWE PAPER 69-APM-17]

18 p3214 A69-34393

Two point tensor function symmetries of nonlocal cohesive finite elastic materials determined from atomic lattice theory, obtaining Green function

19 p3444 A69-36798

Continuous particle media on basis of microstructure, discussing granular media deformation, elastic media dilatation, turbulent flow and dilute suspensions

19 p3446 A69-36833

Adjoint system for determining equilibrium stability of elastic continuum subjected to follower type surface tractions

19 p3446 A69-36835

Grade three strain-gradient elastic materials, deriving general solution to linearized field equations

20 p3621 A69-37073

Linearly elastic medium supersonic flow past rigid wedge, considering longitudinal and transverse perturbations interactions, dry friction, adhesion, slip and wedge physicochemical properties

20 p3515 A69-37439

Semiinverse method for elastic nonhomogeneity problems, considering case of seismic wave propagation

20 p3624 A69-37589

Superposition principle extended for wave propagation in composite materials /nonhomogeneous elastic media/

20 p3627 A69-37765

Dynamic stress concentrations and rigid body response of cylinder imbedded in elastic medium subjected to compressional wave

21 p3840 A69-39300

Linear elastic isotropic materials for model tests, describing properties of material composed of Araldite B and air

21 p3844 A69-39319

Overall elastic moduli evaluation for solid composite materials comprising matrix of homogeneous elastic materials embedded with cylindrical shape inclusions

24 p4396 A69-42731

Initially sharp plane pressure pulse propagation through linear elastic composite material, determining wave front shape change and stresses behind front [ASME PAPER 69-APMW-11]

24 p4401 A69-43103

Stress wave propagation in nonhomogeneous elastic media, considering curvilinear characteristics transformation into equal slope straight lines by change of independent variable

24 p4403 A69-43574

ELASTIC MODULUS

U MODULUS OF ELASTICITY

ELASTIC PLATES

Equations of linear theory of anisotropic elastic plates including Reissner-Green bending equations

01 p0168 A69-10387

Stroboscopic technique for obtaining interferential holograms of vibrating transparent and reflecting plates

02 p0251 A69-12561

Stresses in infinite elastic plate containing rigid rectangular inclusion subject to uniform stress field, using complex variable method and Schwartz-Christoffel conformal mapping

02 p0348 A69-12796

Stresses around two reinforced circular openings in thin elastic plate of isotropic material under biaxial loads

02 p0349 A69-12799

Mathematical models to investigate transient plane bending wave propagation in elastic plates, using elasticity and plate theories

03 p0525 A69-13606

Elastic equilibrium stress condition of anisotropic plates with circular isotropic inclusions

04 p0667 A69-14264

Photoelastic analysis of HF stress waves propagating in bars and plates subjected to damped sinusoidal loading [ASME PAPER 68-WA/APM-27]

04 p0669 A69-14397

Stress field for skew hole determined from plane stress field for equivalent right hole, considering elastic plate penetrated by oblique circular cylinder

04 p0674 A69-14589

Large finite deflections of clamped thin elastic circular plate subject to transverse concentrated load at center solved by power series

04 p0675 A69-14596

Plate thickness effect on bending of elastic plate with crack, investigating stress distribution
04 p0678 A69-14890

Bending theory for sandwich plates with layers having different elastic properties using asymptotic integration of three dimensional equations
04 p0684 A69-15534

Pointwise limitation of field dislocation and bending moments in elastic plates
05 p0831 A69-15599

Stress-strain state for two dimensional physically nonlinear multiply connected elastic regions, noting plate with two identical circular holes
05 p0841 A69-16203

Stress distribution in infinite strip with equally spaced identical semicircular notches on one edge and subject to transverse bending
05 p0842 A69-16643

Stresses in finite width infinite elastic isotropic strip with equally spaced identical semicircular notches under uniform tension or pure bending
05 p0843 A69-16644

Vibration response of thin elastic plates to random loads
05 p0844 A69-16741

Nonlinear constrained optimization by nonrandom complex method demonstrated by minimum weight structural analysis of elastic ring and plate
06 p1022 A69-17366

Transient nonaxisymmetric elastic wave propagation in infinite isotropic elastic plate, using linear elasticity theory
06 p1024 A69-17509

Computer analysis for optimizing size and shape of thin walled axisymmetric elastic rings, plates and shells with respect to tension, rigidity and weight
06 p1026 A69-18017

Plate theories of linearly elastic materials under free undamped vibration, giving 500 references
[AIAA PAPER 69-24] 06 p1027 A69-18061

Fiber geometry and partial debonding effects on bond stress distributions around single rigid fiber in infinite elastic plate subject to tensile stress
07 p1170 A69-18717

Finite aspect ratio sandwich plates flutter in supersonic gas flow analyzed by differential equation describing plates elastic equilibrium
08 p1412 A69-20324

Stability and bending of flexible plates and shallow shells obeying hereditary relations solved by singular kernel functions
08 p1413 A69-20335

Forced vibration of thin elastic plate resting on elastic foundation and subjected to time dependent loads and external damping
08 p1416 A69-20692

Monograph on plane problem and bending problem for infinite elastic plate with doubly periodic set of circular holes
08 p1416 A69-20709

Inhomogeneous half planes equilibrium bonded by elastic layer, noting tangential stresses at interfaces
09 p1611 A69-21482

Complex variable theory solution of eigenvalue problem governing elastic stability of thin elastic plate subjected to hydrostatic in-plane compression
09 p1615 A69-21921

Finite element analysis of large deflections in thin elastic plates subjected to transverse loading, including nonlinear geometric effects
09 p1615 A69-21924

Flexible circular plate on elastic support connected at free edge, noting stress independent of working load
09 p1618 A69-22239

Boundary layer suction sound emission, analyzing turbulent flow past elastic plate with reinforced slots performing flexural and torsional vibrations
09 p1483 A69-22638

Elastic Cosserat plate and shell theory, considering constitutive equations imitating transversely isotropic material and elastic deformations
10 p1798 A69-23147

Natural frequencies and associated composite loss factor for laminated plate with alternate elastic and viscoelastic layers, deriving partial differential equations
[ASME PAPER 69-VIBR-68] 10 p1805 A69-24158

Propagation of extensional cylindrical waves in elastic plates with free boundaries, considering plane stress and Lamb dispersion
11 p1969 A69-24414

Elastic unbounded isotropic plane weakened by doubly periodic system of identical holes, noting solution involving Cauchy type integral
11 p1972 A69-24652

Stress distribution around holes in thin shells and plates during large elastic displacements, considering hole size, loading and shallow spherical shells
11 p1972 A69-24654

Two dimensional problems solutions by contour smoothing methods, considering stress concentrations in reinforced or perforated thin elastic plates
11 p1973 A69-24661

Two dimensional elasticity and plate bending theories for calculating elastic isotropic panels and thin reinforced plates
11 p1974 A69-24664

Book on statics and dynamics of anisotropic and heterogeneous elastic structures covering thin heterogeneous anisotropic panels, elastic and sandwich plates, etc
11 p1986 A69-25236

Viscous flow-induced vibrations of elastically restrained flat plates in narrow channel, considering one dimensional viscous flow theory
11 p1991 A69-25515

Monochromatic waves propagation in infinite micropolar elastic plate, treating Lamb and Love waves
11 p1995 A69-25605

Thermal stresses in infinite elastic plates containing insulated circular holes, using two dimensional bipolar coordinates
12 p2180 A69-26267

Transverse symmetrical vibrations of thin elastic plates under Jacobi pressure distribution, giving displacement and velocity plots
12 p2180 A69-26271

Elastic mirror flexure and distortion patterns, considering periodic nature of load in polar coordinates, second flexure mode avoidance and friction elimination
12 p2056 A69-26407

Antiflexure cylinder for large astronomical mirror, noting support by astatic counterpoint levers and simple flanges
12 p2056 A69-26409

Mathematical bending theory for three layer elastic plates containing light or rigid fillers
12 p2182 A69-26678

Turbulent boundary layer sound emission effect on elastic plate, discussing pressure pulsation spectrum reflection
13 p2246 A69-27538

Stresses in elastic half plane with bonded disk of same elastic properties, describing stress production by expansion of disk
13 p2363 A69-28132

Thin elastic plates buckling under small normal load and external edge force
14 p2531 A69-28810

Bending of elastic triangular plates with free and supported corners under uniformly distributed transverse load determined using Ritz method
14 p2535 A69-29410

Stroboscopic technique for obtaining interferential holograms of vibrating transparent and reflecting plates
15 p2608 A69-30258

Equations for bending of elastic cantilever plate with parallelogram shape in oblique angle coordinate system, constructing functions satisfying Poisson conditions at contour
15 p2710 A69-30861

Elastic anisotropic panels mechanics analyzed using differential equations stressing transverse displacements, anisotropic thermal expansion, shape imperfections and slip deformations
15 p2711 A69-30904

Variational principles and differential equations of thin elastic panels mechanics for aerospace structures
15 p2712 A69-30974

Linear bending theory of elastic anisotropic sandwich plates with strong and weak cores
15 p2713 A69-31025

Unsteady oscillations after rupture in thin homogeneous isotropic elastic plate, assuming deflection amplitude smaller than thickness
16 p2873 A69-32033

Finite aspect ratio sandwich plates flutter in supersonic gas flow analyzed by differential equation describing plates elastic equilibrium
17 p3058 A69-33317

Infinite isotropic elastic plate vibration under vertical harmonic load, deriving vertical displacement at center of loaded area
17 p3058 A69-33408

Noise transmission from turbulent boundary layer through flexible plate into closed cavity, emphasizing nonlinear plate stiffness and mutual interaction between plate and airflow
17 p3006 A69-33409

Elastic sandwich structures design for maximum strength, using potential energy functional to derive governing equations
17 p3062 A69-33708

Error estimation in thin elastic plate bending problem approximate solution by equal deflection lines method, constructing two sided bound for boundary value problems
17 p3062 A69-33713

Von Karman equations in dimensionless and finite difference forms for deflections of elastic circular plate with central hole under load solved by iteration
[ASME PAPER 69-APM-20] 18 p3214 A69-34395

Elastic beam-plate vibration natural frequency and dynamic instability in transverse static or oscillating magnetic field
[ASME PAPER 69-APM-B] 18 p3215 A69-34400

Elastic circular cylindrical panel behavior in fluid with acoustic shock wave, allowing for propagation waviness of elastic stresses
18 p3216 A69-34579

Critical stresses and crack development near holes in compressed elastic plate
18 p3218 A69-34603

Transient processes of strain wave propagation in elastic shells and plates under time varying loads
18 p3224 A69-35321

Engineering equations for elastic thin plate oscillations of materials with properties described by linear integral Volterra-Boltzmann operators
19 p3437 A69-35989

Elliptic system of twelfth order equations describing elastic equilibrium of plate with kinematic functions analyzed by integration procedure
19 p3438 A69-36203

Coupled dilatational and equivoluminal modes of free vibration for elastic prisms and polygonal plates, using Poisson ratio and wave path construction
19 p3444 A69-36801

Swept cantilever thin elastic plates bending analyzed by power series representing deflection in oblique coordinate system
20 p3621 A69-37207

Stability loss nonaxisymmetric distribution in elastic annular plates under axisymmetric heating, using Ritz method to determine critical temperature
20 p3623 A69-37327

Turbulent boundary layer sound emission effect on elastic plate, discussing pressure pulsation spectrum reflection
20 p3518 A69-38204

Nonlinearly elastic plates with reinforced edges, deriving differential equations for boundary conditions
21 p3833 A69-38574

Stress analysis of circular elastic plate buckling under radial compression, noting Kirchhoff hypothesis influence on critical value of thickness-to-radius ratio
21 p3834 A69-38722

Deformation of uniformly thick elastic circular plates containing circular holes reinforced by thin rigid elastic rings
21 p3846 A69-39713

Stress concentration in elastic plate reinforced at edge by straight rib analyzed in finite form by Cauchy integrals and Fourier transforms
22 p4041 A69-40114

Network method for stability of thin nonlinearly elastic compressible material plates, noting difference operators for rigidly clamped plates
23 p4230 A69-42003

Force maintaining rigid inclusion embedded in elastic plate with rigid boundaries
23 p4235 A69-42465

Real space-time Green functions applied to turbulence induced infinite thin elastic plate vibration, analyzing mechanical dissipation effects
24 p4395 A69-42597

Forced symmetrical vibrations of circular elastic plate analyzed by applying Gaussian hypergeometric, Legendre functions and Jacobi polynomial
24 p4397 A69-42746

ELASTIC PROPERTIES

NT AEROELASTICITY	
NT AEROTHERMOELASTICITY	
NT ANELASTICITY	
NT DYNAMIC MODULUS OF ELASTICITY	
NT ELASTOPLASTICITY	
NT HYDROELASTICITY	
NT MAGNETOSTRICTION	

NT MODULUS OF ELASTICITY
 NT PHOTOELASTICITY
 NT PHOTOVISCOELASTICITY
 NT THERMOELASTICITY
 NT THERMOVISCOELASTICITY
 NT VISCOELASTICITY

Charge materials purity found to increase beta-Ti alloys properties

01 p0094 A69-10216

Stress function formulas in asymmetric theory of elasticity obtained by completeness method

01 p0167 A69-10325

Upper and lower bounds for static or geometric field in two and three dimensional elasticity theory, using Green functions

01 p0167 A69-10328

Flexural vibration of unbalanced rotating shaft with nonlinear characteristic of elasticity and damping, using equations of motion

01 p0168 A69-10329

Elastic anisotropy and polycrystalline orientations in cold rolled titanium sheets investigated by Fourier series method, discussing Young modulus values

01 p0094 A69-10431

Two dimensional structural model of micropolar continuum involving orientable points joined by extensible and flexible rods

01 p0169 A69-10810

Elastic properties of epoxy resins, deriving relation by considering different shear properties in tension and compression

01 p0103 A69-11268

Differential equations for dynamical problems in plates obtained by symbolic approach involving power series substitution into linear elasticity dynamical equations

01 p0172 A69-11282

Uniqueness formulation of concentrated load problem in linear theory of couple-stress elasticity

02 p0338 A69-11720

Modified Galerkin method applied to approximate solutions of two dimensional elasticity equations of equilibrium

02 p0338 A69-11748

Expandable D 21 airlock scheduled for testing on NASA Orbital Workshop Flight based on elastic materials technique, noting more complex chemically rigidized concept [IAF PAPER SD-49]

02 p0334 A69-11949

Equilibrium problem of elastic medium with stress couples in linearized elasticity theory, representing biharmonic function with aid of analytical functions

02 p0340 A69-12035

Elastic constants of point defects for bcc and fcc crystals with vacancies and interstitials calculated by Born-Huang method for nonprimitive lattices

02 p0267 A69-12186

Two dimensional elasticity problem for two zero tangential stresses, expressing stress-strain states by biharmonic and harmonic functions

02 p0341 A69-12198

Kinetic theory of fracture initiation, discussing changes in relative orientation distribution of network chains

02 p0345 A69-12401

Elastic analogue in creep stress analysis under time dependent boundary conditions and strain hardening theory

02 p0345 A69-12418

Numerical solutions of elastic problems by conformal mapping and finite difference method applied to circumferentially grooved shafts in torsion

02 p0346 A69-12419

Temperature dependence of elastic constants of highly and weakly doped n- and p-type GaAs

03 p0484 A69-13282

General solutions of three dimensional elasticity theory applied to isotropic disks and plates, emphasizing homogeneous solutions

03 p0526 A69-13738

Computerized solution of three dimensional problems of elasticity theory using Ritz method

03 p0527 A69-13743

Two dimensional problem of elasticity by numerical solution, outlining program for computer

03 p0527 A69-13750

Integral equations solved numerically for general nonhomogeneous elastic inclusion problem, using linear elasticity theory

03 p0530 A69-14064

Elastodynamic boundary value problem solution for stability in linear elasticity

03 p0530 A69-14066

Elastohereditary characteristics of composite materials with random inhomogeneities based on Volterra principle

04 p0667 A69-14263

Stress distribution near circular hole in elastic layer

04 p0667 A69-14266

Plane problem of asymmetric elasticity based on biharmonic and Helmholtz equation for stress functions

04 p0667 A69-14267

Thermal stress determination in two dimensional problem of theory of elasticity, using stress simulation by thin plate bending

04 p0668 A69-14272

Variational principle for solving nonlinear equations in elasticity theory, theoretical mechanics and mathematical physics

04 p0668 A69-14273

Adiabatic elastic constants of molybdenum-rich rhenium alloys, studying concentration effects on bulk modulus, Debye temperatures and interatomic forces

04 p0613 A69-14455

Stored energy function of hyperelastic material by Lie group extension of Truesdell theorem on symmetry groups

04 p0680 A69-14945

Soviet handbook on elasticity, plasticity and creep theories, emphasizing stresses and strains in solid thin walled shells and plates under bending, tension and torsion

04 p0683 A69-15499

Linear theory applied to anisotropic elastic materials, discussing transition from compressible to incompressible elastic materials

05 p0834 A69-15795

Stresses in cylindrical shell with elastic core loaded on curved surface solved, using elasticity theory for core and membrane solutions for shell

05 p0835 A69-15871

Plastic moments calculation of continuous steel beams under various loading patterns

05 p0837 A69-16035

Elastic plastic stress distribution in compressed ring determined with postyield strain gages and stress-strain relationship from uniaxial tensile test

05 p0837 A69-16063

Variational principles for differential equations and initial and boundary value problems in dynamic geometrically nonlinear elasticity theory

05 p0840 A69-16202

Circular inclusion effect on stresses around line crack in sheet under tension based on elasticity theory

05 p0841 A69-16432

Mechanical anisotropy of polyethylene terephthalate and relation to molecular structure and cold drawing

05 p0785 A69-16489

Plane problem of moment theory of elasticity for stress concentration near circular hole

05 p0842 A69-16502

Stress-strain state of infinite plate with two holes of different diameter solved, using integral equation derived for two dimensional problem in elasticity theory for anisotropic medium

05 p0843 A69-16680

Asymptotic integration of equations in theory of elasticity to develop approximate theory of momentless shells

05 p0843 A69-16689

Book on continuum mechanics covering elasticity, fluid mechanics, plasticity and viscoelasticity, emphasizing basic concepts

05 p0843 A69-16713

Compressional and shear wave velocities vs porosity for sintered perlitic bricks

06 p1000 A69-17009

Elastic stability of three dimensionally reinforced composite cylindrical shells [AIAA PAPER 69-122]

06 p1029 A69-18216

Stresses and displacement around crack under various conditions using two dimensional elasticity theory, deriving complex potentials for various loading types

07 p1231 A69-18269

Elastic limit of lunar outer layer determined from analysis of lunar crater dimensions variations as functions of diameter

07 p1212 A69-18600

Cylindrically orthotropic hollow cylinder elastic properties determination using experimental test for production of stress and strain states and end effects

07 p1232 A69-18718

Complementary variational principles for boundary value problems in continuum mechanics of solids, obtaining generalized Hamilton canonical formalism

07 p1232 A69-19173

Elastic constants of composite materials by dispersion relation of sound waves for long wavelength, assuming periodicity in three dimensional rectangular lattice

07 p1236 A69-19457

Temperature dependence of single crystal elastic constants of nickel aluminide determined by ultrasonic wave propagation measurement

08 p1332 A69-20288

Elastic potential for obtaining localized strain theory, describing deformation characteristics of compressible and incompressible orthotropic materials with physical nonlinearity

08 p1412 A69-20328

Complementary plastic work theorems in piecewise-linear elastoplasticity applied to plastic and nonlinear elastic problems

08 p1414 A69-20528

Dislocation model of strength of elastically inhomogeneous crystalline materials based on elastic interactions between dislocations and periodic fluctuations of shear modulus

08 p1333 A69-20557

Two dimensional problems in classical theory of elasticity concerning zero normal stress and zero tangential stresses, noting formulas for right cylinder

08 p1415 A69-20660

Elastic stability of one dimensional structures analyzed by energy method, discussing deformable line, conservative forces and linear stability

08 p1418 A69-20846

Asymptotic two dimensional moment theory of elasticity, analyzing stress concentration at curvilinear holes and fluctuating boundary loads

09 p1614 A69-21884

Error estimates of stress concentration at free hole determined by two dimensional elasticity theory of thick plates

09 p1614 A69-21885

Complex variable theory solution of eigenvalue problem governing elastic stability of thin elastic plate subjected to hydrostatic in-plane compression

09 p1615 A69-21921

Part-through and through-thickness fatigue crack growth observations in glassy plastics, using linear elastic fracture mechanics [SESA PAPER 1348]

09 p1617 A69-22013

Micropolar elasticity using Green functions to solve wave equations in unbounded medium, noting effects of concentrated force and body couples

09 p1618 A69-22261

Elasticity theory upper and lower bounds for two and three dimensional inhomogeneous problems and applications to plates

10 p1794 A69-22889

Pointwise bounding of eigenfunctions in vibration and stability problems in elasticity theory

10 p1794 A69-22925

Cosserat continuum and elasticity models of dynamics of composite materials, analyzing dispersive longitudinal waves

10 p1798 A69-23148

Stress concentration in Cosserat continua based on model of six elastic constants in linear isotropic and notch case

10 p1799 A69-23150

Dual continuum model of nonelastic processes in elasticity and dislocation theory, including incompatibility effects of interaction forces between structural elements

10 p1799 A69-23152

Continuum theory of dislocations and internal stresses in generalized Cosserat continuum as theoretical model for crystals

10 p1799 A69-23153

Numerical orthonormalized system of functions for formulating functional equations in potential and elasticity theory, considering boundary value problems

10 p1801 A69-23687

Integral transform solutions for Griffith cracks in brittle fracture theory, discussing disk and penny shaped cracks in cylinders and thick plates

10 p1801 A69-23688

Energy theorem for time dependent materials, deriving convexity conditions for minimum work and maximum complementary work functions

11 p1969 A69-24412

Modified Rayleigh-Ritz method for prediction of stress concentration in elastostatic problems for elastic continua, noting plate bending

11 p1969 A69-24413

Asymptotic methods for integral equations of plane mixed problems of elasticity theory for nonclassical regions

11 p1971 A69-24647

- Nonlinear elasticity theories emphasizing quadratic approximation of stress concentration
11 p1973 A69-24660
- Conformal mappings for solving boundary value problems in elasticity and plasticity theories for regions having singular points
11 p1973 A69-24662
- Two dimensional elasticity and plate bending theories for calculating elastic isotropic panels and thin reinforced plates
11 p1974 A69-24664
- Micropolar elasticity theory for materials exhibiting granular structure and microstructure, discussing deformation geometry and measurement, strain kinematics, microstrains, thermodynamics, etc
11 p1975 A69-24674
- Partial derivatives of harmonic and biharmonic functions at surface of cylinder for three dimensional problem in elasticity theory, considering displacement vector
11 p1976 A69-24777
- Two dimensional elastic reinforcements effects on stress, strain and elasticity of quasi-homogeneous anisotropic elastic medium
11 p1981 A69-24941
- Three dimensional problem of elasticity for transversely isotropic medium with cylindrical anisotropy, using partial differential equations for unknown functions
11 p1983 A69-25091
- Flat bar optimal cross section under tensile stress applied to minimize stress in large structural components using elasticity theory
11 p1986 A69-25203
- Dynamic stability of elastic beam type structures, using electronic simulation based on finite element approach
11 p1986 A69-25344
- Classification of second order quasi-linear partial differential equations with two independent variables in structural dynamics with emphasis on elastic structures
11 p1991 A69-25513
- Theorem for integral expansion applied to boundary value problems of mathematical physics and elasticity theory for single sheet hyperboloids of revolution
11 p1910 A69-25731
- Stress distribution in elements of unidirectionally fiber reinforced composite materials analyzed as function of fiber content and fiber-matrix elastic properties
12 p2180 A69-26263
- Volterra operator algebra for boundary value problems involving linear viscoelasticity with continuous relaxation time and delay time spectra
12 p2182 A69-26677
- Orthotropic properties and stress fields for configurations of fiber or whisker reinforced composite materials subjected to nonaxial loading, considering infinite elastic matrix
12 p2186 A69-26824
- Monograph on shell calculations by linear three dimensional elasticity theory, relating displacements and stresses
12 p2188 A69-26902
- Variational principle for admissible functions partial solution in elasticity theory involving solid bodies with cracks
13 p2359 A69-27290
- Elastic directed curves dynamic theory, considering Hamilton principle, mass conservation and behavior of action density function under rigid body variations
13 p2360 A69-27321
- Plane problem for inhomogeneous elastic media based on assumption of elastic coefficients as functions of two variables defined in domain occupied by medium
13 p2362 A69-27977
- Classical plasticity theory modified to include finite elastic and plastic strain components by considering thermoelasticity and plastic work irreversible processes
13 p2362 A69-28119
- Polyharmonic Gq functions derivation and applicability to three dimensional elasticity theory equations solutions
13 p2369 A69-28522
- Elastic medium properties recovered from reflected or transmitted plane waves at normal incidence, obtaining computational procedures and analytical solution from Schroedinger equation
13 p2300 A69-28664
- End loaded two layer laminated elastic strip stress concentration and self equilibrating traction distribution analyzed by eigenvalue equation
13 p2370 A69-28672
- Three dimensional equations of elasticity reduced to two dimensional equations of shell theory, discussing stressed states of thin elastic bodies
14 p2531 A69-28807
- Plane mixed boundary value problem in elasticity theory for infinite wedge
14 p2531 A69-28809
- Fracture mechanics based on linear elasticity for evaluating crack propagation resistance, presenting plane strain fracture toughness test results for high strength alloys
[ASME PAPER 69-DE-10] 14 p2461 A69-28842
- Integral equations for classical elasticity boundary value problems, stressing analogous Stokes flow hydrodynamic equations
14 p2535 A69-29361
- Working fluids elastic characteristics variability effect on hydraulic actuator dynamics, studying adiabatic and isothermal conditions
14 p2405 A69-29423
- Difference schemes for elasticity theory plane dynamic problem with mixed boundary conditions, establishing scheme absolute stability
14 p2536 A69-29474
- Iterative solution for difference equations approximating displacement vector determination problem in theory of elasticity, investigating algorithm convergence
14 p2536 A69-29479
- Temperature dependence of elastic constants of highly and weakly doped n- and p-type GaAs
14 p2508 A69-29655
- Differential equations for elastic stress distribution in thin rotating shell with arbitrary profile, obtaining analytical dimensionless solutions for potential profiles
15 p2703 A69-30158
- Charge materials purity found to increase beta-Ti alloys properties
15 p2638 A69-30272
- Longitudinal internal cracks in deformed Al alloys initiated by elastic stress concentration in areas of highest flow rate gradient
15 p2638 A69-30277
- Plane contact problems in elasticity theory allowing for cohesive forces solved by integral and differential equations
15 p2706 A69-30578
- Infinite strip plane elastic problem reduced to Hilbert problem by employing multiply connected region and biharmonic solutions
15 p2707 A69-30625
- Coaxial deviator theory of nonlinear elasticity, applying deformation theory variant to shell theory
15 p2592 A69-31058
- Integral representation of p-analytic functions of complex variable, applying axisymmetric boundary value problems of elasticity theory for cylindrical surfaces and paraboloid of revolution
15 p2714 A69-31191
- Analogy between Timoshenko plate theory and moment theory of elasticity achieved by reducing Timoshenko equations to biharmonic and Helmholtz equation
15 p2715 A69-31205
- Potential functions applications to three dimensional static elasticity problems of parallelepipeds, using general stress solution
15 p2715 A69-31216
- Polycrystalline BeO sound velocities determined as function of pressure and temperature using pulse superposition method
16 p2802 A69-32338
- Transient stress waves due to inputs of various types and time dependence in plates and revolving shells, discussing applications of elasticity theory analysis methods
16 p2876 A69-32785
- Two dimensional plate theory with moment stress considerations derived from three dimensional elasticity theory, discussing reduction of equilibrium and compatibility equations
16 p2876 A69-32786
- Composition effect on tensile and flexural moduli of composites containing randomly distributed fibrous strands, establishing strength-composition relationships
17 p2991 A69-32960
- Soviet collection of articles on hydroaeromechanics and elasticity theory, number 7
17 p3054 A69-33121
- Random oscillations of elastoacoustic systems, obtaining solution for spherical shell containing acoustic medium
17 p3057 A69-33199
- Static implications of strong ellipticity condition in linearized elasticity theory, exemplifying homogeneous deformations
17 p3058 A69-33415
- Fracture processes in high strength materials, considering effect of stored elastic energy, component geometry, fracture toughness and environment
17 p2988 A69-33553
- Filamentary composites elastic constants calculation extended to hexagonal symmetry by long waves method
17 p3061 A69-33666
- Complete spherical shells transverse frequency analysis, comparing results of elastic theory and classical, improved and membrane shell theories
17 p3061 A69-33705
- Orthogonal polynomials for solving plane elasticity theory boundary value problems without constructing mapping functions, noting applications
17 p3067 A69-34144
- Pressurized cylindrical shell creep analysis by elastic procedure extension using computer program
17 p3067 A69-34211
- Book on numerical methods in applied theory of elasticity, discussing oscillations of twisted rods for theory of steam and gas turbine blades
18 p3211 A69-34331
- Temperature dependence of metal elastic properties including thermal strains effect on stress field, yield stress changes and elastic modulus variations
18 p3212 A69-34353
- Plane problems of elasticity theory solved numerically using conformal mapping
18 p3219 A69-34709
- Spherical shells axisymmetric equilibrium properties under uniformly distributed external compression
18 p3224 A69-35318
- Fredholm integral equation solution of circularly axisymmetric stress state for bodies of revolution
18 p3226 A69-35375
- Silicon carbide coated boron fiber reinforced /Bor-sic/ Al composites tensile strength and elastic properties
19 p3344 A69-35926
- Plate material Poisson ratio determined by application of holographic interferometry to plate pure bending deformation contour lines
19 p3312 A69-36206
- Volume prediction of human body exposed to vacuum based on animal skin elasticity and anatomical features
19 p3258 A69-36456
- Generalized Love functions in axisymmetric micropolar elasticity, deriving stress functions expressing all state components
19 p3440 A69-36585
- Variational principle for Fredholm integral equations applied to inclusion and indentation problems in elasticity
19 p3440 A69-36589
- Elastic stability theory from thermodynamic viewpoint, considering postulates and energy equations
19 p3442 A69-36796
- Linear-elastic fracture mechanics applied to environment enhanced crack growth /stress corrosion cracking/
19 p3349 A69-36888
- Stiffness matrices in plane elasticity problems by Galerkin method, leading to simultaneous expressions related to finite element method
20 p3619 A69-36951
- Grade three strain-gradient elastic materials, deriving general solution to linearized field equations
20 p3621 A69-37073
- Thin circular cylindrical shells elastic equilibrium under loads producing deflection, elongation or contraction described by integrating equilibrium equations with constant coefficient
20 p3621 A69-37076
- Fourier transform methods in elasticity problems, considering three dimensional equilibrium equations in elastostatics in terms of displacements
20 p3622 A69-37282
- Elastic properties of hot pressed polycrystalline quartz and rutile as function of pressure, obtaining pressure coefficients of compressional and shear wave velocities
20 p3583 A69-37502
- Collection of papers on mechanics including quantum theory, mechanics of micropolar continua, elasticity and plasticity, rheology, etc
20 p3623 A69-37580
- Elastic constants of composite containing parallel cylindrical fibers, discussing disturbance in stress field
20 p3626 A69-37759

Analog method for determining structural creep displacement by setting up boundaries for linear elasticity and perfect plasticity

20 p3628 A69-37915

Shell elasticity calculation method, discussing stress state model, equilibrium conditions, shell geometry, etc

21 p3832 A69-38419

Nonlinear theory of elastic membranes accounting for thickness effects, obtaining field equations and constitutive relations for various cases

21 p3832 A69-38465

Composites elastic behavior, considering stress-strain in anisotropic lamina, composite plates and shells theory, thermal stresses and buckling for improving heterogeneous structures design

21 p3836 A69-38931

Diffusion layers and elasticity-dependent interdiffusion coefficients of Ti binary systems, using X rays

21 p3745 A69-38954

Asymptotic solution, existence and uniqueness of integral equations occurring in elasticity theory and mathematical physics

21 p3772 A69-39618

Soviet collection of papers on static and dynamic problems in elasticity and plasticity theory covering plates, shells, beams, etc

22 p4038 A69-39911

Strain anisotropy matrices behavior along strain trajectories of arbitrary curvature, studying matrices and elastic constants dependence

22 p4039 A69-39914

Strain anisotropy matrix construction for various strain trajectories from elastic properties of expression relating stress and elastic strain deviators

22 p4039 A69-39915

Airway distensibility effect on elastic behavior of human lungs, noting compliance and resistance at different breathing frequencies for diseased lungs

22 p3873 A69-40205

Variational method using Hamilton principle and calculus of variations to determine elastic curve and internal forces in static or dynamic loaded beam

22 p4043 A69-40459

Elasticity boundary value problems solution based on equilibrating method and differential equation

22 p4046 A69-40967

Mechanical properties of fiberglass reinforced textile at normal temperature, noting applicability of elasticity formulas

23 p4179 A69-41994

Three dimensional mixed boundary value problem in elasticity by dominant states method, examining generalized Fourier series feature in Legendre polynomials

23 p4229 A69-41998

Nonlinear formulation for rigid jointed space frame comprised of prismatic linear elastic members, using Newton-Raphson and successive substitution methods

23 p4232 A69-42142

Fcc metals higher order elastic constants calculated by Morse potential function, considering atomic interactions truncation and pressure derivatives

23 p4233 A69-42337

Soviet book on resistance of materials to deformation and fracture in complex stress states covering elasticity, mechanical theories of limiting stress state, experimental verification, etc

24 p4402 A69-43233

Orthotropic fiberglass/epoxy faced honeycomb aircraft type sandwich structure elastic properties by edgewise compression test

24 p4403 A69-43443

ELASTIC SCATTERING

Soviet book on atomic collisions and elementary processes in plasma covering atomic interactions, elastic and inelastic collisions, negative ions, autoionization, ion mobility and recombination

01 p0132 A69-11200

Many valley n-type Ge and Si semiconductors dissipative current breakdown effects, noting dependence on symmetry of valleys and phonon scattering pattern

02 p0298 A69-12098

Elastic and inelastic collisions between deformable bodies, using Michelson interferometer with He-Ne laser as source

02 p0282 A69-12607

Elastic scattering cross section for low energy electrons on metastable He atoms, using polarized orbital method

03 p0469 A69-12922

Elastic scattering of slow electrons by negative H and positive Li ions, calculating differential cross sections and phase shifts

03 p0469 A69-12924

Differential cross sections for elastic scattering of 600 Mev protons from He 3 between 19 and 45 degrees

03 p0472 A69-13464

Transport phenomena analysis in n-InSb semiconductors during elastic/inelastic current carrier scattering

03 p0492 A69-14171

Elastic scattering of electrons from argon atoms in argon air plasmas by shock tube microwave reflection method, measuring power reflection coefficient

[AIAA PAPER 68-138] 04 p0632 A69-14701

Angular distribution of reactive elastic scattering analyzed by opacity function /reaction probability/

04 p0554 A69-14859

Elastic bodies collisions in presence of thermoelastic effects, investigating local inertial and thermoelastic forces effect on compression region shape

05 p0841 A69-16207

Vibrational excitation by electron impact in kinetic energy range 30-60 eV studied for water vapor and carbon dioxide, determining intensities relative to elastic scattering

06 p0960 A69-17108

Energy spectra of muons determined from knock-on electrons projected angles of emission in C, Al and Cu

06 p0991 A69-17305

Cross section calculations for elastic and inelastic electron collisions with atoms, ions and molecules and ionization of atomic systems by electrons and photons

07 p1187 A69-19660

Electron transport parameters in noble gases at low electric field intensities, elastic and inelastic scattering and Boltzmann transport equation

08 p1362 A69-20285

Quantum theory of line broadening and shift, relating adiabatic and diabatic collisions to elastic and inelastic scattering of perturbers

08 p1363 A69-20464

Channel coupling effects in elastic electron-atom collisions involving electric dipole transitions, noting phase shifts and differential cross section

09 p1542 A69-21623

Exact solutions for two state potential curve crossing in subexcitation molecular collisions in terms of various decoupling schemes

12 p2131 A69-25983

Elastic proton scattering measurements, noting consistency with statistical theory when diffraction is taken into account

13 p2302 A69-28368

Elastic and inelastic elementary particle collisions described by Feinman diagrams, discussing computer results for high energy particle interactions

13 p2303 A69-28369

Elastic collision effect on gas laser atoms velocity distribution and gain factor determined for strong collision model

14 p2459 A69-29388

Resonances in elastic cross section for electron/hydrogen atom scattering noting wide structure

15 p2657 A69-31265

Elastic collision operator for relativistic Lorentz gas converted to differential form using Fokker-Planck limit for anisotropy segments

16 p2817 A69-31668

Elastic scattering cross sections of negative pions by deuterons compared with Glauber model calculations

17 p3007 A69-32885

Gas laser power dip in presence of elastic collisions, using equilibrium equations for particles velocity distribution function

17 p2983 A69-33972

Quasi-plastic impact resulting from incomplete elastic collision of two material points in presence of dry Coulomb friction, noting engineering role in pneumatic equipment

18 p3215 A69-34568

Elastic scattering cross sections for 21-Mev incident protons measured for nuclei differing in mass, determining optical model potential

18 p3179 A69-35489

Heated supersonic beam study of He-Ar intermolecular potential, determining total elastic collision cross section as function of velocity in scattering chamber

19 p3377 A69-36183

Energy dependence of elastic total collision cross section of identical He molecules, using velocity selected primary beams at low target temperature

19 p3378 A69-36186

Differential cross sections for elastic scattering of protons by Ar atoms in energy range 12.7-44.1 eV, estimating internuclear separation

20 p3580 A69-37499

Wave scattering in elastic medium by discontinuity line or finite crack, noting dynamic stress intensity dependence on incident wavelength and Poisson ratio

21 p3840 A69-39293

Proton-antiproton high energy elastic scattering by bosons exchange, introducing vertex functions for non-local Lagrangian

21 p3775 A69-39467

Diatomic molecules rotational excitation calculated from electron molecule elastic scattering parameters in fixed nuclei approximation

21 p3775 A69-39665

Stueckelberg formulation for transition probabilities to interpret perturbation effects in elastic scattering differential cross section measurements

22 p3987 A69-41005

Shape resonances in low energy elastic scattering of electrons by C, N and O, discussing ground state configurations and close coupling equations corrections

23 p4193 A69-41452

Negative pions elastic scattering from hydrogen, confirming differential cross section minimum for specific incident momentum-scattering angle region

24 p4352 A69-43049

Intermediate energy protons elastic and quasi-elastic scattering from light nuclei, correlating p-D, p-He-3, p-p and p-He-4 data with various scattering models

24 p4352 A69-43123

Differential cross section and polarization measurements for elastic scattering of high energy protons from light nuclei

24 p4352 A69-43125

Elastic differential Li ion scattering cross sections on helium, nitrogen and oxygen

24 p4354 A69-43817

Elastic electron scattering by metastable states of rare gases, using effective potential matching experimental binding energy of negative ions

24 p4354 A69-43818

ELASTIC SHEETS

Stress distribution near circular hole in elastic layer

04 p0667 A69-14266

Load diffusion from transverse tension bar into semiinfinite elastic sheet, considering line and area contact methods of stringer attachment

[ASME PAPER 68-WA/APM-15] 04 p0669 A69-14396

Turbulent skin friction on compliant skins stretched over damping fluid in shallow bath in flat plate

[AIAA PAPER 69-164] 06 p0914 A69-18163

Boundary determination for separating elastic and plastic regions of infinite perforated sheet with triangular network of circular holes

11 p1996 A69-25736

Plane stress theory for large elastic deformations of isotropic thin sheets, outlining successive substitutions method for neoHookean materials static and dynamic problems

13 p2359 A69-27320

Two dimensional stress analyzed near crack in infinite elastic sheet, considering crack shape and Young modulus

19 p3440 A69-36638

Turbulent skin friction on compliant skins stretched over damping fluid in shallow bath in flat plate

[AIAA PAPER 69-164] 24 p4306 A69-43683

ELASTIC SHELLS

Elastic shell nonlinear theory, introducing nonsymmetric stress tensor and principles of virtual work and objectivity

01 p0166 A69-10166

Predeformations of thin walled elastic isotropic spherical shells analyzed using Vlasov shell bending theory

02 p0336 A69-11555

Three dimensional elastic theory using parametric expansion method developed for cylindrical translation shell profiles

02 p0338 A69-11718

Existence and uniqueness of weak solutions in linear theory of stable equilibrium position for inhomogeneous elastic thin walled shells

02 p0340 A69-12036

Critical points separating stable and unstable branches of equilibrium curve of nonlinear elastic systems, discussing flexible shallow conical shell in temperature field

02 p0341 A69-12256

Matrix displacement method for nonlinear elastic analysis of shells of revolution under symmetrical and asymmetrical loadings

02 p0346 A69-12511

Postbuckling behavior of elastic spherical shells from pressure and volume-displacement instrumentation and photography

03 p0524 A69-13062

Stress diffusion from axially loaded stiffeners into cylindrical elastic shells

03 p0530 A69-14065

Elastic noncircular orthotropic conical shell stress-strain state, obtaining differential equations reducible to integrodifferential equations solvable by iteration

04 p0673 A69-14494

Variational theorems for stress function formulation of boundary value problems in linear theory of thin elastic shells

04 p0678 A69-14894

Kirchhoff-Love hypothesis error dependence on stressed state variability index in theory of elasticity for closed spherical shell under uniform surface load

04 p0680 A69-14927

Stability of circular cylindrical viscoelastic and elastic shells with local effects due to radial load on circumference or thermally induced tangential stress

04 p0680 A69-14928

Poincare sphere representation of polarized light used to predict rotation effect on optical observations in photoelastic shell analysis

04 p0683 A69-15495

Elastic stability of thin circular cylindrical shell with elastic core, longitudinal and transverse reinforcement ribs, initial defects and under large strains

05 p0832 A69-15691

Bending equations for shallow elastic three layer asymmetric shell with different isotropic layers and transversely isotropic rigid filler at various temperatures

05 p0840 A69-16197

Three layer structure theory, discussing thin elastic sandwich shells with middle layer susceptible to transverse shear

06 p1025 A69-17615

Computer analysis for optimizing size and shape of thin walled axisymmetric elastic rings, plates and shells with respect to tension, rigidity and weight

06 p1026 A69-18017

Local stability of thin walled elastic shells of revolution subjected to external pressure

07 p1237 A69-19686

Finite elements for analysis of flexible shells, considering Kirchhoff theory for transverse shear deformation and problems involving rotations and buckling

08 p1411 A69-20142

Surrounding fluid effects on free axisymmetric vibrations of thin elastic spherical shells, studying irrotational motions in compressible and incompressible ideal fluids

09 p1613 A69-21720

Axisymmetric dynamic snap through critical load analysis for elastic clamped shallow spherical shells, considering impulsive and step loads

09 p1616 A69-21977

Elastic Cosserat plate and shell theory, considering constitutive equations imitating transversely isotropic material and elastic deformations

10 p1798 A69-23147

Stress concentration at holes and cavities in thin elastic shells under static and dynamic loads, considering physical nonlinearities of material

11 p1974 A69-24665

Static and dynamic stability of flexible shallow spherical shell under axisymmetric load and elastically hinged along contours

11 p1976 A69-24763

Thin elastic shell interior equations based on stress and strain, discussing shell description, strain derivatives plate deformation into cylindrical shells, etc

11 p1977 A69-24802

Thin elastic shell theory, using iterative process to develop differential equation integrals for interior state of stress

11 p1977 A69-24804

Nonlinear theories of deformable surfaces as two dimensional generalized continua applied to elastic shells, emphasizing elastic Cosserat surface

11 p1978 A69-24805

Consistent elastic shell theory based on expansion of sought solutions in power series over distance between point and middle surface

11 p1978 A69-24806

Continuum theory for thin elastic shells with local structural effects, emphasizing shell constituted by Cosserat material

11 p1978 A69-24809

Asymptotic methods for three dimensional equations in thin and thick elastic shell theory for determining two dimensional systems

11 p1978 A69-24810

Linear thin shell theory in complex dependent variable form for determining fourth order partial differential equations, considering elastic shells with edge loads

11 p1978 A69-24811

Thin conical elastic shell stress-strain state calculated by computer for arbitrary thicknesses and loading conditions, considering temperature and edge forces effects

11 p1981 A69-24943

Thin elastic conical shells asymmetric deformation under stresses and strains, deriving asymptotic solution

11 p1983 A69-25090

Book on statics and dynamics of anisotropic and heterogeneous elastic structures covering thin heterogeneous anisotropic panels, elastic and sandwich plates, etc

11 p1986 A69-25236

Stochastic problems in thin elastic shell theory solved by equations obtained by linearizing shell equations near initial state of stress

11 p1996 A69-25732

Nonlinear equations solvability for elastic cylindrical shells found existing for arbitrary load and clamping conditions

12 p2177 A69-25881

Quasi-shallow shells theory applicability to thin elastic shallow shells, emphasizing use of function W/δ

12 p2178 A69-26001

Postcritical deformations of thin conical elastic shells hinged along edges under external pressure using Pogorelov method for cylindrical shells

12 p2181 A69-26609

Axisymmetric elastic stresses in ring stiffened segmented shells of revolution, noting finite difference method for nonlinear analysis and computer program

12 p2185 A69-26818

Plane strain solution for thick walled viscoelastic cylinder bonded to thin elastic shell from deformation rate and strain, including inertia effects

16 p2871 A69-31876

Approximate analytic solution to transient response of infinitely long cylindrical shell surrounded by viscoelastic medium, discussing composite and elastic shells

16 p2871 A69-31877

Elastic spheroidal shell of revolution under external pressure described by buckling and postbuckling theory

16 p2874 A69-32162

Damped vibrations of elastic open cylindrical shell under arbitrary loading, obtaining mean square of bending from correlation theory

17 p3054 A69-33094

Local stability of viscoelastic shells of revolution under axisymmetric loads, discussing asymmetric snapthrough of dome

18 p3216 A69-34573

Collocation method applied to solving contact thermoelasticity problem for short thick walled hollow cylinder attached to thin elastic shell in axisymmetric temperature field

18 p3217 A69-34595

Growth rate of stability loss intrinsic modes in elastic shells under severe load, discussing stress distribution during buckling

18 p3217 A69-34598

Nonlinear axisymmetric oscillations and motion stability of cylindrical wound elastic glassfiber shell under time dependent uniform internal pressure

18 p3222 A69-34975

Initial deflection effect on elastic cylindrical shell stability under compression, finding critical load by determining limiting point in successive loading

18 p3224 A69-35319

Transient processes of strain wave propagation in elastic shells and plates under time varying loads

18 p3224 A69-35321

Weak moment shells made from materials with different elastic moduli, developing theory based on undeformable normals

18 p3225 A69-35367

Resonant oscillations amplitude of nonlinearly elastic hinged cylindrical shell determined with cubic equation taking into account Hooke law, linear stresses, shell theory displacements, etc

19 p3435 A69-35843

Contact problem of two thin elastic shells within Kirchhoff-Love theory, discussing constitutive equations

19 p3438 A69-36305

Thin elastic shells internal stress state by iteration of two dimensional equation of general linear theory

19 p3443 A69-36790

Elastic shell theory to regularize singular integrodifferential equation, investigating load transfer from reinforcing ribs to circular cylindrical shell and numerical solution correlation

19 p3443 A69-36792

Elastic closed and truncated conical shell stability with initial deflections under dynamic critical loading

21 p3834 A69-38716

Asymmetrical oscillations of cylindrical shell with elastic bottom containing liquid, discussing liquid level influence on natural oscillation frequencies

21 p3834 A69-38718

Linear hydrodynamic equations describing inviscid fluid flow past thin elastic cylindrical shells in circle with motions described by shallow shell equations

21 p3834 A69-38719

Stability loss for hinged circular cylindrical elastic shells reinforced by thin walled closed profile ribs, proposing minimum weight design method

21 p3835 A69-38723

Strain rate-load relations in elastoplastic shells reaching yield point, discussing variational method applicability

21 p3838 A69-39189

General system of equations derived for nonaxisymmetric oscillations of elastic spherical shells, obtaining expressions for oscillations from torsion, tension and bending

21 p3839 A69-39199

Deformation of orthotropic layered elastic shells based on linear elasticity theory, assuming surface and stress constraints

23 p4226 A69-41535

Computer program for natural oscillations of plates and shells, deriving differential equations of motion for thin elastic shell by variational method

23 p4230 A69-42004

Dynamic response of anisotropic elastic cylindrical and spherical shells determined by application of Hankel transforms, considering time dependence of loads

23 p4235 A69-42481

Transverse acoustic wave excitation of elastic circular cylindrical sandwich shell submerged in infinite fluid medium, describing simultaneous equations development for modal response

[ASME PAPER 69-APMW-17]

Axisymmetric vibration of shallow spherical caps, using nonlinear dynamic equations and associated variational equation of motion for elastic spherical shells

[ASME PAPER 69-APMW-6]

24 p4401 A69-43100

ELASTIC STABILITY
U DAMPING

ELASTIC SYSTEMS
Normal modes and natural frequencies of combined linear elastic structures resting on immovable base

04 p0678 A69-14870

Natural longitudinal single frequency oscillations of system of n material points connected in series by nonlinear elastic threads and with energy dissipation

05 p0832 A69-15687

Maximum index of exponential growth of solution of linear Hamiltonian equation with periodic operator coefficient encountered in dynamic stability of elastic systems

07 p1231 A69-18501

Random oscillations of nonlinear elastic system described by nonlinear partial differential equations

11 p1918 A69-24781

Linear differential equation solution for elastic systems stability problems, discussing applications to heated rectangular plates

11 p1982 A69-24950

Gradient iterative methods for finite element eigenvalue problem associated with stability and vibrations of elastic systems based on Rayleigh quotient

16 p2871 A69-31898

Holor algebra with tensor notations applied to elastic structures/discrete systems/, discussing inertia and stiffness tensors

21 p3831 A69-38415

Damping effects on elastic systems stability under nonconservative forces, correlating stability and quasi-stability regions

22 p4040 A69-39981

Matrix method for analyzing elastic structures linear transient response to time dependent loads and temperature change

24 p4399 A69-42988

ELASTIC WAVES
NT AEROYNAMIC NOISE

ELASTICITY

NT AIRCRAFT NOISE
 NT BAROCLINIC WAVES
 NT COHERENT ACOUSTIC RADIATION
 NT COMPRESSION WAVES
 NT DETONATION WAVES
 NT ELECTROACOUSTIC WAVES
 NT ELECTROSTATIC WAVES
 NT ENGINE NOISE
 NT GRAVITY WAVES
 NT IONIC WAVES
 NT JET AIRCRAFT NOISE
 NT LAMB WAVES
 NT LOVE WAVES
 NT MACH CONES
 NT MAGNETOACOUSTIC WAVES
 NT MAGNETOELASTIC WAVES
 NT MAGNETOHYDRODYNAMIC STABILITY
 NT MAGNETOHYDRODYNAMIC WAVES
 NT NOISE [SOUND]
 NT NORMAL SHOCK WAVES
 NT OBLIQUE SHOCK WAVES
 NT PHONON BEAMS
 NT PHONONS
 NT PLASMA WAVES
 NT POLARIZED ELASTIC WAVES
 NT RAYLEIGH WAVES
 NT RIEMANN WAVES
 NT S WAVES
 NT SEISMIC WAVES
 NT SHOCK WAVES
 NT SONIC BOOMS
 NT SOUND WAVES
 NT STRESS WAVES
 NT THERMAL NOISE
 NT TOLLMEIN-SCHLICHTING WAVES
 NT ULTRASONIC RADIATION
 NT UNLOADING WAVES
 Spikes on sonic boom pressure waveforms due to simultaneous focusing and diffraction of planar N wave by inhomogeneous atmosphere layer
 01 p0011 A69-11280
 Hydraulic analogy for shock and expansion waves arising in supersonic compressors due to three dimensionality of flow
 [ONERA-TP-598]
 02 p0187 A69-11621
 Elastic-plastic wave profiles in Al alloy under uniaxial strain load, investigating sensitivity to various strain rates
 02 p0344 A69-12289
 Elastic/viscoplastic wave propagation in thin tubes under combined stress of tension and torsion, using viscoplastic constitutive equations
 02 p0344 A69-12293
 HF pressure waves dispersion in blood vessels ascribed to viscoelastic behavior of walls
 02 p0204 A69-12602
 Wave structure for moving load on surface of anisotropic material in plane stress investigated for stable elastic wave propagation
 02 p0348 A69-12609
 Longitudinal elastic wave damping, excitation and propagation in lithium niobate crystals at frequencies from 200 to 2000 MHz
 03 p0487 A69-13729
 Longitudinal thermoelastic wave propagation in infinite body, proving generalized Kirchhoff theorem
 03 p0528 A69-13924
 Longitudinal and transverse elastic waves propagation in medium with random inhomogeneities, deriving scattering coefficients in Born approximation for Fraunhofer region
 04 p0667 A69-14262
 Legendre transformation application to plane elastoplastic loading waves, examining shock front formation in interaction region
 04 p0673 A69-14495
 Torsional elastic wave scattering from penny shaped crack, determining local dynamic stress field
 04 p0678 A69-14872
 Flexural wave reflection from corner joint between plates, establishing reflection coefficient dependence on wave frequency
 04 p0679 A69-14903
 Monochromatic flexural waves passage through elastic insert between plates, determining wave absorptivity dependence on wave frequency
 04 p0679 A69-14906
 Plane shear pressure wave propagation in elastoplastic half space for various combined normal and shearing loadings
 05 p0835 A69-15798
 Rotation wave propagation in elastic homogeneous isotropic centrosymmetric body in asymmetric elasticity theory
 05 p0843 A69-16645
 Dynamic response of semiinfinite circular cylindrical shells to traveling load
 06 p1021 A69-17148

Apparatus for generating HF shock fronted pressure waves in resonant tube
 06 p0906 A69-17149
 Transient nonaxisymmetric elastic wave propagation in infinite isotropic elastic plate, using linear elasticity theory
 06 p1024 A69-17509
 Interaction of laminar hypersonic boundary layer and supersonic corner expansion wave, discussing upstream influence, transverse pressure gradients and external flow
 [AIAA PAPER 69-137]
 06 p0913 A69-18078
 HF instability of steady combustion process with allowance for elastic strains in chamber walls
 07 p1242 A69-18993
 Forced vibrations in semibounded elastic bar with various moduli of elasticity, discussing reversing longitudinal force and elastic waves propagation
 10 p1799 A69-23155
 Elastic release wave and pressure drop measurement in 2024-T4 aluminum at 313 kb for dynamic yield strength, considering surface velocity and stress
 10 p1712 A69-23665
 Elastic waves propagation in inhomogeneous composite media, considering coefficient of structural stress concentration
 11 p1972 A69-24649
 Two dimensional contained plastic deformation in asymmetrical elasticity theory based on Cosserat medium, examining boundary value problems, stress concentration and elastic wave propagation at holes
 11 p1973 A69-24659
 Elastic waves propagation in micropolar cylinder, treating longitudinal and torsional monochromatic waves in Cosserat medium
 11 p1995 A69-25606
 Flexural wave reflection from corner joint between plates, establishing reflection coefficient dependence on wave frequency
 12 p2182 A69-26656
 Monochromatic flexural waves passage through elastic insert between plates, determining wave absorptivity dependence on wave frequency
 12 p2182 A69-26659
 Thermoelastic waves in stretched circular cylindrical bar, analyzing displacements, secondary pressure and temperature field by using Frobenius method
 12 p2189 A69-27115
 Pressure waves interaction with solid fuel hot surface at HF based on linear theory of acoustic instability in condensed systems
 13 p2371 A69-27383
 High purity beryllium dynamic tests, determining Hugoniot equation of state, shock profile and spall threshold/onset of microcracking/for elastic pulses
 [AIAA PAPER 69-360]
 13 p2283 A69-28293
 Couple stresses effect on dynamic stress concentrations, considering elastic compressional wave diffraction by cylindrical discontinuity
 13 p2369 A69-28351
 Elastic microwaves propagation attenuation along lithium niobate crystals trigonal axis at various temperatures
 15 p2665 A69-30040
 Maser amplification of 9.5 GHz longitudinal elastic waves in divalent nickel impurity ions doped sapphire by stimulated emission from inverted spin population
 16 p2795 A69-31554
 Inhomogeneity effects on elastic waves generated by impulsive loading of surface using asymptotic method, discussing high stress intensification regions
 16 p2873 A69-32157
 Elastic wave reflection and refraction around cracks, considering plane harmonic compressional and vertically-horizontally polarized shear waves
 17 p3053 A69-32986
 Schlieren method for visualization of refractive index changes in transparent materials, discussing application to study of elastic wave fields
 17 p2973 A69-33322
 Canonical forms for three dimensional diffraction problem of elastic harmonic waves propagating along circular cylinders infinite array
 19 p3437 A69-36144
 Finite chemical reaction rate detonation wave interaction with rarefaction wave, noting mixture activation energy and heating power influence
 19 p3298 A69-36384
 Microwave elastic propagation in single crystal specimen of yttrium-iron-garnet ferrite, discussing attenuation
 21 p3780 A69-38774
 Air pressure wave forces on missile from silo wall motion resulting from close nuclear blast, using acoustic wave equation for concentric cylinder flow
 21 p3691 A69-39765

Plane double front detonation wave attenuation by pursuing rarefaction waves, analyzing oscillations, onset mechanism and stability during transition to Chapman-Jouguet mode
 22 p3929 A69-40112
 Turbomachinery periodic structures design to improve tolerance to inflow distortion and resonant oscillatory flows, considering large amplitude pressure waves propagation
 [SAE PAPER 690388]
 23 p4201 A69-41666
 Longitudinal elastic waves produced in truncated hollow Al cone due to steel spheres impact
 [ASME PAPER 69-APMW-15]
 24 p4401 A69-43101
 Three dimensional and shell theory analysis of nonaxisymmetric harmonic elastic wave propagation in hollow elastic sphere
 [ASME PAPER 69-APMW-7]
 24 p4402 A69-43105
 Computerized spectral analysis of vibrational frequency due to elastic waves in isotropic hollow spherical shells
 [ASME PAPER 69-APMW-8]
 24 p4402 A69-43106
ELASTICITY
U ELASTIC PROPERTIES
ELASTICIZERS
U PLASTICIZERS
ELASTODYNAMICS
NT ELASTIC DAMPING
NT ELASTOHYDRODYNAMICS
 Dynamical strength of solid cylinder under axial loads increasing in time at given rate, using constitutive equations of thermodynamic theory
 02 p0342 A69-12278
 Elastodynamic boundary value problem solution for stability in linear elasticity
 03 p0530 A69-14066
 Reissner variational principle extended to cover elastodynamics, discussing relation with Hamiltonian function
 05 p0835 A69-15870
 Uniqueness theorem for equations of dynamics of viscoelastic bodies, using energy and hereditary elasticity considerations
 08 p1415 A69-20658
 Vibrations of thick walled shallow circular cylinder with thickness change in time, applying dynamic elasticity and Volterra equations
 14 p2533 A69-28985
 Axisymmetric impact of circular cylindrical plates, obtaining two dimensional dynamic stress distributions for materials of linear elastic compressibility and plastic behavior in shear
 14 p2534 A69-29027
 Wing elastic strains effect on vertical velocity in downwash, noting wing tail combination
 18 p3086 A69-34999
 Completeness and relations between potentials and stress functions in micropolar elasticity and thermoelasticity
 19 p3439 A69-36476
 Continuous dependence of boundary value problems of linear elastic body in smooth three dimensional region on force, elasticity and initial data
 24 p4397 A69-42750
 Mathematical flow graphs application in analysis and design of elastomechanical structural systems
 [AAS PAPER 69-151]
 24 p4339 A69-42816
ELASTOHYDRODYNAMICS
 Inertia effect of flow between eccentric cylinders with rotating outer cylinder, calculating pressure and shearing distribution and force on inner cylinder
 01 p0059 A69-10307
 Elastohydrodynamic lubrication, discussing film thickness and dependence on fluid hydrodynamics and contact zone deformation
 01 p0088 A69-11324
 Elastohydrodynamic lubrication of square section high pressure face seals mounted on rigid housings, considering design charts for load and leakage
 [ASLE FICFS PREPRINT 16]
 15 p2621 A69-30493
 Elastohydrodynamic lubrication film thickness in finite elliptical contact determined by two dimensional Reynolds equation in inlet region, using finite difference approximation
 [ASME PAPER 69-LUBS-17]
 18 p3120 A69-34379
 Elastohydrodynamic solution for ball torque spinning without rolling in nonconforming groove, showing increase in torque with stress and spinning and decreasing conformity
 [ASME PAPER 69-LUBS-11]
 18 p3140 A69-34381

Elastohydrodynamic theory of spherical bodies in normal approach contact, discussing lubrication and elasticity equations
[ASME PAPER 69-LUBS-3]

18 p3213 A69-34384

Cage and roller slip in high speed roller bearings over steady radial loads by measurement and theory

20 p3547 A69-37066

Surface texture effects, discussing metallic and elastomeric contacts, measurement, profile, model parameters, adhesion, hysteresis, lubrication, squeeze films, macroelastohydrodynamics and randomness

23 p4170 A69-42359

Elastohydrodynamic lubrication of cylindrical rubber surface sliding over glass plate, using optical interference technique

23 p4171 A69-42531

Undissolved air effects on working fluids elastodynamics in aircraft hydraulic actuators

24 p4255 A69-43076

ELASTOMERS

NT THIOPLASTICS

Elastomeric bearings for support of heavy loads and accommodation of oscillatory motions, considering molded type for helicopter tail rotor

01 p0085 A69-10406

Seal swell prediction methods extended to include three dimensional solubility parameter concept
[ASLE PAPER 68-LC-21]

07 p1171 A69-19306

Crack propagation in crosslinked glassy polymers, noting effects of added elastomers molecular weight

08 p1338 A69-20492

In situ vacuum testing requirement for valid measurement of vacuum induced changes in mechanical and thermal properties of various filled elastomers

09 p1477 A69-22008

Elastomeric solid propellant grains viscoelastic flow, analyzing stresses and strains under various operating conditions and rocket engine geometry effect

10 p1801 A69-23702

Elastomeric adhesives diffusion theory, tack increasing methods, cast polymer films, properties and applications in shoe manufacturing and sealants

14 p2468 A69-29341

Elastomer hardness criteria ensuring maximum life and performance of rotary shaft seals

16 p2794 A69-32432

Fuel resistant elastomers evaluated for seal compounds for low temperature capability, noting epichlorohydrin-ethylene oxide as promising sealant

19 p3356 A69-35534

Polyperfluoroalkyleneimideolperfluoroalkylene-amine synthesized by reaction of perfluoroalkane dinitriles with ammonia or diamidine, giving elastomers of varying strength and elongation, noting thermal stability

19 p3264 A69-35535

Elastomeric thermosetting one part silicone encapsulant environmental tests, checking physical and electrical properties stability under temperature and relative humidity conditions

19 p3281 A69-35549

Elastomeric and coating materials for aerospace systems, considering temperature, rain, sand erosion, propellant and radiation resistant properties

19 p3357 A69-35586

Molecular engineering of high organic polymers, discussing molecular weight, crystallization, elastomers, fiber formers and building construction materials

20 p3566 A69-37598

Surface texture effects, discussing metallic and elastomeric contacts, measurement, profile, model parameters, adhesion, hysteresis, lubrication, squeeze films, macroelastohydrodynamics and randomness

23 p4170 A69-42359

Elastomers for SST aircraft applications, discussing properties evaluation, material selection, sealant requirements, etc

24 p4338 A69-43455

ELASTOPLASTICITY

Temperature evolution velocity parameter effect on behavior of elastoviscoplastic solids, noting demonstration by work hardening tests at variable temperatures
[ONERA-TP-644]

01 p0164 A69-10036

Microscopic cleavage strength of high nitrogen steel notched bars determined from critical tensile stress criteria using elastoplastic analysis method

01 p0169 A69-10765

Elastoplastic stress-strain behavior of concentric composite cylinders under uniaxial tension using analytical model, predicting transverse stresses during axial loading

01 p0171 A69-11263

Paradoxes associated with elastic-plastic limit load analysis of material satisfying Drucker stability postulates

02 p0337 A69-11562

Dynamic behavior of elastoplastic beam column model with one degree of freedom subjected to axial compressive force

02 p0337 A69-11717

Critical loads in elastoplastic buckling of cylindrical shells analyzed using power series

02 p0340 A69-12058

Elastic-plastic wave profiles in Al alloy under uniaxial strain load, investigating sensitivity to various strain rates

02 p0344 A69-12289

Numerical solutions elastoplastic torsion of circumferentially grooved shafts based on flow and deformation type theories

02 p0346 A69-12420

Internal elastoplastic stress distribution within reinforced plastics subjected to force normal to internal filaments direction

02 p0347 A69-12513

Spherical elastic-plastic stress wave propagation analysis via finite difference procedure

02 p0348 A69-12610

Rapid uniform expansion of spherical cavity in compressible elastic-plastic solid, obtaining similarity solution

03 p0528 A69-13798

Elastoplastic bending of plates with nonlinear stress-strain diagram

04 p0667 A69-14269

Elastic-plastic boundaries velocities for combined longitudinal and torsional plastic wave propagation in thin walled tube during unloading
[ASME PAPER 68-WA/APM-7]

04 p0670 A69-14403

Elastic-plastic thin walled cylindrical shell axisymmetric behavior under radial pressure difference, noting load for collapse
[ASME PAPER 68-APM/AA]

04 p0670 A69-14404

One dimensional wave propagation analysis for zero value stress time derivatives on both sides of elastic-plastic boundary

04 p0670 A69-14407

Legendre transformation application to plane elastoplastic loading waves, examining shock front formation in interaction region

04 p0673 A69-14495

Stability of elastoplastic clamped free rod, noting compressive force for production of new equilibrium state and occurrence of transition to state

04 p0679 A69-14925

Book on thermal time independent plastic and time dependent creep strains in structures through analogy permitting inelastic structures analysis

04 p0681 A69-15200

Plane shear pressure wave propagation in elastic-plastic half space for various combined normal and shearing loadings

05 p0835 A69-15798

Elastoplastic element structural growth induced by thermal cycling analyzed as function of temperature and sustained axial load
[ASME PAPER 68-WA/MET-14]

05 p0837 A69-16067

Impulse loaded elastic-plastic beam response approximate solutions based on uniqueness proof
[ASME PAPER 68-WA/APM-23]

05 p0840 A69-16188

Elastoplastic stress-strain state of asymmetric profile thin walled beam under mobile load

05 p0841 A69-16205

Statically indeterminate elastoplastic problem under condition of complex shear

05 p0843 A69-16691

Circular bar elastoplastic behavior under combined axial force and torque in strain hardening range, noting elastic compressibility effects

06 p1023 A69-17371

Iterative solution of integral equation and uniform convergence conditions of function sequence approximating incremental stress distribution in elastic-plastic structures

06 p1024 A69-17510

Automatic data processing method for analyzing multiply connected elastoplastic shells of revolution

06 p1025 A69-17614

Initial defects influence on equilibrium states of compressed elastoplastic plates

06 p1025 A69-17684

Snapping and buckling of simple elastic structures under dynamic load, noting influence of structural geometry and load duration
[AIAA PAPER 69-22]

06 p1029 A69-18206

Crack growth during cyclic loading in elastoplastic bodies

07 p1232 A69-18992

Minimum theorems in elastoplastic theory extended to continua for plastic strains governed by holonomic and nonholonomic stress-strain laws

07 p1235 A69-19442

Quadratic programming and theory of elastic perfectly plastic structures under holonomic laws, proving theorems of limit analysis

07 p1235 A69-19443

Unstable elastoplastic brittle fracture criterion based on energy balance considerations

07 p1238 A69-19693

Complementary plastic work theorems in piecewise-linear elastoplasticity applied to plastic and nonlinear elastic problems

08 p1414 A69-20528

Quasi-linear differential constitutive equation of work hardenable elastoviscoplastic material in case of plane wave propagation in half space

08 p1415 A69-20662

Matrix displacement method for nonlinear elastoplastic two or three dimensional structures or continua, discussing strain distribution

08 p1416 A69-20705

Axisymmetric elastoplastic bending theory for cylindrical shell by applying Saint Venant plasticity conditions, determining stress distribution

08 p1419 A69-21179

Duality between effect and influence problems in linear elastoplasticity, obtaining rules for influence functions plotting

09 p1612 A69-21604

Elastoplastic response of intersecting hemispherical/cylindrical shell structures compared with plastic deformation predictions

09 p1615 A69-21922

Elastoplastic stress in notch as cause of decreased lifetime of aircraft components, analyzing stress reversal and displacement during takeoff and landing

09 p1620 A69-22576

Nonwork hardening elastic plastic material fracture criteria for antiplane strain, noting plastic zone shape effect on zone size and crack opening

10 p1795 A69-23064

Continuum theory of dislocations and plasticity in crystals, analyzing stress fields in elastoplastic materials

10 p1799 A69-23154

Plastic energy dissipation and crack surface displacement of penny shaped crack in elastoplastic material

10 p1803 A69-24030

Moire patterns for photoelastic strain analysis noting applications to elasticity, plasticity and creep problems

11 p1882 A69-24944

Plastic strains in aluminum alloy under biaxial tensile and combined tensile and torsion tests, discussing small elastoplastic deformation theory

11 p1905 A69-24948

Bent plates elastoplastic stress-strain state determination by elastic solution and finite differences, considering linear strengthening under uniform distribution of load

11 p1985 A69-25175

Elastic and elastoplastic strains in materials under various loadings, determining temperature variations by thermoelectric method and verifying by tensile tests

11 p1985 A69-25178

Transverse impact along flexible couplings, deriving motion equations in presence of elastoplastic deformation

12 p2178 A69-26034

Elastoplastic stress wave generation by penetration of impulsive electromagnetic radiation through thin surface layer of solid

12 p2179 A69-26215

Computationally stable solution of finite element analysis of elastic-plastic response of nonlinear discrete structures loaded beyond yield load

12 p2185 A69-26819

Incompressible elastic-plastic solid flow through rough converging conical channel analyzed using Mises yield condition and Prandtl-Reuss equations

12 p2063 A69-27114

Perturbation theory of antiplane elastoplastic deformations based on plasticity theory, considering circular hole in body under uniform shear

13 p2359 A69-27263

Elastoplastic cylindrical shell instability determination under axial compression applied to inelastic solids

13 p2363 A69-28124

Plane elastoplastic shock waves propagation due to combined shear loadings assuming elastic isotropic work hardening materials

13 p2368 A69-28346

Minimum theorems for plastic strain rates and plastic strains governed by holonomic elastoplastic theory utilizing quadratic functions

13 p2370 A69-28629

Elastic-plastic bending of rectangular plates with asymmetrically inhomogeneous material in plastic range, using modified Ritz method

14 p2533 A69-28984

Elastoplastic continua fire resistance at high temperatures, establishing plasticity condition and stress-strain relationships

14 p2536 A69-29598

Device for elastic-plastic circular bending with constant bending moment and angular strain for low cycle fatigue testing

15 p2583 A69-30207

Elastoplastic matrix for stress increments for yield surfaces with associated flow rule, considering initial stress computation

15 p2706 A69-30433

Elastic and elastoplastic bodies, showing vector field for surface condition as sufficient condition for stability

15 p2707 A69-30621

Plane strain and stress compared for elastoplastic cracked plate in work hardening tension

15 p2710 A69-30811

Elastoplastic strains in thin walled beams subjected to oblique bending by mobile loads of coupled concentrated forces, calculating deflections and plastic region distribution

15 p2711 A69-30971

Thomas fracture theory and compatibility conditions for fracture surface of elastic-plastic rotating hollow shaft, discussing plastic equilibrium

15 p2712 A69-31017

Stress waves propagation through elastic-plastic medium with uniaxial displacement, discussing wave interactions and interface conditions

16 p2870 A69-31809

Compressibility of material in stability problems of elastoplastic plates and shells

16 p2875 A69-32292

Stresses and displacements in elastoplastic cantilever beams and beams fastened at both ends calculated by stress-strain diagrams of material

17 p3056 A69-33191

Plane wave propagation due to combined compressive and shear stresses in half space, assuming elastoplastic material
[ASME PAPER 69-APM-12]

18 p3213 A69-34388

Elastoplastic boundaries of wave propagation of combined longitudinal and torsional stresses at tube end
[ASME PAPER 69-APM-13]

18 p3213 A69-34389

Load analysis for elastoplastic bodies by Prandtl-Reuss theory and Mises yield condition, considering avoidance of difficulties associated with nonlinear partial differential equation solution

18 p3216 A69-34571

Two dimensional elastoplastic problems in static condition, discussing analytical, variational and finite difference methods

18 p3217 A69-34594

Buckling in process of loading idealized elastoplastic Shanley column, noting continuous increase possibility

18 p3217 A69-34596

Quadratic programming method for equations of elastic perfectly plastic solid applied to stress distribution in plate torsion and bending

18 p3218 A69-34661

Elastoplastic flow equations formulation, inverting flow rule to relate stress rates to strain rates and instantaneous stresses, noting Navier equations

18 p3219 A69-34666

Stress-strain state of elastoplastic material subjected to quasi-static uniaxial tension and compression, considering Bauschinger type effects by scalar parameters

18 p3222 A69-34909

Constrained elastoplastic torsion of closed thin walled cylindrical shells, analyzing tangential and normal stress by using equilibrium equations

18 p3222 A69-34978

Reflection of spherical stress wave against smooth in-deformable plane in elastoviscoplastic medium, discussing Taylor series expansions for displacement, velocity and stress fields

18 p3226 A69-35463

Stochastic models for calculating optimal elastoplastic one dimensional systems

19 p3438 A69-36313

Elastoplastic state of composite structures with applicability of elasticity law and yield conditions illustrated by reinforced plate under plane stress

19 p3444 A69-36808

Equations of deformation for elastoviscoplastic bodies with different properties under loading and unloading conditions

19 p3445 A69-36812

Buckling behavior of idealized Shenley rod consisting of linearly reinforced elastoplastic materials under compression, formulating constraints for stability

19 p3446 A69-36846

Stress strain state in thin circular elastoplastic disks under axially symmetric transient temperature distribution, noting moving annular plastic deformation region

20 p3629 A69-38028

Mathematical models and solution techniques for calculating optimal elastoplastic structures by computer, discussing methods for displacements preceding plastic failure

21 p3831 A69-38414

Elastic-plastic torsion over complex polygonal domains without symmetry axis, using Sobolev space completeness characteristic to solve minimum variational problem

21 p3832 A69-38427

Stress-strain state of thin spherical shell of variable thickness in elastoplastic equilibrium, using Meissner variables to reduce equilibrium equations

21 p3834 A69-38717

Stress-strain state of thick and thin walled closed shells of variable thickness during elastoplastic torsion developing in aircraft component production

21 p3835 A69-38882

Strain rate-load relations in elastoplastic shells reaching yield point, discussing variational method applicability

21 p3838 A69-39189

Small parameter method applied to axisymmetric problems of elastoplastic nearly spherical bodies undergoing exponential hardening process, deriving linearized expressions for boundary conditions

21 p3839 A69-39198

Elastoplastic analysis of thin plates deformation, discussing loading conditions effects

22 p4041 A69-40064

Book on convergence in calculation of elastoplastically deformable aircraft structures and continua, covering matrix displacement method and stepwise linearized computational technique

22 p4044 A69-40619

Energy equilibrium for crack growth in elastoplastic media, analyzing crack behavior during plastic deformation concentrated at edge of propagating crack

22 p4046 A69-41060

Thermodynamics of elastoplastic materials with dislocation motion related to internal state variables, including case of rate independent plasticity

23 p4226 A69-41537

Yield condition for elastic-plastic medium, considering pure torsion-associated second order effects and dissimilarity between stress and strain increment Mohr circles

23 p4234 A69-42409

Cylindrical steel specimens high strain rate tensile tests, using Malvern theory for ideal elastoplastic and work hardened materials

23 p4236 A69-42529

Elastoplastic boundary dynamic behavior in strip with crack determined by solving boundary value problem in elliptic integrals form

24 p4395 A69-42591

Reflection of spherical stress wave against plane clamped partition in elastoviscoplastic medium, investigating three dimensional problem by infinitesimal deformations theory

24 p4406 A69-43732

ELASTOSTATICS

Stress concentration around centrally placed circular bolt in axially loaded bar, using theory of infinite systems of linear equations

04 p0681 A69-15195

Uniqueness theorem validity for boundary value problem in linear elastostatics for homogeneous media

05 p0844 A69-16739

Korn constant for boundary value problem of linear elastostatics applied to circular ring domain

05 p0844 A69-16740

Fundamental problems of plane elastostatics with stress couples reduced to solution of integral equations, noting uniqueness theorem in plate bending theory

07 p1233 A69-19328

Static axisymmetric deformation of elastic paraboloid of revolution, using integration of equilibrium equation in Lamé displacement

09 p1613 A69-21631

Modified Rayleigh-Ritz method for prediction of stress concentration in elastostatic problems for elastic continua, noting plate bending

11 p1969 A69-24413

Stresses and displacements in half plane with edge crack given as eigenfunction expansions using Wiener-Hopf technique

11 p1987 A69-25438

Bending of weightless thin elastic beams clamped to circular template by external force

12 p2181 A69-26572

Existence theorems for partial differential equations theory for traction boundary value problem of linearized elastostatics

12 p2188 A69-26928

Finite difference treatment of mixed boundary value problems in two dimensional elastostatics, using first derivatives of displacement components at grid points

15 p2706 A69-30432

Static implications of strong ellipticity condition in linearized elasticity theory, exemplifying homogeneous deformations

17 p3058 A69-33415

Green functions theory for finite integral Lebedev-Kantorovich transforms derivation, with application to elastostatics boundary value problems

17 p3067 A69-34148

Fourier transform methods in elasticity problems, considering three dimensional equilibrium equations in elastostatics in terms of displacements

20 p3622 A69-37282

Statics of axisymmetric deformation of cylindrical and conical shells of revolution of moderate thickness under uniformly and nonuniformly distributed loads

23 p4226 A69-41705

ELDO LAUNCH VEHICLE

Solid propellant rocket engine designs for ELDO-PAS apogee motors, discussing use of advanced materials to improve mass ratio and strap-on boosters

03 p0495 A69-12890

European launcher program analyzed from point of view of telecommunication and cost

03 p0520 A69-13593

Electric propulsion for payload transfer from low to synchronous orbit of ELDO launch vehicles

03 p0496 A69-13994

European launch vehicle development program, discussing economic limitations and employment possibilities

04 p0665 A69-14808

Platform system of ELDO launch vehicle and necessary test and alignment equipment, discussing inertial platform system for future space projects

04 p0629 A69-14809

Inertial guidance system for ELDO launch vehicles

07 p1176 A69-18491

In-flight testing of second and third stages of F 7 section of Europa 1 satellite booster, noting third stage explosion

08 p1410 A69-21144

Separation systems in Europa 1 booster vehicle, discussing thrust decay, ignition and control system characteristics

08 p1410 A69-21145

ELDO Europa 1 Fairings Jettisoning System and explosive devices, discussing heat shield structure and safety regulations

10 p1635 A69-23027

Aerodynamic heating of ELDO-A booster rocket, calculating flow field, heat transfer and conduction by method of characteristics and thermal models

11 p1966 A69-25433

ELDO/PAS rocket motor for satellite launching from elliptic orbit apogee to synchronous orbit powered by ammonium perchlorate with organic binder and Al

17 p3022 A69-33604

ELDO booster/EUROPA 1/ third stage management and construction problems

17 p3050 A69-33701

Microminiature Elliott MCS 920 M digital computer for inertial guidance of CECLES-ELDO launcher, discussing construction, code, interrupt, guidance system and functions

20 p3501 A69-37391

ELDO radio guidance station at Gove, discussing propulsion stage tracking and instruction transmitted to vehicle

22 p3919 A69-39920

Programming and checkout of computer for ELdo inertial guidance system, including flight simulation and autopilot tests
[AIAA PAPER 69-961]

22 p3978 A69-40342

ELECTRIC ANALOGIES

U ANALOGIES

ELECTRIC ARCS

NT CARBON ARCS
NT MERCURY ARCS

Heat transfer between arc column and discharge chamber wall of vortex linear plasmatron, using approximate similitude method

01 p0125 A69-10091

Electric arc properties, investigating volt-ampere characteristics by approximate similitude and dimensional analysis

01 p0125 A69-10099

Bilateral plasma outflow plasmatron with variable electrode diameter, discussing efficiency, current-voltage characteristics and size

01 p0125 A69-10102

Sparks from laser induced air breakdown due to focusing of laser beam, noting evidence for initiation by self focusing

01 p0092 A69-11246

Solar copper abundance determined from measuring Cu 1 and 2 and resonance lines transition probabilities in electric arc emission under LTE conditions

02 p0204 A69-11456

Electric discharge in gas flow with magnetic field, showing varying charged particle density as function of argon-cesium pressure

02 p0285 A69-11570

Magnetic confinement of electric arc in alkali metal vapor containing gas flow, considering degree of ionization

02 p0286 A69-11585

DC argon arc electrical and thermal parameters and optical properties at high pressure, using spherical anode

02 p0291 A69-12482

Ion and atom temperature distribution for two fluid model of Ar plasma in cylindrically symmetrical wall stabilized electric arc column

03 p0481 A69-14155

Low temperature plasma electric arc source operation describing current voltage characteristics and potential distribution

05 p0802 A69-15902

Plasma characteristics in thermionic converter operating under low voltage arc conditions obtained by computer, probes and spectral techniques

06 p0963 A69-16910

Retrograde motion of electric arcs in transverse magnetic fields, using multifluid equation to predict inclination and properties

[AIAA PAPER 69-45] 06 p0971 A69-18091

Temperature profile calculations for high pressure electric arcs using diffusion approximation for radiant flux density, taking energy transfer into account

08 p1420 A69-20148

Experimental and theoretical investigation of mass injection effect on high current MPD arc

[AIAA PAPER 69-266] 09 p1564 A69-21242

Plasma column of free burning electric arc, deriving temperature, electron concentration and electric field radial distributions

09 p1545 A69-21431

Electric arc interaction with turbulent boundary layer in vortex stabilized plasmatron, noting variation in arc intensity

09 p1545 A69-21432

Device for producing high current high pressure arc discharge using water cooled chamber and Be bronze electrodes

09 p1547 A69-21593

Low power gradient uniform electric arc column in cross flow and transverse magnetic field, analyzing temperature, velocity, pressure and magnetic field distribution

11 p1933 A69-25556

Plasma physics of electric arc transition from conducting plasma to insulating gas in electric circuit interruption, noting interrupter interaction with power system

12 p2133 A69-25905

Dynamic energy balance in positive column of electric arc, integrating expression to determine temperature time dependence

12 p2137 A69-26535

Knudsen arcs in argon showing potential well presence with anode barrier and cathode potential drop, establishing slow electrons thermal equilibrium

12 p2137 A69-26536

Semiconductor thin films analysis using mass spectrometer with spark source

13 p2316 A69-27293

Electric arc and hydrogen flow interaction at high pressure, showing radiation role in heat exchange

13 p2305 A69-27387

Current, magnetic field, flow velocity and plasmatron dimensions effects on arc voltage in coaxial plasmatron

13 p2306 A69-27388

Tangential drag measurements at electrodes of arc in plasma accelerator, ion current partitioning at cathode and electrode damage

[AIAA PAPER 67-657] 13 p2312 A69-28219

Electric arc structure in hydrogen magnetic annular discharge computed using nonequilibrium hydrodynamics to analyze supersonic and subsonic processes

13 p2312 A69-28221

Two chamber DC arc heater with vortex stabilization, determining current-voltage characteristics and efficiency

13 p2244 A69-28557

Low voltage arc in cesium thermionic converter, investigating current-voltage characteristics, electron temperature, electron density and plasma potentials in ignited mode

14 p2401 A69-29231

Low voltage arc in thermionic cesium vapor diode with lengthy electrodes and temperature variations along emitter, discussing plasma and current density distributions

14 p2402 A69-29244

Argon electric arc axis temperature measurements, showing current and tube diameter ratio dependence

15 p2662 A69-30977

Air plasma electrical and thermal conductivity coefficients measured in wall stabilized DC arc at atmospheric pressure and high temperatures

15 p2663 A69-30979

Electric arc plasma generator efficiency analysis including supply voltage, working current, current-source impedance, ballast resistor and optimum voltage-current selection

15 p2664 A69-31177

Microwave breakdown dependence on elevated gas temperature in electric arc shock tube, considering air, nitrogen and argon

16 p2749 A69-31693

Mode transition characteristics of free burning argon electric arc with transpiration cooled anode, noting current blowing parameter

[AIAA PAPER 69-696] 17 p3011 A69-33451

Electric arc stabilization in crossed convective and magnetic fields, discussing column slanting relationship to widening near downstream electrode

[AIAA PAPER 68-709] 24 p4359 A69-43572

Anode fall measurements with Langmuir probe in coaxial arcs in Ar compared with anode energy balance values

24 p4256 A69-43695

ELECTRIC BATTERIES

NT ALKALINE BATTERIES

NT DRY CELLS

NT NICKEL CADMIUM BATTERIES

NT SILVER CADMIUM BATTERIES

NT SILVER ZINC BATTERIES

NT STORAGE BATTERIES

NT THERMAL BATTERIES

Spacecraft voltage-limited charging system for sealed secondary batteries, discussing operating characteristics and battery parameters

01 p0013 A69-11010

Water and heat removal unit for hydrogen/oxygen fuel cell systems, discussing temperature distribution, heat and liquid transport

05 p0704 A69-15676

High energy density lithium/dichloroisocyanuric acid battery system discharging under constant voltage and load conditions

[ECS PAPER 15] 05 p0706 A69-16231

Power supply subsystem for TD1/TD2 satellites with solar cells, discussing design including standby battery for solar eclipse periods

13 p2209 A69-28481

Aircraft secondary power sources reliability dependence on electric loads, charge control and maintenance, discussing hermetically sealed batteries features

17 p2905 A69-34113

Secondary power sources for space applications in solar arrays, static and dynamic thermal systems, high power batteries and fuel cells, discussing NASA machinery procurement

19 p3255 A69-36323

Computer simulation of satellite electric power systems concerning solar array, thermal, battery and charge models for end-of-mission-life orbits

23 p4068 A69-42241

Solar cell power systems for manned space stations, summarizing studies of battery power system designs

23 p4068 A69-42242

Battery subsystems optimization for earth satellite lifetimes greater than 5 years, analyzing flexibility, weight and reliability

23 p4068 A69-42243

Fuel cell/battery and solar array/battery systems for manned Apollo Applications Program /AAP/ space vehicles, considering mission and power requirements

23 p4069 A69-42244

Research and development programs leading to heat sterilizable spacecraft battery separator material, describing bench tests

23 p4072 A69-42284

Battery/fuel cell hybrid power source, discussing fast transient response

[SAE PAPER 690205] 24 p4255 A69-42889

ELECTRIC BRIDGES
NT WHEATSTONE BRIDGES
NT WIRE BRIDGE CIRCUITS

Bridge circuit n-type conductivity converter with internal compensation of parasitic effects

05 p0727 A69-15641

Distance measurement by distance relay circuit composed of intermediate current transformers and rectifier bridges

05 p0765 A69-16746

Balanced diode shunt bridges with electronically tunable carrier selection high-Q N-path filter from 0 to 200 kHz, using single integrated module

07 p1089 A69-18249

Integrated four transistor bridge network used for self neutralized active element in tuned RLC amplifier design

07 p1103 A69-18884

Equivalent circuit synthesis with six reactances- two terminal network bridges

08 p1295 A69-21166

RLC two terminal bridge network synthesis, considering two reactances, three resistances and constraints

09 p1464 A69-22291

Equivalence and stability for negative impedance converter of bridge circuits by symmetrical amplifier design

09 p1467 A69-22559

Parametric frequency converter consisting of mixer head in bridge circuit with varactors for 12 GHz TV transmitters

11 p1854 A69-25614

Linear bridge circuits design having proportional output signal to first or second derivative of input signal envelope

12 p2037 A69-25962

Design and operation of two frequency phase meter for plasma diagnostics, using frequency modulation of microwave oscillator and waveguide bridge

14 p2451 A69-29798

Tubes faults monitoring in three phase Graetz converter bridges by measuring voltage across DC smoothing inductor

15 p2575 A69-30180

Electrical conductivity in wake neck measured using RF bridge on boom extending from reentry vehicle

21 p3724 A69-39030

Carrier frequency monitoring amplifier with automatic bridge tuning for coupling to passive sensors including strain gages, inductive transmitters, etc

22 p3915 A69-40937

ELECTRIC CELLS

Integral cell-level electronic charge controls for secondary batteries, emphasizing performance, reliability and power system interfaces

23 p4076 A69-42542

ELECTRIC CHARGE

NT ELECTROSTATIC CHARGE

NT ION CHARGE

NT SPACE CHARGE

NT TRAVELING CHARGE

Spacecraft voltage-limited charging system for sealed secondary batteries, discussing operating characteristics and battery parameters

01 p0013 A69-11010

Plasma generator for maintenance of space vehicle electrical neutrality during ejection of high velocity electron pulses

[AIAA PAPER 69-273] 09 p1567 A69-21263

Rechargeable nickel cadmium batteries state of charge determination by monitoring capacitance

09 p1435 A69-21425

FET memory element charge storage two layer model for thin film dielectrics noting charge/discharge times

10 p1742 A69-22947

Design aspects and relation to optimum operation on overcharge in Ni-Cd cells

10 p1639 A69-23991

ELECTRIC CHOPPERS

Signal electrode charge control of sealed Ni-Cd batteries, discussing signal voltage for overcharge control 10 p1640 A69-23993

Maintenance free high rate sealed Ni-Cd battery power system compatible with existing aircraft electrical systems 10 p1640 A69-23994

Electrically charged earth satellite motion under action of Lorentz force produced by geomagnetic field interaction, relating field trajectories to acceleration 19 p3431 A69-36615

Integral cell-level electronic charge controls for secondary batteries, emphasizing performance, reliability and power system interfaces 23 p4076 A69-42542

ELECTRIC CHOPPERS

Tunnel diode univibrator, noting polarization influence on recovery time and pulse length stabilization dependence on resistive load 04 p0578 A69-15069

Regulated voltage converter systems for onboard spacecraft electric power supplies, noting chopper circuits with rectifiers 12 p2015 A69-25867

ELECTRIC CIRCUITS

U CIRCUITS

ELECTRIC COILS
NT MAGNETIC COILS

Pulse transformer design relationships and definitions, discussing core and winding structure choice 08 p1285 A69-20382

Lumped element construction technique involving crossed coils to reduce ferrite produced heat in resonance isolators, using substituted YIG 11 p1856 A69-25632

ELECTRIC CONDUCTORS

Hybrid microstrip integrated microwave circuits, discussing substrate and conductor materials and fabrication processes 01 p0040 A69-10199

Reflection of plane electromagnetic wave from conducting plane covered with moving uniaxial sheath 02 p0209 A69-12334

HF approximations, discussing plane wave diffraction by conducting circular cylinder using Watson transform 03 p0384 A69-12903

Scattering from thin conducting sheet obstacle on cylindrical surface 03 p0399 A69-14253

Relativistic analysis of far zone electromagnetic scattering by conducting sphere moving through incident plane wave, calculating scattering cross section 04 p0559 A69-15212

Flat cable terminating techniques for electric and electronic systems 04 p0578 A69-15217

Hydromagnetic laminar natural convection flow and heat transfer of nonNewtonian fluid between parallel electrically conducting walls 10 p1728 A69-23237

Two dimensional inhomogeneous conductors resistance determined by interchanging equipotential and flow lines 14 p2422 A69-29554

Superconducting leads with small electrical resistance and low thermal conductance for cryogenic applications, noting manganin wires coated with Pb-Sn alloy 22 p3997 A69-41236

Self consistent fields in waveguides containing thin conductors, expanding induced field into Fourier series in normal waves for series coefficients 23 p4123 A69-41942

ELECTRIC CONNECTORS

Air gap isolated microcircuit beam-lead devices fabrication, operation, electrical performance and radiation resistance 02 p0221 A69-12469

Flat cable terminating techniques for electric and electronic systems 04 p0578 A69-15217

Laws of wear and average life, noting application to electric connector reliability 04 p0579 A69-15320

Coupled and uncoupled terminals series connection for reactive multiport network determined by transforming scattering matrix columns into coordinate vectors 07 p1100 A69-18529

Spacecraft component heat sterilization, discussing heat effects on electrical connections, polymers and adhesives 08 p1284 A69-20267

Wire, lead frame, direct bonding and beam lead techniques for interconnecting active elements into hybrid circuits 09 p1508 A69-22338

Critical signal assignments optimization in electrical/electronic connectors, considering bent pins, signal cross talk, adjacency requirements and corona 19 p3284 A69-36030

Environmentally sealed connector for avionics packaging with die-cast Al alloy shell meeting specification ARINC 404 requirements 22 p3910 A69-39946

High density environment-resistant circular connectors, discussing design, applications, test and performance data compliance with MIL-C-81511 specifications 22 p3910 A69-39947

ELECTRIC CONTACTS

Space charge limited currents in SbSI single crystals with gallium electrodes during phase transition, discussing sticking probability and photoconductivity 01 p0137 A69-10258

Flat cable terminating techniques for electric and electronic systems 04 p0578 A69-15217

Braze bonds of refractory electrical contacts using induction heating 04 p0607 A69-15218

Multiple high field domain nucleation in GaAs, discussing dependence on contact inhomogeneities 05 p0807 A69-15959

Pyrolusite samples high dielectric and ferroelectric properties value ascribed to parasitic effects occurring in commonly used contacts 05 p0809 A69-16374

Electron and phonon tunneling spectroscopy in metal Ge contacts, noting improved agreement with one electron model 06 p0982 A69-18234

Dry sliding friction and wear in ultrahigh vacuum, emphasizing slip rings and brushes for space applications [IME PAPER 7] 07 p1138 A69-18561

Electron-electron interaction effect on I-V characteristic and equivalent circuit of metal-semiconductor contact, noting conductivity and rectifying properties 07 p1107 A69-19162

Differential capacity of Li doped zinc oxide single crystals between vapor deposited asymmetrical In electrode contacts 08 p1371 A69-19883

Semiconductor current fluctuations associated with generation, recombination and annihilation of random electron-hole pairs at ohmic contacts 08 p1372 A69-20545

Differential capacitance of n-n heterojunction calculated by metal semiconductor contact method 09 p1555 A69-21476

Space charge limited currents in SbSI single crystals with gallium electrodes during phase transition, discussing sticking probability and photoconductivity 09 p1559 A69-22651

Emission and diffusion theories of metal-semiconductor contacts for describing current characteristics of abrupt isotype nGe-nGaAs heterojunction 11 p1938 A69-25115

Current-voltage characteristics for double injection processes in nonideal contact p-i-n semiconductors operating in ohmic relaxation mode 13 p2323 A69-28524

Erosion of contacts under capacitive loads noting cable length, arc duration and battery voltage 13 p2269 A69-28608

Differential capacitance of n-n heterojunction calculated by metal semiconductor contact method 15 p2669 A69-30721

Optimum metal contact stripe width for CW operation of GaAs junction lasers bonded on copper heat sink 16 p2796 A69-31698

Cost optimization in converting brush type to brushless aircraft AC power systems, using analog computer to determine modifications 17 p2905 A69-34109

Gold/polycrystalline cadmium selenide film contact found ohmic in darkness and barrier in light, noting potential distribution, electron concentration and energy gap 19 p3384 A69-36480

Metal-semiconductor contact current-voltage characteristic derived from modified diode theory taking into account electron distribution function 19 p3391 A69-36608

Metal semiconductor contact resistance determination from measuring voltage drop in current passing through contact and second metallic contact 21 p3780 A69-39046

Corrosion of Ni through porous Au plate in humid sulfur dioxide atmospheric environments, analyzing product deposits and contact properties 23 p4176 A69-41534

STAR/Stud and Rocker Panel/ four couple section improved by incorporating bonded tungsten electrical contacts for PbTe thermoelectric elements 23 p4188 A69-42261

ELECTRIC CONTROL

Electrically controlled heat transfer between flat parallel flow hydrocarbon diffusion flame and walls of combustion chamber 02 p0353 A69-12324

Electrically controlled broadband microwave phase shifter consisting of coaxial line with varactors or ferroelectrics 03 p0408 A69-13987

Electrohydraulic guidance of second stage of Diamant rocket used for orbiting satellites employing thrust vector orientation 04 p0551 A69-15183

Electric position servosystems for 50 ton telemetry reception antenna and 1200 ton loading turntable of nuclear power plant 04 p0585 A69-15184

Electrohydraulic radar antenna telecontrol system, discussing pump assembly, hydraulic motor and pump control servojack 04 p0551 A69-15185

Electrohydraulic attitude servomechanism for controlling movements of pilot training cabin, describing hydraulic system and electric control circuit 06 p0906 A69-16966

Transverse AC current influence on longitudinal current induced by constant electric field in anisotropic semiconductor 06 p0978 A69-16991

Book on feedback control theory for engineering and applied physics noting signal theory, servomechanisms, transfer functions, system stability and Nyquist diagrams 08 p1295 A69-19841

Aircraft electrohydraulic primary control systems including electrical signal transmission, engine failure detection, signal structure and digital systems 08 p1347 A69-20872

Electrohydraulic vibration isolation systems with feedback, considering band and notch isolation, system stability and adjustable frequency response [ASME PAPER 69-VIBR-40] 10 p1641 A69-24178

Electric outside-in attitude gyro display system prototype tested and compared with contemporary inside-out display [SAE PAPER 690326] 11 p1890 A69-24507

Electrohydraulic servosystem to counteract atmospheric turbulence effects on B-52 global bombers, noting reduction in aircraft fatigue and structural damage 20 p3467 A69-38184

ELECTRIC CORONA

Lightning strikes to aircraft, discussing corona discharge, electric fields and meteorological measurements during thunderstorm in cumulonimbus 03 p0458 A69-13031

Counter rotating vertical vortices produced by corona discharge on heated flat plate under free convection conditions [ASME PAPER WA/HT-9] 05 p0846 A69-16117

Corona and breakdown voltage in helium-oxygen atmospheres, analyzing conditions for manned space flight vehicles 05 p0730 A69-16241

Supersonic airplane high temperature wire tests, detecting corona onset voltage /COV/ or voltage breakdown 05 p0731 A69-16245

ELECTRIC CURRENT

NT ALTERNATING CURRENT

NT ARC DISCHARGES

NT AURORAL ELECTROJETS

NT BEAM CURRENTS

NT BRILLOUIN FLOW

NT CARBON ARCS

NT DIRECT CURRENT

NT EDDY CURRENTS

NT ELECTRODELESS DISCHARGES

NT EQUATORIAL ELECTROJET

NT GAS DISCHARGES

NT GLOW DISCHARGES

NT HIGH CURRENT

NT IONOSPHERIC CURRENTS

- NT LIGHTNING
NT LINE CURRENT
NT MERCURY ARCS
NT MULTIPACTOR DISCHARGES
NT PENNING DISCHARGE
NT RADIO FREQUENCY DISCHARGE
NT RING CURRENTS
NT RING DISCHARGE
NT TELLURIC CURRENTS
NT THRESHOLD CURRENTS
NT TOWNSEND DISCHARGE
- Gate current measurement of p-n junction during ultralow current operation of junction field effect transistor (JFET)
01 p0038 A69-10122
- Electromagnetic wave propagation in superconductors, noting transmission line structure variation with magnetic fields and current and suitability for parametric amplifiers
01 p0135 A69-10176
- Silicon p-n junction avalanche current temperature dependence calculation by considering space charge current and multiplication factor as function of temperature
01 p0136 A69-10245
- Forward current shot noise in parametric amplifiers using GaAs varactors, noting additional noise due to stored minority carriers current
01 p0048 A69-11137
- Dipole antenna current distribution, deriving simple, accurate formula for infinite, semiinfinite and finite cases
02 p0218 A69-12330
- Step voltage transient behavior of electron-hole plasma injected into Ge, noting current time dependence
02 p0301 A69-12651
- Laser oscillation frequency shift dependence on discharge current in 6328 Å He-Ne laser
02 p0260 A69-12658
- High power sinusoidal pulsed current generator using Si controlled rectifiers /thyristors/ as switches
03 p0404 A69-13262
- Josephson current dependence on nonmagnetic impurity concentration in pure and highly contaminated superconductor
03 p0484 A69-13284
- Critique of paper on theory of gradient instability in semiconductor currents, questioning boundary value problems solution validity
03 p0487 A69-13728
- Electrostatic potential generated by rockets on space vehicles, noting source of electric current in exhaust plumes and effect on instrumentation
03 p0522 A69-13903
- Magnetic field dependences of Josephson critical current in high and low current Josephson junctions, discussing influence of induced self field
04 p0640 A69-14437
- Current nature on infinite cylindrical antenna in compressible anisotropic lossy plasma medium, noting characteristic waves on infinite cylinder
04 p0578 A69-15215
- Equation for analyzing radiation produced by current passing through filament situated over anisotropically conducting plane in flat waveguide
05 p0718 A69-15647
- Small scale filament structure of current systems in earth magnetosphere, noting coherence of magnetic disturbances in conjugate regions
05 p0753 A69-16049
- Surface recombination rate effect on lux-ampere characteristic of photomagnetic effect in CdS single crystals of low and high photosensitivity
05 p0809 A69-16377
- Equivalent capacitance derivation of space charge limited current from filamentary cathode
05 p0734 A69-16567
- Thermal and excess currents in GaSb tunnel diodes
05 p0734 A69-16570
- Electromagnetic properties associated with presence of overlapping bands in pure superconductors, discussing temperature dependence
05 p0810 A69-16802
- Temperature dependence of Josephson critical current in superconductor model having anisotropic energy gap
05 p0810 A69-16803
- Transverse AC current influence on longitudinal current induced by constant electric field in anisotropic semiconductor
06 p0978 A69-16991
- Solar flare eruptions due to current disruption, leading to magnetic energy transfer from whole current circuit to very small volume
06 p0995 A69-17444
- Backscattering due to collisions for electrons from emitter accelerated through positive ion sheath into plasma in thermionic diodes
06 p0898 A69-17773
- Wide range current-to-frequency converter with pulse frequency linear to input current
07 p1107 A69-19170
- Coupled wave equation solution based on spectral resolution for longitudinal components of electric and magnetic fields when source currents are present in compressible anisotropic plasma
08 p1274 A69-20031
- Semiconductor current fluctuations associated with generation, recombination and annihilation of random electron-hole pairs at ohmic contacts
08 p1372 A69-20545
- Resonances in plasma column monitored by frequency and current modulation methods
08 p1365 A69-20552
- Internal electric field effect of diode with inhomogeneously doped base on lifetime of strong reverse current generated during instantaneous switching
08 p1287 A69-20890
- Hall current influence on plasma jet interaction with space periodic magnetic field created by system of coaxial coils with alternating current directions
08 p1370 A69-21017
- Time dependent recoverable isothermal decrease of photocurrent in CdS crystals in vacuum, noting trap mechanism involving electron redistribution
08 p1374 A69-21187
- Plasma acceleration by induced Hall currents, discussing Hall-to-current ratio maximum at critical magnetic field
[AIAA PAPER 69-280]
09 p1562 A69-21228
- Segmented anode current and heat distribution in MPD engine measured with current shunts and calorimetric methods
[AIAA PAPER 69-244]
09 p1566 A69-21260
- Modified first order theory of magnetosphere boundary shape incorporating effects of neutral sheet currents of extended geomagnetic tail
09 p1488 A69-21661
- Near cathode magnetic field effect on instability in linear Hall current accelerators, using geometry of field extending from anode to cathode region
[AIAA PAPER 69-381]
09 p1568 A69-21731
- Current oscillations in semiinsulating O and Cr doped GaAs samples at room temperature, noting photoconductivity excitation spectra
09 p1557 A69-21753
- Electric current spoke in MPD operation, using segmented anode and image converter methods with argon and helium propellant gases
09 p1548 A69-21962
- Current instability in H plasma in electric field of large amplitude fast magnetosonic wave, noting plasma heating
09 p1552 A69-22526
- Impulse induction MHD generator with cylindrical channel, finding differential equations for velocity and current
10 p1638 A69-23484
- Parametric amplification in beam plasma system, analyzing amplification of electron current component dependent on second order terms of velocity and charge density
10 p1740 A69-23791
- Electrical conductivity of impurity semiconductors containing variable current carrier concentrations, discussing current-voltage characteristics
11 p1937 A69-24909
- Current flow coefficient of high pervance three electrode electron guns with longitudinal compression
11 p1849 A69-24911
- Magnetospheric substorm as discharge process of associated electric current system, discussing relaxation processes, explosive release of energy, etc
11 p1879 A69-25249
- Electric field penetration into homogeneous plasma at frequencies near Langmuir frequency and current at surface of thin cylindrical antenna in plasma
11 p1853 A69-25551
- Emitter current density dependence on distance from center of drift transistor circular emitter, obtaining distributed base resistance in presence of arbitrary base current
11 p1853 A69-25565
- Correlation functions and spectral density of current fluctuations in weakly ionized plasma flows
11 p1934 A69-25715
- Si IMPATT diode current and voltage waveforms of oscillation, noting small signal theory inapplicability
12 p2036 A69-25914
- High speed photography of W strip fracture, considering electric current effects and electric circuit interruption by fracture
12 p2113 A69-26195
- Computer analysis on ideal step recovery diode frequency multipliers for optimum efficiencies
12 p2039 A69-26378
- Current to frequency converter for astronomical photometry, discussing oscillator drift, linearity characteristics and feedback pulse counting
12 p2040 A69-26479
- Carbon dioxide dissociation in carbon dioxide laser gas discharge plasma for various flow rates, pressures, discharge current densities and tube diameters
12 p2107 A69-26540
- Subtraction procedure for feedpoint singularity in current on axially symmetric antenna with slice generator
12 p2041 A69-26864
- Azimuthal electric currents generation by Coriolis forces in hot stars with intensive radial flows in convective zones
13 p2350 A69-27862
- Dispersion relations in semiconductors in magnetic field indicating current anisotropic instability association with excessive noise
13 p2317 A69-27876
- Fluctuations in electric field induced by plasma flow in constant magnetic field, performing spectral analysis of voltage and current fluctuations in plasma
13 p2310 A69-28029
- MOS transistor Hall voltage, mobility and constant verified by magnetoelectric measurements of Si p-inversion layer
13 p2323 A69-28331
- Current harmonics in triode klystron for frequency multipliers, noting modulation voltage
13 p2234 A69-28510
- Forward current decrease in Si mesa diodes under fast neutron irradiation ascribed to increase in base resistance
13 p2236 A69-28549
- Thermionic converters with matrix circuit connections, considering current flow patterns in matrices to evaluate electrical failure spreading
14 p2400 A69-29225
- Electrodynamics law between current elements consistent with Newtonian dynamics, noting consequences in discharge and plasma control
14 p2485 A69-29320
- Secular terms for parallel component of electric current parallel to permanent magnetic field in toroidal MHD oscillations
14 p2492 A69-29369
- Two dimensional inhomogeneous conductors resistance determined by interchanging equipotential and flow lines
14 p2422 A69-29554
- Josephson current dependence on nonmagnetic impurity concentration in pure and highly contaminated superconductor
14 p2508 A69-29656
- Slow neutrons irradiation compensated high resistivity p-InSb current instability
15 p2666 A69-30058
- Current effects on quantum efficiency of gallium phosphide junction diodes emitting red light
15 p2575 A69-30174
- Point discharge measuring based on pulsed nature of discharge current, outlining field experiment results
15 p2610 A69-30698
- Disturbance currents from penetration of acoustic waves in weakly ionized gas, analyzing wave interaction with DC glow discharge
15 p2665 A69-31547
- Hall current effect on thermal instability explaining nonself gravitating astronomical objects, discussing current effects on propagation modes
16 p2854 A69-31649
- Screw pinch stability explained by strong force free current carried by magnetic field around central plasma column
16 p2821 A69-32037
- IR quenching of photocurrent under field effect in CdS crystal
16 p2827 A69-32044
- Equation for analyzing radiation produced by current passing through filament situated over anisotropically conducting plane in flat waveguide
16 p2762 A69-32504
- Partially conserved axial vector currents and current algebra to obtain vertex functions at point having zero mass by extrapolations
17 p3008 A69-33004

Thin metal antenna average current and effective impedance in randomly inhomogeneous medium, discussing cases of strong and weak permittivity fluctuations

17 p2927 A69-33858

Electron current flow from metal target in gas due to laser radiation, showing increased dependence on gas pressure

18 p3152 A69-35124

Time dependent recoverable isothermal decrease of photocurrent in CdS crystals in vacuum, noting trap mechanism involving electron redistribution

18 p3183 A69-35156

Current generator circuit designed for semiconductor laser excitation with pulses modulated by sinusoidal signals at 4.75 MHz

18 p3153 A69-35256

Solar flare model based on force-free currents in solar atmosphere, noting rapid energy release due to exceeding current density critical limit

18 p3188 A69-35392

Multiphoton luminescence and photocurrent excitation by ruby and neodymium laser beams of KCl-Eu single crystals, noting brightness dependence on laser beam power

19 p3335 A69-36165

Energy spectrum and transport mechanism for current carriers in amorphous-crystalline semiconductors, measuring thermally stimulated conductivity, induced photoconductivity, optical quenching, etc

19 p3391 A69-36558

High resistivity gallium arsenide single crystal LF current oscillations at low temperature, investigating electron heating effect and mechanisms

19 p3391 A69-36609

HCN laser line gain measurements during continuous excitation as function of current and pressure for acetonitrile and water mixtures

19 p3339 A69-36695

Optical and thermal attenuation of current induced by low energy electron bombardment in CdS crystal

19 p3392 A69-36727

Magnetic field variation rates characteristics during magnetic storms investigated for longitudinal dependence and influence of equatorial electric current

20 p3520 A69-37037

Astronomical observatory photomultiplier cell dark current fluctuations, showing statistical resemblance to binomial distribution

20 p3599 A69-37470

Small scale filament structure of current systems in earth magnetosphere, noting coherence of magnetic disturbances in conjugate regions

20 p3532 A69-37958

Three dimensional current systems constructed semiquantitatively for polar magnetic substorms based on magnetic field distribution on earth surface

20 p3533 A69-38085

Radiation sources fields and propagation in homogeneous lossy magnetoplasma, deducing wave equations for electric and magnetic current electron flux and mechanical body force sources

21 p3775 A69-38434

Dispersion relations in semiconductors in magnetic field indicating current anisotropic instability association with excessive noise

21 p3782 A69-39142

Galvanostatic anodic and cathodic currents effect on stress corrosion of Be sheet in aerated synthetic sea water at 72 F

21 p3747 A69-39436

Theory for current magnetic field characteristics of Penning discharge valid to extinction point

22 p3991 A69-40865

Edge diffracted fields by conical body frustums evaluated, including equivalent currents for caustic regions

23 p4136 A69-41583

Solid cylindrical antenna current and admittance calculation, considering reflection coefficient and multiple reflection phenomena at antenna ends

23 p4142 A69-42336

Solar quiet and lunar electric current systems deduced from geomagnetic data, discussing electrical conductivities and wind models in dynamo region

23 p4160 A69-42427

ELECTRIC DIPOLES

Dipole shielding factor in coupled Hartree-Fock approximation for atomic S state

02 p0281 A69-12179

Bound motion for particle in point electric dipole field, noting features of motion common to spherical pendulum motion

03 p0473 A69-14109

Oscillating electric dipole in cold plasma with ideal conductivity along lines of force of external magnetic field

06 p0921 A69-17743

Paraelectric resonance spectroscopy on KCl, using bistable dipole model

06 p0982 A69-18235

Horizontal electric dipole excitation of spherical guide waves between earth and ionosphere, discussing TM and TE modes and ELF and VLF range

08 p1273 A69-20023

Power radiated by oscillating magnetic and electric dipoles in cold streaming plasma calculated by Poynting vector method

09 p1544 A69-21329

Field patterns for wave radiation from electric dipole immersed in anisotropic plasma column excited by longitudinal DC magnetic field

12 p2034 A69-27103

Radiation pattern of electric and magnetic dipole on flat semiinfinite impedance system edge found similar

13 p2236 A69-28546

Molecular hydrogen electron scattering, optical refractivity and molecular anisotropy used to construct model dipole spectrum consistent with oscillator strength rules

14 p2488 A69-29094

Resonance effects between H levels by induced electric dipole transitions, using spatially periodic potential barriers

18 p3179 A69-35488

Electromagnetic field of horizontal LF electric dipole formed by thin ionosphere layer between anisotropic planes

20 p3521 A69-37047

Helium sequence ions spin forbidden transitions electric dipole oscillator strengths and transition probabilities evaluated by variational procedure

20 p3577 A69-38171

Effective Gaunt factors for threshold excitation of positive ions by electron collisions for 23 dipole transitions in 15 isoelectronic sequences

20 p3581 A69-38175

Radiation field several wavelengths from dipole above plane earth, specifying rigorous integral expression for Hertz vector by method of operators

21 p3770 A69-38748

Electromagnetic radiation characteristics from vibrating electrons or electric dipole moving in compressible isotropic plasma and from stationary dipole in moving medium, emphasizing Doppler effects

23 p4114 A69-41359

Hydromagnetic radiation characteristics of electric and magnetic dipoles in homogeneous anisotropic cold plasma, obtaining field components and wave propagation modes

24 p4307 A69-42905

ELECTRIC DISCHARGES

NT ARC DISCHARGES

NT CARBON ARCS

NT ELECTRODELESS DISCHARGES

NT GAS DISCHARGES

NT GLOW DISCHARGES

NT LIGHTNING

NT MERCURY ARCS

NT MULTIPACTOR DISCHARGES

NT PENNING DISCHARGE

NT RADIO FREQUENCY DISCHARGE

NT RING DISCHARGE

NT TOWNSEND DISCHARGE

HF plasma ionic composition dependence on discharge conditions and ions translational energy

01 p0129 A69-10682

MHD instability in current discharges in magnetic field stabilized by current frequency modulation higher than perturbation increment of plasma column

04 p0635 A69-14549

Equilibrium and stability of strong current discharge in dense optically transparent plasma, determining cause of instability

04 p0636 A69-14983

Continuous emission spectrum and continuous plasma absorption spectral coefficients for optically dense quasi-steady state electrical discharge plasma in sulfur capillary

06 p0964 A69-17251

Forward velocity of Bostick plasmoids demonstrated proportional to mean surge current through button source

06 p0964 A69-17480

Lorentz force sustained energy discharge, discussing cesium added argon flow across magnetic field in disk channel

06 p0969 A69-17910

Heat transfer from unseeded DC augmented propane air flame to water cooled probe placed beyond discharge zone

06 p1035 A69-17934

Zeta discharge in low density regime characterized by strong turbulence, rapid loss of plasma, resistance higher than predicted and high ion temperature

06 p0970 A69-17955

Converging cylindrical shock waves produced by discharging condenser bank into single turn coil surrounding gas container /theta pinch discharge/

10 p1678 A69-22933

Primary explosives tested for effects of shock, friction, heat and electrical discharges

10 p1750 A69-23010

Neon discharge positive column at medium gas pressures, discussing calculated and experimental data concerning diffusion theory to interpret parameters

10 p1740 A69-23723

Sulfur dioxide-helium laser pulsed and CW submillimeter outputs

10 p1706 A69-24005

Magnetospheric substorm as discharge process of associated electric current system, discussing relaxation processes, explosive release of energy, etc

11 p1879 A69-25249

Neutron emission anisotropies in capacitor discharge produced plasma focus, detailing coaxial plasma gun energy spectrum and flux measurement

11 p1930 A69-25321

Aerospace applications of electric discharge interaction with fluid motion including sonic boom reduction, high lift devices, reentry vehicle pitch control, etc

12 p2136 A69-26405

Oscillating electron ion discharge in magnetic field in system of alternating positive and negative electrodes to obtain fast neutral particle fluxes

13 p2311 A69-28109

Electrical breakdown voltage and voltage-current characteristics of uncooled coplanar carbon electrodes in walls of supersonic conical and rectangular nozzles [AIAA PAPER 68-713]

13 p2249 A69-28231

Spectral lines emitted from low voltage discharge in cesium filled diode with hot cathode, giving current-voltage characteristics as function of pressure and temperature

14 p2491 A69-29260

Duoplasmatron charged particles energy spectra analyzed as function of discharge parameters

14 p2501 A69-29955

Point discharge measuring based on pulsed nature of discharge current, outlining field experiment results

15 p2610 A69-30698

Discharge parameters modulation caused by acoustic wave propagating in partially ionized plasma, deriving perturbation current density and irradiated light intensity

16 p2752 A69-32364

Atmospheric ozone production by silent discharges near ground level during first stage of storm cell development

16 p2785 A69-32623

Materials fracture electrically induced including arc and spark discharges, dielectric breakdown, electrolysis, etc

17 p2989 A69-33558

Electrical discharge machining effect on heat resistant alloys surface finish, noting volt-ampere characteristics

18 p3147 A69-34547

Capacitor discharge stud welding on Ti alloys, discussing weld zone microstructure, arc and mechanical properties

18 p3151 A69-35431

He-Ne laser light noises due to discharge current fluctuations and random mode beat

19 p3330 A69-35760

Parameters of DC discharge between concentric cylinders calculated for plasma probes by pressure theory, noting ion neutral collisions and magnetic field effects

21 p3776 A69-38712

Electrical excitation discharge effect on molecular composition of flowing carbon dioxide gas laser, noting dissociation characteristics

21 p3736 A69-38940

Shadow photography study of electrical discharge set off by laser spark

21 p3740 A69-39552

Methyl alcohol, ether and acetone vapors decomposition in microwave discharge, obtaining H and CO in addition to solid polymeric films

22 p3895 A69-40103

- Electromagnetic radiation below 1 GHz from gap type electrical discharges on electric power distribution lines
23 p4126 A69-42218
- Electrothermal waves in nonequilibrium electrical discharge in potassium seeded argon plasma
24 p4359 A69-43645
- ### ELECTRIC ENERGY STORAGE
- Stark effect meter for electric field measurement in space, discussing absorption cell development
03 p0429 A69-13222
- Automatic device for charging storage capacitors in plasma devices provides voltage and operational frequency control
04 p0580 A69-14493
- Inverted transistor parameters required for accurate prediction of electrical and radiation storage time, discussing computer predictions of radiation responses
06 p0977 A69-16884
- Erosion type plasma accelerator using inductive energy storage compared with capacitive energy storage
13 p2311 A69-28110
- Storage batteries for satellite electrical power sources emphasizing operation in overcharged state
16 p2735 A69-31729
- ### ELECTRIC EQUIPMENT
- Electrical explosive devices for space applications including explosive bolts, primers and igniters
01 p0141 A69-10544
- Reliability terms for electrical apparatus, equipment and systems, indicating need for international standardization
08 p1292 A69-21108
- Electrical analogs with passive elements in combination with stepping switches for simulation of plants with distributed parameters
09 p1471 A69-21436
- Type 2 ceramic capacitor manufacture, selection and control in Concerto space program
11 p1853 A69-25393
- Resistance type bonded strain gages for seven adverse environments, discussing installations and transducers
12 p2099 A69-27165
- Airborne electric power systems maintenance aids, describing design and operation of annunciator for establishment and display of system failure causes
17 p2905 A69-34112
- ### ELECTRIC EQUIPMENT TESTS
- Supersonic airplane high temperature wire tests, detecting corona onset voltage (COV) or voltage breakdown
05 p0731 A69-16245
- Design and tests of cable assemblies for F-111 aircraft
05 p0731 A69-16246
- Computer programs for linear systems fault isolation, discussing technique theory and limitations
12 p2040 A69-26568
- Fluidic curved-wall electropneumatic converter optimization, presenting steady state, step and pulse mode responses for various positions and lengths of resistive heaters
15 p2553 A69-31298
- Soviet book on testing aircraft electrical equipment covering climatic and mechanical tests, malfunction detection, etc
20 p3464 A69-37237
- Electrical sliprings assembly development with low dynamic resistance and long lifetime for space simulation testing, noting wear rate of rings and brushes [AIAA PAPER 69-1035]
22 p3925 A69-40402
- ### ELECTRIC FIELD STRENGTH
- Microwave instabilities in bulk GaAs under strong electric fields, considering characteristics connected with structural properties and contact formation conditions
01 p0136 A69-10256
- Dielectric constants of barium titanate single crystals as function of electric field intensity at different frequencies
01 p0139 A69-10889
- Electron drift velocity, diffusion coefficient and trapping time in GaAs, measuring variation with electric field
01 p0140 A69-11255
- Advanced potentials method to determine electric field intensity tangential component on surface of cylindrical radiator
03 p0408 A69-14131

- Electric field strength and helix pitch in induced cholesteric-nematic phase transitions, noting activation energy for charge carrier production
04 p0555 A69-14964
- Homogeneous electroluminescence at 77 K in n-type GaAs single crystals without artificial p-n junctions, noting effects of electric field strength and Zn doping
04 p0644 A69-15271
- Multiple high field domain nucleation in GaAs, discussing dependence on contact inhomogeneities
05 p0807 A69-15959
- Electric field growth directional effect on avalanche breakdown conditions in p-n junctions
06 p0981 A69-17828
- Electrostatic field strength and conductivity dependence of expansion and contraction of space charge cloud in process of discharging during static electrification
06 p0959 A69-18219
- Electron transport parameters in noble gases at low electric field intensities, elastic and inelastic scattering and Boltzmann transport equation
08 p1362 A69-20285
- Temperature stability of slightly ionized gas for arbitrary collision cross sections, discussing electron temperature variation as function of electric field strength
09 p1551 A69-22039
- Microwave instabilities in bulk GaAs under strong electric fields, considering characteristics connected with structural properties and contact formation conditions
09 p1559 A69-22649
- Electromagnetic wave transmission through anisotropic plasma, discussing incident wave field strength effects near cyclotron frequency
10 p1728 A69-23167
- Cs and K ions drift velocity calculations in vapors of own atoms under various electric field strengths effect
11 p1922 A69-24226
- Relation between electric field strength and mean energy for electron swarms in oxygen determined, using Boltzmann transport equation
11 p1921 A69-24419
- Neutral gas flow transport velocity and Mach number effects on critical electric field strength and direction in formation of self sustained discharge
11 p1933 A69-25545
- Charged aerosols production for electrohydrodynamic processes by spraying liquids through capillary at high electric field strengths into high pressure air flows
12 p2138 A69-26631
- Charged particles generation by liquid subjected to high electric field for efficient bipolar microthruster [AIAA PAPER 67-728]
13 p2325 A69-28220
- Electric field distribution in focal region of finite off-set paraboloid reflector illuminated by linearly polarized plane wave
13 p2234 A69-28427
- Spectral distribution of fluctuations in stable plasma in absence of external fields, emphasizing electric field fluctuations, quasi-steady states, isotropic plasmas and thermodynamic equilibrium
14 p2490 A69-29103
- Plasma arc characteristic and radiation at high pressure and temperature showing strong electrical field strength and radiation increases with pressure
15 p2659 A69-30377
- Relative dielectric constant and permeability of inhomogeneously filled rectangular waveguide filling medium expanded into trigonometric series to calculate cut-off frequencies and field patterns
15 p2577 A69-30627
- Fluctuation kinetics of electron system in nonequilibrium state arising in semiconductor in strong electric field, considering lattice and interelectron scattering
16 p2824 A69-31569
- Yttrium desorption from W wire by strong electric field, noting electron work function or temperature increase effects on desorption field
17 p3015 A69-33631
- Anomalous absorption of electromagnetic wave in collisionless dense cylindrical plasma beam in circular waveguide, noting electric field strength for energy transfer
18 p3101 A69-34621
- Dielectric constants of barium titanate single crystals as function of electric field intensity at different frequencies
18 p3182 A69-34720
- Electromagnetic shaping of metallic parts using equations describing magnetic and electric field intensity

- as function of blank profile and cylindrical blank wall thickness
18 p3151 A69-35456
- Cumulus and cumulonimbus clouds electrical and microphysical properties measured by instrumented aircraft
20 p3572 A69-37907
- Artificial ion plasma cloud experiment for studying auroral electric fields
21 p3710 A69-38507
- Horizontal and vertical magnetospheric electric fields measured by balloon, determining average field strength for quiet and active periods
22 p3939 A69-40514
- Analyzing conditions for variable magnetic and electric noise occurrence at input of nuclear precession magnetometer used in field strengths measurements
23 p4165 A69-41852
- Electron density in positive column of Cs vapor discharge related to current and gas pressure, discussing field strength effects on drift velocities
23 p4196 A69-42197
- Fluctuating electric fields relations to MHD bow shock structure, using LF fluxgate magnetometer aboard OGO 5
24 p4306 A69-42693
- ### ELECTRIC FIELDS
- Temperature dependence of hot electron drift velocity in silicon at high electric fields, using space charge perturbation theory
01 p0135 A69-10120
- Electric field control of growth rates of insulating organic crystals from vapor phase
01 p0135 A69-10140
- Weak alternating electric field effects on human circadian rhythms
01 p0013 A69-10167
- Microwave second harmonic, sum and difference frequencies generation for two different microwaves normally incident on low temperature semiconductor slab in DC field
01 p0137 A69-10334
- Numerical solution method for equation of electric field affected by permanent flux of identical ions
01 p0128 A69-10364
- Electric field effects on flame temperature variation, suggesting electrons active role in flame combustion reactions
01 p0176 A69-10389
- Symmetrically truncated right angle E-plane corner, placing electric and magnetic walls in symmetry plane, solving resulting boundary value problems
01 p0044 A69-10624
- Electrohydrodynamic analogies to known MHD effects studied by differential equations for hydrodynamic and electric field energy relations
01 p0131 A69-10775
- Electrostatic polarization field formation by acoustic wave propagation through ionosphere, calculating effect on ionization drift velocity
01 p0068 A69-11110
- Sporadic E layer formation, considering ion convergence effects due to neutral wind shears and drift ionization due to electrostatic field
01 p0072 A69-11174
- Growth rate of wave instability in conducting liquid jet in perpendicular electric field and accelerating under gravity
01 p0062 A69-11207
- One dimensional Vlasov plasma nonlinear response to external electric field varying in space and time
01 p0133 A69-11214
- VLF electric field measurements from 1 AU heliocentric orbit, noting field oscillations in solar wind and large amplitude HF noise bursts
01 p0035 A69-11224
- Electric field in plasma half space determined by longitudinal wave normal mode analysis, using BKG particle conserving collision model
01 p0134 A69-11287
- Carrier mobility variation with electric field related to structure of epitaxial field effect transistors
02 p0294 A69-11541
- Plasma discharge energy balance analysis to determine discharge power and temperature as function of electric field parameters
02 p0286 A69-11572
- Characteristics of electrovortices and auroral electrojets of polar disturbance field, discussing dynamics during geomagnetic storms
02 p0240 A69-11723

Electric field induced IR absorption and Raman scattering by optical phonons in centrosymmetric crystals, discussing tensor coefficients

02 p0295 A69-11779

Positive ion beam probe for approximate static electric field distribution in low pressure RF discharges, analyzing deflection data for potential distributions

02 p0287 A69-11838

Holtzmark plasma microfield, discussing neglect of term comparable to dipole moment during Fourier transform development for long range Coulomb field

02 p0287 A69-11871

Traveling high electric field domains in bulk semiconductors use in high speed integrated electronics, noting domain properties of GaAs and CdS

02 p0216 A69-12144

Dipole shielding factor in coupled Hartree-Fock approximation for atomic S state

02 p0281 A69-12179

Wave measurements of normal electric field and tangential magnetic field over microwave disk antenna surfaces

02 p0219 A69-12342

Photoelectric effect of thin gold film under electric field, noting work function dependence on film thickness exhibits extremum

02 p0300 A69-12631

Optical modulation near intrinsic edge in n-type bulk GaAs due to Franz-Keldysh effect, noting carrier production by photon initiated excitation

02 p0300 A69-12650

Green tensor for collisionless plasma, emphasizing relations between outgoing and ingoing electric fields

02 p0293 A69-12745

Transport phenomena in crossed electric and strong magnetic fields, developing semiclassical and quantum treatments

03 p0473 A69-12926

Scattering of energetic charged particles in weakly unstable plasma for integrated spectrum of plasma electric field autocorrelation function

03 p0475 A69-13151

Electron beam meter application as lunar surface electric field detector, discussing breadboard model and performance characteristics

03 p0429 A69-13221

Stark effect meter for electric field measurement in space, discussing absorption cell development

03 p0429 A69-13222

Electric effect in ruby, discussing resonance magnetic field and transition

03 p0485 A69-13320

Helium plasma ion oscillations damping by external RF electric field at sheath-plasma resonance condition

03 p0476 A69-13323

Perfect piezosemiconductor resonator /phaser/ with CdSe/CdS crystal, discussing vibration excitation in wurtzite type crystal in electric field of electron drift

03 p0431 A69-13930

Reduction of optical breakdown threshold in laser focus by superimposed microwave field

03 p0441 A69-13997

Frequency of damped oscillations in plasma in DC field, noting variation with electron density and DC field

03 p0479 A69-14050

Transport phenomena in semiconductors in strong DC field, emphasizing electrical conductivity as function of crystallographic orientation

03 p0491 A69-14097

Bound motion for particle in point electric dipole field, noting features of motion common to spherical pendulum motion

03 p0473 A69-14109

Explosive detonated in external electric field to obtain data on gas state behind shock wave

04 p0634 A69-14430

Electric field and energy dispersion law effects on plasma oscillations in semiconductors, calculating composite oscillation frequency

04 p0642 A69-14554

Detection of electric field turbulence in earth bow shock, noting wave amplitude correlation with magnetic field structure

04 p0592 A69-14681

High power waveguide tuner for use in traveling wave resonator to tune out reflections in resonant ring

04 p0576 A69-14759

Surface wave stability for horizontal layer of incompressible dielectric fluid in electric field, noting viscosity effect

04 p0638 A69-15193

Drifting temperature fluctuations in semiconductors in presence of strong electric field

04 p0643 A69-15256

Electric field influence on fluid oscillation modes for Korteweg-Helmholtz force density on incompressible dielectric liquid immersed in electric field

04 p0591 A69-15504

Boltzmann equation for weakly ionized gas electron component, solved by transformation to integral equation, applied to Lorentz gas in alternating electric field

05 p0795 A69-15619

Lamination influence on traveling wave tube performance, showing negative effect of radial variations in electric field

05 p0727 A69-15642

Electron bunching improvement by combined effect of space charge and inhomogeneous electrostatic field on velocity modulated electron flux in microwave devices

05 p0799 A69-15646

Charged particle motion in constant direction magnetic field varying exponentially with time, discussing electric field effect on particle motion

05 p0801 A69-15744

Stationary solutions of Vlasov equation with external electric fields and BGK collision terms, using perturbation theory in moving frame

05 p0801 A69-15745

Ultrasound propagation amplification coefficient in high permittivity semiconductors with electric field based electron-phonon interaction

05 p0809 A69-16372

Whistler mode propagation in homogeneous electron plasma situated in longitudinal electrostatic field, using Fokker-Planck model

05 p0758 A69-16417

Electric field effects on thermal annealing of electron irradiation damage in p-channel MOSFET device

05 p0733 A69-16562

Electrogas dynamics /EGD/ engineering, discussing generators and compressors

05 p0804 A69-16586

Electron distribution function for homogeneous weakly ionized gas in presence of alternating electric field, discussing solution of Boltzmann equations

05 p0797 A69-16604

Coaxial Hall plasma accelerator, noting interaction between radial applied magnetic field and axial applied electric field

05 p0806 A69-16734

Electromagnetic waves transformation and scattering in plasma in electric field, showing abrupt increase at certain critical value

06 p0886 A69-16894

Hydrodynamic and lattice vibrations equations for coupled waves in ion semiconductors in external electric and magnetic fields, observing sound amplification

06 p0978 A69-16897

Gunn effect verification using n-type semiconductor single crystals in DC field, noting microwave field polarization plane rotation

06 p0978 A69-16902

Molecular and atomic beam focusing in electric and magnetic fields with helical symmetry of specified type

06 p0959 A69-16917

General theorem of isotropic microwave waveguide junction ports imposed by reflection symmetry

06 p0893 A69-16935

Static problem of electric field intensity and space charge density distribution in semiconductor with hot electrons and holes

06 p0978 A69-16989

Temperature dependence of n-InSb Hall coefficient and resistivity, noting increase in conductivity with degree of compensation associated with electrical breakdown

06 p0978 A69-16990

Longitudinal acoustic waves propagation in partially ionized gas in external electric field, taking into account ionic collisions with electrons and neutral particles

06 p0963 A69-17079

Ambipolar motion of light injected photocarriers in cadmium-mercury-telluride in terms of diffusion and drift in electric fields

06 p0979 A69-17154

Parametric instability of horizontal surface of ideally conducting or very high dielectric constant liquid in varying perpendicular electric field

06 p0957 A69-17542

Electrothermal domains in semiconductors, examining domain velocity of motion under external potential

06 p0981 A69-17880

Rates of charging of thermionically emitting particles in space charge

06 p1035 A69-17928

Dispersion relation for longitudinal oscillations of one component weakly ionized plasma without inter-carrier collisions in uniform constant electric field

06 p0970 A69-17957

Electromagnetic ion acceleration in steady electric and magnetic fields chosen to match fields of Alkali Plasma Hall Accelerator /ALPHA/ [AIAA PAPER 69-111]

06 p0985 A69-18175

Strong electrostatic fields effects on burning rates of double base and composite propellants [WSCI PAPER 68-24]

07 p1241 A69-18366

Nonlinear coupling between background illumination and illumination signal producing lateral electrical fields in p-n junction, noting effect on sensitivity of position sensor

07 p1101 A69-18654

MHD models for analysis of nonhomogeneous magnetized plasma stability with regard to perturbations having electrical field as potential field

07 p1190 A69-18694

Laser light scattering with orientation saturation of microsystems by electric field, noting application to optical anisotropy of macromolecules and colloidal particles

07 p1149 A69-18900

Maxwell equations solution for linear induction MHD machine coil area field components, allowing for finiteness of magnetic permeability of iron

07 p1059 A69-19028

Magnetospheric and high latitude ionospheric disturbances, bulk motion /convective/ flow pattern and electric field distribution

07 p1128 A69-19370

Gas breakdown in HF uniform electric field with/without steady transverse magnetic field

07 p1194 A69-19415

Complex microwave incremental conductivity of InSb at 77 K in steady electric field using displaced Maxwellian distribution function

07 p1200 A69-19447

Dynamics of pulsed microwave breakdown in nonuniform field at waveguide fed mica aperture, noting electric field distribution change due to initial plasma configuration

07 p1107 A69-19448

Electric fields and conductivity in thunderclouds by parachuting rotating differential electric field mills

08 p1345 A69-19813

Kinetic theory for plasma, considering electric field fluctuations time evolution simultaneously with one particle distribution time evolution and Landau damping in wave equation

08 p1360 A69-19991

Horizontal electric dipole excitation of spherical guide waves between earth and ionosphere, discussing TM and TE modes and ELF and VLF range

08 p1273 A69-20023

Bounds on electric field outside radiating system determined for application to UHF and VHF systems design, considering microwave breakdown

08 p1273 A69-20026

Diffusion coefficient, velocity distribution function and velocity averages for gaseous ions moving in strong electric fields, considering ion-gas molecule charge transfer collisions

08 p1355 A69-20209

Solution of equations of motion of charged particles in constant magnetic field and variable electric field

08 p1361 A69-20213

High Q capacitance loaded coaxial cavity resonator for study of electric susceptibility of ionized gas

08 p1313 A69-20214

Time dependent velocity distribution functions for carriers calculated in weakly ionized plasma in external electric field

08 p1362 A69-20265

Distribution and carrier type in germanium bar in electric field, relating distribution obtained by using Hall effect to avalanche phenomenon

08 p1372 A69-20277

Inertia of electrically charged spherical body calculated on basis of relativistic stress energy

08 p1352 A69-20756

Linear perturbation theory to predict instability threshold conditions caused by electric field in poorly conducting liquid subject to vertical temperature gradient

08 p1352 A69-20790

Electroconvective instability produced by uniform electric field in poorly conducting fluid under stabilizing

ing vertical temperature gradient, noting heat flow increase

08 p1352 A69-20791

Interfacial charge relaxation overstability in tangential electrical field, discussing electromechanical polarization surface waves propagation and dielectrophoretic orientation of liquids in zero gravity space

08 p1353 A69-20792

Heating of collisionless plasma in magnetic mirror by random electric field transverse to magnetic field

08 p1368 A69-20805

Trapped particles drift velocity in time dependent meridional magnetic and perpendicular electric field

08 p1368 A69-20809

Internal electric field effect of diode with inhomogeneously doped base on lifetime of strong reverse current generated during instantaneous switching

08 p1287 A69-20890

Thin semiconductor plates negative differential resistance associated with captures at surface, describing electron gas by electron temperature

08 p1374 A69-21081

Population inversion in semiconductors obtained by applying electric field through dielectric sphere /field effect/

08 p1374 A69-21082

Charged liquid droplets generator and acceleration through electric field for thrust vectoring, analyzing beam focusing and deflection

[AIAA PAPER 69-283]

09 p1563 A69-21230

Coaxial electrodes with electric and magnetic fields to study instability in MPD arcs

[AIAA PAPER 69-230]

09 p1563 A69-21231

Electrothermal instabilities for explanation of MPD arc thruster rotating spoke phenomenon, noting agreement with experimental results

[AIAA PAPER 69-231]

09 p1566 A69-21254

Electron multiplication during ionized H plasma exposure to annular electric field and magnetic field, including microwave diagnostics

09 p1543 A69-21299

Plasma column of free burning electric arc, deriving temperature, electron concentration and electric field radial distributions

09 p1545 A69-21431

Charged particles concentration change during vertical propagation of acoustic wave in F layer found transforming electric field into circularly polarized wave

09 p1484 A69-21528

Plasma conductivity tensor components in crossed fields calculated by Boltzmann kinetic equation, noting influence of magnetic field presence

09 p1546 A69-21565

Electromagnetic wave fluctuations and scattering in plasma in strong electric and magnetic fields at magnetoacoustic frequencies

09 p1453 A69-21569

Nighttime electric fields and vertical ionospheric drifts near magnetic equator concurrent measurements

09 p1489 A69-21705

Reflected particle acceleration at magnetospheric bow shock front attributed to interplanetary electric field

09 p1577 A69-21714

Shock wave structure problems in plasma, including plasma particles random motion in term representing electric field

09 p1551 A69-22032

Faraday dark space geometries in glow discharge, using superposition principle to divide electric field for transition visualization

09 p1540 A69-22099

Static characteristics of transistors dependence on current carriers surface recombination in inactive base region, noting strong electric field influence

09 p1464 A69-22287

Current instability in H plasma in electric field of large amplitude fast magnetosonic wave, noting plasma heating

09 p1552 A69-22526

Space electric fields research by artificial clouds of vaporized barium launched by rockets, noting neutral atmosphere and ionospheric results

09 p1492 A69-22800

Book on thermodynamics of charged and polarized layers covering matter in electric fields, general framework theory, applications, etc

10 p1724 A69-23159

Field distribution in insulated gate FET determined by numerical solution of Poisson equation

10 p1662 A69-23170

Closed cycle MPD experiments with applied electric and magnetic fields emphasizing current leakage, segmentation, relaxation and aerodynamic effects

10 p1738 A69-23479

MHD generator performance operating on nonequilibrium Ar plasma with K additions in presence of electric fields

10 p1637 A69-23480

Nonequilibrium ionization effects on performance of subsonic constant area MHD generator, using closed cycle blowdown loop facility

10 p1637 A69-23481

Two dimensional flow of unipolar medium in electrogasdynamic power generation channel, discussing stationary model, electric field and ion density distributions

10 p1638 A69-23486

Pulse and CW breakdown criteria for plasmas subject to spatially nonuniform electric fields, using variational formulation

10 p1739 A69-23650

Pulsed glow discharges in He and He-H mixtures for high current density, noting electric field and wall potential distributions

10 p1739 A69-23660

Small signal HF conductivity of GaAs calculated for arbitrary frequency and DC field, considering subcritical Gunn devices

10 p1747 A69-23694

Rotating plasma behavior in magnetic mirror trap, using radial electric field

10 p1740 A69-23716

Transport and balance coefficients in ionized neon and helium plasmas in homogeneous electric field, calculating electron mobility, diffusion coefficient, energy and collision parameters

10 p1740 A69-23722

Field effect on positive column plasma of glow discharge in air, analyzing near wall potential and conductivity

10 p1741 A69-23946

Landau type interaction between electron beam and whistler/helicon/ wave electric field within semiconductor /InSb/

10 p1742 A69-24107

Longitudinal electric field distribution and charged particle density in magnetic mirror under potential difference between magnetic equator and plane

10 p1689 A69-24204

One dimensional electrostatic plasma oscillations in alternating external electric field, noting plasma stability and electron-electron two stream instability

11 p1924 A69-24298

Electric field fluctuations in inhomogeneous plasma calculated by test particle method, interpreting results in convective modes terms in plasma control and stability

11 p1924 A69-24301

Photoconductivity of semiconductors with multilevel electron energy and isotropic hole spectra, discussing nonlinearity of field dependence

11 p1937 A69-24913

Complete electric field of idealized infinite slot antenna with uniform excitation in infinite conducting plane

11 p1851 A69-24994

Electric field vertical and radial components for time harmonic electric line sources with piecewise sinusoidal current distribution

11 p1836 A69-24995

Tonks-Dattner resonances in plasma column, using linearized Vlasov equation for coupling to plasma waves of time varying electric fields

11 p1929 A69-25266

Electric field measurements for turbulence in collision-free shocks, noting power spectra of magnetic and electric fluctuations and electron density

11 p1930 A69-25276

Convective drift and flute instabilities of plasma stabilized by exerting HF forces on electrons, determining required HF field amplitudes

11 p1932 A69-25538

Electric field penetration into homogeneous plasma at frequencies near Langmuir frequency and current at surface of thin cylindrical antenna in plasma

11 p1853 A69-25551

Flute oscillation instability of dense plasma cylinder under nonuniform electric field, analyzing oscillation spectrum properties

11 p1934 A69-25707

Flow in linear MHD channel with two permeable electrodes, solving Riemann boundary value problem for electric field in channel

11 p1934 A69-25727

Paraxial electron beams from Pierce gun and spreading due to thermal velocities and space charge in nonuniform potential

12 p2036 A69-25920

Electric fields effect on flame front propagation structure and velocity, obtaining color topolegrams by high speed photography

12 p2190 A69-26192

Electric vector transformation for three dimensional photoelastic medium irradiated by light in reverse direction, noting optical systems of birefringent plates and rotators

12 p2180 A69-26339

One dimensional stationary flow of medium consisting of charged and neutral components within electrohydrodynamic limits in AC and DC electric fields

12 p2135 A69-26398

Radial electric field effect on pressure drop in isothermal laminar flow of dielectric liquid through stainless steel tube, considering ion drag

12 p2136 A69-26401

Electrically driven thin fluid jet stability in longitudinal field between two plate electrodes, discussing role of Ohm law in calculating jet potential

12 p2136 A69-26402

Plasma instability in magnetic and HF electric fields, observing aperiodic short wave and oscillatory instabilities

12 p2136 A69-26526

Electromagnetic waves directional velocity, plasma temperature and particle density determined from analyzing electric field fluctuations amplification near body in plasma

12 p2137 A69-26531

Solution for kinetic energy equation for organic semiconductors with narrow conduction band situated in strong electric field

12 p2144 A69-26673

Longitudinal electric field penetration into semibounded plasma using kinetic approximation, assuming diffusive plasma particles reflection from plasma boundary

12 p2138 A69-26711

Joint probability distributions of electric microfield in hot ionized plasma consisting of noninteracting particles

12 p2139 A69-26871

Inhomogeneous permittivity and boundary effects influence on electric fields of laser with open cavity containing inhomogeneous active medium

12 p2110 A69-26908

Atmospheric electricity and space charges ionization and equilibrium in earth atmosphere, discussing electric fields in lower atmosphere, ionosphere and magnetosphere

12 p2076 A69-27105

Infinitely long journal bearing using ionized gas lubricant with magnetic field applied axially and electric field applied transversely to fluid film

[ASME PAPER 68-LUBS-30]

13 p2267 A69-27287

Magnetic and electric fields influence on gas lubrication of bearings

[ASME PAPER 68-LUBS-26]

13 p2267 A69-27288

Alternating electric field parametric effects on inhomogeneous plasma in magnetic field, obtaining electrostatic wave coupling dispersion relation by density gradients considerations

13 p2304 A69-27298

Stationary magnetic field effect on sum and difference frequency generation due to nonuniform RF electric fields applied externally to plasma

13 p2305 A69-27376

Transport equation describing drift, diffusion and reaction of iron swarm influenced by electric field in gas

13 p2306 A69-27457

Polarization stabilization times dependence on risetime of external field pulse leading edge for semiconductor crystal, determining field concentration

13 p2317 A69-27880

Capture levels at photosensitive CdS crystals surface determined by studying field effect mobility dependence on electric field

13 p2318 A69-27884

Electric drift instability in semiconductors with hot electrons, discussing diffusion, electron heat conduction, energy transfer, space charge density, etc

13 p2318 A69-27891

Semiconductor luminescent devices and laser pumping by solar radiation modulated to interact resonantly with solid state plasma oscillations and electric field in crystal

13 p2272 A69-27969

Fluctuations in electric field induced by plasma flow in constant magnetic field, performing spectral analysis of voltage and current fluctuations in plasma
13 p2310 A69-28029

Gas laser modulation steady state characteristics with KDP crystal in cavity, noting output power dependence on applied electric field
13 p2273 A69-28432

Electric field frequency effect on cyclotron resonance during gas discharge, establishing causes of discrepancy between theory and experiments
13 p2315 A69-28577

Electric field distribution in TWT electron beam deflection system determined, accounting for current-voltage characteristics dependence on electromagnetic field distribution
13 p2237 A69-28582

Potassium plasma drift instability suppression by applied external HF electric field, noting plasma diffusion decrease toward container wall
14 p2489 A69-28740

Electrothermal domains in semiconductors, examining domain velocity of motion under external potential
14 p2503 A69-28789

Time dependent convection electric fields as agents for diffusing trapped magnetospheric radiation inward toward earth, discussing one dimensional diffusion equation
14 p2510 A69-28936

Diffusion of equatorial particles in outer radiation zone caused by expansions and contractions of permanently compressed magnetosphere, obtaining electric fields
14 p2510 A69-28937

Effects of cold electron and light emission centers from dispersed Au films in electric field, as universal qualities characterizing dispersed metal films
14 p2504 A69-28992

Galvanomagnetic characteristics of n-type semiconductor subjected to perpendicular electric and magnetic fields, noting electron temperature
14 p2505 A69-29037

Low energy charged particle motion parallel with magnetic force lines analyzed in magnetosphere model with constant electric field
14 p2512 A69-29040

Electric field determination from charged particle concentration in wake of body moving in rarefied plasma, noting hydrodynamics similarity
14 p2517 A69-29068

Horizontal electric fields relations to charged particle fluxes in polar auroral ionosphere
14 p2437 A69-29070

Electromagnetic energy spectra of lightning expressed as function of electric field spectral density of atmospheric
14 p2437 A69-29076

Longitudinal electric field penetration into plasma slab in constant magnetic field
14 p2493 A69-29665

Ionospheric models for motion of slightly ionized homogeneous cold plasma influenced by electrostatic field and neutral particles flow, considering geomagnetic effects
14 p2499 A69-29863

Compressible gas MHD steady one dimensional flow in electric and magnetic fields
14 p2500 A69-29905

Velocity distribution effect on electric field at walls for axisymmetric flow of electrolyte in circular channel in magnetic field of E shaped inductor
14 p2501 A69-29915

Density fluctuations effect on fully ionized plasma electrical conductivity in large or zero frequency external electric fields
14 p2502 A69-29990

Integral formulation of scattering theory extended to Coulomb interactions by expanding Green function and treating kernel singularities
14 p2489 A69-29995

Boltzmann equation for hot electron distribution functions in GaAs and threshold field in Gunn effect
15 p2665 A69-30025

Secondary effects role in n-GaAs crystals electrical reflection spectra with low free carrier concentration at room temperature in external electric field
15 p2666 A69-30061

Resonance cones in angular distribution of short antenna RF electric field in anisotropic plasma noting variation with incident, cyclotron and plasma frequency
15 p2659 A69-30876

Plane incompressible fluid interface stability in presence of transverse electric field, deriving equation of motion for perturbation amplitude
15 p2652 A69-30911

Energy absorption by cold nonuniform plasma from externally driven electric field, noting relation between plasma and driving frequencies
15 p2661 A69-30922

Molecular beam behavior in constant electric and magnetic fields, applying laser frequency dependence on magnetic field orientation to resonator
15 p2655 A69-30943

Interferometer for measuring electric fields spatial correlation function at camera aperture, describing laser light coherence measurements after propagation through turbulent atmosphere
15 p2653 A69-31164

Plasma modes, critical fluctuations and optical properties electric field dependence in two valley model of Gunn instability semiconductors
15 p2581 A69-31240

Alternating electric field effects on circadian rhythms in men, discussing period shortening and internal desynchronization
15 p2557 A69-31461

Controlled electric field capacitance probes for non-destructive testing, discussing field projection pattern and direction effective depth of field, applications, etc.
15 p2616 A69-31503

Low density cold plasma effect on stability of cylindrical layer of charged particles against electrostatic perturbations in uniform magnetic field
16 p2816 A69-31635

Nonlinear theory of $E \times B$ instability for weakly ionized plasma in presence of density gradient and parallel electric field perpendicular to magnetic field
16 p2819 A69-31682

Nonlinear generation of sum and difference frequency components in magnetoplasma current density due to alternating electric fields, electron density and temperature gradients
16 p2821 A69-32036

Lamination influence on traveling wave tube performance, showing negative effect of radial variations in electric field
16 p2762 A69-32499

Electron bunching improvement by combined effect of space charge and inhomogeneous electrostatic field on velocity modulated electron flux in microwave devices
16 p2823 A69-32503

Charged particles concentration change during vertical propagation of acoustic wave in F layer found transforming electric field into circularly polarized wave
16 p2783 A69-32523

Linearized motion equations for conducting gas in magnetic and electric field solved for coaxial channel and free jet, assuming small Reynolds number and parallel flow
17 p3010 A69-33016

Atmospheric aerosols influence on electric field in ground layer to account for ionization, demonstrating number and turbulent exchange coefficient relationship
17 p2996 A69-33036

Triple probes behavior in plasmas under AC electric field perturbations
17 p2920 A69-33592

Electromagnetic fields theory simultaneously determining vector electric and magnetic field aspects in terms of operator Green functions
17 p2924 A69-33833

Vertical distribution of ionospheric drift velocity in auroral zone, evaluating role and intensity of electric field formed in dynamo region
17 p2964 A69-33964

Level crossing signal obtained by magnetic/electric field modulation, tabulating corrections to widths and centers for distortions
17 p3009 A69-34155

HF electromagnetic waves penetration into slightly ionized plasma analyzed by Maxwell and kinetic equations, giving penetrating electric field by WKB formula
17 p2932 A69-34220

Pulse propagation through antipode, calculating time domain response of fields near axial caustic
18 p3100 A69-34233

Dawn-dusk electric field in outer radiation zone associated with magnetospheric plasma convection, comparing electron densities for magnetically quiet periods
18 p3128 A69-34942

Microfluctuations frequency and wavelength of electromagnetic, electric and magnetic field distributions in plasma shock wave front found consistent with ion-acoustic origin hypothesis
18 p3180 A69-35017

Conducting medium steady one dimensional motions determined by assuming space charge-electric field interaction, considering electrohydrodynamic behavior of medium
18 p3181 A69-35315

Refractive index profiles yielding wave functions expressed in terms of standard transcendental functions for electric fields in spherically stratified isotropic media
19 p3372 A69-35618

Near and antipodal fields in earth-ionosphere waveguide using mode theory, ray theory, zonal harmonics series and method of images to derive field representations
19 p3283 A69-35931

Electric fields and electron work functions, surface potentials and number density distributions in selected metals surfaces determined using free electron model
19 p3382 A69-36045

Longitudinal electric field, electron density and temperature in positive column of low pressure Cs-Ar DC arc discharge, discussing Cs vapor depletion
19 p3380 A69-36441

OGO 5 spacecraft detector instrumentation for measuring electrostatic and electromagnetic waves electric fields with coupled antennas, describing in-flight operation
19 p3315 A69-36683

Lower ionosphere electric fields and currents vertical profiles above geomagnetic equator under quiet geomagnetic conditions from rocket data
20 p3521 A69-37053

Electric field correlation to magnetic fields in quantum theory of coherence, deriving dynamical equations governing space-time development of correlation matrix
20 p3575 A69-37304

Retarding potential analyzers to measure rocket vehicle potentials and ambient electric fields in active auroras
20 p3542 A69-37793

VLF electric and magnetic fields observed in auroral zone with Javelin 8.46 sounding rocket, noting HF electrostatic noise bursts
20 p3533 A69-38080

Ion density, electric field and electron temperature responses to gas density perturbation calculated for acoustic wave propagation in gas discharge using hydrodynamic equations
20 p3578 A69-38243

Ionospheric currents geophysical DC electric fields measurement from sounding rockets, indicating anticorrelation with auroral luminosity
21 p3710 A69-38508

Electrostatic charge formations in atmosphere, discussing atmospheric electricity during precipitation and thunderstorms
21 p3758 A69-38785

Microwave breakdown characteristics predictable for circular loop antennas from near electric field analysis
21 p3683 A69-39281

MHD energy converters electric fields and current distributions, analyzing MHD flow problems
21 p3777 A69-39480

Nonlinear electron conductivity of Lorentz plasma subjected to frequency modulated electric field
21 p3778 A69-39573

Laminar burning rate of premixed propane-air flames at one atmospheric pressure in DC electric fields, using cooled porous plug burned method
21 p3852 A69-39596

Temperature measurement in and near opposed-jet diffusion flame subjected to electric field, discussing flame behavior at low mass flow rate
21 p3852 A69-39597

Accelerating electric field model to interpret energy and angular distribution of auroral particles, noting electric potential limitations
22 p3938 A69-40445

Injun 5 satellite VLF electric and magnetic fields observations, discussing antenna operation, Poynting flux and noise band measurements
22 p3938 A69-40503

Horizontal and vertical magnetospheric electric fields measured by balloon, determining average field strength for quiet and active periods
22 p3939 A69-40514

Homogeneous conducting moon-solar wind interactions, describing time dependent lunar magnetic and electric fields induced by interplanetary magnetic field variations
22 p4023 A69-40518

Electric field regions of p-n junctions using electron beam deflection measurement, noting application to Si specimens
22 p3994 A69-40752

Midlatitude F region continuity equation solutions, including east-west electric field effects on electron density
22 p3941 A69-40917

Dirac equation in external electromagnetic fields, deriving solution for constant orthogonal electric and magnetic fields encountered in plasma transport
23 p4190 A69-41357

Oscillatory electric field disturbances monitored near human body concurrent with heart beat and respiration, showing signals unrelated to blood flow or streaming potentials
23 p4101 A69-41449

Electric fields reducing recombination radiation intensity from bulk ionized GaAs and InP and shifting spectrum to lower energies, discussing self absorption
23 p4198 A69-41499

Liquid drop in electric field numerically analyzed for disintegration dynamics and instability through cross section computation at time intervals
23 p4151 A69-41694

Impedance of inhomogeneous earth from magnetic and electric fields and geomagnetic potential measurements
23 p4157 A69-41867

Wideband vertical electric field noise reduction in ELF/VLF atmospheric receiving systems using bucking, delayed feedback and frequency rejection units
23 p4128 A69-42504

Transverse plasma waves propagating along parallel static electric and magnetic fields may lead to instabilities regardless of carriers sign
24 p4355 A69-42923

Sounding rocket measurements of electric and magnetic fields near auroral electrojet
24 p4310 A69-43188

ELECTRIC FILTERS
NT CRYSTAL FILTERS
NT DIGITAL FILTERS
NT IMAGE FILTERS
NT RADIO FILTERS
NT TRACKING FILTERS
NT WAVEGUIDE FILTERS

Active RC low pass filters sensitivity to component changes, discussing effect of below minimum limit value
04 p0578 A69-15070

Zero sensitivity integrated RC filter circuits design, exploiting capacitors and resistors property of having same temperature coefficient
08 p1300 A69-21174

Damping accuracy sensitivity to circuit element tolerances in polynomial filters
11 p1850 A69-24970

Transfer function parameters identification by fault isolation technique using white noise stimulus and processor matrix of orthogonal filters
11 p1865 A69-25077

Laser Doppler particle sensor to measure velocities in rocket exhausts, using He-Ne laser light source and Fabry-Perot interferometer frequency filter
[AIAA PAPER 68-723] 12 p2094 A69-26783

Distributed RC networks combined with lumped passive and active elements to produce distributed-lumped-active (DLA) networks for filter requirements
23 p4144 A69-41401

ELECTRIC FUSES
Exploding wire self healing fuse feasibility demonstrated with Hg, noting dynamics of conversion of electric to mechanical energy
01 p0120 A69-10677

ELECTRIC GENERATORS
NT AC GENERATORS
NT ALKALINE BATTERIES
NT DIRECT POWER GENERATORS
NT DRY CELLS
NT DYNAMOMETERS
NT FUEL CELLS
NT HYDROGEN OXYGEN FUEL CELLS
NT MAGNETOHYDRODYNAMIC GENERATORS
NT PHOTOELECTRIC GENERATORS
NT RADIOISOTOPE BATTERIES
NT REGENERATIVE FUEL CELLS
NT SNAP 10A
NT SNAP 13
NT SNAP 21
NT SNAP 27
NT SOLAR AUXILIARY POWER UNITS
NT SOLAR CELLS
NT SOLAR GENERATORS
NT THERMAL BATTERIES
NT THERMIONIC CONVERTERS
NT THERMOELECTRIC GENERATORS
NT TURBOGENERATORS

Gunn generator efficiency dependence on diode and regime parameters using computer model
01 p0042 A69-10319

Storm-Shattuck and push-pull tunnel diode DC-to-DC converters suitable for spacecraft power supplies
01 p0013 A69-10750

Hydrocarbon-air fuel cell producing electric power automatically for five days
01 p0013 A69-10965

Miniaturized X band IMPATT microstrip power sources based on Si avalanche transit time diodes integrated with microstrip oscillator circuits
02 p0216 A69-12146

Onboard electric power systems of transport aircraft, analyzing constant frequency systems for supersonic aircraft
02 p0196 A69-12166

Charge accumulation elimination on dielectric electrodynamic channel walls, comparing resistive wall channel to high internal impedance generator
02 p0291 A69-12506

High power sinusoidal pulsed current generator using Si controlled rectifiers /thyristors/ as switches
03 p0404 A69-13262

Transient stability of AC generator analyzed by Liapunov direct method, considering effects of flux decay, speed governor and voltage regulator
07 p1058 A69-18644

Caterpillar diesel electric sets for powering NASA tracking station in Australia during Apollo 8 flight
07 p1117 A69-19632

Sawtooth generators production based on equivalent circuit theory, calculating linearity errors in voltages
08 p1296 A69-20105

Electrical energy production on board space vehicles including solar batteries, chemical reagents and possible nuclear energy utilization
08 p1259 A69-21036

Electrochemical generators using zinc electrode in alkaline medium, noting weight consideration of zinc/air or zinc/oxygen cells
08 p1261 A69-21049

High energy-density electrochemical generators using lithium anode and copper sulfide cathode in nonaqueous media
08 p1261 A69-21056

Thermodynamic cycle and optimum conditions of electric power source of MHD generator in combination with thermocompressor
09 p1435 A69-21592

Power converter design for electrically propelled spacecraft, discussing weight, reliability, and thrustor load requirements
[AIAA PAPER 69-240] 09 p1568 A69-21732

Lumped element line generators for high power pulsed sinusoidal oscillations utilizing recurrent triggering system, noting use in plasma physics experiments
10 p1662 A69-23344

Electrical power requirements in spacecraft, discussing communication, engine and control systems, data processing, electrochemical and nuclear sources
12 p2015 A69-25863

Regulated voltage converter systems for onboard spacecraft electric power supplies, noting chopper circuits with rectifiers
12 p2015 A69-25867

Satellite and spacecraft power supply and power converters
13 p2209 A69-27917

Single phase bidirectional AC/DC power convertor based on back-to-back SCR hybrid bridge
13 p2209 A69-28178

Thermionic reactor design for electric propulsion with emphasis on reactor power and fuel energy and fast neutron flux
14 p2509 A69-29184

Thermionic electrical power generation from reentry plasmas with nose cone as emitter and vehicle afterbody as collector
14 p2399 A69-29194

Power conversion efficiency of frequency doubler using ideal nonlinear capacitance with arbitrary output phase angle
14 p2421 A69-29537

Power generating unit operating on air bearings
15 p2629 A69-31028

Aircraft generator weight in relation to system performance requirements, using digital computer to study generator design
17 p2904 A69-34087

Electric power quality effects on aircraft electronic utilization equipment, discussing characteristics of

variable speed constant frequency /VSCF/ generating system
17 p2905 A69-34091

Electric power system selection for long duration manned space station
[AIAA PAPER 68-1034] 22 p3869 A69-40549

Duty cycle IC generator for switching regulators, discussing construction, resistive and dielectric films fabrication, applications, etc
23 p4073 A69-42293

ELECTRIC IGNITION
Electrical devices for detonation initiation in pyrotechnic equipment for space applications, tabulating characteristics
10 p1749 A69-23006

Igniferous materials for electrical initiation of explosive in extreme conditions, considering nitrophenol salts and pyrotechnics
10 p1750 A69-23015

Soviet book on electric ignition systems for piston and jet engines and design aspects of different types of ignition systems
12 p2146 A69-26756

Inverse current in ignited mode diode linearly related to spacing, noting emitter sheath
14 p2401 A69-29230

AC ignitor priming of quartz-chlorine gas discharge X band waveguide limiter with fast recovery used as radar receiver protector
15 p2573 A69-30035

ELECTRIC MOMENTS
Benzene quadrupole moment estimates from second virial coefficient data with polarizability in intermolecular potential function and from molecular susceptibility anisotropy
01 p0124 A69-10687

ELECTRIC MOTORS
NT SYNCHRONOUS MOTORS
NT TORQUE MOTORS

Graetz-connection frequency converter and three phase shunt-connection commutatorless motor, noting speed control performed by electronic circuit
01 p0012 A69-10064

Magnetic core logic circuit system for bidirectional stepping motor drive voltage power supply control in proper phase and time sequence
01 p0047 A69-11000

DC servo system with torque feedback to ensure insensitivity to load variation and provide optimal performance
05 p0736 A69-15659

Motor design for operation in ultrahigh vacuum, discussing absence of convection cooling, outgassing avoidance, lubrication impossibility and oxygen absence as design parameters
08 p1377 A69-21028

DC/AC collectorless step electric motors operation and commutation circuits
09 p1442 A69-21860

Brushless DC motor with commutation control by magnetic position sensor scanned at HF
12 p2017 A69-26894

Hall generator DC brushless motors for aerospace use, discussing speed control and motor design
18 p3094 A69-35074

Advanced reaction wheel controller for spacecraft attitude control, discussing brushless DC motor role in weight and power reduction and control precision
[AIAA PAPER 69-855] 21 p3822 A69-39383

Tensor analysis of brushless DC motor controlled by transistors, discussing torque phase, torque variation phase and efficiency phase characteristics
24 p4255 A69-42678

ELECTRIC NETWORKS
Full multiplier design based on stable iterative array cells interconnected to provide logical functions, noting capabilities for binary numbers
01 p0048 A69-11138

Frequency controlled time delay network for broadband phased array antenna steering
04 p0580 A69-15469

Ultimate state periodic analysis of nonlinear electric systems by approximation methods in calculus of variations, discussing functional concept
09 p1474 A69-22448

Transmission line all pass equalizers theory and design for operation in TEM, TE or TM modes
13 p2233 A69-28065

State variables with delta functions for electrical network with discontinuously variable components, discussing application to parametron
19 p3287 A69-36763

- Distributed RC networks combined with lumped passive and active elements to produce distributed-lumped-active/DLA networks for filter requirements
23 p4144 A69-41401
- ELECTRIC POTENTIAL**
 NT BIOELECTRIC POTENTIAL
 NT CONTACT POTENTIALS
 NT COULOMB POTENTIAL
 NT LIENARD POTENTIAL
 NT LOW VOLTAGE
 NT PHOTOVOLTAGES
 NT SPIKE POTENTIALS
- Sensitivity of voltage transfer function relative to variation in value of components of resistance terminated reciprocal reactive network
01 p0049 A69-10069
- Amplifier with logarithmic transfer function noting use as null detector
01 p0038 A69-10075
- Capacitance-voltage relationships for PETN initiation by various diameter gold exploding bridgewires, noting optimum capacitance dependence on energy transfer efficiency
01 p0141 A69-10679
- Rarefied plasma flow interactions with conductors having cross sections equal to Debye radius, noting production of self consistent electrostatic potential
01 p0134 A69-11307
- Electric potential effects on heat transfer from plasma to solid wall, measuring heat input rates
02 p0290 A69-12423
- Electron flow in stable negative electrostatic potential well produced by electronic injection at center of hollow open spherical anode
03 p0475 A69-13153
- Electric potential for axisymmetric equilibrium electron density distribution, solving Poisson equation in closed form
03 p0476 A69-13159
- Potential energy functions based on electronegativities instead of spectroscopic parameters for Li and K molecules
03 p0472 A69-13805
- Electric potential distribution in coaxial quasi-stationary plasma injector
03 p0478 A69-13838
- Galvanostatic transients of iron passive in 2N sulfuric acid, noting space charge effects and zero field current variation
[ECS PAPER 84] 03 p0382 A69-13858
- Electrostatic potential generated by rockets on space vehicles, noting source of electric current in exhaust plumes and effect on instrumentation
03 p0522 A69-13903
- Potential distribution approximations for junction semiconductor devices, noting application to barrier layers and electron tunneling
03 p0408 A69-14107
- Advanced potentials method to determine electric field intensity tangential component on surface of cylindrical radiator
03 p0408 A69-14131
- Uniform external magnetic field effect on electric potential distribution within ion-electron beams near planar emitting surface
03 p0482 A69-14214
- Transient electro-osmosis of water in capillary tubes for pumping and generation modes, analyzing response to step change in pressure or voltage change under external loading
04 p0555 A69-14862
- Surface potential measurements for flat conductors or semiconductors using scanned electron beam probe
04 p0601 A69-15115
- Electric quadrupole parameters, discussing relationship between voltages at terminals
04 p0579 A69-15228
- N-type Si surface photopotential, conductivity and capacitance during anodic oxidation in absolute ethylene glycol
04 p0643 A69-15260
- Supply voltage limits for transistor amplifier circuit, examining processes during supply voltage variation
05 p0729 A69-16083
- Alkali metals thermoelectric power and energy dependence of Heine-Abarankov pseudopotential, taking into account anisotropy effects
05 p0809 A69-16507
- Gamma radiation effects on gate threshold voltages in modified oxide insulators in MOS structures
06 p0976 A69-16876
- Immobile space charge in MOS semiconductors as function of external voltage
06 p0979 A69-17153

Voltage divider network board composed of composite carbon resistors for measurement of terminal voltage of 3 Mev Dynamitron electron accelerator recalibration
06 p0907 A69-17705

Current-voltage characteristic of tunnel diodes, with curve approximation by even degree polynomials of voltage, discussing quasi-linear analysis
06 p0898 A69-17802

Voltage dependence of depletion layer width, maximum electric field and capacitance of Gaussian diffused plane, cylindrical and spherical p-n junctions
07 p1196 A69-18242

Potential barrier curvature influence in aluminum trioxide tunnel junctions, noting ionic space-charge effect on shape
07 p1196 A69-18243

Oxide impurity effects causing potential shifts in Si covered by thick oxide layer studied with metal-oxide-Si electrical measurement and radiochemical analysis
07 p1072 A69-18272

Forward transient response characteristics of high resistivity, long base, low lifetime p-n-n silicon diodes doped with Au, noting voltage oscillations
07 p1101 A69-18652

Direct method determination of pinch-off voltage in depletion mode FET
07 p1102 A69-18861

Potential effect on wetting of platinum electrodes in acid electrolytes noting drainage role
08 p1268 A69-20362

LF electric potential oscillation of discharge plasma, describing oscillation behavior by theory of dissipative drift instability of weakly ionized plasma
08 p1370 A69-21020

Fluctuation voltage mean square value at polar dielectric capacitor terminals determined by applying stochastic properties of Poisson point processes to statistical model
08 p1295 A69-21151

Electron irradiation effect on surface potential of thermally grown silicon dioxide layers, noting conductivity and annealing effects
09 p1557 A69-21743

Cathode material effects on temperature coefficients for glow discharge tubes, noting running voltage pressure characteristics
09 p1468 A69-22602

Specifying electrical isolation and error signals suppression due to presence of common mode voltage in passive signal handling and conditioning equipment
10 p1654 A69-23272

Spherical and rod-plate spark gap response voltage as function of sawtooth wave, cosmic, gamma and UV radiation
11 p1851 A69-25086

Si IMPATT diode current and voltage waveforms of oscillation, noting small signal theory inapplicability
12 p2036 A69-25914

Differential capacitance, diffusion voltage and exponent alpha of hyperabrupt junction varactor
12 p2039 A69-26375

Multielectrode plasma probe with potential negative with respect to plasma, noting effect of microoptical features of probe on accuracy of I-V measurements
12 p2138 A69-26538

Collector supply voltage and base width effects on transistor amplification and frequency characteristics at microampere currents
12 p2042 A69-26879

Voltage characteristics in MHD generator with water cooled segmented electrodes using potential probes, considering forced convection heat transfer
12 p2017 A69-27178

CdS acoustoelectric oscillator steady state oscillation frequency dependence on voltage and conductivity compared with linear acoustoelectric amplification theory
13 p2227 A69-27244

Uninsulated in-core thermionic reactor design permitting diode series connections to build output voltage
14 p2398 A69-29186

Linear analog computing elements realizing voltage transfer function with poles and zeros independently controlled, basing method on dummy variable technique
14 p2422 A69-29551

Current and electroluminescence brightness dependence on reverse voltage in n-SiC diodes including tunnel and avalanche processes
15 p2573 A69-30062

Complex load impedance determination by measuring maximum, minimum and load voltages in line, including error analysis
15 p2582 A69-30123

Three dimensional effects of potential minimum near cathode emitting axisymmetric beam, relating electric fields distribution to noise reduction coefficient
15 p2568 A69-30794

Solid electrolyte tantalum condensers reliability under repeated service voltage applications for calculating defective condenser probability
15 p2626 A69-30836

Flush electrostatic probe edge effect, considering Couette flow of weakly ionized compressible gas past discontinuous wall potential
15 p2653 A69-30912

Vibrational excess entropy in dilute solid solutions alloys calculated by changes in potential fields surrounding impurity atoms
16 p2798 A69-31706

Semiconductor impressed voltage preconditioning, considering problems involving surface properties
16 p2758 A69-31713

Hall effect and transverse voltages in type II superconductors in mixed state, considering cold rolled Nb-Zr alloys
16 p2827 A69-31827

Electron trap behavior on charged spacecraft, obtaining expressions for current to aperture and internal retarding electrodes for all apertures and spacecraft potentials
16 p2849 A69-31976

Radar control system based on load waveform monitoring by coupled control and modulating circuits
16 p2753 A69-32439

Stabilized DC to DC converter advantages in output voltage, overall dimensions and efficiency for battery driven mobile equipment
16 p2765 A69-32443

Surface state density determination as function of surface potential in MIS capacitors, discussing MIS capacitance method theory and computer programs
16 p2827 A69-32556

Electron heat transfer and spherical probe characteristics in moving nonequilibrium plasma analyzed at stagnation region as function of solid surface potential [AIAA PAPER 69-699]
17 p3011 A69-33475

Electrode potentials of pure metals, Ni-Cr and Ni base alloys in molten salts applied to corrosion studies
17 p2990 A69-33650

Bernoulli distribution and Monte Carlo method for electrical load analysis in designing electric power generation and distribution
17 p2905 A69-34090

Electrode potential measurements for corrosion study of metals and alloys in aqueous solutions, molten salts and gaseous atmospheres
18 p3150 A69-35412

IR detector limiting noise voltage /photon noise/ due to photon arrival fluctuations at responsive element determined using Planck radiation law
19 p3309 A69-36059

Current-voltage characteristics of umtron with metal-dielectric-semiconductor structure /MOSFET/ taking into account substrate potential effect
19 p3284 A69-36592

Multiple electrode probe characteristics in rarefied plasma flow created by ion source, noting electrode potential role
19 p3314 A69-36622

Electric models optimization for heat exchange systems based on mathematical similarity between equations describing temperature and electrical potential fields
19 p3256 A69-36717

Voltage variation frequency analysis for narrow-band sweep oscillators circuit design
20 p3486 A69-37010

Negative electric potential effect on deposition rate of Mo from molybdenum carbonyl and on deposit chemical composition during pyrolysis
20 p3559 A69-37016

Computerized design parameters for realizable over-driven bimode varactor frequency doubler based on charge-voltage relationship at break point
20 p3505 A69-37299

Josephson frequency-voltage relation at microwave and far IR frequencies compared, using radiation induced steps
20 p3583 A69-37418

Dielectric response of semiinfinite metal surface to external point charge in linearized Fermi-Thomas approximation, discussing potential in metal and vacuum
20 p3583 A69-37498

Metal insulator semiconductor volt-capacitance changes due to light flux, introducing surface recombination rate to improve model
20 p3585 A69-38273

- Steady state vertical distribution of small ions in ground layer assuming atmospheric dynamic and thermal sublayers, calculating air resistance and electric field potential
21 p3715 A69-38836
- Molecular hydrogen-CO fuel cells operation, studying internal voltage oscillations due to repeated electrode poisoning and reactivation
22 p3896 A69-40738
- Electric potential measuring device for frog isolated skeletal muscle fiber mounted on micromanipulator
23 p4111 A69-42058

ELECTRIC POWER

- VHF transistor power output capability, discussing limitation by RF saturation resistance and current crowding by large current densities and high frequencies
07 p1101 A69-18653
- MHD power plant research and development, discussing shock wave electric power generators and modulated systems
11 p1925 A69-24469
- Piston-like laminar liquid metal flow in MHD generator to increase thermodynamic efficiency of cycle and to generate electricity by synchronous principle
13 p2206 A69-27491
- Thermionic electrical power generation - Conference, Stresa, Italy, May 1968
14 p2394 A69-29172
- Scientific satellite 1 solar cell panels power output dependence on temperature and spin calculated and compared with results for outdoor sunlight
15 p2552 A69-30072
- Electric power quality effects on aircraft electronic utilization equipment, discussing characteristics of variable speed constant frequency /VSCF/ generating system
17 p2905 A69-34091
- Optimum power allocation for RF carrier phase error and synchronization error in two channel system
19 p3274 A69-36283
- Sealed Ni-Cd battery with bipolar construction to reduce internal resistance and increase power bursts capacity, emphasizing electrical characteristics and economic considerations
23 p4072 A69-42283

ELECTRIC POWER PLANTS

- NT NUCLEAR POWER PLANTS**
- Mission model construction for power limited systems, discussing flight concepts, propulsion mixes and electric propulsion
09 p1584 A69-21205
- Bernoulli distribution and Monte Carlo method for electrical load analysis in designing electric power generation and distribution
17 p2905 A69-34090
- Electrical power system synthesis for manned lunar base for surface explorations of increasing energy requirements and duration, discussing thermal control, reliability, etc
23 p4076 A69-42541

ELECTRIC POWER TRANSMISSION

- Surface structure effect on flux penetration and AC losses in superconductive niobium
02 p0298 A69-12031
- Electromagnetic radiation below 1 GHz from gap type electrical discharges on electric power distribution lines
23 p4126 A69-42218

ELECTRIC PROPULSION

- NT ELECTROMAGNETIC PROPULSION**
- NT ELECTROSTATIC PROPULSION**
- NT ION PROPULSION**
- NT PLASMA PROPULSION**
- NT RESISTOJET ENGINES**
- Book on electric propulsion systems for spacecraft covering thermoelectric, electromagnetic, electrostatic, plasmacore, thermonuclear and photon systems
02 p0305 A69-12233
- Electropropulsion by thruster using colloidal carbon particles charged by electron bombardment to provide thrust, noting specific impulse
03 p0495 A69-13396
- Electric propulsion for payload transfer from low to synchronous orbit of ELDO launch vehicles
03 p0496 A69-13994
- French research on electric propulsion dealing with plasma dynamics, discussing traveling wave accelerators, pulsed plasma guns, ion thrusters, etc
[AIAA PAPER 67-740] 03 p0496 A69-13995
- Electric space propulsion systems and auxiliary power sources development in West Germany, noting solar cells, isotope generators and reactors with conversion systems
03 p0496 A69-13996

- Electrical propulsion for space maneuvers, discussing interrelationship of orbital changes, payloads and time
06 p0998 A69-16858
- Multimission interplanetary probe using solar electric propulsion
06 p0984 A69-17593
- Advanced electrical and nuclear propulsion systems for European launchers, comparing performances with chemical propulsion
06 p0984 A69-17628
- Electric propulsion research in Japan, considering cesium ion thruster, plasma acceleration and thrust by electric explosion of fine wires
06 p0984 A69-17629
- Electric propulsion - AIAA Conference, William-sburg, March 1969
09 p1584 A69-21201
- Spacecraft electric propulsion parameters and launching vehicle characteristics in low thrust mission simulation, discussing spacecraft path
09 p1584 A69-21202
- Electric propulsion missions analysis for spacecraft design engineer, discussing out-of- ecliptic and Jupiter flyby probes
09 p1584 A69-21203
- Pre-design and mission analysis software capability for sizing, design, fabrication and developmental testing of flight hardware for electrically propelled interplanetary spacecraft
09 p1585 A69-21210
- Experimental program for tests to identify primary electric propulsion system integration problems and solutions, emphasizing design and initial testing
[AIAA PAPER 69-236] 09 p1560 A69-21213
- Pulsed MPD arc jet electric propulsion system requirements, examining physical constraints, pulse duration, duty cycle, power network structural details, etc
[AIAA PAPER 69-269] 09 p1560 A69-21215
- NASA program in electric propulsion, noting applications for spacecraft position control and for small automated interplanetary spacecraft
[AIAA PAPER 69-248] 09 p1561 A69-21216
- Cesium electron bombardment microthruster system, discussing ion engine, feed, discharge neutralizer, power conditioning and control electronics
[AIAA PAPER 69-293] 09 p1561 A69-21223
- Space charge sheath electric thruster principles, construction and performance using laboratory test model
[AIAA PAPER 69-282] 09 p1563 A69-21235
- British electric propulsion research, discussing electron bombardment ion engines, conical theta pinch and rail devices and test facilities
[AIAA PAPER 69-299] 09 p1564 A69-21241
- Advanced reconnaissance electric planetary spacecraft /AREPS/ concept for repeated coverage of Mars or Venus surface, using solar-photovoltaic system
[AIAA PAPER 69-253] 09 p1585 A69-21244
- Solar electric propulsion mission simplification by staging concept, discussing thrust combination, weight tradeoffs, design and Jupiter flyby probe
[AIAA PAPER 69-251] 09 p1586 A69-21245
- Liquid mercury cathode thrusters characteristics satisfying constraints imposed by solar flux variations with distance from sun
[AIAA PAPER 69-237] 09 p1565 A69-21246
- Ion thrusters and various microthrusters /electron bombardment ion and pulsed plasma/ for proposed European missions
[AIAA PAPER 69-274] 09 p1565 A69-21250
- NASA long range planning of primary electric propulsion for automated space program
[AIAA PAPER 69-247] 09 p1565 A69-21251
- Propellant condensation on surfaces near electric rocket exhaust, calculating particle arrival rates, backflow and desorption energies
[AIAA PAPER 69-270] 09 p1565 A69-21252
- Synchronous orbit attainment with continuous electric propulsion, noting payload ratio dependence on various parameters and changing orbit inclination
[AIAA PAPER 69-275] 09 p1586 A69-21265
- Scientific data acquisition and interpretation effects on electric spacecraft plasmas and field directions, noting electron interchange reactions effect
[AIAA PAPER 69-276] 09 p1568 A69-21727
- Spacecraft design, trajectory and mission analyses for multipurpose solar electric propulsion missions, emphasizing modular ion engine and fixed attitude spacecraft designs
[AIAA PAPER 69-252] 09 p1568 A69-21729
- Liquid mercury cathode electron bombardment thrusters applicability to electric propulsion missions
[AIAA PAPER 69-302] 09 p1569 A69-21876
- Electric propulsion design, considering effects of weight, impedance matching, beam voltage regulation

- and operating point variations in formulating system mass and reliability
[AIAA PAPER 69-254] 09 p1569 A69-21879
- Book on theory and design of jet, rocket, nuclear, ion and electric propulsion systems noting combustion, detonation, fluid injection and space mission applications
11 p1943 A69-25582
- Electric and ion propulsion with solar array or nuclear reactor energy sources, discussing thermal thrusters, electrostatic thrusters and plasma thrusters
11 p1944 A69-25592
- Electric propulsion systems characteristics, examining sputtering of metallic targets as thrust augmentor
11 p1944 A69-25598
- Thermionic reactor design for electric propulsion with emphasis on reactor power and fuel energy and fast neutron flux
14 p2509 A69-29184
- Electrically propelled TV satellite control maneuvers to reach target position in synchronous circular orbit from spiral ascent trajectory
16 p2868 A69-31935
- Electric propulsion, discussing plasma research, MPD thruster and arcs, ion thruster research and spacecraft integration
[AIAA PAPER 69-497] 16 p2838 A69-32655
- Solar electric propulsion system performance consisting of thrusters with thrust vector aligning actuators, switching network and flight type power conditioner
[AIAA PAPER 69-498] 16 p2843 A69-32708
- Solar and nuclear electric power technology for electric propulsion
[AIAA PAPER 69-826] 16 p2741 A69-32709
- Minimal electric propulsion systems for interplanetary spacecraft, discussing payload, reduced trip time and low thrust systems for Jupiter flyby
[AIAA PAPER 69-499] 16 p2844 A69-32714
- Charged colloids generation by electrostatic spraying for thruster concept, subjecting metal capillary needles to AC voltage
[AIAA PAPER 69-495] 16 p2846 A69-32773
- Electric propulsion systems for manned planetary exploration flights, discussing arc jet, ion and plasma engines
18 p3185 A69-35108
- Solar electric thrust system technology concerning performance, thruster control system stability and method for solution
19 p3394 A69-35941
- Soviet monograph on electrical rocket engines covering basics of nuclear, electrothermal, plasma and ion engines
20 p3586 A69-37236
- Trajectory requirements and performance comparisons of single stage electrically propelled space vehicles
[AAS PAPER 68-106] 21 p3819 A69-39204
- High voltage power supply electronic subsystem for electric propulsion of ATSD satellite, describing packaging, temperature control and performance in simulated space environment
22 p3999 A69-39948
- Spacecraft electric propulsion research in France, Great Britain and Germany
24 p4363 A69-42668

ELECTRIC PULSES

- Passive circuit to transform voltage of indefinitely repeated positive or negative pulses using transistors, diodes and magnetic cores
01 p0043 A69-10564
- High voltage controlled amplitude rectangular pulse generators having nanosecond buildup time
04 p0597 A69-14849
- Electric signals by shock and detonation waves, describing detection technique
[WSCJ PAPER 68-44] 07 p1240 A69-18360
- Failure mechanism in high-voltage semiconductor diodes explained by effect of reverse voltage pulses, considering design reliability
08 p1294 A69-21116
- Current controlled negative differential resistivity observed during current-voltage measurements made with p-type Te at 77 K
09 p1557 A69-21747
- Cesium ions decay time in thermionic converter operating in gas kinetic mode by pulse ionization, noting dependence on interelectrode potential distribution
14 p2403 A69-29252
- Plasma energy and energy replacement time dependent on discharge pulse shape and magnitude
14 p2499 A69-29848

Solid electrolyte tantalum condensers reliability under repeated service voltage applications for calculating defective condenser probability
15 p2626 A69-30836

Welding technique using pulsed current supply to achieve smooth metal transfer on thin sections in various positions
18 p3150 A69-35418

Pulses and sine waves coupling between parallel transmission lines obtained using Oliver elementary coupling theory
19 p3266 A69-35768

Stimulated emission at current pulse end ascribed to external resonator turn-on time delay effects with GaAs injection lasers at room temperature
21 p3734 A69-38408

Electric responses of anterior and posterior gyrus cinguli to stimuli of sciatic nerve in cats
22 p3886 A69-41175

Holographic storage of electric signals in wideband pulsed carrier radar communications, noting Fourier transform in ultrasonic light modulator
23 p4164 A69-41626

Luminescence, I-V and pulse characteristics of high resistivity Ni doped GaAs single crystals, noting injection conductivity
24 p4362 A69-43734

ELECTRIC RELAYS

Distance measurement by distance relay circuit composed of intermediate current transformers and rectifier bridges
05 p0765 A69-16746

Steady modes of operation analysis for optimal single channel differential relay system with inertial controlled plant, assuming constant rate varying plant input
12 p2052 A69-26278

Operational O factor of optimal differential relay system with inertial plant during tracking process, noting cadence pulses high repetition rate influence
12 p2052 A69-26279

Relay control systems limit cycle calculations, comparing classical differential equation, Laplace transformation and state and phase space analysis methods
13 p2238 A69-27396

Relays - Conference, Oklahoma State University, April 1969
13 p2230 A69-28042

Relay reliability cost vs failure cost in spacecraft applications
13 p2231 A69-28044

Electric relays reliability requirements, discussing specifications, minimum current, load and frequency effects, etc
13 p2231 A69-28045

Electric relays requirements for spacecraft with magnetic field constraints
13 p2231 A69-28046

Latching high-voltage reed relays in satellite instrumentation systems
13 p2231 A69-28047

Sealed and unsealed relay coils temperature rise at simulated outer space air pressure levels
13 p2231 A69-28048

Microminiature latching relay design and manufacturing cost
13 p2232 A69-28049

Optimal control with computer prediction for inertial linear plants relay system containing time lag
24 p4295 A69-43706

ELECTRIC ROCKET ENGINES

NT ARC JET ENGINES
NT CESIUM ENGINES
NT ELECTROSTATIC ENGINES
NT ELECTROTHERMAL ENGINES
NT ION ENGINES
NT PLASMA ENGINES
NT RESISTOJET ENGINES

SERT 2 thruster hollow cathode durability tested in bell jar
[AIAA PAPER 69-304] 09 p1562 A69-21224

Power converter design for electrically propelled spacecraft, discussing weight, reliability, and thruster load requirements
[AIAA PAPER 69-240] 09 p1568 A69-21732

Ion spacecraft propulsion systems, discussing components and characteristics of reaction type rocket engines and electrical thrust devices
11 p1944 A69-25593

Mercury electron bombardment thrusters, discussing mission, design, ground tests, components and thrust vectoring
12 p2148 A69-26787

Electric and chemical rocket propulsion systems
13 p2325 A69-28255

Liquid, solid, hybrid propellant and nuclear, electric and air breathing rocket engines, discussing orbiting payload cost, controllability, operating environments, velocity, etc
19 p3395 A69-36321

Soviet monograph on electrical rocket engines covering basics of nuclear, electrothermal, plasma and ion engines
20 p3586 A69-37236

ELECTRIC SPARKS

Exploding wire discharges similarity with underwater sparks for understanding water breakdown and parallel discharges
01 p0117 A69-10657

Sparks from laser induced arc breakdown due to focusing of laser beam, noting evidence for initiation by self focusing
01 p0092 A69-11246

Sparks four meters long in atmospheric air, noting image converter photographs, electrical measurements, light output, spectra and energy balance
02 p0281 A69-12406

Spark ignition of liquid fuel droplets atomized in air analyzed by spark discharge visualization for two phase mixture
09 p1623 A69-22220

Dwell time of sample particles in plasma excitation zone, noting effect on spectral analysis of sample materials injected into spark discharge plasma
11 p1926 A69-24624

Vacuum spark light source for extreme UV noting mechanical trigger, compatibility with clean vacuum system and magnetic confinement of ions
11 p1885 A69-24839

Photoelectronic high speed image intensifier framing camera, showing single shot synchronized photography of electric spark in air
12 p2082 A69-26137

Nanosecond time variations in current-voltage characteristics of gas discharge in air, taking into account discharge circuit resistance and discharge space capacitance
12 p2137 A69-26534

Statistical analysis of operation of precision electric spark machine servosystems with RC generator based on working pulse peak voltage distribution
23 p4168 A69-41307

Automation of single pass electric spark machining of high alloy steels and hard alloys, including anodic-mechanical profiling, cutting and drilling
23 p4168 A69-41308

ELECTRIC STIMULI

Response rates of rats to periodic shocking for food reinforcement with added clock cue stimuli
10 p1644 A69-23304

Penile erection electrically evoked from Macaca mulatta forebrain, measuring density and distribution of responding points
12 p2018 A69-25775

Ventral posterolateral potentials in anesthetized immobilized cats in response to electric stimulation of mesenteric nerves and mechanoreceptors, studying thalamus nucleus role
12 p2020 A69-26562

Electrode stimulated hypothalamic drinking in rats compared with drinking induced by water deprivation, noting difference in consumption
17 p2910 A69-33750

Lateral hypothalamic stimulation bound eating motivation in animals, comparing electrical stimulation and hunger elicited eating
17 p2910 A69-33752

Electrical stimulation effect on drive specificity in lateral hypothalamus area of satiated rat, suggesting fallacy in previous conclusion concerning appetite
22 p3876 A69-40269

Anesthetized cats with electrodes in visual cerebral cortex, investigating stimulation of conditioned alimentary reflexes in response to light signals by electric signals
22 p3885 A69-41066

Functional relation between primary response in individual phases and neurons activity in cats cerebral cortex
22 p3886 A69-41067

Mapping of biological potentials evoked in primary somatosensory fields by electrical signals on dorso-lateral surface of brain cortex of cats
22 p3886 A69-41121

Electrical self stimulation adaptability of hypothalamus or instrumental self reinforcing reaction in rats using skinner box technique
23 p4091 A69-42052

Self rhythms of low audio frequencies in motor nerves under electric pulses influence at VLF related to viscosity changes of nerve substance
23 p4092 A69-42051

Sinusoidal pressure electric stimuli frequency effects in isolated carotid sinus on canine peripheral blood pressure, determining dynamic characteristics from observation data
23 p4092 A69-42051

Electrical stimulation effects of carotid sinus on sinoatrial and atrioventricular conduction for vagi and sympathetic nerves interruption to heart in dogs
24 p4257 A69-42625

ELECTRIC STRAIN GAGES

U STRAIN GAGES

ELECTRIC SWITCHES
NT CRYOTRONS
NT THERMOSTATS

Fast reversible switching between highly resistive and conductive states in various disordered semiconductor devices, using electric field
01 p0140 A69-11246

High power sinusoidal pulsed current generated using Si controlled rectifiers/thyristors/as switches
03 p0404 A69-13266

Hollow charge pyrotechnic circuit closer, noting on piece construction, transportability, safety, quick action and reproducible delay
10 p1635 A69-23033

Pyrotechnic circuit closer using jet to achieve conduction between hollow charge lining and coaxial electrode
10 p1635 A69-23033

Gallium arsenide Fe-doped diodes efficiency as high speed switches from measured current-voltage characteristics at various temperatures
13 p2319 A69-27899

Latching high-voltage reed relays in satellite instrumentation systems
13 p2231 A69-28044

ELECTRIC TERMINALS

Signal detection by four terminal receiver network optimal for background Gaussian noise
04 p0557 A69-14774

Flat cable terminating techniques for electric and electronic systems
04 p0578 A69-15217

Electric quadrupole parameters, discussing relationship between voltages at terminals
04 p0579 A69-15223

Coupled and uncoupled terminals series connection for reactive multiport network determined by transforming scattering matrix columns into coordinate vectors
07 p1100 A69-18522

Equivalent circuit synthesis with six reactances-two terminal network bridges
08 p1295 A69-21166

Computer program for generation of test patterns for multiterminal devices and networks
21 p3679 A69-39604

ELECTRIC WELDING

NT ARC WELDING
NT ELECTRON BEAM WELDING
NT ELECTROSLAG WELDING
NT GAS TUNGSTEN ARC WELDING
NT PLASMA ARC WELDING

Resistance welding monitoring systems including thermal expansion slow scan ultrasonic and electric energy monitor/limiter systems
02 p0253 A69-11866

Welding technique using pulsed current supply to achieve smooth metal transfer on thin sections in various positions
18 p3150 A69-35418

ELECTRIC WIRE

NT EXPLODING WIRES

Stability of compound superconducting cables under conditions of controlled heat transfer from cable surface to liquid He
[IEEE PAPER 13.5] 01 p0176 A69-10711

Very thin short metallic filament scattering and absorption cross sections for various values of filament conductivity
03 p0395 A69-13622

Mini trend hookup copper wire insulation performance evaluation
05 p0730 A69-16244

Flat conductor cable technology, discussing design manufacture, specifications, etc
[ASME PAPER 69-DE-8] 14 p2393 A69-28855

Pulsed ruby lasers for welding fine wires for electrical interconnections, considering laser energy and pulse duration effects
15 p2617 A69-30099

- Solid rocket motor ignition system based on exothermic alloying of bimetallic wire constituents [AIAA PAPER 69-425] 16 p2832 A69-32653
- Radiated interference and susceptibility prediction for unshielded wires in near field of vertical rod antenna 23 p4141 A69-42225
- Stability criteria for electrical interconnection in parallel operating valve controlled hydraulic servomotors applied to gimbaled system 24 p4256 A69-43310
- ELECTRIC WIRING**
U WIRING
- ELECTRICAL CONDUCTIVITY METERS**
Electrical conductivity standards and eddy current measurements noting calibration facility 01 p0081 A69-10830
- Laboratory atmospheric electrical conductivity meter, discussing structural elements 04 p0600 A69-15106
- ELECTRICAL ENERGY**
U ELECTRIC POWER
- ELECTRICAL FAULTS**
NT SHORT CIRCUITS
- Planar transistor micromode operation during collector junction avalanche breakdown 01 p0047 A69-10884
- Many valley n-type Ge and Si semiconductors dissipative current breakdown effects, noting dependence on symmetry of valleys and phonon scattering pattern 02 p0298 A69-12098
- RF voltage breakdown in solid state telemetry transmitters on sounding rocket, noting glow discharge initiated by energetic dissociated electrons 02 p0222 A69-12691
- Tunnel breakdown in p-n junctions used to generate microwave oscillations, discussing Si and Ge properties 03 p0492 A69-14163
- Conductivity in p-n junctions during avalanche breakdown at HF calculated, noting agreement with experiments 03 p0492 A69-14164
- Schottky barrier mixer diodes and point contact diodes failure, discussing criterion for degradation of noise figure, 1/f noise and reverse breakdown voltage 04 p0574 A69-14352
- P-n junction breakdown, discussing local regions of overheating and increased current density, differential resistance frequency dependence and breakdown region temperature 04 p0577 A69-14782
- Corona and breakdown voltage in helium-oxygen atmospheres, analyzing conditions for manned space flight vehicles 05 p0730 A69-16241
- Controlled factorial experiments on high voltage vacuum breakdown, using Yates algorithm analysis on computer 05 p0731 A69-16244
- Supersonic airplane high temperature wire tests, detecting corona onset voltage /COV/ or voltage breakdown 05 p0731 A69-16245
- Peripheral surface damage effects on epitaxial GaAs bulk diodes breakdown characteristics, noting measurements on mechanically and chemically prepared elements 05 p0733 A69-16561
- Threshold failure levels of semiconductor diodes and transistors due to pulse voltages 06 p0977 A69-16883
- Requirements for analysis and synthesis of diagnostic tests for detecting faults in combinational logic circuit 06 p0892 A69-17408
- Electric field growth directional effect on avalanche breakdown conditions in p-n junctions 06 p0981 A69-17828
- Destructive breakdown in Schottky barrier diodes by evaporating contact metal through mask onto silicon, showing local heating by thin wax layer 08 p1286 A69-20860
- Synthetic circuit equipment for semiconductor rectifier life testing with built-in fault analyzer for indicating shorted and broken diodes 08 p1293 A69-21113
- Second breakdown in semiconductors, studying thermal feedback connected with temperature time dependence of junction electrical properties 08 p1294 A69-21115
- Failure mechanism in high-voltage semiconductor diodes explained by effect of reverse voltage pulses, considering design reliability 08 p1294 A69-21116
- Failure mechanisms in semiconductors, discussing imperfections, fabrication errors and electrical, thermal and mechanical stresses 08 p1294 A69-21117
- Second breakdown mechanisms in transistors, describing electrical and physical characteristics and effects of design and structural defects on resistance to initiation 08 p1294 A69-21120
- Gas breakdown model for analyzing breakdown of Ce vapor filled crack in thermionic trilayer insulator 09 p1441 A69-21840
- RF voltage breakdown in air for 50 ohm coaxial transmission line configuration [JPL-TR-32-1379] 09 p1470 A69-22790
- Breakdown voltage and avalanche drift instability factors in planar passivated p-n junctions as function of oxide thickness and mobile charge 10 p1743 A69-23174
- Transfer function parameters identification by fault isolation technique using white noise stimulus and processor matrix of orthogonal filters 11 p1865 A69-25077
- Plasma physics of electric arc transition from conducting plasma to insulating gas in electric circuit interruption, noting interrupter interaction with power system 12 p2133 A69-25905
- Electrical breakdown between cold electrodes in contact with flowing plasma produced by electromagnetic shock tube 12 p2134 A69-26098
- Computer programs for linear systems fault isolation, discussing technique theory and limitations 12 p2040 A69-26568
- Planar transistor micromode operation during collector junction avalanche breakdown 12 p2041 A69-26648
- Electrical breakdown mechanism in semiconductors determined by measuring Zener current in avalanche breakdown 13 p2317 A69-27660
- Dielectric constant, loss and breakdown of electrical insulation materials, discussing atomic and molecular models and effects of polarizations, environment and manufacturing procedures 13 p2230 A69-27983
- Prebreakdown and breakdown electrical properties of thin film capacitors with certain oxides, fluorides and Teflon dielectrics 13 p2322 A69-28012
- Electrical breakdown voltage and voltage-current characteristics of uncooled coplanar carbon electrodes in walls of supersonic conical and rectangular nozzles [AIAA PAPER 68-713] 13 p2249 A69-28231
- Optical maser induced electrical breakdown interaction with superhigh pressure ionized gases, using optical interferometry and holography 13 p2273 A69-28464
- Thermionic converters with matrix circuit connections, considering current flow patterns in matrices to evaluate electrical failure spreading 14 p2400 A69-29225
- Oscillation breakdown of varactor diodes in parametric amplifiers from studying I-V characteristics, noting resonant circuit retuning effect 15 p2574 A69-30127
- Tubes faults monitoring in three phase Graetz converter bridges by measuring voltage across DC smoothing inductor 15 p2575 A69-30180
- Third generation computer reliability including preparation and test of integrated logic circuits 15 p2626 A69-30832
- Solid electrolyte tantalum condensers reliability under repeated service voltage applications for calculating defective condenser probability 15 p2626 A69-30836
- Arbitrary single gate failures diagnosis in combinational logic circuits not requiring fault table construction 15 p2583 A69-31112
- Second breakdown and other thermal instabilities analyzed by heat flow equation, obtaining stability criteria predicting reduced power dissipation for transistor at low currents 16 p2758 A69-31618
- Prebreakdown and breakdown electrical properties and light emission during destructive breakdown in thin film capacitors 16 p2761 A69-32323
- InSb instabilities and time dependence of transverse breakdown, performing Hall effect measurements on n-type InSb at 77 K 19 p3389 A69-36546
- Electrical failures in aircraft due to static electrification of electrically heated windscreens, noting materials for reducing surface resistivity 19 p3256 A69-36769
- Gunn oscillators protection from catastrophic breakdown phenomena, using carrier velocity saturation in n-type Ge 21 p3682 A69-38777
- MOS arrays failure mechanisms, discussing oxide defects, contamination and metal migration due to mode of operation and fabrication techniques 21 p3684 A69-39605
- Hybrid microelectronic circuit failure mechanisms for thick and thin film resistors, conductors and capacitors, noting packaging contributions 22 p3910 A69-39954
- Digital data systems fault detection and isolation, describing diagnostic programs and hardware [AIAA PAPER 69-967] 22 p3906 A69-40348
- RF voltage breakdown facility for studying spacecraft antenna characteristics in space and planetary atmosphere environments [AIAA PAPER 69-1028] 22 p3924 A69-40397
- Gas velocity and pressure influence on electrical breakdown potential of Ar, N and He between parallel flat plate and concentric electrodes 24 p4359 A69-43693
- Anisotropic carrier distribution effect on polarization of spontaneous recombination radiation during GaAs breakdown in electric field 24 p4362 A69-43736
- ELECTRICAL IMPEDANCE**
NT CONTACT RESISTANCE
NT LC CIRCUITS
NT REACTANCE
- Modified admittance yielding Kubo admittance at nonzero frequencies, discussing transformation of correlations of Ising model 01 p0115 A69-10019
- Transistorized feedback amplifier for data transmission over high voltage lines in conveyed wave systems 01 p0038 A69-10074
- Small signal impedance of subcritically doped gallium arsenide Gunn diodes, using drift velocity vs electric field relationship 01 p0038 A69-10121
- Multistub filter for microstripline using shorted and open stubs 01 p0041 A69-10200
- Planar arrays of linear antennas above stratified medium, showing antenna impedance and current distribution expressed in terms of free space environment 01 p0042 A69-10343
- Fourier transformation method for current distribution and driving point admittance of coupled antennas in dissipative medium 02 p0215 A69-11946
- Reflection of plane electromagnetic wave from impedance cylinder in vacuum, using ray expansion method 02 p0217 A69-12262
- Admittance of parallel plate waveguide aperture with infinite flange illuminating metal sheet, using wedge diffraction theory and integral transform method 02 p0218 A69-12328
- C and S band waveguide impedance measurements taken in flight in reentry plasma, noting results for plasma 02 p0218 A69-12333
- End correction for input admittance of electrically thick monopole antenna with arbitrary radius driven from coaxial line 02 p0219 A69-12346
- Linear transistor models synthesis based on measured characteristics of four terminal admittance parameters 03 p0404 A69-13596
- Active and reactive impedance components of plane capacitor immersed in plasma and at LF noting dependence on plasma conductivity 03 p0477 A69-13713
- Electrodeless conductivity probe impedance in anisotropic plasma computed on basis of Maxwell equation 03 p0483 A69-14252
- Driving point admittance of radiating aperture in infinite periodic planar phased array, determining coefficients of waveguide modal expansion and Floquet series 04 p0571 A69-14315
- Surface impedance variation effect on surface wave propagation along rod waveguide 04 p0576 A69-14761

Input impedance of slot antenna in primary resonance region
04 p0577 A69-14784

Corrugated impedance antennas synthesized, using model in impedance surface form
04 p0577 A69-14786

Input admittance of cylindrical dipole antenna immersed in cold isotropic lossless plasma medium and insulated by ion sheath or unit permittivity dielectric
04 p0580 A69-15490

Equivalent circuit diagrams for impedance of plasma column in low current low pressure glow discharge
05 p0800 A69-15742

Input admittance of confocal Fabry-Perot resonator, with waveguide coupled infinitely long conic-section cylindrical reflectors, taking into account diffraction and resistive losses
05 p0731 A69-16295

Admittance between terminals measured for stabilizing single loop negative feedback transistor amplifier
05 p0739 A69-16341

Composite equivalent circuits method for complex waveguide-resonator couplings based on variational principle for admittance matrices of electromagnetic volume couplings
05 p0736 A69-16785

Solar flares, discussing transformation of magnetic energy into ion and electron kinetic energy by acceleration in high impedance region in current filaments
06 p0995 A69-17445

Residue contributions to integrals associated with admittance of plasma or dielectric covered circular aperture antenna used to calculate surface wave contribution to waveguides
06 p0896 A69-17477

Characteristic impedance of rectangular waveguide computation curve explained on basis of computer program for cascade of transmission line sections
06 p0897 A69-17490

Numerical values for cylindrical antenna admittance in uniaxial plasma, considering plasma compressibility and vacuum sheath
06 p0965 A69-17513

Plasma impedance effect on time variation of inverse pinch
06 p0967 A69-17716

Circular antenna array consisting of identical centered cylindrical dipoles placed tangential to and in plane of circle and with equal spacing
06 p0898 A69-17765

External impedance controlled nucleation of Gunn effect domains studied theoretically by Nyquist criterion
06 p0981 A69-18217

Electrical impedance of semiconductor supporting two waves contains entire complex transcendental function with complex parameter and infinity of zeros in left half z plane
07 p1196 A69-18268

Frequency dependence of input impedance of voltage controlled bootstrap amplifier stages
07 p1090 A69-18294

IMPATT diode microwave oscillator, discussing large signal characterization and model for efficiency dependence on load conductance and admittance plane characteristics
07 p1101 A69-18650

Antenna impedances in cold plasma with perpendicular static magnetic field
08 p1281 A69-20029

Cylindrical antenna input impedance in isotropic plasma, assuming weak three dimensional plasma diffusion
08 p1285 A69-20428

Converging solutions for imaginary admittance and current distribution in linear cylindrical antennas
08 p1295 A69-21165

Noise factor of two port in terms of various sets of noise parameters and source immittances, giving table for conversion formulas
09 p1455 A69-21897

Complex admittances and impedances of various networks determined by impedance bridge, describing frequency dependent limits of measurement parameters
09 p1501 A69-22578

Micromin alumina substrates design data, determining dielectric constant, impedance vs line width and wavelength vs frequency
09 p1460 A69-22792

Electromagnetic wave propagation over constant impedance flat earth, using electromagnetic compensation theorem
10 p1655 A69-23422

Current distribution and impedance of insulated cylindrical antenna embedded in dielectric cylinder immersed in compressible electron plasma
10 p1663 A69-23423

High gain proportional and bistable fluidic amplifier design, noting high impedance role in pressure sensing and computer circuits in aircraft engine control
10 p1638 A69-23555

Coupling coefficient and impedance for excitation of isotropic plasma column by ring of magnetic current outside plasma, noting surface wave resonance effect
10 p1659 A69-24064

Input admittance response characteristics and input susceptance and input conductance of resonant reactive modulator with varactors and nonlinear losses
10 p1665 A69-24066

Rectangular RC distributed circuits with shaped electrodes, analyzing short circuit admittance parameters
11 p1858 A69-24938

Load admittance effect on low pass voltage transfer characteristics of RC lines, analyzing shaped lines at open circuit under terminated conditions
11 p1859 A69-24939

Air gap tolerances effect on admittance of TEM mode dielectric and plasma coated slot antennas determined by variational method
11 p1851 A69-24986

Induced EMF method for calculation of antenna impedance, discussing effects of approximations in calculation
11 p1851 A69-24997

Electromagnetic scattering from thin wire loops under various impedance loadings, considering positive and negative resistors effect combined with reactive networks
11 p1837 A69-25000

Resonant load impedance effects on Gunn diode oscillators output fluctuations, noting maximum power conditions
11 p1853 A69-25609

RF measurement techniques and interpretation of bonding impedance characteristics through VHF region
12 p2040 A69-26472

Power spectral analysis feasibility for data reduction for medical interpretation of changes in pulmonary impedance pneumograph in remote monitoring
12 p2024 A69-26558

Dielectric coated finite cylindrical antennas, using numerical and Wiener-Hopf methods to obtain input admittance and current distribution
12 p2041 A69-26604

Horseshoe electromagnet sensors above ferromagnetic plate, analyzing electromagnetic properties of plate and coil impedance
12 p2094 A69-26719

Steady state small signal input impedance of low power planar transistor as function of temperature and operation mode
12 p2042 A69-26878

Input impedance of quarter wavelength antenna in anisotropic plasma, discussing plasma parameters role and use of probe antenna in plasma diagnostics
12 p2044 A69-27071

High resistivity GaAs impedance with nonlinear I-V characteristics, showing appreciable reactive component
13 p2317 A69-27881

Low resistance Bi thin film complex electrical impedance in IR range, stating methods and equivalent circuits for determining impedance
13 p2322 A69-28011

Synthesis for asymmetrical branch guide directional coupler-impedance transformers, noting application in antenna design
13 p2233 A69-28069

Characteristic impedance determination for transmission lines cascades terminated by resistor using recurrent relations, discussing reflection coefficient
13 p2221 A69-28074

Admittance of radiating elements in circular array with longitudinal slots on conducting cylinder, taking into account element interactions
13 p2234 A69-28505

Radiation pattern of electric and magnetic dipole on flat semiinfinite impedance system edge found similar
13 p2236 A69-28546

Surface impedance of spherical earth isolated by nonconducting atmosphere from ionospheric currents producing alternating electromagnetic field
14 p2438 A69-29082

Transistors transfer admittances measured indirectly, evaluating mean square error for transfer parameters
14 p2420 A69-29396

Impedance eigenvalues for eigenmodes of multiconductor transmission lines, discussing transverse field distributions along conical line
14 p2423 A69-29756

Complex load impedance determination by measuring maximum, minimum and load voltages in line, including error analysis
15 p2582 A69-30123

Frequency effects on Gunn oscillator modulation sensitivity, discussing microwave-frequency deviation and diode impedance
15 p2577 A69-30614

Plane electromagnetic wave propagation normal and parallel to magnetic field in plasma analyzed by equivalent circuits and impedances
15 p2659 A69-30799

Approximate solution for coupled microstrip transmission lines in integrated circuits, discussing impedance, capacitance and testing
15 p2580 A69-31078

Linearly tapered transmission line equation and transfer matrix parameters, considering input impedances and microwave application
16 p2749 A69-31582

Diffraction of electromagnetic waves produced by vertical dipole on impedance sphere of large radius in isotropic medium, using moment method
16 p2751 A69-32028

Warm plasma probe, describing transit electrons interaction with electric field and generation of electroacoustic waves radiation
16 p2824 A69-32611

Thin metal antenna average current and effective impedance in randomly inhomogeneous medium, discussing cases of strong and weak permittivity fluctuations
17 p2927 A69-33858

Driving point admittance of radiating aperture in infinite periodic phased array, determining Floquet series and coefficients of waveguide modal expansion
17 p2938 A69-33876

Plane screen electrical shielding effectiveness calculation, using incident wave impedances associated with current loop and magnetic dipoles in transmission line equations
19 p3267 A69-35932

Current distribution and input impedance of cylindrical antenna enclosed in uniaxial crystal and oriented along optical axis from thin antenna theory
19 p3285 A69-36878

Active admittance, realized gain and linear polarization degradation vs scan angle for infinite periodic phased arrays of circular apertures
20 p3507 A69-37844

Admittance of infinite cylindrical antennas driven from coaxial line
20 p3507 A69-37846

Multiplexer network synthesis based on arbitrary divisibility of frequency range and obtainability of input impedance at all frequencies
21 p3681 A69-38530

Mutual impedances of radiators in periodic and doubly periodic rod antenna arrays with orthogonal harmonics current distribution, noting diffraction theory applications
21 p3682 A69-39126

High resistivity GaAs impedance with nonlinear I-V characteristics, showing appreciable reactive component
21 p3782 A69-39143

VHF cavity backed cylindrical gap antenna input tuning impedance and equatorial radiation patterns controlled by cavity adjustments
22 p3914 A69-40698

Radiation and impedance characteristics of spherically capped conical and monopole antennas protruding from spherical vehicle related to cone height, angle and vehicle diameter
22 p3908 A69-40699

Waveguide fed rectangular aperture antenna with dielectric plug load, describing admittance resonant perturbation due to excited TE mode
23 p4136 A69-41589

Impedance of inhomogeneous earth from magnetic and electric fields and geomagnetic potential measurements
23 p4157 A69-41867

Decoupling structures, deriving expressions for infinitely long grooves self and mutual impedance
23 p4138 A69-41938

Solid cylindrical antenna current and admittance calculation, considering reflection coefficient and multiple reflection phenomena at antenna ends
23 p4142 A69-42336

S-band pin-diode switch for high CW power satellite and deep space probe communication, using multiple quarter-wave transformers to stepdown diode impedance
23 p4143 A69-42518

Small signal amplitude/frequency response or transfer gain of volume-terminated pneumatic lines with circular and rectangular cross sections
24 p4301 A69-43288

ELECTRICAL INSULATION

Input admittance of cylindrical dipole antenna immersed in cold isotropic lossless plasma medium and insulated by ion sheath or unit permittivity dielectric
04 p0580 A69-15490

Electrical insulation - IEEE Conference, Los Angeles, December 1968
05 p0730 A69-16240

Mini trend hookup copper wire insulation performance evaluation
05 p0730 A69-16242

Solid insulator performance in vacuum, analyzing breakdown factors
05 p0731 A69-16243

Controlled factorial experiments on high voltage vacuum breakdown, using Yates algorithm analysis on computer
05 p0731 A69-16244

Design and tests of cable assemblies for F-111 aircraft
05 p0731 A69-16246

Insulated gate tetrode with high drain breakdown potential and low Miller feedback capacitance, noting V-I characteristics
05 p0733 A69-16556

Steady rotation of insulating body of revolution in unbounded electrically conducting fluid permeated by applied axial magnetic field
07 p1190 A69-18814

Power losses in MHD channel due to longitudinal end effects related to finite dimensions of electrodes and terminal insulators
07 p1193 A69-19030

Aircraft radomes lightning protection, discussing evaluation by experimental methods and simulation
07 p1142 A69-19535

Electroexplosive devices protection by nonconducting composition against premature ignition by RFI in spacecraft environment, noting Apollo Standard Initiators
10 p1751 A69-23018

Supplementary bibliography of papers on metal insulator semiconductor theory and technology
10 p1743 A69-23169

Specifying electrical isolation and error signals suppression due to presence of common mode voltage in passive signal handling and conditioning equipment
10 p1654 A69-23272

TWT heat pipe cooled depressed collector designed as compact heat transfer device and electrical insulator
11 p1847 A69-24746

Plastics for electrical insulation - Conference, New York, January 1967
13 p2285 A69-27982

Dielectric constant, loss and breakdown of electrical insulation materials, discussing atomic and molecular models and effects of polarizations, environment and manufacturing procedures
13 p2230 A69-27983

Dielectric properties measurement of plastics for electrical insulation, stressing techniques for complex dielectric constants in various frequency ranges
13 p2285 A69-27984

Polymeric insulation materials, discussing intrinsic properties dependence on temperature and atmosphere, stressing effect on aging
13 p2285 A69-27985

Polymer structure relationship to thermal, mechanical and chemical properties of electrical insulating materials
13 p2285 A69-27986

Fabrication techniques for plastic insulation in electronics, discussing packaging, low pressure molding, casting, etc
13 p2285 A69-27987

Heat resistant polyamides and polyimides for electrical insulation, discussing properties and applications under extreme temperatures and basic reactions
13 p2286 A69-27988

Fiber polymer composite flexible insulating materials properties and applications stressing synthetic organic fibers
13 p2286 A69-27989

Silicone polymers and polymer formations for electrical applications including silicones for molded devices and components, potting resins, dielectric gel, RTV rubbers, etc
13 p2286 A69-27990

Uninsulated in-core thermionic reactor design permitting diode series connections to build output voltage
14 p2398 A69-29186

Ceramic and cermet materials insulating, physical and mechanical properties for use in thermionic converters
14 p2467 A69-29214

Harmonic analysis for computing diffusing matter with periodically varying surface concentration applied to electrical insulants degradation by atmospheric moisture
15 p2592 A69-31057

MHD flow of incompressible viscous fluid between rotating electrical insulator disks
24 p4354 A69-42599

ELECTRICAL LEADS
U ELECTRIC CONDUCTORS

ELECTRICAL MEASUREMENT
NT POLAROGRAPHY

Amplifier with logarithmic transfer function noting use as null detector
01 p0038 A69-10075

Time dependent functions integration by glow discharge tube and oscillator, discussing device for voltage measurement and applications in meteorology and geophysics
02 p0251 A69-12773

Surface potential measurements for flat conductors or semiconductors using scanned electron beam probe
04 p0601 A69-15115

Differential thermistor gauge using Wheatstone bridge for use in free molecule pressure probe measurement of macroscopic velocity in rarefied gases
04 p0601 A69-15117

Cathode emission site analysis by measuring prebreakdown current under ultrahigh vacuum conditions
05 p0800 A69-15740

Simultaneous and independent measurement of thermal conductivity, thermoelectric power and electric resistivity, applying method to cadmium arsenide-zinc arsenide system
05 p0764 A69-16338

Si transistor I sub CE sub 0 characteristics measurement on curve tracer, discussing generation of loop by junction capacitances and emitter base diode
05 p0734 A69-16569

Voltage divider network board composed of composite carbon resistors for measurement of terminal voltage of 3 Mev Dynamitron electron accelerator recalibration
06 p0907 A69-17705

Direct method determination of pinch-off voltage in depletion mode FET
07 p1102 A69-18861

GP zones study in aluminum alloys during fatigue process by electrical measurement, discussing resistivity, cyclic deformation, loading and unloading
07 p1166 A69-18962

Temperature effect on phase stability and electrical length of braided coaxial cables, considering dielectric constant and mechanical length
08 p1283 A69-20225

Segmented anode current and heat distribution in MPD engine measured with current shunts and calorimetric methods
[AIAA PAPER 69-244] 09 p1566 A69-21260

Moderately ionized plasma electrical conductivity calculated by generalized Ohm law and measured along with other plasma properties
[AIAA PAPER 69-277] 09 p1543 A69-21264

High time resolution electrical conductivity measurement of ionized plasma gas flow, using changes in Q of circuit
09 p1546 A69-21585

DC electrical resistance of magnetosphere between two satellites with sheaths and current voltage relation of satellite sheath
09 p1489 A69-21710

Electrical testing of six converter solar energy thermionic generator, discussing overheating and dual current mode anomalies
09 p1439 A69-21823

Y-circulators specified, measured and calculated values correlated as function of leakage matrix elements and terminating dipoles reflection
09 p1473 A69-22114

Capacitance methods for measuring adhesives mechanical properties in thin film bonded joints, noting results for tension, compression and shear loading
09 p1500 A69-22309

Current-voltage characteristics of combustion driven shock tube generated argon plasma
10 p1737 A69-23466

Voltage drop measurement across plasma anodized germanium film to determine anodization constant
10 p1742 A69-24004

Solar cell equation series resistance and junction recombination parameters determination, considering I-V characteristics
11 p1826 A69-25395

Mismatch correction in microwave power measurements based on directional coupler techniques
12 p2038 A69-26055

Electrical conductivity measurements combined with indentation hardness measurements for non-destructive evaluation of commercial precipitation hardenable aluminum alloys
12 p2114 A69-26307

Photoconductor open circuit voltage determination, calculating responsivity and sensitivity of actual and ideal cases
12 p2093 A69-26481

Barrier capacitance measurement in mm wavelength parametric and multiplication diodes eliminating socket capacitance influence, describing oscilloscope and indicator methods
12 p2043 A69-26885

Field distribution in HF flame discharges by measuring electrical and geometrical parameters of discharge channel
12 p2140 A69-27128

Electrical properties of p-type indium antimonide, noting effects of deep level compensation on ev values
13 p2318 A69-27895

Dielectric properties measurement of plastics for electrical insulation, stressing techniques for complex dielectric constants in various frequency ranges
13 p2285 A69-27984

Epitaxial layers impurity concentration and resistivity measurements by capacitive and three point probe methods
13 p2323 A69-28641

Point discharge measuring based on pulsed nature of discharge current, outlining field experiment results
15 p2610 A69-30698

Electrical parameters measurement for homogeneous batches of planar silicon transistors subjected to cobalt 60 gamma rays, considering isochronal and isothermal annealing
15 p2625 A69-30827

Diode burn-in dissipation measurement for reliability testing
15 p2579 A69-31043

Prebreakdown currents measurement in H and N for deducing ionization coefficients via Townsend and Lucas equations respectively, noting validity by digital computer technique
16 p2815 A69-32574

Thermal contact resistance measurement at various ambient pressures compared with theoretical predictions with each parameter analyzed over interface by computer program
[AIAA PAPER 69-629] 17 p3073 A69-33299

Kinetic inductance measurements in linear circular and rectangular cylindrical superconductors, giving inductance temperature dependence for wires and both thick and thin films
17 p3016 A69-33783

Ta type I and II wire resistance in transverse magnetic field during superconducting to normal transition, discussing strain and impurity effects
17 p3016 A69-33791

Bessel functions new addition theorem suggested from mathematical investigation of ideal discriminator output voltage
19 p3266 A69-35767

Saturated liquid oxygen dielectric constant measurements to calculate polarizability
[NAS-NRC PAPER D-3] 22 p3998 A69-40620

Dependence of cochlear microphonics and summing potential on endocochlear potential
23 p4085 A69-41574

ELECTRICAL PROPERTIES
NT CAPACITANCE
NT CARRIER MOBILITY
NT CHARGE DISTRIBUTION
NT CONTACT RESISTANCE
NT DIELECTRIC PROPERTIES
NT DIELECTRIC MOMENTS
NT ELECTRON MOBILITY
NT ELECTROSTRICTION

NT FERROELECTRICITY
 NT HOLE MOBILITY
 NT INDUCTANCE
 NT IONOSPHERIC CONDUCTIVITY
 NT LC CIRCUITS
 NT MAGNETORESISTIVITY
 NT PHOTOCONDUCTIVITY
 NT PHOTOVOLTAIC EFFECT
 NT PIEZOELECTRICITY
 NT PLASMA CONDUCTIVITY
 NT POLARIZATION CHARACTERISTICS
 NT PYROELECTRICITY
 NT REACTANCE
 NT SUPERCONDUCTIVITY

Lossy and lossless fluidic transmission line theory to estimate downstream conditions having known upstream system
 01 p0012 A69-10153

Integrated operational amplifiers for control systems, noting high stability and linearity through negative feedback
 01 p0039 A69-10169

Dielectric surface coatings effect on transmission and loss properties of silicon-microstrip microwave transmission lines
 01 p0041 A69-10201

Soviet book on semiconductor compounds, production and properties covering crystal structures, phase diagrams, etc
 01 p0137 A69-10353

Electrical properties of gold-gallium arsenide n-type junctions investigated for influence of crystallographic orientation of surface and charge carrier density
 01 p0138 A69-10432

Gunn effect application in fast logic circuit devices including comparators, adder and shift register circuits
 01 p0042 A69-10438

Electrical equation of state of metals determination from density, conductivity, energy and metal vapor velocity measurements in wire explosions
 01 p0117 A69-10659

Microscopic theory of superconductivity, considering quantitative physical properties of low temperature electric current flow
 02 p0293 A69-11432

Lunar electrical parameters range determination using models
 [AAS PAPER 68-199]
 02 p0312 A69-11477

Test procedure for obtaining large signal S characterization of nonlinear power transistors
 02 p0214 A69-11600

Electrical properties of p-n junctions of diffused Cd or Zn in indium phosphide
 02 p0294 A69-11628

Shockley theory of field effect transistors, calculating characteristics in miniaturization problems by removing geometric constraints with aid of electric analog
 02 p0215 A69-11781

Hot pressed boron nitride properties and fabrication, noting low moisture absorptivity and aerospace applications
 02 p0270 A69-11802

Electrical properties of vacuum deposited Bi, noting association of negative temperature coefficient of resistance in Bi thin films with grain-boundary effects
 02 p0296 A69-11878

Plastic material requirements for semiconductor device encapsulation noting electrical compatibility, mechanical and environmental protection and costs
 02 p0270 A69-12161

DC argon arc electrical and thermal parameters and optical properties at high pressure, using spherical anode
 02 p0291 A69-12482

Conduction mechanism in unstable range of Au doped double injection Ge diode at 77 K
 02 p0222 A69-12686

Carrier generation-recombination in space charge region of asymmetrical p-n junction, noting experimental results for InSb diodes
 03 p0487 A69-13641

MOST devices characteristics at cryogenic temperatures, studying variation in gain over audio frequency range
 03 p0405 A69-13642

Electrical properties of edge and screw type dislocations in germanium, using bilateral microscopy
 03 p0488 A69-13761

Surface and interface phenomena in engineering technology, determining mechanical or electronic properties
 03 p0434 A69-13868

Electrical, optical, magnetic and structural properties of titanium oxide, stressing transition difference with vanadium oxide
 03 p0490 A69-13923

Vapor grown GaP electrical and optical properties, considering undoped and Se or S doped samples on GaAs and GaP substrates
 04 p0640 A69-14438

Electrical properties of crystals relation to variations of electron or hole distributions, discussing inhomogeneities
 04 p0641 A69-14506

P-type GaSb crystals with various impurity concentrations noting conductivity, transverse magnetoresistance, Hall effect and acceptor band width and conductivity
 04 p0643 A69-15259

Semiinsulating GaAs mobile electric domains, determining electric field strength from electrooptical effect measurements
 04 p0643 A69-15261

Fe doped Ga-as p-i-n structure electrical conductivity, Hall effect, thermally induced currents, space charge bounded currents and current instability
 04 p0643 A69-15263

Temperature dependence of electrical properties of In and Cu doped CdSb single crystals prepared by zone refining
 04 p0643 A69-15264

Electrical properties of xenon pulse plasmas with high power dissipation, measuring discharge pressure and radiation distribution as function of voltage drop
 05 p0801 A69-15746

Five layer thin film band elimination filters amplitude and phase frequency characteristics
 05 p0729 A69-16088

Deep trapping levels caused by ion implantation doping, discussing level effects on electrical characteristics of zinc implanted GaAs diodes
 05 p0808 A69-16287

Pyrolusite samples high dielectric and ferroelectric properties value ascribed to parasitic effects occurring in commonly used contacts
 05 p0809 A69-16374

Si transistor I sub CE sub 0 characteristics measurement on curve tracer, discussing generation of loop by junction capacitances and emitter base diode
 05 p0734 A69-16569

Physical and physicochemical properties of anodic silica obtained by silicon oxidation in organic bath, discussing possible applications
 05 p0810 A69-16589

BiTeBr semiconductor band structure determined from electrical and optical properties
 05 p0810 A69-16609

Disordered regions in electron irradiated silicon noting defect clusters concentration effect on electrical properties
 06 p0974 A69-16866

Nearly abrupt X band Si avalanche IMPATT diodes irradiated by fast neutrons, noting effects on DC and microwave characteristics
 06 p0976 A69-16874

Intervalley scattering model for Gunn domain dynamics, noting effects comparable to diffusion
 06 p0893 A69-16937

Structural and electrical properties of indium antimonide and arsenide films, noting dependence of electron concentration and mobility on thickness
 06 p0981 A69-17892

Periodic electrostatic focusing structures in microwave tubes, evaluating properties by action function method
 07 p1102 A69-18659

Longitudinal edge effect in primary circuit of open loop linear MHD induction machines, determining forward, reverse and zero sequence currents and voltages
 07 p1058 A69-19027

Radomes design and manufacture for high speed flight vehicles, discussing interactions between aerodynamic and electrical requirements with reference to mechanism of aberration
 07 p1141 A69-19510

Alumina radomes fabrication and control techniques to assure reproducibility of electrical and mechanical properties, detailing finished product inspection methods
 07 p1142 A69-19529

Spherical sandwich radomes designs, discussing aerodynamic loads, wind pressure effect, electrical properties and mountings
 07 p1112 A69-19538

Adaptor circuits for MOSFET electrical properties measurement
 07 p1113 A69-19780

Electrical characteristics of linear Faraday generator using binary mixture of noble gases with nonequilibrium ionization
 08 p1359 A69-19880

Linville model for describing elementary phenomena of electronic equipment in terms of physical data applied to irradiated semiconductor diode and transistor
 08 p1280 A69-19974

Controlled charge models for computer calculation of electronic circuits, discussing tunnel diode static characteristics and equivalent transistor circuits
 08 p1280 A69-19975

Passive circuit components electrical properties at HF using equivalent circuit
 08 p1283 A69-20131

High Q capacitance loaded coaxial cavity resonator for study of electric susceptibility of ionized gas
 08 p1313 A69-20214

Quasars optical and electrical properties, distance, nature and role in cosmology
 08 p1390 A69-20377

Second breakdown in semiconductors, studying thermal feedback connected with temperature time dependence of junction electrical properties
 08 p1294 A69-21115

Glass science and technology noting optical, electrical and mechanical properties, forming techniques, structure, ionic properties, high pressure effects and glass ceramics
 08 p1341 A69-21126

Transforming equivalent circuits, keeping electrical characteristics defined by network functions within prescribed limits
 09 p1472 A69-21784

Oxide coated thermionic cathodes, noting semiconducting properties of alkaline earth oxides, particularly barium oxide and adsorption and optical properties
 09 p1470 A69-22700

Pseudoexact bandpass filter response curves and electrical characteristics based on ripple Chebyshev responses
 09 p1470 A69-22794

Busbar effect on interaction between conducting fluid flow and traveling wave magnetic field created by long line with concentrated inductance and capacitance, deriving line gain
 10 p1727 A69-23101

Transient response of MOS capacitance caused by mechanisms dependent on electric field distribution between silicon and oxide
 10 p1744 A69-23176

Schottky barriers on n-type GaAs, measuring forward current characteristics for various electron concentrations and temperatures
 10 p1745 A69-23358

Effective Ohm law for inhomogeneous weakly ionized gas and Hartmann flow analysis, noting electron density fluctuation effect on conductivity
 10 p1735 A69-23462

Electronic properties of beryllium doped silicon studied with IR absorption spectroscopy and electrical measurements, describing Be thermal diffusion
 10 p1747 A69-23989

Maintenance free high rate sealed Ni-Cd battery power system compatible with existing aircraft electrical systems
 10 p1640 A69-23994

Forward and reverse current-voltage characteristics and reverse biased capacitance for nZnSe-pGe emitter base diodes of heterojunction transistors
 11 p1851 A69-25114

Electrical properties of tetracyanoquinodimethane (TCNQ) complexes representing unit segments of non-conjugated and conjugated polymers
 11 p1832 A69-25675

P-n-p planar epitaxial germanium microwave transistor used as amplifier in 1-4 GHz range and as high speed switch, summarizing design, fabrication and characterization
 12 p2037 A69-25940

Nanosecond time variations in current-voltage characteristics of gas discharge in air, taking into account discharge circuit resistance and discharge space capacitance
 12 p2137 A69-26534

UHF transistor small signal internal behavior, using computer simulation for deriving current gain alpha locus, current gain and f sub T
 13 p2227 A69-27241

Two dimensional flow of conducting gas dynamic and electrical parameters in MGD generator channel, considering magnetic field and plasma conductivity
 13 p2305 A69-27386

Inductive converters accuracy calculation by statistical method based on probability theory
 13 p2259 A69-27424

- Electrical, thermal and thermoelectronic properties of refractory oxide materials including lanthanum chromite and strontium zirconate, discussing Hall effect, IR absorption, mixtures, etc
13 p2316 A69-27470
- Nonconducting vanes end effects on electrical characteristics of MHD channels, analyzing current density, Joule losses and finite length vanes
13 p2306 A69-27497
- Organic semiconductors physical properties and intermolecular charge transfer between donor and acceptor
13 p2317 A69-27799
- Dielectric thin film electrical and mechanical properties and preparation for semiconductor devices, emphasizing Si compounds
13 p2286 A69-28004
- Electrical properties of electron beam evaporated Ti, Zr and Hf films as function of substrate temperature, material and film thickness
13 p2321 A69-28010
- Prebreakdown and breakdown electrical properties of thin film capacitors with certain oxides, fluorides and Teflon dielectrics
13 p2322 A69-28012
- Correlation functions of fluctuations in electrical characteristics of nonequilibrium electron gas during scattering, determining spectral densities and populations by kinetic equation Green function
13 p2314 A69-28445
- Ga phosphide p-n junctions formation from GaP- Ga solution, discussing electrical and luminescence properties
13 p2323 A69-28642
- Thermionic converter stability as function of cesium pressure, heat input, reservoir temperature, load voltage or resistance
14 p2402 A69-29236
- Electrical and photoelectrical properties of semiconductor heterojunctions prepared by Ge epitaxy on gallium arsenide bases, showing dependence on base surface treatment
15 p2667 A69-30078
- Hall generator electrical characteristics, discussing plasma homogeneity, stability and shock tube priming
15 p2658 A69-30298
- Flexible aluminum elliptical waveguide design, discussing installation, economy and electrical characteristics
15 p2578 A69-30798
- Multicomponent semiconductor compounds of non-stoichiometric composition, studying structure, behavior and correlation between electrical properties and phase diagrams
15 p2670 A69-31243
- Ni-Cd and Ag-Cd storage batteries for space applications, discussing performance, life and reliability
16 p2740 A69-32422
- Stagnation point electrostatic probe for measuring local electrical properties of solid propellant rocket exhausts
[AIAA PAPER 69-573] 16 p2840 A69-32677
- Test structure model for studying semiconductor-insulator interface related failure mechanisms in large scale integrated circuitry
17 p2936 A69-32894
- Atmospheric ion concentration increment by electrostatic lens to facilitate electrical properties measurements of charged particles in submicroscopic range
17 p2971 A69-32928
- Electrical characteristics of equilibrium plasma sheaths at stagnation point of blunt body in high speed air, considering current collection regimes
[AIAA PAPER 69-702] 17 p3011 A69-33473
- Materials fracture electrically induced including arc and spark discharges, dielectric breakdown, electrolysis, etc
17 p2989 A69-33558
- Monograph on GaAs injection laser electrical and optical properties during crystallization out of solution covering principle, p-n junction fabrication, I-V characteristics, doping effect, etc
17 p2982 A69-33571
- Thermoplastic polyarylsulfone thermal and electrical properties at over 500 F, noting resistance to thermal oxidative attack
19 p3355 A69-35527
- Manufacturing ultrahigh purity aluminum strip for cryogenic magnets, discussing ingot preparation, rolling, chemical milling and cleaning, arc welding, annealing and sampling
19 p3318 A69-35541
- Resistivity, layer thickness, postbarrier heat treatment and impurity effects on cadmium sulfide-copper sulfide solar cell
19 p3250 A69-35685
- Ion beam sputtering, evaporation and electrical degradation of Al contacted Si solar cells observed in high temperature cyclic tests
19 p3250 A69-35686
- Electrochemically passivated Ti/Pd/Ag contacts for Si solar cells tested in humidity stress and temperature cycling
19 p3250 A69-35687
- Bonded solderless solar cell panel prototype withstanding high annealing temperature and thermal shock without electrical or mechanical degradation
19 p3251 A69-35688
- InSb single crystals impurities incorporation and distribution, concluding electrical properties vary with homogeneity or heterogeneity of dopant microdistribution
19 p3389 A69-36547
- InSb-InAs, InSb-GaSb, InP-GaAs and InP-GaP quaternary systems solid solutions optical and electrical properties, determining energy gap change as function of composition
19 p3390 A69-36554
- Electronic properties changes in amorphous CdGeAs caused by long range order loss studied by measuring optical and transport properties
19 p3390 A69-36557
- Optical and electrical properties of thin amorphous films of glass-forming oxide, using X ray diffraction and electron microscopy for structural features
19 p3391 A69-36561
- Thin PbTe semiconductor films electrical properties measured in air and vacuum, showing dependence on thickness and conditions of preparation
21 p3782 A69-39242
- Electrical properties of passive line elements of hybrid integrated circuits on insulating substrates for radio systems
21 p3684 A69-39563
- Two dimensional analysis of junction transistor electrical behavior, analyzing DC and AC crowding effects, conduction and impedance of base and collector
22 p3911 A69-40011
- Photovoltaic cells electrical characteristics, discussing Cd sulfide, single crystal Si and dendritic type Si cells for spacecraft power
22 p3868 A69-40130
- Electrical properties of semiconductors in HF electromagnetic field, showing Debye type EMF dependence on carrier response to field inhomogeneity
22 p3993 A69-40605
- Piezoelectric transducer transient electrical response due to shock loaded stress using transform calculus
22 p3947 A69-40863
- Electric properties and domain structure changes of polycrystalline Ba titanate and other ferroelectrics characterized by high dielectric nonlinearity
22 p3996 A69-41166
- Sealed Ni-Cd battery with bipolar construction to reduce internal resistance and increase power bursts capacity, emphasizing electrical characteristics and economic considerations
23 p4072 A69-42283
- Boron tribromide-oxygen reaction kinetics effects on IC base diffusion uniformity, correlating uniformity with electrical properties
24 p4360 A69-42760
- Electrical and optical properties correlation of air in fog, discussing droplets distribution with regard to dimensions
24 p4347 A69-43506
- ELECTRICAL RESISTANCE**
NT CONTACT RESISTANCE
NT LC CIRCUITS
- Fatigue-damage evaluation system for transport aircraft, noting use of cumulative strain gauge that stores strain history
01 p0165 A69-10118
- Hall effect in ferrites, determining classical and spontaneous Hall coefficients, electrical resistance, temperature effects and current carrier properties
01 p0135 A69-10185
- Aluminum alloy with lithium and magnesium noting mechanical properties and electrical and corrosion resistance
03 p0443 A69-13026
- Electrical resistance temperature dependence below room temperature for polycrystalline epitaxially grown Au and Ag films, noting effects of alpha irradiation
03 p0486 A69-13582
- Low temperature conductance peaks observed in tunneling measurements on aluminum-phosphosilicate glass-degenerate silicon sandwich structures
03 p0493 A69-14183
- Voltage variable resistor MOST, noting channel resistance controllability
04 p0574 A69-14351
- Resistance change arising from transverse straining of single conductor derived in terms of measurable filament and adhesive parameters
04 p0603 A69-15433
- Finite conductivity or ohmic resistance effect on stationary axisymmetric self constricting MHD flow
06 p0966 A69-17548
- Voltage divider network board composed of composite carbon resistors for measurement of terminal voltage of 3 Mev Dynamitron electron accelerator recalibration
06 p0907 A69-17705
- Harmonic oscillations in tunnel diode circuits for three intersection points of loadline with characteristic curve, discussing larger total positive circuit resistance case
06 p0898 A69-17801
- Electrical resistance and Hall coefficient measurement in InAs-GaAs solid solutions system, giving temperature dependence of electron mobility
07 p1199 A69-18689
- Thermal instability in power transistor structures, considering effects of design, emitter and base resistance at high currents
08 p1373 A69-20858
- DC electrical resistance of magnetosphere between two satellites with sheaths and current voltage relation of satellite sheath
09 p1489 A69-21710
- Forward volt-ampere characteristics and differential resistance peak of Schottky barrier diode on doped Si
09 p1557 A69-21744
- Very low temperature dependence of thin single crystal Al plates electrical resistance, noting Umklapp processes contribution
10 p1711 A69-23620
- Input admittance response characteristics and input susceptance and input conductance of resonant reactive modulator with varactors and nonlinear losses
10 p1665 A69-24066
- Tunnel diode test circuit, measuring differential resistances and bias voltages on loss resistance and of socket capacitance
10 p1665 A69-24215
- Solar cell equation series resistance and junction recombination parameters determination, considering I-V characteristics
11 p1826 A69-25395
- Emitter current density dependence on distance from center of drift transistor circular emitter, obtaining distributed base resistance in presence of arbitrary base current
11 p1853 A69-25565
- Current driven AGC effectiveness in selective amplifiers, including conductance variation effect on pass-band instability and frequency response
12 p2043 A69-26887
- Low resistance Bi thin film complex electrical impedance in IR range, stating methods and equivalent circuits for determining impedance
13 p2322 A69-28011
- Two dimensional inhomogeneous conductors resistance determined by interchanging equipotential and flow lines
14 p2422 A69-29554
- Electrical resistance and temperature coefficient dependence on phase composition of Ti, Zr and Nb carbides
15 p2641 A69-31047
- Temperature dependence of resistivity of zirconium oxide with copper oxide additions indicates suitability as heat sensitive resistor material in 300 to 1000 degree C range
16 p2827 A69-32482
- Optimum ballast resistance of thin film heat transfer gage producing shock arrival time, thickness and structure data of low pressure shock tube
18 p3117 A69-34470
- Plasma thermionic diode figure of merit based on Hatsopoulos model altered to include thermal conduction and electrical resistance
22 p3869 A69-40134
- Seizing characteristics of metals using electrical resistance as measure of lattice imperfection density due to friction
22 p3957 A69-41111
- Time varying resistance wire to arrest oscillations in pulsed capacitor discharge circuit, deriving over, under and critical damping conditions
22 p3917 A69-41228
- ELECTRICAL RESISTIVITY**
NT IONOSPHERIC CONDUCTIVITY
NT MAGNETORESISTIVITY
NT PHOTOCONDUCTIVITY
NT PLASMA CONDUCTIVITY
NT SUPERCONDUCTIVITY

Semiconducting diode base Dember effect impedance studied for recombination rates approaching zero or infinity

01 p0137 A69-10260

Space charge limited operation of insulated gate field effect transistors, discussing maximum transconductance and minimum parasitic capacitances

01 p0042 A69-10322

Liquid copper electrical conductivity temperature dependence at very high temperatures from magnetic diffusion and flux penetration measurements, noting exploding wires role

01 p0119 A69-10673

Fast reversible switching between highly resistive and conductive states in various disordered semiconductors, using electric field

01 p0140 A69-11248

Recombination effects in high resistivity Cu doped gallium arsenide single crystals determined by photoconductivity methods

02 p0294 A69-11627

Electron transfer through metal/semiconductor contact surfaces, measuring electrical conductivity on sintered cylinders with or without silver addition

02 p0296 A69-11790

Granite compressional wave velocity and electrical resistivity variations with depth, explaining discrepancy between in situ and laboratory measurements on dry samples

02 p0241 A69-11806

Electrical conductivity of sintered polycrystalline cubic and monoclinic europium sesquioxide from DC current-voltage characteristics obtained in air at various pressures

02 p0296 A69-11874

Solid solutions microstructure and electrical conductivity in InAs-CdS and InAs-CdS and InAs-CdSe systems

02 p0297 A69-11882

Chromium bronze blanks compacted from granules for hardness and electrical conductivity, noting improved high strength characteristics over conventional production methods

02 p0266 A69-12127

Surface layer effects on conductivity of vacuum deposited gold films, studying resistance variations with film thickness

02 p0300 A69-12625

Ti alloys anomalous variations in physical properties measuring electrical, thermal conductivity and thermal EMF

03 p0443 A69-13029

Electromagnetic induction theory for spherical earth model involving conducting core with radial conductivity variation and concentric nonconducting mantle

03 p0423 A69-13523

Electrical resistivity of sintered high melting point metal oxides, noting width of semiconductor forbidden band

03 p0445 A69-13570

Electrical resistivity, composition, and physical properties of titanium carbide, titanium oxide and titanium-oxygen-carbon alloys

03 p0446 A69-13575

Transport phenomena in semiconductors in strong DC field, emphasizing electrical conductivity as function of crystallographic orientation

03 p0491 A69-14097

Li and Cs electrical conductivity measured from 300-1200 K, obtaining interpolation formulas by least squares method

03 p0481 A69-14148

Conductivity in p-n junctions during avalanche breakdown at HF calculated, noting agreement with experiments

03 p0492 A69-14164

Resistivity and Hall mobility periodic change effect on probe measurements in semiconductors

04 p0642 A69-14534

Electrical conductivity of high resistance epitaxial semiconducting films measured by three probe method

04 p0597 A69-14538

Semiconductor resistivity, discussing resonator field structure and specimen position effects on measurement errors by contactless method

04 p0642 A69-14853

Direct reading instrument using four point probe and two analog computing circuits for Si and Ge resistivity measurements

04 p0599 A69-15019

Active RC low pass filters sensitivity to component changes, discussing effect of below minimum limit value

04 p0578 A69-15070

Weighting functions effect in calculating average scalar electrical conductivity in Lorentzian gas

04 p0638 A69-15317

Hall effect current influence on conductance of high current arcs

05 p0803 A69-15999

Electrical conductivity anisotropy in isotropic germanium and silicon semiconductors, noting effect of metallic contact insertion

05 p0808 A69-16216

Incremental conductance of heavily doped n-type Si semiconductor barrier tunneling as function of bias voltage, indicating Fermi level dependence on dopants

05 p0808 A69-16285

Simultaneous and independent measurement of thermal conductivity, thermoelectric power and electric resistivity, applying method to cadmium arsenide-zinc arsenide system

05 p0764 A69-16338

Electrical properties of n-type Cd tin arsenide single crystals with impurity concentrations at various temperatures

05 p0809 A69-16375

Approximate functions for tunnel diode dynamic conductance in three voltage ranges and Fourier conductance terms for tunnel diode frequency converters

05 p0735 A69-16647

Neutron irradiation produced defects in p-type Si at 76 K, measuring Hall effect and electrical conductivity

06 p0975 A69-16868

Barium, oxygen and BaO adsorption influence on Mo and Ti thin films conductivity and work functions

06 p0978 A69-16900

Hall effect and resistivity of n-type gallium arsenide phosphides doped with Te and Se

06 p0978 A69-16988

Temperature dependence of n-InSb Hall coefficient and resistivity, noting increase in conductivity with degree of compensation associated with electrical breakdown

06 p0978 A69-16990

Charge carrier lifetime measured in intrinsic conductivity range of Cd doped InAs to define recombination mechanism, relating temperature dependence to surface impurities recombination

06 p0979 A69-16997

Two section model of saturation drain conductance of MOS transistors

06 p0893 A69-17155

Chemiluminescence and chemionization in flames, considering electrically conducting properties and spectral analysis

06 p1032 A69-17423

Mathematical theory of electromagnetic induction for physical model of earth with conductivity distribution given by sine function

06 p0921 A69-17739

Combustion mixture composition dependence on electrical conductivity of products with potassium additive, discussing hydrocarbon fuels

06 p0870 A69-17908

Electrostatic field strength and conductivity dependence of expansion and contraction of space charge cloud in process of discharging during static electrification

06 p0959 A69-18219

Superconducting flux-flow resistivity minimum in Pb-Ti alloy, discussing thermal dissipation associated with temperature gradients across moving fluxoid

07 p1198 A69-18642

Lunar core electrical conductivity determination based on induced magnetic field arising from time varying interplanetary magnetic field associated with solar wind plasma

07 p1215 A69-18832

Impurity atoms effects on Cu diffusion and solubility in GaAs, determining Hall coefficient temperature dependence and conductivity

07 p1199 A69-19009

Lunar depth profiles of conductivity, dielectric constant and magnetic permeability from radar, radiothermic and magnetic measurements, discussing lunar models

07 p1216 A69-19221

Soil resistivity survey at earth telecommunication installation site to determine optimal grounding or electrode system

07 p1117 A69-19348

Chemisorbed oxygen effect on electrical conductivity of zinc doped polycrystalline tin oxides

07 p1201 A69-19478

Electrical conductivity in interior of earth stressing electromagnetic induction method, discussing mantle conductivity distribution value

08 p1306 A69-19825

Electrical resistivity of commercial nickel base alloys containing iron, chromium and molybdenum, noting anomaly in 20 percent chromium alloy

08 p1329 A69-20003

Alkali metals electrical resistivity variation with temperature calculated in free electron approximation with the Kubel model for phonon spectrum

08 p1372 A69-20224

Flow rates characteristic of trapezoidal geometries encountered after schematization of noneylindrical ducts involving irrotational flow, leakage, heat exchanges and electrical conduction phenomena

08 p1303 A69-20270

Hydrogen-oxygen fuel cells with conducting and nonconducting hydrophobic electrode matrices

08 p1261 A69-21055

CdS single crystals excess conductivity observed at room temperature

08 p1374 A69-21083

Temperature dependence of conductivity and Hall constant of GaAs single crystals with nickel impurity, noting diode structure and I-V curve shapes

09 p1555 A69-21475

Thermal conductivity, electrical resistivity and degree of blackness of refractory metals at high temperatures measured by Bode and Eger-Disselhorst methods

09 p1522 A69-21589

Turbulent heat transfer in conducting fluid flow through circular tube in longitudinal magnetic field and constant wall heat flux, using Lyon relation

09 p1621 A69-21590

Electrical conductivity and Hall effect in thin evaporated bismuth films under vacuum using three point method in variable temperature cryostat

09 p1557 A69-21692

Carbides and silicides temperature coefficient of electrical resistivity and Hall constant plotted as function of metal carbides solid solutions concentration

09 p1523 A69-21740

Effective cross sections of electron-neutron interaction in photosphere and sunspots, calculating electric conductivity and anisotropy coefficient

09 p1579 A69-22175

Semiconducting diode base Dember effect impedance studied for recombination rates approaching zero or infinity

09 p1559 A69-22653

Weak discontinuities in wave propagation, studying ionized gas nonsteady flow having electrical conductivity in magnetic field

10 p1727 A69-22916

Electrical resistivity of epitaxial CdTe films produced by vacuum sublimation on hot orienting mica and single crystal substrates

10 p1742 A69-23001

Three layer vacuum deposited silicon monoxide films current voltage and conduction current density temperature dependence

10 p1745 A69-23324

Pd-D resistivity variation with D concentration at room and liquid He temperatures, discussing structural resistivity

10 p1745 A69-23357

Moving conducting media velocity measurement using Reynolds number and electrical conductivity values, based on magnetic field distortion

10 p1731 A69-23435

Ar-K plasma studied as possible MHD generator working fluid by investigating influence of emission and external magnetic field on nonequilibrium electrical conductivity

10 p1732 A69-23441

Electrical conductivity, electron density and population temperature as functions of current density in Cs-He thermal plasma studied with nonequilibrium ionization model

10 p1732 A69-23443

Small signal HF conductivity of GaAs calculated for arbitrary frequency and DC field, considering subcritical Gunn devices

10 p1747 A69-23694

Viscosity and electrical conductivity effects on axisymmetric instabilities of current carrying annular cylinder of mercury

11 p1923 A69-24292

Electrical conductivity of partially ionized noble gases Ar, He, Xe and Kr, considering electron temperature and electron-electron interactions

11 p1923 A69-24295

Electrical resistivity and magnetization saturation in cobalt alloys during formation of modulated structures

11 p1904 A69-24707

Electrical conductivity of impurity semiconductors containing variable current carrier concentrations, discussing current-voltage characteristics
11 p1937 A69-24909

Electrical conductivity of space charge surface layer in semiconductors with many-valley energy spectra of current carriers, discussing scalar relaxation time
11 p1937 A69-24915

Electrical conductivity of air behind incident and reflected shock wave fronts as function of temperature and Mach numbers measured by electrode method
11 p1888 A69-25220

Electrical conductivity radial distribution in plasma flux from changes in Q factor and circuit inductance in presence and absence of skin effect
11 p1928 A69-25221

Sb addition effect on electrical conductivity and Hall effect in PbTe single crystals over temperature range
11 p1939 A69-25706

Electrical conductivity measurements combined with indentation hardness measurements for non-destructive evaluation of commercial precipitation hardenable aluminum alloys
12 p2114 A69-26307

Scale effect on gold films electrical conductivity, analyzing film thickness and electron parameters of mean free path, concentration and surface reflection
12 p2143 A69-26459

Gases effect on electrical conductivity of vacuum deposited thin films of Cr, Be, Ni, Au and Ge at different thickness and low pressure
12 p2143 A69-26460

Microminiature five point measuring head with linear point design for resistivity measurement of semiconductor films, noting four point head capabilities
12 p2099 A69-27104

CdS acoustoelectric oscillator steady state oscillation frequency dependence on voltage and conductivity compared with linear acoustoelectric amplification theory
13 p2227 A69-27244

Effective electrical conductivity of two phase vapor-potassium flow in flat duct at flow temperature 800 C, showing dependence on volumetric vapor content
13 p2306 A69-27480

Electrical end losses in liquid-metal MHD generators with variable conductivity, noting working fluids and aspect ratios
13 p2206 A69-27493

Nonequilibrium conductivity and radiation of CdS, GaAs and PbS single crystals in waveguide cell under electron beam
13 p2318 A69-27886

Coaxial three coil probe measuring local electrical conductivity and velocity in plasma streams, discussing operations in electrolytes and axisymmetric plasma stream [AIAA PAPER 69-327]
13 p2313 A69-28264

Epitaxial layers impurity concentration and resistivity measurements by capacitive and three point probe methods
13 p2323 A69-28641

Magnetovariational sounding procedure for determining vertical distribution of earth mean electrical conductivity using geomagnetic field spatial derivatives for spherical earth
14 p2438 A69-29081

Electrical resistivity decrease in niobium-hydrogen alloys during isothermal aging at low temperature attributed to hydride precipitation, noting reaction rate and activation energy
14 p2463 A69-29288

Flow phenomena associated with electrically conducting boundary layer jet injection through slot into uniform slipstream in presence of transverse magnetic field
14 p2501 A69-29917

CoO complex defects indicated by negative enthalpy of formation, considering isobaric electrical conductivity measurements at various temperatures and oxygen pressures
14 p2508 A69-29925

Electrical conductivity ratio of weakly ionized turbulent gas to quiescent gas as function of electron temperature
14 p2502 A69-29991

Electrical conductivity and optical spectra changes of strontium titanate single crystals under constant electric field action
15 p2666 A69-30043

Indium arsenide electrical parameters analyzed by kinetic effects, considering conductivity, thermal and magnetothermal EMF and transverse Nerst-Ettingshausen effect
15 p2666 A69-30066

Cold worked high purity Mo wire recovery after plastic deformation at room temperature, considering electrical resistivity decrease as function of annealing temperature
15 p2636 A69-30082

P-type zinc-tin-antimonide crystals electric conductivity, Hall coefficient and thermal EMF found similar to p-type diamond-like semiconductors properties
15 p2667 A69-30197

Semiconductor resistivity, discussing resonator field structure and specimen position effects on measurement errors by contactless method
15 p2667 A69-30245

Nb and Ti carbides investigated for lattice parameters, microhardness and resistivity in homogeneity domain
15 p2638 A69-30282

Temperature dependence of conductivity and Hall constant of GaAs single crystals with nickel impurity, noting diode structure and I-V curve shapes
15 p2669 A69-30720

Ion-acoustic oscillations effect on weakly ionized plasma electrical conductivity, using BGK collision integral model
15 p2662 A69-30970

Induced high pressure HF discharge parameters computed for Ar, O and N by using electrical and thermal conductivity functions
15 p2662 A69-30976

Air plasma electrical and thermal conductivity coefficients measured in wall stabilized DC arc at atmospheric pressure and high temperatures
15 p2663 A69-30979

Nonuniform electrical resistivity distribution in InSb single crystals as function of growth direction
15 p2670 A69-31049

Electrical resistivity of aluminum oxide films deposited on tubular substrates by plasma and gas flame spraying, noting dependence on film thickness and substrate
15 p2630 A69-31179

Electrical conductivity and thermoelectromotive force of bismuth telluride and bismuth telluride-bismuth selenide alloys obtained by sintering, hot pressing and annealing
15 p2670 A69-31248

Lunar dynamic response to discontinuities in interplanetary magnetic field to determine electrical conductivity and internal temperature
15 p2700 A69-31442

Multiple repair welding effects on AL welds tensile strength, using conductivity measurements to monitor strength
15 p2631 A69-31509

Electrical conductivity, hardness, ultimate tensile strength and yield strength correlations of age hardenable Al alloys by eddy current methods
15 p2641 A69-31513

Electrical conductivity of cesium iodide single crystals with anion and cation impurities noting temperature dependence
16 p2824 A69-31573

Electrical and thermal conductivities of high pressure arc plasmas from I-V characteristics and radial temperature profile
16 p2817 A69-31644

Electrical switching in thin film arsenic selenium telluride semiconducting glass diodes, observing formation of liquid phase and conducting filaments
16 p2760 A69-32017

Wave front resistivity in laser produced plasma interacting with magnetic field enhanced by two stream instability
16 p2823 A69-32564

Thermal EMF, electrical conductivity and Peltier effect in sintered refractory oxides at high temperature in air and in Ar
17 p3068 A69-32990

Ion density, electrical conductivity and weighted mean mobility deduced from Gordien capacitor I-V characteristics used in balloon sounding of stratosphere
18 p3130 A69-34970

Solid solutions microstructure and electrical conductivity in InAs-CdS, InAs-CdS and InAs-CdSe systems
18 p3182 A69-35042

Finite electrical conductivity effect on sun angular momentum loss due to solar wind
18 p3189 A69-35398

Adhesive bonding of Al sheets for honeycomb sandwich material, using electrical conductivity to measure sheets age hardening progress during high temperature curing
19 p3321 A69-35565

Transient recombination lifetimes in n-type float zone Si from 4.2 K to room temperature, obtaining electrical and photoconductivity values
19 p3383 A69-36447

Anomalous phenomenon in resistance and magnetoresistance of cleaved InAs surface, plotting temperature and magnetic field variation effects, proposing explanation of anomaly
19 p3388 A69-36543

Transport properties of liquid semiconductors, using model for liquid mercury with minimum state density
19 p3391 A69-36560

Nb-Ti-C alloys electrical resistivity and thermal EMF noting nearly linear variations with temperature
20 p3558 A69-36976

Nonferrous metals and alloys conductivity standards development program resulting in fabrication, calibration and certification of 16 primary reference standards
20 p3537 A69-37008

Melting points, electrical conductivity, Hall constants, magnetic susceptibility, density, bending strength, microhardness and elastic modulus of zirconium nitride in homogeneity range
20 p3558 A69-37014

Terrestrial electrical conductivity measurement from electromagnetic field variations determination by geomagnetic sounding
20 p3522 A69-37058

Structure of isolated MHD shock wave in viscous heat-conducting radiating gas finite electrical conductivity and transverse magnetic field
20 p3581 A69-37189

Electrical conductivity anisotropy in isotropic germanium and silicon semiconductors, noting effect of metallic contact insertion
20 p3584 A69-37786

Hall coefficient and conductivity measured as function of temperature for liquid Au, Cu and Ag tellurides and liquid alloy systems Bi-Te and Ti-Te
20 p3584 A69-38024

Carbides and silicides temperature coefficient of electrical resistivity and Hall constant plotted as function of metal carbides solid solutions concentration
20 p3585 A69-38216

Conducting and insulating construction materials at high temperatures for MHD conversion nozzles, noting lifetimes
21 p3751 A69-38456

Semiconductor properties of indium telluride alloys, conductivity and Hall effect
21 p3779 A69-38580

Negative ion influence on electrical conductivity of partially ionized multicomponent gas mixtures, basing analysis on thermodynamic calculations of composition
21 p3774 A69-38867

Two dimensional numerical solution for Faraday DC MHD generators with variable conductivity, velocity and magnetic field
21 p3649 A69-39027

Electrical conductivity in wake neck measured using RF bridge on boom extending from reentry vehicle
21 p3724 A69-39030

S doped GaSb single crystals prepared by Crochral-ski method studied for temperature dependence of resistivity and Hall coefficient
21 p3781 A69-39048

Electrical conductivity of rare earth metals La, Ce, Pr and Nd in solid and liquid states by rotating magnetic field method
21 p3781 A69-39070

Nernst effect in pyrolytic graphite at low temperatures including thermal EMF, electrical conductivity, thermal conductivity and magnetoresistance coefficients
21 p3753 A69-39562

Thermoelectric power generator with variable thermal conductivity and electrical resistivity, obtaining steady state temperature distribution, power output and thermal efficiency
22 p3868 A69-40131

Metals conductivity under high pressure, giving theories for electrons scattering cross sections on ions and for Debye temperature
22 p3980 A69-40187

Electrical conductivity of uppermost lunar surface layers, indicating dry powdered rocks with frequency independent dielectric loss tangent
22 p4023 A69-40570

Engineering alloys electrical resistivities measurement at various temperatures, noting temperature and heat treatment effects [NAS-NRC PAPER D-5]
22 p3970 A69-40633

Radioactive decay and conductivity changes with time in high and low resistivity CdS single crystals after irradiation with 14 Mev and reactor fast neutrons
22 p3993 A69-40728

Microwave reflection technique for transient and quiescent electrical conductivity of Si, noting nonohmic contacts
22 p3997 A69-41226

Praseodymium germanides resistivity and thermal EMF temperature dependence determined, discussing Hall effect, thermal expansion coefficient, melting point microhardness, etc
23 p4199 A69-42467

Structural features and electrical resistivity of siliconated pyrolytic graphite, analyzing dependence on preparation conditions using X ray diffraction measurements
24 p4335 A69-42926

Stored energy of cold work and electrical resistivity of Ag-Mg solid solution alloys measured as functions of strain, Mg concentration and initial state of order
24 p4332 A69-43029

Air electrical conductivity reduction in fog ascribed to small ions concentration, increase in droplets capture efficiency and particle concentration
24 p4347 A69-43509

ELECTRICALLY SUSPENDED GYROSCOPES

U ELECTROSTATIC GYROSCOPES

ELECTRICITY

NT ALTERNATING CURRENT
NT ATMOSPHERIC ELECTRICITY
NT AURORAL ELECTROJETS
NT EQUATORIAL ELECTROJET
NT GEOELECTRICITY
NT IONOSPHERIC CURRENTS
NT STATIC ELECTRICITY
NT TELLURIC CURRENTS

Electricity from MHD - Conference, Warsaw, July 1968, Volume 6
21 p3777 A69-39477

ELECTRIFICATION

Electrostatic field strength and conductivity dependence of expansion and contraction of space charge cloud in process of discharging during static electrification
06 p0959 A69-18219

ELECTRO-OPTICAL EFFECT

Laser beam spectra for modulation by electrooptic Doppler shift, considering sawtooth and triangular functions for applied electric field
01 p0091 A69-10843

Transverse electro-optical effect in piezoelectric crystals, using light modulation
04 p0639 A69-14427

Gallium arsenide electro-optic switch measuring signal time response to radiation step of homogeneously broadened carbon dioxide, He and nitrogen laser amplifier
05 p0773 A69-16293

Electro-optical effect in Cr-doped GaAs single crystals at room temperature, discussing carbon dioxide laser radiation modulation by GaAs
06 p0934 A69-17466

Signal conversion by multiple modulation in optical communication system, discussing electrooptic modulators and modulation spectrum
07 p1075 A69-18472

Electro-optical and magneto-optical effects in solids, noting high sensitivity and resolution in application to spectroscopic investigation of absolute spectra
08 p1371 A69-20217

Laser radiation modulation at EHF by linear electro-optical effect of KDP and ADP crystals
19 p3334 A69-35884

Electro-optical effect in Cr-doped GaAs single crystals at room temperature, discussing carbon dioxide laser radiation modulation by GaAs
20 p3555 A69-37949

Electro-optical tuning effect on frequency of parametric laser with KDP crystal, noting Curie point
20 p3555 A69-38003

Metal insulator semiconductor volt-capacitance changes due to light flux, introducing surface recombination rate to improve model
20 p3585 A69-38273

ELECTRO-OPTICAL PHOTOGRAPHY

Automatic laser tracker system for close-up photographic coverage of rocket test
[SMPTE PREPRINT 101-91]
07 p1116 A69-18949

Electron-optical image converter camera for wide time intervals, considering nanosecond electronic control and high voltage stabilized power supply
12 p2083 A69-26140

Nanosecond electron-optical image converter multiframing camera designed for reducing frame exposure time
12 p2083 A69-26141

Image intensifier cascade tubes and slit type electronic cameras with high sensitivity multiple integral images, exemplifying projectile velocity measurements
12 p2083 A69-26143

Ultrahigh speed photographic cameras with exposure times between 5 and 500 nsec, using image tube and high voltage pulse generator
12 p2083 A69-26146

Q switched ruby laser stroboscope for high speed photography, using electro-optical crystals for Q switch
12 p2086 A69-26167

Generalized quantum yield for sensitivity of photoelectric devices, considering multistage image converter and photomultiplier
14 p2496 A69-29788

Computer graphics technique for reducing photographic data from optical device to replace time consuming visual methods
18 p3134 A69-34373

Solar image selection device based on statistical analysis of photospheric contrast, noting use for electronic photography and location impaired observatory
23 p4213 A69-41697

ELECTRO-OPTICS

Electro-optic Q switch using lithium niobate as electro-optic material, comparing performance to conventional device using potassium deuterium phosphate
01 p0089 A69-10184

Electro-optical measurements to determine intermolecular interaction temperatures in organic liquids compressed by shock waves
02 p0230 A69-11979

Electro-optical device using KDP crystal for laser beam deflection at temperatures near Curie point
03 p0435 A69-12984

Q switched lasers powerful outputs obtainable at sum frequency, discussing frequency mixing in nonlinear dispersive media
03 p0438 A69-13047

Analog FM subcarrier modulation selected for real time TV picture transmission via electro-optic space communication system
04 p0562 A69-15474

Electro-optical tracking devices for displacement and/or dislocation measurement without physical contact
05 p0763 A69-15986

Electro-optic properties of tungsten-bronze niobate ferroelectric crystals
[IEEE PAPER F-7]
05 p0808 A69-16313

Fast digitalized scan laser using Nd-YAG as active medium and containing crossed array of lithium niobate electro-optic switches for mode selection
[IEEE PAPER R-2]
05 p0775 A69-16326

Time stabilization method for lasing in electro-optically Q switched ruby laser with saturable absorber in cavity
07 p1147 A69-18531

Coherent emission from rare earth ions in electro-optic crystals, noting oscillations and electric field modulation occurrence
09 p1514 A69-21339

Nonlinear optical properties of barium sodium niobate in ferroelectric tetragonal phase above room temperature, noting spontaneous parametric emission
09 p1515 A69-21354

Electro-optical shutter for Nd-glass laser with high peak power pulses, discussing switching time, contrast ratio and synchronizaton
09 p1493 A69-21422

Optical pulse compression experiment illustrating performance of electro-optical Doppler shifter as linearly time varying frequency shift production device
09 p1519 A69-22445

Optoelectronic spectrum analyzer with raster illuminator for producing two dimensional Fourier transform to analyze two dimensional functions
10 p1725 A69-22301

Electro-optical tracking device with pyramidal reflector for field of view dissection, determining dead zones and trajectories for pointing error correction
10 p1698 A69-24219

Lasers and opto-electronics - Conference, University of Southampton, England, March 1969
11 p1897 A69-25034

Electro-optic broadband laser light modulator designs and modulation characteristics, computing curve set for evaluation of various materials
11 p1897 A69-25039

Electro-optically Q switched Nd doped calcium tungstate laser for producing two controlled pulses, noting application to other solid state lasers
11 p1899 A69-25052

Kerr constant verification device to study electrooptic liquids properties
12 p2084 A69-26148

Electro-optical scanning device and electro-optical matrix for mechanization of difference measurements in automatic photointerpretation of surveillance maps
12 p2090 A69-26302

Optical alignment for lasers with electro-optical Q switching and mutually misaligned ruby rod, KDP crystal and polarizing prism
12 p2107 A69-26589

Giant pulses from laser with electro-optical quartz shutter, noting advantageous optical and mechanical properties of quartz
12 p2108 A69-26591

Electrooptical ADP modulator design for use with helium-neon laser, considering temperature stability and crystal faces parallelism
13 p2272 A69-28191

Optophotovoltaic pickup design for angular displacement measurements, considering application of moire pattern produced by radial diffraction gratings
14 p2447 A69-29327

Directional properties of electro-optical goniometric system based on known design parameters
14 p2420 A69-29332

Electro-optical Q switched lasers with prismatic reflectors and phase shifter studied using Johns matrices for polarizer, Kerr cell and Porro prism elements
14 p2459 A69-29390

Electro-optical automatic gain control system to reduce atmospheric turbulence produced fluctuations in received optical signal strength
14 p2459 A69-29491

Electro-optical measurements to determine intermolecular interaction temperatures in organic liquids compressed by shock waves
15 p2561 A69-30264

Spontaneous self pulsing and cavity dumping in carbon dioxide laser Q switched by internal GaAs electro-optic cell without saturable absorber
16 p2797 A69-32014

Electronically tunable lithium niobate optical filter utilizing collinear acousto-optic diffraction in anisotropic medium
17 p2943 A69-34157

Electrooptical distance measurement based on laser pulse traveling time and phase measurements to determine satellite range
18 p3103 A69-35199

Electro-optical crystals resonance modulator for coherent light beams and microwave frequencies, describing application to multichannel TV transmission system
19 p3266 A69-35763

Ruby laser Q switching with electro-optical shutter based on Li metaniobate crystals by applying static, single pulse or periodic potential to Pockels cell
19 p3336 A69-36346

He-Ne laser subnanosecond intracavity coupler consisting of coaxial krytron pulse generator and electrooptic modulator
19 p3339 A69-36823

Single crystal line block electro-optical shutter reflector operation based on double reflection and birefringence in anisotropic media, noting application to Nd glass laser
20 p3554 A69-37611

Pointing vector and angular rate relationships for various optical elements, discussing analytical models development for precision electro-optical stabilization systems
23 p4131 A69-42544

ELECTROACOUSTIC TRANSDUCERS

NT HYDROPHONES

Electroacoustic transducers interaction effects in multibeam acoustical reflector type receiving antennas
13 p2227 A69-27536

Ultrasonic probe selection and standardization for nondestructive testing, discussing instrument sensitivity and probe losses
15 p2617 A69-31517

ELECTROACOUSTIC WAVES

Model for fast randomization of electron gas by trapped electroacoustical waves
02 p0289 A69-12236

Acoustoelectric domains in CdS, making time evolution visible by means of modified optical strain birefringence and stroboscopic illumination
02 p0258 A69-12618

- Electrostatic acoustic wave mode with plasma motion in magnetic surfaces perpendicular to field in toroidal systems with geodesic curvature
03 p0475 A69-13147
- Acoustoelectric domain propagation in N-type GaAs, noting flux influence on peak acoustic density
05 p0806 A69-15815
- Threshold velocities of acoustoelectric current oscillations in elemental piezo- and nonpiezoelectric semiconductors, taking into account amplification and losses of phonons
05 p0807 A69-15956
- Interacting carriers acoustoelectric waves in semiconductors with high dielectric constant, analyzing dispersion equation
13 p2317 A69-27878
- Current oscillations in n-type gallium arsenide related to electroacoustic domains motions, noting oscillation period dependence on voltage
13 p2318 A69-27892
- Warm plasma probe, describing transit electrons interaction with electric field and generation of electroacoustic waves radiation
16 p2824 A69-32611
- Plasma electroacoustic resonance in reentry sheath of Trailblazer 2 vehicle excited by nonradiating coaxial antenna, deducing electron density gradient at vehicle surface
17 p3010 A69-32915
- Electroacoustic-electromagnetic waves nonlinear coupling in compressible isotropic plasma, comparing slowly varying and resonant interaction approaches
17 p2928 A69-33870
- ELECTROCARDIOGRAMS**
U ELECTROCARDIOGRAPHY
ELECTROCARDIOGRAPHY
- Electrocardiographic tests to study changes in electropotentials of heart in flying personnel after flight, noting changes in myocardium
03 p0378 A69-14207
- Vectorometric EKG analysis of cardiac activity during hypokinesia with and without exercise and medication
05 p0710 A69-16519
- Automatic processing of electrocardiograms recorded during space flight by computer
05 p0715 A69-16524
- Electrocardiographic T-wave changes related to bradycardia in healthy individuals, discussing T-wave inversion in people with vagotonia
09 p1445 A69-22557
- Electrocardiograms of homeothermic animal, hibernator, warm and cool climate poikilothermic animals compared for hypothermia, considering metabolic changes contributing to EKG changes
10 p1643 A69-23123
- Vectorometric EKG analysis of cardiac activity during hypokinesia with and without exercise and medication
18 p3096 A69-34738
- Automatic processing of electrocardiography recorded during space flight by computer
18 p3098 A69-34743
- EKG during electrical defibrillation of heart in immobilized dogs
19 p3257 A69-36168
- EKG signal transmission to hospital during cardiac patient transportation by emergency vehicle, noting prototype system construction and tests
19 p3262 A69-36271
- Automated computer network analyzing electrocardiograms, using telephone lines for bidirectional communications between cardiac data acquisition stations and computer center
19 p3262 A69-36273
- Recording instrument paper speed effect on pulse wave measurements precision, discussing multiple observer studies of left ventricular ejection time
19 p3258 A69-36449
- Electrocardiographic and heart rate data recording of crew members during transatlantic helicopter flight and normal daily routine
19 p3263 A69-36451
- Abnormalities of routine electrocardiograms in medical certification of pilots, indicating errors in screening
19 p3263 A69-36462
- Electrocardiographic changes during gravitational stress
21 p3660 A69-39178
- Low noise physiological recording with dry electrodes, discussing material, construction, preamplifier design and experimental data in electrocardiography
21 p3666 A69-39441
- QRS complex detection time error in noisy electrocardiograms
21 p3667 A69-39442
- Device producing step-like output representing amplitude of ECG R-wave on beat by beat basis
21 p3667 A69-39443
- Arrhythmia diagnosis instruction aided by cardiac pacemaker digital simulation, discussing clinical electrocardiograms generation mechanisms
21 p3667 A69-39606
- Algorithmic approach to nonlinear signal estimation problem useful in fetal electrocardiography
21 p3668 A69-39866
- Serial ECG change from normal conduction to right bundle branch block in 59 patients without overt cardiac disease
23 p4085 A69-41677
- Muscle function measurement in astronauts using electromyogram, electrocardiogram and isometric tension at fixed percentage of maximum voluntary contraction
23 p4103 A69-41684
- EKG data telemetry from personnel to receiver located within same closed metallic chamber, discussing FM/AM and FM/FM systems
23 p4103 A69-41766
- Computer assisted electrocardiography, discussing multipole analog simulation of heart electrical activity and vectorcardiogram recording
23 p4105 A69-41784
- Test animals prolonged deep submersion in water, in mixed oxygen-H atmosphere at elevated pressure, noting EEG and EKG activities
24 p4262 A69-43025
- ELECTROCATALYSTS**
- Electrocatalysts for direct electrochemical oxidation on n-octane in fuel cells, discussing platinum consumption reduction
[ECS PAPER 8] 03 p0368 A69-13856
- Electrochemical oxidation of fuels in liquid ammonia, evaluating electrode surfaces as catalysts
[ECS PAPER 212] 03 p0382 A69-13857
- Oxidizer reducing and fuel oxidizing catalysts role in large current densities production at electrodes of low temperature carbon fuel cells
08 p1259 A69-21037
- Platinum based metal binary catalysts as anodes for hydrogen/carbon monoxide fuel mixtures oxidation, discussing alloy surface chemisorption of CO
12 p2026 A69-25937
- Thin film metallic oxide catalysts for oxidation in low temperature cells using hydrogen and hydrocarbons and for oxygen reduction in acid electrolyte
16 p2738 A69-32408
- ELECTROCHEMICAL CELLS**
NT ALKALINE BATTERIES
NT DRY CELLS
NT ELECTRIC BATTERIES
NT FUEL CELLS
NT HYDROGEN OXYGEN FUEL CELLS
NT NICKEL CADMIUM BATTERIES
NT REGENERATIVE FUEL CELLS
NT SILVER CADMIUM BATTERIES
NT SILVER ZINC BATTERIES
NT STORAGE BATTERIES
NT THERMAL BATTERIES
- Dual gas reference electrode system for molten carbonate cells with immobilized electrolyte
05 p0706 A69-16237
- Solid state electrochemical cells, discussing electrodes composition, battery construction and low, medium and high drainage under temperature extremes
[AIChE PAPER 22D] 08 p1256 A69-19848
- Electrochemical generators for space applications - Conference, Paris, December 1967
08 p1258 A69-21034
- Electrochemical generators using zinc electrode in alkaline medium, noting weight consideration of zinc/air or zinc/oxygen cells
08 p1261 A69-21049
- High energy-density electrochemical generators using lithium anode and copper sulfide cathode in nonaqueous media
08 p1261 A69-21056
- Solid state battery utilizing high conductivity solid electrolytes /metal silver iodide/, demonstrating cell performance improvements
10 p1640 A69-23998
- Solid electrolyte batteries development and current research, detailing Sprague cell and iodine complexes
10 p1640 A69-23999
- Electrochemical energy storage and conversion for space flight, emphasizing hydrogen oxygen and silver zinc batteries, Gemini and Apollo programs, etc
12 p2015 A69-25866
- Electrochemical generators for space applications - Conference, Paris, December 1967
16 p2736 A69-32405
- Electrochemical generators space applications, discussing nuclear, solar and rechargeable cells
16 p2737 A69-32407
- Lateral diffusion gas electrodes for electrochemical generators compared with classical electrodes
16 p2739 A69-32415
- Electrochemical generators utilizing anodically polarized zinc associated with oxygen, mercuric oxide or silver oxide for space power sources
16 p2739 A69-32420
- Nonaqueous lithium anode high energy density electrochemical primary generators, considering energy factors and electrolytic couples
16 p2740 A69-32427
- High temperature electrochemical high performance batteries
17 p2904 A69-33663
- Calorimetric methods for battery and cells testing, discussing heat generation data correlation
18 p3093 A69-34780
- ELECTROCHEMICAL CORROSION**
- Corrosive characteristics of jet fuels near condensing water studied by weight loss method, using copper alloy plates
01 p0142 A69-11099
- Nickel maraging steel polarization behavior in acidic solutions, noting corrosion potential dependence on pH
13 p2282 A69-28188
- Titanium alloys stress corrosion cracking in presence of chloride, bromide and iodide under potentiostatic conditions, postulating electrochemical kinetic and mass transport model
19 p3351 A69-36901
- Corrosion kinetics in metals using electrochemistry, stressing polarization techniques
21 p3749 A69-39494
- Molybdenum disulfide influence on electrochemical corrosion of metals
21 p3733 A69-39804
- ELECTROCHEMICAL MACHINING**
- Electrochemical grinding application to metal cutting of refractory alloys in aircraft jet engine overhaul
[SAE PAPER 680662] 03 p0433 A69-13453
- Electrochemical shaping of turbine blades under symmetric cycle conditions, showing role of experimental functions for optimum regime
04 p0605 A69-14560
- Electrode gap change in one dimensional steady state electrochemical machining
[ASME PAPER 68-WA/PROD-16] 05 p0768 A69-16193
- Kinematics of electrochemical machining defined as quasi-steady process
[ASME PAPER 68-WA/PROD-22] 05 p0769 A69-16194
- Book on electrochemical machining methods, theory, working gap, tool design and power supply
06 p0932 A69-17857
- Electrode gap calculations in intricate surfaces in electrochemical machining, discussing tool electrode
08 p1321 A69-20726
- Metal electrolyte system for electrochemical machining in sodium chloride solution for achieving dimensional control
13 p2268 A69-27521
- Tungsten surfaces with high work functions generated by electrochemical etching, discussing effects of heat treatment in vacuum
14 p2506 A69-29267
- Electrochemical dimensional machining of metals and alloys with rotating cathode in parts manufacture from mechanically intractable materials
23 p4168 A69-41309
- Metal removal mechanisms during electrochemical milling for moving electrodes, noting equations of motion of point for nonmoving electrodes
23 p4168 A69-41310
- Step cathodic flux cleaning of furnace brazed Al assemblies used in combination with ultrasonic and chemical conversion coating techniques
24 p4319 A69-42938

ELECTROCHEMICAL OXIDATION

Electrocatalysts for direct electrochemical oxidation on n-octane in fuel cells, discussing platinum consumption reduction
[ECS PAPER 8] 03 p0368 A69-13856

Electrochemical oxidation of fuels in liquid ammonia, evaluating electrode surfaces as catalysts
[ECS PAPER 212] 03 p0382 A69-13857

Electrochemical oxidation of n-octane based fuels containing aromatic, olefinic and naphthenic components
[ACS PAPER 93] 05 p0716 A69-16234

Long term electrochemical oxidation performance of n-octane based fuels containing aromatic, olefinic and naphthenic components
[ACS PAPER 94] 05 p0716 A69-16235

Physical and physicochemical properties of anodic silica obtained by silicon oxidation in organic bath, discussing possible applications
05 p0810 A69-16589

Zinc oxidation in weakly alkaline media, discussing basic properties of electrochemical cells containing zinc
08 p1268 A69-21050

Adsorption kinetics of hydrocarbon oxidation on platinum electrode
08 p1268 A69-21052

Hydrogen peroxide electrode cathodic polarization studied for liquid oxidant use in methanol fuel cells
11 p1825 A69-24523

Alloying effect on surface oxides determined from photoelectric polarization measurements for Ti-Nb and Ti-Ni
13 p2275 A69-27292

Electrochemical synthesis of chlorine pentafluoride formation from chlorine trifluoride-anhydrous hydrogen fluoride-sodium fluoride system
13 p2217 A69-28134

Chlorine pentafluoride formation from chlorine in anhydrous hydrogen fluoride in electrochemical cell, noting formation rate
13 p2217 A69-28135

Cyclohexane and benzene anodic oxidation at fuel cell electrodes, noting cathodic desorption products as function of potential and reactant
[ECS PAPER 330] 15 p2562 A69-31540

Electrochemical oxidation of hydrocarbons on platinum electrode, discussing adsorption kinetics
16 p2740 A69-32423

ELECTROCHEMISTRY

NT COULOMETRY

Ozonesonde based on modified Brewer electrochemical sonde
01 p0079 A69-10218

Galvanostatic transients of iron passive in 2N sulfuric acid, noting space charge effects and zero field current variation
[ECS PAPER 84] 03 p0382 A69-13858

Porous gas diffusion electrodes design for electrochemical energy converters, noting contribution of theory of electrode kinetics
04 p0551 A69-15309

Passive current maxima during anodic polarization of stainless steel in sulfuric acid, using electrochemical and electron microprobes
06 p0944 A69-17853

Electrochemical kinetic and mass transport model for studying stress corrosion crack propagation in Ti
[ECS PAPER 147] 08 p1332 A69-20359

Platinum electrode study of electrochemical oxygen reduction in nonaqueous media, including kinetic effects of different water concentration levels
[ECS PAPER 7] 08 p1268 A69-20361

Book on thermodynamics of charged and polarized layers covering matter in electric fields, general framework theory, applications, etc
10 p1724 A69-23159

Sandwich electrode for direction and magnitude measurement of velocity gradients at wall for flow around cylinder at high Reynolds numbers
11 p1872 A69-25132

Electrolytic hydrogen evolution reaction on Al covered by thin oxide in aqueous buffered acetate solutions
11 p1832 A69-25674

Electrochemical test predicting stress corrosion performance of 2219 aluminum alloy in T851 and T87 tempers
16 p2798 A69-31716

Medium temperature fuel cells advantages including improved electrochemical reaction kinetics, water and heat removal
16 p2739 A69-32417

Electrochemically passivated Ti/Pd/Ag contacts for Si solar cells tested in humidity stress and temperature cycling
19 p3250 A69-35687

Electrochemical analysis of stress corrosion cracking in Al-Zn-Mg alloy, noting oxide film growth at grain boundary
19 p3351 A69-36899

Austenitic stainless steels nonreproducible passivating tendencies, determining electrochemical and corrosion characteristics, discussing critical anodic current density role
20 p3562 A69-37750

C content and microstructure effect on electrochemical parameters of Fe and steels in dilute sulfuric acid, discussing Tafel constants and current density
20 p3563 A69-38002

Porous hydrophilic oxygen electrodes behavior, showing electrochemical reaction influence on shape of current density vs voltage curves
20 p3484 A69-38071

Titanium alloys hardness indirect measurement by determining electrochemical potential
23 p4177 A69-41598

ELECTRODE FILM BARRIERS

Collector efficiency limitation of surface barrier-limited photoconductors attributed to photogenerated carrier diffusion into electrode
20 p3583 A69-37732

ELECTRODELESS DISCHARGES

Spectroscopic investigation of emission of air plasma in HF electrodeless plasmatron, analyzing near IR, UV and visible spectra
07 p1191 A69-18995

Electron temperature and electron density variations with radial distance in 10 MHz electrodeless ring discharge in H, noting electric field
08 p1361 A69-20230

RF ion thrusters using self sustaining electrodeless discharge
[AIAA PAPER 69-285] 09 p1565 A69-21247

Theta pinch plasma microwave emission from electrodeless inductive discharge at low pressures recorded at near plasma frequencies
09 p1549 A69-22017

Electron concentration at front of anisotropic plasma expanding in axial direction in electrodeless induction discharge from measurements of reflected microwaves
09 p1550 A69-22027

Electrodeless plasmatron coupled with oscillator operating at 5-30 kHz, discussing parameters effect on operation mode and performance
12 p2140 A69-27123

One dimensional theory for cylindrical low pressure electrodeless discharge, predicting electron number density and temperature as function of applied fields
[AIAA PAPER 69-703] 17 p3011 A69-33479

Volatile oxygen organic compounds subjected to RF electrodeless discharge, explaining product distribution in terms of reaction sequences
21 p3670 A69-39737

High temperature equilibria from hydrocarbon plasma sources subjected to 3000 W RF electrodeless discharge
21 p3670 A69-39738

ELECTRODEPOSITION

NT ELECTROPLATING

Electrolytic deposits of titanium, vanadium and alloys from molten salts, discussing formation conditions, velocity and properties
03 p0446 A69-13574

Absolute short term current efficiency of aluminum electrolytic cell, stressing aluminum amount determination in cathode
06 p0869 A69-17233

Electrodeposition of Te-containing Permalloy films with uniaxial magnetic anisotropy, noting electrolyte composition and film structure
11 p1935 A69-24332

Prototype system for continuous dielectrophoretic deposition and alignment of micron sized ultrahigh strength whisker reinforced composites
13 p2269 A69-28676

Electrodeposits on molybdenum alloys in high temperature oxidizing environments, noting performance of Cr-Ni-Cr composite coating
14 p2466 A69-29934

Molybdenum coatings electrodeposition from fused salt system
18 p3156 A69-35001

Electroforming of Al matrix composites by codeposition of short graphite fibers, obtaining increased strength and elastic modulus
19 p3318 A69-35510

Titanium diboride electrodeposition on Inconel from molten salt electrolyte at high temperatures noting electrolyte metabolites and coating thickness range
22 p3970 A69-40735

Soviet collection of papers on bright electrolytic coatings including physicochemical principles of deposition
22 p3958 A69-41261

Physicochemical principles of electrolysis and electrodeposition of metals for obtaining bright galvanic coatings
22 p3958 A69-41262

Bright chromium electrodeposition principles and properties of coatings
22 p3958 A69-41263

Bright nickel plating, examining brighteners and anti-tipping additions effect on deposition mechanism
22 p3959 A69-41264

Bright cobalt plating electrolytic processes, examining brighteners and formation mechanism of deposits
22 p3959 A69-41265

Bright cadmium plating by electrolysis, describing processes during electrodeposition from sulfate electrolytes
22 p3959 A69-41266

ELECTRODERMAL RESPONSE

U GALVANIC SKIN RESPONSE

ELECTRODES

NT ANODES

NT CATHODES

NT CELL ANODES

NT CELL CATHODES

NT COLD CATHODE TUBES

NT DIFFUSION ELECTRODES

NT DYNODES

NT GLASS ELECTRODES

NT HOT CATHODES

NT PHOTOCATHODES

NT PHOTOMULTIPLIER TUBES

NT PHOTOTUBES

NT PLASMA ELECTRODES

NT THERMIONIC CATHODES

NT TUBE CATHODES

NT TUBE GRID

Electron density in arc discharge between carbon electrodes and in discharge with Na vapor, noting relation to temperature and current
01 p0128 A69-10433

Electrode indentation in resistance spot welds related to weld strength for titanium, steel and aluminum alloy
01 p0086 A69-10538

Neutral buoyancy microelectrode for prolonged recording from single nerve units
02 p0202 A69-11865

Gas flow model of coaxial electromagnetic plasma gun front profiles and speeds for operation with positive central electrode
02 p0288 A69-12032

Electrochemical oxidation of fuels in liquid ammonia, evaluating electrode surfaces as catalysts
[ECS PAPER 212] 03 p0382 A69-13857

Fully austenitic stainless steel welding electrodes for welds in cryogenic or high temperature applications, noting creep rupture test results
04 p0607 A69-15220

Porous gas diffusion electrodes design for electrochemical energy converters, noting contribution of theory of electrode kinetics
04 p0551 A69-15309

Design theory for electron guns using three high permeance electrodes demonstrated with gun model
05 p0730 A69-16211

Dual gas reference electrode system for molten carbonate cells with immobilized electrolyte
05 p0706 A69-16237

Platinum electrode study of electrochemical oxygen reduction in nonaqueous media, including kinetic effects of different water concentration levels
[ECS PAPER 7] 08 p1268 A69-20361

Potential effect on wetting of platinum electrodes in acid electrolytes noting drainage role
08 p1268 A69-20362

Electrode gap calculations in intricate surfaces in electrochemical machining, discussing tool electrode
08 p1321 A69-20726

Electrochemical characteristics of lateral diffusion gas electrodes for fuel cells, noting electrodes fabrication by pulverizing on nickel sheet
08 p1260 A69-21044

Fuel cell oxygen ionization on nickel, silver and nickel-silver disk electrodes

08 p1260 A69-21045

Thermodynamics and polarization of zinc electrode in alkaline media, discussing anodic dissolution and passivation

08 p1268 A69-21048

Coaxial electrodes with electric and magnetic fields to study instability in MPD arcs [AIAA PAPER 69-230]

09 p1563 A69-21231

Electron bombardment thrusters for low specific impulse operation, discussing electrode structures fabrication by bonding alumina disk to metal electrode [AIAA PAPER 69-301]

09 p1568 A69-21730

Gunn effect domains propagation calculated for nonuniform diodes of annular geometry, obtaining frequency variation

09 p1464 A69-22159

Signal electrode charge control of sealed Ni-Cd batteries, discussing signal voltage for overcharge control

10 p1640 A69-23993

Zinc electrode cycle life improvement by reducing change in electrode shape, noting effectiveness of teflonation

10 p1640 A69-23995

Highly resistant separator performance in Zn-Ag oxide battery, discussing zinc electrode limitations on battery performances

10 p1640 A69-23996

Linear MHD generator power characteristics at large magnetic Reynolds numbers, analyzing magnetic field distribution for sectioned and solid electrodes

11 p1824 A69-24224

Hydrogen peroxide electrode cathodic polarization studied for liquid oxidant use in methanol fuel cells

11 p1825 A69-24523

Image tube storage target mesh electrode structure and transmission data for electron beams of various velocities, noting secondary electron redistribution control

11 p1848 A69-24749

Rectangular RC distributed circuits with shaped electrodes, analyzing short circuit admittance parameters

11 p1858 A69-24938

Rare earths additives effects on arc instability and weld puddle fluidity of stainless steel bare wire electrodes

12 p2103 A69-26623

Oxide and carbide high-melting-point materials for MHD generator electrode walls

13 p2284 A69-27471

Oscillating electron ion discharge in magnetic field in system of alternating positive and negative electrodes to obtain fast neutral particle fluxes

13 p2311 A69-28109

Tangential drag measurements at electrodes of arc in plasma accelerator, ion current partitioning at cathode and electrode damage [AIAA PAPER 67-657]

13 p2312 A69-28219

Electrode surface bismuth coating selected for reducing electrostatic analyzers photocurrents

14 p2446 A69-29048

Cyclohexane and benzene anodic oxidation at fuel cell electrodes, noting cathodic desorption products as function of potential and reactant [ECS PAPER 330]

15 p2562 A69-31540

Electrodes for fuel cells with liquid electrolytes, discussing problems under weightless and high gravity situations

16 p2738 A69-32409

Fuel cell oxygen electrode problems, noting oxygen ionization reaction and disk electrodes role

16 p2739 A69-32416

Thermodynamics and polarization of Zn electrode in alkaline medium for electric generators

16 p2739 A69-32419

Electrochemical generators utilizing anodically polarized zinc associated with oxygen, mercuric oxide or silver oxide for space power sources

16 p2739 A69-32420

Electrochemical oxidation of hydrocarbons on platinum electrode, discussing adsorption kinetics

16 p2740 A69-32423

Hydrogen oxygen fuel batteries with hydrophobic porous film electrodes and alkaline electrolyte

16 p2740 A69-32426

Electrode potentials of pure metals, Ni-Cr and Ni base alloys in molten salts applied to corrosion studies

17 p2990 A69-33650

Structural parameters selection for thermocouples with butt-weld electrodes, developing mathematical

basis for thermoelectrode length to measure unstable gas temperatures

19 p3311 A69-36197

Porous hydrophilic oxygen electrodes behavior, showing electrochemical reaction influence on shape of current density vs voltage curves

20 p3484 A69-38071

Pt electrode as detector of red blood cell oxygenation, attempting Fc value dependence on flow velocity determination

20 p3480 A69-38283

Low noise physiological recording with dry electrodes, discussing material, construction, preamplifier design and experimental data in electrocardiography

21 p3666 A69-39441

Self consistent flow calculation in dense space charge beams, including electrode design for portions isolation

22 p3985 A69-40668

Metal removal mechanisms during electrochemical milling for moving electrodes, noting equations of motion of point for nonmoving electrodes

23 p4168 A69-41310

Clark oxygen electrode calibration by preparation of oxygen standard aqueous solutions, noting repair by ammonium hydroxide treatment

23 p4101 A69-41451

Capacitance sensor of vertical with flexible mobile electrode, describing diagram and operation

23 p4163 A69-41550

Ion sputtering method for making electrodes in thermionic energy converters, discussing alumina and W surface layers preparation

23 p4170 A69-42259

ELECTRODIALYSIS

Justi-Winsel extraction process by electrodialysis for removing product water from electrochemical reaction in H-O fuel cells

08 p1260 A69-21043

Optimization of electrolytic extraction process of water from H-O fuel cells through choice of current density as function of electrolyte concentration

16 p2738 A69-32414

Electrodialysis method for depleting positive Na, K, Ca and Mg ions from Anabaena flos-aquae A-37, noting algae survival rate

23 p4079 A69-41387

ELECTRODISSOLUTION

Stress corrosion cracking of metals related to surface phenomena involving surface reaction layer ruptures or selective electrochemical dissolution along defects

19 p3349 A69-36885

ELECTRODYNAMICS

NT ELECTROHYDRODYNAMICS

NT ELECTROMECHANICS

NT QUANTUM ELECTRODYNAMICS

Hydrodynamics-electrodynamics analogies for electromagnetic flight

01 p0121 A69-11134

Atomic electron spontaneous transition in theory of direct particle interaction, considering electrodynamic field zero-point oscillations role

03 p0468 A69-13773

Electrodynamics of turbulent conducting media based on nonrelativistic MHD

03 p0479 A69-13972

Total conserved momentum-energy of electromagnetic interaction of system of point charges in Wheeler-Feynman theory, noting mass defect of connected system

04 p0631 A69-15058

Interaction between point charges in Wheeler-Feynman electrodynamics, noting impossibility of deducing momentum and energy conservation from variational principle

04 p0631 A69-15059

Field theories and direct interparticle action theories of classical electrodynamics, establishing general correspondence between formalisms

04 p0631 A69-15189

Geometrical optics approximation of Maxwell equations for electrodynamics of inhomogeneous anisotropic media

07 p1076 A69-18519

Waveguide Y circulator electrodynamic parameters by design algorithm and computer programs

10 p1661 A69-23108

Inhomogeneous permittivity and boundary effects influence on electric fields of laser with open cavity containing inhomogeneous active medium

12 p2110 A69-26908

Theoretical model describing electrodynamic plasma properties of HF flame discharge in air, heating

discharge envelopes by heat diffusion from discharge channel surface

12 p2140 A69-27125

Electrodynamic model applicability to HF flame discharge for case of flame discharge stabilization by axial air injection

12 p2140 A69-27126

Electrodynamic law between current elements consistent with Newtonian dynamics, noting consequences in discharge and plasma control

14 p2485 A69-29320

Energy relations and conversion for electrodynamic plasma acceleration with allowance for mass transfer processes resulting from recombination, diffusion and electrode erosion

15 p2664 A69-31176

Reciprocity method for absolute calibration of piezoelectric accelerometer mounted on electrodynamic shaker table

15 p2615 A69-31283

Earth ionosphere and magnetosphere electrodynamic state analyzed as function of neutral gas small scale motions, considering magnetic disturbances and ionospheric discontinuities

20 p3519 A69-37026

Approximate boundary conditions in electrodynamics of stratified tensor media estimated for ferrite layers

21 p3675 A69-39282

Time symmetric electrodynamics for various cosmological models, discussing position and negative space curvature

22 p4022 A69-40469

Intrinsic transport theorem for electrodynamics of continuous media, using Cartan method of exterior differential forms

24 p4350 A69-43368

ELECTRODYNAMOMETERS

U DYNAMOMETERS

ELECTROENCEPHALOGRAPH

U ELECTROENCEPHALOGRAPHY

ELECTROENCEPHALOGRAPHY

Human psychological factors involved in genesis of contingent or conative negative variation using EEG activity measurements

01 p0015 A69-10904

Head injury clinical and laboratory long term follow-up data, discussing conscious state alterations, focal neurological deficit, EEG abnormalities, etc

01 p0022 A69-11346

Increasing hypoxia effects on rabbit EEG and light flash conditioned alimentary reflex for simulated altitude ascent, noting subcortical stimulation

02 p0197 A69-11492

Flexible printed circuitry electrode arrays fabrication for surface cortical potentials recording in animals

02 p0204 A69-12601

Prolonged bed rest effect on brain bioelectrical activity from EEG reactions of subjects to acoustic signals followed by light signals

05 p0710 A69-16520

Standards for EEG in pilot flight examinations, analyzing effects of total flying hours

06 p0875 A69-18021

Resting EEG and parieto-occipital response changes evoked by slowly repeated flashes in case of severe hypothyroidism secondary to panhypopituitarism

07 p1064 A69-18634

High oxygen concentration effect on conditioned reflex and associated EEG responses to light flash in rabbits occurs in well defined sequences

07 p1065 A69-18976

EEG lead sensitivity to location and orientation of sources in brain by applying reciprocity theorem

10 p1648 A69-23186

EEG, heart beat, respiration rates, body temperature, motor activity, physical and mental efficiency of man during anechoic chamber confinement

10 p1646 A69-23510

EEG monitor helmet for aircraft or flight simulator programs, discussing sensing and transmitting system

12 p2023 A69-26553

Computer analysis of EEG recording, presenting model studies under rest and performance conditions

15 p2560 A69-31232

EEG and pilots flight performance relations, discussing in-flight telemetric measurements from ground station

15 p2560 A69-31233

EEG electrode stimulated simian mental activity in problem solving during simulated space flight, discussing skull implantation and EEG recordings of hippocampus activity

17 p2910 A69-33749

- Prolonged bed rest effect on brain bioelectrical activity from EEG reactions of subjects to acoustic signals followed by light signals
18 p3096 A69-34739
- EEG monitoring during decompression illness /bends/ treatment by hyperbaric procedure using small multichannel telemetry pack
19 p3261 A69-36268
- Electrical response of frog and human visual cortex neurons to thermal vestibular and light flash stimulation
20 p3469 A69-37242
- Human sleep during prolonged rotation, discussing electroencephalograms, acoustic signal frequency producing waking reaction, cutaneous galvanic reflex and deepness of sleep
20 p3472 A69-37261
- High oxygen concentration effect conditioned reflex and associated EEG responses to light flash in rabbits occurring in well defined sequences
20 p3479 A69-38224
- Ultrasound-echo-encephalography in diagnosis of posttraumatic intracranial hemorrhage of skull and brain trauma, noting neuroradiological techniques
21 p3652 A69-38790
- EEG patterns evoked from left and right cerebral hemisphere by visual and verbal stimuli, showing asymmetrical role of hemispheres in governing cognitive behavior
21 p3656 A69-38976
- Hyperbaric oxygen convulsions origin and site, studying pressure effect on brain electrical activity in rabbit by EEG
21 p3656 A69-38977
- EEG with combined multichannel radiotelemetry and telephone for onward data transmission
21 p3664 A69-38978
- EEG patterns computerized spatio-temporal display technique using CRT and motion picture camera
21 p3668 A69-39864
- Radiotelemetric EEG recording variation possibility, examining dynamic behavior of human cerebral rhythms
22 p3889 A69-40158
- Image disappearance or reappearance time controlled by inducing changes in alpha occurrence probability, executing on-line closed loop program detecting alpha rhythm
22 p3871 A69-40159
- Age and carbon dioxide tension effects on EEG of adolescents and adults, discussing end-tidal carbon dioxide during routine hyperventilation
22 p3872 A69-40162
- Meaningful comparisons between single stimulus EEG records and average evoked potential
22 p3890 A69-40163
- EEG alpha activity relationship to laterality of reflective eye movements, indicating physiological correlates of hypnotizability
22 p3887 A69-41213
- Equal bandwidth multichannel FM/FM EEG telemetry system using subcarrier frequencies and HF modulation via varactor diodes
23 p4106 A69-41802
- EEG, ocular movements, gastric mobility and pH during human sleep from data transmitted by swallowed radio transmitter
23 p4093 A69-42063
- Occipital eeg activity slowing and physiological changes during prolonged immobilization plus perceptual deprivation of human beings
24 p4256 A69-42554
- Test animals prolonged deep submersion in water, in mixed oxygen-H atmosphere at elevated pressure, noting EEG and EKG activities
24 p4262 A69-43025
- Lambda waves EEG recording for evaluating eye movements during pattern vision
24 p4268 A69-43401
- ELECTROEROSION**
U SPARK MACHINING
- ELECTROEXPLOSIVE DEVICES**
U INITIATORS [EXPLOSIVES]
- ELECTROFORMING**
Buckling of electroformed thin conical shells under hydrostatic pressure, proving theory for cones of large taper ratio
02 p0347 A69-12515
- Electroplating solutions test for filament winding and electroforming process used in fabricating fiber reinforced metal composites
11 p1890 A69-24337

- Electroforming methods in design and fabrication of liquid propellant rocket motor injectors and composite thrust chambers
[AIAA PAPER 69-583] 16 p2794 A69-32757
- Electroforming of Al matrix composites by codeposition of short graphite fibers, obtaining increased strength and elastic modulus
19 p3318 A69-35510

ELECTROGENERATORS

U ELECTRIC GENERATORS

ELECTROHYDRAULIC CONTROL

U ELECTRIC CONTROL

U HYDRAULIC CONTROL

ELECTROHYDRODYNAMICS

- Electrohydrodynamic analogies to known MHD effects studied by differential equations for hydrodynamic and electric field energy relations
01 p0131 A69-10775

- Instabilities for two highly conducting finite length streams in relative motion and coupled by transverse electric or longitudinal magnetic fields
01 p0062 A69-11208

- Charge accumulation elimination on dielectric electrodynamic channel walls, comparing resistive wall channel to high internal impedance generator
02 p0291 A69-12506

- Dynamic properties of electrohydraulic servomechanisms having variable structure analyzed by analog computer
03 p0368 A69-13686

- Stationary, moving and pulsating electrohydrodynamic flow between parallel dielectric plates and Couette flow, noting reaction concentration near wall
03 p0419 A69-13919

- Electrodynamic generator for direct conversion of moving dielectric medium potential or thermal energy to electric power
03 p0369 A69-14153

- Electrostatics /EGD/ engineering, discussing generators and compressors
05 p0804 A69-16586

- Electrodynamic gas flow in one dimensional approximation for transition through speed of sound, discussing flow parameters profile and dynamic efficiency
06 p0964 A69-17326

- Flapper-nozzle type electrohydraulic amplifier design with emphasis on elements and subsystems
08 p1256 A69-20459

- Dynamic behavior of electrohydraulic servomotors over wide range of loads using differential equations of motion
08 p1256 A69-20718

- Electrohydrodynamics - Conference, Cambridge, Mass., March-April 1969
12 p2135 A69-26397

- One dimensional stationary flow of medium consisting of charged and neutral components within electrohydrodynamic limits in AC and DC electric fields
12 p2135 A69-26398

- Electrohydrodynamic equations and transfer coefficients for multicomponent plasma with volumetric charge in electric field, discussing Ohm law and equations for plasma motion
12 p2135 A69-26399

- Electrohydrodynamic channel flow using boundary problem and approximations corresponding to flow of unipolarly charged and polarized media
12 p2135 A69-26400

- Electrically driven thin fluid jet stability in longitudinal field between two plate electrodes, discussing role of Ohm law in calculating jet potential
12 p2136 A69-26402

- Electrohydrodynamic instability of incompressible conducting cylindrical viscous jet in external magnetic field, noting viscosity role in oscillation modes and growth rate
12 p2136 A69-26403

- Virtual power principles applied to solving force acting on fluid consisting of colloidal suspension of polarized particles in neutral vehicle
12 p2136 A69-26404

- Aerospace applications of electric discharge interaction with fluid motion including sonic boom reduction, high lift devices, reentry vehicle pitch control, etc
12 p2136 A69-26405

- Charged aerosols production for electrohydrodynamic processes by spraying liquids through capillary at high electric field strengths into high pressure air flows
12 p2138 A69-26631

- Electrohydrodynamic flows at large electric Reynolds numbers, obtaining Bernoulli and Cauchy-Lagrange integrals
13 p2305 A69-27379

- Partially ionized multicomponent gas mixture kinetics in strong electromagnetic field, determining magnetic field, stress tensors and transfer coefficients
14 p2492 A69-29610

- Hydraulic regenerative servoamplifier system for electrohydraulic actuator design, discussing specifications and test results
15 p2553 A69-31294

- Small amplitude motions of plane interface between fluids stressed by initially perpendicular electric field, modeling fluids as ohmic conductors
16 p2811 A69-31667

- Electrohydrodynamics of fluids having uniform electrical properties, emphasizing shear effects for interfacially confined electromechanical coupling
18 p3123 A69-34919

- Conducting medium steady one dimensional motions determined by assuming space charge-electric field interaction, considering electrohydrodynamic behavior of medium
18 p3181 A69-35315

- Electrohydrodynamic subsonic flow of isothermal charged gas over wavy insulator wall by perturbation method, calculating surface pressure, streamlines and electric lines of force
19 p3297 A69-35837

- Electrohydrodynamic supersonic flow over wavy wall by oscillating piston model, calculating streamlines and density distributions
19 p3297 A69-35838

- Electrohydrodynamic Rayleigh-Taylor bulk instability in initially static stratified fluid under electric stress
20 p3578 A69-38235

- Dielectrophoretic zero gravity cryogenic liquid expulsion using lightweight high voltage ribbon electrode conduits and electrohydrodynamic bang-bang field effect
24 p4300 A69-43237

ELECTROJETS

U AURORAL ELECTROJETS

U EQUATORIAL ELECTROJET

ELECTROKINETICS

- Electrokinetic converter of biochemical parameters for diagnosis and control of organism behavior, noting biomechanical utility
14 p2409 A69-29471

- Fluctuation kinetics of electron system in nonequilibrium state arising in semiconductor in strong electric field, considering lattice and interelectron scattering
16 p2824 A69-31569

ELECTROLUMINESCENCE

- Display techniques, discussing cold cathode luminous gas discharge /plasmas/ tube, electroluminescence and cathode ray tube
04 p0600 A69-15029

- Homogeneous electroluminescence at 77 K in n-type GaAs single crystals without artificial p-n junctions, noting effects of electric field strength and Zn doping
04 p0644 A69-15271

- Electrical polarization effect on electroluminescence brightness waves in zinc sulfide films
05 p0807 A69-16213

- Polarization effect on electroluminescent properties of zinc sulfide films
05 p0807 A69-16214

- Diffused Si and GaAs diodes electroluminescence and current-voltage characteristics
06 p0893 A69-16898

- Impact ionization and tunneling effect during electroluminescence of zinc sulfides
06 p0980 A69-17261

- Optimal electroluminescent efficiencies for vapor grown gallium arsenide phosphide diodes, analyzing current spreading, absorption, impurity and composition effects
[ECS PAPER 103] 08 p1284 A69-20366

- Voltage dependence of red and green electroluminescence in GaP diodes prepared by growing n-type liquid epitaxial layer on p-type solution grown substrate
10 p1663 A69-23664

- Soviet book on electroluminescent devices covering panels, indicator contrast levels, control, multicolor indicators, image conversion and storage and optoelectrical systems
11 p1850 A69-24976

- Electroluminescence and electroluminescent devices, considering semiconductor lasers, radiation sources and image amplifiers
11 p1899 A69-25198

Negative resistance in GaP electroluminescent diodes with p-i-n structure at low temperatures, noting oxygen role
13 p2226 A69-27194

Electroluminescence of p-GaAs diodes analyzed over temperature range of linear dependence of lasing on injection current
13 p2230 A69-27887

SiC and GaP diodes used as low power light sources, studying electroluminescence in p-n region under pulsed excitation
14 p2419 A69-29325

Current and electroluminescence brightness dependence on reverse voltage in n-SiC diodes including tunnel and avalanche processes
15 p2573 A69-30062

Optical and electrical properties of electroluminescent diffused gallium arsenide phosphide diodes with low donor concentrations, analyzing spectral emission and fabrication effects
16 p2758 A69-31699

Continuous IR radiation source using electrically heated Mo ribbon, comparing emission from V shape and flat portions
19 p3313 A69-36491

Electroluminescence of p-GaAs diodes, analyzing temperature range of linear dependence of lasing on injection current
21 p3682 A69-39145

Ball lightning as positively charged region of electroluminescent air maintained in dynamic structure and molecular composition by atmospheric electric field
22 p3940 A69-40536

Hybrid display for data visual display using electroluminescent and thermochromic technologies for wide range of ambient illumination
24 p4313 A69-42899

Colors production on electroluminescent display using phosphors impressed-frequency/emission-color relationships together with chromatic biasing
24 p4286 A69-42900

Luminescence, I-V and pulse characteristics of high resistivity Ni doped GaAs single crystals, noting injection conductivity
24 p4362 A69-43734

Diagonal tunneling and radiation polarization in doped heterojunctions and p-n junctions of GaAs, using electroluminescence spectrum analysis
24 p4362 A69-43737

Electroluminescence in doped p-type GaAs single crystal diodes ascribed to double injection of nonequilibrium current carriers
24 p4288 A69-43739

ELECTROLUMINESCENT LAMPS
U ELECTROLUMINESCENCE

ELECTROLYSIS
NT COULOMETRY

Water electrolysis, discussing oxygen generators for spacecraft prototype cells and testing
03 p0379 A69-12987

Charge and degree of ionization of nickel alloyed with molybdenum analyzed by electrolytic ion migration method
07 p1159 A69-18535

Electrochemical synthesis of chlorine pentafluoride formation from chlorine trifluoride- anhydrous hydrogen fluoride-sodium fluoride system
13 p2217 A69-28134

Physicochemical principles of electrolysis and electrodeposition of metals for obtaining bright galvanic coatings
22 p3958 A69-41262

ELECTROLYTES

NT ELECTRIC CONDUCTORS
NT ELECTRIC CONNECTORS
NT ELECTRIC WIRE
NT EXPLODING WIRES
NT ION EXCHANGE MEMBRANE ELECTROLYTES
NT MOLTEN SALT ELECTROLYTES
NT PHOTOCONDUCTORS
NT SUPERCONDUCTORS

Electrolytic marking process for aircraft component identification without use of stamping or engraving
02 p0253 A69-12065

Water removal unit design for electrolyte reaction accumulation in hydrogen oxygen fuel cell systems
04 p0552 A69-15316

Oxygen reclamation from carbon dioxide using solid oxide electrolyte, noting water vapor catalytic effect
07 p1071 A69-19423

Electrolytic bubble level during wind tunnel tests for aircraft model attitude
10 p1672 A69-23268

Metal fluoride compounds as cathodes for use with mixed fluoride electrolyte /LiF-NaF-KF eutectic/ in thermal batteries
10 p1640 A69-23997

Solid state battery utilizing high conductivity solid electrolytes /metal silver iodide/, demonstrating cell performance improvements
10 p1640 A69-23998

Solid electrolyte batteries development and current research, detailing Sprague cell and iodine complexes
10 p1640 A69-23999

Metal electrolyte system for electrochemical machining in sodium chloride solution for achieving dimensional control
13 p2268 A69-27521

Velocity distribution effect on electric field at walls for axisymmetric flow of electrolyte in circular channel in magnetic field of E shaped inductor
14 p2501 A69-29915

Solid electrolyte tantalum condensers reliability under repeated service voltage applications for calculating defective condenser probability
15 p2626 A69-30836

Removal rate of reaction water from fuel cells by diffusion-condensation procedure as function of temperature and electrolyte concentration
16 p2736 A69-32200

Electrodes for fuel cells with liquid electrolytes, discussing problems under weightless and high gravity situations
16 p2738 A69-32414

Optimization of electrolytic extraction process of water from H-O fuel cells through choice of current density as function of electrolyte concentration
16 p2740 A69-32421

Electrochemical couples of zinc-metallic oxides or O used in battery with water electrolyte
16 p2740 A69-32421

Hydrogen oxygen fuel batteries with hydrophobic porous film electrodes and alkaline electrolyte
16 p2740 A69-32426

Nonaqueous lithium anode high energy density electrochemical primary generators, considering energy factors and electrolytic couples
16 p2740 A69-32427

Titanium diboride electrodeposition on Inconel from molten salt electrolyte at high temperatures noting electrolyte metabolates and coating thickness range
22 p3970 A69-40735

Bright cadmium plating by electrolysis, describing processes during electrodeposition from sulfate electrolytes
22 p3959 A69-41266

ELECTROLYTIC CELLS

Secondary cells with liquid lithium anodes and immobilized fused salt electrolytes
04 p0552 A69-15330

Absolute short term current efficiency of aluminum electrolytic cell, stressing aluminum amount determination in cathode
06 p0869 A69-17233

Electrodes behavior for fuel cells with liquid electrolyte under high-g and weightlessness conditions, discussing spontaneous liquid motion
08 p1259 A69-21038

Cold hydrogen and basic electrolyte cells at CGE research center, discussing single cell batteries, reagent chambers and auxiliary control systems
08 p1259 A69-21039

Electrochemical characteristics of lateral diffusion gas electrodes for fuel cells, noting electrodes fabrication by pulverizing on nickel sheet
08 p1260 A69-21044

Proton electrolyte application to fuel cells, discussing proton diffusion in solids and materials with vacancies /proton conductors/ in structures
08 p1269 A69-21053

Polishing-etching cell permitting continuous sample surface observation for use with inverted stage microscopes
13 p2281 A69-28156

Electrolytic vertical indicators response errors, discussing nonlinear properties of transducer steady state characteristics
14 p2446 A69-28925

Oxygen isotope separation magnitude in zirconia electrolytic cells found proportional to mobility difference of isotopes
15 p2552 A69-30701

Hydrogen and basic electrolyte cold cells, studying control systems for reactants supply, current, reaction by-products, etc
16 p2738 A69-32410

ELECTROMAGNETIC ABSORPTION

Oxygenator for weightlessness operation, generating oxygen electrolytically and passing oxygen through membrane for animal experiments
17 p2903 A69-33039

Cathode materials role in high temperature zirconia electrolyte fuel cell performance, discussing metals, collector-embedded and electronically conducting oxides properties
22 p3869 A69-40734

High pressure hydrogen-oxygen reversible fuel cells using calcia stabilized porous zirconia as membrane and aqueous KOH as electrolyte
23 p4076 A69-42308

ELECTROLYTIC GRINDING

U ELECTROCHEMICAL MACHINING

ELECTROLYTIC POLARIZATION

Thermodynamics and polarization of Zn electrode in alkaline medium for electric generators
16 p2739 A69-32419

Electrochemical generators utilizing anodically polarized zinc associated with oxygen, mercuric oxide or silver oxide for space power sources
16 p2739 A69-32420

ELECTROLYTIC POLISHING

U ELECTROPOLISHING

ELECTROMAGNETIC ABSORPTION

NT AURORAL ABSORPTION
NT MOLECULAR ABSORPTION
NT PHOTOABSORPTION
NT POLAR CAP ABSORPTION
NT X RAY ABSORPTION

Absorption of linearly polarized light in reflecting surface layer of collisionless plasma, calculating layer lifetime for reflection of light
01 p0127 A69-10283

Radio wave abnormal absorption in auroral zone of ionosphere, investigating index of frequency dependence in absorption vs frequency relation
01 p0063 A69-10425

Signal absorption in negative ionospheric ions effect on maximal frequency for space radio communication [UN PAPER 68-95272]
01 p0029 A69-10529

Probabilities of error, correct reception and signal cancellation in radio communication systems channels with signal absorption fading
01 p0030 A69-10592

Intense laser emission interaction with current carriers in semiconductors, analyzing dependence of thermoelectric field produced by light absorption on intensity, frequency and temperature
01 p0139 A69-10895

Optical absorption coefficients for triphenylmethylarsonium tetracyanoquinodimethan complex single crystal, evaluating reflectance
01 p0140 A69-10934

Ionosphere formed waveguide electromagnetic field determined by expression, accounting for radio wave absorption during communications via artificial satellites
02 p0206 A69-11661

Sudden cosmic noise absorption in ionosphere confirms relationship with solar chromospheric flares
02 p0306 A69-11667

Terrain roughness effect on ionospheric radio wave absorption measurement data compared with theoretical results
02 p0207 A69-11669

Electric field induced IR absorption and Raman scattering by optical phonons in centrosymmetric crystals, discussing tensor coefficients
02 p0295 A69-11779

Performance characteristics of 300 GHz Dicke type superheterodyne radiometer receiver for measuring atmospheric attenuation of electromagnetic waves
02 p0209 A69-12336

Diffraction by rocket exhausts, discussing electromagnetic signal attenuation based on two dimensional straight edge diffraction model
02 p0209 A69-12352

Ruby laser output energy degradation due to pump light absorption by color centers of ruby rod
02 p0256 A69-12358

Linear absorption coefficient of seminsulating Cr doped GaAs for IR carbon dioxide laser radiation, discussing lattice absorption mechanism
02 p0258 A69-12619

Ionospheric absorption measurements using beacon satellite emission compared to Kazantsev results
02 p0246 A69-12742

Sunrise effects in lower D region by solar eclipse, discussing anomaly in ionospheric absorption due to negative ion factor or recombination coefficient
02 p0246 A69-12767

Narrowing of ionospheric absorption anomaly in D region during solar eclipses in long and medium wave ranges due to recombination equation variability
02 p0246 A69-12770

Two photon absorption and stimulated emission mechanism of CdS-CdSe mixed crystals investigated by ruby laser output
03 p0438 A69-13052

Q switched ruby laser nonlinear absorption in optically transparent organic liquids attributed to two quantum process with large cross section
03 p0439 A69-13055

Ionospheric midday radio wave absorption as function of geomagnetic latitude, season and solar activity from pulsed vertical radar sounding data
03 p0394 A69-13521

Radio wave absorption in ionosphere at five fixed frequencies for determining correlation with changes in sporadic E layer parameters
03 p0423 A69-13539

Very thin short metallic filament scattering and absorption cross sections for various values of filament conductivity
03 p0395 A69-13623

Pulsed electromagnetic signal reflection from plane boundary of absorbing medium
03 p0397 A69-13711

Temperature dependent far IR absorption of ferroelectric sodium nitrite, discussing single and multiphonon processes
03 p0490 A69-13940

Optical absorption of vacuum deposited thin rubidium films, noting similarity to sodium and potassium
03 p0491 A69-14114

Carrier scattering mechanisms in n-type GaP, measuring IR radiation absorptivity in Te doped GaP
03 p0492 A69-14168

Photoionization of donor impurities during absorption of IR radiation in n-type Te doped GaP at low temperatures
03 p0492 A69-14169

Quadratic and cubic response in photoelectric emission in potassium antimonide under laser irradiation observed with measurement of energy distribution of excited electrons
05 p0771 A69-15813

Conversion of emission from pulse tube using neodymium laser with luminophor solution filled active element, discussing pumping nonlinear absorption kinetics
05 p0777 A69-16373

Light absorption in semiconductors with electron hole pair formation noting conduction and valence band
06 p0978 A69-16901

Magnetobremstrahlung /synchrotron/ and Cerenkov radiation of ultrarelativistic particles, radiation reabsorption and magnetic field measurement
06 p0962 A69-17245

Ionospheric D layer electron concentration profile from radio wave absorption frequency dependence
06 p0920 A69-17729

Mechanism for laser surface damage of glasses working through optical absorption, fluorescence, chemical reaction by quenching and breakdown
06 p0935 A69-17771

Collisionally induced microwave absorption by non-polar gases, discussing dimer absorption
06 p0962 A69-17816

Absorption edge broadening by electric field in Gunn domain of N-GaAs crystals
07 p1197 A69-18454

Interstellar light absorption in Milky Way region of Cepheus analyzed by excess color technique
07 p1216 A69-18855

Laser beam absorption induced index changes associated with thermal blooming observed in iodine doped carbon tetrachloride, using Mach-Zehnder interferometer
07 p1149 A69-18899

Milky Way local spiral arm 10 MHz absorption, noting interstellar absorption effect and evidence for cool electron gas
08 p1383 A69-19900

Optical absorption index for molten beryllium oxide based on measurements of small beryllium/ solid propellant rocket motor exhaust plumes
08 p1351 A69-20149

Picosecond light pulse measurement by two photon excitation of photographic film
08 p1313 A69-20165

Atmospheric propagation properties of laser light, discussing particle absorption, gaseous absorption and refractive index disturbance effects
09 p1518 A69-22129

Ferromagnetic composite materials for microwave absorption and shielding over frequency band 0.3 to 10.0 GHz
09 p1510 A69-22352

Probabilities of error, correct reception and signal cancellation in radio communication systems channels with signal absorption fading
10 p1653 A69-23106

Error analysis of Hubble galaxies count to resolve contradiction of values for average optical half thickness tau of galactic absorbing layer
10 p1779 A69-23609

Gas laser with nonlinear absorbing cell in resonator, discussing effective gain dependence on squared field amplitude, hysteresis phenomena and output power
10 p1704 A69-23625

Low energy particle effects on midlatitude lower ionosphere conditions after July 7, 1966 proton flare, using ground based measurement
10 p1684 A69-23782

Light absorption of In and Ga thin films in various gaseous media, noting displacement of irregular absorption band
10 p1747 A69-23792

Midlatitude ionospheric disturbances accompanied by auroral type radio absorption observed by radio astronomy and probes during May 26, 1967 storm
10 p1688 A69-23935

Xenon pulse discharge plasma temperature distribution, spectral brightness density and light absorption across quartz tube section, noting temperature drop near wall
10 p1742 A69-24081

Polarized Hartree-Fock model computing photoionization cross sections for Li isoelectronic sequence, listing phase shifts for partial waves of scattered electrons
11 p1922 A69-25260

Centrifugal instability of plasma column generated by cyclotron absorption of microwave power in magnetic mirror field
11 p1931 A69-25366

Reflection and absorption characteristics of two dimensional array of magnetic dipoles for microwaves, considering element orientation and distribution
12 p2035 A69-25901

Reabsorption effect of emitted quantum on lifetime of excited levels in gas laser, determining capture factor
12 p2104 A69-26028

Laser beam damage in glass blocks, noting high speed photographic study and absorption of light by inclusions
12 p2117 A69-26193

Elastoplastic stress wave generation by penetration of impulsive electromagnetic radiation through thin surface layer of solid
12 p2179 A69-26215

Pulsar distances estimated from neutral hydrogen absorption, using observations from 140 ft telescope
12 p2156 A69-26224

Optical constants of bulk diamonds compared with interstellar extinction, calculating extinction curves for diamond particles from Mie theory
12 p2157 A69-26230

Optical absorption cell with variable path length and temperature for measuring absorption coefficients of gases at low and high temperatures
12 p2093 A69-26482

Ionosphere formed waveguide electromagnetic field determined by expression, accounting for radio wave absorption during communications via artificial satellites
13 p2224 A69-28692

Sudden cosmic noise absorption in ionosphere confirming relationship with solar chromospheric flares
13 p2334 A69-28698

Terrain roughness effect on ionospheric radio wave absorption measurement data compared with theoretical results
13 p2224 A69-28700

Seasonal variation in ionospheric radiation absorption related to time variation between sunrise and constant angle attainment of sun
14 p2437 A69-29072

Radio wave absorption coefficient in lower ionosphere related to total radiation absorption and electron concentration profile
14 p2411 A69-29075

UV radiation decreased transmittance through quartz exposed to plasma at high temperature and pressure, showing dependence on heated surface layer absorption
14 p2490 A69-29159

Ionospheric radio wave absorption at midlatitude, noting mesospheric zonal wind inversion
14 p2441 A69-29418

Neodymium laser having adjustable pulse duration and homogeneous spatial radiation structure developed by two photon absorption
14 p2460 A69-29670

Frequency dependence of light absorption by excitons obtained for allowed and forbidden zone transfers in semiconductors
15 p2632 A69-30057

Interstellar absorption and spatial distribution in northern Aquila with absence of early O-B2 stars, including luminosity function
15 p2683 A69-30513

CNA and geomagnetic pulsations observed by ground based instruments in southern auroral region occurring near geomagnetic noon, noting electron precipitation role
15 p2597 A69-30697

Two photon absorption excitation of luminescence in ruby crystals by neodymium laser radiation, determining luminous intensity dependence on pumping intensity
15 p2634 A69-30731

Pressure and wavelength dependence of molecular O absorption coefficient near 1215 A, utilizing UV emission from crossed beam atomic collision
15 p2656 A69-31031

Nonresonant absorption and dispersion of microwaves by gases, studying gaseous mixtures, relaxation parameters, anomalous dispersion and temperature effects
15 p2654 A69-31219

Solar X rays intensity and spectrum effects on e layer critical frequency and D region ionospheric absorption
15 p2677 A69-31346

Laser radiation absorption by inhomogeneous overdense plasma, discussing effects of plasma expansion on energy coupling efficiency
16 p2818 A69-31679

Ruby laser output energy degradation due to pump light absorption by color centers, discussing roles of defects and impurities in center formation
16 p2795 A69-31697

Magnetotransport-electric effect, analyzing center motion of cyclotron orbit during photon and phonon absorption and current quantity
16 p2826 A69-31823

LF ground based absorption results compared with rocket measured D region electron density profiles
16 p2778 A69-32188

Increase or decrease in light absorption by plasma particles found dependent on laser intensity level
16 p2797 A69-32382

Spontaneous and stimulated aspects of light scattering by absorbing media, relating refraction index to temperature variations and external stresses
16 p2798 A69-32449

Ionospheric winter anomaly duration in height range of mesopause region based on zenith angle dependence of absorption at LF
16 p2782 A69-32456

Radio waves ionospheric absorption dependence on equivalent frequency, showing marked difference for summer and winter conditions
17 p2918 A69-32927

Cosmic radio emission absorption during IQSY at 24.6 MHz, relating diurnal variation of absorption and geomagnetic index F scatter occurrence
17 p2968 A69-33992

Ionospheric absorption and virtual heights relationships for electron density distribution in lower ionosphere, computing model profiles
18 p3125 A69-34248

Optical parametric oscillator output /signal/ frequency locked to absorbing atomic transition, discussing effective linewidth
18 p3133 A69-34263

Anomalous absorption of electromagnetic wave in collisionless dense cylindrical plasma beam in circular waveguide, noting electric field strength for energy transfer
18 p3101 A69-34621

Photodestruction rate of H molecules by absorption of Lyman or Weber band radiation in interstellar space calculated at various distances from early stars
18 p3204 A69-35351

Reflection and transmission measurements on as grown surfaces of tetracyanoquinodimethane, obtaining optical constants by Kramer-Kronig method
18 p3183 A69-35477

Plane electromagnetic wave diffraction on conducting sphere situated in absorbing nonuniform plasma layer
19 p3275 A69-36340

Electroabsorption oscillations in CdTe films compared with results of interband transitions theory
19 p3386 A69-36523

Hot electrons effect on Fe-doped CdTe optical absorption by measuring optical transmission vs photon wavelength at liquid helium temperatures
19 p3389 A69-36551

Optical and thermal attenuation of current induced by low energy electron bombardment in CdS crystal
19 p3392 A69-36727

Ruby laser-ultrahigh vacuum device for studying electron and ion emissions and light absorption of materials, noting influence of adsorbed gas layers
20 p3553 A69-37406

Lower ionosphere radiation absorption at 4.01 MHz determined using A-3 method in measuring radio wave field between radio transmitters
20 p3528 A69-37675

Cosmic radio emission absorption in D, E region and in F 2 layer above and below electron concentration maximum from vertical ionospheric sounding 1959 over Moscow
20 p3590 A69-37676

Ionospheric radio wave absorption seasonal and diurnal variations over Tiflis from pulsed ionospheric sounding at 2.2 MHz
20 p3491 A69-37677

Lower ionospheric effective electron collision number from cosmic noise recordings and radio wave absorption data obtained by vertical sounding rocket
20 p3528 A69-37679

Frequency dependence of radio wave absorption in ionosphere at 2.2-4 MHz by impulse method, noting effect of sporadic layer
20 p3491 A69-37680

Cepheus light attenuation curve explained by applying polymodal particle size distribution, obtaining interstellar dust density
20 p3608 A69-38048

Emission kinetics of passive Q switched laser without constraints on relaxation time and switching characteristics of absorption centers and medium
21 p3740 A69-39550

Spectral dependence of optical absorption in InSb thin films under conditions of quantum dimensional effect, considering allowance for nonparabolic conduction zone
21 p3783 A69-39560

Spectrophotometric analysis of interstellar absorption in direction of IC 1805 cluster, noting anomalies
21 p3814 A69-39576

Absorption spectra from excited metastable states in tunable dye laser pumped atomic Ca, using fast flashlamp continuum
21 p3775 A69-39740

Corpuscular radiation intensity measurements in upper atmosphere at midlatitudes by meteorological probe during geomagnetic storm, noting radio wave absorption
22 p4008 A69-41104

Absorption coefficient measurement for hydrocarbon gases for He-Ne laser beam at 3.39 microns, tabulating coefficients, noting variations from spectroscopic data
23 p4174 A69-42192

Approximate expressions derived from Appleton-Hartree magnetoionics formula tested for validity in computation of radio wave absorption in model ionospheric layers
23 p4126 A69-42354

Ionospheric radio waves constant absorption term obtained from sunrise and sunset data
23 p4127 A69-42424

Ionospheric nondeviative radio wave absorption, noting roles of collisional and working frequencies and solar zenith angle
23 p4127 A69-42425

Laser hazard probability assessment in various applications, discussing power characteristics, attenuation by absorption and scattering and radiant energy spatial distribution
24 p4327 A69-42576

Ionospheric absorption relationship to major stratospheric sudden warmings, considering regional coincidence and interaction mechanism
24 p4306 A69-42680

Auroral vLF emission bursts simultaneous with sharp ionospheric absorption dip and SC deflections in geomagnetic H, noting corpuscular ionization
24 p4308 A69-43001

ELECTROMAGNETIC COMPATIBILITY

Pulse shape influence on electromagnetic compatibility and transmitter efficiency, discussing trapezoidal, raised-sine, sliced and complete error function shapes
01 p0030 A69-10631

Compatibility requirements and considerations of range telemetry tape crossplay operations, discussing major classes
07 p1133 A69-19117

Magnetic field susceptibility testing method as defined in DOD Electromagnetic Compatibility Control documents MIL-STD-461 and MIL-STD-462
17 p2947 A69-34133

Electromagnetic compatibility /EMC/ hardware design, discussing NDC 1060 computer configuration, requirements and service environment
17 p2947 A69-34136

Integrated systems testing for unmanned spacecraft electromagnetic compatibility, discussing identification and elimination of interference sources
21 p3683 A69-39438

High sensitivity communication system design consisting of radome enclosed steerable antenna, 500 kw transmitter and microwave configuration compatible with low noise receivers
23 p4149 A69-42131

Electromagnetic compatibility, - IEEE Conference, Asbury Park, New Jersey, June 1969
23 p4140 A69-42215

Natural and man-made radio noise measurements, including formula for calculating signal strength of coherent interference
23 p4126 A69-42217

Electromagnetic compatibility /EMC/ quantification in system effectiveness by decision analysis technique, constructing conceptual model
23 p4145 A69-42227

Colocated radio equipment time-sharing scheme for interference avoidance, describing switching method and sampling signal shape
23 p4142 A69-42228

Receivers EMC, discussing single parameter to evaluate susceptibility to desensitization, cross modulation and intermodulation
23 p4142 A69-42232

Electromagnetic compatibility /EMC/ filter design and test methods to achieve effectiveness and reliability, emphasizing transfer impedance characteristics
23 p4142 A69-42233

Airplane structure electromagnetic compatibility engineering problem including bonding, electrointerference suppression and static control considerations
23 p4063 A69-42234

ELECTROMAGNETIC CONTROL

U ELECTROMAGNETS

U REMOTE CONTROL

ELECTROMAGNETIC DEDUCTION

U MAGNETIC INDUCTION

ELECTROMAGNETIC FIELDS

NT FAR FIELDS

Einstein-Maxwell equations corresponding to superposed electric and magnetic fields stationary solutions, noting singularities in metric tensor
01 p0115 A69-10020

Multiphoton ionization cross section of atom via perturbed Green function, considering light wave electromagnetic field perturbing effects on atomic levels
02 p0283 A69-11539

Symmetric tensor of time averaged stresses for collisionless plasma in oscillating field derived by Maxwell equations
02 p0286 A69-11588

Electromagnetic fields in vacuum extended to fields in presence of matter, deriving field equations covariant under Lorentz proper and improper transformations
02 p0281 A69-12196

Light-light interaction in homogenous media ascribed to multilevel atomic system simultaneous excitation by both fields
02 p0258 A69-12637

Transverse radiation field distribution in CW laser found by geometrical optics approximation, assuming active two level medium and mode close to threshold
02 p0258 A69-12642

Electromagnetic oscillations in ionized plasma, assuming higher oscillation frequency than collision frequency
02 p0292 A69-12643

Electric field, current density and magnetic induction of plasma flow measured, obtaining plasma conductivity and flow velocity for electron temperature and density
03 p0473 A69-12877

Electromagnetic diffraction theory for radar cross section of aircraft, missiles and satellites, discussing mathematical representation of electromagnetic field for extreme wavelengths
03 p0383 A69-12902

Wave fields and coupling of RF power to ion cyclotron waves in finite length thermal collisional plasma column
03 p0474 A69-13114

Plasma equation of motion in external electromagnetic field analyzed as generalization of Bernoulli equation in relativistic MHD
03 p0476 A69-13385

Electromagnetic and gravitational tensor fields in Riemannian space, generalizing Maxwell and Bel-Robinson tensors
03 p0467 A69-13755

Electromagnetic theory of gravitational forces unifying electromagnetic, meson and gravitational fields
03 p0469 A69-14096

Trouton-Noble experiment to detect motion of earth through ether by electromagnetic torque on charged suspended parallel plate capacitor, explaining null results
03 p0517 A69-14106

Driving point admittance of radiating aperture in infinite periodic planar phased array, determining coefficients of waveguide modal expansion and Floquet series
04 p0571 A69-14315

Electromotive force along magnetic field induced by liquid metal flow /alpha effect/, giving foundation for self excitation of electromagnetic field
04 p0635 A69-14547

Space-frequency correlation relationship of complex field fluctuations, amplitude and intensity to levels and phases of waves propagating in medium of random inhomogeneities
04 p0557 A69-14774

Noise stability of phase and amplitude information of regular interference pattern of electromagnetic field
04 p0557 A69-14775

Field theories and direct interparticle action theories of classical electrodynamics, establishing general correspondence between formalisms
04 p0631 A69-15189

Waveguide field of arbitrary cross section determined on models with quasi-static fields
05 p0717 A69-15635

Equations for frequency portions of electron-velocity distribution function in Lorentz plasma under influence of time periodic electromagnetic fields with two fundamental frequencies
05 p0800 A69-15743

Feynman rules for electromagnetic and Yang-Mills fields from gauge independent path dependent field formalism
05 p0794 A69-16363

Coupled waves in ferromagnetic and antiferromagnetic semiconductors in constant electric and magnetic fields, discussing spin, electromagnetic and plasma waves dispersion
05 p0809 A69-16548

Kinetic equation for plasma in external inhomogeneous nonstationary electromagnetic field, noting perturbation theory and Vlasov approximation
05 p0805 A69-16700

Electric and magnetic fields of narrow coherent polarized light beam in free space, noting longitudinal field components due to beam narrowness
05 p0777 A69-16789

Electromagnetic properties associated with presence of overlapping bands in pure superconductors, discussing temperature dependence
05 p0810 A69-16802

Mathematical description of electromagnetic field containing plasma, discussing energy transfer modes between plasma and containing field
06 p0965 A69-17517

Earth electromagnetic field micropulsations associated with proton flare, evaluating data from polar caps, auroral zones and midlatitudes
06 p0996 A69-17754

Resonant frequencies and fields in circular cylindrical microwave cavity containing cold uniform magnetoplasma dielectric
06 p0968 A69-17763

Electromagnetic field induced energy and momentum changes effects on pressure, temperature and particle velocity of flows behind propagating gaseous detonation waves
06 p0970 A69-18084

Domain oscillations removal in n-type gallium arsenides by externally applied microwave field, noting doping effect on LSA conversion efficiency
07 p1196 A69-18446

Hydrogen arc in axially parallel magnetic field produces higher plasma temperatures by reduced thermal conductivity coefficient
07 p1189 A69-18489

Electromagnetic field strength of narrow polarized monochromatic light beam, noting spatial curvature and twisting in beam current line
07 p1147 A69-18524

Field diffraction at finite metallic surface represented in eigenfunctions of discrete spectrum, considering forced oscillations of open circuit
07 p1463 A69-19151

Electron anomalous magnetic moment effect on nonlinear Lagrangian of electromagnetic field, deriving additional nonlinear corrective term
08 p1353 A69-19781

Double diurnal oscillation of atmospheric pressure and vertical gradient of electromagnetic field, noting agreement between diagrams and role of atmospheric tides
08 p1306 A69-19866

Corrections to relativistic plasma thermodynamic functions associated with electromagnetic field effect, demonstrating inapplicability of Darwin Hamiltonian to problem
08 p1359 A69-19953

Electromagnetic fields and magnetic and dielectric constants in fiberglass reinforced polymers determined by treating polymers as ideal dielectrics
08 p1336 A69-20336

Electromagnetic field of infinite helical sheath, basing calculations on previous helical antenna studies
09 p1463 A69-21682

Temporal and spatial coherence effects of optical fields and relationship to multipole coherence effect
09 p1540 A69-22083

Magnetic field plane radiation patterns for tapered dielectric rod antennas computed by Schelkunoff principle, noting taper angle effect on lobes
09 p1464 A69-22097

Geometrized theory of combined gravitational and electromagnetic fields, using metric tensor of four dimensional Riemannian continuum to describe both fields
09 p1540 A69-22134

Maxwellian field and second order invariant system in vacuum in three dimensional Riemannian space with positive-definite metric, discussing Lorentz invariant equations
09 p1541 A69-22392

Cosmic charged particle acceleration in electromagnetic field described by vector and scalar potentials, constituting plane electromagnetic wave propagating along z axis
10 p1756 A69-22816

Solar activity effect on interplanetary electromagnetic field according to cosmic ray modulation data, noting ineffective correlation and solar wind effects
10 p1759 A69-22841

Relativistic energy momentum tensor of electromagnetic field in moving multicomponent dispersive media and instability of wave
10 p1653 A69-23193

Slow electromagnetic wave propagation along cold collisionless cylindrical plasma in axial magnetic field, noting surface wave metamorphosis into bulk waves
10 p1739 A69-23659

Earth electromagnetic micropulsations in connection with July 7 1966 proton flare, discussing peculiarities in occurrence of pearls before and after flare
10 p1683 A69-23779

Matrix formulation of electromagnetic field equations and nonlinear conservation laws for measurable quantities
10 p1725 A69-24049

Weakly ionized gas in crossed electromagnetic fields, formulating Ohm law from Ginzburg equations
11 p1925 A69-24319

Coherence theory of electromagnetic field from classical/wave/ or quantum/particle/ standpoint, stressing information theory
11 p1915 A69-24455

Adiabatic theory of charged particle motion in electromagnetic field, applying asymptotic methods of nonlinear oscillations theory
11 p1948 A69-24857

External modulated currents induced electromagnetic field effect on density distribution of bounded plasma, discussing fluctuations in various configurations
11 p1927 A69-24910

Statistical properties of electromagnetic field diffracted by illuminated plane aperture studied in Fresnel zone on basis of partial coherence theory
11 p1836 A69-24978

Propagated ray paths plotted as functions of frequency and launch angle to predict signal dispersions
11 p1837 A69-25003

Charged particle motion in periodic electromagnetic field, constructing dynamic variables describing motion
11 p1927 A69-25100

Radiation emission by scalar particle in field of two plane linearly polarized electromagnetic waves propagating toward each other
11 p1900 A69-25568

Electromagnetic fields in cylindrically symmetrical microwave resonator filled with premagnetized ferrite along cylinder axis
11 p1855 A69-25625

Electromagnetic field penetration into plasma cylinder having electron mean free path comparable with plasma diameter, noting anomalous skin effect
12 p2133 A69-25833

Saddle point analysis of electromagnetic ground wave propagation in source excited field in waveguide formed by two parallel plate dielectrics
12 p2028 A69-25898

Steady equilibrium collisionless plasma in oscillating electromagnetic field, describing formalism for linear relation between perturbation and charges and currents induced in plasma
12 p2135 A69-26284

Laser active media polarization in strong electromagnetic fields, solving boundary value problems
12 p2110 A69-26907

Two photon and resonance parametric lasers nonlinear polarization theory, deriving equations for electromagnetic field oscillations
12 p2110 A69-26910

Electromagnetic field in idealized medium of uniformly curved gas lens for light beam waveguide, describing lens radius effects on incident beam spot
12 p2270 A69-27181

Radio wave propagation in anisotropic inhomogeneous medium, obtaining reflection and conversion coefficients and electromagnetic field distribution
13 p2218 A69-27182

Vlasov equations solved for electrons and ions in electromagnetic field, coupling electric field to density oscillation modes of plasma
13 p2306 A69-27461

Electromagnetic field induced plasma oscillation amplitude dependence on field frequency as function of field amplitude and discharge current at low N pressures
13 p2313 A69-28332

Variational method for time invariant states of collisionless plasma in oscillating electromagnetic field
13 p2314 A69-28365

Unified geometric description of gravitational and electromagnetic fields, determining electromagnetic field influence on geometry from dimensional constant
13 p2300 A69-28450

Electric field distribution in TWT electron beam deflection system determined, accounting for current-voltage characteristics dependence on electromagnetic field distribution
13 p2237 A69-28582

Surface impedance of spherical earth isolated by nonconducting atmosphere from ionospheric currents producing alternating electromagnetic field
14 p2438 A69-29082

Time averaged stress tensor for ionized plasma in HF electromagnetic field, considering collisions
14 p2493 A69-29649

Si III and O II spectral lines distortion in pulse HF plasma in rotating electromagnetic field, showing particle rotational speed dependence on discharge chamber radius
14 p2497 A69-29791

Boundary problems solution for electromagnetic field two dimensional distributions in MHD channels at arbitrary magnetic Reynolds numbers, considering longitudinal terminal effects
14 p2500 A69-29906

Field equations for plane-parallel induction MHD machines with allowance for winding zone thickness and magnetic permeability of iron
14 p2405 A69-29914

Theory of field distribution in antenna aperture extended to scanning with desired shape beam
15 p2578 A69-30634

Integral equation for diffraction from infinitely extended grating as mixed boundary problem of electromagnetic field, discussing single anomaly
15 p2568 A69-30795

Plane monochromatic and pulsed electromagnetic waves penetration into metal cylindrical shells, deriving equations for electromagnetic field in interior
15 p2569 A69-30950

Weakly ionized plasma electron heating by interaction with HF electromagnetic field calculated using Boltzmann transport equation
15 p2665 A69-31480

Quasi-linear theory of waves in collisionless plasma in absence of external fields, relating wave energy growth and decay to plasma stability
16 p2817 A69-31646

Waveguide bends fields expressed in coupled local annular modes derived by evaluating differential scattering coefficients
16 p2760 A69-31943

Parametric interaction of electromagnetic field with spherical cavity having time variable radius, considering wave diffraction and TM oscillations
16 p2751 A69-32029

Electromagnetic fields in closed one dimensional resonators with oscillating boundary, analyzing amplitude buildup
16 p2751 A69-32030

Electromagnetic wave diffraction in plasma cylinder of small nonuniform radius, analyzing interior field and radio wave reflection
16 p2751 A69-32031

Waveguide field of arbitrary cross section determined on models with quasi-static fields
16 p2762 A69-32493

Electromagnetic field eigenvalues along conductive circular cylinder in magnetoionic medium, assuming lossless medium and field frequency not equal to cyclotron frequency
16 p2754 A69-32568

Laboratory plasma produced by electromagnetically generated shock front propagation through ionized hydrogen [AIAA PAPER 69-693]
17 p2945 A69-33447

Electromagnetic fields theory simultaneously determining vector electric and magnetic field aspects in terms of operator Green functions
17 p2924 A69-33833

Propagation in inhomogeneous and dispersive media, noting potential functions for vector electromagnetic field
17 p2924 A69-33838

Arbitrary electromagnetic field prediction based on spherical harmonics expansion method using field points measurement data, determining electromagnetic properties of environments
17 p2929 A69-33881

Electromagnetic field formulation of eigenvalue problem for optical coaxial dielectric waveguide, using computer root searching method
17 p2930 A69-33892

Polar ionosphere investigation based on vertical sounding and riometric observations, earth electromagnetic field and polar auroras spectrum intensity variations
17 p2963 A69-33950

Linear irreversible thermodynamics theory as applied with conservation principles and Maxwell relations to charged particle motion in electromagnetic field, noting Onsager coefficients role
17 p3075 A69-34142

Electromagnetic induction in concentric thin shell-enclosed solid conducting sphere immersed in varying electromagnetic field [AFCRL-69-0082]
18 p3101 A69-34803

Microfluctuations frequency and wavelength of electromagnetic, electric and magnetic field distributions in plasma shock wave front found consistent with ion-acoustic origin hypothesis
18 p3180 A69-35017

Semiconductor plasma DC overheating instability in electric and magnetic fields, determining growth increments of oscillation amplitude
18 p3182 A69-35022

Radiation emission by molecules in electromagnetic field, considering cavity resonators and waveguides excitation
18 p3178 A69-35404

Hyperbolic EM microwave field used for contactless measurements of parabolic antenna surfaces
19 p3281 A69-35766

Ponderomotive forces and sudden irregularities in earth rotation, discussing core-mantle electromagnetic coupling and toroidal field induction effects
19 p3302 A69-35769

Parametric conversion kinetics of monochromatic light waves in nonlinear crystals, using quantized electromagnetic field to study amplification and generation
19 p3332 A69-35870

Wave equation of electromagnetic field of optical resonator with arbitrary mirrors, utilizing Schroedinger equation and equivalent mechanical system
19 p3333 A69-35880

Microwave holograms generated by spinning dipole field perturbation technique, showing zone plates and moire fringe resolution

19 p3315 A69-36824

Electromagnetic field of horizontal LF electric dipole formed by thin ionosphere layer between anisotropic planes

20 p3521 A69-37047

Terrestrial electrical conductivity measurement from electromagnetic field variations determination by geomagnetic sounding

20 p3522 A69-37058

Stationary electromagnetic wave fields LF behavior, discussing integral operators, incident and tangential fields, single valued solutions, etc

20 p3487 A69-37071

Singular electromagnetic field rectilinear and elliptical polarization in general relativity, calculating light plane rotation in Schwarzschild space

20 p3576 A69-37431

Vertically moving ionospheric disturbances altitude estimated from geomagnetic pulsations in earth electromagnetic field

20 p3528 A69-37686

Received electromagnetic fields fluctuations due to transhorizon propagation, emphasizing fading- tropospheric turbulence correlation and rapid fluctuations due to small scale index variations

20 p3494 A69-37810

Electromagnetic waves attenuation and field structure within gas filled dielectric waveguide tube, tube walls and waveguide surroundings

21 p3674 A69-39123

Synoptic study of worldwide VLF electromagnetic wave fields distribution above ionosphere from Ariel 3 observations

21 p3717 A69-39262

Constitutive equations for homogeneous viscous fluid and Kelvin-Voigt viscoelastic solid in electromagnetic field, using linear irreversible thermodynamics and continuum mechanics

21 p3851 A69-39289

Field equations for electromagnetic radiation propagation in accelerated systems including dispersive and nonisotropic media

21 p3772 A69-39466

Level shifts and spontaneous transitions in steady state of universe by path integral method of first quantization, considering time symmetric electromagnetic theory

22 p3980 A69-40169

Electrical properties of semiconductors in HF electromagnetic field, showing Dember type EMF dependence on carrier response to field inhomogeneity

22 p3993 A69-40605

Electron-positron pair formation in electromagnetic field created by coherent laser light focused into vacuum with ideal lens

22 p3965 A69-41116

Parametric losses in nonlinear centrosymmetrical ferroelectric ceramic in strong microwave field at temperatures above Curie point

22 p3996 A69-41164

Dirac equation in external electromagnetic fields, deriving solution for constant orthogonal electric and magnetic fields encountered in plasma transport

23 p4190 A69-41357

Rumanian book on MHD covering electromagnetic field theory, motion equations, laminar flow, MHD generators, fluid motion past thin airfoils, shock waves, etc

23 p4195 A69-41363

Accelerated motion influence on onboard vertical gyro with design based on free astatic gyro with electromagnetic compensation

23 p4163 A69-41553

Ionosphere reflected radio waves field strength measurements, obtaining formula for ground wave discrimination

23 p4123 A69-41861

Ridge-slot-ridge slow-wave structures used in multibeam TWT/traveling wave tube/, analyzing E type electromagnetic dispersion as function of system parameters

23 p4140 A69-42049

High intensity electromagnetic fields generation equipment for calibrating field intensity monitors, discussing anechoic chamber, transmitting antenna, etc

24 p4312 A69-42577

ELECTROMAGNETIC INTERACTIONS

NT PLASMA-ELECTROMAGNETIC INTERACTION

Resonance energy transfer mechanism in Forster-Dexter theory of electron energy transfer by resonance

interaction in condensed media, using many particle treatment

01 p0121 A69-11257

Electromagnetic waves parametric interactions during unsteady Josephson effect as function of wavelength ratio, magnetic field penetration and contact dimensions

02 p0293 A69-11464

Electromagnetic field interaction with polarizable elastic medium in gravitation theory resolves definition of electromagnetic energy in matter

02 p0279 A69-11537

Weak signal interaction between electron beam and microwave resonators, obtaining electron conductance, gain and transfer admittance

02 p0208 A69-12265

Light-light interaction in homogenous media ascribed to multilevel atomic system simultaneous excitation by both fields

02 p0258 A69-12637

Unsteady phenomena during light pulses interaction in media with polarization, considering group delay, dispersion spreading and space-time analogy

02 p0259 A69-12646

Generation of UHF space charge waves by nonlinear interaction of two microwave signals in magnetoplasma, predicting optical mixing

03 p0475 A69-13146

Model for predicting characteristics of short duration intense microwave pulse propagating in heated high temperature air

04 p0634 A69-14453

Total conserved momentum-energy of electromagnetic interaction of system of point charges in Wheeler-Feynman theory, noting mass defect of connected system

04 p0631 A69-15058

Interaction between point charges in Wheeler-Feynman electrodynamics, noting impossibility of deducing momentum and energy conservation from variational principle

04 p0631 A69-15059

Field theories and direct interparticle action theories of classical electrodynamics, establishing general correspondence between formalisms

04 p0631 A69-15189

Multielement antenna array radiators interaction taking into account edge effects

05 p0727 A69-15638

Modulation of galactic cosmic rays due to electromagnetic conditions of interplanetary space, considering time variations and Parkers model

06 p0989 A69-17287

Small signal coupled mode analysis including relativistic effects for studying spiraling electron beam interaction with fast wave circuits

07 p1114 A69-18436

S matrix theory of electromagnetic interactions, obtaining equivalence of results with quantum electrodynamics by choice of subtraction constants

08 p1351 A69-20211

Collective interactions of electromagnetic waves in plasma, discussing light scattering from electron fluctuations, stimulated emission and anomalous absorption

08 p1361 A69-20220

Slow distribution function of magnetoactive plasma, deriving kinetic equation in quasi-linear approximation for analyzing particle-HF electromagnetic wave interactions

08 p1365 A69-20550

Plasma transport properties derived from Boltzmann equation using Debye shielded Lande potential to represent collisions, noting viscosity and thermal conductivity

09 p1553 A69-22539

Busbar effect on interaction between conducting fluid flow and traveling wave magnetic field created by long line with concentrated inductance and capacitance, deriving line gain

10 p1727 A69-23101

Total energy-momentum interaction of system with mass defect in Wheeler-Feynman theory of electromagnetic interaction, demonstrating existence of gauge invariance

11 p1915 A69-24326

Pulsed molecular nitrogen laser positive UV and IR systems interaction under varying gas pressure, applied voltage and tube diameters

11 p1893 A69-24346

Quantum oscillators interaction with two level molecules system in circular laser

11 p1899 A69-25325

Laser active media polarization in strong electromagnetic fields, solving boundary value problems

12 p2110 A69-26907

Two photon and resonance parametric lasers nonlinear polarization theory, deriving equations for electromagnetic field oscillations

12 p2110 A69-26910

Model for perturbations in earth rotation and geomagnetic core-mantle coupling, discussing electromagnetic restoring torque

12 p2077 A69-27110

Shear stress and velocity profile in MHD duct, examining turbulence damping by electromagnetic coupling

13 p2309 A69-28024

Optical maser induced electrical breakdown interaction with superhigh pressure ionized gases, using optical interferometry and holography

13 p2273 A69-28464

Weakly divergent intense light beam propagation in laminar optically inhomogeneous medium with self focusing possibility analyzed by perturbation theory

13 p2223 A69-28568

Current distribution along linear antenna array taking into account interaction between neighboring elements and effect on antenna radiation characteristics

13 p2236 A69-28572

Spatial harmonic spectrum and tangential field distributions in microwave devices showing separation of higher harmonics through delay structure

13 p2236 A69-28576

Equations describing interaction between HF and LF waves propagating in nonlinear dispersive medium, obtaining approximate solutions

15 p2568 A69-30733

Electromagnetic muon-nucleon interaction explanation for observed horizontal air showers, reexamining shower data in view of triplet particles

15 p2678 A69-31498

Injection semiconductor lasers emission characteristics, discussing gallium arsenide diodes, nonlinear losses in pulsed mode, laser interactions, etc

16 p2796 A69-31949

Electromagnetic vibration exciters based on permanent magnet and AC coil interaction

16 p2790 A69-32077

Spontaneous and stimulated aspects of light scattering by absorbing media, relating refraction index to temperature variations and external stresses

16 p2798 A69-32449

Multielement antenna array radiators interaction taking into account edge effects

16 p2762 A69-32496

Current distribution and scattering cross section of missile with plume/ionized trail/of tapered conductivity due to plane wave electromagnetic excitation

17 p2921 A69-33671

Nonresonance parametric phenomena in distributed systems, discussing interaction between signal and parameter wave at superlight velocity

17 p2928 A69-33868

Electromagnetic and cyclotron waves interaction across opaque boundary in moving plasma in one dimensional approximation

18 p3181 A69-35027

Mathematical methods for quantum mechanical problems caused by electromagnetic field interaction with matter

18 p3175 A69-35402

Plane electromagnetic wave interaction with moving conductive dielectric medium to obtain reflection and transmission coefficients, noting energy transfer

18 p3105 A69-35486

Coherent radiation generation using gas lasers, analyzing interaction between EM radiation and matter

19 p3335 A69-36067

Cs jet device eliminating wall influence in nonlinear radiation-atom interaction phenomena

19 p3376 A69-36174

Soviet book on quantum electronics covering electronic devices, nonrelativistic quantum mechanics, radiation field and matter interaction, black body radiation spectra, etc

20 p3556 A69-38210

Transverse wave-beam interaction propagation in fast wave structure in finite homogeneous magnetostatic field, deriving wave-beam equation for nonrelativistic beams

21 p3672 A69-38435

Interaction between modes of radiation field and active medium in laser with nonresonant feedback, discussing amplitude stabilization of total radiation

21 p3735 A69-38581

ELECTROMAGNETIC INTERFERENCE

Dimensionless coupling constants predicted from causal relationship among strong, electromagnetic, weak and gravitational interactions in fluid region of universe
22 p3981 A69-40416

Quantum optics or electronics, discussing electromagnetic waves control and interactions with matter, maser oscillators theory and characteristics, nonlinear optics, induced transparency, etc
23 p4174 A69-42315

Coil under alternating current interacting with laminated conducting structure, giving recurrence formula for calculating deflector voltage
24 p4296 A69-42653

ELECTROMAGNETIC INTERFERENCE

NT ATMOSPHERICS
NT BLACKOUT [PROPAGATION]
NT COSMIC NOISE
NT CROSSTALK
NT DAWN CHORUS
NT HISS
NT IONOSPHERIC CROSS MODULATION
NT IONOSPHERIC NOISE
NT IONOSPHERICS
NT JAMMING
NT POLAR RADIO BLACKOUT
NT RADIO FREQUENCY INTERFERENCE
NT SHOT NOISE
NT SUDDEN ENHANCEMENT OF ATMOSPHERICS
NT THERMAL NOISE
NT WHISTLERS
NT WHITE NOISE

Phase locked loop demodulators for binary PSK signals compared with and without decision directed feedback in presence of CW interference
03 p0409 A69-13201

Sunrise modal interference patterns for VLF propagation, analyzing variations with latitude
03 p0396 A69-13628

Uniform asymptotic expansion series for saddle point integrals applied to probability distribution in noise interference problems
03 p0398 A69-13832

Noise stability of phase and amplitude information of regular interference pattern of electromagnetic field
04 p0557 A69-14775

Decoupling techniques for antennas on aerospace vehicles, noting effects on far field radiation pattern and antenna gain
05 p0729 A69-15977

Nonpolarized single frequency gas laser radiation produced by interferential effects in complex resonator
07 p1149 A69-18936

Electromagnetic interference (EMI) created by noise coupling through conductive paths, discussing responsibility for control within systems management
07 p1079 A69-18944

Thermal noise and other disturbances from mismatched two port isolator in low power microwave transmission antenna noise between generators and leads
07 p1108 A69-19486

Signal interference criteria in considering frequency sharing between communication satellite systems and terrestrial radio services
09 p1449 A69-21273

Earth station antenna radiation patterns for studying mutual interference effects between radio relay stations and communication satellite earth stations
09 p1461 A69-21282

Constant amplitude in-band additive interference for analysis of PSK signals in Gaussian noise, discussing coherent and differential detection
09 p1455 A69-21848

Equal inclination interference fringes effects on laser beam reflection from plane parallel glass plates, evaluating angular distance between adjacent fringes
11 p1896 A69-24840

Graphs determining interference levels for optimum shielding, suppression, signal parameters and waveforms for pulses, step functions, CW signals and for military technology
12 p2030 A69-26471

Received signal phase angle error probability in coherent PSK system in Gaussian noise and interference
13 p2219 A69-27665

Limiting incoherent or coherent interference signals at frequency of biphasic or quadriphase digital signal
14 p2413 A69-29483

Calibration of interference measuring instruments, stressing input impedance calibration of field intensity meters
15 p2577 A69-30375

Electromagnetic interference correction for airborne telemetry, illustrating actual and simulated data for interfering source signatures identification
16 p2754 A69-32575

Active antenna impedance matching network constituting low noise device for electromagnetic interference measurements useful for automatic or manual scanning
17 p2943 A69-34131

Airborne communication receiver solid state interference blanker circuitry comprising black box insertable between antenna and RF input
17 p2943 A69-34132

Interference filter design for IR devices on Fresnel equation basis, analyzing plane electromagnetic wave propagation through stratified dielectric multilayer
19 p3373 A69-36053

Integrated systems testing for unmanned spacecraft electromagnetic compatibility, discussing identification and elimination of interference sources
21 p3683 A69-39438

Electromagnetic waves emission intensity in one dimensional resonator, allowing for wave interference effects
22 p3966 A69-41172

Recursion formula for multilayer interferometer derived, with allowance for multiwave interference, to calculate resonant circuit maxima and minima
23 p4165 A69-41729

Linear filtering effects in channel with binary direct sequence antipodal biphasic modulation in presence of white noise and sinusoidal interference, noting variance
23 p4122 A69-41774

Electromagnetic interference (EMI) characteristics of various digital logic ICs
23 p4141 A69-42219

HF receiver interference blanker, discussing limiter-blanker system, integration, effectiveness and squelch circuit
23 p4141 A69-42221

Interference prediction models of equipment emissions and susceptibility thresholds based on limited spectrum signature data
23 p4126 A69-42223

Aircraft antenna-coupled electromagnetic interference analysis, describing mathematical model for frequency coincidence, power levels and receiver thresholds
23 p4141 A69-42224

Phase-lock loop demodulator ability to acquire and remain locked on signal under noise and pulse interference
23 p4145 A69-42230

ELECTROMAGNETIC MEASUREMENT

Continuous laser beam power output meter based on wire resistance thermometry method
01 p0081 A69-10822

Lunar electrical parameters range determination using models [AAS PAPER 68-199]
02 p0312 A69-11477

Wave measurements of normal electric field and tangential magnetic field over microwave disk antenna surfaces
02 p0219 A69-12342

Electromagnetic phase measurement for determining integrated air density near earth surface
04 p0598 A69-14910

Disturbing TM mode generation effect on attenuation measurement accuracy in TE mode attenuators
08 p1283 A69-20126

Large aperture satellite communication antenna gain measurement technique, using extraterrestrial radio wave source or satellite
09 p1456 A69-22116

One way measurement of dual inband frequency diversity improvement on HF ionospheric path with frequency division multiplexed FSK modulation
10 p1656 A69-23536

Red shift hypothesis postulated on perfect cosmological principle and uniqueness of electromagnetic wavelength measurements, showing agreement with astronomical data
11 p1961 A69-25108

Precision electromagnetic measurements - IEEE Conference, Boulder, June 1968
12 p2037 A69-26046

Microwave measurement methods, discussing uses of digital computers and sampling techniques
13 p2223 A69-28605

Varactor diode parameters measurements by microwave power reflection method
13 p2237 A69-28645

Incoming IR flux measurements at high altitude, noting flux increase due to water vapor condensation in troposphere
13 p2256 A69-28647

Line of sight atmospheric path measurements for atmospheric inhomogeneities, using phase quadrature, microwave and near IR techniques
14 p2415 A69-29516

Worldwide observation of atmosphere with occultation satellites, correcting orbit perturbations to obtain air pressure
14 p2447 A69-29517

Radio pulse sounding of ionospheric structure and motions, discussing digital ionosonde, data analysis methods, etc
14 p2415 A69-29519

FM measurements of angle distortion introduced by single pole bandpass filters compared to theoretical distortion
14 p2416 A69-29552

Design and electrical features of microwave measurement system for solid state spectroscopy, discussing waveguides, signal source, detector, etc
15 p2610 A69-30709

Electromagnetic accelerometer with symmetrically placed photocells detecting small steel ball position
17 p2971 A69-32897

Cosmic X rays diffused component absolute intensity measurement using rotating collimator borne on sounding rocket, noting flat spectrum and Sco X-1 intensity variation
17 p3023 A69-33068

Arbitrary electromagnetic field prediction based on spherical harmonics expansion method using field points measurement data, determining electromagnetic properties of environments
17 p2929 A69-33881

Active antenna impedance matching network constituting low noise device for electromagnetic interference measurements useful for automatic or manual scanning
17 p2943 A69-34131

Pulsar PSR 0833-45 polarization structure frequency dependence measurement leading to model implying radiation emanated from magnetic poles neighborhood
18 p3202 A69-35215

Tunnel diode coupling with spheroidal resonant cavity, describing method of measuring elements for interpretation
19 p3283 A69-35998

Telemetry transmitter-receiver RF links quality determination, emphasizing nonlinear effects measurement by notch noise tests
19 p3270 A69-36239

Radio measurement methods and standards including measurements of attenuation, phase shift, time delay, impedance, field strength, antenna characteristics, RF properties of materials, etc
19 p3276 A69-36426

OGO-F electric and electromagnetic fields measurement for ionosphere using dipole antenna, emphasizing broadband observation covering whistler mode waves
19 p3284 A69-36677

Sequential filter equations for nonlinear system dynamics and observational model with linear estimator, comparing difference between white and colored noise filter results [AIAA PAPER 69-840]
21 p3686 A69-39371

Electromagnetic catheter flowmeter with flexible sensor suitable for branch and artery application to minimize surgical intervention
22 p3889 A69-40058

Electromagnetic cascade showers transition effect in various materials, measuring energy deposition as function of position
22 p3987 A69-41003

Accuracy standards for diffraction measurements of electromagnetic waves incident on periodic arrays, using monochromatic field and plane phase wavefront
23 p4139 A69-42042

Near field effects on accuracy of LF shielded enclosure measurements compared to open field environment
23 p4141 A69-42226

Air density determination using transit time method involving microwave phase measurements
24 p4313 A69-42898

ELECTROMAGNETIC NOISE

NT ATMOSPHERICS
NT COSMIC NOISE
NT DAWN CHORUS
NT HISS
NT IONOSPHERIC NOISE
NT IONOSPHERICS
NT SHOT NOISE

NT SUDDEN ENHANCEMENT OF ATMOSPHERICS
NT THERMAL NOISE
NT WHISTLERS

Direct couplings of autonomous noisy quadrupoles used for noise matching

01 p0043 A69-10591

Digital matched filtering technique for RF interferometer employing carrier modulated by pseudonoise sequence, discussing applications to antenna arrays

01 p0048 A69-11003

VLF electric field measurements from 1 AU heliocentric orbit, noting field oscillations in solar wind and large amplitude HF noise bursts

01 p0035 A69-11224

RF feedback amplifier analytical design, deriving open and closed loop feedback noise figure expressions by use of equivalent noise model

02 p0217 A69-12150

Microwave transistor noise figure, power gain and noise measure as function of source admittance and source reflection coefficient in L and S bands

02 p0219 A69-12427

Noise performance of broadband traveling wave masers with longitudinal or transverse stagger tuned magnetic field

02 p0257 A69-12428

Simultaneous measurement of gain and noise of linear two port device using noise generators as signal sources

02 p0210 A69-12430

Radiometric measurement of attenuation, emission and noise fluctuations due to earth atmosphere in 4 cm to 8 mm range

02 p0210 A69-12432

Calibration of coaxial line noise sources in terms of rectangular waveguide standard, discussing use of adapter for comparison

02 p0210 A69-12436

X band radiometer to minimize errors in calibration of microwave noise sources

02 p0220 A69-12440

Matrix representation of linear active two port noise figures and charts in terms of power wave variables

02 p0211 A69-12444

AM and FM noise in mutually synchronized oscillators

02 p0220 A69-12449

Microwave oscillator AM and FM noise measurement using Schottky barrier diode detector, discriminator, storage oscilloscope and wave analyzer

02 p0220 A69-12453

AM/PM noise conversion in solid state FM microwave signal sources, relating baseband noise power contribution to PM baseband noise power

02 p0212 A69-12462

Clutter rejection using coded burst waveform for airborne early warning /AEW/ and airborne attack type radars

03 p0388 A69-13185

Noiseproof ionization manometer with ion current dual modulation for ultrahigh vacuum measurement in magnetic field with extraneous charged particles interference

03 p0429 A69-13263

Time dependent photoelectron multiplier with low noise for recording long wave laser light pulses

03 p0440 A69-13264

Wide signal and noise statistics range to determine noise rejection characteristics of communication system used for single path and diversity reception

03 p0394 A69-13376

Atmospheric noise amplitude distribution relation to rms phase errors in frequency components of VLF timing pulse

03 p0396 A69-13629

Sensitivity of radio receiver detecting weak sinusoidal and noise signals by counting zero crossings by envelope or phase of signal sum

03 p0405 A69-13717

Multiplication effects on noise in Si avalanche diodes, noting high resolution apparatus for measurement of spatial variations

04 p0573 A69-14332

Schottky barrier mixer diodes and point contact diodes failure, discussing criterion for degradation of noise figure, 1/f noise and reverse breakdown voltage

04 p0574 A69-14352

Onsager reciprocity relations applied to thermodynamics of nonlinearity and noise in diodes

04 p0574 A69-14435

Noise stability of phase and amplitude information of regular interference pattern of electromagnetic field

04 p0557 A69-14775

Etched manganin gauge for shock pressure measurement in high noise environments containing radiation and electromagnetic effects

04 p0603 A69-15431

Low noise shaped beam Cassegrain antenna design for space communications earth station service, noting gain/noise temperature figure and antenna construction

05 p0728 A69-15669

Traveling wave maser and cooled parametric amplifier for ultralow noise preamplification in satellite communication earth terminal installations

05 p0728 A69-15670

Expression derived for correlation function and power spectrum of bearing of set of point radiators, taking into account receiver internal noise

05 p0719 A69-16219

Noise sources representation in pumped nonlinear systems simplifies noise analysis and noise propagation

05 p0720 A69-16345

Measurement methods at IF and baseband sections of microwave links, calculating noise superimposed on each swept measurement curve

05 p0722 A69-16728

Noise measure formula for negative resistance amplifiers imbedded in lossy passive network

05 p0735 A69-16731

Noise description of linear n ports obtainable from spot noise parameters of two ports formed from n port

05 p0741 A69-16732

Noise generation mechanism of Read microwave avalanche diode under large signal conditions

06 p0895 A69-17472

Error and noise sources in analog differentiators, discussing signal distortion minimization techniques and augmentation with linear phase filter

06 p0897 A69-17702

Probe noise in quiescent plasmas investigated using back diffusion type discharge tubes producing low density plasmas and positive plasma columns

06 p0967 A69-17715

Cosmic radio noise absorption in ionosphere, discussing diurnal, seasonal and longer variations of integral absorption

06 p1008 A69-17727

Silicon double injection diode, discussing HF noise measurement, Nyquist noise equivalent circuit for double injection process and source of LF noise

06 p0898 A69-17762

Q factors dependence of IMPATT diode oscillator FM noise, noting excess noise temperature correlation with diode current

06 p0899 A69-17826

Fluctuation phenomena in electromagnetic field in optical spectral region and coherence characteristics of optical fields, analyzing quantum noise

06 p0937 A69-18011

Noise characteristics of transistorized feedback amplifier stages for application in amplifier design

07 p1090 A69-18284

Transistor HF noise factor measurement by semiautomatic device with saturated diode comparison noise source heater current automatically controlled

07 p1090 A69-18292

FM noise in two and three chamber klystron oscillators, discussing tubes to reduce noise and relative merits of active or passive stabilization circuits

07 p1096 A69-18438

Wideband uncooled two stage reflecting parametric amplifiers with low noise temperature, noting application to space stations for telecommunications by satellites

07 p1099 A69-18463

Statistical study of solar radio flux fluctuations incidence, observing absorption and polarization effects

07 p1215 A69-18819

Injection locking method for reducing FM noise in Gunn effect oscillators

07 p1102 A69-18862

Linear noisy two port preceded by nonreciprocal lossless network analyzed, showing existence of associated quantity invariant under lossless transformation

07 p1104 A69-18891

Q switched laser quasi-periodic short pulse emission pattern evolution from broadband noise source, using fluctuating dipole model

07 p1149 A69-18897

Electromagnetic interference /EMI/ created by noise coupling through conductive paths, discussing responsibility for control within systems management

07 p1079 A69-18944

Radio noise generation in topside ionosphere, noting Cerenkov radiation from intense soft fluxes of auroral electrons

07 p1127 A69-19257

Semiconductor diode noise experimental measurements indicating fluctuation-dissipation theorem /FDT/ inapplicability to all quasi-equilibrium systems

07 p1113 A69-19596

Spectral distribution of intermodulation noise of AM and FM transmission systems calculated by probability theory

08 p1271 A69-19916

Thermal feedback generation of 1/f-flicker noise in bipolar transistors, deriving formula for flicker noise voltage of emitter junction

08 p1283 A69-20129

Interference noise in communication satellite receivers and terrestrial radio relay receivers, noting interference reduction transfer factor

09 p1450 A69-21279

Microwave power and low noise transistors, noting continuous wave output and circuit design

09 p1462 A69-21407

Optical parametric noise in water by ruby laser beam for phase matched four photon process

09 p1539 A69-21751

Book on communication theory principles covering Fourier transformation, signal transmission, electromagnetic noise, amplitude, phase, frequency and pulse modulation, etc

09 p1454 A69-21801

Noise factor of two port in terms of various sets of noise parameters and source immittances, giving table for conversion formulas

09 p1455 A69-21897

Tunnel diode amplifier operation in presence of noise

09 p1469 A69-22630

Sporadic noise, false fronts and other noise effects on phase of output oscillations of resonance apparatus

09 p1460 A69-22641

Noise in instrumentation systems, considering coupling and current noise source and reduction by isolation and filtering

10 p1691 A69-23231

Zero crossing statistics measurements for 1/f noise, noting statistically stationary character of probability density distributions of interval spacings between zero crossings

10 p1656 A69-23657

Variance fluctuations of 1/f noise and relation to sample number and lower cut-off frequency, noting nonstationarity hypothesis

10 p1656 A69-23661

Output pulse duration calculation for compressing filter in presence of pulse or continuous FM noise, using parallelogram of arguments method

11 p1844 A69-24445

DC conversion amplifier commutation induced noise and signal ratio as function of shunt capacitance across vibrator load investigated for increased noise stability

11 p1845 A69-24555

Energy gain during diversity reception in presence of random noise calculated, considering signal and noise amplitudes Rayleigh fluctuations

11 p1835 A69-24968

Transmitter frequency increase effect on production of artificial stimulated VLF emissions in magnetosphere

11 p1878 A69-25156

Microwave amplifiers and receivers noise performance factors measurement noting thermal noise, definitions of noise temperatures and noise figure, noise generators, etc

11 p1840 A69-25301

Kalman equations of optimal recursive filter for linear discrete system extended to continuous system through limiting procedure

11 p1859 A69-25408

Intermodulation noise distorting arbitrary frequency-modulated multicarrier microwave signal in satellite transponder, emphasizing nonlinear energy dissipation and AM-FM conversion

11 p1841 A69-25634

LF noise mechanism for forward biased semiconductor p-n junction, noting charge carrier capture in electron traps of carrier depleted region

11 p1857 A69-25705

Laser emission noise and voltage noise cross correlation coefficient for CW GaAs laser diodes at 77 K, noting strong dependence on bias current

12 p2038 A69-26328

Up-converter IR detector noise characteristics for pulse and CW signal detection compared with photoconductive detector

12 p2029 A69-26329

Noise sensitivity of space diversity reception system with narrow beam electrically switchable antennas for incomplete beam separation

12 p2030 A69-26485

LF generation-recombination noise in MOS transistors with depletion region impurity centers, analyzing noise resistance saturation and drain-voltage dependence
12 p2041 A69-26627

LF wave propagation and emission in magnetosphere, discussing steady noise and discrete emissions
12 p2072 A69-26745

Microwave radiometric brightness temperature relationship to soil moisture content for estimating bearing strength
12 p2099 A69-27008

Dispersion relations in semiconductors in magnetic field indicating current anisotropic instability association with excessive noise
13 p2317 A69-27876

Nuclear explosions electromagnetic effects on electronic systems, considering signals emitted from fireball and signal attenuation by changed atmospheric propagation
13 p2234 A69-28344

Noise stability of nonoptimal radar detection system for noise and FM signals, deriving expressions for optimal spectral width
13 p2222 A69-28508

Algorithm for hypothesis optimal tests by series during signal detection in presence of noise
13 p2222 A69-28509

Wide signal and noise statistics range to determine noise rejection characteristics of communication system used for single path and diversity reception
14 p2410 A69-28826

Radio noise of auroral origin analyzed from Northern and Southern Hemisphere reports indicating correlation with auroras, magnetic activity, sunspot cycles and synchrotron radiation
14 p2411 A69-29108

FM discriminator click widths probability distribution function, defining click widths duration from input noise considerations
14 p2422 A69-29553

Frequency distribution and statistical characteristics of high level RF noise produced by high pervance electron beam of magnetron injection gun (MIG)
14 p2449 A69-29558

Electromagnetic noise radiation structure during lightning flash by measuring time duration distribution between pulses
14 p2445 A69-29885

Noise fluctuations transport in convergent flow crossed field electron guns using Monte Carlo method for two dimensional computerized gun simulation
15 p2572 A69-30031

Potential noise stability of reception in binary communications system with active pause in channel for unknown signal arrival time
15 p2563 A69-30134

Pulsed noise sensitivity in radar receivers having noise limiter for simple and complex signals
15 p2563 A69-30137

Noise parameters at output of logarithmic detector separating two AM signals with overlapping spectra
15 p2564 A69-30148

Correlated noise effect on accuracy of suboptimal servosystem velocity measurements from recording Doppler frequencies
15 p2567 A69-30341

Three dimensional effects of potential minimum near cathode emitting axisymmetric beam, relating electric fields distribution to noise reduction coefficient
15 p2568 A69-30794

Noise signals in earth magnetosheath interpreted as electromagnetic waves propagating in whistler mode
16 p2774 A69-31985

Electromagnetic noise in current sheet in geomagnetic tail, discussing effects on distribution function [AFCLR-69-0395]
16 p2781 A69-32317

System noise parameters derivation, using standard IRE definition as foundation and amplifier noise measurement as example for error analysis
16 p2755 A69-32800

Geomagnetic field effects on microwave noise spectrum in earth-ionosphere resonator, calculating field energy spectrum near resonance maximum, discussing excitation by lightning
17 p2918 A69-33034

Noise levels due to long range tropospheric transmission calculated for microwave radio systems
17 p2919 A69-33146

VHF band surface incidental radio noise levels over metropolitan areas compared with airborne data
17 p2921 A69-33672

Cryogenic applications to low noise reception development in radio astronomy, planetary radar and communication with deep space probes
17 p2921 A69-33685

State space structure of model reference adaptive control and parameter tracking systems subject to noise
18 p3111 A69-34686

Terrestrial radio noise source aspects including atmospheric, propagation influence, lightning-generated noise and whistlers, radio interference, etc
19 p3276 A69-36434

He-Ne laser discharges noise and oscillations classified, investigating interaction between intrinsic oscillations
19 p3338 A69-36605

O stars spectrograms study for luminosity and temperature criteria
20 p3598 A69-37463

Optical parameters of Martian surface and temperature, discussing brightness distribution along diameter in red spectral region, based on photoelectric cross sections
20 p3608 A69-38050

Dispersion relations in semiconductors in magnetic field indicating current anisotropic instability association with excessive noise
21 p3782 A69-39142

Transistorized low noise reception antennas with built-in amplifying elements, discussing radiation patterns and noise problems
21 p3683 A69-39264

Sequential filter equations for nonlinear system dynamics and observational model with linear estimator, comparing difference between white and colored noise filter results
21 p3686 A69-39371

Handbook of radar measurement covering noise measurement, error analysis, antenna performance, etc
21 p3678 A69-39668

Radio emission data from 20 May 1966 partial solar eclipse, giving radio noise and brightness distribution data
22 p4010 A69-39986

Discrete delay line measuring FM noise, discussing special case of narrow band cavity resonator method
23 p4137 A69-41606

Analyzing conditions for variable magnetic and electric noise occurrence at input of nuclear precession magnetometer used in field strengths measurements
23 p4165 A69-41852

Noise elimination by filtering in high power microwave transmitters, noting practical design tradeoffs
23 p4142 A69-42235

ELECTROMAGNETIC PROPERTIES

NT ABSORPTANCE
NT ABSORPTIVITY
NT BIREFRINGENCE
NT BRIGHTNESS
NT COLOR
NT DICHROISM
NT FARADAY EFFECT
NT KERR MAGNETOOPTICAL EFFECT
NT LUMINOSITY
NT OPACITY
NT OPTICAL PROPERTIES
NT OPTICAL REFLECTION
NT PHOSPHORESCENCE
NT PHOTOCONDUCTIVITY
NT PHOTOELASTICITY
NT PHOTOELECTRIC EFFECT
NT PHOTOELECTRIC EMISSION
NT PHOTOIONIZATION
NT PHOTOVOLTAICITY
NT PHOTOVOLTAIC EFFECT
NT RADIANCE
NT REFLECTANCE
NT REFRACTIVITY
NT SKY BRIGHTNESS
NT SPECTRAL REFLECTANCE
NT STELLAR LUMINOSITY
NT TRANSMISSIVITY
NT TRANSMITTANCE
NT TRANSPARENCY
NT TURBIDITY

Electromagnetic properties of bounded isotropic plasma in kinetic approximation
03 p0477 A69-13712

Two band model for determining linear and nonlinear electromagnetic responses of small band gap semiconductors in magnetic field
03 p0487 A69-13753

Electromagnetic field strength of narrow polarized monochromatic light beam, noting spatial curvature and twisting in beam current line
07 p1147 A69-18524

VLF wave electromagnetic properties in magnetosphere, noting whistler mode propagation and refractive index and electron density of medium
08 p1306 A69-20180

Intensity distribution in principal mode of TEM oscillations at various gain amplification levels, plotting intensity distribution generated by argon ion CW laser
09 p1520 A69-22685

Radiative heat transfer, discussing electromagnetic theory, transfer between surfaces and simultaneous conduction, convection and radiation
13 p2376 A69-28140

Electromagnetic wave scattering from conducting bodies of arbitrary shape and electromagnetic properties
17 p2918 A69-33002

Arbitrary electromagnetic field prediction based on spherical harmonics expansion method using field points measurement data, determining electromagnetic properties of environments
17 p2929 A69-33881

Lunar Explorer 35 measurements of lunar surface electromagnetic properties, magnetic fields and solar wind-moon interactions
21 p3794 A69-38379

ELECTROMAGNETIC PROPULSION

Electromagnetic thrust equations for coaxial MPD accelerator, noting role of externally applied magnetic field [AIAA PAPER 69-108]
06 p0972 A69-18197

Electric rocket propulsion, discussing roles of plasma and gas discharge physics in development of electromagnetic, electrostatic and thermoelectric nuclear systems
13 p2325 A69-28253

Nuclear rocket propulsion operation, design, properties and performance of electrostatic, electrothermal and electromagnetic systems
13 p2297 A69-28254

Helicopter powering and positioning by CW microwave beam, describing antenna and sensor arrays, feasibility experiments, system applications, etc
23 p4063 A69-42534

ELECTROMAGNETIC PULSES

Plane monochromatic and pulsed electromagnetic waves penetration into metal cylindrical shells, deriving equations for electromagnetic field in interior
15 p2569 A69-30950

Atomic coherence and inhomogeneous broadening effects on laser amplifier ultrashort electromagnetic high peak power pulses
15 p2635 A69-31239

Electromagnetic echo generation in collisionless spatially homogeneous plasma dependence on velocity distribution and magnetic interaction
16 p2818 A69-31677

Laser amplifier nonlinear losses effect on light beam propagation, studying arbitrary waveform development into asymptotic steady state pulse /SSP/
16 p2797 A69-32043

Gravitational effect of electromagnetic radiation evaluated on test particle using Einstein field equations
16 p2812 A69-32049

Impulsive radio emission from CP 0950 by Mark I telescope, plotting mean and interpulse profiles
17 p3036 A69-33638

Observed and computed radio pulse profiles of white dwarfs, noting resemblance of emissivity variation with latitude to magnetic field distribution on sun
17 p3037 A69-33644

Distortion of electromagnetic pulse propagating through inhomogeneous plasma medium with linear electron density variation
20 p3496 A69-38030

Bloch wall motion along hard direction of Permalloy films due to fast rising hard-axis pulses
20 p3584 A69-38191

Multistable logic circuitry with 10 stability levels based on phased pulse principle, noting efficiency and complexity in man machine interface
21 p3686 A69-39065

Response of three level particles system with equidistant spectrum under resonant action of acoustic and electromagnetic pulses sequence with different frequencies
21 p3737 A69-39068

Holographic interferometry by single two wavelength laser pulse exposure, discussing variable sensitivity techniques
21 p3725 A69-39448

ELECTROMAGNETIC PUMPS

Soviet monograph on design and theory of linear induction pumps for liquid metals covering electromagnetic phenomena, optimized dimensions, etc
13 p2209 A69-27926

Plane linear induction pump design optimization without short circuiting bus bars, allowing for MHD effects induced by traveling magnetic field
14 p2405 A69-29913

Electromagnetic field pumping effects in electrically conductive gas lubricants, producing gas film between surfaces without external pressurization
15 p2629 A69-31003

ELECTROMAGNETIC RADIATION
NT AIRGLOW
NT BLACK BODY RADIATION
NT BREMSSTRAHLUNG
NT CERENKOV RADIATION
NT COHERENT ELECTROMAGNETIC RADIATION
NT COHERENT LIGHT
NT CYCLOTRON RADIATION
NT DAYGLOW
NT DECA-METRIC WAVES
NT EXTRA-TERRESTRIAL RADIO WAVES
NT FAR INFRARED RADIATION
NT FAR ULTRAVIOLET RADIATION
NT GALACTIC RADIO WAVES
NT GAMMA RAY BEAMS
NT GAMMA RAYS
NT GEGENSCHN
NT GEOCORONAL EMISSIONS
NT H WAVES
NT INFRARED RADIATION
NT LIGHT [VISIBLE RADIATION]
NT LIGHT BEAMS
NT LONG WAVE RADIATION
NT LYMAN ALPHA RADIATION
NT LYMAN BETA RADIATION
NT MICROWAVES
NT MILLIMETER WAVES
NT MODULATED CONTINUOUS RADIATION
NT MONOCHROMATIC RADIATION
NT NEAR INFRARED RADIATION
NT NEAR ULTRAVIOLET RADIATION
NT NIGHTGLOW
NT NONEQUILIBRIUM RADIATION
NT PHONON BEAMS
NT PHOTON BEAMS
NT PHOTONS
NT PLANETARY RADIATION
NT POLARIZED ELECTROMAGNETIC RADIATION
NT POLARIZED LIGHT
NT RADIO BURSTS
NT RADIO EMISSION
NT RADIO WAVES
NT SHORT WAVE RADIATION
NT SKY RADIATION
NT SKY WAVES
NT SOLAR RADIO BURSTS
NT SOLAR RADIO EMISSION
NT SOLAR X-RAYS
NT SUBMILLIMETER WAVES
NT SUNLIGHT
NT SYNCHROTRON RADIATION
NT TERRESTRIAL RADIATION
NT THERMAL RADIATION
NT TWILIGHT GLOW
NT TYPE 2 BURSTS
NT TYPE 3 BURSTS
NT TYPE 4 BURSTS
NT TYPE 5 BURSTS
NT ULTRAVIOLET RADIATION
NT X RAYS
NT ZODIACAL LIGHT

Approximate integrals of Einstein equations for dipole and quadrupole electromagnetic radiation
01 p0115 A69-10263

Waves in inhomogeneous warm magnetoplasmas with static pressure gradients, applying dyadic to planar stratified plasma case
01 p0129 A69-10561

Analytical expressions for transfer function matrices of four terminal signal shaping networks, assuming rational matrix spectral density of randomly polarized signal
01 p0031 A69-10880

Soviet investigations of solar and cosmic electromagnetic and charged particle radiations by balloon, rocket and satellite measurements
01 p0145 A69-10945

Electromagnetic waves trajectory distortion in moving plasma due to additional time delay noting propagation of pearl pulsations, whistling atmospherics and proton whistlers
01 p0068 A69-11114

Electromagnetic wave path emitted by artificial satellites across anisotropic ionosphere due to geomagnetic field determined by computer program
01 p0068 A69-11115

Charged particle motion caused by ELF electromagnetic waves in presence of constant magnetic field, noting earth ionosphere application
02 p0240 A69-11712

Electromagnetic wave propagation problems, using asymptotic solutions of differential and integral equations in domains containing transition points
02 p0208 A69-12130

Reflection of plane electromagnetic wave from impedance cylinder in vacuum, using ray expansion method
02 p0217 A69-12262

Iris satellite experiments in astrophysics including nuclear and solar induced electromagnetic radiation
03 p0427 A69-12849

Procedure and apparatus for integral microwave and X ray and spectral measurements of quasi-steady plasma radiation
03 p0473 A69-12897

Outer space electromagnetic radiation transfer in turbulent plasma with allowance for polarization effects, describing polarization induced changes in Stokes parameters
03 p0506 A69-13083

Green functions associated with electromagnetic radiation in moving medium, finding time dependent and harmonic Green functions
03 p0466 A69-13352

Nonlinear interaction of steady state circularly polarized electromagnetic wave with cold plasma in constant longitudinal magnetic field
03 p0476 A69-13381

Electromagnetic wave diffraction at uniformly expanding sphere solved by Kirchhoff method
03 p0397 A69-13719

Plane reflector with variable reflection coefficient for electromagnetic centimeter waves, consisting of plane grating of semiconductor diodes mounted in waveguide
03 p0406 A69-13938

Emissivity and other radiative characteristics of stainless steel oxides heated to various temperatures in air
03 p0453 A69-14157

Viscoelasticity effect on tensile stress in absorption layer for free surface uniaxial motion
04 p0676 A69-14705

Artificial lunar satellite orbital motion calculated by numerical integration, including solar and lunar electromagnetic radiation pressure effects
04 p0662 A69-15251

Electromagnetic radiation from solar flares based on rocket and satellite observations of 10-100 kev X ray emission and ground observation of cm-wavelength bursts
05 p0813 A69-15603

Biological effects of VHF electromagnetic radiation from radar antennas
05 p0715 A69-16701

Diffraction of plane electromagnetic waves obliquely incident on conducting rotated periodically tapered grating structure formed of infinite metal strips
05 p0723 A69-16788

Electromagnetic waves transformation and scattering in plasma in electric field, showing abrupt increase at certain critical value
06 p0886 A69-16894

Spatial dispersion of electromagnetic waves reflection from moving plasma layer in magnetic field, determining transmission and energy absorption coefficients
06 p0886 A69-16895

Hydrodynamic and lattice vibrations equations for coupled waves in ion semiconductors in external electric and magnetic fields, observing sound amplification
06 p0978 A69-16897

Gunn effect verification using n-type semiconductor single crystals in DC field, noting microwave field polarization plane rotation
06 p0978 A69-16902

Electromagnetic wave refraction angles in earth atmosphere, noting effect of stratified discontinuities on angle magnitude
06 p0887 A69-17450

Diffuse reflection of electromagnetic waves by rough random surface using probabilistic method and statistical distributions
07 p1075 A69-18280

Electromagnetic waves excitation during interaction between density modulated beam and plasma in magnetic field, analyzing instabilities
07 p1189 A69-18508

Focused electromagnetic beam interferometers and antenna parameters for measuring electron density in plasma diagnostics
07 p1132 A69-18865

Relaxation theory of highly ionized hydrogen plasma noting applications to stimulated emission, radiation source development and electromagnetic radiation amplification
07 p1191 A69-18996

Initial equations for plane wave diffraction at grids of squared beams, calculating transmission and reflection coefficients by reflection method and computer
07 p1084 A69-19149

Plane electromagnetic wave diffraction at oblique screen of circular cross section conducting wires solved, assuming smaller wire radius than grid spacing and wavelength
07 p1084 A69-19150

Thin electron flux interaction with electromagnetic wave in open waveguide, discussing nonlinear theory and performance of gyroresonance transverse wave tube
07 p1107 A69-19159

Radiation resistance of short dipole immersed in cold magnetoionic medium, using polarized wave modes
07 p1107 A69-19226

Hamilton-Jacobi equations of motion for classical electron in presence of traveling pulse of electromagnetic radiation, solving radiation pulse shape orbits
08 p1377 A69-19790

Rays associated Fokker-Planck relation for isotropic turbulence diffusion equation, discussing logarithmic refractive index, moments and path length
08 p1272 A69-20021

Horizontal electric dipole excitation of spherical guide waves between earth and ionosphere, discussing TM and TE modes and ELF and VLF range
08 p1273 A69-20023

Ultrashort optical pulses of coherent light, discussing propagation in inhomogeneously broadened medium of two level systems
08 p1324 A69-20083

Electromagnetic waves and photons coexistence, discussing wave mechanics and guidance of particles, photon guidance and corpuscular magnitudes, etc
08 p1351 A69-20117

Time-averaged value of forces of electromagnetic wave falling from vacuum and acting on magnetoactive plasma
08 p1361 A69-20200

Collective interactions of electromagnetic waves in plasma, discussing light scattering from electron fluctuations, stimulated emission and anomalous absorption
08 p1361 A69-20220

Radiation spectrum in nonrelativistic fully ionized gas in thermal equilibrium, obtaining dispersion relation for transverse electromagnetic waves and dielectric constant
08 p1357 A69-20748

MPD plasma acceleration in West Germany, discussing Hall acceleration, electrodeless plasma acceleration by electromagnetic waves and space charge neutralized Hall ion thruster [AIAA PAPER 69-279]
09 p1564 A69-21238

Cylindrical electromagnetic waves diffraction at impedance wedge in anisotropic cold plasma, using Maxwell equation and double contour integral
09 p1545 A69-21505

Electromagnetic wave fluctuations and scattering in plasma in strong electric and magnetic fields at magnetoacoustic frequencies
09 p1453 A69-21569

Dispersion equation to describe spectrum of LF density perturbations by pumping plane electromagnetic wave in transparent homogeneous plasma or fluid media
09 p1453 A69-21570

Lower ionosphere effect on LF electromagnetic disturbances, comparing propagation and damping of clockwise and counterclockwise polarized waves
09 p1487 A69-21637

Solar electromagnetic radiation spectral distribution from ground level, rocket and satellite observations to obtain value of energy received at top of atmosphere
09 p1575 A69-21645

Electromagnetic wave reflection from subrefractive layers in inhomogeneous region
09 p1454 A69-21679

Coupling electromagnetic power to beam plasma amplifiers without use of helices and cavities, discussing modes of interaction, gap coupling and Cerenkov coupling
09 p1463 A69-21805

Electromagnetic diffraction for waves generated by electric quadrupole on perfectly conducting wedge, discussing finiteness and radiation emission
09 p1455 A69-22082

Electromagnetic wave diffraction on conducting sphere in inhomogeneous medium with given refractive index variation law, using asymptotic solution for boundary value problem
09 p1459 A69-22628

Second harmonic generation by electromagnetic wave incident on inhomogeneous plasma, determining power output
10 p1653 A69-23133

Reflection coefficient of electromagnetic wave reflected from thin ionization layer, using frequency dependence of amplitude to estimate ionospheric layer thickness
10 p1686 A69-23912

Plasma wave conversion into electromagnetic waves in strong magnetic field, studying nonlinear coalescence and scattering on thermal and epithermal ions
11 p1922 A69-24245

Electromagnetic wave buildup by induced Compton effect as possible radio emission source, considering data for quasars and pulsars
11 p1957 A69-24402

Diffraction of plane electromagnetic wave incident on conducting sphere segment, deriving secondary electromagnetic field equations in geometrical optics approximation
11 p1846 A69-24613

Scattering of spherical electromagnetic wave emitted by electric and magnetic dipoles with equal moments at truncated infinitely thin ideally conducting paraboloid of revolution
11 p1846 A69-24614

High energy cosmic ray origin and acceleration by LF electromagnetic radiation produced by pulsars, noting maximum energy for protons
11 p1950 A69-24927

Magnetospheric plasma heating by magnetosheath generated electromagnetic waves
11 p1950 A69-25149

Multiple scattering in Kapitza-Dirac effect describing electron scattering by standing electromagnetic wave, noting transition probability less than unity
11 p1919 A69-25323

LF electromagnetic waves stability and propagation conditions in plasma confined in central-conductor configuration measured, noting agreement with wave equation solution
11 p1931 A69-25362

Critical condition for electromagnetic radiation generation by energetic electrons gyrating in dense magnetized plasma, proposing plasma instability mechanism
11 p1931 A69-25363

Directional coupler for TEM waves composed of two waveguides and having locally dependent coupling function
11 p1855 A69-25629

Transformation of longitudinal plasma wave into electromagnetic wave during collision with dielectric in plasma
11 p1934 A69-25708

Time harmonic electromagnetic waves diffraction by circular aperture in conducting plane screen between different media, using Hertz vector formulation
12 p2030 A69-26463

Surface waves effect on electromagnetic waves incoherent reflection from plasma-vacuum boundary, describing polarization and angular and spectral distributions
12 p2031 A69-26530

Analytical expressions for transfer function matrices of four terminal signal shaping networks, assuming rational matrix spectral density of randomly polarized signal
12 p2031 A69-26644

Plane transient electromagnetic wave from cold lossless plasma half space and slab
12 p2033 A69-26865

Field patterns for wave radiation from electric dipole immersed in anisotropic plasma column excited by longitudinal DC magnetic field
12 p2034 A69-27103

Electromagnetic step-function plane waves propagation in ionosphere using Fourier transform and Bessel functions
12 p2034 A69-27132

Electromagnetic flux from nonlinear self interaction of electron plasma waves in far field of perturbation under anisotropic electron pressures
12 p2141 A69-27147

Simultaneous Wiener-Hopf equations for electromagnetic wave diffraction, giving cyclic matrix solutions for Dirichlet and Neumann mixed boundary value problems
13 p2287 A69-27299

Electromagnetic and plasma waves scattering by space vehicle excited by ground source in isotropic warm plasma, obtaining radar cross sections
13 p2221 A69-27965

Finite difference solution to TEM mode transmission line cross section for defining continuous potential function leading to capacitance upper bound
13 p2221 A69-28064

TEM mode networks design for producing phase coherent pulse modulated microwave signals through spectrum S band
13 p2234 A69-28073

High energy electrons producing electromagnetic cascades in electron photon showers in lead measured by scintillation detectors
13 p2332 A69-28419

Whistler type electromagnetic waves excitation by electron beam in plasma, noting intensity dependence on electron frequency
13 p2314 A69-28443

Outer space electromagnetic radiation transfer in turbulent plasma with allowance for polarization effects, describing polarization induced changes in Stokes parameters
14 p2515 A69-28765

Reflection and absorption coefficients analyzed for obliquely incident electromagnetic wave from magnetoactive plasma in constant parallel magnetic field
14 p2411 A69-28997

Electromagnetic energy spectra of lightning expressed as function of electric field spectral density of atmospheric
14 p2437 A69-29076

Current oscillations and electromagnetic radiation in low pressure cesium thermal emission converters using glass diode with plate geometry metal electrodes
14 p2402 A69-29246

Subroutines for computing characteristics of electromagnetic radiation scattered by absorbing and homogeneous sphere employing logarithmic derivative method
14 p2412 A69-29283

Book on depolarization of electromagnetic waves covering interface reflection and diffraction, scattered waves, anisotropic media, random scattering, Fresnel coefficients, Brewster angle, etc
14 p2412 A69-29315

Asymptotic expansions for Einstein-Maxwell field representing gravitational and electromagnetic radiation from finite source of matter and charge
14 p2486 A69-29635

Reflection of electromagnetic wave from magnetoactive plasma at inclined incidence, finding reflection and absorption coefficients
14 p2417 A69-29661

Plasma density and conductivity radio interferometry during ultrarapid disturbances based on electromagnetic wave phase shift dependence on density
14 p2498 A69-29803

Passive electric microwave probe with balancing capacitance for studying waveguide fields at high microwave power levels in radiative plasma accelerators
14 p2498 A69-29807

Incident electromagnetic waves Raman scattering at turbulent plasma oscillations, obtaining plasma intrinsic radiation spectrum
15 p2659 A69-30728

Nonlinear mixing of Ar plasma ion wave and externally applied electromagnetic wave
16 p2820 A69-31769

Electromagnetic fields in closed one dimensional resonators with oscillating boundary, analyzing amplitude buildup
16 p2751 A69-32030

Gravitational effect of electromagnetic radiation evaluated on test particle using Einstein field equations
16 p2812 A69-32049

Diffraction of axisymmetric electromagnetic wave at surface discontinuity of impedance cylinder forming core of coaxial waveguide
16 p2761 A69-32479

Electromagnetic /ULF, VLF/ and light emissions development during magnetic substorms, discussing varied pulsations present in development phases
16 p2788 A69-32648

Electromagnetic waves - Conference, Stresa, Italy, June 1968
17 p2922 A69-33832

Deformation of amplitude and frequency envelopes of plane modulated electromagnetic waves with dispersion in isotropic dielectric with cubic nonlinearity
17 p2928 A69-33869

Electromagnetic wave scattering in two angled rectangular waveguides filled with isotropic homogeneous medium
17 p2930 A69-33887

HF electromagnetic waves penetration into slightly ionized plasma analyzed by Maxwell and kinetic equations, giving penetrating electric field by WKB formula
17 p2932 A69-34220

Macroscopic roughness effect on surface radiation characteristics for special cases
18 p3229 A69-34711

Reflection coefficient of symmetric parallel plate waveguide operating in TEM mode illuminating lossless dielectric layer, using wedge diffraction and geometrical optics methods
18 p3108 A69-34802

Algebraic formulation of electromagnetic diffraction, discussing propagation of positive and negative time frequency components by dual operators
18 p3172 A69-35010

Electromagnetic wave effect on electron in homogeneous magnetic field, noting relativistic momenta of dragged electrons
18 p3181 A69-35497

Electromagnetic field signatures in optical IR spectrum of satellite-borne sensors, analyzing spectral, spatial and temporal distributions, polarization and phase
19 p3309 A69-36060

Stationary electromagnetic wave fields LF behavior, discussing integral operators, incident and tangential fields, single valued solutions, etc
20 p3487 A69-37071

Electromagnetic radiation in moving uniaxially anisotropic medium, obtaining time dependent solutions for oriented magnetic dipole current distribution density
20 p3576 A69-37578

Electromagnetic radiation detectors in nonphotographic sensing systems, describing performance as function of time constant, spectral response, cooling requirements and signal handling
20 p3540 A69-37736

Electromagnetic radiation from slot excited ground plane covered by inhomogeneous plasma layer, considering far field radiation pattern
20 p3495 A69-37852

Electromagnetic wave refraction angles in earth atmosphere, noting effect of stratified discontinuities on angle magnitude
20 p3496 A69-37935

Induced Compton scattering of plasma and electromagnetic waves under astrophysical conditions, discussing HF radio emission spectra from cosmic objects and quasar
20 p3607 A69-38035

Auroras and VLF emissions observations at ground stations to correlate emissions with auroral displays, noting low ionospheric absorption role
21 p3708 A69-38494

Simultaneous ground and Alouette 2 satellite measurements of enhanced electromagnetic band emission in 500-1000 Hz range
21 p3708 A69-38496

Interaction between modes of radiation field and active medium in laser with nonresonant feedback, discussing amplitude stabilization of total radiation
21 p3735 A69-38581

X ray sources and diffuse background radiation observed in gamma and X ray spectral regions, considering electromagnetic waves attenuation by interstellar matter
21 p3789 A69-38817

Electromagnetic wave diffraction in three dimensional space divided by dielectric orthogonal half planes/wedges/, using contact boundary value problem
21 p3673 A69-39012

Electromagnetic radiation measurements in shielded enclosures, describing equipment and effects of frequency
21 p3683 A69-39439

Absolute and convective instability criteria of interacting electromagnetic waves in waveguide systems involving parametric oscillators and amplifiers
21 p3677 A69-39555

Coupled acoustic and spiral EM waves drift instabilities in bounded plasma of solid body found to be convective
21 p3782 A69-39556

Electromagnetic radiation and scattering from conducting bodies of revolution, obtaining formulation in integrodifferential equation from potential integrals and boundary conditions
22 p3899 A69-40014

Transverse mode selection in rotating mirror neodymium doped calcium tungstate laser by inserting slit and edge into resonator
22 p3961 A69-40316

- Diffuse reflection of electromagnetic longitudinal wave from magnetoactive plasma in oblique incidence
22 p3990 A69-40788
- Aperture distortions and spectral line shapes of electromagnetic radiation diffused by plasma
22 p3982 A69-40799
- Reflection and transmission coefficients for harmonic electromagnetic wave incident at parabolic layer of stratified isotropic plasma
22 p3901 A69-41020
- Monte Carlo methods for electromagnetic showers simulation, noting electron track length distribution in Pb glass absorber
22 p4007 A69-41057
- Electromagnetic waves emission intensity in one dimensional resonator, allowing for wave interference effects
22 p3966 A69-41172
- Electromagnetic radiation characteristics from vibrating electrons or electric dipole moving in compressible isotropic plasma and from stationary dipole in moving medium, emphasizing Doppler effects
23 p4114 A69-41359
- Electromagnetic backscattering by perfectly conducting prolate spheroid, predicting echo signal in resonance region
23 p4115 A69-41584
- Radiation scattering by thick planetary atmosphere according to Rayleigh law, considering luminance variation and absorption ray polarization
23 p4213 A69-41698
- Electromagnetic wave diffraction normally incident on symmetrical five element metallic array
23 p4123 A69-42029
- Plane electromagnetic wave diffraction by screened periodic metallic strips array with real ferrite transversely magnetized to saturation
23 p4124 A69-42032
- Linear diffraction equations in electronics in self consistent formulation reduced to complex transcendental equations, using perturbation method
23 p4124 A69-42033
- Space charge wave propagation induced by electron beam moving in annular waveguide, considering radiated field and current redistribution
23 p4124 A69-42034
- Electromagnetic wave diffraction by multielement periodic metallic strips arrays positioned transversely in rectangular waveguide
23 p4124 A69-42035
- Time dependent natural oscillations of plane open resonators infinite periodic sequence, considering electromagnetic energy transfer into ambient medium
23 p4139 A69-42039
- Plane polarized electromagnetic wave diffraction incident on skewed metal ribbons array
23 p4125 A69-42043
- Diffraction characteristics of electromagnetic wave by periodic two element arrays, noting amplitude measurement of harmonics in millimeter wavelength range
23 p4139 A69-42044
- Electromagnetic radiation below 1 GHz from gap type electrical discharges on electric power distribution lines
23 p4126 A69-42218
- Radiated interference and susceptibility prediction for unshielded wires in near field of vertical rod antenna
23 p4141 A69-42225
- Quantum optics or electronics, discussing electromagnetic waves control and interactions with matter, maser oscillators theory and characteristics, nonlinear optics, induced transparency, etc
23 p4174 A69-42315
- Electromagnetic wave buildup by induced Compton effect as possible radio emission source, considering data for quasars and pulsars
24 p4391 A69-43792

ELECTROMAGNETIC SCATTERING

- NT HALOS
- NT IONOSPHERIC F-SCATTER PROPAGATION
- NT LIGHT SCATTERING
- NT MICROWAVE SCATTERING
- NT MIE SCATTERING
- NT RAMAN SPECTRA
- NT RAYLEIGH SCATTERING
- NT X RAY SCATTERING
- Geometric optics inverse scattering method for smooth conducting convex bodies of revolution, demonstrating bounds on size and shape
02 p0280 A69-11929
- Electromagnetic wave scattering by turbulent plasma pulsations in external magnetic field
02 p0289 A69-12174

- Reflection of plane electromagnetic wave from conducting plane covered with moving uniaxial sheath
02 p0209 A69-12334
- Scattering from coated absorbing conducting bodies, considering flat plane and curved surfaces in Rayleigh region
03 p0384 A69-12908
- Radar cross section enhancement effect of corner reflectors, multiple reflectors and dielectric lenses
03 p0384 A69-12909
- Missile radar cross section based on modeling from simple forms, noting computer program
03 p0384 A69-12910
- Plane electromagnetic wave scattering from slightly rough surface tilted away from reference plane, noting polarization effects
03 p0395 A69-13625
- Transport equation for electromagnetic waves multiple scattering by turbulent plasma
03 p0478 A69-13959
- Scattering data for optical diagnostic measurements on two component suspensions or gases, using random distributions of spheres
04 p0555 A69-14282
- Moment method used to determine pulsed radiation instability propagating in luminescent scattering medium
04 p0610 A69-14425
- Quasi-specular bistatic radar measurements of oblique scattering properties of lunar surface using telemetry carrier from Explorer 35 as lunar orbiting radar beacon
04 p0655 A69-14657
- Relativistic analysis of far zone electromagnetic scattering by conducting sphere moving through incident plane wave, calculating scattering cross section
04 p0559 A69-15212
- Scattering of electromagnetic waves from rough surface moving with uniform velocity
04 p0560 A69-15213
- Bounded and perfectly conducting object embedded in Euclidean 3-space, discussing electromagnetic inverse scattering problem
05 p0719 A69-15929
- Electromagnetic wave scattering in ferromagnetic crystals with anisotropy, discussing correlation functions of characteristics fluctuations and magnetoacoustic resonance
05 p0809 A69-16547
- Scattering and diffraction of plane electromagnetic wave incident on conducting cylinder coated with moving anisotropic medium
07 p1086 A69-19469
- Electromagnetic waves attenuation and scattering by rainfalls calculated using droplet distribution function
08 p1275 A69-20430
- HF electromagnetic wave scattering at small scale plasma turbulence in magnetic fields, discussing interactions in frequent collisions region
08 p1275 A69-20435
- Scattering and transformation of electromagnetic waves in plasma in crossed electric and magnetic fields showing radiation spectrum maxima due to ion-acoustic oscillations propagation
08 p1277 A69-21080
- Radio waves polarization scattered at ionospheric discontinuities analyzed for vertical incidence, determining modulus distributions and polarization factor argument
09 p1453 A69-21527
- Electromagnetic wave fluctuations and scattering in plasma in strong electric and magnetic fields at magnetoacoustic frequencies
09 p1453 A69-21569
- Dispersion equation to describe spectrum of LF density perturbations by pumping plane electromagnetic wave in transparent homogeneous plasma or fluid media
09 p1453 A69-21570
- Bose condensation and shock waves in photon spectrum during scattering for equilibrium state of ionized plasma and radiation
09 p1546 A69-21574
- Gamma ray scattering gauge design optimum parameters to measure Mars atmospheric density
09 p1495 A69-21842
- Electromagnetic wave diffraction on conducting sphere in inhomogeneous medium with given refractive index variation law, using asymptotic solution for boundary value problem
09 p1459 A69-22628
- Energy spectra and angular dependence characteristics of electromagnetic wave scattered on statistically uneven surface studied by vector form of Kirchhoff integral
09 p1459 A69-22635
- Solar Lyman alpha radiation scattering into antisolar geocorona, noting inaccessibility of region to solar wind
09 p1583 A69-22760
- Surface currents, scattered field and scattering cross section for perfectly conducting cylinder found by reducing two dimensional problem to solving coupled differential equations
10 p1657 A69-23860
- Scattering of spherical electromagnetic wave emitted by electric and magnetic dipoles with equal moments at truncated infinitely thin ideally conducting paraboloid of revolution
11 p1846 A69-24614
- Lunar surface pore water /or ice/ detection by active orbital or surface electromagnetic experiments, noting water effect on reflection coefficient
11 p1958 A69-24693
- Electromagnetic plane wave scattering from slender semiinfinite cone, obtaining contribution to tip return arising from direct diffraction
11 p1836 A69-24988
- Electromagnetic scattering from thin wire loops under various impedance loadings, considering positive and negative resistors effect combined with reactive networks
11 p1837 A69-25000
- Transformation of Q switched neodymium laser radiation into Stokes component during stimulated combination scattering in liquid nitrogen
11 p1900 A69-25751
- Atmospheric models for electromagnetic scattering of monochromatic IR and microwave radiation by natural suspensions as hazes clouds and precipitation
12 p2030 A69-26467
- Book on depolarization of electromagnetic waves covering interface reflection and diffraction, scattered waves, anisotropic media, random scattering, Fresnel coefficients, Brewster angle, etc
14 p2412 A69-29315
- Transistor scatter and admittance differential parameters measurements graphically correlated
14 p2420 A69-29397
- Multiple scattering of electromagnetic waves in underdense plasma, deriving transport equation for radar backscatter
14 p2412 A69-29453
- Electromagnetic scatter from perturbed continuous medium, expressing problem in terms of periodic functions instead of conventional power series
14 p2414 A69-29513
- Atmospheric multifrequency probing accuracy limitation imposed by irregularities based on scatter theory
14 p2449 A69-29535
- Monograph on wave propagation and multiple scattering in random continuum, emphasizing scalar wave equation solutions
15 p2564 A69-30150
- Electromagnetic field TM and TE modes uncoupling during oblique incidence scattering from radially inhomogeneous cylinders
15 p2565 A69-30170
- Plane electromagnetic wave refraction and scattering in solar corona during eclipsed observations of cosmic sources, calculating angular distribution of radiation intensity
15 p2688 A69-30555
- Incident electromagnetic waves Raman scattering at turbulent plasma oscillations, obtaining plasma intrinsic radiation spectrum
15 p2659 A69-30728
- Nonlinear boundary value problems for isotropic plasma with known magnetic field, examining electromagnetic waves scattering at magnetic fluctuations
15 p2569 A69-30938
- OGO 5 satellite measurements of intensity and width of Lyman alpha line scattered by hydrogen geocorona
15 p2699 A69-31412
- Scattering of line focused electromagnetic waves by infinite cylinders obtained by modification of plane wave theory
15 p2664 A69-31478
- Scattering by cylindrical pool of complex permittivity /plasma/ in rectangular waveguide, calculating reflection, transmission and absorption coefficients by computer
16 p2756 A69-31578
- Scattering of time harmonic linearly polarized plane electromagnetic wave by uniformly axially moving cylinder, analyzing first order velocity effects
16 p2748 A69-31579

Partially coherent radiation scattering determined using Heisenberg operator, noting radiation absorption dependence on interference band coherence
16 p2797 A69-32050

Radio waves polarization scattered at ionospheric discontinuities analyzed for vertical incidence, determining modulus distributions and polarization factor argument
16 p2754 A69-32522

Inverse scattering technique for electromagnetic bistatic scattering by expressing field produced by incident plane wave as sum of incident field and Fourier transform
16 p2754 A69-32569

Electromagnetic wave scattering from conducting bodies of arbitrary shape and electromagnetic properties
17 p2918 A69-33002

Holography of intensities, discussing recording of self luminous body by modulation of scattered radiation using optical Q switch
17 p2973 A69-33113

Wave diffraction problem solution method based on Rayleigh hypothesis equivalent to extended boundary condition method
17 p2920 A69-33422

Dyadic Green function technique extended to problems of electromagnetic scattering in inhomogeneous media with spherical symmetry
17 p2924 A69-33837

Electromagnetic scattering theory, defining areas of current importance and surveying recent papers
17 p2930 A69-33884

Diffraction of skew incident plane electromagnetic wave by perfectly conducting right angled wedge embedded in uniaxially anisotropic medium
17 p2930 A69-33889

Integral equation method for electromagnetic scattering by perfectly conducting obstacles modified for volume scattering regions involving disparities in dielectric constant, permeability or conductivity
17 p2930 A69-33890

Electromagnetic wave scattering and depolarization by horizontally weakly inhomogeneous medium, using small perturbation method
18 p3101 A69-34788

Scattering of electromagnetic waves obliquely incident on inhomogeneous plasma column of parabolic radial density distribution, noting applications to ionospheric irregularities
18 p3102 A69-34963

Plane electromagnetic wave scattering by motion of small ellipsoid in vacuum, noting total scattering and radar cross sections dependence on ellipsoid velocity
18 p3105 A69-35485

Scattered field of linear array of center loaded cylindrical elements illuminated by plane electromagnetic wave
20 p3494 A69-37838

Electromagnetic wave scattering from rough layer with plane and rough interfaces, determining scattering cross sections from electrical field and power density
21 p3677 A69-39459

Computer simulation of radiation scattering of spherical nebula with central isotropic star, discussing proposed program and parameters
21 p3816 A69-39723

Electromagnetic radiation and scattering from conducting bodies of revolution, obtaining formulation in integrodifferential equation from potential integrals and boundary conditions
22 p3899 A69-40014

Spatiotemporal signal distortions for multiple scattering from unsteady radiant energy transfer equations
22 p3899 A69-40247

Plane electromagnetic wave scattering on turbulent fluctuations in electron density of finite volume ionized plasma, evaluating Booker-Gordon relation
23 p4116 A69-41587

Electromagnetic waves scatter propagation in isotropic plasma in plane waveguide, noting electron charge density fluctuations role
23 p4125 A69-42040

Fluctuations in 3K radiation, considering scattering effect on gravitational fields of galactic clusters and large coherence or wavelength scattering by gravitational radiation
23 p4222 A69-42401

Laser hazard probability assessment in various applications, discussing power characteristics, attenuation by absorption and scattering and radiant energy spatial distribution
24 p4327 A69-42576

Electromagnetic scattering by small plasma ellipsoid moving in vacuum through external steady magnetic field, analyzing resonance phenomena
24 p4282 A69-42979

ELECTROMAGNETIC SHIELDING NT RADIO FREQUENCY SHIELDING

Computer program for electromagnetic wave metal shielding evaluation
03 p0398 A69-13901

Corrosion problems associated with electromagnetic shielding gaskets noting galvanic corrosion, corrosion prevention and insulation of gasket from mating surface
05 p0779 A69-15979

Graphs determining interference levels for optimum shielding, suppression, signal parameters and waveforms for pulses, step functions, CW signals and for military technology
12 p2030 A69-26471

Shields frequency ranges analysis to determine frequencies and parameters for electrostatic and magnetostatic modes transition to electromagnetic and microwave modes
15 p2562 A69-30120

Shield facility and Helmholtz coil system used to investigate chronic effects on man of zero magnetic field regulated to cancel geomagnetic field variations
15 p2586 A69-30382

Proton dose in receiver behind combination electromagnetic and material shield, calculating dose for Van Allen and solar proton event spectra
15 p2652 A69-31522

Plane screen electrical shielding effectiveness calculation, using incident wave impedances associated with current loop and magnetic dipoles in transmission line equations
19 p3267 A69-35932

Electromagnetic radiation measurements in shielded enclosures, describing equipment and effects of frequency
21 p3683 A69-39439

Dispersion and resonant properties of electromagnetic waves propagating along plane metallic strip array with shield and dielectric
23 p4124 A69-42038

Diffusion times for saturated region in Hipernom tubes measured for various exciting magnetic fields and pulse duration
23 p4141 A69-42222

Beam wave propagation in conducting hollow circular cylinder applied to shielding cylinders design for aperture antenna transmission
24 p4282 A69-42987

ELECTROMAGNETIC SHOCK TUBES U SHOCK TUBES

ELECTROMAGNETIC SPECTRA

NT BALMER SERIES
NT D LINES
NT ELECTRONIC SPECTRA
NT FRAUNHOFER LINES
NT H ALPHA LINE
NT H BETA LINE
NT H GAMMA LINE
NT H LINES
NT INFRARED SPECTRA
NT K LINES
NT LINE SPECTRA
NT LYMAN SPECTRA
NT MICROWAVE SPECTRA
NT PASCHEN SERIES
NT RADIO SPECTRA
NT RAMAN SPECTRA
NT RYDBERG SERIES
NT SOLAR SPECTRA
NT STELLAR SPECTRA
NT TELLURIC LINES
NT UV SPECTRA
NT ULTRAVIOLET SPECTRA
NT VIBRATIONAL SPECTRA

Spectrum distortion of intermediate frequency signal in coherent Doppler navigation radar
01 p0034 A69-11013

Scattering and transformation of electromagnetic waves in plasma in crossed electric and magnetic fields showing radiation spectrum maxima due to ion-acoustic oscillations propagation
08 p1277 A69-21080

Lunar photon leakage spectrum due to photons from capture and inelastic scattering of neutrons by galactic cosmic rays
09 p1597 A69-22088

Earth resource satellites, discussing mapping, land evaluation, geological observation, agricultural and hydrological applications, electromagnetic spectrum information, sensors and photographs
16 p2881 A69-31763

Solar cells designed to survive exposure to fission/fusion neutrons and electromagnetic spectrum products of nuclear weapon detonation
19 p3251 A69-35689

N-type GaAs optical properties after proton irradiation, noting transmission spectra dependence on initial electron concentration and irradiation dose
20 p3582 A69-36969

Earth resources observation technology from satellites, reviewing sensors and methods, electromagnetic spectrum, atmospheric attenuation and windows, passive-active devices
21 p3720 A69-38624

Spectroscopic observations of optical pulsar NE 0532, using technique permitting phase resolution of spectra of main pulse and interpulse
21 p3799 A69-38646

ELECTROMAGNETIC WAVE FILTERS

NT INFRARED FILTERS
NT MICROWAVE FILTERS
NT OPTICAL FILTERS
NT RADAR FILTERS
NT ULTRAVIOLET FILTERS
NT WAVEGUIDE FILTERS

Transversal filters for equalization of data channels with pulse amplitude modulation, discussing pulse equalizability and convergence criteria for iterative search routine
01 p0027 A69-10251

Mean error rates in microwave PCM systems with wave distortion due to multipath propagation
02 p0208 A69-12307

Frequency locked loop /FLL/ to optimize loop filter and quantization of amplitude channel
03 p0390 A69-13202

Analysis and design of synchronous filter compatible with microelectronics requirements, switching N monolithic RC thin film devices to signal source of resistance
03 p0403 A69-13206

Fourier synthesis procedure optimized to design of large time bandwidth product dispersive filters employing nondispersive tapped delay lines
03 p0403 A69-13217

Waveform distortion resulting from adjacent channel crosstalk and from amplitude and phase nonlinearity in channel filters in DSB/SC telemetry link
07 p1083 A69-19130

Finite IF filter bandwidth degradation of SNR of receiver for biphasic modulated signals using integrate and dump filter
08 p1270 A69-19851

Filters for sampled signals sequences using design simplicity and signal to noise ratio for evaluation and comparison factors
08 p1274 A69-20127

Transfer function and frequency response of notch filters used to achieve notch filter dimensioning and design
08 p1284 A69-20379

Chebyshev filter design problems including minimum highest dissipation loss, bandwidth, resonators, etc
10 p1665 A69-23875

Self tuning in active filter for detection of weak LF signals in noisy background
11 p1845 A69-24548

Stochastic optimal control of continuous time systems with unknown gain, discussing filtering-control interaction and computer experiments
11 p1860 A69-25442

Narrow band LC 70 MHz IF filter design method
12 p2036 A69-25915

Mismatch between signal and filter effect on output response of matched filter for pseudorandom phase-manipulated signals in receiver
12 p2031 A69-26487

Transistorized LF-HF RC filters and current amplifiers design, exhibiting polynomial type characteristics
12 p2040 A69-26488

Optimized receivers synthesized for narrow band radio signal filtration, comparing noise rejection properties of various pulse modulation types during speech transmission
14 p2413 A69-29464

Notch filter construction by single operational amplifier, adjusting notch bandwidth by varying ratio of resistors and capacitors
14 p2421 A69-29550

Shock wave radiation screening by thermodynamically unstable gas, discussing brightness and gas temperature relative to shock wave front position
14 p2493 A69-29673

- Instrumental accuracy of discrete filter during measurement of initial phase of signal dependent on phase structure
15 p2574 A69-30139
- Photoelectric comet observation techniques, tabulating narrow and wideband filter combinations for determining parameter Q for various cometary spectral emissions
15 p2684 A69-30522
- Channel dropping filter for millimeter wave in low loss circular waveguide for overland telecommunications in bandwith over 10 GHz
17 p2936 A69-33032
- Coupled Fabry-Perot interferometer for microwave spectra to improve selectivity of interference filter
22 p3947 A69-40800

ELECTROMAGNETIC WAVE TRANSMISSION

- NT AUTOMATIC PICTURE TRANSMISSION
NT DOUBLE SIDEBAND TRANSMISSION
NT HALOS
NT IONOSPHERIC F-SCATTER PROPAGATION
NT IONOSPHERIC PROPAGATION
NT LIGHT SCATTERING
NT LIGHT TRANSMISSION
NT MANDELSTAM REPRESENTATION
NT MICROWAVE ATTENUATION
NT MICROWAVE TRANSMISSION
NT MULTIPATH TRANSMISSION
NT RADAR ATTENUATION
NT RADAR TRANSMISSION
NT RADIO ATTENUATION
NT RADIO TRANSMISSION
NT SCATTER PROPAGATION
NT SHORT WAVE RADIO TRANSMISSION
NT SINGLE SIDEBAND TRANSMISSION
NT TELEVISION TRANSMISSION
NT TRANSEQUATORIAL PROPAGATION
- Electromagnetic wave propagation in superconductors, noting transmission line structure variation with magnetic fields and current and suitability for parametric amplifiers
01 p0135 A69-10176
- Pulsar radiation origin related to electromagnetic wave distortion during propagation through resonant media
01 p0149 A69-10272
- Coupled wave equations for propagation transverse to magnetostatic field in horizontally stratified and magnetized gyrotropic warm plasma
01 p0129 A69-10611
- Propagation in waveguides filled with moving media, discussing first order theory
01 p0030 A69-10630
- IR reflection and transmission properties of various semiconductor compounds, rubidium halides, strontium titanate, BN and Te
01 p0139 A69-10840
- Finsler geometric apparatus applied to electromagnetic wave propagation in media having refractive index varying with position and time, calculating errors
01 p0031 A69-10879
- Spectral lines source functions for formation in multilevel atom and radiative transfer in atmosphere of three level Na atoms and four level O atoms
01 p0124 A69-10962
- Multifrequency three layer sandwich radomes design for reflectionless sandwich at second frequency
01 p0034 A69-11037
- Moderately strong electromagnetic wave propagation in fully ionized plasma, noting nonlinear effects for frequency near plasma frequency
01 p0133 A69-11213
- Electromagnetic wave propagation across magnetic field under relative streaming motion, noting plasma frequency cut-off
01 p0134 A69-11247
- Normally incident linearly polarized electromagnetic wave reflection and transmission by semiinfinite longitudinally drifting magnetoplasma in static magnetic field
01 p0134 A69-11290
- Electromagnetic waves propagation in cylindrical waveguide containing plasma column along axis in absence of constant magnetic field
02 p0285 A69-11463
- Magnetoionic propagation of signals in magnetosphere using Maxwell equations and tensor quantities, linking to Hall, transverse and longitudinal conductivities
[ONERA-TP-593] 02 p0236 A69-11617
- Transhorizon UHF energy transmission via tropospheric scatter, using propagation path model
02 p0209 A69-12350
- Electromagnetic wave propagation in metals in magnetic field, noting helicon waves, magnetoplasma

- waves, waves with discrete spectrum or near cyclotron resonance and quantum phenomena
02 p0299 A69-12565
- Electromagnetic wave dispersion and damping in mixed molecular crystal, relating refractivity, wave absorption and concentration shift of bottom of exciton band to other parameters
03 p0484 A69-13279
- Cold plasma motion caused by electromagnetic wave pressure propagating along uniform magnetic field
03 p0477 A69-13413
- Electromagnetic wave propagation and amplification in periodic structures, including travel wave and parametric amplifiers, reactance diodes, lasers and quantum amplification
03 p0396 A69-13701
- Electromagnetic wave propagation in nonlinear media with permittivity dependent on modulus of magnetic field
03 p0396 A69-13707
- Electromagnetic wave passage through plane gyrotropic layer of magnetized plasma, analyzing polarization and energy transfer
03 p0397 A69-13709
- Dislocation effects on intensity jumps near K edge of absorption, using interferential transmission of X rays in Ge
03 p0490 A69-13944
- Plasma density spatial distribution determined from HF electromagnetic wave phase shifts without assuming axisymmetry
03 p0480 A69-14138
- Plasma waveguide properties during high intensity electromagnetic wave propagation, discussing microwave waveguide coupling
03 p0482 A69-14228
- Scattering from thin conducting sheet obstacle on cylindrical surface
03 p0399 A69-14253
- Moment method used to determine pulsed radiation instability propagating in luminescent scattering medium
04 p0610 A69-14425
- Dispersion relations for propagation of quasi-TEM mode and higher order symmetric modes in longitudinally magnetized ferrite filled coaxial waveguide
04 p0575 A69-14751
- Moving media influence on transient electromagnetic modal wave propagation in dispersive waveguides
04 p0557 A69-14752
- Electromagnetic wave propagation in moving isotropic refractive media, giving Maxwell-Minkowski and EM wave equations
04 p0557 A69-14760
- Dielectric waveguide propagation, impedance and attenuation characteristics and insertion loss and launching efficiency of mode transducer
04 p0577 A69-14971
- Nonlinear damping of circularly polarized electromagnetic wave propagating in plasma along magnetic field, noting particle motion in resonance region
04 p0558 A69-14982
- Electromagnetic wave propagation in uniform anisotropic plasma, considering wave vectors perpendicular to magnetic field
04 p0637 A69-15048
- Doubly infinite sets of simultaneous linear equations used in electromagnetic boundary value problems solved by Asymptotic Anticipation Method
04 p0560 A69-15214
- Electromagnetic wave propagation in spherically stratified isotropic media, presenting generalized refractive index profiles for electric type fields
04 p0563 A69-15492
- Dispersive properties of axial and annular longitudinally magnetized plasma waveguides
05 p0802 A69-15925
- Formulas describing reflection and transmission coefficients of plasma for plane electromagnetic wave, using Maxwell equations in variable medium
05 p0805 A69-16608
- Polarization tensor variation due to Faraday effect and differential absorption of ordinary and extraordinary waves for radiation propagating in magnetoactive cosmic plasma
05 p0805 A69-16650
- Characteristic waves in gas-dielectric beamguides, calculating attenuation dependence on frequency
05 p0736 A69-16783
- Propagation constant and radiation of center fed linear antenna with feed points displaced transverse to antenna axis and immersed in warm compressible plasma
06 p0896 A69-17476

- Controllability of deep space electromagnetic wave propagation in nonvacuum by calculating optimum values of control parametric functions
06 p0888 A69-17622
- Numerical methods for VLF electromagnetic wave propagation in earth-ionosphere waveguide, discussing boundary conditions assignment effect at ionosphere on eigenvalues
06 p0920 A69-17732
- Electromagnetic wave transmission and reflection at boundary of relativistic collisionless plasma, using Laplace transformation
06 p0968 A69-17783
- Transmission coefficient of plane electromagnetic wave obliquely incident on perforated metal screen in frequency range near primary resonance of structure
07 p1076 A69-18527
- Diffractional crosstalk in optical beam waveguide during simultaneous multibeam transmission arising from beam coupling by aperture diffraction
07 p1100 A69-18648
- Acoustic and electromagnetic energy propagation in lower ionosphere and atmosphere for energy pulse generation by chemical explosion
07 p1078 A69-18844
- Real and imaginary parts of homogeneous isotropic electron plasma complex refractive index, noting application to plane electromagnetic wave propagation
07 p1193 A69-19183
- Electromagnetic windows - Conference, University of Paris, September 1967
07 p1108 A69-19507
- Proportionality between log-amplitude variance and 7/6 power of wavenumber for horizontal propagation from spherical wave transmitter to point detector
07 p1157 A69-19641
- Plane electromagnetic wave reflection and transmission by semiinfinite moving compressible plasma fluid, noting interaction of transmitted H wave
08 p1360 A69-20097
- Electromagnetic microinstabilities of plasmas associated with transverse waves propagating perpendicular to external uniform magnetic induction, noting allowable frequencies
08 p1368 A69-20804
- Loss cones effect of anisotropic Maxwellian velocity distribution on EM waves propagating perpendicular to magnetic field in infinite plasma
08 p1369 A69-20820
- Differential equations for normal propagation of plane electromagnetic waves in isotropic stratified inhomogeneous gyration medium, discussing boundary conditions and reflection properties
08 p1353 A69-21000
- Electromagnetic wave attenuation propagating along external magnetic field ascribed to cyclotron wave energy absorption by resonant plasma particles
08 p1277 A69-21077
- Transverse density nonuniformity effect on electromagnetic wave propagation in cylindrical plasma waveguide immersed in magnetic field, noting frequency increase
09 p1545 A69-21348
- Kinetic theory of electromagnetic wave passage through magnetoactive plasma, discussing dispersion and specular and diffuse reflection
09 p1550 A69-22022
- Kinetic theory of electromagnetic wave propagation in infinite laminated plasma with different dielectrics, determining attenuation
09 p1550 A69-22023
- Electromagnetic wave propagation direction in vacuum for reflection from semiinfinite plasma, noting effects of nonlinear transverse wave excitation
09 p1459 A69-22529
- Cosmic charged particle acceleration in electromagnetic field described by vector and scalar potentials, constituting plane electromagnetic wave propagating along z axis
10 p1756 A69-22816
- Electromagnetic wave transmission through anisotropic plasma, discussing incident wave field strength effects near cyclotron frequency
10 p1728 A69-23167
- Electromagnetic wave propagation over constant impedance flat earth, using electromagnetic compensation theorem
10 p1655 A69-23422
- Dynamic mode electromagnetic surface waves on axially magnetized single crystalline YIG and polycrystalline ferrite rods
10 p1746 A69-23513

Slow electromagnetic wave propagation along cold collisionless cylindrical plasma in axial magnetic field, noting surface wave metamorphosis into bulk waves
10 p1739 A69-23659

Electromagnetic wave propagation along longitudinally magnetized plasma column surrounded by isotropic dielectric medium, without making quasi-static assumption
10 p1658 A69-24061

Radiation probability of transmission through intervening galaxy and screening of quasar emission in universes with positive cosmological constant
10 p1790 A69-24135

Anisotropic plasma density measurement by launching circularly polarized plane electromagnetic wave at small angles to magnetic field direction
11 p1930 A69-25286

Electromagnetic wave propagation in rectangular waveguide containing uniaxial anisotropic birefringent medium, deriving field equations
11 p1853 A69-25350

Radiation emission by scalar particle in field of two plane linearly polarized electromagnetic waves propagating toward each other
11 p1900 A69-25568

TEM-DUAL surface wave propagation in coaxial cable with stratified dielectric structure to reduce attenuation calculated by addition theorem to Bessel functions
11 p1856 A69-25659

Calculation method for electromagnetic wave supplementary attenuation due to auroral absorption for distances up to 4000 km
11 p1841 A69-25760

Saddle point analysis of electromagnetic ground wave propagation in source excited field in waveguide formed by two parallel plate dielectrics
12 p2028 A69-25898

Electromagnetic wave propagation cut-off in slightly noncompensated electron hole plasma, discussing wave evanescence above critical magnetic field value
12 p2133 A69-25926

Electromagnetic waves directional velocity, plasma temperature and particle density determined from analyzing electric field fluctuations amplification near body in plasma
12 p2137 A69-26531

Spectral transmission curves in near UV for optical glasses
12 p2130 A69-26599

Finsler geometric apparatus applied to electromagnetic wave propagation in media having refractive index varying with position and time, calculating errors
12 p2031 A69-26642

Elliptical waveguide design dimensions for minimum attenuation in fundamental mode, giving formulas for attenuation constant and minor-major axis ratio
12 p2044 A69-27070

Guided waves in circular cylindrical radially inhomogeneous medium, using vector theory based on Maxwell equations
13 p2221 A69-28062

Interaction between shock tube gas discharge plasma and fast electrons ionized stationary gas, noting luminous discontinuities propagation
14 p2490 A69-28998

Electromagnetic wave phase characteristics after free space passage through statistical medium with wave disturbance producing density and ionization fluctuations
14 p2435 A69-29049

Monochromatic plane waves propagation in anisotropic homogeneous cold plasmas, treating dispersion surface, reflection, refraction and waveguide applications
14 p2492 A69-29399

Electromagnetic wave propagation through magnetolectric media in circular waveguide
14 p2416 A69-29540

Amplitude modulation of electromagnetic waves by modulated magnetic fields for communications through rocket exhausts and reentry plasma sheaths during blackout
14 p2417 A69-29591

Successive approximations method applied to system of independent equations describing electromagnetic wave propagation in space with gravitational wave metric
14 p2487 A69-29669

Dispersion of electromagnetic wave propagating along ferrite loaded wire, calculating tuning curves and three port waveguide circulator modes
14 p2417 A69-29755

Quasi-optical oversize waveguide directional coupler with two prisms interface matched by Brewster angle effect
14 p2424 A69-29764

Plasma electron density measurement from phase shifts of electromagnetic wave groups propagation
14 p2497 A69-29796

Monograph on wave propagation and multiple scattering in random continuum, emphasizing scalar wave equation solutions
15 p2564 A69-30150

Waveguide mode propagation theory for determining earth-ionosphere spherical waveguide upper boundary height diurnal variation for VLF waves
15 p2595 A69-30224

Electromagnetic waves as data carriers for earth resources and technology satellite sensors
15 p2607 A69-30231

Plane electromagnetic wave propagation normal and parallel to magnetic field in plasma analyzed by equivalent circuits and impedances
15 p2659 A69-30799

Te waves propagation along plasma sheet between conducting plates, determining vertical plasma density distribution
15 p2569 A69-30939

Electromagnetic wave propagation in anisotropic inhomogeneous media by geometric optics approximation, obtaining equations for beam trajectories in spherically symmetrical medium
15 p2569 A69-30949

Doppler geodetical measurements, emphasizing relative orientation between station and orbit influence on coordinates determination accuracy, presenting electromagnetic wave propagation theory
15 p2601 A69-31375

Scattering of line focused electromagnetic waves by infinite cylinders obtained by modification of plane wave theory
15 p2664 A69-31478

Coupled TEM lines arrays analysis in terms of odd and even modes, computing equivalent circuit elements, impedances and admittances
15 p2581 A69-31525

Electromagnetic wave propagation in transversely magnetized warm plasma filled rectangular waveguide, analyzing TE and TM modes
16 p2756 A69-31581

Atmospheric IR spectra determination from transmission functions overlapping effects of atmospheric gases
16 p2814 A69-31792

Noise signals in earth magnetosheath interpreted as electromagnetic waves propagating in whistler mode
16 p2774 A69-31985

Diffraction of electromagnetic waves produced by vertical dipole on impedance sphere of large radius in isotropic medium, using moment method
16 p2751 A69-32028

Electromagnetic cavity resonances in rotationally induced gravitational field by relativistic approach
16 p2812 A69-32048

Electromagnetic wave propagation in plasmas and plasma instabilities due to oscillations, deriving equations for frequency distributions in various plasma compositions
16 p2823 A69-32243

Numerical method based on thin film optics to determine ionospheric electromagnetic transmission and reflection coefficients for vertical incidence
16 p2752 A69-32392

Thin film optical method generalization accounting for intermode coupling and oblique incidence in plane stratified magnetoionic medium applied to ionospheric LF and hydromagnetic propagation
16 p2753 A69-32393

VLF and ULF whistler propagation in magnetosphere for remote sensing magnetospheric plasma parameters, exhibiting characteristic patterns and interaction with plasma
17 p2962 A69-33712

Slow electromagnetic wave propagation in superconducting thin film transmission lines, noting phase velocity dependence on film thickness and spacing
17 p2938 A69-33785

Electromagnetic waves radiation in general time invariant linear media with general boundary conditions, using Green function
17 p2924 A69-33834

Electromagnetic transient wave propagation and reflection in lossless isotropic stratified ionized media, discussing time variations of fields due to incident plane unit step wave
17 p2924 A69-33839

Ray methods application to partial differential equations for electromagnetic wave propagation in ionosphere, discussing strongly and weakly anisotropic inhomogeneous plasma
17 p2925 A69-33840

Electromagnetic beam propagation in anisotropic media, discussing quasi-optical beam divergence
17 p2925 A69-33845

Electromagnetic wave propagation in anisotropic media analyzed for wave packet behavior function stressing waveguide theories
17 p2926 A69-33847

Continuity conditions for drifting magnetoplasma without ionic effects, discussing eigenvalue equation refractive index and electromagnetic modes propagation
17 p2926 A69-33851

Horizontally stratified ionosphere radio wave reflection and transmission properties, calculating full wave by differential equations
17 p2927 A69-33862

Reflection and transmission coefficient matrices for stratified magnetoionic medium determined by thin film optical technique and iteration procedure
17 p2927 A69-33863

Complex refractive index profiles and wave polarizations calculated for electromagnetic waves transmission through ionosphere at micropulsation frequencies
17 p2927 A69-33864

Physical mechanisms for nonlinearities in electromagnetic wave propagation, analyzing plane wave instability, self focused beams propagation and laser oscillations
17 p2928 A69-33867

Electromagnetic wave diffraction in vacuum by equidistant conducting grating, deriving integrodifferential equations for calculating amplitudes
17 p2930 A69-33886

HF electromagnetic waves penetration into slightly ionized plasma analyzed by Maxwell and kinetic equations, giving penetrating electric field by WKB formula
17 p2932 A69-34220

Geomagnetic field latitudinal variation effect on cut-off frequencies of proton whistlers, discussing LF electromagnetic wave propagation in cold multicomponent plasma
18 p3100 A69-34253

Electromagnetic wave propagation in unbounded compressible plasma under drift velocity and magnetic field, obtaining dispersion equation for current density
18 p3179 A69-34261

ELF wave propagation in earth-ionosphere waveguide, considering ionospheric vertical inhomogeneity and models for ambient and disturbed /PCA/ conditions
18 p3101 A69-34949

Scattering of electromagnetic waves obliquely incident on inhomogeneous plasma column of parabolic radial density distribution, noting applications to ionospheric irregularities
18 p3102 A69-34963

Plane electromagnetic wave interaction with moving conductive dielectric medium to obtain reflection and transmission coefficients, noting energy transfer
18 p3105 A69-35486

Transverse electromagnetic wave propagation in cylindrically stratified axially magnetized plasma, obtaining plasma properties profiles from method for isotropic media
19 p3266 A69-35619

Interference filter design for IR devices on Fresnel equation basis, analyzing plane electromagnetic wave propagation through stratified dielectric multilayer
19 p3373 A69-36053

Soviet book on electromagnetic wave theory, discussing plane, cylindrical and spherical waves, complex media, wave damping in waveguides and transmission lines, etc
20 p3487 A69-37239

Distortion of electromagnetic pulse propagating through inhomogeneous plasma medium with linear electron density variation
20 p3496 A69-38030

Monochromatic electromagnetic field in resonant medium, examining linear, incoherent and coherent nonlinear propagations and resonant scattering
21 p3769 A69-38382

Atmospheric transmission determined in submillimeter solar radiation spectra using Bouguer law, identifying absorption lines in nocturnal and diurnal spectra
21 p3796 A69-38472

Electromagnetic wave reflection and transmission from boundary between semiinfinite plasma and air by applying static magnetic field
21 p3672 A69-38743

Plane electromagnetic waves penetration into ferromagnetic medium with permeability increasing with magnetic field, showing nonlinearity effect

21 p3771 A69-39109

Electromagnetic waves attenuation and field structure within gas filled dielectric waveguide tube, tube walls and waveguide surroundings

21 p3674 A69-39123

Nonlinear electromagnetic wave propagation by perturbation method previously employed to treat nonlinear boundary value problems involving partial differential equations

21 p3677 A69-39465

Field equations for electromagnetic radiation propagation in accelerated systems including dispersive and nonisotropic media

21 p3772 A69-39466

Electromagnetic wave propagation in nonlinear media, considering evolution and decay of electromagnetic shocks

21 p3697 A69-39670

Electromagnetic wave propagation in semiconductor plate under constant electric field, studying nonstandard carrier energy dispersion law effects on refractive index

22 p3994 A69-40751

Diffraction of plane polarized electromagnetic wave incident on dielectric wedge formulated as singular integral equation, discussing electric field amplitude

22 p3903 A69-41258

Plane EM wave transmission and reflection by semiinfinite isotropic plasma moving in arbitrary direction parallel to boundary, using Lorentz transformation

23 p4114 A69-41360

Electromagnetic propagation in infinite rectangular waveguide surrounded by dielectric medium described by Green dyadic

23 p4115 A69-41570

Earth sphericity and earth-ionosphere waveguide effects on terrestrial atmospherics, deriving form by computer

23 p4157 A69-41860

Dielectric materials permittivity determined by measuring amplitude ratios of reflected and transmitted plane electromagnetic waves

23 p4123 A69-41950

Electromagnetic oscillations emission by monochromatic electron beam in infinite waveguide formed by periodic diffracting array with energy losses, determining radiated power

23 p4124 A69-42031

Electromagnetic wave propagation in rectangular and plane parallel waveguides coupled by common wall with periodic transverse slots

23 p4124 A69-42037

Dispersion and resonant properties of electromagnetic waves propagating along plane metallic strip array with shield and dielectric

23 p4124 A69-42038

Accuracy standards for diffraction measurements of electromagnetic waves incident on periodic arrays, using monochromatic field and plane wavefront

23 p4139 A69-42042

IR radiation transmission in pulsed carbon dioxide discharge as function of time, proposing pumping and relaxation mechanism model

23 p4174 A69-42196

Terrain surface irregularities influencing electromagnetic wave propagation in inhomogeneous atmosphere, using perturbation calculation

24 p4281 A69-42611

Electromagnetic waves incident upon anisotropic plasma, determining transmission and power reflection coefficients

24 p4282 A69-42978

Electromagnetic waveguides direction-changing capability, deriving expressions for permitted bending radius with respect to mode conversion

24 p4288 A69-43331

Electromagnetic theory of surface radiation properties, analyzing specular reflectance of optically smooth surfaces

04 p0684 A69-14357

Monograph on classical electromagnetism via relativity, developing Maxwell equations from Coulomb law

07 p1180 A69-18404

Electromagnetic processes analysis in autonomous inverters simplified by linear graph method to derive characteristic equation

24 p4255 A69-42571

ELECTROMAGNETS

NT HIGH FIELD MAGNETS

NT SUPERCONDUCTING MAGNETS

Soviet collection of papers on electric circuits and electromagnetic systems

01 p0046 A69-10744

Horseshoe electromagnet sensors above ferromagnetic plate, analyzing electromagnetic properties of plate and coil impedance

12 p2094 A69-26719

Electromagnetic attitude control system for Lincoln Experimental Satellite 5 in near-synchronous equatorial orbit, noting onboard error detection in closed control loop

21 p3827 A69-39755

ELECTROMECHANICAL DEVICES

Electromechanical retracting pedestal for solid target injection into vacuum system and ionization by focused Q switched laser beam

03 p0439 A69-13105

Longitudinal edge effect in primary circuit of open loop linear MHD induction machines, determining forward, reverse and zero sequence currents and voltages

07 p1058 A69-19027

Electrical servopositioning of telemetry reception antenna for tracking satellites, considering weight, stability, etc

11 p1852 A69-25118

Failure engineering analysis of electromechanical switching devices, discussing preanalysis planning, open-ended data sheets, etc

13 p2231 A69-28043

Temperature behavior of resonant and antiresonant frequencies as function of electromechanical coupling and overtone order in piezoelectric resonators

14 p2421 A69-29542

Business aircraft electrical power sources, discussing electromechanical constant speed drive /EMCSD/ and comparison with DC/inverter and hydraulic CSD [SAE PAPER 690346]

15 p2552 A69-30091

Dynamic parameters of full scale and equivalent structures of electromechanical transducer circuits determined experimentally

22 p3869 A69-40249

Electric dose variometer principles, emphasizing differential pressure meter, differential capacitor and capacitor meter

24 p4315 A69-43143

ELECTROMECHANICS

Instabilities for two highly conducting finite length streams in relative motion and coupled by transverse electric or longitudinal magnetic fields

01 p0062 A69-11208

Dynamics of conducting fluid stream coupled to elastic medium by transverse electric or parallel magnetic field, considering stability of system

11 p1923 A69-24289

Electrohydrodynamics of fluids having uniform electrical properties, emphasizing shear effects for interfacially confined electromechanical coupling

18 p3123 A69-34919

Photomechanical and electromechanical effects in semiconductors, considering indentation microhardness decrease caused by light irradiation or electric field

19 p3386 A69-36526

Electromechanical effect dependence on CdS semiconductor surface state, noting relationship between microhardness and discharge current

21 p3781 A69-39072

ELECTROMETERS

Logarithmic response electrometer for upper atmosphere satellite measurements using subminiature vacuum tube

12 p2092 A69-26476

ELECTROMIGRATION

Dielectric overcoating effects on electromigration Al interconnections, showing dependence on thickness and surface passivation

17 p2935 A69-32889

Electromigration role in material accumulation and depletion forming regions in Au film conductors, discussing regions origin from and correlation with thermal gradients along conductor

17 p2936 A69-32896

ELECTROMOTIVE FORCES

NT PONDEROMOTIVE FORCES

Thermal EMF in indium phosphide crystals as function of temperature, electron concentration and magnetic field strength, determining effective mass of electrons

03 p0489 A69-13889

Electromotive force along magnetic field induced by liquid metal flow /alpha effect/, giving foundation for self excitation of electromagnetic field

04 p0635 A69-14547

Photocells with p-n heterojunctions from sintered CdS, describing spectral sensitivity and temperature dependence of no-load photo EMF

08 p1374 A69-21084

Thermal EMF in epitaxial films, analyzing potential distribution in p-n junction with temperature gradients and film thickness effects

09 p1555 A69-21473

Spontaneous reverse current due to Brillouin EMF observed in diode in thermal noise range

10 p1661 A69-22950

Weak magnetic field dynamics in bounded conducting medium having turbulent motion induced under zero boundary conditions

11 p1922 A69-24240

Induced EMF method for calculation of antenna impedance, discussing effects of approximations in calculation

11 p1851 A69-24997

Thermal EMF in indium phosphide crystals as function of temperature, electron concentration and magnetic field strength, determining effective mass of electrons

11 p1939 A69-25690

Solar quiet currents in three dimensional ionosphere, considering ionospheric conductivity and horizontal layer equations

12 p2074 A69-26955

Indium arsenide electrical parameters analyzed by kinetic effects, considering conductivity, thermal and magnetothermal EMF and transverse Nerst-Ettingshausen effect

15 p2666 A69-30066

P-type zinc-tin-antimonide crystals electric conductivity, Hall coefficient and thermal EMF found similar to p-type diamond-like semiconductors properties

15 p2667 A69-30197

Thermal EMF in epitaxial films, analyzing potential distribution in p-n junction with temperature gradients and film thickness effects

15 p2669 A69-30718

Electrical conductivity and thermoelectromotive force of bismuth telluride and bismuth telluride-bismuth selenide alloys obtained by sintering, hot pressing and annealing

15 p2670 A69-31248

Physical process providing EMF for maintaining electrical structure of stratosphere and mesosphere shown to center in lower ionospheric thermally driven tidal motions

18 p3130 A69-35103

Nb-Ti-C alloys electrical resistivity and thermal EMF noting nearly linear variations with temperature

20 p3558 A69-36976

Transverse thermomagnetic EMF and Nerst-Ettingshausen coefficient in GaSb semiconductor with double conduction band and strong degeneracy of current carriers

21 p3783 A69-39558

Electrical properties of semiconductors in HF electromagnetic field, showing Dember type EMF dependence on carrier response to field inhomogeneity

22 p3993 A69-40605

Thermal EMF in cadmium arsenide specimens with various electron concentrations determined to verify parabolic subband structure of conduction band

22 p3993 A69-40607

Praseodymium germanides resistivity and thermal EMF temperature dependence determined, discussing Hall effect, thermal expansion coefficient, melting point microhardness, etc

23 p4199 A69-42467

ELECTROMYOGRAMS

U ELECTROMYOGRAPHY

ELECTROMYOGRAPHS

U ELECTROMYOGRAPHY

ELECTROMAGNETICS

U ELECTROMAGNETISM

ELECTROMAGNETISM

NT MAGNETOSTATICS

Solar, interplanetary and magnetospheric electromagnetic events before and during magnetic storm from ground observatory and earth satellite data

01 p0156 A69-11120

Electromagnetic forming principles and applications describing large capacitor bank facility design for multipurpose research

[ASTME PAPER MR68-418]

02 p0252 A69-11798

ELECTROMYOGRAPHY

ELECTROMYOGRAPHY

Miniaturized transmitter for single channel biotelemetric system to transmit electromyograms incorporating thin film components

08 p1265 A69-19836

Human operator as servo system element of subassemblies in tracking and equilibrium tasks, stressing results of electromyographic analysis

12 p2025 A69-27081

Surface electromyography/EMG/frequency analysis of normal and pathological muscle or nerve contraction as diagnostic tool for industrial physician

21 p3664 A69-38920

Muscle function measurement in astronauts using electromyogram, electrocardiogram and isometric tension at fixed percentage of maximum voluntary contraction

23 p4103 A69-41684

ELECTRON ACCELERATORS

NT BETATRONS

Sudden acceleration of electrons in magnetosphere and magnetic tail related to magnetic bays, noting acceleration occurrence first in magnetosphere during polar substorm

04 p0594 A69-15122

Voltage divider network board composed of composite carbon resistors for measurement of terminal voltage of 3 Mev Dynamitron electron accelerator recalibration

06 p0907 A69-17705

Electron acceleration in microtron through injection from low pressure gas discharge plasma

08 p1279 A69-19803

Plasma wave excitation and dissipation in fast thetatron discharge, indicating electron nonadiabatic inductive acceleration without equilibrium orbit

09 p1552 A69-22046

Outer radiation zone electron intensities during magnetic storms for morphology of zone electron acceleration mechanisms

11 p1950 A69-25147

Auroral electrons intensity modulation by source at L equals 6 magnetic shell on geomagnetic equator, noting dispersion effects

12 p2065 A69-26108

Potential mechanisms of electron acceleration inside magnetosphere, measuring power spectrum of X rays by electron braking in upper atmosphere

12 p2066 A69-26295

Mercury electron bombardment thrusters, discussing mission, design, ground tests, components and thrust vectoring

12 p2148 A69-26787

Artificial aurora generated at 100 km altitude by electron beam fired downward from aerobee 350 rocket above 230 km along earth magnetic field lines

18 p3127 A69-34365

Nanosecond photography with superradiant light source, X rays or electrons using multipurpose electron accelerator, obtaining stop motion pictures

19 p3305 A69-35721

Ultrarelativistic electron acceleration in Crab Nebula maintaining synchrotron spectrum, obtaining power from compressional motion damping, gyrorelaxation effect and pitch angle anisotropy removal

19 p3424 A69-36336

Low energy electron accelerator to produce measurable small fluxes through photoelectric effect from Au cathode UV irradiation to achieve high flux stability

19 p3313 A69-36492

Continuous electron acceleration in astrophysics, discussing Crab Nebula X ray flux and galactic and extragalactic radio source power law spectra

24 p4355 A69-42696

ELECTRON ATTACHMENT

NT NUCLEOPHILES

Double probe characteristics in flame with electronegative gas injection interpreted in terms of conduction of ions in ionized medium

01 p0176 A69-10385

Chemical reaction fluctuations and oxygen electron attachment omission effects on density fluctuations in turbulent wakes, noting electron density fluctuation, bimodal model, etc

02 p0233 A69-12538

Negative ion-molecule reactions in nitrous oxide using mass spectrometer, noting negative ion concentration pressure dependence

06 p0960 A69-17106

Flame inhibition with electron attachment observed using halogenated hydrocarbons

06 p1034 A69-17926

Ionization and attachment coefficients in oxygen at low pressures, noting Paschen curves near minimum sparking potential and secondary ionization coefficient

08 p1354 A69-20099

Region of transition from laminar to turbulent flow in meteor trains, suggesting electron attachment processes to molecular oxygen in presence of third body

08 p1393 A69-20608

Radiative capture of electrons by chlorine, bromine and iodine atoms in shock heated plasma seeded with sodium halides from absolute intensities in continuous emission

08 p1355 A69-20735

Electron detachment cross sections for negative atomic and molecular O ions with incident energies between 3 and 100 ev

09 p1542 A69-21625

Oxygen and NO ions yields produced by dissociative attachment of electrons to nitrogen dioxide as function of electron energy, considering electron affinities lower limits

13 p2301 A69-27363

Ionization and attachment of thermal electrons in oxygen and airlike nitrogen-oxygen mixtures during electron irradiation

13 p2302 A69-27456

ELECTRON AVALANCHE

Avalanche multiplication in abrupt silicon p-n junctions analyzed using ionization coefficient measurements for holes and electrons

01 p0135 A69-10038

Silicon p-n junction avalanche current temperature dependence calculation by considering space charge current and multiplication factor as function of temperature

01 p0136 A69-10245

Planar transistor micromode operation during collector junction avalanche breakdown

01 p0047 A69-10884

Current-voltage characteristics of avalanche transistors, noting impact ionization

02 p0218 A69-12266

Conductivity in p-n junctions during avalanche breakdown at HF calculated, noting agreement with experiments

03 p0492 A69-14164

Electric field growth directional effect on avalanche breakdown conditions in p-n junctions

06 p0981 A69-17828

Microwave spectrum of n-InSb avalanche plasmas under magnetic field, considering dynamic current-voltage characteristics, hole wave instabilities and microwave emission processes

07 p1197 A69-18466

Breakdown voltage and avalanche drift instability factors in planar passivated p-n junctions as function of oxide thickness and mobile charge

10 p1743 A69-23174

Avalanche transistor pulse circuits temperature increase due to power dissipation, noting effects of external resistance grounding base and pinch in

11 p1845 A69-24570

Planar transistor micromode operation during collector junction avalanche breakdown

12 p2041 A69-26648

Angular distribution function calculations for avalanche electrons at various stages of cascade development, discussing electron energies and primary electron roles

13 p2303 A69-28414

Current and electroluminescence brightness dependence on reverse voltage in n-SiC diodes including tunnel and avalanche processes

15 p2573 A69-30062

ELECTRON BEAM WELDING

High strength steel welding with physical properties equal to parent metal, discussing gas tungsten-arc, electron beam and plasma arc techniques

01 p0088 A69-11399

Electron beam welding of beryllium, discussing procedures, weld quality and tensile strength efficiencies

02 p0252 A69-11863

Electron beam welding procedure planning and production shop control parameters

04 p0605 A69-14529

Electron beam welding using glow discharge as source of electrons, noting hollow anode gun design and electrode geometry influence on beam shape

04 p0608 A69-15480

Electron beam process application to welding, machining and assembling in automobile mass production

04 p0608 A69-15484

Weldability of thermally stable titanium alloy, noting properties of electron beam and submerged arc welding

06 p0940 A69-17092

Welding methods used for Ti and Ti alloys and difficulties encountered

07 p1139 A69-18789

Energy consideration in electron beam welding, obtaining expression for penetration decrease in terms of thermal diffusivity

08 p1320 A69-20360

Metallic systems microbonding and joining reliability, noting electron and laser beam welding and deposited film connections

09 p1510 A69-22348

Electron beam welding of Lunar Module Descent Engine, emphasizing variable area injector element and manifold assembly problems and techniques

12 p2102 A69-26621

Electron beam welding characteristics for aircraft components and design noting limitations

15 p2617 A69-30089

Electron beam welding method for very thin foils, discussing welding of pinhole free Ni, Cu and stainless steel foils

17 p2977 A69-32854

Electron beam welds orientation effects on tensile and deformation properties of strengthened and welded austenitic stainless steels

18 p3151 A69-35432

Plasma electron beam for welding, deriving beam current from secondary emission by ion bombardment, discussing gas pressure, equipment and applications

19 p3320 A69-35555

Electron beam welding for repair and production, discussing application to Ti VHF antennas, Concorde switchgears and nuclear reactor loading tubes

20 p3550 A69-37451

Electron beam welding machine modifications for welded airframe components production, discussing work chamber, vacuum system and workpiece mounting

20 p3550 A69-37455

Electron beam welding for fabrication of aircraft structures, discussing fatigue strength of Ti and Al alloys and marring and low alloy steels

20 p3550 A69-37456

Fracture and tensile properties of electron beam welded Al alloy for pressure vessels compared to gas tungsten arc welding results

24 p4319 A69-42941

ELECTRON BEAMS

Weak signal interaction between electron beam and microwave resonators, obtaining electron conductance, gain and transfer admittance

02 p0208 A69-12265

Scanning electron beam display of space charge of defects and junction behavior of edge dislocation array in Ge and Si monocrystals

02 p0301 A69-12661

Temperature dependence of electron beam pumped GaAs laser threshold current density and emission spectra, noting doping effects

02 p0260 A69-12683

Electron beam meter application as lunar surface electric field detector, discussing breadboard model and performance characteristics

03 p0429 A69-13221

Modulated photocurrent in CdS crystal obtained by irradiation with intensity modulated electron beam, noting relaxation time and trap concentration

03 p0490 A69-13946

Experimental equipment and procedure to investigate defocusing of electron beam directly in cavity beam hole of TWT amplifier

03 p0407 A69-13975

Nonlinear cross sectional space charge density distribution in electron beam of traveling wave tube

03 p0407 A69-13984

Equations for self oscillating mode of operation for O-type backward wave generator with electrostatically focused electron beam and finite values of amplification parameter

03 p0407 A69-13986

Interaction between surface waves propagating along plane plasma boundary and parallel low density electron beam, noting wave amplification and excitation

03 p0480 A69-14135

Temperature rise of micron sized silver particles on carbon film due to electron beam heating, setting up heat balance equation

04 p0640 A69-14449

Pulsations of relativistic and nonrelativistic narrow /paraxial/ electron beams with spatial axis curved ac-

cording to various laws, deriving approximate descriptive equations

04 p0632 A69-14981

Smear out electron beam generation for experiments on weak plasma turbulence by passing beam through aluminum foils

04 p0636 A69-15020

HF interaction of relativistic electron beam and plasma extended to include arbitrary variation of plasma density

04 p0637 A69-15046

Surface potential measurements for flat conductors or semiconductors using scanned electron beam probe

04 p0601 A69-15115

Electron cyclotron instability and HF ionization in beam-plasma experiment using electron beam guided by magnetic field through He gas

05 p0798 A69-15612

Focusing of relativistic cylindrical electron beam in static axial electric and magnetic fields, using least action principle to derive trajectory differential equation

05 p0796 A69-15715

Electron beam modulation of germanium reflectance

05 p0807 A69-15816

RF electron heating by beam-plasma interaction in uniform magnetic field

05 p0804 A69-16458

Velocity distribution of plasma electrons in electron beam generated He plasma using Boltzmann equation, neglecting electron-electron collisions

05 p0805 A69-16705

Wave dispersion analysis for amplification in cold plasma filled cylindrical waveguide penetrated by electron beam of same radius

05 p0736 A69-16790

Light valving techniques applied to large screen display of computer generated video information, noting electron beam control mechanism for transmitted light

06 p0928 A69-17922

Beam modulation resynchronization at large signal levels by TWT circuit wave to enhance efficiency

07 p1094 A69-18423

Traveling wave amplifiers beam defocusing by RF circuits and space charge fields under large signal operating conditions, discussing magnetic field strength

07 p1094 A69-18424

High power microwave interactions in pulsed electron beam plasma klystron

07 p1095 A69-18433

Small signal coupled mode analysis including relativistic effects for studying spiraling electron beam interaction with fast wave circuits

07 p1114 A69-18436

Microwave oscillations during interaction between electron beam and plasma in electron tube

07 p1189 A69-18504

Wave propagation on cylindrical electron beam in vacuum and in plasma background, including relativistic effects

07 p1189 A69-18657

Periodic electrostatic focusing structures in microwave tubes, evaluating properties by action function method

07 p1102 A69-18659

Thin electron flux interaction with electromagnetic wave in open waveguide, discussing nonlinear theory and performance of gyroresonance transverse wave tube

07 p1107 A69-19159

Cold plasma stability during traversing by electron beams in presence of external magnetic field, obtaining dispersion relations for longitudinal and transverse modes

07 p1195 A69-19465

High energy particles obtained by accelerating plasma with frozen-in magnetic field to relativistic velocities during scattering of fast electron beam

08 p1358 A69-19805

GaAs laser employing external resonator with thin film active substance, noting output power and emission thresholds during electron beam excitation

08 p1326 A69-20543

Analog study of periodic permanent magnet focusing, considering ray equation, beam radius dependence on distance, amplitude variations, etc

08 p1285 A69-20555

Contour of axisymmetric holes in dimensional electron-beam machining calculated from density distribution of transmitted energy

08 p1321 A69-20727

Finite ion mass effect on stability of space charge neutralized electron beam

09 p1545 A69-21342

Electrons resonant heating in beam plasma discharge, discussing ion cyclotron wave excitation in hot electron plasma produced by electron beam

09 p1549 A69-22016

Optimal working parameters and operational characteristics of laboratory electron gun, examining beam shape, convergence and current density distribution

09 p1464 A69-22243

High temperature electron component of plasma produced by strong electron beam in adiabatic magnetic trap, deriving turbulent diffusion coefficient dependence

09 p1553 A69-22657

Quasi-linear relaxation of electron beam in magnetoactive plasma, noting instability of plateau in velocity distribution function

09 p1553 A69-22659

Combined electron microprobe and ellipsometric study of thin silicon dioxide films on silicon, noting reliability and accuracy

10 p1742 A69-22946

Plasma electron beam nonlinear interaction, considering equations of motion of electron distribution function, plasma wave spectrum and mode coupling effects

10 p1729 A69-23407

Electron beam addressed electrooptic light valve used as spatial filter, discussing electronic control and optical processing in real time

10 p1697 A69-23870

Landau type interaction between electron beam and whistler/helicon wave electric field within semiconductor /InSb/

10 p1742 A69-24107

Collection of papers on electron beam and laser beam technology covering cold electron emitters, space charge flow, gas lasers, microelectronics, thin polycrystalline films

11 p1846 A69-24596

Unrippled space-charge flow in dense axially symmetric electron beams as basis for electron gun design

11 p1846 A69-24598

Thin polycrystalline film structure and formation, using electron beam instrument

11 p1936 A69-24601

Image tube storage target mesh electrode structure and transmission data for electron beams of various velocities, noting secondary electron redistribution control

11 p1848 A69-24749

Linear interaction of electron beam and plasma in magnetic field noting convective wave instability, wave dispersion and properties behavior

11 p1929 A69-25267

Synchrotron radiation amplification by monoenergetic electron stream helically gyrating in static magnetic field of cold plasma, discussing amplification rate frequency dependence

11 p1931 A69-25361

HF electrostatic waves propagation excited by electron beam in hot inhomogeneous plasma in magnetic field, studying wave transformation and absorption

11 p1931 A69-25364

Paraxial electron beams from Pierce gun and spreading due to thermal velocities and space charge in nonuniform potential

12 p2036 A69-25920

Direct electron beam shadowgraph photographic /betagraphy/ technique for recording small high speed objects with 3 nanosecond exposure time

12 p2086 A69-26164

Continuous polarized electron beam produced from spin conversion in ionizing reactions involving optically pumped metastable atoms in He discharge

12 p2130 A69-26312

Plasma-electron beam interaction induced HF oscillations, obtaining nearly noise free oscillations

12 p2137 A69-26529

DC to RF energy conversion in ungridded klystron gaps, calculating efficiency and optimum load conductance as function of gap dimensions

12 p2041 A69-26629

LF oscillations nonlinear excitation increment in plasma by electron beam found proportional to reciprocal of wave potential

12 p2138 A69-26709

Two beam electron flux instability in crossed magnetic and inhomogeneous electric fields using linearized hydrodynamic and Lagrangian formalism approximation

12 p2133 A69-26714

Instabilities related to particles transit time in system of two counterstreaming electron beams of finite length, noting wave dispersion

12 p2141 A69-27179

Metastable molecules and fragments produced by electron excitation of nitrogen, hydrogen, carbon dioxide and nitrous oxide, noting excitation functions, kinetic energy, etc

13 p2301 A69-27362

Photon loss coefficients in electron beam pumped GaAs laser showing dependence on doping type and impurity concentration, noting threshold current density measurement

13 p2271 A69-27467

Plasma lens device for focusing ion or plasma beams with closed electron drift

13 p2307 A69-27658

Nonequilibrium conductivity and radiation of CdS, GaAs and PbS single crystals in waveguide cell under electron beam

13 p2318 A69-27886

Nonmagnetic ionization gage consisting of quadrupole lens systems excited at HF, discussing electron focusing during operation

13 p2263 A69-28084

Microwave and LF oscillations interactions in plasma beam system, showing oscillation amplitude dependence on frequency relationships

13 p2312 A69-28111

Waves propagating along rotating electron beam and interacting with magnetized plasma waveguide slow waves

13 p2312 A69-28118

Time varying flow properties effects on hypersonic wind tunnel spectroscopic measurements, considering direct emission and electron beam techniques

13 p2242 A69-28267

Spatial harmonics of harmonic frequency instabilities of cyclotron half frequency in system of two symmetrical electron beams confined by magnetic field

13 p2314 A69-28364

Whistler type electromagnetic waves excitation by electron beam in plasma, noting intensity dependence on electron frequency

13 p2314 A69-28443

Magnetized plasma waveguide dispersion characteristics using Maxwell equations, stressing interaction of electron beam with wave modes

13 p2315 A69-28571

Double beam parametric electron amplifier with compensation of difference channel, noting beams noise removal

13 p2237 A69-28578

Electric field distribution in TWT electron beam deflection system determined, accounting for current-voltage characteristics dependence on electromagnetic field distribution

13 p2237 A69-28582

Frequency distribution and statistical characteristics of high level RF noise produced by high perveance electron beam of magnetron injection gun /MIG/

14 p2449 A69-29558

Energy resolution improvement in cylindrical electrostatic energy selector by focusing and limiting electron beam before entrance into monochromator

14 p2450 A69-29572

Small signal analysis of processes in klystron resonators involving beam-field interaction

15 p2573 A69-30117

Molecular benzene emission spectra excited by electron beams in RF modulated source, tabulating lifetime measurements

15 p2562 A69-30468

Ionization within intersecting alkali atomic and slow electron beams, observing ionization cross sections increment near ionization threshold

15 p2655 A69-30726

Three dimensional effects of potential minimum near cathode emitting axisymmetric beam, relating electric fields distribution to noise reduction coefficient

15 p2568 A69-30794

Radial self focusing of low density electron beam by interaction with plasma in presence of beam plasma instability

15 p2662 A69-30964

Electron beam exposure system to photoetch integrated circuit patterns without photomasks, using electronic computer for automatic pattern generation and registration

15 p2579 A69-31039

Electronic-ultrasonic amplifiers with external electron stream and longitudinal or surface wave studied for damping influence, deriving dispersion equation

16 p2761 A69-32061

Electron beam rotational temperature, noting discrepancies between experimental values and iterative calculations due to secondary electron effects

16 p2814 A69-32175

Turbulent heating of ions and electrons by interaction between magnetically collimated electron beam and electron beam self generated plasma
17 p3014 A69-33827

Plasma generation and heating by electron beam-plasma interactions, discussing HF fields excitation and absorption
17 p3014 A69-33828

Time resolved beam distribution functions resulting from cyclotron instability and harmonics in electron injection machine during beam-plasma experiment
17 p3014 A69-33829

Plasma-cyclotron interaction wave coupling mechanism in symmetrical double beam system in uniform magnetic field leading to unstable wave excitation along beam
17 p3015 A69-33831

Artificial aurora generated at 100 km altitude by electron beam fired downward from aerobee 350 rocket above 230 km along earth magnetic field lines
18 p3127 A69-34365

Electron beam fluorescence probe and afterglow investigation for hypersonic He flow visualization, observing qualitative structure
19 p3291 A69-35722

Quantitative photographs of low density flowfields during shock tunnel tests using electron beam excitation with image intensifier tube detector
19 p3292 A69-35723

Axially symmetric magnetic fields for constant radius annular electron beams reflection, applying results to design of reflex klystron millimeter oscillator
19 p3267 A69-35930

TV camera tubes with electron beam scanning adapted to IR imaging, emphasizing vidicon
19 p3311 A69-36069

Jet and Mach disk density measured by fluorescence electron beam technique, calculating Mach disk thickness from density profiles
19 p3239 A69-36396

Vibrational temperature of low density nitrogen measured by electron beam method, discussing relationship to ratio of integrated vibrational band intensities
20 p3579 A69-37222

Solar bremsstrahlung intensity dependence on heliographic longitude, noting maximum intensity shift toward electron beam direction
20 p3589 A69-37552

Ambient atmospheric temperature and molecular nitrogen density measured simultaneously by rocket-borne electron beam luminescence method
20 p3543 A69-37799

Dynamic electron beam devices for refractory materials evaporation, discussing electron guns and vaporization film data
[ASM PAPER D8-22.2] 20 p3551 A69-38131

Luminous tenuous collimated electron beam from plume of MPD arc in fiberglass vacuum tank, examining beam trajectory in geomagnetic fields
20 p3582 A69-38236

Electron beam pumped semiconductor laser light beam amplitude and phase distribution, studying effects of inhomogeneous excitation by model
21 p3737 A69-39041

Changes in CdS crystals spontaneous and coherent emissions caused by electron beam radiation damage, determining intensity and spectral composition dependence
21 p3780 A69-39047

Electron beam pumped dislocation free GaAs lasers filamentary and nonuniform emission characteristics from X ray topographs before and after bombardment
22 p3963 A69-40565

Linear self consistent diffraction emission theory and relationship to electron beam propagation
22 p3899 A69-40615

Self consistent flow calculation in dense space charge beams, including electrode design for portions isolation
22 p3985 A69-40668

Electric field regions of p-n junctions using electron beam deflection measurement, noting application to Si specimens
22 p3994 A69-40752

Electron beam injection into magnetic trap, obtaining plasma by ionization of supersonic argon flow passing through system
22 p3990 A69-40791

Electronically controlled microwave phasers and time delay elements design and operation, discussing beam width, steering and effects, directivity and planar arrays
23 p4135 A69-41353

S band phased array receiver developed to track automatically moving telemetry transmitter by electronic beam steering
23 p4120 A69-41751

Electromagnetic oscillations emission by monochromatic electron beam in infinite waveguide formed by periodic diffracting array with energy losses, determining radiated power
23 p4124 A69-42031

Space charge wave propagation induced by electron beam moving in annular waveguide, considering radiated field and current redistribution
23 p4124 A69-42034

Atmospheric gases emission spectra excited by electron beam as function of pressure
24 p4353 A69-43698

ELECTRON BOMBARDMENT

High energy neutral molecule beam for gas-surface interaction studies generated in electron bombardment ion source
19 p3376 A69-36176

Effective Gaunt factors for threshold excitation of positive ions by electron collisions for 23 dipole transitions in 15 isoelectronic sequences
20 p3581 A69-38175

Cations desorption from O, H and N films adsorbed at graphite surface under electron bombardment, studying desorption cross sections discrepancies
22 p3972 A69-39957

Proton ejection as hydrogen ion clusters by low energy electron bombardment of solid hydrogen
24 p4389 A69-43747

ELECTRON BUNCHING

Power saturation in isochronal traveling wave tube explained by motion of electron bunches relative to waves
01 p0047 A69-10882

Klystron bunching analysis, adding electron overtaking formulation to existing nonlinear space-charge wave theory
02 p0215 A69-11939

Electron bunching improvement by combined effect of space charge and inhomogeneous electrostatic field on velocity modulated electron flux in microwave devices
05 p0799 A69-15646

Relation between electric field strength and mean energy for electron swarms in oxygen determined, using Boltzmann transport equation
11 p1921 A69-24419

Power saturation in isochronal traveling wave tube explained by motion of electron bunches relative to waves
12 p2041 A69-26646

Electron bunching improvement by combined effect of space charge and inhomogeneous electrostatic field on velocity modulated electron flux in microwave devices
16 p2823 A69-32503

ELECTRON CAPTURE

Trapping parameters of Fe doped GaAs-GaP, measuring thermally stimulated conductivity and space charge limited currents
02 p0296 A69-11789

Energy distribution and capture cross section ratio limiting factors in semiconductors with deep energy levels
02 p0299 A69-12562

Spectroscopy of fast atoms resulting from fast ion impact with gas targets and electron capture into excited state
03 p0471 A69-13162

Polar auroral region cosmic radio noise absorption bays diurnal variations attributed to drift of electrons captured in magnetosphere
03 p0423 A69-13520

Region of plasma electron capture during cyclotron electron resonance in magnetic trap with mirrors
03 p0478 A69-13849

Collection efficiency of continuous dynode electron multiplier arrays, discussing incident electron current
06 p0897 A69-17699

Thin semiconductor plates negative differential resistance associated with captures at surface, describing electron gas by electron temperature
08 p1374 A69-21081

Photoelectric ejection of grain electrons by solar quanta balance with solar wind electron capture by grain for interplanetary grain equilibrium potential
09 p1593 A69-21655

Surface charge exchange in metal oxide silicon capacitors generated at low temperatures by surface state free carrier trapping
10 p1744 A69-23179

High latitude capture region boundary for electrons in upper radiation belt determined relative to current electrojets in ionosphere from satellite observations
13 p2327 A69-27700

Capture levels at photosensitive CdS crystals surface determined by studying field effect mobility dependence on electric field
13 p2318 A69-27884

Electron reactivity of one equivalent oxidizing agents at ZnO surface by electrochemical reduction
19 p3392 A69-36731

Galactic X ray flux from H I region low energy cosmic ray nuclei, studying electron capture effects on line intensities
24 p4367 A69-43048

ELECTRON CLOUDS

Variable radio sources observation at 9.55 mm wavelength, discussing flux density and electron cloud expansion
13 p2334 A69-27309

ELECTRON COUNTERS

Low energy electrons on day side of magnetosphere observed with MIT electron detector on OGO 3 satellite
03 p0503 A69-14027

Photoelectron counting in extreme UV using windowless photomultiplier detectors as photon counters
04 p0595 A69-14277

Satellite-borne auroral particle spectrometer calibration to minimize uncertainty in measuring absolute particle flux of electrons and protons
04 p0599 A69-15022

Electron detector for OGO-E to measure flux and energy spectrum of electrons in primary cosmic rays [IEEE PAPER 3C-4]
07 p1135 A69-19198

Solid state detector for electron spatial distribution measurements on OGO-F satellite, discussing design emphasizing reliability
19 p3284 A69-36676

Planar thermal ion and electron trap experiments on Explorer 31 satellite, measuring ion and electron density and temperature and ionic composition
20 p3544 A69-37878

ELECTRON DECAY RATE

Inhomogeneous distribution of nonequilibrium current carrier concentrations in semiconductors with electrons and holes of different lifetimes, noting instability
15 p2665 A69-30041

Air afterglows electron loss mechanisms, measuring electron densities decay rates after microwave ionization
22 p4006 A69-40527

ELECTRON DENSITY [CONCENTRATION]

NT IONOSPHERIC ELECTRON DENSITY

NT MAGNETOSPHERIC ELECTRON DENSITY

Recombination rate dependence on nonequilibrium charge carriers concentration at semiconducting surface
01 p0136 A69-10253

Generalized pair of space correlation and wave number spectrum functions applied to plasma electron density fluctuations and velocity fluctuations of background fluid
01 p0127 A69-10339

Dense plasmas produced by explosions of wires and mercury filaments, discussing plasma conductivities
01 p0128 A69-10391

Exosphere diurnal and latitudinal variations in electron and proton content, ion composition, and electron, proton and positive O ion densities
01 p0063 A69-10422

Electron density in arc discharge between carbon electrodes and in discharge with Na vapor, noting relation to temperature and current
01 p0128 A69-10433

Galactic H II regions morphology from high resolution radio observations, noting variation of electron density with region size
01 p0151 A69-10552

Spectroscopic investigation of high density plasma from Li exploded wires
01 p0129 A69-10662

End holes and glass tube effects in TM 010 mode measurements of average electron number density in cylindrical plasmas
01 p0131 A69-10812

Differential Faraday technique to determine electron content latitude dependence in Northern Hemisphere during magnetically disturbed periods in March 1966
01 p0146 A69-11128

Solar corona electron density, polarization, temperature and monochromatic emission during November 1966 eclipse
02 p0310 A69-11457

- Capillary arc source spectroscopy, determining plasma temperature and pressure dependence on capillary geometry and discharge current
02 p0286 A69-11573
- Alpha recombination coefficient of molecular helium ions measured in helium afterglow plasmas as function of electron density and gas temperature
02 p0283 A69-11834
- Scaling laws for RF discharge experiments in ionized environments, considering proper limit variables for simulation of electron density
02 p0283 A69-12241
- Electron density measurement technique for dense thick steady state plasmas using swept microwave interferometer
02 p0290 A69-12349
- Chemical reaction fluctuations and oxygen electron attachment omission effects on density fluctuations in turbulent wakes, noting electron density fluctuation, bimodal model, etc
02 p0233 A69-12538
- Solar corona delay effects on pulsar signals due to inhomogeneities in coronal electron density
02 p0328 A69-12727
- Electric field, current density and magnetic induction of plasma flow measured, obtaining plasma conductivity and flow velocity for electron temperature and density
[ONERA-TP-649]
03 p0473 A69-12877
- Emitted light and excited state populations resulting from two electron collisional radiative recombination related to free electron density
03 p0469 A69-12923
- Average plasma electron density measurement by feedback oscillator to determine dielectric constant
03 p0473 A69-13103
- Automatic recording of neutral atom temperature and free electron density of partially ionized gas by Fabry-Perot interferometer
03 p0428 A69-13111
- Nighttime sporadic E layer occurrence due to ionization redistribution established, noting concurrent F region electron concentration decrease
03 p0423 A69-13536
- Thermal EMF in indium phosphide crystals as function of temperature, electron concentration and magnetic field strength, determining effective mass of electrons
03 p0489 A69-13889
- Low energy electrons on day side of magnetosphere observed with MIT electron detector onOGO 3 satellite
03 p0503 A69-14027
- Frequency of damped oscillations in plasma in DC field, noting variation with electron density and DC field
03 p0479 A69-14050
- Time resolved electron number density and electron temperature in decaying plasma using laser interferometer
03 p0432 A69-14187
- Discontinuities in plasma situated in magnetic field, noting drift of quasi-neutral inhomogeneities of electron and ion density
04 p0634 A69-14431
- Electron density variation in region of change of regime in gas discharge excited by HF capacitance and external electrode
04 p0637 A69-15060
- Ultrahigh speed holographic interferometry for studying plasmas produced by focused laser beam, noting electron density evolution in deuterium plasma
05 p0760 A69-15587
- Electron density measurement in rapidly varying plasma, using improved Mach-Zehnder interferometer
05 p0760 A69-15613
- Low dispersion spectrograph for temperature and electron density determination in plasma beam
05 p0803 A69-15997
- Electron concentration in pulsed plasma measured with Fabry-Perot interferometer and laser radiation source
06 p0963 A69-16911
- Ionization index, electron formation and effective recombination coefficient in E 2 layer, noting solar activity effect
06 p0920 A69-17725
- Theta pinch plasma electron density and temperature distributions measured using Thompson scattering of laser light and plasma bremsstrahlung
06 p0972 A69-18220
- Focused electromagnetic beam interferometers and antenna parameters for measuring electron density in plasma diagnostics
07 p1132 A69-18865
- Whistlers and VLF emissions from ground based and satellite measurements, applying results to electron density mapping and ion detection
07 p1127 A69-19354
- Three dimensional Fourier synthesis at low resolution for calculating ribosome electron density distribution in chromatoid bodies
07 p1074 A69-19394
- Free fall theory for afterglow decay of average electron density and temperature in pulsed cylindrical mercury vapor discharge plasma
08 p1358 A69-19811
- Plasma electron density and collision frequency determination, using CW maser interferometer
08 p1359 A69-19987
- Electron density measurement in solar flare spray using discrepancy between measured and theoretical polarization
08 p1378 A69-20244
- Population densities of UV bound resonance lines of neutral helium for 41-level model atom, discussing optical thickness and electron temperature and density
08 p1390 A69-20392
- Ambipolar diffusion in electron concentration inhomogeneities of weakly ionized plasma in magnetic field analyzed by linearized quasi-hydrodynamic equations
08 p1362 A69-20426
- Spectroscopic diagnostics for determining temperatures, electron densities and line shapes in optically thick plasmas
08 p1363 A69-20466
- White dwarfs transfer to superconducting state, using BCS theory for superconducting transition temperature dependence on electron density
08 p1391 A69-20546
- Dimensions, temperature and electron density of quiet solar corona from radio interferometer measurements, noting activity and temperature at solar maximum and minimum
08 p1393 A69-20573
- Pulsar distance estimates, discussing effect of interstellar electron and H densities and temperature dependence of H density-electron density ratio within disk
08 p1397 A69-20698
- Laser produced blast wave expansion measured by microwave technique, obtaining surface temperature and electron density
09 p1514 A69-21324
- Voltage dependence of mobility limited electron current density in gas filled diode for collision frequency proportional to electron speed
09 p1462 A69-21326
- Forward and backscattering of radio waves at electron concentration discontinuity near reflecting ionospheric layer with vertical nonuniformity
09 p1453 A69-21525
- Vertical transport rate of charged particles in F region, allowing for vertical velocity gradients
09 p1485 A69-21529
- Electron content of earth-Venus interplanetary medium measured by observing relative propagation time of radar pulses to Venus
09 p1594 A69-21697
- HgTe-CdTe single crystals homogeneity and Cd distribution obtained by Bridgman and/or zone melting studied for carrier concentration and electron mobility
09 p1557 A69-21737
- Valence electrons mean density stability in Ti and V monoxides, describing mechanism for filling M vacancies with simultaneously forming O vacancies
09 p1523 A69-21738
- Spectroscopic measurements of electron density and temperature for quasi-saturation region of ignited mode plasma in planar thermionic converter
09 p1439 A69-21826
- Fission fragment generated plasma applicability to thermionic energy converters from electron density, temperature and transport studies
09 p1440 A69-21829
- Strongly doped n-type indium antimonide, determining dependence of limiting electron concentration on dopant impurity nature
09 p1558 A69-21869
- Electron density fluctuations in turbulent wakes of hypersonic projectiles in ballistic ranges, discussing use of cylindrical Langmuir probe for direct measurement
09 p1496 A69-21934
- Electron concentration at front of anisotropic plasma expanding in axial direction in electrodeless induction discharge from measurements of reflected microwaves
09 p1550 A69-22027
- Structure and properties of high heat resistant alloys based on high melting point metals with bcc lattice explained by electron theory
09 p1525 A69-22139
- Recombination rate dependence on nonequilibrium charge carriers concentration at semiconducting surface
09 p1559 A69-22646
- Electron density and collision frequency of MHD plasma determined directly by measuring phase shift and attenuation of propagating laser microwave signal
10 p1731 A69-23436
- Electrical conductivity, electron density and population temperature as functions of current density in Cs-He thermal plasma studied with nonequilibrium ionization model
10 p1732 A69-23443
- K coronameter observations used to construct electron density models of corona above proton flare region of July 1966
10 p1763 A69-23733
- Polarization measurements of July 1966 proton flare, considering electron scattering and density
10 p1764 A69-23740
- Ionization instability in low temperature magnetized plasma, analyzing electron concentration perturbation caused by Joule heating during electron-ion collisions
10 p1741 A69-23962
- Electron concentration and temperature dependence on gas temperature as factor determining He-Ne laser output at 6328 Å
10 p1706 A69-24078
- Thermodynamic stability of dense plasma consisting of electrons and charged ions, plotting ionization potential as function of electron density and temperature
11 p1922 A69-24232
- Ion and electron temperature and density measurement by Thomson scattering with low resolution monochromator for Salpeter parameter near unity
11 p1925 A69-24310
- Electron number density LF oscillations for ionized gas identified with periodic solutions to neutral and charged particle plasma continuity equations
11 p1925 A69-24315
- Solar flare and magnetic storm signals from ATS 1 geostationary satellite on May 28, 1967, deriving total electron content
11 p1951 A69-25161
- Temperature and electron concentration in plasma spark obtained in air by focusing Q switched laser radiation
11 p1928 A69-25235
- Free electron density upper limits in plasma attributed to negative ion formation, noting effect on ionization equilibrium calculations for stellar atmospheres
11 p1928 A69-25255
- Thermal EMF in indium phosphide crystals as function of temperature, electron concentration and magnetic field strength, determining effective mass of electrons
11 p1939 A69-25690
- Resonance radiation output effect on electron distribution according to energies and concentration in low temperature plasma, solving relevant kinetic equations
11 p1935 A69-25757
- Electron concentrations in steady Ar and Ar-He plasma jets measured with microwave Fabry-Perot interferometer and Stark broadening of H beta line
12 p1237 A69-26537
- RF synchrotron radiation emitted by electrons trapped in geomagnetic fields above auroral zones, discussing electron flux and cosmic background
12 p1251 A69-26949
- Unified model for spatial distribution of transpolar exospheric electron density for polar plasma study
12 p1251 A69-26952
- NGC 4151 bright lines intensity, electron density, temperature and ions quantity evaluation from spectrograms with 140 Å/mm dispersion
12 p1264 A69-27021
- Rocket observations of visible and UV dayglow, using electron density and temperature measurements for emission rates of various excitation mechanisms
12 p2076 A69-27108
- Carbon dioxide laser as light source in Michelson interferometer for plasma electron density measurement
12 p2100 A69-27177
- Ultimate resolvable line dependence of Balmer series on electron density, considering line broadened by Stark and Doppler effects
13 p2351 A69-27865

Longitudinal magnetoresistance oscillations in n-type GaSb single crystals associated with electron concentrations minima

13 p2319 A69-27900

Dissipative drift instability due to electron density gradient and dissipative mechanism /neutral-electron and ion-electron collisions/ in plasma in constant magnetic field

13 p2308 A69-27979

Primary particle energy and extensive air shower electron density relationship derived from vertical spectral profiles

13 p2331 A69-28396

Proton initiated nuclear cascade in atmosphere calculated using Monte Carlo method, relating electron number to primary proton energy

13 p2331 A69-28397

Electron concentration enhancement in upper atmosphere at polar latitudes, noting three independent zones and relation to magnetic local time

14 p2510 A69-28938

Equatorial electrojet VHF radar observations indicating nontwo stream electron concentration irregularities related to electron drift velocity

14 p2511 A69-28953

Free electron model for electron work functions and number density distributions and surface potentials in metals

14 p2504 A69-29009

Low voltage arc in cesium thermionic converter, investigating current-voltage characteristics, electron temperature, electron density and plasma potentials in ignited mode

14 p2401 A69-29231

RF impedance method for electron density and collision frequency in plasma

14 p2492 A69-29352

Electron density, temperature and dimensions of helium breakdown induced by Q switched ruby laser beam as function of space and time

14 p2492 A69-29636

Polychromator measurement of hydrogen plasma electron density produced by normal ionizing shock wave, using Stark broadening study of H beta line

14 p2494 A69-29767

Fabry-Perot interferometer employing gas laser for plasmoid electron concentrations measurement at 3.39 micron wavelength

14 p2451 A69-29778

Helium plasma electron temperature and concentration measured in arc in magnetic field by laser light scattering at electrons

14 p2496 A69-29780

Electron temperature and concentration in plasma determined by measuring diamagnetic signal and IR radiation intensity, emphasizing usefulness in plasmoid head portion

14 p2496 A69-29785

Plasma electron density measurement from phase shifts of electromagnetic wave groups propagation

14 p2497 A69-29796

Three channel microwave FM phase meter for studying plasma electron concentrations directional distribution without interferences between channels

14 p2497 A69-29799

FM homodyne phase meter with klystron oscillator for measuring plasma electron concentration, giving block diagrams of meter, detector and oscillator

14 p2451 A69-29800

Amplitude and scale of microscopic fluctuations of electron density within M8 from brightness ratios of O II lines, using multiple shell model

14 p2514 A69-29949

Radiative instability problem of stream plasma system in kinetic regime, discussing Fung letter

14 p2502 A69-29960

Electron densities measurement in plasmas in magnetic fields from profiles of spectral lines, noting Stark and Zeeman effect

15 p2657 A69-30027

Burstein-Moss effect observed in studying n-GaAs crystals electrical reflection spectra with large free carrier concentration at two temperatures and low energy levels

15 p2666 A69-30060

Secondary effects role in n-GaAs crystals electrical reflection spectra with low free carrier concentration at room temperature in external electric field

15 p2666 A69-30061

Argon afterglow microwave and spectroscopic studies, monitoring time-varying electron density and temperature and extracting electron-ion recombination coefficients

15 p2658 A69-30173

Electronic density of collisional cesium plasma, comparing measurements made by Langmuir and HF spherical probes

15 p2659 A69-30300

Free electron concentrations and dispersion in H I regions noting ionized interstellar gas components role

15 p2681 A69-30420

Radial self focusing of low density electron beam by interaction with plasma in presence of beam plasma instability

15 p2662 A69-30964

Electron concentration in low temperature nonequilibrium steady state plasma, including Saha equation applicability criterion

15 p2662 A69-30975

Temperature and electron number density behind reflected shock in helium gas in T tube, noting Z pinch discharges

15 p2593 A69-31161

Electron and ion density distributions in propagating current sheet in Z pinch discharge in argon obtained by microwave reflection interferometer

16 p2816 A69-31639

Steady state density profile dependence on electron density dependence of net volume ionization rate by analyzing ambipolar diffusion in RF excited magnetized plasmas

16 p2818 A69-31672

Microwave field-plasma slab nonlinear interaction in rectangular waveguide, analyzing current and electron density and second harmonic TE and TM power

16 p2749 A69-31703

Heat treatment effects on Te-doped GaAs, using photoluminescence and carrier concentration measurements to study defects formed

16 p2825 A69-31708

Density ratios of H ions to H atoms in ground state calculated as function of quasi-neutral plasma electron density

16 p2820 A69-31770

High temperature ionized turbulent argon jet gasdynamics noting electron density

16 p2770 A69-31889

Spectral density function derivation for energy scattered from underdense turbulent wake

16 p2732 A69-31893

Electron concentration and mass density behind reflected shock in ionizing argon, using time resolved two wavelength interferometry

16 p2771 A69-31918

Plasma magnetic field and electron density measured by Faraday rotation using resonant gas laser radiation

16 p2822 A69-32041

Forward and backscattering of radio waves at electron concentration discontinuity near reflecting ionospheric layer with vertical nonuniformity

16 p2754 A69-32520

Vertical transport rate of charged particles in F region, allowing for vertical velocity gradients

16 p2783 A69-32524

Electron density measurement method in plasma or vacuum based on refraction index in optical frequency range using laser interferometer mismatch as criterion

16 p2798 A69-32583

Hydrogen line profiles, equivalent widths and electron densities for peculiar alpha 2 CVn and gamma Lyr stars

16 p2864 A69-32594

Faraday effect and permittivity of hydrogen plasma measured simultaneously, determining electron density and collision frequency

17 p2919 A69-33394

Electron temperature and number density measured at atmospheric pressure in plasma thermal laminar boundary layer adjacent to cooled wall

17 p3011 A69-33446

Interferometric study of electron concentration and mass density profiles through ionized argon thermal end-wall layer formed in shock tube

17 p3074 A69-33477

One dimensional theory for cylindrical low pressure electrodeless discharge, predicting electron number density and temperature as function of applied fields

17 p3011 A69-33479

Energy dissipation in collisionless shock waves generated in plasmas with 1-500 trillion/cm electron density by theta pinch, measuring axial ionic energy spectrum

17 p3013 A69-33820

Coupling between electric dipoles in warm plasma, determining electron density and temperature from resonance peak of mutual impedance at electron plasma frequency

17 p2925 A69-33846

Microwave propagation inside hollow cylinder using model plasma as dielectric, deriving relationship between phase shift and free electron density

17 p2932 A69-34218

Quiet solar wind model with magnetic field numerically calculated, obtaining coronal electron densities and angular momentum near earth

18 p3186 A69-34300

Heated Hg shock tube construction and operation, application to high electron density plasmas and problem of shock bifurcation in Hg monatomic gas

18 p3116 A69-34453

Dawn-dusk electric field in outer radiation zone associated with magnetospheric plasma convection, comparing electron densities for magnetically quiet periods

18 p3128 A69-34942

Electron intensities in Starfish belt /1963- 1965/, discussing radial diffusion loss mechanism and pitch-angle diffusion

18 p3187 A69-34945

Electron temperature, density and magnetic disturbances measurements at 1000 km compared with visual observations during 25-26 May 1967 magnetic storm and aurora

18 p3129 A69-34954

Low density plasma electrical conductivity determined by temperature and electron density measurements, using Ohm law

18 p3181 A69-35072

High electron density in transient mercury vapor plasma determined using He-Ne laser interferometer measurements

18 p3153 A69-35307

White light solar corona brightness distribution observations /1964-1967/, considering solar radio flux relationship and equatorial electron densities

18 p3205 A69-35394

Solar radio emission during quiet sun years 1964-1965 mapped using Stanford spectroheliograph, attributing slowly varying component to electron density enhancement

18 p3188 A69-35395

Be 7 stability in galactic cosmic radiation, noting lifetime dependence on electron density around nucleus

18 p3189 A69-35482

Electron concentration in hypersonic nonequilibrium shock layer flow by two wavelength laser interferometry, noting wavelength dependence of refractivity

19 p3306 A69-35742

Electric fields and electron work functions, surface potentials and number density distributions in selected metals surfaces determined using free electron model

19 p3382 A69-36045

Electron density and electron temperatures determine in planetary nebulae, using maximum number of observed forbidden transitions

19 p3423 A69-36224

Electron temperatures and densities in interelectrode plasma of close spaced high current cesium plasma diode

19 p3380 A69-36415

Longitudinal electric field, electron density and temperature in positive column of low pressure Cs-Ar DC arc discharge, discussing Cs vapor depletion

19 p3380 A69-36441

Electron effective mass, density and mobility in /000, and /111/ conduction band minima in Te-doped degenerate GaSb-InSb single crystals

19 p3390 A69-36555

Solar corona Fe XII emission spectral lines relative intensity analyzed as function of temperature electron density

20 p3603 A69-37548

Solar microwave emission relationship to geomagnetic activity, analyzing statistically source intensity and model of coronal condensation associated with sunspots based on electron densities

20 p3589 A69-37557

Plasma ion and electron concentration perturbations in wake of body moving at high velocity in collisionless plasma under steady magnetic field

20 p3459 A69-37659

Cosmic radio emission absorption in D, E region and in F 2 layer above and below electron concentration maximum from vertical ionospheric sounding 1959 over Moscow

20 p3590 A69-37676

Flux magnitude and pitch angle distribution relationship for postsubstorm auroral electrons, noting particle precipitation and acceleration models

20 p3592 A69-38082

HgTe-CdTe single crystals homogeneity and Cd distribution obtained by Bridgman and/or zone melting studied for carrier concentration and electron mobility 20 p3584 A69-38215

Precursors ahead of pressure driven shock waves in Ar, considering electron diffusion, temperature a density 20 p3518 A69-38237

Precursor electrons due to photoionization ahead of pressure driven shock waves, presenting electron temperature and density theoretical analysis 20 p3511 A69-38238

Upper atmosphere particles, luminosity and electron concentration measurements documented in input, storage and energy radiation classes, determining recombination coefficients 21 p3707 A69-38491

Current carrier concentration and magnetic field as factors influencing laser frequency resonance mixing in semiconductors with narrow forbidden bands 21 p3737 A69-38998

Attachment coefficients for negative oxygen ion formation in low energy electron swarms over various voltage/pressure ratios 21 p3774 A69-39238

Radio wave reflection from irregularly ionized meteor trains, discussing decay time scatter and electron line density 22 p3899 A69-39969

Live retinal photoreceptors studied by low angle X ray reflection, proposing electron density model 22 p3871 A69-40057

Power per unit volume of UV and forbidden lines emitted by ionized C, N, O and Ne as function of electron temperature and density 22 p3984 A69-40157

Arc-heated plasma jet wind tunnel flow properties in plenum chamber by spectroscopic techniques, measuring electron excitation, temperature and densities 22 p3990 A69-40596

Stark broadening of H-gamma for electron density measurement in plasma, noting temperature range 22 p3985 A69-40664

Electron and ion Stark broadening of allowed and forbidden, triplet and singlet transitions in neutral He at low electron densities, noting Doppler broadening 22 p3985 A69-40665

Ionic excited states statistical equilibrium populations calculated for various electron densities and temperatures including effects of dielectronic, radiative and three body recombinations 22 p3985 A69-40666

High radial velocity matter of bright region near Trapezium in Orion Nebula, determining electron density lower limit and mean velocity 22 p4029 A69-40769

Laser radiation power and electron concentration in He-Ne plasma measured by microwave diagnostics 22 p3964 A69-40794

Mach-Zehnder laser interferometer for measurements of electron density in transient Hg vapor plasma, noting agreement with microwave measurements 22 p3965 A69-40924

Multifrequency dispersion interferometers applicability in plasma diagnostics, considering integral electron concentration measurements 22 p3947 A69-40959

Electron density decrease in F 2 layer ascribed to 9 July 1962 thermonuclear explosion, noting dissociative recombination role 22 p3942 A69-41098

Plane electromagnetic wave scattering on turbulent fluctuations in electron density of finite volume ionized plasma, evaluating Booker-Gordon relation 23 p4116 A69-41587

Integral electron concentration in column of space between earth satellite and ground determined by integral equation, assessing errors minimization methods 23 p4157 A69-41858

Blunt body stagnation point air ionization by chemical nonequilibrium thin viscous shock layer analysis, predicting electron density 23 p4060 A69-41917

Electron density in positive column of Cs vapor discharge related to current and gas pressure, discussing field strength effects on drift velocities 23 p4196 A69-42197

Electron density fluctuations in transition region of turbulent plasma jet, noting spiky waveform [AIAA PAPER 68-685] 24 p4360 A69-43697

Atomic nitrogen collisional ionization and recombination rates under assumed quasi-steady nonequilibrium distribution of electron state populations 24 p4353 A69-43700

ELECTRON DENSITY PROFILES

Vertical wind profiles and electron density profiles in E region, determining time dependence and ionization drift velocity 01 p0072 A69-11172

LF continuous wave rocket propagation in D region presented in terms of electron density profiles 01 p0076 A69-11232

Temperature and electron density distribution during late phase of wire explosion, analyzing optically thin plasma column by quantitative spectroscopy 02 p0286 A69-11711

Plasma column density profile measurement by means of two resonant cavity modes for low pressure discharge in small diameter tubes 02 p0290 A69-12403

Electron radial distribution determination in positive Hg plasma column using simultaneous measurements with two different microwave cavities 02 p0290 A69-12404

Electric potential for axisymmetric equilibrium electron density distribution, solving Poisson equation in closed form 03 p0476 A69-13159

Electron temperature and concentration and solar UV absorption data from sounding rockets, estimating ion exchange rate, recombination coefficient and heat flux 03 p0422 A69-13508

Nighttime variations of F region electron density profiles at Puerto Rico, discussing seasonal and solar cycle variations in temperature and vertical drift velocity 03 p0503 A69-14017

Transpolar exospheric electron concentration distributions along earth-sun line parallel path of Alouette 1 satellite 03 p0425 A69-14018

Error introduced into total electron content data by changes in ionospheric layer height 05 p0816 A69-16281

Rocket measured profiles of electron density and ion abundances in E region, discussing role of minor atmospheric constituents 05 p0757 A69-16408

Radial electron concentration profile determination by spectroscopic examination of continuous plasma radiation of pulsed discharge in capillary 06 p0964 A69-17253

Ionospheric D layer electron concentration profile from radio wave absorption frequency dependence 06 p0920 A69-17729

Electron density shock layer profiles measured by Langmuir probe in hypersonic tunnel on blunt body for air flows and gas densities [AIAA PAPER 69-81] 06 p0863 A69-18101

Nonequilibrium electron temperature, concentration and reflection in reentry boundary layers, discussing heat transfer and ionization energy diffusion [AIAA PAPER 69-82] 06 p0915 A69-18190

Electron density distribution stationary with respect to sun determined by Alouette 1 measurements over winter pole, noting relation to high density plasma 06 p0922 A69-18224

Electron momentum density in diamond, graphite and carbon black from Compton profile measurement by X ray scattering vector 06 p0982 A69-18233

Single polynomial analysis of ionograms, determining electron density profiles from small number of measured heights 07 p1125 A69-18915

Faraday rotation measurements using incoherent scatter to obtain ionospheric electron density profiles 07 p1085 A69-19223

D region electron density vertical profiles measured using partially reflected echoes from lower ionosphere 08 p1307 A69-20189

Electron temperature and electron density variations with radial distance in 10 MHz electrodeless ring discharge in H, noting electric field 08 p1361 A69-20230

Plasma column of free burning electric arc, deriving temperature, electron concentration and electric field radial distributions 09 p1545 A69-21431

Maximum ionization altitude, thickness, electron density profile and temperature mean variations in summer of IGY and IQSY at Moscow station 09 p1486 A69-21544

VLF emissions intensity and spectra variations compared with energetic electron fluxes variations during magnetosphere storm periods 09 p1488 A69-21698

Electrothermal instabilities of ionization region of nonequilibrium MHD generator in presence of magnetic field 09 p1548 A69-21919

Electron density profile from oblique ionogram calculated by iteration, assuming concentric spherically stratified ionosphere 10 p1684 A69-23826

Topside ionospheric electron density profiles compared for magnetically quiet and disturbed periods surrounding December 17, 1962 magnetic storm 10 p1685 A69-23835

VHF radar observations of electron density irregularity in nighttime equatorial electrojet, comparing day and night time electron drift rates and directions 10 p1769 A69-23837

Radio nebula NRAO 591/593, discussing thermal and nonthermal source and models based on electron density distribution 10 p1790 A69-24136

Seasonal variations of electron density profiles in lower ionosphere measured by differential absorption using partial reflections 14 p2438 A69-29109

Electron temperature and density distributions across cesium converter interelectrode gap determined spectroscopically, noting maxima toward emitter 14 p2491 A69-29259

Boltzmann equation for hot electron distribution functions in GaAs and threshold field in Gunn effect 15 p2665 A69-30025

Time resolved Stark broadened spectral profiles for Na I 5682-88 A and 4978-82 A lines of plasma, comparing electron densities 15 p2656 A69-31155

Magnetospheric equatorial electron density profile estimated from midlatitude whistler observations, determining paths from dispersion data 15 p2677 A69-31357

E region ionization redistribution by neutral winds, comparing calculated vertical drift velocities to observed electron density profiles 15 p2677 A69-31395

Ground based partial reflection and cross modulation or wave interaction techniques compared for studying D region electron densities 15 p2606 A69-31537

Nonlinear generation of sum and difference frequency components in magnetoplasma current density due to alternating electric fields, electron density and temperature gradients 16 p2821 A69-32036

Nighttime decreases in F 2 layer heights at near conjugate stations in low latitudes, using electron density profiles 16 p2778 A69-32186

Maximum ionization altitude, thickness, electron density profile and temperature mean variations in summer of IGY and IQSY at Moscow station 16 p2783 A69-32539

Plasma electroacoustic resonance in reentry sheath of Trailblazer 2 vehicle excited by nonradiating coaxial antenna, deducing electron density gradient at vehicle surface 17 p3010 A69-32915

Precursor plasma electron number densities calculations for blunt reentry vehicles, analyzing extreme UV radiation emanating from bow shock [AIAA PAPER 69-718] 17 p2893 A69-33487

Ionospheric absorption and virtual heights relationships for electron density distribution in lower ionosphere, computing model profiles 18 p3125 A69-34248

Radio meteor ionization profiles, discussing electron line density measurements by backscatter system 19 p3283 A69-35992

Solid state detector for electron spatial distribution measurements onOGO-F satellite, discussing design emphasizing reliability 19 p3284 A69-36676

Electron density distribution in laminar air boundary layer on sharp wedges and cones predicted by reducing chemical kinetic model to ordinary differential equations [AIAA PAPER 68-733] 20 p3458 A69-37181

Pulsar distance determined by electron content in line of sight to pulsar compared with neutral H amount integrated through galaxy in pulsar direction 20 p3597 A69-37409

Electron density distribution in northern and southern polar regions ionosphere based on 1958 and 1959 observations at high geomagnetic relatively low geographic latitudes 20 p3526 A69-37664

ELECTRON DIFFRACTION

Topside ionogram reduction for ionospheric electron density determination, using geomagnetic strength at all heights, iteration and change of variables
20 p3529 A69-37864

Electron density profiles from topside ionograms compared to ground based sounding results, discussing error corrections
20 p3495 A69-37865

Computer aided data interpretation system converting ionograms to vertical electron density profiles
20 p3504 A69-37866

Global electron density distribution morphology in topside ionosphere during sunspot minimum from Alouette 1 and 2 ionograms
20 p3530 A69-37867

High latitude limit of closed geomagnetic field lines indicated by high latitude electron boundary in outer radiation zone during Alouette satellite energy particle experiment
20 p3531 A69-37875

Birefringent element within Fabry-Perot cavity for identification of direction of electron density change in z-pinch discharge
22 p3946 A69-40438

Operational characteristics of multiple arcjet wind tunnel for time varying mass flow rate programs, calculating isentropic core densities and velocities [AIAA PAPER 68-229]
22 p3927 A69-40541

LF oscillations in electron number density of ionized deuterium, Ne and He identified from particle continuity equation
22 p3986 A69-40759

Midlatitude ionospheric electron density rocket data survey, including nighttime and daytime N/h profiles for specific solar activities
23 p4155 A69-41563

Ionospheric electron content and distribution at low altitudes from satellite S 66 data, describing seasonal variations of equatorial anomaly peak
24 p4367 A69-43010

Ionization rate limiting processes behind strong shock waves in pure N₂, plotting electron density profile diagrams
24 p4302 A69-43367

Near wake electron density distribution for reentry configuration models in shock tunnel with minimum flow interference [AIAA PAPER 68-161]
24 p4248 A69-43643

ELECTRON DIFFRACTION

Surface structures determination by energy analysis and low energy electron diffraction of scattered electrons
09 p1554 A69-21340

Back scattered electron inelastic LEED spectra of cesium plasma in W/100-Cs system, noting strong loss peak
12 p2132 A69-26116

Low energy electron diffraction oxygen adsorption kinetics on planes of tungsten at coverages below monolayer and work function measurements
18 p3183 A69-35106

Carbonaceous meteorites mineralogically identified by selected-area electron diffraction, suggesting formation from minerals mixtures
19 p3311 A69-36111

Linear self consistent diffraction emission theory and relationship to electron beam propagation
22 p3899 A69-40615

ELECTRON DIFFUSION

Electron drift velocity, diffusion coefficient and trapping time in GaAs, measuring variation with electric field
01 p0140 A69-11255

Diffusion process in dislocation-free doped and undoped GaAs single crystals
02 p0296 A69-11792

Radial diffusion coefficient for trapped electrons moving across field lines, obtaining time dependent solutions of Fokker-Planck equation
03 p0502 A69-14002

Transport diffusion cross sections of slow electrons during scattering at inert gas atoms by microwave method, calculating electron transfer coefficients
03 p0481 A69-14143

Nonlinear and second order thermal diffusion of electrons in ionized gas
04 p0636 A69-14878

Drift and diffusion of electron pulse advancing through gas, providing physical basis for Townsend ionization coefficient
04 p0633 A69-15443

Unique solution for radial diffusion coefficient applicable to equatorially trapped electrons in artificial radiation belt
05 p0816 A69-16279

Radial diffusion of high energy electrons in outer radiation belts, determining statistically delay time between electron intensity variations
06 p0919 A69-17720

Recombination coefficients for dense weakly ionized cesium plasma, treating recombination process as diffusion generated by electron collisions
08 p1359 A69-19844

Fast electron diffusion in stochastic magnetic field, obtaining diffusion coefficient as function of ratio of correlation time to Larmor period
08 p1368 A69-20807

Bimodal diffusion mechanism for acceleration of trapped electrons and protons in earth radiation belts, noting particle intensity profiles and energy spectra
09 p1576 A69-21708

Relativistic solar electron detection in interplanetary space during July 7, 1966 proton flare event, noting energy spectrum and time history
10 p1767 A69-23766

Diffusion of ion-electron pairs produced by photoionization upstream of strong shock waves to shock tube walls based on particle flux and Poisson equations
11 p1866 A69-25275

Nighttime maxima anomaly in electron concentration of ionospheric F layer at midlatitudes, considering diffusion and recombination
12 p2064 A69-26007

Ions and electrons in ionosphere diffusion tensor components and ambipolar diffusion coefficient expressions derived for nonisothermal plasma
12 p2071 A69-26700

Particle fluxes in outer radiation belt and unstable radiation zone of outer geomagnetic field, discussing electron diffusion into magnetosphere and magnetic disturbances
12 p2150 A69-26744

Pitch angle diffusion of trapped electrons in terrestrial radiation zones, discussing diffusion theory based on Fokker-Planck equation, atmospheric Coulomb scattering mechanism, etc
12 p2150 A69-26746

Electron and ion separation as function of plasma potential drop in Langmuir cathode layer in arc regime
14 p2490 A69-29237

Electron intensities in Starfish belt /1963- 1965/, discussing radial diffusion loss mechanism and pitch-angle diffusion
18 p3187 A69-34945

Radial motion of trapped electrons caused by pitch angle scattering in distorted geomagnetic field, noting diffusion coefficient
20 p3593 A69-38104

Precursors ahead of pressure driven shock waves in Ar, considering electron diffusion, temperature a density
20 p3518 A69-38237

Electron recombination and diffusion in afterglow following short pulsed DC discharge in CO₂, using microwave diagnostic techniques
22 p3984 A69-40478

Magnetospheric instabilities and whistler mode turbulence relationship to loss of high energy electrons from Van Allen belts
24 p4306 A69-42692

ELECTRON DISTRIBUTION

Electron impact ionization cross sections and rate coefficients from ground state given for free atoms and ions from hydrogen to calcium
01 p0125 A69-10992

Cosmos satellites monitoring electrons distribution in inner radiation belt suggest intensity stability for solar activity cycle
01 p0147 A69-11309

Nonlinear interaction between longitudinal Langmuir waves and parallel wave vectors in heated plasma study, based on Cauchy problem of kinetic equation for electron distribution
02 p0285 A69-11461

Electron distribution function of isotropic homogeneous Lorentzian plasma subjected to frequency modulated electric field calculated by successive approximation method
02 p0285 A69-11543

Ionization and recombination in low temperature plasmas, noting fast electron distribution function deviation from Maxwellian form and calculation for Cs plasma
02 p0292 A69-12559

Surface layer effects on conductivity of vacuum deposited gold films, studying resistance variations with film thickness
02 p0300 A69-12625

Exciton distribution in semiconductors below Bose condensation temperature differing from diffusion distribution
03 p0486 A69-13415

Nighttime sporadic E layer occurrence due to ionization redistribution established, noting concurrent F region electron concentration decrease
03 p0423 A69-13536

Nonlinear effect of triggering pulse on electron distribution for triggering of VLF emissions
03 p0399 A69-14022

Ionized medium effect on polarization of synchrotron radiation from monoenergetic distribution of electrons
04 p0648 A69-14420

UHF discharge plasma, electron distribution over bound states and ionization stages
04 p0634 A69-14442

Electrical properties of crystals relation to variations of electron or hole distributions, discussing inhomogeneities
04 p0641 A69-14506

Distribution functions for fast electrons near anode calculated by kinetic theory, assuming weakly ionized plasma with smaller Debye length than collision mean free path
04 p0635 A69-14764

Electron distribution function effect on microwave emission and HF conductivity of weakly ionized discharge plasma
05 p0799 A69-15734

Charge carrier concentration determination by double probe in plasma with Druyvesteyn distribution of incident electron flow
05 p0800 A69-15737

Solar wind electron component detection by plasma experiment on Pioneer 6, particularly class 2B flare and quiet period
05 p0816 A69-16275

Particles nonlinear motion in plasma in magnetic field with arbitrary electron velocity distribution, discussing wave discontinuity patterns
05 p0804 A69-16370

Electron distribution function for homogeneous weakly ionized gas in presence of alternating electric field, discussing solution of Boltzmann equations
05 p0797 A69-16604

Solar type 4 bursts characteristics accounted for by cyclotron mechanism, assuming models of spot magnetic field configuration and electron density distribution
07 p1205 A69-18959

Limiting speed for target tracking hypersonic vehicle due to electrons formation through aerodynamic heating, calculating allowable flow conditions, maximum speeds and electron distribution
07 p1086 A69-19509

Complex microwave transmission coefficient of nominal cut-off plasma for several different types of electron distribution, noting discharge characteristics for cut-off
08 p1366 A69-20759

Electron drainage currents from dilute streaming plasmas to positively biased silicon and cadmium sulfide solar cell arrays [AIAA PAPER 69-262]
09 p1436 A69-21726

Scientific data acquisition and interpretation effects on electric spacecraft plasmas and field directions, noting electron interchange reactions effect [AIAA PAPER 69-276]
09 p1568 A69-21727

Hard X ray event spectrum representation by thermal bremsstrahlung spectrum emitted by energetic electrons, determining various physical parameters of source
09 p1579 A69-22180

D-2 satellite radiation dose based on upper atmosphere electron and proton distribution model, simulating electron bombardment and aging of materials and subsystems
11 p1949 A69-24869

Resonance radiation output effect on electron distribution according to energies and concentration in low temperature plasma, solving relevant kinetic equations
11 p1935 A69-25757

Relativistic electrons synchrotron radiation by calculating magnetoactive plasma permittivity tensor, determining normal waves polarization characteristics
13 p2315 A69-28451

- Fabry-Perot interferometer for studying spatial distribution of plasma electron concentration, discussing resolution using solid state gas laser light source
14 p2451 A69-29777
- Ionization and recombination in low temperature plasmas, noting fast electron distribution function deviation from Maxwellian form and calculation for Cs plasma
15 p2658 A69-30256
- Linearized kinetic equation for perturbed electron distribution function, detailing plasma oscillations along magnetic field by Landau collision term
16 p2818 A69-31674
- Electron distribution function for weakly ionized plasma under alternating electric and circularly polarized rotating magnetic field, noting cyclotron resonance
16 p2820 A69-31753
- Ion and electron distributions in chemical nonequilibrium boundary layer flow over hypersonic reentry vehicle, discussing plasma sheath and boundary layer thickness relations
16 p2769 A69-31874
- Time resolved beam distribution functions resulting from cyclotron instability and harmonics in electron injection machine during beam-plasma experiment
17 p3014 A69-33829
- Differential cross sections for secondary electron production in atomic ionization by charged particle impact, using classical binary encounter approximation
17 p3009 A69-34189
- Lorentz gas approximation to Boltzmann collision operator generalized for heavy molecule nonMaxwellian gas distribution function, obtaining equilibrium distribution applicable to ionized gas
18 p3179 A69-34438
- Metal-semiconductor contact current-voltage characteristic derived from modified diode theory taking into account electron distribution function
19 p3391 A69-36608
- Temperature effect on electron concentration steady distribution in F 2 layer
20 p3525 A69-37657
- Flux magnitude and pitch angle distribution relationship for poststorm auroral electrons, noting particle precipitation and acceleration models
20 p3592 A69-38083
- Drift shell splitting in nondipolar distorted magnetosphere tested with data from electron spectrometer on ATS 1 and OGO 3 satellites
22 p4005 A69-40508
- Strong doping criterion for Si with deep level impurity centers based on electron spectra of fast surface traps
22 p3992 A69-40604
- Pitch angle distribution of cosmic ray electrons in decreasing magnetic field for waves in ionized plasma, noting anisotropy due to synchrotron radiation
22 p4006 A69-40642
- Extensive air showers temporal distribution of electrons by diffusion equations in A approximation compared with experiments and Monte Carlo calculations
22 p4007 A69-41054
- Boltzmann equation for electron distribution function of Lorentzian plasma traversed by transverse traveling wave, showing existence and uniqueness of solution
24 p4354 A69-42675
- ELECTRON EMISSION**
NT FIELD EMISSION
NT PHOTOELECTRIC EMISSION
NT SECONDARY EMISSION
- Spherical and cylindrical probes emitting electrons and ions in unbounded plasma, deriving I-V characteristics equations
02 p0247 A69-11569
- Radiation and electrical precursor effects in expansion tube of electromagnetic shock tube, discussing primary causes
02 p0229 A69-11936
- Electron emitter cooling and plasma heating of thermionic converters noting effects of plasma density, diode spacing, etc
03 p0368 A69-13127
- Spectrum and yield of emitted electrons resulting from passage of heavy ions through metal films
03 p0471 A69-13164
- Electron production and loss rates in F region from measurements of Faraday rotation imposed on VHF telemetry transmissions from geostationary satellite
03 p0503 A69-14016
- Electron emission into vacuum from forward biased Schottky barrier consisting of cesiated thin layer of Pt on n-type ZnS
03 p0493 A69-14186
- Electron emission from metal foils used to study lifetime, concentration and mean ion energy of hot plasma
03 p0481 A69-14211
- Ion and electron contaminating currents removal in vacuum evaporating devices, using biased field plates
04 p0577 A69-14875
- Cathode emission site analysis by measuring prebreakdown current under ultrahigh vacuum conditions
05 p0800 A69-15740
- Thermionic electron emission from Mo and W targets irradiated by CW carbon dioxide laser beam
05 p0771 A69-15812
- Cosmic X rays, gamma rays and electron production under astrophysical conditions, noting potential use in supernova and quasar research
07 p1204 A69-18391
- Electron emission of probe caused by impinging ions and photons, discussing model for low plasma densities
08 p1361 A69-20232
- Photoelectric ejection of grain electrons by solar quanta balance with solar wind electron capture by grain for interplanetary grain equilibrium potential
09 p1593 A69-21655
- Saturation electron emission characteristics from incompletely outgassed Ta wire emitters immersed in Cs vapor using plasma anode technique, noting oxygen effects
09 p1437 A69-21812
- Semiempirical relation for electron cooling modified by plasma heating of thermionic converters, including effects of plasma density, diode spacing and surface potential difference
09 p1440 A69-21831
- Peaked electron emission from nickel surface with large work function under laser radiation, discussing emission pulses, electron currents and surface temperature time variations
10 p1703 A69-23572
- Cold electron emitters and operational principles, discussing thin film tunnel emitter, Schottky barrier emitters, MgO type emitter, etc
11 p1846 A69-24597
- I-V characteristics of electron emitting satellite in ionosphere, analyzing spherical Langmuir probe in collisionless plasma in magnetic field
14 p2511 A69-28956
- Effects of cold electron and light emission centers from dispersed Au films in electric field, as universal qualities characterizing dispersed metal films
14 p2504 A69-28992
- Cs mixture effects with Ba and I on cathode electron emission in thermionic converter
14 p2402 A69-29239
- High energy electrons emission during alloy evaporation on hot metal filaments used for thin film deposition
16 p2827 A69-32016
- Ionospheric processes associated with changes in polar aurora height, noting glow in E layer and soft electron emission into earth atmosphere
17 p2964 A69-33957
- Atomic H ionization by proton impact analyzed to calculate ejected electrons angular and energy distributions by extending Rudge and Seaton theory
19 p3375 A69-35911
- Electron ejections from nuclei of radio galaxies and quasars explained on basis of plasma stability, discussing role of relativistic electrons and resulting unstable pinch
20 p3606 A69-38032
- Electron emitters tested for gas laser operations, discussing nonreactive and reactive gases cases, matrix structures containing BaSrO and barium zirconate cathodes
23 p4172 A69-41394
- ELECTRON ENERGY**
- Electron thermal relaxation length in positive column determined by plasma parameters variations in small amplitude moving striations
01 p0127 A69-10341
- Electron density and temperature, ion density, composition and temperature and plasma space potential relative to space vehicle potential measured by spherical probe assembly
01 p0065 A69-10549
- Meteorological rocket measurement of ionizing radiation flux in upper atmosphere, noting flux decrease with increasing electron energy
01 p0144 A69-10586
- Spacecraft ionospheric probe for simultaneous measurement of electron temperature and density, plasma space potential, ion composition, etc
01 p0081 A69-10760
- Neutral gas temperature variations effect on electron-ion temperature height profile in tidally generated sporadic E layer with wind shear of gravity wave origin
01 p0073 A69-11176
- Electron flux intensities and energy spectra in inner radiation zone, noting decay constants
01 p0147 A69-11235
- Resonance energy transfer mechanism in Forster-Dexter theory of electron energy transfer by resonance interaction in condensed media, using many particle treatment
01 p0121 A69-11257
- Auroral emission rates and heating effects as function of altitudes
02 p0235 A69-11426
- Alkali metal quadrupole spectral doublets used as diagnostic for determining alkali-metal plasma electron temperature
02 p0286 A69-11584
- Polar ionosphere heating by spill-over electron energy during strong geomagnetic disturbances, giving mathematical representation
02 p0237 A69-11664
- Electron measurements at 18 earth radii in Vela satellite program
02 p0307 A69-11735
- Measured noise temperature in argon tubes vs theoretical electron temperature for gas discharge noise sources
02 p0210 A69-12437
- Diffusion effect on particle buildup in deionizing steady plasma flux linked to plasma concentration in presence of electron temperature gradients
02 p0291 A69-12483
- Radiation effect enhancement in supersonic plasma jet cooled by rapid expansion, giving energy equation for electron cooling rates to analyze electron temperature
02 p0292 A69-12557
- Oxygen electron cooling effect on ionospheric electron temperatures, noting discrepancy removal throughout day at all altitudes
02 p0245 A69-12739
- Electric field, current density and magnetic induction of plasma flow measured, obtaining plasma conductivity and flow velocity for electron temperature and density
03 p0473 A69-12877
- Electron temperature and concentration and solar UV absorption data from sounding rockets, estimating ion exchange rate, recombination coefficient and heat flux
03 p0422 A69-13508
- Fast type r moving striations in plasmas and dependence of ionization frequency on electron mean energy
03 p0477 A69-13801
- High latitude electrons boundary dependent on geomagnetic axis orientation, noting role of coupling between solar wind and magnetosphere
03 p0502 A69-14003
- Nocturnal electron concentrations and temperature at Manitoba measured by rocket-borne Langmuir probe, compared with F 1 region
03 p0502 A69-14008
- Time resolved electron number density and electron temperature in decaying plasma using laser interferometer
03 p0432 A69-14187
- Electron radiation temperature measurement in carbon dioxide laser with N and He additions by microwave technique, noting average electron energy and optical gain
04 p0611 A69-14445
- Effect of dipole/dipole resonance interaction between excited and nonexcited atoms on gas thermodynamic properties, showing unstable quasi-molecules formation
04 p0632 A69-14551
- Nonlinear electron oscillations in plasma, deriving asymptotic expression for plasma perturbation
04 p0635 A69-14552
- Electron, ion and neutral particle temperatures of upper atmosphere
04 p0592 A69-14975
- Inelastic collisions effect on electron energy distribution in low temperature diffusion dominated discharges
04 p0637 A69-15047
- Electron temperature time variation measurement in plasma-beam discharge by method based on single spectral line
04 p0638 A69-15368
- Ionospheric electron temperature probe analysis based on Japanese Kappa rocket data
05 p0761 A69-15701

Field strength, electron temperature and ion concentration fluctuations in axial direction determined from measurements between homogeneous and stratified plasma columns
05 p0800 A69-15736

Equations for frequency portions of electron-velocity distribution function in Lorentz plasma under influence of time periodic electromagnetic fields with two fundamental frequencies
05 p0800 A69-15743

Radiation intensity distribution from first negative and positive nitrogen system in equilibrium gas flow behind propagating shock front, discussing kinetics mechanism and electronic states
05 p0745 A69-15890

Electron cooling rates in midlatitude and auroral zone thermosphere measured by probe rockets
05 p0755 A69-16267

Auroral electron energy spectrum observed by sounding rocket reveals smooth continuum with peak to produce auroral arcs
05 p0756 A69-16274

Langmuir probe experiment measurement of upper region electron temperature on Explorer 32 conflict with Jicamarca Radar Observatory measurements
05 p0756 A69-16283

Langmuir probe to determine helium plasma density effect on electron temperature from relation between spectral line intensities
05 p0804 A69-16376

Electron temperature relation to population ratio in Gunn effect
05 p0810 A69-16576

Galactic magnetic field estimation obtained from cosmic ray electron spectrum and radio data
05 p0828 A69-16612

Velocity distribution of plasma electrons in electron beam generated He plasma using Boltzmann equation, neglecting electron-electron collisions
05 p0805 A69-16705

Relation between energy spectrum and potential drop in plasma expelled from hot cathode tube into vacuum derived by electrostatic analyzer
06 p0963 A69-16899

Primary electrons implications on cosmic ray confinement in Galaxy, astrophysical aspects and problems of energy spectrum
06 p0991 A69-17308

Electronic charge variations with cosmic time determined from geochronological data
06 p1003 A69-17323

Cosmic ray electron energy spectrum compared with galactic radio noise for estimating galactic magnetic field
06 p0992 A69-17377

Ground state energy of Anderson Hamiltonian calculated by cluster variation for cases of infinite d-d correlation energy
06 p0958 A69-17712

Electron temperatures and optical depths for planetary nebulae outer regions derived using radio spectra and Balmer line isophotes
06 p1009 A69-17962

Nonequilibrium electron temperature, concentration and reflection in reentry boundary layers, discussing heat transfer and ionization energy diffusion [AIAA PAPER 69-82]
06 p0915 A69-18190

Nonequilibrium of electron and gas temperatures and reaction process for force-free plasma parallel beam produced in burner by expansion of argon plasma [DVL-875]
07 p1188 A69-18277

Surface UV irradiated MgO powder catalytic activity for hydrogen-deuterium exchange reaction
07 p1073 A69-18374

Field effect in p-type gallium arsenide single crystals as characteristic of surface electron energy state spectrum
07 p1199 A69-18686

Differential energy spectrum of protons and helium nuclei using lithium drifted silicon detectors and scintillator-Cerenkov counter
07 p1204 A69-18833

High electron-proton temperature ratios effect on solar wind double shock wave structure, using one dimensional and two fluid models
07 p1205 A69-18849

Local interstellar electron spectrum limits from measurements of cosmic ray electrons, nonthermal galactic radio emission and solar modulation effects
07 p1206 A69-19269

Energy transfer through ionospheric electrons, discussing degradation of fast electrons and role of neutral gas motion in ionospheric currents
07 p1128 A69-19369

Low energy electrons in magnetosphere from OGO-1 and OGO-3 observations, discussing plasma sheet, magnetic bay activity, electron pressure, temperature and density gradient
07 p1209 A69-19373

Rosette Nebula structure from high resolution observations at 178 MHz of galactic plane, deriving 8600 K electron temperature for Nebula, discussing Monoceros Nebulosity
07 p1223 A69-19625

Nonlinear modulation distortions of high power radio waves propagating in ionosphere, noting electron temperature increase from radio wave
07 p1088 A69-19746

Electron energy distribution measurements in carbon dioxide laser discharges noting similarity of distribution for nitrogen
08 p1323 A69-19801

Free fall theory for afterglow decay of average electron density and temperature in pulsed cylindrical mercury vapor discharge plasma
08 p1358 A69-19811

Electron temperature and electron density variations with radial distance in 10 MHz electrodeless ring discharge in H, noting electric field
08 p1361 A69-20230

Population densities of UV bound resonance lines of neutral helium for 41-level model atom, discussing optical thickness and electron temperature and density
08 p1390 A69-20392

Electron energy distribution function in plasma heated by electron-cyclotron resonance in adiabatic trap determined from bremsstrahlung spectrum
08 p1365 A69-20547

Electron temperatures and internal turbulence in H II regions of Sagittarius arm measured by high resolution interference method
08 p1392 A69-20566

Recombination rate of electrons in high pressure helium-like plasma with gas temperature fixed at 300 K and electron temperature varied between 300-2000 K
08 p1356 A69-20742

Electron temperature of Orion Nebula at 6750 K from intensities of hydrogen n alpha lines, discussing Stark broadening
08 p1398 A69-20776

Time harmonic, spherical harmonic and power series expansion of Boltzmann equation
08 p1353 A69-20793

Plasma stream behavior emerging from magnetic field, noting transverse velocity imparted to electrons by field
08 p1368 A69-20808

Rotational energy conversion of neutron star into relativistic electrons energy suggested by increasing period of pulsating radio source in Crab Nebula
09 p1591 A69-21454

Impurities effect on electron energy spectrum in semiconductors at zone boundary and arbitrary doping levels, using Green function
09 p1554 A69-21467

Type 3 solar radio noise bursts at hectometer wavelengths, deducing coronal electron temperatures from decay rates
09 p1594 A69-21665

Heat sources in E region from electron temperature data analysis recorded by rockets during eclipses in July 1963
09 p1490 A69-21771

Electron gas heating at E region altitudes as function of ionization of atmospheric gases, noting rocket experiments during solar eclipse
09 p1490 A69-21772

Spectroscopic measurements of electron density and temperature for quasi-saturation region of ignited mode plasma in planar thermionic converter
09 p1439 A69-21826

Electrons resonant heating in beam plasma discharge, discussing ion cyclotron wave excitation in hot electron plasma produced by electron beam
09 p1549 A69-22016

Nonlinear longitudinal oscillations in nonisothermal electron plasma with Maxwellian distribution in velocity space and different temperatures of electrons and ions
09 p1550 A69-22025

Stochastic model of electron cyclotron heating, calculating energy gain during transit of magnetic mirror field in presence of microwave electric field
09 p1551 A69-22038

Temperature stability of slightly ionized gas for arbitrary collision cross sections, discussing electron temperature variation as function of electric field strength
09 p1551 A69-22039

Electrons velocity-space instability in plasma column, analyzing unstable wave and dispersion characteristics
09 p1552 A69-22041

Solar moving type 4 burst emitting synchrotron radiation, noting electron acceleration in collisionless shock wave in corona
09 p1578 A69-22058

Synchrotron and X ray emission generation from upper chromosphere electrons during solar flares
09 p1580 A69-22203

Energy distribution in electron gun with single crystal spherical cathode, noting work function, space charge cloud and beam overlapping effects
09 p1464 A69-22396

Cosmic ray electrons and gamma quanta at lower atmosphere recorded with balloon equipment, plotting vertical profiles of electron energy spectra
10 p1758 A69-22830

Electrical conductivity, electron energy balance, ionization equilibrium time and channel parameters in pulse discharge nonequilibrium Cs plasma containing inert gas addition
10 p1731 A69-23439

Nitrogen impurities effect on electron energy balance in DC arc burning in inert gas
10 p1732 A69-23442

Excitation and ionization relaxation of cesium seeded argon gas computed for stepwise increase of electron temperature
10 p1732 A69-23444

Electron temperature distributions in Ar-K plasma of simulated Faraday type MHD generator for current distributions, determining current density distribution experimentally
10 p1734 A69-23453

Conductivity and electron temperature in coaxial MHD generator plasma with magnetic field, studying Joule heating effect on performance
10 p1735 A69-23463

One dimensional analysis of stationary argon flow in linear Hall generator from continuity, momentum and energy equations, discussing electron heating and nonequilibrium ionization
10 p1736 A69-23465

Nonequilibrium electron heating effect on inert gas plasma conductivity during shock wave movement across magnetic field
10 p1737 A69-23470

MHD conversion experiments using rare gas, considering Typhee loop, electron heating and correction effects
10 p1738 A69-23475

Entrainment and acoustothermal effect in piezoelectric semiconductors having electrons with different energy
10 p1746 A69-23573

Bright emission nebula components and electron temperature determined by radio telescope observation
10 p1778 A69-23603

Fast electron energy distribution function and atom concentration in first excited level in weakly ionized plasma, considering transitions between excited levels
10 p1739 A69-23628

Energetic particles observed during proton flare noting relativistic electrons, protons to alpha particles ratio, low energy particles and bidirectional proton stream
10 p1768 A69-23785

Moving striations in plasmas, presenting measurements of relative phases of electron temperature, plasma potential and luminous intensity near Pupp current limit
10 p1741 A69-23859

Ionospheric measurements of electron density, electron and ion temperature profiles from strength of incoherent radio wave scattering
10 p1686 A69-23910

Auroral electron energy diurnal variation, noting ground observations of polar auroras, riometric absorption, vertical changes in ionization layer maximum position, etc
10 p1687 A69-23915

Electron concentration and temperature dependence on gas temperature as factor determining He-Ne laser output at 6328 Å
10 p1706 A69-24078

Nebular abundances allowing for temperature variations in nebula along line of sight, correcting changes in electron temperature along path of observation
10 p1787 A69-24116

- Electron-ion temperature relaxation near interface of two semiinfinite nonmagnetized different temperature plasmas brought into thermal contact
11 p1923 A69-24296
- Ion and electron temperature and density measurement by Thomson scattering with low resolution monochromator for Salpeter parameter near unity
11 p1925 A69-24310
- Resonances in cross sections for electron impact excitation of forbidden lines in oxygen molecular ion at near threshold energies for astrophysical applications
11 p1921 A69-24417
- Relation between electric field strength and mean energy for electron swarms in oxygen determined, using Boltzmann transport equation
11 p1921 A69-24419
- Cold electron emitters and operational principles, discussing thin film tunnel emitter, Schottky barrier emitters, MgO type emitter, etc
11 p1846 A69-24597
- Monograph on internal structure of sun corona covering variations in intensity and width of coronal lines, inhomogeneity, quasi-homogeneous and anisothermal coronas, etc
11 p1961 A69-25103
- Optical and radio measurements of electron temperature of H II regions obtained from brightness ratio of hydrogen line and continuum, considering isothermal model
11 p1950 A69-25110
- Radar backscatter and rocket profiles of ionospheric electron temperature, noting agreement in daytime flight measurements
11 p1951 A69-25162
- Ionization equilibrium for ions of solar abundant elements between C and Ni calculated as function of electron temperature
11 p1928 A69-25262
- Critical condition for electromagnetic radiation generation by energetic electrons gyrating in dense magnetized plasma, proposing plasma instability mechanism
11 p1931 A69-25363
- Recombination emission spectrum relation to plasma recombination coefficient, determining plasma electron temperature from continuous spectrum intensity
11 p1934 A69-25566
- Molecular vibration absorption spectra from variation of field emitted electron energy distribution due to inelastic electron-molecule interaction at metal-vacuum interface
12 p2132 A69-26097
- Knudsen arcs in argon showing potential well presence with anode barrier and cathode potential drop, establishing slow electrons thermal equilibrium
12 p2137 A69-26536
- NGC 4151 bright lines intensity, electron density, temperature and ions quantity evaluation from spectrograms with 140 Å/mm dispersion
12 p2164 A69-27021
- Diffusion and mass flow in steady state magnetically stabilized helium arc plasma effects on spectroscopic determinations of electron temperature, discussing degree of ionization
12 p2141 A69-27146
- Plasma ion oscillations excited in plasma consisting of ion beam and thermal electrons produced by back diffusion sources
13 p2304 A69-27301
- Oxygen and NO ions yields produced by dissociative attachment of electrons to nitrogen dioxide as function of electron energy, considering electron affinities lower limits
13 p2301 A69-27363
- Global coverage of positive ion composition and temperature, and electron density and temperature measurements during AURORAE mission of ESRO 1 satellite
13 p2253 A69-27753
- Electrical properties of p-type indium antimonide, noting effects of deep level compensation on cv values
13 p2318 A69-27895
- Collective scattering of light from ruby laser by cold dense deuterium plasma produced by electrical discharge, deducing density and electron temperature
13 p2273 A69-28366
- Primary particle energy and extensive air shower electron density relationship derived from vertical spectral profiles
13 p2331 A69-28396
- Angular distribution function calculations for avalanche electrons at various stages of cascade development, discussing electron energies and primary electron roles
13 p2303 A69-28414
- Polar ionosphere heating by spill-over electron energy during strong geomagnetic disturbances, giving mathematical representation
13 p2257 A69-28695
- Ionospheric electron and ion temperatures correlated with electron concentration profile as measured by rockets and satellites
14 p2510 A69-28942
- Two fluid continuum theory of incoherent scattering extended to include unequal electron and ion temperatures, considering backscatter power dependency on collision frequencies
14 p2510 A69-28946
- Suprathermal electrons energy distributions as function of magnetic latitude in polar ionosphere obtained by Explorer 31 satellite observation
14 p2512 A69-28963
- Low energy electron precipitation data at northern high latitudes obtained from satellite low altitude polar orbit
14 p2512 A69-28964
- Electron and ion temperatures height variations in sporadic E layers, noting effects of neutral gas temperature changes
14 p2440 A69-29127
- Radiative and collisional ionization of H and He in planetary nebulae, discussing dielectronic recombination at high electron temperatures
14 p2518 A69-29133
- Plasma screening effect on energy spectra of electrons localized at surface charges in weakly doped unipolar n-type semiconductor
14 p2505 A69-29170
- Low voltage arc in cesium thermionic converter, investigating current-voltage characteristics, electron temperature, electron density and plasma potentials in ignited mode
14 p2401 A69-29231
- Low voltage arc discharge characteristics in cesium vapor, considering energy balance, electron temperature, energy losses, volt-ampere characteristics, ignition, cathode temperatures, etc
14 p2401 A69-29234
- Cesium plasma electron temperature in narrow electrode space of thermionic converter determined using electrode and changeable space diode
14 p2491 A69-29243
- Electron energy distribution function and nonequilibrium ionization rate in near cathode layer of thermionic converter
14 p2404 A69-29255
- Electron temperature and density distributions across cesium converter interelectrode gap determined spectroscopically, noting maxima toward emitter
14 p2491 A69-29259
- Energy resolution improvement in cylindrical electrostatic energy selector by focusing and limiting electron beam before entrance into monochromator
14 p2450 A69-29572
- Electron energy distribution functions and energy transfer rates to inelastic levels of carbon dioxide and nitrogen in laser
14 p2460 A69-29603
- Electron density, temperature and dimensions of helium breakdown induced by Q switched ruby laser beam as function of space and time
14 p2492 A69-29636
- Linear approximation of electron temperature increment and electron mobility in nondegenerate polar semiconductor in crossed fields
14 p2508 A69-29662
- Rare gases total excitation cross sections absolute values measured in collision chamber, noting energy distribution of exciting electron beam, fine structure, etc
14 p2493 A69-29693
- Helium plasma electron temperature and concentration measured in arc in magnetic field by laser light scattering at electrons
14 p2496 A69-29780
- Plasma electron temperatures from electron bremsstrahlung spectra measurements in X ray region
14 p2496 A69-29783
- Electron temperature and concentration in plasma determined by measuring diamagnetic signal and IR radiation intensity, emphasizing usefulness in plasmoid head portion
14 p2496 A69-29785
- Plasma electron temperature determination by line intensity ratio of beryllium-like ions, noting excitation functions
14 p2496 A69-29789
- Three component fast neutral beam for hydrogen plasma ion density and electron temperature determination, improving accuracy and reliability
14 p2452 A69-29812
- Radio observations of emission nebulae for flux densities, deriving electron temperatures
[ASME PAPER 69-DE-46] 14 p2527 A69-29941
- Electrical conductivity ratio of weakly ionized turbulent gas to quiescent gas as function of electron temperature
14 p2502 A69-29991
- Fermi acceleration of energetic electrons trapped within dipole magnetic field analyzed to obtain quantitative results for wave-particle interaction within complex magnetospheric configuration
15 p2594 A69-30095
- Calorimetric measurement of electron temperature in collisionless shock wave propagating in plasma column, discussing role of H beta line Stark broadening
15 p2657 A69-30104
- Argon afterglow microwave and spectroscopic studies, monitoring time-varying electron density and temperature and extracting electron-ion recombination coefficients
15 p2658 A69-30173
- Radiation effect enhancement in supersonic plasma jet cooled by rapid expansion, giving energy equation for electron cooling rates to analyze electron temperature
15 p2658 A69-30254
- Negative curvature electron energy spectrum of discrete radio source model, assuming acceleration by Fermi mechanism and energy loss by synchrotron radiation
15 p2687 A69-30540
- Electron energy distribution determination from electron synchrotron radiation spectrum for various magnetic field configurations within radio source
15 p2655 A69-30546
- Impurities effect on electron energy spectrum in semiconductors at zone boundary and arbitrary doping levels, using Green function
15 p2669 A69-30712
- Meteorological rocket measurement of ionizing radiation flux in upper atmosphere, noting flux decrease with increasing electron energy
15 p2675 A69-30756
- Electron temperature relaxation in shock heated Ar plasma, measuring plasma microwave radiation
15 p2663 A69-30995
- Resonances in elastic cross section for electron/hydrogen atom scattering noting wide structure
15 p2657 A69-31265
- Magnetic storm effects on electrons and protons in outer belt, using satellite data for intensity and differential energy spectra
15 p2676 A69-31314
- Electron temperature observation in daytime ionosphere, considering energy loss to ions and neutral particles
15 p2603 A69-31402
- Morning, daytime and nighttime rocket measurements of electron flux in upper atmosphere at 80-165 km altitudes, noting energy flux
15 p2677 A69-31413
- Simultaneous middle and low latitude Thomson scatter measurements, comparing electron density, temperature and exospheric temperature data on quiet and disturbed days
15 p2604 A69-31418
- Gyropasma probe data from rocket observations, determining winter ionospheric electron density profiles, electron temperature and electrostatic cyclotron waves effect
15 p2606 A69-31446
- Weakly ionized plasma electron heating by interaction with HF electromagnetic field calculated using Boltzmann transport equation
15 p2665 A69-31480
- Linearized Boltzmann equation in kinetic theory for weakly ionized plasma electrons under alternating electric and circularly polarized magnetic field, noting higher harmonics generation
16 p2820 A69-31752
- Lasing influence on electron energy distribution in gas discharge measured with Langmuir probe, showing electron-electron interaction insufficient to maintain equilibrium
16 p2796 A69-31772
- Metagalactic electrons inverse Compton effect on relic radiation to interpret cosmic isotropic X radiation entire energy spectrum
16 p2847 A69-31800
- Nonequilibrium plasma boundary layer along channel insulator wall, noting different electron and heavy particle temperatures
[AIAA PAPER 68-134] 16 p2821 A69-31873
- Rocket measurements of upper F region electron temperature and density profiles, for particle and ener-

gy balance of ionosphere topside, noting diffusive equilibrium 16 p2848 A69-31975

Electron cooling rates due to vibrational excitation of molecular oxygen calculated as function of electron temperature in E region 16 p2774 A69-31982

Ion, electron and neutral temperatures from ion composition distribution, assuming no change in vertical distribution within horizontal distance between upleg and downleg measurements 16 p2849 A69-31990

Numerical analysis of charged particles radial distribution in radiation belts extended to geomagnetic tail for low energy auroral electrons 16 p2850 A69-32102

Electron temperature time variation measurement in plasma-beam discharge by method based on single spectral line 16 p2822 A69-32115

Energy spectrum of secondary electrons and fluorescent efficiency in 3914 Å band, obtaining ionization cross section 16 p2850 A69-32315

Cosmic ray electron spectrum data obtained by balloon flights, showing electron flux reduction above 500 Mev with increasing solar activity 16 p2851 A69-32566

NonMaxwellian electron velocity distribution influence on ionospheric measurements by Thompson scattering, explaining disagreement between scattering and probe measurements of electron temperature 16 p2788 A69-32647

Electron energy effects on reflectance degradation and recovery of thermal control materials in vacuum, reporting test results for various protective coatings [AIAA PAPER 69-643] 17 p3005 A69-33306

Electron temperature and number density measured at atmospheric pressure in plasma thermal laminar boundary layer adjacent to cooled wall [AIAA PAPER 69-692] 17 p3011 A69-33446

Electron heat transfer and spherical probe characteristics in moving nonequilibrium plasma analyzed at stagnation region as function of solid surface potential [AIAA PAPER 69-699] 17 p3011 A69-33475

One dimensional theory for cylindrical low pressure electrodeless discharge, predicting electron number density and temperature as function of applied fields [AIAA PAPER 69-703] 17 p3011 A69-33479

Coupling between electron dipoles in warm plasma, determining electron density and temperature from resonance peak of mutual impedance at electron plasma frequency 17 p2925 A69-33846

Lower ionosphere electron concentration confirmed as function of electron and ion temperature by satellite and probe data 17 p2966 A69-33981

Optically thin gas surrounding X ray source, plotting electron temperature and ionization equilibrium of hydrogen, He, carbon, nitrogen, oxygen and neon 18 p3186 A69-34295

Recombination coefficients of oxygen and nitrogen ions with electrons related to electron temperature, using microwave afterglow/mass spectrometer 18 p3176 A69-34789

Electron temperature, density and magnetic disturbances measurements at 1000 km compared with visual observations during 25-26 May 1967 magnetic storm and aurora 18 p3129 A69-34954

Electronic levels excitation in S I and II by beam foil method 18 p3177 A69-35015

Electromagnetic wave effect on electron in homogeneous magnetic field, noting relativistic momenta of dragged electrons 18 p3181 A69-35497

Atomic H ionization by proton impact analyzed to calculate ejected electrons angular and energy distributions by extending Rudge and Seaton theory 19 p3375 A69-35911

Electron density and electron temperatures determination in planetary nebulae, using maximum number of observed forbidden transitions 19 p3423 A69-36224

M8 electron temperature and internal kinematics from photoelectric Fabry-Perot spectrometric recording of H alpha line profiles and N II 19 p3424 A69-36334

Electron temperatures and densities in interelectrode plasma of close spaced high current cesium plasma diode 19 p3380 A69-36415

Longitudinal electric field, electron density and temperature in positive column of low pressure Cs-Ar DC arc discharge, discussing Cs vapor depletion 19 p3380 A69-36441

Electron energy distribution for Cs plasma in emitter region of ignited mode thermionic converter, noting nonequilibrium ionization effect 19 p3380 A69-36442

High resistivity gallium arsenide single crystal LF current oscillations at low temperature, investigating electron heating effect and mechanisms 19 p3391 A69-36609

Electron band forces probable values of Meinel system positive N molecules and first positive system of nitrogen molecules at high temperatures 20 p3579 A69-37307

Rarefied nonmagnetic plasma in wake of body moving at higher than electron and ion thermal velocities 20 p3525 A69-37660

Retarding potential analyzers to measure rocket vehicle potentials and ambient electric fields in active auroras 20 p3542 A69-37793

Cylindrical electrostatic probes on Alouette 2 and Explorer 31 satellites used in intersatellite comparison of directly measured ionospheric electron temperature and density 20 p3544 A69-37876

Ionospheric parameters of ion and electron density and temperature and ionic species compared by direct measurement probes on Explorer 31 satellite 20 p3531 A69-37882

Ionospheric electron and ion concentration and temperature by Langmuir plate and spherical ion probe on Explorer 31 and ionosonde on Alouette 2 20 p3531 A69-37883

Ionic composition determined by combining Alouette topside sounder electron density profiles with electron and ion temperatures measured by ground based Thomson scatter sounder 20 p3532 A69-37898

Simultaneous observations of 5 to 15 second period modulated energetic electron fluxes at synchronous altitude and auroral zone 20 p3592 A69-38082

Precursors ahead of pressure driven shock waves in Ar, considering electron diffusion, temperature a density 20 p3518 A69-38237

Precursor electrons due to photoionization ahead of pressure driven shock waves, presenting electron temperature and density theoretical analysis 20 p3511 A69-38238

Shock and current sheet separation in magnetic shock tubes, determining electron temperature behind shock and within current layer 20 p3511 A69-38241

Ion density, electric field and electron temperature responses to gas density perturbation calculated for acoustic wave propagation in gas discharge using hydrodynamic equations 20 p3578 A69-38243

Electron momentum transfer cross sections by numerically solving electron energy distribution function from Boltzmann equation in Lorentz approximation 21 p3773 A69-38396

Rocket measurements indicating auroral electrons modulation near equatorial plane, noting intensity changes as function of rocket flight time and altitude 21 p3709 A69-38499

Optical data supporting satellite observations of soft electron precipitation on poleward side of normal auroral zone 21 p3709 A69-38501

Cosmic ray electron recorder for measuring intensity, energy spectrum and angular distribution of electron fluxes within specific energy range 21 p3724 A69-39074

Ariel 3 satellite observations, including topside ionospheric variations with time and solar activity, electron density, temperature measurements, etc 21 p3716 A69-39257

Electron temperature profile across shock wave in weakly ionized nonequilibrium argon by numerical integration of energy conservation equation, noting three body recombination 21 p3698 A69-39791

Electron energy loss spectrum of nitrogen, suggesting atmospheric auroral nitrogen emissions compatibility with low energy electron impact excitation mechanisms 22 p3935 A69-39970

Power per unit volume of UV and forbidden lines emitted by ionized C, N, O and Ne as function of electron temperature and density 22 p3984 A69-40157

Ionospheric electron temperature profiles for mid-day equinoctial conditions noting protonospheric and conjugate heating effects 22 p3939 A69-40506

Splash and return albedo electrons in cosmic ray electron spectrum between 12 Mev-1 Gev measured by high altitude balloon flight 22 p4005 A69-40510

Daily variation of trajectory derived high latitude vertical cut-off rigidities in magnetospheric model consistent with proton and electron experiments 22 p4005 A69-40513

Boltzmann equation analysis used to study near surface electron temperature for weakly ionized plasmas, showing nonequilibrium absorption layer governing electron temperature profile 22 p3989 A69-40528

Arc-heated plasma jet wind tunnel flow properties in plenum chamber by spectroscopic techniques, measuring electron excitation, temperature and densities 22 p3990 A69-40596

Radio recombination line data from H II regions interpreted in terms of single electron temperature, considering non-LTE /local thermodynamic equilibrium/ and clumping 22 p4025 A69-40645

Rocket measurements of plasma densities and temperatures in visual aurora using electrostatic onboard and ejected Langmuir probes, observing hyperthermal electron 23 p4167 A69-42334

Topside ionosphere response to magnetic storms, using Explorer 22 satellite electron concentration and temperature measurements 23 p4161 A69-42438

Electron energy measurement accuracy in carbon dioxide laser plasma by S band radiometer 24 p4327 A69-42613

Plasma microinstabilities due to ion and electron anisotropic velocity distributions, considering frequencies near harmonics of ion cyclotron frequency 24 p4355 A69-42686

Low energy electrons energy loss by inelastic collisions in moving through atmosphere, estimating cross sections and loss rates 24 p4351 A69-42763

Conjugate regions 6300 Å airglow enhancement during predawn, noting photoelectrons role in heating dark ionosphere region by producing fast electron flux 24 p4308 A69-43011

Cosmic ray electron energy spectrum and intensity measurements indicating time variations attributed to solar modulation effects 24 p4367 A69-43175

Nighttime protonosphere thermal balance from Alouette 2 electrostatic probe measurements of electron temperature and concentration in magnetosphere 24 p4310 A69-43181

Isotropic cosmic X rays measured by balloon-borne scintillation telescope, discussing agreement with electron energy spectral distribution 24 p4368 A69-43185

Magnetic and electron temperature interaction effects in fast MHD shock waves in slightly ionized plasma 24 p4356 A69-43361

Electron temperature distribution across shock wave in weakly ionized plasma, noting variable ionization across wave 24 p4356 A69-43362

Electron temperature and density of inviscid free molecular nozzle flow of shock tunnel measured with thin wire Langmuir probes 24 p4317 A69-43648

ELECTRON FLUX

U ELECTRONS

U FLUX [RATE]

ELECTRON FLUX DENSITY

Solar proton event generating sudden commencement magnetic storm, discussing effects on outer belt electrons as observed by Explorer 26 and time delay 01 p0146 A69-11124

Electron flux intensities and energy spectra in inner radiation zone, noting decay constants 01 p0147 A69-11235

Electron intensity diagram of diurnal trapped electron variation from Cosmos 5 satellite data, including harmonic analysis of data 01 p0147 A69-11321

Ionospheric electron content, slab thickness and scintillation occurrence measurements at low latitude stations

02 p0235 A69-11427

Photometric measurement of atomic oxygen green line emissions and high energy electron flux using twilight sounding rocket

02 p0309 A69-12743

Magnetic retuning of resonator with helical electron flux /gyromonoton/ in starting and prestarting modes

03 p0407 A69-13979

Energetic electron fluxes measured at 2000 km over auroral and polar regions and at 17 earth radii in magnetotail plasma sheet

03 p0503 A69-14013

Cosmic ray electron flux and energy spectrum from balloon data obtained at Palestine, Texas, monitoring proton flux periodically

05 p0815 A69-16250

Energetic electrons of terrestrial origin behind bow shock and upstream in solar wind

05 p0815 A69-16253

Drift periodic echoes in outer zone electron flux due to magnetospheric disturbance

05 p0815 A69-16259

Hydrogen, helium and electron flux measurements by differential detectors at Fort Churchill in 1967

05 p0756 A69-16277

Cut-off boundary latitude and electron flux changes in midnight sector of outer radiation belt during magnetic bay periods from Injun 4 satellite data

07 p1204 A69-18836

Particle measurements by Vela nuclear test detection satellites /2A and 2B/ noting plasma sheet in center of magnetotail

07 p1208 A69-19362

Electron fluxes energy spectra determined from simultaneous photometric and riometric observations in polar regions

09 p1485 A69-21530

Auroral electron flux from particle fluxes measured with shielded Geiger-Muller telescopes mounted in rocket launched into diffuse aurora

09 p1576 A69-21663

Flux and energy spectrum of secondary electrons at balloon altitude in atmosphere, correcting Beedle and Webber plotting error

09 p1490 A69-21914

Energetic proton and electron fluxes spatial gradients after July 7, 1966 solar flare, noting satellite observations and injection mechanism geometry

10 p1767 A69-23767

Satellite measurements of suprathermal electrons at conjugate sunrise, indicating photoelectron escape from production level and movement along geomagnetic lines into conjugate ionosphere

11 p1950 A69-25144

Outer radiation zone electron intensities during magnetic storms for morphology of zone electron acceleration mechanisms

11 p1950 A69-25147

Auroral electrons intensity modulation by source at L equals 6 magnetic shell on geomagnetic equator, noting dispersion effects

12 p2065 A69-26108

Inner radiation zone including data on electrons, protons and heavier particles and results from high altitude nuclear tests

12 p2152 A69-27144

Integral particle flux of protons and electrons in upper atmosphere, discussing energy and angular distribution

13 p2328 A69-27757

Low energy electron precipitation data at northern high latitudes obtained from satellite low altitude polar orbit

14 p2512 A69-28964

Electron flux-atmosphere interaction solved by numerical integration on computer, discussing auroral ionosphere

14 p2513 A69-29069

Sporadic electron flux contribution to high latitude geomagnetic disturbances at outer radiation belt boundary estimated from Elektron 1 and 2 observations

14 p2438 A69-29079

Electron current, space potential and ionic composition obtained by Langmuir type probes on Explorer 31 for disturbance region dependence on ionic composition

14 p2518 A69-29122

Electron fluxes energy spectra determined from simultaneous photometric and riometric observations in polar regions

16 p2783 A69-32525

Cosmic ray electron spectrum data obtained by balloon flights, showing electron flux reduction above 500 Mev with increasing solar activity

16 p2851 A69-32566

Precipitated low energy protons and electrons measurements during breakup aurora, discussing fluxes and poleward boundaries

18 p3187 A69-34946

Periodic fading in 42 MHz auroral backscatter by high speed polarization measurements, discussing scatter bursts and pulsating primary electron flux relationship

18 p3102 A69-34950

Westward traveling auroral surge associated with electron flux during absence of H beta emission

18 p3130 A69-35189

Lithium doped solar cell irradiation by strontium 90 radioisotope, discussing electron flux rate, spectrum and recovery rates

19 p3251 A69-35693

Low energy electron accelerator to produce measurably small fluxes through photoelectric effect from Au cathode UV irradiation to achieve high flux stability

19 p3313 A69-36492

Ion and electron fluxes and drag force dependence on electrostatic charge and velocity of interstellar dust particle

19 p3425 A69-36562

Electron and gamma quanta concentrations measurements by high altitude balloon, noting fluctuations at various altitudes

20 p3587 A69-37046

Suprathermal electron flux in lower latitudes and polar region analyzed from measurements by retarding potential analyzers on Explorer 31 satellite

20 p3590 A69-37880

Simultaneous observations of 5 to 15 second period modulated energetic electron fluxes at synchronous altitude and auroral zone

20 p3592 A69-38082

Radiation sources fields and propagation in homogeneous lossy magnetoplasma, deducing wave equations for electric and magnetic current electron flux and mechanical body force sources

21 p3775 A69-38434

Cosmic ray electron recorder for measuring intensity, energy spectrum and angular distribution of electron fluxes within specific energy range

21 p3724 A69-39074

IMP 4 satellite measurements of cosmic ray electrons in interplanetary space compared to predictions of electron intensity from interstellar proton-electron collisions

24 p4365 A69-42667

Conjugate regions 6300 A airglow enhancement during predawn, noting photoelectrons role in heating dark ionosphere region by producing fast electron flux

24 p4308 A69-43011

Magnetospheric electron sudden intensity increases correlated with magnetic substorms occurrence at midnight meridian from ATS 1 observation

24 p4367 A69-43173

Electron temperature and density of inviscid free molecular nozzle flow of shock tunnel measured with thin wire Langmuir probes

24 p4317 A69-43648

ELECTRON GAS

High temperature, fully ionized plasma equation of state, using quantum statistical theory of low density electron-ion plasma in thermal equilibrium

01 p0128 A69-10346

Model for fast randomization of electron gas by trapped electroacoustical waves

02 p0289 A69-12236

Electron fluid compression coefficient from simultaneous measurement and correlation of absolute magnitudes of ion acoustic wave potential and accompanying plasma density perturbation

03 p0475 A69-13148

Quantum theory of electron gas with anomalous magnetic moments in intense magnetic fields, noting pair creation from thermodynamic energy in system

08 p1353 A69-19782

Electron gas heating at E region altitudes as function of ionization of atmospheric gases, noting rocket experiments during solar eclipse

09 p1490 A69-21772

Plasma decay coefficient, charge recombination coefficient and electron scattering in cooling electron gas of quasi-steady cesium discharge plasma under high pressure

10 p1733 A69-23448

Specific heat of electron gas at temperatures approaching absolute zero, using method of displacements and collective variables

11 p1927 A69-24918

Thermodynamic approach to equation of state of magnetized Fermi gas, deriving energy eigenvalues of free electron in magnetic field

11 p1961 A69-25107

Fresnel dragging effect on 3 cm microwaves by electron gas drift in low pressure glow discharge, noting electron density and excitation modes

12 p2133 A69-25766

Ionosphere temperature profiles, discussing heating and cooling of electron gas and ion gases and thermal balance

12 p2063 A69-25903

Polarization of continuum background of planetary nebulae in window in visible spectrum from scattering of nucleus star radiation by electron gas

13 p2339 A69-27567

Electron gas behavior in nondegenerate envelope of magnetic white dwarf, discussing increased opacity due to magnetic fields

13 p2343 A69-27624

Correlation functions of fluctuations in electrical characteristics of nonequilibrium electron gas during scattering, determining spectral densities and populations by kinetic equation Green function

13 p2314 A69-28445

Electron shielding in heavily doped many valley semiconductors, discussing Thomas-Fermi screening and Mott transition

13 p2324 A69-28683

Neutrino-pair bremsstrahlung for hot degenerate electron gas during Coulomb scattering on imbedded nuclei in stellar regimes including lattice structure effects

18 p3176 A69-35004

Ferromagnetism stable state in degenerate electron gas and magnetic fields in gravitationally collapsed bodies based on total microscopic magnetic moments associated with Landau level electrons

21 p3798 A69-38600

Solar atmosphere radio emission generation by hydrodynamic shock wave interaction with coronal plasma, treating corona as ideal gas consisting of protons and electrons

22 p4009 A69-39984

ELECTRON GUNS

Electron gun with plasma cathode consisting of gas discharge chamber, electron ejecting component and focusing system

04 p0598 A69-14857

Electron beam welding using glow discharge as source of electrons, noting hollow anode gun design and electrode geometry influence on beam shape

04 p0608 A69-15480

Design theory for electron guns using three high-perveance electrodes demonstrated with gun model

05 p0730 A69-16211

Beam transmission in electron guns having single apertured control grid, studying ratio of target current to cathode current

05 p0734 A69-16566

Convergent high-perveance electron gun design for use in microwave tubes, reducing anode aperture effect on current density

07 p1101 A69-18658

Optimal working parameters and operational characteristics of laboratory electron gun, examining beam shape, convergence and current density distribution

09 p1464 A69-22243

Energy distribution in electron gun with single crystal spherical cathode, noting work function, space charge cloud and beam overlapping effects

09 p1464 A69-22396

Unrippled space-charge flow in dense axially symmetric electron beams as basis for electron gun design

11 p1846 A69-24598

Current flow coefficient of high perveance three electrode electron guns with longitudinal compression

11 p1849 A69-24911

Paraxial electron beams from Pierce gun and spreading due to thermal velocities and space charge in nonuniform potential

12 p2036 A69-25920

Frequency distribution and statistical characteristics of high level RF noise produced by high perveance electron beam of magnetron injection gun/MIG/

14 p2449 A69-29558

Noise fluctuations transport in convergent flow crossed field electron guns using Monte Carlo method for two dimensional computerized gun simulation

15 p2572 A69-30031

- Electron microprobe to produce plane grating X ray hologram based on Lloyd mirror experiment principle
17 p2977 A69-34160
- Dynamic electron beam devices for refractory materials evaporation, discussing electron guns and vaporization film data
[ASM PAPER D8-22.2] 20 p3551 A69-38131
- ELECTRON IMPACT**
- Electron impact ionization cross section in cesium vapor measured with Tate-Smith apparatus
01 p0137 A69-10285
- Electron impact spectrometer for obtaining molecular energy loss spectra used to investigate scattering cross sections for optically allowed and forbidden transitions
01 p0123 A69-10620
- Electron impact ionization cross sections and rate coefficients from ground state given for free atoms and ions from hydrogen to calcium
01 p0125 A69-10992
- Electron impact excitation of Lyman alpha emission from 2p state of atomic H, noting discrepancy below 50 Mev
02 p0283 A69-12466
- Collisional ionization cross section for Fe ions evaluated to estimate solar corona temperature
04 p0651 A69-14365
- Emission cross sections of first negative band system of nitrogen under electron impact excitation
05 p0795 A69-15617
- Ion current output vs gas component partial pressure determined to measure ion source efficiency employing electron impact ionization
06 p0960 A69-16919
- Vibrational excitation by electron impact in kinetic energy range 30-60 eV studied for water vapor and carbon dioxide, determining intensities relative to elastic scattering
06 p0960 A69-17108
- Electron impact excitation cross sections for emission from first negative bands of positive N molecule ion
06 p0961 A69-17135
- Spectral line shapes broadened by electron impacts, taking into account contribution of radiation produced by perturbing electrons
06 p0961 A69-17136
- Electron impact ionization cross sections for second quantum level of atomic H, using Born exchange approximation and Vainshtein approximation
06 p0961 A69-17138
- Polarization of diatomic molecular line radiation excited by electron impact
06 p0961 A69-17140
- Angular dependence of low energy electron impact excitation cross section of lowest molecular hydrogen triplet states
06 p0962 A69-17820
- Back bombardment of magnetron cathode as single surface multiplier, noting effects of cathode grooves and output loading
07 p1101 A69-18656
- Electron impact induced fragmentation of ring D in steroids involving loss of carbon atoms analyzed by mass spectrometry
07 p1069 A69-19497
- Plasma spectral line shifting and broadening under ion and electron impact
07 p1187 A69-19720
- Absolute excitation cross sections for emission of second positive bands of nitrogen under electron impact
08 p1355 A69-20208
- Hydrogenic atoms ionization by high energy electrons, discussing cross sections for ejected electrons and total energy
08 p1356 A69-20738
- Electron impacts role on dissociation rates of CO molecules in upper layers of solar photosphere
09 p1590 A69-21376
- Kinetic coefficients of carrier motion in semiconductor obtained by Boltzmann equation, considering impacts between carriers
09 p1554 A69-21468
- Electron impact ionization of negative H ions computed by wave expansion methods and compared with experiments
09 p1542 A69-21622
- Electron impact cross sections for diatomic molecule ionization and excitation from modified Gryzinski theory, discussing results from molecular models
09 p1542 A69-22249

- Optical cross section measurements for electron excitation from ground state of nitrogen
12 p2132 A69-26246
- Nonequilibrium radiation from first negative band of molecular nitrogen ion excited by shock wave electron impact
13 p2245 A69-27380
- Binary encounter model for ionization by charged particle impact modified to evaluate cross section for ionization of positive ions by electron impact
14 p2489 A69-29996
- Mass spectra peaks of N-Acyl-2-indolinols fragmentation processes upon electron impact, noting compounds predominance in open chain tautomer gas phase
15 p2561 A69-30407
- Electron impact field ionization source for mass measurement of molecular ions, noting organic geochemistry applications
15 p2608 A69-30428
- Kinetic coefficients of carrier motion in semiconductor obtained by Boltzmann equation, considering impacts between carriers
15 p2669 A69-30713
- Electron impact broadening of isolated spectral lines emitted by neutral atoms in plasma
16 p2823 A69-32468
- Electron impacts role on dissociation rates of CO molecules in upper layers of solar photosphere
18 p3198 A69-34764
- Stark broadened H gamma profile, considering effect of strong collisions in electron perturbation and electron impact broadening of lower levels
20 p3579 A69-37305
- Spectral line broadening and shift due to electron and ion shocks in impact theory
20 p3580 A69-37828
- Primary excitation mechanism in pulsed carbon dioxide lasers found to be electron impact
20 p3556 A69-38122
- Coupled equations for determining cross sections for rotational transitions in CN induced by low energy electron impact
21 p3773 A69-38476
- Luminous efficiency for electron induced molecular nitrogen bands, discussing thick- and thin-target measurements of fluorescent efficiencies
21 p3774 A69-38521
- Semiempirical electron impact cross sections and energy loss functions applied to dayglow and auroral intensities calculation, discussing atomic and aeronomic implications
21 p3713 A69-38527
- ELECTRON-ION RECOMBINATION**
- NT RADIATIVE RECOMBINATION**
- Emitted light and excited state populations resulting from two electron collisional radiative recombination related to free electron density
03 p0469 A69-12923
- Relaxation method for separation of continuous electron/ion recombination spectrum from electron spectrum in nonequilibrium gas discharge plasma
04 p0639 A69-15369
- Photoionization cross section measurements for sodium line by analyzing electron-ion recombination radiation from sodium seeded plasma, determining electron temperatures and concentrations
07 p1184 A69-19164
- Ionization relaxation in atmospheric pressure Ar-Cs plasma, considering two and three body recombination and O impurity effects
10 p1733 A69-23445
- Electron-ion recombination coefficient for triple collisions in dense low temperature plasma, deriving finite electron Fokker-Planck equation
11 p1933 A69-25541
- Collisional radiative electron-ion recombination rates measured in decaying rare gas plasmas produced by transient discharge
12 p2134 A69-25981
- Effective recombination coefficient in lower ionosphere determined from charged particle spectra obtained by rocket sounding in Canada
14 p2511 A69-28960
- Argon afterglow microwave and spectroscopic studies, monitoring time-varying electron density and temperature and extracting electron-ion recombination coefficients
15 p2658 A69-30173
- Electron ion recombination role in atomic collision process in rare gases ionization path, considering scintillation mechanism
15 p2655 A69-30961

- Relaxation method for separation of continuous electron/ion recombination spectrum from electron spectrum in nonequilibrium gas discharge plasma
16 p2822 A69-32116
- Green line suppression in type B aurorae based on negative ion-electron chemistry below O transition region
16 p2778 A69-32191
- Recombination coefficients of oxygen and nitrogen ions with electrons related to electron temperature, using microwave afterglow/mass spectrometer
18 p3176 A69-34789
- Gold donor level impurity photovoltaic effect in silicon, noting solar cell efficiency reduction due to minority carrier recombination
19 p3381 A69-35679
- Nighttime F region nonlinear recombination and variable drift effects, suggesting empirical model
21 p3715 A69-38559

ELECTRON IONIZATION**U IONIZATION****ELECTRON IRRADIATION**

- Irradiation influence on yield stress of Ni-Al intermetallics noting temperature dependence and electron dosage
01 p0095 A69-10608
- Electron irradiation induced damage in undoped GaSb single crystals at 77 K, noting dependence on energy and orientation
01 p0141 A69-11256
- Fluorescence efficiency of air under electron bombardment measured at low pressure
02 p0284 A69-12734
- High current electron bombardment ion source for production of low energy ion beams without metastable contamination
03 p0428 A69-13106
- Electropulsion by thruster using colloidal carbon particles charged by electron bombardment to provide thrust, noting specific impulse
03 p0495 A69-13396
- Free radicals produced in ribonuclease, lysozyme and trypsin during exposure in vacuum and various temperatures to electron and heavy ion irradiation
03 p0372 A69-13484
- Modulated photocurrent in CdS crystal obtained by irradiation with intensity modulated electron beam, noting relaxation time and trap concentration
03 p0490 A69-13946
- Cathodoluminescence of n-type GaAs with various carrier concentration bombarded with 24-keV electrons, studying emission spectrum for radiative transition
04 p0639 A69-14436
- Fermi level in n- and p-type Ge after irradiation by 50 Mev electrons determined by temperature dependence of carrier concentration
04 p0640 A69-14444
- Temperature rise of micron sized silver particles on carbon film due to electron beam heating, setting up heat balance equation
04 p0640 A69-14449
- High voltage mercury electron bombardment ion thruster power efficiency
[ECS PAPER 170D] 05 p0812 A69-16233
- Electric field effects on thermal annealing of electron irradiation damage in p-channel MOSFET device
05 p0733 A69-16562
- Recovery of carrier concentration and lifetime in n- and p-type Si during annealing after irradiation by 10 Mev electrons, noting impurities effects
06 p0974 A69-16865
- Disordered regions in electron irradiated silicon noting defect clusters concentration effect on electrical properties
06 p0974 A69-16866
- Recovery rate at room temperature in Li-doped p-n Si diodes and solar cells after 1 Mev electron irradiation, noting capacitance changes
06 p0974 A69-16867
- Electron radiation damage in MOSFET devices using bias temperature treatments
06 p0976 A69-16877
- GaAs laser excited by fast electrons exhibiting high efficiency and output power at room and liquid nitrogen temperatures
06 p0933 A69-16994
- Electron irradiation annealing and modification of 35 and 65 K defects in n-type Ge induced by 1 Mev electrons at low temperature
06 p0980 A69-17757
- Electron bombardment ion source generated Ar plasma beam to study wakes of disks and spheres, considering plasma interaction with bodies
[AIAA PAPER 69-79] 06 p0865 A69-18200

- Majority carrier concentration changes in P-doped n-type Si during fast electron bombardment, discussing relative effect of A and E centers
07 p1199 A69-18684
- Cross sections computed for excitation and ionization of atoms and ions by electrons, using peaking approximation to evaluate Coulomb-Born matrix approximation
08 p1355 A69-20206
- Electron bombardment effects on performance characteristics of UV gratings
08 p1318 A69-21097
- Electron bombardment mercury ion thruster plasma properties and performance, computing ion beam current, discharge losses and propellant utilization efficiency [AIAA PAPER 69-256]
09 p1560 A69-21214
- Electron bombardment thrusters for low specific impulse operation, discussing electrode structures fabrication by bonding alumina disk to metal electrode [AIAA PAPER 69-301]
09 p1568 A69-21730
- Electron irradiation effect on surface potential of thermally grown silicon dioxide layers, noting conductivity and annealing effects
09 p1557 A69-21743
- Liquid mercury cathode electron bombardment thrusters applicability to electric propulsion missions [AIAA PAPER 69-302]
09 p1569 A69-21876
- Causes and magnitudes of thrust misalignment of Kaufman type electron bombardment ion thruster [AIAA PAPER 69-303]
10 p1753 A69-23362
- Electron bombardment produced clustered displacements, paired vacancies and interstitial atoms in Si, discussing possible mechanism for developing defects
10 p1747 A69-23713
- Diffusion processes during annealing of metals irradiated by electrons and neutrons, discussing crystal damage, recovery and recrystallization
11 p1891 A69-24800
- Electron and proton radiation doses impinging on orbiting satellites computed using orbit calculation and B, L coordinates
11 p1949 A69-24862
- Computer program for electron and proton fluxes impinging on spacecraft, performing computation for Van Allen belts and solar flares
11 p1949 A69-24863
- Electron, proton and gamma ray radiation effects on thin film CdS, GaAs and CdTe solar cells
11 p1825 A69-24872
- Drift and tunnel effect of MOS transistors under ionizing electron and X ray irradiation, considering fabrication, electrical characteristics and D-2 satellite tests
11 p1848 A69-24873
- Ionization and attachment of thermal electrons in oxygen and airlike nitrogen-oxygen mixtures during electron irradiation
13 p2302 A69-27456
- Internal friction, Young modulus and resistivity measurements for stage I interstitials in electron irradiated tungsten
13 p2284 A69-28682
- High temperature effects on electron and X ray irradiated MOS transistors for space charge analysis and defects in silica films
15 p2625 A69-30828
- Logic family with low power consumption subjected to 1 Mev electrons analyzed within telemetry circuit concept for space application
15 p2625 A69-30830
- Discharge chamber plasma processes in electron bombardment ion thrusters, considering factors affecting thruster performance [AIAA PAPER 69-494]
16 p2845 A69-32735
- Luminescence spectra of aromatic polymers, monomers and dimers under high energy electron excitation using molecular resonance model
16 p2828 A69-32792
- Electron energy effects on reflectance degradation and recovery of thermal control materials in vacuum, reporting test results for various protective coatings [AIAA PAPER 69-643]
17 p3005 A69-33306
- Unfilled Pyrrone prepared from powder into molded parts for flexural tests at elevated temperatures observed for stability to electron irradiation in air
19 p3356 A69-35529
- Imperfection photoconductivity in electron irradiated Li-doped Si annealed at room temperature, noting level rearrangement in O rich material
19 p3382 A69-35696
- Photoresponse and minority carrier diffusion length long term stability of Li doped solar cells after proton, neutron and electron irradiation
19 p3252 A69-35697
- Injection level effects on minority carrier lifetimes in lithium-doped devices and solar cells irradiated by electrons and reactor neutrons
19 p3252 A69-35698
- Proton and electron auroral ovals, deriving H alpha intensity and frequency distributions as function of geomagnetic latitude and time from patrol spectrographs in Canada
19 p3302 A69-35993
- Coherent recombinational radiation of semiconductors excited by electron beam
19 p3387 A69-36539
- Lithium doped silicon acceptor concentration resulting from electron irradiation damage decreased by annealing at 300 degrees K
23 p4197 A69-41498
- Electron irradiation-temperature dependence of introduction rate and room temperature annealing of carrier-removal defects in Li-doped Si
24 p4360 A69-42647
- ### ELECTRON MASS
- Faraday effect of free carriers on n-type GaSb at 20 K, determining mass and mobility of electrons from Hall effect and conductivity
02 p0298 A69-12039
- Richardson constant and tunneling effective mass for thermionic and thermionic field emission in Schottky barrier diodes
07 p1089 A69-18247
- Energy separation and electrons effective mass ratio of conduction bands of tellurium doped GaSb obtained by free carrier Faraday rotation measurements
07 p1201 A69-19464
- Effective masses of electrons and holes in HgSe and HgTe characterized by narrow forbidden bands and high charge carrier mobility
11 p1937 A69-24920
- Zr doped superconducting ceramic strontium titanate, noting effective electron mass variations and transition temperature
13 p2316 A69-27400
- Cadmium arsenide carriers effective mass under strong transverse magnetic field, noting restricted role of thermal EMF and Hall coefficients
13 p2318 A69-27897
- Electron effective mass, density and mobility in /000/ and /111/ conduction band minima in Te-doped degenerate GaSb-InSb single crystals
19 p3390 A69-36555
- Polarons large to nearly small transitions, studying ground state mass dependence on bare electron mass, electron-phonon interactions model, superconducting strontium titanate, etc
20 p3583 A69-37280
- ### ELECTRON MICROSCOPES
- Sliding surface tracks from hardened steel sliders on flat PTFE examined for molecular orientation with electron microscope
01 p0085 A69-10369
- Pedoscope use in soil microbiological studies including ecology, infection susceptibility, etc
01 p0021 A69-11092
- Crystal structure of boron filaments vapor deposited on tungsten wire substrate, using X ray diffraction and transmission-electron microscopy
02 p0268 A69-12405
- Electroerosion effect on fabrication of small disks for direct examination by electron microscopy, using refined and heat treated aluminum
03 p0427 A69-12880
- Magnified image of Al-Mg specimen microanalyzed during examination by electron microscope, studying segregation and initial precipitation at grain boundaries
03 p0442 A69-12894
- Temperature rise of micron sized silver particles on carbon film due to electron beam heating, setting up heat balance equation
04 p0640 A69-14449
- Ultrahigh vacuum electron microscope using differential sputter ion pumps to obtain low contamination environment
04 p0599 A69-15016
- Electron fractography techniques and fracture modes in metallic materials interpretation, giving special attenuation to classical fracture replication and shadowing techniques
04 p0619 A69-15395
- Bioadhesive investigation in echinoderms extended to class Holothuroidea, using electron microscope with correlative light microscopy for tube feet of sea cucumbers
05 p0708 A69-15984
- Plastic yielding and strain distribution in Al reinforced with stainless steel wires determined by electron microscopy
06 p0940 A69-16947
- X ray fluorescence and electron microprobe for determining thin film thickness
07 p1113 A69-19582
- Dislocations effect on intermediate body centered tetragonal phase precipitation in Fe-Ni-Cr-Be alloy using transmission electron microscopy
08 p1333 A69-20447
- Plastic backing films removal from carbon electron microscope replicas by maintaining specimens in horizontal position
09 p1495 A69-21651
- Inhomogeneity distribution of carrier concentration and electrovoltaic effect in GaAs devices analyzed by scanning electron microscope
09 p1557 A69-21746
- Electron microscopy for continuous observation and recording of dynamic reactions in high temperature materials
09 p1499 A69-22304
- Thin foil preparation technique for transmission electron microscopy and selected etch pitting technique for CoO single crystals
12 p2112 A69-25944
- Dislocations observations in fracture study of crystals, considering etching, decoration technique, X ray topography and diffraction electron microscopy
13 p2316 A69-27223
- Microscopic mechanisms in fracture surface markings, using electron fractography cleavage, fatigue, stress corrosion cracking, microvoid coalescence and tear ridge formation
13 p2274 A69-27224
- Wear-resistant hard thin layers deposited on various base material surfaces analyzed by electron microprobe
13 p2282 A69-28164
- Electron microscope fractographic studies to determine service failure causes, detecting grinding and quench cracks, hydrogen flakes and embrittlement fractures, etc
13 p2269 A69-28181
- Electron fractography used in machine parts failure analysis to detect internal and surface cracks, forging defects, stress corrosion, fluid leakage sources, etc
13 p2269 A69-28182
- Scanning electron microscopy to study device failure and performance, discussing limitations and progress
17 p2936 A69-32890
- Scanning electron mirror microscope advantages over electron mirror and scanning electron microscopes for examining integrated circuits
17 p2971 A69-32891
- Scanning electron microscopy of dehydrifying solder glass seals for hermetic packages, biased integrated circuits and metallization corrosion
17 p2936 A69-32892
- Scanning electron microscopy for reliability studies in semiconductor devices
19 p3382 A69-35788
- Cultured mammalian cell growth morphology studied in situ with scanning electron microscope, discussing surface morphology changes during mitotic cycle of Chang liver cells
20 p3467 A69-37100
- Recovery process observation in pure binary Al-Cu alloy and commercial Al-Cu-Mg-Pb alloy, noting electron microscope applicability
22 p3968 A69-40062
- ### ELECTRON MOBILITY
- Electron transport theory for pure and doped low mobility semiconductors and for impurity conduction in disordered semiconductors, noting related optical phenomena
01 p0135 A69-10047
- Electron-hole collisions effect on drift and electron and hole diffusion in semiconductors at high injection levels
01 p0137 A69-10257
- Power saturation in isochronal traveling wave tube explained by motion of electron bunches relative to waves
01 p0047 A69-10882
- Magnetoplasma wave propagation in periodic conducting solid, calculating electron drift effect on space harmonics
02 p0287 A69-11945
- Faraday effect of free carriers on n-type GaSb at 20 K, determining mass and mobility of electrons from Hall effect and conductivity
02 p0298 A69-12039

Electron flow in stable negative electrostatic potential well produced by electronic injection at center of hollow open spherical anode

03 p0475 A69-13153

Perfect piezosemiconductor resonator /phaser/ with CdSe/CdS/ crystal, discussing vibration excitation in wurtzite type crystal in electric field of electron drift

03 p0431 A69-13930

Epitaxial GaAs films with high electron mobility, noting radiation recombination spectra dependence on substrate orientation

03 p0492 A69-14172

Electron vs phonon superconductivity mechanism conditions for semiconductors, semimetals and molecular crystals

03 p0492 A69-14176

Fresnel drag produced by relativistic addition of electron velocities in semiconductors measured by changes in refractive index

05 p0807 A69-16026

Critical electron drift velocity threshold in surface wave amplification in semiconductor in magnetic field, noting partial effect of diffusion

05 p0810 A69-16648

Magnetic field generation in nonuniformly rotating plasma by current density from electron drift relative to positive ion gases due to viscous forces

06 p1009 A69-17966

Voltage dependence of mobility limited electron current density in gas filled diode for collision frequency proportional to electron speed

09 p1462 A69-21326

Kaufman thruster with predominant radial field, noting electron mobility across ion extraction screen and advantages of uniform plasma distribution [AIAA PAPER 69-259]

09 p1569 A69-21877

Electron-hole collisions effect on drift and electron and hole diffusion in semiconductors at high injection levels

09 p1559 A69-22650

Acoustic wave amplification and generation in piezoelectric semiconductors and semimetals by supersonic carrier drift currents

11 p1926 A69-24641

Vapor phase epitaxial production of indium arsenic phosphide crystalline layers, discussing electron mobilities, electrical resistivities and doping

12 p2142 A69-25934

Power saturation in isochronal traveling wave tube explained by motion of electron bunches relative to waves

12 p2041 A69-26646

Electron motion effects along magnetic field lines on axisymmetric torsional hydromagnetic oscillations in inhomogeneous low beta plasma, discussing resonance trapping

12 p2076 A69-27107

Linear approximation of electron temperature increment and electron mobility in nondegenerate polar semiconductor in crossed fields

14 p2508 A69-29662

Langmuir probe measurements leading to electron groups composition of electron velocity distribution function in negative glow light

14 p2493 A69-29694

Electron and ion mobility in multiple cusp magnetic fields related to Polytron experiment

14 p2499 A69-29852

Faraday rotation measurements in ionosphere by geostationary satellite ATS-3 as evidence of considerable nighttime electron transport

17 p2959 A69-32926

Electron transport initiated by radiant energy absorption or by reducing suitable electron acceptor as source of energy for extraterrestrial life

17 p2908 A69-32973

InSb thin films prepared by flash evaporation, discussing Hall measurements at various temperatures and electron mobility dependence on film thickness

18 p3182 A69-34348

Ion density, electrical conductivity and weighted mean mobility deduced from Gerden capacitor I-V characteristics used in balloon sounding of stratosphere

18 p3130 A69-34970

Electron effective mass, density and mobility in /000/ and /111/ conduction band minima in Te-doped degenerate GaSb-InSb single crystals

19 p3390 A69-36555

Radiation fields from energetic electron moving in helical orbit in magnetoactive plasma, using Maxwell equations

22 p4008 A69-39965

Electron transport chain of monovalent and divalent cations and of polyamines, studying effects on

menadione reductase activity to determine salt dependence

22 p3886 A69-41077

ELECTRON MULTIPLIERS U PHOTOMULTIPLIER TUBES ELECTRON OPTICS

Trajectory equations for outermost electron on beam in TWT operating in dynamic mode for Brillouin flux

03 p0406 A69-13974

Design and principles of operation of SHF electron-optical multiply stable storage elements with dynamic attributes of states

03 p0441 A69-13982

Advances in electronics and electron physics, Volume 25, covering linear ion accelerators, Hall effect, VLF propagation, thermionic cathodes and electron microscopy

09 p1469 A69-22696

Soviet book on electroluminescent devices covering panels, indicator contrast levels, control, multicolor indicators, image conversion and storage and optoelectrical systems

11 p1850 A69-24976

Lasers and opto-electronics - Conference, University of Southampton, England, March 1969

11 p1897 A69-25034

Energy resolution improvement in cylindrical electrostatic energy selector by focusing and limiting electron beam before entrance into monochromator

14 p2450 A69-29572

Axially symmetric magnetic fields for constant radius annular electron beams reflection, applying results to design of reflex klystron millimeter oscillator

19 p3267 A69-35930

Optical instruments as visual aids in scientific detecting including electron optical image converters detecting emissions invisible to human eye

22 p3943 A69-39974

Electron optical techniques for failure analysis involving brittle fracture, corrosion fatigue, stress corrosion, welding and surface phenomenon

24 p4313 A69-42768

ELECTRON ORBITALS

Polarized orbital method for calculating electron-atom scattering amplitudes, noting discontinuous wave function, nonvariational technique and strong dependence on parameter

02 p0284 A69-12702

Linear combination of atomic orbitals-molecular orbitals self consistent fields calculation on beryllium dihydride, using Gaussian basis functions

05 p0811 A69-15910

Incoherent wave scattering of particle orbits as nonlinear effect of LF instabilities

08 p1367 A69-20801

Thermionic emission from bare and Cs-covered metal surfaces, calculating current and work function by employing localized electron orbital model

14 p2505 A69-29264

Atomic size and outer electron effect on Fe, Co and Mn polymorphism, noting change in crystal lattices

15 p2638 A69-30321

Hartree-Fock calculations for wavelengths of K alpha X ray transitions, tabulating configuration and term energies, dipole integrals and relative multiplet strengths

22 p3984 A69-40156

Self consistent field molecular orbital method in LCAO/linear combination of atomic orbitals/ approximation applied to LiH ground state for potential energy curve

22 p3985 A69-40721

ELECTRON OSCILLATIONS

Shock tube and samples of fluoroethylene, difluorodichloroethylene and fluoromethane in argon diluent used to prepare carbon difluoride, discussing electronic oscillator strengths

04 p0632 A69-14944

LF electric potential oscillation of discharge plasma, describing oscillation behavior by theory of dissipative drift instability of weakly ionized plasma

08 p1370 A69-21020

Oscillating electron ion discharge in magnetic field in system of alternating positive and negative electrodes to obtain fast neutral particle fluxes

13 p2311 A69-28109

Electron velocity distribution function in gaseous plasma with known collective oscillations and frequency/wave number relationship

13 p2313 A69-28327

Push-pull circuit configurations for GaAs transferred electron oscillators, discussing CW X band and pulsed L band devices operation

15 p2574 A69-30168

Bayard-Alpert type ionization gage for low pressures with and without modulation, discussing role of electron oscillations

20 p3464 A69-37407

Response of pi electrons in large organic molecule to scalar field for coronene, showing oscillator strength enhancement near single particle excitation band

20 p3580 A69-37497

Electromagnetic radiation characteristics from vibrating electrons or electric dipole moving in compressible isotropic plasma and from stationary dipole in moving medium, emphasizing Doppler effects

23 p4114 A69-41359

ELECTRON PARAMAGNETIC RESONANCE

Perhydroxyl radical electron spin resonance spectrum in solution of hydrogen peroxide and water at 77 K, noting g factor, hyperfine splitting and molecular structure

01 p0024 A69-10683

EPR spectra and thermal conductivity measurement in excited organic semiconductor salt derivatives of tetracyanoquinodimethane

03 p0484 A69-13278

Electric effect in ruby, discussing resonance magnetic field and transition

03 p0485 A69-13320

Benzene anion radical in solid solution ESR spectrum, noting removal of orbital degeneracy at 4.2 degrees K

03 p0382 A69-13379

UV induced excited-state properties of DNA using optical emission and electron spin resonance methods

03 p0372 A69-13488

Region of plasma electron capture during cyclotron electron resonance in magnetic trap with mirrors

03 p0478 A69-13849

EPR investigation of free radicals formed during mechanical fracture and gamma irradiation, discussing recombination rate and reaction rate with oxygen

03 p0434 A69-13871

Gamma irradiated silver carbonate EPR at liquid nitrogen temperatures

05 p0716 A69-15915

Ferroelectric Li niobate single crystals internal magnetic field analysis by acoustic EPR, establishing field induced hypersound resonance absorption in spin systems

09 p1556 A69-21563

Ion pairing effects of cyclooctatetraene anion radical, studying electron spin resonance spectra temperature dependence

10 p1651 A69-22938

Angular dependence of EPR line widths of trivalent Cr ions in zinc tungstate in rotating magnetic field, noting spin-phonon mechanism

10 p1743 A69-23131

EPR spectra and thermal conductivity measurement in excited organic semiconductor salt derivatives of tetracyanoquinodimethane

14 p2508 A69-29652

Parametron preamplifier for X band superheterodyne ESR spectrometer, noting sensitivity and SNR

14 p2423 A69-29757

Pulse radar quantum paramagnetic amplifier protection from saturation by transmitter power, using linear electrical bias of EPR line

15 p2579 A69-30956

Electric quadrupole coupling for N 14 in amidinofluorite studied by observation of second order transitions in electron spin resonance spectra

18 p3178 A69-35474

Electron spin resonance spectra of gamma irradiated single crystals of 9-methyladenine, analyzing H abstraction radical and temperature effects

19 p3264 A69-35974

ESR comparative study of selenoamino acids and S analog radical formation and radiation resistance, noting selenium groups ability as acceptors for unpaired electrons

21 p3668 A69-38425

Electron paramagnetic resonance line splitting between two nondegenerate Zeeman levels, using ruby laser as pumping source

21 p3735 A69-38582

Gamma radiolysis of silver nitrate ice forming neutral Ag in magnetically distinct sites, discussing water dipoles rotation and electron paramagnetic resonance

22 p3992 A69-40574

Electron spin resonance /ESR/ of polycrystalline Mo(V) complexes with dipyrindyl and phenanthroline, observing hyperfine interaction due to odd numbered isotopes

22 p3897 A69-40971

- Defect structure of ceramic Ba titanate doped with Cr ions, evaluating visible, IR and EPR spectra
22 p3996 A69-41160
- ELECTRON PHONON INTERACTIONS**
- Phonon capture by electrons in semiconductors with high permittivity in external electric field
03 p0489 A69-13891
- Localized umklapp scattering effect on galvanomagnetic properties of nearly free electron bcc metal with spherical Fermi surface
03 p0493 A69-14240
- Electron phonon coupling in barriers of GaAs Schottky diodes, noting first and second derivatives of I-V characteristic in n-type GaAs-Pd Schottky diode
03 p0493 A69-14242
- Superconductivity and band structure from pseudopotential for zinc and cadmium, analyzing values of electron phonon mass enhancement
04 p0642 A69-14965
- Phonon capture by electrons in semiconductors with high permittivity in external electric field
11 p1939 A69-25692
- Electrons and optical phonons interaction effects on optical and photoconducting properties of semiconductors, discussing phonon cyclotron resonance and oscillatory and magneto-oscillatory photoconductivity
19 p3385 A69-36517
- Polarons large to nearly small transitions, studying ground state mass dependence on bare electron mass, electron-phonon interactions model, superconducting strontium titanate, etc
20 p3583 A69-37280
- Nonlinear interaction of electron-acoustic oscillations in plasma, allowing for decay and inductive scattering in equation derivation for wave packet intensity
21 p3776 A69-38584
- ELECTRON PHOTOGRAPHY**
- Electron microautoradiograph preparation determining trace element amount and distribution by utilizing radioactive isotopes and high resolution of electron micrographs
13 p2263 A69-28168
- ELECTRON PHOTON CASCADES**
- Generation process in three stage He-Ne cascade laser with wideband resonance, using simplified energy level scheme
06 p0934 A69-17496
- High energy electron photon cascades event recorded with X ray photography, discussing origin in related atmospheric cosmic ray showers component subgroups
13 p2331 A69-28398
- Nuclear active cosmic ray component particle energy spectrum and nuclear cascade avalanches curves, using ionization calorimeter with Pb absorber
13 p2303 A69-28399
- Stable particles heavier than nucleons in extensive cosmic ray showers detected by delayed coincidences relative to shower electron photon component
13 p2331 A69-28402
- High energy ionization bursts in cosmic ray showers electron photon component, obtaining bursts power spectrum and component energy dependence
13 p2332 A69-28404
- Sea level fluctuations of electron-photon, muon and active nuclear components of extensive cosmic ray showers determined, obtaining shower parameters
13 p2332 A69-28406
- Inverse problem method for reconstructing electrons differential spectral cross sections and photon pair formation in electron photon cascade
13 p2303 A69-28415
- Primary electrons and gamma quanta generated electron photon cascades in Pb, obtaining error free cascade curves
13 p2304 A69-28416
- Electron photon cascades energy dependence on primary particle energy determined in lead by various instruments
13 p2304 A69-28418
- High energy electrons producing electromagnetic cascades in electron photon showers in lead measured by scintillation detectors
13 p2332 A69-28419
- Cosmic ray particle Pb nucleus interaction energy transfer to electron photon cascade in first inelastic collision, noting dependence on particle energy
17 p3008 A69-33387
- Electromagnetic cascade showers transition effect in various materials, measuring energy deposition as function of position
22 p3987 A69-41003

ELECTRON PLASMA

- Light scattering from plasmas embedded in homogeneous magnetic field, discussing solid state and high temperature gas plasmas
01 p0125 A69-10015
- Electron plasma wave dispersion along cylindrical plasma column in magnetic field
01 p0126 A69-10277
- Statistical analysis of polarization of semiinfinite electron/ion plasma bounded by dielectric or conducting solid wall, deriving steady state and space potential
02 p0286 A69-11706
- Statistical analysis of polarization of two component nonisothermal electron-ion Coulomb gas plasma containing microfluxes
02 p0286 A69-11707
- Electron plasmas near plane metallic surfaces, determining transmittance and reflectance of incident light waves and surface waves dispersion characteristics
02 p0286 A69-11788
- Standing ion-acoustic wave excitation in weakly ionized plasma, noting isothermal compression of electron gas
02 p0292 A69-12555
- Dipole and quadrupole bremsstrahlung and damping of electron plasma oscillations, finding negative k-square collisional electron-ion contribution
03 p0475 A69-13149
- Enhanced bremsstrahlung from supraluminous and sublumines waves in thermal isotropic homogeneous Maxwellian electron plasma, noting applicability to Crab Nebula
03 p0507 A69-13150
- Electron plasma oscillations diffusion due to scattering by large amplitude ion wave background, noting electron wave spectrum evolution
03 p0483 A69-14256
- Monograph on electron waves and resonances in bounded plasmas covering theoretical and experimental methods, metallic and dielectric resonance probes, etc
04 p0633 A69-14296
- Nonlinear electron oscillations in plasma, deriving asymptotic expression for plasma perturbation
04 p0635 A69-14552
- Kinetic theory to determine wave increments propagating across magnetic field in system of relativistic electrons in cold plasma
04 p0635 A69-14555
- Kinetic model equation for electron plasma incorporating collision terms for model scattering
04 p0636 A69-15042
- Plasma instabilities produced by beam plasma discharge in mirror magnetic trap
05 p0803 A69-16212
- Potential functions to solve coupled wave equations for compressible anisotropic plasma with electric and magnetic current sources
05 p0803 A69-16350
- Whistler mode propagation in homogeneous electron plasma situated in longitudinal electrostatic field, using Fokker-Planck model
05 p0758 A69-16417
- Collision induced instability of partially ionized gases having large Ramsauer effect in external magnetic field, analyzing nonlinear characteristics
05 p0804 A69-16441
- Electron plasma interaction with transverse EM wave propagating along magnetic field, calculating permittivity, density, field strength and applied frequency
05 p0805 A69-16699
- Spatial and temporal characteristics of two component electron-ion nonisothermal plasma and penetration of external LF electric field into plasma
05 p0806 A69-16745
- Electron concentration in pulsed plasma measured with Fabry-Perot interferometer and laser radiation source
06 p0963 A69-16911
- Resonant four wave interaction for nonlinear energy transfer in electron plasma oscillations
06 p0963 A69-17143
- Surface plasmons microscopic theory based on modified random phase approximation
06 p0967 A69-17711
- Model for phase transition mechanism quantum-Coulomb plasmas, finding transition temperature for white dwarfs
06 p0968 A69-17785
- Real and imaginary parts of homogeneous isotropic electron plasma complex refractive index, noting application to plane electromagnetic wave propagation
07 p1193 A69-19183

- Plasma column radial density profile measurement by electron plasma waves propagation in presence of strong magnetic field
07 p1194 A69-19323
- Low energy electrons in magnetosphere fromOGO-1 and OGO-3 observations, discussing plasma sheet, magnetic bay activity, electron pressure, temperature and density gradient
07 p1209 A69-19373
- Electron plasma and magnetic field effects on polaritons in semiconducting GaAs studied by Raman scattering of light at small angles
07 p1200 A69-19401
- HF wave propagation in unbounded electron-plasma systems using moment equations, discussing collisions effect and dispersion relation
07 p1086 A69-19468
- Nonlinear behavior of two stream instability between cold electron and ion streams
08 p1367 A69-20800
- Nonlinear longitudinal oscillations in nonisothermal electron plasma with Maxwellian distribution in velocity space and different temperatures of electrons and ions
09 p1550 A69-22025
- Integrodifferential equations describing longitudinal oscillation properties in nonlinear region of electron Maxwellian plasma waves and two cold electron beams
09 p1550 A69-22026
- Current distribution and impedance of insulated cylindrical antenna embedded in dielectric cylinder immersed in compressible electron plasma
10 p1663 A69-23423
- Ground wave propagation attainment of electron plasma resonance of F region, stressing need of wave vector orientation toward magnetic north
10 p1684 A69-23828
- Laser radiation spectrum scattered by low temperature plasma electrons at atmospheric pressure
11 p1922 A69-24233
- Electron confinement in magnetic mirror geometry supplemented with RF quasi-potential barriers, considering gas scattering
11 p1924 A69-24306
- Computer calculated phase velocities for surface wave and waveguide modes given for circular waveguide filled with inhomogeneous electron plasma
11 p1844 A69-24437
- Electromagnetic flux from nonlinear self interaction of electron plasma waves in far field of perturbation under anisotropic electron pressures
12 p2141 A69-27147
- Electron velocity distribution function in gaseous plasma with known collective oscillations and frequency/wave number relationship
13 p2313 A69-28327
- Linearized dispersion equation for electron oscillations in isotropic plasma with known electron velocity distribution function
13 p2313 A69-28328
- Magnetic and electric field effects on undamped electron-hole LF frequency plasma oscillations in spatially homogeneous nonpolar semiconductor
13 p2323 A69-28581
- Electron plasma oscillations and electron whistler of solar wind near Jupiter orbit
14 p2513 A69-29115
- Plasma electron temperature determination by line intensity ratio of beryllium-like ions, noting excitation functions
14 p2496 A69-29789
- Standing ion-acoustic wave excitation in weakly ionized plasma, noting isothermal compression of electron gas
15 p2658 A69-30252
- Plane electromagnetic wave propagation normal and parallel to magnetic field in plasma analyzed by equivalent circuits and impedances
15 p2659 A69-30799
- Wave regeneration by resonant particles interaction in inhomogeneous plasma of electrons confined in quadratic potential solved in WKB approximation
15 p2660 A69-30918
- Hot electron plasma formation by injecting megaelectron volt ion beams followed by Lorentz trapping, noting advantages of DC operation
15 p2661 A69-30925
- Transverse instabilities in collisionless electron plasma in absence of permanent magnetic field with spheroidal velocity distribution, noting application to shock theory
16 p2817 A69-31645
- Equivalent dielectric tensor for warm drifting electron plasma using model
16 p2820 A69-31701

Normal modes of electrons-electromagnetic field coupled system for many valley semiconductors, calculating dielectric constant for electron gas for ellipsoidal energy surfaces
16 p2826 A69-31821

He-Ne laser plasma behavior, establishing parameters for electron gas, cross sections of formation and annihilation and excited states lifetimes
17 p2982 A69-33390

Precursor plasma electron number densities calculations for blunt reentry vehicles, analyzing extreme UV radiation emanating from bow shock
[AIAA PAPER 69-718] 17 p2893 A69-33487

Oscillations excitation between ion cyclotron and electron plasma frequency in He ion beam generated plasma
17 p3014 A69-33830

Damping of plane sinusoidal wave in cold collisionless plasma, studying supercritical amplitude oscillatory process
18 p3180 A69-34703

Plasma instabilities produced by beam plasma discharge in mirror magnetic trap
20 p3581 A69-37784

Linearized dispersion equation for isotropic electron plasma without external fields solved by harmonic function model
21 p3775 A69-38564

Electron plasma velocity distribution function determined from dispersion equation by harmonic function analog
21 p3776 A69-38565

Relativistic solution by Landau procedure of initial value problem for one dimensional electron plasma wave coexisting with charged immobile background
21 p3778 A69-39579

Microwave power coupling to high density plasmas for electrons heating, using dielectric plates
21 p3779 A69-39746

Stark broadening of H-gamma for electron density measurement in plasma, noting temperature range
22 p3985 A69-40664

Multifrequency dispersion interferometers applicability in plasma diagnostics, considering integral electron concentration measurements
22 p3947 A69-40959

Acoustic wave propagation in plasma, analyzing ionic and electron sound caused by oscillation and relaxation processes using Landau and Vlasov kinetic equations
23 p4196 A69-41726

Holographic interferometry for determining total free electrons in plasma produced by irradiating solid hydrogen foils with giant pulse ruby laser
24 p4314 A69-42980

ELECTRON PRECIPITATION

Magnetosphere studies in France noting magnetosphere characteristics, wave propagation, charged particles, particle precipitation mechanisms in auroral zones and polar caps
02 p0242 A69-11904

High latitude outer zone electrons boundary region during geomagnetically quiet periods
03 p0502 A69-14004

East-West aligned fast auroral waves, suggesting origin in hydromagnetic processes occurring near equatorial plane
04 p0594 A69-15123

High resolution electron and proton energy measurements by sounding rockets indicating plasma sheet as source of energetic auroral electrons
05 p0756 A69-16273

Satellite scintillation at high latitudes and possible relation to soft particle precipitation
05 p0757 A69-16406

Correspondence between HF radar backscatter, optical aurora and electron precipitation, noting application to gross tracking of auroral oval
06 p0918 A69-17383

Radio noise generation in topside ionosphere, noting Cerenkov radiation from intense soft fluxes of auroral electrons
07 p1127 A69-19257

Auroral electron penetration into atmosphere analyzed on basis of independent electron particle motion, using auroral electron angular distributions and energy spectra above atmosphere
07 p1128 A69-19368

Nocturnal auroral electron showers configuration and displacement determined from sounding balloon measurement of X rays due to showers braking in upper atmosphere
08 p1308 A69-20281

Auroral electrons intensity modulation by source at L equals 6 magnetic shell on geomagnetic equator, noting dispersion effects
12 p2065 A69-26108

Production source of ionization due to low energy electron influx and inclusion in ionospheric continuity equation, noting quiet ionosphere
12 p2066 A69-26112

ESRO 1 satellite measuring proton intensities and energy spectra of precipitated and magnetically trapped electrons
13 p2327 A69-27754

Electron and proton spectra in 1-13 kev range relative to geomagnetic field lines measured by ESRO 1 satellite during Aurorae mission
13 p2328 A69-27755

Low energy electron precipitation data at northern high latitudes obtained from satellite low altitude polar orbit
14 p2512 A69-28964

Auroral substorms concept extended to include associated effects at all local times throughout magnetosphere, considering particle precipitation influence on substorms in midnight sector
15 p2593 A69-30008

Low energy electron and proton precipitation, discussing acceleration mechanisms and periodicity in relation to auroras and airglows
15 p2594 A69-30018

CNA and geomagnetic pulsations observed by ground based instruments in southern auroral region occurring near geomagnetic noon, noting electron precipitation role
15 p2597 A69-30697

He I/1.083 mu/ and O I/5577 A/ absolute brightness measured in sunlit aurora for various shadow heights of solar radiation, considering primary electron precipitation
16 p2780 A69-32311

Precipitated low energy protons and electrons measurements during breakup aurora, discussing fluxes and poleward boundaries
18 p3187 A69-34946

Auroral displays photographed by all-sky cameras at magnetically conjugate stations, morphological similarities and electron precipitation role
20 p3535 A69-38187

Lower thermosphere ion and neutral minor constituent concentrations in nighttime auroral zone, considering ionization due to electron precipitation and bremsstrahlung
21 p3704 A69-38365

Auroral zone geomagnetic pulsations on nightside and dayside of earth related to magnetospheric substorm and particle precipitation
21 p3708 A69-38497

Auroral electron and proton fluxes precipitation measurements by satellite, studying data in terms of spatial, energy and angular distributions
21 p3709 A69-38500

Optical data supporting satellite observations of soft electron precipitation on poleward side of normal auroral zone
21 p3709 A69-38501

Particle precipitation into auroral zone and plasma-energetic particle relationship in geomagnetic tail, discussing plasma sheet extent, energetic electron fluxes, etc
21 p3711 A69-38510

Dungey reconnection model of magnetosphere with dayside current sheet and pseudotrapping region compared with dayside observations of precipitation regions
21 p3711 A69-38511

Satellite observations of auroral particle precipitations indicating latitude dependence of auroral electrons averaged pitch angle and energy spectral distributions
22 p3938 A69-40502

ELECTRON PRESSURE

Hydrogen to He ratio effect on stellar atmospheric structure, considering flux relations, UVB color indices, H line profiles, electron and gas pressures
13 p2339 A69-27562

ELECTRON PROBES

Electron microprobe analysis of potassium feldspar in Weekeroo Station meteorite
04 p0659 A69-14979

Surface potential measurements for flat conductors or semiconductors using scanned electron beam probe
04 p0601 A69-15115

Tantalum diffusion layer on refractory cobalt and nickel base alloys analyzed by electron microprobe
[ONERA-TP-665] 06 p0941 A69-17097

Passive current maxima during anodic polarization of stainless steel in sulfuric acid, using electrochemical and electron microprobes
06 p0944 A69-17853

Electron microprobe analysis of vanadium in presence of titanium by compositional measurement of chromite in chondritic meteorites
07 p1073 A69-18419

Electron probe analysis of olivine and pyroxene in LL-group chondrites, discussing iron and fayalite composition and unequilibrated stones
08 p1406 A69-20931

Impurity heterogeneities in oxidized and oxidized silicon slices from electron probe X ray microanalyzer, discussing thermal oxidation effects
10 p1743 A69-23171

Wear-resistant hard thin layers deposited on various base material surfaces analyzed by electron microprobe
13 p2282 A69-28164

Relativistic electron confinement within geomagnetic tail neutral sheet measured by Pioneer 7 deep space probe, confirming kinetic energy observations of IMP 1 satellite
14 p2433 A69-28934

Electron beam fluorescence probe and afterglow investigation for hypersonic He flow visualization, observing qualitative structure
19 p3291 A69-35722

ELECTRON RADIATION NT BETA PARTICLES

Silicon n-p solar cell behavior during electron radiation, describing radiation resistant solar cell
11 p1825 A69-24871

Angular distribution of electrons leaving plasma at electrode boundary, using kinetic Boltzmann equation with scattering function and specular reflection
11 p1933 A69-25546

Electron photon cascades energy dependence on primary particle energy determined in lead by various instruments
13 p2304 A69-28418

Radiative scattering cross sections of electrons from neutral O and atomic and molecular N using rapid scanning spectrometer for bremsstrahlung intensity
15 p2657 A69-31160

Criticism of Chiu theory on radio emission from pulsars supposing electron radiation
16 p2865 A69-32802

Cosmic ray electron role in energetics of solar flares, stellar flares and explosions, galactic eruptions and quasars
21 p3790 A69-38823

Cosmic ray electrons component measurements at balloon altitudes with electron spectrometers
22 p4002 A69-40091

Pulsar CP 0328 radiation mechanism, considering relativistic effects of rapid rotation
22 p4035 A69-41206

ELECTRON RECOMBINATION NT RADIATIVE RECOMBINATION

Alpha recombination coefficient of molecular helium ions measured in helium afterglow plasmas as function of electron density and gas temperature
02 p0283 A69-11834

Electrons relaxation caused by ionization and recombination in nonequilibrium plasma, using Kerrebrock model
03 p0477 A69-13609

Recombination rate of electrons in high pressure helium-like plasma with gas temperature fixed at 300 K and electron temperature varied between 300-2000 K
08 p1356 A69-20742

Static characteristics of transistors dependence on current carriers surface recombination in inactive base region, noting strong electric field influence
09 p1464 A69-22287

Metallic impurities effect on Ge surface charge and recombination properties, noting fast and slow electron density changes by forbidden band penetration
11 p1939 A69-25703

Nighttime maxima anomaly in electron concentration of ionospheric F layer at midlatitudes, considering diffusion and recombination
12 p2064 A69-26007

Relaxation oscillations in field ionized epitaxial n-GaAs Gunn oscillators on seminsulating substrates, discussing recombination of excess electrons and holes
13 p2207 A69-27236

Dielectric recombination in plasma, considering role in populating highly excited levels
20 p3580 A69-38016

- Electron recombination and diffusion in afterglow following short pulsed DC discharge in CO, using microwave diagnostic techniques
22 p3984 A69-40478
- Tabulated numerical values of Burgess general formula for computing dielectronic recombination rates
23 p4207 A69-41281
- ### ELECTRON SCATTERING
- Bragg reflection of electrons by standing light waves of giant pulse laser
02 p0255 A69-11833
- Polarized orbital method for calculating electron-atom scattering amplitudes, noting discontinuous wave function, nonvariational technique and strong dependence on parameter
02 p0284 A69-12702
- Elastic scattering cross section for low energy electrons on metastable He atoms, using polarized orbital method
03 p0469 A69-12922
- Elastic scattering of slow electrons by negative H and positive Li ions, calculating differential cross sections and phase shifts
03 p0469 A69-12924
- Carbon dioxide laser for observing nonlinear effects related to electron interaction with lattice vibration within semiconductors
03 p0437 A69-13041
- Ionizing shock front structure in monatomic gas, considering atom-atom and electron-atom collisional ionization rates
03 p0414 A69-13138
- Electron scattering by neutral acceptors in semiconductors, noting relaxation time for Ge at very low temperatures
03 p0484 A69-13280
- Radiative transfer equations solved for electron scattering stellar atmosphere, using transformation of integrodifferential transfer equations into singular integral equations
03 p0466 A69-13351
- InSb semiconductors electron scattering analysis at ionized impurities and optical and acoustical lattice vibrations with various polarizations
03 p0492 A69-14170
- Superconductivity of electron beam evaporated tungsten films by X ray and electron diffraction techniques, discussing temperature dependence of energy gap
04 p0640 A69-14447
- Elastic scattering of electrons from argon atoms in argon air plasmas by shock tube microwave reflection method, measuring power reflection coefficient [AIAA PAPER 68-138]
04 p0632 A69-14701
- Kinetic model equation for electron plasma incorporating collision terms for model scattering
04 p0636 A69-15042
- Quantum electrodynamics of radiation scattering from ionized interacting plasma, considering electron interactions
04 p0636 A69-15044
- Electron backscattering from cathode to cathode due to collisions with molecules, assuming isotropy of scattering
05 p0800 A69-15738
- Bounce resonant scattering of auroral zone electrons, noting contribution to microbursts and mirror point diffusion
05 p0754 A69-16260
- Zone behind reflected shock wave in shock tube using electron beam scattering, showing flow spectra and attenuation region of wave
05 p0752 A69-16688
- Carrier scattering from defects in neutron irradiated semiconductors, noting mobility and relaxation time
06 p0974 A69-16864
- Physics of plasmas, Volume 2, Weakly ionized gas, covering inelastic collision, free electron scattering, intermediary plasmas, etc
06 p0963 A69-17165
- Ionizing electron collisions with He, determining energies and angular correlation distributions of scattered and ejected electrons
06 p0962 A69-17191
- Formation dynamics of thin sporadic layers of E region, determining maximum ionization and electron concentration and electron-neutral atoms collision frequency
06 p0922 A69-17751
- Chemisorption of H onto Nb (110) surface, measuring low energy electron diffraction and inelastic electron scattering from clean and H-covered surfaces
06 p0980 A69-17758
- Backscattering due to collisions for electrons from emitter accelerated through positive ion sheath into plasma in thermionic diodes
06 p0898 A69-17773
- Ratios of gas kinetic electron-atom collision integrals of Ramsauer for Ar
06 p0963 A69-17822
- Differential thermal EMF at room temperature in p-InSb as function of concentration for different electron and hole scattering mechanisms
06 p0981 A69-17881
- Equations for electron scattering by sound in n-type semiconductors, giving corrections to sound propagation velocity during interactions
07 p1199 A69-18680
- Electron-electron interaction effect on I-V characteristic and equivalent circuit of metal-semiconductor contact, noting conductivity and rectifying properties
07 p1107 A69-19162
- Low pressure measurement by electron scattering using Born approximation
07 p1181 A69-19218
- Solar X ray bursts decay curves and spectra in 10 to 150 keV range interpreted as hot coronal condensation during flare and electron bremsstrahlung
07 p1206 A69-19250
- Cyclotron- and bounce-resonance scattering of electrons trapped in geomagnetic field for pitch-angle scattering, noting whistler mode disturbances
07 p1208 A69-19367
- Physics of electronic and atomic collisions - Conference, Leningrad, July 1967
07 p1186 A69-19651
- Cross sections for inelastic interactions of electrons with atoms and heavy impurity ions and processes of atomic excitation
07 p1195 A69-19652
- Population inversion mechanism based on electron collisional excitation cross sections for molecular vibrational levels in carbon dioxide lasers
07 p1157 A69-19655
- Electron collisional excitation cross sections for upper states in Ar ion lasers
07 p1157 A69-19656
- Electron collisional excitation cross section calculations for atoms and ions using modified Born approximation taking into account three physical effects
07 p1187 A69-19658
- Cross section calculations for elastic and inelastic electron collisions with atoms, ions and molecules and ionization of atomic systems by electrons and photons
07 p1187 A69-19660
- Atomic and electronic collisions experimental study techniques, noting three data logging systems
07 p1187 A69-19662
- Electron collision excitation of positive ions, calculating collision cross sections for transitions between levels of P term
07 p1187 A69-19714
- Recombination coefficients for dense weakly ionized cesium plasma, treating recombination process as diffusion generated by electron collisions
08 p1359 A69-19844
- He concentration measurement in transient He-air mixture by spectroscopic analysis of fluorescence excited by high energy electron beam
08 p1312 A69-19860
- Electron-ion collisions during forbidden lines excitation in gaseous nebulae, using Hartree-Fock functions and variational principles
08 p1391 A69-20530
- Surface structures determination by energy analysis and low energy electron diffraction of scattered electrons
09 p1554 A69-21340
- Tables of effective electron cross sections and macroscopic coefficients, Volume 1, covering hydrogen and rare gas molecular and atomic interactions with electrons
09 p1541 A69-21579
- Electron impact ionization of negative H ions computed by wave expansion methods and compared with experiments
09 p1542 A69-21622
- Channel coupling effects in elastic electron-atom collisions involving electric dipole transitions, noting phase shifts and differential cross section
09 p1542 A69-21623
- Inverse Compton scattering of far IR background radiation proposed as explanation of high energy gamma ray flux
09 p1580 A69-22296
- Polarization measurements of July 1966 proton flare, considering electron scattering and density
10 p1764 A69-23740
- Thin film thickness and composition determination through scattered electron and characteristic X ray radiation recording
10 p1747 A69-23847
- Electrons resonance scattering by diatomic molecules from elastic and inelastic channel measurements in transmission
11 p1921 A69-24418
- Multiple scattering in Kapitza-Dirac effect describing electron scattering by standing electromagnetic wave, noting transition probability less than unity
11 p1919 A69-25323
- Auroral electrons intensity modulation by source at L equals 6 magnetic shell on geomagnetic equator, noting dispersion effects
12 p2065 A69-26108
- Inelastic interactions cross sections of slow electrons with adsorbed particles on W surface as function of temperature in surface bond vibrational region
12 p2132 A69-26114
- Average ionization cross sections of atomic and molecular H and He beams ionized by plasma electrons with Maxwellian velocity distribution
12 p2138 A69-26542
- Polarization of continuum background of planetary nebulae in window in visible spectrum from scattering of nucleus star radiation by electron gas
13 p2339 A69-27567
- Energy loss during inelastic collisions between electrons and ionospheric particles, determining ionospheric heating by UV radiation
13 p2252 A69-27614
- Transverse quantum thermogalvanomagnetic phenomena in thin semiconducting films, noting effects of inelastic electron scattering at acoustic lattice vibrations
13 p2318 A69-27890
- Cadmium arsenide carriers effective mass under strong transverse magnetic field, noting restricted role of thermal EMF and Hall coefficients
13 p2318 A69-27897
- Electronic structure of clean metallic interfaces, considering electron, ion and surface interactions for metal-vacuum interface
13 p2321 A69-28008
- Nonmagnetic quadrupole ionization gauge, discussing systems design and electron oscillations
13 p2262 A69-28020
- Correlation functions of fluctuations in electrical characteristics of nonequilibrium electron gas during scattering, determining spectral densities and populations by kinetic equation Green function
13 p2314 A69-28445
- Differential thermal EMF at room temperature in p-InSb as function of concentration for different electron and hole scattering mechanisms
14 p2503 A69-28790
- Molecular hydrogen electron scattering, optical refractivity and molecular anisotropy used to construct model dipole spectrum consistent with oscillator strength rules
14 p2488 A69-29094
- Thomson scatter probes for diurnal variations of daytime atmospheric density at 100 km altitude
14 p2440 A69-29125
- RF impedance method for electron density and collision frequency in plasma
14 p2492 A69-29352
- Electron scattering by neutral acceptors in semiconductors, noting relaxation time for Ge at very low temperatures
14 p2508 A69-29653
- Rare gases total excitation cross sections absolute values measured in collision chamber, noting energy distribution of exciting electron beam, fine structure, etc
14 p2493 A69-29693
- Free electron concentrations and dispersion in H I regions noting ionized interstellar gas components role
15 p2681 A69-30420
- Metagalactic electrons and relic radiation interaction calculations allowing for universe expansion, space curvature and X ray absorption
15 p2687 A69-30541
- Electron scattering due to Kapitza-Dirac effect in laser standing wave field
15 p2634 A69-30736
- Low energy neutral bremsstrahlung cross sections for Ne, Ar and Xe, using rapid scanning spectrometer
15 p2657 A69-31159
- Fluctuation kinetics of electron system in nonequilibrium state arising in semiconductor in strong electric field, considering lattice and interelectron scattering
16 p2824 A69-31569

Perturbation theory for nonlinear oscillations in ionized plasma, treating electron-neutral collisions effect by Boltzmann-Vlasov equation relaxation term, noting distribution function

16 p2820 A69-31702

Partial reflections method of Gardner and Pawsey for determining vertical profile of electron collision frequencies in lower ionosphere and upper D layer

16 p2775 A69-32034

Electronic collision frequency measurement at F layer peak near ground sunrise time

16 p2779 A69-32197

Ionosonde electric circuit modified to permit radio wave absorption measurements over wide frequency range, calculating electron collision frequencies in F region

17 p2968 A69-33994

X ray absorption in surrounding gas sphere as function of continuous absorption, electron scattering and diffuse ionizing radiation, using radiative transfer theory

18 p3186 A69-34296

Atomic excitation and ionization by thermal electrons, using Monte Carlo trajectories to determine adiabatic collisions effects on energy transfer near dissociation limit

18 p3176 A69-34790

Long lived highly excited atoms production in electron collisions with CO, O and N molecules

18 p3177 A69-35125

Lower ionospheric effective electron collision number from cosmic noise recordings and radio wave absorption data obtained by vertical sounding rocket

20 p3528 A69-37679

Radial motion of trapped electrons caused by pitch angle scattering in distorted geomagnetic field, noting diffusion coefficient

20 p3593 A69-38104

Diatomic molecules rotational excitation calculated from electron molecule elastic scattering parameters in fixed nuclei approximation

21 p3775 A69-39665

Exact solution of macroscopic line transfer equation including electron scattering terms for Milne-Eddington model atmosphere, discussing electron scattering effect on growth curves

22 p4007 A69-40903

Electron collisions effect on polarization of waves reflected from ionosphere

22 p3941 A69-40922

Shape resonances in low energy elastic scattering of electrons by C, N and O, discussing ground state configurations and close coupling equations corrections

23 p4193 A69-41452

Low energy electrons energy loss by inelastic collisions in moving through atmosphere, estimating cross sections and loss rates

24 p4351 A69-42763

Lyman alpha radiation from electron collisions with simple H-containing molecules, finding dissociative excitation cross section role

24 p4351 A69-43033

Diffuse cosmic X rays from Compton collisions between galactic leakage electrons and extragalactic background photons to verify microwave blackbody radiation properties

24 p4368 A69-43202

Solar X ray bursts decay curves and spectra in 10 to 150 keV range interpreted as hot coronal condensation during flare and electron bremsstrahlung

24 p4372 A69-43613

Elastic electron scattering by metastable states of rare gases, using effective potential matching experimental binding energy of negative ions

24 p4354 A69-43818

ELECTRON SOURCES

Electron gun with plasma cathode consisting of gas discharge chamber, electron ejecting component and focusing system

04 p0598 A69-14857

Cesium plasma produced inside hot cylindrical tantalum cavity at 1400 K by contact ionization at wall while obtaining electrons from internal filament

06 p0927 A69-17707

Diurnal variation of D region electron production rates, discussing Lyman alpha ionization of nitric oxide

09 p1577 A69-21717

Semiautomatic recording device to determine gas discharge ion and electron sources operation modes optimum parameters

15 p2658 A69-30237

ELECTRON SPIN

Acoustic paramagnetic resonance in arsenic doped germanium, measuring spin-lattice relaxation

02 p0296 A69-11835

Synchrotron radiation excitation in system of relativistic monoenergetic electrons rotating in cold magnetoactive plasma

03 p0476 A69-13383

Ground state energy of Anderson Hamiltonian calculated by cluster variation for cases of infinite d-d correlation energy

06 p0958 A69-17712

Spin-other-orbit matrix elements for F super 3 electron configurations

06 p0962 A69-17819

Electronegativity and work function relationship from thermodynamic and quantum mechanics standpoint, describing electrons structure by spin orbitals localized around lattice sites

14 p2505 A69-29263

Spin compensated state of localized magnetic impurity moment in space, calculating size range of magnetic impurity spin/conduction electron spin correlation function

22 p3983 A69-40061

Electron spin memory in optical pumping cycle of potassium halides F centers, measuring relaxed excited state g factors and spin resonance line widths

23 p4198 A69-42419

ELECTRON STATES

Electron states at deep levels in InSb by deriving equations for Bloch wave functions of conduction and valence bands

09 p1556 A69-21508

High temperature gas mixture plasmas thermodynamical properties, emphasizing Debye electrostatic interactions and electron states

10 p1810 A69-23794

Beam-foil technique for measuring radiative lifetimes of excited electronic states in ionic species of O, including transition probabilities

13 p2301 A69-27452

Electronic states of semiconductor acceptor centers at forbidden band deep levels, considering inner electron shell excitation in impurity ion

15 p2665 A69-30039

LTE departure calculated for He I in hot star model atmospheres for effects on populations of singlet and triplet states

21 p3801 A69-38761

Forbidden absorption bands of diatomic O in Ar continuum region, determining rotational constants of upper electronic states

22 p3896 A69-40479

ELECTRON SWEEPING

U SWEEP FREQUENCY

ELECTRON TELESCOPES

U PARTICLE TELESCOPES

ELECTRON TRAJECTORIES

Trajectory equations for outermost electron on beam in TWT operating in dynamic mode for Brillouin flux

03 p0406 A69-13974

Hamilton-Jacobi equations of motion for classical electron in presence of traveling pulse of electromagnetic radiation, solving radiation pulse shape orbits

08 p1377 A69-19790

Numerical integration of motion equations of electrons subject to electrostatic waves, considering turbulent heating

08 p1368 A69-20806

Electromagnetic field penetration into plasma cylinder having electron mean free path comparable with plasma diameter, noting anomalous skin effect

12 p2133 A69-25833

Surface resistivity oscillatory dependence on magnetic field in single crystal metals, examining electron trajectories, energy levels and wave functions

13 p2316 A69-27641

Nonmagnetic quadrupole ionization gauge, discussing systems design and electron oscillations

13 p2262 A69-28020

ELECTRON TRANSFER

Electron drift velocity, diffusion coefficient and trapping time in GaAs, measuring variation with electric field

01 p0140 A69-11255

F 2 layer cut-off frequency predawn increase caused by sunrise, resulting in photoelectrons transfer along force lines at magnetically conjugate point

02 p0238 A69-11681

Electron transfer through metal/semiconductor contact surfaces, measuring electrical conductivity on sintered cylinders with or without silver addition

02 p0296 A69-11790

Gunn effect and resulting electron transfer mechanism in semiconductor devices

03 p0486 A69-13610

Transport diffusion cross sections of slow electrons during scattering at inert gas atoms by microwave method, calculating electron transfer coefficients

03 p0481 A69-14143

Electron temperature relation to population ratio in Gunn effect

05 p0810 A69-16576

Frequency and power stable backward wave oscillators as energy pumps for molecular and wideband parametric amplifiers used in satellite receivers

07 p1095 A69-18430

Oscillators and amplifiers based on intervalley electron transfer in bulk GaAs

07 p1096 A69-18442

Current and voltage waveforms of transit time, resonant domain and LSA modes of operation of transferred-electron oscillators

07 p1097 A69-18443

Enthalpies determination of adduct formation of sulfoxides, sulfanilamides and thionylamides with trimethylalane, noting replacement effect on electron donating ability of oxygen

07 p1074 A69-18631

Electron transport of Halobacterium cutirubrum, discussing spectrophotometric identification of cytochromes

07 p1068 A69-19481

Electron transport parameters in noble gases at low electric field intensities, elastic and inelastic scattering and Boltzmann transport equation

08 p1362 A69-20285

F 2 layer cut-off frequency predawn increase caused by sunrise, resulting in photoelectrons transfer along force lines magnetically conjugate point

13 p2257 A69-28712

Pseudospin splitting/peroxide mechanism for O reduction at fuel cell cathodes, analyzing O molecule adsorption, H bonding and electron transfer at surface

16 p2748 A69-32809

Interface electron transport phenomena in stress corrosion, expressing defect movements in terms of electron energy dynamics

19 p3349 A69-36889

Flavoprotein/cytochrome b/559/ role as branch of Halobacterium electron transport in DPNH oxidase determined by salt dependence of reduced DPNH

20 p3484 A69-37101

Photon induced precursor ionization and electron produced wave separation from electrical shock tubes

20 p3511 A69-38240

Electron transport coefficients determined for weakly and fully ionized gases under various conditions

23 p4195 A69-41517

ELECTRON TRANSITIONS

Organic dye lasers energy characteristics excited by monochromatic radiation, investigating radiation absorption during transitions from lower to higher electron-vibrational levels

01 p0090 A69-10381

Coulomb approximation for dipole and quadrupole transitions, calculating tables for radial matrix elements

01 p0124 A69-10901

Ar atom transition probabilities in 5000-6000 angstrom range, noting effect of nonuniform source temperature

01 p0125 A69-10963

GaAs photoemissive yield spectrum analysis, discussing transition energies and energy band structure models

01 p0140 A69-11254

Radiative lifetimes for four N II excited states emitting UV during transition to lower level

02 p0280 A69-11928

Laser transition and photon energy of lightly doped GaAs, showing many body electron-hole-lattice interactions

02 p0257 A69-12615

Induced combinational scattering /ICS/ on IR active transitions, deriving equations with allowance for population variation

02 p0282 A69-12636

High power output CW laser oscillation measured at 4416 A laser transition in Cd 2 using single isotope of Cd 114

02 p0259 A69-12653

Electronic transition moment for C /Swan/ bands measured in shock tube in carbon dioxide and argon mixtures

02 p0285 A69-12833

Molybdenum interband transitions noting low energy optical property anomalies and origin of two absorption bands

03 p0442 A69-12986

- Semiconductor nonlinear electron polarizability, using model to obtain correct order of magnitudes 03 p0483 A69-13035
- F values for Ti II, Cr II and Fe II by empirical astrophysical line strength analysis, discussing f value determination from stellar growth curve 03 p0508 A69-13175
- Electron transition probability of oxygen molecule determined using weak bands telluric lines photoelectric recordings 03 p0420 A69-13276
- Doublet electronic states of benzyl radical, discussing configuration-interaction calculations and transition predictions 03 p0472 A69-13321
- Atomic electron spontaneous transition in theory of direct particle interaction, considering electrodynamic field zero-point oscillations role 03 p0468 A69-13773
- Electrical, optical, magnetic and structural properties of titanium oxide, stressing transition difference with vanadium oxide 03 p0490 A69-13923
- Autoionizing states effects on absorption cross sections for ejection of outer subshell electron from atomic oxygen 04 p0633 A69-15127
- Franck-Condon factors in radiative, excitation and ionization molecular transitions of oxygen, carbon monoxide, nitric oxide, etc 05 p0795 A69-15664
- Vibrational excitation by electron impact in kinetic energy range 30-60 eV studied for water vapor and carbon dioxide, determining intensities relative to elastic scattering 06 p0960 A69-17108
- Semiconductor lasers, discussing electron transitions, radiative band-band transitions, emission and absorption spectra, recombination rates, carrier lifetime and lasing conditions 06 p0937 A69-18009
- Plasma ionization enhancement by laser line radiation matched to specific atomic transitions [AIAA PAPER 69-47] 06 p0972 A69-18186
- Experiments on Josephson tunneling junctions and superconducting contacts to demonstrate quantum electronic properties of superconductors [IEEE PAPER D-7] 07 p1200 A69-19052
- Enhanced two photon emission between 6S and 4S levels of K, discussing stimulated three photon Raman scattering and four photon parametric coupling processes [IEEE PAPER S-8] 07 p1154 A69-19080
- Level crossing effect in stimulated emission and application to determination of hyperfine splitting in Xe 129 excited electronic state during laser transition 07 p1156 A69-19398
- Ligand field transitions in tertiary phosphine and arsine complexes of ruthenium and osmium 07 p1075 A69-19483
- Electron collisional excitation cross section calculations for atoms and ions using modified Born approximation taking into account three physical effects 07 p1187 A69-19658
- Atomic excitation and ionization involving inner shell electrons during collisions between atoms and ions, examining photoabsorption by inner shell electrons 07 p1187 A69-19659
- Electron collision excitation of positive ions, calculating collision cross sections for transitions between levels of P term 07 p1187 A69-19714
- Degree of population inversion and inverse temperature measurement in medium 07 p1137 A69-19761
- Vacuum UV perturbation spectroscopy compatibility with resonance transitions in Ar ion laser 08 p1324 A69-20161
- Mutual influence of two laser modes, showing reduced transition rates due to perturbation of lower level 08 p1325 A69-20283
- Mutual influence of two different laser modes corresponding to two transitions with same ground level, using He-Ne DC laser 08 p1325 A69-20284
- Emission spectrum of laser employing electron-vibrational transitions in samarium doped calcium difluoride crystal, noting spectrum shift with increasing crystal temperature 08 p1326 A69-20544
- Self consistent field calculations of effective quantum numbers for nd, nf and ng electrons for atomic configurations from 2-126 Z 08 p1355 A69-20734
- Oscillator forces and photoionization and photorecombination cross sections of electron transitions in hydrogen atom, considering approximation for total radiation probability 09 p1588 A69-21365
- Galactic and intergalactic ionic fine structure transitions effect on background microwave radiation intensity 09 p1590 A69-21445
- Temperature effect on pulsed laser action on electron transitions in diatomic molecules for rotational relaxation, discussing excitation mechanisms 09 p1520 A69-22654
- Triplet-triplet transitions for Q switching, examining organics for passive Q switches 09 p1520 A69-22682
- Transitions between heavy hole and spin orbit split bands in uniaxially stressed Ge and GaAs, noting spectra for various temperatures and valence band parameters 10 p1745 A69-23359
- Simultaneous action of RF perturbation between Zeeman sublevels of atomic transition sustaining gas laser oscillations, discussing single pi mode laser operation 10 p1704 A69-23808
- Gas laser transitions and power broadening, analyzing saturation and gain profiles of He-Ne laser by light probe 11 p1898 A69-25046
- Multiple scattering in Kapitza-Dirac effect describing electron scattering by standing electromagnetic wave, noting transition probability less than unity 11 p1919 A69-25323
- Thermosphere radiative cooling by atomic O 62 micron line, noting cooling and heating rates 12 p2064 A69-26009
- Organic dye lasers energy characteristics excited by monochromatic radiation, investigating radiation absorption during transitions from lower to higher electron-vibrational levels 12 p2109 A69-26676
- Hydrogenic transition derived excitation temperatures for Wolf-Rayet stars of WC sequence 12 p2160 A69-26904
- Oscillator strengths and wavelengths of X ray and EUV transitions in highly ionized iron line spectra 13 p2326 A69-27554
- Relative transition probabilities for visible Si atom lines, noting disagreement with LS coupling predictions and solar Si abundance determination 13 p2340 A69-27580
- Far IR electronic and vibronic transitions in single crystals of Nd ions in tysonite lanthanide fluorides 13 p2316 A69-27628
- Electron and proton components contribution to reverse current production after particle shower through upper Cu wall of ionization chamber with lower Pb wall 13 p2304 A69-28417
- Excited hydrogen RF spectral lines from nebula NGC 6618, calculating frequency for transitions by Balmer formula 13 p2353 A69-28433
- Electron transition probability of oxygen molecule determined using weak bands telluric lines photoelectric recordings 14 p2487 A69-28784
- Single crystals garnets Raman spectra using laser radiation, separating phonon spectra of host lattices from electronic Raman effect 14 p2507 A69-29334
- Partial wave description for calculating cross sections of fine structure transitions of Na in collision with He, discussing shape resonances 15 p2655 A69-30198
- Transition probabilities of spectral lines in helium-like ions estimated from hydrogen magnetic dipole transitions, discussing single photon decay 15 p2695 A69-30892
- Electron excitation and phase shift method for radiative lifetimes of Ar II UV transitions 15 p2656 A69-31034
- Oscillator strengths calculated for transitions in Si III using dipole length and velocity matrix elements, comparing many electron correlation problem approximations 15 p2656 A69-31158
- Magneto-optical oscillation of absorption coefficient in semiconductors during direct electron transitions 16 p2824 A69-31574
- Laser action and spontaneous emission at atomic oxygen transition, discussing pulsed emission mode in argon-oxygen laser 17 p2982 A69-33633
- Shock tube application to transition probability measurements with emphasis on thermodynamic state of radiating gas, noting temperature dependence of level population 18 p3176 A69-34446
- Oscillator forces and photoionization and photorecombination cross sections of electron transitions in hydrogen atom, considering approximation for total radiation probability 18 p3197 A69-34755
- Computer program to predict spectra from electronic transitions of diatomic molecules and atoms, noting line intensity distribution by Voigt profile 18 p3177 A69-35239
- Resonance effects between H levels by induced electric dipole transitions, using spatially periodic potential barriers 18 p3179 A69-35488
- Self mode locking of carbon dioxide laser with high order transverse mode oscillations in vibrational-rotational transitions of P branch 19 p3330 A69-35602
- Laser emission theory for indirect band-band transitions, considering light absorption by free carriers in semiconductors with polar and unpolar scattering 19 p3332 A69-35873
- Frequency shift dependence in transition of Rb 87 atoms on pulsed pumping intensity, discussing continuous and pulsed indication and peak determination 19 p3336 A69-36345
- Electroreflection study of inversion asymmetry and warping induced interband magneto-optical transitions in InSb, employing low temperature electric field modulation technique 19 p3386 A69-36521
- Fe-doped p-type gallium arsenide single crystal radiative recombination emission during current carriers transition from deep acceptor level into valence band 19 p3392 A69-36611
- Rotational analysis of O_2 band of gamma-prime system of TiO molecule, considering transition to ground state 20 p3577 A69-38170
- Effective Gaunt factors for threshold excitation of positive ions by electron collisions for 23 dipole transitions in 15 isoelectronic sequences 20 p3581 A69-38175
- Unquantized field calculations extended to include atomic field effect on atom, predicting spontaneous decay rate from excited state and light frequency time dependence 21 p3769 A69-38578
- Thermally insensitive technique for atomic transition probability measurement 22 p3983 A69-40100
- Hydrogen high level transition probabilities formula, giving two tables of oscillator strengths [AFCLR-69-0301] 22 p3983 A69-40149
- Level shifts and spontaneous transitions in steady state of universe by path integral method of first quantization, considering time symmetric electromagnetic theory 22 p3980 A69-40169
- Molecular N UV spectrum at various pressures, showing absorption band dependence on pressure induced dipole transitions 22 p3986 A69-40723
- Off-diagonal matrix elements of Breit interaction between singlet-triplet transitions for helium isoelectronic sequences 22 p3986 A69-40783
- Chemical high pressure laser action produced by stimulated phototransition of electrons at contact moment between pair of reacting nonexcited gas molecules 22 p3965 A69-41117
- Pulsed Hg ion-He laser operation, revealing transition in near IR 23 p4171 A69-41393
- Hydrogen fluoride chemical laser emission spectrum, studying rotational-vibrational transition of molecules triggered optically or electrically 23 p4172 A69-41493
- Autoionized resonance transitions of He at 206.2-192.2 Å using He continuum produced by capillary spark, also producing He II line spectra 23 p4191 A69-42149
- Transitions competition in He-Ne laser pulse operating in single mode with nonuniform gain saturation 24 p4328 A69-43165

ELECTRON TUBES

NT BACKWARD WAVE TUBES
 NT CAMERA TUBES
 NT CARCINOTRONS
 NT CATHODE RAY TUBES
 NT CESIUM DIODES
 NT COLD CATHODE TUBES
 NT GAS DISCHARGE TUBES
 NT HELITRONS
 NT IMAGE DISSECTOR TUBES
 NT IMAGE ORTHICONS
 NT IMAGE TUBES
 NT KLYSTRONS
 NT MAGNETRONS
 NT MICROWAVE TUBES
 NT PHOTOMULTIPLIER TUBES
 NT PHOTOTUBES
 NT PICTURE TUBES
 NT PLANOTRONS
 NT THERMIONIC DIODES
 NT THYRATRONS
 NT TRAVELING WAVE TUBES
 NT VACUUM TUBE OSCILLATORS
 NT VACUUM TUBES
 NT VIDICONS

Electron tubes in phased array radar systems, discussing replacement limits by solid state devices, reliability and cost reduction

01 p0048 A69-11040

Transistors vs electron tubes as microwave power sources in UHF phased array radars, noting transistor cost competitive limit

01 p0048 A69-11041

Tube and transistor type quartz crystal FM oscillators circuitry and operating characteristics, discussing generation of three frequencies

05 p0732 A69-16532

Electronic tubes utilization in space flight, summarizing characteristics and satellite applications

07 p1093 A69-18421

Inertia limited flow transition to mobility limited flow in gas diodes by taking velocity moments of Boltzmann equation for electron velocity distribution function

09 p1462 A69-21325

TR tubes spurious harmonic power generation investigated for intersystem interference reduction and design criteria, discussing effects of incident power, gas pressure and tube geometry

15 p2573 A69-30032

Tubes faults monitoring in three phase Graetz convertor bridges by measuring voltage across DC smoothing inductor

15 p2575 A69-30180

Unsuccessful space charge noise suppression measurements on field emission tubes, obtaining diffusion and shot noise measurements at high currents

16 p2752 A69-32384

Far IR radiation generation, considering incoherent sources, harmonic generators, electron tubes, relativistic electrons and quantum oscillators

22 p3982 A69-40669

Heat pipe design for electron tubes cooling at various temperatures, including dielectric heat pipes and traveling wave tubes
 [ASME PAPER 69-HT-25]

24 p4412 A69-43543

ELECTRON TUNNELING

WKB approximation for metal-semiconductor junction tunneling and transmission coefficient of parabolic barrier, discussing density of states in degenerate semiconductors

02 p0301 A69-12652

Superconductor tunnel junction with noise, calculating frequency pulling, radiation linewidth and voltage power spectrum in AC Josephson effect

03 p0486 A69-13387

Tunnel breakdown in p-n junctions used to generate microwave oscillations, discussing Si and Ge properties

03 p0492 A69-14163

Low temperature conductance peaks observed in tunneling measurements on aluminum-phosphosilicate glass-degenerate silicon sandwich structures

03 p0493 A69-14183

Electron phonon coupling in barriers of GaAs Schottky diodes, noting first and second derivatives of I-V characteristic in n-type GaAs-Pd Schottky diode

03 p0493 A69-14242

Incremental conductance of heavily doped n-type Si semiconductor barrier tunneling as function of bias voltage, indicating Fermi level dependence on dopants

05 p0808 A69-16285

Impact ionization and tunneling effect during electroluminescence of zinc sulfides

06 p0980 A69-17261

Electron and phonon tunneling spectroscopy in metal Ge contacts, noting improved agreement with one electron model

06 p0982 A69-18234

Richardson constant and tunneling effective mass for thermionic and thermionic field emission in Schottky barrier diodes

07 p1089 A69-18247

Surface plasmon excitation by tunneling electrons in GaAs-Pb junctions, discussing conductance at bias voltages, plasmon energy and concentration

07 p1200 A69-19402

Radiative tunneling shifting peak spectra in abrupt asymmetrically doped GaAs junctions

09 p1544 A69-21336

Stationary Josephson effect used to determine fluctuations influence on superconducting tunneling

09 p1556 A69-21669

Trapping state effect on tunneling probability in Schottky barriers, discussing current-voltage characteristics

09 p1557 A69-21748

Josephson effects in superconductivity and superfluidity including electron tunneling DC and AC effects, basic and double junctions

11 p1938 A69-25240

Current and electroluminescence brightness dependence on reverse voltage in n-SiC diodes including tunnel and avalanche processes

15 p2573 A69-30062

Superconductive tunneling measurements on thin Al films, discussing enhanced transition temperatures, energy gap dependence on temperature, electron microscope observation of crystallites, etc

16 p2825 A69-31634

Field ionization at metal surfaces as rearrangement collision, considering anisotropic electron tunneling probabilities produced by Fermi surface

17 p3015 A69-32821

Electron-plasmon interaction in degenerate semiconductors, using mathematical model for rectifying metal contacts tunneling characteristics

19 p3382 A69-36049

Diagonal tunneling and radiation polarization in doped heterojunctions and p-n junctions of GaAs, using electroluminescence spectrum analysis

24 p4362 A69-43737

ELECTRONIC AMPLIFIERS
U AMPLIFIERS

ELECTRONIC CONTROL

Mechanically and electronically despun spacecraft antennas, comparing designs and projected performances for spin stabilized Intelsat 3 satellite

06 p0897 A69-17590

Electronic controller with integrated circuits and inexpensive SCR as coupler or interface between card reader and frequency synthesizer designed for unattended operation

06 p0897 A69-17704

Direct coupled monolithic IF amplifier with active gain control, analyzing large signal response, stability, available gain and noise behavior

07 p1104 A69-18885

Electron-optical image converter camera for wide time intervals, considering nanosecond electronic control and high voltage stabilized power supply

12 p2083 A69-26140

Transistorized VOR system using electronic goniometer and fixed antennas, describing power supply, transmitter, goniometer, antenna and design

16 p2827 A69-31938

Beam control of optically fed two axis airborne electronically scanned phased arrays by on-array and off-array processing

17 p2942 A69-34085

Air traffic control/electronics automation developments and controllers responsibilities in Great Britain and Netherlands

18 p3168 A69-34805

Concorde Olympus 593 engines electronic control and adjustment devices

19 p3395 A69-36706

Servovalves with fluidic and electrical inputs compared for gas servoamplifiers performance, considering use as sensors in closed-loop hydraulic circuit

19 p3255 A69-36711

Thermostatic electronic control device of birefringent filter in Wroclaw Observatory coronagraph during prominence observations

22 p3943 A69-40000

Electronic measurement and control in industry - Conference, Budapest, 1969

22 p3915 A69-40934

Electronically controlled microwave phasers and time delay elements design and operation, discussing beam width, steering and effects, directivity and planar arrays

23 p4135 A69-41353

Integral cell-level electronic charge controls for secondary batteries, emphasizing performance, reliability and power system interfaces

23 p4076 A69-42542

Tensor analysis of brushless DC motor controlled by transistors, discussing torque phase, torque variation phase and efficiency phase characteristics

24 p4255 A69-42678

Mechanization of analog electrical-to-fluidic transducer using carrier circuit techniques and piezoelectric bender drive assembly

24 p4315 A69-43026

ELECTRONIC COUNTERMEASURES

NT CHAFF

Soviet book on electronic countermeasures and intelligence covering jamming methods for automatic systems

03 p0385 A69-12927

Radar or ECM/ECCM system simulation by digital computer, using signal and jamming spectral inputs

03 p0400 A69-13200

Avionics and electronic countermeasures equipment design, development, installation and application problems for high performance military aircraft to meet hostile electronic environment
 [AIAA PAPER 69-822]

19 p3243 A69-35599

Microcircuit phased array electronic countermeasures system design and hardware techniques for aerospace applications, analyzing adaptive, retrodirective and combination array systems

24 p4287 A69-43110

ELECTRONIC EQUIPMENT

NT AVALANCHE DIODES
 NT CRYOTRONS
 NT CRYSTAL RECTIFIERS
 NT GALLIUM ARSENIDE LASERS
 NT GERMANIUM DIODES
 NT JUNCTION DIODES
 NT JUNCTION TRANSISTORS
 NT METAL OXIDE SEMICONDUCTORS
 NT MICROMODULES
 NT PARAMETRIC DIODES
 NT PHOTODIODES
 NT PHOTOVOLTAIC CELLS
 NT RUBY LASERS
 NT SEMICONDUCTOR DEVICES
 NT SEMICONDUCTOR LASERS
 NT SILICON TRANSISTORS
 NT SOLID STATE DEVICES
 NT SOLID STATE LASERS
 NT THERMISTORS
 NT THYRISTORS
 NT TRANSISTOR AMPLIFIERS
 NT TRANSISTORS
 NT VARACTOR DIODES

Cloud pictures from weather satellites reception according to automatic picture transmission /APT/ system, discussing design and field strength measurements

[UN PAPER 68-95451]

01 p0108 A69-10458

Small earth stations in future communication satellite systems, discussing applications, characteristics and equipment

[UN PAPER 68-95751]

01 p0028 A69-10492

Chemical phenomena during explosions of wires in various gaseous atmospheres, using apparatus with electronic crowbar for current flow regulation

01 p0081 A69-10680

Electronic device networks periodic structures accuracy estimated by automatic measurement of complete error spectrum of network spacings

01 p0045 A69-10732

Variable impedance matching device employing lumped and homogeneous circuit elements and stub line technique

01 p0046 A69-10740

Electronics and aerospace systems - IEEE Conference, Washington, D.C., September 1968

03 p0385 A69-13176

Avionics, discussing use of electronics in control of aerospace vehicles

03 p0431 A69-14085

Electronic scanning radar systems design, discussing beam types, bandwidth, tracking, target acquisition, etc

04 p0556 A69-14301

Time averaged products and squares of fluid turbulence signals at LF, using Hall effect multiplier device and integrating voltmeter

04 p0601 A69-15116

Flat cable terminating techniques for electric and electronic systems

04 p0578 A69-15217

Solid state precision frequency standard for L multiplex carrier equipment, using four precision quartz crystal oscillators

04 p0561 A69-15451

Ground station electronic environment, telemetry encoding and radio links for spacecraft communications and tracking

06 p0886 A69-16860

Transversal equalizer circuit consisting of delay line and variable sampler and reinjection coupler for microwave frequencies

07 p1102 A69-18671

Computer aided design methods for electronic and mechanical materials, discussing basic concepts and problems

08 p1278 A69-19971

Thermal stabilization and ethylene oxide effect on spaceborne electronic component sterilization and decontamination

08 p1283 A69-20266

Automation and instrumentation - Conference, Milan, November 1968, Volume 1

08 p1296 A69-20301

Ultrahigh speed systems and logic circuits specifications implementation into electrical design, discussing circuit selection, line propagation delays, noise margins and temperature effects [AGARDOGRAPH-114]

08 p1298 A69-20985

Electronic terminal guidance requirements for all-weather VTOL operations, suggesting future first generation landing system

08 p1348 A69-21064

Assessing cost effectiveness of reliability and quality of semiconductor products, using mathematical models

08 p1292 A69-21102

Electronic components reliability tests, determining correlation between material quality and failure

08 p1293 A69-21109

Process control data in acceptance procedures for high reliability electronic components, discussing supplier and user cooperation

08 p1293 A69-21110

Conventional electronic and microelectronic circuits reliability, discussing external stress effects on improvement in avionics and rocket applications

08 p1293 A69-21112

Integrated semiconductor circuits reliability in electronics and microelectronics, discussing hybrid and monolithic circuits in thin/thick film design and on Si monocrystals

08 p1294 A69-21118

Large scale electronic systems configuration compatibility concept, discussing modular line replaceable units [LRU/ assigned set of numbers

08 p1322 A69-21154

Soviet book on electronics and radio instruments of flight vehicles, covering radars and antennas, automatic pilots and design

09 p1463 A69-21930

Accelerated reliability tests of electronic capacitors using voltage as main forcing factor, establishing correlations between lifetimes in accelerated and long term tests

09 p1464 A69-22244

Thick film hybrid circuit technology and equipment reviewing conductors, resistors, and insulator inks

09 p1508 A69-22337

Polyimide materials, discussing lamination and applications in electronic circuitry such as interconnection cables and multilayer interconnection boards

09 p1511 A69-22354

Digital computer simulation as maintainability design and prediction tools, discussing fault localization in complex electronics systems

10 p1668 A69-22974

Electronic circuit analysis by computer programming including system and program commands, network data, output control, discussing steady state circuit programming

10 p1659 A69-23143

Skorsky HH-3F helicopters electronic equipment, discussing communication and navigation aids, search and recovery missions, etc

10 p1662 A69-23222

Reliability function for electronic device during initial period of operation, based on use of lower bound

10 p1662 A69-23318

Digital design techniques for electronic equipment including measuring instruments, generators, synthesizers, etc

10 p1664 A69-23796

High energy radiation effects on electronic components in space missions, noting simulation tests and shielding

11 p1946 A69-24521

Real time electronically scanned radar control using digital computer with input and output conversion for information handling, noting interface equipment

11 p1834 A69-24544

Soviet book on electroluminescent devices covering panels, indicator contrast levels, control, multicolor indicators, image conversion and storage and optoelectrical systems

11 p1850 A69-24976

Modular designed automatic test system consisting of central computer controlled system with multiplexed remote test stations for depot level maintenance

11 p1864 A69-25067

Computer simulation application to electronic systems, discussing design, performance optimization, implementation and environmental effects

11 p1843 A69-25319

Reliability planning role in directing business functions to quality efforts integration in engineering, production and testing of electronic equipment

12 p2102 A69-25971

Digital computer-aided reliability engineering methods for electronic equipment design and analysis

12 p2037 A69-25973

Nuclear explosions electromagnetic effects on electronic systems, considering signals emitted from fireball and signal attenuation by changed atmospheric propagation

13 p2234 A69-28344

Parameters optimization in electronic equipment design, considering parameters and efficiency criteria as additive elements functions of dimensional chain

14 p2418 A69-28835

Quartz oscillator with electronic temperature compensation, noting reduced size, weight and power consumption

14 p2420 A69-29398

Electronic systems packaging substitution method for optimized malfunction isolation at succeeding levels to final discard-at-failure

14 p2420 A69-29494

Reliability of electronic components for space - Conference, Grenoble, November 1968

15 p2622 A69-30816

Computer aided design [CAD/ of component selection for circuit optimization applied to circuit performance and sensitivity calculations

15 p2628 A69-30849

Automatic hybrid apparatus for solving linear equations, using Gauss-Seidel iterative method and stressing control arrangement, communication circuits, etc

15 p2572 A69-31089

Electronic equipment for data acquisition in extraterrestrial experiments including low noise charge amplifiers, discriminator, pulse lengthener, linear gate and logarithmic amplifier

16 p2759 A69-31857

Polish electronic measurement devices operating principles and specifications including vibration, frequency and pressure meters, fatigue testing machines, etc

16 p2790 A69-32076

Thermal silicone grease type filler materials for heat transfer across bolted or clamped sheet metal surfaces in electronic equipment for space applications

16 p2794 A69-32560

Integrated circuits effect on electronic equipment design and production technology

16 p2762 A69-32578

Wire-wrap solderless joints production technology in electronic equipment

16 p2763 A69-32579

Electronic device utilizing scanning beam to evaluate limb photographs, reducing errors by introducing second generator with frequency proportional to deflecting potential variation

17 p2970 A69-32884

Cosmic ionizing radiation effects on electronic elements operation based on radiation and matter interaction principles

17 p2937 A69-33583

Automatic device for logarithmic damping decrement measurement from vibrograms, showing structural arrangement and electrical circuitry

17 p2976 A69-33931

Electric power quality effects on aircraft electronic utilization equipment, discussing characteristics of variable speed constant frequency [VSCF/ generating system

17 p2905 A69-34091

Series 3 Skyvan design, describing controls, electric and electronics equipment, weather protection, environmental and fuel systems

17 p2906 A69-34194

Development, manufacturing and logistic costs of reliability improvement in electronic equipment design

18 p3231 A69-34485

Physics of Control program for electronic devices reliability, discussing qualified parts, chemical, physical and electrical properties, parameter ranges, specifications and corrective action

18 p3143 A69-34488

Radiation resistant devices for minimizing neutron and gamma radiation effects on military electronic components, discussing selection features and sampling lot sizes

18 p3144 A69-34491

Prefailure detection of unreliable electronics parts from random samples of received parts lots, noting cost reductions

18 p3146 A69-34508

Equipment maintainability demonstration technique, discussing simulation, repair time rates mathematical distribution, range and limits

18 p3117 A69-34530

Apollo 10 lunar landing module, detailing weight, shape, electronic system and rendezvous radar

18 p3207 A69-34629

Book on digital electronics for scientists covering digital circuits and instruments for measurement, control or computation

18 p3112 A69-34915

Fire-retardant thermoplastic and thermosetting materials for electronics industry use including blending of fire-retardant additives into plastics

18 p3162 A69-35273

Electronics applications of superconductivity including inductors for energy storage, computer elements and magnets, cavities for microwave circuits, signal generators and detectors, etc

19 p3382 A69-35807

IEEE Conference - San Antonio, April 1969

21 p3676 A69-39437

Electronic terminal guidance requirements for all-weather VTOL operations, suggesting future first generation landing system

22 p3978 A69-39875

Thermal protection for air-launched missile electronics during carry and free flight, considering active, passive and combination systems and weight penalties

22 p4049 A69-39943

Electronic equipment thermal control, describing design and use of heat pipes

22 p4049 A69-39944

Techniques to control, measure and assure reliability of electronics systems and equipment, emphasizing Thorndike chart and Molina tables

22 p3953 A69-40026

Reliability testing and parts screening of electronic systems for best parts selection

22 p3953 A69-40029

Electronic equipment environmental cooling by controlled airflow systems, reviewing systems designs, control problems, etc

22 p3954 A69-40035

Electronic measurement and control in industry - Conference, Budapest, 1969

22 p3915 A69-40934

Digital signal processing electronic device for linearizing signals from sensors with nonlinear frequency output by modifying time signal frequency

22 p3915 A69-40935

Two channel electronic system with one redundant channel for automatic replacement in case of failure evaluated for operational preparedness

23 p4136 A69-41559

Equipment reliability determination from relations for efficiency characteristics of stochastic queueing system with finite number of sources having Markov character

24 p4287 A69-43129

ELECTRONIC EQUIPMENT TESTS

Test procedure for obtaining large signal S characterization of nonlinear power transistors

02 p0214 A69-11600

Electronic system checkout in SAAB 37 Viggen, using computer controlled test equipment

05 p0726 A69-16767

Synthetic circuit equipment for semiconductor rectifier life testing with built-in fault analyzer for indicating shorted and broken diodes

08 p1293 A69-21113

Automatic transistor reliability testing system based on measured data and reliability research
08 p1294 A69-21119

Reliability in microelectronics estimated from failures expected during lifetime, describing various test methods
08 p1294 A69-21121

Computer controlled flight line tester performing automatic real time testing of aircraft avionics systems on flight line or hanger
11 p1864 A69-25060

Computer controlled testing of commercial aircraft avionics systems for automatic, semiautomatic and manual operation to perform repair and calibration tasks
11 p1864 A69-25061

Single purpose, multipurpose and multistation automatic test systems for production and maintenance
11 p1864 A69-25068

In-circuit diodes testing by semiautomatic low current regulated voltage test set
12 p2035 A69-25835

Plasma diagnostics FM phase meter circuits tests, considering raster phase indicators, phase detectors and frequency integrators
14 p2497 A69-29797

Scientific satellite 1 solar cell panels power output dependence on temperature and spin calculated and compared with results for outdoor sunlight
15 p2552 A69-30072

Pulse generator to accommodate electronic system testing to shock response spectrum by simulating real world shock environment
15 p2585 A69-30360

Flight worthiness of mishandled electronic equipment, analyzing fragility and performance of shock exposed components and connections
15 p2576 A69-30362

Integrated circuit failure analysis in military and space applications utilizing type-test programs
15 p2624 A69-30820

Electronic components reliability by failure rates and drift behavior, assuming probabilities product rule and exponential law of life distribution
15 p2626 A69-30835

Radiology and thermography in nondestructive reliability testing of electronic equipment
15 p2610 A69-30850

Reliability testing of development models during production, considering short term and large batch tests
15 p2579 A69-31036

Semiconductor rectifiers economic life testing with synthetic circuits utilizing thyristor switch
15 p2579 A69-31041

Diode burn-in dissipation measurement for reliability testing
15 p2579 A69-31043

Electronic hardware optimum quality assurance selected by dynamic programming in terms of failure mechanism detection efficiency per source allocation
15 p2722 A69-31127

Quality control of high volume microelectronic circuit assembly of military computer emphasizing preventive action
15 p2580 A69-31129

Integrated circuits screens, developing sequence of life and environmental tests to remove units of potential reliability hazards
15 p2580 A69-31130

Large scale integrated MOS devices tests for space applications, establishing quality specifications
15 p2580 A69-31131

Failure analysis techniques in electronic component reliability laboratory, discussing electrical and physical tests to detect weaknesses in manufacturing and design
15 p2722 A69-31133

Electronic component life test sampling plans based on lognormal distribution and instantaneous failure rate or hazard rate criterion
15 p2630 A69-31137

Semiconductor devices leak testing methods including liquids, helium mass spectrometer, Radflo and hermetic seal tests
16 p2758 A69-31712

Metal oxide semiconductor integrated circuits, showing failure rates and degradation causes
16 p2759 A69-31851

Aircraft solid state electric system logic level tested functionally by built-in test equipment (BITE) operated on ground during preflight tests
17 p2977 A69-34110

Electromagnetic compatibility (EMC) hardware design, discussing NDC 1060 computer configuration, requirements and service environment
17 p2947 A69-34136

AGREE /Advisory Group on Reliability of Electronic Equipment/ testing philosophy, emphasizing environmental tests
18 p3143 A69-34481

Failure analyses of semiconductor devices for military use, suggesting modifications to MIL-STD reliability screen tests
18 p3108 A69-34499

Reliability prediction in electronics, discussing basics, advances, limitations, etc
18 p3146 A69-34514

Leak tests for sealed electronic circuits using helium mass spectrometer
18 p3138 A69-35271

Materials evaluation for devices with long term underground exposure, including field tests at tropical locations
19 p3321 A69-35568

Communication equipment reliability improvement through testing and failure analysis
19 p3282 A69-35783

Integrated circuits failure analysis techniques utilizing pin-to-pin curve tracer tests and thermal measurements
19 p3282 A69-35786

Bayesian reliability demonstration tests for predetermining sample size producer and consumer risks for equipment with exponential and binomial failure distributions
19 p3327 A69-36039

Visual inspection, thermal and mechanical shock, burn-in and hermeticity tests of microelectronic equipment, reviewing test methods and procedures of MIL-STD-883 program
19 p3284 A69-36043

Hazard and renewal rate and bathtub curves for electronic equipment reliability, noting single and multiple probability densities
20 p3504 A69-37070

MIL-STD-781B reliability tests with standard based on exponential distribution for equipment exhibiting constant failure rate, noting sampling
20 p3551 A69-38289

Metallurgical, chemical and mechanical analyses and high stress tests application to verification of electronic device reliability, noting failure modes and rate
22 p3953 A69-40030

MERA /Molecular Electronics for Radar Applications/ modules testing in planar array simulator, measuring far field amplitude patterns in transmitting and receiving modes
22 p3912 A69-40067

Solar array configurations and performance on Martian surface, including hard lander design and surviving shock levels
23 p4073 A69-42289

Quality and reliability of electronic spacecraft devices and structural components produced in limited quantity, discussing documentation of production and testing
23 p4171 A69-42474

All-equipments reliability test improved by removing usual truncation and extending accept- reject lines of test plan MIL-STD-781
24 p4321 A69-43203

Microelectronics test program consisting of four reliability screening levels based on Mil-Std 883
24 p4287 A69-43205

ELECTRONIC FILTERS

Integrated circuit digital filters design characterized by weight coefficients containing Lanczos factor for application to processing of signal transmitted from space vehicles
01 p0038 A69-10071

Multistub filter for microstripline using shorted and open stubs
01 p0041 A69-10200

Nonreciprocal tunable yttrium-iron garnet microstrip filter design through generation of circularly polarized field
01 p0041 A69-10202

Optimal predictor design by comparison of statistical input models, measuring signal filter performance by root-mean-squared errors
01 p0043 A69-10558

Digital matched filtering technique for RF interferometer employing carrier modulated by pseudonoise sequence, discussing applications to antenna arrays
01 p0048 A69-11003

Miniaturized adding sample and hold device with adjustable delay applied to digital filters
04 p0574 A69-14350

Line filter compression and positioning of bipolar video pulse trains for conjunctive use with moving target indicator in echo elimination
04 p0558 A69-15071

High speed modular multiplier and digital filter for LSI development
04 p0567 A69-15354

Digital filter transfer functions design by sampled data transformation, noting role of analog filters
04 p0584 A69-15461

Special purpose computer for implementing programmable digital filter used in sampled data control systems
04 p0569 A69-15462

Digital filters for moving target indicator radars compared with analog filter systems
04 p0580 A69-15463

Interpolation filters with restricted transmission zeros in transmission function capable of reconstructing continuous function from equidistant sample values
05 p0735 A69-16617

Expressions for calculating filtering errors resulting from insufficient information about useful signal and noise characteristics
05 p0740 A69-16668

Balanced diode shunt bridges with electronically tunable carrier selection high-Q N-path filter from 0 to 200 kHz, using single integrated module
07 p1089 A69-18249

Random filters and stabilization of periodic signals mixed with noise, establishing second order statistics at output
07 p1089 A69-18281

Parasitic reactance disturbing attenuation and return loss of reactance filters, discussing correction of numerator polynomial of characteristic function
08 p1283 A69-20128

Spherical electronically tunable multiresonator YIG filters design using filter tables and coupling bandwidth charts
08 p1292 A69-21006

Chebyshev error norms of polynomial approximations for ideal filter minimized by emphasizing role of transfer function even and odd parts
08 p1299 A69-21168

Filter design using transformed frequency variables suitable for computer programs
08 p1300 A69-21172

Insertion-loss synthesis of narrow band crystal band-elimination filters, using narrow band approximation and pseudoreactance theory
08 p1300 A69-21173

Equal element elliptic function filters, noting lower dissipation loss when applied to bandpass and bandstop filters
08 p1300 A69-21175

Discrete predicting filter optimal synthesis in terms of rms error by solving normal Gaussian equations
09 p1473 A69-21858

Precision trimmed RC active networks for high selectivity microelectronic filter fabrication for frequency division multiplex applications
09 p1466 A69-22452

Joint filter optimization in combination analog-digital hybrid multilevel transmission system
09 p1457 A69-22465

Signal conditioning amplifiers covering carrier and DC amplifiers, differential amplifiers, charge amplifiers and active filters
10 p1691 A69-23230

Noise in instrumentation systems, considering coupling and current noise source and reduction by isolation and filtering
10 p1691 A69-23231

Output pulse duration calculation for compressing filter in presence of pulse or continuous FM noise, using parallelogram of arguments method
11 p1844 A69-24445

Recursive estimation of noisy nonlinear multivariable systems in white noise by Kalman, second order nonlinear and iteration filters
12 p2046 A69-26062

Optimal filtering of linear distributed parameter systems corrupted by boundary and/or volume stochastic disturbances
15 p2565 A69-30183

Feedback realization of continuous optimal filter applied to designing servomechanisms with stochastic inputs and disturbances
18 p3110 A69-34673

- Single loop directional stripline filters synthesis, including general expression for frequency characteristics based on wave matrices
19 p3284 A69-36570
- Transmission filter to improve voice communication intelligibility and SNR, describing applications to nonlinear circuits
20 p3505 A69-37293
- Electromagnetic compatibility (EMC) filter design and test methods to achieve effectiveness and reliability, emphasizing transfer impedance characteristics
23 p4142 A69-42233
- Recursive estimation of noisy nonlinear multivariable systems in white noise by Kalman, second order nonlinear and iteration filters
23 p4146 A69-42447

ELECTRONIC LEVELS
U ELECTRON ENERGY
U ENERGY LEVELS

ELECTRONIC MODULES
NT MICROMODULES

- Electronic module testing with integrated hardware/software system, noting module test console and manual capabilities
11 p1864 A69-25065
- Semiautomatic and automatic off-line module testing machines, comparing costs for different test populations
11 p1865 A69-25076
- Spacecraft integration electronics modular packaging, discussing slice housing concept and design criteria including environmental resistance, reliability, performance, etc
22 p3910 A69-39949
- Modular configuration of recoverable scientific MAP/Modular Auroral Probe/ payloads aboard Nike-Apache rockets, discussing payload design concepts
23 p4223 A69-41763
- Modularized static AC and DC inverters and converters for aerospace electrical power conditioning systems, discussing circuit functions and performance tests
23 p4073 A69-42292

ELECTRONIC PACKAGING

- Electronic packaging techniques for long life spacecraft, discussing effects of mechanical and electrical stress, temperature cycling, vacuum, radiation and contamination
01 p0038 A69-10145
- Integrated circuits technology, discussing thin film, monolithic compatible and hybrid circuit techniques
02 p0216 A69-12050
- Plastics in electronic packaging - Conference, Binghamton, New York, October 1968
04 p0620 A69-14953
- Electric components encapsulation by combining liquid resin techniques and transfer molding
04 p0607 A69-14955
- Medium scale integration for packaging hybrid electronic monolithic systems
05 p0735 A69-16752
- Semiconductor device failure modes temperature dependence, discussing bonds, metallization and packaging
06 p0894 A69-17218
- Spacecraft component heat sterilization, discussing heat effects on electrical connections, polymers and adhesives
08 p1284 A69-20267
- Hybrid circuit technology application to packaging electronic systems
09 p1508 A69-22336
- Low temperature low cost dip brazing technique for light weight magnesium alloy electronic packaging structures, noting distortion
09 p1509 A69-22346
- Flat flexible printed circuitry in AWG-10 missile control system on F-4J, regarding wire harness packaging
09 p1511 A69-22356

- Electronic systems partitioning in preparation for MOS large scale integration for system performance and cost improvement
09 p1466 A69-22451
- Electrical, thermal and mechanical requirements in design of Landing Radar Electronic Assembly for Apollo Lunar Module
10 p1663 A69-23537
- Integrated circuits, discussing development from transistors and vacuum tubes, operation, fabrication and applications
12 p2038 A69-26331

- Fabrication techniques for plastic insulation in electronics, discussing packaging, low pressure molding, casting, etc
13 p2285 A69-27987
- Doppler radar clearance hole packaging method for ruggedized dual in-line integrated circuits with conventional etching, tooling and double-sided printed wiring techniques
14 p2419 A69-29102
- Electronic systems packaging substitution method for optimized malfunction isolation at succeeding levels to final discard-at-failure
14 p2420 A69-29494
- Engineering problems in IC microminiaturization, dividing devices according to suitability for microminiaturization
15 p2576 A69-30352
- Large scale integration /LSI/ and medium scale integration /MSI/ circuits evolution and requirements, noting onboard computers and space applications
15 p2625 A69-30825
- Epoxy encapsulated transistors reliability, data from long term maximum rated life and accelerated tests
18 p3145 A69-34498
- Leak tests for sealed electronic circuits using helium mass spectrometer
18 p3138 A69-35271
- Seam and stitch welding in miniaturized semiconductor package fabrication, including leak rate tables
18 p3149 A69-35272
- Epoxy molding compounds performance on DIP integrated circuits, determining comparative moisture protection provided by encapsulants
19 p3280 A69-35546
- Glass encased electronic components with conformal coatings, considering glass breakage at low temperature
19 p3281 A69-35547
- Transfer molded epoxy dielectrics, comparing encapsulation rate, pressure and cure times to compression molding
19 p3281 A69-35548
- Microelectronics role in maintenance and maintainability of subminiature solid state components, emphasizing functional packaging at module level
19 p3283 A69-36021
- Electronic packaging and production - Conference, Anaheim, February 1969 and Philadelphia, June 1969
22 p3909 A69-39941
- Environmentally sealed connector for avionics packaging with die-cast Al alloy shell meeting specification ARINC 404 requirements
22 p3910 A69-39946
- High voltage power supply electronic subsystem for electric propulsion of ATS-D satellite, describing packaging, temperature control and performance in simulated space environment
22 p3999 A69-39948
- Spacecraft integration electronics modular packaging, discussing slice housing concept and design criteria including environmental resistance, reliability, performance, etc
22 p3910 A69-39949
- Dual role core /Ducor/ memory system with unique core stack assembly feature to achieve cost reduction and structural integrity for severe environmental conditions
22 p3903 A69-39950
- Flexible circuitry for reliable spaceborne data processing equipment electronic packaging
22 p3903 A69-39951
- Hybrid microelectronic modules, using basic thermal design guidelines
22 p3910 A69-39952
- Encapsulation effects on piece parts in high density package, considering unexpected part failures elimination in Lunar Module Signal Conditioning Electronic Assembly
22 p3910 A69-39953
- Handbook of electronic packaging including rigid and flexible printed wiring, soldering and mechanical interconnections, bonding, computer and military applications, etc
22 p3911 A69-40046
- Micromodule unsteady thermal behavior reduced to calculating linear heat flux for boundary conditions containing temporal and spatial derivatives
23 p4136 A69-41558

ELECTRONIC PHOTOGRAPHY
U ELECTRO-OPTICAL PHOTOGRAPHY
ELECTRONIC RECORDING SYSTEMS

- Portable amplitude and frequency recording system for studying ionosphere by radio signals from artificial satellites
04 p0597 A69-14748

- Diffraction pattern recording technique and application to thin film measurements
09 p1499 A69-22303
- Electronic data processing facilitating engineering design development work, including computer programming
18 p3106 A69-34838

ELECTRONIC SIGNAL MEASUREMENT
U SIGNAL MEASUREMENT
ELECTRONIC SPECTRA

- Relation between energy spectrum and potential drop in plasma expelled from hot cathode tube into vacuum derived by electrostatic analyzer
06 p0963 A69-16899
- Impurities effect on electron energy spectrum in semiconductors at zone boundary and arbitrary doping levels, using Green function
09 p1554 A69-21467
- Inverse problem method for reconstructing electrons differential spectral cross sections and photon pair formation in electron photon cascade
13 p2303 A69-28415
- Impurities effect on electron energy spectrum in semiconductors at zone boundary and arbitrary doping levels, using Green function
15 p2669 A69-30712
- Cosmic ray electron spectrum data obtained by balloon flights, showing electron flux reduction above 500 Mev with increasing solar activity
16 p2851 A69-32566
- Rocket instrumentation for electron and proton spectra measurement in aurora borealis
17 p2972 A69-33038

ELECTRONIC STRUCTURE
U ATOMIC STRUCTURE
ELECTRONIC SWITCHES
U SWITCHING CIRCUITS
ELECTRONIC TRANSDUCERS

- Design and development of electrical transducer and associated instrumentation for fluid pressure measurement
03 p0427 A69-12914
- Onboard aircraft weighing system /OBAWS/ for accurate gross weight and CG measurements, describing axle shear deflection transducer system
10 p1693 A69-23276
- HF electromagnetic decoupling pressure gage, using transducer with solid state strain gages as sensing elements
15 p2611 A69-31029
- Differential capacitance transducer measuring small displacements in heated transformer oil, air, castor oil or glycerin
22 p3946 A69-40439
- Capacitance sensor of vertical with flexible mobile electrode, describing diagram and operation
23 p4163 A69-41550

ELECTRONICS

- Physical electronics, discussing gas discharges, semiconductor devices, electron emission, noise in electronic devices and masers and lasers
05 p0735 A69-16666
- NASA civil aviation electronics research program, discussing feasibility of V/STOL aircraft all-weather operations
05 p0850 A69-16718
- Photoelectronic imaging systems in space exploration emphasizing acquisition time, storage capacity and transmission time
07 p1136 A69-19591
- Reliability in electronics - Conference, Budapest, October 1968, Volume A
08 p1321 A69-21098
- Reliability in electronics - Conference, Budapest, October 1968, Volume D
08 p1292 A69-21105
- Reliability in electronics - Conference, Budapest, October 1968, Volume B
08 p1293 A69-21111
- Advances in electronics and electron physics, Volume 25, covering linear ion accelerators, Hall effect, VLF propagation, thermionic cathodes and electron microscopy
09 p1469 A69-22696
- Cryogenic applications including maser amplification, IR detection and superconductivity, discussing systems optimization and cost reduction
10 p1665 A69-24017
- Space electronics, telemetry, antennas, computers - IEEE Conference, Cocoa Beach, Florida, November 1968
11 p1837 A69-25288

Astronautics - Conference Braunschweig, West Germany, October 1968, Volume 1, Flight control and electronics

12 p1217 A69-25870

Photoelectronic image devices, discussing detectors, electronography, Lallemand camera, spectracon and electron image multipliers

12 p2082 A69-26136

Photoelectronic high speed image intensifier framing camera, showing single shot synchronized photography of electric spark in air

12 p2082 A69-26137

Electronics - Conference, Rome, March 1969

14 p2422 A69-29685

Quantum electronics, Volume 2, Maser amplifiers and oscillators

17 p2982 A69-33687

Aerospace electronics - IEEE Conference, Dayton, May 1969

17 p2939 A69-34056

Book on solid state electronics, discussing quantum mechanical approach, Fermi-Dirac statistics, electron theory of metals, semiconductors and magnetism

18 p3182 A69-34653

Soviet collection of papers on quantum electronics covering ruby laser actions, harmonic generation, laser outputs, etc

19 p3330 A69-35862

Soviet book on quantum electronics covering electronic devices, nonrelativistic quantum mechanics, radiation field and matter interaction, black body radiation spectra, etc

20 p3556 A69-38210

Book on electronics and electron physics covering electron beams, far IR radiation, electron microscopy, scintillation detectors and breakdown in solids

22 p3981 A69-40667

ELECTRONOGRAPHY

Thin CuAs selenide films by vacuum deposition, electronographic study proves cubic sphalerite phase existence

02 p0298 A69-12045

Electronographic determination of ternary alloys of germanium antimony tellurides noting hexagonal laminary with cell periods

02 p0298 A69-12046

Asymmetrical profiles of 4430 A interstellar absorption band, discussing stellar and electronographic spectra

10 p1781 A69-23676

Photoelectronic image devices, discussing detectors, electronography, Lallemand camera, spectracon and electron image multipliers

12 p2082 A69-26136

Magnetically focused electronographic image converters in far UV photography and spectroscopy in space astronomy applications

17 p2972 A69-33084

UBV photometry of faint stars, discussing photographic plate effect on accuracy, emulsion standardization and use of electronography

17 p3031 A69-33099

ELECTRONS

NT CONDUCTION ELECTRONS

NT FREE ELECTRONS

NT HIGH ENERGY ELECTRONS

NT HOT ELECTRONS

NT NEGATRONS

NT PHOTOELECTRONS

NT PI-ELECTRONS

NT POLARONS

Gravitational force measurement on electrons and positrons in free fall through vertical metal tubes at low temperatures

01 p0125 A69-10979

Solar X ray control of D layer based on Explorer 33 data, computing electron production rates due to typical X ray flux

03 p0500 A69-13224

Linear analysis of operation of multistage magnetron amplifiers using injected electron flux and stepwise varying dimensions of interaction space

03 p0407 A69-13977

Electron viscosity coefficient in weakly turbulent plasma in strong magnetic field, noting electrical and thermal conductivity

03 p0480 A69-14136

Electron detector for OGO-E to measure flux and energy spectrum of electrons in primary cosmic rays [IEEE Paper 3C-4]

07 p1135 A69-19198

Long lived streams of low energy solar electrons and protons and association with bright flares or solar active regions

07 p1206 A69-19249

Electron anomalous magnetic moment effect on nonlinear Lagrangian of electromagnetic field, deriving additional nonlinear corrective term

08 p1353 A69-19781

Trapped electron belts formation and storm time behavior assuming presence of bimodal diffusion from low energy source at magnetosphere outer edge

08 p1307 A69-20184

Components relationships in binary phase diagrams of IIIa and VIa transition metals on basis of electronic structure

08 p1331 A69-20191

Electron flux parameters determination from ionograms and reflected signal amplitudes between 120-130 km, considering electron collision frequencies

10 p1688 A69-23931

Two beam electron flux instability in crossed magnetic and inhomogeneous electric fields using linearized hydrodynamic and Lagrangian formalism approximation

12 p2133 A69-26714

Ionization processes in Seyfert galaxies, considering thermal electrons, superthermal protons and electrons and nonthermal UV radiation

13 p2346 A69-27710

Earth radiation belt data, discussing origin, density, distribution, etc, of protons, electrons and alpha particles

15 p2674 A69-30016

Aurora electron and proton excitation patterns determined spectroscopically, discussing ground based observations of emission geomagnetic latitude-time distribution

15 p2593 A69-30017

Phonons, electrons and protons in ferro-paramagnetics and hydrogen bonded ferroelectrics, examining higher frequency optical and lower frequency dielectric properties

16 p2827 A69-32262

Auroral electrons measurement by rocket, discussing difficulties due to secondary electrons and method permitting primary electrons detection threshold determination as function of rocket position

16 p2785 A69-32617

Thermodynamic properties of hydrogen atoms, protons and electrons, using canonical group analysis to determine bound and free states

21 p3850 A69-38964

Diurnal variations of electron flux based on balloon observations near polar cap consistent with geomagnetic cut-off variations of magnetospheric models

22 p4005 A69-40511

Electron-positron pair formation in electromagnetic field created by coherent laser light focused into vacuum with ideal lens

22 p3965 A69-41116

ELECTROPHORESIS

Prototype system for continuous dielectrophoretic deposition and alignment of micron sized ultrahigh strength whisker reinforced composites

13 p2269 A69-28676

Dielectrophoretic zero gravity cryogenic liquid expulsion using lightweight high voltage ribbon electrode conduits and electrohydrodynamic bang-bang field effect

24 p4300 A69-43237

ELECTROPHOTOMETERS

Photoelectric photometry of Mercury, Venus, Mars, Jupiter and Saturn /1963-1965/, determining phase curves and monochromatic albedos

04 p0663 A69-15383

Photoelectric equipment for nephelometric simulation studies of light scattering by cloud particles

06 p0953 A69-17993

Absolute magnitudes and intrinsic color photoelectric observations of Wolf-Rayet stars in Magellanic Clouds and Galaxy

07 p1221 A69-19583

Galactic dust layer spatial structure and relation to brightness of Milky Way based on analysis of photoelectric color excesses in Aql and Cyg stars

09 p1590 A69-21381

Rocket-borne photoelectric photometers for UV observations of Saturn, using interference filters

09 p1602 A69-22216

Transistorized electrophotometer for polarimetric and photometric analysis of weak light fluxes, noting pulse amplifying and shaping circuits

11 p1884 A69-24735

Radioactive light sources in photoelectric photometry, analyzing characteristics, brightness and stability of light flux and energy spectrum

11 p1951 A69-25421

Plasma velocity measurement by Doppler shifts of spectral lines with photoelectric recording, using Fabry-Perot interferometer

12 p2079 A69-26021

Photoelectric recorder with timebase image converter tube for investigating ultrashort light pulse transient response of laser

12 p2083 A69-26139

Spectral reflectivity differences of selected dark and bright regions of Mars observed with double beam photometer

13 p2338 A69-27553

Photoelectric scanning of CH Cygni spectrum calibrated and compared with 45 Arietis, discussing high dispersion, excess blue and UV continua, H beta emission, etc

13 p2338 A69-27557

Photoelectric observations of blue light minima of U Geminorum variable Ex Hydrae indicating no change in orbital period

13 p2338 A69-27558

Photoelectric photometry of artificial satellites noting equipment, Pegasus satellite observations and light curves from Cosmos 151, 192 and 220

15 p2616 A69-31391

Photoelectric observations of color and titanium oxide in M7 giants in nuclear bulge of Galaxy compared with late giants near sun

16 p2863 A69-32396

Atmospheric extinction determined by monochromatic photometry in Chile in 3000 to 6000 A range, discussing components

17 p3031 A69-33100

UBV photoelectric investigation on southern globular clusters NGC 2808 and 1851, presenting star magnitudes and colors in tabular form and estimating reddening

18 p3190 A69-34290

Galactic dust layer spatial structure and relation to brightness of Milky Way based on analysis of photoelectric color excess in Aql and Cyg stars

18 p3198 A69-34769

Astronomical data collection and evaluation, discussing digital distance measurement, photoelectric photometry, servocontrols and electronic computers suited for Schmidt telescope output

20 p3539 A69-37525

Automatic planetary electrophotometer designed for earth atmosphere and lunar photometry, noting operational data

20 p3547 A69-38310

Astronomical photoelectric photometry system, describing telescope and photometer, coldboxes, analog integrators, digital recording equipment and computer programs

24 p4318 A69-43805

ELECTROPHOTOMETRY

Rocket IR astronomy in support of big bang hypothesis, considering photoelectric detectors and instrument system

10 p1772 A69-22868

A and B stars near North Galactic Pole and with magnitudes from 5 to 14.5, noting photoelectric UBV and four color photometric measurements

10 p1773 A69-22963

Yellow and blue photoelectric observations of eclipsing binary CO Lac

10 p1775 A69-23202

Crab Nebula pulsar NP 0532 photoelectric spectrophotometry results, noting main pulse and interpulse spectral energy distributions similarity to extended synchrotron radiation

13 p2335 A69-27317

Photoelectric search for delta Scuti variables in Coma and NGC 752 clusters, discussing short period variability of B, A and F stars

13 p2343 A69-27620

Solar flares associated with intensive sodium D lines emission observed photoelectrically with telescope in unperturbed region, analyzing possibilities of comets solar origin

15 p2674 A69-30506

Photoelectric comet observation techniques, tabulating narrow and wideband filter combinations for determining parameter Q for various cometary spectral emissions

15 p2684 A69-30522

Photometry methods for spacecraft brightness in dynamical states of rapid spin and tumble

21 p3671 A69-38340

ELECTROPHYSICS

NT MOLECULAR ELECTRONICS

P-type zinc-tin-antimonide crystals electric conductivity, Hall coefficient and thermal EMF found similar to p-type diamond-like semiconductors properties
15 p2667 A69-30197

ELECTROPHYSIOLOGY

Tape recorder for simultaneous double channel recording of physiological experiments, describing circuit modifications and additional circuits
07 p1131 A69-18640

Graphical method for plotting electrophysiological observations, showing hodographs application in biopotential studies of cortical reactions
11 p1829 A69-24540

Peak amplitude selector for electrophysiological phenomena analysis, describing memory schemes, threshold crossing detectors and display, input and output circuits, timing, etc
15 p2612 A69-31266

Electrophysiological /electrospinalhogram/ medical data transmission via satellite from France to U.S. for real time computer processing
16 p2746 A69-32070

Soviet book on nervous mechanisms of vestibular reactions emphasizing mathematical description of operation, neurohythmic changes in cerebral cortex and oculomotor activity modeling
16 p2746 A69-32605

Electrophysiological data for directionally sensitive units in optic tectum of mammals, indicating midbrain as site for rotating spiral motion aftereffects
20 p3480 A69-38264

Visual retroactive perceptual masking effect in monkeys pretrained in visual discrimination task, interpreting electrical potentials recorded along optic pathways
22 p3876 A69-40265

Supraventricular arrhythmias after acute myocardial infarction, noting benefit of early DC shock
24 p4262 A69-42729

ELECTROPLATING

Graphite fiber electroplating with nickel on continuous basis for ribbon like continuous flexible twist free yarn
09 p1512 A69-22362

Electroplating solutions test for filament winding and electroforming process used in fabricating fiber reinforced metal composites
11 p1890 A69-24337

Plating wear resistant electrodeposits of Ag, Cu, Ni and Cr on Ti, noting adhesion tests
18 p3148 A69-34654

Electroplating method for local stress concentrations determination, discussing measurement techniques, metal fatigue failure prediction, etc
19 p3441 A69-36751

Soviet collection of papers on bright electrolytic coatings including physicochemical principles of deposition
22 p3958 A69-41261

Bright nickel plating, examining brighteners and anti-tipping additions effect on deposition mechanism
22 p3959 A69-41264

Bright cobalt plating electrolytic processes, examining brighteners and formation mechanism of deposits
22 p3959 A69-41265

ELECTROPLETHYSMOGRAPHY

Blood circulation in brain during acceleration analyzed by tensometric sensors and electroplethysmography, noting intracranial sensitivity to gravitational changes
06 p0874 A69-17646

ELECTROPOLISHING

Polishing-etching cell permitting continuous sample surface observation for use with inverted stage microscopes
13 p2281 A69-28156

Electrolytic and mechanical polishing techniques for metallographic specimens of beryllium
13 p2281 A69-28161

Automatic electropolisher for copper disks
21 p3720 A69-38597

ELECTRORETINOGRAPHY

Dark adaptation mechanisms studied from light intensity recovery after experimental flash, using electroretinography methods
10 p1647 A69-23588

Stiles-Crawford effect measurements before and following eye movements to determine retina shearing during eye movements
15 p2555 A69-31035

Local electroretinogram responses produced in cats by light intensity incremental changes
22 p3878 A69-40835

Electroretinogram a-wave relationship to early inhibition and excitation of retinal ganglion cells produced by flash superimposition in rabbits
22 p3878 A69-40836

Cat intraretinal DC component and b-wave separation based on sensitivity to visual stimuli, discussing electroretinogram recorded with microelectrodes
22 p3883 A69-40881

High intensity flash effects on local electroretinogram, late receptor and slow potentials and ganglion cell activity in area centralis of cat retina
22 p3883 A69-40882

Human electroretinogram /ERG/ physiological variations as function of stimulation energy and wavelength
22 p3884 A69-40884

Pigeon visual adaptation to flickering light, attributing ERG b-wave postadaptation rebound to retina bipolar cells inhibition
23 p4084 A69-41463

Rabbits long term reversible retinal function changes due to short high intensity light flashes, noting ERG suppression
23 p4084 A69-41468

Rhythmic wavelets electroretinogram recorded from rabbit retina in vitros preparation indicating dominant relatively low voltage waves compared to in vivos waves
23 p4101 A69-41471

Electroretinogram and visually evoked cortical potential as response potentials in human visual system
24 p4271 A69-42644

ELECTROSEISMIC EFFECT

U ELECTRIC CURRENT
U SEISMIC WAVES

ELECTROSLAG REFINING

Pitting corrosion resistance improvement in austenitic stainless steels with added molybdenum through electroslog resmelting
05 p0781 A69-16499

ELECTROSLAG WELDING

Welding methods used for Ti and Ti alloys and difficulties encountered
07 p1139 A69-18789

Electroslog welding using plasma jets with powdered material, discussing various parameters
08 p1321 A69-20766

Covered electrode, submerged arc, electroslog, gas metal arc, gas tungsten arc and plasma arc welding processes application to high strength steels
12 p2100 A69-25828

ELECTROSTATIC CHARGE

Electrostatic potential generated by rockets on space vehicles, noting source of electric current in exhaust plumes and effect on instrumentation
03 p0522 A69-13903

Aircraft instrumentation for measuring aircraft electrostatic charge, atmospheric electric field intensity and currents of aircraft
04 p0549 A69-15107

Aircraft charge measurements in stratus clouds, noting charge sign is independent of cloud space charge
04 p0549 A69-15108

Photoelectric ejection of grain electrons by solar quanta balance with solar wind electron capture by grain for interplanetary grain equilibrium potential
09 p1593 A69-21655

Interfacial charges in MOS transistors determined as function of surface potential by measuring channel conductance as function of temperature
10 p1744 A69-23178

LF electrostatic oscillations of inhomogenous solid state plasma with small number of current carriers in parallel external electric and magnetic fields
15 p2665 A69-30042

Ion and electron fluxes and drag force dependence on electrostatic charge and velocity of interstellar dust particle
19 p3425 A69-36562

Steady state sunlit lunar surface electrostatic charge and potential distributions, noting electrons photoemission and solar wind particles collection
20 p3609 A69-38077

Electrostatic charge formations in atmosphere, discussing atmospheric electricity during precipitation and thunderstorms
21 p3758 A69-38785

ELECTROSTATIC ENGINES

Electrostatic electron bombardment ion thruster with magnetoelectrostatically contained plasma
[AIAA PAPER 69-260] 09 p1567 A69-21262

Electrostatic rocket exhaust condensation on spacecraft solar electric panels cover glasses, noting deleterious effects
[AIAA PAPER 69-271] 09 p1569 A69-21874

Electric rocket propulsion, discussing roles of plasma and gas discharge physics in development of electromagnetic, electrostatic and thermoelectric nuclear systems
13 p2325 A69-28253

Nuclear rocket propulsion operation, design, properties and performance of electrostatic, electrothermal and electromagnetic systems
13 p2297 A69-28254

ELECTROSTATIC EROSION

U SPARK MACHINING

ELECTROSTATIC FIELDS

U ELECTRIC FIELDS

ELECTROSTATIC GYROSCOPES

Strapdown electrostatic aerospace navigator /SEAN/ using electrostatically suspended gyros /ESG/ for inertial reference, including drift and computer tests
19 p3369 A69-35802

ELECTROSTATIC PLASMA

U PLASMAS [PHYSICS]

ELECTROSTATIC PRECIPITATORS

Rocket measurements of primary auroral particles energy spectra indicating spectral structure acceleration peaks associated with electrostatic fields
21 p3707 A69-38490

ELECTROSTATIC PROBES

Wake structure behind spherical bodies in rarefied plasma flow by measuring plasma parameters and disturbances with probes
01 p0134 A69-11308

Barium plasma density measurements by Langmuir, microwave probes and resonance fluorescence scattering compared in Q device
02 p0288 A69-12172

Plasma diagnostics in magnetic field with thin cylindrical probe based on Langmuir method
02 p0292 A69-12556

Nocturnal electron concentrations and temperature at Manitoba measured by rocket-borne Langmuir probe, compared with F1 region
03 p0502 A69-14008

Multielectrode analyzers for measuring properties of ionospheric charged particles
05 p0761 A69-15702

Langmuir probe to determine helium plasma density effect on electron temperature from relation between spectral line intensities
05 p0804 A69-16376

Qualitative mechanisms to explain Langmuir paradox, discussing wall mechanism for Maxwellian distribution formation in low pressure discharges
06 p0960 A69-16922

Stagnation point electrostatic probe measurements of flowing partially ionized high density monatomic gases
06 p0964 A69-17196

Weakly ionized gas flow past discontinuous wall potential used to study edge effects and interaction problems for single and multiple flush electrostatic probes
[AIAA PAPER 69-80] 06 p0972 A69-18191

Space plasma potential measurement based on RF impedance of plasma sheath/probe system
07 p1130 A69-18300

Analytic integration of Langmuir equation for spherical space charge flow obtained in terms of Airy equation or Bessel functions solution
07 p1115 A69-18864

Spacecraft applications of Langmuir probes, obtaining data from current-voltage characteristics for electron/ion concentrations, ion mass spectra and charged particle energy distribution
08 p1316 A69-20474

Current fluctuations in Langmuir probe in turbulent plasma measured for various pressures, frequency bands, etc, noting plasma density fluctuations role
08 p1364 A69-20517

Integrated charged particle energy spectra from gridded electrostatic analyzers, relating retarding potential curve to particle floating potential, kinetic temperature, etc
08 p1364 A69-20521

Moderately ionized plasma electrical conductivity calculated by generalized Ohm law and measured along with other plasma properties
[AIAA PAPER 69-277] 09 p1543 A69-21264

Electron density fluctuations in turbulent wakes of hypersonic projectiles in ballistic ranges, discussing use of cylindrical Langmuir probe for direct measurement
09 p1496 A69-21934

Electrostatic probe measurements in gas warmer than probe, demonstrating applicability of continuum theory for highly negative probe

11 p1930 A69-25274

Electrostatic charge distribution on ultrahigh vacuum cleaved silicates including instrumentation, UV irradiation, half life, Paschen relation, etc

13 p2322 A69-28018

I-V characteristics of electron emitting satellite in ionosphere, analyzing spherical Langmuir probe in collisionless plasma in magnetic field

14 p2511 A69-28956

Electrode surface bismuth coating selected for reducing electrostatic analyzers photocurrents

14 p2446 A69-29048

Spherical plate electrostatic analyzer transmission characteristics, emphasizing angular response to external particle sources as functions of angular coordinates and particle energy

14 p2449 A69-29560

Langmuir probe measurements leading to electron groups composition of electron velocity distribution function in negative glow light

14 p2493 A69-29694

Plasma diagnostics in magnetic field with thin cylindrical probe based on Langmuir method

15 p2658 A69-30253

Electronic density of collisional cesium plasma, comparing measurements made by Langmuir and HF spherical probes

15 p2659 A69-30300

Flush electrostatic probe edge effect, considering Couette flow of weakly ionized compressible gas past discontinuous wall potential

15 p2653 A69-30912

Vaporization rates of Ti, Zr, Hf, Nb and Ta carbides at high temperatures measured by Langmuir method

15 p2640 A69-30983

Plasma parameters, except ion temperature, obtained from current-voltage characteristics of flowing plasma measured by electrostatic probes in low density wind tunnel

16 p2816 A69-31637

Stagnation point electrostatic probe for measuring local electrical properties of solid propellant rocket exhausts

[AIAA PAPER 69-573]

16 p2840 A69-32677

Data distortion elimination by improved superimposing of sinusoidal audio frequency signal on DC voltage of automatic Langmuir probe second derivative plotters

17 p2970 A69-32855

Langmuir probe to determine space vehicle orientation in ionospheric or interplanetary plasma, discussing apparatus, accuracy and application

17 p3001 A69-33222

Collisionless cylindrical Langmuir probe response in turbulent plasma for mean and statistical properties

[AIAA PAPER 69-698]

17 p3010 A69-33438

Surface type airborne electrostatic probes in ambipolar diffusion flux, measuring ion saturation current, discussing electrode contamination and temperature and ablation tests

[AIAA PAPER 69-700]

17 p2974 A69-33443

Shock structure in RF heated partially ionized Ar plasma jet, using cylindrical free molecule Langmuir probe

[AIAA PAPER 69-697]

17 p3011 A69-33466

Positive ion concentration in D region, using spherical stationary electrostatic probe in weakly ionized collision dominated gas

18 p3128 A69-34804

Plasma parameters relationship with double electrostatic probe volt-ampere characteristics, applying corrected formulas for temperature, ion density, etc, to flame diagnostics

18 p3137 A69-34932

Biased electrostatic probes determining free stream charge density and ionization risetime in supersonic flows in arc heated pressure driven shock tube

19 p3291 A69-35715

Electrostatic probes in nonequilibrium collision dominated ionized gas flow ballistic ranges

19 p3291 A69-35716

Electrostatic probes calibration and use for hypersonic wakes behind projectiles in ballistic range

19 p3291 A69-35717

Ion collecting cylindrical electrostatic probes as flow field tracing instruments in low density slightly ionized flows

19 p3291 A69-35718

Small continuum electrostatic probes calibration and operation in ionized plasma flow with sheath dimensions larger than boundary layer dimensions

19 p3304 A69-35719

High speed analog to digital multiple channel wide-band data acquisition system designed for short pulse Doppler radar and probe measurements

19 p3307 A69-35745

Spherical, cylindrical and toroidal electrostatic analyzers with symmetrical angular characteristics for solar wind investigations

19 p3396 A69-36632

Cylindrical electrostatic probes on Alouette 2 and Explorer 31 satellites used in intersatellite comparison of directly measured ionospheric electron temperature and density

20 p3544 A69-37876

Cylindrical electrostatic probe measurements on Alouette 2 and Explorer 31, considering implications for future missions

20 p3544 A69-37877

Langmuir plate and spherical ion probe experiments aboard Explorer 31, measuring concentrations and temperatures of thermal electrons and ions

20 p3545 A69-37881

Langmuir probe immersed in plasma RF response over range of signal amplitude and frequency and plasma electron density, showing sheath capacitance role

21 p3723 A69-38939

Anode fall measurements with Langmuir probe in coaxial arcs in Ar compared with anode energy balance values

24 p4256 A69-43695

ELECTROSTATIC PROPULSION ION PROPULSION

West German activity in field of electrostatic propulsion, discussing ion thrusters, colloid thruster development and mission analysis

09 p1565 A69-21248

Research and development program in annular slit colloid thruster technology, proving thruster feasibility by performance tests

[AIAA PAPER 69-287]

09 p1566 A69-21257

Electrostatic thrusters using RF ion sources to optimize payload ratios, terminal velocities, propellants, life span and efficiencies

09 p1568 A69-21489

Development and applications of ion propulsion covering electrostatic acceleration of particles, Cs contact and electron bombardment ion thrusters, space missions, etc

17 p3020 A69-33354

ELECTROSTATIC SHIELDING

Dipole shielding factor in coupled Hartree-Fock approximation for atomic S state

02 p0281 A69-12179

Electron shielding in heavily doped many valley semiconductors, discussing Thomas-Fermi screening and Mott transition

13 p2324 A69-28683

Electrostatic screening in isothermal symmetrically charged and quasi-neutral plasmas, noting confinement in electrostatic trap

14 p2490 A69-29035

Electrostatic control for portable clean rooms, describing fabrication, assembly and checkout problems with Instrument Unit (IU) control center for Saturn launch vehicles

19 p3428 A69-35550

ELECTROSTATIC WAVES

Ionospheric plasma electrostatic resonances from Alouette satellite signal observations

01 p0067 A69-10983

Electrostatic plasma wave instabilities in ionosphere along auroral field lines, noting critical electron flux and subsequent acceleration of electrons

01 p0075 A69-11222

Nonlinear large amplitude electrostatic and electromagnetic oscillations in cold plasma having one dimensional spatial variations and fixed neutralized ion background

02 p0288 A69-12171

Acceleration of charged particles in strong DC magnetic field by electrostatic waves with spatially varying phase velocities integrated numerically on IBM 360/65

03 p0479 A69-14028

LF electrical resonance oscillations in nonisothermal plasma jet flow, noting pressure and magnetic field effects on amplitude and frequency

04 p0638 A69-15174

Electrostatic ionospheric waves excited around lower hybrid resonance frequency by high energy electrons

06 p0918 A69-17381

Electrostatic waves interaction to electrons in plasma characterized by bump-in-tail distribution function, deducing mechanism of wave particle interaction

06 p0966 A69-17521

Electrostatic waves in inhomogeneous plasma in finite magnetic field, noting dispersion relation for cold plasma and stabilization of instability

06 p0967 A69-17761

Longitudinal electrostatic oscillations in plasma with Fermi distribution of energies, noting oscillation frequency dependence on electron density

08 p1359 A69-19985

Ion cyclotron resonance acceleration and higher harmonic acceleration in axially nonuniformly magnetized plasma under influence of RF electric field

08 p1360 A69-20079

Numerical integration of motion equations of electrons subject to electrostatic waves, considering turbulent heating

08 p1368 A69-20806

Current instability in H plasma in electric field of large amplitude fast magnetosonic wave, noting plasma heating

09 p1552 A69-22526

Unstable transverse potential oscillations in plasma with beam anisotropy and initial density modulation and analogy with known electrostatic oscillations

10 p1727 A69-23092

One dimensional electrostatic plasma oscillations in alternating external electric field, noting plasma stability and electron-electron two stream instability

11 p1924 A69-24298

Electrostatic wave dispersion relation in uniformly rotating plasma cylinder used in interpreting Q machine experiments

11 p1924 A69-24300

HF electrostatic waves propagation in nonuniform plasma in uniform magnetic field, obtaining solutions of dispersion relation

11 p1931 A69-25360

HF electrostatic waves propagation excited by electron beam in hot inhomogeneous plasma in magnetic field, studying wave transformation and absorption

11 p1931 A69-25364

Electrostatic drift wave dissipative instability in framework of macroscopic theory, accounting for resistivity and viscosity using WKB method

11 p1934 A69-25655

Alternating electric field parametric effects on inhomogeneous plasma in magnetic field, obtaining electrostatic wave coupling dispersion relation by density gradients considerations

13 p2304 A69-27298

Ballistic wake structure and jump conditions for plane plasma shock waves with electrostatic turbulence

15 p2660 A69-30914

Critical study of Tidman model for turbulent electrostatic shock wave structure in plasmas, noting velocity distribution function role

15 p2661 A69-30927

Propagation and linear transformation of HF electrostatic waves in hot magnetoactive radially inhomogeneous plasma, noting wavelength shortening

16 p2816 A69-31638

Wave damping in current sheet in geomagnetic tail by radiating energy from sheet sides by electrostatic waves

[AFCRL-69-0396]

16 p2781 A69-32318

LF electrical resonance oscillations in nonisothermal plasma jet flow, noting pressure and magnetic field effects on amplitude and frequency

18 p3180 A69-34716

Magnetospheric disturbances effect on radio wave propagation, discussing wave-particle interactions, VLF emissions and electrostatic waves

19 p3303 A69-36429

ELECTROSTATICS

Mixed boundary value problem of elastostatics for isotropic elastic cylinder containing strip crack opened by internal pressure, using auxiliary functions

01 p0167 A69-10317

Nonexistence of Biota-Cloud recontamination hazard for planetary lander proved by analysis of interactions between small particles and physical fields around vehicle

02 p1201 A69-11771

Electron flow in stable negative electrostatic potential well produced by electronic injection at center of hollow open spherical anode

03 p0475 A69-13153

Fiber optic electrostatically focused image intensifier tube for recording star spectra with reduced exposure time

[WERL-68-1C2-TAEC-P1]

04 p0603 A69-15444

Electrostatic storage display tube characteristics, construction, applications and reliability

07 p1101 A69-18655

Periodic electrostatic focusing structures in microwave tubes, evaluating properties by action function method
07 p1102 A69-18659

Shock-like solutions of electrostatic Vlasov and Poisson equations, assuming zero temperature of positive ions and increasing electrostatic potential
08 p1359 A69-19982

Atmospheric ion concentration increment by electrostatic lens to facilitate electrical properties measurements of charged particles in submicroscopic range
17 p2971 A69-32928

Electrostatically focused klystron /EFSK/ small signal gain calculations based on lens cell space charge wave analysis
18 p3109 A69-35294

Ionospheric VLF electrostatic noise observed by sounding rocket, noting proton gyrofrequency harmonics effects within emission attenuation bands
21 p3714 A69-38550

ELECTROSTRICTION

Kerr effect and electrostriction during self focusing of high power laser beam in gases and liquids
04 p0611 A69-14792

ELECTROTHERMAL ENGINES

NT ARC JET ENGINES
NT PLASMA ENGINES
NT RESISTOJET ENGINES

Multijet electrothermal systems for attitude control and stationkeeping of synchronous communications satellite
[AIAA PAPER 67-723] 02 p0305 A69-12375

Performance analysis for electrothermal thruster using lithium propellant with supersonic heat addition
[AIAA PAPER 69-286] 09 p1567 A69-21267

Electric rocket propulsion, discussing roles of plasma and gas discharge physics in development of electromagnetic, electrostatic and thermoelectric nuclear systems
13 p3235 A69-28253

Nuclear rocket propulsion operation, design, properties and performance of electrostatic, electrothermal and electromagnetic systems
13 p2297 A69-28254

Fast heat-up electrothermal ammonia thruster role in development of hybrid resistojet in millipound thrust range
[AIAA PAPER 69-496] 16 p2838 A69-32649

Refractory metals in rocket propulsion devices, applying tungsten in uncooled rocket nozzles and tungsten and rhenium to electrothermal propulsion
23 p4177 A69-42161

ELEKTRON SATELLITES

Elektron satellite recorded sporadic radio emission noting relationship to geomagnetic disturbances and dependence on satellite position
05 p0824 A69-16059

Elektron satellite recorded sporadic radio emission noting relationship to geomagnetic disturbances and dependence on satellite position
20 p3606 A69-37969

ELEKTRON 4 SATELLITE

Elektron 4 satellite radio emission data transmitted from July to December 1964, noting month-to-month variations in mean radiation level
09 p1578 A69-21776

ELEMENT ABUNDANCE

U ABUNDANCE

ELEMENTARY EXCITATIONS

NT EXCITONS
NT MAGNONS
NT PHONON BEAMS
NT PHONONS
NT PLASMONS
NT POLARONS

Low field helicon wave transmission through n-type Ge at liquid He temperature, noting cyclotron resonance damping
02 p0295 A69-11787

Quasi-phonon model for acoustic scattering and diffraction from rigid real obstacle in fluid medium
05 p0797 A69-16649

ELEMENTARY PARTICLE INTERACTIONS

NT ELECTRON CAPTURE

Light tachyons, tachyon velocity and relation to gravitational quanta
02 p0282 A69-12746

Strong interactions at energies above 100 Gev, examining use of cosmic ray experiment for qualitative studies of interaction process
03 p0498 A69-12939

High energy cosmic ray research facility at mountain altitudes, noting nucleon-proton interactions, particle identification and momentum analysis
03 p0499 A69-12942

Field theories and direct interparticle action theories of classical electrodynamics, establishing general correspondence between formalisms
04 p0631 A69-15189

Upper limit estimated for anomalous interaction between cosmic muons with greater than 100 Bev energy
06 p0986 A69-17246

Weak interaction theory modifications needed for high energy cosmic ray muons to not violate conservation of probability
09 p1583 A69-22758

Book on stellar, galactic and nucleosynthetic evolution covering nuclear, Fermi, electromagnetic and gravitational interactions roles
11 p1964 A69-25413

Photoemulsion stacks irradiated by protons in magnetic field, determining nuclear isobar generation during quasi-nucleon interactions
13 p2303 A69-28373

ELEMENTARY PARTICLES

NT ALPHA PARTICLES
NT ANTINEUTRINOS
NT ANTINUCLEONS
NT ANTIPARTICLES
NT ANTIPROTONS
NT BARYONS
NT BETA PARTICLES
NT BOSONS
NT COLD NEUTRONS
NT CONDUCTION ELECTRONS
NT DEUTERONS
NT ELECTRONS
NT FAST NEUTRONS
NT FERMIONS
NT FREE ELECTRONS
NT HADRONS
NT HIGH ENERGY ELECTRONS
NT HOT ELECTRONS
NT HYPERONS
NT K-MESONS
NT KAONS
NT LEPTONS
NT LIGHT BEAMS
NT MESON RESONANCES
NT MESONS
NT MUONS
NT NEGATONS
NT NEUTRINOS
NT NEUTRONS
NT NUCLEONS
NT PHOTOELECTRONS
NT PHOTON BEAMS
NT PHOTONEUTRONS
NT PHOTONS
NT PI-ELECTRONS
NT PIONS
NT POLARONS
NT POSITRONS
NT PROTONS
NT QUARKS
NT SOLAR PROTONS
NT THERMAL NEUTRONS

Elementary particles and cosmic radiation, discussing current state of knowledge and observational techniques
02 p0307 A69-11907

Light tachyons, tachyon velocity and relation to gravitational quanta
02 p0282 A69-12746

Static formations in general theory of relativity and plankions
05 p0793 A69-15776

Cosmic rays, elementary particle physics and astrophysics - Conference, Aligarh, India, December 1967
06 p0986 A69-17268

Einstein space time concepts for unified formalism of matter interactions from elementary particles to astronomical bodies, discussing relativity theory
08 p1352 A69-20730

Universe origin, discussing big bang theory, effects of expansion time and temperature on elementary particles, RF quanta, etc
11 p1953 A69-24352

Validity of Lorentz invariance, discussing nuclear magnetic resonance test on torque for spin of electrons, muons and neutrons
18 p3176 A69-35007

Static formations in general theory of relativity and plankions
18 p3173 A69-35029

Cosmological constant and elementary particle theory
20 p3606 A69-38013

Unified theory of elementary particles assuming quantum mechanics as consequence of changes in time within microcosmos and particle-universe interaction
21 p3816 A69-39622

Magnetic monopole search using synchrotrons and cosmic radiation to destroy ferromagnetic materials binding in rocks, meteorites and deep sea sediments
22 p3981 A69-40197

ELEMENTS

Stellar abundance and origin of elements, discussing stellar atmospheres and gaseous nebulae spectral determination, chronology of galactic halo, etc
09 p1587 A69-21306

Quantitative separation of elements in gamma prime from precipitation hardened high temperature nickel-base alloys by anodic dissolution
13 p2277 A69-27408

Relative element abundances in Cyg, Her and Boo atmospheres, calculating curves of growth by Planck gradient method for stellar spectra
14 p2519 A69-29356

Nucleosynthesis based on stellar spectra and nuclear reactions data, discussing elements in sun and stars, meteorites, solar neutrinos, etc
14 p2529 A69-29985

Abundance compilations of elements due to nuclear processes, discussing carbonaceous chondrites character
21 p3789 A69-38812

ELEVATION ANGLE

Wavefront Wilkins-Minnis, null selection and elevation scanning techniques for measuring radio signals elevation angles with vertical antenna arrays
08 p1275 A69-20293

Mathematical expressions for measuring heights of vertical and nonvertical features with both slant and ground range radar images
13 p2263 A69-28198

Ground backscatter elevation angle recorded by phase comparison method, postulating ionospheric tilts to interpret data
20 p3535 A69-38188

ELEVATORS [CONTROL SURFACES]

Aerodynamic stick force and speed characteristics of various horizontal tails and elevator trimmers, noting zero stick force case
09 p1434 A69-22597

ELEVATORS [LIFTS]

Stress-strain state of shells of multicable elevator pulleys under asymmetric load for various friction coefficients and pulley shell lengths and widths
06 p1026 A69-18016

ELEVONS

Concorde elevons sandwich construction to meet sonic environment, discussing core, adhesive, design and fabrication
24 p4403 A69-43429

ELLIPSES

Hankel functions and vibration equations solutions, discussing asymptotic behavior and monotonic properties in neighborhood of ellipses
08 p1416 A69-20714

Elastohydrodynamic lubrication film thickness in finite elliptical contact determined by two dimensional Reynolds equation in inlet region, using finite difference approximation
[ASME PAPER 69-LUBS-17] 18 p3120 A69-34379

Visual ellipse phenomena excitation by sinusoidal stimulating currents, noting frequency effects on ellipse shape
23 p4095 A69-42077

ELLIPSOIDS

Earth oblateness, discussing geometric interpretation and direct measurement
01 p0064 A69-10447

Three body problem, discussing impossibility of libration points of gravitating ellipsoid
01 p0155 A69-10957

Stress-strain state of thin elliptical shell of revolution under rapidly varying cyclic edge loads
05 p0832 A69-15686

Circumferential buckling of ellipsoid of revolution due to internal pressure, assuming linear deflection and uniform thin shell
[ASME PAPER 68-WA/PVP-12] 05 p0840 A69-16190

Wall temperature and Mach number effect on heat flux distribution at spreading line of flow for supersonic gas on ellipsoid of revolution
06 p0858 A69-17331

Asymmetric supersonic air flow at 60 degree angle of attack past ellipsoid with frontal spike creating separation area
06 p0858 A69-17337

Mixed three dimensional separation of boundary layer on ellipsoid of revolution at ten degree angle of attack, ignoring heat flux
08 p1251 A69-19876

Morphology of E and SO galaxies in terms of equilibrium isopleths within general relativity
08 p1395 A69-20636

Aerodynamic forces causing deformation and breakup of liquid droplet with ellipsoid of revolution form in constant velocity gas flow
11 p1875 A69-25466

Analytic model resembling thick walled ellipsoid of revolution incorporating three dimensional shape of human left ventricle and ventricular wall thickness effects
12 p2022 A69-26235

Coupling geodetic systems of coordinates linked to reference ellipsoids from determination of angle of inclination relative to earth rotation axis and equatorial plane
12 p2068 A69-26426

Residual field in inner airspace of magnetostatic shielding thin walled stretched ellipsoids of revolution
13 p2237 A69-28610

Close binary system components approximated by two nonsimilar ellipsoids, obtaining interpretation of light curves
15 p2695 A69-30957

Three dimensional periodic boundary layer on ellipsoid in harmonic motion at given angle of attack, using successive approximations
15 p2548 A69-31008

Geopotential represented in ellipsoidal harmonics, discussing Lamé functions generation and rectangular-ellipsoidal coordinates relation and orbital elements perturbations
15 p2599 A69-31333

Earth ellipsoid determination by satellite observations, noting accuracy of polar flattening measurement on basis of perturbation or perigee argument
18 p3131 A69-35195

H II regions radial velocities ellipsoidal distribution in M 33 explained as distribution with minor axis in direction of rotation
21 p3797 A69-38538

Inertial motions, equipotential surfaces and Coriolis forces on earth ellipsoid, discussing pendulum-like oscillations
24 p4346 A69-43156

ELLIPSOMETERS

Ellipsometric dimensions calculations with aid of laser radiation, stressing formulas for compensator and polarizer assemblies
15 p2636 A69-31474

Ellipsometric liquid immersion method for optical parameters determination of system with nonabsorbing surface film on absorbing substrate
24 p4316 A69-43321

Ellipsometer measurements for oxidation rates of binary Ti-Al alloys in vacuum and in pure and premixed gases, using in situ test cell
24 p4316 A69-43322

ELLIPTIC DIFFERENTIAL EQUATIONS

Differentiability of fundamental solution to elliptic equations based on exact theorems of smoothness
01 p0106 A69-10955

Upper semicontinuity of subsolutions of second order elliptic partial differential equations in divergence form with discontinuous coefficients
02 p0270 A69-11548

Normal derivative of solutions to Dirichlet problem for elliptic quasi-linear equation and construction of given mean curvature hyperspace in curved space
02 p0272 A69-12221

Soviet book on linear and quasi-linear second order elliptic equations, emphasizing boundary value problems in various functional spaces
02 p0273 A69-12566

Dirichlet problem for degenerating elliptical equations with nonlinear low order terms
03 p0456 A69-13601

Dirichlet problem for elliptical system, showing solvability of inhomogeneous system with uniform boundary values for half plane and circle cases
03 p0456 A69-13602

Dirichlet problem deviation from Bitsadze system with Noetherian properties, giving Hausdorff normal solvability conditions for inhomogeneous problem
03 p0456 A69-13603

Second order elliptical operator for m-dimensional Euclidian space with open region bounded by closed surface
03 p0456 A69-13604

Discretization error of Dirichlet problem analyzed in plane region with corners, discussing error in numerical solution of elliptic differential equations
03 p0457 A69-13741

Quantitative form of maximum principle for elliptic partial differential equations
03 p0457 A69-13826

Numerical solution of elliptic equations by iteration result in convergence prevention and solution of Laplace and Poisson equations with singular Laplace operator
04 p0625 A69-15133

Solution regularity for class of quasi-linear second order elliptic systems, applying results to regularity of extremals of particular integral
05 p0786 A69-15927

Asymptotic expansion of solution to linear singular perturbation problem of elliptic type in bounded strictly convex domain
05 p0786 A69-15928

Boundary value problems for second order degenerate elliptic equations, formulating and proving theorems for existence of generalized solutions
05 p0786 A69-16422

Boundary value problems for unstable quasi-linear elliptic differential operator class, proving theorems on properties of quasi-linear elliptic-parabolic equations in bounded space
05 p0787 A69-16424

N-dimensional analog of Fragmen-Lindelof theorem applied to solving partial differential elliptic equation
06 p0947 A69-17393

Elliptic equation solution of Dirichlet problem with zero boundary condition, examining dependence of modulus of continuity of solution on boundary properties
07 p1173 A69-18498

Dirichlet problem for nonuniformly second order elliptic quasi-linear equation for case of arbitrary coefficient growth
07 p1173 A69-18500

Existence and uniqueness of Dirichlet problem solutions for elliptic type equations with measurable and bounded coefficients
08 p1343 A69-20659

Singular perturbation problem for elliptic linear partial differential equation, studying asymptotic expansion of solution in vicinity of singular points in nonconvex domain
08 p1352 A69-20751

Difference schemes for approximating boundary value problems of elliptic equation free of mixed derivatives in rectangular region
09 p1532 A69-21788

Linear elliptic partial differential equations, deriving sufficient conditions on coefficients for equations to be oscillatory in certain unbounded domains
09 p1533 A69-22771

Boundary value problems solutions for quasi-linear elliptic and parabolic equations of arbitrary order applied to nonlinear differential equations
10 p1717 A69-22809

Scheme for choosing approximating system of difference equations for degenerate linear and nonlinear elliptic boundary value problems
10 p1719 A69-23515

Boundary value problem for elliptic-parabolic partial differential equations in theory of random processes, obtaining analytical solution in terms of hypergeometric functions
10 p1719 A69-23516

Factorization procedure for iterative solution of systems of algebraic equations from discretization of elliptic boundary value problems
10 p1719 A69-23520

Nonlinear A/x operators in reflexive Banach space Y characterized by weak closure of values, defining solvability conditions for equations having such operator
10 p1720 A69-23563

Elliptic equation of degenerating order in neighborhood of degeneration hyperplane, discussing solution behavior
11 p1908 A69-24696

Oscillation theorems for linear self adjoint elliptic equations of even order 2m, discussing proofs dependence on Swanson comparison theorem
11 p1909 A69-24882

Dynamic programming approach to numerical solution of elliptic boundary value problems, using Laplace equations
11 p1910 A69-25411

Dirichlet problem solution for Volterra elliptic integrodifferential equation, considering existence theorem hypotheses
12 p2121 A69-26468

Boundary value problems of thermoelasticity, discussing existence and uniqueness theorems, ellipticity, thermoelastopotentials, Liapunov-Tauber theorem, Fredholm theorems, etc
12 p2182 A69-26726

Dirichlet problem for elliptic second order differential equations with constant coefficients in region of Euclidean space of two real variables bounded by ellipses
12 p2123 A69-26728

Dirichlet problem of linear degenerate second order differential elliptic systems with independent variables
12 p2123 A69-26729

Elliptic second order equation showing nonequivalent regularity conditions for Laplace and continuous coefficient equations
13 p2288 A69-27743

Variational difference method application to second order elliptic equations with inhomogeneous boundary conditions, applying results to boundary value problems in elasticity theory
13 p2289 A69-28318

Pointwise estimate for gradient of solution of first boundary value problem /Dirichlet problem/ for second order elliptic equation
13 p2289 A69-28319

Algorithm for solving Dirichlet problem of nonlinear elliptical differential equations representing atmospheric dynamics balance equation
14 p2470 A69-29401

Monograph on Dirichlet problem for quasi-linear elliptic differential equations with many independent variables
14 p2471 A69-29599

Mixed boundary problem for elliptic equations with variable coefficients reduced to finite system of algebraic equations
16 p2804 A69-32062

Static implications of strong ellipticity condition in linearized elasticity theory, exemplifying homogeneous deformations
17 p3058 A69-33415

Convergence rate estimates for singular perturbations solutions of linear elliptic boundary value problems
19 p3360 A69-35899

Elliptic system of twelfth order equations describing elastic equilibrium of plate with kinematic functions analyzed by integration procedure
19 p3438 A69-36203

Large atmospheric motions analyzed by elliptic partial differential equation and hydrostatic and quasi-geostrophic approximations
19 p3364 A69-36504

Book on heat and mass transfer in recirculating flows, presenting elliptic differential equations and numerical solutions by computer
21 p3691 A69-38333

Partial difference methods from parabolic, elliptic and hyperbolic equations solved by splittings of locally one dimensional nature
21 p3754 A69-38745

Resistor network electric analog consisting of arithmetic units block, proposing procedure for elliptic equation solution
21 p3680 A69-39854

Normal derivative of solutions to Dirichlet problem for elliptic quasi-linear equation and construction of given mean curvature hyperspace in curved space
23 p4182 A69-41972

ELLIPTIC FUNCTIONS

Nonlinear time dependent parameters systems, analyzing governing differential equations in terms of elliptic functions
01 p0050 A69-10237

Canonical forms for second order elliptic systems with constant coefficients, studying Dirichlet problem solvability for systems reduced to canonical forms
07 p1174 A69-19476

Sobolev type boundary value problems for elliptic operators using manifold theory
08 p1344 A69-21157

Equal element elliptic function filters, noting lower dissipation loss when applied to bandpass and bandstop filters
08 p1300 A69-21175

- Elliptic complexes over compact manifolds without boundary, discussing general theory of elliptic operators in vector bundles
09 p1532 A69-21733
- Higher order Rayleigh-Ritz approximations to eigenvalues and eigenfunctions of elliptic boundary value problem
09 p1534 A69-22798
- Generalized solutions of elliptic boundary value problems by applying Green functions
10 p1718 A69-23207
- Elliptic integrals to determine orbital elements time dependence in three body problem, estimating satellite lifetime
10 p1791 A69-24196
- Evolutionary hypoelliptic equations with real variable coefficients, analyzing positive solutions and application to parabolic equations
11 p1908 A69-24534
- Elliptic boundary value problem for differential equation and pseudodifferential boundary conditions, obtaining Green formula from formulated conjugate problem
12 p2121 A69-26200
- Homeomorphism theorem for Petrovskii and homogeneous elliptic systems applied to boundary value problems and Green formula
13 p2287 A69-27515
- Density distribution in axisymmetrical gravitating systems with ellipsoidal velocity distribution function, using integral equation of state for effective radii of cylindrical configurations
14 p2486 A69-29465
- Applied function theory, Volume 6, Tables of theta functions and elliptical functions with examples, Part 1
14 p2471 A69-29774
- Sobolev type boundary value problems for elliptic operators using manifold theory
15 p2645 A69-31250
- Stepped digital narrow band pass microwave elliptic function filters design and construction
16 p2759 A69-31939
- Generalized solutions of elliptic boundary value problems by applying Green functions
21 p3756 A69-39148
- Evolutionary hypoelliptic equations with real variable coefficients, analyzing positive solutions and application to parabolic equations
21 p3756 A69-39151

ELLIPTICAL CYLINDERS

- Elliptic cylindrical chambers optimum design for optical pumping of solid state lasers, discussing transfer efficiency and approximation by circular cylindrical chambers
10 p1706 A69-24010
- Radiation fields induced by constant current in elliptic ring, discussing analysis results applicability to elliptic capacitive antennas and annular slot
11 p1850 A69-24981
- Radiation field patterns from metal wall aperture in waveguide with rectangular cross section determined using elliptic cylinder
11 p1850 A69-24982
- Channel wall effect on gain of apparent mass of cylindrical and elliptical bodies floating in channel and subject to vertical impact
11 p1875 A69-25487
- Steady state problems of elastic orthotropic cylinder solutions applicable to boundary value problems of laminar orthotropic elliptical cylinders
13 p2369 A69-28528
- Unsteady heat conduction equations for elliptic cylinder with convection solved by point matching
16 p2879 A69-32171
- Stationary elliptic cylinders in subcritical flow, determining Strouhal number, pressure fluctuations and wake geometry as functions of angle of attack
18 p3084 A69-34412

ELLIPTICAL ORBITS

- NT INTERPLANETARY TRANSFER ORBITS
- NT PERIHELIONS
- NT TRANSFER ORBITS
- Stability of elliptical Venus orbits with solar gravitational perturbations, using equation accuracy and influence on mission planning
02 p0331 A69-12819
- Release windows for auxiliary body ejection from satellite in eccentric orbit, discussing visibility, celestial body interference, etc
03 p0505 A69-13003
- Rendezvous maneuvers for vehicle and elliptically orbiting targets, formulating relative motion of two bodies
04 p0658 A69-14828

- Roll dynamics of spinning axisymmetric satellite in elliptical orbit, discussing eccentricity and gravity gradient torque effect
05 p0830 A69-16397
- Molniya 1 communication satellite using elliptical orbit to provide radio, telephone and TV service [UN PAPER 68-95771]
06 p1013 A69-17044
- Braking and acceleration speeds and maximum magnitude during transfer from circular orbit having earth center as focus to elliptical orbit within circular orbit
06 p1007 A69-17578
- Rendezvous maneuvers for fixed elliptical target orbit, discussing numerical solution of problem and suitability of various points of target ellipse for rendezvous
09 p1538 A69-21649
- Earth gravitational field effect on satellite orbits, noting elliptical motion in central force field, energy criteria and rotational ratios
10 p1776 A69-23295
- Perturbing body influence on motion near triangular Lagrangian solutions of restricted elliptical three body problem applied to earth-moon system under solar perturbations
10 p1779 A69-23612
- Relation between planets axial moments and protoplanetary particles orbital eccentricity as explanation of outward winding of planets
12 p2154 A69-25818
- Linear dynamic stability of spinning satellite in elliptic orbit, applying perturbation method to determine Floquet solutions
14 p2534 A69-29318
- Provisional elliptic orbit computed for asteroid Floirac using Gauss-Encke and least squares method, tabulating residuals and ephemeris
14 p2521 A69-29585
- Discrepancy between Kepler first two laws and corresponding Newton propositions, noting necessary substitution of ovals for elliptical orbits
15 p2695 A69-31011
- Optimal rendezvous maneuver of pursuing vehicle with minimum fuel expenditure in approach stage on elliptic and hyperbolic orbits
15 p2701 A69-31548
- Equatorial moderately elliptical satellite orbit perturbations calculated in local invariants, assuming state vector dependence of acceleration
17 p3039 A69-33796
- Orbit computation by means of predictor-corrector algorithms based on nonpolynomial functions, including numerical results for two body elliptic motion
19 p3397 A69-35611
- Optimal fuel transfers between coplanar and noncoplanar coaxial elliptical orbits determined by Pontryagin maximum principle, using digital program for Hamiltonian equations solutions
19 p3399 A69-35670
- Minimum impulse transfer between circular and nearby noncoplanar elliptic orbit, applying Pontryagin principle
19 p3400 A69-35675
- Stability of periodic orbits in elliptic restricted three body problem [AAS PAPER 68-086]
20 p3595 A69-37172
- Time-independent feedback attitude control system for high accuracy earth pointing motion of stable and unstable satellites in elliptic orbits
21 p3804 A69-39020
- Daily communication link geometry between spacecraft in elliptical orbit and landed capsule, establishing spacecraft visibility contours for landing site latitude [AAS PAPER 68-110]
21 p3805 A69-39223
- Recurrence formulas for calculating Fourier expansions in elliptic motion in terms of eccentric and mean anomaly [AIAA PAPER 69-910]
21 p3807 A69-39342
- Gravity gradient perturbing torque cast in terms of perturbing Hamiltonian, deriving long term changes in rotational motion of tumbling triaxial satellite in elliptical orbit [AIAA PAPER 69-922]
21 p3821 A69-39353

ELLIPTICAL POLARIZATION

- Frequency discrimination characteristics of elliptically polarized dual polarization gas laser, discussing intensity crossover phenomenon and frequency stabilization application [IEEE PAPER P-5]
07 p1153 A69-19074
- Radio waves polarization scattered at ionospheric discontinuities analyzed for vertical incidence, determining modulus distributions and polarization factor argument
09 p1453 A69-21527
- Elliptical polarization in ultrabroadband YIG pulse compression networks, using reflections at rod faces
13 p2230 A69-27680

- Radio waves polarization scattered at ionospheric discontinuities analyzed for vertical incidence, determining modulus distributions and polarization factor argument
16 p2754 A69-32522
- Singular electromagnetic field rectilinear and elliptical polarization in general relativity, calculating light plane rotation in Schwarzschild space
20 p3576 A69-37431
- Polarization ellipse orientation at source from Faraday fringes on Jupiter decametric radio bursts swept frequency records
20 p3594 A69-38169
- Poincare sphere properties representing birefringent behavior of materials and qualitative measurement technique for elliptically polarized light
21 p3844 A69-39318
- Statistical analysis of random production errors on phasing section polarization field of antenna with elliptical polarization
23 p4125 A69-42041

ELLIPTICITY

- Ellipticity of trajectory of free motions of pole of revolution of earth, using harmonic analysis of motion amplitudes and phases
06 p0919 A69-17536
- Photometric over dynamical ellipticity excess attributed to gravitational darkening in eclipsing binaries of W Ursae Majoris type
10 p1776 A69-23217
- Plane stress solution for stresses due to concentrated couple acting at any point on elliptic plate with fixed edge
15 p2712 A69-31014
- Rapid orbit prediction method for planning satellite observation programs, considering oblateness and radiation pressure effects
15 p2697 A69-31310

ELONGATION

- Surfaces role in superplasticity, demonstrating rate of neck growth dependence on surface irregularities
03 p0449 A69-13879
- Elongational viscosity coefficient determined from tensile measurements of materials under applied stress
10 p1681 A69-23976
- Stress-strain relation in crystalline media for pure tension and elongation epsilon several times conventional elastic limit, verifying by testing Al alloy [ONERA-TP-695]
11 p1975 A69-24754
- Strain rate and temperature effects on sintered molybdenum sheets strength and elongation characteristics
14 p2464 A69-29322

EMANATION

U EMISSION

EMBEDDING

- Necessary and sufficient conditions for Einstein spaces of second embedding class
06 p0957 A69-17547
- Direct epoxy embedding of monolayer cells cultured on millipore filter and fixed, dehydrated and microscoped before immersion
10 p1649 A69-23404
- Strain gage embedding techniques and applications
21 p3725 A69-39327

EMBOLISMS

- Decompression gas emboli detection while moving in flow streams of arteries and veins using ultrasonic Doppler shift principle and square-wave electromagnetic flowmeter
21 p3663 A69-38914
- Ultrasonic Doppler flowmeter for detection of circulating gas emboli of animal blood vessels during decompression
21 p3663 A69-38915
- Intravascular gas emboli literature critique covering early nonclinical decompression experiments, clinical use of intravenous gas emboli, etc
21 p3655 A69-38916

EMBRITTELEMENT

- High pressure hydrogen environment on tensile properties of stainless steel with and without strain induced martensite
01 p0093 A69-10062
- Welding with aluminum-zinc-magnesium alloys, discussing stress corrosion, embrittlement, compositions, heat treatment, material production and fabrication
02 p0266 A69-12063
- Liquid metal adsorption induced embrittlement, noting bond strength reduction and grain boundaries penetration
03 p0448 A69-13872

Hydrogen effect on interatomic bonds of Ti beta alloy and Young modulus, noting measurements at various temperatures

04 p0618 A69-15178

Metals hydrogen embrittlement theory, discussing role of dynamic strain aging hypothesis in overcoming theory defects

09 p1523 A69-21849

Pressure vessel design to alleviate hydrogen embrittlement of steels for shock tunnel drivers [AIAA PAPER 68-367]

09 p1477 A69-21993

Nb H alloys embrittlement, discussing hydride formation and resistance variation with temperature

10 p1707 A69-22989

Brittle fracture at high temperatures in titanium alloys using scanning electron beam microanalysis, noting reaction diffusion with atmosphere and grain boundaries destruction

10 p1713 A69-23823

Ductile metal clads and coatings of silicides, aluminides and noble metals to protect Cr alloys against nitrogen embrittlement and air oxidation

12 p2114 A69-26495

Hydrogen embrittlement of stainless steel and effects on mechanical properties, discussing martensitic phase role

12 p2115 A69-26616

Sigma phase and temperature effects on toughness of austenitic stainless steel weldments

18 p3150 A69-35429

Hydrogen effect on embrittlement of Cr-Ni stainless steel from viewpoint of corrosion cracking, using reverse bending apparatus

19 p3358 A69-35774

Ti-Al alloys yield and fracture characteristics as function of high exposure temperatures, studying causes of embrittlement

19 p3344 A69-35927

Hydrogen embrittlement mechanism in steel based on modified pressure theory, discussing crack propagation mechanisms and stress corrosion cracking

19 p3350 A69-36894

EMBRYOLOGY

Weightlessness effects on fertilized frog egg development on board Gemini 8 and 12 manned orbital flights, discussing cell division, differentiation and embryogenesis

01 p0017 A69-11084

EMERALD

U BERYL

EMERGENCY LIFE SUSTAINING SYSTEMS

Physiological approach to tests and evaluation of aviation survival equipment, noting human reactions study under extreme conditions

06 p0877 A69-16953

Automatic inflators for life jackets and survival gear in emergencies activated after submersion in water

06 p0877 A69-16955

Small column insulated delay /SCID/ aircraft seat ejection systems, illustrating weight saving

06 p0877 A69-16957

Survival of aircrew after successful ejection over water and boarding life raft

06 p0878 A69-16958

FAA regulations for improvements on crashworthiness and emergency evacuation from viewpoint of plastic applications and fire safety in aircraft

08 p1254 A69-20497

Emergency escape and personnel recovery systems including F-111 explosive system, midair deployed buoyancy aerostat and fly-away flexible wing rotor

15 p2551 A69-30853

Gangrene and caisson disease due to diving accidents, discussing emergency treatment with hyperbaric oxygen

17 p2911 A69-33775

Aircrew Arctic survival situation simulation experiments with survivors staying close to aircraft and walking across difficult terrain from emergency location

23 p4088 A69-41810

EMISSION

NT BIOLUMINESCENCE
NT CHEMILUMINESCENCE
NT ELECTROLUMINESCENCE
NT ELECTRON EMISSION
NT FIELD EMISSION
NT FLUORESCENCE
NT ION EMISSION
NT LIGHT EMISSION
NT LUMINESCENCE
NT LUNAR LUMINESCENCE
NT NEUTRON EMISSION
NT OPTICAL RESONANCE
NT PARTICLE EMISSION
NT PHOSPHORESCENCE

NT PHOTOELECTRIC EFFECT
NT PHOTOELECTRIC EMISSION
NT PHOTOIONIZATION
NT PHOTOLUMINESCENCE
NT RADIO BURSTS
NT RADIO EMISSION
NT SECONDARY EMISSION
NT SHOCK WAVE LUMINESCENCE
NT SOLAR RADIO BURSTS
NT SOLAR RADIO EMISSION
NT SPECTRAL EMISSION
NT SPONTANEOUS EMISSION
NT STIMULATED EMISSION
NT THERMAL EMISSION
NT THERMIONIC EMISSION
NT THERMOLUMINESCENCE
NT TYPE 2 BURSTS
NT TYPE 3 BURSTS
NT TYPE 4 BURSTS
NT TYPE 5 BURSTS
NT X RAY FLUORESCENCE

Emission and diffusion theories of metal-semiconductor contacts for describing current characteristics of abrupt isotype nGe-nGaAs heterojunction

11 p1938 A69-25115

Radiation absorption and emission problem for material of unit density at rest solved by finite difference scheme

21 p3773 A69-39666

EMISSION SPECTRA

IR emission in NGC 7027 spectrum and role of discrete line emissions, discussing magnetic dipole transitions, temperature and density

01 p0148 A69-10051

GaP p-n structures creation for diode sources of green and red radiation, comparing diffusion and epitaxial methods

01 p0137 A69-10259

Adsorbed gas influence on X ray emission from exploding tungsten wires noting ungassed and degassed specimens in vacuum

01 p0118 A69-10668

Red shift pattern in quasar emission spectra consistent with fractional screening charges on emitting atom nuclei

01 p0153 A69-10855

Europium complexes high resolution emission spectra in relation to molecular configuration

01 p0024 A69-10893

Free bounded continuum processes effect in nonequilibrium gases of finite continuous opacity, noting curves of growth for finite plane parallel layer emission lines

01 p0121 A69-10959

Auroral emission rates and heating effects as function of altitudes

02 p0235 A69-11426

Polarization of nightglow, line vs continuum

02 p0235 A69-11428

Ebert spectrometric experiment during Mars flyby aimed at detecting upper atmosphere atoms, ions and molecules in 1100-4300 angstrom spectral range [AAS PAPER 68-184]

02 p0311 A69-11469

Ionized metals emission lines intensity in chromosphere observed with coronagraph, determining hydrogen concentration

02 p0314 A69-11635

Absorption and emission redshift distribution in quasars, N systems and similar compact and radio galaxies

02 p0325 A69-12591

Temperature dependence of electron beam pumped GaAs laser threshold current density and emission spectra, noting doping effects

02 p0260 A69-12683

Spectrophotometric studies of planetary NGC 6543 gaseous nebula, measuring emission line intensities, electron density and temperature [ARL-68-0200]

02 p0327 A69-12708

Antennas with vertical radiation patterns to measure frequency spectrum of distributed cosmic radio emission between 6.3-40 MHz

03 p0500 A69-13080

Interstellar gas masers account for properties of 18 cm emission lines from OH molecules

03 p0511 A69-13465

Photoluminescence spectra of n-type GaAs films grown by gas transport reactions and from solution melt, noting recombination emission

03 p0488 A69-13887

Diurnal variations of low latitude VLF emissions observed at Hiraio, Japan

03 p0398 A69-13900

GaAs diode laser short wave emission, discussing coherent radiation and photon energy

03 p0441 A69-14165

Epitaxial n-GaAs photoluminescence obtained from p-GaAs, considering emission intensity

03 p0492 A69-14167

Luminescence spectra due to radiative recombination of optically injected carriers in Co 60 gamma ray and neutron irradiated Si at low temperature

03 p0494 A69-14243

Microwave excited argon discharge emission spectrum analysis, suggesting possible laser action in microwave discharges

04 p0609 A69-14346

Interatomic collisions effect on multimode He-Ne lasers output power and spectral composition

04 p0610 A69-14383

Cathodoluminescence of n-type GaAs with various carrier concentration bombarded with 24-keV electrons, studying emission spectrum for radiative transition

04 p0639 A69-14436

Gas laser generation frequency control by emission absorption saturation effect, inserting neon filled emission absorbing cell into resonator

04 p0611 A69-14550

Radio emission spectra of radio galaxies from 3CR catalog

04 p0661 A69-15234

Emission lines structure in quasar spectra, analyzing problem of weak absorption lines identification

04 p0662 A69-15236

Coronal X ray emission near limbs in 16-40 A during solar eclipse

04 p0650 A69-15531

Emission cross sections of first negative band system of nitrogen under electron impact excitation

05 p0795 A69-15617

Parameters and relative errors tabulated from IR spectral emittance of Mo, Nb, Zr and Ta near 1400 K

05 p0846 A69-15903

Frequency and polarization selection of neodymium glass laser oscillators by directing secondary radiation into laser cavity and duplicating spectral properties [IEEE PAPER P-3]

05 p0775 A69-16324

Continuous emission spectrum and continuous plasma absorption spectral coefficients for optically dense quasi-steady state electrical discharge plasma in sulfur capillary

06 p0964 A69-17251

Lasing threshold and spectral characteristics of organic dye solutions, using excitation of second harmonic of monopulse ruby laser

06 p0933 A69-17255

Identification of emission lines from 3200 to 7000 A in Eta Carinae spectrum, noting P Cygni-like absorption lines

06 p1002 A69-17263

Mass motion in solar flares, discussing loop flares from emission line profile characteristics

06 p0993 A69-17429

Mass motions in flares and moustaches indicated by spectral features, discussing red asymmetry of line emission

06 p0994 A69-17432

Time dependent emission spectra from flashlamp pumped organic dye lasers recorded with image converter, comparing dyes characteristics

06 p0936 A69-17901

Emission line profiles in spherical atmosphere expanding with constant radial velocity computed by Monte Carlo methods

06 p1009 A69-17965

Semiconductor lasers, discussing electron transitions, radiative band-band transitions, emission and absorption spectra, recombination rates, carrier lifetime and lasing conditions

06 p0937 A69-18009

Helium-neon laser radiation of given spectral compositions, noting relation between spatial coherence and controlled number of frequencies

07 p1148 A69-18803

Radio telescope survey of intense emission regions along galactic plane, considering antenna temperatures, spectrum and steps of observed emission

07 p1216 A69-19138

Induced emission cross section of neodymium glass laser in quasi-steady mode measured as function of rod section, mirror reflectivity and output

07 p1156 A69-19161

Band profiles and emission spectra of shock heated AlO compared for self absorption of blue-green system, discussing electronic transition moment

07 p1184 A69-19163

Absorption and emission spectra of ruthenium 2 complexes dissolved in rigid glasses, discussing crystal field theory and luminescence

07 p1200 A69-19219

- Spectrum data of Nova Vulpeculae /1968/ summarized concerning dispersion figures
07 p1220 A69-19337
- Ligand field transitions in tertiary phosphine and arsine complexes of ruthenium and osmium
07 p1075 A69-19483
- Emission spectrum analysis of faint solar prominences noting kinetic temperature, turbulent velocity and electron density
07 p1210 A69-19718
- UV emission spectrum of double star Boss 1985, excitation potential effect on Fe II lines and table identifying emission lines
08 p1385 A69-20060
- Absolute excitation cross sections for emission of second positive bands of nitrogen under electron impact
08 p1355 A69-20208
- Carbon dioxide absorption and emission in mesosphere, discussing vibrational relaxation time and radiative heating rate
08 p1308 A69-20308
- Emission spectrum of laser employing electron-vibrational transitions in samarium doped calcium difluoride crystal, noting spectrum shift with increasing crystal temperature
08 p1326 A69-20544
- Neutral hydrogen asymmetry in Galaxy M101 as evidence for tidal effects due to nearby companions, noting hydrogen emission spectra
08 p1394 A69-20625
- Color index and mean light curves constructed for Cepheid Variables
08 p1395 A69-20635
- Laser rubies emission characteristics operating at different temperatures in common resonator, studying kinetics for pumping powers
08 p1327 A69-21076
- Emission line galaxy NGC 5253, discussing radial velocity, line width and excitation and similarity to Seyfert galaxies
08 p1407 A69-21132
- Laser stimulated gamma-optical transitions illustrated by gamma-optical absorption detection in dysprosium ethyl sulfate
08 p1328 A69-21185
- Luminescence spectra of molecular gases excited by fast electrons in infrared spectral region, noting H alpha line
09 p1590 A69-21382
- OH emission source in constellation Canis Major discovered with interferometer in October 1968, noting nearby IR object
09 p1591 A69-21448
- Detection of micron Ne emission line from planetary nebula IC 418 using IR spectrometer
09 p1591 A69-21452
- Cosmos 92 satellite observation of night airglow flare, discussing NO bands emission and origin
09 p1485 A69-21533
- Emission spectra of BaO during barium release compared with computed spectra for upper atmosphere temperatures evaluation
09 p1488 A69-21664
- Frequency fluctuations in mode coupled gas laser used to determine natural emission line width
09 p1516 A69-21670
- VLF emissions intensity and spectra variations compared with energetic electron fluxes variations during magnetosphere storm periods
09 p1488 A69-21698
- Hydrogen beta emission profiles for pole-on type Be stars, measuring stellar rotational velocity by Huang-Struve method
09 p1596 A69-22052
- Hydrogen alpha emission nebulae catalog in western half of Cygnus X region, obtaining interstellar absorption from nebular distances determination
09 p1596 A69-22053
- Further microwave emission lines and ammonia clouds in Sagittarius region, tabulating relevant transitions in ammonia and water
09 p1597 A69-22150
- Outstanding solar type 4 radio burst from spectrographic records at metric and decametric wavelengths from Weissenau Observatory
09 p1578 A69-22157
- Solar far UV emissions observed from OSO-C by grazing incidence grating spectrometer, noting temporal variations and atmospheric absorption characteristics
09 p1578 A69-22168
- Solar X ray and extreme UV spectra during flares, attributing intense emissions to optical transitions
09 p1578 A69-22169
- Red shifts of radio sources obtained with Carnegie image tube spectrograph, noting quasi-stellar objects and galaxies
09 p1602 A69-22224
- Iron line absence in emission spectrum of thermal X ray sources, constraining proposed thermal models
09 p1580 A69-22231
- Ratio of volume emission rates of 5577 A and band of positive N molecular ion first negative system for use in auroral observations
09 p1491 A69-22607
- GaP p-n structures creation for diode sources of green and red radiation, comparing diffusion and epitaxial methods
09 p1559 A69-22652
- IR emissivities of powdered silicates and cloudy atmosphere model of spectral emission for radiative transfer in condensed powder
10 p1778 A69-23414
- IR radiation effects in cadmium sulfide crystals with green edge emission at low temperatures, discussing luminescence, photoconductivity and conductivity glow curves
10 p1746 A69-23565
- Laser emission lines produced by pulsed electrical discharge through ammonia
10 p1704 A69-23666
- Simultaneous photometric observations of coronal emission lines during July 1966 solar proton flare plotted on synoptic charts
10 p1763 A69-23731
- Auroral H beta intensities determined from photographs by image intensifier, describing equipment and data reduction method
10 p1684 A69-23824
- Nuclear sizes, emission line widths and densities in Sc galaxy M 51 and Seyfert galaxy NGC 4151, noting similarities and difference between nuclei
10 p1785 A69-24089
- Spectra of low energy X ray source at position of Large Magellanic Cloud, noting flux
10 p1770 A69-24093
- Models for emission line region of 3C 273, considering ionization distributions for estimation of relative abundances
10 p1790 A69-24137
- Tunable Fabry-Perot interferometer for photoelectric measurements of absorption and emission line contours and line center particle concentrations
10 p1698 A69-24212
- UV, visible and near IR spectral characteristics of hydrocarbon-air flames with particulate Al, Mg and B, noting hot metal continuum and oxide emissions
11 p1940 A69-24483
- Solar spectra of Mg II doublet lines during September 22, 1968 eclipse, considering chromospheric activity effects on emission peaks
11 p1958 A69-24591
- B star HD 191980 spectral variations from B-3 to B-8 noting helium to carbon line intensity ratio, interstellar D line strength and radial velocity measurements
11 p1958 A69-24594
- Specific level role in emission of optical radiation by ruby laser stimulated calcium fluoride crystals doped with divalent Dy ions
11 p1894 A69-24618
- Hydroxyl microwave emission sources in Cygnus not connected with continuum emission
11 p1964 A69-25403
- Magnetic fields, green corona emission and filaments relationship at high solar latitudes using synoptic charts
11 p1964 A69-25416
- Photospheric magnetic fields, coronal emission and filaments distribution relationship with 1420 MHz radio emission, noting brightness and plasma density increase
11 p1964 A69-25417
- Free emission spectrum analysis of ruby laser with external mirrors and elimination of axial mode discrimination
11 p1900 A69-25547
- Recombination emission spectrum relation to plasma recombination coefficient, determining plasma electron temperature from continuous spectrum intensity
11 p1934 A69-25566
- Photoluminescence spectra of n-type GaAs films grown by gas transport reactions and from solution melt, noting recombination emission
11 p1939 A69-25688
- Spectral brightness temperature of shock waves in air measured at 220-800 nm, obtaining 9-14 km/sec shock waves by detonating explosives
11 p1877 A69-25755
- Emission spectrum of ruby laser as function of relative orientation of resonator and active crystal axes, noting spectrum width
12 p2104 A69-26029
- Emission from solutions of organic luminophores excited by harmonics of Q switched neodymium laser
12 p2104 A69-26030
- Simultaneous HCN and HOH laser emission in pulsed discharge through mixture containing H, C, N and O
12 p2107 A69-26330
- H alpha line photograph in M 82 spectra, giving equivalent radiating area and total ionized hydrogen mass
12 p2171 A69-27067
- Thermal and free-free emission from planetary nebulae based on graphite grain model, discussing IR fluxes
12 p2172 A69-27158
- Spectrum analysis of radio galaxy M82 nucleus, noting H alpha emission lines from analysis of IR photograph
13 p2335 A69-27310
- Scorpius XR-1 X ray emission spectra, discussing Fe emission line near 7 keV plasma models, supernova mass and cosmic abundance
13 p2325 A69-27313
- Ultrasonic vibrations effect on emission of ruby laser with externally mounted mirrors
13 p2271 A69-27534
- NGC 4194 galaxy emission line spectrum analysis showing presence of highly excited gas in nucleus and in bright central region similar to NGC 7714
13 p2339 A69-27571
- Chromospheric heating and polarization in late stars, considering association with Ca II K line emission cores
13 p2340 A69-27579
- Radio emission from high level transitions in hydrogen calculated by superposing emission lines on background continuum, using Gaunt factor for free-free emission
13 p2327 A69-27596
- IR extragalactic radio sources including normal radio galaxies, quasars and Seyfert galaxies
13 p2342 A69-27597
- Ruby and neodymium glass traveling wave laser free generation spectra kinetics, noting mode transitions as function of pumping levels
13 p2271 A69-27655
- Markarian galaxies with strong UV continuum, observing emission lines differing from each other
13 p2351 A69-27866
- Active medium temperature effect on semiconductor laser emission spectra composition, discussing amplification coefficient frequency dependence at various temperatures
13 p2271 A69-27888
- Single frequency ruby laser emission spectrum coincidence with interacting laser radiation at instant of Q switching
13 p2272 A69-27911
- CW lasers based on composite yttrium fluoride type crystals, noting large number of intense emission bands
13 p2273 A69-28316
- HF emission spectra of radio pulses from cosmic ray showers confirming Dublin group observations
13 p2333 A69-28471
- Intratomic collisions effect on multimode He-Ne lasers output power and spectral composition
14 p2456 A69-28756
- Antennas with vertical radiation patterns to measure frequency spectrum of distributed cosmic radio emission between 6.3-40 MHz
14 p2509 A69-28762
- Rocket observations of Lyman alpha anisotropic galactic radiation, noting distribution of neutral interstellar hydrogen near sun
14 p2516 A69-28952
- Weak superconducting contacts volt-ampere characteristics current steps and emission spectra, showing singularities due to superconducting current nonharmonicity
14 p2504 A69-28994
- Blue continuum emission from hot carbon dioxide measured in shock tube, discussing applications to temperature measurement of gases containing carbon dioxide
14 p2427 A69-29014
- Solar cosmic ray flare of 28 January 1967 observed by neutron monitors, determining emission and particle spectrum at atmosphere boundary
14 p2513 A69-29066
- Galactic OH emission sources time variations found in W49 and W75
14 p2517 A69-29085

Pulsars dynamic spectra, suggesting inadequacy of interstellar scintillation models to explain observed dependence of decorrelation band widths on frequency
14 p2517 A69-29087

Interstellar gas radio and optical spectral lines of neutral H compared with Ca and neutral Na, discussing critically low velocity gas distribution
14 p2519 A69-29135

CdS crystals emission spectrum during two photon excitation by ruby laser, noting dependence on pump power
14 p2458 A69-29167

Emission spectrum width of solid state lasers as function of temperature, investigating effects of active medium parameters, pumping and cavity
14 p2459 A69-29389

Late type stars with emission peak wavelength approximating graphite Debye frequency induced by graphite impurity atoms
14 p2521 A69-29586

High speed photographs of plasma emission spectra in UV and soft X radiation spectrum regions, discussing theory, design and operation of facilities
14 p2496 A69-29784

Emissivity of two photons decay from metastable 2s level of pure hydrogen gaseous nebula, noting radiative and collisional excitation
14 p2529 A69-29975

Airglow research, discussing emission features, observation methods and instruments, ground station network, etc
15 p2594 A69-30020

Gas laser secondary modes emission and beat frequency spectrum widths, using results of Lamb lasers theory
15 p2633 A69-30121

Molecular benzene emission spectra excited by electron beams in RF modulated source, tabulating lifetime measurements
15 p2562 A69-30468

Solar flares associated with intensive sodium D lines emission observed photoelectrically with telescope in unperturbed region, analyzing possibilities of comets solar origin
15 p2674 A69-30506

Spectral emission of active prominences, showing looplike lines during quiet phases and differences in turbulent velocities magnitude
15 p2674 A69-30510

Photoelectric comet observation techniques, tabulating narrow and wideband filter combinations for determining parameter Q for various cometary spectral emissions
15 p2684 A69-30522

Neutron star atmosphere and X ray emission spectrum, computing incident protons mean free path for two assumptions
15 p2686 A69-30535

Neutral hydrogen in dark dust clouds in 21 cm line, showing hydrogen excesses and deficiencies
15 p2691 A69-30763

Transition probabilities for radiative lifetime of Swan and Mulliken diatomic C bands calculated from lifetime data using Franck-Condon factors
15 p2694 A69-30789

Unsaturable frequency discriminator influence in semiconductor laser feedback loop on laser emission spectrum
15 p2635 A69-30967

Atmospheric hydrogen and helium atoms emission in geomagnetic poles and winter hemisphere, comparing thermal dissipation and migration of light atoms
15 p2599 A69-31322

IR horizon of earth from ionospheric IR emission spectra obtained by sounding capsule, discussing earth geometric horizon and particular spectral bands [ONERA-TP-709]
15 p2601 A69-31370

Balmer alpha emission for abundance and distribution of hydrogen around earth, relating temporal variations to azimuth
15 p2700 A69-31437

Supernovae spectra observation suggesting tracing as broad band interstellar absorption rather than emission features on continuum
15 p2701 A69-31534

Optical and electrical properties of electroluminescent diffused gallium arsenide phosphide diodes with low donor concentrations, analyzing spectral emission and fabrication effects
16 p2758 A69-31699

Spectral characteristics of B stars group, reviewing causes of spectral line profile deformation
16 p2855 A69-31828

Intensity and rotational temperature seasonal variations of hydroxyl emission at different latitudes in upper atmosphere
16 p2775 A69-32081

Chromospheric spectrum outside of eclipse, wave lengths 3040 to 9266 Å, listing emission lines taken at McMath solar telescope
16 p2861 A69-32257

Cosmos 92 satellite observation of night airglow flare, discussing NO bands emission and origin
16 p2783 A69-32528

Vertical ozone distribution from emission and absorption in 9.6 μ band determined during IGY in Switzerland
16 p2785 A69-32625

Emission intensity ratio change as function of polar auroral height compared to variation in atmospheric concentration ratio of oxygen to nitrogen
17 p2963 A69-33956

GaAs semiconductor laser emission band homogeneity and continuous energy spectrum levels contribution to induced optical transitions
17 p2984 A69-34161

Thermal emission and spectral degree of blackness of W derived from electron motion equation
18 p3156 A69-34715

Luminescence spectra of molecular gases excited by fast electrons in IR spectral region, noting H alpha line
18 p3176 A69-34770

Neodymium laser emission temporal structure in mode self locking regime with Q switching by saturable filter
18 p3152 A69-35016

Spectral inhomogeneity effect on spectrum of modes emitted by semiconductor p-n junction/laser
18 p3152 A69-35023

Laser stimulated gamma-optical transitions illustrated by gamma-optical absorption detection in dysprosium ethyl sulfate
18 p3152 A69-35154

Water vapor microwave emission measurement from galactic hydroxyl sources
18 p3205 A69-35435

Laser emission in system of four level centers, determining nonuniform emission line broadening due to disturbed quasi-equilibrium distribution of electron subsystem elementary excitations
19 p3333 A69-35877

Single and two mode laser emission dependence on pumping power distribution between four level active centers of different types
19 p3333 A69-35878

High velocity interstellar gas in H I and H II regions, emphasizing observations of neutral atomic hydrogen in and far from galactic plane
19 p3402 A69-35962

Emission line spectrum for ionization and excitation in solar coronal structures, tabulating intensities from ground based eclipses observations
19 p3422 A69-36217

Forbidden lines emitted by gaseous nebulae, emphasizing relative intensities of O II and O III lines
19 p3422 A69-36220

Forbidden emissions in CH Cygni and VV Cephei noting symbiotic star
19 p3423 A69-36228

Intensity variations of Eta Carinae emission lines
19 p3423 A69-36231

Forbidden transitions in emission line spectra of variables near minimum light, finding origin in hot chromosphere
19 p3424 A69-36232

MH alpha 328-116 spectral characteristics noting weak continuum, emission lines from forbidden transitions and absence of absorption
19 p3424 A69-36233

Forbidden emission lines used to study interstellar gas, discussing gas ionization, neutral hydrogen, calcium lines, etc
19 p3424 A69-36235

Forbidden emission lines in spectra of normal, radio and Seyfert galaxies and quasars, giving information about quasi-stellar mean densities, temperatures, ionization, etc
19 p3424 A69-36236

Water vapor laser submillimeter emission spectra, considering rotational and vibrational lasing transitions due to electron impact and molecular interactions
19 p3336 A69-36349

Pulsed water vapor laser high power operation and strongest component wavelength measurement
19 p3337 A69-36416

Power, efficiency and temperature dependence of emission spectra and threshold current density in electron beam pumped GaAs laser, noting doping concentration
19 p3338 A69-36538

Undoped n-type gallium arsenide single crystals edge emission spectral band shape dependence on crystal type and ambient temperature
19 p3392 A69-36610

Gallium arsenide junction lasers operating above threshold, showing resonant modes dependence of steady state gain function and frequency dependence of spatial gain distribution
19 p3338 A69-36691

Carbon dioxide lasers near IR spontaneous emission spectra
19 p3339 A69-36697

Monochromatic coronal emission line photographs improved by composite technique
20 p3539 A69-37547

Solar corona Fe XII emission spectral lines relative intensity analyzed as function of temperature electron density
20 p3603 A69-37548

H alpha line for emission nebulae analyzed by Fabry-Perot etalon, noting Doppler profile
20 p3607 A69-38039

Doppler broadened atomic O emission line measurement providing indication of exospheric temperature storm-time variations
20 p3546 A69-38099

Solar UV emission lines from high resolution rocket observations
20 p3612 A69-38167

Ce II line reversal from absorption to emission in solar spectrum, noting reversal position dependence on wavelength and line source function scattering term
20 p3613 A69-38168

Ultrasonic vibrations effect on emission of ruby laser with externally mounted mirrors
20 p3556 A69-38201

Simultaneous ground and Alouette 2 satellite measurements of enhanced electromagnetic band emission in 500-1000 Hz range
21 p3708 A69-38496

Intensity changes of OI nightglow emission at 100 km by transport associated with tides, gravity waves and turbulent mixing
21 p3713 A69-38526

Emission band intensities of carbonyl fluoride in 2.0-6.0 micron region with scanning spectrometer, comparing results for room and shock temperature with theoretical data
21 p3669 A69-38759

Helium-neon laser radiation of given spectral compositions, noting relation between spatial coherence and controlled number of frequencies
21 p3736 A69-38948

Spectral characteristics of Q switched single frequency ruby laser with tunable emission frequency in giant pulse mode
21 p3737 A69-38991

Active medium temperature effect on semiconductor laser emission spectra composition, discussing amplification coefficient frequency dependence at various temperatures
21 p3738 A69-39146

Pumping and excitation spectra of solid solutions of cryptocyanine in glycerine irradiated by ruby laser, discussing population inversion and scattering and vibrational transitions
21 p3740 A69-39546

Spectral, angular and temporal characteristics of traveling wave mode ruby laser emission, noting high transverse divergence effect on mode operation
21 p3741 A69-39554

Lunar surface IR emissivity comparison spectra including proposed Apollo landing sites, indicating Si-O ratio difference for Plato crater
21 p3815 A69-39587

Ti emission and absorption K spectra in Ti-Al intermetallics, suggesting hypothesis concerning long wave and fundamental subbands origin
21 p3749 A69-39787

Solar flares and prominences emission lines equivalent width correlated with relative differential velocity between filaments
22 p4001 A69-39994

Singlet-singlet energy transfer kinetics dependence on emission and absorption spectra overlap via dipole-dipole interaction
22 p3895 A69-40056

- Radiation emission and ionization in precursor and nonequilibrium region behind shock wave during approach to equilibrium in argon-like gas
22 p4006 A69-40526
- Mars upper atmosphere ionized carbon dioxide and CO emission spectra in 1900-4300 Å region measured by Mariner 6, observing atomic hydrogen and oxygen lines
22 p4023 A69-40568
- Emission dynamics and fine pulse structure in GaAs injection lasers, determining pulse duration and amplitude dependence on current and resonator length
22 p3963 A69-40603
- K-alpha band characteristics of N spectra stimulated in nitrides of transition metals by X rays
22 p3974 A69-41118
- Radiative properties of Ta, Mo, Nb, graphite and niobium carbide at high temperatures
23 p4175 A69-41331
- Hydrogen fluoride chemical laser emission spectrum, studying rotational-vibrational transition of molecules triggered optically or electrically
23 p4172 A69-41493
- IC 3258 emission line spectrum observations, discussing blueshift, extragalactic location, possible nature, etc
23 p4219 A69-42374
- Daylight observations of Comet Ikeya-Seki 1965-f at perihelion passage, discussing resulting emission line spectra within comet head
23 p4221 A69-42386
- Forbidden O I 5577 Å dayglow emission equatorial measurements with rocket photometer, discussing altitude profiles and excitation mechanism
24 p4314 A69-43005
- Upper atmosphere OH molecules vibrational temperature and total emission energy, measuring average seasonal variations
24 p4308 A69-43007
- Emission spectrum of nonself locked He-Ne ring laser, deriving phase relations for LF intermode oscillations
24 p4328 A69-43159
- Atmospheric gases emission spectra excited by electron beam at angles of pressure
24 p4353 A69-43698
- EMISSION**
- Emissivity and other radiative characteristics of stainless steel oxides heated to various temperatures in air
03 p0453 A69-14157
- Emissivity of rough metallic surfaces with preserved profile similarity, showing independence to roughness height
05 p0845 A69-15894
- Emissivity of high temperature air and carbon dioxide-nitrogen mixtures in two diaphragm shock tube
06 p0911 A69-17348
- IR radiative heat transfer in nongray gases for non-black bounding surfaces, considering diatomic gases with single vibration rotation band
06 p1033 A69-17559
- Oxidation influence on molybdenum disilicide coatings, determining degree of blackness over thermal stability range
09 p1522 A69-21588
- High altitude radiant emittance of cirrus clouds and cloudless sky for IR transmissivity based on aircraft measurements
09 p1536 A69-21641
- Integral normal emissivity of electrically conducting materials heated to high temperatures by HF field of inductor, discussing measurement procedure and equipment
11 p1888 A69-25230
- Radiative heat transfer calculations between parallel surfaces, applying approximations based on total emissivities to known spectral emissivities
14 p2539 A69-29223
- Integral normal emissivity of Ta and Hf carbides at temperatures from 1300 to 3000 K measured by radiation method in vacuum
15 p2640 A69-30984
- Flight instrument package for change of energy absorption and energy radiation of vehicle surfaces during various phases of space vehicle mission
15 p2613 A69-31269
- Balmer line H alpha emission and absorption coefficients measured with hydrogen plasma generated in high current low voltage free burning arc
16 p2822 A69-32040
- Emissivity of high melting point compounds measured, considering electronic structure and atomic weight
18 p3158 A69-35260
- Spectral absorption coefficients and emissivities of thermodynamic equilibrium mixture of various combustion products at high temperatures, based on graphs
19 p3266 A69-36840
- Emissivity of nitrogen, oxygen and air plasmas in vacuum UV region of spectrum by photographic measurement, using He recombination radiation as brightness standard
21 p3774 A69-38944
- Corrections for eliminating anomalous skin effect on IR emissivity for Ag, Cu, Au and Al
23 p4177 A69-42212
- EMISSOGRAPHS**
U ACTINOMETERS
U RECORDING INSTRUMENTS
- EMITTANCE**
- Solar absorptance, total hemispherical emittance and absorptance/emittance ratio for metals at cryogenic temperatures measured simultaneously with sinusoidally perturbed incident radiation
01 p0176 A69-10847
- Total and spectral emittance of cobalt surfaces conditioned by evaporating some cobalt from surface at high temperature in vacuum
05 p0716 A69-16447
- Solar absorptance and hemispherical emittance of metals at space conditions determined with cyclic incident radiation technique
06 p0945 A69-18154
- Guarded disk type emissometer for hemispherical emittance measurements of sample materials in 88 to 420 K range based on steady state calorimetry
17 p2973 A69-33280
- Normal and directional emittance for two dimensional emitting, absorbing and scattering semiinfinite plane slab based on Monte Carlo method compared with Bobco approximation
17 p3005 A69-33301
- IR directional and hemispherical emittance of spacecraft thermal control coatings, comparing values determined by various measurement techniques
23 p4164 A69-41633
- EMITTERS**
NT THERMIONIC CATHODES
- Emitter base lateral diode carrier injection effect on current gain properties of small area double diffused planar transistors
05 p0728 A69-15808
- Finned radiation emitter tube unsteady state temperature field as function of working body temperature and emitter geometry
05 p0846 A69-15898
- Thermal instability in power transistor structures, considering effects of design, emitter and base resistance at high currents
08 p1373 A69-20858
- Lanthanum hexaboride single crystal field emitters for vacuum devices, describing construction and performance
09 p1468 A69-22601
- Emitter current density dependence on distance from center of drift transistor circular emitter, obtaining distributed base resistance in presence of arbitrary base current
11 p1853 A69-25565
- Emitter self bias in power stages of transistor transmitters, considering transistor parameters dispersion
13 p2226 A69-27217
- EMOTIONAL FACTORS**
- Psychiatric study of master attack carrier aviators inability to fly, considering adult situational reaction diagnosis
03 p0369 A69-12883
- Isolation effects on higher nervous activity, motor and vegetative reactions, muscular strength and emotional state
03 p0377 A69-14202
- Recorded vocal reactions of humans analyzed as characteristic of positive and negative emotions
05 p0709 A69-16518
- Professional activity of cosmonauts, considering training, mental and physical qualities and engineering background
06 p0879 A69-17036
- Time perception capacity of astronauts and jet pilots during brief weightlessness, noting emotional state effects
07 p1065 A69-18981
- Recorded vocal reactions of humans analyzed as characteristic of positive and negative emotions
18 p3096 A69-34737
- Time perception capacity of astronauts and jet pilots during brief weightlessness, noting emotional state effects
20 p3480 A69-38229
- Male patients urine tests during sinusoidal vibration, noting catecholamine excretion as criterion of emotional stress under various environmental conditions
21 p3654 A69-38909
- Heart rate measurements in ski jumpers with radio telemetric system revealing tachycardia during climbing and emotional stress
23 p4078 A69-41313
- Psychological stress effect on human convergent and divergent thinking after presentation of disturbing or benign control films
24 p4269 A69-42555
- Supersonic flying effect on urinary catecholamine excretion rates in pilots, noting emotional state
24 p4265 A69-43370
- EMPHYSEMA**
- Pulmonary emphysema effect on expiratory flow limitation from static pressure-volume and flow volume curves during natural and forced deflation of hamster lungs
23 p4082 A69-41442
- EMPLOYMENT**
- Industrial loyalty and trade secrets, discussing preservation of forms of intellectual property posed by mobile employee and management policies
01 p0180 A69-10991
- Occupational attrition estimation methods for determining personnel separation through marriage, death, retirement and transfer applied to engineering and nursing
07 p1245 A69-19728
- Organizational identification of scientists as professional employees, exploring degree of loyalty and perceived self prestige
21 p3855 A69-38765
- EMULSIONS**
NT NUCLEAR EMULSIONS
NT PHOTOGRAPHIC EMULSIONS
- JP-4 fuel emulsions properties, handling characteristics and safety performance, noting satisfactory shelf life and thermal stability
06 p0982 A69-17190
- Fuel control systems using emulsified fuel, noting exposure effects and temperature and pressure characteristics
09 p1571 A69-22486
- Two phase MHD generator with gas in liquid metal emulsions, discussing loops efficiency
13 p2306 A69-27479
- ENCAPSULATING**
- Plastic material requirements for semiconductor device encapsulation noting electrical compatibility, mechanical and environmental protection and costs
02 p0270 A69-12161
- Electric components encapsulation by combining liquid resin techniques and transfer molding
04 p0607 A69-14955
- Gallium arsenide materials technology, discussing solution and vapor-phase epitaxy and liquid encapsulation as related to crystal growth and purification
12 p2141 A69-25834
- Elastomeric thermosetting one part silicone encapsulant environmental tests, checking physical and electrical properties stability under temperature and relative humidity conditions
19 p3281 A69-35549
- Encapsulation effects on piece parts in high density package, considering unexpected part failures elimination in Lunar Module Signal Conditioning Electronic Assembly
22 p3910 A69-39953
- ENCKE METHOD**
- Encke type analytical-numerical integration for solving differential equations of modified set of Lagrange planetary equations, obtaining satellite ephemeris for orbit prediction
21 p3807 A69-39340
- Multispacecraft simultaneous simulation on hybrid computer using Encke perturbation method for translational motion and Hamilton quaternion method for inertial transformations
22 p4036 A69-40320
- ENCODERS**
U CODERS
- ENCODING**
U CODING
- ENCOUNTERS**
- Distributions of close planet-comet encounters for various orbital elements, calculating trajectory by conic matching
18 p3195 A69-34433

END PLATES

END PLATES

Atomic flux from Cs and K ion recombination on hot end plates of Q machine measured, noting contribution to total plasma end loss rate
08 p1358 A69-19810

Cesium plasma confinement time improvement in symmetrically heated tungsten end plates of Q machine
11 p1925 A69-24314

End constraints and length/width ratio influence on composites off axis tensile tests, considering rigid clamping with/without end rotation
13 p2286 A69-28667

End loaded two layer laminated elastic strip stress concentration and self equilibrating traction distribution analyzed by eigenvalue equation
13 p2370 A69-28672

Spanwise velocity correlations of turbulent vortices shed by two dimensional bluff body of D section with different aspect ratios, noting end plates effect
23 p4234 A69-42397

ENDFIRE ARRAYS

NT YAGI ANTENNAS

Superdirective aerial endfire array of four unequally spaced half wave dipoles and only one fed element, calculating and measuring maximum gain
09 p1468 A69-22603

Electromagnetic plane wave scattering from slender semiinfinite cone, obtaining contribution to tip return arising from direct diffraction
11 p1836 A69-24988

Gain optimization for dipole endfire array through orthogonalization of element directivity noting effects of element spacing, element gain and mutual coupling
13 p2226 A69-27186

ENDOCRINE GLANDS

- U ADRENAL GLAND
- U PINEAL GLAND
- U PITUITARY GLAND
- U THYROID GLAND

ENDOCRINE SECRETIONS

- NT ALDOSTERONE
- NT CORTISONE
- NT HORMONES
- NT PITUITARY HORMONES

Human endocrine-metabolic response to sequential decompression exposure during simulated orbital flight or extravehicular activity
01 p0022 A69-11337

F-102 pilot anticipatory and flight stress, noting endocrine-metabolic hyperactivity
12 p2023 A69-26552

European pilots accustomed to equatorial climate tested during regular flying missions, discussing heat effects on urinary steroids
12 p2024 A69-26560

Rats adrenal corticosterone concentrations changes in response to ACTH, determining response sensitivity dependence on time after hypophysectomy
22 p3870 A69-39871

ENDOCRINE SYSTEMS

Pituitary-adrenocortical axis and neuro-endocrine functions in animals maintained in oxygen atmosphere, discussing norepinephrine and epinephrine excretion values, etc
01 p0019 A69-11343

Glucose, lactate, free fatty acids, hepatic glycogen and endocrine activity in fasting hibernating dormouse and rat in deep hypothermia
10 p1642 A69-23118

Urinalysis of crew members of first transatlantic helicopter flight indicating interindividual endocrine-metabolic variability and circadian trends modification
19 p3263 A69-36452

ENDOGENOUS CONDITIONS

U PHYSIOLOGY

ENDOTHERMIC REACTIONS

Temperature profiles in laminar boundary layer with endothermal reaction investigated using nitrogen plasma jet in rarefied gas wind tunnel
16 p2821 A69-31833

Packed bed catalytic reactors cooling capacity in promoting endothermic reactions of hydrocarbon fuels, using computerized temperature and composition profiles
[AIAA PAPER 69-588] 17 p3071 A69-33265

ENDURANCE

Maximum voluntary isometric muscle strength relation to endurance time in static work during partial curarization
22 p3890 A69-40213

ENERGETIC PARTICLE EXPLORER D

U EXPLORER 26 SATELLITE

ENERGY

Energy definition in relativity for steady state universes, particularly Schwarzschild universes
05 p0792 A69-15683

ENERGY ABSORPTION

- NT AURORAL ABSORPTION
- NT ELECTROMAGNETIC ABSORPTION
- NT MOLECULAR ABSORPTION
- NT NEUTRON THERMALIZATION
- NT PHOTOABSORPTION
- NT POLAR CAP ABSORPTION
- NT SELF ABSORPTION
- NT THERMAL ABSORPTION
- NT THERMALIZATION [ENERGY ABSORPTION]
- NT X RAY ABSORPTION

Nonequilibrium carriers during semiconductor depolarization, noting microwave oscillation energy absorption in silicon and zinc sulfide crystals
01 p0138 A69-10434

Approximation formulas of Appleton-Hartree equations for nighttime medium wave frequency absorption in E region of ionosphere, discussing electron density
07 p1122 A69-18295

Electromagnetic wave attenuation propagating along external magnetic field ascribed to cyclotron wave energy absorption by resonant plasma particles
08 p1277 A69-21077

Self focusing of CW argon laser beam due to absorptive heating in crown glass, emphasizing time dependence of beam diameter as function of distance
10 p1706 A69-24009

Radiant power flow, transmittance and absorbance of absorbing thin film multilayer in terms of characteristic matrix and admittance of surrounding media
11 p1896 A69-24850

Nuclear component energy flux absorption in Fe measured with ionization calorimeter
13 p2330 A69-28386

Shock load protection through energy absorption and dissipation in primary or composite structures, listing honeycomb, cellular plastics and rubber mechanical properties
[ASME PAPER 69-DE-37] 14 p2531 A69-28846

Disaccommodation component of magnetic aftereffect causing dynamic absorption of HF magnetic energy in ferrites
15 p2665 A69-30038

Quality assurance impact energy attenuation testing of U.S. Army flyer protective helmet, considering combined interaction of shell, foam liner and plastic pads
15 p2559 A69-30851

Energy absorption by cold nonuniform plasma from externally driven electric field, noting relation between plasma and driving frequencies
15 p2661 A69-30922

Pumping energy absorbed by active element of neodymium glass during laser emission related to activator concentration
15 p2635 A69-31104

Flight instrument package for change of energy absorption and energy radiation of vehicle surfaces during various phases of space vehicle mission
15 p2613 A69-31269

Ultrasonics for wrought and cast aluminum alloys nondestructive testing, discussing ultrasonic energy damping measurements
16 p2800 A69-31778

Electron transport initiated by radiant energy absorption or by reducing suitable electron acceptor as source of energy for extraterrestrial life
17 p2908 A69-32973

Radiative heat transfer in nonisothermal media composed of spherical particles with complex refractive index emitting absorbing and scattering energy anisotropically, considering various geometries
[AIAA PAPER 69-626] 17 p3073 A69-33297

Generalized energy absorption coefficient effect on vibration mode of specimen on vibration test bench
17 p3062 A69-33718

Neodymium activated glass laser efficiency as function of absorption of pumping and emission energy by glass
22 p3964 A69-40797

Plasma dielectric constant and RF wave energy and power absorption in anomalous dispersion region, noting plasma permittivity inverse relation to absorption band frequency
23 p4195 A69-41385

Molecular radiobiology, discussing physicochemical processes caused by energy absorption in targets, leading to inactivation under various circumambient conditions
23 p4090 A69-41963

Microwave absorption by biological materials, noting energy distribution between reflected, transmitted and absorbed radiation as function of medium physical properties
24 p4270 A69-42574

ENERGY ABSORPTION FILMS

Oscillation mode selection in gas lasers by thin film absorber in resonator, using standing wave electric fields periodicity
04 p0610 A69-14384

Solar irradiance spectral distribution data normalized and combined with spectral absorbance of satellite surface coatings, obtaining absorbed energy for spectral range
09 p1576 A69-21644

Oscillation mode selection in gas lasers by thin film absorber in resonator, using standing wave electric fields periodicity
14 p2456 A69-28757

ENERGY BANDS

- NT BLOCH BAND
- NT CONDUCTION BANDS
- NT FORBIDDEN BANDS

Ionization losses of Ge 72 atoms stopping in Ge, noting no cut-off indicative of energy gap effects
01 p0140 A69-11245

GaAs photoemissive yield spectrum analysis, discussing transition energies and energy band structure models
01 p0140 A69-11254

Intensity ratio of first negative nitrogen band and oxygen line varies in auroral displays
02 p0235 A69-11425

Auroral emission rates and heating effects as function of altitudes
02 p0235 A69-11426

Electron band structure of copper-nickel alloys, discussing thermoelectric properties, energy ranges and effect of alloying additions
02 p0301 A69-12765

Molybdenum interband transitions noting low energy optical property anomalies and origin of two absorption bands
03 p0442 A69-12986

Impurity profiles and energy band diagram for cuprous sulfide-CdS heterojunction based on capacitance, Hall and electron microprobe measurements
03 p0368 A69-13075

Superconductor energy spectrum gap, discussing temperature dependence, anisotropy, thermodynamic and kinetic properties and relation to Fermi surface and phonon spectrum
03 p0485 A69-13331

Light absorption in semiconductors with electron hole pair formation noting conduction and valence band
06 p0978 A69-16901

Superconductors with overlapping energy bands studied by nuclear magnetic resonance method
07 p1198 A69-18513

Cyclotron resonance measurements of quantum effects in Ge valence bands by CW molecular gas laser, developing tunable submillimeter maser
[IEEE PAPER C-6] 07 p1150 A69-19051

Nonequilibrium radiation from first negative band of molecular nitrogen ion excited by shock wave electron impact
13 p2245 A69-27380

Band structure for narrow energy gaps of GeTe and SnTe by perturbation model, noting constant free path and relaxation time
19 p3385 A69-36516

Electroabsorption oscillations in CdTe films compared with results of interband transitions theory
19 p3386 A69-36523

Low temperature energy band gap in n-type single semiconductor crystals of In-Sb-Bi alloys analyzed by measuring Hall constant and optical absorption coefficient
19 p3390 A69-36552

Energy band gap variation as function of composition in In-Ga-P semiconductor crystals
19 p3390 A69-36553

GaAs injection laser properties calculation with doping levels for exponential band tails formation, deriving threshold currents, lasing frequencies, I-V characteristics, etc
22 p3959 A69-40012

ENERGY BUDGETS

- NT ATMOSPHERIC HEAT BUDGET
- NT HEAT BUDGET

Turbulence characteristics up to 150 m above ground, noting surface roughness length directional de-

pendence, longitudinal turbulence spectra and turbulent energy budget

01 p0110 A69-10695

Plasma discharge energy balance analysis to determine discharge power and temperature as function of electric field parameters

02 p0286 A69-11572

Surface radiation balance measurements in India during IQSY, discussing diurnal, seasonal and spatial variations of net radiation

02 p0307 A69-11820

DC arc plasma torch as heat source in plasma tunnel, discussing nonuniformity of plasma flame

02 p0291 A69-12424

Statistical energy approach for analyzing steady state vibration distribution in composite structures in terms of energy balances

04 p0675 A69-14687

Energy metabolism changes during weightlessness, considering effects on basal and nonbasal requirements connected with added increments for activity

06 p0872 A69-17014

Computer simulations, comparing self adaptive/neutron/ control of spacecraft energy allocation subsystem to programmed control

07 p1058 A69-18389

Terrestrial and Cytherean atmospheres evolution based on gray atmosphere model, surface energy budget and partition of water and carbon dioxide

07 p1213 A69-18608

Exchange coefficient of energy balance of earth surface for propagation studies of entrained atmospheric contaminants

09 p1535 A69-21514

Nitrogen impurities effect on electron energy balance in DC arc burning in inert gas

10 p1732 A69-23442

Reactors technical characteristics for high temperature mineralization of closed life systems biological wastes, deriving equations to estimate energy balance

10 p1649 A69-23504

Open loop suboptimal control for linear time dependent tradeoff between energy expenditure and probability of target set entry

11 p1860 A69-25443

Dynamic energy balance in positive column of electric arc, integrating expression to determine temperature time dependence

12 p2137 A69-26535

Soviet book on combustion, detonation and explosive energy of condensed systems covering stable/unstable processes

12 p2190 A69-26757

Kinetic energy balance equation of mean zonal flow in symmetrical polar cap derived from basic concepts of mechanics, discussing relative coordinate system rotation

15 p2595 A69-30219

Energetics relations of limited atmospheric region to global energy budget, discussing interaction, potential energy, generation, boundary flux and conversion terms

15 p2648 A69-30220

Energy budget equations applicable to limited atmospheric region using available potential energy concept, discussing relation to global energy

15 p2648 A69-30221

Air masses transformation, solving nonlinear simultaneous system of equations of motion, heat influx and turbulent energy balance

15 p2649 A69-30647

Food intake changes of female rats in response to changes in energy balance, discussing steroids as physiological tracer

15 p2555 A69-30693

Radiative luminescence of gas discharge plasmas in channel with substantial radial heat transfer determined from energy balance measurement

15 p2662 A69-30978

Electron temperature observation in daytime ionosphere, considering energy loss to ions and neutral particles

15 p2603 A69-31402

Rocket measurements of upper F region electron temperature and density profiles, for particle and energy balance of ionosphere topside, noting diffusive equilibrium

16 p2848 A69-31975

Dislocation and energy balance analysis of ductile and brittle metal cracks for determining metal fracture strength from plastic deformation

17 p3052 A69-32984

Critical review of Deriugin theory of scattering from rough lamellar surfaces using separation of variables method, discussing energy conservation violation

17 p2930 A69-33885

Magnetic storm energy balance, assessing solar corpuscular flux energy consumption in and beyond magnetosphere

17 p2964 A69-33959

Floating body attitude and stability analysis based on system potential energy balance, considering Archimedes principle, torques, equilibrium conditions, body shape, etc

[SAWE PAPER 773] 18 p3172 A69-34874

Energy balance equation for two phase liquid-gas mixture ignition process, deriving formula for speed of combustion zone movement

18 p3231 A69-35123

Meridional circulations in kinetic energy budget of Northern Hemisphere troposphere based on winter and summer climatic mean data, noting Hadley circulation

20 p3523 A69-37505

Components of turbulent energy balance at 1 and 4 meter heights, discussing average motion energy transformation into turbulent energy

20 p3571 A69-37696

Geophysical aspects of earth chemical composition, structure and energy balance

22 p4032 A69-40983

ENERGY CONVERSION

Exploding wire discharges similarity with underwater sparks for understanding water breakdown and parallel discharges

01 p0117 A69-10657

Direct energy conversion and materials limitations, discussing thermoelectricity, solar cells, thermionics and fuel cells

02 p0194 A69-11801

Satellite power generation and transmission system for solar energy conversion, noting estimates of surface area and weight of collectors

02 p0323 A69-12296

Electrostatic generator for direct conversion of moving dielectric medium potential or thermal energy to electric power

03 p0369 A69-14153

Porous gas diffusion electrodes design for electrochemical energy converters, noting contribution of theory of electrode kinetics

04 p0551 A69-15309

Electrostatics/EGD/ engineering, discussing generators and compressors

05 p0804 A69-16586

Solar flares, discussing transformation of magnetic energy into ion and electron kinetic energy by acceleration in high impedance region in current filaments

06 p0995 A69-17445

Plasma oscillation modes perpendicular to magnetic field used to study energy conversion by wave coupling across density discontinuity

08 p1367 A69-20795

Pure fluid amplifying logic and energy converting elements, discussing parameters, characteristics and working principles

[AGARDOGRAPH-118] 08 p1257 A69-20951

Rotational energy conversion of neutron star into relativistic electrons energy suggested by increasing period of pulsating radio source in Crab Nebula

09 p1591 A69-21454

Side wall currents in unignited hardware type thermionic energy converters, discussing work function and heat choke

09 p1439 A69-21822

Isothermal diode as study basis for internal complex controlling thermionic energy conversion

09 p1439 A69-21827

Local creation of mass in steady state universe as source of static field energy propagating away at speed of light

09 p1601 A69-22212

Second harmonic generation by electromagnetic wave incident on inhomogeneous plasma, determining power output

10 p1653 A69-23133

MHD generators with segmented electrodes at high Hall parameters, noting electron density, conductivity and Hall field reduction factor

10 p1637 A69-23476

Nonequilibrium ionization effects on performance of subsonic constant area MHD generator, using closed cycle blowdown loop facility

10 p1637 A69-23481

ENERGY CONVERSION EFFICIENCY

MHD blowdown loop facility for alkali seeded noble gas MHD energy conversion, noting performance and plasma insulation from ground

10 p1674 A69-23482

Closed loop magnetoplasmadynamic energy conversion system design, operation and duct section

10 p1638 A69-23483

Energy release in quasars through nonmassive gravitational collapse compared with local objects, noting cosmological luminosities

10 p1785 A69-24091

Plasma wave conversion into electromagnetic waves in strong magnetic field, studying nonlinear coalescence and scattering on thermal and epithermal ions

11 p1922 A69-24245

Electrochemical energy storage and conversion for space flight, emphasizing hydrogen oxygen and silver zinc batteries, Gemini and Apollo programs, etc

12 p2015 A69-25866

Turbomachinery buffer seals, buffer gas regulation and cleanup systems for operation of closed Brayton cycle power conversion system with gas cooled nuclear reactor

13 p2268 A69-27367

Segmented-electrode and Hall ducts tested on supersonic magnetoaerodynamic conversion rig, defining electrical model for boundary layer losses at electrode surfaces

13 p2311 A69-28034

Book on elements of solid state energy conversion covering quantum mechanics, thermodynamics, thermoelectricity and photovoltaic energy conversion

13 p3222 A69-28038

Convective instability by active stress, discussing composition dependent stress fields in continuous and mechanically isolated material and chemical to kinetic energy conversion

14 p2540 A69-29634

Laser radiation conversion during induced combination scattering, discussing stabilization of emission mode of first Stokes component

14 p2460 A69-29648

Kinetic energy conversion into heat in moving viscous media, formulating equations as volume integrals of spherical harmonics products

14 p2487 A69-29980

Energetics relations of limited atmospheric region to global energy budget, discussing interaction, potential energy, generation, boundary flux and conversion terms

15 p2648 A69-30220

Solar simulator with xenon and krypton lamps designed for thermal balance tests, power conversion and material degradation experiments

15 p2586 A69-30383

Planetary jetstream and general circulation energy transformations, applying circulation model results to specific weather situations

17 p3000 A69-33758

Laboratory device for investigating thermionic energy converters and measuring current-voltage characteristics by static/dynamic methods

18 p3136 A69-34700

Energy conversion - Conference, Washington, D.C., September 1969

23 p4064 A69-42236

Three phase DC-AC inverter with low harmonic distortion, good efficiency and packaging capability, stabilizing frequency by crystal controlled clock oscillator

23 p4074 A69-42294

ENERGY CONVERSION EFFICIENCY

Limited space-charge accumulation mode efficiency for gallium-arsenide diodes, taking into account electron-lattice relaxation processes

01 p0137 A69-10321

Thermodynamic comparison of MHD generators using Brayton and Rankine cycles, showing Rankine cycle conversion at higher channel Mach numbers for nonequilibrium ionization

03 p0369 A69-14154

Heat pipe for thermal control of terrestrial and aerospace energy conversion systems

06 p1030 A69-17189

Thermionic energy converter theory and efficiency, discussing design considerations to improve performance

07 p1057 A69-18255

Second harmonic generation conversion efficiencies at 5300 A with KDP and lithium niobate crystals, using Nd-glass laser of high radiance and narrow bandwidth

09 p1514 A69-21333

Optical motor system to efficiently convert laser energy into mechanical rotational energy, giving equations for controlling motor speed

09 p1442 A69-22457

Gunn effect cavity controlled generator oscillations, noting phase trajectory closing conditions dependence on resonant mode parameters

09 p1468 A69-22596

Closed loop cycle converter, composed of MHD generator and compressor consuming thermal energy, exhibiting moderate cycle efficiency decreases

11 p1824 A69-24223

Minimum conversion loss in general mixer circuit configuration, noting dependence on time varying resistance and equal terminating impedances

11 p1845 A69-24550

Thermodynamics of sinusoidal steady state energy converters governed by Onsager reciprocal relation, determining maximum conversion efficiency

11 p1826 A69-25396

Thermionic converter SD-4 design and performance tests covering emitter, collector and Cs reservoir temperatures and power efficiency

11 p1827 A69-25398

Constant and traveling magnetic fields MHD converters induction and finite dimensions influence analyzed by conformal mapping, separation, Fourier and finite difference methods

11 p1827 A69-25399

Arc mode thermionic Cs converter nonlinear I-V characteristics explained by current-dependent temperature and potential fields in plasma

11 p1827 A69-25400

DC to RF energy conversion in ungridded klystron gaps, calculating efficiency and optimum load conductance as function of gap dimensions

12 p2041 A69-26629

Synchronized microwave harmonic energy generation by filtering using DC step source feeding modified pulse forming network

12 p2041 A69-26630

Thermodynamic atomization in MHD energy conversion through convergent-divergent nozzles, noting nozzle efficiency and droplet size

13 p2245 A69-27477

Energy conversion with liquid metal working fluids in MHD generators, discussing single stage fully Carnotized process

13 p2372 A69-27482

Liquid metal multistage injection efficiency with sodium and potassium working fluids, noting preheating

13 p2372 A69-27483

Liquid metal two phase flow MHD generators efficiency prediction, discussing end losses and flow velocity

13 p2205 A69-27485

Optimal cycle parameters for liquid metal single component MHD cycle, employing condensing ejector in front of generator

13 p2205 A69-27488

Liquid metal MHD generator cycles thermodynamic analysis, considering multicycle operation improvement with heat regeneration

13 p2372 A69-27489

Liquid-metal MHD space power generation system using intermittent vaporization slugs shooting at 2700 R peak temperature

13 p2206 A69-27492

Liquid metal MHD induction generators design and performance, considering effect of geometry, operating conditions, fluid properties and power level on efficiency

13 p2207 A69-27503

Liquid metal induction MHD generator I-V characteristics at no load permitting self excitation with capacitors

13 p2208 A69-27509

Induction, helical and straight through liquid metal MHD generators tested under independent and self excitation conditions

13 p2208 A69-27512

Three phase high temperature liquid metal induction MHD generator performance, noting velocity profile nonuniformity influence

13 p2208 A69-27513

Two chamber DC arc heater with vortex stabilization, determining current-voltage characteristics and efficiency

13 p2244 A69-28557

Reliability and efficiency improvements for thermionic converters at JPL, giving failure analyses

14 p2397 A69-29175

SNAP 13 generator designs to develop technology for isotope heated thermionic converters, describing tests, efficiencies, power outputs and life times

14 p2481 A69-29191

Output current and efficiency of vapor thermionic converters obtained in terms of electrodes and interelectrode gas parameters, exemplifying nuclear fuel element

14 p2400 A69-29222

Noble gas thermionic converters, discussing auxiliary discharge compensation of negative space charge, I-V characteristics, efficiency and comparison to ignited mode cesium vapor converter

14 p2403 A69-29249

Rare gases effect on thermionic converters volt-ampere characteristics, noting gas pressure, oxygen contamination and performance relations

14 p2403 A69-29251

Soviet research on thermionic energy conversion, advantages and applicability in various fields

14 p2405 A69-29279

Energy relations and conversion for electrodynamic plasma acceleration with allowance for mass transfer processes resulting from recombination, diffusion and electrode erosion

15 p2664 A69-31176

Electric arc plasma generator efficiency analysis including supply voltage, working current, current-source impedance, ballast resistor and optimum voltage-current selection

15 p2664 A69-31177

Laser effect in neodymium glass, estimating efficiency of light energy output vs electric energy input

17 p2979 A69-32828

Rotary power transformer design for spin stabilized spacecraft power system, discussing efficiency and advantages

17 p3050 A69-34111

Thermal cycle for direct flow supersonic compressorless MHD generator without heat regeneration and high temperature exchange

18 p3093 A69-34714

Mechanical work recoverable from stored energy and heat absorbed by taking material through closed cycle in strain and entropy space

20 p3575 A69-37074

MHD losses in liquid metal converters due to nonideal magnetic field profile and to flow hydraulics

21 p3649 A69-39483

Rocket motor combustion efficiency evaluated by chemical energy conversion to equilibrium, applicable to fuels, oxidizers and combustors at subsonic or supersonic velocity

23 p4239 A69-41919

Radioisotope thermoelectric generators /RTG/ design and performance analysis method applied to generators using Si-Ge Air-Vac type thermocouples

23 p4188 A69-42260

Performance degradation in cadmium sulfide solar cells, discussing cause identification technique, I-V curve parameter changes, etc

23 p4070 A69-42271

Brayton-B generator for 2-10 kwe production, describing design, heat source/rejection, efficiencies and preliminary test data analysis

23 p4071 A69-42278

Spacecraft solar cell near-maximum power operation by tracking optimum value with array temperature sensor

23 p4075 A69-42303

ENERGY CONVERTERS

U DIRECT POWER GENERATORS

ENERGY DENSITY

U FLUX DENSITY

ENERGY DISSIPATION

NT VISCOUS DAMPING

Energy dissipation at rounded pipe entrance in viscous fluid, showing relation between entrance loss and radius of roundness

01 p0059 A69-10308

Energy gap behavior and thermodynamic properties of anomalous superconductors noting sensitivity to phonon spectrum

01 p0138 A69-10436

Barrier penetration depth by meteorite particles at prethreshold impact velocities, taking into account energy dissipation on shock wave front

01 p0152 A69-10579

Electron impact spectrometer for obtaining molecular energy loss spectra used to investigate scattering cross sections for optically allowed and forbidden transitions

01 p0123 A69-10620

Ionization losses of Ge 72 atoms stopping in Ge, noting no cut-off indicative of energy gap effects

01 p0140 A69-11245

Energy characteristics of laser with passive Q switch, taking into account internal reflections

02 p0256 A69-11999

Ruby laser limiting gain, stimulated emission loss, noise loss and spectral distribution determined by radiation intensity, pumping power and mirror reflection

02 p0256 A69-12000

Photoelectron energy loss mechanisms in planetary atmospheres, considering possible constituents in Mars and Venus upper atmospheres

02 p0321 A69-12118

Ruby laser output energy degradation due to pump light absorption by color centers of ruby rod

02 p0256 A69-12358

Angular distribution of radiation scattered by microscopic polyvinyl toluene sphere monolayer, noting intensity distribution approximation using Mie theory [AIAA PAPER 68-30]

02 p0282 A69-12503

Single degree of freedom structural damping estimations from viscous and hysteretic energy dissipation data

03 p0523 A69-12947

Nonlinear influence of resonator losses on stimulated emission of ruby laser, noting cut-off action

03 p0439 A69-13058

Aperiodic hydrodynamic beam instability development and energy losses, discussing plasma oscillation enhancement and nonlinearities

03 p0480 A69-14137

Q switched Ruby laser metastable state population kinetics and resonator losses, discussing internal energy redistribution with subsequent absorption spectrum changes

04 p0610 A69-14381

Electric field and energy dispersion law effects on plasma oscillations in semiconductors, calculating composite oscillation frequency

04 p0642 A69-14554

Energy dissipation effects on attitude stability of dual-spin satellites with damping mechanism on rotating sections

04 p0665 A69-14703

Average energy dissipation in MHD duct flow of arbitrary cross sectional shape, evaluating bulk temperature, net wall heat flux and pressure gradient

04 p0635 A69-14724

Twin differential calorimeter for measuring heat dissipation by wire specimen under fatigue tests, using semiconductor thermopiles

04 p0618 A69-15205

Asymptotic stability of gyroscopic systems equilibria with partial dissipation used for motion stability analysis

04 p0631 A69-15537

Three energy dependent quantities examined for gases, describing relation between ionization yields, cross section and loss functions

05 p0795 A69-15660

Conical diffuser/exit duct performance and model for estimating energy losses, discussing inlet flow and Reynolds number [ASME PAPER 68-WA/FE-45]

05 p0698 A69-16112

Sounding energy optimum spatial distribution during scanning and detection of several signals, noting reduction of mean energy losses

05 p0723 A69-16786

Magnetosonic waves absorption in plasmas, studying collisions leading to HF energy resonant absorption at lower hybrid frequency

06 p0963 A69-16904

Thermal considerations of spacecraft external panel effects on specular lower systems, discussing heat dissipation and computer program [AIAA PAPER 69-26]

06 p1037 A69-18097

Spherical and single axis passive oscillation energy dampers for gravity gradient oriented satellites, utilizing earth gravity field or solar pressure

07 p1229 A69-18347

Energy losses of clusters of charged particles moving through unbounded isotropic plasma manifesting nonlinearity in interaction of particle generated fields

07 p1189 A69-18528

Superconducting flux-flow resistivity minimum in Pb-Tl alloy, discussing thermal dissipation associated with temperature gradients across moving fluxoid

07 p1198 A69-18642

Atmospheric circulation intensity measurement, using potential energy conversion to kinetic or kinetic energy dissipation by friction

07 p1175 A69-18947

- Power losses in MHD channel due to longitudinal end effects related to finite dimensions of electrodes and terminal insulators
07 p1193 A69-19030
- Diffusion coefficient of interstitial oxygen atoms in tantalum by elastic energy dissipation measurements as temperature function, discussing relaxation effect
07 p1168 A69-19452
- Earth and planets shallow seas tidal dissipation reflected in Q values, noting larger planet pressure effect
08 p1393 A69-20581
- Equal element elliptic function filters, noting lower dissipation loss when applied to bandpass and bandstop filters
08 p1300 A69-21175
- Carrier energy dispersal in communication satellite telephony and TV systems, noting attendant RF bandwidth increase as function of distortion
09 p1450 A69-21277
- Star collapse under energy losses due to neutrino emission, analyzing self similar asymptotic solutions
09 p1587 A69-21359
- Type two superconductors physical properties, discussing magnetic flux lines interaction with structural defects
09 p1555 A69-21490
- Energy characteristics of exploding wires considered as shock wave source
09 p1539 A69-21560
- Galactic cosmic ray scattering and energy loss through solar wind interaction
09 p1580 A69-22202
- Damping criteria for satellite vibration based on energy dissipation by material hysteresis, friction in viscous flow, magnetic hysteresis and eddy currents
10 p1791 A69-22921
- Polymeric composites mechanical energy dissipation dependence on dimensions of interfacial region between matrix and filler phases, considering particle size and strain magnification
10 p1794 A69-23037
- Increased energy losses and microwave emission at cyclotron frequency harmonics during plasma electron heating at cut-off plasma concentrations in magnetic trap
10 p1728 A69-23130
- Differential energy losses of fission fragments in thin carbon films as function of mass and initial energy mapped by time of flight method
10 p1694 A69-23348
- Cosmic protons interaction with interplanetary plasma, analyzing beam energy loss due to excitation of longitudinal electrostatic oscillations
10 p1760 A69-23617
- Summation curves method for development of active region and time dependence of energy loss during proton flare
10 p1764 A69-23743
- Plastic energy dissipation and crack surface displacement of penny shaped crack in elastoplastic material
10 p1803 A69-24030
- Force-free magnetic field integral properties, obtaining rate of decrease limitation via virial theorem
11 p1951 A69-24239
- Thermal balance of intergalactic gas, discussing plasma energy losses due to He emission and reverse Compton electron scattering and rapid cooling effect
11 p1954 A69-24381
- Output power losses in lasers with inhomogeneous active rods, deriving formulas for losses in ruby and Nd-glass laser rods
11 p1926 A69-24603
- Energy dissipation in freely oscillating bodies under static stresses described by differential equation, assuming elliptical hysteresis loop
11 p1919 A69-25092
- Hysteresis loop contour equation derivation based on energy dissipation dependence on stress amplitude in cyclically deformed vibrating system
11 p1985 A69-25176
- Intermodulation noise distorting arbitrary frequency-modulated multicarrier microwave signal in satellite transponder, emphasizing nonlinear energy dissipation and AM-FM conversion
11 p1841 A69-25634
- Energy loss during turbulent plasma heating by current in open magnetic trap, attributing heating to ion-acoustic instability in plasma
11 p1935 A69-25753
- Viscoelastic models for solving longitudinal oscillations of one degree of freedom system under dynamic load, taking into account energy dissipation
12 p2177 A69-25995
- Noise sensitivity of space diversity reception system with narrow beam electrically switchable antennas for incomplete beam separation
12 p2030 A69-26485
- Energy dissipation and fatigue in metals under cyclic static loads, determining logarithmic decrements of vibrations and Bauschinger effect
12 p2181 A69-26612
- Standard phenomenological laser rate equations for population inversion and light intensity generalized by considering intensity dependent losses and Einstein coefficients
12 p2110 A69-27014
- Radiative energy losses in nonequilibrium plasmas, considering plasma geometries and distributions of Plancks function
13 p2305 A69-27374
- Electrical end losses in liquid-metal MHD generators with variable conductivity, noting working fluids and aspect ratios
13 p2206 A69-27493
- Linear inductive MHD converters, reducing effects of losses due to finite length of converter by cylindrical construction
13 p2207 A69-27505
- Radiative relaxation of relativistic particle distribution undergoing synchrotron radiation and reabsorption, discussing self absorbed radio source model
13 p2327 A69-27572
- Energy loss during inelastic collisions between electrons and ionospheric particles, determining ionospheric heating by UV radiation
13 p2252 A69-27614
- Resonance tube excitation from energy depletion in central part of subsonic jet supplying tube
13 p2247 A69-27738
- Dielectric constant, loss and breakdown of electrical insulation materials, discussing atomic and molecular models and effects of polarizations, environment and manufacturing procedures
13 p2230 A69-27983
- Radiative thermal losses of K in gases for MHD flow
13 p2308 A69-28022
- Output power and loss analysis of 2 n injection locked oscillators combined through magic tee hybrids
13 p2232 A69-28061
- Muon energy losses due to pair formation taking into account nucleus screening by electrons
13 p2304 A69-28423
- Two chamber DC arc heater with vortex stabilization, determining current-voltage characteristics and efficiency
13 p2244 A69-28557
- Q switched ruby laser metastable state population kinetics and resonator losses, discussing internal energy redistribution with subsequent absorption spectrum changes
14 p2456 A69-28754
- Shock load protection through energy absorption and dissipation in primary or composite structures, listing honeycomb, cellular plastics and rubber mechanical properties
[ASME PAPER 69-DE-37] 14 p2531 A69-28846
- Low voltage arc discharge characteristics in cesium vapor, considering energy balance, electron temperature, energy losses, volt-ampere characteristics, ignition, cathode temperatures, etc
14 p2401 A69-29234
- External and internal energy dissipation coefficients in vibrating aerodynamic rod structures
14 p2537 A69-29748
- Hydrogen gas role in galaxy formation, estimating quantity needed to dissipate gas cloud contraction energy, discussing formation mechanics of molecular hydrogen
15 p2680 A69-30204
- Thermistor thermometer with low energy dissipation for flow measurements, discussing design considerations
15 p2608 A69-30296
- Back pressure control system for heat leak evaluation tests of cryogenic containers, discussing component selection and error analysis
15 p2702 A69-30397
- Seal selection criteria based on maintaining fluid film between faces, discussing facial heat generation and dissipation, speed and size effects, etc
[ASLE FICF5 PREPRINT 25] 15 p2620 A69-30488
- Unsteady nonadiabatic shock waves in stellar gas dynamics, analyzing energy losses due to ionization at shock fronts by extended Chiznell-Wisem method
15 p2682 A69-30508
- Barrier penetration depth by meteorite particles at prethreshold impact velocities, taking into account energy dissipation on shock wave front
15 p2709 A69-30749
- Stellar energy diffusion processes studied to determine energy transfer time scale between stellar layers
15 p2692 A69-30767
- Nova outburst dynamics investigation by time dependent hydrodynamics computer program including energy transport by radiation and convection
15 p2692 A69-30769
- Energy transfer during fast electrons and photons interactions, indicating Compton energy losses related to space X ray and gamma radiation sources
15 p2676 A69-30953
- Diode burn-in dissipation measurement for reliability testing
15 p2579 A69-31043
- Electron temperature observation in daytime ionosphere, considering energy loss to ions and neutral particles
15 p2603 A69-31402
- Waveguide capacitive screw tuners effects on dissipative loss, discussing microwave measurements with copper screw tuners
16 p2757 A69-31586
- Energy release efficiency in gravitational collapse, estimating rest energy fraction from energy conservation, neutron star stability and spherically symmetrical systems collapse considerations
16 p2853 A69-31594
- Second breakdown and other thermal instabilities analyzed by heat flow equation, obtaining stability criteria predicting reduced power dissipation for transistor at low currents
16 p2758 A69-31618
- Ruby laser output energy degradation due to pump light absorption by color centers, discussing roles of defects and impurities in center formation
16 p2795 A69-31697
- Plasma experiments with TM-3 apparatus under stable discharge conditions in H, discussing energy loss mechanisms, transport coefficients, reciprocal lifetime, etc
16 p2820 A69-31795
- Far field energy radiated by two body system using approximation method in general relativity and Minkowski gravitation theory
16 p2812 A69-31836
- Laser amplifier nonlinear losses effect on light beam propagation, studying arbitrary waveform development into asymptotic steady state pulse /SSP/
16 p2797 A69-32043
- Incident energy transfer to particles due to nonlinear interactions during passage of intense light beam through plasma, considering decay into plasma waves
16 p2822 A69-32046
- Transistor temperature and power limitations and thermal resistance calculation, discussing heat sink surface optimum design for power losses
16 p2760 A69-32047
- Nonlinear mechanical systems vibrations damping emphasizing energy dissipation
16 p2874 A69-32245
- Turbulence dissipation rate in clouds and precipitations determined from rms width of vertical sounding radar signal fluctuation spectra, distinguishing gravity and turbulence effects
16 p2807 A69-32273
- Thermal contacts effects on optimum operating conditions of solar thermoelectric power generator, discussing losses due to low thermal conductivity coefficient of insulating layers
16 p2741 A69-32797
- Linear pyrolysis of condensed materials in presence of heat loss into ambient medium expressed in terms of thermoneutral and thermal reactions
17 p3069 A69-33134
- Radiative heat transfer in nonisothermal media composed of spherical particles with complex refractive index emitting absorbing and scattering energy anisotropically, considering various geometries
[AIAA PAPER 69-626] 17 p3073 A69-33297
- Combustion and exhaust losses in gas turbines, recommending pulsating combustion for increased useful energy
17 p3021 A69-33360
- Energy dissipation in collisionless shock waves generated in plasmas with 1-500 trillion/cm electron density by theta pinch, measuring axial ionic energy spectrum
17 p3013 A69-33820
- Soviet collection of papers on energy dissipation during vibrations of mechanical systems, covering elastic

oscillations, nonlinear systems, energy frequency characteristics, etc
17 p3062 A69-33912

Nonlinear differential equations of mechanical systems with restoring forces approximated by odd power displacement functions and energy dissipation approximated by displacement and velocity functions
17 p3007 A69-33914

Oscillations of nonlinear dissipative mechanical system with two degrees of freedom, possessing structural damping at joints between moving masses and base
17 p3064 A69-33915

Forced oscillations of resonance machine elements represented by truss of concentrated masses and external forces, taking into account aerodynamic energy dissipation
17 p3064 A69-33916

Axisymmetric bending oscillations of thin circular plates of constant thickness with allowance for energy dissipation in material, analyzing resonance and phase amplitude characteristics
17 p3064 A69-33919

Energy dissipation influence on elastic elements random vibrations, obtaining relations between displacements rms value and random disturbance intensity
17 p3064 A69-33921

Energy-frequency characteristics of vibrating machines obtained as spatial curves relating energy dissipation to system vibrations frequency
17 p3065 A69-33922

Energy dissipation in elastic systems as function of limiting damping characteristics of oscillations
17 p3065 A69-33923

Energy dissipation in vibrating warped turbine blades subject to complex stress-strain rate produced by simultaneous bending, torsional and tensile stresses
17 p3065 A69-33924

Facility for determining energy dissipation in materials under cyclic stresses or strains for wide range of temperatures
17 p2946 A69-33925

Facility for studying energy dissipation in refractory materials during fatigue tests in vacuum at various temperatures, describing principal components
17 p2947 A69-33926

Scale factor determination for energy dissipation at clamped ends, analyzing geometric parameter and clamping force effect on oscillation damping constant
17 p3065 A69-33927

Test facility to determine factors influencing aerodynamic energy dissipation of cantilever rods oscillating in airstream
17 p2947 A69-33928

Stationary liquid under pressure effect on energy dissipation of rectilinear pipelines under pure bending
17 p2904 A69-33930

Static tensile stresses effect on energy dissipation in alloys used in compressor blades found dependent on composition and heat treatment
17 p2991 A69-33934

Energy dissipation in fiberglass reinforced plastics subjected to axially induced sinusoidal stresses, noting absorption coefficient and hysteresis heating
17 p2993 A69-33937

Energy dissipation in bonded structures, analyzing vibration damping, hysteresis loop and absorption coefficient dependence on deformation energy
17 p3066 A69-33943

Aerodynamic energy dissipation during vibrations of bars in airstreams characterized by energy loss per cycle and logarithmic decrement
17 p3066 A69-33948

Magnetic storm energy balance, assessing solar corpuscular flux energy consumption in and beyond magnetosphere
17 p2964 A69-33959

Dynamic model of bodies with microstructure and nondissipative energy motion, discussing action steadiness, invariance conditions and Galilean relativity
17 p3067 A69-34149

Plastic energy dissipation rate during stable crack growth in sheet under uniaxial tension
18 p3212 A69-34345

Networks of ideal inductors, capacitors and periodically operated switches with no energy loss, deriving frequency-power formulas from response functions
18 p3111 A69-34682

Star collapse under energy losses due to neutrino emission, analyzing self similar asymptotic solutions
18 p3197 A69-34749

Climatological patterns of atmospheric kinetic energy dissipation in free atmosphere derived from upper

wind statistics of Northern Hemisphere, using Kolmogoroff functions
18 p3166 A69-34825

Earth bow shock electrical conductivity estimation from macroscopic equations without knowing microscopic dissipation processes
18 p3131 A69-35191

Hexagonal and nonhexagonal cell phenolic honeycomb design as energy dissipating material noting processing, composite constituents, cell configuration and usage environment
19 p3353 A69-35503

Energy dissipation of solder-covered and solderless solar cells with TiAg contacts as function of storage time, temperature and humidity
19 p3253 A69-35706

Ruby laser resonator losses resulting from changes in mirror transmittance or inclination, or introduction of bleachable absorbers
19 p3331 A69-35863

Acoustic measurements at room temperature for determining losses in rocket chamber during combustion instability, using small scale model
19 p3394 A69-35946

Energy dissipation near tropopause determined from measured clear air turbulence spectra and probabilities
19 p3303 A69-36407

NonNewtonian power law fluids flow behavior in circular pipe entry region, taking into account energy loss due to viscous dissipation in boundary layer
19 p3240 A69-36472

Nondestructive test method using transducer action of flow in stress field causing plastic deformation with energy release as acoustic emission
19 p3314 A69-36634

Inductively coupled RF excited toroidal Ar ion laser, confining current discharge by strong axial magnetic field to reduce wall losses
19 p3338 A69-36690

Energy losses due to drag in unstable laminar fluid flow in tube
20 p3513 A69-36973

Mechanical loss factors calculated by approximation formula from resonance curves of Voigt-Kelvin and Maxwell models
20 p3623 A69-37435

Aluminum doped silicon solar cell energy loss coefficient under proton and high energy electron irradiation
20 p3465 A69-37911

Photospheric radiation field role in temperature inversion of stellar chromospheres with dominant H ion opacity, postulating mechanical energy dissipation
20 p3613 A69-38173

Semiempirical electron impact cross sections and energy loss functions applied to dayglow and auroral intensities calculation, discussing atomic and aeronomic implications
21 p3713 A69-38527

Heat loss from cylinders at low Reynolds numbers in N-He and N-Ne binary mixtures
21 p3848 A69-38706

Scalar conductivity as governing parameter in determining current sheet diffusion and energy dissipation in MHD shock producing devices
21 p3776 A69-38708

Fluid loop rotational kinetic energy dissipator reducing time required for reaching WRESAT 1 satellite spin stabilization axis
21 p3828 A69-39767

Electron energy loss spectrum of nitrogen, suggesting atmospheric auroral nitrogen emissions compatibility with low energy electron impact excitation mechanisms
22 p3935 A69-39970

Differential approximation for radiant energy loss in nonequilibrium plasma generated from truncated Taylor series expansion of radiation source function
22 p3988 A69-40102

Seasonal effects on energy expenditure during rest and exercise at controlled ambient temperatures, noting effects on heart rate
22 p3890 A69-40211

Small losses measurement in circulators and reciprocal quadrupoles, using scattering matrix to eliminate mismatch errors
22 p3875 A69-40259

Radiant energy diffusion from spherical expanding matter for masses and velocities of model supernova outbursts, discussing thermonuclear and neutron star origins of supernovae
22 p4026 A69-40649

Parametric losses in nonlinear centrosymmetrical ferroelectric ceramic in strong microwave field at temperatures above Curie point
22 p3996 A69-41164

Power flow relations between randomly vibrating systems with weak linear elastic or dissipative coupling
23 p4227 A69-41877

Average total losses of H waves transmitted over waveguide communication lines by nanosecond pulse sequences
23 p4123 A69-41949

Electromagnetic oscillations emission by monochromatic electron beam in infinite waveguide formed by periodic diffracting array with energy losses, determining radiated power
23 p4124 A69-42031

Energy cost of muscular exercise in gastrocnemius muscle of dogs anesthetized with morphine, chloralose and urethane
23 p4093 A69-42065

Antenna losses produced by metal space frame radome determined by considering end effects, member junctions circulating currents, mutual scattering and near field effects
23 p4149 A69-42127

Integral energy loss spectrum of extensive air showers recorded by Haverah Park 50-m array
23 p4207 A69-42499

Hemolysis rates in various blood flows, considering effects on energy dissipation
23 p4100 A69-42533

Low energy electrons energy loss by inelastic collisions in moving through atmosphere, estimating cross sections and loss rates
24 p4351 A69-42763

Stellar neutrino energy loss due to electron-electron neutrino bremsstrahlung in nondegenerate gas determined from transition probability for charged baryons or leptons interaction
24 p4351 A69-42794

Thermal nonequilibrium state and effective collision frequency between protons and electrons in solar wind plasma, explaining abnormal dissipation
24 p4368 A69-43187

Energy dissipation in oscillating sphere filled with viscous fluid, giving fluid response by solving Navier-Stokes equation
24 p4305 A69-43587

Solar flare models in terms of energy storage and release mechanisms
24 p4374 A69-43622

Thermal balance of intergalactic gas, discussing plasma energy losses due to He emission and reverse Compton electron scattering and rapid cooling effect
24 p4389 A69-43771

ENERGY DISTRIBUTION

NT SPECTRAL ENERGY DISTRIBUTION

Proton energy distributions for passage through NaCl, KCl, KBr, Si and Ge single crystals at various angles relative to /100/ and /110/ crystallographic planes
01 p0140 A69-11109

Total energy of plasma wave from second order energy, showing close approximation to wave packet energy
02 p0287 A69-11876

Energy distribution and capture cross section ratio limiting factors in semiconductors with deep energy levels
02 p0299 A69-12562

Positive Ar ion energy distribution for beam extracted from nonmagnetic hot cathode gas discharge ion source under various source conditions
03 p0427 A69-13102

Energy distribution among products of reactive collision of atomic H with Br molecule yielding HBr and Br atom, using perturbed Morse oscillator approximation
03 p0472 A69-13316

Energy partition between mechanical and magnetic modes in turbulent plasma in external field
03 p0476 A69-13384

Trouton-Noble experiment to detect motion of earth through ether by electromagnetic torque on charged suspended parallel plate capacitor, explaining null results
03 p0517 A69-14106

Statistical energy approach for analyzing steady state vibration distribution in composite structures in terms of energy balances
04 p0675 A69-14687

Inelastic collisions effect on electron energy distribution in low temperature diffusion dominated discharges
04 p0637 A69-15047

Variable energy blast waves analysis with reference to cylindrical spark channel formation, noting shock front velocity approximation
04 p0590 A69-15203

Low collision energy charge transfer and dissociative charge transfer between rare gas ions and molecular

- nitrogen, measuring nitrogen ion kinetic energy distributions
05 p0796 A69-15909
- Sounding energy optimum spatial distribution during scanning and detection of several signals, noting reduction of mean energy losses
05 p0723 A69-16786
- Mass spectrometric measurements to determine energy distributions of ions produced in dissociative photoionization of O molecules
06 p0960 A69-17110
- Ground state energy of Anderson Hamiltonian calculated by cluster variation for cases of infinite d-d correlation energy
06 p0958 A69-17712
- Energy fluxes statistical distribution produced by random and regular energy sources
07 p1076 A69-18510
- Pulsation energy balance of turbulent jet of conducting fluid expanding in longitudinal magnetic field
07 p1192 A69-19021
- Statistical theory of ionization for magnetoactive plasma with nonequilibrium concentration level and nonequilibrium energy distribution
07 p1193 A69-19142
- Energy separation and electrons effective mass ratio of conduction bands of tellurium doped GaSb obtained by free carrier Faraday rotation measurements
07 p1201 A69-19464
- Energy deposits from decay of tritium incorporated into bacteria, using computer simulation for radiation dose distribution
07 p1068 A69-19490
- Tropospheric energy cycle interannual variability and quasi-biennial oscillation from geostrophic computations of eddy kinetic energy, energy transfer and internal redistribution
07 p1129 A69-19628
- Unstable elastoplastic brittle fracture criterion based on energy balance considerations
07 p1238 A69-19693
- Electron energy distribution measurements in carbon dioxide laser discharges noting similarity of distribution for nitrogen
08 p1323 A69-19801
- Micromachining with laser beam, choosing mirrors and lenses of optical system to provide uniform energy distribution for microwelding or hole boring
08 p1324 A69-19980
- Electron energy distribution function in plasma heated by electron-cyclotron resonance in adiabatic trap determined from bremsstrahlung spectrum
08 p1365 A69-20547
- Energy density and transport velocity of RF wave in plasma in damped oscillations region, discussing resonance
08 p1365 A69-20553
- Atmospheric structure and energy distribution of planetary nebulae central stars
08 p1393 A69-20570
- Contour of axisymmetric holes in dimensional electron-beam machining calculated from density distribution of transmitted energy
08 p1321 A69-20727
- Optical systems with quasi-monochromatic partially coherent illumination, discussing energy distribution computation program
08 p1353 A69-21096
- Temperature dependence of energy gap in gallium arsenide and gallium phosphide from absorption measurements
09 p1553 A69-21330
- Surface structures determination by energy analysis and low energy electron diffraction of scattered electrons
09 p1554 A69-21340
- Ultrashort light pulses problems in measurements of time characteristics and instantaneous power of laser radiation
09 p1516 A69-21575
- Circular central shading effect on energy distribution parameters of paraboloidal mirrors, noting reflected radiant flux power limitation
09 p1436 A69-21804
- Energy distribution in electron gun with single crystal spherical cathode, noting work function, space charge cloud and beam overlapping effects
09 p1464 A69-22396
- Computation and optimization of energy distribution over randomly oriented elements of radiation receiving surface of hollow collector of concentrator type solar device
09 p1442 A69-22534
- Angular energy distribution in gamma quanta beam during collision between laser photons and relativistic electrons
10 p1701 A69-23132
- Fast electron energy distribution function and atom concentration in first excited level in weakly ionized plasma, considering transitions between excited levels
10 p1739 A69-23628
- Stratified atmosphere mean vertical flux due to ground disturbances, obtaining results for various wind and temperature profiles
10 p1685 A69-23856
- Microscale fluctuations in interplanetary magnetic field, considering proton thermal energy and magnetic field energy densities
10 p1785 A69-24100
- Mean absolute solar spectrum energy distribution from 1800 Å to 4 mm, noting solar constant and radiation intensity determination
11 p1951 A69-24242
- Molecular vibration absorption spectra from variation of field emitted electron energy distribution due to inelastic electron-molecule interaction at metal-vacuum interface
12 p2132 A69-26097
- Light scattering from high reflectivity dielectric mirrors, measuring angular power distribution from beam axis by scanning with narrow slit
13 p2298 A69-27663
- Maxwellian velocity distributions simulated in one, two and three dimensions by superposition of N monoenergetic isotropic distributions, noting application to kinetic theory computation
13 p2313 A69-28222
- Half wave dipole antenna operational factors analyzed for RF radiation spatial power distribution from atmospheric cosmic ray showers
13 p2332 A69-28408
- Cosmic ray showers components relationships, analyzing superhigh energy nuclear cascade development, discussing components distribution function at constant proton energy
13 p2332 A69-28410
- Cosmic ray showers electron, positron and photon energy distribution functions calculated, considering positron annihilation, Compton effect and relativistic electrons formation
13 p2303 A69-28413
- Cosmic ray muons energy and angular distribution measurements, obtaining curve with respect to projection angles
13 p2332 A69-28420
- Bayes theory and nonclassical variation method to solve optimal energy distribution available for identifying weak signals in background noise
14 p2410 A69-28817
- Suprathermal electrons energy distributions as function of magnetic latitude in polar ionosphere obtained by Explorer 31 satellite observation
14 p2512 A69-28963
- Low voltage arc discharge characteristics in cesium vapor, considering energy balance, electron temperature, energy losses, volt-ampere characteristics, ignition, cathode temperatures, etc
14 p2401 A69-29234
- Electron energy distribution function and nonequilibrium ionization rate in near cathode layer of thermionic converter
14 p2404 A69-29255
- Energy momentum tensor in Einstein field equations derived from covariant field equations for vector meson
14 p2486 A69-29452
- Space radiometers energy characteristics calculation taking into account reflecting surface roughness and antennas directional patterns
15 p2575 A69-30338
- Comet Ikeya-Seki tail spectra from nebular spectrograph, tabulating energy distribution in comet tail, noting similarity to solar spectrum
15 p2685 A69-30524
- Electron energy distribution determination from electron synchrotron radiation spectrum for various magnetic field configurations within radio source
15 p2655 A69-30546
- Spatial and energy characteristics of laser with nonuniform transmittance across resonator mirrors, analyzing transverse modes interaction
15 p2634 A69-30962
- Lasing influence on electron energy distribution in gas discharge measured with Langmuir probe, showing electron-electron interaction insufficient to maintain equilibrium
16 p2796 A69-31772
- Earth-reflected solar energy /albedo energy/ distribution model, assuming isotropic scattering by homogeneous atmosphere
17 p2961 A69-33292
[AIAA PAPER 69-591]
- Solar power concentrator-absorber system, discussing flux distribution in focal plane and cavity heater optimization
17 p3022 A69-33795
- Ion energy distribution function and density profile in strong implosion wave generated by theta pinch discharge, investigating compression wave in deuterium
17 p3013 A69-33821
- Molecular gas absorption coefficient dependence on laser emission energy density, considering disturbed equilibrium distribution of molecules
17 p2983 A69-33973
- Bernoulli distribution and Monte Carlo method for electrical load analysis in designing electric power generation and distribution
17 p2905 A69-34090
- Differential cross sections for secondary electron production in atomic ionization by charged particle impact, using classical binary encounter approximation
17 p3009 A69-34189
- IR and optical measurement of Crab pulsar NP 0532, analyzing energy density per pulse and smoothness of visual data
18 p3191 A69-34318
- Light curve of pulsar NP 0532 represented with oblique rotator hypothesis, assuming concentrated emission at opposite spots on star
18 p3192 A69-34321
- Gaseous and solid phase properties of atomic and molecular systems, treating statistical energy distribution, kinetics, excited states and relaxation
18 p3178 A69-35406
- Single and two mode laser emission dependence on pumping power distribution between four level active centers of different types
19 p3333 A69-35878
- Atomic H ionization by proton impact analyzed to calculate ejected electrons angular and energy distributions by extending Rudge and Seaton theory
19 p3375 A69-35911
- Electron energy distribution for Cs plasma in emitter region of ignited mode thermionic converter, noting nonequilibrium ionization effect
19 p3380 A69-36442
- Electron momentum transfer cross sections by numerically solving electron energy distribution function from Boltzmann equation in Lorentz approximation
21 p3773 A69-38396
- Auroral electron and proton fluxes precipitation measurements by satellite, studying data in terms of spatial, energy and angular distributions
21 p3709 A69-38500
- Ionization wavefronts nonlinear analysis including energy effects and ionization wave structure, discussing Joule heating due to transverse electric field
22 p3990 A69-40758
- Electromagnetic cascade showers transition effect in various materials, measuring energy deposition as function of position
22 p3987 A69-41003
- Pulsed energy balance expressions for turbulent characteristics of incompressible circular flow in channel with inserted rotating cylinder
22 p3933 A69-41028
- Distribution function of output energies of polycrystalline metal surface used as plasma probe, considering homogeneous plasma flow and isotropic particle velocity distribution
23 p4196 A69-41696
- Microwave absorption by biological materials, noting energy distribution between reflected, transmitted and absorbed radiation as function of medium physical properties
24 p4270 A69-42574
- Energetics of planetary boundary layer /Prandtl layer/ from system of hydrodynamic equations, discussing flux divergence term importance in free-windless convection transition region
24 p4309 A69-43148

ENERGY EQUIPARTITION
U EQUIPARTITION THEOREM

- ENERGY LEVELS
NT ATOMIC ENERGY LEVELS
NT ELECTRON STATES
NT GROUND STATE
NT INTERMOLECULAR FORCES
NT MOLECULAR ENERGY LEVELS

Saturation peak half widths on Ne energy level population inside single frequency Michelson-type He-Ne

laser by tuned differential spectrometry, observing power broadening 01 p0089 A69-10182

Satellite optimal transfers from elliptic to parabolic orbits within set time 01 p0157 A69-11306

Energy distribution and capture cross section ratio limiting factors in semiconductors with deep energy levels 02 p0299 A69-12562

Inverse population of vibrational levels generation in polyatomic molecules 02 p0259 A69-12647

Mean life measurement of excited ions electronic levels using beam foil light source, emphasizing beam particle monitoring and theoretical equations 04 p0595 A69-14278

Radiation intensity distribution from first negative and positive nitrogen system in equilibrium gas flow behind propagating shock front, discussing kinetics mechanism and electronic states 05 p0745 A69-15890

Deep trapping levels caused by ion implantation doping, discussing level effects on electrical characteristics of zinc implanted GaAs diodes 05 p0808 A69-16287

Relaxation time of carbon dioxide laser levels as function of water vapor, CO and Xe gas pressure measured by afterglow pulse gain technique [IEEE PAPER G-1] 05 p0774 A69-16314

Angular dependence of low energy electron impact excitation cross section of lowest molecular hydrogen triplet states 06 p0962 A69-17820

Radio recombination lines in populations of highly excited states of hydrogen, discussing collisional transition effects 06 p1010 A69-17970

Lasers, reviewing phenomenology, physical and theoretical fundamentals, quantized energy levels, population of energy levels and laser components 06 p0936 A69-18003

Field effect in p-type gallium arsenide single crystals as characteristic of surface electron energy state spectrum 07 p1199 A69-18686

Hole concentration at deep energy levels in p-type indium antimonide single crystals containing structural defects 07 p1199 A69-18687

Optical excitation process of energy states by light pulses of short duration compared to relaxation time, predicting Raman echoes [IEEE PAPER H-3] 07 p1152 A69-19062

Degree of population inversion and inverse temperature measurement in medium 07 p1137 A69-19761

Mutual influence of two different laser modes corresponding to two transitions with same ground level, using He-Ne DC laser 08 p1325 A69-20284

Relaxation times of carbon dioxide laser levels induced by radiation 09 p1515 A69-21488

Quark model to account for enormous energy from quasars 09 p1597 A69-22084

Recombination parameters and depth of levels of p-n junctions in semiconductor photocells determined from position of maximum spectral sensitivity 09 p1560 A69-22718

Interfacial charges in MOS transistors determined as function of surface potential by measuring channel conductance as function of temperature 10 p1744 A69-23178

Electronic states and minority carrier transport in mixed semiconductors with graded composition, noting position dependent band gaps and effective masses 10 p1745 A69-23360

Shallow impurity states in semiconductors, calculating bulk and surface energy eigenvalues in Si and Ge 10 p1745 A69-23361

Level degeneracy effect on nonlinear interactions between traveling waves of different planes of polarization 10 p1705 A69-23815

Reabsorption effect of emitted quantum on lifetime of excited levels in gas laser, determining capture factor 12 p1204 A69-26028

Anomalous interaction of argon and krypton ion laser lines, considering connecting radiative transitions and cross modulation 13 p2270 A69-27204

Radio emission from high level transitions in hydrogen calculated by superposing emission lines on background continuum, using Gaunt factor for free-free emission 13 p2327 A69-27596

Surface resistivity oscillatory dependence on magnetic field in single crystal metals, examining electron trajectories, energy levels and wave functions 13 p2316 A69-27641

Electrical properties of p-type indium antimonide, noting effects of deep level compensation on ν values 13 p2318 A69-27895

Monte Carlo method used to calculate probability of muon penetration to deep underground levels with sea level energies 13 p2333 A69-28424

Emissivity of two photons decay from metastable 2s level of pure hydrogen gaseous nebula, noting radiative and collisional excitation 14 p2529 A69-29975

Burstein-Moss effect observed in studying n-GaAs crystals electrical reflection spectra with large free carrier concentration at two temperatures and low energy levels 15 p2666 A69-30060

Human locomotion analysis, measuring metabolic expenditure and mechanical energy levels of principal body segments during walking 15 p2558 A69-30587

Beam foil technique to measure energy transition levels radiative lifetime for nitrogen ions 17 p3009 A69-34154

Mean life of D energy level in N IV, discussing Be I isoelectronic sequence 17 p3009 A69-34187

Energy level NMR spectral analysis for spin systems with sets of magnetically nonequivalent chemical-shift equivalent nuclei 20 p3579 A69-37348

Differential equations for field amplitude and level populations applicable to solid state lasers output power pulsations 20 p3554 A69-37726

He-Ne laser oscillation frequency shifts with variations in DC discharge ascribed to changes in populations of He and Ne levels 20 p3556 A69-38124

Stellar nuclear reactions at low energies studied to provide predictions of cross sections in carbon burning 20 p3612 A69-38164

Optical pumping and selective population applications, considering double magneto-optic resonance and inelastic interatomic collisions 21 p3735 A69-38454

Exponential decay and mean lives of lowest P levels in N V measured with beam foil source, noting agreement with theories taking configuration interaction into account 21 p3774 A69-38760

Energy levels of multicharge acceptor centers and level splitting in InSb and GaAs deformed crystals, using multizone approximation 21 p3781 A69-39067

Response of three level particles system with equidistant spectrum under resonant action of acoustic and electromagnetic pulses sequence with different frequencies 21 p3737 A69-39068

Population and excitation rates of working levels of carbon dioxide laser calculated on basis of emission power, amplification coefficient and spontaneous emission intensity 22 p3964 A69-40795

Approximations for meson-nucleus scattering length from energy level measurements on mesonic atoms, emphasizing formula for negative pi mesonic atoms 22 p3987 A69-41004

Prebiological chemical evolution, studying synthesis and degradation rates relationship at primitive environment energy levels 24 p4269 A69-43514

ENERGY METHODS

NT BERNSTEIN ENERGY PRINCIPLE

NT STRAIN ENERGY METHODS

Electrical equation of state of metals determination from density, conductivity, energy and metal vapor velocity measurements in wire explosions 01 p0117 A69-10659

Structural designs for minimum flexibility or weight using energy intensity per unit mass parameter 02 p0345 A69-12380

Rayleigh-Ritz finite element method for approximate solution of nonlinear energy functional describing large deflection bending behavior of uniform beam under point loads 05 p0833 A69-15711

Generation process in three stage He-Ne cascade laser with wideband resonance, using simplified energy level scheme 06 p0934 A69-17496

Incremental complementary energy method of stress analysis of orthotropic nonlinear materials having different behavior in tension and compression [AIAA PAPER 69-119] 06 p1028 A69-18159

Elastic stability of one dimensional structures analyzed by energy method, discussing deformable line, conservative forces and linear stability 08 p1418 A69-20846

Matrix elements for asymmetric rotors using rigid rotor reduced energies, describing computations method 09 p1614 A69-21913

Energy theorem for time dependent materials, deriving convexity conditions for minimum work and maximum complementary work functions 11 p1969 A69-24412

Solution for kinetic energy equation for organic semiconductors with narrow conduction band situated in strong electric field 12 p2144 A69-26673

Energy detection of random processes in colored Gaussian noise, discussing filtering, threshold detection, false alarm, probability distribution and density 13 p2220 A69-27937

Kolmogorov-Prandtl turbulence energy hypothesis extended from turbulent region of one dimensional flow to laminar sublayer, obtaining numerical solutions for Couette flow 13 p2250 A69-28339

Energy separability method for linear systems in transient evolution using two new identities 13 p2370 A69-28634

Atmospheric circulation by energy concepts, giving quantitative analysis of interaction between upper and lower atmosphere 14 p2477 A69-29825

Energy principle applied to Astron type device stability based on model with rigid E layer electrons, finding critical pressure expression for ballooning modes 16 p2821 A69-32035

Energy method determining sufficient conditions for fluid motion stability described by infinitesimal theory of viscoelasticity, restricting analysis to confined fluids or periodic velocity field 17 p2949 A69-33015

Perturbation procedures applied to energy computation for ground and first excited state of hydrogen molecule at large separation 17 p3009 A69-34170

Quasi-static crack growth in viscous bodies analyzed by continuum mechanics, rheological models and energy equation, discussing fine structure 18 p3215 A69-34570

Structural vibrations characteristics using expression of complex energy applied to structure, discussing coupling between damping modes [ONERA-TP-724] 18 p3218 A69-34639

Active attitude control method with energy increases and decreases induced to modify attitude motions for particles and rigid bodies 19 p3429 A69-35958

Uniqueness theorems for energy methods solution of equations of dynamic thermoelasticity and viscoelasticity 19 p3439 A69-36470

Energy criteria inconsistency in evaluating frequency band changes attributed to simultaneous narrowing and broadening of different signal power bands 19 p3278 A69-36716

Bending of normally loaded simply supported rectangular plates in large deflection range solved by nonlinear differential equations and minimum potential energy principle 19 p3445 A69-36828

Interface electron transport phenomena in stress corrosion, expressing defect movements in terms of electron energy dynamics 19 p3349 A69-36889

Rotta analysis for linear flow transformation into turbulent flow, discussing Reynolds numbers 20 p3513 A69-37086

Energy formulation extended for plane anisotropic rectangular plates, handling nonuniform properties and loadings 20 p3627 A69-37766

Postbuckling of filled circular cylindrical shell using Ritz energy method for load deformation relation, discussing stabilizing effect of core 22 p4038 A69-39895

- Natural frequency equations for torsional vibration of fixed/fixed and fixed simply supported uniform thin walled beams of open section based on energy method
22 p0400 A69-39935
- Pulsed energy balance expressions for turbulent characteristics of incompressible circular flow in channel with inserted rotating cylinder
22 p3933 A69-41028
- Potential energy modeling method for optimal design of structural systems with diverse performance criteria, giving truss design example
23 p4228 A69-41923
- Large deflection of three dimensional bar structures stability analyzed by potential energy minimization method, considering radome design
23 p4232 A69-42141

ENERGY OF FORMATION

- Linear elastic theory for calculating monovacancies entropy and energy of formation in metals
24 p4360 A69-42649

ENERGY REQUIREMENTS

- Photoionization curves and threshold energies for fluorocarbon and trifluoromethyl halide molecules and ions, calculating ionic heats of formation and bond dissociation energies
02 p0205 A69-12464
- Self oscillations of dynamic systems representing space vehicles, considering periodic motions stability, bifurcation curves and energy consumption requirement limit
03 p0519 A69-13068
- Wall attachment type fluidic logic devices with low power consumption requirements, noting monostable and bistable devices
05 p0704 A69-16002
- Radar signal parameters measurements consisting of SNR estimation and optimum energy supply determination from SNR estimation
07 p1085 A69-19153
- Self oscillations of dynamic systems representing space vehicles, considering periodic motions stability, bifurcation curves and energy consumption requirement limit
14 p2530 A69-28750
- Energy cost of piloting helicopters and fixed wing aircraft calculated from expired minute volume and air oxygen content measured during basal state and flight
22 p3891 A69-40218
- Regression relations for energy expenditure in work predicted from heart rate and pulmonary ventilation in volunteers carrying loads upstairs
22 p3891 A69-40220
- Eddy current plasmoids formation in potential magnetokinematic plasma flux found economical in terms of energy requirements
23 p4214 A69-41834

ENERGY SOURCES

- Hydrocarbon-air fuel cell producing electric power automatically for five days
01 p0013 A69-10965
- Energy source specifications and control techniques evaluated for microwave amplifier arrays, discussing use of common power supply and energy storage bank
01 p0047 A69-10998
- Liquid lasers compound range of organic type, circulating system of inorganic type and power peaks
01 p0092 A69-11194
- Technique for combining large numbers of solid state energy sources by using dense array of radiating elements
02 p0217 A69-12148
- Energy sources and properties of quasars and radio galaxies by X ray astronomy
02 p0310 A69-12793
- Homopolar generator as energy store for large laser pumping
04 p0612 A69-15151
- Oxygen supply inert diluent impurities effect on hydrogen-oxygen fuel cell performance
04 p0551 A69-15310
- Gas accretion on neutron star surface as energy source for X ray radiation
05 p0814 A69-15847
- High energy density lithium/dichloroisocyanuric acid battery system discharging under constant voltage and load conditions [ECS PAPER 15]
05 p0706 A69-16231
- Plasma instability role in radiant energy release from astronomical objects, noting plasma instabilities in solar system, cosmic rays, galactic and extragalactic objects
06 p1009 A69-17967

- Electronic circuits power supply onboard space vehicle, discussing chemical, solar and nuclear energy sources
07 p1225 A69-18251
- Energy fluxes statistical distribution produced by random and regular energy sources
07 p1076 A69-18510
- Gamma heating rate measured by aqueous dosimeter converted to rate in thin tungsten detector in water shield through transport theory calculations, obtaining correction factors
07 p1178 A69-18825
- Two dimensional flat geometry for initial solar flare development stage, discussing tearing mode energy source for solar flares and plasma compressibility effects
09 p1583 A69-22757
- Microwave solid state power sources including transistors, varactor harmonic generator chains, tunnel diodes, avalanche transit time devices, etc
10 p1662 A69-23144
- Astronautics - Conference, Braunschweig, West Germany, October 1968, Volume 2, Energy sources
12 p2014 A69-25862
- Cadmium sulfides thin film solar cells for supplying power to instrumentation and data telemetry on longer lived balloons
15 p2553 A69-31287
- Satellite solar power station proposed for power generation for future requirements, discussing world energy needs and finiteness of fossil fuel reserves
16 p2867 A69-31817
- Multispectral imaging remote sensors, analyzing energy sources affecting systems synthesis
17 p2977 A69-34064
- Acoustic gravity waves generated in isothermal atmosphere by ground energy source calculated using stationary phase method and kinematic theory
18 p3129 A69-34953
- Nova luminosity sources during premaximum, considering stellar shell separation and intense ejection of matter
19 p3426 A69-36574
- High energy phosphate splitting flux energy requirements not met by oxidation during supermaximal exercise, noting glycogen splitting into lactic acid after phosphate exhaustion
23 p4100 A69-41443
- Book on interaction between oscillatory systems and energy source of limited capacity, examining stability and resonance phenomena
23 p4170 A69-42166
- Radioisotope thermal energy (RITE) source for integrated life support systems for two man 180 day space station mission, determining optimum material selection and design details
23 p4189 A69-42268
- Solar flares energy supply origin from studying magnetic field behavior, flare position and initial evolution
24 p4366 A69-42687
- Magnetic field energy supply to solar flares from consideration of energies in solar active regions
24 p4370 A69-43606
- Solar flare energy source derived from energetic protons trapped in sunspot magnetic field prior to flare occurrence
24 p4374 A69-43623

ENERGY SPECTRA

NT ELECTRONIC SPECTRA
NT NEUTRON SPECTRA

- Continuous random process spectral density at PAM system output
01 p0050 A69-10211
- Equation of characteristic functional for Burgers one dimensional model fluid turbulence using logarithmic expansion method, discussing change in time of energy spectrum
01 p0059 A69-10338
- Energetic X ray intensities from large and small Magellanic clouds investigated by balloon flight sky survey, noting energy flux upper limits
01 p0150 A69-10370
- Silicon doped p-n GaAs single crystals and epitaxial layers energy spectrum, studying shift in position of emission band maximum
01 p0139 A69-10833
- March 1966 Forbush decrease observed in underground meson component at 70 mwe compared with neutron and sea level meson intensity variations
01 p0146 A69-11129
- Electron flux intensities and energy spectra in inner radiation zone, noting decay constants
01 p0147 A69-11235

- Longitudinal correlation lengths in grid turbulence air flow transport subjected to planar deformation measured from energy spectra of velocity fluctuations
02 p0192 A69-12626
- Superconductor energy spectrum gap, discussing temperature dependence, anisotropy, thermodynamic and kinetic properties and relation to Fermi surface and phonon spectrum
03 p0485 A69-13331
- Absolute cross sections for coincidence detection of deuteron breakup by 42 Mev alpha particles, showing He 5 and Li 5 final state interaction peaks
03 p0472 A69-13469
- Galactic cosmic rays energy modulation spectrum in interplanetary space, showing influence of solar wind velocity and diffusion coefficient dependence
03 p0501 A69-13527
- Polar aurora incident energetic particles spectroscopic analysis, showing system of lines and bands intensity dependence on particle energy spectrum and magnetic activity
05 p0752 A69-15799
- High energy proton and neutron fluxes and spectra from nuclear emission stacks on Cosmos satellites, calculating cosmic radiation doses
05 p0814 A69-16051
- Cosmic ray electron flux and energy spectrum from balloon data obtained at Palestine, Texas, monitoring proton flux periodically
05 p0815 A69-16250
- Auroral electron energy spectrum observed by sounding rocket reveals smooth continuum with peak to produce auroral arcs
05 p0756 A69-16274
- Energy spectrum and intensities of medium and very heavy nuclei in primary cosmic radiation
05 p0816 A69-16365
- Heavy nuclei energy spectrum in primary cosmic rays explained by assuming two component charged nuclei
05 p0816 A69-16366
- Secondary particle spectra from proton-proton interactions analyzed in two temperature statistical model, considering momentum distributions
05 p0797 A69-16368
- Galactic magnetic field estimation obtained from cosmic ray electron spectrum and radio data
05 p0828 A69-16612
- Temperature dependence of Josephson critical current in superconductor model having anisotropic energy gap
05 p0810 A69-16803
- Relation between energy spectrum and potential drop in plasma expelled from hot cathode tube into vacuum derived by electrostatic analyzer
06 p0963 A69-16899
- Optical mean energy distribution of quasars, discussing red shift effects, significance of physical origin of optical continuum radiation and K-term magnitude determination
06 p0999 A69-16975
- Low energy diffuse cosmic X radiation, considering adequacy of single exponent power law spectrum [ISAS-428]
06 p0986 A69-17024
- Cosmic radiation propagation in interstellar space, discussing differential kinetic energy spectra of protons, He, C and O nuclei and Fe
06 p0988 A69-17269
- Cosmic ray propagation model, considering determination of He interstellar spectrum and amount of matter traversed at low energies
06 p0988 A69-17270
- Heavy nuclei abundances and energy spectra in primary cosmic rays, using blob gap parameter as measure of primary ionization
06 p0988 A69-17274
- Charge and energy composition of particles in solar flare, discussing rigidity spectra of singly and multiply charged nuclei
06 p0989 A69-17280
- Galactic cosmic rays anisotropies due to density gradient perpendicular to ecliptic plane studied, using diurnal and semidiurnal component and intensity deficiency
06 p0990 A69-17289
- Astrophysical aspects of primary energy spectrum deduced from shower size spectra and high energy interactions of extensive air showers
06 p0990 A69-17298
- Extensive air shower high energy muons measurements noting energy spectrum, lateral spread and dependence on shower size
06 p0990 A69-17300

Energy spectra of muons determined from knock-on electrons projected angles of emission in C, Al and Cu
06 p0991 A69-17305

Primary electrons implications on cosmic ray confinement in Galaxy, astrophysical aspects and problems of energy spectrum
06 p0991 A69-17308

Low energy photon spectrum at balloon altitudes, noting small geomagnetic latitude dependence
06 p0992 A69-17313

Nonadiabatic particle losses effect on integral proton flux in inner radiation belt, discussing proton energy spectrum
06 p0921 A69-17742

Electron and phonon tunneling spectroscopy in metal Ge contacts, noting improved agreement with one electron model
06 p0982 A69-18234

Field effect in p-type gallium arsenide single crystals as characteristic of surface electron energy state spectrum
07 p1199 A69-18686

Differential energy spectrum of protons and helium nuclei using lithium drifted silicon detectors and scintillator-Cerenkov counter
07 p1204 A69-18833

Electron detector for OGO-E to measure flux and energy spectrum of electrons in primary cosmic rays [IEEE PAPER 3C-4]
07 p1135 A69-19198

Local interstellar electron spectrum limits from measurements of cosmic ray electrons, nonthermal galactic radio emission and solar modulation effects
07 p1206 A69-19269

Arrival time distribution and energy content of extensive air shower at large core distances, discussing photon energy spectra and Monte Carlo calculation
07 p1186 A69-19410

Cosmic ray nuclei energy spectra and abundances above 20 Mev/nucleon determined by OGO-1 satellite experiment, considering He, B, C, N, O, Ne, Mg, Si, Mn, Fe, Co and Ni
08 p1378 A69-20067

Energy dissipation of solar particles in atmosphere for 3914 and 5577 Å bands, computing light emissions associated with PCA
08 p1378 A69-20186

Energy spectrum of primary cosmic ray helium nuclei from nuclear emulsion stacks exposed in sounding rocket flights
08 p1378 A69-20264

Integrated charged particle energy spectra from gridded electrostatic analyzers, relating retarding potential curve to particle floating potential, kinetic temperature, etc
08 p1364 A69-20521

Energy spectra of carbon and oxygen nuclei in primary cosmic radiation, comparing results to earlier measurements and satellite observation
08 p1380 A69-20632

Cosmic ray Li, Be and B nuclei measurements, analyzing differential energy spectra, L-M ratio, atmospheric and solar modulation
08 p1380 A69-20638

Radiative tunneling shifting peak spectra in abrupt asymmetrically doped GaAs junctions
09 p1544 A69-21336

Oscillator forces and photoionization and photorecombination cross sections of electron transitions in hydrogen atom, considering approximation for total radiation probability
09 p1588 A69-21365

Electron fluxes energy spectra determined from simultaneous photometric and riometric observations in polar regions
09 p1485 A69-21530

Anomalous magnetic field energy spectrum obtained from aeromagnetic survey and approximation valid for earth crust and upper mantle
09 p1487 A69-21554

Solar protons in magnetospheric tail after flare of July 7, 1966 with isotropic pitch angle distribution, expressing energy spectrum as exponential in rigidity
09 p1576 A69-21699

Power spectrum of nonstationary processes with periodicity in two dimensional autocorrelation function based on Fourier transform
09 p1455 A69-21847

Mean and turbulent energies and energy spectra of large scale wind velocity pulsations, analyzing annual variation for fixed wave numbers
09 p1536 A69-21861

Flux and energy spectrum of secondary electrons at balloon altitude in atmosphere, correcting Beedle and Webber plotting error
09 p1490 A69-21914

Photometric standard based on calibration of Vega by Hayes compared with six color magnitudes
09 p1603 A69-22233

Energy spectra and angular dependence characteristics of electromagnetic wave scattered on statistically uneven surface studied by vector form of Kirchhoff integral
09 p1459 A69-22635

Cosmic rays origin, measurements of energy spectrum and stellar diurnal variations
10 p1757 A69-22823

Forbush decreases spectra in low energy region from satellite measurements of neutron and hard component of cosmic rays
10 p1758 A69-22829

Cosmic ray electrons and gamma quanta at lower atmosphere recorded with balloon equipment, plotting vertical profiles of electron energy spectra
10 p1758 A69-22830

Slow atmospheric neutron energy spectrum determined by resonance detectors and $1/\nu$ detectors, measuring cadmium ratio dependence on longitude and latitude
10 p1758 A69-22831

Solar protons balloon measurements following flare, noting integral proton flux and energy spectra
10 p1767 A69-23763

Silicon doped p-n GaAs single crystals and epitaxial layers energy spectrum, studying shift in position of emission band maximum
11 p1936 A69-24700

Radioactive light sources in photoelectric photometry, analyzing characteristics, brightness and stability of light flux and energy spectrum
11 p1951 A69-25421

Correlation functions and spectral density of current fluctuations in weakly ionized plasma flows
11 p1934 A69-25715

Solar radio emission bursts periodicity relation to burst intensity
12 p2157 A69-26234

Atmospheric turbulent energy spectra in boundary surface layer, considering homogeneous axisymmetric model in presence of temperature and velocity gradients
12 p2067 A69-26355

Primary cosmic ray energy spectrum studies during 11-year cycle based on changes in intensity at various altitudes
12 p2149 A69-26682

Solar wind plasma observations in geomagnetospheric wake compared at 1000 and 500 earth radii, considering ion energy spectra and geomagnetic tail
12 p2151 A69-26943

Interplanetary plasma measurements by Luna, Mars 1, Zond 2 and Venera 3 probes, including solar plasma flux energy spectra diagram
13 p2336 A69-27354

ESRO 1 satellite measuring proton intensities and energy spectra of precipitated and magnetically trapped electrons
13 p2327 A69-27754

Electron and proton spectra in 1-13 keV range relative to geomagnetic field lines measured by ESRO 1 satellite during Aurorae mission
13 p2328 A69-27755

Radiative heat transfer of materials, discussing spectrum characteristics
13 p2373 A69-27768

Cosmic ray postinteraction nuclear active particle energy spectrum measurements with ionization calorimeter, noting energy underrating
13 p2331 A69-28392

Nuclear active cosmic ray component energy spectrum determined from calorimetric ionization burst measurements, discussing nuclear particle interactions absorption coefficients
13 p2331 A69-28393

High energy nuclear active particles and muons studied with calorimeters, noting cascades muon origin and muon energy spectra
13 p2331 A69-28395

Nuclear active cosmic ray component particle energy spectrum and nuclear cascade avalanches curves, using ionization calorimeter with Pb absorber
13 p2303 A69-28399

High energy muons energy spectrum in extensive cosmic ray showers from spectrum study of ionization bursts due to penetrating component
13 p2332 A69-28403

Cosmic ray chain reaction particles energy spectrum determination in heavy media, discussing cascade parameter application in showers development
13 p2303 A69-28412

Monte Carlo method used to calculate probability of muon penetration to deep underground levels with sea level energies
13 p2333 A69-28424

Continuous random process spectral density at PAM system output
14 p2424 A69-28748

Electromagnetic energy spectra of lightning expressed as function of electric field spectral density of atmospheric
14 p2437 A69-29076

Plasma screening effect on energy spectra of electrons localized at surface charges in weakly doped unipolar n-type semiconductor
14 p2505 A69-29170

Soviet book on solar cosmic rays covering origin, propagation, energy spectrum, diffusion dependence on particle energy and distance, solar flares, etc
14 p2514 A69-29816

Duoplasmatron charged particles energy spectra analyzed as function of discharge parameters
14 p2501 A69-29955

IQSY low energy galactic and solar cosmic ray observations made by various satellites and space probes, including hydrogen and helium energy spectra
15 p2673 A69-30014

Negative curvature electron energy spectrum of discrete radio source model, assuming acceleration by Fermi mechanism and energy loss by synchrotron radiation
15 p2687 A69-30540

X ray energy spectrum from Crab Nebula and diffuse background on celestial sphere near galactic anticenter, noting spectral index
15 p2675 A69-30759

Eigenfrequency spectrum and stability of perfectly conducting inviscid incompressible fluids in cylindrical channels and twisted magnetic fields, noting flowfields and critical wavelengths
15 p2664 A69-31063

Photometric rocket measurements in hydrogen auroras, finding vertical H beta emission profile estimate of proton energy spectrum for H beta production cross section
15 p2598 A69-31307

Rocket observations of protons and alpha particles energy spectra after solar flares, noting riometer and magnetometer recordings
15 p2677 A69-31329

Ground level muon density of extensive air showers related to threshold energy and zenith angle for primary particles
15 p2678 A69-31483

Pulsar NP 0532 in Crab Nebula observed by rocket and telescope showing strong pulsed X ray signal
15 p2679 A69-31529

Kovaszny spectral theory of turbulence, discussing energy spectrum decrease in viscous subrange
16 p2768 A69-31686

Metagalactic electrons inverse Compton effect on relict radiation to interpret cosmic isotropic X radiation entire energy spectrum
16 p2847 A69-31800

Energy spectrum of secondary electrons and fluorescent efficiency in 3914 Å band, obtaining ionization cross section
16 p2850 A69-32315

Electron fluxes energy spectra determined from simultaneous photometric and riometric observations in polar regions
16 p2783 A69-32525

Anomalous magnetic field energy spectrum obtained from aeromagnetic survey and approximation valid for earth crust and upper mantle
16 p2784 A69-32549

Spatial and temporal dependence of trapped particle energy spectra on basis of bimodal diffusion
16 p2852 A69-32619

He II excitation spectrum for interparticle potential using pair Hamiltonian with repulsive core and attractive well
17 p3008 A69-33118

GaAs semiconductor laser emission band homogeneity and continuous energy spectrum levels contribution to induced optical transitions
17 p2984 A69-34161

Solar thermonuclear reactions studied by emitted neutrinos detection, plotting energy spectra for sensitivity of Cl 37 detection system
18 p3185 A69-34278

Oscillator forces and photoionization and photorecombination cross sections of electron transitions in hydrogen atom, considering approximation for total radiation probability
18 p3197 A69-34755

- Energy spectrum of Fe group heavy nuclei from fossil track densities depth variation in hypersthene and oligoclase crystals from meteorite Saint-Severin, noting ablation
19 p3410 A69-36095
- Hydromagnetic wave-charged particle resonant interaction described by diffusion equation in momentum space, deriving diffusion coefficients and time evolution ultrarelativistic particle energy spectrum
19 p3424 A69-36335
- Turbulence energy spectra in free atmosphere with convective layer surmounted by inversion layer, noting power law followed by velocity components
19 p3362 A69-36406
- Energy spectrum and transport mechanism for current carriers in amorphous-crystalline semiconductors, measuring thermostimulated conductivity, induced photoconductivity, optical quenching, etc
19 p3391 A69-36558
- Ensembles of random Hermitian cyclic matrices in statistical theory of complex systems energy level spectra, noting Gaussian density function of eigenvalues
20 p3567 A69-36988
- High energy proton and neutron fluxes and spectra from nuclear emulsion stacks on Cosmos satellites, calculating cosmic radiation doses
20 p3591 A69-37961
- Energy spectrum, spatial characteristics and displacements of auroral zone X rays from X ray spectrometry
21 p3787 A69-38359
- Rocket measurements of primary auroral particles energy spectra indicating spectral structure acceleration peaks associated with electrostatic fields
21 p3707 A69-38490
- Energy spectra measurements of turbulent velocities behind grids of different geometries noting relation to deviation from isotropy
21 p3693 A69-38704
- One dimensional model and equation of energy spectrum function solved in studying turbulent diffusion in fluid at rest
21 p3693 A69-38749
- Meteoritic compositions used to determine prehistoric cosmic rays composition and energy spectrum
21 p3789 A69-38815
- High energy cosmic rays primary spectrum determined from observations of secondary components including gamma rays, muons and air showers
21 p3790 A69-38822
- Approximate formula for energy spectrum of isotropic turbulence at large wave numbers, showing agreement with Gaussian exponential form
21 p3694 A69-38834
- Cosmic ray electron recorder for measuring intensity, energy spectrum and angular distribution of electron fluxes within specific energy range
21 p3724 A69-39074
- Galactic cosmic rays, discussing chemical composition, isotopic separation, proton and alpha particles energy spectra, propagation, interactions, etc
21 p3791 A69-39502
- Electron energy loss spectrum of nitrogen, suggesting atmospheric auroral nitrogen emissions compatibility with low energy electron impact excitation mechanisms
22 p3935 A69-39970
- Sco X-1 X-ray source energy spectrum and time variation from rocket flights in India
22 p4030 A69-40774
- Neutrons energy spectrum at sea level calculated and proved consistent with satellite cosmic ray data
23 p4205 A69-41701
- Integral energy loss spectrum of extensive air showers recorded by Haverah Park 50-m array
23 p4207 A69-42499
- Low energy galactic cosmic ray spectrum determined from ionization rate per hydrogen atom, correlating peak intensity with stellar particle emission high energy portion
24 p4365 A69-42608
- N II 4176 A emission line occurrence in connection with type B auroras, studying secondary electrons energy spectra
24 p4309 A69-43012
- Horizontal wind speeds kinetic energy spectrum near surface, discussing diurnal variations
24 p4343 A69-43063
- H beta production in hydrogen aurora measured during rocket flight, obtaining proton energy spectrum
24 p4309 A69-43170
- Cosmic ray electron energy spectrum and intensity measurements indicating time variations attributed to solar modulation effects
24 p4367 A69-43175
- Crossed beam apparatus /evatron/ for studying energy spectra of crossed positive ethylene ion beams and neutral ethylene molecule beams
24 p4280 A69-43813
- ENERGY STORAGE**
NT ELECTRIC ENERGY STORAGE
NT HEAT STORAGE
- Energy source specifications and control techniques evaluated for microwave amplifier arrays, discussing use of common power supply and energy storage bank
01 p0047 A69-10998
- Stored energy function of hyperelastic material by Lie group extension of Truesdell theorem on symmetry groups
04 p0680 A69-14945
- Line broadening possibility for Q switched iodine laser with aid of magnetic effect /Zeeman effect/, noting energy storage capability increase
05 p0773 A69-16288
- Electrochemical energy storage and conversion for space flight, emphasizing hydrogen oxygen and silver zinc batteries, Gemini and Apollo programs, etc
12 p2015 A69-25866
- Transient temperature response of cylindrical composite energy storage devices with thermal conductivity, density and specific heat independent of temperature
22 p3868 A69-40132
- Solar flare models in terms of energy storage and release mechanisms
24 p4374 A69-43622
- ENERGY TRANSFER**
NT COUPLING CIRCUITS
- Sensitivity of voltage transfer function relative to variation in value of components of resistance terminated reciprocal reactive network
01 p0049 A69-10069
- Mass or energy transfer in reinforced media, discussing components characteristics and role of diffusion processes
01 p0173 A69-10079
- Excitation heating energy pumping mechanism for explaining dynamic equilibrium in C rich arc plasmas with high ion temperature/electron temperature ratio
01 p0126 A69-10276
- Quasi-monochromatic wave dispersion relation and energy transfer in inhomogeneous anisotropic medium
01 p0126 A69-10278
- Nonradiative transfer of excitation energy between mixed trinuclear complexes of Tb and Eu ions with lactose in aqueous solution
01 p0023 A69-10288
- Thermal model for interaction of exploding wires with methane atmosphere, discussing energy transfer efficiency in high temperature pyrolyses near explosion
01 p0119 A69-10674
- Intermolecular collision induced vibration to vibration energy transfer in nitrous oxide in various gas mixtures, measuring fluorescence and relaxation rates
01 p0123 A69-10684
- Power spectrum for energy transfer region in HF turbulent plasma by nonlinear equations, with results applied to subcosmic ray acceleration
01 p0145 A69-10790
- Solar flare mechanism from analysis of energy transfer in quiet solar atmosphere, discussing convection, radiation, mechanical and MHD waves and thermal conduction
01 p0145 A69-10990
- Turbulent flow between parallel plates, discussing turbulence generation by energy addition
01 p0061 A69-10993
- Energy transport in atmosphere studied by considering sphere in isotropic fluid in infinite field without gravity, using first law of thermodynamics
01 p0067 A69-11032
- Resonance energy transfer mechanism in Forster-Dexter theory of electron energy transfer by resonance interaction in condensed media, using many particle treatment
01 p0121 A69-11257
- Mathematical models of energy and mass transfer processes in closed loop multicomponent life support systems
01 p0021 A69-11316
- Transhorizon UHF energy transmission via tropospheric scatter, using propagation path model
02 p0209 A69-12350
- Wave fields and coupling of RF power to ion cyclotron waves in finite length thermal collisional plasma column
03 p0474 A69-13114
- Energy transfer and viscosity coefficients during gas molecular interactions, using spherical monatomic gas molecules model
03 p0415 A69-13419
- Conceptual problems of quantum optics, considering quantum mechanical and classical descriptions of effect of field on matter for damped and undamped modes
03 p0467 A69-13474
- Energy transfer in circulatory force fields, noting mechanism changes for simultaneously operative original field and adjoint field energy sources
04 p0671 A69-14415
- Laser with combined active medium resulting from investigation of autoresonant energy transfer in composite crystals with optical centers
04 p0611 A69-14546
- Motion of vapor derived from solid material vaporization and subsequent heating by nonequilibrium continuum radiation, noting continuity equations and energy transfer
04 p0686 A69-14985
- Turbulent transport of energy in atmospheric boundary layer near earth surface resulting from forced convection
04 p0627 A69-15087
- Perturbation method determination of gravitational induction for quasi-static axisymmetric systems
04 p0661 A69-15190
- Internal gravity waves propagation in shear flow, detailing interaction stress in incompressible stratified Boussinesq liquid, conservation energy exchange and radiation stress
05 p0788 A69-15721
- Energy transfer from radiating sphere to medium with molecular heat conduction
05 p0845 A69-15782
- Diagrams for power transfer parameters between double tuned bandpass filters with arbitrary coupling
05 p0729 A69-15964
- Relaxation time of carbon dioxide laser levels as function of water vapor, CO and Xe gas pressure measured by afterglow pulse gain technique [IEEE PAPER G-1]
05 p0774 A69-16314
- Stimulated Compton effect for energy transfer between relativistic electrons and radio photons in quasi-stellar objects
05 p0828 A69-16652
- Cross field energy transfer in collisionless plasma across earth magnetospheric boundary, using computer and one dimensional sheet model simulation [ISAS-429]
06 p0916 A69-17023
- Resonant four wave interaction for nonlinear energy transfer in electron plasma oscillations
06 p0963 A69-17143
- Solar flare eruptions due to current disruption, leading to magnetic energy transfer from whole current circuit to very small volume
06 p0995 A69-17444
- Mathematical description of electromagnetic field containing plasma, discussing energy transfer modes between plasma and containing field
06 p0965 A69-17517
- Life support system energy efficiency, treating transfer equations of closed space regeneration systems
06 p0882 A69-17644
- Power flow in cyclotron and plasma modes propagating in waveguide filled with cold collisionless axially magnetized plasma
06 p0897 A69-17760
- Vibrational excitation in diatomic gas mixtures by translation to vibration energy conversion in simple collisions and by vibrational energy exchange between components
06 p0962 A69-17821
- Zeta discharge in low density regime characterized by strong turbulence, rapid loss of plasma, resistance higher than predicted and high ion temperature
06 p0970 A69-17955
- Energy transfer from pulse network to mass associated with propagating current sheet in linear pinch discharge, discussing pulsed plasma accelerator efficiency [AIAA PAPER 69-113]
06 p0971 A69-18123
- Surface parameters influence on energy transfer to arc jet anode, discussing work function, accommodation coefficient and diffuse reflection coefficient of electrons [AIAA PAPER 69-107]
06 p1039 A69-18185
- Radiation transfer in resonance lines and in recombination continuum in plasma, discussing frequency redistribution during reradiation and optically dense systems
07 p1188 A69-18282
- Laser excited vibrational fluorescence for determining vibrational energy transfer rates in HCl-carbon dioxide, HCL-HI and HI-carbon dioxide
07 p1144 A69-18289

Radiative transfer problems in inhomogeneous anisotropically scattering plane parallel planetary atmospheres with internal source distributions solved by recursive method
07 p1213 A69-18610

Meteorological satellites observation of energy exchange between earth and space, discussing planetary albedo, energy absorption and source and sink regions
07 p1127 A69-19261

Geomagnetic field line stretching outward due to energy entry in form of large number of charged particles or increase in particle temperature/inflation/
07 p1127 A69-19357

Energy transfer through ionospheric electrons, discussing degradation of fast electrons and role of neutral gas motion in ionospheric currents
07 p1128 A69-19369

Discrete ordinate difference equations of radiative transfer for slab using invariant method, noting storage and computing time advantages
07 p1183 A69-19623

Tropospheric energy cycle interannual variability and quasi-biennial oscillation from geostrophic computations of eddy kinetic energy, energy transfer and internal redistribution
07 p1129 A69-19628

Nonlinear interactions of positive and negative energy electrostatic modes of plasma immersed in magnetic field, discussing instability criterion and Landau damping [IAEA PAPER CN-24/E-13]
07 p1196 A69-19768

Exact solution to kinetic equation for resonant three wave coupling in weakly turbulent plasmas, assuming only single triplet of modes interaction
08 p1360 A69-19989

Radiative transfer by doubling very thin layers in problem of diffuse reflection from plane-parallel atmosphere eliminates numerically solving transfer equation
08 p1420 A69-20064

Radiative transfer equation solution for spectral line formed in two dimensionally varying atmosphere extended to continuum radiation in inhomogeneous atmospheres
08 p1386 A69-20077

Temperature profile calculations for high pressure electric arcs using diffusion approximation for radiant flux density, taking energy transfer into account
08 p1420 A69-20148

Drift measurements of rate constants for charge transfer in ion-molecule processes
08 p1355 A69-20210

Meridional flow, angular momentum and energy flux in atmosphere calculated from IGY data
08 p1346 A69-20312

Energy consideration in electron beam welding, obtaining expression for penetration decrease in terms of thermal diffusivity [ECS PAPER 144]
08 p1320 A69-20360

Green function in closed form for energy transport equation solution in axisymmetric Oseen flow
08 p1305 A69-20850

Near resonant transfer of vibrational energy from carbon dioxide nu 3 mode to N 14 and N 15 molecules in collisions
08 p1358 A69-21011

Energy transfer in gases transmitting heat by interaction of thermal conduction and IR radiation
09 p1621 A69-21442

Momentum and energy transfers analogy in turbulent convection fluid flow emphasizing difficulties in case of liquid metals
09 p1480 A69-21687

Pure ammonium perchlorate single crystal self deflagration, determining energy transfer mechanisms from pressure effects, combustion characteristics and subsurface profile [AIAA PAPER 69-142]
09 p1560 A69-21900

Variational principle to obtain variational estimate of arbitrary functional of solution to radiative transfer equation
09 p1541 A69-22253

Eddington approximation to radiative transfer equation extended to time dependent multifrequency problems
09 p1541 A69-22254

Algorithm for mean energy transmission coefficient of fundamental mode in beam guide with given inhomogeneities, discussing mode conversions
09 p1469 A69-22629

Early disturbances in active migration of potassium 42 ions in irradiated erythrocytes in rats, showing relation between influx and energy exchange in cells
10 p1647 A69-23966

Vibrational energy transfer computed for processes in carbon dioxide-nitrogen laser based on vibrational relaxation data
10 p1706 A69-24083

Radiative transfer equation in nonuniform magnetoactive medium derived from continuity equation for radiative energy density in space of coordinates and wave vectors
10 p1742 A69-24143

Monte Carlo method application to heat transfer analysis including radiation, rarefied gas energy transfer and conduction
11 p1997 A69-24457

Multiple scattering of solar radiation in turbid atmosphere, considering equations of sky radiation and radiative transfer
11 p1911 A69-24587

Radiant power flow, transmittance and absorbance of absorbing thin film multilayer in terms of characteristic matrix and admittance of surrounding media
11 p1896 A69-24850

Solar wind particles acceleration and transformation into radiation belt particles
11 p1948 A69-24855

Resonant vibrational energy transfer between specific mode of carbon dioxide and N molecules at high temperatures, monitoring IR emission
12 p1313 A69-25984

Translational-vibrational energy transfer value between atom and diatomic molecule determined using steric factor with repulsive interaction potential
12 p1334 A69-25988

Energy exchange between LF waves and magnetospheric energetic particle population by bounce resonant interaction
12 p2073 A69-26946

Spectral line formation in nonlinear multilevel atom line transfer problems, considering radiation transfer through plane parallel atmospheres of H and Mg atoms
12 p1333 A69-26967

Energy transfer mechanisms between translational, rotational, vibrational, chemical and electronic degrees of freedom in hypersonic shock wave in high temperature air
12 p2063 A69-26969

Resonance line radiation transfer in finite homogeneous cylinders of various shapes and optical thicknesses using Monte Carlo method
12 p191 A69-26970

Vibrational energy exchange between diatomic molecules by IR emission of CO fundamental behind shock waves
13 p2301 A69-27361

Heat transfer in solid bodies, deriving thermal conductivity equation and surface boundary conditions in presence of radiative energy transfer
13 p2373 A69-27584

Acoustic power transferred to plane homogeneous elastic structures and cylindrical shells by neighboring sound sources
13 p2363 A69-28186

Energy transfer by simultaneous conduction and radiation between two media in intimate contact, detailing numerical solution method for resulting coupled nonlinear integrodifferential equations
13 p2378 A69-28340

Transistorized DC amplifier circuit with reversible and controllable transfer constant based on voltage conversion principle
13 p2235 A69-28511

Energy exchange of rare earth ions in uranyl phosphate liquids and glasses, studying sensitized luminescence origin
14 p2485 A69-29034

Gas-surface interaction for trapping and energy exchange, comparing continuum and discrete lattice models for solids
14 p2409 A69-29092

Energy transport between vortices in turbulent flow calculated from vortex stability study
14 p2430 A69-29508

Self resonant energy transfer mechanisms in active media for lasers investigated by two methods
14 p2460 A69-29644

Energy exchange between active centers in silicate and phosphate glass, comparing luminescent and lasing properties
15 p2632 A69-30053

Wave energy flux and correlation wave energy flux relationship to energy transport, noting applicability to fluids
15 p2595 A69-30218

Cosmic ray particle Pb nucleus interaction energy transfer to electron photon cascade in first inelastic collision, noting dependence on particle energy
17 p3008 A69-33387

Half space applications regarding equation of transfer for planetary atmosphere
18 p3191 A69-34306

Radiation gas dynamics in shock tube, studying radiation coupled flows with flow field affected by radiant energy transport
18 p3116 A69-34447

Prestressed ceramic driver chamber energy efficiency for arc driven shock tube by pressure measurements with piezoelectric probe
18 p3116 A69-34456

Atomic excitation and ionization by thermal electrons, using Monte Carlo trajectories to determine adiabatic collisions effects on energy transfer near dissociation limit
18 p3176 A69-34790

Balmer alpha and Lyman beta intensities for multiple scattering calculated for hydrogen geocorona models by radiative transfer equations, discussing radiation transport through earth hydrogen atoms
18 p3128 A69-34943

Energy transfer from radiating sphere to medium with molecular heat conduction
18 p3230 A69-35034

Moment and discrete ordinate methods in radiative transfer problems in planar, radiating and nonscattering media, noting conical transformation of moment equations
18 p3174 A69-35237

Temperature distribution around radiating sphere in homogeneous gas medium with molecular heat transfer, solving energy transport equation
18 p3231 A69-35325

Solar flare model based on force-free currents in solar atmosphere, noting rapid energy release due to exceeding current density critical limit
18 p3188 A69-35392

Stored energy release in exploding wire circuit during divergent detonation wave ignition in propane-oxygen mixture in circular sector
19 p3451 A69-36365

Hypervelocity ionized gas flow analysis, allowing for finiteness of energy exchange duration between electrons and ions
19 p3379 A69-36383

Gas-surface energy transfer experiment on OGO-F satellite, measuring upper atmosphere kinetic energy flux to determine accommodation and drag coefficients, density, etc
19 p3255 A69-36680

Stochastic motion in linear lattice of coupled harmonic oscillators analyzed by Schroedinger coordinates and Bessel functions for time behavior, energy flow and impurity effect
19 p3374 A69-36752

Homogeneous isotropic turbulence spectrum asymptotic behavior for various spectral energy transfer models
19 p3301 A69-36818

Active center chemical bond alteration influences on luminescence characteristics of phosphate glasses, noting quick energy transfer via ions
20 p3552 A69-37017

Radiative energy transport quantities for hydrogen plasma including Plank and Rosseland mean absorption coefficients, discussing line and continuum radiation and optical limits
20 p3581 A69-37306

Kinetic energy of sunspot rotational motion transferred to electromagnetic energy in filamentary currents, noting time variations in solar atmosphere preconditioning for flare
20 p3589 A69-37550

Radiative transport equation solution in two flow approximation for plane layer, considering absorption and dispersion characteristics dependence on radiation density
20 p3553 A69-37608

Power spectrum for energy transfer region in HF turbulent plasma by nonlinear equations, with results applied to subsonic ray acceleration
20 p3591 A69-38008

Negative energy waves presence, showing qualitative difference on theoretically derived parametric amplification in plasmas
20 p3582 A69-38244

Polarization effect on diffusion equations of radiative transfer, noting anisotropy in Rayleigh scattering
21 p3847 A69-38473

DC MHD generator using gas plasma as working fluid, discussing fundamental principle, components interactions and energy conversion
21 p3777 A69-39165

Transformer for unilateral energy transfer using single domain uniaxial Permalloy film
21 p3684 A69-39454

Singlet-singlet energy transfer kinetics dependence on emission and absorption spectra overlap via dipole-dipole interaction
22 p3895 A69-40056

Spatiotemporal signal distortions for multiple scattering from unsteady radiant energy transfer equations
22 p3899 A69-40247

Radiation transfer in circumstellar dust envelopes, considering thin and opaque clouds
22 p4027 A69-40655

Emission lines in optical spectra of radio galaxy nuclei, considering time dependent energy release nature
22 p4034 A69-41174

Electron excitation and collisional energy transfer processes in laser level of pure carbon dioxide fill and carbon dioxide-water vapor mixture
23 p4171 A69-41390

Thermotidal energy transfer from lower neutral atmosphere to and above lower ionosphere, considering tidal wave transmission mechanism
23 p4155 A69-41561

Monte Carlo method for energy transfer efficiency of ruby laser pumping cavities by helical flash lamps, noting dependence on ruby parameters
23 p4173 A69-41630

Interplanetary magnetic field role in interaction between terrestrial magnetosphere, solar plasma and solar flux energy transfer
23 p4214 A69-41865

Power flow relations between randomly vibrating systems with weak linear elastic or dissipative coupling
23 p4227 A69-41877

Parametric differentiation applied to radiation gas dynamics equations solution, considering energy transfer by thermal radiation in high speed reentry
[AIAA PAPER 68-668] 23 p4059 A69-41892

Arc heating of shock tube driver gas, describing radiative energy transfer mechanism
23 p4147 A69-41895

Time dependent natural oscillations of plane open resonators infinite periodic sequence, considering electromagnetic energy transfer into ambient medium
23 p4139 A69-42039

Optimum functions for mass and energy flow during spacecraft orbital transfer, emphasizing time behavior of propulsion variables
24 p4382 A69-42921

Oscillatory convection, energy transport and structure of sunspots, suggesting fast changes in equilibrium conditions for magnetic reconstruction and solar flares origin
24 p4374 A69-43624

Transmission functions probabilistic model for solving radiative transfer problems in spherical shell medium surrounding emitting black core or point source, using integrodifferential equations
24 p4415 A69-43637

ENGINE ANALYZERS

Maintenance process simulation for engine and major components to provide routine material usage forecast and policies
09 p1503 A69-21802

Howell engine hot section analyzer/HSA/ developed to improve maintenance, flight safety and costs of jet aircraft engines
10 p1671 A69-23263

Sonic diagnostic engine analyzer for detecting jet engine malfunctions prior to failure
24 p4312 A69-42758

ENGINE CONTROL

NT ROCKET ENGINE CONTROL

NT TURBOJET ENGINE CONTROL

Pneumatic pressure ratio sensing element and associated high pressure switches and amplifiers for gas turbine engine control systems
02 p0249 A69-12088

Fluidic system controlling inlet guide vanes to high pressure compressor of two spool jet engine, using digital elements to drive hydraulic servosystem
02 p0305 A69-12090

Digital electronic computer technique for control of aircraft power plant, describing self adaptive control
03 p0496 A69-14091

Aircraft turbine engines operation and control, discussing technology, simulation and system developments
05 p0812 A69-16528

Aircraft gas turbine engines control systems capabilities and future requirements, considering maximum propulsion system performance with minimum fuel consumption
[ASME PAPER 68-GT-62] 08 p1376 A69-19846

Digital computer simulation and analysis of control loops for ion thruster control
[AIAA PAPER 69-239] 09 p1564 A69-21240

30 cm diameter mercury bombardment low impulse thruster development for potential space applications, discussing performance and control
[AIAA PAPER 69-238] 09 p1566 A69-21256

Gas turbine engines control and fuel systems integration, considering weight reduction
[ASME PAPER 69-GT-49] 09 p1571 A69-22483

Fluidic overspeed sensor for small turboshaft power turbine, discussing requirements, circuit and system design, packaging, reliability and maintainability
[ASME PAPER 69-GT-17] 09 p1571 A69-22500

Compressor inlet Mach number choice to control high performance variable stator compressors geometry
[ASME PAPER 69-GT-14] 09 p1571 A69-22502

Fluidic compressor bleed control unit for TF-30 jet engine to prevent stall at low rpm operation
10 p1753 A69-23559

Flow control valve for hydraulic motor speed regulation operated by remote pressure signal
11 p1827 A69-25646

Control technology advancement effects on gas turbine design and application, integrating control scheme, modularization and commonality, system design and energy input and load control
12 p2146 A69-25786

Gas turbine fuel and control systems for two and three shaft engines in military and civilian aircraft including helicopters
[IME PAPER 12] 12 p2147 A69-25796

Blade material temperature variation observed in turbojet engine during air bleed of varying intensity and duration
13 p2325 59-27444

Digital computers for aircraft engine control, discussing economic assessment, advantages basic control system
15 p2671 At 30323

Aircraft engine accessories for engine control monitoring and protection, discussing transducer redesign, equipment range for Concorde, small engine design, etc
16 p2789 A69-31813

Integrated propulsion control system for ramjet Hypersonic Research Engine to operate at 3-8 Mach numbers
[AIAA PAPER 69-546] 16 p2845 A69-32744

Helicopter engine dynamic analysis, discussing modeling techniques, rotor responses and turbine speed control simulations and transition from mathematical models to hardware components
[AHS PAPER 332] 17 p2946 A69-33531

Digital computer for aircraft engine control covering in-flight health monitoring, automatic flight checkout, diagnostic failure routines, etc
17 p3022 A69-33603

Monograph on control dynamics of gas turbines with adjustable guide vanes, using methods of control theory and applied mathematics
21 p3784 A69-38449

JT9D engine fuel and vane control systems for Boeing 747, noting computing system positioning of throttle valve for fuel flow control
[SAE PAPER 69-0405] 23 p4201 A69-41658

Engine fuel and geometry control design for large high bypass aircraft turbofan engines used for airbus powering
[SAE PAPER 69-0403] 23 p4201 A69-41659

Digital computers effect on aircraft automatic power unit controls, discussing safety, reliability, self monitoring and redundant computer systems
24 p4253 A69-43113

ENGINE COOLANTS

Diathermal regenerative cooling of combustion chambers and engine nozzles with supercritical heat transfer mode
03 p0495 A69-12970

NERVA engine cooldown system for emergency shutdowns using high pressure liquid H followed by gaseous H warmup and liquid N cooldown
[AIAA PAPER 69-512] 16 p2810 A69-31846

Heat pipes design for rocket engines cooling, discussing connections to space radiator and to heat rejection device and heat transfer capability
[AIAA PAPER 69-582] 16 p2839 A69-32668

Turbine rotors temperature reducible by increasing air cooling system flow rate
24 p4364 A69-43081

Foamed liquid as potential coolants in rocket engine to overcome low efficiency and streaky coverage of conventional liquid film cooling
24 p4408 A69-43127

Scramjet engine active cooling with regenerative system using superalloy heat exchangers and hydrogen fuel as coolant
[AIAA PAPER 68-1091] 24 p4365 A69-43725

ENGINE DESIGN

Brushless DC torqued motor using reluctance magnetic circuit and toroidally distributed coil winding
01 p0012 A69-10154

Engine air intake design and development for Concorde aircraft, discussing design constraints
[AIAA PAPER 67-752] 01 p0006 A69-11014

Human reaction to aircraft engine noise, evaluating effective perceived noise level and constraints on engine design
02 p0204 A69-12766

CF6 turbofan engine technology program for improvement in performance, weight, durability, noise, etc
[SAE PAPER 68-0691] 03 p0496 A69-13446

Aerothermodynamics of subsonic-aircraft propulsion, analyzing performance of bypass engine, fuel consumption and specific weight
05 p0695 A69-15551

High bypass turbofan design, discussing JT9D engine combustion, materials and cooling
05 p0811 A69-15552

Engines for V/STOL application, discussing aerodynamics of thrust lift and lift jet engines
05 p0811 A69-15553

Soviet book on design of aircraft engine component and subsystem elements, emphasizing aligning, locking and sealing methods, torque transmission, etc
05 p0812 A69-15864

Similarity conditions in turbine engine tests, analyzing flight speed, Reynolds number, combustion efficiency, heat changes, inlet turbulence and outlet nozzle
05 p0742 A69-16028

Transpiration air cooled blading to test and design small gas turbine at 2500 F inlet, discussing cascade and full stage component
[SAE PAPER 69-0035] 07 p1203 A69-18310

Optimum fixed geometry ramjet in Mach range of 3 to 7 with successively subsonic and supersonic combustion
[ONERA-TP-656E] 07 p1203 A69-18415

T-53 engine operation in U.S. Army helicopters noting design problems from compressor blade failure, sand and dust erosion and bearing and lubrication malfunctions
[AHS PAPER 215] 07 p1203 A69-18867

Instrumentation design problems connected with NERVA, considering high gamma and neutron radiations and temperature environments
[IEEE PAPER 2D-5] 07 p1134 A69-19189

Material design problems in small gas turbines, discussing engine performance sensitivity, thinness of rotor-blade and stator-vane trailing edges, dimensional tolerances, etc
[ASM PAPER D8-16.2] 07 p1204 A69-19668

Titanium alloys role in turbofan and turbojet engine design, noting use in components and introduction in manufacturing techniques
[ASM PAPER D8-26.4] 07 p1143 A69-19673

Supercharged bypass engines for possible application in light aircraft, noting payload fractions and total takeoff weights values
08 p1254 A69-20168

Three shaft turbofan engines for 1970s noting thermodynamic and propulsive efficiencies, fuel consumption, weight, noise reduction, etc
08 p1376 A69-20627

Motor design for operation in ultrahigh vacuum, discussing absence of convection cooling, outgassing avoidance, lubrication impossibility and oxygen absence as design parameters
08 p1377 A69-21028

Dual-rotor high-bypass-ratio CF6 turbofan engine design and development programme and growth
08 p1377 A69-21163

Experimental program for tests to identify primary electric propulsion system integration problems and solutions, emphasizing design and initial testing
[AIAA PAPER 69-236] 09 p1560 A69-21213

Extraction and acceleration mechanism in RF ion motors, fixing plasma potential with extraction anode [AIAA PAPER 69-284] 09 p1564 A69-21237

RF ion thrusters using self sustaining electrodeless discharge [AIAA PAPER 69-285] 09 p1565 A69-21247

Radiation cooled MPD arc thruster design and performance, noting specific impulse relation to arc spoke rotation frequencies [AIAA PAPER 69-245] 09 p1566 A69-21259

Power systems for future aircraft emphasizing growth in performance and reduction in weight 09 p1567 A69-21387

Hollow cathode mercury electron bombardment thruster design, emphasizing low specific impulse operation and discharge chamber improvements [AIAA PAPER 69-300] 09 p1569 A69-21880

Composite materials and alloys for jet turbine components in 1970s, discussing anticipated temperatures and material properties 09 p1523 A69-22061

Design, metallurgical and manufacturing problems of titanium application in superjet C5 and SST engines 09 p1570 A69-22062

High recovery inlet design for Boeing 747 high bypass ratio fan engine, considering throat Mach number, lip losses and auxiliary passage losses [ASME PAPER 69-GT-41] 09 p1570 A69-22482

Fan compressor noise reduction indicating effects of design, number of blades, vane/blade ratio, aerodynamic parameters and blade spacing [ASME PAPER 69-GT-9] 09 p1571 A69-22505

High bypass ratio compound fan shaft engine design and performance for convertible rotary wing aircraft [ASME PAPER 69-GT-51] 09 p1572 A69-22511

Baseline requirements for commercial aircraft propulsion systems, stressing engine installation in aircraft [ASME PAPER 69-GT-57] 09 p1572 A69-22514

JT15D business aircraft turbofan engine, discussing low costs and fuel consumption, maintenance, reliability, installation, etc [ASME PAPER 69-GT-119] 09 p1572 A69-22524

Compressor to inlet distortion tolerance design techniques for gas turbine compressors, noting rotor matching, blade chord length, blade geometry, etc [ASME PAPER 69-GT-115] 09 p1572 A69-22525

Combustion chamber design for advanced gas turbines, noting influence of fuel air mixing and air flow distribution 09 p1573 A69-22612

Film cooling injection slots number and position over flame tube and minimum cooling airflow in aircraft gas turbines 09 p1625 A69-22623

Gas turbine engine development data system based on test stands subsystems and central computer 10 p1660 A69-23284

Aircraft engines future specifications as affected by expanding market, noting speed requirements and thrusts 11 p1942 A69-25215

Aerodynamic design of axial flow compressors and turbines, using aerothermodynamic equations for compressible flow analysis 11 p1821 A69-25585

Hybrid chemical rocket theory and design noting radiation effects, regression and convective heat transfer 11 p1944 A69-25589

Nuclear rocket propulsion, discussing solid core and fluid core systems for reactors, nozzles, feed systems, control, component design and performance 11 p1914 A69-25590

Control technology advancement effects on gas turbine design and application, integrating control scheme, modularization and commonality, system design and energy input and load control 12 p2146 A69-25786

Radial gas turbine design and performance including nozzle and rotor loss, mechanical and thermal stresses and manufacturing methods and materials [IME PAPER 7] 12 p2146 A69-25787

Aerodynamic and thermal considerations in axial flow turbine blade design, discussing internal air cooling [IME PAPER 2] 12 p2146 A69-25788

Gas turbine combustion chamber design factors including combustion volume, burning zone, dilution zone, pressure drop, fuel preparation, injection and ignition, exhaust smoke, etc [IME PAPER 3] 12 p2146 A69-25789

Tubular gas turbine combustion chamber design for optimum mixing performance using flow and mixing data of cold air injection into hot gas stream [IME PAPER 15] 12 p2147 A69-25793

Concorde SST turbojet engine integrated assembly consisting of air inlet, gas generator, reheater and convergent-divergent nozzle 12 p2147 A69-26357

Thin ring-strut structure resting on elastic foundation, analyzing deformation taking warping effects into account, noting applicability to engine design 12 p2184 A69-26812

CF6 turbofan engine technology program for improvement in performance, weight, durability, noise, etc 13 p2324 A69-27331

Gas turbine compressor end seals, discussing air leakage paths, primary and secondary seals, design and efficiency [ASLE PREPRINT 68AM 4B-4] 13 p2267 A69-27366

Shorter combustors for high temperature jet engines of high speed aircraft, considering lifetime, shroud scoops, overheating, warpage, etc 14 p2509 A69-29433

Jet engine intershaft bearing oil feed design, discussing use of nonrotating feed link and improvement of oil scavenging at high altitudes 15 p2671 A69-30702

Aircraft gas turbine parts design and fabrication, discussing role of welding techniques 15 p2629 A69-30928

Europa 1 booster supplementing with perigee-apogee system for development of Europa 2, noting payload launching capability into 24-hr circular orbit 15 p2671 A69-31051

Subsonic transport high bypass ratio engine evaluation in terms of fuel consumption, size, thrust-weight ratio, noise and price 16 p2835 A69-31803

Aircraft engine accessories for engine control, monitoring and protection, discussing transducer redesign, equipment range for Concorde, small engine design, etc 16 p2789 A69-31813

CF6 turbofan engine technology program for improvement in performance, weight, durability, noise, etc [SAE PAPER 680691] 16 p2837 A69-32367

Fast heat-up electrothermal ammonia thruster role in development of hybrid resistojet in millipound thrust range [AIAA PAPER 69-496] 16 p2838 A69-32649

High temperature radial turbine design for small gas turbine engines, discussing aerodynamic, structural and thermal analyses [AIAA PAPER 69-524] 16 p2838 A69-32662

Systems approach in turbofan engine design acoustic evaluation, discussing noise sources and radiation patterns [AIAA PAPER 69-491] 16 p2839 A69-32667

L-500 inlet development program, discussing external forebody design, entry lip and diffuser geometries, configuration and technology developments, experimental techniques and test equipment [AIAA PAPER 69-448] 16 p2733 A69-32684

M 3.5 two dimensional mixed compression inlet system with self restart using flexible variable ramp system [AIAA PAPER 69-447] 16 p2845 A69-32732

Self contained lift fan concept and circulation controlled rotor aircraft power plants for high speed VTOL transports 17 p2897 A69-33208

High bypass ratio engine influence on short range civil aircraft design, considering performance, noise, engine location, etc 17 p2897 A69-33212

Aircraft auxiliary power system influence on power plant installation and aerodynamic design 17 p3017 A69-33216

Aircraft auxiliary power systems, discussing weight and power requirements, component design, driving methods and influence on power plant design 17 p3018 A69-33217

Liquid oxygen and hydrogen rocket engine HM4 design and operation, discussing fuel, low temperatures and heat exchange 17 p3020 A69-33345

Gas turbine engines smoke reduction, aerated fuel sprays for smoke control on engine design and factors affecting visibility of exhaust plumes 17 p3020 A69-33350

Propulsion power plant arrangements for rotary wing aircraft with thrust producer for forward flight, considering convertible fan/shaft engine configurations [AHS PAPER 333] 17 p3021 A69-33529

Vertical takeoff aircraft propeller/rotor design and performance prediction, discussing vortex model, wake contraction, blade element aerodynamic properties, etc [AHS PAPER 325] 17 p2894 A69-33534

Aircraft engine lubrication system design, discussing bearings reduction, oil compartment scavenging, sealing, cooling, pressurization, etc 18 p3185 A69-35244

Low smoke emission combustors for aircraft turbine engines, discussing effects on ignition and exit temperature distribution [AIAA PAPER 69-493] 19 p3394 A69-36299

Jet engine compressors and fans, combustors, turbines and composite materials in evaluating thrust-weight ratio, engine size, weight and life, etc 19 p3395 A69-36322

Pressure sensors, strakes, removal of full length guide vanes indicate possible difficulties with thrust of NK-8-2 turbofans in Tu-154 19 p3395 A69-36757

Turbine engine monitoring during operation, discussing automatic monitoring systems and engine design 19 p3329 A69-36873

Lift engine inlet development for XV-4B aircraft, discussing tests, pressure distortion and recovery during simulated hover and transitional flight [AIAA PAPER 68-636] 20 p3585 A69-37150

Rolls-Royce RB.211 turbofan engine development, discussing three shaft design, engine performance, testing program, etc 20 p3640 A69-37927

Superalloy technology applications to gas turbine engines 21 p3785 A69-38928

RB 202 self contained lift fan engine design for high speed interurban civil VTOL operations, considering weight, cost, noise and fuel consumption 22 p3862 A69-39933

Wakkel engine development in Poland for powered military gliders at 18 hp and 5500 rpm 22 p3999 A69-40006

Building block approach to turbofan engine design, discussing fuel consumption, noise and component research [RAES PAPER 14] 22 p3999 A69-40493

Aircraft engine technology, discussing turbine entry temperatures, reheat temperatures, high pressure spools, high temperature materials and small blades fabrication [RAES PAPER 20] 22 p4000 A69-40499

TF39 high bypass ratio engine design, development and tests, noting low smoke combustor [RAES PAPER 21] 22 p4000 A69-40622

Dynamic simulation for gas turbine engine components design to assure stable operation and rapid response characteristics [SAE PAPER 690386] 23 p4200 A69-41655

Large fan blade design, discussing aerodynamic design and rig test program supporting fan definition [SAE PAPER 690387] 23 p4200 A69-41656

Engine fuel and geometry control design for large high bypass aircraft turbofan engines used for airbus powering [SAE PAPER 690403] 23 p4201 A69-41659

Douglas DC-10 aircraft design programs and methods stressing power plant reliability, maintainability and costs [SAE PAPER 690391] 23 p4201 A69-41664

Lockheed 1011 propulsion system design relating to system and component maintainability, reliability, performance and noise [SAE PAPER 690390] 23 p4201 A69-41665

Optimization of RF ion thruster cluster engines for ascending trajectory, discussing unfolding mechanism of solar cell panels [DGLR-69-022] 23 p4203 A69-41933

Rankine cycle power systems with reciprocating engines using organic working fluids, discussing engine development, system characteristics, etc 23 p4067 A69-42237

Computerized design of potassium vapor turbine with supersaturation effects compared with equilibrium flow turbine design 23 p4187 A69-42251

Positive displacement Rankine cycle rotary wet steam engine design compared with piston type, noting simplified evaporator and tests 23 p4069 A69-42252

Rolls-Royce-Bristol/SNECMA M45H medium power turbojet for VFW 614 aircraft
24 p4363 A69-42566

Turbofan jet engine research, discussing future compression and bypass ratios, weight and noise reduction, maintenance and reliability, temperature effects, etc
24 p4363 A69-42569

Aircraft engine lubrication system design, discussing bearings reduction, oil compartment scavenging, sealing, cooling, pressurization, etc
24 p4363 A69-42780

Engine design program for TF34-GE2 high bypass ratio turbofan military aircraft engine, outlining estimating procedures for thrust, fuel consumption and weight requirements
24 p4364 A69-43042

Monitoring devices and modular construction features of Rolls-Royce RB.211 three shaft turbofan engine, discussing maintainability
24 p4321 A69-43112

ENGINE FAILURE

Titanium alloy stress corrosion behavior in atmospheric salt environments at elevated temperatures related to aircraft engine part failures
01 p0099 A69-11056

T-53 engine operation in U.S. Army helicopters noting design problems from compressor blade failure, sand and dust erosion and bearing and lubrication malfunctions
[AHS PAPER 215] 07 p1203 A69-18867

Helicopter flight safety as function of service duration, performance limitations and propulsion failure
07 p1054 A69-19313

Engine usage indicator to cumulate small gas turbine engine exposure to certain deterioration, presenting circuit logic block diagram
[ASME PAPER 69-GT-69] 09 p1572 A69-22519

Monitors to detect incipient failure during turbine engine development, describing servocontrol
10 p1692 A69-23253

Spectrometric oil analysis procedure /SOAP/ for predicting failure of oil wetted parts in small turboprop aircraft engines
[SAE PAPER 690325] 11 p1941 A69-24508

Steady state and dynamic distortion influence on performance and stall of turbofan engine, discussing compressor instrumentation, tests and simulation data
18 p3185 A69-35175

Computer program using system simulation and Monte Carlo techniques to assess turbojet engine compressor disk reliability, discussing maintenance policy and engine design effects
19 p3394 A69-36042

Flight vehicle motion optimization taking into account random failures of sectioned power plant with limited capacity and independent parallel units
21 p3647 A69-38893

Engine oil analysis applied to commercial airline operations, ensuring lubricating qualities retention and detecting oil-wetted component failures
[SAE PAPER 690423] 23 p4169 A69-41647

Solid rocket motors failure during static firing, discussing sequence of events
24 p4365 A69-43260

ENGINE INLETS

NT HYPERSONIC INLETS

Engine inlet thermal antiicing analysis, detailing computer programs to determine air flow velocity, water impingement and thermal requirements
01 p0055 A69-11045

Turbine powered helicopter engine inlet air filtration system utilizing direct-connect S-bend duct
01 p0143 A69-11054

Vitiated inlet air effects on J60-P-6 turbojet engine performance at sea level for various simulated flight Mach numbers
01 p0143 A69-11063

Analytical design of SH-3 helicopter engine inlet ice deflector shield interior surfaces, defining potential flow pattern and moisture droplet trajectories
01 p0011 A69-11064

Fluidic system controlling inlet guide vanes to high pressure compressor of two spool jet engine, using digital elements to drive hydraulic servosystem
02 p0365 A69-12090

Pressure oscillation production in wind tunnel by hinged plates in test section walls to test jet engine inlets under controlled conditions
02 p0229 A69-12537

Jet engine inlet noise control by modification of inlet guide vanes
05 p0811 A69-15622

C-5 engine inlet development, presenting two phase nacelle forebody and five phase model tests, scale corrections inlet/cowl optimization and prototype tests
[ASME PAPER 69-GT-52] 09 p1570 A69-22481

High recovery inlet design for Boeing 747 high bypass ratio fan engine, considering throat Mach number, lip losses and auxiliary passage losses
[ASME PAPER 69-GT-41] 09 p1570 A69-22482

Compressor inlet temperature /CIT/ sensors, describing bimetal strip and liquid expansion aspirated types
[ASME PAPER 69-GT-18] 09 p1571 A69-22499

Compressor inlet Mach number choice to control high performance variable stator compressors geometry
[ASME PAPER 69-GT-14] 09 p1571 A69-22502

Compressor to inlet distortion tolerance design techniques for gas turbine compressors, noting rotor matching, blade chord length, blade geometry, etc
[ASME PAPER 69-GT-115] 09 p1572 A69-22525

Inlet produced dynamic distortion and effects on stall margin of J-85 turbojet engine from supersonic wind tunnel tests
[AIAA PAPER 69-487] 16 p2840 A69-32676

L-500 inlet development program, discussing external forebody design, entry lip and diffuser geometries, configuration and technology developments, experimental techniques and test equipment
[AIAA PAPER 69-448] 16 p2733 A69-32684

Fluidic temperature sensors for measuring turbine inlet temperature on large turbine engine
[AIAA PAPER 69-544] 16 p2792 A69-32692

Aircraft wing aerodynamic forces and moments due to lifting engine air intake simulated by wind tunnel experiment
19 p3239 A69-36400

Lift engine inlet development for XV-4B aircraft, discussing tests, pressure distortion and recovery during simulated hover and transitional flight
[AIAA PAPER 68-636] 20 p3585 A69-37150

ENGINE MONITORING INSTRUMENTS

Engine usage indicator to cumulate small gas turbine engine exposure to certain deterioration, presenting circuit logic block diagram
[ASME PAPER 69-GT-69] 09 p1572 A69-22519

Multichannel miniature telemetry for vibration, strain and temperature measurements in high speed machinery by solid state encapsulated devices
10 p1654 A69-23251

Aircraft engine accessories for engine control, monitoring and protection, discussing transducer redesign, equipment range for Concorde, small engine design, etc
16 p2789 A69-31813

C-141 engine health monitoring program, applying results to maintenance costs reduction
[AIAA PAPER 69-775] 19 p3244 A69-35646

Turbine engine monitoring during operation, discussing automatic monitoring systems and engine design
19 p3329 A69-36873

Jet fleet engine performance monitoring program, discussing systems design and resultant management planning
22 p3999 A69-39922

ENGINE NOISE

Aircraft engine noise reduction in test runs by sound insulating hangar
01 p0054 A69-10033

Aircraft noise suppression, discussing community aspects of jet and fan noise and physical mechanisms of jet noise
01 p0009 A69-10349

Human reaction to aircraft engine noise, evaluating effective perceived noise level and constraints on engine design
02 p0204 A69-12766

Soviet MI-8 and MI-4 passenger helicopters noise characteristics with turboprop and piston engines and during landing takeoff and horizontal flight
03 p0366 A69-13417

Power generation in combat environment by tested self contained organic Rankine silent engine, discussing working fluid properties
[SAE PAPER 690062] 07 p1058 A69-18309

Concorde jet engine silencer concept and characteristics
[AIAA PAPER 67-391] 12 p2148 A69-26759

Rolls Royce noise and compressor test facility for continual lowering of engine sound pressure levels, considering sound generating mechanisms
13 p2240 A69-27616

Equipment and test installations for turbojet noise studies, discussing noise from rotating parts, pure jet noise and air propagation of noise
13 p2325 A69-28589

Aircraft noise control at source through high bypass ratio engine modification, FAA decibel standards and higher capacity aircraft for increased traffic density
14 p2509 A69-29156

Systems approach in turbofan engine design acoustic evaluation, discussing noise sources and radiation patterns
[AIAA PAPER 69-491] 16 p2839 A69-32667

Test rig vehicle design for noise research on single stage high bypass ratio fans for quieter turbofan powerplants
[AIAA PAPER 69-492] 16 p2767 A69-32727

Real time analyzers of acoustic signals for aircraft engine noise, noting automatic test
20 p3462 A69-37756

Jet engine noise technology evaluation, noting effects on airport neighbor
[RAES PAPER 13] 22 p3999 A69-40492

Sonic diagnostic engine analyzer for detecting jet engine malfunctions prior to failure
24 p4312 A69-42758

ENGINE PARTS

Protective coatings for gas turbine engine components in marine environments, considering corrosion of diffuser, impeller, compressor case and turbine blades
01 p0099 A69-11057

Soviet book on design of aircraft engine component and subsystem elements, emphasizing aligning, locking and sealing methods, torque transmission, etc
05 p0812 A69-15864

Maintenance process simulation for engine and major components to provide routine material usage forecast and policies
09 p1503 A69-21802

Composite materials and alloys for jet turbine components in 1970s, discussing anticipated temperatures and material properties
09 p1523 A69-22061

Potential usage of titanium in cast parts for gas turbine engines, emphasizing alloys development
[ASME PAPER 69-GT-24] 09 p1513 A69-22494

Radiographic, ultrasonic, thermographic and leak test quality control for brazed liquid propellant rocket engine components
10 p1699 A69-23054

Spectrometric oil analysis procedure /SOAP/ for predicting failure of oil wetted parts in small turboprop aircraft engines
[SAE PAPER 690325] 11 p1941 A69-24508

Explosive fabrication of aircraft components including turbine engine exhaust components, door seals, etc
[SAE PAPER 690316] 11 p1890 A69-24510

Fabricable materials with low plastic deformation for gas turbine components, noting strength vs temperature for alloys, fiber composites and ceramics
[IME PAPER 8] 12 p2147 A69-25791

Small gas turbine Brayton cycle analysis treating component efficiencies as dependent variables in examining single stage radial compressor and turbine aerodynamic configuration
[IME PAPER 5] 12 p2147 A69-25794

Cast high temperature alloys for gas turbine components, discussing production, temperature capability, composition, oxidation, hot corrosion and weldability
[IME PAPER 10] 12 p2147 A69-25795

Statistical theory of cumulative wear of machine parts with application to engine parts of passenger aircraft, automobiles, tractors, etc
13 p2268 A69-28052

Aircraft gas turbine parts design and fabrication, discussing role of welding techniques
15 p2629 A69-30928

Forced oscillations of three layer plate used as vibration dampers for engine components
16 p2873 A69-32143

Molded composites application to engine components, discussing turboprop reduction gear case design using polymer matrix boron composite
[AIAA PAPER 69-466] 16 p2795 A69-32763

Vernier motor for Europa 1 rocket third stage, discussing component design, system performance and fuel composition
17 p3018 A69-33328

Aircraft turbines mechanical parts reliability tests, discussing examples of blade fatigue rupture and rotor disk fatigue
17 p3020 A69-33347

ENGINE STARTERS

Holography application in gas turbine components stress and vibration analysis, discussing techniques and apparatus usable by nonspecialist and measurement accuracy 17 p2974 A69-33351

Mechanical components life or cycles to failure probability distributions determined by Monte Carlo method, comparing theory with aircraft engine parts field data 19 p3327 A69-36031

Jet engine compressors and fans, combustors, turbines and composite materials in evaluating thrust-weight ratio, engine size, weight and life, etc 19 p3395 A69-36322

Airbreathing gas turbines construction materials including composites and Ti and austenitic alloys [ASM PAPER D8-25.2] 20 p3586 A69-38133

Building block approach to turbofan engine design, discussing fuel consumption, noise and component research [RAES PAPER 14] 22 p3999 A69-40493

Numerical control as manufacturing tool, with application to aircraft engine precision components 24 p4318 A69-42710

Carbon fibers and resin composites used as rocket motor systems ablative liners and structures, noting role in motor weight reduction 24 p4336 A69-43210

ENGINE STARTERS

Solid propellant cartridges, discussing uses for starting large engines and providing auxiliary power in missiles or actuating devices 02 p0302 A69-11524

M 3.5 two dimensional mixed compression inlet system with self restart using flexible variable ramp system [AIAA PAPER 69-447] 16 p2845 A69-32732

ENGINE TESTING LABORATORIES

Blow-down facility for hypersonic testing of air breathing engines, describing test cell, air heating system, exhausters and data system 02 p0227 A69-11756

Turbine engine in-flight operating conditions simulated on test stand 11 p1942 A69-24528

ENGINE TESTS

NT COLD FLOW TESTS

NT SPACE ELECTRIC ROCKET TESTS

NT STATIC FIRING

Nondestructive testing of brazed liquid propellant rocket engine components and assemblies, describing radiographic, ultrasonic, thermographic, and leak test methods 01 p0085 A69-10534

Steam ingestion tests on carrier aircraft gas turbine engines, analyzing inlet pressure and temperature distortion in steam-air environment 01 p0143 A69-11062

Pressure oscillation production in wind tunnel by hinged plates in test section walls to test jet engine inlets under controlled conditions 02 p0229 A69-12537

Weapons propulsion system off-design engine performance, noting installation loss effects [SAE PAPER 680712] 03 p0496 A69-13445

Quantitative amounts of contaminants oil from piston engine and life of oil lubricant in engine 04 p0604 A69-14500

Similarity conditions in turbine engine tests, analyzing flight speed, Reynolds number, combustion efficiency, heat changes, inlet turbulence and outlet nozzle 05 p0742 A69-16028

Transpiration air cooled blading to test and design small gas turbine at 2500 F inlet, discussing cascade and full stage component [SAE PAPER 690035] 07 p1203 A69-18310

Concorde testing program, detailing materials, structure, systems, engine, wind tunnel and flight tests 07 p1054 A69-19294

Computer simulation on engines dynamic behavior covering thrust transfer functions, time behavior and engine and fuel controller operation 08 p1301 A69-20167

C-5 engine inlet development, presenting two phase nacelle forebody and five phase model tests, scale corrections inlet/cowl optimization and prototype tests [ASME PAPER 69-GT-32] 09 p1570 A69-22481

Transpiration cooling effect on turbine stator blade performance determined by annular cascade tests, using data to establish empirical correlation for loss coefficient [ASME PAPER 69-GT-39] 09 p1432 A69-22487

Miniature fluidic oscillator temperature sensors evaluated in gas turbine engine nozzle, discussing temperature control and related signal error compensation and temperature averaging [ASME PAPER 69-GT-70] 09 p1572 A69-22512

Radial inflow gas turbine engine performance testing, discussing instrumentation, recording systems and calibration techniques [ASME PAPER 69-GT-104] 09 p1501 A69-22522

Fuel concentration effect on turbojet engine reheat jet pipe vibrations via tests 09 p1573 A69-22616

Bearing deposition test for evaluating degradation characteristics of aircraft gas turbine engine lubricants 10 p1700 A69-24070

Turbine engine in-flight operating conditions simulated on test stand 11 p1942 A69-24528

Aircraft test setup design and techniques to simultaneously measure engine thrust and engine thrust minus drag, noting nozzle configurations variations effect [AIAA PAPER 68-395] 12 p2059 A69-26769

Thrust balance for scale model of powered nacelle fan jet engine from drag analysis in wind tunnel, deriving fan nozzle velocity coefficient 13 p2199 A69-27446

Thermocouples precision used for measuring metal temperatures of cooled jet engine turbine buckets 15 p2613 A69-31274

Analog computer for design of control systems used in nonnuclear testing of nuclear rocket engine components and subsystems 15 p2589 A69-31289

Stator setting effect on single stage turbine performance, considering blade loss and surface velocity distribution [AIAA PAPER 69-525] 16 p2841 A69-32686

Flox/methane pump fed engine, discussing RL-10-1-A engine tests and optimized 5000 lb thrust engine design [AIAA PAPER 69-510] 16 p2741 A69-32720

Interagency Chemical Rocket Propulsion Group method of treating measurement error for liquid rocket engine performance parameters, using uncertainty model [AIAA PAPER 69-734] 16 p2846 A69-32781

Nondestructive ultrasonic, spectroscopic and TV test methods reducing time for inspection and increasing reliability of turbines 17 p2978 A69-33330

Twin spool hydrogen turbopump performance at zero net positive suction pressure (NPSF) saturated fluid in propellant tank, including steady state and simulated transient engine tests [AIAA PAPER 69-550] 18 p3140 A69-34414

Supersonic aircraft and power plant structural members operating under cyclic stress at elevated temperatures tested by various methods for interaction between creep and fatigue 20 p3620 A69-37001

Monograph on jet turbine with small hub ratio for cases of complete and partial admission, considering masking effects, flow measurements, etc 20 p3586 A69-37924

Rolls-Royce RB.211 turbofan engine development, discussing three shaft design, engine performance, testing program, etc 20 p3640 A69-37927

RB 202 self contained lift fan engine design for high speed interurban civil VTOL operations, considering weight, cost, noise and fuel consumption 22 p3862 A69-39933

LM descent engine behavior upon contact with lunar surface simulated, basing test condition on statistical trajectory analysis indicating fire until touchdown possibility [AIAA PAPER 69-1020] 22 p3923 A69-40391

Cs contact ion engine with tubular W ionizer tested for performance and reliability in vacuum chamber 22 p4000 A69-40592

Solid rocket motor static firing tests in low pressure environment, presenting data concerning vacuum chamber pressure, diffusers pressure distribution, chamber wall temperature distribution, etc 22 p4000 A69-40593

TF39 high bypass ratio engine design, development and tests, noting low smoke combustor [RAES PAPER 21] 22 p4000 A69-40622

Performance test of German MPD plasma rocket engine with augmented magnetic field and 5-10 kw output, describing integral measurement procedure and observed phenomena [DGLR-69-024D] 23 p4202 A69-41927

ENGINEERING

Physical electronics, discussing gas discharges, semiconductor devices, electron emission, noise in electronic devices and masers and lasers 05 p0735 A69-16666

Society of American Value Engineers Conference, San Diego, April 1969 13 p2382 A69-28092

Value engineering application to engineer recruiting phase of industrial relations 13 p2382 A69-28093

Aircraft design cost control emphasizing engineering performance direct inclusion in design costs including tooling, testing, etc 13 p2382 A69-28094

Value engineering proposal costs sustained by maintenance and overhaul industry in government contract negotiations, discussing reimbursement and proposed central agency 13 p2383 A69-28099

Value engineering ultimate objectives in industry, discussing engineering and procurement role in prorating goal to applicable departments 13 p2383 A69-28101

NASA Pilot Program in instructional monographs to provide up-to-date material from current research for engineering education 18 p3236 A69-35078

IEEE Conference - San Antonio, April 1969 21 p3676 A69-39437

Book on matrix-computer methods in engineering covering matrix algebra and calculus, computer programming, Fourier transforms, etc 23 p4234 A69-42421

ENGINEERING DEVELOPMENT U PRODUCT DEVELOPMENT ENGINEERING DRAWINGS

Three dimensional computer graphic modeling program, discussing SIGHT and LEGER programs 05 p0724 A69-16383

Computer aided automatic drawing of printed circuits, including design and manufacture of films for engraving 08 p1296 A69-19979

Computerized system-safety fault trees, discussing drawing, configuration control and simulation program 19 p3280 A69-36029

ENGINES

NT AIR BREATHING ENGINES

NT AIRCRAFT ENGINES

NT ARC JET ENGINES

NT AUTOMOBILE ENGINES

NT BOOSTER ROCKET ENGINES

NT BRISTOL-SIDDELEY OLYMPUS 593 ENGINE

NT CESIUM ENGINES

NT DUCTED FAN ENGINES

NT ELECTRIC ROCKET ENGINES

NT ELECTROSTATIC ENGINES

NT ELECTROTHERMAL ENGINES

NT EXTERNAL COMBUSTION ENGINES

NT F-1 ROCKET ENGINE

NT GAS TURBINE ENGINES

NT HELICOPTER ENGINES

NT HOT WATER ROCKET ENGINES

NT HYBRID PROPELLANT ROCKET ENGINES

NT HYDRAZINE ENGINES

NT HYDROGEN OXYGEN ENGINES

NT INTERNAL COMBUSTION ENGINES

NT ION ENGINES

NT J-79 ENGINE

NT J-85 ENGINE

NT JET ENGINES

NT LIQUID PROPELLANT ROCKET ENGINES

NT M-1 ENGINE

NT MICROROCKET ENGINES

NT NUCLEAR ENGINE FOR ROCKET VEHICLES

NT NUCLEAR ROCKET ENGINES

NT PISTON ENGINES

NT PLASMA ENGINES

NT PULSED JET ENGINES

NT PULSEJET ENGINES

NT RAMJET ENGINES

NT RESISTOJET ENGINES

NT RESTARTABLE ROCKET ENGINES

NT RL-10-A-1 ENGINE

NT SOLID PROPELLANT ROCKET ENGINES

NT SUPERSONIC COMBUSTION RAMJET ENGINES

NT T-53 ENGINE

NT TURBINE ENGINES

NT TURBOFAN ENGINES

NT TURBOJET ENGINES

NT TURBOPROP ENGINES

NT ULLAGE ROCKET ENGINES

NT VERNIER ENGINES

NT WANKEL ENGINES

- Kaufman thruster performance dependence on transmission of ion extraction optics and magnetic field shape [AIAA PAPER 69-257] 09 p1569 A69-21878
- Thermodynamic analysis of engines and heat pumps operating within negative absolute temperatures, noting work increase by throttling 09 p1623 A69-22219
- Temperature and pressure relations in power plant with closed gas cycles with radiative heat transfer, noting radiation area reduction influence 20 p3464 A69-37603
- ENGRAVING**
U PHOTOENGRAVING
- ENLARGING**
U EXPANSION
- ENSKOG-CHAPMAN THEORY**
U CHAPMAN-ENSKOG THEORY
- ENSTATITE**
Carbonaceous, enstatite and stony meteorite classification on basis of siderophilic, chalcophilic and lithophilic element proportions or isotope composition, discussing thermodynamic equilibrium 01 p0025 A69-11368
- Enstatite chondrites structure and mineral content and composition using microscopic and X ray analysis, grouping parameters in distinguishing types 02 p0317 A69-12016
- Shocked Bamle enstatite transformed to disordered enstatite, noting Debye-Scherrer patterns similarity 21 p3792 A69-38321
- ENTHALPY**
Nitrogen compressibility and thermodynamic functions up to 10,000 atm pressure and 400 C 01 p0175 A69-10366
- Vibrational relaxation of diatomic gases behind shock waves, with variable heat bath temperature extended to constant enthalpy and constant total enthalpy conditions 01 p0061 A69-11204
- Formation energy of heat vacancies in molybdenum and temperature dependence of concentration determined on basis of enthalpy data 02 p0266 A69-12184
- Semiperfect gases with enthalpy dependent only on temperature, discussing validity of concept and Joule experiment on equivalence of heat and work 05 p0848 A69-16336
- Plane reaction cell unit for use in differential flux calorimeters and devices for differential enthalpy analysis 05 p0764 A69-16607
- High enthalpy, Mach and Reynolds number flight studies on ballistic ranges, describing launchers, flight simulation, measuring and recording techniques 06 p0860 A69-17632
- Enthalpies determination of adduct formation of sulfonides, sulfanilamides and thionylamides with trimethylalane, noting replacement effect on electron donating ability of oxygen 07 p1074 A69-18631
- Local enthalpy measurements in atmospheric argon arc plasma jet at various arc currents, comparing calorimetric and spectrometric methods 09 p1547 A69-21602
- Enthalpy distribution in plasma tube arc heater inlet flow region with hot and cold gas core boundary in presence of electric field 09 p1553 A69-22538
- Enthalpy excess thermodynamic functions of binary gas mixtures based on stationary diffusion thermoeffect in tube 11 p2003 A69-25552
- CoO complex defects indicated by negative enthalpy of formation, considering isobaric electrical conductivity measurements at various temperatures and oxygen pressures 14 p2508 A69-29925
- Multimegawatt arc heater for hypersonic continuous flow high enthalpy wind tunnel 15 p2586 A69-30378
- Water cooled split-flow probe measuring enthalpy of high temperature subsonic streams 15 p2614 A69-31275
- Solid W enthalpy from 2800 K to melting point measured with drop calorimeter, tabulating heat capacity, entropy and free energy function 17 p2987 A69-33075
- High energy recovery pressure and enthalpy sensor /HERPES/ for flow measurements in aerospace simulation facilities 19 p3307 A69-35750
- Enthalpy and heat capacity of high melting point homogeneous Ti, Zr and Nb carbides, analyzing influence of Me-Me bonds and carbon sublattice defects 21 p3742 A69-38614
- Uniform flow and wall boundary layer growth measurement in conical nozzle of reflected shock tunnel operating at high enthalpy conditions 24 p4247 A69-43575
- High enthalpy shock tube and nozzle gas flows for incident shock Mach numbers analyzed for laminar boundary layers and boundary layer transitions 24 p4305 A69-43664
- ENTIRE FUNCTIONS**
Tabulation of definite and indefinite integrals of products of error function with elementary and transcendental functions 12 p2121 A69-26395
- Computer implementation of Bergman solution to initial value problem for partial differential equation of compressible fluid flow 18 p3164 A69-34614
- Polya concept of maximum and minimum densities of series applied to entire functions of finite order with positive zeros 20 p3568 A69-37442
- ENTRAINMENT**
Coanda nozzle entrainment and flow augmentation approximating numerical stability by finite differences 05 p0746 A69-16021
- Solid cylindrical body entrainment by viscous incompressible fluid flow in tube under constant pressure gradients and absence of gravitational force 10 p1678 A69-23366
- Entrainment and acoustothermal effect in piezoelectric semiconductors having electrons with different energy 10 p1746 A69-23573
- Entrainment of viscous electrically conducting liquid in long duct with narrow rectangular cross section and movable walls in magnetic induction field 16 p2816 A69-31606
- Turbulent boundary layer on disk rotating in free air, using circumferential and radial momentum integral equations and entrainment equation 17 p2957 A69-33601
- Turbulent boundary layer growth predicted for adverse pressure gradients, using entrainment theory for two dimensional and axisymmetric flows [ASME PAPER 69-FE-16] 20 p3517 A69-37991
- Diurnal entrainment deviations and atmospheric turbulence effects on flash photographs from Geos I 21 p3793 A69-38339
- ENTROPY**
Nitrogen compressibility and thermodynamic functions up to 10,000 atm pressure and 400 C 01 p0175 A69-10366
- Unsteady aerodynamics of ablating flared reentry body, noting complications due to blunted nose shear flow and entropy gradient effects 02 p0189 A69-12524
- Thermodynamics of directed continuous media, discussing kinematics, equations of state, entropy inequality and material objectivity principle 02 p0354 A69-12611
- Physical mechanism of stability loss in nonvortical flows of uniformly dense ideal fluids, discussing entropy production 06 p0911 A69-17498
- Hypersonic flow past blunt body near stagnation point, noting surface layer characterized by increased density and decreased entropy of gas 07 p1050 A69-18755
- Hydrodynamic stability and entropy decrease in flow in three dimensional space, using irreversible thermodynamics principles 10 p1808 A69-22892
- Lagrangian evolution criterion for electromagnetic conducting fluid and MHD flow, defining generalized fluxes and forces 10 p1727 A69-22904
- Mach wave and anisentropic supersonic flow interaction, considering constant entropy along streamline and layer of entropy discontinuities/interfaces 10 p1631 A69-22906
- Molar heat and entropy of adsorption and activity coefficient of adsorbed phase for methane-ethane-silica gel system 10 p1652 A69-23370
- Growth rates for convective disturbances propagation in atmosphere with linear entropy variation, noting WKB approximation 11 p1957 A69-24422
- Entropy minimization in feature extraction by dimensionality reduction with linear transformation of pattern vectors, noting recognition time and storage space savings 11 p1909 A69-25291
- Thermomechanical theory for nonreacting binary fluid mixtures, discussing free energy function, entropy flux vector, equations of motion, constraints, etc 12 p2191 A69-26927
- Fundamental principles of thermodynamics incorporation into general relativity and geometrodynamics, interpreting entropy growth in terms of space dynamics 14 p2538 A69-29019
- Spatial supersonic ideal gas flows past blunt bodies analyzed by numerical finite difference methods, discussing flow fields and entropy 14 p2390 A69-29616
- Supersonic jet flow with separated shock wave flowing past infinite wedge using Chapplygin method, assuming negligible entropy variations 14 p2391 A69-29619
- Vibrational excess entropy in dilute solid solutions alloys calculated by changes in potential fields surrounding impurity atoms 16 p2798 A69-31706
- Communication channel information capacity determination through particle ensembles entropy analysis 19 p3334 A69-35885
- Amplitude equations for magnetoacoustic and entropy waves diverging from normal MHD shock, obtaining energy flux ratios associated with incident and transmitted waves 20 p3582 A69-38242
- Universal dependence of density fluctuations on specific entropy derived from equation describing material composed of neutral particles and equal number of charged and antiparticles 21 p3771 A69-38995
- Physics of massive starlike objects, discussing high entropy requirement, eventual nonrelativistic collapse and gravitational fields produced by low entropy equilibrium 21 p3811 A69-39516
- Parameter estimation using entropy of error as criterion function compared with mean square error analysis 21 p3757 A69-39664
- Relativistic thermodynamics using entropy principle to find restrictions on constitutive functions 22 p4050 A69-40451
- Book on entropy gradient effect on laminar hypersonic boundary layers, covering external frictionless flow calculations based on momentum and energy integral theorems 22 p3930 A69-40618
- Entropy definition for nonequilibrium states, using mathematical theory of stability of motion applied to kinetic equations of irreversible processes 23 p4238 A69-41366
- Linear elastic theory for calculating monovacancies entropy and energy of formation in metals 24 p4360 A69-42649
- ENVELOPES**
Weak signal optimization of multilevel quantization and corresponding detection performance, discussing asymptotic limits 09 p1456 A69-22293
- Galactic novae observational data and theoretical interpretations, considering envelope detachment from star, luminosity, motion and emission line intensities 17 p3032 A69-33103
- Envelope detection threshold levels definition for low input SNR based on apparent modulation depth reduction 22 p3902 A69-41225
- ENVIRONMENT MODELS**
RF synchrotron emission from electrons trapped in earth magnetic field observed by satellite, using magnetospheric environment model 18 p3128 A69-34948
- ENVIRONMENT SIMULATION**
NT ACOUSTIC SIMULATION
NT ALTITUDE SIMULATION
NT SPACE ENVIRONMENT SIMULATION
NT THERMAL SIMULATION
NT WEIGHTLESSNESS SIMULATION
- Passive ice protection of aerodynamic surfaces by icephobic coating, measuring removal of ice under simulated conditions in tunnel tests 01 p0056 A69-11047
- Automatic life support system tried on leeches for space applications 01 p0021 A69-11080

Pituitary-adrenocortical axis and neuro-endocrine functions in animals maintained in oxygen atmosphere, discussing norepinephrine and epinephrine excretion values, etc

01 p0019 A69-11343

Mathematical simulation of temperature and humidity changes in compartments of hermetically sealed space vehicle cabins

02 p0200 A69-11489

Closed system toroidal electrodynamic facility proposed for reentry simulation, discussing velocity generation

04 p0585 A69-15323

Lunar environment simulation, discussing space suit encumbrances on astronaut performance, gravity effects, surface texture, illumination, confinement and isolation

06 p0906 A69-17388

Oxygen-helium cabin atmosphere effect on speech communication analyzed during simulated space mission

07 p1066 A69-19420

Prolonged hypokinesia effects on white rats resistance to convulsions induced by high altitude simulation

08 p1262 A69-19929

Environmental simulation in aircraft engineering, tests concerning aerodynamic conditions and simulator design

08 p1301 A69-20603

Vacuum engineering problems during booster rocket engine ground tests, simulating flight environment [TR-781-O]

09 p1570 A69-22300

Near field repeatable stimulator of infrared earth horizon sensors in variable environments and test levels, noting orbital conditions [AIAA PAPER 69-322]

09 p1478 A69-22376

Nitrogen dilution low pressure simulation technique for subsonic flow flame stabilization of bluff bodies

09 p1624 A69-22614

Lunar visual environment effects on astronaut control manipulation task performance, discussing solar illumination simulation facility

12 p2059 A69-26554

Vibration machine as vibration environment simulation for product reliability testing, analyzing spectrum of acceleration waveforms

12 p2060 A69-26940

Real time pressure simulation chambers for testing space vehicles, discussing slow and rapid evacuation and pumping systems

13 p2240 A69-28077

Gravity preference tests on rats subjected to simulated Aerobee 150 A rocket launching and flight in ground based spiral centrifuge

13 p2213 A69-28090

Superconductivity methods to neutralize ambient magnetic field by free electrons motion for nonmagnetic environments

13 p2244 A69-28604

Selectively pumped thermal vacuum test chamber for orbital heat transfer and environment simulation for flight vehicle performance prediction

15 p2587 A69-30392

Saturn 5 boost phase environment simulation on Apollo stages, discussing fixtures, load devices, instrumentation and ground test

15 p2588 A69-30405

Swept frequency microwave measurements in simulated reentry environments using dielectric layers, glow discharge plasma and aperture antenna-plasma layer model

[AIAA PAPER 69-701]

17 p2920 A69-33461

Medical and biological laboratory ground experiments role in development of life support systems and suitable environments for prolonged manned space flights

18 p3098 A69-35165

Random vibratory environment simulation for spectra, noting electrodynamic generator employed to excite electric field force

19 p3294 A69-35904

Onboard computer and environment simulation for real time programs development, discussing instructions analysis, variables extraction and values and peripheral components

20 p3502 A69-37395

Thermal control coatings, windows and mirrors for 1973 Mars Viking Lander vehicles under simulated Martian surface conditions

[AIAA PAPER 69-1023]

22 p3923 A69-40393

Aircrew Arctic survival situation simulation experiments with survivors staying close to aircraft and walking across difficult terrain from emergency location

23 p4088 A69-41810

Swept frequency X band reflectometer for measuring antenna properties in simulated reentry environments

[AAS PAPER 69-282]

24 p4313 A69-42861

ENVIRONMENT SIMULATORS

NT HIGH VACUUM ORBITAL SIMULATOR

NT LUNAR GRAVITY SIMULATOR

NT SOLAR SIMULATORS

NT SPACE SIMULATORS

Lunar gravity simulation effect on human performance, discussing fidelity requirements, self locomotion, metabolic rate and psychomotor task decrement

02 p0203 A69-12217

Martian entry test facility for real size entry systems, discussing design, fabrication and operation

15 p2587 A69-30390

Motion cues simulation system with seat of six differentially inflatable sections, discussing DYNASEAT

17 p2947 A69-34007

Space environmental simulation facilities, discussing digital computers and equipment for simulating oxygen atmosphere, vacuum, heating and cooling, etc

19 p3295 A69-36326

Test facility for space vehicles simulating outer space gas pressure, heat sink behavior and relative motion to sun, detailing design and operation

21 p3689 A69-38420

ENVIRONMENTAL CHAMBERS

U TEST CHAMBERS

ENVIRONMENTAL CONTROL

Biological aspects of space exploration, analyzing human response to artificial environment in prolonged space missions

[UN PAPER 68-95715]

06 p0873 A69-17035

Pollution control forecast, contamination control specialist and systems approach

08 p1265 A69-19808

High bay clean room design with laminar air flow, discussing air filtration, sound attenuation, construction, illumination, etc

10 p1673 A69-23354

Biaxial stress effect on creep properties of thin walled tubes of polymethyl methacrylate at controlled temperature and humidity

10 p1717 A69-24216

Bleed air environmental system utilizing air to air jet pumps as flow multipliers for cabin pressurization air supply in commercial turboprop aircraft

[SAE PAPER 690331]

11 p1941 A69-24494

Pressurized Navajo aircraft environmental system, discussing ventilation, pressurization, heating and air cooling systems

[SAE PAPER 690330]

11 p1829 A69-24504

Manned space stations for future space exploration, discussing earth-like environment, artificial gravity, human factors and time dependence

11 p1965 A69-25644

Space flight research programs including stellar and biological evolutions and environmental control

12 p2155 A69-26005

Remote sensing of environment - Conference, University of Michigan, Ann Arbor, April 1968

12 p2094 A69-26974

Theoretical model of homogeneous solid propellant ignition in neutral nonflow environment, discussing ignition time

13 p2324 A69-28218

Climatic environments development for physiological studies, considering ambient temperature, radiated heat and air velocity and movement

13 p2215 A69-28594

Airport noise control responsibility for airport and community planners using perceived noise level, noise and number index and community annoyance index as planning criteria

14 p2541 A69-29506

Aircraft noise environmental problem, discussing improvement through source, transmission and receiver control options

15 p2585 A69-30373

Microbiology quality assurance program for planetary mission, considering spacecraft sterilization during fabrication, test and launch site activities

15 p2559 A69-31124

Avionics clean room workshops, discussing turbulent and laminar flow rooms and contamination monitoring of controlled environment facility

16 p2767 A69-32369

Ti corrosion resistance improved in special environments by oxidizing agents heavy metal ions and alloying

16 p2802 A69-32436

Optimal design for improving thermal performance of existing spacecraft thermally actuated lower system by increasing open-to-closed emittance ratio

[AIAA PAPER 69-627]

17 p3071 A69-33269

Mars lander thermal control system design parameters including environment, power duty cycle and lander size and weight

[AIAA PAPER 69-610]

17 p3072 A69-33274

Apollo Lunar Module Environmental Control System /LM/ECS/ steady state performance simulation techniques, discussing vacuum chamber data of LTA-8/LM-3

[AIAA PAPER 69-616]

17 p2903 A69-33307

Habitat modification for airport bird population control, discussing draining of wet areas, waste control, etc

17 p2915 A69-33368

Flight recorder program determining combat operating environments of CH-46D helicopters analyzed and compared with aircraft design criteria

[AHS PAPER 375]

17 p3059 A69-33513

Organic Rankine cycle system using heat absorption from turbine exhaust to provide increased electrical output and to power air conditioning

23 p4070 A69-42267

ENVIRONMENTAL ENGINEERING

Space photography to provide synoptic sedimentary environmental data analysis, discussing orbital sensing advantages

05 p0753 A69-15993

Displacement pumps and fluids for extreme environments, discussing fluid types and operational parameters such as speed, pressure, temperature, power, displacement and size

06 p0931 A69-17188

Test program for solid propellant rockets capability to withstand space environments

06 p0982 A69-17594

Mercury atmospheric models for preliminary environmental criteria to be used in spacecraft design and engineering trade-off studies

[AIAA PAPER 69-54]

06 p1010 A69-18042

Venusian atmosphere model developed from satellite and earth based radar data for environmental criteria in spacecraft design and mission planning

[AIAA PAPER 69-51]

06 p1011 A69-18096

IR camera determining surface temperatures, discussing construction and space applications

08 p1315 A69-20455

Field noise reduction frequency spectra afforded by spacecraft shroud, basing estimating criterion on flight test data

09 p1609 A69-21892

Surveyor electronic engineering design for lunar environment, discussing vacuum and temperature effects

11 p1958 A69-24633

Remote sensing of urban environments for metropolitan information systems noting photographic, thermal IR, radar and microwave applications

12 p2193 A69-27012

Environmental studies - Conference, Paris, March-April 1969

13 p2214 A69-28587

Man and environment - Conference, Anaheim, California, April 1969

15 p2584 A69-30356

Transient and long lasting space environment stresses, discussing accelerations, vibrations, shocks, rapid descent in vacuum, temperature variations, gravity, etc

15 p2625 A69-30824

Equipment environmental conditions tabulated to assist engineer in preliminary design considerations and in planning test programs for specimens

17 p2910 A69-33661

High density environment-resistant circular connectors, discussing design, applications, test and performance data compliance with MIL-C-81511 specifications

22 p3910 A69-39947

Dynamic power and life support systems electrical/thermal integration for manned spacecraft using low temperature Rankine cycle generator

23 p4189 A69-42269

Closed Brayton cycle power systems for space, lunar, terrestrial and undersea environmental conditions, discussing design and performance

23 p4071 A69-42277

Commercial aircraft environmental compatibility planning, considering problems of airport traffic growth and restrictive air traffic control regulations

[AAS PAPER 69-326]

24 p4252 A69-42808

ENVIRONMENTAL LABORATORIES

Book on groups under stress covering psychological research in SEALAB 2, emphasizing planning of data collection and experimental results
04 p0552 A69-14533

Equipment testing, discussing collaboration between government agencies and independent environmental testing laboratories
15 p2720 A69-30398

Lunar conditions differing from simulations in laboratories, examining surface, physicochemical properties and friction
18 p3113 A69-34241

Medical and biological laboratory ground experiments role in development of life support systems and suitable environments for prolonged manned space flights
18 p3098 A69-35165

ENVIRONMENTAL TEMPERATURE

U AMBIENT TEMPERATURE

ENVIRONMENTAL TESTS

NT CORROSION TESTS

NT HIGH TEMPERATURE TESTS

NT LOW TEMPERATURE TESTS

NT SALT SPRAY TESTS

NT THERMAL VACUUM TESTS

NT UNDERWATER TESTS

High pressure hydrogen environment on tensile properties of stainless steel with and without strain induced martensite
01 p0093 A69-10062

Pressure and temperature dependence of slow crack growth in hardened steel in gaseous hydrogen environment
01 p0096 A69-10612

Structural testing in aircraft design, discussing costs, environmental conditions, test rigs and apparatus
01 p0170 A69-10864

Environmental effects on aircraft and propulsion systems - Conference, Bordentown, New Jersey, October 1968
01 p0055 A69-11043

Permissible JP-5 fuel sulfur content effect on hot corrosion of protective coated Ni-base superalloys in marine environment, noting atmospheric sea salt role
01 p0141 A69-11059

Resistance of animal organisms and cells to extreme environmental conditions discussing exobiological implications for extraterrestrial life systems
01 p0017 A69-11083

Titanium-base alloys resistance to atmospheric corrosion based on weight change measurements and tensile tests after multicyclic exposures
01 p0100 A69-11351

Atmospheric stress corrosion tests of aluminum alloys in various environments, comparing aging results with accelerated laboratory tests
01 p0100 A69-11352

Space lubrication system for Orbiting Solar Observatory program, discussing theoretical high vacuum principles and flight performance and environmental test data
02 p0252 A69-11766

Environmental tests of space vehicles, determining parameter effects on ground storage and transportation, launching and orbital life
02 p0228 A69-11918

Surface effects on mechanical properties of crystalline and vitreous materials, considering environmental effects on dislocation mobility
03 p0454 A69-13870

Manual performance relationship to men exposed to cold, thermal neutral and hot environments, discussing finger dexterity and motor coordination tests
03 p0381 A69-14074

Hypoxia effect on animal brain gamma-aminobutyric acid levels
04 p0552 A69-14482

Atmospheric exposure chamber design for small animals, discussing dynamic and recirculating operations and gas scrubbing system
04 p0584 A69-14678

Graphite ablation in high pressure environments, extending existing analysis of thermochemical and thermomechanical behavior to include allotropic features [AIAA PAPER 68-1153]
04 p0686 A69-14873

Temperature, acoustic, vibration and shock environment effects on pure fluid bistable and proportional amplifiers [ASME PAPER 68-WA/FE-31]
05 p0705 A69-16104

Sensible heat exchange from Gemini and Apollo space suits determined in environmental test facilities, presenting data for heat flux distributions
06 p0880 A69-17089

Graphite ablation in air, N₂, Ar and He assuming chemical equilibrium, equal diffusion coefficients and steady state ablation [AIAA PAPER 69-148]
06 p0947 A69-18155

Lunar shelter regenerative life support system performance and manned test
07 p1071 A69-19427

Shock ignition procedure to keep pyrotechnic composition in optimum condition in space environment, describing test layouts and theory
10 p1749 A69-23007

Environment influence on fatigue crack propagation mechanisms in aluminum alloys in vacuum, ambient air and distilled and sea water
10 p1710 A69-23084

Environmental requirements of military specifications tabulated according to tests for altitude, temperature, vibration, shock, humidity, temperature/altitude, etc
11 p1862 A69-24331

Low energy charged particle detectors reliability, analyzing windowless electron multipliers and effects of secondary emission layers on sensitivity
11 p1848 A69-24868

Single crystal solar cell degradations in space, duplicating radiation effect on minority carriers lifetime by laboratory tests
11 p1826 A69-24876

Ablation test specimen environment at high temperature, analyzing laboratory heating, pyrolysis gas diffusion, convective heating, critical stress and temperature profiles, etc
12 p2191 A69-26815

Ablation wedge model design for testing in wave superheater under controlled pressure gradients and constant temperature
12 p2059 A69-26816

Transistorized amplifiers reliability estimated from step by step failures during operation in intense external environment
12 p2043 A69-26886

Procedures and facilities applicable to sonic environmental testing of flight vehicles, discussing sonic energy sources in vehicles and potential failure modes
12 p2060 A69-26939

Polymeric insulation materials, discussing intrinsic properties dependence on temperature and atmosphere, stressing effect on aging
13 p2285 A69-27985

One inch ceramic vidicon with slow scan photoconductor, electrostatic focusing and magnetic deflection to withstand sterilization and environmental testing for space applications
13 p2234 A69-28262

Accelerometer force balance used in measuring forces and moments acting on models in short duration rocket plume tests at simulated high altitude [AIAA PAPER 69-351]
13 p2264 A69-28285

Meteoroid perforation effects on space cabin design, discussing simulated destructive environmental tests [AIAA PAPER 69-365]
13 p2357 A69-28297

Climatic environments development for physiological studies, considering ambient temperature, radiated heat and air velocity and movement
13 p2215 A69-28594

Helicopter climatic testing, discussing component, systems and field tests and facilities
14 p2427 A69-29505

Space environment simulation tests of cadmium sulfide thin film solar cells, noting output loss
14 p2405 A69-29538

Continuous-channel electron multipliers degradation in spacecraft environment simulation laboratory equipment
14 p2449 A69-29565

Pulse generator to accommodate electronic system testing to shock response spectrum by simulating real world shock environment
15 p2585 A69-30360

Solar simulator with xenon and krypton lamps designed for thermal balance tests, power conversion and material degradation experiments
15 p2586 A69-30383

Space Environment Simulation (SES)/ facility at Goddard Space Flight Center, discussing operations and maintenance
15 p2586 A69-30386

Vibration/acoustics environmental testing, discussing advantages of digital computer control system and digital noise generation techniques
15 p2586 A69-30387

Vibration/acoustics digitally controlled environmental testing, describing random test signal generation and random vibration tests
15 p2587 A69-30389

Integrated structural and dynamic testing plans for proposed large interplanetary spacecraft, discussing acoustic testing, testing environments and flight environment transformation into laboratory
15 p2588 A69-30399

Integrated circuits screens, developing sequence of life and environmental tests to remove units of potential reliability hazards
15 p2580 A69-31130

Large scale integrated MOS devices tests for space applications, establishing quality specifications
15 p2580 A69-31131

Titanium alloy tensile specimens tests in air, methanol and anhydrous methanol environments at known stress-strain-time relations examined by fractography and high resolution electron diffraction
16 p2799 A69-31718

Static, transient and in-space environmental tests at satellite structures and heat shield test facilities in Italy
16 p2765 A69-31750

Gas environment effect on catabolic activities and enzymatic reactions of trachoma and meningopneumonia agents of genus Chlamydia
16 p2747 A69-31865

Urine excretion following water load in male subjects exposed to normal, hot/dry and comfortable/dry environment applied to airline crews
17 p2914 A69-33182

Hand movements in water environment, weightlessness and normal gravity conditions, discussing inner coordinative structure and muscular efforts
17 p2915 A69-33385

Acoustic spectrum averager for Mariner spacecraft environmental tests, calculating rms average 1/3 octave spectrum bands in real time [JPL-TR-32-1442]
17 p2946 A69-33658

Equipment environmental conditions tabulated to assist engineer in preliminary design considerations and in planning test programs for specimens
17 p2910 A69-33661

Test program simulating solar wind outside magnetosphere to evaluate high melting point high density ceramic oxides as white thermal control coating pigments [AIAA PAPER 69-641]
17 p2993 A69-33762

AGREE /Advisory Group on Reliability of Electronic Equipment/ testing philosophy, emphasizing environmental tests
18 p3143 A69-34481

Environmental testing role in qualification, acceptance, burn-in and reliability demonstration tests
18 p3143 A69-34482

Thermal and mechanical properties UV of diazadiphenoxides, carbodiimides and phosphorus amide epoxies resins composites for use in environmental extremes
19 p3356 A69-35528

Future combined environment space simulation tests duplicating environment interaction encountered during earth orbits, deep space probes and manned flights
19 p3288 A69-35531

Elastomeric thermosetting one part silicone encapsulant environmental tests, checking physical and electrical properties stability under temperature and relative humidity conditions
19 p3281 A69-35549

Military storage and environment effects on strength of filament wound glass reinforced epoxy structures, tested on plastic motor case and pressure vessels
19 p3321 A69-35567

Materials evaluation for devices with long term underground exposure, including field tests at tropical locations
19 p3321 A69-35568

Tilt wing V/STOL aircraft spray circulation characteristics in overwater operation, examining forces, moments and generated environmental conditions [AIAA PAPER 69-791]
19 p3243 A69-35638

Thin silicon solar cells environmental tests, evaluating temperature and humidity effects on various contacts and coatings
19 p3252 A69-35699

Environmental testing of space hardware, discussing failure detection by thermal vacuum tests and mechanical signature analysis
19 p3430 A69-36009

Apollo spacecraft equipment qualification program for margin assurance, discussing ground and flight tests
19 p3430 A69-36015

Surveyor thermal vacuum test data comparison with flight results indicating performance prediction reliability of earth-based tests for vacuum and lunar environments
19 p3430 A69-36016

Environment effect on scientific and telecommunication equipment mounted on exploratory probe during Venus atmosphere entry for acceleration loading in design

19 p3431 A69-36037

Environmental crowding effect on individual and group behavior in rat colony, using implanted passive resonant circuits for identification and passage information

19 p3257 A69-36243

Stress corrosion cracking of stainless steels and Incoloy and Inconel alloys in chloride, caustic, oxygenated and miscellaneous environments

19 p3349 A69-36890

Ti alloy stress corrosion susceptibility in salt water, alcohols and alkanes, comparing stress intensity for crack propagation in dry air

19 p3353 A69-36907

Stress corrosion cracking of alpha and alpha-beta Ti alloys in aqueous environment at ambient temperature, noting Al content and microconstituents

21 p3743 A69-38663

Handbook of solar simulation for thermal vacuum testing, discussing space environment, thermal control coatings, radiation sources, optical components, etc

21 p3690 A69-38894

Space simulation facility assembly and operational testing

22 p3919 A69-39959

Reliability test program based on MIL-STD-781 B specification, noting test environments with AGREE chamber

22 p3953 A69-40027

Environmental neutron flux measured by various techniques, studying effects of soil and moisture on density

22 p4002 A69-40094

Operational reliability verification of Apollo real time mission program and testing structure, discussing environment, processing, controls, response criteria, etc

[AIAA PAPER 69-981]

22 p3907 A69-40361

Manned testing of EVA equipment in thermal-vacuum environment for qualification of Apollo extravehicular mobility unit, using lunar surface thermal simulator

[AIAA PAPER 69-992]

22 p3893 A69-40370

Mariner Mars 1969 TV system environmental test and calibration program

22 p3920 A69-40372

Orbiting Astronomical Observatory thermal test and evaluation program, discussing equipment and role in experimental design

[AIAA PAPER 69-995]

22 p3920 A69-40373

Mission sequential environment effects on Dacron parachute material mechanical properties

[AIAA PAPER 69-1018]

22 p3923 A69-40390

Ceramic-sealed Ni-Cd secondary batteries space environmental behavior testing to determine heat dissipation during spaceborne operation

22 p3869 A69-40591

Corrosion of Ni through porous Au plate in humid sulfur dioxide atmospheric environments, analyzing product deposits and contact properties

23 p4176 A69-41534

Heart rate responses and corresponding tolerance tests in trained athletes and nonathletes during simulated environmental extremes

23 p4102 A69-41683

Large reflector paraboloid antenna performance under environmental loads

23 p4231 A69-42132

Closed Brayton cycle power systems for space, lunar, terrestrial and undersea environmental conditions, discussing design and performance

23 p4071 A69-42277

Design, fabrication and evaluation of lunar base solar array power modules, emphasizing structural/dynamic, thermal vacuum and acoustic tests

23 p4072 A69-42288

Solar array configurations and performance on Martian surface, including hard lander design and surviving shock levels

23 p4073 A69-42289

Fuel cells construction materials selecting and optimizing techniques using diffusion block and differential corrosion concepts

23 p4075 A69-42299

Stress corrosion cracks propagation from fatigue precrack in Al alloy exposed to organic liquid environments

23 p4178 A69-42452

Test animals prolonged deep submersion in water, in mixed oxygen-H atmosphere at elevated pressure, noting EEG and EKG activities

24 p4262 A69-43025

Solid film lubricants deposited by DC triode sputtering on Ni, Ni-Cr and Nb surfaces friction tested under ultrahigh vacuum conditions

24 p4321 A69-43126

Behavioral patterns and physiological parameters of medical leech Hirudo medicinalis determined in natural environment prior to biological experiment in space

24 p4268 A69-43402

Environmental stress effects on medical leech studied to determine tolerance to spacecraft launching, orbiting and reentry

24 p4268 A69-43403

ENVIRONMENTS

NT AEROSPACE ENVIRONMENTS
NT ARTIFICIAL RADIATION BELTS
NT CHROMOSPHERE
NT CISLUNAR SPACE
NT D REGION
NT DEEP SPACE
NT E-2 LAYER
NT E REGION
NT EARTH ATMOSPHERE
NT EXOSPHERE
NT EXTRATERRESTRIAL ENVIRONMENTS
NT F REGION
NT F 1 REGION
NT F 2 REGION
NT FREE ATMOSPHERE
NT HIGH ALTITUDE ENVIRONMENTS
NT HIGH GRAVITY ENVIRONMENTS
NT HIGH TEMPERATURE ENVIRONMENTS
NT INNER RADIATION BELT
NT INTERPLANETARY SPACE
NT INTERSTELLAR SPACE
NT IONOSPHERE
NT JUPITER ATMOSPHERE
NT LOW TEMPERATURE ENVIRONMENTS
NT LOW TEMPERATURE PHYSICS
NT LOWER ATMOSPHERE
NT LOWER IONOSPHERE
NT LUNAR ATMOSPHERES
NT LUNAR ENVIRONMENT
NT MAGNETOPAUSE
NT MAGNETOSPHERE
NT MARS ATMOSPHERE
NT MARS ENVIRONMENT
NT MESOPAUSE
NT MESOSPHERE
NT MIDLATITUDE ATMOSPHERE
NT OUTER RADIATION BELT
NT OZONOSPHERE
NT PLANETARY ATMOSPHERES
NT PLANETARY ENVIRONMENTS
NT PROTON BELTS
NT RADIATION BELTS
NT ROTATING ENVIRONMENTS
NT SOLAR ATMOSPHERE
NT SOLAR CORONA
NT SPACECRAFT ENVIRONMENTS
NT SPORADIC E LAYER
NT STELLAR ATMOSPHERES
NT THERMAL ENVIRONMENTS

Crash protection of flight data recorders, aircraft accident investigation, systems analysis, environment and enclosures

10 p1691 A69-23248

Altered gaseous environments effect /parabrosis/ on interferon production in mice injected with Newcastle disease virus, noting hypoxia role

24 p4262 A69-42888

ENZYME ACTIVITY

Tyrosine transaminase activity estimation by radioactive isotopic assay method, discussing application to rat liver and other organs

01 p0014 A69-10902

Glycolysis rate role in regulation of substrate inhibition of dehydrogenases

01 p0015 A69-10931

Insignificant or recoverable changes observed in blood acetylcholine content and cholinesterase activity of rabbits subjected to 8 g acceleration

02 p0197 A69-11491

1.5 g angular acceleration effects on acetylcholine metabolism in guinea pig brains and hearts

02 p0198 A69-11505

Ribulose diphosphate carboxylase and phosphoribulokinase activity in chemosynthetic autotrophs Thiobacillus thioautotrophicus and Thiobacillus neapolitanus, noting sedimentation and gel filtration characteristics

02 p0199 A69-11866

Phosphodiesterase activity of anterior pituitary, median eminence, heart and cerebral cortex of rat, studying effects of caffeine, theophylline and hydrocortisone

02 p0199 A69-11885

Lactodehydrogenase activity and LDG isoenzymes ratio in various tissues of rats during exposure to prolonged hypoxia at simulated heights

02 p0199 A69-11982

Slow proton irradiation of ribonuclease thin layers, determining differential inactivation cross section for various proton energies

03 p0371 A69-13482

Inactivation by heavy ions of esterase activity of dried trypsin as function of temperature during irradiation

03 p0372 A69-13483

Free radicals produced in ribonuclease, lysozyme and trypsin during exposure in vacuum and various temperatures to electron and heavy ion irradiation

03 p0372 A69-13484

Long lived radicals produced in crystalline ribonuclease and lysozyme by 120-Mev protons studied by ESR spectroscopy

03 p0372 A69-13485

Trapped radical relationship to inactivation of trypsin exposed to UV by measuring radical concentration and inactivation degree

03 p0372 A69-13486

Substrate and subunit interactions influence of beta 2 protein of Escherichia coli tryptophan synthetase on fluorescence properties of pyridoxal phosphate prosthetic groups

04 p0553 A69-15304

Cellular localization of acetyl-coenzyme A synthetase in yeast, noting enzyme distribution during aerobic growth on glucose

04 p0554 A69-15333

Brain norepinephrine effect on daily rhythmic changes in activity of tyrosine transaminase in livers of starved adrenalectomized rats

05 p0707 A69-15582

Identity between growth hormone degrading activity of pituitary gland and plasmin

06 p0873 A69-17105

Amino acid biosynthesis control in microorganisms by end product /feedback/ inhibition of enzyme action

06 p0876 A69-18238

Escherichia coli WWU multiautotrophic revertants with nonsense suppression, noting role in aberrant morphology and in catabolizing thymidine for energy and carbon

07 p1069 A69-19503

Enzymic decomposition of urea in urine, noting production of ammonia and effect of urea components on hydrolysis rate

08 p1265 A69-19834

Adrenal epinephrine and phenylethanolamine n-methyl transferase /PNMT/ activity in rat bearing transplantable pituitary tumor

08 p1263 A69-20374

Cation concentration requirement of halophilic NADH dehydrogenase for stability and maximum activity

10 p1651 A69-23127

Repeated blood sampling effect on plasma cholinesterase, acid phosphatase, alkaline phosphatase and hematocrit ratios in domestic chickens

10 p1644 A69-23158

Epinephrine forming enzyme phenylethanolamine-N-methyl transferase /PNMT/ in various brain regions of rats, cats, hens and turtles

10 p1644 A69-23303

Acceleration effects on cellular and subcellular structures enzyme activity in humans and animals, noting changes resulting from changed permeability of membranes

10 p1645 A69-23496

Transverse accelerations effect on dogs gastrointestinal tract secretory activity, noting central nervous system role

10 p1645 A69-23498

Rats tolerance to impact accelerations from blood enzyme activity providing safety limits for living organisms

10 p1645 A69-23500

Poly A-poly U synthesized by Azotobacter Vinelandi RNA polymerase in unprimed reaction containing ATP and UTP, following short lag period

10 p1647 A69-24185

DNA replication in vivo as function of temperature sensitive polynucleotide ligase mutant Th, tsA80 in strand synthesis

10 p1647 A69-24188

Tryptic digestion of C terminal tritiated peptides analyzed with Scenedesmus ferredoxin, noting use for protein structural study

10 p1648 A69-24190

Oxidative and dephosphorylating enzymes and esterases in rat and squirrel monkey cerebral cortexes, noting neuron activity

12 p2018 A69-25773

Histochemical studies on nucleus basalis of Meynert of squirrel monkey

12 p2018 A69-25774

Histochemical tests on enzymes distribution in rhesus and squirrel monkeys intrafusal and extrafusal muscle fibers

12 p2018 A69-25777

Lactate dehydrogenase and monoamine oxidase distribution in medulla oblongata and cerebellum of squirrel monkey

12 p2018 A69-25778

NADH stimulation of ATP dependent carbon dioxide fixation in crude extracts of Hydrogenomonas facilis, considering allosteric regulation of phosphoribulokinase activity

15 p2554 A69-30036

Proline residue effects on hydrolysis of peptide bonds by thermolysin

15 p2561 A69-30083

Histological and histochemical studies of dephosphorylating enzyme distribution in muscle spindle capsule of guinea pig thigh muscles and cat calf muscles

15 p2554 A69-30406

High vacuum effects on oxidative processes in bacteria and physiological activities of enzymes

15 p2557 A69-31354

Gas environment effect on catabolic activities and enzymatic reactions of trachoma and meningopneumonitis agents of genus Chlamydia

16 p2747 A69-31865

Hepatic tyrosine transaminase rhythm in rats under various conditions of lighting, food consumption and dietary protein content

17 p2910 A69-33755

Urease activity determined by using C 14 urea in stored, preserved /Permafrost/ and irradiated soils

18 p3095 A69-34543

Salts and organic solvents effect on halophile Halobacterium cutirubrum catalase, noting enzyme activity inhibition by cation and anion

18 p3096 A69-35291

Flavoprotein/cytochrome b/559/ role as branch of Halobacterium electron transport in DPNH oxidase determined by salt dependence of reduced DPNH

20 p3484 A69-37101

Substrate specificity of cathepsin C derived from rat liver, describing polymeric structure and behavior as acidic protein

20 p3473 A69-37577

Enzymes distribution in subformal organ in squirrel monkey

20 p3478 A69-37934

Biological experiments on cells with/without suppressors, discussing RNA, DNA, enzymatic and UAA codon activities

20 p3480 A69-38265

Organism growth physiology based on decisive enzyme reactions, considering synthesis of biological proteins from DNA and molecular life processes

21 p3652 A69-38787

Single large X ray dose depressive effect on aminotransferase activity in rabbit blood serum, liver, kidney, heart, spleen, lungs, etc

21 p3657 A69-39051

Nerve tissue oxidation processes relation to nervous system radiation sensitivity in dogs with cerebellum X rayed after enzyme poisons administration

21 p3658 A69-39053

Enzyme activity changes in liver, heart and cerebrum of X ray exposed rats and rabbits, noting individual enzyme differences in same X rayed organ

21 p3658 A69-39054

Single X ray dose effect on alpha-amylase and alpha-glucanophosphorylase in rabbit liver tissues and blood serum

21 p3658 A69-39055

Brain weight and cholesterase activity in rats after exposures to acoustic and light stimuli

21 p3662 A69-39627

Enzyme transitions in RNA polymerase state during unprimed synthesis of r(t/c) copolymer, noting dimer-monomer pattern during lag phase

22 p3895 A69-40050

Sympathetic nerve liberated noradrenaline increasing melatonin synthesis, using C 14 tracer for monitoring

22 p3871 A69-40051

DNA and d(A-T) oligomers enzyme binding to DNA polymerase by sucrose density gradient centrifugation

22 p3898 A69-41075

Electron transport chain of monovalent and divalent cations and of polyamines, studying effects on menadione reductase activity to determine salt dependence

22 p3886 A69-41077

Anoxia effect on succinic dehydrogenase and lactic dehydrogenase activities in digestive glands and organs sensitive to oxygen tension changes

22 p3887 A69-41193

Compensatory hypertrophy effects on adrenal phenylethanolamine n-methyl transferase /PNMT/ activity in rats

23 p4080 A69-41404

Enzymatic processes of glucose metabolism in immature rats lymphatic tissues during exercise- induced elevated corticosteroid secretion

23 p4080 A69-41405

Cardiac myosin characteristics obtained from dogs with naturally occurring heart failure, showing reduced adenosinetriphosphatase activity as compared with normal dogs

24 p4258 A69-42630

Experimental myocardial infarction in dogs, examining lysosomal enzymes activity changes in soluble and particle-bound fraction

24 p4259 A69-42636

Chlorella enzymes activity in reducing nitrate to nitrite and nitrite to ammonia

24 p4263 A69-43136

ENZYMES

NT CATALASE

NT CHOLINESTERASE

NT COENZYMES

NT LYSOZYME

NT OXIDASE

NT TRYPSIN

Enzymes in simulated Martian environment exhibit higher resistance than in earth atmosphere at 4 C

07 p1065 A69-18974

Enzymes in simulated Martian environment exhibit higher resistance than in earth atmosphere at 4 C

20 p3479 A69-38222

Catalytic, physical and chemical properties of enzyme lactate dehydrogenase isolated from lobster tail muscle

22 p3897 A69-41069

DNA polymerase from Escherichia coli, discussing physical and chemical properties of enzyme and polypeptide chain consistency

22 p3898 A69-41070

Chemical modifications effects on Escherichia coli, DNA polymerase, including Hg atom addition to sulfhydryl group of enzyme

22 p3898 A69-41071

Properties, relative magnitudes and relationship of pyrophosphate exchange reactions catalyzed by DNA polymerase from Escherichia coli

22 p3898 A69-41072

Exonuclease function of DNA polymerase from Escherichia coli, discussing hydrolysis of polydeoxyribonucleotides and resistancy of oligonucleotides

22 p3898 A69-41073

Deoxyribonucleoside triphosphate substrate binding to Escherichia coli DNA polymerase, conducting equilibrium dialysis

22 p3898 A69-41074

Amino acid sequence of dogfish lactic dehydrogenase, isolating acylated amino-terminal peptide and arginine residues, indicating four polypeptide chain composition

24 p4280 A69-43051

ENZYMOLGY

Pyridine nucleotide-linked D-lactate dehydrogenase stereospecificity in various species of invertebrates

01 p0018 A69-11198

Ribulose diphosphate carboxylase and phosphoribulokinase activity in chemosynthetic autotrophs Thiobacillus thioarus and Thiobacillus neapolitanus, noting sedimentation and gel filtration characteristics

02 p0199 A69-11866

Lactodehydrogenase activity and LDG isoenzymes ratio in various tissues of rats during exposure to prolonged hypoxia at simulated heights

02 p0199 A69-11982

Uptake, metabolism and enzymatic synthesis of adrenaline in mammalian brain

07 p1066 A69-19260

EOSINOPHILS

Vestibular stimulation effect on human blood composition during rocking test indicating blood eosinophile content as function of hypophysis and adrenal cortex reactions

20 p3473 A69-37268

EPE-D

U EXPLORER 26 SATELLITE

EPHEMERIDES

NT PLANET EPHEMERIDES

Computer program in ALGOL for computing satellite ephemerides applicable to satellites with direct or retrograde motion observed in Northern or Southern Hemispheres

12 p2159 A69-26448

Gauss method for Kepler equation ephemeris computation in nearly parabolic orbits, using expansions suitable for high speed computers

12 p2171 A69-27154

Provisional elliptic orbit computed for asteroid Floirac using Gauss-Encke and least squares method, tabulating residuals and ephemeris

14 p2521 A69-29585

Satellites meridian and extrameridian observations by transit instrument, examining errors in ephemerides of bulletins

16 p2858 A69-32211

Epochs and ephemerides of asteroid Amor for 1916, 1924 and 1972, noting unfavorable observing conditions in future

17 p3038 A69-33723

Book on Messier nebulae and star clusters covering current astronomical ideas, star maps, identification diagrams, telescope illustrations and astronomical data

18 p3206 A69-35471

Orbital elements of visual binaries Don 91 and ADS 9756 derived graphically, tabulating observations with ephemerides

20 p3600 A69-37480

Encke type analytical-numerical integration for solving differential equations of modified set of Lagrange planetary equations, obtaining satellite ephemeris for orbit prediction [AIAA PAPER 69-908]

21 p3807 A69-39340

Pluto positions /1930-1965/ from photographic observations, ascribing declination errors to atmospheric dispersions

22 p4025 A69-40612

EPHEMERIS TIME

Ephemeris Time and Atomic Clock Time roles in astronomy, discussing errors in daylength determination for mechanical, Shortt and atomic clocks, UT and Ephemeris Time

01 p0156 A69-10989

Ephemeris of comet Grigg-Skjellerup for reappearance in 1971/72, based on equations of motion integration and perturbations

17 p3044 A69-34183

Lunar occultations analyzed to determine Moon position and ephemeris time, confirming adopted values of node and perigee motions

20 p3601 A69-37494

Bright lunar limb zenith distances measured by equal altitudes method, deriving Ephemeris- Atomic Time A3 and Ephemeris-TU2 time relations

23 p4208 A69-41289

EPIDEMIOLOGY

Epidemiology of aerial application accidents analyzed in groups of high and low wing monoplanes, biplanes and helicopters

09 p1447 A69-22554

EPIDERMIS

Dermal injury predictability for exposure to thermal radiation based on mathematical model using temperature-time histories

06 p0875 A69-17840

EPILEPSY

Epilepsy acquired by 25 year old jet fighter pilot, noting cardiovascular abnormalities

09 p1446 A69-22728

EPINEPHRINE

Uptake, metabolism and enzymatic synthesis of adrenaline in mammalian brain

07 p1066 A69-19260

Sympathetic neurohormones measurement in plasma of race car drivers

07 p1067 A69-19424

Adrenal epinephrine and phenylethanolamine n-methyl transferase /PNMT/ activity in rat bearing transplantable pituitary tumor

08 p1263 A69-20374

Epinephrine forming enzyme phenylethanolamine-N-methyl transferase /PNMT/ in various brain regions of rats, cats, hens and turtles

10 p1644 A69-23303

Social and visual isolation effect on rat blood pressure, pulse pressure, heart rate, behavior and response to epinephrine

14 p2407 A69-29296

Mammalian brain epinephrine metabolism data after isotonic saline perfusion into cranial vasculature
21 p3650 A69-38323

Aminazine and adrenaline effects on adrenocortical function in patients with diencephalic syndrome
22 p3888 A69-41272

Increased oxygen tension adaptation and effects on adrenocortical and sympatho-adreno-medullary activity in rats, indicating toxic conversion of epinephrine to indoles
23 p4087 A69-41791

EPITAXY

Gallium arsenide single crystal epitaxy with doping/concentrations into semiinsulating microwave circuits
01 p0040 A69-10196

Carrier mobility variation with electric field related to structure of epitaxial field effect transistors
02 p0294 A69-11541

Fundamental microwave oscillations at high frequencies in GaAs epitaxial sandwich layers, using space charge growth control
02 p0297 A69-11941

Photoluminescence spectra of n-type GaAs films grown by gas transport reactions and from solution melt, noting recombination emission
03 p0488 A69-13887

Power epitaxial GaAs tunnel diodes grown from solution in tin with tellurium
03 p0489 A69-13895

Coherent emission in epitaxial structures with heterojunctions in AlAs-GaAs system
03 p0489 A69-13896

Relaxation effect in epitaxial silicon MOS structures, formulating differential equation for doping distribution in epitaxial layer
03 p0490 A69-13947

Epitaxial GaAs films with high electron mobility, noting radiation recombination spectra dependence on substrate orientation
03 p0492 A69-14172

Electrical conductivity of high resistance epitaxial semiconducting films measured by three probe method
04 p0597 A69-14538

Red light emitting p-n junctions in GaP fabricated by epitaxial growth
06 p0979 A69-16999

Solution regrowth method to prepare epitaxial GaAs for Gunn effect devices
07 p1197 A69-18451

Epitaxially grown guard rings for GaAs p-n junction and Schottky barrier avalanche diodes
08 p1284 A69-20368

Vapor deposition of high purity epitaxial layers of n-type gallium arsenide, noting resistivity and Hall coefficient measurements [ECS PAPER 62]
08 p1373 A69-21067

Thermal EMF in epitaxial films, analyzing potential distribution in p-n junction with temperature gradients and film thickness effects
09 p1555 A69-21473

Electrical resistivity of epitaxial CdTe films produced by vacuum sublimation on hot orienting mica and single crystal substrates
10 p1742 A69-23001

Hetero-epitaxial germanium films on GaAs by germanium condensation from molecular beams in vacuum, obtaining p-type conductivity
11 p1938 A69-25033

Photoluminescence spectra of n-type GaAs films grown by gas transport reactions and from solution melt, noting recombination emission
11 p1939 A69-25688

Power epitaxial GaAs tunnel diodes grown from solution in tin with tellurium
11 p1939 A69-25696

Coherent emission in epitaxial structures with heterojunctions in AlAs-GaAs system
11 p1939 A69-25697

Gallium arsenide materials technology, discussing solution and vapor-phase epitaxy and liquid encapsulation as related to crystal growth and purification
12 p2141 A69-25834

Vapor phase epitaxial production of indium arsenic phosphide crystalline layers, discussing electron mobilities, electrical resistivities and doping
12 p2142 A69-25934

Substructural patterns of epitaxial PbTe films obtained by condensation of vaporized PbTe on NaCl crystal surfaces, discussing formation kinetics and morphology
12 p2144 A69-26675

Vapor phase growth of epitaxial single crystalline GaAs-GaSb alloys using arsine and stibine
12 p2145 A69-26920

Epitaxial layers impurity concentration and resistivity measurements by capacitive and three point probe methods
13 p2233 A69-28641

Thermal EMF in epitaxial films, analyzing potential distribution in p-n junction with temperature gradients and film thickness effects
15 p2669 A69-30718

Semiconductor films synthesis and properties, discussing single crystal films, epitaxial nucleation, nuclei surface distribution, layer kinetics, doping and film-substrate interface
15 p2670 A69-31046

EPITHELIUM

Corneal epithelium chromosome rearrangements in gamma irradiated white adult mice, noting radiation dosage and duration
17 p2907 A69-32944

EPOCHS

U TIME MEASUREMENT

EPOXIDES

U EPOXY COMPOUNDS

EPOXY COMPOUNDS

NT ETHYLENE OXIDE

Susceptibility of high modulus graphite and boron fiber epoxy composites to lightning damage, noting degradation by pulse current
08 p1338 A69-20486

Rotational spectrum of ethylene episulfide to determine molecular structure, particularly orientation of C sub 2 S ring
08 p1268 A69-20535

Boron epoxy strut prototype for support system of advanced nuclear flight stage with nonintegral cryogenic tankage configuration, achieving weight reduction
19 p3354 A69-35516

EPOXY RESINS

Elastic properties of epoxy resins, deriving relation by considering different shear properties in tension and compression
01 p0103 A69-11268

Mechanical and optical viscoelastic characterization of Hysol 4290 epoxy polymer as function of time and temperature, using creep test data
03 p0524 A69-13064

Phenolic and epoxy adhesives for metal-metal and honeycomb bonding, discussing cold cure adhesives for aircraft structures and aircraft floor sandwich design optimization
04 p0606 A69-14845

Epoxy molding compounds characterization and classification for development and evaluation of raw materials
04 p0620 A69-14954

Cryogenic mechanical properties of epoxy resins and glass/epoxy composites
05 p0785 A69-16491

Temperature dependence of dynamic viscoelastic properties of plasticized epoxy resins
06 p0946 A69-17125

Compressive strength of boron fiber-epoxy matrix composite, noting matrix support of fibers against buckling
07 p1170 A69-18713

Anisotropic glass fiber reinforced epoxy resin composite under biaxial and uniaxial loads, noting isochromatics and isoclinics in photoelastic analysis
07 p1170 A69-18715

Multidirectional boron-epoxy laminates shear strengths and elastic moduli, calculating in-plane tension and compression
08 p1337 A69-20484

Loading rate effects on fracture energy in carboxy terminated liquid Hycar toughened cantilever cleaved epoxy resin
08 p1338 A69-20491

Crack propagation in crosslinked glassy polymers, noting effects of added elastomers molecular weight
08 p1338 A69-20492

Tensile strength of glass-fiber reinforced epoxy resin laminates subjected to fluctuating tension, discussing crack density dependence on fatigue stress cycles
08 p1338 A69-20494

Tensile characteristics of discontinuous unidirectional fiber reinforced glass-epoxy composites and filament wound material, discussing alignment and interfacial bonding
08 p1339 A69-20496

Matched metal molding of short graphite fiber composites
08 p1339 A69-20502

Fire retardant brominated epoxy systems for wet filament winding process, noting viscosity, pot life and NOL ring mechanical properties
08 p1340 A69-20507

Mechanical properties of cast epoxy resins correlation with corresponding composites strength under static and dynamic fatigue stressing
08 p1340 A69-20510

Boron-epoxy composites applications and properties, comparing strength to weight and stiffness to weight ratios with aluminum, titanium and beryllium
09 p1529 A69-22068

Prepreg based on S glass with HTS finish and B staged epoxy resin, discussing tensile strength and moisture exposure
09 p1530 A69-22327

Compressive behavior of uniaxial filament reinforced epoxy tubes for aerospace structures, using hand layup method with Teflon mandrel and sleeve
09 p1508 A69-22339

Boron filaments reinforced epoxy aircraft landing gear structure prototype, discussing development, fabrication, and testing
09 p1508 A69-22340

Subscale aircraft fuselage section fabricated with lightweight graphite fiber/epoxy resin composite material
09 p1509 A69-22341

Static and dynamic strength tests and modulus data for graphite fiber/epoxy composite yarn, noting ply winding and dimensions [ASME PAPER 69-GT-114]
09 p1531 A69-22520

Temperature and strain rates effect on delayed yield and failure of plasticized epoxy resin
10 p1717 A69-24218

High temperature organic sealants for repairing small gas leakages in vacuum devices, tabulating test results for alkyd, epoxy, silicone and polyimide resins
11 p1907 A69-24742

Graphite and B filament-epoxy resin composites application to aeroelastic scaled dynamic models, analyzing weight savings, fabrication and component stiffness
11 p1990 A69-25508

Fabrication, machining and contouring of boron-epoxy composite for sandwich type aircraft structure, noting F-5 supersonic fighter main landing gear strut door
12 p2103 A69-26826

Rigid structures high damping without loss of rigidity achieved by epoxy resin dampers, noting moderate cost
13 p2370 A69-28601

Uniaxial compressive stability of rectangular boron-epoxy laminated plates clamped on loaded edges, determining buckling loads by Southwell plots
13 p2287 A69-28669

Short fiber composites flow orientation in system of high volume glass fibers in epoxy resin measured by glass rheometer
13 p2287 A69-28670

Shrinkage stresses in two phase materials, analyzing stress distribution in epoxy inclusions in plasticized matrix during curing by photoelastic method
13 p2371 A69-28675

Epoxy adhesives physical chemistry, curing processes, formulation, surface application methods, testing and health hazards
14 p2468 A69-29339

Interlaminar shear strength development for utilization of unidirectional strength and stiffness of graphite fibers, discussing epoxy resin-fiber interface improvement
15 p2642 A69-30312

High temperature structural adhesives at temperatures of 350 F and higher including epoxies, polyimides, amide-imides and polybenzimidazoles
15 p2642 A69-30329

Low endurance fatigue in aluminum, Nylon 66 and epoxy resin compared, considering stress-strain relationships, fatigue damage, failure mechanisms and crack propagation
18 p3155 A69-34633

High modulus graphite epoxy composite material laminates fabricated and tested, correlating filament strength variation effect with composite tensile strength
19 p3354 A69-35518

Thermal and mechanical properties UV of diazadiphenetides, carbodiimides and phosphorus amide epoxies resins composites for use in environmental extremes
19 p3356 A69-35528

Flexible-rigid hybrid polyimide-epoxy glass multilayer board to fill gap between all flexible and all rigid circuit boards

19 p3319 A69-35545

Epoxy molding compounds performance on DIP integrated circuits, determining comparative moisture protection provided by encapsulants

19 p3280 A69-35546

Transfer molded epoxy dielectrics, comparing encapsulation rate, pressure and cure times to compression molding

19 p3281 A69-35548

Glass fiber with epoxy resins compared to polyester resins, discussing chemical reactions, bonding and strength relations

19 p3358 A69-35902

Glass fiber laminates based on epoxy organosilicon resins, discussing various hardeners effects on strength, etc

19 p3358 A69-35903

Photochromic panel for flash blindness protection using epoxy plastic plates containing aromatic hydrocarbon compounds excited to triplet states

21 p3668 A69-39783

Photoelastic and micromechanics studies of epoxy resins of varying Young moduli by simultaneous stress analysis of FRP and matrix materials

21 p3846 A69-39796

Epoxy resin materials assessed for model materials for three dimensional photoelasticity

22 p4042 A69-40311

Beta-thiodiglycol effect on hardening of epoxy resin with stoichiometric amounts of maleic anhydride and methyltetrahydrophthalic anhydride

22 p3973 A69-40677

Photographic study of epoxy resin breakdown kinetics under pulsed laser beams, showing crack area as function of time

22 p3973 A69-40743

Boron fiber reinforced composite materials in aircraft structures, comparing rigidity with glass fiber plastics and weight gains

23 p4179 A69-42155

Large contoured nozzle fabrication using liquid epoxy as casting material, presenting molding process based on experimental data

24 p4318 A69-42643

Redesigned Al wing structure using B-epoxy composite applied to pressurized fuel carrying section, including material, fabrication and test data

24 p4323 A69-43418

Boron epoxy composites evaluation for use in aircraft dynamic components, considering fatigue failure mechanism identification

24 p4337 A69-43450

Gel permeation chromatography to measure rate of adhesive aging and curing in one shot epoxy tapes, noting handling techniques and space applications

24 p4338 A69-43463

EQUATIONS OF MOTION

NT EULER EQUATIONS OF MOTION
NT HELMHOLTZ VORTICITY EQUATION
NT HYDRODYNAMIC EQUATIONS
NT KINEMATIC EQUATIONS
NT KINETIC EQUATIONS
NT NAVIER-STOKES EQUATION
NT REYNOLDS EQUATION

Equations of motion for kinematics of complex mechanisms, noting methods and relations

01 p0115 A69-10165

Vector potential used to express equations of incompressible fluid motion in form suitable for digital solution, discussing boundary conditions

01 p0058 A69-10228

Natural vibration properties of elastic free-free body obeying Hooke law analysis from equilibrium and motion equations, determining Green tensor

01 p0167 A69-10323

Flexural vibration of unbalanced rotating shaft with nonlinear characteristic of elasticity and damping, using equations of motion

01 p0168 A69-10329

Unsteady laminar boundary layer near thermally insulated rotating disk, establishing solutions describing motion

01 p0059 A69-10361

Equations of motion of point restricted tethered parafoil for investigating longitudinal and lateral dynamic stability

01 p0009 A69-10415

Equations of motion of satellite in rotating coordinate system, noting effects of precession and nutation on transformation of orbital elements

01 p0150 A69-10445

Optimal control system sensitivity definitions, analysis methods and design techniques, discussing equations of motion of dynamical system satisfying vector differential equation

01 p0051 A69-10553

Theory for stability of steady motions of system with cyclic coordinates applicable to total damping

01 p0151 A69-10567

Forced oscillations of unbalanced rotor on elastic bearings with nonlinear characteristics investigated for resultant forces and amplitude using motion equations

01 p0170 A69-10824

Matrix technique for transformation of equation of motion into first order equation in analyzing perturbation forces producing mechanical oscillations

01 p0170 A69-10827

Flight simulator based on analog computer simulating six linearized equations of motion and aircraft model, discussing design and applications

01 p0057 A69-11300

Idealized delta wing free-free oscillations determination by deriving equations of motion for flexibility and rigidity and formulating boundary value problems

01 p0172 A69-11358

Group invariant solutions of differential equation systems applied to quasi-linear partial differential equations of motion of air masses

02 p0274 A69-11444

Motion, field momentum and field kinetic energy equations of concentrated dislocations based on Zorski field theory of defects

02 p0336 A69-11556

Pressure to density ratio to analyze one dimensional high temperature gas flows with heat transfer, considering motion equations

02 p0350 A69-11576

Periodic cubic differential equation of motion solved with special reference to location of fixed points and stability of solutions

02 p0280 A69-11816

Linear integrodifferential motion equations for turbulent flow within Heisenberg statistical turbulence theory

02 p0230 A69-11869

Plane shock wave interaction with elastic shallow spherical shell in compressible fluid, formulating equations of motion

02 p0339 A69-11977

Computer solution of six degrees of freedom flight equations, discussing advantages of using flight path axes for translational equations of motion

02 p0212 A69-11998

Motion stability of two tethered unsymmetrical earth pointing bodies in circular orbit, presenting nine degrees of freedom differential equations of motions

02 p0324 A69-12507

Time dependent tube wall radial displacement during explosive welding as function of distance from initial explosion

02 p0254 A69-12675

Equations of motion for arbitrary first order perturbations around any spherically symmetric metric

02 p0328 A69-12730

Lie groups for equations of motion in quantum mechanics or field theory determined by operator analysis

02 p0282 A69-12840

Differential equations of motion for holonomic system of points with variable mass

03 p0465 A69-12965

Vehicle trajectory motion in transition region of three body problem, noting equations of motion, first order solutions, etc

03 p0505 A69-13001

Cold plasma motion caused by electromagnetic wave pressure propagating along uniform magnetic field

03 p0477 A69-13413

Kinematic parameters for elastic slender body aid in description of motion of body

04 p0668 A69-14271

Steady state plasma flows stability equations, using variational principle for analyzing toroidal plasmas

04 p0635 A69-14556

Beam vibration problems with mixed response-excitation input information solved by recasting equations of motion

[AIAA PAPER 68-319] 04 p0676 A69-14711

Simulation of flight dynamic equations of motion for fixed wing aircraft, using variable analog computer with gimballed and servocontrolled aircraft model

04 p0585 A69-14829

Separation of center of mass and rotational coordinates from N electron diatomic Schroedinger equation

04 p0554 A69-14861

Motion of vapor derived from solid material vaporization and subsequent heating by nonequilibrium continuum radiation, noting continuity equations and energy transfer

04 p0686 A69-14985

Equations of motion derived for incompressible and irrotational viscous fluids in special relativity

05 p0792 A69-15682

Game interception of motions, obtaining proof for extremal aiming scheme

05 p0793 A69-15777

Equations of motion of nonholonomic mechanical systems in Poincare-Chetaev variables

05 p0793 A69-15778

Nonlinear steady state vibration of single degree of freedom system, obtaining relationships between non-dimensional pi parameters of differential equation of motion

[ASME PAPER 68-WA/DE-7] 05 p0839 A69-16172

Integrability of equations for problem of motion of heavy solid body about fixed point

05 p0794 A69-16206

Equations formulated for space vehicle reaction to rotating machinery and internal mass motion, evaluating dynamics of cylindrical space station rotating about major axis

05 p0827 A69-16476

Integrability of equations of motion of gyrostat about fixed point inertial moments varying identically in time

05 p0764 A69-16504

Energy integral of equations used in studying atmospheric motions in quasi-geostrophic approximation

05 p0759 A69-16641

Energy integral for holonomic system of points of variable mass, transforming Lagrangian form via Hamiltonian function

05 p0794 A69-16685

Equations of motion solved for solid body with ellipsoidal cavity containing ideal incompressible fluid in uniform eddy motion

06 p0957 A69-16823

Equation for charged particle motion in electromagnetic wave field propagated along magnetic field applied to nonlinear wave propagation in plasma near cyclotron resonance

06 p0963 A69-16905

Simple dipolar stresses, noting effect of antisymmetry on equations of motion and energy equation

06 p1022 A69-17239

Nonlinear equations of motion for rendezvous in circular orbits, pursuer using minimum fuel and pursued having no propulsion

06 p1014 A69-17571

Optimality criterion and equations of motion determined for fixed time impulsive trajectory to minimize total characteristic velocity

06 p1007 A69-17575

Gradient method solution for class of optimal control problems, minimizing root mean square value of finite state components of object in motion

06 p0904 A69-17886

Rolling ballistic vehicles mass and aerodynamic characteristics determined from dynamic motion data by performing Fourier analysis on roll axis equation of motion

[AIAA PAPER 69-102] 06 p0862 A69-18039

Computing optimum flight profiles by Balakrishnan epsilon method, including equations of motion constraint in cost function to be minimized

[AIAA PAPER 69-75] 06 p0868 A69-18058

Nonlinear equations of motion approximate solution, determining ordnance weapons aerodynamic stability coefficients from angular motion as functions of angle of attack

[AIAA PAPER 69-135] 06 p0863 A69-18120

Aerodynamic coefficients from observed motion of body in flight, eliminating need for closed form solutions by employing numerical solutions to equations of motion

[AIAA PAPER 69-134] 06 p0864 A69-18161

Simplification of equations of two temperature plasma composed of electrons, singly charged ions and neutral atoms, noting effect of viscosity and thermal force

07 p1190 A69-18693

Group analysis of MHD equations, determining group properties of motion equations of compressible fluid, obtaining invariant solutions

07 p1191 A69-18994

Two dimensional flow of conducting fluid in channels with longitudinal transverse magnetic field and Hall effect, discussing gas motion equations linearization

07 p1192 A69-19015

Hydraulic drag coefficient in MHD fluid flows in traveling magnetic field from motion equations for turbulent flows, considering velocity profiles
07 p1192 A69-19017

Pulsation energy balance of turbulent jet of conducting fluid expanding in longitudinal magnetic field
07 p1192 A69-19021

Charged particle motion in electromagnetic field from basic equation of motion for magnetosphere, discussing dipolar magnetic field, Stormer trapped particle theory, etc
07 p1208 A69-19355

Circular cylindrical spinning shells vibrations by gyroscopically induced inertia loads, formulating equations of motion based on shallow shell theory
07 p1236 A69-19459

Traveling waves on elastic spherical shells derived from dynamic equations of motion, including transverse shear and rotatory inertia effects
07 p1236 A69-19460

Composition effect of flight path measurements on correction of space vehicles flight path, discussing single parameter correction of motion in force free field
07 p1178 A69-19607

Damping flywheel to stabilize permanent rotation of weightless solid body moving by inertia, obtaining differential equations of motion
07 p1183 A69-19678

Hamilton-Jacobi equations of motion for classical electron in presence of traveling pulse of electromagnetic radiation, solving radiation pulse shape orbits
08 p1361 A69-19790

Mathematical theory generalization for smooth materially uniform simple bodies, discussing elastic body structure, material tangent bundle and index bundle, motion equations, etc
08 p1410 A69-19822

Solution of equations of motion of charged particles in constant magnetic field and variable electric field
08 p1361 A69-20213

Stability and instability conditions derived for undisturbed motion of system over finite period of time
08 p1351 A69-20321

Trajectory calculation of unguided meteorological rocket by digital computers and by equations of motion, discussing wind influence on ceiling and horizontal ranges
08 p1409 A69-20457

Dynamic behavior of electrohydraulic servactuators over wide range of loads using differential equations of motion
08 p1256 A69-20718

Numerical integration of motion equations of electrons subject to electrostatic waves, considering turbulent heating
08 p1368 A69-20806

Steady motion through rarefied gas of circular cylinder due to surface temperature difference
08 p1305 A69-20888

Hydromagnetic steady forced flow against porous rotating disk, integrating equations of motion by Karman-Pohlhausen and series methods
08 p1370 A69-21005

Lateral stability of glider towed by cable in steady rectilinear horizontal flight, deriving motion equations as ordinary differential equations
09 p1433 A69-21498

Charged particles equations of motion in earth magnetosphere in polar storms, considering auroral zone, diurnal variations and electron and proton velocities
09 p1485 A69-21535

Integration time reduction for equations of motion of vehicle center of mass during parabolic reentry, using Runge principle
09 p1532 A69-21763

Motion stability over finite interval of time for perturbed mechanical systems
09 p1539 A69-21881

Final motions of Hamiltonian conservative systems, analyzing Liouville type, homogeneous and similar systems
09 p1540 A69-21882

Bubble spiral path motion toward axis of rotation of liquid rotating at constant angular velocity
09 p1483 A69-22006

Structural damping coefficient for free vibrations of one degree freedom general systems motion
09 p1617 A69-22076

High sensitivity gyroscopic HF angular acceleration sensor using special differentiator, obtaining motion equations and dynamic response
09 p1498 A69-22109

Differential equation for droplet motion along ballistic trajectory in gas flow, noting applicability to solid bodies via computer programming
09 p1483 A69-22222

Gunn effect cavity controlled generator oscillations, noting phase trajectory closing conditions dependence on resonant mode parameters
09 p1468 A69-22596

Relativistically corrected Vlasov equation solved as approximate solution of exact relativistic equations of motion for low density media
10 p1724 A69-22924

Invariant transformation of equations for ideal gas plane steady motions, noting application to gas flows with shock waves and eddies
10 p1680 A69-23709

Rigid body rotational simultaneous equations of motion transformed into explicit form for digital simulation
10 p1661 A69-23855

Rotatory inertia and shear deformation effects on natural frequency and bending mode shape in equations of motion of rotating turbomachine blade [ASME PAPER 69-VIBR-50]
10 p1804 A69-24148

Nonlinear confining and deconfining forces of laser light interaction with inhomogeneous plasma, analyzing macroscopic motion based on ponderomotive force description
11 p1923 A69-24297

Turbulent flow velocity field evolution in presence of random forces using equation of motion
11 p1867 A69-24628

Formula in Prandtl-Batchelor theory describing motion of incompressible fluid in sphere interior verified experimentally
11 p1868 A69-24755

Differential equations for effect of sinusoidal force with slowly varying frequency on dynamic behavior of nonlinear vibrator, using phase surface technique
11 p1916 A69-24760

Dynamic stability of double pendulum with vibrating point of suspension, obtaining differential equations of motion by Lagrange equations application in averaging method
11 p1884 A69-24768

Kowalewski solution for motion of heavy body with fixed point, noting hodographs
11 p1917 A69-24776

Variational equations for rotation of heavy solid body with fixed point about horizontal axis, noting mass distribution
11 p1917 A69-24778

Steady state solutions of differential equations of motion for body with fixed point, considering Kharlamov cone for rotation of heavy gyrost
11 p1917 A69-24780

Distribution of steady state solutions for equations of helical motion of body in infinite fluid, noting coaxial control surfaces
11 p1868 A69-24782

Kinematic equations of motion of body about fixed point, considering Steklov solution
11 p1918 A69-24791

Finite difference solutions for time dependent equations of motion for steady flow around cylinder at large Reynolds numbers
11 p1872 A69-25133

Radial hydrostatic bearing parameters calculated by pressure distribution diagram in bipolar coordinates, obtaining equations of motion
11 p1892 A69-25341

Motion equations for conducting paramagnetic fluid in magnetic field derived, including MHD equations and equation determining magnetic moment variation rates
11 p1932 A69-25465

Motion equations for ideal transonic gas flow, applying solutions to flow with incident shock waves of various profiles
11 p1820 A69-25468

Transverse pulsating motion of spherical particle in turbulent flow, considering differential equation of motion transformation
11 p1876 A69-25489

Space vehicle docking dynamics and matrix equations of motion amenable to numerical solution on digital computer, using Hamilton principle and Lagrange multipliers
11 p1967 A69-25501

Elastic free-free body deformation during motion based on equations of motion valid for rigid body, noting dynamic Green tensor
11 p1994 A69-25604

Covariant equations of motion of body of variable mass in general relativity, considering Schwarzschild field, rotating mass field and Einstein static universe
11 p1965 A69-25744

Motion of heavy body with gyroscope, using coordinate system to reduce problem to linear second order differential equation
11 p1920 A69-25746

Equations of motion of body with fixed point, deriving solutions representable as segments of trigonometric series in variable related to time differentially
11 p1920 A69-25748

Observation process optimization in system described by linear differential equations of motion reducible to optimal control problem
12 p2027 A69-25882

Jet flows instabilities with vertical and horizontal velocity drifts from numerical integration of atmospheric motion equations linearized with respect to small perturbations
12 p2125 A69-25950

Boussinesq approximation for compressible fluids, discussing perturbation pressure and velocities and vertical scale motions
12 p2061 A69-26013

Monograph on rapid rotations of aircraft with fixed controls, covering spin and roll movements differential equations
12 p2013 A69-26118

Linearized steady state equations of motion solved for boundary conditions of fluid lying between horizontal planes with temperature varying horizontally
12 p2066 A69-26134

Electrohydrodynamic equations and transfer coefficients for multicomponent plasma with volumetric charge in electric field, discussing Ohm law and equations for plasma motion
12 p2135 A69-26399

Potential error source in VTOL aircraft dynamics analysis suggested by dual function of symbol used in perturbation equations of motion
12 p2014 A69-26776

Orbit determination from satellite using linear combinations of time of flight measurements and based on expansion of satellite law of motion
12 p2159 A69-26778

Thermomechanical theory for nonreacting binary fluid mixtures, discussing free energy function, entropy flux vector, equations of motion, constraints, etc
12 p2191 A69-26927

Controllable motions of compressible homogeneous isotropic solids, anisotropic solids and fluids with memory under constant body force
12 p2189 A69-27118

Microstructured mixtures theory including energy balance, mass and momentum equations and entropy production inequality for structured fluids in motion
13 p2371 A69-27318

Particle volume role in normal shockwave structure in gas-particle mixtures, discussing equations of motion formulation
13 p2244 A69-27327

Equations of motion computerized simulation for attitude stabilization of orbiting telescope coupled to crew compartment
13 p2261 A69-27952

Equations of motion of compressible fluid with non-zero resistivity near thin foil, solving supersonic and subsonic flow by Fredholm integral equations
13 p2200 A69-28360

Circular membranes vibrational and stability characteristics under simultaneous constant spin and precessional motions, obtaining Hill equation for motion amplitude coefficients
13 p2370 A69-28665

Energy integral of equations used in studying atmospheric motions in quasi-geostrophic approximation
14 p2433 A69-28797

Periodic solutions for small nutation angle of quasi-linear autonomous system of equations of motion of heavy solid body moving around fixed point
14 p2445 A69-28896

Rigid obstacle unsteady motion in compressible fluid with load applied to surface layer, deriving numerical solution of pressure expansion
14 p2430 A69-29480

Relativistic behavior of electromagnetic multipolar nongravitating particle, discussing integrability of field equations
14 p2486 A69-29594

Quasi-distribution function differential equation for laser field with nonMarkoffian character derived from density matrix master equation
14 p2486 A69-29633

Soviet book on partially liquid filled solid body dynamics from viewpoint of space and aircraft applications

14 p2530 A69-29815

Plane shock wave interaction with elastic shallow shell in compressible fluid, formulating equations of motion

15 p2704 A69-30262

Master equation in quantum optics phase-space formulation based on Schroedinger equation of motion, noting application to Volterra integral equation and Born approximation

15 p2633 A69-30307

Air masses transformation, solving nonlinear simultaneous system of equations of motion, heat influx and turbulent energy balance

15 p2649 A69-30647

Theory for stability of steady motions of system with cyclic coordinates applicable to total damping

15 p2690 A69-30737

Dynamic stability of elastic bodies with motion described by partial differential equation

15 p2652 A69-30860

Plane incompressible fluid interface stability in presence of transverse electric field, deriving equation of motion for perturbation amplitude

15 p2652 A69-30911

Stress distribution in isotropic spherical shell rotating uniformly about diametral axis, deriving equilibrium equations

15 p2712 A69-31005

Integrable cases of equations of motion of solid body around fixed point located in potential field of elastic supports

15 p2653 A69-31194

Magnetothermoelasticity equations, uniqueness and reciprocity theorems and solutions emphasizing moving media

15 p2715 A69-31215

Dynamics of spin stabilized satellite with long crossed dipoles or slender beams, including linearized equations of motion

15 p2703 A69-31332

Equations for gradually changing motion by differentiating momentum and energy equations with respect to abscissa noting wall resistance, viscosity, turbulence and Coriolis coefficients

15 p2593 A69-31489

Eigenvalue bounds for amplification rates, wave speeds and linear stability conditions for Orr-Sommerfeld equation governing parallel flow in boundary layer and round pipes

16 p2768 A69-31591

D-stationary principle to determine optimum hypersurfaces in configuration space containing optimal motion trajectories

16 p2811 A69-31625

Motion equations for dynamics of aircraft control surface controlled by autopilot with rigid feedback

16 p2809 A69-32134

Mechanical systems modeling modification to include mobile coordinates, introducing gyroscopic and pseudogyroscopic terms into motion equations

16 p2875 A69-32246

Motion of two rigid spheroids with mutual gravitational attraction based on Hamilton-Jacobi theory applicable to binary stars

16 p2863 A69-32402

Charged particles equations of motion in earth magnetosphere in polar storms, considering auroral zone diurnal variations and electron and proton velocities

16 p2783 A69-32530

Fluid filled spherical shell axisymmetric nontorsional motion analysis via differential equations obtained by Hamilton principle

17 p3051 A69-32956

Mechanical systems differential equations of motion solution behavior, discussing program constraints

17 p3053 A69-33017

Wave generation in infinite micropolar elastic solid body analyzed by linearized equations of motion

17 p3053 A69-33018

Subsonic thermal convection or internal gravity waves from formal scale analysis of equations of motion in plane parallel atmosphere

17 p2960 A69-33155

Rotational equations of motion for two body spacecraft on common spin axis required for simulated gravity environment or gyroscopic stability augmentation

17 p3047 A69-33227

Stability and instability conditions derived for undisturbed motion of system over finite period of time

17 p3005 A69-33314

Exact similarity solutions of hypersonic small disturbance equations for steady flow, discussing equations of state and motion and dissociating gas flow [AIAA PAPER 69-707]

17 p2953 A69-33448

Lifting rotors with thrust or tilting moment feedback control, deriving blade equations of motion [AHS PAPER 340]

17 p2899 A69-33510

Two dimensional incompressible flow past circular cylinder at moderate Reynolds number, reducing partial differential equations of motion by series truncation for flow field

17 p2896 A69-33600

Gyrocompass differential equations of motion reduced to Volterra integral equation, proposing solution algorithm

17 p2995 A69-33617

Natural frequencies and vibration modal shapes of asymmetrical airfoil blades analyzed by differential equations of motion, noting flexure coordinates center variations effect

17 p3067 A69-34053

Circular cylindrical shell nonlinear response to uniform radial impulsive pressure, noting inextensibility constraint and equations of motion roles [ASME PAPER 69-APM-26]

18 p3214 A69-34399

Orbit determination for short and long period comets using equations of motion including terms for radial components of nongravitational force

18 p3195 A69-34432

Drift of two connected gyroscopes, discussing equations of motion assuming unperturbed rotation and weightlessness

18 p3135 A69-34561

Longitudinal oscillations of homogeneous elastic rod under nonconservative force at one end, deriving equations of motion and stability conditions

18 p3216 A69-34578

Equations of motion of rapidly rotating spacecraft, considering deformations of long elastic booms

18 p3207 A69-34582

Fixed point reaction force in mobile system of solids coupled kinematically, examining zero dynamic components

18 p3172 A69-34590

Equations of motion for plate vibration derived by complementary variational principle, including boundary conditions and thin plate transverse vibrations

18 p3218 A69-34626

Thermal emission and spectral degree of blackness of W derived from electron motion equation

18 p3156 A69-34715

Game interception of motions, obtaining proof for extremal aiming scheme

18 p3173 A69-35030

Periodic solution of boundary value problem involving motion equation of viscous fluid

18 p3123 A69-35053

Spiral disk galaxies stability analysis assuming centrifugal force balancing self gravitation, transforming linearized equations of motion into eigenvalue equations

18 p3200 A69-35131

Quadratic approximation at matrix level of dynamic equations for rotating bodies applied to gravity gradient satellite exhibiting nonlinear resonances

18 p3174 A69-35298

Protosun and solar system angular momentum losses analyzed from equations for convective star rotation change, noting almost total protosun initial momentum loss possibility

18 p3203 A69-35346

Polar coordinates in Euclidean space applied to theory of satellite moving in gravitational field of spherically symmetrical body, introducing equipotential surfaces

19 p3397 A69-35610

Equations of motion for axisymmetric elastic deformation of inhomogeneous body of revolution subjected to torsion and steady oscillations

19 p3436 A69-35845

Linearization of equations of motion for three body problem, emphasizing lunar far side libration point as related to possible landing

19 p3402 A69-35961

Nonlinear free motion of conservative oscillator with one degree of freedom calculated by collocation method

19 p3438 A69-36308

Gas dynamics of material slab under radiation impact assuming thermal equilibrium reemission, discussing equations of motion and mean free path as function of frequency

19 p3449 A69-36355

Long term integration of fluid motion equations with finite difference scheme using hexagonal grid system to avoid nonlinear computational instability

19 p3564 A69-36508

Numerical integration of atmospheric motion equations in global domain using hexagonal grid, including sphericity corrections and Coriolis term

19 p3564 A69-36509

Motion equations of holonomic system of elastic bodies subjected to scleronomic, ideal and statically determinate constraints, using Green tensor

19 p3374 A69-36584

Gyrostatt satellite equilibrium positions in circular equatorial orbit under action of gravitational magnetic and aerodynamic moments based on gyrostatically stabilized satellite equations of motion

19 p3432 A69-36620

Group properties of adiabatic motion equations of medium in relativistic hydrodynamics, including solutions of subgroups applicable to multiple particle production

19 p3301 A69-36843

Translating Tolman problem of cosmic dust motion into centrally symmetrical reading system, showing relativistic and Newtonian motion laws coincidence

20 p3594 A69-37079

Stability of periodic orbits in elliptic restricted three body problem [AAS PAPER 68-086]

20 p3595 A69-37172

Perturbation matrix derivation in rectangular coordinates using Sitarsky two body variational equation for all motions

20 p3568 A69-37200

Numerical solution of equations of motion of rocket under thrust in inverse square force field, discussing effects of initial acceleration

20 p3595 A69-37203

Asymptotic stability of null solution of matrix differential equation, considering linearized equations of rotational motion for hinged two body gravity gradient satellite orbit

20 p3575 A69-37212

Numerical integration of lunar motion equations to investigate lunar theory for high precision applications and to examine motion departures from gravitational theory

20 p3603 A69-37560

Hydromagnetic waves equations of motion for non-relativistic case, discussing particle and fluid flow models

20 p3616 A69-38317

Equations of motion for optimal attitude of suborbital aircraft regarding time and distance range

21 p3795 A69-38440

Jupiter mass determined by applying Cowell numerical integration to equations of motion for ninth satellite

21 p3795 A69-38468

Literat solution to equations of motion applied to lunar theory using electronic computer with series convergence

21 p3796 A69-38474

Magnetospheric electromagnetic phenomena explained by equations of motion for particle acceleration, forbidden regions and MHD processes

21 p3707 A69-38485

Steady motions stability of gyroscope in Cardan suspension, deriving equations of motions with rectangular coordinate system

21 p3723 A69-38851

Time optimal control for second order automatic system with motion described by differential equations

21 p3770 A69-38856

Near resonant and nonresonant solutions of nonlinear equation describing rotating pendulum motion under periodic disturbance

21 p3771 A69-39004

Reaction forces calculated for system of connected solid bodies of various composition during accomplishment of given motion

21 p3771 A69-39085

Integrals of motion for minimum fuel rocket trajectories in inverse square field calculated for constant power and constant exhaust rockets [AIAA PAPER 69-904]

21 p3806 A69-39336

Vector integral extension to optimal trajectory coordinate multiplier systems with constant of motion demonstrated for coast-arc problem [AIAA PAPER 69-907]

21 p3807 A69-39339

Inertial motion of body produced by revolving uniformly deformed configuration, showing constant semiaxes without kinetic energy losses

21 p3772 A69-39620

Equation of motion for determining nonlinear vibration of rod pendulum in viscous flow of varying velocity

21 p3773 A69-39679

Equations of motion of elastic dumbbell satellite and two-mass spring-connected satellite in orbit, using energy and Floquet theory to investigate spinning motion stability

21 p3817 A69-39759

Optimal flight regime determination for variable mass body pursuing target by straddling method, presenting motion equations and approximate solutions

21 p3818 A69-39819

General control theory for spacecraft motions, deriving dynamic equations of motion about center of mass for holonomic and nonholonomic control programs

21 p3829 A69-39829

Controlled motion of space vehicle about center of mass analyzed by equation expressing nutation angle invariance

21 p3830 A69-39839

Minimization of motion deviation from prescribed motion analyzed as differential game of converging motions using equations of motion

22 p3980 A69-40105

Equations of motion of holonomic and non-holonomic mechanical systems obtained by displacement operators

22 p3980 A69-40106

Motion of body with cavity completely filled with viscous fluid about center of mass in potential mass-force field, applying small parameter method

22 p3980 A69-40109

Flexible string extraction from bobbin through nozzle, solving equations of motion by neglecting bending rigidity, extensibility, drag, internal friction, etc

22 p3930 A69-40585

Equations of motion of unguided rocket under wind effect, calculating launch angles for wind compensation

22 p4037 A69-40815

Artificial satellite motion analysis and perturbation function, considering disturbances due to second satellite or sun

22 p4030 A69-40906

Positive solutions of parabolic and hyperbolic partial differential equations arising as viscoelastic media equations of motion, noting maximum principle utilization

22 p3976 A69-41035

Nonlinear model including rocket rotary and forward motion inside smoothbore launcher utilizing dynamic friction coefficient

22 p4037 A69-41038

Integral equations of motion for plane steady flow of viscous incompressible electrically conducting fluid around flat plate

22 p3992 A69-41109

Crack development in solid body, considering condition at crack tip not derivable from equation of motion and strain equation

22 p4047 A69-41123

Quantum mechanical systems dynamics in diagonal coherent state representation, discussing applications

22 p3983 A69-41259

Metal removal mechanisms during electrochemical milling for moving electrodes, noting equations of motion of point for nonmoving electrodes

23 p4168 A69-41310

Book on porous bodies hydrodynamics covering motion equations for free, filtration, perfect and Newtonian fluids

23 p4150 A69-41501

Differential equations of motion and associated boundary condition for axisymmetric flexural vibration of cylindrically anisotropic circular plate, using variational calculus

23 p4228 A69-41911

Computer program for natural oscillations of plates and shells, deriving differential equations of motion for thin elastic shell by variational method

23 p4230 A69-42004

Motion equations of quasi-linear nonautonomous systems with many degrees of freedom, obtaining periodic solutions by asymptotic integration

23 p4183 A69-42477

Ballistic equations for mass center movement in vertical plane defined by projectile initial velocity

23 p4183 A69-42482

Mathematical model for ascent and descent of high altitude tethered balloon, developing computer program and deriving differential equations of motion [AIAA PAPER 68-942]

24 p4254 A69-43722

EQUATIONS OF STATE

NT HUGONOT EQUATION OF STATE

High temperature, fully ionized plasma equation of state, using quantum statistical theory of low density electron-ion plasma in thermal equilibrium

01 p0128 A69-10346

Electrical equation of state of metals determination from density, conductivity, energy and metal vapor velocity measurements in wire explosions

01 p0117 A69-10659

MHD equations describing interactions between gases and magnetic fields solved by finite difference method

01 p0129 A69-10722

Thermodynamics of directed continuous media, discussing kinematics, equations of state, entropy inequality and material objectivity principle

02 p0354 A69-12611

General theory of relativity equations for homogeneous anisotropic three dimensional space with matter, deriving ultrarelativistic equation of state

03 p0466 A69-13423

Active circuit analysis by state variable method, defining state vector as set of voltages between nodes and reference node

03 p0410 A69-13831

Thermodynamic theory of strain rate sensitive plastic material within framework of thermodynamics of materials with internal state variables

05 p0834 A69-15792

Three atom interaction contribution to nonideal dissociating gas state equation, determining quantum correction for third virial coefficient

05 p0796 A69-15893

State variable techniques applied to optimal continuous linear feature extraction for binary Gaussian pattern recognition or detection problem

05 p0740 A69-16577

State variables of ideal gas in two phase region, discussing determination from equations of state and equation for internal energy and Maxwell criterion inapplicability

06 p1030 A69-17170

Continuous time nonlinear dynamical system state variables estimated suboptimally from discrete noisy measurements with second order nonlinear filter, deriving dynamical equations

06 p0904 A69-17939

Schwarzschild perfect fluid spheres stability to radial perturbations, noting fluid adiabatic index relation to critical value

07 p1221 A69-19585

Consistency of high temperature equation of state of solids, considering Grüneisen parameter and lattice dynamics

08 p1419 A69-19814

Finite elastic locking medium, discussing equation of state for thermodynamic variables and applications to thermoelasticity [IS-ERI-70]

09 p1612 A69-21561

Thermal models for Jupiter and Saturn corresponding to completely convective structure, using De Marcus state equations

09 p1607 A69-22428

Self similar solutions for collapse of empty cylindrical cavity in gas with given equation of state, describing gas motion past cavity

10 p1679 A69-23367

Thermodynamic approach to equation of state of magnetized Fermi gas, deriving energy eigenvalues of free electron in magnetic field

11 p1961 A69-25107

Specific isochoric heat capacity of pure fluids, considering thermal equation of state, vapor pressure and boundary conditions at critical point

11 p2001 A69-25201

Ferromagnetic transition in superdense nuclear matter and neutron stars, developing relativistic equation of state

11 p1965 A69-25564

Rational transfer function matrix realization into irreducible Jordan canonical form state equation by nonsingular transformations

12 p2122 A69-26511

Lumped linear system state estimation with optimal linear smoothing instead of filtering, noting smoothing lag and variance

12 p2122 A69-26524

Equations of state for continuous media, using variational principles within framework of relativity theory

12 p2131 A69-26972

Computer determination of symbolic state equations for nonlinear circuits using FORTRAN notation

12 p2055 A69-27097

Polynomial and nonlinear equations of state for solids and liquids analyzed using uncommon statistical and least squares methods

14 p2486 A69-29470

Shock attenuation and equation of state of polyurethane based on aquarium technique and free surface velocity measurement

16 p2828 A69-31810

Exact similarity solutions of hypersonic small disturbance equations for steady flow, discussing equations of state and motion and dissociating gas flow [AIAA PAPER 69-707]

17 p2953 A69-33448

Plate dynamics generalized equations independent of plate theory hypotheses, discussing algorithm and initial and boundary conditions

18 p3226 A69-35376

Nondissociating vibrationally excited dense N₂, analyzing compressibility factor, internal energy, enthalpy, entropy, sound speed and specific heat by state equations

20 p3631 A69-37214

Thomas-Fermi approximation applied to calculation of equations of state and thermodynamic functions at high pressure from differential equations of statistical atom model

22 p3984 A69-40186

Equation of state measurements of earth materials by shock wave techniques, applying to olivine for earth mantle constitution problem

22 p3937 A69-40188

Linear partial differential equations derived from thermodynamic identities integrated by method of characteristics for relationships between temperature and pressure incomplete equations of state

23 p4239 A69-41569

Fully dispersed wave reflection from plane wall in stable relaxing gas, obtaining canonical equation of state

24 p4299 A69-42717

Liapunov functionals for time delay systems by path integrals in state space, using convolution equations involving distributions with compact support

24 p4295 A69-43317

EQUATORIAL ELECTROJET

Equatorial and auroral electrojets, discussing origin theories and ionospheric irregularities

02 p0236 A69-11433

Diurnal variation in horizontal magnetic component of South American stations close to electrojet during IGY

02 p0246 A69-12771

Symmetric baroclinic instability role in Jupiter equatorial acceleration

03 p0508 A69-13347

Equatorial hourly storm time part of disturbances field for 1958, discussing magnetic storm effects

07 p1124 A69-18822

Equatorial counter-electrojet and inverse quiet day solar diurnal variation current layers, noting regular diurnal variation horizontal component and latitude effect

08 p1306 A69-19884

Toroidal magnetic fields in ionosphere associated with solar quiet daily variations producing electric current and equatorial auroral electrojets

10 p1681 A69-22805

VHF radar observations of electron density irregularity in nighttime equatorial electrojet, comparing day and night time electron drift rates and directions

10 p1769 A69-23837

Equatorial electrojet role in electromagnetic induction at magnetic dip equator, applying Price theory for space gradients

13 p2252 A69-27519

Equatorial electrojet VHF radar observations indicating nontwo stream electron concentration irregularities related to electron drift velocity

14 p2511 A69-28953

Diurnal change in equatorial electrojet parameters observed by magnetometers on Nike Apache rockets

15 p2598 A69-31320

Equatorial electrojet north-south cross sections in Pacific observed by airborne equipment during magnetically quiet day, moderately disturbed day and solar eclipse

16 p2777 A69-32182

Equatorial electrojet current distribution determined using equivalent circuit method and magnetic force model, noting electron density profile influence on current density

18 p3130 A69-35186

Model equatorial electrojet with meridional current system constructed by spherical harmonic expansion for geomagnetic field, noting current loops

20 p3533 A69-38084

Atmospheric gravity waves amplitude generated in equatorial electrojets and polar regions

20 p3593 A69-38107

Daytime drift velocities and signal fading characteristics of equatorial and blanketing sporadic E layer irregularities, noting independence of electrojet intensity
23 p4160 A69-42429

Ionospheric F region equatorial anomaly in electron density showing high correlation with equatorial electrojet range and poor correlation with Fuquene range
23 p4160 A69-42432

Two stream plasma instability in equatorial electrojet extended to nonlinear domain by nonlinear treatment of ion kinetic equation
24 p4310 A69-43182

EQUATORIAL ORBITS
NT STATIONARY ORBITS

Attitude control system for gravity gradient stabilized satellite in synchronous and near synchronous equatorial orbits, discussing libration damping methods
03 p0504 A69-12857

Magnetic sample-and-hold damping using geomagnetic field for libration damping of gravity gradient stabilized satellite in near synchronous equatorial orbit
07 p1227 A69-18337

Magnetic field at synchronous equatorial orbit by analyzing magnetometer data recorded by ATS 1 satellite during magnetic storms, geomagnetic substorms and quiet times
07 p1123 A69-18343

Earth quadrupole moment effects on precession of gyroscope in satellite in equatorial orbit
17 p2972 A69-33072

Equatorial moderately elliptical satellite orbit perturbations calculated in local invariants, assuming state vector dependence of acceleration
17 p3039 A69-33796

Global communication satellite system with 12 to 16 hour period equatorial orbit, discussing satellite daily switchings, motions relative to earth, etc
20 p3497 A69-38189

F region atmospheric density measurements obtained from aerodynamic drag on San Marco 2 satellite in equatorial orbit, comparing data with San Marco 1
21 p3704 A69-38369

Electromagnetic attitude control system for Lincoln Experimental Satellite 5 in near-synchronous equatorial orbit, noting onboard error detection in closed control loop
21 p3827 A69-39755

EQUATORS
NT MAGNETIC EQUATOR

Solar eclipse effect on geomagnetic field at and near dip equator observed at Huancayo Observatory, Peru
02 p0241 A69-11727

Hydrodynamic model of atmospheric circulation in equatorial region, using group invariant method
03 p0462 A69-13931

F2 layer diffusion and sporadic E layer characteristics from equatorial ionosphere soundings on Zaria schooner
09 p1486 A69-21548

Cosmic ray equators from trajectory tracing procedure for computing vertical cut-off rigidities with two different geomagnetic field simulations compared to experimental equators
14 p2511 A69-28961

F 2 layer diffusion and sporadic E layer characteristics from equatorial ionosphere soundings on Zaria schooner
16 p2784 A69-32543

Equinox and equator corrections of orientation elements of FK3 and FK4 catalogs based on meridian solar observations
17 p3027 A69-32871

Ionization irregularities in equatorial E region observed in various scale sized by rocket-borne Langmuir and plasma-noise probes
23 p4160 A69-42430

Equatorial anomaly during declining solar activity, treating seasonal and daily variations, longitude dependence and geomagnetic storm-time distortions
23 p4161 A69-42436

Equatorial anticyclones over eastern Pacific caused by large scale cross-equatorial flows determined by ATS-1 photographs, noting frictional convergence factor
24 p4342 A69-42895

Equator-to-pole temperature gradient relation with planetary pressure belts, comparing observational data with theoretical circulation criterion
24 p4345 A69-43149

EQUILIBRIUM

Elastic shell nonlinear theory, introducing nonsymmetric stress tensor and principles of virtual work and objectivity
01 p0166 A69-10166

Weakly interacting neutrinos in anisotropic cosmological models with emphasis on equilibrium period, noting energy increment
01 p0123 A69-10348

Equilibrium problem of elastic medium with stress couples in linearized elasticity theory, representing biharmonic function with aid of analytical functions
02 p0340 A69-12035

Asymptotic stability of gyroscopic systems equilibria with partial dissipation used for motion stability analysis
04 p0631 A69-15537

Initial defects influence on equilibrium states of compressed elastoplastic plates
06 p1025 A69-17684

Inhomogeneous half planes equilibrium bonded by elastic layer, noting tangential stresses at interfaces
09 p1611 A69-21482

Holonomic and scleronomic dynamic systems steady state motion stability under effect of generalized forces derived on basis of Liapunov theory
10 p1724 A69-22929

Nonlinear systems of differential equations to free oscillations about equilibrium, obtaining periodic solutions
18 p3172 A69-34591

EQUILIBRIUM DIAGRAMS
U PHASE DIAGRAMS
EQUILIBRIUM EQUATIONS

Elliptic system of twelfth order equations describing elastic equilibrium of plate with kinematic functions analyzed by integration procedure
19 p3438 A69-36203

Equilibrium equations for longitudinally hinged nonshallow cylindrical shells transformed into coupled equations with constant coefficients
19 p3439 A69-36581

Nonlinear shell theory for thin elastic circular cylinders, obtaining equations for investigating equilibrium configurations of postbuckled states
19 p3440 A69-36636

Thin circular cylindrical shells elastic equilibrium under loads producing deflection, elongation or contraction described by integrating equilibrium equations with constant coefficient
20 p3621 A69-37076

Equilibrium equations reduced to single partial differential equation for membrane theory of shells having coefficients of first quadratic form and specified curvature radius
20 p3622 A69-37220

Equilibrium and stability of axisymmetric gaseous polytropes in toroidal magnetic fields, calculating harmonic oscillations by virial tensor method
21 p3797 A69-38534

Stress-strain state of thin spherical shell of variable thickness in elastoplastic equilibrium, using Meissner variables to reduce equilibrium equations
21 p3834 A69-38717

Gaseous mixtures for hypervelocity applications, studying equilibrium conditions and thermodynamic properties for shock and constant volume heating processes
22 p4049 A69-40266

Dynamic stability of circular isotropic plate with central hole subjected to torsional moment uniformly distributed over both edges by equilibrium equation
22 p4043 A69-40455

Natural torsional-flexural vibrations of bars with single symmetry, using matrix equations of equilibrium, displacements and natural coupled vibrations
22 p4043 A69-40456

Homogeneous equilibrium equations of nonlinear shallow shell theory, obtaining six stress function solutions for strain measures
22 p4048 A69-41199

Stress analysis in elastic bodies induced by axisymmetric strains in presence of mass forces and temperature gradients, obtaining equilibrium equation
23 p4229 A69-41997

Takeoff indicator design based on solution of equilibrium equation for forces acting on aircraft along drag axis
24 p4253 A69-43085

EQUILIBRIUM FLOW
NT FROZEN EQUILIBRIUM FLOW

Equilibrium turbulent boundary layer prediction for proposed Prandtl mixing length distribution
03 p0419 A69-13992

Steady state plasma flows stability equations, using variational principle for analyzing toroidal plasmas
04 p0635 A69-14556

Numerical solution of chemically reacting boundary layer equations, noting loss of accuracy due to numerical cancellations
04 p0588 A69-14737

Linear theory of equilibrium and nonequilibrium gas flows applied to steady two dimensional nonequilibrium flow of inviscid nonheat-conducting gas
06 p0909 A69-17327

Natural modes and eigenfunctions of low amplitude oscillation determined by Ritz averaging method for ideal fluid with equilibrium surface in weak force field
07 p1119 A69-18746

Laminar boundary layer flow on sphere in hypersonic flow of equilibrium dissociating air
07 p1050 A69-18756

Equilibrium theory of parametric pump using cyclic flow of binary mixture through column with heated and cooled bed of solid absorbent
09 p1481 A69-21910

Axisymmetric flow theory for turbomachine of non-free vortex design in distributed equilibrium state, considering boundary conditions and blade leading edges [ASME PAPER 69-GT-10]
09 p1432 A69-22504

Turbulent boundary layers behavior near flow separation, obtaining equations for equilibrium layers
15 p2591 A69-30638

Adiabatic compressible turbulent equilibrium boundary layer integral method analysis extended to study nonequilibrium laminar flows, deriving dissipation integrals, presenting numerical solutions [AIAA PAPER 69-689]
17 p2955 A69-33481

Fully developed whirls steady state structure, discussing tornadoes maximum azimuthal speed, hurricanes rotational speed, model for mature hurricane and numerical computation [AIAA PAPER 69-671]
17 p2997 A69-33499

Equilibrium Couette flow of ionized multicomponent ideal gas between moving catalytic plates, obtaining thermal flow formulas and thermal conductivity coefficient
19 p3240 A69-36403

Computerized design of potassium vapor turbine with supersaturation effects compared with equilibrium flow turbine design
23 p4187 A69-42251

EQUILIBRIUM METHODS

Natural vibration properties of elastic free-free body obeying Hooke law analysis from equilibrium and motion equations, determining Green tensor
01 p0167 A69-10323

Modified Galerkin method applied to approximate solutions of two dimensional elasticity equations of equilibrium
02 p0338 A69-11748

Stress discontinuity surface of three dimensional rigid plastic body arbitrary yield condition, considering equilibrium of regular four sided pyramid
11 p1996 A69-25738

Equilibrium paths in initial postbuckling of elastic structural systems, discussing stability boundaries and relationships between imperfections and critical loads
13 p2359 A69-27261

Inverse deformation in elastic materials, using variational principle to obtain equilibrium equations properties
13 p2360 A69-27324

Effective tensors of elastic moduli and yielding of composite materials, considering multiparticle interactions and use of equilibrium and incompatibility equations
13 p2360 A69-27382

Love stress function derivation from equilibrium equations
13 p2364 A69-28233

Higher order difference method for equilibrium and eigenvalue problems of two dimensional structures using iterative solution
13 p2365 A69-28239

Finite element analysis of flat rectangular panels, developing equilibrium equations based on specified displacement modes
15 p2708 A69-30667

Equilibrium equations for elastic medium with stress couples, presenting first term of asymptotic expansion of solution for disk and simply connected region
16 p2871 A69-31830

Linear theory of elastic stability of structures, discussing deformation kinematics, perturbed and neutral equilibria and solutions for buckling of beams, plate, shells, etc
17 p3054 A69-33042

EQUINOXES

EQUINOXES

Equinox and equator corrections of orientation elements of FK3 and FK4 catalogs based on meridian solar observations

17 p3027 A69-32871

Ionospheric electron temperature profiles for mid-day equinoctial conditions noting protonospheric and conjugate heating effects

22 p3939 A69-40506

EQUIPARTITION THEOREM

Klein theorem kinetic energy corrections taking into account breakdown of equipartition theorem

16 p2823 A69-32469

EQUIPMENT SPECIFICATIONS

Fluidic element design calculations, noting flow characteristic differences

02 p0195 A69-12074

Precision coaxial connectors, giving IEEE standard mechanical, electrical and environmental specifications for general precision connectors using coplanar butt joints

02 p0222 A69-12757

Large area proportional counter for cosmic ray design, construction and specifications

03 p0427 A69-12979

Economic planning of satellite earth station equipment in relation to expected traffic demand, emphasizing specifications for communication via Intelsat 2 and 3 satellites

07 p1117 A69-19347

Avionic systems development, discussing criteria for realization of operational requirement and engineering product satisfying requirement [AGARDOGRAPH-114]

08 p1317 A69-20982

Microminiature system mechanical design for aerospace environment, considering guidelines for implementation of requirements [AGARDOGRAPH-114]

08 p1291 A69-20986

Process control data in acceptance procedures for high reliability electronic components, discussing supplier and user cooperation

08 p1293 A69-21110

Maintenance process simulation for engine and major components to provide routine material usage forecast and policies

09 p1503 A69-21802

Environmental requirements of military specifications tabulated according to tests for altitude, temperature, vibration, shock, humidity, temperature/altitude, etc

11 p1862 A69-24331

Equipment life cycle costs computer simulation for design and changes evaluation, including maintenance analysis example

15 p2723 A69-31138

Polish electronic measurement devices operating principles and specifications including vibration, frequency and pressure meters, fatigue testing machines, etc

16 p2790 A69-32076

Light aircraft emergency downed position indicators installation program, discussing transmitter minimum performance standards, listening watch insurance, etc

17 p2931 A69-34102

Physics of Control program for electronic devices reliability, discussing qualified parts, chemical, physical and electrical properties, parameter ranges, specifications and corrective action

18 p3143 A69-34488

Reliability demonstration by MIL-STD-781 for equipment failure and success, proposing useful alternatives

18 p3145 A69-34507

Reliability prediction limited to approximations related to past experience on similar equipment

18 p3147 A69-34517

MIL-STD-781B reliability tests with standard based on exponential distribution for equipment exhibiting constant failure rate, noting sampling

20 p3551 A69-38289

High density environment-resistant circular connectors, discussing design, applications, test and performance data compliance with MIL-C-81511 specifications

22 p3910 A69-39947

MIL-STD-781A vibration requirements, using mechanical shakers for AGREE vibration testing

22 p3954 A69-40036

Hungarian-made semiconductor silicon-base strain gages meeting specifications at half world market price

22 p3947 A69-40938

All-equipments reliability test improved by removing usual truncation and extending accept-reject lines of test plan MIL-STD-781

24 p4321 A69-43203

Radiation hard device specifications, comparing data with environmental considerations

24 p4287 A69-43204

Microelectronics test program consisting of four reliability screening levels based on Mil-Std 883

24 p4287 A69-43205

EQUIPOTENTIALS

Earth equipotential surface shape determination from satellite orbit dynamics, obtaining triaxial ellipsoid

09 p1487 A69-21635

Equilibration potentials between dense thrust beam and dilute space plasma measured in wind tunnel [AIAA PAPER 69-263]

09 p1568 A69-21728

Theory for describing rotating fluid planets external geometry in state of hydrostatic equilibrium, noting role of equipotential surfaces

20 p3594 A69-37077

Inertial motions, equipotential surfaces and Coriolis forces on earth ellipsoid, discussing pendulum-like oscillations

24 p4346 A69-43156

EQUIVALENCE

Equivalence principle application to gyroscope motion in uniform gravitational field to obtain precessional angular velocity

05 p0764 A69-16367

Space-frequency equivalence between monochromatic correlator interferometer using directional antennas and wideband correlator interferometer using isotropic antennas

07 p1132 A69-18917

Space time structure conditions derived for compatibility with simultaneous fulfillment of causality and equivalence principles

08 p1351 A69-19948

Equivalence of initial boundary value problem and integral equations obtained by regularization using potential theory

10 p1721 A69-23959

Penfield-Haus solution to magnetodynamic effect problem as inertial effect of orbital angular momentum, deriving Bohr magneton formula from Einstein equivalence principle

11 p1919 A69-25098

Thermodynamic equivalence of limit theorems for canonical and grand canonical ensembles, discussing Massieu-Planck function analog relation by Legendre transformation

12 p2191 A69-27148

Sinusoidal or random excitations equivalence from point of view of rupture risks, considering industrial applications

13 p2370 A69-28602

Algorithms for equivalence equation to approximate transient processes in higher order linear system by transient processes of lower order linear models

19 p3286 A69-36191

Two procedures for processing statistical data concerning Gaussian processes made exchangeable by manageable formula

19 p3361 A69-36646

Equivalence of initial boundary value problem and integral equations obtained by regularization using potential theory

21 p3756 A69-39150

Two level systems with overall performance as explicit function of first level performance, defining equivalence condition to prove coordinability for nonadditive case

24 p4294 A69-43308

EQUIVALENT CIRCUITS

DC biased microwave bolometer/barretter/detector, describing small signal dynamic equivalent circuit for output voltage

01 p0044 A69-10626

Semiconductor switching diode, evaluating operation with nonlinear time delay equivalent circuit

01 p0046 A69-10747

Transistor parameters for operation as minority carrier charge controlled device, developing equivalent circuit for computer calculation of transient response

01 p0046 A69-10748

Equivalent circuits for transient characteristics approximation of distributed RC circuits

01 p0046 A69-10779

Shockley theory of field effect transistors, calculating characteristics in miniaturization problems by

removing geometric constraints with aid of electric analog

02 p0215 A69-11781

Working equivalent circuits for fluidic transverse impact modulator in LF and IF range

02 p0196 A69-12082

Diffraction of cylindrical and plane waves in system of two parallel circular cylinders, using equivalent circuit method

02 p0217 A69-12261

Dielectric dispersion in inhomogeneous dielectrics and semiconductors, discussing three layered equivalent circuit

02 p0301 A69-12837

Impedance matching selection for phased array element, using element impedance data and equivalent circuit

04 p0572 A69-14323

Equivalent circuit of varactor with open p-n junction used as frequency multiplier

04 p0575 A69-14465

Varactor Q calculation from impedance vs bias measurements, circumventing circuit loss problem by procedure based on Weissfloch equivalent circuit of lossy two port network

04 p0575 A69-14753

Equivalent generator approach to facilitate scattering matrix analysis of complicated microwave circuit

04 p0582 A69-14755

Equivalent circuit for parallel conductor array based on array capacitance matrix

04 p0576 A69-14756

Small signal field effect transistor model at saturation and Borel equivalent scheme, giving evidence of internal feedback

04 p0579 A69-15226

Equivalent circuit diagrams for impedance of plasma column in low current low pressure glow discharge

05 p0800 A69-15742

Equivalent noise circuit for resonant transistor amplifier, deriving expression for noise factor

05 p0729 A69-16084

Stability of linear passive time variable circuits, discussing validity of circuit elements replacement by gyrator equivalents

05 p0739 A69-16348

Equivalent circuit for microwave point diode noting waveform calculations, frequency dependent elements and recovery phenomena

05 p0735 A69-16605

Composite equivalent circuits method for complex waveguide-resonator couplings based on variational principle for admittance matrices of electromagnetic volume couplings

05 p0736 A69-16785

Silicon double injection diode, discussing HF noise measurement, Nyquist noise equivalent circuit for double injection process and source of LF noise

06 p0898 A69-17762

Electron-electron interaction effect on I-V characteristic and equivalent circuit of metal-semiconductor contact, noting conductivity and rectifying properties

07 p1107 A69-19162

MOS transistor equivalent circuit for computer aided calculations with IMAG I program, noting versatility of model

08 p1280 A69-19978

Equivalent network representation of feedthrough lens array taking into account mutual coupling between elements to predict performance characteristics

08 p1280 A69-20014

Sawtooth generators production based on equivalent circuit theory, calculating linearity errors in voltages

08 p1296 A69-20105

Passive circuit components electrical properties at HF using equivalent circuit

08 p1283 A69-20135

Equivalent circuit synthesis with six reactances-two terminal network bridges

08 p1295 A69-21166

Insertion-loss synthesis of narrow band crystal band-elimination filters, using narrow band approximation and pseudoreactance theory

08 p1300 A69-21173

Transforming equivalent circuits, keeping electrical characteristics defined by network functions within prescribed limits

09 p1472 A69-21784

Steady state operation of atomic hydrogen maser by analogy with electronic circuits, calculating atomic magnetic susceptibility using density matrix and deriving equivalent circuits

09 p1517 A69-22093

HF excess noise and equivalent circuit representation of MOSFET with n-type channel, noting local mobility fluctuations effect

09 p1463 A69-22094

Equivalence and stability for negative impedance converter of bridge circuits by symmetrical amplifier design

09 p1467 A69-22559

Glass covered microwire technology to realize RC element, analyzing equivalent element errors by simulating irrational transfer functions

09 p1476 A69-22677

Polar geomagnetic disturbances global current systems representation by prototypes of equivalent current systems

10 p1688 A69-23937

Microstripline circuit for stabilizing oscillating frequency of Gunn diodes prepared with GaAs slices

12 p2036 A69-25924

Multivariable automatic control system consisting of similar local subsystems studied by transforming system equations into equivalent diagonal form

12 p2048 A69-26076

Equivalent subsystems for designing multivariable linear automatic control system

12 p2052 A69-26280

Electrical equivalent circuit for piezoelectric generation and detection of transient and sinusoidal ultrasonic waves by interdigital electrodes

12 p2039 A69-26376

Common source and common gate FET connections showing equivalent noise figures

13 p2227 A69-27237

Multiperture waveguide directional couplers analyzed by four port equivalent circuits, discussing synthesis method for optimizing coupling directivity

13 p2228 A69-27669

Delta modulated control system model for determining oscillation modes at sampling instants

13 p2221 A69-27962

Two idler parametric amplifiers bandwidth properties investigated using equivalent circuit, noting role of idler circuit design

13 p2233 A69-28066

Small signal, HF equivalent circuit for intrinsic metal oxide semiconductor field effect transistor, considering nonpinchoff and pinchoff modes

13 p2238 A69-28429

Reactive parameter scatter effect on amplitude frequency characteristics of regenerative reflection amplifiers based on equivalent circuit

13 p2235 A69-28515

Capacitors pi network representation of series gap in center conductor of matched coaxial transmission line

14 p2424 A69-29766

Transit time effects in silicon space charge limited diodes, studying frequency characteristics of small signal equivalent circuit

15 p2575 A69-30181

VHF and uHF MOS tetrode minimum noise factor computed as function of frequency by adding thermal noise sources to resistive parts of equivalent circuit

15 p2577 A69-30603

Equivalent circuit of single winding transformer, using distributed constant theory

15 p2578 A69-30793

Plane electromagnetic wave propagation normal and parallel to magnetic field in plasma analyzed by equivalent circuits and impedances

15 p2659 A69-30799

Equivalent circuits of dielectric loaded and unloaded rectangular waveguide Esaki diode reflection amplifier

15 p2578 A69-30801

Wind effects on ionospheric electric currents, using equivalent circuits to study tidal modes and current patterns

16 p2775 A69-32087

German monograph on theoretical and experimental investigations of tubes and lumped fluidic elements covering equivalent circuit

17 p2903 A69-33573

Superconducting antenna factors and matching circuit equivalents developed for predicting efficiency and Q increase on basis of Pb surface resistance

17 p2937 A69-33784

Fluierics /no moving part fluidics/, discussing diodes, capacitors, logic elements, temperature sensors, systems design, environmental factors, etc

17 p2904 A69-34067

Equatorial electrojet current distribution determined using equivalent circuit method and magnetic force model, noting electron density profile influence on current density

18 p3130 A69-35186

Equivalent circuit demonstrating noise reduction through input transistor integration into passive receiving antenna, stressing circuit loss control and preamplification role

19 p3281 A69-35764

Equivalent circuit for microwave cavity containing active GaAs device applied to waveguide and radial mode cavity design

20 p3508 A69-37900

Generation-recombination noise due to trapped charge fluctuation at impurity centers in Si junction gate field effect transistors transition regions, using lumped equivalent circuit

22 p3911 A69-40009

Equivalent circuit technique for dispersion equation and coupling impedance of slow wave structures of ring-rod systems, noting retardation

23 p4139 A69-41944

ERBIUM

Paramagnetic resonance of Er ion in calcium tungstate single crystal, determining spin-Hamiltonian parameters

04 p0643 A69-15141

Absorption and fluorescent spectra, relaxation times and quantum efficiencies measured for glasses doped with trivalent erbium, reviewing spectroscopic parameters involved with laser effect

22 p3962 A69-40476

ERECTION

U CONSTRUCTION

ERGODIC PROCESS

Delay method of finite ergodic Markov chains, analyzing first moments of state probabilities with aid of asymptotic equation

04 p0624 A69-15002

Time dependent statistical equilibrium equations solutions for describing time development of atomic populations by means of ergodic Markov chain

09 p1542 A69-22218

Stochastic and ergodic aspects of magnetic lines of force, discussing cosmic ray diffusion in interplanetary magnetic field

10 p1770 A69-24111

Accuracy and variance of nonergodicity estimates for random processes associated with radiophysical applications

15 p2582 A69-30946

ERGOMETERS

Bicycle ergometer combined with induction clutch, investigating effect of eccentric dynamic work with arms and legs

21 p3663 A69-38902

ERGONOMICS

U HUMAN FACTORS ENGINEERING

EROS PROJECT

U EXPERIMENTAL REFLECTOR ORBITAL SHOT PROJ

EROSION

NT WATER EROSION

Erosion damage of bearing alloy lining in thin lubricating oil film, considering Cu-Pb alloy and tin base white metal

01 p0094 A69-10313

Aircraft gas turbine compressor parts erosion tests

01 p0099 A69-11058

Wind tunnel investigation of damage to aircraft radomes by water droplet encounter during cloud passage and gaseous molecule friction in air

07 p1054 A69-19541

Trajectories of particles entrained by gas flow in nozzles for study of erosion damage during passage of gas-particle mixture

11 p1818 A69-25355

Erosion type plasma accelerator using inductive energy storage compared with capacitive energy storage

13 p2311 A69-28110

Hypersonic wind tunnel for erosion test of multiple particle impacts, considering dust on cork, carborazole and silicone rubber

13 p2243 A69-28277

Erosion of contacts under capacitive loads noting cable length, arc duration and battery voltage

13 p2269 A69-28608

Erosion wear of graphitic and mica-ceramic materials used for sealing turbine compressors at high temperatures, including test installation

15 p2643 A69-31186

Solid materials erosion rate as function of cumulative damage generated by liquid droplets impingement

16 p2794 A69-31904

Airborne particle size influence on gas turbine parts erosion, with attempts to relate to filtration and engine life

16 p2794 A69-32026

Ground jet suppression fences for VTOL aircraft prepared pads, investigating erosion reduction and particle entrainment

[AIAA PAPER 68-639] 17 p2902 A69-34028

Tungsten carbide erosion resistant coatings, discussing optimum plasma deposition process and coating characteristics

20 p3561 A69-37373

Lunar surface erosion processes revealed by Lunar Orbiter photographs of boulder concentrations

21 p3794 A69-38378

Crater formation by gas erosion in vent of 4.3 kiloton nuclear explosion detonated at 280 ft depth in layered trachytic volcanic rocks

22 p3937 A69-40409

Module landing effects on lunar surface, deriving erosion law from Surveyor 5 engine firing test and vacuum test data

23 p4211 A69-41388

Graphite rocket engine nozzles chemical erosion at various temperatures, comparing reaction and diffusion rates

23 p4180 A69-42156

Sand erosion behavior of metals and plastics in air blast rig under varying exposure time, angles of impact and tensile stress

24 p4363 A69-42787

ERROR ANALYSIS

Root-mean-square error determination in automatic control system by digital computer for realizing control function, investigating harmonic and random input effects

01 p0050 A69-10208

Error and sensitivity analysis of on-line algorithms for fixed point linear smoothing

01 p0050 A69-10238

A priori and a posteriori estimates of direct methods accuracy in solving linear algebraic equations

01 p0105 A69-10727

Electronic device networks periodic structures accuracy estimated by automatic measurement of complete error spectrum of network spacings

01 p0045 A69-10732

Minimum measurement time of dynamic transmission coefficient of system by FM method, calculating error

01 p0031 A69-10785

Ephemeris Time and Atomic Clock Time roles in astronomy, discussing errors in daylight determination for mechanical, Short and atomic clocks, UT and Ephemeris Time

01 p0156 A69-10989

Multiple light scattering and reflection elimination from observed light brightness indicatrix to obtain true light scattering indicatrix, discussing error analysis

01 p0074 A69-11184

Atmospheric transmission factor and optical stability determination by photometer, estimating error due to solar aureole

01 p0075 A69-11193

Exponential approximation with piecewise linear error criteria for continuous function over interval

01 p0107 A69-11415

Error probability distribution density at output of optimal Gaussian random signal detection, using approximate solution of integral equations

02 p0206 A69-11605

Algorithms for error analysis, optimum filtering sensitivity and fixed interval smoothing solutions to linear estimation problems

02 p0224 A69-11961

Errors arising from inaccurate insertion of initial conditions in autonomous determination of coordinates of object moving along surface of spherical earth

02 p0281 A69-12137

Rms approximation validity limits for satellite temperature variances by deriving equations for thin insulated plate in space

02 p0352 A69-12211

Error reduction in initial azimuth alignment and azimuth and level axis gyro drifts in long range air transport gyro accelerometer inertial systems

02 p0278 A69-12361

Space surveillance radar system sensor missassociation of one space object for another, noting applicability to sonar and optical sensors

02 p0210 A69-12388

Errors in wind data due to wind response of parachute-borne sensor corrected with radar tracking, comparing corrected and uncorrected data

02 p0276 A69-12700

Planetary atmosphere determination error analysis using Kalman filter, noting results of simulated Martian atmosphere entry

02 p0331 A69-12806

Mission capability differences between direct and orbital Mars missions as to launch period selection, targeting capability and error analysis
02 p0331 A69-12821

Working breadboard model of planet tracker under various illuminating conditions, discussing hardware and closed loop tracking error analysis accounting for signal to noise effects
03 p0463 A69-13214

VOR path course errors, emphasizing effects of propagation and receiver processing
03 p0392 A69-13245

Error analysis of orientation methods for extraterrestrial stereophotogrammetric mapping
[JPL-TR-32-1344] 03 p0429 A69-13299

Chebyshev polynomials maximum property, examining effect of roundoff errors in Horner scheme for floating point arithmetic
03 p0456 A69-13553

Approximation for discretization error of discrete analog of Bergman harmonic kernel, discussing discretization error in Dirichlet and Neumann problems for Laplace equation
03 p0456 A69-13555

Two dimensional flow of incompressible fluid near sharp leading edge of plate at zero incidence, discussing approximation error and friction stress
03 p0415 A69-13651

Upper and lower bounds on mean reduced error of pulse code telemetering systems operating by binary code
03 p0396 A69-13687

Discretization error of Dirichlet problem analyzed in plane region with corners, discussing error in numerical solution of elliptic differential equations
03 p0457 A69-13741

Impulse bandwidth measurement error determination by trapezoidal numerical integration
03 p0398 A69-13902

Errors of wavemeter employing open resonator with spherical mirrors
03 p0407 A69-13983

Circuit for accurate division of attenuation and phase shift changes, noting calculation errors
04 p0573 A69-14337

Daily solar indices monthly averages errors due to evaluation for days presenting favorable weather conditions
04 p0657 A69-14700

Kirchhoff-Love hypothesis error dependence on stressed state variability index in theory of elasticity for closed spherical shell under uniform surface load
04 p0680 A69-14927

Gaussian channels capacity, studying supremum of information transmission rates with small error probability
04 p0558 A69-15006

Error distribution maps for measurements of parameters epsilon, F and E of geomagnetic potential in Northern and Southern Hemispheres
04 p0627 A69-15031

Transistor scattering matrix parameters determination, emphasizing directional coupler errors and impedance mismatches
04 p0582 A69-15067

Boundary condition description effect on numerical accuracy of series solution to boundary value problem by direct method
04 p0681 A69-15283

Errors in amplitudes and phases recorded by earth tide recording equipment determined, using special multiflex galvanometer
04 p0601 A69-15305

Photographic plates based parallax determinations of nearby stars weights, relative and absolute values, probable error and observation interval
04 p0663 A69-15381

Spectroscopic charged particle concentration determination, discussing error and limits of applicability in low temperature plasma
05 p0762 A69-15899

Parameters and relative errors tabulated from IR spectral emittance of Mo, Nb, Zr and Ta near 1400 K
05 p0846 A69-15903

First order linear differential equations having complementary solutions of exponential type to determine effective initial and boundary conditions
05 p0786 A69-15926

Probable errors in FK4 catalog of star positions and proper motions determined by Scott method
05 p0823 A69-16041

IR radiation in upper atmosphere, indicating sources of error in data
05 p0753 A69-16058

Sonic nozzle mass flow measurement errors at high supply pressures and moderate temperatures due to real gas effects
[ASME PAPER 68-WA/FM-4] 05 p0699 A69-16114

Error introduced into total electron content data by changes in ionospheric layer height
05 p0816 A69-16281

Error analysis methods for inherent errors in analog, digital and linkage equipment of typical hybrid computer configuration
05 p0725 A69-16472

Expressions for calculating filtering errors resulting from insufficient information about useful signal and noise characteristics
05 p0740 A69-16668

Meteorological satellites data for quantitative weather forecasts, discussing error effects due to data treatment in adiabatic approximation
06 p0949 A69-17032

Error probability vs SNR and power spectrum of PCM/FM signal with small phase deviation, noting applications in satellite tracking
06 p0889 A69-17656

Error origin and control in high gain operational amplifier in time differentiation of voltage signal used for photoemission studies
06 p0897 A69-17700

Error and noise sources in analog differentiators, discussing signal distortion minimization techniques and augmentation with linear phase filter
06 p0897 A69-17702

Antenna transmission and receiving system effects on radio brightness temperature measurements by airborne equipment
06 p0929 A69-18000

Nonsteady combustion models for gases, liquid fuels and solid propellants, reviewing errors in physics and mathematics
[AIAA PAPER 69-178] 06 p1037 A69-18100

Bit error probability for noncoherent binary FSK link involving Rician interfering signal
07 p1080 A69-19095

Single channel binary PSK communication systems performance influenced by degree of RF coherence between transmitter and receiver
07 p1082 A69-19109

Bit error probability estimation of NRZ PCM synchronizer and detector operating in presence of fluctuating data frequency source
07 p1083 A69-19121

Waveform distortion resulting from adjacent channel crosstalk and from amplitude and phase nonlinearity in channel filters in DSB/SC telemetry link
07 p1083 A69-19130

Most probable position /MPP/ choosing methods accuracy, investigating relative effects of dead reckoning /DR/ and celestial lines of position /LOP/ errors
07 p1177 A69-19214

Radome induced distortions of radioelectric axis analyzed by sectional phase analysis
07 p1110 A69-19521

Radome axis error due to phase /dielectrics/ and metallic obstacles
07 p1112 A69-19542

Truncation error reducing scheme for balanced forecast models
07 p1176 A69-19629

Errors estimation in determination of radio signal source flux density, position and recorded half power widths
07 p1088 A69-19722

Subjective and objective upper air forecasts for aviation comparison by isobaric pressure height fields, discussing error analysis
08 p1345 A69-19886

Synchronization errors effects on performance of compression-line demodulator, increasing mean-square error in measuring instantaneous frequency and locking probability
08 p1271 A69-19920

Sawtooth generators production based on equivalent circuit theory, calculating linearity errors in voltages
08 p1296 A69-20105

Error in receiver sensitivity calculation using approximate equation for noise power at input
08 p1275 A69-20226

Total error of minimization of differentiable functionals based on gradient projection procedures
08 p1342 A69-20319

Coincidence error between star image and planet edge for entrance pupil and telescope magnification
08 p1314 A69-20383

Error bounds and variational methods for nonlinear boundary value problems for ordinary differential equations
08 p1343 A69-20536

Weather forecasts range and accuracy, outlining procedure for estimating growth rate of atmospheric behavior
08 p1346 A69-20600

Error estimation technique for Chebyshev series solution to ordinary differential equations
08 p1344 A69-20828

Response optimization of feedback control systems with reference to single settlement time-constant ideal determined for error evaluation
08 p1298 A69-20855

Chebyshev error norms of polynomial approximations for ideal filter minimized by emphasizing role of transfer function even and odd parts
08 p1299 A69-21168

Error probability for transmission of one of M orthogonal, equally likely, equal energy signals over generalized incoherent channel
09 p1452 A69-21314

Separation of normal geomagnetic field component from limited length measurements by moving averages, considering error and inhomogeneity of anomalous field
09 p1486 A69-21537

Error analysis of high resolution balloon-borne temperature sensor and comparison of temperature data with simultaneous rawinsonde measurements
09 p1494 A69-21642

Spacecraft trajectory optimal determination without knowing measurements error distribution function, examining computer solution properties of linear programming
09 p1595 A69-21757

Optimal moments for trajectory parameters measurements determined by linear analysis to minimize error for initial conditions
09 p1495 A69-21758

Coding schemes for memoryless Gaussian channels with feedback considering error probabilities
09 p1454 A69-21794

Digital information transmission error characteristics determining error distribution over time and relation to distribution function of intervals between errors
09 p1454 A69-21795

Atmospheric density profile from satellite measurements of light wave phase and refraction angles, discussing ionospheric, water vapor and diffraction effects on errors
09 p1490 A69-21862

Error estimates of stress concentration at free hole determined by two dimensional elasticity theory of thick plates
09 p1614 A69-21885

Trajectory error propagation upper bounds in many body field for impulsive initial error, relating error to mission tolerances
09 p1595 A69-21937

Microwave interferometer circuits errors, considering interferometers with phase detector, logic counting circuits, frequency conversion and amplitude modulation
09 p1496 A69-22029

Refraction errors in plasma density measurement by microwave interferometry
09 p1496 A69-22031

Subjective and objective upper air forecasts compared for error analysis of headwinds, noting influence of geographical location
09 p1536 A69-22074

Error bounds for estimation error covariance matrix of fixed point smoothing and fixed interval smoothing algorithms for optimum linear estimation
09 p1533 A69-22436

Glass covered microwire technology to realize RC element, analyzing equivalent element errors by simulating irrational transfer functions
09 p1476 A69-22677

Saint Venant torsion and flexure of prismatic bars analysis in polar coordinates, discussing boundary errors
09 p1621 A69-22770

Minimum measurement time of dynamic transmission coefficient of system by FM method, calculating error
10 p1653 A69-23114

Apollo LM and CSM tracking systems boresight shift reducible by decreasing modulation indices or scaling factor alpha
10 p1672 A69-23277

- Mississippi Test Facility /MTF/ hardware data acquisition system error analysis from extensive simulated static firing tests
10 p1673 A69-23287
- Systematic errors caused by planet asphericity in measurements of orientation and motion parameters of orbiting object compensated by scanning navigation system
10 p1693 A69-23320
- Stability and error bounds in numerical integration of ordinary differential equations, determining highest possible degree of stable finite difference form
10 p1719 A69-23518
- Riemann sum definition and development of bounds for error in approximating integral, showing quadrature formulas as Riemann sums
10 p1719 A69-23521
- Multichannel bit error probability for FSK and DPSK obtained for slow nonselective-fading multipath as function of multipath parameters and diversity order
10 p1656 A69-23533
- Error analysis of Hubble galaxies count to resolve contradiction of values for average optical half thickness tau of galactic absorbing layer
10 p1779 A69-23609
- Infinite diameter detonation velocity vs loading density curve for ammonium perchlorate, finding quadratic mean error
11 p1940 A69-24486
- HF measurements by phase and amplification control of signal in impulse oscillography, noting accuracy in nanosecond range and signal distortion
11 p1880 A69-24541
- ELDO satellite command decoder performance in presence of noise, evaluating PDM bit decoder bit error probability and false command probability
11 p1834 A69-24563
- Jittering delay of triggering circuit driven by ramp signals of different finite slopes, noting tunnel diode discriminators and regenerative feedback loop circuits
11 p1858 A69-24568
- Error probability distribution density at output of optimal Gaussian random signal detection, using approximate solution of integral equations
11 p1835 A69-24712
- Shell theory foundations and basic equations, discussing classical shell equations asymptotic nature and errors
11 p1978 A69-24808
- Minimum test error probability test limits for known test equipment and signal tolerances, developing semi-graphically single equation for calculation
11 p1865 A69-25079
- Error analysis in conversion of two port scattering parameters used in microwave transistor characterization
11 p1852 A69-25200
- Comparison of errors obtained by using linearly gliding and rotating strengthening moduli in stress-strain state on basis of linear stepwise approximation
11 p1986 A69-25342
- Inertial navigation systems error analysis based on method of state variables
11 p1914 A69-25434
- Modeling errors in linear discrete stochastic system effects on Kalman filter state estimates
11 p1860 A69-25448
- Numerical prediction for nonlinear transient response of structures, considering geometric and material nonlinearities in systems with line elements
11 p1993 A69-25526
- Numerical computation method for evaluating transition matrix of linear time invariant system, estimating error propagated in transient response
11 p1910 A69-25660
- Computer controlled network analyzer performing automatic microwave measurements of passive and active networks, based on signal splitting and detecting
12 p2037 A69-26048
- Quantization error reduction for stochastic signals processing problems
12 p2051 A69-26201
- Error bounds for orthogonal signals in additive white Gaussian noise channels for class of generalized decision strategies permitting variable-size list decoding
12 p2029 A69-26204
- Atmospheric turbulence effects on detection and resolution of incoherent objects, discussing error probabilities of threshold and maximum-likelihood systems
12 p2029 A69-26252
- Satellite position errors due to atmospheric instability, discussing altitude-temperature relation and stellar scintillation synchronism for stars at small angular distances
12 p2158 A69-26445
- Error due to amplitude quantization and design of digital control systems in discrete time optimum control theory
12 p2053 A69-26507
- Asymptotic sampling error in closed loop hybrid systems, noting dependence on sampling period and execution time
12 p2053 A69-26508
- Potential error source in VTOL aircraft dynamics analysis suggested by dual function of symbol used in perturbation equations of motion
12 p2014 A69-26776
- Satellite positions measurements by laser compared with radar and photographic methods, considering measurement errors
12 p2110 A69-27149
- Errors in Appleton-Baynon equation for skip distance of radio waves in ionosphere
13 p2218 A69-27214
- Numerical methods for time integrating first order differential equations, emphasizing atmospheric oscillations in baroclinic model, evaluating errors
13 p2290 A69-27636
- Rms error for reproduction of satellite signal transmitted through continuous Gaussian channel assessed by numerical calculation
13 p2219 A69-27697
- Thermocouples dynamic response attached to thin skinned model under constant heating rate, considering error reduction in temperature measurement
13 p2375 A69-27785
- Automatic processing and error analysis of horizontal, vertical, static and geostrophic wind data by U.S.S.R. Hydrometeorological Service
13 p2292 A69-27839
- Trajectory terminal state error analysis using adjoint-generated sensitivities in nonlinear time-varying systems
13 p2296 A69-27940
- Radar SEP /spherical error probable/ for defining error ellipsoid in three dimensional accuracy and CEP /circular error probable/ for defining two dimensional accuracy
13 p2221 A69-27963
- Error analysis involved in calculating tangent functions defined by nonlinear differential equation solution, using digital differential analyzer
13 p2225 A69-27968
- Ferrite parameters measurement in alternating fields based on continuous analysis of magnetic, magnetizing and measuring circuits for assessing errors
13 p2320 A69-27996
- Variational method used to determine accuracy of approximation technique for dielectric slab on sidewall of rectangular waveguide
13 p2233 A69-28072
- Power spectrum of random process from discrete sequence of instantaneous values, assessing error
13 p2239 A69-28514
- Root-mean-square error determination in automatic control system by digital computer for realizing control function, investigating harmonic and random input effects
14 p2424 A69-28744
- High energy scattering approximation valid from small to large angles, discussing errors and proton scattering by He
14 p2487 A69-29008
- SNR improvement during low level turbulence measurements, examining correlation between hot-wire anemometers, including error analysis
14 p2446 A69-29018
- Semiempirical parameters in streamline division and momentum integral analyses for separated flows, using error function velocity profile and spreading parameter sigma
14 p2389 A69-29028
- Wentzel-Kramers-Brillouin approximation validity determined by sufficiency conditions based on differential equations series solution
14 p2471 A69-29454
- Long distance VLF multirange navigation fix errors as function of angles of cut of position lines and range errors, presenting error isograms
14 p2478 A69-29484
- Ground testing method to evaluate inertial navigation systems dynamic errors by programmed platform drift rates, position output comparisons and error source identification
14 p2479 A69-29490
- Photoelectric observation of passage of stars through meridian, detailing error sources and corrective technique
14 p2521 A69-29507
- Error analysis in efficiency measurement of gas turbines, considering thermodynamics and power output
14 p2509 A69-29509
- Error bounds for covariance matrix used in optimum filtering and smoothing algorithms for control and communications systems operation
14 p2416 A69-29549
- Minimum error criteria for shock wave structure determined by applying Mott-Smith distribution to Boltzmann equations for rigid sphere gas
14 p2431 A69-29579
- Chopper modulated IR detection system error analysis through minimizing mean square error of approximating output function
14 p2450 A69-29639
- Dynamic instrumental errors of quasi-steady state mechanical meters approximated by graph analytical method
14 p2451 A69-29747
- Plasma microwave measurement error allowance for multiple reflection of waves from vacuum chambers dielectric walls
14 p2498 A69-29806
- Variational principle for solving boundary value problems and reciprocal formula for error estimation, discussing applicability to general transport phenomena problems
15 p2716 A69-30022
- Complex load impedance determination by measuring maximum, minimum and load voltages in line, including error analysis
15 p2582 A69-30123
- Algorithm for optimal digital processing of pulse signals during multilevel quantization in Markov noise, including error analysis
15 p2571 A69-30126
- Logarithmic amplifiers amplitude characteristics accuracy obtained by gain variations or successive summation of voltages, plotting curves illustrating error variations vs gain
15 p2574 A69-30128
- Signal phase measurement accuracy by discrete phase technique ensured by using wideband signals and automatic control of input SNR
15 p2574 A69-30130
- Orthogonal signal recognition in set of false signals by resolving devices with limited sensitivity, giving design formulas for error probability
15 p2563 A69-30135
- Instrumental accuracy of discrete filter during measurement of initial phase of signal dependent on phase structure
15 p2574 A69-30139
- Linear distortions effect on signals detection in binary communication channel with fluctuating noise, determining error probability
15 p2564 A69-30146
- Errors in magnitude equation and atmospheric dispersion calculated for 400 mm astrophotograph, emphasizing constant errors due to objective
15 p2646 A69-30162
- Perturbation analysis for error estimates in algebraic eigenvalues and eigenvectors problems for solving skewed membrane vibrations
15 p2703 A69-30211
- Bearing errors from radio beacons with rotating or multilobe radiation patterns
15 p2567 A69-30343
- Subtractor performance for processing correlated random signals with different spectral widths in signal delay time indicator, discussing errors
15 p2572 A69-30346
- Spacecraft radar altimetry with application to geodesy, discussing orbital and tracking errors
15 p2609 A69-30460
- Error assessment for 20 May 1966 annular eclipse observation point and observation time determination
15 p2686 A69-30533
- Geopotential determination from gravity force measurements at known surface and error assessment for earth model with aid of spherical harmonic expansion
15 p2689 A69-30567
- Creep rates measurement errors at low stresses in intermediate temperature range, examining log creep rate vs log stress plot in Cr-Mo steel
15 p2639 A69-30599
- Time delay errors compensation methods in analog-digital computation loops, finding digital scheme inferior to analog
15 p2572 A69-30618

Runge-Kutta type method truncation error estimation, discussing validity conditions, evaluation processes and numerical tests

15 p2644 A69-30672

Antenna, frequency converter and automatic spectrum recorder system for closest approach times prediction and satellite identification, discussing errors

15 p2569 A69-30800

Reliability of integrated circuits with emphasis on errors

15 p2626 A69-30831

Initial uncertainties role in weather forecasting, discussing errors as represented by rms deviation of ensemble members from mean

15 p2649 A69-30894

Systematic error pattern in raw data obtained during tracking ROSE balloons by two radar systems, estimating range resolver error

15 p2649 A69-30897

Reflecting or reradiating obstacle proximity as cause of siting errors in azimuth radio measurements, discussing omnidirectional obstacles effect

15 p2651 A69-31090

Algorithm for calculating recognition error by applying pattern vectors having two multivariate Gaussian distribution to optimum Bayes classifier

15 p2572 A69-31113

System estimation methods compared for rational boundaries of lower confidence limit, discussing variables/attributes error propagation

15 p2722 A69-31135

Clevis design for reduced friction errors associated with round hole clevis in plane strain fracture toughness measurements

15 p2612 A69-31150

Satellite trajectory determination and expected errors for OGO 4 and Geos 1 orbits, noting geopotential, aerodynamic drag and integration contributions

15 p2698 A69-31331

Literal algebra /KSPASM/ computer program critical verification of Kozai short period lunar perturbations, discussing errors

15 p2699 A69-31381

Israel research on space data for meteorological purposes, describing automatic picture transmission data and errors in surface temperature determination by satellite radiometry

15 p2650 A69-31422

Carrier lifetime in p-n-u-n diodes, discussing error of forward pulsed diode method by Wilson and alternative model

16 p2757 A69-31615

Microwave power loss and semiconductor conductivity relationship measured for carrier lifetime and mobility, noting nonlinearity and accuracy

16 p2825 A69-31617

Three antenna interferometer angle measurement accuracy dependent on antenna spacing, deriving optimal spacing value

16 p2758 A69-31730

Thermocouple probe measurement error evaluation by parallel plate analytical model

16 p2789 A69-31903

Differential coefficients applied to Izsak-Borchers ballistic trajectory and errors produced by perturbations of initial vectors, applying results to data capsule recovery

16 p2857 A69-32156

Numerical estimates of momentum integral error in applying locally similar solutions to nonsimilar problems, assuming two dimensional or axisymmetric flow

16 p2772 A69-32174

Satellites meridian and extrameridian observations by transit instrument, examining errors in ephemerides of bulletins

16 p2858 A69-32211

Error analysis of one bit autocorrelation method of spectral estimation, noting decrease in spectral variance with increased sampling rate

16 p2752 A69-32390

Separation of normal geomagnetic field component from limited length measurements by moving averages, considering error and inhomogeneity of anomalous field

16 p2783 A69-32532

Interagency Chemical Rocket Propulsion Group method of treating measurement error for liquid rocket engine performance parameters, using uncertainty model

[AIAA PAPER 69-734] 16 p2846 A69-32781

System noise parameters derivation, using standard IRE definition as foundation and amplifier noise measurement as example for error analysis

16 p2755 A69-32800

Knife-edge obstacle diffraction of nonisotropic transmitter analyzed via isotropic source model propagation path noting accuracy

17 p2917 A69-32847

Voltage standing wave ratio measurement technique at low power level, including tolerated errors, compared with Roberts-von Hippel method

17 p2918 A69-33031

Equipment- and program-type methods for solving automatic digital control systems synthesis problems, evaluating efficiency based on accuracy

17 p2933 A69-33120

Lunar surface thermal characteristics revised from analysis of error sources in daytime lunar surface temperatures derived from Surveyor 5 compartment data [AIAA PAPER 69-594]

17 p3033 A69-33287

Data inaccuracy used for calculating forecasts of reliability analyzed by Monte Carlo simulation

17 p2937 A69-33389

Nitrogen density measurements up to 4000 atm and 1000 C, examining possible error sources

17 p3073 A69-33393

Error estimation in thin elastic plate bending problem approximate solution by equal deflection lines method, constructing two sided bound for boundary value problems

17 p3062 A69-33713

Monograph on solar system space flight trajectory calculations covering solutions to differential equations, error analysis and gravitational effects

17 p3039 A69-33798

Ionospheric parameter recording accuracy by vertical sounding, discussing errors in frequency-height curve

17 p2969 A69-34002

Antenna three dimensional radiation patterns, describing error analysis of various pattern measurement techniques

17 p2942 A69-34086

Measurement errors and geometry effects on navigational accuracy, determining maximum allowable error for measuring devices employed

17 p3002 A69-34098

Turbulence measurement errors with inclined hot wires described by equations, assuming normal component cooling includes greater tangential cooling

18 p3134 A69-34442

Vibrations damping coefficient for asymptotic stability of inertial navigation system platform, determining stabilization errors

18 p3134 A69-34555

Inertial characteristics determination error influence of solid body on damping system parameters

18 p3171 A69-34562

Vibration-proof devices obtained by relating variance determination errors in selective filter response, modulating process bandwidth and spectral analyzer passband

18 p3109 A69-34584

Meteorological forecasting as problem in fluid mechanics and thermodynamics, discussing accuracy and electronic computer role in classical or mathematical methods

18 p3166 A69-34694

Range effects on apparent height and frequency biases of radar precipitation echoes determined by regression technique for several stations

18 p3101 A69-34826

Inertial aircraft navigation, describing instruments and error analyses with regard to simulation, error propagation and total system error

18 p3169 A69-34850

Automatic celestial navigation, discussing star trackers design, mathematics of celestial fix and relationship to errors and physical and environmental constraints

18 p3169 A69-34852

Dynamic balance for rotating aerospace vehicles, discussing error in principal axis location between rotor on machine and free body in space

[SAWE PAPER 740] 18 p3137 A69-34887

Weight estimation inaccuracies due to use of quickie equations, discussing error and extrapolation avoidance in wing weight study

[SAWE PAPER 794] 18 p3222 A69-34904

Radiant heat transfer integral equations solutions accuracy determined from differences between geometric and resolving angular emission factors

18 p3230 A69-35119

Venusian cloud layer radius, discussing error in determination of occultation level height of Regulus by Venus

18 p3203 A69-35331

Wind profile data measured by AN/FPS-16 radar/suppression balloon system, noting error sources

18 p3139 A69-35428

Error analysis for pressure measurements in blow-down supersonic tunnel

19 p3292 A69-35728

Error sources in forecasts for heights of isobaric surfaces obtained by numerical integration of prognostic equations of equivalent barotropic models

19 p3361 A69-35770

Ordinary differential equations integration method, presenting algorithm based on double constraint of maximum accuracy and stability

19 p3279 A69-35805

Directional couplers design considerations for use in microwave power meters, analyzing directivity and mismatch effect on system error

19 p3282 A69-35826

Digital data compression system transmission error statistical analysis, emphasizing addressing schemes effect on compression ratio

19 p3272 A69-36261

Maximum rms error comparison of redundancy reduction techniques, emphasizing limiting slope technique and worst case interpolation error

19 p3273 A69-36264

Digital data transmission by pulse code modulation considered for minimum mean square error

19 p3274 A69-36282

AC technique using lock-in power amplifier SNR for measuring galvanomagnetic and Shubnikov-de Haas effects, noting error reduction

19 p3312 A69-36375

Abnormalities of routine electrocardiograms in medical certification of pilots, indicating errors in screening

19 p3263 A69-36462

High index frequency modulated waveform spectrum analysis including upper bound on approximation error to avoid fallacy of Woodward theorem [IEEE PAPER 68-TP-74-COM1]

19 p3276 A69-36485

Finite difference analogs with increasing error terms applied to simple differential Laplace operator for accuracy determination

19 p3365 A69-36510

Approximation error involved in difference optimal control problem substitution for differential optimal control problem based on functional minimization

20 p3509 A69-36989

Relative displacement spectra analysis illustrating shock spectra errors, comparing real system response with simple single degree of freedom system response

20 p3548 A69-37301

Cramer-Rao and split-beam tracker techniques compared for optimum bearing error attainable with linear passive sonar array in spatially incoherent noise environment

20 p3576 A69-37322

Spectral calculation deformations and errors estimation using Blackman-Tukey spectral formulas

20 p3571 A69-37697

Wind speed and direction determination accuracy of radar or theodolite methods

20 p3572 A69-37698

Pilot balloon observation errors due to inaccurate balloon height determination, relating error determination to wind speed and direction errors

20 p3572 A69-37699

Minimax error technique used with finite difference methods to estimate error in approximations to functions defined by nonlinear differential equations

20 p3568 A69-37832

FM data transmission distortion noise and error rate compared with AM and phase step modulation, noting role of bandwidth

20 p3496 A69-37905

IR radiation in upper atmosphere, indicating sources of error in data

20 p3533 A69-37968

Atmospheric predictability as revealed by naturally occurring analogs, noting superposed error

20 p3573 A69-38057

Inertial navigation systems trajectory parameters errors due to inaccurate initial coordinates input, deriving trigonometric functions for autonomous error determination

21 p3760 A69-38572

Balloon location by low orbit meteorological satellites, discussing balloon movement due to wind and geometric and nongeometric effects on errors

21 p3760 A69-38618

Differential curve-of-growth analysis of late type giant stars yielding chemical compositions, discussing nature and size of uncertainties in estimates

21 p3800 A69-38700

Error function for boundary methods

21 p3755 A69-39008

Residual analysis prior to statistical tests on experimental data
21 p3755 A69-39120

Lunar Orbiter missions pre- and postflight error analyses compared to estimate dispersions from reference trajectory
[AAS PAPER 68-108] 21 p3805 A69-39220

Correlation role in navigation satellite analysis noting reduction in ephemeris error effects
[AAS PAPER 68-145] 21 p3761 A69-39222

Error propagation and tolerance analysis in design and reliability engineering and stress analysis
21 p3842 A69-39303

Satellite orbit determination errors attributed to Gaussian noise effect on tracking measurements, assuming known Gaussian probability error distribution
[AIAA PAPER 69-911] 21 p3807 A69-39343

Statistical error analysis of autonomous manned spacecraft navigation in long duration eccentric Mars orbits
[AIAA PAPER 69-880] 21 p3763 A69-39406

Mathematical formulation and error analysis of two rotor gyroorbit used in plotting orbital system of satellite coordinates
21 p3765 A69-39636

Parameter estimation using entropy of error as criterion function compared with mean square error analysis
21 p3757 A69-39664

Handbook of radar measurement covering noise measurement, error analysis, antenna performance, etc
21 p3678 A69-39668

Isoclinic angle errors effects on photoelastic fringe order measurements accuracy
22 p3945 A69-40082

Correction to circuit theory textbooks concerning observable but not controllable modes and stability
22 p3917 A69-40135

Probability characteristics of total error in vertical gyroscope evaluated from component errors along suspension axes
22 p3946 A69-40251

Pluto positions /1930-1965/ from photographic observations, ascribing declination errors to atmospheric dispersions
22 p4025 A69-40612

Mars positions determined from photographic observations by zone astrophot, establishing rms errors and objective centering error
22 p4025 A69-40613

Error probability of Gaussian signal detector in Gaussian noise background determined from quadratic form of probability distribution density
22 p3901 A69-40955

Errors in determining controlled satellite rotation periods, proposing scheme for corrected trajectory calculation of small eccentricity orbits
22 p4033 A69-41086

Satellite trajectory parameters estimation by maximum likelihood method applied to continuous satellite observations assuming random Gaussian process as measurement error
22 p3979 A69-41087

Thermal conductivity measurements of fluids, considering contribution of radiation, convection, temperature jump and experimental arrangement eccentricity to errors
23 p4237 A69-41325

Delay line MTI receivers performance calculation accuracy, discussing error for general and restricted number of pulses from single and double cancellation at IF
23 p4117 A69-41605

Tradeoff between Doppler measurement capability and subcarrier demodulation in coherent digital communication system quantitatively presented for various SNR
23 p4122 A69-41771

Errors due to neutron counter radioactivity in cosmic rays nucleon measurements analyzed in reducing readings to barometric pressure
23 p4206 A69-41855

Integral electron concentration in column of space between earth satellite and ground determined by integral equation, assessing errors minimization methods
23 p4157 A69-41858

Image recognition algorithms estimated for effectiveness by formulas minimizing classification error probability
23 p4134 A69-41954

Statistical analysis of random production errors on phasing section polarization field of antenna with elliptical polarization
23 p4125 A69-42041

Antenna pointing and tracking accuracy by identifying error sources in servo, structural, mechanical and alignment factors
23 p4125 A69-42126

Rigid shaft dynamics in hinged and elastic bearings, eliminating inaccuracy by limiting analysis to forced vibration
23 p4171 A69-42483

Error probability bounds for self synchronized binary PSK communication systems, simulating decision feedback, phase doubling and maximum likelihood systems
23 p4128 A69-42501

Correcting deficiencies in parametric expressions for rate distortion function of Gaussian process under weighted square error criterion
24 p4281 A69-42722

Errors in estimating cardiac function from aortic and peripheral pulses, using cadaver experiments
24 p4262 A69-42728

Osculatory interpolation explicit method demonstration with error terms determination
24 p4341 A69-43230

Atlas/Centaur/Surveyor flights guidance accuracy, discussing postflight analysis of injection errors due to hardware, software and propulsion system
[AIAA PAPER 68-842] 24 p4348 A69-43239

Geodetic and geophysical random uncertainties as fundamental limitations on terrestrial inertial navigation accuracy
[AIAA PAPER 68-847] 24 p4348 A69-43240

Optimization problems solution applied to separable but bounded state variable problem, providing control over commercial errors
24 p4292 A69-43286

Error sources in magnetic field measurements using magnetic probes in high temperature plasmas, discussing detection, correction and elimination
[AIAA PAPER 68-727] 24 p4316 A69-43571

Unmodeled errors detection in recursive flight trajectory estimation, deriving equations for unmodeled parameters
24 p4387 A69-43585

Astatic gyro motion with horizontal rotor axis, defining suspension error with allowance for external force moments
24 p4317 A69-43707

ERROR BAND
U ACCURACY

ERROR CORRECTING DEVICES

Atmospheric temperature corrections for measurements by rocketsonde and balloonsonde with thermistor, noting dissipation factors and thermal time constants
01 p0081 A69-10697

Automatic control systems correction by compensating for nonlinear statistical dynamic characteristics with aid of nonlinear devices
01 p0053 A69-10801

Errors in wind data due to wind response of parachute-borne sensor corrected with radar tracking, comparing corrected and uncorrected data
02 p0276 A69-12700

Error correcting coding on DCSF satellite channels, discussing single access communication through wideband SHF repeaters in synchronous earth orbit
03 p0387 A69-13177

Short baseline radiating satellite interferometer concept for reducing satellite navigation systematic errors for aircraft and ships
03 p0463 A69-13208

Transatlantic aircraft cross-track air navigation error reducible by augmenting Doppler system with satellite ranging system
03 p0464 A69-13237

Topological principles of gate and contact self correcting circuits not using self correcting codes
03 p0410 A69-13421

Dynamic behavior of large steerable radio telescope, showing structural resonance influence on error detection system
03 p0412 A69-14093

Book on information coding and transmission and error detection and correction
04 p0558 A69-15066

Errors in amplitudes and phases recorded by earth tide recording equipment determined, using special multiflex galvanometer
04 p0601 A69-15305

Hybrid computational method for partial differential equations to reduce time of solution and error propagation
04 p0566 A69-15347

Strapdown gyros in back to back connection for reduction of component cross coupling errors
04 p0603 A69-15473

Quasi-optical transmission lines having composite correction devices with/without phasing devices
05 p0723 A69-16784

L-step orthogonalization of Bose-Chaudhuri-Hocquenghem codes
06 p0903 A69-17532

Sectoral hoghorn as line feed for correcting spherical aberration in offset spherical reflector antennas
06 p0898 A69-17823

Error correcting codes - Conference, University of Wisconsin, May 1968
06 p0890 A69-17861

Linear recurring sequences over finite fields, discussing application to error correcting codes
06 p0948 A69-17863

Sequences with small correlation functions as error correcting codes in word separation, synchronization and pulse compression systems
06 p0948 A69-17868

Line reversal temperature measurement technique, calculating error and outlining correction methods for flames with cool boundary layers and flames containing solid particles
06 p1035 A69-17929

Vertistat H gravity gradient configuration prevents elastic deformation, permitting high pointing accuracy at synchronous altitudes
07 p1229 A69-18351

Swept-frequency complex return-gain response of injection locked oscillator over locking bandwidth, detecting and correcting phase errors between injection-locked diode oscillators
07 p1100 A69-18645

FET sample and hold circuit using error corrective feedback
08 p1298 A69-20837

Binary block codes for correction of substitution and synchronization errors
09 p1452 A69-21316

Error control coding noting cyclic codes, binary shift registers, shift register circuits, encoding and decoding
09 p1461 A69-21893

Thrust vectoring system using accelerometer displacement to reduce alignment errors in multiaperture electron bombardment ion engines
[AIAA PAPER 68-543] 09 p1570 A69-21985

Dual inertia magnetic tape recorder/reproducer combining low wideband flutter and low time base errors
10 p1693 A69-23289

Telemetry data channel gain and phase correction with frequency response calibration technique using digital filtering
10 p1654 A69-23291

Spectral baseline instability correction for time of flight mass spectrometer operating at source pressures up to one torr
10 p1693 A69-23345

Error correction of digital data with cyclic codes and probability function set extended to Bose-Chaudhuri-Hocquenghem codes and P super M codes
10 p1655 A69-23529

Tandem interleaved cyclic codes for digital HF communication with improved error rate at reduced decay time
10 p1655 A69-23530

Cyclic vector amplitude error from noisy data corrected for calculating geophysical lunar tidal effects
12 p2033 A69-26956

Error correction for correlation coefficient between satellite data of earth radiation intensity and satellite vision field shift
14 p2435 A69-29043

Automatic control circuit zero drift compensation during external disturbance, using algorithm for computer minimizing of losses caused by control and response inaccuracy
14 p2425 A69-29140

Optimum time for telemetry data transmission by system using feedback combined with error correcting codes
14 p2412 A69-29428

Bearing errors reduction in vertical loop HF direction finders for ionospherically propagated signals in dual channel system
14 p2413 A69-29493

Structural influence coefficients from vibration test modes and frequencies, eliminating errors by Gram-Schmidt orthogonalization
16 p2872 A69-31916

Electromagnetic interference correction for airborne telemetry, illustrating actual and simulated data for interfering source signatures identification
16 p2754 A69-32575

Data distortion elimination by improved superimposing of sinusoidal audio frequency signal on DC voltage of automatic Langmuir probe second derivative plot-
17 p2970 A69-32855

Ammonia jet device to stabilize telecommunication satellites consisting of electric heating element, ejection nozzle and thermal screens
17 p3018 A69-33236

Integrated trajectory error display /ITED/ for flight path control of helicopters and VTOL, describing principles governing display synthesis
[AHS PAPER 314] 17 p3001 A69-33541

Analog correction method to suppress pilot maneuver effects during analysis of aircraft accelerations induced by atmospheric turbulence
[ICAS PAPER 68-39] 17 p2901 A69-33590

Temperature correction procedures for line-blanked model atmospheres modified, noting effect on convergence to flux constancy
17 p3039 A69-33730

Observer theory application to hybrid inertial navigation systems, discussing error estimation and correction, real time mechanization, eigenvalues, etc
17 p3003 A69-34099

Computer aided design of machines with custom LSI arrays, describing error detection procedures and MOS logic circuits
17 p2942 A69-34121

Taylor series expansion used in correcting quantized digital coefficient errors in hybrid feedback control system
18 p3111 A69-34687

Controlled vehicle disturbed trajectory multiple correction, considering constrained control or limited accessible coordinates for observations
18 p3174 A69-35316

Meteorological corrections of meson megatelescope data based on hourly ground-level pressures and temperatures, considering vector and regression analyses
19 p3308 A69-35991

Mathematical basis for inertial vertical gyro development, considering Schuler conditions fulfillment with integral position correction
19 p3311 A69-36193

Buffer shift register with feedback control during tape recorder playback to obtain variable delay to compensate for recorder time base error
19 p3312 A69-36284

Surrounding masses gravitational field effect on gravitational constant determination by torsional oscillations method, considering oscillation amplitude stability to eliminate errors
19 p3374 A69-36468

Red leak corrections for UV filter on color UV indices for stars of various spectral types using wintereddened response curve
19 p3426 A69-36566

Contactless correcting devices based on magnetic moments for automatic control
21 p3685 A69-38453

Satellite phase and aberration corrections in processing photographic observations for geodetic purposes
21 p3720 A69-38606

Control system generating compensating reactions for correcting trajectory deviations due to uncontrollable random factors, discussing linear automatic control system optimization
21 p3770 A69-38853

Digital computers used in error calculation in calibration curves of turboengines and other pneumatic devices
21 p3724 A69-39100

Electromagnetic attitude control system for Lincoln Experimental Satellite 5 in near-synchronous equatorial orbit, noting onboard error detection in closed control loop
21 p3827 A69-39755

Temperature control instrumentation accuracy in terms of static errors and dynamic errors minimizing costs
22 p3954 A69-40037

Error correction of strain gage/cement combination reading relaxation under prolonged steady loading at elevated temperature
22 p4042 A69-40313

Algebraic decoding techniques, discussing channel models, errors correction, hardware and software, etc
23 p4119 A69-41746

Wideband telemetry recording error compensator for reducing flutter and interchannel time-base error in magnetic tape instrumentation
23 p4137 A69-41775

Surface accuracy of large diameter radio telescopes maintained by uncoupling reflector surface from backup structure, using active compensation
23 p4149 A69-42136

Corrections for eliminating anomalous skin effect on IR emissivity for Ag, Cu, Au and Al
23 p4177 A69-42212

Ionospheric range difference errors after correction for position fixing from satellite, considering elevation angle, latitude, day time, spatial and time electron content correlation
23 p4128 A69-42505

Iterative and vectoral methods for correcting computed direction cosine matrix errors
23 p4134 A69-42543

Correction coefficients for time response of hybrid control systems with digital feedback elements containing quantized coefficients
24 p4293 A69-43302

Scale error correction technique for structural impact modeling using dissimilar materials, involving permanent deformation of spherical caps impacted into liquids
24 p4406 A69-43692

ERROR DETECTION CODES

Book on error detecting logic for digital computers covering error detection codes, logic circuits, checkers in data paths, etc
02 p0212 A69-11453

Book on information coding and transmission and error detection and correction
04 p0558 A69-15066

L-step orthogonalization of Bose-Chaudhuri-Hocquenghem codes
06 p0903 A69-17532

Linear recurring sequences over finite fields, discussing application to error correcting codes
06 p0948 A69-17863

Binary block codes for correction of substitution and synchronization errors
09 p1452 A69-21316

Error control coding noting cyclic codes, binary shift registers, shift register circuits, encoding and decoding
09 p1461 A69-21893

Decoding procedure for error locating binary code indicating location of single subblock containing errors in code word, employing feedback shift registers
11 p1857 A69-24549

Airborne computer controlled data acquisition system for real time fault detection and isolation in avionics
11 p1843 A69-25082

Cross correlation and probability metric in coded sequential detection telemetry system, giving optimum parameters, overflow and error probabilities using computer simulations
19 p3273 A69-36266

Spacecraft onboard computer for prelaunch targeting constants verification through checksum equation and error detection scheme, using generated number sequences
[AIAA PAPER 69-946] 22 p3974 A69-40329

Tree codes for memoryless time discrete sources with bounded fidelity criterion
24 p4284 A69-42720

Algorithm for constructing random error correcting convolutional codes
24 p4284 A69-42723

ERROR FUNCTIONS

Error reduction in identifying pilot describing function from flight test data by shifting input signal by pilot delay time in simulated computer model
02 p0202 A69-11950

Mean error rates in microwave PCM systems with wave distortion due to multipath propagation
02 p0208 A69-12307

Closed form solution for two input correlator processing gain with error function transfer characteristics and operating in Gaussian environment
03 p0403 A69-13253

Error probability for discriminator detection of wideband PCM/FM, considering IF bandwidth/bit duration product and low pass filtering effect
08 p1271 A69-19864

Signal correlation functions measurement errors due to randomly fluctuating delay, investigating additive and multiplicative noise with periodic and random signals
08 p1296 A69-19923

Tabulation of definite and indefinite integrals of products of error function with elementary and transcendental functions
12 p2121 A69-26399

Error function for boundary methods
21 p3755 A69-39008

ERROR SIGNALS

Error reduction in identifying pilot describing function from flight test data by shifting input signal by pilot delay time in simulated computer model
02 p0202 A69-11950

Specifying electrical isolation and error signals suppression due to presence of common mode voltage in passive signal handling and conditioning equipment
10 p1654 A69-23272

Control moment gyro /CMG/ and use in space vehicle attitude control system, emphasizing control laws [AIAA PAPER 67-589]
12 p2129 A69-26777

Nonlinear control systems error signals convergence to steady states in frequency domain, applying step or ramp functions to single feedback system
13 p2237 A69-27188

Received signal phase angle error probability in coherent PSK system in Gaussian noise and interference
13 p2219 A69-27665

Omega/VLF transmission range rate measurements for satellite Doppler navigation to provide velocity and location data, noting propagation error
14 p2479 A69-29857

Phase locked loop with flip-flop error detector compared to analog loop, discussing signal to noise ratio
17 p2931 A69-34115

Closed loop target tracking system generating error signals for aligning target with tracking axis
19 p3310 A69-36063

ERRORS

NT INSTRUMENT ERRORS
NT PHASE ERROR
NT PILOT ERROR
NT POSITION ERRORS
NT RANDOM ERRORS
NT RANGE ERRORS
NT ROOT-MEAN-SQUARE ERRORS
NT TRUNCATION ERRORS
NT VELOCITY ERRORS

Averaging error of system of nonlinear differential equations with time periodic right-hand sides
04 p0624 A69-15097

Thin foil heat flux sensor for radiative and convective heating rates over wide range and dynamic response, noting error mechanisms, calibration and accuracy
04 p0602 A69-15426

Computer program reliability enhancement, discussing significance of underestimation
08 p1278 A69-19845

Straight line method for boundary problems solutions with errors for partial differential equations
22 p3976 A69-41110

ERYTHROCYTES

NT RETICULOCYTES
In vivo hyperbaric hyperoxia effect on erythrocytes unsaturated fatty acid composition alterations of tocopherol deficient mice
03 p0375 A69-14070

Hemoglobin diffusion influence on oxygen uptake and release by red cells solved by calculus of finite differences
05 p0707 A69-15677

Structural and functional changes in cells as result of freezing of muscular tissue or suspension of erythrocytes
10 p1642 A69-23117

Early disturbances in active migration of potassium 42 ions in irradiated erythrocytes in rats, showing relation between influx and energy exchange in cells
10 p1647 A69-23966

High positive g sub x acceleration effects on red cells destruction rate, measuring endogenous CO production of Gemini astronauts
17 p2908 A69-33176

Pt electrode as detector of red blood cell oxygenation, attempting Fc value dependence on flow velocity determination
20 p3480 A69-38283

Oxygen replacement rate by CO from combination with oxyhemoglobin in cells at various temperatures
21 p3650 A69-38385

Erythroblasts fractionating method based on size, density and resistance of immature erythroblasts which change during maturation
22 p3877 A69-40761

- Oxygen steady state transfer across thin layers of centrifuged erythrocytes at 37 degrees C before and after hemoglobin saturation with CO
23 p4093 A69-42064
- Human blood viscosity measurement over wide range of shear rates, obtaining rheological data, suggesting osmotic red cell crenation role
23 p4095 A69-42078
- Microrheological property of blood measured with microglass fiber viscosimeter, noting sensitivity to intercellular friction of erythrocytes
23 p4098 A69-42100
- ESAKI DIODES**
U TUNNEL DIODES
- ESCAPE CAPSULES**
Three valve manifold for five self righting inflation bags in escape capsule on F-111, providing one directional flow and pressure relief and shutoff
20 p3467 A69-38185
- ESCAPE SYSTEMS**
Emergency escape and personnel recovery systems including F-111 explosive system, midair deployed buoyancy aerostat and fly-away flexible wing rotor
15 p2551 A69-30853
Descent device for emergency egress from jumbo jets based on centrifugal brake, including test data on C-5 fuselage section
19 p3255 A69-36146
Flexible parawing lifting decelerator research data from wind tunnel and flight tests, noting manned space vehicle recovery and aircraft escape systems [AIAA PAPER 68-967]
24 p4254 A69-43715
- ESCAPE VELOCITY**
Biological systems response to inertial environment, escape from earth gravity, planetary gravity and artificial gravity
06 p0872 A69-17011
Spacecraft range control algorithm during reentry at parabolic velocity into atmosphere with varying parameter distributions
13 p2355 A69-27682
Tabulation of basic solar system data and formulas concerning trajectory length, escape velocity, orbits, etc
16 p2856 A69-32074
Stars kinetic energy and escape rates from isolated cluster with arbitrary stellar mass distributions, assuming spherical symmetry and velocity distribution isotropy
17 p3038 A69-33721
Parking orbit optimal orientation for minimal impulsive maneuvers total velocity increment in three dimensional capture-escape mission [AIAA PAPER 69-918]
21 p3808 A69-39347
- ESCHERICHIA**
Escherichia coli detection and differentiation from other bacteria by direct gas chromatographic analysis of culture media
03 p0382 A69-13550
Substrate and subunit interactions influence of beta 2 protein of Escherichia coli tryptophan synthetase on fluorescence properties of pyridoxal phosphate prosthetic groups
04 p0553 A69-15304
Escherichia coli WWU multiauxotrophic revertants with nonsense suppression, noting role in aberrant morphology and in catabolizing thymidine for energy and carbon
07 p1069 A69-19503
Escherichia coli B/r survival in high vacuum at different temperatures irradiated with UV or X rays tested as colony forming ability
15 p2557 A69-31388
Escherichia coli B/r cells plasmolyzed in sucrose observed under phase contrast, noting plasmolysis reduction in ions presence
19 p3257 A69-35973
DNA polymerase from Escherichia coli, discussing physical and chemical properties of enzyme and polypeptide chain consistency
22 p3898 A69-41070
Chemical modifications effects on Escherichia coli, DNA polymerase, including Hg atom addition to sulfhydryl group of enzyme
22 p3898 A69-41071
Properties, relative magnitudes and relationship of pyrophosphate exchange reactions catalyzed by DNA polymerase from Escherichia coli
22 p3898 A69-41072
Exonuclease function of DNA polymerase from Escherichia coli, discussing hydrolysis of polydeoxyribonucleotides and resistancy of oligonucleotides
22 p3898 A69-41073
- Deoxyribonucleoside triphosphate substrate binding to Escherichia coli DNA polymerase, conducting equilibrium dialysis
22 p3898 A69-41074
- ESG [GYROSCOPES]**
U ELECTROSTATIC GYROSCOPES
- ESOPHAGUS**
Increased gravitational stress effects on esophageal sphincter pressures and gastroesophageal reflux in rhesus monkeys, noting cardia competence
06 p0874 A69-17838
- ESRO 1 SATELLITE**
Esro 1 satellite program management, discussing scientific mission, structure, tracking system and history
13 p2355 A69-27360
Esro 1/Aurorae project for ionospheric phenomena connected with incoming protons and electrons, describing orbit and alignment with geomagnetic field
13 p2356 A69-27747
Auroral phenomena investigation by ESRO 1 satellite, measuring particle flux arriving at auroral height
13 p2381 A69-27748
Esro 1 communication system and telemetering system compared to ESRO 2
13 p2220 A69-27749
Esro 1 project management and organization, discussing cost control, time saving, program evaluation and review system /PERT/, etc
13 p2382 A69-27750
Ground station network and facilities for control of and acquisition and processing data from ESRO 1 satellite
13 p2220 A69-27751
Auroral luminosity determination by two photometers on ESRO 1 satellite
13 p2253 A69-27752
Esro 1/Aurorae scientific satellite for ionospheric phenomena observation, discussing management structure and development process
15 p2702 A69-31080
Esro 1/Aurorae satellite for Arctic ionosphere and aurorae observation, discussing electrons and protons measurements and auroral photometry
15 p2702 A69-31081
Esro 1 satellite design coordination, assembly and tests
15 p2702 A69-31082
Esro 1 satellite centralized control system, discussing housekeeping system responsible for task execution in connection with power supply
15 p2702 A69-31083
Esro 1/Aurorae satellite telemetry system constraints, discussing encoder, pulsed operation and integrated circuit assembly
15 p2702 A69-31085
Esro 1 and 2 satellites onboard remote control system, discussing tone digital standard code and equipment design features
15 p2702 A69-31086
Magnetometers role in Aurorae satellite attitude stabilization, discussing operation principle, characteristics and performances
15 p2611 A69-31087
- ESRO 2 SATELLITE**
International Radiation Investigation Satellite /IRIS/ mission, structural design, power supply and control systems
01 p0162 A69-11101
Scientific mission of ESRO 2/IRIS satellite, study of X rays and particles from sun and galaxy and primary cosmic ray electron measurement
01 p0163 A69-11102
Transmitting systems of ESRO 2/IRIS satellite for ground station contact, discussing telemetry system, mission requirements and telecontrol
01 p0034 A69-11103
Esro 2/IRIS satellite launching checkout, count-down and breakdown of operations
01 p0163 A69-11104
Status of European Space Operations Center /ESOC/ with ESRO 2/IRIS launching
01 p0163 A69-11105
Orbiting ESRO 2/IRIS energy measuring experiments, satellite stabilization, power source, communications and data recovery
01 p0156 A69-11108
Esro 1 and 2 satellites onboard remote control system, discussing tone digital standard code and equipment design features
15 p2702 A69-31086
- ESRO SATELLITES**
NT HEOS A SATELLITE
NT HEOS SATELLITES
- ESRO satellites power supply design, operation and characteristics
05 p0829 A69-15919
Data handling during ESRO satellite testing and launching, describing checkout equipment and programming of satellite computers
05 p0727 A69-16771
European Space Research Organization projects including satellites and sounding rocket launchings for various missions
12 p2175 A69-26922
Power supply subsystem for TD1/TD2 satellites with solar cells, discussing design including standby battery for solar eclipse periods
13 p2209 A69-28481
Short term plan of European electronic component selection for ESRO satellite without established guaranteed failure rate
15 p2624 A69-30823
ESRO Aurorae satellite telecommunication system, detailing information nature, PCM telemetry and remote control system standard
15 p2702 A69-31084
TD-1 astrophysical satellite and future ESRO projects, considering HEOS-0A2 and TD-2
17 p3051 A69-34217
ESRO Large Astronomical Satellite /LAS/ observatory in orbit, discussing operation, design and instrument settings in scientific package
18 p3208 A69-34793
- ESSA SATELLITES**
Satellites in meteorological service, describing TOS, ESSA and Nimbus satellites operation methods
08 p1409 A69-19960
TIROS global weather satellite system performance, reviewing TIROS and ESSA satellites, APT camera and ground stations and projected TIROS M/ITOS satellite
10 p1722 A69-23145
Tiros-ESSA satellite operations, describing first and second generation systems
19 p3433 A69-36909
- ESTERS**
NT ACRYLATES
NT CELLULOSE NITRATE
NT CHLOROFORMATE
NT ISOCYANATES
NT LACTATES
NT LEAD ACETATES
NT NITROGLYCERIN
NT PETN
NT POLYCARBONATES
NT POLYESTERS
NT POLYETHYLENE TEREPHTHALATE
NT URETHANES
Analytical, IR absorption and polarographic analysis of cyclic niobium /V/ and tantalum /V/ esters
11 p1832 A69-24575
Physicochemical and operational properties of trimethylol propane esters as lubricating oils under static and dynamic conditions
12 p2103 A69-27090
Reaction kinetics between hydrazine and esters in benzene solution at 55° C, using amides as catalytic agents
14 p2409 A69-29033
Oxygen concentration effects on oxidation of synthetic paraffinic and type II ester lubricants determined from ball bearing tests at 400 and 450 degrees F
18 p3149 A69-35177
Sequence preparation of protected peptide polymer bond with anion exchange resin using solid phase transesterification
24 p4279 A69-42713
Transesterification of amino acid peptide alkyl and fatty acid esters by treatment with anion-exchange resin
24 p4280 A69-43513
- ESTIMATES**
NT COST ESTIMATES
A priori and a posteriori estimates of direct methods accuracy in solving linear algebraic equations
01 p0105 A69-10727
Continuous time nonlinear dynamical system states variables estimated suboptimally from discrete noisy measurements with second order nonlinear filter, deriving dynamical equations
06 p0904 A69-17939
Postselection estimation of component reliability in multicomponent systems, considering cases of binomial and exponential distributions of random variables
08 p1322 A69-21099
Distribution function of SNR from coherent optimal estimate of signal amplitude
15 p2564 A69-30149

ESTIMATING

- Chetaev /A, lambda/ estimates of approximate integrations of system of ordinary differential equations, analyzing stability with aid of Liapunov functions
15 p2644 A69-30664
- Accuracy and variance of nonergodicity estimates for random processes associated with radiophysical applications
15 p2582 A69-30946
- System estimation methods compared for rational boundaries of lower confidence limit, discussing variables/attributes error propagation
15 p2722 A69-31135

ESTIMATION

- Simultaneous estimation of parameters in multiple equation regression model arising from radioactive tracer experiments using compartmental models
01 p1006 A69-10926
- Bayes estimator in decision directed adaptive detection problem, noting allowance for decision errors
05 p0740 A69-16583
- Optimal estimation of sampled stochastic process with finite state unknown parameters
06 p0901 A69-17362
- Optimal estimation of conditional mean of posterior probability density function in multistage nonlinear filters, using Monte Carlo techniques and Bayes theorem
10 p1667 A69-24039
- Adaptive optimal estimation of sampled stochastic process with finite state unknown parameters, using separation technique
11 p1858 A69-24935
- Estimation system distinction from adaptive system, discussing network of adaptive estimation systems
11 p1858 A69-24937
- Runge-Kutta type method truncation error estimation, discussing validity conditions, evaluation processes and numerical tests
15 p2644 A69-30672
- Book on estimation theory and applications covering stochastic processes, linear estimators and recursive formulations
16 p2764 A69-32386
- Automatically controlled dynamic systems reliability estimation; in terms of failure probability illustrated with autopilot-aircraft case
17 p3001 A69-33144
- Ammonium perchlorate melting point estimate taking into account theory of corresponding states encompassing two sets of experimental independent data
20 p3585 A69-37217
- Data acquisition amount estimation technique for vertical panoramic sounding of ionosphere
20 p3492 A69-37692
- Nonlinear estimation with noisy data, considering least squares fit, sequential /Kalman/ estimate and iterated sequential scheme
21 p3686 A69-39370
- Nonlinear filter for optimal estimation of mean, covariance and third central moments of system, noting simulation tests stability for orbital navigation [AIAA PAPER 69-852]
21 p3686 A69-39380
- Gaussian type density estimates by representing unknown density in terms of convolution expansion of Gaussian probability density and arbitrary distribution, discussing convergence rates
21 p3756 A69-39499
- General linear state estimation from algebraic viewpoint without probability theory concepts, establishing least squares parameter estimation
23 p4182 A69-41880

ESTIMATORS

- Orthogonal projection derived equation to optimally estimate state of nonstationary linear discrete systems with time delay, developing Kalman type filter
09 p1473 A69-22437
- Asymptotic stability of discrete homogeneous linear minimum-variance estimation formulas
11 p1860 A69-25449
- Optimal linear recursive estimators for uncertain observation, considering false alarm probability
20 p3485 A69-36922
- Optimal explicit method for parameters estimation not restricted to linear Gaussian problem derived in canonical form [AIAA PAPER 69-947]
22 p3975 A69-40330
- Optimal scheme of combining moment estimators set derived for computational simplicity and asymptotic efficiency
24 p4342 A69-43704

ETCHANTS

- Structural imperfections of CdSb single crystals undoped and doped with tellurium and indium noting etching techniques, grain boundaries and impurities
11 p1938 A69-25030

Nital etchant and sodium bisulfite stain for morphology of quenched dilute alloy Fe-Ni martensite
13 p2282 A69-28166

ETCHING

- Stacking faults in Ge epitaxial layers revealed by etching reagents and X ray diffraction with photographic recording
02 p0297 A69-11880
- Electrolytic marking process for aircraft component identification without use of stamping or engraving
02 p0253 A69-12065
- Etching techniques for revelation and viewing of fossil charged particle tracks in meteoritic and terrestrial minerals
02 p0245 A69-12569
- RF sputter etching of microcircuits and components
04 p0606 A69-14874
- Selective etching process for microminiaturization of special circuits for aerospace
05 p0736 A69-16753
- Selective etching technique in study of dislocations in epitaxial layers of gallium arsenide
06 p0981 A69-17891
- Etch pits behavior during diffusion and rediffusion of copper in low dislocation crystals of gallium arsenide, demonstrating vacancy nature
11 p1937 A69-25029
- Thin foil preparation technique for transmission electron microscopy and selected etch pitting technique for CoO single crystals
12 p2112 A69-25944
- Etching, spray etching and photo-resist methods for producing CrNi steel heating elements for propeller deicing
12 p2102 A69-26370
- Dislocations observations in fracture study of crystals, considering etching, decoration technique, X ray topography and diffraction electron microscopy
13 p2316 A69-27223
- Polishing-etching cell permitting continuous sample surface observation for use with inverted stage microscopes
13 p2281 A69-28156
- Anodic stain etching technique for carbide precipitates of niobium-base alloy Cb 132, noting X ray diffraction
13 p2282 A69-28162
- Tungsten surfaces with high work functions generated by electrochemical etching, discussing effects of heat treatment in vacuum
14 p2506 A69-29267
- Flux grown magnetic garnet crystal internal defects analyzed by etching and Lang X ray transmission topography, revealing tubular structural deviations
16 p2825 A69-31692
- Alpha alumina whiskers grown by vapor reaction examined by X ray microtopography and etching
16 p2802 A69-32341
- Crystallization front topography and stratified structure of melt extracted n-type GaAs single crystals from anodic etching method
20 p3582 A69-37013
- Germanium single crystals etching with water vapor and hydrogen sulfide in hydrogen flow system, studying concentration, pressure and temperature effects on surface reactions
22 p3970 A69-40737

ETHANE

- Molar heat and entropy of adsorption and activity coefficient of adsorbed phase for methane-ethane-silica gel system
10 p1652 A69-23370
- Ethylene oxide and ethane low pressure fuel-rich flames mass spectrometry, analyzing composition and temperature profiles and OH radical role
11 p1831 A69-24478
- Barrier to internal rotation from PMR spectrum for 1, 2-disubstituted ethanes, studying vicinal coupling parameters dependence
12 p2132 A69-25987
- Nucleate boiling burnout heat flux data for ethane, ethylene and ethane-ethylene mixtures at various pressures, discussing applicability of Noyes equations
15 p2671 A69-31118

ETHERS

- NT POLYPHENYL ETHER
- Lewis acidity of alanes, discussing interactions of trimethylalane with amines, ethers and phosphines
07 p1074 A69-18630
- Methyl alcohol, ether and acetone vapors decomposition in microwave discharge, obtaining H and CO in addition to solid polymeric films
22 p3895 A69-40103

ETHYL ALCOHOL

- General aviation accidents and hazards presented by drugs, ethyl alcohol, pesticides and carbon monoxide
07 p1068 A69-19435
- Isothiocyanates and phenyl isocyanate reaction with hydrazinoethanol and hydrazinoethyl hydrogen sulfate
16 p2747 A69-31808
- Alcohol and drug intake effects on drivers control of motor vehicles, describing postrotatory nystagmus test for toxicity measurement
21 p3652 A69-38791
- Pilots and automobile drivers functional impairment due to alcohol and drugs
21 p3663 A69-38792
- Cavitation flow of water and ethyl alcohol in venturi tube, noting effect of varying vapor concentration and thermodynamic properties
21 p3696 A69-39101
- Alcoholic hangover effects on human balance system from flying demands viewpoint, discussing ocular-vestibular system disturbances
23 p4089 A69-41817

ETHYLENE

- Nucleate boiling burnout heat flux data for ethane, ethylene and ethane-ethylene mixtures at various pressures, discussing applicability of Noyes equations
15 p2671 A69-31118
- Low pressure ethylene decomposition on high temperature W ribbon surface
19 p3265 A69-36729
- Low pressure ethylene decomposition on high temperature Re ribbon surface
19 p3266 A69-36730
- Oxygen influence on low pressure ethylene decomposition on high temperature tungsten and Re ribbons surface
19 p3266 A69-36732
- Crossed beam apparatus /evatron/ for studying energy spectra of crossed positive ethylene ion beams and neutral ethylene molecule beams
24 p4280 A69-43813

ETHYLENE COMPOUNDS

- Aluminum corrosion and inhibition mechanisms in ethylene glycol/water solutions, using controlled powder immersion tests
02 p0265 A69-11895
- Hypergolic filling materials for solid fuels with hybrid propellant combinations, discussing ignition and combustion of ethyleneimine derivatives
10 p1753 A69-24023
- Flame velocities of stable premixed tetrafluorethylene-oxygen mixture flames measured with bunsen-cone method
11 p1940 A69-24485
- Aluminum corrosion in ethylene glycol-water systems, discussing protection mechanisms of adsorption-type inhibitors and additives effects on corrosion rate
14 p2466 A69-29932

ETHYLENE OXIDE

- Ethylene oxide sterilization rate dependence on temperature, gas concentration, relative humidity and medium surrounding microorganisms
05 p0707 A69-15940
- Formic acid catalytic action on sterilizing effectiveness of ethylene oxide
05 p0713 A69-15945
- Ethylene oxide and ethane low pressure fuel-rich flames mass spectrometry, analyzing composition and temperature profiles and OH radical role
11 p1831 A69-24478
- Fuel resistant elastomers evaluated for seal compounds for low temperature capability, noting epichlorohydrin-ethylene oxide as promising sealant
19 p3356 A69-35534

ETIOLOGY

- Valsalva maneuver produced abrupt onset of ptosis and proptosis caused by ethmoidal air cell rupture, discussing etiologies
17 p2909 A69-33186
- In-flight illnesses in French Air Force, emphasizing psychological failures in etiology
21 p3666 A69-39270

EUCLIDEAN GEOMETRY

- NT ANGLES [GEOMETRY]
NT BRAGG ANGLE
NT BREWSTER ANGLE
NT CARTESIAN COORDINATES
NT CHORDS [GEOMETRY]
NT CIRCLES [GEOMETRY]
NT CYCLOIDS
NT ELLIPSES
NT GREAT CIRCLES
NT HYPERBOLAS

NT LINES [GEOMETRY]
 NT LOCI
 NT MERCATOR PROJECTION
 NT OBLATE SPHEROIDS
 NT OCTAHEDRONS
 NT PARABOLAS
 NT PARALLELEPIPEDS
 NT PARALLELOGRAMS
 NT POINTS [MATHEMATICS]
 NT POLYHEDRONS
 NT PROJECTIVE GEOMETRY
 NT PROLATE SPHEROIDS
 NT RADII
 NT RECTANGLES
 NT S CURVES
 NT SPHEROIDS
 NT SQUARES [MATHEMATICS]
 NT TANGENTS
 NT TETRAHEDRONS
 NT TORUSES
 NT TRIANGLES
 NT TRIGONOMETRY

Bifurcation of closed orbits from equilibrium points of autonomous differential system
 02 p0281 A69-12133

Second order elliptical operator for m-dimensional Euclidean space with open region bounded by closed surface
 03 p0456 A69-13604

Bounded and perfectly conducting object embedded in Euclidean 3-space, discussing electromagnetic inverse scattering problem
 05 p0719 A69-15929

Majority logic decoding of Euclidean or projective geometry codes in two steps
 06 p0891 A69-17867

Boundary value problems solutions for quasi-linear elliptic and parabolic equations of arbitrary order applied to nonlinear differential equations
 10 p1717 A69-22809

Perturbations of Volterra integral equation with vectors in n-dimensional real or complex Euclidean space, comparing solution with linear system solution
 11 p1909 A69-24886

Instability criterion for motion differing from criteria of Liapunov and Chetaev
 18 p3174 A69-35317

Polar coordinates in Euclidean space applied to theory of satellite moving in gravitational field of spherically symmetrical body, introducing equipotential surfaces
 19 p3397 A69-35610

Stability criteria for integral manifold formed by intersection of hypersurfaces in Euclidean n-dimensional space
 21 p3770 A69-38850

Integral transformation applicability to inverse problems concerning interaction potential energy between particle pairs in n-dimensional Euclidean space
 23 p4182 A69-41960

EUGLENA
 Euglena gracilis grown heterotrophically, investigating respiratory physiology as function of glucose, acetate or ethanol growth supporting carbon source
 10 p1647 A69-24186

Continuous culture device for controlled growth of Euglena gracilis
 15 p2555 A69-30445

EULER BUCKLING
 Thin walled channel columns section stability analyzed in terms of overall Euler and local buckling
 13 p2361 A69-27440

EULER EQUATIONS OF MOTION
 Gyroscope with rotational symmetry subjected to random input torques analyzed by Euler equation of motion
 01 p0079 A69-10236

Solid body motion about fixed point representable by two dimensional motion of two points on complex plane
 01 p0116 A69-10356

Euler-Lagrange relationship from equations of motion of tagged particle in turbulent velocity field consisting of random dispersive waves
 01 p0121 A69-11202

Differential equations of rotational motion of systems of rigid bodies in gravitational field derived with Lagrange equation
 06 p0957 A69-17130

Euler rotational equations for bodies with variable inertia tensor subjected to extreme variations of mass distribution and mass loss
 09 p1616 A69-21956

Existence of motions of second type in explicit self similar strong shock solutions of Euler equations when velocity is linear function of coordinate
 10 p1680 A69-23789

Invariant transformation of Euler equations of motion for plane steady flows of perfect compressible fluid
 11 p1877 A69-25739

Dynamic meteorology quasi-stable problems solved using sequential approximations solution for barotropic model of Euler equations
 14 p2476 A69-29821

Coupling conditions by distinct equations for two laminar flow regions, studying near wake and considering Euler, Navier-Stokes and Prandtl correlations [ONERA-TP-738]
 19 p3299 A69-36649

Coordinate transformation of Euler equations governing precession and nutation of self gravitating bodies of viscous fluid in inertial coordinates
 21 p3797 A69-38539

Euler equation in variational problems for optimized process described by ordinary differential equations, deriving final extremal relationship
 21 p3829 A69-39825

Spacecraft spherical motion about mass center under inertial force using Euler differential equations
 21 p3830 A69-39838

Eulerian equations for precession and nutation of self gravitating fluid globes of arbitrary structures in inertial coordinates, discussing coplanar case, tidal breathing, etc
 22 p4030 A69-40904

Helicopter rotors trailing vortices by flow visualization, comparing Euler and Runge-Kutta iterative solutions
 23 p4150 A69-41376

Absolute atmospheric kinetic energy, comparing equations deduced from Euler equations with equations deduced from equations of motion for inertial system
 24 p4345 A69-43151

EULER-LAGRANGE EQUATION
 Euler-Lagrange relationship from equations of motion of tagged particle in turbulent velocity field consisting of random dispersive waves
 01 p0121 A69-11202

Particle motion, deriving Lagrangian formalism equivalent to Schroedinger equation for random motion theory
 07 p1182 A69-19455

Electron anomalous magnetic moment effect on nonlinear Lagrangian of electromagnetic field, deriving additional nonlinear corrective term
 08 p1353 A69-19781

Perturbing body influence on motion near triangular Lagrangian solutions of restricted elliptical three body problem applied to earth-moon system under solar perturbations
 10 p1779 A69-23612

Hamilton principle for inviscid compressible fluid in Euler coordinates, analyzing shortcomings found in variational principles and model in Lagrangian coordinates
 11 p1875 A69-25483

Encke type analytical-numerical integration for solving differential equations of modified set of Lagrange planetary equations, obtaining satellite ephemeris for orbit prediction [AIAA PAPER 69-908]
 21 p3807 A69-39340

Motion and stability of rotating connected two body space station satellite system, developing Lagrangian equations of motion and optimizing damping system parameters [AIAA PAPER 69-919]
 21 p3820 A69-39349

Cylindrical shells vibrations using Lagrangian based on Fluegge system of stress-strain relations
 22 p4039 A69-39924

EUROPA LAUNCH VEHICLES
 Solid, liquid and advanced propulsion techniques in France, discussing Diamant program and Europa booster
 02 p0334 A69-11919

EUROPA 1 LAUNCH VEHICLE
 ELDO Europa 1 Fairings Jettisoning System and explosive devices, discussing heat shield structure and safety regulations
 10 p1635 A69-23027

Europa 1 booster supplementing with perigee-apogee system for development of Europa 2, noting payload launching capability into 24-hr circular orbit
 15 p2671 A69-31051

Europa 1 first stage attitude control system adaptation to Europa 2 requirements, discussing design modifications and improvements and inertial guidance system introduction
 16 p2866 A69-31726

Vernier motor for Europa 1 rocket third stage, discussing component design, system performance and fuel composition
 17 p3018 A69-33328

ELDO booster/EUROPA 1/ third stage management and construction problems
 17 p3050 A69-33701

Pyrotechnical gas generator performance tests during Europa 1 rocket second and third stage separation, including generator design, ground and flight tests
 23 p4224 A69-42153

EUROPA 2 LAUNCH VEHICLE
 Satellite communications with emphasis on European programs, discussing synchronous satellites, Europa 2 rocket and Saros and Symphonie projects
 02 p0207 A69-11910

Europa 1 booster supplementing with perigee-apogee system for development of Europa 2, noting payload launching capability into 24-hr circular orbit
 15 p2671 A69-31051

Europa 1 first stage attitude control system adaptation to Europa 2 requirements, discussing design modifications and improvements and inertial guidance system introduction
 16 p2866 A69-31726

Orbital and attitude control tests for PAS /two stage perigee-apogee synchronous satellite/ in conjunction with booster Europa 2, discussing functional configuration
 17 p3048 A69-33238

EUROPA 3 LAUNCH VEHICLE
 Europa 3 rocket design, comparing 2 ton geostationary satellites and 700 kg satellite conceptions
 17 p3045 A69-33095

EUROPE
 Multiengine helicopter scheduled passenger service operations in Europe
 11 p2004 A69-24378

Air transport prediction for West Europe by 1980
 11 p2004 A69-25216

Axial counterweight lateral support system with ternary symmetry for European Southern Observatory telescope mirror
 12 p2058 A69-26419

U.S.-Europe air traffic, attributing European lag to dense air route duplication, load factors, etc
 13 p2381 A69-27338

Spatial geodesy results from European data, discussing accuracy of geodetical European network and geocentric coordinate computation
 15 p2601 A69-31369

Book on competition in North Atlantic commercial air transport covering passengers, freight and mail from supply, demand and market point of view
 16 p2881 A69-31866

Geomagnetic normal field of vertical component for Central Europe, discussing influence of local factors on observational data
 16 p2782 A69-32461

Daily European weather surveys based on meteorological satellite pictures transmitted during third quarter 1967
 17 p3000 A69-33769

Daily European weather surveys based on pictures transmitted by satellite during fourth quarter 1967
 17 p3000 A69-33778

Relative technological standing of U.S. and Europe, discussing meaning and existence of technology gap
 17 p3076 A69-34040

Supersonic transport aircraft impact on air traffic control in Eurocontrol area, discussing climb, acceleration, cruise and descent
 19 p3370 A69-36653

Eurocontrol Experimental Data Processor for automation in air traffic control, discussing system size configuration and environment
 19 p3280 A69-36654

EUROPEAN SPACE PROGRAMS
 British contributions to communication satellite earth station technology covering antennas, low noise amplifiers, traveling wave tubes and threshold extension demodulators [UN PAPER 68-95843]
 01 p0054 A69-10507

San Marco project, discussing Italian Space Commission and NASA cooperation, equatorial range concept and development [UN PAPER 68-95862]
 01 p0180 A69-10518

Diapason satellite geodetic results concerning measurement accuracy, terrestrial potential models and station synchronization
 01 p0065 A69-10543

Status of European Space Operations Center /ESOC/ with ESRO 2/IRIS launching
 01 p0163 A69-11105

Collection of papers on French space effort covering space sciences and applications, vehicles and boosters, launch sites, tracking, international cooperation, etc
02 p0315 A69-11901

French solar research program, emphasizing photosphere-chromosphere transition zone
02 p0316 A69-11905

French radio astronomy, presenting sky background radiation and solar emission results from Rubis 02 and 04 rockets
02 p0316 A69-11908

French applied and basic research in space biology including manned space flight, deep space problems, weightlessness and cosmic heavy ion radiation effects
02 p0199 A69-11909

Satellite communications with emphasis on European programs, discussing synchronous satellites, Europa 2 rocket and Saros and Symphonie projects
02 p0207 A69-11910

Satellites use in French space meteorology, discussing evolution, achievements, Eole project, etc
02 p0275 A69-11911

French geodetic work with aid of artificial satellites, describing equipment, mounting, observation technique and laser telemetry experiments
02 p0228 A69-11913

Balloon, rocket probe and satellite payloads, noting French contributions and CNES role
02 p0333 A69-11914

French /LRBA, ONERA and Sud-Aviation/ sounding rocket design emphasizing meteorological rockets and standard equipment
02 p0333 A69-11916

French satellites structure, power and communications systems, stabilization and detector groups
02 p0333 A69-11917

Solid, liquid and advanced propulsion techniques in France, discussing Diamant program and Europa booster
02 p0334 A69-11919

French space center in Guiana, discussing geographic location advantages for payload, rocket launching, space rendezvous, etc
02 p0228 A69-11920

Temporary launching sites for rocket probes, discussing CNES activity, Dragon and Titus programs and mobile launching units
02 p0228 A69-11921

CNES worldwide network of tracking stations, describing equipment, location, organization and center of operations
02 p0228 A69-11922

Turquoise satellite booster, using stages of SBSBs and MSBS ballistic missiles
02 p0334 A69-12232

Increased payload in orbit capability for future versions of Black Arrow vehicle, discussing propellant
02 p0335 A69-12681

European space programs requirements for satellite launch autonomy/independence from U.S. and U.S.S.R., discussing satellite applications for resource surveys, weather forecasting, etc
02 p0335 A69-12682

Iris satellite experiments in astrophysics including nuclear and solar induced electromagnetic radiation
03 p0427 A69-12849

Angular motion during first stage cut-off of Europa 1 launch vehicle from flight tests compared with theoretical predictions
03 p0519 A69-12856

Economic importance of European communications satellite system development
03 p0535 A69-13583

European space research program, discussing government, science and industry in developing satellites and sounding rockets
03 p0520 A69-13584

European regional satellite communication systems, discussing EUROVISION TV program broadcasting and multiple access telephony
03 p0395 A69-13585

U.S.-European cooperation in space activities, discussing implementation by COSPAR and jointly owned industrial corporations
03 p0535 A69-13586

Application satellites for air traffic control, meteorology and earth resources, considering European participation
03 p0520 A69-13587

Cooperation in developing space programs between Western Europe and U.S.
03 p0535 A69-13588

Cooperation between U.S. and Europe in space programs, discussing contracts and conditions
03 p0535 A69-13590

Cooperation between U.S. and Europe in communication satellite programs
03 p0535 A69-13591

Intelsat application satellites, considering economy and global telecommunication
03 p0535 A69-13592

European launcher program analyzed from point of view of telecommunication and cost
03 p0520 A69-13593

Topics and objectives of Third Eurospace U.S.-European Conference, Munich, June 1968
03 p0535 A69-13594

U.S.-European cooperation, stressing unsatisfactory role of European industry and governments in space projects
03 p0536 A69-13595

French research on electric propulsion dealing with plasma dynamics, discussing traveling wave accelerators, pulsed plasma guns, ion thrusters, etc
[AIAA PAPER 67-740] 03 p0496 A69-13995

Electric space propulsion systems and auxiliary power sources development in West Germany, noting solar cells, isotope generators and reactors with conversion systems
03 p0496 A69-13996

European launch vehicle development program, discussing economic limitations and employment possibilities
04 p0665 A69-14808

Platform system of ELDO launch vehicle and necessary test and alignment equipment, discussing inertial platform system for future space projects
04 p0629 A69-14809

Space research from European point of view, discussing research history and satellite orbit inclination
04 p0658 A69-14882

Facilities at High Down Test Site for testing Black Arrow launch vehicles, discussing mechanical and electrical equipment test procedures
04 p0585 A69-15041

HM 4 rocket motor for second stage of Diogene booster, using LOX and hydrogen propellants
04 p0647 A69-15064

Regulated high voltage DC to DC converter with output voltage programmable numerically, noting application on board HEOS A satellite
04 p0602 A69-15400

Spacecraft propulsion - ELDO Conference, Paris, October 1967
05 p0791 A69-15593

Polonium 210 production for radiothermal propulsion via bismuth irradiation in graphite gas power reactor
05 p0791 A69-15594

Radioisotopic propulsion stage design with liquid hydrogen working fluid, stressing tank insulation and hydrostatic flight behavior
05 p0811 A69-15595

Isotopic propulsion engine development problems, emphasizing single channel thermal power engine with hydrogen working fluid
05 p0811 A69-15596

Thorium 228 production and shaping for radiothermal propulsion, discussing transformation from radium 226, irradiated target processing, etc
05 p0791 A69-15597

ESRO satellites power supply design, operation and characteristics
05 p0829 A69-15919

Data handling during ESRO satellite testing and launching, describing checkout equipment and programming of satellite computers
05 p0727 A69-16771

French and German cooperative program Project Symphonie to develop telecommunications satellite for radio and TV broadcasting
05 p0830 A69-16817

UK space research in 1970s emphasizing solar observations in UN, cosmic X ray astronomy, solar space astronomy and ionospheric investigation
06 p0997 A69-16853

Suborbital probes, discussing UK sounding rockets Skylark, Petrel and Skua configurations, capabilities and performances
06 p1012 A69-16859

German-American interplanetary vehicle to investigate interplanetary space and solar characteristics
06 p1012 A69-16970

French geodetic satellites tracking operations, on-board equipment and ground stations
[UN PAPER 68-95835] 06 p1013 A69-17065

French program of space geodesy, discussing spatial triangulation, telemetry, dynamic geodesy, Diapason and Diademe experiments
[UN PAPER 68-95834] 06 p0917 A69-17071

Project Symphonie, discussing stationary communication satellite, coverage, frequencies and characteristics
06 p0886 A69-17072

Eole meteorological satellite secondary use, discussing cosmic rays monitoring, navigation purposes and oceanographic research
[UN PAPER 68-95833] 06 p1013 A69-17077

Dynamic stability tests of tilt winged V-STOL aircraft model in ultralow speed range, discussing apparatus for stability derivatives
06 p0866 A69-17091

Cloud features produced by European tropospheric low pressure areas observed by meteorological satellite photographs, noting cyclonic systems development
06 p0950 A69-17619

Advanced electrical and nuclear propulsion systems for European launchers, comparing performances with chemical propulsion
06 p0984 A69-17628

West German test facility for simulating artificial satellite rotation about center of mass
07 p1116 A69-18260

Traveling wave tubes for Symphonie Communication Satellite, discussing design, performance and efficiency
07 p1095 A69-18429

Inertial guidance system for ELDO launch vehicles
07 p1176 A69-18491

Satellite communications antenna system at Fucino earth station, describing transmitting and receiving equipment, facilities, power supply, etc
07 p1075 A69-18493

European research on ultrahigh vacuum lubrication in space environments, emphasizing friction of materials under various loadings and temperatures
[IME PAPER 10] 07 p1138 A69-18564

ONERA vertical bench for dynamometric calibration to 20 tons used for engine and rocket thrust measurement
07 p1116 A69-19217

AZUR satellite movement simulator for thermal control tests, describing assembly
08 p1300 A69-20095

NERO thrust power measurement, discussing electromagnetic and strain-gage test stands
08 p1301 A69-20156

Long range HF propagation in equatorial zone observed with San Marco 2 satellite, discussing overall conditions of ionosphere
08 p1276 A69-20593

Nuclear power supply with in-core thermionic reactor for space power source and use in satellite TV, discussing theory, design and components
08 p1350 A69-20871

British electric propulsion research, discussing electron bombardment ion engines, conical theta pinch and rail devices and test facilities
[AIAA PAPER 69-299] 09 p1564 A69-21241

West German activity in field of electrostatic propulsion, discussing ion thrusters, colloid thruster development and mission analysis
[AIAA PAPER 69-288] 09 p1565 A69-21248

Ion thrusters and various microthrusters /electron bombardment ion and pulsed plasma/ for proposed European missions
[AIAA PAPER 69-274] 09 p1565 A69-21250

Auroral French rocket probe in Norway, studying low energy particles, relations between electron showers and high altitude electric fields, etc
09 p1498 A69-22160

Belier rocket launching facilities in Guiana, describing pads, tracking system, telecommunications network, etc
09 p1477 A69-22161

Vacuum engineering problems during booster rocket engine ground tests, simulating flight environment
[TR-781-O] 09 p1570 A69-22300

Automatic flight control system /AOOSY/ for German Azur satellite
09 p1459 A69-22563

Space stage separation qualification of ONERA rocket vehicles based on angular perturbation measurements during variable roll speeds
10 p1669 A69-23005

ELDO Europa 1 Fairings Jettisoning System and explosive devices, discussing heat shield structure and safety regulations
10 p1635 A69-23027

Pyrotechnics applications to Skylark upper atmosphere sounding rocket, discussing payload heads, nose cones, sensor covers, etc

10 p1792 A69-23029

Nose cone ejecting system with pyrotechnic devices for two stage Centaur rockets /Sud-Aviation/ with RF mass spectrometer

10 p1635 A69-23034

European space research program, discussing government, science and industry in developing satellites and sounding rockets

11 p1966 A69-25102

Type 2 ceramic capacitor manufacture, selection and control in Concerto space program

11 p1853 A69-25393

Calibration and accuracy check of measuring instruments at National Center of Space Studies in France, emphasizing reference instruments

12 p2080 A69-26123

Traveling wave tube for European communication satellite power amplifiers, showing nonlinear distortions dependence on RF input/output power and helix voltage [AIAA PAPER 68-430]

12 p2041 A69-26786

AZUR German research satellite main structure dynamic characteristics, solar panels, yo-yo despin system, electronic ignition devices and magnetometer boom

12 p2175 A69-26875

AZUR satellite structural development static and dynamic considerations, discussing center of gravity, notching technique and test results

12 p2187 A69-26876

European Space Research Organization projects including satellites and sounding rocket launchings for various missions

12 p2175 A69-26922

ESRO 1/Aurora project for ionospheric phenomena connected with incoming protons and electrons, describing orbit and alignment with geomagnetic field

13 p2356 A69-27747

Auroral phenomena investigation by ESRO 1 satellite, measuring particle flux arriving at auroral height

13 p2381 A69-27748

ESRO 1 project management and organization, discussing cost control, time saving, program evaluation and review system /PERT/, etc

13 p2382 A69-27750

Satellite networks for air traffic control and aircraft communications in North Atlantic

13 p2296 A69-27831

European earth resource satellite systems technology, applications and costs

13 p2356 A69-27833

Application satellites effects on European economy

13 p2382 A69-27834

Three meter spherical volume heat balance test facility for space vehicles at European Space Technology Center, describing vacuum system, solar simulation, etc

13 p2241 A69-28080

Scientific aims, optical design, instrument data, control and orbit operation of European Large Astronomical Satellite used in UV observations

13 p2264 A69-28477

European space program developmental and fabrication problems in satellite structure development covering booster constraints, mission constraints, tolerances, etc

13 p2357 A69-28479

Power supply subsystem for TD1/TD2 satellites with solar cells, discussing design including standby battery for solar eclipse periods

13 p2209 A69-28481

German solar and space probe Hora, discussing payload and propellant

13 p2357 A69-28638

Control system design for Black Arrow satellite launch vehicle based on Black Knight test vehicle system

14 p2530 A69-29630

Computer program for STV-F9 satellite communication parameters, using ELDO forecasting values as input data

14 p2530 A69-29689

Communications mission of Symphonie project and satellite communications subsystem design

15 p2562 A69-30084

Short term plan of European electronic component selection for ESRO satellite without established guaranteed failure rate

15 p2624 A69-30823

Ceramic condensers with very high reliability mass produced for Concerto program, describing component characteristics and production methods

15 p2627 A69-30844

Europa 1 booster supplementing with perigee-apogee system for development of Europa 2, noting payload launching capability into 24-hr circular orbit

15 p2671 A69-31051

Photoelectric photometry of artificial satellites noting equipment, Papego satellite observations and light curves from Cosmos 151, 192 and 220

15 p2616 A69-31391

Finnish space research covering satellite tracking and telemetry facilities, different Faraday and Doppler measurements with Explorer 22 signals, etc

15 p2723 A69-31426

Swiss space research report to COSPAR covering upper atmosphere studies, solar wind, etc

15 p2723 A69-31427

Austrian space research covering satellite observation, receiving and evaluating picture transmissions, theoretical investigations, etc

15 p2724 A69-31432

Polish report on space sciences activities to COSPAR covering satellite position observations, geodesy, space physics, mechanics, computations, meteorology, etc

15 p2724 A69-31433

Report on East German space activities to COSPAR covering ionospheric research, geomagnetism, solar activity, solar radio astronomy and international cooperation

15 p2724 A69-31453

Swedish space research report to COSPAR covering organization and publications

15 p2724 A69-31454

Centro Ricerche Aerospaziali objectives, equipment and activities in aerospace research, including space flight simulation facilities and scientific satellite launching range

15 p2724 A69-31456

British rocket and satellite experiments in space research, considering neutral atmosphere, ionosphere and solar radiation, orbital analysis, etc

15 p2724 A69-31463

Netherlands space research covering solar and stellar research, cosmic radiation, photometry and satellite geodesy

15 p2725 A69-31464

Italian space research report to COSPAR covering international cooperation, extrasolar X rays, electron density measurements with San Marco 2 satellite, etc

15 p2725 A69-31465

German space research organizations, rocket ascents and programs including meteorology, aeronomy, ionospheric physics, magnetosphere, solar radiation and solar wind, astronomy, etc

15 p2725 A69-31467

French space program report to COSPAR covering orbiting satellites, rocket launchings, cosmic rays, space biology, geodesy, meteorology, etc

15 p2725 A69-31473

Automatic quantitative checkout equipment for telemetry circuit of Diamant satellite booster before launching

16 p2750 A69-31727

Bipropellant propulsion systems using Aerozine 50 and nitrogen tetroxide for Symphonie telecommunications satellite

16 p2828 A69-31733

Power supplies for balloon-borne instruments, describing light flexible NiCd batteries and solar cells used in EOLE project

16 p2736 A69-31745

French space research center in Toulouse, discussing organization and activities involving satellites, rocket probes, balloons and environmental tests

16 p2765 A69-31758

AZUR research satellite HF communications system, describing telemetry transmitter, command receiver and data transmission

16 p2759 A69-31854

German ground station commercial receiving system for satellite broadcast reception

16 p2766 A69-31855

Ground station command transmission equipment for German AZUR satellite, describing components based on NASA Tone Digital Command System

16 p2759 A69-31856

Reentry flight test vehicle development for West German space program, using hypersonic model to determine controllability and aerodynamic stability

16 p2867 A69-31934

Permanent magnets optimal design and properties for attitude control of German research satellite Azur, considering environmental influences

16 p2868 A69-31936

Project Symphonie German-French communication satellite mission and technical data

16 p2868 A69-32055

D-2 satellite stabilization system design and development, noting mission to determine hydrogen distribution around earth

17 p3046 A69-33223

Numerical integration of Eole satellite attitude equations compared with results obtained by analog simulation or hybrid computation

17 p3048 A69-33232

Orbital and attitude control tests for PAS /two stage perigee-apogee synchronous satellite/ in conjunction with booster Europa 2, discussing functional configuration

17 p3048 A69-33238

German rocket engine industry reliability and performance, discussing solid fuel, two component fuel, single fuel hydrazine, mixed fuel and ramjet engines

17 p3021 A69-33361

French space geodesy since Space Age, detailing Diapason and Diademe satellites program, techniques and results

17 p2961 A69-33382

European highly eccentric orbit satellite /HEOS/ cislunar probe to explore interplanetary space for magnetic fields, cosmic radiation, solar wind and earth shock wave

17 p3050 A69-33397

European launcher system based on modular principle for low orbit, geostationary and space probe missions payload requirements

17 p3050 A69-33428

Kaufman ion thruster ESKA 18 operation principles and design compared to RIT 10 and SERT 2, discussing discharge and focusing characteristics and propulsion parameters

17 p3022 A69-33605

International organization and project management procedures in design and construction of Heos 1 satellite for measuring charged particles energy distribution outside geomagnetic field

17 p3050 A69-33699

German research satellite Azur design and production management

17 p3050 A69-33700

TD-1 astrophysical satellite and future ESRO projects, considering HEOS-0A2 and TD-2

17 p3051 A69-34217

European Space Research Program report on HEOS-A satellite, noting planetary physics research particularly in magnetic fields, cosmic radiation and solar wind

18 p3207 A69-34628

TD1/TD2 satellites power supply subsystem, stressing high power requirements and significant design features regarding battery and solar array controls

18 p3093 A69-34791

Cassiopee device for spacecraft or sounding rocket attitude control, describing gyroscopic control unit, sensor element and jet control devices [ONERA-TP-707]

19 p3432 A69-36686

ESRO and legal liability in damage suits concerning satellite protection and environmental control

20 p3635 A69-37108

Swedish satellite onboard computer for particle experiment, discussing functional design based on buffer unit for experimental data

20 p3501 A69-37386

Onboard data processor design for Swedish satellite to study spatial and temporal variations of auroral particles

20 p3501 A69-37387

Onboard satellite computer for project Roseau experiments for magnetosphere study, discussing program switches, monitors and data compilers

20 p3501 A69-37388

Auroral sounding rocket research and instrumentation in Scandinavia, discussing auroral particles, optical measurements, probe experiments and scientific objectives

20 p3542 A69-37794

High quality castings unified standards for European aerospace industry

20 p3551 A69-38029

Magnetic test facilities at ESTEC consisting of system for geomagnetic field compensation and facility for magnetization and demagnetization, testing ESRO satellite models

20 p3512 A69-38279

Monte Cardiga telemetry station associated with sounding rocket range at Salto di Quirra, Sardinia, describing equipment, telemetry system capabilities and flexibility

20 p3512 A69-38280

German ground station radio communications via Intelsat satellites, discussing transmitting facilities, TV picture and sound signals, etc

22 p3902 A69-41249

Aircraft navigation by geostationary satellites, discussing Dioscures project

24 p4280 A69-42568

Spacecraft electric propulsion research in France, Great Britain and Germany

24 p4363 A69-42668

Communication satellites european development, discussing economic and technological problems, stressing color TV and SHF/FM transmission, compared to conventional ground station transmission

24 p4393 A69-43133

EUROPEAN SPACE RESEARCH ORGANIZATION SAT

NT ESRO 1 SATELLITE

NT ESRO 2 SATELLITE

Subsystems of ESRO research satellites Td 1 and Td 2, discussing telecommunication, attitude control, power supply and temperature control design and functions

01 p0160 A69-10031

EUROPEAN 1 SPACECRAFT

Europe 1 carrier rocket prelaunch wind load calculations as base for launch or delay decision

01 p0160 A69-10032

In-flight testing of second and third stages of F 7 section of Europa 1 satellite booster, noting third stage explosion

08 p1410 A69-21144

Separation systems in Europa 1 booster vehicle, discussing thrust decay, ignition and control system characteristics

08 p1410 A69-21145

Europa 1 launch clearance procedure based on wind load precalculations from weather balloon determined wind profiles

20 p3619 A69-38281

EUROPIUM

Nonradiative transfer of excitation energy between mixed trinuclear complexes of Tb and Eu ions with lactose in aqueous solution

01 p0023 A69-10288

Meteoritic materials investigated for Sc, Ce and Eu content and distribution in various phases, using neutron activation analysis

01 p0026 A69-11376

EUROPIUM COMPOUNDS

Europium complexes high resolution emission spectra in relation to molecular configuration

01 p0024 A69-10893

Electrical conductivity of sintered polycrystalline cubic and monoclinic europium sesquioxide from DC current-voltage characteristics obtained in air at various pressures

02 p0296 A69-11874

Temperature dependence of semiconductivity of sintered polycrystalline EuO from current-voltage characteristics, measuring activation energy

02 p0296 A69-11875

Multiphoton luminescence and photocurrent excitation by ruby and neodymium laser beams of KCl-Eu single crystals, noting brightness dependence on laser beam power

19 p3335 A69-36165

EUTECTIC ALLOYS

Plastic deformation in hypoeutectoid and hypereutectoid Ni-Ti alloys studied by compressive stress-strain analysis and transmission electron microscopy

06 p0941 A69-17222

Controlled microstructures of eutectic aluminum-copper aluminides produced for mechanical properties studies

06 p0942 A69-17227

Fatigue characteristics of unidirectionally solidified Al-intermetallic aluminum nickel eutectic alloy consisting of discontinuous Al-Ni intermetallic whiskers in Al matrix

08 p1329 A69-20006

Eutectic anisotropic InSb-NiSb crystals applied to IR detection, noting sensitivity to carbon dioxide lasers

08 p1373 A69-20866

Microstructure and crystallography of lamellar eutectic alloy of Ni and intermetallic Ni-Ti compound

10 p1707 A69-22986

Unidirectionally solidified eutectic composite of Al and Cu-Al intermetallic, noting tensile properties at room and high temperatures

10 p1708 A69-22995

Zirconium-rhenium-carbon ternary system, determining resistivity of melted alloys, discussing eutectic quasi-binary compounds

10 p1715 A69-24055

Crystal microstructure and mechanical properties of unidirectionally solidified Ni-Ni-Nb intermetallic eutectic alloy at high temperature, examining deformation and fracture modes

13 p2276 A69-27402

Temperature effects on mechanical properties and fracture behavior of lamellar Ni-nickel titanide intermetallic eutectic alloy showing dependence on intermetallic constituent

13 p2277 A69-27406

Composition, gamma structure and mechanical properties of three unidirectionally solidified eutectics within Ni-Al-Cb, Ni-Al-Zr and Ni-Al-Ti systems

13 p2277 A69-27407

Eutectoid pearlite growth by pure iron-carbon specimen heat treatment

13 p2281 A69-28158

Turbine blades materials with emphasis on oriented solidification of eutectic alloys, discussing blades cooling by thermosiphons or ducts

17 p2978 A69-33334

Orientation relationships between phases in Co-TaC pseudobinary eutectic alloy, discussing Co fcc-hep allotropic transformation

17 p2988 A69-33395

Directionally solidified Co-Nb eutectic alloys mechanical properties and magnetic performance for elevated temperature space applications

19 p3341 A69-35542

Ni-Cr alloy unidirectionally solidified, grain and eutectic structure and alloy strength

19 p3343 A69-35921

Cu, Ni, Co, Cr and Ti effect on high temperature mechanical properties and stability after prolonged annealing of Al-Si alloy with added 1 percent Mg

22 p3968 A69-40063

EUTECTIC DIAGRAMS

U PHASE DIAGRAMS

EUTECTICS

NT EUTECTIC ALLOYS

Directional solidification of multicomponent metal alloys for matrix in fiber reinforced composites, using monovariant eutectic reactions

07 p1166 A69-19145

TiC-Re phase diagram over wide range of temperatures and chemical compositions

15 p2641 A69-31247

EVACUATING [TRANSPORTATION]

Navigation techniques for emergency helicopter services in medical evacuation and air/sea rescue missions, discussing displays and search patterns

02 p0279 A69-12363

Electronic stethoscopes for use in high background noise environments for patients on air evacuation flights

21 p3667 A69-39444

Patient transportation and evacuation system at disposal of Paris hospital, using short and long haul aircraft, turbojets and helicopters

23 p4105 A69-41785

Helicopter evacuation role in mortality rate among wounded in battle in Korea and Vietnam, discussing air ambulance unit organization

23 p4107 A69-41809

Medical aid, equipment and organization for injured passengers in large aircraft accidents at airports and immediate neighborhood

24 p4270 A69-42602

Air evacuation of maxilla-facially wounded persons from place of accident, noting helicopter use

24 p4270 A69-42603

Algorithm for aeromedical airlift system stop selection and sequencing, minimizing patient in-system time and aircraft flight distance

24 p4251 A69-42804

EVACUATING [VACUUM]

Gas parameters in collisionless region during discharge into vacuum, considering plane and axisymmetric cases and free molecular boundary region

02 p0234 A69-12583

Gas pressure differential across multilayer insulation blanket during rapid evacuation predicted, using one dimensional flow theory

17 p3072 A69-33275

EVALUATION

Central test evaluation group as part of systems engineering of large systems

05 p0742 A69-15803

Evaluation technique for astronautics subsystems in automated spacecraft designed for interplanetary missions, considering operation times, navigation updating and midcourse correction

21 p3764 A69-39408

EVANESCENCE

Resonance frequency behavior of waveguide cavity with evanescent air gap symmetrically loaded with dielectric

22 p3900 A69-40925

EVAPORATION

NT PROPELLANT EVAPORATION

NT TRANSPIRATION

Ion and electron contaminating currents removal in vacuum evaporating devices, using biased field plates

04 p0577 A69-14875

Vacuum equipment for evaporation or sputtering in semiconductor industry

04 p0598 A69-14876

Vaporization of mist of small droplets by intense light beam for droplet extinction rate proportional to absorbed radiant energy

09 p1539 A69-21346

Laser evaporation vapors from refractory materials to produce surface temperature for carrying out reactions in gaseous phase and thin film preparation

09 p1519 A69-22476

Size and velocity measurements of particles suspended in gas expanding from nozzle into vacuum simulating cometary two phase flow with evaporation

10 p1674 A69-23686

Holographic interference method for measuring film height in analyses of fluid film vaporization under blowing hot gas

12 p2088 A69-26178

Vacuum evaporation effects on internal macrostresses in deposited metal films based on X ray analysis, showing substrate temperature contribution

12 p2143 A69-26457

Pressure balance and maximum power density at evaporation from heat pipe experiments, deriving maximum heat flux densities

14 p2538 A69-29204

Ion beam sputtering, evaporation and electrical degradation of Al contacted Si solar cells observed in high temperature cyclic tests

19 p3250 A69-35686

Open cycle air evaporation technique selected for water recovery from human urine, based on tradeoff studies

19 p3258 A69-36455

Dynamic electron beam devices for refractory materials evaporation, discussing electron guns and vaporization film data

20 p3551 A69-38131

EVAPORATION RATE

Evaporation rate measurements in fog during carbon dioxide laser radiation, obtaining correlation to describe visibility improvement

02 p0258 A69-12622

Mechanical properties of titanium physically vapor deposited by electron beam high rate evaporation, noting results of tension testing

03 p0443 A69-13117

Condensation-enhanced vaporization rates in nonisothermal systems, noting fume nucleation augmentation of rates into cooler environments

03 p0532 A69-13122

Bulk aerodynamic method for heat and water vapor fluxes from data obtained at Chiba /1966/, introducing modified integral diffusivity

07 p1176 A69-18965

Elastic and inelastic evolution of concentrated gravitational systems, discussing stellar diffusion, evaporation, halos and rotating systems

15 p2687 A69-30548

Test methods for lubricants vapor pressure and flash point determination

15 p2642 A69-30607

Vaporization rates of Ti, Zr, Hf, Nb and Ta carbides at high temperatures measured by Langmuir method

15 p2640 A69-30983

Metal particles evaporation kinetics in plasma arc, determining total and unsteady evaporation time by spectroscopy and absorption radiography

15 p2663 A69-30990

Evaporation rate of liquid sprays involving atomization, droplets ballistics, drop size distribution, turbulence effects, etc

18 p3119 A69-34246

Heat transfer characteristics in evaporative, transpiration cooled porous systems
21 p3851 A69-39037

EVAPORATIVE COOLING
NT FILM COOLING
NT SWEAT COOLING
Ruby laser boring and welding apparatus cooled by evaporated nitrogen gas, suitable for diamond boring
03 p0434 A69-13720
Heat pipe boil-off control system for reducing cryogenic boil-off during long term space storage
12 p2191 A69-26793
Evaporation of liquid droplets from heating wall observed cinematographically, noting heat transfer by violent film boiling and conduction through thin vapor layer
15 p2718 A69-31117

EVAPORATORS
Evaporographic converter to test for striations /schlieren/ in materials used in IR
08 p1314 A69-20384

EVASIVE ACTIONS
Tactical aspects of pursuit and evasion, emphasizing analysis of conceptual framework and construction of analytic models
03 p0457 A69-13898
Optimum evasion tactics for aircraft pursued by missile, using steepest ascent method for maximization of distance of closest approach
06 p0866 A69-17401
Policies and controller design for pursuing vehicle developed in terms of pursuit-evasion differential games
24 p4341 A69-43295

EVECTION
U LUNAR ORBITS
U ORBIT PERTURBATION
U SOLAR GRAVITATION

EVOLUTION
Organic matter signals in carbonaceous meteorites, discussing possible relation to extraterrestrial life and origin
11 p1953 A69-24342

EVOLUTION [DEVELOPMENT]
NT ABIOTIC EVOLUTION
NT BIOLOGICAL EVOLUTION
NT GALACTIC EVOLUTION
NT LUNAR EVOLUTION
NT PLANETARY EVOLUTION
NT STELLAR EVOLUTION
Lagrangian evolution criterion for electromagnetic conducting fluid and MHD flow, defining generalized fluxes and forces
10 p1727 A69-22904
Proton flare event of July 1966, summarizing active region birth, evolution of spots, configuration and activity of center and general development
10 p1766 A69-23760
Energy separability method for linear systems in transient evolution using two new identities
13 p2370 A69-28634
Cosmic X rays diffuse component possible origin, discussing galactic gamma ray flux and disagreement with measured isotropy
18 p3185 A69-34275
C3 and C4 carbonaceous chondrites origin, evolution and classification based on mineralogic and petrologic data
19 p3413 A69-36109
Evolution of diffuse nebulae, considering gas dynamic equations, shock and ionization fronts, models and numerical methods, radiation pressure, interstellar magnetic field, etc
21 p3810 A69-39504
Cometary and asteroidal orbital differences and similarities, emphasizing limiting cases to study orbital evolution of meteors
23 p4208 A69-41284

EVOLUTION [LIBERATION]
U GAS EVOLUTION

EXAMINATION
U EYE EXAMINATIONS

EXCHANGING
U CHARGE EXCHANGE
U GAS EXCHANGE
U ION EXCHANGING

EXCITATION
NT ACOUSTIC EXCITATION
NT ATOMIC EXCITATIONS
NT HARMONIC EXCITATION
NT SELF EXCITATION
NT WAVE EXCITATION
Ionization cross sections of excited states of hydrogen atoms and hydrogenoids calculated by Monte Carlo method
01 p0122 A69-10040
Lanthanum isotopes beta decay, analyzing excitation of near spherical daughter nuclei of barium isotopes
01 p0122 A69-10100
Excitation heating energy pumping mechanism for explaining dynamic equilibrium in C rich arc plasmas with high ion temperature/electron temperature ratio
01 p0126 A69-10276
Preionization of gases by laser beam using theory based on molecular equilibrium concentration and collision excitation
02 p0283 A69-11703
EPR spectra and thermal conductivity measurement in excited organic semiconductor salt derivatives of tetracyanoquinodimethane
03 p0484 A69-13278
Doublet electronic states of benzyl radical, discussing configuration-interaction calculations and transition predictions
03 p0472 A69-13321
UV induced excited-state properties of DNA using optical emission and electron spin resonance methods
03 p0372 A69-13488
Nanosecond range flash photolysis technique and application to absorption spectra of excited singlet states
05 p0760 A69-15608
Hydrogen ions collision-induced dissociation cross section angular dependence measured, showing qualitative agreement with theoretical predictions
05 p0798 A69-16698
Electron impact excitation cross sections for emission from first negative bands of positive N molecule ion
06 p0961 A69-17135
Polar molecule rotational excitation diffusion cross sections for electron scattering
06 p0961 A69-17139
Vibrational excitation in diatomic gas mixtures by translation to vibration energy conversion in simple collisions and by vibrational energy exchange between components
06 p0962 A69-17821
Gas lasers principles of operation, discussing population mechanism, lifetime conditions, excitation processes, electron velocity distribution and types of discharges
06 p0937 A69-18008
Collisional excitation and ionization rates comparison in statistical equilibrium model atmosphere calculations
08 p1385 A69-20065
Electron-ion collisions during forbidden lines excitation in gaseous nebulae, using Hartree-Fock functions and variational principles
08 p1391 A69-20530
Direct nonresonance excitation of rotational and vibrational states of diatomic molecular ions by electrons in Born-Coulomb approximation
10 p1726 A69-23627
Spontaneous magnetic field excitation in turbulent plasma noting possible instability
10 p1740 A69-23715
Nitrogen, oxygen and air luminescence spectra excited by fast electrons at low gas pressures in IR spectral region compared with polar auroral spectra
10 p1687 A69-23916
Coupling coefficient and impedance for excitation of isotropic plasma column by ring of magnetic current outside plasma, noting surface wave resonance effect
10 p1659 A69-24064
Damping of solid state laser relaxation oscillations in power output due to diffusion of excitation
10 p1706 A69-24079
Single circuit parametric oscillator excitation by small external narrow band signal, using method of slowly varying amplitudes
11 p1845 A69-24453
Vibrationally excited nitrous oxide formation in reaction of N atoms with nitrogen dioxide, noting IR emission and vibrationally excited nitric oxide
11 p1832 A69-24880
Excitation of plane plasma layer in magnetic field perpendicular to wave vector of excitation wave in gyrotronic waveguide
11 p1927 A69-24916
Excitation coefficients of waves subjected to sudden expansion in radiating waveguide using integral relations, noting convergence
11 p1855 A69-25621

Steady state solution of periodically excited circuit, constructing Green function for use in convolution integral
12 p2036 A69-25918
Optical cross section measurements for electron excitation from ground state of nitrogen
12 p2132 A69-26246
Sinusoidal or random excitations equivalence from point of view of rupture risks, considering industrial applications
13 p2370 A69-28602
EPR spectra and thermal conductivity measurement in excited organic semiconductor salt derivatives of tetracyanoquinodimethane
14 p2508 A69-29652
Rare gases total excitation cross sections absolute values measured in collision chamber, noting energy distribution of exciting electron beam, fine structure, etc
14 p2493 A69-29693
Aurora electron and proton excitation patterns determined spectroscopically, discussing ground based observations of emission geomagnetic latitude-time distribution
15 p2593 A69-30017
Electronic states of semiconductor acceptor centers at forbidden band deep levels, considering inner electron shell excitation in impurity ion
15 p2665 A69-30039
Excited cyanide molecules concentration in arc discharge determined from spectral bands absolute intensities during electron transition
15 p2654 A69-30080
Excitation sources distribution in chromosphere from observed H alpha line contour, considering resonant scattering and internal excitation
15 p2683 A69-30509
Steady state solutions for parametric excitations in various limits in plasmas, allowing for higher order mode coupling
15 p2661 A69-30919
Optimal parameters of cuvette for use with helium-neon laser as excitation source to record combination light scattering spectra of powdery materials
15 p2635 A69-31105
Electron cooling rates due to vibrational excitation of molecular oxygen calculated as function of electron temperature in E region
16 p2774 A69-31982
He-Ne laser plasma behavior, establishing parameters for electron gas, cross sections of formation and annihilation and excited states lifetimes
17 p2982 A69-33390
Earth-ionosphere waveguide excitation by lightning discharges and geomagnetic field influence on ELF noise spectrum
17 p2928 A69-33865
Rate coefficients for chemiluminescent reactions of excited He with N, O, carbon monoxide and dioxide determined from spatial dependence of visible emission
20 p3483 A69-36936
Absorption spectrum of diatomic oxygen excited by AC silent discharge photographed with vacuum spectrograph, associating lines with Schumann-Runge band
20 p3581 A69-38276
Diatomic molecules rotational excitation calculated from electron molecule elastic scattering parameters in fixed nuclei approximation
21 p3775 A69-39665
Population and excitation rates of working levels of carbon dioxide laser calculated on basis of emission power, amplification coefficient and spontaneous emission intensity
22 p3964 A69-40795

EXCITED STATES
U EXCITATION

EXCITONS
Recombination radiation from excitons and free carriers in epitaxial GaAs with impurities at liquid He temperatures
01 p0140 A69-11253
Exciton distribution in semiconductors below Bose condensation temperature differing from diffusion distribution
03 p0486 A69-13415
Exciton spectrum for limiting case of large radius leading to Wannier-Mott equation with static dielectric permeability
03 p0486 A69-13416
Bound excitons spectra in CdS, semiconductor band structure and tabulating positions of lines identified with excitons
03 p0488 A69-13784

Interaction between semiconductor excitons, obtaining formulas for exciton concentrations ground state energy and dispersion, noting association with Pauli statistics
08 p1371 A69-19955

Localized plasmons and optical phonons occurrence on local plasma levels, noting role of impurity atom in localized exciton-plasma resonance
09 p1548 A69-21674

Excitation of ultrathin Cd/Se/Si platelets with mode locked He-Ne laser for excitons formation, discussing time delay
10 p1703 A69-23512

Coulomb interaction during optical transitions between Landau subbands of Ge semiconductor valence and conduction bands in magnetic field, observing diamagnetic excitons
11 p1936 A69-24640

Photosimulation of electron hole and exciton mechanisms of NaI-Tl and KI-Tl single crystal scintillations
12 p2144 A69-26722

Frequency dependence of light absorption by excitons obtained for allowed and forbidden zone transfers in semiconductors
15 p2632 A69-30057

Bound excitons spectra in Cu doped gallium arsenide crystals, analyzing line absorption structure and uniaxial compression effect
16 p2824 A69-31571

CaO and MgO reflectance spectra measurements at high resolution and at low temperature including exciton spectra at 25 K, obtaining fine structure
18 p3181 A69-34274

Exciton line broadening in II-VI compound semiconductors, discussing thermal broadening of n equals one exciton associated with LO phonon-induced scattering
19 p3386 A69-36524

Photosimulation of electron hole and exciton mechanisms of NaI-Tl and KI-Tl single crystal scintillations
21 p3781 A69-39135

EXCRETION

Renal effects of moderate hypoxia exposure in mice as reflected in urine volume and electrolyte excretion patterns during four days at simulated altitude
01 p0015 A69-10921

Rapid global transportation effect on circadian rhythmic patterns in human body functions, discussing kidney excretion and pituitary adrenal cortical system
09 p1444 A69-22545

Physical factors affecting proximal and distal tubular sodium reabsorption in dogs undergoing water diuresis
13 p2210 A69-28482

Male patients urine tests during sinusoidal vibration, noting catecholamine excretion as criterion of emotional stress under various environmental conditions
21 p3654 A69-38909

EXECUTIVE AIRCRAFT

U GENERAL AVIATION AIRCRAFT

U PASSENGER AIRCRAFT

EXERCISE [PHYSIOLOGY]

Respiratory gas exchange in exercise during He-O breathing, analyzing effects on O consumption, carbon dioxide production and minute ventilation of human subjects
17 p2910 A69-33751

Reticulocyte count comparison on trained and sedentary college male subjects before and after strenuous exercise, noting role in oxygen uptake
21 p3654 A69-38907

Exercise-temperature regulation in men under constant submaximal workload at various simulated altitudes, discussing exercise core temperature equilibrium level setting mechanisms
22 p3891 A69-40219

Enzymatic processes of glucose metabolism in immature rats lymphatic tissues during exercise-induced elevated corticosteroid secretion
23 p4080 A69-41405

EXERTION

U PHYSICAL WORK

EXHAUST DIFFUSERS

Gas turbine exhaust silencer performance correlated in laboratory and in service
[ASME PAPER 68-WA/GT-9]
05 p0812 A69-16144

Ejector-diffuser performance improvement by reduction of backflow with orifice plate installed at inlet of straight diffuser duct
11 p1819 A69-25382

EXHAUST FLOW SIMULATION

Radar backscattering from turbulent rocket exhaust plumes
[AIAA PAPER 69-71] 06 p0891 A69-18071

Ingestion and flow field characteristics of interaction of two heated parallel air jets; discussing VTOL exhaust ingestion tests
[AIAA PAPER 68-79] 12 p2012 A69-26761

Hydrogen and methane combustion to simulate expansion of storable propellants
[AIAA PAPER 68-635] 20 p3631 A69-37188

Outer space rocket plumes simulation facility combining low density wind tunnel and molecular sink properties, discussing role of liquid nitrogen cooled diffuser-precooler
22 p3928 A69-40731

EXHAUST GASES

Cylindrical afterbodies at free stream Mach 2 with hot argon gas ejection, discussing flow rate influence on base pressure
02 p0190 A69-12533

Jet engine exhaust composition and methods for reducing smoke emission through burner design changes, noting primary zone fuel and airflow pattern
[SAE PAPER 680348] 03 p0495 A69-13350

Monograph on exhaust gases mixing with cold airstream in ducted fanjet engine, noting thrust and efficiency increase
03 p0496 A69-14048

Soviet book on turbojet engine reverse thrust systems and systems for deflection of jet stream covering aircraft braking efficiency
04 p0647 A69-14934

Nuclear rocket engine exhaust gas cooling by injecting water jet eliminates need for secondary cooling
[AIAA PAPER 68-604] 04 p0591 A69-15516

Control methods and designs for limiting atmospheric pollution emitted by aircraft gas turbine engines
[SAE PAPER 680347] 07 p1204 A69-19729

Real time real temperature exhaust gas reingestion and structural heating test facility for jet lift V/STOL configurations
[AIAA PAPER 69-310] 09 p1479 A69-22388

Gas turbine engines smoke emission, considering smoke measurement, flame structure, carbon production, pressure effects fuel-air ratio, etc
09 p1573 A69-22622

Control methods and designs for limiting atmospheric pollution emitted by aircraft gas turbine engines
12 p2147 A69-26236

Exhaust gas recirculation for VTOL aircraft
[AIAA PAPER 67-439] 12 p2013 A69-26760

Test programs utilizing pitot probes to map exhaust plumes from liquid bipropellant engines in low ambient pressures conducted to verify calculations
[AIAA PAPER 69-575] 16 p2869 A69-32746

Noise abatement and smoke emission reduction from aircraft engines
[AIAA PAPER 69-489] 16 p2746 A69-32764

Optimum adaptation of propulsion gas generators to power jet driven rotors with blown flap control, considering jet engine, fanjet and engine driven compressor
17 p3020 A69-33344

Density profiles in far field of reaction control system plumes in vacuum obtained by method eliminating difficulties encountered by continuum method
19 p3238 A69-35954

Water injection cooling of exhaust gases during stage testing of NERVA engine, discussing exhaust duct configuration and flow characteristics, spray nozzle geometry, etc
[AIAA PAPER 69-514] 19 p3372 A69-36301

Aerated fuel spray effect on smoke reduction from high pressure ratio aircraft gas turbines engines, including smoke measurement and visibility
19 p3395 A69-36770

Chemical and thermal behavior of materials corrosion in propellant exhaust gases with analysis of reactions involving hydrogen, nitrogen, water, carbon dioxide, etc
21 p3784 A69-39489

Organic Rankine cycle system using heat absorption from turbine exhaust to provide increased electrical output and to power air conditioning
23 p4070 A69-42267

EXHAUST NOZZLES

NT CONVERGENT-DIVERGENT NOZZLES

NT PLUG NOZZLES

Three dimensional scramjet exhaust nozzle flow fields by second order method of characteristics
[AIAA PAPER 69-5] 06 p0862 A69-18048

Collimated nozzle beam for probing low density gas flows, discussing transition from free molecular to isentropic flow and Knudsen numbers
07 p1136 A69-19467

Solid propellant motors nozzle design, analyzing structural and material problems, high temperature exhaust gases effects, thermal insulation, etc
10 p1716 A69-23403

Aircraft test setup design and techniques to simultaneously measure engine thrust and engine thrust minus drag, noting nozzle configurations variations effect
[AIAA PAPER 68-395] 12 p2059 A69-26769

Exhaust nozzle/airframe interference test evaluation for twin engine supersonic fighter
[AIAA PAPER 69-430] 16 p2733 A69-32730

Local external flow variations effect on blow-in-door nozzle performance in transonic flight regime
[AIAA PAPER 69-428] 16 p2733 A69-32731

Location effect of power plants on aft-mounted supersonic cruise exhaust nozzles at transonic speeds in flight and wind tunnel
[AIAA PAPER 69-427] 16 p2734 A69-32769

Directional thrust control for solid propellant rockets, describing swinging, bent rotating nozzles and secondary injection
17 p3019 A69-33332

Flow field of two dimensional nozzle exhausting to vacuum, describing computer program based on BGK equation and plotting exhaust region density, temperature and velocity
[AIAA PAPER 69-658] 17 p2893 A69-33490

Nitrogen and water vapor effects on hydrogen-oxygen system recombination, using shock tubes for design of exhaust nozzles for hypersonic flow vehicles
21 p3669 A69-38801

EXHAUST SYSTEMS

Flight vehicle cabins ventilation for undesirable gas contaminants removal, discussing contaminant concentration calculation and automatic control
02 p0200 A69-11512

Air backflow in nuclear exhaust system duct for ground testing of NERVA engines, noting overpressure effect
[AIAA PAPER 69-325] 09 p1479 A69-22390

Exhaust gas reingestion and inlet flow distortion in V/STOL lift engines, discussing static and wind tunnel testing using fighter configuration models
[AIAA PAPER 68-78] 12 p2012 A69-26762

EXHAUST VELOCITY

Axial velocities in ammonia MPD thruster exhaust by measuring Doppler shifts of spectral lines emitted by plasma constituents
16 p2835 A69-31890

EXHAUSTION

Exhaustion time extension in rats by altitude acclimation, noting adaptation loss resulting from physical exercise discontinuation
23 p4086 A69-41787

EXISTENCE

Existence and uniqueness of weak solutions in linear theory of stable equilibrium position for inhomogeneous elastic thin walled shells
02 p0340 A69-12036

Quadratic Liapunov function existence for exponentially stable linear system with varying coefficients described by vector differential equations
19 p3359 A69-35617

EXISTENCE THEOREMS

Boundary value problems for steady, three dimensional MHD flow of viscous incompressible conducting fluid past various bodies, proving existence of solutions
01 p0126 A69-10164

Geometrical existence proof of elastically coupled nonlinear systems normal mode vibrations demonstrated by existence of extremal arcs in Riemann space
01 p0166 A69-10232

Existence of smooth solution for system of equations describing nonlinear oscillations of thin plate and shallow shell
02 p0337 A69-11654

Existence of periodic solutions by Whittaker criterion to equations describing motion of satellite of spheroidal planet in planetocentric coordinate system
02 p0317 A69-11959

Existence theorems for solutions to second order ordinary differential equations
02 p0272 A69-12129

Uniqueness and existence theorem concerning stability of solutions of mixed nonlinear boundary value problem, discussing generalized heat transfer phenomena
02 p0352 A69-12255

Bounded solutions for systems of ordinary second order differential equations
03 p0455 A69-13257

Ordinary nonlinear differential equations with linear boundary conditions, discussing formulation and proof of lemma and theorems to demonstrate existence
04 p0621 A69-14416

Boundary value problem of hyperbolic equation with discontinuous boundary conditions
04 p0622 A69-14617

First-kind operator equation solution by reduction to dual extremum problem, proving existence and convergence
04 p0622 A69-14622

Asymptotic oscillation results for solutions to first order nonlinear differential-difference equations, obtaining existence-uniqueness theorems
04 p0624 A69-14950

Existence theorem for periodic solutions of parabolic boundary value problem for infinite space time cylinder
04 p0624 A69-15004

Boundary value problems for second order degenerate elliptic equations, formulating and proving theorems for existence of generalized solutions
05 p0786 A69-16422

Existence and uniqueness theorem for functional equation of optimal control problems, noting stability of solution
06 p0949 A69-17889

Complex variable theory usefulness in investigating existence and uniqueness of solutions for boundary values in partial differential equation
07 p1173 A69-18731

Periodic asymptotically stable MHD motions, proving uniqueness and existence theorems
07 p1194 A69-19437

Existence and uniqueness of Dirichlet problem solutions for elliptic type equations with measurable and bounded coefficients
08 p1343 A69-20659

Almost periodic systems stability criteria derived from differential inequalities and Liapunov function, considering existence and uniqueness
09 p1532 A69-21612

Decrease existence at t approaching infinity solution of Sobolev linear partial differential equations describing rotating fluid small oscillations
09 p1481 A69-21899

Existence and uniqueness to boundary layer continuation problem based on flow equation for steady gas flow
10 p1679 A69-23569

Existence and oscillation of initial and boundary value problems solutions for real scalar second order differential equations
10 p1720 A69-23637

Existence and uniqueness for nonlinear boundary value problems satisfying Lipschitz condition
10 p1721 A69-23640

Solution existence of nonlinear two point boundary value problems from uniqueness
11 p1909 A69-24883

Existence and completeness of eigenfunctions for boundary value problem arising in theory of small amplitude motions of stratified polytropic gas
11 p1868 A69-24884

Existence theorems for hyperbolic genuinely nonlinear systems of conservation laws, studying Cauchy problem
11 p1909 A69-25163

Dirichlet problem solution for Volterra elliptic integrodifferential equation, considering existence theorem hypotheses
12 p2121 A69-26468

Existence theorems for partial differential equations theory for traction boundary value problem of linearized elastostatics
12 p2188 A69-26928

Sufficient conditions for periodic motion existence of autonomous nonlinear feedback systems derived in terms of linear system frequency response
13 p2238 A69-27923

Singularity-free global solutions to nonlinear differential equations associated with variational principles, deriving necessary condition for existence from dilatation invariance considerations
14 p2470 A69-29367

Monograph on Dirichlet problem for quasi-linear elliptic differential equations with many independent variables
14 p2471 A69-29599

Von Karman swirling flow problem differential equations solved by extending Serrin existence theorems
14 p2432 A69-29676

Conduction solution to generalized nonlinear Benard problem showing existence of bifurcation and analyticity of convective motion
14 p2540 A69-29679

Necessary and sufficient conditions for solution existence to second order boundary value problems, considering second order differential equation involving function of three variables
14 p2471 A69-29951

Necessary and sufficient conditions for existence of smooth solution to quasi-linear partial differential equation
17 p2994 A69-32843

Classical solution existence to mixed boundary value problems for second order hyperbolic operators obtained by Laplace transforms
18 p3165 A69-35313

Existence and uniqueness theorems for operator equation in differential equations theory for application to boundary value problem
19 p3360 A69-36373

Fixed point existence in study nonlinear mapping determined on semiordeired Banach space, noting results applicability to integral equations and boundary value problems
19 p3361 A69-36640

Existence theorem for limits of minimizing sequences in optimal control problems, applying results to systems governed by partial differential equations
19 p3287 A69-36724

Heat transfer problem involving temperature determination of body and ambient medium, deriving existence and uniqueness theorems for boundary value problems in curvilinear regions
20 p3631 A69-36991

Method of straight lines applied to two phase Stefan type problem for quasi-linear parabolic equation, obtaining existence and uniqueness of solutions
20 p3567 A69-36992

Continuous optimal control problems, proving direct solutions existence for case of differential equations system linearity in control and state variables
21 p3684 A69-38431

Existence theorem for linear stochastic systems optimal control described by differential equation with random coefficients, providing rms stabilization
22 p3917 A69-40116

Existence conditions of critical points for autonomous differential equations in bounded flows
22 p3975 A69-40571

Existence theorem for Markov chain finite state stochastic games applied to saddle point and optimal strategy or epsilon-optimal strategy pairs
22 p3975 A69-41010

Existence theorem for relation between solutions of systems of ordinary differential equations
23 p4182 A69-41959

Decrease existence at approaching infinity solution of Sobolev linear partial differential equations describing rotating fluid small oscillations
23 p4152 A69-41975

EXO BIOLOGY

Space controlled microbiology, discussing telemetry control of waste material conversion in air and water pollution
[UN PAPER 68-95861] 01 p0014 A69-10456

Space biology, discussing U.S. research program, emphasizing gravity/organism reactions, biochronology and exobiology
[UN PAPER 68-95345] 01 p0014 A69-10486

Cosmic radiation genetic, cytological and histological changes, particularly of pathological nature, on ecological systems employed in long duration Soviet manned flights
01 p0016 A69-10948

Biological life support system based on continuous algae seaweed cultivation as link of closed ecological system, discussing design and performance
01 p0020 A69-11077

Resistance of animal organisms and cells to extreme environmental conditions discussing exobiological implications for extraterrestrial life systems
01 p0017 A69-11083

Mathematical models for Chlorella cell and biomass growth under illumination during space flight, noting ionizing radiation presence
02 p0198 A69-11508

Extraterrestrial life possibility in solar system, noting Martian atmosphere and terrestrial life adaption to Mars simulations
02 p0198 A69-11770

French applied and basic research in space biology including manned space flight, deep space problems, weightlessness and cosmic heavy ion radiation effects
02 p0199 A69-11909

Space radiation biology - NASA Conference, Berkeley, September 1965
03 p0370 A69-13476

Mars biological exploration, discussing life detection, chemical and biological experimental strategy [AIAA PAPER 68-1122] 03 p0375 A69-13700

Biological space research, discussing microecology and weightlessness effects on human space flight [DVL-847] 04 p0553 A69-14811

Microbial contaminants on space hardware, discussing detection and enumeration techniques
05 p0714 A69-15954

Life probability and origin on Milky Way planets with emphasis on solar system, discussing molecular biology role
05 p0707 A69-15966

Animals in weightless state, noting vigilance, attention, sensorial and motor reaction time, muscular tone at rest and muscles electrical activity in movement
09 p1445 A69-22721

Primates for space research, discussing selection, purchase, handling and use as controls in observations of disorders experienced by man
09 p1445 A69-22723

Soviet book on space radiobiology, discussing somatic effects, influence of flight factors, relative biological effectiveness of various radiations and radiation safety
11 p1827 A69-24263

Bioorganic comparative analysis of desert soils, Precambrian shales and meteorites by automated pyrolysis-gas chromatography-mass spectrometry system for future Mars soil analysis [JPL-TR-32-1368] 11 p1832 A69-25640

Space biological tests performed on lower animals and vegetables relating to higher organisms reactions during prolonged manned space flights, reviewing Nasa experiments
12 p2019 A69-26494

Soviet space biology and medicine, discussing ecological physiology, closed system ecology, exobiology and medical tests on cosmonauts
13 p2209 A69-27356

Weightlessness, increased gravitational fields and radiation effects on biological systems at organismal, cellular and subcellular levels, discussing biosatellite experiments
14 p2406 A69-29097

Exobiology, Search for extraterrestrial life - AAS-AAAS Conference, New York, December 1967
17 p2907 A69-32967

Solar system physical environments surveyed from exobiological viewpoint
17 p2907 A69-32968

Origin of microbial life on earth and implications for extraterrestrial forms
17 p2907 A69-32972

UFOs from sociological viewpoint, stressing need for international cooperation in exobiological research
17 p3076 A69-32974

Radiation effects on microorganisms and plants during space flight on Biosatellite 2 and Gemini 11 missions
20 p3476 A69-37617

Insects mutational responses to space flight and associated radiation on biosatellite 2 compared with ground based controls
20 p3476 A69-37618

Physical and life supporting properties of hypothetical Martian biosphere, considering organism adaptation theories
22 p3876 A69-40271

Mars exploration for life by Mariner flybys and orbiters and 1973 Viking landers
23 p4212 A69-41611

Bulk, selective particulate and hard rock samplers for landed extraterrestrial geological and biological instruments performing on-site analysis
23 p4146 A69-41620

Extraterrestrial optical microscopy, discussing experiment, telemetry, data interpretation and instrument characteristics concerning biological, cytochemical and petrographic microscopes
23 p4164 A69-41621

Optical activity measurement for exobiology applications, considering polarimetry, gas-liquid chromatography, mass spectrometry and radioactivity detection
23 p4213 A69-41622

EXOSPHERE

Exosphere diurnal and latitudinal variations in electron and proton content, ion composition, and electron, proton and positive O ion densities
01 p0063 A69-10422

Venus exospheric temperature for various composition models, discussing carbon dioxide concentration effects
02 p0319 A69-12109

Propagation of long electromagnetic waves in ionosphere and exosphere, discussing thunderstorm noise spectrum
03 p0396 A69-13702

Lateral transport of constituents in planetary exospheres, considering planetary rotation
03 p0515 A69-14010

Transpolar exospheric electron concentration distributions along earth-sun line parallel path of Alouette 1 satellite
03 p0425 A69-14018

Semiannual variations in exospheric density near 1100 km derived from Echo 2 orbit, noting phases during solar cycle
06 p0918 A69-13785

Cyclotron instability of outer radiation belt protons, taking into account data on spatial distribution and ion composition of exospheric plasma
06 p0919 A69-17721

D/H ratio in Venus exosphere, discussing isotopic fractionation mechanisms and Lyman alpha data from Mariner 5
11 p1962 A69-25145

Model ion-exosphere for nonrotating planet with static dipole magnetic field generalized by permitting density and temperature variations over baropause
11 p1879 A69-25284

Atmospheric models for exospheric temperatures of Mars and Venus based on photoionization heating efficiency
12 p2155 A69-26020

Unified model for spatial distribution of transpolar exospheric electron density for polar plasma study
12 p2151 A69-26952

Polar exosphere near solar maximum investigation by Explorer 19 and Explorer 24 drag satellites, considering density and atomic oxygen concentration measurements
15 p2600 A69-31351

Exospheric temperature variations by Thomson scattering related to solar and geomagnetic activity, discussing seasonal effect on thermospheric variables
15 p2604 A69-31409

Simultaneous middle and low latitude Thomson scatter measurements, comparing electron density, temperature and exospheric temperature data on quiet and disturbed days
15 p2604 A69-31418

Ion depletion in high latitude exosphere, considering OGO 2 simultaneous observations of positive ion concentration, VLF signal propagation and whistlers
18 p3187 A69-34939

Primitive earth upper atmosphere thermal models, considering roles of exospheric temperature and free hydrogen availability in methane dominated environment
20 p3608 A69-38056

Doppler broadened atomic O emission line measurement providing indication of exospheric temperature storm-time variations
20 p3546 A69-38099

Neutral exosphere model for nonrotating planet permitting barosphere uniform rotation at certain angular velocity, determining velocity distribution and density
22 p4023 A69-40524

H and He atoms escape from atmosphere under MHD waves action at exosphere boundary
23 p4156 A69-41847

EXOTHERMIC REACTIONS

Exothermal effects during sintering of nickel-aluminum powder mixture
02 p0269 A69-12838

Exothermal effects during sintering of nickel-aluminum powder mixture, showing role of liquid phase decomposition and intermetallics
02 p0269 A69-12843

Thermal explosion criterion used for explosion/ignition delay of exothermic material surrounding heated wires having good thermal conductivity
[WSCIPAPER 68-23] 07 p1240 A69-18359

Ammonium perchlorate exothermic decomposition control noting effects of preheating and ammonium fluoroborate additives
[WSCIPAPER 68-25] 07 p1202 A69-18363

Dynamic differential thermal analysis of dried plant and animal specimens and related substances yielding discrete decomposition peaks of exothermic type
15 p2555 A69-31000

Solid rocket motor ignition system based on exothermic alloying of bimetallic wire constituents
[AIAA PAPER 69-425] 16 p2832 A69-32653

Ammonium and magnesium perchlorate mixture thermal stability study with differential scanning calorimetry, noting exothermic decomposition of AP
[AIAA PAPER 69-500] 16 p2833 A69-32661

Premature exothermic decomposition suppression in propellant grade ammonium perchlorate, using differential thermal analysis
[AIAA PAPER 69-503] 16 p2833 A69-32688

Criteria to predict flow instabilities triggered by exothermic reaction presence in high temperature reaction kinetic shock tube studies
18 p3116 A69-34462

Combustible mixtures flow past bodies, discussing equation for shock polar for exothermal discontinuities at subsonic and supersonic velocities
19 p3241 A69-36780

EXPANDABLE STRUCTURES

NT BALLOONS

NT BEACON SATELLITES

NT BELLOWS

NT EXPLORER 22 SATELLITE

NT HIGH ALTITUDE BALLOONS

NT INFLATABLE STRUCTURES

NT METEOROLOGICAL BALLOONS

NT TETHERED BALLOONS

Expandable D 21 airlock scheduled for testing on NASA Orbital Workshop Flight based on elastic materials technique, noting more complex chemically rigidized concept
[IAF PAPER SD-49] 02 p0334 A69-11949

Foldable tubular connection application to expandable lattice structure, analyzing cross sectional distortions
06 p1024 A69-17608

Resin impregnated fiber reinforced expandable structures used for automatic cure or rigidizing in space and initially small compact packages on earth
19 p3433 A69-35585

Dynamic uniaxial tensile stress-strain data obtained at high rates by measuring kinematics of symmetrically expanding thin ring specimens
24 p4330 A69-42735

EXPANSION

NT GAS EXPANSION

NT PRANDTL-MEYER EXPANSION

Observations indicating slow earth expansion
22 p4018 A69-40179

Earth gravitational potential energy changes in examining expanding earth theory
22 p3936 A69-40180

Graphical method for two dimensional supersonic expansion flow with subsonic reaction front around corner compared to existing iteration method
23 p4061 A69-42411

EXPANSION WAVES

U ELASTIC WAVES

EXPECTANCY HYPOTHESIS

Expected occurrences mathematical model for flight system availability under uncertainty
18 p3210 A69-35083

EXPECTATION

Areas of expectation for single radar automatic tracking of flying objects derived on basis of equation of circle in polar coordinates
01 p0035 A69-11296

EXPERIMENTAL DESIGN

Phased array antenna radiator element design, emphasizing configuration selection and reflection loss for beam steering
04 p0572 A69-14321

Diffraction limited telescope fine guidance experiment to improve pointing stability in space, noting attitude control system and nonmechanical suspension
08 p1317 A69-21072

Thermionic space power reactor design, detailing Critical Experiment problems
09 p1441 A69-21835

Antenna for lunar occultation observations at 81.5 MHz, detailing experimental procedure and data reduction
10 p1779 A69-23606

Einstein second postulate concerning invariability of light vector in vacuum experimented for validity, using earth and moon as light rays launching and reflecting media
13 p2354 A69-28650

Book on integrated circuits covering fabrication techniques, basic semiconductor theory, thin film, monolithic, compatible circuits, packaging, etc
14 p2419 A69-29002

Gas laser design utilizing internal window mirrors deposited with dielectric coating outside resonator
14 p2457 A69-29160

Foil bearings design, fabrication, applications to flexible material transport, rotor support, etc
15 p2618 A69-30327

Solar simulator with xenon and krypton lamps designed for thermal balance tests, power conversion and material degradation experiments
15 p2586 A69-30383

Microwave strip transmission line, discussing evolutionary improvements, computerized design, materials, semiconductors, packaging, reliability, etc
15 p2721 A69-31074

Nonlinear regression techniques for statistical simultaneous measurement of thermal properties including convergence criterion
[AIAA PAPER 69-602] 17 p3070 A69-33260

Lunar based physics and chemistry, discussing exploration of and survival in lunar environment
18 p3112 A69-34235

Molecular beam experiments on moon, noting lunar environmental advantages for studies of beam-beam scattering, beam-surface interactions, beam-field deflection, etc
18 p3113 A69-34240

Space exploitation for experimental research - AAS Conference, Dedham, Mass., May 1968, Volume 24
18 p3193 A69-34367

Semiconductor reliability evaluation program for economical experimental design, noting stress tests
18 p3232 A69-34496

OGO triaxial search coil magnetometer for measuring earth magnetic fluctuations, discussing design rationale and observation results
19 p3284 A69-36675

Fabry-Perot interferometer with Al coating reflecting surface deposited on unbaked thin films
20 p3536 A69-36933

Apollo 11 passive seismic experiment design and objectives, describing seismometer characteristics and lunar interior
20 p3539 A69-37516

Digital data analysis systems role in experimentation and R and D
21 p3843 A69-39315

Interactive experimenter computer system software and hardware design considerations based on astronaut-machine/experimenter question-answer interactions
[AIAA PAPER 69-953] 22 p3904 A69-40335

Troposphere fine scale properties, comparing simultaneous results of five experimental methods
22 p3941 A69-40914

Space experimental design based on manned vs unmanned spacecraft value for multipurpose low cost flexible space station in low earth orbit
23 p4223 A69-42457

Ergonomic study of experimental tests design for comparing equipments efficiency with man
24 p4275 A69-43023

EXPERIMENTAL REFLECTOR ORBITAL SHOT PROJ

Multispectral photographic determination of reflectance of environmental features from aerial spectral photographs, noting EROS program application
11 p1880 A69-24266

EXPIRATION

Sequential lung emptying at varying expiratory flow rates at increasing acceleration levels using expired nitrogen analysis
23 p4083 A69-41448

EXPLODING CONDUCTOR CIRCUITS U CIRCUITS

EXPLODING WIRES

Exploding wire - Conference, Boston, October 1967
01 p0116 A69-10654

Nonlinear circuit equations describing initial phase of exploding wire, noting solution for wire resistance variation with internal energy
01 p0117 A69-10656

Exploding wire discharges similarity with underwater sparks for understanding water breakdown and parallel discharges
01 p0117 A69-10657

Exploding wires as light source for quantitative spectroscopy, noting optically thin plasma clouds with radial symmetry
01 p0117 A69-10658

Electrical equation of state of metals determination from density, conductivity, energy and metal vapor velocity measurements in wire explosions
01 p0117 A69-10659

Axial magnetic field effect on exploding wire phenomenon, studying direct interaction
01 p0118 A69-10660

Ministriations in frequency graphs as evidence of standing waves in electrically exploded iron wires
01 p0118 A69-10661

Spectroscopic investigation of high density plasma from Li exploded wires
01 p0129 A69-10662

Faraday rotation of plane polarized microwave beam for measuring precursor ionization from exploding wire discharge in various gases
01 p0129 A69-10663

Continuous and time-resolved absorption and emission spectra studies produced by exploding wires in gases, discussing effects of environment, pressure and electrical energy
01 p0118 A69-10664

Copper exploding wire Kerr-cell time-resolved absorption spectra analysis, considering copper atom transition
01 p0118 A69-10665

Exploding wire heating technique using combination of focused laser beam electric field intensity and pulsed power electric current
01 p0090 A69-10666

High temperature plasmas generation by exploding gold wires in vacuum, using time of flight technique for plasma densities and flow velocities
01 p0129 A69-10667

Adsorbed gas influence on X ray emission from exploding tungsten wires noting ungasged and degassed specimens in vacuum
01 p0118 A69-10668

Current sheath surrounding exploding copper wire in vacuum, plotting current distribution as function of time and radius
01 p0119 A69-10669

Exploding wire phenomenon during early expansion from time correlated X ray and optical streak photographs in vacuum chamber
01 p0119 A69-10670

Time resolved spectroscopy of exploding wire plasmas in visible spectrum of various elements, determining plasma characteristics
01 p0119 A69-10671

Exploding wire detonators noting dependence of threshold burst current on bridgewire length and diameter, explosive surface, density, etc
01 p0119 A69-10672

Liquid copper electrical conductivity temperature dependence at very high temperatures from magnetic diffusion and flux penetration measurements, noting exploding wires role
01 p0119 A69-10673

Thermal model for interaction of exploding wires with methane atmosphere, discussing energy transfer efficiency in high temperature pyrolyses near explosion
01 p0119 A69-10674

Hydrocarbon formation mechanisms under conditions resulting from graphite filament explosions in hydrogen atmospheres, emphasizing stepwise radical formation and methane role
01 p0120 A69-10675

Exploding wire detonators without primary explosive, discussing high precision fabrication, safety aspects and firing circuit
01 p0120 A69-10676

Exploding wire self healing fuse feasibility demonstrated with Hg, noting dynamics of conversion of electric to mechanical energy
01 p0120 A69-10677

Slowly exploding wires for igniting self sustaining deflagrations in PETN, RDX, HMX and tetryl, comparing circuit parameters for detonation initiation
01 p0141 A69-10678

Capacitance-voltage relationships for PETN initiation by various diameter gold exploding bridgewires, noting optimum capacitance dependence on energy transfer efficiency
01 p0141 A69-10679

Chemical phenomena during explosions of wires in various gaseous atmospheres, using apparatus with electronic crowbar for current flow regulation
01 p0081 A69-10680

Wires electrical explosion applications used to study equilibrium characteristics of metals and alloys at high temperatures
02 p0280 A69-11581

Temperature and electron density distribution during late phase of wire explosion, analyzing optically thin plasma column by quantitative spectroscopy
02 p0286 A69-11711

Dense plasma radiation, analyzing spectrographically initial stages of wire explosion in vacuum
03 p0482 A69-14227

Electric propulsion research in Japan, considering cesium ion thruster, plasma acceleration and thrust by electric explosion of fine wires
06 p0984 A69-17629

Gasdynamic flow shock wave phenomena during exploding wire dwell time inside metal vapor cylinder, noting effect on reignition
07 p1188 A69-18275

Thermal explosion criterion used for explosion/ignition delay of exothermic material surrounding heated wires having good thermal conductivity
[WSCJ PAPER 68-23] 07 p1240 A69-18359

Energy characteristics of exploding wires considered as shock wave source
09 p1539 A69-21560

Secondary explosives ignition by primers and other explosive wire devices on missiles, discussing circuitry and resistance to severe climatic and electrical environments
10 p1751 A69-23021

Expansion velocity of discharge plasma in exploding wires measured by X ray flash and streak photography, noting discrepancy
11 p1926 A69-24472

Flash radiography technique using tungsten wire explosion in vacuum to obtain ultrafast reproducible X ray pulse
12 p2092 A69-26480

Optical and spectral properties of dense plasma expanding after exploding electric wire in vacuum using high speed photography
12 p2137 A69-26533

Digital computers for aircraft engines control, discussing economic assessment, advantages and basic control system
15 p2671 A69-30323

Pressure behind spherically divergent shock wave produced by explosion of metal wire measured and compared with calculated values
16 p2769 A69-31837

Micrometeorite simulation by wire explosion plasma, discussing energy requirements and simulator performance
16 p2821 A69-31839

Exploding bridgewire /EBW/ systems compared to hot-wire initiators for Mars space probe
17 p2905 A69-34108

Cumulative shock waves in vaporized products of electrical explosion of conical copper wire configuration, discussing atmospheric ionized vertical configuration formation
19 p3372 A69-35823

Stored energy release in exploding wire circuit during divergent detonation wave ignition in propane-oxygen mixture in circular sector
19 p3451 A69-36365

Conductor material thermal conductivity contribution to self similar explosion in strong magnetic field, determining critical field strength
22 p3982 A69-41019

EXPLORATION

U LUNAR EXPLORATION
U SPACE EXPLORATION

EXPLORER SATELLITES

NT IMP
NT MICROMETEOROID EXPLORER SATELLITES
NT RADIO ASTRONOMY EXPLORER SATELLITE

Upper atmospheric models, considering satellite orbital and solar panel torques, prediction, atmospheric density and composition measurements, etc
[AIAA PAPER 69-50] 06 p1011 A69-18085

Magnetopause, magnetosheath, bow shock and adjoining interplanetary domain study by IMP-1 satellite, discussing macroscopic plasma variables and fluid model for solar wind
07 p1129 A69-19374

EXPLORER 1 SATELLITE

Lifetime of artificial satellites by approximate integration method with application to Explorer 1, comparing analytical prediction
22 p4036 A69-39973

EXPLORER 16 SATELLITE

Meteoroid flux measured by Explorer 16 and Lunar Orbiter, analyzing penetration rate, average velocity and consistency with photographic meteors
13 p2349 A69-27820

EXPLORER 18 SATELLITE

IMP-1 experiment, describing design and applications of SDP-3 computer
19 p3280 A69-36265

EXPLORER 20 SATELLITE

Explorer 20 satellite for obtaining fixed frequency pulse soundings of ionospheric topside, discussing transceiver-dipole antenna instrumentation and payload
20 p3618 A69-37857

EXPLORER 22 SATELLITE

Scintillation index variations based on 40 MHz Explorer 22 satellite signals recorded in Germany
12 p2034 A69-27094

Radio signal amplitude changes from Explorer 22 beacon satellite attributed to wave diffraction by tropospheric structures
14 p2411 A69-29107

Explorer 22 observations of ionosphere electron content, describing measuring equipment and data evaluation
22 p3935 A69-39977

EXPLORER 26 SATELLITE

Explorer 26 observations of solar proton penetration inside trapped radiation near geomagnetic equator
01 p0146 A69-11122

EXPLORER 29 SATELLITE

Satellite trajectory determination and expected errors for OGO 4 and Geos 1 orbits, noting geopotential, aerodynamic drag and integration contributions
15 p2698 A69-31331

Optical observations of Geos 1 over North America in short arc reduction to improve tracking stations survey coordinates, discussing dependence on earth gravity and mass
15 p2599 A69-31342

EXPLORER 30 SATELLITE

Solar flux variations in 44-60 A band during ascent of current solar cycle /Number 20/ measured by Solrad 8 satellite
04 p0650 A69-15530

Explorer 30 satellite monitoring of solar X ray emission during July 1-15 1966, noting plage region activation with increasing emission
10 p1763 A69-23736

Geomagnetic storm induced temporary radiation zones located by determining Explorer 30 attitude and spin axis orientation
14 p2514 A69-29384

Anomalous X ray signals from Explorer 30 satellite showing saturation in ionization chamber possibly due to enhanced solar and atmospheric X rays
21 p3792 A69-39808

EXPLORER 31 SATELLITE

Cylindrical electrostatic probes on Alouette 2 and Explorer 31 satellites used in intersatellite comparison of directly measured ionospheric electron temperature and density
20 p3544 A69-37876

Cylindrical electrostatic probe measurements on Alouette 2 and Explorer 31, considering implications for future missions
20 p3544 A69-37877

Planar thermal ion and electron trap experiments on Explorer 31 satellite, measuring ion and electron density and temperature and ionic composition
20 p3544 A69-37878

Langmuir plate and spherical ion probe experiments aboard Explorer 31, measuring concentrations and temperatures of thermal electrons and ions
20 p3545 A69-37881

Plasma temperature and ion concentration profiles determined from simultaneous measurements by Alouette 2 and Explorer 31 satellites of electron density, temperature and ion abundance
20 p3532 A69-37896

EXPLORER 33 SATELLITE

Explorer 33 and 35 satellites reliability achievement by design via AIMP program
03 p0519 A69-13232

Anisotropic fluxes of energetic particles in and near distant trapping region encountered by Explorer 33 satellite in outer magnetosphere
11 p1950 A69-25146

EXPLORER 35 SATELLITE

Explorer 33 and 35 satellites reliability achievement by design via AIMP program
03 p0519 A69-13232

Lunar magnetic moment and surface field, discussing Explorer 35 field measurements
03 p0514 A69-14005

Picogram dust particle flux in selenocentric space measurement by Lunar Explorer 35, showing enhancement during meteor showers
15 p2699 A69-31396

Lunar Explorer 35 measurements of lunar surface electromagnetic properties, magnetic fields and solar wind-moon interactions 21 p3794 A69-38379

EXPLORER 38 SATELLITE

RAE satellite boom deployment to achieve gravity gradient capture 07 p1228 A69-18346

EXPLORER 40 SATELLITE

Explorer 40 satellite mathematical model and verification testing for close spacecraft flight temperature predictions [SAE PAPER 690202] 07 p1239 A69-18305

EXPLOSIONS

NT AERIAL EXPLOSIONS
NT CHEMICAL EXPLOSIONS
NT GAS EXPLOSIONS
NT NUCLEAR EXPLOSIONS
NT THERMONUCLEAR EXPLOSIONS
NT UNDERGROUND EXPLOSIONS

Centimeter radio wave reflections from explosion region produced by TNT and hexogen charge 02 p0282 A69-12415

Supercooled water drop frozen and observed to undergo explosive shattering and ejection of ice splinters 02 p0275 A69-12693

Medium heating by explosion in presence of allotropic changes and thermochemical reactions concerning temperature field determination 03 p0534 A69-14159

Explosive detonated in external electric field to obtain data on gas state behind shock wave 04 p0634 A69-14430

Deficiencies in two hazard classification system for detonating and fire producing materials from analysis of chemical industry accident fatality statistics 04 p0645 A69-14471

Characteristics of liquid propellant explosions, analyzing detonation, shock wave formation and deflagration 04 p0645 A69-14474

Saturn fireball thermal environment associated with liquid propellant explosions, using analytical model 04 p0645 A69-14475

Structures response to explosive blast, discussing damage criterion in terms of blast wave impulse and critical time 04 p0671 A69-14476

Thermal explosion criterion used for explosion/ignition delay of exothermic material surrounding heated wires having good thermal conductivity [WSCI PAPER 68-23] 07 p1240 A69-18359

Fragmentation behavior of small thin walled metal cylinders during explosions as function of expansion velocity and material parameters 09 p1611 A69-21352

Unsteady gas dynamics of explosions and detonation theory, noting applications to rocket propulsion systems performance 11 p1876 A69-25595

Holographic position and velocity measurement techniques for high speed objects from explosions 12 p2087 A69-26174

Physical and physiological hazards of cryogenic liquids, emphasizing fire and explosion problems associated with storage and handling 17 p3017 A69-33684

Gas dynamics of explosions - IAA Conference, Brussels, September 1967 19 p3448 A69-36351

Numerical program for gas dynamics of hydrodynamic flow and radiation transport in diffusion and grey body approximations 19 p3450 A69-36356

Explosions mechanism in radio galaxies and quasars mechanism based on observed phenomena, emphasizing galactic flares 24 p4378 A69-42698

EXPLOSIVE DECOMPRESSION

Invertebrates resistance to explosive decompression and low end pressure, noting hypoxia and freezing as cause of death 07 p1059 A69-18537

EXPLOSIVE DEVICES

NT DETONATORS
NT INITIATORS [EXPLOSIVES]
NT PRIMERS [EXPLOSIVES]
NT SHAPED CHARGES

Explosive devices to sabotage aircraft in flight, discussing evidence of sabotage in aircraft wreckage and detection of explosives before loading 04 p0549 A69-14943

Pyrotechnic and explosive elements in space systems - Conference, Tarbes, France, July 1968 10 p1748 A69-23003

General and classical statistical techniques for cutting effectiveness and operational reliability of cutting fuses 10 p1749 A69-23004

Space vehicle explosive components, discussing identification, screening and final qualification of explosives and severe environment simulation methods 10 p1749 A69-23008

Explosive and pyrotechnical elements for Grillo 1, Grillo 2 and Trigone 1 hot water rockets, detailing nozzle closure and chemical reaction activation 10 p1753 A69-23028

Emergency escape and personnel recovery systems including F-111 explosive system, midair deployed buoyancy aerostat and fly-away flexible wing rotor 15 p2551 A69-30853

EXPLOSIVE FORMING

Time dependent tube wall radial displacement during explosive welding as function of distance from initial explosion 02 p0254 A69-12675

Explosive forming process to shape aircraft structural parts, advantages and potentials [ASM PAPER C7-2.4] 04 p0604 A69-14524

Explosive welding application to dissimilar metals and tube to tube plate welding, noting influence of detonation and sound bulk velocity 04 p0608 A69-15481

Air cushion effect on dimensional accuracy in explosive forming of metal sheet 06 p0930 A69-17001

Air cushion effect in explosive forming of metal sheets, considering simple geometrical shape 06 p0931 A69-17526

Metals structure and mechanical properties after hydroexplosive forming analyzed by X ray diffraction 09 p1503 A69-21851

Explosive forming, discussing optimum parameters for model and prototype parts and subscale forming criteria for aluminum ellipsoidal domes 09 p1512 A69-22371

Explosive fabrication of aircraft components including turbine engine exhaust components, door seals, etc [SAE PAPER 690316] 11 p1890 A69-24510

Fusion and solid state welding of steels, considering electron beam, HF resistance, friction and explosive welding 12 p2100 A69-25830

Explosive compacting of aluminum powder, describing operational and experimental techniques, compacts hardness and density, mass production feasibility, etc 16 p2793 A69-31790

Explosive forming theory and experience including explosives characteristics, dimensional relations, hold-down pressure, economics and applications 24 p4320 A69-43038

EXPLOSIVE GASES

U FLAMMABLE GASES

EXPLOSIVE WELDING

Explosive bonding technique, discussing choice of explosive and geometrical parameters to match material parameters [ASME PAPER 69-DE-47] 14 p2454 A69-28849

Explosives parameters effect on metal sheet velocity during explosive welding, considering load density and explosive force 18 p3149 A69-35279

Explosive welding principles, applications, materials limitations and advantages, stressing safeness and low cost 18 p3151 A69-35479

Tensile data and photomicrographs of explosively bonded metal matrix composites interfaces 24 p4326 A69-43452

EXPLOSIVES

NT CELLULOSE NITRATE

NT RDX

NT TETRYL

Megagauss magnetic field generation methods, discussing high explosives, initial field, flux compression, capacitor discharges and applications 01 p0115 A69-10049

Electrical explosive devices for space applications including explosive bolts, primers and igniters 01 p0141 A69-10544

Powders and explosives - Conference, Brussels, September 1966 02 p0301 A69-11519

Shock sensitivity of solid explosives and propellants, using calibrated gap testing techniques 02 p0302 A69-11520

Remotely controlled explosives processing facility for handling unfamiliar sensitive materials, noting safety aspects and inspection, testing, transporting and destroying techniques 02 p0226 A69-11521

Detonation wave structure in solid cylindrical shell explosive, noting attainment of steady state structure 02 p0349 A69-11526

Detonation generation in granular explosive subjected to different shock wave intensities due to variable impact velocity 02 p0349 A69-11527

Compatibility of inorganic azides with organic explosives from elevated temperature interactions using trinitrobenzene as model 02 p0304 A69-12499

Ultrahigh pressure test vessel for determining pressure vs burning rate characteristics of propellants and explosives 04 p0645 A69-14472

Explosives and propellants sensitivity to fragment impact, establishing threshold detonation velocity 04 p0645 A69-14473

Wedge shaped charge technique for evaluation of detonation hazards of liquid explosives 04 p0646 A69-14479

Explosive containment capsule for nuclear reactor irradiation 04 p0629 A69-14480

Liquid explosive testing from point of view of liquid mobility 04 p0646 A69-14481

Insensitive explosive trigger or initiator consisting of metal/metal oxide powder with low shock sensitivity and high thermal stability 04 p0646 A69-15300

Liquid phase radical oxidation with intermediate and end products in same phase, discussing products, hydroperoxidation and liquid systems explosiveness 06 p1032 A69-17425

Fragments and markings produced on aircraft aluminum by explosion as means of detecting sabotage in crashes 06 p0868 A69-17833

Explosive acrylic polymers properties and preparation methods, noting chemical reactions and structure 08 p1376 A69-21152

Aminotetrazole preparation to obtain tetrazole derivatives and explosive salts 10 p1651 A69-23013

Heat resistant DIPAM and HNS explosives in aerospace applications, considering mild detonating fuse and core loading 10 p1750 A69-23014

Igniferous materials for electrical initiation of explosive in extreme conditions, considering nitrophenol salts and pyrotechnics 10 p1750 A69-23015

Shock initiation and sensitivity of granular explosives, noting heterogeneity effect in ammonium perchlorate 10 p1751 A69-23016

Initiation of priming explosives by electrons, photons, electrical discharges and laser radiation 10 p1751 A69-23017

Combustion mechanism of condensed inflammable systems such as gunpowder and other explosives, discussing combustion stability 11 p2000 A69-25187

Soviet book on combustion, detonation and explosive energy of condensed systems covering stable/unstable processes 12 p2190 A69-26757

Aluminum capsule used in test reactor to irradiate explosive and propellant samples, determining radiation effects 17 p3004 A69-32945

Irregular pressure profiles and pressure-time histories when using octofluorocyclobutane and sulfur hexafluoride in explosive driven shock tube [AIAA PAPER 68-730] 24 p4297 A69-43577

EXPONENTIAL FUNCTIONS

NT LOGARITHMS

Linear ordinary differential equations with exponential coefficients, giving solutions asymptotic behavior for large values of independent variable 01 p0103 A69-10231

Distribution of moment of first passage through positive level for homogeneous process with independent increments and exponential characteristic function, constructing integral equation 01 p0104 A69-10265

Exponential distributions in Markov chain models for communication channels, considering error free runs of tropospheric systems
01 p0027 A69-10267

Divergent-convergent and convergent-divergent cascaded exponential lines, determining equivalent length of uniform transmission line
01 p0044 A69-10623

Exponential approximation with piecewise linear error criteria for continuous function over interval
01 p0107 A69-11415

First order linear differential equations having complementary solutions of exponential type to determine effective initial and boundary conditions
05 p0786 A69-15926

Large displacement bending of rods for constant deformation cross section, negligible shearing forces and exponential stress-strain relation
05 p0843 A69-16682

Hyperbolic sine creep law, discussing limiting stresses for approximation by linear or exponential relationship
07 p1235 A69-19384

Cumulative probability distribution of positive random variable from moment generating function, exemplifying exponential and Poisson functions
12 p2120 A69-25927

Negative exponential solution of matrix Riccati equation associated with linear optimal regulator and filter problems for time invariant plants
12 p2122 A69-26513

Linear difference equations with exponential coefficients for numerical methods of integrating differential equations
13 p2288 A69-27526

Leonid meteoroids mass distribution law exponent evaluation based on unstable meteoric radio echo durations integral distribution
18 p3203 A69-35334

Partial prior information utilization via confidence intervals for mean time to failure of exponential reliability model
19 p3360 A69-36038

Distribution of moment of first passage through positive level for homogeneous process with independent increments and exponential characteristic function, constructing integral equation
19 p3360 A69-36200

Drag minimization as extremization of products integrals powers, noting application to optimum wings and fuselages
19 p3242 A69-36800

Generalized limit theorem for reliability replacing Drenick exponential theorem
20 p3547 A69-37068

Table of definite and indefinite integrals of products of exponential integrals with elementary or transcendental functions
24 p4341 A69-43324

EXPONENTS
Leonid meteoroids mass distribution law exponent evaluation based on unstable meteoric radio echo durations integral distribution
18 p3203 A69-35334

EXPOSURE
Life raft thermal protection against exposure of aircrews to cold, noting chemically fueled heaters and IR reflective liners
06 p0883 A69-17841

Hologram storing on photochromic film, obtaining equations for optimal exposure time
[IEEE PAPER F-1]
07 p1133 A69-19053

Electron beam exposure system to photoetch integrated circuit patterns without photomasks, using electronic computer for automatic pattern generation and registration
15 p2579 A69-31039

EXPRESSIONS [MATHEMATICS]
U FORMULAS [MATHEMATICS]

EXPULSION
Damped mass expulsion for space vehicle attitude control reducing propellant consumption and pulsing frequency
[AIAA PAPER 67-535]
09 p1610 A69-21986

Propellant orientation and expulsion methods in space vehicle tankage, discussing ullage rockets system, bladders and diaphragms, dielectrophoretic expulsion, etc
16 p2736 A69-31734

EXTENSIONS
Antisymmetric cross ply and angle ply laminated plates deflection under transverse loading with coupling between bending and middle-plane extension
07 p1231 A69-18711

EXTENSOMETERS
Four specimen vacuum device for simultaneous tensile creep tests at 1200 C, discussing linear and thermal expansion
07 p1116 A69-19318

Capacitance methods for measuring adhesives mechanical properties in thin film bonded joints, noting results for tension, compression and shear loading
09 p1500 A69-22309

Automatic recording inverted dilatometer employing fused quartz vertical pedestal and yoke type pushrod
15 p2607 A69-30153

High temperature capacitance strain gage development, discussing extensometer prototype systems
15 p2614 A69-31278

EXTERNAL COMBUSTION ENGINES
External burning ramjets in supersonic stream noting applications to drag reduction, lift-drag ratio and attitude control
11 p1941 A69-24261

EXTINCTION
Borrmann effect and abnormal transmission and extinction observed by reconstruction of images of holograms recorded in three dimensional photosensitive medium
09 p1494 A69-21492

Atmospheric extinction function in Chile by using photoelectric spectrum scans, observing neutral component, Rayleigh scattering and ozone absorption variations
10 p1777 A69-23386

Interstellar extinction models of classical Mie particles and quantum mechanical polycyclic aromatic molecules
10 p1781 A69-23679

Extinction kinetics of monopropellant droplet burning in inert gas reservoir with atmospheric temperature lower than adiabatic combustion temperature
13 p2378 A69-28250

Equations for steady state combustion of fuel drops in oxidizing atmosphere integrated numerically, obtaining ignition and extinction conditions
13 p2379 A69-28456

Monograph on interstellar extinction computations covering theoretical curves for spherical metal and graphite particles, albedo, optical constants, normalization, temperature dependence, etc
14 p2516 A69-28901

Extinction efficiency of graphite core interstellar grains with solid hydrogen and ice mantles, using theoretical models
14 p2486 A69-29587

Efficient extinction in optically coupled GaAs injection lasers achieved by selecting quenching radiation frequency close to operating frequency
15 p2633 A69-30059

Positively charged diatomic hydrogen molecules interstellar extinction and photodissociation cross section in terms of formation mechanisms
24 p4375 A69-42610

EXTINGUISHERS
U FIRE EXTINGUISHERS

EXTINGUISHING
Solid propellant motor extinction by depressurization, determining extinction conditions by electrical analogy
17 p3021 A69-33355

Solid propellant motor extinction by depressurization, determining extinction conditions by electrical analogy
[ONERA-TP-722]
18 p3184 A69-34637

EXTRACTION
NT ION EXTRACTION

Organic compounds /mctabolites/ extracting technique from nutrient media of Chlorella cultures indicate unsaturated amine and phenol composition
08 p1262 A69-19833

Dispersion-strengthened alloys from extraction replicas, determining volume fraction and spacing of dispersed phase particles
13 p2282 A69-28167

Ti determination in presence of Nb or Ta by extraction-photometric method with diantipyryl methane and thiocyanate
20 p3544 A69-37812

EXTRAGALACTIC LIGHT
U EXTRATERRESTRIAL RADIATION
U LIGHT [VISIBLE RADIATION]

EXTRAPOLATION
Extrapolation and interpolation for data compression including polynomial concept
12 p2027 A69-25877

Extrapolation of aperiodic step responses
12 p2051 A69-26237

Technological forecasting by intuitive forecasts, consensus methods, analogy, trend extrapolation and structural models
13 p2382 A69-28040

Unlimited extrapolation into infinity to determine ranges of applicability of theories in relativistic cosmology noting paradoxes
14 p2516 A69-28867

Trajectory models accuracy beyond tracking intervals, studying roles of extrapolation and independent measurements number and accuracy
22 p4032 A69-41015

EXTRATERRESTRIAL ENVIRONMENTS
NT CHROMOSPHERE
NT CISLUNAR SPACE
NT DEEP SPACE
NT INTERPLANETARY SPACE
NT INTERSTELLAR SPACE
NT JUPITER ATMOSPHERE
NT LUNAR ATMOSPHERES
NT LUNAR ENVIRONMENT
NT MARS ATMOSPHERE
NT MARS ENVIRONMENT
NT PLANETARY ATMOSPHERES
NT PLANETARY ENVIRONMENTS
NT SOLAR ATMOSPHERE
NT SOLAR CORONA
NT STELLAR ATMOSPHERES
NT VENUS ATMOSPHERE

Extraterrestrial vestibular research, discussing human otolithic apparatus regulation subjected to change from geocentric to heliocentric orientation
[UN PAPER 68-95389]
01 p0014 A69-10508

Spacecraft sterilization techniques efficiency in terrestrial and extraterrestrial environments noting dry heat, radiation, ethylene oxide, isopropanol and formaldehyde in methanol
05 p0712 A69-15937

Space photography as sedimentological research tool demonstrated by space photographs application to projected Mars mission
09 p1490 A69-21797

Electronic equipment for data acquisition in extraterrestrial experiments including low noise charge amplifiers, discriminator, pulse lengthener, linear gate and logarithmic amplifier
16 p2759 A69-31857

Venusian atmospheric features obtained from Venus 5 and 6 and Mariner 5 observations, indicating extremely high temperatures and pressures
19 p3401 A69-35840

EXTRATERRESTRIAL LIFE
Soviet literature on extraterrestrial life and civilization emphasizing establishment of contact by radio and laser sources
01 p0016 A69-10953

Resistance of animal organisms and cells to extreme environmental conditions discussing exobiological implications for extraterrestrial life systems
01 p0017 A69-11083

Planetary quarantine and biological search strategy, discussing Voyager-Mars mission configuration, sterilization, back contamination and decisions
01 p0021 A69-11090

Soil, moisture and other requirements for microorganism survival in simulated Martian environment
01 p0018 A69-11091

Pedoscope use in soil microbiological studies including ecology, infection susceptibility, etc
01 p0021 A69-11092

Extraterrestrial life detection methods based on soil or atmospheric sampling, discussing enzyme activity, DNA determination, microbial growth, etc
01 p0021 A69-11093

Extraterrestrial life possibility in solar system, noting Martian atmosphere and terrestrial life adaption to Mars simulations
02 p0198 A69-11770

NASA Planetary Exploration Program to gather data on origin of solar system and life, discussing planetary evolution and extraterrestrial life
02 p0200 A69-12804

Product assurance role in spacecraft sterilization to maintain planetary biological environments integrity in space programs for extraterrestrial life determination
03 p0379 A69-13400

Mars biological exploration, discussing life detection, chemical and biological experimental strategy
[AIAA PAPER 68-1122]
03 p0375 A69-13700

Life probability and origin on Milky Way planets with emphasis on solar system, discussing molecular biology role
05 p0707 A69-15966

Organic matter signals in carbonaceous meteorites, discussing possible relation to extraterrestrial life and origin
11 p1953 A69-24342

- Hypothesis for intelligent life existence in universe
13 p2353 A69-28435
- Integrated device to detect biological growth and catabolic and anabolic activity in extraterrestrial exploration
15 p2556 A69-31306
- Life detection for space missions based on detecting optical asymmetry in biogenic molecules by gas chromatography involving diastereomeric esters synthesis
15 p2556 A69-31315
- Biochemiluminescent luminol-peroxide reaction to detect iron porphyrin proteins in microorganisms for extraterrestrial life search, discussing reaction kinetics
15 p2556 A69-31325
- Exobiology, Search for extraterrestrial life - AAS-AAAS Conference, New York, December 1967
17 p2907 A69-32967
- Solar system physical environments surveyed from exobiological viewpoint
17 p2907 A69-32968
- Experiments integrated into single automated laboratory to detect extraterrestrial life through measuring metabolism and growth in planetary surface material
17 p2912 A69-32969
- Extraterrestrial life detection experiments integrated into single multipurpose space laboratory, including chemical analyses, metabolism identification, observation for molecular and/or cellular growth and replication
17 p2912 A69-32970
- Interstellar communication in search for extraterrestrial intelligence, discussing radio objects, OH emission regions and pulsating stars
17 p3028 A69-32971
- Origin of microbial life on earth and implications for extraterrestrial forms
17 p2907 A69-32972
- Electron transport initiated by radiant energy absorption or by reducing suitable electron acceptor as source of energy for extraterrestrial life
17 p2908 A69-32973
- Earth ecosystem chemical composition compared with Mars and Venus ecosystems to determine presence of life
18 p3193 A69-34361
- Soviet book on cosmos and microorganism utilization for creating regenerative life support in spacecraft
20 p3467 A69-37230
- Probability of biological development leading to human life on another planet
21 p3652 A69-38786
- Sporopollenin content of Orgueil and Murray meteorites as evidence for extraterrestrial life
21 p3662 A69-39617
- Meteorites pigments identification as porphyrins for extraterrestrial life evidence, noting sample analyses of Orgueil, Murray, Cold Bokkeveld and Mokoia carbonaceous chondrites
22 p4008 A69-39889
- Physical and life supporting properties of hypothetical Martian biosphere, considering organism adaptation theories
22 p3876 A69-40271
- Ecological foundations of Haldane metalaw and implications of interstellar golden rule, discussing social interaction with alien life forms
23 p4240 A69-41304
- Mars exploration for life by Mariner flybys and orbiters and 1973 Viking landers
23 p4212 A69-41611
- Life on Mars, past and future missions, possibilities of metabolic system and analysis methods
23 p4212 A69-41612
- Spaceborne planetary UV spectroscopic search for atoms and molecules basic to life, specifically molecular N and water vapor photodissociation products
23 p4113 A69-41616
- Extraterrestrial optical microscopy, discussing experiment, telemetry, data interpretation and instrument characteristics concerning biological, cytochemical and petrographic microscopes
23 p4164 A69-41621
- Optical activity measurement for exobiology applications, considering polarimetry, gas-liquid chromatography, mass spectrometry and radioactivity detection
23 p4213 A69-41622
- Sequential analyses of planetary surface sample for extraterrestrial life detection, discussing chemistry, morphology, growth and metabolism for life attributes
23 p4213 A69-41623
- Human habitation conditions on moon from viewpoint of solar and lunar radiation, vacuum and gravitation effects including solar energy utilization
23 p4111 A69-42213

EXTRATERRESTRIAL MATTER

- NT COSMIC GASES
NT COSMIC PLASMA
NT INTERPLANETARY GAS
NT INTERSTELLAR GAS
- Meteoritic extraterrestrial materials sampling for chemical, petrographic and metallurgical analyses, discussing microstructure and optimum specimen weight for representative analysis
[UN PAPER 68-95381] 01 p0150 A69-10480
- Methods and conclusions for rate of influx to earth of extraterrestrial material
03 p0511 A69-13467
- Satellite data for reevaluating extraterrestrial particles origin found in polar ice, atmosphere and terrestrial surface collections
04 p0654 A69-14655
- Galaxies classified by matter content of nucleus, discussing evolution
11 p1953 A69-24351
- Black magnetite spherules electromagnetically separated from residue of Permian rock salt, determining content and properties of extraterrestrial material
12 p2154 A69-25821
- Spiral galaxies rotation curve fluctuations attributed to kinematic properties of galactic matter and gas components
12 p2170 A69-27062
- Earth contamination by returned lunar or Martian material, discussing extraterrestrial biota survival on earth
13 p2210 A69-28467
- Noctilucent clouds total or partial extraterrestrial origin, deriving minimum particulate influx from satellite and rocket data
21 p3702 A69-38347
- Universe evolution from hot initial state, discussing element synthesis, quanta, radiation particles, etc
21 p3795 A69-38401
- Extraterrestrial matter - Conference, Argonne, Illinois, March 1968
22 p4011 A69-40083
- Tektite origin theories, discussing Surveyor experiments effects on lunar geology and Tektite origin
22 p4012 A69-40086
- Lunar regolith from Surveyor Program pictorial data of lunar maria
22 p4012 A69-40087
- Thermal conduction by electrons in stellar matter, presenting opacity tables for H, He, C and red giant cores and solar composition
22 p4014 A69-40147
- EXTRATERRESTRIAL RADIATION
NT COSMIC NOISE
NT GALACTIC RADIATION
NT GALACTIC RADIO WAVES
NT GEGENSCHLEIN
NT INTERSTELLAR RADIATION
NT LUNAR RADIATION
NT PLANETARY RADIATION
NT PRIMARY COSMIC RAYS
NT RADIO BURSTS
NT SOLAR CORPUSCULAR RADIATION
NT SOLAR COSMIC RAYS
NT SOLAR PROTONS
NT SOLAR RADIATION
NT SOLAR RADIO BURSTS
NT SOLAR RADIO EMISSION
NT SOLAR WIND
NT SOLAR X-RAYS
NT STELLAR RADIATION
NT STELLAR WINDS
NT SUNLIGHT
NT TYPE 2 BURSTS
NT TYPE 3 BURSTS
NT TYPE 4 BURSTS
NT TYPE 5 BURSTS
NT ZODIACAL LIGHT
- Space X ray background measurements, considering relativistic electrons Compton emission and metagalactic gas bremsstrahlung as possible sources
01 p0147 A69-11310
- Cosmic rays properties and sources, considering origin in supernovae, galaxies, quasars and unknown sources
02 p0308 A69-12158
- Outer space electromagnetic radiation transfer in turbulent plasma with allowance for polarization effects, describing polarization induced changes in Stokes parameters
03 p0506 A69-13083
- Space radiation biology - NASA Conference, Berkeley, September 1965
03 p0370 A69-13476
- Extraterrestrial background gamma radiation /0.3-2 Mev/ observations used to derive upper limits for

cosmic ray protons and CNO nuclei in interstellar space

03 p0501 A69-13934

Proton beams uniformity available at NASA synchrocyclotron designed for radiation biology research by simulating space radiation environment

05 p0742 A69-15992

Intergalactic continuum study showing universe behavior like black body with 2.7 K radiation temperature, noting cosmological and cosmogonic importance

05 p0827 A69-16593

Nuclear and space radiation effects - IEEE Conference, University of Montana, July 1968

06 p0973 A69-1686

X ray astronomy use for probing hot regions of outer space and high energy electrons

06 p0991 A69-17307

Space radiation effect on spacecraft components and materials simulated by proton and fast electron bombardment of silicon, glass and skin materials

06 p0906 A69-17612

Particle flux and dose rates in Jupiter Van Allen belts based on assumed synchrotron radiation from trapped electrons in dipole magnetic field [AIAA PAPER 69-18]

06 p0997 A69-18129

Discrete extragalactic X ray sources model for explanation of diffuse X ray background, noting evolutionary aspects

07 p1206 A69-19255

Compton scattering of microwave radiation on cosmic ray electrons proposed as mechanism generating 100 Mev cosmic gamma rays

09 p1580 A69-22295

Celestial X ray source positions from rotating modulation collimator, predicting performance of collimator

10 p1722 A69-23328

Extragalactic gamma ray fluxes predicted, discussing collisions, matter-antimatter annihilation and cosmological implications

11 p1946 A69-24466

Calculation of radiation doses in space - Conference, Toulouse, France, February 1968

11 p1947 A69-24854

Space radiation phenomena, discussing auroral precipitations and characteristics and solar flare particle ejection

11 p1948 A69-24859

Extragalactic radio sources parameters analyzed for distinguishing quasars from dominant luminous radio galaxies by radio spectra

13 p2348 A69-27801

Outer space electromagnetic radiation transfer in turbulent plasma with allowance for polarization effects, describing polarization induced changes in Stokes parameters

14 p2515 A69-28765

Scientific equipment on Cosmos 237 satellite for recording extraterrestrial radiation data, discussing specifications, operation and mission purpose

14 p2446 A69-29047

Extragalactic research to solve problems in cosmological and cosmogonic theory, including relativistic cosmology and observations

15 p2681 A69-30436

Energy transfer during fast electrons and photons interactions, indicating Compton energy losses related to space X ray and gamma radiation sources

15 p2676 A69-30953

Extraterrestrial X ray galactic and extragalactic sources research fields, emphasizing identification with optical objects

15 p2696 A69-31213

Metagalactic electrons inverse Compton effect on relic radiation to interpret cosmic isotropic X radiation entire energy spectrum

16 p2847 A69-31800

600 Mev proton synchrocyclotron at Space Radiation Effects Laboratory for space radiation environment simulation, discussing beam energy spread

16 p2814 A69-32201

Corrections to previous papers on extragalactic gamma rays, discussing effects on various cosmological models

17 p3025 A69-34168

Photodisintegration of ultrahigh energy cosmic rays by universal radiation field, analyzing implications on origin and propagation time

18 p3188 A69-35006

Instruments for gamma ray astronomy including Ranger low energy detector, howitzer detector and cosmic spark chamber

18 p3138 A69-35135

Radio and radar astronomy with reference to extragalactic sources and solar system, noting astronomical instrumentation
19 p3425 A69-36430

Linear and circular integrated polarization of extragalactic radio sources measured by two element interferometer at Owens Valley Radio Observatory
20 p3610 A69-38139

Soft x ray extragalactic background flux measurements, considering correction for absorption by interstellar medium
21 p3788 A69-38541

Particles integral and differential fluxes spectral distribution calculation for determining radiation load for synchronous satellite
22 p4035 A69-39909

Extragalactic universe major constituents and physical properties of normal, radio and compact galaxies, discussing missing matter existence
23 p4217 A69-42317

High energy astronomical diffuse radiation component properties tabulated, discussing power law and thermal X ray background, gamma rays, etc
23 p4207 A69-42319

EXTRATERRESTRIAL RADIO WAVES

NT COSMIC NOISE

NT GALACTIC RADIO WAVES

NT RADIO BURSTS

NT SOLAR RADIO BURSTS

NT SOLAR RADIO EMISSION

NT TYPE 2 BURSTS

NT TYPE 3 BURSTS

NT TYPE 4 BURSTS

NT TYPE 5 BURSTS

Radiation due to collective effects in plasma physical aspects of astrophysics, discussing synchrotron radiation and bremsstrahlung
02 p0310 A69-12792

Antennas with vertical radiation patterns to measure frequency spectrum of distributed cosmic radio emission between 6.3-40 MHz
03 p0500 A69-13080

Linear polarization of cosmic radio emission, discussing original measurement method and revised version based on discrimination of useful signal
03 p0501 A69-13705

F cosine i theorem validity for VLF radio wave absorption in ionosphere tested using exponential electron density models, noting Brewster angle influence on reflection coefficient
13 p2222 A69-28473

Antennas with vertical radiation patterns to measure frequency spectrum of distributed cosmic radio emission between 6.3-40 MHz
14 p2509 A69-28762

Sky cosmic radio emission absolute temperature measured at decimeter wavelengths and at two zenith angles to minimize atmospheric influence
15 p2687 A69-30544

Interstellar radio absorption influence on spatial distribution of cosmic radio emission observations with fixed multiple dipole antenna arrays
15 p2687 A69-30545

EXTRATERRESTRIAL RESOURCES

1967 space Treaty Article 11, discussing provisions concerning private exploitation and supernational body authority
20 p3635 A69-37107

Multiple use doctrines in space law for resource utilization, discussing formation of planning commissions and licensing agencies
20 p3639 A69-37133

Planetary resources control and use from legal and policy standpoints, discussing space treaty effects on international law
20 p3639 A69-37134

Bulk, selective particulate and hard rock samplers for landed extraterrestrial geological and biological instruments performing on-site analysis
23 p4146 A69-41620

Manned facilities design, construction and maintenance on extraterrestrial bodies, discussing astrophysical and lunar surface data requirements [AAS PAPER 69-208]
24 p4296 A69-42875

EXTRAVEHICULAR ACTIVITY

Soviet book on human movements coordination during space flight covering space walks, lunar surface photographs, space docking, weightlessness, etc
01 p0018 A69-11180

Prolonged decompression stress effects on humans in simulated orbital flight or extravehicular activity, investigating endocrine-metabolic disturbance by urinalysis
01 p0022 A69-11336

Voskhod 1 and 2 crew performance, orientation and motor activity analysis indicating time increment for task performance, psychophysiological irregularities and visual analysors impaired functioning
02 p0203 A69-12123

Hard space suit for use on planetary surfaces and extravehicular activity, discussing design, fabrication and mobility
03 p0379 A69-12993

Portable astronaut life support systems for extravehicular activities [AICHE PAPER 42C]
04 p0554 A69-14511

Soviet astronaut experiences and visual impressions during space walk outside Voskhod 2, noting dominance of optical analyzer in space perception and orientation [UN PAPER 68-95717]
06 p1000 A69-17049

Astronaut extravehicular protection systems, discussing space suit, life support and thermal control subsystems and micrometeoroid protection
06 p0882 A69-17643

Space suit meteoroid protection for extravehicular activity, discussing Gemini and lunar surface EVA suits and bumper concept [AIAA-PAPER-69-366]
13 p2213 A69-28298

Dynamic characteristics of model of spacecraft-astronaut-tether system during approach, deriving kinetic potential
15 p2696 A69-31064

Physiological effects on men of 10 hour exposure to nitrogen-oxygen mixture followed by pure oxygen 4 hour exposure, simulating conditions during EVA
17 p2912 A69-32940

Cooling system control system for astronaut thermal equilibrium and work output maximization during extravehicular space missions [AIAA PAPER 69-617]
17 p2914 A69-33278

Lithium peroxide utilization feasibility for oxygen supply and carbon dioxide control in extravehicular portable life support systems [AIAA PAPER 69-620]
17 p2914 A69-33303

Space docking, personnel placement on space stations, rescue stations, etc
18 p3196 A69-34630

Relative motion of two bodies linked by flexible weightless tether in artificial earth satellite orbit, simulating extravehicular walk
19 p3427 A69-36618

Mathematical model of astronaut motion and spacecraft angular control during tethered reentry, discussing conditions preventing spinning and collisions
21 p3667 A69-39630

Manned testing of EVA equipment in thermal-vacuum environment for qualification of Apollo extravehicular mobility unit, using lunar surface thermal simulator [AIAA PAPER 69-992]
22 p3893 A69-40370

Apollo Extravehicular Communication Telemetry System for monitoring astronaut portable life support system, space suit performance and body functions on lunar surface
23 p4121 A69-41767

Orbital EVA, discussing technology associated with Apollo Applications Program [AAS PAPER 69-517]
24 p4272 A69-42841

Two degrees of freedom control moment gyro for astronaut attitude control during EVA, discussing muscle-controlled shoe-mounted stilts and precessional feedback forces [AAS PAPER 69-472]
24 p4272 A69-42846

EVA/IVA fluid umbilical improved stowability and flexibility, discussing cross section development and tests [AAS PAPER 69-470]
24 p4272 A69-42847

Unstabilized astronaut, hand-held and integrated life support EVA maneuvering units tested in gimbaled six degree of freedom servo driven moving base simulator [AAS PAPER 69-516]
24 p4272 A69-42850

EXTREMA

U RANGE [EXTREMES]

EXTREMELY HIGH FREQUENCIES

Digital transmission at 35 GHz, noting atmospheric and rainfall effect on terrestrial millimeter wave propagation
03 p0389 A69-13192

CW klystron amplifiers design limitations at Ku and Ka bands, discussing operation characteristics
03 p0405 A69-13724

Temperature dependence of conversion coefficients and sensitivity of n-type InSb detectors in millimeter and submillimeter ranges
07 p1199 A69-18683

High CW power K-band Gunn oscillators attained through control over doping level, profile and GaAs epitaxial layer thickness
12 p2036 A69-25907

Broadband plasma waveguide switch application extended to 26-40 GHz range, discussing isolation, cold loss, switching time, trigger signal and ionized plasma
12 p2036 A69-25938

Zenith atmospheric attenuation in 183-325 GHz region measured by wideband Ge bolometer detector and spectral convolution technique
23 p4115 A69-41586

EXTREMELY LOW RADIO FREQUENCIES

ELF radio wave propagation characteristics using two layered ionospheric model, noting deeper penetration than VLF
03 p0421 A69-13326

Ionospheric LF radio noise cut-off near proton gyrofrequency, discussing satellite ELF and VLF observations
03 p0399 A69-14021

ELF radio waves reflection coefficients calculated from two layer ionospheric model, noting ion collision frequency effect in Schumann resonance frequency band
07 p1124 A69-18820

Magnetospheric ELF noise, discussing OGO 3 spectrum analysis
07 p1124 A69-18834

Scanning Fabry-Perot interferometer with ultralow modulation frequencies, obtaining inverse piezoelectric effect curves of ceramic element
15 p2611 A69-31107

Earth-ionosphere waveguide excitation by lightning discharges and geomagnetic field influence on ELF noise spectrum
17 p2928 A69-33865

ELF wave propagation in earth-ionosphere waveguide, considering ionospheric vertical inhomogeneity and models for ambient and disturbed /PCA/ conditions
18 p3101 A69-34949

ELF radio wave propagation characteristics analyzed by two layer ionosphere model
20 p3488 A69-37285

ELF atmospheric propagation, determining slow tail atmospheric group velocity, relating characteristics to spectral characteristics of lightning
23 p4114 A69-41362

EXTREMUM VALUES

NT LIMITS [MATHEMATICS]

NT MINIMA

Book on variational methods in optimum control theory covering necessary and sufficient conditions for extremum and functional constraints
01 p0053 A69-11107

Boundedness theorem for all solutions of class of nonlinear second order differential equations
02 p0271 A69-11549

Extremum problems from functional-analytic point of view, discussing methods of solving and convergence conditions
03 p0456 A69-13403

Ionospheric beam deflection maximum and minimum levels, deriving equations for maximum usable frequency at given ionization conditions and radiation angles
03 p0424 A69-13540

Upper bound for free energy of nonlocal superconductor in magnetic field, using variational method and perturbation theory
03 p0491 A69-13971

First-kind operator equation solution by reduction to dual extremum problem, proving existence and convergence
04 p0622 A69-14622

Optimum control problems solved numerically on computer, noting multivalence of extremal solutions and application to orbital transfer in central gravitational field
06 p0903 A69-17539

Bounds on scattering lengths, phase shifts and other scattering parameters determining cross sections, noting variational bounds for zero incident energy
07 p1186 A69-19657

Optimizer for shaping control signal of hunting type system with plant in form of nonlinear inertialess element, examining inadequacy for system operation
07 p1115 A69-19757

Infinite tree code ensemble upper bound on moments derived for sequential decoding governed by Fano algorithm
09 p1471 A69-21318

Trajectory error propagation upper bounds in many body field for impulsive initial error, relating error to mission tolerances

09 p1595 A69-21937

Minimal distance of image boundary from origin and second coefficient of univalent function in unit disk

10 p1718 A69-22860

General extremality for optimal controls with restricted phase coordinates and with unorthodox criterion function, discussing hypotheses for deriving necessary conditions

10 p1721 A69-23864

Extremal controlled plants identification by Chebyshev orthogonal polynomials, comparing results with regression analysis

11 p1861 A69-25713

Bounding technique of first excursion probability for random vibration, considering relation to reliability of mechanical and structural systems under random disturbances

13 p2361 A69-27438

Sinusoidal perturbation extremal control system stability, using harmonic balance principle to obtain periodic solutions of system differential equations

15 p2582 A69-30616

Singular and sliding modes/unique extremals/ in calculus of variations for optimal control problems with nonlinear equations and linear control

16 p2764 A69-31629

Received radar signal power maximizing problems in planetary exploration, analyzing abelian group real line and circle problems

17 p2993 A69-32831

Robust detection of binary signal in additive noise, using extreme value theory /EVT/ to estimate probability density function and system error and threshold

17 p2944 A69-33624

Drag minimization as extremization of products integrals powers, noting application to optimum wings and fuselages

19 p3242 A69-36800

Discrete extremum problems solution convergence to optimal control continuous problem as functional optimal value and optimal control

21 p3684 A69-38430

Euler equation in variational problems for optimized process described by ordinary differential equations, deriving final extremal relationship

21 p3829 A69-39825

Monotonic minimization algorithm for nonsmooth extremal problems of mathematical programming, game theory, approximations and optimal control in arbitrary Banach space

23 p4181 A69-51524

Deceleration parameter lower and upper limits for zero pressure big bang cosmological Friedmann models imposed by density parameter, Hubble constant and universe age

23 p4219 A69-42373

Extreme value statistics used to determine minimum acceptable tensile strength of wire command links in TOW antitank missiles

24 p4318 A69-42642

EXTRUDING

Hydroextrusion effect on Mo structure and mechanical properties, noting improved ductility after high temperature annealing

02 p0267 A69-12189

Extrusion processes used for aluminum, magnesium and titanium extrusions, presenting die configurations

04 p0604 A69-14526

Slip band extrusions in hexagonal close packed Cd, Mg and Ti subject to cyclic stresses, noting microstructure changes

12 p2116 A69-26912

Moire and gridwork methods of plastic strain analysis with application to plane strain and axisymmetric extrusion

13 p2359 A69-27256

Hydrostatic tube extrusion, discussing equipment, techniques and commercial applications

[SAE PAPER 690319] 15 p2617 A69-30093

Hot extrusion process for steel and various metals in U.S. semifinished product industry, considering lubrication problems, research centers and development

15 p2618 A69-30228

Hydroextrusion influence on mechanical properties of powder compacts of sintered Mo rods

16 p2803 A69-32491

Disk type or elastic melt extruders development based on Weissenberg effect permitting near uniform extrusion

18 p3148 A69-34612

Hydraulically extruded Mo properties after annealing, showing reduction in stability and hardness and varying nature of change in plasticity

18 p3156 A69-34719

Wide panel Ti structural extrusions with integral stiffeners, discussing material, sizes, properties and tolerances

19 p3319 A69-35552

Processing variables influence on microstructure of extruded Ti-Al-Sn alloy, noting deformation by slip over temperature range

20 p3557 A69-36955

Extrusion variables influence on microstructure and hardness level of Ti-Al-Sn compared with recrystallization behavior after cold swaging

[ASM PAPER W9-8.2] 21 p3729 A69-38660

Optimal conditions for extrusion compacting of hard alloy mixtures plasticized with paraffin, determining plasticizer content, upsetting, pressure and temperature

22 p3956 A69-40635

Ti alloy aircraft components and equipment production, considering roles of temperature, deformation rate and thermal conductivity in drop forging and extrusion processes

[DGLR-69-003] 23 p4170 A69-42162

EYE [ANATOMY]

NT CHOROID MEMBRANES

NT CORNEA

NT FOVEA

NT OCULOMOTOR NERVES

NT RETINA

Analytical model for frog retinal bug detector cell to make possible signal measurement in frog optic fibers

07 p1070 A69-18383

Oculomotor muscular tonus of rabbit during rocket flight acceleration and weightlessness

07 p1062 A69-18590

Classical and differential eyelid conditioning for truth or falsity of visually presented verbal statements

07 p1064 A69-18632

Clinicomorphological changes in rabbit eyes vascular system by exposing transverse accelerations

08 p1262 A69-19832

Pulsed and CW microwave power effects on rabbit eyes, noting lens opacities produced

10 p1648 A69-23185

Ocular injuries during bailout from Vampire aircraft, noting hemorrhages

10 p1649 A69-23380

Photography role in experimental research with applications to flight analysis and comparison with human visual accuracy

11 p1881 A69-24573

Probability of ocular damage for illumination by pulsed laser beam transmitted through atmosphere, developing safety nomograph for eye hazard analysis

11 p1830 A69-24843

Circadian rhythm of optic nerve impulses in isolated eye of sea hare *Aplysia californica* in total darkness

14 p2406 A69-28870

Darkness adaptation, observing relationship between left and right eye

16 p2745 A69-32448

Valsalva maneuver produced abrupt onset of ptosis and proptosis caused by ethmoidal air cell rupture, discussing etiologies

17 p2909 A69-33186

Damage thresholds to ocular tissues from laser radiation, presenting comparative theoretical curves and recommended safe working levels

18 p3097 A69-34312

Eye elemental response to individual frequency jumps in oscillations of light, noting transient effect polarity

21 p3650 A69-38320

Cytoplasmic and ciliary connections between inner and outer segments of mammalian visual receptors

22 p3881 A69-40857

Eye optical system spherical aberration measured by knife-edge method derived from Foucault test, investigating retinal image quality

22 p3882 A69-40873

Blue cone mechanism contribution to mesopic function in producing Purkinje shift with luminance decrease, measuring sensitivity by flicker technique

22 p3883 A69-40880

Human eye modulation transfer function in reflected light by analyzing depolarized and polarized components emerging from eye

22 p3884 A69-40888

Liquid filled adjustable optical analog of human eye for aligning, calibrating and systems testing of automatic IR optometers

22 p3888 A69-41231

Pigeon visual adaptation to flickering light, attributing ERG b-wave postadaptation rebound to retinal bipolar cells inhibition

23 p4084 A69-41465

Senior commercial jet pilots ability to visualize flight instruments

23 p4089 A69-41822

Rod signals elicited by flashes in human eye measured, deriving relation between nerve signal size and rods and flashes energy

23 p4099 A69-42119

EYE DISEASES

NT ASTIGMATISM

NT CATARACTS

NT GLAUCOMA

Human body responses to microwave irradiation, discussing thermal and nonthermal effects and damage to eyes and to information storage in living systems

23 p4111 A69-42216

EYE EXAMINATIONS

Pilots myopia incidence statistical study after initial medical examination, emphasizing skiagram value in prognosis

24 p4267 A69-43400

EYE MOVEMENTS

Cerebral cortical neurons response to visual stimuli during stationary and rapid eye movement

03 p0369 A69-13360

Ocular motor failures in pilots due to convergent and divergent strabismus, discussing low pressure chamber tests and blood pressure effects on cranial nerve

03 p0370 A69-13470

Oculomotor activity of cosmonauts during orbital flight, analyzing electrooculograms taken during vestibular tests

07 p1063 A69-18594

Classical and differential conditioning of eyelid response with correctness of solutions of arithmetic problems as discriminandum

07 p1064 A69-18637

Small eye movements measurement and retinal image stabilization based on tracking edge of blood vessel in optic disk

09 p1446 A69-21908

Electrooculographic method to study eye movements control system for fixation on stationary point of following discretely or continuously moving target

09 p1447 A69-22675

Coriolis effect in rotating spacecraft simulation, discussing optokinetic reflex responses as function of head turning angle with spin axis

14 p2409 A69-29300

Stiles-Crawford effect measurements before and following eye movements to determine retina shearing during eye movements

15 p2555 A69-31035

Apparent movement in peripheral vision induced by sequential flashing of spatially unresolved two dots, studying dynamics of illusion

16 p2746 A69-31556

Vestibular reactions in rats under hypothermal conditions by measuring postrotatory nystagmus beats number and duration, respiration rates and rectal temperature

17 p2906 A69-32934

Cortical auditory-evoked response during eye movement in cats, discussing relation to central mechanism

17 p2911 A69-34171

Phase and tonic activity of oculomotor apparatus of rabbits during vestibular reflexes and postrotational nystagmus

20 p3469 A69-37243

Multilevel mathematical model of oculomotor apparatus using neuron networks and complex activators, including computer analysis

20 p3470 A69-37245

Single flash and rhythmic light stimuli effect on nystagmus of patients with tumoral posterior cranial fossa, recorded electroencephalographically

20 p3470 A69-37250

Threshold variations in caloric nystagmus in pigeons subjected to accelerations in head to tail direction in centrifuge at various temperatures

20 p3471 A69-37252

Otolith apparatus functioning under weightlessness and accelerations in test stand experiments, discussing measuring techniques and nystagmic reaction durations

20 p3471 A69-37253

Combined angular and centrifugal acceleration effects on human and animal eyes motion studied to explain weightlessness effects on humans

20 p3471 A69-37257

Nystagmus reactions in rabbits subjected to rotating vestibular tests, noting decrease following previous adaptation to stimulus

20 p3473 A69-37267

Rapid component of nystagmus using photostagmography, noting dependence on afferent pulse of ampullar apparatus

20 p3481 A69-37272

Electronystagmographic method of eye movement recording, noting applications to vestibular and visual analysis and study of oculomotor nuclei-vegetative centers relations

20 p3481 A69-37273

Isometric tensions of detached lateral rectus muscles measured during strabismus surgery for mechanical components of human eye movements, giving muscle tone range

22 p3872 A69-40200

Target distance and direction monocular estimates with stabilized and nonstabilized retinal images, finding eye movements not improving spatial judgment accuracy

22 p3878 A69-40838

Visual suppression association with smooth following and saccadic eye movements in tracking slow moving target

22 p3879 A69-40842

Horizontal tracking eye movements response to unpredictable constant velocity target motions with or without saccadic position corrections recorded by contact lens optical lever

22 p3881 A69-40856

Visual stimuli initiating horizontal eye vergence movement in human subjects, noting cerebral conditions for convergence

22 p3881 A69-40859

Angular velocity of visual stimulus effect on human torsional eye movements using sectorized disks

22 p3883 A69-40874

Eye movement control mechanisms during binocular fixation used to determine corrective roles of flicks and drifts

22 p3883 A69-40876

EEG alpha activity relationship to laterality of reflective eye movements, indicating physiological correlates of hypnotizability

22 p3887 A69-41213

EEG, ocular movements, gastric mobility and pH during human sleep from data transmitted by swallowed radio transmitter

23 p4093 A69-42063

Retinal eccentricity effects on horizontal-vertical illusion magnitude, considering eye flattening and astigmatic properties

24 p4263 A69-43117

Lambda waves EEG recording for evaluating eye movements during pattern vision

24 p4268 A69-43401

EYE PROTECTION

Laser radiation hazards due to direct or reflected viewing determined by evaluating output characteristics and environmental factors effects

02 p0204 A69-12497

Laser radar eye hazard for fixed and variable transmitter intensities, considering eye damage magnitude and successful detection magnitude of transmitter intensity

11 p1830 A69-24845

Photochromic panel for flash blindness protection using epoxy plastic plates containing aromatic hydrocarbon compounds excited to triplet states

21 p3668 A69-39783

EYRING THEORY

Failure distribution functions based on Eyring component aging model, including failure probability density function for Weibull and gamma type distributions

08 p1322 A69-21104

F

F CENTERS

U COLOR CENTERS

F REGION

Enhanced 6300 angstrom emission from F region auroral latitudes in terms of reaction between oxygen ions and atoms

01 p0062 A69-10137

Ionospheric irregularities height measurement using spaced receivers for recording satellite signals

01 p0064 A69-10428

Latitudinal variations in auroral and subauroral region F layer diurnal and magnetic storm pattern shown by scintillation measurements

01 p0069 A69-11127

Unusual stratification of F region during solar activities, noting role of traveling inhomogeneities

02 p0237 A69-11663

Seasonal variations in thickness of ionospheric E-F interlayer region during daylight and maximum integral ionization values

02 p0239 A69-11682

Algorithm for N/h ionospheric profiles calculations using both x and o magnetoionic components, taking into account interlayer and underlying ionization influence

02 p0239 A69-11687

Tropical night F layer maintenance mechanism, noting airglow enhancement and ionization source association with plasma drifts

02 p0242 A69-11825

Fading characteristics of radio waves reflected from two different heights in F region over Ahmedabad, India

03 p0385 A69-12915

Latitude variation of time of occurrence of maximum F height and maximum spread F probability

03 p0420 A69-13305

F layer disturbance showing pronounced difference in corpuscular flux effect on day and nighttime ionosphere

03 p0512 A69-13517

Radio waves diffusive and oblique reflections from F region, noting diffusive properties decrease during magnetic storms, especially during maximum solar activity

03 p0423 A69-13529

Electron concentration profile change in ionospheric F region in auroral zone during negative magnetic bay disturbances

03 p0423 A69-13530

Nighttime sporadic E layer occurrence due to ionization redistribution established, noting concurrent F region electron concentration decrease

03 p0423 A69-13536

Electron production and loss rates in F region from measurements of Faraday rotation imposed on VHF telemetry transmissions from geostationary satellite

03 p0503 A69-14016

Nighttime variations of F region electron density profiles at Puerto Rico, discussing seasonal and solar cycle variations in temperature and vertical drift velocity

03 p0503 A69-14017

Mechanism for noon electron concentration maximum in F region at midlatitudes found to be recombination process

05 p0753 A69-16031

Gravity waves observed by ionospheric temperature measurements in F region

05 p0754 A69-16262

Diurnal variations of neutral and charged particle temperatures in equatorial F region

05 p0755 A69-16270

Internal atmospheric gravity waves in F region observed with electron density profiles deduced from vertical incidence ionograms, obtaining phase velocities

05 p0756 A69-16402

F region seasonal and magnetic storm behavior from region daily behavior showing global upper atmospheric circulation

05 p0757 A69-16404

F region equatorial irregularity belt observed from satellite transmission scintillation, noting north-south elongated patches

05 p0758 A69-16418

Reaction rates coefficients of oxygen ions with molecular oxygen and nitrogen in nighttime F region over Moscow based on loss coefficient estimate

06 p0919 A69-17724

Charged particles concentration change during vertical propagation of acoustic wave in F layer found transforming electric field into circularly polarized wave

09 p1484 A69-21528

Vertical transport rate of charged particles in F region, allowing for vertical velocity gradients

09 p1485 A69-21529

Aeronomic parameters effect on ionospheric effect of SC magnetic storm, calculating maximum ionization levels, F layer ionization and vertical ionization profile parameters

09 p1486 A69-21546

F region response to solar proton flare characterized by two phase ionospheric storm as measured at ground

base stations

10 p1684 A69-23783

Incoherent scatter measurements of F region electron concentrations at solar activity minimum

10 p1684 A69-23825

Ground wave propagation attainment of electron plasma resonance of F region, stressing need of wave vector orientation toward magnetic north

10 p1684 A69-23828

Thomson scatter bistatic sounder data on ionization transports in F region, describing diurnal variations by hourly values of velocities

10 p1685 A69-23830

Nonlinear charge exchange and dissociative recombination effects on night F region decay compared with linear theory

10 p1685 A69-23832

Nighttime ionospheric recombination studies by model reference heights varying diurnally, seasonally and with solar flux and geographic location

10 p1685 A69-23834

Ionospheric slopes and range frequency characteristics obtained from oblique incidence sounding of horizontally nonuniform ionosphere

10 p1686 A69-23914

Hourly N/h profiles of F region calculated from ionograms by normal integral method during magnetic disturbance, measuring region temperature

10 p1687 A69-23928

Nighttime maxima anomaly in electron concentration of ionospheric F layer at midlatitudes, considering diffusion and recombination

12 p2064 A69-26007

Theories for universal time controlled polar F region reevaluated in light of satellite low energy charged particle observations

12 p2065 A69-26103

Autocorrelation and cross correlation analysis of rapid density variations in F region determined from satellite deceleration and geomagnetic data

12 p2069 A69-26436

Vertical ionization drift in F region as function of electron density, ionization coefficient and recombination coefficient

12 p2070 A69-26584

Neutral gas motions causing plasma motions in F region, obtaining vertical plasma velocity component pronounced diurnal variations

12 p2070 A69-26684

Vertical drift velocity of ionospheric F region during eclipse and on control day based on chemical reaction coefficients models, discussing electron density distribution

12 p2077 A69-27109

Magnetospheric corpuscular fluxes night ionization role in E and D region, considering precipitation from outside, trapped and dumped particles of radiation belts

13 p2254 A69-28333

Unusual stratification of F region during solar activities, noting role of traveling inhomogeneities

13 p2256 A69-28694

Seasonal variations in thickness of ionospheric E-F interlayer region during daylight and maximum integral ionization values

13 p2257 A69-28713

Algorithm for N/h ionospheric profiles calculations using both x and o magnetoionic components, taking into account interlayer and underlying ionization influence

13 p2258 A69-28718

Ion drag effects on acoustic gravity waves propagation in isothermal F region, discussing indicated wave damping

14 p2434 A69-28944

Vertical motion of ionized formations in ionospheric F region related to sporadic E layer

14 p2437 A69-29074

Zonal drift influence on morning ionization anomaly in F region, noting shifts to West with increasing height and electron production rate

14 p2442 A69-29732

RF mass spectrometric measurements of diurnal variation of thermosphere and ionospheric E and F regions composition, noting oxygen concentration

15 p2601 A69-31371

Rocket measurements of upper F region electron temperature and density profiles, for particle and energy balance of ionosphere topside, noting diffusive equilibrium

16 p2848 A69-31975

Simultaneous solution of continuity and heat conduction equations for ionospheric electrons, ions and neutral species for studying F region magnetic storm

F 1 REGION

behavior

16 p2775 A69-32083

Ion-neutral air motion in F region under time dependent electric and constant magnetic field effect, using partial differential equations

16 p2777 A69-32181

Horizontal magnetic variation peak at eight degree dip latitude, noting F region contribution to magnetic tubes of force integrated transverse conductance

16 p2778 A69-32189

Correlation between F region electrons vertical motion velocity variations and E region electrons horizontal motions in equatorial ionosphere

16 p2779 A69-32193

F 2 critical frequency data at Hawaii for clarifying total electron content data obtained by geostationary satellite measurement of Faraday signal rotation

16 p2779 A69-32196

Electronic collision frequency measurement at F layer peak near ground sunrise time

16 p2779 A69-32197

Ionization density, velocity and temperatures oscillations revealed by Thomson scatter observations of gravity waves in F regions

16 p2779 A69-32198

Pressure gradients and moving ions driven neutral-air winds in F region, using asymmetric pressure model

16 p2779 A69-32302

Atomic oxygen density role in ionospheric E and F region magnetic stability, noting heat loss effect of atomic excitation

16 p2780 A69-32314

Charged particles concentration change during vertical propagation of acoustic wave in F layer found transforming electric field into circularly polarized wave

16 p2783 A69-32523

Vertical transport rate of charged particles in F region, allowing for vertical velocity gradients

16 p2783 A69-32524

Aeronomical parameter effect on ionospheric effect of SC magnetic storm, calculating maximum ionization levels, F layer ionization and vertical ionization profile parameters

16 p2783 A69-32541

Lunar tidal oscillations in F 2 layer critical frequency and F region minimum virtual height at Huancayo during IGY/IGC to study solar cycle effects

16 p2784 A69-32613

F region stratification during solar minimum and maximum, discussing regularities of plasma frequencies and diurnal variations

17 p2959 A69-33005

Annual variations of postsunset altitude peak of equatorial F region noting correlation with solar activity

17 p2966 A69-33983

F region during earth passage through solar corpuscular stream, analyzing critical frequencies, virtual height, magnetogram H component and ionospheric storm effects attributed to downward drift

17 p2967 A69-33989

Reflection and ionization heights diurnal variations in F region, obtaining data for sporadic E formation

17 p2968 A69-33995

Vertical ionization displacements in F region as trace distortions on ionograms observed at low, mid and high altitudes during daytime

17 p2969 A69-33998

Space diversity reception and diurnal variations of F region ionospheric motions, comparing IQSY program

17 p2969 A69-33999

Vertical ionospheric perturbations shown responsible for Z component in F region

17 p2969 A69-34000

Radio echo from south showing origin from irregularities in F but not E region, discussing propagation modes for particular record

18 p3125 A69-34252

Reexamination of polar F region electron density diurnal variation data contradicting King-Kohl theory of rotating neutral winds role

18 p3125 A69-34255

Anomaly of F region electron content vs polar geographic latitude and local mean time

18 p3126 A69-34257

Radiative recombination of atomic oxygen ions in nighttime F region UV radiation detected by polar-orbitingOGO 4 satellite

18 p3129 A69-34957

Field aligned ionospheric F layer ion density irregularities, using simultaneous hourly radar echo and spread F data and detailed ray path calculations

18 p3129 A69-34958

Ionospheric radio propagation, considering D and F region theory and ionospheric disturbances

19 p3303 A69-36428

Wind velocity components calculation at F-sphere maximum level, taking into account electrodynamic drift of ionospheric plasma and ion motion

20 p3519 A69-36972

F region electron and ion concentration vertical distribution, discussing various ionization reactions

20 p3520 A69-37030

Nighttime ionospheric F region velocity component and recombination coefficient computer calculation

20 p3521 A69-37049

F zero layer occurrence relation to solar, magnetic and ionospheric activity levels variations from Ashkhabad observations/1958-1964/

20 p3527 A69-37671

Vertically moving disturbances relationship to behavior of E and F layers over Tiflis, noting sporadic E layers formation

20 p3528 A69-37685

F layer penetration frequencies predictions compared with Alouette topside data

20 p3530 A69-37871

Alouette topside ionograms of ionospheric storms at midlatitudes indicating critical frequencies difference between F 1 and F 2 layers

20 p3532 A69-37894

Equilibrium velocity distributions of F region photoelectrons produced by solar ionizing radiation, discussing dayglow as impact result

20 p3591 A69-38061

Ionospheric scintillation power spectrum measurements from radio star and satellites related to F region radio refractive index fluctuations

20 p3534 A69-38093

F region vertical density profiles for positive ions and neutral molecules of various gases determined from rocket-borne mass spectrometer data

21 p3702 A69-38354

F region atmospheric density measurements obtained from aerodynamic drag on San Marco 2 satellite in equatorial orbit, comparing data with San Marco 1

21 p3704 A69-38369

Ionosphere characteristics in terms of airglow, describing daytime F/D layers formation model provided by photoionization, loss processes and ambipolar diffusion

21 p3712 A69-38517

Nocturnal electron/ion density balance in F region ionosphere from examining 6300 A emission

21 p3712 A69-38518

Nighttime F region nonlinear recombination and variable drift effects, suggesting empirical model

21 p3715 A69-38559

Midlatitude F region continuity equation solutions, including east-west electric field effects on electron density

22 p3941 A69-40917

Lunar semimonthly variations in noon values of F region absorption at Singapore, noting opposite phases of lunar tides in D and F regions

22 p4035 A69-41211

F region dynamic model, including variations in temperature, electron and molecular ion concentrations, etc

23 p4156 A69-41843

Nighttime F region time-altitude variations in aeronomical parameters calculated under conditions close to solar activity maximum

23 p4156 A69-41844

VHF radio propagation over transequatorial circuit related to equatorial anomaly in F layer, suggesting F2/F2 propagation mode role

23 p4127 A69-42431

Ionospheric F region equatorial anomaly in electron density showing high correlation with equatorial electrojet range and poor correlation with Fuquene range

23 p4160 A69-42432

F 1 REGION

Criticism of overlay analysis method for F 1 region ionograms

05 p0757 A69-16403

Maximum ionization altitude, thickness, electron density profile and temperature mean variations in summer of IGY and IQSY at Moscow station

09 p1486 A69-21544

Solar flare X ray and extreme UV radiation contribution to E and F1 region ionospheric effects observed by sudden frequency deviations

11 p1950 A69-25160

Overlay technique for analysis of F region transition

into F1 and F2, noting ionization and recombination

12 p2065 A69-26102

F 1 layer formation relationship to height variations in ionic concentrations, determining different ion concentration combinations

12 p2071 A69-26702

Maximum ionization altitude, thickness, electron density profile and temperature mean variations in summer of IGY and IQSY at Moscow station

16 p2783 A69-32539

F 1 layer observation at 80-87 degree solar zenith angles explained by additional ionization maximum development in presence of temperature gradients

17 p2967 A69-33985

Latitudinal variations in conditions for F 1 layer occurrence probability and stability during solar activity minimum period

20 p3527 A69-37669

Diurnal F 1 layer development over Irkutsk, Siberia, during minimum and maximum solar activity, using semiquantitative method

20 p3527 A69-37670

F 2 REGION

Lunar tidal effects on F 2 critical frequency and height maximum, evaluating variations with altitude

01 p0063 A69-10424

Tropical 6300 angstrom red oxygen nightglow enhancements related to variations in height of nighttime F 2 layer, noting implications for layer structure and physics

01 p0068 A69-11113

Relation between north-south asymmetry of F 2 region critical frequencies and geomagnetic axis inclination angle, establishing increase in asymmetry during increased solar activity

02 p0237 A69-11662

Ion formation rate in F 2 layer in southern polar cap, noting effect of season, latitude and solar activity

02 p0238 A69-11679

11-year solar cycle influence on F 2 region critical frequency, investigating correlation coefficient between mean monthly values of F 2 variations and respective sunspot numbers

02 p0238 A69-11680

F 2 layer cut-off frequency predawn increase caused by sunrise, resulting in photoelectrons transfer along force lines at magnetically conjugate point

02 p0238 A69-11681

Statistical characteristics of magnetoionic components of obliquely incident waves, obtaining envelope distribution of signal reflected from F 2 layer

02 p0314 A69-11691

Computer program for calculating density distribution of deviation of F 2 layer critical frequency from median value

02 p0239 A69-11692

Plasma drift global distribution due to neutral gas motion in F 2 region, noting effect on electron concentration distributions

03 p0422 A69-13513

F 2 layer critical frequencies variation coefficients, analyzing variation and root-mean-square deviations in terms of geomagnetic latitude and Wolf number

03 p0422 A69-13514

F 2 layer equatorial anomaly at local noon, discussing position of trough center in latitudinal distribution of ionization

03 p0422 A69-13515

Diurnal variation of variation coefficient of F 2 critical frequency for steady and unsteady primary ionizing fluxes simulated on computer

03 p0423 A69-13516

Ionospheric F 2 layer following SSC magnetic storm, noting similarity with polar aurora region

03 p0423 A69-13531

Ionospheric parameters variation during SC effect as function of solar and magnetic activities

03 p0423 A69-13534

Time dependence of relation between sunspot number and ionospheric index IF 2, noting hysteresis characteristic and changes for different solar cycles

03 p0424 A69-13632

F 2 layer formation and fast neutral particles ionization source due to charge exchange between solar wind protons and moving interstellar hydrogen

04 p0592 A69-15009

Day and night reversals in NmF2 north-south asymmetry related to neutral wind direction

06 p0918 A69-17384

Synoptic observations of F 2 layer in magnetically conjugate regions, comparing critical frequencies

06 p0919 A69-17723

Optimum length of Fourier time series approximation

ing diurnal F 2 critical frequency variation on planetary scale

06 p0921 A69-17746

Simultaneous solution of time-dependent momentum and continuity equations for ions and neutral air in midlatitude F 2 region conditions

07 p1123 A69-18818

Ionospheric plasma flute instability considered as possible cause of occurrence of elongated small scale inhomogeneities in F 2 layer

08 p1309 A69-20425

Analytical description of planetary distribution of space-time variations of fOF2, deriving Fourier series as function of UT

09 p1486 A69-21545

F2 layer diffusion and sporadic E layer characteristics from equatorial ionosphere soundings on Zaria schooner

09 p1486 A69-21548

F 2 layer drift relation to current systems of dynamo region confirmed at middle and high latitudes

10 p1682 A69-23611

Luni-solar tide interpretation in F2 critical frequency based on sum and difference frequencies production by nonlinear atmospheric response to forces

10 p1685 A69-23829

F 2 layer state prediction as function of solar activity by series expansion for describing space-time variations of monthly F 2 medians critical frequencies

10 p1687 A69-23927

Overlay technique for analysis of F region transition into F1 and F2, noting ionization and recombination

12 p2065 A69-26102

Diurnal and seasonal variations in drift velocity vector of small scale inhomogeneities in F 2 region

12 p2070 A69-26688

Mean annual characteristics of F 2 layer ionization state, using results of worldwide observation station system

12 p2071 A69-26701

Correlation coefficient between changes in F 2 layer critical frequency and sporadic E layer maximum frequency

13 p2254 A69-28330

Relation between north-south asymmetry of F 2 region critical frequencies and geomagnetic axis inclination angle, establishing increase in asymmetry during increased solar activity

13 p2256 A69-28693

Ion formation rate in F 2 layer in southern polar cap noting effect of season, latitude and solar activity

13 p2257 A69-28710

11-year solar cycle influence on F 2 region critical frequency, investigating correlation coefficient between mean monthly values of F 2 variations and respective sunspot numbers

13 p2257 A69-28711

F 2 layer cut-off frequency predawn increase caused by sunrise, resulting in photoelectrons transfer along force lines magnetically conjugate point

13 p2257 A69-28712

Statistical characteristics of magnetoionic components of obliquely incidence waves, obtaining envelope distribution of signal reflected from F 2 layer

13 p2355 A69-28722

Computer program for calculating density distribution of deviation of F 2 layer critical frequency from median value

13 p2258 A69-28723

Drift of F 2 layer inhomogeneities compared for IGY and IQSY

14 p2443 A69-29866

F 2 region small scale inhomogeneities drift observations showing seasonal and diurnal velocity and direction changes

14 p2444 A69-29868

Tide dependent variations of critical frequencies of ionospheric layers minimal heights and maximum height of F 2 layer reflection

14 p2444 A69-29871

Spectrometric rocket measurements of ion concentrations between 200 and 630 km

16 p2774 A69-31974

Ionization troughs below F 2 layer maximum due to ionospheric disturbances detected by Antarctica ionograms direction of arrival data

16 p2775 A69-32080

Lunar tidal variations of electron concentration in F 2 region near magnetic equator showing large latitudinal dependence

16 p2776 A69-32090

Nighttime decreases in F 2 layer heights at near conjugate stations in low latitudes, using electron density

profiles

16 p2778 A69-32186

Combined midlatitude neutral air wind and equatorial electrodynamic drift effect on F 2 layer diurnal variations

16 p2781 A69-32316

Analytical description of planetary distribution of space-time variations of fOF2, deriving Fourier series as function of UT

16 p2783 A69-32540

F 2 layer diffusion and sporadic E layer characteristics from equatorial ionosphere soundings on Zaria schooner

16 p2784 A69-32543

Synoptic observations of F 2 region in magnetically conjugate regions of Kerguelen and Archangel, comparing critical frequencies during magnetic and ionospheric disturbances

16 p2784 A69-32612

Horizontal drifts and anisotropy of irregularities in ionospheric F 2 region by pulse fading drift records

17 p2960 A69-33164

Unsteady model taking into account photoionization, neutralization and diffusion, describing electron concentration diurnal and seasonal variations in ionosphere F 2 region at midlatitudes

17 p2966 A69-33978

Effective rate coefficients of ion-molecular processes, dissipative recombination and ion production in F 2 layer at midlatitudes

17 p2966 A69-33979

Geomagnetic control of geographic distribution of F 2 layer midday ionization based on data from ionospheric vertical sounding stations

17 p2966 A69-33982

Postsunset apparent reflection height and electron density variability in equatorial F 2, discussing singularities of diurnal variation in November-January

17 p2967 A69-33984

Radio wave trajectories for waves emitted at 15, 20 and 25 kHz within spherically stratified ionosphere below F 2 maximum

17 p2969 A69-34001

Magnetic declination effect on F 2 layer critical frequency diurnal variations attributed to vertical ionospheric drift due to neutral air winds

18 p3126 A69-34256

Nighttime F 2 region temperature distribution under geomagnetically calm and disturbed conditions calculated from Alouette 1 satellite data

19 p3304 A69-36623

Positive and negative correlations in F 2 layer perturbations observed by network of paired conjugate ionospheric stations at low latitude

20 p3521 A69-37050

Global distribution of F 2 layer critical frequencies by expanding empirical function of diurnal variations into natural orthogonal components

20 p3521 A69-37051

Predawn F 2 layer critical frequency enhancement at Johannesburg, discussing electron density hump from corpuscular ionization increase

20 p3523 A69-37576

Electron-ion gas ambipolar diffusion effect on F 2 layer electron density vertical distribution variations

20 p3525 A69-37655

Temperature effect on electron concentration steady distribution in F 2 layer

20 p3525 A69-37657

F 2 critical frequency meridional cross sections latitude profiles based on global network ionospheric stations observations, confirming daytime Northern Hemisphere ionization maximum

20 p3526 A69-37661

Altitude variations at and near maximum electron concentration in quiet F 2 layer during solar activity maximum from sounding at southern geomagnetic pole

20 p3526 A69-37662

Solar activity effect on F 2 layer geometrical parameters, plotting prognostic maps using nomographic methods

20 p3526 A69-37663

F 2 region critical frequencies obtained during winter at Northern and Southern Hemisphere stations located in auroral and polar zones, correlating changes with ionization

20 p3526 A69-37665

F 2 layer seasonal anomaly, discussing global distribution observed by network of ionospheric stations

20 p3526 A69-37666

Seasonal anomaly of F 2 layer critical frequency in Northern and Southern Hemispheres during high and low solar activity, discussing geomagnetic effect

20 p3526 A69-37667

F 2 layer midlatitude positive disturbances observed

during IGY on quiet and disturbed days, noting positive to negative transition latitudes

20 p3527 A69-37674

Causal and semiphenomenological theories concerning equatorial F 2 region, discussing electrodynamic drift theory and transequatorial winds

20 p3531 A69-37888

Critical frequency variations of F 2 layer and M/3000/F 2 with sunspot number for 19th solar cycle, noting dependence on geomagnetic latitude

21 p3715 A69-38560

Magnetic declination effect on altitude of top of F 2 ionospheric layer at midlatitudes using M/3000/F 2 transmission factor

21 p3717 A69-39577

Electron density decrease in F 2 layer ascribed to 9 July 1962 thermonuclear explosion, noting dissociative recombination role

22 p3942 A69-41098

Diurnal variation of Pc type geomagnetic pulsations correlation with F 2 layers critical frequency diurnal variations

23 p4161 A69-42441

F- 2 AIRCRAFT

Lifting body type M2-F1 and M2-F2 aircraft enabling astronauts to make own landings at choice airport

03 p0366 A69-13367

F- 4 AIRCRAFT

Duplex servoactuator package sized for stabilator channel of F-4 aircraft providing compact integrated control surface positioning

19 p3249 A69-35640

F- 5 AIRCRAFT

Northrop F-5-21 fighter design, avionics, performance and operational existence

21 p3646 A69-38732

F- 104 AIRCRAFT

Maintenance system in Germany for F-104-G Starfighter planes noting disassembling, system testing and test flight

17 p2979 A69-33703

F- 106 AIRCRAFT

NF106B-VST model follower flight control system, discussing design criteria/performance index, rigid/elastic math model development, flight test evaluation, hardware design, etc

21 p3764 A69-39412

F- 111 AIRCRAFT

Design and tests of cable assemblies for F-111 aircraft

05 p0731 A69-16246

F-111 interdiction capability, discussing avionics subsystems for low level penetration flying and Vietnam performance

07 p1052 A69-18550

Emergency escape and personnel recovery systems including F-111 explosive system, midair deployed buoyancy aerostat and fly-away flexible wing rotor

15 p2551 A69-30853

Jet engine compressor stalls in-flight investigation up to Mach 2 on F-111A by pressure sensors, noting steady state distortion role

16 p2843 A69-32706

Three valve manifold for five self righting inflation bags in escape capsule on F-111, providing one directional flow and pressure relief and shutoff

20 p3467 A69-38185

Vacuum cured glass-reinforced polyimide laminate tests for use at elevated temperatures on F-111 aircraft

24 p4335 A69-42933

F-111D computer complex to provide selective functional redundancy and flexibility to accommodate mechanization changes

24 p4285 A69-43719

F-J ROCKET ENGINE

Saturn F-1 rocket engine as generator of infrasonic waves and magnetic fluctuations, noting ignition and cut-off signal characteristics

24 p4365 A69-43415

FAB [PROGRAMMING LANGUAGE]

U FORTRAN

FABRICATION

Fabrication of large parts in aircraft and space industry, discussing extrusion, forging, explosive forming and diffusion bonding

01 p0088 A69-11400

Welding with aluminum-zinc-magnesium alloys, discussing stress corrosion, embrittlement, compositions, heat treatment, material production and fabrication

02 p0266 A69-12063

P-i-n structure isolation method for fabricating monolithic integrated circuits

02 p0222 A69-12471

Beam-lead fabrication on dual Schottky barrier diodes for low noise integrated microwave mixers

02 p0222 A69-12474

Fabrication of large arched bottoms for pressure vessels from aluminum alloys, discussing sheet cutting and welding, annealing, machining, etc

02 p0254 A69-12678

Loss factors effects on substrate choice in production of microwave printed circuit components

04 p0578 A69-15199

MOSFET fabrication by ion implantation using gate metal as mask, noting source and drain alignment with gate and low feedback capacitance

05 p0734 A69-16563

Processing techniques for fabrication of ceramic radomes from alumina and silica

07 p1142 A69-19527

Thick film hybrid circuit technology and equipment reviewing conductors, resistors, and insulator inks

09 p1508 A69-22337

Compressive behavior of uniaxial filament reinforced epoxy tubes for aerospace structures, using hand layup method with Teflon mandrel and sleeve

09 p1508 A69-22339

Subscale aircraft fuselage section fabricated with lightweight graphite fiber/epoxy resin composite material

09 p1509 A69-22341

Hollow turbine disks for provision of coolant to high performance aircraft gas turbine engines, fabricating disk in two axial halves

09 p1509 A69-22345

Whisker metal matrix composite fabrication, discussing aligned whisker distribution without degrading strength or fracturing and detailing extrusion process

09 p1511 A69-22361

Laser application to welding, drilling and other processes involving material removal for microelectronic circuits and components fabrication

11 p1846 A69-24600

Fabrication procedure for microwave epitaxial GaAs diodes applicable for switching purposes

12 p2035 A69-25831

Fabrication techniques for plastic insulation in electronics, discussing packaging, low pressure molding, casting, etc

13 p2285 A69-27987

Book on integrated circuits covering fabrication techniques, basic semiconductor theory, thin film, monolithic, compatible circuits, packaging, etc

14 p2419 A69-29002

Boron filament wound composite structures fabrication noting physical properties

14 p2455 A69-29413

Metal film resistor reliability for conventional and space use, outlining guidelines for fabrication and quality control

15 p2628 A69-30847

JT8D turbofan engine composite fan blades design and fabrication methods using aluminum-Borsic fiber, noting direct and indirect weight reduction

[AIAA PAPER 69-465] 16 p2842 A69-32698

Small penetration aid rocket motors fabrication, discussing axial- and tangential-thrust integral assembly, impulse levels, delay line connection for igniters, production evolution, etc

[AIAA PAPER 69-520] 16 p2795 A69-32779

Be/Al cast duplex alloy with Be embedded as discrete particles in Al matrix, detailing fabrication techniques and mechanical properties

19 p3340 A69-35524

Fabrication effects on high strength Al alloy plate properties, comparing texture, plane strain fracture toughness, yield stress, ultimate tensile stress and elongation

19 p3346 A69-36437

Seam welded Al alloy aircraft structure fabrication problems, emphasizing stress corrosion

[SBAC PAPER 5] 20 p3550 A69-37454

Graphite fiber reinforced graphite composites fabrication, discussing spray forming and physical and mechanical properties

[ASM PAPER W9-20.4] 21 p3730 A69-38671

Economic effectiveness of design and fabrication changes in aircraft construction industry for profitable operation of commercial transport aircraft

21 p3855 A69-38874

Heat pipe development and fabrication in various sizes and shapes for operation over range of temperatures and power levels, noting applications

23 p4074 A69-42296

Materials research structural design cycle, discussing simultaneous optimization, constituent materials, fabrication process, load environment and mission constraints

24 p4399 A69-42991

Silicon nitride ceramics fabrication technology and dimensional stability during nitridation, discussing applicability to aerospace precision or joined ceramic shapes

24 p4336 A69-43211

FABRICS

NT DACRON [TRADEMARK]

NT GAUZE

NT PARACHUTE FABRICS

Organic and inorganic fabric reinforcements effects on thermal properties of composites noting thermal conductivity, diffusivity, specific heat constants and temperature ranges

15 p2642 A69-30466

FABRY-PEROT INTERFEROMETERS

Plasma density dynamic measurements by Fabry-Perot microwave resonator, discussing resonator and coupling problems

01 p0080 A69-10318

Fabry-Perot etalon for obtaining monochromatic weak solar prominences

02 p0248 A69-11634

Automatic recording of neutral atom temperature and free electron density of partially ionized gas by Fabry-Perot interferometer

03 p0428 A69-13111

Microwave Fabry-Perot resonator for anisotropic plasma diagnostics in presence of static magnetic field

04 p0635 A69-14757

Nonadjustable Fabry-Perot scanning interferometer for gas laser spectra analysis, using barium titanate piezoceramic elements

04 p0598 A69-14854

Electron concentration in pulsed plasma measured with Fabry-Perot interferometer and laser radiation source

06 p0963 A69-16911

Strain distribution at crack base measured by Fabry-Perot interferometer and photoelastic coating

06 p1020 A69-17127

Instrument profile of grating spectrograph determined by applying He-Ne laser mode separated in Fabry-Perot interferometer

07 p1131 A69-18405

Multibeam Fabry-Perot interferometers for aerodynamics measurements of rarefied gas flows, determining density distribution, shape, structure and detachment of shock waves

08 p1314 A69-20385

Fabry-Perot fringes maxima in frequency response of laser interferometer, describing passive technique using eight wave plate

09 p1517 A69-21915

Tunable Fabry-Perot interferometer for photoelectric measurements of absorption and emission line contours and line center particle concentrations

10 p1698 A69-24212

Active scanning Fabry-Perot interferometer interaction with mode matched laser resonator, analyzing phase and intensity of reflected wave of active three mirror resonator

11 p1886 A69-25047

Electron concentrations in steady Ar and Ar-He plasma jets measured with microwave Fabry-Perot interferometer and Stark broadening of H beta line

12 p2137 A69-26537

Fabry-Perot interferometer for studying spatial distribution of plasma electron concentration, discussing resolution using solid state gas laser light source

14 p2451 A69-29777

Fabry-Perot interferometer employing gas laser for plasmodion electron concentrations measurement at 3.39 micron wavelength

14 p2451 A69-29778

Nonadjustable Fabry-Perot scanning interferometer for gas laser spectra analysis, using barium titanate piezoceramic elements

15 p2608 A69-30246

Filamentary nebula IC 443 observation by Fabry-Perot etalon with image converter, determining radial, expansion velocities and H alpha line half width

15 p2686 A69-30538

Scanning Fabry-Perot interferometer with ultralow modulation frequencies, obtaining inverse piezoelectric effect curves of ceramic element

15 p2611 A69-31107

Aberrations of Fabry-Perot interferometers with small nonuniformities in plate spacing used as spectral and optical filters

17 p2972 A69-33081

Fabry-Perot interferometer with Al coating reflecting surface deposited on unbacked thin films

20 p3536 A69-36933

H alpha auroral activity on Jupiter isolated by using Fabry-Perot etalons, showing photograph reproductions

20 p3598 A69-37414

Birefringent element within Fabry-Perot cavity for identification of direction of electron density change in z-pinch discharge

22 p3946 A69-40438

Coupled Fabry-Perot interferometer for microwave spectra with improved selectivity of interference filter

22 p3947 A69-40800

Recursion formula for multilayer interference derived, with allowance for multiwave interference, to calculate resonant circuit maxima and minima

23 p4165 A69-41729

Scanning Fabry-Perot interferometer interaction with laser source, calculating laser intensity and oscillation frequency changes for weak mode coupling

24 p4329 A69-43756

Thermally scanned Fabry-Perot interferometer in flat-flat resonator configuration, featuring high transmission and large usable apertures, used for spectral analysis

24 p4329 A69-43757

FABRY-PEROT LASERS

U LASERS

FABRY-PEROT SPECTROMETERS

Rapid scanning Fabry-Perot spectrometers, considering time resolution, wavelength resolution, wavelength interval size, aperture diameter and limitations of mechanical components

01 p0082 A69-10837

Carbon dioxide abundance in Mars atmosphere measured with three etalon Fabry-Perot spectrometer

09 p1607 A69-22427

Venus atmosphere radial mass velocities measured spectrographically with Fabry-Perot interferometer, noting retrograde rotation

10 p1778 A69-23409

FACE [ANATOMY]

NT FOREHEAD

Air evacuation of maxilla-facially wounded persons from place of accident, noting helicopter use

24 p4270 A69-42603

FACE CENTERED CUBIC LATTICES

Substructures around fatigue cracks in fcc metals and alloys, noting relation between structural formation and crack propagation

02 p0260 A69-11826

Fatigue mechanism in fcc metals at ultrasonic frequencies, comparing microstructural changes in copper and alpha-brass

04 p0613 A69-14448

Nickel-cobalt fcc alloys rolling and recrystallization textures established with filtered Aco K-alpha radiation, considering stacking fault energy effects

04 p0615 A69-14643

Work hardening of fcc single crystals, emphasizing transmission electron microscopy of thin foils, X ray topography and etch pitting techniques

05 p0778 A69-15753

Dislocation distributions in cold worked fcc, bcc and hcp metals, discussing dislocation structures in deformed single crystals and work hardening theories

05 p0778 A69-15754

Unified theory of stress-strain curve of fcc metal crystals in Stages II and III of work hardening

05 p0778 A69-15755

Structural characteristics of Ni-Mo alloys analyzed using electron microscopy and X ray diffusion scattering

05 p0782 A69-16808

Fatigue hardening in fcc metals, discussing dislocation distribution in unidirectionally deformed single crystals

06 p0944 A69-17503

Fcc metals cyclic deformation and fatigue dependence on cross slip of screw dislocations, considering strain hardening and crack propagation

11 p1906 A69-25389

Heat treatment effect on Ti-Mn alloy microstructure, discussing fcc martensite transformation into alpha, beta and intermediate phases as function of aging

11 p1906 A69-25578

Martensite transformation with fcc lattice in Ti alloys containing 5.9 percent Fe analyzed as function of cooling rate using X ray analysis

15 p2636 A69-30105

- Tungsten influence on morphology and lattice parameter of fcc gamma prime phase in Ni-Cr-Ti-Al alloys
20 p3558 A69-36962
- Impurities effects on single crystal film formation of fcc metals on alkali-halide cleavage planes, stressing stacking fault energy importance
22 p3992 A69-39899
- Fcc metals higher order elastic constants calculated by Morse potential function, considering atomic interactions truncation and pressure derivatives
23 p4233 A69-42337
- FACETS**
U FLAT SURFACES
- FACSIMILE COMMUNICATION**
NT AUTOMATIC PICTURE TRANSMISSION
- TV picture and newspaper pages simultaneous transmission via earth satellite /Orbit/ system, measuring SNR and crosstalk
19 p3277 A69-36567
- FACTOR ANALYSIS**
- Factorizability of Einstein field equations in two dimensional spinor formulation
03 p0468 A69-13759
- Factor analysis applied to identifying extremal plants, presenting regression analysis based on least squares techniques to calculate mathematical model coefficients
05 p0737 A69-15888
- Pattern recognition method dependent on preselection of good variables, discussing SELFIC and relationship to Karhunen-Loeve expansion and factor analysis
07 p1088 A69-18386
- Integral representation for Wiener Hopf factorization of functions of complex variables for numerical processing of radiation problems
11 p1851 A69-24998
- Mathematical index model based on weighted factor analysis to facilitate management and technical decisions concerning achievement of numerous tasks with fixed funds
18 p3232 A69-34504
- Factor analysis of complex perceptual-motor performance of man, measuring speed, flexibility, balance and strength
18 p3098 A69-35085
- FACTORIES**
U INDUSTRIAL PLANTS
- FACULAE**
- Microwave spectra of peak flux of solar radio bursts of March and July 1966, relating plage regions to spectral characteristics
01 p0069 A69-11121
- Turbulent velocity in faculae and photosphere obtained from IR triplet of oxygen analysis
02 p0314 A69-11646
- Longitudinal component of solar facula magnetic field measured by high resolution spectograms
04 p0651 A69-14368
- Solar flares and plages free energy origin in magnetic field dissipation
06 p0996 A69-17446
- Synoptic charts of chromosphere, giving position and magnitude of sunspots, faculae and prominences during synodic revolution of sun
08 p1379 A69-20378
- Alpha hydrogen plage 20934 /McMath no. 8362/ associated with July 1966 proton flare development and configuration along sunspot group axis
10 p1762 A69-23728
- Two component calcium plage associated with proton flare of July 1966, describing initial development in old region periphery and component merging
10 p1763 A69-23729
- Explorer 30 satellite monitoring of solar X ray emission during July 1-15 1966, noting plage region activation with increasing emission
10 p1763 A69-23736
- Variable solar X ray emission from subflare activity in plage region producing polar cap absorption proton flare of July 7, 1966
10 p1764 A69-23745
- Variations in active region around McMath plage 8362 prior to proton flare, noting disk structure and nearby prominence modification
10 p1765 A69-23747
- Solar X ray flare of July 7, 1966 with Explorer 33 satellite attributed to McMath plage region 8362, discussing solar and cosmic radio noise
10 p1766 A69-23754
- Solar polar faculae observations, discussing relation to general solar magnetic field and coronal properties, solar high latitude rotation and susceptibility to atmospheric conditions
12 p2160 A69-26897
- Solar Ca chromospheric plage decay curves obtained from area measurements, showing similarity and exponential mean curve
16 p2859 A69-32222
- Slowly varying component of solar radio emission /S component/, correlating 35 GHz S component flux and corresponding plage, discussing magnetic fields and electron density
17 p3030 A69-33056
- Molecular concentration-optical depth curves for combinations of two photospheric and two facular models, noting lines contrast dependence on dissociation energy
18 p3204 A69-35391
- Magnetic measurements of active regions at various levels of solar atmosphere, discussing chromospheric cold and hot region, faculae magnetic fields, etc
22 p4010 A69-39991
- Core profiles of H alpha, H beta, H and K from spectrograms of plages
22 p4010 A69-39993
- Geomagnetic disturbances and cosmic ray storm of 25-26 May 1967 caused by McMath plage region 8818, noting Forbush decreases and ring current effect
22 p4004 A69-40307
- FADING**
U SELECTIVE FADING
U SIGNAL FADING
U SIGNAL FADING RATE
- FAHRENHEIT TEMPERATURE SCALE**
U TEMPERATURE SCALES
- FAIL-SAFE SYSTEMS**
- Airline pilot incapacitation by death or terminal collapse due to organic causes while on duty, noting incidence and resulting accidents
06 p0883 A69-17849
- Fail-safe design principles and criteria for helicopter structures to prevent operational failure arising from undetected fatigue damage
[AIAA PAPER 69-213] 07 p1054 A69-19549
- Fail-safe goals, design criteria, analytical methods and test procedures to achieve reliable damage tolerant dynamic rotating parts for V/STOL and helicopter transports
[AIAA PAPER 69-215] 07 p1237 A69-19569
- System safety analysis for V/STOL aircraft, discussing fault-tree technique role in fail-safe design
[AIAA PAPER 69-216] 07 p1056 A69-19575
- NASA flight safety research, discussing size effects on aircraft handling and built-in response to failure modes
07 p1057 A69-19764
- On-off multiple tank fuel systems for single and twin engine light aircraft, noting fail-safe design
[SAE PAPER 690334] 11 p1825 A69-24502
- Fatigue crack propagation and fail-safe design for stiffened large Al alloy panels with crack stoppers, using residual strength analysis method
12 p2186 A69-26835
- Trident 2E and 3B structural design and fail-safe tests, noting difference in fuselage length
13 p2202 A69-27972
- NERVA engine cooldown system for emergency shutdowns using high pressure liquid H followed by gaseous H warmup and liquid N cooldown
[AIAA PAPER 69-512] 16 p2810 A69-31846
- V/STOL fatigue design parameters, balancing fail-safe and safe-life design procedures
[AHS PAPER 376] 17 p2900 A69-33512
- Stability augmentation system for CX-84 tilt wing V/STOL aircraft, using redundancy techniques to achieve fail operational performance with two active channels
[AHS PAPER 310] 17 p2901 A69-33545
- Navigation and guidance systems for low altitude aircraft flight safety noting position determination, cockpit environment and fail-safe operation
17 p3002 A69-34080
- Fail-soft operation in array processor with cellular redundancy, discussing cellular autonomy, long life and ultrareliability
[AIAA PAPER 69-965] 22 p3906 A69-40346
- Fatigue collapse probability of fail-safe structure compared to safety factor design
22 p4045 A69-40820
- Two channel electronic system with one redundant channel for automatic replacement in case of failure evaluated for operational preparedness
23 p4136 A69-41559
- L-1011 fail operative automatic landing system design, operational characteristics and test programs [SAE PAPER 690407] 23 p4185 A69-41657
- Automatic, semiautomatic and manually operated parachute release systems used in Switzerland
24 p4252 A69-42911
- FAILURE**
NT ENGINE FAILURE
NT STRUCTURAL FAILURE
NT SYSTEM FAILURES
- Schottky barrier mixer diodes and point contact diodes failure, discussing criterion for degradation of noise figure, 1/f noise and reverse breakdown voltage
04 p0574 A69-14352
- Random variables generation from distribution having given failure rate function
12 p2102 A69-26571
- FAILURE ANALYSIS**
- Airline aircraft maintenance programs, discussing objectives, procedures and failure analysis models
15 p2549 A69-30209
- Space equipment reliability, discussing manufacturing defects, design faults, component failures, maintenance, overloads, accidents and operating errors
15 p2624 A69-30817
- Integrated circuit failure analysis in military and space applications utilizing type-test programs
15 p2624 A69-30820
- Screening techniques for semiconductor devices, considering component classification with respect to population strength distribution
15 p2627 A69-30840
- Arbitrary single gate failures diagnosis in combinational logic circuits not requiring fault table construction
15 p2583 A69-31112
- Electronic hardware optimum quality assurance selected by dynamic programming in terms of failure mechanism detection efficiency per source allocation
15 p2722 A69-31127
- Integrated circuits failure analysis in space program applications, describing electrical analog for notification, fact gathering, part analysis and corrective action functions
15 p2580 A69-31132
- Failure analysis techniques in electronic component reliability laboratory, discussing electrical and physical tests to detect weaknesses in manufacturing and design
15 p2722 A69-31133
- Electronic component life test sampling plans based on lognormal distribution and instantaneous failure rate or hazard rate criterion
15 p2630 A69-31137
- Aerodynamic failure investigation of Black Brant 2 single stage sounding rockets
15 p2703 A69-31545
- Device quantity failure kinetics or time dependence effect on time-to-failure distribution resulting from given device degradation coefficients distribution
17 p2936 A69-32895
- Shear stress theory of fatigue failure of ductile materials based on crystallographic orientation and probability of slip of neighboring crystals
18 p3211 A69-34344
- Soviet book on reliability of semiconductor radio devices of flight vehicles covering failures through production errors, power source instability, environment induced changes, etc
18 p3108 A69-34350
- Fault tree for hardware multiple failure safety analysis and reliability analysis for single failure analysis, illustrating comparative advantages
18 p3142 A69-34479
- Spacecraft and aircraft components failure analysis for ensuring high reliability of final products
18 p3143 A69-34483
- Quantitative and qualitative reliability programs for commercial and aerospace products, considering Failure Effect Management System
18 p3143 A69-34486
- Failure mechanisms time and stress dependence relations
18 p3144 A69-34490
- Mechanical failure technology, describing programs of government coordinated Mechanical Failure Working Group /MFWG/
18 p3144 A69-34492
- Beam lead sealed junction transistor and integrated circuits reliability, describing test conditions and failure mechanisms
18 p3145 A69-34497

- Failure analyses of semiconductor devices for military use, suggesting modifications to MIL-STD reliability screen tests
18 p3108 A69-34499
- Flight failure analysis, discussing methods and restrictions due to hardware unavailability, minimum data, urgency and publicity
18 p3145 A69-34502
- Prefailure detection of unreliable electronics parts from random samples of received parts lots, noting cost reductions
18 p3146 A69-34508
- Accelerated temperature tests, calculating temperature behavior of hazard rates and activation energy from failure data using computer simulation
18 p3117 A69-34509
- Failure detection methods, discussing percent checkout, failure sensitivity, undetectable failures, etc
18 p3146 A69-34511
- Hazard plot analysis of incomplete data involving times to failure for failed units and running times on unfailed units
18 p3147 A69-34515
- Failure rate data role in reliability analysis and design optimization
18 p3147 A69-34516
- OGO program failure rate analysis with respect to cost, schedule and performance tradeoffs, considering component and systems design and reliability, prelaunch feedback, etc
18 p3207 A69-34519
- Failure mode and effect analysis integrating design and reliability engineering, discussing management controls and interdisciplinary coordination
18 p3147 A69-34526
- Statistical testing techniques using small sample size at low component levels to predict product performance
18 p3117 A69-34528
- Equipment maintainability demonstration technique, discussing simulation, repair time rates mathematical distribution, range and limits
18 p3117 A69-34530
- Slide methods for duplex parallel and switchover redundant mission availabilities based on cost, reliability and maintainability
18 p3147 A69-34531
- Low endurance fatigue in aluminum, Nylon 66 and epoxy resin compared, considering stress-strain relationships, fatigue damage, failure mechanisms and crack propagation
18 p3155 A69-34633
- Low cycle fatigue leading to failure on AISI 321 stainless steel as function of elevated temperature and straining frequency
18 p3219 A69-34834
- Stochastic failure models based on stress peak distributions, including randomly deteriorating strength model and increasing hazard reliability functions
18 p3148 A69-35079
- Collection of articles on physical nature of plastic deformation and failure of metals
18 p3159 A69-35451
- Low temperature bond failures of room temperature vulcanizing methyl-phenyl adhesive bonds attributed to thermal stress cracking of primer, presenting in-process tests
19 p3321 A69-35563
- Failure analysis - IEEE Conference, Philadelphia, May 1969
19 p3281 A69-35781
- System reliability evaluation based on failure analysis illustrated with examples covering initial requirement through parts production monitoring and control
19 p3454 A69-35782
- Communication equipment reliability improvement through testing and failure analysis
19 p3282 A69-35783
- Closed-loop system for test, failure analysis and corrective action in avionics reliability growth, showing cost effectiveness relationship to test program
19 p3282 A69-35784
- Microwave equipment reliability considered in terms of various subsystems and components, showing carefully formulated and executed test program as essential
19 p3282 A69-35785
- Integrated circuits failure analysis techniques utilizing pin-to-pin curve tracer tests and thermal measurements
19 p3282 A69-35786
- Failure mechanisms and analyses of large scale integrated circuits based on bipolar and MOS transistors, describing measurement and probing techniques
19 p3282 A69-35787
- Environmental testing of space hardware, discussing failure detection by thermal vacuum tests and mechanical signature analysis
19 p3430 A69-36009
- Integrated test program based on mission requirements, failure mode and effects analysis with feedback from testing to design and development functions
19 p3327 A69-36014
- Hydraulic systems incipient failure detection, discussing destructive cavitation, component defects, human error, etc
19 p3255 A69-36018
- Intermediate level mathematical reliability model relating failure mechanism, part strength and interaction of application stresses to parts failure rates, with emphasis on microcircuits
19 p3283 A69-36019
- Reliability study of launch support equipment, presenting failure data for mechanical and electromechanical components
19 p3295 A69-36023
- Computerized system-safety fault trees, discussing drawing, configuration control and simulation program
19 p3280 A69-36029
- Mechanical components life or cycles to failure probability distributions determined by Monte Carlo method, comparing theory with aircraft engine parts field data
19 p3327 A69-36031
- Time-dependent failures of components subjected to fatigue loading analyzed for reliability prediction
19 p3437 A69-36032
- Partial prior information utilization via confidence intervals for mean time to failure of exponential reliability model
19 p3360 A69-36038
- Bayesian reliability demonstration tests for predetermining sample size producer and consumer risks for equipment with exponential and binomial failure distributions
19 p3327 A69-36039
- Sequential Bayes procedure demonstrating mean time to failure exceeding acceptable value with given confidence coefficient
19 p3327 A69-36040
- Nonlinear rotational viscoelastic membranes creep rupture and failure found dependent on function of accumulated energy and power dissipation during deformation
19 p3444 A69-36806
- Integer programming method for optimizing constrained reliability problems with several system failure modes
20 p3504 A69-37069
- Component hazard rate distribution functions from unit time and failure analysis, noting confidence statements and simulation studies
20 p3548 A69-37158
- Failure test algorithm for sequential units with delay lines of control digital computers, detecting replacement of output terminals by sensitive paths
20 p3502 A69-37394
- Weld defect data analysis in relation to aerospace structure performance, emphasizing effect on fatigue behavior and acceptance standard [SBAC PAPER 17]
20 p3550 A69-37450
- Multiply censored data plotting on various type hazard papers for engineering information on time to failure distribution
20 p3567 A69-38288
- MIL-STD-781B reliability tests with standard based on exponential distribution for equipment exhibiting constant failure rate, noting sampling
20 p3551 A69-38289
- Flight vehicle motion optimization taking into account random failures of sectioned power plant with limited capacity and independent parallel units
21 p3647 A69-38893
- Deformation rates effect on failure of cast aluminum alloys under various loading rates for tension and compression
21 p3746 A69-38958
- MOS arrays failure mechanisms, discussing oxide defects, contamination and metal migration due to mode of operation and fabrication techniques
21 p3684 A69-39605
- Mean time between failures/MTBF/ for component, equipment or system subjected to total unit test hours at various confidence levels
21 p3684 A69-39700
- Hybrid microelectronic circuit failure mechanisms for thick and thin film resistors, conductors and capacitors, noting packaging contributions
22 p3910 A69-39954
- Failure analysis of corrosion products in hybrid thin film circuits, discussing detection technique, instrumentation and results
22 p3911 A69-39955
- Reliability incentive programs, considering linear and nonlinear curves for mean time before failure/MTBF/ vs incentive dollars and negative MTBF vs penalty dollars
22 p3952 A69-40024
- Metallurgical, chemical and mechanical analyses and high stress tests applied to verification of electronic device reliability, noting failure modes and rate
22 p3953 A69-40030
- Failure analysis on semiconductor devices and integrated circuits, discussing procedure for factual information representing present condition of device
22 p3953 A69-40032
- Continuum fracture concept indicating essential surface energy interpretation difference in otherwise similar adhesive and cohesive failures
22 p3974 A69-40760
- Safety engineering programs for aircraft design, discussing organizational relations, failure and operational safety analyses
22 p3867 A69-41132
- Performance degradation in cadmium sulfide solar cells, discussing cause identification technique, I-V curve parameter changes, etc
23 p4070 A69-42271
- Postbuckling analysis by equilibrium solutions of conservative system near critical point, considering stability failure in elastic structure under increasing load
24 p3496 A69-42730
- Safety and failure of components - Conference, Brighton, England, September 1969
24 p3497 A69-42767
- Electron optical techniques for failure analysis involving brittle fracture, corrosion fatigue, stress corrosion, welding and surface phenomenon
24 p3413 A69-42768
- NDT techniques relation to engineering design problems with failure potential, discussing management planning and cost analysis
24 p3418 A69-42769
- Fatigue crack initiation mechanism as used in design to prevent fatigue failures in service
24 p3497 A69-42770
- Structural materials deformation response to loading conditions and stress or strain cycle analysis to predict failure, including creep and stress relaxation
24 p3498 A69-42771
- Diagnosis of service failures and reasons for primary failure isolation from secondary damage
24 p3498 A69-42772
- Gas turbine engine problem causing component failures, considering alternative replacement strategies
24 p3418 A69-42774
- Engineering components service failures involving fatigue crack propagation, analyzing causes
24 p3498 A69-42775
- Component reliability effect on airline operation of VC 10 aircraft, investigating failure modes and maintenance
24 p3418 A69-42776
- Management activities related to economics of failure in aerospace industry
24 p4416 A69-42777
- Management role in ensuring products and components quality and reliability, analyzing failure reasons
24 p4416 A69-42778
- Civil aircraft structural components failure analysis, discussing fatigue failures and fail-safe design for accident prevention
24 p4251 A69-42779
- Automatic system failure sequence statistical analysis, considering randomly time variable external effects
24 p4289 A69-42953
- Static mechanical strength of syntactic foam tested by generating failure conditions based on combined biaxial and triaxial stress [ASME PAPER 69-APMW-24]
24 p3436 A69-43095
- Solid rocket motors failure during static firing, discussing sequence of events
24 p3465 A69-43260
- Structural analysis and statistical fracture approach to design and testing for polycrystalline ceramic materials, including combined stress testing and load redistribution models
24 p3433 A69-43339
- Aerospace systems failures caused by stress corrosion, fatigue, overload, improper designing or inadequate processing control
24 p3432 A69-43428

Boron epoxy composites evaluation for use in aircraft dynamic components, considering fatigue failure mechanism identification
24 p4337 A69-43450

FAIRCHILD-HILLER AIRCRAFT
U JET AIRCRAFT
U XC-142 AIRCRAFT

FAIRCHILD MILITARY AIRCRAFT
U MILITARY AIRCRAFT

FAIRINGS
ELDO Europa 1 Fairings Jettisoning System and explosive devices, discussing heat shield structure and safety regulations
10 p1635 A69-23027
Test facility for qualification of satellite fairings jettisoning system, describing accelerating tower and recording and control instrumentation
16 p2765 A69-31739

FALKNER-SKAN EQUATION
Particular solutions and quasi-linearization combined to solve nonlinear two point boundary value problems, illustrating method with Falkner-Skan equation
20 p3515 A69-37532

FALLOUT
Nuclear radiation dose rate and atmospheric ionization from radioactive fallout and natural sources, discussing fallout effect on population
01 p0145 A69-10982
Stratospheric air sampling reliability instrumentation as part of radioactivity fallout detection program
05 p0766 A69-16751
Radioactive debris distribution in space from 9 July 1962 thermocuclear explosion over Johnston island recorded by Cosmos 6 satellite
23 p4205 A69-41836

FAN IN WING AIRCRAFT
Hovering fan powered V/STOL aircraft effects on objects on ground, discussing related dust and debris problems
05 p0701 A69-15565
High bypass ratio compound fan shaft engine design and performance for convertible rotary wing aircraft [ASME PAPER 69-GT-51]
09 p1572 A69-22511

FANLIFT DEVICES
U LIFT FANS

FAR FIELDS
Frequency independent antenna far field radiation approximated for gain, polarization, field amplitude and phase, defining omnidirectional antenna with wide-band goniometry
08 p1295 A69-21149
Two dimensional signal analog correlation in noise background using optical spatial filtering Fraunhofer hologram and input as functions
09 p1499 A69-22276
Antenna array models with different emitters to investigate characteristics of radiation patterns in near and far fields
11 p1844 A69-24451
Fraunhofer hologram as interference pattern between Fraunhofer diffraction pattern and coherent background, noting role of distance in image deterioration
11 p1882 A69-24678
Statistical gain characteristics of radar antennas at very short Fresnel zone ranges compared to Fraunhofer zone
12 p2040 A69-26470
Electromagnetic flux from nonlinear self interaction of electron plasma waves in far field of perturbation under anisotropic electron pressures
12 p2141 A69-27147
Irradiance distribution in far field diffraction patterns of partially coherent light diffracted by annular aperture, using Fourier transformation relationship of Schell
14 p2460 A69-29640
Far field energy radiated by two body system using approximation method in general relativity and Minkowski gravitation theory
16 p2812 A69-31836
Mode patterns and far field distribution for gas lasers operated in lowest order Gaussian transverse mode
17 p2981 A69-33090
Far and near field solutions for one dimensional unsteady flows in general inviscid relaxing gas, obtaining flow field structure by matching techniques
17 p2957 A69-33599
Noise intensity measurements in far field of circular nozzle for jet noise composition
17 p2957 A69-33602

Far field of line source in medium with sinusoidally stratified dielectric constant, studying diffraction effects due to Bragg mechanism
17 p2925 A69-33842
On-course monitoring for instrument landing system glide path operating with far field samples
17 p3003 A69-34105
Far field helicopter rotor noise radiation, analyzing blade slap, rotation noise, vortex noise effects and loading harmonics utilizing computer program
18 p3090 A69-34322
Density profiles in far field of reaction control system plumes in vacuum obtained by method eliminating difficulties encountered by continuum method
19 p3238 A69-35954
Analysis theory of shaped beam doubly curved reflector antenna, computing far field patterns by determining current density distribution on nonanalytic surface
20 p3506 A69-37835
Radiation field produced by parasitic loop counterpoise antenna, obtaining far field from geometrical diffraction theory
20 p3507 A69-37840
Electromagnetic radiation from slot excited ground plane covered by inhomogeneous plasma layer, considering far field radiation pattern
20 p3495 A69-37852
Dornier Do 31 VTOL jet aircraft noise alleviation in far field, discussing shielding, interference, ground attenuation and reflection
22 p3862 A69-39932
Fraunhofer hologram of glass fiber by Be X rays reconstructed using He-Ne laser light
24 p4314 A69-42973

FAR INFRARED RADIATION
Microwave and far IR molecular rotational absorption spectra investigated for measuring concentrations of reacting molecular and atomic species in hypersonic projectile wakes
01 p0006 A69-10961
Far IR rocket observations of night sky background radiation
01 p0121 A69-11249
Very far IR techniques applications in molecular and solid state spectroscopy and relationship with impurity band conduction
02 p0296 A69-11791
Far IR background due to superposition of IR galaxies, noting galaxies contribution to extragalactic radio background
02 p0308 A69-12128
Temperature dependent far IR absorption of ferroelectric sodium nitrite, discussing single and multiphonon processes
03 p0490 A69-13940
Balloon observations of solar far IR spectrum and brightness temperature
04 p0652 A69-14419
Far IR observations of atmospheric molecular lines, using high altitude aircraft platforms
04 p0628 A69-15146
Frequency and stability measurements in far IR laser region
07 p1146 A69-18482
Stimulated Compton scattering for laser action, noting voltage tunability and gain at far IR wavelengths [IEEE PAPER S-9]
07 p1154 A69-19081
High responsivity high speed performance Ge bolometer detector for very far IR region, discussing performance theory and noise equivalent power
08 p1313 A69-20132
Far IR laser pulse shape and duration
09 p1515 A69-21424
Free carrier magnetoplasma effect used for far IR phase matched difference frequency generation in semiconductors, discussing carbon dioxide laser transitions
09 p1556 A69-21578
Far IR source in galactic center detected at 100 microns, noting thermal emission of interstellar dust grains as possible mechanism
09 p1603 A69-22264
Inverse Compton scattering of far IR background radiation proposed as explanation of high energy gamma ray flux
09 p1580 A69-22296
Far IR CW gas laser design for maximum output, discussing pulsed operation, wavelength measurement and radiation detection
11 p1898 A69-25051
Electron cyclotron resonance measurement in n-type indium antimonide using far IR emission from HCN

FAR ULTRAVIOLET RADIATION
and water vapor lasers, noting magnetic field strength effects
13 p2270 A69-27200
Far IR and millimeter solar continuum, analyzing flatness of limb darkening curves and brightness temperature near minimum
13 p2341 A69-27591
Balloon-borne instrumentation for detection of far IR extended emission regions and bright point sources, describing results of initial flights
13 p2342 A69-27599
IR astronomy and cosmology, considering cosmic microwave background and isotropic radiation significance in distant IR
13 p2342 A69-27601
Far IR electronic and vibronic transitions in single crystals of Nd ions in tysonite lanthanide fluorides
13 p2316 A69-27628
Night sky far IR observation by rocket-borne telescope, discussing minimum signal detection and origin
16 p2781 A69-32445
Tunable far IR radiation generated from difference frequency between two Q switched ruby lasers using lithium niobate and quartz as mixing crystals
16 p2798 A69-32603
High energy cosmic ray proton, electron and photon propagation through cosmic microwave background, discussing mean free paths
16 p2852 A69-32819
Sunspot of 28 December 1967 studied by far IR scanning with interference and Reststrahlen filters defining bandpass, obtaining umbral temperature
17 p3029 A69-33050
Long path difference vacuum Michelson interferometer application to far IR and IR laser wavelength measurements compared with 6328 A He-Ne wavelength
17 p3006 A69-33405
Far IR angular scattering observations as diagnostic tool to examine microstructure of high altitude cirrus clouds
18 p3126 A69-34281
Regenerative Josephson effect detector with feedback-narrowed far IR response as tunable millimeter and submillimeter wave radiation detector
19 p3313 A69-36417
Intensities of translational lattice mode absorptions of alpha phase solid molecular nitrogen in far IR, noting temperature dependence
20 p3579 A69-37346
Josephson frequency-voltage relation at microwave and far IR frequencies compared, using radiation induced steps
20 p3583 A69-37418
Horizon definition for Apollo space navigation references from examining earth atmosphere visible and far IR spectrum [AIAA PAPER 69-869]
2 p3763 A69-39395
Construction and components of laboratory water vapor laser emitting coherent radiation in far IR
2 p3738 A69-39446
Grating spectrometer for far IR, discussing light source, reflection gratings, filters, etc
21 p3726 A69-39682
Far IR nightglow emission from atomic oxygen observed by rocket-borne liquid He-cooled telescope
22 p3940 A69-40521
Far IR radiation generation, considering incoherent sources, harmonic generators, electron tubes, relativistic electrons and quantum oscillators
22 p3982 A69-40669
Far IR gas laser with linearly polarized radiation output obtained by using echelette reflection grating in place of end mirror
23 p4172 A69-41400
Strong IR millimeter wave emission from galactic center due to interstellar dust grains resembling semiconductor structure
23 p4215 A69-42115

FAR ULTRAVIOLET RADIATION
NT LYMAN ALPHA RADIATION
NT LYMAN BETA RADIATION
Far UV spectra of O and B stars in Orion photographed from Aerobee rocket, describing wavelength measurements and line identifications
02 p0327 A69-12712
Solar coronal ion abundance analyses from extreme UV emission lines
02 p0327 A69-12719
EUV emission line radiative lifetime measurement by foil-excitation technique, noting correction for cascading, He II and transition probabilities for N II and O III
03 p0471 A69-13165

Line identification methods in solar extreme UV and X ray regions 03 p0507 A69-13171

Gas phase photolysis of carbon dioxide in far UV, searching for carbon trioxide 03 p0381 A69-13318

Photoelectron counting in extreme UV using windowless photomultiplier detectors as photon counters 04 p0595 A69-14277

Hydrogen molecular action in vacuum UV region during high current discharge 05 p0771 A69-15814

Absolute sensitivity of Soviet UTs-3 photographic emulsion to vacuum UV radiation by method involving absolute calibration of photocathodes 07 p1136 A69-19620

Vacuum UV perturbation spectroscopy compatibility with resonance transitions in Ar ion laser 08 p1324 A69-20161

Transmission and reflection properties of materials for vacuum UV spectroscopy, using LTE plasmas for calibrating UV intensities 08 p1315 A69-20468

Polar auroral far UV spectra using Ebert-Fastie monochromator flanked by photometers with same visual field 08 p1311 A69-21026

Solar far UV emissions observed from OSO-C by grazing incidence grating spectrometer, noting temporal variations and atmospheric absorption characteristics 09 p1578 A69-22168

Solar X ray and extreme UV spectra during flares, attributing intense emissions to optical transitions 09 p1578 A69-22169

Fourth positive carbon monoxide system observed in absorption in vacuum UV region, discussing rotational and vibrational band structure 09 p1607 A69-22429

Solar research from rockets and satellites, considering solar instruments including EUV spectrographs 10 p1772 A69-22867

Far UV stellar astronomy, concerning very hot stars and interstellar gas composition studies 10 p1772 A69-22870

Diffusion pump oil reflectance and absorption coefficients measured in three thicknesses using light source, monochromator and detector 10 p1725 A69-23647

Far UV spectra of zeta Puppis and gamma super two Velorum with 1.6 A resolution photographed with all reflective objective spectrograph on Aerobee rocket 10 p1788 A69-24120

Vacuum spark light source for extreme UV noting mechanical trigger, compatibility with clean vacuum system and magnetic confinement of ions 11 p1885 A69-24839

Solar flare X ray and extreme UV radiation contribution to E and F1 region ionospheric effects observed by sudden frequency deviations 11 p1950 A69-25160

Forbidden solar corona lines transition probability in vacuum UV region 12 p2157 A69-26334

Oscillator strengths and wavelengths of X ray and EUV transitions in highly ionized iron line spectra 13 p2326 A69-27554

Nighttime molecular O densities between 100- 130 km determined from Schumann-Runge absorption data for successive far UV spectra of hot star 14 p2435 A69-28959

Coronal limb enhancement photometric study by spectroheliograms, comparing maximum brightness profiles in lines of different temperature in extreme UV 15 p2693 A69-30781

Magnetically focused electronographic image converters for far UV photography and spectroscopy in space astronomy applications 17 p2972 A69-33084

Solar photography at extreme UV wavelengths using pinhole camera instrumentation on stabilized Skylark rocket 20 p3539 A69-37545

Solar far UV images systematic photometry for thin solar models in terms of quiet sun intensity 20 p3603 A69-37546

Magnetically focused electronographic image converters for far UV photography and spectroscopy from sounding rockets, discussing stellar observations 20 p3543 A69-37801

Solar cycle variation of extreme UV radiation from total solar disk under nonflare conditions by photoelectric measurements 20 p3592 A69-38103

Vacuum UV flux along T type shock tube axis and measurements of He I line precursor emission, indicating ionizing radiation contributions to precursor ionization and excitation 20 p3511 A69-38239

Emissivity of nitrogen, oxygen and air plasmas in vacuum UV region of spectrum by photographic measurement, using He recombination radiation as brightness standard 21 p3774 A69-38944

Rocket measurement of far UV spectral intensity of theta Orionis for far UV interstellar extinction law in Orion nebula region 22 p4030 A69-40770

Diurnal and solar cycle variations of thermospheric density and temperature generated by solar EUV input and tidal wave, using two dimensional model 24 p4367 A69-43003

Solar flare soft X ray and EUV emission spectra data obtained on OSO-3 satellite compared with centimetric radio bursts 24 p4371 A69-43609

Optical design of double monochromator for use in EUV, describing astigmatism and transmission properties 24 p4351 A69-43758

FARADAY DARK SPACE

Faraday dark space geometries in glow discharge, using superposition principle to divide electric field for transition visualization 09 p1540 A69-22099

FARADAY EFFECT

Negative Faraday effect and Doppler line width measurements for He-Ne IR gas laser tube by producing beat frequencies in ring laser system 01 p0088 A69-10028

Faraday angle of rotation of radio signals polarization plane from satellites and celestial bodies 01 p0030 A69-10574

Faraday rotation of plane polarized microwave beam for measuring precursor ionization from exploding wire discharge in various gases 01 p0129 A69-10663

Symmetrical design of short ferrite Faraday rotator using matrix representation, noting matching to rectangular waveguide 01 p0048 A69-11034

Differential Faraday technique to determine electron content latitude dependence in Northern Hemisphere during magnetically disturbed periods in March 1966 01 p0146 A69-11128

Ionospheric electron density determined from Faraday effect, using ATS-3 radio signals 02 p0237 A69-11660

Faraday effect of free carriers on n-type GaSb at 20 K, determining mass and mobility of electrons from Hall effect and conductivity 02 p0298 A69-12039

Laser with passive Q switching with Faraday cell switch, studying induced recombination and Mandelsham-Brillouin scattering 03 p0435 A69-12983

Electron concentration in lower ionosphere based on measurement of Faraday rotation of polarization plane of radio waves scattered by meteor trail 03 p0423 A69-13535

Radio waves Faraday rotation measured from pulsars by recording difference in received power 03 p0513 A69-13771

Electron production and loss rates in F region from measurements of Faraday rotation imposed on VHF telemetry transmissions from geostationary satellite 03 p0503 A69-14016

Free carrier Faraday effect in piezoelectric semiconductors investigated for microwave frequencies, low temperatures, mixed deformation potential and piezoelectric scattering 04 p0643 A69-15201

Ionospheric electron content and slab thickness changes during magnetic storm in June 1965 using Faraday rotation and critical frequencies 05 p0759 A69-16420

Faraday effect at free carriers in indium antimonides and gallium arsenides, analyzing frequency dependence of rotation angle 06 p0979 A69-16996

Suppressed rotation reciprocal ferrite phase shifter theory explained in terms of nonreciprocal coupling of cross polarized waveguide modes 06 p0896 A69-17484

Faraday rotation measurements using incoherent scatter to obtain ionospheric electron density profiles 07 p1085 A69-19223

Energy separation and electrons effective mass ratio of conduction bands of tellurium doped GaSb obtained by free carrier Faraday rotation measurements 07 p1201 A69-19464

Linear polarized emission from pulsar CP 0328 dependent on frequency, discussing model for source with constant Faraday rotation 08 p1382 A69-19817

Electrical characteristics of linear Faraday generator using binary mixture of noble gases with nonequilibrium ionization 08 p1359 A69-19880

Orbiter and rotator models of pulsating radio sources, considering relationship between lack of Faraday rotation and similar polarization in decametric radiation from Jupiter 08 p1397 A69-20688

Near IR radiation magneto-optic light modulators using Faraday effect in yttrium-iron garnet and in related compounds 11 p1886 A69-25057

Lead factor role in nonequilibrium ionization process in Faraday-type generator, determining relationship with conductivity 13 p2314 A69-28361

Ionospheric electron density determined from Faraday effect, using ATS-3 radio signals 13 p2256 A69-28691

Faraday effect for magnetic properties of chromium tribromide along various isotherms near critical point, confirming scaling laws 15 p2668 A69-30686

Faraday angle of rotation of radio signals polarization plane from satellites and celestial bodies 15 p2568 A69-30744

Integral charge neutrality effect on local space charge density of MHD generator channel, examining electrode couple for Faraday generators 15 p2664 A69-31055

Pioneer 6 S band telemetry carrier Faraday rotation during corona occultation measured by deep space tracking antenna 15 p2700 A69-31419

Faraday rotation measurements of signals from Explorer 22 analyzed to determine scintillation boundary in auroral ionosphere 15 p2605 A69-31443

Plasma magnetic field and electron density measured by Faraday rotation using resonant gas laser radiation 16 p2822 A69-32041

Second order correction to first order Faraday rotation equation for quasi-transverse propagation of ionospheric radio waves obtained from Appleton-Hartree equation 16 p2777 A69-32101

Satellite signal probability density determined from scintillation plus Faraday effect in statistical terms 16 p2751 A69-32103

Faraday rotation measurements in ionosphere by geostationary satellite ATS-3 as evidence of considerable nighttime electron transport 17 p2959 A69-32926

Rocket-borne AM radio receiver for Faraday rotation experiments to measure lower ionosphere electron density, giving circuit diagrams 17 p2936 A69-33062

Faraday effect and permittivity of hydrogen plasma measured simultaneously, determining electron density and collision frequency 17 p2919 A69-33394

Quasi-transverse /Q-T/ point time lag on Faraday rotation records at widely spaced frequencies during satellite pass explained by refraction theory 18 p3100 A69-34251

Faraday rotation in NP 0527 and CP 0328, measuring angular velocity and mean longitudinal magnetic fields 18 p3192 A69-34319

Magneto-optical constants and conduction band parameters of GaAs by coherent radiation at high temperatures, measuring Faraday rotation 19 p3386 A69-36522

Ionospheric electron content and concentration variations analysis based on data of radio waves propagating from satellite, considering Doppler shift and Faraday effect 20 p3486 A69-37027

Polarization ellipse orientation at source from Faraday fringes on Jupiter decametric radio bursts swept frequency records 20 p3594 A69-38169

Two dimensional numerical solution for Faraday DC MHD generators with variable conductivity, velocity and magnetic field 21 p3649 A69-39027

Ionospheric vertical columnar electron content at midlatitudes near solar cycle minimum based on Faraday rotation data from Explorer 22
22 p3939 A69-40505

Faraday effect measurements by polar orbiting satellites for vertical distribution of ionospheric electron density
22 p3941 A69-40718

Galactic magnetic field existence arguments, discussing general and optical evidences, radio emissions, Faraday rotation from extragalactic sources and from pulsars, etc
23 p4217 A69-42321

Faraday rotation diurnal variation plotted by analyzing radio transmissions from Canary Bird geostationary satellite, considering ionospheric electron density peak
23 p4160 A69-42433

Ionospheric electron content measurement from Faraday fading on satellite BE-B, using computer program for data reduction as function of latitude
23 p4160 A69-42434

Mean and variance of Faraday rotation and pulsar signal dispersion in galactic turbulent structure, applying to statistically homogeneous disk model of Galaxy
24 p4375 A69-42659

Optimization of Faraday MHD generators with nonequilibrium ionization and plasma turbulence, assuming electrons at Saha equilibrium at elevated temperatures
24 p4256 A69-43682

FARM CROPS
NT POTATOES

Plant and soil thermal behavior for various conditions of crop species, plant spacing, tillage, irrigation and aerial thermal scanner imagery
12 p2075 A69-26989

Remote sensing technology application to improving range resource inventories, discussing aerial photography, optical, IR and radar scanning, etc
12 p2098 A69-26992

Automated crop surveys from integrating observations made at different times /time dimensioning/ during growing season, noting earth resources satellites role
18 p3126 A69-34337

Automated air photo identification of crop types, utilizing stereo height as discriminating variable
23 p4155 A69-41721

FAST NEUTRONS

Fast neutron fluxes at various atmospheric levels and geomagnetic northern midlatitudes measured by proportional counters using boron trifluoride
03 p0501 A69-13528

Radiation tests on Ovonic threshold switches performed with fast neutrons and broadband X rays
06 p0978 A69-16891

MOS and junction transistors damage due to radiation, noting decrease in collector current under fast neutron dose
13 p2227 A69-27514

Forward current decrease in Si mesa diodes under fast neutron irradiation ascribed to increase in base resistance
13 p2236 A69-28549

Fast atmospheric neutrons flux and spectrum measurement during two balloon flights, tabulating results and evaluating albedo flux during quiet sun period
16 p2851 A69-32616

Fast neutron irradiation effect on niobium nitride current carrying capacity, showing enhancement
17 p3008 A69-33765

Fast neutron spectrum for subcritical section of homogeneous U 235-polyethylene thermionic critical assembly measured by pulsed source time- of-flight method
18 p3170 A69-34313

RBE of fast neutrons on mice, rats and guinea pigs, discussing suppression of mitosis in isolated cells
20 p3478 A69-37629

Fast neutron irradiation effect in Ge crystals, using X ray diffraction and volumetric measurements
20 p3584 A69-38125

Histological changes in internal organs of rats after exposure to 400 r fast neutron dose, showing destructive processes followed by compensation reactions of cellular proliferation
21 p3659 A69-39062

Radioactive decay and conductivity changes with time in high and low resistivity CdS single crystals after irradiation with 14 Mcv and reactor fast neutrons
22 p3993 A69-40728

Fast neutron irradiation effect on IR absorption in single crystal GaAs for various fluences
23 p4198 A69-41540

FAST NUCLEAR REACTORS

Safety problems associated with transient boiling of liquid metals in fast nuclear reactors, emphasizing behavioral differences between liquid metals and water
08 p1420 A69-20101

Fast and thermal thermionic reactor systems characteristics including fissile material, components mass, power output and flattening and design features
14 p2480 A69-29182

FASTENERS
NT BOLTS
NT NUTS [FASTENERS]
NT PINS
NT RIVETS
NT SCREWS

Aluminum coatings compared with cadmium coatings for aerospace fasteners, discussing plating methods
[ASM PAPER D8-5.2] 07 p1142 A69-19663

Ultrasonically assisted installation of fasteners for weight savings in aircraft/spacecraft structures
09 p1478 A69-22373

Machined fastened joints for airframe structural parts, discussing fatigue life, strength and fastener hole preparation
19 p3319 A69-35553

Ti-Al-V fasteners heat treated in beta field, showing superior mechanical properties to samples treated in alpha plus beta field
21 p3729 A69-38661

Aircraft fastening systems guidelines based on mechanical strength, weight, cost and joint efficiency, discussing hole preparation and expansion design
22 p3956 A69-40822

Mechanical properties of aircraft fasteners high temperature materials
22 p3956 A69-40823

Titanium alloys for strength and weight saving in aircraft fasteners operating at cryogenic or elevated temperatures, discussing corrosion and notch sensitivity
22 p3956 A69-40824

Galvanic corrosion prevention measures for airframe fasteners, discussing crevice sealants, primers, zinc chromate, cadmium and aluminum coatings
22 p3957 A69-40825

Aircraft fastener fatigue-acceptance criteria compared with actual tests, considering unusual service conditions
22 p4045 A69-40826

Interference fit fasteners role in improving aircraft structure fatigue life through preload barrier against fatigue stresses
22 p3957 A69-40830

Clamping and sealing fastener for single direction installation consisting of pin, collar and sealing collar with insert
22 p3957 A69-40831

Titanium stress pin with headed straight-shank pin and collar for reducing fatigue stress around holes
22 p3957 A69-40832

Structural airframe fasteners, reviewing systems for fatigue critical wing/fuselage structures, honeycomb panel attachments and data on fatigue life
24 p4325 A69-43437

Various fasteners influence on fatigue life of bolted joints, noting high clamping force beneficial effect
24 p4325 A69-43438

Aerospace fastener systems standardization proposal to reduce inventories, simplify design and provide extended structural life
24 p4325 A69-43439

Aerospace fastening system requirements to lower in-place costs, extend service life and reduce weight of aircraft
24 p4325 A69-43440

Fastener materials selection for high temperature aircraft structures, considering various physical properties influence
24 p4325 A69-43441

Aircraft fastener corrosion control with emphasis on surrounding joint and structure, discussing test programs, Al coatings, etc
24 p4334 A69-43442

FATIGUE [BIOLOGY]
NT FLIGHT FATIGUE
NT MUSCULAR FATIGUE

Psychophysical method of studying heart rate as indication of physiological fatigue
17 p2911 A69-34013

Glider pilots fatigue attributed to nutritional habits
23 p4106 A69-41796

Psychophysiological effects of fatigue and correlation with somatic parameters following circadian rhythm
24 p4268 A69-43407

FATIGUE [MATERIALS]
NT BENDING FATIGUE
NT METAL FATIGUE
NT THERMAL FATIGUE

Fatigue-damage evaluation system for transport aircraft, noting use of cumulative strain gauge that stores strain history
01 p0165 A69-10118

Fretting effect on fatigue of press fitted axle assemblies, analyzing relative slip amplitude dependence on size, shape, clamping pressure, nominal stress and cycles
01 p0167 A69-10305

Handbook on fatigue properties for product design covering metals stress conditions, machine parts load and stress determination, cyclic stress, etc
01 p0170 A69-10918

Fatigue properties and failure mechanisms of glass reinforced plastics based on chopped strand mat polyester resin laminates
02 p0269 A69-11795

Fiberglass reinforced plastic laminates failure under biaxial compression due to layer separation with strain energy as endurance criterion
02 p0270 A69-12142

Strain multiplier device for fatigue sensors for totalizing resistance change from aircraft service load parameters
02 p0250 A69-12230

Strain induced deformational instability of aluminum alloys
03 p0447 A69-13818

Cumulative damage theories application to fatigue data for high strength materials, discussing stress levels
04 p0668 A69-14379

Stress variation cycles pattern effects on fatigue strength of materials, discussing results of low- carbon steel tests under sinusoidal loading
04 p0673 A69-14535

General linear theory of isotropic cumulative failure involving phenomenological consideration of fatigue damage accumulation
[ASME PAPER 68-WA/MET-6]
05 p0838 A69-16149

Crack nucleation in high strain fatigue based on plastic instability model
05 p0780 A69-16430

Superimposed stress of higher frequency and rotating bending stress effects on aluminum alloy
06 p0941 A69-17121

Stress direction and mean stress effects on fatigue properties of fiberglass reinforced plastics
06 p0945 A69-17124

Photographic observations of fatigue fracture of heat treated polycarbonate
06 p0946 A69-17205

Polycarbonate surface stiffness increase associated with fatigue induced by repetition of loads
06 p0946 A69-17206

Device for measurement of time to failure of brittle materials in thermal-endurance testing, noting shock wave
06 p0927 A69-17690

Fatigue gauge for plastic deformation based on plastic strain rates, cycles, temperature, etc
07 p1135 A69-19216

Strain concentration design factors for notch effect in low cycle fatigue and crack propagation conditions
07 p1235 A69-19383

Surface environment effects on mode of microcrack formation during fatigue of Al single crystals, noting surface void formation mechanism
07 p1235 A69-19387

Tensile strength of glass-fiber reinforced epoxy resin laminates subjected to fluctuating tension, discussing crack density dependence on fatigue stress cycles
08 p1338 A69-20494

Fatigue behavior of composite disk modified from previously evaluated boron epoxy reinforced titanium compressor disk
09 p1619 A69-22323

Electron fractographic study of fatigue cracks in wrought beryllium sheet, noting transgranular and intergranular modes on fracture surface
09 p1500 A69-22324

Aluminum alloy crack propagation and fracture patterns as function of temperature under high strain amplitude and low strain rate
10 p1709 A69-23071

Fatigue behavior of plastics classified noting temperature rises, crack initiation, etc
10 p1716 A69-23394

Fatigue growth of disk shaped crack in infinite body, noting dependence on fourth power of stress intensity factor
10 p1802 A69-24028

Metals with combined high damping and good mechanical properties for solving fatigue, noise and vibration problems
10 p1715 A69-24044

Polymer fatigue model from low cycle analysis of dynamic and thermal properties in structural plastics
10 p1717 A69-24217

Dynamic IR inspection to detect fatigue cracks in aircraft and missile structure from distance
11 p1861 A69-24262

Hydrostatic pressure-cycling technique for controlled fatigue precracking of spin burst fracture toughness specimens, noting ultrasonic flaw detection
11 p1995 A69-25650

Material selection criteria for low cycle fatigue resistance in components design determined from tensile test and incremental step test curves
[ASME PAPER 69-DE-59] 14 p2461 A69-28852

Book on fatigue strength in construction covering structural strength and stability, load design, metal physical properties, elasticity and plasticity theories, stress concentration, strain buildup, etc
14 p2534 A69-29333

General linear theory of isotropic cumulative failure involving phenomenological consideration of fatigue damage accumulation
[ASME PAPER 68-WA/MET-6] 14 p2535 A69-29436

Fatigue design procedures - Conference Munich, June 1965
15 p2705 A69-30355

Uniaxial stress effects on molecular breakage rate, relating structure-sensitive parameter to elastic modulus
15 p2709 A69-30807

Fatigue cracks growth rate under combined static and cyclic stresses
15 p2709 A69-30808

Fatigue crack propagation caused by cumulative damage due to strain cycling at crack tip, relating resistance to cyclic ductility
15 p2710 A69-30812

Shear stress theory of fatigue failure of ductile materials based on crystallographic orientation and probability of slip of neighboring crystals
18 p3211 A69-34344

Low endurance fatigue in aluminum, Nylon 66 and epoxy resin compared, considering stress-strain relationships, fatigue damage, failure mechanisms and crack propagation
18 p3155 A69-34633

Mechanical machine for fatigue testing flat samples of thin walled structures under tension and at various frequency ranges
18 p3118 A69-34833

Stress-strain state of elastoplastic material subjected to quasi-static uniaxial tension and compression, considering Bauschinger type effects by scalar parameters
18 p3222 A69-34909

Fatigue fracture due to heat generation in polycarbonate subjected to pulsating tensile load, presenting temperature change per unit stress increase
18 p3163 A69-35498

Ultrasonic nondestructive testing technique for fatigue induced damage location and criticality in filament wound fiberglass cylinders, correlating damage to residual life
19 p3322 A69-35577

Reactivity of hydrogen with surface of Ti-Al-V alloy under fatigue cycling at ambient and cryogenic temperatures
20 p3557 A69-36960

Fatigue endurance determined from thermal stresses by balancing elastic strain rates, creep relaxation and mechanical cyclic loading with triangular waveform, discussing nonsteady creep
21 p3843 A69-39310

Fatigue collapse probability of fail-safe structure compared to safety factor design
22 p4045 A69-40820

Scale factor in designing uniform strength structures for dynamic load effects determined by recording fatigue limit and failure location, using variable cross section samples
23 p4225 A69-41422

Nondestructive testing for fatigue cracks, considering X ray, magnetic particle, penetrant, ultrasonic and eddy current inspection techniques
23 p4234 A69-42451

Structural materials deformation response to loading conditions and stress or strain cycle analysis to predict failure, including creep and stress relaxation
24 p4398 A69-42771

FATIGUE DIAGRAMS U S-N DIAGRAMS

FATIGUE LIFE

Low cycle fatigue life of aluminum alloy in reversed biaxial bending
01 p0093 A69-10116

Hollow rolling elements for reducing centrifugal load on high performance bearings, discussing production, fatigue life, etc
01 p0085 A69-10294

Fatigue life, kinematics, dynamics, etc, of thrust loaded ball bearings, considering inertial effects of hollow balls
01 p0087 A69-10908

Stress peak distribution effects on random load fatigue investigated for one and two degree of freedom systems
01 p0172 A69-11355

Shot peening effect on fatigue properties of maraging and Al-Zn-Mg alloy steel welds, using repeated tensile tests
02 p0253 A69-12061

Plastic fatigue life of steel under rotary bending, proposing fracture criterion based on strain amplitude for low cycle stress levels
02 p0346 A69-12421

Notch stress procedure to predict low cycle fatigue life of specimens with fabrication flaws, discussing crack initiation and propagation lives effects
[ASME PAPER 68-PVP-15] 03 p0523 A69-12997

Butt weld fatigue properties improvement in maraging steels, using shot peening and prestretching
03 p0434 A69-13762

Fatigue endurance of structural elements determined from stress rupture strength under high and low loading rates
04 p0673 A69-14536

Random cumulative damage theory for fatigue failure of steel under sinusoidal loading taking into account randomness of time to failure and possession of memory
04 p0680 A69-15154

Fatigue life reduction in Al alloy specimens with stress concentrations due to notches
05 p0843 A69-16696

Superimposed stress of higher frequency and rotating bending stress effects on aluminum alloy
06 p0941 A69-17121

Delamination effects on strength degradation of filament wound composites
06 p0946 A69-17126

Fatigue life in nonstationary cyclic loading above endurance limit, describing methods of shortened fatigue tests for fatigue life
07 p1231 A69-18403

Atmospheric influence on friction endurance of solid powdered lubricants at constant layer thickness
[IME PAPER 3] 07 p1138 A69-18563

Metal fatigue simulation by Monte Carlo method, showing programmed fatigue tests in form of life distribution functions
07 p1233 A69-19314

Stress analysis split method for determining residual strength and fatigue crack life of damaged or initially cracked VTOL structures
[AIAA PAPER 69-214] 07 p1237 A69-19576

Matrix properties related to torsional fatigue life of fiberglass reinforced NOL rings, using polyester and epoxy resins as model systems
08 p1339 A69-20495

Aircraft structural aluminum alloy fatigue life, considering atmospheric relative and absolute humidity
09 p1521 A69-21390

Weld discontinuities effects on fatigue strength of Al welds tested to determine unaffected defect size and severity of discontinuities
09 p1527 A69-22372

Fatigue strength research - Conference, Darmstadt, West Germany, May 1968
09 p1619 A69-22570

Fatigue strength and aircraft structural standards based on experimentally determined safety factors
09 p1619 A69-22571

Fatigue strength and stress-time functions obtained by programmed fatigue tests under time variable loads
09 p1620 A69-22572

Fatigue life evaluation by programmed fatigue strength tests, using frequency distribution of load sequence amplitudes
09 p1620 A69-22573

Material selection for structures under vibration loads, analyzing fatigue strength on basis of stress susceptibility and relationship with tensile strength
09 p1620 A69-22574

Elastoplastic stress in notch as cause of decreased lifetime of aircraft components, analyzing stress reversal and displacement during takeoff and landing
09 p1620 A69-22576

Strain fatigue mechanism of crack propagation in ductile metals, considering distribution of plastic cohesive stresses at crack tip
10 p1795 A69-23059

Existing predictive methods for determining high temperature low cycle fatigue life reexamination based on experiments on nickel
10 p1796 A69-23068

Low cycle fatigue of metals under biaxial strain, considering specimen life and strain amplitude correlation
10 p1797 A69-23083

Progressive accelerated fatigue testing for reliability in determining fatigue limits
10 p1800 A69-23349

Potential testing methods for corrosion induced changes in materials, discussing mechanical properties, corrosion fatigue and cracking and creep
10 p1713 A69-23822

Notched members fatigue life prediction from smooth specimen fatigue data and Neuber rule application
10 p1715 A69-23984

Structural fatigue life evaluation as cumulative damage analysis for irregularly varying loads
[DVL-780] 10 p1802 A69-24020

Tresca shear stress fatigue failure criterion and experimental data for combined bending and torsion acting out of phase
11 p1984 A69-25140

Aircraft structures fatigue life determination based on Kordonskii method, comparing steel tests result with linear summation theory
11 p1987 A69-25345

Fatigue strength reduction in Ti alloy in sliding friction contact with metallic materials caused by fretting corrosion
12 p2113 A69-26125

Fatigue life of Al alloy thin laminated sheets, considering cyclic frequency and temperature effects
12 p2180 A69-26359

Fatigue crack propagation laws determined by material yielding at crack tips, stress intensity and exponential crack growth law
12 p2187 A69-26846

Tension-compression fatigued alpha Ti twin formation contribution to fatigue damage during cyclic loading
12 p2116 A69-26913

Oxygen content effect on tension-compression fatigue of alpha Ti alloys, discussing internal damage associated with twin formation
12 p2116 A69-27134

Crack initiation prediction in high temperature components subjected to arbitrary thermal-mechanical cycling
13 p2365 A69-28252

Physical limit model of fatigue in metals and alloys to determine stress producing plastic flow in surface layer
14 p2461 A69-28913

S-N fatigue life small bondable resistance sensor, discussing random response data interpretation with emphasis on use of strain multipliers
15 p2613 A69-31270

Fatigue life gage on operational aircraft providing in situ monitoring of fatigue damage prior to and during propagation of running fatigue cracks
15 p2613 A69-31271

Fatigue data adapted to conditions of specific design part including fatigue limits, S-N curves and various failure diagrams
16 p2794 A69-32433

Secondary fatigue curves slope variation to determine preloaded materials fatigue life under unstationary loading
17 p3052 A69-32976

Fatigue life estimation for irregularly varying loads with emphasis on ground-air-ground stress cycles in aircraft
17 p3052 A69-32977

- Short life fatigue data for metals, noting applications in design
17 p3052 A69-32978
- Random stress statistical properties and relationship to fatigue life, discussing Fuller prediction, comparison with test data, and vehicle design evaluation
17 p3053 A69-32988
- Mechanical and resistance type fatigue life indicator, comparing operating and performance characteristics [AHS PAPER 378]
17 p3059 A69-33511
- V/STOL fatigue design parameters, balancing fail-safe and safe-life design procedures [AHS PAPER 376]
17 p2900 A69-33512
- Maximum helicopter level flight speed loads spectrum shape and severity related to rotor component fatigue design strength [AHS PAPER 372]
17 p3059 A69-33516
- Mean stresses effect on fatigue strength by specimens vibratory/tensile mean stress diagram combining Goodman line and Gerber parabola merits with increased accuracy
17 p3067 A69-34197
- Stress field in elastic contact area vicinity of hollow sphere subjected to normal load through flat plate, noting contact life [ASME PAPER 69-LUBS-5]
18 p3212 A69-34383
- Reinforced plastics static fatigue strength under various loads including thin walled tubes long term tests under constant internal pressure
18 p3162 A69-35353
- Machined fastened joints for aircraft structural parts, discussing fatigue life, strength and fastener hole preparation
19 p3319 A69-35553
- Stress coining methods for improving aircraft structure fatigue life by controlling material yielding inside holes and materials surrounding holes and slots [AIAA PAPER 69-761]
19 p3433 A69-35659
- Cyclic stress frequency on mild steel corrosion fatigue tests, showing strength dependence on potential and stress current
19 p3342 A69-35775
- Fatigue life testing apparatus with computerized simulation of random load maxima and minima, describing rotating bend test application
19 p3434 A69-35777
- Electroplating method for local stress concentrations determination, discussing measurement techniques, metal fatigue failure prediction, etc
19 p3441 A69-36751
- Relationship between chronological and fatigue life in airframes, showing fatigue life dependence on operating conditions, pilot techniques and maintenance and inspection quality
20 p3461 A69-36920
- Apparent dynamic modulus and damping under multilevel loading during fatigue cycling to estimate stainless steel specimens cumulation fatigue lives
20 p3620 A69-36997
- S/N fatigue life gage response to constant frequency random amplitude input strain
20 p3537 A69-37007
- Electron beam welding for fabrication of aircraft structures, discussing fatigue strength of Ti and Al alloys and margining and low alloy steels [SBAC PAPER 12]
20 p3550 A69-37456
- Fatigue crack initiation in relation to contact stresses due to fretting, studying causes of strength reduction and crack inclination to surface
20 p3563 A69-38110
- Fatigue resistance of bimetallic sheets of steel and Al alloys by fatigue resonant machine, analyzing lifetime distribution and failure probability
21 p3835 A69-38773
- Stress concentration and surface strain hardening effects on fatigue strength of refractory alloy specimens with and without cut
21 p3745 A69-38875
- Optimum number of test aircraft in test program to predetermine endurance and service life of same aircraft in serial production
21 p3647 A69-39098
- Ti-Al-V forgings macro /prior beta/ grain size and in-process thermal treatment effects on fatigue life [AIME PAPER S69-2]
21 p3732 A69-39470
- Static and fatigue strength of end-closed filament-wound vessels under internal pressure
21 p3846 A69-39797
- Estimation of program fatigue life curves from equivalent load program using Miner law
21 p3846 A69-39810
- Damaging effects of vibration on materials and parts to estimate fatigue life, considering periodic and non-periodic stress vs time relationships
22 p4041 A69-40167
- Large diameter bolts in aircraft structures resisting hydrogen embrittlement and stress corrosion, noting fatigue properties
22 p3957 A69-40827
- Interference fit fasteners role in improving aircraft structure fatigue life through preload barrier against fatigue stresses
22 p3957 A69-40830
- Creep strength as function of oxygen pressure for Ni at 510 and 600 C, dropping creep rupture life to plateau of nearly constant life
23 p4176 A69-41504
- Notch effect on corrosion fatigue behavior of high strength Al alloy under bending and direct stresses
24 p4330 A69-42553
- Fatigue crack initiation mechanism as used in design to prevent fatigue failures in service
24 p4397 A69-42770
- Engineering components service failures involving fatigue crack propagation, analyzing causes
24 p4398 A69-42775
- Structural airframe fasteners, reviewing systems for fatigue critical wing/fuselage structures, honeycomb panel attachments and data on fatigue life
24 p4325 A69-43437
- Various fasteners influence on fatigue life of bolted joints, noting high clamping force beneficial effect
24 p4325 A69-43438
- Relative slip effect on fretting fatigue strength, deriving stress initiating fatigue cracks
24 p4404 A69-43628
- Deferred rupture as function of applied load noting test methods
24 p4407 A69-43801
- Rotational bending fatigue strength of plain and notched conventional and maraging steels, evaluating gas nitriding effects
24 p4335 A69-43802
- FATIGUE TESTING MACHINES**
- Torsion bar with two inertia masses attached used to determine damping capacity and torsional fatigue strength
03 p0431 A69-13917
- Fatigue gauge for plastic deformation based on plastic strain rates, cycles, temperature, etc
07 p1135 A69-19216
- Sample changer for metal fatigue studies under ultrahigh vacuum conditions, noting successive testing in same vacuum
08 p1302 A69-20877
- Testing system stiffness effect on sheet fracture, discussing notch strength dependence on stiffness
10 p1796 A69-23075
- Thermal fatigue testing system for martensitic steels using fluidized bed heating and cooling, specimen manipulation means, cycle control, data evaluation, etc
10 p1714 A69-23979
- Mechanical machine for fatigue testing flat samples of thin walled structures under tension and at various frequency ranges
18 p3118 A69-34833
- Fatigue life testing apparatus with computerized simulation of random load maxima and minima, describing rotating bend test application
19 p3434 A69-35777
- FATIGUE TESTS**
- Ultrasonic detection and measurement of fatigue cracks in notched cylinders subjected to reversed axial cyclic loading
01 p0078 A69-10113
- Crack initiation and propagation in Ti alloys during thermal cyclic heating, noting influence of gas saturation
01 p0094 A69-10215
- Moisture effects on crack propagation in high strength aluminum alloys studied by fatigue tests
01 p0098 A69-10766
- Strain multiplier device for fatigue sensors for totalizing resistance change from aircraft service load parameters
02 p0250 A69-12230
- Stress variation cycles pattern effects on fatigue strength of materials, discussing results of low-carbon steel tests under sinusoidal loading
04 p0673 A69-14535
- Fatigue endurance of structural elements determined from stress rupture strength under high and low loading rates
04 p0673 A69-14536
- Residual gas effect on fatigue behavior of pure iron subjected to alternating bending load in ultrahigh vacuum
04 p0616 A69-14846
- Twin differential calorimeter for measuring heat dissipation by wire specimen under fatigue tests, using semiconductor thermopiles
04 p0618 A69-15205
- Linear cumulative damage theory defining low cycle fatigue region of classic S-N curve, providing biaxial strain mode by centrifugally loading rotors [ASME PAPER 68-WA/MET-8]
05 p0838 A69-16151
- Device based on stroboscopic effect for observing crack propagation on rotating specimens during fatigue tests
05 p0843 A69-16665
- Fatigue life reduction in Al alloy specimens with stress concentrations due to notches
05 p0843 A69-16696
- Fatigue performance of composites consisting of W or Mo helical coils embedded in Cu matrix, discussing evaluation from microstructural behavior
06 p0940 A69-16951
- Fatigue life in nonstationary cyclic loading above endurance limit, describing methods of shortened fatigue tests for fatigue life
07 p1231 A69-18403
- Metal fatigue simulation by Monte Carlo method, showing programmed fatigue tests in form of life distribution functions
07 p1233 A69-19314
- Fatigue tests on steel of various diameters using standard and accelerated methods
07 p1233 A69-19315
- Chromium steel /E1961/ susceptibility to structural damage under cyclic loads by nondestructive inspection of magnetic hysteresis and eddy current losses
07 p1141 A69-19316
- Impact cyclic loading fatigue tests of smooth and notched duralumin, discussing increased impact strength resulting from initial underloading
07 p1167 A69-19317
- Multiloop control plant described by Jacobian transfer matrix to control spectral characteristics of random processes
08 p1296 A69-20233
- Flexural fatigue of glass-reinforced thermoplastics as function of various parameters, discussing test for autogenous dissipative heating
08 p1337 A69-20481
- Mechanical properties of cast epoxy resins correlation with corresponding composites strength under static and dynamic fatigue stressing
08 p1340 A69-20510
- Fatigue strength of gears with integrally forged, cut and ground teeth, discussing pancake forgings [SAE PAPER 680632]
08 p1321 A69-20732
- Crack propagation properties of polymethyl methacrylate during bending and tension, noting temperature and loading time effect on crack size
09 p1529 A69-21854
- Part-through and through-thickness fatigue crack growth observations in glassy plastics, using linear elastic fracture mechanics [SESA PAPER 1348]
09 p1617 A69-22013
- Weld discontinuities effects on fatigue strength of Al welds tested to determine unaffected defect size and severity of discontinuities
09 p1527 A69-22372
- Fatigue strength and stress-time functions obtained by programmed fatigue tests under time variable loads
09 p1620 A69-22572
- Fatigue life evaluation by programmed fatigue strength tests, using frequency distribution of load set amplitudes
09 p1620 A69-22573
- Progressive accelerated fatigue testing for reliability in determining fatigue limits
10 p1800 A69-23349
- Aluminum plates bending fatigue tests, discussing mechanical properties, structural failure, grain size, strain hardening, stress-strain-time relations, heat treatment, etc
10 p1711 A69-23356
- Surface temperature rise of solution treated austenitic steel measured during double repeated rotating bending fatigue tests at room and elevated temperatures
10 p1711 A69-23393
- Fatigue behavior of plastics classified noting temperature rises, crack initiation, etc
10 p1716 A69-23394
- Elastic-plastic deformations /strains/ amplitudes measured at high cycle temperatures in thermal fatigue tests
10 p1801 A69-23844

Aircraft structures fatigue strength determination, discussing test procedures, sample preparation, strength prediction, etc

11 p1970 A69-24525

Rod load capacity changes due to random overloads constituting upper limit of stress probability distribution density function used in programmed fatigue tests

11 p1985 A69-25180

Aircraft structures fatigue life determination based on Kordonskii method, comparing steel tests result with linear summation theory

11 p1987 A69-25345

Inclination effect of fatigue cracks on plane strain fracture toughness of 7075-T651 Al alloy, discussing cantilever bending

12 p2177 A69-25958

Bolt materials selection criteria in design of high strength lightweight joints, showing fatigue curves and temperature effects

13 p2268 A69-27758

Material selection criteria for low cycle fatigue resistance in components design determined from tensile test and incremental step test curves [ASME PAPER 69-DE-59]

14 p2461 A69-28852

Ultrasonic detection and measurement of fatigue cracks in notched cylinders subjected to reversed axial cyclic loading

14 p2445 A69-28882

Linear cumulative damage theory defining low cycle fatigue region of classic S-N curve, providing biaxial strain mode by centrifugally loading rotors [ASME PAPER 68-WA/MET-8]

14 p2535 A69-29438

Device for elastic-plastic circular bending with constant bending moment and angular strain for low cycle fatigue testing

15 p2583 A69-30207

Device for fatigue testing turbine disk models in unsteady temperature fields with radial and axial nonuniformity produced by HF heating

15 p2583 A69-30208

Titanium alloys fatigue properties at various temperatures using notched and unnotched specimens, considering vibrational fatigue strength and notch sensitivity

15 p2637 A69-30227

Crack initiation and propagation in Ti alloys during thermal cyclic heating noting influence of gas saturation

15 p2637 A69-30271

Structural fatigue-inducing random load spectrum analyzed and computed for laboratory simulation

15 p2705 A69-30363

Thick walled pressurized cylinder fatigue test results compared with axial tension and rotating beam tests on same material

15 p2709 A69-30676

Automated IR fatigue crack detection in sonic test facility capable of subjecting large aircraft or missile structures to intense sound fields

15 p2631 A69-31505

Rotating bending fatigue tests on aluminum alloys based on statistical analysis for material strength

17 p3052 A69-32979

Random stress statistical properties and relationship to fatigue life, discussing Fuller prediction, comparison with test data, and vehicle design evaluation

17 p3053 A69-32988

Cumulative metal fatigue damage gauges, analyzing resistance change properties by using strain amplitude tests

17 p3053 A69-32989

Aircraft turbines mechanical parts reliability tests, discussing examples of blade fatigue rupture and rotor disk fatigue

17 p3020 A69-33347

Fatigue test loading spectra calculation methods, discussing helicopter rotating and nonrotating components tests [AHS PAPER 373]

17 p2945 A69-33515

Fatigue strength of highly loaded gears and stress measurements by strain gauges [AHS PAPER 371]

17 p3060 A69-33517

Fatigue properties and test procedures for glass reinforced plastic rotor blades used in twin engine helicopter [AHS PAPER 370]

17 p3060 A69-33518

Facility for studying energy dissipation in refractory materials during fatigue tests in vacuum at various temperatures, describing principal components

17 p2947 A69-33926

Statistical characteristics stabilization of random loads in fatigue tests, noting transfer function of testing machine and spring stiffness

18 p3215 A69-34544

Nondestructive eddy current testing of chromium steel for early stage fatigue damage of aircraft components

18 p3136 A69-34777

Graphite fiber NOL rings and biaxial wound pressurized cylinders tested at ambient and cryogenic temperatures for tensile and cyclic fatigue properties

19 p3355 A69-35521

Ultrasonic nondestructive testing technique for fatigue induced damage location and criticality in filament wound fiberglass cylinders, correlating damage to residual life

19 p3322 A69-35577

Fatigue characteristics of Al alloys by fatigue tests with complex stress patterns, finding secondary stress wave effects

19 p3342 A69-35772

Cyclic stress frequency on mild steel corrosion fatigue tests, showing strength dependence on potential and stress current

19 p3342 A69-35775

Multidimensional discrete control systems for spectral characteristics of random processes in vibrational and fatigue strength testing of machines and equipment

19 p3286 A69-35890

Time-dependent failures of components subjected to fatigue loading analyzed for reliability prediction

19 p3437 A69-36032

Axial load fatigue crack propagation tests on Al alloy sheets for stress ratio effects

19 p3346 A69-36435

Fatigue strength tests of steels simulating boiler installation operating conditions, reproducing corrosion characteristics of water

19 p3347 A69-36741

Supersonic aircraft and power plant structural members operating under cyclic stress at elevated temperatures tested by various methods for interaction between creep and fatigue

20 p3620 A69-37001

Polarizable ions effect on glass fibers strength retention, noting fatigue tests for hydrolytic stress corrosion

20 p3567 A69-37769

Concorde structural tests emphasizing problems associated with thermal cycle, including fatigue test setup on complete airframe [RAES PAPER 16]

22 p4043 A69-40495

Summation methods for multiple damages caused by static fatigue in glass fiber reinforced plastics under stepwise loads

22 p3974 A69-40748

Aircraft fastener fatigue-acceptance criteria compared with actual tests, considering unusual service conditions

22 p4045 A69-40826

Nonmetallic inclusions effect on steels cyclic strength dependence on inclusion composition and metallic matrix properties, derived from fatigue tests

22 p4047 A69-41064

Fatigue tests with cylindrical samples for observation of macrocrack formation and propagation at bottom of notches, discussing kinetics of fatigue failure

23 p4225 A69-41425

Structural changes in subsurface layer and surface microgeometry factors of metal fatigue failure, explaining crack formation and propagation

24 p4395 A69-42559

Civil aircraft structural components failure analysis, discussing fatigue failures and fail-safe design for accident prevention

24 p4251 A69-42779

Long term fatigue tests of wooden gliders, discussing structural materials fatigue strength and glider strain spectra

24 p4398 A69-42912

Static and cyclic tensile fatigue of alumina by ring test method, measuring time to failure

24 p4334 A69-43343

Low cycle fatigue strength tested on notched and unnotched round steel bars, distinguishing between fatigue lives for crack initiation and propagation

24 p4404 A69-43627

FATS

NT CHOLINE

Exercise effects on hepatic cholesterol of rats on diets high in saturated or unsaturated fats

21 p3653 A69-38903

FATTY ACIDS

In vivo hyperbaric hyperoxia effect on erythrocytes unsaturated fatty acid composition alterations of tocopherol deficient mice

03 p0375 A69-14070

Fatty acids in blue-green algae related to phylogenetic position

05 p0707 A69-15751

Glucose, lactate, free fatty acids, hepatic glycogen and endocrine activity in fasting hibernating dormouse and rat in deep hypothermia

10 p1642 A69-23111

Normal, isoprenoid, dicarboxylic, keto and various aromatic acids isolated from controlled stepwise degradation of Green River kerogen by successive chromic acid oxidations

15 p2606 A69-31523

Acetate-2-C 14 conversion to C 14 carbon dioxide and C 14 fatty acids in rats with 2/3 of liver removed

19 p3257 A69-35970

Sediments and crude oils analyzed for fatty acids considering abiological or bacterial origin of acids

20 p3523 A69-37531

FAULT MECHANICS

U FRACTURE MECHANICS

FAULTS

Masking and standby redundancy approach to fault tolerance in space navigation computers with illustrations, discussing automatic maintenance

19 p3279 A69-35798

FAYALITE

Mossbauer spectra of shocked and unshocked iron meteorite and fayalite

03 p0517 A69-14231

Olivine-bronzite chondrite fragments found near Oshkosh, Wisconsin, in fall of 1961

22 p4021 A69-40413

FBFM [MODULATION]

U FEEDBACK FREQUENCY MODULATION

FCC LATTICES

U FACE CENTERED CUBIC LATTICES

FECES

Integrated Waste Management/Rocket Propulsion System, using human feces as propellant component [SAE PAPER 680717]

03 p0495 A69-13442

FEDERATIONS

U BUREAU [ORGANIZATIONS]

FEED SYSTEMS

Pressure and flow transients in liquid rocket engine feed systems predicted by method of characteristics

03 p0495 A69-12991

LOX prevalue accumulator system with He pressurant for prevention of Pogo effect on Saturn 5

04 p0666 A69-15298

Jet engine intershaft bearing oil feed design, discussing use of nonrotating feed link and improvement of oil scavenging at high altitudes

15 p2671 A69-30702

Rocket engines propellant feed systems dynamics analyzed by model using linear methods with distributed-parameter pipe representation [ASME PAPER 69-FE-6]

20 p3586 A69-37987

Liquid hydrogen pumping for Phoebus reactor, discussing feed systems, nozzles, configurations, design, testing, etc [AIAA PAPER 67-478]

21 p3769 A69-39751

Portable multiunit low pressure chamber with locks, permitting water replenishment, feeding of animals under continuous pressure and gas mixtures

22 p3891 A69-40217

Parabolic antenna properties generated by dual band circularly polarized focused two channel monopulse feed system, discussing tracking data from helicopter, Apollo 8 and Cassiopeia A

23 p4120 A69-41752

FEEDBACK

NT NEGATIVE FEEDBACK

NT NONLINEAR FEEDBACK

NT POSITIVE FEEDBACK

NT SENSORY FEEDBACK

Sequential signal design for feedback channels, emphasizing single set subject to peak and average power constraints in time continuous transmission

03 p0408 A69-12868

Recirculator with sign variable feedback coefficient for delay line passband increase

04 p0575 A69-14464

Small signal field effect transistor model at saturation and Borel equivalent scheme, giving evidence of internal feedback

04 p0579 A69-15226

Upper and lower bounds for feedback decoding and definite decoding minimum distances of binary convolutional codes

06 p0904 A69-17865

Frequency domain stability criterion for pulse width modulated feedback

06 p0904 A69-17942

Nonlinear feedback shift register circuit design by logical sequences

08 p1298 A69-20835

- Decoupling by state variable feedback and determination of inverse extended to linear time varying multivariable system
09 p1472 A69-21680
- DC/AC collectorless step electric motors operation and commutation circuits
09 p1442 A69-21860
- Complete observability in linear time invariant systems decoupled via state-variable feedback, deriving sufficient conditions
12 p2053 A69-26514
- Apollo-Saturn 5 propulsion and structure feedback loop, analyzing Pogo components and Nyquist plot application [AIAA PAPER 69-877]
21 p3824 A69-39403
- Feedback effects and social facilitation of human vigilance performance, evaluating mere coaction vs potential evaluation
24 p4271 A69-42751
- Isolation technique using exploding mirror shutter in multistage high gain laser system to overcome amplified target feedback during pulse lasing of reflective targets
24 p4330 A69-43762
- FEEDBACK AMPLIFIERS**
- Transistorized feedback amplifier for data transmission over high voltage lines in conveyed wave systems
01 p0038 A69-10074
- Partial avoidance of jump resonance in nonlinear feedback system, applying procedure to feedback amplifier circuit
01 p0051 A69-10442
- Frequency domain stability criterion for nonlinear feedback system consisting of nonlinear amplifier, linear dynamical system and transducer with backlash
02 p0225 A69-11968
- RF feedback amplifier analytical design, deriving open and closed loop feedback noise figure expressions by use of equivalent noise model
02 p0217 A69-12150
- Transistorized two stage amplifiers with common feedback operating under steady conditions and for short times
04 p0575 A69-14466
- Admittance between terminals measured for stabilizing single loop negative feedback transistor amplifier
05 p0739 A69-16341
- Noise characteristics of transistorized feedback amplifier stages for application in amplifier design
07 p1090 A69-18284
- Integrated frequency selective amplifier design for radio frequencies based on feedback configuration with positive real zero in loop transmission function
07 p1104 A69-18886
- Feedback amplifier with transfer function poles on parabola, discussing small rise time with small overshoot combined in transient response
08 p1282 A69-20111
- Operational amplifier integrated circuits applications, discussing simple and transducer amplifiers, operational circuits, wave shapers and generators and power supplies
11 p1857 A69-25665
- Wideband inverter operational amplifier frequency response, open and closed loop transfer functions, beta, settling time and slew rate limits, discussing HF performance prediction
11 p1857 A69-25666
- Book on industrial control engineering covering mathematics, semiconductor devices, feedback amplifier theory, closed loop systems, frequency response diagrams
12 p2051 A69-26244
- Two stage amplifier with two differential feedbacks, investigating tuning sensitivity
14 p2426 A69-29147
- Negative resistance converter with single differential input operational amplifier, discussing input and output signal
15 p2580 A69-31091
- X band avalanche diode oscillator operated as super-regenerative amplifier, noting frequency response characteristics ascribed to diode susceptance modulation
16 p2757 A69-31585
- Regenerative amplifier to counteract cable damping due to narrow bandwidth in PCM systems
16 p2755 A69-31860
- Fluidic feedback oscillator performance from fluid density effects analysis including supply jet, feedback line dynamics and load and control port impedances [ASME PAPER 69-FLCS-39]
20 p3465 A69-37984
- Proportional fluid amplifiers analysis in cascade and with feedback by extended lumped parameter method, discussing dynamic characteristics of analog amplifiers with air
24 p4255 A69-43268
- FEEDBACK CIRCUITS**
- Microwave selective filter using resonant cavity with single coupling component in feedback circuit of amplifier traveling wave tube or klystron
01 p0042 A69-10384
- Partial avoidance of jump resonance in nonlinear feedback system, applying procedure to feedback amplifier circuit
01 p0051 A69-10442
- Broadband null balancing microwave scanning radiometer using diode in feedback loop as reference noise source
02 p0221 A69-12457
- Soviet book on impulse generators in transistors covering multivibrators and pulse generators with timer circuits, crystal controlled frequency and delayed feedback
04 p0578 A69-15053
- Stability of nonlinear time varying feedback systems, using passive operator technique
04 p0583 A69-15110
- Time domain synthesis of multivariable automatic control with predetermined output signal shape, allowing for internal cross coupling effects
05 p0737 A69-15887
- Stability analysis of nonlinear and time varying discrete feedback systems
05 p0740 A69-16600
- Optimum linear feedback code for additive noise systems with average power constraint on transmitter to increase channel capacity
07 p1085 A69-19181
- Feedback systems analysis, considering single phase and polyphase coupled and uncoupled commutation networks in forward loop and linear transfer function feedback loop
08 p1295 A69-19853
- Thermal feedback generation of 1/f-flicker noise in bipolar transistors, deriving formula for flicker noise voltage of emitter junction
08 p1283 A69-20129
- Single purpose analog computer with analog and hybrid elements for calculating Nyquist diagrams for feedback circuits
08 p1278 A69-20397
- Round trip delay effect on probability of error in uncertainty feedback communication systems operating at channel capacity
09 p1453 A69-21322
- Feedback design for monotonically stabilized linear sampled data control system
12 p2045 A69-25961
- Voltage amplitude for combination frequency of small signal transistor amplifier calculated from feedback dependence
13 p2226 A69-27218
- Unsaturation frequency discriminator influence in semiconductor laser feedback loop on laser emission spectrum
15 p2635 A69-30967
- Negative resistance converter with single differential input operational amplifier, discussing input and output signal
15 p2580 A69-31091
- Amplitude-frequency characteristic and noise bandwidth of electron tube reflex autodyne operating in over or under voltage mode and including IR feedback
16 p2761 A69-32477
- Linear feedback additive noise communication systems formulated in terms of arbitrary operations at transmitting and receiving points
17 p2944 A69-33626
- Multiloop feedback in active distributed RC networks for low parameter sensitivity with low amplifier gain compared to single loop circuits
18 p3111 A69-34679
- Noiseless feedback schemes for digital and analog transmission over additive white Gaussian noise channels
21 p3671 A69-38405
- Interaction between modes of radiation field and active medium in laser with nonresonant feedback, discussing amplitude stabilization of total radiation
21 p3735 A69-38581
- Phase-pulse multistable circuit reliability improvement by additional negative feedback increasing parametric variation tolerance, feeding voltages and temperature
23 p4143 A69-42338
- Analog feedback system for digital data transmission, describing feedback channel, error rate and SNR effects
24 p4289 A69-42977
- State variable feedback design of m-input, m-output time invariant linear systems requiring noninertion and exact transfer functions, considering coupled core nuclear reactor
24 p4294 A69-43315
- FEEDBACK CONTROL**
- NT CASCADE CONTROL**
- Integrated operational amplifiers for control systems, noting high stability and linearity through negative feedback
01 p0039 A69-10169
- Monolithic sense amplifier for laminated-ferrite memories including provision for strobing, detecting, pulse forming and internal inversion logic using thermal feedback control
01 p0039 A69-10174
- Nonlinear negative definite feedback control systems governed by parabolic partial differential equation, deriving asymptotic stability
01 p0050 A69-10239
- Computational algorithm for determining piecewise-constant feedback gains for linear system optimal control
02 p0224 A69-11964
- Frequency domain stability criterion for nonlinear feedback system consisting of nonlinear amplifier, linear dynamical system and transducer with backlash
02 p0225 A69-11968
- Off-axis circle criterion for frequency domain stability of feedback systems with single monotonic nonlinearity, noting relation to Popov criterion
02 p0225 A69-11969
- Power advantage of optimum system achieved with suboptimum feedback function for sequential binary detection system
02 p0225 A69-11996
- Correlation of overshoot with gain crossover frequency, phase crossover frequency, phase margin and velocity error constant for linear feedback control systems
02 p0225 A69-12026
- Constant thrust deceleration formula for gravity turn soft landing maneuvers expressed in elementary and trigonometric functions of initial conditions for descent
02 p0335 A69-12531
- Dynamic mode locking of CW He-Ne laser by external regenerative feedback using RF beats between axial modes
02 p0260 A69-12657
- Stability properties of discrete-continuous feedback control systems with signal dependent sampling
02 p0226 A69-12733
- Logarithmic variation criteria for stability of feedback systems with time varying gains
03 p0409 A69-13073
- Stability criteria for closed rigid feedback systems with stable linear part connected in series with parametric quick response nonlinear element
03 p0410 A69-13683
- Global and nonglobal stability of continuous systems with multiplicative feedback
04 p0583 A69-15112
- Dynamics of single loop nonlinear sampled data systems with integrator, deriving equations of periodic motions and stability conditions by means of point transformations
04 p0583 A69-15135
- Servosystems and control, discussing open and closed loops and parallel, decoupling, multivariable and adaptive control
04 p0550 A69-15180
- DC servo system with torque feedback to ensure insensitivity to load variation and provide optimal performance
05 p0736 A69-15659
- Periodic cycles in linear closed loop integral pulse FM systems, discussing existence conditions, periodic formulae and stability criterion
05 p0737 A69-15865
- Minimum sensitivity deadbeat sampled data control system design by frequency domain technique, using two controllers [ASME PAPER 68-WA/AUT-15]
05 p0738 A69-16177
- Sensitivity matrix in multivariable feedback control systems, discussing loop gain matrix design to achieve desired insensitivity to system error sources [ASME PAPER 68-WA/AUT-9]
05 p0738 A69-16179

Optimization of bounded feedback gains with respect to arbitrary integral performance criterion, using nonlinear programming [ASME PAPER 68-WA/AUT-8] 05 p0738 A69-16180

Admittance between terminals measured for stabilizing single loop negative feedback transistor amplifier 05 p0739 A69-16341

Root sensitivity of linear feedback control systems calculated with signal flow graph and transforming circle 05 p0740 A69-16588

Combined neutron degradation and gamma induced effects on closed loop system simulated by SECURE program 06 p0899 A69-16889

Settling time estimation method for class of time varying feedback control systems of linear, nonlinear and multivariable natures 06 p0902 A69-17399

M measurement optimal feedback control algorithm for stochastic discrete time systems, considering nonlinear plant, constrained controls, nonquadratic cost and simulations 06 p0902 A69-17402

Optimal control of linear systems with state variables generated by linear feedback from output variables, considering time variance 06 p0903 A69-17406

L super P stability conditions for nonlinear time varying feedback systems derived with transformation technique and small gain theorem 06 p0903 A69-17411

Automatic closed loop distortionless control of magnetic field modulation using light sensitive resistor as one leg of attenuator 06 p0897 A69-17708

Rearrangement inequalities for positivity of nonquadratic transformations, discussing stability of nonlinear feedback loop described by difference equations 06 p0904 A69-17943

Linear state variable feedback to obtain asymptotic stabilization of linear dynamic systems 06 p0905 A69-17947

Absolute stability of dynamic control systems with single nonlinear element function of two feedback state variables, giving sufficient conditions 06 p0905 A69-17948

Circle criterion for stability of nonlinear time varying systems, considering integrator and infinite sequence of impulses in impulse response 06 p0905 A69-17949

Linear closed loop control system poorly damped response to deterministic inputs improved by stability constraint for minimization of mean squared error 06 p0905 A69-17950

Closed loop time optimal control achieved by exploiting generalization properties of threshold logic networks [AIAA PAPER 69-77] 06 p0905 A69-18092

Linear equivalent gain matrix of multivariable nonlinearity evaluated with equivalent gain concept for monovariable nonlinear stochastic process 07 p1114 A69-18286

Root-locus curve characterization of dynamic behavior of nonlinear control system, considering effects of changes in perturbing variable or reference input 07 p1114 A69-18290

DC servo system with torque feedback, discussing bang-bang system comparison, analog simulation, damping and quasi-optimum behavior 07 p1059 A69-19229

Closed loop and electronically calibrated radome measurement systems for beam deflection, boresight shift and transmission loss measurements 07 p1109 A69-19517

Book on feedback control theory for engineering and applied physics noting signal theory, servomechanisms, transfer functions, system stability and Nyquist diagrams 08 p1295 A69-19841

Feedback systems analysis, considering single phase and polyphase coupled and uncoupled commutation networks in forward loop and linear transfer function feedback loop 08 p1295 A69-19853

Multiloop control plant described by Jacobian transfer matrix to control spectral characteristics of random processes 08 p1296 A69-20233

Nonlinearities identification in closed loop systems using harmonic balance principle for transforming measured block diagram into diagram of simple form 08 p1297 A69-20302

Response optimization of feedback control systems with reference to single settlement time-constant ideal determined for error evaluation 08 p1298 A69-20855

Fluidic devices for closed loop control of gas turbines [AGARDOGRAPH-118] 08 p1258 A69-20956

Intermittent feedback channel for transmitter using orthogonal signals, noting smaller error probability and improved communication reliability 09 p1452 A69-21315

Optimal closed loop control system for linear time varying system with two independent parameters, noting trajectory sensitivity in large launch booster 09 p1473 A69-22439

Closed loop regulated flyback DC to DC converter using constant frequency generator for duty cycle control 09 p1442 A69-22454

Transient behavior of DC measuring amplifiers with time variable feedback, using matrix method and Laplace transform 09 p1467 A69-22560

Analog multiplier with controlled current splitting devices and feedback technique for stabilization of transfer characteristics, noting implementation in bipolar transistor 09 p1475 A69-22584

Aircraft modal control systems synthesis to improve response characteristics by altering pairs of complex conjugate and real eigenvalues simultaneously 09 p1435 A69-22779

Geometrical stability criterion similar to Popov criterion for single loop time varying nonlinear control systems analysis 09 p1476 A69-22784

Suboptimum decision feedback communications systems incorporating simple digital processing compared with optimum Wald scheme 10 p1656 A69-23534

Time varying linear optimal control system sensitivity obtained by comparing closed loop with open loop sensitivity to parameter variations 10 p1667 A69-24058

Active feedback control of distributed parameter systems including elastic airplane and missile structures, noting feedback loop coupling problem [ASME PAPER 69-VIBR-61] 10 p1668 A69-24145

Active broadband vibration isolation of human subjects from severe vertical dynamic excitations experienced in low level high speed flight [ASME PAPER 69-VIBR-65] 10 p1650 A69-24157

Electrohydraulic vibration isolation systems with feedback, considering band and notch isolation, system stability and adjustable frequency response [ASME PAPER 69-VIBR-40] 10 p1641 A69-24178

Dynamic programming determining optimal feedback control policies for optimal trajectories based on invariant imbedding 11 p1910 A69-25410

Feedback control law preserving optimality for systems with unknown parameters, discussing optimally adaptive performance index 11 p1860 A69-25441

Stability of systems with sector nonlinearities determined by converting feedback equation into positive operators equation and by introducing appropriate multiplier 11 p1860 A69-25450

Optimal controllers analytical design for closed loop systems with pure time delay in actuating mechanism using differential equations 12 p2045 A69-25959

Frequency stability of He-Ne laser with nonresonant feedback, noting spectral line width dependence on number of interacting modes 12 p2105 A69-26049

Optimal communication by signal feedback link between transmitter and receiver based on optimum control and dynamic programming 12 p2046 A69-26060

Computer aided design of linear multivariable control systems applied to VTOL aircraft stability augmentation 12 p2013 A69-26068

Third order multivariable control systems calculation with linear differential equations describing plant for design and digital optimization 12 p2049 A69-26085

Book on industrial control engineering covering mathematics, semiconductor devices, feedback amplifier theory, closed loop systems, frequency response diagrams 12 p2051 A69-26244

Hydraulic servo actuators load effect included in control loop actuator simulation 12 p2016 A69-26265

Feedback control of linear systems subject to sudden changes in parameter values 12 p2052 A69-26502

Near optimum regulator design technique for high order linear systems, using singular perturbation method to reduce system order 12 p2052 A69-26503

Hysteresis of on-off element with proportional feedback around element, noting autooscillations and results for electromagnetic relay 12 p2053 A69-26506

Asymptotic sampling error in closed loop hybrid systems, noting dependence on sampling period and execution time 12 p2053 A69-26508

Linear, quadratic, optimal control problems solved by sweep method, discussing time role, feedback control law and use of matrix equations 12 p2053 A69-26512

Space vehicle angular velocities reduced to zero through linear and nonlinear optimal feedback control systems 12 p2054 A69-26516

Feedback controller compensator for invariant linear systems having unstable modes 12 p2054 A69-26517

Linear closed loop control systems with periodically varying parameters analyzed by harmonics method using Fourier transforms 12 p2054 A69-26720

Helicopter stabilization systems design using optimal control theory to obtain multivariable feedback controller 12 p2014 A69-26764

Asymptotically stable discrete time closed loop linear systems synthesis, presenting feedback matrix as illustration 13 p2287 A69-27238

Passive adaptive sampled data control system with conditional feedback, discussing transfer function role and minimization of external disturbances and internal parameter variations effects 13 p2238 A69-27394

Stability test for linear unit feedback control system with second order lag and dead time compensated by PIO controller 13 p2238 A69-27395

Delta modulated control system model for determining oscillation modes at sampling instants 13 p2221 A69-27962

Population feedback control in planarians by fission suppression by brain near other planarians 14 p2406 A69-28871

Compensating /feedback/ loops determination method for linear two dimensional control system achieving self regulation 14 p2425 A69-28908

Trajectory sensitivity analysis of open and closed loop optimal control systems, demonstrating previous analysis inaccuracy 14 p2427 A69-29539

Multivariable linear time-variant systems noninteracting control problem, discussing realization by state variable feedback 15 p2582 A69-30024

Hybrid computer system for real time optimum feedback controller using iterative algorithms with rapid convergence, discussing simulation and performance 15 p2582 A69-30071

Time delay errors compensation methods in analog-digital computation loops, finding digital scheme inferior to analog 15 p2572 A69-30618

Turbojet engine open and closed loop boundary control systems performance during maximum penetration of prohibited operating area induced by HF external disturbances [AIAA PAPER 69-543] 16 p2841 A69-32681

Lifting rotor dynamics and undesirable characteristics reduction, discussing feedback control systems for pitch and roll [AHS PAPER 340A] 17 p2899 A69-33509

Lifting rotors with thrust or tilting moment feedback control, deriving blade equations of motion [AHS PAPER 340] 17 p2899 A69-33510

Stability augmentation system for CX-84 tilt wing V/STOL aircraft, using redundancy techniques to achieve full operational performance with two active channels [AHS PAPER 310] 17 p2901 A69-33545

Linear computer-controlled closed loop systems sensitivity analysis, deriving estimation error incremental covariance to demonstrate quality deterioration under perturbed initial conditions, parameters, etc 17 p2944 A69-33742

Multiple input and output nonlinear time invariant feedback system under almost constant inputs 17 p2944 A69-33743

Automatic tuning of superconducting cavity resonant frequency using optical feedback, discussing phase error processing and frequency deviation 17 p2937 A69-33781

Solid state single unit digital control computer performing stability augmentation, pilot relief functions and generating minimum fuel flight paths for VTOL landing 17 p2934 A69-34075

Book on elements of optimal control covering methods for deterministic problems including calculus of variations, Pontryagin principle, dynamic programming, feedback control, etc 18 p3109 A69-34532

Filtering and optimal control problems for discrete stochastic dynamical systems, describing various feedback controls and midcourse guidance optimization 18 p3109 A69-34660

Feedback realization of continuous optimal filter applied to designing servomechanisms with stochastic inputs and disturbances 18 p3110 A69-34673

Suboptimal closed loop control of nonlinear systems subject to quadratic performance indices by invariant imbedding concepts and maximum principle 18 p3111 A69-34678

Taylor series expansion used in correcting quantized digital coefficient errors in hybrid feedback control system 18 p3111 A69-34687

Algorithm for minimizing expected value of quadratic performance index in closed loop optimal control of linear time varying systems 18 p3111 A69-34688

Closed-loop system for test, failure analysis and corrective action in avionics reliability growth, showing cost effectiveness relationship to test program 19 p3282 A69-35784

Closed loop target tracking system generating error signals for aligning target with tracking axis 19 p3310 A69-36063

Buffer shift register with feedback control during tape recorder playback to obtain variable delay to compensate for recorder time base error 19 p3312 A69-36284

Servovalves with fluidic and electrical inputs compared for gas servoamplifiers performance, considering use as sensors in closed-loop hydraulic circuit 19 p3255 A69-36711

C-5 aircraft stability augmentation and autopilot development with consideration for unusual design required by takeoff weight, inertia and low approach speed 20 p3461 A69-36927

Trajectory sensitive vector introduction into closed loop linear optimal control, considering linear or nonlinear formulations 20 p3509 A69-37141

Differential synthesis technique application to design of multiaxis stability augmentation systems for aerospace vehicles [AIAA PAPER 68-834] 20 p3616 A69-37156

Stability augmentation system for B-52, noting flight test performance evaluation for structural vibrations and rigid body motions of aircraft [AIAA PAPER 68-1068] 20 p3461 A69-37157

Existence and uniqueness of optimal feedback control proved for autonomous nonlinear differential equations, allowing any finite number of variables 21 p3685 A69-38433

Linear nonstationary system with singular point analyzed for stability necessary and sufficient conditions using Riemann-Mellin conversion integrals and Laplace transforms 21 p3685 A69-38451

Large parameter variations effect on linear feedback control systems performance, optimal or suboptimal 21 p3685 A69-38726

Time-independent feedback attitude control system for high accuracy earth pointing motion of stable and unstable satellites in elliptic orbits 21 p3804 A69-39020

Lifting body stability augmentation systems design, development, ground tests and flight data including frequency response, limit cycle and structural resonance [AIAA PAPER 69-887] 21 p3647 A69-39413

Neighboring optimum feedback guidance to motivate min-distance lookup parameter determined by minimizing metric function of perturbed state and reference trajectory [AIAA PAPER 69-888] 21 p3765 A69-39414

Optimum filter design for noisy analog feedback system with forward and feedback disturbances, using mean square error criterion between signal and data 21 p3687 A69-39449

Stability of nonlinear systems with state variable feedback applied to fuel valve servomechanism 21 p3687 A69-39460

Second order suboptimal control systems with time varying coefficients, calculating switching curves for quadratic cost functional 21 p3825 A69-39634

Two-pulse limit cycle oscillation stability relation to physical parameters of pulse modulated feedback system used for satellite attitude control 21 p3688 A69-39756

Aperiodic feedback substitution for angular velocity component of control signal in stabilization systems of oriented satellites 21 p3829 A69-39832

Satellite attitude stabilization systems transient response optimization using combined feedback 21 p3830 A69-39833

Computerized algorithm facilitating automatic synthesis of time invariant linear compensation for highly complex multiloop control systems [AIAA PAPER 69-941] 22 p3917 A69-40324

Controllability and linear closed-loop controls in linear periodic systems 22 p3917 A69-40572

Suboptimal linear regulators design method yielding feedback controller for multivariable linear systems subject to parameter variations 22 p3918 A69-41012

Nonlinear time varying feedback control system stability applied to damped Mathieu equation 23 p4146 A69-42473

Frequency condition for ensuring stochastic stability of one dimensional discrete feedback control system containing linear dynamic part and inertialess nonlinear component 24 p4288 A69-42670

Manual vehicle control analysis based on feedback systems analysis and mathematical models for human operators engaged in control tasks 24 p4274 A69-43021

Bellman equation analyzed for higher derivatives, suggesting bounded partial derivatives of optimal feedback control function 24 p4341 A69-43234

Optimal deterministic estimation and feedback control for linear nonstationary process and measurement systems defined by Riccati equations, including Kalman-Bucy filter 24 p4291 A69-43276

Quadratic optimization applied to helicopter flight control design, assuming constant feedback gains and command step input with zero steady state error 24 p4253 A69-43279

Quasi-optimum control law for aircraft landing control system design based on Friedland technique, evaluating effectiveness by computer simulation 24 p4253 A69-43280

Suboptimal closed loop controller for linear time varying process subject to additive random disturbances and measurement noises 24 p4292 A69-43285

Fluid logic feedback control circuit synthesis using synthesis table, describing procedure to assign memory valves and switching signals 24 p4292 A69-43290

Feedback controller for linear stationary differential systems with time lag and fixed unknown parameters, noting closed loop transfer function role 24 p4293 A69-43293

Correction coefficients for time response of hybrid control systems with digital feedback elements containing quantized coefficients 24 p4293 A69-43302

Minimal time closed loop controller design for linear systems with bounded control amplitudes and rates 24 p4293 A69-43304

General purpose computer program for synthesis of multivariable systems decoupled by state feedback 24 p4294 A69-43307

Stability of linear systems with convolution operator in forward loop and time-varying gain in feedback loop analyzed for frequency- and time- domain conditions 24 p4295 A69-43316

Pulse modulated feedback system for satellite attitude control, analyzing relationship between physical parameters to ensure two pulse limit cycle oscillation stability 24 p4295 A69-43318

Parameter identification algorithm identifying linear dynamic systems by digital computer used to identify human operator characteristics in closed loop control situation 24 p4276 A69-43320

FEEDBACK FREQUENCY MODULATION

Frequency feedback receiver capabilities as low threshold demodulator in frequency modulated frequency division multiplexing satellite system 01 p0034 A69-11141

Phase locked loop demodulators for binary PSK signals compared with and without decision directed feedback in presence of CW interference 03 p0409 A69-13201

Signal/noise performance of frequency locked loop FM threshold extension demodulator compared to phase locked loop demodulator and conventional FM discriminator 06 p0886 A69-16934

Frequency modulation feedback demodulator design procedure for satellite communications, noting importance of nonideal implementation 09 p1457 A69-22464

FEEDING [SUPPLYING]

Aircraft and fuel supply system functional compatibility requirements and analysis noting gasolines, fuel tanks, valves, fuel transfer and metering [SAE PAPER 690308] 11 p1825 A69-24503

Social entrainment of feeding rhythms in Rhesus monkeys with light, temperature and sound held constant 24 p4260 A69-42704

FEEDING DEVICES

U ANTENNA FEEDS

FEEL

U SENSORY FEEDBACK

FELDSPARS

Electron microprobe analysis of potassium feldspar in Weekeroo Station meteorite 04 p0659 A69-14979

Chemical compositions and structural states of feldspar in recrystallized /Type 6/ chondrite meteorites, using electron microprobe analysis and X ray diffraction techniques 05 p0819 A69-15626

Meteorite minerals as detectors for studying fossil record of cosmic ray nuclei, emphasizing feldspars and pyroxenes 20 p3590 A69-37568

Primitive low energy Fe-group nuclei irradiation of meteoritic crystals from studies of pyroxene and feldspar from meteorites, discussing astrophysical implications 20 p3590 A69-37569

FELSITE

U IGNEOUS ROCKS

FENCES [BARRIERS]

Pressure fluctuations in separated flow region behind thin fence, determining recombination point position, noise sources and frequency spectra variations 04 p0544 A69-14868

Ground jet suppression fences for VTOL aircraft prepared pads, investigating erosion reduction and particle entrainment [AIAA PAPER 68-639] 17 p2902 A69-34028

FERMI-DIRAC STATISTICS

U QUANTUM STATISTICS

FERMI STATISTICS

U QUANTUM STATISTICS

FERMI SURFACES

Fermi level in n- and p-type Ge after irradiation by 50 Mev electrons determined by temperature dependence of carrier concentration 04 p0640 A69-14444

Surface photovoltaic effect in copper electroplated single crystal CdS solar cells, discussing Fermi level and Hall effect 05 p0704 A69-15958

Incremental conductance of heavily doped n-type Si semiconductor barrier tunneling as function of bias voltage, indicating Fermi level dependence on dopants 05 p0808 A69-16285

Fermi surface topology effects on Nernst-Ettingshausen coefficient from measurements in magnetic fields to 3.3 tesla and 1.2-4.2 K temperatures in metallic tin
05 p0808 A69-16357

Equations for pn junction behavior valid at impurity concentrations beyond nondegenerate range, noting contact potential and carrier density
11 p1938 A69-25306

Fermi surface data of alkali metals interpreted in terms of interaction between conduction electrons and ionic lattice for deducing partial wave phase shifts
13 p2304 A69-28681

X pocket Fermi surface of ferromagnetic Ni, considering magnetic breakdown effects
15 p2668 A69-30687

Field ionization at metal surfaces as rearrangement collision, considering anisotropic electron tunneling probabilities produced by Fermi surface
17 p3015 A69-32821

Amplification coefficient, luminescence power and spacing between Fermi quasi-levels in GaAs diode injection lasers, using spectral absorption dependence
22 p3965 A69-40801

FERMIONS

NT ANTINEUTRINOS

NT BARYONS

NT HYPERONS

NT LEPTONS

NT MESONS

NT NEUTRONS

NT PROTONS

NT THERMAL NEUTRONS

Bogoliubov transformations effect on quasi-free translationally invariant states of fermion fields, using Clifford algebra based on Hilbert space
03 p0455 A69-13364

Superfluidity and superconductivity under cosmic conditions, discussing Bose-Einstein condensation, Fermi particles, boson systems, neutron stars, etc
16 p2853 A69-31595

FERRIC ION

Trivalent iron doped andalusite crystals dielectric and maser properties, investigating spin-lattice relaxation, cross relaxation times and inversion ratio [IEEE PAPER C-2]
07 p1150 A69-19049

Excitation cross sections of Fe XIV lines in solar coronal spectra, comparing computations with Coulomb-Born approximation
08 p1392 A69-20563

FERRIMAGNETIC MATERIALS

Tunable ferrimagnetic bandpass filter using magic T configuration to permit low magnetic field strength and retain nonstacked configuration advantages
04 p0573 A69-14343

High pressure synthesis of dense ferrimagnetic perovskite allotropic form of yttrium-iron garnet
08 p1372 A69-20372

FERRIMAGNETISM

YIG single crystal resonator tuning of Gunn diode in coaxial line circuit
01 p0042 A69-10320

Time dependences of retardation effect, reversible magnetic permeability and magnetic viscosity during pulse magnetization of ferrite cores
13 p2319 A69-27993

Ferrites dynamic characteristics in alternating magnetization pulse with variable amplitude indicating linearity loss in strong fields
13 p2320 A69-27994

Exchange interactions in lithium ferrite aluminates, measuring spontaneous magnetization by ballistic technique from 77 K to Curie point
13 p2320 A69-27995

FERRITES

Hall effect in ferrites, determining classical and spontaneous Hall coefficients, electrical resistance, temperature effects and current carrier properties
01 p0135 A69-10185

Performance characteristics of microstrip ferrite devices for hybrid microwave integrated circuit systems, including meander line phase shifters and YIG elements
01 p0040 A69-10191

Thin ferrite use in microwave integrated circuits including phase shifters, latching circulators, isolators and phase and amplitude modulators
01 p0040 A69-10192

Voltage tunable magnetron used in conjunction with ferrite circulator as phase locked amplifier
01 p0045 A69-10632

Delayed response in threshold switching from reset state in ferrite memory cores consisting of magnesium compounds [IEEE PAPER 16.4]
01 p0045 A69-10719

Procedure accounting for variable thermal conductivity and internal heat generation in temperature distribution prediction for waveguide ferrite slabs
02 p0215 A69-11877

Ferrite and sigma phase formation in austenitic stainless steels with nickel and chromium content
02 p0269 A69-12764

X ray study of scandium containing ferrites, establishing lattice stresses due to ion replacement in octahedral interstices
03 p0491 A69-14053

Reciprocal latching ferrite phase shifters application to lightweight scanned phased arrays, noting quasi-circularly polarized modes with lowest insertion loss
04 p0572 A69-14320

Ferrite core temporary storage unit with 500 nsec cycle time
04 p0564 A69-15222

Resonance rotation of polarization plane in circular waveguide with ferrite resonator
05 p0718 A69-15640

Ferrite materials characteristics related to choice for use in waveguide devices, noting importance of low HF magnetic losses and thermal stability
05 p0810 A69-16792

High Q magnetically tunable microwave filters using magnetodynamic modes in ferrite spheres
06 p0892 A69-16831

Scattering matrix for internal diffraction in rectangular waveguide with transversely magnetized ferrite core
06 p0895 A69-17455

Suppressed rotation reciprocal ferrite phase shifter theory explained in terms of nonreciprocal coupling of cross polarized waveguide modes
06 p0896 A69-17484

Ferrite microstrips substrates role in integrated circuits, noting application of hybrid technology
07 p1090 A69-18399

Ferrite Y junction E plane circulator for airborne high power X band radar
07 p1100 A69-18639

Band three port Y junction stripline circulator with triangular ferrite
08 p1286 A69-20838

Reciprocal and nonreciprocal electronically adjustable ferrite phase shifters and application in scanning leaky wave antennas
08 p1290 A69-20979

Dynamic mode electromagnetic surface waves on axially magnetized single crystalline YIG and polycrystalline ferrite rods
10 p1746 A69-23513

Electromagnetic fields in cylindrically symmetrical microwave resonator filled with premagnetized ferrite along cylinder axis
11 p1855 A69-25625

Magnetically selective microwave filters using magnetodynamic natural oscillations in premagnetized ferrite sphere at cavity center
11 p1855 A69-25626

Neutron irradiation and temperature effects on ferrite and Permalloy memory cores hysteresis loops
12 p2142 A69-26259

Magnetic crystallographic anisotropy of Li-Ga ferrite single crystals at temperature range measured by ferromagnetic resonance techniques
12 p2144 A69-26721

Control signal correction in microwave ferrite modulators, eliminating losses due to screening effect of feeder
13 p2226 A69-27216

Applied magnetic field effects on longitudinally magnetized reciprocal ferrite phase shifters, showing shift type dependence on guide electrical thickness
13 p2229 A69-27673

High power ferrite latching switch with forced air cooling, discussing nonreciprocal phase shifter materials and configurations
13 p2229 A69-27674

Physical and physicochemical properties of ferrites - Conference, Minsk, Belorussian SSR, 1967
13 p2319 A69-27991

Polycrystalline Fe-Ni, Fe-Ni-Co ferrites structure, magnetostriction, magnetization curves and hysteresis prior and after thermomagnetic treatment
13 p2319 A69-27992

Time dependences of retardation effect, reversible magnetic permeability and magnetic viscosity during pulse magnetization of ferrite cores
13 p2319 A69-27993

Ferrites dynamic characteristics in alternating magnetization pulse with variable amplitude indicating linearity loss in strong fields
13 p2320 A69-27994

Exchange interactions in lithium ferrite aluminates measuring spontaneous magnetization by ballistic technique from 77 K to Curie point
13 p2320 A69-27995

Ferrite parameters measurement in alternating fields based on continuous analysis of magnetic, magnetizing and measuring circuits for assessing errors
13 p2320 A69-27996

Artificial aging effect on spinel structure and properties of ferrites using X ray analysis, neutron diffraction and electron microscopy
13 p2320 A69-27997

Bismuth oxide introduction into Y and Y-Al garnets, noting effect on formation and properties
13 p2320 A69-27998

Polycrystalline Ca-V garnets and Mg-Cr ferrites magnetic properties after adding rare earth elements
13 p2320 A69-27999

Substituted lithium ferrites analyzed to obtain materials with small initial magnetic losses at different microwave ranges
13 p2320 A69-28000

Magnetic properties of ferrites with garnet structure, discussing temperature effect on magnetic states of Gd, Li, Y and Lu sublattices
13 p2323 A69-28564

Ferrite core storages characteristics with rectangular hysteresis loop for digital control units, discussing optimal selection method
14 p2418 A69-29145

Tunable band stop filter realization from characteristic equation solution for propagation modes by magnetized ferrite slab placed in rectangular waveguide
14 p2422 A69-29751

Dispersion of electromagnetic wave propagating along ferrite loaded wire, calculating tuning curves and three port waveguide circulator modes
14 p2417 A69-29755

Disaccommodation component of magnetic aftereffect causing dynamic absorption of HF magnetic energy in ferrites
15 p2665 A69-30038

Ferrite frequency mixers used with heterodyne receiver, studying combination and cross noise rejection efficiency
15 p2574 A69-30129

Time logarithmic switching to explain anomalous delay in threshold response of MgMnZn ferrite memory cores
15 p2668 A69-30688

Wave reflection in laser resonators with ferrite end faces, determining oscillation spectra and wave amplitudes
15 p2579 A69-30954

Structural formula of slowly cooled Mg and Al-Mg microwave ferrites, noting ion mobility during cooling
15 p2670 A69-31184

Crystallographic classes of ferrites for microwave devices, discussing magnetic properties, applications and work on polycrystalline yttrium-calcium iron-vanadium-indium garnet
15 p2670 A69-31208

Magnetic anisotropy and porosity from approach to saturation of polycrystalline ferrites based on magnetization measurement
16 p2825 A69-31700

Resonance rotation of polarization plane in circular waveguide with ferrite resonator
16 p2762 A69-32498

Synthetic ferrites and sulfides of Ni and Co sulfated in presence of molten sodium pyrosulfate and sodium bisulfate
16 p2747 A69-32567

Line source excited ferrite layer radiation pattern reduced to one dimensional form by Fourier transform, obtaining angle of maximum leaky wave radiation
17 p2926 A69-33852

X ray study of scandium containing ferrites, establishing lattice stresses due to ion replacement in octahedral interstices
18 p3182 A69-35046

Microwave elastic propagation in single crystal specimen of yttrium-iron-garnet ferrite, discussing attenuation
21 p3780 A69-38774

Parametric excitation of spin waves during parallel pumping of rubidium nickel fluoride ferrite, relating relaxation time and temperature
21 p3781 A69-39069

Magnetic crystallographic anisotropy of Li-Ga ferrite single crystals measured by ferromagnetic resonance techniques
21 p3781 A69-39134

- Approximate boundary conditions in electrodynamics of stratified tensor media estimated for ferrite layers
21 p3675 A69-39282
- Ultrasonic oscillations effects on magnetic permeability of ferrite circuit components
23 p4138 A69-41873
- Transient processes in microwave quadrupoles with ferrite resonators
23 p4139 A69-41948
- Plane electromagnetic wave diffraction by screened periodic metallic strips array with real ferrite transversely magnetized to saturation
23 p4124 A69-42032

Ferroelectricity

- Symmetrical design of short ferrite Faraday rotator using matrix representation, noting matching to rectangular waveguide
01 p0048 A69-11034
- Ferroelectric strontium barium niobate as sensitive detector of single pulse IR radiation, noting application to Q switched carbon dioxide laser output
02 p0300 A69-12623
- Ferroelectric domain structure in twinband intersections in mechanically deformed lithium niobate
03 p0486 A69-13618
- Temperature dependent far IR absorption of ferroelectric sodium nitrite, discussing single and multiphonon processes
03 p0490 A69-13940
- Electrically controlled broadband microwave phase shifter consisting of coaxial line with varactors or ferroelectrics
03 p0408 A69-13987
- Ferroelectric transition of barium titanates doped in OH or oxygen vacancies, using pyroelectric method
03 p0491 A69-14059
- Electro-optic properties of tungsten-bronze niobate ferroelectric crystals [IEEE PAPER F-7]
05 p0808 A69-16313
- Ferroelectric Li niobate single crystals internal magnetic field analysis by acoustic EPR, establishing field induced hypersound resonance absorption in spin systems
09 p1556 A69-21563
- Quadrupole splitting of Na 23 nuclear magnetic resonance (NMR) to investigate spontaneous polarization, coercive field and domain characteristics in Rochelle salt ferroelectric phase
09 p1559 A69-22283
- Phonons, electrons and protons in ferro-paraelectrics and hydrogen bonded ferroelectrics, examining higher frequency optical and lower frequency dielectric properties
16 p2827 A69-32262
- Ferroelectric transducer for heat transfer rates and flow measurement in gaseous systems with autostabilized temperature, noting film coefficient
19 p3307 A69-35749
- Ferroelectricity - Conference, Riga, May 1968
22 p3994 A69-41155
- Spontaneous polarization onset in perovskite ferroelectrics, analyzing influence of Curie point, Jahn-Teller effect and atomic structure
22 p3995 A69-41159
- Temperature dependence of heat capacity of Ba and Sr titanate solid solutions in ferroelectric phase transition region
22 p3996 A69-41162
- Parametric losses in nonlinear centrosymmetrical ferroelectric ceramic in strong microwave field at temperatures above Curie point
22 p3996 A69-41164
- Electric properties and domain structure changes of polycrystalline Ba titanate and other ferroelectrics characterized by high dielectric nonlinearity
22 p3996 A69-41166
- Polycrystalline ferroelectrics dielectric dispersion region in decimeter-centimeter wavelength range using waveguide resonance method employing wideband strip line
22 p3997 A69-41167
- Ferroelectric Films**
- Magnetic reversible phase holograms on thin film Mn-Bi by Curie-point writing technique
10 p1706 A69-24007
- Magnetic domain structure in supercritical ferromagnetic films with perpendicular anisotropy
12 p2143 A69-26458

Ferromagnetic Materials

- NT MAGNETITE
NT PERMALLOYS [TRADEMARK]

- Heisenberg ferromagnet dynamics at low temperatures, calculating spectral weight function and other properties with low density expansion
01 p0135 A69-10016
- Magnon density of states of ferromagnetic gadolinium trichloride in magnetic field, using high resolution optical spectroscopy
03 p0494 A69-14257
- Ferromagnetic composite materials for microwave absorption and shielding over frequency band 0.3 to 10.0 GHz
09 p1510 A69-22352
- Nonlinear DC magnetic fields for nonhomogeneous isotropic current free regions in presence of ferromagnetic materials, discussing analytic solutions of boundary value problems
11 p1888 A69-25311
- Horseshoe electromagnet sensors above ferromagnetic plate, analyzing electromagnetic properties of plate and coil impedance
12 p2094 A69-26719
- X pocket Fermi surface of ferromagnetic Ni, considering magnetic breakdown effects
15 p2668 A69-30687
- Narrow band gap alloys and ferromagnetic semiconductors, using transport properties for characterization
19 p3388 A69-36541
- Plane electromagnetic waves penetration into ferromagnetic medium with permeability increasing with magnetic field, showing nonlinearity effect
21 p3771 A69-39109
- Magnetic monopole search using synchrotrons and cosmic radiation to destroy ferromagnetic materials binding in rocks, meteorites and deep sea sediments
22 p3981 A69-40197
- Ferromagnetic Resonance**
- Electromagnetic wave scattering in ferromagnetic crystals with anisotropy, discussing correlation functions of characteristics fluctuations and magnetoacoustic resonance
05 p0809 A69-16547
- Resonators made of YIG single crystals exhibiting lowest linewidth in ferromagnetic resonance at microwave frequencies
11 p1855 A69-25627
- Nonlinear homogeneous uniaxial ferromagnetic resonance, analyzing stationary regime lifetime and vibrational spectrum
14 p2503 A69-28989
- Ferromagnetism**
- Ferromagnetic ordering effect on gadolinium dialuminide thermoelectric power, measuring temperature dependence of power and electrical resistivity
03 p0485 A69-13322
- Lenz-Ising model of ferromagnetism noting mathematical methods used to investigate model properties
03 p0488 A69-13785
- Stainless steel sensitization analyzed using Mossbauer spectroscopy and X ray diffraction, noting ferromagnetic phase
06 p0944 A69-17852
- Induced magnetic fields determination in linear DC MHD generators with ferromagnetic and nonmagnetic walls, using Fredholm equation
10 p1636 A69-23454
- Microwave magnetoelastic wave propagation in ferromagnet subjected to pulsed magnetic field using coupled mode approach
10 p1746 A69-23655
- Ferromagnetic transition in superdense nuclear matter and neutron stars, developing relativistic equation of state
11 p1965 A69-25564
- Electron magnon interaction in ferromagnetic and antiferromagnetic semiconductors, showing conduction band and electron effective mass and magnetic moment dependences on temperature and spin direction
14 p2504 A69-28991
- High field susceptibility in Fe and Ni and high field Mossbauer study in Fe relating results to band structure and models of ferromagnetism
19 p3383 A69-36050
- Ferromagnetism stable state in degenerate electron gas and magnetic fields in gravitationally collapsed bodies based on total microscopic magnetic moments associated with Landau level electrons
21 p3798 A69-38600

Ferry Spacecraft

- Vehicles for lunar surface exploration and transportation including flying machines and wheeled vehicles
13 p2352 A69-27908

- Crew and passenger transportation to and from space station orbits, discussing cost reduction possibilities with current or future technology
21 p3827 A69-39691
- Low cost efficient shuttle system for personnel and cargo transport to earth orbit for NASA and DOD needs
21 p3827 A69-39695
- Manned transport into orbit and manned orbital operations systems, considering systems selection factors and mission and cost influences
21 p3857 A69-39696
- NASA programs for space stations and base development, discussing housing and equipment capacity, manned and unmanned stations and shuttlecraft for interstation travel
23 p4224 A69-42456

FET [TRANSISTORS]

U FIELD EFFECT TRANSISTORS

Feynman Diagrams

- Feynman rules for electromagnetic and Yang-Mills fields from gauge independent path dependent field formalism
05 p0794 A69-16363
- Feynman rules for gravitational field from coordinate independent field theoretic formalism, expressing path dependent Green functions in path independent functions
05 p0794 A69-16364
- Dielectric constant of liquid metals emphasizing Green function techniques for Wick theorem, Feynman diagrams, Dyson equation and diagrams in impulse space
07 p1196 A69-18298
- Elastic and inelastic elementary particle collisions described by Feynman diagrams, discussing computer results for high energy particle interactions
13 p2303 A69-28369
- Particle diffusion and wave spectrum in unstable plasma calculated using Feynman diagrams, considering quasi-linear growth, resonant three wave coupling and nonlinear Landau damping
15 p2660 A69-30915

FIAT Aircraft

U G-91 Aircraft

FIAT G-91 Aircraft

U G-91 Aircraft

Fiber Optics

- Glass fiber optical angular displacement noncontacting nonloading transducer suitable for measuring torsional vibrations
06 p0923 A69-16929
- Fiber optics - Conference, Baltimore, April 1968
06 p0958 A69-17674
- Fiber optics evolution, discussing industrial and medical applications
06 p0958 A69-17675
- Fiber optics technology, discussing fabrication and applications involving light carrying (incoherent/ and image carrying/coherent) fibers
06 p0958 A69-17676
- High transmittance long fiber optics, presenting data on special transmission as function of temperature
06 p0958 A69-17677
- Optical commutation to permit multifield monitoring and recording with one sensor by employing high resolution imaging fiber optics elements feeding common focusing lens
06 p0926 A69-17678
- Supersonic aircraft fire detection using coherent fiber bundles
06 p0926 A69-17679
- Fiber optics application to fiberscopes and fused fiber optic plates, noting surface coating for light scattering prevention
12 p2084 A69-26150
- Flame propagation velocity for different gas mixtures enclosed in glass tube determined by fiber optics devices
16 p2789 A69-31764
- Flexible glass fiber optics, discussing total internal reflection, light and image transmission, digit display and waveguide for laser communication
16 p2789 A69-31933
- HF data transmission system unaffected by high energy electromagnetic fields using GaAs IR emitting diode, glass fiber optic light guide and photomultiplier tube
23 p4121 A69-41768
- Fiber optics interferometers, analyzing light propagation along dielectric light pipes and wave interference
24 p4315 A69-43162

FIBER STRENGTH

FIBER STRENGTH

Fiber-fiber interaction effect on stress distribution and tensile strength of discontinuous aligned fiber composites

01 p0171 A69-11261

High temperature tensile strengths of uncoated boron filament and filament coated with silicon carbide

02 p0270 A69-12731

NonHookian behavior of stiff strong carbon fibers under stress

03 p0454 A69-13937

Twisted yarns composed of continuous viscoelastic filaments dynamic response under periodic strain effect on dynamic modulus

04 p0619 A69-14686

Fiberglass reinforced plastics modulus of elasticity and Poisson ratio determined by strain gauges and frequency and resistivity measurements

08 p1335 A69-20330

Chemical composition effect on glass fibers strength, discussing reasons for increased surface layer strength

10 p1717 A69-24045

Unidirectional fibrous materials stability, finding characteristic equation in form of infinite determinant by solving three dimensional stability of reinforcing fibers in binder

11 p1985 A69-25172

Interlaminar shear strength development for utilization of unidirectional strength and stiffness of graphite fibers, discussing epoxy resin-fiber interface improvement

15 p2642 A69-30312

High strength fibers and composite materials for structural design, considering anisotropy and low ultimate tensile strain

16 p2802 A69-32380

Surface chemistry of plastics-reinforced with strong fibers, stressing need for investigating coupling films, catalysts and metallic ions role in coupling compounds chemisorption

17 p2992 A69-33655

Measuring elastic modulus and tensile strength of high modulus graphite fibers including comparative data, error sources and full strand test

19 p3355 A69-35520

Graphite fiber NOL rings and biaxial wound pressurized cylinders tested at ambient and cryogenic temperatures for tensile and cyclic fatigue properties

19 p3355 A69-35521

Polymer fibers tensile strength improved using sectional orientation strengthening at controlled temperature and tension conditions

19 p3358 A69-35984

Geometry effects on stresses in discontinuous composite materials, studying fiber spacing, failure and discontinuities size and nature

20 p3565 A69-36942

Strength characteristics of high performance fibers and application to reinforced composite materials noting whiskers, polycrystalline and vitreous fibers

20 p3567 A69-37748

Polarizable ions effect on glass fibers strength retention, noting fatigue tests for hydrolytic stress corrosion

20 p3567 A69-37769

Metal matrix compatibility of metal coated graphitized, silicon carbide and boron fibers, discussing fiber weakening processes

21 p3751 A69-38670

Tensile strength of glass and graphite fibers for fiber reinforced plastics /FRP/ tested with modified balance type and strain gage type tensile testers

21 p3753 A69-39799

Carbon fibers and resin composites used as rocket motor systems ablative liners and structures, noting role in motor weight reduction

24 p4336 A69-43210

FIBERGLASS

U GLASS FIBERS

FIBERS

NT DACRON [TRADEMARK]
NT GLASS FIBERS
NT MICROFIBERS
NT REINFORCING FIBERS
NT SYNTHETIC FIBERS

Fiber-matrix interfacial bond function and bond strength role in fiber composites mechanical behavior

03 p0450 A69-13881

NonHookian behavior of stiff strong carbon fibers under stress

03 p0454 A69-13937

Evaluation tests of fixed frequency variable tension vibroscope for filaments and wires, noting instrument errors and corrections

04 p0599 A69-15018

Equation for analyzing radiation produced by current passing through filament situated over anisotropically conducting plane in flat waveguide

05 p0718 A69-15647

Stimulated emission properties of active fibers obtained from photomultipliers transmitting pulses to oscillograph

05 p0761 A69-15657

Crack propagation through layer of viscous fibers joining orthotropic elastic half planes

10 p1803 A69-24029

Book on design procedures for modern fibrous composites emphasizing stiffness properties and calculations, covering laminates orthotropic lamina, etc

12 p2179 A69-26238

Fiber axis distribution resulting from mechanical working deformation of matrix containing initially randomly oriented fibers

12 p2188 A69-26933

Equation for analyzing radiation produced by current passing through filament situated over anisotropically conducting plane in flat waveguide

16 p2762 A69-32504

Stimulated emission properties of active fibers obtained from photomultipliers transmitting pulses to oscillograph

16 p2792 A69-32514

Carbon fibers fine structure graphitized at high temperatures studied by X ray diffraction and electron microscopy

16 p2803 A69-32572

Thermal analysis of opacified fibrous insulation systems, discussing heat transmission, heat transfer and thermal conductivity relations to compression load and temperature

17 p3072 A69-33282

Micell type optimum fiber arrangement for transferring torque across annulus, considering single straight, double and multiple annular arrays under single load system

19 p3447 A69-36851

Static theory of fibrous surface media based on continuum mechanics, neighboring fibers noninteraction principle and additivity of mechanical properties

19 p3447 A69-36858

FIBRILLATION

Hypokinesis effects on transversostriated muscle fibers of mice, noting changes in myofibrillar apparatus, mitochondria and sarcoplasm

13 p2212 A69-28616

EKG during electrical defibrillation of heart in immobilized dogs

19 p3257 A69-36168

Corneal stroma collagen fibrils and ground substance refractive indices, discussing corneal transparency and clouding

22 p3884 A69-40886

FIBRINOGEN

Yield stress of normal human blood related to endogenous fibrinogen concentration as function of total protein concentration, proposing fibrinogen adsorption and coupling model

22 p3874 A69-40223

FIBROBLASTS

U COLLAGENS

FIBROSIS

Fibrosis histological patterns of left ventricular papillary muscles from comparison of hearts with myocardial infarction, noting acute and healed mural lesions

24 p4261 A69-42724

FIBROUS MATERIALS

U FIBERS

FICKS EQUATION

Cardiac output during space flight based on rebreathing method for estimation of gas tension in mixed venous blood and Fick equation

01 p0151 A69-10527

FIDELITY

U ACCURACY

FIELD COILS

Decoupling force exerted by magnetic forming Be coil assembly on metallic plate during forming

11 p1888 A69-25310

FIELD EFFECT TRANSISTORS

Gate current measurement of p-n junction during ultralow current operation of junction field effect transistor /JFET/

01 p0038 A69-10122

MOSFET drivers for low current memory fabricated in 64 unit monolithic strips, discussing driver performance data

01 p0039 A69-10172

Space charge limited operation of insulated gate field effect transistors, discussing maximum transconductance and minimum parasitic capacitances

01 p0042 A69-10322

Carrier mobility variation with electric field related to structure of epitaxial field effect transistors

02 p0294 A69-11541

Thin film transistors prepared from spray deposited cadmium sulfide, discussing carrier mobility and low stability

02 p0214 A69-11596

Heterojunction band model and carrier transport mechanisms emphasizing applications to heterophotodiodes, solar cells and hetero field effect transistors

02 p0294 A69-11598

Shockley theory of field effect transistors, calculating characteristics in miniaturization problems by removing geometric constraints with aid of electric analog

02 p0215 A69-11781

Analog sampled data simulator using field effect transistors and single value of holding capacitor for covering sample frequency variation

03 p0405 A69-13600

Plane of symmetry determination for generalized junction gate field effect transistors extended to include impurity profiles and bias voltage conditions

04 p0574 A69-14344

Small signal field effect transistor model at saturation and Borel equivalent scheme, giving evidence of internal feedback

04 p0579 A69-15226

Electric field effects on thermal annealing of electron irradiation damage in p-channel MOSFET device

05 p0733 A69-16562

MOSFET fabrication by ion implantation using gate metal as mask, noting source and drain alignment with gate and low feedback capacitance

05 p0734 A69-16563

Neutron radiation effects on MOSFET, presenting model for neutron produced ionization in oxide layer

06 p0976 A69-16875

Electron radiation damage in MOSFET devices using bias temperature treatments

06 p0976 A69-16877

Refractory metal silicon device technology noting high temperature diffusion masking properties for possible use in MOSFET technology

06 p0930 A69-17152

Junction gate field effect transistor design covering geometries and impurity profiles

06 p0893 A69-17197

Field effect in Ge and Si, noting relation between dependence of space charge on surface level charge and on surface potential

07 p1199 A69-18682

Field effect in p-type gallium arsenide single crystals as characteristic of surface electron energy state spectrum

07 p1199 A69-18686

Direct method determination of pinch-off voltage in depletion mode FET

07 p1102 A69-18861

Monolithic operational amplifier design combining junction FET with n-p-n transistor

07 p1103 A69-18876

Optimized gain control configuration using field effect transistor with broadband control to maintain high signal to noise ratio with low distortion

07 p1115 A69-18889

IMP F and G solar cosmic ray spectrometer utilizing FET analog multiplier for onboard particle identification data processing

07 p1135 A69-19197

Adapter circuits for MOSFET electrical properties measurement

07 p1113 A69-19780

FET sample and hold circuit using error corrective feedback

08 p1298 A69-20837

Field effect transistors with Schottky-barrier gates using epitaxial layers of silicon on substrates and gallium arsenide on seminsulating substrates

08 p1286 A69-20863

HF excess noise and equivalent circuit representation of MOSFET with n-type channel, noting local mobility fluctuations effect

09 p1463 A69-22094

FET memory element charge storage two layer model for thin film dielectrics noting charge/discharge times

10 p1742 A69-22947

- Field distribution in insulated gate FET determined by numerical solution of Poisson equation
10 p1662 A69-23170
- Design of 126 channel PCM telemetry unit for C-5 aircraft flight test, discussing FET analog multiplexing
10 p1693 A69-23275
- Device to simultaneously observe integral and differential field effect curves on oscilloscope screen as function of continuously varying field
10 p1698 A69-24210
- Temperature effects on noise levels in field effect transistors, discussing Lorentz spectrum
11 p1853 A69-25391
- LF generation-recombination noise in MOS transistors with depletion region impurity centers, analyzing noise resistance saturation and drain-voltage dependence
12 p2041 A69-26627
- Common source and common gate FET connections showing equivalent noise figures
13 p2227 A69-27237
- MOS and junction transistors damage due to radiation, noting decrease in collector current under fast neutron dose
13 p2227 A69-27514
- Small signal, HF equivalent circuit for intrinsic metal oxide semiconductor field effect transistor, considering nonpinch-off and pinch-off modes
13 p2238 A69-28429
- MOS unitoron switching circuit operation subjected to nonlinear load, using analytic approximations of current-voltage characteristics
13 p2234 A69-28507
- Amplitude modulator with field effect tetrode transistor /FETT/, discussing linear mode operation of modulator circuit
14 p2420 A69-29459
- MOSFET /unitoron/ switching circuits classification in terms of load curve shapes obtained with different output connections of load elements
15 p2574 A69-30122
- Integrated nonvolatile read-write memory with addressing using variable threshold field effect transistor including cell operation, channel shielding and circuit
17 p2942 A69-34120
- Current-voltage characteristics of unitoron with metal-dielectric-semiconductor structure /MOSFET/ taking into account substrate potential effect
19 p3284 A69-36592
- Book on field effect and bipolar junction transistors and microcircuits, covering ideal and practical amplifiers, circuit characteristics, etc
20 p3505 A69-37147
- MOS threshold voltages calculations, considering fixed bulk and oxide charges and difference in work function between metal and semiconductor, considering MOS-FET devices
20 p3506 A69-37779
- Generation-recombination noise due to trapped charge fluctuation at impurity centers in Si junction gate field effect transistors transition regions, using lumped equivalent circuit
22 p3911 A69-40009
- Thin film field effect transistors and integrated microcircuits, investigating active and passive elements fabrication
24 p4419 A69-42908
- FIELD EMISSION**
- Field ion microscope study of imaging solute atoms of dilute Pt-based W, Pd, Co, Ni and Au alloys
01 p0092 A69-10055
- Field distribution and potential drop in semiconducting field emitter, noting nonlinear effects in indium trisulfide, electron mobility and multiplication factor
05 p0806 A69-15630
- Field aligned Birkeland currents generation at auroral latitudes
05 p0755 A69-16266
- Pulse generation in Q switched traveling wave laser, noting effect of field amplification [IEEE PAPER Q-5]
07 p1154 A69-19077
- Lanthanum hexaboride single crystal field emitters for vacuum devices, describing construction and performance
09 p1468 A69-22601
- Heat treatment effects on molybdenum-rhenium alloy field emission and surface structure in alpha and sigma phase regions
12 p2113 A69-26041
- Molecular vibration absorption spectra from variation of field emitted electron energy distribution due to inelastic electron-molecule interaction at metal-vacuum interface
12 p2132 A69-26097
- Cineradiography based on repetitive flashes drawn from single field emission X ray tube energized by high voltage pulse generator
12 p2086 A69-26163
- CO adsorption on tungsten, determining work function changes and Fowler-Nordheim preexponentials on field emitter single crystal faces
14 p2409 A69-29093
- Unsuccessful space charge noise suppression measurements on field emission tubes, obtaining diffusion and shot noise measurements at high currents
16 p2752 A69-32384
- FIELD INTENSITY METERS**
- Calibration of interference measuring instruments, stressing input impedance calibration of field intensity meters
15 p2577 A69-30375
- FIELD MODE THEORY**
- Transient nonlinear mode partially responsible for anomalous operation of IMPATT diodes below transit time cut-off frequency
01 p0043 A69-10559
- Mode coefficients for geometrical optics field expansion at waveguide feed junction of sectoral horn
09 p1468 A69-22590
- FIELD STRENGTH**
- NT ELECTRIC FIELD STRENGTH**
- NT MAGNETIC FLUX**
- Lower ionosphere vertical motions found responsible for nighttime variation of radio waves total field strength
02 p0207 A69-11689
- Rotating bodies stability conditions relative to radial disturbances found to be field strength dependence on internal mass at any point
02 p0317 A69-11978
- Satellite TV transmitter power requirements for adequate direct broadcasting field strength in existing UHF TV bands
03 p0394 A69-13578
- Propagation tests of skywave field strength reduction by orthogonal transmission
03 p0395 A69-13597
- Waveguide field of arbitrary cross section determined on models with quasi-static fields
05 p0717 A69-15635
- Field strength, electron temperature and ion concentration fluctuations in axial direction determined from measurements between homogeneous and stratified plasma columns
05 p0800 A69-15736
- Probability distribution of field strength fluctuations in p-n junctions taking into account impurities distribution
05 p0807 A69-16000
- Electromagnetic field strength of narrow polarized monochromatic light beam, noting spatial curvature and twisting in beam current line
07 p1147 A69-18524
- Geometric optics and polarization properties of spherical reflector for integral representation of focal region fields, discussing stationary phase and field points
08 p1272 A69-20017
- Atmospheric radio noise at 27 kc measured at European stations, showing field strength variations, latitude dependence and amplitude distribution
09 p1491 A69-22163
- Quasi-static modified field distributions in inhomogeneously filled cavities and waveguide tubes, comparing with homogeneously filled cavities and obtaining matrix eigenvalues
09 p1467 A69-22561
- OMEGA VLF navigational transmission phase delay variations and field strength measurements on transatlantic propagation path, noting effect of directional change
09 p1538 A69-22595
- Static ferromagnetic frequency doubler graphic design, considering magnetic field strength and flux density, energy cycle and energy transfer
10 p1663 A69-23566
- Fading velocity short period characteristics and duration and depth of field strength variations over transhorizon path compared with corresponding atmospheric parameters
12 p2028 A69-25897
- Iono-index about hard emission of solar active regions, analyzing field fluctuations and SID in D region under daytime conditions
12 p2148 A69-26107
- Microwave propagation in Venusian atmosphere, analyzing refraction angles, attenuation and field strength fluctuations
13 p2223 A69-28567
- Lower ionosphere vertical motions found responsible for nighttime variation of radio waves total field strength
13 p2224 A69-28720
- Rotating bodies stability conditions relative to radial disturbances found to be field strength dependence on internal mass at any point
15 p2680 A69-30260
- UHF propagation in spherically stratified superrefractive troposphere with trapping surface layer, discussing distant field strength dependence on refractivity profile
16 p2752 A69-32388
- Waveguide field of arbitrary cross section determined on models with quasi-static fields
16 p2762 A69-32493
- Field strength determination at reception point for long range short wave paths, taking into account multiple ray paths and antenna radiation patterns
20 p3520 A69-37035
- Ionosphere reflected radio waves field strength measurements, obtaining formula for ground wave discrimination
23 p4123 A69-41861
- FIELD THEORY [ALGEBRA]**
- U CUBIC EQUATIONS**
- U QUADRATIC EQUATIONS**
- FIELD THEORY [PHYSICS]**
- NT ELECTRIC FIELDS**
- Killing fields applied to nonsymmetric spaces specify coordinate lines with slowest possible metric tensor variation and gravitational radiation
01 p0115 A69-10018
- Einstein-Maxwell equations corresponding to superposed electric and magnetic fields stationary solutions, noting singularities in metric tensor
01 p0115 A69-10020
- Gravitation theory similar to special relativity and Newtonian theories, noting gravitational potential, metric and Newtonian charts
01 p0115 A69-10340
- Field theory of gravitation, discussing consequence of universality of gravitation /space-time geometry determination/
01 p0116 A69-10443
- Motion, field momentum and field kinetic energy equations of concentrated dislocations based on Zorski field theory of defects
02 p0336 A69-11556
- Gaussian type microfield formation in plasma by placing constraints on plasma particles displacements
02 p0285 A69-11568
- General structure of magnetic surfaces of 3-turn helical magnetic field with axial current flow, noting closed magnetic trap production
02 p0288 A69-12168
- Electromagnetic fields in vacuum extended to fields in presence of matter, deriving field equations covariant under Lorentz proper and improper transformations
02 p0281 A69-12196
- N body systems with/without external field, noting galactic field effect on system flattening
02 p0322 A69-12270
- General covariant quantization of gravitation and cosmology
02 p0326 A69-12640
- High energy strong interaction theory in cosmic ray physics, discussing Regge model, fireball production and quark problem
03 p0469 A69-12940
- Bogoliubov transformations effect on quasi-free translationally invariant states of fermion fields, using Clifford algebra based on Hilbert space
03 p0455 A69-13364
- Gravitational field representation based on linear spin-two field without direct self interaction, using divergence free nonlocal projection of matter stress tensor
03 p0466 A69-13388
- Electromagnetic and gravitational tensor fields in Riemannian space, generalizing Maxwell and Bel-Robinson tensors
03 p0467 A69-13755
- Conformal change and connection relations in Einstein unified field theory, noting tensor applications
03 p0467 A69-13756
- Factorizability of Einstein field equations in two dimensional spinor formulation
03 p0468 A69-13759
- Shape and stability of interface between liquids subjected to surface tension and mass force field in vessel
03 p0417 A69-13809

Electromagnetic theory of gravitational forces unifying electromagnetic, meson and gravitational fields
03 p0469 A69-14096

Field theories and direct interparticle action theories of classical electrodynamics, establishing general correspondence between formalisms
04 p0631 A69-15189

Nonlinear field theories for continuum mechanics noting heat, kinematics, isotropic materials, viscometric flows, elastic bodies, thermodynamics and wave motion
05 p0792 A69-15768

Asymptotic formulas for field diffracted by conducting wedge illuminated by line source usable for self consistent field analyses
05 p0720 A69-16344

Feynman rules for electromagnetic and Yang-Mills fields from gauge independent path dependent field formalism
05 p0794 A69-16363

Feynman rules for gravitational field from coordinate independent field theoretic formalism, expressing path dependent Green functions in path independent functions
05 p0794 A69-16364

Regularization of perturbed Keplerian motion in three dimensional space by means of Levi-Civita transformation generalized to three dimensions
05 p0827 A69-16602

Satellite orbit evolution under effect of small perturbing force with constant magnitude and direction
05 p0829 A69-16672

Motion stability of gyroscope in universal suspension with spring restraints and damper in gravitational field extended to include Newtonian central force field
05 p0765 A69-16684

Vehicle motion parameters in Newtonian central force field determined, using geometrical structures devised from properties of velocity hodograph
05 p0765 A69-16686

Asymptotic wave equation application conditions in describing field behavior near caustic surface, using Airy functions
07 p1076 A69-18520

Finite formulation of field theory applied to quantum electrodynamics, assuming Bogoliubov causality and TCP invariance of S operator
07 p1181 A69-18957

Quantum mechanical perturbation treatment of optical parametric luminescence in nonlinear lithium niobate crystals, noting applications to noncolinear phase matching problems
[IEEE PAPER K-8] 07 p1152 A69-19067

Relativistic systems and relativistic Hamiltonian systems defined by second order equation, discussing canonical transformations conserving vector field Hamiltonian character
07 p1182 A69-19331

Magnetic energy relationships in magnetosphere, discussing confinement energy of magnetic dipole field, energy of transient compression and zero order energy of trapped particles
07 p1128 A69-19359

Gravitational and inertial field equations of Maxwellian form leading to gravitation theory consistent with special relativity
07 p1182 A69-19408

Riemann metric leading to empty flat space from Rainich equations of already unified field theory
07 p1182 A69-19418

Gravitational field in static spherical shell of matter in vacuum, deducing exact junction conditions for thin shell
07 p1182 A69-19453

Radiation pattern solved for antenna enclosed in radome, deriving exact formulas for scalar field
07 p1112 A69-19543

Ray path geometry derived by Poynting vector to calculate surface fields due to creeping waves in sphere planes
08 p1274 A69-20046

Interlocking systems within Galaxy, deducing gravitational theory accounting for galactic spiral patterns
08 p1387 A69-20136

Linear approximation of Moller condition for reference frames interpretable as linear approximation of field equation in tetrad theory of gravitation
08 p1351 A69-20287

General theory of relativity and tensor field equations relating space time characteristics to local properties of matter and vacuum, using Palatini Lagrangian method
09 p1593 A69-21572

Counterexample to Tangherlini argument, discussing inconsistency of postulates leading to Schwarzschild metric without field equations
09 p1540 A69-22100

Einstein cosmological field equations solved after subjecting electromagnetic null field metric tensor to Einstein gravitational field equations, noting coordinates significance
10 p1778 A69-23406

Matrix formulation of electromagnetic field equations and nonlinear conservation laws for measurable quantities
10 p1725 A69-24049

Metal surface distribution of electromagnetic field from striding transducer in eddy current flow detection, calculating magnetic field component
10 p1697 A69-24071

Mechanical model for oscillatory motion of solid body in Newtonian central force field
11 p1919 A69-25179

TEM-WAVE propagation between parallel conducting planes, stressing changes in curved waveguide sections
11 p1841 A69-25619

Conservative system /with two degrees of freedom/ motion in plane harmonic force field with potential satisfying Laplace equation, discussing graphic trajectory construction
11 p1920 A69-25745

Field distribution in HF flame discharges by measuring electrical and geometrical parameters of discharge channel
12 p2140 A69-27128

Exterior field equations for radiating spheres with zero limb darkening in relativity and Bondi coordinates, determining radiative flux and pressures
13 p2339 A69-27566

Unified geometric description of gravitational and electromagnetic fields, determining electromagnetic field influence on geometry from dimensional constant
13 p2300 A69-28450

Quasi-integral analytic continuation operator applicability to potential field approximated by certain truncated series expansion
14 p2470 A69-29032

Gravitational recoil, showing integration of Einstein equations in axisymmetric case reduced to integration of equations for Fourier coefficients
14 p2485 A69-29358

Energy momentum tensor in Einstein field equations derived from covariant field equations for vector meson
14 p2486 A69-29452

First order approximation to spherically symmetric solution of Einstein equations, noting gravitational and cosmic lambda force potentials
14 p2521 A69-29455

Asymptotic expansions for Einstein-Maxwell field representing gravitational and electromagnetic radiation from finite source of matter and charge
14 p2486 A69-29635

Discontinuities in interplanetary magnetic field direction presented on mesoscale from Pioneer 6 observation, emphasizing distribution in time
14 p2528 A69-29970

Junction diode field factor, comparing results of dynamic impedance and distortion measurement methods with deduced values of static characteristic
15 p2575 A69-30301

Uniform approximation mathematical theory applied to wave propagation problems, considering cylindrical waves and rainbows and glory scattering
15 p2653 A69-31165

Neutral point theory applied to solar wind and magnetospheric physics, discussing magnetic field reconstructions
16 p2846 A69-31596

Einstein field equations solutions generated via static spherically symmetric mass and charge distributions
16 p2812 A69-32053

Inertial navigation system theory that uses increased numbers of newtonometers /force measuring devices/ in place of gyroscopic sensitive elements
16 p2791 A69-32283

Conservation laws in general relativity, discussing Noether theorem, Bianchi identities, superpotential, Einstein-Klein theorem, momentum method and outgoing radiation
16 p2813 A69-32362

Einstein equations for empty space applied to degenerate gravitational fields with twisting rays, admitting shear-free twisting congruence of null geodesics
17 p3004 A69-32832

Quantum electronics theory, Volume 1, covering radiation-matter interactions, relaxation processes, spontaneous and stimulated emission, etc
17 p2982 A69-33686

Angular spectrum representation of diffracted wave fields expressible by plane wave expansions containing only homogeneous waves
17 p3007 A69-34153

Einstein gravitational field equations series expansion in powers of gravity constant by Bondi method for gravitational waves
18 p3173 A69-35146

Burger condition for distortion field of dislocation lines in continuous medium, considering arbitrary shape in arbitrary motion
19 p3439 A69-36477

Space transitions identified with asymptotic solutions at system field equations transition points
19 p3445 A69-36811

Stationary electromagnetic wave fields LF behavior, discussing integral operators, incident and tangential fields, single valued solutions, etc
20 p3487 A69-37071

Response of pi electrons in large organic molecule to scalar field for coronene, showing oscillator strength enhancement near single particle excitation band
20 p3580 A69-37497

Force fields to establish nature and position of remotely located conditions, discussing radiated power, electromagnetic waves, black body radiation, etc
20 p3494 A69-37747

Atomic sources local multipolar field in anisotropic dielectrics determined from magnetic dipole radiation spatial distribution measurements
21 p3779 A69-38531

Unquantized field calculations extended to include atomic field effect on atom, predicting spontaneous decay rate from excited state and light frequency time dependence
21 p3769 A69-38578

Linear field gravitation theories, discussing spin dynamics
22 p3979 A69-39976

Lagrange formulation of gravitation finite range theory compared with Einstein theory
22 p4027 A69-40656

Natural frequencies of N open dielectric waveguides system, obtaining fields expressions and dispersion equation for propagation constants
22 p3901 A69-40954

Field theories of gravitation and experimental survey of general relativity theory, discussing red shift, Mercury orbit rotation, light deflection, solar oblateness, etc
23 p4192 A69-42330

Gravitational field quantization according to Einstein theory using classical Hamiltonian dynamics and quantum rules for constraints
23 p4192 A69-42332

Particle creation and quantized fields in expanding universe using covariant generalization of special relativistic free field equations, studying zero- and arbitrary-spin particles
24 p4352 A69-43193

General relativity uniqueness established by postulating derivability of equations of motion from gravitational field equations
[AIAA PAPER 67-481] 24 p4365 A69-43668

FIGHTER AIRCRAFT

NT F-2 AIRCRAFT

NT F-4 AIRCRAFT

NT F-104 AIRCRAFT

NT F-106 AIRCRAFT

NT F-111 AIRCRAFT

NT G-91 AIRCRAFT

NT JAGUAR AIRCRAFT

NT P-1127 AIRCRAFT

NT SAAB 37 AIRCRAFT

VFX fighter aircraft, discussing U.S. Navy requirements influence in VFX-1 and VFX-2 design
03 p0367 A69-13675

Airframe/propulsion blending in high performance fighter aircraft, discussing thrust augmentation, fuel consumption, induction system and exhaust nozzle balance with airframe
03 p0364 A69-13676

Swing wings on combat aircraft and SST, discussing suitability for aircraft carriers and problems in aerodynamic balance
03 p0367 A69-13677

Tactical support aircraft size, economy and flexibility requirements based on Vietnam experience
04 p0549 A69-15486

Engine air intake for operational Harrier V/STOL strike/reconnaissance fighter, describing intake instrumentation ring, temperature and pressure probe development and pressure recording
05 p0767 A69-16773

First flight test phase of multipurpose Viggen aircraft designed as basic platform for attack, trainer, reconnaissance and fighter versions
06 p0867 A69-17662

Mass distribution and inertia characteristics influence on spin susceptibility and spin recovery characteristics for eight current fighter aircraft [AIAA PAPER 69-188]
06 p0868 A69-18057

Military applications of VTOL aircraft, discussing role in battle area with restricted surface transportation [AIAA PAPER 69-326]
07 p1055 A69-19556

Fighter aircraft design and performance criteria including acceleration, maneuvering, interception and turning combat capabilities
14 p2393 A69-29700

Frequency hopping technique applied to multiple access air-to-air/ground communication for tactical fighters, noting additive recognition
17 p2931 A69-34117

Tactical fighter aircraft avionics technical risk and integration, considering initial and operating costs, combat sequence and weapon control
17 p2902 A69-34128

Gross weight and aircraft size estimates for configuration design of fighter aircraft [SAWE PAPER 760]
18 p3220 A69-34880

Design iteration loop calculations related to fighter aircraft weight growth factor, noting asymptotic aircraft performance and strength [SAWE PAPER 732]
18 p3221 A69-34893

Computerized air combat simulation with comparison of analog and digital approaches, noting Air to Air Combat/Fort Worth [AIAA PAPER 69-811]
19 p3289 A69-35629

Fighter aircraft higher order control system dynamics effects on longitudinal handling qualities evaluated by in-flight simulator for role of pilot induced oscillations tendencies [AIAA PAPER 69-768]
19 p3245 A69-35655

System engineering to select hydraulics subsystem for advanced fighter aircraft by cost effectiveness analysis, noting maintainability and reliability
19 p3254 A69-36012

Wind tunnel tests of swept wing fighter aircraft for transonic buffet onset lift coefficient resulting from camber and leading and trailing edge deflection [AIAA PAPER 69-793]
19 p3238 A69-36297

Onboard radar for light interceptor aircraft /Aida II/, discussing navigation, low altitude penetration and air to air missile interception
19 p3278 A69-36701

Northrop F-5-21 fighter design, avionics, performance and operational existence
21 p3646 A69-38732

Fighter pilot teeth loss prevention and curative treatments, describing various suitable dentures
21 p3661 A69-39277

Background flying experience of tactical fighter aircraft pilots accident potential, comparing accident and nonaccident groups
23 p4103 A69-41685

MIG-21 fighter aircraft development, characteristics and technical and operational data
24 p4251 A69-42795

FIGURE OF MERIT

Figures of merit for polycrystalline uniaxial antiferromagnetic materials, for nonreciprocal devices at millimeter and submillimeter wavelengths, calculated from perturbation theory [IEEE PAPER 17.11]
01 p0045 A69-10720

Undetected defects and false alarm probabilities for automatic test equipment, emphasizing quality and confidence limits
03 p0428 A69-13187

Single mode intensity measured for 0.6328 micron He-Ne laser as function of cavity Q, using Lamb semiclassical theory
07 p1157 A69-19414

Wideband 4 GHz Esaki diode injection locked oscillator, noting locking figure of merit and locking bandwidth
09 p1470 A69-22785

Telemetry system sensitivity as function of noise figure, noting SNR and noise and bandwidth effects on system information handling capability
11 p1840 A69-25300

Analog correlator performance interpreted as output SNR dependence on input signals and integrating

system characteristics, covering filters and finite time integrators
14 p2413 A69-29485

Plasma thermionic diode figure of merit based on Hatsopoulos model altered to include thermal conduction and electrical resistance
22 p3869 A69-40134

FILAMENT WINDING

Glass, boron and graphite filament wound resin composites and liners for cryogenic pressure vessels
05 p0785 A69-16488

Delamination effects on strength degradation of filament wound composites
06 p0946 A69-17126

Axial loading of unidirectional composite with hexagonal array of isotropic circular filaments generalized for filament anisotropy, discussing matrix elastic modulus and Poisson ratio
07 p1170 A69-18724

Filament winding process variables effect on carbon or fiberglass reinforced composites, determining mechanical properties
08 p1338 A69-20489

Tensile characteristics of discontinuous unidirectional fiber reinforced glass-epoxy composites and filament wound material, discussing alignment and interfacial bonding
08 p1339 A69-20496

Laminates and filament wound structures using carbon fibers with silicon carbide whiskerized surfaces, noting compositing and laminating techniques
08 p1339 A69-20501

Fire retardant brominated epoxy systems for wet filament winding process, noting viscosity, pot life and NOL ring mechanical properties
08 p1340 A69-20507

Planar ribbon winding for buildup control of material near polar openings of filament wound vessels, discussing ribbon width and density
09 p1507 A69-22328

Compressive behavior of uniaxial filament reinforced epoxy tubes for aerospace structures, using hand layup method with Teflon mandrel and sleeve
09 p1508 A69-22339

Boron filaments reinforced epoxy aircraft landing gear structure prototype, discussing development, fabrication, and testing
09 p1508 A69-22340

Electroplating solutions test for filament winding and electroforming process used in fabricating fiber reinforced metal composites
11 p1890 A69-24337

Residual stresses and strains in wound reinforced plastic fiber cylinders subjected to polymerization by heat treating
11 p1907 A69-25679

Glass finish and glass resin chemical bond adhesion roles in filament wound structures response, failure and filament strength
14 p2468 A69-29345

Boron filament wound composite structures fabrication noting physical properties
14 p2455 A69-29413

Nondestructive tests for glass filament wound composites void content, considering test methods and mechanical properties prediction role
17 p2979 A69-33656

High modulus filament wound composites used for propellant and pressurization tanks, discussing overwrap and liner permeability, porosity, weight, etc
19 p3354 A69-35513

Military storage and environment effects on strength of filament wound glass reinforced epoxy structures, tested on plastic motor case and pressure vessels
19 p3321 A69-35567

Axially symmetric distribution of residual strain in multilayered filament wound ring analyzed and compared with experimental results
20 p3628 A69-37774

Filament wound composites for structures, discussing fabrication, properties and aerospace applications
21 p3753 A69-39496

Fracture strength of glass fiber-reinforced cylinders made by unidirectional filament winding predicted by analyzing three dimensional stress distributions
21 p3846 A69-39795

Static and fatigue strength of end-closed filament-wound vessels under internal pressure
21 p3846 A69-39797

Ultrasonic method for detecting strength defects in filament wound materials
21 p3733 A69-39798

Initial stress dependence on tensile load in glass fiber reinforced plastic rings during winding
22 p4045 A69-40749

FILAMENTS

Crystal structure of boron filaments vapor deposited on tungsten wire substrate, using X ray diffraction and transmission-electron microscopy
02 p0268 A69-12405

Very thin short metallic filament scattering and absorption cross sections for various values of filament conductivity
03 p0395 A69-13623

Boron carbide continuous filaments preparation and properties, discussing use in resin and metal composites [ECS PAPER 210]
05 p0783 A69-16236

Spatial structure of solar proton flare of 5 April 1960, discussing top ascending emission filament velocity in H alpha and coronal lines
17 p3025 A69-34224

Macrostructural differences between filaments of B and SiC vapor deposited onto small diameter W wire, discussing radial cracks due to dilatation
18 p3160 A69-34266

Random arrays representing random filament packing of actual composite materials, discussing effects on transverse stiffness
20 p3626 A69-37758

B composite materials in helicopter development, including B and C filament production and B filament applications
22 p3971 A69-40899

Cassiopeia A luminous filaments motion study noting stellar remnant magnitude
24 p4389 A69-43746

FILLERS

Filler metals for HY steels, discussing tensile and yield strength, elongation and area reduction of butt welds deposited
08 p1320 A69-20406

Bulk weld filler metals, discussing granular compositions, electrodes and iron, nickel and cobalt base deposits
11 p1891 A69-24931

Dielectric constants of nonconducting composite suspensions of spheres and parallel cylinders in terms of filler particles, matrix and volume fraction
13 p2287 A69-28677

Transverse bending of asymmetric sandwich plates with rigid filler taking into account stresses and strains in filler
17 p3055 A69-33129

Damping constant of sandwich samples with foam plastic filler subjected to torsional and flexural vibrations determined for aircraft design applications
17 p2993 A69-33942

Hollow thin walled carbon spheres developed as filler material for resins in low weight high temperature applications
19 p3355 A69-35522

Dual filler metals for increasing joint efficiency by changing fusion zone composition, discussing mechanical properties in Ti and Al plates welding
22 p3956 A69-40462

FILM BOILING

Silicon carbide deposition from liquid organic compounds using film boiling applied on heated tungsten wire substrate
02 p0252 A69-11804

Liquid nitrogen dispersed flow film boiling data accounting for droplet breakup by vapor acceleration, drag coefficient and heat transfer from wall [ASME PAPER 68-HT-44]
02 p0351 A69-12203

Heat release during boiling of downward flowing liquid oxygen film
04 p0687 A69-15161

Film boiling of subcooled liquid nitrogen in turbulent flow tubes, using one dimensional mathematical model of rod-flow regime
07 p1243 A69-19737

Film and transition boiling as functions of critical temperature, discussing role of heat transfer and vapor production
11 p1997 A69-24458

Heat transfer and skin friction in convective and stagnation flow laminar film boiling in boundary layer flows with appreciable radiation
11 p1873 A69-25242

Creeping flow model of Leidenfrost boiling with moving surface, discussing vaporization time for equivalent drop film boiling on stationary surface [AIChE PAPER 20]
15 p2718 A69-31116

Evaporation of liquid droplets from heating wall observed cinematographically, noting heat transfer by

FILM CONDENSATION

violent film boiling and conduction through thin vapor layer

15 p2718 A69-31117

Film vaporization of fuel in combustion chambers of aircraft turbines, determining concentration and velocity distributions of fuel and air

20 p3633 A69-37921

Hydrodynamic inlet conditions effect on film boiling and near critical hydrogen heat transfer, using data from electrically heated various geometry test sections [ASME PAPER 69-HT-27]

24 p4412 A69-43541

Film-nucleate boiling transition for liquid nitrogen in vertical forced flow in electrically heated tube, discussing conduction model and agreement with visual experiment

[ASME PAPER 69-HT-26]

24 p4412 A69-43542

FILM CONDENSATION

Outgassed condensation effects in vacuum on magnesium difluoride overcoated UV irradiated Al mirrors, including temperature effects, Lyman alpha reflectance and IR analysis of deposits

13 p2299 A69-28015

Condensation dynamics of atom by solid body model consisting of one dimensional chain of harmonic oscillators

21 p3775 A69-39557

FILM COOLING

Film cooling by subsonic gas injection of air through porous flat plate into 2.9 Mach air flow, noting wall temperatures

03 p0413 A69-12994

Gaseous film cooling at various hot gas acceleration rates and free stream turbulence levels

06 p1033 A69-17557

Film cooling design criteria for small rocket engines [AIAA PAPER 68-617]

09 p1570 A69-21978

Film cooling injection slots number and position over flame tube and minimum cooling airflow in aircraft gas turbines

09 p1625 A69-22623

Velocity and temperature profiles in gaseous turbulent boundary layer above liquid surface used to study liquid film cooling heat transfer

13 p2375 A69-27792

Mass transfer cooling data correlation for estimating mass injection effect on slender cone drag

13 p2199 A69-28224

Thermal shielding effectiveness of flat wall behind tangential blowing slit, considering case of quasi-isothermal homogeneous turbulent boundary layer

14 p2537 A69-28971

Injection film cooling effect on surface heat transfer downstream of flush nontangential injection holes and slots in turbine applications [AIAA PAPER 69-523]

16 p2843 A69-32703

Film cooling slot adiabatic wall effectiveness measurement in two dimensional constant property flow, showing role of lip thickness and injection angle

20 p3585 A69-37082

Flat surfaces downstream of heated section and porous strip, determining film cooling effectiveness and heat flux from heat transfer coefficients ratios

20 p3631 A69-37096

Foamed liquid as potential coolants in rocket engine to overcome low efficiency and streaky coverage of conventional liquid film cooling

24 p4408 A69-43127

FILM THICKNESS

Erosion damage of bearing alloy lining in thin lubricating oil film, considering Cu-Pb alloy and tin base white metal

01 p0094 A69-10313

Radial face seals lubricating mechanism noting surface waviness effect on film thickness fluctuations

01 p0087 A69-10910

Elastohydrodynamic lubrication, discussing film thickness and dependence on fluid hydrodynamics and contact zone deformation

01 p0088 A69-11324

Surface layer effects on conductivity of vacuum deposited gold films, studying resistance variations with film thickness

02 p0300 A69-12625

Photoelectric effect of thin gold films on silver and quartz substrates, analyzing work function dependence on thickness of deposited metal

02 p0300 A69-12630

Photoelectric effect of thin gold film under electric field, noting work function dependence on film thickness exhibits extremum

02 p0300 A69-12631

Nondestructive measurement of thin transparent film thickness by interference method, noting diffusion profiles

03 p0430 A69-13634

Space charge layer thickness determination in plasma filled capacitor by capacitance measurement, noting thickness dependence on plasma potential

03 p0477 A69-13714

Rayleigh step journal bearings, considering pressure distribution, load capacity and attitude angle and optimal film thickness ratio for incompressible fluid lubrication

04 p0605 A69-14587

Structural and electrical properties of indium antimonide and arsenide films, noting dependence of electron concentration and mobility on thickness

06 p0981 A69-17892

Film thickness effect on wear life of resin bonded solid lubricant film compared for various load test conditions

[ASLE PREPRINT 68AM 7C-4]

07 p1139 A69-18624

X ray fluorescence and electron microprobe for determining thin film thickness

07 p1113 A69-19582

Integrated semiconductor circuits reliability in electronics and microelectronics, discussing hybrid and monolithic circuits in thin/thick film design and on Si monocrystals

08 p1294 A69-21118

Temperature profiles and heat transfer coefficients in two phase liquid-liquid stratified laminar flow of variable immiscible film thickness with surface evaporation

09 p1622 A69-21904

Photocell base thickness for optimal power to weight ratio, noting photons spectral distribution and absorption coefficient dependence on frequency

09 p1443 A69-22719

Thin film thickness and composition determination through scattered electron and characteristic X ray radiation recording

10 p1747 A69-23847

Holographic interference method for measuring film height in analyses of fluid film vaporization under blowing hot gas

12 p2088 A69-26178

Scale effect on gold films electrical conductivity, analyzing film thickness and electron parameters of mean free path, concentration and surface reflection

12 p2143 A69-26459

Gases effect on electrical conductivity of vacuum deposited thin films of Cr, Be, Ni, Au and Ge at different thickness and low pressure

12 p2143 A69-26460

Electrical properties of electron beam evaporated Ti, Zr and Hf films as function of substrate temperature, material and film thickness

13 p2321 A69-28010

Light sensitivity dependence of semiconductor-metal systems on layer thickness

14 p2508 A69-29666

Absorption band edge position in p type indium antimonide thin films after heating, showing forbidden bandwidth function relationship to film thickness

15 p2666 A69-30044

Thin film thickness determined by weighing film and substrate in liquid having same density as substrate material

15 p2607 A69-30239

Eccentric face seal with tangentially varying film thickness, analyzing leakage flow proportional to eccentricity and surface waviness

[ASLE FICFS PREPRINT 15B]

15 p2620 A69-30484

Load support and leakage from microasperity lubricated face seals, developing hydrodynamic lubricant films

[ASLE FICFS PREPRINT 21]

15 p2622 A69-30500

Electrical resistivity of aluminum oxide films deposited on tubular substrates by plasma and gas flame spraying, noting dependence on film thickness and substrate

15 p2630 A69-31179

Dielectric overcoating effects on electromigration Al interconnections, showing dependence on thickness and surface passivation

17 p2935 A69-32889

Elastohydrodynamic lubrication film thickness in finite elliptical contact determined by two dimensional Reynolds equation in inlet region, using finite difference approximation

[ASME PAPER 69-LUBS-17]

18 p3120 A69-34379

Silicon carbide compact coatings deposition on graphite by silicon tetrachloride, H and benzene gaseous mixture, relating layer thickness to temperature and process duration

20 p3566 A69-37368

Chalcogenide semiconductor film switches time parameters, showing delay time decrement with thickness decrease and voltage increase

21 p3780 A69-39045

Film thickness and normal load effect in thin films solid friction, noting dependence on deformation at contact

22 p3955 A69-40407

F-111 sandwich structure adhesive joints glue lines, describing thickness measurement techniques and acceptance criteria

24 p4403 A69-43461

Centrifugal forces effect on stability of inviscid liquid film over rotating cylinder away from stagnation region, noting film thickness stabilization effect

24 p4305 A69-43597

FILMS

Convective heat transfer across fluid film limited by right sections of two parallel circular hollow steel cylinders

01 p0176 A69-11135

FILTERING

U FILTRATION

FILTERS

Frequency selective mechanical filter and LCR circuits and applications, noting inductances in solid state and thin film technology

09 p1467 A69-22558

Filter network synthesis for realization of rational functions, discussing numerator polynomial inclusion by choice of divisor polynomial and branch introduction and parallel systems

10 p1667 A69-24038

Surface wave study techniques, discussing digital moving window analysis of group and phase velocity and use of time variable filters

16 p2784 A69-32576

Acoustic filters performance determination, standing wave tube and anechoic termination methods

20 p3464 A69-37321

Isotropic ideal bidimensional filter in interpretation of anomalous gravity fields, especially for separating local and regional effects

21 p3724 A69-39246

FILTRATION

NT SPATIAL FILTERING

Algorithms for error analysis, optimum filtering sensitivity and fixed interval smoothing solutions to linear estimation problems

02 p0224 A69-11961

Singularities of optimal filtration for random signals given by differential equations with variable coefficients and white noise

13 p2218 A69-27251

Airborne particle size influence on gas turbine parts erosion, with attempts to relate to filtration and engine life

16 p2794 A69-32026

On-board digital filtering applied to spectral estimation and data compression, discussing theory, techniques, computerized implementation and prototype design

[AIAA PAPER 69-969]

24 p4285 A69-43510

FIN STABILIZERS

U FIN

U STABILIZERS [FLUID DYNAMICS]

FINE STRUCTURE

Fine structure of vibrational spectra of molecular H and O, water and deuterium oxide, using molecular photoelectron spectrometer

01 p0023 A69-10141

Spectral fine structure in emission from pulsars, noting correlation between fading and spectral change

01 p0150 A69-10273

Polar aurorae fine scale structure interpretation based on plasma instabilities characteristics

02 p0239 A69-11693

Interactions of moving solar plasmas and solar magnetic fields, discussing solar velocity fields and fine structure observations

02 p0329 A69-12784

Turbulent mixing of scalar fields such as temperature or concentration noting fine structure, number and distribution of zero gradient points and minimal gradient surfaces

03 p0414 A69-13134

Solar chromosphere dark mottles size, shape and evolution, using high resolution photography near solar disk center

03 p0515 A69-14038

Chromosphere fine structure in Lyman alpha intensity, compiling isophote map

03 p0515 A69-14039

Effective slip systems in hexagonal close packed magnesium alloy under static and hydroexplosive loading, examining flow mechanism for fine structure formation

04 p0615 A69-14639

Atmospheric fine structure studied by amplitude distribution and autocorrelation functions for different heights of scatter volume in microwave range

04 p0628 A69-15306

Bright streaks in H alpha disk chromosphere, noting predominantly horizontal loop structures

04 p0664 A69-15525

Fine structure and geology of lunar surface from Luna, Ranger, Surveyor and Orbiter data

07 p1212 A69-18547

Three dimensional Fourier synthesis at low resolution for calculating ribosome electron density distribution in chromatoid bodies

07 p1074 A69-19394

Diffuse interstellar absorption bands and doublet line, noting large intensities of forbidden transitions

08 p1395 A69-20639

Galactic and intergalactic ionic fine structure transitions effect on background microwave radiation intensity

09 p1590 A69-21445

Interplanetary scintillation of radio sources to determine size and motion of plasma irregularities in solar wind for fine structure

09 p1594 A69-21658

Fine structure of absorption lines of circumstellar Ca ejected from Nova Delphini 1967, determining ejection dates and photospheric radius

13 p2346 A69-27709

E layer fine scale structure, F1 reactions and F2 reflected signals analysis during 20 May 1966 solar eclipse

13 p2255 A69-28541

Polar aurorae fine scale structure interpretation based on plasma instabilities characteristics

13 p2258 A69-28724

Partial wave description for calculating cross sections of fine structure transitions of Na in collision with He, discussing shape resonances

15 p2655 A69-30198

Ca XV spectrum in vacuum UV under laboratory conditions, discussing fine structure of ground level of Ca XV and coronal lines

15 p2688 A69-30553

Collision free earth shock wave gross and fine structure deduced from OGO 5 plasma diagnostics [AIAA PAPER 69-676]

17 p2961 A69-33452

Solar radio bursts spectra fine structure, discussing observations of fast drift storm, drift pair and split pair bursts

17 p3024 A69-33607

Fine structure of 9 June 1968 solar flare related to nonflare chromosphere in active regions

17 p3024 A69-33802

CaO and MgO reflectance spectra measurements at high resolution and at low temperature including exciton spectra at 25 K, obtaining fine structure

18 p3181 A69-34274

Transition probabilities of N I far UV multiplets, comparing experimental and theoretical results

18 p3178 A69-35413

Spectral lines due to magnetic dipole transitions in fine structure levels in collisionally excited neutral H clouds, discussing theoretical difficulties in interpretation

19 p3379 A69-36225

Abrasion and corrosion resistant Cr-Co-B cast alloys in aggressive media, concluding resistance is due to chromium boride and fine dendritic structure

19 p3347 A69-36742

4 October 1965 type IV solar burst, studying acceleration mechanisms for fast electrons by comparing fine structure at various frequencies

22 p4001 A69-39983

Solar magnetic field measurements for fine structure of magnetic asymmetry at different heights and within sunspots, discussing asymmetry for corona and interplanetary space

22 p4010 A69-39990

Emission dynamics and fine pulse structure in GaAs injection lasers, determining pulse duration and amplitude dependence on current and resonator length

22 p3963 A69-40603

V contents influence on high temperature strength and fine structure interrelation in low alloy CrMoWV steels

22 p3972 A69-41083

FINENESS RATIO

Minimal interference thin metal strap support system for dynamic stability tests of high fineness ratio wind tunnel models

[AIAA PAPER 69-350] 13 p2243 A69-28284

FINES

Lunar rocks and fines samples physical, chemical, mineralogical and biological preliminary analysis at Lunar Receiving Laboratory

24 p4382 A69-42935

FINISHES

U GLAZES

FINITE DIFFERENCE THEORY

Boundary value bending problem for anisotropic shells of revolution under asymmetrical loading solved by finite difference technique

01 p0165 A69-10088

Finite difference method for boundary value problem for second order differential equation, demonstrating convergence

01 p0105 A69-10721

MHD equations describing interactions between gases and magnetic fields solved by finite difference method

01 p0129 A69-10722

N dimensional extensions of finite difference scheme for solution of differential heat conduction equation, noting practical limit by truncation error considerations

01 p0107 A69-11365

Eigenvalue problem for Laplace operator for two dimensional region with boundary composed of piecewise-analytical simple closed curves solved by finite difference method

02 p0271 A69-11650

Finite difference schemes for axisymmetric oscillations of shells of revolution filled with liquid

03 p0523 A69-12951

Finite difference solution of time dependent Navier-Stokes equation for incompressible fluids, using velocities and pressure as variables

03 p0415 A69-13369

Finite difference method for symmetric positive linear differential equations, discussing methods to solve finite difference equations generated

03 p0455 A69-13370

Finite element solution of Helmholtz equation and application to waveguides with complicated boundaries

03 p0404 A69-13598

Analysis of solution of Navier-Stokes equations describing two dimensional flow of viscous incompressible fluid by finite difference techniques and introduction of curl

03 p0416 A69-13652

Finite difference schemes to solve fundamental equations in boundary layer flow theory

03 p0416 A69-13655

Implicit finite difference scheme to integrate unsteady boundary layer equations for compressible gas

03 p0416 A69-13656

Survey of papers on computer calculation of two and three dimensional gas flows, emphasizing method of characteristics and finite difference techniques

03 p0363 A69-13657

Finite difference methods to solve Cauchy problem for three dimensional Laplace equation

03 p0424 A69-13661

Slow nonNewtonian flow in separation zone analyzed using finite difference scheme

04 p0587 A69-14594

Boundary value problem of hyperbolic equation with discontinuous boundary conditions

04 p0622 A69-14617

Difference approximation with second order accuracy of numerical solution for parabolic type equations

04 p0622 A69-14618

Transformations useful for finite difference solution of differential equations with infinite regions, considering flow problems application

04 p0588 A69-14717

Finite difference approximation for numerical solution of periodic parabolic problem subject to nonlinear boundary condition

04 p0625 A69-15131

Difference schemes implementation through fractional time step and phase error methods reduce dispersion

04 p0591 A69-15282

Finite differences for identifying partial differential equations and associated boundary conditions of distributed parameter system [ASME PAPER 68-WA/AUT-1]

05 p0738 A69-16185

Three dimensional boundary layer problems analyzed by exact numerical method [AIAA PAPER 69-138]

06 p0911 A69-18041

Chemical kinetic model for hydrocarbon fuels combustion and application to multidimensional finite difference mixing analyses in hypersonic engines and nozzles [AIAA PAPER 69-86]

06 p1037 A69-18119

Spherical caps axisymmetric static and dynamic buckling under load, using axisymmetric nonlinear elastic shell theory approximation and finite difference equations [AIAA PAPER 69-89]

06 p1028 A69-18133

Finite difference computations for calculating two dimensional natural convection, deriving requirements for numerical stability

07 p1242 A69-19397

Stability of cylindrical shells under concentrated annular loads using finite difference method, discussing critical loads, moments and errors

07 p1238 A69-19688

Axisymmetric jet impingement against solid plane from tube at finite distance, using nonlinear partial differential equation in finite difference form [AICHE PAPER 31F]

08 p1302 A69-19847

Finite difference numerical solutions to free streamline axisymmetric potential fluid flow, noting independent and dependent variables consideration in boundary value problem

09 p1481 A69-21920

Constant property turbulent boundary layer flow, developing finite difference solution for prediction of velocity profiles and skin friction coefficient

09 p1482 A69-21950

Validity of finite difference approximations for barotropic instability of zonal currents

09 p1537 A69-22298

Requirements for numerical solution of Navier-Stokes equations by finite difference method found limited to Re values with no turbulence

10 p1678 A69-22917

Finite difference schemes of high order of accuracy for Strum-Liouville and boundary value problems with regular singularity

10 p1719 A69-23365

Finite difference approximation to degenerate Dirichlet problem, obtaining a priori estimate to prove convergence

10 p1719 A69-23517

Stability and error bounds in numerical integration of ordinary differential equations, determining highest possible degree of stable finite difference form

10 p1719 A69-23518

Finite difference technique for numerical computation of steady supersonic two dimensional gas flows, with or without diffusion normal to mean flow streamlines

10 p1679 A69-23595

Finite difference method for transient and steady state response of vibrating plates, considering explicit and implicit formulas

11 p1983 A69-25020

Finite difference solutions for time dependent equations of motion for steady flow around cylinder at large Reynolds numbers

11 p1872 A69-25133

Finite difference method for heat transfer for developing laminar flow at inlet of circular uniformly heated and isothermal tube, determining Nusselt number

12 p2062 A69-26242

Waveguide higher order modes solved by finite difference method, employing successive overrelaxation to compute field potentials at discrete points in arbitrary guide shapes

13 p2228 A69-27670

Parameter identification in linear dynamical systems with transport lags, discussing linear differential-difference equations and finite difference theory

13 p2289 A69-27945

Finite difference solution to TEM mode transmission line cross section for defining continuous potential function leading to capacitance upper bound

13 p2221 A69-28064

Laminar boundary layer studies by finite difference computer program for Mach numbers up to 15

13 p2248 A69-28173

Finite difference Newton-Raphson algorithm extension to solve variational equations for simultaneous optimization of trajectories and associated parameters [AIAA PAPER 68-115]

13 p2353 A69-28203

Differential equation with finite jump type discontinuities

14 p2424 A69-28811

Finite difference treatment of mixed boundary value problems in two dimensional elastostatics, using first derivatives of displacement components at grid points
15 p2706 A69-30432

Taylor expansion applied to solution of nonlinear simultaneous algebraic equations in analyses of nonlinear structural systems using finite differences or elements
15 p2711 A69-30871

Godunov finite difference method modified for steady or unsteady flowfields about planar axisymmetric blunt bodies, presenting body pressures and shock shapes
16 p2732 A69-31886

Linear static deformation and buckling of shallow spherical shells under asymmetric load by solving two dimensional finite difference equations
16 p2871 A69-31897

Book on three dimensional flow of ideal gases past smooth bodies, emphasizing utility of finite difference methods
16 p2771 A69-32003

Potential and kinetic energy of cylindrical thin shell with cutout approximated by two dimensional finite difference methods, obtaining eigenvalue problem
[AIAA PAPER 68-318] 16 p2874 A69-32158

Generalized finite difference approximations of linear partial differential operators in space based on functional approximations
16 p2756 A69-32552

Mixed supersonic/subsonic type steady wake flow fields in flat based slender bodies, using finite difference method
[AIAA PAPER 69-649] 17 p2892 A69-33468

Finite difference schemes for barotropic fluid free surface model primitive equations tested for numerical integration stability and accuracy
17 p2997 A69-33691

Natural longitudinal oscillations of variable cross section straight rods, assessing errors due to use of finite difference schemes
18 p3217 A69-34581

Convergence properties of finite difference approximations to solutions of Dirichlet problem for Poisson equation
18 p3164 A69-34840

Finite difference scheme for primitive equation model, emphasizing two grid internal noise suppression to improve gradient force expression accuracy
19 p3364 A69-36507

Long term integration of fluid motion equations with finite difference scheme using hexagonal grid system to avoid nonlinear computational instability
19 p3364 A69-36508

Finite difference analogs with increasing error terms applied to simple differential Laplace operator for accuracy determination
19 p3365 A69-36510

Plane elastic deformation in isotropic homogeneous medium using displacement vector, discussing finite difference equations and application to rectangular boundary
19 p3441 A69-36719

Rectangular plate bending element corresponding to finite difference method use, deriving stiffness matrix from strain energy approximation
20 p3619 A69-36949

Radiation absorption and emission problem for material of unit density at rest solved by finite difference scheme
21 p3773 A69-39666

Natural convection in rectangular cavity with nonuniform lateral surfaces temperature, using finite difference scheme with numerical analysis
21 p3855 A69-39853

Radial and tangential stress analysis of rotating disk during steady state creep, using equations solved by finite difference method
22 p4043 A69-40458

Finite-difference grid procedure for predicting friction heat and mass transfer in two dimensional boundary layers
22 p3932 A69-40939

Boundary layer separation and free mixing phenomena between streams behind thin flat plate by finite difference methods and Prandtl exchange coefficient
23 p4060 A69-41912

Boundary conditions for Tricomi equation in symmetric positive form, showing analytical and finite difference solutions
24 p4339 A69-42792

Iterative finite difference method for initial value problems applied to hyperbolic system representing

one dimensional time dependent flow of compressible polytropic gas
24 p4340 A69-43226

FINITE ELEMENT METHOD

Finite element method in stress analysis for axisymmetric rotors design, describing computer program and applications
19 p3445 A69-36826

Finite element displacement method using elastic analogy applied to viscoelastic materials plane stress analysis
19 p3445 A69-36830

Finite elements general theory applied to wave propagation, gas kinetics, nonlinear partial differential equations, continuum mechanics and fluid dynamics
20 p3567 A69-36948

Stiffness matrices in plane elasticity problems by Galerkin method, leading to simultaneous expressions related to finite element method
20 p3619 A69-36951

Finite element discretization technique extended to time dependent processes emphasizing dynamics and heat conduction, discussing applications to aircraft transient response
20 p3575 A69-37204

Transverse stiffness and strength of unidirectional fiber-reinforced composites determined as function of fiber volume content, using finite element method and stress functions
20 p3623 A69-37354

Finite element analysis and strain gage results to verify end constraint on off-axis tensile coupons and to design test specimen
20 p3628 A69-37775

Computerized aircraft structural analysis system, adopting finite element technique /direct stiffness method/ based on COSMOS system
21 p3842 A69-39307

Finite element relaxation method for computing stress distribution in thin walled structure, considering computer program, storage and solving time
21 p3843 A69-39313

Isoparametric finite element system for stress analysis, with examples for arch dam, impeller and cellular structure, illustrating shells of revolution
21 p3732 A69-39314

Finite element method application to minimum principle for incompressible lubrication problem, noting flow boundary conditions and squeeze film effects
22 p3955 A69-40406

Cylindrical shells bending by finite element /cylindrical strips/ method, considering shells of arbitrary shape and variable thickness
22 p4046 A69-40968

Curved rectangular elements stiffness matrices derived for finite element analysis of cylindrical shells bending
22 p4046 A69-40969

Natural coordinates in finite element method, giving formulas for straight or curved element analysis and polynomial integration
23 p4182 A69-41901

ASTRA /advanced structural analyzer/ based on stiffness approach to finite element method, generating mathematical model for stresses and deflections
23 p4232 A69-42144

Triangular plate bending element using Herrmann variational method, deriving matrices for finite elements
24 p4404 A69-43591

FINITE-STATE MACHINES

U TURING MACHINES

FINLAND

Finnish space research covering satellite tracking and telemetry facilities, different Faraday and Doppler measurements with Explorer 22 signals, etc
15 p2723 A69-31426

FINNED BODIES

Finned tube radiators optimum design for waste heat removal from space power plants
02 p0354 A69-12664

Finned radiation emitter tube unsteady state temperature field as function of working body temperature and emitter geometry
05 p0846 A69-15898

Local film heat transfer coefficients variations effect on longitudinal constant area fin surface under turbulent flow
[ASME PAPER 68-HT-20] 13 p2373 A69-27770

Finned tube radiators with constant longitudinal specific heat flow, determining thermal efficiency and optimal thermal and structural parameters
20 p3631 A69-36978

FINS

NT COOLING FINS

Constant thickness fin with arbitrarily distributed heat sources optimized using approximate physical model and closed form solution of field equation
[SAE PAPER 690198] 07 p1239 A69-18302

Temperature variation and heat transfer in fins and relations between heat-flux-density and temperature difference
12 p2190 A69-25763

FIRE CONTROL

Military rotor blade radar antennas for all-weather low level flight and fire control
04 p0559 A69-15197

Airborne IR line scanning systems for latent forest fire detection, discussing discrimination module for automatic identification of hot targets
12 p2193 A69-26994

Airborne IR remote sensing techniques for fire detection, considering marginal and submarginal targets
12 p2098 A69-26995

Multifunction helicopter rotor blade radar for navigation, IFR approach and fire control, including flight test results
[AHS PAPER 315] 17 p2920 A69-33535

Helicopter fire control systems evaluation by computer model for hit probability and impact point sensitivity to various parameters
[AHS PAPER 316] 17 p2933 A69-33540

AH-56A Cheyenne integrated avionics, armament and fire control system for precise weapons delivery and navigation
[AHS PAPER 312] 17 p2903 A69-33542

Onboard hybrid computer for helicopter fire control system, generating turret pointing angles and corrections
17 p2934 A69-34074

FIRE EXTINGUISHERS

Flame extinguishing potential of various substances for low pressure premixed and diffusion flames
13 p2380 A69-28460

Halon 1301 fire extinguisher for burning spilled hypergol on Apollo/Saturn LM adapter, discussing concentration requirements and exposure hazards
18 p3094 A69-35062

Halon 1301 /bromotrifluoromethane/ concentration for inerting Aerozine-50 spills or extinguishing fires, noting joint use of carbon dioxide and water
18 p3094 A69-35090

Manual extinguisher using bromochlorodifluoromethane /BCF/ for aircraft cabin fire protection, discussing design and low toxicity, corrosiveness and cost
19 p3256 A69-36863

FIRE FIGHTING

Concorde SST fire protection equipment, discussing fire and overheat detectors, fire extinguisher, crash fire protection, explosion suppression equipment, etc
19 p3256 A69-36864

FIRE PREVENTION

Flammability handbook for plastics noting characteristics, behavior under fire conditions and various fire hazard reduction mechanisms, tables, drawings, manufacturers, suppliers, etc
04 p0620 A69-14952

Supersonic aircraft fire detection using coherent fiber bundles
06 p0926 A69-17679

Apollo spacecraft fire, presenting recommendations for power supply, cabin atmosphere and safety measures
07 p1071 A69-18970

FAA regulations for improvements on crashworthiness and emergency evacuation from viewpoint of plastic applications and fire safety in aircraft
08 p1254 A69-20497

Foam carpet and airport equipment to prevent fires and explosions from retracted gear landings
10 p1674 A69-23708

Polyurethane with additives for fuel fire control in aircraft structures, achieving desired protection without impairing foams mechanical properties
15 p2561 A69-30311

Physical and physiological hazards of cryogenic liquids, emphasizing fire and explosion problems associated with storage and handling
17 p3017 A69-33684

Fire-retardant thermoplastic and thermosetting materials for electronics industry use including blending of fire-retardant additives into plastics
18 p3162 A69-35273

Ignition hazards in electrical circuits contaminated by glycol fluids, describing hazard detection by RF

- methods, decontamination procedures, safety checks, etc
19 p3359 A69-36028
- Manual extinguisher using bromochlorodifluoromethane /BCF/ for aircraft cabin fire protection, discussing design and low toxicity, corrosiveness and cost
19 p3256 A69-36863
- Concorde SST fire protection equipment, discussing fire and overheat detectors, fire extinguisher, crash fire protection, explosion suppression equipment, etc
19 p3256 A69-36864
- Fire hazard in closed chamber associated with intestinal hydrogen and methane formed by space diets, comparing Gemini-type and bland diets
20 p3482 A69-37622
- Apollo spacecraft fire, presenting recommendations for power supply, cabin atmosphere and safety measures
20 p3483 A69-38218
- Space cabin and suit pressures for decompression sickness avoidance and fire hazard alleviation
22 p3890 A69-40212
- Ignition of aircraft fluids leaked onto hot turbofan engine surfaces, considering cooling air direction, surface temperature, nacelle engine compartment ventilation, engine power, etc [SAE PAPER 690436]
23 p4200 A69-41653
- Flame resistant organic fiber in cross linked polymer structure, discussing properties and aerospace applications
24 p4337 A69-43424
- FIREBALLS**
Bolide fireball radiation maximum efficiency from observed spectra, using monochromatic radiation efficiency data for rarefied atoms and ions in meteor comas
03 p0512 A69-13692
- Nuclear explosions electromagnetic effects on electronic systems, considering signals emitted from fireball and signal attenuation by changed atmospheric propagation
13 p2234 A69-28344
- Fireball events, isobars and meson resonances in very high energy nuclear interactions, discussing dispersion and four momenta transfer methods
13 p2303 A69-28380
- Meteorite orbits analysis with emphasis on recovered meteorites, noting fireballs and hyperbolic orbits
19 p3414 A69-36115
- Photographic networks for meteors orbits and trajectories and meteorites impact points during nighttime, discussing fireball occurrence
19 p3415 A69-36120
- Network for fireball trajectories rapid analysis to recover meteorites and obtain orbital elements data, noting role of planetariums
19 p3295 A69-36121
- Transverse momentum of fireball particles emitted in high energy inelastic collision related to emission angle and energy in accelerators
19 p3396 A69-36644
- FIREBEE 2 TARGET DRONE AIRCRAFT**
Firebee 2 /BQM-34E/ turbojet-propelled recoverable supersonic aerial target construction, performance prediction and missions
09 p1434 A69-21901
- FIRES**
Deficiencies in two hazard classification system for detonating and fire producing materials from analysis of chemical industry accident fatality statistics
04 p0645 A69-14471
- Closed compartment fire mathematical model to analyze combustion parameter effects, atmosphere pressure and temperature during fire [AIAA PAPER 69-618]
17 p3074 A69-33704
- FIREFORKS**
U PYROTECHNICS
- FIRING [IGNITING]**
NT RETROFIRING
NT ROCKET FIRING
NT STATIC FIRING
NT TEST FIRING
- Exploding wire detonators without primary explosive, discussing high precision fabrication, safety aspects and firing circuit
01 p0120 A69-10676
- Initiation of detonation by incident shock waves in hydrogen-oxygen-argon mixtures
02 p0304 A69-12313
- Igniter formulations characteristics, discussing desirable properties
10 p1750 A69-23009
- Simplified model of ignition tests with liquid propellant rocket engines under high vacuum conditions, giving possible parameter for evaluation of simulation of real conditions [DVL-831]
10 p1754 A69-24022
- FIRING TIME**
U BURNING TIME
- FIRST AID**
Medical aid organization after aircraft accidents at airports, examining injury probability by statistical methods
23 p4107 A69-41812
- Medical aid, equipment and organization for injured passengers in large aircraft accidents at airports and immediate neighborhood
24 p4270 A69-42602
- FISH**
U FISHES
- FISHES**
Blind goldfish behavioral responses to short lowered gravitational force cycles during vertical flight classified as vestibular reflexes resulting from otolith displacement
11 p1828 A69-25464
- Amino acid sequence of dogfish lactic dehydrogenase, isolating acylated amino-terminal peptide and arginine residues, indicating four polypeptide chain composition
24 p4280 A69-43051
- FISHTAILING**
U YAW
- FISSION MATERIALS**
U FISSIONABLE MATERIALS
- FISSION**
Population feedback control in planarians by fission suppression by brain near other planarians
14 p2406 A69-28871
- Correction of thermally lowered fission track ages of australites
15 p2696 A69-31140
- FISSION ELECTRIC CELLS**
U SNAP 8
U SNAP 10A
- FISSION PRODUCTS**
Uranium content in fragments from iron meteorites determined by fission fragment track recording
01 p0026 A69-11377
- Fission fragment generated plasma applicability to thermionic energy converters from electron density, temperature and transport studies
09 p1440 A69-21829
- Differential energy losses of fission fragments in thin carbon films as function of mass and initial energy mapped by time of flight method
10 p1694 A69-23348
- Lithium 6 and 7 fission following pion capture, searching for H 4 and 5
12 p2132 A69-26296
- Postirradiation investigation of uranium dioxide fuelled thermionic emitters by evaluating released fission gases, noting different neutron fluxes metallic effects
14 p2481 A69-29200
- Geochemistry of fission Xe component in chondrites, suggesting Xe derivation from superheavy elements with Z 112 to 119
15 p2681 A69-30325
- Spontaneous symmetric fission of superheavy elements near doubly magic nucleus as explanation for Xe and Kr isotopic composition anomalies in meteorites
20 p3601 A69-37503
- FISSIONABLE MATERIALS**
Thermionic reactor systems, discussing fissionable material content, power output, specific power, component mass, total mass and design
02 p0279 A69-12662
- Nuclear particle plastic dielectric track detectors to record distribution of fissionable and heavy elements in nature and cosmic radiation
08 p1401 A69-20899
- Fissioning plasma generated in shock tube with 235 uranium hexafluoride gas, selecting tube diameter, reflector depth and initial gas density for specific neutron multiplication
18 p3180 A69-34455
- FITNESS**
U FLIGHT FITNESS
U PHYSICAL FITNESS
- FITTINGS**
Flow in square to rectangular constant area transition piece having straight walls with outlet aspect ratio of 5 fitted with exit duct
02 p0189 A69-12412
- Fittings stress distribution determined for optimization of material utilization
23 p4169 A69-41418
- FIXED POINTS [MATHEMATICS]**
Error and sensitivity analysis of on-line algorithms for fixed point linear smoothing
01 p0050 A69-10238
- Solid body motion about fixed point representable by two dimensional motion of two points on complex plane
01 p0116 A69-10356
- Orbits with small eccentricities and inclinations in generalized problem of two fixed centers, showing osculating elements relationship to intermediate orbit elements
10 p1779 A69-23613
- Two fixed centers with force function approximating earth gravitational potential, deducing formula for gravity distribution at level surface
11 p1952 A69-24254
- Kowalewski solution for motion of heavy body with fixed point, noting hodographs
11 p1917 A69-24776
- Steady state solutions of differential equations of motion for body with fixed point, considering Kharlamov cone for rotation of heavy gyrost
11 p1917 A69-24780
- Stability of uniform rotations of gyrost with fixed point in potential force field, considering Routh rule
11 p1918 A69-24786
- Kinematic equations of motion of body about fixed point, considering Steklov solution
11 p1918 A69-24791
- Equations of motion of body with fixed point, deriving solutions representable as segments of trigonometric series in variable related to time differentially
11 p1920 A69-25748
- Fixed point reaction force in mobile system of solids coupled kinematically, examining zero dynamic components
18 p3172 A69-34590
- Fixed point existence in study nonlinear mapping determined on semiordered Banach space, noting results applicability to integral equations and boundary value problems
19 p3361 A69-36640
- Point mapping in optimal control, describing maximum principle, dynamic programming and substitution of variables
21 p3688 A69-39860
- FIXED-WING AIRCRAFT**
U AIRCRAFT CONFIGURATIONS
U FIXED WINGS
- FIXED WINGS**
Airframe subsonic aerodynamic problems for fixed wing aircraft under low speed/high lift conditions
05 p0695 A69-15542
- Design of high lift devices in relation to fixed wing subsonic transport aircraft, considering lift, drag, stability and control
05 p0695 A69-15544
- Compound rotorcraft VTOL vehicle current programs
05 p0703 A69-16394
- Large and small fixed wing airplane crashworthiness requirements, noting occupant protection in survivable crash environment and rapid safe evacuation [SAE PAPER 690321]
11 p2004 A69-24509
- Economics evaluation for operation of commercial fixed wing aircraft at aft center of gravity position, noting fuel saving from drag reduction [SAWE PAPER 806]
18 p3091 A69-34902
- Schweikhard method for measuring changes in lift, drag and pitching moment of fixed wing aircraft as function of distance from ground
20 p3462 A69-37423
- FLAGELLATA**
Photoinhibition of cell division and growth in Euglenoid flagellates by fluorescent and incandescent visible light
01 p0014 A69-10903
- FLAME HOLDERS**
Flame stabilization by jet flame holders for case of different composition of jets and incident flow
03 p0531 A69-12956
- Nitrogen dilution low pressure simulation technique for subsonic flow flame stabilization of bluff bodies
09 p1624 A69-22614
- Hydrogen diffusion flames stabilization by flame holders in supersonic flow at low stagnation temperature, measuring burning limits [DVL-813]
09 p1624 A69-22615

Turbulent premixed ammonia-air flame stabilization on flameholders, discussing secondary oxygen injection into circulation zone at blowoff limits
21 p3849 A69-38808

FLAME INTERACTION

U CHEMICAL REACTIONS

FLAME IONIZATION

Double probe characteristics in flame with electronegative gas injection interpreted in terms of conduction of ions in ionized medium
01 p0176 A69-10385

Electrically controlled heat transfer between flat parallel flow hydrocarbon diffusion flame and walls of combustion chamber
02 p0353 A69-12324

Chemiluminescence and chemionization in flames, considering electrically conducting properties and spectral analysis
06 p1032 A69-17423

Flame inhibition with electron attachment observed using halogenated hydrocarbons
06 p1034 A69-17926

Positive ion concentration in subsonic high velocity laminar flames determined by interpreting kinetic and diffusion factors of adding cesium to flame
13 p2380 A69-28463

Major ions in chemi-ionization of hydrocarbon flames determined for heats of formation by photoionization mass spectrometer
22 p3896 A69-40727

FLAME PROBES

Double probe characteristics in flame with electronegative gas injection interpreted in terms of conduction of ions in ionized medium
01 p0176 A69-10385

Chemiluminescence and chemionization in flames, considering electrically conducting properties and spectral analysis
06 p1032 A69-17423

Heat transfer from unseeded DC augmented propane air flame to water cooled probe placed beyond discharge zone
06 p1035 A69-17934

Thermocouple and optical methods for temperature profile measurement in slow burning flat hydrogen-nitrogen-oxygen flame at atmospheric pressure
07 p1242 A69-19489

Induction period of reactions behind incident shock waves traveling through undiluted high temperature CO and molecular oxygen mixtures, using CO flame spectra
16 p2877 A69-31768

Plasma parameters relationship with double electrostatic probe volt-ampere characteristics, applying corrected formulas for temperature, ion density, etc, to flame diagnostics
18 p3137 A69-34932

FLAME PROPAGATION

Gas combustion stability with respect to one dimensional perturbations, considering flow compressibility stabilizing effect
01 p0174 A69-10107

Detonation wave initiation in gaseous media, noting transition process for flames accelerating to detonation and explosions behind reflected shock wave
02 p0350 A69-11530

Flame zone development of monopropellant droplets during heat-up period
02 p0352 A69-12310

Hydrogen bromide, HI and HCl effects on hydrogen-air mixtures flammability, discussing flame propagation inhibition efficiency
02 p0304 A69-12315

Spherical flames of spark-ignited dust clouds, discussing streak film photographs, flame propagation, particle burnout time and burning velocities
02 p0353 A69-12323

Chemical reaction scheme effect on hot zone structure of hydrogen-oxygen diffusion flame, considering influence of hydroxyl radical
03 p0531 A69-12895

Inflammable gas mixtures and deflagrations noting self ignition temperature, flame propagation, flame front structure and flame stability
06 p1031 A69-17417

Flame establishment and propagation in gas phase taking into account aerodynamic and chemical kinetics
06 p1031 A69-17418

Reciprocal interaction of combustion wave and field of turbulence, discussing aerodynamic principles, turbulence effect on flame propagation speed and measuring methods
06 p1032 A69-17420

Laminar and turbulent regimes of flame propagation studied by blowing explosive gas mixture through porous wall, determining Reynolds number by hot-wire anemometer
06 p1034 A69-17626

Impinging jet flames on furnace hearth, analyzing thermal boundary layer characteristics and convective heat transfer rates
06 p1035 A69-17933

Heat conduction equation for convective flow applied to gunpowder combustion under harmonic pressure variation
07 p1241 A69-18708

Chemical reactions in boundary layer on porous plate in oxygen stream, discussing similar solution of laminar boundary layer equations with flame front
07 p1119 A69-18735

Homogeneous turbulent gas flame front location as function of caloric value of mixture and flow velocity
08 p1420 A69-19998

Flame front instability in air-propane mixtures established by motion picture study
08 p1421 A69-20344

Thermal approach to pulsating combustion, determining temperature-time variation, frequency and pressure from mathematical model
09 p1625 A69-22694

Flame propagation normal velocity evaluated with heat transfer equation at flame front taking into account temperature, pressure and inert gas percentage
09 p1625 A69-22695

Steady flames transition into spherical detonation in various gas mixtures using high speed photography in sealed volumes
10 p1810 A69-23897

Turbulent flame propagation velocity in homogeneous premixed combustible gas, using one dimensional inviscid flame model
11 p1998 A69-24473

Cool flames nonisothermal two-stage ignition of neopentane-oxygen mixtures, discussing chain propagation due to isomerization
11 p1940 A69-24477

Turbulent flame propagation described by turbulence intensity and integral scale and fuel properties including laminar flame velocity and equivalence ratio
11 p1999 A69-24482

Hydrodynamic effects in flame spreading, ignitability and steady burning of liquid fuels, using analogy of films floating on water
11 p1999 A69-24484

Flame velocities of stable premixed tetrafluoroethylene-oxygen mixture flames measured with bunsen-cone method
11 p1940 A69-24485

Steady propagation of flame front initiated by local ignitor /spark/ in gas mixture, discussing critical requirements, boundary conditions, etc
11 p2001 A69-25190

Flame front propagation over solid fuel surface with hot igniting material injected into end-to-end cavity, discussing heat transfer by convection and radiation
11 p2001 A69-25193

Electric fields effect on flame front propagation structure and velocity, obtaining color toepolograms by high speed photography
12 p2190 A69-26192

Steel cylinder wall materials effects on flame propagation at constant volume of propane-air mixtures
13 p2379 A69-28363

Turbulent burning velocity definition for one dimensional turbulent flow and average flame orientation perpendicular to flow direction, discussing transient flames in turbulent environment
13 p2379 A69-28452

Thermal ignition of methane-oxygen mixture, observing flame propagation
13 p2380 A69-28459

Supersonic combustible gas mixture flow around circular cone, discussing ignition by shock wave and flow modification by conical flame front
15 p2548 A69-31007

Self excited vibrating laminar diffusion flames, discussing coupling, jet spacing radial heat transfer and boundary layer interaction
16 p2876 A69-31711

Flame propagation velocity for different gas mixtures enclosed in glass tube determined by fiber optics devices
16 p2789 A69-31764

Initial temperature effects on flame propagation velocity in turbulent flow of homogeneous gasoline-air mixture under realistic conditions
16 p2837 A69-32138

Two phase detonations of fuel in liquid layer on shock tube wall with gaseous oxidizer, presenting one dimensional approximation for film detonation propagation
16 p2879 A69-32151

Additives effect on flame propagation velocity and stability in N diluted hydrogen-chlorine propellants, noting entrained air role [WSC1 PAPER 69-13]
16 p2831 A69-32353

Flame propagation in narrow slit and fine hole of solid propellant grain [AIAA PAPER 69-561]
16 p2833 A69-32680

Monograph on turbulent isothermal swirl-free jets and turbulent swirling flames, studying mixture and propagation in free space
17 p3068 A69-32996

Flame front structure and combustion rates of gases as function of temperature dependence of thermal conductivity, diffusion coefficients, density and molecular weight
17 p3069 A69-33136

Normal flame speed during gas combustion in calorimetric bomb with constant combustion volume calculated by approximate equations
17 p3069 A69-33137

Computer calculation of kinetic characteristics of normal flame propagation during gas combustion, constructing physical model and differential equation system
17 p3069 A69-33138

Temperature and pressure effects on flame propagation rates, burning time and combustion zone length in turbulent flows of homogeneous gas mixtures
17 p3069 A69-33140

Flame propagation mechanism on plastic fuel in oxygen-nitrogen atmospheres with variable pressures and at different initial fuel temperatures, discussing safety and ignition problems
17 p3074 A69-33662

Turbulent velocity of flame propagation in supersonic stream of hydrogen-air mixture determined by velocity distribution, exchange coefficient and burning time
19 p3448 A69-35854

Flame and pressure /or velocity/ oscillations interaction in unstable combustion regimes, considering tubes with propane-air mixtures
19 p3450 A69-36357

Flame acceleration data applied to unburnt gas boundary layer analysis, discussing velocity and temperature profiles, layer thickness variation and expansion phase backflow
19 p3450 A69-36359

Transverse and longitudinal velocity components of detonation waves in stoichiometric hydrogen-oxygen propagating in fundamental mode in square section tube
19 p3451 A69-36367

Flow induced by plane flame traveling supersonically or subsonically at constant speed through long tube studied for flow field steadiness in flame fixed coordinates [ASME PAPER 69-FE-33]
20 p3460 A69-37993

Propagation characteristics of steady adiabatic one dimensional laminar flames in premixed gases, considering activation energy and Lewis number
21 p3849 A69-38802

Flame pressure drop and burning velocity related, discussing stream tube area expansion error
21 p3849 A69-38806

Ammonia addition effect on laminar flame speeds of propane-air mixtures
21 p3849 A69-38809

Combustion turbulence effect on flame propagation velocity taking into account flame-generated pulsation velocity as function of temperature and flame velocity
21 p3850 A69-38861

Interferometric study of cool flame propagation in equimolar propane-oxygen mixtures, observing refractive index and temperature distribution changes
21 p3852 A69-39595

Book on rate constants of chemical reactions from flames covering flame propagation, mass spectroscopy, electron spin resonance, particles diffusion, combustion physics, etc
22 p3895 A69-40318

Aircraft fuel vent line sensitivity to lightning hazards, using flame propagation and arrester experiments with high voltage and high current facilities [SAE PAPER 690434]
23 p4062 A69-41651

FLAME QUENCHING

U EXTINGUISHING

U QUENCHING [COOLING]

FLAME SPRAYING

- Alumina radomes manufacture by flame spraying process, discussing raw materials quality control, spraying operation, sintering and final inspection
07 p1142 A69-19528
- Electrical resistivity of aluminum oxide films deposited on tubular substrates by plasma and gas flame spraying, noting dependence on film thickness and substrate
15 p2630 A69-31179
- Metal or ceramic layers application to substrate by flame spraying process
21 p3731 A69-38938

FLAME STABILITY

- Gas combustion hydrodynamic stability using feedback equation and theorems for variations in mass and momentum vector
01 p0173 A69-10087
- Stabilized low temperature ignition of cyclohexane using vertical flow reactor
02 p0304 A69-12314
- Flame stabilization on rectangular burners, discussing blow-off limits correlation by velocity gradients close to corners
02 p0353 A69-12320
- Combustion and flame stabilization in axisymmetric laminar or turbulent H flows, noting combustion rates and flame breakdown conditions
02 p0355 A69-12673
- Flame stabilization by jet flame holders for case of different composition of jets and incident flow
03 p0531 A69-12956
- Air jet high temperature and low pressure influence on combustion stability in ramjet engine
03 p0531 A69-12968
- Unsteady motions of diffusion flame sheet due to perturbations of reactant concentration, approximating species and energy conservation requirements
03 p0532 A69-13014
- Inflammable gas mixtures and deflagrations noting self ignition temperature, flame propagation, flame front structure and flame stability
06 p1031 A69-17417
- Activation energies in baffle stabilized flame deduced from reaction zone using gas chromatography
06 p1035 A69-17930
- Turbulent premixed flames stabilization, determining gas flow velocity, turbulence intensity, flame thickness and burning velocity relation to intensity
06 p1035 A69-17931
- Flame front instability in air-propane mixtures established by motion picture study
08 p1421 A69-20344
- Nitrogen dilution low pressure simulation technique for subsonic flow flame stabilization of bluff bodies
09 p1624 A69-22614
- Hydrogen diffusion flames stabilization by flame holders in supersonic flow at low stagnation temperature, measuring burning limits
09 p1624 A69-22615
- Ethylene oxide and ethane low pressure fuel-rich flames mass spectrometry, analyzing composition and temperature profiles and OH radical role
11 p1831 A69-24478
- Stability of slow combustion in viscous gas mixture, showing viscosity as principal stabilizing factor
11 p1999 A69-24554
- Hydrodynamic instability of normal flame and turbulent combustion of gas mixtures, considering surface and volume combustion models
11 p2000 A69-25186
- Electrodynamic model applicability to HF flame discharge for case of flame discharge stabilization by axial air injection
12 p2140 A69-27126
- Flame extinguishing potential of various substances for low pressure premixed and diffusion flames
13 p2380 A69-28460
- Turbulent jet theory, thermal ignition theory and flameout characteristics of bluff body flame stabilizers
16 p2879 A69-32141
- Sound effects on turbulent flame in gasoline-air mixture jet in Toepfer device with pulsed light source, measuring ionization in combustion zone
17 p3069 A69-33141
- Diffusion flame stability at inlet of fuel stream into oxidizer, showing ignition coordinates dependence on fuel, oxidizer and ratio of burning flow rate
19 p3448 A69-35855
- Detonation in unbounded gas mixture starting from spherical flame, discussing stability of gasdynamic discontinuities and cellular structure
19 p3450 A69-36358

- Propagation characteristics of steady adiabatic one dimensional laminar flames in premixed gases, considering activation energy and Lewis number
21 p3849 A69-38802
- Temperature and concentration measurements of H radical in hydrogen flames
21 p3669 A69-38807
- Turbulent premixed ammonia-air flame stabilization on flameholders, discussing secondary oxygen injection into circulation zone at blowoff limits
21 p3849 A69-38808
- Temperature influence of homogeneous kerosene-air mixture on flame stabilization by mechanical and gas dynamic baffle systems
21 p3850 A69-38859
- Discontinuity characteristics of trough-shaped flame stabilizers for combustion in wake of poorly streamlined body during period of ignition arrest
21 p3851 A69-39092
- Monograph on electrically heated turbulent flames in cylindrical combustion chamber, investigating temperature distribution and stability
21 p3853 A69-39707
- Turbulence characteristics of flow influence on critical flameout conditions of disk shaped flame stabilizer, circulation zone length and combustion efficiency by bluff body
24 p4408 A69-43078

FLAME TEMPERATURE

- Electric field effects on flame temperature variation, suggesting electrons active role in flame combustion reactions
01 p0176 A69-10389
- Line reversal and excitation temperatures in low pressure flames
02 p0350 A69-11709
- Line reversal temperature measurement technique, calculating error and outlining correction methods for flames with cool boundary layers and flames containing solid particles
06 p1035 A69-17929
- Heat transfer from unseeded DC augmented propane air flame to water cooled probe placed beyond discharge zone
06 p1035 A69-17934
- Solid propellant burning rate behavior during abrupt environmental pressure excursions, using transient combustion model
[AIAA PAPER 69-172] 06 p1036 A69-18046
- Thermocouple and optical methods for temperature profile measurement in slow burning flat hydrogen-nitrogen-oxygen flame at atmospheric pressure
07 p1242 A69-19489
- Isothermal theory of cool flames, discussing oscillations-fuel consumption relations, kinetics, etc
11 p1970 A69-24476
- Chemical mechanism of two stage spontaneous ignition controlled by cool flames of alkane-air mixtures under engine conditions to avoid knocking
11 p1998 A69-24479
- Monograph on comparison of various methods for experimental determination of temperature fields in laminar burner flames
11 p1999 A69-24635
- Interferometric study of cool flame propagation in equimolar propane-oxygen mixtures, observing refractive index and temperature distribution changes
21 p3852 A69-39595
- Monograph on electrically heated turbulent flames in cylindrical combustion chamber, investigating temperature distribution and stability
21 p3853 A69-39707

FLAMEOUT

- Extinction by depressurization of AP composite solid propellants theory to predict rate of pressure decrease required to achieve flameout
[AIAA PAPER 69-176] 06 p0983 A69-18102
- Flame burnout of atomized hydrocarbon fuel in gas turbine combustion chambers as function of ratio of time to total burnout time
08 p1420 A69-19999

FLAMES

- NT DIFFUSION FLAMES
- NT PREMIXED FLAMES
- Diffusional, thermal diffusional and thermal fluxes in multicomponent flames, discussing flame structure and reaction kinetics
01 p0175 A69-10144
- Microcalorimetric measurement of radiation flux of flames of condensed burning material, noting surface temperature distribution
02 p0355 A69-12671

- Equilibrium between H and OH radicals in turbulent H flames, noting component concentrations in H-O-N flames of different composition
11 p1999 A69-24487
- HO₂ radical detection in rarefied H flame produced by HF discharges, recording high amplitude signals
15 p2716 A69-30054
- Monograph on static pressure and turbulence in free jets and jet flames covering radial velocity oscillations with and without chemical reactions, confined jets turbulence, etc
15 p2719 A69-31190
- Spectroscopic quantitative analytical method for measuring atomic absorption in flame based on determining integral absorption magnitude during evaporation
20 p3539 A69-37605

FLAMMABILITY

- Burning ability and inflammability of mixtures of powdered Mg, Al, Mg alloys or Al alloys and C-H-O organic compounds
02 p0355 A69-12669
- Detonation capacity of mixture of ammonium perchlorate base and polymethyl methacrylate and polystyrene, noting critical particle size dependence on composition
02 p0305 A69-12674
- Flammability handbook for plastics noting characteristics, behavior under fire conditions and various fire hazard reduction mechanisms, tables, drawings, manufacturers, suppliers, etc
04 p0620 A69-14952
- Oxygen index test for precise flammability ratings of plastics on numerical basis, eliminating drawbacks of ignition, end point and nonequilibrium conditions operation
04 p0621 A69-14957
- Oxygen index test for precise flammability ratings of plastics on numerical basis, eliminating drawbacks of ignition, end point and nonequilibrium conditions operation
08 p1335 A69-20114
- Flammability control for aerospace avionics systems safety, considering risk, test method, acceptability criteria, confidence level and ignition source
24 p4336 A69-43422
- Hazard rating for flammability of aerospace materials in air and oxygen environments applied to J-2 rocket engine insulation
24 p4336 A69-43423
- Flame resistant organic fiber in cross linked polymer structure, discussing properties and aerospace applications
24 p4337 A69-43424

FLAMMABLE GASES

- One dimensional unsteady flows of combustible gas mixture with finite chemical reaction rates, considering piston motion, igniting shock wave propagation and point explosion
06 p0909 A69-17325
- Inflammable gas mixtures and deflagrations noting self ignition temperature, flame propagation, flame front structure and flame stability
06 p1031 A69-17417
- Gas dynamics effects of hot spot in explosive gas mixture using kinetic rate equations, discussing composition, enthalpy and time dependence
[WSCI PAPER 68-53] 07 p1240 A69-18322
- Nonequilibrium chemical reaction effect on decay in spontaneous explosion for reactive expelled gas and inert expelling gas
07 p1119 A69-18705
- Turbulent flame propagation velocity in homogeneous premixed combustible gas, using one dimensional inviscid flame model
11 p1998 A69-24473
- Hydrodynamic instability of normal flame and turbulent combustion of gas mixtures, considering surface and volume combustion models
11 p2000 A69-25186
- Flame acceleration data applied to unburnt gas boundary layer analysis, discussing velocity and temperature profiles, layer thickness variation and expansion phase backflow
19 p3450 A69-36359

FLANGES

- Symmetric and asymmetric metal flanges effects on radiation patterns of H plane sectoral horns, noting theoretical explanation and applications
02 p0216 A69-12027
- Asymmetric excitation of conducting flanges by primary aperture antenna and consequent radiation pattern
02 p0217 A69-12246

FLAP CONTROL

Rectangular shock tube for use with pressure and vacuum, discussing sealing of circular end flanges to buildup tube
06 p0906 A69-16928

Metal flanges position effect on radiation patterns of H-plane sectoral horn radiators
08 p1285 A69-20554

Gyromotor flanges axial rigidity measuring methods based on axial deflection of flange or natural frequency of oscillating system
09 p1513 A69-22704

Conducting flanges effects on H plane radiation patterns of E plane sectoral horns, noting improved beam width and gain and H plane beam tilting
10 p1665 A69-24063

Flanges flexural rigidity effect on load carrying capacity, failure mechanism and postbuckling behavior of webs in shear, noting permissible load
18 p3227 A69-35492

Asymmetric metal flanges effect on beam tilt of aperture antennas
24 p4288 A69-43765

FLAP CONTROL

U AIRCRAFT CONTROL
U FLAPS [CONTROL SURFACES]

FLAPPING

Hingeless fiberglass rotary wings dynamics, discussing effects of in-plane bending to flapping frequency ratio
[AIAA PAPER 69-204] 07 p1054 A69-19548

Lifting rotor blades flapping response to atmospheric turbulence, discussing time averaging and perturbation schemes
[AIAA PAPER 69-206] 07 p1057 A69-19577

Flapper valves in high pressure hydraulic aircraft systems, with hydrodynamic equations and charts for design and performance characteristics
09 p1435 A69-21296

FLAPS [CONTROL SURFACES]

NT JET FLAPS
NT LEADING EDGE SLATS
NT TRAILING-EDGE FLAPS
NT WING FLAPS

Aerodynamics of flap balanced swivel airfoils, discussing lift curve slope, incidence change response and application of control forces and movements
03 p0364 A69-13908

Lifting reentry dynamic stability of flare stabilizers and flap controls
[AIAA PAPER 69-182] 06 p1017 A69-18053

Hypersonic laminar boundary layers on compression corner model, studying flap lengths effects and mass transfer
[AIAA PAPER 69-36] 06 p0866 A69-18214

Lift augmentation by lateral blowing over lifting surface, discussing wind tunnel pressure tests on wings, flaps and stabilizers
[AIAA PAPER 69-193] 07 p1051 A69-19554

Spoiler effect on aerodynamic characteristics of airfoil with hinged flap in inviscid fluid plane flow
15 p2549 A69-31223

Optimum adaptation of propulsion gas generators to power jet driven rotors with blown flap control, considering jet engine, fanjet and engine driven compressor
17 p3020 A69-33344

FLARED BODIES

Unsteady aerodynamics of ablating flared reentry body, noting complications due to blunted nose shear flow and entropy gradient effects
02 p0189 A69-12524

Lift efficiency of and stabilization by square flare on high speed missile, comparing wind tunnel measurements with circular conical flare
02 p0190 A69-12544

Wind tunnel tests for static stability of Black Brant 4 vehicle second stage with flare and two fin flare combinations at supersonic speed
17 p2948 A69-34212

Supersonic aerodynamic characteristics of flared cones with various flare angles studied by schlieren photography, showing geometrical parameters influence on flow patterns
19 p3239 A69-36387

Supersonic flow past segmented and blunt bodies, investigating flow characteristics
19 p3242 A69-36783

FLARES

YZ Canis Minoris red dwarf star flare event observation record, noting optical spectrum energy output and slow decay
17 p3043 A69-34165

Meteor flakes nature and statistics from studying 318 meteors characterized by irregular brightness curve
18 p3203 A69-35333

Mayeda flare observed on Mars on 4 June 1937, suggesting oriented reflection of solar rays from ice crystals cloud or Martian surface feature
20 p3608 A69-38049

FLASH

Physiological effects of intermittent light stimulation during helicopter flight, discussing visual and electric cortical functions at critical frequency threshold of subjective fusion
13 p2211 A69-28595

Circadian rhythm phase shifts during ontogenesis produced by hormone concentration changes resulting from light variations
22 p3872 A69-40198

Psychophysical threshold changes during subliminal monocular and interocular stimulation, studying conditioning flash size effects on temporal summation
22 p3881 A69-40860

High intensity flash effects on local electroretinogram, late receptor and slow potentials and ganglion cell activity in area centralis of cat retina
22 p3883 A69-40882

FLASH BLINDNESS

Electroretinogram a-wave relationship to early inhibition and excitation of retinal ganglion cells produced by flash superimposition in rabbits
22 p3878 A69-40836

FLASH LAMPS

High repetition rate pulsed illuminator using electrodeless halogen discharge for rapid light extinction
04 p0599 A69-15021

Approach light efficiency, discussing Calvert bar system and strobe flash on basis of pilot questionnaire polling
06 p0884 A69-18029

Xenon flash lamps with electrolytic capacitors designed for photographic studies of laminar flows of viscous fluids
07 p1116 A69-18259

High oxygen concentration effect on conditioned reflex and associated EEG responses to light flash in rabbits occurs in well defined sequences
07 p1065 A69-18976

Stroboscopic generator of trains of high brightness light flashes for hydrodynamic and gas dynamic research, noting electronic control and thyatron circuits
11 p1879 A69-24235

Flash radiography technique using tungsten wire explosion in vacuum to obtain ultrafast reproducible X ray pulse
12 p2092 A69-26480

Kr and Ar flash lamps pumping efficiencies compared for Nd-doped YAG and glass lasers
17 p2980 A69-32958

High speed photography for hypervelocity aerobalistic ranges, using giant pulse ruby laser for front lighting
19 p3306 A69-35732

High oxygen concentration effect conditioned reflex and associated EEG responses to light flash in rabbits occurring in well defined sequences
20 p3479 A69-38224

Flashlamp-excited organic dye lasers capable of tunable emission throughout most of visible spectrum
22 p3966 A69-41219

Monte Carlo method for energy transfer efficiency of ruby laser pumping cavities by helical flash lamps, noting dependence on ruby parameters
23 p4173 A69-41630

Flash lamp for biological applications, discussing control unit circuitry, pulse duration, frequency and color, flash-dark ratio, etc
23 p4110 A69-42054

FLASH POINT

Test methods for lubricants vapor pressure and flash point determination
[ASLE PAPER 68-LC-23] 15 p2642 A69-30607

FLASHBACK

Flame stabilization on rectangular burners, discussing blow-off limits correlation by velocity gradients close to corners
02 p0353 A69-12320

FLASHING [VAPORIZING]

Laser produced Sb and Te vaporization near critical point, using time of flight mass spectrometer
22 p3993 A69-40719

FLAT LAYERS

Gases emissivity at high temperatures calculated for different gas layer thicknesses and atmospheric pressures, giving results in tabular form
02 p0285 A69-11567

Radiative-conductive heat transfer in plane layer of gray heat conducting medium, solving energy equation
09 p1621 A69-21433

Diffuse reflection of monochromatic radiation by semiinfinite plane layer in case of isotropic scattering, reducing problem to power series
11 p1960 A69-24732

Brightness coefficients for isotropic scattering of homogeneous plane layer in turbid medium, using Legendre polynomials
11 p1960 A69-24733

FLAT PLATES

Viscous electrically conducting fluid with aligned magnetic field flowing past flat plate at nonzero angle of attack
01 p0126 A69-10163

Free convection from partially uniformly heated and partially insulated vertical flat plate, discussing dimensionless velocity, temperature, heat flux and axial length parameters
01 p0175 A69-10331

Time history of unsteady heat transfer in laminar boundary layer over semiinfinite flat plate due to step change in wall temperature or wall flow
01 p0177 A69-11401

Plate temperature oscillation effects on forced convection laminar viscous incompressible MHD boundary layer flow from semiinfinite flat plate
02 p0288 A69-12143

Transient laminar boundary layer development on flat plate following impulsive start of surrounding fluid motion, obtaining temperature and velocity distribution relationship
[ASME PAPER 68-HT-10] 02 p0232 A69-12208

Accelerated plate motion effect on flow of electrically conducting viscous incompressible fluid past infinite flat plate in uniform magnetic field
02 p0289 A69-12237

Surface temperature of flat plate cooled convectively and insulated by circular spot, determining effects of spot radius and Biot number
03 p0531 A69-12863

Transpiration cooling of porous flat plate by injection of carbon dioxide or air into carbon dioxide and air free streams
03 p0413 A69-12996

Boundary layer equations for uniform motion of semiinfinite flat plate through incompressible conducting fluid at rest and in magnetic field, using numerical method
03 p0477 A69-13794

Laminar two dimensional viscous wake behind finite flat plate, investigating upstream and downstream flow field of trailing edge region for high Reynolds numbers
[ASME PAPER 68-WA/APM-20] 04 p0541 A69-14387

Conically bent plate cross section distortion analysis employing von Karman large deflection theory, noting effect of tapering
[ASME PAPER 68-APM/Y] 04 p0670 A69-14402

Unsteady compressible laminar boundary layer flow over insulated or isothermal flat plate moving with arbitrary time variant velocity in viscous fluid
04 p0588 A69-14715

Thermal and ablative lag induced by periodic heat input to oscillating flat plate in high velocity flow, showing crossover from dynamically stabilizing to destabilizing condition as oscillation frequency increases
[AIAA PAPER 67-336] 04 p0685 A69-14720

Hypersonic boundary layer on flat plate with strong hypersonic viscous interaction and uniform surface blowing distribution
04 p0588 A69-14722

Rarefied hypersonic flow model for sharp flat plate in strong interaction regimes, discussing inviscid and viscous shock and merged layers subregimes
04 p0589 A69-14747

Transverse normal waves excitation in flat plate by applying piezoelectric plate or comb shaped emitter to surface or end face
04 p0678 A69-14901

Natural convection heat transfer through enclosed horizontal layer of supercritical carbon dioxide, discussing flat plate configuration data
04 p0688 A69-15398

Stability functions for local buckling of long thin flat walled structures loaded for longitudinal compression and shear
05 p0833 A69-15709

Laminar flow of stably stratified fluid with uniform upstream velocity and density gradient past thin flat plate, discussing upstream wake and boundary layer
05 p0745 A69-15724

Time dependent two dimensional incompressible laminar boundary layers analysis, discussing application to transient flow over semiinfinite flat plate
[ASME PAPER 68-FE-10] 05 p0748 A69-16076

Counter rotating vertical vortices produced by corona discharge on heated flat plate under free convection conditions
[ASME PAPER WA/HT-9] 05 p0846 A69-16117

Elastic-plastic analysis of flat plates in membrane stretching and flexure, using method of initial strains
[ASME PAPER 68-WA/PVP-10] 05 p0840 A69-16191

Circular inclusion effect on stresses around line crack in sheet under tension based on elasticity theory
05 p0841 A69-16432

Boundary layer on flat plate with homogeneous suction, discussing dimensionless displacement/ momentum thickness and wall shearing stress
05 p0752 A69-16744

Heat and mass transfer by catalytic effect at wall, noting interaction of laminar boundary layer on flat plate
06 p1030 A69-17115

Boundary layer transition detection at supersonic speeds, using thin film gages to infer local laminar and turbulent supersonic skin friction
[AIAA PAPER 69-9] 06 p0912 A69-18075

Radiation profiles in ablating flat plate air- Teflon laminar boundary layer, discussing visible, UV and IR wavelengths
[AIAA PAPER 69-99] 06 p1037 A69-18086

Finite plate length effect on two dimensional supersonic turbulent boundary layer with large distributed surface injection
[AIAA PAPER 69-162] 06 p0864 A69-18138

Flow near leading edge of sharp insulated and cooled flat plates, using Monte Carlo direct molecular simulation
[AIAA PAPER 69-141] 06 p0866 A69-18208

Differential equations governing free convection boundary layer flow past isothermal semiinfinite vertical flat plate solved for large Prandtl numbers by matched asymptotic expansions
07 p1239 A69-18266

Plane anisotropic rectangular plates with various boundary conditions, analyzing stability, natural frequencies, mode shapes and displacement under lateral loads
07 p1232 A69-18719

Discontinuity effect on Ekman layer development at leading edge of flat plate
07 p1120 A69-19044

Transition boundary layer on flat plate in subsonic wind tunnel measured by hot-wire method, obtaining velocity fluctuation distribution and turbulence intensity
07 p1121 A69-19329

Analytical solution for plate velocity statistics of turbulent-flow-excited rectangular flat plate, discussing vibration excitation
07 p1236 A69-19461

Circular turbulent air jet from flat plate into deflecting stream analyzed with potential flow model, noting applicability to V/STOL aircraft technology
[AIAA PAPER 69-223] 07 p1051 A69-19557

Numerical method for three dimensional boundary layer equations, applying perturbation technique and independence principle to rotating flat blade
[AIAA PAPER 69-227] 07 p1051 A69-19560

Liquid flow field about oscillating flat plate, comparing visualization results with numerical solution of Navier-Stokes equations
[AIAA PAPER 69-226] 07 p1121 A69-19565

Dynamic stability of thin flat plates and applications in ship and aircraft deck construction, studying dynamic buckling for rectangular plate
08 p1415 A69-20665

Supersonic jet impingement on flat plate, showing shock wave profiles and slipstream surface at stations parallel to nozzle axis
08 p1252 A69-20841

Transient free convection laminar boundary layer equations for heat transfer from vertical semiinfinite flat plate
08 p1305 A69-20842

Hot air open circuit wind tunnel for testing vaporized fuel films heat and mass transfer over flat plates
08 p1302 A69-20878

Power series solutions of MHD boundary layer equations for flat plate with transverse magnetic field and arbitrary pressure gradient, discussing skin friction
09 p1545 A69-21396

Free transverse vibrations of rectangular flat plate simply supported along periphery and rigidly connected to interior columns
[ASCE PAPER 739] 09 p1616 A69-21928

Local heat transfer coefficients in oscillating turbulent boundary layer over flat plate
[ASME PAPER 69-GT-34] 09 p1623 A69-22490

Wall temperature and Prandtl number effects on turbulent boundary layer thicknesses and shape factors for subsonic compressible gas flow over flat plate
[ASME PAPER 69-GT-55] 09 p1432 A69-22513

Thermal shock stresses in flat plates, solids and hollow cylinders, noting geometry, wall thickness, heat transfer characteristics and material properties effects
[ASME PAPER 69-GT-107] 09 p1619 A69-22523

Large amplitude free vibration of isosceles right angled triangular plate with simply supported edges
10 p1800 A69-23236

Heat transfer at plate in hydrodynamically stabilized turbulent boundary layer region, obtaining formulas for calculating transfer coefficients
10 p1809 A69-23427

Temperature field calculation in infinite plate with heat transfer coefficient and ambient temperature arbitrary functions of time
10 p1809 A69-23430

Laminar flow stream containing periodic fluctuation of mass fraction of chemical species over flat plate with reactive surface
11 p1831 A69-24284

Elastic unbounded isotropic plate weakened by doubly periodic system of identical holes, noting solution involving Cauchy type integral
11 p1972 A69-24652

Turbulent boundary layer velocity distributions in uniform/accelerated compressible flow over flat plate, using change of variables based on mixing length formula
[ONERA-TP-693] 11 p1867 A69-24752

Shock induced boundary layer flow establishment on semiinfinite flat plate, measuring heat transfer rates and transition to turbulence
11 p1869 A69-24890

Velocity profiles in unsteady laminar incompressible boundary layer over flat plate in shock tube by two parameter integral method
11 p1871 A69-25026

Velocity distributions and skin friction coefficients in turbulent boundary layers over flat plate with injection or suction through porous wall
11 p1871 A69-25027

Buckling of long flat panel in combined compression and shear with sinusoidal edge moments and support on two edges and on point supports
11 p1984 A69-25138

Elastic bending moments and shear forces uniformly loaded flat plate structures with rectangular symmetry, using collocation technique and complex variable methods
11 p1986 A69-25241

Free convection boundary layer flow past vertical flat plate analyzed for nonlinear wall temperature distributions using series solutions
11 p2002 A69-25243

Buoyancy effect on boundary layer flow over semiinfinite vertical plate heated to constant temperature in uniform free stream
11 p1874 A69-25352

Free vibration frequencies of simply supported parallelogrammic plates, noting skew angle splitting of degenerate frequencies and frequency crossing of modes
11 p1987 A69-25379

Flat plate in two dimensional low density hypersonic flow wind tunnel tested for aerodynamic effects on spacecraft reentry
11 p1819 A69-25424

Aerodynamic characteristics of flat plate in viscous hypersonic flow incident at zero or small angle of attack, using numerical integration
11 p1820 A69-25471

Viscous flow-induced vibrations of elastically restrained flat plates in narrow channel, considering one dimensional viscous flow theory
11 p1991 A69-25515

Flutter analysis of plates with inplane boundary support flexibility exposed to transverse pressure loading or buckled by uniform thermal expansion
11 p1992 A69-25523

Heat and mass transfer in laminar boundary layer on porous flat plate with variable suction or injection velocity and constant wall temperature
12 p2061 A69-25947

Fracture surfaces of thermally toughened glass plates using Crazz-Schardin spark camera, confirming internal front lead over front in surface layers
12 p2118 A69-26194

Transverse normal waves excitation in flat plate by applying piezoelectric plate or comb shaped emitter to surface or end face
12 p2182 A69-26654

Pressure and heating rate correlations for rocket exhausts impinging on flat plates and curved panels, generating axisymmetric real gas exhaust plumes
12 p2190 A69-26781

Cylinder buckling and other boundary value problems, applying inverse differential operators to solution of integrodifferential equations
12 p2186 A69-26841

Thermal stability of power transistor plates calculation using equivalent body with equivalent heat source at upper surface
12 p2042 A69-26881

Thermal stability of complex transistorized structures determined by extending method of single heat source equivalence to several interacting sources
12 p2042 A69-26882

Thermal radiation effects on laminar free convection boundary layer of vertical flat plate, studying absorbing and nonabsorbing gases
[ASME PAPER 68-HT-43] 13 p2373 A69-27772

Free convection heat transfer from heated inclined flat plate in air, studying effects of angular positions
13 p2375 A69-27794

Incompressible uniform shear flows merging behind trailing edge of semiinfinite flat plate, using inner-outer expansion method based on Navier-Stokes equation
13 p2248 A69-28223

Numerical solutions of equations for high Prandtl number boundary layers in two dimensional flat plate incompressible flow with mass injection
13 p2249 A69-28238

Loitsianski method of parametric approximation extended to include flat plate with constant surface suction and flow past circular cylinder
13 p2249 A69-28247

Angle of attack and blunting effect on aerodynamic lift and drag coefficients of flat plates in hypersonic flow at low Reynolds number
13 p2200 A69-28358

Temperature factor effect on transition from laminar to turbulent flow in boundary layer of plate
13 p2251 A69-28558

Flat plate turbulent boundary layer, noting Navier-Stokes equations solutions and formation of rotations to determine velocity field
13 p2251 A69-28632

Flow structure in conical shock wave-sharp flat plate interaction zone in supersonic flow, noting turbulent boundary layer before separation
14 p2428 A69-28897

Three dimensional laminar boundary layer on semiinfinite permeable flat plate in viscous incompressible fluid flow, calculating velocity profiles and skin friction components
14 p2433 A69-29898

Power law fluids boundary layer near flat plate studied by series expansion and steepest descent methods, determining velocity gradient and skin friction coefficient
15 p2589 A69-30002

Steady natural oscillations of unbounded brittle plane with cut under edge load, showing decreased critical load in presence of inertial effect
15 p2703 A69-30050

Heat and mass transfer interaction at wall for laminar boundary layer on flat plate, considering catalytic effect of wall in atomic nitrogen recombination
15 p2716 A69-30415

Normal modes stability analysis of fluid layer adjacent to flat plate submerged in liquid, considering effects of interfacial surface tension and buoyant forces
[AIAA PAPER 69-386] 15 p2590 A69-30476

Uncoupled dynamic thermal stresses and displacements by heat generation in infinite flat plates, using classical thermoelasticity theory for infinitesimal displacements
15 p2709 A69-30669

Exact static exterior and interior solution of Einstein equations for thick plane plate, discussing surface energy-momentum tensor
15 p2654 A69-31477

Vortex shedding and wake formation behind inclined flat plate at low Reynolds number, using dye injector method for streak line observation
16 p2768 A69-31767

Boundary layer over impulsively started flat plate, describing flow transition from unsteady /Rayleigh/ to steady /Blasius/ state by iterative methods
16 p2769 A69-31812

Stress waves analysis in laminates design, assuming one dimensional linear elastic response to plane stress pulse on flat laminated plate surface
16 p2872 A69-31923

Temperature field in plate heated at one end and situated in solidifying gas, leading to gas layer formation by sublimation
16 p2878 A69-31957

Heat transfer in laminar separated flows with flat plate segment connections, indicating correlation between local heat transfer rates for successive regions
16 p2879 A69-32169

Free flow field from underexpanded rocket motor nozzle and impingement effects of pressure and heat transfer to flat plate
[AIAA PAPER 69-568] 16 p2842 A69-32693

Two dimensional plate theory with moment stress considerations derived from three dimensional elasticity theory, discussing reduction of equilibrium and compatibility equations
16 p2876 A69-32786

Monograph on Navier-Stokes equations with integral relations approximate solution and application to flow around flat plate of finite length
17 p2949 A69-32993

Blockage effects of flat plates and solid bluff bodies in closed wind tunnels compared concerning drag coefficient values
17 p2890 A69-33245

Temperature determination of thick flat plate rotating in space in solar flux with one surface insulated compared with Apollo heat shield results
[AIAA PAPER 69-614] 17 p3071 A69-33266

Air resistance effect on transverse vibration damping of flat specimens of heat resistant alloy, duraluminum, Ti, Mo and Nb
17 p2991 A69-33947

Discrete element displacement method applied to buckling analysis of flat rectangular plates under arbitrary membrane loading, calculating critical load intensities
17 p3066 A69-34048

Stress field in elastic contact area vicinity of hollow sphere subjected to normal load through flat plate, noting contact life
[ASME PAPER 69-LUBS-5] 18 p3212 A69-34383

Three dimensional incompressible wake behind blunt obstacle at leading edge of flat plate compared with mathematical model by Oseen linearization
18 p3083 A69-34403

Boundary layer transition from laminar to turbulent flow on flat plate, considering supersonic and hypersonic flow, pressure gradients, surface curvature and roughness, etc
18 p3123 A69-34920

Standing twin vortices in wake behind thin flat plate normal to flow visualized by Al dust, noting Karman vortex street
18 p3086 A69-35167

Boundary layer equation for steady incompressible flow past flat plate with parabolic leading edge, obtaining series solution in inverse powers of Reynolds number
18 p3124 A69-35270

Accelerometer force balance method for measuring aerodynamic rocket plume forces acting on flat plate model in short duration shock tunnel test environments
19 p3292 A69-35737

Hypersonic rarefied gas flow past flat plate with sharp leading edge and past circular cylinder, noting wake structure similarity to viscous theory prediction
19 p3294 A69-35755

Boundary conditions of incompressible fluid viscous flow on semiinfinite plate edge defined using difference methods for Navier-Stokes equations
19 p3299 A69-36394

Heat flux densities and Reynolds potentials in turbulent boundary layer on heated flat plate with wall suction
19 p3452 A69-36722

Incompressible fluid flow of given density and kinematic viscosity near trailing edge of flat plate
20 p3458 A69-37098

Surface pressure, skin friction and heat transfer measurements on sharp flat plates and wedges in low density hypersonic flow, noting slip velocity
20 p3458 A69-37186

Monte Carlo simulation for studying rarefied hypersonic gas flow about slender cones and flat plates
20 p3459 A69-37902

Unsteady boundary layer flows of compressible fluid over semiinfinite flat plate, discussing heat transfer rate
20 p3518 A69-38318

Momentum and energy equations for fluctuating flow of viscous incompressible conducting fluid past flat plate with time dependent suction under transverse magnetic field
21 p3691 A69-38445

Turbulent skin friction coefficients of compliant surfaces on flat plates determined as function of speed for different materials
21 p3695 A69-39039

Velocity and temperature profiles at Prandtl number values obtained for unsteady laminar free convection on infinite vertical plate with stepwise varying temperature
21 p3853 A69-39681

Thermal boundary layer formed during laminar jet flow over flat porous plate, discussing temperature distribution and mass transfer at plate surface
21 p3854 A69-39846

Velocity profile and skin friction in boundary layer on flat plate with periodic vorticity near leading edge
22 p3929 A69-40015

Laminar viscous flow and skin friction near trailing edge of flat plate analyzed by modified Oseen approximation, noting accuracy for high Reynolds numbers
22 p3930 A69-40683

Unsteady viscous flow past flat plate based on Stokes approximation, calculating shear stress
22 p3931 A69-40684

Forced convection liquid flow past heated flat plate with variable viscosity and thermal conductivity, analyzing velocity and temperature distribution in boundary layer
22 p4051 A69-40685

Strong interaction between hypersonic boundary layer over flat plate and associated inviscid flow, discussing heating and vorticity effects, boundary layer edge, etc
22 p3860 A69-40896

Space-time behavior of random pressure field of turbulent boundary layer on plane plate surface
22 p3933 A69-41027

Nonlinear random vibrations excitation in rectangular flat plate with initial imperfection by white noise, assuming clamped boundary conditions
22 p4048 A69-41183

Unsteady periodic boundary layer stability on flat plate, presenting model for disturbance wave packet propagation streamwise pressure gradients effects in transition flow
23 p4152 A69-41888

Hypersonic turbulent flow heat transfer and pressure data for flat plate containing steps and cavities obtained in hypersonic wind tunnel
[AIAA PAPER 68-673] 23 p4060 A69-41902

Boundary layer separation and free mixing phenomena between streams behind thin flat plate by finite difference methods and Prandtl exchange coefficient
23 p4060 A69-41912

Natural vibrational frequencies of uniform thin elastic isotropic flat plates, investigating rectangular and parallelogram plates with various edge conditions
23 p4233 A69-42348

Flat square plates loaded along two opposite straight edges, analyzing postbuckling behavior and geometric imperfections effects
23 p4234 A69-42395

Hypersonic viscous interaction, studying axisymmetric flow over slender sharp nose cones at zero angle of attack and three dimensional flow over sharp flat plate
24 p4248 A69-43579

Mean velocity and pressure fields in turbulent boundary layer on flat plate at Mach 2 investigated for ratios of mass flow
[AIAA PAPER 68-129] 24 p4304 A69-43581

Compressible laminar boundary layer behind shock or thin expansion wave past moving flat plate solved by transforming governing equations into Blasius equation
24 p4305 A69-43596

Quasi-steady laminar flat plate boundary layer in shock tube determined by reducing boundary layer equations to linear differential equations
24 p4305 A69-43632

Wake development from turbulent boundary layers on both sides of thin flat plate
24 p4249 A69-43694

Jet dynamic characteristics injected into supersonic air slipstream incident on flat body, calculating configuration, shock wave geometry and parameters distribution in flow field
24 p4250 A69-43710

FLAT SURFACES

Directly backscattered light /echoes/ from dielectric plane surface with roughness and volume scattering, comparing indicatrices with moon echo
06 p0887 A69-17173

Electromagnetic wave propagation over constant impedance flat earth, using electromagnetic compensation theorem
10 p1655 A69-23422

Plane contact problems in elasticity theory allowing for cohesive forces solved by integral and differential equations
15 p2706 A69-30578

Flat surfaces downstream of heated section and porous strip, determining film cooling effectiveness and heat flux from heat transfer coefficients ratios
20 p3631 A69-37096

Circular liquid jet oblique impingement on flat surface, noting dry zone occurrence at small angles due to lateral flow deflection
21 p3691 A69-38551

Three dimensional turbulent boundary layer over flat surface in incompressible flow calculated by finite difference method based on time averaged motion equations integration
21 p3693 A69-38767

FLATTENING

Earth ellipsoid fundamental parameters for calculation of earth flattening and normal acceleration due to gravity
09 p1487 A69-21633

Plastic bending of thin walled pipes taking into account cross section flattening
21 p3835 A69-38868

FLATWORMS

Population feedback control in planarians by fission suppression by brain near other planarians
14 p2406 A69-28871

FLAW DETECTION

U NONDESTRUCTIVE TESTS

FLAWS

U DEFECTS

FLEXIBILITY

Spacecraft control system and flexible structures interactions, discussing transient phenomena, limit-cycle oscillations and instabilities
[AIAA PAPER 69-116] 06 p1019 A69-18187

Field approach for stress and deflection analysis in rectangular plates reinforced by straight ribs, noting kernel function
11 p1983 A69-25019

Linearized theory for stability of self acting gas journal bearings with noncircular members and elements of flexibility and damping, noting three lobed rotor
[ASME PAPER 68-LUBS-45] 13 p2266 A69-27277

Flanges flexural rigidity effect on load carrying capacity, failure mechanism and postbuckling behavior of webs in shear, noting permissible load
18 p3227 A69-35492

Unfilled Pyrrone prepared from powder into molded parts for flexural tests at elevated temperatures observed for stability to electron irradiation in air
19 p3356 A69-35529

Flexible-rigid hybrid polyimide-epoxy glass multilayer board to fill gap between all flexible and all rigid circuit boards
19 p3319 A69-35545

Flexible circuitry for reliable spaceborne data processing equipment electronic packaging
22 p3903 A69-39951

FLEXIBLE BODIES

Flexible finite cylindrical shell undergoing arbitrary temporal and spatial motion, determining fluid /aerodynamic/ forces acting on shell
01 p0005 A69-10229

Structural designs for minimum flexibility or weight using energy intensity per unit mass parameter
02 p0345 A69-12380

Flexible vehicle control, using cybernetic model for system design and response
[AIAA PAPER 69-115] 06 p1018 A69-18088

Nonlinear large amplitude vibrations of flexible beam with pinned ends supported simply on rigid base noting frequencies, modes, waveforms and stress distribution
[ASME PAPER 69-VIBR-43] 10 p1807 A69-24181

Flexible cylinder vibration in nominally axial flow, discussing length, mass, flexural rigidity and diameter variation effects on vibration amplitude
11 p1984 A69-25166

- Dynamic modeling for spin stability of satellites with flexible parts, noting torques induced by attitude control
11 p1994 A69-25533
- Flexible skirt design for air cushion vehicle consisting of semicylindrical elements and permitting horse power and cost reductions
13 p2203 A69-28179
- Linear analysis of damped flexibly mounted rolling element bearings influence on dynamic rotor unbalance response, including optimum support characteristics
[ASME PAPER 69-LUBS-8]
18 p3212 A69-34382
- Lumped parameter simulation model, based on vector mechanics for flexible spinning bodies, to study spin stabilized spacecraft or turbine rotors
19 p3280 A69-35990
- Liapunov stability theory for motion of spacecraft with flexible and moving parts in force free space
[AAS PAPER 68-125]
20 p3617 A69-37180
- Peristaltic pumping in circular cylindrical tube, discussing viscous fluid flow induced by axisymmetric traveling sinusoidal wave imposed on flexible tube wall
[ASME PAPER 69-APMW-3]
24 p4275 A69-43108
- FLEXIBLE WINGS**
NT PARAWINGS
- Velocity field generated by vibrations propagating at finite velocity over elastic wing surface
02 p0190 A69-12571
- Root locus method applied to longitudinal and lateral stability of aircraft with flexible fuselage and wing
04 p0677 A69-14835
- NASA research on flexible and stiffened flexible wings, discussing range of applicability, aerodynamic characteristics and wind tunnel results
05 p0701 A69-15568
- FLEXING**
- Flexural waves passage through obstacles in infinite plate, determining vibration arresting properties of rigid ribs, elastic inserts and hinged couplings
04 p0678 A69-14902
- Flexural wave reflection from corner joint between plates, establishing reflection coefficient dependence on wave frequency
04 p0679 A69-14903
- Anodizing effect on flexural properties of Al-aluminum oxide sandwich composites, emphasizing properties of oxide coatings as function of thickness
07 p1159 A69-18723
- Conformal mapping method for flexure function determination, discussing shear coefficients for arbitrary cross section beams in Timoshenko beam theory
09 p1612 A69-21611
- Four point flexure, ring flexure and NOL ring tension tests for evaluation of composite material mechanical properties
09 p1499 A69-22308
- Electric analogy technique for torsion and flexure functions of uniform beams with terminal loads, considering Neumann boundary value problem
11 p1195 A69-25649
- Elastic mirror flexure and distortion patterns, considering periodic nature of load in polar coordinates, second flexure mode avoidance and friction elimination
12 p2056 A69-26407
- Antiflexure cylinder for large astronomical mirror, noting support by astatic counterpoint levers and simple flanges
12 p2056 A69-26409
- Flexural waves passage through obstacles in infinite plate, determining vibration arresting properties of rigid ribs, elastic inserts and hinged couplings
12 p2182 A69-26655
- Flexural wave reflection from corner joint between plates, establishing reflection coefficient dependence on wave frequency
12 p2182 A69-26656
- Woven roving construction and fill/warp ratio effects on flexural strengths of four ply laminates
14 p2469 A69-29414
- Membrane analogy for flexure of prismatical beams with square cross section and longitudinal cavities, employing Saint-Venant solution
15 p2704 A69-30288
- Flexure of Ta and Nb thin rectangular specimens during high temperature oxidation, showing stress generation due to O dissolution into metal surface
[ECS PAPER 87]
15 p2641 A69-31541
- Flexure functions of triangular sections under terminal loads, using electric analogy to study function effect on section shape and material Poisson ratio
17 p3066 A69-34050
- Structural flexure center position from shear stress analysis showing nondependence on Poisson ratio
20 p3622 A69-37213
- Deformation tractions in undeformed and curved cuboid flexure and inverse flexure determined by stress-strain relations for homogeneous isotropic compressible materials
23 p4226 A69-41521
- FLEXURE**
U FLEXING
- FLICKER**
- Ohz intensity variation in bright homogeneous auroras prior to and during breakup observed visually and with image orthicon TV systems
04 p0594 A69-15129
- Painted helicopter rotor blades ruled out as cause of flicker induced vertigo, reporting pilots psychophysiological responses to formation flying
17 p2913 A69-33175
- Flicker characteristics of eye color receptive systems by measuring modulation thresholds for sinusoidal flicker of color superimposed on complementary color background
22 p3880 A69-40851
- Hue shift and brightness enhancement of flickering light measured as function of illuminance, wavelength and target size
22 p3882 A69-40871
- FLICKER FUSION FREQUENCY**
U CRITICAL FLICKER FUSION
- FLIGHT ALTITUDE**
- Optimum cruise altitude, block time and fuel relations for Convair 600/640 aircraft for various temperatures, segment distances and weight
08 p1255 A69-21007
- Fast and slow neutron latitude variation at aircraft altitudes during solar minimum, noting environment effects on measurement
09 p1574 A69-21402
- Supersonic flight altitude stability, studying effects of velocity, lift-drag ratio, thrust law, wind direction, engine unstarts, etc
[AIAA PAPER 69-813]
19 p3366 A69-35627
- STOL takeoff optimal trajectory maximizing altitude at given runway distance, using aircraft models
[AIAA PAPER 69-935]
21 p3649 A69-39427
- Flight altitude effects on pilot performance with comparison of sensory and mental functions, considering oxygen use and flight safety
23 p4106 A69-41794
- Atmospheric variability at proposed flight levels, analyzing meteorological requirements of SST operations, discussing annual cycles in stratospheric circulation
24 p4251 A69-42711
- FLIGHT CHARACTERISTICS**
- Boeing 747 characteristics for passenger and cargo service noting economic gain, operational performance, control cabin, engine, etc
[AIAA PAPER 67-397]
01 p0010 A69-10636
- Flight vehicle dynamics, discussing classical mechanics, fluid dynamics, structural dynamics and thermodynamics
02 p0193 A69-11985
- Flying qualities considerations in design and development of Huey Cobra for helicopter attack mission, describing stability and control augmentation systems
[AHS PAPER 217]
07 p1053 A69-18871
- Coaxial multipurpose KA-26 helicopter design, discussing cruising speed, passenger capacity, range, flight ceiling, gross weight and piston engines
07 p1053 A69-18969
- Bow shock wave position and shape in rectilinear flight with constant acceleration
09 p1433 A69-21386
- Schleicher glider AS-W15 prototype tests, discussing balsa sandwich structure and flight characteristics
10 p1633 A69-22872
- Approximation formula for calculating descent speed and lift-drag ratio
10 p1633 A69-22873
- VTOL aircraft flight control systems, considering computerization and automation approach with human pilot serving as monitor and emergency system
11 p1823 A69-25387
- Digital computerized analysis and characteristics of variable stability aircraft, examining digital control system
15 p2549 A69-30229
- Bow shock wave during rectilinear flight with varying acceleration, describing sonic boom loop mechanism
16 p2734 A69-32005
- Flight performance prediction for throttling bipropellant rocket engine utilizing ablative combustion chamber throat, discussing lunar module descent engine
[AIAA PAPER 69-452]
16 p2841 A69-32690
- Running test facility for study of aerodynamics and flight dynamics of V/STOL aircraft models
17 p2944 A69-32851
- Military V/STOL aircraft flying qualities specification, considering structure, hover and low speed requirements, forward flight, transition maneuverability and control
[AHS PAPER 363]
17 p2900 A69-33520
- Mission task performance oriented approach to winged helicopters flying and handling qualities, considering wings and horizontal stabilizers influence
[AHS PAPER 360]
17 p2900 A69-33522
- Interim revision of military flying qualities specifications according to experimental data and characteristics of existing aircraft
[AIAA PAPER 68-245]
17 p2902 A69-34026
- Performance capabilities and handling quality characteristics of aircraft equipped for in-flight thrust reversing
[AIAA PAPER 68-880]
17 p2902 A69-34031
- Aerodynamic and flight characteristics of variable geometry entry spacecraft during subsonic wing deployment and landing
[AIAA PAPER 69-742]
18 p3084 A69-34407
- Flight performance analysis of space systems, discussing preparation, implementation and communication
18 p3206 A69-34501
- Longitudinal flying qualities evaluation by pilots in carrier approach flight simulation, describing experiment apparatus, procedures and results
[AIAA PAPER 69-895]
21 p3648 A69-39419
- Aircraft flying qualities research program, discussing Navy test pilot evaluations and longitudinal handling characteristics for simulated carrier landing task
[AIAA PAPER 69-897]
21 p3648 A69-39421
- Longitudinal flying qualities of aircraft, comparing attitude and altitude control data
[AIAA PAPER 69-898]
21 p3648 A69-39422
- Wind tunnel tests determining propeller slipstream effect on roll-damping derivative in transitional flight region, estimating STOL aircraft characteristics
22 p3863 A69-40145
- Flight range and fuel consumption formulas of power gliders used for transportation compared with automobiles
24 p4253 A69-43142
- Measurement methods for quantitative character of aircraft pilot rating scales for vehicle flying qualities, considering wording ambiguity, dual mission character, etc
24 p4276 A69-43326
- FLIGHT CLOTHING**
- Liquid fluidic amplifiers combined into controller for modulating coolant temperature to control flight suit temperature automatically
02 p0202 A69-11923
- Quality assurance impact energy attenuation testing of U.S. Army flyer protective helmet, considering combined interaction of shell, foam liner and plastic pads
15 p2559 A69-30851
- FLIGHT CONDITIONS**
- Weightlessness effects on organism in space flight along parabolic trajectories, discussing interaction between analysts
02 p0197 A69-11499
- Mission requirements influence on aerothermodynamic environment for vehicle entering Venus atmosphere, considering different entry modes
02 p0332 A69-12823
- Aircraft reports of high level turbulence on European and Atlantic routes, noting rapid changes in large scale flow pattern occurring locally
12 p2127 A69-26901
- Flight and piloting influence on morbidity of civil aviation personnel, noting incidence of enteric, hemorrhoidal and respiratory diseases
18 p3098 A69-35303
- Illumination effect on air navigation chart reading during flight, using questionnaire data
24 p4271 A69-42605
- Human circulatory reactions to cumulative flight vegetative stimuli evaluated by cumulative stress simulation method
24 p4266 A69-43375
- FLIGHT CONTROL**
NT AUTOMATIC FLIGHT CONTROL

NT AUTOMATIC LANDING CONTROL NT THRUST VECTOR CONTROL

Airline area navigation system functions for developing map type pictorial display system including digital computer, cockpit control unit and microfilm charts
01 p0112 A69-10453

Hydraulic powered flight control system for Jaguar supersonic military training aircraft
01 p0012 A69-10634

Optimal flight stabilization of VTOL aircraft in hovering mode based on linear rotation dampers system
05 p0702 A69-16024

Variable properties aircraft for flying simulator, discussing flight control system and stability behavior
07 p1052 A69-18254

Direction changing of large solid propellant motors by changing jets angle or gas injection
07 p1230 A69-19291

Rocket vehicle inertial attitude reference system, discussing flight control
09 p1609 A69-21618

Helicopter all-weather flight control system, using autostabilization and artificial horizon
09 p1435 A69-22778

Astronautics - Conference Braunschweig, West Germany, October 1968, Volume 1, Flight control and electronics
12 p2127 A69-25870

Hypersonic vehicles multivariable flight control systems, analyzing flight path in terms of equation of motion of longitudinal mode
12 p2128 A69-26066

Dynamic analysis methods for airframe flight control design noting equations of motion, system criteria and analysis and synthesis methods
[AIAA PAPER 68-832] 12 p2174 A69-26758

Helicopter stabilization systems design using optimal control theory to obtain multivariable feedback controller
12 p2014 A69-26764

GHOST Balloon Project, emphasizing launch and ascent control and location and life expectancy of superpressurized balloons in tropical stratosphere
15 p2551 A69-31361

Flight and space mechanics problems from engineer standpoint, discussing flight path calculation, stability and control characteristics and experimental techniques for high reliability
17 p3076 A69-33041

VTOL variable stability system /VSS/ for XV-4B lift jet for flight control and handling verification
17 p2902 A69-34066

Solid state single unit digital control computer performing stability augmentation, pilot relief functions and generating minimum fuel flight paths for VTOL landing
17 p2934 A69-34075

Optimum automatic system for controlling helicopter formation flight, stressing transient response Q factor and transmission ratios
18 p3090 A69-34656

Flight control systems influence on military aircraft design and performance, discussing static stability, ride quality, flutter margin and maneuver load controls
[AIAA PAPER 68-767] 19 p3245 A69-35656

Mars autonomous entry navigation, discussing flight path angle control with onboard sensors using realistic sun, Canopus and planet line of sight tracker accuracies
19 p3368 A69-35790

Computerized clock sequenced ATC system, area navigation /R Nav/ systems and STOL flight control
19 p3370 A69-36317

Flight control and stability of STOL transport aircraft with powered-lift boundary layer control system augmented lift
20 p3462 A69-37513

Design concepts and principles of systems for monitoring of Concorde flight control actuators, considering servo control, control interconnections and control input system
20 p3467 A69-38190

Titan 3C launch vehicle digital flight control system using flight equations time-shared with guidance equations
[AIAA PAPER 69-878] 21 p3824 A69-39404

Model performance index /PI/ providing criterion for approximating one dynamic flight control system by another based on geometrical representation of linear autonomous systems
[AIAA PAPER 69-885] 21 p3764 A69-39410

NF106B-VST model follower flight control system, discussing design criteria/performance index,

rigid/elastic math model development, flight test evaluation, hardware design, etc
[AIAA PAPER 69-886] 21 p3764 A69-39412

Real time operating system /RTOS/ 360 for spaceflight control, describing hardware, applications, task management and capacity, etc
21 p3679 A69-39602

Design criteria for Concorde SST servoflight control system reliability and safety
21 p3650 A69-39697

Atlas/Centaur/Surveyor flights guidance accuracy, discussing postflight analysis of injection errors due to hardware, software and propulsion system
[AIAA PAPER 68-842] 24 p4348 A69-43239

Quadratic optimization applied to helicopter flight control design, assuming constant feedback gains and command step input with zero steady state error
24 p4253 A69-43279

FLIGHT CREWS

Airline crew training, requalification, recurrent, upgrading and aircraft transition training for crew and pilot
01 p0019 A69-10450

Psychological aspects of crew members resistance to eject from aircraft in trouble
06 p0877 A69-16956

Survival of aircrew after successful ejection over water and boarding life raft
06 p0878 A69-16958

Psychophysiologic factors in USAF aircraft mishaps involving ground egress
06 p0878 A69-16959

Clinical analysis of combat and noncombat ejection experience of USAF
06 p0878 A69-16960

Hand operated visual signaling devices, discussing Mini Signals and cartridge load aerial signals
06 p0878 A69-16962

Cardiovascular disease incidence among airline flight deck personnel in relation to increase in average age of personnel
06 p0875 A69-17848

Psychological study of stewardesses for depressive, neurotic and psychosomatic episodes, discussing psychopathological structures corresponding to etiological sequences
07 p1067 A69-19434

Head injuries evaluation in aircrew, noting motor cycle accidents
10 p1649 A69-23378

Aircrew incapacitation during high altitude flying following partial gastrectomy, discussing aeromedical evaluation
10 p1645 A69-23381

Traditional flight crew organization relevance to current and developing flight systems, discussing inadequacies, anachronisms and safety threats
12 p2023 A69-26555

Computer simulation models for prediction of individual and crew performance in man machine environments
12 p2026 A69-27087

Psychophysiologic factors in USAF aircraft mishaps involving ground egress
15 p2558 A69-30462

Problems connected with rescue of crew members ejected over water
15 p2551 A69-30866

Concorde aircrew seats design for electric operated tracking and lift, vertical movement accommodation seat and back tilt
15 p2553 A69-31167

Diurnal periodicity of physiological functions of flight crews flying through several time zones found to correspond to time zone of permanent residence
17 p2906 A69-32935

Optimized flight crew training, evaluating safety, flight simulator efficiency, takeoff/landing practice and line experience based on test results
[AIAA PAPER 69-771] 19 p3245 A69-35653

Flight surgeon observations of stress and fatigue effects on aircrew of first nonstop transatlantic helicopter flight, discussing fatigue ratings, sleep patterns, etc
19 p3262 A69-36450

Electrocardiographic and heart rate data recording of crew members during transatlantic helicopter flight and normal daily routine
19 p3263 A69-36451

Urinalysis of crew members of first transatlantic helicopter flight indicating interindividual endocrine-metabolic variability and circadian trends modification
19 p3263 A69-36452

Vestibular function tested with angular acceleration, applying semicircular canal reflexes for flight crew selection and appraisal
20 p3481 A69-37271

Cabin personnel occupational strain in civil aviation, relating heart rate to aerobic power while working during flight
21 p3665 A69-39180

Statistics on airline flight crew members grounding due to psychic disorders
21 p3665 A69-39181

Mandrax and barbiturates effects on aircrew reaction time, response time and tracking ability
21 p3661 A69-39274

Cosmic radiation exposure of passengers and crew in supersonic transport at high altitude
22 p4002 A69-40093

Computerized crewstation geometry evaluation and design optimization using 23-pin-joint man-model
[AIAA PAPER 69-977] 22 p3892 A69-40357

Pilots and flight crews screening and training by supplemental air carriers
22 p4054 A69-41148

Air traffic safety enhanced through flight crew awareness of hazards, clear air turbulence detection and avoidance, collision avoidance, etc
22 p3868 A69-41151

Flying effects on air hostesses, considering questionnaire data for various psychophysiological factors and flight modes
23 p4086 A69-41688

Psychotherapeutic treatment of depressions and neuroses in flight crews, noting face to face method effectiveness
23 p4086 A69-41690

SST flight crew operational requirements to achieve maximum human efficiency and man/machine compatibility, discussing pilot role, advanced flight instrumentation, etc
23 p4107 A69-41820

Renal calculus incidence among aircrews of long and short haul airlines, considering effects of dry cabin environment and dehydration
23 p4108 A69-41826

Flight personnel hearing tests per ICAO recommendations and flight safety requirements, using tonal audiogram and vocal audiometric test
24 p4277 A69-43377

Psychiatric morbidity as absenteeism cause among ground and flight personnel in civil aviation, recommending psychotherapy and chemotherapy
24 p4266 A69-43378

In-flight medical disorders sustained by crew members of various aircraft in French Air Force correlated with aircraft accidents, flight experience and age
24 p4277 A69-43383

Airline pilots simulated incapacitation involving myocardial infarction or cerebrovascular accident, discussing effect on crew behavior during flight task performance
24 p4277 A69-43386

Medical wastage of military and civil aviators in Great Britain /1963-1968/, discussing cardiovascular disease, fatal flying accidents and psychiatric disease
24 p4277 A69-43391

Hyperventilation effect on flight personnel, discussing oxygen and carbon dioxide partial pressures, symptoms and clinical signs
24 p4269 A69-43410

FLIGHT FATIGUE

Helicopter flight loads spectra data compared on statistical basis to establish component service lives
[AHS PAPER 301] 17 p2901 A69-33548

Flight surgeon observations of stress and fatigue effects on aircrew of first nonstop transatlantic helicopter flight, discussing fatigue ratings, sleep patterns, etc
19 p3262 A69-36450

Aircrew fatigue and sleep loss factors, discussing transition through various time zones and flying through normal sleeping times
21 p3666 A69-39275

FLIGHT FITNESS

Cardiovascular disease incidence among airline flight deck personnel in relation to increase in average age of personnel
06 p0875 A69-17848

Airline pilot incapacitation by death or terminal collapse due to organic causes while on duty, noting incidence and resulting accidents
06 p0883 A69-17849

Standards for EEG in pilot fitness examinations, analyzing effects of total flying hours
06 p0875 A69-18021

Blood pressure fluctuations in multiple extra systoles during tilt table studies for flying fitness of pilot
10 p1645 A69-23379

Aircrew incapacitation during high altitude flying following partial gastrectomy, discussing aeromedical evaluation
10 p1645 A69-23381

Passenger aircraft flight readiness verification, discussing flaw and corrosion detection and rivet joint inspection methods
11 p1822 A69-24526

Astronauts physical training for space flight requirements
13 p2215 A69-28611

Visual, auditory and reaction-time responses in aging pilots, determining continuing capacity for choice and discrimination with advancing age
14 p2408 A69-29307

Physical exercises to increase cosmonaut space environment tolerance, discussing effects of acceleration, altitude and hypoxia
15 p2560 A69-31460

Pilots mental and physical welfare, discussing roles of mental hygiene and preventive medicine in flight surgeons programs
18 p3097 A69-35301

Boeing 747 design, fitting to operation, airline planning for flight training, airport facilities, ground equipment, service functions, etc
[RAES PAPER 12]
22 p3864 A69-40621

Serial ECG change from normal conduction to right bundle branch block in 59 patients without overt cardiac disease
23 p4085 A69-41677

Civil pilots medical certification after head trauma, evaluating current methods efficiency
23 p4086 A69-41687

Senior commercial jet pilots ability to visualize flight instruments
23 p4089 A69-41829

Flight personnel hearing tests per ICAO recommendations and flight safety requirements, using tonal audiogram and vocal audiometric test
24 p4277 A69-43377

FLIGHT HAZARDS
NT METEOROID HAZARDS

Flight accident rate of U.S. physician pilots noting relation to number of takeoffs and landings
01 p0022 A69-11344

Physiological effects of space cabin environment variables during long and hazardous space missions with regard to engineering constraints and radiobiology
03 p0380 A69-13504

Light aircraft hazards due to trailing vortex generated by heavy transport aircraft, suggesting specific procedures for takeoff, landing and flight phase
[SAE PAPER 680220]
04 p0549 A69-14930

Explosive devices to sabotage aircraft in flight, discussing evidence of sabotage in aircraft wreckage and detection of explosives before loading
04 p0549 A69-14943

Frequencies and natural oscillation modes in sporting gliders, demonstrating horizontal oscillation induced aileron suspension brackets destruction
04 p0549 A69-15416

Concorde and Boeing supersonic transport overland sonic booms, discussing social, political and legal reactions
06 p0868 A69-17899

Aircraft safety hazards due to birds, discussing radar role in plotting bird migrations
11 p1837 A69-25247

Physiological effects of intermittent light stimulation during helicopter flight, discussing visual and electric cortical functions at critical frequency threshold of subjective fusion
13 p2211 A69-28595

Interspecific synthetic signals research for effective bioacoustic bird scaring techniques including optical signals
17 p2914 A69-33364

Airfield bird scaring methods including Very pistol shell cracker firing and broadcast calls on civilian and military airfields
17 p2915 A69-33365

Radar cross section of bird represented as unit density dielectric spheroid for bird hazard monitoring, discussing meteorological, insect and bird echoes
17 p2919 A69-33366

Bird warning and forecast systems based on radar data covering 50 mile radius from airport
17 p2899 A69-33367

Radiation exposure during orbital flight assessed for adverse effect on space stations and laboratories personnel, discussing shielding and dose rate tables
20 p3481 A69-37339

Infectious diseases in space flight, considering environment role in infection transmission, occurrence and severity
20 p3479 A69-37973

Flying effects on air hostesses, considering questionnaire data for various psychophysiological factors and flight modes
23 p4086 A69-41688

Military pilots cervical spine dynamic X ray studies, comparing spine curvature and rectitude of jet and nonjet pilots and nonflying personnel
23 p4087 A69-41798

Contact lenses hazards during high altitude aircraft piloting analyzed via bubble development
23 p4106 A69-41806

FLIGHT INSTRUMENTS
NT APPROACH INDICATORS
NT ATTITUDE INDICATORS
NT AUTOMATIC PILOTS
NT HORIZON SCANNERS
NT RADIO ALTIMETERS

Head-Up Display /HUD/ flight information applied to civil aviation, noting operational safety improvement and pilot work load reduction
01 p0020 A69-10635

In-flight measurement of shock and vibration effects on aircraft and propulsion systems
01 p0084 A69-11051

Aircraft cockpit displays design for flight control and navigation, discussing integration, pictorial realism, moving part, pursuit tracking, frequency separation and optimum scaling
02 p0203 A69-12213

Engine air intake for operational Harrier V/STOL strike/reconnaissance fighter, describing intake instrumentation ring, temperature and pressure probe development and pressure recording
05 p0767 A69-16773

Flight deck equipment guidelines in aircraft, discussing pilots natural senses, visual information, displays, logic and memory capable computers and ground controller
08 p1266 A69-20450

Air data system consisting of aerodynamic and thermodynamic sensors and computer calculating flight parameters for automatic flight control
18 p3169 A69-34854

Situation displays and flight instrument development including head-up, vertical tape and map systems
18 p3170 A69-34858

Cumulative error in flight vehicle position determination by inertial navigation system, showing dependence on constant acceleration components
22 p3978 A69-40252

Flight indicators monitoring by pilots, describing physiological and psychotechnical criteria for dials and clocks arrangement to improve efficiency
23 p4108 A69-41827

FLIGHT LOAD RECORDERS

Aircraft reliability under cyclic loads in flight taking into account stress fluctuations
08 p1322 A69-21106

Strain gages to measure flight loads in high temperature environment, discussing selection, calibration techniques and performance characteristics
15 p2614 A69-31277

Helicopter flight loads spectra data compared on statistical basis to establish component service lives
[AHS PAPER 301]
17 p2901 A69-33548

FLIGHT MECHANICS
Hydrodynamics-electrodynamics analogies for electromagnetic flight
01 p0121 A69-11134

Atmospheric turbulence effects on aircraft flight noting causes of turbulence
11 p1911 A69-24527

Book on aerodynamics of aircraft flight covering air flow, wing geometry, forces on wings, etc
11 p1817 A69-24583

Monograph on flight mechanics and control technology of low flight vehicles at high flight velocities, discussing altitude control design, power spectra, etc
11 p1823 A69-24638

Flight dynamics problems, determining extremum of functional by graph-analytical method and with aid of Pontryagin maximum principle
11 p1823 A69-25343

Mechanical engineering applications to aerospace flight, discussing stability and piloting problems and experimental methods
11 p1824 A69-25672

Flight and space mechanics problems from engineer standpoint, discussing flight path calculation, stability and control characteristics and experimental techniques for high reliability
17 p3076 A69-33041

Book on flight mechanics of aircraft and missiles covering mass, propulsion and aerodynamic forces, TOL problems, optimization problems, etc
17 p2898 A69-33319

Torque calculations about joints of rigidly chain-like arranged clusters of flying bodies
18 p3208 A69-34776

Nervous system relations to insect flight musculature of lift and thrust mechanism
21 p3651 A69-38780

Computer program /TACTICS/ for simulating three vehicles simultaneous motion in space, considering interceptor-target guidance and intercept trajectories
[AIAA PAPER 69-890]
21 p3678 A69-39415

Collection of papers on space flight mechanics covering trajectories, motion about center of mass, optimization, control systems
21 p3828 A69-39816

Flight dynamics boundary value problem for spacecraft trajectories optimization, using variational method
21 p3817 A69-39817

Variational problem involving winged flight vehicles ascending and descending flight optimal program determination, considering necessary extremal conditions
21 p3767 A69-39823

Optimal gain theory for input vector and application to regulator problem describing aircraft dynamics
24 p4293 A69-43305

FLIGHT OPTIMIZATION

Aircraft and engine parameters for maximum theoretical range of turbojet for given cruising speed
03 p0366 A69-12950

Optimal circular satellite orbits for planetary surface mapping mission minimizing overlap
03 p0518 A69-14247

Computing optimum flight profiles by Balakrishnan epsilon method, including equations of motion constraint in cost function to be minimized
[AIAA PAPER 69-75]
06 p0868 A69-18058

Air navigation and economics, discussing air traffic control and traffic density effects on fuel consumption and engine life
07 p1052 A69-18661

Optimum cruise altitude, block time and fuel relations for Convaiv 600/640 aircraft for various temperatures, segment distances and weight
08 p1255 A69-21007

Optimal control-computation technique and application to minimal time flight profile optimization and isoperimetric problem of Lagrange with equality constraints
09 p1595 A69-21798

Vehicles optimal flights with controlled or boundary level thrust in circular orbit neighborhood, using linearized equations of motion
19 p3427 A69-36612

Flight vehicle motion optimization taking into account random failures of sectioned power plant with limited capacity and independent parallel units
21 p3647 A69-38893

Jet aircraft quasi-level flight above flat earth, deriving equation of path minimizing linear combination of fuel consumption and flight time
21 p3647 A69-39006

Interplanetary midcourse velocity correction schedules optimization, discussing timing equations modifications, mission simulation and role of earth based radar
21 p3766 A69-39646

FLIGHT PATHS
NT GLIDE PATHS

Vertical flight path navigation requirements for supersonic aircraft based on computer simulated flights of Mach 2 Concorde
02 p0277 A69-11590

Computer solution of six degrees of freedom flight equations, discussing advantages of using flight path axes for translational equations of motion
02 p0212 A69-11998

Relative weight of fuel required for flight along prescribed flight trajectory
03 p0519 A69-12964

FLIGHT PLANS

OMEGA radio navigation system optimization, emphasizing implementation of phase modulation to ensure lane identification 03 p0463 A69-13212

Navigation computer utilizing current integrators and step motors to record flight path 03 p0404 A69-13431

Air density fluctuation effects on aircraft dynamic stability around center of gravity during climbing and diving maneuvers, discussing atmospheric pressure and flight path angle 04 p0548 A69-14825

Computing optimum flight profiles by Balakrishnan epsilon method, including equations of motion constraint in cost function to be minimized [AIAA PAPER 69-75] 06 p0868 A69-18058

Optimum approach and departure paths for VTOL aircraft simulated by hybrid computer under constraints [AIAA PAPER 69-209] 07 p1178 A69-19570

Composition effect of flight path measurements on correction of space vehicles flight path, discussing single parameter correction of motion in force free field 07 p1178 A69-19607

Air traffic lateral separation assurance over North Atlantic for increased routes capacity without safety reduction 08 p1349 A69-21200

Scientific report of Rockwell polar flight, November 14-17, 1965 09 p1484 A69-21401

Polar flight navigation charts showing feasibility of three dimensional celestial positioning 09 p1538 A69-21406

Meteorological data for flight path climatologies, analyzing annual frequency distribution of maximum wind velocities 09 p1535 A69-21519

Black arrow rocket vehicle flight path computer programming, discussing geographical restrictions on design 09 p1593 A69-21616

Discrete variable approximation for computation of flight path optimization, discussing constrained and unconstrained minimizations 09 p1538 A69-22090

Hypersonic vehicles multivariable flight control systems, analyzing flight path in terms of equation of motion of longitudinal mode 12 p2128 A69-26066

Conjugate gradient methods for optimization problems with terminal constraints, noting minimum time paths for V/STOL aircraft climb phase 12 p2013 A69-26763

Complex climatological cloud profiles structural characteristics along given air traffic routes prepared for practical aviation problems 12 p2127 A69-26899

Multiple drone aircraft automatic control system, discussing preprogrammed mission path and controls of altitude, plan position and velocity 14 p2392 A69-29495

Position determination from radio bearings using complex numbers, noting application to reconnaissance flight path 14 p2479 A69-29499

Air lane longitudinal separation distance reduction for accommodating increased traffic using airborne computers for single file system 15 p2651 A69-30293

Aircraft constant altitude-pressure flight navigation attained using Bellamy formula and loxodromic route for drift compensation 15 p2651 A69-30294

Statistical correlation of temperature and tail-wind data for London-New York route at 50 mb for SST operation 15 p2651 A69-30690

Flight and space mechanics problems from engineer standpoint, discussing flight path calculation, stability and control characteristics and experimental techniques for high reliability 17 p3076 A69-33041

Integrated trajectory error display /ITED/ for flight path control of helicopters and VTOL, describing principles governing display synthesis [AHS PAPER 314] 17 p3001 A69-33541

Pictorial display area navigation system for air traffic control in terms of cockpit utilization, interface with ground navigation aids, parallel multiple routes, etc [AIAA PAPER 69-798] 19 p3367 A69-35632

Airborne astatic vertical gyro motion found dependent on aircraft motion along trajectory 19 p3311 A69-36194

Terminal air traffic management in future noting transition airspace, approach and departure paths and airport capacity [AIAA PAPER 68-1101] 20 p3573 A69-37160

Jet aircraft quasi-level flight above flat earth, deriving equation of path minimizing linear combination of fuel consumption and flight time 21 p3647 A69-39006

Aircraft navigation system requiring computer and display for approach guidance to circular orbit over fixed ground area [AIAA PAPER 69-986] 22 p3978 A69-40366

Optimal control computing method applied to minimal time flight profile optimization 24 p4383 A69-42954

FLIGHT PLANS

Great circle route determination based on celestial spherical triangulation 02 p0278 A69-12360

Soviet book on aeronautical climatologies covering methodology of climatologic indices useful for airfields, pilots and flight routes evaluation 04 p0627 A69-14935

Subjective and objective upper air forecasts for aviation comparison by isobaric pressure height fields, discussing error analysis 08 p1345 A69-19886

Optimal control computation technique and application to minimal time flight profile optimization and isoperimetric problem of Lagrange with equality constraints 09 p1595 A69-21798

Computer uses for air traffic control in Germany including flight plans and weather report data processing 15 p2650 A69-30230

Weights study of V/STOL aircraft types for similar mission and payload requirements with different propulsion systems and flight profiles [SAWE PAPER 783] 18 p3091 A69-34869

Expected occurrences mathematical model for flight system availability under uncertainty 18 p3210 A69-35083

Subsonic civil air transport navigation systems, discussing flight routes redistribution across North Atlantic to meet increased traffic 20 p3574 A69-37417

FLIGHT RECORDERS

Navigation computer utilizing current integrators and step motors to record flight path 03 p0404 A69-13431

Digital adaptive recording system /DARS/ 12 channel flight recorder 05 p0766 A69-16754

Government flight recorder regulations, detailing approved systems 10 p1691 A69-23246

Flight data recorders history and regulations, discussing parameters and design of systems 10 p1691 A69-23247

Crash protection of flight data recorders, aircraft accident investigation, systems analysis, environment and enclosures 10 p1691 A69-23248

Onboard flight data recorder as integrated system for investigating aircraft accidents, describing German LEADS 200 model 17 p2974 A69-33429

Flight performance analysis of airline pilot group related to flight recording monitoring system 22 p3868 A69-41145

FLIGHT RULES

U INSTRUMENT FLIGHT RULES

FLIGHT SAFETY

Medicinal therapy and flight safety of pilots and astronauts, discussing drug use, self treatment, tolerance and environmental factors 01 p0014 A69-10583

Light aircraft all-weather flight feasibility, discussing storm and clear air turbulence detection and icing prevention 01 p0111 A69-11049

Correlation between CAT and thermal gradient increase at standard isobaric levels found to be potential forecasting tool 02 p0275 A69-11818

Alpha numerical and symbolic information combined for head up display /HUD/ systems, providing pilot with takeoff director 03 p0379 A69-12885

Aircraft flight safety, discussing structural and aerodynamic concepts, maintenance and operations 03 p0365 A69-12886

Air safety - Conference, Dallas, April 1968 06 p1040 A69-16834

Government role in air transportation policy, considering growing demands on air traffic control 06 p1040 A69-16835

Air safety, emphasizing misunderstandings or unresolved problems in accident prevention connected with law/safety interface 06 p1040 A69-16837

FAA aviation safety program design standards, maintenance and inspection procedures and assessment of accidents 06 p1041 A69-16839

Airline safety programs focused on developing reliable automatic landing system, realistic pilot training and airborne monitoring/recording system 06 p1041 A69-16840

Aviation safety information dissemination to improve accident and incident prevention 06 p1041 A69-16841

Manned space flight safety, discussing astronaut exposure to danger on ground, in training and in space mission 06 p0882 A69-17650

Flying safety and human factors relationships from job classification survey oriented toward social psychology 06 p0884 A69-18035

Apollo spacecraft fire, presenting recommendations for power supply, cabin atmosphere and safety measures 07 p1071 A69-18970

System reliability influence on air accidents resulting from pilot errors, unforeseen obstacles, breakdowns and atmospheric effects 07 p1054 A69-19288

Helicopter flight safety as function of service duration, performance limitations and propulsion failure 07 p1054 A69-19313

Pilot protection against laser hazards, discussing protective eyeglasses, fireproof clothing and materials 07 p1072 A69-19436

Permissible irradiation doses established for spacecraft crews making short and long flights, considering roles of life span, somatic effects, leukemia and genetics 07 p1069 A69-19618

NASA flight safety research, discussing size effects on aircraft handling and built-in response to failure modes 07 p1057 A69-19764

STOL and V/STOL role in eliminating air traffic congestion at U.S. and West European airports and in short haul and municipal routes 08 p1254 A69-20093

Analog video processor in omnidirectional radar system for flight safety, discussing construction, transistorization and circuitry 08 p1276 A69-20605

Aircraft reliability under cyclic loads in flight taking into account stress fluctuations 08 p1322 A69-21106

Howell engine hot section analyzer /HSA/ developed to improve maintenance, flight safety and costs of jet aircraft engines 10 p1671 A69-23263

Cockpit TV-radar for providing pilots with navigation, weather and traffic data, discussing safety factor and radar picture transmission quality [SAE PAPER 690327] 11 p1833 A69-24506

Collision avoidance system for air traffic, discussing false signal discrimination via electronic measurement of light pulse duration from aircraft Xenon discharge beacon lamp 12 p2129 A69-26772

Air Canada flight safety system including company philosophy, safety activities, incident and accident handling and information schemes 13 p2201 A69-27541

Flight regularity and safety in complex meteorological situations, noting synoptic forecasting advantages over inertial forecasting 14 p2475 A69-29740

Flight worthiness of mishandled electronic equipment, analyzing fragility and performance of shock exposed components and connections 15 p2576 A69-30362

Medicinal therapy and flight safety of pilots and astronauts, discussing drug use, self treatment, tolerance and environmental factors 15 p2555 A69-30753

Flying offenses committed by private and professional pilots in Great Britain, discussing role of authorities involved 17 p3077 A69-34202

Aviation health service for flight safety problems with emphasis on accident prevention, emphasizing physician role in man-machine relationship of personnel surveillance

18 p3098 A69-35305

Manual extinguisher using bromochlorodifluoromethane (BCF) for aircraft cabin fire protection, discussing design and low toxicity, corrosiveness and cost

19 p3256 A69-36863

Apollo spacecraft fire, presenting recommendations for power supply, cabin atmosphere and safety measures

20 p3483 A69-38218

System analysis in aerospace software including ground checkout software, command and control software and onboard programs

[AIAA PAPER 69-962] 22 p3905 A69-40343

Air safety - Conference, Anaheim, October 1968

22 p3866 A69-41127

Accident prevention program of Bureau of Aviation Safety, discussing probable cause analysis and function in feedback loop, hazard analysis and accident data center

22 p3867 A69-41140

SST stratospheric environment problems, discussing temperature effects on fuel consumption and convective turbulence effect on flight safety and efficiency

22 p3867 A69-41141

Aircraft pilots medical disabilities as potential flight safety hazard, discussing aerospace medical specialist role and pilot education in symptoms evaluation

22 p3894 A69-41146

Air traffic control transoceanic satellite system for minimizing navigation errors forcing wide separations, providing VHF voice communication and position surveillance

22 p3901 A69-41147

Airline management service to cockpit team for safe operation providing safety information sources and transmission channels and undesirable trend detection and correction

22 p4054 A69-41149

Air traffic safety enhanced through flight crew awareness of hazards, clear air turbulence detection and avoidance, collision avoidance, etc

22 p3868 A69-41151

Orbital biomedical laboratory for in-flight measurement to assure human safety and optimize astronauts performance in extended space mission

23 p4223 A69-41801

Space station safety, discussing damage containment and control, escape and rescue, etc

[AAS PAPER 69-518] 24 p4392 A69-42842

Crew survival ensurance under emergency situations during manned space flight, discussing Apollo abort system refinements

24 p4272 A69-42848

Systems safety for unmanned spacecraft, considering power supply, equipment operation, trajectory correction, etc

[AAS PAPER 69-520] 24 p4392 A69-42849

Management system for safety in NASA Manned Space Flight Program, discussing hazard analyses and reduction precedence sequence

24 p4418 A69-42851

FLIGHT SIMULATION

NT ATMOSPHERIC ENTRY SIMULATION

Vitiated inlet air effects on J60-P-6 turbojet engine performance at sea level for various simulated flight Mach numbers

01 p0143 A69-11063

Human endocrine-metabolic response to sequential decompression exposure during simulated orbital flight or extravehicular activity

01 p0022 A69-11337

Vertical flight path navigation requirements for supersonic aircraft based on computer simulated flights of Mach 2 Concorde

02 p0277 A69-11590

Validation study of pilots visual sampling behavior, using queueing model based on instrument and eye movement data from Link trainer mission flights

02 p0202 A69-11954

Computer solution of six degrees of freedom flight equations, discussing advantages of using flight path axes for translational equations of motion

02 p0212 A69-11998

Digital computers in space flight simulation and vehicle performance optimization, examining mission analysis

04 p0652 A69-14519

Large subsonic wind tunnels for correct simulation of V/STOL powered flight by minimizing wall constraint effects on flow field

05 p0741 A69-15573

Test facilities and techniques for low speed flight problems of aircraft handling qualities, stability, control and performance

05 p0741 A69-15575

Digital simulation of vehicle motion and control for six degree of freedom simulations of Gemini reentry and aircraft, missile control, etc

05 p0725 A69-16477

Simulation in design of automated flight test data system

05 p0743 A69-16759

Electrohydraulic attitude servomechanism for controlling movements of pilot training cabin, describing hydraulic system and electric control circuit

06 p0906 A69-16966

High enthalpy, Mach and Reynolds number flight studies on ballistic ranges, describing launchers, flight simulation, measuring and recording techniques

06 p0860 A69-17632

AZUR satellite movement simulator for thermal control tests, describing assembly

08 p1300 A69-20095

Spacecraft electric propulsion parameters and launching vehicle characteristics in low thrust mission simulation, discussing spacecraft path

09 p1584 A69-21202

Low thrust mission simulation dependence on hardware definition, discussing power plant characteristics, jet velocity and thrustor efficiency

09 p1584 A69-21204

Interplanetary low thrust mission analysis model, discussing major elements interactions

09 p1585 A69-21206

Man in loop computer facility for programmers to check out flight programs in simulated space flight environment

[AIAA PAPER 69-324] 09 p1479 A69-22384

Turbine engine in-flight operating conditions simulated on test stand

11 p1942 A69-24528

Complex piloting simulation including fatigue for optimizing man machine synergy, emphasizing human adaptability and computer precision and speed

12 p2025 A69-27083

Concorde thermal fatigue resistance tested by alternate heating and cooling cycles simulating supersonic flight profile

13 p2241 A69-28102

Selectively pumped thermal vacuum test chamber for orbital heat transfer and environment simulation for flight vehicle performance prediction

15 p2587 A69-30392

Air transport industry safety record and variable stability research planes to simulate aircraft airborne behavior and handling qualities

15 p2558 A69-30453

Supersonic combustion for high Mach number high altitude flight, discussing laboratory simulation for actual flight condition and chamber design

[AIAA PAPER 69-458] 16 p2880 A69-32743

CH-46 helicopter flight simulation program for pilot response to large perturbation maneuvers, using six degrees of freedom mathematical models

[AHS PAPER 361] 17 p2946 A69-33521

AH-56A helicopter manual and automatic terrain following and manual terrain avoidance systems, discussing nap-of-earth flight, design and simulation

[AHS PAPER 311] 17 p3002 A69-33544

Computer graphics engineering applications in line drawing displays for industry, including design programs and color TV flight simulation

18 p3106 A69-34659

Autopilot for flight simulation of stability and control of pilot-airframe combined performance on reentry missions, using airborne analog computer for vehicle response

18 p3208 A69-35000

Aircraft terrain-following algorithm for use with airborne general purpose digital computer, discussing simulation techniques and test results

[AIAA PAPER 69-817] 19 p3366 A69-35625

Tilt wing V/STOL aircraft spray circulation characteristics in overwater operation, examining forces, moments and generated environmental conditions

[AIAA PAPER 69-791] 19 p3243 A69-35638

Aircraft wing aerodynamic forces and moments due to lifting engine air intake simulated by wind tunnel experiment

19 p3239 A69-36400

Aircraft simulation, discussing flight simulation, real time computer assembly operation, computer-auxiliary interfaces, etc

19 p3296 A69-36707

Apollo translunar injection burn simulation, analyzing polynomial solutions of optimum geometry and characteristic velocity

[AAS PAPER 68-150] 21 p3820 A69-39225

Mission analysis and trajectory simulation (MATS) program, discussing computer controls, modular design, integration evaluation

[AIAA PAPER 69-939] 22 p3904 A69-40322

Mission simulation testing in thermal vacuum environment for Apollo Lunar Module, noting conformal skin heaters

[AIAA PAPER 69-991] 22 p3920 A69-40369

Three axis motion simulator for in-orbit spacecraft attitude control evaluation using earth, sun and star sensor references

[AIAA PAPER 69-1029] 22 p3924 A69-40398

Molecular beams for simulating orbital flight through planetary atmospheres, considering various nozzle beam systems

[AIAA PAPER 69-1031] 22 p3926 A69-40437

Flight simulation requirements for reducing aircraft training flight time, discussing control system and instrument motion characteristics, visual simulation and critical maneuvers motion

22 p3928 A69-41139

Decreasing barometric pressure effects on abdominal gas volume in military men under simulated flight conditions, noting abdominal fullness and pain

23 p4076 A69-41291

Decompression sickness in simulated zoom flights, discussing bubble formation probability and instantaneous surface tension effect on bends resistance

23 p4077 A69-41292

Central nervous, cardiovascular and metabolic data of Macaca nemestrina during simulated Biosatellite flight, testing data acquisitions systems

24 p4260 A69-42703

Space and missile guidance performance analysis through automatic generation of mission performance sensitivity with respect to error sources from Monte Carlo simulation

[AAS PAPER 69-404] 24 p4347 A69-42836

Airline pilots simulated incapacitation involving myocardial infarction or cerebrovascular accident, discussing effect on crew behavior during flight task performance

24 p4277 A69-43386

FLIGHT SIMULATORS

NT COCKPIT SIMULATORS

Flight simulator based on analog computer simulating six linearized equations of motion and aircraft model, discussing design and applications

01 p0057 A69-11300

Dynamic flight simulators fidelity assessment, discussing hybrid method based on pilot psychomotor responses

02 p0203 A69-12215

Business jet aircraft use for air transport pilot training instead of simulating devices, noting pilot cabins

03 p0366 A69-13643

Simulation of flight dynamic equations of motion for fixed wing aircraft, using variable analog computer with gimbal and servocontrolled aircraft model

04 p0585 A69-14829

Digitally controlled flight systems simulators, noting design improvements over conventional trainers

05 p0742 A69-15884

West German test facility for simulating artificial satellite rotation about center of mass

07 p1116 A69-18260

Test techniques for X-22A VTOL research aircraft during ground simulator work and actual flight test, describing stability and control characteristics

[AIAA PAPER 69-319] 10 p1633 A69-23044

Flight testing and preflight simulated testing of Lockheed C-5 Galaxy transport aircraft

10 p1634 A69-23599

Human pilot adaptation in simulated multiloop VTOL hovering task with series loop closure model

10 p1650 A69-23878

Intermittent flow facilities for ballistic and lifting reentry flight simulation including shock tubes, ballistic ranges and shock and gun tunnels

11 p1863 A69-25016

NASA manned aerospace simulation techniques and equipment as used at Ames Research Center, noting applications to various types of manned vehicles

[ASME PAPER 69-DE-56] 14 p2427 A69-28844

Centro Ricerche Aerospaziali objectives, equipment and activities in aerospace research, including space flight simulation facilities and scientific satellite launching range

15 p2724 A69-31456

Ground simulations data of jet lift V/STOL compared with visual flight results, studying hover, lateral quick start and stop maneuver
[AHS PAPER 362] 17 p2946 A69-33519

Artificial horizon indicator design modifications to facilitate maintaining horizontal aircraft position, discussing automatic pilot advantages in turbulence and flight simulators
17 p2903 A69-34214

Air Transport Total In-Flight Simulator-707/AT/TIFS-707/ concept for pilot training, stressing airframe and major flight systems
[SAWE PAPER 747] 18 p3118 A69-34884

Optimized flight crew training, evaluating safety, flight simulator efficiency, takeoff/landing practice and line experience based on test results
[AIAA PAPER 69-771] 19 p3245 A69-35653

Manned aircraft air to air combat capabilities evaluated by simulator using two cockpits, digital computer and collimated displays
[AIAA PAPER 68-253] 20 p3510 A69-37159

Rotary actuator to create realistic control effects in hydraulic loading system of jet flight- training simulators
20 p3511 A69-38182

Spacecraft wide angle attitude control system stability analysis, using air bearing table simulation
[AIAA PAPER 69-856] 21 p3823 A69-39384

Piloted ground-based flight simulators role in tactical and VTOL aircraft design, describing simulation devices, computer programs and design information
[RAES PAPER 10] 22 p3927 A69-40490

Flight training using digital simulators, including maneuver analysis for TWA 707 program
22 p3928 A69-41137

Human factors methods importance in nonmilitary flight simulation training, discussing cost factors and skills evaluation
22 p3894 A69-41138

Flight simulators role in airline pilot training, discussing skilled learning, performance measurements and future developments
23 p4112 A69-42366

Flight simulator with large lateral motion for large and supersonic transport aircraft, emphasizing reproduction of cockpit accelerations due to supersonic engine thrust loss
24 p4297 A69-43044

FLIGHT STABILITY TESTS

Strip method for prediction of subcritical frequency and damping characteristics for subsonic wind tunnel and flight flutter tests
11 p1987 A69-25368

Jet influence and aerodynamic force changes on V/STOL aircraft in transitional and high speed flight investigated in wind tunnel tests for fighter aircraft
16 p2734 A69-31937

Stratospheric balloon vertical oscillations and gondola attitude during long flights
19 p3248 A69-36689

FLIGHT STRESS

Psychic stress effect on physiological parameters of helicopter pilots during critical flight situations, considering biotelemetric examination of heart and circulatory systems
11 p1829 A69-24347

F-102 pilot anticipatory and flight stress, noting endocrine-metabolic hyperactivity
12 p2023 A69-26552

FLIGHT STRESS [BIOLOGY]

NT SPACE FLIGHT STRESS

Respiratory disturbances relationship to experience and attitudes toward gas anesthesia and response to different types of face mask
03 p0378 A69-12884

Electrocardiographic tests to study changes in electropotentials of heart in flying personnel after flight, noting changes in myocardium
03 p0378 A69-14207

Biochemical indicators of pilot reactions to flights complicated by unexpected autopilot failures, using postflight chemical analysis of blood and urine
05 p0710 A69-16525

Asthmatic attacks in military air crews, discussing flight stress factors including altitude, ventilation and insecurity as possible causes
05 p0710 A69-16624

Telemetric system for in-flight measurements of jet pilot heart and circulatory system to determine flight stresses leading to pilot failure
05 p0715 A69-16707

Predictive scale of aircraft emergencies, analyzing human error rate under stress
06 p0880 A69-17208

Blood glucose measured before, during and after high performance aircraft flight for occurrence of fasting hypoglycemia
09 p1445 A69-22555

EEG and pilots flight performance relations, discussing in-flight telemetric measurements from ground station
15 p2560 A69-31233

Long distance air flights through different time zones, discussing circadian physiological cycles, light-dark ratio shifts effects and methods of lessening desynchronization effects
16 p2745 A69-32444

Inflight spontaneous pneumothorax case of civilian pilot lung collapse experience during exposure to reduced ambient pressure, discussing etiology, incidence, treatment and disposition
17 p2909 A69-33183

Biochemical indicators of pilot reactions to flights complicated by unexpected autopilot failures, using postflight chemical analysis of blood and urine
18 p3096 A69-34744

Flight surgeon observations of stress and fatigue effects on aircrew of first nonstop transatlantic helicopter flight, discussing fatigue ratings, sleep patterns, etc
19 p3262 A69-36450

Cabin personnel occupational strain in civil aviation, relating heart rate to aerobic power while working during flight
21 p3665 A69-39180

Jet flying effects on air hostess menstrual function, considering cycle length, duration, regularity, dysmenorrhoea and flow severity
23 p4103 A69-41689

Flight altitude effects on pilot performance with comparison of sensory and mental functions, considering oxygen use and flight safety
23 p4106 A69-41794

Adrenosympathetic reaction in flight, studying contributions of physical and nervous stresses in physically trained and untrained persons
23 p4099 A69-42363

Urine sampling conditions for kidney function circadian rhythm during global flight, considering food and water intake, sampling intervals and body position
24 p4266 A69-43374

Stillbirth and neonatal death in stressed rats exposed to mild and acute gravitational loads in automobile ride and aircraft flight
24 p4266 A69-43381

Urinary excretion of hormonal metabolites in intercontinentally flown test subjects, using gas chromatographic procedure for steroid identification
24 p4268 A69-43404

FLIGHT SURGEONS

Pilots mental and physical welfare, discussing roles of mental hygiene and preventive medicine in flight surgeons programs
18 p3097 A69-35301

Aviation health service for flight safety problems with emphasis on accident prevention, emphasizing physician role in man-machine relationship of personnel surveillance
18 p3098 A69-35305

Flight surgeon observations of stress and fatigue effects on aircrew of first nonstop transatlantic helicopter flight, discussing fatigue ratings, sleep patterns, etc
19 p3262 A69-36450

Vestibulometric test program for flight surgeon appraisal of flying personnel, emphasizing singling out persons prone to illusory sensations
20 p3473 A69-37277

Vestibulometric tests for flight surgeon appraisal of applicants in flying profession, comparing Coriolis forces cumulative load tests with conventional tests
20 p3481 A69-37278

FLIGHT TEST INSTRUMENTS

Cloud instrumentation for measurement of icing conditions of airplane flight tests
01 p0055 A69-11044

FLIGHT TEST VEHICLES

Flight test evaluation of small one man lunar flying device /POGO/, discussing vehicle control, pressure suit factors and piloting differences
[AIAA PAPER 68-240] 02 p0229 A69-12379

Procedures and facilities applicable to sonic environmental testing of flight vehicles, discussing sonic energy sources in vehicles and potential failure modes
12 p2060 A69-26939

Rentry flight test vehicle development for West German space program, using hypersonic model to determine controllability and aerodynamic stability
16 p2867 A69-31934

FLIGHT TESTS

Aircraft flight testing for determining airframe, engine and pilot degradation, examining flutter, handling characteristics, water ballast, propulsion, etc
01 p0054 A69-10292

T63 regenerative helicopter engine program, noting operational performance and engine-aircraft compatibility
[AHS PAPER 212] 01 p0143 A69-10410

Paraglider as recoverable sounding rocket dropped from helicopter, describing system design and flight tests
[UN PAPER 68-95445] 01 p0161 A69-10465

Error reduction in identifying pilot describing function from flight test data by shifting input signal by pilot delay time in simulated computer model
02 p0202 A69-11950

Angular motion during first stage cut-off of Europa 1 launch vehicle from flight tests compared with theoretical predictions
03 p0519 A69-12856

Soviet book on aircraft flight tests, discussing determination of maximum speed, climbing rate, flying range, takeoff and landing, controllability, maneuverability and recovery
03 p0365 A69-12900

Boundary layer transition measurements on flight tests of experimental 22 degree conical reentry vehicle with Be heat shield and graphite nose
[AIAA PAPER 68-1152] 03 p0362 A69-13648

Flight tests in wide Mach number range of blunt nosed flare stabilized hypersonic reentry nose cone, deducing drag and stability coefficients
[AIAA PAPER 68-1145] 03 p0521 A69-13668

Lifting body entry vehicles in low speed flight test program for determining handling qualities, discussing M2-F2 glide flights
05 p0702 A69-15571

Factors influencing development of both wind tunnel and flight test technology for determining aerodynamic derivatives of aircraft motions
05 p0741 A69-15572

Flight test support design, developing measure of performance of test environments stated in weapon or space system terms
05 p0742 A69-15804

On-line ground flight test data processing system
05 p0725 A69-16757

Flight test data reduction on time sharing general purpose computer, noting hardware link between airborne equipment and computer
05 p0726 A69-16758

Simulation in design of automated flight test data system
05 p0743 A69-16759

Army engineering flight testing of OH-6A helicopter, presenting test program and results
06 p0867 A69-17659

First flight test phase of multipurpose Vigen aircraft designed as basic platform for attack, trainer, reconnaissance and fighter versions
06 p0867 A69-17662

C-5A transport flight test and progress report, discussing taxi runs, first flights and flight-flutter program
06 p0867 A69-17665

Flight evaluation of direct lift control on DC-8 super 63 jet transport
06 p0867 A69-17666

General aviation flight testing philosophy and origin
06 p1043 A69-17667

LR-1 prototype design criteria and flight testing, discussing Model 99 airliners for commuter airlines
06 p0867 A69-17668

Lifting Body Test Program at Edwards AFB compared with flight testing standards of high performance aircraft, discussing testing philosophy
06 p1017 A69-17671

Mass distribution and inertia characteristics influence on spin susceptibility and spin recovery characteristics for eight current fighter aircraft
[AIAA PAPER 69-188] 06 p0868 A69-18057

Atmospheric entry testing in terms of velocity-altitude duplication, suggesting multistage rocket propelled aeroballistic range type testing
[AIAA PAPER 69-166] 06 p0907 A69-18189

Naval Research Laboratory experience with two and three axis gravity gradient satellites stabilization systems
07 p1228 A69-18344

Self excited rotor blade oscillation at high subsonic Mach numbers during flight tests of Sikorsky NH-3A compound helicopter
07 p1053 A69-18870

UHF telemetry flight tests at White Sands Missile Range, discussing multipath and target scintillation problems

07 p1082 A69-19116

Wind tunnel rain erosion testing of components of aircraft or missiles flying at high speed

07 p1117 A69-19534

Engineering testing of aerodynamic efficiency of helicopter rotors during hovering with and without ground effect

08 p1254 A69-20169

STOL aircraft intercity test flights emphasizing curved ILS approach, using onboard computer for altitude and distance data

08 p1347 A69-20602

Optical design of Wolter type 1 glancing incidence X ray telescope for 6-100 Å wavelength region, describing results of laboratory and rocket flight tests of prototype

08 p1318 A69-21087

In-flight testing of second and third stages of F 7 section of Europa 1 satellite booster, noting third stage explosion

08 p1410 A69-21144

Flight test performance of airborne Omega radio navigation system capable of worldwide coverage, discussing diurnal variations effects in phase velocity

08 p1348 A69-21191

Ammonia resistojet stationkeeping subsystem on-board ATS 4 satellite, noting flight test data agreement with ground tests

[AIAA PAPER 69-296] 09 p1560 A69-21212

Newton-Raphson technique development for determining stability derivatives from flight data, noting use of a priori wind tunnel information

[AIAA PAPER 69-315] 09 p1434 A69-22379

Thermal and pressure environments analysis in Saturn S-1C stage base during flight tests, noting base gas flowfield and heating

[AIAA PAPER 69-318] 09 p1611 A69-22383

Flight test evaluation program for airborne multisensor electro-optical display systems performance in TV mode under variety of optical conditions

[AIAA PAPER 69-317] 09 p1500 A69-22387

Onboard test and fault isolation design for airborne systems considering tradeoff parameters for optimum reliability, performance and cost

[AIAA PAPER 69-306] 09 p1434 A69-22389

Schleicher glider AS-W15 prototype tests, discussing balsa sandwich structure and flight characteristics

10 p1633 A69-22872

Test techniques for X-22A VTOL research aircraft during ground simulator work and actual flight test, describing stability and control characteristics

[AIAA PAPER 69-319] 10 p1633 A69-23044

Flight test telemetry data processing system designed for C-5

10 p1660 A69-23269

Ground station integrated flight test data system with interactive data input terminals, on-line assembly and responsive program development

10 p1633 A69-23271

Design of 126 channel PCM telemetry unit for C-5 aircraft flight test, discussing FET analog multiplexing

10 p1693 A69-23275

Lockheed XV-4B Hummingbird 2 VTOL aircraft propulsion, control, escape systems, with tests

10 p1634 A69-23597

Flight testing and preflight simulated testing of Lockheed C-5 Galaxy transport aircraft

10 p1634 A69-23599

Hypersonic flight test data of Berenice missile compared to wind tunnel test data, discussing in-flight flow separation, Mach-Reynolds torque, etc

10 p1632 A69-23842

Flight tests of deployment of 20 ft diam ribbon parachute at high dynamic pressures and supersonic speeds

11 p1823 A69-25383

Engineering assessment and flight testing of aircraft systems in UK, discussing operational reliability, etc

13 p2201 A69-27539

X-22A VSTOL aircraft testing, discussing control sensitivity, dutch roll mode period and performance test planning based on characteristics prediction

14 p2392 A69-29699

Multiple shaker ground vibration test system for confidence in helicopter designs before flight testing and evaluation of force balancers

15 p2585 A69-30357

Location effect of power plants on aft-mounted supersonic cruise exhaust nozzles at transonic speeds in flight and wind tunnel

[AIAA PAPER 69-427] 16 p2734 A69-32769

Rotary wing aircraft height-velocity testing, analyzing engine-out landing by combining flight tests with mathematical simulation model

[AHS PAPER 353] 17 p2900 A69-33524

Canadair CL-84 two propeller V/STOL utility tilt wing vehicle development program and flight tests to assess military potential of aircraft

17 p3077 A69-34065

Aerodynamic characteristics of ballistic reentry vehicles from flight test dynamic measurements, illustrating results

18 p3085 A69-34670

Biosatellite attitude control systems design development and flight test results for payload perturbing effects, discussing simulation activity

18 p3210 A69-35094

Computerized prediction of RF instrumentation system signal margins for missile flight tests based on trajectory and range balance equation

18 p3103 A69-35097

V/STOL wind tunnel data at low forward speeds, discussing test limit dependence on model size, downwash angle and tunnel geometry

18 p3119 A69-35229

Operational flight tests of IR atmospheric turbulence detection system

[AIAA PAPER 69-799] 19 p3367 A69-35631

Laboratory and flight tests of airborne solid state UHF telemetry transmitter, discussing miniaturized coaxial hardware from RF power conservation viewpoint

19 p3267 A69-35996

Apollo spacecraft equipment qualification program for margin assurance, discussing ground and flight tests

19 p3430 A69-36015

C-5 air force logistic transport, discussing structural design, configuration, payload, aerodynamics and flight testing

[AIAA PAPER 69-758] 19 p3248 A69-36295

Gust absorber system configuration flight tests and analysis, emphasizing application to delta wing aircraft

[ONERA-TP-698] 20 p3462 A69-37753

STOL airline operation test programs involving aircraft, navigation equipment, systems and ATC

21 p3646 A69-38731

Lifting body stability augmentation systems design, development, ground tests and flight data including frequency response, limit cycle and structural resonance

[AIAA PAPER 69-887] 21 p3647 A69-39413

In-flight test to determine variation effects in bank angle control parameters on cruise flight handling qualities, considering spiral stability

[AIAA PAPER 69-893] 21 p3648 A69-39425

Guidance and navigation flight tests, demonstrating system performance improvements by onboard inertial system communicating with external navigation aid

[AIAA PAPER 69-842] 21 p3765 A69-39429

Pioneer 9 deep space probe with telemetry link operated in coded mode with sequential decoding, discussing ground and flight test data

23 p4131 A69-42522

V/STOL aircraft radar inertial navigation system, describing approach and landing phase flight test results

[AAS PAPER 69-401] 24 p4252 A69-42831

Training missions and military exercises to field test weapons system models

[AAS PAPER 69-478] 24 p4296 A69-42884

Flight tests in wide Mach number range of blunt nosed flare stabilized hypersonic reentry nose cone, deducing drag and stability coefficients

[AIAA PAPER 68-1145] 24 p4394 A69-43250

High speed compound helicopter rotor loads flight test program, discussing measured parametric effects

[AIAA PAPER 68-980] 24 p4250 A69-43712

FLIGHT TIME

Variational calculus applied to time optimal trajectories between two points in range altitude space, discussing aircraft thrust and drag laws

01 p0009 A69-10414

Circadian rhythms disruption during long distance flights, discussing adverse effects on pilot and passenger performance

03 p0378 A69-14260

Radar round trip time of flight measurements to Venus for three month interval about inferior conjunction of August 1968

04 p0663 A69-15384

Conjugate gradient methods for optimization problems with terminal constraints, noting minimum time paths for V/STOL aircraft climb phase

12 p2013 A69-26763

Orbit determination from satellite using linear combinations of time of flight measurements and based on expansion of satellite law of motion

12 p2159 A69-26778

Time of flight measurement for velocity of micron sized particles in two phase flow by light transmission method

13 p2263 A69-28243

Minimum fuel multiple impulse orbital rendezvous for fixed transfer time near circular orbits

16 p2857 A69-32161

Flight times compared for intercept and pure pursuit missile trajectories

20 p3618 A69-37716

Flight simulation requirements for reducing aircraft training flight time, discussing control system and instrument motion characteristics, visual simulation and critical maneuvers motion

22 p3928 A69-41139

FLIGHT TRAINING

NT SPACE FLIGHT TRAINING

Airline crew training, requalification, recurrent, upgrading and aircraft transition training for crew and pilot

01 p0019 A69-10450

Annual general aviation aircraft accident rate variation related to annual variations in pilot flight training activity

19 p3262 A69-36448

Human factors methods importance in nonmilitary flight simulation training, discussing cost factors and skills evaluation

22 p3894 A69-41138

Flight simulation requirements for reducing aircraft training flight time, discussing control system and instrument motion characteristics, visual simulation and critical maneuvers motion

22 p3928 A69-41139

Annual general aviation accident rate prediction from annual flight training variations

23 p4062 A69-41793

Algorithm minimizing personnel number and training costs to meet uncertain skill requirements, applying to army aviation contingency force training composition

[AAS PAPER 69-116] 24 p4271 A69-42818

FLIGHT VEHICLES

Flight vehicle dynamics, discussing classical mechanics, fluid dynamics, structural dynamics and thermodynamics

02 p0193 A69-11985

Book on flight structure theory and analysis covering methods for digital computers, differential equations for equilibrium boundary value problems, etc

03 p0525 A69-13266

Time difference position determination system for space, surface and airborne vehicles, describing application to satellite navigation and air traffic control

08 p1348 A69-21066

Soviet book on radio navigation of flight vehicles covering systems classification, operational characteristics, satellite navigation, etc

12 p2129 A69-27076

Fracture design for aircraft vehicles, discussing crack strength requirements and method for serviceability prediction

17 p3060 A69-33563

Soviet book on flight vehicles astronaut navigation covering automatic equipment accuracy, changes in spherical coordinates, time measuring, etc

18 p3168 A69-34355

Optimal control of flight vehicle consisting of long thin elastic body under torsional deformations, solving by method of successive approximations

21 p3760 A69-38852

Optimal control of rotational and transversal motions of elastic flight vehicles, considering torsional and flexural deformations

21 p3760 A69-38890

Time optimal control for torsional vibrations of flight vehicle for limited energy case, illustrating uniform wing of constant rigidity

21 p3686 A69-38891

Soviet book on flight vehicle design dynamics, discussing lift effectiveness and rigidity as function of internal stresses during ground and flight operations

21 p3825 A69-39533

Flight vehicle motion in high density medium reacting with static, vortex and dynamic forces analyzed for optimal regime via Lagrange-Euler equation

21 p3768 A69-39824

Flow stability regions at surface of flight vehicle, considering boundary layer flow of incompressible fluid

21 p3645 A69-39827

FLIP-FLOPS

Time difference position determination system for space, surface and airborne vehicles, describing application to satellite navigation and air traffic control
22 p3977 A69-39874

Cumulative error in flight vehicle position determination by inertial navigation system, showing dependence on constant acceleration components
22 p3978 A69-40252

HF vibrations effect on motion of gyroscopic linear acceleration integrator, showing additional error in flight vehicle acceleration measurements
22 p3946 A69-40253

Digital computer program for determining flight vehicle telemetry antenna performance from ground test readings
23 p4133 A69-41754

FLIP-FLOPS

Performance characteristics of variable geometry bistable fluid amplifiers
[ASME PAPER 68-WA/FE-18]
05 p0748 A69-16094

Temperature, acoustic, vibration and shock environment effects on pure fluid bistable and proportional amplifiers
[ASME PAPER 68-WA/FE-31]
05 p0705 A69-16104

Flip-flops built with complementary symmetry MOS, discussing power, noise and load stability due to n and p channel series transistors
07 p1113 A69-19766

Nonlinear discrete on-off system phase plane system analysis by motion separation method
16 p2763 A69-31628

Phase locked loop with flip-flop error detector compared to analog loop, discussing signal to noise ratio
17 p2931 A69-34115

Current mode gates and flip-flops with subnanosecond propagation delay for integrated logic circuits, discussing memories dimensions, LSI arrays, etc
20 p3505 A69-37342

Classification of switching process in bistable fluid amplifiers with illustration of fluid oscillator, discussing capacitor and bleeds
[ASME PAPER 69-FLCS-28]
20 p3465 A69-37977

Integrated TTL flip-flop circuits, describing functional principles of circuits with DC and capacitive coupling
24 p4287 A69-43130

FLOATS

Magnetic masses of differentiating or integrating floating gyroscope effect on gyro moment sensor performance, examining utilization of multiple permanent magnet
09 p1497 A69-22102

Operational errors of floating gyroscopes with hydrostatic unloading of bearings, establishing eccentricity tolerances, axes misalignment and temperature field nonuniformity
09 p1497 A69-22103

Centering force and initial rigidity of magnetically suspended bearings of integrating floating gyroscope with allowance for mutual inductance of exciting coils
09 p1497 A69-22104

Channel wall effect on gain of apparent mass of cylindrical and elliptical bodies floating in channel and subject to vertical impact
11 p1875 A69-25487

Floating body attitude and stability analysis based on system potential energy balance, considering Archimedes principle, torques, equilibrium conditions, body shape, etc
[SAWE PAPER 773]
18 p3172 A69-34874

FLOQUET THEOREM

Determining transfer matrix and comparing solution of homogeneous differential equation to Floquet theory results
10 p1666 A69-22928

Unforced periodically varying systems, developing approximate solutions with Floquet theory
11 p1909 A69-25289

Linear dynamic stability of spinning satellite in elliptic orbit, applying perturbation method to determine Floquet solutions
14 p2534 A69-29318

Driving point admittance of radiating aperture in infinite periodic phased array, determining Floquet series and coefficients of waveguide modal expansion
17 p2938 A69-33876

FLORA

U PLANTS [BOTANY]

FLOTATION

Flotation technique for laboratory calibration of low level accelerometers, noting accuracy dependence on flotation fluid density stability
[AIAA PAPER 68-874]
24 p4315 A69-43242

FLOTATION SYSTEMS

U FLOATS

FLOW CHAMBERS

Coaxial flow jet chamber flow patterns dependence on inlet gas velocity, density and length/diameter ratio
[AICHE PAPER 25B]
04 p0587 A69-14509

Flow velocity, density, temperature, dryness and pressure in mixing chamber of MHD vaporizer
06 p0871 A69-17919

FLOW CHARACTERISTICS

NT BOUNDARY LAYER STABILITY

NT FLAME STABILITY

NT MAGNETOHYDRODYNAMIC STABILITY

Steady three dimensional flow through impeller of turbines with small number of blades and with edge cut hub, noting inefficiency of flow without impact
01 p0142 A69-10309

Steady state three dimensional MHD flow in variable profile channels calculated by reducing problem to two dimensional approximation using curvilinear coordinate system
01 p0131 A69-10776

Electromagnetic fields effect on turbulent boundary layer characteristics of compressible fluid on insulating wall of MGD channel
01 p0131 A69-10777

Cryogenic expansion to pressures below triple point and resulting formation of solid-vapor mixtures, discussing flow and heat transfer characteristics in heated tubes
01 p0176 A69-11146

Expression derived for flow characteristics in smooth pipe for entire Reynolds number range
02 p0230 A69-11870

Fluidic element design calculations, noting flow characteristic differences
02 p0195 A69-12074

Turbulent gas flow characteristics obtained by extremal hypothesis, using maximum perturbation stability in formulating variational problem and computer algorithm
02 p0232 A69-12354

Strain rate and temperature effect on flow stress of 7075 aluminum bars
03 p0443 A69-13120

Heat input influence on hypersonic flows past sphere and circular cylinder
[DVL-844]
03 p0364 A69-13663

Slow nonNewtonian flow in separation zone analyzed using finite difference scheme
04 p0587 A69-14594

Flow characteristics and sound velocity in two temperature plasma
05 p0802 A69-15796

Flow characteristics about curved lateral jet, discussing effect of pitot tube nozzle shape and turbulence
05 p0746 A69-16017

Circular cylinder near wake in cross flow measured with hot-wire anemometry for various Reynolds numbers, noting data processing on digital computer
[ASME PAPER 68-FE-5]
05 p0747 A69-16068

Liquid flow systems dynamic response to periodic disturbances of system structural supports
05 p0747 A69-16073

Turbulent free shear layers in isoenergetic flow, correlating theory and experiment
[ASME PAPER 68-FE-9]
05 p0748 A69-16077

Shock tube investigation of formation and flow characteristics of impulsively generated vortex street recorded interferometrically, using high speed framing camera
[ASME PAPER 68-FE-32]
05 p0748 A69-16079

Argon flow characteristics in converging nozzle in continuum, slip and free molecular regimes
[ASME PAPER 68-WA/FE-9]
05 p0698 A69-16089

Filtration and flow characteristics of wire cloths used in hydraulic systems described by expressions from measured properties
[ASME PAPER 68-WA/FE-39]
05 p0750 A69-16111

Smith correlation of turbine stage efficiency for relating achievable efficiency to stage loading and flow factors used for total pressure loss coefficient data
[ASME PAPER 68-WA/GT-5]
05 p0812 A69-16140

Quasi-method of characteristics with application to fluid lines with frequency dependent wall shear and heat transfer
[ASME PAPER 68-WA/AUT-7]
05 p0750 A69-16181

Fluctuation velocity, apparent kinematic viscosity and turbulent shear stress in isothermal homogeneous free jets
06 p0909 A69-17169

Flow velocity, density, temperature, dryness and pressure in mixing chamber of MHD vaporizer
06 p0871 A69-17919

Electromagnetic field induced energy and momentum changes effects on pressure, temperature and particle velocity of flows behind propagating gaseous detonation waves
[AIAA PAPER 69-44]
06 p0970 A69-18084

Mathematical model for flow within external target type thrust reverser, assuming inviscid incompressible two dimensional flow
[AIAA PAPER 69-3]
06 p0985 A69-18124

Steady flow circuit characteristics in square cross section channels of planar geometry fluid control elements in case of laminar flow
07 p1118 A69-18293

Flow in impellers of mixed and radial flow compressors for jet engines, turbochargers and automotive gas turbines, discussing velocity, load distribution, etc
[SAE PAPER 690033]
07 p1049 A69-18312

Nonstationary flow past spheres and cylinders in electromagnetic shock tube, determining time required for flow to become stationary
07 p1119 A69-18744

MHD flow in channels with abruptly widening sections and finned walls under transverse magnetic field, discussing effects on drag
07 p1192 A69-19016

Grain size dependence of yield, flow and fracture stresses of Fe-Co-V alloy for 77-298 K
07 p1166 A69-19264

Thermally activated processes influence on dislocation interaction and on temperature dependence of flow stress in niobium single crystals
08 p1333 A69-20446

Transonic flow around airfoils with constant curvature in uniform asymptotic stream, studying leading edges in exact form
09 p1429 A69-21606

Characteristic equation obtained by considering world line vector, basic thermodynamic variables and metric tensor as functions of Lichnerowicz class
09 p1480 A69-21614

Stationary shock wave formation onset in Meyer-Prandtl flow, obtaining Marchal number for plane flow
09 p1429 A69-21688

Expansion tube modification incorporating nozzle plate at secondary diaphragm for reducing flow nonuniformity and contamination
[AIAA PAPER 68-371]
09 p1477 A69-21960

Diagnostic techniques to identify flow regimes of high enthalpy shock tunnel
[AIAA PAPER 68-729]
09 p1477 A69-21970

Thin jet-flapped airfoil flow analysis in ground proximity at small angle of incidence, assuming inviscid incompressible flow
09 p1431 A69-22275

Incompressible fluid flow engine spiral casing, considering flow as potential flow
10 p1632 A69-22914

Laminar boundary steady two dimensional constant velocity flow over curved surface equation derived from Navier-Stokes equation
11 p1867 A69-24375

Convection heat transfer and flow in rotating bodies, discussing laminar, turbulent and mixed flow in cones and disks, spheres and cylinders
11 p1998 A69-24459

Viscous effects of wall boundary layer behind primary shock wave on flow in shock tube, noting pressure and temperature changes
11 p1870 A69-25010

Intermittent flow facilities for ballistic and lifting reentry flight simulation including shock tubes, ballistic ranges and shock and gun tunnels
11 p1863 A69-25016

Hot wire sensitivity to velocity, temperature and density fluctuations of temperature varying flow field, discussing calibration curves and special cases
11 p1886 A69-25088

Friction coefficients for turbulent flow through smooth pipes, considering average and friction velocity relations, fluid velocity measurements and flow Reynolds number
11 p1874 A69-25429

Flow models for externally pressurized gas bearings, discussing pressure distributions, load capacity and flow rate
[ASME PAPER 68-LUBS-2] 13 p2267 A69-27285

Discontinuity coefficient on boundaries of mixing zone of plane jet, observing homogeneity of thermal and kinematic structures 13 p2247 A69-27978

Gas-liquid critical flows, considering compressibility, rate of momentum, mass and heat transfer, etc 13 p2376 A69-28144

Combined free and forced convection flows in parallel channel systems and in single channels, discussing metastable flow regimes, single phase laminar flows, etc 13 p2377 A69-28152

Stationary radial source flow of liquid particles into vacuum, discussing boundary value problem equations, parameters effects on flow structure and flow field characteristics 13 p2248 A69-28210

Boundary layer characteristics of incompressible flow in wind tunnel with asymmetric two dimensional contraction, discussing flow profiles 13 p2249 A69-28235

Small disturbances distribution in flow parameters along two dimensional combustion zone of finite width using thermal diffusion theory 14 p2537 A69-28986

Argon flow characteristics in converging nozzle in continuum, slip and free molecular regimes
[ASME PAPER 68-WA/FE-9] 14 p2390 A69-29445

Displacement of liquid by insoluble liquid from horizontal circular tube during laminar flow, analyzing flow characteristics 14 p2431 A69-29607

Shock wave velocity and gas flow parameters in shock tube with noninstantaneously opening diaphragm calculated by method of characteristics 14 p2432 A69-29623

Turbulence constant for flows near walls, analyzing viscosity dependence on wall distance by utilizing maximum stability principle 15 p2590 A69-30048

Turbulent gas flow characteristics obtained by extremal hypothesis, using maximum perturbation stability in formulating variational problem and computer algorithm 15 p2590 A69-30263

Turbulent boundary layers behavior near flow separation, obtaining equations for equilibrium layers 15 p2591 A69-30638

Thermal radiation effects on subsonic flow of ideal gray gas, calculating streamwise variations of flow properties 15 p2717 A69-30908

Two dimensional laminar convection cells asymptotic behavior for high Rayleigh number, discussing Robinson and Pillow models for fluid between horizontal plates heated from below 16 p2767 A69-31588

Supersonic compressor blade sections performance prediction near maximum pressure ratio and efficiency by analyzing flow processes 16 p2843 A69-32711

Local external flow variations effect on blow-in-door nozzle performance in transonic flight regime
[AIAA PAPER 69-428] 16 p2733 A69-32731

Nonequilibrium ionized gas flow past insulated wall with corners under magnetic field, discussing flow characteristics 17 p3010 A69-32865

Hele-Shaw and porous medium fuel tank systems behavior in simulated low gravity environment, studying sloshing, wetting, funnelling and fuel-driver gas interface stability
[AIAA PAPER 69-678] 17 p3021 A69-33444

Flow simulation on wind tunnel test models for aerodynamic characteristics of aircraft design, discussing boundary layer and external flow coupling
[AIAA PAPER 69-660] 17 p2945 A69-33471

Conducting fluid and plasma rotation between concentric cylinders due to crossed fields, determining velocity distribution, induced magnetic field and kinetic energy
[AIAA PAPER 69-726] 17 p3011 A69-33472

Shock tube calibration for aerodynamic loading, determining flow parameters by observing particle trajectories with high speed photography of smoke tracers 18 p3085 A69-34469

Statistical dynamics and structure of turbulent shear flows in incompressible fluids of constant density, discussing Reynolds stress at critical layers 18 p3123 A69-34922

Optimum efficiency of turbines with small volumetric flow rate, determining height of air-gas flow, partial admittance and flow angle in clearance 18 p3184 A69-34983

Working fluid flow parameters compensation by expelled cooling air in air-gas flow area of turbine stage 18 p3184 A69-34985

Double knife-edged double-crossing schlieren apparatus analyzed for operation principle and applied to measure hypersonic wake characteristics in hotshot tunnel 19 p3293 A69-35740

Servovalve orifice characteristics described by discharge, flow or loss coefficients for laminar and turbulent flow, noting use of Mises model 19 p3256 A69-36712

Boundary layer formed in miniature nozzle studied for effect on jet spreading discharged into space at high Mach numbers 19 p3395 A69-36760

Gas ionizing shock waves structure in arbitrary magnetic field, considering greater magnetic viscosity than dissipative coefficients 19 p3381 A69-36773

Supersonic flow past segmented and blunt bodies, investigating flow characteristics 19 p3242 A69-36783

Statistical equations for compressible gas, discussing turbulent quantities separated into fluctuating and macroscopic parts 19 p3300 A69-36784

Cold subsonic coaxial jets observed for relationship between noise output and flow characteristics, showing effect of relative annular and central jet velocities 20 p3513 A69-37063

Film cooling slot adiabatic wall effectiveness measurement in two dimensional constant property flow, showing role of lip thickness and injection angle 20 p3585 A69-37082

Flow characteristics and wall heat transfer in separated flow region of annular cavity at free stream hypersonic speed and high gas temperature
[AIAA PAPER 68-672] 20 p3458 A69-37185

Electromagnetic effects on pressure, temperature and particle velocity in flow behind propagating gaseous detonation waves based on one dimensional flow field model 20 p3514 A69-37190

Rarefied molecular gas flow past permeable surface, determining reflection law and flow parameters 20 p3459 A69-37438

Simultaneous lateral skewing regions existence in low speed three dimensional turbulent incompressible boundary layer flow
[ASME PAPER 69-FE-24] 20 p3517 A69-37998

Compressible fluid flow characteristics in turbomachine stage, discussing simplified radial equilibrium method as basis for design 21 p3643 A69-38457

Computational method for nonlinear two and three dimensional disturbances in plane parallel flows applied to transverse disturbances in plane Poiseuille flow 21 p3691 A69-38464

Gas flow characteristics in shrouded and unshrouded turbine wheel assemblies, emphasizing radial flow role in efficiency 21 p3785 A69-38865

Membrane vibration problems for combined free and forced laminar convection through vertical ducts, obtaining expressions for velocity, temperature and Nusselt numbers 21 p3851 A69-38974

Circular baffle mounted above flat-bottomed cylindrical tank outlet, discussing effect on remaining tank fluid volume and flow behavior under low gravity conditions 21 p3696 A69-39232

Skin friction results from free stream velocity boundary layers with varying injection and suction wall conditions, describing flow characteristics 21 p3696 A69-39431

Free stream dispersion without permeation using nonporous glass beads and solutes, examining flow rate, particle size distribution, solute diffusivity, etc 22 p3894 A69-39873

Arc-heated plasma jet wind tunnel flow properties in plenum chamber by spectroscopic techniques, measuring electron excitation, temperature and densities 22 p3990 A69-40596

Cooldown of vacuum insulated transfer lines using liquid N and H, discussing flow characteristics reproduction by digital computer program
[NAS-NRC PAPER I-1] 22 p4050 A69-40625

Liquid solid mixtures of parahydrogen flow characteristics in pipe, globe valve, orifices and venturi, determining pressure loss
[NAS-NRC PAPER F-5] 22 p3998 A69-40626

Pulsatile blood flow physical characteristics in short vascular segments 22 p3878 A69-40785

Pulsed energy balance expressions for turbulent characteristics of incompressible circular flow in channel with inserted rotating cylinder 22 p3933 A69-41028

Ionized He and Ar plasmas nonequilibrium nozzle flows, noting temperature difference between electron gas and atom-ion gas, calculating flow parameters 22 p3861 A69-41047

Flow and thermodynamic variables of Ar-Cs mixture behind normal shock in shock tube at various temperatures and pressures 23 p4150 A69-41335

Mean flow properties of incompressible turbulent three dimensional jets and wakes, treating flow within boundary layer theory context 23 p4060 A69-41908

Serrated flow characteristics in gold-indium solid solutions at various strain rates and temperatures 24 p4361 A69-43028

Wiener-Hermite truncated stochastic expansion used for velocity and concentration fields in turbulent flow convecting passive scalar, determining diffusivity and spectrum function 24 p4302 A69-43359

Flow discharge characteristics of nozzle during swirling shock flow ejection, considering isentropic and isothermal limiting cases 24 p4247 A69-43499

Bubble flow evolution at various pressures up to critical value
[ASME PAPER 69-HT-30] 24 p4411 A69-43529

Air flow laminarizing turbulent boundary layer, determining velocity, turbulence intensity, temperature profiles and local heat transfer coefficients
[ASME PAPER 69-HT-10] 24 p4413 A69-43558

Physical flow characteristics with self similar laminar boundary layers, performing inverse transformation of Falkner-Skan equation 24 p4304 A69-43586

FLOW CHARTS

Computer systems definition, terminology and functional description, discussing engineering problems, flow charts, programming and techniques 04 p0563 A69-14515

Space-time evolution of one Petrov type into another, obtaining algorithm, flow diagram and discontinuous hypersurfaces results 08 p1350 A69-19789

Minimal representation in state variables for multivariable control system, discussing algorithms, identification methods and flow graph techniques 12 p2047 A69-26070

Procurement procedures in management planning, discussing document flow charts, contract negotiation, etc 15 p2719 A69-30314

Programming aspects of computer uses in civil engineering, stressing engineer-coder communication via flow diagrams 22 p3903 A69-40138

FLOW COEFFICIENTS

NT DISCHARGE COEFFICIENT

Boundary layer effect on flow coefficient of fluid amplifier feed nozzle, noting flow uniformity, incompressibility, velocity and velocity distribution assumptions 07 p1059 A69-19320

Current flow coefficient of high pervance three electrode electron guns with longitudinal compression 11 p1849 A69-24911

Turbulent viscosity and thermal conductivity coefficients for entire cross section of fluid flow including wall boundary layers 11 p1873 A69-25228

Two phase two dimensional turbulent jet analysis for predicting uncertainty in measured value of mixing coefficient 13 p2247 A69-27787

Discontinuity coefficient on boundaries of mixing zone of plane jet, observing homogeneity of thermal and kinematic structures 13 p2247 A69-27978

Turbulent gas coaxial mixing theory, deriving eddy viscosity model and semiempirical expressions for velocity, temperature and density fluctuations [AIAA PAPER 69-682] 17 p2952 A69-33434

Anisotropy of derivatives of transverse velocity fluctuations in grid turbulence subjected to plane deformation, determining dimensionless coefficient 19 p3299 A69-36647

FLOW DEFLECTION

Soviet book on turbojet engine reverse thrust systems and systems for deflection of jet stream covering aircraft braking efficiency 04 p0647 A69-14934

Axial deviation of gas flow resulting from mixing turbulent gas jets 04 p0591 A69-15411

Base pressure calculation in initial turbulent boundary layer of supersonic flow about two dimensional backward facing step, using mass conservation conditions 07 p1119 A69-18747

Supersonic flows past slender bodies, calculating pressure by means of moving singularities 08 p1252 A69-20721

Fluidic jet beam deflection amplifier, discussing basic principles, operating characteristics and design criteria 10 p1638 A69-23554

Oblique shock wave properties with free stream Mach number and flow deflection angle as independent variables, noting explicit solution 11 p1819 A69-25378

Different pressure and deflection measurements coherence in vortex flows verified assuming radial equilibrium conditions 12 p2012 A69-26362

Electrically driven thin fluid jet stability in longitudinal field between two plate electrodes, discussing role of Ohm law in calculating jet potential 12 p2136 A69-26402

Displaced layer thickness dependence on air injection parameters measured in wind tunnel 13 p2245 A69-27385

Displacement of liquid by insoluble liquid from horizontal circular tube during laminar flow, analyzing flow characteristics 14 p2431 A69-29607

Extension of Helmholtz classical problem of flows with discontinuous surfaces, considering two sources and transverse plane 14 p2433 A69-29683

Gas flow deflection at centrifugal pump wheel outlet for wheels having different inlet and outlet vane angles 15 p2547 A69-30571

Alpine effects on wind field at synoptic scale using potential-vorticity equation, discussing deflection angle dependence on potential temperature distribution 15 p2650 A69-31445

Pressure distribution in wake produced by obstacle with secondary fluids injection into boundary layer, obtaining coefficient governing resistance of obstacle to forward motion 16 p2768 A69-31604

Nonequilibrium ionized gas flow past insulated wall with corners under magnetic field, discussing flow characteristics 17 p3010 A69-32865

Hydraulic tank for visualizing flows around stationary models, noting absence of wall effects [ONERA-TP-708] 17 p2956 A69-33588

Viscous electrically conducting fluid flow around thin profiles for equal Reynolds and magnetic Reynolds numbers, using Oseen method to linearize equations 18 p3124 A69-35285

Linearly elastic medium supersonic flow past rigid wedge, considering longitudinal and transverse perturbations interactions, dry friction, adhesion, slip and wedge physicochemical properties 20 p3515 A69-37439

Circular liquid jet oblique impingement on flat surface, noting dry zone occurrence at small angles due to lateral flow deflection 21 p3691 A69-38551

Forces on stationary cylinder under sinusoidal flow, considering symmetrically located vortex pairs and flowfield [ASME PAPER 69-FE-13] 21 p3643 A69-38601

LF switching in wall attachment type digital fluid amplifiers, studying visual and quantitative values for switch pressure and flow as function of geometric variables [ASME PAPER 69-FLCS-31] 21 p3649 A69-38604

Fluidic angular rate sensor, obtaining rate information by sensing laminar jet flow deflection from nozzle, discussing advantages over mechanical rate sensors 21 p3722 A69-38766

Incompressible viscous fluid flow past sphere at low Reynolds number, evaluating stream function and drag on sphere 21 p3694 A69-38771

Jet deflection in drifting subsonic gas flow 21 p3644 A69-39096

Axisymmetric and two dimensional flows over blunt bodies at high Mach numbers by integral relations method 21 p3645 A69-39790

Shock wave detachment distance in front of spheres and cylinders in hypersonic flow, using magnetic shock tubes and Mach 5 and 18 wind tunnels 22 p3931 A69-40710

Transient flow resulting from plane shock diffraction by analytic blunt body, basing analysis on Taylor series expansions in space and time variables 22 p3860 A69-40895

Supercavitating flow past thin hydrofoils, determining flow velocity or acceleration potential near free surface 22 p3933 A69-41023

Integral equations of motion for plane steady flow of viscous incompressible electrically conducting fluid around flat plate 22 p3992 A69-41109

Asymptotic description of laminar hypersonic boundary layer acceleration approaching sharp corner, assuming small interaction with outer inviscid flow [AIAA PAPER 68-67] 23 p4059 A69-41883

Two dimensional diverging flow of ideal compressible fluid past slender profile, using Prandtl-Glauert rule and linearized equation 24 p4243 A69-42584

Supersonic rarefied gas flow past circular cylinder, studying flow and shock parameters by multiple wave interferometry 24 p4244 A69-43070

Boundary layer separation zones in laminar, transition and turbulent fluid flows past conical bodies with widening skirts 24 p4245 A69-43481

Hydrogen-air combustion in supersonic flow past sphere determined with allowance for chemical reactions nonequilibrium rates at high pressure and temperature 24 p4408 A69-43488

Supersonic viscous flow around sharp corner at various expansion angles, giving pressure distributions and velocity profiles role [ASME PAPER 69-HT-14] 24 p4247 A69-43555

FLOW DIRECTION INDICATORS
NT WIND VANES

Heat transfer dependence on direction of heat flow in stainless steel/aluminum interfaces, showing surface roughness and flatness influence 01 p0177 A69-11406

Fixed position pressure probe for measuring subsonic flow direction over range of Reynolds number, Mach number and flow angle 17 p2973 A69-33107

FLOW DISTORTION

Flexural waves passage through obstacles in infinite plate, determining vibration arresting properties of rigid ribs, elastic inserts and hinged couplings 04 p0678 A69-14902

Acoustic streaming near small spherical obstacles, obtaining stream functions 04 p0631 A69-14904

Two dimensional supersonic rotational flow around convex corner solved using coordinate system consisting of left running characteristics and streamlines 05 p0697 A69-15722

Perturbed wake behind spherical models in rarefied plasma flow, noting effects of electron temperature and electric potential of models 05 p0803 A69-16048

Oblique shock wave propagation through two dimensional steady nonuniform inflow, discussing higher order theory via irrotational or rotational disturbances of arbitrary amplitude [AIAA PAPER 69-39] 06 p0913 A69-18103

Exact partial solutions to transonic gas flow equations used to describe flow around shape streamlined by supersonic flow with additional shock wave 07 p1118 A69-18698

Steady conical compressed flows in nonaxisymmetric ring nozzles characterized by discontinuities 07 p1120 A69-18989

Wake deformation for horizontal and vertical cylinders present in wake of hovering rotor, using flow visualization technique [AIAA PAPER 69-228] 07 p1051 A69-19551

Helicopter rotor wake distorted geometry prediction by analytical method, noting experimental results for rotor in forward flight [AIAA PAPER 69-196] 07 p1051 A69-19553

Large amplitude waves in inviscid flows of stably stratified fluids over barriers with constant density upstream constructed from vortex pairs and doublets 08 p1346 A69-20313

Rotor downwash in ground effect in presence of step, using two dimensional analysis for flow field calculation [AIAA PAPER 69-225] 08 p1253 A69-21032

Lift engine model compressor response to inlet pressure distortion to determine nature and extent of critical area of spoiling for axial flow compressors [ASME PAPER 69-GT-29] 09 p1571 A69-22493

Two dimensional stratified flow over obstacle in finite height channel, noting lee waves and drag increase with decreasing speed 11 p1869 A69-24892

Interference between bodies of revolution and wings in supersonic flow, using Volterra method for calculation 11 p1820 A69-25476

Thin deformable body motion in disturbed potential flow of ideal incompressible fluid 11 p1876 A69-25488

Flexural waves passage through obstacles in infinite plate, determining vibration arresting properties of rigid ribs, elastic inserts and hinged couplings 12 p2182 A69-26655

Acoustic streaming near small spherical obstacles, obtaining stream functions 12 p2131 A69-26657

Subsonic wind tunnel solid and ventilated wall interference on air flow around aerodynamic models, discussing data corrections and slotted wall tests [AIAA PAPER 68-360] 12 p2059 A69-26766

Ideal compressible fluid motion and heat transfer, noting convective heat transfer intensification with increased twisting velocity of flow 13 p2251 A69-28559

Hypersonic wakes interference effects induced by facility instrumentation, discussing results of wind/shock tunnel investigations 15 p2588 A69-30475

Flow disturbances in supersonic rocket nozzles due to secondary injection analyzed by effective body approximation, including side forces [AIAA PAPER 69-443] 16 p2839 A69-32666

Inlet produced dynamic distortion and effects on stall margin of J-85 turbojet engine from supersonic wind tunnel tests [AIAA PAPER 69-487] 16 p2840 A69-32676

Velocity and static pressure redistribution in distorted flow field upstream of axial flow compressors [AIAA PAPER 69-485] 16 p2842 A69-32694

Subsonic diffuser design, discussing flow distortion and turbulence levels and pressure loss characteristics [AIAA PAPER 69-449] 16 p2843 A69-32700

Free stream disturbances influence on hypersonic boundary layer transition Reynolds number in heated and unheated flows [AIAA PAPER 69-704] 17 p2953 A69-33453

Velocities and pressure in twisted jet in unbounded space containing same fluid as jet 19 p3298 A69-36388

Nonuniform supersonic flow of ideal inviscid gas impinging on plane obstacle, discussing flowfields and shock wave production in impact 19 p3239 A69-36397

Stratified fluid flow past obstacle, considering steady inviscid flow with nonlinear convection and vertical acceleration 19 p3240 A69-36474

Anisotropy of derivatives of transverse velocity fluctuations in grid turbulence subjected to plane deformation, determining dimensionless coefficient 19 p3299 A69-36647

Perturbed wake behind spherical models in rarefied plasma flow, noting effects of electron temperature and electric potential of models 20 p3581 A69-37957

Convergence of axes of plane-parallel jets due to reciprocal ejection effect, analyzing deformation of jet, rarefaction coefficient for air between jets, etc 21 p3696 A69-39095

Boundary value problem solution for inviscid fluid flow past compliant body with analytical behavior of flow discontinued at points 23 p4151 A69-41525

- Turbomachinery periodic structures design to improve tolerance to inflow distortion and resonant oscillatory flows, considering large amplitude pressure waves propagation
[SAE PAPER 690388] 23 p4201 A69-41666
- Supersonic flows around slender bodies calculated by method of moving singularities
23 p4061 A69-42407
- Transonic flow around profiles with heat input, showing drag reduction in supersonic part of flow field
23 p4061 A69-42414
- Aerodynamics of twisted jet propagating in same fluid by asymptotic expansion, analyzing twist influence on heat transfer
24 p4244 A69-43057

FLOW DISTRIBUTION

- Kernel function applied to compressible fluid flow computation for linear procedure to determine subsonic flow patterns
01 p0058 A69-10225
- Inertia effect of flow between eccentric cylinders with rotating outer cylinder, calculating pressure and shearing distribution and force on inner cylinder
01 p0059 A69-10307
- Gas jet interaction with supersonic flow during injection from orifice of flat body, investigating Mach number, orifice diameter and jet effects on flow pattern near injection
01 p0005 A69-10357
- Vortex method within slender body theory for aerodynamic interference between missile in both captive and dropped positions and carrying aircraft
01 p0007 A69-11026
- Laminar flow of anisotropic Erickson fluid near wall at large Reynolds numbers, discussing Newtonian behavior, viscosity coefficient and particle orientation
02 p0231 A69-12141
- Ground simulation of reentry observables with ablation, studying ablation products interaction with flow field of wave superheater hypersonic tunnel
02 p0229 A69-12502
- Hypersonic surface measurements and flowfield properties about slender cones in hypersonic viscous interaction regime
[AIAA PAPER 68-2] 02 p0189 A69-12520
- Hypersonic flow distribution and separation types over highly swept delta wings with trailing edge flaps at Mach 6
[AIAA PAPER 68-97] 02 p0189 A69-12522
- Three dimensional wakes and jets, discussing centerline velocity, half width growth and velocity irregularities
02 p0190 A69-12549
- Self similar solutions uniqueness of three dimensional laminar boundary layer equations for conical flow determined by supplementary conditions derived from flow pattern
02 p0233 A69-12572
- Hypersonic flow past delta wings with attached shock wave, analysis leads to determination of closed flow pattern
02 p0191 A69-12577
- Photographic flow patterns of separated flows with vortex formation obtained in wind tunnel for different aerodynamic configurations of revolution
02 p0191 A69-12586
- Velocity measurement and flow pattern determination of plane shock waves during passage through channel diaphragm
02 p0234 A69-12589
- Nonlinear weak shock wave diffraction around convex angled corners in polytropic inviscid thermally nonconducting gas
03 p0412 A69-12848
- Circumferential inhomogeneity of flow through impeller blades of axial flow compressor
03 p0361 A69-12954
- Pressure and flow transients in liquid rocket engine feed systems predicted by method of characteristics
03 p0495 A69-12991
- Jet engine exhaust composition and methods for reducing smoke emission through burner design changes, noting primary zone fuel and airflow pattern
[SAE PAPER 680348] 03 p0495 A69-13350
- Flow rate effect on flow pattern of gas escaping through lateral hole of arbitrary depth
04 p0586 A69-14274
- Laminar two dimensional viscous wake behind finite flat plate, investigating upstream and downstream flow field of trailing edge region for high Reynolds numbers
[ASME PAPER 68-WA/APM-20] 04 p0541 A69-14387
- Coaxial flow jet chamber flow patterns dependence on inlet gas velocity, density and length/diameter ratio
[AIChE PAPER 25B] 04 p0587 A69-14509

- Rarefied flow past sphere, analyzing collisionless flowfield structure and development as density increases
04 p0542 A69-14731
- Flow field of impulsively started circular cylinder, noting drag due to nonlinear convection
04 p0544 A69-14897
- Boundary layer flow of viscous incompressible liquid past wedge embedded circular cylinder
04 p0590 A69-15276
- Flow pattern induced by oscillatory point source in rotating inviscid liquid
04 p0591 A69-15279
- Static and dynamic performance of pancake vortex flow field and application to signal amplification
05 p0704 A69-16001
- Suction effect on incompressible flow through step expansion in circular pipe through sudden enlargement, considering inlet flow with thin boundary layer
[ASME PAPER 68-FE-11] 05 p0748 A69-16074
- Flow field in fluidic temperature sensor using schlieren and shadowgraph techniques
[ASME PAPER 68-WA/FE-29] 05 p0763 A69-16102
- Mach number effects on pattern of vortex flow past delta wing and circular cones at various Reynolds numbers
06 p0858 A69-17339
- Visual investigation of flow field at swept wing, measuring pressure distribution at stall fence and vortices formation
06 p0858 A69-17341
- Flow fields about upswept rear fuselages of rear loading cargo transport aircraft
06 p0859 A69-17492
- Kinetic theory of sharp leading edge parallel to supersonic flow using Boltzmann equation, determining flow field
06 p0861 A69-17637
- Laminar constant pressure gradient flow of viscous incompressible conducting fluid through rotating straight circular pipe with perpendicular magnetic field
06 p0967 A69-17718
- Three dimensional scramjet exhaust nozzle flow fields by second order method of characteristics
[AIAA PAPER 69-5] 06 p0862 A69-18048
- Mixing and combustion of gaseous and particle laden jets in air stream, analyzing turbulent, coaxial and jet mixing flows
[AIAA PAPER 69-33] 06 p1038 A69-18146
- Flow field for single or multiple jets firing forward into oncoming supersonic free stream, noting effect of forward extending cylindrical body
[AIAA PAPER 69-69] 06 p0864 A69-18164
- Method of characteristics for nonequilibrium internal flow fields in propulsion systems, discussing focusing, shock wave and accuracy
06 p0915 A69-18170
- Linearized unsteady nonequilibrium flows produced by unsteady motion of thin foil or circular cylindrical shell in compressible gas
07 p1119 A69-18738
- Performance of short supersonic nozzles producing expansion and density jumps in flow, noting efficiency in obtaining maximum driving effect
07 p1050 A69-18753
- Mach number distribution along axes of underexpanded supersonic jets measured in wind tunnel experiments
07 p1050 A69-18922
- Similarity of mean flow patterns of natural local wind to model wind in wind tunnel
07 p1176 A69-18964
- Viscous hydrodynamical equations for flow field exterior to obstacle moving with constant velocity, discussing force relationships, drag invariance and integral representations
07 p1121 A69-19298
- Magnetospheric and high latitude ionospheric disturbances, bulk motion/convection flow pattern and electric field distribution
07 p1128 A69-19370
- Wake deformation for horizontal and vertical cylinders present in wake of hovering rotor, using flow visualization technique
[AIAA PAPER 69-228] 07 p1051 A69-19551
- Computer programmed momentum theory for induced flow field of helicopter rotor in forward flight
[AIAA PAPER 69-224] 07 p1052 A69-19562
- Liquid flow field about oscillating flat plate, comparing visualization results with numerical solution of Navier-Stokes equations
[AIAA PAPER 69-226] 07 p1121 A69-19565

- Shockload on axial intake fan leading edge of radial flow compressor, calculating flow field
08 p1251 A69-20604
- Displacement effect due to subsonic reaction heat front behind shock wave in two dimensional supersonic flows
08 p1252 A69-20691
- Rotor downwash in ground effect in presence of step, using two dimensional analysis for flow field calculation
[AIAA PAPER 69-225] 08 p1253 A69-21032
- Three dimensional flow field of incompressible fluid with purely axial development in conical ducts and turbomachines
09 p1480 A69-21597
- Diagnostic techniques to identify flow regimes of high enthalpy shock tunnel
[AIAA PAPER 68-729] 09 p1477 A69-21970
- Fluid injection into flowfield from porous forward portion of blunt body in stagnation region flow, determining reservoir pressure and mass flow rate
09 p1430 A69-21973
- Unsteady relative flow in centrifugal impeller passage running at part capacity and zero flow observed by hydrogen bubble flow visualization method
[ASME PAPER 69-GT-35] 09 p1432 A69-22489
- Turbulent circular wall air jet trajectory and spreading in perpendicular crossflow of constant and varying velocities
[ASME PAPER 69-GT-33] 09 p1483 A69-22491
- Finite difference method computer programs for calculation of velocities and streamlines on blade to blade surface of revolution of turbomachine
[ASME PAPER 69-GT-48] 09 p1432 A69-22495
- Mach wave and anisotropic supersonic flow interaction, considering constant entropy along streamline and layer of entropy discontinuities/interfaces
10 p1631 A69-22906
- Noninterfering instrumentation techniques to measure hypersonic flowfield parameters in wind tunnels, measuring flight time of pulsed laser generated spark for velocity
10 p1672 A69-23266
- Thin wall flow of circular jets in bounded transverse flow, showing hydrodynamical parameter of mixture effect on jets dimensionless path
10 p1679 A69-23567
- Singular integral equation for velocity in linearized Rayleigh problem in rarefied gas flow field solved by applying Luke weight coefficients
10 p1679 A69-23596
- Air flow distribution and wind velocities in cyclones constructed from Cosmos 122 TV cloud images
11 p1912 A69-24825
- Hot wire sensitivity to velocity, temperature and density fluctuations of temperature varying flow field, discussing calibration curves and special cases
11 p1886 A69-25088
- Spherically blunted 15 degree semivertex angle cone flow field parameters at Mach 8.6, measuring pitot pressure and shock shape
11 p1818 A69-25143
- Asymptotic theory for obtaining nearly free molecular flow solutions uniformly valid throughout flow field based on linearized Boltzmann equation
11 p1818 A69-25283
- Wing geometry and wing lower surface boundary layer effects on rolled-up tip vortices geometry and strength
11 p1819 A69-25372
- Aerodynamic heating of ELDO-A booster rocket, calculating flow field, heat transfer and conduction by method of characteristics and thermal models
11 p1966 A69-25433
- Supersonic nozzle design ensuring desirable flow field in inviscid core of viscous gas flow, using boundary layer equations
11 p1820 A69-25473
- Steady flow field for viscous incompressible fluid in rotating pipe with porous walls determined from Navier-Stokes equations
11 p1875 A69-25481
- Flow field structure involving supersonic secondary jet interactions and separated regions in thrust vector control system
11 p1944 A69-25594
- Spool valve flow patterns within hysteresis region, discussing effects of valve geometry, Reynolds and cavitation numbers
11 p1827 A69-25645
- Flow field over plain or complex bodies with pressure density changes, using high speed schlieren apparatus with color strip filter
12 p2088 A69-26183

FLOW DISTRIBUTION

Aerodynamic field around symmetric profile two dimensional plates, visualizing velocity fields with Al particles

12 p2011 A69-26288

Steady state flow of viscous conducting liquid in inlet of channel with or without transverse magnetic field, emphasizing approach to Hartmann- Poiseuille patterns downstream

12 p2138 A69-26626

Exhaust gas recirculation for VTOL aircraft [AIAA PAPER 67-439]

12 p2013 A69-26760

Ingestion and flow field characteristics of interaction of two heated parallel air jets, discussing VTOL exhaust ingestion tests [AIAA PAPER 68-79]

12 p2012 A69-26761

Imaging for flowfield of nonuniform parallel streams with thin airfoil represented by vorticity distribution, noting change of lift and moment

12 p2012 A69-26775

Aircraft reports of high level turbulence on European and Atlantic routes, noting rapid changes in large scale flow pattern occurring locally

12 p2127 A69-26901

Nonuniform flowfield from supersonic penetration of plane shock by three dimensional pointed planar wing, using integral transform method to study field perturbation pressure

13 p2199 A69-27323

Flow field instability over concave bodies in supersonic free stream computed by integration of gasdynamic equations, noting application to supersonic parachutes [AIAA PAPER 68-946]

13 p2199 A69-28228

Pulsed laser holographic interferometry of density field created by high speed projectile motion in air [AIAA PAPER 69-347]

13 p2263 A69-28282

Characteristics method for stress waves from hypervelocity impact of circular cylinder on half space, discussing numerical diffusion effect on pressure and flow fields [AIAA PAPER 69-355]

13 p2365 A69-28287

Numerical method for time dependent compressible Navier-Stokes equations applied to axisymmetric flow field produced by hypervelocity impact, examining viscous effects [AIAA PAPER 69-354]

13 p2366 A69-28288

Analytical model for free convection heat transfer from vertical plates with nonhorizontal leading edges, discussing flow field

13 p2379 A69-28342

Plasma rotation by Lorentz force in homopolar gas discharge device, considering centrifugal forces effect on flow pattern

13 p2315 A69-28556

Short fiber composites flow orientation in system of high volume glass fibers in epoxy resin measured by glass rheometer

13 p2287 A69-28670

Spherical symmetric unsteady conservation equations describing transient burning of volatile fuel droplets, obtaining time dependent fuel and heat distribution in flow field

14 p2537 A69-29016

Spatial supersonic ideal gas flows past blunt bodies analyzed by numerical finite difference methods, discussing flow fields and entropy

14 p2390 A69-29616

Air mass analysis, discussing homogeneity, quasi-barotropic fluids, noise elimination to arrive at smooth flow pattern, etc

15 p2647 A69-30193

Flow and pressure fields for spiral grooved pumping seal with specified groove dimensions and Reynolds number [ASLE FICFS PREPRINT 30]

15 p2619 A69-30481

Supersonic flow past cone in presence of blowing normal to cone surface, calculating flow field parameters behind conical shock wave

15 p2548 A69-31175

Solid rocket propellants tests, considering propulsion performance measurements, altitude simulation problems, internal flow patterns, nozzle geometry, etc

16 p2765 A69-31751

Two dimensional analysis of isentropic perfect gas flow fields in axisymmetric nozzles for transonic two phase flow initial values, calculating particle trajectories [AIAA PAPER 69-572]

16 p2731 A69-31847

Water vapor recondensation effect on structure of liquid particle flow into vacuum

16 p2769 A69-31869

Godunov finite difference method modified for steady or unsteady flowfields about planar axisymmet-

ric blunt bodies, presenting body pressures and shock shapes

16 p2732 A69-31886

Flow field around sharp slender cones with surface mass transfer at zero angle of attack in low density supersonic and hypersonic flow [AIAA PAPER 68-66]

16 p2732 A69-31887

Plasma flow pattern in twilight regions of earth magnetosheath from positive ion observations of twin Vela 3 satellites

16 p2773 A69-31961

Flow field of highly ionized arc heated supersonic free jet, using continuous flow test facility [AIAA PAPER 68-135]

16 p2772 A69-32153

Free flow field from underexpanded rocket motor nozzle and impingement effects of pressure and heat transfer to flat plate [AIAA PAPER 69-568]

16 p2842 A69-32693

Velocity and static pressure redistribution in distorted flow field upstream of axial flow compressors [AIAA PAPER 69-485]

16 p2842 A69-32694

Rocket exhaust plume flow fields studied for vehicle effects taking into account nozzle boundary layer, coalescence shock and nonisentropic flow [AIAA PAPER 69-569]

16 p2842 A69-32696

Three dimensional supersonic nozzle flow field calculations using second order numerical method of characteristics and computer programmed for internal flows [AIAA PAPER 69-463]

16 p2734 A69-32766

Deflection effect on flow and mixing process in flames covering enclosed turbulent diffusion flames in combustion chamber

17 p3068 A69-32966

Monograph on interaction between flow and sound fields as singular perturbation problem, using matched asymptotic expansion

17 p2949 A69-32998

Separated flow patterns in base flow at body recesses, emphasizing shock wave boundary layer interaction, laminar flow and flow in front of recess

17 p2949 A69-33124

Constitutive equation variation effect on near wall flow pattern of dilute polymer solutions

17 p2951 A69-33257

Nongray absorption and radiation cooling on smooth symmetric blunt bodies included in modified Maslen flow field method for radiation and large blowing [AIAA PAPER 69-637]

17 p2891 A69-33290

Flow field pressure distribution due to plane shock wave impinging by thin wing moving in opposite direction, discussing mathematical formulation, analytic solution and applications [AIAA PAPER 69-647]

17 p2891 A69-33459

Supersonic leading edge problem using nonlinear Boltzmann equation with clipsoidal model, calculating molecular distribution functions for flow field [AIAA PAPER 69-652]

17 p2892 A69-33464

Mixed supersonic/subsonic type steady wake flow fields in flat based slender bodies, using finite difference method [AIAA PAPER 69-649]

17 p2892 A69-33468

Flow field of two dimensional nozzle exhausting to vacuum, describing computer program based on BGK equation and plotting exhaust region density, temperature and velocity [AIAA PAPER 69-658]

17 p2893 A69-33490

Flow field study of merging between bow shock and viscous layer upstream of highly cooled axisymmetric blunt body in rarefied hypersonic stream [AIAA PAPER 69-656]

17 p2893 A69-33498

Flow measurements about high Mach number low Reynolds number laminar wake behind spherically blunted cones, including surface and wake flow field data, radial wake profiles, etc [AIAA PAPER 69-714]

17 p2894 A69-33500

Far and near field solutions for one dimensional unsteady flows in general inviscid relaxing gas, obtaining flow field structure by matching techniques

17 p2957 A69-33599

Two dimensional incompressible flow past circular cylinder at moderate Reynolds number, reducing partial differential equations of motion by series truncation for flow field

17 p2896 A69-33600

Flow structure in wake of blunt bodies placed perpendicular in parallel airstream determined from hot-wire anemometry [AIAA PAPER 69-746]

18 p3084 A69-34409

Laminar recompression behavior downstream of stagnation point behind hypersonic slender body, obtaining finite difference numerical solutions for near wake flow field [AIAA PAPER 69-713]

18 p3085 A69-34417

Mean patterns of meridional interhemispheric flow for 40 degree equatorial sector, calculating mean air mass transport in lower troposphere over western Indian Ocean

18 p3166 A69-34420

Turbomachinery aerodynamics, discussing secondary flow in blading and digital computer applications to annulus flow field

18 p3086 A69-34925

Shock wave structure in single component monatomic gas by expanding Boltzmann equation distribution function in terms of Hermite polynomial

18 p3124 A69-35170

Gas core reactor curved porous walls geometry tested with clear and smoky air injection, noting mass flow ratio in reactor cavity

18 p3171 A69-35181

Rotating static thrust propeller or hovering rotor flow field study by schlieren photography, considering vortex field, tip flow and shock wake formation

18 p3087 A69-35218

Flow field throughout wind tunnel containing rotor with sharply deflected blades, noting reversed flow effect in front of wake

18 p3119 A69-35228

Systematic mathematical ordering of knowledge concerning three dimensional flow patterns around blunt bodies, emphasizing high speed computers role

18 p3089 A69-35269

Molten iron plane melt flow duration and mass in bimetallic castings production determined using nomogram

18 p3149 A69-35289

Secondary flow consisting of longitudinal vortices superposed on convection flow on inclined plate, obtaining flow pattern through flow visualization

18 p3124 A69-35383

Ion collecting cylindrical electrostatic probes as flow field tracing instruments in low density slightly ionized flows

19 p3291 A69-35718

Fraunhofer holography for measurement of three dimensional flowfield velocity components, investigating rectangular channel flow

19 p3305 A69-35729

Holographic velocimetry data reduction applicable to flow field holograms, using singlet interference pattern for spherical and plane wave illumination

19 p3305 A69-35730

Static temperature measurement in arc-tunnel tests producing high velocity air streams by duplex scanning IR spectrometer

19 p3294 A69-35752

Axial stagnation point flow in shock wave reflected from sphere or circular cylinder, determining velocity time variation, enthalpy pressure and reflection

19 p3298 A69-36385

Supersonic aerodynamic characteristics of flared cones with various flare angles studied by schlieren photography, showing geometrical parameters influence on flow patterns

19 p3239 A69-36387

Hydrogen jet structure ejected into vacuum from Laval nozzle at supersonic velocity, considering separation point from diffuser wall

19 p3240 A69-36601

Conducting gas flow parameters in coaxial duct, considering magnetic nonuniformity, Hall currents and fields distortion near electrodes

19 p3381 A69-36772

Ordered sets of Massieu thermodynamic characteristic speeds for reacting gas mixtures relevant to nonequilibrium flow fields compared to Laplacian and Newtonian speeds

19 p3452 A69-36802

Heat transfer coefficient and flow patterns of horizontal circular plate for various Rayleigh numbers, noting surface temperature

20 p3632 A69-37523

Flow induced by plane flame traveling supersonically or subsonically at constant speed through long tube studied for flow field steadiness in flame fixed coordinates [ASME PAPER 69-FE-33]

20 p3460 A69-37993

N strip algorithm of integral relations to analyze flow around circular cone at incidence in supersonic flow

20 p3460 A69-38128

Computer solutions for nonlinear partial differential equations governing compressible flow patterns with shocks, using Lagrange coordinates

20 p3569 A69-38212

Forces on stationary cylinder under sinusoidal flow, considering symmetrically located vortex pairs and flowfield [ASME PAPER 69-FE-13]

21 p3643 A69-38601

Flow field induced by spiral vortex sheet, noting existence of radial velocity component
21 p3692 A69-38610

Laminar free convection from horizontal infinite strip with downward facing thermally insulated vertical walls at edges, noting boundary layer thickness and flow pattern
21 p3853 A69-39672

Small particle holography technique extended for dynamic properties of particle fields, determining velocity and density field, size distribution, flow structure and diffusion rate
21 p3726 A69-39776

Flow structure in wake behind cylinder in plane channel, discussing circulation zone variation and velocity and turbulence distribution at various channel cross sections
21 p3698 A69-39850

Mach 8 flow field effects and forces on small delta tail surfaces mounted on body of revolution at various angles of attack
[AIAA PAPER 68-891] 22 p3859 A69-40539

Base pressure of peripheral jet ground effect machines in heaving motion, discussing flow patterns
22 p3866 A69-40817

Flowfield properties of two dimensional supersonic jet near sonic nozzle exit by numerical method of characteristics
22 p3860 A69-40920

Stratified blood flow distribution in lung lobe from analyzing breath-holding changes on expired Ar and nitrous oxide tension plateaus during rest and exercise
23 p4078 A69-41315

Alaska sled dogs cardiovascular performance and flow distribution during cross country runs
24 p4256 A69-42624

Fluid mechanical structure of laminar hypersonic wake behind sharp circular cone, investigating flow field at zero angle of attack and adiabatic wall temperature
24 p4247 A69-43576

Reverse flow profiles in turbulent free jet mixing with streamwise pressure gradient
24 p4306 A69-43684

LF approximation in predicting unsteady aerodynamic forces affecting large aircraft stability, analyzing velocity potential of oscillating wings
24 p4250 A69-43729

FLOW EQUATIONS
NT HELMHOLTZ VORTICITY EQUATION
NT VON KARMAN EQUATION
NT VORTICITY EQUATIONS

Lossy and lossless fluidic transmission line theory to estimate downstream conditions having known upstream system
01 p0012 A69-10153

Asymptotic solution of Orr-Sommerfeld equation by multiple scales method for linear and general velocity profile
01 p0059 A69-10332

MHD boundary layer equations in Blasius problem reduced to differential equations and solved by Laplace transform
01 p0127 A69-10337

Indeformable gravity waves in horizontal cylindrical channel, using first and second order approximations for nearly uniform flow equations solutions
01 p0060 A69-10392

Shock layer gas radiation influence on deep space missile shape, noting evaluation by flow equations
01 p0007 A69-11070

General theory of constitutive equations for rational mechanics of deformation and flow
02 p0341 A69-12251

Meksyn method application to problems of jet mixing and jet reattachment
02 p0233 A69-12530

Unsteady incompressible boundary layer flow over leading edge boundary layer calculated by three dimensional time dependent equations
02 p0233 A69-12543

Self similar solutions uniqueness of three dimensional laminar boundary layer equations for conical flow determined by supplementary conditions derived from flow pattern
02 p0233 A69-12572

Geostrophic wind direct computation from grid point analysis of observed winds, using balance equation
04 p0626 A69-14913

Variable energy blast waves analysis with reference to cylindrical spark channel formation, noting shock front velocity approximation
04 p0590 A69-15203

Flow of two conducting immiscible liquids between parallel porous moving plates under transverse magnetic field
05 p0743 A69-15600

Source and sink method application to direct axisymmetric problems of hydrodynamics
05 p0747 A69-16039

Model kinetic integral equation for describing flow in transition region at leading edge of tapered body in rarefied gas
05 p0697 A69-16040

Simulation of two and three dimensional fluid transients by use of one dimensional equations in lattice-work of piping elements
05 p0747 A69-16071

Interaction between supersonic jet and counterflow of ideal compressible fluid
05 p0751 A69-16501

Two dimensional aligned field MGD flows analyzed using corresponding basic equations
05 p0806 A69-16735

Magnetoplasticity induced in metal by high magnetic fields, examining stationary flow in two dimensional deformation
05 p0844 A69-16804

Approximate solution of equations for boundary layer flow of conducting medium on insulating and electrode walls of MHD generator channel
06 p0871 A69-17914

Viscid-inviscid equations solution, describing flows with coupled mixing, combustion and lateral pressure gradients
[AIAA PAPER 69-83] 06 p1037 A69-18109

Computer solution of incompressible two dimensional time dependent Navier-Stokes equations for oscillating body with rectangular boundaries
[AIAA PAPER 69-185] 06 p0914 A69-18135

Parasitic eigenvalue in integration of equations governing one dimensional flow of chemically reactive gas
07 p1118 A69-18317

Approximation of Chaplygin plane motion equations of gas flow at high supersonic velocities
07 p1120 A69-18754

Three dimensional vector fields and flows geometry, discussing vector lines as geodesics on surfaces of normal congruence and flat vector fields
08 p1302 A69-19823

Clebsch transformation application to equations describing viscous fluid, deducing canonical equations equivalent to Navier-Stokes equations
08 p1303 A69-20125

Approximate equations for transonic viscous heat conducting gas flow past finite body of revolution
08 p1251 A69-20322

Transformation of laminar stationary incompressible boundary layer equations for body of revolution in incident flow, using difference method
08 p1252 A69-20703

Frequency response from linearized dynamic equations for viscous incompressible fluid flow in viscoelastic tubes, discussing transfer gain
08 p1304 A69-20704

Gas kinetics application to various flow problems by solving Boltzmann equation for monoatomic single component gas
08 p1351 A69-20708

Singular perturbation problem for elliptic linear partial differential equation, studying asymptotic expansion of solution in vicinity of singular points in nonconvex domain
08 p1352 A69-20751

Fluid equations for collisionless plasma including finite ion Larmor radius and finite beta effects
08 p1368 A69-20802

Flow equations of rheological media derived using thermodynamics, assuming nonlinear stress-strain relation in incompressible medium
08 p1419 A69-21074

Rarefied gases back diffusion between parallel plates used for studying diffusion in capillaries, deriving volume flow equation valid for any density
10 p1677 A69-22903

MHD first order partial differential equations used to investigate wave front between perturbed and unperturbed flow regions in magnetosonic propagation through homogeneous medium
10 p1727 A69-23090

Optimum operation modes of MHD converter
10 p1636 A69-23095

Three dimensional MHD flow near forward stagnation point magnetic fields with large induction values described by differential equations, showing tendency towards two dimensional flow
10 p1727 A69-23100

Similarity solutions of laminar boundary layer equations for three dimensional flows of incompressible power law fluids
10 p1678 A69-23235

Existence and uniqueness to boundary layer continuation problem based on flow equation for steady gas flow
10 p1679 A69-23569

Laminar boundary steady two dimensional constant velocity flow over curved surface equation derived from Navier-Stokes equation
11 p1867 A69-24375

Shock wave propagation in gravitational field with pressure and density gradients, considering nonlinear equations of fluid flow
11 p1961 A69-25106

Iterative solutions of nonlinear integrodifferential dynamical equation for two point velocity correlation tensor in incompressible fluid turbulence studies
12 p2062 A69-26602

Nonlinear periodic wave propagation at angle to magnetic field in collisionless plasma studied by two fluid plasma equations
13 p2304 A69-27297

Unique solution proven for laminar boundary layer equations of flow of revolution in unsteady state
13 p2248 A69-28195

Stationary radial source flow of liquid particles into vacuum, discussing boundary value problem equations, parameters effects on flow structure and flow field characteristics
13 p2248 A69-28210

Boundary layer equation of viscous incompressible fluid with moment stresses, noting flow around thin plate and submerged jet problems
14 p2428 A69-28815

Model equation for Reynolds stress in turbulent two dimensional shear flow
14 p2428 A69-29000

Unsteady pressure on oscillating slender cone in hypersonic flow derived by expanding flow equations in powers of shock density parameter
14 p2389 A69-29020

Kelvin-Helmholtz instability noting effects of oblique magnetic field and rotation, deriving dispersion relation
14 p2491 A69-29335

MHD equations system in intrinsic form, establishing conditions of integrability
14 p2492 A69-29593

Radiating gray gas laminar jet in thermodynamic equilibrium ejected from plane nozzle into wake analyzed using boundary layer, divergence and transfer equations
14 p2432 A69-29612

Von Karman swirling flow problem differential equations solved by extending Serrin existence theorems
14 p2432 A69-29676

Riemann problem with arbitrary jump data for extended hyperbolic systems of equations, showing conditions for unique solution
14 p2433 A69-29678

Extension of Helmholtz classical problem of flows with discontinuous surfaces, considering two sources and transverse plane
14 p2433 A69-29683

Cosmic shock waves simulation through correlations between shock equations in classical and relativistic fluid dynamics, using shock tube tests
14 p2433 A69-29981

Boundary value problem for quasi-linear equation of unsteady transonic gas flows, including linear model and operators for group of transformations
15 p2590 A69-30049

Incompressible two dimensional turbulent boundary layer equations with arbitrary pressure distribution solved by weighted residual method
[AIAA PAPER 69-397] 15 p2591 A69-30478

Rate equation for effective turbulent viscosity variations, considering effects of generation, convection, diffusion and decay in quasi-parallel shear flows
15 p2591 A69-30905

Pressure fluctuation relaxation model to close turbulent distribution function equations at one point level, solving equation for rectilinear flows and periodic wake decay
15 p2591 A69-30906

Similarity solutions for laminar compressible boundary layer with reverse flow, considering various wall/stagnation temperature ratios
15 p2591 A69-30907

Hamiltonian variational principle for stationary bounded MHD flows, choosing suitable functions and rigid conducting boundary location
15 p2660 A69-30910

Laminar boundary layer equation solution representing velocity profile by fourth degree polynomial
15 p2593 A69-31263

Two phase flow mixing shocks, obtaining expressions for pressure and entropy changes, discussing shock stability and gas entrapment mechanism
16 p2768 A69-31589

Eigenvalue bounds for amplification rates, wave speeds and linear stability conditions for Orr-Sommerfeld equation governing parallel flow in boundary layer and round pipes
16 p2768 A69-31591

Mean velocity distribution prediction in turbulent shear flows of variable density by coordinate stretching method
[AIAA PAPER 68-41] 16 p2770 A69-31888

Monograph on solutions to equations for unsteady flow of ideal gases, with applications to hypersonic flows, based on three space coordinates and time
16 p2773 A69-32428

Compressor surge effect on mixed compression inlet flow from numerical solution of one dimensional unsteady inviscid flow equations in variable area duct
[AIAA PAPER 69-484] 16 p2841 A69-32682

Approximate equations for transonic viscous heat conducting gas flow past finite body of revolution
17 p2891 A69-33312

Adiabatic compressible turbulent boundary layer equations for two dimensional and axisymmetric flows, discussing methods of solution based on eddy viscosity formulation
[AIAA PAPER 69-687] 17 p2955 A69-33470

Flow field of two dimensional nozzle exhausting to vacuum, describing computer program based on BGK equation and plotting exhaust region density, temperature and velocity
[AIAA PAPER 69-658] 17 p2893 A69-33490

Elastoplastic flow equations formulation, inverting flow rule to relate stress rates to strain rates and instantaneous stresses, noting Navier equations
18 p3219 A69-34666

Similarity solutions of viscous transonic equation describing spiral and radial flows, containing shock-like transitions of corresponding inviscid solutions
18 p3121 A69-34787

Magnetic fields and electrically conducting fluids interaction with emphasis on magnetodynamics equations, investigating rectilinear flows in pipes and nozzles, shock waves, etc
19 p3379 A69-35804

Gas dynamics equations solution applied to Cauchy problem
19 p3297 A69-35861

Asymptotic form of axisymmetric solution with Dirichlet integral for Navier-Stokes equations applied to flow past bodies of revolution with smooth surfaces
19 p3298 A69-36143

Finite difference scheme for primitive equation model, emphasizing two grid internal noise suppression to improve gradient force expression accuracy
19 p3364 A69-36507

Series expansion for exponent of singularity of Laplace equation for flow near apex of plane delta wing
19 p3240 A69-36590

Coupling conditions by distinct equations for two laminar flow regions, studying near wake and considering Euler, Navier-Stokes and Prandtl correlations
[ONERA-TP-738] 19 p3299 A69-36649

Momentum and energy equations for fluctuating flow of viscous incompressible conducting fluid past flat plate with time dependent suction under transverse magnetic field
21 p3691 A69-38445

Boundary layer flow past permeable surface, generalizing integral equations for case with suction
21 p3691 A69-38573

Sedov canonic equations for supersonic gas flow solved by applying Chaplygin function to determination of Riemann function for potential and stream function equations
21 p3643 A69-38637

Blast angle effect on fanjet gas dynamics in crosswind, using equations for free lateral flow trajectories and reverse flow regions
21 p3850 A69-38863

Equations governing steady diabatic gas flows in Crocco velocity vector field, discussing changes in total pressure
21 p3695 A69-39007

Existence conditions of critical points for autonomous differential equations in bounded flows
22 p3975 A69-40571

Friction, heat transfer and mass transfer theory of flow represented by two dimensional parabolic boundary layer equations
22 p3933 A69-40940

Second order differential equations of supersonic flows past bodies at small angles of attack, showing linearized characteristics method applicability for conical nose
24 p4243 A69-42581

Two dimensional diverging flow of ideal compressible fluid past slender profile, using Prandtl-Glauert rule and linearized equation
24 p4243 A69-42584

Book on flow equations for composite gases derived from Boltzmann equation, BGK approximation application, etc
24 p4299 A69-42766

Unsteady axisymmetric potential flow of ideal incompressible fluid with free surfaces, deriving differential equations for gas bubble dynamics and surface geometry
24 p4302 A69-43500

Numerical program solving partial differential equations parabolic system for internal turbulent gas flow extended to flows undergoing circular tube laminarization by heating
[ASME PAPER 69-HT-52] 24 p4409 A69-43520

FLOW GEOMETRY

Flow in square to rectangular constant area transition piece having straight walls with outlet aspect ratio of 5 fitted with exit duct
02 p0189 A69-12412

Surface geometry of three dimensional inviscid hypersonic flows, developing tensor equations for geodesic, steepest descent and pressure approximations
04 p0542 A69-14718

Ducted turbulent mixing and burning of coaxial streams, presenting experimental results for rocket-air mixing system
[AIAA PAPER 69-85] 06 p0984 A69-18082

Heat transfer coefficients for supersonic open cavity flow recompression steps noting influence of step and flow shapes
13 p2375 A69-27786

Gas turbine areas calculation of through flow cross sections for temperature deformations and blades elongation
18 p3184 A69-34987

Hydrodynamic equations of laminar plane flow of incompressible viscous fluid in rectangular region, calculating velocity field by equivalent network and integration
19 p3297 A69-35853

Divergence losses of noncircular C-D nozzles based on approximation by spherical source flows
19 p3238 A69-35960

Multistep axisymmetrical supersonic exit cones optimum geometry design diagram based on external oblique and normal compression shock
21 p3785 A69-39104

Secondary flow occurrence and geometry in viscous turbulent flow in square channel, using iterative solution
24 p4303 A69-43501

Local Nusselt number beyond abrupt circular channel expansion tested for Reynolds numbers with air as working fluid
[ASME PAPER 69-HT-35] 24 p4411 A69-43532

FLOW GRAPHS

Compressible fluid two dimensional supersonic and one dimensional unsteady flows similarities shown graphically, discussing hodograph-speedgraph relationship
19 p3300 A69-36777

Mathematical flow graphs application in analysis and design of elastomechanical structural systems
[AAS PAPER 69-151] 24 p4339 A69-42816

FLOW MEASUREMENT

Leak flow rates of nitrogen and helium at various pressure gradients measured by gas chromatography and mass spectroscopy
01 p0079 A69-10297

Discharge coefficient nondependence on Reynolds number demonstrated by measurement at orifices with sharp edges
01 p0006 A69-10362

Flow nonuniformity measured in shock tubes by determining heat transfer rate to fine wire probes
01 p0062 A69-11219

Pressure gain estimates in analog jet amplifier based on total pressure measurements in main jet interaction region
02 p0195 A69-12076

Discharge coefficients for Herschel type smooth venturimeters, analyzing influence of transport coefficients, convergence angles and contraction ratios
02 p0250 A69-12414

Wind tunnel and test equipment for studying flow in straight airfoil lattices at Reynolds numbers 50,000-1,200,000 and Mach numbers 0.1-1.0
03 p0412 A69-13789

Laminar and turbulent flow measurement in variety of tube diameters, using ring laser without insertion of mechanical probe
04 p0596 A69-14281

Open circuit wind tunnel experiment to measure properties of two dimensional plane turbulent wall jet in moving stream
[ASME PAPER 68-WA/APM-13] 04 p0586 A69-14390

Inclined hot-wire and hot-film anemometers parameter dependent on length-to-diameter ratio used to describe deviations from cosine law
[ASME PAPER 68-WA/APM-16] 04 p0596 A69-14391

Current mode amplifier circuit used with carbon resistors for measuring low flow rates of liquid hydrogen from small containers
04 p0577 A69-15025

Primary flow measuring element based on Chebyshev principle, noting differential pressure output loss and resistance to accumulation of contaminants
04 p0600 A69-15030

Nondirectional probe for mean velocity measurement in turbulent flow, determining reduced velocity profiles in interior of free flow
04 p0600 A69-15056

Sonic nozzle mass flow measurement errors at high supply pressures and moderate temperatures due to real gas effects
[ASME PAPER 68-WA/FM-4] 05 p0699 A69-16114

Venturi meter with separable diffuser and radial outward step at transition from throat to diffuser, noting effect of step on efficiency
[ASME PAPER 68-WA/FM-2] 05 p0763 A69-16135

Flow measurements in near wake of 7 degree half angle cone at free stream Mach number 4.3, noting pressure measurements
[AIAA PAPER 69-186] 06 p0863 A69-18068

Turbulent density fluctuations in near wake of hypersonic axisymmetric slender body measured photometrically with near UV absorption of sulfur dioxide in flow
[AIAA PAPER 69-70] 06 p0864 A69-18158

Book on fundamentals of temperature, pressure and flow measurements covering standards, calibration, moving fluid effects, transient effects and installations in fluids and solids
07 p1131 A69-18410

Flow diagnostics for high enthalpy nonequilibrium gas flows in shock tubes using long pulse ionized Ar gas laser
08 p1323 A69-1979

Multibeam Fabry-Perot interferometers for aerodynamics measurements of rarefied gas flows, determining density distribution, shape, structure and detachment of shock waves
08 p1314 A69-20385

Highly turbulent boundary layers on walls in channels using laser light sources
09 p1515 A69-21434

Spatial distribution of velocity, spatial correlation and ergodicity of turbulent flow, using spectrum of intensity fluctuations of scattered laser light
09 p1493 A69-21491

Impurity concentrations in expansion tube flow, measuring radiation intensities
[AIAA PAPER 68-371] 09 p1477 A69-21961

Diagnostic techniques to identify flow regimes of high enthalpy shock tunnel
[AIAA PAPER 68-729] 09 p1477 A69-21970

Bloodless heart flow measurement methods, noting simultaneous external recording of carotid and femoral pulses and impedance plethysmography
09 p1448 A69-22730

Flow and heat transfer measurements for heated air in subsonic flow through contraction section connecting tube to conical section
[JPL-TR-32-1348] 10 p1809 A69-23194

Mean flow measurements in supersonic wake of slender two dimensional body at zero incidence and heat transfer rate, noting predictability from similarity analysis
11 p1817 A69-24281

Nonorientable five channel adapter with spherical measuring head for three dimensional gas flow mea-

surement, noting sensitivity to mechanical disturbances in calibration

11 p1888 A69-25340

Laser Doppler flowmeter for heterodyne detection of laser light scattered from moving fluid applied to fluid velocity and velocity distribution measurements

12 p2093 A69-26546

Radial liquid flow between flat annular rings /face seals/, discussing film cavitation

13 p2267 A69-27365

Shock wave gas flow density behind shock tube calculated by shadows measurements using interferometric techniques

13 p2245 A69-27384

Effective electrical conductivity of two phase vapor-potassium flow in flat duct at flow temperature 800 C, showing dependence on volumetric vapor content

13 p2306 A69-27480

Construction and calibration of combined temperature and pressure probe for compressible flow

13 p2242 A69-28226

Monograph on velocity distribution function in turbulent boundary layer, discussing hot wire anemometer for mean velocity, turbulence intensity and higher order moments determination

13 p2250 A69-28336

Venturi meter with separable diffuser and radial outward step at transition from throat to diffuser, noting effect of step on efficiency
[ASME PAPER 68-WA/FM-2]

14 p2447 A69-29447

Axial and radial turbulence intensities for flow through smooth round tubes, measuring velocity profiles and drag coefficients

15 p2590 A69-30003

Thermistor thermometer with low energy dissipation for flow measurements, discussing design considerations

15 p2608 A69-30296

Shock tube hot flow duration, contact surface configuration and boundary layer thickness

15 p2590 A69-30297

Fluid flow velocity measurements by Doppler shift of laser light scattered from moving fluid, determining beat frequencies

15 p2616 A69-31291

Hydrodynamic parameters of annular Couette flow in longitudinal magnetic field for variable Reynolds and Mach numbers

16 p2821 A69-31953

Leak rate measurement accuracy of rate-of-rise technique for nitrogen, methane and He between millionth and thousandth torr

16 p2791 A69-32326

Temperature and flow measurements in jet engine combustion chamber, discussing design and calibration of gasdynamic thermometer, double thermocouple and flow probe

17 p2945 A69-32947

Flow measurements about high Mach number low Reynolds number laminar wake behind spherically blunted cones, including surface and wake flow field data, radial wake profiles, etc
[AIAA PAPER 69-714]

17 p2894 A69-33500

Constant pressure adiabatic turbulent boundary layer characteristics measurements correlated in incompressible reference frame, using modified Mager compressibility transformation

17 p2958 A69-34051

Fluctuating heat transfer and flow measurements for circular cylinder in crossflow with simultaneously imposed transverse standing sound field

18 p3124 A69-35384

Ferroelectric transducer for heat transfer rates and flow measurement in gaseous systems with autostabilized temperature, noting film coefficient

19 p3307 A69-35749

High energy recovery pressure and enthalpy sensor /HERPES/ for flow measurements in aerospace simulation facilities

19 p3307 A69-35750

Book on flow measurement techniques, considering forces, pressures, temperatures, boundary layers, wakes, turbulence, streamlines, etc

19 p3313 A69-36381

Liquid mercury flow turbulent intensity measured by quartz insulated Pt hot-film sensors, discussing calibration equation and measurement techniques

21 p3722 A69-38769

Monograph on hot wire anemometer measurements of velocity and temperature turbulence, discussing flow characteristics, calibration, etc

22 p3951 A69-41256

Gilson cuvette densitometer used for blood flow measurement in canine forelimb and human forearm and hand during constant intrabrachial arterial dye infusion

23 p4077 A69-41294

Pump system to obtain indocyanine green dye dilution curves without blood loss in small animals and infants

23 p4101 A69-41450

Discrepancy between theoretical and experimental coefficients of friction losses on blades of centrifugal compressor impeller wheels, using lattice theory

23 p4058 A69-41727

Internal flow measurements in transonic region of supersonic nozzle with small throat radius of curvature compared with prediction data

23 p4060 A69-41900

Stewart-Hamilton formula for cardiac output measurements and regional blood flow determination

24 p4271 A69-42784

Two dimensional incompressible inviscid fluid flow problems solution by conducting-paper analog with electrical equipotentials tracing, based on Laplace equation applicability

24 p4299 A69-43024

Fluid flow around sphere at high Reynolds number by measuring pressure distribution, considering boundary layer separation, tunnel blockage, etc
[ASME PAPER 69-APMW-26]

24 p4245 A69-43093

Transition from turbulent to laminar regime as consequence of high heating rates for internal convective flow, noting roles of Nusselt numbers and friction factors

24 p4304 A69-43559

FLOW REGULATORS

NT FUEL FLOW REGULATORS

Ejector-diffuser performance improvement by reduction of backflow with orifice plate installed at inlet of straight diffuser duct

11 p1819 A69-25382

Spiral grooved turbulent screw seal /viscoseal/ analysis, combining results of spiral grooved journal bearing study with turbulent fluid film theory
[ASLE FICFS PREPRINT 32]

15 p2619 A69-30482

Distributed boundary layer suction effectiveness for controlling supersonic transitional flow separation

16 p2772 A69-32149

Pt wire detector for flow regulation of atomic hydrogen beam, noting hydrogen maser application

22 p3950 A69-41232

FLOW RESISTANCE

NT AERODYNAMIC DRAG

NT FRICTION DRAG

NT SUPERSONIC DRAG

NT VISCOUS DRAG

Energy dissipation at rounded pipe entrance in viscous fluid, showing relation between entrance loss and radius of roundness

01 p0059 A69-10308

Laval nozzle resistance as result of friction and under expansion of gas, noting flow and pressure recovery coefficients

03 p0361 A69-12967

Incompressible turbulent boundary layer with near zero wall friction at circular cylinder situated longitudinally in flow

03 p0416 A69-13664

Ellipsoids of revolution in viscous flow at very low Reynolds number, determining optimum shapes and minimum resistance values

06 p0911 A69-17780

Approximate solution for turbulent jet expansion in opposing stream, discussing hydraulic drag coefficient formula derivation

07 p1118 A69-18396

Pressure distribution on star-shaped bodies in wind tunnel at Mach 4 and Reynolds number .000006

07 p1050 A69-18703

Wall friction influence on three dimensional flow in axial flow turbomachines, introducing shear stresses between flow planes

08 p1252 A69-20724

Equilibrium dissociating gas laminar flow in circular tube calculated for heat transfer and hydraulic resistance, using boundary layer equations

10 p1679 A69-23426

Plenum chamber obstructions influence on hovercraft lift fan performance, discussing tests and losses due to flat plate at impeller outlet

13 p2202 A69-27546

Heat flow resistance between solid bodies in contact in vacuum

13 p2378 A69-28338

Diffuser inlet geometry, studying effects of straight section length on flow pattern and diffuser resistance

14 p2391 A69-29899

Gas ducted flow at subsonic inlet velocity and critical outlet Reynolds numbers, proposing surface friction relation to Mach number

16 p2771 A69-31956

Hydrogen check valve with low cracking pressure and flow pressure drop for hydrogen vent system at Saturn launch pad
[AIAA PAPER 69-578]

16 p2845 A69-32738

Heat transfer and hydrodynamic resistance for turbulent gas flow in longitudinal positive and negative pressure gradients analyzed using Reynolds number data

21 p3848 A69-38635

Hydraulic resistance of pipes with flow vorticity produced by helical swirlers

21 p3695 A69-38862

Turbulent Hartmann flow between rough walls in transverse magnetic field, determining field influence on resistance coefficient

22 p3989 A69-40255

Wave processes in pipelines during fluid filling, studying effects of flow resistance due to pumps and nozzles

24 p4300 A69-43075

Choking and shock in flashing single component two phase flow in tube, including vibrational effects, predicting minimum stagnation pressure loss
[ASME PAPER 69-HT-61]

24 p4303 A69-43535

Heat transfer and fluid friction of hydrogen and helium gas flows undergoing turbulent to laminar flow transition in heated pipe
[ASME PAPER 69-HT-54]

24 p4303 A69-43539

FLOW SEPARATION

U BOUNDARY LAYER SEPARATION

U SEPARATED FLOW

FLOW STABILITY

NT BOUNDARY LAYER STABILITY

NT FLAME STABILITY

NT MAGNETOHYDRODYNAMIC STABILITY

Couette flow stability in axial magnetic field, considering time bounded perturbation energy during increasing angular velocity in radial direction

01 p0059 A69-10233

Linear stability of steady and time dependent plane Poiseuille flow

01 p0175 A69-10333

Stabilization of plane parallel MHD flow at inlet and outlet of flat rectangular tube with transverse magnetic field

01 p0130 A69-10770

Linear stability of parallel flow in concentric annulus for infinitesimal axisymmetric disturbances

01 p0061 A69-11201

Instabilities for two highly conducting finite length streams in relative motion and coupled by transverse electric or longitudinal magnetic fields

01 p0062 A69-11208

Coaxial jet mixing regimes in jet engines, determining requirements for compatibility by applying aerodynamic theory of ejectors
[ONERA-TP-599]

02 p0187 A69-11619

Turbulent gas flow characteristics obtained by extremal hypothesis, using maximum perturbation stability in formulating variational problem and computer algorithm

02 p0232 A69-12354

Algorithm for Orr-Sommerfeld equation applied to stability of laminar flow, noting profile resembling mean velocity profile of turbulent flow in flat tube

02 p0233 A69-12573

Barotropic instability analyses by method of jet stream like fields and energy transport from zonal current to wave disturbances based on vorticity equation

02 p0276 A69-12758

Viscous liquid layer flow down inclined plane under boundary conditions, taking into account drag and penetration at porous bed surface

02 p0234 A69-12774

Plane Couette flow stability in heated nonlinear viscous fluid flowing between horizontal plates heated to different temperatures

02 p0235 A69-12828

Solute vertical stabilizing gradient inhibition of thermal convection of fluid layer under temperature gradient, discussing effects on two dimensional flows motion

03 p0532 A69-13012

Cylindrical jet stability of perfectly conducting, incompressible and inviscid fluid in presence of axial magnetic field

03 p0474 A69-13142

Neutrally stable disturbances for nonplanar parallel shear flow with continuously varying mean velocity
03 p0415 A69-13155

Eigenvalues for Orr-Sommerfeld equation by difference technique for Reynolds number range 5780-729000, determining Poiseuille flow stability in plane channel
03 p0416 A69-13654

Sufficient conditions for stability of compressible atmospheric flows for rigid lid types of upper boundary condition
03 p0417 A69-13796

Instability and disturbance amplification in external laminar natural convection boundary layer over vertical flat surface with uniform heat flux
03 p0533 A69-13951

Stability of nondissipative stratified rotating flows with constant density to axisymmetric disturbances
04 p0588 A69-14740

Stabilizing influence of axial magnetic field on confined vortex flow of aqueous electrolytic conductor generated by two dimensional wall jets
05 p0798 A69-15611

Coanda nozzle entrainment and flow augmentation approximating numerical stability by finite differences
05 p0746 A69-16021

Laminar flow stability parameter presenting coupling ratio between angular momentum change and loss rate by frictional drag
05 p0750 A69-16187

Laminar flow stability along flexible boundary, using broken linear velocity profile instead of boundary layer profile
06 p0909 A69-17207

Secular equation for Couette flow stability in incompressible viscoelastic fluid
06 p0909 A69-17240

Inviscid incompressible fluid flow stability against helical disturbances in circular cylinder
06 p0910 A69-17332

Physical mechanism of stability loss in nonvortical flows of uniformly dense ideal fluids, discussing entropy production
06 p0911 A69-17498

Current sheet pattern and gas flow stabilization in pulsed plasma accelerators
[AIAA PAPER 69-112] 06 p0971 A69-18140
Natural frequency of fluid oscillations in complex pipelines
07 p1119 A69-18745

Stability of rotating liquid mass held together by surface tension
07 p1121 A69-19268

Combined effect of short wavelengths associated Kelvin-Helmholtz instability and long wavelengths associated gravitational instability on self gravitating fluid layer, discussing kinetic energy
07 p1182 A69-19276

Corrected stability limit for Poiseuille flow in pipes, annuli and channels, discussing flow between cylinders
07 p1121 A69-19475

Stability of plane vortex sheet in magnetic fields, noting stabilization effect of compressibility for nonmagnetic case
08 p1358 A69-19797

Electroconvective instability produced by uniform electric field in poorly conducting fluid under stabilizing vertical temperature gradient, noting heat flow increase
08 p1352 A69-20791

Nonlinear behavior of two stream instability between cold electron and ion streams
08 p1367 A69-20800

Stability of unsymmetrical plane flow noting velocity profile effect
08 p1304 A69-20812

Stability of inviscid swirling flow with finite axial velocity components and nonvanishing radial density gradients, noting criterion for infinitesimal disturbances
08 p1305 A69-20851

Hydrodynamic stability and entropy decrease in flow in three dimensional space, using irreversible thermodynamics principles
10 p1808 A69-22892

Incompressible Newtonian flow between two parallel planes, noting marginal stability condition, mean velocity profile and turbulence
10 p1673 A69-22909

Weak discontinuities in wave propagation, studying ionized gas nonsteady flow having electrical conductivity in magnetic field
10 p1727 A69-22916

Flow instability of incompressible nonconducting fluid in thin cylindrical conducting elastic pipe in constant uniform magnetic field
10 p1798 A69-23094

Laminar turbulent transition conditions in MHD channel flow
10 p1727 A69-23097

Long and ultralong waves in baroclinic zonal current, investigating current stability and wave perturbation characteristics by applying linearized perturbation equations to multilayer model
10 p1682 A69-23325

MHD boundary layer nonlinear instability, treating laminar to turbulent flow transition as reversible process
10 p1734 A69-23452

Dynamics of conducting fluid stream coupled to elastic medium by transverse electric or parallel magnetic field, considering stability of system
11 p1923 A69-24289

Viscosity and electrical conductivity effects on axisymmetric instabilities of current carrying annular cylinder of mercury
11 p1923 A69-24292

Parallel flow of viscous liquid film with free surface down inclined plane, noting growth of initially infinitesimal amplitude waves and finite amplitude wave stability
11 p1869 A69-24891

Charge bunching approach for gravitational hydrodynamic instability of infinite uniform self gravitating system in translational motion, using conservation laws
11 p1961 A69-25105

Gravitational stability of spheroidal expansions of rotating gas masses in astronomy, noting mechanism for fragmentation in cosmology
11 p1962 A69-25112

Viscous flow stability in rotating pipe, giving velocity components in cylindrical polar coordinates
11 p1871 A69-25125

Degree of knottedness of tangled vortex lines, discussing vorticity distribution for inviscid flow and MHD invariants
11 p1872 A69-25126

Low Reynolds number stability of incompressible fluid half jet flow, investigating free laminar boundary layer instability
11 p1874 A69-25280

Thin spherical layer flow stability with respect to small disturbances, showing unsteady motion above critical Reynolds numbers and secondary flow features
11 p1875 A69-25486

Buoyancy-driven system instability mechanism, showing Prandtl number increment effect and relation to Coriolis-driven instability of rotating fluids
11 p1876 A69-25559

Two dimensional convective flow stability for arbitrary Rayleigh numbers in horizontal layer, assuming large Prandtl number and free boundary conditions
11 p2003 A69-25657

Holographic interference method for measuring film height in analyses of fluid film vaporization under blowing hot gas
12 p2088 A69-26178

Electrohydrodynamic instability of incompressible conducting cylindrical viscous jet in external magnetic field, noting viscosity role in oscillation modes and growth rate
12 p2136 A69-26403

Flow stability of axisymmetric jet with parabolic velocity profile in fluid at rest, calculating critical Reynolds numbers
13 p2244 A69-27300

Rayleigh-Taylor instability in synchronous liquid metal MHD generators, showing stabilization by channel positioning and threshold power rating
13 p2307 A69-27508

Perturbations stabilization in electrically conducting fluid by distributed automatic control system, determining feedback operators via boundary value problem
13 p2311 A69-28105

Flow field instability over concave bodies in supersonic free stream computed by integration of gasdynamic equations, noting application to supersonic parachutes
[AIAA PAPER 68-946] 13 p2199 A69-28228

Time varying flow properties effects on hypersonic wind tunnel spectroscopic measurements, considering direct emission and electron beam techniques
[AIAA PAPER 69-331] 13 p2242 A69-28267

Two dimensional Couette flow analysis showing stability at Reynolds number tending to infinity
14 p2428 A69-28802

Flow stability of one dimensional Cartesian and cylindrical incompressible inviscid flows with no body forces and interfaces
14 p2429 A69-29013

Energy transport between vortices in turbulent flow calculated from vortex stability study
14 p2430 A69-29508

Ideal fluid unsteady rectilinear plane-parallel flow stability, calculating shear layers before breakdown by using modified Rayleigh method
14 p2431 A69-29606

General atmospheric circulation instability factors for statistical weather forecasting, considering atmosphere as nonlinear oscillating system, analyzing relaxation time
14 p2476 A69-29820

Convective and nonconvective two stream instability for hot plasmas, approximating equilibrium distribution function for given temperature by resonance functions
14 p2499 A69-29844

Two piston flow stability separated by thin wall in traveling magnetic field, finding piston inertia centers velocity equal to field velocity
14 p2500 A69-29903

Turbulent gas flow characteristics obtained by extremal hypothesis, using maximum perturbation stability in formulating variational problem and computer algorithm
15 p2590 A69-30263

Dynamic behavior of dissociating homonuclear diatomic gas, deriving instability equations, proposing stability loss in transonic region
15 p2548 A69-31065

Eigenvalues for class of nonself adjoint differential equations system treated as small perturbation of norm epsilon, assuming perturbation expansion
16 p2812 A69-31811

Linear amplification, nonlinear limiting and secondary instability induced by unsteady effects illustrated for various transitional flows, including roughness and streamwise vorticity
17 p2950 A69-33248

Turbulence origin and structure in stably stratified media for finite disturbance instability in sloping flows experimentally observed with visualization techniques
17 p2999 A69-33735

Minimum Reynolds number and Malkus theory of turbulent channel flow, discussing stability, equilibrium flow, and stationary turbulence via variational theorem
17 p2957 A69-33764

Asymptotic theory of Orr-Sommerfeld problem for symmetric channel flow stability
17 p2958 A69-34151

Criteria to predict flow instabilities triggered by exothermic reaction presence in high temperature reaction kinetic shock tube studies
18 p3116 A69-34462

Shock tunnel steady flow starting process in two dimensional reflection nozzle, using multiple shadowgraphs and interferograms, noting nozzle geometry influences
18 p3085 A69-34471

Hydrodynamic stability of solid fuel combustion in presence of acoustic disturbances in gas phase, considering material erosion and particle dispersion
18 p3231 A69-35150

Flow breakdown in wind tunnel tests of high disk loading systems at low forward speeds, investigating downwash distribution effect using disk loading and airfoil models
18 p3119 A69-35230

Atmospheric flow with respect to mesoscale disturbances, examining conditions for hydrodynamic stability
18 p3167 A69-35343

Hydrodynamic stability of incompressible fluid boundary layer flow during blowing or suction through porous surface, determining Reynolds number lower bounds
18 p3124 A69-35381

Viscous fluid secondary flow stability between coaxial rotating cylinders, using nonlinear differential equations derived from equations of motion
19 p3299 A69-36391

Energy losses due to drag in unstable laminar fluid flow in tube
20 p3513 A69-36973

Stability theory formulation for evaluation of boundary layer transition from laminar to turbulent states
[AIAA PAPER 68-669] 20 p3514 A69-37184

External natural convection flows, studying laminar instability, transition and turbulence in boundary layer flow
20 p3633 A69-37718

Flow induced by plane flame traveling supersonically or subsonically at constant speed through long tube studied for flow field steadiness in flame fixed coordinates [ASME PAPER 69-FE-33] 20 p3460 A69-37993

Unsteady boundary layer flows of compressible fluid over semiinfinite flat plate, discussing heat transfer rate 20 p3518 A69-38318

Naimark theorem extended to class of nonself-adjoint eigenvalue problems in hydrodynamic stability, considering Orr-Sommerfeld equation and Taylor stability problem 21 p3754 A69-38426

Fluid motion in free falling partially filled cylindrical vessel due to sudden vertical velocity change, considering free surface disturbances 21 p3692 A69-38684

Small amplitude acoustic waves propagating in compressible fluid with parallel shear flow and within constant gravitational field 21 p3772 A69-39241

Channel flows energy stability, discussing Couette and plane Poiseuille flows, velocity profiles, vorticity maxima, etc 21 p3697 A69-39675

Parallel shear flow equilibrium in inviscid nonheat-conducting incompressible fluid with density varying as function of vertical coordinate 21 p3697 A69-39743

Flow stability regions at surface of flight vehicle, considering boundary layer flow of incompressible fluid 21 p3645 A69-39827

Interaction between boundary layer and external vortex flows and stability transitions of heated rotating fluid annulus 21 p3698 A69-39869

Linear normal mode instability of three dimensional laminar and turbulent shear layers, analyzing relations between velocity profile, eddy viscosity and oscillations 22 p3932 A69-40893

Linear stability criteria for two dimensional wave perturbations effects on nonNewtonian fluid flow between parallel plates 22 p3933 A69-41108

Turbulence theory in laminar-turbulent flow transition, nonlinear stability for flows with Reynolds number higher than critical and fully developed turbulence 23 p4152 A69-42313

Parallel magnetic field effect on free boundary layer type flows stability of low Reynolds number between parallel streams of viscous incompressible conducting fluid 24 p4298 A69-42596

Tristable fluid amplifiers, analyzing J functions of staticized variable, ternary logical characteristics, input equations, flow stability and switching measurements 24 p4255 A69-43298

Nonlinear finite-amplitude instability of two dimensional compressible laminar wake flows, using Fourier expansion and Landau equation 24 p4245 A69-43357

Solution stability and secondary solutions growth beyond critical points investigation for Burgers equations for laminar-turbulent transition 24 p4302 A69-43360

Natural convection flow, discussing initial instability of laminar flow, disturbance amplification and transition to turbulent flow [ASME PAPER 69-HT-29] 24 p4411 A69-43531

Plane Poiseuille flow with nonlinear temperature distribution, studying vortex type secondary flow onset due to buoyant forces [ASME PAPER 69-HT-37] 24 p4411 A69-43533

Supersonic flow stability with energy input applied to reaction kinetics of processes in aircraft and rocket combustion chambers 24 p4248 A69-43642

FLOW THEORY

NT MIXING LENGTH FLOW THEORY

Gravity waves train propagation in cylindrical channel, discussing derivation by three dimensional flow analysis method 01 p0059 A69-10382

Semiempirical theory of turbulent MHD tube flow at small Reynolds numbers taking into account magnetic field presence 01 p0130 A69-10769

Turbulent flow between parallel plates, discussing turbulence generation by energy addition 01 p0061 A69-10993

Turbulent boundary layer theory, discussing effective viscosity, numerical integration, mixing length flow theory and wall jets 02 p0231 A69-11987

Statistical model of turbulent flow confirms Kolmogoroff hypothesis of equilibrium zone at large Reynolds numbers 03 p0413 A69-12949

Unperturbed tube flow theory extended to flow through short axisymmetric tube 03 p0419 A69-13969

Second order difference scheme for calculation of plane or rotational compressible flow, investigating stationary flow as asymptotic limit of unsteady flow [ONERA-TP-652] 03 p0419 A69-14111

Transformations useful for finite difference solution of differential equations with infinite regions, considering flow problems application 04 p0588 A69-14717

Stationary velocity profile near jet driven vortex tube outer wall calculated by laminar boundary layer flow theory, neglecting wall curvature effects 05 p0798 A69-15610

NonNewtonian hydrodynamics equations for non-linearly viscous and viscoelastic media, analyzing dependence on rheological model 05 p0745 A69-15786

Time dependent two dimensional incompressible laminar boundary layers analysis, discussing application to transient flow over semiinfinite flat plate [ASME PAPER 68-FE-10] 05 p0748 A69-16076

Pressure distribution across short vortex chamber to exit radius with known inlet geometry based on incompressible flow model and visualization photographs [ASME PAPER 68-WA/FE-17] 05 p0748 A69-16093

Flow theories of fluids with elastic deformation of substructure, treating suspensions of irregularly shaped deformable particles 05 p0752 A69-16738

Linear theory of equilibrium and nonequilibrium gas flows applied to steady two dimensional nonequilibrium flow of inviscid nonheat-conducting gas 06 p0909 A69-17327

Universal equations for three dimensional laminar boundary layer of incompressible fluid on walls of axisymmetric channel with vortical external flow 06 p0909 A69-17328

Isoenergetic two dimensional supersonic turbulent base flow, noting boundary layer separation properties upstream and downstream [AIAA PAPER 69-68] 06 p0864 A69-18137

Theory of unsteady one dimensional motion of ideal compressible fluid, discussing equation of state 07 p1119 A69-18750

Green function in closed form for energy transport equation solution in axisymmetric Oseen flow 08 p1305 A69-20850

Interplanetary plasma flow simulation around earth magnetosphere and planets not considering initial conditions influence 09 p1577 A69-21768

Axisymmetric flow theory for turbomachine of non-free vortex design in distributed equilibrium state, considering boundary conditions and blade leading edges [ASME PAPER 69-GT-10] 09 p1432 A69-22504

Unrippled space-charge flow in dense axially symmetric electron beams as basis for electron gun design 11 p1846 A69-24598

Formula in Prandtl-Batchelor theory describing motion of incompressible fluid in sphere interior verified experimentally 11 p1868 A69-24755

Asymptotic theory for obtaining nearly free molecular flow solutions uniformly valid throughout flow field based on linearized Boltzmann equation 11 p1818 A69-25283

Universal laminar boundary layer equations, analyzing form of Prandtl equations not containing external flow velocity 11 p1876 A69-25490

Viscous flow-induced vibrations of elastically restrained flat plates in narrow channel, considering one dimensional viscous flow theory 11 p1991 A69-25515

Similarity solutions for incompressible, steady hydrodynamic and thermal boundary layers on longitudinally curved walls, allowing for displacement and curvature effects 12 p2060 A69-25761

Book on negative turbulent viscosity theory covering laboratory analysis and applications to earth and solar atmospheres, oceanic circulations, spiral galaxies and solar nebula 12 p2131 A69-26868

Smooth solutions to Navier-Stokes equation obtained by imposing bound on associated pressure pertaining to weak solution 12 p2124 A69-26971

Wall pressure fluctuations due to turbulent boundary layer flow, calculating statistical properties [AIAA PAPER 68-642] 13 p2244 A69-27246

Microstructured mixtures theory including energy balance, mass and momentum equations and entropy production inequality for structured fluids in motion 13 p2371 A69-27318

Two dimensional flow through nonuniform gauze by computerized analysis based on linearized theory 13 p2248 A69-28174

Loitsianski method of parametric approximation extended to include flat plate with constant surface suction and flow past circular cylinder 13 p2249 A69-28247

Rate equation for effective turbulent viscosity variations, considering effects of generation, convection, diffusion and decay in quasi-parallel shear flows 15 p2591 A69-30905

Compressible shear flow linear theory applied to transonic flow past thin airfoil, determining pressure distribution, discussing compressibility effects of nonuniform Mach number 16 p2731 A69-31593

Molecular flow network theory applicable to volumes interconnected by small orifices or porous membranes for transient pressure measurements 16 p2813 A69-32325

Monograph on Navier-Stokes equations with integral relations approximate solution and application to flow around flat plate of finite length 17 p2949 A69-32993

Incompressible turbulent boundary layer analysis by two region characterization for eddy viscosity, using Spalding generalized function and Prandtl free shear flow model 17 p2951 A69-33255

Normal stress effects in viscoelastic fluid theories applied to one dimensional Burgers model of weak turbulence predicting drag reduction 17 p2951 A69-33256

Constitutive equation variation effect on near wall flow pattern of dilute polymer solutions 17 p2951 A69-33257

Gas pressure differential across multilayer insulation blanket during rapid evacuation predicted, using one dimensional flow theory [AIAA PAPER 69-608] 17 p3072 A69-33275

Three dimensional hypersonic laminar boundary layer subdivided into inner and outer regions, obtaining flow description by matching inner and outer solutions [AIAA PAPER 69-710] 17 p2955 A69-33467

Aerodynamic control surface/trim tab coupling coefficients in subsonic two dimensional unsteady flow using matrix method valid for motion involving harmonic oscillations 17 p2895 A69-33597

Kim-Anderson flux flow theory for materials with kappa nearly equal to 1, discussing pinning forces and sites 17 p3016 A69-33754

Flow mechanics applications to medicine, discussing vascular and technical systems and measuring equipment adaptation to human organisms 17 p2915 A69-33771

Leading edge vortices and shock detachment flow over delta wings, discussing drag reduction due to lift 17 p2896 A69-34025

Constant pressure adiabatic turbulent boundary layer characteristics measurements correlated in incompressible reference frame, using modified Mager compressibility transformation 17 p2958 A69-34051

Galerkin-Kantorovich-Dorodnitsyn/GKD/ multimoment integral method improved reversed flow formulation for lower branch similar flows 17 p2958 A69-34054

Pressure distribution in two dimensional incompressible potential flow on Joukowski airfoils with normal upper surface spoilers, emphasizing potential flow theory [AIAA PAPER 69-737] 18 p3083 A69-34402

Micropolar liquid basic flows, considering case with coupling constant relating microstructure to macroscopic flow greater than viscosity coefficient 18 p3121 A69-34786

Transformed Navier-Stokes equations for incompressible fluids flow, deriving forces acting on surface of bounded region 18 p3122 A69-34830

Higher order boundary layer theory development from Prandtl simplification of Navier-Stokes equations to successive approximations for incompressible and compressible flows 18 p3123 A69-34923

FLOW VELOCITY

Turbulent wake and ambient flow interaction analysis based on integral methods in boundary layer theory
19 p3299 A69-36390

Mean parameters calculation between widening of turbulent flow and point of reattachment, including similarity hypothesis concerning velocity profile
19 p3299 A69-36648

Reducibility conditions of flow theory for smooth and piecewise smooth yield surfaces to relations of small elastoplastic deformations
19 p3443 A69-36794

Heuristic process for constructing similarity parameters approximation solution of laminar and turbulent boundary layers equations
19 p3301 A69-36799

Second order theory for steady or unsteady subsonic flow past slender lifting bodies of finite thickness
[AIAA PAPER 68-75] 20 p3458 A69-37182

Reynolds analogy factor approximate calculation for turbulent boundary layer with pressure gradient
20 p3514 A69-37183

Potential flow theory applied to determination of airfoil separated vortex flow and maximum lift and Reynolds number dependence
20 p3459 A69-37421

Laminar jet mixing of incompressible viscous fluid issuing from rectangular nozzle into uniform stream, considering various boundary conditions
[ASME PAPER 69-FLCS-22] 20 p3516 A69-37976

Slip ratios in annular two phase flow for case of laminar flow in film and no entrainment of liquid in vapor
[ASME PAPER 69-FE-43] 20 p3517 A69-37995

Computational method for nonlinear two and three dimensional disturbances in plane parallel flows applied to transverse disturbances in plane Poiseuille flow
21 p3691 A69-38464

Nonlinear incompressible potential flow with unbounded free surfaces, analyzing singularities in finite part of space
21 p3696 A69-39295

Soviet book on hydrodynamic cascade theory covering mathematical methods and numerical solutions for ideal fluid flow problems
21 p3696 A69-39527

Prandtl boundary layer theory problems, considering solution uniqueness and stability, unsteady flow, boundary layer separation, existence conditions, etc
21 p3697 A69-39698

Rumanian book on MHD covering electromagnetic field theory, motion equations, laminar flow, MHD generators, fluid motion past thin airfoils, shock waves, etc
23 p4195 A69-41363

Forced flow against infinite rotating disk, showing von Karman similarity equations solution for axial flow at large distances toward disk
24 p4244 A69-42718

Slot type jet interaction flow tests at free stream Mach 4 and 5, describing equipment, procedure and results
24 p4249 A69-43686

FLOW VELOCITY

Leak flow rates of nitrogen and helium at various pressure gradients measured by gas chromatography and mass spectroscopy
01 p0079 A69-10297

Laser Doppler velocity profile measurement at localized points in flow stream without disturbing flow
01 p0090 A69-10298

Confined vortex in air tangential and axial velocity distribution based on smoke profile pictures
01 p0060 A69-10413

Steady state circular motion of fluid with variable rheological characteristics between coaxial cylindrical surfaces, obtaining velocity distribution
01 p0061 A69-10733

Condensing injector cycles internal efficiency for high velocity liquid metal flows in closed cycle MHD power plants
02 p0194 A69-11582

Boron diffusion in silicon, using nitrogen carrier and boron trichloride diffusant at high temperature for determination of critical oxygen flow rate
02 p0297 A69-11994

Two dimensional unsteady Rayleigh flow velocity of conducting and nonconducting viscous fluid past porous plate, analyzing suction and magnetic field effects
02 p0232 A69-12156

Cylindrical afterbodies at free stream Mach 2 with hot argon gas ejection, discussing flow rate influence on base pressure
02 p0190 A69-12533

Discrete vortices in two dimensional subsonic and supersonic wake, determining Strouhal numbers, frequencies and flow velocities with aid of HF cinematography
02 p0191 A69-12587

Similarity law for channel wall influence in wind tunnels valid for all flow velocities
02 p0192 A69-12830

Electric field, current density and magnetic induction of plasma flow measured, obtaining plasma conductivity and flow velocity for electron temperature and density
[ONERA-TP-649] 03 p0473 A69-12877

Fluid flow velocity measurements by optical device having trigonal rectangular glass prisms and microscope objective
03 p0427 A69-12969

Similar solutions of boundary layer equations for compressible model fluid adjacent to wall, discussing velocity overshoot dependence on wall temperature
03 p0413 A69-13013

Flow rate effect on flow pattern of gas escaping through lateral hole of arbitrary depth
04 p0586 A69-14274

Reynolds number similarity argument, establishing relation between mean velocity at pipe or channel center and shear stress at wall
04 p0589 A69-14895

Optical signal frequency method for measuring velocity of fluid flow
04 p0598 A69-14995

Current mode amplifier circuit used with carbon resistors for measuring low flow rates of liquid hydrogen from small containers
04 p0577 A69-15025

Thermal diffusion coefficient and composition of gas mixtures by measuring gas flow rate in capillary tube as function of viscosity
04 p0688 A69-15410

Round air jet projected parallel to wall, analyzing velocity profiles, decay and growth rate
04 p0591 A69-15487

Entry region flow and convective heat transfer prediction in cooled vertical pipe open at both ends, considering wall temperature
05 p0845 A69-15717

Micro and macroturbulent motions velocity in solar photosphere based on Fraunhofer lines analysis
05 p0823 A69-16014

Coanda nozzle entrainment and flow augmentation approximating numerical stability by finite differences
05 p0746 A69-16021

Two dimensional incompressible laminar boundary layer on curved wall for potential velocity inversely proportional to distance along origin
[ASME PAPER 68-WA/FE-20] 05 p0749 A69-16096

Gas flow rate predictions for long and short tubes and annuli and at densities between laminar-continuum and free molecular regimes
[ASME PAPER 68-WA/PID-5] 05 p0750 A69-16166

Rotating hot wire and five hole pressure probes for determining complete velocity vector in subsonic flow
05 p0764 A69-16398

Turbulence hypothesis for velocity of laminar fluid flow at dividing line, considering base pressure and adiabatic mixing zones
06 p0910 A69-17330

Stability of tangential velocity discontinuity between two media with different densities situated in acoustic field
06 p0910 A69-17344

Gaseous film cooling at various hot gas acceleration rates and free stream turbulence levels
06 p1033 A69-17557

Turbulent premixed flames stabilization, determining gas flow velocity, turbulence intensity, flame thickness and burning velocity relation to intensity
06 p1035 A69-17931

Transformation theory for compressible turbulent boundary layer with arbitrary pressure gradient
[AIAA PAPER 69-160] 06 p0912 A69-18073

Velocities of neutral and ionic species in MPD flow determined from Doppler shift of selected spectral lines
[AIAA PAPER 69-109] 06 p0971 A69-18116

Initial stage of motion in Rayleigh problem, calculating time variable velocity of tangential stress on and velocity of gas near plate
07 p1118 A69-18701

High velocity subsonic flow past wedge in wind tunnel with perforated walls, applying solution to optimum parameter determination of suction system
07 p1050 A69-18741

Nonstationary aerodynamic load for harmonically oscillating body in fluid flow with constant mean velocity measured, determining errors as functions of system parameters
07 p1050 A69-18752

One dimensional flow of conducting inviscid compressible fluid in channel in presence of transverse fields, discussing steady velocity flows
07 p1191 A69-19014

Hydraulic drag coefficient in MHD fluid flows in traveling magnetic field from motion equations for turbulent flows, considering velocity profiles
07 p1192 A69-19017

Unsteady conducting incompressible viscous fluid flow past plate in magnetic field, analyzing surface friction reduction
07 p1192 A69-19018

Magnetic knots /intergranular space strong small scale magnetic fields near sunspot/, longitudinal and transversal fields and radial velocities
07 p1217 A69-19244

Boundary layer effect on flow coefficient of fluid amplifier feed nozzle, noting flow uniformity, incompressibility, velocity and velocity distribution assumptions
07 p1059 A69-19320

Solution velocity and turbulence effects on solvent cleaning of corrosion resistant steel tubing, discussing fluidity forces and cleaning formulation
08 p1318 A69-19807

Semilogarithmic law of velocity and temperature for turbulent flow in circular channel, examining analogy between momentum and energy transfer
08 p1420 A69-19877

Homogeneous turbulent gas flame front location as function of caloric value of mixture and flow velocity
08 p1420 A69-19998

Flow rates characteristic of trapezoidal geometries encountered after schematization of noncylindrical ducts involving irrotational flow, leakage, heat exchanges and electrical conduction phenomena
08 p1303 A69-20270

Stability of unsymmetrical plane flow noting velocity profile effect
08 p1304 A69-20812

Jet engine gas flow, temperature, velocity and pressure measurements by analog and digital systems
08 p1316 A69-20869

Convective MHD channel flow in vertical channel, subjected to temperature and pressure gradients, discussing wall conductances effects on flow rate and heat transfer
09 p1545 A69-21441

Spatial distribution of velocity, spatial correlation and ergodicity of turbulent flow, using spectrum of intensity fluctuations of scattered laser light
09 p1493 A69-21491

MHD oscillatory flow along infinite plane porous wall with variable suction velocity, obtaining expressions for velocity and magnetic fields in boundary layer
09 p1547 A69-21607

Velocity and temperature fields in Newtonian fluid in motion past stationary obstacle in gravitational field, noting similarity parameters reduction
09 p1429 A69-21686

Turbulent circular wall air jet trajectory and spreading in perpendicular crossflow of constant and varying velocities
[ASME PAPER 69-GT-33] 09 p1483 A69-22491

Finite difference method computer programs for calculation of velocities and streamlines on blade to blade surface of revolution of turbomachine
[ASME PAPER 69-GT-48] 09 p1432 A69-22495

Bloodless heart flow measurement methods, noting simultaneous external recording of carotid and femoral pulses and impedance plethysmography
09 p1448 A69-22730

Impulse induction MHD generator with cylindrical channel, finding differential equations for velocity and current
10 p1638 A69-23484

Vortex incompressible flow in thin cylindrical chamber, analyzing outer and inner region and interface tangential velocity, shear and static pressures
10 p1679 A69-23557

Excess velocity and temperature decay laws in axisymmetric jet in transverse flow obtained via jet momentum and heat conservation equations
10 p1679 A69-23568

Finite difference method for calculating lee waves incident on obstacle with arbitrary vertical distribution of main flow horizontal velocity and temperature
10 p1722 A69-23967

Velocity profiles of turbulent plasma flow in circular tube during application of longitudinal homogeneous magnetic field
11 p1922 A69-24234

Turbulent flame propagation described by turbulence length and integral scale and fuel properties including laminar flame velocity and equivalence ratio
11 p1999 A69-24482

Turbulent flow velocity field evolution in presence of random forces using equation of motion
11 p1867 A69-24628

Holographic recording of three dimensional flow field velocities, applying theory of particle size assessment via Fraunhofer holography
11 p1884 A69-24691

Viscous flow stability in rotating pipe, giving velocity components in cylindrical polar coordinates
11 p1871 A69-25125

Pressure and flow rate variations at any point of manifold with control units calculated using transfer functions
11 p1942 A69-25335

Neutral gas flow transport velocity and Mach number effects on critical electric field strength and direction in formation of self sustained discharge
11 p1933 A69-25545

Low power gradient uniform electric arc column in cross flow and transverse magnetic field, analyzing temperature, velocity, pressure and magnetic field distribution
11 p1933 A69-25556

Helmholtz resonance in rocket injectors as function of frequency response of interaction between chamber pressure and dissolved gas-fuel injection flow rate
12 p2148 A69-26806

Incompressible conducting fluid turbulent flow velocity distribution in transverse magnetic field at small magnetic Reynolds numbers and constant MHD interaction frequency
13 p2246 A69-27498

Variable fluid and field velocity HF induction generator, determining interaction between fluid dynamic forces and magnetic field and kinetic energy
13 p2207 A69-27502

Velocity potential function for flow over disk shaped wing near screen, noting aerodynamic lift and drag
13 p2199 A69-27524

Vibrating camera for photographic measurement of flow velocities and trajectories of bodies marked by light spots
13 p2261 A69-27913

Monograph on return currents produced by confined jet of incompressible fluid with low initial ambient fluid velocity
13 p2250 A69-28335

Plane shock layer structure in pseudoMaxwellian monatomic gas, integrating Krook equation for gas molecule velocity
14 p2432 A69-29613

Turbulent Hartmann flow between planes in perpendicular magnetic field including flow velocity profile measurements
14 p2500 A69-29908

Power law fluids boundary layer near flat plate studied by series expansion and steepest descent methods, determining velocity gradient and skin friction coefficient
15 p2589 A69-30002

Longitudinal internal cracks in deformed Al alloys initiated by elastic stress concentration in areas of highest flow rate gradient
15 p2638 A69-30277

Fluid flow velocity measurements by Doppler shift of laser light scattered from moving fluid, determining beat frequencies
15 p2616 A69-31291

Mean velocity distribution prediction in turbulent shear flows of variable density by coordinate stretching method
[AIAA PAPER 68-41] 16 p2770 A69-31888

Density and velocity fluctuations in hypersonic turbulent boundary layer based on Wallace data
16 p2770 A69-31908

Streamline flow of ideal stable gas with constant ratio of specific heats around conical body with arbitrary taper, determining flow velocity components
16 p2732 A69-32126

Velocity field in turbulent flow based on momentum transfer, determining velocity distribution for flow near solid surface
16 p2772 A69-32128

Reaction rate constants of ion-molecule interchange reaction as function of temperature, flow velocity, activation energy and constant part of steric factor P
16 p2747 A69-32312

Hot-wire anemometers calibration technique providing accurate and direct velocity measurements in slow moving liquids
17 p2971 A69-32901

Transverse turbulent pipe flow, obtaining limiting behavior of time averaged velocity gradient at wall
17 p2949 A69-33013

Liquid draining motion from transversely moving cylindrical tank in time varying gravity field with outlet pipe at bottom, discussing flow rate and free surface
[AIAA PAPER 69-679] 17 p2953 A69-33440

Turbulent velocity distribution and wall friction calculated from eddy viscosity distribution for concentric annulus
17 p2956 A69-33575

Flow rate in ascending aorta, stroke volume and cardiac output determination by ballistocardiography, calculations based on Hagen-Poiseuille theory
17 p2915 A69-33772

Microturbulence velocity estimation method for solar type stars using low dispersion spectra of narrow band photometry
17 p3044 A69-34178

Flow rate effect of oxygen-argon mixture on Zr oxidation studied to determine exclusion as factor in Zr weight increase
18 p3154 A69-34272

Fluidic sensor for measuring gas and liquid velocities, describing design and principles of operation
18 p3133 A69-34308

Static and impact pressure distributions for Mach number and velocity profiles of supersonic to subsonic flow transition in tube at low Reynolds numbers
[ASME PAPER 69-APM-23] 18 p3120 A69-34397

Conservation theorems for energy and mean circulation in inviscid rotating fluid, noting inertial wave spectrum continuity
18 p3121 A69-34550

Fluid velocities at earth core surface inferred from magnetic data, considering velocity constraints and diffusion contributions to secular change
18 p3129 A69-34951

Ducted fan engine turbine air flow rate and frontal gas temperature determined from air temperature/pressure measurements behind compressor and engine fuel flow
18 p3086 A69-34986

Static temperature measurement in air-tunnel tests producing high velocity air streams by duplex scanning IR spectrometer
19 p3294 A69-35752

Flow rate of ideal fluid ejected from swirl injector taking into account radial component of flow velocity at nozzle exit
19 p3297 A69-35820

Thermoanemometer filament frequency response measured by generator of velocity pulsations compared with conventional methods
19 p3308 A69-35856

High velocity interstellar gas in H I and H II regions, emphasizing observations of neutral atomic hydrogen in and far from galactic plane
19 p3402 A69-35962

Flow velocity, flow Mach number and weak disturbance velocity behind shock wave measured for nitrogen, oxygen and carbon dioxide
19 p3298 A69-36362

Velocities and pressure in twisted jet in unbounded space containing same fluid as jet
19 p3298 A69-36388

Tangential and radial velocities in vortex boundary layer flow, relating diminishing amplitudes to increasing height using iterative method
19 p3363 A69-36499

Anisotropy of derivatives of transverse velocity fluctuations in grid turbulence subjected to plane deformation, determining dimensionless coefficient
19 p3299 A69-36647

Mean parameters calculation between widening of turbulent flow and point of reattachment, including similarity hypothesis concerning velocity profile
19 p3299 A69-36648

Sedov formula for complex velocity of arbitrary circulation in two dimensional theory of small curvature thin wings
19 p3242 A69-36795

Boundary layer velocity distribution in turbulent swirling pipe flow produced by twisted tape inserts
[ASME PAPER 69-FE-14] 20 p3516 A69-37990

Simultaneous lateral skewing regions existence in low speed three dimensional turbulent incompressible boundary layer flow
[ASME PAPER 69-FE-24] 20 p3517 A69-37998

Axial velocity and static pressure for incompressible fluid flow through straight smooth porous tube
[ASME PAPER 69-FE-44] 20 p3517 A69-38000

Flow field induced by spiral vortex sheet, noting existence of radial velocity component
21 p3692 A69-38610

Continuous cavitation model for incompressible fluid one dimensional unsteady motion
21 p3693 A69-38752

Shaft speed limitations on close clearance seals, using test data on changes in fluid viscosity causing contact and damage
[ASLE PAPER 68-LC-13] 21 p3731 A69-38763

Two dimensional numerical solution for Faraday DC MHD generators with variable conductivity, velocity and magnetic field
21 p3649 A69-39027

Finite difference method for calculating Lee waves incident on obstacle with arbitrary vertical distribution of main flow horizontal velocity and temperature
21 p3759 A69-39653

Channel flows energy stability, discussing Couette and plane Poiseuille flows, velocity profiles, vorticity maxima, etc
21 p3697 A69-39675

Equation of motion for determining nonlinear vibration of rod pendulum in viscous flow of varying velocity
21 p3773 A69-39679

Fluid velocity in starting flow in circular tube using Laplace transform
22 p3931 A69-40688

Skin friction and mean velocity profiles measured for fully developed 1000-10,000 Reynolds number flows in pipes and channels
22 p3932 A69-40897

Supercavitating flow past thin hydrofoils, determining flow velocity or acceleration potential near free surface
22 p3933 A69-41023

Distributed suction effect on boundary layer structure of water flow from turbulence measurements, determining velocity and pulsation intensity distributions
22 p3933 A69-41029

Stroboscope method for measuring pulsating flow transient velocity based on hot-wire chromometric recording of small ion clouds emitted during pulsation
22 p3951 A69-41257

Constant temperature thermoanemometer design and subsystem operation applied to measurements of turbulent flow velocity and pulse characteristics
24 p3311 A69-42558

Perturbation velocity potential of unsteady potential flow of barotropic gas past cascade of thin blades oscillating harmonically
24 p4244 A69-42716

Air bubbles rise velocity and path in water based on time measurement of bubble traversing two light beams, describing electronic recording system
24 p4299 A69-42918

Turbine rotors temperature reducible by increasing air cooling system flow rate
24 p4364 A69-43081

Total load factor static vertical component and lubricant flow rate square related to pocketed hydrostatic journal bearing revolutions
24 p4321 A69-43091

Hot-wire anemometer calibration technique for measuring velocity of very slowly moving liquids
[ASME PAPER 69-HT-A] 24 p4316 A69-43527

Heat transfer capability and startup behavior of sodium heat pipes, studying heat transfer limit due to vapor velocity at evaporator end
[ASME PAPER 69-HT-21] 24 p4412 A69-43547

Gas velocity and pressure influence on electrical breakdown potential of Ar, N and He between parallel flat plate and concentric electrodes
24 p4359 A69-43693

FLOW VISUALIZATION

Schlieren method for studying rotating sphere heat transfer during natural convection
01 p0174 A69-10095

Luminous flow in front of sphere and behind cylinder under high temperature and low density conditions, discussing profiles of shock waves
02 p0189 A69-12182

Photographic flow patterns of separated flows with vortex formation obtained in wind tunnel for different aerodynamic configurations of revolution
02 p0191 A69-12586

Boundary layer effects on shadow deformation, emphasizing two dimensional flow with image projected by parallel light beams perpendicular to flow plane
03 p0364 A69-13787

Pressure distribution across short vortex chamber to exit radius with known inlet geometry based on incompressible flow model and visualization photographs [ASME PAPER 68-WA/FE-17]

05 p0748 A69-16093

Visual investigation of flow field at swept wing, measuring pressure distribution at stall fence and vortices formation

06 p0858 A69-17341

High speed streak camera synchronization with shock tube process involving nonreacting gases or mixtures in pressure chamber

06 p0926 A69-17499

Xenon flash lamps with electrolytic capacitors designed for photographic studies of laminar flows of viscous fluids

07 p1116 A69-18259

Kine films of gas flows within highly luminous transient arc taken by laser schlieren technique

08 p1316 A69-20615

Flow visualization tracer for quantitative measurements for laminar and turbulent flow, discussing mean velocity and shear stress

09 p1495 A69-21911

Unsteady relative flow in centrifugal impeller passage running at part capacity and zero flow observed by hydrogen bubble flow visualization method [ASME PAPER 69-GT-35]

09 p1432 A69-22489

Q switched ruby laser application to high speed shadow photography and holography in study of gas flow around ballistic body

12 p2088 A69-26177

Quantitative analysis of differential interferometer photographs using Wollaston prism with beam separation, applying method to sphere in low density hypersonic flow

12 p2089 A69-26187

Optical methods in three dimensional gas flow research, noting role in density field determination and conjunctive use with gas dynamics equations

12 p2011 A69-26191

Aerodynamic field around symmetric profile two dimensional plates, visualizing velocity fields with Al particles

12 p2011 A69-26288

Imaging for flowfield of nonuniform parallel streams with thin airfoil represented by vorticity distribution, noting change of lift and moment

12 p2012 A69-26775

Shadow, schlieren and interferometric methods for study of transonic, supersonic and hypersonic fields of aerodynamics, using refractivity variations in heterogeneous medium

12 p2060 A69-26934

Supersonic wake flow visualization, obtaining direct photographs of various smoke streamlines [AIAA PAPER 69-346]

13 p2200 A69-28281

Laminar to turbulence transition in submerged and bounded jets, using schlieren visualization for compressible flow and birefringent visualization for incompressible flow

14 p2428 A69-28876

Direct simulation Monte Carlo method for hypersonic rarefied gas flow past solids, modeling on digital computer

14 p2390 A69-29580

Hydraulic tank for visualizing flows around stationary models, noting absence of wall effects [ONERA-TP-708]

17 p2956 A69-33588

Visual observation of pipe wall regions in turbulent flow by suspending colloidal size particles and photographing with high speed motion picture camera

17 p2956 A69-33598

Turbulence origin and structure in stably stratified media for finite disturbance instability in sloping flows experimentally observed with visualization techniques

17 p2999 A69-33735

Flow structure in wake of blunt bodies placed perpendicular in parallel airstream determined from hot-wire anemometry

18 p3084 A69-34409

Streak photographs by differential interferometer to study head wave standoff in shock tubes as function of time

18 p3085 A69-34473

Secondary flow consisting of longitudinal vortices superposed on convection flow on inclined plate, obtaining flow pattern through flow visualization

18 p3124 A69-35383

Electron beam fluorescence probe and afterglow investigation for hypersonic He flow visualization, observing qualitative structure

19 p3291 A69-35722

Quantitative photographs of low density flowfields during shock tunnel tests using electron beam excitation with image intensifier tube detector

19 p3292 A69-35723

Karman vortex street formation indicated by smoke visualization method study of laminar wake behind single cylinder

21 p3644 A69-38687

One dimensional spectra of turbulent wakes behind circular cylinders, discussing isotropy, anisotropy and Reynolds number

21 p3693 A69-38705

Rotor aerodynamics research in terms of theoretical and experimental data comparison, rotor blade flow visualization and blade section camber

23 p4057 A69-41372

Helicopter rotors trailing vortices by flow visualization, comparing Euler and Runge-Kutta iterative solutions

23 p4150 A69-41376

Axisymmetric separated flow in Chapman model shown nonexistent by flow visualization technique

23 p4060 A69-41905

Low Reynolds number unsteady wake flows, using hydrogen bubble flow visualization in high concentration glycerine mixtures

24 p4298 A69-43691

FLOWMETERS

NT HOT-WIRE FLOWMETERS

NT RHEOMETERS

Primary flow measuring element based on Chebyshev principle, noting differential pressure output loss and resistance to accumulation of contaminants

04 p0600 A69-15030

Nondirectional probe for mean velocity measurement in turbulent flow, determining reduced velocity profiles in interior of free flow

04 p0600 A69-15056

Venturi meter with separable diffuser and radial outward step at transition from throat to diffuser, noting effect of step on efficiency

[ASME PAPER 68-WA/FM-2]

05 p0763 A69-16135

Venturi meter design, discussing effects of turbulent velocity fluctuations, hole size and internal geometry on differential pressure measurement

11 p1880 A69-24468

Induction flowmeters design, discussing materials and structural details of sensor and transducer elements

11 p1887 A69-25208

Laser Doppler flowmeter for heterodyne detection of laser light scattered from moving fluid applied to fluid velocity and velocity distribution measurements

12 p2093 A69-26546

Dynamic gas flowmeter for ultrahigh vacuum based on transmission characteristics of diffuser screens and associated pressure drops

13 p2263 A69-28087

Venturi meter with separable diffuser and radial outward step at transition from throat to diffuser, noting effect of step on efficiency

[ASME PAPER 68-WA/FM-2]

14 p2447 A69-29447

Inlet shape and Reynolds number effects on entrance flow development, using laser flowmeter based on Doppler effect to obtain laminar velocity profiles

15 p2589 A69-30001

Nuclear magnetic resonance flowmeter operating from outside pipe walls, discussing operating principles and applications

15 p2616 A69-31290

Laser flowmeter for pulse flow of highly corrosive rocket fuels and oxidizers with measured rise times less than 10 msec

15 p2616 A69-31292

Maintaining of flow similarity in calibration of nozzle type water meters for study of working processes of pumps

16 p2772 A69-32145

Decompression gas emboli detection while moving in flow streams of arteries and veins using ultrasonic Doppler shift principle and square-wave electromagnetic flowmeter

21 p3663 A69-38914

Ultrasonic Doppler flowmeter for detection of circulating gas emboli of animal blood vessels during decompression

21 p3663 A69-38915

Electromagnetic catheter flowmeter with flexible sensor suitable for branch and artery application to minimize surgical intervention

22 p3889 A69-40058

Venturi low resistance flowmeter for ventilatory measurements during rest and exercise on humans, noting suitability for analog integrator computation of tidal volumes

22 p3894 A69-40979

Flow profile effect on signal of Doppler ultrasonic flowmeter, noting limited application to quantitative blood circulation measurements

23 p4166 A69-42085

FLOX

Safety planning for use of reactive cryogenics in large volume, noting FLOX and liquid fluorine

04 p0645 A69-14468

Space storable regenerative cooling with FLOX/methane under conditions for small pump fed engine, describing injector and chamber design [AIAA PAPER 69-509]

16 p2844 A69-32718

Flox/methane pump fed engine, discussing RL-10-1-A engine tests and optimized 5000 lb thrust engine design [AIAA PAPER 69-510]

16 p2741 A69-32720

Space storable hydrocarbon fuel blended FLOX propellant performance with coaxial injector including characteristic velocity, chamber geometry, pressure and heat flux distribution [AIAA PAPER 69-507]

16 p2835 A69-32772

High energy oxygen-free hybrid propulsion system using polyethylene propellant and F oxygen mixture as oxidizer [DGLR-69-017]

23 p4202 A69-41930

FLUCTUATION

U VARIATIONS

FLUCTUATION THEORY

Variational methods for nonequilibrium thermodynamic processes noting fluctuation theory introduction

04 p0551 A69-15314

Quasi-periodic variations of solar radio emission intensity related to solar activity variations

07 p1211 A69-18516

Period fluctuations in ionospheric plasma resonance amplitude, proposing hypothesis in terms of quasi-electrostatic surface waves guided by antenna wire

07 p1125 A69-18847

Intensity fluctuations of single frequency gas laser at 3.39 microns, discussing fluctuation minimization methods

11 p1900 A69-25750

Cosmic radiation origin in terms of sudden injection of particles in time, momentum and space, considering statistical fluctuations role in observed spectrum

12 p2148 A69-26206

Linear extrapolation of stationary stochastic process predicting fluctuations of minimum and maximum periods in solar cycle

12 p2149 A69-26221

Velocity fluctuation amplitude in potential cone of plane jet compared to properties of irrotational fluctuations induced by flow boundaries

13 p2247 A69-27736

Kinetic theory of fluctuations in turbulent plasmas based on construction of many particle distribution functions

14 p2502 A69-29989

Fluctuation spectra of monatomic gases, using two time probability distributions for distribution function autocorrelations

16 p2817 A69-31669

Source requirements for cosmic radiation origin model, noting fluctuations in momentum changing process

18 p3188 A69-35005

Microwave background angular fluctuations investigated for relationship between whirl motion velocity and temperature dispersion, noting role of scattering by moving plasma

18 p3188 A69-35208

Fluctuating heat transfer and flow measurements for circular cylinder in crossflow with simultaneously imposed transverse standing sound field

18 p3124 A69-35384

Scalar waves propagation in bounded randomly fluctuating media, emphasizing interface effects on coherent wave motion

21 p3675 A69-39283

Einstein development of theory of fluctuations applied to homogeneous nucleation, calculating activation energy, liquid drop-vapor system equilibrium state peculiarity, etc

22 p3938 A69-40448

Transverse spectra and structural functions of fluctuations for plane waves of different frequencies propagating in isotropic turbulent medium

23 p4117 A69-41728

Fluctuations in 3K radiation, considering scattering effect on gravitational fields of galactic clusters and large coherence or wavelength scattering by gravitational radiation

23 p4222 A69-42401

**FLUID AMPLIFIERS
NT JET AMPLIFIERS**

Liquid fluidic amplifiers combined into controller for modulating coolant temperature to control flight suit temperature automatically

02 p0202 A69-11923

Switching action mechanism in wall attachment fluid amplifier, outlining theory based on turbulent jet entrainment

02 p0195 A69-12073

Fluid amplifier signal noise sources, using large scale model for investigating jet-knife edge interaction

02 p0195 A69-12078

Vortex controlled fluid amplifiers, discussing static and dynamic performance characteristics

02 p0195 A69-12081

Curved wall fluid amplifier performance under high or low supply pressure

02 p0196 A69-12083

Pneumatic pressure ratio sensing element and associated high pressure switches and amplifiers for gas turbine engine control systems

02 p0249 A69-12088

Static and dynamic performance of pancake vortex flow field and application to signal amplification

05 p0704 A69-16001

Fluid amplifiers, discussing digital and proportional jet-interaction devices and circuits

05 p0704 A69-16004

Vortex value and angular rate sensor based on amplification of tangential velocity component of swirl achieved by control jet or rotation

05 p0746 A69-16006

Beam deflection fluid amplifiers dynamic properties determined by random signal testing

05 p0705 A69-16010

Turbulent free jet at miniature nozzle exit, analyzing wall attachment fluid amplifier and flow characteristics

05 p0746 A69-16012

Performance characteristics of variable geometry bistable fluid amplifiers
[ASME PAPER 68-WA/FE-18]

05 p0748 A69-16094

Temperature, acoustic, vibration and shock environment effects on pure fluid bistable and proportional amplifiers
[ASME PAPER 68-WA/FE-31]

05 p0705 A69-16104

Fluid amplifier linear transfer functions at signal levels on order of internal noise identified by random signal testing method
[ASME PAPER 68-WA/AUT-2]

05 p0706 A69-16184

Boundary layer effect on flow coefficient of fluid amplifier feed nozzle, noting flow uniformity, incompressibility, velocity and velocity distribution assumptions

07 p0159 A69-19320

Fluidic power control switch for supersonic fluid amplifier, presenting performance data and possible industrial applications

08 p1256 A69-20304

Pure fluid amplifying logic and energy converting elements, discussing parameters, characteristics and working principles
[AGARDOGRAPH-118]

08 p1257 A69-20951

Vortex valves and amplifiers small signal analysis using mathematical model to describe quantitative effects of vortex parameter changes
[AGARDOGRAPH-118]

08 p1257 A69-20953

Peripheral fluidic devices for sequencing and monitoring machinery in hazardous areas, describing circuits
[AGARDOGRAPH-118]

08 p1257 A69-20954

Fluidic devices, including amplifiers, bistable elements, modulators, gates, etc

09 p1443 A69-22535

Discontinuous vortex power amplifier and diode design, noting supply regulator effects and load matching

09 p1443 A69-22737

Vortex amplifiers small signal analysis based on mathematical model and network theory

09 p1443 A69-22739

Vortex amplifiers design and performance, noting nonvented and vented amplifiers and fluid valving applications

09 p1443 A69-22741

Fluidic jet beam deflection amplifier, discussing basic principles, operating characteristics and design criteria

10 p1638 A69-23554

High gain proportional and bistable fluidic amplifier design, noting high impedance role in pressure sensing and computer circuits in aircraft engine control

10 p1638 A69-23555

Vortex amplifier as active element in analog circuits

10 p1639 A69-23556

Large signal vortex amplifier analysis using load lines to evaluate series orifice and vortex flow control valve characteristics

10 p1639 A69-23558

Hybrid fluidic pressure regulator combining vortex amplifier and confined-jet amplifier with performance upgrading moving metering element, noting greater efficiency and reliability

10 p1639 A69-23560

Sound amplification role in increasing spread of bounded two dimensional smoke jet studied for application to fluid amplifiers
[ASME PAPER 69-VIBR-3]

10 p1640 A69-24161

Gas jets collision flowing from parallel wall channels, applying solution to calculating geometrical characteristics of fluid jet amplifiers

12 p2016 A69-25879

Attachment and separation of free jet from wall, discussing model equations for wall attachment fluid amplifier

14 p2428 A69-28877

Counter for decimal counting and numeric display applications using integrated fluid logic elements

15 p2616 A69-31295

Linear fluid amplifier with beam-deflection proportional active element, discussing optimum maximally flat frequency response

15 p2553 A69-31299

Fluidic operational amplifier design and applications

15 p2554 A69-31300

Fluidic digital position sensor consisting of fluidic monostable amplifier, analyzing operation by characteristics method

15 p2554 A69-31301

Self contained remote sense remote control pressure regulator using pure fluid amplifiers, controlling large or small flow over wide pressure range

15 p2554 A69-31303

Fluid amplifier with sudden widening applied to various computer tasks, utilizing for detection and measurement of viscosity, temperature and sonic or rotational velocity

17 p2903 A69-33010

Switching time of transient two dimensional fluidic bistable wall attachment amplifiers based on mathematical model and separation bubble control

17 p2904 A69-34068

Servovalves with fluidic and electrical inputs compared for gas servoamplifiers performance, considering use as sensors in closed-loop hydraulic circuit

19 p3255 A69-36711

Fluid amplifiers for gas turbojet engines control, discussing hydraulic control and relationship between turbine rpm, fuel consumption and operating temperature

20 p3585 A69-36944

Classification of switching process in bistable fluid amplifiers with illustration of fluid oscillator, discussing capacitor and bleeds
[ASME PAPER 69-FLCS-28]

20 p3465 A69-37977

Model predicting steady state input-output characteristics of vortex amplifiers operating in incompressible flow regime, correlating model with experimental data
[ASME PAPER 69-FLCS-20]

20 p3465 A69-37980

Fluidic feedback oscillator performance from fluid density effects analysis including supply jet, feedback line dynamics and load and control port impedances
[ASME PAPER 69-FLCS-39]

20 p3465 A69-37984

LF switching in wall attachment type digital fluid amplifiers, studying visual and quantitative values for switch pressure and flow as function of geometric variables
[ASME PAPER 69-FLCS-31]

21 p3649 A69-38604

Fluidic amplifiers development and logic applications, describing various elements and circuits

22 p3870 A69-41239

Proportional fluid amplifiers analysis in cascade and with feedback by extended lumped parameter method,

discussing dynamic characteristics of analog amplifiers with air

24 p4255 A69-43268

Tristable fluid amplifiers, analyzing J functions of staticized variable, ternary logical characteristics, input equations, flow stability and switching measurements

24 p4255 A69-43298

Design of vortex fluid amplifiers operating in incompressible flow regime, based on fluid properties and geometry effects on amplifier behavior

24 p4256 A69-43299

FLUID BOUNDARIES

NT GAS-SOLID INTERFACES

NT JET BOUNDARIES

NT LIQUID-LIQUID INTERFACES

NT LIQUID-SOLID INTERFACES

NT LIQUID-VAPOR INTERFACES

Transonic flow around profile in blocked plane channel and in free jet, noting channel wall and jet edge effects on flow along profile

03 p0361 A69-13018

Laminar flow stability along flexible boundary, using broken linear velocity profile instead of boundary layer profile

06 p0909 A69-17207

Kelvin-Helmholtz instability for interface between two uniform superposed fluids with constant densities and velocities in horizontal motion in oblique magnetic field

07 p1182 A69-19274

Continuum flow boundary in freely expanding jet estimated from molecular mean free path and modulus of random motion mean velocity

10 p1679 A69-23425

Free periods of oscillation of incompressible rotating fluid bounded by rigid concentric spheres, using Longuet-Higgins solution of Laplace tidal equation

11 p1876 A69-25558

Linearized steady state equations of motion solved for boundary conditions of fluid lying between horizontal planes with temperature varying horizontally

12 p2066 A69-26134

Surface equilibrium configurations and bifurcation points for rotating homogeneous right fluid cylinder confined by surface tension forces

14 p2428 A69-28816

Small amplitude motions of plane interface between fluids stressed by initially perpendicular electric field, modeling fluids as ohmic conductors

16 p2811 A69-31667

Shear layer effect on plane sound waves, discussing reflection and refraction at velocity discontinuity between two regions of fluid

17 p3005 A69-32954

Thermal convection in horizontal fluid layer heated from below, with zero shear boundaries above and below, noting critical Rayleigh number measured value

20 p3518 A69-38234

Boundary layer development on body accelerating in viscous incompressible fluid, using straight lines approximation and asymptotic expansions

22 p3929 A69-40110

FLUID DYNAMICS

NT AERODYNAMICS

NT AEROTHERMODYNAMICS

NT ELASTOHYDRODYNAMICS

NT ELECTROHYDRODYNAMICS

NT GAS DYNAMICS

NT HYDRODYNAMICS

NT HYPERSONICS

NT MAGNETOHYDRODYNAMICS

NT RAREFIED GAS DYNAMICS

NT ROTOR AERODYNAMICS

Collection of papers on computational fluid dynamics

01 p0061 A69-10916

Turbulent flow between parallel plates, discussing turbulence generation by energy addition

01 p0061 A69-10993

Two dimensional compressible inviscid laminar gas flows unsteady processes studied by extending method of characteristics

01 p0008 A69-11360

Heat conduction in viscous fluid flows with large concentration of suspended solid particles

02 p0351 A69-12052

Noninstantaneous, nonlocal nonlinear responses of momentum and energy flows to thermodynamic forces in single component simple fluid with memory

03 p0413 A69-12921

Finite difference solution of time dependent Navier-Stokes equation for incompressible fluids, using velocities and pressure as variables

03 p0415 A69-13369

Bubble motion inside liquid in spherical cavity, allowing for bubble surface deformation
03 p0418 A69-13813

Axisymmetric vortex free motion of ideal fluid in conical container with spherical bottom under axial acceleration
06 p0910 A69-17335

Superlayer structure in turbulent boundary layer without pressure gradient, using constant temperature linearized hot wire anemometers
07 p1118 A69-18299

Flow in impellers of mixed and radial flow compressors for jet engines, turbochargers and automotive gas turbines, discussing velocity, load distribution, etc [SAE PAPER 690033]
07 p1049 A69-18312

NonNewtonian effects in axisymmetric rotational flows of elastico-viscous liquids
07 p1180 A69-18815

Combined effect of short wavelengths associated Kelvin-Helmholtz instability and long wavelengths associated gravitational instability on self gravitating fluid layer, discussing kinetic energy
07 p1182 A69-19276

Schlieren optics study of omega wave in water filled cuvette, noting propagation by wall reflected water wave
08 p1350 A69-19889

Statistical dynamics of turbulent incompressible fluid, discussing harmonic function in Navier-Stokes equation
08 p1303 A69-20323

Frequency response from linearized dynamic equations for viscous incompressible fluid flow in viscoelastic tubes, discussing transfer gain
08 p1304 A69-20704

Fluid equations for collisionless plasma including finite ion Larmor radius and finite beta effects
08 p1368 A69-20802

Fluid flow induced by horizontally moving bodies in stratified and rotating fluids determined by matched asymptotic expansion theory
08 p1253 A69-20997

Surrounding fluid effects on free axisymmetric vibrations of thin elastic spherical shells, studying irrotational motions in compressible and incompressible ideal fluids
09 p1613 A69-21720

Draining liquid surface dip formation in tanks of arbitrary shapes and drain hole positions
09 p1483 A69-21999

Fluid dynamical aspect of Schrodinger quantum mechanics and thermal equilibrium
09 p1541 A69-22394

Circle theorem extensions and applications to mechanics of continua, noting supersonic and subsonic compressible fluid flow
10 p1723 A69-22877

Incompressible fluid flow engine spiral casing, considering flow as potential flow
10 p1632 A69-22914

Dynamics of conducting fluid stream coupled to elastic medium by transverse electric or parallel magnetic field, considering stability of system
11 p1923 A69-24289

Numerical method for coupled moments of inertia and integral equations of boundary value problems for fluid in moving cavities
11 p1868 A69-24774

Motion of body with cavity containing liquid based on Kharlamov solution, noting gyrostatic moment and liquid sloshing effect
11 p1868 A69-24775

Distribution of steady state solutions for equations of helical motion of body in infinite fluid, noting coaxial control surfaces
11 p1868 A69-24782

Friction coefficients for turbulent flow through smooth pipes, considering average and friction velocity relations, fluid velocity measurements and flow Reynolds number
11 p1874 A69-25429

Flow field structure involving supersonic secondary jet interactions and separated regions in thrust vector control system
11 p1944 A69-25594

Iterative solutions of nonlinear integrodifferential dynamical equation for two point velocity correlation tensor in incompressible fluid turbulence studies
12 p2062 A69-26602

Microstructured mixtures theory including energy balance, mass and momentum equations and entropy production inequality for structured fluids in motion
13 p2371 A69-27318

Monograph on return currents produced by confined jet of incompressible fluid with low initial ambient fluid velocity
13 p2250 A69-28335

Diffusion characteristics of turbulent flow produced by square mesh grid in low speed wind tunnel
13 p2250 A69-28496

Eddy diffusivities ratio for heat and momentum by mixing length theory, using Mach-Zehnder interferometer for temperature profiles
13 p2380 A69-28497

Dissipative fluid sphere motion due to impulsive point source calculated by finite difference scheme, assuming Voigt and Maxwell type internal friction mechanisms limitations
14 p2485 A69-29026

Parametric resonance motion in viscous fluid column in communicating vessels during vertical oscillations, calculating critical accelerations over viscosity range
14 p2432 A69-29628

Cosmic shock waves simulation through correlations between shock equations in classical and relativistic fluid dynamics, using shock tube tests
14 p2433 A69-29981

Noncontacting minimum leakage dynamic seal requiring liquid-vapor interface with leakage tolerance [ASLE FICFS PREPRINT 40]
15 p2620 A69-30485

Fluid filled spherical shell axisymmetric nontorsional motion analysis via differential equations obtained by Hamilton principle
17 p3051 A69-32956

Statistical dynamics of turbulent incompressible fluid, discussing harmonic function in Navier-Stokes equation
17 p2952 A69-33313

Fluid dynamic simulation of gas core nuclear rocket chamber for separating light and heavy gas via centrifugal force produced by MHD-driven rotational flow [AIAA PAPER 69-727]
17 p3004 A69-33483

Computer simulation of numerical fluid dynamic problems for compressible and incompressible flows, noting Marker and Cell method
18 p3106 A69-34665

Fluid-shell interactions, using piston theory and cylindrical-wave approximations
18 p3223 A69-35174

Finite elements general theory applied to wave propagation, gas kinetics, nonlinear partial differential equations, continuum mechanics and fluid dynamics
20 p3567 A69-36948

Turbomachine blade thickness effect on meridional flow disturbances analyzed through blade geometry using differential equations
20 p3457 A69-37084

Rocket engines propellant feed systems dynamics analyzed by model using linear methods with distributed-parameter pipe representation [ASME PAPER 69-FE-6]
20 p3586 A69-37987

Differential equations for variable mass solid body motion about fixed point having cavities filled with ideal fluid
21 p3771 A69-39106

Homogeneous dynamo in cylindrically symmetric volume with symmetrically moving fluid and large magnetic Reynolds number, demonstrating first and second approximations using Braginskii method
22 p3989 A69-40192

Eulerian equations for precession and nutation of self gravitating fluid globes of arbitrary structures in inertial coordinates, discussing coplanar case, tidal breathing, etc
22 p4030 A69-40904

Friction, heat transfer and mass transfer theory of flow represented by two dimensional parabolic boundary layer equations
22 p3933 A69-40940

Anisotropic porous media model for fluid motion in rectangular fuel cell cavities, analyzing pressure, velocity, stream functions and purge time
23 p4075 A69-42300

Angular grid spacing resolution near poles effect tests in global prediction model for geophysical fluid dynamics, investigating forecast height and wind fields
24 p4344 A69-43066

Fluid flow around sphere at high Reynolds number by measuring pressure distribution, considering boundary layer separation, tunnel blockage, etc [ASME PAPER 69-APMW-26]
24 p4245 A69-43093

Dynamic models for viscous fluid transmission lines using distributed parameter for accuracy and rational approximate form to avoid computational difficulty
24 p4301 A69-43289

FLUID FILTERS

NT AIR FILTERS

Filtration and flow characteristics of wire cloths used in hydraulic systems described by expressions from measured properties [ASME PAPER 68-WA/FE-39]
05 p0750 A69-16111

Aircraft hydraulic equipment ultrafine filters effect on component life and system reliability
15 p2552 A69-30069

Liquid filter cells design with emphasis on filters usable for inorganic and organic liquids
21 p3770 A69-38679

Protective layer material for high sludge capacity filters for fine purification of liquids used in aircraft hydraulic system
22 p3869 A69-40637

FLUID FLOW

NT ADIABATIC FLOW
NT AIR CURRENTS
NT AIR FLOW
NT AIR JETS
NT ANNULAR FLOW
NT AXIAL FLOW
NT AXISYMMETRIC FLOW
NT BAROTROPIC FLOW
NT BASE FLOW
NT BLASIUS FLOW
NT BLOOD FLOW
NT BOUNDARY LAYER FLOW
NT BOUNDARY LAYER SEPARATION
NT CAPILLARY FLOW
NT CASCADE FLOW
NT CAVITATION FLOW
NT CHANNEL FLOW
NT COAXIAL FLOW
NT COMBUSTIBLE FLOW
NT COMPRESSIBLE FLOW
NT CONTINUUM FLOW
NT CONVECTIVE FLOW
NT CORE FLOW
NT COUETTE FLOW
NT COUNTERFLOW
NT CRITICAL FLOW
NT DUCTED FLOW
NT EQUILIBRIUM FLOW
NT EQUIPOTENTIALS
NT FREE FLOW
NT FREE MOLECULAR FLOW
NT FROZEN EQUILIBRIUM FLOW
NT FUEL FLOW
NT GAS FLOW
NT HARTMANN FLOW
NT HEAD FLOW
NT HELICAL FLOW
NT HYPERSONIC FLOW
NT HYPERVELOCITY FLOW
NT INCOMPRESSIBLE FLOW
NT INLET FLOW
NT INVISCID FLOW
NT ION INJECTION
NT ISOTHERMAL FLOW
NT JET FLOW
NT JET MIXING FLOW
NT JET STREAMS [METEOROLOGY]
NT KNUDSEN FLOW
NT LAMINAR FLOW
NT LIQUID FLOW
NT MAGNETOHYDRODYNAMIC FLOW
NT MASS FLOW
NT MERIDIONAL FLOW
NT MOLECULAR FLOW
NT MULTIPHASE FLOW
NT NONEQUILIBRIUM FLOW
NT NONNEWTONIAN FLOW
NT NONUNIFORM FLOW
NT NOZZLE FLOW
NT ONE DIMENSIONAL FLOW
NT OPEN CHANNEL FLOW
NT ORIFICE FLOW
NT OSCILLATING FLOW
NT PERIPHERAL JET FLOW
NT PIPE FLOW
NT PLASTIC FLOW
NT POTENTIAL FLOW
NT PROPELLANT TRANSFER
NT RADIAL FLOW
NT REATTACHED FLOW
NT RECIRCULATIVE FLUID FLOW
NT REVERSED FLOW
NT SECONDARY FLOW
NT SEPARATED FLOW
NT SHEAR FLOW
NT SLIP FLOW
NT STAGNATION FLOW
NT STEADY FLOW
NT STEAM FLOW
NT STOKES FLOW
NT STRATIFIED FLOW
NT SUBCRITICAL FLOW
NT SUBSONIC FLOW

NT SUPERCAVITATING FLOW
 NT SUPERCRITICAL FLOW
 NT SUPERSONIC FLOW
 NT SUPERSONIC JET FLOW
 NT THREE DIMENSIONAL FLOW
 NT TRANSITION FLOW
 NT TRANSONIC FLOW
 NT TRESCA FLOW
 NT TURBULENT FLOW
 NT TWO DIMENSIONAL FLOW
 NT TWO PHASE FLOW
 NT UNIFORM FLOW
 NT UNSTEADY FLOW
 NT VERTICAL AIR CURRENTS
 NT VISCOUS FLOW
 NT WALL FLOW
 NT WATER FLOW
 NT WEDGE FLOW

Relationship between cooled surface temperature and pressure self oscillation frequency during heat transfer to turbulent fluid flow, showing temperature variations

01 p0173 A69-10094

Immersion depth influence on hydrofoil for flow of arbitrary depth with bottom consisting of free surface or solid wall

01 p0007 A69-11132

Hall effect in unperturbed flow of fluids near thin profiles at infinity

01 p0132 A69-11133

Collection of Soviet articles on computer methods and programming covering fluid flow by numerical methods

03 p0362 A69-13649

Kinematic and dynamic relations determined for vortex flow of ideal incompressible fluid past circular cylinder, noting use for calibrating cylindrical adapters

04 p0541 A69-14484

Optical signal frequency method for measuring velocity of fluid flow

04 p0598 A69-14995

Ideal plane incompressible fluid flow past airfoil noting hydrodynamic effects, assuming presence of constant eddy

04 p0589 A69-14996

Induced flow determination in pulsejet ejector, solving momentum and continuity equations by method of characteristics and mathematical model
 [ASME PAPER 68-WA/FE-33]

05 p0812 A69-16106

Stagnation pressure losses of adiabatic flow of compressible fluids through abrupt area expansion and contraction in subsonic range, discussing base pressure
 [ASME PAPER 68-WA/FE-46]

05 p0750 A69-16113

Flow theories of fluids with elastic deformation of substructure, treating suspensions of irregularly shaped deformable particles

05 p0752 A69-16738

Inviscid incompressible fluid flow stability against helical disturbances in circular cylinder

06 p0910 A69-17332

Laminar natural convection in enclosed rectangular cavity, discussing temperature gradient effects

06 p1033 A69-17556

Fluid flow longitudinal temperature profiles for inclusion in heat transfer computer program
 [AIAA PAPER 69-30]

06 p1038 A69-18174

AC fluidics for pressure pulse frequency control and monitoring in flow, discussing design and application to steam turbine speed control

07 p1058 A69-18938

Nondimensional Jeffreys number as ratio of Reynolds to Froude number for gravitational motion of viscous masses, with application to lunar maria and plastic ice

07 p1218 A69-19262

Fluid motion and MHD disturbances in viscous incompressible fluid of finite electrical conductivity, studying axis of oscillating dipole perpendicular to exciting field

07 p1195 A69-19451

Large amplitude waves in inviscid flows of stably stratified fluids over barriers with constant density upstream constructed from vortex pairs and doublets

08 p1346 A69-20313

Fluid flow induced by horizontally moving bodies in stratified and rotating fluids determined by matched asymptotic expansion theory

08 p1253 A69-20997

Turbulent diffusion from point source in boundary layer, discussing horizontal and vertical effects

09 p1535 A69-21513

Equilibrium theory of parametric pump using cyclic flow of binary mixture through column with heated and cooled bed of solid absorbent

09 p1481 A69-21910

Viscous fluids rotational flow in cylindrically symmetrical vessels, circumventing Navier-Stokes equations of motion by Wedemeyer approximation

10 p1677 A69-22896

Test stand final control element for fluid flow application, noting analog control valve with digital to analog conversion and digital actuator

10 p1671 A69-23259

Network rupture hypothesis and molecular structure considerations used in obtaining constitutive equations for flow of polymer melts and solutions
 [AICHE PAPER 42C]

10 p1800 A69-23369

Finite difference method for calculating lee waves incident on obstacle with arbitrary vertical distribution of main flow horizontal velocity and temperature

10 p1722 A69-23967

Longitudinal vibrations induced by internal flow in metal bellows resembling vortex shedding excitations of elastically restrained cylinders, discussing spring mass mechanical model
 [ASME PAPER 69-VIBR-5]

10 p1805 A69-24163

Similarity solution for flow of fluid-particle suspension over disk rotating at constant velocity, solving differential equations for flow velocity distributions

11 p1867 A69-24280

Diffusive flow with isopycnic lateral boundaries in porous medium and density distribution of diffusive motion, noting exact solution equivalence to previous solution

11 p1869 A69-24887

Model evolution of flow in fluid layer suddenly heated from below at Rayleigh number convection sufficient for turbulence

11 p1874 A69-25351

Flow control valve for hydraulic motor speed regulation operated by remote pressure signal

11 p1827 A69-25646

Linearized steady state equations of motion solved for boundary conditions of fluid lying between horizontal planes with temperature varying horizontally

12 p2066 A69-26134

Holographic interference method for measuring film height in analyses of fluid film vaporization under blowing hot gas

12 p2088 A69-26178

Ray tracing techniques applied to internal gravity waves in fluid with spatially varying mean flows

12 p2067 A69-26345

Aerospace applications of electric discharge interaction with fluid motion including sonic boom reduction, high lift devices, reentry vehicle pitch control, etc

12 p2136 A69-26405

Self controlled vibration of elastically supported cylinder in fluid stream due to von Karman shedding, considering fluidelastic interaction, structural deformation and natural frequency

13 p2360 A69-27437

Variable fluid and field velocity HF induction generator, determining interaction between fluid dynamic forces and magnetic field and kinetic energy

13 p2207 A69-27502

Heat transfer coefficient deterioration between fluid and tube wall at supercritical pressure and high heat fluxes
 [ASME PAPER 68-HT-39]

13 p2373 A69-27771

Heat transfer involving particulate suspension, discussing characteristics of flowing suspension, inertia effects, impingement, deposition, radiation and electric charges

13 p2377 A69-28151

Computer program for compressible fluid flows with space and time dependent variables, discussing hypervelocity impact
 [AIAA PAPER 69-353]

13 p2365 A69-28286

Ideal compressible fluid motion and heat transfer, noting convective heat transfer intensification with increased twisting velocity of flow

13 p2251 A69-28559

Boundary layer equation of viscous incompressible fluid with moment stresses, noting flow around thin plate and submerged jet problems

14 p2428 A69-28815

Axial and radial turbulence intensities for flow through smooth round tubes, measuring velocity profiles and drag coefficients

15 p2590 A69-30003

Turbulence constant for flows near walls, analyzing viscosity dependence on wall distance by utilizing maximum stability principle

15 p2590 A69-30048

Self contained remote sense remote control pressure regulator using pure fluid amplifiers, controlling large or small flow over wide pressure range

15 p2554 A69-31303

Bubble boiling onset in forced fluid flow, deriving equations for calculating minimum temperature difference between wall and fluid, discussing applicability range

16 p2878 A69-31954

Fluid flow problems during orbital refueling vehicle maneuvers and system operations in propellant transfer, including disturbances, liquid-vapor interface instability, vapor ingestion, etc
 [AIAA PAPER 69-567]

16 p2868 A69-32721

Fluid transfer in orbit under low or zero g, stressing orientation
 [AIAA PAPER 69-565]

16 p2865 A69-32770

Book on gas dynamics of two phase media for thermal power engineering equipment, discussing phase transformations, condensation in high velocity flows, etc

17 p2948 A69-32951

Monograph on interaction between flow and sound fields as singular perturbation problem, using matched asymptotic expansion

17 p2949 A69-32998

Model calculations for movement of barotropic and initially symmetric vortices in rotating fluids with Coriolis parameter or fluid depth varying horizontally

17 p3000 A69-33761

Computer implementation of Bergman solution to initial value problem for partial differential equation of compressible fluid flow

18 p3164 A69-34614

Transformed Navier-Stokes equations for incompressible fluids flow, deriving forces acting on surface of bounded region

18 p3122 A69-34830

Axissymmetric laminar and turbulent wakes of body in flow with streamline pressure gradient, discussing velocity defects and profiles

19 p3296 A69-35762

Least squares method application to boundary value problem approximate solution for plane, axisymmetric, creeping and incompressible irrotational flows

19 p3299 A69-36475

Long term integration of fluid motion equations with finite difference scheme using hexagonal grid system to avoid nonlinear computational instability

19 p3364 A69-36508

Static and dynamic characteristics of pressure compensated oil-hydraulic flow control valves and relief valves with emphasis on linearized effects

19 p3256 A69-36713

Laser Doppler velocimeter (LDV) for fluid velocity measurements, noting advantages

20 p3552 A69-37004

Pressure increment due to inertia of rotating fluid film at journal bearing periphery theoretically estimated and measured

20 p3548 A69-37085

Incompressible fluid flow of given density and kinematic viscosity near trailing edge of flat plate

20 p3458 A69-37098

Hydromagnetic waves equations of motion for non-relativistic case, discussing particle and fluid flow models

20 p3616 A69-38317

Compressible fluid flow characteristics in turbomachine stage, discussing simplified radial equilibrium method as basis for design

21 p3643 A69-38457

Finite difference method for calculating Lee waves incident on obstacle with arbitrary vertical distribution of main flow horizontal velocity and temperature

21 p3759 A69-39653

Temperature-vorticity analogy for viscous two dimensional fluid flow extended to compressible flows, noting enthalpy and shear stress analogy

22 p3929 A69-39892

MHD dynamo construction with emphasis on fluid motion effect on magnetic field, considering spatially periodic dynamo derivation from kinematic considerations

22 p3989 A69-40196

Fluid velocity in starting flow in circular tube using Laplace transform

22 p3911 A69-40688

EVA/IVA fluid umbilical improved stowability and flexibility, discussing cross section development and tests

24 p4272 A69-42847

Fluid flow around sphere at high Reynolds number by measuring pressure distribution, considering boundary layer separation, tunnel blockage, etc
 [ASME PAPER 69-APMW-26]

24 p4245 A69-43093

FLUID INJECTION
 NT GAS INJECTION

NT LIQUID INJECTION NT WATER INJECTION

Plane MHD jets with variable conductivity, showing effective mixing length as function of distance

01 p0130 A69-10773

Structure of shock waves from MHD jet injected into zero viscosity, finite thermal and electrical conductivity medium analyzed by nonlinear differential equation system

01 p0130 A69-10774

Steady laminar flow in two dimensional channel with different permeability porous walls and large injection at both walls

03 p0417 A69-13795

Plasma transverse injection into toroidal magnetic field created by linear current leads to plasma confinement along magnetic force lines

03 p0478 A69-13837

Electric potential distribution in coaxial quasi-stationary plasma injector

03 p0478 A69-13838

Secondary injection effect on supersonic parallel diffuser, analyzing flow patterns, pressure distribution and recovery and heat transfer

03 p0365 A69-13991

Mean temperature distribution through inner and outer regions of turbulent boundary layer with injection through heated porous wall

04 p0685 A69-14729

Heat transfer, suction and injection in plane Couette flow analyzed for Rivlin-Ericksen fluid, using perturbation method

04 p0589 A69-14970

Source and sink method application to direct axisymmetric problems of hydrodynamics

05 p0747 A69-16039

Uniform hot fluid injection effect on heat transfer in constant property turbulent boundary layer [ASME PAPER 68-WA/HT-24]

05 p0847 A69-16126

Pressurized fluid journal bearing with fluid fed into space between shaft and shell from plenum chamber in bearing housing through circumferential slots

06 p0931 A69-17529

Impurity elimination from hydrogen plasma jets injected from coaxial source normal to octupole magnetic field

08 p1370 A69-21016

Experimental and theoretical investigation of mass injection effect on high current MPD arc [AIAA PAPER 69-266]

09 p1564 A69-21242

Krause numerical solution applied to normal injection in three dimensional incompressible laminar boundary layer [DVL-902]

09 p1482 A69-21971

Fluid injection into flowfield from porous forward portion of blunt body in stagnation region flow, determining reservoir pressure and mass flow rate

09 p1430 A69-21973

Static pressure measurements at surface of sharp plate in supersonic flow during gas/liquid jet injection

11 p1821 A69-25479

Liquid metal multistage injection efficiency with sodium and potassium working fluids, noting preheating

13 p2372 A69-27483

Steam-water convergent condensing injector with supersonic inlet vapor, discussing axial pressure profiles and discharge pressure

13 p2372 A69-27486

Thermodynamic efficiency of MHD cycles for liquid Na with multistage injection and injection condensation

13 p2205 A69-27487

Wet steam injector power losses in nozzle as function of humidity, noting compensation of nozzle throat diameter and fluid flow rates

13 p2246 A69-27490

Numerical solutions of equations for high Prandtl number boundary layers in two dimensional flat plate incompressible flow with mass injection

13 p2249 A69-28238

Pressure distribution in wake produced by obstacle with secondary fluids injection into boundary layer, obtaining coefficient governing resistance of obstacle to forward motion

16 p2768 A69-31604

Two dimensional turbulent mixing with surface mass injection at supersonic and hypersonic speeds, noting velocity and temperature distributions [AIAA PAPER 68-130]

16 p2170 A69-31883

Compressible flow over finite porous plate in supersonic stream with massive injection over surface analyzed using inviscid vortical flow model

16 p2770 A69-31884

Incompressible attached wall jet/Coanda flow/over circular cylinder with finite incompressible injection normal to surface

16 p2772 A69-32148

Injection film cooling effect on surface heat transfer downstream of flush nontangential injection holes and slots in turbine applications [AIAA PAPER 69-523]

16 p2843 A69-32703

Orbital refueling techniques, discussing vapor-liquid interface stability, pressurant requirements, transfer line chilldown, propellant transfer dynamics, dielectrophoresis, suction speed estimating and system tradeoffs [AIAA PAPER 69-564]

16 p2869 A69-32733

Skin friction drag reducing high polymer solution injected into turbulent boundary layer to test effectiveness on marine vehicles

17 p2951 A69-33254

Jet injection into free circular cross section cross wind using curvilinear dynamic model, assuming negligible Archimedean forces effect

18 p3124 A69-35149

Flow rate of ideal fluid ejected from swirl injector taking into account radial component of flow velocity at nozzle exit

19 p3297 A69-35820

Laminar flow in porous circular pipe with constant suction or injection applied at wall

24 p4298 A69-42618

Turbulent flow in circular porous tube laminarized by uniform mass injection through tube wall, measuring velocity and turbulence intensity by impact probe [ASME PAPER 69-HT-57]

24 p4303 A69-43537

FLUID JET AMPLIFIERS

U JET AMPLIFIERS

FLUID JETS

NT AIR JETS

NT FREE JETS

NT GAS JETS

NT HYDRAULIC JETS

NT VAPOR JETS

Jet line in rotational incompressible plane flows around shrouded propeller blade, using electrical analog

01 p0058 A69-10037

Growth rate of wave instability in conducting liquid jet in perpendicular electric field and accelerating under gravity

01 p0062 A69-11207

Instabilities for two highly conducting finite length streams in relative motion and coupled by transverse electric or longitudinal magnetic fields

01 p0062 A69-11208

Pressure gain estimates in analog jet amplifier based on total pressure measurements in main jet interaction region

02 p0195 A69-12076

Cylindrical jet stability of perfectly conducting, incompressible and inviscid fluid in presence of axial magnetic field

03 p0474 A69-13142

Flow characteristics about curved lateral jet, discussing effect of pitot tube nozzle shape and turbulence

05 p0746 A69-16017

Wall attachment phenomenon/Coanda effect/ basis for jet elements in digital and/or pulse-mode systems

10 p1638 A69-23553

Hybrid fluidic pressure regulator combining vortex amplifier and confined-jet amplifier with performance upgrading moving metering element, noting greater efficiency and reliability

10 p1639 A69-23560

Fuel jet shape in air stream/mechanical atomization calculated as function of stream and fuel injection parameters

11 p2002 A69-25336

Electrically driven thin fluid jet stability in longitudinal field between two plate electrodes, discussing role of Ohm law in calculating jet potential

12 p2136 A69-26402

Electrohydrodynamic instability of incompressible conducting cylindrical viscous jet in external magnetic field, noting viscosity role in oscillation modes and growth rate

12 p2136 A69-26403

Flow phenomena associated with electrically conducting boundary layer jet injection through slot into uniform slipstream in presence of transverse magnetic field

14 p2501 A69-29917

Vortex ring production in liquid jet by vibration induced pressure pulses at orifice, discussing plates formed under high g vibration [AIAA PAPER 68-132]

16 p2770 A69-31880

Cylindrical viscous jet transition points from stable to unstable modes of oscillation found same as for inviscid jet

16 p2773 A69-32570

Evaporation rate of liquid sprays involving atomization, droplets ballistics, drop size distribution, turbulence effects, etc

18 p3119 A69-34246

Jet injection into free circular cross section cross wind using curvilinear dynamic model, assuming negligible Archimedean forces effect

18 p3124 A69-35149

Aerodynamic characteristics of plane inviscid fluid jets expanding over curvilinear surface, deriving force equations for surfaces in jet and rocket engines

19 p3296 A69-35815

Velocities and pressure in twisted jet in unbounded space containing same fluid as jet

19 p3298 A69-36388

Circular liquid jet oblique impingement on flat surface, noting dry zone occurrence at small angles due to lateral flow deflection

21 p3691 A69-38551

Jet efflux from two dimensional symmetric nozzles of arbitrary shape determined using conformal mapping and Riemann-Hilbert solution to mixed boundary value problem

21 p3692 A69-38686

Convergence of axes of plane-parallel jets due to reciprocal ejection effect, analyzing deformation of jet, refraction coefficient for air between jets, etc

21 p3696 A69-39095

FLUID LOGIC

Variable time delay achievement in fluid logic circuits based on Coanda effect devices

02 p0196 A69-12085

Wall attachment type fluidic logic devices with low power consumption requirements, noting monostable and bistable devices

05 p0704 A69-16002

Fluidic logic elements using suction to influence main jet, outlining operation principles

16 p2736 A69-31835

Fluidic logic for high speed pneumatic stepping motor for high radiation environments, discussing bellows pressure sequencing by open-loop counter, signal conversions and performance

18 p3092 A69-34310

Fluid logic feedback control circuit synthesis using synthesis table, describing procedure to assign memory valves and switching signals

24 p4292 A69-43290

FLUID MECHANICS

NT AERODYNAMICS

NT AEROTHERMODYNAMICS

NT ELASTOHYDRODYNAMICS

NT ELECTROHYDRODYNAMICS

NT GAS DYNAMICS

NT HYDRODYNAMICS

NT HYDROSTATICS

NT HYPERSONICS

NT MAGNETOHYDRODYNAMICS

NT MAGNETOHYDROSTATICS

NT RAREFIED GAS DYNAMICS

NT ROTOR AERODYNAMICS

Asymptotic solution of Orr-Sommerfeld equation by multiple scales method for linear and general velocity profile

01 p0059 A69-10332

Equation of characteristic functional for Burgers one dimensional model fluid turbulence using logarithmic expansion method, discussing change in time of energy spectrum

01 p0059 A69-10338

Fluid mechanics of one stage momentum flueric diode

02 p0195 A69-12071

Fluid mechanics of supersonic flow separation and reattachment in fluidic devices

02 p0231 A69-12077

Equilibrium problem for fluid subjected to gravitational forces and surface tension, proposing algorithm for numerical solution

03 p0417 A69-13810

Inviscid cavity and wake flows behind submerged bodies, analyzing mathematical and theoretical models

04 p0587 A69-14608

Difference schemes implementation through fractional time step and phase error methods reduce dispersion

04 p0591 A69-15282

Laminar compressible viscous boundary layer with arbitrary external pressure distribution, using implicit multiple difference method

04 p0591 A69-15294

Viscous incompressible fluid motion in two or more dimensions and with zero fluid velocity on domain boundary, determining lower bounds and uniqueness for solutions

04 p0626 A69-15311

Ornstein-Zernike relation for homogeneous fluid relating direct and indirect correlation functions

04 p0591 A69-15435

Laminar flow of nonNewtonian fluids described via rheological three parameter model

05 p0744 A69-15678

Analog simulation of water hammer type phenomena governed by linear constant coefficient partial differential equations

05 p0751 A69-16475

Class of uniform motions of continuous media and rarefied gases

05 p0751 A69-16677

Asymptotic solutions of Grad system of kinetic moments

05 p0752 A69-16678

Book on continuum mechanics covering elasticity, fluid mechanics, plasticity and viscoelasticity, emphasizing basic concepts

05 p0843 A69-16713

Thermodynamics of fluid materials and characterization of thermodynamics of irreversible processes, using constitutive equations

06 p0959 A69-18222

Book on fluid mechanics fundamentals and applications covering incompressibility and compressibility effects, viscosity, hydrostatics, aerostatics, one dimensional, potential, turbulent flow and boundary conditions

07 p1121 A69-19376

Statistical theory of fluids in equilibrium based on correlation functions for pair interactions between constituent molecules, invoking superposition closure approximation

08 p1350 A69-19868

Computer study of analytical model of boundary layer transition from laminar to turbulent flow [AIAA PAPER 68-38]

09 p1482 A69-21945

Turbulent transport processes mathematical model, determining upper and lower bounds

10 p1677 A69-22895

Short memory elasticoviscous fluid motion in and around oscillating spherical shell

10 p1800 A69-23240

Simple fluids viscosity dependence on density analyzed by molecular theory, exemplifying with liquid argon

13 p2299 A69-28036

Fluids structural relaxation analyzed by nonequilibrium thermodynamics and molecular kinetic theory, considering Brownian motion

13 p2299 A69-28037

Horizontal shear flow effect on linear geostrophic adjustment in unbounded barotropic fluid, discussing gravity waves, vorticity equations, available energy, etc

15 p2648 A69-30217

Leakage prediction through mechanical seal by theoretical equation developed from basic fluid mechanics [ASLE FICFS PREPRINT 17]

15 p2621 A69-30499

Kovaszny spectral theory of turbulence, discussing energy spectrum decrease in viscous subrange

16 p2768 A69-31686

Gaseous reactor fluid mechanics for nuclear rocket engines, discussing experiments on geometries used in open cycle engine for acceptable uranium loss rate [AIAA PAPER 69-477]

16 p2811 A69-32728

Book on mechanics of deformable media covering fluid and solid mechanics and applications to irrotational flows of compressible and incompressible fluids

16 p2813 A69-32789

Switching time of transient two dimensional fluidic bistable wall attachment amplifiers based on mathematical model and separation bubble control

17 p2904 A69-34068

State space procedure for mixed boundary value problems applied to structural analysis, fluid mechanics and eigenvalues for deformable bodies

18 p3164 A69-34685

Meteorological forecasting as problem in fluid mechanics and thermodynamics, discussing accuracy and electronic computer role in classical or mathematical methods

18 p3166 A69-34694

Collection of papers on fluid mechanics, Volume 1, covering buoyant plumes and thermals, laminar separation, electrohydrodynamics, boundary layer transition, hydrodynamic noise, etc

18 p3122 A69-34916

Applied mechanics - Conference, Waterloo, Ontario, Canada, May 1969

19 p3374 A69-36655

Thomas wave equation in fluid mechanics, examining coordinates system with normal hyperbolic metric of universe tube having given signature

20 p3598 A69-37430

Continuum mechanics of micropolar fluids and solids, discussing thermodynamical restrictions on elasticity and viscosity coefficients, deriving field equations and boundary conditions

20 p3624 A69-37582

One dimensional model and equation of energy spectrum function solved in studying turbulent diffusion in fluid at rest

21 p3693 A69-38749

Interaction between boundary layer and external vortex flows and stability transitions of heated rotating fluid annulus

21 p3698 A69-39869

Volterra problem with given singularities for exterior of circle applied to fluid mechanics

24 p4339 A69-42679

FLUID POWER

Compact hydraulic power transfer units in aircraft with common connecting shaft for pump/motor elements, discussing integrated power package

06 p0930 A69-17168

Fluid power - Conference, London, September 1968

19 p3255 A69-36710

Pneumatic control circuits design based on logic functions and truth tables, noting fluid logic application

19 p3256 A69-36714

FLUID ROTOR GYROSCOPES

Unconventional two axis gyroscopes using fluids, determining precession moments and gyroscopic effects of medium [DVL-848]

04 p0597 A69-14831

FLUID SWITCHING ELEMENTS

Fluid mechanics of one stage momentum fluric diode

02 p0195 A69-12071

Switching action mechanism in wall attachment fluid amplifier, outlining theory based on turbulent jet entrainment

02 p0195 A69-12073

Fluidic element design calculations, noting flow characteristic differences

02 p0195 A69-12074

Pneumatic pressure ratio sensing element and associated high pressure switches and amplifiers for gas turbine engine control systems

02 p0249 A69-12088

Wall attachment type fluidic logic devices with low power consumption requirements, noting monostable and bistable devices

05 p0704 A69-16002

Fluidics research and development of control elements and components

05 p0704 A69-16003

Vortex devices and turbulence amplifiers, describing circuits, operating principles and performance

05 p0705 A69-16005

Fluidic power control switch for supersonic fluid amplifier, presenting performance data and possible industrial applications

08 p1256 A69-20304

Design criteria for pneumatic servo controls with fluidic elements stressing final transient, pilot circuits and amplifier elements

08 p1256 A69-20305

Fluidic devices, including amplifiers, bistable elements, modulators, gates, etc

09 p1443 A69-22535

Switching time of transient two dimensional fluidic bistable wall attachment amplifiers based on mathematical model and separation bubble control

17 p2904 A69-34068

Discharge coefficient and opening time of pneumatic and hydraulic systems incorporating disks, nozzles and valves

18 p3094 A69-34981

Classification of switching process in bistable fluid amplifiers with illustration of fluid oscillator, discussing capacitor and bleeds [ASME PAPER 69-FLCS-28]

20 p3465 A69-37977

Fluidic amplifiers development and logic applications, describing various elements and circuits

22 p3870 A69-41239

FLUID TRANSMISSION LINES

Lossy and lossless fluidic transmission line theory to estimate downstream conditions having known upstream system

01 p0012 A69-10153

Liquid flow systems dynamic response to periodic disturbances of system structural supports

05 p0747 A69-16073

Natural frequency of fluid oscillations in complex pipelines

07 p1119 A69-18745

Reliable fluid transmission systems by brazed joints, noting base and filler metals, fitting designs and various processes

09 p1507 A69-22333

Cerebral circulation arterial system pulsatile flow flexible vessel digital simulation models distribution

19 p3264 A69-36867

Acoustic frequency response of unsteady turbulent flow in transmission lines, considering effects of small amplitude disturbances and heat transfer [ASME PAPER 69-FE-11]

20 p3516 A69-37988

Dynamic models for viscous fluid transmission lines using distributed parameter for accuracy and rational approximate form to avoid computational difficulty

24 p4301 A69-43289

FLUID TRANSPIRATION

U TRANSPARATION

FLUIDICS

Lossy and lossless fluidic transmission line theory to estimate downstream conditions having known upstream system

01 p0012 A69-10153

Fluidic display systems, discussing thermochromic modules and decoder with miniature components

01 p0078 A69-10155

Fluidics - Conference, London, November 1968

02 p0194 A69-12070

Fluidic element design calculations, noting flow characteristic differences

02 p0195 A69-12074

Fluid mechanics of supersonic flow separation and reattachment in fluidic devices

02 p0231 A69-12077

Vortex valve characteristics, noting Reynolds number and geometry effects on flow and turndown ratio

02 p0195 A69-12079

Malfunction elimination in asynchronous fluidic switching circuit by locating static hazards

02 p0195 A69-12080

Working equivalent circuits for fluidic transverse impact modulator in LF and IF range

02 p0196 A69-12082

Fluid logic circuits miniaturization for flow in straight and curved channels of various cross sections

02 p0196 A69-12084

Fluidic pulse time modulated angular position sensor for two axis hydrostatically supported gyroscope

02 p0249 A69-12087

Fluid temperature sensor generating output differential pressure proportional to temperature of fluid entering device

02 p0249 A69-12089

Fluidic acceleration sensor based on vibrating string principle, discussing design, suspension system, driving-oscillator circuit, beat frequency circuit and detection circuits

02 p0249 A69-12091

Pneumatic elements, discussing development from process control via modules systems to logic elements and fluid sensors

02 p0197 A69-12795

Fluidic numerical controls of linear or rotating motors, discussing pneumatic, hydraulic, hybrid logic components and amplifiers

04 p0550 A69-15082

Comparison of electric, electronic and fluidic logic circuits

04 p0583 A69-15083

Fluidics research and development of control elements and components

05 p0704 A69-16003

Vortex devices and turbulence amplifiers, describing circuits, operating principles and performance

05 p0705 A69-16005

Fluidic component descriptions and systems synthesis, discussing mathematical, graphical and linear models

05 p0705 A69-16007

Breadboard technique and interconnection for fluidic circuits in large systems

05 p0705 A69-16009

Theory of capillary flow for fluidic resistor design
05 p0705 A69-16011

Wall jet type fluidic elements subjected to hydroacoustic dynamic effects, discussing use of boundary layer flow properties
05 p0705 A69-16016

Bistable fluid device utilizing Coanda effect along convex surface for wall attachment
[ASME PAPER 68-WA/FE-27] 05 p0749 A69-16101

Flow field in fluidic temperature sensor using schlieren and shadowgraph techniques
[ASME PAPER 68-WA/FE-29] 05 p0763 A69-16102

Synthesis of simulated aircraft cabin pure fluidic temperature control system
[ASME PAPER 68-WA/FE-30] 05 p0705 A69-16103

Fluidic proportional thruster system for sounding rocket control
[ASME PAPER 68-WA/FE-32] 05 p0763 A69-16105

Hazards in pneumatic fluidic sequential circuits caused by delays in pneumatic tubing
[ASME PAPER 68-WA/AUT-18] 05 p0706 A69-16174

Fluidic systems with long lines simulated by transmission lines of OR/NOR oscillator
[ASME PAPER 68-WA/AUT-12] 05 p0706 A69-16178

Fluidic type temperature sensor for total temperature measurement for hypersonic aircraft in atmosphere
05 p0766 A69-16755

Book on fluidics applications analyzing world literature dealing with fluidic devices
06 p0869 A69-17171

Fluidic vortex valve warm gas flow control for rocket application
[AIAA PAPER 69-118] 06 p0872 A69-18147

Steady flow circuit characteristics in square cross section channels of planar geometry fluid control elements in case of laminar flow
07 p1118 A69-18293

AC fluidics for pressure pulse frequency control and monitoring in flow, discussing design and application to steam turbine speed control
07 p1058 A69-18938

Fluidic devices application to attitude and guidance control of satellites, rockets and space probes
07 p1230 A69-19292

Sensor suspension, damping and signal readout through use of fluids with applications to rate and acceleration sensors
[AGARDOGRAPH-118] 08 p1257 A69-20949

Gas servo design utilizing floating flapper disk switching valves and pulse-length modulated pressure waves to actuate on-off switch
[AGARDOGRAPH-118] 08 p1257 A69-20950

Fluidics in UK, discussing digital control elements and systems and transmission lines in alternating flow hydraulics
[AGARDOGRAPH-118] 08 p1257 A69-20952

Peripheral fluidic devices for sequencing and monitoring machinery in hazardous areas, describing circuits
[AGARDOGRAPH-118] 08 p1257 A69-20954

Fluidic devices for closed loop control of gas turbines
[AGARDOGRAPH-118] 08 p1258 A69-20956

Fluidic component application to propellant tank pressurization and controller design
[AIAA PAPER 68-629] 09 p1442 A69-21980

Fluic light-off detector (FLOD) for sensing and indicating minimum light-off or blow out conditions in turbojet engine afterburner
[ASME PAPER 69-GT-36] 09 p1501 A69-22488

Air powered fluid jet engine compressor bleed control stressing closing, reset and override operations
[ASME PAPER 69-GT-19] 09 p1571 A69-22498

Fluidic overspeed sensor for small turboshaft power turbine, discussing requirements, circuit and system design, packaging, reliability and maintainability
[ASME PAPER 69-GT-17] 09 p1571 A69-22500

Miniature fluidic oscillator temperature sensors evaluated in gas turbine engine nozzle, discussing temperature control and related signal error compensation and temperature averaging
[ASME PAPER 69-GT-70] 09 p1572 A69-22512

Fluidic devices, including amplifiers, bistable elements, modulators, gates, etc
09 p1443 A69-22535

Vortex fluidic devices - Conference, Philadelphia, January-February, 1967
09 p1443 A69-22736

Vortex valve pure fluid modulators steady state characteristics, analyzing geometry of exit, control and supply areas and chamber
09 p1443 A69-22738

Vortex fluid devices in control systems, considering electrical, mechanical and hydraulic systems
09 p1443 A69-22740

Fluidics technology including applications, construction and mountings
10 p1636 A69-23401

Fluidic control technology compared to other control modes, describing fluidic functions and devices
10 p1636 A69-23402

Wall attachment phenomenon /Coanda effect/ basis for jet elements in digital and/or pulse-mode systems
10 p1638 A69-23553

Fluidic jet beam deflection amplifier, discussing basic principles, operating characteristics and design criteria
10 p1638 A69-23554

Fluidic compressor bleed control unit for TF-30 jet engine to prevent stall at low rpm operation
10 p1753 A69-23559

Fluidic secondary injection thrust vector control systems for solid propellant and hydrogen-oxygen rocket engines
10 p1753 A69-23561

Jet fluidic differential amplifier transfer function determination, describing interconnection dynamics
11 p1824 A69-24350

Passive structural units in fluidic circuits, discussing tesla diode and proportional amplifier
11 p1825 A69-24542

Fluidic quantities analogous to electrical properties of lumped circuit elements in DC networks, noting validity of Kirchhoff node and mesh theorems
11 p1861 A69-25676

Analog jet elements of pneumonics operating on direct interaction between streams, calculating static characteristics for analog jet amplifying element
14 p2393 A69-28746

Fluidic systems for automatic control of fuel supply to ramjet engine combustor, coolant rationing and distribution to engine structure and performance efficiency maintenance
14 p2508 A69-28875

Hydraulic resistance, capacitance and inductance of fluidic element derived by analogy with electric circuits
15 p2552 A69-31060

Optimizing control system design using fluidic digital circuitry and FM type transducers
15 p2583 A69-31296

Fluidic control systems for industrial applications, discussing fluidic solutions to process problems
15 p2553 A69-31297

Acoustic fluidic sensor /sonicell/ combining sonic generator based on edgetone principles with sensor dependent on laminar stream acoustic disturbance
15 p2616 A69-31302

Fluidic temperature sensors for measuring turbine inlet temperature on large turbine engine
[AIAA PAPER 69-544] 16 p2792 A69-32692

Fluidic sensors for jet engine control, analyzing convergent divergent nozzles, vortex and acoustic oscillators for pressure and gas temperature measurements
[AIAA PAPER 69-542] 16 p2843 A69-32699

Fluidics for satellite and rocket attitude control and guidance, discussing computing block function and components, system reliability and resistance to aging, etc
17 p3049 A69-33243

Fluidic thrust reversal control system for turbojet achieving cost and weight reduction, illustrating fluidic circuit and noting circuit reliability
17 p3018 A69-33329

German monograph on theoretical and experimental investigations of tubes and lumped fluidic elements covering equivalent circuit
17 p2903 A69-33573

Fluidics /no moving part fluidics/, discussing diodes, capacitors, logic elements, temperature sensors, systems design, environmental factors, etc
17 p2904 A69-34067

Fluidic attitude control systems performance prediction from conventional control analysis emphasizing steady state positioning accuracy
17 p2904 A69-34069

Fluidic system applications to turbojet propulsion control, thrust stabilization control, temperature sensing, normal shock sensing, pressure ratio sensing, supersonic air inlet control and flight control
17 p2904 A69-34070

Fluidic sensor for measuring gas and liquid velocities, describing design and principles of operation
18 p1313 A69-34308

Fluidic pressure ratio computing device based on two free jets interaction principle, describing prototype system design and analysis, electronics and overall error
18 p3133 A69-34309

Servovalves with fluidic and electrical inputs compared for gas servoamplifiers performance, considering use as sensors in closed-loop hydraulic circuit
19 p3255 A69-36711

Coanda effect of separated jets reattachment to wall at high Knudsen number in pneumatic fluidic devices, discussing Reynolds and Mach numbers effect
[ASME PAPER 69-FLCS-37] 21 p3692 A69-38602

Fluidic pressure signal generator for use in fluidic system frequency response studies, considering design and performance
[ASME PAPER 69-FLCS-40] 21 p3649 A69-38603

Fluidic angular rate sensor, obtaining rate information by sensing laminar jet flow deflection from nozzle, discussing advantages over mechanical rate sensors
21 p3722 A69-38766

Fluidic proportional level control and density control systems, discussing advantages of low initial and maintenance cost, long life and temperature, shock, radiation resistance, etc
22 p3870 A69-41241

Fluidic servoactuator controlled by hydraulic vortex valves using mechanical signals for helicopter stability augmentation system
24 p4255 A69-42800

Mechanization of analog electrical-to-fluidic transducer using carrier circuit techniques and piezoelectric bender drive assembly
24 p4315 A69-43026

Parallel wire array fluidic sun sensor for solar pointing fluidic attitude control, discussing design and breadboard test
24 p4348 A69-43297

Static and dynamic characteristics of fluid pressure signal transmitter between members with relative rotary motion
24 p4256 A69-43300

FLUIDIZED BED PROCESSORS

Hydrodynamics of turbulent gas flow through powder layer for vapor phase coating of particles, noting fluidized bed
20 p3548 A69-37363

Heat transfer mechanisms between fluidized beds and wall surfaces by application of film penetration theory of mass transfer, noting bubbling bed model
20 p3632 A69-37519

FLUIDS

Heat transfer coefficients for free convection from single horizontal cylinder to fluids computed from empirical correlation
09 p1625 A69-22693

Specific isochoric heat capacity of pure fluids, considering thermal equation of state, vapor pressure and boundary conditions at critical point
11 p2001 A69-25201

Thermal conductivity measurements of fluids, considering contribution of radiation, convection, temperature jump and experimental arrangement eccentricity to errors
23 p4237 A69-41325

FLUORESCENCE

NT PHOSPHORESCENCE

NT X RAY FLUORESCENCE

Fluorescence spectroscopy of proteins, analyzing polarity, distances between groups, flexibility and conformational transitions
01 p0023 A69-10291

Interactions between intermediate fluorescence quenching trapping center and associated electron acceptor of oxygen evolving photosynthetic spinach chloroplast photosystem
01 p0024 A69-10928

Fluorescence efficiency of air under electron bombardment measured at low pressure
02 p0284 A69-12734

Fluorescence and phosphorescence from tryptophan powders stimulated at low temperatures with UV, vacuum UV, fast electrons and X rays
03 p0372 A69-13487

Substrate and subunit interactions influence of beta 2 protein of Escherichia coli tryptophan synthetase on fluorescence properties of pyridoxal phosphate prosthetic groups
04 p0553 A69-15304

Hydrogen adaptation effect on fluorescence of normal and Mn deficient algae, noting system II photosynthesis
04 p0554 A69-15325

Upper limit of nonradiative relaxation time between specific states of absorption bands and fluorescence state emitting R lines in ruby laser

05 p0777 A69-16335

Mechanism for laser surface damage of glasses working through optical absorption, fluorescence, chemical reaction by quenching and breakdown

06 p0935 A69-17771

Laser excited vibrational fluorescence for determining vibrational energy transfer rates in HCl-carbon dioxide, HCL-HI and HI-carbon dioxide

07 p1144 A69-18289

Hydrogen molecule spectroscopy in vicinity of ionization limit, determining absorption and ionization cross sections and fluorescence

07 p1184 A69-18490

Fluorescent light polarization of neon atoms subjected to gas discharge, static magnetic field and laser beam [IEEE PAPER T-9]

07 p1155 A69-19084

Iodine fluorescence spectra excited by krypton ion laser, analyzing spectral series and vibrational rotational levels

07 p1156 A69-19304

Ruby absorption, fluorescence and lasing properties, calculating polarization effect on relative intensities and forms of R1 and R2 bands in macroscopic theory

07 p1201 A69-19646

Ce activated garnet crystals optical properties, noting IR and near UV absorption spectra and room and low temperature fluorescence

07 p1201 A69-19647

Cometary magnetic fields by measuring depolarization of molecular resonance fluorescence

09 p1603 A69-22234

Intensity interferometry by two photon excitation of fluorescence trace for three mode laser under phase locking, free running and FM-like conditions

10 p1705 A69-23811

Mode locked lasers for measuring fast radiative decay in fluorescent systems

12 p2105 A69-26310

Intense ultrashort pulse widths determination by two photon fluorescence patterns, using model of partial laser mode locking

13 p2270 A69-27198

Neodymium laser emission of organic molecules in UV region noting molecular absorptivity and fluorescence

13 p2271 A69-27657

Fluorescence stimulated by high energy electron and ion beams, determining vibrational temperature and concentration of molecular oxygen in high enthalpy wind tunnel flows

13 p2302 A69-28265

Radiative decay of polyatomic molecules, applying Green function form for transition probability to decay of manifold of closely spaced coupled levels

14 p2488 A69-29924

Fluorescence noise in Q switched ruby laser at-mospheric backscattering experiments, noting relation to optical radar spurious and enhanced returns

16 p2777 A69-32183

Energy spectrum of secondary electrons and fluorescent efficiency in 3914 A band, obtaining ionization cross section

16 p2850 A69-32315

Mossbauer spectroscopy, discussing nuclear resonance fluorescence and equipment

18 p3099 A69-34622

GaAs laser used as optical sweep generator for display of Cs 133 spectral line shape, studying fluorescence and radiation lifetime

19 p3339 A69-36696

Luminous efficiency for electron induced molecular nitrogen bands, discussing thick- and thin-target measurements of fluorescent efficiencies

21 p3774 A69-38521

Density, ion temperature, electron temperature and ion drifts in Ba or Ba doped plasmas determined by resonance fluorescence and optical pumping

22 p3962 A69-40532

Fluorescence properties of nucleotides, polynucleotides and phosphorylated derivatives as function of temperature, pH and ionic strength

22 p3898 A69-41078

Detection and spectral examination of trace porphyrin complexes by demetalation with methanesulfonic acid and spectrofluorometry, compared to absorption spectrophotometry

24 p4279 A69-42557

Laser cavity modes phase equality demonstrated by oscilloscope trace in two photon fluorescent method

24 p4327 A69-42981

Optical properties of neodymium-doped YAG and glass laser materials including fluorescence lifetime and conversion efficiency, absorption spectra, sensitization effects, etc

24 p4329 A69-43751

FLUORESCENT EMISSION U FLUORESCENCE

FLUORIDES

NT BERYLLIUM FLUORIDES
NT BORON FLUORIDES
NT CALCIUM FLUORIDES
NT CHLORINE FLUORIDES
NT CRYOLITE
NT HYDROFLUORIC ACID
NT LANTHANUM FLUORIDES
NT LITHIUM FLUORIDES
NT NICKEL FLUORIDES
NT NITROGEN FLUORIDES
NT OXYFLUORIDES
NT OXYGEN FLUORIDES
NT SULFUR FLUORIDES
NT URANIUM FLUORIDES

Chemical vapor deposition of W-Mo-Re ternary alloys from hydrogen reduction of fluorides on Cu or Mo substrates

01 p0096 A69-10642

Pressure properties of fluorides and silicofluorides as cutting and grinding lubricants for titanium [ASLE PAPER 68-LC-20]

07 p1141 A69-19311

Metal fluoride compounds as cathodes for use with mixed fluoride electrolyte /LiF-NaF-KF eutectic/ in thermal batteries

10 p1640 A69-23997

Far IR electronic and vibronic transitions in single crystals of Nd ions in tysonite lanthanide fluorides

13 p2316 A69-27628

Fluorides or AMOX increased concentrations effect on thyroid growth rate, uptake and adrenal weight in rats

14 p2406 A69-29291

Emission band intensities of carbonyl fluoride in 2.0-6.0 micron region with scanning spectrometer, comparing results for room and shock temperature with theoretical data

21 p3669 A69-38759

FLUORINATION

Remotely operated open-cup impact tester for studying impact initiation of reaction of various liquid fluorinating agents with metals and plastics

06 p0907 A69-17876

Elemental fluorine reactions with Ni, Cu, Fe, Ti, Be, Al, Zr and Ag, giving reaction rate constants, activation energies, etc

21 p3670 A69-39706

FLUORINE

Solubility of helium in liquid fluorine increases with temperature exhibiting reverse order

01 p0142 A69-11258

High thrust fluorine engines and propellants

03 p0494 A69-12889

Safety planning for use of reactive cryogenics in large volume, noting FLOX and liquid fluorine

04 p0645 A69-14468

Galvanic corrosion couples of metals and alloys tested in liquid fluorine, determining corrosion rates for possible missile components application

06 p0944 A69-17854

Bellows sealed valve for measurement of fluorine thermodynamic properties at moderately high pressures

09 p1493 A69-21428

Fluorine nuclei in primary cosmic radiation identified by counter telescope measurements on Pioneer 8 spacecraft

15 p2676 A69-30886

Analytical model for liquid fluorine non-vent loading operations noting application to flightweight upper stage systems [AIAA PAPER 69-579]

16 p2767 A69-32715

Fluorine injectors for main tank injection of space vehicle liquid hydrogen tank, including study of hypergolicity and reaction product freezing [AIAA PAPER 69-528]

16 p2767 A69-32717

Mean lives of 1s super 2 2p super 2 super 1D level in F VI and O V measured by beam foil technique

17 p3009 A69-34188

Beryllium fluoride heat of formation from heat of combustion of Be-polytetrafluoroethylene mixture in fluorine

21 p3853 A69-39703

Vapor pressure measurements on liquid fluorine from triple to critical point at one degree K intervals [NAS-NRC PAPER H-2]

22 p3998 A69-40624

FLUORINE COMPOUNDS

NT BERYLLIUM FLUORIDES

NT BORON FLUORIDES
NT CALCIUM FLUORIDES
NT CHLORINE FLUORIDES
NT CRYOLITE
NT FLUORIDES
NT FLUORITE
NT FLUORO COMPOUNDS
NT FLUOROCARBONS
NT FLUOROHYDROCARBONS
NT HYDROFLUORIC ACID
NT LANTHANUM FLUORIDES
NT LITHIUM FLUORIDES
NT NICKEL FLUORIDES
NT NITROGEN FLUORIDES
NT OXYFLUORIDES
NT OXYGEN FLUORIDES
NT POLYTETRAFLUOROETHYLENE
NT SULFUR FLUORIDES
NT TETRAFLUOROHYDRAZINE
NT URANIUM FLUORIDES

Pulsed laser emission from carbon dioxide collisionally pumped by vibrationally excited DF produced by reacting fluorine oxide with deuterium

12 p2104 A69-25986

Fluosilicic acid in chemical milling of Ti and Ti alloys

21 p3669 A69-38966

Impurities effect-on corrosion of fluorine containing propellant oxidizer systems, noting aqueous and anhydrous hydrogen fluoride corrosion

21 p3784 A69-39487

FLUORINE-LIQUID OXYGEN U FLOX

FLUORINE ORGANIC COMPOUNDS

NT FLUOROCARBONS
NT FLUOROHYDROCARBONS

Fluorinated polyurethanes synthesis for liquid oxygen environments and cryogenic structural utility, noting structural effects on LOX compatibility

05 p0717 A69-16498

Organic fluorine chemistry, discussing synthesis reactions and reaction of polyfluorocycloalkenes with various nucleophiles

08 p1269 A69-21129

Flame velocities of stable premixed tetrafluoroethylene-oxygen mixture flames measured with bunsen-cone method

11 p1940 A69-24485

Sugars identification as trifluoroethylacetyl polyol derivatives by gas-liquid chromatography

15 p2558 A69-31539

FLUORITE

CW lasers based on composite yttrifluorite type crystals, noting large number of emission bands

13 p2273 A69-28316

Fluorite crystal laser activated by divalent samarium, discussing characteristics in pulsed operation mode

14 p2458 A69-29328

FLUORO COMPOUNDS

NT CRYOLITE
NT FLUORINE ORGANIC COMPOUNDS
NT FLUOROCARBONS
NT FLUOROHYDROCARBONS
NT POLYTETRAFLUOROETHYLENE

Wear resistance of briquetted lubricants from fluoroplast and molybdenum disulfide under pressure

21 p3733 A69-39805

FLUOROCARBONS

Fracture process in composite films of stressed tetrafluoroethylene and fluorinated ethylene propylene

02 p0270 A69-12368

Photoionization curves and threshold energies for fluorocarbon and trifluoromethyl halide molecules and ions, calculating ionic heats of formation and bond dissociation energies

02 p0205 A69-12464

Shock tube and samples of fluoroethylene, difluorodichloroethylene and fluoromethane in argon diluent used to prepare carbon difluoride, discussing electronic oscillator strengths

04 p0632 A69-14944

Combustion bomb testing of propellants containing fluorocarbon binder and ammonium perchlorate, noting unique ignition, combustion and extinction properties [WSCI PAPER 69-9]

16 p2831 A69-32349

Steel ball bearing high temperature fatigue life tested with synthetic paraffinic oil, fluorocarbon and polyphenyl ether [ASME PAPER 69-LUBS-18]

18 p3140 A69-34378

Low molecular weight fluorocarbons pyrolysis and oxidation in single pulse shock tubes, using vapor phase chromatography and mass spectral analyses

18 p3099 A69-34467

FLUOROHYDROCARBONS

Perfluorocyclobutane-oxygen mixture combustion, measuring burning velocities and adiabatic equilibrium flame temperatures 21 p3852 A69-39594

FLUOROHYDROCARBONS

Polyfluoroethylene resin breakdown under uniaxial tension, considering continuity disruption 13 p2286 A69-28321

Halon 1301 /bromotrifluoromethane/ concentration for inerting Aerozine-50 spills or extinguishing fires, noting joint use of carbon dioxide and water 18 p3094 A69-35090

Integral fuel tank sealant based on various hydrofluorocarbon polymers prepared, tested and compared for physical properties 19 p3356 A69-35533

FLUOROMICA

U MICA

FLUOROSCOPY

Dynamic roentgenology of cervical spine noting ease of use in neutral profile, hyperflexion and hyperextension for aeronautical medicine 23 p4087 A69-41797

Military pilots cervical spine dynamic X ray studies, comparing spine curvature and rectitude of jet and nonjet pilots and nonflying personnel 23 p4087 A69-41798

FLUSHING

Ram recovery of flush intake for air cushion vehicles noting influence of intake geometry, placement and incidence angle 01 p0005 A69-10026

FLUTING

U GROOVING

FLUTTER

NT PANEL FLUTTER
NT SUBSONIC FLUTTER
NT SUPERSONIC FLUTTER

Pseudorandom scanned TV signal distortion due to flutter and skew introduced by tape recorder, computing system SNR for distortion as additive random noise 01 p0033 A69-10999

Spadoryc slide rule for damping determination from vibration decay traces, noting use in flight flutter tests 01 p0087 A69-11029

Dual inertia magnetic tape recorder/reproducer combining low wideband flutter and low time base errors 10 p1693 A69-23289

Servocontrol to delay flutter onset of aeroelastic structures, discussing rapid amplitude and phase changes near instability point, wind tunnel models, instrumentation, analog simulation 11 p1992 A69-25518

Self excited vibration of flowing medium and infinite cylindrical duct wall in primary magnetic field, discussing vibration stability and critical speeds 18 p3226 A69-35462

Aeroelasticity of supersonic aircraft in flight, discussing buffeting, wing flutter and control surface flutter 22 p3862 A69-40003

FLUTTER ANALYSIS

Supercritical flow effects on unsteady aerodynamic coefficients used for subsonic aircraft flutter analysis, emphasizing changes due to shock and flow separation 01 p0007 A69-11020

Flutter vibration of sails fixed along edge and single wing weather vanes in supersonic flows 02 p0192 A69-12824

Flutter vibration in subsonic flows, analyzing critical velocity for membrane and damping destabilizing effects in nonconservative system 02 p0192 A69-12825

Eigenvectors utilized in flutter computation for couplings [ONERA-TP-650] 03 p0522 A69-12878

Energy transfer in circulatory force fields, noting mechanism changes for simultaneously operative original field and adjoint field energy sources 04 p0671 A69-14415

Early design stage flutter analysis for variable sweep aircraft, using subsonic flutter model 04 p0677 A69-14834

Boom flutter effects on attitude dynamics of OV1-10 satellite, noting introduction of angular momentum by tip mass elliptical vibration 04 p0666 A69-15520

Stability of three layer cylindrical shell in gas stream, analyzing oscillation mode and critical flutter dependence on filler resistance to transverse shear 05 p0843 A69-16683

Unsteady supersonic flow around thin circular cylinder representing rocket stage, calculating flutter and response to random environment 06 p0857 A69-17098 [ONERA-TP-666]

Tandem airfoils wing-tail interaction flutter analysis, using three dimensional vortex lattice aerodynamic theory [AIAA PAPER 69-57] 06 p1028 A69-18105

Thermally induced vibration and flutter of flexible spacecraft boom, discussing stability by considering boom as cantilever beam [AIAA PAPER 69-21] 06 p0869 A69-18144

Anomalous spacecraft OGO-D motion explained by open section boom thermally induced oscillations, discussing corrective measures 07 p1231 A69-18331

Effects, measurement and analysis of flutter in instrumentation recorders 07 p1133 A69-19118

Tape flutter and additive noise time base errors in coherent demodulation of suppressed carrier AM multiplex 07 p1082 A69-19119

Finite aspect ratio sandwich plates flutter in supersonic gas flow analyzed by differential equation describing plates elastic equilibrium 08 p1412 A69-20324

Hydrofoil vehicle flutter investigations including simple foils and struts, geometrical parameters, finite span, cavitation, etc 09 p1614 A69-21898

Flow instability of incompressible nonconducting fluid in thin cylindrical conducting elastic pipe in constant uniform magnetic field 10 p1798 A69-23094

Semiautuator disk method for boundary layers and velocity of stall flutter cascade blades vibrating in transient mode, considering nonstall flutter 11 p1818 A69-25028

Strip method for prediction of subcritical frequency and damping characteristics for subsonic wind tunnel and flight flutter tests 11 p1987 A69-25368

Aircraft structure geometry design for minimizing total mass concerning flutter requirements 11 p1989 A69-25493

Critical flutter behavior of variable geometry aircraft with wing of 70 degree leading edge sweep, noting wing-tail interference 11 p1991 A69-25517

Flutter analysis of plates with inplane boundary support flexibility exposed to transverse pressure loading or buckled by uniform thermal expansion 11 p1992 A69-25523

Flutter design charts for isotropic panels stressed to verge of buckling for typical values of structural damping 11 p1992 A69-25524

Collection of papers on aerodynamic flutter covering airfoils, flow theory, aircraft structures, etc 13 p2358 A69-27234

Numerical procedure to optimize complex structures by determining relative proportions of selected elements attaining flutter speed with minimum total mass 16 p2874 A69-32163

Finite aspect ratio sandwich plates flutter in supersonic gas flow analyzed by differential equation describing plates elastic equilibrium 17 p3058 A69-33317

Spacecraft booms thermally induced vibration and flutter, considering damping and solar exposure effects 22 p4043 A69-40545

Semiempirical stability boundary for flutter of simply supported cylinders for various length- radius and radius-thickness ratios 23 p4228 A69-41914

FLUX [RATE]

NT HEAT FLUX
NT MAGNETIC FLUX
NT SOLAR FLUX

Intensity ratio of first negative nitrogen band and oxygen line varies in auroral displays 02 p0235 A69-11425

Linear analysis of operation of multistage magnetron amplifiers using injected electron flux and stepwise varying dimensions of interaction space 03 p0407 A69-13977

Mixing effect on solar neutrino fluxes, assuming solar convective core with rapid thorough mixing 06 p1001 A69-17192

Electron detector for OGO-E to measure flux and energy spectrum of electrons in primary cosmic rays [IEEE PAPER 3C-4] 07 p1135 A69-19198

Electron flux parameters determination from ionograms and reflected signal amplitudes between 120-130 km, considering electron collision frequencies 10 p1688 A69-23931

Two beam electron flux instability in crossed magnetic and inhomogeneous electric fields using linearized hydrodynamic and Lagrangian formalism approximation 12 p2133 A69-26714

Simultaneous particle flux and VLF noise spectrum measurements by rocket sounding, discussing equipment, telemetry and calibration systems and experimental data 15 p2605 A69-31423

Kim-Anderson flux flow theory for materials with kappa nearly equal to 1, discussing pinning forces and sites 17 p3016 A69-33754

Diurnal variations of electron flux based on balloon observations near polar cap consistent with geomagnetic cut-off variations of magnetospheric models 22 p4005 A69-40511

Reentrant albedo flux and singly charged particles directional asymmetry in upper atmosphere estimated from oriented telescope observations over Hyderabad 22 p4005 A69-40519

FLUX DENSITY

NT CURRENT DENSITY
NT ELECTRON FLUX DENSITY
NT ILLUMINANCE
NT IRRADIANCE
NT LUMENS
NT LUMINANCE
NT LUMINOUS INTENSITY
NT NEUTRON FLUX DENSITY
NT PARTICLE FLUX DENSITY
NT PHOTON DENSITY
NT PROTON FLUX DENSITY
NT RADIANCE
NT RADIANT FLUX DENSITY
NT SOLAR CONSTANT
NT SOLAR FLUX DENSITY
NT SOUND INTENSITY

Ring current particle energy density distribution for symmetric portion of magnetic storm derived from current magnetic field profile measurements 01 p0147 A69-11227

Free convective heat transfer in liquid filled spherical volume with constant thermal flux density at boundary 04 p0686 A69-14992

Flux equivalences of reflected and transmitted radiation among Rayleigh, isotropic and other scattering models 04 p0687 A69-15281

Acoustoelectric domain propagation in N-type GaAs, noting flux influence on peak acoustic density 05 p0806 A69-15815

High energy density lithium/dichloroisocyanuric acid battery system discharging under constant voltage and load conditions [ECS PAPER 15] 05 p0706 A69-16231

Energy flux into earth atmosphere due to fast corpuscular neutrals arising from charge transfer collisions between solar protons and neutral interstellar H 05 p0817 A69-16654

Frequency structure of pulse energy or pulsar intensity, emphasizing total energy density received per pulse 05 p0828 A69-16660

Lunar occultations of radio source Sagittarius A observed at various frequencies between 230 and 2400 MHz, obtaining diameter, position and decimeter band flux densities 06 p1009 A69-17960

Temperature profile and power density distribution in metastable level of ruby laser rod during pumping in air 07 p1150 A69-18937

Radio sources flux densities from fan beam survey using Molongo radio telescope compared to flux densities of Parkes catalog, presenting revised spectra 07 p1218 A69-19278

Errors estimation in determination of radio signal source flux density, position and recorded half power widths 07 p1088 A69-19722

Radio spectra of normal galaxies noting transition in spectrum 08 p1398 A69-20777

Fluorescer-photomultiplier mobile telescope for measurement of vertical cosmic ray intensity and equator points in atmosphere 09 p1493 A69-21420

Taurus A flux density measurement at 4.3 mm with 36-ft antenna at National Radio Astronomy Observatory to determine spectrum unambiguously
09 p1591 A69-21450

Cross-spectral density of pressure induced on lifting surface by isotropic atmospheric turbulence, solving integral equation
[ONERA-TP-681] 09 p1613 A69-21689

Corpuscular radiation contributions to D layer ionization determined from intensity measurements
09 p1577 A69-21770

Gamma ray luminosity of typical type I supernovae remnant computed by assuming Ni 56 radioactive decay energy origin of optical luminosity
09 p1581 A69-22409

Constant envelope threshold detection for establishing signal energy in presence of input noise power density variations
09 p1459 A69-22474

Anomalous Forbush decrease observations in November 1960 demonstrating cosmic ray flux anisotropy near earth
09 p1582 A69-22753

Satellite data on relative flux and group composition of heavy nuclei in primary cosmic rays
10 p1756 A69-22820

Absolute flux density of five radio sources and relative flux densities of 37 sources defining absolute flux density scale for Southern Hemisphere
10 p1772 A69-22857

Effect of degree of expansion of ionized gas in nozzle on specific power of MHD generator
10 p1636 A69-23103

Earth currents and magnetic field variations recording in period range 10-200 sec, computing power density spectra on analog computer
10 p1682 A69-23593

Sagittarius A occultation by moon, determining peak brightness and flux density of radio source
11 p1958 A69-24592

Sound field generation by isotropic turbulence through finite strength shock, estimating acoustic energy flux from supersonic jet containing shock waves
11 p1872 A69-25130

Temperature variation and heat transfer in fins and relations between heat-flux-density and temperature difference
12 p2190 A69-25763

IR radiative temperature changes as function of latitude, season and height in region 30-110 km
12 p2064 A69-26008

Charged particles influx from cusp shaped regions of stagnant plasma trapped in vicinity of two magnetic cusps on polar magnetopause
12 p2151 A69-26945

Quasar spectra changes observed from 1962 to 1966 including flux density and antenna temperature for 3C 279 at cm wavelengths
12 p2167 A69-27043

Hydrogen to He ratio effect on stellar atmospheric structure, considering flux relations, UVB color indices, H line profiles, electron and gas pressures
13 p2339 A69-27562

Model atmosphere source function, mean intensity and flux by matrix methods
13 p2288 A69-27564

Night sky background observation by near IR radiation flux, using rocket-borne telescope and ground based equipment
13 p2342 A69-27600

Molecular gas flows in containers for space environment simulation, discussing flux distribution
13 p2241 A69-28081

Transverse particle and energy fluxes in toroidal magnetic traps magnetic fields with ionized plasmas, discussing particle diffusion coefficient and thermal conductivity
13 p2314 A69-28446

Riometric data processing method for radio wave absorption measurement, considering nighttime cosmic radio emission intensity
14 p2436 A69-29056

Pulsar dispersion-removing technique, discussing pulsar mean flux density decrease with age
14 p2517 A69-29091

Pressure balance and maximum power density at evaporation from heat pipe experiments, deriving maximum heat flux densities
14 p2538 A69-29204

Radio observations of emission nebulae for flux densities, deriving electron temperature
[ASME PAPER 69-DE-46] 14 p2527 A69-29941

High energy gamma rays detection by balloon near geomagnetic equator, observing enhanced flux from galactic disk
15 p2675 A69-30695

Radiative energy transfer through nongray absorbing and emitting medium generating heat with graphical presentation of temperature distribution and flux
15 p2718 A69-31153

Radiative scattering cross sections of electrons from neutral O and atomic and molecular N using rapid scanning spectrometer for bremsstrahlung intensity
15 p2657 A69-31160

Solar wind speed transverse variation effect on cosmic ray intensity at earth analyzed using mathematical model
16 p2849 A69-32088

Aircraft measurements and computer calculations of downward and upward solar radiation fluxes related to albedo, altitude and sun angle
17 p3023 A69-33158

Shock waves propagation in inhomogeneous gases, considering time development and energy flux during point explosion in plane layers by quasi-stationary approximation
17 p2952 A69-33383

Saturn emission peak and flux density at 408 MHz determined by cross telescope, discussing mechanism for enhanced radiation at long wavelengths
17 p3041 A69-33813

Monochromatic energy flux measurement in H and forbidden lines of planetary nebulae indicating ionization level and optical depth
19 p3423 A69-36223

Heat flux densities and Reynolds potentials in turbulent boundary layer on heated flat plate with wall suction
19 p3452 A69-36722

Amplitude equations for magnetoacoustic and entropy waves diverging from normal MHD shock, obtaining energy flux ratios associated with incident and transmitted waves
20 p3582 A69-38242

Primary H nuclei flux and spectrum near geomagnetic equator, discussing emulsion stack exposure
22 p4005 A69-40520

Radio source Cassiopeia A flux density in terms of expanding radio source theory, noting frequency and time correlation with flux density changes
23 p4215 A69-42112

Extragalactic radio sources flux densities at 5009 MHz tabulated, ascribing accuracy variations to uncertainty in receiver gain and dish efficiency
24 p4382 A69-42922

Average meteorite flux at Martian surface estimated by generating flux distribution for Martian atmosphere top and adjusting for mass loss and deceleration
24 p4387 A69-43351

FLUX MAPPING

U MAPPING

FLUX QUANTIZATION

Methods and conclusions for rate of influx to earth of extraterrestrial material
03 p0511 A69-13467

FLUXES

Oxygen free fluxes for fusion welding titanium alloys, discussing weld structure and properties
06 p0930 A69-17093

Step cathodic flux cleaning of furnace brazed Al assemblies used in combination with ultrasonic and chemical conversion coating techniques
24 p4319 A69-42938

FLUXMETERS

U MAGNETIC MEASUREMENT

U MEASURING INSTRUMENTS

FLYBY MISSIONS

NT SWINGBY TECHNIQUE

Ebert spectrometric experiment during Mars flyby aimed at detecting upper atmosphere atoms, ions and molecules in 1100-4300 angstrom spectral range
[AAS PAPER 68-184] 02 p0311 A69-11469

Benefits accruing from swingby operation, considering space flights past Jupiter, Saturn and other planets
02 p0326 A69-12663

Planetary swingby theory mechanics and applications for optimization of interplanetary trajectories
02 p0331 A69-12818

Interplanetary transportation network involving numerous spacecraft on various planetary flyby trajectories, discussing integration of gravity thrust, braking and scramjet concept
03 p0511 A69-13402

Aeroshell structural development for Mars flyby and entry landing mission compatible with Atlas/Centaur launch vehicle
[AIAA PAPER 68-1159] 03 p0521 A69-13667

Orbital trajectories about Mars or Venus, considering reentry to earth, planet perturbation effect, total mission time and orbital distance from planet
05 p0823 A69-16042

Optimum low thrust interplanetary transfers involving swingby trajectory past intermediate planet analyzed, assuming impulsive velocity change at planet
06 p1006 A69-17572

Jupiter unmanned flyby probes trajectory and mission analysis, considering planetary gravitational field role for trajectory shaping and flight times
06 p1007 A69-17598

Midcourse maneuvers in interplanetary guidance, considering spin stabilized spacecraft flyby for Jupiter mission
13 p2354 A69-28504

Mars exploration by 1969 Mariner 6 and 7 flyby, discussing mission and instrumentation
18 p3201 A69-35141

Narrow angle high resolution TV camera design and testing for Mariner 6 and 7 Mars flyby missions, noting computer drawn spot diagrams
19 p3307 A69-35808

Mission windows for single and multiple planet swingbys past Jupiter to outer planets
[AAS PAPER 68-115] 19 p3402 A69-35936

Scientific findings from interplanetary spacecraft radio propagation experiments, particularly Mariner 5 data
19 p3267 A69-35940

Orbital trajectories about Mars or Venus, considering reentry to earth, planet perturbation effect, total mission time and orbital distance from planet
20 p3606 A69-37951

Spacecraft guidance analysis of multiple outer planet mission utilizing gravity assist swingbys to achieve planetary flybys with single spacecraft
[AAS PAPER 68-109] 21 p3761 A69-39205

Triple planet ballistic flybys, discussing mission opportunities and launch windows
[AAS PAPER 68-114] 21 p3805 A69-39206

Direct flight and Jupiter swingby heliocentric trajectory modes of elliptic capture orbits compared for unmanned missions to outer planets
[AAS PAPER 68-105] 21 p3805 A69-39221

Interplanetary periodic orbits and flyby dates for multiple Earth-Venus swingby missions, describing various iterative solutions for trajectory
[AIAA PAPER 69-931] 21 p3809 A69-39359

Halley Comet rendezvous mission, comparing low thrust mode with ballistic Jupiter or Saturn swingby mode
[AIAA PAPER 69-933] 21 p3809 A69-39360

Perturbative effects of Jupiter moons on spacecraft flyby and postencounter heliocentric trajectories, noting precision targeting
[AIAA PAPER 69-932] 21 p3809 A69-39361

Manned flyby/orbiter of Mars providing scientific information at low incremental cost
[AAS PAPER 69-180] 24 p4379 A69-42813

Venus swingby and direct Mercury trajectories analysis for optical imaging from flyby missions
[AAS PAPER 69-258] 24 p4380 A69-42860

Reconnaissance missions for outer planets exploration, discussing spacecraft design constraints, multiple planet fly-by, planetary orbiter, etc
[AAS PAPER 69-291] 24 p4381 A69-42864

Space mission opportunities selection from analysis of short period comet perihelia, discussing flyby and rendezvous mission payloads
[AAS PAPER 69-320] 24 p4381 A69-42866

Mars and Venus flyby missions and Mercury planetary exploration plans, discussing future conditions permitting Jupiter, Saturn, Uranus, Neptune, Pluto flybys
24 p4384 A69-43137

FLYING PERSONNEL

NT AIRCRAFT PILOTS

NT ASTRONAUTS

NT COSMONAUTS

NT FLIGHT CREWS

NT SPACECREWS

NT TEST PILOTS

Electrocardiographic tests to study changes in electropotentials of heart in flying personnel after flight, noting changes in myocardium
03 p0378 A69-14207

Asthmatic attacks in military air crews, discussing flight stress factors including altitude, ventilation and insecurity as possible causes
05 p0710 A69-16624

Pulmonary mouth pressure and heart rate in Flack test for flight personnel by simultaneous double recordings
05 p0710 A69-16626

Corneal greyish opaque arc as warning of atherosclerosis in flight crews
05 p0711 A69-16631

Convective heat exchange coefficients for human organism in aircraft surroundings under homogeneous temperature conditions, deriving acclimatization equations [AGARDOGRAPH-111]
08 p1266 A69-20673

Amplitude variations in ULF ballistocardiograms of young normal airline stewardesses and applicants, discussing cardiovascular reactivity
09 p1444 A69-22544

Systolic murmurs and flight personnel evaluation, noting phonocardiographic definition and tracings of specific systolic murmurs
09 p1445 A69-22726

Parasitic calcifications of soft parts in flight personnel studied radiologically, noting filariasis, bilharziasis and worms
09 p1446 A69-22729

Aeronautical health service problems relating to efficiency of military and civil aviation personnel of all nations
12 p2023 A69-26490

Body composition of USAF flying personnel, evaluating obesity by using radioactive potassium /K-40/ method
14 p2409 A69-29295

Clinical data on ambulant airmen with complete left bundle branch block discovered on electrocardiogram, finding majority with evidence of organic heart disease
19 p3263 A69-36463

Vestibulometric test program for flight surgeon appraisal of flying personnel, emphasizing singling out persons prone to illusory sensations
20 p3473 A69-37277

Vestibulometric tests for flight surgeon appraisal of applicants in flying profession, comparing Coriolis forces cumulative load tests with conventional tests
20 p3481 A69-37278

In-flight illnesses in French Air Force, emphasizing psychological failures in etiology
21 p3666 A69-39270

Cardiovascular illnesses incidence among airline flight personnel, discussing coronary insufficiency detection
21 p3661 A69-39271

Aircrew fatigue and sleep loss factors, discussing transition through various time zones and flying through normal sleeping times
21 p3666 A69-39275

Jet flying effects on air hostess menstrual function, considering cycle length, duration, regularity, dysmenorrhea and flow severity
23 p4103 A69-41689

Aircrew Arctic survival situation simulation experiments with survivors staying close to aircraft and walking across difficult terrain from emergency location
23 p4088 A69-41810

Brain atrophy clinical diagnosis aided by biochemical analyses, including age frequencies and symptoms to control incidence among aviation personnel
23 p4089 A69-41816

Urinary lithiasis frequency among aircrews, reviewing etiology, symptomatology, therapeutics and prevention
24 p4267 A69-43388

Norms for quantitative vectorcardiography derived from statistical analysis of results from healthy young subjects, emphasizing medical evaluation of flying personnel
24 p4277 A69-43390

FLYING PLATFORM STABILITY
U AERODYNAMIC STABILITY

FLYING PLATFORMS

Remote sensing platform requirements for oceanographic and meteorologic observations, discussing orbital and aircraft platforms [AIAA PAPER 69-154]
06 p1044 A69-18122

Atmospheric measurements and experiments using aircraft as platforms, noting aircraft operation in severe weather, electrical supply problem and aircraft wake problem [AIAA PAPER 69-157]
06 p0869 A69-18153

FLYING QUALITIES

U FLIGHT CHARACTERISTICS

FLYWHEELS

Damping flywheel to stabilize permanent rotation of weightless solid body moving by inertia, obtaining differential equations of motion
07 p1183 A69-19678

Numerical solution for changing satellite orientation within circular orbit plane by applying force of onboard flywheel
10 p1792 A69-24194

Space vehicle attitude stabilization based on rotating flywheel resistance to changes in rotation axis attitude, noting grease lubricated hydrodynamic bearing system
12 p2175 A69-26893

Magnetic desaturation of inertia flywheels of satellite in equatorial or slightly inclined orbit, discussing satellite stabilization
13 p2357 A69-28476

Satellite three axis attitude control analysis showing rolling and longitudinal stabilization possibility by flywheel, with validity tested by analog simulation
17 p3048 A69-33240

Flywheels desaturated by magnetic action for optimizing stabilization system of satellite in circular orbit [ONERA-TP-732]
17 p3049 A69-33241

Satellite attitude stabilization synthesis by flywheels allowing independent control of angular motions, assessing perturbation type influence
21 p3768 A69-39831

FOAMS

Uniaxial strain static and gas gun compression tests result compared for syntactic foam
02 p0345 A69-12295

Inhomogeneous dielectric filling to simulate curvature in model earth-ionosphere waveguide
05 p0732 A69-16346

Foam carpet and airport equipment to prevent fires and explosions from retracted gear landings
10 p1674 A69-23708

Local failure of axially loaded plastic foam core sandwich panels, using face wrinkling analysis procedures
13 p2357 A69-27207

Syntactic foam low density thermoplastic microspheres as hollow spherical filler in polyester matrix, noting applications
14 p2467 A69-29285

Damping constant of sandwich samples with foam plastic filler subjected to torsional and flexural vibrations determined for aircraft design applications
17 p2993 A69-33942

Syntactic foam prepreg for low density laminate construction, presenting design and mechanical test data
19 p3353 A69-35512

Static mechanical strength of syntactic foam tested by generating failure conditions based on combined biaxial and triaxial stress [ASME PAPER 69-APMW-24]
24 p4336 A69-43095

Foamed liquid as potential coolants in rocket engine to overcome low efficiency and streaky coverage of conventional liquid film cooling
24 p4408 A69-43127

FOCUSING

NT DEFOCUSING

NT SELF FOCUSING

Ruby laser light beam self focusing in sodium chloride and potassium bromide crystals
03 p0438 A69-13051

Horizon focusing gain for radio waves reflected obliquely from ionosphere, noting effects of transmitter location and ionosphere geometry
03 p0395 A69-13627

Focusing of relativistic cylindrical electron beam in static axial electric and magnetic fields, using least action principle to derive trajectory differential equation
05 p0796 A69-15715

Astronomical two mirror telescope with aplanatic secondary focus, describing prime and secondary focus field correctors
05 p0761 A69-15733

Molecular and atomic beam focusing in electric and magnetic fields with helical symmetry of specified type
06 p0959 A69-16917

Directional mirror antenna parameters measurement by finite focusing of radiating element
06 p0895 A69-17453

Periodic electrostatic focusing structures in microwave tubes, evaluating properties by action function method
07 p1102 A69-18659

Focusing effect on far field directional pattern shifting of array normal, noting electronic scanning properties
08 p1285 A69-20400

Analog study of periodic permanent magnet focusing, considering ray equation, beam radius dependence on distance, amplitude variations, etc
08 p1285 A69-20555

Charged liquid droplets generator and acceleration through electric field for thrust vectoring, analyzing beam focusing and deflection [AIAA PAPER 69-283]
09 p1563 A69-21230

Double focus lens holography for diffusely reflecting surface deformation recording, discussing gas lasers, Polaroid photographic materials, etc
11 p1880 A69-24467

Power transmission efficiency between arbitrarily focused circular antennas with Gaussian amplitude illumination in Fresnel region for various phase illuminations and Fresnel numbers
11 p1851 A69-24991

Neutron emission anisotropies in capacitor discharge produced plasma focus, detailing coaxial plasma gun energy spectrum and flux measurement
11 p1930 A69-25321

Ruby laser light scattered at 90 degrees by dense plasma focus, analyzing signal detection
11 p1899 A69-25324

Holographic in-focus projection of images on three dimensional focal planes of arbitrary shape, noting moire pattern strain analysis
11 p1889 A69-25653

Double focalization in atomic hydrogen maser by hexapolar magnets selecting hyperfine energy transitions
12 p2105 A69-26050

Focusing factor in stratified medium with refractive index depending exponentially on height
12 p2029 A69-26100

Diode type image shutter tube with proximity focusing for high speed photography
12 p2083 A69-26145

Focusing power of hyperbolic gas lens for light beam waveguides, noting temperature distribution measurements and pole separation
12 p2107 A69-26392

Plasma lens device for focusing ion or plasma beams with closed electron drift
13 p2307 A69-27658

Forward and backscatter soundings compared to verify focusing mechanism of HF sky waves
14 p2435 A69-28967

Radial self focusing of low density electron beam by interaction with plasma in presence of beam plasma instability
15 p2662 A69-30964

Angular structure of second optical harmonic for cylindrical lens focusing of ND laser beam into negative KDP crystal
17 p2981 A69-33110

Laser emission spatial structure transformation determined from ratio between focused spot radius and distance between lens and output mirror
17 p2981 A69-33111

Night sky Cerenkov light detectors observations of pulsars CP 1133, NP 0532 and NP 0527, noting instrumental limitation in detecting ultrashort light pulses
18 p3200 A69-34994

Spherical aberration effect on atomic beam focusing in six pole magnetic system
19 p3380 A69-36602

Perturbed ionospheric regions acting as radio wave focusing lens, discussing frequency, power and pattern selection
20 p3486 A69-37048

Directional mirror antenna parameters measurement by finite focusing of radiating element
20 p3508 A69-37938

Coherent light focusing by helicoidal guide- extension to particle focusing, discussing analogy between index distribution for classical optics and potential distribution for electronic optics
22 p3981 A69-40475

Focus broadening by astigmatism of large microwave parabolic antennas, discussing large span surface deformations caused by astigmatic aberration
23 p4140 A69-42188

FOG

Airport warm fog dispersal, discussing full scale aircraft seeding of polyelectrolyte materials, noting ground dispenser
01 p0054 A69-10149

Visibility improvement in warm fog by seeding with micron size hygroscopic particles, noting results for NaCl
01 p0111 A69-10696

Thermodynamics in homogeneous steady state fog over rough terrain representing absolutely absorbing surface

02 p0274 A69-11442

Evaporation rate measurements in fog during carbon dioxide laser radiation, obtaining correlation to describe visibility improvement

02 p0258 A69-12622

Polarization of laser radiation scattered forward and back in artificial fog and smoke

03 p0393 A69-13275

Temperature change and fog forecasting diagram modified by Swinbank relation in place of Brunt formula

03 p0462 A69-13965

Liquefied propane fog dispersal at Medford- Jackson airport, Oregon

04 p0585 A69-14918

Cloud and fog droplet spectra due to condensation of water vapor on nuclei solved by partial differential equation

12 p2126 A69-26017

Polarization of laser radiation scattered forward and back in artificial fog and smoke

14 p2410 A69-28783

Short laser pulses reflection from artificial fog and smoke, showing dependence on reflecting medium attenuation coefficient

15 p2562 A69-30077

Fog removal by high power carbon dioxide lasers, evaluating possibility of clearing airport runways [AIAA PAPER 69-670]

17 p2945 A69-33449

Visibility changes in fog at London airport determined by transmissometer records

18 p3167 A69-35266

He-Ne laser emission attenuation coefficient relation to water content of artificial fogs for 0.63, 1.15 and 3.39 microns

21 p3738 A69-39118

F-5 cockpit fogging during low flights and dive bombing in South Vietnam attributed to hot humid weather, recommending cockpit temperature control and pilot diet

24 p4277 A69-43376

Angular distribution of He-Ne laser beam scattered by artificial fog from data by light detection devices at various angles

24 p4328 A69-43503

Electrical and optical properties correlation of air in fog, discussing droplets distribution with regard to dimensions

24 p4347 A69-43506

Air electrical conductivity reduction in fog ascribed to small ions concentration, increase in droplets capture efficiency and particle concentration

24 p4347 A69-43509

FOIL BEARINGS

Foil bearings design, fabrication, applications to flexible material transport, rotor support, etc

15 p2618 A69-30327

High speed rotors with air lubricated foil bearings, studying motion in pressurized and self acting modes

22 p3955 A69-40405

FOILS

Arbitrary stationary foil in perfect incompressible fluid moving at constant velocity at infinity assuming plane, steady and irrotational flow

08 p1303 A69-20272

FOILS [MATERIALS]

NT METAL FOILS

Beam-foil spectroscopy - NASA Conference, University of Arizona, November 1968, Volume I

03 p0470 A69-13160

Beam-foil spectroscopy problems noting light collection, spectrograph design, broadening of spectral lines by Doppler effect and other complications

03 p0470 A69-13161

Beam-foil spectroscopy above 5.5 Mev for multiply ionized atoms, noting use of Tandem accelerator, spectral resolution, beam intensity and Doppler effect

03 p0471 A69-13163

Beam foil spectroscopy for measuring wavelengths and spectral line intensities

04 p0595 A69-14276

Mean life measurement of excited ions electronic levels using beam foil light source, emphasizing beam particle monitoring and theoretical equations

04 p0595 A69-14278

Static beam deflection in beam foil spectroscopy for determining parent ionization stage of emitting ions

04 p0595 A69-14279

Surface density of carbon foils measured accurately by determining trapped carbon dioxide pressure after burning in pure oxygen

10 p1746 A69-23663

Outgassing rates of multifoil insulation materials for sealed vacuum systems measured over temperature range as function of pumping time

13 p2299 A69-28016

Circular curved foil steady oscillations near screen in semiinfinite space filled with incompressible fluid transformed into equivalent linearized problem

15 p2547 A69-30576

Electrostatically accelerated iron spheres interaction with thin metal and nitrocellulose foils to develop detectors for cosmic dust collection and recording

21 p3719 A69-38344

FOKKER BOND TESTERS

U ADHESION TESTS

FOKKER-PLANCK EQUATION

Random motion of particle with nonlinear damping, obtaining velocity spectrum by solving associated nonstationary Fokker-Planck equation and using equivalent linearization technique

04 p0561 A69-15454

Normal multimode laser action with and without phase locking, using exact steady state solution of Fokker-Planck equation

08 p1325 A69-20291

Density functions analytic solution for Fokker-Planck equation representing cascaded phase locked loops

09 p1474 A69-22450

Asymptotic solution for Fokker-Planck equation at low collision frequency, studying electron-ion collisions effect on universal instability in inhomogeneous plasma

11 p1930 A69-25358

Approximate solution of boundary value problems for Fokker-Planck equation to determine probability of exceeding limits in nonlinear automatic control systems

12 p2054 A69-26653

Mathematical model of mechanical wear in surface friction based on approximation of cross section profiles, using Fokker-Planck equation for distribution function

14 p2455 A69-29331

Galactic cosmic rays and Alfvén waves interaction, considering gyration frequency resonance, wave growth, Fokker-Planck equation and diffusion model

15 p2675 A69-30761

Elastic collision operator for relativistic Lorentz gas converted to differential form using Fokker-Planck limit for anisotropy segments

16 p2817 A69-31668

Fokker-Planck equation applied to probability density for finding rays larger than correlation distance during propagation in random medium

17 p2926 A69-33854

Kinetic equations for fully ionized plasmas and approximate derivation method for generalized Fokker-Planck equation including nonadiabatic effect

23 p4195 A69-41515

Fokker-Planck plasma collision equation derived from Boltzmann equation, Markov process and Liouville equation

23 p4195 A69-41516

FOLDING

Crimping method for preventing nuts loosening, discussing elliptical deformation and point crimp for obtaining maximum interference fits

22 p3957 A69-40828

FOLDING STRUCTURES

Testing program using electrical measurements for determining adequacy of erectable parabolic reflector for space missions

02 p0223 A69-12812

Foldable tubular connection application to expandable lattice structure, analyzing cross sectional distortions

06 p1024 A69-17608

Folding propotor VTOL aircraft configuration analytical and experimental investigations to study design requirements for cruise speeds to Mach 0-75 [AIAA PAPER 69-220]

10 p1635 A69-24087

Aluminum models of single cell simply supported folded plates to study instability phenomena possibly occurring in actual structure

15 p2709 A69-30679

Folding propotor V/STOL aircraft characteristics, showing configuration effects on performance and optimization of rotor, wing and propulsion systems [AHS PAPER 302]

17 p2901 A69-33547

Elastic stiffness, kinematically equivalent loads and initial loads due to initial strains of FUGA 6 element, describing program for matrices generation

19 p3447 A69-36852

FOLIAGE

Previsual detection of vigor loss and mortality signs in ponderosa pine trees subject to bark beetle attack

12 p2098 A69-26993

FOOD

Hydrogenomonas eutropha as means of protein food source independent of conventional agriculture for animal feed supplement

10 p1644 A69-23306

Prolonged dehydrated food diet effect on metabolism of humans, noting complete adaptation after three or four months

13 p2212 A69-28624

Food-borne diseases prevention in civil aviation, reporting gastroenteritis cases during flight

24 p4278 A69-43392

FOOD INTAKE

Short latency antidiuresis following initiation of food ingestion by food deprived rats, noting possible signaling factor

01 p0014 A69-10860

Fiddler crab absorption of DDT residues from organic detritus in estuaries, discussing DDT residue entrance into diverse food chains

14 p2406 A69-28872

Space flight food evaluation by metabolic balance techniques during space flight simulation, considering food consumption during weightlessness

15 p2560 A69-31470

Human performance assessed by pulse rate increment at onset of exercise on bicycle ergometer and decrement during recovery after fasting

21 p3655 A69-38910

Pigeon accelerated performance patterns as function of contiguity of brief visual stimuli and food reinforcement, noting pattern absence during stimuli omission

23 p4081 A69-41436

Cerebrospinal fluid /CSF/ formation in male monkeys as function of fluid pressure at third ventricle level following temperature stress and feeding

23 p4084 A69-41469

Constant illumination intensity effects fixed ratio lever pressing behavior for appetitive reinforcement with chimpanzee in temperature and humidity controlled environment

24 p4260 A69-42702

FORBIDDEN BANDS

Astronomical needs for atomic spectra, discussing emissions in Wolf-Rayet lines and O-F stars and forbidden lines in absorption in sun and F-K stars

03 p0508 A69-13172

Electrical resistivity of sintered high melting point metal oxides, noting width of semiconductor forbidden band

03 p0445 A69-13570

Energy structure parameters for ZnTe-CdTe and ZnSe-ZnTe crystals, obtaining forbidden bandwidth dependence on composition

03 p0492 A69-14173

Forbidden resonance line of Ca II in Arcturus from spectrograms at widely different times of year

08 p1392 A69-20558

Continuum emission and forbidden lines in helium plasma in linear Z-pinch tube, noting plasma electron density

08 p1369 A69-20887

Dipole magnetosphere model with cylindrical or spherical forbidden band for studying plasma motion in quasi-hydrodynamic approximation

10 p1769 A69-23901

Resonances in cross sections for electron impact excitation of forbidden lines in oxygen molecular ion at near threshold energies for astrophysical applications

11 p1921 A69-24417

Ca II forbidden lines in photospheric spectrum identified with weak Fraunhofer line by photoelectric spectrometer scans

14 p2528 A69-29962

Electronic states of semiconductor acceptor centers at forbidden band deep levels, considering inner electron shell excitation in impurity ion

15 p2665 A69-30039

Absorption band edge position in p type indium antimonide thin films after heating, showing forbidden bandwidth function relationship to film thickness

15 p2666 A69-30044

Frequency dependence of light absorption by excitons obtained for allowed and forbidden zone transfers in semiconductors

15 p2632 A69-30057

- GaAs zinc gallium selenide solid solutions properties, analyzing lattice constant, microhardness, forbidden zone and concentration relationships
15 p2670 A69-31050
- Fe II forbidden lines profiles and equivalent widths prediction for solar photospheric spectrum, deducing photospheric Fe abundance
16 p2854 A69-31652
- Vertical wind effects in atmosphere on 5577 A radiance, showing dependence on atomic oxygen density
16 p2778 A69-32185
- ZnS-CdS crystals luminescence during varied forbidden bandwidth, discussing two photon and ruby laser excitation and temperature dependence
19 p3331 A69-35866
- Forbidden lines in solar corona, discussing ionization equilibrium and excitation of levels in highly ionized atoms
19 p3422 A69-36216
- Forbidden lines emitted by gaseous nebulae, emphasizing relative intensities of O II and O III lines
19 p3422 A69-36220
- Collisional excitation of forbidden lines in planetary nebulae from 5537/5517 intensity ratio measurements, noting density and intensity relationship
19 p3422 A69-36221
- Forbidden lines of O I, O II, S II, N II and A III in red and near IR spectra of NGC 1976, IC 418 and IC 4997
19 p3422 A69-36222
- Monochromatic energy flux measurement in H and forbidden lines of planetary nebulae indicating ionization level and optical depth
19 p3423 A69-36223
- Forbidden emissions in CH Cygni and VV Cephei noting symbiotic star
19 p3423 A69-36228
- Forbidden lines in slow nova RR Tel spectrum, comparing ionization rate with RR Pic
19 p3423 A69-36230
- Forbidden emission lines used to study interstellar gas, discussing gas ionization, neutral hydrogen, calcium lines, etc
19 p3424 A69-36235
- Forbidden emission lines in spectra of normal, radio and Seyfert galaxies and quasars, giving information about quasi-stellar mean densities, temperatures, ionization, etc
19 p3424 A69-36236
- WY Gem star spectroscopic observation showing peculiarity about forbidden and absorption spectra superposition
20 p3598 A69-37464
- Invalidity of Pagel method for intrinsic and interstellar reddening for peculiar objects, discussing excitation mechanism for forbidden lines of ionized Fe for Eta Carinae
21 p3815 A69-39616
- Power per unit volume of UV and forbidden lines emitted by ionized C, N, O and Ne as function of electron temperature and density
22 p3984 A69-40157
- Forbidden absorption bands of diatomic O in Ar continuum region, determining rotational constants of upper electronic states
22 p3896 A69-40479
- Photoionization model of Seyfert galaxy extended to calculate temperatures, luminosities and sizes of zones emitting forbidden Fe X /6374 A/ and Fe XIV /5303 A/
22 p4024 A69-40581
- Forbidden O I 5577 A dayglow emission equatorial measurements with rocket photometer, discussing altitude profiles and excitation mechanism
24 p4314 A69-43005

FORBIDDEN TRANSITIONS

- Electron impact spectrometer for obtaining molecular energy loss spectra used to investigate scattering cross sections for optically allowed and forbidden transitions
01 p0123 A69-10620
- Solar Fe abundance from photospheric permitted Fe and forbidden Fe II lines, noting equivalent widths of two Fe II lines
03 p0515 A69-14036
- Planetary nebulae NGC 7662 and IC 418 forbidden line spectra compared with computer model predictions, noting evidence for dynamical effects and filamentary structure
06 p1009 A69-17963
- Forbidden S I lines due to transitions within ground configuration identified in Fraunhofer spectrum of sun, noting photospheric abundance of S
07 p1217 A69-19237
- Hartree-Fock calculations of coronal forbidden transition lines in Ar I isoelectronic sequence, obtaining

wavelengths, magnetic dipole and electric quadrupole transition probabilities
08 p1385 A69-20071

Diffuse interstellar absorption bands and doublet line, noting large intensities of forbidden transitions
08 p1395 A69-20639

Present state of abundance determination in solar corona, discussing forbidden and UV lines analysis
08 p1402 A69-20907

Physical conditions in nuclei of various Seyfert galaxies deduced from line intensities, noting permitted and forbidden lines formation in different regions
09 p1596 A69-22056

Helium I line profiles including forbidden component, discussing electron and ion Stark broadening and thermal Doppler broadening
09 p1601 A69-22209

Intrinsic absorption temperature dependence in doped p-InSb, discussing forbidden transitions
09 p1559 A69-22648

Forbidden solar corona lines transition probability in vacuum UV region
12 p2157 A69-26334

Forbidden NI transitions in nighttime upper atmosphere observed with Fabry-Perot spectrometer
14 p2440 A69-29120

Forbidden transition probabilities of solar corona lines in vacuum UV range
14 p2519 A69-29355

Forbidden transitions in stellar spectra - Conference, Liege, Belgium, June 1968
19 p3420 A69-36211

Celestial spectra forbidden lines tabulated by element and ionization stages, describing laboratory spectrum analysis programs
19 p3421 A69-36212

Forbidden transitions in diatomic molecules with nonzero spin and zero orbital angular momentum, stressing application in outer planets and M stars hydrogen spectra
19 p3421 A69-36213

Forbidden atomic transitions involving metastable species in upper atmosphere, tabulating permitted and forbidden molecular band systems
19 p3421 A69-36214

Forbidden transitions in absorption spectra of sun and normal and peculiar stars
19 p3422 A69-36215

Intensity ratios effect of forbidden Fe and Ca transitions in solar corona on Fe/Ca ratio, noting cascading configurations
19 p3422 A69-36219

Electron density and electron temperatures determination in planetary nebulae, using maximum number of observed forbidden transitions
19 p3423 A69-36224

Forbidden emission transition probabilities in high excitation symbiotic stars, novae, Cygni stars and peculiar binaries
19 p3423 A69-36227

Forbidden transitions in emission line spectra of variables near minimum light, finding origin in hot chromosphere
19 p3424 A69-36232

MH alpha 328-116 spectral characteristics noting weak continuum, emission lines from forbidden transitions and absence of absorption
19 p3424 A69-36233

Helium sequence ions spin forbidden transitions electric dipole oscillator strengths and transition probabilities evaluated by variational procedure
20 p3577 A69-38171

Electron and ion Stark broadening of allowed and forbidden, triplet and singlet transitions in neutral He at low electron densities, noting Doppler broadening
22 p3985 A69-40665

FORBUSH DECREASES

- March 1966 Forbush decrease observed in underground meson component at 70 mwe compared with neutron and sea level meson intensity variations
01 p0146 A69-11129
- Anisotropies in Forbush decreases in March 1966, noting dependence on interplanetary magnetic field structure
06 p0990 A69-17290
- Recurrent Forbush decrease association with proton enhancement, discussing energetic storm particle events
09 p1582 A69-22752
- Anomalous Forbush decrease observations in November 1960 demonstrating cosmic ray flux anisotropy near earth
09 p1582 A69-22753

Satellite data on galactic cosmic ray variations near magnetosphere and in interplanetary space, discussing Forbush decreases
10 p1756 A69-22819

Forbush decreases spectra in low energy region from satellite measurements of neutron and hard component of cosmic rays
10 p1758 A69-22829

Forbush effects energy spectra and cosmic ray anisotropy beyond magnetosphere analyzed during solar activity minimum, using data from neutron monitors global network
10 p1758 A69-22835

Cosmic ray absorption and modulation in lower ionosphere at midlatitudes, considering 11 year variations, Forbush effects and solar radiation on electron concentration
10 p1759 A69-22840

Time dependence, anisotropy and spectral composition of cosmic radiation generated during series of flares during July 5-20, 1966 by Pioneer 6 observations
10 p1768 A69-23769

Forbush decrease associated with July 7 1966 proton event from cosmic ray intensity variation measurements by neutron monitors
10 p1768 A69-23774

Muonic component diurnal wave trains at 70 mwe during cosmic ray decreases, discussing Forbush decay as result of shock front advance
14 p2511 A69-28962

Cosmic ray intensity preceding Forbush effects as function of chromospheric flares solar longitude and solar wind velocity
14 p2512 A69-29044

Frequency distribution of sudden cosmic ray intensity increases, considering Forbush phenomenon
14 p2514 A69-29773

Geomagnetic storms and Forbush decreases accounted for by interplanetary solar corpuscular streams effects described by interplanetary magnetic field structure, noting independence of flares
18 p1817 A69-34937

Stream structure in interplanetary magnetic field during 1966, analyzing geomagnetic activity and solar particles and Forbush decrease anisotropy
18 p3199 A69-34938

Charged particle acceleration in interplanetary plasma from analysis of cosmic ray intensity increases accompanied by SC magnetic storms and Forbush effects
21 p3788 A69-38587

Short lived Forbush decreases, discussing phase differences between stations due to asymptotic directions changed by geomagnetic field and spatial anisotropy
23 p4204 A69-41480

Geomagnetic disturbances relations to cosmic ray diurnal variation phase and amplitude, including Forbush decreases
23 p4204 A69-41483

FORCE

- Torkington progressive rigidity model with successive minimum requirements relation to diagonal matrix elements of molecular force constants
17 p3068 A69-34230
- Force maintaining rigid inclusion embedded in elastic plate with rigid boundaries
23 p4235 A69-42465

FORCE DISTRIBUTION

- Forced oscillations of unbalanced rotor on elastic bearings with nonlinear characteristics investigated for resultant forces and amplitude using motion equations
01 p0170 A69-10824
- Stress transfer from loaded matrix to single fiber in composite materials determined by series and step formulations
01 p0172 A69-11271
- Electric field influence on fluid oscillation modes for Korteweg-Helmholtz force density on incompressible dielectric liquid immersed in electric field
04 p0591 A69-15504
- Accuracy of deformation theory in case of simple loading, analyzing external forces under conditions not satisfying loading theorem
07 p1237 A69-19684
- Multicomponent force transducer for measuring track generated forces acting on rocket sled, discussing combined load and vibration tests [ASME PAPER 69-VIBR-21]
10 p1698 A69-24168
- Bending of weightless thin elastic beams clamped to circular template by external force
12 p2181 A69-26572

Macroscopic crack extension force, critical flaw size and minimum fracture strength calculated from microscopic quantities

13 p2275 A69-27227

Galactic force law from observed stellar velocity and space density distribution

13 p2348 A69-27802

Accelerated boundary layers classified in terms of integral balance of pressure, inertia, wall friction forces and entrainment momenta [AIAA PAPER 69-666]

17 p2955 A69-33462

Forced oscillations of resonance machine elements represented by truss of concentrated masses and external forces, taking into account aerodynamic energy dissipation

17 p3064 A69-33916

Side force problem for shallow helicoidal shell, shown as static geometric analog of pure bending problem, solved by applying duality [ASME PAPER 69-APM-11]

18 p3213 A69-34387

Force on circular plate near screen due to incident potential incompressible jet flow

19 p3297 A69-35816

Monograph on forces exerted by air during yawing motion of sharp cones in supersonic and hypersonic flows by semilinear method

20 p3460 A69-37919

Forces on stationary cylinder under sinusoidal flow, considering symmetrically located vortex pairs and flowfield [ASME PAPER 69-FE-13]

21 p3643 A69-38601

Forces on aircraft during ground roll with slick runway surface and cross wind for deceleration and control on ground [SAE PAPER 690375]

23 p4062 A69-41652

Force acting on multipole in external magnetic field, noting dependence on multipole axes

23 p4158 A69-42172

Gas concentration liberated during each revolution in atmospheres of short period comets to explain impulsive forces upon nuclei, noting diatomic carbon density

23 p4221 A69-42387

FORCE FIELDS

U FIELD THEORY [PHYSICS]

FORCE-FREE MAGNETIC FIELDS

Force free magnetic fields and solar filaments, describing model for explaining filament characteristics

02 p0329 A69-12787

Composition effect of flight path measurements on correction of space vehicles flight path, discussing single parameter correction of motion in force free field

07 p1178 A69-19607

Force-free magnetic field integral properties, obtaining rate of decrease limitation via virial theorem

11 p1951 A69-24239

FORCED CONVECTION

Heat transfer rates from high temperature spheres into subcooled liquid sodium during forced convection, noting surface vapor formation [ASME PAPER 67-WA/HT-32]

02 p0351 A69-12202

Turbulent transport of energy in atmospheric boundary layer near earth surface resulting from forced convection

04 p0627 A69-15087

Forced convection heat transfer coefficient invariance to flow reversal in Stokes and potential streaming flows past isothermal particles of arbitrary shape

04 p0590 A69-15274

Surface vibrations effect on forced convection heat transfer normal to cylinder, discussing convective coefficients dependence on Reynolds number [ASME PAPER 68-WA/HT-5]

05 p0846 A69-16116

Forced laminar flow convection in horizontal tube with variable viscosity and free convection effects [ASME PAPER 68-WA/HT-20]

05 p0847 A69-16123

Simultaneous natural and forced convection flow around wall, analyzing perturbations of hydrodynamic elements due to obstacle

06 p1030 A69-17095

Heat exchangers in cryogenic fluids in free and forced convection, discussing measurements in liquid H, D, Ne and N

08 p1420 A69-19914

Acceleration effects on forced convection in turbulent boundary layer, noting heat transfer history and rates prediction

09 p1480 A69-21480

Horizontal surface heat transfer coefficient under simultaneous free and forced convection calculated as function of temperature head, air flow velocity and area

10 p1810 A69-24085

Forced heat convection in steady turbulent air flow in circular cross sectioned tubes, noting laminar sublayer in wall regions

11 p2000 A69-25096

Oxygen effects in Type 316 stainless steel, Nb-Zr alloy liquid potassium system, discussing thermal convection and forced circulation loops and corrosion rates

12 p2112 A69-25943

Forced convection in atmospheric boundary layer above nonuniformly heated earth surface, noting roles of wind and stratification parameters

12 p2126 A69-26579

Surface vibrations effect on forced convection heat transfer normal to cylinder, discussing convective coefficients dependence on Reynolds number [ASME PAPER 68-WA/HT-5]

13 p2374 A69-27781

Liquid fuel droplets combustion under free and forced convection noting combustion rate

15 p2719 A69-31174

Forced laminar flow convection in horizontal tube with variable viscosity and free convection effects [ASME PAPER 68-WA/HT-20]

17 p3068 A69-32902

Combined free and forced convection hydromagnetic flow and heat transfer of electrically conducting fluid subjected to temperature variations in vertical channel

19 p3380 A69-36304

Forced convection liquid flow past heated flat plate with variable viscosity and thermal conductivity, analyzing velocity and temperature distribution in boundary layer

22 p4051 A69-40685

Forced convection heat transfer coefficient for fully developed turbulent flow in circular tube with time-varying circumferential heat flux

22 p4051 A69-40921

Gaseous absorption cell variable attenuator for carbon dioxide laser radiation at specific wavelength, using forced convection to eliminate thermal defocusing effects

23 p4172 A69-41396

Induced convection effect on peak pool-boiling heat flux under variable gravity, pressure and size conditions and various boiled liquids

24 p4409 A69-43516

Laminar flow in horizontal circular tubes with uniform heat flux, analyzing combined free and forced convection effects on secondary flow

24 p4409 A69-43519

24 p4409 A69-43519

24 p4409 A69-43519

24 p4409 A69-43519

24 p4409 A69-43519

24 p4409 A69-43519

24 p4409 A69-43519

24 p4409 A69-43519

24 p4409 A69-43519

24 p4409 A69-43519

24 p4409 A69-43519

24 p4409 A69-43519

24 p4409 A69-43519

24 p4409 A69-43519

24 p4409 A69-43519

24 p4409 A69-43519

24 p4409 A69-43519

24 p4409 A69-43519

24 p4409 A69-43519

24 p4409 A69-43519

24 p4409 A69-43519

24 p4409 A69-43519

24 p4409 A69-43519

24 p4409 A69-43519

24 p4409 A69-43519

24 p4409 A69-43519

24 p4409 A69-43519

24 p4409 A69-43519

24 p4409 A69-43519

24 p4409 A69-43519

24 p4409 A69-43519

24 p4409 A69-43519

24 p4409 A69-43519

24 p4409 A69-43519

24 p4409 A69-43519

24 p4409 A69-43519

24 p4409 A69-43519

24 p4409 A69-43519

24 p4409 A69-43519

24 p4409 A69-43519

24 p4409 A69-43519

24 p4409 A69-43519

24 p4409 A69-43519

24 p4409 A69-43519

Dynamic response of anisotropic circular cylinders to uniformly distributed pressure varying periodically with time analyzed using Laplace transformation

09 p1611 A69-21440

Generalized orthogonality principles and expansion schemes for forced response of partial differential equations, noting applicability to rodlike structures

09 p1533 A69-21975

Forced vibrations in semibounded elastic bar with various moduli of elasticity, discussing reversing longitudinal force and elastic waves propagation

10 p1799 A69-23155

Forced vibrations of elastic beam covered by viscoelastic layer subjected to transverse harmonic excitation

10 p1800 A69-23241

Forced torsional vibrations of turbine blades calculated by computer using mathematical models for resonance frequencies and tangential stresses

10 p1803 A69-24076

Longitudinal vibrations induced by internal flow in metal bellows resembling vortex shedding excitations of elastically restrained cylinders, discussing spring mass mechanical model [ASME PAPER 69-VIBR-5]

10 p1805 A69-24163

Superimposed tool vibration function in deep drawing, ironing and cold forging, discussing equipment instrumentation, emphasizing dynamic force measurement [ASME PAPER 69-VIBR-8]

10 p1700 A69-24164

Mechanical model for oscillatory motion of solid body in Newtonian central force field

11 p1919 A69-25179

Amplitudes of forced bending vibrations of frames with superfluous elastohysteretic couplings by dynamic compliances method

11 p1986 A69-25333

Forced discontinuous vibrations of liquid in conduit experimentally analyzed, discussing test devices and procedures

11 p1875 A69-25485

Viscous flow-induced vibrations of elastically restrained flat plates in narrow channel, considering one dimensional viscous flow theory

11 p1991 A69-25515

Zero Gaussian curvature rib reinforced shells free oscillations reduced to nonreinforced shell forced oscillations under cyclic loads

12 p2177 A69-25996

Self and forced oscillations in multivariable relay control system, considering relays with hysteresis and dead band and stability of periodic states

12 p2049 A69-26084

Monograph on nonlinear servosystems covering nonlinearity with/without inertia, self oscillations, linearization by forced oscillations, stability theorems and Liapunov function choice

12 p2054 A69-26966

Torsional oscillation of cylindrical shell of non-homogeneous material under periodic shearing force

13 p2361 A69-27462

Vibrating camera for photographic measurement of flow velocities and trajectories of bodies marked by light spots

13 p2261 A69-27913

Free and forced vibrations of elastic layer, using iteration procedure based on asymptotic integration of linear theory of elasticity dynamic equations

13 p2363 A69-28126

Differential equations of single loop parametric amplifier response, analyzing forced oscillations

13 p2234 A69-28329

Bladed disk assemblies vibrational properties, discussing dynamic characteristics of system with pairs of close natural frequency modes under forced vibration

15 p2704 A69-30304

Finite integral transform determination for solving circular plates forced vibrations with time dependent conditions

15 p2704 A69-30306

Laminar thin orthotropic cylindrical shells natural and forced oscillations and dynamic deflection coefficient

15 p2715 A69-31202

Boundedness in mean square of solutions derived for linear differential equations forced oscillations with nonwhite Gaussian random functions parameters

16 p2873 A69-32058

Forced oscillations of three layer plate used as vibration dampers for engine components

16 p2873 A69-32143

Distribution function, harmonic and statistical linearization methods applied to study forced oscillations in nonlinear oscillatory system
16 p2813 A69-32284

Force resonance oscillations of one degree of freedom system with randomly time varying natural frequency
16 p2813 A69-32285

Amplitude maxima for nonstationary oscillations of dynamic system with multiple degrees of freedom
16 p2876 A69-32296

Forced oscillations of resonance machine elements represented by truss of concentrated masses and external forces, taking into account aerodynamic energy dissipation
17 p3064 A69-33916

Forced harmonic oscillations of one dimensional mechanical girder systems allowing for nonlinear resisting forces calculated by boundary value problem reduction to Cauchy problem
17 p3064 A69-33917

Secondary vortex generation in near wake of circular cylinders under forced oscillation, analyzing motion dependent transition regimes using hydrogen bubbles flow visualization
[AIAA PAPER 69-755] 18 p3084 A69-34411

Forced vibration testing of complex continuous systems, demonstrating suppression of certain resonant frequencies due to laboratory techniques
18 p3114 A69-34422

Periodic motions in single mass impact vibration system by point transformations method, noting complexity characteristics
18 p3172 A69-34565

Parametric and forced oscillations analogy for analyzing dynamic behavior of oscillatory systems with time dependent parameters
18 p3175 A69-35322

Linear oscillations of sphere in compressible viscous fluid with slip at surface, noting drag variation
19 p3297 A69-35836

Vibrational displacement phase measurement by Michelson interferometer with laser source
20 p3538 A69-37320

Monograph on frequency response characteristics of mechanical oscillator chains, calculating forced vibrations in linear systems
20 p3577 A69-37920

Tensional and torsional forced vibration tester for viscoelastic plastic materials under tensile strain
21 p3720 A69-38591

Combination resonance and instability regions of second type for parametrically excited oscillations with nonlinear/cubic/damping
23 p4230 A69-42107

Rigid shaft dynamics in hinged and elastic bearings, eliminating inaccuracy by limiting analysis to forced vibration
23 p4171 A69-42483

Real space-time Green functions applied to turbulence induced infinite thin elastic plate vibration, analyzing mechanical dissipation effects
24 p4395 A69-42597

Forced symmetrical vibrations of circular elastic plate analyzed by applying Gaussian hypergeometric, Legendre functions and Jacobi polynomial
24 p4397 A69-42746

Asymmetric dynamic response to free and forced vibrations of thin membrane shells at given stress state due to previous loads
24 p4399 A69-42990

Cylindrical shell with supersonic nozzle end, describing axisymmetric oscillations forced by burning filler in gas stream
24 p4300 A69-43073

Forced parametrically excited periodic vibration of finite length plate in plane supersonic flow, considering periodic forces applied at edges
24 p4407 A69-43733

FOREARM

Rheography of blood circulation of forearm after tightening with pneumatic cuff, analyzing amplitude increase and information about vascular system
21 p3653 A69-38838

Arterial and deep venous blood from human forearm analyzed following rest and rhythmic exercise on ergometer in hyperbaric oxygen chamber
22 p3878 A69-40834

Forearm skin capacity vessels tonus as function of intrapulmonary pressure during positive and negative pressure breathing
23 p4093 A69-42068

FOREBODIES

NT ABLATIVE NOSE CONES
NT NOSE CONES

NT NOSES [FOREBODIES]
NT ROCKET NOSE CONES

Flow field for single or multiple jets firing forward into oncoming supersonic free stream, noting effect of forward extending cylindrical body
[AIAA PAPER 69-69] 06 p0864 A69-18164

C-5 engine inlet development, presenting two phase nacelle forebody and five phase model tests, scale corrections inlet/cowl optimization and prototype tests
[ASME PAPER 69-GT-52] 09 p1570 A69-22481

FORECASTING

NT LONG RANGE WEATHER FORECASTING
NT NUMERICAL WEATHER FORECASTING
NT PERFORMANCE PREDICTION
NT STATISTICAL WEATHER FORECASTING
NT WEATHER FORECASTING

Geomagnetic disturbance activity forecasting method using solar coronal streams, noting reliability of test forecasts
01 p0150 A69-10372

Long range management forecasting by Delphi technique, describing expert panel selection, composite group replies and successive revisions
01 p0180 A69-11250

Technological forecasting role in company growth planning via Delphi technique
06 p1044 A69-17871

Gravity gradient stabilization role in space missions in 1970s and 1980s
07 p1229 A69-18348

Solar activity forecasting methods
10 p1777 A69-23312

Design management in next century covering computer methods, market needs, etc
11 p2004 A69-24371

Technological forecasting by intuitive forecasts, consensus methods, analogy, trend extrapolation and structural models
13 p2382 A69-28040

Solar activity forecasting methods based on sunspots and flares
13 p2333 A69-28657

Delphi technique of technological forecasting used for R and D planning
20 p3639 A69-37353

Top-down initiating technique for forecasting future decade major systems requirements based on information progression
[AAS PAPER 69-409] 24 p4417 A69-42803

Air traffic growth forecasting, describing various mathematical econometric models
[AAS PAPER 69-329] 24 p4417 A69-42807

Technological forecasting as aid to aerospace planner in optimizing R and D resources allocation
[AAS PAPER 69-105] 24 p4417 A69-42819

Solar activity long term forecasts determined from comparison between Mount Wilson magnetic field synoptic chart latitude zones and sunspot groups
24 p4374 A69-43625

Interplanetary and geophysical conditions forecast- ing based on repetitions of low latitude photospheric background magnetic field patterns during solar activity cycles
24 p4387 A69-43626

FORECASTS

U FORECASTING

FOREHEAD

Cutaneous receptor response to microwave irradiation, measuring warmth sensory effects in human forehead with radiometer
[AGARDOGRAPH-111] 08 p1266 A69-20677

FOREIGN POLICY

U INTERNATIONAL COOPERATION

FORESTS

Avionics in forest resource inventories management, noting design of radar altimeter for low level aerial photography
01 p0080 A69-10352

Aerospace research applications in agriculture and forestry, discussing information acquisition for worldwide coverage
[UN PAPER 68-95393] 01 p0065 A69-10504

Remote sensing and forest survey sampling designs, discussing nonstereo stratification, conventional photography and IR or radar imagery
12 p2097 A69-26991

Statistical properties of spatial radiance distribution of sky and forest backgrounds in IR, noting one dimensional Wiener spectra
12 p2131 A69-27072

Agricultural and forestry applications of tethered balloons, discussing observation angle effect on spectral signature response and signal preprocessing
22 p4053 A69-40805

Earth orbital remote sensing applications to forest and range resources management, discussing conventional aerial photography
[AAS PAPER 69-059] 24 p4307 A69-42823

FORGING

Cold drawing workability of Nb, Mo and Ta using dies with lubrication for metal sheets
03 p0452 A69-14124

Large hydraulic press forgings for light metals, discussing 50,000 ton machine used for Al alloys, tooling and die considerations
[ASM PAPER C7-5.1] 04 p0604 A69-14521

Hydraulic press large closed die forging of various alloys and refractory materials, evaluating mechanical and metallurgical problems
[ASM PAPER C7-5.4] 04 p0604 A69-14521

Closed die development for forging very large and complex parts to meet needs of high Mach aircraft
04 p0604 A69-14523

Fatigue strength of gears with integrally forged, cut and ground teeth, discussing pancake forgings
[SAE PAPER 680632] 08 p1321 A69-20732

Forging techniques for forming Be into cylinders, rings, shafts and disks, investigating controlled texture forging for turbine engine components
09 p1504 A69-22073

Structural inhomogeneity of Ti alloys cause increased susceptibility to production of sheets, forgings and drop forgings
11 p1902 A69-24276

Cast and forged steel mechanical properties noting starting materials and production methods roles in cast steel improvement
11 p1904 A69-24644

Ti alloy forgings production for optimal mechanical properties by cross section and structural condition selection and avoidance of oxygen, nitrogen and hydrogen pickup
16 p2801 A69-31785

Forge to determine refractory metals formability and ductility at high temperature in protective pressure
17 p2945 A69-33419

Plane strain forging of pure Al and Al-Cu alloy at low strain rates and elevated temperatures, in constant velocity compression test
17 p2979 A69-34137

Ti structural components for forgings, noting problems facing die-forging industry and machining equipment
21 p3728 A69-38459

Powder metallurgy all inert processing method for producing nickel base superalloys forgings, discussing microstructure, reproducibility, mechanical properties, etc
[ASM PAPER GG-8-3-3] 21 p3745 A69-38929

Ti-Al-V forgings macro/prior beta/ grain size and in-process thermal treatment effects on fatigue life
[AIME PAPER S69-2] 21 p3732 A69-39470

Ti alloy aircraft components and equipment production, considering roles of temperature, deformation rate and thermal conductivity in drop forging and extrusion processes
[DGLR-69-003] 23 p4170 A69-42162

FORM

U SHAPES

FORM PERCEPTION

U SPACE PERCEPTION

FORMALDEHYDE

Sterilization without damage by mixing steam and formaldehyde at 80 C under subatmospheric pressure, noting thorough penetration
05 p0713 A69-15946

Molecule reorientation and transition probability in molecular beam maser using formaldehyde
07 p1158 A69-19760

Aluminum effect on ammonium percholate/ polyformaldehyde mixtures combustion properties noting heat transfer decrease into k phase
08 p1375 A69-20338

Interstellar formaldehyde detection in absorption against galactic and extragalactic radio sources, discussing chemical evolution
10 p1786 A69-24108

Total gasification heat measurement during pyrolysis of polymethyl methacrylate and paraformaldehyde, discussing method and calorimetric equipment
17 p3069 A69-33133

Molecular collision pumping mechanism for anomalous microwave absorption by formaldehyde rotational transition in Galaxy dust cloud
22 p4029 A69-40768

Carbon isotopes compared in interstellar formaldehyde transition for galactic nucleosynthesis,
22 p4029 A69-40768

- discussing spectrum analysis of radio astronomical telescope observations
23 p4220 A69-42376
- FORMAT**
Flexible format generator for manned spacecraft data management system designed with memory for data sampling formats, emphasizing software counters and power strobing
23 p4133 A69-41762
- FORMATES**
U CHLOROFORMATE
- FORMATION HEAT**
U HEAT OF FORMATION
- FORMIC ACID**
Formic acid catalytic action on sterilizing effectiveness of ethylene oxide
05 p0713 A69-15945
- FORMING TECHNIQUES**
NT AUSFORMING
NT BLANKING [CUTTING]
NT CASTING
NT COINING
NT COLD ROLLING
NT COLD WORKING
NT ELECTROFORMING
NT EXPLOSIVE FORMING
NT EXTRUDING
NT FORGING
NT HOT WORKING
NT INVESTMENT CASTING
NT MAGNETIC FORMING
NT METAL DRAWING
NT PRESSING [FORMING]
NT PROPELLANT CASTING
NT ROLL FORMING
NT SLIP CASTING
Fabrication of large parts in aircraft and space industry, discussing extrusion, forging, explosive forming and diffusion bonding
01 p0088 A69-11400
Shot impact shaping of parts made of monolithic panels, relating curvature of profile to parameters of process
03 p0433 A69-12963
Tubular metal parts and assemblies, discussing flaring, forming, beading, tapering and step drawing
03 p0435 A69-13918
Diffusion bonding and forming of large and complex Ti structures, noting advantages in freedom of design and in economy
[ASM PAPER C7-2.3] 04 p0604 A69-14525
Titanium hot forming and sizing die fabrication concepts for aircraft structures
[ASM PAPER D8-26.1] 07 p1143 A69-19671
Pressure formed parabolic reflectors for millimeter waves, discussing electrical measurements at 30 GHz
08 p1282 A69-20039
Glass science and technology noting optical, electrical and mechanical properties, forming techniques, structure, ionic properties, high pressure effects and glass ceramics
08 p1341 A69-21126
Metal castings around ceramic cores for economic manufacture of jet engines
09 p1503 A69-21907
Forging techniques for forming Be into cylinders, rings, shafts and disks, investigating controlled texture forging for turbine engine components
09 p1504 A69-22073
Whisker metal matrix composite fabrication, discussing aligned whisker distribution without degrading strength or fracturing and detailing extrusion process
09 p1511 A69-22361
Superimposed tool vibration function in deep drawing, ironing and cold forging, discussing equipment instrumentation, emphasizing dynamic force measurement
[ASME PAPER 69-VIBR-8] 10 p1700 A69-24164
Aspherical surfaces formation from spherical by removing part of substrate by means of tool mask for lapping nonuniform wear of surface
12 p2102 A69-26597
Slow forming forging and extrusion required for Ti alloys, discussing mechanical properties as function of beta transformation temperature
16 p2793 A69-31786
Forge to determine refractory metals formability and ductility at high temperature in protective pressure
17 p2945 A69-33419
Forming and heat treatment process for stainless steel pressure containers using liquid N, discussing austenite-martensite transformation role
18 p3161 A69-34605
- Stiffened integrally formed panel stability evaluation based on compression structural efficiency and manufacturing costs
[AIAA PAPER 69-760] 19 p3434 A69-35660
Electrochemical dimensional machining of metals and alloys with rotating cathode in parts manufacture from mechanically intractable materials
23 p4168 A69-41309
Forming techniques to overcome pressing behavior of maraging steels, noting tendency to thin during stretching and reluctance to stretch
23 p4170 A69-42157
Explosive forming theory and experience including explosives characteristics, dimensional relations, hold-down pressure, economics and applications
24 p4320 A69-43038
- FORMULAS [MATHEMATICS]**
Transposition formula for finite displacements of solid body having fixed point relative to fixed axes
18 p3172 A69-34589
Natural coordinates in finite element method, giving formulas for straight or curved element analysis and polynomial integration
23 p4182 A69-41901
Formulas for discriminant and regressive weather analysis for computer calculations under operational weather forecasting conditions
23 p4184 A69-42490
- FORTRAN**
JFIP computer language /Jet Propulsion Laboratory FORTRAN language with Intervals Preprocessor/ for extending FORTRAN 4 to utilize subroutines performing interval arithmetic
01 p0036 A69-10710
FORTRAN Deductive System to find solutions to theorem proving problems, discussing computer implementation
01 p0037 A69-10806
System/360 Continuous Modeling Program, detailing input language, user-defined functions and documentation
05 p0723 A69-16196
Book on FORTRAN computer programming language
06 p0891 A69-17364
Argon plasma composition in Saha equilibrium, using FORTRAN 4 program
07 p1193 A69-19168
Fortran 4 program for computation of equilibrium compositions of gas mixtures at high temperatures
08 p1278 A69-20154
Numerical methods for solving steady state and transient heat transfer problems suitable for high speed digital computer
13 p2376 A69-28141
Polygonal approximation to functional equation solution by using search algorithms, listing FORTRAN IV programs
15 p2644 A69-30424
FORTRAN program for calculation of magnitude and phase of digital filter transfer functions and power spectra of periodic waveforms
15 p2567 A69-30612
FORTRAN computer program for quality control and calculation of total ozone measurements and lamp tests for Dobson ozone spectrophotometer
16 p2787 A69-32644
Man-computer interactive Terminal Interface System /TITS/ compatible for programming graphics, character scopes and typewriter using FORTRAN
[AIAA PAPER 69-955] 22 p3905 A69-40337
- FORWARD SCATTERING**
Forward and backward scattered modes over frequency range in multimode nonuniform waveguide, transforming coupled modes telegraphist equations into Volterra equations
01 p0043 A69-10621
Polarization of laser radiation scattered forward and back in artificial fog and smoke
03 p0393 A69-13275
Hologram form of forward scatter bistatic radar or sonar
07 p1078 A69-18866
Forward scattering of metastable and ground state argon atoms after argon ion-atom charge transferring collisions, discussing excitation resonances
08 p1354 A69-19809
Forward and backscattering of radio waves at electron concentration discontinuity near reflecting ionospheric layer with vertical nonuniformity
09 p1453 A69-21525
Polarization of laser radiation scattered forward and back in artificial fog and smoke
14 p2410 A69-28783
- Forward and backscatter soundings compared to verify focusing mechanism of HF sky waves
14 p2435 A69-28967
Forward and backscattering of radio waves at electron concentration discontinuity near reflecting ionospheric layer with vertical nonuniformity
16 p2754 A69-32520
Two polarization light interference scattered by moving and fixed atoms, obtaining forward scattered light intensity
17 p3005 A69-33109
Plane wave scattering by semiinfinite turbulent dielectric slab, using Born approximation to develop asymptotic series for stochastic components of forward scattered field
[OSA PAPER WH-16] 18 p3174 A69-35245
- FOSSIL METEORITE CRATERS**
U FOSSILS
U METEORITE CRATERS
- FOSSILS**
Etching techniques for revelation and viewing of fossil charged particle tracks in meteoritic and terrestrial minerals
02 p0245 A69-12569
Energy spectrum of Fe group heavy nuclei from fossil track densities depth variation in hypersthene and oligoclase crystals from meteorite Saint-Severin, noting ablation
19 p3410 A69-36095
Densities and angular distributions of fossil tracks in meteorites produced by slowing down heavy primary cosmic ray nuclei
19 p3410 A69-36096
Meteorite minerals as detectors for studying fossil record of cosmic ray nuclei, emphasizing feldspars and pyroxenes
20 p3590 A69-37568
Paleozoic plant fossils carbohydrate content
21 p3669 A69-39333
Carbohydrate analyses of upper carboniferous plant fossils in England, noting monosaccharides separation
21 p3661 A69-39534
Amino acid components in paleozoic plant fossils and rock samples noting glycine, serine and glutamic acid
21 p3662 A69-39535
Prokaryotic and eucaryotic nanofossils localized in prePaleozoic microflora, noting radiometric age and association with stromatolites
22 p3935 A69-40052
Microstructure of Proterozoic nanofossils bracketed by dated granitic events compared with living Eucapsis of blue green Chroococcaceae algal family
22 p3936 A69-40059
Early Precambrian Onverwacht microstructures studied in petrographic thin sections and powdered preparations for possibility of oldest terrestrial fossils
24 p4263 A69-43221
- FOUNDATIONS**
Undamped rigid rotor critical speed analysis for firm and flexible foundations, discussing effect of center of gravity and rotor shapes
[ASME PAPER 69-VIBR-49] 10 p1808 A69-24184
- FOUR BODY PROBLEM**
Numerical solution on UNIVAC 1107 for model describing symmetrical gravitational collision of two four body systems
02 p0322 A69-12269
Hill surfaces in triangular restricted four body problem, deriving equation of surface of zero relative velocity
04 p0660 A69-15038
- FOURIER ANALYSIS**
Output power of Gunn effect microwave diode using equal area analysis and Fourier transforms
01 p0049 A69-11195
Fourier synthesis procedure optimized to design of large time bandwidth product dispersive filters employing nondispersive tapped delay lines
03 p0403 A69-13217
Infrasonic waves recordings from Saturn 5 vehicle, observing signal reversal occurrence
03 p0509 A69-13358
Impacting oscillatory devices for use as mechanical frequency dividers
07 p1136 A69-19458
Real time Fourier spectroscopic system for synthesis of spectrum of interferogram, noting polystyrene IR transmission spectra
11 p1884 A69-24837

FOURIER SERIES

Book on random signal analysis covering Fourier analysis, circuit analysis, Fourier transform theory, operators, probability, random variables, stochastic processes

12 p2031 A69-26632

Fourier analysis of pseudorandom binary sequences, noting relation of sequence sampling properties to interchange of phase angles of sequence harmonic components

13 p2287 A69-27245

Fourier analysis of ionospheric wave reflection pulses for frequency contents and relative phase angles

14 p2440 A69-29351

Generalized Fourier analysis for satellite motion deviations from arbitrarily chosen reference orbit generated analytically or numerically, determining equations for potential coefficients

15 p2697 A69-31323

Interdependent behavior of Fourier solutions to sets of partial differential equations with variable coefficients

16 p2804 A69-32252

Modulation transfer function based on Fourier techniques, discussing nonlinear film development process

17 p3005 A69-33080

Orbit parameters identification method based on given tracking data span applied to lunar orbiter tracking using Fourier analysis

19 p3401 A69-35916

Fourier spectrum analysis of solar line oscillation sequences, discussing power spectra and lifetime of oscillation phase

22 p4019 A69-40286

ELF atmospherics excitation, discussing cloud to ground and intracloud lightning discharges Fourier integration and current moment spectrum

23 p4115 A69-41562

FOURIER SERIES

Incompressible fluid steady motion in curved tube investigated by Fourier series, solving coupled nonlinear equations numerically

01 p0058 A69-10142

Fast Fourier transform, discussing algorithms for sampled Fourier spectra and FORTRAN programs

04 p0625 A69-15223

One to one mappings of Fourier series of analytic almost periodic functions and Dirichlet series, discussing satisfaction of functional equation

05 p0786 A69-15882

Optimum length of Fourier time series approximating diurnal F 2 critical frequency variation on planetary scale

06 p0921 A69-17746

Nonaxisymmetric temperature field of unbounded hollow cylinder with moving heating boundary, expanding surface temperature into Fourier series

07 p1241 A69-18924

NERVA transfer functions evaluation by computer data processing, using Fourier algorithm [IEEE PAPER 2B-2]

07 p1179 A69-19187

Analytical description of planetary distribution of space-time variations of f_0F_2 , deriving Fourier series as function of UT

09 p1486 A69-21545

Single and double transformed Fourier series reduced to forms satisfying certain definite conditions, even with finite number of terms series

09 p1533 A69-22258

MHD generator analysis, formulating boundary value problem for ion diffusion and Fourier series solution for end effect of electrodes pair

13 p2208 A69-27613

Stationary vibration modes of systems subject to nonlinearities using finite sums of Fourier series

13 p2361 A69-27615

Localization and convergence of Fourier series for fundamental systems of functions of Laplace operator, including eigenfunctions and trigonometric systems

15 p2644 A69-30287

Relativistic generalization for polar Sommerfeld rosette of Fourier series expansions by Lagrange and Bessel for particle motion in Keplerian field

16 p2811 A69-31607

Analytical description of planetary distribution of space-time variations of f_0F_2 , deriving Fourier series as function of UT

16 p2783 A69-32540

Recurrence formulas for calculating Fourier expansions in elliptic motion in terms of eccentric and mean anomaly [AIAA PAPER 69-910]

21 p3807 A69-39342

Fourier series solution of finite range Wiener Hopf equation, determining coefficients from Wiener Hopf procedure

23 p4181 A69-41608

Self consistent fields in waveguides containing thin conductors, expanding induced field into Fourier series in normal waves for series coefficients

23 p4123 A69-41942

FOURIER TRANSFORMATION

Holtmark plasma microfield, discussing neglect of term comparable to dipole moment during Fourier transform development for long range Coulomb field

02 p0287 A69-11871

Fourier transformation method for current distribution and driving point admittance of coupled antennas in dissipative medium

02 p0215 A69-11946

Digital modified discrete Fourier transform Doppler radar processor for tactical aircraft

03 p0389 A69-13196

Fast Fourier-Hadamard transform for digitized signal representation, classification, discrimination and efficiency

03 p0392 A69-13249

Optical imaging systems achieving aperture synthesis by lensless Fourier transform holography, noting X ray astronomy, ultrasonic and space applications

03 p0430 A69-13324

Fourier transform solution for cylindrical antennas of arbitrary length, discussing simplification and applications to solid antennas and antenna in conducting media

03 p0405 A69-13624

Fourier transform method to measure two point correlations in grid generated turbulence

03 p0419 A69-13950

Fourier coding method for coding images for digital transmission, achieving bandwidth reduction for televised images

04 p0556 A69-14429

Fast Fourier transform, discussing algorithms for sampled Fourier spectra and FORTRAN programs

04 p0625 A69-15223

Algorithm for calculating discrete Fourier transform by computer

04 p0565 A69-15336

Arbitrary factor technique to derive fast Fourier transform, evaluating recursive properties of trigonometric functions

04 p0565 A69-15337

Digital spectra analysis by Fourier transform and comb filter for determination of voltage and power spectra

05 p0722 A69-16762

Optical Fourier transform applied to structural analysis of catalase crystalline media by gas laser

06 p0928 A69-17890

Fourier transform algorithm introduction leading to image coding technique with image transformed by Hadamard matrix operator

07 p1078 A69-18859

Adaptive primary feed system for wide angle beam scanning from parabolic reflector antenna, using Fourier transformation to obtain uniform power distribution

08 p1279 A69-19908

Interferometric measurement of polarization distributions in Crab Nebula and 3C 315 radio sources by Fourier synthesis, discussing complex brightness

08 p1390 A69-20389

Kinetic theory for weak shock generation by impulsive piston, using Fourier and Laplace transforms to solve BGK equation

08 p1304 A69-20783

Book on communication theory principles covering Fourier transformation, signal transmission, electromagnetic noise, amplitude, phase, frequency and pulse modulation, etc

09 p1454 A69-21801

Power spectrum of nonstationary processes with periodicity in two dimensional autocorrelation function based on Fourier transform

09 p1455 A69-21847

Complex spatial filtering by holographic Fourier transform subtraction

10 p1690 A69-22953

Optoelectronic spectrum analyzer with raster illuminator for producing two dimensional Fourier transform to analyze two dimensional functions

10 p1725 A69-23301

Discrete Fourier transforms, discrete linear filters and spectrum weighting for purpose of sidelobe reductions

10 p1666 A69-23888

Cepstrum /Fourier transform of log-spectrum of signal/ as model for prediction of perception of pitches in harmonic residue /ambiguity of pitch/

11 p1834 A69-24571

Fourier transform holography lensless recording using spherical wave as reference beam

11 p1882 A69-24677

Fourier transform holograms by Fresnel zone-plate fringe interferometer, discussing source size and bandwidth

12 p2090 A69-26249

Electromagnetic step-function plane waves propagation in ionosphere using Fourier transform and Bessel functions

12 p2034 A69-27132

Fast Fourier transform algorithm for low storage capacity computer programs

15 p2572 A69-31092

Langevin equation for interacting molecule system derived by Fourier transformation of Hamiltonian, noting physical correspondence to equation for shear viscosity in monatomic liquids

16 p2815 A69-32370

Multiple reference sources to improve field of view of lensless Fourier transform holography limitation due to modulation transfer function of film and turbulence

17 p2971 A69-32920

Numerical Fourier transform and inversion in random vibration performed on computer, noting use for stochastic structural dynamic analysis of complex structures

17 p2996 A69-33710

Transient vibration linear analysis using Duhamel integral and Fourier and Laplace transformations, deriving receptances and application to aeroelastic systems

18 p3211 A69-34326

Fourier transform laboratory spectroscopy for absorption near earth atmosphere millimeter wave spectrum, discussing integrated absorption strength and dimeric effect

18 p3177 A69-35240

Elastic oscillations of inhomogeneous orthotropic ring under time-variable axisymmetrical load analyzed by Fourier method

19 p3434 A69-35828

Fourier transform techniques applications in optics, converting optical signal amplitude and phase information into electrical signal information

19 p3374 A69-36737

Fourier transform methods in elasticity problems, considering three dimensional equilibrium equations in elastostatics in terms of displacements

20 p3622 A69-37282

Linear radar system theory including Fourier transforms, linear superposition and input/output ratio for deterministic and random signals, discussing filter and sampling theory

20 p3489 A69-37633

Soviet book on antenna synthesis theory for application to antenna radiation patterns with allowance for Fourier transforms limitations

20 p3508 A69-38208

Image deblurring and aperture synthesis using a posteriori processing by Fourier transform holographic spatial filtering

21 p3722 A69-38793

Cosserat theory on couple stresses applied to stress distribution in semiinfinite plate, using Fourier transform method

22 p4038 A69-39902

Extended source Fourier transform holography for single image synthesis of multiple identical images produced by multiple pinhole camera in X ray astronomy

22 p3943 A69-40019

Motion-distorted photograph deblurring method using extended range holographic Fourier transform division

22 p3944 A69-40020

Holographic storage of electric signals in wideband pulsed carrier radar communications, noting Fourier transform in ultrasonic light modulator

23 p4164 A69-41626

Fast Fourier Transform connection with circulant and permutation matrices for case with discrete time sample number equal to discrete frequency samples

23 p4182 A69-41761

Carroll Fourier transform method applied to stellar spectra lines to determine small rotational velocities

23 p4222 A69-42404

FOVEA

High oxygen concentration breathing effect on foveal thresholds, using sea level tests on trained observers

02 p0203 A69-12216

Foveal luminances for chromatic and absolute thresholds for hue identification in case of small targets
07 p1183 A69-19649

Tritanope and trichromat experiments for parafoveal visual response of tritanope, measuring spectral sensitivity and absolute threshold values
22 p3882 A69-40869

FRACTIONATION

Lead isotope composition and concentrations of U, Th, Ra, total Pb and Pb 210 in recent volcanic rocks, noting disequilibrium due to chemical fractionations
04 p0593 A69-15011

Discrete fractional steps method for approximate solution to Navier-Stokes equations, noting perturbation
18 p3165 A69-35278

Eclogite fractionation role in creation and spreading of suboceanic lithospheric plate, discussing density determination at 100 km depth
18 p3132 A69-35434

Meteorite and primordial matter composition related to possible fractionation processes influence, discussing nuclear species abundance
19 p3406 A69-36073

Fractionation of abundant lithophile element ratios of Si, Mg, Ca, Al and Ti in carbonaceous, common and enstatite chondrites
19 p3409 A69-36087

Erythroblasts fractionating method based on size, density and resistance of immature erythroblasts which change during maturation
22 p3877 A69-40761

FRACTOGRAPHY

Fracture surface topography and applications to fracture analysis of laboratory and service failures, describing fracture models
04 p0619 A69-15394

Electron fractography techniques and fracture modes in metallic materials interpretation, giving special attenuation to classical fracture replication and shadowing techniques
04 p0619 A69-15395

Electron fractographic study of fatigue cracks in wrought beryllium sheet, noting transgranular and intergranular modes on fracture surface
09 p1500 A69-22324

Electron fractography of aluminum alloy fatigue for intermetallic particles and inclusions effects on crack growth
10 p1795 A69-23065

Electron microscope fractographic studies to determine service failure causes, detecting grinding and quench cracks, hydrogen flakes and embrittlement fractures, etc
13 p2269 A69-28181

Electron fractography used in machine parts failure analysis to detect internal and surface cracks, forging defects, stress corrosion, fluid leakage sources, etc
13 p2269 A69-28182

Interferometric technique for studying fracture specimens plastic zone using laser holography
15 p2609 A69-30681

Titanium alloy tensile specimens tests in air, methanol and anhydrous methanol environments at known stress-strain-time relations examined by fractography and high resolution electron diffraction
16 p2799 A69-31718

Microfractographic observations of Al, Al alloy, Nimonic 90 and austenitic steel 18/10 after creep rupture
17 p2986 A69-32910

Fracture surfaces of stress corrosion cracks in Fe-Cr-Ni alloys studied by electron microfractography, noting cleavage fracture
19 p3350 A69-36891

Fractography of compact fracture toughness specimens failure, noting stress at fracture origin and crack growth rate
20 p3557 A69-36957

Spherulite boundaries and interspherulite breakdown in polyethylene, considering structure control by varying macromolecular microstructure
22 p3973 A69-40740

Room temperature tensile tests determining failure modes and defect influence on diffusion welds of unalloyed Ti, using electron microscopy and fractography
24 p4331 A69-42939

FRACTURE MECHANICS

Bursts of high speed rotor occurring at diametric cross section and around hub as function of hub size
01 p0142 A69-10306

Natural aging effects on fracture characteristics of aluminum weldments, investigating precracked Charpy impact toughness
01 p0086 A69-10537

Strain distribution for fracture initiation and steady state crack propagation in plane strain tension of plastic materials
01 p0169 A69-10764

Low stress fracture criteria for large elastic structures and small brittle laboratory specimens below transition temperature
01 p0169 A69-10768

Dynamic mechanical behavior of metal at tip of plain strain crack, discussing fracture strength relation to triaxial plastic stability
02 p0343 A69-12284

Fracture process in composite films of stressed tetrafluoroethylene and fluorinated ethylene propylene
02 p0270 A69-12368

Spin tests to determine brittle fracture under plane strain, using cyclic thermal stress or hydrostatic pressure to generate fatigue crack in rotor blank
03 p0524 A69-13060

Plane strain yielding, stresses and fracture about notches and cracks in terms of flow and fracture stresses and crack tip radii
03 p0528 A69-13876

Fatigue endurance of structural elements determined from stress rupture strength under high and low loading rates
04 p0673 A69-14536

Shear type fracture formation mechanism in tensile test specimens of Ti alloys, noting transition in macrogeometry
04 p0617 A69-15076

Fracture surface topography and applications to fracture analysis of laboratory and service failures, describing fracture models
04 p0619 A69-15394

Griffith biaxial fracture criterion for porous brittle materials based on continuum model with random infinitely sharp cracks
[ASME PAPER 68-WA/MET-12]
05 p0838 A69-16152

Fracture propagation in organic glasses, considering density of hyperbolic markings in polymethyl methacrylate and Dugdale model
05 p0784 A69-16429

Fracture mechanics and data from instrumented Charpy impact test
05 p0780 A69-16431

Simulated crack experiment illustrating Griffith energy balance fracture criterion
05 p0842 A69-16438

Photographic observations of fatigue fracture of heat treated polycarbonate
06 p0946 A69-17205

Stresses and displacement around crack under various conditions using two dimensional elasticity theory, deriving complex potentials for various loading types
07 p1231 A69-18269

Crack front and zone in brittle elastic body under high pressure at wall inside body
07 p1231 A69-18699

Laminated composite fracture statistical theory with stress enhancements in elements next to primary fracture, comparing elastic and plastic matrices
07 p1170 A69-18712

Fracture mechanics for predicting crack propagation rate in rotor spars
07 p1053 A69-18872

Flow fracture and rheological properties of viscoelastic material under biaxial loading
07 p1202 A69-19386

Prandtl brittle fracture model modified for semi-infinite crack in infinite body, discussing microscopic and macroscopic relation and crack propagation kinetics
07 p1237 A69-19682

Brittle crack theory analyzed to justify Irwin criterion at crack ends, dismissing Kristianovich-Barenblatt assumption and solutions for elastic problems
07 p1238 A69-19689

Critical analysis of Sedov contention of infinite stress development at ends of brittle cracks
07 p1238 A69-19690

Unstable elastoplastic brittle fracture criterion based on energy balance considerations
07 p1238 A69-19693

Loading rate effects on fracture energy in carboxy terminated liquid Hycar toughened cantilever cleaved epoxy resin
08 p1338 A69-20491

Fracture energy of unidirectional laminated composites related to diameter, debonding energy and strength of reinforcing filaments
08 p1414 A69-20493

Ductile fracture behavior of two phase stainless steel examined by straining smoothed and notched tensile and Charpy impact specimens
08 p1333 A69-20574

Failure causes for planetary reduction gear tooth for adjustment of radio telescopic antennas, studying fracture characteristics, working conditions and loading moments
08 p1321 A69-20853

Fragmentation behavior of small thin walled metal cylinders during explosions as function of expansion velocity and material parameters
09 p1611 A69-21352

Displacements and stress intensity as function of crack length for compact tension specimen, considering load line and crack edge
09 p1503 A69-21392

Crystallographic fracture path of stress corrosion cracks in austenitic stainless steels using scanning electron microscopy
09 p1522 A69-21486

Polymethyl methacrylate rupture time under stress determined from short and long time strength tests, noting relation to crack propagation time
09 p1528 A69-21853

Crack propagation properties of polymethyl methacrylate during bending and tension, noting temperature and loading time effect on crack size
09 p1529 A69-21854

Quasi-brittle fracture of plastic materials based on Griffith theory and crack propagation, analyzing real surface energy and work of plastic strain
09 p1614 A69-21883

Part-through and through-thickness fatigue crack growth observations in glassy plastics, using linear elastic fracture mechanics
[SESA PAPER 1348]
09 p1617 A69-22013

Crack stability under mechanical and thermal stresses, noting critical tensile stress and thermal insulating character of crack
10 p1794 A69-22890

Crack propagation velocity in titanium alloys over varying stress intensities under adverse environment
10 p1709 A69-23058

Substructural changes during fatigue due to stacking fault energy variations related to morphology of fracture surface in solid solution Ni-Co alloys
10 p1795 A69-23060

Nonwork hardening elastic plastic material fracture criteria for antiplane strain, noting plastic zone shape effect on zone size and crack opening
10 p1795 A69-23064

Relaxation method for configurations and energies of atoms and stress induced crack opening displacements in crystalline solids
10 p1796 A69-23067

Aluminum alloy crack propagation and fracture patterns as function of temperature under high strain amplitude and low strain rate
10 p1709 A69-23071

High temperature effect on fatigue deformation and fracture of nickel base superalloy in single crystal and columnar grained forms
10 p1709 A69-23073

Testing system stiffness effect on sheet fracture, discussing notch strength dependence on stiffness
10 p1796 A69-23075

Plastic crack propagation in nonstrain hardening doubly grooved bending specimens with two surface slip, discussing crack angles, crack ductilities and fatigue striations
10 p1797 A69-23077

Low cycle fatigue fracture behavior at high temperatures, noting fatigue crack behavior and crack density concept
10 p1797 A69-23081

Fracture surfaces of Ti and Ti-Sn alloys for stress corrosion cracking in methanol with HCl and in aqueous chloride solutions
10 p1710 A69-23085

Composition and sintering temperature cooling effects on fracture properties of W-Ni-Fe alloys, using electron microscope fractography
10 p1711 A69-23333

Integral transform solutions for Griffith cracks in brittle fracture theory, discussing disk and penny shaped cracks in cylinders and thick plates
10 p1801 A69-23688

Beta parameter in exponential stress dependences of high temperature steady state creep rate and time to rupture of creep resistant alloys
10 p1712 A69-23719

Potential functions for three dimensional problems of elliptical crack in elastic solid
10 p1802 A69-24026

Time dependence criterion in dynamic fracture determined by spall stress relation to stress pulse duration during plate impact

10 p1803 A69-24032

Brittle fracture of steel analyzed using statistical model, attributing occurrence to coalescence of arrested cracks initiated at different points

10 p1803 A69-24033

Collection of papers on fracture, Volume 2, Mathematical fundamentals

11 p1974 A69-24667

Mathematical theory of equilibrium cracks in stressed bodies with minimum loading for crack extension, analyzing crack tip zone and force transmission

11 p1974 A69-24668

Strain energy for two and three dimensional crack systems subjected to varying loads, detailing loading and crack geometry effects on fracture criterion

11 p1974 A69-24669

Continuum mechanics analysis of fractures and crack extension, discussing solids elasticity, plasticity, boundary value problems, etc

11 p1974 A69-24670

Macroscopic states of stress criteria for plastic flow initial yielding, plastic flow and brittle fracture of ductile and brittle metals

11 p1975 A69-24671

Dynamic and fatigue crack propagation theories for brittle and quasi-brittle solids and plates

11 p1975 A69-24672

Probability models used in statistical approach to fracture mechanics, noting role of weakest link model in representing brittle fracture

11 p1975 A69-24673

Fractures in refractory metals surface layers due to Q switched laser pulses

11 p1899 A69-25402

High speed photography of W strip fracture, considering electric current effects and electric circuit interruption by fracture

12 p2113 A69-26195

Fatigue crack propagation laws determined by material yielding at crack tips, stress intensity and exponential crack growth law

12 p2187 A69-26846

Fracture mechanics of polymers and fiberglass reinforced plastics, indicating microcracking under static and cyclic loading due to resin phase brittleness and low strength

12 p2120 A69-26849

Crack growth and crack initiation in cylindrical specimens subject to low cycle strain controlled tension-compression induced fatigue, noting measurement techniques

12 p2188 A69-26914

Crack opening displacements of stationary and running cracks and of inclined stationary cracks in centrally notched plates, noting normal strain fields

12 p2189 A69-27163

Book on microscopic and macroscopic fundamentals of fracture of solids covering structural, metallographic and physical aspects, dislocations, brittle fracture, etc

13 p2274 A69-27220

Solid state physics applications to fracture problems and structure of solids, considering crystallography, lattice vibrations, defects, electron bands, alloys and surface physics

13 p2316 A69-27221

Fracture and equilibrium position of dislocations in discrete and continuously distributed dislocations arrays including stress due to crack, energy considerations and crack initiation

13 p2358 A69-27222

Dislocations observations in fracture study of crystals, considering etching, decoration technique, X ray topography and diffraction electron microscopy

13 p2316 A69-27223

Microscopic mechanisms in fracture surface markings, using electron fractography cleavage, fatigue, stress corrosion cracking, microvoid coalescence and tear ridge formation

13 p2274 A69-27224

Metallographic aspects of fracture, analyzing very brittle solids, Griffith cracks, ductile solids and ductile to brittle transition

13 p2274 A69-27225

Structural modes of fracture, analyzing brittle, ductile, fatigue and stress corrosion fractures using fractography

13 p2274 A69-27226

Stress waves analysis of brittle fractures, considering loading time role and cavitation of viscous fluids relation to fracture incipience

13 p2275 A69-27229

Variational principle for admissible functions particular solution in elasticity theory involving solid bodies with cracks

13 p2359 A69-27290

Fracture of bumper protected fuel tanks subjected to hypervelocity meteoroid impact, applying method of characteristics to stress wave propagation in tank walls [AIAA PAPER 69-369]

13 p2367 A69-28301

Sinusoidal or random excitations equivalence from point of view of rupture risks, considering industrial applications

13 p2370 A69-28602

Fracture mechanics based on linear elasticity for evaluating crack propagation resistance, presenting plane strain fracture toughness test results for high strength alloys [ASME PAPER 69-DE-10]

14 p2461 A69-28842

Rolling direction tensile tests of alloy steel plate displaying various fracture configurations over distinct temperature ranges, noting stress state, void formation and anisotropy [ASME PAPER 68-WA/MET-1]

14 p2464 A69-29440

Three dimensional problem in crack theory for brittle body, determining stress concentration and critical loads

15 p2708 A69-30658

Uniaxial stress effects on molecular breakage rate, relating structure-sensitive parameter to elastic modulus

15 p2709 A69-30807

Griffith crack in thin plate opened by uniform tension at infinity, discussing effect of ties on stress intensity factor

15 p2710 A69-30809

Pop-in mode of fracture obtained during investigation of fracture strength of glassy plastics, discussing mechanics

15 p2642 A69-30814

Thomas fracture theory and compatibility conditions for fracture surface of elastic-plastic rotating hollow shaft, discussing plastic equilibrium

15 p2712 A69-31017

Cost effective pressure vessel design using fracture mechanics, discussing fabrication costs, service life requirements, etc

16 p2870 A69-31740

Unstable metal deformation, discussing volume displacement in necking leading to fracture, homogeneous total deformation and torsion

17 p3053 A69-32987

Alloying elements effects on low temperature metal fracture, considering changes in ductile-brittle transition flow due to solute

17 p2988 A69-33551

Fracture processes in high strength materials, considering effect of stored elastic energy, component geometry, fracture toughness and environment

17 p2988 A69-33553

Fracture strength of Al alloys, discussing tests for tensile properties, linear elastic fracture mechanics techniques, yield strength, corrosive media, etc

17 p2989 A69-33555

Refractory metals fracture, discussing interstitial impurity addition effects in Group 5a and 6a metals

17 p2989 A69-33556

Arrest mechanisms to halt crack before gross failure, involving material toughness exploitation and subduing stress by structural configuration

17 p3060 A69-33560

Rotating machinery fracture and design approach based on effect of detailed stress and strain duty on imperfect materials metallurgical behavior

17 p3060 A69-33561

Fracture safe design practices for pressure vessels and piping, stressing transition temperature and proof testing roles

17 p3060 A69-33562

Fracture design for aircraft vehicles, discussing crack strength requirements and method for serviceability prediction

17 p3060 A69-33563

Engineering fracture design noting temperature effects, brittleness, plane strain fracture toughness, fracture test evaluation

17 p2989 A69-33564

Fracture tests evaluated for transition temperature welding procedures, residual stress, flaws and instrumentation

17 p2989 A69-33565

Fracture kinetics of biaxial oriented polymethyl methacrylate, discussing crack development and propagation as compared to unoriented polymer

18 p3162 A69-35354

Ti-6Al-4V alloy general and stress corrosion behavior in Freon environments, discussing fracture mechanics

18 p3150 A69-35411

High speed brittle fracture of polycarbonate resin subjected to static bending in liquid nitrogen determined from crack propagation speed of surface coating

19 p3358 A69-35776

Fracture mechanics application to pressure vessel design and analysis, reviewing nondestructive inspection techniques

19 p3439 A69-36438

Fracture mechanics applied to cylindrical pressure vessels containing longitudinal defects for fracture behavior prediction from fracture toughness or stress intensity factor

19 p3439 A69-36439

Stress corrosion cracking mechanisms in liquid-solid metal combinations and solvent exposed plastics, discussing adsorption processes and cathodic polarization inhibition

19 p3349 A69-36887

Linear-elastic fracture mechanics applied to environment enhanced crack growth /stress corrosion cracking/

19 p3349 A69-36888

Computed and experimental displacement distribution curves compared for anisotropic material concerning creep rate enhancement by small cracks

20 p3620 A69-36965

Al alloys properties evaluated to determine tensile and static fracture behavior

21 p3743 A69-38668

Fracture mechanics concepts for cost effective booster pressure vessel design and fabrication from commercial steels using boiler plate techniques and minimal NDT quality control

21 p3837 A69-39028

Scattered light mean intensity determination in twilight aerosol atmosphere from satellite observations, formulating boundary value problem

21 p3717 A69-39656

Mohr tensor representation and Mohr theorem proof developed for general problem in structural engineering

22 p4038 A69-39903

Metal fatigue crack nucleation at stresses below static fracture strength, determining local plastic strain under cyclic loading

22 p4041 A69-40053

Anodic Al oxide films mechanical and fracture properties, studying roles of environmental water vapor and film thickness [ECS PAPER 81]

22 p3973 A69-40736

Photographic study of epoxy resin breakdown kinetics under pulsed laser beams, showing crack area as function of time

22 p3973 A69-40743

Continuum fracture concept indicating essential surface energy interpretation difference in otherwise similar adhesive and cohesive failures

22 p3974 A69-40760

Loading rate effects on fracture characteristics of unidirectional fiber reinforced materials, discussing fiber-resin interface strength

22 p3974 A69-41212

Stressed state of thin plate with circular hole under normal and breaking force applied over hole perimeter

23 p4233 A69-42341

Time and plasticity effects on fracture determining solids strength as function of crack dimension

23 p4236 A69-42530

Electron optical techniques for failure analysis involving brittle fracture, corrosion fatigue, stress corrosion, welding and surface phenomenon

24 p4313 A69-42768

Stress analysis in design techniques taking into account failure of flawed structures, discussing fracture mechanics

24 p4398 A69-42773

Model for estimating creep life of material containing wedge crack growth

24 p4399 A69-43032

Soviet book on resistance of materials to deformation and fracture in complex stress states covering elasticity, mechanical theories of limiting stress state, experimental verification, etc

24 p4402 A69-43233

FRACTURE STRENGTH
Fracture toughness concept in predicting failure of materials due to sharp notches or cracks

02 p0336 A69-11431

Dynamic mechanical behavior of metal at tip of plain strain crack, discussing fracture strength relation to triaxial plastic stability
02 p0343 A69-12284

Pre-cracked ceramic rocket nozzle throat inserts, discussing improved thermal displacement accommodation, load transmission, fracture tolerance, articulation capability, etc
02 p0334 A69-12369

Plane strain yielding, stresses and fracture about notches and cracks in terms of flow and fracture stresses and crack tip radii
03 p0528 A69-13876

Fracture toughness of Ni maraging steel weldments, using bending tests
[AIAA PAPER 68-507] 03 p0450 A69-13910

Brittle fracture resistance of low carbon maraging and martensitic steels with cracks established by crack growth measurements during tensile and impact tests
04 p0615 A69-14647

Long term strength of Ni-Cr-Al-Ti alloys, studying gamma particles size and distribution effect
04 p0616 A69-14651

Fracture toughness measurements by means of dimensionless fracture toughness parameters, noting results for materials with very different elastic moduli
05 p0780 A69-16080

Statistical model for tensile fracture of parallel fiber composites based on stress criterion for crack propagation
[ASME PAPER 68-WA-RP-7] 05 p0783 A69-16159

Fracture mechanics and data from instrumented Charpy impact test
05 p0780 A69-16431

Elastic displacements for edge cracked plate specimens used as crack extension indicator in plane strain fracture toughness measurements
05 p0841 A69-16433

Deformation and fracture of Be bicrystals grown by seeding and floating zone melting method from Be single crystal
06 p0942 A69-17225

Ultrahigh strength steel susceptibility to brittle fracture, describing methods of testing rupture toughness and stress intensity factor
07 p1158 A69-18402

Grain size dependence of yield, flow and fracture stresses of Fe-Co-V alloy for 77-298 K
07 p1166 A69-19264

Brittle fracture models compared with experimental stress analysis results, noting plane strain and plane stress fracture toughness
07 p1234 A69-19379

TIG welding introduced residual stresses amplitude and distribution in Ti sheets, studying effects on mechanical properties
[ASM PAPER GG8-6.2] 07 p1169 A69-19674

Brittle fracture criterion for small steel specimens based on interaction between stress concentration of initial crack and nearby slip band
07 p1238 A69-19694

Cr-Ni-Mo steel toughness with strain induced austenite to martensite transformation by TRIP /transformation induced plasticity/
08 p1330 A69-20012

Temperature dependence of polymethylmethacrylate deformation, yield and fracture in constant strain rate compressive and tensile tests
08 p1335 A69-20215

Crack propagation in crosslinked glassy polymers, noting effects of added elastomers molecular weight
08 p1338 A69-20492

Liquid surface active media /kerosene, water, castor oil/ effect on strength of V notched polymethyl methacrylate specimens
09 p1528 A69-21852

Fracture toughness of laminated adhesive bonded structures and monolithic aluminum, considering fracture stresses and ductile and brittle failure
09 p1526 A69-22318

Plain strain fracture toughness tests on two inch thick maraging steel plates of various strengths, using bend and compact tension tests
10 p1795 A69-23057

Stress intensity magnification factors in surface flawed tension plates and notched round tension bars, evaluating fracture toughness
10 p1797 A69-23080

Ceramics strength and fracture behavior in terms of modified Griffith equation, discussing effective surface energy and initial crack size
11 p1907 A69-25238

Hydrostatic pressure-cycling technique for controlled fatigue precracking of spin burst fracture toughness specimens, noting ultrasonic flaw detection
11 p1995 A69-25650

Tensile strength and failure loading evaluation for structure, discussing stresses in neighborhood of crack, crack toughness measurement and fracture mechanics
12 p2176 A69-25861

Inclination effect of fatigue cracks on plane strain fracture toughness of 7075-T651 Al alloy, discussing cantilever bending
12 p2177 A69-25958

Plane strain fracture toughness tests on maraging steel plates for various yield strengths and large dimensions
12 p2114 A69-26496

Tempered glass plates strength nondestructive testing by scattered light photoelastic method, discussing application to aircraft windshield sandwich structures
[AIAA PAPER 68-323] 12 p2118 A69-26768

Macroscopic crack extension force, critical flaw size and minimum fracture strength calculated from microscopic quantities
13 p2275 A69-27227

Fracture mechanics based on linear elasticity for evaluating crack propagation resistance, presenting plane strain fracture toughness test results for high strength alloys
[ASME PAPER 69-DE-10] 14 p2461 A69-28842

Pop-in mode of fracture obtained during investigation of fracture strength of glassy plastics, discussing mechanics
15 p2642 A69-30814

Crack growth monitoring and recording techniques during fracture testing, using foil gauge, potential flow and acoustic pickup methods
15 p2713 A69-31109

Clevis design for reduced friction errors associated with round hole clevis in plane strain fracture toughness measurements
15 p2612 A69-31150

Fracture toughness of AlZnMgCu alloys, employing sharp notch tension, tear and precracked Charpy impact tests
16 p2800 A69-31780

Biaxial stress strain properties of graphite base refractory composites noting fracture strength predictions
[AIAA PAPER 68-337] 16 p2803 A69-32150

Brittle toughness determination method compared with Robertson and notch impact tests, evaluating steel susceptibility to brittle failure propagation
16 p2795 A69-32796

Dislocation and energy balance analysis of ductile and brittle metal cracks for determining metal fracture strength from plastic deformation
17 p3052 A69-32984

Fracture strength of Al alloy in biaxial stress field, considering strain rate influence on material toughness
17 p2986 A69-32985

Microstructural factors role in metal fracture toughness, considering effects of deformation processing and heat treatment, grain size, structural refinement, fibering, etc
17 p2988 A69-33552

Fracture processes in high strength materials, considering effect of stored elastic energy, component geometry, fracture toughness and environment
17 p2988 A69-33553

Fracture toughness of structural steels, discussing evaluation methods for brittle fracture resistance, toughness values and ratings correlation, etc
17 p2989 A69-33554

Fracture strength of Al alloys, discussing tests for tensile properties, linear elastic fracture mechanics techniques, yield strength, corrosive media, etc
17 p2989 A69-33555

Plane strain fracture toughness determined for crack notched bend specimens using standard test procedure for specific metallic material property
17 p2989 A69-33566

Temperature effects on fracture of various alloys, presenting strength and toughness values tested at cryogenic temperatures
17 p2990 A69-33567

Nickel maraging steel weld metal impact strength and fracture toughness improved by heat treatment
18 p3151 A69-35430

Minimum cost design /MCD/ of space launch vehicle, discussing material and process selection based on fracture-safe conditions
19 p3433 A69-35587

Plane strain fracture toughness of high strength steels and Ti alloy from precracked notched bend test method
19 p3346 A69-36436

Fabrication effects on high strength Al alloy plate properties, comparing texture, plane strain fracture toughness, yield stress, ultimate tensile stress and elongation
19 p3346 A69-36437

Multiaxial stress effect at room temperature on fracture strength of silicon carbide tubular specimens
20 p3565 A69-36939

Alloying elements effect on low temperature notch-bend fracture toughness of martensitic high strength steels, noting transition temperature
20 p3556 A69-36952

Phase transformations and strengthening mechanisms in Ti-Al-V alloy
20 p3556 A69-36954

Fractography of compact fracture toughness specimens failure, noting stress at fracture origin and crack growth rate
20 p3557 A69-36957

Yield strength, deformation modes and fracture characteristics of Ti-Al alloys, examining strength and fracture characteristics as function of structure and chemical composition
20 p3557 A69-36959

Axial through-cracks extension criteria in cylindrical pressure vessels, considering fracture toughness and plastic flow stress
[ASM PAPER W9-13.3] 21 p3833 A69-38658

Inconel and aluminum tested in pressurized hydrogen at room temperature, using surface flawed fracture toughness specimens and preflawed pressure vessels
21 p3730 A69-38666

Al alloys sheet, plate and weldments crack behavior and fracture toughness at cryogenic temperatures, using notched and surface flawed plane strain specimens
[ASM PAPER W9-19.3] 21 p3743 A69-38669

Alpha-beta Ti-Al-V-Mo-Zr alloy with high strength, fracture toughness and crack propagation resistance, low density and adequate ductility, discussing test results
[AIME PAPER S69-3] 21 p3747 A69-39472

Stress corrosion cracking in aerospace situations, discussing corrective measures emphasizing fracture toughness criteria
21 p3748 A69-39491

Fracture strength of glass fiber-reinforced cylinders made by unidirectional filament winding predicted by analyzing three dimensional stress distributions
21 p3846 A69-39795

Axial through-cracks extension criteria in cylindrical pressure vessels, considering fracture toughness and plastic flow stress
22 p4046 A69-41040

Aluminum alloys fracture strength tabulated data showing trends regarding yield strength, specimen orientation effects and product size
23 p4175 A69-41476

Fracture toughness and crack propagation in annealed aircraft titanium alloys tested per ASTM procedure, comparing results with high strength steels and aluminum alloys
23 p4177 A69-42165

Plane strain fracture toughness of S-200 grade Be for 77-533 K temperature range, noting effects of loading, heat treatment and neutron irradiation
23 p4178 A69-42450

Traction stresses distribution over contact surfaces using photoelastic frozen stress model
23 p4235 A69-42461

Fracture and tensile properties of electron beam welded Al alloy for pressure vessels compared to gas tungsten arc welding results
24 p4319 A69-42941

Beryllium R and D emphasizing brittleness and fracture toughness for safe working stress levels of structurally loaded components
24 p4332 A69-43208

Al-B composites fracture toughness obtained by comparing notched tensile data with unnotched specimens
24 p4335 A69-43451

Deferred rupture as function of applied load noting test methods
24 p4407 A69-43801

FRACTURES [MATERIALS]

Heavy titanium carbide precipitation on fatigue slip zones of stainless steel, noting rupture produced crystallographic facets
03 p0447 A69-13605

FRACTURING

Plastic fractures of age hardened aluminum alloys analyzed by tensile tests and electron fractography, considering stresses, surface and intergranular effects
07 p1166 A69-18961

Liquid crystal coatings for determining fracture initiation flaws in material structures, considering stress concentration and hysteresis heating
10 p1699 A69-23053

Micromechanism of crack propagation in brittle fracture, considering kinematics for steady state crack in plane strain and energy dissipation
10 p1796 A69-23070

Brittle fracture at high temperatures in titanium alloys using scanning electron beam microanalysis, noting reaction diffusion with atmosphere and grain boundaries destruction
10 p1713 A69-23823

Temperature effect on tensile brittle fracture stress of polycrystalline tungsten
12 p2116 A69-27135

Continuum mechanics for brittle fracture analysis in metal structures, discussing plastic limit loads
13 p2275 A69-27228

Temperature effects on mechanical properties and fracture behavior of lamellar Ni-nickel titanide intermetallic eutectic alloy showing dependence on intermetallic constituent
13 p2277 A69-27406

Electron microscope fractographic studies to determine service failure causes, detecting grinding and quench cracks, hydrogen flakes and embrittlement fractures, etc
13 p2269 A69-28181

Materials and structural failures under short time compressive loadings, showing structural response to tensile stresses produced by rarefaction waves
15 p2639 A69-30364

Collection of papers on fracture, Volume 6, Fracture of metals
17 p2988 A69-33550

Laser technology and effects on materials fracture
17 p2989 A69-33557

Materials fracture electrically induced including arc and spark discharges, dielectric breakdown, electrolysis, etc
17 p2989 A69-33558

Papers on fracture, Volume 5, Fracture design of structures
17 p3060 A69-33559

Glass encased electronic components with conformal coatings, considering glass breakage at low temperature
19 p3281 A69-35547

Microbial contamination release from impact-fractured solids, examining bacterial spores growth in fractured methyl methacrylate plastic for application to space exploration
20 p3475 A69-37614

Stress rupture parameters for refractory metals and alloys from Larson-Miller, Dorn and Manson-Haferd constants, noting optimization procedure
[ASM PAPER D8-3.4] 20 p3564 A69-38135

Polymer films damage due to supersonic plasma jets, comparing fracture relief of oriented and unoriented polymers
21 p3752 A69-39081

Damping effects of vibration on materials and parts to estimate fatigue life, considering periodic and non-periodic stress vs time relationships
22 p4041 A69-40167

Structural analysis and statistical fracture approach to design and testing for polycrystalline ceramic materials, including combined stress testing and load redistribution models
24 p4333 A69-43339

FRACTURING

EPR investigation of free radicals formed during mechanical fracture and gamma irradiation, discussing recombination rate and reaction rate with oxygen
03 p0434 A69-13871

Snap through in thin shells with initial irregularities during creep, determining critical time to failure by analyzing undisturbed buckling process
21 p3838 A69-39188

FRAGMENTATION

Frequency occurrence of small particles in meteor showers, discussing fragmentation and cosmic erosion as primary effects in small particle development
01 p0154 A69-10872

Supercooled water drop frozen and observed to undergo explosive shattering and ejection of ice splinters
02 p0275 A69-12693

Electron impact induced fragmentation of ring D in steroids involving loss of carbon atoms analyzed by mass spectrometry
07 p1069 A69-19497

Fragmentation behavior of small thin walled metal cylinders during explosions as function of expansion velocity and material parameters
09 p1611 A69-21352

High velocity gas stream induced shattering of liquid drops, disintegration rate and breakup time
[AIAA PAPER 68-83] 09 p1482 A69-21947

Mass spectral fragmentation of substituted aliphatic glycols and hydroxylated carbon-carbon bond
09 p1448 A69-22551

Statistical analysis of photometric curves for meteors undergoing fragmentation at onset of vaporization
12 p2154 A69-25819

Freezing of water droplets in thermal equilibrium with gas mixtures, considering droplet shattering and gas volume
12 p2126 A69-26018

Mass spectra peaks of N-Acyl-2-indolinols fragmentation processes upon electron impact, noting compounds predominance in open chain tautomer gas phase
15 p2561 A69-30407

Hybrid propulsion chemical and technical problems, discussing solid fuel fragmentation and defining typical combustion modes
17 p3021 A69-33358

Meteor dynamical and photometrical analyses compared quantitatively, determining mass loss value from fragmentation model
17 p3045 A69-34223

Ion cyclotron double resonance technique to identify collision-induced ion fragmentation pathways illustrated with p-chloroethylbenzene
19 p3265 A69-36292

Data on mass distribution of terrestrial fragmented rocks to interpret lunar rock samples, noting origin of asteroids and meteorites
20 p3613 A69-38250

Solar radiation pressure windmill effect in rotational bursting and elimination from solar system of small magnetic celestial bodies
21 p3814 A69-39584

FRAGMENTS

Explosives and propellants sensitivity to fragment impact, establishing threshold detonation velocity
04 p0645 A69-14473

Fragments and markings produced on aircraft aluminum by explosion as means of detecting sabotage in crashes
06 p0868 A69-17833

Nonmesonic to mesonic decay ratio estimated for delta hydrogen hyperfragments
12 p2133 A69-26298

FRAME PHOTOGRAPHY

Electronically controlled spark gap system for HF optical frame separation based on Cranz-Schardin principle
05 p0763 A69-15985

Nanosecond electron-optical image converter multiframe camera designed for reducing frame exposure time
12 p2083 A69-26141

Multiframe image converter registration of space-time ruby laser spot structure changes in Q switched regime prior to giant pulse formation
12 p2083 A69-26142

Rotating mirror framing camera with continuous access at f/18 aperture, discussing image transfer system, frame rate and capacity, etc
12 p2085 A69-26157

High speed continuous access framing camera design noting velocity doubler, parallax free aperture stop and polaroid film capability
12 p2085 A69-26158

Multiple lens high speed camera with mechanical shutter for investigating AC arc in circuit breaker during zero current, noting framing rate and capacity
12 p2085 A69-26159

Selective stroboscope with explosive bright light source and microsecond pulse duration for short flash period over large area, noting single frame separation method
12 p2086 A69-26162

Shadow and schlieren photography, interferometry and quantitative data treatment obtainable by high speed multiframe photographic arrangement, using laser beam
12 p2086 A69-26165

Ultrahigh speed multiple framing photography system using sequentially modulated ruby laser and smear type camera applied to dynamic photoelasticity
12 p2086 A69-26166

FRAMES

NT AIRFRAMES

NT UNDERCARRIAGES

Amplitudes of forced bending vibrations of frames with superfluous elastohysteretic couplings by dynamic compliances method
11 p1986 A69-25333

Optimal design of rectangular frames for stability
13 p2358 A69-27209

Stress distribution in variable rigidity reinforcing frame of circular cylindrical shell using strain energy method
17 p3055 A69-33131

Thin walled rods for girder and frame systems designed by matrix method, solving differential equations for tension, compression, bending and torsion
23 p4230 A69-42005

Metal space frame radome design, considering electromagnetic performance, structural integrity, cost, membrane structures stability, etc
23 p4231 A69-42139

Nonlinear formulation for rigid jointed space frame comprised of prismatic linear elastic members, using Newton-Raphson and successive substitution methods
23 p4232 A69-42142

Space frame radome model elastic buckling tests for load deflection and maximum load predictions, considering individual beam failure and complex instability
23 p4232 A69-42143

FRAMING CAMERAS

Photoelectronic high speed image intensifier framing camera, showing single shot synchronized photography of electric spark in air
12 p2082 A69-26137

Multiple frame camera with image compensation as ballistic phototheodolite
12 p2084 A69-26153

Rotating mirror turbine with air cushion floating shaft for use in streak and framing cameras, noting framing rate
12 p2085 A69-26156

Rotating mirror framing camera with continuous access at f/18 aperture, discussing image transfer system, frame rate and capacity, etc
12 p2085 A69-26157

Framing device capable of producing four pictures within 5 nsec, using Q switch laser for light source
12 p2086 A69-26168

Ultrahigh speed cinematographic materials, discussing mirror turbines, streak and synchronized framing cameras
12 p2090 A69-26197

FRANCE

Preparation of refractory alloys in powders, fibers and sintered billets by thermochemical method
[ONERA-TP-636] 02 p0251 A69-11625

Collection of papers on French space effort covering space sciences and applications, vehicles and boosters, launch sites, tracking, international cooperation, etc
02 p0315 A69-11901

Satellites use in French space meteorology, discussing evolution, achievements, Eole project, etc
02 p0275 A69-11911

French geodetic work with aid of artificial satellites, describing equipment, mounting, observation technique and laser telemetry experiments
02 p0228 A69-11913

French/LRBA, ONERA and Sud-Aviation/ sounding rocket design emphasizing meteorological rockets and standard equipment
02 p0333 A69-11916

French air transport and airports covering aviation enterprises, air traffic density, airport activities, traffic flow, etc
04 p0689 A69-15479

French geodetic satellites tracking operations, on-board equipment and ground stations
[UN PAPER 68-95835] 06 p1013 A69-17065

Dynamic stability tests of tilt winged V/STOL aircraft model in ultralow speed range, discussing apparatus for stability derivatives
06 p0866 A69-17091

French air cushion vehicle technology for water and land, outlining principles of lift, propulsion and control and specifications of several craft
08 p1254 A69-20198

Laser control of French rocket head guidance system, discussing gyroscopic master, stellar or solar detectors, etc
09 p1518 A69-22162

French space program report to COSPAR covering orbiting satellites, rocket launchings, cosmic rays, space biology, geodesy, meteorology, etc
15 p2725 A69-31473

French space research center in Toulouse, discussing organization and activities involving satellites, rocket probes, balloons and environmental tests
16 p2765 A69-31758

French helicopter industry projected development for existing types, production models or final development and long range design programs
19 p3248 A69-36848

European cooperation in aircraft industry and application to Anglo-French helicopter program
19 p3456 A69-36849

In-flight medical disorders sustained by crew members of various aircraft in French Air Force correlated with aircraft accidents, flight experience and age
24 p4277 A69-43383

FRANCK-CONDON PRINCIPLE

Franck-Condon factors in radiative, excitation and ionization molecular transitions of oxygen, carbon monoxide, nitric oxide, etc
05 p0795 A69-15664

Franck-Condon factors for high rotational levels of nitrogen calculated in Morse potential approximation for application to plasma diagnostics
07 p1185 A69-19169

Franck-Condon factors for band systems of molecular hydrogen, computing wave functions for vibrational levels using potential energy function, Part I
15 p2656 A69-31156

Franck-Condon factors for band systems of molecular hydrogen, computing wave functions for vibrational levels using potential energy function, Part II
15 p2656 A69-31157

Franck-Condon factors for band systems of molecular hydrogen, computing wave functions for each electronic state by numerical solutions of radial Schroedinger equation
21 p3774 A69-38758

FRAUNHOFER LINES

Time compression system with ultrasonic diffraction cell allows coherent light optical spectrum analyzer to function at audiofrequencies
01 p0035 A69-11283

Fraunhofer lines hyperfine structure effect on solar abundances of V, Mn, Co, Cu and Ba, calculating equivalent line widths by ALGOL program
02 p0311 A69-11458

Fraunhofer lines in solar spectrum in 2950-8770 A wavelength region, noting 8000 additional unidentified lines
03 p0507 A69-13170

Submicron particles spatial location in three dimensional volume detected by Fraunhofer holography
04 p0596 A69-14292

Inner corona Fraunhofer lines invisibility at solar eclipses, emphasizing uncertainty of photospheric absorption lines appearance as electron scattering
04 p0654 A69-14628

Photospheric network obtained by spectroheliograms, discussing Fraunhofer lines weakening, nonsunspot magnetic fields and Zeeman sensitivity
04 p0664 A69-15523

Micro and macroturbulent motions velocity in solar photosphere based on Fraunhofer lines analysis
05 p0823 A69-16014

Local solar magnetic fields longitudinal component correlation with central intensities in various Fraunhofer lines, noting chromospheric levels effect
07 p1219 A69-19285

Central Fraunhofer line intensities near solar minimum compared to Soviet results for possible solar cycle variation
08 p1386 A69-20075

Fraunhofer line distortion on scattering from zodiacal dust cloud for various particle density and size distributions, discussing Keplerian orbits
08 p1308 A69-20391

Solar photosphere abundances of various heavy elements from photoelectric spectrometer measurements of equivalent width of known Fraunhofer lines
08 p1390 A69-20393

Rotational Raman scattering in planetary atmospheres, analyzing spectra of deep solar Fraunhofer lines
09 p1601 A69-22207

Source functions of IR Fraunhofer lines obtained using solar disk equivalent width method, noting LTE role
14 p2528 A69-29961

Ca II forbidden lines in photospheric spectrum identified with weak Fraunhofer line by photoelectric spectrometer scans
14 p2528 A69-29962

Photoelectric photometric stellar spectroscopy for calculating metal abundance from Fraunhofer absorption lines, relating results to star age
17 p3043 A69-34140

Fraunhofer holography for measurement of three dimensional flowfield velocity components, investigating rectangular channel flow
19 p3305 A69-35729

Limb effect of solar Fraunhofer lines determined by telescope equipped with autocollimated type diffraction spectrograph
20 p3607 A69-38044

Solar Fraunhofer spectrum, observing Fe 5576 and 6678, K 7699 and Ni 5436, 6129, 5847 and 6130 A lines
20 p3615 A69-38297

Neutral titanium Fraunhofer lines 4534, 4562, 5210 and 5238 A, investigating profiles and asymmetries using spectrophotoelectrical methods
21 p3795 A69-38467

Sunspot penumbra model in hydrostatic equilibrium accounting for continuum and Fraunhofer lines observations
22 p4019 A69-40290

Sunspot spectra near solar limb for difference between Fraunhofer line continuum and line core formation levels, finding geometrical height scale and pressure equilibrium
22 p4019 A69-40292

FRAUNHOFER REGION
U FAR FIELDS

FREDHOLM EQUATIONS

Initial value method applied to Fredholm integral equation for radiative transfer, neutron transport and multiple scattering, verifying invariant imbedding method
01 p0103 A69-10002

Unstable Volterra integral equation reduced to finding solutions for Fredholm integral equation by restricting solutions to closed ball in Hilbert space
01 p0103 A69-10004

Three dimensional stress concentration around cylindrical hole in semiinfinite elastic body loaded at infinity, using Fredholm integral equation
01 p0172 A69-11332

Arbitrary phase shift vibrations of airfoil profiles in incompressible flow reduced to Fredholm equations, allowing for trailing vortices influence
02 p0190 A69-12574

Lift from unsteady flow past cascade of slender profiles with stagger angle reduced to solution of Fredholm integral equation
02 p0190 A69-12575

Linear differential system with boundary conditions, obtaining equivalent Fredholm integral equation and perturbation theorem
07 p1173 A69-18729

Fredholm equations from dual integral equations for studying penny shaped crack response to incident harmonic shear wave in elastic medium
07 p1233 A69-19175

Problems using Fredholm integral equations providing unique solution
08 p1418 A69-21004

Induced magnetic fields determination in linear DC MHD generators with ferromagnetic and nonmagnetic walls, using Fredholm equation
10 p1636 A69-23454

Satellite mounted radiometers for determining albedo variations, using Fredholm equation with allowance for instrument errors
10 p1689 A69-23969

Boundary value problems of thermoelasticity, discussing existence and uniqueness theorems, ellipticity, thermoelastopotentials, Liapunov-Tauber theorem, Fredholm theorems, etc
12 p2182 A69-26726

Equations of motion of compressible fluid with non-zero resistivity near thin foil, solving supersonic and subsonic flow by Fredholm integral equations
13 p2200 A69-28360

Temperature distribution in shadowed lunar craters formulated in Fredholm integral equations, showing constant temperature and correction for soil thermal inertia
17 p3033 A69-33291

Fredholm integral equation solution of circularly axisymmetric stress state for bodies of revolution
18 p3226 A69-35375

Variational principle for Fredholm integral equations applied to inclusion and indentation problems in elasticity
19 p3440 A69-36589

Satellite mounted radiometers for determining albedo variations, using Fredholm equation with allowance for instrument errors
21 p3717 A69-39655

Fredholm integral equation for source function of Greenhouse effect and finite atmospheres solved by computational algorithm
23 p4239 A69-41607

FREDHOLM OPERATORS
U OPERATORS [MATHEMATICS]

FREE ATMOSPHERE

Boundary layer effect on large scale atmospheric processes from analyzing two layer free atmosphere model, plotting weather forecast charts
02 p0273 A69-11435

Free atmospheric turbulence theory extended to include ionosphere, deriving equations for horizontal ionospheric wind together with turbulence coefficient
02 p0274 A69-11678

Horizontal wind velocity energy spectra, attributing free atmosphere meso and microscale turbulence to meso and micrometeorological processes
12 p2070 A69-26575

Soviet book on temperature regime of free atmosphere above Northern Hemisphere covering aerological data processing, statistical estimates, latitudinal and seasonal variations
13 p2294 A69-27934

Free atmospheric turbulence theory extended to include ionosphere, deriving equations for horizontal ionospheric wind and turbulence coefficient
13 p2295 A69-28709

Atmospheric motions equations in mesometeorology prognostic problems taking into account free atmosphere and boundary layer interactions
15 p2646 A69-30107

Lagrangian solution for air mass element trajectory in free atmosphere using vortex invariant, noting application to atmospheric transport of contamination
16 p2805 A69-31611

Soviet monograph on turbulence in free atmosphere covering measurement and statistical techniques, tropospheric and stratospheric disturbances, wind pulsations, effects on aircraft flights, etc
18 p3165 A69-34351

Turbulence energy spectra in free atmosphere with convective layer surmounted by inversion layer, noting power law followed by velocity components
19 p3362 A69-36406

Energy density distribution in power spectra of turbulence in long wave region in free atmosphere
24 p4346 A69-43155

FREE BOUNDARIES

Free surface in supercritical regime downstream of valve submerged in MHD flow, noting effects of horizontal and vertical magnetic induction fields
15 p2659 A69-30299

Nonlinear free surface effects in low gravity tank draining, finding domains of validity for linearized and nonlinear analyses
17 p2953 A69-33450

FREE CONVECTION

Schlieren method for studying rotating sphere heat transfer during natural convection
01 p0174 A69-10095

Free convection from partially uniformly heated and partially insulated vertical flat plate, discussing dimensionless velocity, temperature, heat flux and axial length parameters
01 p0175 A69-10331

Laminar natural convection of electrically conducting fluid under magnetic field, noting temperature profiles
01 p0134 A69-11407

Transverse pressure gradient and streamwise derivatives effect on free convection laminar heat transfer on isothermal vertical plate at low Prandtl numbers
01 p0177 A69-11409

Natural convection boundary layer stability on heated isothermal vertical plane wall, discussing Grashof number as laminar to turbulent flow transition criterion
02 p0188 A69-12038

Solute vertical stabilizing gradient inhibition of thermal convection of fluid layer under temperature gradient, discussing effects on two dimensional flows motion
03 p0532 A69-13012

Thermal convection in rotating fluid annulus, discussing suppression of frictional constraint on lateral boundary

03 p0460 A69-13339

Environmental temperature and water vapor increases associated with ascending thermals estimated by penetrative convection

03 p0460 A69-13340

Instability and disturbance amplification in external laminar natural convection boundary layer over vertical flat surface with uniform heat flux

03 p0533 A69-13951

Pressure induced variations in stability constant characterizing bubble structure in two phase boundary layer of several liquids during boiling with natural convection

03 p0534 A69-14149

Approximate method for finding solution of weak free convection in partially filled vessel in gravitational field

04 p0685 A69-14619

Free convective heat transfer in liquid filled spherical volume with constant thermal flux density at boundary

04 p0686 A69-14992

Natural convection heat transfer through enclosed horizontal layer of supercritical carbon dioxide, discussing flat plate configuration data

04 p0688 A69-15398

Stability of laminar natural convection boundary layer flow, discussing thermal capacity coupling between fluid and wall and Prandtl number

05 p0744 A69-15719

Free convective heat transfer of cylinder in rarefied gas yielding Nusselt number as function of Grashof, Prandtl and Knudsen numbers

05 p0846 A69-15904

Heat transfer through vertical plane layer for various Prandtl numbers, discussing velocity and temperature profiles and effects of aspect ratio, Grashof and Rayleigh numbers [ASME PAPER 68-WA/HT-4]

05 p0846 A69-16115

Counter rotating vertical vortices produced by corona discharge on heated flat plate under free convection conditions [ASME PAPER WA/HT-9]

05 p0846 A69-16117

Forced laminar flow convection in horizontal tube with variable viscosity and free convection effects [ASME PAPER 68-WA/HT-20]

05 p0847 A69-16123

Natural convection heat transfer for incipient vapor formation in liquid H and N and for nucleate boiling of liquid H [ASME PAPER 68-WA/PID-4]

05 p0848 A69-16165

Simultaneous natural and forced convection flow around wall, analyzing perturbations of hydrodynamic elements due to obstacle

06 p1030 A69-17095

Laminar natural convection in enclosed rectangular cavity, discussing temperature gradient effects

06 p1033 A69-17556

Modified schlieren interferometer for quantitative investigation of free convection boundary layer temperature profiles

07 p1130 A69-18263

Differential equations governing free convection boundary layer flow past isothermal semiinfinite vertical flat plate solved for large Prandtl numbers by matched asymptotic expansions

07 p1239 A69-18266

Convection in planetary interiors produced by combined thermal and nonthermal mechanisms, noting self gravitating homogeneous nonrotating compressible fluid spheres

07 p1214 A69-18613

Convection in conducting fluid filled cavities with variable wall temperature due to magnetic field, with results applicable to rheological systems

07 p1241 A69-18921

Heat convection coefficient for wires enclosed in cylindrical tubes filled with water or ethanol, showing dependence on inclination angle

07 p1242 A69-18926

Finite difference computations for calculating two dimensional natural convection, deriving requirements for numerical stability

07 p1242 A69-19397

Heat exchangers in cryogenic fluids in free and forced convection, discussing measurements in liquid H, D, Ne and N

08 p1420 A69-19914

Transient free convection laminar boundary layer equations for heat transfer from vertical semiinfinite flat plate

08 p1305 A69-20842

Unsteady free convection in incompressible viscous fluid having internal thermal source contained in bounded volume

09 p1621 A69-21792

Heat transfer coefficients for free convection from single horizontal cylinder to fluids computed from empirical correlation

09 p1625 A69-22693

Thermal convection in earth mantle with temperature and pressure dependent viscosity, considering mechanisms for fluid-like mantle

10 p1682 A69-23412

Thermal diffusion and free thermal convection in fluids by diffraction interferometer, using laser for light source

10 p1702 A69-23431

Horizontal surface heat transfer coefficient under simultaneous free and forced convection calculated as function of temperature head, air flow velocity and area

10 p1810 A69-24085

Free convection boundary layer flow past vertical flat plate analyzed for nonlinear wall temperature distributions using series solutions

11 p2002 A69-25243

MHD free convection from horizontal isothermal plate in vertical uniform magnetic field, considering boundary layer thickness

11 p1930 A69-25277

Oxygen effects in Type 316 stainless steel, Nb-Zr alloy liquid potassium system, discussing thermal convection and forced circulation loops and corrosion rates

12 p2112 A69-25943

RR Lyrae gap stellar model atmospheres including radiation spectra, temperature radiation and convection, etc

13 p2338 A69-27561

Planetary interior convection analysis extended to include variable viscosity, heat source distribution, thermal expansion and diffusivity, etc

13 p2344 A69-27646

Free convection heat transfer from heated inclined flat plate in air, studying effects of angular positions

13 p2375 A69-27794

Analytical model for free convection heat transfer from vertical plates with nonhorizontal leading edges, discussing flow field

13 p2379 A69-28342

Similar solution for free convective flow past vertical porous wall and unsteady flow past porous wall with dissipation term, using group transforms

15 p2592 A69-31010

Liquid fuel droplets combustion under free and forced convection noting combustion rate

15 p2719 A69-31174

Magnetic field effect on thermal convection onset in compressible polytropic atmosphere compared with results from thin layer approximation

16 p2855 A69-31658

Forced laminar flow convection in horizontal tube with variable viscosity and free convection effects [ASME PAPER 68-WA/HT-20]

17 p3068 A69-32902

Two term expansion for Nusselt number for laminar natural convection about isothermal horizontal cylinder in fluid with vanishingly small Prandtl number

17 p3068 A69-33014

Subsonic thermal convection or internal gravity waves from formal scale analysis of equations of motion in plane parallel atmosphere

17 p2960 A69-33155

Combined free and forced convection hydromagnetic flow and heat transfer of electrically conducting fluid subjected to temperature variations in vertical channel

19 p3380 A69-36304

Surface tension gradients caused thermocapillary convection solved for spherical fluid film under weightlessness conditions

19 p3452 A69-36392

Thermal convection in horizontal fluid layer heated from below, with zero shear boundaries above and below, noting critical Rayleigh number measured value

20 p3518 A69-38234

Heat and mass transfer coefficients in binary laminar boundary layer during natural convection obtained with integral equations and Karman-Pohlhausen method

21 p3848 A69-38633

Heat transfer coefficients, boundary layer thicknesses and temperature and velocity distributions in free convection boundary layer in closed axisymmetric volumes

21 p3848 A69-38634

Free convection boundary layer singular character at low Prandtl numbers, deriving expression for Nusselt-Grashof relation

21 p3849 A69-38772

Simultaneous equations for natural convection from horizontal cylinder at moderate Grashof numbers, using iteration digital computer method for boundary values

21 p3851 A69-38975

Velocity and temperature distribution curves in turbulent boundary layer formed by natural convection on isothermal vertical plate, using Prandtl and Nusselt numbers

21 p3852 A69-39430

Laminar free convection from horizontal infinite strip with downward facing thermally insulated vertical walls at edges, noting boundary layer thickness and flow pattern

21 p3853 A69-39672

Velocity and temperature profiles at Prandtl number values obtained for unsteady laminar free convection on infinite vertical plate with stepwise varying temperature

21 p3853 A69-39681

Free convection of capillary fluid at vertical plate, allowing for temperature dependence of viscosity coefficient

21 p3854 A69-39843

Natural convection in rectangular cavity with nonuniform lateral surfaces temperature, using finite difference scheme with numerical analysis

21 p3855 A69-39853

Dynamic processes in upper earth mantle, discussing thermal convection currents and stress propagation

22 p3937 A69-40184

Free convection from vertical surface using perturbation method

24 p4407 A69-42916

Rectangular fins arrangement on horizontal surfaces for optimum free convection heat transfer coefficient, considering fin weight, height and spacing effects [ASME PAPER 69-HT-44]

24 p4409 A69-43517

Laminar flow in horizontal circular tubes with uniform heat flux, analyzing combined free and forced convection effects on secondary flow

24 p4409 A69-43519

Transverse curvature effect on laminar free convection heat transfer from vertical isothermal cylinders [ASME PAPER 69-HT-G]

24 p4410 A69-43522

Heat transfer data for laminar, transition and turbulent natural convection boundary layers from water experiment on constant heat flux vertical plate [ASME PAPER 69-HT-D]

24 p4410 A69-43525

FREE ELECTRONS

Critical values of laser formed solid angle determined in plasma diagnostics of scattering spectrum density distribution

02 p0251 A69-12416

Radiative transfer equations solved for electron scattering stellar atmosphere, using transformation of integrodifferential transfer equations into singular integral equations

03 p0466 A69-13351

Free electron kinetic equation including inelastic electron-atom collisions derived for nonequilibrium low temperature plasma, showing interrelated electronic and atomic energy distribution

05 p0802 A69-15889

Highly ionized plasma acceleration by intrinsic radiation achieved by deep cooling of free electrons

07 p1195 A69-19595

Microwave absorption by free carriers in c domain barium titanate crystals inserted in waveguide during polarization reversal

08 p1374 A69-21189

Electron injection into ZnO from aqueous solutions of stable substances, correlating injection with oxidation potential of substance

10 p1651 A69-22940

Cold electron emitters and operational principles, discussing thin film tunnel emitter, Schottky barrier emitters, MgO type emitter, etc

11 p1846 A69-24597

Thermodynamic approach to equation of state of magnetized Fermi gas, deriving energy eigenvalues of free electron in magnetic field

11 p1961 A69-25107

Free electron density upper limits in plasma attributed to negative ion formation, noting effect on

ionization equilibrium calculations for stellar atmospheres

11 p1928 A69-25255

Free electron model for electron work functions and number density distributions and surface potentials in metals

14 p2504 A69-29009

Burstein-Moss effect observed in studying n-GaAs crystals electrical reflection spectra with large free carrier concentration at two temperatures and low energy levels

15 p2666 A69-30060

Secondary effects role in n-GaAs crystals electrical reflection spectra with low free carrier concentration at room temperature in external electric field

15 p2666 A69-30061

Free electron concentrations and dispersion in H I regions noting ionized interstellar gas components role

15 p2681 A69-30420

Microwave absorption by free carriers in c domain barium titanate crystals inserted in waveguide during polarization reversal

18 p3183 A69-35158

Electric fields and electron work functions, surface potentials and number density distributions in selected metals surfaces determined using free electron model

19 p3382 A69-36045

Free electrons influence on reflection coefficient of semiconductor in IR spectra, showing selective modulation with change in carrier concentration

20 p3583 A69-37610

Holographic interferometry for determining total free electrons in plasma produced by irradiating solid hydrogen foils with giant pulse ruby laser

24 p4314 A69-42980

FREE ENERGY

Stability of weakly inhomogeneous plasmas with free energy available for nonlinear resonant three wave interactions

01 p0133 A69-11212

Thermodynamic analysis of refractory compounds vapor transport conditions, illustrating integral free energy diagrams

03 p0453 A69-13619

Upper bound for free energy of nonlocal superconductor in magnetic field, using variational method and perturbation theory

03 p0491 A69-13971

Wagon rolling toward piston executing HF oscillations, discussing periodic solutions of equations of motion corresponding to piston phase at collision

04 p0630 A69-14893

Free energy of low density quantum plasmas derived statistically from exact two particle scattering phase shifts

05 p0799 A69-15629

Free energy in linear viscoelastic solids

06 p1022 A69-17241

Solar flares and plagues free energy origin in magnetic field dissipation

06 p0996 A69-17446

Rhenium effect on lattice solid solubility of oxygen in tungsten, calculating rhenium-oxygen cluster minimum binding free energy

08 p1329 A69-20007

Relative free energies of crystal zones of tungsten using field electron microscope, determining surface energy anisotropy from Wulff construction

08 p1330 A69-20139

Correlation between interfacial tension in binary and ternary systems and reciprocal solubility of bulk phases, assuming concentration as function of thickness

09 p1448 A69-21909

Lame problem for elastic isotropic medium having free energy dependent on medium deformation and deformation gradients, estimating minimum surface curvature

11 p1970 A69-24632

High temperature plasma quasi-classical pseudopotential, binary function and free energy derived, using displacement and collective variable methods

11 p1934 A69-25701

Isoperimetric plasma thermodynamics problems, including plasma free energy and relativistic plasma density fluctuations energy

12 p2138 A69-26603

Thermomechanical theory for nonreacting binary fluid mixtures, discussing free energy function, entropy flux vector, equations of motion, constraints, etc

12 p2191 A69-26927

Surface free energy of solid Mo measured by Udin zero-creep method at high temperatures, noting low value due to residual impurity adsorption

12 p2117 A69-27137

Dielectric polarization of barium titanate and barium strontium titanate in pulsed fields in paraelectric phase, analyzing coefficient B in free energy function and equilibrium state

22 p3996 A69-41165

FREE FALL

Gravitational force measurement on electrons and positrons in free fall through vertical metal tubes at low temperatures

01 p0125 A69-10979

Self balancing single degree of freedom free fall space environment simulator, discussing coincidence of mass and rotation centers

04 p0586 A69-15468

Free fall vehicle dynamics for wind tunnel measurements of research shapes used in computer simulation of vehicle trajectories

[AIAA PAPER 69-229] 06 p0864 A69-18130

Luminous spherical fog layer surrounding burning zirconium droplet during free fall through oxygen containing atmosphere, noting effect on mass and heat transfer processes

13 p2380 A69-28462

Laser ignited Zr droplet free fall combustion in oxygen, analyzing metal conservation and luminosity correlation assuming reflux action from fog layer

[WSCI PAPER 69-1] 16 p2830 A69-32342

Fluctuations evolution in density perturbations analyzed to obtain free fall and free expansion universe models, showing no difference between expanding and static Newtonian universes

18 p3203 A69-35347

Two body mechanical system operating within dynamics laws simulating backward and forward bending motions of falling cat

19 p3259 A69-36832

Fluid motion in free falling partially filled cylindrical vessel due to sudden vertical velocity change, considering free surface disturbances

21 p3692 A69-38684

FREE FLIGHT

Multichannel telemetering device for magnetically suspended or free flight wind tunnel models noting strain gage pickups, switching and auxiliary circuits

[ONERA-TP-643] 02 p0226 A69-11623

Free flight static, dynamic stability and drag data for 10 degree semiangle cone obtained at 8-16 Mach numbers

[AIAA PAPER 69-133] 06 p0862 A69-18050

Autorotation characteristics of various shapes in subsonic and hypersonic flows for mechanics of free flight reentry to earth impact

[AIAA PAPER 69-132] 06 p0863 A69-18062

Free flight sharp cone drag measurements in rarefied hypersonic flow

13 p2199 A69-28244

Dynamic plasticity of nonsymmetrical free flight collision impact of crystalline solids, using linear temperature dependent stress-strain function and finite amplitude wave expansion

21 p3840 A69-39298

Free flight telemetry base pressure measurements on slender cones and domed afterbodies in hypersonic laminar flow, using shock tunnel test facility

[AIAA PAPER 68-698] 24 p4249 A69-43675

FREE FLIGHT TEST APPARATUS

Free flight telemetered base pressure test data correlation for high Mach numbers, noting facilities and instrumentation

20 p3458 A69-37196

FREE FLOW

Hydromagnetic stability of free boundary layer between two uniform streams in presence of aligned uniform magnetic field at large Reynolds number

02 p0287 A69-11832

Gray radiation and conductive heat transfer in Oseen-like free mixing flow, computing temperature distribution by inversion integral

02 p0354 A69-12504

Turbulent free shear layers in isoenergetic flow, correlating theory and experiment

[ASME PAPER 68-FE-9] 05 p0748 A69-16077

Gaseous film cooling at various hot gas acceleration rates and free stream turbulence levels

06 p1033 A69-17557

Free stream turbulence influence on stagnation zone heating in arc heated hypersonic facilities, obtaining stagnation point heating rates

[AIAA PAPER 69-167] 06 p1039 A69-18198

Free turbulent mixing, emphasizing flowing gas mixtures with and without chemical reaction

[AIAA PAPER 69-31] 06 p0915 A69-18223

Stagnation point heat transfer sensitivity to free stream turbulence attributed to external vorticity, noting correlation with Prandtl number

09 p1622 A69-21905

Buoyancy effect on boundary layer flow over semi-infinite vertical plate heated to constant temperature in uniform free stream

11 p1874 A69-25352

Free transonic gas flow incident on symmetrical profile at angle of attack with given velocity at infinity calculated using difference scheme

11 p1820 A69-25469

Laminar temperature and velocity profiles near plane rectangular surface for free supersonic flow, solving partial differential equations for mass, momentum and energy conservation

13 p2309 A69-28025

Flow field instability over concave bodies in supersonic free stream computed by integration of gasdynamic equations, noting application to supersonic parachutes

[AIAA PAPER 68-946] 13 p2199 A69-28228

Extension of Helmholtz classical problem of flows with discontinuous surfaces, considering two sources and transverse plane

14 p2433 A69-29683

Transport properties interrelationship in turbulent pipe flow and free turbulence

15 p2591 A69-30792

One dimensional free expansion of collisionless plasma tested as function of thermal equilibrium and confinement, using Vlasov equations and computer

16 p2819 A69-31685

Shock tunnel facility generating short duration high velocity high density air flow with equilibrium chemical simulation of free stream flight conditions

[AIAA PAPER 68-17] 16 p2766 A69-32167

Free flow field from underexpanded rocket motor nozzle and impingement effects of pressure and heat transfer to flat plate

[AIAA PAPER 69-568] 16 p2842 A69-32693

Conducting fluid incompressible flow in entrance of MHD channel by momentum integral method, permitting edge stress existence at boundary layer free stream interface

[AIAA PAPER 69-724] 17 p2952 A69-33436

Free stream disturbances influence on hypersonic boundary layer transition Reynolds number in heated and unheated flows

[AIAA PAPER 69-704] 17 p2953 A69-33453

Turbulent kinetic energy equation for determining turbulent flow fields applied to free mixing problem of constant density streams

[AIAA PAPER 69-683] 17 p2956 A69-33492

Transport properties of free turbulent mixing of subsonic coaxial streams by introducing environmental distributions in integrals of momentum, energy and species continuity equations

[AIAA PAPER 69-681] 17 p2956 A69-33495

Nonequilibrium, real gas and nose bluntness effects on hypersonic slender body flows, analyzing similitudes, free stream temperature, velocity and relaxation

[AIAA PAPER 69-708] 17 p2894 A69-33501

Jet injection into free circular cross section cross wind using curvilinear dynamic model, assuming negligible Archimedean forces effect

18 p3124 A69-35149

Gas dynamics in transition regime between continuum motion at high gas density and free particle motion at low density limit

19 p3300 A69-36658

Fluid motion in free falling partially filled cylindrical vessel due to sudden vertical velocity change, considering free surface disturbances

21 p3692 A69-38684

Nonlinear incompressible potential flow with unbounded free surfaces, analyzing singularities in finite part of space

21 p3696 A69-39295

Reentry Vehicle Altitude-Velocity Sensor for continuously measuring hypersonic vehicles free stream density and velocity in atmosphere at low angle of attack

[AIAA PAPER 69-866] 21 p3725 A69-39392

Heat transfer from spheres in free finite width flow, determining heat transfer coefficient distribution as function of flow width and Reynolds number

21 p3855 A69-39849

Free stream dispersion without permeation using nonporous glass beads and solutes, examining flow rate, particle size distribution, solute diffusivity, etc

22 p3894 A69-39873

FREE JETS

- Free stream velocity in high enthalpy arc heated wind tunnel by measuring imposed temperature modulation apparent phase shift, describing circuit diagrams 22 p3926 A69-40444
- Supersonic free stream flow past finite conical body with subsonic surface gas injection 23 p4059 A69-41884
- Slot type jet interaction flow tests at free stream Mach 4 and 5, describing equipment, procedure and results 24 p4249 A69-43686
- Free convection flows about inclined infinite cylinders with isothermal surfaces 24 p4416 A69-43687

FREE JETS

- Viscous effects on impact pressure measurements in free jet low density gas flows at high Mach numbers 02 p0234 A69-12633
- Transonic flow around profile in blocked plane channel and in free jet, noting channel wall and jet edge effects on flow along profile 03 p0361 A69-13018
- Laminar two dimensional free jet outflow of incompressible nonNewtonian pseudoplastic fluid from orifice into mass of same fluid 04 p0586 A69-14406
- Turbulent free jet at miniature nozzle exit, analyzing wall attachment fluid amplifier and flow characteristics 05 p0746 A69-16012
- Heat transfer, temperature and velocity profiles in circular free jet can be described by heat conduction type equations 05 p0747 A69-16032
- Fluctuation velocity, apparent kinematic viscosity and turbulent shear stress in isothermal homogeneous free jets 06 p0909 A69-17169
- Stream function for plane free sonic gas jet flowing past profile 07 p1050 A69-18740
- Nongray radiation effects on compressible turbulent free jet mixing of nonsimilar gases, using stepwise spectral absorption coefficient and Beer law 08 p1253 A69-20844
- Closed form solution for boundary shape of underexpanded axisymmetric jet in still air 09 p1482 A69-21968
- Supersonic free jet with real gas effects and chemical reactions calculated by approximation 10 p1631 A69-22898
- Continuum flow boundary in freely expanding jet estimated from molecular mean free path and modulus of random motion mean velocity 10 p1679 A69-23425
- Attachment and separation of free jet from wall, discussing model equations for wall attachment fluid amplifier 14 p2428 A69-28877
- One dimensional approximation for free jet nozzle flow in perpendicular magnetic field, calculating velocity distributions 14 p2501 A69-29910
- Numerical analysis for spreading of free turbulent gas jets with arbitrary uneven initial distribution of momentum and heat and mass fluxes 15 p2590 A69-30157
- Monograph on static pressure and turbulence in free jets and jet flames covering radial velocity oscillations with and without chemical reactions, confined jets turbulence, etc 15 p2719 A69-31190
- Flow field of highly ionized arc heated supersonic free jet, using continuous flow test facility [AIAA PAPER 68-135] 16 p2772 A69-32153
- Combustion effects on mixing of axisymmetric supersonic and turbulent free jets to obtain species concentrations, pitot pressures and temperatures [AIAA PAPER 69-538] 16 p2843 A69-32705
- German monograph on turbulence in isothermal free jets and free jet flames covering local flow variations, Reynolds number effects, exchange processes, etc 17 p3068 A69-32991
- Fluidic pressure ratio computing device based on two free jets interaction principle, describing prototype system design and analysis, electronics and overall error 18 p3133 A69-34309
- Free jet shock wave structure penetrated by surrounding pure gas molecules 18 p3086 A69-34819
- Rarified gas dynamics of blunt and sharp-pointed slender bodies in supersonic stream and free jet sonic expansion into high vacuum 18 p3123 A69-34924

- Pure gas suction through free jet shock structure, analyzing aerodynamic effect of molecular separation 19 p3240 A69-36650
- Free jet boundary layer in mixing zone of hypersonic gas flow past body 20 p3513 A69-37094
- Low density free jet properties, discussing velocity distribution perpendicular to axis and correlation of all terminal parallel Mach numbers for monatomic gases 20 p3514 A69-37206
- Carbon dioxide free jet expanding from conical nozzle into low density atmosphere, using freeze up method 22 p4000 A69-40594
- Mixing spread of hydrogen plumes and air pollutants exhausted into open atmosphere, predicting subsonic free round jets air entrainment 24 p4300 A69-43257
- Reverse flow profiles in turbulent free jet mixing with streamwise pressure gradient 24 p4306 A69-43684

FREE MOLECULAR FLOW

- Monte Carlo direct simulation for treating rarefied supersonic flows about bodies in transitional regime between continuum and free molecular flow 02 p0189 A69-12523
- Closed form solution of convective heat transfer to yawed concave hemisphere in free molecule flow 02 p0354 A69-12529
- Gas parameters in collisionless region during discharge into vacuum, considering plane and axisymmetric cases and free molecular boundary region 02 p0234 A69-12583
- Time independent flow of highly rarefied neutral gas past finite cone at zero angle of attack with freestream, noting molecular distribution function 04 p0541 A69-14712
- Argon flow characteristics in converging nozzle in continuum, slip and free molecular regimes [ASME PAPER 68-WA/FE-9] 05 p0698 A69-16089
- Weakly ionized wakes study in free quasi-molecular regime of supersonic flow, using Langmuir probe in wind tunnels, discussing ion density distribution 06 p0966 A69-17639
- Transmission and reflection coefficients of cylindrical tubes moving in free molecular gas flow determined by Monte Carlo method 06 p0911 A69-17877
- Heat transfer to wedge in nearly free-molecular hypersonic flow of strongly rarefied gas 07 p1050 A69-18707
- Complex bodies aerodynamic characteristics in free molecular gas flow by applying Monte Carlo method 09 p1430 A69-21793
- Asymptotic theory for obtaining nearly free molecular flow solutions uniformly valid throughout flow field based on linearized Boltzmann equation 11 p1818 A69-25283
- Mass flow rates for nearly free molecular flow through two dimensional slit for several tank pressure ratios 11 p1874 A69-25357
- Argon flow characteristics in converging nozzle in continuum, slip and free molecular regimes [ASME PAPER 68-WA/FE-9] 14 p2390 A69-29445
- Effective heat transfer coefficient lambda for microscopic Fe particles traversing rarefied air, oxygen and Ar target gases 16 p2769 A69-31870
- Thermal accommodation coefficients determination, comparing techniques based on free molecule flow heat flux data 18 p3230 A69-35071
- Homogeneous deformations of space and Cauchy problem for homogeneous free molecular motions, considering velocity fields and accelerations 19 p3444 A69-36803
- Density field surrounding leaking circular hatch of spacecraft treated as free molecular flow from annulus, superposing far field of effusive orifice flow 21 p3695 A69-39035
- Aerodynamic characteristics of moving and rotating bodies of revolution in free molecular rarefied gas flow, assuming Maxwellian thermal velocity distribution and diffuse specular interaction 24 p4243 A69-42583
- Varying ratio between mean free path and spherical particle radius at 0-10 km, discussing free molecular flow effects in cloud physics 24 p4345 A69-43145

- Monte Carlo calculation of free molecular flow over concave spherical surface, considering partial diffuse reflection and imperfect energy accommodation 24 p4248 A69-43592
- Electron temperature and density of inviscid free molecular nozzle flow of shock tunnel measured with thin wire Langmuir probes 24 p4317 A69-43648
- Shear stress and free molecular drag for gas flow along concave cylindrical surface oriented at angle of attack, analyzing multiple surface collisions effect 24 p4249 A69-43660

FREE RADICALS

- Perhydroxyl radical electron spin resonance spectrum in solution of hydrogen peroxide and water at 77 K, noting g factor, hyperfine splitting and molecular structure 01 p0024 A69-10683
- Radio signals from hydroxyl radicals by maser action in early stars, noting emission magnitude and intensity spectrum dissimilarity at different frequencies 02 p0324 A69-12493
- Doublet electronic states of benzyl radical, discussing configuration-interaction calculations and transition predictions 03 p0472 A69-13321
- Free radicals produced in ribonuclease, lysozyme and trypsin during exposure in vacuum and various temperatures to electron and heavy ion irradiation 03 p0372 A69-13484
- Long lived radicals produced in crystalline ribonuclease and lysozyme by 120-Mev protons studied by ESR spectroscopy 03 p0372 A69-13485
- Trapped radical relationship to inactivation of trypsin exposed to UV by measuring radical concentration and inactivation degree 03 p0372 A69-13486
- EPR investigation of free radicals formed during mechanical fracture and gamma irradiation, discussing recombination rate and reaction rate with oxygen 03 p0434 A69-13871
- Photometric methods for determination of H atom and hydroxyl radical concentrations in hot gases in convergent-divergent nozzles, noting Li/LiOH lithium hydroxide absorption 09 p1496 A69-21952
- Equilibrium between H and OH radicals in turbulent H flames, noting component concentrations in H-O-N flames of different composition 11 p1999 A69-24487
- Kinetics of combustion promotion of hydrogen-hydrocarbon mixtures by active particles, free atoms and free radicals using differential equations 17 p3069 A69-33139
- Electric quadrupole coupling for N 14 in aminedissulfonate studied by observation of second order transitions in electron spin resonance spectra 18 p3178 A69-35474
- Electron spin resonance spectra of gamma irradiated single crystals of 9-methyladenine, analyzing H abstraction radical and temperature effects 19 p3264 A69-35974
- Free radicals destruction rates by gamma irradiation at 77 K measured as first order function of dosage, using electron spin resonance spectroscopy 19 p3265 A69-36376
- Temperature and concentration measurements of H radical in hydrogen flames 21 p3669 A69-38807
- Cometary nuclei composition as last samples of early solar system composition, discussing dirty snowball model and radical lifetime problem 22 p4013 A69-40097

FREE VIBRATION

- Simultaneous partial integro-differential equations governing natural vibrations of arbitrary cross section cylindrical tubes, suggesting Fourier series solution 01 p0164 A69-10065
- Spacecraft periodic motion near center of mass determined by point transformation combined with bifurcation theory, studying stability and parametric dependence 01 p0161 A69-10205
- Idealized delta wing free-free oscillations determination by deriving equations of motion for flexibility and rigidity and formulating boundary value problems 01 p0172 A69-11358
- Ultraspherical potential approximation in nonlinear symmetric free oscillations applied to systems with hardening and softening cubic nonlinearities 01 p0107 A69-11418
- Modal substitution method for free vibration analysis of large discrete undamped dynamic systems 02 p0338 A69-11747

- Spectral peaks for torsional oscillations of earth, estimating free periods from observations at six stations around earth
02 p0243 A69-12007
- Longitudinal stress pulse propagation in finite length free-free bar with variable cross section, noting stresses in projectile impacting plane target
04 p0671 A69-14412
- Natural vibrations of cylindrical panels analyzed on basis of Lamé parameters, shell equations and energy method
04 p0674 A69-14592
- Temperature distributions, thermal stresses and natural frequencies of radial vibrations in thin circular cylindrical shells
04 p0675 A69-14704
- Asymptotic solutions of linear difference equations, discussing applications to eigenvalue problems of free oscillations of model galaxies
04 p0623 A69-14946
- Frequencies and natural oscillation modes in sporting gliders, demonstrating horizontal oscillation induced aileron suspension brackets destruction
04 p0549 A69-15416
- Free vibration of thin laminated orthotropic cylindrical shells
06 p1020 A69-17145
- Natural frequencies and modes of skew membranes obtained by Rayleigh-Ritz method
06 p1021 A69-17146
- Ritz method for natural oscillations of ideal liquid in spherical vessel with various filling levels, considering vertical perturbing force
06 p0910 A69-17333
- Plate theories of linearly elastic materials under free undamped vibration, giving 500 references
[AIAA PAPER 69-24] 06 p1027 A69-18061
- Free vibrations of plates and beams of pyrolytic graphite type materials, analyzing transverse shear deformation and rotary inertia
[AIAA PAPER 69-55] 06 p1027 A69-18070
- Radial vibrations of thin cylindrical shells subjected to thermal loadings, discussing temperature distributions, thermal stresses and natural frequencies
[AIAA PAPER 69-59] 06 p1028 A69-18143
- Dynamic tests of mechanical properties of polyamide Tarlon X-A using free and resonant vibrations methods
09 p1528 A69-21496
- Free vibration frequencies and mode shapes for thin orthotropic oblate spheroidal shells, noting isotropic oblate spheroidal shell and isotropic spherical shell
09 p1613 A69-21719
- Surrounding fluid effects on free axisymmetric vibrations of thin elastic spherical shells, studying irrotational motions in compressible and incompressible ideal fluids
09 p1613 A69-21720
- Self gravitating incompressible fluid sphere free oscillations, deriving characteristic equations for arbitrary viscosities
09 p1481 A69-21790
- Self excited aeroelastic galloping oscillations of long prismatic bodies subjected to wind velocity, noting effect of aerodynamically unstable cross sections
09 p1615 A69-21923
- Free transverse vibrations of rectangular flat plate simply supported along periphery and rigidly connected to interior columns
[ASCE PAPER 739] 09 p1616 A69-21928
- Structural damping coefficient for free vibrations of one degree freedom general systems motion
09 p1617 A69-22076
- Large amplitude free vibration of isosceles right angled triangular plate with simply supported edges
10 p1800 A69-23236
- Natural frequencies and associated composite loss factor for laminated plate with alternate elastic and viscoelastic layers, deriving partial differential equations
[ASME PAPER 69-VIBR-68] 10 p1805 A69-24158
- Free vibrations in axisymmetrically loaded orthotropic circular conical shells with longitudinal and circumferential stiffening based on linearized theory, considering shear deformation and inertia
11 p1969 A69-24327
- Transverse beam natural vibration frequency evaluation method from Timoshenko theory
11 p1970 A69-24581
- Numerical analysis of natural oscillations of three layer sandwich plates of rectangular planform, considering end conditions
11 p1976 A69-24773
- Free vibration modes of infinite uniform plate in linear coupled theory of thermoelasticity, considering heat transfer conditions
11 p1976 A69-24793
- Nonlinear free vibration of beams with clamped and supported ends subjected to axial load, considering symmetric and antisymmetric modes
11 p1983 A69-25024
- Energy dissipation in freely oscillating bodies under static stresses described by differential equation, assuming elliptical hysteresis loop
11 p1919 A69-25092
- Unforced periodically varying systems, developing approximate solutions with Floquet theory
11 p1909 A69-25289
- Free vibration frequencies of simply supported parallelogramic plates, noting skew angle splitting of degenerate frequencies and frequency crossing of modes
11 p1987 A69-25379
- Inplane and rotary inertia effects on free vibration frequencies of circular cylindrical shells eccentrically stiffened by orthogonal set of stringers and/or rings
11 p1992 A69-25520
- Free vibration of discretely stiffened cylindrical shells with arbitrary end conditions programmed for digital computer, considering flexure, extension, torsion and nonsymmetric stiffener cross section
11 p1992 A69-25521
- Free periods of oscillation of incompressible rotating fluid bounded by rigid concentric spheres, using Longuet-Higgins solution of Laplace tidal equation
11 p1876 A69-25558
- Magnetically selective microwave filters using magnetodynamic natural oscillations in premagnetized ferrite sphere at cavity center
11 p1855 A69-25626
- Zero Gaussian curvature rib reinforced shells free oscillations reduced to nonreinforced shell forced oscillations under cyclic loads
12 p2177 A69-25996
- Regulated pulse lasers under free oscillation for photographing distant objects by illumination with shortened light pulses
12 p2089 A69-26190
- Free vibration fundamental natural frequency of shallow shell or dished plate with simply supported square boundary
12 p2179 A69-26211
- Natural vibration modes of linearly tapered rectangular plates, approximating plate characteristic shapes with series of products of beam characteristic shapes
13 p2358 A69-27211
- Vibration modes in four lowest natural frequencies of clamped rectangular plates with linear thickness variation, using Ritz method
13 p2361 A69-27442
- Free and forced vibrations of elastic layer, using iteration procedure based on asymptotic integration of linear theory of elasticity dynamic equations
13 p2363 A69-28126
- Sine series solution for flexural vibration of rectangular isotropic plates applied to free vibration of orthotropic plates
13 p2363 A69-28128
- Free vibrations of laminated anisotropic rectangular plates with clamped edges analyzed by Rayleigh-Ritz energy method
13 p2371 A69-28673
- Spacecraft periodic motion near center of mass determined by point transformation combined with bifurcation theory, studying stability and parametric dependence
14 p2530 A69-28741
- Uncoupled field equations for free large amplitude axisymmetric transverse vibrations of spinning membrane disks
15 p2704 A69-30303
- Oscillations of freely supported cylindrical shell of arbitrary cross section with breaks along generatrix, determining eigenvalue of infinite matrix with normal determinant
15 p2707 A69-30581
- Laminar thin orthotropic cylindrical shells natural and forced oscillations and dynamic deflection coefficient
15 p2715 A69-31202
- Natural vibration of isotropic plates in temperature field with nonuniform distribution over plate
16 p2871 A69-31891
- Transverse free vibration of slender cantilever subjected to compressive follower force
16 p2871 A69-31899
- Calculation of natural twisting and bending vibrations of beam with characteristics varying along length
16 p2873 A69-32130
- Anisotropic conical shells free vibrations analyzed by Galerkin and operator-matrix methods, neglecting transverse shear deformation and rotatory inertia effects
16 p2874 A69-32165
- Free vibrations of thin truncated circular conical shell and reinforcing rings and stringers, determining resonant frequencies for stiffened and unstiffened configurations
17 p3051 A69-32955
- Free-free transverse vibration damping phenomena, calculating strain amplitude dependence of internal friction at various frequencies
17 p3051 A69-32961
- Planetary free vibrations, discussing models for earth, moon, Venus and Mars, rotation and ellipticity effects and measurement on seismometers, gravimeters and magnetometers
17 p3031 A69-33097
- Frequency and mode shapes of conical shell free oscillations related to shell parameters and boundary conditions
17 p3058 A69-33201
- Test stand for free oscillations frequencies and mode shapes of truncated conical shells of revolution with clamped edges and one free edge
17 p3058 A69-33202
- Transverse shear deformation and rotatory inertia effects on large amplitude lateral free vibrations of transversely isotropic plates
[ASME PAPER 69-APM-10] 18 p3213 A69-34386
- Supported shafts natural vibration frequencies determined by averaging shaft parameters, noting suitability in HF ranges
18 p3147 A69-34546
- Natural longitudinal oscillations of variable cross section straight rods, assessing errors due to use of finite difference schemes
18 p3217 A69-34581
- Nonlinear systems of differential equations to free oscillations about equilibrium, obtaining periodic solutions
18 p3172 A69-34591
- Free oscillations of rigidly clamped circular plate carrying concentrated masses, deriving frequency equation and value of lower roots
18 p3226 A69-35377
- Plane LF oscillations of eccentric cylinder under harmonic pressure applied to lateral surfaces, noting natural oscillations
18 p3226 A69-35380
- Natural oscillations and flutter of three layer cylindrical shell in supersonic gas flow analyzed by semimomentless theory, discussing boundary value problems, damping effects, etc
19 p3437 A69-36201
- Nonlinear free motion of conservative oscillator with one degree of freedom calculated by collocation method
19 p3438 A69-36308
- Free oscillation period of nonlinear oscillators with one degree of freedom, discussing approximation method
19 p3373 A69-36310
- Coupled dilatational and equivoluminal modes of free vibration for elastic prisms and polygonal plates, using Poisson ratio and wave path construction
19 p3444 A69-36801
- Free vibrational characteristics of thin walled circular cylindrical shells with layers of anisotropic elastic material laminated about middle surface
20 p3627 A69-37767
- Cold disk galactic models free short wavelength oscillations, obtaining asymptotic approximations for eigenfrequencies and eigenfunctions of bending and planar modes
20 p3611 A69-38151
- Natural oscillations of loaded strings, membranes and geometric bodies with distributed loads treated as material discontinuities
20 p3578 A69-38292
- Natural oscillations of end-hinged solid beam with variable parameters and concentrated masses, determining natural frequencies
21 p3833 A69-38575
- Natural oscillations of free surface liquid and elastic bottom of cylindrical cavity determined by integrodifferential equations based on liquid level
21 p3693 A69-38720

Free vibration of thin cylindrical shells with thickness discontinuity, considering natural frequencies and mode shapes dependence on thick/thin ratio
21 p3836 A69-38984

Curvilinear planform plates natural oscillations, assuming small elastic bending strain obeying Hookes law
22 p4038 A69-39912

Harmonic linearization for analyzing dry friction effect on gyroscopic stability with free play in mechanical couplings, showing effective damping of natural oscillations
23 p4163 A69-41554

Computer program for natural oscillations of plates and shells, deriving differential equations of motion for thin elastic shell by variational method
23 p4230 A69-42004

Rectangular waveguide with periodic array of infinitely thin metallic strips, studying intrinsic oscillations critical frequencies and amplitude spectrum
23 p4124 A69-42036

Time dependent natural oscillations of plane open resonators infinite periodic sequence, considering electromagnetic energy transfer into ambient medium
23 p4139 A69-42039

Density model for free oscillations of earth, noting dependence on core radius and S wave velocity at top and bottom of D layer
23 p4158 A69-42117

Asymmetric dynamic response to free and forced vibrations of thin membrane shells at given stress state due to previous loads
24 p4399 A69-42990

FREEDOM FIGHTER AIRCRAFT U F-5 AIRCRAFT

FREEZING NT ZONE MELTING

Microscopic time lapse movies in solid/liquid interface profile during melting and freezing of materials for spacecraft thermal control as reversible heat sink [AIAA PAPER 69-95]
06 p1038 A69-18126

Invertebrates resistance to explosive decompression and low end pressure, noting hypoxia and freezing as cause of death
07 p1059 A69-18537

Vacuum, radiation and freeze drying effects on survival rate of microorganisms, noting influence of protective materials on extent of damage
07 p1064 A69-18943

Structural and functional changes in cells as result of freezing of muscular tissue or suspension of erythrocytes
10 p1642 A69-23117

Freezing of water droplets in thermal equilibrium with gas mixtures, considering droplet shattering and gas volume
12 p2126 A69-26018

FREEZING POINTS U MELTING POINTS

FREIGHT U CARGO

FREIGHT COSTS

Air cargo traffic increase, discussing technical and economical prospects, use of intermodal containers and transportation automation tendency
01 p0008 A69-10030

Legal consequences of discrepancies between freight rates for airline tickets and bills of lading and actual invoices, discussing liability areas and regulated tariff
07 p1244 A69-19232

Handling and processing function in air freight transportation, discussing system design approaches, cargo terminals, materials handling systems and containerization
22 p4053 A69-40483

FRENCH GUIANA

French space center in Guiana, discussing geographic location advantages for payload, rocket launching, space rendezvous, etc
02 p0228 A69-11920

FRENCH SATELLITE NT DIADEME SATELLITE

French satellites structure, power and communications systems, stabilization and detector groups
02 p0333 A69-11917

D-2 satellite radiation dose based on upper atmosphere electron and proton distribution model, simulating electron bombardment and aging of materials and subsystems
11 p1949 A69-24869

FRENKEL DEFECTS

Poole-Frenkel model for internal field assisted thermal emission with compensation for relative densities of donor and acceptor sites
04 p0640 A69-14450

Approximate solution to differential equations describing primary radiation defects transformation into secondary defects in semiconductors
07 p1199 A69-18679

Frenkel defects in light irradiated p-type InSb single crystals at subthreshold radiation energies
13 p2318 A69-27885

Frenkel defects in light irradiated p-type InSb single crystals at subthreshold radiation energies
21 p3782 A69-39144

FREON

Halocarbon solvent for application of chlorosilane finish to heat cleaned glass fabric for reinforcement of plastic, noting relative humidity effect
08 p1341 A69-20513

Freons applications to radiation detector cooling, calculating specific volumes and compressibility factors for Freon 14
14 p2447 A69-29330

Toxic effects of Freon R FE 1301 on animals and human beings at different concentrations, assessing judgement, alertness and neuromuscular skill
18 p3098 A69-35061

Ti-6Al-4V alloy general and stress corrosion behavior in Freon environments, discussing fracture mechanics
18 p3150 A69-35411

Freon boiler designed for Rankine cycle heater fired on hydrocarbons with over 2000 F flame front temperature, considering radiant/convective heat transfer
23 p4068 A69-42239

FREQUENCIES

NT AUDIO FREQUENCIES

NT BEAT FREQUENCIES

NT BROADBAND

NT C BAND

NT CARRIER FREQUENCIES

NT CRITICAL FLICKER FUSION

NT CRITICAL FREQUENCIES

NT CYCLOTRON FREQUENCY

NT EXTREMELY HIGH FREQUENCIES

NT EXTREMELY LOW RADIO FREQUENCIES

NT FREQUENCY ASSIGNMENT

NT HIGH FREQUENCIES

NT INFRASONIC FREQUENCIES

NT IONIZATION FREQUENCIES

NT LOW FREQUENCIES

NT LOW FREQUENCY BANDS

NT MAXIMUM USABLE FREQUENCY

NT MICROWAVE FREQUENCIES

NT NYQUIST FREQUENCIES

NT PLASMA FREQUENCIES

NT RADIO FREQUENCIES

NT RESONANT FREQUENCIES

NT SUPERHIGH FREQUENCIES

NT SWEEP FREQUENCY

NT ULTRAHIGH FREQUENCIES

NT VERY HIGH FREQUENCIES

NT VERY LOW FREQUENCIES

Small signal characteristics and frequency response of diode-stabilized integrated linear circuits, discussing feedback, impedance, bias-diode, etc
01 p0041 A69-10204

Dynamic polarizability at imaginary frequencies, deriving upper and lower variational bounds with functionals containing trial functions
01 p0122 A69-10284

Second order nonlinear coefficient measurement for optical generation of millimeter wave difference frequencies in GaAs waveguide, using carbon dioxide laser
06 p0928 A69-17903

Frequency dependence of input impedance of voltage controlled bootstrap amplifier stages
07 p1090 A69-18294

Two and three frequency techniques for measuring group delay time of communication channels
07 p1076 A69-18557

Dielectric radome designs for operation at harmonically unrelated frequencies in C and K bands, discussing sandwich structure of A and B types
07 p1110 A69-19523

Ionospheric plasma density vertical profile by measuring reflected radio waves phase frequency characteristics
12 p2070 A69-26685

Pulse frequency integral estimate devices with integrating chemotron tetrodes for automatic systems metering applications
13 p2227 A69-27522

Reactive parameter scatter effect on amplitude frequency characteristics of regenerative reflection amplifiers based on equivalent circuit
13 p2235 A69-28515

Frequency time dispersion of storm sudden commencement micropulsations, noting polarization effects
14 p2440 A69-29129

FREQUENCY AMPLIFIERS U AMPLIFIERS

FREQUENCY ANALYZERS

Computer analysis of linear active nontime varying circuits by two graph topological approach based on Binet-Cauchy theorem
01 p0037 A69-11349

Filter uncertainty for time or frequency resolution in analysis of waveform, decomposing characteristic functions and determining least uncertain realizable filter
02 p0226 A69-12306

Simultaneous passage of useful and noise signals through differential frequency discriminator, determining spectrum by phase detection and detuned circuits
04 p0556 A69-14462

Transistorized frequency detector for sensing system load changes affects speeds of control valves of prime movers
06 p0896 A69-17478

Multichannel HF resolution spectral analyzer of pulses reflected from ionosphere applied to dependence of cross correlation coefficient on frequency separation
06 p0897 A69-17740

High speed photodetector frequency characteristics using multimode gas laser and Kerr cell
10 p1707 A69-24211

Simultaneous passage of useful and noise signals through differential frequency discriminator, determining spectrum by phase detection and detuned circuits
14 p2410 A69-28833

Ferrite frequency mixers used with heterodyne receiver, studying combination and cross noise rejection efficiency
15 p2574 A69-30129

Oscillators frequency instability theories emphasizing difference between concepts of frequency instability and spectral purity
22 p3900 A69-40930

Frequency response of control systems analyzed by digital computer using operational arrays, noting extensions to time response and root locus computation
22 p3909 A69-41255

FREQUENCY ASSIGNMENT

Signal interference criteria in considering frequency sharing between communication satellite systems and terrestrial radio services
09 p1449 A69-21273

Coordination distances and interference probabilities to control interference in frequency sharing between communication satellite systems and terrestrial radio services
09 p1450 A69-21280

Frequency bands allocations for space research and radio astronomy development, noting Inter Union Commission of Frequency Allocations recommendations
18 p3100 A69-34376

Satellite systems for air traffic control, navigation, communications and telemetry in view of regulations of frequency allocations
18 p3103 A69-35089

ITU space communication projects, discussing frequency registration, progress reports from member countries and committees, UN resolutions, communication satellites, etc
19 p3456 A69-36821

Frequency assignment methods for Intelsat 2 and 3 communication satellites [AIAA PAPER 68-454]
21 p3674 A69-39226

Three phase DC-AC inverter with low harmonic distortion, good efficiency and packaging capability, stabilizing frequency by crystal controlled clock oscillator
23 p4074 A69-42294

NASA program for radio spectrum utilization in aerospace communication systems
23 p4128 A69-42502

FREQUENCY BANDS U FREQUENCIES

FREQUENCY COMPRESSION DEMODULATORS

Synchronization errors effects on performance of compression-line demodulator, increasing mean-square error in measuring instantaneous frequency and locking probability
08 p1271 A69-19920

FREQUENCY CONTROL

NT AUTOMATIC FREQUENCY CONTROL

Frequency dependences of induced HF and high pressure discharge parameters, noting optimal frequency

cy range independence from particular gas and gas flow rate
03 p0481 A69-14144

Harmonic balance method to investigate phase locked oscillator stationary modes
04 p0559 A69-15138

Optical performance of coupled Fabry-Perot resonators with additional mirrors, determining frequency separation parameters due to third mirror
04 p0612 A69-15372

Frequency controlled time delay network for broadband phased array antenna steering
04 p0580 A69-15469

Gas laser frequency stabilization, considering electromechanical control systems
05 p0773 A69-16230

Frequency and polarization selection of neodymium glass laser oscillators by directing secondary radiation into laser cavity and duplicating spectral properties [IEEE PAPER P-3]
05 p0775 A69-16324

Selective resonators for laser emission spectral structure control, proposing dispersion power increase by inserting telescopic system
05 p0777 A69-16371

Helium-neon laser radiation of given spectral compositions, noting relation between spatial coherence and controlled number of frequencies
07 p1148 A69-18803

Multistage amplifier design with frequency compensation by eliminating stages in HF region
07 p1103 A69-18877

Carbon dioxide laser radiation frequency controlled by varying boron trichloride pressure in cell inserted in resonator
08 p1323 A69-19804

Center feed system for broadening frequency bandwidth in X-band edge slotted waveguide array antenna
08 p1286 A69-20836

Carbon dioxide laser with two gas absorption cells in cavity for emission wavelength control and HF pulsed mode of operation
08 p1327 A69-21088

Frequency selective mechanical filter and LCR circuits and applications, noting inductances in solid state and thin film technology
09 p1467 A69-22558

Singular integral method in approximation for synthesizing sequence of functions with spectrum of limited length
09 p1460 A69-22642

Frequency retuning characteristics of oscillator employing avalanche transit-time diode with complementary varactor subject to current or voltage variation
11 p1844 A69-24449

Voltage amplitude for combination frequency of small signal transistor amplifier calculated from feedback dependence
13 p2226 A69-27218

Frequency selector for gas laser, considering monochromatic emission and multimode oscillation
16 p2795 A69-31608

Optical performance of coupled Fabry-Perot resonators with additional mirrors, determining frequency separation parameters due to third mirror
16 p2797 A69-32119

Solid state CW laser frequency control during operation, discussing emission properties and laser applications
19 p3331 A69-35864

Solid state laser emission frequency control and retuning using dispersive resonators, analyzing interference methods for wavelength measurement
19 p3331 A69-35865

Frequency controlled unmodulated laser for long path interferometry, noting servoloop correction of frequency relative to Lamb dip
20 p3553 A69-37303

Resonant parametric oscillator stable and random phases, considering smooth frequency tuning and two quantum luminescence laser construction
20 p3554 A69-37723

Single mode He-Ne laser frequency stabilization by Zeeman effect
20 p3554 A69-37729

He-Ne laser emission tuning with thin absorbing metallic film situated near reflecting mirror
20 p3555 A69-37730

Eye elemental response to individual frequency jumps in oscillations of light, noting transient effect polarity
21 p3650 A69-38320

Helium-neon laser radiation of given spectral compositions, noting relation between spatial coherence and controlled number of frequencies
21 p3736 A69-38948

Spectral characteristics of Q switched single frequency ruby laser with tunable emission frequency in giant pulse mode
21 p3737 A69-38991

Reflex klystron with closed electron flux in crossed electric and magnetic fields permitting inertialess frequency returning
21 p3682 A69-39128

Periodic solutions of differential equation as example of locking in of frequencies, developing mapping procedure for perturbation methods application
22 p3979 A69-39894

FREQUENCY CONVERTERS
NT DOWN-CONVERTERS
NT PARAMETRIC FREQUENCY CONVERTERS

Graetz-connection frequency converter and three phase shunt-connection commutatorless motor, noting speed control performed by electronic circuit
01 p0012 A69-10064

Thermal and shot noise in pumped resistive diode for frequency conversion, analyzing equivalent circuits
03 p0406 A69-13828

Frequency conversion in sheath capacitance of glow discharge plasma contained within metallic coaxial cylinders
04 p0634 A69-14456

Single band millimeter wave amplitude modulator for phase meters with homodyne frequency conversion
04 p0577 A69-14850

Transistorized single sideband detector-converter operation in presence of large signal and heterodyne voltage levels, deriving equation for transmission coefficient
05 p0730 A69-16220

VHF to UHF conversion, noting modular UHF telemetry transmitter, miniature UHF special purpose transmitter, RF power amplifiers and telemetry receiver
05 p0732 A69-16305

Conversion of range telemetry systems /CORTS/ program noting installations and standardization
05 p0743 A69-16306

Tunable Raman upconverter as coherent light generator, using Q switched Nd-YAG laser beam [IEEE PAPER B-2]
05 p0774 A69-16309

Approximate functions for tunnel diode dynamic conductance in three voltage ranges and Fourier conductance terms for tunnel diode frequency converters
05 p0735 A69-16647

IR radiation at 10.6 micron from two point sources mixed with collimated ruby laser radiation in proustite, obtaining visible image
06 p0928 A69-17904

Wide range current-to-frequency converter with pulse frequency linear to input current
07 p1107 A69-19170

Microwave converters structural characteristics, calculating noise figure
08 p1285 A69-20594

Nonlinear capacitive parallel frequency converter circuit stability, using filtered circuit method
08 p1299 A69-21148

Autodyne frequency converters minimum noise and conversion factor calculation and optimal mode determination
09 p1469 A69-22631

Frequency conversion in microwave crystal mixer with EMF amplitude fluctuations in heterodyne
09 p1469 A69-22644

Visible imaging of IR objects by conversion of IR frequency to visible with sum-frequency generation within nonlinear dielectric medium
11 p1897 A69-25037

Microwave filters with lumped capacitances and coupled waveguides derived by frequency conversion from lumped filters circuits
11 p1855 A69-25628

Angle-to-code converter designed on basis of quantum magnetometers frequency sensors, transforming vector sum of bias magnetic fields into pulse repetition rates
12 p2016 A69-25963

Current to frequency converter for astronomical photometry, discussing oscillator drift, linearity characteristics and feedback pulse counting
12 p2040 A69-26479

Nd-doped glass pulsed laser with selected second harmonic radiation and KDP crystal frequency converter operating T 12Hz and 530 nm
12 p2108 A69-26594

FREQUENCY DISTRIBUTION

Multiband frequency conversion in filters or correcting circuits with four terminal networks, noting prototypes
13 p2235 A69-28519

Power conversion efficiency of frequency doubler using ideal nonlinear capacitance with arbitrary output phase angle
14 p2421 A69-29537

Homodyne frequency converter design using microwave oscillator with bitonal frequency modulation
14 p2451 A69-29801

CdS films vacuum deposited on optically polished single crystals used for converting microwave radio signals into hypersonic waves
15 p2575 A69-30236

Single band millimeter wave amplitude modulator for phase meters with homodyne frequency conversion
15 p2575 A69-30242

Varactors for frequency conversion circuits, discussing efficiency and output power
15 p2578 A69-30797

Negative resistance converter with single differential input operational amplifier, discussing input and output signal
15 p2580 A69-31091

IR radiation detection sensitivity emphasizing frequency up-conversion
17 p2969 A69-32839

Noise during frequency combination and conversion in mixer
17 p2931 A69-33911

He speech processor for aerospace applications, discussing He speech distortion nature
17 p2911 A69-34095

Solid state S band to VHF converter design to obtain optimum system noise for radio telemetry, discussing cost effectiveness and system performance
19 p3270 A69-36238

Solid state traveling wave optical quantum amplifier for conversion of modulated signal carrier frequency, applying to frequency conversion in laser communication links
21 p3739 A69-39540

X ray scintillation spectrometers temperature stabilizing circuit, describing amplitude-frequency conversion technique for position stability
21 p3727 A69-39856

Symmetrically regulated AC/DC converters power characteristics improved by switching in phase rectifiers twice during control cycle
24 p4254 A69-42570

FREQUENCY DISTRIBUTION

Generalized pair of space correlation and wave number spectrum functions applied to plasma electron density fluctuations and velocity fluctuations of background fluid
01 p0127 A69-10339

Minimum measurement time of dynamic transmission coefficient of system by FM method, calculating error
01 p0031 A69-10785

Particle size frequency distributions and lunar surface materials, showing impossibility of distinguishing between impact fragmentation of surface and pyroclastic rock deposition
02 p0325 A69-12567

Phonon states effective density in neodymium trichloride from vibronic spectra accompanying electronic transitions in trivalent Pr and Nd ions
03 p0473 A69-13907

Space-frequency correlation relationship of complex field fluctuations, amplitude and intensity to levels and phases of waves propagating in medium of random inhomogeneities
04 p0557 A69-14774

Frequency distribution of wind velocity as function of height, averaging time and thermal stratification
04 p0628 A69-15088

Blade natural frequency distribution around rotor and mechanical coupling between blades effects on flexing amplitudes under forced vibration [ASME PAPER 68-WA/GT-3]
05 p0837 A69-16139

Numerical determination of Doppler effect and reduced Doppler frequency difference for two coherent radio waves emitted from earth satellite
07 p1087 A69-19610

Frequency and radial velocity for various cepheid binaries, discussing hot companions detection through photometry
07 p1223 A69-19627

Propagation induced phase fluctuations reduction in widely separated oscillators, presenting microwave and optical methods
08 p1273 A69-20022

FREQUENCY DIVIDERS

Self damped pneumatic vibration isolators by modifying characteristics throughout frequency range, noting inertia block for improving HF behavior
08 p1301 A69-20398

Frequency distribution curves of spot groups according to area, confirming existence of stable stages in evolution of sunspots
08 p1379 A69-20612

One and two dimensional frequency distributions for probability estimates of climatological quantities, discussing temperature and interdiurnal changes
09 p1535 A69-21520

Frequency effects in laser with nonlinearly absorbing gas cell inserted in resonator, noting self stabilization of generation frequency
09 p1520 A69-22661

Minimum measurement time of dynamic transmission coefficient of system by FM method, calculating error
10 p1653 A69-23114

Geomagnetic field pulsations frequency changes in relation to geomagnetic and solar activity level
10 p1689 A69-23939

Sunspot lifetime, maximum area and cyclic variations recorded in photoheliographic results of Greenwich, discussing frequency distribution and mean
10 p1770 A69-24000

Analytic investigation of spectrum of electrical signals induced by spherical defects in ferroprobe sensors
10 p1675 A69-24072

Periodic solutions of quasi-linear self contained system with several degrees of freedom in case of commensurate frequencies, showing coordinates functions breakdown
11 p1920 A69-25749

Descriptive statistics in quality control dealing with variability and probability, discrete and continuous variables, frequency distributions and measures of central tendency and dispersion
12 p2100 A69-25846

Phase pulsations between normal frequencies and combination tones in CW gas laser output, analyzing observations by scanning interferometer
12 p2108 A69-26635

Statistical distribution of instantaneous frequency and power of signal associated with Doppler spectrum for exponentially distributed and determinate frequencies
12 p2032 A69-26863

Amplitude and frequency spectra for Ipc pulsations during geomagnetic storms
14 p2441 A69-29417

Frequency distribution and statistical characteristics of high level RF noise produced by high permeance electron beam of magnetron injection gun/MIG/
14 p2449 A69-29558

Sporadic E layer frequency characteristics dependence on reflected signal fading, showing fine structure influence and maximum value of mean electron concentration
14 p2442 A69-29733

Frequency distribution of sudden cosmic ray intensity increases, considering Forbush phenomenon
14 p2514 A69-29773

Temperature, velocity and density perturbation propagation as heat convection wave in viscoelastic thermally compressible heat conducting fluid, analyzing damping and frequency spectra
16 p2878 A69-31952

Electromagnetic wave propagation in plasmas and plasma instabilities due to oscillations, deriving equations for frequency distributions in various plasma compositions
16 p2823 A69-32243

Frequency distribution of star masses formed from solid H grains clouds, noting agreement with Salpeter initial mass function
16 p2862 A69-32372

Radiation diffusion in plane-parallel isothermal gas layer of two and three level atoms, considering stimulated emission and frequency redistribution
16 p2864 A69-32587

Solar image motion frequency spectra analysis via photoelectric equipment, showing influence on photographic pictures, spectra and modulation transfer functions for diffraction telescope
17 p3029 A69-33047

Spatial frequency distribution of linear array with randomly located elements from probabilistic analysis
17 p2929 A69-33873

Thin disk galactic models small oscillations, discussing frequency spectra and types of continua
18 p3196 A69-34551

Occurrence frequency distributions at microwave frequencies as function of peak intensity and directivities of solar bursts
18 p3187 A69-34969

Statistical characteristics of wind wave development in initial stage, obtaining distribution functions and frequency spectrum for various velocities and temperatures
18 p3167 A69-35341

Optical frequencies mixing based on photoelectric effect in metals and semiconductors, noting internal photoconductivity
19 p3332 A69-35871

Energy criteria inconsistency in evaluating frequency band changes attributed to simultaneous narrowing and broadening of different signal power bands
19 p3278 A69-36716

Frequency spectra of Pi2 geomagnetic field pulsations, noting effects of auroral zone location, configuration and structure
20 p3520 A69-37038

Qualitative interpolation formula for phonon frequency spectrum of mass disordered alloys three dimensional systems at high concentrations
20 p3583 A69-37279

F 2 critical frequency meridional cross sections latitude profiles based on global network ionospheric stations observations, confirming daytime Northern Hemisphere ionization maximum
20 p3526 A69-37661

Sideband structure of transmitted frequency spectrum exhibited by plasma wave features on topside ionograms, noting harmonic resonances
20 p3496 A69-37891

Current carrier concentration and magnetic field as factors influencing laser frequency resonance mixing in semiconductors with narrow forbidden bands
21 p3737 A69-38998

Statistical analysis of wind velocity measurements at floating buoy stations, presenting velocity power spectra for different frequency bands
21 p3758 A69-39111

Natural frequency equations for torsional vibration of fixed/fixed and fixed/simply supported uniform thin walled beams of open section based on energy method
22 p4040 A69-39935

Statistical analysis of chromospheric flares connections with sunspots, using frequency distributions of flares occurrences in sunspot groups
22 p4001 A69-39996

Magnetic fluctuations in various frequency ranges, associated with earth bow shock, detected with search coil magnetometer on OGO 3
22 p3938 A69-40501

Frequency discrimination in optical harmonic generators, discussing spectral width of wideband laser for supershort pulses and spectral device, using frequency dependence of mode locking direction
22 p3965 A69-40964

Time domain expression derived for frequency varying nonperiodic square wave in FDM and FM systems, using orthogonal functions to obtain frequency spectrum
24 p4281 A69-42623

Heart murmurs frequency analysis on patients to improve detection of aortic insufficiency in presence of mitral stenosis
24 p4279 A69-43800

FREQUENCY DIVIDERS

Optimal coherent reception of frequency diversity signals in multipath channels investigated for noise immunity
01 p0028 A69-10375

Coherent diversity reception of discrete signals in presence of concentrated noise investigated for use of optimal solution circuits for noise elimination
01 p0028 A69-10376

Parametric frequency divider using reverse biased hyperabrupt junction diodes to provide nonlinear capacitance
02 p0217 A69-12152

Correlation coefficient between frequency diversified signals amplitudes estimated by approximation for two beam short wave radio channels
04 p0560 A69-15401

Transistor-transistor logic switching circuits design for use in frequency dividers with variable division ratios in frequency processing systems
05 p0729 A69-15963

Response curves of frequency changer circuits /multipliers and dividers/ using reactive nonlinearity calculated as function of filter mismatch
07 p1114 A69-18279

Natural amplitude and phase fluctuations of originally monochromatic oscillations at output of regenerative frequency divider with thermal and shot noise
07 p1099 A69-18526

Impacting oscillatory devices for use as mechanical frequency dividers
07 p1136 A69-19458

Antenna switch for cascading and separating RF channels of high power wideband broadcasting systems
11 p1854 A69-25617

System switch, separating RF bands according to frequency and polarization for simultaneous transmission from parabolic horn antenna
11 p1854 A69-25618

FREQUENCY DIVISION MULTIPLEXING

Dynamic tracking filter analysis and capabilities as low threshold demodulator in frequency modulated frequency division multiplexing satellite system
01 p0034 A69-11140

Electronically steered and shaped beams for linear and ring phased array antennas by sampling element signals multiplexed into single channel
04 p0570 A69-14307

Frequency division multiplex telemetry technique with double sideband-quadrature carrier multiplexing system, discussing data signals, channels and distortion
07 p1084 A69-19131

Multiple access techniques in civil satellite communications systems, noting proposed digital time and frequency division methods
08 p1272 A69-19959

Preemphasis applications compared in active communication satellite systems for frequency division multiplex telephony and for TV
09 p1449 A69-21275

Precision trimmed RC active networks for high selectivity microelectronic filter fabrication for frequency division multiplex applications
09 p1466 A69-22452

One way measurement of dual inband frequency diversity improvement on HF ionospheric path with frequency division multiplexed FSK modulation
10 p1656 A69-23536

Optimum thermal and nonlinear noise intensities distributions in frequency division multiplex satellite communications systems, relating relay station power, frequency band and channels
14 p2412 A69-29426

Communication satellite frequency and time divisions multiple access problem, detailing microwave multiplexers design
14 p2417 A69-29688

Wideband multiplexers design with directional filters, discussing operational characteristics
15 p2581 A69-31524

Demand assigned frequency division multiple access-PCM system designed by COMSAT for satellite communication
16 p2749 A69-31602

Multiplexer network synthesis based on arbitrary divisibility of frequency range and obtainability of input impedance at all frequencies
21 p3681 A69-38530

Time domain expression derived for frequency varying nonperiodic square wave in FDM and FM systems, using orthogonal functions to obtain frequency spectrum
24 p4281 A69-42623

FREQUENCY MEASUREMENT

Methodological problems in studying ionosphere by phase measurements without taking into account geomagnetic field, noting value of main results
02 p0237 A69-11668

Mass effect on frequency tested during approach of pulsar to sun
02 p0323 A69-12298

Beam laser as frequency standard, considering wavelength and molecular transfer constraints imposed by technology limitations and frequency stability requirements
03 p0440 A69-13715

Errors of wavemeter employing open resonator with spherical mirrors
03 p0407 A69-13983

Approximation formulas of Appleton-Hartree equations for nighttime medium wave frequency absorption in E region of ionosphere, discussing electron density
07 p1122 A69-18295

Frequency and stability measurements in far IR laser region
07 p1146 A69-18482

Frequency response from linearized dynamic equations for viscous incompressible fluid flow in viscoelastic tubes, discussing transfer gain
08 p1304 A69-20704

Automatic level measuring system, consisting of decade control oscillator, digital level generator and selective level meter for 200Hz-2MHz range
09 p1501 A69-22577

LF measurements with positive or negative temperature coefficient resistors based on current-voltage characteristics
11 p1845 A69-24522

Transverse beam natural vibration frequency evaluation method from Timoshenko theory
11 p1970 A69-24581

Characteristic frequencies approximation formula for gas bubbles in liquids compared with exact solutions
11 p1915 A69-24582

Count rate meter for statistical frequency of signals applied to input of trigger with Poisson distribution of pulse intervals
11 p1884 A69-24734

Radio signal carrier frequency and arrival time measurements, deriving expressions for phase amplitude distortions effects
11 p1835 A69-24959

Frequency measurement of moving spacecraft RF carrier waves at low SNR by analog recording of noisy signal and HF trigger tone, noting data processing and signal fading rate
12 p2038 A69-26051

High sensitivity LF and HF frequency deviation meter with resonant RC amplifiers for frequency discrimination and filtering
12 p2038 A69-26337

Methodological problems in studying ionosphere by phase measurements without taking into account geomagnetic field, noting value of main results
13 p2257 A69-28699

Atmospheric multifrequency probing accuracy limitation imposed by irregularities based on scatter theory
14 p2449 A69-29535

Shields frequency ranges analysis to determine frequencies and parameters for electrostatic and magnetostatic modes transition to electromagnetic and microwave modes
15 p2562 A69-30120

Atomic and astronomical time and frequency measurement via Loran C and VLF/Omega phase tracking receivers
15 p2615 A69-31285

Laser harmonic frequency measurement application to absolute frequency determination of 84 micron heavy water laser
17 p2982 A69-33406

Beat frequency measurements in far IR due to harmonic mixing of klystrons, discussing noise role
17 p3006 A69-33674

Energy-frequency characteristics of vibrating machines obtained as spatial curves relating energy dissipation to system vibrations frequency
17 p3065 A69-33922

Microwave frequency measuring instruments design solutions for electric measurements reduction to length measurement
21 p3720 A69-38563

Resonance frequency behavior of waveguide cavity with evanescent air gap symmetrically loaded with dielectric
22 p3900 A69-40925

Thermonuclear explosion Operation Starfish effect on ionospheric state from recording in Central Kazakhstan, studying frequency characteristics
22 p3942 A69-41097

Empirical determination of equivalent frequency characteristics of nonlinear system in random noise, assessing measurement errors
24 p4289 A69-42950

FREQUENCY MODULATION
NT FEEDBACK FREQUENCY MODULATION
NT PULSE FREQUENCY MODULATION
NT PULSE FREQUENCY MODULATION
TELEMETRY

Frequency diversity for communication in fading environment, relating performance variance to between channel correlation variance
01 p0026 A69-10177

Injection locked oscillator FM receiver consisting of linear mixer and negative resistance oscillator in phase locked configuration, solving receiver output differential equation
01 p0042 A69-10247

Radar FM signal design with zigzag frequency variation, discussing relation between waveform characteristics and associated ambiguity function features
01 p0033 A69-11001

Electron distribution function of isotropic homogeneous Lorentzian plasma subjected to frequency modulated electric field calculated by successive approximation method
02 p0285 A69-11543

Superposition of discrete number of collinear amplitude modulated harmonic oscillations
02 p0281 A69-12252

AM and FM noise in mutually synchronized oscillators
02 p0220 A69-12449

Injection phase locking for synchronizing oscillators and reducing FM noise
02 p0220 A69-12450

Microwave measurements of AM and FM noise spectra with video frequency and RF coverage flexibility and high sensitivity
02 p0221 A69-12455

AM/PM noise conversion in solid state FM microwave signal sources, relating baseband noise power contribution to PM baseband noise power
02 p0212 A69-12462

Frequency locked loop /FLL/ to optimize loop filter and quantization of amplitude channel
03 p0390 A69-13202

Optimum demodulation of PAM-FM signal for case of minimum mean square error as performance criterion
03 p0392 A69-13250

MHD instability in current discharges in magnetic field stabilized by current frequency modulation higher than perturbation increment of plasma column
04 p0635 A69-14549

Digital nth order phase locked loop for FM demodulation
04 p0561 A69-15452

Frequency stabilization and noise suppression in argon FM laser
[IEEE PAPER P-7] 05 p0775 A69-16325

Nonlinear distortion of FM signal during passage through multipath medium, using analysis of linear passive four terminal network
05 p0721 A69-16531

Tube and transistor type quartz crystal FM oscillators circuitry and operating characteristics, discussing generation of three frequencies
05 p0732 A69-16532

Microwave generator of FM oscillations using two reflex klystrons and modified by wideband regenerative amplifier to minimize intrinsic AM
05 p0736 A69-16791

Statistical aspects of uncertainty function of linearly frequency modulated signals for nonstationary random process of phase errors
06 p0889 A69-17798

Incidental modulation effect on accuracy, signal loss and sensitivity of pseudorandom code systems
06 p0890 A69-17824

Q factors dependence of IMPATT diode oscillator FM noise, noting excess noise temperature correlation with diode current
06 p0899 A69-17826

External and internal modulation methods in lasers noting phase, amplitude and frequency modulation, birefringence, electrooptics and Stark and Zeeman effects
06 p0937 A69-18010

High power microwave oscillator /carpitron/ for pure or FM signal amplification, noting low output noise level
07 p1096 A69-18437

FM noise in two and three chamber klystron oscillators, discussing tubes to reduce noise and relative merits of active or passive stabilization circuits
07 p1096 A69-18438

Frequency modulated signal envelope passage through bandpass filter of inductively coupled circuits described by differential equation
07 p1100 A69-18555

AC fluidics for pressure pulse frequency control and monitoring in flow, discussing design and application to steam turbine speed control
07 p1058 A69-18938

OMEGA 4 100-k Hz ground station telemetry system for acquiring and processing outputs up to 23 FM and two TDM signals applied simultaneously from instrumentation recorder
07 p1105 A69-19103

Digital FM techniques, signal spectral properties, discrimination detection, phenomenological model, etc
07 p1081 A69-19105

Bit probability of PCM/FM for receiver with IF bandwidth equal to or greater than data rate, limiter-discriminator detection and postdetection filter
07 p1082 A69-19106

Smooth limiter effect on output of SNR for unbalanced and balanced FM discriminators, noting role of error function
07 p1106 A69-19127

Frequency feed forward open loop technique for lowering threshold and linearity of FM demodulators
07 p1106 A69-19128

Double sideband suppressed carrier FM telemetry system as airborne data recorder, discussing noise, environmental conditions, laboratory and flight tests
07 p1084 A69-19132

Frequency modulation of CW mm-wave IMPATT diode oscillator with wide band tunability and related harmonic generation effects
07 p1106 A69-19146

Error probability for discriminator detection of wide-band PCM/FM, considering IF bandwidth/bit duration product and low pass filtering effect
08 p1271 A69-19864

Resonances in plasma column monitored by frequency and current modulation methods
08 p1365 A69-20552

Frequency modulation methods and multiple access for communication satellite systems, considering bandwidth for space station transponder
09 p1449 A69-21274

Preemphasis applications compared in active communication satellite systems for frequency division multiplex telephony and for TV
09 p1449 A69-21275

Structure of quasi-linear and wideband satellite transponders, discussing possible improvements
09 p1609 A69-21619

Thermal effects on modulation sensitivity and inherent AM percentage as functions of modulation frequency in IMPATT oscillators
09 p1468 A69-22588

Noise rejection in multichannel telephone signal reception with FM and multiplexing, determining SNR dependence on SNR at receiver input
09 p1459 A69-22640

Envelope shock waves transitions between modulated wave amplitude and frequency in dispersive medium with relaxing nonlinearity
09 p1483 A69-22660

Magnetic tape recorder/reproducer for FM analog test data
10 p1691 A69-23233

Circuit for generation of square wave with frequency as sum or difference of two periodic signal frequencies, discussing SSB modulation
10 p1665 A69-24047

Injection locked oscillator FM demodulator, analyzing signal distortion, intermodulation noise, differential gain and differential phase
11 p1845 A69-24565

Signal to noise ratio in spectral composition of FM signals in magnetic recorder channels, taking into account parasitic FM and AM
11 p1834 A69-24612

Step-up mixer converting modulated IF signal to HF level by HF high power oscillator signal, discussing efficiency
11 p1854 A69-25615

Intermodulation noise distorting arbitrary frequency-modulated multicarrier microwave signal in satellite transponder, emphasizing nonlinear energy dissipation and AM-FM conversion
11 p1841 A69-25634

Permutation modulation for waveform transmission of quantized bandlimited signal, deriving signal to noise ratio
12 p2030 A69-26386

Monograph on discrete signals transmission by FM, considering secondary signal compression device and wire communication channels
12 p2033 A69-26866

Analytic expressions for predicted widths of AM and FM mode locked pulses in homogeneous lasers
13 p2270 A69-27191

Pseudorandom FM waveforms for simultaneous range and Doppler shift radar measurements
13 p2221 A69-27944

FM laser pulse formation time characteristics noting modulated resonator losses
13 p2272 A69-28114

Phase distortion, conversion of delay coefficients into channel noise and determination of waveguide delay coefficients for FM satellite communication systems
[IEEE PAPER 68-TP-382-COM] 13 p2222 A69-28153

FREQUENCY MULTIPLIERS

Noise stability of nonoptimal radar detection system for noise and FM signals, deriving expressions for optimal spectral width

13 p2222 A69-28508

Carrier disappearance method for FM telemetry transmitter characteristics measurements including frequency deviation sensitivity, linearity and frequency response

14 p2411 A69-28881

Oscillation spectrum with harmonic phase or frequency modulation, analyzing structural dependence on initial phase

14 p2412 A69-29427

Performance of oscillating limiter driven by noise corrupted FM signals covering frequency deviations, carrier to noise ratio, etc

14 p2413 A69-29497

FM measurements of angle distortion introduced by single pole bandpass filters compared to theoretical distortion

14 p2416 A69-29552

FM discriminator click widths probability distribution function, defining click widths duration from input noise considerations

14 p2422 A69-29553

Time domain method for hybrid simulation to compute interchannel distortions due to linear transducers in FM systems

14 p2417 A69-29556

Plasma diagnostics FM phase meter circuits tests, considering raster phase indicators, phase detectors and frequency integrators

14 p2497 A69-29797

Three channel microwave FM phase meter for studying plasma electron concentrations directional distribution without interferences between channels

14 p2497 A69-29799

FM homodyne phase meter with klystron oscillator for measuring plasma electron concentration, giving block diagrams of meter, detector and oscillator

14 p2451 A69-29800

Homodyne frequency converter design using microwave oscillator with bitonal frequency modulation

14 p2451 A69-29801

FM oscillations spectral width during modulation by finite sequences of multiple and nonmultiple frequencies

15 p2562 A69-30116

Residual phase term influence on compressed signal shape, analyzing linearly frequency modulated signal spectrum and sidelobe suppression in pulsed radar

15 p2564 A69-30143

Noise stability of FM receiver with automatic control of IF amplifier resonance frequency in presence of weak noise

15 p2564 A69-30144

Noise sensitivity of FM discriminator/limiter in digital binary communication system with FM/PCM-FM/

15 p2564 A69-30145

Frequency effects on Gunn oscillator modulation sensitivity, discussing microwave-frequency deviation and diode impedance

15 p2577 A69-30614

Scanning Fabry-Perot interferometer with ultralow modulation frequencies, obtaining inverse piezoelectric effect curves of ceramic element

15 p2611 A69-31107

Optimizing control system design using fluidic digital circuitry and FM type transducers

15 p2583 A69-31296

FM/FM telemetry system for high altitude rocket research, using independent subcarrier oscillator for each measurement transmitted with individual frequency modulation

16 p2750 A69-31853

Long distance FM radar signal relating to central station image processing, showing wideband sum signal especially suitable for transmission

16 p2750 A69-31862

Nonlinear distortion of FM signal during passage through multipath medium, using analysis of linear passive four terminal network

16 p2753 A69-32473

Maximum a posteriori estimate of modulation on carrier with noise, discussing iterative technique and FM test

17 p2994 A69-32917

FM detecting resolution using free running multimode uniphase Ar laser with Doppler broadened bandwidth

17 p2981 A69-33091

Broadband intracavity SHF modulation of He-Ne laser emission in 10 cm band, showing agreement with calculations

17 p2981 A69-33112

Short term frequency stability measured for Doppler radar and space tracking communication applications, reviewing FM theory for spectral purity relationship

18 p3100 A69-34277

Neumann-Lommel formula generalization for obtaining Bessel functions product sums illustrated with FM wave distortion calculation in multichannel system

18 p3101 A69-34625

Preemphasis analysis for FM system optimization to maintain constant output signal to noise ratio throughout baseband

18 p3103 A69-35088

Electro-optical crystals resonance modulator for coherent light beams and microwave frequencies, describing application to multichannel TV transmission system

19 p3266 A69-35763

Encoding and decoding in IR tracking system, analyzing chopping rotating FM reticle pattern

19 p3268 A69-36058

Phase locked loop design of desensitized monolithic integrated circuits for FM multiplex signal filtering and demodulation, describing external tuning

19 p3273 A69-36274

Computer program designing multiplex taper to minimize FM/FM telemetry system carrier threshold SNR, examining noise behavior of multiplex system stages for system performance

19 p3273 A69-36275

Baseband automatic gain control in AM/FM systems, determining time constant and steady state and tracking error

19 p3274 A69-36276

High index frequency modulated waveform spectrum analysis including upper bound on approximation error to avoid fallacy of Woodward theorem [IEEE PAPER 68-TP-74-COM]

19 p3276 A69-36485

FM radioaltimeter for Concorde aircraft, describing autocorrelation and automonitoring device, signal characteristics, reliability, etc

19 p3315 A69-36699

Analog telemetry signals generalizing frequency and pulse position modulations over coherent channels, noting added degrees of freedom function

20 p3492 A69-37713

FM data transmission distortion noise and error rate compared with AM and phase step modulation, noting role of bandwidth

20 p3496 A69-37905

Radio relay FM channel data transmission, evaluating cumulative thermal noise due to IF amplification at each station

21 p3672 A69-38653

Nonlinear electron conductivity of Lorentz plasma subjected to frequency modulated electric field

21 p3778 A69-39573

Real time FM-to-digital converter for measuring periods of demodulated FM/FM data, discussing systems design

22 p3903 A69-39923

Frequency modulating transducers advantages in process control by overcoming information loss due to series and shunt resistance, avoiding mains interference, easing commutation, etc

22 p3946 A69-40309

PCM role in FDM-FM short haul low density cable communications systems used in exchange area and tactical military systems

22 p3900 A69-40678

Nonlinearity effect on spectral shape and bandwidth in connection with frequency modulation by noise

22 p3900 A69-40923

Digital signal processing electronic device for linearizing signals from sensors with nonlinear frequency output by modifying time signal frequency

22 p3915 A69-40935

Discrete delay line measuring FM noise, discussing special case of narrow band cavity resonator method

23 p4137 A69-41606

Tradeoff between Doppler measurement capability and subcarrier demodulation in coherent digital communication system quantitatively presented for various SNR

23 p4122 A69-41771

Equal bandwidth multichannel FM/FM EEG telemetry system using subcarrier frequencies and HF modulation via varactor diodes

23 p4106 A69-41802

Time domain expression derived for frequency varying nonperiodic square wave in FDM and FM systems, using orthogonal functions to obtain frequency spectrum

24 p4281 A69-42623

FREQUENCY MULTIPLIERS

Efficiency curve for step recovery diode frequency multipliers, using analog computer simulation

02 p0215 A69-11947

Microwave frequency multipliers for radio relay systems based on VHF transistors and varactor diodes

02 p0216 A69-12097

Frequency mixing of organic dye solution laser radiation with ruby laser radiation, showing broader UV spectrum

04 p0610 A69-14424

Equivalent circuit of varactor with open p-n junction used as frequency multiplier

04 p0575 A69-14465

Correlation function and spectrum analysis of passage of random noise and signal through multistage frequency multiplier

04 p0557 A69-14777

Laser radiation influence on effectiveness of frequency doubling in KDP crystal

04 p0612 A69-15375

Response curves of frequency changer circuits/multipliers and dividers/ using reactive nonlinearity calculated as function of filter mismatch

07 p1114 A69-18279

Emission of Nd giant pulse laser with high repetition rate and peak power to generate second harmonic radiation in lithium niobate single crystals

07 p1144 A69-18469

Frequency doubling due to nonlinear response from Zeeman levels of ruby, discussing output and paramagnetic resonance

07 p1144 A69-18471

Two signal four quadrant multiplier design having subnanosecond response

07 p1103 A69-18879

Analog multiplier using differential transistor pairs, discussing FM/AM detection, suppressed carrier modulation and TV chroma demodulation

07 p1103 A69-18880

Frequency doubling of laser light with variable Q switched resonator

07 p1158 A69-19753

Phase synchronized oscillators in microwave frequency multipliers with improved SNR

09 p1464 A69-22113

Static ferromagnetic frequency doubler graphic design, considering magnetic field strength and flux density, energy cycle and energy transfer

10 p1663 A69-23566

Storage varactors and frequency dependent diode input power for multiplier cascades control, discussing series connections and limitations by thermal noise

11 p1841 A69-25607

Computer analysis on ideal step recovery diode frequency multipliers for optimum efficiencies

12 p2039 A69-26378

Power losses of varactor frequency multipliers with series connected circuits including open circuit tuned to second harmonic

12 p2043 A69-26888

Current harmonics in triode klystron for frequency multipliers, noting modulation voltage

13 p2234 A69-28510

Laser radiation influence on effectiveness of frequency doubling in KDP crystal

16 p2797 A69-32122

Quantum mechanical microwave frequency doubling in ruby, discussing output power variation with orientation

17 p3015 A69-33024

Computerized design parameters for realizable over-driven bimode varactor frequency doubler based on charge-voltage relationship at break point

20 p3505 A69-37299

Step recovery diode principle and operation mode as frequency multiplier explained by models

21 p3684 A69-39736

Push-pull pentode frequency multipliers with sinusoidal undistorted outputs, studying grid bias effects on operating characteristics

22 p3912 A69-40260

FREQUENCY RANGES

NT RADIO RANGE

Quasi-sinusoidal tunnel diode oscillator studied for frequency and amplitude of harmonic voltage components

01 p0038 A69-10070

Signal absorption in negative ionospheric ions effect on maximal frequency for space radio communication [UN PAPER 68-95272] 01 p0029 A69-10529

Dielectric constants of barium titanate single crystals as function of electric field intensity at different frequencies 01 p0139 A69-10889

Working equivalent circuits for fluidic transverse impact modulator in LF and IF range 02 p0196 A69-12082

Anisotropically conducting spiral cone current phase distribution applied to frequency independent antennas analysis, discussing spiral motion and field azimuthal dependence effects 03 p0408 A69-14133

Frequency dependences of induced HF and high pressure discharge parameters, noting optimal frequency range independence from particular gas and gas flow rate 03 p0481 A69-14144

Interatomic collisions effect on multimode He-Ne lasers output power and spectral composition 04 p0610 A69-14383

Multivibrator with two widely different zones of discontinuous oscillation 06 p0896 A69-17474

Radio sources detected in HF surveys not listed in 4C catalog 06 p1010 A69-17974

Symmetrical three layer A and B type sandwich reflectionless radomes design for multifrequency operation and insertion phase delay 07 p1110 A69-19522

Magnetic probes characteristics measurement for frequency range from 10 kc to 50 mc, using quenching resistors 08 p1313 A69-20120

Wullenweber arrays with extended frequency ranges, discussing design considerations and performance characteristics 08 p1288 A69-20962

Argon laser frequency spectrum instability caused by competing axial oscillations 08 p1327 A69-21023

Frequency fluctuations in mode coupled gas laser used to determine natural emission line width 09 p1516 A69-21670

Small signal HF conductivity of GaAs calculated for arbitrary frequency and DC field, considering subcritical Gunn devices 10 p1747 A69-23694

Ionospheric slopes and range frequency characteristics obtained from oblique incidence sounding of horizontally nonuniform ionosphere 10 p1686 A69-23914

He-Ne laser radiation frequency spectrum as function of transverse magnetic field determined by photoheterodyne method 11 p1894 A69-24622

Space and carrier frequency diversity determination for mutually interfering microwave radio equipments 11 p1835 A69-24952

Dielectric properties measurement of plastics for electrical insulation, stressing techniques for complex dielectric constants in various frequency ranges 13 p2285 A69-27984

Automatic device for impedances and complex transmission factors measurement at meter and decimeter wavelengths, noting reflection factor 13 p2235 A69-28520

Interatomic collisions effect on multimode He-Ne lasers output power and spectral composition 14 p2456 A69-28756

Microwave filter tailored for frequency response in L through S band regions for high range resolution radar receiver 14 p2423 A69-29759

Adapter between dielectrically loaded waveguides with different cut-off frequencies and sizes for pulse compression systems 14 p2423 A69-29760

Frequency diversity reception system for drift of small scale ionospheric inhomogeneities, noting circuit diagrams 14 p2452 A69-29875

Earth Resources Technology Satellites design for complete spectrum of frequencies 14 p2453 A69-29952

Efficient extinction in optically coupled GaAs injection lasers achieved by selecting quenching radiation frequency close to operating frequency 15 p2633 A69-30059

FM oscillations spectral width during modulation by finite sequences of multiple and nonmultiple frequencies 15 p2562 A69-30116

Shields frequency ranges analysis to determine frequencies and parameters for electrostatic and magnetostatic modes transition to electromagnetic and microwave modes 15 p2562 A69-30120

Pulsar NP 0532 period measurements at various frequencies, obtaining accuracy in timing data reduction by linking pulse arrivals over interval of months 15 p2680 A69-30232

Relative dielectric constant and permeability of inhomogeneously filled rectangular waveguide filling medium expanded into trigonometric series to calculate cut-off frequencies and field patterns 15 p2577 A69-30627

Solar flares and bursts correlation, taking into account sunspot type associated with flare and frequency range of bursts 16 p2850 A69-32213

Lumped element circuit producing directional coupling by electric and magnetic coupling of reactance quadrupoles, discussing insufficient coverage of calculated frequency range 16 p2763 A69-32581

Ionosonde electric circuit modified to permit radio wave absorption measurements over wide frequency range, calculating electron collision frequencies in F region 17 p2968 A69-33994

Bandwidth limitations for phase steered planar arrays in satellite applications, discussing weight reduction by modulo 2 pi beam steering 17 p2941 A69-34082

Geomagnetic field latitudinal variation effect on cut-off frequencies of proton whistlers, discussing LF electromagnetic wave propagation in cold multicomponent plasma 18 p3100 A69-34253

Supported shafts natural vibration frequencies determination by averaging shaft parameters, noting suitability in HF ranges 18 p3147 A69-34546

Dielectric constants of barium titanate single crystals as function of electric field intensity at different frequencies 18 p3182 A69-34720

Mechanical machine for fatigue testing flat samples of thin walled structures under tension and at various frequency ranges 18 p3118 A69-34833

Reflected signals detection with limited frequency spectrum and minimum velocity resolution considered, analyzing signal properties 18 p3104 A69-35265

Single loop directional stripline filters synthesis, including general expression for frequency characteristics based on wave matrices 19 p3284 A69-36570

Spectral density of outgoing radiation in 0.6-0.8 micron frequency range, noting reflected radiation and cloud fields correlation functions 19 p3366 A69-36672

OGO-F electric and electromagnetic fields measurement for ionosphere using dipole antenna, emphasizing broadband observation covering whistler mode waves 19 p3284 A69-36677

Holographic image range contouring produced by multifrequency emission from resonant output reflector in pulsed ruby laser cavity 20 p3540 A69-37733

Multiplexer network synthesis based on arbitrary divisibility of frequency range and obtainability of input impedance at all frequencies 21 p3681 A69-38530

Frequency domain and Liapunov instability criteria for attitude control system design of large booster, noting nonlinear feedback [AIAA PAPER 69-853] 21 p3687 A69-39381

Electromagnetic radiation measurements in shielded enclosures, describing equipment and effects of frequency 21 p3683 A69-39439

Sensors array to determine propagation wave vector velocity via high resolution frequency wavenumber spectrum analysis, emphasizing seismic applications 22 p3902 A69-41220

Sweep tuning gas laser and output power vs frequency characteristics, demonstrating tuning ability within entire Doppler bandwidth 23 p4174 A69-41635

Type 4 bursts maximum intensities at different frequencies compared for centimeter and decimeter waves 24 p4366 A69-42964

FREQUENCY RESPONSE

Modified admittance yielding Kubo admittance at nonzero frequencies, discussing transformation of correlations of Ising model 01 p0115 A69-10019

Amplifying channel processes of DC amplifier, discussing relations to couple channel with HF channels of operational operators and to synthesize amplifier frequency characteristics 01 p0053 A69-10802

TAF /time and frequency/ code written in FORTRAN language for computing steady state, frequency and time response from nonlinear simultaneous differential equations 04 p0565 A69-15341

Transfer function coefficients from frequency response data determined to obtain information about dynamic system characteristics 05 p0844 A69-16764

Spectral response of fast GaAs point-contact diode in mm and submillimeter wavelength ranges 06 p0893 A69-16939

Steady state frequency response of conical and cylindrical shells under lateral excitation 06 p1021 A69-17147

Validity of formula for oscillation frequency of nearly sinusoidal tunnel diode oscillator extended to operation in nonsinusoidal regime 08 p1279 A69-19924

Pseudoexact Chebyshev response curves for band-pass filter design, discussing phase response and time delay characteristics 08 p1283 A69-20227

Transfer function and frequency response of notch filters used to achieve notch filter dimensioning and design 08 p1284 A69-20379

Interference capability of noise of different frequency bandwidths, comparing weighted sound pressure to loudness level 08 p1276 A69-20857

Fabry-Perot fringes maxima in frequency response of laser interferometer, describing passive technique using eight wave plate 09 p1517 A69-21915

IR He-Ne laser frequency response determined with inherently swept frequency modulator based on rotating corner reflector 10 p1702 A69-23347

Frequency response dynamics of beam type periodic structures on elastic supports typical in flight vehicle designs [ASME PAPER 69-VIBR-17] 10 p1804 A69-24150

Modal coupling in thermally stressed plates, obtaining solution for frequencies and stiffness 11 p1990 A69-25509

Wideband inverter operational amplifier frequency response, open and closed loop transfer functions, beta, settling time and slew rate limits, discussing HF performance prediction 11 p1857 A69-25666

Book on industrial control engineering covering mathematics, semiconductor devices, feedback amplifier theory, closed loop systems, frequency response diagrams 12 p2051 A69-26244

Sufficient conditions for periodic motion existence of autonomous nonlinear feedback systems derived in terms of linear system frequency response 13 p2238 A69-27923

Two stage tunnel diode amplifier synthesis with gain stabilization circuit widening passband, discussing operating frequency and maximally flat amplitude frequency response 13 p2236 A69-28575

Wideband transistorized amplifier frequency response analysis by simplified approximations, subdividing operational frequency range 15 p2573 A69-30113

Frequency response of MIS capacitance beyond inversion voltage, discussing recombination rate and generation-recombination current in space charge region 15 p2565 A69-30179

FORTRAN program for calculation of magnitude and phase of digital filter transfer functions and power spectra of periodic waveforms 15 p2567 A69-30612

- Linear fluid amplifier with beam-deflection proportional active element, discussing optimum maximally flat frequency response 15 p2553 A69-31299
- Mechanical single degree of freedom system mean square response to AM random noise, considering frequency response, input excitation spectrum, etc [ASME PAPER 69-APM-25] 18 p3214 A69-34398
- Human ear frequency discrimination, discussing nonlinear functional modeling systems 18 p3097 A69-35440
- Thermoanemometer filament frequency response measured by generator of velocity pulsations compared with conventional methods 19 p3308 A69-35856
- Helicon wave dimensional resonance in n-InSb plasma waveguides at different wavelengths relative to wall thickness 19 p3383 A69-36479
- Acoustic and internal dampings in freely supported uniform beams of circular and rectangular section, showing frequency dependence and vacuum effect 20 p3620 A69-37062
- Ordinary coherence functions for computing frequency response in mechanical systems under random excitation 20 p3537 A69-37162
- Solar atmosphere line source function showing frequency dependence as consequence of spectral line disappearance at solar limb 20 p3588 A69-37540
- Nonmonochromatic laser emission frequency characteristics, studying second harmonic generation in nonlinear KDP crystal 20 p3554 A69-37727
- Monograph on frequency response characteristics of mechanical oscillator chains, calculating forced vibrations in linear systems 20 p3577 A69-37920
- Acoustic frequency response of unsteady turbulent flow in transmission lines, considering effects of small amplitude disturbances and heat transfer [ASME PAPER 69-FE-11] 20 p3516 A69-37988
- Fluidic pressure signal generator for use in fluidic system frequency response studies, considering design and performance [ASME PAPER 69-FLCS-40] 21 p3649 A69-38603
- Quadrupole network transfer matrix calculation from known octupole matrix, describing frequency response determination of coupled transmission lines 22 p3912 A69-40257
- Frequency response transient vibration testing of standing man, discussing data analysis procedure, test stand, and Welch correction for instrument dynamics 23 p4101 A69-41494
- Frequency response of thin film thermal detectors, discussing steady state harmonic response proportionality to film thickness and thermal conductivity 23 p4163 A69-41549
- Frequency and space averaging effect on variability and standard deviation of multimode media transmission responses, with application to reverberant media 23 p4115 A69-41576
- Aerodynamic frequency response calibration measurements of wind anemometer by input velocity and output drag values under unsteady flow conditions 24 p4315 A69-43262
- Dynamic pressure response of viscous compressible fluids in rigid tubes with dead ended volume termination, testing Ibrall theorem as function of Stokes number 24 p4301 A69-43287
- Small signal amplitude/frequency response or transfer gain of volume-terminated pneumatic lines with circular and rectangular cross sections 24 p4301 A69-43288
- ### FREQUENCY SCANNING
- Electronic scanning radar systems design, discussing beam types, bandwidth, tracking, target acquisition, etc 04 p0556 A69-14301
- CRT direction finder with linear scanning to determine statistical data for azimuthal distribution of atmospheric 04 p0600 A69-15104
- Pulsed ultrasonic flaw detectors resolving power enhancement by shunting semiconductor diodes across piezoelectric elements of scanning heads to shorten scan pulse duration 18 p3137 A69-35112
- Voltage variation frequency analysis for narrow-band sweep oscillators circuit design 20 p3486 A69-37010
- Semiconductor phase shifting for inertialess antenna scanning at microwave to millimeter wavelengths, describing diode construction with emphasis on solving insertion loss [ONERA-TP-712] 23 p4143 A69-42519
- ### FREQUENCY SHIFT
- Temperature dependent isomer shift and anharmonic binding of Sn 119 in niobium stannide, measuring Mossbauer recoil free fraction 01 p0134 A69-10009
- Emission and frequency shift angles of antiStokes radiation from trapped filaments of laser light in liquids 01 p0114 A69-10012
- Radar FM signal design with zigzag frequency variation, discussing relation between waveform characteristics and associated ambiguity function features 01 p0033 A69-11001
- Amplification process for VLF whistler mode radio signals observed in study of magnetosphere frequency shifting mechanism 01 p0077 A69-11241
- Pulsar frequency Doppler shift due to general relativistic corrections to optical path of photons in field of sun 02 p0315 A69-11836
- Pulsar CP 1133 pulse duration increase with decreasing RF from analysis of pulse shape data 02 p0318 A69-12093
- Frequency difference of traveling waves in accelerated rotating ring laser 02 p0257 A69-12417
- Dye solution laser wavelength shift and simultaneous oscillations at different wavelength ranges for pumping by another dye laser 02 p0258 A69-12620
- Laser oscillation frequency shift dependence on discharge current in 6328 A He-Ne laser 02 p0260 A69-12658
- Light wave propagation in gyrotropic crystals, examining laser frequency shift circularly polarized by modulating field 03 p0436 A69-13037
- High range resolution by pulse to pulse frequency shifting, utilizing existing low resolution equipment by adding signal processing capability to receiver 03 p0388 A69-13181
- Pumping light filtration conditions effect on transition frequency of rubidium atoms 04 p0611 A69-14779
- Taurus A 21 cm absorption line frequency decrease during optical path approach to sun, discussing gravitational and electromagnetic origin 04 p0661 A69-15148
- Frequency variation during oscillation pulse in avalanche transit time diodes, discussing related thermally dependent diode voltage rise 07 p1098 A69-18459
- Frequency transformation coefficients in titanium oxide-chromide traveling wave maser 07 p1146 A69-18481
- Helium-Ne laser beat frequencies between neighboring axial modes shifting linearly with inserted cavity loss 07 p1156 A69-19412
- Frequency transformation allowing comb-line filters of narrow and wide bandwidth, using resonance type filters with lumped elements 07 p1108 A69-19487
- Peak acoustic attenuation frequency shifts and peak power insertion losses in air flow ducts related to air specific weight changes 07 p1117 A69-19700
- Frequency shift and Q change of microwave cavity caused by lossy dielectrics and plasmas, examining perturbing volume requirements for conductor behavior 09 p1544 A69-21323
- Optical pulse compression experiment illustrating performance of electro-optical Doppler shifter as linearly time varying frequency shift production device 09 p1519 A69-22445
- Rubidium vapor laser pumping induced frequency shifts eliminated by detuning resonator without decreasing output power 09 p1520 A69-22636
- High density plasma in resonant cavity obtained by frequency shifting power source 10 p1727 A69-22955
- Optical modulation through Doppler frequency shift obtained by rotating radial diffraction grating [AOLR-69-1] 11 p1889 A69-25394
- High sensitivity LF and HF frequency deviation meter with resonant RC amplifiers for frequency discrimination and filtering 12 p2038 A69-26337
- Horizontal gradients below satellite orbit effect on reduced and minimum difference in Doppler frequency shifts of coherent radio waves from satellite in inhomogeneous ionosphere 13 p2219 A69-27701
- Frequency shifts of Lamb dip minimum in helium-neon laser, considering effects of discharge tube parameters and gas pressure 14 p2457 A69-28929
- Design and operation of two frequency phase meter for plasma diagnostics, using frequency modulation of microwave oscillator and waveguide bridge 14 p2451 A69-29798
- First order Doppler shift in ionosphere and horizontal gradients influence, discussing total electron content determination method made from geodetic satellites using two coherent frequencies 16 p2755 A69-32614
- Frequency agility techniques applied to target detection in noncoherent pulsed radar systems 17 p2917 A69-32919
- Repetitively Q switched ruby laser applied to frequency conversion, stimulated Raman scattering and vacuum UV generation 17 p2980 A69-33027
- Frequency hopping technique applied to multiple access air-to-air/ground communication for tactical fighters, noting additive recognition 17 p2931 A69-34117
- Light induced shift of Rb 87 vapor laser emission frequency during modulated optical pumping, discussing elimination by filter temperature and tuning 19 p3336 A69-36344
- Frequency shift dependence in transition of Rb 87 atoms on pulsed pumping intensity, discussing continuous and pulse indication and peak determination 19 p3336 A69-36345
- Frequency shifts observed in Alouette 2 cyclotron harmonic plasma resonances, noting antenna length and direction 20 p3496 A69-37892
- He-Ne laser oscillation frequency shifts with variations in DC discharge ascribed to changes in populations of He and Ne levels 20 p3556 A69-38124
- Hue shift and brightness enhancement of flickering light measured as function of illuminance, wavelength and target size 22 p3882 A69-40871
- Amplitrons use as broadband microwave amplifiers in high power radar systems with frequency agility, involving modified high vacuum tube modulator and modulator circuit 23 p4135 A69-41384
- Nonlinear theory of optically excited semiconductor laser for conditions of self excitation, steady state lasing amplitude and lasing frequency shift 23 p4174 A69-41733
- Rotating mirrors used for light signal Doppler frequency shifting 24 p4351 A69-43806
- ### FREQUENCY SHIFT KEYING
- Bit error probability for noncoherent binary FSK link involving Rician interfering signal 07 p1080 A69-19095
- Incoherent m-ary frequency shift keying (MFSK)/system analysis concerning automatic time synchronization 08 p1274 A69-20133
- Coherent FSK LF/VLF radio communication modem with large predetection bandwidth for improvement of reception in atmospheric noise 09 p1458 A69-22473
- Multichannel bit error probability for FSK and DPSK obtained for slow nonselective-fading multipath as function of multipath parameters and diversity order 10 p1656 A69-23533
- One way measurement of dual band frequency diversity improvement on HF ionospheric path with frequency division multiplexed FSK modulation 10 p1656 A69-23536
- Binary error investigation in noncoherent FSK communication link with nonselective fading, noting Doppler shift 14 p2414 A69-29498
- Compression capabilities of combined frequency and phase shift keying in radar and sonar pulse modulation using binary noise codes 15 p2568 A69-30628
- Split phase PCM code modulated carrier transmission characteristics determined for amplitude, phase and frequency shift keying, assuming random bit pattern and noncoherent modulation 21 p3676 A69-39451

FREQUENCY STABILITY

Combustion instabilities in solid propellant rocket engines, emphasizing acoustic types for longitudinal and tangential modes

02 p0303 A69-11531

Frequency domain stability criterion for nonlinear feedback system consisting of nonlinear amplifier, linear dynamical system and transducer with backlash

02 p0225 A69-11968

Off-axis circle criterion for frequency domain stability of feedback systems with single monotonic nonlinearity, noting relation to Popov criterion

02 p0225 A69-11969

Solid propellant combustion instability models describing combustion zone dynamics applied to acoustic and nonacoustic instability in LF regime [WSCI PAPER 67-13]

02 p0352 A69-12311

F 2 layer critical frequencies variation coefficients, analyzing variation and root-mean-square deviations in terms of geomagnetic latitude and Wolf number

03 p0422 A69-13514

Hydrogen maser oscillations with external gain, noting frequency stability

04 p0611 A69-14443

Self adaptive systems stability analyzed using filter and correlation methods, considering higher harmonics at rectifier and synchronous detectors output

04 p0582 A69-14796

Weak magnetic fields effect on molecular oscillator frequency taking into account Zeeman sublevels

05 p0727 A69-15643

Rb 87 vapor laser short term frequency stability independent of vapor concentration, noting use as frequency standard

05 p0770 A69-15656

Gas laser frequency stabilization, considering electromechanical control systems

05 p0773 A69-16230

Visible laser frequency stabilization scheme and simultaneous determination of frequency in terms of time standard

05 p0773 A69-16291

Frequency stabilization and noise suppression in argon FM laser [IEEE PAPER P-7]

05 p0775 A69-16325

Stabilization method for composite cavity single frequency laser, noting insensitivity to oscillation power level variations

05 p0776 A69-16333

Frequency and noise characteristics of gyrator circuits, analyzing Q factor, stability and oscillation sensitivity

05 p0735 A69-16621

Frequency domain stability criterion for pulse width modulated feedback

06 p0904 A69-17942

Stabilized frequency single mode ionized argon laser, discussing intensity of electric field in cavity and mode selector

07 p1145 A69-18475

Frequency and stability measurements in far IR laser region

07 p1146 A69-18482

Emission frequency stabilizing effect in concentric sapphire-coated ruby laser, noting frequency independence from temperature fluctuations and thermal stresses

07 p1147 A69-18543

Frequency-stable tunnel diode oscillator loaded with transmission line

07 p1104 A69-18890

Frequency reproducibility of He-Ne laser, using absorption dependence on frequency in strong field standing wave limit to provide stabilization [IEEE PAPER P-4]

07 p1153 A69-19073

Frequency discrimination characteristics of elliptically polarized dual polarization gas laser, discussing intensity crossover phenomenon and frequency stabilization application [IEEE PAPER P-5]

07 p1153 A69-19074

Upper and lower frequency stability bounds using hydrogen masers, studying signal power and relaxation rate as function of resonator effective field

08 p1327 A69-20715

Incoherent wave scattering of particle orbits as nonlinear effect of LF instabilities

08 p1367 A69-20801

Argon laser frequency spectrum instability caused by competing axial oscillations

08 p1327 A69-21023

Gas laser frequency stabilization by coupled oppositely circularly polarized components of single cavity mode in axial magnetic field

08 p1327 A69-21090

Stability of systems with periodic parameters, relation to automatic control systems and frequency characteristics role

09 p1473 A69-21855

Gunn effect domains propagation calculated for nonuniform diodes of annular geometry, obtaining frequency variation

09 p1464 A69-22159

Frequency domain stability criteria accuracy for application to fourth order nonlinear position control system

09 p1475 A69-22591

Intrinsic amplitude and frequency fluctuations in transistor autooscillator, examining natural additive noise influence

09 p1469 A69-22632

Optical frequency standards, discussing lasers VHF stability, RF and optical ranges, long and short term effects, etc

10 p1702 A69-23299

Ruby laser unsteady modes with ruby filter, discussing conditions for pulsed, monopulse and steady mode transitions, with formulas for steady emission

11 p1894 A69-24619

Amplification factor of He-Ne traveling wave light amplifier, discussing frequency stability and telescopic wave front broadening for uniform radiation distribution

11 p1894 A69-24623

Laser frequency drift effect on operation of three mirror interferometer, noting wave reflection by two compounded mirrors

11 p1895 A69-24720

HF instability of low pressure discharge in magnetic field, discussing plasma diffusion and oscillations

11 p1927 A69-24912

Frequency noises suppression in Gunn diode oscillators by frequency stabilization, using high Q external cavity

11 p1853 A69-25608

Frequency stabilization of He-Ne laser, using external Ne absorption tube in variable magnetic field as frequency standard

11 p1900 A69-25678

Upconverter with gain and stabilized frequency, using sideband locking of IMPATT diode oscillator

12 p2036 A69-25909

Multivibrator circuit for generation of oscillations with frequency stability against transistor ambient temperature changes

12 p2036 A69-25919

Microstripline circuit for stabilizing oscillating frequency of Gunn diodes prepared with GaAs slices

12 p2036 A69-25924

Frequency stability of He-Xe laser with nonresonant feedback, noting spectral line width dependence on number of interacting modes

12 p2105 A69-26049

Laser output power amplitude fluctuations effect on beat frequency stability for traveling waves in annular laser with broadened Doppler emission line

12 p2107 A69-26541

Spatial harmonics of harmonic frequency instabilities of cyclotron half frequency in system of two symmetrical electron beams confined by magnetic field

13 p2314 A69-28364

Three level He-Ne laser, showing nonlinear interference effects on gain line shape and use in magnetic field and frequency stabilization

14 p2460 A69-29671

Reference oscillator frequency instability effect on radio signals phase shift in ionosphere measurements, evaluating errors

14 p2444 A69-29873

Quartz oscillator amplitude and frequency fluctuations due to elements tolerance fluctuations, examining oscillator parameters contributions to spectral line width

15 p2579 A69-30944

Weak magnetic fields effect on molecular oscillator frequency taking into account Zeeman sublevels

16 p2762 A69-32500

Rb 87 vapor laser short term frequency stability independent of vapor concentration, noting use as frequency standard

16 p2798 A69-32513

Relativistic effect detection on pulsar frequencies by general relativity theory, assuming pulsars are orbiting objects

17 p3037 A69-33645

General relativity theory test using earth orbital motion and solar gravitational field effects on pulsars frequency stability

17 p3037 A69-33646

Short term frequency stability measured for Doppler radar and space tracking communication applications, reviewing FM theory for spectral purity relationship

18 p3100 A69-34277

Single hyperfine-state atomic beam selector effect on hydrogen maser stability, discussing DC magnetic field variation

18 p3153 A69-35306

Gyrator stability and frequency behavior obtained by controlled sources selection

19 p3287 A69-36739

Pulse-to-pulse carrier frequency stability of microwave radar transmitter tube for fixed target suppression

20 p3485 A69-36943

Emission frequency stabilizing effect in concentric sapphire-coated ruby laser, noting frequency independence from temperature fluctuations and thermal stresses

21 p3735 A69-38695

Frequency stabilization in He-Ne three mode laser by stabilizing LF oscillations via automatic adjustment of laser resonator length

21 p3738 A69-39078

Automatic frequency control circuit for stabilizing beat emissions of coupled multifrequency gas lasers

21 p3738 A69-39079

Free space to dielectric waveguide millimeter wavelength ratio as function of frequency, discussing equipment and procedure

21 p3674 A69-39130

Superconducting cavity X band oscillator designed for study of stability and spectral purity dependence on temperature

21 p3683 A69-39453

Accuracy and frequency stability of H masers in terms of wall collision effect and cavity resonator tuning

21 p3741 A69-39685

Oscillators frequency instability theories emphasizing difference between concepts of frequency instability and spectral purity

22 p3900 A69-40930

Frequency and phase instability characteristics of negative resistance amplifier due to changes in circuit parameters

22 p3916 A69-40962

Three phase DC-AC inverter with low harmonic distortion, good efficiency and packaging capability, stabilizing frequency by crystal controlled clock oscillator

23 p4074 A69-42294

Short term frequency stability and spectral purity measurements of ATS 1 multiple access communication system

23 p4129 A69-42509

Short term frequency fluctuations of CW HCN masers reduced to 10 kHz by improving plasma stability

24 p4327 A69-42614

Frequency domain stability criteria for open and closed loop distributed parameter linear time invariant systems

24 p4294 A69-43309

FREQUENCY STANDARDS

Beam laser as frequency standard, considering wavelength and molecular transfer constraints imposed by technology limitations and frequency stability requirements

03 p0440 A69-13715

Varian cesium resonator as prime frequency testing standard with accuracy dependent on electronic system for quartz slaving

04 p0600 A69-15068

Solid state precision frequency standard for L multiplex carrier equipment, using four precision quartz crystal oscillators

04 p0561 A69-15451

Rb 87 vapor laser short term frequency stability independent of vapor concentration, noting use as frequency standard

05 p0770 A69-15656

Visible laser frequency stabilization scheme and simultaneous determination of frequency in terms of time standard

05 p0773 A69-16291

Absolute wavelength standard using saturated molecular absorption in methane inside He-Ne laser cavity [IEEE PAPER P-1]

05 p0775 A69-16323

Laboratory equipment for atomic and astronomical time and frequency measurement

05 p0827 A69-16582

Atomic clocks frequency standards, discussing masers, atomic beam resonators and gas cells and various applications 09 p1501 A69-22598

Optical frequency standards, discussing lasers VHF stability, RF and optical ranges, long and short term effects, etc 10 p1702 A69-23299

Frequency stabilization of He-Ne laser, using external Ne absorption tube in variable magnetic field as frequency standard 11 p1900 A69-25678

Rb 87 vapor laser short term frequency stability independent of vapor concentration, noting use as frequency standard 16 p2798 A69-32513

FREQUENCY SYNCHRONIZATION

Q switched lasers powerful outputs obtainable at sum frequency, discussing frequency mixing in nonlinear dispersive media 03 p0438 A69-13047

Sampled data delay-lock loop for synchronizing pulsed envelope RF signals, using digital circuitry 03 p0390 A69-13216

Incoherent m-ary frequency shift keying (MFSK)/system analysis concerning automatic time synchronization 08 p1274 A69-20133

Two oscillator signal combiner based on mutual synchronization, providing output signal free of phase jumps or amplitude fluctuations 11 p1849 A69-24928

Tunnel diode self excited SHF oscillators synchronization, deriving single frequency generation conditions 11 p1849 A69-24955

Transient responses of mutually synchronized signal systems, obtaining design parameters 12 p2030 A69-26388

Discrete information transmission synchronization in communication systems concerning optimal signal detection, HF, phase and coded synchronization, etc 18 p3104 A69-35264

Bethenod pendulum behavior using coupled nonlinear differential equations, discussing synchronization methods 24 p4349 A69-42673

FREQUENCY SYNTHESIZERS

Electronic controller with integrated circuits and inexpensive SCR as coupler or interface between card reader and frequency synthesizer designed for unattended operation 06 p0897 A69-17704

Difference frequency generation by multiple quantum transition from laser medium considered as resonant optical frequency mixing device 07 p1144 A69-18470

Free carrier magnetoplasma effect used for far IR phase matched difference frequency generation in semiconductors, discussing carbon dioxide laser transitions 09 p1556 A69-21578

Microwave frequency synthesizer for digitally tuned UHF and microwave superheterodyne receivers, considering phase locking voltage-tuned transistor oscillator 12 p2030 A69-26390

Digital frequency synthesizer design parameter selection, giving expressions for output frequency and division coefficient variations 19 p3284 A69-36594

FRESNEL DIFFRACTION

Fresnel pulse holograms of three dimensional diffuse objects by single mode ruby laser with or without Q switching 07 p1132 A69-18801

Ray tracing application to evaluating aberrations produced by Fresnel holograms for optimizing design of aplanatic lens holography system 11 p1885 A69-24848

Statistical properties of electromagnetic field diffracted by illuminated plane aperture studied in Fresnel zone on basis of partial coherence theory 11 p1836 A69-24978

Diffraction theory of schlieren photometric slot and wire methods for cylindrical light wave of even order, discussing Fresnel diffraction for spherical wave 12 p2088 A69-26180

Fourier transform holograms by Fresnel zone-plate fringe interferometer, discussing source size and bandwidth 12 p2090 A69-26249

Fresnel irregularities calculated from radio wave partial reflection from lower ionosphere measured by rocket probes 15 p2604 A69-31420

Amplitude and intensity distributions of plane periodic Fresnel diffraction grating calculated by Fraunhofer theory, noting applicability to spectrometric and meteorological instruments 19 p3372 A69-35906

X ray heliography by Fresnel-Soret type zoneplate camera to obtain solar photographs from rockets 20 p3544 A69-37803

Fresnel pulse holograms of three dimensional diffuse objects by single mode ruby laser with or without Q switching 21 p3724 A69-38946

Planetary atmosphere effect on Fresnel diffraction of ultrashort radio waves determined from short wave approximation of damping function 22 p3901 A69-40948

Optical ultrashort pulse compression with paired diffraction gratings in terms of phase shift frequency dependence and Fresnel diffraction analogy 23 p4171 A69-41392

FRESNEL REGION

Power transmission efficiency between arbitrarily focused circular antennas with Gaussian amplitude illumination in Fresnel region for various phase illuminations and Fresnel numbers 11 p1851 A69-24991

Statistical gain characteristics of radar antennas at very short Fresnel zone ranges compared to Fraunhofer zone 12 p2040 A69-26470

Fresnel zone plate as converging and diverging lens in holographic image reconstruction, noting sine wave zone plate 22 p3947 A69-40864

Asymptotic approximation formulas to compute on-axis Fresnel region fields for coupling between two large aperture antennas 23 p4136 A69-41582

FRETTING

Hydrogen effects on ELI Ti-Al-Sn alloy, conducting tensile, fretting and abrasion tests on stressed and thermal cycled specimens [AIAA PAPER 69-585] 16 p2803 A69-32760

Relative slip effect on fretting fatigue strength, deriving stress initiating fatigue cracks 24 p4404 A69-43628

FRETTING CORROSION

Fretting effect on fatigue of press fitted axle assemblies, analyzing relative slip amplitude dependence on size, shape, clamping pressure, nominal stress and cycles 01 p0167 A69-10305

Fretting fatigue prevention in Al alloys, noting strength reduction due to fretting 09 p1526 A69-22148

Fatigue strength reduction in Ti alloy in sliding friction contact with metallic materials caused by fretting corrosion 12 p2113 A69-26125

Modes and mechanisms of wear covering adhesive, abrasive and corrosive wear, surface fatigue and fretting corrosion 13 p2265 A69-27231

Fatigue crack initiation in relation to contact stresses due to fretting, studying causes of strength reduction and crack inclination to surface 20 p3563 A69-38110

Mean stresses effects on fatigue crack initiation and propagation under controlled fretting slip amplitude 20 p3563 A69-38111

FRICTION

NT AERODYNAMIC DRAG
NT DRY FRICTION
NT FLOW RESISTANCE
NT INTERNAL FRICTION
NT KINETIC FRICTION
NT SKIN FRICTION
NT SLIDING FRICTION
NT STATIC FRICTION
NT SUPERSONIC DRAG
NT VISCOUS DRAG

Forced flexural vibrations of elastic truss systems with allowance for hysteresis friction 03 p0432 A69-12953

Laval nozzle resistance as result of friction and under expansion of gas, noting flow and pressure recovery coefficients 03 p0361 A69-12967

Atmospheric influence on friction endurance of solid powdered lubricants at constant layer thickness [IME PAPER 3] 07 p1138 A69-18563

European research on ultrahigh vacuum lubrication in space environments, emphasizing friction of materials under various loadings and temperatures [IME PAPER 10] 07 p1138 A69-18564

Short cylinder of perfectly plastic Coulomb yield conditions compressed between rigid plates, discussing cylinder-plate interface frictions, angles of internal friction and cohesion 08 p1410 A69-19890

Mathematical model of mechanical wear in surface friction based on approximation of cross section profiles, using Fokker-Planck equation for distribution function 14 p2455 A69-29331

Interface friction and adhesion of alloys workpieces and die materials under pressure and temperatures typical of plastic deformation 15 p2629 A69-30902

Viscous friction damping effect on impact vibrator stability, analyzing boundary region of multiply periodic single impact motion by point mapping 18 p3172 A69-34588

Friction and orography effects on vertical currents in planetary boundary layer and numerical forecasting of baric field 21 p3758 A69-38837

FRICTION COEFFICIENT

U COEFFICIENT OF FRICTION

FRICTION DRAG

NT AERODYNAMIC DRAG
NT SUPERSONIC DRAG
NT VISCOUS DRAG

Laminar flow stability parameter presenting coupling ratio between angular momentum change and loss rate by frictional drag 05 p0750 A69-16187

Incompressible laminar boundary layer with normal suction or blowing, discussing approximate method for evaluating laminar friction on wing contour 06 p0911 A69-17781

Polyvinyl chloride coating for reducing aerodynamic skin friction drag, noting water saturation effect on polyurethane foam [AIAA PAPER 69-165] 06 p0912 A69-18043

Stationary viscous incompressible fluid flow past rough surface, noting solution stability and friction stress determination for given pressure gradient 07 p1119 A69-18751

Skin friction drag coefficient for right circular cylinder calculation coefficient on basis of Blasius solution for flow 11 p1819 A69-25384

Rotating cylinder or vortex motion in shear flow with friction, noting drag and rotor force combined influence 17 p2950 A69-33151

Skin friction drag reducing high polymer solution injected into turbulent boundary layer to test effectiveness on marine vehicles 17 p2951 A69-33254

Preston probe measurement of friction drag on subsonic and supersonic nozzle wall including effects of heat transfer, compressibility and pressure gradient [AIAA PAPER 69-648] 17 p2893 A69-33496

Skin friction drag formula for tapered and delta wings with allowance for coefficient variation and Reynolds number dependence on chord length 17 p2896 A69-34037

Parametric variations of nonlinear system moving in medium with nonlinear drag, using Bogoliubov-Krylov asymptotic method 18 p3171 A69-34564

Turbulent skin friction coefficients of compliant surfaces on flat plates determined as function of speed for different materials 21 p3695 A69-39039

FRICTION FACTOR

Viscoseal sealing coefficient and friction factor under turbulent flow conditions [ASLE PREPRINT 68AM 5B-1] 01 p0087 A69-10911

Resisting forces produced by transverse vibration of rotating disks in viscous fluid 02 p0232 A69-12257

Frictional forces and collision frequencies for ions moving in neutral gases 03 p0421 A69-13328

Two dimensional flow of incompressible fluid near sharp leading edge of plate at zero incidence, discussing approximation error and friction stress 03 p0415 A69-13651

Frictional losses in straight tubing and effect of system on ball type valve, using polyurethane foam damped flexible silastic tube 04 p0608 A69-15331

Equations for instability of stabilized platform of inertial navigation system with viscous friction in accelerometers

06 p0954 A69-16824

Oil lubricant vapors under frictional working conditions in vacuum analyzed by mass spectrometer and gas-liquid chromatography concerning molecular weight and composition
[IME PAPER 11]

07 p1137 A69-18558

Wind tunnel investigation of damage to aircraft radomes by water droplet encounter during cloud passage and gaseous molecule friction in air

07 p1054 A69-19541

Dynamical friction on star in postNewtonian approximation of general relativity

08 p1386 A69-20072

Wall friction influence on three dimensional flow in axial flow turbomachines, introducing shear stresses between flow planes

08 p1252 A69-20724

Primary explosives tested for effects of shock, friction, heat and electrical discharges

10 p1750 A69-23010

Axial vibration effects on frictional losses in gear systems under dry friction or boundary lubrication conditions
[ASME PAPER 69-VIBR-15]

10 p1701 A69-24169

Friction and wear characteristics of ceramics and cermets as bearing materials, with tabulation of room temperature hardness and maximum service temperatures

13 p2284 A69-27232

Earth mantle and core friction interaction suggested as cause of secular change in orbital motion obliquity

13 p2253 A69-27821

Relative variations of wall friction and thermal flux for laminar incompressible flow of constant volume mass

13 p2250 A69-28357

Reynolds number, incident flow turbulence and interblade channels roughness effects on friction losses in axial flow turbines

15 p2547 A69-30074

Mach numbers effect on pressure distribution and friction moment in nonisothermal layer of gas lubricant, using power series

15 p2629 A69-31021

Friction effects on friction couples made of two different nonferrous alloys, discussing temperature regime difference effects on microgeometry and structure

15 p2629 A69-31027

Inertia, compressibility and viscous friction effects on dynamic response of long fluid line, constructing models

16 p2771 A69-32066

Friction and wind relationships expressing actual and geostrophic wind as complex numbers or by corresponding vectors in Gauss-Argand diagram

16 p2808 A69-32455

Friction characteristics during diamond honing of different steel grades, determining lubricating and cooling liquids effect on friction coefficient

22 p3958 A69-41170

Discrepancy between theoretical and experimental coefficients of friction losses on blades of centrifugal compressor impeller wheels, using lattice theory

23 p4058 A69-41727

Microrheological property of blood measured with microglass fiber viscosimeter, noting sensitivity to intercellular friction of erythrocytes

23 p4098 A69-42100

Prandtl number influence on heat transfer and pressure drop characteristics of roughened channels, determining friction factor

24 p4407 A69-42915

Transition from turbulent to laminar regime as consequence of high heating rates for internal convective flow, noting roles of Nusselt numbers and friction factors
[ASME PAPER 69-HT-9]

24 p4304 A69-43559

FRICION MEASUREMENT

Internal friction measurement apparatus for non-metallic solids, noting variations of Young modulus in extremely low loss materials

03 p0428 A69-13108

Thin film heated Pt resistance thermometer for skin friction or velocity measurements in air, water or blood

04 p0601 A69-15118

Solid lubricant compacts for ball bearing separator materials, describing fabrication, design and friction and wear properties in air and vacuum
[ASLE PAPER 68-LC-16]

07 p1139 A69-18626

Friction and wear tests of synthetic rutile single crystals against diamond styli and spherical sliders of ruby, sapphire and hardened steel
[ASLE PAPER 68-LC-3]

07 p1140 A69-19307

Physical sputtering deposition of molybdenum disulfide films as solid lubricant on rotating and sliding components, discussing lubrication properties in vacuum
[ASLE PAPER 68-LC-15]

07 p1140 A69-19308

Floating element skin friction meter designed for adverse pressure gradients, discussing wall shear stress measurement

11 p1889 A69-25557

Friction resistance between steel and ground basalt in ultrahigh vacuum, showing increase by adhesion

13 p2298 A69-28014

Skin friction measurement in aerodynamic tests using thin liquid crystal coatings with changes in maximum light scattering wavelength in response to shear forces

14 p2427 A69-29029

Calculated and experimental surface wear damage data correlated for materials under friction conditions

15 p2618 A69-30106

Sliding friction tests of Cu and Cu-Be alloy plates in contact with various alloy sliders in air and vacuum
[ASLE PAPER 68-LC-5]

15 p2622 A69-30610

Contact conformity effects on spinning torque and friction coefficient in angular contact ball bearings from lubricated and unlubricated tests
[ASME PAPER 68-LUB-10]

15 p2628 A69-30901

Three dimensional effects on Stanton tube data for skin friction determination for small protuberances drag immersed in turbulent boundary layer

16 p2771 A69-31920

External friction of refractory materials at high temperature in vacuum, discussing testing machine and methods including metallographic, X ray, spectral and electron diffraction analyses

21 p3690 A69-39154

Friction tests for Mariner Mars 1969 spacecraft mechanisms in ultrahigh vacuum molecular sink chamber, noting increased friction attributed to vacuum environment
[AIAA PAPER 69-996]

22 p3920 A69-40374

Finite-difference grid procedure for predicting friction heat and mass transfer in two dimensional boundary layers

22 p3932 A69-40939

Wear resistance and antifriction measurement device for polymer coatings in high vacuum, various gases and during exposure to electron radiation

23 p4169 A69-41599

Aircraft braking, discussing systems, brakes, tires, runway interface, heat sink materials, friction measurements, skid control, cooling and recovery equipment
[SAE PAPER 690376]

23 p4063 A69-41671

FRICION PRESSURE DROP U SKIN FRICION

FRICION REDUCTION

Unsteady conducting incompressible viscous fluid flow past plate in magnetic field, analyzing surface friction reduction

07 p1192 A69-19018

Axial vibration effects on frictional losses in gear systems under dry friction or boundary lubrication conditions
[ASME PAPER 69-VIBR-15]

10 p1701 A69-24169

Plain and rolling metal bearings manufacture and use, discussing materials structure and properties, operating conditions, lubrication, etc

11 p1903 A69-24517

Friction damping properties of deployed structures vibrating in weightless state compared to damping in space for true determination

12 p2183 A69-26792

Collection of Soviet papers on wear and antifriction properties of materials

13 p2268 A69-28050

Antifriction characteristics of hard lubricating coatings based on molybdenum disulfide and graphite in inert gas atmosphere and vacuum, determining thermal stability temperature ranges

13 p2269 A69-28053

Dry dynamic friction of brass disk against steel surface reduced using ultrasonic oscillations creating air gap

18 p3135 A69-34587

Aircraft onboard weighing system, eliminating o ring seal friction to permit accurate measurement of oleo strut pressure
[SAWE PAPER 748]

18 p3137 A69-34883

Solid film lubricants deposited by DC triode sputtering on Ni, Ni-Cr and Nb surfaces friction tested under ultrahigh vacuum conditions

24 p4321 A69-43126

FRINGE PATTERNS U DIFFRACTION PATTERNS

FROGS

Weightlessness effects on fertilized frog egg development on board Gemini 8 and 12 manned orbital flights, discussing cell division, differentiation and embryogenesis

01 p0017 A69-11084

Analytical model for frog retinal bug detector cell to make possible signal measurement in frog optic fibers

07 p1070 A69-18383

Simulated weightlessness used in determining ontogenesis of otolith organ in tadpoles and eggs as function of acceleration forces
[DVL-855]

10 p1647 A69-24021

Static pressure-diameter measurements on small pulmonary blood vessels of frogs, analyzing capillary septal area as function of intravascular pressures noting high compliance

22 p3885 A69-40974

Optic nerve spikes elicited by acetylcholine application on isolated perfused retina of frog, varying response by prostigmine and atropine

23 p4084 A69-41465

Electric potential measuring device for frog isolated skeletal muscle fiber mounted on micromanipulator

23 p4111 A69-42058

FRONTAL AREAS [METEOROLOGY] U FRONTS [METEOROLOGY]

FRONTS [METEOROLOGY]

Frequency of cold front passages during year in French part of Switzerland and times of occurrence during day

04 p0628 A69-15089

Satellite radiation maps for synoptic analysis regarding world weather maps, discussing front, intertropical convergence zones and typhoon location

14 p2473 A69-29729

Relation between radar echoes spatial extent and synoptic conditions with reference to various fronts, noting significance for aviation

14 p2474 A69-29738

Low level jet stream near meso-low on stationary front in Japanese rainy season analyzed from radar echoes, noting appearance of vertical current

16 p2809 A69-32601

Variable scatter mechanism in turbulent tropospheric propagation medium, employing dynamic meteorology concepts for frontal disturbances effect on scatter volume

17 p2927 A69-33856

FROST

Dew /or frost/ point determination method for low temperature humidity measurement

09 p1502 A69-22691

Vertical wind velocity profiles approximation accuracy determined by linear, exponential and logarithmic functions of altitude during ice and frost

13 p2293 A69-27846

IR reflection spectra agreement for frost particles and Venus clouds, noting ice as clouds constituent

18 p3190 A69-34282

Minimum air temperature forecast by terrestrial thermal or long wave radiation balance measurement, using radiometer data

23 p4184 A69-42211

FROUDE NUMBER

Hydrofoils fully submerged in seaway at up to 140 knots and constant Froude number, discussing foils lift/drag ratios as function of speed and submergence

11 p1871 A69-25122

Froude number for scaling wind stress at air-water interface, verifying logarithmic wind profile and relating shear velocity to surface roughness

17 p2996 A69-33152

FROZEN EQUILIBRIUM FLOW

Frozen shock in steady one dimensional compression flow of relaxing gases weaker than equilibrium shock

08 p1304 A69-20785

Electrical characteristics of equilibrium plasma sheaths at stagnation point of blunt body in high speed air, considering current collection regimes
[AIAA PAPER 69-702]

17 p3011 A69-33473

FROZEN FOODS

Astronaut feeding in space and NASA criteria for space foods, eliminating foods in metal tubes and directing development efforts to dehydrated foods

15 p2560 A69-31459

FRUSTUMS

Geometrical diffraction theory for bistatic scattering of plane wave by conducting frustum, calculating scattering matrix

11 p1837 A69-24999

Bending theory for truncated multilayer anisotropic conical shells, defining relations between displacements and external forces

11 p1984 A69-25141

Axisymmetric vibration modal properties /frequencies and mode shapes/ of thin conical shell frustums, considering dimensional and boundary condition influences

11 p1992 A69-25519

Surface wave patterns of truncated conical shells with free edges attributed to mechanical properties

12 p2178 A69-26002

Longitudinal elastic waves produced in truncated hollow Al cone due to steel spheres impact

[ASME PAPER 69-APMW-15]

24 p4401 A69-43101

FUEL-AIR RATIO

Coal grain combustion rate and duration at finite air excess coefficient, solving combustion process equations under steady state assumption

04 p0687 A69-15168

Photochemical ignition of low pressure fuel-oxidizer mixtures applied to unsensitized stoichiometric mixtures of methane-oxygen and hydrogen-oxygen

[WSCI PAPER 68-42]

06 p1034 A69-17791

Ducted turbulent mixing and burning of coaxial streams, presenting experimental results for rocket-air mixing system

[AIAA PAPER 69-85]

06 p0984 A69-18082

Hydrogen-air supersonic combustion at low densities, discussing laboratory computer simulation based on boundary layer concepts and finite rate chemistry

[WSCI PAPER 68-29]

07 p1240 A69-18358

Spark ignition of liquid fuel droplets atomized in air analyzed by spark discharge visualization for two phase mixture

09 p1623 A69-22220

Combustion chamber design for advanced gas turbines, noting influence of fuel air mixing and air flow distribution

09 p1573 A69-22612

Gas turbine engines smoke emission, considering smoke measurement, flame structure, carbon production, pressure effects fuel-air ratio, etc

09 p1573 A69-22622

Gas turbine engines smoke reduction, aerated fuel sprays for smoke control on engine design and factors affecting visibility of exhaust plumes

17 p3020 A69-33350

Kinetic model and steepest descent method to optimize one dimensional combustor

[AIAA PAPER 68-644]

19 p3448 A69-35943

FUEL CAPSULES

Multifuel-capsule radioisotope thermoelectric generator design procedure, applying statistical environment definition

24 p4349 A69-43191

FUEL CELL CATALYSTS

U ELECTROCATALYSTS

FUEL CELLS

NT HYDROGEN OXYGEN FUEL CELLS

NT REGENERATIVE FUEL CELLS

Hydrocarbon-air fuel cell producing electric power automatically for five days

01 p0013 A69-10965

Direct energy conversion and materials limitations, discussing thermoelectricity, solar cells, thermionics and fuel cells

02 p0194 A69-11801

Electrocatalysts for direct electrochemical oxidation on n-octane in fuel cells, discussing platinum consumption reduction

[ECS PAPER 8]

03 p0368 A69-13856

Secondary cells with liquid lithium anodes and immobilized fused salt electrolytes

04 p0552 A69-15330

Low temperature hydrogen fuel cells and basic electrolyte batteries design, discussing electrolyte concentration regulation by elimination of water formed

08 p1258 A69-21027

Manned spacecraft electrical power systems requirements, noting Gemini and Apollo fuel cell system design and configuration

08 p1259 A69-21035

Oxidizer reducing and fuel oxidizing catalysts role in large current densities production at electrodes of low temperature carbon fuel cells

08 p1259 A69-21037

Electrodes behavior for fuel cells with liquid electrolyte under high-g and weightlessness conditions, discussing spontaneous liquid motion

08 p1259 A69-21038

Cold hydrogen and basic electrolyte cells at CGE research center, discussing single cell batteries, reagent chambers and auxiliary control systems

08 p1259 A69-21039

ABEPAC fuel cell with ion exchange membrane electrolyte impregnated with sulfuric acid solution, describing electrodes and bipolar collectors

08 p1259 A69-21040

Ion exchange fuel cells for emitter-receiver on atmospheric constant ceiling balloon, stressing pressure effect on operation and fuel storage

08 p1260 A69-21042

Electrochemical characteristics of lateral diffusion gas electrodes for fuel cells, noting electrodes fabrication by pulverizing on nickel sheet

08 p1260 A69-21044

Fuel cell oxygen ionization on nickel, silver and nickel-silver disk electrodes

08 p1260 A69-21045

Medium temperature fuel cells, noting reliability and high efficiency leading to selection for lunar exploration vehicle of Apollo project

08 p1260 A69-21046

Fuel cell system using double skeleton catalyst gas diffusion electrodes, discussing design, mode of operation and performance

08 p1261 A69-21047

Proton electrolyte application to fuel cells, discussing proton diffusion in solids and materials with vacancies /proton conductors/ in structures

08 p1269 A69-21053

Fuel cells utilizing direct electrochemical conversion of energy of radioactive elements

08 p1269 A69-21054

Hydrogen peroxide electrode cathodic polarization studied for liquid oxidant use in methanol fuel cells

11 p1825 A69-24523

Cyclohexane and benzene anodic oxidation at fuel cell electrodes, noting cathodic desorption products as function of potential and reactant

[ECS PAPER 330]

15 p2562 A69-31540

Removal rate of reaction water from fuel cells by diffusion-condensation procedure as function of temperature and electrolyte concentration

16 p2736 A69-32200

Manned spacecraft fuel cell selection and design, discussing Gemini ion exchange membrane and Apollo Bacon cell systems

16 p2737 A69-32406

Thin film metallic oxide catalysts for oxidation in low temperature cells using hydrogen and hydrocarbons and for oxygen reduction in acid electrolyte

16 p2738 A69-32408

Electrodes for fuel cells with liquid electrolytes, discussing problems under weightless and high gravity situations

16 p2738 A69-32409

Hydrogen and basic electrolyte cold cells, studying control systems for reactants supply, current, reaction by-products, etc

16 p2738 A69-32410

Power source with electrolyte consisting of ion exchange membrane in aqueous solution of sulfuric acid

16 p2738 A69-32411

Fuel cell oxygen electrode problems, noting oxygen ionization reaction and disk electrodes role

16 p2739 A69-32416

Medium temperature fuel cells advantages including improved electrochemical reaction kinetics, water and heat removal

16 p2739 A69-32417

Double skeleton catalyst type VARTA fuel cell system for space power, using potassium hydroxide as electrolyte

16 p2739 A69-32418

Fuel cells with solid membranes with ion conductivity, discussing proton electrolyte

16 p2740 A69-32424

Low temperature fuel cell with mixed oxidizer and fuel and fuel cell based on water radiolysis under alpha and gamma radiation

16 p2740 A69-32425

Irreversibility resulting from composition changes in operating fuel cell anode and cathode chambers and cell geometry influence

18 p3093 A69-34781

Secondary power sources for space applications in solar arrays, static and dynamic thermal systems, high power batteries and fuel cells, discussing NASA machinery procurement

19 p3255 A69-36323

Fuel cells ionic concentration changes across porous matrix during operation, measuring voltage losses due to pH changes and liquid junction potentials

[ECS PAPER 335]

20 p3466 A69-38069

Cathode materials role in high temperature zirconia electrolyte fuel cell performance, discussing metals, collector-embedded and electronically conducting oxides properties

22 p3869 A69-40734

Molecular hydrogen-CO fuel cells operation, studying natural voltage oscillations due to repeated electrode poisoning and reactivation

22 p3896 A69-40738

Fuel cell /battery and solar array/ battery systems for manned Apollo Applications Program /AAP/ space vehicles, considering mission and power requirements

23 p4069 A69-42244

Fuel cells construction materials selecting and optimizing techniques using diffusion block and differential corrosion concepts

23 p4075 A69-42299

Anisotropic porous media model for fluid motion in rectangular fuel cell cavities, analyzing pressure, velocity, stream functions and purge time

23 p4075 A69-42300

Battery/fuel cell hybrid power source, discussing fast transient response

[SAE PAPER 690205]

24 p4255 A69-42889

FUEL COMBUSTION

Sulfur organic compound formation effect on composition and structure of solid phase formed during hydrocarbon jet fuels oxidation

01 p0142 A69-11097

Gas turbine alloys composition role in high temperature corrosion resistance under high sulfur diesel fuel combustion

03 p0444 A69-13309

Ducted turbulent mixing and burning of coaxial streams, presenting experimental results for rocket-air mixing system

[AIAA PAPER 69-85]

06 p0984 A69-18082

Nonsteady combustion models for gases, liquid fuels and solid propellants, reviewing errors in physics and mathematics

[AIAA PAPER 69-178]

06 p1037 A69-18100

Quasi-steady combustion model of fuel droplet with convection, including pressure effect

[AIAA PAPER 69-147]

06 p1037 A69-18114

Chemical kinetic model for hydrocarbon fuels combustion and application to multidimensional finite difference mixing analyses in hypersonic engines and nozzles

[AIAA PAPER 69-86]

06 p1037 A69-18119

Fuel mixing mechanism in diffusion type supersonic combustion, noting influence of combustor configuration and fuel density

[AIAA PAPER 69-32]

07 p1242 A69-19266

Petroleum sulfides advantageous effect on oxygen consumption during combustion

07 p1202 A69-19456

Kerosene droplets combustion stability studied by motion pictures, discussing pressure, temperature and O concentrations effects in turbulent carbon dioxide flow

08 p1421 A69-20345

Rolls Royce Spey engine combustion system development, emphasizing carbon formation, exhaust smoke, fuel injection, increased area interconnector, and overheating

09 p1573 A69-22613

Hydrodynamic effects in flame spreading, ignitability and steady burning of liquid fuels, using analogy of films floating on water

11 p1999 A69-24484

Unsteady heating of fuel mixture in vertical cylindrical container with Arrhenius heat source, discussing heat conduction equations and wall temperature effects

11 p2001 A69-25192

Acoustic frequency of longitudinal self oscillations during vibrational fuel combustion in afterburner, taking into account nonlinear properties of heat supply zone

11 p2002 A69-25339

Tubular gas turbine combustion chamber design for optimum mixing performance using flow and mixing data of cold air injection into hot gas stream

[IME PAPER 15]

12 p2147 A69-25793

Platinum based metal binary catalysts as anodes for hydrogen/carbon monoxide fuel mixtures oxidation, discussing alloy surface chemisorption of CO

12 p2026 A69-25937

Transverse wave spacings for self sustaining detonations in oxygen and diluents mixtures with hydrogen, methane, acetylene or ethylene fuel, noting dilution

13 p2378 A69-28217

Equations for steady state combustion of fuel drops in oxidizing atmosphere integrated numerically, obtaining ignition and extinction conditions
13 p2379 A69-28456

Spherical symmetric unsteady conservation equations describing transient burning of volatile fuel droplets, obtaining time dependent fuel and heat distribution in flow field
14 p2537 A69-29016

Liquid fuel droplets combustion under free and forced convection noting combustion rate
15 p2719 A69-31174

Fuel drop combustion under unsteady conditions at high pressure in unlimited and limited air volume
15 p2719 A69-31476

Semiempirical correlation of characteristic velocity for Otto Fuel II during monopropellant combustion, assuming droplet vaporization as rate controlling process [AIAA PAPER 69-419]
16 p2877 A69-31843

Two phase detonations of fuel in liquid layer on shock tube wall with gaseous oxidizer, presenting one dimensional approximation for film detonation propagation
16 p2879 A69-32151

Hydrodynamic stability of solid fuel combustion in presence of acoustic disturbances in gas phase, considering material erosion and particle dispersion
18 p3231 A69-35150

Fuel droplet evaporation and combustion in still air as unsteady diffusion controlling phenomenon, basing calculations on flame front model
20 p3632 A69-37520

Film vaporization of fuel in combustion chambers of aircraft turbines, determining concentration and velocity distributions of fuel and air
20 p3633 A69-37921

Film vaporizing gas turbine combustor design including performance tests and combustion physics
21 p3784 A69-38607

Thermal stability of reactive spherical shell, investigating spontaneous ignition of volatile fuel drop exposed to hot oxidizing environment
21 p3849 A69-38804

Temperature influence of homogeneous kerosene-air mixture on flame stabilization by mechanical and gas dynamic baffle systems
21 p3850 A69-38859

Nonstationary solid rocket fuel combustion scheme, using unsteady combustion model for quantitative analysis of rocket engine irregularities attributed to excessive fuel
22 p4050 A69-40457

Supercritical burning of liquid fuel droplets in stagnant environment, using flame sheet model to obtain heat and mass fields
24 p4415 A69-43600

FUEL CONSUMPTION

Optimum control with respect to minimum fuel and power consumption involving constraints based on Kuhn-Tucker conditions and saddle point theorem
02 p0223 A69-11564

Hydrostatic journal gas bearings calculations for carrying capacity, gas consumption and optimal dimensions for maximum lifting capacity
03 p0432 A69-12960

Hovercraft range operating at constant speed as function of design efficiency, power apportionment, fuel consumption and initial specific resistance
03 p0367 A69-13909

Minimum fuel attitude control of spacecraft by Pontryagin principle and extended steepest descent method
03 p0522 A69-14100

Book on planetocentric, lunar and interplanetary transfer techniques covering communications and coordinate system selection, minimum fuel and time transfer and rendezvous, etc
04 p0652 A69-14458

Aerothermodynamics of subsonic-aircraft propulsion, analyzing performance of bypass engine, fuel consumption and specific weight
05 p0695 A69-15551

Minimum fuel consumption for low thrust jet engine propelled space vehicles maneuvering in circular trajectories
05 p0829 A69-15879

Minimum fuel rendezvous maneuver for two space vehicles in circular orbit, considering propelled tracking equipment nonlinear equations of motion
05 p0823 A69-16036

Optimization procedure developed and applied to minimum fuel midcourse guidance of spacecraft, discussing optimal closed loop control of linear stochastic systems
06 p0955 A69-17576

Minimum fuel control of spacecraft orbital elements for transfers between elliptical orbits by low variable thrust propulsion, noting interplanetary trajectory optimization
06 p0955 A69-17579

Suboptimal guidance corrections for continuous thrust vehicle disturbances during minimum fuel rendezvous in Martian orbit, discussing physical and modified cost functional [AIAA PAPER 69-76]
06 p0956 A69-18081

Linearized theory for minimum fuel guidance in neighborhood of minimum fuel space trajectory, unrestricted thrust magnitude and allowances for mid-course impulses [AIAA PAPER 69-74]
06 p0956 A69-18183

Optimum approach and departure paths for VTOL aircraft simulated by hybrid computer under constraints [AIAA PAPER 69-209]
07 p1178 A69-19570

Aircraft gas turbine engines control systems capabilities and future requirements, considering maximum propulsion system performance with minimum fuel consumption [ASME PAPER 68-GT-62]
08 p1376 A69-19846

Optimum cruise altitude, block time and fuel relations for Conqair 600/640 aircraft for various temperatures, segment distances and weight
08 p1255 A69-21007

Damped mass expulsion for space vehicle attitude control reducing propellant consumption and pulsing frequency [AIAA PAPER 67-535]
09 p1610 A69-21986

Space flight fuel consumption optimization as function of acceleration of nozzle control
10 p1666 A69-22919

Propulsion optimization for various vehicles, considering power plant weight, specific fuel consumption, power and thrust ratios, etc
11 p1941 A69-24462

Isothermal theory of cool flames, discussing oscillations-fuel consumption relations, kinetics, etc
11 p1970 A69-24476

Spacecraft attitude control with minimum energy control logic for small constant disturbance torques, considering reaction jet torquers and fuel consumption
11 p1966 A69-25446

Thrust, bank angle and angle of attack of aircraft minimum fuel lateral turns at constant altitude and specified velocities
13 p2203 A69-28245

Turbofan engines impact on aircraft engineering development emphasizing large performances, high fan flow rates and low fuel consumption
15 p2550 A69-30322

Optimal rendezvous maneuver of pursuing vehicle with minimum fuel expenditure in approach stage on elliptic and hyperbolic orbits
15 p2701 A69-31548

Rendezvous maneuver with minimum fuel in circular orbit solved without restrictive conditions for accelerations due to approach thrust
16 p2852 A69-31558

Minimum fuel multiple impulse orbital rendezvous for fixed transfer time near circular orbits
16 p2857 A69-32161

Nitrogen reaction with excess fuel in ramjet engines, noting kinetic limitations in applications [WSCI PAPER 69-12]
16 p2831 A69-32351

Gas phase ignition shock tube analysis of solid propellant taking into account changing surface temperature and fuel vapor consumption
18 p3183 A69-34463

Time and fuel optimization of angular momentum alignment and nutation elimination of spin stabilized bodies with inertial reference direction
18 p3208 A69-34775

Economics evaluation for operation of commercial fixed wing aircraft at aft center of gravity position, noting fuel saving from drag reduction [SAWE PAPER 806]
18 p3091 A69-34902

Computer-generated airline fleet performance data on B-720, B-727 and DC-8 aircraft, attributing deterioration to increased drag and fuel consumption [AIAA PAPER 69-770]
19 p3245 A69-35651

Minimum fuel guidance from hyperbolic into specified circular orbit
19 p3367 A69-35663

Optimal fuel transfers between coplanar and non-coplanar coaxial elliptical orbits determined by Pontryagin maximum principle, using digital program for Hamiltonian equations solutions
19 p3399 A69-35670

Numerical integration of plane orbital transfers with multiple powered arcs, minimizing propellant expenditure of small thrust chemical rocket
19 p3400 A69-35673

Coplanar impulsive transfers and second variation test, using maximum principle and Lagrangian multiplier technique for propellant expenditure minimization
19 p3400 A69-35676

Stream surface characteristics as criteria for hypersonic lifting bodies shapes for optimal aerodynamic and fuel performance
19 p3248 A69-36399

Automatic stationkeeping/geosynchronization/ for maintaining satellite in circular synchronous orbit at all geocentric longitudes for prolonged time with low fuel consumption
21 p3805 A69-39213

Integrals of motion for minimum fuel rocket trajectories in inverse square field calculated for constant power and constant exhaust rockets [AIAA PAPER 69-904]
21 p3806 A69-39336

Closed form solution for minimum fuel constant thrust trajectories for vehicle transfer in vacuum between arbitrary boundary conditions [AIAA PAPER 69-905]
21 p3806 A69-39337

Minimum fuel thrust limited transfer trajectories computation for coplanar elliptic orbits [AIAA PAPER 69-914]
21 p3808 A69-39344

Analytic approximation for initial adjoint vector for optimal/minimum propellant/ space trajectories [AIAA PAPER 69-916]
21 p3808 A69-39345

Fuel-time optimal retrothrust control for vertical and gravity turn ballistic trajectories of soft landing nonlifting bodies based on Pontryagin principle [AIAA PAPER 69-868]
21 p3809 A69-39394

Building block approach to turbofan engine design, discussing fuel consumption, noise and component research [RAES PAPER 14]
22 p3999 A69-40493

Optimal minimum fuel rendezvous maneuver variational problem, generalizing circular orbit results to conical orbits
22 p4028 A69-40754

SST stratospheric environment problems, discussing temperature effects on fuel consumption and convective turbulence effect on flight safety and efficiency
22 p3867 A69-41141

Thrust increase methods for air breathing turbojet engines analyzed with respect to effectiveness, taking into account environmental supporting mass and fuel expenditures
23 p4199 A69-41578

Flight range and fuel consumption formulas of power gliders used for transportation compared with automobiles
24 p4253 A69-43142

FUEL CONTAMINATION

Propellants volatile fraction removal followed by gas chromatographical determination, noting use of heating method
02 p0302 A69-11522

Oxygen supply inert diluent impurities effect on hydrogen-oxygen fuel cell performance
04 p0551 A69-15310

Petroleum sulfides advantageous effect on oxygen consumption during combustion
07 p1202 A69-19456

Aircraft design, fabrication and finish techniques taking into account aircraft integral fuel tank corrosion due to contaminants associated with microbiological debris [NACE PAPER 49]
08 p1320 A69-20599

Contaminants formation during pulse mode operation of liquid bipropellant attitude control rocket engine, discussing exhaust plume effects [AIAA PAPER 69-574]
16 p2870 A69-32774

Hydrogen fluoride corrosive effects in cryogenic propellant, emphasizing contamination by particulate matter from corrosion products
21 p3783 A69-39486

FUEL CONTROL

Computer simulation on engines dynamic behavior covering thrust transfer functions, time behavior and engine and fuel controller operation
08 p1301 A69-20167

Fuel control systems using emulsified fuel, noting exposure effects and temperature and pressure characteristics [ASME PAPER 69-GT-40]
09 p1571 A69-22486

Differential game for determining singular fuel optimal control of plant with uncertainty in dynamic equation
10 p1667 A69-24041

Gas turbine fuel and control systems for two and three shaft engines in military and civilian aircraft including helicopters
[IME PAPER 12] 12 p2147 A69-25796

Fluidic systems for automatic control of fuel supply to ramjet engine combustor, coolant rationing and distribution to engine structure and performance efficiency maintenance
14 p2508 A69-28875

Hydrostatic stability and damping characteristics of perforated plates and screens for passive propellant control schemes from drop tower tests
[AIAA PAPER 69-531] 16 p2833 A69-32691

Capillary barriers to provide propellant positioning, expulsion capability and slosh dampening for spacecraft propulsion systems during rotational maneuvers
[AIAA PAPER 69-529] 16 p2868 A69-32713

Cost optimization of mixture ratio control systems for liquid propellant launch vehicles, considering open and closed loop systems
[AIAA PAPER 69-441] 16 p2870 A69-32775

Hele-Shaw and porous medium fuel tank systems behavior in simulated low gravity environment, studying sloshing, wetting, funneling and fuel-driver gas interface stability
[AIAA PAPER 69-678] 17 p3021 A69-33444

Minimum-fuel controls in multidimensional optimum transfer problems
19 p3400 A69-35677

Acoustic pumping system for propellant control at zero gravity, describing system operation by hydraulic analogy for liquid sloshing prevention
20 p3548 A69-37294

Trajectory optimization of second state of rocket launched into earth circular orbit in gravitational field by stepwise fuel control, using Pontryagin maximum principle
21 p3829 A69-39818

JT9D engine fuel and vane control systems for Boeing 747, noting computing system positioning of throttle valve for fuel flow control
[SAE PAPER 69-0405] 23 p4201 A69-41658

Engine fuel and geometry control design for large high bypass aircraft turbofan engines used for airbus powering
[SAE PAPER 69-0403] 23 p4201 A69-41659

FUEL CORROSION

Corrosive characteristics of jet fuels near condensing water studied by weight loss method, using copper alloy plates
01 p0142 A69-11099

Additions of dialkyl and diaryldithiophosphates of Ba, Ca, Zn, Pb and Ni as antioxidants and corrosion inhibitors for hydrocarbons
12 p2027 A69-27091

Dynamic hot corrosion rig test for operating environment and alloy composition effect on sulfidation attack during gas turbine fuel combustion
23 p4150 A69-42448

FUEL ELEMENTS [NUCLEAR REACTORS]

U NUCLEAR FUEL ELEMENTS

FUEL FLOW

NT PROPELLANT TRANSFER

Concorde fuel management, discussing trim, fuel as coolant and booster pumps
07 p1057 A69-19705

Fuel jet shape in air stream/mechanical atomization calculated as function of stream and fuel injection parameters
11 p2002 A69-25336

Laser flowmeter for pulse flow of highly corrosive rocket fuels and oxidizers with measured rise times less than 10 msec
15 p2616 A69-31292

Gas core reactor curved porous walls geometry tested with clear and smoky air injection, noting mass flow ratio in reactor cavity
18 p3171 A69-35181

Fueling process in internal combustion engines having fuel admission systems with different flow cross sections
19 p3393 A69-35824

Diffusion flame stability at inlet of fuel stream into oxidizer, showing ignition coordinates dependence on fuel, oxidizer and ratio of burning/flow rate
19 p3448 A69-35855

FUEL FLOW REGULATORS

Fluidic vortex valve to modulate solid propellant generated hot gas flow
[AIAA PAPER 69-424] 16 p2844 A69-32723

Stochastic fuel regulator problem investigated by optimal and self organizing techniques, emphasizing realizability of resulting controllers
24 p4292 A69-43284

FUEL GAGES

Aircraft nucleonic fuel gauging system, using radioactive gas to emit gamma rays for fuel mass sensing
18 p3139 A69-35468

FUEL INJECTION

Combustion in high power jet engine combustion chamber in case of continuous and intermittent liquid fuel injection
08 p1421 A69-20762

Fuel concentration effect on turbojet engine reheat jet pipe vibrations via tests
09 p1573 A69-22616

Film cooling injection slots number and position over flame tube and minimum cooling airflow in aircraft gas turbines
09 p1625 A69-22623

Leading edge conditions of obstacle exuding fuel into oxidizer stream, using Oseen equations in parabolic coordinate system
11 p1997 A69-24307

Injected propellant behavior during one dimensional passage through rocket combustion gas chamber, considering Reynolds number and propellant characteristics
11 p1941 A69-24329

Fuel jet shape in air stream/mechanical atomization calculated as function of stream and fuel injection parameters
11 p2002 A69-25336

Helmholtz resonance in rocket injectors as function of frequency response of interaction between chamber pressure and dissolved gas-fuel injection flow rate
12 p2148 A69-26806

Fuel injector-induced mass flux and mixture ratio distributions effects on combustion performance, chamber volume and stability, discussing combustion oscillation avoidance
16 p2877 A69-31731

Liquid propellant injector design for rocket thrust chambers, discussing mass and mixture ratio regulation
16 p2836 A69-31999

Oxygen difluoride-diborane propellant injector and chamber design criteria applied to unmanned spacecraft rocket engine development
[AIAA PAPER 69-508] 16 p2839 A69-32671

Integrated double oblique shock scramjet for supersonic combustion tests and instrumentation development, discussing fuel injection through sonic orifices, combustion data, etc
[AIAA PAPER 69-827] 16 p2840 A69-32673

Combustion of pure crystalline boron single particles injected into hot oxidizing gases streams at atmospheric pressure
[AIAA PAPER 69-562] 16 p2880 A69-32741

Rocket performance optimization by extending injector design technology to high performance injectors for space storable FLOX/LPG propellants
[AIAA PAPER 69-506] 16 p2846 A69-32778

Vortex motion enhancement of jet penetration and spreading in supersonic fuel injection into large diameter combustors
[AIAA PAPER 69-664] 17 p2953 A69-33437

Li-F-H tripropellant study, discussing injection method variations and thrust chamber configuration effects on characteristic velocity efficiency and heat flux measurement
24 p4362 A69-43128

Intermediate hydrazine-RFNA reaction product formed on injector nozzle and combustion chamber surfaces after fuel injection without ignition analyzed by various methods
24 p4365 A69-43669

FUEL OILS

Displacement pumps and fluids for extreme environments, discussing fluid types and operational parameters such as speed, pressure, temperature, power, displacement and size
06 p0931 A69-17188

Fuel requirements for flights up to Mach 3.5, discussing heat stable mineral oil based SST fuels
11 p1941 A69-25422

FUEL PUMPS

Liquid hydrogen circulation pump design emphasizing heat leaks
01 p0087 A69-11148

Liquid hydrogen and LOX boost pump design for Centaur missile and liquid hydrogen and LOX chill-down pump design for Saturn 4B missile
01 p0087 A69-11149

Vane type fuel pump designed for small gas turbine engines, describing design analysis and laboratory evaluation
[ASME PAPER 69-GT-45] 09 p1513 A69-22485

Fueling procedures for Boeing 747 aircraft, discussing design and operation of large capacity fuel trucks
10 p1674 A69-23631

Fueling procedures for Boeing 747 aircraft, discussing design of high rate mobile fuel dispensers
10 p1674 A69-23633

Close coupled accumulators for suppressing missile longitudinal oscillations (POGO) developed for Gemini and Titan 3, including pump interaction
[AIAA PAPER 69-547] 16 p2869 A69-32729

Transient performance of full flow hydraulic turbine driven two speed pump inducer system, formulating computer model
[AIAA PAPER 69-551] 18 p3140 A69-34415

FUEL SPRAYS

Gas turbine engines smoke reduction, aerated fuel sprays for smoke control on engine design and factors affecting visibility of exhaust plumes
17 p3020 A69-33350

Aerated fuel spray effect on smoke reduction from high pressure ratio aircraft gas turbine engines, including smoke measurement and visibility
19 p3395 A69-36770

Fuel droplet evaporation and combustion in still air as unsteady diffusion controlling phenomenon, basing calculations on flame front model
20 p3632 A69-37520

FUEL SYSTEMS

NT AIRCRAFT FUEL SYSTEMS

Gas turbine engines control and fuel systems integration, considering weight reduction
[ASME PAPER 69-GT-49] 09 p1571 A69-22483

On-off multiple tank fuel systems for single and twin engine light aircraft, noting fail-safe design
[SAE PAPER 69-0334] 11 p1825 A69-24502

Gaseous He bubbles injection into liquid propellant launch vehicle fuel lines to reduce vehicle pogo oscillations by lowering feed system natural frequencies
11 p1967 A69-25498

AH-56A Cheyenne armed compound helicopter designed to operate from unimproved bases with minimum support equipment, noting on-board fueling capacity
[AIAA PAPER 68-560] 12 p2017 A69-26770

Fueling process in internal combustion engines having fuel admission systems with different flow cross sections
19 p3393 A69-35824

Aircraft fuel vent line sensitivity to lightning hazards, using flame propagation and arrester experiments with high voltage and high current facilities
[SAE PAPER 69-0434] 23 p4062 A69-41651

FUEL TANK PRESSURIZATION

Model describing outflow of cryogenic propellant tank pressurized by pressurizing gas, predicting pressurant mass, gas and wall temperature distribution, inlet flow rate, etc
01 p0163 A69-11147

Volatile liquid pressurization, discussing pressurants, heat sources and system design
[AIAA PAPER 68-630] 02 p0232 A69-12382

Pressurization system for liquid rockets, analyzing inert weight and complexity reduction using Saturn 5 S-4B stage
02 p0305 A69-12386

Liquid nitrogen inertant for continuous suppression of pressurized fuel tank explosion
05 p0703 A69-16505

Fluidic component application to propellant tank pressurization and controller design
[AIAA PAPER 68-629] 09 p1442 A69-21980

Propellant pressurization system for British Black Arrow composite vehicle, describing valve design and performance
14 p2509 A69-29629

Liquid expulsion by direct pressurization of propellant tank in spinning missile system, demonstrating feasibility with subscale hardware
[AIAA PAPER 69-527] 16 p2838 A69-32651

Fluorine injectors for main tank injection of space vehicle liquid hydrogen tank, including study of hypergolicity and reaction product freezing
[AIAA PAPER 69-528] 16 p2767 A69-32717

Pressurant gas requirements for pressurized discharge of liquid hydrogen from propellant tanks for optimum pressurization system designs
[AIAA PAPER 69-526] 16 p2845 A69-32737

Main tank injection for packaged liquid missiles, discussing propulsion system design, pressurization, packaging and screen reservoir
[AIAA PAPER 68-627] 19 p3429 A69-35947

FUEL TANKS
NT WING TANKS
Axisymmetric vortex free motion of ideal fluid in conical container with spherical bottom under axial acceleration 06 p0910 A69-17335
HORA, flexible upper rocket stage, noting variable fuel tank capacity and high energy propulsion 08 p1409 A69-20094
Aircraft design, fabrication and finish techniques taking into account aircraft integral fuel tank corrosion due to contaminants associated with microbiological debris
[NACE PAPER 49] 08 p1320 A69-20599
Draining liquid surface dip formation in tanks of arbitrary shapes and drain hole positions 09 p1483 A69-21999
On-off multiple tank fuel systems for single and twin engine light aircraft, noting fail-safe design
[SAE PAPER 690334] 11 p1825 A69-24502
Fiber reinforced space vehicle combustion chambers and cryogenic fuel tanks, discussing design and elastomechanical problems 12 p2176 A69-25860
Stress corrosion cracking of titanium alloys in contact with high temperature fuel tank sealants 12 p2112 A69-25945
Aircraft integral fuel tanks corrosion causes and prevention, discussing microorganisms, maintenance and cleaning procedures, anticorrosive additives, etc 12 p2013 A69-25946
Fracture of bumper protected fuel tanks subjected to hypervelocity meteoroid impact, applying method of characteristics to stress wave propagation in tank walls
[AIAA PAPER 69-369] 13 p2367 A69-28301
Hele-Shaw and porous medium fuel tank systems behavior in simulated low gravity environment, studying sloshing, wetting, funnelling and fuel-driver gas interface stability
[AIAA PAPER 69-678] 17 p3021 A69-33444
Tank configurations allowing for sloshing in liquid fuel reaction control system in spinning satellite 18 p3219 A69-34796
Microbiological corrosion and degradation of aircraft metals and organic materials in fuel tanks 19 p3341 A69-35569

FUEL TESTS
Jet fuel lubricity evaluation by ball-on-cylinder device
[ASLE PREPRINT 68AM 4A-2] 01 p0083 A69-10914
Laboratory test stands for ignition, combustion and expansion processes experiments in hypergolic liquid fuels, noting minimal recombination gains 08 p1301 A69-20170
Hot air open circuit wind tunnel for testing vaporized fuel films heat and mass transfer over flat plates 08 p1302 A69-20878
Fuel requirements for flights up to Mach 3.5, discussing heat stable mineral oil based SST fuels 11 p1941 A69-25422
Turbine and jet engines kerosene fuels tests in small and medium size laboratory combustion chambers 13 p2240 A69-27932

FUEL VALVES
LOX preclude accumulator system with He pressurant for prevention of Pogo effect on Saturn 5 04 p0666 A69-15298
Propellant pressurization system for British Black Arrow composite vehicle, describing valve design and performance 14 p2509 A69-29629
Fluidic vortex valve to modulate solid propellant generated hot gas flow
[AIAA PAPER 69-424] 16 p2844 A69-32723
Hydrogen check valve with low cracking pressure and flow pressure drop for hydrogen vent system at Saturn launch pad
[AIAA PAPER 69-578] 16 p2845 A69-32738
Stability of nonlinear systems with state variable feedback applied to fuel valve servomechanism 21 p3687 A69-39460

FUELING
U REFUELING

FUELS
U AEROZINE
U AIRCRAFT FUELS
U CHEMICAL FUELS
U CRYOGENIC ROCKET PROPELLANTS
U DOUBLE BASE ROCKET PROPELLANTS

U FUEL OILS
U GELLED ROCKET PROPELLANTS
U HYDROCARBON FUELS
U HYDROGEN FUELS
U HYPERGOLIC ROCKET PROPELLANTS
U JET ENGINE FUELS
U JP-4 JET FUEL
U LIQUID ROCKET PROPELLANTS
U METAL FUELS
U METAL PROPELLANTS
U MONOPROPELLANTS
U NUCLEAR FUELS
U SOLID ROCKET PROPELLANTS

FULL SCALE FATIGUE TESTS
U FATIGUE TESTS
FULL SCALE TESTS
Full scale and transonic wind tunnel store separation characteristics, outlining uses of heavy and light scaling methods 17 p2896 A69-34035
Helicopter rotors forward-flight noise characteristics determined by wind tunnel tests compared to rotor noise during flyover 18 p3119 A69-35225
V/STOL model small scale tests compared with full scale tunnel or flight tests, considering normal differences in parameters and rotor instability 18 p3119 A69-35227

FUMES
Monograph on spreading of explosive vapor/air mixtures during aircraft fueling, covering underlying flow technology principles 15 p2551 A69-30930

FUNCTION GENERATORS
Zener diode function generators used in analog computers for solution of complex problems involving nonlinear relationship 02 p0214 A69-11595
Dynamic programming application to function generation, determining breakpoints for best linear approximation of one dimensional function 03 p0401 A69-13765
Interpolation filters with restricted transmission zeros in transmission function capable of reconstructing continuous function from equidistant sample value 05 p0735 A69-16617
Function generator for approximating function of many variables without recourse to multiplication, providing continuous functions representation 08 p1278 A69-20235
Pneumatic diode function generator for simulating nonlinear control systems, discussing operating characteristics and programming methods 11 p1858 A69-24580
Cumulative probability distribution of positive random variable from moment generating function, exemplifying exponential and Poisson functions 12 p2120 A69-25927
Time-pulse function generator with piecewise parabolic approximation for converting value given by DC voltage or time interval into DC voltage for arbitrary functional relation 12 p2079 A69-25968
Energy metric algorithm for Liapunov functions generation, discussing stability conditions in Wall and Moe work 12 p2122 A69-26521
Random variables generation from distribution having given failure rate function 12 p2102 A69-26571
Function generator internal storage and dimensions diminished, approximating functions of several variables by hyperplane strip 14 p2425 A69-29142
Theory, function generator routine and testing for six node 18 degree of freedom triangular element for plate bending 15 p2706 A69-30430
Recognition system for discrete decision function generation to select one out of two classes of objects, deriving solutions for selection probability 17 p2932 A69-33119
Threshold logic for LSI to realize broad range of functions noting signal control, gate characteristics, weighting, etc 17 p2943 A69-34122
Planar distributed function generator for analog computing scheme, considering operation, cosine circuit and temperature error 17 p2934 A69-34123
Random function output current obtained in phototube and scintillation detector including amplitude distribution, time measurements and pulse shape discrimination 22 p3947 A69-40670

Minimization algorithm for switching systems synthesis, describing design of mass spectrometer curve function generator and autonomous shift register 23 p4146 A69-42535

FUNCTION SPACE
NT BANACH SPACE
NT HILBERT SPACE
Integral operators on space of Borel measurable functions bounded considering weight function, giving condition for infinite complex matrices, mapping analytic sequence spaces 01 p0107 A69-11244
Nonlinear programming of optimization of parameters and control functions of dynamic systems 03 p0408 A69-12974
Matrix theorem giving necessary and sufficient conditions for leaving cone invariant, considering finite dimensional spaces 04 p0624 A69-15003
Volterra equation generalization extended and applied to functional Volterra equations, proving theorem dealing with topological, quasi-compact and uniform spaces 08 p1342 A69-20268
Functional equations of physical systems in strong coupling solved by quantum theory model of anharmonic oscillator, discussing relativistic invariant field theories 09 p1541 A69-22393
Nondifferential function minimization on entire vector space or bounded subset for application to minimax problems in function spaces, time optimal control, etc 10 p1721 A69-23863
Differential equations describing system stability with delay in functional space 11 p1919 A69-25093
Topologies introduced on state space for differential equations to obtain dynamical systems 11 p1909 A69-25409
Parametric variations method for solving nonlinear algebraic and transcendental equations, determining number of solutions in complex space 12 p2123 A69-26608
Regional boundaries in control-parameter space constructed by computer algorithm, involving parameter vibration direction changes in parameter plane 13 p2225 A69-27967
Algebra of quasi-homogeneous pseudodifferential operators applied to lateral boundary values of solutions of parabolic differential equations, discussing function spaces 17 p2994 A69-32842
Eigenvalue conversion of second variation test for algebraic and differential constraints to Jacobi accessory minimum problem by introducing norm in coordinate perturbation space 19 p3400 A69-35672
Ordinary differential equations in linear topological space extended from Fattorini investigation, emphasizing use of linear operator 19 p3360 A69-36599
Computer-algorithm elements required for engineering design and invention problems including design requirements, selection of spaces for variables using computerized heuristics, etc 19 p3280 A69-36666
Stability criteria for integral manifold formed by intersection of hypersurfaces in Euclidean n-dimensional space 21 p3770 A69-38850
Asymptotic stability of differential equations solutions in linear normalized spaces via Liapunov theorems extension 21 p3755 A69-39105

FUNCTION TESTS
U TESTS

FUNCTIONAL ANALYSIS
NT BANACH SPACE
NT CONVOLUTION INTEGRALS
NT FOURIER TRANSFORMATION
NT FREDHOLM EQUATIONS
NT HARMONIC ANALYSIS
NT HILBERT SPACE
NT HILBERT TRANSFORMATION
NT INTEGRAL EQUATIONS
NT INTEGRAL TRANSFORMATIONS
NT LAPLACE TRANSFORMATION
NT SINGULAR INTEGRAL EQUATIONS
NT TESSERAR HARMONICS
NT VOLTERRA EQUATIONS
NT WIENER HOPF EQUATIONS
NT ZONAL HARMONICS
Sobolev first embedding theorem providing relationship between global and local properties of functions in theory of differential equations 01 p0103 A69-10005

Book on approximate representation of regular functions of complex variable, discussing Faber polynomials, best approximation theorems, etc
01 p0104 A69-10616

Controllability of dynamic systems obtained by studying vector function increments along system trajectories
01 p0051 A69-10698

Finite f function computation by d/r circuit, discussing computation time
01 p0105 A69-10734

Unstable minimization problem of functional, examining construction of sequences and stability
02 p0271 A69-11648

Mathematical analysis to determine complete characteristic of functions tolerating polynomial approximation in mean in crescent type noncaratheodory domains
02 p0272 A69-12164

Extremum problems from functional-analytic point of view, discussing methods of solving and convergence conditions
03 p0456 A69-13403

Rayleigh-Ritz finite element method for approximate solution of nonlinear energy functional describing large deflection bending behavior of uniform beam under point loads
05 p0833 A69-15711

Functions satisfying mixed boundary conditions derived for boundary value problems involving regions of complex form
05 p0787 A69-16455

Optimal approximation of functional matrix, giving upper bounds for deviations of general matrices from closest special matrices
06 p0948 A69-17495

Cauchy problem for nonstationary linearized Navier-Stokes equations for fixed container partially filled with liquid
06 p0959 A69-17888

Cosserat functions for homogeneous isotropic elastic body filling finite domain with sufficiently smooth boundaries, noting eigenfunctions for first and second boundary value problems
07 p1173 A69-18499

Uniqueness conditions of expansions in series of functions stressing Jacobi series applied to singular partial differential equations
07 p1174 A69-18805

Volterra equation generalization extended and applied to functional Volterra equations, proving theorem dealing with topological, quasi-compact and uniform spaces
08 p1342 A69-20268

Total error of minimization of differentiable functionals based on gradient projection procedures
08 p1342 A69-20319

Second order tensor describing deformation of particles of continuum determined by functional, noting invariance restrictions
08 p1416 A69-20690

Iterative method for least square polynomial curve fitting with abscissas and ordinates subject to error
08 p1343 A69-20827

Singular integral method in approximation for synthesizing sequence of functions with spectrum of limited length
09 p1460 A69-22642

Tricomi theorem extension concerning intermediate value property of continuous real valued functions of real variable
09 p1533 A69-22797

Book on special functions and approximations covering differential and integral equations and attendant theories arising in mathematical physics analysis
10 p1717 A69-22801

Minimal distance of image boundary from origin and second coefficient of univalent function in unit disk
10 p1718 A69-22860

Numerical orthonormalized system of functions for formulating functional equations in potential and elasticity theory, considering boundary value problems
10 p1801 A69-23687

Liapunov functions generation for deterministic ordinary differential equations, discussing integral methods, quadratic forms, partial differential equations, canonical forms, etc
11 p1908 A69-24317

Flight dynamics problems, determining extremum of functional by graph-analytical method and with aid of Pontryagin maximum principle
11 p1823 A69-25343

Parabolic interpolation method for values of function given for certain values of argument and of first derivative, including numerical examples
12 p2121 A69-26434

Analog simulation of nonlinear functions of single independent variable compared digital to analog representation principles
13 p2224 A69-27531

Book on calculus of variations and optimal control theory, discussing functional analysis for use in space science
13 p2289 A69-28054

Inequality theorems for multidimensional functional Volterra equations formulated and proved, deriving upper and lower solutions
13 p2290 A69-28684

Applied function theory, Volume 6, Tables of theta functions and elliptical functions with examples, Part I
14 p2471 A69-29774

Functional analysis methods to solve Cauchy problem for linear nonhomogeneous differential equations with delayed argument
15 p2643 A69-30101

Soviet monograph on projective-iterative methods of solving operator equations in generalized metric and structurally normalized spaces
16 p2805 A69-32366

Thermoelectric converter systems optimization by geometry independent functions
18 p3093 A69-34782

Cauchy problem for homogeneous linear difference scheme with constant complex coefficients, giving stability lemmas
18 p3165 A69-35049

Simplification of linear equation of first kind with Tikhonov smoothing functionals
18 p3165 A69-35052

Autonomous functional differential equations with finite time interval dependent derivatives, resulting in periodicity theorem applicable to difference equations
19 p3361 A69-36600

Approximation error involved in difference optimal control problem substitution for differential optimal control problem based on functional minimization
20 p3509 A69-36989

Algorithm for Chernousko local variation method during application to solution of variational problems involving nonadditive functionals, assessing convergence
20 p3513 A69-36990

Ordinary coherence functions for computing frequency response in mechanical systems under random excitation
20 p3537 A69-37162

Discrete extremum problems solution convergence to optimal control continuous problem as functional optimal value and optimal control
21 p3684 A69-38430

Partial differential equation initial value problems analyzed by ordinary differential equations via functional approximation method
21 p3756 A69-39132

Variational problem for nonlinear functionals connected with finite plasticity, extending existence and uniqueness theorems to limit analysis
21 p3837 A69-39157

Minimization of unconstrained function of several variables by gradient dependent techniques, discussing applications to boundary value problems in optimal control
22 p3975 A69-40333

Uniqueness theorem and successive approximations for delay functional differential equations, noting scalar problems
24 p4341 A69-43236

FUNCTIONAL INTEGRATION

Representation for real functions of quantum mechanical momentum operator obtained by functional integration in phase space
01 p0106 A69-10930

FUNCTIONS [MATHEMATICS]

NT AIRY FUNCTION
NT ANALYTIC FUNCTIONS
NT APERIODIC FUNCTIONS
NT ASYMPTOTES
NT BOOLEAN FUNCTIONS
NT CONFORMAL MAPPING
NT COORDINATE TRANSFORMATIONS
NT DELTA FUNCTION
NT DISCRETE FUNCTIONS
NT DISTRIBUTION FUNCTIONS
NT DISTURBING FUNCTIONS
NT ELLIPTIC FUNCTIONS
NT ENTIRE FUNCTIONS
NT ERROR FUNCTIONS
NT EXPONENTIAL FUNCTIONS
NT FOURIER TRANSFORMATION
NT GAMMA FUNCTION
NT GREEN FUNCTION
NT HAMILTONIAN FUNCTIONS
NT HANKEL FUNCTIONS

NT HARMONIC FUNCTIONS
NT HYPERBOLIC FUNCTIONS
NT HYPERGEOMETRIC FUNCTIONS
NT KERNEL FUNCTIONS
NT LAME FUNCTIONS
NT LAPLACE TRANSFORMATION
NT LEGENDRE FUNCTIONS
NT LIAPUNOV FUNCTIONS
NT LINEAR TRANSFORMATIONS
NT LOGARITHMS
NT LORENTZ TRANSFORMATIONS
NT MATHIEU FUNCTION
NT MAXWELL-BOLTZMANN DENSITY FUNCTION
NT MELLIN TRANSFORMS
NT MONOTONE FUNCTIONS
NT NORMAL DENSITY FUNCTIONS
NT ORTHOGONAL FUNCTIONS
NT ORTHONORMAL FUNCTIONS
NT PEARSON DISTRIBUTIONS
NT PERIODIC FUNCTIONS
NT POISSON DENSITY FUNCTIONS
NT PROBABILITY DENSITY FUNCTIONS
NT PROBABILITY DISTRIBUTION FUNCTIONS
NT RATIONAL FUNCTIONS
NT RAYLEIGH DISTRIBUTION
NT RECURSIVE FUNCTIONS
NT SINE SERIES
NT SPACE-TIME FUNCTIONS
NT SPHERICAL HARMONICS
NT STEP FUNCTIONS
NT STRESS FUNCTIONS
NT TANGENTS
NT TIME FUNCTIONS
NT TRANSCENDENTAL FUNCTIONS
NT TRIGONOMETRIC FUNCTIONS
NT WEIBULL DENSITY FUNCTIONS
NT WEIGHTING FUNCTIONS
NT WHITTAKER FUNCTIONS

Displacement function selection in calculating rubber-metal valve design, considering boundary conditions of material deformation
01 p0087 A69-10829

Expanded describing functions used in studying nonlinear control systems with multiplication points, considering systems with/without integral response
01 p0054 A69-11359

Sunspots autocorrelation functions in sunspot area on solar disk, tabulating extremal values
02 p0314 A69-11677

Existence theorems for solutions to second order ordinary differential equations
02 p0272 A69-12129

Necessary and sufficient conditions for solution boundedness for Lienard equation with forcing function
02 p0272 A69-12132

Minimal conditions for association of binary variables, studying nondecreasing functions and equivalence in coherent binary systems theory
04 p0624 A69-15007

Book on computer evaluation of mathematical functions, discussing errors, square and cube root, Chebyshev polynomials, approximation, rational function, asymptotic expansions, etc
05 p0723 A69-15955

Motion stability analysis of system represented by differential equation having continuously differentiable functions as continuously acting disturbances
05 p0794 A69-16450

Difference iteration method for solving three dimensional Dirichlet problem presented as system of plane Dirichlet problems
05 p0787 A69-16457

Uniform matched asymptotic approximations derived for various functions, with application to boundary value problem for ordinary differential equation with turning point
07 p1180 A69-18810

Symmetry considerations method for determination of Walsh function values independent of previously computed functions
09 p1452 A69-21321

Duality between effect and influence problems in linear elastoplasticity, obtaining rules for influence functions plotting
09 p1612 A69-21604

Ultimate state periodic analysis of nonlinear electric systems by approximation methods in calculus of variations, discussing functional concept
09 p1474 A69-22448

Perturbation solution for propagation of fourth order coherence function in random medium extended to larger field fluctuations, deriving integrodifferential equation
10 p1724 A69-23042

Correction of linear functional differential equations with time delay showing error due to incorrect in-

terchange of order of integration involving Stieltjes integral
10 p1721 A69-23642

General extremality for optimal controls with restricted phase coordinates and with unorthodox criterion function, discussing hypotheses for deriving necessary conditions
10 p1721 A69-23864

Potential functions for three dimensional problems of elliptical crack in elastic solid
10 p1802 A69-24026

Optimal controls for differential system nonlinear in state function and linear in control function
10 p1667 A69-24057

Integral representation for Wiener Hopf factorization of functions of complex variables for numerical processing of radiation problems
11 p1851 A69-24998

Computational method for quasi-optimal control with parameter sensitivity function, noting application to dynamical system model
11 p1859 A69-25165

Eigenvalue approximation for first order systems by introducing artificial periodicity through successive impulse functions of alternate sign
13 p2287 A69-27242

Model atmosphere source function, mean intensity and flux by matrix methods
13 p2288 A69-27564

Variational principle for finite element method restricting deflection shapes to small region of model surrounding single element
13 p2364 A69-28229

Sunspots autocorrelation functions in sunspot area on solar disk, tabulating extremal values
13 p2355 A69-28708

Wentzel-Kramers-Brillouin approximation validity determined by sufficiency conditions based on differential equations series solution
14 p2471 A69-29454

Source functions of IR Fraunhofer lines obtained using solar disk equivalent width method, noting LTE role
14 p2528 A69-29961

Master equation in quantum optics phase-space formulation based on Schrodinger equation of motion, noting application to Volterra integral equation and Born approximation
15 p2633 A69-30307

Polygonal approximation to functional equation solution by using search algorithms, listing FORTRAN IV programs
15 p2644 A69-30424

Recognition systems nonlinear discriminant function for separating linear inseparable patterns, describing orthogonal representation, correlation ratio and average variance criteria
15 p2645 A69-30806

Random functions applications to random vibrations, discussing spectral power density, ergodic steady functions, etc
17 p3054 A69-33063

Function theoretic solution of dual integral equations applied to boundary value problem of supersonic flow over infinite span thin wing
19 p3239 A69-36311

Minimax error technique used with finite difference methods to estimate error in approximations to functions defined by nonlinear differential equations
20 p3568 A69-37832

Relation between smoothed and filtered linear least squares estimates of signal process in white noise from deriving resolvent identity of covariance function
21 p3754 A69-38432

Extremal trajectory formulations for state variable inequality constrained optimization problems, forming augmented functional
23 p4182 A69-41907

Complex configuration shells described by single analytical expression using R-conjunctive and R-disjunctive functions yielding boundary equations
23 p4229 A69-41991

FUNGI

NT MICROSPORES
NT NEUROSPORA
NT SPORES
NT YEAST

Aluminum corrosion by fungi isolated from jet fuel system with predominance of Cladosporium resinae, noting protective coatings
04 p0616 A69-14765

Aluminum corrosion by fungus culture isolated from jet fuel system
06 p0941 A69-17123

FUNGICIDES

U URIC ACID

FUNNELS

Laminar boundary layer on funnel wall, considering internal vortical and radial flow
21 p3692 A69-38611

FURAN RESINS

U POLYAMIDE RESINS

FURNACES

NT SOLAR FURNACES
NT VACUUM FURNACES

Impinging jet flames on furnace hearth, analyzing thermal boundary layer characteristics and convective heat transfer rates
06 p1035 A69-17933

Molten high melting compounds obtained by arc furnace with consumable electrode and adjustable protecting atmosphere
12 p2055 A69-26264

Furnace for automatic high temperature cycling in controlled oxidizing environment
12 p2093 A69-26483

FUSELAGE MOUNTING

U AIRCRAFT PRODUCTION

FUSELAGES

Flow fields about upswept rear fuselages of rear loading cargo transport aircraft
06 p0859 A69-17492

Vibration characteristics of rectangular plate with fatigue crack and subject to tensile load, applying results to crack propagation in fuselage panels
08 p1413 A69-20399

Subscale aircraft fuselage section fabricated with lightweight graphite fiber/epoxy resin composite material
09 p1509 A69-22341

Titanium fuselage skin contouring to shallow compound curvature of supersonic aircraft by elastic draping, shotpeen forming and cold stretching, discussing residual stresses
09 p1512 A69-22374

SST fuselage response to reverberant and turbulent boundary layer noise calculated for computing equivalent reverberant acoustic fields
15 p2549 A69-30302

Fixed weight aircraft growth factor variation with location of initial weight penalty along fuselage station, using static stability margin and trim capability [SAWE PAPER 796]
18 p3220 A69-34862

Forced pressure fluctuations in hydraulic systems of aircraft fuselages and engines, taking into account square law of losses at resistance points
18 p3094 A69-34991

Fuselage corrosion effect on structure and skin of older aircraft with emphasis on pressurized aircraft
21 p3646 A69-38392

FUSES [ORDNANCE]

General and classical statistical techniques for cutting effectiveness and operational reliability of cutting fuses
10 p1749 A69-23004

Detonating fuses for separation of missile and rocket stages, noting separation ease, aftereffects, priming capability and fabrication
10 p1752 A69-23023

FUSIBILITY

Presprayed metal films influence on visibility and contact resistance of GaAs prior to fusing in Sn, In and lead contacts
10 p1748 A69-24214

Fusibility diagrams for Ti-Ta-Cr by determining specimens melting points after homogenization at various temperatures in argon
22 p3969 A69-40075

FUSIFORM SHAPES

U CONES

FUSION [MELTING]

Powder metallurgy, fusion and chemical vapor deposition techniques in manufacturing tungsten base alloys
07 p1165 A69-18792

Thermodynamic consequences of Lindemann mechanism for fusion of pure body, discussing application to isolated equilibrium system of solid and liquid phases
07 p1242 A69-19322

Continental diabases and oceanic tholeiites in light of rare earth and barium abundances and partition coefficients indicating fusion process
08 p1310 A69-20945

FUSION WELDING

NT ARC WELDING
NT BRAZING

NT ELECTRON BEAM WELDING
NT ELECTROSLAG WELDING
NT GAS TUNGSTEN ARC WELDING
NT GAS WELDING
NT LOW TEMPERATURE BRAZING
NT PLASMA ARC WELDING

Fusion, resistance and pressure welding of titanium, discussing shielding, brazing, diffusion and adhesive bonding
02 p0253 A69-12064

Oxygen free fluxes for fusion welding titanium alloys, discussing weld structure and properties
06 p0930 A69-17093

Wrought superalloys fusion welding behavior, discussing hot cracking, hot microfissuring and strain age cracking [SAE PAPER 690102]
09 p1503 A69-21558

Microcracking susceptibility studies of Inconel 718 weld heat affected zones, noting hot ductibility, weld circle patch and fillerless fusion welding tests
11 p1905 A69-24933

Fusion and solid state welding of steels, considering electron beam, HF resistance, friction and explosive welding
12 p2100 A69-25830

High power pulsed laser welding system for structural alloys and parts, discussing pulse length, repetition rate, shielding and applicability
19 p3320 A69-35556

Al alloy application to welded primary airframe structures, discussing welding processes with emphasis on fusion welding [SBAC PAPER 4]
20 p3549 A69-37445

Quality control and dimensional accuracy in airframe structures fusion welding
20 p3549 A69-37446

Fusion welding for thin gauge corrugated core sandwich airframe structures capable of operating at sand temperature, discussing equipment, techniques and quality control [SBAC PAPER 9]
20 p3549 A69-37448

H concentration and pore formation in Ti fusion welds
24 p4319 A69-42885

Seam welding processes and power supply effects on control efficiency based on electrode displacement for Al-Mg alloys
24 p4319 A69-42919

F4H AIRCRAFT

U F-4 AIRCRAFT

G

G FORCE

U ACCELERATION [PHYSICS]

G-91 AIRCRAFT

Fiat G.91Y subsonic light tactical fighter, discussing fixed armaments and weapons facilities
02 p0193 A69-12679

GADOLINIUM

High temperature research on systems formed by zirconium dioxide with samarium and gadolinium sesquioxides near melting point
01 p0101 A69-10044

Ferromagnetic ordering effect on gadolinium dialuminide thermoelectric power, measuring temperature dependence of power and electrical resistivity
03 p0485 A69-13322

Magnon density of states of ferromagnetic gadolinium trichloride in magnetic field, using high resolution optical spectroscopy
03 p0494 A69-14257

Magnetic sublattices interactions in gadolinium ferrite garnet, estimating magnetization level temperature dependence
08 p1374 A69-21186

Gadolinium-cobalt system investigation by X ray diffraction thermoanalysis and metallography for intermetallic compounds, noting structure transformation and homogeneity
11 p1903 A69-24574

Magnetic sublattices interactions in gadolinium ferrite garnet, estimating magnetization level temperature dependence
18 p3183 A69-35155

GAGES

U MEASURING INSTRUMENTS

GAIN [AMPLIFICATION]

U AMPLIFICATION

GALACTIC EVOLUTION

Collisionless computer model performing gravitational experiments with two dimensional galaxy
02 p0322 A69-12271

Interstellar gas field dynamic instability, discussing enhanced ambipolar diffusion in twisted field
02 p0326 A69-12707

Evolutionary theory of origin and properties of Seyfert galaxies and quasars, postulating collisions within superdense clusters leading to supermassive stars and supernovas
05 p0819 A69-15703

Quasar and radio galaxy evolution, discussing energy release rate and particle acceleration effects on radio and optical emissions
05 p0822 A69-15852

MHD quasar model consisting of galaxy with supermassive plasma nucleus moving in magnetic field
05 p0822 A69-15853

Cosmology, discussing big bang and steady state models, arrow of time, red shift/distance relation, background radiation, etc
07 p1210 A69-18390

Galactic model with differential rotation, discussing experiments on bar and cylindrical galaxy and spiral and loop structures formation
07 p1216 A69-19204

Origin of galaxies, discussing initial conditions of formation including density, kinematic and composition inhomogeneities, time effect, etc
07 p1218 A69-19280

Evolution of galaxies, considering masses, gas masses, luminosities, spectra and motions
07 p1219 A69-19297

Critical density ratio concept introduced into cosmological models for matter concentration into galaxies in expanding universe
08 p1381 A69-19794

Physical conditions of intergalactic space in Local Group using virial theorem and assuming energy equipartition, discussing temperature, ionized hydrogen density, turbulent motions, etc
08 p1381 A69-19795

Galactic angular momentum of rotation, applying rotation theory to gravitational instability model of galactic formation
08 p1383 A69-20050

Galactic halo chronology determination by positron component flux measurement in primary cosmic rays
08 p1386 A69-20084

Morphology of E and SO galaxies in terms of equilibrium isopleths within general relativity
08 p1395 A69-20636

Galaxy formation from elements primeval abundance viewpoint stressing initial helium abundance
08 p1400 A69-20894

Stellar abundance and origin of elements, discussing stellar atmospheres and gaseous nebulae spectral determination, chronology of galactic halo, etc
09 p1587 A69-21306

Photon whirls and formation of protogalaxies, discussing density inhomogeneities in hot model of universe in terms of pregalactic structure dynamics
09 p1587 A69-21355

Quasi-stellar radio sources /QSS/ and radio galaxies structure and evolution, discussing nucleus nonuniform model
09 p1592 A69-21500

Cosmology, reviewing Friedman and Lemaitre model, big bang model, primeval fireball hypothesis for residual black body radiation and galactic origin theories
09 p1608 A69-22715

Solid hydrogen condensation on graphite grains for microwave background, discussing hydrogen grain promotion of galactic and stellar formation
10 p1776 A69-23216

Magnetic field and magnetic energy evolution in infinitely conducting homogeneous isotropic turbulent medium, applying results to galactic magnetic field model
10 p1783 A69-23793

Infinitesimal bending oscillations and/or responses of thin rotating disks applied to thin disk galaxies, discussing Magellanic Cloud passage near galactic center
10 p1786 A69-24110

Chemical compositions and ages of M67 and NGC 188 determined from color-magnitude diagrams, noting stellar distribution near gap in diagram and He content
10 p1789 A69-24128

Galaxies classified by matter content of nucleus, discussing evolution
11 p1953 A69-24351

Universe origin, discussing big bang theory, effects of expansion time and temperature on elementary particles, RF quanta, etc
11 p1953 A69-24352

Pulsed radio source near Crab Nebula studied to estimate age of longer period pulsars and frequency of pulsar-producing events in galactic history
11 p1963 A69-25252

Book on stellar, galactic and nucleosynthetic evolution covering nuclear, Fermi, electromagnetic and gravitational interactions roles
11 p1964 A69-25413

Cosmogonic nature of galactic nuclei activity, emphasizing streamers ejection and new formations in galaxies
12 p2163 A69-27016

Statistical data on space density of bright elliptical galaxies, radio galaxies, quasars, noting relation between space density and age
12 p2165 A69-27033

Isotropic 3 K black body radiation implications for hot cosmological model, formation of galaxies, existence of superdense bodies and density nonuniformity during prestellar stage
12 p2167 A69-27047

Interacting NGC 4485 and 4490 galaxies instability, establishing early stage of evolution from morphological and spectroscopic results of photographic observations
12 p2169 A69-27056

Intergalactic matter capture by NGC 1614 nucleus, stellar ejection from galaxies, explosive separation of close binary and other unsteady phenomena in galaxies
12 p2169 A69-27061

Galactic formation by massive matter cloud passage through antimatter cloud, discussing radio sources genesis
12 p2170 A69-27064

Gasdynamic phenomena during subsonic or supersonic motion of isothermal gas under action of gravitational forces in flatten axisymmetric galaxy containing spiral density waves
12 p2170 A69-27065

Spiral arms as wakes of gravitational shock waves arising at galactic nucleus boundary and propagating outward through interstellar gas
12 p2170 A69-27066

Galactic force law from observed stellar velocity and space density distribution
13 p2348 A69-27802

Twelve color stellar photometry for studying galaxy synthesis, relating observations to temperature, luminosity and metal abundance
13 p2348 A69-27804

Galactic formation in Lemaitre universe from statistically probable density fluctuations, using perturbation theory and Newtonian cosmology
14 p2520 A69-29373

Close galactic encounters in dense galactic clusters, discussing effects on internal motions dispersion and stellar dissipation
14 p2521 A69-29461

Polarization characteristics of quasars, radio galaxies and galactic objects suggesting separate evolutionary processes
14 p2526 A69-29771

Galactic nuclei nature, activity, evolution and classification
14 p2527 A69-29896

Low density Friedmann universe models with non-zero cosmological constant and long ages, deducing galaxy evolution rates from magnitude-red shift relations
14 p2527 A69-29944

Hydrogen gas role in galaxy formation, estimating quantity needed to dissipate gas cloud contraction energy, discussing formation mechanics of molecular hydrogen
15 p2680 A69-30204

Diatomic hydrogen abundance evolution in uniform medium, discussing photodissociation effects and galactic evolution
15 p2680 A69-30205

Symmetry between koinomatter and antimatter in universe, discussing koinonucleons production, big bang theory, protogalaxy model, quasi-stellar objects, galaxy evolution, etc
15 p2690 A69-30670

Galaxies formation from superstars ascribed to superstar instabilities
15 p2696 A69-31151

Viscous and thermal generators applicability to production of spin generated galactic magnetic fields in primordial fireball
16 p2866 A69-32812

Supernovae research, discussing supernovae classes and connections with cataclysmic processes in galactic evolution
17 p3044 A69-34173

Aligned galaxies, discussing possible formation by consecutive explosive ejections of new galaxies from parent galaxy
17 p3044 A69-34175

Dwarf elliptical galaxies of local group, discussing star distribution and orbits, formation process, origin and distribution about Milky Way
18 p3194 A69-34424

Photon whirls and formation of protogalaxies, discussing density inhomogeneities in hot model of universe in terms of pregalactic structure dynamics
18 p3197 A69-34745

Spiral arms interpreted and derived as consequences of galactic nuclei explosion
20 p3599 A69-37468

Universe evolution from hot initial state, discussing element synthesis, quanta, radiation particles, etc
21 p3795 A69-38401

Density fluctuations in universe during early stages, using hot big bang cosmological model
21 p3814 A69-39571

Gaseous self gravitating mass equations applied to galactic evolution and star formation
23 p4213 A69-41716

Radio studies of galactic structure, discussing Milky Way origin and formation
23 p4217 A69-42320

Galactic evolution using concept of stellar populations and correlation with metal and He abundances
23 p4218 A69-42323

Carbon isotopes compared in interstellar formaldehyde transition for galactic nucleosynthesis, discussing spectrum analysis of radio astronomical telescope observations
23 p4220 A69-42376

Density fluctuations during later stages of formation of universe, emphasizing problems of galactic cluster formation
23 p4221 A69-42390

Fluctuations in 3K radiation, considering scattering effect on gravitational fields of galactic clusters and large coherence or wavelength scattering by gravitational radiation
23 p4222 A69-42401

Galactic magnetic field origin from galactic turbulence, calculating individual Fourier components in random turbulent velocity
24 p4375 A69-42658

Book on physics and evolution of galaxies covering properties, stellar content, interstellar matter, high energy particles and radio galaxies
24 p4384 A69-43167

GALACTIC MAGNETIC FIELDS

U INTERSTELLAR MAGNETIC FIELDS

GALACTIC RADIATION

Energetic X ray intensities from large and small Magellanic clouds investigated by balloon flight sky survey, noting energy flux upper limits
01 p0150 A69-10370

Cosmic ray neutron integrated flux measurements up to 350 km for energies to 15 Mev, determining neutron leakage flux
01 p0146 A69-11223

Free access of low energy galactic particles to solar wind lines of force due to stochastic nature of lines
01 p0147 A69-11238

Solar and galactic cosmic rays measurement data to investigate variation in time of relations between cosmic rays modulation amplitude and solar activity variations
02 p0306 A69-11658

UV and X ray radiations of stars and interstellar gas of Milky Way and remote galaxies
02 p0316 A69-11906

Galactic Jupiter Probes investigating Jupiter atmosphere and emissions and deep space cosmic radiation
02 p0324 A69-12303

Normal galaxies radio emission and brightness of metagalactic radio background
02 p0325 A69-12564

Optical radiation from galaxies, discussing starlight, nonthermal flux and radiation from hot gas
02 p0326 A69-12706

Galactic X ray sources, discussing location along spiral arms, age and properties of stars responsible for emission

03 p0497 A69-12930

Galactic cosmic ray modulation by interplanetary magnetic fields, discussing compatibility of several models with experimental data

03 p0498 A69-12933

Numerical calculation of trajectories of high energy cosmic rays in galactic disk, using quasi-longitudinal model of magnetic field

03 p0501 A69-13960

Public health aspects of galactic radiation exposure at supersonic transport altitudes

03 p0375 A69-14072

Cosmic ray time variation and anisotropies near earth, discussing galactic and solar cosmic rays, trajectories in geomagnetic field, etc

03 p0504 A69-14236

Planetary nebulae as possible low energy galactic X ray source

04 p0661 A69-15144

Seyfert galaxies nuclear regions, noting multicolor photometric measurements between 0.3 and 1.6 micron and measurements of M87 jet at 1.55 micron

04 p0663 A69-15386

X ray emission from Seyfert galaxy nuclei, noting model with bremsstrahlung from hot source

04 p0649 A69-15387

Supernova remnant theories used to interpret results of 1-mile Molonglo cross type radio telescope survey of nonthermal galactic sources

04 p0664 A69-15441

X ray and gamma astronomy, discussing galactic gamma radiation source and diffuse X ray background radiation

06 p0998 A69-16969

Modulation of galactic cosmic rays due to electromagnetic conditions of interplanetary space, considering time variations and Parkers model

06 p0989 A69-17287

Galactic cosmic rays anisotropies due to density gradient perpendicular to ecliptic plane studied, using diurnal and semidiurnal component and intensity deficiency

06 p0990 A69-17289

Radio spectrum and cosmic ray electron data evaluated concerning conditions in Galaxy, deducing mean magnetic fields

06 p0991 A69-17309

Particle radiations and magnetic fields in metagalaxy, discussing galactic injection spectrum problems

06 p0991 A69-17310

Electron formation in lower ionosphere due to cosmic ray-atmosphere interaction, analyzing ionization of subrelativistic and relativistic solar and galactic cosmic rays

06 p0920 A69-17726

Radio spectra analyzed for NGC 1052 and NGC 4278 elliptical galaxies, discussing 178 MHz flux density, anomalies and radiation absorption mechanisms

06 p1009 A69-17959

Galactic soft X rays observation with two rocket-borne gas filled counters, noting source near Wolf-Rayet star Gamma Velorum in Vela

07 p1204 A69-18599

Cosmic ray astrophysics, discussing chemical composition, energy spectrum and galactic sources

07 p1205 A69-18909

Absolute isophotometry of hydrogen alpha photographs of bright galactic H II regions, attributing difference between theoretical and observed ratio to interstellar absorption

07 p1217 A69-19231

Astronomical unit determined by measuring Doppler shift of spectral features of galactic hydrogen

07 p1222 A69-19590

Rosette Nebula structure from high resolution observations at 178 MHz of galactic plane, deriving 8600 K electron temperature for Nebula, discussing Monoceros Nebulosity

07 p1223 A69-19625

Solar activity modulation of galactic cosmic rays with more than 1 Gev energy

08 p1378 A69-20224

Low latitudes observations of 21 cm line of H I in galactic center direction, giving contours maps of brightness temperature

08 p1392 A69-20562

Sky background of soft X ray emission in spectral band explained by emission lines from galaxies

08 p1380 A69-20769

Galactic H 56 alpha recombination radio line observation in Omega Nebula in millimeter band with radio telescope, obtaining electron temperature

08 p1397 A69-20771

Wideband 1665 MHz OH emission source in Carina region of galaxy in weak continuous radiation region with low degree of polarization

08 p1397 A69-20772

Radio spectra of normal galaxies noting transition in spectrum

08 p1398 A69-20777

Emission line galaxy NGC 5253, discussing radial velocity, line width and excitation and similarity to Seyfert galaxies

08 p1407 A69-21132

Astronomical data on background radiation examined for existence of galactic radio halo

09 p1590 A69-21395

Galactic and intergalactic ionic fine structure transitions effect on background microwave radiation intensity

09 p1590 A69-21445

Approximate solution of nonlinear differential equation describing interaction between galactic cosmic rays and solar wind, obtaining four domains

09 p1575 A69-21524

Further microwave emission lines and ammonia clouds in Sagittarius region, tabulating relevant transitions in ammonia and water

09 p1597 A69-22150

Galactic cosmic ray scattering and energy loss through solar wind interaction

09 p1580 A69-22202

Centaurus constellation search for gamma rays using balloons, discussing radio and X ray luminosity

09 p1580 A69-22269

Solar modulation of galactic cosmic rays, discussing disagreements between convection diffusion theory and observation

09 p1581 A69-22744

X rays from galactic center and Centaurus regions, discussing Cen X-2 flux

09 p1583 A69-22765

Radioactivity levels estimation at surface and in bulk of solar system planets caused by galactic and solar cosmic rays

10 p1756 A69-22813

Quasars and explosive processes in galaxies as cosmic ray sources in expanding universe, studying relation between galactic and metagalactic cosmic rays

10 p1756 A69-22815

Satellite data on galactic cosmic ray variations near magnetosphere and in interplanetary space, discussing Forbush decreases

10 p1756 A69-22819

Galactic cosmic ray modulation and solar activity analyzed on basis of cosmic ray measurement in stratosphere

10 p1758 A69-22832

Galactic and solar cosmic ray modulation in interplanetary space during different phases of 11 year solar activity cycle

10 p1758 A69-22833

Metallicity index Q value difference between cluster and noncluster galaxies determined from UV, blue and violet observation data

10 p1774 A69-22964

Qualitative considerations of color indices grouping for Abell-1781 cluster of galaxies, table of data and identification charts

10 p1775 A69-23204

Position and polarization of 1720 MHz OH emission from W28, W44 and galactic center, considering unresolved concentrations of shell type nonthermal sources

10 p1776 A69-23220

RF spectroscopy of OH molecule, RF absorption by galactic OH and radio emission from OH in dust clouds

10 p1781 A69-23671

Diffuse galactic radiation reinterpretation by solving same transfer problem exactly for properties of interstellar particles

10 p1782 A69-23680

Nuclear sizes, emission line widths and densities in Sc galaxy M 51 and Seyfert galaxy NGC 4151, noting similarities and difference between nuclei

10 p1785 A69-24089

Position of OH sources near seven galactic radio sources determined with two element variable-base-line interferometer, noting strong circular polarization

10 p1787 A69-24114

Radio brightness map at 22.25 MHz of galactic plane including H II regions IC 1805 and IC 1848, discussing LF absorption

10 p1787 A69-24115

Biological radiation doses and protection from galactic, solar particle and trapped radiation in space, noting secondary radiation and bremsstrahlung in absorber

11 p1831 A69-24866

Hydroxyl microwave emission sources in Cygnus not connected with continuum emission

11 p1964 A69-25403

Spheroidal galaxies with early type spectra distinguished by UV continuum, discussing telescopic spectral and color observations

12 p2159 A69-26663

Radio galaxies luminosities distribution and spectral indices, galactic structures and diameters, considering relations between radio emission parameters

12 p2165 A69-27031

Radio galaxy identification and luminosity measurement, noting limitations of red shift observation methods

12 p2165 A69-27032

X ray emission from radio galaxies as possible bremsstrahlung radiation of hot gas, noting Crab Nebula

12 p2166 A69-27037

Blue, UV and yellow spectral observations of M 82 /NGC 3034/, obtaining polarization dependence on reciprocal of wavelength, polarization and color characteristics

12 p2169 A69-27057

H alpha line photograph in M 82 spectra, giving equivalent radiating area and total ionized hydrogen mass

12 p2171 A69-27067

Cosmic rays suggested as origin of interstellar grain alignment, discussing galactic central radiation, gas collisions and isotropic bombardment

13 p2333 A69-28469

Galactic and relativistic and subrelativistic solar cosmic rays effect on electron production rate in ionosphere, detailing low energy SCR-atmosphere interactions

13 p2333 A69-28544

Solar and galactic cosmic rays measurement data used to investigate variation in time of relations between cosmic rays modulation amplitude and solar activity variations

13 p2333 A69-28689

Rocket observations of Lyman alpha anisotropic galactic radiation, noting distribution of neutral interstellar hydrogen near sun

14 p2516 A69-28952

Galactic anticenter region surveyed at 13.1 MHz, observing ionized hydrogen concentrations in galactic plane

14 p2519 A69-29370

Annihilation gamma ray spectra from equilibrium spectra of secondary galactic positrons

14 p2514 A69-29948

High energy gamma rays detection by balloon near geomagnetic equator, observing enhanced flux from galactic disk

15 p2675 A69-30695

Galactic cosmic rays and Alfvén waves interaction, considering gyration frequency resonance, wave growth, Fokker-Planck equation and diffusion model

15 p2675 A69-30761

Energetic gamma ray emission from Cygnus A and X-1, describing high altitude balloon telescope observation and gamma ray emulsion process

15 p2676 A69-30888

Extraterrestrial X ray galactic and extragalactic sources research fields, emphasizing identification with optical objects

15 p2696 A69-31213

Matter traversal of high energy primary galactic cosmic ray protons from antiproton flux and energy measurements

15 p2678 A69-31491

Approximate solution of nonlinear differential equation describing interaction between galactic cosmic rays and solar wind, obtaining four domains

16 p2851 A69-32519

RF spectral line detection from ortho hydrogen ions in Omega Nebula and NML Cygnus

16 p2864 A69-32571

Irregular dwarf galaxies as source of faint objects in close galactic groups

16 p2864 A69-32597

Origin of galactic gamma rays, discussing evidence in support of interstellar gas in galactic disk and production of neutral pions and bremsstrahlung

16 p2852 A69-32806

Earth motion relation to cosmic background radiation excess determined from radiometer study of galactic radiation

17 p3022 A69-32864

Galactic novae observational data and theoretical interpretations, considering envelope detachment from star, luminosity, motion and emission line intensities
17 p3032 A69-33103

Optical spectrum of galaxy NGC 3031 nucleus, considering emission and absorption lines and continuum
17 p3034 A69-33396

Red shift table for six galaxies near Coma Cluster from spectrograms of absorption lines
17 p3044 A69-34182

Cosmic X rays diffuse component possible origin, discussing galactic gamma ray flux and disagreement with measured isotropy
18 p3185 A69-34275

Cosmic ray propagation equilibrium model for rays origin and storage in galaxy, considering energy dependence of nuclei relative abundances
18 p3185 A69-34276

Extragalactic radiation depolarization through Milky Way transit determined from linear polarization and flux density measurements of discrete radio sources at 21.2 cm
18 p3190 A69-34287

Cosmic ray approach directions computation for high latitude stations, discussing results for low rigidity galactic cosmic rays and solar corpuscular events detection
18 p3187 A69-34940

Low energy cosmic ray density in Galaxy due to pulsar PSR 0833-45 caused by mass ejection
18 p3187 A69-34995

Milky Way continuum radiation at 4170 MHz using parabolic antenna, mapping discrete sources concentration at galactic equator
18 p3200 A69-34996

Radio emission attributed to galactic nebula NGC 6857, suggesting origin in high density H II regions excited by OB star clusters
18 p3202 A69-35209

Search for diffuse galactic light component between 2100-2800 Å by rocket measurements of night sky brightness, showing low albedo of interstellar dust
18 p3202 A69-35210

Water vapor microwave emission measurement from galactic hydroxyl sources
18 p3205 A69-35435

Be 7 stability in galactic cosmic radiation, noting lifetime dependence on electron density around nucleus
18 p3189 A69-35482

Red shift-distance relation for galaxies, discussing time dependence
20 p3597 A69-37411

Photographic photometry investigation of Light distribution in spiral galaxies NGC 681, 972 and 1084, discussing mass distribution
20 p3599 A69-37476

M-87 X ray luminosity from balloon-borne detectors, considering background counting rate relation to azimuth
20 p3588 A69-37488

Power spectra of interplanetary magnetic field fluctuations determined from Pioneer 6 satellite data, relating results to galactic cosmic rays modulation
20 p3603 A69-37554

Unresolved background radiation at 2695 MHz surveyed for galactic wing extent determination
20 p3606 A69-37830

Twenty year wave in diurnal anisotropy component of galactic cosmic rays arriving at earth from asymptotic direction east of sun interpreted as magnetic reconnection
20 p3592 A69-38098

Andromeda galaxy brightness distribution, discussing nuclear region, energy distribution, surface brightness, brightness profile, etc
20 p3610 A69-38141

Spectra of peculiar S zero galaxy NGC 7625 with irregular dust distribution, discussing central spheroidal rotation and mass
20 p3610 A69-38142

Galactic X ray source spectral data observed by rocket, presenting graph with corrections
20 p3594 A69-38172

Galactic nucleus observations in 1.65-19.5 micron range with evidence for strong radiation at 10 and 20 microns, noting mechanisms for IR radiation
21 p3799 A69-38650

Cosmic ray electron role in energetics of solar flares, stellar flares and explosions, galactic eruptions and quasars
21 p3790 A69-38823

Galactic cosmic rays, discussing chemical composition, isotopic separation, proton and alpha particles energy spectra, propagation, interactions, etc
21 p3791 A69-39502

Galactic nuclei as collapsed old quasars from dynamics of gas cloud collection in galactic nucleus, discussing cosmic radiation emission from synchrotron mechanism
21 p3815 A69-39610

Milky Way galactic diffuse radiation photometric study using Schmidt camera, stressing Northern Coal-sack commencement region
21 p3817 A69-39725

Chemical composition of galactic and solar cosmic rays, discussing differences from universal cosmic abundances, using Cerenkov counters, emulsions, etc
22 p4002 A69-40090

Diffuse galactic radiation intensity and distribution from photoelectric measurements compared with radiative transfer calculations using various interstellar dust models
22 p4013 A69-40096

Extragalactic radio sources linear polarized radiation distribution at 1418 MHz indicating ordered magnetic fields often oriented differently
22 p4015 A69-40155

RF high resolution observations of edge on spiral galaxy NGC 4631, noting radio halo and spur absence, nonthermal radio emission region, etc
22 p4022 A69-40463

Photoionization model of Seyfert galaxy extended to calculate temperatures, luminosities and sizes of zones emitting forbidden Fe X /6374 Å/ and Fe XIV /5303 Å/
22 p4024 A69-40581

Radio observations of elliptical and spiral noncluster galaxies, noting correlation between magnitude and radio emission in elliptical galaxies
22 p4025 A69-40639

Galactic center observations over various wavelengths including polarization, diameter, flux measurements and power output
22 p4029 A69-40767

Galactic mass model and interstellar dust scattering data used to examine high latitude nebulae illumination possibility by integrated galactic light
22 p4033 A69-41059

Stellar and diffuse galactic radiation intensity observations to obtain albedo values of interstellar dust particles
22 p4034 A69-41112

Emission lines in optical spectra of radio galaxy nuclei, considering time dependent energy release nature
22 p4034 A69-41174

Strong IR millimeter wave emission from galactic center due to interstellar dust grains resembling semiconductor structure
23 p4215 A69-42115

Galactic X ray sources observed in EM spectrum high energy region, discussing hot plasma cloud thermal radiation and electrons synchrotron radiation as emission sources
23 p4206 A69-42318

Galactic magnetic field existence arguments, discussing general and optical evidences, radio emissions, Faraday rotation from extragalactic sources and from pulsars, etc
23 p4217 A69-42321

Low energy galactic cosmic ray spectrum determined from ionization rate per hydrogen atom, correlating peak intensity with stellar particle emission high energy portion
24 p3465 A69-42608

Fire hose instability growth rate in relativistic plasma with anisotropic pressure, discussing importance to cosmic ray liberation and isotropization at galactic halo
24 p4376 A69-42660

Cosmic rays properties and dynamical effects in Galaxy disk including origin, lifetime, magnetic field instability, etc
24 p4366 A69-42695

Milky Way hydrogen line survey with Parkes telescope, giving velocity-longitude control maps and tabulated data covering galactic equator
24 p4383 A69-42961

Galactic X ray flux from H I region low energy cosmic ray nuclei, studying electron capture effects on line intensities
24 p4367 A69-43048

Seyfert galaxies IR radiation attributed to dust grains thermal emission of energy absorbed from galactic nucleus
24 p4374 A69-43741

GALACTIC RADIO WAVES

Galactic H II regions morphology from high resolution radio observations, noting variation of electron density with region size
01 p0151 A69-10553

Compact high-gain chromium doped rutile traveling wave masers for Onsala radio telescope for galactic and extragalactic microwave emission studies
02 p0257 A69-12463

Linear polarization of cosmic radio emission measured near galactic anticenter at centimetric wavelengths
03 p0501 A69-13704

Space radio astronomy techniques for problems in galactic radio emission, solar studies and planetary observations
05 p0821 A69-15844

Cosmic ray electron energy spectrum compared with galactic radio noise for estimating galactic magnetic field
06 p0992 A69-17377

Galactic H 2 regions radio observation using Cassegrain antenna and Dicke radiometer
06 p1008 A69-17696

Ground based radio telescope sensitivity to radio emission from earth atmosphere and galactic sources
07 p1099 A69-18515

Radio telescope survey of intense emission regions along galactic plane, considering antenna temperatures, spectrum and steps of observed emission
07 p1216 A69-19138

Local interstellar electron spectrum limits from measurements of cosmic ray electrons, nonthermal galactic radio emission and solar modulation effects
07 p1206 A69-19269

Inverse Compton effect and universal black body radiation from less energetic radio photons of galactic and metagalactic origin
08 p1381 A69-19786

Nonthermal cosmic radio emission spectral index angular variations during scanning of sky by receiver antenna, analyzing dependence on galactic latitude
10 p1784 A69-23940

LF observations of complex galactic radio source W51, discussing structure and radio spectra of resolved components
12 p153 A69-25807

Radio emission from 18 galaxies noting accompaniment of optical spectrum emission and enhancement due to production of relativistic electrons in active nuclei
12 p164 A69-27026

Interacting galaxies theories, characteristics and terminology, discussing galactic radio sources and properties of matter
12 p169 A69-27055

Radio emitting clouds properties as function of distance to parent galaxy nucleus
13 p2352 A69-27874

Irregular galaxies of type M 82 with weak condensation central parts and diffuse edges, considering radio emission spectrum
16 p2865 A69-32598

Radio wave absorption in interstellar H I regions, considering mean absorption coefficient dependence on height above galactic plane, evaluating planar electron density
17 p3034 A69-33608

Galactic plane at 9.26 cm between longitudes of 32 to 49 degrees, tabulating contour map of antenna temperature and sources
18 p3195 A69-34426

Galactic radio emission and magnetic field strength and structure, using radio surveys to obtain information on cosmic rays
21 p3790 A69-38820

Radio background radiation produced by Galaxy, considering energy, isotropy of radiation and black body character
21 p3790 A69-38821

Cosmic radio background noise spectrum near north galactic pole based on Radio Astronomy Explorer satellite experiments
23 p4219 A69-42375

GALAXIES

NT ANDROMEDA GALAXIES
NT MILKY WAY GALAXY
NT RADIO GALAXIES
NT SPIRAL GALAXIES

Book on cosmic radiation origin and expansion of universe, covering astrophysical reasons for electric charging of galaxies in range of galactic and metagalactic dimensions
02 p0315 A69-11713

Far IR background due to superposition of IR galaxies, noting galaxies contribution to extragalactic radio background

02 p0308 A69-12128

IR and violet sulfur lines for Seyfert galaxies, noting substantial reddening in nuclei

02 p0325 A69-12593

Plasmas in galaxies, spiral structures and radio galaxies, discussing quasar line and continuum spectra

02 p0329 A69-12790

Solar motion in distant objects kinematics, suggesting simultaneous solutions of local motion and galactic rotation parameters

04 p0654 A69-14627

Asymptotic solutions of linear difference equations, discussing applications to eigenvalue problems of free oscillations of model galaxies

04 p0623 A69-14946

Primary electrons implications on cosmic ray confinement in Galaxy, astrophysical aspects and problems of energy spectrum

06 p0991 A69-17308

Relative number of galactic pairs and distribution of linear separation of components determined from Palomar Observatory maps

07 p1214 A69-18663

Element synthesis in stars of galactic halo as possible explanation for heavy elements presence in supermassive objects

07 p1219 A69-19296

Absolute magnitudes and intrinsic color photoelectric observations of Wolf-Rayet stars in Magellanic Clouds and Galaxy

07 p1221 A69-19583

Neutral hydrogen distribution and dynamics in galaxies, discussing observations by spectrographic transit telescope, data processing and profiles

07 p1224 A69-19711

Bright galaxies observed at 408 MHz with fan beam of east-west arm of cross-type radio telescope for correlations between radio and optical properties

08 p1386 A69-20087

Neutral hydrogen asymmetry in Galaxy M101 as evidence for tidal effects due to nearby companions, noting hydrogen emission spectra

08 p1394 A69-20625

Morphology of E and SO galaxies in terms of equilibrium isopleths within general relativity

08 p1395 A69-20636

Galaxies classification using rectified images, noting pitch and inclination angles

08 p1408 A69-21135

Water molecules radio spectral lines from microwave emission sources in Galaxy studied for variability, size and polarization

09 p1587 A69-21307

Galactic clusters absorption, discussing optical thickness in blue and red light

09 p1587 A69-21356

Physical conditions in nuclei of various Seyfert galaxies deduced from line intensities, noting permitted and forbidden lines formation in different regions

09 p1596 A69-22056

Half intensity angular diameter upper limit of Seyfert galaxy NGC 4151 nucleus, considering nonthermal continuum

09 p1602 A69-22227

Galaxies and galactic clusters regarded as particles in kinetic theory of cosmology, discussing distribution function choice and red shift

09 p1605 A69-22410

Age of Galaxy from decay of uranium, assuming prompt synthesis

09 p1605 A69-22414

X ray universe, considering contribution of X ray astronomy to phenomena of big bang, supernovae, neutron stars, exploding galaxies, etc

10 p1760 A69-22869

Metallicity index Q value difference between cluster and noncluster galaxies determined from UV, blue and violet observation data

10 p1774 A69-22964

Abell 2199 cluster of galaxies, discussing population contours, volume density function, structure and other static properties

10 p1774 A69-22965

Supernova frequency in galactic clusters, 45 supernovae in 2144 galaxies and average frequency of one supernova per galaxy per 316 years

10 p1774 A69-22966

Double galaxies consisting of components moving away from each other with hyperbolic velocities from statistical tests of hypotheses

10 p1775 A69-23203

Qualitative considerations of color indices grouping for Abell-1781 cluster of galaxies, table of data and identification charts

10 p1775 A69-23204

Galactic discontinuity near longitude 140 degrees attributed to stars deficiency in anticenter quadrant or interstellar cloud obscuration

10 p1776 A69-23215

Error analysis of Hubble galaxies count to resolve contradiction of values for average optical half thickness tau of galactic absorbing layer

10 p1779 A69-23609

Nuclear sizes, emission line widths and densities in Sc galaxy M 51 and Seyfert galaxy NGC 4151, noting similarities and difference between nuclei

10 p1785 A69-24089

Spectroscopic observations of faint quasar near double galaxy NGC 3561, noting red shifts

10 p1785 A69-24092

Interstellar formaldehyde detection in absorption against galactic and extragalactic radio sources, discussing chemical evolution

10 p1786 A69-24108

Chemical compositions and ages of M67 and NGC 188 determined from color-magnitude diagrams, noting stellar distribution near gap in diagram and He content

10 p1789 A69-24128

Dynamical model for spherical inhomogeneity in mean mass density of universe to predict velocity dispersion observed for Coma Cluster

10 p1789 A69-24133

Microphotometer for stellar magnitudes of galaxies determination from photographs

11 p1879 A69-24256

Galaxies classified by matter content of nucleus, discussing evolution

11 p1953 A69-24351

Intergalactic gas temperature and density reevaluated, considering neutral hydrogen distribution in galaxies peripheries and metagalactic background of ionizing UV radiation

11 p1946 A69-24589

Magellanic Clouds color composite photographs prepared from negatives taken in blue and IR light

12 p2152 A69-25801

Correlation of stellar surface density distribution of young stars and neutral hydrogen gas in Small Magellanic Cloud

12 p2152 A69-25802

Planetary nebulae radial velocities in large and small Magellanic Clouds compared with young objects rotational pattern and interstellar gas densities and velocities

12 p2155 A69-25891

Observed frequencies of number of members in multiple systems of galaxies

12 p2156 A69-26222

Spheroidal galaxies with early type spectra distinguished by UV continuum, discussing telescopic spectral and color observations

12 p2159 A69-26663

Galactic descriptive functions and empirical model construction methods for determining mass distribution

12 p2160 A69-26852

Unsteady phenomena in galaxies - Conference, Buirakhan, Armenian SSR, May 1966

12 p2161 A69-27015

Cosmogonic nature of galactic nuclei activity, emphasizing streamers ejection and new formations in galaxies

12 p2163 A69-27016

Lallemand electronic camera application for spectroscopic observations of unsteady phenomena in galactic nuclei at 4000 A, noting radial velocities

12 p2163 A69-27017

Rotating central disk in galactic plane observed by radio telescope, assessing relation between expanding gas of disk and high velocity stream from center

12 p2163 A69-27018

Instability phenomena encountered in galaxies determined based on classification of galaxies according to mass and brightness

12 p2163 A69-27019

M 31 galaxy ionized gas region high resolution spectroscopy, emphasizing radial velocities in O II lines at various distances from nucleus

12 p2163 A69-27020

NGC 4151 bright lines intensity, electron density, temperature and ions quantity evaluation from spectrograms with 140 A/mm dispersion

12 p2164 A69-27021

Successive explosions produced two gas systems observed in six Seyfert galaxy nuclei by spectrophotometry, using diffraction spectrographs

12 p2164 A69-27022

NGC 4151 absolute intensities of wide emission of weak isolated and IR lines determined from photoelectric spectrophotometric measurements

12 p2164 A69-27023

Rotation curve peculiarities of Sc type galaxy NGC 3432 ascribed to noncircular gas motions

12 p2164 A69-27024

Colorimetric studies of galaxies exhibiting red shift with increasing radial distance from center

12 p2164 A69-27025

Photographic magnitudes of galactic nuclei, presenting plots for stellar magnitude distribution of galactic nuclei

12 p2165 A69-27029

Velocity distribution and density of neutral hydrogen in southern portions of M 31 and Sc- type galaxy M 33 by 75 m radio telescope

12 p2166 A69-27038

Radio emission correlation to nuclei shape in normal galaxies

12 p2166 A69-27040

Interacting galaxies theories, characteristics and terminology, discussing galactic radio sources and properties of matter

12 p2169 A69-27055

Interacting NGC 4485 and 4490 galaxies instability, establishing early stage of evolution from morphological and spectroscopic results of photographic observations

12 p2169 A69-27056

Blue, UV and yellow spectral observations of M 82 /NGC 3034/, obtaining polarization dependence on reciprocal of wavelength, polarization and color characteristics

12 p2169 A69-27057

Galaxies NGC 4402 and NGC 4438 structure, luminosity and color from two color photometric study of Virgo cluster center

12 p2169 A69-27058

Photometric and spectroscopic analysis of southern peculiar galaxy NGC 6438, discussing isophotes, color distribution and radial velocity

12 p2169 A69-27059

NGC 4038-9 velocity field from spectrum obtained at McDonald Observatory, suggesting existence of two centers of matter ejection

12 p2169 A69-27060

Photographic studies of unsteady features of galaxies, discussing spectra, color, spiral arm instability and extragalactic H II regions

12 p2170 A69-27063

NGC 4194 galaxy emission line spectrum analysis showing presence of highly excited gas in nucleus and in bright central region similar to NGC 7714

13 p2339 A69-27571

Ionization processes in Seyfert galaxies, considering thermal electrons, superthermal protons and electrons and nonthermal UV radiation

13 p2346 A69-27710

Ionized hydrogen regions in NGC 4449 from H alpha photography through narrow band interference filter, obtaining radial velocities

13 p2347 A69-27714

Markarian galaxies with strong UV continuum, observing emission lines differing from each other

13 p2351 A69-27866

Photometric data and law of rotation in symmetry plane for constructing mathematical model of mass and luminosity distribution in M 31

13 p2351 A69-27870

Emission line fluxes of southern planetary nebulae in Magellanic Clouds and Galaxy measured photoelectrically, giving upper limit to H beta emission of Magellanic planetary

14 p2520 A69-29376

Radial velocities of planetary nebulae in Magellanic Clouds and Galaxy, discussing Population I and II kinematics

14 p2520 A69-29377

Planetary nebulae nuclei magnitudes in Magellanic Clouds and Galaxy measured photoelectrically, discussing early evolution

14 p2520 A69-29378

Variable stars in Large Magellanic Cloud from photoelectric measurements obtained in blue and violet, including periods of Cepheids and some period amplitude differences

14 p2526 A69-29853

Cosmic dust role in determining structure and dimensions of Galaxy

14 p2527 A69-29897

GALAXY AIRCRAFT

- Excited hydrogen radio lines observations, analyzing neutral and excited hydrogen distribution in galaxies 15 p2682 A69-30502
- Optical and radio estimations of galactic masses, analyzing radius of rotation curve inflection point 15 p2687 A69-30547
- Neutral hydrogen high velocity clouds as possible extragalactic objects in Local Group not contracted to galactic dimensions or densities 15 p2694 A69-30785
- Quasar multiple absorption red shift lines caused by gas in extended galaxy halos, assuming broadened galactic cross section area 15 p2695 A69-30884
- Doppler effect significance in radio astronomy including galaxies relative motion and information concerning isolated hydrogen clouds between galaxies 16 p2853 A69-31565
- Spectrophotometry of elliptic galaxy NGC 1052 nucleus from 3400 to 6300 Å for relating radio properties and optical characteristics 16 p2853 A69-31610
- Magellanic-like galaxy NGC 4631 observed in H alpha light through narrow band interference filter, detecting and cataloging 88 H II regions 16 p2854 A69-31647
- Four color photoelectric photometry of bright galaxies in Virgo Cluster, analyzing properties in nuclear regions 16 p2860 A69-32230
- Galaxies clusters spatial distribution based on crude distance estimates, discussing serial correlation of counts and interpreting results 16 p2862 A69-32371
- Stellar system stability for corresponding stable barotropic gaseous system, discussing Schroedinger operator role 16 p2862 A69-32374
- Giant galaxy classified in terms of stellar population, discussing Orion, intermediate amorphous and combination categories 16 p2862 A69-32395
- Photoelectric observations of color and titanium oxide in M7 giants in nuclear bulge of Galaxy compared with late giants near sun 16 p2863 A69-32396
- Irregular galaxies of type M 82 with weak condensation central parts and diffuse edges, considering radio emission spectrum 16 p2865 A69-32598
- Line widths of 48 galaxies at 21 cm and spectroscopic data, estimating masses and angular momenta, finding mass-angular momentum relation 16 p2866 A69-32818
- Stationary galaxy dynamical theory, assuming constant velocity body of physically homogeneous star subsystems in space 17 p3031 A69-33102
- Optical spectrum of galaxy NGC 3031 nucleus, considering emission and absorption lines and continuum 17 p3034 A69-33396
- Proper motions, color magnitude and distance modulus of stars in galactic cluster in direction of Large Magellanic Cloud using Cape wide angle photometry 17 p3034 A69-33411
- Accurate positions at 2700 MHz and optical identification of radio sources with galaxies and quasi-stellar objects 17 p3035 A69-33611
- Aligned galaxies, discussing possible formation by consecutive explosive ejections of new galaxies from parent galaxy 17 p3044 A69-34175
- Red shift table for six galaxies near Coma Cluster from spectrograms of absorption lines 17 p3044 A69-34182
- H II regions distribution in nearby irregular I galaxies, attributing asymmetry to localized bursts of star formation 18 p3190 A69-34289
- Dwarf elliptical galaxies of local group, discussing star distribution and orbits, formation process, origin and distribution about Milky Way 18 p3194 A69-34424
- Thin disk galactic models small oscillations, discussing frequency spectra and types of continua 18 p3196 A69-34551
- Galactic clusters absorption, discussing optical thickness in blue and red light 18 p3197 A69-34746
- Galactic rotation in Cassiopeia region, studying O, B and A stars circular velocities as function of distance from galactic center 18 p3201 A69-35142

Magellanic clouds positions, associated gases, evolution, etc 19 p3401 A69-35757

Variable star in Large Magellanic Cloud having unusual light curve with complex maximum lasting 300 days 19 p3403 A69-35965

Forbidden emission lines in spectra of normal, radio and Seyfert galaxies and quasars, giving information about quasi-stellar mean densities, temperatures, ionization, etc 19 p3424 A69-36236

Markarian galaxies with strong UV continua, discussing emission spectra, red shift, absolute magnitudes, etc 19 p3426 A69-36577

Pulsar distance determined by electron content in line of sight to pulsar compared with neutral H amount integrated through galaxy in pulsar direction 20 p3597 A69-37409

Spectroscopic and photographic observations of compact galaxies, discussing distances, absolute magnitudes, linear dimensions, Hubble diagram position and correlations with objects showing similar characteristics 20 p3600 A69-37483

Galactic mass relativistic distribution calculated, considering spherically symmetric model differential rotation near sun 20 p3600 A69-37484

Irregular galaxy NGC 3077 with interstellar dust, measuring velocity field by spectroscopy 20 p3610 A69-38144

Cold disk galactic models free short wavelength oscillations, obtaining asymptotic approximations for eigenfrequencies and eigenfunctions of bending and planar modes 20 p3611 A69-38151

Stars of spectral class F 2 and earlier, brighter than magnitude 11.5, found in four regions of intermediate galactic latitude 20 p3612 A69-38162

Discreteness of distances to extragalactic objects, tabulating red shift values from Wilson formula for galaxy clusters 21 p3802 A69-38843

Statistical analysis of galactic structures subject to Newton gravitation covering globular clusters and spiral disk and rotating bar galaxies 21 p3803 A69-38924

Atlas of H II regions in 20 nearby galaxies 22 p4015 A69-40153

Finding list of spectral type A7 stars and earlier in region at south galactic pole compiled from prism survey data 22 p4021 A69-40436

Variational principle for stability of galaxies models, developing perturbation potential in terms of operator similar to Hartree-Fock exchange operator 22 p4022 A69-40468

Projected surface density upper limit of neutral atomic H between M31 and M33 galaxies, noting brightness temperature between NGC 4631 and 4656 22 p4024 A69-40578

Nonexistence of second order clustering of galaxies and relationship to gravitational cut-off, relativistic cosmologies and red shifted light by exponential decay of photon energy 22 p4024 A69-40579

Quasar association with galactic clusters, noting red shift and spectral correspondence 22 p4029 A69-40763

Absolute magnitude dispersion of galactic cluster brightest members as normally distributed random variable independent of cluster richness or faint members luminosity 23 p4215 A69-42113

Extragalactic universe major constituents and physical properties of normal, radio and compact galaxies, discussing missing matter existence 23 p4217 A69-42317

Observational cosmology in terms of relation between red shift and apparent luminosity of galaxies /Hubble relation/ 23 p4219 A69-42328

IC 3258 emission line spectrum observations, discussing blueshift, extragalactic location, possible nature, etc 23 p4219 A69-42374

Transient sources of cosmic rays, discussing possible time variable intensity and momentum spectrum of Galaxy 24 p4367 A69-43006

Book on physics and evolution of galaxies covering properties, stellar content, interstellar matter, high energy particles and radio galaxies 24 p4384 A69-43161

Elements origin and development in universe, discussing energy generation, structure and population of stars in Galaxy 24 p4386 A69-43333

Pulsars turn off time compared to Galaxy age, discussing physical theory and pulsar models 24 p4389 A69-43741

GALAXY AIRCRAFT
U C-5 AIRCRAFT

GALERKIN METHOD

Radiation from isothermal sphere in vacuum having spherical scattering indicatrix solved by Bubnov-Galerkin method with allowance for scattering 01 p0174 A69-10104

Approximate solution for Dirichlet problem for linear Karman differential equation used in thin plate deflections obtained by Bubnov-Galerkin method 01 p0105 A69-10700

Approximate solution convergence for linear operator equation in Hilbert space by least squares method 01 p0105 A69-10728

Modified Galerkin method applied to approximate solutions of two dimensional elasticity equations of equilibrium 02 p0338 A69-11748

Nonlinear boundary value problems direct generalized solutions based on linearization of Bubnov-Galerkin and Ritz method 02 p0272 A69-12136

Generalized Galerkin functions for asymmetric thermoelasticity, considering separation of coupled equations 03 p0525 A69-13608

Vibration analysis of plates with discrete mass distribution based on Galerkin approach 04 p0682 A69-15293

Equations for nonshallow spherical shell deformations derived by Bubnov-Galerkin method 04 p0684 A69-15539

Mathematical problem of MHD thermal entrance regions for parallel plate channel solved by Galerkin method [ASME PAPER 68-WA/HT-10] 05 p0803 A69-16118

Functions satisfying mixed boundary conditions derived for boundary value problems involving regions of complex form 05 p0787 A69-16455

Convergence of Grammel and Galerkin methods allows use of modified Green function 06 p1020 A69-17132

Stress concentration at circular hole in orthotropic cylindrical shell, using coordinates system and Bubnov-Galerkin method 06 p1021 A69-17180

Galerkin method of moments applied to stochastic bounded linear operator equation, discussing statistically homogeneous operator case and electric field in dielectric 07 p1174 A69-19477

Convergence of Bubnov-Galerkin method in complex separable Hilbert space, proving theorems for sufficient conditions 12 p2123 A69-26607

Nonlinear Galerkin analysis of curved plate flutter using shallow shell/von Karman equations and quasi-steady aerodynamic theory 13 p2364 A69-28207

Galerkin method applied to axial, transverse and three dimensional linear combustion instability problems in liquid propellant rocket motors 14 p2538 A69-2902

Galerkin-Kantorovich-Dorodnitsyn /GKD/ multiment integral method improved reversed flow formulation for lower branch similar flows 17 p2958 A69-34055

Modified Bubnov-Galerkin-Ritz method for determining approximation coefficients in stress and displacement analysis, using mixed variational principle of elasticity theory 18 p3215 A69-34561

Structural damping effects on semilinear panel boundary aeroelastic limit by Galerkin variations method 19 p3437 A69-36141

Stiffness matrices in plane elasticity problems by Galerkin method, leading to simultaneous expression related to finite element method 20 p3619 A69-36951

Nonlinear stability of shallow elliptical paraboloidal dome under uniformly distributed compression, solving by Bubnov-Galerkin method on computer
21 p3838 A69-39186

Galerkin method application to solve differential equation and boundary value conditions for elastic stability of bars, showing linear relation between critical loads
21 p3845 A69-39678

GALLATES

Propyl gallate radiation shielding effect variations with proton and gamma ray bombardment, noting growth and development of potato tuber eyes
08 p1262 A69-19927

GALLIUM

Homogenous mechanical stresses in amorphous and crystalline gallium films during vacuum deposition and annealing
01 p0141 A69-11420

Light absorption of In and Ga thin films in various gaseous media, noting displacement of irregular absorption band
10 p1747 A69-23792

Gallium distribution in YIG single crystals by X ray spectral analysis, observing concentration fluctuations
13 p2321 A69-28002

GALLIUM ALLOYS

Contact resistance of In or In-Ga on CdS single crystals
03 p0487 A69-13638

GALLIUM ANTIMONIDES

Electron irradiation induced damage in undoped GaSb single crystals at 77 K, noting dependence on energy and orientation
01 p0141 A69-11256

Faraday effect of free carriers on n-type GaSb at 20 K, determining mass and mobility of electrons from Hall effect and conductivity
02 p0298 A69-12039

GaSb-ZnTe heterojunction fabrication method, noting photoresponse, fluorescence and light transmission
02 p0299 A69-12408

IR absorption and reflection in doped n-GaSb, obtaining absorption coefficient for various impurity concentrations
03 p0492 A69-14174

P-type GaSb crystals with various impurity concentrations noting conductivity, transverse magnetoresistance, Hall effect and acceptor band width and conductivity
04 p0643 A69-15259

Uniaxial compression load effect on activation energy in p-type GaSb single crystals
04 p0644 A69-15269

Thermal and excess currents in GaSb tunnel diodes
05 p0734 A69-16570

Energy separation and electrons effective mass ratio of conduction bands of tellurium doped GaSb obtained by free carrier Faraday rotation measurements
07 p1201 A69-19464

Face effect in p- and n-type gallium antimonide single crystals doped with zinc and tellurium
09 p1558 A69-21870

Drawn n-p and p-n junctions obtained in Te and Zn doped GaSb single crystals prepared in pure He atmosphere by Czochralski method
10 p1745 A69-23329

Microstructural analysis, determining junction orientation polarity effect on draw junction structure in GaSb crystals at room temperature
10 p1745 A69-23330

Repeated stepwise annealing process to obtain homogenized InSb-GaSb alloys continuous solid solutions
10 p1745 A69-23331

Tellurium doping effect on phonon diffusion in GaSb, discussing thermal conductivity at low temperatures
12 p2142 A69-26294

Vapor phase growth of epitaxial single crystalline GaAs-GaSb alloys using arsine and stibine
12 p2145 A69-26920

Conduction band structure in GaSb noting temperature dependence
13 p2319 A69-27899

Longitudinal magnetoresistance oscillations in n-type GaSb single crystals associated with electron concentrations minima
13 p2319 A69-27900

Band structure and optical constants of InSb, InAs and GaSb, calculating linear momentum matrix elements and state density with spin-orbit effects included
19 p3385 A69-36515

GaSb p-n injection laser output at 4.2 K in strong transverse magnetic field, deducing effective mass and g-factor from stimulated emission peak shift
19 p3387 A69-36530

Electron effective mass, density and mobility in /000/ and /111/ conduction band minima in Te-doped degenerate GaSb-InSb single crystals
19 p3390 A69-36555

Tunnel p-n junctions preparation by diffusing Zn into degenerate Te doped n-type GaSb between 580-600 C, measuring volt-ampere and capacitance characteristics
21 p3780 A69-39043

S doped GaSb single crystals prepared by Crochral-ski method studied for temperature dependence of resistivity and Hall coefficient
21 p3781 A69-39048

Transverse thermomagnetic EMF and Nernst-Ettingshausen coefficient in GaSb semiconductor with double conduction band and strong degeneracy of current carriers
21 p3783 A69-39558

Selenium distribution along GaSb single crystals during oriented crystallization determined by radiometry
23 p4198 A69-41725

GALLIUM ARSENIDE LASERS

Optically bistable operation of continuous wave GaAs p-n junction laser at 20 K
01 p0090 A69-10565

Continuous wave GaAs injection lasers operation at high temperatures shown possible by using available threshold current densities with suitable heat sink materials
02 p0255 A69-11710

Laser transition and photon energy of lightly doped GaAs, showing many body electron-hole-lattice interactions
02 p0257 A69-12615

Temperature dependence of electron beam pumped GaAs laser threshold current density and emission spectra, noting doping effects
02 p0260 A69-12683

GaAs injection laser transmission losses and threshold current density under influence of external optical coupling with spherical mirror
02 p0260 A69-12687

Clamp type diode holders for obtaining CW coherent emission from gallium arsenide injection lasers
03 p0435 A69-12985

Uniaxial pressure applied to p-n junction of GaAs injection laser, discussing effects on threshold current and wavelength
03 p0441 A69-13848

GaAs diode laser short wave emission, discussing coherent radiation and photon energy
03 p0441 A69-14165

Bistable operating mode of GaAs semiconductor laser involving light emission shifts
03 p0441 A69-14175

Spectral output time variation of GaAs diode laser operating in Fabry-Perot modes
05 p0772 A69-15961

Gallium arsenide injection lasers properties, analyzing band structure, optical transitions, recombination lifetimes, conduction band states, optical gain, etc
05 p0772 A69-16228

GaAs injection diode laser cooled by closed cycle gas refrigeration system, noting time required to reach laser operating temperature
05 p0777 A69-16793

GaAs laser excited by fast electrons exhibiting high efficiency and output power at room and liquid nitrogen temperatures
06 p0933 A69-16994

Gradual output degradation mechanism in GaAs injection lasers, attributing internal radiative quantum efficiency reduction to nonradiative recombination centers formation
07 p1148 A69-18857

GaAs lasers radiation power hysteresis manifested in generating starts and stops at different injection current levels
07 p1157 A69-19593

GaAs laser employing external resonator with thin film active substance, noting output power and emission thresholds during electron beam excitation
08 p1326 A69-20543

Emission intensity and beam divergence of p-n junction GaAs laser with nonlinear passive element in resonator
09 p1515 A69-21474

Picosecond structure of low power laser signals using calcite beam splitter and potassium diphosphate second harmonic generator
09 p1516 A69-21742

Microwave modulation of GaAs injection laser radiation, using Zaleskii recording method and liquid nitrogen to cool laser diode
12 p2105 A69-26031

Laser emission noise and voltage noise cross correlation coefficient for CW GaAs laser diodes at 77 K, noting strong dependence on bias current
12 p2038 A69-26328

Gallium arsenide junction laser resonant modes from theoretical model, calculating frequency separation
12 p2108 A69-26637

P-type GaAs-Ge lasing on band to band or conduction band to acceptor impurity transitions or on both transitions simultaneously
13 p2270 A69-27193

Temperature effects on polarization degree, threshold current and delay of radiation from GaAs laser diodes with diffused Zn
13 p2227 A69-27328

Photon loss coefficients in electron beam pumped GaAs laser showing dependence on doping type and impurity concentration, noting threshold current density measurement
13 p2271 A69-27467

Laser diodes p-n junctions obtained by Zn diffusion into Ga arsenide, stressing junction flatness problem and arsenic vapor pressure effect
13 p3323 A69-28640

Close confinement GaAs p-n junction lasers with reduced optical loss at room temperature
14 p2457 A69-28893

Gallium arsenide injection laser for communication systems with pulse frequency modulation, noting power output dependence on crystal quality
14 p2459 A69-29349

Efficient extinction in optically coupled GaAs injection lasers achieved by selecting quenching radiation frequency close to operating frequency
15 p2633 A69-30059

Emission intensity and beam divergence of p-n junction GaAs laser with nonlinear passive element in resonator
15 p2633 A69-30719

Optimum metal contact stripe width for CW operation of GaAs junction lasers bonded on copper heat sink
16 p2796 A69-31698

OgaAs platelet laser modes time behavior, discussing control by electron-hole pair density
16 p2796 A69-31704

Injection semiconductor lasers emission characteristics, discussing gallium arsenide diodes, nonlinear losses in pulsed mode, laser interactions, etc
16 p2796 A69-31949

GaAs laser diode radar system for incremental range profiles
17 p2980 A69-32921

GaAs dual diode laser structure used to give electrical control of laser threshold and permit study of optical flux and current density role
17 p2980 A69-32959

GaAs diode laser pulse train emission during pumping near threshold
17 p2982 A69-33421

Monograph on GaAs injection laser electrical and optical properties during crystallization out of solution covering principle, p-n junction fabrication, I-V characteristics, doping effect, etc
17 p2982 A69-33571

GaAs semiconductor laser emission band homogeneity and continuous energy spectrum levels contribution to induced optical transitions
17 p2984 A69-34161

Radiation dynamics of semiconductor GaAs injection laser with pulsed and continuous modes operation of diodes
18 p3154 A69-35495

Amplitude and output spectra of optical quantum amplifier based on GaAs injection laser, noting values in traveling wave and regeneration mode
19 p3336 A69-36348

Magnetic field effects on emission line shift, threshold current and power output of GaAs injection laser, discussing spontaneous radiation in magnetic field
19 p3387 A69-36529

GaAs lasers emission dynamics, considering threshold amplification, spontaneous noise, nonlinear operation, etc
19 p3337 A69-36534

Radiation dynamics of GaAs injection semiconductor laser, plotting spike period dependence on resonator length
19 p3337 A69-36535

- GaAs-P injection laser time delay measured from start of current flow in p-n junction diode, studying effects of memory, temperature and reverse bias
19 p3387 A69-36536
- Power, efficiency and temperature dependence of emission spectra and threshold current density in electron beam pumped GaAs laser, noting doping concentration
19 p3338 A69-36538
- Gallium arsenide junction lasers operating above threshold, showing resonant modes dependence of steady state gain function and frequency dependence of spatial gain distribution
19 p3338 A69-36691
- GaAs laser used as optical sweep generator for display of Cs 133 spectral line shape, studying fluorescence and radiation lifetime
19 p3339 A69-36696
- Stimulated emission at current pulse end ascribed to external resonator turn-on time delay effects with GaAs injection lasers at room temperature
21 p3734 A69-38408
- GaAs laser tracking system for space guidance, describing equipment and operations
[AIAA PAPER 69-870] 21 p3763 A69-39396
- GaAs injection laser properties calculation with doping levels for exponential band tails formation, deriving threshold currents, lasing frequencies, I-V characteristics, etc
22 p3959 A69-40012
- Spiking behavior detection in Q switched light output from GaAs pulsed junction laser, noting width at high pumping levels
22 p3963 A69-40563
- Electron beam pumped dislocation free GaAs lasers filamentary and nonuniform emission characteristics from X ray topographs before and after bombardment
22 p3963 A69-40565
- Emission dynamics and fine pulse structure in GaAs injection lasers, determining pulse duration and amplitude dependence on current and resonator length
22 p3963 A69-40603
- Lasing properties of Ni-doped GaAs diodes evaluated by plotting resonance, mode amplitudes and frequencies for various bias currents and external capacitance
22 p3912 A69-40606
- Amplification coefficient, luminescence power and spacing between Fermi quasi-levels in GaAs diode injection lasers, using spectral absorption dependence
22 p3965 A69-40801
- Intensity of optical pulses from CW GaAs injection lasers observed with fast sampling techniques
23 p4173 A69-41500
- Oscillographic recording of GaAs laser ultrashort radiation pulses, using isolated injection regions and semiconductor photodiode as photoelectric converter
24 p4329 A69-43740
- GaAs laser diodes differential external quantum efficiency and gain per unit length dependence on laser reflectivity, taking into account optical losses
24 p4330 A69-43766
- GaAs laser diodes differential external quantum efficiency and gain per unit length dependence on laser resonator length, taking into account optical losses
24 p4330 A69-43767
- GaAs junction laser total stimulated light power dependence on resonator length taking into account optical losses
24 p4330 A69-43768
- GALLIUM ARSENIDES**
- Small signal impedance of subcritically doped gallium arsenide Gunn diodes, using drift velocity vs electric field relationship
01 p0038 A69-10121
- Gallium arsenide single crystal epitaxy with doping/concentrations into semiinsulating microwave circuits
01 p0040 A69-10196
- Microstrip transmission line integrated circuits on semiinsulating GaAs substrates, showing feasibility at millimeter wave frequencies
01 p0040 A69-10197
- Microwave instabilities in bulk GaAs under strong electric fields, considering characteristics connected with structural properties and contact formation conditions
01 p0136 A69-10256
- Limited space-charge accumulation mode efficiency for gallium-arsenide diodes, taking into account electron-lattice relaxation processes
01 p0137 A69-10321

- Electrical properties of gold-gallium arsenide n-type junctions investigated for influence of crystallographic orientation of surface and charge carrier density
01 p0138 A69-10432
- Negative differential resistance effect producing relaxation type oscillations in n-type gallium arsenide
01 p0138 A69-10557
- Current/field characteristic of n-type GaAs, using high power microwave techniques in presence and absence of transverse magnetic field
01 p0139 A69-10819
- Forward current shot noise in parametric amplifiers using GaAs varactors, noting additional noise due to stored minority carriers current
01 p0048 A69-11137
- Specific heats of Cu, GaAs, GaSb, InAs and InSb measured over low temperature ranges
01 p0140 A69-11252
- Recombination radiation from excitons and free carriers in epitaxial GaAs with impurities at liquid He temperatures
01 p0140 A69-11253
- GaAs photoemissive yield spectrum analysis, discussing transition energies and energy band structure models
01 p0140 A69-11254
- Electron drift velocity, diffusion coefficient and trapping time in GaAs, measuring variation with electric field
01 p0140 A69-11255
- Recombination effects in high resistivity Cu doped gallium arsenide single crystals determined by photoconductivity methods
02 p0294 A69-11627
- Photoelectric properties of n-n junction interfaces in gallium phosphide and arsenide semiconductors
02 p0294 A69-11630
- Trapping parameters of Fe doped GaAs-GaP, measuring thermally stimulated conductivity and space charge limited currents
02 p0296 A69-11789
- Diffusion process in dislocation-free doped and undoped GaAs single crystals
02 p0296 A69-11792
- Injection laser emission from gallium arsenide base films grown epitaxially from gas phase in moist hydrogen atmosphere
02 p0255 A69-11879
- Gunn domains reduction in sheet type GaAs oscillators by spreading of field lines out of active region
02 p0215 A69-11933
- Cavity excitation and support of limited space-charge accumulation mode oscillations in n-GaAs epitaxial diode
02 p0297 A69-11940
- Fundamental microwave oscillations at high frequencies in GaAs epitaxial sandwich layers, using space charge growth control
02 p0297 A69-11941
- GaAs Gunn diode oscillators operating at Q band frequencies
02 p0297 A69-11944
- GaAs injection lasers noting spectral function, I-V characteristics and relations among lasing wavelength, threshold current density and impurity concentration
02 p0256 A69-11993
- Nonisothermal space charge wave analysis of transit time mode oscillations in bulk GaAs, studying device reactance at given negative resistance
02 p0299 A69-12240
- Mechanical thermal stresses effects during laser flash illumination of GaAs, discussing temperature dependence of radiative recombination
02 p0256 A69-12245
- Localized vibration modes of defects and IR absorption bands in compensated Si doped GaAs
02 p0299 A69-12402
- Linear absorption coefficient of semiinsulating Cr doped GaAs for IR carbon dioxide laser radiation, discussing lattice absorption mechanism
02 p0258 A69-12619
- Optical modulation near intrinsic edge in n-type bulk GaAs due to Franz-Keldysh effect, noting carrier production by photon initiated excitation
02 p0300 A69-12650
- Epitaxial GaAs transferred electron oscillators pulsed operation at bias voltage ten times threshold voltage, noting power output and efficiency
03 p0402 A69-12854
- Minority carriers lifetime measurement in degenerate GaAs, showing dependence on current density and operating temperature
03 p0483 A69-12917

- Temperature dependence of elastic constants of highly and weakly doped n- and p-type GaAs
03 p0484 A69-13282
- Gunn effect in bulk GaAs, noting microwave oscillator applications
03 p0484 A69-13292
- Tellurium-doped gallium arsenides stacking-faults transmission electron microscopic study
03 p0486 A69-13614
- Photoluminescence spectra of n-type GaAs films grown by gas transport reactions and from solution melt, noting recombination emission
03 p0488 A69-13887
- Photoluminescence measurement of distribution of majority carrier concentration in GaAs
03 p0489 A69-13893
- Power epitaxial GaAs tunnel diodes grown from solution in tin with tellurium
03 p0489 A69-13895
- Heat capacity of diamond-like semiconducting Si, GaAs and GaP calculated on basis of quasi-chain dynamics of covalent crystals
03 p0490 A69-13943
- Epitaxial n-GaAs photoluminescence obtained from p-GaAs, considering emission intensity
03 p0492 A69-14167
- Epitaxial GaAs films with high electron mobility, noting radiation recombination spectra dependence on substrate orientation
03 p0492 A69-14172
- N-type GaAs single crystal magnetoresistivity, noting charge carrier scattering mechanisms
03 p0492 A69-14177
- Electron phonon coupling in barriers of GaAs Schottky diodes, noting first and second derivatives of I-V characteristic in n-type GaAs-Pd Schottky diode
03 p0493 A69-14242
- Small transverse dimensions effect and domain formation criterion for surface oriented Gunn diodes prepared on thin epitaxial GaAs layers
04 p0639 A69-14335
- Hybrid Gunn domain and LSA mode operation in oversized bulk and epitaxially grown GaAs, noting large signal impedance data
04 p0639 A69-14339
- Photoluminescence measurements of p-type thermal conversion in GaAs grown from silica boats, noting compensation by copper and shallow acceptors
04 p0639 A69-14434
- Cathodoluminescence of n-type GaAs with various carrier concentration bombarded with 24-kv electrons, studying emission spectrum for radiative transition
04 p0639 A69-14436
- Angular distribution of particles sputtered from GaAs and GaP single crystals, bombarding faces with Ar ions at low energy
04 p0640 A69-14452
- Temperature dependence of partial pressure of saturated As vapor over solid solutions of InAs-GaAs of different composition
04 p0642 A69-14938
- Semiinsulating GaAs mobile electric domains, determining electric field strength from electrooptical effect measurements
04 p0643 A69-15261
- Fe doped GaAs p-i-n structure electrical conductivity, Hall effect, thermally induced currents, space charge bounded currents and current instability
04 p0643 A69-15263
- Te and Zn doped p-type GaAs single crystals optical homogeneity, using interferometry
04 p0644 A69-15266
- Homogeneous electroluminescence at 77 K in n-type GaAs single crystals without artificial p-n junctions, noting effects of electric field strength and Zn doping
04 p0644 A69-15271
- Similarity between characteristics of T layers in oxygen discharge positive column and Gunn instabilities in GaAs, noting role of negative O ions
05 p0800 A69-15739
- Acoustoelectric domain propagation in n-type GaAs, noting flux influence on peak acoustic density
05 p0806 A69-15815
- Impurity transfer in doped and undoped epitaxially grown GaAs films, studying substrate dopants effect on carrier concentration profiles
05 p0807 A69-15957
- Multiple high field domain nucleation in GaAs, discussing dependence on contact inhomogeneities
05 p0807 A69-15959
- Recombination radiation of tellurium and zinc doped GaAs alloy type diodes, discussing luminescence spec-

tra, current-voltage characteristics and temperature effects

05 p0729 A69-16210

Microwave diodes on GaAs base, determining basic parameters and effects on crystal formation and device construction

05 p0730 A69-16222

Deep trapping levels caused by ion implantation doping, discussing level effects on electrical characteristics of zinc implanted GaAs diodes

05 p0808 A69-16287

High temperature effects on gallium arsenide crystals current carriers lifetime, discussing recombination characteristics and impurity photoconductivity

05 p0809 A69-16551

Peripheral surface damage effects on epitaxial GaAs bulk diodes breakdown characteristics, noting measurements on mechanically and chemically prepared elements

05 p0733 A69-16561

Limited space charge accumulation /LSA/ oscillations in GaAs, noting frequency independent power interrelationships

05 p0810 A69-16568

Low power RF signal triggering of self sustaining Gunn oscillations in GaAs samples

05 p0734 A69-16575

Neutron and X ray radiation effects upon gallium arsenide devices including Gunn oscillators, transistors, Schottky barrier diodes and optoelectronic pulse amplifiers

06 p0978 A69-16890

Spectral response of fast GaAs point-contact diode in mm and submillimeter wavelength ranges

06 p0893 A69-16939

Hall effect and resistivity of n-type gallium arsenide phosphides doped with Te and Se

06 p0978 A69-16988

Injection characteristics of n-aluminum gallium arsenides-p-GaAs heterojunctions from recombination radiation spectra

06 p0979 A69-16993

Faraday effect at free carriers in indium antimonides and gallium arsenides, analyzing frequency dependence of rotation angle

06 p0979 A69-16996

Gallium arsenide double injection diode using vacuum deposited film electrode on single crystal substrate, noting current controlled negative resistance

06 p0893 A69-17156

GaAs IR emitters efficiency due to semiconductor material band structure

06 p0894 A69-17248

Electro-optical effect in Cr-doped GaAs single crystals at room temperature, discussing carbon dioxide laser radiation modulation by GaAs

06 p0934 A69-17466

Tunnel junctions of narrow gap GeTe and wide gap GaAs, noting current voltage characteristics similar to those in Schottky barrier

06 p0980 A69-17770

Stability of negative differential conductivity state with respect to small disturbances, based on hydrodynamic equations for two valley GaAs semiconductors

06 p0981 A69-17879

Selective etching technique in study of dislocations in epitaxial layers of gallium arsenide

06 p0981 A69-17891

Second order nonlinear coefficient measurement for optical generation of millimeter wave difference frequencies in GaAs waveguide, using carbon dioxide laser

06 p0928 A69-17903

Oscillators and amplifiers based on intervalley electron transfer in bulk GaAs

07 p1096 A69-18442

Oversized GaAs Gunn effect diodes operated in L and S bands at harmonics of fundamental transit time frequency with high power and efficiency

07 p1196 A69-18444

Pulse power from X band LSA devices at centimeter through millimeter wavelengths

07 p1097 A69-18445

Domain oscillations removal in n-type gallium arsenides by externally applied microwave field, noting doping effect on LSA conversion efficiency

07 p1196 A69-18446

Stable negative RF conductance and oscillation conditions for n-GaAs crystals of low $n \times L$ product

07 p1197 A69-18448

Solution regrowth method to prepare epitaxial GaAs for Gunn effect devices

07 p1197 A69-18451

Microwave oscillation and amplification in long bulk GaAs with barium titanate sheets on surface due to differential negative resistance across terminals

07 p1197 A69-18452

Absorption edge broadening by electric field in Gunn domain of N-GaAs crystals

07 p1197 A69-18454

Epitaxial GaAs IMPATT diodes for generating CW X band power, noting high efficiencies and low noise characteristics

07 p1102 A69-18660

Field effect in p-type gallium arsenide single crystals as characteristic of surface electron energy state spectrum

07 p1199 A69-18686

Electrical resistance and Hall coefficient measurement in InAs-GaAs solid solutions system, giving temperature dependence of electron mobility

07 p1199 A69-18689

Impurity atoms effects on Cu diffusion and solubility in GaAs, determining Hall coefficient temperature dependence and conductivity

07 p1199 A69-19009

Magnetic susceptibility of InP-GaAs solid solutions at various temperatures and for varying GaP content

07 p1200 A69-19013

Electron plasma and magnetic field effects on polaritons in semiconducting GaAs studied by Raman scattering of light at small angles

07 p1200 A69-19401

Surface plasmon excitation by tunneling electrons in GaAs-Pb junctions, discussing conductance at bias voltages, plasmon energy and concentration

07 p1200 A69-19402

Dielectric surface loading on GaAs for suppressing traveling high field domain mode oscillations

08 p1371 A69-19911

Quenched multiple domain mode oscillations in GaAs microwave diodes noting relationships between efficiency, power output, negative resistance and bias voltage

08 p1282 A69-20107

Optimal electroluminescent efficiencies for vapor grown gallium arsenide phosphide diodes, analyzing current spreading, absorption, impurity and composition effects

[ECS PAPER 103] 08 p1284 A69-20366

Epitaxially grown guard rings for GaAs p-n junction and Schottky barrier avalanche diodes

08 p1284 A69-20368

Properties of ion implanted GaAs diodes fabricated at room temperature, analyzing light emission, resistance and breakdown voltage

[ECS PAPER 172] 08 p1284 A69-20369

Magnetophonon oscillations of transverse magnetoresistance of n-type epitaxial GaAs in pulsed magnetic field

08 p1373 A69-20760

Field effect transistors with Schottky-barrier gates using epitaxial layers of silicon on substrates and gallium arsenide on seminsulating substrates

08 p1286 A69-20863

Vapor deposition of high purity epitaxial layers of n-type gallium arsenide, noting resistivity and Hall coefficient measurements

[ECS PAPER 62] 08 p1373 A69-21067

Temperature dependence of energy gap in gallium arsenide and gallium phosphide from absorption measurements

09 p1553 A69-21330

Ag-GaAs Schottky barrier photodiodes, describing fabrication and use as UV radiation detectors

09 p1462 A69-21334

Radiative tunneling shifting peak spectra in abrupt asymmetrically doped GaAs junctions

09 p1544 A69-21336

Copper diffusion coefficient in undoped n-type gallium arsenide measured by ultrasonic method

09 p1555 A69-21471

Temperature dependence of conductivity and Hall constant of GaAs single crystals with nickel impurity, noting diode structure and I-V curve shapes

09 p1555 A69-21475

Inhomogeneity distribution of carrier concentration and electrovoltaic effect in GaAs devices analyzed by scanning electron microscope

09 p1557 A69-21746

Current oscillations in seminsulating O and Cr doped GaAs samples at room temperature, noting photoconductivity excitation spectra

09 p1557 A69-21753

Microwave instabilities in bulk GaAs under strong electric fields, considering characteristics connected with structural properties and contact formation conditions

09 p1559 A69-22649

Schottky barriers on n-type GaAs, measuring forward current characteristics for various electron concentrations and temperatures

10 p1745 A69-23358

Transitions between heavy hole and spin orbit split bands in uniaxially stressed Ge and GaAs, noting spectra for various temperatures and valence band parameters

10 p1745 A69-23359

Quenched one dimensional bulk GaAs oscillators with linearly increasing and decreasing concave and convex doping gradients, showing profiles

10 p1663 A69-23667

Small signal HF conductivity of GaAs calculated for arbitrary frequency and DC field, considering subcritical Gunn devices

10 p1747 A69-23694

Presprayed metal films influence on visibility and contact resistance of GaAs prior to fusing in Sn, In and lead contacts

10 p1748 A69-24214

Alloying additions effect on plastic deformation anisotropy in GaAs single crystals, determining dislocation activation energies from creep tests

11 p1936 A69-24537

Etch pits behavior during diffusion and rediffusion of copper in low dislocation crystals of gallium arsenide, demonstrating vacancy nature

11 p1937 A69-25029

Photoluminescence spectra of n-type GaAs films grown by gas transport reactions and from solution melt, noting recombination emission

11 p1939 A69-25688

Photoluminescence measurement of distribution of majority carrier concentration in GaAs

11 p1939 A69-25694

Power epitaxial GaAs tunnel diodes grown from solution in tin with tellurium

11 p1939 A69-25696

Fabrication procedure for microwave epitaxial GaAs diodes applicable for switching purposes

12 p2035 A69-25831

Gallium arsenide materials technology, discussing solution and vapor-phase epitaxy and liquid encapsulation as related to crystal growth and purification

12 p2141 A69-25834

High CW power K-band Gunn oscillators attained through control over doping level, profile and GaAs epitaxial layer thickness

12 p2036 A69-25907

Etched surfaces inhomogeneity of n-type GaAs single crystals, noting oxide layers formation

12 p2142 A69-25980

Carbon dioxide rotational constants from CW beat measurement in bulk GaAs mixer between carbon dioxide vibrational-rotational laser lines

12 p2105 A69-26311

Gallium arsenide thermometer calibration in 1 to 100 K range using interpolation formula derived from p-n junction diode equation

12 p2093 A69-26484

GaAs crystallization for various deviations of melt from stoichiometric state, noting concentration supercooling at phase boundary layer

12 p2144 A69-26586

Vapor phase growth of epitaxial single crystalline GaAs-GaSb alloys using arsine and stibine

12 p2145 A69-26920

Avalanche Schottky barrier photodiodes fabricated by plating GaAs with thin Pt layer and forming proton radiation guard ring, discussing gain bandwidth and SNR

13 p2226 A69-27195

Relaxation oscillations in field ionized epitaxial n-GaAs Gunn oscillators on seminsulating substrates, discussing recombination of excess electrons and holes

13 p2227 A69-27236

GaAs photoelectric devices for radiation detection and light to electric energy conversion, considering photoresistors, photodiodes and solar cells

13 p2203 A69-27465

Se activation energy dependence on crystals composition and Se concentration, based on Hall coefficient temperature dependence in gallium arsenic phosphides

13 p2317 A69-27875

High resistivity GaAs impedance with nonlinear I-V characteristics, showing appreciable reactive component

13 p2317 A69-27881

Nonequilibrium conductivity and radiation of CdS, GaAs and PbS single crystals in waveguide cell under electron beam

13 p2318 A69-27886

Electroluminescence of p-GaAs diodes analyzed over temperature range of linear dependence of lasing on injection current

13 p2230 A69-27887

Current oscillations in n-type gallium arsenide related to electroacoustic domains motions, noting oscillation period dependence on voltage

13 p2318 A69-27892

Gallium arsenide diode nonequilibrium carriers absorption of He-Ne laser radiation under emission conditions

13 p2272 A69-27893

Supplementary absorption and Hall effect temperature dependence in solid solutions of gallium arsenic phosphide

13 p2318 A69-27894

Gallium arsenide Fe-doped diodes efficiency as high speed switches from measured current-voltage characteristics at various temperatures

13 p2319 A69-27898

Stability of negative differential conductivity state with respect to small disturbances, based on hydrodynamic equations for two valley GaAs semiconductors

14 p2503 A69-28788

GaAs photoelectric emission at different activation degrees by adsorbed Cs and BaO layers, noting spectral response characteristics differences and causes

14 p2504 A69-28993

Temperature dependence of elastic constants of highly and weakly doped n- and p-type GaAs

14 p2508 A69-29655

Boltzmann equation for hot electron distribution functions in GaAs and threshold field in Gunn effect

15 p2665 A69-30025

Majority carrier lifetime temperature dependence obtained from photoconductivity measurements of p-type GaAs crystals doped with Ge

15 p2666 A69-30056

Burstein-Moss effect observed in studying n-GaAs crystals electrical reflection spectra with large free carrier concentration at two temperatures and low energy levels

15 p2666 A69-30060

Secondary effects role in n-GaAs crystals electrical reflection spectra with low free carrier concentration at room temperature in external electric field

15 p2666 A69-30061

Gunn effect GaAs oscillators with p-n junctions, studying electrical characteristics, threshold voltages and currents during breakdown and p-n junctions injection

15 p2666 A69-30065

Spectral distribution of photosensitivity for p-n junctions in silicon doped GaAs, showing agreement with state density model and absorption data

15 p2666 A69-30067

Electrical and photoelectrical properties of semiconductor heterojunctions prepared by Ge epitaxy on gallium arsenide bases, showing dependence on base surface treatment

15 p2667 A69-30078

Push-pull circuit configurations for GaAs transferred electron oscillators, discussing CW X band and pulsed L band devices operation

15 p2574 A69-30168

Copper diffusion coefficient in undoped n-type gallium arsenide measured by ultrasonic method

15 p2669 A69-30716

Temperature dependence of conductivity and Hall constant of GaAs single crystals with nickel impurity, noting diode structure and I-V curve shapes

15 p2669 A69-30720

Diffuse Zn layers structure in GaAs single crystals, showing dislocations formation by anomalous Zn diffusion

15 p2670 A69-31048

GaAs zinc gallium selenide solid solutions properties, analyzing lattice constant, microhardness, forbidden zone and concentration relationships

15 p2670 A69-31050

Bound excitons spectra in Cu doped gallium arsenide crystals, analyzing line oscillation structure and uniaxial compression effect

16 p2824 A69-31571

Optical and electrical properties of electroluminescent diffused gallium arsenide phosphide diodes with low donor concentrations, analyzing spectral emission and fabrication effects

16 p2758 A69-31699

Heat treatment effects on Te-doped GaAs, using photoluminescence and carrier concentration measurements to study defects formed

16 p2825 A69-31708

Pulse duration control by two photon absorption, using GaAs as nonlinear element inserted in neodymium-glass laser cavity

16 p2796 A69-31798

Zinc diffused GaAs avalanche diode high CW power and efficiency in normal mode

16 p2760 A69-32015

Alloying pairs of metal pellets to n and p type semi-insulating GaAs, discussing photo effects

17 p3015 A69-32824

Magneto-optical constants and conduction band parameters of GaAs by coherent radiation at high temperatures, measuring Faraday rotation

19 p3386 A69-36522

Radiative recombination in GaAs, giving edge radiation spectra in p and n type crystals and photoluminescence method for measuring junction carrier concentration distribution

19 p3386 A69-36525

Voltage and temperature dependence of zero-bias anomaly in GaAs p-n junction at 0.40-60 K, investigating voltage dependence of differential resistance

19 p3388 A69-36542

Minority carriers penetration depth in solid aluminum gallium arsenide solutions with variable forbidden bandwidth determined from recombination radiation spectra

19 p3391 A69-36606

High resistivity gallium arsenide single crystal LF current oscillations at low temperature, investigating electron heating effect and mechanisms

19 p3391 A69-36609

Undoped n-type gallium arsenide single crystals edge emission spectral band shape dependence on crystal type and ambient temperature

19 p3392 A69-36610

Fe-doped p-type gallium arsenide single crystal radiative recombination emission during current carriers transition from deep acceptor level into valence band

19 p3392 A69-36611

GaAs IMPATT diodes breakdown voltage, impurity density and outer layer thickness compared with Si IMPATT diodes

20 p3504 A69-36914

N-type GaAs optical properties after proton irradiation, noting transmission spectra dependence on initial electron concentration and irradiation dose

20 p3582 A69-36969

Crystallization front topography and stratified structure of melt extracted n-type GaAs single crystals from anodic etching method

20 p3582 A69-37013

Recombination radiation of tellurium and zinc doped GaAs alloy type diodes, discussing luminescence spectra, current-voltage characteristics and temperature effects

20 p3506 A69-37783

Equivalent circuit for microwave cavity containing active GaAs device applied to waveguide and radial mode cavity design

20 p3508 A69-37900

Electro-optical effect in Cr-doped GaAs single crystals at room temperature, discussing carbon dioxide laser radiation modulation by GaAs

20 p3555 A69-37949

Temperature dependence of stimulated light power from GaAs junction lasers operated at constant bias current above threshold

21 p3734 A69-38437

Radiative recombination in GaAs p-n structures having region with concentrations of Ge atoms

21 p3780 A69-39044

Energy levels of multicharge acceptor centers and level splitting in InSb and GaAs deformed crystals, using multizone approximation

21 p3781 A69-39067

Microwave oscillations amplification in bulk GaAs, discussing experimental verification of small signal theory

21 p3781 A69-39127

Se activation energy dependence on crystals composition and Se concentration, based on Hall coefficient temperature dependence in gallium arsenic phosphides

21 p3782 A69-39141

High resistivity GaAs impedance with nonlinear I-V characteristics, showing appreciable reactive component

21 p3782 A69-39143

Electroluminescence of p-GaAs diodes, analyzing temperature range of linear dependence of lasing on injection current

21 p3682 A69-39145

Solid state SHF transmission amplifiers design using rectangular waveguides and biased bulk GaAs

21 p3683 A69-39452

Triode with emitter controlled negative resistance of GaAs as oscillator for microwave applications

22 p3911 A69-40010

Electric fields reducing recombination radiation intensity from bulk ionized GaAs and InP and shifting spectrum to lower energies, discussing self absorption

23 p4198 A69-41499

Fast neutron irradiation effect on IR absorption in single crystal GaAs for various fluences

23 p4198 A69-41540

Ultrahigh vacuum cleaved GaAs-Cs and GaAs-cesium monoxide photoemission acceptor densities, noting crystal parameters role

23 p4198 A69-41548

Temperature gradients effects on GaAs crystals grown by Bridgman method

23 p4199 A69-42469

Luminescence, I-V and pulse characteristics of high resistivity Ni doped GaAs single crystals, noting injection conductivity

24 p4362 A69-43734

Anisotropic carrier distribution effect on polarization of spontaneous recombination radiation during GaAs breakdown in electric field

24 p4362 A69-43736

Diagonal tunneling and radiation polarization in doped heterojunctions and p-n junctions of GaAs, using electroluminescence spectrum analysis

24 p4362 A69-43737

Electroluminescence in doped p-type GaAs single crystal diodes ascribed to double injection of nonequilibrium current carriers

24 p4288 A69-43739

GALLIUM COMPOUNDS

NT GALLATES

Heat conductivity of liquid and solid gallium telluride in steady state regime, using graphite cylindrical device

16 p2824 A69-31572

GaAs-GaP heterojunctions, analyzing continuous conduction band, capacitance and current-voltage characteristics, photoresponse and modulation effect

21 p3779 A69-38424

GALLIUM PHOSPHIDES

GaP p-n structures creation for diode sources of green and red radiation, comparing diffusion and epitaxial methods

01 p0137 A69-10259

Photoelectric properties of n-n junction interfaces in gallium phosphide and arsenide semiconductors

02 p0294 A69-11630

Trapping parameters of Fe doped GaAs-GaP, measuring thermally stimulated conductivity and space charge limited currents

02 p0296 A69-11789

Gallium phosphide luminescence near indirect transition during multiphoton excitation by Q switched ruby and Nd laser beams

03 p0489 A69-13892

Heat capacity of diamond-like semiconducting Si, GaAs and GaP calculated on basis of quasi-chain dynamics of covalent crystals

03 p0490 A69-13943

Carrier scattering mechanisms in n-type GaP, measuring IR radiation absorptivity in Te doped GaP

03 p0492 A69-14168

Photoionization of donor impurities during absorption of IR radiation in n-type Te doped GaP at low temperatures

03 p0492 A69-14169

Vapor grown GaP electrical and optical properties, considering undoped and Se or S doped samples on GaAs and GaP substrates

04 p0640 A69-14438

Angular distribution of particles sputtered from GaAs and GaP single crystals, bombarding faces with Ar ions at low energy

04 p0640 A69-14452

Spectral study of crystal lattice of gallium phosphides for influence of vacancies and impurities on band formation

04 p0643 A69-15258

Hall effect and resistivity of n-type gallium arsenide phosphides doped with Te and Se

06 p0978 A69-16988

Red light emitting p-n junctions in GaP fabricated by epitaxial growth

06 p0979 A69-16999

Temperature dependence of energy gap in gallium arsenide and gallium phosphide from absorption measurements
09 p1553 A69-21330

Structural and optical properties of vacuum deposited GaP films at below 240-850 C
09 p1554 A69-21332

Hole density/Zn concentration ratio in Zn doped solution grown p-type GaP, noting anomalous electrical properties
09 p1557 A69-21750

GaP p-n structures creation for diode sources of green and red radiation, comparing diffusion and epitaxial methods
09 p1559 A69-22652

Voltage dependence of red and green electroluminescence in GaP diodes prepared by growing n-type liquid epitaxial layer on p-type solution grown substrate
10 p1663 A69-23664

Gallium phosphide luminescence near indirect transition during multiphoton excitation by Q switched ruby and Nd laser beams
11 p1939 A69-25693

Negative resistance in GaP electroluminescent diodes with p-i-n structure at low temperatures, noting oxygen role
13 p2226 A69-27194

Se activation energy dependence on crystals composition and Se concentration, based on Hall coefficient temperature dependence in gallium arsenic phosphides
13 p2317 A69-27875

Supplementary absorption and Hall effect temperature dependence in solid solutions of gallium arsenic phosphide
13 p2318 A69-27894

Depth and planarity of zinc diffused junctions in GaP using temperature, phosphorus overpressure and time as independent variables
13 p2322 A69-28136

Ga phosphide p-n junctions formation from GaP. Ga solution, discussing electrical and luminescence properties
13 p2323 A69-28642

SiC and GaP diodes used as low power light sources, studying electroluminescence in p-n region under pulsed excitation
14 p2419 A69-29325

Current effects on quantum efficiency of gallium phosphide junction diodes emitting red light
15 p2575 A69-30174

Gallium phosphide Schottky barrier diodes, discussing construction and metals used, barrier height relationships to impurity concentration and temperature, rectifying characteristics and internal quantum efficiency
16 p2757 A69-31613

Schottky barrier diodes for high temperature operation prepared on n type GaP single crystals, studying I-V and C-V characteristics
19 p3381 A69-35681

IR absorption in n-type gallium phosphide doped with telluride or Si in 1.5-2.0 micron range, analyzing wavelength dependence
19 p3385 A69-36518

GaAs-P injection laser time delay measured from start of current flow in p-n junction diode, studying effects of memory, temperature and reverse bias
19 p3387 A69-36536

Energy band gap variation as function of composition in In-Ga-P semiconductor crystals
19 p3390 A69-36553

Se activation energy dependence on crystals composition and Se concentration, based on Hall coefficient temperature dependence in gallium arsenic phosphides
21 p3782 A69-39141

GALLIUM SELENIDES
GaAs zinc gallium selenide solid solutions properties, analyzing lattice constant, microhardness, forbidden zone and concentration relationships
15 p2670 A69-31050

GALVANIC CELLS
U ELECTROLYTIC CELLS

GALVANIC SKIN RESPONSE
Stability and habituation of nonspecific galvanic skin responses during light and sound stimulation periods in medical students
03 p0380 A69-13462

GALVANOMAGNETIC EFFECTS
.NT NERNST-ETTINGSHAUSEN EFFECT

Many valley n-type Ge and Si semiconductors dissipative current breakdown effects, noting dependence on symmetry of valleys and phonon scattering pattern
02 p0298 A69-12098

Conduction band anisotropy in n-type cadmium tin arsenides, analyzing galvanomagnetic tensor and distribution of isoenergetic surfaces for electrons
03 p0488 A69-13888

Localized umklapp scattering effect on galvanomagnetic properties of nearly free electron bcc metal with spherical Fermi surface
03 p0493 A69-14240

Anomalous size effects in galvanomagnetic properties of zinc crystal samples caused by compensation
06 p0981 A69-18232

Hall effect theory and devices, noting application to measurement of several physical quantities and sources of errors in devices
09 p1541 A69-22698

Conduction band anisotropy in n-type cadmium tin arsenides, analyzing galvanomagnetic tensor and distribution of isoenergetic surfaces for electrons
11 p1939 A69-25689

Transverse quantum thermogalvanomagnetic phenomena in thin semiconducting films, noting effects of inelastic electron scattering at acoustic lattice vibrations
13 p2318 A69-27890

Transport processes under adiabatic conditions between external magnetic field and thermal and electrical gradients in solid, defining galvanomagnetic and thermomagnetic effects
13 p2299 A69-28129

Galvanomagnetic characteristics of n-type semiconductor subjected to perpendicular electric and magnetic fields, noting electron temperature
14 p2505 A69-29037

AC technique using lock-in power amplifier SNR for measuring galvanomagnetic and Shubnikov-de Haas effects, noting error reduction
19 p3312 A69-36375

GALVANOMAGNETISM
U GALVANOMAGNETIC EFFECTS

GALVANOMETERS
Errors in amplitudes and phases recorded by earth tide recording equipment determined, using special multiflex galvanometer
04 p0601 A69-15305

GAME THEORY
NT MINIMAX TECHNIQUE
NT SADDLE POINTS [GAME THEORY]

Game interception of motions, obtaining proof for extremal aiming scheme
05 p0793 A69-15777

Differential pursuit games solved by integrating Bellman equation for value function and determining set of possible positions in game with prescribed duration
05 p0788 A69-16536

Differential games method solving pursuit problem for pursuer with greater maneuverability than pursued
09 p1476 A69-22671

Fuel optimal control for second order system determined by game theory approach
10 p1667 A69-24040

Differential game for determining singular fuel optimal control of plant with uncertainty in dynamic equation
10 p1667 A69-24041

Differential games solution value function constructible from solutions to associated one player optimal control problems
10 p1667 A69-24059

Synthesis for nonlinear second order differential equations with terms satisfying Lipschitz condition, using two person games optimal strategy
11 p1910 A69-25602

Nondeterministic differential games with imperfect state information, emphasizing linear system with quadratic cost functional and additive white Gaussian noise
12 p2053 A69-26505

Differential approach game for unfavorable pursued motion, examining optimum control laws
13 p2288 A69-27525

Pursuit problem involving controllable pursuing plant, deriving condition for engagement with prescribed period of time
14 p2482 A69-28800

Differential games theory with nonzero sum for application to economic analysis, discussing Nash equilibrium, minimax and noninferior strategies set
15 p2645 A69-31237

Nonzero-sum differential games characteristics, generalizing optimal control concepts, discussing Nash equilibrium and noninferior set solutions
17 p2943 A69-32834

Stochastic differential game theory, discussing nonlinear partial differential equations for solution, dynamic programming validity conditions, finite difference scheme, etc
17 p2994 A69-32844

Game interception of motions, obtaining proof for extremal aiming scheme
18 p3173 A69-35030

Two player zero-sum differential games with emphasis on play with state determined by differential equations, noting optimal solutions
19 p3359 A69-35665

Minimization of motion deviation from prescribed motion analyzed as differential game of converging motions using equations of motion
22 p3980 A69-40105

Existence theorem for Markov chain finite state stochastic games applied to saddle point and optimal strategy or epsilon-optimal strategy pairs
22 p3975 A69-41010

Risk taking under uncertainty in individual and group decisions, analyzing gambling and group discussion situations
23 p4091 A69-42016

Differential games derived for conjugate-point necessary conditions and definitions for minimum and maximum problems
24 p4340 A69-42959

Policies and controller design for pursuing vehicle developed in terms of pursuit-evasion differential games
24 p4341 A69-43295

Linear-quadratic pursuit-evasion game with dynamics perturbed by additive white Gaussian noise, obtaining linear minimax solutions
24 p4341 A69-43296

GAMETOCYTES

Recessive lethal mutations frequency in gametes of male and female *Drosophila melanogaster* onboard Vostok spacecraft
07 p1063 A69-18598

Lignin presence in New Zealand moss gametophytes observed for characteristic color reaction and UV spectra, noting contrast with north temperate species
17 p2912 A69-34176

Insect gametes response to space flight and radiation in reduced gravity including plants and microorganisms
23 p4091 A69-42050

GAMMA FUNCTION

Tabulation of high accuracy gamma function values for some rational arguments, noting applications to Gaussian quadrature formulas, fractional Bessel functions and Airy functions
03 p0455 A69-13375

Failure distribution functions based on Eyring component aging model, including failure probability density function for Weibull and gamma type distributions
08 p1322 A69-21104

GAMMA GLOBULIN

Tryptic pentapeptide Asp-Glu-Leu-Thr-Lys synthesis showing relation to Gm/a/ antigen of human gamma g-globulin
24 p4279 A69-42712

GAMMA RAY BEAMS

Angular energy distribution in gamma quanta beam during collision between laser photons and relativistic electrons
10 p1701 A69-23132

GAMMA RAYS

Solar X-ray high activity level during spring 1966 connected with gamma type magnetic solar regions and correlated with ionospheric effects
01 p0146 A69-11119

Scintillation gamma spectrometer on Luna 10, eliminating charged particle background by fabricating detector from NaI single crystal in scintillating plastic container
01 p0084 A69-11314

Chronic gamma radiation biological damage in rats exposed to maximum nonlethal to minimum lethal doses for various periods
02 p0197 A69-11494

Pulsar CP 1133 high energy gamma ray emission, using atmospheric Cerenkov detection technique for high energy neutral cosmic rays
02 p0307 A69-11823

Radioactive decay of neutral pions generated in metagalactic cosmic ray interactions as source of high energy isotropic gamma rays observed by OSO-3
02 p0308 A69-12092

GAMMA RAYS

Neutron and gamma irradiation effects on CdS crystals structure and properties, outlining electron energy level scheme
02 p0298 A69-12119

Gamma ray astronomy, noting fluxes above 100 Mev from strong radio sources and intensities of Crab Nebula
03 p0497 A69-12931

Angular correlation of inelastically scattered alpha particles and gamma rays emitted from 2-plus state of Sn 120
03 p0469 A69-13098

Angular correlation between inelastically scattered 42 Mev alpha particles and emitted gammas from 2-plus Ni 58
03 p0470 A69-13100

Biological effects on rhesus monkeys of high energy protons compared to effects of cobalt 60 gamma radiation
03 p0374 A69-13498

Gamma ray fluxes from pulsating radio sources, using detection of Cerenkov light generated by energetic particles in atmosphere
03 p0513 A69-13772

EPR investigation of free radicals formed during mechanical fracture and gamma irradiation, discussing recombination rate and reaction rate with oxygen
03 p0434 A69-13871

Extraterrestrial background gamma radiation /0.3-2 Mev/ observations used to derive upper limits for cosmic ray protons and CNO nuclei in interstellar space
03 p0501 A69-13934

Burning rate of composite propellant with gamma irradiated ammonium perchlorate, noting enhancement at atmospheric pressure
04 p0647 A69-15519

Gamma radiation effects on transistors and diodes, discussing dosage and thermal changes within operational temperature range of germanium devices
05 p0728 A69-15695

Solar gamma rays measurement role in knowledge of solar flares, discussing simultaneous satellite and ground based observations
05 p0814 A69-15863

Gamma irradiated silver carbonate EPR at liquid nitrogen temperatures
05 p0716 A69-15915

Polymer films tensile properties after exposure to gamma radiation in vacuum, noting chain scission and cross linking
[ASME PAPER 68-WA/RP-6]
05 p0783 A69-16160

Radiosensitivity of potatoes to gamma ray and proton irradiation applied to whole tubers and to isolated eyes before planting
05 p0709 A69-16511

Gamma ray production and high energy electrons in cosmic radiation
05 p0817 A69-16712

Gamma radiation effects on gate threshold voltages in modified oxide insulators in MOS structures
06 p0976 A69-16876

Recovery and long term reliability of Si n-p-n transistors subject to gamma radiation, using military specifications for failure
06 p0976 A69-16878

Gain degradation under applied voltage and injection current during low dose gamma irradiation by Co-60 source for bipolar transistors
06 p0977 A69-16880

Combined neutron degradation and gamma induced effects on closed loop system simulated by SECURE program
06 p0899 A69-16889

X ray and gamma astronomy, discussing galactic gamma radiation source and diffuse X ray background radiation
06 p0998 A69-16969

Low energy photon spectrum at balloon altitudes, noting small geomagnetic latitude dependence
06 p0992 A69-17313

Cosmic X rays, gamma rays and electron production under astrophysical conditions, noting potential use in supernova and quasar research
07 p1204 A69-18391

Gamma heating rate measured by aqueous dosimeter converted to rate in thin tungsten detector in water shield through transport theory calculations, obtaining correction factors
07 p1178 A69-18825

Instrumentation design problems connected with NERVA, considering high gamma and neutron radiations and temperature environments
[IEEE PAPER 2D-5]
07 p1134 A69-19189

Gamma ray telescope development for balloon-borne astronomy in search for discrete gamma sources and supernova explosions
[IEEE PAPER 3A-5]
07 p1134 A69-19192

Onboard calibration system for gamma ray spectrometers and X ray detector in earth satellites, describing fabrication and test results for radioactive sources
[IEEE PAPER 3A-6]
07 p1134 A69-19193

X ray proportional counter, analog to digital converter and power supply for gamma ray spectrometry used in satellite applications
[IEEE PAPER 3A-7]
07 p1134 A69-19194

Inhibition of gamma ray induced DNA degradation by infection with bacteriophage
07 p1069 A69-19709

Cosmic gamma radiation with energies above 100 Mev in southern sky, discussing results of balloon-borne spark chamber flight
08 p1377 A69-19787

Very high energy gamma rays from pulsars, considering implications of various gamma ray production processes
08 p1377 A69-19897

Cosmic gamma ray generation by Compton scattering in discrete sources, applying formulas to M87, Crab Nebula, M82, Cen A, Ngc 1275, and Cas A
08 p1377 A69-20053

Chondrite meteorite fall /1969/ in Mexico, noting opaque and microcrystalline matrices and gamma rays from short lived isotopes
08 p1396 A69-20686

Discrete source hypothesis for interpreting high energy cosmic gamma ray measurements obtained by OSO-3 spacecraft
08 p1380 A69-20699

Laser stimulated gamma-optical transitions illustrated by gamma-optical absorption detection in dysprosium ethyl sulfate
08 p1328 A69-21185

Cosmic gamma ray spectra from metagalactic proton-antiproton annihilation
09 p1574 A69-21459

Gamma ray scattering gauge design optimum parameters to measure Mars atmospheric density
09 p1495 A69-21842

High energy protons, helium and gamma rays observed by particle telescope on board OSO-C, obtaining integral rigidity spectra of proton and helium nuclei
09 p1579 A69-22172

Centaurus constellation search for gamma rays using balloons, discussing radio and X ray luminosity
09 p1580 A69-22269

Compton scattering of microwave radiation on cosmic ray electrons proposed as mechanism generating 100 Mev cosmic gamma rays
09 p1580 A69-22295

Inverse compton scattering of far IR background radiation proposed as explanation of high energy gamma ray flux
09 p1580 A69-22296

Gamma ray luminosity of typical type I supernovae remnant computed by assuming Ni 56 radioactive decay energy origin of optical luminosity
09 p1581 A69-22409

Cosmic ray electrons and gamma quanta at lower atmosphere recorded with balloon equipment, plotting vertical profiles of electron energy spectra
10 p1758 A69-22830

Phonon interactions with recoilless gamma rays, considering usability of Mossbauer effect as probe for VHF acoustic experiments
10 p1724 A69-23088

High altitude balloon measurements of secondary gamma quanta intensity vertical distribution, using scintillation counter with CsI/Tl crystal
10 p1770 A69-23924

Line spectrum of flare gamma radiation due to atmosphere nuclei excitation by high energy proton acceleration
11 p1945 A69-24241

Extragalactic gamma ray fluxes predicted, discussing collisions, matter-antimatter annihilation and cosmological implications
11 p1946 A69-24466

Northern sky scan for discrete sources of gamma rays in 240 to 1000 kev energy region by telescope on balloon flight
11 p1946 A69-24593

Electron, proton and gamma ray radiation effects on thin film CdS, GaAs and CdTe solar cells
11 p1825 A69-24872

Lasers applied to simulation of effects of X ray or gamma ray bursts on semiconductor devices
11 p1896 A69-24877

Shrinkage and heat release of polyglycol maleinate binder during gamma radiation consolidation compared with thermochemical consolidation
12 p2117 A69-25991

X ray polarization from Sco X-1, noting spurious instrumental polarization due to cosmic ray anisotropy using X ray polarimeter
12 p2149 A69-26315

Gamma quanta produced during high energy nucleon-nuclei interaction of air atoms recorded with X ray film
13 p2303 A69-28376

High energy nuclear interactions in graphite block at high altitude, recording gamma quanta produced
13 p2330 A69-28377

Gamma quantum spectrum shape from high altitude X ray film and nuclear emulsion blackening, discussing high energy pion production
13 p2330 A69-28378

Primary electrons and gamma quanta generated electron photon cascades in Pb, obtaining error free cascade curves
13 p2304 A69-28416

Lunar surface gamma radiation observed by Luna 10 spectrometer, suggesting basalt-like minerals composition of lunar maria
13 p2333 A69-28635

Annihilation gamma ray spectra from equilibrium spectra of secondary galactic positrons
14 p2514 A69-29948

Mortality kinetics of Drosophila melanogaster, comparing effects of gamma radiation-induced life shortening and natural aging
15 p2555 A69-30444

High energy gamma rays detection by balloon near geomagnetic equator, observing enhanced flux from galactic disk
15 p2675 A69-30695

Energetic gamma rays emission from radio source Cassiopeia A by high altitude balloon observations, using high resolution telescope
15 p2675 A69-30760

Electrical parameters measurement for homogeneous batches of planar silicon transistors subjected to cobalt 60 gamma rays, considering isochronal and isothermal annealing
15 p2625 A69-30827

Energetic gamma ray emission from Cygnus A and X-1, describing high altitude balloon telescope observation and gamma ray emulsion process
15 p2676 A69-30888

Diurnal variations in gamma rays produced by proton bombardment ascribed to geomagnetic time dependence for low energy solar proton cut-off
16 p2850 A69-32308

Origin of galactic gamma rays, discussing evidence in support of interstellar gas in galactic disk and production of neutral pions and bremsstrahlung
16 p2852 A69-32806

Low level beta, X and gamma radiation detector incorporating Geiger, proportional and scintillation counting features in various modes suiting radionuclide decay scheme
17 p2975 A69-33747

Corrections to previous papers on extragalactic gamma rays, discussing effects on various cosmological models
17 p3025 A69-34168

Radiation resistant devices for minimizing neutron and gamma radiation effects on military electronic components, discussing selection features and sampling lot sizes
18 p3144 A69-34491

Radiosensitivity of potatoes to gamma ray and proton irradiation applied to whole tubers and to isolated eyes before planting
18 p3095 A69-34730

Instruments for gamma ray astronomy including Ranger low energy detector, howitzer detector and cosmic spark chamber
18 p3138 A69-35135

Laser stimulated gamma-optical transitions illustrated by gamma-optical absorption detection in dysprosium ethyl sulfate
18 p3152 A69-35154

Aircraft nucleonic fuel gauging system, using radioactive gas to emit gamma rays for fuel mass sensing
18 p3139 A69-35468

Radiation damage and recovery of lithium-diffused silicon p-n solar cells, measuring photovoltaic parameters as function of gamma radiation fluence
19 p3251 A69-35694

Electron spin resonance spectra of gamma irradiated single crystals of 9-methyladenine, analyzing H abstraction radical and temperature effects

19 p3264 A69-35974

Free radicals destruction rates by gamma irradiation at 77 K measured as first order function of dosage, using electron spin resonance spectroscopy

19 p3265 A69-36376

Supralethal doses of pulsed mixed gamma-neutron radiations from TRIGA reactor administered to unshielded, head shielded and trunk shielded beagles

19 p3259 A69-36459

Electron and gamma quanta concentrations measurements by high altitude balloon, noting fluctuations at various altitudes

20 p3587 A69-37046

Gamma ray flux from processes associated with high energy electrons from pulsar NP 0532, noting light polarization

20 p3588 A69-37410

Gamma ray emission of meteorite of 25 April 1969 measured by scintillation spectrometry, attributing peaks to annihilation radiation, Cs 137, Mn 54, etc

20 p3590 A69-37571

Neutron activation analysis for oxygen determination in Be by gamma emission intensity from nitrogen 16, noting bound oxygen

20 p3544 A69-37811

Gamma radiation effects on behavior of nickel and cadmium electrodes in alkaline solution

20 p3466 A69-38072

NASA lunar receiving laboratory for lunar rock samples examination by gamma ray spectrometry for induced radioactive nuclides and naturally occurring isotopes

20 p3512 A69-38271

X ray sources and diffuse background radiation observed in gamma and X ray spectral regions, considering electromagnetic waves attenuation by interstellar matter

21 p3789 A69-38817

X rays and gamma rays extragalactic components, calculating background component intensity for given model of universe

21 p3789 A69-38818

Nuclear gamma ray astronomy utilization for stellar interior detection, showing identification of key radioactive nuclei of supernova at explosion time

21 p3792 A69-39572

Survival rates of continuously cultivated *Chlorella* plants in air-carbon dioxide atmosphere after single exposure to gamma radiation, using microcolony counting technique

22 p3876 A69-40275

Positive effect of shielding and cystamin administration on tonic and evacuator functions of rats gastrointestinal tract after gamma irradiation

22 p3877 A69-40285

Solar flare optical, neutron and gamma emission, discussing ionization losses and nuclear interaction of accelerated particles in flares

22 p4003 A69-40296

Gamma radiolysis of silver nitrate ice forming neutral Ag in magnetically distinct sites, discussing water dipoles rotation and electron paramagnetic resonance

22 p3992 A69-40574

Cosmic gamma rays spectrum from neutral pions production and decay in metagalactic cosmic ray p-p collisions, deriving models based on Einstein general relativity theory

22 p4006 A69-40641

Relative abundances U-235/U-238, Th-232/U-238, Pu-244/U-238 and I-129/I-127 at solar system formation time to obtain time evolution of gamma process nuclei

22 p3986 A69-40766

Restoration processes in *Chlorella pyrenoidosa* to distinguish intense and less intense gamma ray irradiations

22 p3878 A69-40792

Air ionization and beta and gamma dose rates measurements for natural radiation from cosmic rays compared to nuclear weapons tests fallout, considering biological effects

22 p4007 A69-40915

Nonresonant and resonant cross sections for gamma ray transitions involving isobaric spin mixed states in Be 8

22 p3987 A69-41043

Bacteriophage desoxyribonucleic acid (DNA) degradation by gamma irradiation in vitro by Co 60, discussing breaks, cross links and molecular weight

23 p4079 A69-41402

Exposure rate influence on mechanical properties of polymer binder cross-linked by gamma radiation exposure from cobalt isotope source

23 p4179 A69-41711

Viruslike particles in fat body cells and oenocytes of *Drosophila melanogaster* imagoes, in glial cells of cephalic ganglionic center of flies and in gamma irradiated cells

23 p4091 A69-42021

High energy astronomical diffuse radiation component properties tabulated, discussing power law and thermal X ray background, gamma rays, etc

23 p4207 A69-42319

Cross sections of charge carrier capture by ions in gamma irradiated P-Al-Si glass with metal oxides additions measured for evaluating radiation stability improvement

23 p4180 A69-42470

Gamma radiation effect on AgCl-Cu redox state in AgCl activated, heat treated Na-Al-B-Si glass, using EPR method

23 p4180 A69-42471

High energy gamma rays point source in Sagittarius indicated from evidence obtained by high altitude balloon flights

24 p4365 A69-42606

Solar high energy gamma ray flux abrupt increase detected by neutral particle plastic scintillators at balloon altitude

24 p4371 A69-43612

GANGLIA

NT NERVES

NT NEURONS

Analytical model for frog retinal bug detector cell to make possible signal measurement in frog optic fibers

07 p1070 A69-18383

Morphological microchanges in solar plexus ganglia of white rats after X irradiation

12 p2019 A69-26347

Pathological changes in solar ganglia cells of white rats following X ray exposure, using electron microscope

21 p3659 A69-39064

Local stress effect on immunocompetent cells differentiation in guinea pigs lymphatic ganglia, showing antibody producing cells number increase

22 p3877 A69-40277

Electroretinogram a-wave relationship to early inhibition and excitation of retinal ganglion cells produced by flash superimposition in rabbits

22 p3878 A69-40836

High intensity flash effects on local electroretinogram, late receptor and slow potentials and ganglion cell activity in area centralis of cat retina

22 p3883 A69-40882

Reflex activity of single preganglionic sympathetic fibers during coronary occlusion in cats, discussing left third thoracic T3/ramus communicans

23 p4084 A69-41460

GAPS

NT SPARK GAPS

Capacitors pi network representation of series gap in center conductor of matched coaxial transmission line

14 p2424 A69-29766

GARNETS

NT YTTRIUM-ALUMINUM GARNET

NT YTTRIUM-IRON GARNET

Polarized low temperature laser excited Raman spectra of thulium gallium garnet

02 p0256 A69-11925

Ce activated garnet crystals optical properties, noting IR and near UV absorption spectra and room and low temperature fluorescence

07 p1201 A69-19647

Alternative explanation of garnet composition in Coorara meteorite, giving probable formula

08 p1382 A69-19819

Magnetic sublattices interactions in gadolinium ferrite garnet, estimating magnetization level temperature dependence

08 p1374 A69-21186

Polycrystalline Ca-V garnets and Mg-Cr ferrites magnetic properties after adding rare earth elements

13 p2320 A69-27999

Magnetic properties of ferrites with garnet structure, discussing temperature effect on magnetic states of Gd, Li, Y and Lu sublattices

13 p2323 A69-28564

Single crystals garnets Raman spectra using laser radiation, separating phonon spectra of host lattices from electronic Raman effect

14 p2507 A69-29334

Flux grown magnetic garnet crystal internal defects analyzed by etching and Lang X ray transmission topography, revealing tubular structural deviations

16 p2825 A69-31692

Magnetic sublattices interactions in gadolinium ferrite garnet, estimating magnetization level temperature dependence

18 p3183 A69-35155

IR lattice spectra of rare earth Al, Ga and Fe garnets, discussing oxygen anion, translational rare earth cation and crystal lattice external motions

24 p4360 A69-42974

GAS ANALYSIS

NT OZONOMETRY

Planetary atmosphere composition determination using mass spectrometry for neutral components, ion spectrometry for ionic components and data system optimization

[AAS PAPER 68-183] 02 p0247 A69-11468

Mass spectrometer residual gas analyzer/RGA for identifying and measuring subliminated substances from spacecraft construction materials, noting applications during vacuum testing

02 p0227 A69-11758

Polymethyl methacrylate irradiated by laser in vacuum to study mechanism responsible for gas formation

02 p0270 A69-11980

Gas adsorption of molecular oxygen and hydrogen on molybdenum surface using collector section of field emission retarding potential analyzer

08 p1268 A69-20179

Residual gas analyzer and leak detector by time of flight measurements on neutral metastable atoms and molecules between pulsed electron gun and auger surface detector

13 p2262 A69-28006

Molecular flow network theory extended to pulsed operation with gases mixtures having various molecular weights

13 p2247 A69-28085

Automatic ultrasonic method for determining dissolved gases content in liquid sample, using increasing acoustic oscillations amplitude for bubble development

19 p3308 A69-35822

Calcium-rich achondrites age distribution determined from inert gas measurements and existing data of eucrites, shergottites and howardites

19 p3413 A69-36107

Computerized mass spectrometer for monitoring atmosphere in astronauts suits and cabin

[AIAA PAPER 69-1016] 22 p3922 A69-40388

Jet engine combustion temperature measurements by thermocouples or gas analysis noting errors involved

23 p4165 A69-41650

GAS BEARINGS

Gas flow analysis for externally pressurized porous journal gas bearing, considering circumferential flow in bearing clearance and porous bushing

01 p0085 A69-10312

Whirl instability of externally pressurized gas journal bearing with peripheral feeding holes, discussing analytical natural frequency of shaft bearing systems

02 p0254 A69-12426

Hydrostatic journal gas bearings calculations for carrying capacity, gas consumption and optimal dimensions for maximum lifting capacity

03 p0432 A69-12960

Digital computer program for gas bearing analysis, discussing Reynolds equation and numerical approximations

04 p0604 A69-14518

Stability of high speed rotors with sliding bearings

04 p0607 A69-15163

Self acting gas lubricated bearings production, discussing manufacture to ultraprecision tolerances by semiskilled labor

[ASME PAPER 68-WA/LUB-4] 05 p0768 A69-16130

Pressurized fluid journal bearing with fluid fed into space between shaft and shell from plenum chamber in bearing housing through circumferential slots

06 p0931 A69-17529

Stability of hydrostatic gas bearings with large clearances

08 p1303 A69-20271

Gas bearings for spool gas generator for aircraft turbine engines, noting rotor bearing stability and LP spool balancing and seal leakage

[ASME PAPER 69-GT-60] 09 p1513 A69-22515

Rotating mirror turbine with air cushion floating shaft for use in streak and framing cameras, noting framing rate

12 p2085 A69-26156

Self acting gas lubricated bearings design procedures and comparison with oil lubricated bearings [ASME PAPER 68-LUBS-10]

13 p2265 A69-27267

Pressure distribution in finite width high speed self acting gas lubricated slider and partial arc bearings, noting trailing edge conditions and side leakage effects [ASME PAPER 68-LUBS-15]

13 p2265 A69-27268

Herringbone grooved gas lubricated journal bearing static and dynamic characteristics analyzed approximately, noting pressure distribution and vibration amplitudes [ASME PAPER 68-LUBS-7]

13 p2265 A69-27269

Matched asymptotic expansions to obtain slider bearing load carrying capacity [ASME PAPER 68-LUBS-18]

13 p2266 A69-27270

Herringbone grooved gas lubricated journal bearing stability, testing effects of geometries and clearances on onset speed for half frequency whirl [ASME PAPER 68-LUBS-25]

13 p2266 A69-27271

Flat disk squeeze film air bearing, determining motion of supported mass by computer program [ASME PAPER 68-LUBS-38]

13 p2266 A69-27272

Lubricant compressibility effect on spiral groove gas bearing load carrying capacity [ASME PAPER 68-LUBS-33]

13 p2266 A69-27274

Design optimization for gas lubricated spiral grooved spool bearing based on narrow groove theory, analyzing static and dynamic characteristics for motion in axial direction [ASME PAPER 68-LUBS-12]

13 p2266 A69-27276

Linearized theory for stability of self acting gas journal bearings with noncircular members and elements of flexibility and damping, noting three lobed rotor [ASME PAPER 68-LUBS-45]

13 p2266 A69-27277

Radial and polar load support of squeeze film gas bearing in form of sphere pulsating radially or moving along polar axis [ASME PAPER 68-LUBS-3]

13 p2266 A69-27279

Flat disk squeeze film air bearing, determining motion of supported mass by computer program [ASME PAPER 68-LUBS-35]

13 p2266 A69-27280

Externally pressurized gas lubricated journal and thrust bearings designs, citing reference literature [ASME PAPER 68-LUBS-8]

13 p2267 A69-27282

Externally pressurized gas lubricated bearings treated theoretically using unevenly distributed supercharging method, noting Reynolds equation numerical integration [ASME PAPER 68-LUBS-44]

13 p2267 A69-27283

Gas lubricated hybrid journal bearings with external pressure, noting load capacity and stability in steady state and dynamic analyses [ASME PAPER 68-LUBS-21]

13 p2267 A69-27284

Flow models for externally pressurized gas bearings, discussing pressure distributions, load capacity and flow rate [ASME PAPER 68-LUBS-2]

13 p2267 A69-27285

Heat transfer between surfaces as secondary effect in gas bearing lubrication from analysis taking into account viscosity variation with temperature [ASME PAPER 68-LUBS-4]

13 p2267 A69-27286

Infinitely long journal bearing using ionized gas lubricant with magnetic field applied axially and electric field applied transversely to fluid film [ASME PAPER 68-LUBS-30]

13 p2267 A69-27287

Magnetic and electric fields influence on gas lubrication of bearings [ASME PAPER 68-LUBS-26]

13 p2267 A69-27288

Rate gyro life and reliability, discussing gas bearings separating rotor from stator by thin gas film with conventional oil film characteristics

15 p2608 A69-30410

Gas lubricated tilting pad thrust bearing analysis and performance, determining optimum hydrodynamic crown profile [ASLE PREPRINT 69AM 3C-2]

15 p2619 A69-30472

Power generating unit operating on air bearings

15 p2629 A69-31028

Self excited vibrations of rotors supported in gas bearings from analyzing solutions to equations of rotor motion

16 p2875 A69-32250

Pressure distribution in gas lubrication layer of infinite radial sliding bearings, approximating differential equation by simple formulas

23 p4168 A69-41412

Self acting gas lubricated bearings production, discussing manufacture to ultraprecision tolerances by semiskilled labor [ASME PAPER 68-WA/LUB-4]

24 p4320 A69-43035

GAS CHROMATOGRAPHY

Leak flow rates of nitrogen and helium at various pressure gradients measured by gas chromatography and mass spectroscopy

01 p0079 A69-10297

Quantitative determination of phenolic content in composite materials by pyrolysis gas chromatography method

01 p0025 A69-11267

Propellants volatile fraction removal followed by gas chromatographical determination, noting use of heating method

02 p0302 A69-11522

Gas chromatography used to determine residual solid propellant stabilizers content and nitro derivatives, including thin film chromatography

02 p0303 A69-11528

Gas chromatography technique for separation and purification of chemical compounds for ionizing radiation detectors

02 p0249 A69-12011

Automatic equipment for sampling and preparing gases by dual column gas chromatography for subsequent mass spectral analysis of carbon isotopes during methane metabolism

02 p0205 A69-12603

Escherichia coli detection and differentiation from other bacteria by direct gas chromatographic analysis of culture media

03 p0382 A69-13550

Gas chromatographic determination of hydrocarbon quantity in methane in parts per billion range

03 p0382 A69-14115

Oil lubricant vapors under frictional working conditions in vacuum analyzed by mass spectrometer and gas-liquid chromatography concerning molecular weight and composition [IME PAPER 11]

07 p1137 A69-18558

Gas-liquid and thin layer chromatographic and nuclear magnetic resonance techniques to steric analysis of diketopiperazines

07 p1075 A69-19498

Reagent menthyl chloroformate use in optical analysis of asymmetric amino and hydroxyl compounds by gas chromatography

07 p1075 A69-19499

Quantitative gas-liquid chromatography of sulfur amino acids trimethylsilyl derivatives

13 p2217 A69-28259

Quantitative gas-liquid chromatographic analysis of nucleic acid components including purine and pyrimidine bases, nucleosides or nucleotides

13 p2217 A69-28260

Quantitative analysis for N-acetylneuraminic acid by gas-liquid chromatography using trimethylsilyl derivative

13 p2217 A69-28315

Gas chromatography based on sampling gas-vapor phase at liquid surface for determining volatile oxygen containing compounds in biological media

13 p2216 A69-28627

Life detection for space missions based on detecting optical asymmetry in biogenic molecules by gas chromatography involving diastereomeric esters synthesis

15 p2556 A69-31315

Sugars identification as trifluoethylacetyl polyol derivatives by gas-liquid chromatography

15 p2558 A69-31539

Gas chromatograph-mass spectrometer combination for in situ analysis of lunar organic matter, describing instrument design and operation

18 p3113 A69-34238

Gaseous diffusion coefficients during argon, krypton, oxygen and nitrogen diffusion into helium measured by gas chromatography

18 p3099 A69-34280

Heats of adsorption of carbon dioxide on silver //I/ oxide and copper //II/ oxide by gas chromatography

20 p3485 A69-38277

Acid fraction extraction of Green River shale identified by gas chromatography-mass spectrometry-computer system, noting trimethyl pentadecanoic acid

21 p3669 A69-38983

GAS COMPOSITION NT CARBON DIOXIDE CONCENTRATION

Volcanic gas from lava lake, noting carbon and sulfur gases depletion during cooling and solidification

02 p0236 A69-11466

Planetary atmosphere composition determination using mass spectrometry for neutral components, ion spectrometry for ionic components and data system optimization [AAS PAPER 68-183]

02 p0247 A69-11468

Optimum proportions of gas mixture components in He-Ne laser related to field distribution in cavity

03 p0441 A69-13847

Composition and thermodynamic properties of gaseous system reacting at low temperatures with condensed phase formation, discussing iterative process convergence in approximation

11 p2001 A69-25223

Gas particle concentrations on moon due to solar wind, surface emissions and atmospheric contamination by lunar operations and rocket motor products

18 p3189 A69-34236

Irreversibility resulting from composition changes in operating fuel cell anode and cathode chambers and cell geometry influence

18 p3093 A69-34781

Diverging nozzle flow of gas mixtures containing solid or liquid particles analyzed by one dimensional approximation separately averaging boundary layer and flow core

19 p3298 A69-36389

Negative ion influence on electrical conductivity of partially ionized multicomponent gas mixtures, basing analysis on thermodynamic calculations of composition

21 p3774 A69-38867

Digital computer program for determining alveolar and capillary blood gas compositions corresponding to ventilation-perfusion values, considering dissolved oxygen and inert gas exchange

22 p3875 A69-40230

EKG, EEG, pneumograms and X ray pictures showed no pathological effect after prolonged confinement in sealed chamber having artificial atmosphere with variable gas composition

22 p3892 A69-40284

Book on flow equations for composite gases derived from Boltzmann equation, BGK approximation application, etc

24 p4299 A69-42766

GAS COOLED REACTORS

Gas core reactor curved porous walls geometry tested with clear and smoky air injection, noting mass flow ratio in reactor cavity

18 p3171 A69-35181

GAS COOLING

Mass transfer cooling of high velocity surfaces in gaseous environment noting applications to atmospheric entry

13 p2377 A69-28146

Closed cycle gas cooling techniques for self contained CW kilowatt carbon dioxide laser, relating output power to flow velocity and input power

23 p4173 A69-41497

GAS DENSITY

Earth atmosphere air density and temperature profiles from drag acceleration measurements in falling sphere experiment

02 p0251 A69-12809

Ideal gas spectra and density fluctuations correlations calculated during Markovian and nonMarkovian wandering of particles

03 p0477 A69-13414

Stagnation point electrostatic probe measurements of flowing partially ionized high density monatomic gases

06 p0964 A69-17196

Nonadiabatic reacting homogeneous system undergoing density changes, predicting chemical reaction rates and intermediate combustion products from chain reaction kinetics [AIAA PAPER 69-87]

06 p1036 A69-18054

Pulsar distance estimates, discussing effect of interstellar electron and H densities and temperature dependence of H density-electron density ratio within disk

08 p1397 A69-20698

Gas transport coefficients dependence on density and temperature, noting experimental results for Ne and molecular N and H

08 p1353 A69-21009

Three body ionic recombination coefficient for moderate and high gas densities, taking into account variability in mean free path and trapping radii

09 p1542 A69-21624

Light polarization from stimulated Brillouin effect in compressed gaseous nitrogen, presenting depolarization variations as function of gas density and laser power

09 p1516 A69-21691

Intergalactic gas temperature and density reevaluated, considering neutral hydrogen distribution in galaxies peripheries and metagalactic background of ionizing UV radiation

11 p1946 A69-24589

Dense real gas thermodynamic relations in piston driven shock tube facilities operation

11 p1862 A69-25011

Correlation of stellar surface density distribution of young stars and neutral hydrogen gas in Small Magellanic Cloud

12 p2152 A69-25802

Pulsed laser holography used in conjunction with schlieren three dimensional system for observing gas density gradients at different test positions

12 p2088 A69-26179

Velocity distribution and density of neutral hydrogen in southern portions of M 31 and Sc-type galaxy M 33 by 75 m radio telescope

12 p2166 A69-27038

Shock wave gas flow density behind shock tube calculated by shadows measurements using interferometric techniques

13 p2245 A69-27384

Polytropic gas spheres static models integral characteristics by nonrelativistic generalized gravitation theory, noting central densities dependence on critical values

13 p2352 A69-27872

Simple fluids viscosity dependence on density analyzed by molecular theory, exemplifying with liquid argon

13 p2299 A69-28036

Constant density heating upstream and constant pressure cooling downstream formulas for radiating shock waves

13 p2249 A69-28240

Collision integral kernels of kinetic equation for single component gas density matrix derived by Bogoliubov-Gubov method

14 p2458 A69-29169

Expression relating gas density, radial velocity and temperature at comet nucleus surface to nucleus surface temperature, applying results to unsteady sublimation process

15 p2684 A69-30521

Final states of density, velocity and pressure in gas, comparing states reached after transition through single oblique hydromagnetic shock and two successive shocks

15 p2664 A69-31217

Conditions behind incident and reflected shock waves in shock tube calculated from initial pressure, density, temperature and shock speed

15 p2593 A69-31487

Q switched laser produced blast waves in low pressure Ar, discussing gas density and time dependence roles

16 p2796 A69-31705

Thick gas model for monochromatic one dimensional radiant flux near diffusely emitting and reflecting boundaries, discussing gray gas and exponential kernel approximations

16 p2769 A69-31871

Approximate expression for temperature dependent radiative heat flux in optically thin gas, considering reentry body hypersonic flight

16 p2877 A69-31892

Electron concentration and mass density behind reflected shock in ionizing argon, using time resolved two wavelength interferometry

16 p2771 A69-31918

Atmospheric gas constituents number densities determined as function of altitude by correlating laser beam scattering and absorption data

16 p2781 A69-32387

Upper atmospheric gas density and temperature distribution diurnal and seasonal variations calculated from satellites orbiting time changes

17 p2959 A69-32924

Galactic X ray sources density nearly proportional to interstellar gas density squared, discussing X ray intensities estimation, galactic age, etc

17 p3030 A69-33069

Flame front structure and combustion rates of gases as function of temperature dependence of thermal conductivity, diffusion coefficients, density and molecular weight

17 p3069 A69-33136

Shock wave structure dissipation in gaseous medium with microscopic particle velocities asymptotically approaching light velocity

17 p2958 A69-34145

Gladstone-Dale constants for dissociating high temperature oxygen determined for molecule and atom from density changes across shock

18 p3176 A69-34452

Gas dynamics in transition regime between continuum motion at high gas density and free particle motion at low density limit

19 p3300 A69-36658

Two dimensional unsteady motion of medium with pressure as linear function of density, analyzing gas expansion into vacuum

20 p3512 A69-36916

F region vertical density profiles for positive ions and neutral molecules of various gases determined from rocket-borne mass spectrometer data

21 p3702 A69-38354

Interstellar absorption of 10 A X rays from sources in Scorpio-Sagittarius region, noting gas density between earth and Crab Nebula

21 p3788 A69-38648

Rocket optical experiment for determining water, methane, nitric oxide and ozone vertical profiles in stratosphere and mesosphere

22 p4035 A69-39910

P-V-T surface of fluids in critical region by dielectric measurements, presenting saturation densities of oxygen

[NAS-NRC PAPER H-5] 22 p4050 A69-40623

Nonlinear relativistic wave velocity distribution within spherical nucleus bounded by shock wave in superdense gas determined by Cauchy problem

22 p3861 A69-41114

Metastable atom detection system for ground state atom beams, measuring Ar beam density five orders lower than background gas density

22 p3950 A69-41230

Gas concentration measurement during injection into laminar boundary layer streaming along porous plate, using quadrupole resonance mass spectrometer

23 p4058 A69-41695

Gas concentration liberated during each revolution in atmospheres of short period comets to explain impulsive forces upon nuclei, noting diatomic carbon density

23 p4221 A69-42387

Gas dynamic functions of axisymmetric supersonic gas flows determined using flow density distribution optical measurements

24 p4247 A69-43496

GAS DETECTORS

Leak detection techniques efficiency determined for airtight atmospheric air sampling devices used at low pressure and concentration

24 p4296 A69-42656

GAS DISCHARGE COUNTERS

U COUNTERS

GAS DISCHARGE TUBES

NT THYRATRONS

Time correlation of photons emitted by krypton gas discharge tube and helium-neon multimode laser

02 p0255 A69-11611

Scaling laws for RF discharge experiments in ionized environments, considering proper limit variables for simulation of electron density

02 p0283 A69-12241

Measured noise temperature in argon tubes vs theoretical electron temperature for gas discharge noise sources

02 p0210 A69-12437

Gas discharge tubes and waveguide mounts as reference noise accuracy standards for S, C and X bands in WR284, WR137 and WR90 waveguides

02 p0210 A69-12439

Waveguide band transition noise of gas discharge source, discussing measurement methods for establishing excess noise ratio

02 p0212 A69-12461

Glass pleats and cold cathodes in laser discharging tube, discussing angular displacements

03 p0435 A69-12981

Parallel and coplanar Brewster angle grinding of maser tube ends

03 p0440 A69-13302

Equivalent pressure concept verification for arc discharge with incandescent cathode in mercury vapor

03 p0478 A69-13843

Absorption coefficients of plasmas in capillary discharge tubes, discussing measurement using gas laser light source

03 p0442 A69-14218

Electron gun with plasma cathode consisting of gas discharge chamber, electron ejecting component and focusing system

04 p0598 A69-14857

Display techniques, discussing cold cathode luminous gas discharge /plasmas/ tube, electroluminescence and cathode ray tube

04 p0600 A69-15029

Electron density measurement in rapidly varying plasma, using improved Mach-Zehnder interferometer

05 p0760 A69-15613

Continuous and pulsed lasing characteristics during discharge in pure oxygen noting ozone formation and removal at tube walls

06 p0932 A69-16923

Probe noise in quiescent plasmas investigated using back diffusion type discharge tubes producing low density plasmas and positive plasma columns

06 p0967 A69-17715

Helium-neon laser output power dependence on spark gap cross section geometry, analyzing diffusion equation and population inversion

07 p1147 A69-18541

Gas segregation in positive column of DC discharge due to axial ion motion analyzed using conservation equation

08 p1361 A69-20145

Striation formation during steady state glow discharge, noting origin in cathode interfacial positive ions

09 p1545 A69-21343

Cathode material effects on temperature coefficients for glow discharge tubes, noting running voltage pressure characteristics

09 p1468 A69-22602

Gas laser output increase by nonconstricted discharge in aluminum tube cathode with mirror resonator

09 p1520 A69-22681

Xenon pulse discharge plasma temperature distribution, spectral brightness density and light absorption across quartz tube section, noting temperature drop near wall

10 p1742 A69-24081

Time correlation of photons emitted by krypton gas discharge tube and helium-neon multimode laser

11 p1895 A69-24718

Plasma rotation by Lorentz force in homopolar gas discharge device, considering centrifugal forces effect on flow pattern

13 p2315 A69-28556

Microwave oscillations in low pressure arc noting long gas discharge in small transverse dimensions

14 p2489 A69-28739

Frequency shifts of Lamb dip minimum in helium-neon laser, considering effects of discharge tube parameters and gas pressure

14 p2457 A69-28929

Pulsed HF discharge analysis in hydrogen based on laser light scattering at plasma electrons, noting presence of satellites

14 p2451 A69-29781

AC ignitor priming of quartz-chlorine gas discharge X band waveguide limiter with fast recovery used as radar receiver protector

15 p2573 A69-30035

Ion nitride hardening of Mo-Ti alloy at 1300 degrees C in cathode glow discharge tube

15 p2637 A69-30212

Argon electric arc axis temperature measurements, showing current and tube diameter ratio dependence

15 p2662 A69-30977

Gas discharge tube graphite hollow cathode geometry leading to abnormal discharge operation under certain pressure conditions

16 p2814 A69-31838

Helium-neon laser output power dependence on spark-gap cross section geometry, analyzing diffusion equation and population inversion

21 p3735 A69-38693

GAS DISCHARGES

NT RING DISCHARGE

Long lived low level chemiluminescence due to gaseous reactions at low concentrations induced by mercury lamp irradiation or Tesla coil discharge

01 p0024 A69-10618

Deuterium plasma evolution and creation modes obtained by short pulse laser discharge in gases, discussing detonation and phase wave ionization mechanisms

02 p0288 A69-12040

Measured noise temperature in argon tubes vs theoretical electron temperature for gas discharge noise sources

02 p0210 A69-12437

DC argon arc electrical and thermal parameters and optical properties at high pressure, using spherical anode

02 p0291 A69-12482

Gas parameters in collisionless region during discharge into vacuum, considering plane and axisymmetric cases and free molecular boundary region

02 p0234 A69-12583

Laser produced sparks in 200 kG magnetic field in air, butane and helium at atmospheric pressure

02 p0260 A69-12659

Positive Ar ion energy distribution for beam extracted from nonmagnetic hot cathode gas discharge ion source under various source conditions

03 p0427 A69-13102

Contact phenomena theory in decaying plasma applied to deionizing mercury vapor diode gas discharge plasma diagnostics

03 p0404 A69-13547

Xe gas discharge plasma resistivity dependence on current density measured in large tubular flash lamps

03 p0478 A69-13846

Plasma decay at high pressure in helium and argon with cesium vapor admixture and pure cesium vapor, using Saha equation

03 p0480 A69-14052

Frequency dependences of induced HF and high pressure discharge parameters, noting optimal frequency range independence from particular gas and gas flow rate

03 p0481 A69-14144

Cascade acceleration of plasma by two stage device noting plasma dispersion, plasma losses and highest final plasma velocity

03 p0482 A69-14215

HF gas discharges, discussing plasma temperature and density, plasmoid length and spectroscopic applications

03 p0482 A69-14217

Microwave excited argon discharge emission spectrum analysis, suggesting possible laser action in microwave discharges

04 p0609 A69-14346

High speed shadow photographs of Q switched laser triggered spark gap air discharge, showing sonic waves and development of discharge channel

04 p0610 A69-14349

UHF discharge plasma, electron distribution over bound states and ionization stages

04 p0634 A69-14442

Toroidal gas discharge in waveguide by coupling of microwave power into gas to heat gas, noting plasma confinement

[IMPI PAPER A4]

04 p0636 A69-14999

High repetition rate pulsed illuminator using electrodeless halogen discharge for rapid light extinction

04 p0599 A69-15021

Inelastic collisions effect on electron energy distribution in low temperature diffusion dominated discharges

04 p0637 A69-15047

Electron density variation in region of change of regime in gas discharge excited by HF capacitance and external electrode

04 p0637 A69-15060

Pressurized spark gap triggered by focused Q switched laser beam introduced along axis

04 p0612 A69-15204

Relaxation method for separation of continuous electron/ion recombination spectrum from electron spectrum in nonequilibrium gas discharge plasma

04 p0639 A69-15369

Electron distribution function effect on microwave emission and HF conductivity of weakly ionized discharge plasma

05 p0799 A69-15734

Similarity between characteristics of T layers in oxygen discharge positive column and Gunn instabilities in GaAs, noting role of negative O ions

05 p0800 A69-15739

Hydrogen molecular action in vacuum UV region during high current discharge

05 p0771 A69-15814

Gas lasers involving gas-discharge collisions, selective pumping or chemical reactions to produce necessary inversion, giving theoretical analysis of excitation mechanisms

05 p0772 A69-16226

Time resolved measurements, microwave interferometer and pulsed double probe for studying collision dominated plasma expansion in inductive HF He discharge

05 p0804 A69-16535

Qualitative mechanisms to explain Langmuir paradox, discussing wall mechanism for Maxwellian distribution formation in low pressure discharges

06 p0960 A69-16922

Radial electron concentration profile determination by spectroscopic examination of continuous plasma radiation of pulsed discharge in capillary

06 p0964 A69-17253

Secondary emission and hollow cathode effects in low pressure hot cathode thyatron filled with hydrogen and with shield surrounded thermionic cathode

06 p0896 A69-17475

Zeta discharge in low density regime characterized by strong turbulence, rapid loss of plasma, resistance higher than predicted and high ion temperature

06 p0970 A69-17955

Gas lasers principles of operation, discussing population mechanism, lifetime conditions, excitation processes, electron velocity distribution and types of discharges

06 p0937 A69-18008

Sonic boom reduction devices, discussing supersonic electroaerodynamic flow with shock waves, gas discharge one dimensional continuum analysis, power expenditure and aerodynamic interaction

[AIAA PAPER 69-38]

06 p0869 A69-18150

Spectroscopic investigation of emission of air plasma in HF electrodeless plasmatron, analyzing near IR, UV and visible spectra

07 p1191 A69-18995

Nonsaturated gain of laser radiation in gas discharge in carbon dioxide with N and He

07 p1151 A69-19060

Electron acceleration in microtron through injection from low pressure gas discharge plasma

08 p1279 A69-19803

Harmonic generation in microwave gas discharge in pure and air mixed gases, noting rare gases failure in power source applications

08 p1283 A69-20177

Discharge structure and stability of nonequilibrium plasma undergoing supersonic flow through linear MHD channel

08 p1366 A69-20788

Transition probabilities in repetitively Q modulated HCN maser radiation dependent on gas discharge current

09 p1516 A69-21626

Laser radiation produced by continuous glow discharge within Al hollow cathode, determining laser power in terms of He-Ne mixture pressures

09 p1519 A69-22245

Formation and acceleration of luminescent current layer in Z pinch discharge, noting density and electron mean free path in cold gas

09 p1552 A69-22397

Velocity and temperature influence on discharge characteristics of K seeded argon plasma flow at 1 atm pressure

10 p1733 A69-23449

Argon discharges in metal capillary cathodes noting effects of electron density, flow velocity, electrode phenomena and gas temperature

10 p1733 A69-23450

Low voltage He-Ne laser, noting outputs for various pressures and grid anode separations

10 p1704 A69-23652

Pulsed glow discharges in He and He-H mixtures for high current density, noting electric field and wall potential distributions

10 p1739 A69-23660

Charge transport in high pressure RF glow discharge in air at atmospheric pressure based on model plasma

10 p1740 A69-23662

Microwave oscillations amplitude spatial distribution in gas discharge plasma excited by electron beam

11 p1933 A69-25542

Neutral gas flow transport velocity and Mach number effects on critical electric field strength and direction in formation of self sustained discharge

11 p1933 A69-25545

Ar plasma diagnostics in pinch-discharge laser, determining electron temperature by spectroscopy and measuring plasma conductivity and ion concentration and temperature

11 p1933 A69-25548

Continuous polarized electron beam produced from spin conversion in ionizing reactions involving optically pumped metastable atoms in He discharge

12 p2130 A69-26312

Spontaneous emission of carbon dioxide lasers, studying emission in Second Positive System of nitrogen as function of discharge current and laser output power

12 p2105 A69-26316

Temperatures and densities of atoms and electrons from spectroscopic methods in gas discharge plasma used for CW ion-argon lasers, evaluating inversion mechanism

12 p2106 A69-26319

Nanosecond time variations in current-voltage characteristics of gas discharge in air, taking into account discharge circuit resistance and discharge space capacitance

12 p2137 A69-26534

Carbon dioxide dissociation in carbon dioxide laser gas discharge plasma for various flow rates, pressures, discharge current densities and tube diameters

12 p2107 A69-26540

Laser interferometer determining spatial distribution of neon metastable state in He-Ne active discharge, discussing lens effects

12 p2108 A69-26636

Soviet papers on physics of gas discharge plasma covering helical discharges, plasma jets, flame discharges, etc

12 p2139 A69-27121

Steady helical discharges /skin effect/ in air and Ar under high pressure without gas injection, discussing discharge stability factors

12 p2140 A69-27122

Parameter measurement technique for low pressure helical pulse plasma discharges, determining spatial distribution of HF electric and magnetic fields and current density

12 p2140 A69-27124

Electrodynamic model applicability to HF flame discharge for case of flame discharge stabilization by axial air injection

12 p2140 A69-27126

Dense plasma jets in flowing HF flame discharges, discussing energy balance and longitudinal and radial temperature distribution

12 p2140 A69-27127

Field distribution in HF flame discharges by measuring electrical and geometrical parameters of discharge channel

12 p2140 A69-27128

Oscillator parameter matching to flame discharge parameters to obtain optimal power for powering flame discharge for plasma jet source

12 p2140 A69-27129

Numerical solution to partial differential equations describing helical discharge in Ar with gas injection, discussing initial temperature distribution and radial distribution effects

12 p2141 A69-27131

Electric field frequency effect on cyclotron resonance during gas discharge, establishing causes of discrepancy between theory and experiments

13 p2315 A69-28577

Interaction between shock tube gas discharge plasma and fast electrons ionized stationary gas, noting luminous discontinuities propagation

14 p2490 A69-28998

Laser emission field effect on discharge current in pure carbon dioxide and mixtures with molecular N and He

14 p2458 A69-29161

Balance equations for axial separation in anisothermic plasma columns with radial variation of neutral gas temperature applied to argon discharge with mercury vapor addition

14 p2493 A69-29690

Moving striations relations to ion acoustic waves in DC discharge in neon at various pressures, discharge currents and measurement excitation modes

14 p2494 A69-29695

Time of flight mass spectrometers for plasmoids generated by theta pinch and discharge over organic glass, showing ion and electron currents oscillograms

14 p2498 A69-29813

HO₂ radical detection in rarefied H flame produced by HF discharges, recording high amplitude signals

15 p2716 A69-30054

Semiautomatic recording device to determine gas discharge ion and electron sources operation modes optimum parameters

15 p2658 A69-30237

Plasma three electrode source ion-optical characteristics, noting beam angular divergence dependence on spacing between discharge cavity and intermediate electrode

15 p2658 A69-30240

Induced high pressure HF discharge parameters computed for Ar, O and N by using electrical and thermal conductivity functions

15 p2662 A69-30976

Radiative luminescence of gas discharge plasmas in channel with substantial radial heat transfer determined from energy balance measurement

15 p2662 A69-30978

Lasing influence on electron energy distribution in gas discharge measured with Langmuir probe, showing

electron-electron interaction insufficient to maintain equilibrium

16 p2796 A69-31772

Relaxation method for separation of continuous electron/ion recombination spectrum from electron spectrum in nonequilibrium gas discharge plasma

16 p2822 A69-32116

Transition probability for 5577 Å auroral green line determined from measuring number density of O atoms in oxygen-helium discharge and emitted line intensity

16 p2781 A69-32319

Plasma decay at high pressure in helium and argon with cesium vapor admixture and pure cesium vapor, using Saha equation

18 p3181 A69-35045

He-Ne laser discharges noise and oscillations classified, investigating interaction between intrinsic oscillations

19 p3338 A69-36605

Ion density, electric field and electron temperature responses to gas density perturbation calculated for acoustic wave propagation in gas discharge using hydrodynamic equations

20 p3578 A69-38243

He-Ne laser heterodyne system for measuring dispersion at 6328 and 6401 Å due to Ne metastable atoms in gas discharge

23 p4172 A69-41397

IR radiation transmission in pulsed carbon dioxide discharge as function of time, proposing pumping and relaxation mechanism model

23 p4174 A69-42196

Electron density in positive column of Cs vapor discharge related to current and gas pressure, discussing field strength effects on drift velocities

23 p4196 A69-42197

Moving striations dispersion and stability theory applied to ionization waves excited in Ar, Ne and Hg-Ar mixture low and medium pressure discharge

24 p4356 A69-43363

Anode fall measurements with Langmuir probe in coaxial arcs in Ar compared with anode energy balance values

24 p4256 A69-43695

GAS DISSOCIATION

Intermolecular interaction potentials for dissociating air components determined by calculating collision integrals for very high temperature gases

02 p0283 A69-11586

Dissociation and recombination of moderately complex molecules, using master equation with transition probabilities and decay rates obtained from reaction rates statistical theory

02 p0283 A69-12181

Dissociative velocity rates of oxygen and ozone in ionosphere obtained by exponential approximation for molecular concentration distribution

02 p0246 A69-12769

Reduction of optical breakdown threshold in laser focus by superimposed microwave field

03 p0441 A69-13997

Dissociating gas as working fluid for space plant, noting role in radiator area reduction

04 p0551 A69-15313

Time dependence of laser output in C and N atoms following dissociative excitation transfer explained in terms of measured populations of excited states

05 p0795 A69-15663

HF plane sound waves in ideal gases with internal dissipation, considering particular applications to dissociating diatomic and vibrational relaxing gases

05 p0792 A69-15723

Three atom interaction contribution to nonideal dissociating gas state equation, determining quantum correction for third virial coefficient

05 p0796 A69-15893

Photoelectric absorption studies on molecular nitrogen indicate predissociation contributing to atomic nitrogen production in upper atmosphere

05 p0756 A69-16282

Recombination constants of dissociated oxygen and nitrogen flow in supersonic nozzle at high temperatures using modified Bray method

06 p1030 A69-17349

Ice nucleus formation in developing comet, discussing dissociation and vaporization characteristics of parent molecules as participants in process

06 p1004 A69-17537

Laminar boundary layer on axisymmetric blunt body in dissociated air taking into account nonequilibrium homogeneous chemical reactions

07 p1050 A69-18734

Laminar boundary layer flow on sphere in hypersonic flow of equilibrium dissociating air

07 p1050 A69-18756

Laser induced gas breakdown by focusing nanosecond pulses in air and deuterium [IEEE PAPER U-3]

07 p1155 A69-19085

Early phase of Stromgren sphere development in interstellar molecular hydrogen cloud, analyzing R-type dissociation-ionization fronts using quasi-steady flow

07 p1218 A69-19281

Dissociation-ionization fronts in interstellar molecular hydrogen clouds, analyzing effects of UV radiation from early stars

07 p1221 A69-19584

HF breakdown of air using Boltzmann equation to determine net ionization frequency relation with electric field strength

08 p1357 A69-20810

TiO gas dissociation energy data discrepancies, discussing high temperature vaporization and thermodynamic properties

08 p1268 A69-21012

Electron impacts role on dissociation rates of CO molecules in upper layers of solar photosphere

09 p1590 A69-21376

Gas breakdown model for analyzing breakdown of Ce vapor filled crack in thermionic trilayer insulator

09 p1441 A69-21840

Nonequilibrium three dimensional boundary layer over slightly yawed cone analyzed for air dissociation and ionization parameters, noting binary scaling application

09 p1430 A69-21965

Multicomponent diffusion coefficients of dissociated air as function of pressure, temperature and concentration, based on simplified model of binary diffusion

09 p1623 A69-22098

D type dissociation ionization front structure and associated shock fronts using quasi-steady flow approximation for Stromgren sphere development in interstellar molecular hydrogen cloud

10 p1772 A69-22858

Equilibrium dissociating gas laminar flow in circular tube calculated for heat transfer and hydraulic resistance, using boundary layer equations

10 p1679 A69-23426

Laser light scattering in radiation driven breakdown waves in He, using high resolution streak photography to obtain diagnostic data

11 p1915 A69-24420

Carbon dioxide temperature distribution, absorption and concentration as functions of molecular dissociation behind shock wave determined by measuring IR bands intensity

11 p1873 A69-25226

Carbon dioxide dissociation in carbon dioxide laser gas discharge plasma for various flow rates, pressures, discharge current densities and tube diameters

12 p2107 A69-26540

Breakdown in air produced by picosecond mode locked laser pulses showing evidence for self focusing

13 p2270 A69-27196

Hayashi effect modifications due to high opacity stellar atmosphere or presence of molecular hydrogen dissociation zone, discussing pressure dissociation role

13 p2342 A69-27594

Oscillations and decomposition of diatomic gas molecules at high temperatures during atom/molecule collisions, deriving kinetic equations for energy level changes

13 p2302 A69-27797

Carbon dioxide dissociation by electron impact, determining reaction rate in positive column of DC glow discharge

14 p2488 A69-29095

Enhanced plasma heating in absorption zone of laser-induced gas breakdown at spherical blast wave shock front

14 p2460 A69-29604

Electron density, temperature and dimensions of helium breakdown induced by Q switched ruby laser beam as function of space and time

14 p2492 A69-29636

Molecular dissociation by line radiation absorption, applying results to hydrogen molecules in H I region dissociated by photons of mean interstellar UV radiation field

15 p2693 A69-30783

Dynamic behavior of dissociating homonuclear diatomic gas, deriving instability equations, proposing stability loss in transonic region

15 p2548 A69-31065

Carbon dioxide dissociation relaxation times measured in shock tube at 1900-2400 K and 1.5-2.5 km/sec

16 p2766 A69-31910

Laser induced gas breakdown covering breakdown mechanism and plasma expansion and decay, with bibliography

17 p2980 A69-33026

Exact similarity solutions of hypersonic small disturbance equations for steady flow, discussing equations of state and motion and dissociating gas flow [AIAA PAPER 69-707]

17 p2953 A69-33448

Gladstone-Dale constants for dissociating high temperature oxygen determined for molecule and atom from density changes across shock

18 p3176 A69-34452

Br molecular dissociation rate in argon excess determined, considering visible emission intensity behind shock front

18 p3176 A69-34465

Population inversion in carbon dioxide laser related to pumping frequency, discussing molecular dissociation effect in gas mixture

18 p3151 A69-34620

Electron impacts role on dissociation rates of CO molecules in upper layers of solar photosphere

18 p3198 A69-34764

Hydrogen bulge above springtime pole indicated by Lyman alpha radiation in earth geocorona, discussing hydrogen horizontal transport and hydrogen compounds dissociation as causes

18 p3129 A69-34956

Ionization effects in hydrodynamic model of radiation driven breakdown wave propagation, obtaining wave velocity and absorbed laser flux density relationship

18 p3174 A69-35286

Difference method for parabolic differential equations solution for Rayleigh boundary layer in dissociating gas, using integral estimates to determine stability

18 p3124 A69-35295

Sulfur hexafluoride dissociation in argon at various temperatures and pressures, using shock tube techniques to determine unimolecular parameters

18 p3100 A69-35475

Nonequilibrium laminar boundary layer of dissociating air on axisymmetric body determined using concentration profiles of oxygen and nitrogen components

19 p3239 A69-36395

Nonequilibrium laminar heat transfer in viscous flow of chemically unstable gases past blunt body and plate

20 p3513 A69-37087

Modified model for vibration-dissociation relaxation coupling phenomena in nonequilibrium high temperature gas flow, discussing parameter U variation with kinetic temperature

20 p3514 A69-37208

Nitrogen gas breakdown threshold dependence on pressure during picosecond ruby laser pulse, discussing photoionization leading to breakdown in electromagnetic wave field

20 p3555 A69-38067

Molecular oxygen rate of dissociation resulting from absorption in Schumann-Runge bands, calculating effects on chemistry of lower thermosphere and upper mesosphere

20 p3534 A69-38089

Carbon monoxide displacement rate of oxygen from combination with oxyhemoglobin solutions from human adult and fetal, horse, goat, dog, cat and rabbit

21 p3650 A69-38384

OH emission rise after sunset and decay at sunrise attributed to strong solar dissociation of ozone

21 p3712 A69-38520

Electrical excitation discharge effect on molecular composition of flowing carbon dioxide gas laser, noting dissociation characteristics

21 p3736 A69-38940

Laser induced multiphoton ionization and cascade breakdown in high pressure gases, considering roles of refractive index, laser nonideal output and beam self focusing

21 p3738 A69-39445

Thermal dissociation of chlorine trifluoride behind incident shock waves as function of temperature using UV absorption spectroscopy

21 p3670 A69-39739

Vibration relaxation time and dissociation rate constant of carbon dioxide in high temperature shock waves, using IR emission

21 p3775 A69-39801

Methyl alcohol, ether and acetone vapors decomposition in microwave discharge, obtaining H and CO in addition to solid polymeric films

22 p3895 A69-40103

Quasi-one dimensional analysis for nonequilibrium flow of dissociated diatomic gas through converging-diverging nozzle, discussing critical mass flow rate

22 p3927 A69-40583

Dissociation energy and ionization potential measured for gaseous SiO and GeO

22 p3896 A69-40725

- Dissociational nonequilibrium transonic flow near nozzle throat analyzed for diatomic gas with equilibrium vibrational energy, using perturbation method
22 p3861 A69-41177
- Nonequilibrium boundary layer of dissociated diatomic gas over catalytic flat plate in hot hypersonic uniform flow
22 p3934 A69-41181
- Carbon monoxide dissociation at high temperatures observed spectroscopically, finding complex reaction chain with diatomic C as intermediate
23 p4113 A69-41692
- Model for human hemoglobin dissociation into subunits taking into account molecular explanation of oxygen dissociation curves
23 p4097 A69-42096
- Hemoglobin O reaction model explaining molecular weight and oxygen dissociation curve dependence on hemoglobin concentration
23 p4097 A69-42097
- Atomic spectrophotometry to monitor O atom formation rate behind shock waves in oxygen-argon mixtures, noting dissociation over 2850-5550 K temperature range
23 p4194 A69-42209
- Blast wave energy determination of laser-induced gas breakdown in hydrogen, nitrogen, helium, argon and xenon in pressure chamber
24 p4299 A69-42651
- Reaction broadening in hydrogen-oxygen diffusion flame for slow hydrogen dissociation, using matched asymptotic expansions
24 p4408 A69-42920
- Lyman alpha radiation from electron collisions with simple H-containing molecules, finding dissociative excitation cross section role
24 p4351 A69-43033
- Molecular vibrational relaxation effect on dissociating airflow behind shock wavefront, giving relations to chemical reaction rates in diffusion approximation
24 p4302 A69-43486
- Viscous shock wave chemical relaxation for diatomic nonequilibrium dissociating gas flow, using Navier-Stokes and chemical kinetics equations
24 p4302 A69-43487
- GAS DYNAMICS**
NT AERODYNAMICS
NT AEROTHERMODYNAMICS
NT HYPERSONICS
NT RAREFIED GAS DYNAMICS
NT ROTAR AERODYNAMICS
- High velocity motions in diffuse nebulae connected with stellar wind, noting wind formation of 2-layer shell between two shocks
01 p0148 A69-10050
- Transport properties of steam, analyzing selection, correlation and prediction using statistical mechanical theories
01 p0174 A69-10110
- Cooled probes for gas measurements in high pressure arc jets, hyperthermal wind tunnels, rocket motors, scramjets and similar severe environments
01 p0078 A69-10150
- Book on mathematical and physical fundamentals of molecular gasdynamics based on statistical mechanics, discussing free molecular flow
01 p0060 A69-10711
- Very high temperature air flow laminar boundary layers on rotating bodies with unsteady chemical reactions, determining flow dynamic behavior
01 p0060 A69-10725
- Difference schemes stability for solving linearized gasdynamic equations obtained by representing transition matrices in form of two matrix sum
01 p0060 A69-10729
- Electrohydrogasdynamic analogies to known MHD effects studied by differential equations for hydrodynamic and electric field energy relations
01 p0131 A69-10775
- Electromagnetic fields effect on turbulent boundary layer characteristics of compressible fluid on insulating wall of MGD channel
01 p0131 A69-10777
- Shock layer gas radiation influence on deep space missile shape, noting evaluation by flow equations
01 p0007 A69-11070
- Krook kinetic relaxation equation generalized to include approximate kinetic equations with velocity independent collision frequency
02 p0234 A69-12582
- Radiation due to collective effects in plasma physical aspects of astrophysics, discussing synchrotron radiation and bremsstrahlung
02 p0310 A69-12792

Nonlinear weak shock wave diffraction around convex angled corners in polytropic inviscid thermally nonconducting gas
03 p0412 A69-12848

Gas dynamic choking limitation on heat transfer capacity of heat pipe operating at low vapor pressures from comparison of theory and experiment
03 p0531 A69-12989

Supersonic flow region about blunt body calculated on basis of gasdynamic equations for steady flow of inviscid nonheat conducting gas
03 p0363 A69-13658

Ideal gas flow near stagnation line for blunt bodies, applying van Dyke series truncation method to numerical solution
03 p0364 A69-13660

Flow rate effect on flow pattern of gas escaping through lateral hole of arbitrary depth
04 p0586 A69-14274

Anisotropic nonlinear wave propagation in arbitrarily moving ideal gas, using singular surface/ray combined theories
04 p0630 A69-14532

Effect of dipole/dipole resonance interaction between excited and nonexcited atoms on gas thermodynamic properties, showing unstable quasi-molecules formation
04 p0632 A69-14551

Monograph on radiation gas dynamics, thermal radiation, applied spectroscopy and ablation and applications in high speed atmospheric entry
04 p0685 A69-14597

One-dimensional self similar motion of relaxing gas, noting ODEs of process and gas dynamic parameters of flow field
04 p0588 A69-14623

Nongray radiation absorption coefficients reformulation employing alternative angular moment averaged absorption coefficients with emission/Planck/
04 p0686 A69-14744

Soviet book on shock waves in real gases covering gas flow patterns in shock tube, perturbations, shock and detonation wave reflection, etc
04 p0589 A69-14937

Two dimensional unsteady flow of inviscid polytropic gas using analysis of similarity solutions in homentropic flow
04 p0590 A69-15191

Soviet book on gas dynamics of solid fuel rocket motors covering combustion chamber flow, nozzle and thrust characteristics, pressure relaxation and channel charge
04 p0647 A69-15493

Thermistor assembly apparatus for measuring coefficient of thermal conductivity of pure and binary mixture of gases
05 p0845 A69-15616

Hyperbolic double waves found in compressible flow problems, presenting method of plotting all waves and determining geometrical characteristics
05 p0751 A69-16646

Supersonic gas dynamics variational problems concerning determination of axisymmetric minimum drag
05 p0699 A69-16675

Electrohydrodynamic gas flow in one dimensional approximation for transition through speed of sound, discussing flow parameters profile and dynamic efficiency
06 p0964 A69-17326

Arc phenomena and gas dynamic effects during shock heated plasma interaction with magnetic field
07 p1188 A69-18273

Steady two dimensional MHD flow in finite region of aligned fields
07 p1188 A69-18274

Gasdynamic flow shock wave phenomena during exploding wire dwell time inside metal vapor cylinder, noting effect on reignition
07 p1188 A69-18275

Gas dynamics effects of hot spot in explosive gas mixture using kinetic rate equations, discussing composition, enthalpy and time dependence [WSCI PAPER 68-53]
07 p1240 A69-18322

Initial stage of motion in Rayleigh problem, calculating time variable velocity of tangential stress on and velocity of gas near plate
07 p1118 A69-18701

Stability of motion of spherically symmetric mass of compressible gas with constant space density in absence of gravitational field
07 p1215 A69-18706

Optimum profile of supersonic nozzle with nonequilibrium flow
07 p1119 A69-18737

Gas dynamic shock wave entry into magnetic field, discussing field distribution behind shock front and diffusion and medium motion effects on penetration depths
07 p1192 A69-19022

Neutral hydrogen distribution and dynamics in galaxies, discussing observations by spectrographic transit telescope, data processing and profiles
07 p1224 A69-19711

Wavelike photodissociation of gas molecules under quasi-monochromatic pulsed radiation, investigating associated supersonic disturbances
08 p1354 A69-19950

Frozen shock in steady one dimensional compression flow of relaxing gases weaker than equilibrium shock
08 p1304 A69-20785

Two fluid kinetic model for analyzing shock wave structure in binary mixtures of monatomic inert gases, noting no overshoot in velocity profiles
08 p1304 A69-20813

Star collapse under energy losses due to neutrino emission, analyzing self similar asymptotic solutions
09 p1587 A69-21359

Energy transfer in gases transmitting heat by interaction of thermal conduction and IR radiation
09 p1621 A69-21442

Book on dynamics and thermodynamics of gas at hypersonic velocities and extremely high altitudes
09 p1483 A69-22400

Steady compression waves properties in relaxing gases found independent of thermodynamic behavior and relaxation process
10 p1631 A69-22893

Phase equilibrium and dynamics of gas volume heated by cosmic rays and cooled by radiation
10 p1760 A69-23136

Laser applications to high temperature, gas dynamical and plasma phenomena
10 p1741 A69-23809

Hydrodynamic equations and conservation laws for nonviscous fluid in post-Newtonian approximation of Brans-Dicke theory applied to gaseous mass dynamic instability
10 p1789 A69-24130

Stroboscopic generator of trains of high brightness light flashes for hydrodynamic and gas dynamic research, noting electronic control and thyatron circuits
11 p1879 A69-24235

Boltzmann equation for system of equations governing evolution of gas of identical particles with discrete velocity distribution, applying Chapman-Enskog method
11 p1921 A69-24325

Characteristic frequencies approximation formula for gas bubbles in liquids compared with exact solutions
11 p1915 A69-24582

Existence and completeness of eigenfunctions for boundary value problem arising in theory of small amplitude motions of stratified polytropic gas
11 p2081 A69-24884

Boltzmann H theorem and related mathematical topics, noting applications to subsonic gas flow and continuum flow around and over body
11 p1870 A69-25008

Dense real gas thermodynamic relations in piston driven shock tube facilities operation
11 p1862 A69-25011

Gas dynamics for supersonic nonequilibrium flows, discussing method for determination of nozzle contours for maximum thrust
11 p1820 A69-25475

Unsteady gas dynamics of explosions and detonation systems performance
11 p1876 A69-25595

Gas motion and heating by radiation behind shock wave front, noting ionization and radiation absorption occurrence
12 p2061 A69-25880

Optical methods in three dimensional gas flow research, noting role in density field determination and conjunctive use with gas dynamics equations
12 p2011 A69-26191

One dimensional stationary flow of medium consisting of charged and neutral components within electrohydrodynamic limits in AC and DC electric fields
12 p2135 A69-26398

Diffusion-stabilized difference schemes for inviscid compressible flow equations in conservation form for arbitrary number of space dimensions
12 p2062 A69-26624

Gasdynamic stability of detonation shock wave in case of arbitrary heat evolution kinetics using detonation model
12 p2062 A69-26672

Two dimensional flow of conducting gas dynamic and electrical parameters in MGD generator channel, considering magnetic field and plasma conductivity
13 p2305 A69-27386

Monograph on gasdynamics and classical theory of shock waves covering viscosity, heat conduction, gas cloud expansion into vacuum, etc
13 p2246 A69-27639

Flux, density and pressure variations with position in vacuum system /nonuniform gas distribution/, discussing causes and consequences
13 p2299 A69-28019

Dynamic gas flowmeter for ultrahigh vacuum based on transmission characteristics of diffuser screens and associated pressure drops
13 p2263 A69-28087

Flow field instability over concave bodies in supersonic free stream computed by integration of gasdynamic equations, noting application to supersonic parachutes [AIAA PAPER 68-946]
13 p2199 A69-28228

Plasma jets from MPD accelerators, analyzing swirl, entrainment and pressure distribution using gasdynamic probes
13 p2313 A69-28242

Reservoir conditions of reflected shock wind tunnel by subjecting gas to direct shock and shock reflected at closed downstream end of shock tube
13 p2243 A69-28359

Two temperature gasdynamics for binary gas mixtures of differing molecular weight components, analyzing ultrasound and shock wave propagation
13 p2250 A69-28447

Turbulent jets of gases in general stream of air spreading in cylindrical chamber, discussing distributions of gas dynamic parameters
13 p2200 A69-28501

Completeness theorem for integrodifferential operator to establish Schwarzschild criterion for stability of gaseous masses
14 p2470 A69-28902

Transport coefficient density expansions obtained from time correlation functions in moderately dense gas with short range repulsive intermolecular forces
14 p2540 A69-29469

Difference schemes for quasi-linear hyperbolic equations, with applications to three dimensional supersonic flow past bodies
14 p2430 A69-29475

Gain and loss collision integrals in Boltzmann equation for rigid sphere gas evaluated for distribution expressed as linear combination of Maxwellians
14 p2431 A69-29578

Partially ionized multicomponent gas mixture kinetics in strong electromagnetic field, determining magnetic field, stress tensors and transfer coefficients
14 p2492 A69-29610

Spatial supersonic ideal gas flows past blunt bodies analyzed by numerical finite difference methods, discussing flow fields and entropy
14 p2390 A69-29616

Boundary layer physical and chemical processes effect on dynamic parameters of high temperature hypersonic gas flow past blunt bodies
14 p2391 A69-29620

Kinetic theory of gases collision cross section definition compared to usual definition, discussing time reversed collisions
14 p2488 A69-29993

Oscillatory relaxation of multiatomic gases and gas mixtures with quantum exchange between oscillators, noting gasdynamic applications
15 p2654 A69-30109

Gasdynamic model of comet nucleus region, discussing molecular collisions, surface brightness distribution and dust particle motion
15 p2684 A69-30520

Book on three dimensional flow of ideal gases past smooth bodies, emphasizing utility of finite difference methods
16 p2771 A69-32003

Book on quasi-linear equations systems and application to gasdynamics, including problems involving systems of quasi-linear hyperbolic equations with two independent variables
16 p2771 A69-32113

Trails arising in wake of fan type jets in transverse gas flow during uniform fuel-air mixture combustion
16 p2879 A69-32140

Book on gas dynamics of two phase media for thermal power engineering equipment, discussing phase transformations, condensation in high velocity flows, etc
17 p2948 A69-32951

Radiation gas dynamics in shock tube, studying radiation coupled flows with flow field affected by radiant energy transport
18 p3116 A69-34447

Star collapse under energy losses due to neutrino emission, analyzing self similar asymptotic solutions
18 p3197 A69-34749

Nonlinear differential equations for nonequilibrium gases with internal degrees of freedom, considering spatially homogeneous gas and oscillatory relaxation in harmonic oscillators
18 p3122 A69-34911

MHD flow, deriving equation system and boundary conditions for gas dynamic process
18 p3181 A69-35054

Computer programs determining gaseous properties and aerodynamic characteristics for missiles, reentry vehicles and spacecraft at angles of attack
18 p3107 A69-35068

Temperature distribution around radiating sphere in homogeneous gas medium with molecular heat transfer, solving energy transport equation
18 p3231 A69-35325

Hydrodynamics of gas flow due to solar flares using point explosion model, determining shock wave travel time to earth orbit
18 p3189 A69-35397

Gas dynamics of interactions of tenuous ionosphere with moving satellites and diagnostic probes, using collision-free plasma kinetics methods
18 p3132 A69-35409

Gas dynamics equations solution applied to Cauchy problem
19 p3297 A69-35861

Gas dynamics of explosions - IAA Conference, Brussels, September 1967
19 p3448 A69-36351

Gas dynamics of material slab under radiation impact assuming thermal equilibrium reemission, discussing equations of motion and mean free path as function of frequency
19 p3449 A69-36355

Numerical program for gas dynamics of hydrodynamic flow and radiation transport in diffusion and grey body approximations
19 p3450 A69-36356

Detonation in unbounded gas mixture starting from spherical flame, discussing stability of gasdynamic discontinuities and cellular structure
19 p3450 A69-36358

Gas dynamics in transition regime between continuum motion at high gas density and free particle motion at low density limit
19 p3300 A69-36658

Comet heads gas dynamics, analyzing coma or head region as continuum source flow of dusty gas
19 p3428 A69-36807

Soviet book on theory and design of turbocompressors covering gas dynamic cascade theory, thermodynamics and aerodynamics, viscous gas flow, etc
20 p3459 A69-37238

Equilibrium and stability of axisymmetric gaseous polytropes in toroidal magnetic fields, calculating harmonic oscillations by virial tensor method
21 p3797 A69-38534

Galactic gaseous disk dynamics, considering interstellar gas behavior and cosmic ray-magnetic field instability
21 p3802 A69-38824

Blast angle effect on fanjet gas dynamics in crosswind, using equations for free lateral flow trajectories and reverse flow regions
21 p3850 A69-38863

Invariant transformations for hodograph matrix equations in gas dynamics
21 p3695 A69-39001

Chemical processes responsible for transformation of vast gas and dust cloud into planetary system
21 p3804 A69-39200

Closed cycle MHD with gaseous working fluids and steady state nonequilibrium ionization
21 p3777 A69-39479

Gas dynamic processes during vaporization of solid material under Nd laser emission, using high speed photography
21 p3740 A69-39551

Dynamics of viscous electrically charged gas using Navier-Stokes equation
22 p3931 A69-40686

Two dimensional gas dynamics differential equations for simple waves, discussing invariant solutions and conditions for group solutions
22 p3933 A69-41030

Kinetic processes in gases and plasmas covering molecular transport equations, transport coefficients, chemical reactions as collision processes, etc
23 p4193 A69-41511

Integro-interpolation difference schemes for gas dynamic equations system satisfying laws of mass, momentum, energy conservation and energy balance
23 p4151 A69-41527

Gaseous self gravitating mass equations applied to galactic evolution and star formation
23 p4213 A69-41716

Parametric differentiation applied to radiation gas dynamics equations solution, considering energy transfer by thermal radiation in high speed reentry [AIAA PAPER 68-668]
23 p4059 A69-41892

Detonation wave instability and damping in gas containing liquid or solid inflammable aerosol, considering atomized propellants
23 p4240 A69-42339

Class of one dimensional nonlinear waves and shock structure reduced to steady flows in radiation gas dynamics
23 p4240 A69-42466

Magnetic field implications in stellar formation mechanism including gravitational collapse, magnetic gas cloud fragmentation and stellar winds magnetic braking
24 p4378 A69-42699

Gas flow past bodies, deriving solution method without partial differential equations for flows with momentum potential
24 p4244 A69-43071

Gas dynamic functions of axisymmetric supersonic gas flows determined using flow density distribution optical measurements
24 p4247 A69-43496

GAS EVACUATING
U EVACUATING [VACUUM]

GAS EVOLUTION
Polymethyl methacrylate irradiated by laser in vacuum to study mechanism responsible for gas formation
02 p0270 A69-11980

Gas vacuoles development in blue green algae by cell transfer from defined medium to distilled water
10 p1644 A69-23184

Electrolytic hydrogen evolution reaction on Al covered by thin oxide in aqueous buffered acetate solutions
11 p1832 A69-25674

Free gas formation in propellant systems and effects on attitude control systems [AIAA PAPER 69-434]
16 p2870 A69-32765

Gas products evolved from selected thermal control coating materials during UV radiation in vacuum, noting permanent reflectance loss [AIAA PAPER 69-640]
17 p2992 A69-33289

Gas concentration liberated during each revolution in atmospheres of short period comets to explain impulsive forces upon nuclei, noting diatomic carbon density
23 p4221 A69-42387

GAS EXCHANGE
Biological life support system for regenerating closed atmosphere by photosynthesis, using gas exchange between man and microalgae
01 p0021 A69-11078

Changes in blood circulation, external respiration and gas exchange rates in humans during prolonged hypodynamia
03 p0377 A69-14204

Pulmonary capillary gas exchange and venous admixture model and inclusion into respiratory system model, discussing pressure and concentration gradients, pathological effects, etc
07 p1068 A69-19482

Weightlessness effects on human external respiration, gas exchange and energy expenditure indices during flight of Voskhod 2
12 p2020 A69-26563

Compensative adaptational reactions to weightlessness, discussing blood supply to thorax area, external respiration, gas exchange and energy loss during parabolic and orbital flights
17 p2909 A69-33384

Respiratory gas exchange in exercise during He-O breathing, analyzing effects on O consumption, carbon dioxide production and minute ventilation of human subjects
17 p2910 A69-33751

Ventilation-perfusion inequality increase effects on lung overall gas exchange, using digital model
21 p3662 A69-38388

Respiratory gas exchange during workloads, comparing values for ventilation, oxygen uptake and carbon dioxide output measured in air and in helium-oxygen mixture
22 p3891 A69-40221

Lower body negative pressure /LBNP/ effects on ventilation and lung volumes, presenting lung model for pulmonary gas exchange changes
22 p3891 A69-40222

Human lung ventilation-perfusion scatter decreasing gas exchange efficiency during high altitude adaptation
22 p3875 A69-40227

Digital computer program for determining alveolar and capillary blood gas compositions corresponding to ventilation-perfusion values, considering dissolved oxygen and inert gas exchange
22 p3875 A69-40230

Aircraft passenger cabins pressure safety limits estimating factors, discussing human respiratory gas exchange mechanism, pressure drop and smoking effects, etc
24 p4269 A69-43411

Isotopic exchange reaction rate between O 18 and CO in shock tube coupled to time of flight spectrometer, noting rate increase with time
24 p4353 A69-43807

GAS EXPANSION

Polar wind, describing upward plasma expansion of topside polar ionosphere and acceleration of positive H and He ions
01 p0077 A69-11239

Radiation effect enhancement in supersonic plasma jet cooled by rapid expansion, giving energy equation for electron cooling rates to analyze electron temperature
02 p0292 A69-12557

Laval nozzle resistance as result of friction and under expansion of gas, noting flow and pressure recovery coefficients
03 p0361 A69-12967

Chemical rockets theory for case of chemical equilibrium and frozen nozzle expansions
03 p0495 A69-13004

Idealized cycle of gas expansion machine with regenerator for cooling radio components
04 p0687 A69-15164

Nonsteady expansion of gas into vacuum in analysis of asymptotic solutions of Sedov
05 p0751 A69-16676

Numerical calculation of density profiles of shock waves in expansion flows
06 p0908 A69-17021

Shock wave profiles in expansion flows determined with static and impact pressure probes, investigating pressure gradient effects
06 p0908 A69-17022

Dynamics of Q spoiled neodymium laser created plasma expanding in vacuum magnetic field
06 p0970 A69-17952

Mach number distribution along axes of under-expanded supersonic jets measured in wind tunnel experiments
07 p1050 A69-18922

Stationary supersonic nonequilibrium plasma source in gas vacuum expansion and nozzle flows
07 p1191 A69-18986

Expanding atmospheres in OB supergiants from radial velocity measurements, proposing tentative temperature and velocity fields
08 p1387 A69-20091

Expansion tube modification incorporating nozzle plate at secondary diaphragm for reducing flow nonuniformity and contamination
[AIAA PAPER 68-371]
09 p1477 A69-21960

Impurity concentrations in expansion tube flow, measuring radiation intensities
[AIAA PAPER 68-371]
09 p1477 A69-21961

Effect of degree of expansion of ionized gas in nozzle on specific power of MHD generator
10 p1636 A69-23103

Size and velocity measurements of particles suspended in gas expanding from nozzle into vacuum simulating cometary two phase flow with evaporation
10 p1674 A69-23686

Gravitational stability of spheroidal expansions of rotating gas masses in astronomy, noting mechanism for fragmentation in cosmology
11 p1962 A69-25112

Optical and spectral properties of dense plasma expanding after exploding electric wire in vacuum using high speed photography
12 p2137 A69-26533

Rotating central disk in galactic plane observed by radio telescope, assessing relation between expanding gas of disk and high velocity stream from center
12 p2163 A69-27018

Soviet book on liquid fuel rocket engines design covering gas expansion in nozzles, mixture formation, heat transfer, injectors and supply systems
12 p2148 A69-27078

Relaxing gas nonequilibrium flow in plane expansion, comparing partial differential equations with method of characteristics
13 p2244 A69-27322

Diagnostic measurements in nonequilibrium nozzle flows compared to finite rate expansion calculations, measuring pressure, temperature and density
[AIAA PAPER 69-328]
13 p2200 A69-28263

Radiation effect enhancement in supersonic plasma jet cooled by rapid expansion, giving energy equation for electron cooling rates to analyze electron temperature
15 p2658 A69-30254

Laser radiation absorption by inhomogeneous over-dense plasma, discussing effects of plasma expansion on energy coupling efficiency
16 p2818 A69-31679

One dimensional free expansion of collisionless plasma tested as function of thermal equilibrium and confinement, using Vlasov equations and computer
16 p2819 A69-31685

Fixed mass of monatomic gas unsteady spherically symmetric expansion into vacuum by asymptotic Boltzmann equation expansion
16 p2772 A69-32168

Steady Prandtl-Meyer expansion of shock heated gases for recombination studies, measuring static pressure, stagnation point heat transfer, IR emission and optical absorption
18 p3228 A69-34466

Subsonic and supersonic turbulent air jets expansion over perpendicularly positioned plane disk obstacle, deriving equations for pressure distribution and stagnation temperature
18 p3123 A69-34990

Relaxation time influence on discharge coefficient of sonic nozzle of revolution, considering expanding polyatomic gas problem
19 p3241 A69-36721

Two dimensional unsteady motion of medium with pressure as linear function of density, analyzing gas expansion into vacuum
20 p3512 A69-36916

Hydrogen and methane combustion to simulate expansion of storable propellants
[AIAA PAPER 68-635]
20 p3631 A69-37188

He and Ar arc-heated flows into reservoir and expansion in converging-diverging supersonic nozzles, considering flow equilibrium effect on heat transfer and enthalpy
20 p3631 A69-37198

Flame pressure drop and burning velocity related, discussing stream tube area expansion error
21 p3849 A69-38806

Pneumatic Vernier engines in aircraft and spacecraft, discussing weight, gas expansion and gas temperature
21 p3785 A69-39093

Carbon dioxide free jet expanding from conical nozzle into low density atmosphere, using freeze up method
22 p4000 A69-40594

Mass diffusion and heterogeneities in compression chamber gas mixture in shock tube ascribable to pressure and temperature gradients
23 p4146 A69-41547

Transonic expansion analysis applied to flow through convergent-divergent nozzles with small throat radius of curvature, noting coordinate system selection
23 p4060 A69-41906

Computer calculation of adiabatic expansion of air, allowing for specific heat ratio and compressibility factor changes
24 p4244 A69-43088

Volatile wall vaporization gas flow expansion into vacuum from tube approximating unsteady mass and energy transfer and pressure at blocked end
24 p4408 A69-43489

GAS EXPLOSIONS

Continuous and time-resolved absorption and emission spectra studies produced by exploding wires in

gases, discussing effects of environment, pressure and electrical energy
01 p0118 A69-10664

Detonation wave initiation in gaseous media, noting transition process for flames accelerating to detonation and explosions behind reflected shock wave
02 p0350 A69-11530

Detonation characteristics of gaseous explosives using equations of state for real gases, noting compressibility effect in mixture of hydrocarbons, O and N
05 p0848 A69-16337

Explosive combustion of hydrogen at high pressures, showing attainment of constant value of hydrogen peroxide
05 p0849 A69-16611

Electromagnetic field induced energy and momentum changes effects on pressure, temperature and particle velocity of flows behind propagating gaseous detonation waves
[AIAA PAPER 69-44]
06 p0970 A69-18084

Gas pressure variations behind autonomous stable detonation fronts in propane-O mixtures, noting effect of diameter tubes and initial pressures
08 p1421 A69-20757

Hot inert gas bubble thermal stability in cool reactive liquid
11 p1998 A69-24475

Explosive reactions between hydrogen and oxygen flashed in presence of nitrogen dioxide, chlorine or bromine as sensitizers, considering thermal contribution
11 p1832 A69-24878

Nova thermal explosion, analyzing hydrogen combustion after penetration from white dwarf shell into degenerate core
15 p2682 A69-30507

Monograph on spreading of explosive vapor/air mixtures during aircraft fueling, covering underlying flow technology principles
15 p2551 A69-30930

Shock waves propagation in inhomogeneous gases, considering time development and energy flux during point explosion in plane layers by quasi-stationary approximation
17 p2952 A69-33383

Wave motion nonsteadiness influence on detonation front thickness using quasi-steady kinetic model of induction process, discussing agreement with experimental observations
17 p2952 A69-33403

Plane, cylindrical and spherical point explosions in combustible gas mixtures for different gas motion models, formulating scaling law for detonation wave model
19 p3449 A69-36353

Continuous explosion laser study of stationary detonation waves to determine conditions leading to partial population inversion and critical population density
19 p3336 A69-36360

Computer program for numerical integration of chemical reaction rate equations behind steady state hydrogen-oxygen shock wave
19 p3451 A69-36366

Detonation wave in gaseous media, current theories on wave initiation, structure and propagation
19 p3452 A69-36370

GAS FLOW

NT AIR CURRENTS
NT AIR FLOW
NT CONTINUUM FLOW
NT EQUILIBRIUM FLOW
NT FREE MOLECULAR FLOW
NT FROZEN EQUILIBRIUM FLOW
NT JET STREAMS [METEOROLOGY]
NT KNUDSEN FLOW
NT MERIDIONAL FLOW
NT MOLECULAR FLOW
NT NONEQUILIBRIUM FLOW
NT SLIP FLOW
NT TRANSITION FLOW
NT VERTICAL AIR CURRENTS

Rib positioning effect on mechanical behavior of cantilevered rectangular plate in gas flow, considering critical flow velocities and rigidity relationships
01 p0165 A69-10085

Heat transfer between arc column and discharge chamber wall of vortex linear plasmatron, using approximate similitude method
01 p0125 A69-10091

Gas combustion stability with respect to one dimensional perturbations, considering flow compressibility stabilizing effect
01 p0174 A69-10107

Combustion response of hydrazine-nitrogen tetroxide hypergolic rocket propellants to transverse gas flows, noting coupled and uncoupled oscillations
01 p0175 A69-10112

Cooled probes for gas measurements in high pressure arc jets, hyperthermal wind tunnels, rocket motors, scramjets and similar severe environments
01 p0078 A69-10150

Hypersonic flow of nonequilibrium diatomic gas on and near wedge, studying shock curvature variations
01 p0005 A69-10161

Gas flow analysis for externally pressurized porous journal gas bearing, considering circumferential flow in bearing clearance and porous bushing
01 p0085 A69-10312

Pressure measurements by gauges in rarefied gas flows past bodies of various shapes, discussing configurations effect on gauge readings
01 p0080 A69-10358

Difference methods in solution of incorrect Cauchy problem simulating ideal gas flow in nozzle
01 p0006 A69-10379

Algorithms for three dimensional supersonic gas flow incident on bodies applied to calculating oxygen flow in asymmetric nozzle
01 p0060 A69-10724

Two dimensional compressible inviscid laminar gas flows unsteady processes studied by extending method of characteristics
01 p0008 A69-11360

Electric discharge in gas flow with magnetic field, showing varying charged particle density as function of argon-cesium pressure
02 p0285 A69-11570

Pressure to density ratio to analyze one dimensional high temperature gas flows with heat transfer, considering motion equations
02 p0350 A69-11576

Hypersonic gas flow past blunt body problem solved by integral correlation method, taking into account radiation effects and gas dynamic parameter distribution in shock wave layer
02 p0188 A69-11651

Soviet book on hypersonic internal and external three dimensional viscous and nonviscous gas flow, emphasizing flow past slender blunted bodies
02 p0230 A69-11775

Gas flow model of coaxial electromagnetic plasma gun front profiles and speeds for operation with positive central electrode
02 p0288 A69-12032

Nonstationary wing motion in gas stream near solid surface, analyzing differential equation for acceleration potential
02 p0188 A69-12134

Turbulent gas flow characteristics obtained by extremal hypothesis, using maximum perturbation stability in formulating variational problem and computer algorithm
02 p0232 A69-12354

Longitudinal short wave stability in conducting quasi-one dimensional gas flow, considering regions of high thermal emission
02 p0233 A69-12487

Boundary layer local densities in high temperature gas flows obtained by measuring monochromatic soft X rays attenuation in layer
02 p0233 A69-12489

Survey of papers on computer calculation of two and three dimensional gas flows, emphasizing method of characteristics and finite difference techniques
03 p0363 A69-13657

Similarity motion of fluid particles in one dimensional gas flow, establishing limits of slip factor value change
03 p0419 A69-13920

Laminar and turbulent flow measurement in variety of tube diameters, using ring laser without insertion of mechanical probe
04 p0596 A69-14281

Dynamic processes of heat and mass transfer in transpiration cooling of gas flow
04 p0684 A69-14355

Difference approximation with second order accuracy of numerical solution for parabolic type equations
04 p0622 A69-14618

Numerical algorithm for supersonic gas flow past blunt bodies with shock wave separation, using Dorodnitsyn method of integral correlation
04 p0587 A69-14621

Quasi-neutral, steady, inviscid and nonheat conducting flow of conducting gas with high magnetic Reynolds number in plane channel with transverse magnetic field
04 p0636 A69-14984

Transverse magnetic field effect on three dimensional nonisothermal lubrication layer of conducting gas at small magnetic Reynolds number
04 p0607 A69-14990

Approximate hydrodynamic equations applied to analysis of heat transfer in real gas flow in tube, taking into account energy transfer by radiation
04 p0686 A69-14993

Steady plane supersonic gas flows with large number of shocks computed on basis of weak solutions of hyperbolic system
04 p0544 A69-15284

Axial deviation of gas flow resulting from mixing turbulent gas jets
04 p0591 A69-15411

Heat transfer between body and gas flow near stagnation point
04 p0544 A69-15412

Shock wave damping at large distances from body situated in ideal gas three dimensional flow
04 p0591 A69-15535

Gas velocity variations in ionizing shock wave propagating along magnetic field applied to conducting piston motion
05 p0801 A69-15787

Unsteady motion of ideally conducting gas flow in transverse magnetic field with allowance for gravitational forces
05 p0802 A69-15789

Thermal entry problem solution for low Reynolds number turbulent gas flow based on Reynolds number dependent velocity profile
05 p0748 A69-16090

Heat transfer in turbulent pipe flow of radiating optically thin gas in circular tube
[ASME PAPER 68-WA/FE-11]
05 p0847 A69-16121

Thermal transpiration for performance prediction and development of gas pump
[ASME PAPER 68-WA/ENER-4]
05 p0706 A69-16162

Gas flow rate predictions for long and short tubes and annuli and at densities between laminar continuum and free molecular regimes
[ASME PAPER 68-WA/PID-5]
05 p0750 A69-16166

Electroaerodynamics /EGD/ engineering, discussing generators and compressors
05 p0804 A69-16586

Peculiarities of aerodynamic characteristics of flow past plate and pointed and blunt slender cones in viscous hypersonic thermodynamically ideal gas
05 p0699 A69-16673

Approximate methods for integration of equations of plane isentropic motion of gas at supersonic velocities
05 p0699 A69-16674

Stability of three layer cylindrical shell in gas stream, analyzing oscillation mode and critical flutter dependence on filler resistance to transverse shear
05 p0843 A69-16683

Nonisentropic simple waves in two dimensional steady flow of ideal gas
05 p0752 A69-16687

Approximate method for calculating subsonic gas flows in curvilinear channels for gas admission control in arc welding
06 p0908 A69-16828

Numerical calculation of density profiles of shock waves in expansion flows
06 p0908 A69-17021

Shock wave profiles in expansion flows determined with static and impact pressure probes, investigating pressure gradient effects
06 p0908 A69-17022

Stagnation point electrostatic probe measurements of flowing partially ionized high density monatomic gases
06 p0964 A69-17196

One dimensional unsteady flows of combustible gas mixture with finite chemical reaction rates, considering piston motion, igniting shock wave propagation and point explosion
06 p0909 A69-17325

Linear theory of equilibrium and nonequilibrium gas flows applied to steady two dimensional nonequilibrium flow of inviscid nonheat-conducting gas
06 p0909 A69-17327

Stream function approximation for plane axisymmetric vortex free transonic inviscid gas flow
06 p0910 A69-17336

Surface roughness influence on interaction between gas flow and solid surface for case of diffuse and specular reflection, noting role of inclination angle
06 p0910 A69-17342

Kinetic boundary value problem of gas flow over plane wall with constant mass-velocity gradient
06 p0910 A69-17346

Hot gas flows turbulence linear component intensity and frequency spectrum using optical measurement of pulse velocities
06 p0926 A69-17540

Three dimensional steady/unsteady flows of conducting inviscid gas in magnetic field, in absence of electric field, solving related Cauchy problem
06 p0966 A69-17541

Dynamic behavior of three layer plates in supersonic gas flow
06 p1024 A69-17552

Aspiration psychrometric probe for measurements of relative humidity of gas-vapor phase of gas flow containing liquid droplets
06 p0927 A69-17689

Transmittance and absorption cross sections of carbon particles suspended in flowing stream of nitrogen gas
06 p1034 A69-17804

Dynamic behavior of shock layer of supersonic rarefied gas flow past disk and sphere
06 p0861 A69-17812

Thermal nonequilibrium of unsteady adiabatic gas flow in nonheat conducting tube with open ends
06 p0911 A69-17813

Air film cooling of rotating turbine disk, suggesting applicability to gas flows
06 p1034 A69-17814

Transmission and reflection coefficients of cylindrical tubes moving in free molecular gas flow determined by Monte Carlo method
06 p0911 A69-17877

Turbulent premixed flames stabilization, determining gas flow velocity, turbulence intensity, flame thickness and burning velocity relation to intensity
06 p1035 A69-17931

Three dimensional boundary layer problems analyzed by exact numerical method
[AIAA PAPER 69-138]
06 p0911 A69-18041

Nonlinear lumped parameter model for long gas filled pressure sensing lines covering steady state, laminar or turbulent gas flow
[AIAA PAPER 69-117]
06 p0913 A69-18106

Current sheet pattern and gas flow stabilization in pulsed plasma accelerators
[AIAA PAPER 69-112]
06 p0971 A69-18140

Experimental and numerical nonequilibrium shock layer around cones in hypersonic pure oxygen flows with simultaneous rotational, vibrational and dissociation relaxation
[AIAA PAPER 69-136]
06 p0864 A69-18141

Fluidic vortex valve warm gas flow control for rocket application
[AIAA PAPER 69-118]
06 p0872 A69-18147

Weakly ionized gas flow past discontinuous wall potential used to study edge effects and interaction problems for single and multiple flush electrostatic probes
[AIAA PAPER 69-80]
06 p0972 A69-18191

Free turbulent mixing, emphasizing flowing gas mixtures with and without chemical reaction
[AIAA PAPER 69-31]
06 p0915 A69-18223

Relaxation equations for oscillatory degrees of freedom of molecular supersonic binary gas flow in Laval nozzle, obtaining population inversion
07 p1118 A69-18540

Exact partial solutions to transonic gas flow equations used to describe flow around shape streamlined by supersonic flow with additional shock wave
07 p1118 A69-18698

Mixed sub- and supersonic gas flow in plane pressure nozzle free of vortex and neglecting viscosity and heat conduction
07 p1050 A69-18739

Approximation of Chaplygin plane motion equations of gas flow at high supersonic velocities
07 p1120 A69-18754

Ellipsoidal gas bubble dissolution in low viscosity fluid, discussing rate of steady motion, deformation degree and diffusion rate
07 p1120 A69-18990

Rise velocity of large gas bubbles in liquid calculated, assuming velocity is determined by propagation of bubble produced wave disturbance
07 p1120 A69-18999

Spherical particle motion in vortex gas flow between planes of turbulence chamber perpendicular to axis of flow rotation, noting collisions effect
07 p1181 A69-19000

Two dimensional flow of conducting fluid in channels with longitudinal transverse magnetic field and

Hall effect, discussing gas motion equations linearization
07 p1192 A69-19015

Energy transfer through ionospheric electrons, discussing degradation of fast electrons and role of neutral gas motion in ionospheric currents
07 p1128 A69-19369

Collimated nozzle beam for probing low density gas flows, discussing transition from free molecular to isentropic flow and Knudsen numbers
07 p1136 A69-19467

Flowing CO-N-He laser with power enhancement and high efficiency, noting role of gases
08 p1324 A69-20163

Approximate equations for transonic viscous heat conducting gas flow past finite body of revolution
08 p1251 A69-20322

Finite aspect ratio sandwich plates flutter in supersonic gas flow analyzed by differential equation describing plates elastic equilibrium
08 p1412 A69-20324

High speed photographic study of finely dispersed Al particles combustion and ignition in high temperature gas flows, noting dependence on oxidizers concentration
08 p1375 A69-20341

Kine films of gas flows within highly luminous transient arc taken by laser schlieren technique
08 p1316 A69-20615

Gas flows in close binary systems of dwarf stars
08 p1396 A69-20648

Boundary layer separation and vortex street buildup conditions of gas flow in circular cylinder wake
08 p1252 A69-20713

Behavior of bounded and free arc discharges under action of transverse magnetic fields and gas flows
08 p1366 A69-20767

Jet engine gas flow, temperature, velocity and pressure measurements by analog and digital systems
08 p1316 A69-20869

Compressible gas flow problem in point body gravitational field solved with reference to sun and interstellar gas
09 p1577 A69-21769

Arc driven shock tube with alumina ceramic liner to reduce driver gas contamination, noting shock speed and test time increase
[AIAA PAPER 68-366] 09 p1570 A69-21957

Steady axisymmetric gas flow from galactic center, determining supersonic to subsonic transition by equations of motion
09 p1599 A69-22189

Differential equation for droplet motion along ballistic trajectory in gas flow, noting applicability to solid bodies via computer programming
09 p1483 A69-22222

Wall temperature and Prandtl number effects on turbulent boundary layer thicknesses and shape factors for subsonic compressible gas flow over flat plate
[ASME PAPER 69-GT-55] 09 p1432 A69-22513

Frequency effects in laser with nonlinearly absorbing gas cell inserted in resonator, noting self stabilization of generation frequency
09 p1520 A69-22661

Steady three dimensional flow of gases with thermodynamic relaxation, noting flow field weak discontinuities and effect of discontinuities in wall curvature
10 p1677 A69-22894

Subsonic channel flow of frictionless barotropic gas through oscillating grid, investigating perturbation velocity field and aerodynamic forces on airfoils
10 p1631 A69-22905

Multidimensional theory of characteristics found applicable to calculating three dimensional time dependent gas flows
10 p1632 A69-22913

Weak discontinuities in wave propagation, studying ionized gas nonsteady flow having electrical conductivity in magnetic field
10 p1727 A69-22916

Carbon dioxide laser combining gas flow with fluid mixing to achieve high gain
10 p1701 A69-22954

General solutions of MHD equations for linear nonsteady and plane steady motions of ideally conducting gas
10 p1727 A69-23096

Self similar solutions for collapse of empty cylindrical cavity in gas with given equation of state, describing gas motion past cavity
10 p1679 A69-23367

Existence and uniqueness to boundary layer continuation problem based on flow equation for steady gas flow
10 p1679 A69-23569

Finite difference technique for numerical computation of steady supersonic two dimensional gas flows, with or without diffusion normal to mean flow streamlines
10 p1679 A69-23595

Nozzle flow temperature patterns of relaxing combustion gases compared at different temperatures and pressures, using kinetic-chemical calculations
[DVL-896] 10 p1809 A69-23644

Ionized gas flow from globule containing atomic H in interstellar space, noting surrounding H II region and radiation at ionization front
10 p1782 A69-23682

Invariant transformation of equations for ideal gas plane steady motions, noting application to gas flows with shock waves and eddies
10 p1680 A69-23709

Second approximation of asymptotic damping of disturbances in viscous heat conducting gas supersonic flow about solid of revolution at critical velocity
11 p1817 A69-24627

Binary gas flow past curved body for stationary problem studied by solving Boltzmann equations in form of matched asymptotic expansions
[ONERA-TP-694] 11 p1867 A69-24753

Viscous effects of wall boundary layer behind primary shock wave on flow in shock tube, noting pressure and temperature changes
11 p1870 A69-25010

Small scale oscillations stability in quasi one dimensional conducting gas flow with longitudinal superimposed magnetic field, noting radiation role in transverse oscillations development
11 p1928 A69-25222

Nonorientable five channel adapter with spherical measuring head for three dimensional gas flow measurement, noting sensitivity to mechanical disturbances in calibration
11 p1888 A69-25340

Aerodynamic forces causing deformation and breakup of liquid droplet with ellipsoid of revolution form in constant velocity gas flow
11 p1875 A69-25466

Motion equations for ideal transonic gas flow, applying solutions to flow with incident shock waves of various profiles
11 p1820 A69-25468

Free transonic gas flow incident on symmetrical profile at angle of attack with given velocity at infinity calculated using difference scheme
11 p1820 A69-25469

Supersonic gas flow past plane and axisymmetric bodies with broken generatrix, determining tangential discontinuities and shock waves shape and position
11 p1820 A69-25470

Hypersonic viscous gas flow past thin bodies, deriving equations for interactions between boundary layer and external flow
11 p1820 A69-25472

Self similar axisymmetric and plane laminar viscous gas channel flows noting exponential or hyperbolic law of decrease in static pressure along channel
11 p1875 A69-25482

Neutral gas flow transport velocity and Mach number effects on critical electric field strength and direction in formation of self sustained discharge
11 p1933 A69-25545

Inviscid reacting flow free of molecular transport analyzed locally near stagnation point, using Lighthill-Freeman gas model
11 p1876 A69-25560

Three dimensional gas flows near characteristic surface extended over homogeneous polytropic gas at rest
11 p1876 A69-25729

Navier-Stokes equations for compressible gas, generalizing viscous channel flow of heat conducting gas to slip flow of rarefied gas
12 p2061 A69-25887

Potential triple traveling space waves in barotropic gas with arbitrary equation of state, analyzing adjacent and three dimensional self similar flows
12 p2061 A69-25889

Optical methods in three dimensional gas flow research, noting role in density field determination and conjunctive use with gas dynamics equations
12 p2011 A69-26191

Exhaust gas recirculation for VTOL aircraft
[AIAA PAPER 67-439] 12 p2013 A69-26760

Rotation curve peculiarities of Sc type galaxy NGC 3432 ascribed to noncircular gas motions
12 p2164 A69-27024

Gasdynamic phenomena during subsonic or supersonic motion of isothermal gas under action of gravitational forces in flattened axisymmetric galaxy containing spiral density waves
12 p2170 A69-27065

Shock wave gas flow density behind shock tube calculated by shadows measurements using interferometric techniques
13 p2245 A69-27384

Two dimensional flow of conducting gas dynamic and electrical parameters in MGD generator channel, considering magnetic field and plasma conductivity
13 p2305 A69-27386

Electric arc and hydrogen flow interaction at high pressure, showing radiation role in heat exchange
13 p2305 A69-27387

Current, magnetic field, flow velocity and plasmatron dimensions effects on arc voltage in coaxial plasmatron
13 p2306 A69-27388

Refractory ceramic materials thermal stability in high temperature subsonic ionized gas flow products, emphasizing zirconia and magnesia
13 p2285 A69-27472

Velocity, enthalpy and mass flux radial distributions in laminar boundary layer from calorimetry of argon subsonic flow
[ASME PAPER 68-HT-16] 13 p2374 A69-27776

Turbulent diffusion and Rayleigh-Taylor instability in inhomogeneous flow of combustion gases circulating through magnetic field
13 p2310 A69-28032

Molecular gas flows in containers for space environment simulation, discussing flux distribution
13 p2241 A69-28081

Electric arc structure in hydrogen magnetic annular discharge computed using nonequilibrium hydrodynamics to analyze supersonic and subsonic processes
13 p2312 A69-28221

High pressure AC arc heater system design criteria, discussing magnetic field, chamber gas flow, stabilizing elements, etc
[AIAA PAPER 69-348] 13 p2243 A69-28283

Turbulent jets of gases in general stream of air spreading in cylindrical chamber, discussing distributions of gas dynamic parameters
13 p2200 A69-28501

Spatial distribution patterns of gaseous argon atoms scattered from solid argon surface
13 p2300 A69-28658

Variational problems associated with supersonic gas flows with foreign particles, considering nozzle designs
14 p2389 A69-28801

Thermal entry problem solution for low Reynolds number turbulent gas flow based on Reynolds number dependent velocity profile
[ASME PAPER 68-WA/FE-11] 14 p2430 A69-29446

Shock wave and blunt faced cylinder interaction in supersonic gas flow in two chamber shock tube observed with high speed photography
14 p2390 A69-29467

Transonic ideal gas flow past semiinfinite bodies, determining flow potentials from body perturbations and surface boundary conditions
14 p2390 A69-29476

Supersonic gas flows in shock layer past blunt bodies taking into account selective radiation and radiative transfer in continuum, applying method of characteristics
14 p2390 A69-29477

Direct simulation Monte Carlo method for hypersonic rarefied gas flow past solids, modeling on digital computer
14 p2390 A69-29580

One dimensional unsteady monotonic Maxwellian gas flow at small Knudsen numbers using Hilbert method, noting validity for shear flows
14 p2432 A69-29611

Heat transfer at gas flow stagnation point past blunt body under radiation from air layer in shock wave wake, using gray gas model
14 p2390 A69-29614

Quasi-steady state supersonic gas flow past two closely spaced coaxial separating bodies at different velocities, showing dependence on separation rates
14 p2391 A69-29617

Boundary layer physical and chemical processes effect on dynamic parameters of high temperature hypersonic gas flow past blunt bodies
14 p2391 A69-29620

Diffuser performance in hypersonic shock wind tunnel for nitrogen flow, discussing steady shock wave and separation zone formation time
14 p2391 A69-29622

- Shock wave velocity and gas flow parameters in shock tube with noninstantaneously opening diaphragm calculated by method of characteristics
14 p2432 A69-29623
- Electrical conductivity ratio of weakly ionized turbulent gas to quiescent gas as function of electron temperature
14 p2502 A69-29991
- Turbulent gas flow characteristics obtained by extremal hypothesis, using maximum perturbation stability in formulating variational problem and computer algorithm
15 p2590 A69-30263
- Gas flow deflection at centrifugal pump wheel outlet for wheels having different inlet and outlet vane angles
15 p2547 A69-30571
- Injected gas flow nonisothermicity and transversity effects on friction, heat transfer and flow parameters at cylindrical tube inlet
15 p2592 A69-30986
- Heat release rate during gas combustion products recombination in supersonic nozzle, using graphic interpolation of flow parameters
15 p2717 A69-30987
- Mass transfer during Cs condensation from moving vapor mixture containing Ar in water-cooled tube
15 p2718 A69-30998
- Dynamic behavior of dissociating homonuclear diatomic gas, deriving instability equations, proposing stability loss in transonic region
15 p2548 A69-31065
- Wind tunnel investigation of turbulent gas flow heat transfer and hydrodynamic drag in variable pressure gradient field of divergent-convergent channel
15 p2548 A69-31173
- Gas ducted flow at subsonic inlet velocity and critical outlet Reynolds numbers, proposing surface friction relation to Mach number
16 p2771 A69-31956
- Streamline flow of ideal stable gas with constant ratio of specific heats around conical body with arbitrary taper, determining flow velocity components
16 p2732 A69-32126
- Convective heat transfer in centrifugal force field of cavity between two rotating disks in turbulent gas flow
16 p2837 A69-32139
- Oscillations and stability of cylindrical shell in gas flow taking into account inertia forces
16 p2875 A69-32287
- Monograph on solutions to equations for unsteady flow of ideal gases, with applications to hypersonic flows, based on three space coordinates and time
16 p2773 A69-32428
- Fluidic vortex valve to modulate solid propellant generated hot gas flow
[AIAA PAPER 69-424] 16 p2844 A69-32723
- Nonequilibrium ionized gas flow past insulated wall with corners under magnetic field, discussing flow characteristics
17 p3010 A69-32865
- Shock detachment distance for flow around cylinders and spheres determined by microphotometric tracing of negatives of photographs of forward stagnation streamlines
17 p2949 A69-32962
- Temperature jumps at gas-solid interface in shock tube calculated by one dimensional approximation of thermal boundary layer behind reflected shock wave
17 p2949 A69-33023
- Axisymmetric supersonic gas flow with attached shock wave past cone, calculating flow parameters between body and shock wave
17 p2890 A69-33123
- Self ignition of solid/fluid particles suspended in gas flow, discussing heat transfer coefficient, critical temperatures, etc
17 p3070 A69-33142
- Approximate equations for transonic viscous heat conducting gas flow past finite body of revolution
17 p2891 A69-33312
- Finite aspect ratio sandwich plates flutter in supersonic gas flow analyzed by differential equation describing plates elastic equilibrium
17 p3058 A69-33317
- Nonlinear rarefied gas flow problems with thermal nonequilibrium solved by numerical methods, considering intermolecular collisions effect
17 p2952 A69-33325
- Turbulent gas coaxial mixing theory, deriving eddy viscosity model and semiempirical expressions for velocity, temperature and density fluctuations
[AIAA PAPER 69-682] 17 p2952 A69-33434
- Hydrodynamic approximation to interplanetary gas motion influenced by solar flare caused perturbations
17 p3035 A69-33627
- Flow rate effect of oxygen-argon mixture on Zr oxidation studied to determine exclusion as factor in Zr weight increase
18 p3154 A69-34272
- Fluidic sensor for measuring gas and liquid velocities, describing design and principles of operation
18 p3133 A69-34308
- Superposition method for predicting tube wall temperatures with gas property and heating rate axial variation, noting application to gas flow problems
18 p3227 A69-34315
- Simple waves in compressible isentropic flows of inviscid nonheat-conducting gas free of shock waves
18 p3121 A69-34534
- Gas velocity variations in ionizing shock wave propagating along magnetic field applied to conducting piston motion
18 p3181 A69-35038
- Unsteady motion of ideally conducting gas flow in transverse magnetic field with allowance for gravitational forces
18 p3181 A69-35040
- Integral relation method analysis of supersonic gas flow past blunt body of revolution
18 p3086 A69-35051
- Dynamic pressure pulsations, temperature distribution and gas concentrations in discrete vortices zone in wake of plate in unbounded flow
18 p3124 A69-35120
- Asymptotic solution of supersonic linearized noneisotropic flow of viscous and heat conducting gas with internal heat sources past cylindrical shell, deriving surface pressure
18 p3089 A69-35460
- Electrostatic probes in nonequilibrium collision dominated ionized gas flow ballistic ranges
19 p3291 A69-35716
- Ferroelectric transducer for heat transfer rates and flow measurement in gaseous systems with autostabilized temperature, noting film coefficient
19 p3307 A69-35749
- Electrohydrodynamic subsonic flow of isothermal charged gas over wavy insulator wall by perturbation method, calculating surface pressure, streamlines and electric lines of force
19 p3297 A69-35837
- Plasma density and potential distributions along circular cylinder surface in weakly ionized high speed low pressure gas flow, noting boundary layer separation point
19 p3380 A69-35839
- Nonuniform gas flow past axisymmetric body from supersonic source simulating jet discharging into vacuum, using power series of stream function
19 p3238 A69-35851
- High velocity interstellar gas in H I and H II regions, emphasizing observations of neutral atomic hydrogen in and far from galactic plane
19 p3402 A69-35962
- Natural oscillations and flutter of three layer cylindrical shell in supersonic gas flow analyzed by semimomentless theory, discussing boundary value problems, damping effects, etc
19 p3437 A69-36201
- Numerical program for gas dynamics of hydrodynamic flow and radiation transport in diffusion and grey body approximations
19 p3450 A69-36356
- Hypervelocity ionized gas flow analysis, allowing for finiteness of energy exchange duration between electrons and ions
19 p3379 A69-36383
- Gas motion behind cylindrical shock wave created by piston motion in gravitating medium
19 p3298 A69-36386
- Turbulent wake and ambient flow interaction analysis based on integral methods in boundary layer theory
19 p3299 A69-36390
- Pressure gradient produced steady plane flow of Maxwellian gas between infinite parallel planes, describing linearized Boltzmann equation solution
19 p3379 A69-36604
- Linearized theory of subsonic gas flow past profile compared with methods based on approximations of relationship between density and pressure
19 p3241 A69-36782
- Statistical equations for compressible gas, discussing turbulent quantities separated into fluctuating and macroscopic parts
19 p3300 A69-36784
- Radiating gas flows during hypersonic planetary reentry, discussing atmospheric composition, shock layer characteristics, nonequilibrium flows, etc
20 p3513 A69-36982
- Hypersonic gas flow past blunt bodies valid for any optical thickness of gas, allowing for absorption coefficients dependence on temperature, pressure and frequency
20 p3457 A69-36993
- Earth ionosphere and magnetosphere electrodynamic state analyzed as function of neutral gas small scale motions, considering magnetic disturbances and ionospheric discontinuities
20 p3519 A69-37026
- Nonequilibrium laminar heat transfer in viscous flow of chemically unstable gases past blunt body and plate
20 p3513 A69-37087
- Unsteady heat transfer between gas flow and solid surface during melting
20 p3631 A69-37088
- Laminar flow of compressible viscous gas in channels of variable cross section
20 p3457 A69-37089
- Turbulent boundary layer problem of gas mixture motion solved by approximate methods
20 p3513 A69-37090
- Turbulent boundary layer gas mixture flow incident to porous plate surface
20 p3513 A69-37093
- Free jet boundary layer in mixing zone of hypersonic gas flow past body
20 p3513 A69-37094
- Heat protection efficiency of plane surface in turbulent boundary layer behind tangential slots, comparing cooling effects of insulating gas films
20 p3631 A69-37095
- Electromagnetic effects on pressure, temperature and particle velocity in flow behind propagating gaseous detonation waves based on one dimensional flow field model
20 p3514 A69-37190
- He and Ar arc-heated flows into reservoir and expansion in converging-diverging supersonic nozzles, considering flow equilibrium effect on heat transfer and enthalpy
20 p3631 A69-37198
- Modified model for vibration-dissociation relaxation coupling phenomena in nonequilibrium high temperature gas flow, discussing parameter U variation with kinetic temperature
20 p3514 A69-37208
- Hydrodynamics of turbulent gas flow through powder layer for vapor phase coating of particles, noting fluidized bed
20 p3548 A69-37363
- Magnetic field and radial gas motion in sunspots from Crimean magnetograph observations at different depths of solar atmosphere
20 p3615 A69-38299
- Heat transfer and hydrodynamic resistance for turbulent gas flow in longitudinal positive and negative pressure gradients analyzed using Reynolds number data
21 p3848 A69-38635
- Sedov canonic equations for supersonic gas flow solved by applying Chaplygin function to determination of Riemann function for potential and stream function equations
21 p3643 A69-38637
- Relaxation equations for oscillatory degrees of freedom of molecular supersonic binary gas flow in Laval nozzle, obtaining population inversion
21 p3693 A69-38692
- Optimal boundary layer control ensuring minimum heat transfer to porous plate from incompressible flow of hot gas of cooling system
21 p3849 A69-38846
- Gas flow characteristics in shrouded and unshrouded turbine wheel assemblies, emphasizing radial flow role in efficiency
21 p3785 A69-38865
- Nonequilibrium processes behind shock wave in shock tube supersonic air and nitrogen flow, using photoelectrical shadow method
21 p3695 A69-38961
- Equations governing steady diabatic gas flows in Crocco velocity vector field, discussing changes in total pressure
21 p3695 A69-39007
- Simultaneous passage of two unmixed gas flows through joint two circuit turbojet nozzle into ambient medium
21 p3785 A69-39094
- Jet deflection in drifting subsonic gas flow
21 p3644 A69-39096
- Turbulent gas jet mixing in chamber with four inlet nozzles
21 p3785 A69-39102

Navier-Stokes equations exact solutions for two dimensional steady flow of compressible viscous heat conducting perfect gas

22 p3929 A69-40117

Pressure measurements and gas flow analysis during thermal vacuum tests of manned spacecraft indicating adequate space vacuum simulation

[AIAA PAPER 69-1033] 22 p3924 A69-40401

Kinetic beam instability development in homogeneous dust /gas/ cylinder rotating in hot invariable medium under arbitrary perturbations

22 p4032 A69-41017

Radiative energy transport in moving gaseous media in local thermodynamic equilibrium, assuming spectral line shifts by temperature and pressure variations

22 p3982 A69-41018

Adiabatic plane ideal gas flow past airfoil, studying shock waves propagation effect on dynamic behavior

22 p3861 A69-41024

Polytropic gas unsteady motion in dihedral piston wake by solving mixed boundary value and Goursat problems

22 p3861 A69-41025

Pt wire detector for flow regulation of atomic hydrogen beam, noting hydrogen maser application

22 p3950 A69-41232

Nitrogen-carbon dioxide-helium lasers CW operation at various pressures and N flow rates

23 p4173 A69-41496

Transonic flows behind separated shock waves of ideal gases past bodies of various geometries

23 p4151 A69-41526

Frictionless supersonic and hypersonic flow of ideal gas of constant specific heat past cone with deformed axis at zero angle of attack

23 p4058 A69-41579

Compressible gas flow into cavity of various volumes in presence of supercritical pressure gradients

24 p4298 A69-42587

Hot gas flow through multilayer cylindrical shells, calculating temperature fields in walls

24 p4407 A69-42588

Perturbation velocity potential of unsteady potential flow of barotropic gas past cascade of thin blades oscillating harmonically

24 p4244 A69-42716

Air bubbles rise velocity and path in water based on time measurement of bubble traversing two light beams, describing electronic recording system

24 p4299 A69-42918

Supersonic rarefied gas flow past circular cylinder, studying flow and shock parameters by multiple wave interferometry

24 p4244 A69-43070

DC argon plasma generator operation, studying effects of gas flow direction and rate

24 p4255 A69-43077

Iterative finite difference method for initial value problems applied to hyperbolic system representing one dimensional time dependent flow of compressible polytropic gas

24 p4340 A69-43226

Nonlinear lumped parameter model for long gas filled pressure sensing lines covering steady state, laminar or turbulent gas flow

[AIAA PAPER 69-117] 24 p4301 A69-43259

Turbulence and laminarity effect on vertical waves development rising in thin layer of heavy viscous fluid in contact with vertical gas flow

24 p4302 A69-43480

Velocity and pressure fields produced by deformable load carrying filament studied for unsteady gas motion past slender body with nonpotential external forces

24 p4246 A69-43483

Convective thermal flux at stagnation point in multicomponent partially ionized gas injected flow past body, considering effective ambipolar diffusion coefficient

24 p4246 A69-43485

Intense heat exchange narrow zones on blunted semicone surfaces in hypersonic gas flows ascribed to large Reynolds numbers

24 p4246 A69-43494

Numerical program solving partial differential equations parabolic system for internal turbulent gas flow extended to flows undergoing circular tube laminarization by heating

[ASME PAPER 69-HT-52] 24 p4409 A69-43520

Eddy diffusivity hypothesis modified to fit observed heat transfer from smooth pipe wall to turbulent gas stream at low Reynolds numbers

[ASME PAPER 69-HT-H] 24 p4303 A69-43523

Heat transfer and fluid friction of hydrogen and helium gas flows undergoing turbulent to laminar flow transition in heated pipe

[ASME PAPER 69-HT-54] 24 p4303 A69-43539

Gas phase self induced pressure field and laminar velocity distribution of working fluid within closed heat pipe channels analyzed by momentum integral method

[ASME PAPER 69-HT-22] 24 p4412 A69-43546

Radiation equilibrium temperature measured downstream of transpiration cooled gas flow near slender cone vertex in continuous flow hypersonic tunnel

24 p4248 A69-43588

Shear stress and free molecular drag for gas flow along concave cylindrical surface oriented at angle of attack, analyzing multiple surface collisions effect

24 p4249 A69-43660

High enthalpy shock tube and nozzle gas flows for incident shock Mach numbers analyzed for laminar boundary layers and boundary layer transitions

24 p4305 A69-43664

GAS-GAS INTERACTIONS

Gas jet interaction with supersonic flow during injection from orifice of flat body, investigating Mach number, orifice diameter and jet effects on flow pattern near injection

01 p0005 A69-10357

Jet perpendicular penetration prediction from holes or tubes, discussing resultant gas stream mixing and temperature profiles

[ASME PAPER 68-WA/GT-8] 05 p0750 A69-16143

Circular turbulent air jet from flat plate into deflecting stream analyzed with potential flow model, noting applicability to V-STOL aircraft technology

[AIAA PAPER 69-223] 07 p1051 A69-19557

Polarization of Lyman alpha radiation in hydrogen rare gas collisions calculated in Born and distortion approximations including rotational coupling

08 p1355 A69-20207

High temperature gas mixture plasmas thermodynamical properties, emphasizing Debye electrostatic interactions and electron states

10 p1810 A69-23794

Cool flames nonisothermal two-stage ignition of neopentane-oxygen mixtures, discussing chain propagation due to isomerization

11 p1940 A69-24477

Chemical mechanism of two stage spontaneous ignition controlled by cool flames of alkane-air mixtures under engine conditions to avoid knocking

11 p1998 A69-24479

Explosive reactions between hydrogen and oxygen flashed in presence of nitrogen dioxide, chlorine or bromine as sensitizers, considering thermal contribution

11 p1832 A69-24878

Combustion chemical reactions kinetics of gaseous phase systems, discussing temperature, reaction rates extrapolation, hydrogen and hydrocarbons

11 p2000 A69-25185

Gas-gas interactions second virial coefficients measured at various temperatures, comparing experimental data with results calculated by Kihara potential

14 p2488 A69-29927

Perturbed molecular distribution in translational and internal degrees of freedom in dilute chemically reacting gases with low ion concentrations

14 p2410 A69-29988

Interaction between two phase dynamical and combustion parameters in one dimensional gas-gas-metal combustion system

[AIAA PAPER 69-540] 16 p2880 A69-32742

Rate coefficients for chemiluminescent reactions of excited He with N, O, carbon monoxide and dioxide determined from spatial dependence of visible emission

20 p3483 A69-36936

Plasma-dynamic forces used to suppress fuel-propellant interface turbulence in coaxial jet gas core reactors

24 p4349 A69-43679

GAS GENERATOR ENGINES

U ENGINES

GAS GENERATORS

Gas bearings for spool gas generator for aircraft turbine engines, noting rotor bearing stability and LP spool balancing and seal leakage

[ASME PAPER 69-GT-60] 09 p1513 A69-22515

Solid state ozone generator for preparing ozone in known concentrations to 1000 ppm in air for laboratory studies

10 p1693 A69-23346

Dense real gas thermodynamic relations in piston driven shock tube facilities operation

11 p1862 A69-25011

Piston driven facilities for hot high pressure gas production including gas tunnels, heavy piston facilities, piston driven shock tunnels and high speed guns

11 p1862 A69-25012

Thrust vector control by secondary gas injection for predicting lateral thrust performance, applying method to rocket engines, secondary gas generator and injector configuration

17 p3019 A69-33333

Optimum adaptation of propulsion gas generators to power jet driven rotors with blown flap control, considering jet engine, fanjet and engine driven compressor

17 p3020 A69-33344

High temperature combustion chamber as high velocity gas generator, noting application to MHD power generator research

18 p3184 A69-34931

Pressure drop in control element of gas generator during readjustment of throttle in hydraulic supply line, noting assumptions

19 p3393 A69-35819

Propulsion performance of XB-70A aircraft calculated by gas generator method

[AIAA PAPER 68-594] 20 p3461 A69-37152

Pyrotechnical gas generator performance tests during Europa 1 rocket second and third stage separation, including generator design, ground and flight tests

23 p4224 A69-42153

GAS GUNS

U LIGHT GAS GUNS

GAS HEATING

DC plasmatron for heating argon with potassium additions at high temperatures and at near atmospheric pressure to obtain argon flow

09 p1547 A69-21596

Enthalpy distribution in plasma tube arc heater inlet flow region with hot and cold gas core boundary in presence of electric field

09 p1553 A69-22538

Phase equilibrium and dynamics of gas volume heated by cosmic rays and cooled by radiation

10 p1760 A69-23136

Interstellar gas model based on calculations of heating by low energy cosmic rays, noting gravitational compression to form clouds

10 p1770 A69-24095

Low energy cosmic rays and plasma turbulence in heating and ionizing interstellar gas, discussing acceleration and galactic sources

11 p1945 A69-24380

Gas motion and heating by radiation behind shock wave front, noting ionization and radiation absorption occurrence

12 p2061 A69-25880

Ionosphere temperature profiles, discussing heating and cooling of electron gas and ion gases and thermal balance

12 p2063 A69-25903

Shock heated gas radiation frequency dependence and UB and B-V color indices determination, studying role in close binary systems luminescence

13 p2350 A69-27860

Plane and cylindrical thermionic converters, considering electricity generation by heating through flame, solar radiation and nuclear flux

14 p2419 A69-29178

Reacting gas ignition by sudden contact with heated noncatalytic surface, deriving heating time and transferred heat amount by Blasius perturbation method

16 p2878 A69-31955

Interstellar H I regions and clouds heating and ionization by low energy cosmic rays from quantitative models, noting pressure equilibrium role

17 p3038 A69-33726

Gas heat transfer on turbine interblade channel surfaces and working blade end surfaces at operating Reynolds and Mach numbers

21 p3849 A69-38858

Unsteady aerodynamic heating at stagnation region including surface combustion in arc heated high enthalpy wind tunnel

22 p3860 A69-40597

Arc heating of shock tube driver gas, describing radiative energy transfer mechanism

23 p4147 A69-41895

Transition from turbulent to laminar regime as consequence of high heating rates for internal convective flow, noting roles of Nusselt numbers and friction factors

[ASME PAPER 69-HT-9] 24 p4304 A69-43559

Low energy cosmic rays and plasma turbulence in heating and ionizing interstellar gas, discussing acceleration and galactic sources

24 p4375 A69-43770

GAS INJECTION

Atmospheric diffusion measurement based on analysis of thoron emitted continuously from point source, permitting study of diffusion in atmospheric boundary layer

01 p0144 A69-10043

Gas jet interaction with supersonic flow during injection from orifice of flat body, investigating Mach number, orifice diameter and jet effects on flow pattern near injection

01 p0005 A69-10357

Double probe characteristics in flame with electronegative gas injection interpreted in terms of conduction of ions in ionized medium

01 p0176 A69-10385

Dynamics of moving gas bubble injected in quiescent liquid, considering velocity, heat flow and mass transfer [ASME PAPER 67-WA/HT-30]

02 p0351 A69-12201

Determining influence of blowing various gases into boundary layer on friction and heat and mass transfer when external flow velocity varies according to power law

02 p0234 A69-12581

Film cooling by subsonic gas injection of air through porous flat plate into 2.9 Mach air flow, noting wall temperatures

03 p0413 A69-12994

Hypersonic boundary layer on flat plate with strong hypersonic viscous interaction and uniform surface blowing distribution

04 p0588 A69-14722

Inert gas discontinuous injection into nonequilibrium laminar boundary layer

06 p0860 A69-17635

Transverse secondary gaseous injection penetration into confined supersonic flow [AIAA PAPER 69-2]

06 p0913 A69-18080

Axisymmetric hypersonic near wake with base injection, discussing zero injection case, jet-plume interaction and mixing region [AIAA PAPER 69-66]

06 p0914 A69-18115

Finite plate length effect on two dimensional supersonic turbulent boundary layer with large distributed surface injection [AIAA PAPER 69-162]

06 p0864 A69-18138

Injectant stagnation temperature and molecular weight variation effect on flow field generated from secondary injection into supersonic stream [AIAA PAPER 69-1]

06 p1039 A69-18196

Direction changing of large solid propellant motors by changing jets angle or gas injection

07 p1230 A69-19291

Ion-molecule reactions constants studied directly in ionosphere, using air injection from geophysical probe and airborne RF mass spectrometer

08 p1311 A69-21159

Global characteristics and similarity of ventilated cavity flows by injecting air behind immersed profiles of symmetrical wedge at zero incidence

10 p1680 A69-23788

Velocity distributions and skin friction coefficients in turbulent boundary layers over flat plate with injection or suction through porous wall

11 p1871 A69-25027

Porous cermet electrodes thermochemical protection by blowing neutral gas into electrode boundary layer, examining effect on volt-ampere characteristics

11 p1826 A69-25232

Initial nonuniformity effect of temperature distribution in main stream on efficiency of cooling by air injection through slit or porous collar

11 p2002 A69-25338

Gaseous He bubbles injection into liquid propellant launch vehicle fuel lines to reduce vehicle pogo oscillations by lowering feed system natural frequencies

11 p1967 A69-25498

Displaced layer thickness dependence on air injection parameters measured in wind tunnel

13 p2245 A69-27385

Mass transfer cooling data correlation for estimating mass injection effect on slender cone drag

13 p2199 A69-28224

Turbulent viscoseals gas ingestion and fluid inertia analysis using stability of dynamic gas-liquid interface between rotating cylinders [ASLE FICFS PREPRINT 31]

15 p2621 A69-30496

Injected gas flow nonisothermicity and transversity effects on friction, heat transfer and flow parameters at cylindrical tube inlet

15 p2592 A69-30986

Finite difference method for turbulent mixing and combustion of hydrogen injected parallel to supersonic air stream, considering vitiated and unvitiated air [AIAA PAPER 69-539]

16 p2877 A69-31844

Flow disturbances in supersonic rocket nozzles due to secondary injection analyzed by effective body approximation, including side forces [AIAA PAPER 69-443]

16 p2839 A69-32666

Analytical evaluation of secondary flow injection effects on rocket engine performance including cold flow and simulated hot flow data [AIAA PAPER 69-473]

16 p2844 A69-32726

Thrust vector control by secondary gas injection for predicting lateral thrust performance, applying method to rocket engines, secondary gas generator and injector configuration

17 p3019 A69-33333

Surface pressure and heat transfer over blunt conical body in hypersonic flow with uniform mass addition of various gases [AIAA PAPER 69-716]

17 p2891 A69-33463

Cone boundary layer transition location and Reynolds number as function of nose bluntness combined effect with Ar, air and He mass injection [AIAA PAPER 67-706]

17 p2955 A69-33476

Rocket nozzle control by side forces produced by secondary gas stream injection observed for relationship with inclination angle to nozzle axis

20 p3457 A69-37065

Turbulent boundary layer of injection gas flow calculated past surfaces with pressure gradient

20 p3513 A69-37091

Rice-Ramsperger-Kassel kinetic theory applied to sulfur hexafluoride injection into boundary layer of high speed reentry vehicle

20 p3514 A69-37226

Law of wall parameters for compressible turbulent boundary layer with air injection through wall determined by analyzing data for hypersonic speeds

21 p3692 A69-38685

Gaseous injection effect on laminar boundary layer hypersonic flow around transpiration-cooled blunt bodies analyzed by integral method and Newtonian model

21 p3644 A69-39014

Gas concentration measurement during injection into laminar boundary layer streaming along porous plate, using quadrupole resonance mass spectrometer

23 p4058 A69-41695

Supersonic free stream flow past finite conical body with subsonic surface gas injection

23 p4059 A69-41884

Convective thermal flux at stagnation point in multicomponent partially ionized gas injected flow past body, considering effective ambipolar diffusion coefficient

24 p4246 A69-43485

Mass injection effects on viscous hypersonic low Reynolds number shock layer downstream and at stagnation point in blunt forebody region analyzed for non-reacting gas

24 p4249 A69-43663

GAS-ION INTERACTIONS

Low density limit to three body ionic recombination coefficients in various gases

04 p0632 A69-14679

Reaction rates coefficients of oxygen ions with molecular oxygen and nitrogen in nighttime F region over Moscow based on loss coefficient estimate

06 p0919 A69-17724

Gas segregation in positive column of DC discharge due to axial ion motion analyzed using conservation equation

08 p1361 A69-20145

Diffusion coefficient, velocity distribution function and velocity averages for gaseous ions moving in strong electric fields, considering ion-gas molecule charge transfer collisions

08 p1355 A69-20209

Nonthermal intergalactic bremsstrahlung model as isotropic X ray background due to submicron electron interactions with thermal ionized gas in expanding universe

11 p1947 A69-24595

Ion-molecule reaction kinetics in nitrogen-hydrogen mixtures using ion cyclotron resonance

12 p2131 A69-25985

Elementary processes cross sections in charged states changes during proton-hydrogen molecule interactions

15 p2655 A69-30963

Ion-molecular reactions measurements in ionosphere by VV type device and RF mass spectrometer

15 p2603 A69-31407

Ion momentum transfer through charge exchange in mixture of ion gases and parent neutral gases under thermal nonequilibrium, noting role of Boltzmann equation

16 p2822 A69-32108

Reaction rate constants of ion-molecule interchange reaction as function of temperature, flow velocity, activation energy and constant part of steric factor P

16 p2747 A69-32312

Hydrogen molecular ion dissociation due to ion-molecule inelastic collisions, comparing measured and calculated velocity distributions of protons produced

19 p3375 A69-35985

Shock ionization by ion impact against triatomic H molecules gas target, showing positive ion production dependence on extraction voltage, collision chamber pressure, etc

19 p3378 A69-36188

Thermal energy rate constants of ion-molecule reactions in gaseous hydrogen, deuterium and HD, using ion cyclotron resonance method

20 p3578 A69-36934

Ion-molecule reaction rate constants measurement by ion cyclotron resonance, assuming no ion and neutral gas molecules collisions

20 p3579 A69-37495

Atmospheric small gaseous ions nature and properties, discussing solid elastic and composite interaction, complex, cluster, intermediate and Langevin ions, etc

22 p3940 A69-40538

GAS IONIZATION

NT ATMOSPHERIC IONIZATION

NT AURORAL IONIZATION

NT FLAME IONIZATION

Sparks from laser induced air breakdown due to focusing of laser beam, noting evidence for initiation by self focusing

01 p0092 A69-11246

Deuterium gas ionization over high pressure range under action of short pulse Q switched neodymium glass laser, noting breakdown wave existence

02 p0255 A69-11545

Carbon dioxide ionization by Q switched laser beam, using proportional counter

02 p0255 A69-11702

Preionization of gases by laser beam using theory based on molecular equilibrium concentration and collision excitation

02 p0283 A69-11703

Deuterium plasma evolution and creation modes obtained by short pulse laser discharge in gases, discussing detonation and phase wave ionization mechanisms

02 p0288 A69-12040

Ionizing shock front structure in monatomic gas, considering atom-atom and electron-atom collisional ionization rates

03 p0414 A69-13138

Empirical growth curve determined by using equivalent widths of absorption lines of quasar 3C 191, concluding ionization is mainly due to collisional processes

03 p0514 A69-13962

Solar wind abundance measurements at earth orbit related to solar corona

03 p0503 A69-14047

Collapsing cylindrical ionizing shock in axial magnetic field, solving governing equations numerically

04 p0637 A69-15049

Drift and diffusion of electron pulse advancing through gas, providing physical basis for Townsend ionization coefficient

04 p0633 A69-15443

Electron cyclotron instability and HF ionization in beam-plasma experiment using electron beam guided by magnetic field through He gas

05 p0798 A69-15612

Three energy dependent quantities examined for gases, describing relation between ionization yields, cross section and loss functions

05 p0795 A69-15660

Noble gas atom simultaneous ionization and excitation by removal of metastable electron in fast collision

06 p0961 A69-17137

Ionizing electron collisions with He, determining energies and angular correlation distributions of scattered and ejected electrons

06 p0962 A69-17191

Early phase of Stromgren sphere development in interstellar molecular hydrogen cloud, analyzing R-type dissociation-ionization fronts using quasi-steady flow

07 p1218 A69-19281

Dissociation-ionization fronts in interstellar molecular hydrogen clouds, analyzing effects of UV radiation from early stars

07 p1221 A69-19584

Plasma waveguide parameter changes due to additional gas ionization from microwave field

07 p1196 A69-19750

- HF breakdown of air using Boltzmann equation to determine net ionization frequency relation with electric field strength 08 p1357 A69-20810
- Fuel cell oxygen ionization on nickel, silver and nickel-silver disk electrodes 08 p1260 A69-21045
- Electron multiplication during ionized H plasma exposure to annular electric field and magnetic field, including microwave diagnostics 09 p1543 A69-21299
- Proportional counter pulse shapes calculation for point and extended ionization tracks, considering electron drift velocity and positive ion mobility 09 p1493 A69-21419
- Electron gas heating at E region altitudes as function of ionization of atmospheric gases, noting rocket experiments during solar eclipse 09 p1490 A69-21772
- Ionic species identification in argon-cesium discharges for thermionic converter design 09 p1440 A69-21830
- Ionization and current growth in discharge in rotating plasma device with mirror shaped magnetic field 09 p1552 A69-22042
- Switch-on ionizing shock waves structure, analyzing condition of downstream state and effect on hydromagnetic wave speed 09 p1552 A69-22045
- D type dissociation ionization front structure and associated shock fronts using quasi-steady flow approximation for Stromgren sphere development in interstellar molecular hydrogen cloud 10 p1772 A69-22858
- Primary specific ionization in noble gases by charged particles 10 p1726 A69-23128
- Nonequilibrium distribution functions for neutral atoms excited states in optically thin low temperature singly ionized plasma containing ions, electrons and neutrals 10 p1731 A69-23437
- Electrical conductivity, electron energy balance, ionization equilibrium time and channel parameters in pulse discharge nonequilibrium Cs plasma containing inert gas addition 10 p1731 A69-23439
- Ionization front propagation rate in crossed electric and magnetic fields in Ar-Cs, Hg-Cs and Ne-Xe discharge plasmas 10 p1733 A69-23447
- Argas test loop as model for MHD power plant study, discussing component testing including channel preionization and relaxation experiments 10 p1673 A69-23478
- Engineering and reactor parameters associated with ionization of gas passing through nuclear reactor used as closed cycle MHD system working fluid 10 p1723 A69-23485
- Ionization and recombination processes in He 3 plasmas produced by neutron irradiation of H 3 10 p1738 A69-23488
- Pulse and CW breakdown criteria for plasmas subject to spatially nonuniform electric fields, using variational formulation 10 p1739 A69-23650
- Relaxation phenomena in ionization process in argon shock front structure, using EM and pressure driven shock tube to drive high speed shock waves 10 p1726 A69-23685
- Ionization-recombination thermodynamic equilibrium upset causing spectral excitation in He arc plasma 10 p1742 A69-24077
- Low energy cosmic rays and plasma turbulence in heating and ionizing interstellar gas, discussing acceleration and galactic sources 11 p1945 A69-24380
- Simultaneous photoexcitation and photoionization of He near threshold at 186 Å, measuring probability 11 p1921 A69-24926
- Radiation studies of pressure driven shock tubes with atomic ionization at high temperatures, discussing thermal light sources, autoionization, etc 11 p1863 A69-25014
- Chain mechanism of arc discharge development in crossed electric and magnetic fields explained by direct ionization of neutral particles by ions 11 p1932 A69-25540
- Gas velocity variation in ionizing shock waves arbitrarily oriented with respect to magnetic field, considering magnetic viscosity and conductive piston 11 p1935 A69-25740
- Gas ionization by UV radiation emitted by pellet, target or portion of gas in laser beam focus, using polished metallic mirrors 11 p1901 A69-25754
- Gas motion and heating by radiation behind shock wave front, noting ionization and radiation absorption occurrence 12 p2061 A69-25880
- Charged state variations during protons and inert gas atoms interactions analyzed by coincidence method 12 p2133 A69-26543
- Diffusion and mass flow in steady state magnetically stabilized helium arc plasma effects on spectroscopic determinations of electron temperature, discussing degree of ionization 12 p2141 A69-27146
- Ionization and attachment of thermal electrons in oxygen and airlike nitrogen-oxygen mixtures during electron irradiation 13 p2302 A69-27456
- Negative charge production by H atoms collisions with rare gases and hydrogen, noting smooth rise of cross section with energy for rare gases 13 p2302 A69-27459
- Ionization processes in Seyfert galaxies, considering thermal electrons, superthermal protons and electrons and nonthermal UV radiation 13 p2346 A69-27710
- Ionization fraction as independent variable in plasma transport correlation, noting role in pressure effect increase 13 p2313 A69-28241
- Neutral gas ionization in lower ionosphere, discussing physicochemical reactions, recombination coefficients, equilibrium processes, etc 13 p2255 A69-28540
- Radiative and collisional ionization of H and He in planetary nebulae, discussing dielectronic recombination at high electron temperatures 14 p2518 A69-29133
- Auxiliary discharge thermionic converter with Penning mixture /Ne-Ar/, discussing pressure and Penning ionization effects, collector current discontinuities, etc 14 p2398 A69-29180
- Rasor phenomenological theory of space ionization in arc mode regime of Cs thermionic converter 14 p2402 A69-29242
- Ionization mechanisms in ignited mode cesium thermionic converter, discussing positive ions production for electron space charge neutralization and ion density calculations 14 p2404 A69-29258
- Lenses spherical aberration role in studying laser induced breakdown of gases, considering intense ionization collinear regions multiplicity along optic axis 15 p2634 A69-30878
- Electron ion recombination role in atomic collision process in rare gases ionization path, considering scintillation mechanism 15 p2655 A69-30961
- Initial ionization processes in strong shock wave in hydrogen, determining ionization relaxation length and cross section of atom-atom excitation collisions 16 p2815 A69-31590
- Microwave induced ionization wave propagation in rare gases, noting rapid electron density increase at wave front and subsequent slow plasma decay 16 p2818 A69-31671
- Steady state density profile dependence on electron density dependence of net volume ionization rate by analyzing ambipolar diffusion in RF excited magnetized plasmas 16 p2818 A69-31672
- Stripping and low-energy collisions of H atoms on O and N molecules, showing target ionization to projectile stripping ratio dependence on ionization potential 16 p2814 A69-31773
- Low temperature method for measuring breakdown threshold parameters of liquid and gaseous He by laser beam, observing stimulated Mandelstam-Brillouin scattering 16 p2796 A69-31799
- Monograph on ionization of Ar-CH mixtures during Townsend discharge, covering metastable Ar atoms lifetime in various pressure ranges 16 p2814 A69-31841
- Correlation coefficient of light fluctuations measured in Ar plasma in positive column of glow discharge, noting ionization wave appearance at critical gas pressure 16 p2822 A69-32039
- Laboratory plasma produced by electromagnetically generated shock front propagation through unionized hydrogen [AIAA PAPER 69-693] 17 p2945 A69-33447
- Interstellar H I regions and clouds heating and ionization by low energy cosmic rays from quantitative models, noting pressure equilibrium role 17 p3038 A69-33726
- Optically thin gas surrounding X ray source, plotting electron temperature and ionization equilibrium of hydrogen, He, carbon, nitrogen, oxygen and neon 18 p3186 A69-34295
- Gas ionization relaxation times from ion density profiles in shock tubes at low Mach numbers, discussing influence of impurities on ionization process 18 p3116 A69-34451
- Normal and transverse ionizing shock, discussing Alfvénic regime for normal shocks and shunting effect in transverse shocks 18 p3180 A69-34454
- Shock wave studies of gaseous NO thermal ionization in Kr as function of temperature, using time-of-flight mass spectrometer 18 p3099 A69-34464
- Ionization effects in hydrodynamic model of radiation driven breakdown wave propagation, obtaining wave velocity and absorbed laser flux density relationship 18 p3174 A69-35286
- Charge exchange cross sections and electron losses in hydrogen ion beam impacting on water vapor molecules 19 p3378 A69-36190
- Gas ionizing shock waves structure in arbitrary magnetic field, considering greater magnetic viscosity than dissipative coefficients 19 p3381 A69-36773
- Vacuum UV flux along T type shock tube axis and measurements of He I line precursor emission, indicating ionizing radiation contributions to precursor ionization and excitation 20 p3511 A69-38239
- Normal ionizing shock waves in H, analyzing shock velocities as function of drive magnetic field using Chapman-Jouguet hypothesis 21 p3691 A69-38332
- Laser induced multiphoton ionization and cascade breakdown in high pressure gases, considering roles of refractive index, laser nonideal output and beam self focusing 21 p3738 A69-39445
- Radiation emission and ionization in precursor and nonequilibrium region behind shock wave during approach to equilibrium in argon-like gas 22 p4006 A69-40526
- Collision processes in gaseous nitrogen leading to production of positive triatomic, diatomic and monatomic nitrogen ions 22 p3986 A69-40722
- Electron beam injection into magnetic trap, obtaining plasma by ionization of supersonic argon flow passing through system 22 p3990 A69-40791
- Ionizing shock wave propagation and reflection in transverse magnetic field based on MHD theory, assuming gas thermal equilibrium 22 p3992 A69-41176
- Atoms and ions collision strengths and photoionization cross sections for nitrogen, oxygen and neon fitted to interpolation formulas for temperature and frequency effects 22 p3988 A69-41244
- Xenon laser CW operation on unclassified spectral lines of high ionization states, using laser induced spectroscopy 23 p4172 A69-41399
- Ionization equilibrium and radiative cooling of high temperature low density plasma, noting cosmic gas cooling curve of line emission from oxygen ion transitions 24 p4376 A69-42661
- Moving striations dispersion and stability theory applied to ionization waves excited in Ar, Ne and Hg-Ar mixture low and medium pressure discharge 24 p4356 A69-43363
- Atomic nitrogen collisional ionization and recombination rates under assumed quasi-steady nonequilibrium distribution of electron state populations 24 p4353 A69-43700
- Low energy cosmic rays and plasma turbulence in heating and ionizing interstellar gas, discussing acceleration and galactic sources 24 p4375 A69-43770

GAS JETS

Gas jet interaction with supersonic flow during injection from orifice of flat body, investigating Mach number, orifice diameter and jet effects on flow pattern near injection

01 p0005 A69-10357

Supersonic gas jet impingement on inclined plane barrier, calculating parameters by approximation

03 p0413 A69-12958

Axial deviation of gas flow resulting from mixing turbulent gas jets

04 p0591 A69-15411

Gas mixture separation in supersonic jet, noting results for hydrogen-nitrogen mixture and diffusion flux

06 p0911 A69-17553

Mixing and combustion of gaseous and particle laden jets in air stream, analyzing turbulent, coaxial and jet mixing flows

[AIAA PAPER 69-33]

06 p1038 A69-18146

Soviet collection of papers on turbulent jets of air, plasma and real gas

07 p1049 A69-18392

Axisymmetric liquid nitrogen turbulent jet propagating under supercritical pressure in gaseous nitrogen medium

07 p1049 A69-18398

Stream function for plane free sonic gas jet flowing past profile

07 p1050 A69-18740

Pyrotechnic circuit closer using jet to achieve conduction between hollow charge lining and coaxial electrode

10 p1635 A69-23031

Gas jets collision flowing from parallel wall channels, applying solution to calculating geometrical characteristics of fluid jet amplifiers

12 p2016 A69-25879

Halley comet abrupt daily motion variation ascribed to solid particles ejection from ice nucleus stimulated by gas outflow

14 p2524 A69-29712

Numerical analysis for spreading of free turbulent gas jets with arbitrary uneven initial distribution of momentum and heat and mass fluxes

15 p2590 A69-30157

Sound effects on turbulent flame in gasoline-air mixture jet in Toepfer device with pulsed light source, measuring ionization in combustion zone

17 p3069 A69-33141

Jet and Mach disk density measured by fluorescence electron beam technique, calculating Mach disk thickness from density profiles

19 p3239 A69-36396

Hydrogen jet structure ejected into vacuum from Laval nozzle at supersonic velocity, considering separation point from diffuser wall

19 p3240 A69-36601

Polytetrafluoroethylene ablation in high temperature argon, nitrogen, air and oxygen jets, discussing electric heater and heat flux measurement

20 p3632 A69-37522

Pulsed performance of saturated steam reaction jet, comparing steam performance to nine gases for equal temperatures and thrust levels

21 p3785 A69-39021

Dynamics of relay gas jet preliminary vibration damping system of gravity gradient stabilized satellite, allowing for sensor limitations and stabilizer flexural vibrations

21 p3826 A69-39638

Coaxial turbulent compressible gas jets propagation, discussing mass buildup data in coaxial jets

21 p3645 A69-39847

Underexpanded plane hypersonic gas jet injection into resting medium from straight nozzle, discussing shock wave formation

24 p4246 A69-43484

GAS LASERS

NT ARGON LASERS

NT CARBON DIOXIDE LASERS

Gas laser amplifier nonlinear behavior in axial magnetic fields and operating with two polarized light signals of strong or weak intensities

01 p0088 A69-10010

Negative Faraday effect and Doppler line width measurements for He-Ne IR gas laser tube by producing beat frequencies in ring laser system

01 p0088 A69-10028

Saturation peak half widths on Ne energy level population inside single frequency Michelson-type He-Ne laser by tuned differential spectrometry, observing power broadening

01 p0089 A69-10182

Carbon dioxide laser stabilization using laser profile and three mirror system

01 p0089 A69-10183

Carbon dioxide laser pulsed mode for generating giant pulses, noting applications and electron impact role

01 p0090 A69-10787

Continuous nonresonant visible radiation from Ar ion laser by utilization of wide bore, wall stabilized gas discharges, noting long time frequency stability

01 p0091 A69-10815

Drilling and welding with sealed-off continuous carbon dioxide gas laser with outgoing beam collimated by Ge lens

01 p0086 A69-10821

Pulsed nitrogen laser design involving gas discharge tube fed by low impedance parallel plate transmission line

01 p0091 A69-10842

Carbon dioxide spectral line broadening and self broadening coefficients, using carbon dioxide laser radiant energy

01 p0091 A69-10844

Elastic and inelastic collisions between deformable bodies, using Michelson interferometer with He-Ne laser as source

02 p0282 A69-12607

Evaporation rate measurements in fog during carbon dioxide laser radiation, obtaining correlation to describe visibility improvement

02 p0258 A69-12622

Laser oscillation frequency shift dependence on discharge current in 6328 A He-Ne laser

02 p0260 A69-12658

Transverse magnetic field influence on power and polarization of helium-neon laser emission

02 p0260 A69-12844

Carbon dioxide laser for observing nonlinear effects related to electron interaction with lattice vibration within semiconductors

03 p0437 A69-13041

Saturation effect theory in gas system, taking into account Doppler expansion and collisions based on density matrix

03 p0437 A69-13042

Single oscillation mode gas laser theory, calculating nonlinear susceptibility, gain profile, power tuning characteristics and oscillation frequency with Bloch equations

03 p0440 A69-13296

Raman effect in liquid glycerol obtained with 4880 A ionized argon laser, determining valence vibrational frequencies

03 p0440 A69-13366

Tradeoffs among beam divergence, power output and mirror alignment tolerances of high power argon ion lasers operating in various low order transverse modes

03 p0440 A69-13549

Technique to obtain desirable longitudinal oscillation mode for radiation of Ne-He laser

03 p0441 A69-13844

Temperature dependence of He-Ne laser output at various wavelengths over low temperature range

03 p0441 A69-13845

Optimum proportions of gas mixture components in He-Ne laser related to field distribution in cavity

03 p0441 A69-13847

Arc and HF discharges in Ne-He lasers, comparing output power, spectral line intensities and reduced electric field vs reduced tube radius plots

03 p0441 A69-14139

Simultaneous phase locking of longitudinal and transverse laser modes in He-Ne laser

03 p0441 A69-14188

Absorption coefficients of plasmas in capillary discharge tubes, discussing measurement using gas laser light source

03 p0442 A69-14218

Superradiant and laser spectroscopy in second positive system of molecular nitrogen

04 p0609 A69-14285

High power output from submillimeter continuous wave gas laser

04 p0609 A69-14289

Chirp pulse generation by carbon dioxide laser, discussing carrier frequency sweep

04 p0609 A69-14333

Microwave excited argon discharge emission spectrum analysis, suggesting possible laser action in microwave discharges

04 p0609 A69-14346

Gases optical pumping by self radiation laser action, discussing high intensity oscillatory transitional wide bands of molecular gases

04 p0610 A69-14382

Interatomic collisions effect on multimode He-Ne lasers output power and spectral composition

04 p0610 A69-14383

Oscillation mode selection in gas lasers by thin film absorber in resonator, using standing wave electric fields periodicity

04 p0610 A69-14384

Maximum inversion density and output power of Ne-He laser, given optimal discharge in hollow cathode

04 p0610 A69-14422

Power and time characteristics of He-Ne laser pumped by microwave pulses

04 p0610 A69-14423

Emission amplification coefficients of gas laser using pure carbon dioxide, carbon dioxide/air mixtures and carbon dioxide/air/helium mixtures

04 p0611 A69-14426

Electron radiation temperature measurement in carbon dioxide laser with N and He additions by microwave technique, noting average electron energy and optical gain

04 p0611 A69-14445

Traveling waves interaction effects on emission modes of gas laser with circular resonator

04 p0611 A69-14545

Gas laser generation frequency control by emission absorption saturation effect, inserting neon filled emission absorbing cell into resonator

04 p0611 A69-14550

Nonadjustable Fabry-Perot scanning interferometer for gas laser spectra analysis, using barium titanate piezoceramic elements

04 p0598 A69-14854

Laser holography using colored KBr crystals subjected to hard gamma radiation as photosensitive material

04 p0598 A69-14855

Helium-neon gas laser cavity beam for automatic high speed particle sizing

04 p0611 A69-15023

Scanned laser beam display techniques based on cathode ray tube technology, noting flying spot scanner and beam deflection

04 p0600 A69-15028

Carbon dioxide laser noting output for added gases, efficiency, energy levels, excitation mechanism and tuning to single line and mode

04 p0612 A69-15173

Submillimeter water vapor laser power output for admixtures of H, N, carbon dioxide, methane, He and Ar, noting buffer effect of H

04 p0612 A69-15175

He/Ne ratio effect on performance of He-Ne laser in annular cavity

04 p0612 A69-15176

Colliding waves synchronization and stability in annular gas laser by electronic simulation

05 p0770 A69-15645

Rb 87 vapor laser short term frequency stability independent of vapor concentration, noting use as frequency standard

05 p0770 A69-15656

Relaxation rates of water vapor laser lines obtained with split discharge laser

05 p0771 A69-15810

Hydrogen molecular action in vacuum UV region during high current discharge

05 p0771 A69-15814

Thermal self focusing of argon laser beam passing through lead glass

05 p0771 A69-15819

Gas laser pulse induced attenuated and nonattenuated plasma radiation recording, determining absorption coefficients

05 p0762 A69-15900

Uranium hexafluoride-hydrogen hydrogen fluoride chemical laser, discussing conditions for negligible collisional deactivation and defined rotational temperature determination

05 p0771 A69-15906

Spectroscopy of potassium vapor using laser induced fluorescence, noting laser line coincides with several molecular transitions

05 p0771 A69-15907

Gas lasers involving gas-discharge collisions, selective pumping or chemical reactions to produce necessary inversion, giving theoretical analysis of excitation mechanisms

05 p0772 A69-16226

Gas laser frequency stabilization, considering electromechanical control systems 05 p0773 A69-16230

Thin film thermocouple detector for molecular lasers operating in middle and far IR range 05 p0773 A69-16284

Buildup modes of He-Ne laser in presence of other strongly oscillating modes, noting gain interaction effects 05 p0773 A69-16289

Self locking of three laser modes in He-Ne laser on basis of Lamb theory 05 p0773 A69-16290

High power stable modes of operation of argon laser, observing stable output spectra 05 p0773 A69-16292

Gallium arsenide electro-optic switch measuring signal time response to radiation step of homogeneously broadened carbon dioxide, He and nitrogen laser amplifier 05 p0773 A69-16293

High power continuous and quasi-continuous wave UV generation by ADP and KDP crystals in argon-ion laser cavity [IEEE PAPER B-1] 05 p0773 A69-16308

Relaxation time of carbon dioxide laser levels as function of water vapor, CO and Xe gas pressure measured by afterglow pulse gain technique [IEEE PAPER G-1] 05 p0774 A69-16314

Continuous UV noble gas ion lasers, noting small signal gain and power output limit at various current densities for strong lines [IEEE PAPER L-1] 05 p0775 A69-16321

Brewster angle window degradation of high power ionized argon gas lasers [IEEE PAPER L-4] 05 p0775 A69-16322

Absolute wavelength standard using saturated molecular absorption in methane inside He-Ne laser cavity [IEEE PAPER P-1] 05 p0775 A69-16323

Frequency stabilization and noise suppression in argon FM laser [IEEE PAPER P-7] 05 p0775 A69-16325

Dynamics of laser response in IR detection by means of optical mixing in He-Ne laser, noting bandwidth 05 p0776 A69-16331

Pulsed water vapor laser with single Brewster window for operation between 20 and 120 microns, comparing performance with ordinary laser 05 p0776 A69-16334

Zeeman effect in He-Ne lasers during simultaneous emissions at various gas pressures and currents in magnetic fields 06 p0932 A69-16912

Continuous and pulsed lasing characteristics during discharge in pure oxygen noting ozone formation and removal at tube walls 06 p0932 A69-16923

Carbon dioxide Q switched laser nonlinear amplification characteristics in vibrational-rotational bands 06 p0933 A69-17118

Integrated circuit interconnection patterns computerized design, discussing automatic laser mask-making control 06 p0931 A69-17199

Computer tape controlled pulsed externally excited gas laser mask making machine with micropositioning coordinate table for integrated circuit fabrication 06 p0931 A69-17200

Pulsed laser emission of atomic N in mixture of molecular N and He, noting effects of pressure and frequency and duration of excitation pulses 06 p0933 A69-17258

Gas laser operating on pure O-He-Ne-Ar mixture at liquid N temperatures, noting atomic O transitions, pulsed operation and energy level populations 06 p0933 A69-17259

He-Ne laser gain dependence on temperature noting influence of pumping conditions, discharge tube filling and geometry 06 p0934 A69-17260

Thermodynamic approach to calculation of molecular lasers, determining various population levels of carbon dioxide molecule by measuring amplification factors for rotational vibrational transitions 06 p0934 A69-17465

Electro-optical effect in Cr-doped GaAs single crystals at room temperature, discussing carbon dioxide laser radiation modulation by GaAs 06 p0934 A69-17466

Alternated magnetic field effects on lasing in ionized Ar 06 p0934 A69-17467

Generation process in three stage He-Ne cascade laser with wideband resonance, using simplified energy level scheme 06 p0934 A69-17496

Gas laser operation at high pressures, examining threshold pumping and power output dependence on pressure to optimize parameters 06 p0934 A69-17680

He-Ne laser with small spark gap optimum parameters dependent on active medium and resonator field structure 06 p0935 A69-17683

Coupled cavity carbon dioxide laser interferometer with feedback for measurement of transient plasma density in theta pinch, noting sensitivity 06 p0935 A69-17706

Inductively excited argon ion laser properties in high current regions 06 p0935 A69-17767

Raman spectra of optical phonons in semiconductors, using reflection techniques and Ar laser excitation 06 p0936 A69-17882

Optical Fourier transform applied to structural analysis of catalase crystalline media by gas laser 06 p0928 A69-17890

High power noble gas CW UV ion laser with W disk structure, showing continuous UV output limitation by optical degradation effects 06 p0936 A69-17900

Second order nonlinear coefficient measurement for optical generation of millimeter wave difference frequencies in GaAs waveguide, using carbon dioxide laser 06 p0928 A69-17903

Gas lasers principles of operation, discussing population mechanism, lifetime conditions, excitation processes, electron velocity distribution and types of discharges 06 p0937 A69-18008

Atomic, ionic and molecular gas lasers applications, population reversal conditions and processing technology 07 p1143 A69-18250

Nonlinear interaction effects on frequency and polarization characteristics of dual polarization gas laser, discussing weak cavity anisotropies 07 p1145 A69-18473

He-Ne laser capillary end contamination with consideration of life lengthening, discussing thermal properties of argon ion laser with pyrolytic graphite 07 p1145 A69-18474

Stabilized frequency single mode ionized argon laser, discussing intensity of electric field in cavity and mode selector 07 p1145 A69-18475

Streaming gas effect on carbon dioxide-nitrogen-helium laser power, discussing gas renewal phenomenon and evacuation rate 07 p1145 A69-18476

Helium-neon laser for optical correction and guide beam techniques 07 p1146 A69-18484

Angular velocity of rotation measurement using angular gas laser undergoing axial torsional vibrations 07 p1147 A69-18523

Helium-neon laser output power dependence on spark-gap cross section geometry, analyzing diffusion equation and population inversion 07 p1147 A69-18541

Output polarization rotation sensitivity to axial magnetic field varied by variable angle quartz flat inside He-Ne laser resonator 07 p1198 A69-18646

Helium-neon laser radiation of given spectral compositions, noting relation between spatial coherence and controlled number of frequencies 07 p1148 A69-18803

Measurement of helium-neon laser radiation divergence emitted in TEM sub nm modes 07 p1148 A69-18804

Saturated absorption by Ne inside 6328 A He-Ne laser, discussing selection of Ne isotopes in gain and loss tubes 07 p1149 A69-18898

Single mode output power from 6328 A He-Ne laser through mode coupling induced by added absorption cell containing excited Ne 07 p1149 A69-18901

Pumping power effect on He-Ne laser amplification factor dependence on temperature and discharge currents 07 p1149 A69-18935

Nonpolarized single frequency gas laser radiation produced by interferential effects in complex resonator 07 p1149 A69-18936

He-Ne and He-Xe laser lines in IR tuned by axial magnetic field, observing Stark patterns of organic molecules [IEEE PAPER C-5] 07 p1150 A69-19050

Cyclotron resonance measurements of quantum effects in Ge valence bands by CW molecular gas laser, developing tunable submillimeter maser [IEEE PAPER C-6] 07 p1150 A69-19051

Pulses from Q switched carbon dioxide laser for studying Q switching techniques [IEEE PAPER G-2] 07 p1150 A69-19054

Competition effects between rotational levels of carbon dioxide rotation-vibration band in traveling and standing wave lasers [IEEE PAPER G-6] 07 p1151 A69-19055

Radiative lifetime for nitrous oxide 001-100 transition, laser level absolute population densities and saturation parameter measured in nitrous oxide-nitrogen-He laser [IEEE PAPER G-10] 07 p1151 A69-19057

Single mode single frequency carbon dioxide laser operating on single rotational-vibrational transition [IEEE PAPER G-11] 07 p1151 A69-19058

He-Ne laser self locking of modes and spectrum weeding out at small absorption [IEEE PAPER G-13] 07 p1151 A69-19059

Population inversion of vibrational levels due to molecular collisions in carbon dioxide lasers, calculating transition probabilities, laser parameters and gain profile [IEEE PAPER G-15] 07 p1151 A69-19061

Continuous wave and pulsed IR signals amplification on carbon dioxide laser amplifiers, discussing design, construction and performance of transmitter [IEEE PAPER J-1] 07 p1152 A69-19064

Time resolved spectrum of high current pulsed argon laser discharge, noting primary laser output and afterglow [IEEE PAPER L-12] 07 p1152 A69-19068

Frequency reproducibility of He-Ne laser, using absorption dependence on frequency in strong field standing wave limit to provide stabilization [IEEE PAPER P-4] 07 p1153 A69-19073

Frequency discrimination characteristics of elliptically polarized dual polarization gas laser, discussing intensity crossover phenomenon and frequency stabilization application [IEEE PAPER P-5] 07 p1153 A69-19074

Single mode carbon dioxide laser Lamb dip and vibration rotation lines absorption coefficients [IEEE PAPER P-6] 07 p1153 A69-19075

Phase locking phenomenon of multitransverse longitudinal modes in He-Ne lasers, discussing mechanism of self locking phenomenon [IEEE PAPER Q-1] 07 p1153 A69-19076

Collision broadened spectral line shape obtained in impact approximation using Anderson formulation compared to output of gas lasers [IEEE PAPER T-6] 07 p1154 A69-19083

Mode power spectra observations for ring and normal He-Ne lasers at 6328 A 07 p1155 A69-19087

Gain enhancement effect of CO on carbon dioxide CW laser performance by accelerating relaxation of bending mode 07 p1155 A69-19088

Gas pressure control in xenon lasers, using variable temperature surface partially insulated from liquid nitrogen coolant 07 p1155 A69-19090

Sealed carbon dioxide lasers life and power outputs with Xe and H additives 07 p1155 A69-19091

Output and beat frequency of carbon dioxide laser with various resonator configurations realizing single mode operation 07 p1156 A69-19157

Iodine fluorescence spectra excited by krypton ion laser, analyzing spectral series and vibrational rotational levels 07 p1156 A69-19304

IR beam profiles of carbon dioxide laser permanently recorded on foamed polystyrene 07 p1156 A69-19305

Optical heterodyning with single mode carbon dioxide laser and triglycine sulfate pyroelectric detector, noting detector sensitivity threshold 07 p1156 A69-19332

Helium-Ne laser beat frequencies between neighboring axial modes shifting linearly with inserted cavity loss 07 p1156 A69-19412

Lamb theory of mode self locking in gas lasers approximated to provide criteria for self locking 07 p1156 A69-19413

Single mode intensity measured for 0.6328 micron He-Ne laser as function of cavity Q, using Lamb semiclassical theory

07 p1157 A69-19414

Proportionality between log-amplitude variance and 7/6 power of wavenumber for horizontal propagation from spherical wave transmitter to point detector

07 p1157 A69-19641

Population inversion mechanism based on electron collisional excitation cross sections for molecular vibrational levels in carbon dioxide lasers

07 p1157 A69-19655

Electron collisional excitation cross sections for upper states in Ar ion lasers

07 p1157 A69-19656

Electron energy distribution measurements in carbon dioxide laser discharges noting similarity of distribution for nitrogen

08 p1323 A69-19801

Carbon dioxide laser excitation by fast proton beams, noting generation power increase

08 p1323 A69-19802

Carbon dioxide laser radiation frequency controlled by varying boron trichloride pressure in cell inserted in resonator

08 p1323 A69-19804

Doped crystal and gas lasers, discussing resonant cavities, axial modes, relaxation oscillation, mode locking and Lamb theory

08 p1323 A69-19869

Flow diagnostics for high enthalpy nonequilibrium gas flows in shock tubes using long pulse ionized Ar gas laser

08 p1323 A69-19879

Li niobate crystal emission excited by Ar laser beam, deriving laser action formulas

08 p1323 A69-19941

Amplification curve change of active substance due to saturation by self field of He-Ar laser, discussing axial operation modes instability

08 p1323 A69-19942

Small signal pulsed gas laser amplification limits, discussing time dependency, temperature effects, relaxation rates and energy transfer

08 p1324 A69-20098

Vacuum UV perturbation spectroscopy compatibility with resonance transitions in Ar ion laser

08 p1324 A69-20161

Flowing CO-Ne He laser with power enhancement and high efficiency, noting role of gases

08 p1324 A69-20163

Gas laser modes strong coupling and single moding induced by saturable absorbing medium within cavity resonator

08 p1324 A69-20166

Collision cross sections between monatomic gas impurities and metastable atoms in He-Ne laser from output curve and impurity partial pressure

08 p1325 A69-20278

Mutual influence of two different laser modes corresponding to two transitions with same ground level, using He-Ne DC laser

08 p1325 A69-20284

Molecular beam gas laser operating at transitions between ground state and resonance excited state of inert gas atom, obtaining population inversion

08 p1325 A69-20325

Natural intensity fluctuations spectrum of He-Ne laser, determining modulation coefficient dependence on output

08 p1325 A69-20431

Gas laser emission natural frequency fluctuations spectral density measured by auxiliary heterodyne laser

08 p1326 A69-20540

Nonlinear optical effects in He-Ne and ruby lasers noting laser gain, frequency splitting, frequency differences in coupled lasers and frequency band narrowing

08 p1327 A69-20768

Eutectic anisotropic InSb-NiSb crystals applied to IR detection, noting sensitivity to carbon dioxide lasers

08 p1373 A69-20866

Helium-neon gas laser as coherent light source for holograms of vaporizing fuel films and by Michelson interferometer

08 p1327 A69-20874

Argon laser frequency spectrum instability caused by competing axial oscillations

08 p1327 A69-21023

Carbon dioxide laser with two gas absorption cells in cavity for emission wavelength control and HF pulsed mode of operation

08 p1327 A69-21088

Gas laser frequency stabilization by coupled oppositely circularly polarized components of single cavity mode in axial magnetic field

08 p1327 A69-21090

Pulse velocity in self locked He-Ne laser, noting air turbulence effects prevention

09 p1514 A69-21347

CW helium-neon laser used to detect and measure vibration frequencies of uniform diffuse surfaces

09 p1515 A69-21430

Relaxation times of carbon dioxide laser levels induced by radiation

09 p1515 A69-21488

Optimal conditions for gas discharge in tubes with hollow cathodes in He-Ne mixture for obtaining lasing at Ne line wavelength

09 p1516 A69-21507

Frequency fluctuations in mode coupled gas laser used to determine natural emission line width

09 p1516 A69-21670

Carbon dioxide-nitrogen-helium laser with RF excitation of discharge plasma, noting high power per unit length

09 p1516 A69-21678

Mode locked He-Ne laser pulses compression by multiple reflections from interferometer after application of linear electro-optic frequency sweep

09 p1516 A69-21745

Gain, output power and radiation directivity of He-Ne traveling wave laser with nonresonant feedback

09 p1517 A69-21796

Gas lasers, discussing amplification, resonance, internal and external mirror lasers, outputs, and He-Ne, carbon dioxide and ion lasers

09 p1517 A69-22121

Laser control of French rocket head guidance system, discussing gyroscopic master, stellar or solar detectors, etc

09 p1518 A69-22162

Laser radiation produced by continuous glow discharge within Al hollow cathode, determining laser power in terms of He-Ne mixture pressures

09 p1519 A69-22245

Heat transfer effect on population inversion time variation in pulsed carbon dioxide laser and molecules excitation rates dependence on gas mixture composition

09 p1519 A69-22289

Distance measurements of several hundred feet to resolution of three millionth of inch by applying He-Ne laser interferometer

09 p1519 A69-22475

Gas laser output increase by nonconstricted discharge in aluminum tube cathode with mirror resonator

09 p1520 A69-22681

Intensity distribution in principal mode of TEM oscillations at various gain amplification levels, plotting intensity distribution generated by argon ion CW laser

09 p1520 A69-22685

Linear dependence of saturation parameter on active medium density of He-Ne laser explained by considering exchange collisions of neon atoms

09 p1521 A69-22687

Carbon dioxide laser upper level rotational relaxation rate constant measurement, observing CW gain

10 p1701 A69-22948

Carbon dioxide laser beam deflection and thermal defocusing due to wind in absorbing medium

10 p1701 A69-22949

Carbon dioxide laser combining gas flow with fluid mixing to achieve high gain

10 p1701 A69-22954

Amplitude fluctuations and line width of traveling wave and standing wave He-Ne laser, considering saturation effects

10 p1701 A69-23135

Far IR radiation from water vapor laser, noting monochromaticity and strong linear polarization

10 p1702 A69-23160

Ceramic substrate cutting with carbon dioxide laser by scribing perforation pattern,

10 p1699 A69-23302

Noble gas additives for triggering stability of pulsed argon ion lasers, discussing repetition rate and power loss

10 p1702 A69-23341

IR He-Ne laser frequency response determined with inherently swept frequency modulator based on rotating corner reflector

10 p1702 A69-23347

Excitation of ultrathin Cd/SeS/ platelets with mode locked He-Ne laser for excitons formation, discussing time delay

10 p1703 A69-23512

Q switching combined with pulsed pumping of carbon dioxide laser for observing optimal Q switching instant, noting pulse energy increase

10 p1703 A69-23619

Gas laser with nonlinear absorbing cell in resonator, discussing effective gain dependence on squared field amplitude, hysteresis phenomena and output power

10 p1704 A69-23625

Low voltage He-Ne laser, noting outputs for various pressures and grid anode separations

10 p1704 A69-23652

Quantum phase noise in He-Ne laser, considering amplitude fluctuation, spontaneous emission and oscillator linewidth

10 p1704 A69-23669

Simultaneous action of RF perturbation between Zeeman sublevels of atomic transition sustaining gas laser oscillations, discussing single pi mode laser operation

10 p1704 A69-23808

Mode interactions in argon lasers between two spectral lines noting effect on output

10 p1705 A69-24003

Sulfur dioxide-helium laser pulsed and CW submillimeter outputs

10 p1706 A69-24005

Far IR lasing lines in hydrogen sulfide, sulfur dioxide and OCS, discussing output

10 p1706 A69-24008

Electron concentration and temperature dependence on gas temperature as factor determining He-Ne laser output at 6328 A

10 p1706 A69-24078

Single mode generation and Lamb dip in argon ion gas laser obtained by thin quartz plate inserted near plane mirror of resonator

10 p1706 A69-24080

Vibrational energy transfer computed for processes in carbon dioxide-nitrogen laser based on vibrational relaxation data

10 p1706 A69-24083

High speed photodetector frequency characteristics using multimode gas laser and Kerr cell

10 p1707 A69-24211

Pulsed molecular nitrogen laser positive UV and IR systems interaction under varying gas pressure, applied voltage and tube diameters

11 p1893 A69-24346

He-Ne laser light coherence distortion by atmospheric turbulence

11 p1894 A69-24452

Q switched carbon dioxide laser power increased by placing bleachable /boron tetrachloride/ filter in resonator

11 p1894 A69-24454

Conventional interferometry advances due to gas laser development, discussing basic concepts and methods of interferometers

11 p1881 A69-24599

He-Ne laser radiation frequency spectrum as function of transverse magnetic field determined by photoheterodyne method

11 p1894 A69-24622

Amplification factor of He-Ne traveling wave light amplifier, discussing frequency stability and telescopic wave front broadening for uniform radiation distribution

11 p1894 A69-24623

Molecular carbon dioxide laser radiation emission in tube containing low pressure atmospheric air, using C cathode and Al cold cathode

11 p1895 A69-24625

Perturbation theory applied to emitting density matrix in nonlinear polarization of resonance media, considering gas laser in coaxial magnetic field

11 p1895 A69-24630

Multicolor hologram recording and reconstruction gas lasers, discussing control of ghosts in three dimensional image

11 p1882 A69-24679

Gas lasers coherence properties and availability for holography, discussing continuous power output of He-Ne, Ar and Kr ion lasers

11 p1895 A69-24680

Single frequency Ar ion laser for deep field holography noting thermal compensation, servo stabilization, operating mode, high power and high coherence

11 p1895 A69-24689

Gas laser materials, fabrication and performance, analyzing gas cleanliness, cathode degradation, bore erosion and optical surface contamination effects
11 p1896 A69-24743

Low order transverse modes in Ar ion lasers, analyzing beam divergence, output, mirror alignment and cavity configurations
11 p1896 A69-24841

Turbulence induced depolarization of linearly polarized He-Ne laser beam at 6328 Å traversing atmosphere near ground level
11 p1896 A69-24842

Calorimeter for IR carbon-dioxide laser output power measurement, noting range calibration and accuracy
11 p1885 A69-24903

Coherence phenomena for gas laser transitions coupled by common level, noting coherent superposition
11 p1898 A69-25045

Gas laser transitions and power broadening, analyzing saturation and gain profiles of He-Ne laser by light probe
11 p1898 A69-25046

He-Ne laser output phase fluctuations between adjacent modes during unlocked and self locked condition, noting cavity optical length short term fluctuations influence
11 p1898 A69-25048

High power CW carbon dioxide laser saturation and discharge conditions analyzed by rate equation
11 p1898 A69-25050

Far IR CW gas laser design for maximum output, discussing pulsed operation, wavelength measurement and radiation detection
11 p1898 A69-25051

Carbon dioxide laser for production of high peak power pulse, discussing mw peak power design and oscillation problem in high gain amplifiers
11 p1899 A69-25053

Carbon dioxide-N-He laser amplifier, noting gain time dependence and thermal relaxation rate after gas heating
11 p1899 A69-25054

Gain decrease due to saturation during amplification of pulses from Q switched carbon dioxide laser oscillator, noting rotational sublevels relaxation rate
11 p1899 A69-25055

Ar plasma diagnostics in pinch-discharge laser, determining electron temperature by spectroscopy and measuring plasma conductivity and ion concentration and temperature
11 p1933 A69-25548

Frequency stabilization of He-Ne laser, using external Ne absorption tube in variable magnetic field as frequency standard
11 p1900 A69-25678

Intensity fluctuations of single frequency gas laser at 3.39 microns, discussing fluctuation minimization methods
11 p1900 A69-25750

Two transverse modes locking with multiple longitudinal modes in He-Ne laser, noting separate locking and alternate quenching
12 p2104 A69-25923

Resonant vibrational energy transfer between specific mode of carbon dioxide and N molecules at high temperatures, monitoring IR emission
12 p2131 A69-25984

Pulsed laser emission from carbon dioxide collisionally pumped by vibrationally excited DF produced by reacting fluorine oxide with deuterium
12 p2104 A69-25986

Power output of He-Ne laser as function of transverse magnetic field strength
12 p2104 A69-26023

Absorption characteristics of thin metallic films in standing light wave for mode selection and conversion in lasers
12 p2104 A69-26024

Reabsorption effect of emitted quantum on lifetime of excited levels in gas laser, determining capture factor
12 p2104 A69-26028

Frequency stability of He-Ne laser with nonresonant feedback, noting spectral line width dependence on number of interacting modes
12 p2105 A69-26049

Carbon dioxide rotational constants from CW beat measurement in bulk GaAs mixer between carbon dioxide vibrational-rotational laser lines
12 p2105 A69-26311

Spontaneous emission of carbon dioxide lasers, studying emission in Second Positive System of nitrogen as function of discharge current and laser output power
12 p2105 A69-26316

Disaligning and velocity changing collisions influence on laser light induced saturation peaks or holes in velocity distribution of Ne atoms
12 p2105 A69-26317

Single mode laser oscillations buildup for 0.633 micron transition of He-Ne laser at levels above threshold using fast intracavity chopper
12 p2105 A69-26318

Temperatures and densities of atoms and electrons from spectroscopic methods in gas discharge plasma used for CW ion-argon lasers, evaluating inversion mechanism
12 p2106 A69-26319

Nonlinear crystal generated second harmonic power measured for multimode He-Ne 0.63 micron self locked laser
12 p2106 A69-26321

Water vapor laser, discussing water vapor molecular structure, population inversion mechanism, perturbation model, etc
12 p2106 A69-26325

Argon ion laser with water cooled mercury pool cathode shielded by U-bent section trap, considering advantages as compared to oxide cathodes
12 p2107 A69-26326

Focusing power of hyperbolic gas lens for light beam waveguides, noting temperature distribution measurements and pole separation
12 p2107 A69-26392

Precision optical systems tests, using two beam interferometer and CW gas laser to examine reflected or transmitted wavefront contours
12 p2092 A69-26421

Carbon dioxide dissociation in carbon dioxide laser gas discharge plasma for various flow rates, pressures, discharge current densities and tube diameters
12 p2107 A69-26540

Contrast interference patterns obtained in Michelson interferometer at various path differences, using He-Ne laser as light source
12 p2108 A69-26593

Phase pulsations between normal frequencies and combination tones in CW gas laser output, analyzing observations by scanning interferometer
12 p2108 A69-26635

Population densities, pumping rates, lifetimes, etc, of singly ionized krypton ion laser
12 p2109 A69-26638

Single frequency sealed off carbon dioxide amplifier, giving saturated gain
12 p2109 A69-26640

Incandescent cathode temperature effect on He-Ne laser output, ascertaining mixture parameters, cathode voltage and power dependence on discharge current
12 p2109 A69-26716

Laser Doppler particle sensor to measure velocities in rocket exhausts, using He-Ne laser light source and Fabry-Perot interferometer frequency filter [AIAA PAPER 68-723]
12 p2094 A69-26783

Gas lasers, including stimulated emission in monochromatic field of traveling and standing plane waves, spontaneous emission with stimulated transitions, etc
12 p2109 A69-26906

Carbon dioxide laser as light source in Michelson interferometer for plasma electron density measurement
12 p2100 A69-27177

Anomalous interaction of argon and krypton ion laser lines, considering connecting radiative transitions and cross modulation
13 p2270 A69-27204

Temporal correlations in light field from laser at threshold of oscillation, measuring He-Ne CW gas laser by photoelectron count
13 p2271 A69-27399

Vertical refraction effect on gas laser beam propagation near earth surface under various meteorological conditions, comparing index for diffuse light
13 p2220 A69-27827

Anemometer based on neon helium ring laser with four mirror resonator
13 p2260 A69-27857

Gallium arsenide diode nonequilibrium carriers absorption of He-Ne laser radiation under emission conditions
13 p2272 A69-27893

He-Ne laser transition line shape and gain curve through width, considering spectral frequency characteristics, output power and gas temperature and concentration
13 p2272 A69-28115

Gas ring lasers, discussing optimal parameters, colliding waves interference, nonmutual effect and radiation polarization
13 p2272 A69-28175

Electrooptical ADP modulator design for use with helium-neon laser, considering temperature stability and crystal faces parallelism
13 p2272 A69-28191

Gas laser modulation steady state characteristics with KDP crystal in cavity, noting output power dependence on applied electric field
13 p2273 A69-28432

Laser based on carbon dioxide molecules formed chemically in electrical discharge studied for designing special carbon electrode laser
13 p2274 A69-28585

Passive Q switching of carbon dioxide laser with mixture of sulfur hexafluoride and chlorotrifluoro-ethylene gases within resonator
13 p2274 A69-28659

Gases optical pumping by self radiation laser action, discussing high intensity oscillatory transitional wide bands of molecular gases
14 p2456 A69-28755

Interatomic collisions effect on multimode He-Ne lasers output power and spectral composition
14 p2456 A69-28756

Oscillation mode selection in gas lasers by thin film absorber in resonator, using standing wave electric fields periodicity
14 p2456 A69-28757

Carbon dioxide band vibration-rotation transitions saturation characteristics, stressing role of collisions in molecular gas lasers
14 p2457 A69-28928

Frequency shifts of Lamb dip minimum in helium-neon laser, considering effects of discharge tube parameters and gas pressure
14 p2457 A69-28929

Polarization dependent gain saturation and nonlinearity induced anisotropy in He-Ne laser amplifier
14 p2457 A69-28931

Gas laser design utilizing internal window mirrors deposited with dielectric coating outside resonator
14 p2457 A69-29160

He-Ne laser traveling wave output power, obtaining end mirror reflection coefficient optimal value
14 p2458 A69-29165

Elastic collision effect on gas laser atoms velocity distribution and gain factor determined for strong collision model
14 p2459 A69-29388

He-Ne lasers operation at 6328 Å, discussing optimum design parameters for power, life and stability
14 p2459 A69-29429

Linear polarization achieved in He-Ne laser by applying external transverse magnetic field to plasma discharge
14 p2459 A69-29569

Continuous IR parametric signal amplification in saturable absorber caused by carbon dioxide laser pumping
14 p2459 A69-29601

Nonlinear interactions of linearly polarized carbon dioxide laser signals in sulfur hexafluoride measured as function of angle between polarization planes
14 p2460 A69-29602

Electron energy distribution functions and energy transfer rates to inelastic levels of carbon dioxide and nitrogen in laser
14 p2460 A69-29603

Log amplitude variance calculation methods compared in statistics of optical scintillation by application to measurements with laser
14 p2486 A69-29642

Three level He-Ne laser, showing nonlinear interference effects on gain line shape and use in magnetic field and frequency stabilization
14 p2460 A69-29671

Laser with molecular H and Cl mixture at HCl vibrational transitions
14 p2461 A69-29672

Fabry-Perot interferometer employing gas laser for plasmodic electron concentrations measurement at 3.39 micron wavelength
14 p2451 A69-29778

Undulation in output waveforms of pulsed water vapor laser observed with In-doped Ge detector
14 p2461 A69-29887

High resolution silver halide photoemulsions analyzed by holographic resolvometry using He-Ne laser to obtain interference patterns
15 p2606 A69-30052

Gas lasers output power calculation based on operating transition with mixed contour due to natural and Doppler broadenings
15 p2633 A69-30079

Gas laser secondary modes emission and beat frequency spectrum widths, using results of Lamb lasers theory

15 p2633 A69-30121

Polarization and angular distribution of 6328 Å He-Ne laser light scattered by latex-sphere hydrosols, comparing coherent and incoherent scattering patterns

15 p2595 A69-30223

Nonadjustable Fabry-Perot scanning interferometer for gas laser spectra analysis, using barium titanate piezoceramic elements

15 p2608 A69-30246

Laser holography using colored KBr crystals subjected to hard gamma radiation as photosensitive material

15 p2608 A69-30247

Interferometric technique for studying fracture specimens plastic zone using laser holography

15 p2609 A69-30681

Solid state and gas lasers operational parameters tabulation including pulse durations, powers, energy flux densities, electric and magnetic field strengths, etc

15 p2633 A69-30708

Hydrogen laser operation time reduction attributed to hydrocarbon formation on inner surface of storage flask, promoting atomic hydrogen recombination

15 p2634 A69-30942

Statistical characteristics of Q switched He-Ne laser emission gain fluctuations during transient process from subthreshold to superthreshold value

15 p2634 A69-30960

Optimal parameters of cuvette for use with helium-neon laser as excitation source to record combination light scattering spectra of powdery materials

15 p2635 A69-31105

Mode competition of 5861 and 6470 Å lines in ionized Kr laser attributed to electronic level excitation processes

15 p2635 A69-31106

Frequency selector for gas laser, considering monochromatic emission and multimode oscillation

16 p2795 A69-31608

Gas laser application to magnetospectroscopy of graphite, Bi, As and pyrolytic graphite single crystals

16 p2796 A69-31822

Ruby and gas lasers operation principles, discussing spatial coherence, frequency stability, energy conservation and concentration, Q spoiling, resonators, etc

16 p2797 A69-32377

Colliding waves synchronization and stability in angular gas laser by electronic simulation

16 p2798 A69-32502

Rb 87 vapor laser short term frequency stability independent of vapor concentration, noting use as frequency standard

16 p2798 A69-32513

Cavity linear phase anisotropy and axial magnetic field effect on single mode Zeeman gas laser

16 p2798 A69-32606

HCN laser line width measurement with high resolution spectrum analyzer indicating spectral widths caused by mechanical instability

17 p2979 A69-32850

Multiple mode phase locking of He-Ne laser with fixed cavity length and laser tube fixed position in cavity, generating high speed optical pulses

17 p2980 A69-32957

Mode patterns and far field distribution for gas lasers operated in lowest order Gaussian transverse mode

17 p2981 A69-33090

FM detecting resolution using free running multimode uniphase Ar laser with Doppler broadened bandwidth

17 p2981 A69-33091

Broadband intracavity SHF modulation of He-Ne laser emission in 10 cm band, showing agreement with calculations

17 p2981 A69-33112

Spontaneous gas laser emission from level coupled by spontaneous transition with emitting level, obtaining atoms interaction with laser field velocity distribution and spectral line width

17 p2981 A69-33116

Molecular beam gas laser operating at transitions between ground state and resonance excited state of inert gas atom, obtaining population inversion

17 p2981 A69-33315

He-Ne laser plasma behavior, establishing parameters for electron gas, cross sections of formation and annihilation and excited states lifetimes

17 p2982 A69-33390

Single frequency lasers using thin metal film mode selection filters, discussing film properties and experiments with Ar ion and Nd-YAG lasers

17 p2982 A69-33399

Long path difference vacuum Michelson interferometer application to far IR and IR laser wavelength measurements compared with 6328 Å He-Ne wavelength

17 p3006 A69-33405

Wave interaction in gas ring laser, delineating single mode emission zones as function of pumping, emission frequency position and Q factor differences

17 p2982 A69-33632

Laser action and spontaneous emission at atomic oxygen transition, discussing pulsed emission mode in argon-oxygen laser

17 p2982 A69-33633

Rb 87 vapor laser output power dependence on magnetic field strength and resonator detuning, discussing laser and atomic transition frequency tuning

17 p2983 A69-33694

Gas laser power dip in presence of elastic collisions, using equilibrium equations for particles velocity distribution function

17 p2983 A69-33972

Reliability block diagrams for laser systems, discussing failure modes of solid state, semiconductor and gas lasers

18 p3151 A69-34523

Submillimeter water vapor laser power output for admixtures of H₂, N₂, carbon dioxide, methane, He and Ar, noting buffer effect of H₂

18 p3152 A69-34717

He/Ne ratio effect on performance of He-Ne laser in annular cavity

18 p3152 A69-34718

Statistical model for coherent functions obtained from laser equation, showing amplitude and frequency coupling of radiation fluctuations

18 p3152 A69-34820

High electron density in transient mercury vapor plasma determined using He-Ne laser interferometer measurements

18 p3153 A69-35307

Gas and solid state lasers optical resonance and radiation generation, frequency properties, frequency shift, spectra and Zeeman effect

18 p3154 A69-35408

He-Ne laser light noises due to discharge current fluctuations and random mode beat

19 p3330 A69-35760

Mode coupling effects in CW gas ring lasers, considering excitation density pulsations, traveling waves dispersion, polarization, etc

19 p3334 A69-36046

Lamb theory of Doppler broadened gas laser extended to arbitrary intensities for single mode operation, calculating detuning curves and inversion densities

19 p3335 A69-36048

Coherent radiation generation using gas lasers, analyzing interaction between EM radiation and matter

19 p3335 A69-36067

Internal modulation of HeNe laser in asynchronous regime, evaluating range and efficiency with regard to external modulation

19 p3335 A69-36341

Rb 87 vapor laser pumping, output, spectral line width and emission frequency approximated in three level system

19 p3335 A69-36342

Rb 87 vapor laser output power and spectral line width dependence on optical pumping intensity and atom density in resonator

19 p3336 A69-36343

Light induced shift of Rb 87 vapor laser emission frequency during modulated optical pumping, discussing elimination by filter temperature and tuning

19 p3336 A69-36344

Water vapor laser submillimeter emission spectra, considering rotational and vibrational lasing transitions due to electron impact and molecular interactions

19 p3336 A69-36349

Gas laser oscillation mode selection and self synchronization based on separation in two mirror cavity with nonlinear absorption

19 p3336 A69-36350

Continuous explosion laser study of stationary detonation waves to determine conditions leading to partial population inversion and critical population density

19 p3336 A69-36360

He-Ne laser discharges noise and oscillations classified, investigating interaction between intrinsic oscillations

19 p3338 A69-36605

Inductively coupled RF excited toroidal Ar ion laser, confining current discharge by strong axial magnetic field to reduce wall losses

19 p3338 A69-36690

HCN laser line gain measurements during continuous excitation as function of current and pressure for acetonitrile and water mixtures

19 p3339 A69-36695

Central tuning dip on rotation-vibration transitions of nitrous oxide and carbon dioxide laser with nitrogen, noting frequency discriminator generation

19 p3339 A69-36698

He-Ne laser communication feasibility experiments, discussing modulation, detection, operating parameters, etc

19 p3279 A69-36756

He-Ne laser subnanosecond intracavity coupler consisting of coaxial krytron pulse generator and electrooptic modulator

19 p3339 A69-36823

Spectrum measurement of He-Ne laser by Fabry-Perot interferometer, determining mirrors flatness

20 p3536 A69-36945

AM phase locked states switching behavior of PM He-Ne lasers, considering isotope mixtures effect

20 p3552 A69-36994

Gas mixtures CW gain characteristics at 337 mμ as function of pressure, current, mixture and flow rate, considering HCN laser systems

20 p3552 A69-36995

He-Ne laser temperature condition optimization based on calculation and experiment

20 p3553 A69-37356

He-Ne laser output intensity saturations in presence of axial magnetic field, noting moving and fixed minima

20 p3553 A69-37433

Backscattering intensity measurements by optical elements at 180 degrees to beam propagation direction, using CW He-Ne laser as radiation source

20 p3554 A69-37609

Threshold power, gain, output power and radiation energy during optical pumping of Q switched molecular laser by black body radiation

20 p3554 A69-37722

Single mode He-Ne laser frequency stabilization by Zeeman effect

20 p3554 A69-37729

He-Ne laser emission tuning with thin absorbing metallic film situated near reflecting mirror

20 p3555 A69-37730

Thermodynamic approach to calculation of molecular lasers, determining various population levels of carbon dioxide molecule by measuring amplification factors for rotational vibrational transitions

20 p3555 A69-37948

Electro-optical effect in Cr-doped GaAs single crystals at room temperature, discussing carbon dioxide laser radiation modulation by GaAs

20 p3555 A69-37949

Alternated magnetic field effects on lasing in ionized Ar

20 p3555 A69-37950

Carbon dioxide laser pulsed mode for generating giant pulses, noting applications and electron impact role

20 p3555 A69-38004

He-Ne laser oscillation frequency shifts with variations in DC discharge ascribed to changes in populations of He and Ne levels

20 p3556 A69-38124

Afterglow decay rates of Zn II laser lines in spontaneous emission measured, indicating thermal energy charge exchange excitation and CW oscillation

21 p3735 A69-38598

Helium-neon laser output power dependence on spark-gap cross section geometry, analyzing diffusion equation and population inversion

21 p3735 A69-38693

Helium-neon laser radiation of given spectral compositions, noting relation between spatial coherence and controlled number of frequencies

21 p3736 A69-38948

Measurement of helium-neon laser radiation divergence emitted in TEM sub nm modes

21 p3736 A69-38949

Frequency stabilization in He-Ne three mode laser by stabilizing LF oscillations via automatic adjustment of laser resonator length

21 p3738 A69-39078

Automatic frequency control circuit for stabilizing beat emissions of coupled multifrequency gas lasers

21 p3738 A69-39079

He-Ne laser emission attenuation coefficient relation to water content of artificial fogs for 0.63, 1.15 and 3.39 microns

21 p3738 A69-39118

Molecular hydrogen, oxygen and deuterium additions effect on CW laser operation with ordinary and heavy water as active medium
21 p3738 A69-39131

Multimode He-Ne laser radiation polarization modulation as function of magnetic field, cavity anisotropy and frequency, using Macaluso-Corbino effect
21 p3739 A69-39447

Annular gas laser cavity designs with additional mirrors for longitudinal oscillation mode selection, noting positive results for He-Ne laser
21 p3740 A69-39553

Peak power ranges of Q switched CO-air-He molecular laser, noting recovery time and CO vibrational temperature
21 p3742 A69-39742

Power density and time history of pulsed molecular nitrogen laser, discussing dependence on fill pressure and electric circuit parameters
21 p3742 A69-39779

Output power of CW lasers employing HCN and water vapor active medium
22 p3959 A69-39958

Spatial coherence of He-Ne laser beam studied in Young interference experiment, noting multimode light percentage attributed to weak transverse modes
22 p3960 A69-40018

Strain measurement by interferometer with gas laser source emphasizing long period measurement problem
22 p3960 A69-40189

Gas lasers development and industrial applications, discussing output power, operation modes, etc
22 p3961 A69-40242

Cavity Q dependence of intensity of single mode He-Ne laser above threshold for quantum and semiclassical theories
22 p3961 A69-40415

Single mode high power He-Ne laser with Michelson interferometer in cavity, describing performance determination method
22 p3962 A69-40473

Frequency locking of HCN laser transition at 890 GHz to harmonic of crystal controlled oscillator
22 p3963 A69-40567

Axial mode frequencies, loss coefficients and optimal parameters of three and four mirror resonators of gas lasers, including designs with maximum selectivity
22 p3964 A69-40796

Spatial coherence of He-Ne laser radiation diffused by turbid medium calculated by using diffraction and interference measurements
22 p3964 A69-40798

Pulsed Hg ion-He laser operation, revealing transition in near IR
23 p4171 A69-41393

Electron emitters tested for gas laser operations, discussing nonreactive and reactive gases cases, matrix structures containing BaSrO and barium zirconate cathodes
23 p4172 A69-41394

He-Ne laser heterodyne system for measuring dispersion at 6328 and 6401 Å due to Ne metastable atoms in gas discharge
23 p4172 A69-41397

Xenon laser CW operation on unclassified spectral lines of high ionization states, using laser induced spectroscopy
23 p4172 A69-41399

Far IR gas laser with linearly polarized radiation output obtained by using echelette reflection grating in place of end mirror
23 p4172 A69-41400

Sweep tuning gas laser and output power vs frequency characteristics, demonstrating tuning ability within entire Doppler bandwidth
23 p4174 A69-41635

Absorption coefficient measurement for hydrocarbon gases for He-Ne laser beam at 3.39 microns, tabulating coefficients, noting variations from spectroscopic data
23 p4174 A69-42192

Portable He-Ne laser design featuring positional adjustment for use in aligning optical systems
24 p4327 A69-42924

Amplified radiation of laser used for coherent optical pumping in two level low pressure gas laser
24 p4327 A69-43067

Emission spectrum of nonself locked He-Ne ring laser, deriving phase relations for LF intermode oscillations
24 p4328 A69-43159

Polarization characteristics of He-Ne ring laser emission with circularly anisotropic resonator, analyzing ellipticity as function of half wave cavity plate
24 p4328 A69-43160

Transitions competition in He-Ne laser pulse operating in single mode with nonuniform gain saturation
24 p4328 A69-43165

Angular distribution of He-Ne laser beam scattered by artificial fog from data by light detection devices at various angles
24 p4328 A69-43503

Tilted etalons to obtain tunable single mode emission from gas lasers noting fabrication simplicity, vibration insensitivity and low insertion loss resulting in high efficiency
24 p4329 A69-43752

GAS LIQUEFACTION U CONDENSING

GAS-LIQUID INTERACTIONS

Time dependent interaction of hot gas bubble with chemically reactive liquid stream, detailing thermal boundary layer theory
01 p0058 A69-10162

Fuel films ignition behind shock waves in air and oxygen
02 p0353 A69-12317

Low temperature simulation of hypersonic melting ablation and wave patterns of gas-liquid interface
06 p0907 A69-18064

Acoustic holographic measurement of surface deformation generated by sound waves impinging on gas-liquid interface, discussing acoustic amplitude components
10 p1695 A69-23542

Hydrogen peroxide electrode cathodic polarization studied for liquid oxidant use in methanol fuel cells
11 p1825 A69-24523

Gas-liquid critical flows, considering compressibility, rate of momentum, mass and heat transfer, etc
13 p2376 A69-28144

Quantitative analysis of interaction between spray and ambient atmosphere, discussing atomization of flat sheet and drop behavior relationship to operating conditions
15 p2717 A69-30465

Turbulent viscoseals gas ingestion and fluid inertia analysis using stability of dynamic gas-liquid interface between rotating cylinders
[ASLE FICFS PREPRINT 31]
15 p2621 A69-30496

Two phase flow mixing shocks, obtaining expressions for pressure and entropy changes, discussing shock stability and gas entrapment mechanism
16 p2768 A69-31589

Two phase detonations of fuel in liquid layer on shock tube wall with gaseous oxidizer, presenting one dimensional approximation for film detonation propagation
16 p2879 A69-32151

Undissolved air effects on working fluids elastodynamics in aircraft hydraulic actuators
24 p4255 A69-43076

Turbulence and laminarity effect on vertical waves development rising in thin layer of heavy viscous fluid in contact with vertical gas flow
24 p4302 A69-43480

GAS LUBRICANTS

Self acting gas lubricated bearings design procedures and comparison with oil lubricated bearings
[ASME PAPER 68-LUBS-10]
13 p2265 A69-27267

Herringbone grooved gas lubricated journal bearing static and dynamic characteristics analyzed approximately, noting pressure distribution and vibration amplitudes
[ASME PAPER 68-LUBS-7]
13 p2265 A69-27269

Gas molecular mean free path effect on performance of spiral grooved thrust bearing, discussing slip flow factor and He Knudsen number
[ASME PAPER 68-LUBS-17]
13 p2266 A69-27273

Lubricant compressibility effect on spiral groove gas bearing load carrying capacity
[ASME PAPER 68-LUBS-33]
13 p2266 A69-27274

Design optimization for gas lubricated spiral grooved spool bearing based on narrow groove theory, analyzing static and dynamic characteristics for motion in axial direction
[ASME PAPER 68-LUBS-12]
13 p2266 A69-27276

Externally pressurized gas lubricated journal and thrust bearings designs, citing reference literature
[ASME PAPER 68-LUBS-8]
13 p2267 A69-27282

Heat transfer between surfaces as secondary effect in gas bearing lubrication from analysis taking into account viscosity variation with temperature
[ASME PAPER 68-LUBS-4]
13 p2267 A69-27282

13 p2267 A69-27286
Infinitely long journal bearing using ionized gas lubricant with magnetic field applied axially and electric field applied transversely to fluid film
[ASME PAPER 68-LUBS-30]

13 p2267 A69-27287
Magnetic and electric fields influence on gas lubrication of bearings
[ASME PAPER 68-LUBS-26]

13 p2267 A69-27288
Electromagnetic field pumping effects in electrically conductive gas lubricants, producing gas film between surfaces without external pressurization
15 p2629 A69-31003

Mach numbers effect on pressure distribution and friction moment in nonisothermal layer of gas lubricant, using power series
15 p2629 A69-31021

Analytical method for designing pressure circular bearings verified by experiments concerning loading capacity
16 p2792 A69-31560

High speed rotors with air lubricated foil bearings, studying motion in pressurized and self acting modes
22 p3955 A69-40405

GAS MASERS

Hydrogen maser oscillations with external gain, noting frequency stability
04 p0611 A69-14443

Two cavity large storage box atomic hydrogen maser, obtaining self excited oscillations coupled with high gain amplifier
[IEEE PAPER C-8]
05 p0774 A69-16310

Molecular interactions in ammonia maser beam, discussing influence on oscillation extinction beyond given flow rate
07 p1145 A69-18478

Plasma electron density and collision frequency determination, using CW maser interferometer
08 p1359 A69-19987

Upper and lower frequency stability bounds using hydrogen masers, studying signal power and relaxation rate as function of resonator effective field
08 p1327 A69-20715

Transition probabilities in repetitively Q modulated HCN maser radiation dependent on gas discharge current
09 p1516 A69-21626

Steady state operation of atomic hydrogen maser by analogy with electronic circuits, calculating atomic magnetic susceptibility using density matrix and deriving equivalent circuits
09 p1517 A69-22093

Double focalization in atomic hydrogen maser by hexapolar magnets selecting hyperfine energy transitions
12 p2105 A69-26050

Atomic beam for H maser operation prepared by using nonadiabatically changing magnetic field in transition region
15 p2635 A69-31103

Water vapor absorption at submillimeter wavelengths in atmospheric window regions related to foreign gas pressure, using HCN maser
18 p3152 A69-35241

Transient oscillations in ammonia maser oscillator observation based on switching achieved by signal injection into cavity at molecular resonance frequency
19 p3339 A69-36825

Protostar chemical processes responsibility for population inversion and properties in OH and water masers
22 p4018 A69-40267

Short term frequency fluctuations of CW HCN masers reduced to 10 kHz by improving plasma stability
24 p4327 A69-42614

GAS-METAL INTERACTIONS

Gas content and impurities in aluminum melts, analyzing oxides and hydrogen interactions
01 p0098 A69-10958

Refractory metals interactions with gases in vacuum and inert gas environment, noting temperature and pressure effects on reactions, extent and kinetics
01 p0099 A69-11042

Centrifugal force field influence on heat exchange between gas and blade cascade studied with noncooled blades at low temperatures
03 p0531 A69-12959

Interaction of gas atoms with solid surface, giving mathematical model assumptions
04 p0632 A69-15008

Nickel structure alterations during interaction with high speed air flow at elevated temperatures
05 p0783 A69-16812

- Dissociation of hydrogen on tantalum using modulated molecular beam mass spectrometry
06 p0960 A69-17107
- Static adhesion of metals in hot oxidizing gas environment, considering dry lubrication to prevent adhesion
[IME PAPER 4] 07 p1139 A69-18567
- Interaction of nitrogen oxides and carbon dioxide on nickel crystal surface using low energy electron diffraction and mass spectrometer, discussing work function
08 p1268 A69-20138
- Gas adsorption of molecular oxygen and hydrogen on molybdenum surface using collector section of field emission retarding potential analyzer
08 p1268 A69-20179
- Hydrogen solubility in solid and liquid phases of nickel-molybdenum and nickel-tungsten alloys at high temperatures
08 p1333 A69-20448
- Refractory metals testing at high temperatures in vacuum, discussing equipment modifications, temperature measurement and residual gas problems
10 p1714 A69-23848
- Desorption kinetics of atomic and oxide phases, analyzing composition of surface film formed from W and Mo single crystals interaction with oxygen
12 p2026 A69-26115
- Adsorption of N, H, O and CO on thick vapor deposited Be films at room temperature
13 p2322 A69-28017
- CO adsorption on tungsten, determining work function changes and Fowler-Nordheim preexponentials on field emitter single crystal faces
14 p2409 A69-29093
- Inert gas diffusion of Xe 133 in aluminum and titanium at various temperature ranges, showing effects of recrystallization, plastic deformation and phase transformations
16 p2800 A69-31775
- Laser ignited Zr droplet free fall combustion in oxygen, analyzing metal conservation and luminosity correlation assuming reflux action from fog layer
[WSCI PAPER 69-1] 16 p2830 A69-32342
- Interaction between two phase dynamical and combustion parameters in one dimensional gas-metal combustion system
[AIAA PAPER 69-540] 16 p2880 A69-32742
- Oxygen adsorption on Mo single crystals /100/ surface as function of temperature using low energy electron diffraction
16 p2748 A69-32795
- Secondary electron emission from gas covered metal surfaces, discussing results of neutral beam investigations
17 p3008 A69-33000
- Tunnel junctions with low background currents made by reacting active gas layer adsorbed on Nb film surface with Pb upper film to form barrier
17 p3016 A69-33788
- Gas-surface energy transfer experiment on OGO-F satellite, measuring upper atmosphere kinetic energy flux to determine accommodation and drag coefficients, density, etc
19 p3255 A69-36680
- Elemental fluorine reactions with Ni, Cu, Fe, Ti, Be, Al, Zr and Ag, giving reaction rate constants, activation energies, etc
21 p3670 A69-39706
- Nb-gaseous Nb chlorides equilibrium from transpiration measurements at 800-1400 C, confirming importance of Nb pentachloride, Nb tetrachloride and Nb trichloride
23 p4112 A69-41339
- Desorption of hydrogen and methane from Al, Mg and Mb under room temperature tensile deformation in ultrahigh vacuum
23 p4176 A69-41541
- GAS MIXTURES**
NT DETONABLE GAS MIXTURES
- Diffusional, thermal diffusional and thermal fluxes in multicomponent flames, discussing flame structure and reaction kinetics
01 p0175 A69-10144
- Heat and mass transfer coefficients derived for reacting gas mixtures by applying variational principle
01 p0006 A69-10400
- Sulfur trioxide production in photolysis of sulfur dioxide at 1849 angstroms, noting oxygen addition effect on quantum yield
01 p0024 A69-10619
- Intermolecular collision induced vibration to vibration energy transfer in nitrous oxide in various gas mixtures, measuring fluorescence and relaxation rates
01 p0123 A69-10684
- Multiple velocity dispersion in normal hydrogen and normal hydrogen-helium mixtures at room temperature using ultrasonic interferometer
01 p0121 A69-11284
- Mass velocity of detonation products of hydrogen-oxygen mixtures measured by simultaneously recording internal resistance and induced voltage in ionized medium
02 p0354 A69-12628
- Optimum proportions of gas mixture components in He-Ne laser related to field distribution in cavity
03 p0441 A69-13847
- Monograph on exhaust gases mixing with cold airstream in ducted fanjet engine, noting thrust and efficiency increase
03 p0496 A69-14048
- Scattering data for optical diagnostic measurements on two component suspensions or gases, using random distributions of spheres
04 p0555 A69-14282
- Thermal diffusion coefficient and composition of gas mixtures by measuring gas flow rate in capillary tube as function of viscosity
04 p0688 A69-15410
- Moment equations for general gas mixture from Boltzmann-like equations, evaluating collision integrals
04 p0633 A69-15436
- Thermistor assembly apparatus for measuring coefficient of thermal conductivity of pure and binary mixture of gases
05 p0845 A69-15616
- Laminar flow of isotropic binary gas mixture in circular cylindrical tube with porous walls, determining concentration field variation with wall suction Reynolds number
05 p0744 A69-15618
- Viscosity of compressed nonreacting gas mixtures at high temperatures, discussing conditions for accurate calculation
05 p0845 A69-15895
- Uranium hexafluoride-hydrogen hydrogen fluoride chemical laser, discussing conditions for negligible collisional deactivation and defined rotational temperature determination
05 p0771 A69-15906
- Detonation characteristics of gaseous explosives using equations of state for real gases, noting compressibility effect in mixture of hydrocarbons, O and N
05 p0848 A69-16337
- Diffusion and thermal diffusion in mixture of Maxwellian gases, analyzing Onsager reciprocity relations
05 p0849 A69-16461
- Pulsed laser emission of atomic N in mixture of molecular N and He, noting effects of pressure and frequency and duration of excitation pulses
06 p0933 A69-17258
- Gas laser operating on pure O-He-Ne-Ar mixture at liquid N temperatures, noting atomic O transitions, pulsed operation and energy level populations
06 p0933 A69-17259
- He-Ne laser gain dependence on temperature noting influence of pumping conditions, discharge tube filling and geometry
06 p0934 A69-17260
- Emissivity of high temperature air and carbon dioxide-nitrogen mixtures in two diaphragm shock tube
06 p0911 A69-17348
- Gas mixture separation in supersonic jet, noting results for hydrogen-nitrogen mixture and diffusion flux
06 p0911 A69-17553
- Laminar and turbulent regimes of flame propagation studied by blowing explosive gas mixture through porous wall, determining Reynolds number by hot-wire anemometer
06 p1034 A69-17626
- Combustion in compressible turbulent mixing flows, discussing mixing facility, experimental results and numerical analysis
[WSCI PAPER 68-28] 06 p0969 A69-17794
- Vibrational excitation in diatomic gas mixtures by translation to vibration energy conversion in simple collisions and by vibrational energy exchange between components
06 p0962 A69-17821
- Spherical deflagration and detonation waves in diluted stoichiometric hydrogen-oxygen mixtures in hemispherical combustion chamber
06 p1034 A69-17927
- Heat transfer from unseeded DC augmented propane air flame to water cooled probe placed beyond discharge zone
06 p1035 A69-17934
- Free turbulent mixing, emphasizing flowing gas mixtures with and without chemical reaction
[AIAA PAPER 69-31] 06 p0915 A69-18223
- Adiabatic kinetic calculations of chemical additive effects on ignition delay of hydrogen-oxygen-argon gas mixtures
[WSCI PAPER 68-52] 07 p1239 A69-18316
- Gas dynamics effects of hot spot in explosive gas mixture using kinetic rate equations, discussing composition, enthalpy and time dependence
[WSCI PAPER 68-53] 07 p1240 A69-18322
- Fuel mixing mechanism in diffusion type supersonic combustion, noting influence of combustor configuration and fuel density
[AIAA PAPER 69-32] 07 p1242 A69-19266
- Diffusion coefficients of H atoms in mixtures of He and Ar with hydrogen by catalytic sink technique, discussing rigid sphere collision diameters
07 p1185 A69-19300
- Kinetic theory development of equations for multicomponent gaseous mixtures symmetric diffusion coefficients
07 p1186 A69-19395
- Oxygen-helium cabin atmosphere effect on speech communication analyzed during simulated space mission
07 p1066 A69-19420
- He concentration measurement in transient He-air mixture by spectroscopic analysis of fluorescence excited by high energy electron beam
08 p1312 A69-19860
- Homogeneous turbulent gas flame front location as function of caloric value of mixture and flow velocity
08 p1420 A69-19998
- Fortran 4 program for computation of equilibrium compositions of gas mixtures at high temperatures
08 p1278 A69-20154
- Flowing CO-N-He laser with power enhancement and high efficiency, noting role of gases
08 p1324 A69-20163
- Harmonic generation in microwave gas discharge in pure and air mixed gases, noting rare gases failure in power source applications
08 p1283 A69-20177
- Laminar heat transmission coefficients in combustion zone for particular oxygen and kerosene mixture
08 p1421 A69-20585
- Monograph on shock wave structure in binary gas mixtures covering gas kinetics and shock tube measurements of heavy component density distribution
08 p1304 A69-20711
- Unsteady flow parameters for reaction products behind spherical detonation wave in gas mixtures based on Taylor solution
08 p1421 A69-20765
- Nongray radiation effects on compressible turbulent free jet mixing of nonsimilar gases, using stepwise spectral absorption coefficient and Beer law
08 p1253 A69-20844
- Optimal conditions for gas discharge in tubes with hollow cathodes in He-Ne mixture for obtaining lasing at Ne line wavelength
09 p1516 A69-21507
- Boundary layer at tube wall behind shock wave propagating in gas-vapor mixture, analyzing condensation rate
09 p1480 A69-21591
- Supersonic free jet with real gas effects and chemical reactions calculated by approximation
10 p1631 A69-22898
- Low voltage He-Ne laser, noting outputs for various pressures and grid anode separations
10 p1704 A69-23652
- Pulsed glow discharges in He and He-H mixtures for high current density, noting electric field and wall potential distributions
10 p1739 A69-23660
- High temperature gas mixture plasmas thermodynamical properties, emphasizing Debye electrostatic interactions and electron states
10 p1810 A69-23794
- Spectral measurement of luminous trails produced by injecting high velocity submicron diameter iron particles into gaseous targets compared with meteor spectra
10 p1790 A69-24142
- Chapman-Enskog procedure extension for binary gas mixtures, obtaining diffusion equation from revised relaxation time of component velocities
11 p1921 A69-24308
- Turbulent flame propagation velocity in homogeneous premixed combustible gas, using one dimensional inviscid flame model
11 p1998 A69-24473

Cool flames nonisothermal two-stage ignition of neopentane-oxygen mixtures, discussing chain propagation due to isomerization
11 p1940 A69-24477

Stability of slow combustion in viscous gas mixture, showing viscosity as principal stabilizing factor
11 p1999 A69-24554

Binary gas flow past curved body for stationary problem studied by solving Boltzmann equations in form of matched asymptotic expansions [ONERA-TP-694]
11 p1867 A69-24753

Combustion chemical reactions kinetics of gaseous phase systems, discussing temperature, reaction rates extrapolation, hydrogen and hydrocarbons
11 p2000 A69-25185

Hydrodynamic instability of normal flame and turbulent combustion of gas mixtures, considering surface and volume combustion models
11 p2000 A69-25186

Steady propagation of flame front initiated by local ignitor /spark/ in gas mixture, discussing critical requirements, boundary conditions, etc
11 p2001 A69-25190

Composition and thermodynamic properties of gaseous system reacting at low temperatures with condensed phase formation, discussing iterative process convergence in approximation
11 p2001 A69-25223

Shock wave structure in gas mixtures, discussing velocity and temperature undershoot and overshoot
11 p1874 A69-25356

Enthalpy excess thermodynamic functions of binary gas mixtures based on stationary diffusion thermoeffect in tube
11 p2003 A69-25552

Diffusion coefficients for laminar multicomponent dissociating boundary layer at surfaces of thermally decomposing protective coatings
12 p2190 A69-25890

Ion-molecule reaction kinetics in nitrogen-hydrogen mixtures using ion cyclotron resonance
12 p2131 A69-25985

Freezing of water droplets in thermal equilibrium with gas mixtures, considering droplet shattering and gas volume
12 p2126 A69-26018

Speech intelligibility in air at ground level and in helium-oxygen mixture at 18,000 ft
12 p2019 A69-26548

Heat and mass transfer coefficients derived for reacting gas mixtures by applying variational principle
12 p2062 A69-26668

Particle volume role in normal shockwave structure in gas-particle mixtures, discussing equations of motion formulation
13 p2244 A69-27327

Steel cylinder wall materials effects on flame propagation at constant volume of propane-air mixtures
13 p2379 A69-28363

Thermal ignition of methane-oxygen mixture, observing flame propagation
13 p2380 A69-28459

Passive Q switching of carbon dioxide laser with mixture of sulfur hexafluoride and chlorotrifluoro-ethylene gases within resonator
13 p2274 A69-28659

Laser emission field effect on discharge current in pure carbon dioxide and mixtures with molecular N and He
14 p2458 A69-29161

Partially ionized multicomponent gas mixture kinetics in strong electromagnetic field, determining magnetic field, stress tensors and transfer coefficients
14 p2492 A69-29610

Laser with molecular H and Cl mixture at HCl vibrational transitions
14 p2461 A69-29672

Oscillatory relaxation of multiatomic gases and gas mixtures with quantum exchange between oscillators, noting gasdynamic applications
15 p2654 A69-30109

Supersonic combustible gas mixture flow around circular cone, discussing ignition by shock wave and flow modification by conical flame front
15 p2548 A69-31007

Radiative scattering cross sections of electrons from neutral O and atomic and molecular N using rapid scanning spectrometer for bremsstrahlung intensity
15 p2657 A69-31160

Nonresonant absorption and dispersion of microwaves by gases, studying gaseous mixtures, relaxation parameters, anomalous dispersion and temperature effects
15 p2654 A69-31219

Mixture ratio distribution, injector/chamber performance and nozzle effects on specific impulse of liquid propellant rocket engine using hydrazine and oxygen
16 p2828 A69-31724

Induction period of reactions behind incident shock waves traveling through undiluted high temperature CO and molecular oxygen mixtures, using CO flame spectra
16 p2877 A69-31768

Monograph on ionization of Ar-CH mixtures during Townsend discharge, covering metastable Ar atoms lifetime in various pressure ranges
16 p2814 A69-31841

Gas environment effect on catabolic activities and enzymatic reactions of trachoma and meningopneumonitis agents of genus Chlamydia
16 p2747 A69-31865

Ion momentum transfer through charge exchange in mixture of ion gases and parent neutral gases under thermal nonequilibrium, noting role of Boltzmann equation
16 p2822 A69-32108

Ablative materials in hydrogen/oxygen thrust chamber using expansion nozzle to substitute regenerative thrust chamber assembly [AIAA PAPER 69-442]
16 p2747 A69-32702

Specific impulse deliverable performance of space storable propellant combination fluorine-oxygen/methane and oxygen difluoride/diborane [AIAA PAPER 69-505]
16 p2845 A69-32762

Ultrasonic velocity dispersion in para hydrogen and mixtures with He, Ne and Ar at 300 K, obtaining rotational relaxation times
16 p2815 A69-32791

Monograph on turbulent isothermal swirl-free jets and turbulent swirling flames, studying mixture and propagation in free space
17 p3068 A69-32996

Temperature and pressure effects on flame propagation rates, burning time and combustion zone length in turbulent flows of homogeneous gas mixtures
17 p3069 A69-33140

Boron nitride synthesis by gas phase reaction of boron chloride or diborane with ammonia, determining purity from equilibrium gas mixture components
17 p2992 A69-33432

Gas bath cryostat to study volumetric properties of gaseous mixtures at low temperature and high pressure
17 p2975 A69-33669

Flow rate effect of oxygen-argon mixture on Zr oxidation studied to determine exclusion as factor in Zr weight increase
18 p3154 A69-34272

Shock wave profiles in molecular N-H gas mixtures in shock tube measured by optical electron beam method, noting disagreement with Navier-Stokes calculations
18 p3134 A69-34458

Criteria to predict flow instabilities triggered by exothermic reaction presence in high temperature reaction kinetic shock tube studies
18 p3116 A69-34462

Population inversion in carbon dioxide laser related to pumping frequency, discussing molecular dissociation effect in gas mixture
18 p3151 A69-34620

Turbulent velocity of flame propagation in supersonic stream of hydrogen-air mixture determined by velocity distribution, exchange coefficient and burning time
19 p3448 A69-35854

Flame and pressure /or velocity/ oscillations interaction in unstable combustion regimes, considering tubes with propane-air mixtures
19 p3450 A69-36357

Diverging nozzle flow of gas mixtures containing solid or liquid particles analyzed by one dimensional approximation separately averaging boundary layer and flow core
19 p3298 A69-36389

Ordered sets of Massieu thermodynamic characteristic speeds for reacting gas mixtures relevant to nonequilibrium flow fields compared to Laplacian and Newtonian speeds
19 p3452 A69-36802

Thermal conductivity calculation for chemically reacting multicomponent gas mixture, comparing results from Brokaw method and simplified formula
20 p3483 A69-36974

Gas mixtures CW gain characteristics at 337 mu as function of pressure, current, mixture and flow rate, considering HCN laser systems
20 p3552 A69-36995

Turbulent boundary layer problem of gas mixture motion solved by approximate methods
20 p3513 A69-37090

Turbulent boundary layer gas mixture flow incident to porous plate surface
20 p3513 A69-37093

Pulse height distribution changes of gas filled proportional counters ascribed to deposit accumulation on anode, using X ray fluorescence analysis
20 p3538 A69-37302

Similarity rule in hydrodynamically transcritical regime in ionized multifluid gas
20 p3515 A69-37559

N and H plasmas and N-H plasma mixtures thermodynamic properties calculation, discussing numerical methods and corrections for electrostatic interactions
21 p3847 A69-38421

Thermal conductivity coefficient of gas mixtures at low temperatures obtained using quantum diffusion model and Chapman-Enskog method for Boltzmann equation
21 p3848 A69-38638

Heat loss from cylinders at low Reynolds numbers in N-He and N-Ne binary mixtures
21 p3848 A69-38706

Equilibrium absorption and desorption rates of carbon dioxide-argon mixtures from silica gel measured as function of temperature using gas dynamics method
21 p3848 A69-38707

Propagation characteristics of steady adiabatic one dimensional laminar flames in premixed gases, considering activation energy and Lewis number
21 p3849 A69-38802

Turbulent premixed ammonia-air flame stabilization on flameholders, discussing secondary oxygen injection into circulation zone at blowoff limits
21 p3849 A69-38808

Negative ion influence on electrical conductivity of partially ionized multicomponent gas mixtures, basing analysis on thermodynamic calculations of composition
21 p3774 A69-38867

Spectral transmittance of mixture of carbon monoxide and nitrous oxide for overlapping absorption bands [AIAA PAPER 67-600]
21 p3819 A69-39013

Molecular hydrogen, oxygen and deuterium additions effect on CW laser operation with ordinary and heavy water as active medium
21 p3738 A69-39131

Computer routines for approximations of thermochemical properties of gas mixtures, using JANAF /Joint Army Navy Air Force/ tables of combustion systems
21 p3670 A69-39591

Respiratory gas exchange during workloads, comparing values for ventilation, oxygen uptake and carbon dioxide output measured in air and in helium-oxygen mixture
22 p3891 A69-40221

Gaseous mixtures for hypervelocity applications, studying equilibrium conditions and thermodynamic properties for shock and constant volume heating processes
22 p4049 A69-40266

Carbon dioxide and carbon dioxide mixture mirror Q switched laser peak power generation, using pulsed excitation
22 p3963 A69-40564

Adsorption kinetics in ternary mixture of nitrogen, methane and hydrogen, using concentration-time /breakthrough/ curves measurement on activated coconut shell charcoal [NAS-NRC PAPER H-4]
22 p3981 A69-40629

Kinetic theory for macroscopic transport phenomena in N-component polyatomic gas mixtures with internal degrees of freedom under nonlocal thermodynamic equilibrium
23 p4238 A69-41435

Mass diffusion and heterogeneities in compression chamber gas mixture in shock tube ascribable to pressure and temperature gradients
23 p4146 A69-41547

Binary gas mixtures transport coefficients approximated by self consistent matrix procedure based on Chapman-Cowling expressions
24 p3452 A69-43135

Heat and mass transfer in gas suspension, studying suspended particles effects on heat transfer by irreversible thermodynamics [ASME PAPER 69-HT-34]
24 p4410 A69-43528

GAS PHASES
U VAPOR PHASES

GAS POCKETS

Gas bubble formation in Ti welding associated with gas nuclei in metal, molten dwell time, gas diffusion coefficients, joint edge conditions, etc
11 p1892 A69-25669

GAS PRESSURE

Electric discharge in gas flow with magnetic field, showing varying charged particle density as function of argon-cesium pressure
02 p0285 A69-11570

Plasma stability under anisotropic pressure in axisymmetric magnetic fields determined by quasi-hydrodynamic approximation
02 p0291 A69-12552

Dilatometer for measuring thermal expansion of solid bodies over temperature range at various gas media pressures
03 p0432 A69-14151

Increasing vortex tubes energetic cooling efficiency for cooling aircraft components by using potential energy of gas emitted from tubes
04 p0684 A69-14488

Ion current output vs gas component partial pressure determined to measure ion source efficiency employing electron impact ionization
06 p0960 A69-16919

Gas laser operation at high pressures, examining threshold pumping and power output dependence on pressure to optimize parameters
06 p0934 A69-17680

Ion laser emission cessation with increasing pressure, magnetic field and current strength due to lower transition level lifetime increase
06 p0934 A69-17682

Dense gas effects in free piston hypersonic wind tunnel, discussing Longshot facility, free piston cycle, reservoir conditions decay and hypersonic nozzle flow [AIAA PAPER 69-169]
06 p0907 A69-18188

Gas pressure control in xenon lasers, using variable temperature surface partially insulated from liquid nitrogen coolant
07 p1155 A69-19090

Electron acceleration in microtron through injection from low pressure gas discharge plasma
08 p1279 A69-19803

Monograph on heat transfer coefficients of polystyrene foams noting contribution of gas conduction, convection and radiation to total heat transfer
08 p1421 A69-20716

Gas pressure variations behind autonomous stable detonation fronts in propane-O mixtures, noting effect of diameter tubes and initial pressures
08 p1421 A69-20757

Stimulated Mandelstam-Brillouin scattering in compressed N and H as function of pressure, using ruby laser pulses
09 p1516 A69-21562

Neon discharge positive column at medium gas pressures, discussing calculated and experimental data concerning diffusion theory to interpret parameters
10 p1740 A69-23723

Nitrogen, oxygen and air luminescence spectra excited by fast electrons at low gas pressures in IR spectral region compared with polar auroral spectra
10 p1687 A69-23916

Gases effect on electrical conductivity of vacuum deposited thin films of Cr, Be, Ni, Au and Ge at different thickness and low pressure
12 p2143 A69-26460

Flow models for externally pressurized gas bearings, discussing pressure distributions, load capacity and flow rate [ASME PAPER 68-LUBS-2]
13 p2267 A69-27285

Copper and aluminum fatigue in vacuum and ultrahigh vacuum, discussing effects of hydrogen, nitrogen and oxygen pressures
13 p2280 A69-28088

Constant density heating upstream and constant pressure cooling downstream formulas for radiating shock waves
13 p2249 A69-28240

Electromagnetic field induced plasma oscillation amplitude dependence on field frequency as function of field amplitude and discharge current at low N pressures
13 p2313 A69-28332

Frequency shifts of Lamb dip minimum in helium-neon laser, considering effects of discharge tube parameters and gas pressure
14 p2457 A69-28929

Gas compressibility influence on laminar to turbulent boundary layer transition determined using Taylor hydrodynamic finite perturbation model
14 p2389 A69-28974

Neutral gas pressure in positive column plasma between two coaxial insulated cylinders as function of cylinders radii
14 p2490 A69-29036

Work function changes of tungsten single crystals as function of oxygen and CO gas pressure at high temperatures, using emission microscope
14 p2506 A69-29272

Plasma stability under anisotropic pressure in axisymmetric magnetic fields determined by quasi-hydrodynamic approximation
15 p2658 A69-30249

Gas barrier seal design producing varying unit loading on conventional contact seal faces, including geometric stability and test results [ASLE FICFS PREPRINT 26]
15 p2621 A69-30495

Leakage in mechanical face seals with hydrodynamic films, noting misaligned seal theories for pumping with cavities and two fluids [ASLE FICFS PREPRINT 19]
15 p2621 A69-30497

Pressure and wavelength dependence of molecular O absorption coefficient near 1215 Å, utilizing UV emission from crossed beam atomic collision
15 p2656 A69-31031

Final states of density, velocity and pressure in gas, comparing states reached after transition through single oblique hydromagnetic shock and two successive shocks
15 p2664 A69-31217

Conditions behind incident and reflected shock waves in shock tube calculated from initial pressure, density, temperature and shock speed
15 p2593 A69-31487

Interstellar cloud models, considering gas pressure, cosmic ray flux, magnetic field values, etc
16 p2853 A69-31599

Ammonium perchlorate sublimation models, discussing low temperature decomposition influence on pressure dependence of sublimation rate [WSCF PAPER 69-22]
16 p2832 A69-32360

Hydrogen-oxygen ion exchange membrane fuel cells for sounding balloons, discussing flight duration and power requirements, gas supply pressure effects, etc
16 p2738 A69-32413

Gas pressure differential across multilayer insulation blanket during rapid evacuation predicted, using one dimensional flow theory [AIAA PAPER 69-608]
17 p3072 A69-33275

Quantitative IR spectral emissivity measurements of NO between 300-800 K made in absorption, correlating observed absorbance with optical path length and gas pressure
17 p3009 A69-34156

Electron current flow from metal target in gas due to laser radiation, showing increased dependence on gas pressure
18 p3152 A69-35124

Water vapor absorption at submillimeter wavelengths in atmospheric window regions related to foreign gas pressure, using HCN maser
18 p3152 A69-35241

Two dimensional unsteady motion of medium with pressure as linear function of density, analyzing gas expansion into vacuum
20 p3512 A69-36916

Supersonic molecular beam relative intensity represented as function of nozzle to collimator distance and gas admission pressure
20 p3579 A69-37432

Temperature and pressure relations in power plant with closed gas cycles with radiative heat transfer, noting radiation area reduction influence
20 p3464 A69-37603

Monograph on forces exerted by air during yawing motion of sharp cones in supersonic and hypersonic flows by semilinear method
20 p3460 A69-37919

Nomograph for rapid estimation of pressure drops across orifices in pneumatic systems using real gas data with illustration for nitrogen
20 p3467 A69-38186

Ammonium chloride thermal decomposition by measuring formed noncondensable gas pressure and weight loss in solid state kinetic investigation
21 p3669 A69-38800

Design features comparison and operation principles of gas strain gauges in application to structures, emphasizing independence of temperature variations in pneumatic circuits
21 p3725 A69-39324

Laser induced multiphoton ionization and cascade breakdown in high pressure gases, considering roles of

refractive index, laser nonideal output and beam self focusing
21 p3738 A69-39445

P-V-T surface of fluids in critical region by dielectric measurements, presenting saturation densities of oxygen [NAS-NRC PAPER H-5]
22 p4050 A69-40623

Creep strength as function of oxygen pressure for Ni at 510 and 600 C, dropping creep rupture life to plateau of nearly constant life
23 p4176 A69-41504

Amplified radiation of laser used for coherent optical pumping in two level low pressure gas laser
24 p4327 A69-43067

GAS REACTORS

Adiabatic stirred reactor, discussing steady state nonlinear equations of reactant gases combustion
02 p0352 A69-12316

GAS-SOLID INTERFACES

Spatial and kinetic distributions of molecules reflected by surface in rarefied atmosphere, discussing mathematical model
01 p0122 A69-10041

Cryogenic expansion to pressures below triple point and resulting formation of solid-vapor mixtures, discussing flow and heat transfer characteristics in heated tubes
01 p0176 A69-11146

Interaction of rarefied gas with solid surface, analyzing accommodation coefficients, energy and impulse exchange as function of atomic bulk size
04 p0632 A69-14991

Surface roughness influence on interaction between gas flow and solid surface for case of diffuse and specular reflection, noting role of inclination angle
06 p0910 A69-17342

Gas adsorption on solids, discussing statistical mechanical theory assuming localized adsorption for first adlayer and nonlocalized mobile layer adsorption on top
06 p0980 A69-17387

Concentration changes in binary metal-gas solutions during simultaneous degassing kinetics and metal evaporation
09 p1528 A69-22732

Particle volume role in normal shockwave structure in gas-particle mixtures, discussing equations of motion formulation
13 p2244 A69-27327

Gas-surface interaction for trapping and energy exchange, comparing continuum and discrete lattice models for solids
14 p2409 A69-29092

Transonic ideal gas flow past semiinfinite bodies, determining flow potentials from body perturbations and surface boundary conditions
14 p2390 A69-29476

Chemical reaction between combustible solid fuel surface and oxidizer-containing gas in space capsule
16 p2877 A69-31896

Temperature field in plate heated at one end and situated in solidifying gas, leading to gas layer formation by sublimation
16 p2878 A69-31957

Temperature jumps at gas-solid interface in shock tube calculated by one dimensional approximation of thermal boundary layer behind reflected shock wave
17 p2949 A69-33023

Thermal accommodation coefficients determination, comparing techniques based on free molecule flow heat flux data
18 p3230 A69-35071

Sublimation of various compressed naphthalene wind tunnel models analyzed in supersonic air flow, discussing effects of temperature and model configurations
18 p3231 A69-35121

High energy neutral molecule beam for gas-surface interaction studies generated in electron bombardment ion source
19 p3376 A69-36176

Low and moderate energy gas molecule-solid surface interactions, using molecular beams
19 p3376 A69-36177

Gas molecules scattering by solid surface for monoenergetic and Maxwellian beams, discussing model with different values for magnitude and velocity direction
19 p3377 A69-36181

Autocorrelation function for unsteady temperature and stress fields in bar located in gas stream leaving combustion chamber
19 p3440 A69-36685

Physical state changes, chemical reactions, gaseous diffusion in solids and solid-gas interactions in vacuum, considering saturated vapor pressure, condensation, evaporation, etc

20 p3576 A69-37408

Destructive interaction of refractory carbides and graphite compositions with chemically active high temperature gas streams

21 p3751 A69-38640

Gases effects on UV irradiated thermal control materials spectral reflectance, discussing tests and photolysis mechanisms [AIAA PAPER 69-1025]

22 p3923 A69-40395

GAS SPECTROSCOPY

Successive explosions produced two gas systems observed in six Seyfert galaxy nuclei by spectrophotometry, using diffraction spectrographs

12 p2164 A69-27022

Atmospheric IR spectra determination from transmission functions overlapping effects of atmospheric gases

16 p2814 A69-31792

Shock tube application to transition probability measurements with emphasis on thermodynamic state of radiating gas, noting temperature dependence of level population

18 p3176 A69-34446

Metallic aerosol generator application in shock tube spectrometric measurements of radiation by molecules occurring as solids before decomposition to vapor phase

18 p3099 A69-34461

Spectroscopic measurements of weakly ionized Ar plasma premixed with diatomic N in plenum chamber, demonstrating role of competitive reactions for metastable Ar atom

21 p3779 A69-39794

GAS STREAMS

Laminar mixing of two semiinfinite parallel streams, deriving equations and boundary conditions by applying perturbation technique

05 p0744 A69-15714

Jet perpendicular penetration prediction from holes or tubes, discussing resultant gas stream mixing and temperature profiles [ASME PAPER 68-WA/GT-8]

05 p0750 A69-16143

Approximate solution for turbulent jet expansion in opposing stream, discussing hydraulic drag coefficient formula derivation

07 p1118 A69-18396

Streaming gas effect on carbon dioxide-nitrogen-helium laser power, discussing gas renewal phenomenon and evacuation rate

07 p1145 A69-18476

Heat transfer to wedge in nearly free-molecular hypersonic flow of strongly rarefied gas

07 p1050 A69-18707

Streamer based on model of perfectly conducting plasma produced on boundaries by entering and departing electrons, discussing streamer thickness and propagation velocity

11 p1935 A69-25759

Rotating central disk in galactic plane observed by radio telescope, assessing relation between expanding gas of disk and high velocity stream from center

12 p2163 A69-27018

High gas stream temperature levels and distributions from transient and intermittent probe measurements

15 p2612 A69-31268

Aeroelastic nonlinear panel stability in supersonic gas stream, defining hazardous conditions of critical flutter boundary

15 p2716 A69-31549

Finite difference method for turbulent mixing and combustion of hydrogen injected parallel to supersonic air stream, considering vitiated and unvitiated air [AIAA PAPER 69-539]

16 p2877 A69-31844

Combustion of pure crystalline boron single particles injected into hot oxidizing gases streams at atmospheric pressure [AIAA PAPER 69-562]

16 p2880 A69-32741

High gas stream temperatures determination from short exposure probe based on inferring temperature from transient response of sensor

20 p3536 A69-37005

Rocket nozzle control by side forces produced by secondary gas stream injection observed for relationship with inclination angle to nozzle axis

20 p3457 A69-37065

Gas concentration measurement during injection into laminar boundary layer streaming along porous plate, using quadrupole resonance mass spectrometer

23 p4058 A69-41695

Contraststreaming self gravitating gas streams stability taking into account thermal conduction and radiation effects

24 p4388 A69-43638

GAS TRANSPORT

Heat transfer between concentric cylinders at different temperatures measured for argon, neon and helium

01 p0177 A69-11403

Diatomic dissociating gas free atoms virial coefficient used to study thermodynamic properties and transport coefficients of gases

02 p0283 A69-11574

Diffusion coefficients for oxygen transport in whole blood, discussing effects of intact red cell concentration

02 p0200 A69-12479

Thermodynamic analysis of refractory compounds vapor transport conditions, illustrating integral free energy diagrams

03 p0453 A69-13619

Water and heat removal unit for hydrogen/oxygen fuel cell systems, discussing temperature distribution, heat and liquid transport

05 p0704 A69-15676

Gas kinetics application to various flow problems by solving Boltzmann equation for monoatomic single component gas

08 p1351 A69-20708

Transport coefficient density expansions obtained from time correlation functions in moderately dense gas with short range repulsive intermolecular forces

14 p2540 A69-29469

Atmospheric hydrogen and helium atoms emission in geomagnetic poles and winter hemisphere, comparing thermal dissipation and migration of light atoms

15 p2599 A69-31322

Column method of measuring thermal conductivity of CO and oxygen in 350-1500 degrees K temperature range, discussing error sources and data reliability [AIAA PAPER 69-603]

17 p3073 A69-33298

X ray absorption in surrounding gas sphere as function of continuous absorption, electron scattering and diffuse ionizing radiation, using radiative transfer theory

18 p3186 A69-34296

Transport processes effect in shock wave on hypersonic flow past blunt body in neighborhood of stagnant point, noting heat transfer

18 p3086 A69-34910

Hydrogen bulge above springtime pole indicated by Lyman alpha radiation in earth geocorona, discussing hydrogen horizontal transport and hydrogen compounds dissociation as causes

18 p3129 A69-34956

Chronic hypoxic hypoxia on oxygen-hemoglobin dissociation curve and respiratory gas transport in man, considering altitude residents and heart and lung diseased patients

21 p3650 A69-38383

Decompression research on inert gas transport in body, discussing solubility factors in decompression damage

21 p3655 A69-38913

Kinetic theory for macroscopic transport phenomena in N-component polyatomic gas mixtures with internal degrees of freedom under nonlocal thermodynamic equilibrium

23 p4238 A69-41435

Transport coefficients in neutral gases, discussing fundamental relations of parameters in viscosity, thermal conductivity and self, pressure and thermal diffusion

23 p4193 A69-41514

Oxygen and carbon dioxide transfer in membrane oxygenators, considering liquid dispersion and membrane diffusion limitations

24 p4279 A69-43799

GAS TUNGSTEN ARC WELDING

High strength steel welding with physical properties equal to parent metal, discussing gas tungsten-arc, electron beam and plasma arc techniques

01 p0088 A69-11399

Sheet steel composition effect on gas-tungsten arc welds porosity

04 p0607 A69-15219

Spot weld strength of tungsten inert gas spot welding on Al-Mg-Si sheets greater than resistance welding, noting crack formation during inert gas welding

05 p0769 A69-16538

TIG welding introduced residual stresses amplitude and distribution in Ti sheets, studying effects on mechanical properties [ASM PAPER GG8-6.2]

07 p1169 A69-19674

Roll planishing and thermal treatments effects on gas tungsten arc welded Ti-6Al-4V alloy on residual stresses, tensile, formability and fracture toughness properties

08 p1319 A69-19960

Weldability of precipitation-hardening stainless steels by gas tungsten arc process, discussing microstructure and shrinkage stress cracking

08 p1320 A69-20409

Welding current pulsation techniques for adaptive control of gas tungsten arc welding processes

09 p1508 A69-22334

Covered electrode, submerged arc, electroslag, gas metal arc, gas tungsten arc and plasma arc welding processes application to high strength steels

12 p2100 A69-25828

Microplasma, W inert gas and submerged arc welding processes for fabrication of rocket motor cases and pressure vessels, discussing material requirements and weldability [SBAC PAPER 7]

20 p3550 A69-37449

Porosity and inclusions effects on Al arc weld fatigue properties at ambient and cryogenic temperatures

24 p4331 A69-42940

GAS TURBINE ENGINES

NT BRISTOL-SIDDELEY OLYMPUS 593 ENGINE

NT DUCTED FAN ENGINES

NT J-79 ENGINE

NT J-85 ENGINE

NT T-53 ENGINE

NT TURBOFAN ENGINES

NT TURBOJET ENGINES

NT TURBOPROP ENGINES

Protective coatings for gas turbine engine components in marine environments, considering corrosion of diffuser, impeller, compressor case and turbine blades

01 p0099 A69-11057

Aircraft gas turbine compressor parts erosion tests

01 p0099 A69-11058

Steam ingestion tests on carrier aircraft gas turbine engines, analyzing inlet pressure and temperature distortion in steam-air environment

01 p0143 A69-11062

Pneumatic pressure ratio sensing element and associated high pressure switches and amplifiers for gas turbine engine control systems

02 p0249 A69-12088

Aircraft gas turbine component pressure data storage and scanning

05 p0726 A69-16768

Transpiration air cooled blading to test and design small gas turbine at 2500 F inlet, discussing cascade and full stage component [SAE PAPER 690035]

07 p1203 A69-18310

Control methods and designs for limiting atmospheric pollution emitted by aircraft gas turbine engines [SAE PAPER 680347]

07 p1204 A69-19729

Aircraft gas turbine engines control systems capabilities and future requirements, considering maximum propulsion system performance with minimum fuel consumption [ASME PAPER 68-GT-62]

08 p1376 A69-19846

Flame burnout of atomized hydrocarbon fuel in gas turbine combustion chambers as function of ratio of time to total burnout time

08 p1420 A69-19999

Composite materials and alloys for jet turbine components in 1970s, discussing anticipated temperatures and material properties

09 p1523 A69-22061

Hollow turbine disks for provision of coolant to high performance aircraft gas turbine engines, fabricating disk in two axial halves

09 p1509 A69-22345

Supersonic axial compressor boost stages for small gas turbine engines, using passage flow approach and passage criteria to design airfoils [ASME PAPER 69-GT-44]

09 p1570 A69-22478

Gas turbine engines control and fuel systems integration, considering weight reduction [ASME PAPER 69-GT-49]

09 p1571 A69-22483

Vane type fuel pump designed for small gas turbine engines, describing design analysis and laboratory evaluation [ASME PAPER 69-GT-45]

09 p1513 A69-22485

Transpiration cooling effect on turbine stator blade performance determined by annular cascade tests, using data to establish empirical correlation for loss coefficient [ASME PAPER 69-GT-39]

09 p1432 A69-22487

Potential usage of titanium in cast parts for gas turbine engines, emphasizing alloys development [ASME PAPER 69-GT-24]

09 p1513 A69-22494

Finite difference method computer programs for calculation of velocities and streamlines on blade to blade surface of revolution of turbomachine
[ASME PAPER 69-GT-48] 09 p1432 A69-22495

Fluidic overspeed sensor for small turboshaft power turbine, discussing requirements, circuit and system design, packaging, reliability and maintainability
[ASME PAPER 69-GT-17] 09 p1571 A69-22500

Miniature fluidic oscillator temperature sensors evaluated in gas turbine engine nozzle, discussing temperature control and related signal error compensation and temperature averaging
[ASME PAPER 69-GT-70] 09 p1572 A69-22512

Gas bearings for spool gas generator for aircraft turbine engines, noting rotor bearing stability and LP spool balancing and seal leakage
[ASME PAPER 69-GT-60] 09 p1513 A69-22515

Engine usage indicator to cumulate small gas turbine engine exposure to certain deterioration, presenting circuit logic block diagram
[ASME PAPER 69-GT-69] 09 p1572 A69-22519

Radial inflow gas turbine engine performance testing, discussing instrumentation, recording systems and calibration techniques
[ASME PAPER 69-GT-104] 09 p1501 A69-22522

Compressor to inlet distortion tolerance design techniques for gas turbine compressors, noting rotor matching, blade chord length, blade geometry, etc
[ASME PAPER 69-GT-115] 09 p1572 A69-22525

Rolls Royce Spey engine combustion system development, emphasizing carbon formation, exhaust smoke, fuel injection, increased area interconnector, and overheating
09 p1573 A69-22613

Gas turbine engines smoke emission, considering smoke measurement, flame structure, carbon production, pressure effects fuel-air ratio, etc
09 p1573 A69-22622

Gas turbine engine development data system based on test stands subsystems and central computer
10 p1660 A69-23284

Bearing deposition test for evaluating degradation characteristics of aircraft gas turbine engine lubricants
10 p1700 A69-24070

Onboard gas turbine auxiliary power units for executive jet transport aircraft
[SAE PAPER 690332] 11 p1824 A69-24501

Gas turbine propulsion engines for small single engine helicopters, discussing costs, performance and FAA tests
[SAE PAPER 690310] 11 p1942 A69-24513

Gas turbine disk calculation and plastic flow theory, considering loading conditions and elastoplastic strains due to centrifugal forces and nonuniform heating
11 p1982 A69-24945

Gas turbine fuel and control systems for two and three shaft engines in military and civilian aircraft including helicopters
[IME PAPER 12] 12 p2147 A69-25796

Control methods and designs for limiting atmospheric pollution emitted by aircraft gas turbine engines
12 p2147 A69-26236

Gas turbine engine shaft face seal with self acting lift augmentation preventing rubbing contact, noting disadvantages of labyrinth and conventional seals
[ASLE FICFS PREPRINT 27] 15 p2621 A69-30492

Aircraft gas turbine parts design and fabrication, discussing role of welding techniques
15 p2629 A69-30928

High temperature radial turbine design for small gas turbine engines, discussing aerodynamic, structural and thermal analyses
[AIAA PAPER 69-524] 16 p2838 A69-32662

Scale models of M-1 rocket engine oxygen and hydrogen pump driven two stage turbines used to determine performance and compact inlet manifolds problems
[AIAA PAPER 69-553] 16 p2840 A69-32678

Gas turbine engine compressor system dynamic representation by one dimensional mathematical model
[AIAA PAPER 69-486] 16 p2842 A69-32697

Injection film cooling effect on surface heat transfer downstream of flush nontangential injection holes and slots in turbine applications
[AIAA PAPER 69-523] 16 p2843 A69-32703

High bypass ratio engine influence on short range civil aircraft design, considering performance, noise, engine location, etc
17 p2897 A69-33212

Gas turbine engines smoke reduction, aerated fuel sprays for smoke control on engine design and factors affecting visibility of exhaust plumes
17 p3020 A69-33350

Holography application in gas turbine components stress and vibration analysis, discussing techniques and apparatus usable by nonspecialist and measurement accuracy
17 p2974 A69-33351

Gas turbine components life prediction, using Weibull distribution and Bayes theorem to estimate probability of crack initiation
19 p3394 A69-36004

Aerated fuel spray effect on smoke reduction from high pressure ratio aircraft gas turbine engines, including smoke measurement and visibility
19 p3395 A69-36770

Boron fiber reinforced Al matrix composite material for high performance aircraft gas turbine engine compressor blading
[AIAA PAPER 68-1037] 20 p3586 A69-37153

Airbreathing gas turbines construction materials including composites and Ti and austenitic alloys
[ASME PAPER D8-25.2] 20 p3586 A69-38133

Gas turbine compressor blade buckling during blade fabrication by hydraulic pellet jet technique eliminated by controlling working pressure of jet
21 p3731 A69-38879

Superalloy technology applications to gas turbine engines
21 p3785 A69-38928

Aircraft gas turbine engine lubricant evaluation and systems design from standpoint of effective oil life and lubricant stability requirements
[SAE PAPER 690424] 23 p4200 A69-41648

Dynamic simulation for gas turbine engine components design to assure stable operation and rapid response characteristics
[SAE PAPER 690386] 23 p4200 A69-41655

Large fan blade design, discussing aerodynamic design and rig test program supporting fan definition
[SAE PAPER 690387] 23 p4200 A69-41656

Dynamic hot corrosion rig test for operating environment and alloy composition effect on sulfidation attack during gas turbine fuel combustion
23 p4150 A69-42448

Thermochemical analysis of hot corrosion during sulfidation-oxidation of superalloy gas turbine engine components using Pourbaix method
23 p4178 A69-42449

Blade and vane wall thickness measurements test methods for gas turbine engine using ultrasonic gage and thermoelectric comparator
24 p4312 A69-42753

Gas turbine engine problem causing component failures, considering alternative replacement strategies
24 p4318 A69-42774

GAS TURBINES

Heat transfer in cooled portion of air gas flow area of high temperature gas turbines
03 p0495 A69-12957

Centrifugal force field influence on heat exchange between gas and blade cascade studied with noncooled blades at low temperatures
03 p0531 A69-12959

Gas turbine alloys composition role in high temperature corrosion resistance under high sulfur diesel fuel combustion
03 p0444 A69-13309

Orifice compensated hydrostatic face seal under pressure and thermal loading for aircraft gas turbine
[ASME PAPER 68-WA/LUB-6] 05 p0768 A69-16131

Small aircraft gas turbine regenerators employing heat pipes, noting excessive cost and weight
[ASME PAPER 68-WA/GT-7] 05 p0812 A69-16142

Gas turbine exhaust silencer performance correlated in laboratory and in service
[ASME PAPER 68-WA/GT-9] 05 p0812 A69-16144

Heat transfer performance of porous nozzle blade cascade represented by two dimensional mathematical model
05 p0812 A69-16400

High turbine inlet temperature technology using thermosiphon cooling for gas turbine, possibly doubling specific horsepower of aircraft
[SAE PAPER 690034] 07 p1203 A69-18311

Material design problems in small gas turbines, discussing engine performance sensitivity, thinness of rotor-blade and stator-vane trailing edges, dimensional tolerances, etc
[ASM PAPER D8-16.2] 07 p1204 A69-19668

Fluidic devices for closed loop control of gas turbines
[AGARDOGRAPH-118] 08 p1258 A69-20956

Deformation processing of superalloy gas turbine components, studying ingot characteristics, alloy segregation effect and thermomechanical properties
[SAE PAPER 690101] 09 p1503 A69-21557

Noncontacting torque meters using magnetoelastic properties of steel shafts, discussing gas turbine and industrial applications
[ASME PAPER 69-GT-64] 09 p1500 A69-22480

High temperature sensors for gas turbines, discussing thermocouples and radiation pyrometer to sense turbine hardware
[ASME PAPER 69-GT-30] 09 p1501 A69-22492

Gas turbine blade materials after long term service, analyzing tensile, impact and stress rupture properties and microstructure
[ASME PAPER 69-GT-12] 09 p1527 A69-22503

Nickel base superalloys for aircraft gas turbines, considering strengthening mechanisms for creep resistance
[ASME PAPER 69-GT-7] 09 p1527 A69-22506

Titanium-boron composites for gas turbines, mechanical properties and service life in high temperature environment
[ASME PAPER 69-GT-1] 09 p1527 A69-22510

Combustion in advanced gas turbine systems - Conference, Cranfield, Bedfordshire, England, April 1967
09 p1624 A69-22611

Combustion chamber design for advanced gas turbines, noting influence of fuel air mixing and air flow distribution
09 p1573 A69-22612

Gas turbine combustion control at high pressure, considering mixing, fuel evaporation, spray penetration and cone angle
09 p1625 A69-22620

Digital computer programs for aerodynamics of subsonic gas turbine combustion systems applicable to incompressible flow with specified flow boundaries, noting vortices distribution
09 p1573 A69-22621

Film cooling injection slots number and position over flame tube and minimum cooling airflow in aircraft gas turbines
09 p1625 A69-22623

Off design performance prediction method for radial inflow turbines compared with experimental results for small turbine and Brayton space power plant
10 p1754 A69-23891

Gas turbine blade vibrations, discussing excitation causes and damping techniques
[ASME PAPER 69-VIBR-59] 10 p1805 A69-24155

Thermodynamic cycle analysis of various gas turbines and air breathing propulsion systems noting regenerators, heat exchangers and pulsejet engine
11 p1943 A69-25584

Aerodynamic design of axial flow compressors and turbines, using aerothermodynamic equations for compressible flow analysis
11 p1821 A69-25585

Control technology advancement effects on gas turbine design and application, integrating control scheme, modularization and commonality, system design and energy input and load control
12 p2146 A69-25786

Radial gas turbine design and performance including nozzle and rotor loss, mechanical and thermal stresses and manufacturing methods and materials
[IME PAPER 7] 12 p2146 A69-25787

Gas turbine combustion chamber design factors including combustion volume, burning zone, dilution zone, pressure drop, fuel preparation, injection and ignition, exhaust smoke, etc
[IME PAPER 3] 12 p2146 A69-25789

Gas turbine centrifugal compressor design considerations for impellers and diffusers, including blade loading and pressure gradients determination and aerodynamics
[IME PAPER 1] 12 p2146 A69-25790

Fabricable materials with low plastic deformation for gas turbine components, noting strength vs temperature for alloys, fiber composites and ceramics
[IME PAPER 8] 12 p2147 A69-25791

Tubular gas turbine combustion chamber design for optimum mixing performance using flow and mixing data of cold air injection into hot gas stream
[IME PAPER 15] 12 p2147 A69-25793

Small gas turbine Brayton cycle analysis treating component efficiencies as dependent variables in examining single stage radial compressor and turbine aerodynamic configuration
[IME PAPER 5] 12 p2147 A69-25794

GAS VALVES

Cast high temperature alloys for gas turbine components, discussing production, temperature capability, composition, oxidation, hot corrosion and weldability [IME PAPER 10] 12 p2147 A69-25795

Chemical composition of cermet material for radial sealing of high temperature gas turbines, ensuring structural stability and oxidation resistance 13 p2275 A69-27344

Temperature measurement for aircraft gas-turbine engine development 14 p2509 A69-28886

Error analysis in efficiency measurement of gas turbines, considering thermodynamics and power output 14 p2509 A69-29509

Bladed disk assemblies vibrational properties, discussing dynamic characteristics of system with pairs of close natural frequency modes under forced vibration 15 p2704 A69-30304

Airborne particle size influence on gas turbine parts erosion, with attempts to relate to filtration and engine life 16 p2794 A69-32026

Axial gas turbine efficiency and work functions, discussing turbine using isothermal high velocity combustor 16 p2837 A69-32064

High temperature radial turbine design for small gas turbine engines, discussing aerodynamic, structural and thermal analyses [AIAA PAPER 69-524] 16 p2838 A69-32662

Combustion and exhaust losses in gas turbines, recommending pulsating combustion for increased useful energy 17 p3021 A69-33360

Optimum efficiency of turbines with small volumetric flow rate, determining height of air-gas flow, partial admittance and flow angle in clearance 18 p3184 A69-34983

Working fluid flow parameters compensation by expelled cooling air in air-gas flow area of turbine stage 18 p3184 A69-34985

Gas turbine areas calculation of through flow cross sections for temperature deformations and blades elongation 18 p3184 A69-34987

Steady state thermal problem of gas turbine hyperbolic profile disk equipped with bandaged blades, solving thermal balance equations 18 p3184 A69-34992

Co base alloy for gas turbines, discussing microstructure, creep, oxidation resistance and hot corrosion properties 18 p3158 A69-35421

Soviet monograph on turbines and jet nozzles for two phase flows covering gas-particle velocity and temperature differences, turbine design, etc 20 p3586 A69-38209

Monograph on control dynamics of gas turbines with adjustable guide vanes, using methods of control theory and applied mathematics 21 p3784 A69-38449

Film vaporizing gas turbine combustor design including performance tests and combustion physics 21 p3784 A69-38607

Cooling air from blades discharged into flow-through part of gas turbine, examining gas mixing with air from blade and effect on turbine efficiency 21 p3785 A69-39090

Natural convective heat transfer to gas turbine rotor blade and thermal resistance of cooling system using centrifugal pump 21 p3785 A69-39103

Holography applied to stress and vibration analysis of gas turbine blades, disks and small components 22 p4040 A69-39960

Computerized design of potassium vapor turbine with supersaturation effects compared with equilibrium flow turbine design 23 p4187 A69-42251

GAS VALVES

Two way pyrotechnic high pressure gas valve for D2 satellite, noting resistance to leakage due to nearly monolithic construction 10 p1635 A69-23033

Controllable sonic flow orifice, discussing mass flow rate, area and upstream stagnation pressure 10 p1693 A69-23343

Protective filter for inspiration valve of oxygen masks in high performance aircraft, reducing respiratory volume exchange with given pressure amplitude 17 p2916 A69-33773

Valving concepts and functional approaches for inert gas attitude control thruster systems providing redundancy safeguards at minimum weight, volume and power costs [AIAA PAPER 69-843] 21 p3786 A69-39373

GAS VISCOSITY

Vertical propagation of acoustic waves in atmosphere without gravitational waves and with height varying atmospheric shear viscosity 02 p0274 A69-11440

Axissymmetric hypersonic flow of model gas over slender bodies with strong viscous interaction and shock wave extended to power law viscosity variation 05 p0744 A69-15720

Viscosity of compressed nonreacting gas mixtures at high temperatures, discussing conditions for accurate calculation 05 p0845 A69-15895

Law of corresponding states applied to temperature dependence of viscosity of rarefied gases 06 p0957 A69-16918

Magnetic field generation in nonuniformly rotating plasma by current density from electron drift relative to positive ion gases due to viscous forces 06 p1009 A69-17966

Viscosity coefficients approximation for chemical compositions in chromosphere and coronal gas 09 p1602 A69-22217

Stability of slow combustion in viscous gas mixture, showing viscosity as principal stabilizing factor 11 p1999 A69-24554

Hydrogen viscosity temperature dependence at constant density below room temperature 11 p2003 A69-25704

Simple fluids viscosity dependence on density analyzed by molecular theory, exemplifying with liquid argon 13 p2299 A69-28036

Gas visco seals performance analyzed for continuum flow regime, noting coefficient agreement with laminar flow analysis [ASLE FICFS PREPRINT 34] 15 p2621 A69-30494

Viscosity, thermal conductivity and diffusion predicted for dilute nonpolar, polar and mixed gases, discussing methods for rotational relaxation collision numbers and resonant correction 21 p3850 A69-38951

GAS WELDING

NT BRAZING

NT LOW TEMPERATURE BRAZING

Narrow gap gas metal arc welding process in spray transfer range for narrow welds in thick plates, discussing equipment and applications 11 p1891 A69-24930

Rare earths additives effects on arc instability and weld puddle fluidity of stainless steel bare wire electrodes 12 p2103 A69-26623

GASEOUS CAVITATION

U CAVITATION FLOW

U GAS FLOW

GASEOUS DIFFUSION

Diffusional, thermal diffusional and thermal fluxes in multicomponent flames, discussing flame structure and reaction kinetics 01 p0175 A69-10144

Boron diffusion in silicon, using nitrogen carrier and boron trichloride diffusant at high temperature for determination of critical oxygen flow rate 02 p0297 A69-11994

Chemical reaction scheme effect on hot zone structure of hydrogen-oxygen diffusion flame, considering influence of hydroxyl radical 03 p0531 A69-12895

Ultrasonic sounding for controlling dispersed gas phase in liquid pipelines under laboratory and practical conditions 04 p0596 A69-14489

Mathematical analysis of oxygen diffusion to coal grains during coal dust combustion, evaluating kinetic constants by burning time 04 p0687 A69-15167

Porous gas diffusion electrodes design for electrochemical energy converters, noting contribution of theory of electrode kinetics 04 p0551 A69-15309

Hemoglobin diffusion influence on oxygen uptake and release by red cells solved by calculus of finite differences 05 p0707 A69-15677

Diffusion and thermal diffusion in mixture of Maxwellian gases, analyzing Onsager reciprocity relations 05 p0849 A69-16461

Tantalum diffusion layer on refractory cobalt and nickel base alloys analyzed by electron microprobe [ONERA-TP-665] 06 p0941 A69-17097

Oxygen diffusion parameters in beta-titanium measured by successive layer removal, noting lattice constant dependence on temperature 07 p1163 A69-18783

Ellipsoidal gas bubble dissolution in low viscosity fluid, discussing rate of steady motion, deformation degree and diffusion rate 07 p1120 A69-18990

Kinetic theory development of equations for multicomponent gaseous mixtures symmetric diffusion coefficients 07 p1186 A69-19395

Electrochemical characteristics of lateral diffusion gas electrodes for fuel cells, noting electrodes fabrication by pulverizing on nickel sheet 08 p1260 A69-21044

Fuel cell system using double skeleton catalyst gas diffusion electrodes, discussing design, mode of operation and performance 08 p1261 A69-21047

Deuterium escape in Venus upper atmosphere to explain anomalous Lyman-alpha glow observed by Mariner 5 [SRCC-91] 09 p1594 A69-21696

Rarefied gases back diffusion between parallel plates used for studying diffusion in capillaries, deriving volume flow equation valid for any density 10 p1677 A69-22903

Annealing effects on titanium oxidation kinetics, indicating no relation between oxide formation and diffusion anisotropy of oxygen 12 p2112 A69-26039

Ammonia gas diffusion from line source in turbulent boundary layer, discussing concentration profile discrepancy due to eddy diffusivity and plume shear 13 p2250 A69-28343

Diffusion equation unsteady solution for flasks of equal volumes connected by capillary, considering end effect and transient processes 13 p2251 A69-28561

Ionic diffusion in topside ionosphere analyzed using multiple gas mixture diffusion formula, noting Coulomb ionic collision role 14 p2441 A69-29381

Inert gas diffusion of Xe 133 in aluminum and titanium at various temperature ranges, showing effects of recrystallization, plastic deformation and phase transformations 16 p2800 A69-31775

Airstream parameters /temperature and velocity/ of turbulence intensity in jet core at tube exit and behind grids measured by He diffusion method 16 p2771 A69-31959

Turbulent heat and mass diffusion in catalytic reactors for hydrazine decomposition, developing computer program to calculate temperature and reactant concentration distributions [AIAA PAPER 69-421] 16 p2846 A69-32768

Gaseous diffusion coefficients during argon, krypton, oxygen and nitrogen diffusion into helium measured by gas chromatography 18 p3099 A69-34280

Diffusion processes during formation of coatings by condensation 20 p3549 A69-37365

Diffusion processes, composition and structure of vapor deposited Ni coatings on Nb substrate, plotting intermetallic compounds growth against temperature 20 p3560 A69-37366

Physical state changes, chemical reactions, gaseous diffusion in solids and solid-gas interactions in vacuum, considering saturated vapor pressure, condensation, evaporation, etc 20 p3576 A69-37408

Viscosity, thermal conductivity and diffusion predicted for dilute nonpolar, polar and mixed gases, discussing methods for rotational relaxation collision numbers and resonant correction 21 p3850 A69-38951

Turbulent Schmidt number as function of ratio between turbulent and molecular kinematic viscosities for He, carbon dioxide and normal octane eddy diffusivities 21 p3852 A69-39432

Diffusion in biological systems by random walks with emphasis on gaseous diffusion in lung, noting probabilistic tree model 22 p3885 A69-40978

Hydrogen permeability in Pd alpha phase measured, coupling with grain size measurements for grain boundary to bulk diffusivity ratio 23 p4175 A69-41502

Transport coefficients in neutral gases, discussing fundamental relations of parameters in viscosity, thermal conductivity and self, pressure and thermal diffusion

23 p4193 A69-41514

Mass diffusion and heterogeneities in compression chamber gas mixture in shock tube ascribable to pressure and temperature gradients

23 p4146 A69-41547

Steady state and time dependent concentration gradients in and around cells due to oxygen diffusion and depletion in radiobiology

23 p4090 A69-41966

Oxygen steady state transfer across thin layers of centrifuged erythrocytes at 37 degrees C before and after hemoglobin saturation with CO

23 p4093 A69-42064

GASEOUS FISSION REACTORS

Cavity reactor consisting of dilute fuel core surrounded by moderating reflector to attain very high temperatures in gaseous cores

07 p1179 A69-18954

Gaseous reactor fluid mechanics for nuclear rocket engines, discussing experiments on geometries used in open cycle engine for acceptable uranium loss rate [AIAA PAPER 69-477]

16 p2811 A69-32728

Plasma-dynamic forces used to suppress fuel-propellant interface turbulence in coaxial jet gas core reactors

24 p3439 A69-43679

GASEOUS ROCKET PROPELLANTS

High thrust fluorine engines and propellants

03 p0494 A69-12889

Thermal-chemical rocket based on thermal heating by energy input from nuclear fission process

03 p0496 A69-13666

Initiation of HF combustion oscillation in premixed gas rocket

[ISAS-430] 06 p1029 A69-17025

Sustained combustion initiation in subatmospheric gaseous fuel-oxidant mixtures by UV radiation at room temperature, measuring parameters as function of mixture pressure

[AIAA PAPER 69-88] 06 p0983 A69-18118

Rocket propulsion with gaseous bipropellant systems and attitude control

08 p1376 A69-20870

Gaseous reactor fluid mechanics for nuclear rocket engines, discussing experiments on geometries used in open cycle engine for acceptable uranium loss rate [AIAA PAPER 69-477]

16 p2811 A69-32728

GASES

NT ARGON
NT ARGON ISOTOPES
NT COLD GAS
NT COSMIC GASES
NT DIATOMIC GASES
NT EXHAUST GASES
NT FLAMMABLE GASES
NT GAS DISSOCIATION
NT GAS MIXTURES
NT GAS STREAMS
NT GRAY GAS
NT HELIUM
NT HELIUM ATOMS
NT HELIUM ISOTOPES
NT HIGH TEMPERATURE AIR
NT HIGH TEMPERATURE GASES
NT HYDROGEN
NT HYDROGEN PLASMA
NT IDEAL GAS
NT INTERPLANETARY GAS
NT INTERSTELLAR GAS
NT IONIZED GASES
NT LIQUEFIED GASES
NT LIQUID AMMONIA
NT LIQUID HELIUM
NT LIQUID HYDROGEN
NT LIQUID NITROGEN
NT LIQUID OXYGEN
NT LORENTZ GAS
NT MOLECULAR GASES
NT MONATOMIC GASES
NT NEON
NT NEON ISOTOPES
NT NONPOLAR GASES
NT POLAR GASES
NT POLYATOMIC GASES
NT RADON
NT RARE GASES
NT RAREFIED GASES
NT REAL GASES
NT RESIDUAL GAS
NT SOLIDIFIED GASES
NT XENON

Characteristic waves in gas-dielectric beamguides, calculating attenuation dependence on frequency

05 p0736 A69-16783

Thermal radiation properties of gases in thermodynamic equilibrium, discussing radiation resulting from electronic, atomic and molecular state transitions

11 p1998 A69-24460

Thermal conductivity relationship to heat transport coefficients for gases and liquids with charged or uncharged particles

23 p4237 A69-41324

GASKETS

Corrosion problems associated with electromagnetic shielding gaskets noting galvanic corrosion, corrosion prevention and insulation of gasket from mating surface

05 p0779 A69-15979

EMI-RFI knitted wire mesh gasket for corrosion prevention, noting use of moisture tight seal

09 p1523 A69-21895

GASTROINTESTINAL SYSTEM

NT INTESTINES
NT RECTUM
NT STOMACH

Space biomedical research trends, noting gastroenterology and lack of research on disease processes during space travel and overemphasis on space physiology

03 p0369 A69-12859

Transverse accelerations effect on dogs gastrointestinal tract secretory activity, noting central nervous system role

10 p1645 A69-23498

Gastric perfusion rate in restrained animals determined by Rb 86 clearance technique

17 p2908 A69-33170

Positive effect of shielding and cystamin administration on tonic and evacuator functions of rats gastrointestinal tract after gamma irradiation

22 p3877 A69-40285

EEG, ocular movements, gastric mobility and pH during human sleep from data transmitted by swallowed radio transmitter

23 p4093 A69-42063

Food-born diseases prevention in civil aviation, reporting gastroenteritis cases during flight

24 p4278 A69-43392

GATES [CIRCUITS]

NT THRESHOLD GATES

Gate current measurement of p-n junction during ultralow current operation of junction field effect transistor (JFET)

01 p0038 A69-10122

Space charge limited operation of insulated gate field effect transistors, discussing maximum transconductance and minimum parasitic capacitances

01 p0042 A69-10322

Universal NOR element design with resistors, determining permissible combinations for static mode of operation by computer method

01 p0037 A69-10746

Silicon nitride gate insulator in metal-insulator-silicon (MIS) devices, noting sandwich structures with thermally grown oxides removes limitations

02 p0299 A69-12244

Insulated gate tetrode with high drain breakdown potential and low Miller feedback capacitance, noting V-I characteristics

05 p0733 A69-16556

Junction gate field effect transistor design covering geometries and impurity profiles

06 p0893 A69-17197

Common source and common gate FET connections showing equivalent noise figures

13 p2227 A69-27237

Tunnel diode slideback sampling gate circuits, discussing response characteristics and operational specifications

13 p2236 A69-28538

Charge flow injection into MOS substrate attributed to gate pulses, correlating charge magnitude with pulse frequency

15 p2573 A69-30033

Linear high resolution gate function in blocking out analog signals or reproducing signal amplitudes at output, noting semiconductor elements utilization

15 p2581 A69-31523

Absolute value type of early-late gate bit synchronizer phase noise performance determined by Fokker-Planck method, comparing results with different circuits performance

19 p3270 A69-36246

PCM bit synchronizer models, discussing phase errors gate and differentiating devices

19 p3271 A69-36249

Current mode gates and flip-flops with subnanosecond propagation delay for integrated logic circuits, discussing memories dimensions, LSI arrays, etc

20 p3505 A69-37342

GAUGE INVARIANCE

Total energy-momentum interaction of system with mass defect in Wheeler-Feynman theory of electromagnetic interaction, demonstrating existence of gauge invariance

11 p1915 A69-24326

GAUSS EQUATION

Einstein equations solution in Gaussian coordinates describing particles gravitational fields including point particles

07 p1180 A69-18507

Discrete predicting filter optimal synthesis in terms of rms error by solving normal Gaussian equations

09 p1473 A69-21858

GAUSS-MARKOV THEOREM

Digital computer simulation of multidimensional stationary or nonstationary Gauss-Markov random processes with specified autocorrelation function, discussing time step choice

12 p2122 A69-26523

GAUSSIAN DISTRIBUTIONS

U NORMAL DENSITY FUNCTIONS

GAUSSIAN NOISE

U RANDOM NOISE

GAUSSMETERS

U MAGNETOMETERS

GAUZE

Two dimensional flow through nonuniform gauze by computerized analysis based on linearized theory

13 p2248 A69-28174

GC-130 AIRCRAFT

U C-130 AIRCRAFT

GCR [REACTORS]

U GAS COOLED REACTORS

GEAR TEETH

Failure causes for planetary reduction gear tooth for adjustment of radio telescopic antennas, studying fracture characteristics, working conditions and loading moments

08 p1321 A69-20853

Fatigue strength of highly loaded gears and stress measurements by strain gauges

[AHS PAPER 371] 17 p3060 A69-33517

GEARS

Differential gearing of aileron movements to reduce control forces in aircraft

03 p0367 A69-13786

Miniature ball and jewel bearings and gear lubrication in ultrahigh vacuum tests for space environment operation

[IME PAPER 6] 07 p1138 A69-18562

Three dimensional reinforcement composites for gear and bearing applications with improved interlaminar shear strength, thermal and wear properties

08 p1340 A69-20509

Fatigue strength of gears with integrally forged, cut and ground teeth, discussing pancake forgings

[SAE PAPER 680632] 08 p1321 A69-20732

Axial vibration effects on frictional losses in gear systems under dry friction or boundary lubrication conditions

[ASME PAPER 69-VIBR-15] 10 p1701 A69-24169

Heat treatable low alloy steels weldability for lightweight ultrahigh strength pressure vessels, gear and shaft fabrication in aerospace applications

12 p2100 A69-25827

Nondeformable closed contour spatial gear kinematics using matrix tensor method suitable for computer programming

15 p2713 A69-31020

Polyphenyl ether lubricants and self lubricating materials compared for antifriction ball bearings in thrust reversing actuator gear box

[SAWE PAPER 68-LC-1] 18 p3148 A69-35003

Controllable process for forming Ti-Ni intermetallic wear resistant coating on Ti alloys, discussing techniques, weight saving advantage, gear tests, etc

19 p3323 A69-35582

Dynamic stability of dual wheel gears for aircraft applications, discussing shimmy, tire characteristics, velocity effects, etc

[AIAA PAPER 69-769] 19 p3245 A69-35654

Minimum radius of three dimensional cam gears calculated from driven element motion and pressure angle

23 p4168 A69-41413

GEGENSCHEIN

Gegenschein measurements for determining upper limit on asteroidal debris spatial density

02 p0324 A69-12545

GEIGER COUNTERS

Photographic investigation of gegenschein and cloud satellites at L sub 5 earth-moon libration point, noting gegenschein intensity peak
07 p1212 A69-18602

GEIGER COUNTERS

Geiger-Muller counter telescopes in conjunction with core selectors for studying geomagnetic effect of extensive air showers
03 p0430 A69-13303

Auroral electron flux from particle fluxes measured with shielded Geiger-Muller telescopes mounted in rocket launched into diffuse aurora
09 p1576 A69-21663

Saturated signals of GM counter from solar radiation monitoring satellite, showing Van Allen belt high energy particle origin
14 p2514 A69-29383

GEIGER-MUELLER TUBES

U GEIGER COUNTERS

GELLED ROCKET PROPELLANTS

Slush H and N gels preparation and characteristics, including measurements of weight bearing capacity of gel as function of percent mass silica gelant
22 p3998 A69-40632

GELS

NT DOUBLE BASE ROCKET PROPELLANTS

Dispersion in gel permeation chromatograph, noting contributions of injection and detection systems to peak broadening and retention time
04 p0555 A69-14884

Gel permeation chromatography of nominally linear aliphatic polyesters, using tetrahydrofuran solvent at 37 degrees C
21 p3670 A69-39806

GEMINI FLIGHTS

Earth orbital satellites for geologic applications, discussing Gemini photograph qualities and influence on Earth Resources Observational Satellite program [UN PAPER 68-95441]
01 p0065 A69-10509

Weightlessness effects on fertilized frog egg development on board Gemini 8 and 12 manned orbital flights, discussing cell division, differentiation and embryogenesis
01 p0017 A69-11084

Space photography for natural resource inventory, describing Gemini photographs role in assessing vegetation, geological, metal and soil resources in Western Hemisphere
12 p2097 A69-26987

Space suit meteoroid protection for extravehicular activity, discussing Gemini and lunar surface EVA suits and bumper concept [AIAA-PAPER-69-366]
13 p2213 A69-28298

Micrometeoroid collections, describing Gemini satellite and Aerobee rocket-borne equipment and experimental results
15 p2700 A69-31440

Pre and postflight leukocyte chromosome aberration analyses of Gemini astronauts
17 p2908 A69-33173

Spacecraft pitch and yaw angles measurement using environmental positive ion probes, discussing Gemini flight tests and attitude control systems
24 p4315 A69-43241

GEMINI PROJECT

Satellite photography applications to geography and cartography based on Gemini 7 photographs [UN PAPER 68-95401]
01 p0178 A69-10489

Stellar UV objective prism spectra from Gemini 11 and 12 manned flights
01 p0153 A69-10870

Gemini and Mercury space flights medical results, summarizing physiological effects noted on body systems
01 p0017 A69-11074

Terrestrial microorganism survival in space aboard Gemini satellite, discussing lethal effects of solar radiation
01 p0018 A69-11087

Systems engineering activities in manned space flight involving design, development, manufacture, test and operation of Mercury, Gemini and Apollo flight systems
06 p1016 A69-17602

Gemini program for geologic orbital photography, discussing equipment used
18 p3131 A69-35274

GEMINI SPACECRAFT

Guidance and control concepts and hardware for atmospheric entry of Mercury, Gemini and Apollo spacecraft
11 p1914 A69-25724

Manned spacecraft fuel cell selection and design, discussing Gemini ion exchange membrane and Apollo Bacon cell systems
16 p2737 A69-32406

Hyperaltitude photographs from Gemini spacecraft for geological mapping
18 p3132 A69-35276

Hyperaltitude photographs for geological mapping from Gemini spacecraft, noting remote sensing imagery
22 p3935 A69-40040

GEMINI 11 FLIGHT

Radiation effects on microorganisms and plants during space flight on Biosatellite 2 and Gemini 11 missions
20 p3476 A69-37617

Primary cosmic ray nuclei studies during Gemini 2 flight by nuclear emulsion detector with time resolution capability, describing experiment design and equipment operation
21 p3787 A69-38350

GENERAL AVIATION AIRCRAFT

Listen-in feature, allowing general aviation aircraft equipment to receive airborne SSR reply signals, provides air to air proximity warning
03 p0464 A69-13247

Business jet aircraft use for air transport pilot training instead of simulating devices, noting pilot cabins
03 p0366 A69-13643

Aeronautics - Conference, Beverly Hills, September 1968
06 p0866 A69-17658

General aviation flight testing philosophy and origin
06 p1043 A69-17667

LR-1 prototype design criteria and flight testing, discussing Model 99 airliners for commuter airlines
06 p0867 A69-17668

Anti-icing system for business jets, noting activation prior to encountering visible moisture
06 p0868 A69-17669

Tilt wing executive transport aircraft designed by postgraduates at College of Aeronautics of UK, discussing costs, construction and marketability
11 p1821 A69-24321

Business aircraft injury protection and impact survival design considerations, stressing upper torso restraint installations [SAE PAPER 690335]
11 p1829 A69-24493

Onboard gas turbine auxiliary power units for executive jet transport aircraft [SAE PAPER 690332]
11 p1824 A69-24501

On-off multiple tank fuel systems for single and twin engine light aircraft, noting fail-safe design [SAE PAPER 690334]
11 p1825 A69-24502

Pressurized Navajo aircraft environmental system, discussing ventilation, pressurization, heating and air cooling systems [SAE PAPER 690330]
11 p1829 A69-24504

Thrust reversers for business jet aircraft, discussing federal aircraft regulation requirements for ground and in-flight qualification [SAE PAPER 690311]
11 p1941 A69-24512

Aviation pathology in aircraft accident investigation of accident survivability features and accident precipitation factors, noting cockpit structures and protective equipment
12 p2021 A69-25841

Low cost inertial measurement unit /IMU/ for commercial and private aircraft, evaluating components and system [SAE PAPER 690337]
15 p2606 A69-30092

Annual general aviation aircraft accident rate variation related to annual variations in pilot flight training activity
19 p3262 A69-36448

Cockpit noise intensity during normal cruising operations at various altitudes for 15 different single engine general aviation light aircraft
23 p4102 A69-41676

Annual general aviation accident rate prediction from annual flight training variations
23 p4062 A69-41793

GENERAL DYNAMICS AIRCRAFT

U CL-84 AIRCRAFT
U CV-990 AIRCRAFT
U F-106 AIRCRAFT
U F-111 AIRCRAFT

GENERAL DYNAMICS MILITARY AIRCRAFT

U MILITARY AIRCRAFT

GENERATORS

Synchronization of generators of finite dimensional forces, discussing mechanism of almost conservative dynamic objects on basis of influence matrix
05 p0793 A69-15779

Synchronization of generators of finite dimensional forces, discussing mechanism of almost conservative dynamic objects on basis of influence matrix
18 p3173 A69-35031

GENETICS

NT MUTATIONS

Cosmic radiation genetic, cytological and histological changes, particularly of pathological nature, on ecological systems employed in long duration Soviet manned flights
01 p0016 A69-10948

Genetic effects in yeast induced by heavy ion radiation, studying lethality, mitotic segregation, allelic recombination and reverse mutation
03 p0373 A69-13491

Circadian rhythm effect between individuals of separate twin pairs, noting application to physiological research in medical genetics and human biometeorology
04 p0553 A69-15152

Fatty acids in blue-green algae related to phylogenetic position
05 p0707 A69-15751

Insect gametes response to space flight and radiation in reduced gravity including plants and microorganisms
23 p4091 A69-42050

GENITOURINARY SYSTEM

U BLADDER

GEOASTROPHYSICS

U ASTROPHYSICS

U GEOPHYSICS

GEOCENTRIC COORDINATES

Rectangular space coordinates for points on earth determined from observations of directions and distances to and from satellites [UN PAPER 68-95265]
06 p0917 A69-17064

Geocentric orientation of quasi-geocentric coordinate network determined from simultaneous photographic satellite observations, using gravity force values
12 p2158 A69-26429

Computer method for solution of Banachiewicz graph analytic equivalent for parabolic orbits determination, noting geocentric distances variation
13 p2336 A69-27448

Spatial geodesy results from European data, discussing accuracy of geodetical European network and geocentric coordinate computation
15 p2601 A69-31369

Photographic observations of Neptune occultation of BD-17 degree 4388, Zodiac Catalog number 2232 in April 1968, noting geocentric separation and planet radius
23 p4221 A69-42388

GEOCHEMISTRY

Geochemistry and cosmology - Conference, Prague, August 1968
07 p1212 A69-18546

Avalanche detector radioisotope X ray fluorescence analyzer development for XRF analysis of potassium and calcium, noting precision [IEEE PAPER 3B-9]
07 p1135 A69-19201

Origin and distribution of elements - Conference, Paris, May 1967
08 p1398 A69-20892

Geochemistry and element abundances for Henbury impact glass, Darwin glass and australites, noting evidence for meteorite impact on sandstone
08 p1407 A69-20937

Trace element geochemistry of calc-alkaline andesites, discussing crustal composition models and trace elements distribution
08 p1309 A69-20940

Continental diabases and oceanic tholeiites in light of rare earth and barium abundances and partition coefficients indicating fusion process
08 p1310 A69-20945

Electron impact field ionization source for mass measurement of molecular ions, noting organic geochemistry applications
15 p2608 A69-30428

Gas chromatographic and mass spectrometric analyses of alicyclic hydrocarbons from Carboniferous organic materials, noting alkane distribution and evolutionary histories
17 p2917 A69-34184

Handbook on geochemistry, Volume 2/1, covering geophysics, cosmochemistry, etc
22 p3897 A69-40890

Handbook on geochemistry, Volume 1, covering meteorite composition, cosmic abundances, earth geophysical structure and composition, data evaluation, etc
22 p3897 A69-40980

- Geophysical aspects of earth chemical composition, structure and energy balance
22 p4032 A69-40983
- Geochemistry of tektites - Conference, Corning, New York, April 1969
23 p4209 A69-41340
- Geochemical synthesis of branched chain acyclic polymers from irradiated isoprene
24 p4269 A69-43750

GEOCHRONOLOGY

- Electronic charge variations with cosmic time determined from geochronological data
06 p1003 A69-17323
- Carbon dioxide pressure in earth atmosphere through geologic time determined by carbon input rate and transfer efficiency to crust
08 p1310 A69-20946
- Microstructure of Proterozoic nanofossils bracketed by dated granitic events compared with living Eucapsis of blue green Chroococcaceae algal family
22 p3936 A69-40059
- Paleogeographical evolution in support of earth expansion, discussing polar wandering, global continental drift and final complete disruption
22 p3936 A69-40181
- Precambrian crustal geotectonic evidence of earth radius expansion based on dated orogenic fold belts distribution
22 p3936 A69-40182

GEOCORONAL EMISSIONS

- Solar hydrogen Lyman alpha line profile measurement by rocket-borne spectrophotograph, obtaining flux available for scattering by atomic hydrogen in geocorona
05 p0815 A69-16254
- Solar Lyman alpha radiation scattering into antisolar geocorona, noting inaccessibility of region to solar wind
09 p1583 A69-22760
- Atomic hydrogen vertical profiles with increased high-low altitude ratio for interpreting observations of thermospheric and exospheric hydrogen abundance
14 p2440 A69-29130
- Solar wind and solar breeze theories distinguished, discussing applications to geocoronal hydrogen emission and solar corona expansion
15 p2676 A69-30858
- Geocoronal Lyman alpha short term and 27-day variations observed by OGO 4 spacecraft attributed to flux variability at solar emission line center
15 p2699 A69-31404
- Balmer alpha and Lyman beta intensities for multiple scattering calculated for hydrogen geocorona models by radiative transfer equations, discussing radiation transport through earth hydrogen atoms
18 p3128 A69-34943
- Hydrogen bulge above springtime pole indicated by Lyman alpha radiation in earth geocorona, discussing hydrogen horizontal transport and hydrogen compounds dissociation as causes
18 p3129 A69-34956

GEODESY

- Gravitational field and earth shape determination by calculating perturbing potential at earth surface and in outer space, using Green functions
01 p0063 A69-10360
- Earth oblateness, discussing geometric interpretation and direct measurement
01 p0064 A69-10447
- Earth surface shape determinations by geodetic networks connecting ground observation points and satellite positions
[UN PAPER 68-95377] 01 p0065 A69-10528
- Satellite geodetic literature in U.S.S.R., discussing space triangulation geometric method and dynamic method for earth parameters and gravitational field
01 p0067 A69-10951
- Equatorial geodesic motion of rotating source in gravitational field, using exact empty space solutions of Einstein equations
01 p0157 A69-11289
- Magnetotelluric method for investigating earth vertical structure with allowance for sphericity
02 p0240 A69-11699
- French geodetic work with aid of artificial satellites, describing equipment, mounting, observation technique and laser telemetry experiments
02 p0228 A69-11913
- International cooperation results in field of optical tracking of satellites for solving problems of atmospheric physics, geophysics and geodesy
06 p1042 A69-17050

- French program of space geodesy, discussing spatial triangulation, telemetry, dynamic geodesy, Diapason and Diademe experiments
[UN PAPER 68-95834] 06 p0917 A69-17071
- Anna 1-B geodetic satellite design, instruments and data acquisition
[UN PAPER 68-96195] 06 p0917 A69-17082
- Royal Belgian Observatory studies on time, meridian, seismological and gravimetric services, latitude variation due to polar motion, terrestrial tides and geodetic satellites
08 p1306 A69-19992
- Earth ellipsoid fundamental parameters for calculation of earth flattening and normal acceleration due to gravity
09 p1487 A69-21633
- Magnetotelluric method for investigating earth vertical structure with allowance for sphericity
13 p2258 A69-28730
- Artificial earth satellites positional observations by graphical smoothing on azimuth and altitude, discussing advantages for space geodesy
15 p2594 A69-30029
- Spacecraft radar altimetry with application to geodesy, discussing orbital and tracking errors
15 p2609 A69-30460
- Geometric conditions selection in directions determination in satellite and rocket aided triangulation, deriving formulas for chords directions of earth ellipsoid
15 p2689 A69-30572
- Classical and relativistic gravitation theories using harmonic coordinate system, interpreting Einstein equations for insular distribution of masses and applications in geodesy
15 p2596 A69-30573
- Laser measurements for DIADEME satellites tracking to reconstruct actual trajectory in semidynamic geodesy
15 p2600 A69-31365
- Spatial geodesy results from European data, discussing accuracy of geodetical European network and geocentric coordinate computation
15 p2601 A69-31369
- Doppler measurements in semidynamical geodesy, processing data from Transit satellites collected at various Mediterranean ground stations
15 p2602 A69-31382
- Earth figure parameters from satellite orbit dynamics, including potential on geoidal surface and scale factor for lengths
15 p2602 A69-31387
- Monograph on photogrammetry in satellite geodesy including photogrammetric measurement of satellite positions, German observation stations and work done in U.S., U.S.S.R. and France
16 p2790 A69-32202
- French space geodesy since Space Age, detailing Diapason and Diademe satellites program, techniques and results
17 p2961 A69-33382
- Figure of earth and refraction - Conference, Vienna, March 1967
18 p3131 A69-35194
- Earth ellipsoid determination by satellite observations, noting accuracy of polar flattening measurement on basis of perturbation or perigee argument
18 p3131 A69-35195
- Scale determination in spatial direction networks, using polygonal transverse measured along continental surfaces and Secor method over water surfaces
18 p3131 A69-35196
- Molodenskii boundary value problem exact solution by successive approximations for determination of earth figure, noting quasi-geoid surface
21 p3716 A69-39248
- Earth shape and areas of anomalous gravity from satellite orbital perturbations, tabulating results from various experimenters
21 p3718 A69-39734
- Observations indicating slow earth expansion
22 p4018 A69-40179
- Earth sphericity and earth-ionosphere waveguide effects on terrestrial atmospherics, deriving form by computer
23 p4157 A69-41860
- Geodetic and geophysical random uncertainties as fundamental limitations on terrestrial inertial navigation accuracy
[AIAA PAPER 68-847] 24 p4348 A69-43240

GEODETIC COORDINATES

- Earth pole coordinates calculated from latitude variations at Pulkovo, Greenwich and Washington, giving components of earth motion
03 p0420 A69-13094

- Coupling geodetic systems of coordinates linked to reference ellipsoids from determination of angle of inclination relative to earth rotation axis and equatorial plane
12 p2068 A69-26426
- Coupled geodetic triangular grids obtained using satellite observations for azimuths
12 p2069 A69-26433
- Earth pole coordinates calculated from latitude variations at Pulkovo, Greenwich and Washington, giving components of earth motion
14 p2433 A69-28776
- Satellite space navigation system providing three component position in geodetic coordinates instantly and accurately on or near earth
15 p2650 A69-30088
- Equations derived for radar image coordinate transition to geodetic coordinates in aerial surveying by side-looking airborne radar
15 p2596 A69-30574
- Comparisons and combinations of geodetic parameters from dynamic and geometric satellite solutions and Mariner flights
15 p2600 A69-31362
- Tesseral harmonics of geopotential and station coordinates based on combined Baker-Nunn, laser and range and rate satellite data
15 p2601 A69-31372
- Doppler geodetic measurements, emphasizing relative orientation between station and orbit influence on coordinates determination accuracy, presenting electromagnetic wave propagation theory
15 p2601 A69-31375
- Neglected gravity coefficients influence on computed satellite orbits and geodetic parameters
22 p4023 A69-40556

GEODETIC SATELLITES

- NT ANNA SATELLITES
NT GEOS 2 SATELLITE
- Earth orbital satellites for geologic applications, discussing Gemini photograph qualities and influence on Earth Resources Observational Satellite program
[UN PAPER 68-95441] 01 p0065 A69-10509
- Earth surveying methods by artificial satellites, discussing applications to undeveloped regions
[UN PAPER 68-95793] 01 p0065 A69-10523
- Diapason satellite geodetic results concerning measurement accuracy, terrestrial potential models and station synchronization
01 p0065 A69-10543
- Satellite geodetic literature in U.S.S.R., discussing space triangulation geometric method and dynamic method for earth parameters and gravitational field
01 p0067 A69-10951
- Earth resource information from spacecraft including landmapping, geological photographs, hydrological and oceanographic data, etc
06 p0916 A69-16855
- French geodetic satellites tracking operations, on-board equipment and ground stations
[UN PAPER 68-95835] 06 p1013 A69-17065
- GEOS 2 attitude stabilization by means of gravity gradient principle and passive energy dissipator, noting effects of orbit eccentricity, thermal distortion, radiation, etc
07 p1229 A69-18349
- Ballistics room of Royal Belgian Observatory for observation of geodetic satellites
08 p1272 A69-19993
- Photogrammetry for three dimensional geodesy, discussing satellite triangular methods, refraction anomalies, error corrections, etc
10 p1682 A69-23390
- Earth gravitational field representation by separating geopotential into normal and disturbing potential for solving geodetic boundary value problem for satellite geodesy
12 p2076 A69-27089
- First order Doppler shift in ionosphere and horizontal gradients influence, discussing total electron content determination method made from geodetic satellites using two coherent frequencies
16 p2755 A69-32614
- French space geodesy since Space Age, detailing Diapason and Diademe satellites program, techniques and results
17 p2961 A69-33382
- Geodetic satellite measurements employing curve fitting approach using least squares analysis to resolve atmospheric refraction and shimmer problem
18 p3104 A69-35202
- Australia spatial triangulation and trilateration using geometric satellite geodesy, including station position accuracy tests
18 p3132 A69-35499

Geodetic satellites transfer between low ellipticity orbits by microthrust
21 p3793 A69-38338

GEODETIC SURVEYS

Satellite triangulation simultaneous and trailing methods, discussing timing devices design
[UN PAPER 68-95285] 01 p0064 A69-10475

Earth surveying methods by artificial satellites, discussing applications to undeveloped regions
[UN PAPER 68-95793] 01 p0065 A69-10523

Earth surface shape determinations by geodetic networks connecting ground observation points and satellite positions
[UN PAPER 68-95377] 01 p0065 A69-10528

Economic and scientific reasons for using artificial satellites to establish continental geodetic network, noting continental displacements and terrestrial pole motion observations
[UN PAPER 68-07445] 06 p0917 A69-17069

Side looking radar for earth resources sensing, discussing geological and hydrographical mapping, oceanography, agricultural and biological phenomena
06 p0923 A69-17119

Survey of six year period of satellite observed tropical Pacific cloud mapping
17 p2996 A69-33001

Gemini program for geologic orbital photography, discussing equipment used
18 p3131 A69-35274

Hyperaltitude photographs from Gemini spacecraft for geological mapping
18 p3132 A69-35276

Errors in sighting and identifying geodetic contour points on aerial photographs, considering stereocomparators parallaxes effect
21 p3719 A69-38404

Satellite phase and aberration corrections in processing photographic observations for geodetic purposes
21 p3720 A69-38606

GEOELECTRICITY

NT TELLURIC CURRENTS

Geoelectric field over polar cap based on proton flux detection
04 p0648 A69-14682

Air-earth current density variations with universal time, noting hemispherical dependence of storm activity effects
10 p1682 A69-23415

GEOGRAPHY

NT OROGRAPHY

Satellite photography applications to geography and cartography based on Gemini 7 photographs
[UN PAPER 68-95401] 01 p0178 A69-10489

Aerial chronophotography of Southern Hemisphere conducted on around world polar flight analyzed for meteorological and geographical aspects and compared with satellite data
09 p1534 A69-21405

GEIDS

Earth oblateness, discussing geometric interpretation and direct measurement
01 p0064 A69-10447

Mass functions of real earth derived from satellite orbital perturbations
[UN PAPER 68-95385] 01 p0064 A69-10460

Boundary value problem solved for free air geoid, developing expressions for height anomaly from free air anomalies
07 p1129 A69-19396

Earth ellipsoid fundamental parameters for calculation of earth flattening and normal acceleration due to gravity
09 p1487 A69-21633

Earth figure parameters from satellite orbit dynamics, including potential on geoidal surface and scale factor for lengths
15 p2602 A69-31387

Moldenskii boundary value problem exact solution by successive approximations for determination of earth figure, noting quasi-geoid surface
21 p3716 A69-39248

Conjugate points along lightlike geodesics in general theory of relativity, deriving existence from vector field matrix properties and Ricci curvature
23 p4213 A69-41724

GEOLOGICAL FAULTS

Velocity distribution in lower mantle, showing second major discontinuity in P wave travel time curve at 24 degrees
07 p1129 A69-19502

Volcano-Tectonic origin of lunar mare terrain from Apollo 8 photograph showing faulting pattern identical with uppermost Pleistocene-Holocene faulting
20 p3604 A69-37570

GEOLOGY

NT GEOCHRONOLOGY

NT GEOMORPHOLOGY

NT GLACIOLOGY

NT LITHOLOGY

NT LUNAR GEOLOGY

NT OROGRAPHY

NT PETROGRAPHY

NT PETROLOGY

NT PHOTOGEOLOGY

NT TECTONICS

NT VOLCANOLOGY

Earth orbital satellites for geologic applications, discussing Gemini photograph qualities and influence on Earth Resources Observational Satellite program
[UN PAPER 68-95441] 01 p0065 A69-10509

X Ray fluorescence of rock samples as applied to geological problems, noting standard deviations for element distribution
01 p0082 A69-10890

Space systems use for planetary geology and geophysics - Conference, Boston, May 1967
03 p0509 A69-13390

Space photography to provide synoptic sedimentary environmental data analysis, discussing orbital sensing advantages
05 p0753 A69-15993

Origin of life in terms of polymers synthesis under thermodynamic and geological conditions
12 p2017 A69-25764

Passive remote sensing at microwave frequencies for meteorology, oceanography and geology, reviewing physics of wave interactions, mathematics of data interpretation, etc
14 p2414 A69-29514

Geological radar in regional and detail studies, discussing area side scanning imagery and lithology changes detection
20 p3491 A69-37652

Atmospheric and hydrospheric evolution on primitive earth from geological point of view
21 p3806 A69-39290

Hyperaltitude photographs for geological mapping from Gemini spacecraft, noting remote sensing imagery
22 p3935 A69-40040

Paleontological evidence to verify varying G constant hypothesis for expanding earth theory, discussing uncertainties of geological dating
22 p4017 A69-40177

Multispectral processing of Apollo 6 earth photograph, evaluating geologic, vegetative and cultural features from red, green and blue portions of visible spectrum
22 p3941 A69-40987

Bulk, selective particulate and hard rock samplers for landed extraterrestrial geological and biological instruments performing on-site analysis
23 p4146 A69-41620

GEOMAGNETIC ANOMALIES

U MAGNETIC ANOMALIES

GEOMAGNETIC CROTCHETS

U SUDDEN IONOSPHERIC DISTURBANCES

GEOMAGNETIC EFFECTS

U MAGNETIC EFFECTS

GEOMAGNETIC EQUATOR

U MAGNETIC EQUATOR

GEOMAGNETIC FIELD

U GEOMAGNETISM

GEOMAGNETIC HOLLOW

Statistical method for calculating upper bound heights of sources responsible for magnetic anomalies
12 p2071 A69-26696

GEOMAGNETIC LATITUDE

Differential Faraday technique to determine electron content latitude dependence in Northern Hemisphere during magnetically disturbed periods in March 1966
01 p0146 A69-11128

Earth pole coordinates calculated from latitude variations at Pulkovo, Greenwich and Washington, giving components of earth motion
03 p0420 A69-13094

Latitude variation of time of occurrence of maximum F height and maximum spread F probability
03 p0420 A69-13305

F 2 layer critical frequencies variation coefficients, analyzing variation and root-mean-square deviations in terms of geomagnetic latitude and Wolf number
03 p0422 A69-13514

F 2 layer equatorial anomaly at local noon, discussing position of trough center in latitudinal distribution of ionization
03 p0422 A69-13515

Diurnal variations of low latitude VLF emissions observed at Hiraiso, Japan
03 p0398 A69-13900

Latitude dependence of 6300 A / O II twilight airglow enhancement attributable to conjugate photoelectrons
05 p0756 A69-16280

Low energy photon spectrum at balloon altitudes, noting small geomagnetic latitude dependence
06 p0992 A69-17313

Pc5 geomagnetic pulsations spatial characteristics, showing localized excitation in space and dependence on geomagnetic latitude
06 p0921 A69-17736

Statistical frequency analysis of power spectrum of geomagnetic pulsations, discussing time and latitude dependence
07 p1122 A69-18297

Time and latitude variations of blanketing sporadic E using wind shear theory, predicting ionization layer formation in ionospheric E layer
07 p1125 A69-18840

Average geomagnetic storm ranges as function of latitude, noting disturbances caused by ring and ionospheric currents
09 p1489 A69-21715

Microstructure of pc 3 and pc 4 geomagnetic pulsations, investigating polarization direction, period duration and latitude dependence
12 p2063 A69-25782

Earth pole coordinates calculated from latitude variations at Pulkovo, Greenwich and Washington, giving components of earth motion
14 p2433 A69-28776

Aurora electron and proton excitation patterns determined spectroscopically, discussing ground based observations of emission geomagnetic latitude-time distribution
15 p2593 A69-30017

Geomagnetic field latitudinal variation effect on cut-off frequencies of proton whistlers, discussing LF electromagnetic wave propagation in cold multicomponent plasma
18 p3100 A69-34253

Electron density distribution in northern and southern polar regions ionosphere based on 1958 and 1959 observations at high geomagnetic relatively low geographic latitudes
20 p3526 A69-37664

F 2 layer midlatitude positive disturbances observed during IGY on quiet and disturbed days, noting positive to negative transition latitudes
20 p3527 A69-37674

Explorer 32 atmospheric density measurements revealing neutral thermosphere latitudinal variations during geomagnetically undisturbed times
20 p3535 A69-38100

Critical frequency variations of F 2 layer and M/3000F 2 with sunspot number for 19th solar cycle, noting dependence on geomagnetic latitude
21 p3715 A69-38560

Latitude variation of radio satellite scintillation related to small scale ionospheric irregularities
22 p3899 A69-39972

Pulsating aurora diurnal variations and dependence on latitude and magnetic activity, photometric observations
24 p4308 A69-43004

GEOMAGNETIC MICROPULSATIONS

Quasi-periodic VLF emissions associated with geomagnetic micropulsation activity in terms of comparable periodicity
01 p0063 A69-10274

Micropulsations at magnetoconjugate points in Arctic and Antarctic, noting diurnal and seasonal variations and latitude dependence
01 p0068 A69-11112

Magnetospheric plasma distribution determination based on analysis of structured elements in micropulsations
01 p0076 A69-11229

Relation between solar activity and cyclic variation of pearl pulsations excitation frequency during sunspot cycle
02 p0239 A69-11696

Dispersion measurements and spectrum variations analysis to study pearl micropulsations frequency variation during sudden deformation of magnetosphere by magnetic storms
02 p0240 A69-11697

Subsolar magnetosphere dimensions from ground observations of geomagnetic micropulsation period changes during magnetosphere deformations caused by solar wind inhomogeneities

02 p0244 A69-12356

Geomagnetic micropulsations mechanism, discussing hydromagnetic waves transmission generated by interface instability between solar wind and magnetosphere, noting transmission path role

02 p0244 A69-12395

Geomagnetic micropulsation theory, discussing mechanisms responsible for amplitude spectrum at earth surface and power spectral density

02 p0244 A69-12396

Pc 1 micropulsation and magnetospheric amplification of hydromagnetic waves

05 p0754 A69-16263

Earth electromagnetic field micropulsations associated with proton flare, evaluating data from polar caps, auroral zones and midlatitudes

06 p0996 A69-17754

Nighttime equatorial Pi 2 micropulsations, noting seasonal and diurnal distributions and dependence on three hour index of magnetic activity

07 p1125 A69-18841

Ground propagation of regular Pc 1 and irregular Pi 1 geomagnetic micropulsations demonstrated by precise time measurement

07 p1127 A69-19338

Geomagnetic field irregular pulsations relationship with polar aurora and ULF radiation pulsations, stressing choruses appearance

09 p1485 A69-21536

Earth currents and magnetic field variations recording in period range 10-200 sec, computing power density spectra on analog computer

10 p1682 A69-23593

F 2 layer drift relation to current systems of dynamo region confirmed at middle and high latitudes

10 p1682 A69-23611

Earth electromagnetic micropulsations in connection with July 7 1966 proton flare, discussing peculiarities in occurrence of pearls before and after flare

10 p1683 A69-23779

Geomagnetic micropulsations fluctuations during solar activity cycle showing changes in excitation frequency with change in corpuscular fluxes parameters

10 p1687 A69-23919

Microstructure of pc 3 and pc 4 geomagnetic pulsations, investigating polarization direction, period duration and latitude dependence

12 p2063 A69-25782

Pi 2 micropulsations at African low latitude stations, considering damping effect on ionospheric micropulsation transmission signal dispersion and SNR

12 p2074 A69-26959

Relation between solar activity and cyclic variation of polar pulsations excitation frequency during sunspot cycle

13 p2258 A69-28727

Dispersion measurements and spectrum variations analysis to study pearl micropulsations frequency variation during sudden deformation of magnetosphere by magnetic storms

13 p2258 A69-28728

Oscillations intervals with diminishing period observed during magnetic storms, noting relationship to midlatitude disturbances in F region

14 p2436 A69-29060

Pc 2-4 geomagnetic pulsations abrupt disappearance on global scale ascribed to magnetosphere boundary stabilization, noting interplanetary magnetic field role

14 p2438 A69-29080

Daytime ionospheric screening effect on low latitude geomagnetic micropulsations estimated using ionosphere model

14 p2441 A69-29380

CNA and geomagnetic pulsations observed by ground based instruments in southern auroral region occurring near geomagnetic noon, noting electron precipitation role

15 p2597 A69-30697

Micropulsation records for full moon effect on hydromagnetic emission activity of magnetosphere, noting W and Kp indices

16 p2774 A69-31979

Geomagnetic field irregular pulsations relationship with polar aurora and ULF radiation pulsations, stressing choruses appearance

16 p2783 A69-32531

Relationship between micropulsation periods and size of magnetosphere expressed in power law form and interpreted with wave propagation

18 p3131 A69-35193

Plasma density in magnetosphere by measuring geomagnetic pi 2 micropulsations in direction related to polar aurora oval southern boundary, determining period of pi 2 oscillations

19 p3303 A69-36205

Geomagnetic field micropulsation observations by U.S.S.R. and possible applications to diagnostics of magnetosphere

19 p3304 A69-36642

Doppler observations of ionospheric motions associated with magnetic micropulsations, noting hydromagnetic and neutral gas waves

20 p3535 A69-38194

Pearl type geomagnetic micropulsation development by studying Alfvén waves cyclotron instability in plasma with hot protons anisotropic distribution

23 p4206 A69-41850

Concurrent geomagnetic micropulsations at equatorial and high latitude stations, discussing magnetospheric sources of Pi and Pc types

23 p4161 A69-42439

Pi 2 micropulsation waveform variation with time from simultaneous observations at low latitude stations, estimating phase velocity of higher frequency component

23 p4161 A69-42440

Diurnal variation of Pc type geomagnetic pulsations correlation with F 2 layers critical frequency diurnal variations

23 p4161 A69-42441

GEOMAGNETIC PULSATIONS

Geomagnetic response asymmetry related to solar direction of polarity in interplanetary magnetic field

01 p0077 A69-11236

Hydromagnetic emissions observed at Antarctic auroral zone, discussing relation to sudden storm commencement

02 p0241 A69-11726

Large amplitude Pc 1 events at College, Alaska, noting more ionospheric cosmic noise absorption accompanying large events

02 p0244 A69-12397

Geomagnetic field topology of nighttime magnetosphere, showing pi 2 pulsations excitation mechanism in terms of Alfvén waves resonance in external cavity

03 p0423 A69-13524

Frequency time displays of geomagnetic pulsations at Kiruna revealing Pc 1 pulsations accompanied by cosmic noise absorption /CNA/ and X ray enhancements

03 p0425 A69-14024

Pc5 geomagnetic pulsations spatial characteristics, showing localized excitation in space and dependence on geomagnetic latitude

06 p0921 A69-17736

Resonance in fundamental harmonic identified with Pc4 and in second harmonic with Pc3 geomagnetic pulsations

06 p0921 A69-17737

Statistical frequency analysis of power spectrum of geomagnetic pulsations, discussing time and latitude dependence

07 p1122 A69-18297

Lunar daily geomagnetic periodicities by periodogram or spectral analysis, comparing amplitudes obtained by spectral analysis to those by harmonic analysis

07 p1123 A69-18817

Transverse LF oscillations in geomagnetic field observed during January 1967, noting possibility of being second harmonic of magnetospheric standing Alfvén waves

07 p1124 A69-18835

Particle dynamics measured by ATS satellite synchronous orbit, discussing flux time variations during geomagnetic disturbances

07 p1209 A69-19371

Geomagnetic field quiet solar variations variability explained by model, noting agreement with observations at various stations

09 p1486 A69-21549

Eleven year cyclicity of geomagnetic activity from Sverdllovsk Observatory data, noting possible relation with structural features of solar activity cycles

09 p1486 A69-21552

Geomagnetic pulsations recorded in equatorial regions of Africa found continuous and not pearl modulated

09 p1491 A69-22051

Toroidal magnetic fields in ionosphere associated with solar quiet daily variations producing electric current and equatorial auroral electrojets

10 p1681 A69-22805

Geomagnetic fluctuations positive and negative correlations at conjugate pair stations Syowa base and Reykjavik

10 p1681 A69-22806

Geomagnetic crochet of July 7, 1966, discussing pulsations, recombination coefficient and electron density of ionospheric D region

10 p1683 A69-23757

Electrical phenomena in upper atmosphere and solar wind may control geomagnetic disturbances and aurorae

10 p1686 A69-23903

Geomagnetic field pulsations frequency changes in relation to geomagnetic and solar activity level

10 p1689 A69-23939

Geomagnetic field Pc 3 and Pc 4 pulsation generation mechanism explained by resonance of MHD waves in force tubes adjoining radiation belt maximum

10 p1689 A69-24206

Stable geomagnetic pulsations related to plasma density shock position in magnetosphere and to magnitude of diurnal variations

13 p2253 A69-27692

Geomagnetic pulsations and hydromagnetic wave propagation in magnetosphere, using geometric optics approximation

13 p2254 A69-28176

Large amplitude pulsations in magnetic field magnitude and proton fluxes observed by satellite during magnetic storm compared with various models

14 p2434 A69-28947

Geomagnetic variability relations to interplanetary magnetic field transverse fluctuations, discussing data from Mariner flights

14 p2510 A69-28948

Geomagnetic field secular variations relation to variations of magnetic field of optimum dipoles, noting earth core role

14 p2436 A69-29061

Amplitude and frequency spectra for Ipc pulsations during geomagnetic storms

14 p2441 A69-29417

Statistical analysis of data for 18-19 June 1936, estimating expressions involving external and internal components of geomagnetic field at storm time disturbances

14 p2444 A69-29883

Interplanetary magnetic fields from Explorer 33 magnetometer relationship to surface geomagnetic variations emphasizing unified view

16 p2862 A69-32309

Geomagnetic field quiet solar variations variability explained by model, noting agreement with observations at various stations

16 p2784 A69-32544

Eleven year cyclicity of geomagnetic activity from Sverdllovsk Observatory data, noting possible relation with structural features of solar activity cycles

16 p2784 A69-32547

Electromagnetic /ULF, VLF/ and light emissions development during magnetic substorms, discussing varied pulsations present in development phases

16 p2788 A69-32648

Polar auroras pulsation attributed to background brightness fluctuations, discussing intensity diurnal variation

17 p2963 A69-33954

Frequency spectra of Pi2 geomagnetic field pulsations, noting effects of auroral zone location, configuration and structure

20 p3520 A69-37038

PPi bursts interpreted as proton beams cyclotron instability in geomagnetic field

20 p3521 A69-37039

Plasma concentration in nondipole magnetosphere model from pc 5 pulsations periods for high geomagnetic latitudes, noting solar winds effect

20 p3521 A69-37043

Geomagnetic pulsations with intensity maximum at midlatitudes, noting north to south decreasing trend

20 p3522 A69-37059

Vertically moving ionospheric disturbances altitude estimated from geomagnetic pulsations in earth electromagnetic field

20 p3528 A69-37686

Optical pulsations in aurora, studying relations to pulsations in geomagnetism, telluric currents, X rays from aurora and variations in primary particles flux

21 p3708 A69-38492

Auroral zone geomagnetic pulsations on nightside and dayside of earth related to magnetospheric substorm and particle precipitation

21 p3708 A69-38497

Book on worldwide occurrence of type pc 4 geomagnetic pulsations covering simultaneous recordings, D/H relations, dependence on geomagnetic latitude, etc
22 p3937 A69-40422

Book on geomagnetic quadrupole field temporal changes and effects on earth rotation, covering physical parameters in earth interior and earth conductivity model correlations
22 p3937 A69-40423

Magnetic fluctuations in various frequency ranges, associated with earth bow shock, detected with search coil magnetometer on OGO 3
22 p3938 A69-40501

GEOMAGNETIC STORMS

U MAGNETIC STORMS

GEOMAGNETIC TAIL

September 14, 1966 magnetic storm observation by Explorer 33 in geomagnetic tail and by polar stations, studying relation in magnetosphere and on earth
14 p2438 A69-29078

Solar energetic proton penetration into magnetotail from proton data collected by Vela 4 energetic particle telescopes, comparing proton fluxes inside and outside magnetotail
16 p2847 A69-31966

Auroral absorption occurrence patterns mappable onto magnetotail developed as function of magnetic activity, discussing magnetotail neutral sheet source width changes
16 p2848 A69-31968

Stochastic heating of protons by random magnetosonic wave propagating normal to magnetic field to explain proton energy excess in magnetotail plasma sheet
16 p2848 A69-31969

Numerical analysis of charged particles radial distribution in radiation belts extended to geomagnetic tail for low energy auroral electrons
16 p2850 A69-32102

Electromagnetic noise in current sheet in geomagnetic tail, discussing effects on distribution function [AFCL-69-0395]
16 p2781 A69-32317

Wave damping in current sheet in geomagnetic tail by radiating energy from sheet sides by electrostatic waves [AFCL-69-0396]
16 p2781 A69-32318

Chapman-Ferraro approximation for magnetic interior field line configuration in plasma flow around two dimensional dipole, allowing for tail formation and neutral sheet
18 p3129 A69-34955

Topology of interplanetary field lines in magnetotail, using solar electrons as tracers with moon as absorber
20 p3609 A69-38078

Particle precipitation into auroral zone and plasma-energetic particle relationship in geomagnetic tail, discussing plasma sheet extent, energetic electron fluxes, etc
21 p3711 A69-38510

Equatorial plasma sheet role in magnetotail assessed from Vela satellite data, noting diurnal density variations
21 p3711 A69-38512

Low energy plasma escape flow from polar region/polar wind, examining H, He and O ions participation in expansion
21 p3713 A69-38528

Long time scale magnetodynamic noise in geomagnetic tail, discussing hourly ranges of fluctuations measured by IMP 1 satellite and planetary K index correlation
22 p3935 A69-39967

Plasma pause form in equatorial plane in presence of magnetospheric tail subsonic potential convective flow
22 p3942 A69-41103

Equilibrium plasma configurations in magnetic field of two dimensional dipole analyzed under similar conditions to magnetospheric tail formation with neutral hot plasma layer
23 p4205 A69-41835

GEOMAGNETICALLY TRAPPED PARTICLES

U RADIATION BELTS

GEOMAGNETISM

Low latitude m arcs in 6300 angstrom emission during intense geomagnetic storm related to auroral red oxygen emission peak
01 p0062 A69-10136

Geomagnetic disturbance activity forecasting method using solar coronal streams, noting reliability of test forecasts
01 p0150 A69-10372

26-month periodicity in quiet day range of geomagnetic field horizontal force, noting similar periodicity in

sunspot number and 16-month oscillation in both phenomena
01 p0063 A69-10427

Topside ionosphere average height distributions of electron density and geomagnetic field intensity from Alouette 2 data over Japan, noting ionic composition
01 p0065 A69-10548

Earth and lunar magnetic field studies in U.S.S.R., discussing Soviet earth satellite and lunar probe data
01 p0066 A69-10943

Equatorial enhancement of storm sudden commencements and sudden impulses in horizontal component in American Zone during IGY/IGC
01 p0068 A69-11116

Magnetic field behavior at synchronous orbit during magnetospheric substorms, interpreting satellite observed data in terms of partial ring currents
01 p0075 A69-11225

Sudden magnetic field increase associated with July 8, 1966 sudden commencement observed by OGO 3 satellite in magnetotail
01 p0075 A69-11226

Solar plasma observations during magnetic storms, emphasizing shocks and tangential discontinuities, geomagnetic variations and He
01 p0076 A69-11234

Secular change examination in cislunar geomagnetic tail field gradient during summers of 1966 and 1967, using Explorer 33 and 35 results
01 p0077 A69-11237

Upper atmosphere oxygen emission and heating during geomagnetic disturbances
02 p0235 A69-11421

Relation between north-south asymmetry of F 2 region critical frequencies and geomagnetic axis inclination angle, establishing increase in asymmetry during increased solar activity
02 p0237 A69-11662

Perturbed geomagnetic field structure during magnetic storm recovery phase calculated by magnetosphere magnetic field model, accounting for various external field sources
02 p0237 A69-11666

Methodological problems in studying ionosphere by phase measurements without taking into account geomagnetic field, noting value of main results
02 p0237 A69-11668

Whistler dynamic spectra variation studies, emphasizing distorted magnetospheric geomagnetic field structure effect
02 p0238 A69-11671

Relationship between polar geomagnetic disturbances and DR variations value of geomagnetic field
02 p0238 A69-11672

Dipole models of geomagnetism at earth surface used to calculate magnetic field in outer space
02 p0238 A69-11673

Geomagnetic field components measurements from moving object, investigating astronomical orientation applicability for three component magnetometer
02 p0277 A69-11674

Geomagnetic field H and Z components measured by proton magnetometer, applying supplementary field method for error correction
02 p0238 A69-11675

Analytical model of geomagnetic field constructed from Cosmos 49 data using spherical analysis
02 p0240 A69-11698

Vertical and horizontal components of geomagnetic storm main phase magnetic variations applied to vertical electromagnetic soundings of earth
02 p0240 A69-11700

Polar geomagnetic disturbance development and decay during solar quiet and moderately disturbed periods
02 p0240 A69-11724

Parameters of solar wind responsible for geomagnetic activity, relating magnetic storm features to physical structure of interplanetary space and solar wind bubbles
02 p0240 A69-11725

Solar eclipse effect on geomagnetic field at and near dip equator observed at Huancayo Observatory, Peru
02 p0241 A69-11727

Solar eclipse effects on ionospheric conductivity and geomagnetic field at and near dip equator observed at Huancayo, Peru
02 p0241 A69-11728

Geomagnetic and interplanetary field variation measurements from Mariners 2, 4 and 5, noting correlation between solar phenomena and geomagnetic storms
02 p0241 A69-11737

Magnetotopometer for measuring torque/proportional to magnetic dipole moment/exerted on object by earth magnetic field
02 p0248 A69-11768

Magnetic paleointensity studies in basalts from Flagstaff, Arizona, noting oxidation effect on magnetic strength after heating
02 p0244 A69-12018

Algorithm computing spherical harmonic coefficients for eccentric geomagnetic dipole potential
02 p0245 A69-12735

World maps highlighting differences in geomagnetic field at conjugate localities
02 p0245 A69-12737

Diurnal variation in horizontal magnetic component of South American stations close to electrojet during IGY
02 p0246 A69-12771

Aurora displays distribution over earth, analyzing magnetosphere dependence on astronomical orientation of geomagnetic field in relation to solar wind
02 p0247 A69-12772

Earth magnetic field variations, discussing source of field, dynamo theory and paleomagnetic evidence for polarity reversals
03 p0420 A69-12935

Geiger-Muller counter telescopes in conjunction with core selectors for studying geomagnetic effect of extensive air showers
03 p0430 A69-13303

Earth ionosphere resonator natural frequencies, considering diurnal variation and geomagnetic field eccentricity
03 p0422 A69-13512

Geomagnetic field quiet day solar variations current system calculated, using 2000 LT as zero level basis
03 p0424 A69-13541

Mathematical dipole model for geomagnetic field to provide main magnetic field source distribution within earth
03 p0424 A69-13543

Dipole model of geomagnetic field in terms of spatial distribution of vertical component, discussing computer program for calculating rectangular components
03 p0424 A69-13544

High latitude electrons boundary dependent on geomagnetic axis orientation, noting role of coupling between solar wind and magnetosphere
03 p0502 A69-14003

Outer magnetosphere average magnetic field configuration between 5 and 18 earth radii, noting various maps in equatorial plane
03 p0425 A69-14012

Energetic electron fluxes measured at 2000 km over auroral and polar regions and at 17 earth radii in magnetotail plasma sheet
03 p0503 A69-14013

Earth magnetic field measurements, attributing field origin to random mechanism
03 p0426 A69-14061

Charged particle motion in time dependent external magnetic field
03 p0504 A69-14235

Cosmic ray time variation and anisotropies near earth, discussing galactic and solar cosmic rays, trajectories in geomagnetic field, etc
03 p0504 A69-14236

Aeromagnetic profiles across Reykjanes ridge southwest of Iceland, noting magnetic anomalies symmetry and ocean floor spreading since Mesozoic
04 p0592 A69-14660

Atmospheric, geomagnetic and interplanetary effects on cosmic ray flow, noting anisotropy and diurnal variation phase and amplitude averages
04 p0649 A69-14683

Error distribution maps for measurements of parameters epsilon, F and E of geomagnetic potential in Northern and Southern Hemispheres
04 p0627 A69-15031

Reversals of earth magnetic field, discussing lavas, deep sea sediments, ocean floor magnetic pattern and dynamo theory
04 p0593 A69-15075

Spatial and temporal conjugacy of visual auroras during magnetically quiet periods
05 p0753 A69-16247

Neutral sheet structure and orientation in geomagnetic tail, computing field lines on basis of Explorer 14 magnetic field measurements
05 p0753 A69-16256

Particle and field environment of earth, discussing solar wind, bow shock, magnetosheath, magnetopause, magnetosphere and particle population
06 p1001 A69-17158

- Cosmic ray daily variations relationship to geomagnetic activity, sector structure of interplanetary magnetic field and unspotted activity
06 p0990 A69-17291
- Soviet and French coordinated geophysical studies at magnetically conjugate points in northern U.S.S.R. and Indian Ocean
06 p0918 A69-17391
- Simulation of solar wind interaction with earth magnetic field, discussing selection of dimensionless parameters
06 p0919 A69-17550
- Cyclotron instability of outer radiation belt protons, taking into account data on spatial distribution and ion composition of exospheric plasma
06 p0919 A69-17721
- Vertically moving ionized formations relation to solar and magnetic activity
06 p0920 A69-17730
- Global geomagnetic anomalies influence on longitudinal pattern of solar quiet day variations and in phases of second harmonics of components
06 p0920 A69-17734
- Magnetic activity dependence of VLF emission properties at magnetically conjugate points
06 p0920 A69-17735
- Spatial structure of residual anomalous magnetic field, determining parameters of eccentric horizontal dipole as main source of geomagnetic field
06 p0922 A69-17755
- Magnetospheric ring current effect on main phase of geomagnetic storms, calculating diurnal storm-time portion of perturbation field
07 p1122 A69-18296
- Magnetic sample-and-hold damping using geomagnetic field for libration damping of gravity gradient stabilized satellite in near synchronous equatorial orbit
07 p1227 A69-18337
- Charged particle environment in synchronous orbit region, discussing electrons and protons under influence of geomagnetic field
07 p1204 A69-18340
- Transverse LF oscillations in geomagnetic field observed during January 1967, noting possibility of being second harmonic of magnetospheric standing Alfvén waves
07 p1124 A69-18835
- Computational techniques for determining magnetic field geometry for backscatter reflections
07 p1125 A69-18850
- Earth dipole magnetic field effect on bearing deviation in HF transionospheric propagation analyzed by computer ray tracing
07 p1086 A69-19224
- Geomagnetic field line stretching outward due to energy entry in form of large number of charged particles or increase in particle temperature/inflation/
07 p1127 A69-19357
- Structure, temporal behavior, shape and length of earth magnetic tail via satellite mapping
07 p1208 A69-19363
- Geomagnetic tail topology, reconnection and interaction with moon from Explorer 33 satellite data
07 p1128 A69-19365
- Bow shock and magnetopause boundary observations with IMP 2 plasma detector
07 p1129 A69-19372
- Angular intensity distribution of corpuscular radiation in time independent geomagnetic field characterized by particle velocity distribution
07 p1210 A69-19619
- Equatorial counter-electrojet and inverse quiet day solar diurnal variation current layers, noting regular diurnal variation horizontal component and latitude effect
08 p1306 A69-19884
- Earth internal magnetic field effects on cosmic ray measurements, dipole approximation and effect of external sources
08 p1378 A69-20219
- Geomagnetic field strength in early Precambrian, discussing thermoremanent normal remnant and saturation inverse remnant magnetization studies of Botswana Modipe gabbro
08 p1309 A69-20580
- Atmospheric humidity effect on efficiency of geomagnetic field scales with taut-strip suspension and temperature fluctuation
09 p1494 A69-21518
- Captured particles magnetic drift envelopes in magnetosphere calculated by model considering perpendicular geomagnetic dipole to solar wind
09 p1574 A69-21521
- Geomagnetic secular variations calculated by comparison of satellite, oceanic and aeromagnetic surveys
09 p1485 A69-21534
- Separation of normal geomagnetic field component from limited length measurements by moving averages, considering error and inhomogeneity of anomalous field
09 p1486 A69-21537
- Magnetic declination from moving objects measured by geomagnetic vector projection in solar direction
09 p1486 A69-21538
- Geomagnetic field quiet solar variations variability explained by model, noting agreement with observations at various stations
09 p1486 A69-21549
- Geomagnetic field mean hourly values continuous smoothing from recordings at drifting arctic stations for determining time variations
09 p1487 A69-21553
- Anomalous magnetic field energy spectrum obtained from aeromagnetic survey and approximation valid for earth crust and upper mantle
09 p1487 A69-21554
- Solar wind-magnetosphere pressure balance and proton density of solar wind
09 p1577 A69-21711
- Real configuration effect of magnetic field in moderately perturbed magnetosphere on whistlers dynamic spectra, stressing geomagnetic perturbation detection
09 p1490 A69-21766
- Geomagnetic activity correlation to cosmic ray solar daily variation underground, observing primary cosmic ray flux with meson telescopes
09 p1583 A69-22755
- VLF polar chorus emission and geomagnetic variations caused by compressions or expansions of magnetosphere
10 p1681 A69-22803
- Auroral electrojet precursors and geomagnetic variations before onset of bays, noting satellite observations
10 p1681 A69-22804
- Daily observational results of solar phenomena, cosmic rays, geomagnetic variations, ionosphere, radio wave propagation and airglow arranged according to solar rotation number
10 p1771 A69-22808
- Charged particles motion in geomagnetic field from analyzing spatial distribution within framework of two dipole magnetosphere model
10 p1756 A69-22818
- Cosmic ray intensity variations by spectrographic method, noting geomagnetic effects
10 p1759 A69-22836
- Electron production rates variations in lower ionosphere cosmic layer related to meteorological, geomagnetic and cosmic conditions
10 p1759 A69-22839
- Geomagnetic field variations in middle and high latitudes during proton flare event, discussing UV radiation and period and energy spectra
10 p1683 A69-23780
- Low energy particles during solar proton flare and effects on magnetosphere, cosmic ray intensity, ionosphere and geomagnetic activity
10 p1768 A69-23786
- Mariner 2 measurements of geomagnetic field and interplanetary plasma parameters for analyzing interaction between interplanetary medium and magnetosphere during decreased solar activity
10 p1769 A69-23900
- Magnetosphere boundary configuration calculated with allowance for geomagnetic dipole inclination to geographic axis and nondipole section of geomagnetic field
10 p1686 A69-23902
- Interplanetary magnetic field sectoral structure effect on diurnal cosmic ray intensity and geomagnetic field, noting field direction influence
10 p1769 A69-23905
- Lunar diurnal variation parameters at Irkutsk determined from IGY data concerning geomagnetic field components
10 p1687 A69-23918
- Secular variations distribution on earth surface, plotting isopore charts from mean annual values of magnetic elements/1960-1965/
10 p1687 A69-23920
- Polar geomagnetic disturbances global current systems representation by prototypes of equivalent current systems
10 p1688 A69-23937
- Harmonic analysis of magnetic storms initial phases having steep leading edges and distinct steady portions, showing homogeneity in first approximation
10 p1688 A69-23938
- Geomagnetic field pulsations frequency changes in relation to geomagnetic and solar activity level
10 p1689 A69-23939
- Stable particle trapping zone in magnetosphere, discussing results of adiabatic theory application to charged particle motion in earth magnetic field
11 p1948 A69-24858
- Satellite measurements of suprathermal electrons at conjugate sunrise, indicating photoelectron escape from production level and movement along geomagnetic lines into conjugate ionosphere
11 p1950 A69-25144
- Magnetic anomalies off Cape Hatteras explained as possible edge effect, discussing ocean and continental magnetic crusts and igneous and magnetic rocks
11 p1879 A69-25405
- Recurrent geophysical disturbances associated with solar active regions and low latitude background field pattern on solar surface magnetic fields
11 p1964 A69-25415
- Geomagnetic field vertical and horizontal intensities measured using proton magnetometer with coil theodolite
11 p1889 A69-25435
- Solar and lunar/solar harmonics determination, noting effects of moon on values of horizontal magnetic component
11 p1965 A69-25555
- Upper atmosphere density variations investigation using Eurobs system, correlating density to geomagnetic activity and 10.7 cm solar radio emission
12 p2069 A69-26437
- Cylindrical satellite drag rotating about transverse axis in earth magnetic field, including aerodynamic and magnetic moments
12 p2174 A69-26443
- Solar wind interaction with geomagnetic field simulation practically unrealizable, discussing partial simulation covering neutral magnetic layer formation on night side
12 p2149 A69-26681
- Geomagnetic field dipole model by extrapolating vertical Z component for 1955 to heights between 500 and 25,000 km
12 p2071 A69-26695
- Cosmic radiation recorder designed for use onboard satellite to measure intensity space-time distribution under geomagnetic effect
12 p2094 A69-26697
- Solar wind interaction with geomagnetic field, considering bow shock, field confinement in magnetosphere and stretching out of lines of force
12 p2072 A69-26735
- Solar plasma flow around magnetosphere, discussing plasma velocity, density and temperature and magnetic field space and time variations
12 p2150 A69-26736
- Laboratory models for solar wind and magnetosphere interactions with similarity laws of Vlasov theory as reference system
12 p2150 A69-26737
- Satellite observations of geomagnetic tail in magnetosphere near midnight meridian plane, discussing formation, shape, plasma sheet and models
12 p2072 A69-26739
- Particle fluxes in outer radiation belt and unstable radiation zone of outer geomagnetic field, discussing electron diffusion into magnetosphere and magnetic disturbances
12 p2150 A69-26744
- Low energy plasma fluxes in magnetosphere, discussing plasmapause position dependence on geomagnetic activity
12 p2150 A69-26747
- Solar wind plasma observations in geomagnetospheric wake compared at 1000 and 500 earth radii, considering ion energy spectra and geomagnetic tail
12 p2151 A69-26943
- Model for self consistent time independent ring current of charged particle distribution under combined field of earth dipole and particle motion current
12 p2151 A69-26948
- Southern radio auroral zone observation with rhombic antennas, noting diffuse and discrete zones associated with proton and electron precipitation
12 p2033 A69-26950
- Sea tides and ionospheric effects on lunar variation of geomagnetic field vertical component
12 p2161 A69-26957
- Computer program for worldwide analysis of mean hourly values of field components into constituent fields and associated ionospheric current systems
12 p2074 A69-26958
- Magnetosphere model for plasma pressure by solar wind, discussing plasma drift from neutral sheet into geomagnetic tail
12 p2076 A69-27106

Electron motion effects along magnetic field lines on axisymmetric torsional hydromagnetic oscillations in inhomogeneous low beta plasma, discussing resonance trapping
12 p2076 A69-27107

Model for perturbations in earth rotation and geomagnetic core-mantle coupling, discussing electromagnetic restoring torque
12 p2077 A69-27110

Drift velocity of earth magnetic field based on spherical harmonic analysis of geomagnetic secular variation
12 p2077 A69-27111

Geomagnetic field daily variations, discussing observational techniques, observation analysis, S-field seasonal changes, equatorial electrojet, solar wind effects, dynamo theory, etc
12 p2077 A69-27143

Soviet satellite and probe studies of earth, moon, Venus and Mars magnetic fields, noting automatic magnetometer
13 p2336 A69-27352

Equatorial electrojet role in electromagnetic induction at magnetic dip equator, applying Price theory for space gradients
13 p2252 A69-27519

Magnetospheric field configuration in midnight meridian, considering cavity boundary surface and trapping region currents and tail sheet current
13 p2252 A69-27532

Relation between north-south asymmetry of F 2 region critical frequencies and geomagnetic axis inclination angle, establishing increase in asymmetry during increased solar activity
13 p2256 A69-28693

Perturbed geomagnetic field structure during magnetic storm recovery phase calculated by magnetosphere magnetic field model, accounting for various external field sources
13 p2257 A69-28697

Methodological problems in studying ionosphere by phase measurements without taking into account geomagnetic field, noting value of main results
13 p2257 A69-28699

Whistler dynamic spectra variation studies, emphasizing distorted magnetospheric geomagnetic field structure effect
13 p2257 A69-28702

Relationship between polar geomagnetic disturbances and DR variations value of geomagnetic field
13 p2257 A69-28703

Dipole models of geomagnetism at earth surface used to calculate magnetic field in outer space
13 p2257 A69-28704

Geomagnetic field components measurements from moving object, investigating astronomical orientation applicability for three component magnetometer
13 p2257 A69-28705

Geomagnetic field H and Z components measured by proton magnetometer, applying supplementary field method for error correction
13 p2257 A69-28706

Analytical model of geomagnetic field constructed from Cosmos 49 data using spherical analysis
13 p2258 A69-28729

Vertical and horizontal components of geomagnetic storm main phase magnetic variations applied to vertical electromagnetic soundings of earth
13 p2258 A69-28731

Power spectrum analysis and linear filtering for 27 day variation amplitude of geomagnetic disturbance subject to semiannual amplitude modulation
14 p2434 A69-28955

Low energy charged particle motion parallel with magnetic force lines analyzed in magnetosphere model with constant electric field
14 p2512 A69-29040

Polar auroral region displacement ascribed to distant magnetic field disturbances, proposing calculation method
14 p2436 A69-29059

Statistical description of geomagnetic field as random vector field, presenting correlation functions from empirical estimates from geomagnetic charts
14 p2437 A69-29062

Geomagnetic normal fields determination using spherical harmonic analysis, including extension to local fields
14 p2437 A69-29063

Magnetic damping of homogeneous cylindrical satellite rotation about transverse axis
14 p2530 A69-29065

Geomagnetic cut-off influence on charged particle dynamics in geomagnetic field, applying charged particle motion theories to magnetosphere fields
14 p2513 A69-29099

Satellite 40 mc signal scintillations near sunspot minimum, noting scintillation index dependence on angle between radio ray and magnetic field
14 p2439 A69-29114

Geomagnetic storms caused by plasma streams impinging on earth related to preceding cosmic flares, discussing polar cap absorption and ground level effects
14 p2514 A69-29416

Remanent magnetization properties in alkaalic igneous complexes at Magnet Cove and Potash Suphur Spring, Ark., calculating paleomagnetic pole during Cretaceous
14 p2445 A69-29884

Absorption coefficient in three microwave lines of O with different rotational quantum numbers calculated, examining Zeeman effect in geomagnetic field
15 p2597 A69-30941

Geomagnetic ring current study, giving exact kinetic description based on Vlasov equation of plasma ring current in dipolar field
15 p2598 A69-31218

Exospheric temperature variations by Thomson scattering related to solar and geomagnetic activity, discussing seasonal effect on thermospheric variables
15 p2604 A69-31409

Atmospheric density dependence on solar and geomagnetic activity at low latitudes, discussing atmospheric expansion
15 p2605 A69-31441

Radar thomson scatter from nonthermal steady state level of plasma waves in ionosphere measured, studying role of angle between wave vector and magnetic field
16 p2818 A69-31678

Book on ionospheric radio waves covering geomagnetism and sun, whistler propagation, oblique propagation, satellite sounding, etc
16 p2749 A69-31715

Worldwide changes in geomagnetic field, determining causes by examining magnetic field and plasma data for solar wind and classifying as SSC or SI
16 p2847 A69-31963

Geomagnetic field westward drift related to earth core rotation from calculating drift at earth surface and at core
16 p2774 A69-31983

Self consistent ring current of radiation belt under combined influence of earth dipole field and field due to currents of particle motions
16 p2776 A69-32096

Geomagnetic normal field of vertical component for Central Europe, discussing influence of local factors on observational data
16 p2782 A69-32461

Magnetized minerals studied to investigate space-time structure and reversal of main geomagnetic field
16 p2782 A69-32462

Captured particles magnetic drift envelopes in magnetosphere calculated by model, considering perpendicular geomagnetic dipole to solar wind
16 p2851 A69-32516

Geomagnetic secular variations calculated by comparison of satellite, oceanic and aeromagnetic surveys
16 p2783 A69-32529

Separation of normal geomagnetic field component from limited length measurements by moving averages, considering error and inhomogeneity of anomalous field
16 p2783 A69-32532

Magnetic declination from moving objects measured by geomagnetic vector projection in solar direction
16 p2783 A69-32533

Geomagnetic field quiet solar variations variability explained by model, noting agreement with observations at various stations
16 p2784 A69-32544

Geomagnetic field mean hourly values continuous smoothing from recordings at drifting arctic stations for determining time variations
16 p2784 A69-32548

Anomalous magnetic field energy spectrum obtained from aeromagnetic survey and approximation valid for earth crust and upper mantle
16 p2784 A69-32549

Polar substorms resulting from interaction between magnetized plasma stream and geomagnetic field in magnetosphere
16 p2852 A69-32620

Solar and terrestrial phenomena correlated for March 1966 events
16 p2852 A69-32621

Magnetic analysis by successive double heat treatment of miocene lava cooled during geomagnetic polarity reversal for determining field intensity
16 p2788 A69-32646

Earth core conductivity effects on ionospheric shielding against geomagnetic changes from external sources, noting earth-ionosphere coupling
17 p2959 A69-32925

Earth-ionosphere waveguide excitation by lightning discharges and geomagnetic field influence on ELF noise spectrum
17 p2928 A69-33865

U shaped polar auroras development, examining relation with magnetic activity and current system configuration in lower ionosphere
17 p2963 A69-33952

Time distribution of commencements of substantial intensity increases of geomagnetic and aeromagnetic phenomena
17 p2964 A69-33958

High latitude geomagnetic field quiet solar diurnal variations during magnetically quiet IGY winter days, relating type and amplitude at low and midlatitudes
17 p2964 A69-33960

Geomagnetic disturbances intensity spatiotemporal distribution at Northern Hemisphere high latitudes during IGY and IQSY
17 p2965 A69-33966

Cosmic radio emission absorption during IQSY at 24.6 MHz, relating diurnal variation of absorption and geomagnetic index F scatter occurrence
17 p2968 A69-33992

Cosmic ray diurnal anisotropy variations, correlating component annual means with magnetic activity
18 p3186 A69-34934

Stream structure in interplanetary magnetic field during 1966, analyzing geomagnetic activity and solar particles and Forbush decrease anisotropy
18 p3199 A69-34938

RF synchrotron emission from electrons trapped in earth magnetic field observed by satellite, using magnetospheric environment model
18 p3128 A69-34948

Antarctic VLF emissions polarization and direction determination, using combination of antennas with planes lying in geomagnetic E-W and N-S directions
18 p3102 A69-34965

Solar microwave emission heliographic distribution during pronounced geomagnetic recurrence, noting brightness temperature nonuniformity due to coronal depression through polytropic models for solar wind
18 p3188 A69-35396

Solar cycle line in horizontal force of earth magnetic field resolved by power spectrum analysis suggesting 80 year cycle
18 p3205 A69-35414

Attitude stabilized rocket-released magnetometer for detection of earth field magnitude and direction changes
19 p3309 A69-35994

Electrically charged earth satellite motion under action of Lorentz force produced by geomagnetic field interaction, relating field trajectories to acceleration
19 p3431 A69-36615

Nighttime F 2 region temperature distribution under geomagnetically calm and disturbed conditions calculated from Alouette 1 satellite data
19 p3304 A69-36623

OGO triaxial search coil magnetometer for measuring earth magnetic fluctuations, discussing design rationale and observation results
19 p3284 A69-36675

Reversal rate of earth magnetic field deduced from observed and theoretical polarity interval length using hydraulic transmission line theory
19 p3304 A69-36869

Lower ionosphere geomagnetic field local gradients determination by partial reflection method
20 p3522 A69-37055

Terrestrial electrical conductivity measurement from electromagnetic field variations determination by geomagnetic sounding
20 p3522 A69-37058

Geomagnetic field lines coordinates calculation based on coefficients obtained in spherical harmonic analysis
20 p3522 A69-37060

Geomagnetic field total vector modulus secular variations from airborne measurements
20 p3522 A69-37061

Geomagnetic field model /POGO/ to confirm eccentric dipole westward velocity secular decrease predicted by day length changes
20 p3523 A69-37490

Solar and geomagnetic activity persistence by variance spectrum analysis, noting sunspot numbers and radiation flux autocorrelation functions
20 p3601 A69-37508

Solar microwave emission relationship to geomagnetic activity, analyzing statistically source intensity and model of coronal condensation associated with sunspots based on electron densities
20 p3589 A69-37557

Seasonal anomaly of F 2 layer critical frequency in Northern and Southern Hemispheres during high and low solar activity, discussing geomagnetic effect
20 p3526 A69-37667

Residual nighttime radio wave absorption in ionosphere, noting absorption-magnetic activity relation existence
20 p3528 A69-37678

High latitude limit of closed geomagnetic field lines indicated by high latitude electron boundary in outer radiation zone during Alouette satellite energy particle experiment
20 p3531 A69-37875

Model equatorial electrojet with meridional current system constructed by spherical harmonic expansion for geomagnetic field, noting current loops
20 p3533 A69-38084

Diffraction pattern of satellite signal field-aligned amplitude scintillation during quiet geomagnetic conditions
20 p3497 A69-38108

Geomagnetic field horizontal component daily variations in relation to solar wind, noting effects of ambient field night side decrease
21 p3714 A69-38549

Radio pulse emission from ionized disk of cosmic ray extensive air showers, noting importance of charge separation in geomagnetic field and selective positron absorption
21 p3792 A69-39614

Satellite stabilization by earth magnetic field through conservative magnetic moments application
21 p3830 A69-39834

Herzenberg geomagnetic dynamo model extensions including rigid rotors calculus, laminated rotors, induction problem and fluid rotors in rigid conductor
22 p3989 A69-40193

Bullard-Gellman dynamo, discussing magnetic field development as series expansion, truncation levels and convergence
22 p4018 A69-40194

MHD dynamo construction with emphasis on fluid motion effect on magnetic field, considering spatially periodic dynamo derivation from kinematic considerations
22 p3989 A69-40196

North Pole trajectories and geomagnetic fields assuming motion of earth mantle and interior
22 p3942 A69-41120

Short lived Forbush decreases, discussing phase differences between stations due to asymptotic directions changed by geomagnetic field and spatial anisotropy
23 p4204 A69-41480

Geomagnetic field spherical analysis from angular data and extrapolated values of time variable field coefficient
23 p4157 A69-41866

Low noise nuclear precession magnetometer noise rejection optimization design specifications for measuring geomagnetic field components
23 p4165 A69-41868

Quartz compasses designed for orientation of electronic devices with respect to magnetic meridians at low horizontal component values
23 p4166 A69-41869

Noncyclic daily solar quiet variation in mean hourly geomagnetic field by including noncyclic variation term in regression model
23 p4158 A69-42170

Geomagnetic multipole parameters changes using spherical harmonic coefficients of geomagnetic potential, relating to secular variation field
23 p4158 A69-42171

Single dipole field approximation of geomagnetic field, minimizing sum of squares of differences between dipole field and geomagnetic field
23 p4158 A69-42173

Two and three dipole approximation of main geomagnetic field based on minimization of sum of squares of differences between dipole and geomagnetic fields
23 p4158 A69-42174

Solar quiet and lunar electric current systems deduced from geomagnetic data, discussing electrical conductivities and wind models in dynamo region
23 p4160 A69-42427

Magnetic dip equator position at E layer and gradient with time and altitude, using geomagnetic field models
23 p4160 A69-42428

Solar wind kinetic energy density using geomagnetic field horizontal component daily variation, treating earth as plasma probe
24 p4308 A69-42968

Geomagnetic zenith calculation at given point based on magnetic field model, using polynomial development
24 p4311 A69-43505

GEOMETRICAL HYDROMAGNETICS
U MAGNETOHYDRODYNAMICS

GEOMETRICAL OPTICS
U OPTICS

GEOMETRODYNAMICS
U RELATIVITY

GEOMETRY
NT ANGLES [GEOMETRY]
NT BRAGG ANGLE
NT BREWSTER ANGLE
NT CARTESIAN COORDINATES
NT CHORDS [GEOMETRY]
NT CIRCLES [GEOMETRY]
NT COLLINEARITY
NT COPLANARITY
NT CURL [VECTORS]
NT CURVATURE
NT CURVES [GEOMETRY]
NT CUSPS [MATHEMATICS]
NT CYCLOIDS
NT DIFFERENTIAL GEOMETRY
NT DOUBLE CUSPS
NT ELLIPSES
NT EUCLIDEAN GEOMETRY
NT FIXED POINTS [MATHEMATICS]
NT FLOW GEOMETRY
NT GREAT CIRCLES
NT HYPERBOLAS
NT IMBEDDINGS [MATHEMATICS]
NT INVARIANT IMBEDDINGS
NT LIE GROUPS
NT LINES [GEOMETRY]
NT LOCI
NT MERCATOR PROJECTION
NT NOZZLE GEOMETRY
NT OBLATE SPHEROIDS
NT OCTAHEDRONS
NT PARABOLAS
NT PARALLELEPIPEDS
NT PARALLOGRAMS
NT POINTS [MATHEMATICS]
NT POLYEDRONS
NT PROJECTIVE GEOMETRY
NT PROLATE SPHEROIDS
NT RADII
NT RECTANGLES
NT RIEMANN MANIFOLD
NT S CURVES
NT SPHEROIDS
NT SPINOR GROUPS
NT SQUARES [MATHEMATICS]
NT TANGENTS
NT TANK GEOMETRY
NT TENSOR ANALYSIS
NT TETRAHEDRONS
NT TOPOLOGY
NT TORUSES
NT TRIANGLES
NT TRIGONOMETRY
NT VECTOR ANALYSIS
NT VORTICITY

Mirror photogrammetry geometric principles, studying photo pairs, mirror reflection and reduction methods
01 p0077 A69-10025

Photomultiplier geometry without use of light pipes for uniform response from large area single and double sheet plastic scintillation detectors
03 p0428 A69-13107

Geometrical and thermomechanical effects on pressure and forces in deformation of thin Ti alloy blanks
03 p0452 A69-14123

Computer programming language for three dimensional geometry at symbolic level, noting use for placement problems
05 p0724 A69-16382

Geometry changes influence on rigid plastic circular plate behavior under two independent distributed pressures
06 p1023 A69-17508

Performance prediction for planar and cylindrical electrode geometry fixed spacing thermionic converters
09 p1438 A69-21814

Single mirror scanning geometry and kinematics, analyzing spatial motion of objects plane mirror image
12 p2091 A69-26367

Unified geometric description of gravitational and electromagnetic fields, determining electromagnetic field influence on geometry from dimensional constant
13 p2300 A69-28450

Liquid sloshing in vessel of complex geometry reduced to boundary value problem
14 p2428 A69-28969

Gas discharge tube graphite hollow cathode geometry leading to abnormal discharge operation under certain pressure conditions
16 p2814 A69-31838

Radiative heat transfer in nonisothermal scattering media of plane, spherical and cylindrical geometries separated by particle cloud
16 p2878 A69-31925

Fracture processes in high strength materials, considering effect of stored elastic energy, component geometry, fracture toughness and environment
17 p2988 A69-33553

Measurement errors and geometry effects on navigational accuracy, determining maximum allowable error for measuring devices employed
17 p3002 A69-34098

Syphon geometry influence on rigidity and strength determined using integrating Meissner type differential equations with finite difference schemes
19 p3358 A69-35849

Geometry effects on stresses in discontinuous composite materials, studying fiber spacing, failure and discontinuities size and nature
20 p3565 A69-36942

Theory for describing rotating fluid planets external geometry in state of hydrostatic equilibrium, noting role of equipotential surfaces
20 p3594 A69-37077

Solar activity effect on F 2 layer geometrical parameters, plotting prognostic maps using nomographic methods
20 p3526 A69-37663

Lunar spherical astronomy, discussing coordinate transformations, precessional and nutational motions, etc
21 p3798 A69-38605

Computerized crewstation geometry evaluation and design optimization using 23-pin-joint man-model [AIAA PAPER 69-977]
22 p3892 A69-40357

GEO MORPHOLOGY
Sand ridge origin and dynamical setting, discussing morphology-tidal current system equilibrium indicated by theory and field measurements
15 p2596 A69-30443

Aerial photography in geomorphological interpretations, noting advantages over conventional maps in slope microreliefs, soil erosion network and karst, glacial, aeolian and shore features
20 p3539 A69-37512

Auroral displays photographed by all-sky cameras at magnetically conjugate stations, morphological similarities and electron precipitation role
20 p3535 A69-38187

GEON [TRADEMARK]
U POLYVINYL CHLORIDE

GEO PHYSICAL OBSERVATORIES
NT OGO
NT OGO-D
NT OGO-E
NT OGO-F

Geophysical investigations on manned orbital space laboratories, discussing space photography, spectrophotometry, terrain pictures and aerosol layers
05 p0759 A69-16633

Multiple ground based geophysical sensors for detecting ionospheric phenomena, discussing continuous magnetic tape data recording, common time base and station operation
14 p2448 A69-29526

GEO PHYSICAL SATELLITES
NT OGO
NT OGO-D
NT OGO-E
NT OGO-F

Imaging radar systems for employment on small spacecraft, fabricating small lightweight radar systems packages with integrated circuit techniques
11 p1835 A69-24695

Soviet rocket and satellite studies of upper atmosphere and ionosphere
13 p2251 A69-27347

Soviet meteorological and geophysical rockets, satellites and techniques in cloud studies and weather forecasting, noting Cosmos results
13 p2290 A69-27348

Satellite radio observation for ionospheric parameters, utilizing Doppler and Faraday phenomena, signals fluctuations and sporadic phenomena
15 p2594 A69-30028

- Spacecraft and boosters for earth resources surveys, discussing design, payloads, orbits, etc
21 p3799 A69-38629
- GEOPHYSICS**
- Solar and geophysical activity during February 1965 and March 1966 indicating geomagnetic activity on 27-day recurrence diagram
01 p0068 A69-11118
- Geophysical effects observed in Northern Hemisphere during low solar activity, discussing polar auroral intensities and positions
02 p0239 A69-11694
- Meteorological instrumentation in India for surface and upper air observation
02 p0248 A69-11817
- Geophysical theory and computers - Conference, University of Trieste, September 1967
02 p0242 A69-12005
- Book containing 1960-1965 /including IQSY/ chronological tables of solar and geophysical events, discussing solar activity, geomagnetic, ionospheric, auroral and cosmic ray research
02 p0321 A69-12165
- Slide wire aircraft vertical velocity meter for application during aerogravimetric mapping, discussing calibration and gravitational force measurement accuracy
03 p0429 A69-13261
- Space systems use for planetary geology and geophysics - Conference, Boston, May 1967
03 p0509 A69-13390
- Detection of electric field turbulence in earth bow shock, noting wave amplitude correlation with magnetic field structure
04 p0592 A69-14681
- International cooperation results in field of optical tracking of satellites for solving problems of atmospheric physics, geophysics and geodesy
06 p1042 A69-17050
- Dynamics and instability of multilayered systems models in field of gravity, noting isostatic adjustment of layered globe
08 p1309 A69-20578
- Conversion of Woollard theory coefficients of tidal irregularity of earth rotation to new system of constants
09 p1484 A69-21383
- Statistical regularization for obtaining a priori probability distribution information on mathematically incorrect inverse geophysical problems, deriving algorithm
10 p1689 A69-23968
- Geophysics - Conference, Naples, May 1967
13 p2255 A69-28646
- Geophysical effects observed in Northern Hemisphere during low solar activity, discussing polar auroral intensities and positions
13 p2258 A69-28725
- Solar-terrestrial physics, Solar aspects - IQSY/COSPAR Conference, London, July 1967, Part 1
15 p2672 A69-30005
- Cosmology and geophysics relationships using initial and boundary conditions concept
16 p2864 A69-32451
- Astronomical and geophysical observations, selecting degree of smoothing via Whittaker method for curve construction
17 p3028 A69-32877
- Conversion of Woollard theory coefficients of tidal irregularity of earth rotation to new system of constants
18 p3127 A69-34771
- Geophysics international dictionary, Volume 1 /A-J/ covering seismology, geomagnetism, aeronomy, oceanography, geodesy, gravity, marine geophysics, meteorology, earth origin and evolution
19 p3303 A69-36511
- Geophysics international dictionary, Volume 2 /K-Z/ covering seismology, geomagnetism, aeronomy, oceanography, geodesy, gravity, marine geophysics, meteorology, earth origin and evolution
19 p3304 A69-36512
- Solar proton flare June 1968 analysis, discussing geophysical effects and possible polar cap absorption
20 p3587 A69-37332
- Radar geoscience application, discussing radar return relation to illuminated terrain in detecting buried river channels
20 p3491 A69-37651
- Soviet book on synoptic climatological and heliogeophysical long term weather forecasts, discussing monthly and seasonal anomalies, sun-earth interrelations, solar corpuscular elements, etc
21 p3759 A69-39523

- Statistical regularization for obtaining a priori probability distribution information on mathematically incorrect inverse geophysical problems, deriving algorithm
21 p3680 A69-39654
- Advances in geophysics, Volume 13, covering airborne geophysical methods, ball lightning structure, lidar, middle atmosphere energetics, etc
22 p3940 A69-40534
- Handbook on geochemistry, Volume 2/1, covering geophysics, cosmochemistry, etc
22 p3897 A69-40890
- Handbook on geochemistry, Volume 1, covering meteorite composition, cosmic abundances, earth geophysical structure and composition, data evaluation, etc
22 p3897 A69-40980
- Geophysical aspects of earth chemical composition, structure and energy balance
22 p4032 A69-40983
- Book on geophysics covering lithosphere, hydrosphere, atmosphere, earth motion and tremors, geomagnetism, water mass circulations, radioactivity, atmospheric electricity, measurement techniques and equipment
23 p4154 A69-41367
- Meteorology and geophysics - Conference, Hamburg, April 1968
24 p4344 A69-43144
- Geodetic and geophysical random uncertainties as fundamental limitations on terrestrial inertial navigation accuracy [AIAA PAPER 68-847]
24 p4348 A69-43240
- Interplanetary and geophysical conditions forecasting based on repetitions of low latitude photospheric background magnetic field patterns during solar activity cycles
24 p4387 A69-43626
- GEOPOTENTIAL**
- Gravitational field and earth shape determination by calculating perturbing potential at earth surface and in outer space, using Green functions
01 p0063 A69-10360
- Diapason satellite geodetic results concerning measurement accuracy, terrestrial potential models and station synchronization
01 p0065 A69-10543
- Six level model for numerical geopotential forecast allowing for quasi-static and quasi-geostrophic approximations
02 p0273 A69-11434
- Interpolation of deflections of vertical from horizontal gravity gradients, discussing potential applications to photogrammetry
02 p0243 A69-12012
- Anomalous gravitational geopotential as function of mass, discussing density anomalies in spherical shells for harmonics as obtained from satellite observations
02 p0244 A69-12178
- Satellite orbit selection for determining geopotential and spherical and tesseral harmonic coefficients, discussing propulsion systems and satellite observation cost feasibility
02 p0331 A69-12807
- Geopotential resonant orbital perturbations of existing satellites, noting high inclination role
03 p0521 A69-13777
- Error distribution maps for measurements of parameters epsilon, F and E of geomagnetic potential in Northern and Southern Hemispheres
04 p0627 A69-15031
- Perturbations of stationary orbital vehicles of arbitrary latitude due to earth triaxiality, noting control by low thrust rocket engine
05 p0823 A69-16037
- Canonical correlations used to analyze relations between values of geopotential field
05 p0789 A69-16637
- Earth ellipsoid fundamental parameters for calculation of earth flattening and normal acceleration due to gravity
09 p1487 A69-21633
- Earth equipotential surface shape determination from satellite orbit dynamics, obtaining triaxial ellipsoid
09 p1487 A69-21635
- Optimum coordination between homogeneous isotropic geopotential field and derivatives, estimating efficiency of geopotential and wind fields simultaneous analysis
12 p2126 A69-26580
- Stratosphere and troposphere processes analyzed, indicating feasibility of forecasting geopotential and wind fields between 12 and 24 km
12 p2126 A69-26581

- Earth gravitational field representation by separating geopotential into normal and disturbing potential for solving geodetic boundary value problem for satellite geodesy
12 p2076 A69-27089
- Gravity perturbations in earth external field, treating anomalous potential using Green integral formula and spherical harmonics
12 p2077 A69-27139
- Regression coefficients obtained from satellite cloud observations applicability in constructing geopotential fields, tabulating coefficients obtained from ground stations
13 p2292 A69-27731
- Satellite and aerological ground station data combined to determine geopotential fields and wind velocity fields for inadequately serviced areas
13 p2292 A69-27732
- Wind velocity, geopotential and atmospheric layer temperature fields constructed from Tiros 9 satellite cloud data using least squares method and trigonometric polynomials
13 p2292 A69-27733
- Geopotential and wind prediction by integration of prognostic equations of single level atmosphere
13 p2294 A69-27852
- Canonical correlations used to analyze relations between values of geopotential field
14 p2472 A69-28793
- Odd zonal harmonics coefficients in earth gravitational potential from analysis of satellite orbital eccentricity variations
14 p2439 A69-29118
- Temperatures and geopotentials of isobaric surfaces in Northern and Southern Hemispheres compared for summer and winter seasons
14 p2473 A69-29724
- Spatial correlation function of Northern Hemisphere geopotential, using model based on random distribution of potential vortex fluctuations for atmospheric circulation
14 p2476 A69-29822
- Normalized correlation functions of dispersion values for pressure fields and geopotential obtained by low latitude stations, noting wind field features
14 p2478 A69-29833
- Earth orography influence on climatological distribution of wind and geopotential fields, stressing central asiatic mountains role in atmospheric circulation
14 p2478 A69-29835
- Geopotential determination from gravity force measurements at known surface and error assessment for earth model with aid of spherical harmonic expansion
15 p2689 A69-30567
- Geopotential represented in ellipsoidal harmonics, discussing Lamé functions generation and rectangular-ellipsoidal coordinates relation and orbital elements perturbations
15 p2599 A69-31333
- Coefficients of zonal spherical harmonics to 21st order in expression for earth gravitational potential
15 p2600 A69-31358
- Tesseral harmonics of geopotential and station coordinates based on combined Baker-Nunn, laser and range and rate satellite data
15 p2601 A69-31372
- Earth figure parameters from satellite orbit dynamics, including potential on geoidal surface and scale factor for lengths
15 p2602 A69-31387
- Satellite orbit evolution data applied to refinement of geophysical parameters, including upper atmosphere parameters and zonal harmonic coefficients in gravitational potential expansion
15 p2604 A69-31417
- Satellite orbital resonances due to geopotential analyzed by asymptotic expansion for nearly circular or equatorial orbits
16 p2863 A69-32401
- Geopotential field forecast for 500 mb surface, comparing results from quasi-solenoidal and quasi-geostrophic models
21 p3758 A69-39110
- Impedance of inhomogeneous earth from magnetic and electric fields and geomagnetic potential measurements
23 p4157 A69-41867
- GEOPOTENTIAL HEIGHT**
- Regression generated radiometric and contour height fields of North American Continent using Nimbus 2 IR equivalent black body temperature and geopotential data
24 p4343 A69-42896

GEOS 2 SATELLITE

Heat pipe system performance of GEOS 2 satellite, noting transponders temperature differences
23 p4224 A69-42082

GEOSTROPHIC WIND

Geostrophic adjustment for neutral and lapse conditions, discussing similarity arguments based on appropriate length and velocity scales
02 p0276 A69-12699

Factors producing wind deviations from geostrophic pattern under various atmospheric conditions
03 p0458 A69-13267

Statistical analysis of data concerning difference between real wind velocity and velocity of gradient wind for winds of various velocities
03 p0458 A69-13268

Geostrophic wind direct computation from grid point analysis of observed winds, using balance equation
04 p0626 A69-14913

Energy integral of equations used in studying atmospheric motions in quasi-geostrophic approximation
05 p0759 A69-16641

Geostrophic trajectories of horizontal diffusivity estimated in midlatitude troposphere and lower stratosphere
08 p1308 A69-20310

Two level quasi-geostrophic model to probe atmospheric general circulation, noting functional dependence of zonal momentum meridional flux
08 p1346 A69-20314

Atmospheric boundary layer mean turbulence and vertical velocity calculations, tabulating layer characteristics for various turbulent heat flux and geostrophic wind velocity values
12 p2126 A69-26578

Automatic processing and error analysis of horizontal, vertical, static and geostrophic wind data by U.S.S.R. Hydrometeorological Service
13 p2292 A69-27839

Energy integral of equations used in studying atmospheric motions in quasi-geostrophic approximation
14 p2433 A69-28797

Horizontal shear flow effect on linear geostrophic adjustment in unbounded barotropic fluid, discussing gravity waves, vorticity equations, available energy, etc
15 p2648 A69-30217

Friction and wind relationships expressing actual and geostrophic wind as complex numbers or by corresponding vectors in Gauss-Argand diagram
16 p2808 A69-32455

Jet stream blocking process simulation using geostrophic system of equations, considering effects of orography and contrast heating due to land-sea distribution
16 p2809 A69-32602

Semidiurnal oscillation in thermalgeostrophic atmosphere examined using atmospheric model for tidal oscillations response study
17 p2959 A69-33148

Thermal wind instability by numerical integration of equations of motion, noting convective cells tilt
17 p2998 A69-33734

Steady state solution of quasi-geostrophic perturbation equations for atmospheric forced response to parametrized heating as global monsoon theory
19 p3362 A69-36405

Atmospheric zonal circulation compatible with meridional obtained from model based on dynamic and heat flux equations and Williams and Davis hypothesis
23 p4183 A69-41522

GEOTROPISM

Gravity effects on plant growth, discussing horizontal clinostat experiments and auxin transport mechanism
15 p2555 A69-30470

Gravity independence of life processes in terrestrial organisms concluded from zero gravity experiments with algae, hatched larvae, etc
18 p3095 A69-34692

Geotropic response reciprocity in oat seedlings grown in two axis clinostat compared with acceleration constraints of biosatellites, considering imposition of centrifugal force
20 p3477 A69-37620

GEP TELESCOPES

U PARTICLE TELESCOPES

GERDIEN ARC HEATERS

U ARC HEATING

U HEATING EQUIPMENT

GERDIEN CONDENSERS

Ion density, electrical conductivity and weighted mean mobility deduced from Gardien capacitor I-V characteristics used in balloon sounding of stratosphere
18 p3130 A69-34970

GERMANIDES

Praseodymium germanides resistivity and thermal EMF temperature dependence determined, discussing Hall effect, thermal expansion coefficient, melting point microhardness, etc
23 p4199 A69-42467

GERMANIUM

Bulk effect germanium hot-carrier microwave modulator for Q band, reducing required applied voltages by using short length semiconductor ships
01 p0043 A69-10563

Ionization losses of Ge 72 atoms stopping in Ge, noting no cut-off indicative of energy gap effects
01 p0140 A69-11245

Planar technology application to germanium electronic components and integrated circuits
02 p0214 A69-11597

Vacancy diffusion in Ge, relation to precipitation of Cu impurities from supersaturated solid solution and determination of monovacancy migration energy
02 p0295 A69-11780

Low field helicon wave transmission through n-type Ge at liquid He temperature, noting cyclotron resonance damping
02 p0295 A69-11787

Acoustic paramagnetic resonance in arsenic doped germanium, measuring spin-lattice relaxation
02 p0296 A69-11835

Stacking faults in Ge epitaxial layers revealed by etching reagents and X ray diffraction with photographic recording
02 p0297 A69-11880

Step voltage transient behavior of electron-hole plasma injected into Ge, noting current time dependence
02 p0301 A69-12651

Electrical properties of edge and screw type dislocations in germanium, using bilateral microscopy
03 p0488 A69-13761

Dislocation effects on intensity jumps near K edge of absorption, using interferential transmission of X rays in Ge
03 p0490 A69-13944

Fermi level in n- and p-type Ge after irradiation by 50 Mev electrons determined by temperature dependence of carrier concentration
04 p0640 A69-14444

Current and voltage dependence of negative differential resistance segment of current-voltage characteristic on nature of m-p contact in germanium p-n-p-m structures
04 p0642 A69-14793

Direct reading instrument using four point probe and two analog computing circuits for Si and Ge resistivity measurements
04 p0599 A69-15019

Photon emission in germanium at high injection levels during uniaxial compression
04 p0643 A69-15255

Hydrothermal investigation of Ge trace quantity distribution between metal, silicate and sulfide phases at controlled oxygen partial pressure by oxygen buffer techniques
05 p0819 A69-15624

Electron beam modulation of germanium reflectance
05 p0807 A69-15816

Electrical conductivity anisotropy in isotropic germanium and silicon semiconductors, noting effect of metallic contact insertion
05 p0808 A69-16216

Double diffused planar Ge n-p-n and p-n-p transistors with high switching speed, noting fabrication and performance
05 p0809 A69-16557

Radiation defects stability in semiconductors, noting low temperature electron irradiation of Ge and effects of annealing
06 p0974 A69-16863

Electron irradiation annealing and modification of 35 and 65 K defects in n-type Ge induced by 1 Mev electrons at low temperature
06 p0980 A69-17757

Lattice location of dopant elements implanted into Ge determined by carbon ion backscattering, noting substitutional concentrations above thermal equilibrium solubilities
07 p1199 A69-18903

Instability in pyrolytic silicon dioxide films on Ge substrate under bias at room temperature consisting of positively charged ion motion
07 p1200 A69-19010

Cyclotron resonance measurements of quantum effects in Ge valence bands by CW molecular gas laser, developing tunable submillimeter maser [IEEE PAPER C-6]
07 p1150 A69-19051

Distribution and carrier type in germanium bar in electric field, relating distribution obtained by using Hall effect to avalanche phenomenon
08 p1372 A69-20277

Germanium solid state triode controlling electron currents of space charge limited regime by means of gate conductors in solid state diode
09 p1462 A69-21353

Transitions between heavy hole and spin orbit split bands in uniaxially stressed Ge and GaAs, noting spectra for various temperatures and valence band parameters
10 p1745 A69-23359

Hetero-epitaxial germanium films on GaAs by germanium condensation from molecular beams in vacuum, obtaining p-type conductivity
11 p1938 A69-25033

Solid state IR imaging using monolithic Ge mosaics of isolated sensor elements, discussing design, structure, fabrication, system readout and operation
11 p1938 A69-25307

Metallic impurities effect on Ge surface charge and recombination properties, noting fast and slow electron density changes by forbidden band penetration
11 p1939 A69-25703

Lattice defects in development of recombination centers on Ge semiconductor surfaces, discussing photoconductivity and field effect
12 p2142 A69-25978

Germanium surface IR radiation absorption in vacuum at low temperatures, obtaining modulated interval reflection spectra
13 p2317 A69-27879

Phase diagram for physicochemical study of CdSb-Ge cross section of Cd-Sb-Ge ternary system, discussing exo-endothermal fusion effects, microstructure, etc
14 p2503 A69-28975

Electrical and photoelectrical properties of semiconductor heterojunctions prepared by Ge epitaxy on gallium arsenide bases, showing dependence on base surface treatment
15 p2667 A69-30078

Optical constants changes in germanium determined by modulation method of measuring light reflected at different angles
18 p3173 A69-35014

Transient calibrations for Ge surface thermocouple heat flux sensors used in hypervelocity impulse tunnel
19 p3292 A69-35725

Transducer with single crystal Ge for high heat flux measurement, noting calibration by direct conduction
19 p3307 A69-35748

Reactive scattering from solid surfaces, discussing atom beam reaction of O with heated Ge and Si single crystals
19 p3377 A69-36178

Transport mechanism in amorphous Ge films deposited on glass substrates studied by measuring piezoresistance as function of temperature during pure nitrogen immersion
19 p3391 A69-36559

Electrical conductivity anisotropy in isotropic germanium and silicon semiconductors, noting effect of metallic contact insertion
20 p3584 A69-37786

Fast neutron irradiation effect in Ge crystals, using X ray diffraction and volumetric measurements
20 p3584 A69-38125

Radiative recombination in GaAs p-n structures having region with concentrations of Ge atoms
21 p3780 A69-39044

Germanium single crystals etching with water vapor and hydrogen sulfide in hydrogen flow system, studying concentration, pressure and temperature effects on surface reactions
22 p3970 A69-40737

Ge films formation by evaporation technique, discussing background O pressure effect
24 p4361 A69-43345

GERMANIUM ALLOYS

Electroreflectance spectra of Ge-Si alloys, noting concentration dependence and band structure of Si and Ge
02 p0295 A69-11784

V phase structure and V and E phase lattice constants for ternary systems /Ti, Zr, Nb or Ta/-Ni, Co or Fe/-Si or Ge/
10 p1708 A69-22992

GERMANIUM COMPOUNDS

NT GERMANIDES

Tunnel junctions of narrow gap GeTe and wide gap GaAs, noting current voltage characteristics similar to those in Schottky barrier
06 p0980 A69-17770

Band structure for narrow energy gaps of GeTe and SnTe by perturbation model, noting constant free path and relaxation time
19 p3385 A69-36516

Electronic properties changes in amorphous CdGeAs caused by long range order loss studied by measuring optical and transport properties
19 p3390 A69-36557

GERMANIUM DIODES

Germanium tunnel diode current-voltage characteristics, proposing expression for approximation of differential conductivity as function of voltage
02 p0214 A69-11613

Germanium tunnel diode capacitance as function of bias voltage and HF signal magnitude, considering circuit design
02 p0214 A69-11614

Conduction mechanism in unstable range of Au doped double injection Ge diode at 77 K
02 p0222 A69-12686

Diffusion current detection method applied to reverse biased volt-ampere characteristics of Ge diodes, noting surface leakage role
07 p1105 A69-19007

Noise generator design employing diffused Ge avalanche transit time diode
07 p1107 A69-19156

Germanium tunnel diode current-voltage characteristics, proposing expression for approximation of differential conductivity as function of voltage
11 p1847 A69-24721

Germanium tunnel diode capacitance as function of bias voltage and HF signal magnitude, considering circuit design
11 p1847 A69-24722

Ultra lowpass filter circuit with two point contact Ge diodes and capacitor
12 p2039 A69-26379

Germanium microwave backward diodes optimum design and performance prediction through computer calculation for important parameters
22 p3916 A69-41224

GERMANIUM OXIDES

Voltage drop measurement across plasma anodized germanium film to determine anodization constant
10 p1742 A69-24004

Dissociation energy and ionization potential measured for gaseous SiO and GeO
22 p3896 A69-40725

GERMANY

Rocket guidance, discussing foreign systems with emphasis on German range miss/gradient orientation scheme used on World War II V-2 rockets
02 p0279 A69-12362

Electric space propulsion systems and auxiliary power sources development in West Germany, noting solar cells, isotope generators and reactors with conversion systems
03 p0496 A69-13996

MPD plasma acceleration in West Germany, discussing Hall acceleration, electrodeless plasma acceleration by electromagnetic waves and space charge neutralized Hall ion thruster
[AIAA PAPER 69-279]
09 p1564 A69-21238

Cartographic representation methods in climatological regional charts, discussing topographical elements, scale, screen patterns and area color
12 p2124 A69-25893

Satellite tracking cameras developed in East Germany, discussing optical systems
13 p2262 A69-27958

German solar and space probe Hera, discussing payload and propellant
13 p2357 A69-28638

Solar telescope in Berlin observatory for prominences and other solar phenomena observations by public
15 p2611 A69-30881

Report on East German space activities to COSPAR covering ionospheric research, geomagnetism, solar activity, solar radio astronomy and international cooperation
15 p2724 A69-31453

German space research organizations, rocket ascents and programs including meteorology, aeronomy, ionospheric physics, magnetosphere, solar radiation and solar wind, astronomy, etc
15 p2725 A69-31467

German VFW 614 short haul commercial jet aircraft design, marketing, etc
16 p2734 A69-31805

German ground station commercial receiving system for satellite broadcast reception
16 p2766 A69-31855

Airport planning, discussing air transportation and city planning problems for Hannover air terminal
16 p2882 A69-32329

German VTOL aircraft development excluding helicopters, discussing technical problems, safety and economy in civil application
17 p2899 A69-33381

GERMICIDES

U BACTERICIDES

GERMINATION

Wheat seedling germination and growth processes in absence of gravitational force onboard Biosatellite 2
01 p0015 A69-10932

GETTERS

Gettering effect in silicon of phosphosilicate glass surface layer and underlying phosphorus layer on gold and copper
03 p0487 A69-13640

Vacuum restoration by laser evaporation of active media /getters/ and vapor condensation on cold substrate applicable to nonmetallic active media /titanium-magnesium oxide/
21 p3735 A69-38590

GIANT STARS

Nonlinear adiabatic pulsations of sequence of massive stars of open clusters, allowing for radiation pressure variations
01 p0149 A69-10266

Electron conductivity in low mass red giant core
02 p0327 A69-12709

Red giants limiting helium core mass dependence on total stellar mass and initial composition from stellar evolutionary models
02 p0327 A69-12710

Kinematic parameters of giant stars and stellar evolution, discussing variations as function of zone position in HR diagram
03 p0517 A69-14095

Open clusters age determination method to study giant star distribution as function of age
08 p1388 A69-20237

Color magnitude distribution as function of age for giant stars of open clusters, discussing error sources
08 p1388 A69-20238

Mass loss in Red Giant stage from statistical analysis of H-R diagrams of galactic clusters
08 p1396 A69-20642

Nucleosynthesis in dynamics of massive star cores, noting element synthesis by neutron capture in supernova explosions
08 p1401 A69-20898

High dispersion classification of early K2-M6 giants of high and low velocity, using titanium oxide band strengths criteria tested by atomic lines estimation
13 p2338 A69-27556

Optical depths of convection related to metal deficiency for main sequence and giant stars
14 p2527 A69-29946

Giant galaxy classified in terms of stellar population, discussing Orion, intermediate amorphous and combination categories
16 p2862 A69-32395

Photoelectric observations of color and titanium oxide in M7 giants in nuclear bulge of Galaxy compared with late giants near sun
16 p2863 A69-32396

Evolutionary tracks along horizontal branch of models for Population II stars in postred giant phase
17 p3030 A69-33071

Fluxes and luminous efficiencies tabulated for main sequence and subgiant stars within reflection effect problem in eclipsing binaries and Chandrasekhar non-gray atmospheric models
20 p3600 A69-37479

Giant stars UVB reddening line slopes determined from photometric data
20 p3608 A69-38047

Interstellar grains formation and composition, suggesting mixture of graphite particles in carbon stars and silicates in oxygen-rich giants
20 p3615 A69-38260

Differential curve-of-growth analysis of late type giant stars yielding chemical compositions, discussing nature and size of uncertainties in estimates
21 p3800 A69-38700

Space density of giant M stars as function of distance at galactic anticenter
22 p4014 A69-40125

C, N and O abundances in K giants alpha Boo, beta Gem and epsilon Peg, noting stellar nuclear burning and evolution
22 p4026 A69-40653

M giant star possible evolution into S star, using high dispersion spectrograms
24 p4387 A69-43349

GIMBALLESS INERTIAL NAVIGATION

Miniature floated ball gimballess inertial platform construction, functions, readout, digital computer coupling, etc
[AIAA PAPER 69-835]
21 p3761 A69-39366

Strapdown gimballess inertial measurement unit with general purpose computer, describing hardware, software and test results
[AIAA PAPER 69-850]
21 p3765 A69-39426

GIMBALS

Gyroscope error due to axial play of inner gimbal or Cardan mounting during base circular vibrations, noting axial clearance reduction
09 p1498 A69-22110

Four gimbal Cardan suspension gyroscope kinematics for nonperpendicular arrangement
09 p1502 A69-22705

Fourth angle driving law for different four gimbal systems used for simulation display and inertial platform isolation
12 p2055 A69-26265

Steady motion stability of satellite with gimbal suspended gyroscope in central gravitational field, showing no effect of satellite perturbations on gyrostatic stability
14 p2530 A69-29481

Gimbal torquing as function of gimbal structure response resulting in free gyro erection system, using any angular momentum at any initial starting angle
16 p2792 A69-32553

Boundary layer theory application to dynamics of gyroscope in gimbal suspension, defining nutational and precessional motion
18 p3135 A69-34559

Dynamic performance accuracy of astatic gyroscope with three degrees of freedom improved by inner gimbal mass increase
19 p3308 A69-35825

Triaxial static gyrostatic drifts, assuming perturbing moment steady centered random force applied along stabilizing gimbal axis
19 p3311 A69-36195

Torqued two axis gimbaled boom actuator satellite attitude control
[AIAA PAPER 68-857]
24 p4348 A69-43245

GIRDERS

Forced harmonic oscillations of one dimensional mechanical girder systems allowing for nonlinear resisting forces calculated by boundary value problem reduction to Cauchy problem
17 p3064 A69-33917

Buckling stresses in thin walled box girder under bending determined using stationary potential energy criterion
18 p3224 A69-35344

Thin walled rods for girder and frame systems designed by matrix method, solving differential equations for tension, compression, bending and torsion
23 p4230 A69-42005

Three dimensional welded structure of thin walled girders with stability loss, discussing welding strain gage measurements and simplified computational procedure
23 p4169 A69-42007

GLACIOLOGY

Earth surface temperature change quantitatively determination due to Milankovitch insolation variations
03 p0426 A69-14232

Various glacial periods mechanism ascribed to combination of long term solar activity cycle and polar migration
11 p1877 A69-24409

GLANDS [ANATOMY]

U ADRENAL GLAND

U PINEAL GLAND

U PITUITARY GLAND

U THYROID GLAND

GLANDS [SEALS]

Glass fiber filled polytetrafluoroethylene materials for piston seals in high pressure oil-free reciprocating air compressors, discussing manufacturing and non-destructive tests
19 p3323 A69-35579

GLASS

NT BOROSILICATE GLASS

NT PYROCERAM [TRADEMARK]

NT S GLASS

NT SILICA GLASS

Dynamic current-voltage characteristics of thin film diodes on chalcogenide glass base
02 p0223 A69-12834

Optical materials behavior after irradiation by high energy electrons, gamma rays or protons
03 p0493 A69-14190

Engineering glass manufacturing, properties and applications in buildings, vehicles, lamp and electronic devices, etc
04 p0619 A69-14585

Transitions in glasses at low temperatures, noting molecular relaxation dependence on copolymer composition
04 p0621 A69-15308

Glass lasers, discussing neodymium properties in glass, flexibility of glass in size, shape and optical excellence, temperature coefficient of index of refraction, etc
05 p0772 A69-16227

Fracture propagation in organic glasses, considering density of hyperbolic markings in polymethyl methacrylate and Dugdale model
05 p0784 A69-16429

Polymer glasses low temperature transitions, relating structure and transition temperature
05 p0717 A69-16493

Semiconductor glasses use for electronic devices
06 p0980 A69-17714

Mechanism for laser surface damage of glasses working through optical absorption, fluorescence, chemical reaction by quenching and breakdown
06 p0935 A69-17771

Halide salts, semiconductors and nonoxide glasses as materials for high power laser windows
07 p1144 A69-18401

Nonlinear amplification of powerful light pulses in Nd glass
08 p1323 A69-19946

Near IR transparent aluminocalcium glasses with improved spectral properties
08 p1336 A69-20386

Geochemistry and element abundances for Henbury impact glass, Darwin glass and australites, noting evidence for meteorite impact on sandstone
08 p1407 A69-20937

Glass science and technology noting optical, electrical and mechanical properties, forming techniques, structure, ionic properties, high pressure effects and glass ceramics
08 p1341 A69-21126

Pulsed and CW lasers glass crystals temperature fields determination, including tangential and axial thermal stresses
10 p1702 A69-23428

Nonlinear susceptibility tensor components and refractive index variations of liquids and glasses in high intensity ruby laser field, using interference methods
10 p1703 A69-23622

Nd glass laser for emission of high radiance diffraction limited pulses, noting long path air breakdown and second harmonic generation
10 p1704 A69-23654

Self focusing of CW argon laser beam due to absorptive heating in crown glass, emphasizing time dependence of beam diameter as function of distance
10 p1706 A69-24009

Surface-active additives effect on crystallization kinetics of silicate type glasses, discussing surface tension
11 p1907 A69-25032

Glass lasers with trivalent rare earth ions noting properties, characteristics and recent developments
11 p1898 A69-25043

Quantitative interferometric analysis of shock induced wavelength variations in glass and polished steel plates using Q switched ruby laser light source
12 p2089 A69-26185

Laser beam damage in glass blocks, noting high speed photographic study and absorption of light by inclusions
12 p2117 A69-26193

Fracture surfaces of thermally toughened glass plates using Cranz-Schardin spark camera, confirming internal front lead over front in surface layers
12 p2118 A69-26194

Spectral transmission curves in near UV for optical glasses
12 p2130 A69-26599

Tempered glass plates strength nondestructive testing by scattered light photoelastic method, discussing application to aircraft windshield sandwich structures [AIAA PAPER 68-323]
12 p2118 A69-26768

Mechanical properties of glass, discussing volume flow, hardness, strength and scratchability
12 p2119 A69-26831

Energy exchange of rare earth ions in uranyl phosphate liquids and glasses, studying sensitized luminescence origin
14 p2485 A69-29034

IR spectral transmittance and physicochemical properties of tellurite glasses with vanadium and cerium oxides, showing polymer chains in structure
14 p2468 A69-29329

Energy exchange between active centers in silicate and phosphate glass, comparing luminescent and lasing properties
15 p2632 A69-30053

Tensile, bending and impact strengths of materials produced by metal porous blank impregnation with molten glass, noting metal density and sintering effects
15 p2643 A69-31188

Electrical switching in thin film arsenic selenium telluride semiconducting glass diodes, observing formation of liquid phase and conducting filaments
16 p2760 A69-32017

Laser effect in neodymium glass, estimating efficiency of light energy output vs electric energy input
17 p2979 A69-32828

Polarized emission from Nd activated glass, establishing S and P polarization component energy dependence on pumping energy
17 p2984 A69-33974

Refractive indices for various glasses obtained as function of wavelengths and temperature, using spectrometer as collimator
17 p3007 A69-34158

Shock tube with cylindrical explosive to implode glass wall and produce high velocity glass particle jet, studying jet velocity and behavior and test gas pressure effects
18 p3116 A69-34460

Hypervelocity micrometeor impact sites identification on aluminized glass, using conchoidal pattern as criterion in analysis
18 p3199 A69-34952

Thermal coefficient of optical glasses refractive index determined by interferometry, noting relation to glass chemical composition
18 p3172 A69-35013

Optimum solar cell cover glass systems selected by studying interplanetary space environment effects of proton impact, temperature and concurrent illumination on radiation damage
19 p3253 A69-35702

Optical and electrical properties of thin amorphous films of glass-forming oxide, using X ray diffraction and electron microscopy for structural features
19 p3391 A69-36561

Glassy semiconductors from metallic alloy binary and ternary systems of sulfide, selenide and telluride noting properties
19 p3392 A69-36641

Active center chemical bond alteration influences on luminescence characteristics of phosphate glasses, noting quick energy transfer via ions
20 p3552 A69-37017

Glass lasers development, operation, composition, applications, etc
21 p3734 A69-38407

Absorption and fluorescent spectra, relaxation times and quantum efficiencies measured for glasses doped with trivalent erbium, reviewing spectroscopic parameters involved with laser effect
22 p3962 A69-40476

Glass filter systems for aerial color photography developed from spectral studies of sunlight, skylight and airlight in Rayleigh atmosphere
22 p3948 A69-40986

Darwin and Macedon impact glasses related to Far Eastern tektites through age determination by fission track technique
23 p4210 A69-41344

Fission track ages of tektites, australites and related glasses, considering errors due to annealing and etch pits
23 p4210 A69-41345

Black magnetite bearing spherules extracted from tektites, and magnetic fractions of impact glasses, determined by reflecting microscope and electron microprobe
23 p4210 A69-41349

Mechanical properties of glass and glass-ceramics products improvement through prestressing
24 p4335 A69-43034

GLASS COATINGS

Glass ceramic coated and bonded silicon semiconductor material in integrated circuits devices fabrication, noting matched thermal expansion
15 p2669 A69-31040

Glass encased electronic components with conformal coatings, considering glass breakage at low temperature
19 p3281 A69-35547

GLASS ELECTRODES

Glass pleats and cold cathodes in laser discharging tube, discussing angular displacements
03 p0435 A69-12981

GLASS FIBERS

Creep and stress rupture strength of unidirectional glass fiber reinforced plastics, using tensile tests
01 p0101 A69-10080

Reinforcing glass fiber fillers in thermoplastic commercial products, noting applicability to high speed fabrication by injection molding processes
02 p0269 A69-11794

Fatigue properties and failure mechanisms of glass reinforced plastics based on chopped strand mat-polyester resin laminates
02 p0269 A69-11795

Fiberglass reinforced plastic laminates failure under biaxial compression due to layer separation with strain energy as endurance criterion
02 p0270 A69-12142

Glass fiber reinforced plastics - Conferences, Freudenstadt, West Germany, October 1968
03 p0453 A69-13819

Knee in stress-strain diagram and crack formation in glass fiber reinforced plastics, discussing effect on construction load capacity
03 p0453 A69-13820

Glass fiber reinforced plastic in aircraft construction, considering cellular weight and economy
03 p0454 A69-13821

Light passenger aircraft of glass fiber reinforced plastic, using hose construction technique
03 p0454 A69-13822

Glass fiber reinforced plastics aging behavior under heat and weathering influence
03 p0454 A69-13823

Damping properties of glass fiber reinforced plastics measured by flexural vibrations
03 p0454 A69-13824

Helicopter rigid rotor system with blades of glass fiber reinforced plastic
04 p0548 A69-14817

Shear strengths of polyimide and polybenzimidazole resin/fiberglass reinforced honeycomb materials compared to previous high temperature materials, noting lightweight sandwich aircraft structures
04 p0620 A69-14844

Piezooptical method applied to anisotropic bodies and reinforced plastics, deriving relation between dielectric tensors and stresses and strains
05 p0837 A69-16038

Cryogenic mechanical properties of epoxy resins and glass/epoxy composites
05 p0785 A69-16491

Stress direction and mean stress effects on fatigue properties of fiberglass reinforced plastics
06 p0945 A69-17124

High transmittance long fiber optics, presenting data on special transmission as function of temperature
06 p0958 A69-17677

Resin bonded glass cloth for large airframe structures rectification
06 p0931 A69-17713

Anisotropic glass fiber reinforced epoxy resin composite under biaxial and uniaxial loads, noting isochromatics and isoclines in photoelastic analysis
07 p1170 A69-18715

Hingeless fiberglass rotary wings dynamics, discussing effects of in-plane bending to flapping frequency ratio [AIAA PAPER 69-204]
07 p1054 A69-19548

Fiberglass reinforced plastics modulus of elasticity and Poisson ratio determined by strain gauges and frequency and resistivity measurements
08 p1335 A69-20330

Structural parameters influence on fiberglass reinforced plastics strength studied for optimal structure selection
08 p1335 A69-20332

Structural residual stresses determination in oriented fiberglass reinforced plastics by models taking into account mutual influence of fibers
08 p1335 A69-20333

Fiberglass reinforced plastic plates strength coupled to elastic base with allowance for tangential shearing stresses
08 p1412 A69-20334

Tensile stress and energy-to-break values compared for glass-fortified thermoplastic resins, discussing notched and unnotched Izod impact
08 p1337 A69-20480

Silane coupling effect on composite properties of glass fiber filled injection molded polypropylene, noting interface phenomenon

08 p1337 A69-20482

Tensile strength of glass-fiber reinforced epoxy resin laminates subjected to fluctuating tension, discussing crack density dependence on fatigue stress cycles

08 p1338 A69-20494

Matrix properties related to torsional fatigue life of fiberglass reinforced NOL rings, using polyester and epoxy resins as model systems

08 p1339 A69-20495

Shop-ready high modulus carbon and fiberglass composite reinforcement system, stressing effect of modulus fibers amount in laminate

08 p1340 A69-20508

Halocarbon solvent for application of chlorosilane finish to heat cleaned glass fabric for reinforcement of plastic, noting relative humidity effect

08 p1341 A69-20513

Direct chemical bonding effect on flexural strength and flexural modulus of glass fiber reinforced plastics, noting degradation reactions

08 p1341 A69-20514

Radial and tangential stresses in double glass fiber assuming different Poisson coefficients, determining conditions for axial stress redistribution prevention

09 p1614 A69-21741

Failure modes in fiberglass reinforced epoxy laminates subjected to compression loadings, discussing cracks formation and delamination at glass-resin interface

09 p1529 A69-22305

Glass fibers size, finish and surface treatment identification by pyrolysis attenuated total reflectance IR spectroscopy

09 p1448 A69-22315

Prepreg based on S glass with HTS finish and B staged epoxy resin, discussing tensile strength and moisture exposure

09 p1530 A69-22327

Polyimide glass fabric laminates with nonflammable characteristics for high O concentration spacecraft environments applications

09 p1531 A69-22366

Strength of laminated glass filament reinforced plastic material in biaxial loading, discussing strength theories

10 p1794 A69-22943

Chemical composition effect on glass fibers strength, discussing reasons for increased surface layer strength

10 p1717 A69-24045

Glass reinforced plastic molding compounds for OV-10A airplane structural components, noting cost savings

[SAE PAPER 690342] 11 p1890 A69-24497

Single and clad glass fibers radii and refractive indices measurements on basis of laser light scattering

11 p1918 A69-25044

Glass fiber reinforced plastics tensile strength at low and high temperatures

11 p1907 A69-25181

Birefringent coatings application to plane stress in orthotropic glass-fiber reinforced plastic materials noting stress-strain relations

11 p1995 A69-25647

Glass fiber reinforced plastics shells stability under external hydrostatic pressure, discussing compression and axial tests for normal elastic modulus, shear modulus and Poisson coefficient

11 p1995 A69-25681

Fracture mechanics of polymers and fiberglass reinforced plastics, indicating microcracking under static and cyclic loading due to resin phase brittleness and low strength

12 p2120 A69-26849

Glass reinforced plastics for Hovermarine HM.2 sidewall hovercraft designed for ferry routes

13 p2201 A69-27542

Short fiber composites flow orientation in system of high volume glass fibers in epoxy resin measured by glass rheometer

13 p2287 A69-28670

Glass finish and glass resin chemical bond adhesion roles in filament wound structures response, failure and filament strength

14 p2468 A69-29345

Tissue-type fiberglass reinforced material properties as prototype of continuous anisotropic hereditary elastic media

15 p2642 A69-30584

Stress concentration on circular holes and notches in anisotropic oriented glass fiber reinforced plastics determined by using photoelastic birefringent coatings

15 p2713 A69-31053

Flexible glass fiber optics, discussing total internal reflection, light and image transmission, digit display and waveguide for laser communication

16 p2789 A69-31933

Composition effect on tensile and flexural moduli of composites containing randomly distributed fibrous strands, establishing strength-composition relationships

17 p2991 A69-32960

Shear modulus of fiberglass reinforced plastics determined from torsional tests on squared beam of orthotropic material, evaluating influence of end conditions

17 p3058 A69-33204

Heat transfer suppression techniques in high temperature low density fiberglass insulation for flight vehicles

[AIAA PAPER 69-606] 17 p3072 A69-33279

Fiberglass reinforced plastics internal heat shielding for isopropyl nitrate rocket combustion chamber, considering lining resistance and safety during repeated firing /Ludion motor/

17 p3019 A69-33343

Wire wound glass fibers for rocket motors, discussing rupture strength

17 p3021 A69-33357

Nondestructive tests for glass filament wound composites void content, considering test methods and mechanical properties prediction role

17 p2979 A69-33656

Energy dissipation in fiberglass reinforced plastics subjected to axially induced sinusoidal stresses, noting absorption coefficient and hysteresis heating

17 p2993 A69-33937

Phenolic resin and silica cloth laminates transparency to IR radiation, noting experimental results

18 p1336 A69-34640

Axissymmetric deformation of cylindrical wound fiberglass reinforced plastic shell analyzed by methods of rigid normals and nonlinearly elastic fiber system

18 p3222 A69-34974

Nonlinear axisymmetric oscillations and motion stability of cylindrical wound elastic glassfiber shell under time dependent uniform internal pressure

18 p3222 A69-34975

Fiberglass reinforced plastics short and long term strength anisotropy, correlating stress and logarithm of time to rupture under tension along different directions

18 p1362 A69-35352

Fiber distribution in oriented fiberglass reinforced plastics, noting statistically isotropical distribution and use for regular structure model

18 p1362 A69-35355

Optimal structure model of fiberglass reinforced materials with polymer matrix, obtaining strength utilization coefficient dependence on length/ diameter ratio

18 p1362 A69-35356

Oriented glassfiber reinforced plastics elastic moduli and tensile strength along anisotropic axes determined nondestructively, considering component content and material porosity

18 p1362 A69-35359

Statistical description of microstructural elements /fibers and fillers/ in unidirectional fiberglass reinforced plastics determined in lattice nodes

18 p1363 A69-35363

Linearity range of viscoelastic properties of fiberglass reinforced plastics, calculating stress-strain state

18 p1363 A69-35364

Longitudinal modulus of interlaminar slip during creep of fiberglass reinforced plastic determined by bending tests of beams under concentrated force

18 p1363 A69-35365

Fiberglass-reinforced plastics longitudinal and transverse strain relations at various temperatures

18 p1363 A69-35366

Phenomenological creep theory for woven fiberglass reinforced plastic under moderate loads

18 p3226 A69-35373

Polyimide resin system for glass reinforced laminates, noting processing characteristics and curing

19 p3353 A69-35505

Military storage and environment effects on strength of filament wound glass reinforced epoxy structures, tested on plastic motor case and pressure vessels

19 p3321 A69-35567

Ultrasonic nondestructive testing technique for fatigue induced damage location and criticality in filament wound fiberglass cylinders, correlating damage to residual life

19 p3322 A69-35577

Glass fiber filled polytetrafluoroethylene materials for piston seals in high pressure oil-free reciprocating

air compressors, discussing manufacturing and non-destructive tests

19 p3323 A69-35579

Creep strength of fiberglass reinforced polyester resins measured on structural components in long term tests under torsion

19 p3358 A69-35830

Design and fabrication of plane and trapezoidal fiberglass wings with laminar plastic profiles for aerodynamic tests, including wing rigging and slotted wing

19 p3324 A69-35831

Glass fiber with epoxy resins compared to polyester resins, discussing chemical reactions, bonding and strength relations

19 p3358 A69-35902

Glass fiber laminates based on epoxy organosilicon resins, discussing various hardeners effects on strength, etc

19 p3358 A69-35903

Storage and loss moduli measurement for laminated glass fiber reinforced epoxy composite beams, discussing moduli prediction

20 p3627 A69-37763

Polarizable ions effect on glass fibers strength retention, noting fatigue tests for hydrolytic stress corrosion

20 p3567 A69-37769

Radial and tangential stresses in double glass fiber assuming different Poisson coefficients, determining conditions for axial stress redistribution prevention

20 p3630 A69-38217

Silico-organic liquid water repellent coatings for increasing binder adhesion to glass fiber in glass fiber reinforced plastic materials of aircraft components

21 p3752 A69-38876

Tensile strength of glass and graphite fibers for fiber reinforced plastics (FRP) tested with modified balance type and strain gage type tensile testers

21 p3753 A69-39799

Residual stress effect on strength of oriented glass fiber reinforced plastics under transverse and longitudinal tension

22 p3973 A69-40745

Stress analysis during solidification of binders in glass fiber reinforced plastic materials, using resin coated glass film simulation

22 p3973 A69-40746

Porosity and composition effects on thermal conductivity of glass fiber reinforced plastics, noting tests of multilayer textolite sheets

22 p3973 A69-40747

Summation methods for multiple damages caused by static fatigue in glass fiber reinforced plastics under stepwise loads

22 p3974 A69-40748

Initial stress dependence on tensile load in glass fiber reinforced plastic rings during winding

22 p4045 A69-40749

Glass fibers strength in relation to surface defects, comparing behavior of flawless and commercial fibers

22 p3974 A69-41039

HF data transmission system unaffected by high energy electromagnetic fields using GaAs IR emitting diode, glass fiber optic light guide and photomultiplier tube

23 p4121 A69-41768

Temperature influence on mechanical properties and creep curves of fiberglass reinforced textolites compared with data from elasticity theory

23 p4179 A69-41993

Mechanical properties of fiberglass reinforced textolite at normal temperature, noting applicability of elasticity formulas

23 p4179 A69-41994

Vacuum cured glass-reinforced polyimide laminate tests for use at elevated temperatures on F-111 aircraft

24 p4335 A69-42933

GLASSWARE

Glass vacuum systems grease free assembly method using heat shrinkable polyolefin sleeve tubing connector for compression of O ring joints

08 p1320 A69-20529

GLAUCOMA

Glaucoma in commercial airline pilots noting value and safety of routine tonometry

03 p0376 A69-14078

Indentation tonometry for occult pathology and glaucoma in commercial pilots

23 p4088 A69-41805

GLAUERT COEFFICIENT

U AERODYNAMIC FORCES

U MACH NUMBER

GLAZES

Apollo 11 observations of lunar surface glazing, considering radiation heating due to solar outbursts, rocket exhaust effects, shock heating or volcanism, erosion, etc 23 p4216 A69-42202

GLIDE LANDINGS

Subsonic glide landing approach guidance for unpowered lifting vehicles, using perturbation feedback and approximation of heading and position coordinates [AIAA PAPER 69-865] 21 p3763 A69-39391

GLIDE PATHS

Hypervelocity glide vehicle optimum maneuvers, finding lift optimal control law for maximization of final velocity or altitude 17 p3025 A69-32836

Vertical path guidance computer, noting applications to feeder airlines and air taxi services operating from airports with VOR/TACAN/only 17 p3003 A69-34104

On-course monitoring for instrument landing system glide path operating with far field samples 17 p3003 A69-34105

Mathematical model of fields reradiated by Huygen sources in front of array for glide path site analysis 17 p3003 A69-34107

Wind shear effects on jet aircraft approach, discussing airspeed and glide path position maintenance requirements [AIAA PAPER 69-796] 19 p3367 A69-35634

Ground based guidance for land-landing manned spacecraft with low velocity descent systems, discussing high and low altitude glide path intercept and spiral [AIAA PAPER 69-864] 21 p3762 A69-39390

GLIDERS
NT FLEXIBLE WINGS
NT HL-10 REENTRY VEHICLE
NT HYPERSONIC GLIDERS
NT PARAGLIDERS

Frequencies and natural oscillation modes in sporting gliders, demonstrating horizontal oscillation induced aileron suspension brackets destruction 04 p0549 A69-15416

Testing techniques and graphical presentation of test results to determine resonant frequencies and oscillation modes in sporting gliders 04 p0549 A69-15420

Open class type glider design, discussing structural materials, dimensions and control 05 p0702 A69-16027

Integrated shrouded propeller as glider thrust source permitting powered takeoffs and updraft independence 05 p0702 A69-16379

Wind tunnel measurements on integrated shrouded propeller model proposed for power gliders 07 p1052 A69-19633

Lateral stability of glider towed by cable in steady rectilinear horizontal flight, deriving motion equations as ordinary differential equations 09 p1433 A69-21498

Schleicher glider AS-W15 prototype tests, discussing balsa sandwich structure and flight characteristics 10 p1633 A69-22872

Approximation formula for calculating descent speed and lift-drag ratio 10 p1633 A69-22873

Monograph on optimal design of free-running drag turbines for boundary layer suction in aircraft, emphasizing gliders performance 12 p2011 A69-26117

Spectral model used for analysis of atmospheric turbulence as related to loads on gliders 12 p2127 A69-26931

Sailplanes design, discussing structural flexibility, deformations, aeroelastic effects and plastics and man-made fibers 15 p2551 A69-30899

Optimum overestimate to obtain bound permitting use as convergence criterion for iterative process in orbital glider reentry trajectory optimization [ONERA-TP-628] 16 p2805 A69-32332

Maximum trajectory for glider entering earth atmosphere at supercircular velocity, subject to maximum altitude constraint 19 p3399 A69-35667

Wakkel engine development in Poland for powered military gliders at 18 hp and 5500 rpm 22 p3999 A69-40006

Glider pilots fatigue attributed to nutritional habits 23 p4106 A69-41796

Long term fatigue tests of wooden gliders, discussing structural materials fatigue strength and glider strain spectra 24 p4398 A69-42912

Flight range and fuel consumption formulas of power gliders used for transportation compared with automobiles 24 p4253 A69-43142

GLIDING

Flight dynamics problems, determining extremum of functional by graph-analytical method and with aid of Pontryagin maximum principle 11 p1823 A69-25343

GLINT

Tracking radar glint analysis model using diffraction theory to evaluate parameters of fields received from scattering centers on target aircraft 01 p0033 A69-11007

GLOBAL TRACKING NETWORK

CNES worldwide network of tracking stations, describing equipment, location, organization and center of operations 02 p0228 A69-11922

International 28-station global instrumentation ground support network for space tracking and data acquisition [UN PAPER 68-95912] 06 p1043 A69-17059

Space communication, discussing global network of Intelsat satellites ground facilities, regional switching, RF channels, etc 06 p0890 A69-17860

Pivotal computer operations in Apollo NASA Communication Network, describing UNIVAC computers in use and design considerations 18 p3100 A69-34267

GLOBULES

Ionized gas flow from globule containing atomic H in interstellar space, noting surrounding H II region and radiation at ionization front 10 p1782 A69-23682

GLOBULINS

U GAMMA GLOBULIN

GLOSSARIES

U DICTIONARIES

GLOTRAC [TRACKING NETWORK]

U GLOBAL TRACKING NETWORK

GLOVES

Finger dexterity in JMG-1 pressure gloves with regard to efficiency associated with fine adjustments 06 p0884 A69-18032

Control operation time found dependent on gloves, physical characteristics of control and type of required operation 10 p1648 A69-23180

Glove characteristics effects on manipulability, finding operation time differences between gloved and barehanded operation dependent on type of required control operation 10 p1648 A69-23181

GLOW

U LUMINESCENCE

GLOW DISCHARGES

Time dependent functions integration by glow discharge tube and oscillator, discussing device for voltage measurement and applications in meteorology and geophysics 02 p0251 A69-12773

Frequency conversion in sheath capacitance of glow discharge plasma contained within metallic coaxial cylinders 04 p0634 A69-14456

Hydrazine decomposition in glow discharge, analyzing emission spectra and threshold level of decomposition by gas chromatography 04 p0646 A69-14860

Electron beam welding using glow discharge as source of electrons, noting hollow anode gun design and electrode geometry influence on beam shape 04 p0608 A69-15480

Oxygen ions motion in oxygen, measuring drift velocities in glow discharge 05 p0795 A69-15662

Equivalent circuit diagrams for impedance of plasma column in low current low pressure glow discharge 05 p0800 A69-15742

Mass spectrometric technique applied to positive column of hydrogen glow discharge for plasma properties, including relative densities of various hydrogen ions 05 p0802 A69-15913

Glow discharge technique for dielectric layer deposition between metal interconnection patterns in mul-

tilayer integrated circuits, noting adhesion and feedthrough problems 06 p0931 A69-17201

Spectroscopic analysis of hydrogen spark plasma discharge parameters at small PD values, discussing shock wave initiation accounting for transition to quasi-stable phases 08 p1360 A69-20100

Striation formation during steady state glow discharge, noting origin in cathode interfacial positive ions 09 p1545 A69-21343

Faraday dark space geometries in glow discharge, using superposition principle to divide electric field for transition visualization 09 p1540 A69-22099

Laser radiation produced by continuous glow discharge within Al hollow cathode, determining laser power in terms of He-Ne mixture pressures 09 p1519 A69-22245

Cathode material effects on temperature coefficients for glow discharge tubes, noting running voltage pressure characteristics 09 p1468 A69-22602

Pulsed glow discharges in He and He-H mixtures for high current density, noting electric field and wall potential distributions 10 p1739 A69-23660

Charge transport in high pressure RF glow discharge in air at atmospheric pressure based on model plasma 10 p1740 A69-23662

Field effect on positive column plasma of glow discharge in air, analyzing near wall potential and conductivity 10 p1741 A69-23946

Fresnel dragging effect on 3 cm microwaves by electron gas drift in low pressure glow discharge, noting electron density and excitation modes 12 p2133 A69-25766

Electromagnetic field induced plasma oscillation amplitude dependence on field frequency as function of field amplitude and discharge current at low N pressures 13 p2313 A69-28332

Screw instability in glowing discharge plasma column in longitudinal magnetic field generalized to instabilities in low pressure arc, Penning and high current discharges 13 p2315 A69-28526

Carbon dioxide dissociation by electron impact, determining reaction rate in positive column of DC glow discharge 14 p2488 A69-29095

Magnitude and type of wall losses from small opening in discharge tube for positive plasma column of low pressure glow discharge in hydrogen 14 p2493 A69-29691

Langmuir probe measurements leading to electron groups composition of electron velocity distribution function in negative glow light 14 p2493 A69-29694

Disturbance currents from penetration of acoustic waves in weakly ionized gas, analyzing wave interaction with DC glow discharge 15 p2665 A69-31547

Correlation coefficient of light fluctuations measured in Ar plasma in positive column of glow discharge, noting ionization wave appearance at critical gas pressure 16 p2822 A69-32039

Light sources in 0.15-20 micron spectral range from published literature, unpublished reports, light source manufacturers and individuals 23 p4191 A69-42190

Mechanism for pink afterglow accompanying microwave discharge in pure nitrogen, emphasizing gas kinetic temperature role 24 p4353 A69-43749

GLUCOSE

Blood glucose measured before, during and after high performance aircraft flight for occurrence of fasting hypoglycemia 09 p1445 A69-22555

Glucose disappearance rate from dogs blood at simulated 27,000 ft altitude compared with tolerance at ground level, discussing chlorpromazine administration effect 14 p2408 A69-29305

Enzymatic processes of glucose metabolism in immature rats lymphatic tissues during exercise-induced elevated corticosteroid secretion 23 p4080 A69-41405

GLUES

GLUES

Glued metal joints under cyclic loading evaluated by change in short term strength as function of time at stress levels

04 p0605 A69-14540

F-111 sandwich structure adhesive joints glueclines, describing thickness measurement techniques and acceptance criteria

24 p4403 A69-43461

GLUTAMIC ACID

Glutamic acid metabolism compartmentation in brain cortex demonstrated in vitro, using isotopic labeling

18 p3096 A69-35172

GLYCERINS

U GLYCEROLS

GLYCEROLS

Raman effect in liquid glycerol obtained with 4880 A ionized argon laser, determining valence vibrational frequencies

03 p0440 A69-13366

Physical and psychic stress effects on phosphatidyl glycerol and related phospholipids concentration in human and rat blood plasma

23 p4088 A69-41815

GLYCINE

Pyroelectric crystals transparent at laser output wavelength used for recording transmitted radiation, noting response of triglycine sulfate crystal

03 p0438 A69-13050

GLYCOLS

Heat transfer principles analyzed in development of new quenchants for aluminum, noting properties of inversely water soluble polyalkalene glycols

01 p0087 A69-10900

Aluminum corrosion and inhibition mechanisms in ethylene glycol/water solutions, using controlled powder immersion tests

02 p0265 A69-11895

Mass spectral fragmentation of substituted aliphatic glycols and hydroxylated carbon-carbon bond

09 p1448 A69-22551

Polydiethylene glycol-bis-allyl carbonate /PBAC/ Hugoniot equation of state, reporting shock data, discussing applications to propellant testing

16 p2879 A69-32179

Ignition hazards in electrical circuits contaminated by glycol fluids, describing hazard detection by RF methods, decontamination procedures, safety checks, etc

19 p3359 A69-36028

Beta-thiodiglycol effect on hardening of epoxy resin with stoichiometric amounts of maleic anhydride and methyltetrahydrophthalic anhydride

22 p3973 A69-40677

GLYCOLYSIS

Glycolysis rate role in regulation of substrate inhibition of dehydrogenases

01 p0015 A69-10931

Glycolysis rate and lactic acid content in rats myocardium during adaptation to hypoxia, using pressure chamber

10 p1645 A69-23501

Glycolysis control by respiration in human leukocytes with and without Pasteur effect conditions

15 p2555 A69-30413

GODDARD EXPERIMENT PACKAGE TELESCOPE

U PARTICLE TELESCOPES

GOLD

Electrical resistance temperature dependence below room temperature for polycrystalline epitaxially grown Au and Ag films, noting effects of alpha irradiation

03 p0486 A69-13582

Gold and iridium concentrations in meteoritic and terrestrial materials by neutron activation, discussing chondrules, meteoritic troilite and metallic spherules

08 p1404 A69-20918

Gold diffusion and solubility in indium phosphide, analyzing temperature and vapor pressure effects

09 p1555 A69-21470

Effects of cold electron and light emission centers from dispersed Au films in electric field, as universal qualities characterizing dispersed metal films

14 p2504 A69-28992

Gold diffusion and solubility in indium phosphide, analyzing temperature and vapor pressure effects

15 p2669 A69-30715

Electromigration role in material accumulation and depletion forming regions in Au film conductors, discussing regions origin from and correlation with thermal gradients along conductor

17 p2936 A69-32896

Gold donor level impurity photovoltaic effect in silicon, noting solar cell efficiency reduction due to minority carrier recombination

19 p3381 A69-35679

Mean adsorption lifetimes and activation energies of Ag and Au on polycrystalline tungsten substrate in ultrahigh vacuum system free of hydrocarbon contamination

23 p4198 A69-41542

GOLD ALLOYS

Treatment and testing of thin platinum and gold alloy wires used in thermoelements for studying liquid fuel vaporization in combustion chambers

07 p1130 A69-18258

Fe-Fe interactions influence on increase in thermoelectric power with applied magnetic field at low temperatures for dilute alloys of Fe in Au

10 p1639 A69-23861

GOLD COATINGS

Surface layer effects on conductivity of vacuum deposited gold films, studying resistance variations with film thickness

02 p0300 A69-12625

Scale effect on gold films electrical conductivity, analyzing film thickness and electron parameters of mean free path, concentration and surface reflection

12 p2143 A69-26459

Gold-underlayer film combinations adhesion to oxide substrates, describing adhesion changes as function of Au and underlayer film thickness, time, environment, etc

13 p2321 A69-28007

Spray deposition of low emittance gold thermal control coatings on aerospace structures

15 p2618 A69-30310

Activation energy of annealing of lattice defects in Au films deposited under irradiation with Au ions

18 p3182 A69-34349

Gold/polycrystalline cadmium selenide film contact found ohmic in darkness and barrier in light, noting potential distribution, electron concentration and energy gap

19 p3384 A69-36480

Corrosion of Ni through porous Au plate in humid sulfur dioxide atmospheric environments, analyzing product deposits and contact properties

23 p4176 A69-41534

GONDOLAS

Stabilization system design for stratospheric balloon gondolas, discussing optimal system with flywheel and weight combination

17 p2898 A69-33242

Stratospheric balloon vertical oscillations and gondola attitude during long flights

19 p3248 A69-36689

Balloon-borne gondola azimuth stabilization using lunar tracker

20 p3538 A69-37300

GONIOMETERS

Directional properties of electro-optical goniometric system based on known design parameters

14 p2420 A69-29332

Transistorized VOR system using electronic goniometer and fixed antennas, describing power supply, transmitter, goniometer, antenna and design

16 p2827 A69-31938

Ruby laser goniometric and telemetric echoes by photographing Geos satellites

21 p3671 A69-38335

GOSS (SUPPORT SYSTEM)

U GROUND OPERATIONAL SUPPORT SYSTEM

GOVERNMENTS

Federal government contracting, discussing legality of NASA service contracts

05 p0850 A69-15987

V/STOL aircraft future, discussing Federal Government policies, economics, airport planning, engineering problems, etc

10 p1811 A69-23221

Government flight recorder regulations, detailing approved systems

10 p1691 A69-23246

Flight data recorders history and regulations, discussing parameters and design of systems

10 p1691 A69-23247

Potential hazards of government sponsored technology, examining SST and fluoridation projects and weather problems

10 p1811 A69-23392

Federal, state and municipal jurisdictional aspects for heliport establishment, detailing regulations

13 p2381 A69-27433

Urban noise control over transportation systems including aircraft and highway traffic operating beyond local noise ordinance purview

14 p2541 A69-29157

Equipment testing, discussing collaboration between government agencies and independent environmental testing laboratories

15 p2720 A69-30398

Flying offenses committed by private and professional pilots in Great Britain, discussing role of authorities involved

17 p3077 A69-34202

Reliability management simulation exercise training technique for government personnel, discussing decision making in development, production, testing and field usage of systems

18 p3117 A69-34487

In-house research on R and D management in government agencies, discussing manning, training, center programs, case studies, etc

20 p3640 A69-38022

Planning for safety of future supersonic air traffic including financing and coordination activity of government and industry

22 p4054 A69-41131

GOVERNORS

U SPEED REGULATORS

GRADE

Runway grade relation to jet aircraft takeoff length

19 p3296 A69-36874

GRADIENTS

NT ELECTRON DENSITY PROFILES

NT POTENTIAL GRADIENTS

NT PRESSURE GRADIENTS

NT TEMPERATURE GRADIENTS

Conjugated gradient components of optimization criterion in automatic control determined by applying sensitivity method to computation

11 p1857 A69-24367

Branched trajectory optimization for split rocket vehicles using projected gradient or steepest descent method

[AIAA PAPER 69-917] 21 p3808 A69-39346

GRADIOMETERS

U MAGNETOMETERS

GRADUATION

U CALIBRATING

GRAIN BOUNDARIES

Slip band continuity across grain boundaries in aluminum bicrystals reexamined for geometrical criteria

01 p0095 A69-10607

Grain boundary gas bubbles growth in chemically vapor deposited tungsten as function of annealing time, temperature and fluorine content

01 p0097 A69-10646

Light austenitic grain boundaries in heat treated Cr-Mo-W-V alloy steels

01 p0100 A69-11295

Magnified image of Al-Mg specimen microanalyzed during examination by electron microscope, studying segregation and initial precipitation at grain boundaries

03 p0442 A69-12894

Mechanical effects of grain boundaries, considering hardening associated with vacancies and vacancy-solute interactions

03 p0449 A69-13875

Interfaces role in Ni-base superalloy, discussing grain boundaries and coherent/incoherent phase boundaries

03 p0449 A69-13878

Grain boundary interaction energy with inclusion of second phase, describing equilibrium and boundary shape

03 p0449 A69-13880

Grain boundary sliding influence on gross mechanical behavior and stress distributions, emphasizing creep behavior

03 p0450 A69-13882

Long term creep behavior of nickel-chromium-molybdenum alloy, noting temperature effect on grain boundaries

05 p0781 A69-16500

Grain strain measurements use in studies of high temperature creep

06 p0943 A69-17231

Grain size dependence of yield, flow and fracture stresses of Fe-Co-V alloy for 77-298 K

07 p1166 A69-19264

Grain boundaries structure in tungsten wire using auto ion microscope, showing misorientation corresponds to high density coincidence site lattices

08 p1329 A69-19943

Grain-size refinement of beryllium castings and extrusions after compression in pressure chamber, determining effect on ductility

08 p1330 A69-20013

Grain morphology and preferred orientation effects on direction and propagation of stress corrosion cracking of aluminum alloy plate

09 p1521 A69-21399

Structure transitions in iron meteorites from Widmanstätten to granular pattern to study Barringer crater and Canon diablo meteorites formation

09 p1597 A69-22154

Thin sections of ringwoodite natural spinel in Tenham meteorite shower, observing various rounded purple isotropic grains

09 p1597 A69-22155

Stress corrosion of nonage-hardenable Al-Mg-Cr alloy investigated for failure in absence of grain boundary precipitate, using notched specimens

10 p1709 A69-23055

Carbide precipitation in stainless steels using metal foil and extraction replicas, discussing grain boundaries corrosion relation

10 p1713 A69-23820

Brittle fracture at high temperatures in titanium alloys using scanning electron beam microanalysis, noting reaction diffusion with atmosphere and grain boundaries destruction

10 p1713 A69-23823

Near boundary zones in VT15 Ti alloy not involved in beta phase decomposition during aging below 500 C attributed to vacancy concentration decrease

11 p1902 A69-24275

Structural imperfections of CdSb single crystals undoped and doped with tellurium and indium noting etching techniques, grain boundaries and impurities

11 p1938 A69-25030

Solid titanium surface energy determination, taking into account grain boundaries effect on accuracy

12 p2113 A69-26045

Grain size effect on room temperature tensile strength of alpha-titanium analyzed by tensile testing and electron transmission

13 p2280 A69-27766

W shear moduli at high temperatures measured by forced torsional vibration in wide frequency ranges, discussing grain boundary effects

14 p2465 A69-29651

Thermal stability of Hastelloy Alloy C-276 determined from time and temperature tests for corrosion and grain boundary precipitation

16 p2799 A69-31719

Grain boundaries contribution to creep deformation, discussing ratio of grain boundary slip strain to total creep strain

17 p2985 A69-32905

Creep behavior of oriented Al bicrystals, emphasizing intergranular creep types and crystal orientation

17 p2985 A69-32906

Creep experiments on Mg alloys, discussing dispersed phases influence on creep cavitation and grain boundaries mobility

17 p2985 A69-32907

Polygonization and strengthening effects simultaneous action at grain boundaries increased thermal stability of thermomechanically treated Ni-Cr alloy

17 p2991 A69-33940

Aluminum oxide relative grain boundary energy and surface diffusion coefficient, considering thermal grooving of bicrystals with symmetrical tilt boundaries

17 p2993 A69-34191

Secondary recrystallization in cold rolled molybdenum foil as function of temperature using electron microscopy and diffraction

18 p3157 A69-35253

Annealing temperature effect on Ni-Ti alloys internal friction, noting peak connected with solid solution grain boundaries

18 p3158 A69-35443

Liquid sodium penetration into stainless steel grain boundaries, using laser microprobe

18 p3154 A69-35473

Aluminum 7 percent Mg alloys stress corrosion cracking, presenting aging kinetics and depletion zone dislocations at grain boundaries

19 p3350 A69-36896

Grain boundary grooving kinetics for Cr, W and Mo in Ar and vacuum, determining interface free energies and surface self diffusion coefficients

21 p3744 A69-38740

Al discontinuous deformation noting role of intergranular boundary surface at low temperatures

21 p3750 A69-39789

Spherulite boundaries and interspherulite breakdown in polyethylene, considering structure control by varying macromolecular microstructure

22 p3973 A69-40740

Hydrogen permeability in Pd alpha phase measured, coupling with grain size measurements for grain boundary to bulk diffusivity ratio

23 p4175 A69-41502

GRAINS

Photographic emulsion layers depth dependence of darkening curve, modulation transfer function and granularity, determining properties by enzymatic and electrolytic treatments

12 p2089 A69-26196

Grains with high defect concentration in circumstellar and interstellar space from energetic particles and photons bombardment, discussing lifetime and optical properties

22 p4023 A69-40472

GRAINS [FOOD]

Wheat seedling germination and growth processes in absence of gravitational force onboard Biosatellite 2

01 p0015 A69-10932

Weightlessness and vibration effects on soft red winter wheat seedlings

15 p2557 A69-31368

GRAMMARS

Algorithm for programming language grammars conversion into pushdown store automata translators

21 p3679 A69-39607

GRANITE

Granite compressional wave velocity and electrical resistivity variations with depth, explaining discrepancy between in situ and laboratory measurements on dry samples

02 p0241 A69-11806

GRANTS

NASA university program, discussing participation in space and aeronautics development based on project oriented research grants and Sustaining University grants

[UN PAPER 68-95413] 01 p0179 A69-10506

GRANULAR MATERIALS

Detonation generation in granular explosive subject to different shock wave intensities due to variable impact velocity

02 p0349 A69-11527

Shock initiation and sensitivity of granular explosives, noting heterogeneity effect in ammonium perchlorate

10 p1751 A69-23016

Interstellar grain model consisting of elongated dielectric particles represented by infinite circular cylinders reproducing observed interstellar extinction in IF far UV spectra

10 p1781 A69-23674

Circumstellar grain compositions of stars with various O to C abundance ratios, calculating molecular equilibrium of condensates and gaseous compounds in stellar atmospheres

10 p1786 A69-24103

Micropolar elasticity theory for materials exhibiting granular structure and microstructure, discussing deformation geometry and measurement, strain kinematics, microstrains, thermodynamics, etc

11 p1975 A69-24674

Bulk weld filler metals, discussing granular compositions, electrodes and iron, nickel and cobalt base deposits

11 p1891 A69-24931

Pressure calcining process in production of fine grained ceramics at low temperatures

12 p2119 A69-26832

Matrix grain size relation to dispersed particle size distribution and Zener-McLean equation description of microduplex structure in superalloy Ni-Fe-Cr alloy

13 p2278 A69-27411

Friction resistance between steel and ground basalt in ultrahigh vacuum, showing increase by adhesion

13 p2298 A69-28014

Focal plane observation of granulation phenomena on scattering surface illuminated by coherent light from gas laser

21 p3741 A69-39575

Laser granularity effects on brightness discrimination

[AAS PAPER 69-464] 24 p4272 A69-42843

Lunar surface material mechanical properties from Surveyor observations, analyzing grain size, rock density, internal friction, cohesion and bulk density compared to Luna observations

24 p4383 A69-42962

GRAPHIC ARTS

Multilevel modeling structure for interactive computer graphic design, discussing conversational display manipulation program and interconnection with analysis program

05 p0724 A69-16381

Three dimensional computer graphic modeling program, discussing SIGHT and LEGER programs

05 p0724 A69-16383

Graphic electronic visualization equipment for computerized design

10 p1660 A69-23795

Computer processed pictures including transformation of graphical material, picture generation from data or abstract rules, discussing procedures, instrumentation, color and applications

11 p1842 A69-24588

Computer driven graphical techniques for aerospace design and analysis

[ASME PAPER 69-DE-27] 14 p2454 A69-28854

Book on Smith chart electronic applications in waveguide, circuit and component analysis and synthesis

22 p3915 A69-40780

GRAPHITE

NT PYROLYTIC GRAPHITE

Chemical vapor deposition of iridium coatings on graphite for high temperature oxidation protection, discussing parameters for iridium compounds and optimum depositing conditions

01 p0097 A69-10643

Hydrocarbon formation mechanisms under conditions resulting from graphite filament explosions in hydrogen atmospheres, emphasizing stepwise radical formation and methane role

01 p0120 A69-10675

Highly oriented graphite crystallites in pyrographites and composite materials, discussing preparation and anisotropy ratios in physical properties

01 p0102 A69-10978

Graphite specific heat temperature dependence at low temperatures, noting Wigner effect for neutron irradiation

02 p0269 A69-11782

Alloy elements effect on spreading of liquid titanium and zirconium alloys on graphite

03 p0446 A69-13573

IR radiation of NML Cygnus with O/C ratio close to unity ascribed to circumstellar shell of graphite particles

03 p0513 A69-13775

Graphite ablation in high pressure environments, extending existing analysis of thermochemical and thermomechanical behavior to include allotropic features

[AIAA PAPER 68-1153] 04 p0686 A69-14873

High temperature physical, mechanical and thermal properties of polycrystalline graphites, relating properties to manufacturing techniques and processing

[AIAA PAPER 68-297] 04 p0621 A69-15329

X ray emission from powdered graphite, diamond and titanium carbides

06 p0946 A69-17545

Graphite ablation in air, N, Ar and He assuming chemical equilibrium, equal diffusion coefficients and steady state ablation

[AIAA PAPER 69-148] 06 p0947 A69-18155

Electron momentum density in diamond, graphite and carbon black from Compton profile measurement by X ray scattering vector

06 p0982 A69-18233

Chemical bond nature and properties in cyclic compounds of carbon and graphite, presenting bond energy computation method

07 p1171 A69-18932

Susceptibility of high modulus graphite and boron fiber epoxy composites to lightning damage, noting degradation by pulse current

08 p1338 A69-20486

Filament winding process variables effect on carbon or fiberglass reinforced composites, determining mechanical properties

08 p1338 A69-20489

Matched metal molding of short graphite fiber composites

08 p1339 A69-20502

Whiskerizing technique for growing small beta SiC single crystals on graphite filament surfaces, noting changes in interface geometry and chemistry

08 p1341 A69-20511

Apparatus for depositing protective coatings on graphite by vacuum method in refractory metal carbonyl and halides mixtures and in molten metals

09 p1528 A69-21850

Boron and graphite fibers role in composites cost feasibility in 1970s

09 p1524 A69-22067

Tensile strengths and elasticity moduli of graphite fibers produced from textile organic thread, discussing application to composites, ablative and fiber reinforced materials

09 p1529 A69-22071

Subscale aircraft fuselage section fabricated with lightweight graphite fiber/epoxy resin composite material

09 p1509 A69-22341

Whiskerized graphite fiber in resin matrix composites, analyzing interstitial growth characteristics, resin infiltration, layup and compaction

09 p1511 A69-22360

Graphite fiber electroplating with nickel on continuous basis for ribbon like continuous flexible twist free yarn

09 p1512 A69-22362

Static and dynamic strength tests and modulus data for graphite fiber/epoxy composite yarn, noting ply winding and dimensions
[ASME PAPER 69-GT-114]

09 p1531 A69-22520

Graphite particle formation in atmosphere of C type Mira variables, calculating particle size distribution by nucleation and coagulation theory

10 p1782 A69-23681

Fiber content by weight of reinforced plastics measured by pyrolysis

10 p1716 A69-23695

Graphite improvement for high temperature applications by computerized properties analysis, failure criterion and improved testing for defective billets

12 p2115 A69-26845

High energy nuclear interactions in graphite block at high altitude, recording gamma quanta produced

13 p2330 A69-28377

Monograph on interstellar extinction computations covering theoretical curves for spherical metal and graphite particles, albedo, optical constants, normalization, temperature dependence, etc

14 p2516 A69-28901

Graphites wear rates and structural changes in machine parts under dynamic stresses in air or vacuum, noting pressure role

14 p2467 A69-28912

Late type stars with emission peak wavelength approximating graphite Debye frequency induced by graphite impurity atoms

14 p2521 A69-29586

Extinction efficiency of graphite core interstellar grains with solid hydrogen and ice mantles, using theoretical models

14 p2486 A69-29587

Interlaminar shear strength development for utilization of unidirectional strength and stiffness of graphite fibers, discussing epoxy resin-fiber interface improvement

15 p2642 A69-30312

Niobium deposition on graphite from vapor-gas phase assuming heterogeneous process

15 p2629 A69-30992

Erosion wear of graphitic and mica-ceramic materials used for sealing turbine compressors at high temperatures, including test installation

15 p2643 A69-31186

Gas discharge tube graphite hollow cathode geometry leading to abnormal discharge operation under certain pressure conditions

16 p2814 A69-31838

Biaxial stress strain properties of graphite base refractory composites noting fracture strength predictions

[AIAA PAPER 68-337]

16 p2803 A69-32150

Load capacities of graphite lined journal bearings, discussing factors affecting wear rates

[SAWE PAPER 68-LC-9]

18 p3148 A69-35002

High modulus graphite epoxy composite material laminates fabricated and tested, correlating filament strength variation effect with composite tensile strength

19 p3354 A69-35518

Fiber reinforced carbon and graphite with application to reentry and propulsion systems and high temperature gas turbines, noting three dimensional woven quartz

19 p3354 A69-35519

Measuring elastic modulus and tensile strength of high modulus graphite fibers including comparative data, error sources and full strand test

19 p3355 A69-35520

Graphite fiber NOL rings and biaxial wound pressurized cylinders tested at ambient and cryogenic temperatures for tensile and cyclic fatigue properties

19 p3355 A69-35521

Niobium carbide formation on graphite from gaseous niobium pentachloride and Ar mixtures, discussing parameters affecting layer growth rate

20 p3566 A69-37367

Silicon carbide compact coatings deposition on graphite by silicon tetrachloride, H and benzene gaseous mixture, relating layer thickness to temperature and process duration

20 p3566 A69-37368

Niobium carbide deposition from gaseous halogen compounds on graphite particles in pseudoliquidified state, noting stoichiometric coatings

20 p3566 A69-37369

Carbide coatings formation on graphite in molten media, determining diffusion coefficient of carbon in molten Zr

20 p3566 A69-37372

Solid para hydrogen coated graphite particles expulsion into interstellar medium from star formation regions, considering mantles stability and particles extinction efficiency, albedo and phase function

20 p3601 A69-37492

Interstellar grains formation and composition, suggesting mixture of graphite particles in carbon stars and silicates in oxygen-rich giants

20 p3615 A69-38260

Diffusion welding and soldering of metallic wire with graphite and graphitized viscose applied to chromel, copel, chromel-alumel, Mo, W and W-Re

21 p3728 A69-38617

High performance graphite fiber reinforced plastic composites development and characterization, discussing fiber property data

[ASM PAPER W9-16.1]

21 p3728 A69-38655

Graphite fiber reinforced graphite composites fabrication, discussing spray forming and physical and mechanical properties

[ASM PAPER W9-20.4]

21 p3730 A69-38671

Chemical bond nature and properties in cyclic compounds of carbon and graphite, presenting bond energy computation method

21 p3752 A69-39153

Tensile strength of glass and graphite fibers for fiber reinforced plastics (FRP) tested with modified balance type and strain gage type tensile testers

21 p3753 A69-39799

Lamellar solids abrasiveness, effects of particle share in graphite and molybdenite samples

22 p3966 A69-39877

Aromatic and nonaromatic hydrocarbon fractions in terrestrial graphite, discussing classification and analysis by chromatography and mass spectrometry

22 p3934 A69-39890

Cations desorption from O, H and N films adsorbed at graphite surface under electron bombardment, studying desorption cross sections discrepancies

22 p3972 A69-39957

Thermodynamic properties of exchange reaction of Ti, Nb, Mo and W disilicides with graphite and pyrographite systems

22 p3970 A69-40638

Graphite rocket engine nozzles chemical erosion at various temperatures, comparing reaction and diffusion rates

23 p4180 A69-42156

Temperature dependence of equilibrium solid solubility of C in Au, Cu and Ag foils with respect to graphite

24 p4334 A69-43413

Postcured low void content graphite fiber reinforced polyimide resin composites fabrication including shear, flexural and tensile strength data

24 p4337 A69-43446

High modulus graphite/asbestos reinforced laminates, noting improved transverse strength and thermal properties

24 p4337 A69-43447

GRAPHITIZATION

Stress graphitizing and boron codeposition effect on dynamic mechanical properties of pyrolytic carbon, noting increase in internal friction and dynamic modulus

10 p1716 A69-23036

Carbon fibers fine structure graphitized at high temperatures studied by X ray diffraction and electron microscopy

16 p2803 A69-32572

GRAPHS [CHARTS]

NT PATTERSON MAP

Graphical and analytical interpolation methods for representing initial compositions in equilibrium thermodynamic systems

01 p0176 A69-10403

Schematic chart prepared for shock wave geometry of Tungusk meteorite, discussing tree felling

01 p0159 A69-11379

Equations, tables and charts for shock drag parameter in determination of shock wave drag of body in supersonic free stream of ideal gas

02 p0188 A69-11862

Charts of horizontal cross sections of radio echo focus for radio echo reflections from cumulonimbus clouds

03 p0459 A69-13281

Graphical representation of stress distributions and forces on dislocations

03 p0529 A69-13973

Self dual graphs and diagraphs enumeration and properties

06 p0947 A69-17410

IR solar spectrum tables and graphs covering 10,657-12,857 Å

06 p1008 A69-17809

Naval Research Laboratory experience with two and three axis gravity gradient satellites stabilization systems

07 p1228 A69-18344

Finding and representing graphically intersections of double curvature surfaces with planes within scope of digital computer design

08 p1278 A69-19921

Integrated charged particle energy spectra from gridded electrostatic analyzers, relating retarding potential curve to particle floating potential, kinetic temperature, etc

08 p1364 A69-20521

Optimal length conditions of liquid rocket combustion chambers, considering propellants, injection conditions, etc, noting graphs and differential equations solutions

08 p1376 A69-20606

Approximate nomography problem solution based on application of graph theory

08 p1343 A69-20663

Brightness curves of eclipsing systems under monotonicity of unknown functions, using stable algorithm

09 p1588 A69-21363

Limb darkening nonlinearity effects on solutions for brightness curves of eclipsing binaries

09 p1588 A69-21364

Graphical methods for photoelastic effect behind system with stresses rotating about direction of light propagation, discussing j circle technique

09 p1617 A69-22011

Optimum selection of modulation indices for multitone phase modulation by graphical method, noting tolerance insensitivity

09 p1457 A69-22463

Graphs of ionospheric measurements by vertical incidence sounding during Antarctic expedition, describing instrumentation and sounding techniques

10 p1681 A69-23315

Graphical method for plotting electrophysiological observations, showing hodographs application in biopotential studies of cortical reactions

11 p1829 A69-24540

Flight dynamics problems, determining extremum of functional by graph-analytical method and with aid of Pontryagin maximum principle

11 p1823 A69-25343

Statistical reliability tools and methods, graphs and charts, estimations, prediction techniques and demonstrations

12 p2101 A69-25847

Automatic plotting devices for graphic readouts in analog and digital computers

12 p2091 A69-26303

Multiinput sine comparators graphical analysis and design considerations, emphasizing semiconductor circuit providing quadrilateral polar characteristic on impedance plane

12 p2039 A69-26350

Graphs determining interference levels for optimum shielding, suppression, signal parameters and waveforms for pulses, step functions, CW signals and for military technology

12 p2030 A69-26471

Photographic magnitudes of galactic nuclei, presenting plots for stellar magnitude distribution of galactic nuclei

12 p2165 A69-27029

Graphical method for plotting contours of Rice distribution function as rocket-borne radar reflection data, determining leakage factor
14 p2416 A69-29536

Algorithm for enumerating all circuits of linear graph, noting suitability for computerization without large computer memory
14 p2421 A69-29541

Observations of 123 southern radio sources made with two element variable spacing interferometer, tabulating and graphing results
15 p2696 A69-31166

Popov type graphic criterion for determining absolute stability of modulation systems
16 p2764 A69-32440

Popov and Sandberg graphic methods for determining absolute stability of nonautonomous systems, noting role of single nonzero eigenvalue in matrix
16 p2765 A69-32441

Brightness curves of eclipsing systems under monotonicity of unknown functions, using stable algorithm
18 p3197 A69-34753

Limb darkening nonlinearity effects on solutions for brightness curves of eclipsing binaries
18 p3197 A69-34754

Tail tip-evacuation limits, calculating aircraft balance effect of passenger relocations by graphical method [SAWE PAPER 765]
18 p3091 A69-34877

Graphical representation of friction stresses produced on mechanical parts surface layers, using mathematical model based on Poisson ratio and friction coefficient
19 p3329 A69-36723

Book on Smith chart electronic applications in waveguide, circuit and component analysis and synthesis
22 p3915 A69-40780

Plane-truss joints displacements determined by graph-analytic method, discussing representation of fictitious forces and moments
23 p4225 A69-41420

Pulmonary emphysema effect on expiratory flow limitation from static pressure-volume and flow volume curves during natural and forced deflation of hamster lungs
23 p4082 A69-41442

Graphical method for two dimensional supersonic expansion flow with subsonic reaction front around corner compared to existing iteration method
23 p4061 A69-42411

Intercity travel demands simulation by linear graph model applied to Windsor-Montreal corridor [AAS PAPER 69-382]
24 p4417 A69-42805

Equal velocity contour diagrams for interstellar matter emission and absorption study in Cassiopeia-Perseus region
24 p4384 A69-43050

Graph analytical method for calculating heat transfer in diathermic exchangers during boiling together with critical thermal loads
24 p4408 A69-43080

Image reconstruction by graphical method for equal wavelengths of recording and reconstructing radiation and equal scales of hologram
24 p4315 A69-43166

Demand curves for VTOL intercity transportation, discussing conventional helicopters, compound helicopters, tilt rotor, tilt wing, stored rotor and fan or jet lift
24 p4254 A69-43721

GRASHOF NUMBER

Natural convection boundary layer stability on heated isothermal vertical plane wall, discussing Grashof number as laminar to turbulent flow transition criterion
02 p0188 A69-12038

Simultaneous equations for natural convection from horizontal cylinder at moderate Grashof numbers, using iteration digital computer method for boundary values
21 p3851 A69-38975

GRASSMANN ALGEBRA
U VECTOR SPACES

GRATINGS

Grating size effect on threshold of grating pattern for various colors of illumination and target orientations
22 p3879 A69-40840

GRATINGS [SPECTRA]

Intracavity laser diffraction gratings for single wavelength output
01 p0092 A69-10897

Submillimeter wave oscillator /orotron/ involving open resonator with mirror having reflection grating period less than wavelength
02 p0250 A69-12248

Pulse compression by optical correlation techniques, discussing laser beam control by diffraction grating in ultrasonic delay line
03 p0397 A69-13732

Bleaching of absorption hologram diffraction gratings for improved light efficiency, discussing bleaching materials results
04 p0596 A69-14284

Diffraction of plane electromagnetic waves obliquely incident on conducting rotated periodically tapered grating structure formed of infinite metal strips
05 p0723 A69-16788

Instrument profile of grating spectrograph determined by applying He-Ne laser mode separated in Fabry-Perot interferometer
07 p1131 A69-18405

Optical modulation through Doppler frequency shift obtained by rotating radial diffraction grating [AOLR-69-1]
11 p1889 A69-25394

Integral equation for diffraction from infinitely extended grating as mixed boundary problem of electromagnetic field, discussing single anomaly
15 p2568 A69-30795

Plane wave scattering by multimode corrugated structure with H mode incidence, revealing theoretically scattering resonance as P type Wood anomalies
17 p2925 A69-33844

Amplitude and intensity distributions of plane periodic Fresnel diffraction grating calculated by Fraunhofer theory, noting applicability to spectrometric and meteorological instruments
19 p3372 A69-35906

Modified residue-calculus technique combined with scattering matrix multiple reflection techniques for boundary value problems in waveguide phased arrays, diffraction gratings, etc
20 p3505 A69-37298

Auroral spectroscopy for high resolution coverage at maximum wavelength range, discussing plane diffraction grating
21 p3707 A69-38486

Grating spectrometer for far IR, discussing light source, reflection gratings, filters, etc
21 p3726 A69-39682

Optical ultrashort pulse compression with paired diffraction gratings in terms of phase shift frequency dependence and Fresnel diffraction analogy
23 p4171 A69-41392

Design and performance of microwave open resonators with diffraction grating in mirror, describing Q factor calculation
23 p4139 A69-42045

GRAVIMETERS

Errors in amplitudes and phases recorded by earth tide recording equipment determined, using special multiflex galvanometer
04 p0601 A69-15305

Gyroplatform to stabilize gravimetric equipment on aircraft, noting channel stabilization by electrohydraulic servomechanism
21 p3723 A69-38885

GRAVIMETRY

Slide wire aircraft vertical velocity meter for application during aerogravimetric mapping, discussing calibration and gravitational force measurement accuracy
03 p0429 A69-13261

Connecting duct influence on slide wire vertical airspeed indicator operating on barometric principle during aerial gravimetric surveying
13 p2260 A69-27828

Monograph on gravity covering gravimetric boundary value problem, iterative solutions, error analysis, gravity reduction, integral equations, etc
13 p2254 A69-27929

Lunar gravimetric data reprocessed to present in usable and readable form, plotting acceleration on Mercator projection of lunar surface
18 p3194 A69-34413

Book on gravimetry covering gravity measurement on land and in ocean, gravity anomalies, isostasy, geodetic applications, Eotvosian measurements and terrestrial tides
21 p3715 A69-39000

Tectonic classification of earth gravitational field based on mean gravity anomalies, correlating positive anomalies with Quaternary volcanism
23 p4154 A69-41318

Three channel inertial ship or aircraft navigator for determining gravity vector, using earth gravity field model
23 p4162 A69-41320

Gravitational constant G determination, describing accuracy enhancement
24 p4350 A69-42944

GRAVIRECEPTORS
NT OTOLITH ORGANS

Motor and tonic reactions in animals during weightlessness, discussing interaction between gravity receptors and visual analyzer
20 p3470 A69-37247

GRAVITATION

NT ARTIFICIAL GRAVITY
NT HIGH GRAVITY ENVIRONMENTS
NT LUNAR GRAVITATION
NT LUNAR GRAVITATIONAL EFFECTS
NT PLANETARY GRAVITATION
NT REDUCED GRAVITY
NT SOLAR GRAVITATION

Secularly stable figures of equilibrium of rotating heterogeneous fluids of planetary size, noting dependence on laws of inertia and gravitation
03 p0513 A69-13780

Coordinate transformations eliminating singularities in gravitational radius of Schwarzschild metric, noting local Lorentz transformations
08 p1351 A69-19952

Geocentric orientation of quasi-geocentric coordinate network determined from simultaneous photographic satellite observations, using gravity force values
12 p2158 A69-26429

Monograph on gravity covering gravimetric boundary value problem, iterative solutions, error analysis, gravity reduction, integral equations, etc
13 p2254 A69-27929

Geopotential determination from gravity force measurements at known surface and error assessment for earth model with aid of spherical harmonic expansion
15 p2689 A69-30567

Surface gravity and temperature model atmospheres for O-type stars with UV line blanketing
15 p2693 A69-30778

GRAVITATION THEORY

Gravitation theory similar to special relativity and Newtonian theories, noting gravitational potential, metric and Newtonian charts
01 p0115 A69-10340

Radiation problem in general theory of relativity investigated by momentum energy tensor, formulating criterion for gravitational radiation
01 p0116 A69-10435

Field theory of gravitation, discussing consequence of universality of gravitation /space-time geometry determination/
01 p0116 A69-10443

Mach principle in scalar-tensor gravitation theory, discussing self energy calculations in canonical formalism for solitary neutral and charged point particles
01 p0120 A69-10858

Conservation laws of energy and linear momentum in general relativity formulated, noting application to radiating gravitational systems
01 p0121 A69-11286

Tensor character of fictitious potential function introduced to approximate locally tangent actual potential function, discussing planetary gravitational anomaly observation from orbiting vehicles [AAS PAPER 68-198]
02 p0312 A69-11476

Electromagnetic field interaction with polarizable elastic medium in gravitation theory resolves definition of electromagnetic energy in matter
02 p0279 A69-11537

Gravitational fields in Hamiltonian formulation of relativistic theory of gravitation, noting geometrical aspects and equivalence to Einstein theory
02 p0280 A69-11715

Lorentz invariant theories of gravitation compared with Einstein general relativity tests with respect to one body motion observations
02 p0318 A69-12094

General covariant quantization of gravitation and cosmology
02 p0326 A69-12640

Invariant theory of gravitational radiation, using impulse energy tensor
02 p0332 A69-12835

Plane front gravitational waves analyzed on basis of gravitational radiation theory, discussing Einstein equations
02 p0332 A69-12836

Gravitational field representation based on linear spin-two field without direct self interaction, using divergence free nonlocal projection of matter stress tensor
03 p0466 A69-13388

Static locally flat solutions of Einstein vacuum field equation with line singularities and global space curvature, noting analogy to electromagnetic fields
03 p0466 A69-13389

First order equations for gravitational field quantized by methods developed for relativistic wave equations, describing elementary particles
03 p0466 A69-13422

General theory of relativity equations for homogeneous anisotropic three dimensional space with matter, deriving ultrarelativistic equation of state
03 p0466 A69-13423

Kerr family of solutions of Einstein and Einstein-Maxwell equations for gravitational field of rotating body, noting global structure and causality
03 p0466 A69-13473

Electromagnetic theory of gravitational forces unifying electromagnetic, meson and gravitational fields
03 p0469 A69-14096

General relativity confirmation, discussing mass equivalence and classical and new experiments such as gravitational shift, rotation effect on perihelion and precession test
04 p0661 A69-15165

Perturbation method determination of gravitational induction for quasi-static axisymmetric systems
04 p0661 A69-15190

Static formations in general theory of relativity and plankions
05 p0793 A69-15776

Lunar laser ranging for testing Einstein and Brans-Dicke gravitational theories, discussing pulse transit time and dominant nonNewtonian correction
05 p0825 A69-16362

Soviet book on theoretical astronomy covering evolution from Ptolemy to Einstein, universal gravitation and principles of celestial mechanics
07 p1211 A69-18544

Gravitational and inertial field equations of Maxwellian form leading to gravitation theory consistent with special relativity
07 p1182 A69-19408

Gravitational field in static spherical shell of matter in vacuum, deducing exact junction conditions for thin shell
07 p1182 A69-19453

Self gravitating medium in quasi-static equilibrium, using phenomenological equilibrium theory and zero time fluctuations
07 p1222 A69-19622

Forces generated by vortex gravitational field coupled to Newtonian field, motion of fluid mass in two gravitational fields and gravitational wave propagation
08 p1382 A69-19881

Interlocking systems within Galaxy, deducing gravitational theory accounting for galactic spiral patterns
08 p1387 A69-20136

Two gravitational fields theory of gravitation in general relativity for flat universe, discussing gravitational wave propagation
08 p1390 A69-20276

Linear approximation of Moller condition for reference frames interpretable as linear approximation of field equation in tetrad theory of gravitation
08 p1351 A69-20287

Early evolution of universe related to present upper bound of primordial black body gravitational radiation temperature
09 p1601 A69-22210

Variable gravitational number kappa, discussing effects on cosmology
09 p1603 A69-22270

Brans-Dicke gravitation theory effects on solar evolution and neutrino flux, discussing solar luminosity
09 p1605 A69-22415

Gravitational analog of Mariot-Robinson theorem, obtaining two related theorems with Newman-Penrose spinor formalism
11 p1919 A69-25097

Gravitational recoil due to gravitational emission of source analyzed in terms of Einstein equations
12 p1310 A69-26338

Quasars and radio-quiet objects numbers and properties, discussing red shifts interpretation by cosmological, gravitational and Doppler theories
12 p2161 A69-26937

Relativistic version of generalized gravitation theory, establishing models to describe gravitars having large gravitational mass defect and red shift
13 p2351 A69-27864

Polytropic gas spheres static models integral characteristics by nonrelativistic generalized gravitation theory, noting central densities dependence on critical values
13 p2352 A69-27872

Philosophical problems of Einstein theory of gravitation and relativistic cosmology - Conference, Kiev, June 1966
14 p2482 A69-28856

Observed values concept applied to general relativity theory, considering gravitational energy problem
14 p2483 A69-28858

Rigid space concept in gravitation theory, discussing reference systems with nonrigid and rigid background
14 p2484 A69-28863

Gravitational recoil, showing integration of Einstein equations in axisymmetric case reduced to integration of equations for Fourier coefficients
14 p2485 A69-29358

Inertial and gravitational mass equality reexamined, considering Galileo, Newton and Eotvos experiments
14 p2486 A69-29647

Density perturbation mode in Lifshitz relativistic theory for expanding universe gravitational instability, adopting Lagrangian coordinate condition to eliminate physically meaningless solution
15 p2652 A69-30203

Classical and relativistic gravitation theories using harmonic coordinate system, interpreting Einstein equations for insular distribution of masses and applications in geodesy
15 p2596 A69-30573

Newtonian invariant mechanics, giving inertial interpretation of gravitation and Hubble expansion of universe
15 p2654 A69-31214

Hall current effect on thermal instability explaining nonself gravitating astronomical objects, discussing current effects on propagation modes
16 p2854 A69-31649

Far field energy radiated by two body system using approximation method in general relativity and Minkowski gravitation theory
16 p2812 A69-31836

Simplified method for derivation of universal gravitation law from Kepler law of planetary orbits
16 p2813 A69-32481

Generalized Newtonian theory of gravitation, stressing internal solutions of gravitational field equations and incompressible fluid configuration in state of equilibrium
16 p2865 A69-32599

Spherically symmetric vacuum solution of Treder gravitational theory with emphasis on gravitational collapse
17 p3029 A69-33011

Hard cosmic radiation hypothesis for Newton gravitation law for neighboring bodies, obtaining gravitational energy quanta and propagation velocity relationship
18 p3172 A69-34627

Physical singularity reduced to imaginary by introducing arbitrary function in form of perturbation into gravitational equations general solution
18 p3173 A69-35018

Static formations in general theory of relativity and plankions
18 p3173 A69-35029

Spiral disk galaxies stability analysis assuming centrifugal force balancing self gravitation, transforming linearized equations of motion into eigenvalue equations
18 p3200 A69-35131

Einstein gravitational field equations series expansion in powers of gravity constant by Bondi method for gravitational waves
18 p3173 A69-35146

Bjerhammer gravity reduction method applied to gravity in space, analyzing two test models with mass focused between topographical and reference surface
18 p3173 A69-35197

Hydrogen atom excess charge creating universal repulsive force in analyzing cosmological gravitational contraction in terms of Newtonian mechanics
18 p3206 A69-35469

Relativistic tensor theories of gravitation in flat space with Neumann and Newton forms of gravitational potential, deriving expressions to estimate differences perceived by observer
19 p3373 A69-36204

Numerical integration of lunar motion equations to investigate lunar theory for high precision applications and to examine motion departures from gravitational theory
20 p3603 A69-37560

Statistical analysis of galactic structures subject to Newton gravitation covering globular clusters and spiral disk and rotating bar galaxies
21 p3803 A69-38924

Linear field gravitation theories, discussing spin dynamics
22 p3979 A69-39976

Variable gravitational constant hypothesis, theories of gravity and gravity laws for earth interior, solar motion, cosmological problem and earth orbit
22 p4017 A69-40174

Dirac hypothesis on varying G constant considered in formulating earth expansion theory without resorting to Ramsey hypothesis
22 p4018 A69-40178

Lagrange formulation of gravitation finite range theory compared with Einstein theory
22 p4027 A69-40656

Stellar evolutionary ages and gravitational theory relations based on initial abundance ratio U 235/U 238 and present interstellar medium heavy element content
23 p4219 A69-42329

Field theories of gravitation and experimental survey of general relativity theory, discussing red shift, Mercury orbit rotation, light deflection, solar oblateness, etc
23 p4192 A69-42330

Einstein general theory of relativity and apparatus for gravitational radiation detection, discussing Dicke experiments and Riemann tensor measurement
23 p4192 A69-42331

GRAVITATIONAL COLLAPSE

Light fluctuations rise time, electron density, emission temperature and peak luminosity estimated for quasars powered by local gravitational collapse events
02 p0325 A69-12590

Relativity and stellar model stability, discussing energetics of quasars and gravitational collapse of supermassive stars
06 p1002 A69-17315

White dwarf general relativistic instability toward dynamic collapse and Type I supernovae
06 p1010 A69-17975

Dynamical stability in premain sequence stars, discussing adiabatic models for pure hydrogen composition and collapse initiation by low opacity
07 p1220 A69-19388

Galactic angular momentum of rotation, applying rotation theory to gravitational instability model of galactic formation
08 p1383 A69-20050

Three color photoelectric observations of stars near Orion Nebula, discussing gravitational contraction stars and color magnitude diagram
08 p1384 A69-20055

Metagalaxy stationary model in terms of relativity theory, investigating radiation pressure balancing of gravitation as imaginary situation
08 p1389 A69-20263

Star collapse under energy losses due to neutrino emission, analyzing self similar asymptotic solutions
09 p1587 A69-21359

Motion and dispersion of peculiar velocities of stars in gravitational condensing interstellar gas
09 p1589 A69-21371

Poincare recurrence theorem applicable to collapsing gravitational system with particles velocity dispersion other than zero
09 p1593 A69-21567

Energy release in quasars through nonmassive gravitational collapse compared with local objects, noting cosmological luminosities
10 p1785 A69-24091

Theoretical models corresponding to initial phases in thermal-gravitational collapse of spherical clouds from interstellar gas for stellar formation
11 p1963 A69-25261

Angular momentum-gravitational field coupling in collapsing star, applying rotational perturbation to spherically symmetric time dependent interior solution of Einstein field equation
14 p2520 A69-29374

Protostars collapse and flare up computations, including radiative and convective energy flow terms in hydrodynamic equations of motion
15 p2680 A69-30206

Relativity theorems applied to collapsing stars and expanding universe noting limitations of general relativity from prediction of singularities
15 p2694 A69-30854

Energy release efficiency in gravitational collapse, estimating rest energy fraction from energy conservation, neutron star stability and spherically symmetrical systems collapse considerations

16 p2853 A69-31594

Spherically symmetric vacuum solution of Treder gravitational theory with emphasis on gravitational collapse

17 p3029 A69-33011

Star collapse under energy losses due to neutrino emission, analyzing self similar asymptotic solutions

18 p3197 A69-34749

Motion and dispersion of peculiar velocities of stars in gravitational condensing interstellar gas

18 p3198 A69-34760

Quarkian core substance in superstars of great masses, discussing existence as primordial state forming baryon and nuclei and origin in stellar gravitational contraction

19 p3401 A69-35912

NonJeans gravitational instability of stars and interstellar gas in Galaxy due to wave interaction with stars having velocity near wave phase velocity

20 p3607 A69-38037

Stellar mass loss in gravitational contraction and variation of rotation law during transition to main sequence

20 p3607 A69-38041

Ferromagnetism stable state in degenerate electron gas and magnetic fields in gravitationally collapsed bodies based on total microscopic magnetic moments associated with Landau level electrons

21 p3798 A69-38600

Quasars observations interpretation, discussing red shift origin, gravitational collapse, lifetime, distribution, cosmological aspects, etc

21 p3802 A69-38825

Physics of massive starlike objects, discussing high entropy requirement, eventual nonrelativistic collapse and gravitational fields produced by low entropy equilibrium

21 p3811 A69-39516

Relativistic star clusters, discussing existence and quasi-static evolution before collapse through gravitational radius

21 p3814 A69-39570

Galactic nuclei as collapsed old quasars from dynamics of gas cloud collection in galactic nucleus, discussing cosmic radiation emission from synchrotron mechanism

21 p3815 A69-39610

Spherically rotating symmetric body gravitational collapse within Schwarzschild radius, presenting trapped surface concept for asymmetrical cases and generalization of space-time singularities

23 p4219 A69-42333

Magnetic field implications in stellar formation mechanism including gravitational collapse, magnetic gas cloud fragmentation and stellar winds magnetic braking

24 p4378 A69-42699

GRAVITATIONAL CONSTANT

Laser beams self focussing interpreted as photon contraction due to equivalent gravitational attraction with gravitational constant proportional to nonlinear refractive index

08 p1324 A69-20085

Surrounding masses gravitational field effect on gravitational constant determination by torsional oscillations method, considering oscillation amplitude stability to eliminate errors

19 p3374 A69-36468

Newton gravitational constant determination from measured acceleration and known magnitude of masses, describing control system

20 p3537 A69-37140

Five dimensional theory applied to Einstein generalized gravity equations for spherically symmetrical gravitational waves, yielding gravity constant variation from Newton approximation

21 p3802 A69-38842

Gravitational constant secular change from considering relativistic cosmology and galactic structure, deriving equations of Newtonian cosmology

22 p4017 A69-40173

Variable gravitational constant hypothesis, theories of gravity and gravity laws for earth interior, solar motion, cosmological problem and earth orbit

22 p4017 A69-40174

Paleontological evidence to verify varying G constant hypothesis for expanding earth theory, discussing uncertainties of geological dating

22 p4017 A69-40177

Dirac hypothesis on varying G constant considered in formulating earth expansion theory without resorting to Ramsey hypothesis

22 p4018 A69-40178

Laser range measurement from earth to lunar retroreflector to study earth tipping and gravitational constant secular decrease

22 p3960 A69-40190

Gravitational constant G determination, describing accuracy enhancement

24 p4350 A69-42944

GRAVITATIONAL EFFECTS

NT LUNAR GRAVITATIONAL EFFECTS

NT SOLAR GRAVITATION

Self gravitating pulsating cylindrical and ring shaped cosmic masses from group theory standpoint compared with oscillating stars

01 p0148 A69-10124

Space biology, discussing U.S. research program, emphasizing gravity/organism reactions, biochronology and exobiology

[UN PAPER 68-95345] 01 p0014 A69-10486

Extraterrestrial vestibular research, discussing human otolith apparatus regulation subjected to change from geocentric to heliocentric orientation

[UN PAPER 68-95389] 01 p0014 A69-10508

General theory of relativity tests with aid of satellites, considering gravitational red shift measurements, light deflection in solar field, etc

01 p0152 A69-10751

Meteorite scattering in geogravitational field and influence on lunar meteorite precipitation distribution

01 p0153 A69-10756

Wheat seedling germination and growth processes in absence of gravitational force onboard Biosatellite 2

01 p0015 A69-10932

Gravitational force measurement on electrons and positrons in free fall through vertical metal tubes at low temperatures

01 p0125 A69-10979

Near circular satellite orbits evolution taking into account gravitational fields zonal harmonics effect on motion

01 p0157 A69-11304

Spacecraft maneuvering by changing spacecraft geometry and utilizing different gravitational forces acting on finitely extended bodies

01 p0158 A69-11318

Mass points substitution for mass of earth, giving gravitational effect equal to observed gravity values corrected for centrifugal acceleration

02 p0243 A69-12008

N body gravitational problem - Conference, Paris, August 1967

02 p0322 A69-12267

Numerical regularization of single binary collision in n body gravitational problem

02 p0322 A69-12268

Numerical solution on UNIVAC 1107 for model describing symmetrical gravitational collision of two four body systems

02 p0322 A69-12269

Collisionless computer model performing gravitational experiments with two dimensional galaxy

02 p0322 A69-12271

Computer study of collisionless self gravitating system using two dimensional model, obtaining gravitational field by solving Poisson equation

02 p0322 A69-12272

Statistical mechanics and thermodynamics for molecular systems applied to gravitational systems, discussing collisionless Boltzmann equation and Chandrasekhar binary collision model

02 p0323 A69-12273

Collective stability of collisionless gravitating systems based on variational principles resembling energy principle

02 p0323 A69-12275

Constant thrust deceleration formula for gravity turn soft landing maneuvers expressed in elementary and trigonometric functions of initial conditions for descent

02 p0335 A69-12531

Stability of elliptical Venus orbits with solar gravitational perturbations, using equation accuracy and influence on mission planning

02 p0331 A69-12819

Interplanetary transportation network involving numerous spacecraft on various planetary flyby trajectories, discussing integration of gravity thrust, braking and scramjet concept

03 p0511 A69-13402

Soviet collection of articles on dynamics of fluid-containing bodies under weightlessness conditions

03 p0417 A69-13808

Light and radial velocity changes in close binary systems, including limb and gravity darkening of distorted stars in analysis of spectroscopic effects

04 p0653 A69-14612

Low degree earth gravity harmonics effect on 12 and 24 hour orbits of high altitude communications satellites

04 p0592 A69-14661

Navier-Stokes equations for self gravitating viscous fluid, discussing generalization based on irreversible thermodynamics

04 p0588 A69-14699

Saturn ring formation by satellite spiral into Roche limit and disintegration

04 p0660 A69-15128

Taurus A 21 cm absorption line frequency decrease during optical path approach to sun, discussing gravitational and electromagnetic origin

04 p0661 A69-15148

Cosmology, experiments on gravitation, space-time theory and model of universal history

04 p0661 A69-15157

Iterative guidance mode /IGM/ applied to effective gravity vector prediction, acceleration measurement of noise sensitivity and energy limitations

[AIAA PAPER 67-620] 04 p0629 A69-15501

Center of gravity of two dimensional gravitating bodies by gravitational anomaly technique, based on conformal mapping of bilinear function

05 p0792 A69-15696

Gravitational instability of rotating anisotropic plasma for longitudinal wave propagation mode, obtaining dispersion by using modified Chew-Goldberger-Low equation

05 p0827 A69-16596

Quasars, stressing local Doppler and gravitational hypotheses for observed red shifts

06 p0998 A69-16968

Biological systems response to inertial environment, escape from earth gravity, planetary gravity and artificial gravity

06 p0872 A69-17011

Weightlessness simulation, discussing mechanics of biological effects, simulation of specific anticipated effects and concept of mechanical acceleration and gravity equivalent effects

06 p0879 A69-17012

Renal excretion response to blood fluid volume shift resulting from altered orientation within gravity or from absence of gravity

06 p0873 A69-17015

Differential equations of rotational motion of systems of rigid bodies in gravitational field derived with Lagrange equation

06 p0957 A69-17130

Large paraboloid radio antennas structural setting for minimizing effects on performance due to deformation of surface by gravitational forces

06 p1023 A69-17372

Blood circulation in brain during acceleration analyzed by tensometric sensors and electrophysiology, noting intracranial sensitivity to gravitational changes

06 p0874 A69-17646

Increased gravitational stress effects on esophageal sphincter pressures and gastroesophageal reflux in rhesus monkeys, noting cardia competence

06 p0874 A69-17838

Complex distribution of quasar red shift interpreted as due to two simple distributions of cosmological and gravitational red shift

06 p1009 A69-17968

Gravitational effects during physiological functions formation of human organism, noting myogenic tonus rearrangement as primary response

07 p1060 A69-18572

Otolith and cupular apparatus interaction in human vestibular analyzer during gravitational changes

07 p1062 A69-18589

Sensory and motor activity of human subjects exposed to reduced gravitation during aircraft motions along parabolic trajectories

07 p1062 A69-18592

Human postural muscle activity, motor reactions and dexterity during gravitational changes

07 p1063 A69-18593

Stability of motion of spherically symmetric mass of compressible gas with constant space density in absence of gravitational field

07 p1215 A69-18706

Nondimensional Jeffreys number as ratio of Reynolds to Froude number for gravitational motion of viscous masses, with application to lunar maria and plastic ice

07 p1218 A69-19262

Combined effect of short wavelengths associated Kelvin-Helmholtz instability and long wavelengths associated gravitational instability on self gravitating fluid layer, discussing kinetic energy

07 p1182 A69-19276

Stars of higher multiplicity, discussing numerical membership and gravitational binding of star clusters and binary stars

07 p1219 A69-19295

Stellar galactic orbit perturbation by irregularities in distribution of gas cloud for motion inclined to galactic plane

07 p1223 A69-19634

Plumb line fluctuations /M sub 2 tide, 1961/ at 135 degree azimuth by Voit method, discussing residual ellipse for Borowiec

08 p1306 A69-19824

General relativistic gravitational red shift effect on frequency transmitted from satellite orbits, noting possibility of measurement

08 p1383 A69-19901

Otolith apparatus response threshold under weightlessness conditions simulated by aircraft flight, measuring galvanic current threshold for banking

08 p1263 A69-19934

Trajectories minimizing missile velocity losses due to gravity by setting boundary conditions and trend of thrust in time

08 p1409 A69-20587

Rotation effect on homogeneous gravitating systems stability, noting lack of unity in approaches to cosmogony by various authors

09 p1589 A69-21372

Uniform gravity load effect on buckling of beam continuously supported by soft foundation and subjected to uniform lateral load

09 p1615 A69-21927

Rotating plasma gravitational instability during discharge as function of centrifugal acceleration, noting Coriolis and Larmor effects

09 p1552 A69-22043

Quasar red shifts due to cosmological and gravitational factors, assuming correlation of QSO intrinsic luminosity with gravitational red shift values

09 p1597 A69-22151

General solution of Liouville equation for collisionless system of gravitationally interacting particles, with distribution function locally isotropic in momentum space

09 p1605 A69-22412

Satellite altitude stabilization by gravity gradient capture in earth elliptical orbit, showing effect of increase in damping

10 p1791 A69-22926

Total planet interaction energy of comets passing through solar system, showing non-Gaussian shape of distribution

10 p1774 A69-22970

Photometric over dynamical ellipticity excess attributed to gravitational darkening in eclipsing binaries of W Ursae Majoris type

10 p1776 A69-23217

Earth gravitational field effect on satellite orbits, noting elliptical motion in central force field, energy criteria and rotational ratios

10 p1776 A69-23295

Finite Larmor radius, finite conductivity, rotation and Hall current effects on Jeans criterion for gravitational instability of plasma

10 p1729 A69-23408

Radial motion of uniform spheres in general relativity, finding conditions for initially inward motion to reverse/bounce/

10 p1779 A69-23607

Simulated weightlessness used in determining ontogenesis of otolith organ in tadpoles and eggs as function of acceleration forces [DVL-855]

10 p1647 A69-24021

Ellipsoidal satellite translational rotational motion under spherical planet and point source sun gravitational fields influence, obtaining approximate solution for three body problem

11 p1956 A69-24399

Gravitational effects on thermodynamic variable equilibrium composition of liquid-vapor binary mixtures near critical point, discussing changes in phase with altitude

11 p1999 A69-24914

Charge bunching approach for gravitational hydrodynamic instability of infinite uniform self gravitating system in translational motion, using conservation laws

11 p1961 A69-25105

Gravitational stability of spheroidal expansions of rotating gas masses in astronomy, noting mechanism for fragmentation in cosmology

11 p1962 A69-25112

Blind goldfish behavioral responses to short lowered gravitational force cycles during vertical flight classified as vestibular reflexes resulting from otolith displacement

11 p1828 A69-25464

Solid body motions containing cavity filled with viscous fluid under influence of gravity, formulating motion equations for fluid and body

12 p2061 A69-25884

Satellite motion short period perturbations by earth gravitational field tesseral and sectoral harmonics

12 p2069 A69-26431

Finite ion Larmor radius effect on gravitational instability of two superposed fluids in uniform rotation, analyzing interchange perturbations and vortex sheet

12 p2062 A69-26461

Weightlessness and higher g values effects on caloric and rotational nystagmus

12 p2020 A69-26551

Friction damping properties of deployed structures vibrating in weightless state compared to damping in space for true determination

12 p2183 A69-26792

Gasdynamic phenomena during subsonic or supersonic motion of isothermal gas under action of gravitational forces in flatten axisymmetric galaxy containing spiral density waves

12 p2170 A69-27065

Self adjusting digital computer method for two dimensional gravitational anomalies

12 p2076 A69-27088

Quasar applications as gravitational lenses within Hoyle-Fowler quasar model

13 p2340 A69-27575

Hydromagnetic stability of spiral arm embedded in gravitating medium from analysis of instability of self gravitating incompressible cylinder

13 p2346 A69-27705

Finite Larmor radius and collision with neutral atoms simultaneous effects on plasma gravitational instability

13 p2346 A69-27708

Lunar astronauts psychological problems, discussing isolation from outside world, gravitational and extreme light effects, protective space suits, etc

13 p2210 A69-27905

Gravity preference tests on rats subjected to simulated Aerobee 150 A rocket launching and flight in ground based spiral centrifuge

13 p2213 A69-28090

Optimal stochastic controller synthesis theory applied to stabilizing and controlling orientation of rotating bodies in central gravitational fields

13 p2300 A69-28326

Satellite motion relative to center of mass and resonances by approximate solutions to motion equations, applying asymptotic methods

13 p2357 A69-28502

Hypokinesia and nutrition deficiency effect on blood coagulation, noting combination with accelerations may lead to hypocoagulation

13 p2212 A69-28625

Dynamics of gyroscope having flexible axis under gravitational force and elastic coupling reactions, deriving motion equations, precessions angular velocities, etc

14 p2445 A69-28798

Density distribution in axisymmetrical gravitating systems with ellipsoidal velocity distribution function, using integral equation of state for effective radii of cylindrical configurations

14 p2486 A69-29465

First order secular and aperiodic perturbations in Keplerian orbital elements of synchronous satellite due to earth gravitational field eccentricity

14 p2521 A69-29466

Gravity effects on plant growth, discussing horizontal clinostat experiments and auxin transport mechanism

15 p2555 A69-30470

Pulsar clock mechanisms on basis of relativistic gravitational effects, considering white dwarfs and neutron stars

15 p2694 A69-30855

Simulated gravitational lens made of Plexiglass for demonstrating stellar gravitational lens phenomena, presenting partial cross section

15 p2653 A69-31163

Satellite motion about center of mass, discussing satellite stabilization and libratory motion in gravitational force field, planet resonances, etc

15 p2703 A69-31411

Gravitational effect of electromagnetic radiation evaluated on test particle using Einstein field equations

16 p2812 A69-32049

Gravitational and magnetic torque effect on rotational motion of triaxial rigid body in regressing orbit about oblate primary mass

16 p2861 A69-32240

Turbulence dissipation rate in clouds and precipitation determined from rms width of vertical sounding radar signal fluctuation spectra, distinguishing gravity and turbulence effects

16 p2807 A69-32273

Motion of two rigid spheroids with mutual gravitational attraction based on Hamilton-Jacobi theory applicable to binary stars

16 p2863 A69-32402

Fluid transfer in orbit under low or zero g, stressing orientation [AIAA PAPER 69-565]

16 p2865 A69-32770

Ground state energy inequalities for N particle non-relativistic quantum mechanical system, showing non-saturating gravitational forces and increasing binding energy per particle

17 p3028 A69-32900

Human motion coordination under acceleration followed by weightlessness during jet flights along Keplerian orbits, discussing initial disturbance and subsequent subsiding

17 p2907 A69-32938

Pulmonary ventilation and perfusion in normal supine subjects before and during exposure to lower body negative pressure measured using Xe-133

17 p2909 A69-33180

Liquid draining motion from transversely moving cylindrical tank in time varying gravity field with outlet pipe at bottom, discussing flow rate and free surface [AIAA PAPER 69-679]

17 p2953 A69-33440

General relativity theory test using earth orbital motion and solar gravitational field effects on pulsars frequency stability

17 p3037 A69-33646

Microwave background anisotropy induced by gravitational effects interpreted using spatially flat Friedmann model for substratum

18 p3190 A69-34286

Gravity independence of life processes in terrestrial organisms concluded from zero gravity experiments with algae, hatched larvae, etc

18 p3095 A69-34692

Rotation effect on homogeneous gravitating systems stability, noting lack of unity in approaches to cosmogony by various authors

18 p3198 A69-34761

Materials processing in space, suggesting electronic single crystals preparation, materials melting and utilization of low g earth orbit environment

19 p3324 A69-35589

Perturbation technique application to stability criterion for rectilinear missile flight with arbitrary inclination, noting mass reduction and flow and gravity effect

19 p3429 A69-35779

Attitude stabilization of symmetrical nonrotating earth satellite using earth-pointing rotor as gravitational anchor

19 p3429 A69-35914

Gravity torque influence on axisymmetric dual spin satellites in fixed attitudes, using attitude stability studies of spinning single rigid bodies

19 p3429 A69-35917

Gas motion behind cylindrical shock wave created by piston motion in gravitating medium

19 p3298 A69-36386

Rats locomotion in centrifugally generated gravity fields determined for in-space behavioral studies of earth organisms gravity requirements

19 p3263 A69-36457

Surrounding masses gravitational field effect on gravitational constant determination by torsional oscillations method, considering oscillation amplitude stability to eliminate errors

19 p3374 A69-36468

Gravitational stability of infinite conducting fluid cylinder in axial magnetic field and surrounded by fluid of different density

19 p3380 A69-36483

Atmospheric entry-capsule dynamics, considering angle of attack motion under gravity forces influence and aerodynamic normal force stability relations

20 p3617 A69-37197

Moon possible origin, discussing spin off from earth, accretion from same dust cloud or formed elsewhere and captured

20 p3603 A69-37559

Hot star photogravitational acceleration determined from difference between apex and antiapex brightness, noting constant magnitude and direction of principal component of apex force

20 p3608 A69-38046

Periodic orbits of Poincare and Schwarzschild types in motion of artificial satellite in disturbed gravitational field of axisymmetric oblate spheroid

21 p3795 A69-38441

Statistical mechanics applied to mechanical properties and thermodynamics studies of rapidly expanding or collapsing self gravitating systems

21 p3801 A69-38702

Two dimensional gravity assisted trajectories for solar probe missions in ecliptic plane, discussing Venus and Jupiter assist missions

21 p3804 A69-39022

Squirrel monkeys escape behavior under centrifuge simulated gravity in excess of earth gravity

21 p3665 A69-39174

Motion sickness susceptibility during parabolic flight, comparing weightlessness and hypergravity effects on normal and labyrinthine-defective subjects

21 p3660 A69-39176

Electrocardiographic changes during gravitational stress

21 p3660 A69-39178

Spacecraft guidance analysis of multiple outer planet mission utilizing gravity assist swingbys to achieve planetary flybys with single spacecraft [AAS PAPER 68-109]

21 p3761 A69-39205

Acceleration effects on solid propellant rocket motors combustion characteristics [AIAA PAPER 68-530]

21 p3786 A69-39217

Exploration capabilities provided by Jupiter gravity assisted trajectories compared to direct ballistic flight trajectories [AAS PAPER 68-116]

21 p3805 A69-39224

Gravitational fields and atmospheric pressure effects on soils subjected to static and dynamic loading, using aircraft parabolic gravity simulation [AIAA PAPER 69-1009]

22 p3921 A69-40382

Responsiveness of cortex and visual pathway during transient hypotension induced by increased gravitational stress, discussing intraocular pressure of cat

22 p3878 A69-40779

Kinetic beam instability development in homogeneous dust /gas/ cylinder rotating in hot invariable medium under arbitrary perturbations

22 p4032 A69-41017

MHD of ideal charged gravitating fluid by variational principle, considering Einstein general relativity theory

22 p3992 A69-41056

Autometric gyro for satellite general relativity experiments, particularly earth orbit measurement of Lense-Thirring precession

23 p4162 A69-41543

Terrestrial type planetary evolution from early history and present internal configuration of earth, discussing gravitational energy associated with earth formation

23 p4212 A69-41613

Hydrodynamic stability of conducting fluid in external magnetic field subject to attraction of external spherically symmetric gravitational field

23 p4213 A69-41717

Spheroidal disturbances theoretical seismograms on surface of gravitating elastic sphere with homogeneous mantle and liquid core, considering gravity and polar radial stress effects

23 p4158 A69-42020

Tiltable conventional radio telescopes possibilities of passing gravitational limit for diameter and shortest wavelength, discussing dead load

23 p4231 A69-42138

Gravitational field structure effects on Alfvén waves propagation in inhomogeneous medium

23 p4223 A69-42478

Gravitational stress effect on heart and venous system, discussing digital computer model simulating pressure changes under head-up and down tilt

24 p4271 A69-42783

Urine osmolality of centrifurged rats compared with ad libitum or pair-fed control animals, indicating enhanced free water excretion and antidiuretic hormone involvement

24 p4262 A69-42904

Quasi-optimum control law for minimum-time bounded acceleration rendezvous in central force field using Friedland technique, with application to lunar flight

24 p4349 A69-43313

Stillbirth and neonatal death in stressed rats exposed to mild and acute gravitational loads in automobile ride and aircraft flight

24 p4266 A69-43381

Contraststreaming self gravitating gas streams stability taking into account thermal conduction and radiation effects

24 p4388 A69-43638

Ellipsoidal satellite translational rotational motion under spherical planet and point source sun gravitational fields influence, obtaining approximate solution for three body problem

24 p4390 A69-43789

GRAVITATIONAL FIELDS

Killing fields applied to nonsymmetric spaces specify coordinate lines with slowest possible metric tensor variation and gravitational radiation

01 p0115 A69-10018

Gravitation theory similar to special relativity and Newtonian theories, noting gravitational potential, metric and Newtonian charts

01 p0115 A69-10340

Stability of gravitating fluid layer of infinite extent but finite thickness including Hall effect

01 p0128 A69-10342

Gravitational field and earth shape determination by calculating perturbing potential at earth surface and in outer space, using Green functions

01 p0063 A69-10360

First approximation stability of single rotation of artificial earth satellite about center of mass in Newtonian gravitational force field

01 p0161 A69-10585

Particle moving in circular orbit perpendicular to axis of cylindrically symmetric magnetic field

01 p0120 A69-10816

Three body problem, discussing impossibility of libration points of gravitating ellipsoid

01 p0155 A69-10957

Equatorial geodesic motion of rotating source in gravitational field, using exact empty space solutions of Einstein equations

01 p0157 A69-11289

Spacecraft maneuvering by changing spacecraft geometry and utilizing different gravitational forces acting on finitely extended bodies

01 p0158 A69-11318

Tensor character of fictitious potential function introduced to approximate locally tangent actual potential function, discussing planetary gravitational anomaly observation from orbiting vehicles

02 p0312 A69-11476

Schuler gyroscopic pendulum, noting magnitude requirement for gravitational field used in inertial navigation

02 p0248 A69-11593

Gravitational fields in Hamiltonian formulation of relativistic theory of gravitation, noting geometrical aspects and equivalence to Einstein theory

02 p0280 A69-11715

Anomalous gravitational geopotential as function of mass, discussing density anomalies in spherical shells for harmonics as obtained from satellite observations

02 p0244 A69-12178

General covariant quantization of gravitation and cosmology

02 p0326 A69-12640

Light tachyons, tachyon velocity and relation to gravitational quanta

02 p0282 A69-12746

Satellite orbit selection for determining geopotential and spherical and tesseral harmonic coefficients, discussing propulsion systems and satellite observation cost feasibility

02 p0331 A69-12807

Invariant theory of gravitational radiation, using impulse energy tensor

02 p0332 A69-12835

Plane front gravitational waves analyzed on basis of gravitational radiation theory, discussing Einstein equations

02 p0332 A69-12836

Saturn ring gravitational field perturbations of space vehicle orbit on flyby mission solved by particle motion perturbation theory

03 p0508 A69-13260

Gravitational field representation based on linear spin-two field without direct self interaction, using divergence free nonlocal projection of matter stress tensor

03 p0466 A69-13388

Static locally flat solutions of Einstein vacuum field equation with line singularities and global space curvature, noting analogy to electromagnetic fields

03 p0466 A69-13389

First order equations for gravitational field quantized by methods developed for relativistic wave equations, describing elementary particles

03 p0466 A69-13422

Kerr family of solutions of Einstein and Einstein-Maxwell equations for gravitational field of rotating body, noting global structure and causality

03 p0466 A69-13473

Electromagnetic and gravitational tensor fields in Riemannian space, generalizing Maxwell and Bel-Robinson tensors

03 p0467 A69-13755

Plasma gravitational stability problem with Hall effect, noting relevance to astrophysical systems

03 p0478 A69-13803

Equilibrium problem for fluid subjected to gravitational forces and surface tension, proposing algorithm for numerical solution

03 p0417 A69-13810

Primary frequency of oscillations of ideal liquid in cylindrical vessel with axially directed weak gravitational field

03 p0418 A69-13812

Electromagnetic theory of gravitational forces unifying electromagnetic, meson and gravitational fields

03 p0469 A69-14096

Approximate method for finding solution of weak free convection in partially filled vessel in gravitational field

04 p0685 A69-14619

Idealized point mass motion in axisymmetric gravitational field, discussing orbital stability about oblate planet

04 p0658 A69-14887

Canonical equations for Lagrangian form of gravitational field equations in empty space

04 p0658 A69-14899

Capture of electrically charged micrometeorites and corpuscles in magnetic field of gravitating dipole, noting necessary condition on particle motion

04 p0659 A69-14962

Soviet book on artificial satellite motion in noncentral gravitational field, discussing celestial axisymmetric planetary orbits, stationary centers, three body problem, etc

04 p0659 A69-15027

Center of gravity of two dimensional gravitating bodies by gravitational anomaly technique, based on conformal mapping of bilinear function

05 p0792 A69-15696

Unsteady motion of ideally conducting gas flow in transverse magnetic field with allowance for gravitational forces

05 p0802 A69-15789

Lagrange multipliers of variational problem of point motion and isochronal derivatives in field of attraction of axisymmetric planet

05 p0823 A69-16015

Perturbations of stationary orbital vehicles of arbitrary latitude due to earth triaxiality, noting control by low thrust rocket engine

05 p0823 A69-16037

Velocity increments for orbital transfer in satellite rendezvous in central Newtonian gravitational field by two impulse ballistic transfer method

05 p0789 A69-16046

Parallel rendezvous of space vehicles in central gravitational field, discussing relative motion of space vehicle and supplementary force required

05 p0789 A69-16047

Feynman rules for gravitational field from coordinate independent field theoretic formalism, expressing path dependent Green functions in path independent functions

05 p0794 A69-16364

Equivalence principle application to gyroscope motion in uniform gravitational field to obtain precessional angular velocity

05 p0764 A69-16367

Satellite relative equilibrium stability under action of gravitational and aerodynamic moments

05 p0830 A69-16503

Motion stability of gyroscope in universal suspension with spring restraints and damper in gravitational field extended to include Newtonian central force field

05 p0765 A69-16684

Alfvén waves observed propagating along lines of force in inhomogeneous plasma in presence of homogeneous gravitational field

05 p0805 A69-16706

Moment equations of Vlasov plasma used for pressure effects on gravitational flute instability of nonuniform plasma

06 p0965 A69-17515

- Ballistic reentry trajectories, considering point mass motion in central force field under tangential thrust action and spherical atmospheric density distribution
06 p1006 A69-17564
- Spherical and single axis passive oscillation energy dampers for gravity gradient oriented satellites, utilizing earth gravity field or solar pressure
07 p1229 A69-18347
- Einstein equations solution in Gaussian coordinates describing particles gravitational fields including point particles
07 p1180 A69-18507
- Viscous gravitating sphere oscillations and velocity field, noting oscillations of Maxwell sphere
07 p1123 A69-18806
- Petrov classification of cylindrically symmetric space-time, giving Weyl conformal curvature tensor and surviving Ricci tensor components
07 p1182 A69-19409
- Ideal fluid interaction with gravitational field, assuming internal energy as function of natural pressure and density
07 p1182 A69-19419
- Steady state motions stability of gyroscope mounted on satellite in gravitational orbit
07 p1137 A69-19679
- Forces generated by vortex gravitational field coupled to Newtonian field, motion of fluid mass in two gravitational fields and gravitational wave propagation
08 p1382 A69-19881
- Landau damping of long wavelength ion acoustic waves in collision-free one dimensional plasma with gravity field
08 p1359 A69-19983
- Two gravitational fields theory of gravitation in general relativity for flat universe, discussing gravitational wave propagation
08 p1390 A69-20276
- Dynamics and instability of multilayered systems models in field of gravity, noting isostatic adjustment of layered globe
08 p1309 A69-20578
- Gravitational wave solution of Einstein field equations, deriving Ricci and Riemann tensors for Einstein space
08 p1352 A69-20755
- Cosmic microwave background variations produced by nonthermal gravitational radiation, imposing limits on equivalent mass density
08 p1398 A69-20773
- Velocity and temperature fields in Newtonian fluid in motion past stationary obstacle in gravitational field, noting similarity parameters reduction
09 p1429 A69-21686
- Compressible gas flow problem in point body gravitational field solved with reference to sun and interstellar gas
09 p1577 A69-21769
- Geometrized theory of combined gravitational and electromagnetic fields, using metric tensor of four dimensional Riemannian continuum to describe both fields
09 p1540 A69-22134
- Early evolution of universe related to present upper bound of primordial black body gravitational radiation temperature
09 p1601 A69-22210
- Gravitational potential of circular rings used to investigate motion stability of Saturn rings
10 p1771 A69-22855
- Generalized gravitational field equations derived on basis of principle of least action, noting vector potential of electromagnetic field
10 p1725 A69-23714
- Quasi-integral operator applicability to analytical continuation of potential field into complex region arising during gravitational and magnetic anomalies interpretation
10 p1689 A69-24082
- Two fixed centers with force function approximating earth gravitational potential, deducing formula for gravity distribution at level surface
11 p1952 A69-24254
- Stability of spherically symmetrical nonrotating mass systems moving in self consistent gravitational Einstein field, considering quasar applicability
11 p1956 A69-24394
- Shock wave propagation in gravitational field with pressure and density gradients, considering nonlinear equations of fluid flow
11 p1961 A69-25106
- Einstein field equations solutions for homogeneous cosmological models, assuming perfect fluid gravitation source and existence of simply transitive surface motions
11 p1919 A69-25245
- Gyrostabilized satellite steady state motions in Newtonian force field having displaced satellite center of mass orbital plane relative to center of attraction
12 p2173 A69-25885
- Density stratified model of troposphere and constant gravity field for ground level pressure perturbations in mesoscale region
12 p2126 A69-26016
- Gravitational recoil due to gravitational emission of source analyzed in terms of Einstein equations
12 p2130 A69-26338
- Pitch angle distribution function of thermal protons in magnetosphere taking into account earth gravitational field
12 p2067 A69-26354
- Relativistic hydrodynamic equations for charged particles interacting in external scalar and gravitational fields, considering particle motion and scalar plasma dispersion
12 p2130 A69-26462
- Nonrelativistic theory of rotating configurations in terms of gravitational potential, center mass density and variable angular velocity
12 p2159 A69-26662
- Spiral arms as wakes of gravitational shock waves arising at galactic nucleus boundary and propagating outward through interstellar gas
12 p2170 A69-27066
- Earth gravitational field representation by separating geopotential into normal and disturbing potential for solving geodetic boundary value problem for satellite geodesy
12 p2076 A69-27089
- Gravity perturbations in earth external field, treating anomalous potential using Green integral formula and spherical harmonics
12 p2077 A69-27139
- Surface gravities and detection of metallic line early A stars from spectral classification using equivalent line widths
12 p2171 A69-27151
- Gravitational parameters of highly condensed objects, considering white dwarf evolutionary stages, density and upper mass limit
13 p2334 A69-27190
- Spacecraft horizontal maneuvers in homogeneous gravitational field to achieve soft landing on planetary surface, including optimal liftoff and orbital transfer
13 p2356 A69-27685
- Finite Larmor radius effects on gravitational instability of rotating anisotropic plasma for transverse wave propagation mode
13 p2346 A69-27704
- Conformally plane solutions to Einstein equations derived with energy momentum tensor characteristic of pulverized material representing gravitational fields
13 p2298 A69-27796
- Internal solution of Einstein equations for steady axisymmetric gravitational fields by integrating differential equations with initial conditions
13 p2351 A69-27863
- Unified geometric description of gravitational and electromagnetic fields, determining electromagnetic field influence on geometry from dimensional constant
13 p2300 A69-28450
- Increases of Newtonian potential, gradient and second derivative on gravitating body, considering positive and negative masses
13 p2300 A69-28545
- Odd zonal harmonics coefficients in earth gravitational potential from analysis of satellite orbital eccentricity variations
14 p2439 A69-29118
- Energy momentum tensor in Einstein field equations derived from covariant field equations for vector meson
14 p2486 A69-29452
- Steady motion stability of satellite with gimbal suspended gyroscope in central gravitational field, showing no effect of satellite perturbations on gyrostaticity
14 p2530 A69-29481
- Asymptotic expansions for Einstein-Maxwell field representing gravitational and electromagnetic radiation from finite source of matter and charge
14 p2486 A69-29635
- Successive approximations method applied to system of independent equations describing electromagnetic wave propagation in space with gravitational wave metric
14 p2487 A69-29669
- Mass point system moving in gravitational field, discussing statistical mechanics, relaxation time and evolution of stellar systems
14 p2530 A69-29987
- Elastic and inelastic evolution of concentrated gravitational systems, discussing stellar diffusion, evaporation, halos and rotating systems
15 p2687 A69-30548
- First approximation stability of single rotation of artificial earth satellite about center of mass in Newtonian gravitational force field
15 p2702 A69-30755
- Simulated gravitational lens made of Plexiglass for demonstrating stellar gravitational lens phenomena, presenting partial cross section
15 p2653 A69-31163
- Weakly damped transverse and thermal waves development and propagation in viscous heat conducting incompressible fluid under temperature and gravitational fields
15 p2718 A69-31168
- Lunar mass and gravitational field determined from lunar satellite dynamics, using potential function in terms of spherical harmonics
15 p2699 A69-31405
- Satellite orbit evolution data applied to refinement of geophysical parameters, including upper atmosphere parameters and zonal harmonic coefficients in gravitational potential expansion
15 p2604 A69-31417
- Electromagnetic cavity resonances in rotationally induced gravitational field by relativistic approach
16 p2812 A69-32048
- Gravitational radiation indicated by coincidences of detector observations over 1000 km, eliminating seismic and electromagnetic effects
16 p2784 A69-32565
- Einstein equations for empty space applied to degenerate gravitational fields with twisting rays, admitting shear-free twisting congruence of null geodesics
17 p3004 A69-32832
- Ground state energy inequalities for N particle non-relativistic quantum mechanical system, showing non-saturating gravitational forces and increasing binding energy per particle
17 p3028 A69-32900
- Particle production by gravitational fields in universe via quantum field theory, considering cosmological models
17 p3008 A69-33003
- Minimum time single axis capture of satellite spinning about pitch axis by low thrust jets, considering gravity gradient phenomenon
17 p3048 A69-33237
- Effective temperature and gravity values for Mn Ap stars by comparing spectrum scans and H line profiles with predictions from atmospheric models
17 p3038 A69-33724
- Earth-moon and moon-earth trajectory parameters related to lunar orbit conditions for synthesizing lunar orbit trajectory
18 p3196 A69-34704
- Capture of electrically charged micrometeorites and corpuscles in magnetic field of gravitating dipole, noting necessary condition on particle motion
18 p3197 A69-34725
- Unsteady motion of ideally conducting gas flow in transverse magnetic field with allowance for gravitational forces
18 p3181 A69-35040
- Einstein gravitational field equations series expansion in powers of gravity constant by Bondi method for gravitational waves
18 p3173 A69-35146
- Polar coordinates in Euclidean space applied to theory of satellite moving in gravitational field of spherically symmetrical body, introducing equipotential surfaces
19 p3397 A69-35610
- Relativistic tensor theories of gravitation in flat space with Neumann and Newton forms of gravitational potential, deriving expressions to estimate differences perceived by observer
19 p3373 A69-36204
- Newtonian and general relativistic orbits of point mass in inverse square law force field, noting radar determination of spacecraft orbits
20 p3595 A69-37176
- Satellite representations of earth gravity field portraying consistent pattern of mass anomalies due to density differences in layers
20 p3523 A69-37566

Velocity increments for orbital transfer in satellite rendezvous in central Newtonian gravitational field by two impulse ballistic transfer method 20 p3574 A69-37955

Parallel rendezvous of space vehicles in central gravitational field, discussing relative motion of space vehicle and supplementary force required 20 p3574 A69-37956

Satellite orbit determination method allowing geogravitational field determination and correction of station coordinates 21 p3793 A69-38337

Infinitesimal mass trajectories and possible double collision in gravitational field of two finite and unequal masses in plane elliptic restricted three body problem 21 p3795 A69-38443

Five dimensional theory applied to Einstein generalized gravity equations for spherically symmetrical gravitational waves, yielding gravity constant variation from Newton approximation 21 p3802 A69-38842

Gravity gradient phenomena in orbiting vehicle used to explore planetary gravity [AIAA PAPER 68-851] 21 p3804 A69-39024

Near equatorial near synchronous satellite orbits determined by supplementing spherical harmonics representation of earth gravitational field with polynomial force model representation [AAS PAPER 68-141] 21 p3806 A69-39234

Isotropic ideal bidimensional filter in interpretation of anomalous gravity fields, especially for separating local and regional effects 21 p3724 A69-39246

Statistical characteristics of linear transformations of gravity field anomalies by linear operators, noting computation of covariance function 21 p3716 A69-39247

Time-similar and isotropic geodetic curves simulating paths of test bodies in Riemann space corresponding to gravitational field 21 p3772 A69-39621

Earth shape and areas of anomalous gravity from satellite orbital perturbations, tabulating results from various experimenters 21 p3718 A69-39734

Variations in gravity, plotting results for U.S., with tables for Alaska, Mexico, India, Africa, etc 21 p3718 A69-39735

Earth gravitational potential energy changes in examining expanding earth theory 22 p3936 A69-40180

Gravitational fields and atmospheric pressure effects on soils subjected to static and dynamic loading, using aircraft parabolic gravity simulation [AIAA PAPER 69-1009] 22 p3921 A69-40382

Dimensionless coupling constants predicted from causal relationship among strong, electromagnetic, weak and gravitational interactions in fluid region of universe 22 p3981 A69-40416

Neglected gravity coefficients influence on computed satellite orbits and geodetic parameters 22 p4023 A69-40556

Nonexistence of second order clustering of galaxies and relationship to gravitational cut-off, relativistic cosmologies and red shifted light by exponential decay of photon energy 22 p4024 A69-40579

Model atmospheres of late type stars with solar abundances, effective temperatures between 2000-4000 K and gravities corresponding to dwarf, giant and supergiant stars 22 p4027 A69-40654

Schwarzschild metric properties in synchronous reference system, using succession of Schwarzschild interval holonomic transformations as function of gravitational radius 22 p3982 A69-41063

Optimal pulsed orbital transfer between close nearly circular orbits in central field of gravity realized by geometrical solution 22 p4033 A69-41085

Tectonic classification of earth gravitational field based on mean gravity anomalies, correlating positive anomalies with Quaternary volcanism 23 p4154 A69-41318

Ionospheric perturbations generation by time variable alternating electrical currents at polar latitudes, constructing radiation patterns for gravitational waves 23 p4155 A69-41842

Einstein general theory of relativity and apparatus for gravitational radiation detection, discussing Dicke experiments and Riemann tensor measurement 23 p4192 A69-42331

Gravitational field quantization according to Einstein theory using classical Hamiltonian dynamics and quantum rules for constraints 23 p4192 A69-42332

Optimal thrust control for plane curvilinear motion of variable mass point in gravitational field 23 p4192 A69-42340

Fluctuations in 3K radiation, considering scattering effect on gravitational fields of galactic clusters and large coherence or wavelength scattering by gravitational radiation 23 p4222 A69-42401

Gravitational field structure effects on Alfvén waves propagation in inhomogeneous medium 23 p4223 A69-42478

Stationary equilibrium of two dimensional plasmas with motion perpendicular to uniform magnetic field and gravitational field, considering resistive diffusion role 24 p4356 A69-43365

Stellar system differential rotation effect on gravitational instability with distribution propagating in rotation axis direction 24 p4388 A69-43639

General relativity uniqueness established by postulating derivability of equations of motion from gravitational field equations [AIAA PAPER 67-481] 24 p4365 A69-43668

Stability of spherically symmetrical nonrotating mass systems moving in self consistent gravitational Einstein field, considering quasar applicability 24 p4390 A69-43784

GRAVITY

U GRAVITATION

GRAVITY GRADIENT SATELLITES

NT APPLICATIONS TECHNOLOGY SATELLITES

NT ORBITAL SATELLITE

Attitude control system for gravity gradient stabilized satellite in synchronous and near synchronous equatorial orbits, discussing libration damping methods 03 p0504 A69-12857

Boom flutter effects on attitude dynamics of OV-10 satellite, noting introduction of angular momentum by tip mass elliptical vibration 04 p0666 A69-15520

Thermoelastic effects on gravity gradient stabilization of artificial satellites, including role of solar activity 06 p1025 A69-17613

ORBIT-CAL designed to achieve three axis orientation to local vertical and velocity vector in eccentric orbit by gravity gradient stabilization 07 p1226 A69-18323

Thermal flutter effect on gravity gradient stabilized spacecraft, noting dependence on sunlight and time 07 p1226 A69-18325

Semipassive attitude control system providing one degree pointing accuracies in all axes 07 p1226 A69-18326

Storable tubular extendible member /STEM/ booms for gravity gradient applications, emphasizing reflective coatings to minimize deflection by solar radiation 07 p1226 A69-18327

RAE-A satellite design, simulation and flight performance, discussing gravity gradient stabilization 07 p1226 A69-18328

Three axis gravity gradient stabilization system to minimize stray magnetic fields 07 p1226 A69-18329

Three axis gravity gradient stabilization systems for OV-1 spacecraft design 07 p1227 A69-18330

Damping boom flutter and magnetic dipoles effects on attitude stability of gravity gradient satellites with three axis stabilization 07 p1227 A69-18332

Semiactive gravity gradient stabilization system design for low altitude earth oriented spacecraft attitude control, using active reaction wheel scanner 07 p1227 A69-18334

Hybrid simulation study of satellite attitude control system to replace momentum wheels and gas jets by commandable gravity gradient boom 07 p1227 A69-18335

Magnetic sample-and-hold damping using geomagnetic field for libration damping of gravity gradient stabilized satellite in near synchronous equatorial orbit 07 p1227 A69-18337

System designs for manned spacecraft gravity gradient stabilization of Saturn S-4B stage at 400 km and lunar module at synchronous altitude 07 p1228 A69-18338

Eddy current damping systems for gravity gradient stabilized satellites, discussing electromagnetic torque and various parametric relationships 07 p1228 A69-18341

Semiactive gravity gradient stabilization system /SAGS/ for active pitch control and semipassive roll/yaw control 07 p1228 A69-18342

Naval Research Laboratory experience with two and three axis gravity gradient satellites stabilization systems 07 p1228 A69-18344

Long life gravity gradient stabilization system using Vee configured control moment gyros to semipassively damp vehicle librations 07 p1228 A69-18345

RAE satellite boom deployment to achieve gravity gradient capture 07 p1228 A69-18346

Spherical and single axis passive oscillation energy dampers for gravity gradient oriented satellites, utilizing earth gravity field or solar pressure 07 p1229 A69-18347

Gravity gradient stabilization role in space missions in 1970s and 1980s 07 p1229 A69-18348

GEOS 2 attitude stabilization by means of gravity gradient principle and passive energy dissipator, noting effects of orbit eccentricity, thermal distortion, radiation, etc 07 p1229 A69-18349

Wire screen deployable boom concept for avoiding thermal bending of slender tubes problem in application to gravity gradient stabilization and antennas of spacecraft 07 p1229 A69-18350

Vertistat H gravity gradient configuration prevents elastic deformation, permitting high pointing accuracy at synchronous altitudes 07 p1229 A69-18351

Digital program containing Eulerian formalism for multiple interconnected rigid members applied to gravity gradient stabilized satellite with flexible booms 11 p1989 A69-25502

Magnetic attitude detection and control system for Radio Astronomy Explorer satellite [AIAA PAPER 68-855] 12 p2174 A69-26779

Satellite gravitational stabilization system with maximum damping rate, discussing orbital plane oscillations 16 p2867 A69-31738

Damping of gravity gradient stabilized satellites by hysteresis of materials, friction of viscous fluids, magnetic hysteresis and Foucault currents 17 p3047 A69-33230

Gravity gradient satellite stabilization and magnetic hysteresis damping systems, outlining energy dissipation device involving torques 17 p3047 A69-33231

Rotor hazards in rotational behavior of gravity stabilized satellites, describing gyrostat applications 17 p3048 A69-33233

Gravity gradient stabilized satellite achieving best theoretical performance through Foucault current and magnetic hysteresis articulations 17 p3048 A69-33234

Quadratic approximation at matrix level of dynamic equations for rotating bodies applied to gravity gradient satellite exhibiting nonlinear resonances 18 p3174 A69-35298

Asymptotic stability of null solution of matrix differential equation, considering linearized equations of rotational motion for hinged two body gravity gradient satellite orbit 20 p3575 A69-37212

Gravity gradient phenomena in orbiting vehicle used to explore planetary gravity [AIAA PAPER 68-851] 21 p3804 A69-39024

Three dimensional coupled flexural and attitude dynamics of libration-damped cruciform gravity gradient satellite, discussing effects of orbital eccentricity, solar radiation pressure, etc [AAS PAPER 68-126] 21 p3819 A69-39211

Radio Astronomy Explorer satellite boom deployment method resulting in gravity gradient capture, emphasizing role of predeployment attitude and antenna Vee angle [AIAA PAPER 69-920] 21 p3821 A69-39350

Capture and gravity gradient stabilization of LIDOS satellite in eccentric orbit [AIAA PAPER 69-921] 21 p3821 A69-39351

Gravity gradient perturbing torque cast in terms of perturbing Hamiltonian, deriving long term changes in

GRAVITY WAVES

rotational motion of tumbling triaxial satellite in elliptical orbit
[AIAA PAPER 69-922] 21 p3821 A69-39353

Aerodynamic and gravitational torque effects on orbiting satellites attitude stability, applying Liapunov direct method in case of conservative aerodynamic torque
[AIAA PAPER 69-832] 21 p3821 A69-39363

Dynamics of relay gas jet preliminary vibration damping system of gravity gradient stabilized satellite, allowing for sensor limitations and stabilizer flexural vibrations 21 p3826 A69-39638

Periodic solutions for gravity-gradient stabilized satellite librating in orbital plane, using elliptic sine function and harmonic balance method 23 p4224 A69-41876

Torqued two axis gimbaled boom actuator satellite attitude control
[AIAA PAPER 68-857] 24 p4348 A69-43245

Stability analysis of periodic solutions associated with planar librations of gravity oriented satellite using linear perturbation analysis 24 p4388 A69-43649

GRAVITY WAVES

NT BAROCLINIC WAVES

Gravity waves train propagation in cylindrical channel, discussing derivation by three dimensional flow analysis method 01 p0059 A69-10382

Indeformable gravity waves in horizontal cylindrical channel, using first and second order approximations for nearly uniform flow equations solutions 01 p0060 A69-10392

Solitary mesoscale waves from air mass motion in troposphere, neglecting Coriolis force and turbulence 02 p0274 A69-11445

Dispersion relation of internal acoustic gravity wave motion in compressible nonviscous and nonheatconducting atmosphere 02 p0242 A69-11868

Viscous damping of internal waves on rotating earth, analyzing spatial propagation attenuation in two layer system 02 p0247 A69-12775

Invariant theory of gravitational radiation, using impulse energy tensor 02 p0332 A69-12835

Plane front gravitational waves analyzed on basis of gravitational radiation theory, discussing Einstein equations 02 p0332 A69-12836

Quasi-biennial oscillation in tropical stratosphere as result of long period gravity waves interaction with zonal wind 03 p0461 A69-13342

Reflectivity of low Richardson number critical levels for internal gravity waves propagating in stably stratified fluids with shear, studying stability numerically 03 p0424 A69-13953

Gravity wave contribution to atmospheric wind motion at 100 km 03 p0426 A69-14031

Irrrotational almost uniform plane flow of two immiscible inviscid liquids on horizontal bottom in channel, noting permanent gravity waves 04 p0590 A69-15055

Long distance propagation of acoustic gravity waves ducted in thermosphere, noting effect of seasonal variations in polar region 04 p0595 A69-15437

Internal gravity waves propagation in shear flow, detailing interaction stress in incompressible stratified Boussinesq liquid, conservation energy exchange and radiation stress 05 p0788 A69-15721

Atmospheric density variation measurements by density gages on Explorer 32 satellite confirm wave propagation in neutral thermosphere as free internal gravity waves 05 p0754 A69-16261

Gravity waves observed by ionospheric temperature measurements in F region 05 p0754 A69-16262

Internal atmospheric gravity waves in F region observed with electron density profiles deduced from vertical incidence ionograms, obtaining phase velocities 05 p0756 A69-16402

Spatial distribution of vertically moving ionized formations in ionosphere suggests acoustic gravity waves excited in polar regions as cause 06 p0922 A69-17749

Brans-Dicke scalar-tensor theory, showing radiative Riemann tensor existence in absence of usual spin-2 gravitational waves 07 p1216 A69-18894

Mass displacement in light path due to interaction with gravitational wave accompanying light pulse, discussing general relativity tests for time delay and starlight bending 09 p1540 A69-22081

Gravitational waves emitted by relativistic, nonrotating, nonradially pulsating stellar model, discussing polarization and energy and momentum transport 09 p1605 A69-22417

Magnetoionic formulas similarity in ionospheric radio propagation and atmospheric acoustic gravity wave propagation above electron gyrofrequency 10 p1655 A69-23419

Data requirements and acquisition for detection and description of tides and gravity waves in upper atmosphere 10 p1685 A69-23833

Dispersion relation for internal gravity wave propagation across exponentially decreasing magnetic field in conducting fluid, noting atmospheric wave propagation in ionosphere 11 p1877 A69-24564

Boundary value problem for gravity induced wave motion of ideal fluid in axisymmetric vessel with annular ribs, noting application to bodies of revolution 11 p1868 A69-24769

Full wave calculation of gravity waves for thermospheric model, describing wave type reflection, transmission, conversion and coupling by scattering matrix elements 11 p1878 A69-25150

Joule heating role in generating internal gravity wave energy in auroral electrojet region, using linear model 12 p2064 A69-26010

Ray tracing techniques applied to internal gravity waves in fluid with spatially varying mean flows 12 p2067 A69-26345

Variational method for weak second order resonant interactions among waves with position and time varying amplitudes and phase angles 13 p2297 A69-27634

Ion drag effects on acoustic gravity waves propagation in isothermal F region, discussing indicated wave damping 14 p2434 A69-28944

Linearized perturbation for photochemical and dynamical effects in internal atmospheric gravity wave production of E region ionospheric irregularities 14 p2440 A69-29128

Nonlinear internal gravity waves in stratified atmosphere of unbounded inviscid incompressible fluid, noting wave amplitude inverse proportion to atmospheric density 14 p2441 A69-29574

Horizontal shear flow effect on linear geostrophic adjustment in unbounded barotropic fluid, discussing gravity waves, vorticity equations, available energy, etc 15 p2648 A69-30217

Internal gravity waves suggested as possible cause for anomalous mesospheric temperatures 15 p2601 A69-31376

Gravity waves in thermospheric heating during magnetic storm, discussing electron density and temperature and ion velocity variations 15 p2605 A69-31435

Strong vertical wind in low ionosphere due to short period reflected gravity waves, obtaining standing wave system 15 p2606 A69-31449

Discrete layers criterion for multilayer approximation to real atmosphere in acoustic gravity wave propagation 16 p2774 A69-31980

Ionization density, velocity and temperatures oscillations revealed by Thomson scatter observations of gravity waves in F regions 16 p2779 A69-32198

Subsonic thermal convection or internal gravity waves from formal scale analysis of equations of motion in plane parallel atmosphere 17 p2960 A69-33155

Lee waves and orographic wind phenomena in Rocky Mountains near Boulder, noting stratospheric standing gravity waves and turbulence sampled by HI-CAT U-2 17 p2999 A69-33738

Traveling ionospheric disturbances in form of large scale electron concentration discontinuities created by propagating internal gravitational waves 17 p2996 A69-33980

Models for pulsars periodicity and period range due to nonradial gravity wave in almost adiabatic matter of degenerate neutron stars 18 p3196 A69-34645

Dispersion relation for gravity waves propagating in atmosphere with horizontal background wind variable with altitude 18 p3128 A69-34801

Acoustic gravity waves generated in isothermal atmosphere by ground energy source calculated using stationary phase method and kinematic theory 18 p3129 A69-34953

Convective momentum exchange in mesoscale gravity wave 20 p3522 A69-37350

Eddy diffusion coefficients due to instabilities in internal gravity waves near mesopause 20 p3534 A69-38090

Atmospheric gravity waves amplitude generated in equatorial electrojets and polar regions 20 p3593 A69-38107

Lunar maria structure and evolution as homologous transient gravity wave systems from impact craters on crust 21 p3803 A69-38982

Small amplitude acoustic waves propagating in compressible fluid with parallel shear flow and within constant gravitational field 21 p3772 A69-39241

Universe expansion model, integrating Einstein gravitation equations with cosmological constant lambda to interpret Hubble effect 22 p4029 A69-40756

Acoustic gravity waves propagation over spherical earth with isothermal windless atmosphere, determining pressure perturbations 23 p4158 A69-42175

Wavelike structure observed near tropopause with sensitive radar system, suggesting clear air turbulence as cause of breakdown of gravitational wave 24 p4342 A69-42893

GRAY GAS

Radiant heat transfer in optically thick gray gas situated between parallel black diffusively emitting walls, using matched asymptotic expansion method 01 p0178 A69-11411

Radiative-convective heat transfer in gray gas plane layer blown into turbulent flow past permeable plate 07 p1242 A69-18991

Radiative transfer iteration for gray medium between concentric spheres and for constant heat generating spherical region imbedded in gray medium 08 p1420 A69-20152

Radiative-conductive heat transfer in plane layer of gray heat conducting medium, solving energy equation 09 p1621 A69-21433

Thermal radiation effects on laminar free convection boundary layer of vertical flat plate, studying absorbing and nonabsorbing gases [ASME PAPER 68-HT-43] 13 p2373 A69-27772

Differential approximation for radiative transfer between concentric spheres enclosing gray gas [ASME PAPER 68-HT-21] 13 p2373 A69-27774

Radiative transfer between two concentric gray opaque spheres separated by radiating gray gas, employing Fredholm equations 13 p2377 A69-28149

Radiating gray gas laminar jet in thermodynamic equilibrium ejected from plane nozzle into wake analyzed using boundary layer, divergence and transfer equations 14 p2432 A69-29612

Substitute kernel approximation for acoustic waves radiative transfer equations for nongray gas near equilibrium 15 p2717 A69-30791

Thermal radiation effects on subsonic flow of ideal gray gas, calculating streamwise variations of flow properties 15 p2717 A69-30908

Nonuniform wall radiation production of radiative equilibrium temperature and flux distributions in gray medium, discussing various approximation methods of solution [AIAA PAPER 69-633] 17 p3072 A69-33294

Atmospheric structure, greenhouse effect and convective instability in window gray and nongray planetary atmospheres 20 p3615 A69-38257

Total band absorptance of nonisothermal IR radiating gas, using wideband formulation of Curtis-Godson approximation and series expansion formulation 22 p3983 A69-40101

Quasi-isotropic semigray radiative transfer prediction using nongray model in bounded plane-parallel geometries for gas with spectrum from free-free processes
24 p4415 A69-43673

GREASES

Ball bearing test apparatus for evaluation of greases and solid lubricants at high temperatures [ASLE PREPRINT 68AM 7C-2]
01 p0087 A69-10912

Thermal silicone grease type filler materials for heat transfer across bolted or clamped sheet metal surfaces in electronic equipment for space applications
16 p2794 A69-32560

GREAT BRITAIN

Weathering tests on wrought aluminum alloys exposed at U.S. sites compared to British industrial atmospheric exposure results
01 p0101 A69-11354

Space science and technology - Conference, London, February 1968
06 p0997 A69-16852

Suborbital probes, discussing UK sounding rockets Skylark, Petrel and Skua configurations, capabilities and performances
06 p1012 A69-16859

Fluidics in UK, discussing digital control elements and systems and transmission lines in alternating flow hydraulics [AGARDOGRAPH-118]
08 p1257 A69-20952

Airport evolution in London, discussing transportation, safety, international trade, economics, aircraft types and noise spectra
09 p1479 A69-22582

Engineering assessment and flight testing of aircraft systems in UK, discussing operational reliability, etc
13 p2201 A69-27539

Synchronous satellite TV broadcasting systems in UK, discussing equipment, transmission problems and economic factors
13 p2220 A69-27830

Vertical takeoff aircraft role in British Government air industry program, noting applications to intercity passenger service
13 p2203 A69-28355

Short takeoff aircraft characteristics, discussing aircraft certification and airfield regulation in Great Britain
13 p2203 A69-28356

British and Soviet D region electron density distributions from same VLF and LF propagation data
14 p2439 A69-29112

Meteorite entering earth atmosphere on 25 April 1969 over England, describing path, size and recovered fragments
15 p2701 A69-31528

Flying offenses committed by private and professional pilots in Great Britain, discussing role of authorities involved
17 p3077 A69-34202

Edwards Inquiry Report into British Civil Air Transport based on cost effective economic study, involving airlines and regulatory system
18 p3231 A69-34311

Visibility changes in fog at London airport determined by transmissometer records
18 p3167 A69-35266

European cooperation in aircraft industry and application to Anglo-French helicopter program
19 p3456 A69-36849

Airport requirements in England, considering various sites, noise nuisance and integration into total transport system
22 p3926 A69-40432

GREAT CIRCLES

Great circle route determination based on celestial spherical triangulation
02 p0278 A69-12360

GREAT POLAR CAPS

U POLAR CAPS

GREEN FUNCTION

Upper and lower bounds for static or geometric field in two and three dimensional elasticity theory, using Green functions
01 p0167 A69-10328

Gravitational field and earth shape determination by calculating perturbing potential at earth surface and in outer space, using Green functions
01 p0063 A69-10360

Multiphoton ionization cross section of atom via perturbed Green function, considering light wave electromagnetic field perturbing effects on atomic levels
02 p0283 A69-11539

Green function for linear antennas in warm plasma fed by coaxial air filled transmission line, computing current distribution and input admittance
02 p0215 A69-11942

Green functions associated with electromagnetic radiation in moving medium, finding time dependent and harmonic Green functions
03 p0466 A69-13352

Second order elliptical operator for m-dimensional Euclidian space with open region bounded by closed surface
03 p0456 A69-13604

Displacement correlations and frequency spectra for mass disordered lattices, deriving cluster expansion for phonon Green function
03 p0493 A69-14241

Book on boundary value problems of mathematical physics emphasizing solutions, Green functions, transforms and variational methods
04 p0625 A69-15233

Green function for computation of stress intensity factors for edge cracks in rectangular plates with arbitrary loadings [ASME PAPER 68-WA/MET-18]
05 p0839 A69-16156

Feynman rules for gravitational field from coordinate independent field theoretic formalism, expressing path dependent Green functions in path independent functions
05 p0794 A69-16364

Convergence of Grammel and Galerkin methods allows use of modified Green function
06 p1020 A69-17132

Dielectric constant of liquid metals emphasizing Green function techniques for Wick theorem, Feynman diagrams, Dyson equation and diagrams in impulse space
07 p1196 A69-18298

Green function applied to isotropic scattering of radiation in three dimensional homogeneous space
07 p1241 A69-18808

Green function method for atomic line broadening in plasma radiation, including electron correlations and quantum effects
08 p1361 A69-20147

Green function in closed form for energy transport equation solution in axisymmetric Oseen flow
08 p1305 A69-20850

Influence function for vertical wind profile from pressure gradient field
09 p1536 A69-21867

Green function type solutions of shell equations by small parameter technique for case of free terms consisting of Dirac delta function
09 p1614 A69-21886

Micropolar elasticity using Green functions to solve wave equations in unbounded medium, noting effects of concentrated force and body couples
09 p1618 A69-22261

Micropolar thermoelasticity using Green functions to solve wave equations in unbounded medium and study displacement, rotation and temperature fields
09 p1618 A69-22262

Diffraction problem on cylindrical bodies of arbitrary shape reduced to integral equations by using Green functions for free spaces
09 p1459 A69-22634

Incompressible fluid nonlinear oscillations in rectangular basin analyzed by Green function for mixed problem, calculating velocity potential and free surface approximations
09 p1483 A69-22711

Generalized solutions of elliptic boundary value problems by applying Green functions
10 p1718 A69-23207

Green function solution to Maxwell equations for interplanetary and coronal magnetic fields above photosphere, considering field at source surface
11 p1958 A69-24429

Green tensor construction for systems of linear differential equations with constant coefficients
11 p1996 A69-25730

Steady state solution of periodically excited circuit, constructing Green function for use in convolution integral
12 p2036 A69-25918

Elliptic boundary value problem for differential equation and pseudodifferential boundary conditions, obtaining Green formula from formulated conjugate problem
12 p2121 A69-26200

Homeomorphism theorem for Petrovskii and homogeneous elliptic systems applied to boundary value problems and Green formula
13 p2287 A69-27515

Nonnegative solutions of second order linear divergence structure parabolic differential equations, discussing Cauchy problem solution, Green function, etc
13 p2290 A69-28539

Green function for boundary value problems of heat conduction equation constructed by heat potentials method
13 p2380 A69-28548

Radiation field from sources on conical surface using Green functions
13 p2223 A69-28569

General formulas, reciprocity theorem and modified Green formula derived from variational principles for mixed problem of wave equation
14 p2485 A69-29354

Integral formulation of scattering theory extended to Coulomb interactions by expanding Green function and treating kernel singularities
14 p2489 A69-29995

Green function construction for boundary value problems of heat conduction on rectilinear segment with dynamic boundaries, using integral equations
15 p2716 A69-30075

Rayleigh assumption validity for wave scattering by analytic periodic surface predicated on solutions analytic continuation across boundary, discussing Green function role
15 p2652 A69-30673

Time dependent Green function method for premature saturation due to parametric amplification of nonuniform spin wave modes by one and two magnon processes
15 p2668 A69-30685

Green functions for Laplace, Poisson and transient heat diffusion equations solved by matrix multiplication
15 p2710 A69-30870

Linear aerospace structures vibrations in randomly distributed pressure field forecasted by applying Green function [ONERA-TP-703]
17 p3054 A69-33064

Electromagnetic fields theory simultaneously determining vector electric and magnetic field aspects in terms of operator Green functions
17 p2924 A69-33833

Electromagnetic waves radiation in general time invariant linear media with general boundary conditions, using Green function
17 p2924 A69-33834

Wave propagation and scattering in anisotropic media, obtaining asymptotic expression for dyadic Green function for infinite space
17 p2924 A69-33835

Dyadic Green function technique extended to problems of electromagnetic scattering in inhomogeneous media with spherical symmetry
17 p2924 A69-33837

Wave scattering from nonplanar periodic structures using periodicity method, including Green function and Mellin transform
17 p2929 A69-33880

Green functions for displacement and rotation fields of infinite homogeneous isotropic centrosymmetric micropolar elastic body subjected to time dependent mass forces and momenta
18 p3226 A69-35459

Motion equations of holonomic system of elastic bodies subjected to scleronomic, ideal and statically determinate constraints, using Green tensor
19 p3374 A69-36584

Generalized solutions of elliptic boundary value problems by applying Green functions
21 p3756 A69-39148

Nonresonant Green functions of auxiliary boundary value problems for deriving integral equations for Dirichlet and Neumann diffractions at open screens
22 p3901 A69-40949

Green matrix for operator M governing steady state wave propagation in inhomogeneous anisotropic media obtained as solution of integral equations system
23 p4180 A69-41368

Green formula and fundamental solution for determining displacements and stresses in contour integral form for plate bending problems
23 p4230 A69-42002

Real space-time Green functions applied to turbulence induced infinite thin elastic plate vibration, analyzing mechanical dissipation effects
24 p4395 A69-42597

GREENHOUSE EFFECT

Greenhouse effect in Venusian atmosphere, discussing cause of vertical temperature distribution established by Venera 4 probe
13 p2345 A69-27690

GRIDS

Nongray greenhouse model of Venus atmosphere possessing IR opacity due to carbon dioxide, water and diatomic N compatible with Mariner 5 and Venera 4 results

20 p3615 A69-38259

Saturn surface spectrum near ring shadow examined for water vapor content in ring and greenhouse effect on surface

20 p3616 A69-38305

Fredholm integral equation for source function of Greenhouse effect and finite atmospheres solved by computational algorithm

23 p4239 A69-41607

GRIDS

Grid method of strain determination, discussing print, record, analysis and application

18 p3134 A69-34423

Finite difference scheme for primitive equation model, emphasizing two grid internal noise suppression to improve gradient force expression accuracy

19 p3364 A69-36507

Numerical integration of atmospheric motion equations in global domain using hexagonal grid, including sphericity corrections and Coriolis term

19 p3364 A69-36509

Energy spectra measurements of turbulent velocities behind grids of different geometries noting relation to deviation from isotropy

21 p3693 A69-38704

Computer program for satellite APT geographical grid production, discussing latitude-longitude intersections transformation to Cartesian coordinates

21 p3718 A69-39749

Grids applied to plastic samples for strain measurement using moire fringe method, comparing tensile test results with Linley extensometer

22 p4042 A69-40312

Gridding technique for satellite APT pictures taken with camera axis perpendicular to earth surface

24 p4314 A69-42992

Angular grid spacing resolution near poles effect tests in global prediction model for geophysical fluid dynamics, investigating forecast height and wind fields

24 p4344 A69-43066

GRIFFITH CRACK

Griffith biaxial fracture criterion for porous brittle materials based on continuum model with random infinitely sharp cracks

[ASME PAPER 68-WA/MET-12]

05 p0838 A69-16152

Simulated crack experiment illustrating Griffith energy balance fracture criterion

05 p0842 A69-16438

Griffith crack in brittle material, discussing validity for rock-like material with nonlinear stress-strain relationship

06 p1020 A69-17128

Quasi-brittle fracture of plastic materials based on Griffith theory and crack propagation, analyzing real surface energy and work of plastic strain

09 p1614 A69-21883

Integral transform solutions for Griffith cracks in brittle fracture theory, discussing disk and penny shaped cracks in cylinders and thick plates

10 p1801 A69-23688

Mathematical theory of equilibrium cracks in stressed bodies with minimum loading for crack extension, analyzing crack tip zone and force transmission

11 p1974 A69-24668

Ceramics strength and fracture behavior in terms of modified Griffith equation, discussing effective surface energy and initial crack size

11 p1907 A69-25238

Metallographic aspects of fracture, analyzing very brittle solids, Griffith cracks, ductile solids and ductile to brittle transition

13 p2274 A69-27225

Stress intensity for Griffith crack with asymmetrical distribution of surface tractions

13 p2369 A69-28352

Griffith crack in thin plate opened by uniform tension at infinity, discussing effect of ties on stress intensity factor

15 p2710 A69-30809

GRINDING [COMMINUTION]

Powdering temperature effect on mesh size, structure and mechanical properties of pressed semifinished sintered Al-Cr and Al-Fe alloys

03 p0452 A69-14119

Thermochemically synthesized high melting micropowders grinding by vibrational method and classification for polishing and finishing applications

12 p2113 A69-26256

GRINDING [MATERIAL REMOVAL]

NT METAL GRINDING

Low temperature grinding technique for IR spectra of propellants and binders in potassium bromide disks

01 p0082 A69-10892

Parallel and coplanar Brewster angle grinding of maser tube ends

03 p0440 A69-13302

Stainless steel biaxial residual surface stresses from grinding and finish machining determined by dissection technique

[ASME PAPER 68-WA/MET-9]

14 p2455 A69-29437

GRINDING MILLS

H release, pressure and oxide layer formed by reaction during ball milling Cr in water

21 p3728 A69-38567

GROOVES

NT V GROOVES

Numerical solutions of elastic problems by conformal mapping and finite difference method applied to circumferentially grooved shafts in torsion

02 p0346 A69-12419

Numerical solutions elastoplastic torsion of circumferentially grooved shafts based on flow and deformation type theories

02 p0346 A69-12420

Elastohydrodynamic solution for ball torque spinning without rolling in nonconforming groove, showing increase in torque with stress and spinning and decreasing conformity

[ASME PAPER 69-LUBS-11]

18 p3140 A69-34381

Keyway stresses in shafts under tension, bending and torsion, using frozen stress photoelastic technique

19 p3445 A69-36827

Tension tests of polycarbonate plates grooved at various angles, demonstrating necking dependence on mechanical instability

21 p3753 A69-39809

GROOVING

Grooved commercial Ti and Ti alloys mechanical properties under uniaxial static tension at low temperatures

03 p0443 A69-13028

Runways slipperiness and grooving, discussing influence of wetness, tire form and speed on friction coefficient

10 p1674 A69-23707

Runway grooving to improve aircraft tire traction in adverse weather tested by F-4D and Convair 990A under wet conditions

[AIAA PAPER 69-773]

19 p3244 A69-35649

Grain boundary grooving kinetics for Cr, W and Mb in Ar and vacuum, determining interface free energies and surface self diffusion coefficients

21 p3744 A69-38740

GROUND-AIR-GROUND COMMUNICATIONS

Optimum modulation technique determination for single channel voice communication under severe noise conditions

[UN PAPER 68-95851]

01 p0029 A69-10526

Ground-air-ground communications system using pseudonoise through satellite and central ground based control facility, discussing system advantages, SNR and modulation schemes

01 p0033 A69-11009

Digital communications between aircraft and flow control computers on ground to avoid runway saturation and automating routing functions

05 p0721 A69-16722

Ground station electronic environment, telemetry encoding and radio links for spacecraft communications and tracking

06 p0886 A69-16860

Satellite communication channel number and distribution optimization, obtaining malfunction probability for telephone service communication system

[UN PAPER 68-95772]

06 p0886 A69-17030

Economic planning of satellite earth station equipment in relation to expected traffic demand, emphasizing specifications for communication via Intelsat 2 and 3 satellites

07 p1117 A69-19347

Design aspects of 20 ft air transportable satellite earth station

08 p1272 A69-19926

Self focusing aerial antenna arrays with full angular coverage for two way airborne communications

08 p1289 A69-20971

RF selection for interspacecraft or earth-spacecraft communication

09 p1449 A69-21270

Propagation and noise effects on frequency choice for communication satellite service to aircraft and

ships, noting tropospheric and ionospheric attenuation considerations

09 p1451 A69-21288

Maintenance telemetering, tracking and telecommand for developmental and operational satellites, discussing possibilities of frequency sharing between satellites and terrestrial services

09 p1451 A69-21290

Technical characteristics of spacecraft telemetering, tracking and telecommand systems, stressing links between earth stations and spacecraft

09 p1451 A69-21291

Orbiting Data Relay Network communications system provides continuous wideband communication between ground and earth orbiting spacecraft via synchronous satellite repeaters

[AIAA PAPER 68-432]

09 p1455 A69-21989

Time function multiplex system for simultaneous communication via satellite between number of stations, considering transmission capacity decrease due to hard limiting amplifier

17 p2919 A69-33320

Frequency hopping technique applied to multiple access air-to-air/ground communication for tactical fighters, noting additive recognition

17 p2931 A69-34117

Pictorial display area navigation system for air traffic control in terms of cockpit utilization, interface with ground navigation aids, parallel multiple routes, etc

[AIAA PAPER 69-798]

19 p3367 A69-35632

Legal principles observed for international telecommunication systems establishment by means of artificial satellites regarding states interests and rights

20 p3638 A69-37124

Daily communication link geometry between spacecraft in elliptical orbit and landed capsule, establishing spacecraft visibility contours for landing site latitude

[AAS PAPER 68-110]

21 p3805 A69-39223

Worldwide communication system via synchronous satellites for aeronautical, maritime and land mobile services

23 p4114 A69-41355

GROUND BASED CONTROL

NT AIR TRAFFIC CONTROL

NT RADAR APPROACH CONTROL

Ground based control system via cockpit PPI display on transponder equipped aircraft broadcast with digital coding

03 p0464 A69-13244

FAA coded broadcasting to transponder equipped aircraft for air traffic control, navigation, collision avoidance and airfield approach

04 p0629 A69-15478

Real time performance, ground control and data processing of Surveyor spacecraft during maneuvers

[AIAA PAPER 67-644]

04 p0586 A69-15502

Digital computer motion pictures generation for ground controlled intercept simulation

06 p0906 A69-17397

Flight deck equipment guidelines in aircraft, discussing pilots natural senses, visual information, displays, logic and memory capable computers and ground controller

08 p1266 A69-20450

Automatic ground traffic control of aircraft on airport taxiway without visual detection, noting induction loop detection in surface traffic control system /STRACS/

11 p1913 A69-24267

Ground controlled remote manipulator spacecraft system to perform unmanned satellite orbital maintenance, discussing refurbishment, laboratory simulation, system cost effectiveness and feasibility

19 p3430 A69-36001

Airborne collision avoidance system based on time-frequency techniques for use within ground based control systems, showing air/ground synchronization and collision geometry

19 p3371 A69-36735

Electron density profiles from topside ionograms compared to ground based sounding results, discussing error corrections

20 p3495 A69-37865

Ground based guidance for land-landing manned spacecraft with low velocity descent systems, discussing high and low altitude glide path intercept and spiral

[AIAA PAPER 69-864]

21 p3762 A69-39390

ELDO radio guidance station at Gove, discussing propulsion stage tracking and instruction transmitted to vehicle

22 p3919 A69-39920

Onboard processor servicing spacecraft sensors, programmable from ground, discussing functions and applications
22 p3903 A69-39921

Mars landing site topography reconstructed via stereoscopic pictures returned by surface-based imaging systems
23 p4164 A69-41618

GROUND CREWS

Psychiatric morbidity as absenteeism cause among ground and flight personnel in civil aviation, recommending psychotherapy and chemotherapy
24 p4266 A69-43378

GROUND EFFECT

Ground effects influence on VTOL aircraft secondary forces during hovering and transitional flight, discussing component dynamic coefficients in wind tunnel [DVL-851]
04 p0547 A69-14813

Testing station design for VTOL aircraft ground effects investigations
08 p1302 A69-20880

Rotor downwash in ground effect in presence of step, using two dimensional analysis for flow field calculation [AIAA PAPER 69-225]
08 p1253 A69-21032

Thin jet-flapped airfoil flow analysis in ground proximity at small angle of incidence, assuming inviscid incompressible flow
09 p1431 A69-22275

Horizontal VLF cylindrical transmission antenna current distribution calculated with allowance for ground reaction, showing exponential decrease with distance
09 p1467 A69-22581

Numerical solutions of thick cambered jet flap in ground effect for flat plate and diamond shaped airfoil [AIAA PAPER 69-738]
18 p3083 A69-34404

Schweikhard method for measuring changes in lift, drag and pitching moment of fixed wing aircraft as function of distance from ground
20 p3462 A69-37423

Thin jet flapped airfoil analysis with wake fully developed from leading edge and jet flow reflected from ground
22 p3861 A69-41184

Solar energetic particle effects during polar cap absorption observed in earth upper atmosphere and at ground level
24 p4373 A69-43618

GROUND EFFECT MACHINES
NT HOVERCRAFT GROUND EFFECT
MACHINES

Ram recovery of flush intake for air cushion vehicles noting influence of intake geometry, placement and incidence angle
01 p0005 A69-10026

Survival analysis based on probability theory for design of air cushion vehicle to determine height for operating over open sea
01 p0008 A69-10027

Hovercraft handling characteristics, seakeeping and maneuverability during English Channel operation
02 p0277 A69-11592

Air cushion landing gear in civil air transport, discussing system concept, advantages and LA 4 aircraft experimental application
02 p0193 A69-12690

Legal problems in hovercraft classification, discussing problems in adapting existing transport legislation to hovercraft operation
04 p0689 A69-14942

Unified design approach for second generation air cushion craft based on existing first generation craft
05 p0701 A69-15567

UK hovercraft research covering internal/external dynamics, propulsion systems and full scale tests
05 p0702 A69-16393

Fixed point support properties of quasi-vertical peripheral jet hovercraft with two pressure stages
06 p0857 A69-16820

Mountbatten class hovercraft for truly amphibious craft
06 p0867 A69-17664

Water jet propulsion for air cushion vehicles, emphasizing inlet shape effect on performance and potential flow theory application to inlet design
08 p1254 A69-20115

French air cushion vehicle technology for water and land, outlining principles of lift, propulsion and control and specifications of several craft
08 p1254 A69-20198

U.S. policy for commercial surface effects ships regulation, discussing operational, construction and design requirements
08 p1254 A69-20199

Monograph on air cushion vehicles /ACV/ in Scandinavian water transport, covering state of the art, technical and economic competitiveness, etc
09 p1434 A69-22075

Skirts on hovercraft, noting rough water drag, plough in and overturning, and skirt oscillation and wear problems
10 p1634 A69-23629

Book on hovercraft design and construction covering aerostatic and aerodynamic craft, cushion performance, ducting, fans, compressors, drag, propulsion, control, stability, economics
12 p2013 A69-26633

Integrated lift, propulsion and control in Aeromobile air cushion vehicle, considering ram wing and gimbal fan plenum chamber vehicles
13 p2201 A69-27543

Canadian air cushion vehicle industry, considering materials, design, production, tests, components and quality control
13 p2381 A69-27544

Multicell air cushion vehicle technology based on 1/4 scale and full scale tests, noting comparison with plenum systems and costs
13 p2202 A69-27547

Flexible skirt design for air cushion vehicle consisting of semicylindrical elements and permitting horse power and cost reductions
13 p2203 A69-28179

Air cushion vehicles tests for public transportation facilities noting operation costs
15 p2550 A69-30409

Mountbatten /SR.N4/ hovercraft development, seakeeping, skirt design and service introduction
15 p2550 A69-30479

Performance potential of high speed ocean-going air cushion vehicles with aircraft nuclear power plants [AIAA PAPER 69-416]
15 p2550 A69-30480

Air cushion vehicle research and development laboratory testing, plans, support equipment, monitoring by TV, etc
15 p2589 A69-30865

Hover and forward speed aerodynamic characteristics of tracked air cushion vehicle /TACV/ models, discussing wind tunnel tests [AIAA PAPER 69-750]
18 p3084 A69-34410

Nuclear powered surface effects machine performance estimates, calculating reactor power and payload fraction for various clearance heights, gross weights and velocities
18 p3171 A69-35180

Air cushion vehicle legal status and cargo and passenger liability
19 p3455 A69-36330

Recirculation concept for air cushion vehicle air curtain evaluated by two dimensional and circular models, discussing optimum cushion area/jet exit area ratio
22 p3866 A69-40816

Base pressure of peripheral jet ground effect machines in heaving motion, discussing flow patterns
22 p3866 A69-40817

Pitching characteristics of three dimensional peripheral jet ground effect machines with compartment partition along pitch axis, considering longitudinal static stability and dynamic pitching motion
22 p3866 A69-40818

GROUND HANDLING

Environmental tests of space vehicles, determining parameter effects on ground storage and transportation, launching and orbital life
02 p0228 A69-11918

Airport facilities planning for conventional jet, STOL and SST aircraft ground handling, stressing facilities economy and transportation subsystems [AIAA PAPER 69-808]
19 p3289 A69-35623

STOL aircraft characteristics emphasizing ground and air space operations requirements and noise levels
22 p3863 A69-40430

Handling and processing function in air freight transportation, discussing system design approaches, cargo terminals, materials handling systems and containerization
22 p4053 A69-40483

Air space saturation, urban surface transport network enlargement necessity and expeditious passenger processing and baggage handling
24 p4296 A69-42567

General aviation airport application as freight consolidation terminals to reduce ground handling costs, circumvent air and ground traffic problems, etc
24 p4419 A69-43047

GROUND OPERATIONAL SUPPORT SYSTEM

Conversion from VHF to UHF at White Sands Missile Range, discussing telemetry acquisition, tracking and receiving systems
07 p1077 A69-18828

Ground data operations system for large astronomical satellite comprising UHF telemetry, PCM telecommand and processing and display equipment
18 p3117 A69-34794

Air travel and population growth requiring larger structures for office buildings, airport passenger terminals and aircraft servicing facilities [AIAA PAPER 69-809]
19 p3289 A69-35622

GROUND RESONANCE

U RESONANCE

GROUND RUN-UP

U ENGINE TESTS

GROUND SQUIRRELS

Specific antibody formation to influenza A virus vaccine /strain PR sub s/ in hibernating ground squirrels /Citellus tridecemlineatus/
08 p1263 A69-20173

GROUND STATE

Ground state population modulation in trivalent rare earth doped single crystals by means of optical double resonance, noting applications
01 p0134 A69-10013

Ground state energies of HeH divalent ion, comparing perturbation calculation values with variation-perturbation technique
01 p0123 A69-10547

Nonequilibrium nitrogen plasma spectral line intensities calculated assuming optically thin plasma
01 p0124 A69-10960

Electron impact ionization cross sections and rate coefficients from ground state given for free atoms and ions from hydrogen to calcium
01 p0125 A69-10992

Thorium and La-compounds retained superconductivity to Pr and Tm concentrations due to crystal field splitting effect producing nonmagnetic singlet ground state
02 p0295 A69-11778

High current electron bombardment ion source for production of low energy ion beams without metastable contamination
03 p0428 A69-13106

Ground state energy for single magnetic impurity dissolved in nonmagnetic metal, applying cluster variation method to s-d interaction Hamiltonian
03 p0485 A69-13298

Dissociation energy and vibrational terms of ground state hydrogen
05 p0796 A69-15908

LCAO-MO-SCF wave functions determined for ground and excited states of nitrogen dioxide at five different ONO angles
06 p0960 A69-17109

Natural orbital expansion coefficients of LCAO-MO-SCF-CI wave functions for ground state of H molecule
06 p0960 A69-17112

Ground state energy of Anderson Hamiltonian calculated by cluster variation for cases of infinite d-d correlation energy
06 p0958 A69-17712

Orientation of diamagnetic ground state Pb 207 atoms with nonzero orbital angular momentum by means of optical pumping and determination of nuclear moment
07 p1156 A69-19399

Interaction between semiconductor excitons, obtaining formulas for exciton concentrations ground state energy and dispersion, noting association with Pauli statistics
08 p1371 A69-19955

Molecular beam gas laser operating at transitions between ground state and resonance excited state of inert gas atom, obtaining population inversion
08 p1325 A69-20325

Electron states at deep levels in InSb by deriving equations for Bloch wave functions of conduction and valence bands
09 p1556 A69-21508

Direct Coulomb interaction matrix elements between hydrogen atoms in ground states calculated, presenting interaction potential
11 p1921 A69-24416

Ca XV spectrum in vacuum UV under laboratory conditions, discussing fine structure of ground level of Ca XV and coronal lines
15 p2688 A69-30553

Lifetime of ground state oxygen molecular ions in sunlight from photodetachment rate by free electron production measurement from ions in buffer gas
16 p2848 A69-31973

Ground state energy inequalities for N particle non-relativistic quantum mechanical system, showing non-saturating gravitational forces and increasing binding energy per particle
17 p3028 A69-32900

Molecular beam gas laser operating at transitions between ground state and resonance excited state of inert gas atom, obtaining population inversion
17 p2981 A69-33315

Perturbation procedures applied to energy computation for ground and first excited state of hydrogen molecule at large separation
17 p3009 A69-34170

Self consistent field molecular orbital method in LCAO (linear combination of atomic orbitals) approximation applied to LiH ground state for potential energy curve
22 p3985 A69-40721

Impact parameter versions of two state and Born approximations to calculate single excitation cross sections of H atoms ground state collisions
22 p3987 A69-41006

Metastable atom detection system for ground state atom beams, measuring Ar beam density five orders lower than background gas density
22 p3950 A69-41230

Shape resonances in low energy elastic scattering of electrons by C, N and O, discussing ground state configurations and close coupling equations corrections
23 p4193 A69-41452

Ultrasonic paramagnetic resonance investigations of Pr ions ground state energy levels in calcium fluoride
24 p4360 A69-42790

GROUND STATIONS

NT DEEP SPACE INSTRUMENTATION FACILITY
NT STADAN [SATELLITE TRACKING NETWORK]

Broadband parametric amplifier used as front amplifier in satellite communication systems ground station receiver, noting cryogenic operation capability
01 p0041 A69-10243

Small earth stations in future communication satellite systems, discussing applications, characteristics and equipment
[UN PAPER 68-95751] 01 p0028 A69-10492

Fucino earth station operation with Early Bird and Intelsat 2-F3 satellites receiving equipment and transmission system
[UN PAPER 68-95455] 01 p0028 A69-10493

British contributions to communication satellite earth station technology covering antennas, low noise amplifiers, traveling wave tubes and threshold extension demodulators
[UN PAPER 68-95843] 01 p0054 A69-10507

Automatic picture transmission station equipment including antenna, cavity filters, tape recorder, oscilloscope, facsimile system and kinescope
[UN PAPER 68-95450] 01 p0054 A69-10522

Ground-air-ground communications system using pseudonoise through satellite and central ground based control facility, discussing system advantages, SNR and modulation schemes
01 p0033 A69-11009

Magnetic field data fromOGO-2 spacecraft and surface magnetic observatories, noting magnetic storm occurrence and magnetosphere inflation and detection of polar ionospheric currents
01 p0069 A69-11125

Radio links between earth and deep space probes, summarizing bistatic radar astronomy results
[AAS PAPER 68-182] 02 p0311 A69-11467

Space observations of solar intermediate corona, discussing balloon and rocket experiments and limitation of ground based observations
[AAS PAPER 68-217] 02 p0313 A69-11483

Monopulse ground station antenna configuration for improvement of sidelobe level in satellite transmission [DVL-856]
02 p0214 A69-11599

Subsolar magnetosphere dimensions from ground observations of geomagnetic micropulsation period changes during magnetosphere deformations caused by solar wind inhomogeneities
02 p0244 A69-12356

Lake Kickapoo Space Surveillance Transmitting Station in Texas, discussing surroundings, equipment, operating range, VHF transmission, etc
03 p0411 A69-13209

Mutual RF interference between satellite and terrestrial telecommunications microwave relay system at shared frequencies
03 p0392 A69-13242

Low noise broadband parametric amplifier for communication satellite ground stations
03 p0406 A69-13733

AN/TSC-54 military satellite communications terminal for contingency deployment, discussing design, system tradeoffs and performance
[AIAA PAPER 68-439] 04 p0579 A69-15367

Earth station system for ground based communications with Intelsats 2 and 3 noting antennas, receivers, transmitters and power supplies
05 p0741 A69-15667

Low noise shaped beam Cassegrain antenna design for space communications earth station service, noting gain/noise temperature figure and antenna construction
05 p0728 A69-15669

UV solar spectra observation, discussing coordination of ground based and satellite programs
05 p0822 A69-15861

Hard solar X ray bursts characteristics and coordination of ground and space observations
05 p0814 A69-15862

On-line ground flight test data processing system
05 p0725 A69-16757

Ground station electronic environment, telemetry encoding and radio links for spacecraft communications and tracking
06 p0886 A69-16860

Earth resource satellites, discussing world ground station network for data reception and information dissemination and training and research center
[UN PAPER 68-95529] 06 p0917 A69-17067

Power traveling wave tubes in ground stations for INTLSAT 3 direction finding system
07 p1094 A69-18426

Satellite communications antenna system at Fucino earth station, describing transmitting and receiving equipment, facilities, power supply, etc
07 p1075 A69-18493

Sensitivity problems in receiving microwave signals from communications satellite at deep space distances, considering noise factors
07 p1077 A69-18669

Economic planning of satellite earth station equipment in relation to expected traffic demand, emphasizing specifications for communication via Intelsat 2 and 3 satellites
07 p1117 A69-19347

Soil resistivity survey at earth telecommunication installation site to determine optimal grounding or electrode system
07 p1117 A69-19348

Measurement bases in general, discussing theoretical data justifying ground level base and measurements results
07 p1136 A69-19516

Water effect on air supported radome of ground station for satellite communication
07 p1111 A69-19533

Design aspects of 20 ft air transportable satellite earth station
08 p1272 A69-19926

Large aperture low noise aerial design for satellite communication earth stations, discussing expected performance of 85-ft antenna at 4 GHz
08 p1279 A69-19956

Reliability effect on operating costs of satellite communications system ground stations, calculating annual cost of channel with continuous time carry-over
08 p1276 A69-20586

Signal interference criteria in considering frequency sharing between communication satellite systems and terrestrial radio services
09 p1449 A69-21273

Multiple access in communication satellite systems for achieving maximum flexibility of interconnection between earth stations
09 p1450 A69-21276

Maximum horizontally radiated power of earth stations in any 4-kHz band for multichannel telephony and TV using satellites
09 p1450 A69-21278

Earth station antennas for communication satellite service, discussing design, fabrication, main lobe gain, side and back lobe suppression and noise performance
09 p1461 A69-21281

Earth station antenna radiation patterns for studying mutual interference effects between radio relay stations and communication satellite earth stations
09 p1461 A69-21282

Antenna noise temperature at earth station due to rain on radomes, solar and cosmic noise, noting SNR degradation
09 p1461 A69-21283

Sensitivity of microwave earth stations for analog and digital communications
09 p1453 A69-21409

Commercial communication satellite earth station at Australia, noting antenna, autotracking capability, preamplifiers, and computer for control and monitoring functions
09 p1458 A69-22469

Low noise wideband amplifier system for commercial satellite communication ground terminal receiver, noting cryogenically cooled parametric amplifier
09 p1458 A69-22470

Geomagnetic fluctuations positive and negative correlations at conjugate pair stations Syowa base and Reykjavik
10 p1681 A69-22804

Power requirements for tracking, telecommand and telemetry of spacecraft over interplanetary distances considering transmission problems, equipment weight and reliability
10 p1652 A69-22984

Ground station integrated flight test data system with interactive data input terminals, on-line assembly and responsive program development
10 p1633 A69-23271

Ground station receiving antenna design and size for indirect distribution of TV programs by geostatic satellites
10 p1654 A69-23389

Ground level solar proton event recorded by neutron monitors
10 p1766 A69-23761

Spatial direction determination from simultaneous photographs of Echo 2 at Nikolaev and Helwan stations, using circle of simultaneity
12 p2068 A69-26427

Budapest University satellite radio observation APT station design, equipment and methods
12 p2059 A69-26449

Number 2 ground communications antenna system on Goonhilly Downs for British Post Office earth station
12 p2044 A69-26923

Ground station network and facilities for control of and acquisition and processing data from ESO 1 satellite
13 p2220 A69-27751

September 14, 1966 magnetic storm observation by Explorer 33 in geomagnetic tail and by polar stations, studying relation in magnetosphere and on earth
14 p2438 A69-29078

Multiple ground based geophysical sensors for detecting ionospheric phenomena, discussing continuous magnetic tape data recording, common time base and station operation
14 p2448 A69-29526

Cosmic ray observations on synoptic scale, discussing equipment and programs of IQSY world array of monitor stations
15 p2673 A69-30012

Airglow research, discussing emission features, observation methods and instruments, ground station network, etc
15 p2594 A69-30020

Satellite triangulation by least squares method based on conditions relating to observing stations coordinates, concerning synchronous observations of directions and distances
15 p2594 A69-30030

Doppler measurements in semidynamical geodesy, processing data from Transit satellites collected at various Mediterranean ground stations
15 p2602 A69-31382

Global satellite communication networks design by computer simulation, discussing politotechnical interface problems, ground stations, atmospheric factors, system optimization, etc
16 p2750 A69-31852

German ground station commercial receiving system for satellite broadcast reception
16 p2766 A69-31855

Ground station command transmission equipment for German AZUR satellite, describing components based on NASA Tone Digital Command System
16 p2759 A69-31856

PDM command coder meeting NASA Tone Digital Command Standard for German central ground station
16 p2755 A69-31859

Long distance FM radar signal relaying to central station image processing, showing wideband sum signal especially suitable for transmission
16 p2750 A69-31862

LF ground based absorption results compared with rocket measured D region electron density profiles
16 p2778 A69-32188

Atmospheric sources automatic location by direction finding network based on triangulation network principle
18 p3102 A69-34961

- Satellites and ground stations system providing transoceanic civil, air and marine traffic control in North Atlantic, discussing position determination, communication and navigation, etc
18 p3170 A69-35065
- Parametric amplifier developed for unattended satellite communication ground stations, featuring low noise broadband characteristics
19 p3270 A69-36240
- Commercial satellite communication ground station at Arvi, India, discussing system design, operation and international standards
19 p3275 A69-36412
- Gokhberg magnetovariational sounding method for single location analysis of magnetic storms early phases, comparing ground station network observations
20 p3521 A69-37040
- Positive and negative correlations in F2 layer perturbations observed by network of paired conjugate ionospheric stations at low latitude
20 p3521 A69-37050
- Short radio wave damping of earth satellite transmitter due to ionospheric diffraction resulting from increasing satellite-ground station distance
20 p3491 A69-37689
- Ground station equipment for studying motions and structure of ionospheric inhomogeneities by combined space-frequency diversity reception, noting altitude dependence of ionospheric parameters
20 p3510 A69-37693
- Near-polar circular orbiting satellite for calibrating and evaluating ground-based radars observing space objects
20 p3617 A69-37714
- Monte Cardiga telemetry station associated with sounding rocket range at Salto di Quirra, Sardinia, describing equipment, telemetry system capabilities and flexibility
20 p3512 A69-38280
- D1A satellite Doppler observations, noting effect of observation grouping on ground stations mutual position
21 p3701 A69-38336
- Image intensifiers and orthicons, plumbicons, vidicons as photoelectric devices in TV auroral observation from ground stations and jet aircraft
21 p3706 A69-38484
- Simultaneous ground and Alouette 2 satellite measurements of enhanced electromagnetic band emission in 500-1000 Hz range
21 p3708 A69-38496
- German ground station radio communications via Intelsat satellites, discussing transmitting facilities, TV picture and sound signals, etc
22 p3902 A69-41249
- Carpitron locked oscillator with wide electronic tuning range, describing CW operation characteristics and application to ground station microwave transmitters
23 p4135 A69-41302
- Cosmic ray diurnal phase and amplitude variations determined using superimposed records of cosmic ray stations inside limited rigidity region
23 p4204 A69-41481
- Traveling wave tubes in satellite earth stations, discussing single carrier tubes and multiple carrier technique
23 p4143 A69-42420
- Envelope characteristics of earth station Cassegrain antenna sidelobes, deriving formulas for central and spar blocking and forward feed spillover
23 p4143 A69-42517
- GROUND SUPPORT EQUIPMENT**
- Airport warm fog dispersal, discussing full scale aircraft seeding of polyelectrolyte materials, noting ground dispenser
01 p0054 A69-10149
- CNES worldwide network of tracking stations, describing equipment, location, organization and center of operations
02 p0228 A69-11922
- Short wave bands for earth-space communications, considering propagation anomalies compensated systems and frequency bands availability
03 p0397 A69-13721
- Tactical airfield/aircraft system effectiveness in terms of ground support resources, aircraft reliability and maximum potential sorties
05 p0743 A69-16238
- Spacecraft onboard checkout systems and design of ground support equipment and software, noting adaptive dynamic analysis and maintenance (ADAM) concept
09 p1478 A69-22382
- General purpose space vehicle ground support equipment adapted from special purpose systems, discussing checkout, launch control and data monitoring requirements
09 p1479 A69-22385
- Transpondersondes for atmospheric measurements, considering ground tracking, radiosondes, rocket-sondes and flight results
10 p1692 A69-23257
- Fueling procedures for Boeing 747 aircraft, discussing design and operation of large capacity fuel trucks
10 p1674 A69-23631
- Fueling procedures for Boeing 747 aircraft, discussing design of high rate mobile fuel dispensers
10 p1674 A69-23633
- Foam carpet and airport equipment to prevent fires and explosions from retracted gear landings
10 p1674 A69-23708
- Ground military equipment hardening against nuclear environment, selecting worst case levels from isodamage curves
15 p2651 A69-30380
- Air traffic control ground equipment developments including radio direction finders, surveillance radar, interconsole marking, etc
18 p3168 A69-34806
- Reliability study of launch support equipment, presenting failure data for mechanical and electromechanical components
19 p3295 A69-36023
- Crawler-Transporter at Kennedy Space Center for moving ground support equipment, Apollo/Saturn space vehicle and mobile launcher, describing design and components
21 p3690 A69-38754
- General purpose space vehicle ground support equipment adapted from special purpose systems, discussing checkout, launch control and data monitoring requirements
22 p3927 A69-40552
- Tracking and data relay satellite system (TDRSS)/compared to ground based mission support, considering altitude coverage capability, economy and communication requirements
23 p4120 A69-41756
- GROUND SUPPORT SYSTEMS**
- International 28-station global instrumentation ground support network for space tracking and data acquisition
06 p1043 A69-17059
- Ground based guidance systems for supplementing onboard guidance of manned space vehicles
06 p0955 A69-17580
- Ground station network and facilities for control of and acquisition and processing data from ESRO 1 satellite
13 p2220 A69-27751
- Space vehicle checkout, launch control and data monitoring by general purpose ground system providing flexible stimuli generation, measurement acquisition, computation and information display
18 p3118 A69-35064
- Real time multiprocessing telemetry ground support integrated system design with expanded definition of hardware/software decision tradeoffs
22 p3907 A69-40351
- Radio astronomy Explorer A attitude determination via disk-oriented programming ground support system for reducing and calibrating telemetry data, attitude prediction and command, etc
22 p3907 A69-40363
- Cape Kennedy Space Center mobile launchers and auxiliary equipment for Saturn vehicles, discussing functions, design and systems
24 p4297 A69-43036
- GROUND TESTS**
- NT COLD FLOW TESTS
- NT PRELAUNCH TESTS
- NT STATIC FIRING
- Concorde structural tests, discussing ground test program for simulating flight temperature and stress conditions at 2.6/2.7 station of wing-fuselage section
02 p0193 A69-11892
- Ground vibration testing of flight and space vehicles, noting structural damping asymmetries and nonlinearities
04 p0585 A69-14833
- Communication satellite ground test programs, discussing structural, electrical integration, thermal control and antenna pattern models for simulation tests
08 p1409 A69-19962
- Vacuum engineering problems during booster rocket engine ground tests, simulating flight environment
09 p1570 A69-22300
- Real time real temperature exhaust gas reingestion and structural heating test facility for jet lift V/STOL configurations
09 p1479 A69-22388
- Air backflow in nuclear exhaust system duct for ground testing of NERVA engines, noting overpressure effect
09 p1479 A69-22390
- Computer controlled flight line tester performing automatic real time testing of aircraft avionics systems on flight line or hanger
11 p1864 A69-25060
- Vitiated air contamination effects on combustion and hypersonic air breathing engine ground tests
13 p2325 A69-28274
- Ground testing method to evaluate inertial navigation systems dynamic errors by programmed platform drift rates, position output comparisons and error source identification
14 p2479 A69-29490
- Multiple shaker ground vibration test system for confidence in helicopter designs before flight testing and evaluation of force balancers
15 p2585 A69-30357
- Saturn 5 boost phase environment simulation on Apollo stages, discussing fixtures, load devices, instrumentation and ground test
15 p2588 A69-30405
- Static structure ground test for Saturn-Apollo vehicle short stack, describing air pressure simulation, data acquisition and readout systems
15 p2589 A69-31079
- Apollo spacecraft equipment qualification program for margin assurance, discussing ground and flight tests
19 p3430 A69-36015
- Vitiated contamination effect on airbreathing engine ground testing, considering equilibrium, vibrational and chemical relaxation, condensation, combustion, mixing and engine performance
19 p3448 A69-36333
- Lifting body stability augmentation systems design, development, ground tests and flight data including frequency response, limit cycle and structural resonance
21 p3647 A69-39413
- Mission simulation testing in thermal vacuum environment for Apollo Lunar Module, noting conformal skin heaters
22 p3920 A69-40369
- Digital computer program for determining flight vehicle telemetry antenna performance from ground test readings
23 p4133 A69-41754
- Diamond shaped surface ablation patterns development mechanism for several ablation materials of ground test and recovered flight vehicles
23 p4059 A69-41891
- Training missions and military exercises to field test weapons system models
24 p4296 A69-42884
- GROUND-TO-AIR MISSILES**
- U SURFACE TO AIR MISSILES
- GROUND TRACKS**
- Representation for computer storage of contour map data for searching problem involving determination of aircraft ground track
01 p0036 A69-10704
- Generalized techniques for contour maps problem solution applied to problem of locating ground track of aircraft from elevation readings obtained during flight
09 p1461 A69-22599
- GROUND WAVE PROPAGATION**
- Terrain influence in ground wave propagation evaluated by two dimensional diffraction and scattering problems, using Airy type wave functions
01 p0033 A69-10970
- Ground wave excited by dipole in conducting half space, discussing lateral wave character and optimum radiation angle
02 p0209 A69-12347
- Ionospheric radio signal reflection measurements based on ground to rocket pulse propagation
02 p0245 A69-12736
- Ground propagation of regular Pc 1 and irregular Pi 1 geomagnetic micropulsations demonstrated by precise time measurement
07 p1127 A69-19338
- VLF electromagnetic wave propagation in earth-ionosphere waveguide with reflections from ionosphere, noting TE and TM mode coupling and mode conversion
09 p1460 A69-22699

GROUP DYNAMICS

- Ground wave propagation attainment of electron plasma resonance of F region, stressing need of wave vector orientation toward magnetic north
10 p1684 A69-23828
- Slow waves contribution to image radiation from array of line sources above ground plane, determining optimum height of lowest element of array
11 p1837 A69-25002
- Saddle point analysis of electromagnetic ground wave propagation in source excited field in waveguide formed by two parallel plate dielectrics
12 p2028 A69-25898
- Ground conductivity effects on MF sky wave transmission strength, discussing transmission over open sea
17 p2918 A69-33029
- Ionosphere reflected radio waves field strength measurements, obtaining formula for ground wave discrimination
23 p4123 A69-41861

GROUP DYNAMICS

- Large scale information displays for group sharing in air traffic control, military operations and organization management
02 p0250 A69-12159
- Book on groups under stress covering psychological research in SEALAB 2, emphasizing planning of data collection and experimental results
04 p0552 A69-14533
- Environmental crowding effect on individual and group behavior in rat colony, using implanted passive resonant circuits for identification and passage information
19 p3257 A69-36243
- Group leadership attempting behavior dependence on situational and perceptual variables
23 p4110 A69-42015
- Risk taking under uncertainty in individual and group decisions, analyzing gambling and group discussion situations
23 p4091 A69-42016
- Group interaction finite Markov chain model, analyzing changes in interpersonal relationships based on balanced dyadic states
23 p4110 A69-42017

GROUP THEORY

- Self gravitating pulsating cylindrical and ring shaped cosmic masses from group theory standpoint compared with oscillating stars
01 p0148 A69-10124
- Lie groups for equations of motion in quantum mechanics or field theory determined by operator analysis
02 p0282 A69-12840
- Lie algebra of second order linear differential equations
02 p0273 A69-12841
- Independent variables reduction in nonlinear partial differential equations, detailing group theory method
03 p0456 A69-13740
- Stored energy function of hyperelastic material by Lie group extension of Truesdell theorem on symmetry groups
04 p0680 A69-14945
- Group classification of solutions to Hopf equation according to type of viscosity coefficient
07 p1118 A69-18700
- Group analysis of MHD equations, determining group properties of motion equations of compressible fluid, obtaining invariant solutions
07 p1191 A69-18994
- Group theory application to multidimensional symmetrical linear dynamic control systems optimization, considering natural vibrations of three material points
12 p2129 A69-26071
- Lower bound for time required for group multiplication by logic circuits, using modified Winograd model for Abelian group
12 p2034 A69-26752
- Nonsingular matrices inversion method by group partitioning applied to noise covariance matrix used in optimal prediction and control
12 p2123 A69-26754
- Systematic formalism specialization of group theory techniques for similarity analysis applied to three dimensional incompressible boundary layer flows
16 p2773 A69-32379
- Received radar signal power maximizing problems in planetary exploration, analyzing abelian group real line and circle problems
17 p2993 A69-32831
- Group properties of adiabatic motion equations of medium in relativistic hydrodynamics, including solu-

- tions of subgroups applicable to multiple particle production
19 p3301 A69-36843
- Generalized Clifford matrix algebra applications, noting relation to generators of special unitary group
20 p3568 A69-37072
- Two dimensional gas dynamics differential equations for simple waves, discussing invariant solutions and conditions for group solutions
22 p3933 A69-41030
- Nondiscrete locally compact group having noncontinuous irreducible representations, proving theorem
23 p4183 A69-42022
- Compact semigroups continuous characters, noting character extension possibilities
24 p4340 A69-42891
- Density matrices of symmetry projected single determinant wave functions for finite groups, considering many particle system
24 p4351 A69-43810

GROUP VELOCITY

- Numerical method for determining group velocity of waves in homogeneous anisotropic medium, using implicit function from dispersion relation
01 p0131 A69-11117
- Anomalous infrasonic signals observed during launching of space vehicles with thrust greater than 200,000 lb, noting supersonic and subsonic group velocity spreads
07 p1078 A69-18853
- Chebyshev filter with flat group delay obtaining transfer function, noting cascade synthesis and extended bisection theorem
08 p1299 A69-21169
- Backward plasma waves in region of anomalous dispersion indicated by opposite directions of RF wave phase and group velocities
11 p1927 A69-25116
- Plasma electron density measurement from phase shifts of electromagnetic wave groups propagation
14 p2497 A69-29796
- Group delay time for dispersive wave propagation velocity determined using correlation method
15 p2562 A69-30094
- Wave propagation at different group velocities along parametric line in traveling wave parametric amplifier
16 p2805 A69-32254
- Surface wave study techniques, discussing digital moving window analysis of group and phase velocity and use of time variable filters
16 p2784 A69-32576
- Superluminal group velocities in relation to causality axion, considering sound propagation in ultradense matter and particles of imaginary mass /tachyons/
21 p3769 A69-38543
- High pass filters reflection group delay compared with low pass filters transmission group delay with Butterworth, Chebyshev and elliptic responses
21 p3686 A69-39139
- ELF atmospheric propagation, determining slow-tail atmospheric group velocity, relating characteristics to spectral characteristics of lightning
23 p4114 A69-41362

GROUP 3A COMPOUNDS

- Collection of papers on III-V compound semiconductors and semimetals covering physical properties, solid solutions and electric field, pressure, radiation and impurity effects
04 p0641 A69-14501
- Diffusion in compounds of elements of groups III-V
04 p0641 A69-14502
- Radiation effects on III-V compounds, considering damage in solar cells and luminescence, light emitting and Esaki diodes
04 p0641 A69-14504
- Phenomena in III-V compounds and III-V compound-other compound solid solutions, examining equilibrium phase diagrams
04 p0641 A69-14505

GROUP 3B COMPOUNDS

- Collection of papers on III-V compound semiconductors and semimetals covering physical properties, solid solutions and electric field, pressure, radiation and impurity effects
04 p0641 A69-14501

GROUP 4A COMPOUNDS

- Group 4A carbides and nitrides formation in Mo by arc melting, determining threshold solute metal-interstitial atom ratios
12 p2117 A69-27136

GROUP 5A COMPOUNDS

- Collection of papers on III-V compound semiconductors and semimetals covering physical properties, solid solutions and electric field, pressure, radiation and impurity effects
04 p0641 A69-14501
- Diffusion in compounds of elements of groups III-V
04 p0641 A69-14502
- Radiation effects on III-V compounds, considering damage in solar cells and luminescence, light emitting and Esaki diodes
04 p0641 A69-14504
- Phenomena in III-V compounds and III-V compound-other compound solid solutions, examining equilibrium phase diagrams
04 p0641 A69-14505

GROUP 5B COMPOUNDS

- Collection of papers on III-V compound semiconductors and semimetals covering physical properties, solid solutions and electric field, pressure, radiation and impurity effects
04 p0641 A69-14501

GROUP 6A COMPOUNDS

- Tungsten replacement by chromium or molybdenum in heavy metals shown possible for binding material of group 6A metals
05 p0780 A69-15991

GROUP 7A COMPOUNDS

U HALOGEN COMPOUNDS

GROUP 8 COMPOUNDS

- Group 7A and group 8 elements alloying effect on Cr dislocation structure and mechanical properties, discussing ductile-brittle transition temperature and electronic theory
18 p3160 A69-35452

GROWTH

- NT CRYSTAL GROWTH
NT CZOCHRALSKI METHOD
NT EPITAXY
NT HYDROTHERMAL CRYSTAL GROWTH
- Vertical vibration stimulation of growth of onion bulbs and mice body weights
01 p0014 A69-10584
- Photoinhibition of cell division and growth in Euglenoid flagellates by fluorescent and incandescent visible light
01 p0014 A69-10903
- Identity between growth hormone degrading activity of pituitary gland and plasmin
06 p0873 A69-17105
- Plants growth from seeds exposed to space environment onboard Cosmos 110 biological satellite compared with control plants
07 p1064 A69-18972
- Vertical vibration stimulation of growth of onion bulbs and mice body weights
15 p2555 A69-30754
- Plants growth from seeds exposed to space environment onboard Cosmos 110 biological satellite compared with control plants
20 p3479 A69-38220
- Organism growth physiology based on decisive enzyme reactions, considering synthesis of biological proteins from DNA and molecular life processes
21 p3652 A69-38787
- Erythroblasts fractionating method based on size, density and resistance of immature erythroblasts which change during maturation
22 p3877 A69-40761
- Compensatory hypertrophy effects on adrenal phenylethanolamine n-methyl transferase /PNMT/ activity in rats
23 p4080 A69-41404

GRUMMAN AIRCRAFT

- U A-6 AIRCRAFT
U E-2 AIRCRAFT
U F-111 AIRCRAFT

GRUMMAN MILITARY AIRCRAFT

U MILITARY AIRCRAFT

GRUNEISEN CONSTANT

- Consistency of high temperature equation of state of solids, considering Gruneisen parameter and lattice dynamics
08 p1419 A69-19814

GUIDANCE [MOTION]

- NT AIRCRAFT GUIDANCE
NT COMMAND GUIDANCE
NT INERTIAL GUIDANCE
NT INJECTION GUIDANCE
NT MAP MATCHING GUIDANCE
NT MIDCOURSE GUIDANCE
NT REENTRY GUIDANCE
NT RENDEZVOUS GUIDANCE
NT SATELLITE GUIDANCE

NT SPACECRAFT GUIDANCE
 NT STRAPDOWN INERTIAL GUIDANCE
 NT TERMINAL GUIDANCE

Nozzle separation for thrust vector control with applications to guidance problems
 01 p0161 A69-10412

Iterative guidance mode /IGM/ applied to effective gravity vector prediction, acceleration measurement of noise sensitivity and energy limitations
 [AIAA PAPER 67-620] 04 p0629 A69-15501

Successive approximation for iterative construction of near optimum guidance
 06 p0954 A69-17573

Diffraction limited telescope fine guidance experiment to improve pointing stability in space, noting attitude control system and nonmechanical suspension
 08 p1317 A69-21072

Guidance law for autoguided system trajectory to impact target, noting kinematic study
 10 p1723 A69-23701

Dynamic vibration effects on guidance and control systems performance determined from spectral densities, cross spectral densities and vibratory environment amplitude distributions
 15 p2608 A69-30367

Lift and drag determination for moving rectangular coils over infinite plane sheet for magnetic suspension and guidance for rocket sleds
 17 p2946 A69-33789

General purpose /GP/, differential digital analyzer /DDA/ and CORDIC /coordinate rotation digital computer/ computers for navigation system computations
 17 p3003 A69-34100

Polynomial approximations in perturbational navigation and guidance schemes including Chebyshev and least square approximations
 19 p3368 A69-35664

GUIDANCE SENSORS

Sensor suspension, damping and signal readout through use of fluids with applications to rate and acceleration sensors
 [AGARDOGRAPH-118] 08 p1257 A69-20949

Satellite attitude control, discussing mission requirements, typical guidance sensors, actuating torque, systems reliability, etc
 09 p1609 A69-21617

Flight test evaluation program for airborne multisensor electro-optical display systems performance in TV mode under variety of optical conditions
 [AIAA PAPER 69-317] 09 p1500 A69-22387

Inertial navigation system sensors including one and two axis, laser, vibratory, gyroflex and free rotor gyros
 12 p2078 A69-25874

Earth sensor for spin stabilized spacecraft to maintain specific orientation with earth, discussing use of blue and red filters
 15 p2609 A69-30593

Tacite rocket probe to study space IR radiation, using passive stellar sensor for recording reference stars positions to recalibrate gyroscope kinetic motion for attitude restoration
 [ONERA-TP-731] 17 p3001 A69-33220

Casing bearings dry friction force moment effect on double rotor gyrocompass sensor motion, showing diminished device accuracy at high latitudes
 18 p3135 A69-34560

Induced-emission oscillator navigation sensor with performance limitations, noting ring laser and nuclear maser gyro and laser accelerometer
 19 p3369 A69-35795

Strapdown redundant experimental sensor inertial navigation package containing gyros and accelerometers, discussing signal real time processing by digital computer
 [AIAA PAPER 69-851] 21 p3762 A69-39379

GUIDANCE STABILITY
 U CONTROL STABILITY

GUIDE VANES
 NT JET VANES

Missile control during propulsion period, emphasizing vane deflection required for lateral wind compensation
 01 p0163 A69-11297

Jet engine inlet noise control by modification of inlet guide vanes
 05 p0811 A69-15622

Flow through turbine stage with inclined guide vanes at moderate Mach numbers, discussing exit blade angle formula for swept cascades
 15 p2547 A69-30570

Blade length effects on performance of flow straightener vanes influenced by secondary flow, noting high deflection and low aspect ratio
 17 p2896 A69-33606

Potential flow interaction effects between blade rows in axial flow compressor stage, emphasizing inlet guide vane-rotor interaction
 21 p3643 A69-38439

Monograph on control dynamics of gas turbines with adjustable guide vanes, using methods of control theory and applied mathematics
 21 p3784 A69-38449

GUIDED MISSILES
 U MISSILES

GUINEA PIGS

1.5 g angular acceleration effects on acetylcholine metabolism in guinea pig brains and hearts
 02 p0198 A69-11505

Acoustical vestibular stimulation in guinea pig, showing activation of receptors
 03 p0376 A69-14076

Histological and histochemical studies of dephosphorylating enzyme distribution in muscle spindle capsule of guinea pig thigh muscles and cat calf muscles
 15 p2554 A69-30406

Decompression sickness prevention in guinea pigs by heparin and papaverine combination nebulized in carbon, discussing nitrogen elimination enhancement
 21 p3655 A69-38917

Cholesterol-protein metabolism in muscles, liver and cerebrum of lethal X ray exposed guinea pigs compared with unexposed group
 21 p3657 A69-39052

Local stress effect on immunocompetent cells differentiation in guinea pigs lymphatic ganglia, showing antibody producing cells number increase
 22 p3877 A69-40277

Albino guinea pigs respiration rates and ear skin histology after exposures to coherent ruby laser light
 24 p4270 A69-42578

GUM VULCANIZATES
 U VULCANIZED ELASTOMERS

GUMBEL THEORY
 U RANGE [EXTREMES]

GUN LAUNCHERS

Ruggedized ballistic range telemetry system survivability and in-flight stability after gun launching, presenting temperature, strain and stagnation point pressure measurements
 10 p1654 A69-23281

GUN PROPELLANTS

Relaxation induced self oscillations during combustion of gunpowder in semiclosed volume, noting combustion instability
 04 p0686 A69-14987

Heat conduction equation for convective flow applied to gunpowder combustion under harmonic pressure variation
 07 p1241 A69-18708

Combustion mechanism of condensed inflammable systems such as gunpowder and other explosives, discussing combustion stability
 11 p2000 A69-25187

Unsteady combustion wave passage through inert obstacle in gunpowder in N filled pressure vessel
 22 p4051 A69-41119

GUN TURRETS

Onboard hybrid computer for helicopter fire control system, generating turret pointing angles and corrections
 17 p2934 A69-34074

GUNN EFFECT

Small signal impedance of subcritically doped gallium arsenide Gunn diodes, using drift velocity vs electric field relationship
 01 p0038 A69-10121

Gunn generator efficiency dependence on diode and regime parameters using computer model
 01 p0042 A69-10319

YIG single crystal resonator tuning of Gunn diode in coaxial line circuit
 01 p0042 A69-10320

Gunn effect application in fast logic circuit devices including comparators, adder and shift register circuits
 01 p0042 A69-10438

Output power of Gunn effect microwave diode using equal area analysis and Fourier transforms
 01 p0049 A69-11195

Gunn domains reduction in sheet type GaAs oscillators by spreading of field lines out of active region
 02 p0215 A69-11933

GaAs Gunn diode oscillators operating at Q band frequencies
 02 p0297 A69-11944

Domain operating point application to Gunn domain buildup including trajectory graphs
 02 p0297 A69-11948

Optical modulation near intrinsic edge in n-type bulk GaAs due to Franz-Keldysh effect, noting carrier production by photon initiated excitation
 02 p0300 A69-12650

Magnetic field effect on amplitude, frequency and form of LF oscillations in Gunn diodes
 02 p0222 A69-12684

Microwave energy generation with solid state equipment, noting Gunn effect diodes, avalanche diodes and limited space charge accumulation /LSA/ devices
 03 p0402 A69-12971

Gunn effect in bulk GaAs, noting microwave oscillator applications
 03 p0484 A69-13292

Gunn effect and resulting electron transfer mechanism in semiconductor devices
 03 p0486 A69-13610

Stray fields and domain dynamics in Gunn effect semiconductors covered with dielectric sheets
 03 p0491 A69-13988

Small transverse dimensions effect and domain formation criterion for surface oriented Gunn diodes prepared on thin epitaxial GaAs layers
 04 p0639 A69-14335

Hybrid Gunn domain and LSA mode operation in oversized bulk and epitaxially grown GaAs, noting large signal impedance data
 04 p0639 A69-14339

Computer simulations defining conditions to produce series operation of Gunn effect diodes
 04 p0573 A69-14340

Similarity between characteristics of T layers in oxygen discharge positive column and Gunn instabilities in GaAs, noting role of negative O ions
 05 p0800 A69-15739

Gunn effect theory, discussing dynamic characteristics and domain propagation for inhomogeneous transmission line profile
 05 p0807 A69-15821

Bibliography on Gunn effect theory, experimental results and applications
 05 p0810 A69-16565

X-band swept frequency oscillator using Gunn diode and ferrite phase shifter
 05 p0734 A69-16573

Low power RF signal triggering of self sustaining Gunn oscillations in GaAs samples
 05 p0734 A69-16575

Electron temperature relation to population ratio in Gunn effect
 05 p0810 A69-16576

Gunn effect verification using n-type semiconductor single crystals in DC field, noting microwave field polarization plane rotation
 06 p0978 A69-16902

Intervalley scattering model for Gunn domain dynamics, noting effects comparable to diffusion
 06 p0893 A69-16937

Gunn effect pulse generator for antenna arrays operating at decimeter wavelengths with external power source
 06 p0895 A69-17459

External impedance controlled nucleation of Gunn effect domains studied theoretically by Nyquist criterion
 06 p0981 A69-18217

Gunn effect diodes application to ultrafast pulse electronic circuitry for computer logic
 07 p1089 A69-18244

Oversized GaAs Gunn effect diodes operated in L and S bands at harmonics of fundamental transit time frequency with high power and efficiency
 07 p1196 A69-18444

High peak power Gunn effect oscillators for low gigahertz frequencies in transit and nontransit time limited modes
 07 p1097 A69-18447

Computer model of Gunn diode, discussing operations under pulse bias voltage and in resonator
 07 p1097 A69-18449

Conditions for existence of stationary high field domain in Gunn diode
 07 p1097 A69-18450

Solution regrowth method to prepare epitaxial GaAs for Gunn effect devices
 07 p1197 A69-18451

Gunn effect pulse devices with resistive loading, discussing logic, circuits and low power consumption
 07 p1097 A69-18453

Absorption edge broadening by electric field in Gunn domain of N-GaAs crystals
 07 p1197 A69-18454

Mechanically and electronically tunable resonator for driving IMPATT and Gunn diodes
 07 p1097 A69-18455

GUNPOWDER

Gunn effect for cathode contacts with interface resistance, developing control characteristic boundary condition concept for explaining cathode fall and other phenomena

07 p1199 A69-18649

Injection locking method for reducing FM noise in Gunn effect oscillators

07 p1102 A69-18862

Degenerate parametric amplifier using self pumping action of oscillating domain capacitance in Gunn effect

07 p1107 A69-19450

Gunn effect memory loop in pulse diodes consisting of two Gunn diodes connected in series

08 p1279 A69-19912

High field domains in Gunn effect diode in transit time mode of operation probed with stroboscopic electron beam in scanning electron microscope

08 p1283 A69-20162

Series operation of Gunn devices with differing threshold currents at SHF

09 p1463 A69-21684

Gunn effect domains propagation calculated for nonuniform diodes of annular geometry, obtaining frequency variation

09 p1464 A69-22159

Gunn diode operating to VHF range with coaxial line to generate rectangular waves and to function as memory element

09 p1467 A69-22587

Pulsed J band Gunn effect oscillators performance, noting hybrid domain mode due to high bias fields

09 p1468 A69-22594

Gunn effect cavity controlled generator oscillations, noting phase trajectory closing conditions dependence on resonant mode parameters

09 p1468 A69-22596

Gunn diode reliability improvement by using device structures preventing high field domains from reaching anode

09 p1470 A69-22788

Gunn diode field distribution with distributed capacitance electrode analyzed with one dimensional computer simulation

09 p1470 A69-22789

Small signal HF conductivity of GaAs calculated for arbitrary frequency and DC field, considering subcritical Gunn devices

10 p1747 A69-23694

Frequency noises suppression in Gunn diode oscillators by frequency stabilization, using high Q external cavity

11 p1853 A69-25608

Resonant load impedance effects on Gunn diode oscillators output fluctuations, noting maximum power conditions

11 p1853 A69-25609

Gunn oscillators synchronizing by injecting HF external signal, discussing oscillator fabrication techniques, phase synchronization, etc

11 p1856 A69-25636

High CW power K-band Gunn oscillators attained through control over doping level, profile and GaAs epitaxial layer thickness

12 p2036 A69-25907

Microstripline circuit for stabilizing oscillating frequency of Gunn diodes prepared with GaAs slices

12 p2036 A69-25924

LF negative resistance of X band Gunn diodes with lumped components, using coaxial circuit

12 p2039 A69-26387

Bias circuit LF oscillations in short Gunn devices, analyzing sinusoidal and relaxation oscillations and stable bias in terms of terminal I-V characteristics

12 p2041 A69-26628

Harmonic generation, using nonlinear current-voltage characteristics of Gunn diodes at 9500 MHz frequency

13 p2226 A69-27235

Relaxation oscillations in field ionized epitaxial n-GaAs Gunn oscillators on seminsulating substrates, discussing recombination of excess electrons and holes

13 p2227 A69-27236

Frequency memory in cavity controlled Gunn oscillators, discussing loop gain and bandwidth dependence on oscillation mode and bias voltage

13 p2229 A69-27677

SHF solid state phased array radar with Gunn effect modular microwave IC design, discussing air and ground applications

14 p2420 A69-29435

Boltzmann equation for hot electron distribution functions in GaAs and threshold field in Gunn effect

15 p2665 A69-30025

Gunn effect GaAs oscillators with p-n junctions, studying electrical characteristics, threshold voltages and currents during breakdown and p-n junctions injection

15 p2666 A69-30065

Waveguide below cut-off resonators for active microwave circuits, describing experiments with avalanche and Gunn diodes

15 p2577 A69-30613

Frequency effects on Gunn oscillator modulation sensitivity, discussing microwave-frequency deviation and diode impedance

15 p2577 A69-30614

Plasma modes, critical fluctuations and optical properties electric field dependence in two valley model of Gunn instability semiconductors

15 p2581 A69-31240

Gunn effect theory and applications, discussing field domains in semiconductors, excited oscillations measurement, oscillators design, computer elements, etc

18 p3183 A69-35160

Gunn effect and devices effective use for specific purposes and as components of microwave systems

18 p3183 A69-35263

Magnetic field effect on Gunn diode vibrations and LF oscillations, noting increase in threshold field and decrease in threshold current

18 p3183 A69-35267

Gunn effect applied to digital electronics, discussing diode characteristics, microwave amplifier design, pattern recognition, analog-numerical conversion, etc

19 p3285 A69-36708

Gunn effect pulse generator for antenna arrays operating at decimeter wavelengths with external power source

20 p3508 A69-37942

Gunn device performance for various oscillator types, discussing cavity oscillator characteristics variation

21 p3681 A69-38394

Gunn oscillators protection from catastrophic breakdown phenomena, using carrier velocity saturation in n-type Ge

21 p3682 A69-38777

GUNPOWDER

U GUN PROPELLANTS

GUNS [ORDNANCE]

Gun projectiles assisted by solid propellant motor to increase range, discussing construction, performance and free-wheeling rotation band use

15 p2702 A69-30592

GUST ALLEVIATORS

Aircraft gust alleviation system for minimizing weighted sum of normal acceleration and pitch rate response by limiting control surface deflections

09 p1434 A69-22279

Gust absorber system configuration flight tests and analysis, emphasizing application to delta wing aircraft [ONERA-TP-698]

20 p3462 A69-37753

GUST LOADS

Low altitude atmospheric turbulence model evaluated from analysis of A-6A aircraft gust load data, comparing model estimates with aircraft response characteristics

01 p0056 A69-11053

Lift fluctuation on airfoil due to transverse and chordwise gusts applied to rotating fan and compressor blade design [ASME PAPER 68-FE-28]

05 p0697 A69-16070

Wing penetration into zone of sharply localized gust, deriving equations for forces and moments acting on wing

07 p1050 A69-18742

Atmospheric gust effect on aircraft flying at Mach one calculated for subsonic and supersonic regions, finding difficulties for transonic calculations

10 p1632 A69-22918

Gust load predictions for aircraft design by treating aircraft load history as linear response to stationary Gaussian process excitation

11 p1823 A69-25504

Turbulence and SST, discussing subsonic accidents, probability of encountering gust induced accelerations, turbulence at cruise altitudes, radar storm return and mountain waves

16 p2808 A69-32368

Random gust design requirement and gust load covariances to define boundaries of gust-loading region for airframes

20 p3621 A69-37167

FAA power spectral gust methods for computing design limit loads on commercial aircraft, noting British investigation

24 p4253 A69-43111

GUSTATORY PERCEPTION
U TASTE

GUSTS

Numerical filtering procedures for gust spectrum analyses compared for gain and phase lag frequency response characteristics, discussing gust acceleration spectra

01 p0084 A69-11052

Pressure oscillation production in wind tunnel by hinged plates in test section walls to test jet engine inlets under controlled conditions

02 p0229 A69-12537

Wind gust simulation procedures, discussing high altitude clear air turbulence and simulation of air perturbations

03 p0461 A69-13647

Gust probes in model of low altitude atmospheric turbulence during USAF research program L.O.-LOCAT, plotting relationship between peak count distribution curves

17 p2999 A69-33737

GYMNASTICS

U EXERCISE [PHYSIOLOGY]

GYNECOLOGY

Jet flying effects on air hostess menstrual function, considering cycle length, duration, regularity, dysmenorrhea and flow severity

23 p4103 A69-41689

GYRATION

NT AUTOROTATION
NT EARTH ROTATION
NT LARMOR PRECESSION
NT MOLECULAR ROTATION
NT PRECESSION
NT ROTATION
NT SATELLITE ROTATION
NT SOLAR ROTATION
NT STELLAR ROTATION

Differential equations for normal propagation of plane electromagnetic waves in isotropic stratified inhomogeneous gyration medium, discussing boundary conditions and reflection properties

08 p1353 A69-21000

GYRATORS

NT MICROWAVE FILTERS

Impedance and gain approximation in transistor configurations, noting gyrator circuit

02 p0213 A69-11532

Stability of linear passive time variable circuits, discussing validity of circuit elements replacement by gyrator equivalents

05 p0739 A69-16348

Controllable gyrator use in nonlinear network synthesis

05 p0735 A69-16620

Frequency and noise characteristics of gyrator circuits, analyzing Q factor, stability and oscillation sensitivity

05 p0735 A69-16621

3-terminal gyrator circuits using operational amplifiers, noting exact cancellation of negative by positive resistance and unattainability of LF unstable modes

06 p0893 A69-16936

Gyrator stability and frequency behavior obtained by controlled sources selection

19 p3287 A69-36739

GYROCOMPASSES

Book on magnetic compasses and magnetometers covering pivoted needle instruments, surveying, transmitting and gyromagnetic compasses, inductor instruments and compass testing

08 p1315 A69-20444

Two rotor gyrocompass oscillations stability during finite time interval, deriving differential equation by suitable quadratic functions

11 p1886 A69-25089

Land gyrocompass on torsional suspensions in liquid filled chamber, considering design and operation in terms of precession theory

13 p2259 A69-27431

Natural oscillation frequency of gyrocompass mounted in torsional suspension, taking into account moments of inertia of sensitive element

16 p2791 A69-32282

Gyrocompass differential equations of motion reduced to Volterra integral equation, proposing solution algorithm

17 p2995 A69-33617

Gyrocompassing precision problems related to gyro drift, input axis deviation and base motion compensation, describing inertial navigation platform alignment to true north

17 p2977 A69-34081

- Casing bearings dry friction force moment effect on double rotor gyrocompass sensor motion, showing diminished device accuracy at high latitudes
18 p3135 A69-34560
- Accuracy improvement of method of averages applied to equations of small motions and disturbances of two rotor gyrocompass on ship performing circular maneuvers
18 p3139 A69-35378
- Precision azimuth reference accuracy standards with confidence limits for gyrocompass evaluation, emphasizing astro and transfer angle repeatability [AIAA PAPER 69-859]
21 p3725 A69-39387
- GYROFREQUENCY**
- Incoherent synchrotron radiation by relativistic electrons gyrating in cold magnetoactive plasma rederived, correcting errors
10 p1741 A69-23858
- Banded chorus, VLF discrete emissions in magnetosphere in single variable frequency band with frequency depending on equatorial electron gyrofrequency
16 p2774 A69-31981
- Natural gyrofrequencies of rigid rotor during slowing/stopping at high forward speed, using simple approximation
17 p2899 A69-33507
- Ionospheric VLF electrostatic noise observed by sounding rocket, noting proton gyrofrequency harmonics effects within emission attenuation bands
21 p3714 A69-38550
- Resonant perturbation response of Vlasov magnetoplasma to source below electron gyrofrequency, explaining fractional resonances in Alouette 2 topside data
22 p4023 A69-40516
- GYROINTERACTION**
U MAGNETIC RIGIDITY
- GYROMAGNETISM**
NT GYROFREQUENCY
- Upper hybrid and modified plasma resonance on basis of rocket-borne gyroplasma probe data
10 p1726 A69-22807
- GYROPLANES**
U HELICOPTERS
- GYROS**
U GYROSCOPES
- GYROSCOPE FLUIDS**
- Sensor suspension, damping and signal readout through use of fluids with applications to rate and acceleration sensors
[AGARDGRAPH-118]
08 p1257 A69-20949
- Operational errors of floating gyroscopes with hydrostatic unloading of bearings, establishing eccentricity tolerances, axes misalignment and temperature field nonuniformity
09 p1497 A69-22103
- GYROSCOPES**
NT ATTITUDE GYROS
NT ELECTROSTATIC GYROSCOPES
NT FLUID ROTOR GYROSCOPES
NT GYROCOMPASSES
NT GYROSCOPIC PENDULUMS
NT GYROSTABILIZERS
NT ROTARY GYROSCOPES
- Gyroscope with rotational symmetry subjected to random input torques analyzed by Euler equation of motion
01 p0079 A69-10236
- Optimal stabilization of free gyrostats using duration of transient processes and functionals of fuel and power requirements as criteria
01 p0079 A69-10261
- Sequential probability ratio test for detecting changes in Gauss-Markov process characteristics, noting application to fault detection in gyro navigational system
01 p0083 A69-11002
- Gyrovibrator /angular rate measuring device/, discussing output signal and natural frequency dependence on moments of inertia
01 p0083 A69-11004
- Laser gyro applications including guidance, navigation and control problems
02 p0248 A69-11741
- Laser gyro in future inertial navigation systems for Category 1 landing without position updating
03 p0463 A69-13210
- Nonorthogonal multisensor strapdown inertial reference unit providing redundant capabilities and optimal performance
03 p0429 A69-13211
- Equilibrium orientations of orbiting gyrostats, giving spectrum of solutions for bodies of varied shape and internal rotor angular momentum
03 p0522 A69-14246
- Invariance of stabilized coordinates in power gyrostabilizers, using matrix equivalent of gyroscopic moments acting on platform
04 p0597 A69-14602
- Dry friction stabilizing effect on motion of astatic gyroscope with quasi-elastic compensation
04 p0597 A69-14605
- Strapdown gyros in back to back connection for reduction of component cross coupling errors
04 p0603 A69-15473
- Equivalence principle application to gyroscope motion in uniform gravitational field to obtain precessional angular velocity
05 p0764 A69-16367
- Integrability of equations of motion of gyrostat about fixed point inertial moments varying identically in time
05 p0764 A69-16504
- Spherical gyroscope servosystem probabilistic synthesis ensuring minimum dispersion of random drift
05 p0764 A69-16669
- Motion of gyroscopic integrator of linear accelerations, analyzing nutational vibrations imposed on precession
06 p0927 A69-17688
- Equilibria of orbiting gyrostat satellite with internal angular momenta along principal axes
07 p1227 A69-18336
- Steady state motions stability of gyroscope mounted on satellite in gravitational orbit
07 p1137 A69-19679
- Collection of papers on designing components of gyroscopic systems covering moment sensors, floating devices, bearings, etc
09 p1497 A69-22101
- Magnetic masses of differentiating or integrating floating gyroscope effect on gyro moment sensor performance, examining utilization of multipole permanent magnet
09 p1497 A69-22102
- Operational errors of floating gyroscopes with hydrostatic unloading of bearings, establishing eccentricity tolerances, axes misalignment and temperature field nonuniformity
09 p1497 A69-22103
- Centering force and initial rigidity of magnetically suspended bearings of integrating floating gyroscope with allowance for mutual inductance of exciting coils
09 p1497 A69-22104
- Rational shape selection for magnetoconductors of centering elements of magnetically suspended bearings, studying effects on initial rigidity
09 p1497 A69-22105
- Earth rotation and aircraft speed effects on vertical gyroscopes during banking, obtaining formulas for gyro errors
09 p1498 A69-22107
- Kinematics of vertical gyroscope mounted in additional servo frame, determining kinematic errors due to rotor axis deviation
09 p1498 A69-22108
- High sensitivity gyroscopic HF angular acceleration sensor using special differentiator, obtaining motion equations and dynamic response
09 p1498 A69-22109
- Drift rate of gyroscopic devices in space based on kinematic theorem, stressing free gyroscope subjected to harmonically varying moment
09 p1498 A69-22111
- Biaxial gyrostabilizers mounting on rocking base, deriving expressions for constant components of stabilizer precession rate
09 p1498 A69-22112
- Stabilized gyroscope platform internal dynamics analysis, outlining optimal orientation for full compensation of cross couplings
09 p1499 A69-22240
- Vibrating momentum exchange device /VMED/ in single axis configuration as competitor for inertia wheel or twin gyro
09 p1538 A69-22435
- Azimuthal drift of rotor axis of directional gyroscope mounted on sloping base, showing vertical component responsibility via truncated equations of motion
09 p1502 A69-22702
- Gyrorotor center axial displacements due to axial load, noting equal load distribution between bearings with resilient cover plates
09 p1502 A69-22703
- Gyromotor flanges axial rigidity measuring methods based on axial deflection of flange or natural frequency of oscillating system
09 p1513 A69-22704
- Tumbling motion for testing gyroscopic devices quality
10 p1689 A69-22927
- Synchronous vibration absorbers using gyroscopic systems, noting antiresonance with Perissogyro [ASME PAPER 69-VIBR-39]
10 p1807 A69-24177
- Dynamics of gyroscopic synchronous servo system intended for remote measurement of spatial orientation coordinates of sensor moving element
11 p1881 A69-24558
- Directional gyroscope accuracy increased by self adaptive systems, based on precession theory and drift amplitude dependence
11 p1881 A69-24559
- Gyroscopes orientation influence on dynamic drift of triaxial power gyrostabilizer on rocking platform, noting optimum orientations
11 p1881 A69-24560
- Constant velocity moving object influence on indications of vertical gyroscope having electromagnetic compensation with residual imbalance of sensor element
11 p1881 A69-24561
- Image motion trajectory in rotating angular mirror having converging reflections from two surfaces, using precession theory of gyroscopes
11 p1881 A69-24562
- Stability of uniform rotations of gyrostat with fixed point in potential force field, considering Routh rule
11 p1918 A69-24786
- Motion of heavy body with gyroscope, using coordinate system to reduce problem to linear second order differential equation
11 p1920 A69-25746
- Inertial navigation system sensors including one and two axis, laser, vibratory, gyroflex and free rotor gyros
12 p2078 A69-25874
- Directional gyroscope with interframe correlation, discussing errors during object pitching and banking
14 p2446 A69-28923
- Inertial navigation system theory that uses increased numbers of newtonometers/force measuring devices/ in place of gyroscopic sensitive elements
16 p2791 A69-32283
- Rotor hazards in rotational behavior of gravity stabilized satellites, describing gyrostat applications
17 p3048 A69-33233
- Gyroscopic apparent rate meters generating steering moments in inertial navigation systems for determining moving object position and course
18 p3134 A69-34556
- Drift of two connected gyroscopes, discussing equations of motion assuming unperturbed rotation and weightlessness
18 p3135 A69-34561
- Dynamic performance accuracy of astatic gyroscope with three degrees of freedom improved by inner gimbal mass increase
19 p3308 A69-35825
- Mathematical basis for inertial vertical gyro development, considering Schuler conditions fulfillment with integral position correction
19 p3311 A69-36193
- Gyroscopic system behavior analyzed for steady state operation following transient period
21 p3723 A69-38832
- Envelope plotting of nutational vibrations of astatic gyroscope under influence of dissipative forces, noting quasi-elastic model
21 p3723 A69-38889
- Hydrodynamic conical and spherical spiral grooved grease bearings replacement of gyro ball bearings for extended space missions [AIAA PAPER 69-836]
21 p3732 A69-39367
- Gyro drift rate mathematical modeling based on stationary and nonstationary time series analysis techniques with random process reduction to white noise residuals [AIAA PAPER 69-838]
21 p3761 A69-39369
- Single degree of freedom gyroscope design factors applicable to strapdown guidance system, discussing torque-to-balance loop, multiple pulse bursting and error sources [AIAA PAPER 69-848]
21 p3762 A69-39378
- Mathematical formulation and error analysis of two rotor gyroorbit used in plotting orbital system of satellite coordinates
21 p3765 A69-39636
- Probability characteristics of total error in vertical gyroscope evaluated from component errors along suspension axes
22 p3946 A69-40251
- HF vibrations effect on motion of gyroscopic linear acceleration integrator, showing additional error in flight vehicle acceleration measurements
22 p3946 A69-40253

GYROSCOPIC COUPLING

Autometric gyro for satellite general relativity experiments, particularly earth orbit measurement of Lense-Thirring precession 23 p4162 A69-41543

Astatic gyro motion with horizontal rotor axis, defining suspension error with allowance for external force moments 24 p4317 A69-43707

GYROSCOPIC COUPLING

Gyrostatic moments effects on critical angular velocities of varying and constant cross section rigidly and elastically supported hinged rotors 09 p1567 A69-21384

Dynamics of gyroscope having flexible axis under gravitational force and elastic coupling reactions, deriving motion equations, precessions angular velocities, etc 14 p2445 A69-28798

Coupled gyroscopic systems two parameter stabilization problem analyzed for steady state characteristics by iterative method 21 p3723 A69-38829

Harmonic linearization for analyzing dry friction effect on gyroscope stability with free play in mechanical couplings, showing effective damping of natural oscillations 23 p4163 A69-41554

GYROSCOPIC DRIFT

U GYROSCOPES

GYROSCOPIC PENDULUMS

Schuler gyroscopic pendulum, noting magnitude requirement for gravitational field used in inertial navigation 02 p0248 A69-11593

Ballistic deviations of gyropendulum vertical damped by astatic gyroscope 06 p0927 A69-17687

Hydropendulum bearing linear horizontal vibration effect on vertex vibration, analyzing zero initial phase using precession theory 10 p1697 A69-24086

Vibrarotor gyroscope operated as rate gyro for simultaneously indicating two components of angular velocity by amplitude and phase of periodic output signal 18 p3139 A69-35299

Motion analysis of symmetrical physical pendulum having mobile fulcrum for geocentric vertical indicator possibility 21 p3727 A69-39830

GYROSCOPIC STABILITY

Optimal stabilization of free gyrostats using duration of transient processes and functionals of fuel and power requirements as criteria 01 p0079 A69-10261

Dynamically symmetric gyrostat steady motion stability in relation to satellite motion 01 p0163 A69-11301

Error reduction in initial azimuth alignment and azimuth and level axis gyro drifts in long range air transport gyro accelerometer inertial systems 02 p0278 A69-12361

Gyroscopically induced vibrational response of rectangular plates and membranes, determining spin and precession effects on natural frequencies 02 p0347 A69-12519

Mathematical modeling of gyro drift rate in inertial navigation based on stationary and nonstationary time series analysis 03 p0463 A69-13213

Equilibrium orientations of orbiting gyrostats, giving spectrum of solutions for bodies of varied shape and internal rotor angular momentum 03 p0522 A69-14246

Invariance of stabilized coordinates in power gyro stabilizers, using matrix equivalent of gyroscopic moments acting on platform 04 p0597 A69-14602

Optimal compensating loop in stabilization circuit of uniaxial gyro stabilizer 04 p0597 A69-14604

Dry friction stabilizing effect on motion of astatic gyroscope with quasi-elastic compensation 04 p0597 A69-14605

Asymptotic stability of gyroscopic systems equilibria with partial dissipation used for motion stability analysis 04 p0631 A69-15537

Equivalence principle application to gyroscope motion in uniform gravitational field to obtain precessional angular velocity 05 p0764 A69-16367

Spherical gyroscope servosystem probabilistic synthesis ensuring minimum dispersion of random drift 05 p0764 A69-16669

Motion stability of gyroscope in universal suspension with spring restraints and damper in gravitational field extended to include Newtonian central force field 05 p0765 A69-16684

Effect of small periodic moment applied to axis of inner gimbal on gyro drift when gyro is mounted on base fluctuating about two mutually perpendicular axes 06 p0924 A69-17183

Ballistic deviations of gyropendulum vertical damped by astatic gyroscope 06 p0927 A69-17687

Special and general relativity theories following Newtonian mechanics and gravitation theories, discussing metric tensor, sun oblateness and experiments with gyroscope spin axis precession 07 p1181 A69-18928

Magnetic masses of differentiating or integrating floating gyroscope effect on gyro moment sensor performance, examining utilization of multiple permanent magnet 09 p1497 A69-22102

Gyroscope error due to axial play of inner gimbal of Cardan mounting during base circular vibrations, noting axial clearance reduction 09 p1498 A69-22110

Drift rate of gyroscopic devices in space based on kinematic theorem, stressing free gyroscope subjected to harmonically varying moment 09 p1498 A69-22111

Single axis gyro stabilizer stability analysis allowing for dry friction in precession axis, noting asymptotic tendency of motions toward steady rotation 09 p1502 A69-22701

Azimuthal drift of rotor axis of directional gyroscope mounted on sloping base, showing vertical component responsibility via truncated equations of motion 09 p1502 A69-22702

Gyrorotor center axial displacements due to axial load, noting equal load distribution between bearings with resilient cover plates 09 p1502 A69-22703

Four gimbal Cardan suspension gyroscope kinematics for nonperpendicular arrangement 09 p1502 A69-22705

Optimization of autonomous system parameters, exemplifying by disturbed motion of gyroscope system 11 p1858 A69-24557

Rotational dynamics equations in linearized matrix form applied to satellite librations in circular orbit and gyroscope motion 11 p1970 A69-24608

Slender elastic rod stability under spatial finite deflection, analyzing critical load by using Kirchhoff analogy and gyroscope motion 11 p1970 A69-24609

Two rotor gyrocompass oscillations stability during finite time interval, deriving differential equation by suitable quadratic functions 11 p1886 A69-25089

Stability of stationary motion, analyzing gyroscopically unstabilizable systems and extension to continuous spectrum case 11 p1919 A69-25437

Dynamics of triaxial gyro stabilizer with additional rotor mounted on base, showing systematic drift 13 p2259 A69-27428

Gyroscope motion with unbalanced rotor in run-down mode, integrating equations for small oscillations 13 p2259 A69-27429

Triaxial gyro stabilizer systematic drifts during rocking at large platform displacement angles, analyzing drift direction and rate dependence 13 p2259 A69-27430

Nonstatic gyroscope nonlinear oscillations caused by swaying of synchronous gyromotor rotor 13 p2264 A69-28438

Instantaneous rotational impulse imparting steady motion of disk determined for coupled gyroscope 13 p2264 A69-28527

Dynamics of gyroscope having flexible axis under gravitational force and elastic coupling reactions, deriving motion equations, precessions angular velocities, etc 14 p2445 A69-28798

Ballistic deviations limits for aircraft vertical gyroscope taking into account aircraft vertical movements, using compensation in system 14 p2445 A69-28899

Dry friction effects on stability of single axis gyro stabilizer 14 p2445 A69-28922

Steady motion stability of satellite with gimbal suspended gyroscope in central gravitational field, showing no effect of satellite perturbations on gyro stability 14 p2530 A69-29481

Modeling nonstationary random processes using linear time-invariant difference equation, with applications to Kalman filtering and gyro drift 14 p2479 A69-29486

Gimbal torquing as function of gimbal structure response resulting in free gyro erection system, using any angular momentum at any initial starting angle 16 p2792 A69-32553

Earth quadrupole moment effects on precession of gyroscope in satellite in equatorial orbit 17 p2972 A69-33072

Cosmos 149 satellite stabilization system, discussing three axis orientation and pitch, yaw and roll stabilizations by aerodynamic and/or gyroscopic moments 17 p3047 A69-33226

Rotational equations of motion for two body spacecraft on common spin axis required for simulated gravity environment or gyroscopic stability augmentation 17 p3047 A69-33227

Gyro controlled rigid rotor dynamic stability studied for stoppable rotor operation, developing analytical expressions for determining stability boundary of constant and rotor speed gyros [AHS PAPER 343] 17 p2899 A69-33508

Gyrocompassing precision problems related to gyro drift, input axis deviation and base motion compensation, describing inertial navigation platform alignment to true north 17 p2977 A69-34081

Rotary motion stability of axisymmetric solid body or gyroscope suspended on string and containing ellipsoidal cavity filled with liquid 18 p3135 A69-34558

Boundary layer theory application to dynamics of gyroscope in gimbal suspension, defining nutational and precessional motion 18 p3135 A69-34559

Casing bearings dry friction force moment effect on double rotor gyrocompass sensor motion, showing diminished device accuracy at high latitudes 18 p3135 A69-34560

Drift of two connected gyroscopes, discussing equations of motion assuming unperturbed rotation and weightlessness 18 p3135 A69-34561

Steady motion stability of satellite gyroscope in Cardan suspension traveling along circular orbit in Newtonian central force field 18 p3135 A69-34585

Mean drift rates of single and two rotor gyroscopic linear acceleration integrators mounted on irregularly rocking base 18 p3135 A69-34586

Optimal asymptotic stabilization of gyrostat relative equilibrium, determining norm constraints for application to global gyrostat attitude control 18 p3210 A69-35145

Accuracy improvement of method of averages applied to equations of small motions and disturbances of two rotor gyrocompass on ship performing circular maneuvers 18 p3139 A69-35378

Asynchronous gyrostat postimpact drift direction found orthogonal with respect to initial impulse by averaging method 19 p3311 A69-36192

Airborne astatic vertical gyro motion found dependent on aircraft motion along trajectory 19 p3311 A69-36194

Triaxial static gyro stabilizer drifts, assuming perturbing moment steady centered random force applied along stabilizing gimbal axis 19 p3311 A69-36195

Gyrostat satellite equilibrium positions in circular equatorial orbit under action of gravitational magnetic and aerodynamic moments based on gyro stabilized satellite equations of motion 19 p3432 A69-36620

Gyroscopic platforms automatic stability relative to inertial reference system, considering functional equations and error computation 21 p3760 A69-38734

Coupled gyroscopic systems two parameter stabilization problem analyzed for steady state characteristics by iterative method 21 p3723 A69-38829

Steady motions stability of gyroscope in Cardan suspension, deriving equations of motions with rectangular coordinate system 21 p3723 A69-38851

Gyro drift rate mathematical modeling based on stationary and nonstationary time series analysis techniques with random process reduction to white noise residuals
[AIAA PAPER 69-838] 21 p3761 A69-39369

Spacecraft attitude acquisition/reorientation and stabilization controller design implemented by control moment gyro, proposing control algorithm using control actuator nonlinearity
21 p3826 A69-39641

Attitude stability of orbiting vehicle containing gyrost, discussing asymptotic stability
22 p4037 A69-40555

Gyroscopic motion with center of mass displaced along suspension axes and kinetic moment varying as power law under linear accelerations
23 p4163 A69-41552

Accelerated motion influence on onboard vertical gyro with design based on free astatic gyro with electromagnetic compensation
23 p4163 A69-41553

Harmonic linearization for analyzing dry friction effect on gyroscope stability with free play in mechanical couplings, showing effective damping of natural oscillations
23 p4163 A69-41554

Optimal control parameters for gyroscopic devices with constrained phase coordinates obtained on analog computer by introducing equivalent phase coordinates system
24 p4317 A69-43708

GYROSTABILIZERS

Invariance principle application in gyrostabilizer systems, noting effect of external disturbances and system noise
04 p0597 A69-14603

Optimal compensating loop in stabilization circuit of uniaxial gyrostabilizer
04 p0597 A69-14604

Biaxial gyrostabilizers mounting on rocking base, deriving expressions for constant components of stabilizer precession rate
09 p1498 A69-22112

Single axis gyrostabilizer stability analysis allowing for dry friction in precession axis, noting asymptotic tendency of motions toward steady rotation
09 p1502 A69-22701

Gyroscopes orientation influence on dynamic drift of triaxial power gyrostabilizer on rocking platform, noting optimum orientations
11 p1881 A69-24560

Gyrostabilized satellite steady state motions in Newtonian force field having displaced satellite center of mass orbital plane relative to center of attraction
12 p2173 A69-25885

Dynamics of triaxial gyrostabilizer with additional rotor mounted on base, showing systematic drift
13 p2259 A69-27428

Triaxial gyrostabilizer systematic drifts during rocking at large platform displacement angles, analyzing drift direction and rate dependence
13 p2259 A69-27430

Spacecraft attitude control and stabilization by three degree of freedom control moment gyro with controllable gyro spin angular velocity
13 p2355 A69-27445

Dry friction effects on stability of single axis gyrostabilizer
14 p2445 A69-28922

Power gyrostabilizer kinematic structure synthesis, applying matrix methods to design variables
14 p2446 A69-28924

Soviet monograph on liquid rocket as controlled plant covering rocket bodies, liquids motion stabilization and gyrosystem positioning
18 p3206 A69-34333

Momentum control system for satellite maneuvering and pointing in pitch and roll developed by modifying existing libration damping gyrostabilizer
18 p3207 A69-34684

Triaxial static gyrostabilizer drifts, assuming perturbing moment steady centered random force applied along stabilizing gimbal axis
19 p3311 A69-36195

Gyrostabilized satellite equilibrium positions in circular equatorial orbit under action of gravitational magnetic and aerodynamic moments based on gyrostabilized satellite equations of motion
19 p3432 A69-36620

Gyroplatform to stabilize gravimetric equipment on aircraft, noting channel stabilization by electrohydraulic servomechanism
21 p3723 A69-38885

Harmonic linearization for analyzing dry friction effect on gyroscope stability with free play in mechanical

couplings, showing effective damping of natural oscillations
23 p4163 A69-41554

GYROSTATS
U GYROSCOPES

GYROTROPISM

Light wave propagation in gyrotropic crystals, examining laser frequency shift circularly polarized by modulating field
03 p0436 A69-13037

Electromagnetic wave passage through plane gyrotropic layer of magnetized plasma, analyzing polarization and energy transfer
03 p0397 A69-13709

Gyrotropically filled waveguides propagation parameters calculation by variational method
05 p0718 A69-15648

Excitation of plane plasma layer in magnetic field perpendicular to wave vector of excitation wave in gyrotropic waveguide
11 p1927 A69-24916

Thermal radiation polarization in anisotropic and gyrotropic media described by Hermitian permittivity tensor, noting linearity
15 p2653 A69-30940

Gyrotropically filled waveguides propagation parameters calculation by variational method
16 p2754 A69-32505

Radio wave propagation in homogeneous turbulent gyrotropic medium, presenting solution for fluctuations in direction of wave scattering by geometrical optics approximation
17 p2927 A69-33861

Biquadratic plane wave dispersion relation for gyrotropic waveguides with dielectric and magnetic properties, discussing associated quartic equation for refractivity
21 p3675 A69-39285

LF hydromagnetic waves propagation along geomagnetic field lines in gyrotropic ionosphere model taking Hall effect into account
23 p4157 A69-41864

H

H ALPHA LINE

H alpha emission symmetrical spatial distribution of night airglow observed with high transmission diffraction spectrographs
01 p0062 A69-10128

Hydrogen alpha line strength in 951 O, B and early A stars from narrow band photoelectric measurements for stellar luminosity
03 p0511 A69-13435

Dynamic H alpha phenomena in projection on solar disk for simultaneously appearing flare and eruptive prominence on January 29, 1968
03 p0516 A69-14043

Instrument profile of birefringent Lyot filter for H alpha line determined from photographic spectra with grating spectrograph
04 p0664 A69-15524

Bright streaks in H alpha disk chromosphere, noting predominantly horizontal loop structures
04 p0664 A69-15525

High resolution H alpha line photographs of solar chromosphere, showing superpenumbra-like dark fibrils around isolated sunspots
04 p0664 A69-15526

Radio bursts at 3.3 mm and H alpha emission during flares, proposing thermal enhancement
04 p0650 A69-15527

Spectrographic H alpha observations indicating effects of rotary mass motion in flares and prominences
06 p0994 A69-17434

Solar moustaches H alpha profiles spectroscopic studies indicating near symmetry
06 p0994 A69-17435

Solar prominence structures observed in H alpha emission, determining radial velocities as function of distance from limb
06 p0994 A69-17436

Jovian limb H alpha line due to auroral emission obtained from high dispersion spectra with long light path through upper atmosphere
07 p1214 A69-18614

Absolute isophotometry of hydrogen alpha photographs of bright galactic H II regions, attributing difference between theoretical and observed ratio to in-

terstellar absorption
07 p1217 A69-19231

Chromospheric velocity field temporal characteristics in quiet region of sun, determining power spectra of Doppler shifts of H alpha spectra
07 p1217 A69-19240

Three dimensional information pictures of chromospheric alpha H line using special camera attached to solar telescope diffraction grating spectrograph
07 p1217 A69-19241

M82 galaxy as Seyfert-like galaxy seen edge-on, using radio and optical data showing H alpha emission collisionally excited, discussing circular polarization
08 p1383 A69-20051

Galactic H 56 alpha recombination radio line observation in Omega Nebula in millimeter band with radio telescope, obtaining electron temperature
08 p1397 A69-20771

Electron temperature of Orion Nebula at 6750 K from intensities of hydrogen n alpha lines, discussing Stark broadening
08 p1398 A69-20776

Spectrophotometry of relics of supernovae, determining H alpha and N II lines intensities radial velocities and velocity dispersion
09 p1587 A69-21357

H alpha emission line in nucleus of Virgo A radio galaxy observed on spectrograph, estimating gas electron density and mass
09 p1588 A69-21360

Luminescence spectra of molecular gases excited by fast electrons in infrared spectral region, noting H alpha line
09 p1590 A69-21382

Hydrogen alpha emission nebulae catalog in western half of Cygnus X region, obtaining interstellar absorption from nebular distances determination
09 p1596 A69-22053

Solar X ray bursts observed by proportional counter on IMP-F satellite to correlate optical H alpha flares and radio bursts
09 p1582 A69-22746

Solid hydrogen mantle condensation accounting for lack of detectable alpha hydrogen in star clusters and OB associations
10 p1776 A69-23214

Alpha hydrogen plage 20934/McMath no. 8362/ associated with July 1966 proton flare development and configuration along sunspot group axis
10 p1762 A69-23728

H alpha, H beta and D sub 3 /helium/ emission photographs of active prominence of July 9, 1966 using monochromatic filters for characteristic emissions from hydrogen and helium
10 p1764 A69-23738

Solar west limb activity observations in H alpha line, noting July 9, 1966 loop system and July 11, 1966 twisted eruptive prominence
10 p1764 A69-23741

H alpha line photograph in M 82 spectra, giving equivalent radiating area and total ionized hydrogen mass
12 p2171 A69-27067

Ionized hydrogen regions in NGC 4449 from H alpha photography through narrow band interference filter, obtaining radial velocities
13 p2347 A69-27714

H II alpha and beta radio recombination lines strengths predicted, noting role of calculations of hydrogen energy levels non-LTE populations
14 p2517 A69-29088

H alpha line emission preceding auroral breakup by data analysis of Antarctica Meinel-type patrol spectrograph, noting magnetic activity role
14 p2441 A69-29386

Solar rotation measured as function of latitude using Doppler compensator with magnetograph, noting daily rotation rate difference in H alpha and metallic lines
14 p2528 A69-29974

Excitation sources distribution in chromosphere from observed H alpha line contour, considering resonant scattering and internal excitation
15 p2683 A69-30509

Filamentary nebula IC 443 observation by Fabry-Perot etalon with image converter, determining radial, expansion velocities and H alpha line half width
15 p2686 A69-30538

Pure hydrogen stellar atmosphere nonLTE models, calculating surface temperature rise due to H alpha line effect on continuum energy balance
15 p2693 A69-30777

Magellanic-like galaxy NGC 4631 observed in H

H BETA LINE

alpha light through narrow band interference filter, detecting and cataloging 88 H II regions
16 p2854 A69-31647

Balmer line H alpha emission and absorption coefficients measured with hydrogen plasma generated in high current low voltage free burning arc
16 p2822 A69-32040

H alpha/D3 intensity ratio variations in peripheral regions of prominences may be due to dynamic conditions of material emitting radiations
17 p3029 A69-33051

Spectrophotometry of relics of supernovae, determining H alpha and N II lines intensities radial velocities and velocity dispersion
18 p3197 A69-34747

H alpha emission line in nucleus of Virgo A radio galaxy observed on spectrograph, estimating gas electron density and mass
18 p3197 A69-34750

Luminescence spectra of molecular gases excited by fast electrons in IR spectral region, noting H alpha line
18 p3176 A69-34770

Balmer alpha and Lyman beta intensities for multiple scattering calculated for hydrogen geocorona models by radiative transfer equations, discussing radiation transport through earth hydrogen atoms
18 p3128 A69-34943

Resonance effects between H levels by induced electric dipole transitions, using spatially periodic potential barriers
18 p3179 A69-35488

Proton and electron auroral ovals, deriving H alpha intensity and frequency distributions as function of geomagnetic latitude and time from patrol spectrograms in Canada
19 p3302 A69-35993

M8 electron temperature and internal kinematics from photoelectric Fabry-Perot spectrometric recording of H alpha line profiles and N II
19 p3424 A69-36334

H alpha auroral activity on Jupiter isolated by using Fabry-Perot etalons, showing photograph reproductions
20 p3598 A69-37414

H alpha filtergrams and spectra of solar corona arch filament systems indicating downward and upward motions produced by magnetic field
20 p3588 A69-37543

H alpha line for emission nebulae analyzed by Fabry-Perot etalon, noting Doppler profile
20 p3607 A69-38039

Upper atmospheric H and He observations, showing Lyman alpha, H alpha measurements and H abundance values relative to Kockarts-Nicolet model
21 p3714 A69-38529

Core profiles of H alpha, H beta, H and K from spectrograms of plagues
22 p4010 A69-39993

Mean intensity profiles of photospheric H alpha radiation illuminating solar prominences moving at different heights
22 p4011 A69-39995

Optical and mechanical systems of Wrocław Observatory Lyot type coronagraph for prominence observations in H alpha line
22 p3943 A69-39999

Sunspot position in H alpha core relative to continuum, discussing height differences between H alpha core and continuum levels
22 p4019 A69-40291

Total solar eclipse of 5 February 1962 observed for spectrophotometry of flash spectrum, finding abnormal intensity gradients of H alpha and D3 lines
24 p4388 A69-43636

H BETA LINE

Hydrogen line profiles in various early stars compared with profiles predicted from model atmosphere calculations for rotating and nonrotating early stars
01 p0154 A69-10876

Hydrogen beta emission profiles for pole-on type Be stars, measuring stellar rotational velocity by Huug-Struve method
09 p1596 A69-22052

H alpha, H beta and D sub 3 /helium/ emission photographs of active prominence of July 9, 1966 using monochromatic filters for characteristic emissions from hydrogen and helium
10 p1764 A69-23738

Auroral H beta intensities determined from photographs by image intensifier, describing equipment and data reduction method
10 p1684 A69-23824

H beta emission line in night sky spectrum measured with gas pressure scanned Fabry-Perot interferometer in Italian alps
12 p2074 A69-26963

H II alpha and beta radio recombination lines strengths predicted, noting role of calculations of hydrogen energy levels non-LTE populations
14 p2517 A69-29088

Polychromator measurement of hydrogen plasma electron density produced by normal ionizing shock wave, using Stark broadening study of H beta line
14 p2494 A69-29767

H beta line for measuring radial temperature distribution in cylindrical hydrogen arc at one atm and to 150 A current in high temperature range
15 p2671 A69-31101

Photometric rocket measurements in hydrogen auroras, finding vertical H beta emission profile estimate of proton energy spectrum for H beta production cross section
15 p2598 A69-31307

Four color and H beta photometry of stars in Coma and Ursa Major clusters compared to standard relations for Hyades Cluster
16 p2860 A69-32234

Westward traveling auroral surge associated with electron flux during absence of H beta emission
18 p3130 A69-35189

Core profiles of H alpha, H beta, H and K from spectrograms of plagues
22 p4010 A69-39993

H beta production in hydrogen aurora measured during rocket flight, obtaining proton energy spectrum
24 p4309 A69-43170

H GAMMA LINE

Stark broadened H gamma profile, considering effect of strong collisions in electron perturbation and electron impact broadening of lower levels
20 p3579 A69-37305

Stark broadening of H-gamma for electron density measurement in plasma, noting temperature range
22 p3985 A69-40664

H LINES

Paschen series line contours for hydrogen in solar spectrum plotted from IR spectrophotometric data
01 p0148 A69-10126

Galactic neutral hydrogen structure in region of Cygnus observed with parabolic antenna and frequency-switched radiometer
08 p1388 A69-20243

Stark broadening of Balmer H alpha, H beta, H gamma and H delta lines in plasma region in strong magnetic fields
09 p1542 A69-22248

Degeneracy of hydrogenic states to sum S-matrix in Stark broadening calculations
09 p1543 A69-22405

Hydrogen balmer lines broadening by Stark and Doppler effects, finding prominences and chromosphere electron concentrations
11 p1955 A69-24389

Ionized gas cloud eruption from galactic nucleus deduced from observed hydrogen line at 5.1 cm
12 p2171 A69-27068

Hydrogen to He ratio effect on stellar atmospheric structure, considering flux relations, UVB color indices, H line profiles, electron and gas pressures
13 p2339 A69-27562

Radio emission from high level transitions in hydrogen calculated by superposing emission lines on background continuum, using Gaunt factor for free-free emission
13 p2327 A69-27596

Hydrogen content in Ia supergiant spectra of type B, noting lack of Stark wings of Balmer lines
13 p2348 A69-27722

Magnetic A star HD 152107 anomalous intensification of Balmer series H lines observed by spectrograms
13 p2352 A69-27873

Excited hydrogen RF spectral lines from nebula NGC 6618, calculating frequency for transitions by Balmer formula
13 p2353 A69-28433

Interstellar gas radio and optical spectral lines of neutral H compared with Ca and neutral Na, discussing critically low velocity gas distribution
14 p2519 A69-29135

21 cm line emission surveyed for spatial distribution of random velocities of neutral hydrogen in solar neighborhood
14 p2520 A69-29371

Excited hydrogen radio lines observations, analyzing neutral and excited hydrogen distribution in galaxies
15 p2682 A69-30502

Radio source W 43 distance determined from analyzing neutral H line profile and radial velocity in excited H line 104 alpha
15 p2687 A69-30543

Photometric calibration correction for B-V/ and U-B/ colors taking into account hydrogen line blocking
15 p2694 A69-30786

Spectroscopic observations of HD 4174 star by superimposition of emission and M-I absorption spectra, revealing intensity and radial velocity variations
16 p2858 A69-32214

He I/1.083 mu/ and O I/5577 A/ absolute brightness measured in sunlit aurora for various shadow heights of solar radiation, considering primary electron precipitation
16 p2780 A69-32311

Hydrogen line profiles, equivalent widths and electron densities for peculiar alpha 2 CVn and gamma Lyr stars
16 p2864 A69-32594

Ca 2 resonance line profiles in large disk flares and in surrounding plage, discussing H and K line behavior
17 p3023 A69-33054

Effective temperature and gravity values for Mn Ap stars by comparing spectrum scans and H line profiles with predictions from atmospheric models
17 p3038 A69-33724

Balmer line spectrum formation in extended atmospheres of Be and shell stars, noting influence of angle of inclination to observer
18 p3204 A69-35349

Photodestruction rate of H molecules by absorption of Lyman or Weber band radiation in interstellar space calculated at various distances from early stars
18 p3204 A69-35351

Chromospheric inhomogeneities rapid changing properties observable in H and K lines above sunspot umbrae
18 p3204 A69-35389

High velocity interstellar gas in H I and H II regions, emphasizing observations of neutral atomic hydrogen in and far from galactic plane
19 p3402 A69-35962

Monochromatic energy flux measurement in H and forbidden lines of planetary nebulae indicating ionization level and optical depth
19 p3423 A69-36223

H II regions radial velocities ellipsoidal distribution in M 33 explained as distribution with minor axis in direction of rotation
21 p3797 A69-38538

Atomic hydrogen departures from LTE computed for models of B star atmospheres, assuming detailed balance in hydrogen lines
24 p4376 A69-42665

Milky Way hydrogen line survey with Parkes telescope, giving velocity-longitude control maps and tabulated data covering galactic equator
24 p4383 A69-42961

Galactic X ray flux from H I region low energy cosmic ray nuclei, studying electron capture effects on line intensities
24 p4367 A69-43048

Hydrogen balmer lines broadening by Stark and Doppler effects, finding prominences and chromosphere electron concentrations
24 p4390 A69-43779

H WAVES

Metal flanges position effect on radiation patterns of H-plane sectoral horn radiators
08 p1285 A69-20554

Wave-mode converter with feed for omnidirectional antenna excitation, discussing H to E wave conversion, waveguides, emitter, etc
11 p1854 A69-25616

Wave reflections due to rotationally symmetrical jump in circular waveguide cross section, using orthogonal expansion to solve resulting boundary value problem
11 p1855 A69-25622

Waveguide cross connection of right-angled waveguides to determine reflection and transmission factors for incidence of H waves
11 p1855 A69-25623

Multiple strip H guide field distribution and low loss wave mode analysis, obtaining approximate thin layer equations
22 p3917 A69-41254

Average total losses of H waves transmitted over waveguide communication lines by nanosecond pulse sequences
23 p4123 A69-41949

H- 34 HELICOPTER

U CH- 34 HELICOPTER

H- 51 HELICOPTER

U XH-51 HELICOPTER

H- 56 HELICOPTER

AH-56A Cheyenne integrated avionics, armament and fire control system for precise weapons delivery and navigation
[AHS PAPER 312] 17 p2903 A69-33542

AH-56A helicopter manual and automatic terrain following and manual terrain avoidance systems, discussing nap-of-earth flight, design and simulation
[AHS PAPER 311] 17 p3002 A69-33544

C-5A transport aircraft airframes manufacture, discussing Lockheed profits, contract disputes and Cheyenne helicopter contract cancellation
20 p3640 A69-37355

HABITABILITY

Human habitation conditions on moon from viewpoint of solar and lunar radiation, vacuum and gravitation effects including solar energy utilization
23 p4111 A69-42213

HABITUATION [LEARNING]

Stability and habituation of nonspecific galvanic skin responses during light and sound stimulation periods in medical students
03 p0380 A69-13462

HADRONS

Three dimensional Monte Carlo calculations for hadronic component of extensive air showers using semiempirical model high energy nuclear interactions
15 p2678 A69-31482

HAFNium

Lanthanum and hafnium effect on transition and recrystallization temperatures of tungsten and tungsten base alloys
05 p0782 A69-16797

Hafnium microstructure and impurity concentrations before and after electron beam melting
23 p4178 A69-42361

HAFNium ALLOYS

Hard metals and materials containing NbC and HfC, noting X ray studies of pseudoternary and pseudoternary systems
14 p2464 A69-29323

Binary Nb-Hf system phase diagram below solidus line noting lattice parameters and oxygen and nitrogen effects on phase equilibrium boundaries
18 p3157 A69-35247

Ti sub 3, Rh sub 5 and Hf sub 3, Rh sub 5 existence and isomorphism confirmed by crystallographic and X ray methods
19 p3343 A69-35920

HAFNium CARBIDES

Hard metals and materials containing NbC and HfC, noting X ray studies of pseudoternary and pseudoternary systems
14 p2464 A69-29323

Integral normal emissivity of Ta and Hf carbides at temperatures from 1300 to 3000 K measured by radiation method in vacuum
15 p2640 A69-30984

HAIl

Origin and mineralogical composition of stones associated with 1824 stone hail near Sterlitamak
01 p0160 A69-11387

HAIlSTONES

U HAIl

HAIf CONES

Transonic dynamic stability of free flight half angle cones in wind tunnel for high drag planetary entry vehicles, discussing Mars entry trajectories
[AIAA PAPER 69-105] 06 p01019 A69-18209

Free flight sharp cone drag measurements in rarefied hypersonic flow
13 p2199 A69-28244

Aerodynamic problems posed by hypersonic flight from Mach 3 to 20, considering relationship to half cone with flat base
16 p2867 A69-31761

HAIf LIFE

Excited atomic H state radiative mean life measurements using beam-foil excitation method
03 p0469 A69-12920

Mean life of D energy level in N IV, discussing Be I isoelectronic sequence
17 p3009 A69-34187

Mean lives of 1s super 2 2p super 2 super 1D level in F VI and O V measured by beam foil technique
17 p3009 A69-34188

Be 7 stability in galactic cosmic radiation, noting lifetime dependence on electron density around nucleus
18 p3189 A69-35482

Exponential decay and mean lives of lowest P levels in N V measured with beam foil source, noting agreement with theories taking configuration interaction into account
21 p3774 A69-38760

HAIf PLANES

Vertical, horizontal and rocking vibrations of body on surface of otherwise unloaded elastic half plane, estimating stiffness for coupled vibrations
[ASME PAPER 68-WA/APM-12] 04 p0668 A69-14393

Load diffusion from transverse tension bar into semiinfinite elastic sheet, considering line and area contact methods of stringer attachment
[ASME PAPER 68-WA/APM-15] 04 p0669 A69-14396

Ground influence on Helmholtz flow in presence of plate perpendicular to stream, reducing problem to mixed Volterra problem in complex half plane
04 p0590 A69-15221

Basic equations describing stress-strain state of anisotropic half planes and anisotropic planes with cuts
06 p1020 A69-16827

Electrical impedance of semiconductor supporting two waves contains entire complex transcendental function with complex parameter and infinity of zeros in left half z plane
07 p1196 A69-18268

Inhomogeneous half planes equilibrium bonded by elastic layer, noting tangential stresses at interfaces
09 p1611 A69-21482

Elastic isotropic half plane weakened by circular hole with concentrated force applied along hole contour, considering stress distribution
11 p1972 A69-24653

Stresses and displacements in half plane with edge crack given as eigenfunction expansions using Wiener-Hopf technique
11 p1987 A69-25438

Stresses in elastic half plane with bonded disk of same elastic properties, describing stress production by expansion of disk
13 p2363 A69-28132

Contact problem for half plane with elastic stiffener reduced to Prandtl integrodifferential equation, determining contact stresses
14 p2531 A69-28804

Stress-strain problem of piecewise-homogeneous plane with cut normal to interface line reduced to Wiener Hopf equation, obtaining solution for arbitrary boundary conditions
14 p2531 A69-28805

Electromagnetic wave diffraction in three dimensional space divided by dielectric orthogonal half planes/wedges/, using contact boundary value problem
21 p3673 A69-39012

Numerical solution by approximation of Wiener-Hopf-Fock equation for diffractions at finite or infinite number of equidistant half planes applied to open-end waveguides
22 p3901 A69-40950

HAIf SPACES

Steady state problem of convective heat transfer in half space with boundary conditions of third kind
01 p0174 A69-10103

Torsional oscillations of elastic half space set up by rigid circular disk examined by integral equation method
01 p0169 A69-10809

Small metallic sphere detection by electromagnetic induction method, emphasizing masking effect of resistive half space below scatterer
01 p0047 A69-10974

Electric field in plasma half space determined by longitudinal wave normal mode analysis, using BKG particle conserving collision model
01 p0134 A69-11287

Thermoviscoelasticity equation solution for class of dynamic problems, giving problem solution for half space with arbitrary temperature field boundary condition
02 p0336 A69-11554

Ground wave excited by dipole in conducting half space, discussing lateral wave character and optimum radiation angle
02 p0209 A69-12347

Cylindrical sound pulse propagation in homogeneous layer under inhomogeneous half space
04 p0630 A69-14531

Viscoelasticity effect on tensile stress in absorption layer for free surface uniaxial motion
04 p0676 A69-14705

Plane shear pressure wave propagation in elastic-plastic half space for various combined normal and shearing loadings
05 p0835 A69-15798

Axially symmetric torsion of finite elastic cylindrical rod partially bonded to elastic half space, discussing coupling between dual Dini series and integral equations
07 p1236 A69-19474

Charged body moving at subsonic velocity normally through stratified elastic half space composed of film on homogeneous half space
08 p1417 A69-20753

Reflection of plane waves from stress free flat surface of micropolar elastic half space, presenting reflection laws and amplitude ratios
15 p2714 A69-31147

Viscoelastic half space properties effect on self excited vibration boundaries determination
16 p2873 A69-32063

Half space applications regarding equation of transfer for planetary atmosphere
18 p3191 A69-34306

Plane wave propagation due to combined compressive and shear stresses in half space, assuming elastoplastic material
[ASME PAPER 69-APM-12] 18 p3213 A69-34388

Heat conduction in thin layer near boundary surface of solid by approximating one dimensional conduction in half space with allowance for curvature
20 p3633 A69-38213

Self similar solution to one dimensional isothermal ionized gas outflow from ionization front in half space filled with neutral gas exposed to quanta flux
21 p3771 A69-38997

Constant surface heating of half space with temperature dependent thermal conductivity
21 p3851 A69-39292

Wave propagation in dynamical theory of thermoelasticity, considering half space subject to step time strain, temperature and stress distributed over free surface
23 p4235 A69-42464

Sphere set in motion at constant velocity by impulsive force submerged in incompressible fluid in half space
24 p4298 A69-42585

HAIlIDES

NT ALKALI HALIDES
NT ALUMINUM CHLORIDES
NT AMMONIUM CHLORIDES
NT BERYLLIUM FLUORIDES
NT BORON CHLORIDES
NT BORON FLUORIDES
NT CALCIUM FLUORIDES
NT CARBON TETRACHLORIDE
NT CESIUM IODIDES
NT CHLORIDES
NT CHLORINE FLUORIDES
NT CHROMIUM BROMIDES
NT HYDROCHLORIC ACID
NT HYDROFLUORIC ACID
NT IRON CHLORIDES
NT LANTHANUM FLUORIDES
NT LITHIUM FLUORIDES
NT MAGNESIUM CHLORIDES
NT METAL HALIDES
NT NICKEL FLUORIDES
NT NITROGEN FLUORIDES
NT OXYFLUORIDES
NT OXYGEN FLUORIDES
NT POTASSIUM BROMIDES
NT POTASSIUM CHLORIDES
NT SILVER HALIDES
NT SILVER IODIDES
NT SODIUM CHLORIDES
NT SULFUR FLUORIDES
NT TITANIUM CHLORIDES
NT URANIUM FLUORIDES

Thermionic converters with chloride and fluoride vapor deposited tungsten emitters, comparing performance characteristics and stability
09 p1438 A69-21819

Titanium alloys stress corrosion cracking in presence of chloride, bromide and iodide under potentiostatic conditions, postulating electrochemical kinetic and mass transport model
19 p3351 A69-36901

HAIlITES

Black magnetite spherules electromagnetically separated from residue of Permian rock salt, determining content and properties of extraterrestrial material
12 p2154 A69-25821

HALL ACCELERATORS

- Coaxial Hall plasma accelerator, noting interaction between radial applied magnetic field and axial applied electric field 05 p0806 A69-16734
- Cusp magnetic field stabilizing superimposition on toroidal plasma discharge in polytron machine, noting role of Hall acceleration mechanism 06 p0965 A69-17514
- Low density Hall ion thruster with application to Van Allen probe and orbit-to-orbit transfer [AIAA PAPER 69-281] 09 p1562 A69-21229
- Coaxial electrodes with electric and magnetic fields to study instability in MPD arcs [AIAA PAPER 69-230] 09 p1563 A69-21231
- MPD plasma acceleration in West Germany, discussing Hall acceleration, electrodeless plasma acceleration by electromagnetic waves and space charge neutralized Hall ion thruster [AIAA PAPER 69-279] 09 p1564 A69-21238
- Hall type electromagnetic plasma accelerator, with thrust affected only by Lorentz forces in external magnetic field, compared to pure Hall accelerator 11 p1866 A69-25214
- HALL CURRENTS**
- U ELECTRIC CURRENT**
- HALL EFFECT**
- Hall effect in ferrites, determining classical and spontaneous Hall coefficients, electrical resistance, temperature effects and current carrier properties 01 p0135 A69-10185
- Stability of gravitating fluid layer of infinite extent but finite thickness including Hall effect 01 p0128 A69-10342
- Hall effect in unperturbed flow of fluids near thin profiles at infinity 01 p0132 A69-11133
- Many valley n-type Ge and Si semiconductors dissipative current breakdown effects, noting dependence on symmetry of valleys and phonon scattering pattern 02 p0298 A69-12098
- Characteristic time on motion of magnetic lines of force in medium with Hall effect 02 p0290 A69-12399
- Hall effect in semiconductors with polarons as majority carriers, noting variation with temperature of magnetic field dependence on Lorentz force 03 p0484 A69-13281
- Plasma gravitational stability problem with Hall effect, noting relevance to astrophysical systems 03 p0478 A69-13803
- Hall effect destabilization influence in Kelvin-Helmholtz problem for ideal plasma, noting instability growth rate 03 p0478 A69-13804
- CdS Hall coefficient, Hall mobility and magnetoresistance coefficient dependence on electric field, magnetic field and scattering mechanisms 03 p0490 A69-13945
- Hall mobility of photoelectrons in cadmium sulfide layers 03 p0491 A69-14055
- MHD generator two dimensional analysis for studying edge effect, taking into account Hall effect 03 p0480 A69-14099
- Resistivity and Hall mobility periodic change effect on probe measurements in semiconductors 04 p0642 A69-14534
- MHD channel flow temperature distributions with Hall effect, using formulation for momentum and energy equations 04 p0635 A69-14746
- Hydromagnetic analogs calculated for Rayleigh-Taylor problem with Hall effect, confirming introduction of plasma instabilities 04 p0637 A69-15050
- Evolutionarity of equations of MHD with Hall effect allowance for nondissipative plasma two dimensional flow 05 p0801 A69-15788
- Hall effect current influence on conductance of high current arcs 05 p0803 A69-15999
- Electrical properties of n-type Cd tin arsenide single crystals with impurity concentrations at various temperatures 05 p0809 A69-16375
- P-n junctions and device structures formed by ion implantation, using Hall effect and channeling techniques to evaluate implanted layer nature 06 p0974 A69-16862
- Neutron irradiation produced defects in p-type Si at 76 K, measuring Hall effect and electrical conductivity 06 p0975 A69-16868

Hall effect and magnetoresistance for compensated n-InP samples, discussing dependence on magnetic field 06 p0978 A69-16987

Hall effect and resistivity of n-type gallium arsenide phosphides doped with Te and Se 06 p0978 A69-16988

Temperature dependence of n-InSb Hall coefficient and resistivity, noting increase in conductivity with degree of compensation associated with electrical breakdown 06 p0978 A69-16990

Electrical resistance and Hall coefficient measurement in InAs-GaAs solid solutions system, giving temperature dependence of electron mobility 07 p1199 A69-18689

Impurity atoms effects on Cu diffusion and solubility in GaAs, determining Hall coefficient temperature dependence and conductivity 07 p1199 A69-19009

Magnetoelectric characteristics of inversion layers below gate region in transistors, noting Hall mobility 08 p1372 A69-20460

Hall current influence on plasma jet interaction with space periodic magnetic field created by system of coaxial coils with alternating current directions 08 p1370 A69-21017

Vapor deposition of high purity epitaxial layers of n-type gallium arsenide, noting resistivity and Hall coefficient measurements [ECS PAPER 62] 08 p1373 A69-21067

Hall effect and mass flow influence on MPD arc jet radial pressure profile calculated as function of pressure and magnetic field [AIAA PAPER 69-246] 09 p1562 A69-21226

Plasma acceleration by induced Hall currents, discussing Hall-to-current ratio maximum at critical magnetic field [AIAA PAPER 69-280] 09 p1562 A69-21228

N type surface layer in p type sample noting effect on Hall constant and relationship to temperature 09 p1555 A69-21472

Temperature dependence of conductivity and Hall constant of GaAs single crystals with nickel impurity, noting diode structure and I-V curve shapes 09 p1555 A69-21475

Nonlinearity of Hall voltage induced in plasma by external magnetic field under various assumptions 09 p1548 A69-21683

Electrical conductivity and Hall effect in thin evaporated bismuth films under vacuum using three point method in variable temperature cryostat 09 p1557 A69-21692

Near cathode magnetic field effect on instability in linear Hall current accelerators, using geometry of field extending from anode to cathode region [AIAA PAPER 69-381] 09 p1568 A69-21731

Carbides and silicides temperature coefficient of electrical resistivity and Hall constant plotted as function of metal carbides solid solutions concentration 09 p1523 A69-21740

Hall effect theory and devices, noting application to measurement of several physical quantities and sources of errors in devices 09 p1541 A69-22698

MHD flows in MHD generator channel under magnetic field, analyzing steady laminar flow during entry and Hall effect on conductivity temperature dependence 10 p1734 A69-23455

Turbulent plasma near stability limit in MHD generator with constant load coefficients, noting effective conductivity and effects of gas temperature 10 p1735 A69-23460

Linear nonequilibrium MHD generator operating at Mach 2 and Hall parameter of 3 using cesium seeded helium as working fluid 10 p1636 A69-23471

Large disk MHD generator operating at high Hall coefficient and driven by cesium seeded argon or molecular gases 10 p1637 A69-23473

MHD generators with segmented electrodes at high Hall parameters, noting electron density, conductivity and Hall field reduction factor 10 p1637 A69-23476

InAs thin film sensors using Hall effect to measure magnetic fields at cryogenic temperatures 10 p1696 A69-23717

Geomagnetic field directed hydromagnetic waves propagation in lower ionosphere, noting inhomogeneous conductivity, Hall effect and lines of forces role 10 p1687 A69-23926

Boundary layers influence on external electrical characteristics of MHD generator 11 p1824 A69-24221

Heat transfer in MHD parallel plate channel flow in entrance regions analyzed by Galerkin method, noting Hall current effect 11 p1923 A69-24290

Sb addition effect on electrical conductivity and Hall effect in PbTe single crystals over temperature range 11 p1939 A69-25706

Se activation energy dependence on crystals composition and Se concentration, based on Hall coefficient temperature dependence in gallium arsenic phosphides 13 p2317 A69-27875

Supplementary absorption and Hall effect temperature dependence in solid solutions of gallium arsenic phosphide 13 p2318 A69-27894

MOS transistor Hall voltage, mobility and constant verified by magnetoelectric measurements of Si p-inversion layer 13 p2323 A69-28331

N-type InSb single crystals with high dislocation density, investigating anisotropy of mobility, Hall effect and transverse and longitudinal magnetoresistance 14 p2503 A69-28734

Hall effect in semiconductors with polarons as majority carriers, noting variation with temperature of magnetic field dependence on Lorentz force 14 p2508 A69-29654

P-type zinc-tin-antimonide crystals electric conductivity, Hall coefficient and thermal EMF found similar to p-type diamond-like semiconductors properties 15 p2667 A69-30197

N type surface layer in p type sample noting effect on Hall constant and relationship to temperature 15 p2669 A69-30717

Temperature dependence of conductivity and Hall constant of GaAs single crystals with nickel impurity, noting diode structure and I-V curve shapes 15 p2669 A69-30720

Current distribution and Hall voltage in crossed fields discharge with split electrodes in nonequilibrium Ar and Cs plasmas 15 p2663 A69-30980

Hall current effect on thermal instability explaining oneself gravitating astronomical objects, discussing current effects on propagation modes 16 p2854 A69-31649

Hall effect and transverse voltages in type II superconductors in mixed state, considering cold rolled Nb-Zr alloys 16 p2827 A69-31827

Diagonal conducting wall /DCW/ MHD generator channel flows in formulation including Hall effect, electrode drop and electrode wall angle 16 p2736 A69-32172

InSb thin films prepared by flash evaporation, discussing Hall measurements at various temperatures and electron mobility dependence on film thickness 18 p3182 A69-34348

Evolutionarity of equations of MHD with Hall effect allowance for nondissipative plasma two dimensional flow 18 p3181 A69-35039

Hall mobility of photoelectrons in cadmium sulfide layers 18 p3182 A69-35048

Hot electron behavior in n-type InSb under magnetic fields at 4.2 and 1.7 K, plotting current-voltage and current-Hall voltage characteristics, etc 19 p3388 A69-36544

InSb instabilities and time dependence of transverse breakdown, performing Hall effect measurements on n-type InSb at 77 K 19 p3389 A69-36546

Conducting gas flow parameters in coaxial duct, considering magnetic nonuniformity, Hall currents and fields distortion near electrodes 19 p3381 A69-36772

Melting points, electrical conductivity, Hall constants, magnetic susceptibility, density, bending strength, microhardness and elastic modulus of zirconium nitride in homogeneity range 20 p3558 A69-37014

Hall coefficient and conductivity measured as function of temperature for liquid Au, Cu and Ag tellurides and liquid alloy systems Bi-Te and Ti-Te 20 p3584 A69-38024

Carbides and silicides temperature coefficient of electrical resistivity and Hall constant plotted as function of metal carbides solid solutions concentration 20 p3585 A69-38216

Semiconductor properties of indium telluride alloys, conductivity and Hall effect 21 p3779 A69-38580

S doped GaSb single crystals prepared by Crochral-ski method studied for temperature dependence of resistivity and Hall coefficient

21 p3781 A69-39048

Se activation energy dependence on crystals composition and Se concentration, based on Hall coefficient temperature dependence in gallium arsenic phosphides

21 p3782 A69-39141

Plasma instabilities in closed cycle MHD generator with gaseous working fluids, discussing effective Hall parameters

21 p3777 A69-39481

HF ion engine RIT 10, Kaufman ion engine ESKA, Hall effect ion engine HIT and MPD engine compared for state of development

[DGLR-69-021] 23 p4202 A69-41928

HALL GENERATORS

Book on Hall generators /magnetically controllable semiconductor elements/, discussing principles of operation, design, manufacture and applications

03 p0406 A69-13954

One dimensional analysis of stationary argon flow in linear Hall generator from continuity, momentum and energy equations, discussing electron heating and nonequilibrium ionization

10 p1736 A69-23465

Hall generator electrical characteristics, discussing plasma homogeneity, stability and shock tube priming

15 p2658 A69-30298

Hall generator for measuring mechanical displacements and vibrations of 10 A, describing operating principles and arrangements

17 p2971 A69-33022

Hall ion thruster prime propulsion system, considering low and high voltage mode in plasma source I-V characteristics

17 p3019 A69-33338

Hall generator DC brushless motors for aerospace use, discussing speed control and motor design

18 p3094 A69-35074

HALO PARACHUTING

U PARACHUTE DESCENT

HALOGEN COMPOUNDS

NT ALKALI HALIDES
NT ALUMINUM CHLORIDES
NT AMMONIUM CHLORIDES
NT AMMONIUM PERCHLORATES
NT BERYLLIUM FLUORIDES
NT BORON CHLORIDES
NT BORON FLUORIDES
NT BROMINE COMPOUNDS
NT CALCIUM FLUORIDES
NT CARBON TETRACHLORIDE
NT CESIUM IODIDES
NT CHLORATES
NT CHLORIDES
NT CHLORINE COMPOUNDS
NT CHLORINE FLUORIDES
NT CHLOROSILANES
NT CHROMIUM BROMIDES
NT CRYOLITE
NT DICHLORODIPHENYLTRICHLOROETHANE
NT FLUORINE ORGANIC COMPOUNDS
NT FLUORITE
NT FLUORO COMPOUNDS
NT FLUOROCARBONS
NT FLUOROXYHYDROCARBONS
NT HALIDES
NT HYDROCHLORIC ACID
NT HYDROFLUORIC ACID
NT HYDROXYLAMMONIUM PERCHLORATES
NT IODIDES
NT IODINE COMPOUNDS
NT IRON CHLORIDES
NT LANTHANUM FLUORIDES
NT LITHIUM FLUORIDES
NT MAGNESIUM CHLORIDES
NT MAGNESIUM PERCHLORATES
NT METAL HALIDES
NT NICKEL FLUORIDES
NT NITROGEN FLUORIDES
NT NITRONIUM PERCHLORATE
NT OXYFLUORIDES
NT OXYGEN FLUORIDES
NT PERCHLORATES
NT POLYTETRAFLUOROETHYLENE
NT POTASSIUM BROMIDES
NT POTASSIUM CHLORIDES
NT POTASSIUM PERCHLORATES
NT SILVER HALIDES
NT SILVER IODIDES
NT SODIUM CHLORIDES
NT SULFUR FLUORIDES
NT TITANIUM CHLORIDES
NT URANIUM FLUORIDES

Hydrogen bromide, HI and HCl effects on hydrogen-air mixtures flammability, discussing flame propagation inhibition efficiency

02 p0304 A69-12315

Halocarbon solvent for application of chlorosilane finish to heat cleaned glass fabric for reinforcement of plastic, noting relative humidity effect

08 p1341 A69-20513

Group 7A and group 8 elements alloying effect on Cr dislocation structure and mechanical properties, discussing ductile-brittle transition temperature and electronic theory

18 p3160 A69-35452

HALOGENATION

NT FLUORINATION

Flame inhibition with electron attachment observed using halogenated hydrocarbons

06 p1034 A69-17926

HALOGENS

NT BROMINE
NT CHLORINE
NT FLUORINE
NT IODINE
NT IODINE ISOTOPES

High repetition rate pulsed illuminator using electrodeless halogen discharge for rapid light extinction

04 p0599 A69-15021

Halogen concentrations in basaltic achondritic meteorites, discussing applications to rare gas and lunar surface studies

24 p4382 A69-42929

HALOPHILES

Cation concentration requirement of halophilic NADH dehydrogenase for stability and maximum activity

10 p1651 A69-23127

Salts and organic solvents effect on halophile Halobacterium cutirubrum catalase, noting enzyme activity inhibition by cation and anion

18 p3096 A69-35291

Flavoprotein/cytochrome b/559/ role as branch of Halobacterium electron transport in DPNH oxidase determined by salt dependence of reduced DPNH

20 p3484 A69-37101

HALOS

Element synthesis in stars of galactic halo as possible explanation for heavy elements presence in supermassive objects

07 p1219 A69-19296

Galactic halo chronology determination by positron component flux measurement in primary cosmic rays

08 p1386 A69-20084

Elastic and inelastic evolution of concentrated gravitational systems, discussing stellar diffusion, evaporation, halos and rotating systems

15 p2687 A69-30548

Quasar multiple absorption red shift lines caused by gas in extended galaxy halos, assuming broadened galactic cross section area

15 p2695 A69-30884

HAMILTON-JACOBI EQUATION

Gravitational fields in Hamiltonian formulation of relativistic theory of gravitation, noting geometrical aspects and equivalence to Einstein theory

02 p0280 A69-11715

Spacecraft optimum low thrust trajectory analyzed by Hamilton-Jacobi perturbation theory, obtaining canonic constants of motion

06 p1007 A69-17574

Hamilton-Jacobi equations of motion for classical electron in presence of traveling pulse of electromagnetic radiation, solving radiation pulse shape orbits

08 p1377 A69-19790

Particular solutions relative to system of invariant relationships in involution

09 p1596 A69-22049

Hamilton-Jacobi equation integrated for Hamiltonians, extending method to more than two variables case

11 p1910 A69-25747

Canonical transformation and Hamilton-Jacobi theories applied to space vehicle trajectory analysis, discussing elliptical coast arc and optimal low thrust problems

13 p2353 A69-28202

HAMILTONIAN FUNCTIONS

Transverse plasma mode excitation by nonlinear interaction analyzed by Hamiltonian function

01 p0127 A69-10280

Matrizants construction for Keplerian motions, discussing Hamiltonian character of variational equations for planar two body problem

03 p0513 A69-13779

Higher dimensional Dirac Hamiltonians from L-matrix hierarchy using dimensional eigenvector

04 p0625 A69-15275

Energy integral for holonomic system of points of variable mass, transforming Lagrangian form via Hamiltonian function

05 p0794 A69-16685

Unperturbed Hamiltonian transformation applied to existing perturbation theories for exchange forces between atoms to obtain correct long range behavior

07 p1184 A69-18288

Maximum index of exponential growth of solution of linear Hamiltonian equation with periodic operator coefficient encountered in dynamic stability of elastic systems

07 p1231 A69-18501

Superconductors with overlapping energy bands studied by nuclear magnetic resonance method

07 p1198 A69-18513

Analytic autonomous Hamiltonian differential equations with two degrees of freedom admitting unstable equilibrium point

07 p1215 A69-18732

Relativistic systems and relativistic Hamiltonian systems defined by second order equation, discussing canonical transformations conserving vector field Hamiltonian character

07 p1182 A69-19331

Final motions of Hamiltonian conservative systems, analyzing Liouville type, homogeneous and similar systems

09 p1540 A69-21882

Particular solutions relative to system of invariant relationships in involution

09 p1596 A69-22049

Canonical invariance of Hamiltonians noting nature of solutions of differential equations, existence of periodic solutions and application to three body problem

10 p1721 A69-23987

Hamilton principle for inviscid compressible fluid in Euler coordinates, analyzing shortcomings found in variational principles and model in Lagrangian coordinates

11 p1875 A69-25483

Hamilton-Jacobi equation integrated for Hamiltonians, extending method to more than two variables case

11 p1910 A69-25747

Autonomous two degrees of freedom Hamiltonian system triangular libration points found stable for all mass ratios in circular restricted three body problem

12 p2155 A69-25883

Eigenvalues of finite matrix Hamiltonian, considering convergence radius of perturbation series, limits and renormalization

14 p2470 A69-29451

Hamiltonian variational principle for stationary bounded MHD flows, choosing suitable functions and rigid conducting boundary location

15 p2660 A69-30910

Langevin equation for interacting molecule system derived by Fourier transformation of Hamiltonian, noting physical correspondence to equation for shear viscosity in monatomic liquids

16 p2815 A69-32370

Hyperfine spectrum analysis of NaCl at low field using molecular beam electric resonance method, discussing Hamiltonian function representation

16 p2815 A69-32794

Differential equations as Hamiltonian function for signal path, travel time and frequency variation in anisotropic nonpermanent absorbing medium

17 p2924 A69-33836

Variational method using Hamilton principle and calculus of variations to determine elastic curve and internal forces in static or dynamic loaded beam

22 p4043 A69-40459

Gravitational field quantization according to Einstein theory using classical Hamiltonian dynamics and quantum rules for constraints

23 p4192 A69-42332

Spin-phonon systems thermal noise, based on combined lattice and spin lattice Hamiltonian densities, applied to acoustic noise field measurements

24 p4350 A69-43061

HAMSTERS

Cultured Chinese hamster cells responses to UV light of different wavelengths indicating photon absorbing molecules inhibition of colony development

07 p1068 A69-19492

Synergistic effects of prolonged heat exposure and whole body irradiation with ionizing radiation on survival time in hamsters

08 p1263 A69-20174

Hamsters responses to helium-oxygen and nitrogen-oxygen at ambient temperatures, comparing respiration rates, weights and body temperatures
10 p1646 A69-23564

Postirradiation growth of cultured Chinese hamster cells exposed to UV light, including comparison with X irradiation
19 p3257 A69-35975

Pulmonary emphysema effect on expiratory flow limitation from static pressure-volume and flow volume curves during natural and forced deflation of hamster lungs
23 p4082 A69-41442

Body weight and organ sizes in hibernating cold and warmth adapted golden hamsters, discussing lungs, heart, kidney, pancreas and liver weight increases
23 p4084 A69-41462

Neodymium laser radiation effect on electrical and histomorphological properties of liver in rats and hamsters
23 p4111 A69-42344

HAND [ANATOMY]

Hand movements in water environment, weightlessness and normal gravity conditions, discussing inner coordinative structure and muscular efforts
17 p2915 A69-33385

Hand and thumb exercise effects on acquisition tracking task performance
23 p4101 A69-41453

HANDBOOKS

Handbook on Soviet space science research covering rockets, satellites, space probes, biomedical investigations, atmospheric composition
01 p0154 A69-10935

Handbook on metabolism and nutrition containing tables, charts and diagrams on food composition, material incorporation into organism, energy exchange and end products
04 p0553 A69-14908

Flammability handbook for plastics noting characteristics, behavior under fire conditions and various fire hazard reduction mechanisms, tables, drawings, manufacturers, suppliers, etc
04 p0620 A69-14952

Soviet handbook on stress analysis of anisotropic three layer reinforced plates and shells and of thick walled cylinders, Volume 2
04 p0683 A69-15500

Handbook of techniques in high pressure research and engineering, discussing construction materials, design and construction methods, measuring techniques, etc
07 p1137 A69-18412

HANDEDNESS

Operator handedness effect on control display movement stereotypes
02 p0203 A69-12212

HANDLING

U MATERIALS HANDLING

HANDLING QUALITIES

U CONTROLLABILITY

HANDWRITING

Manual performance of aircraft pilots under sustained acceleration using measurements of handwriting pressure
06 p0884 A69-18030

HANGARS

Aircraft engine noise reduction in test runs by sound insulating hangar
01 p0054 A69-10033

HANKEL FUNCTIONS

Hankel functions and vibration equations solutions, discussing asymptotic behavior and monotonic properties in neighborhood of ellipses
08 p1416 A69-20714

HANSEN LUNAR THEORY

Hansen planetary theory basic function, discussing perturbations expansion into trigonometric series
03 p0514 A69-13781

Satellite position perturbation due to earth oblateness using Hansen method [AIAA PAPER 69-909]
21 p3807 A69-39341

HARDENERS

Glass fiber laminates based on epoxy organosilicon resins, discussing various hardeners effects on strength, etc
19 p3358 A69-35903

Beta-thiodiglycol effect on hardening of epoxy resin with stoichiometric amounts of maleic anhydride and methyltetrahydrophthalic anhydride
22 p3973 A69-40677

HARDENING [MATERIALS]

NT CARBURIZING

NT HOT PRESSING

NT NITRIDING

NT PRECIPITATION HARDENING

NT PULSE HEATING

NT SHOT PEENING

NT SILICONIZING

NT STRAIN HARDENING

NT WORK HARDENING

Cycle dependent fatigue hardening and softening of metals in terms of crystal structure and stress amplitude
01 p0165 A69-10133

Mechanical effects of grain boundaries, considering hardening associated with vacancies and vacancy-solute interactions
03 p0449 A69-13875

Hardenability of ShKh-15 steel, establishing relationship of porosity to sintering method
04 p0619 A69-15390

Yield to ultimate tensile strength ratio of titanium alloys subjected to thermomechanical treatment
11 p1906 A69-25683

Shock hardening in Ni at high pressure observed by electron microscopy showing dominating thermal effects on microstructure
15 p2637 A69-30225

TiNi compound alloying with Al and Fe, considering effect on hot hardness at various temperatures
18 p3157 A69-35249

Titanium alloys case hardened by diffusion of various metals at high temperatures, measuring increase in wear resistance
19 p3344 A69-36153

Texture hardening combined with age hardening for biaxial strength improvement of Ti-Al-V alloy, discussing applications to spherical pressure vessels
21 p3729 A69-38662

Plastic deformation in hardened Ti alloys with thermally unstable beta phase under static compression and tensile loads by electron microscope
21 p3746 A69-39161

Creep theory with anisotropic hardening during early creep stages based on analogy with plastic flow theory
21 p3839 A69-39196

Small parameter method applied to axisymmetric problems of elastoplastic nearly spherical bodies undergoing exponential hardening process, deriving linearized expressions for boundary conditions
21 p3839 A69-39198

Enlargement of circular hole in disk with kinematic hardening and Tresca yield function compared with isotropic hardening
21 p3840 A69-39297

Bifurcation and hardening rate of rigid-plastic bodies presented on buckling of rectangular plate with lateral restraint
21 p3840 A69-39299

Strain induced creep equation for hardened materials for fixed temperature and stresses range, noting application to steel and Al alloys
22 p3971 A69-41033

Niobium solution hardening by nitrogen and oxygen, noting grain size effects in electron beam refining
23 p4178 A69-42362

HARDNESS

NT MICROHARDNESS

Al/Zn/Mg alloys preprecipitation, discussing Guinier-Preston and critical zone sizes and reversible vacancy trap
03 p0447 A69-13613

Hardness reference data for metals and nonmetals, using hardness test results for data reliability
04 p0617 A69-15033

Diamond pyramid hardness dependence on grain size of recrystallized alpha titanium
06 p0943 A69-17235

Surface finish and hardness effects on wear life of inorganic solid lubricant film [ASLE PREPRINT 68AM 7C-3]
07 p1139 A69-18623

Hard metals and materials containing NbC and HfC, noting X ray studies of pseudoternary and pseudoternary systems
14 p2464 A69-29323

Electrical conductivity, hardness, ultimate tensile strength and yield strength correlations of age hardenable Al alloys by eddy current methods
15 p2641 A69-31513

Elastomer hardness criteria ensuring maximum life and performance of rotary shaft seals
16 p2794 A69-32432

Extrusion variables influence on microstructure and hardness level of Ti-Al-Sn compared with recrystallization behavior after cold swaging [ASM PAPER W9-8.2]
21 p3729 A69-38660

HARDNESS TESTS

Structural transformations of quenched Fe-Ni-Nb austenitic alloy from X ray diffraction microstructure examination and hardness measurements
01 p0095 A69-10603

Silica glass hardness relationship to pressure induced densification at low temperatures
03 p0453 A69-13616

Hardness reference data for metals and nonmetals, using hardness test results for data reliability
04 p0617 A69-15033

Impact hardness of materials determined by Droz method of static hardness determination, noting tests on steel
10 p1801 A69-23850

Electrical conductivity measurements combined with indentation hardness measurements for non-destructive evaluation of commercial precipitation hardenable aluminum alloys
12 p2114 A69-26307

Mechanical properties of glass, discussing volume flow, hardness, strength and scratchability
12 p2119 A69-26831

Ni-Ti maraging steel hardness impact strength and thermal EMF changes during quenching
19 p3345 A69-36154

Titanium alloys hardness indirect measurement by determining electrochemical potential
23 p4177 A69-41598

HARDWARE

Low thrust mission simulation dependence on hardware definition, discussing power plant characteristics, jet velocity and thruster efficiency
09 p1584 A69-21204

Hardware and software as single entity in small scale programs, describing English language oriented program code of Controller/Programmer/Evaluator
11 p1864 A69-25062

Electronic module testing with integrated hardware/software system, noting module test console and manual capabilities
11 p1864 A69-25065

Hardware-software interface defined for design of computer controlled test system, discussing criteria for designing economical systems
11 p1842 A69-25071

Hardware limitations on communications, instrumentation and data handling for manned deep space missions
13 p2219 A69-27666

Avionic subsystems warranty costs estimates, considering reliability prediction and hardware recycling
18 p3232 A69-34506

Environmental testing of space hardware, discussing failure detection by thermal vacuum tests and mechanical signature analysis
19 p3430 A69-36009

Computer memory reduction through Fortran higher level language, discussing tradeoff between costs saved and additional logic hardware [AIAA PAPER 69-963]
22 p3905 A69-40344

Software/hardware interface testing of real time system, including possible improvements to computer program management flow
22 p3908 A69-40364

HARMONIC ANALYSIS

NT TESSERAL HARMONICS

NT ZONAL HARMONICS

Algorithm computing spherical harmonic coefficients for eccentric geomagnetic dipole potential
02 p0245 A69-12735

Matrix-harmonic method for vibration study of mechanisms and machines
03 p0468 A69-13860

Matrix-harmonic method of vibration study extended to include autonomous vibrations of single degree of freedom machines
03 p0468 A69-13861

Fourier transform method to measure two point correlations in grid generated turbulence
03 p0419 A69-13950

Harmonic balance method to investigate phase locked oscillator stationary modes
04 p0559 A69-15138

Harmonic analysis of magnetic storms initial phases having steep leading edges and distinct steady portions, showing homogeneity in first approximation
10 p1688 A69-23938

Nonpolar LF latitude variations based on spectroscopic and harmonic analysis of zenith telescope and prismatic astrolabe observations
11 p1956 A69-24401

Resonance circuit application to harmonic analysis of periodic functions on analog computer, considering transient period and sequential order
12 p2123 A69-26718

Linear closed loop control systems with periodically varying parameters analyzed by harmonics method using Fourier transforms
12 p2054 A69-26720

Drift velocity of earth magnetic field based on spherical harmonic analysis of geomagnetic secular variation
12 p2077 A69-27111

Lunar topography harmonic analysis, noting sample point density and evenness variations effects on estimated coefficients
13 p2344 A69-27647

Three dimensional harmonic dispersion analysis of incremental waves in uniaxially prestressed plastic and viscoplastic bars, plates and unbounded media
13 p2363 A69-28125

Spatial harmonic spectrum and tangential field distributions in microwave devices showing separation of higher harmonics through delay structure
13 p2236 A69-28576

Atmospheric pressure variation coefficients computation based on harmonic analysis of wave behavior
13 p2295 A69-28648

Geomagnetic normal fields determination using spherical harmonic analysis, including extension to local fields
14 p2437 A69-29063

Moon figure determined by DOD-66 Selenodetic Control System compared with second surface harmonic using computer analysis
14 p2527 A69-29942

Sinusoidal perturbation extremal control system stability, using harmonic balance principle to obtain periodic solutions of system differential equations
15 p2582 A69-30616

Harmonic analysis for computing diffusing matter with periodically varying surface concentration applied to electrical insulants degradation by atmospheric moisture
15 p2592 A69-31057

Geopotential represented in ellipsoidal harmonics, discussing Lamé functions generation and rectangular-ellipsoidal coordinates relation and orbital elements perturbations
15 p2599 A69-31333

Solar quiet day geomagnetic variations harmonic analysis with respect to time intervals centered around noon, defining parameters responsible for modulated Sq
16 p2781 A69-32452

Higher harmonic pitch angle inputs to eliminate oscillatory helicopter blade root shear determined through teetering rotor model
18 p3089 A69-35233

First harmonic approximation method reformulated to interpret nonlinear characteristic directly, discussing oscillation stability of servosystems
19 p3287 A69-36709

Geomagnetic field lines coordinates calculation based on coefficients obtained in spherical harmonic analysis
20 p3522 A69-37060

Self excited oscillations in systems with one linearity symmetrical with origin determined by harmonic balance method
21 p3685 A69-38463

Diurnal variations of cosmic ray neutrons corrected for barometric and temperature effects by harmonic analysis
21 p3791 A69-38840

Rectangular dielectric waveguide propagation modes, describing computer analysis based on electromagnetic field expansion in circular harmonics series terms
24 p4288 A69-43330

Nonpolar LF latitude variations based on spectroscopic and harmonic analysis of zenith telescope and prismatic astrolabe observations
24 p4391 A69-43791

HARMONIC EXCITATION

High efficiency punch-through avalanche transit time diode for generating microwaves over three octaves
07 p1098 A69-18457

Forced vibrations of elastic beam covered by viscoelastic layer subjected to transverse harmonic excitation
10 p1800 A69-23241

Nonstationary vibrations of mechanical systems subjected to harmonic or external limited energy source excitations
11 p1975 A69-24739

Linear automatic control system floating response to harmonic effects achieved by coinciding open loop system transfer function poles with disturbance pattern poles
12 p2045 A69-25967

Emission from solutions of organic luminophores excited by harmonics of Q switched neodymium laser
12 p2104 A69-26030

Infinite isotropic elastic plate vibration under vertical harmonic load, deriving vertical displacement at center of loaded area
17 p3058 A69-33408

Nonlinear flexural vibrations excitation in cylindrical shell by longitudinal harmonic load, discussing solution of partial differential equations of motion
17 p3064 A69-33920

Single freedom vibratory system response to imposed displacement harmonic excitation, analyzing response in terms of constrained system modes
17 p3067 A69-34139

DYDRA data logger for dynamic measurements of pressure distributions on harmonically excited wind tunnel models, noting use as general transfer function analyzer
19 p3293 A69-35746

Numerical method for solution of nonlinear systems applied to damped and undamped motion with symmetrical and asymmetrical elasticity under harmonic excitation
22 p4040 A69-39937

Three layered circular plate under harmonic excitation, analyzing forced vibrational characteristics by variational principle and Ritz method
23 p4236 A69-42495

HARMONIC FUNCTIONS

Two dimensional elasticity problem for two zero tangential stresses, expressing stress-strain states by biharmonic and harmonic functions
02 p0341 A69-12198

Green functions associated with electromagnetic radiation in moving medium, finding time dependent and harmonic Green functions
03 p0466 A69-13352

Approximation for discretization error of discrete analog of Bergman harmonic kernel, discussing discretization error in Dirichlet and Neumann problems for Laplace equation
03 p0456 A69-13555

Statistical dynamics of turbulent incompressible fluid, discussing harmonic function in Navier-Stokes equation
08 p1303 A69-20323

Partial derivatives of harmonic and biharmonic functions at surface of cylinder for three dimensional problem in elasticity theory, considering displacement vector
11 p1976 A69-24777

Conservative system /with two degrees of freedom/ motion in plane harmonic force field with potential satisfying Laplace equation, discussing graphic trajectory construction
11 p1920 A69-25745

Cauchy problem for initial functionals, determining spherical limiting harmonic function for solution stabilization
13 p2375 A69-27795

Polyharmonic Gq functions derivation and applicability to three dimensional elasticity theory equations solutions
13 p2369 A69-28522

Statistical dynamics of turbulent incompressible fluid, discussing harmonic function in Navier-Stokes equation
17 p2952 A69-33313

Linearized dispersion equation for isotropic electron plasma without external fields solved by harmonic function model
21 p3775 A69-38564

Electron plasma velocity distribution function determined from dispersion equation by harmonic function analog
21 p3776 A69-38565

HARMONIC GENERATIONS

Optimum coupling for intracavity second harmonic generation in multilevel lasers
01 p0089 A69-10181

Microwave second harmonic, sum and difference frequencies generation for two different microwaves normally incident on low temperature semiconductor slab in DC field
01 p0137 A69-10334

Efficient conversion of Q switched neodymium-glass laser output into second harmonic obtained for low output levels at fundamental frequency
03 p0437 A69-13046

Q switched neodymium-glass laser output conversion into second optical harmonic by passing beam through double Galilean telescope with adjustable focus
03 p0438 A69-13048

Aperture effects in nonlinear optical processes associated with second harmonic and parametric generation of light
03 p0439 A69-13056

Second optical harmonic generation in uniaxial negative potassium dihydrogen phosphate, noting influence of generating process on angular structure and output power
03 p0439 A69-13057

Second harmonic generation in ternary semiconductor compounds
03 p0489 A69-13894

Nonlinear optics noting harmonic generation of light, optical modulation, parametric oscillators, stimulated scattering, self focusing of light and resonance phenomena
05 p0770 A69-15704

Harmonic generation of S band signal inside plasma column at resonance
06 p0965 A69-17488

Emission of Nd giant pulse laser with high repetition rate and peak power to generate second harmonic radiation in lithium niobate single crystals
07 p1144 A69-18469

Phase matched optical harmonic generation by anomalous dispersion in liquid media, using dye fuchsin red
07 p1155 A69-19086

Frequency modulation of CW mm-wave IMPATT diode oscillator with wide band tunability and related harmonic generation effects
07 p1106 A69-19146

Impacting oscillatory devices for use as mechanical frequency dividers
07 p1136 A69-19458

Second harmonic generation in laser crystals by Gaussian beams of finite aperture
07 p1158 A69-19756

Harmonic generation in microwave gas discharge in pure and air mixed gases, noting rare gases failure in power source applications
08 p1283 A69-20177

Second harmonic generation conversion efficiencies at 5300 A with KDP and lithium niobate crystals, using Nd-glass laser of high radiance and narrow bandwidth
09 p1514 A69-21333

Nonlinear control theory for constant temperature hot-wire anemometers with large velocity fluctuations, noting second harmonic generation
09 p1493 A69-21421

Picosecond structure of low power laser signals using calcite beam splitter and potassium diphosphate second harmonic generator
09 p1516 A69-21742

Laser pulse picosecond substructure measurements, using pulse compression and second harmonic generation techniques
10 p1703 A69-23514

Second harmonic generation in ternary semiconductor compounds
11 p1939 A69-25695

Microwave harmonic generation in plasma capacitor, considering power resonances dependence on electron temperature and density
12 p2037 A69-25939

Second harmonic conversion of giant pulse Nd laser emission related to beam divergence and space-time distribution of radiation, noting energy relationship
12 p2104 A69-26022

Cyclotron harmonic waves /CHW/ nonlinear decay instability and parametric amplification, considering applicability to practical amplifiers
12 p2135 A69-26314

Nonlinear crystal generated second harmonic power measured for multimode He-Ne 0.63 micron self locked laser
12 p2106 A69-26321

Harmonic generation, using nonlinear current-voltage characteristics of Gunn diodes at 9500 MHz frequency
13 p2226 A69-27235

Nonlinear generation of sum and difference frequencies in ionized plasma current densities by nonuniform microwave fields noting electron scattering
14 p2507 A69-29350

Laser-nonlinear crystal dynamical interactions, studying saturation and coherence properties of second harmonic wave generated inside laser cavity
15 p2632 A69-30026

TR tubes spurious harmonic power generation investigated for intersystem interference reduction and design criteria, discussing effects of incident power, gas pressure and tube geometry

15 p2573 A69-30032

Capacitive parametric modulator transient processes and second harmonic effect analysis, obtaining transient response and recovery time

15 p2574 A69-30125

Mesa-structure varactors /p-n junction generating harmonics by nonlinear capacity variation/reliability, determining selection criterion and optimal test duration period

15 p2627 A69-30839

Microwave field-plasma slab nonlinear interaction in rectangular waveguide, analyzing current and electron density and second harmonic TE and TM power

16 p2749 A69-31703

Linearized Boltzmann equation in kinetic theory for weakly ionized plasma electrons under alternating electric and circularly polarized magnetic field, noting higher harmonics generation

16 p2820 A69-31752

Cosmic ray second harmonic daily variations explainable by symmetrical gradient rising away from solar equatorial plane

16 p2850 A69-32304

Nonlinear Maxwell equations applied to non-monochromatic emission for nonlinear crystal situated in resonator, examining generation of second optical harmonic

19 p3332 A69-35869

Second harmonic generation in media with center of inversion following deformation by laser beam or static pressure

19 p3332 A69-35872

Optical mixing and harmonic generation in semiconductors, discussing magnetoconductivity tensors and magneto-optical phenomena due to free carriers

19 p3385 A69-36519

Second harmonic radiation generation in nonlinear dielectric by broadband short pulse optical signals

19 p3278 A69-36693

Second harmonic emission in KDP crystal using ruby rod as active material, discussing difficulties encountered by diffused reflector

20 p3552 A69-36970

Nonmonochromatic laser emission frequency characteristics, studying second harmonic generation in nonlinear KDP crystal

20 p3554 A69-37727

Simultaneous mode locking of Nd YAG laser and intracavity second harmonic generation in high temperature Li niobate or BaNa niobate

20 p3555 A69-37731

Time characteristics and second harmonic of radiation of Nd laser containing lens systems, producing second harmonic in KDP crystal

21 p3740 A69-39544

Second harmonic influence on traveling wave amplifier operation employing distributed nonlinear active medium

22 p3916 A69-40963

Beam divergence and multimode laser visible emission influence on power and angular structure of second optical harmonic generated in KDP crystals

24 p4328 A69-43161

Ruby laser second harmonic generation statistical characteristics with dielectric surface scatterer, showing variety of modes and high cross sectional stability

24 p4328 A69-43164

HARMONIC GENERATORS

Second harmonic generation by electromagnetic wave incident on inhomogeneous plasma, determining power output

10 p1653 A69-23133

Synchronized microwave harmonic energy generation by filtering using DC step source feeding modified pulse forming network

12 p2041 A69-26630

Far IR radiation generation, considering incoherent sources, harmonic generators, electron tubes, relativistic electrons and quantum oscillators

22 p3982 A69-40669

Frequency discrimination in optical harmonic generators, discussing spectral width of wideband laser for supershort pulses and spectral device, using frequency dependence of mode locking direction

22 p3965 A69-40964

HARMONIC MOTION

NT SIMPLE HARMONIC MOTION

Three dimensional periodic boundary layer on ellipsoid in harmonic motion at given angle of attack, using successive approximations

15 p2548 A69-31008

Wave propagation in rectangular guides, determining dispersion curves by continued fractions method allowing for infinite set of time-space harmonics

17 p2925 A69-33843

Reflection and transmission coefficients for harmonic electromagnetic wave incident at parabolic layer of stratified isotropic plasma

22 p3901 A69-41020

HARMONIC OSCILLATION

Self sustained oscillations of piston type valving system with conduit line at upstream and capacity at downstream

01 p0012 A69-10310

Single frequency oscillations in stochastic quasilinear differential equations with delay

01 p0170 A69-10825

Superposition of discrete number of collinear amplitude modulated harmonic oscillations

02 p0281 A69-12252

Statistical characteristics of random phase quasi-harmonic process investigated for application of mathematical representation

02 p0208 A69-12263

Pulsar hypothesis based on oscillating white dwarf surrounded by hot rarefied corona to explain radio emission

03 p0505 A69-13077

Time harmonic vibrations and wave propagation in laminated plate, using elasticity theory equations and continuum theory for layered medium

04 p0675 A69-14685

Blade oscillations in cascade flow of axial turbomachinery calculated as function of pitch ratio, stagger angle, angle of attack and camber [ASME PAPER 68-FE-7]

05 p0837 A69-16069

Ion plasma oscillations harmonics in helium plasma produced by back diffusion source, relating harmonics amplitude to electron density

05 p0804 A69-16459

Harmonic oscillations for systems of two differential equations, analyzing relative and global boundedness for solutions

05 p0788 A69-16479

Harmonic oscillations in tunnel diode circuits for three intersection points of loadline with characteristic curve, discussing larger total positive circuit resistance case

06 p0898 A69-17801

Frequency doubling due to nonlinear response from Zeeman levels of ruby, discussing output and paramagnetic resonance

07 p1144 A69-18471

Nonstationary aerodynamic load for harmonically oscillating body in fluid flow with constant mean velocity measured, determining errors as functions of system parameters

07 p1050 A69-18752

Space harmonics effect on helical TWT design, discussing operating voltage, beam radius, perveance and maximum allowable gain

07 p1105 A69-18950

Diurnal thermal wave form driven by harmonically oscillating ground temperature in nongray atmosphere, calculating results for terrestrial and Martian atmospheres

07 p1126 A69-19036

Anharmonic lattice vibrations, specific heats and coefficient of linear expansion of solids at high temperatures, noting interatomic spacing

10 p1809 A69-23653

Tracking filter steady state oscillation amplitude and phase distributions determined from Fokker-Planck equation for high and low noise levels

11 p1844 A69-24441

Solar atmosphere five minute oscillations observed by Frazer divided into two harmonic atmospheric model for studying oscillation region height and mean temperature

13 p2343 A69-27627

Minimum weight design of structures excited to harmonic vibrations by given single load, with intensity dependent on time

13 p2369 A69-28350

Spatial harmonics of harmonic frequency instabilities of cyclotron half frequency in system of two symmetrical electron beams confined by magnetic field

13 p2314 A69-28364

Current harmonics in triode klystron for frequency multipliers, noting modulation voltage

13 p2234 A69-28510

Pulsar hypothesis based on oscillating white dwarf surrounded by hot rarefied corona to explain radio emission

14 p2515 A69-28759

Inelastic scattering cross sections calculated, comparing results for various nuclear states expressed as Wood-Saxon radial and harmonic oscillator functions

14 p2504 A69-29001

Oscillation spectrum with harmonic phase frequency modulation, analyzing structural dependence on initial phase

14 p2412 A69-29421

Plasma surface HF harmonic oscillations amplitude determined by comparing side frequencies intensities of reflected microwave signal

14 p2497 A69-29770

Circular curved foil steady oscillations near screen in sem infinite space filled with incompressible fluid transformed into equivalent linearized problem

15 p2547 A69-30577

Calculation of natural twisting and bending vibrations of beam with characteristics varying along length

16 p2873 A69-32131

Aerodynamic forces acting on harmonically oscillating thin profile in stalled plane parallel flow of ideal incompressible fluid

16 p2732 A69-32141

Aircraft and missile dynamic characteristics for heavy loads and large heat flux, noting small harmonic vibrations of heated structures in plastic domain [ICAS PAPER 68-38]

17 p3061 A69-33588

Forced harmonic oscillations of one dimensional mechanical girder systems allowing for nonlinear resisting forces calculated by boundary value problem reduction to Cauchy problem

17 p3064 A69-33917

Higher harmonic pitch angle inputs to eliminate oscillatory helicopter blade root shear determined through teetering rotor model

18 p3089 A69-35233

Plane LF oscillations of eccentric cylinder under harmonic pressure applied to lateral surfaces, noting natural oscillations

18 p3226 A69-35388

Electrohydraulic servomechanism harmonic response showing nonlinear behavior, including jump resonance, analyzed by mathematical model and analog simulation

20 p3464 A69-36999

Slender profile oscillations in subsonic flow near solid boundary, calculating pressure gradients by dipole method

23 p4058 A69-41717

HARMONIC OSCILLATORS

Quasi-sinusoidal tunnel diode oscillator studied for frequency and amplitude of harmonic voltage components

01 p0038 A69-10076

Transition probabilities for collinear collision of particle with harmonic oscillator, noting reasons for discrepancy in Jackson and Mott form

01 p0124 A69-10681

Nonisothermal space charge wave analysis of transit time mode oscillations in bulk GaAs, studying device reactance at given negative resistance

02 p0299 A69-12240

Unsteady hydromagnetic flow of viscous electrically conducting incompressible liquid over infinite conducting harmonically oscillating plate

04 p0638 A69-15091

Synchronization problem for quasi-harmonic oscillator with nonlinearity in form of cubic parabola discussing existence and stability of periodic solutions

04 p0578 A69-15131

Temperature sensitivity of frequency of integrated oscillators, giving design method for achieving temperature compensation

07 p1103 A69-18888

Gunn effect cavity controlled generator oscillations noting phase trajectory closing conditions dependence on resonant mode parameters

09 p1468 A69-22559

Tunnel diode harmonic mode mixer having IF oscillator with single and double resonant circuit

14 p2424 A69-29766

Computer model for avalanche transit time diode oscillator with single and double resonant circuit

15 p2577 A69-30611

Nonlinear differential equations for nonequilibrium gases with internal degrees of freedom, considering spatially homogeneous gas and oscillatory relaxation in harmonic oscillators

18 p3122 A69-34911

Stochastic motion in linear lattice of coupled harmonic oscillators analyzed by Schroedinger coordinates and Bessel functions for time behavior, energy flow and impurity effect

19 p3374 A69-36757

Condensation dynamics of atom by solid body model consisting of one dimensional chain of harmonic oscillators
21 p3775 A69-39557

HARMONIC RADIATION

Electron cyclotron harmonic waves in magnetoplasma irradiated by external microwaves
01 p0127 A69-10335

Laser based on xanthene series dyes and excited by neodymium laser second harmonic radiation, noting radiation spectra
06 p0932 A69-16914

Harmonic ion cyclotron waves shown to possess stop and passband characteristics, supporting quasi-static ion cyclotron mode theory
06 p0970 A69-17953

Epithermal microwave radiation from plasma produced by PIG Reflex in magnetic field with mirror geometry, discussing radiation at harmonics of electron cyclotron frequency
08 p1370 A69-21019

Nd-doped glass pulsed laser with selected second harmonic radiation and KDP crystal frequency converter operating T 12Hz and 530 nm
12 p2108 A69-26594

Angular structure of second optical harmonic for cylindrical lens focusing of ND laser beam into negative KDP crystal
17 p2981 A69-33110

ELF noise band observed by Alouette 2 receiver interpreted in terms of electrostatic proton cyclotron harmonic waves, using digital power spectrum techniques
20 p3497 A69-38079

Layer model of random discrete inhomogeneities used to derive harmonic wave one dimensional scattering field and mean square of field
21 p3673 A69-38993

Mutual impedances of radiators in periodic and doubly periodic rod antenna arrays with orthogonal harmonics current distribution, noting diffraction theory applications
21 p3682 A69-39126

HARMONICS

NT HARMONIC EXCITATION
NT HARMONIC GENERATIONS
NT HARMONIC OSCILLATION
NT SIMPLE HARMONIC MOTION
NT SPHERICAL HARMONICS
NT SUPERHARMONICS
NT TESSERAL HARMONICS
NT ZONAL HARMONICS

Second harmonic cosmic ray daily variation, discussing density gradient model with particle diffusion along field direction
02 p0305 A69-11422

Uniaxial loading effect determination by change of harmonics amplitude of inductive pickup signal
05 p0763 A69-15995

Resonance in fundamental harmonic identified with Pc4 and in second harmonic with Pc3 geomagnetic pulsations
06 p0921 A69-17737

Base pressure fluctuations behind cone in supersonic gas flow, noting complicated superposition of harmonics associated with various factors
09 p1431 A69-22237

Solar and lunar/solar harmonics determination, noting effects of moon on values of horizontal magnetic component
11 p1965 A69-25555

Laser harmonic frequency measurement application to absolute frequency determination of 84 micron heavy water laser
17 p2982 A69-33406

Ionospheric VLF electrostatic noise observed by sounding rocket, noting proton gyrofrequency harmonics effects within emission attenuation bands
21 p3714 A69-38550

Modulation envelopes, tables of profiles and harmonic components for modulated waves in electrical and communications problems
21 p3673 A69-38778

HARTMANN FLOW

Axisymmetric MHD flow in turbulence chamber at large Hartmann numbers studied for flow boundary layer effects
01 p0130 A69-10772

Axial magnetic field effect on steady linear Ekman boundary layer
03 p0474 A69-13141

Prigogine evolution criterion extended to MHD, considering Hartmann flow
07 p1188 A69-18267

Effective Ohm law for inhomogeneous weakly ionized gas and Hartmann flow analysis, noting electron density fluctuation effect on conductivity
10 p1735 A69-23462

Hartmann problem for motion of electroconductive fluid in homogeneous porous medium, modifying classical MHD equations by introduction of velocity of filtration
11 p1925 A69-24324

Steady state flow of viscous conducting liquid in inlet of channel with or without transverse magnetic field, emphasizing approach to Hartmann- Poiseuille patterns downstream
12 p2138 A69-26626

Laminar-turbulent transition in MHD channel in transverse and longitudinal magnetic fields, discussing Reynolds equation for large Hartmann numbers
13 p2307 A69-27500

Turbulent Hartmann flow between planes in perpendicular magnetic field including flow velocity profile measurements
14 p2500 A69-29908

Temperature distributions and heat transfer in thermal entrance region for Hartmann liquid flows under constant pressure gradient between parallel electrically conducting walls at rest
21 p3847 A69-38442

Turbulent Hartmann flow between rough walls in transverse magnetic field, determining field influence on resistance coefficient
22 p3989 A69-40255

HARTREE-APPLETON APPROXIMATION
U HARTREE APPROXIMATION

HARTREE APPROXIMATION
Dipole shielding factor in coupled Hartree-Fock approximation for atomic S state
02 p0281 A69-12179

Approximation formulas of Appleton-Hartree equations for nighttime medium wave frequency absorption in E region of ionosphere, discussing electron density
07 p1122 A69-18295

Hartree-Fock calculations of coronal forbidden transition lines in Ar I isoelectronic sequence, obtaining wavelengths, magnetic dipole and electric quadrupole transition probabilities
08 p1385 A69-20071

Polarized Hartree-Fock model computing photoionization cross sections for Li isoelectronic sequence, listing phase shifts for partial waves of scattered electrons
11 p1922 A69-25260

Upper bounds for electromagnetic transition rates for Ne 20 determined using Hartree-Fock wave functions
18 p3177 A69-35166

Hartree-Fock calculations for wavelengths of K alpha X ray transitions, tabulating configuration and term energies, dipole integrals and relative multiplet strengths
22 p3984 A69-40156

Variational principle for stability of galaxies models, developing perturbation potential in terms of operator similar to Hartree-Fock exchange operator
22 p4022 A69-40468

Approximate expressions derived from Appleton-Hartree magnetospheric formula tested for validity in computation of radio wave absorption in model ionospheric layers
23 p4126 A69-42354

HARTREE-FOCK APPROXIMATION
U HARTREE APPROXIMATION

HASTELLOY (TRADEMARK)
Time and temperature effects on corrosion and structure of Hastelloy alloy C-276
14 p2466 A69-29930

Thermal stability of Hastelloy Alloy C-276 determined from time and temperature tests for corrosion and grain boundary precipitation
16 p2799 A69-31719

Minor elements effect on cracking sensitivity of weld heat affected zone in Hastelloy alloy X, noting hot tearing and midrange cracking
22 p3967 A69-39881

HAWAII
Seismic refraction study of internal structure of volcanic cinder cone
02 p0236 A69-11465

HAWKER HUNTER AIRCRAFT
U F-2 AIRCRAFT

HAWKER P-1127 AIRCRAFT
U P-1127 AIRCRAFT

HAWKER SIDDELEY AIRCRAFT
NT BUCCANEER AIRCRAFT
NT DH 121 AIRCRAFT

NT F-2 AIRCRAFT
NT P-1127 AIRCRAFT

Nimrod maritime reconnaissance aircraft, discussing high speed high altitude transit flights
05 p0702 A69-15885

HAWKEYE AIRCRAFT
U E-2 AIRCRAFT

HAZARDS
NT AIRCRAFT HAZARDS
NT FLIGHT HAZARDS
NT METEOROID HAZARDS
NT OPERATIONAL HAZARDS
NT RADIATION HAZARDS
NT TOXIC HAZARDS

Emergency oxygen supply systems for aircraft, discussing simplicity, standardization, safety, reliability and maintenance
01 p0013 A69-11025

Deficiencies in two hazard classification system for detonating and fire producing materials from analysis of chemical industry accident fatality statistics
04 p0645 A69-14471

Wedge shaped charge technique for evaluation of detonation hazards of liquid explosives
04 p0646 A69-14479

Tires tested for road hazards, noting correlation to population density and rainfall
09 p1480 A69-22735

Qualitative and quantitative hazards analysis of potential accidents/incidents in Post Boost Propulsion System with hypergolic propellants, considering recovery
10 p1753 A69-22972

Safety requirements of test ranges, considering RF hazards to electroexplosive devices
10 p1751 A69-23019

Noise as public health hazard - Conference, Washington, D.C., June 1968
14 p2541 A69-29149

Noise measurement and scales in studying psychological and nonauditory physiological effects on human functioning
14 p2485 A69-29150

Physical and physiological hazards of cryogenic liquids, emphasizing fire and explosion problems associated with storage and handling
17 p3017 A69-33684

Accelerated temperature tests, calculating temperature behavior of hazard rates and activation energy from failure data using computer simulation
18 p3117 A69-34509

HAZE
Atmospheric haze effect on Umkehr measurements, considering computation from direct sounding of vertical ozone distribution and from model atmospheres
08 p1308 A69-20316

Radiation attenuation in hazy lower atmosphere, calculating attenuation coefficients and using spherical model of haze particles and empirical formula for haze spectra
11 p1913 A69-25571

Multiple light scattering solutions accuracy by diffraction peak omission from cloud and haze analytic phase functions compared for optically thick and thin planetary atmospheres
17 p3032 A69-33159

HC-1 HELICOPTER
U CH-47 HELICOPTER

HD-1 GROUND EFFECT MACHINES
U HOVERCRAFT GROUND EFFECT MACHINES

HEAD (ANATOMY)
NT CRANIUM
NT OCCIPITAL LOBES
NT SKULL

Head injury clinical and laboratory long term follow-up data, discussing conscious state alterations, focal neurological deficit, EEG abnormalities, etc
01 p0022 A69-11346

Head injuries evaluation in aircraft, noting motor cycle accidents
10 p1649 A69-23378

Civil pilots medical certification after head trauma, evaluating current methods efficiency
23 p4086 A69-41687

HEAD (FLUID MECHANICS)
Jet pump head rise deterioration parameter for prediction of cavitation
05 p0745 A69-15791

HEAD (PRESSURE)
U PRESSURE HEADS

HEAD FLOW

HEAD FLOW

Streak photographs by differential interferometer to study head wave standoff in shock tubes as function of time
18 p3085 A69-34473

HEAD MOVEMENT

Head movements controlled for rapid vestibular adaptation in slow rotation room (SRR), preventing motion sickness
17 p2908 A69-33178

Spacecraft rotation and astronaut head and body motion as stimuli for vestibular analyzer function study during weightlessness
20 p3473 A69-37275

Hearing movement affecting visual and kinesthetic localization accuracy, discussing free and fixed head conditions
24 p4275 A69-43118

HEALTH

NT MENTAL HEALTH

Aeronautical health service problems relating to efficiency of military and civil aviation personnel of all nations
12 p2023 A69-26490

Physical activity programs in industry for selected employees as routine component of occupational health programs
21 p3663 A69-38919

HEARING

NT ACOUSTIC FATIGUE

Hearing errors in voice communication with radio telephone, noting effects of mean syllable number and consonants per syllable in pilots and controllers
06 p0891 A69-18034

Auditory analyzer functional changes due to prolonged slow rotation
20 p3470 A69-37251

Hearing at LF, comparing noise and tone thresholds
21 p3664 A69-38986

Human hearing and vision mathematical simulation, relating signal perception parameters to corresponding adaptation processes
23 p4109 A69-41979

Dynamic reactions of mathematical model representing vision and hearing process adaptation
23 p4110 A69-41984

Hearing adaptation measurements after aircraft noise stresses for estimation of induced noise damage
23 p4110 A69-42051

Stimulus correlated with neuronal discharge periodicities in colliculus inferior, deriving structure models, discussing acoustic channel below geniculum mediale
23 p4096 A69-42089

Sound evoked DC changes on intact skull of adult humans using data from AgCl electrodes, investigating intensity function, analyzing data by computer
23 p4098 A69-42101

Flight personnel hearing tests per ICAO recommendations and flight safety requirements, using tonal audiogram and vocal audiometric test
24 p4277 A69-43377

HEARING LOSS

U AUDITORY DEFECTS

HEART

NT CARDIAC AURICLES

NT CARDIAC VENTRICLES

NT MYOCARDIUM

Phosphodiesterase activity of anterior pituitary, median eminence, heart and cerebral cortex of rat, studying effects of caffeine, theophylline and hydrocortisone
02 p0199 A69-11885

Analytic model resembling thick walled ellipsoid of revolution incorporating three dimensional shape of human left ventricle and ventricular wall thickness effects
12 p2022 A69-26235

EKG during electrical defibrillation of heart in immobilized dogs
19 p3257 A69-36168

Hypoxia tolerances in nitrogen dilution chamber of chickens at sea level and high altitudes, discussing role of hematocrit and heart mass
22 p3874 A69-40214

Physical exercise effect on adolescent males, comparing oxygen uptake, heart volume and height in training and nontraining groups
23 p4077 A69-41312

Critical oxygen pressure dependence on buffer in diluted heart muscle sarcosome suspensions and effect of hemoglobin or myoglobin
23 p4080 A69-41427

Noradrenalin release from hearts of open chest dogs given artificial respiration upon occlusion of left descending coronary artery
23 p4092 A69-42053

Gravitational stress effect on heart and venous system, discussing digital computer model simulating pressure changes under head-up and down tilt
24 p4271 A69-42783

Pneumatic driving system for heart assist or total replacement pumps, discussing design features and performance characteristics
24 p4273 A69-42983

HEART DISEASES

Cardiovascular disease incidence among airline flight deck personnel in relation to increase in average age of personnel
06 p0875 A69-17848

Airline pilot incapacitation by death or terminal collapse due to organic causes while on duty, noting incidence and resulting accidents
06 p0883 A69-17849

EKG signal transmission to hospital during cardiac patient transportation by emergency vehicle, noting prototype system construction and tests
19 p3262 A69-36271

Increased tolerance of orthostatic stress in heart failure patients
19 p3258 A69-36374

Coronary angiography for evaluating cardiac problems of aircrew, giving case histories and clinical and laboratory findings
19 p3263 A69-36461

Clinical data on ambulant airmen with complete left bundle branch block discovered on electrocardiogram, finding majority with evidence of organic heart disease
19 p3263 A69-36463

Cardiovascular illnesses incidence among airline flight personnel, discussing coronary insufficiency detection
21 p3661 A69-39271

Chronic congestive heart failure in dogs compared to pulmonary system, discussing effect on cardiac lymphatics
23 p4078 A69-41364

Reflex activity of single preganglionic sympathetic fibers during coronary occlusion in cats, discussing left third thoracic /T3/ ramus communicans
23 p4084 A69-41460

Serial ECG change from normal conduction to right bundle branch block in 59 patients without overt cardiac disease
23 p4085 A69-41677

Cardiac myosin characteristics obtained from dogs with naturally occurring heart failure, showing reduced adenosinetriphosphatase activity as compared with normal dogs
24 p4258 A69-42630

Blood viscosity as possible key factor in physiology and pathology of circulation, suggesting causes of myocardial infarction and coronary occlusion
24 p4261 A69-42725

Abnormally slow ultrasound diastolic slope detected by mitral valve motion study in patients with clinically pure mitral insufficiency
24 p4261 A69-42727

Risk factors in coronary diseases modified to provide base for estimating achievable mortality magnitude reduction
24 p4262 A69-43059

Airline pilots simulated incapacitation involving myocardial infarction or cerebrovascular accident, discussing effect on crew behavior during flight task performance
24 p4277 A69-43386

Heart murmurs frequency analysis on patients to improve detection of aortic insufficiency in presence of mitral stenosis
24 p4279 A69-43800

HEART FUNCTION

Left ventricle rapid filling period measurement from rapid filling wave of apexcardiogram, noting possible influences of age and sex
03 p0376 A69-14081

Bloodless heart flow measurement methods, noting simultaneous external recording of carotid and femoral pulses and impedance plethysmography
09 p1448 A69-22730

Psychic stress effect on physiological parameters of helicopter pilots during critical flight situations, considering biotelemetric examination of heart and circulatory systems
11 p1829 A69-24347

Myocardial changes in rabbits after general chronic ionizing irradiation attributed to lower cardiac activity, hypotrophy and dystrophy
17 p2906 A69-32929

Heart electrical activity time sequence estimation based on multiple dipole binary model, deriving algorithm
21 p3668 A69-39865

Rebreathing method for determining mixed venous oxygen pressure and cardiac output during rest and exercise in trained athletes
23 p4078 A69-41316

Cat papillary muscle length-tension curves before and after inotropic intervention, noting optimal length changes
23 p4084 A69-41461

Nonsurgical methods of cardiac output measurement in aerospace medicine, considering simultaneous recording of carotid and femoral pulses and impedance plethysmography
23 p4088 A69-41813

Acceleration effect on greyhound cardiac output and regional blood flow from Sapienstein radioisotope uptake technique, studying blood, skin, skeletal muscle, etc
23 p4089 A69-41823

Cat hearts ventricular pressure curves dv/dt and dp/dt correlated with left heart ventricle mechanical performance
23 p4095 A69-42076

Myocardium protein metabolism and heart physiology and pathophysiology, examining contractile function and energy transformation in hyperfunction, hypertrophy and heart failure
24 p4259 A69-42637

Errors in estimating cardiac function from aortic and peripheral pulses, using cadaver experiments
24 p4262 A69-42728

HEART RATE

NT ARRHYTHMIA

NT BRADYCARDIA

NT SYSTOLE

NT TACHYCARDIA

Cerebral circulation under longitudinal acceleration, discussing rheoplethysmographic measurements of heart rate
05 p0710 A69-16625

Pulmonary mouth pressure and heart rate in Flack test for flight personnel by simultaneous double recordings
05 p0710 A69-16626

Autonomic nervous system in control of heart rate in acceleratively stressed monkeys, discussing sympathetic, parasympathetic and bradycardiac influence
06 p0875 A69-17844

Abrupt deceleration effects on monkey heart rate, noting occurrence of relative bradycardia
06 p0876 A69-18031

Astronauts increased heart beat, respiration rates and higher blood pressure subsides during repeated weightlessness tests
07 p1061 A69-18582

Pneumograms and EKG used to determine heart beat, respiration rates and systolic index of cosmonauts during Voskhod 2 flight
07 p1062 A69-18585

Telemetering aortic blood pressure and heart rate from dogs under various physical activities and emotional stress
07 p1071 A69-19133

Tilt-table and acceleration tolerance of athletes and inactive students, comparing cardiovascular responses, heart rate and blackout level [DVL-834]
09 p1444 A69-21304

Physiological effects of breathing cool dehumidified air in hot humid environment, tabulating tolerance time, heart rate, temperature changes and sweat loss
09 p1446 A69-22543

Dogs orthostatic tolerance and resistance to transverse acceleration after 14-day hypodynamia, studying tachycardia and arterial pressure
10 p1645 A69-23499

Bed rest effect on orthostatic tolerance of patients with acute myocardial infarction and without heart failure
10 p1648 A69-24189

Heart rate and bodily fluid changes in acclimating desert anurans, discussing weight loss and metabolism reduction
11 p1827 A69-24923

Heart rate and respiratory response correlations in men during surface and underwater work, showing reasonable approximations of workload in surface-equivalent terms
14 p2406 A69-29293

Telemetry techniques, based on pulse rate measurements, permitting continuous examination of humans under natural working conditions

15 p2559 A69-31228

Psychophysical method of studying heart rate as indication of physiological fatigue

17 p2911 A69-34013

Electrocardiographic and heart rate data recording of crew members during transatlantic helicopter flight and normal daily routine

19 p3263 A69-36451

Noise influence on heart rate and oxygen consumption of young male subjects under simultaneous physical stress

21 p3654 A69-38908

Seasonal effects on energy expenditure during rest and exercise at controlled ambient temperatures, noting effects on heart rate

22 p3890 A69-40211

Regression relations for energy expenditure in work predicted from heart rate and pulmonary ventilation in volunteers carrying loads upstairs

22 p3891 A69-40220

Oxygen uptake and circulatory response in human male subjects during maximal treadmill and bicycle exercise

22 p3874 A69-40226

Real time metabolic rate analysis of suited astronaut using heart rate and O methods during thermal vacuum and extravehicular mobility tests [AIAA PAPER 69-993]

22 p3893 A69-40371

Heart beat rate, arterial pressure, blood volume and peripheral blood pressure increase observed in dogs running 7 min at 10 km/hr

22 p3885 A69-40966

Heart rate respiratory control model with inclusion of pressoreceptor feedback, considering posture effect in transient envelope alteration

22 p3894 A69-41202

Arterial pressure and heart rate responses to increased intrapulmonary pressure in anesthetized dogs via simulated Valsalva tests

23 p4078 A69-41365

Telemetered heart rate response to progressively increased distance swimming competition compared with equidistance running events for change patterns, magnitude and recovery

23 p4100 A69-41444

Pulmonary capillary blood flow, stroke volume and heart rate measured in tilted and supine subjects during respiration, discussing tourniquets and intravenous atropine effects

23 p4082 A69-41445

Physiological response to steady state hypoxia from exposure to 12 percent oxygen atmosphere, noting minimal heart rate and blood pressure changes

23 p4085 A69-41673

Heart rate responses and corresponding tolerance tests in trained athletes and nonathletes during simulated environmental extremes

23 p4102 A69-41683

Arterial oxygen partial pressures and heart beat rates measured in humans during acute hypoxia after altitude and ergometer training, noting sensorimotor performance

23 p4086 A69-41788

Aortic pressure effect on left ventricular function, emphasizing effect of heart rate hematocrit and oxygen consumption

23 p4092 A69-42061

Diurnal rhythms of heart rate and blood pressure reactions to posture changes on tilt table, finding orthostatic lability maxima

23 p4094 A69-42072

Human heart rate changes resulting from diving and breath holding exercises

23 p4095 A69-42083

Venous tone, peripheral venous pressure, skin and muscle blood flow, alterations of heart rate and respiration in men during leg exercise

23 p4096 A69-42090

Isolated pacemaker tissue from rabbit heart under dynamic and static stretching, discussing spontaneous frequency phenomena

23 p4096 A69-42092

Respiration effects on heart rhythm emphasizing direct mechanical influences

23 p4097 A69-42093

Oxygen consumption, ventilation and cardiac frequency relationship to body weight during submaximal exercise in normal human beings

23 p4099 A69-42169

Refractory period adaptation to sudden heart rate changes in dogs

24 p4257 A69-42628

Contraction frequency increment effects on myocardial oxygen consumption in dogs determined for various heart rate levels, using isovolumic left ventricular preparation

24 p4258 A69-42634

Circadian rhythm phase relationships between photoperiodism and heart rate, locomotor activity and deep body temperature /DBT/ in unrestrained monkeys

24 p4260 A69-42706

Frequency analysis of second heart sound splitting in patients with coronary artery disease assessed clinically and by phonocardiography

24 p4261 A69-42726

HEARTHS

Direct bead sampling by aspiration of molten metal in open hearth furnaces and converters

07 p1141 A69-19341

HEAT

U DRY HEAT

U NUCLEAR HEAT

HEAT ACCLIMATIZATION

U ACCLIMATIZATION

HEAT BALANCE

Operational and integral heat balance method to obtain exact and approximate solution for monotonic heating of two layer unbounded plate

01 p0174 A69-10097

Posistors heat capacity investigated as temperature function, showing maximum heat balance corresponds to Curie temperature

01 p0038 A69-10098

Oxygen electron cooling effect on ionospheric electron temperatures, noting discrepancy removal throughout day at all altitudes

02 p0245 A69-12739

Mean and eddy terms contribution to momentum and heat balance of troposphere and lower stratosphere at solstices, describing zonal wind equations

08 p1308 A69-20318

Thermal balance of intergalactic gas, discussing plasma energy losses due to He emission and reverse Compton electron scattering and rapid cooling effect

11 p1954 A69-24381

Particle, momentum and heat balance of static and rotating magnetized plasmas in terms of macroscopic equations

11 p1928 A69-25248

Steady state thermal problem of gas turbine hyperbolic profile disk equipped with banded blades, solving thermal balance equations

18 p3184 A69-34992

Ariel 3 satellite shape and systems including heat balance, data storage and compatibility problems

21 p3820 A69-39256

Radiative heat input to artificial satellite in orbit due to solar and earth radiations calculated and presented in graphs for satellite temperature calculation

22 p4006 A69-40589

Nighttime protonosphere thermal balance from Alouette 2 electrostatic probe measurements of electron temperature and concentration in magnetosphere

24 p4310 A69-43181

Thermal balance of intergalactic gas, discussing plasma energy losses due to He emission and reverse Compton electron scattering and rapid cooling effect

24 p4389 A69-43771

HEAT BUDGET

NT ATMOSPHERIC HEAT BUDGET

Equation for calculating meteor shielded tubular panel heat radiators emissivity and weight optimization, considering surface thermal balance and temperature distribution

05 p0846 A69-15897

HEAT CAPACITY

U SPECIFIC HEAT

HEAT CONDUCTION

U CONDUCTIVE HEAT TRANSFER

HEAT CONTENT

U ENTHALPY

HEAT DISSIPATION

U COOLING

HEAT DISSIPATION CHILLING

U COOLING

HEAT EFFECTS

U TEMPERATURE EFFECTS

HEAT ENGINES

U ENGINES

HEAT EQUATIONS

U THERMODYNAMICS

HEAT EXCHANGERS

NT TUBE HEAT EXCHANGERS

Finned tube radiators optimum design for waste heat removal from space power plants

02 p0354 A69-12664

Heat exchangers in cryogenic fluids in free and forced convection, discussing measurements in liquid H, D, Ne and N

08 p1420 A69-19914

Flow rates characteristic of trapezoidal geometries encountered after schematization of noncylindrical ducts involving irrotational flow, leakage, heat exchanges and electrical conduction phenomena

08 p1303 A69-20270

Roll diffusion bonding technique for permitting complex design of coldplates and radiators of spacecraft electronic equipment

09 p1504 A69-22066

Cryogenic heat exchanger design and application including vaporizers, recuperators, regenerators, reversing exchangers, nonsteady state flow and thermoelectric techniques

17 p3074 A69-33681

Electric models optimization for heat exchange systems based on mathematical similarity between equations describing temperature and electrical potential fields

19 p3256 A69-36717

Book on mathematical model for heat and material exchange in bubbles covering bubble formation, transition period and quasi-stationary bubble rise

21 p3847 A69-38448

Heat flow in belt-type heat transport device allowing for conductive and mass transport effects, deriving expression for heat transfer capability

22 p4050 A69-40554

Graph analytical method for calculating heat transfer in diathermic exchangers during boiling together with critical thermal loads

24 p4408 A69-43080

Heat pipe coupled to air cooled heat exchanger to cool high power airborne radio component by dissipating thermal load into ambient air [ASME PAPER 69-HT-16]

24 p4413 A69-43552

HEAT FLUX

Diffusional, thermal diffusional and thermal fluxes in multicomponent flames, discussing flame structure and reaction kinetics

01 p0175 A69-10144

Free convection from partially uniformly heated and partially insulated vertical flat plate, discussing dimensionless velocity, temperature, heat flux and axial length parameters

01 p0175 A69-10331

Flow nonuniformity measured in shock tubes by determining heat transfer rate to fine wire probes

01 p0062 A69-11219

Electric potential effects on heat transfer from plasma to solid wall, measuring heat input rates

02 p0290 A69-12423

Downstream radiation flux distribution calculated for blunt entry bodies, considering self absorption effects

02 p0354 A69-12547

Relationships derived by dimensional arguments connecting vertical heat fluxes and horizontal momentum in constant flux layer with other relevant variables

02 p0275 A69-12692

Stress and heat flux cospectra estimation using Busch-Panofsky observations

02 p0276 A69-12698

Surface temperature thermal fluxmeters used in measurements of shock tubes [ONERA-TP-648]

03 p0427 A69-12876

Vertical wind velocity structure and turbulent heat flux temperature measurements over steppe and sea, noting underlying surface influence

03 p0458 A69-13270

Long wave radiative heat flux in boundary layers of cloud during solid overcast, discussing dependence on various cloud and atmospheric parameters

03 p0458 A69-13271

Stationary and nonstationary weak discontinuity surfaces propagation for ideal and viscous compressible conductive atmosphere with regard to heat flux, using Hadamard method

03 p0422 A69-13511

Theory of heat conduction with finite wave speeds for materials with memory

03 p0533 A69-13956

Free convective heat transfer in liquid filled spherical volume with constant thermal flux density at boundary

04 p0686 A69-14992

HEAT GAIN

Covariances of temperature and meridional wind component and relation to northward flux of sensible heat due to transient eddies in stratosphere
04 p0627 A69-15084

Thin foil heat flux sensor for radiative and convective heating rates over wide range and dynamic response, noting error mechanisms, calibration and accuracy
04 p0602 A69-15426

Fast response thin skinned calorimeters for high heat flux profiles of arc jet flows
04 p0602 A69-15427

Nucleate pool boiling heat transfer data extended to relate effect of heating surface characteristics [ASME PAPER 68-WA/HT-22]
05 p0847 A69-16125

Plane reaction cell unit for use in differential flux calorimeters and devices for differential enthalpy analysis
05 p0764 A69-16607

Sensible heat exchange from Gemini and Apollo space suits determined in environmental test facilities, presenting data for heat flux distributions
06 p0880 A69-17089

Prigogine evolution criterion extended to MHD, considering Hartmann flow
07 p1188 A69-18267

Solid body surface temperature relation to heat flux during cooling by fluid flow solved on computer
07 p1241 A69-18923

Bulk aerodynamic method for heat and water vapor fluxes from data obtained at Chiba /1966/, introducing modified integral diffusivity
07 p1176 A69-18965

Fabrication welding with maraging steels with emphasis on minimizing heat input
08 p1320 A69-20407

Plasma sheath-boundary interactions, analyzing emission, reflection and surface ionization effects on current densities and heat fluxes for cesium and argon
08 p1369 A69-20818

Heat flux effect on laminar boundary layer separation in supersonic flow stressing free interaction zone
09 p1429 A69-21690

Emissivity of screened tube in presence of heat conducting connecting pieces between tube and screen
11 p1997 A69-24229

Heat flux toward electrodes measured under high current discharge, showing conductive heat transfer and erosion effect
11 p1928 A69-25227

Temperature variation effects on heat transfer in laminar tube flow, taking into account constant wall temperature and heat flow density
12 p2189 A69-25762

Temperature variation and heat transfer in fins and relations between heat-flux-density and temperature difference
12 p2190 A69-25763

Atmospheric energy budget of latent and sensible heat and potential energy between equator and 60 degree N
12 p2066 A69-26132

Heat flux in two dimensional laminar separation zone in supersonic flow, measuring convection coefficient and wall pressure
12 p2011 A69-26289

Radiation measurements by Cosmos 122 satellite over various regions, determining radiation temperature, long wave heat flux and albedo
13 p2291 A69-27726

Heat transfer coefficient deterioration between fluid and tube wall at supercritical pressure and high heat fluxes
[ASME PAPER 68-HT-39] 13 p2373 A69-27771

Unsteady temperature distribution in solid sphere with variable internal heat source and surface subjected to variable heat flux
13 p2373 A69-27773

Optical constants of soot applied to heat flux calculations, discussing soot particles concentration determination in hydrocarbon combustion products [ASME PAPER 68-HT-13] 13 p2374 A69-27777

Conducting liquid boundary layer flow and heat flux on electrodes of MHD generator, including one dimensional flow outside boundary layer
13 p2309 A69-28028

Functionality between heat flux and imposed operating conditions during nucleate pool boiling
13 p2376 A69-28142

Relative variations of wall friction and thermal flux for laminar incompressible flow of constant volume mass
13 p2250 A69-28357

Vertical wind velocity structure and turbulent heat flux temperature measurements over steppe and sea, noting underlying surface influence
14 p2471 A69-28778

Long wave radiative heat flux in boundary layers of cloud during solid overcast, discussing dependence on various cloud and atmospheric parameters
14 p2471 A69-28779

Materials compatibility and maximum heat flux capability of heat pipes emphasizing thermionic conversion
14 p2538 A69-29202

Pressure balance and maximum power density at evaporation from heat pipe experiments, deriving maximum heat flux densities
14 p2538 A69-29204

Radiation method for temperature and heat flux measurement, discussing transducer with thermopile as sensor
15 p2607 A69-30154

Surface temperature measurements to deduce surface heat fluxes, noting dependence on environment and sensor characteristics
15 p2716 A69-30379

Periodic radial heat flux in infinite cylinder with varying heat sources, assuming time variable heat exchange on surface
15 p2717 A69-30575

Turbulent heat and momentum fluxes spectra measured in atmospheric ground layer, describing changes as function of height and stratification conditions
15 p2649 A69-30648

Atmospheric radiative balance measurement on board Cosmos 149, describing design and operation of device
15 p2597 A69-30652

Heat release rate during gas combustion products recombination in supersonic nozzle, using graphic interpolation of flow parameters
15 p2717 A69-30987

Nucleate boiling burnout heat flux data for ethane, ethylene and ethane-ethylene mixtures at various pressures, discussing applicability of Noyes equations
15 p2671 A69-31118

Wall pressure and heat flux distribution in hypersonic flow on delta wings at variable angle of attack for low Reynolds numbers
16 p2731 A69-31605

Compressible turbulent accelerating boundary layer flow model for convective heat transfer from rocket combustion gases, noting heat flux
16 p2878 A69-32000

Linear heat flux in thin composite plate with internal point source, assuming no heat transfer at surface and neglectable temperature changes
17 p3068 A69-33126

Nonuniform wall radiation production of radiative equilibrium temperature and flux distributions in gray medium, discussing various approximation methods of solution
[AIAA PAPER 69-633] 17 p3072 A69-33294

Radiative heat transfer in nonisothermal media composed of spherical particles with complex refractive index emitting absorbing and scattering energy anisotropically, considering various geometries
[AIAA PAPER 69-626] 17 p3073 A69-33297

Heat transfer in evacuated multilayer insulation by radiation and conduction, considering optically thin media separating reflective layers
[AIAA PAPER 69-607] 17 p3073 A69-33300

Tropical circulation long term mean values of wind and temperature fields, momentum and heat fluxes from weather stations data, noting consistent pattern and energy source
18 p3165 A69-34418

Convective heat flux from nonisothermal surface by temperature superimposition method with Spalding function as turbulent heat transfer coefficient, noting wall temperature
18 p3229 A69-34836

Transient calibrations for Ge surface thermocouple heat flux sensors used in hypervelocity impulse tunnel
19 p3292 A69-35725

Transducer with single crystal Ge for high heat flux measurement, noting calibration by direct conduction
19 p3307 A69-35748

Heat flux densities and Reynolds potentials in turbulent boundary layer on heated flat plate with wall suction
19 p3452 A69-36722

Homogeneous heat flux effect on limit load of isotropic plate with rectilinear through crack, noting conditions for crack propagation
19 p3441 A69-36744

Flat surfaces downstream of heated section and porous strip, determining film cooling effectiveness and heat flux from heat transfer coefficients ratios
20 p3631 A69-37096

Polytetrafluoroethylene ablation in high temperature argon, nitrogen, air and oxygen jets, discussing electric heater and heat flux measurement
20 p3632 A69-37522

Heat influx equation coupling in the thermoviscoelasticity, considering internal forces dissipation and stress-strain operators
22 p4044 A69-40741

Forced convection heat transfer coefficient for fully developed turbulent flow in circular tube with time-varying circumferential heat flux
22 p4051 A69-40921

Micromodule unsteady thermal behavior reduced to calculating linear heat flux for boundary conditions containing temporal and spatial derivatives
23 p4136 A69-41558

Heat flux applied to infinite plate contacting semiinfinite body determined from plate unsteady temperature, allowing for calorimeter heat losses
24 p4407 A69-42589

Li-F-H tripropellant study, discussing injection method variations and thrust chamber configuration effects on characteristic velocity efficiency and heat flux measurement
24 p4362 A69-43128

Induced convection effect on peak pool-boiling heat flux under variable gravity, pressure and size conditions and various boiled liquids
24 p4409 A69-43516

Heat transfer during nitrogen tetroxide nucleate boiling at various pressures and heat fluxes [ASME PAPER 69-HT-58] 24 p4411 A69-43536

Wick capillary pressure, permeability and burnout heat flux measurements to provide data for heat pipe design [ASME PAPER 69-HT-18] 24 p4412 A69-43548

Rotating wickless hollow shaft heat pipe utilizing centrifugal acceleration for return pumping of condensate and transferring high heat fluxes [ASME PAPER 69-HT-19] 24 p4413 A69-43550

Heat finite propagation velocity effects on temperature distribution and heat flux for step temperature change at semiinfinite body surface [ASME PAPER 69-HT-1] 24 p4414 A69-43564

Solid propellant flame zone radiant energy flux emitted through side port of internal burning cylindrical rocket motor related to total heat flux at burning surface
24 p4415 A69-43595

HEAT GAIN

U HEATING

HEAT GENERATION

Procedure accounting for variable thermal conductivity and internal heat generation in temperature distribution prediction for waveguide ferrite slabs
02 p0215 A69-11877

Plastic deformation wave propagation and heat generated near yield point of annealed aluminum
02 p0342 A69-12280

Heat production rate equivalence to heat removal rate during ignition of ballistite powder by incandescent wires
02 p0354 A69-12668

Burning ability and inflammability of mixtures of powdered Mg, Al, Mg alloys or Al alloys and C-H-O organic compounds
02 p0355 A69-12669

Steady state temperature distribution in heat generating fluid in plug flow in circular tube with arbitrary inlet and wall temperature distribution
03 p0530 A69-12862

Variational technique for determination of temperature fields due to nonuniform heat transfer over surface of heat producing body
03 p0531 A69-12864

Heating effects produced by periodic stresses in viscoelastic bodies with resonance dispersion, considering torsional oscillations of viscoelastic cylinders
06 p1019 A69-16826

Transient heat evolution response to reapplied stress of alloys plastically predeformed at 4.2 K attributed to thermally softened defect structures
07 p1165 A69-18906

Heat generation effects by plastic deformations at tip of propagating crack in quasi-brittle materials, considering elastic stress field and crack velocity
08 p1412 A69-20144

Radiative transfer iteration for gray medium between concentric spheres and for constant heat generating spherical region imbedded in gray medium
08 p1420 A69-20152

Liquid crystal coatings for determining fracture initiation flaws in material structures, considering stress concentration and hysteresis heating
10 p1699 A69-23053

Equation for one dimensional heat conduction with nonlinear heat generation transformed from boundary to initial value problem
10 p1809 A69-23689

Heat generation in thin viscoelastic cylindrical shell with relaxation and resonance dispersion during torsional vibration
11 p2000 A69-25168

Seal selection criteria based on maintaining fluid film between faces, discussing facial heat generation and dissipation, speed and size effects, etc
[ASLE FICFS PREPRINT 25]
15 p2620 A69-30488

Uncoupled dynamic thermal stresses and displacements by heat generation in infinite flat plates, using classical thermoelasticity theory for infinitesimal displacements
15 p2709 A69-30669

Calorimetric methods for battery and cells testing, discussing heat generation data correlation
18 p3093 A69-34780

Fatigue fracture due to heat generation in polycarbonate subjected to pulsating tensile load, presenting temperature change per unit stress increase
18 p3163 A69-35498

Heat generation in meteorites by radioactive isotopes generated by early solar proton irradiation prior to solar system solidification
19 p3411 A69-36098

Earth temperature distribution using various models, noting excess of total heat production in interior vs heat flow during planet history
21 p3718 A69-39732

HEAT MEASUREMENT

Surface temperature thermal fluxmeters used in measurements of shock tubes
[ONERA-TP-648]
03 p0427 A69-12876

Twin differential calorimeter for measuring heat dissipation by wire specimen under fatigue tests, using semiconductor thermopiles
04 p0618 A69-15205

Plane reaction cell unit for use in differential flux calorimeters and devices for differential enthalpy analysis
05 p0764 A69-16607

Homogeneous turbulent gas flame front location as function of caloric value of mixture and flow velocity
08 p1420 A69-19998

Segmented anode current and heat distribution in MPD engine measured with current shunts and calorimetric methods
[AIAA PAPER 69-244]
09 p1566 A69-21260

Pyroelectric thermometry for measurements at low temperatures with emphasis on calorimetry, discussing pyroelectric coefficients, dielectric constants and resistivities
09 p1493 A69-21423

Local enthalpy measurements in atmospheric argon arc plasma jet at various arc currents, comparing calorimetric and spectrometric methods
09 p1547 A69-21602

Calorimetric measurement of electron temperature in collisionless shock wave propagating in plasma column, discussing role of H beta line Stark broadening
15 p2657 A69-30104

Radiation method for temperature and heat flux measurement, discussing transducer with thermopile as sensor
15 p2607 A69-30154

Calorimetric measurement of source and broadband spectral absorptances of spacecraft thermal control coatings during exposure to UV in vacuum environment
16 p2789 A69-31815

Composite solid propellant combustion using differential scanning calorimeter and mechanical model of steady state combustion
[AIAA PAPER 69-504]
16 p2833 A69-32679

Solid W enthalpy from 2800 K to melting point measured with drop calorimeter, tabulating heat capacity, entropy and free energy function
17 p2987 A69-33075

Total gasification heat measurement during pyrolysis of polymethyl methacrylate and paraformaldehyde, discussing method and calorimetric equipment
17 p3069 A69-33133

Guarded disk type emissometer for hemispherical emittance measurements of sample materials in 88 to 420 K range based on steady state calorimetry
[AIAA PAPER 69-600]
17 p2973 A69-33280

Earth surface heat flow pattern measurement and distribution techniques, considering relation to surface features and tectonic movements of crust
[AIAA PAPER 69-589]
17 p2961 A69-33284

Steady state performance of multistrand superconducting compound conductors in current sharing state, using heat measurement from metal surface to He bath
17 p3016 A69-33786

Ti thermal diffusivity and conductivity at high temperatures measured from heat wave phase shift
18 p3156 A69-34699

Calorimetric methods for battery and cells testing, discussing heat generation data correlation
18 p3093 A69-34780

Heats of adsorption of carbon dioxide on silver /I/ oxide and copper /II/ oxide by gas chromatography
20 p3485 A69-38277

Calorimetry-thermometry discrepancy during prolonged exercise in hot dry environment, measuring rectal temperature with increasing exposure time
23 p4098 A69-42104

Heat flux applied to infinite plate contacting semi-infinite body determined from plate unsteady temperature, allowing for calorimeter heat losses
24 p4407 A69-42589

HEAT OF COMBUSTION

Combustion products temperature and composition in chamber or at nozzle exit calculated for fuels containing excess oxidizer ratios greater than unity
04 p0684 A69-14486

Thermodynamic computations for combustion product temperature and flow rate as function of pressure in burner and excess air ratio
04 p0684 A69-14487

Heat release in combustion chambers of propulsion and lift engines considering various parameters of materials and design problems
09 p1625 A69-22619

Solution of confluence in three dimensional shock and detonation polars for spinning detonation
11 p2002 A69-25353

HEAT OF FORMATION

Formation energy of heat vacancies in molybdenum and temperature dependence of concentration determined on basis of enthalpy data
02 p0266 A69-12184

Photoionization curves and threshold energies for fluorocarbon and trifluoromethyl halide molecules and ions, calculating ionic heats of formation and bond dissociation energies
02 p0205 A69-12464

Relative heats of formation and reduced melting temperatures of lanthanide compounds correlated to lanthanide contraction
07 p1168 A69-19597

High pressure combustion of ortho-barenes /carboranes/, determining formation heat and amounts of boric acid and carbon dioxide
21 p3670 A69-39625

Beryllium fluoride heat of formation from heat of combustion of Be-polytetrafluoroethylene mixture in fluorine
21 p3853 A69-39703

Major ions in chemi-ionization of hydrocarbon flames determined for heats of formation by photoionization mass spectrometer
22 p3896 A69-40727

HEAT OF SOLUTION

Heat of solution and diffusivity of nitrogen in molybdenum analyzed by quenching technique and resistivity measurements at liquid helium temperature
02 p0267 A69-12188

Heats of solution of Ag and Cu in dilute Ag-Cu-Sn alloys at 720 K, using liquid metal-solution calorimeter
13 p2279 A69-27759

Heats of solution of Au and Cu in dilute Au-Cu-Sn alloys determined using liquid metal solution calorimeter, calculating self interaction coefficients
17 p2987 A69-33077

HEAT OF VAPORIZATION

Vaporization waves in metals, discussing thermodynamic function of carrying liquid metal through successive states on liquidus line in two phase region
01 p0117 A69-10655

Gas film protection of quartz tube wall transparency loss due to hot plasma contact used to study UV emission during high power pulse discharges
11 p1926 A69-24616

Heats of condensation and vaporization of W, Re and Mo cathodes of thermoelectric converter with Cs arc for various output powers and Cs vapor pressure
12 p2017 A69-26544

Vaporizer temperature and collision efficiency correlation data for magnesium oxide-argon dilute diffusion flames studied for determining inverse temperature dependence
13 p2380 A69-28461

Total gasification heat measurement during pyrolysis of polymethyl methacrylate and paraformaldehyde, discussing method and calorimetric equipment
17 p3069 A69-33133

Latent heat of condensation related to atmospheric dynamics in cloud formation processes with allowance for moisture exchange
17 p2997 A69-33188

HEAT PIPES

Out-of-core thermionic space power generators using heat pipes, discussing feasibility in geometry, heat pipes, reactor, shield, heat exchanger and radiator
08 p1256 A69-19856

Lithium vapor fueled applied field MPD arc jet performance using open end heat pipe vaporizer and hollow cathode
[AIAA PAPER 69-241]
09 p1561 A69-21222

Heat pipes for thermionic converters, wicks development, high temperature life testing and performance
09 p1440 A69-21833

Out-of-core thermionic reactor power increase by using central heat pipe in coaxial cavity
09 p1441 A69-21836

TWT heat pipe cooled depressed collector designed as compact heat transfer device and electrical insulator
11 p1847 A69-24746

High power TWT tube cooling in space vehicle, discussing thermal control system based on heat pipe radiator
11 p1847 A69-24747

Vacuum tube with cathode heated directly by external radioisotope source, noting heat pipe providing isothermal heat transfer
11 p1848 A69-24748

Out-of-core thermionic reactor concept for space power supply using lithium heat pipes in crossed layers
14 p2480 A69-29187

Out-of-core thermionic systems with heat pipes usable in space applications, meeting advanced auxiliary power and nuclear propulsion requirements
14 p2480 A69-29188

European heat pipe research emphasizing transportable heat quantities, heating rate and life duration
14 p2538 A69-29201

Materials compatibility and maximum heat flux capability of heat pipes emphasizing thermionic conversion
14 p2538 A69-29202

Corrosion mechanism in high temperature Nb-Zr/Li and Ta/Li heat pipes and heat transfer measurements, noting oxygen content of wall material
14 p2462 A69-29203

Pressure balance and maximum power density at evaporation from heat pipe experiments, deriving maximum heat flux densities
14 p2538 A69-29204

Limiting heat power transported by sodium heat pipes dependent on capillary network geometry, inclination angle and operating temperature
14 p2538 A69-29205

Dimensionless approach to maximum flow in heat pipes and optimization of capillary structure
14 p2539 A69-29206

Liquid-vapor interaction in loop plates with different heat pipe capillary geometries using water as heat transporting medium
14 p2539 A69-29207

Heat pipes for heating emitters of thermionic converters at high temperatures, noting capillary optimization and thermal resistance values
14 p2539 A69-29208

Cell current and calorimetric measurements of electrical power and heat generation with heat pipe thermionic converter
14 p2402 A69-29238

Heat pipes design for rocket engines cooling, discussing connections to space radiator and to heat rejection device and heat transfer capability
[AIAA PAPER 69-582]
16 p2839 A69-32668

Constant temperature heat pipe for thermal control of spacecraft components by direct coupling to external radiator
[AIAA PAPER 69-632]
17 p3070 A69-33262

Two component heat pipe operating characteristics on basis of thermodynamic phase equilibrium for binary mixtures
[AIAA PAPER 69-631]
17 p3071 A69-33268

- Heat pipe application to thermal equalization around ATS-E solar cell mounting panels, comparing predicted and actual performance [AIAA PAPER 69-630] 17 p3072 A69-33277
- Heat pipe devices applied to radiative body heat transfer in space suit temperature control [AIAA PAPER 69-619] 17 p2914 A69-33293
- Heat pipes for isothermal and adaptable energy transfer for space applications, discussing temperature control by fluid choice 21 p3852 A69-39475
- Electronic equipment thermal control, describing design and use of heat pipes 22 p4049 A69-39944
- Sonic vapor flow heat transfer limitations in heat pipes for Na, K and Cs, showing strong influence of temperature and working fluid 23 p4239 A69-41719
- Heat pipe system performance of GEOS 2 satellite, noting transponders temperature differences 23 p4224 A69-42082
- Heat pipe thermionic converters, discussing heat transport, heating rate, pipe lifetime, etc 23 p4074 A69-42295
- Heat pipe development and fabrication in various sizes and shapes for operation over range of temperatures and power levels, noting applications 23 p4074 A69-42296
- Li, Na and K heat pipes for high temperature emitter and low temperature collector thermionic applications 23 p4074 A69-42297
- Pumping pore size and permeability of wicks as part of heat pipes design 23 p4074 A69-42298
- Space radiator system with hybrid, water heat pipes to transport waste heat from radioisotopic thermoelectric generator 23 p4190 A69-42304
- Heat pipes design for avionic applications, using wicking bench tests 23 p4075 A69-42305
- Two fluid heat pipe performance, measuring temperatures and condenser end vapor pressures for two thermal power input conditions 23 p4240 A69-42306
- Temperature control by heat pipe using noncondensing gas with methanol to vary thermal resistance and mathematical model to describe heat source temperature variations 23 p4240 A69-42307
- Heat pipe design for electron tubes cooling at various temperatures, including dielectric heat pipes and traveling wave tubes [ASME PAPER 69-HT-25] 24 p4412 A69-43543
- Nucleate boiling effect on operation of low temperature heat pipes, using everted stainless steel to permit visualization of wick structure and bubble nucleation [ASME PAPER 69-HT-24] 24 p4412 A69-43544
- Temperature distributions in heat pipe wicks as function of liquid thermal conductivity [ASME PAPER 69-HT-23] 24 p4412 A69-43545
- Gas phase self induced pressure field and laminar velocity distribution of working fluid within closed heat pipe channels analyzed by momentum integral method [ASME PAPER 69-HT-22] 24 p4412 A69-43546
- Heat transfer capability and startup behavior of sodium heat pipes, studying heat transfer limit due to vapor velocity at evaporator end [ASME PAPER 69-HT-21] 24 p4412 A69-43547
- Wick capillary pressure, permeability and burnout heat flux measurements to provide data for heat pipe design [ASME PAPER 69-HT-18] 24 p4412 A69-43548
- Wick-limited heat pipe performance, discussing maximum, steady heat transfer rate and transient response [ASME PAPER 69-HT-20] 24 p4413 A69-43549
- Rotating wickless hollow shaft heat pipe utilizing centrifugal acceleration for return pumping of condensate and transferring high heat fluxes [ASME PAPER 69-HT-19] 24 p4413 A69-43550
- Heat pipe wick materials liquid transport properties analysis, using water and Freon 113 as working fluids [ASME PAPER 69-HT-17] 24 p4413 A69-43551
- Heat pipe coupled to air cooled heat exchanger to cool high power airborne radio component by dissipating thermal load into ambient air [ASME PAPER 69-HT-16] 24 p4413 A69-43552
- Performance curves of cylindrical water heat pipe for performance map, observing free hydrogen accumulation [ASME PAPER 69-HT-15] 24 p4413 A69-43554

HEAT PUMPS

- Thermodynamic analysis of engines and heat pumps operating within negative absolute temperatures, noting work increase by throttling 09 p1623 A69-22219
- Cascade thermoelectric heat pump reducing temperature gradient in legs of element near cold junction and reducing Joule heating in cold junction area 22 p3869 A69-40133

HEAT RADIATORS

NT SPACECRAFT RADIATORS

- Space radiators for heat rejection from nuclear powered spacecraft doubling as primary structures to save weight, discussing conical or cylindrical configurations 01 p0160 A69-10151
- Equation for calculating meteor shielded tubular panel heat radiators emissivity and weight optimization, considering surface thermal balance and temperature distribution 05 p0846 A69-15897
- Optimized radiative heat transfer systems performance, comparing tubular radiators with various fin geometries and systems with belt radiator 06 p1033 A69-17600
- Optimizing radiating system consisting of radially diverging conical heat removing projections attached to cooled isothermal sphere 06 p1033 A69-17603
- Constant temperature heat pipe for thermal control of spacecraft components by direct coupling to external radiator [AIAA PAPER 69-632] 17 p3070 A69-33262
- Finned tube radiators with constant longitudinal specific heat flow, determining thermal efficiency and optimal thermal and structural parameters 20 p3631 A69-36978
- Absorptivity of nonuniformly heated thin walled cylindrical radiator with central radiating hole, calculated by forward-reverse and integral methods 23 p4238 A69-41332

HEAT REGULATION

U TEMPERATURE CONTROL

HEAT RESISTANCE

U THERMAL RESISTANCE

HEAT RESISTANT ALLOYS

- NT MOLYBDENUM ALLOYS
- NT NIMONIC ALLOYS
- NT NIOBIUM ALLOYS
- NT REFRACTORY METAL ALLOYS
- NT RHENIUM ALLOYS
- NT TANTALUM ALLOYS
- NT TUNGSTEN ALLOYS
- NT WASPALOY
- Dendrite formation and solidification relationship in highly alloyed materials from quantitative determination of controlling factors for segregation 01 p0098 A69-10899
- Permissible JP-5 fuel sulfur content effect on hot corrosion of protective coated Ni-base superalloys in marine environment, noting atmospheric sea salt role 01 p0141 A69-11059
- Temperature dependence of thermal conductivity coefficient and specific heat of sublimating heat proof materials 02 p0350 A69-11580
- Gas turbine alloys composition role in high temperature corrosion resistance under high sulfur diesel fuel combustion 03 p0444 A69-13309
- Interfaces role in Ni-base superalloy, discussing grain boundaries and coherent/incoherent phase boundaries 03 p0449 A69-13878
- Structural stability of cobalt base superalloy at high temperature prolonged exposure under stress 05 p0781 A69-16448
- Sigma formation effects on cast nickel-based superalloys properties, discussing sigma occurrence prevention for longer service life of gas turbines 06 p0942 A69-17223
- Ti-Al-V alloys phase diagrams for isothermal cross sections and polythermal cross sections with constant Al/V ratios 07 p1161 A69-18768
- Ti rich Ti-Al-Mo-Zr alloys phase diagrams at high temperatures, noting presence of solid solutions 07 p1161 A69-18769
- Heat resistance of Ti-Al-Mo-Zr alloys analyzed by bend tests, discussing phase diagrams 07 p1163 A69-18779
- Chemical composition relationship to heat resistance of titanium alloys, using diagrams for establishing composition of new multicomponent alloys 07 p1163 A69-18780

- Columbium alloys properties, discussing creep strength, oxidation resistance, costs, production, etc 07 p1164 A69-18797
- Czechoslovakian heat resistant iron-carbon-aluminum alloy Pyroferal, properties and applications 07 p1168 A69-19388
- Elevated temperature mechanical properties data for commercially produced super-strength alloys supplemented by product description tables 08 p1328 A69-19919
- Ductility as principal cause of postweld heat treatment stress relaxation cracking in nickel based Waspaloy alloy 718 08 p1318 A69-19994
- Statistical techniques to develop nickel base superalloy with high temperature capabilities for jet engine turbine bucket applications 08 p1329 A69-20001
- Monograph on precipitation hardening and mechanical properties of various heat resistant alloys with Co contents to 35 percent 08 p1334 A69-20765
- Sulfidation attack and structural stability of nickel base superalloy [SAE PAPER 690103] 09 p1522 A69-21550
- Deformation processing of superalloy gas turbine components, studying ingot characteristics, alloy segregation effect and thermomechanical properties [SAE PAPER 690101] 09 p1503 A69-21550
- Wrought superalloys fusion welding behavior discussing hot cracking, hot microfissuring and strain age cracking [SAE PAPER 690102] 09 p1503 A69-21550
- Heat resistant nickel alloys for castings, tabulating chemical composition, mechanical properties, heat treatment, weldability, etc 09 p1522 A69-21604
- Heat resistant nickel alloys static and dynamic properties at high temperature, creep-fatigue interactions etc 09 p1523 A69-21604
- Soviet collection of articles on physicochemical studies of heat resistant alloys 09 p1524 A69-22133
- Vacuum melting effect on O concentration in heat resistant alloys, outlining conditions for nitrides formation in equilibrium with melt 09 p1524 A69-22133
- Heat resistant materials based on high melting point metals, summarizing achievements of chemical technology and vacuum metallurgy 09 p1524 A69-22133
- Structure and properties of high heat resistant alloys based on high melting point metals with bcc lattice explained by electron theory 09 p1525 A69-22139
- Heat resistance preservation in heat resistant alloys by inhibiting dislocation motion during operation at high temperatures 09 p1525 A69-22144
- Heat resistant alloying of niobium with group 4A, 5A and 6A elements, studying elements diffusion mobility dependence on melting point 09 p1525 A69-22144
- Heat resistant alloys plastic deformation, studying stress/strain systems, strain divisibility, strain rate and temperature effects, etc 09 p1504 A69-22144
- Mechanical properties of welds of niobium and Ni-base heat resistant alloys and susceptibility to crack formation at high temperatures 09 p1504 A69-22144
- Nickel base superalloys for aircraft gas turbines, considering strengthening mechanisms for creep resistance [ASME PAPER 69-GT-7] 09 p1527 A69-22506
- Heat release in combustion chambers of propulsion and lift engines considering various parameters of materials and design problems 09 p1625 A69-22619
- Oxidation effects on creep and fatigue properties of metals noting time and temperature roles 10 p1708 A69-22998
- Chemical composition of chromium steels for optimum heat resistance properties, noting effects of nickel, nitrogen and ferrite and austenite-forming elements 10 p1708 A69-23000
- High temperature effect on fatigue deformation and fracture of nickel base superalloy in single crystal and columnar grained forms 10 p1709 A69-23073
- Beryllium cermet compositions, discussing beryllium oxide content, mechanical strength and elastic and shear moduli 10 p1711 A69-23334

Solid propellant motors nozzle design, analyzing structural and material problems, high temperature exhaust gases effects, thermal insulation, etc
10 p1716 A69-23403

Nickel base wrought and cast superalloys examined to determine minor phases and microstructure thermal stability in high temperature heat treated condition
10 p1714 A69-23977

Cobalt base high chromium carbide strengthened superalloy, evaluating physical and mechanical properties
11 p1901 A69-24259

Weld cracking sensitivity of Inconel 713C investigated for determining aluminum content effect on weldability of nickel base heat resistant alloys
11 p1906 A69-25577

Fabricable materials with low plastic deformation for gas turbine components, noting strength vs temperature for alloys, fiber composites and ceramics
[IME PAPER 8] 12 p2147 A69-25791

Cast high temperature alloys for gas turbine components, discussing production, temperature capability, composition, oxidation, hot corrosion and weldability
[IME PAPER 10] 12 p2147 A69-25795

Book on hard alloy properties, discussing bending and compression properties, tensile, torsional and impact strength, wear resistance and thermal shock resistance
12 p2111 A69-25902

Soviet monograph on nuclear radiation effect on structure and properties of metals and alloys covering electron, gamma and neutron radiation
12 p2114 A69-26469

Crystal microstructure and mechanical properties of unidirectionally solidified Ni-Ni-Nb intermetallic eutectic alloy at high temperature, examining deformation and fracture modes
13 p2276 A69-27402

Nickel base superalloys long time carbide and intermetallic phases stability at high temperatures
13 p2277 A69-27405

Microstructural stability Fe-Ni base heat resistant alloy Pyromet 860 during long time creep-rupture testing
13 p2279 A69-27764

Spacecraft construction materials and strength problems including stress-strain determination, thin shell structural stability, dynamic loads, heat resistance, fiber-reinforced composites, ablation materials, etc
13 p2362 A69-27920

Ni alloys phase precipitation and Fe substitution effects on heat resistant alloys
13 p2283 A69-28488

Thoria strengthened Ni-Cr alloys high temperature stability, noting thoria particle size influence
14 p2465 A69-29682

High temperature properties relationship to microstructure of Co base superalloys and strengthening methods
14 p2465 A69-29891

Casting variables of Co base superalloys, discussing variables effects on ultimate mechanical properties, investment casting, etc
14 p2456 A69-29893

VM-1 alloy investigated for creep mechanisms and ultimate strength for applications in reactors, rockets and aircraft construction
15 p2638 A69-30284

Heat resistant Fe and Cu alloys creep index affected by temperature, testing time and specimen grain size
15 p2639 A69-30569

Heat resistant fiber composites produced by oriented eutectic crystallization in Co and Ni quaternary alloys [ONERA-TP-710] 16 p2799 A69-31765

Carbidothemic process for high melting metals and alloys production stressing Ti alloys
16 p2800 A69-31777

Precipitation processes and effect on properties of Cr-Ni-W-Ti heat resistant austenitic steel, using electron diffraction and transmission electron microscopy
17 p2984 A69-32833

Machine for testing high temperature creep under variable tensile-compressive stress while maintaining specimen stability, noting discrepancy between creep strains in heat resistant alloy
17 p3054 A69-33044

Welding research program at Polish Institute of Aviation concerning electron beam, AR shielded arc, resistance welding and soldering of heat resistant alloys
17 p2979 A69-33688

Static tensile stresses effect on energy dissipation in alloys used in compressor blades found dependent on composition and heat treatment
17 p2991 A69-33934

Polygonization and strengthening effects simultaneous action at grain boundaries increased thermal stability of thermomechanically treated Ni-Cr alloy
17 p2991 A69-33940

Electrical discharge machining effect on heat resistant alloys surface finish, noting volt-ampere characteristics
18 p3147 A69-34547

Co base alloy for gas turbines, discussing microstructure, creep, oxidation resistance and hot corrosion properties
18 p3158 A69-35421

Full circle Be brake disks in C-5 aircraft, discussing properties at elevated temperature and fastening of friction lining
18 p3095 A69-35424

Soviet collection of papers on strength and plasticity of Ni and Ti and alloys covering high temperature internal friction, deformation and creep characteristics
18 p3158 A69-35442

Tensile and stress rupture strengths of diffusion bonded Ni superalloys, using spin tests of simulated hollow turbine disks
19 p3320 A69-35559

Stress relaxation of heat-resistant steels as function of equal stress during different elevated temperatures, applying results to time residual stress prediction
19 p3342 A69-35778

Nickel base superalloy high temperature fatigue properties, comparing crack initiation and propagation in directionally solidified and conventionally cast forms
19 p3342 A69-35919

Ni base superalloy stacking fault energy, studying effects of various solute additions
19 p3343 A69-35925

Al effect on B and Cr diffusion in protective coating on Cr-Ni heat resistant alloy, noting thermochemical kinetics for homogeneous layers
19 p3345 A69-36157

Book on high temperature materials covering creep phenomena, design considerations, load and temperature effects, various steels, superalloys, refractory metals, etc
20 p3559 A69-37148

Repair welding methods for trailing edge cracks in nickel base superalloy used in turbine vanes, emphasizing plasma arc fusion welding
[ASM PAPER D8-16.3] 20 p3551 A69-38137

Heat resistance and strength properties of porous Ni-base cermet materials with mica additions under high temperature oxidation
21 p3751 A69-38615

Slip band etching procedure revealing Ni-base superalloy plastic deformation, accentuating slip bands and subgrain boundaries by electropolishing
21 p3744 A69-38741

Superalloy technology applications to gas turbine engines
21 p3785 A69-38928

Powder metallurgy all inert processing method for producing nickel base superalloys forgings, discussing microstructure, reproducibility, mechanical properties, etc
[ASM PAPER GG-8-3.3] 21 p3745 A69-38929

Phase softening transformations heat resisting alloys during cyclic heating, using X ray and electron microscope analyses
21 p3746 A69-38957

Minor element influence on high temperature weldability of high Ni alloys and weld quality
22 p3967 A69-39879

C and B influence on heat affected zone hot cracking and postweld heat treatment on Ni base superalloys
22 p3967 A69-39880

Minor elements effect on weld-metal cracking resistance of wrought Ni-base heat resistant alloy by Circular Patch Test
22 p3967 A69-39882

Short period creep and relaxation in various heat resistant alloys under heat treatments and loads, determining temperature dependence of cyclic thermal instability
22 p3969 A69-40071

Titanium alloys for strength and weight saving in aircraft fasteners operating at cryogenic or elevated temperatures, discussing corrosion and notch sensitivity
22 p3956 A69-40824

Ce, Zr, Nb and B effect on heat resistance and structure of low alloy CrMoWV steels (type CSN 41 5335/
22 p3972 A69-41079

Ni based superalloy mechanical properties, determining chromium carbide discontinuous precipitation effects at various temperatures
23 p4176 A69-41507

Structural aircraft design requirements for high flight speeds stressing aerodynamic heating, heat resistant materials, weight and geometry problems
23 p4233 A69-42164

Thermochemical analysis of hot corrosion during sulfidation-oxidation of superalloy gas turbine engine components using Pourbaix method
23 p4178 A69-42449

Cobalt-base superalloys analysis for temperature stability, corrosion resistance, creep, fatigue and strength in aircraft structures and parts applications
24 p4334 A69-43427

Protective coatings on Ni base superalloys for gas turbine engine blade and vane components for hot corrosion and oxidation resistance
[SAE PAPER 690480] 24 p4335 A69-43515

HEAT SHIELDING NT REENTRY SHIELDING

Ablative heat shield materials for Mars and Venus atmospheric entries
02 p0333 A69-11750

Rapidly heated ablative reinforced plastics strength and stress-strain properties, considering heat shield designs
02 p0347 A69-12512

Porous ceramic heat shields for lifting reentry vehicles, noting crack propagation resistance and load redistribution
[SAE PAPER 680643] 03 p0453 A69-13457

Blunt and conical body optimum heat shield shapes for Jupiter atmospheric entry, noting shallow flight path
[AIAA PAPER 68-1150] 03 p0520 A69-13565

Active cooling systems for high performance reentry vehicles in thermal and shear stress environments
[AIAA PAPER 68-1154] 03 p0533 A69-13669

Atmospheric gas composition effects on shock layer radiative heat transfer and heat shield response in Venus entry simulated by earth reentry
[AIAA PAPER 68-1148] 03 p0412 A69-13672

Make wire, light pipe and spring wire ablation sensors development for measuring parameters of heat shield materials for reentry vehicles
04 p0602 A69-15428

Inflatable solar shields for thermal protection of space vehicles utilizing cryogen propellants
06 p1017 A69-17609

Charring phenolic nylon ablator material pyrolysis and surface recession for cyclic and constant combined convective and radiative heating
[AIAA PAPER 69-151] 06 p1036 A69-18055

Ablative and insulative performance of reference heat shield materials under transient heating simulating ballistic vehicle reentry trajectory, using plasma jet facility
[AIAA PAPER 69-150] 06 p0907 A69-18110

Thermochemical and mechanical ablation mechanisms for Apollo heat shield material, comparing surface thermochemistry computer program and arc plasma tunnel data
[AIAA PAPER 69-98] 06 p1038 A69-18149

Microwave techniques for bondline defects and thickness of reentry elastomeric heat shield material bonded to titanium alloy
09 p1499 A69-22306

Initial nonuniformity effect of temperature distribution in main stream on efficiency of cooling by air injection through slit or porous collar
11 p2002 A69-25338

Ablation cooling application to aerodynamic heat shielding, discussing various materials, sublimation, rocket probe ascents, satellites and experimental aircraft
12 p2011 A69-25854

Ablation characteristics of heat shield materials measured in arc heated wind tunnels, considering influence of model scale, heating rate and pressure level
12 p2119 A69-26813

Time and temperature dependence of plastic properties of fiber reinforced phenolic heat shield materials
12 p2119 A69-26825

Dynamic response of distended carbon materials to shock loading defined by measuring equation of state, unloading behavior and spallation strength
12 p2119 A69-26847

Heating facility for testing ablative heat shield material models in combined convective and radiative heating environment with constant or transient heating conditions
[AIAA PAPER 69-342] 13 p2243 A69-28278

Thermal shielding effectiveness of flat wall behind tangential blowing slit, considering case of quasi-isothermal homogeneous turbulent boundary layer
14 p2537 A69-28971

Static, transient and in-space environmental tests at satellite structures and heat shield test facilities in Italy
16 p2765 A69-31750

Temperature determination of thick flat plate rotating in space in solar flux with one surface insulated compared with Apollo heat shield results
[AIAA PAPER 69-614] 17 p3071 A69-33266

Heat transfer suppression techniques in high temperature low density fiberglass insulation for flight vehicles
[AIAA PAPER 69-606] 17 p3072 A69-33279

Lunar module multilayer radiation insulation for thermal control, testing aluminum coated Mylar and Kapton sheets
[AIAA PAPER 69-609] 17 p3073 A69-33304

Fiberglass reinforced plastics internal heat shielding for isopropyl nitrate rocket combustion chamber, considering lining resistance and safety during repeated firing /Ludion motor/
17 p3019 A69-33343

Ablation heat shields, emphasizing dielectric low cost fabrication and application to entry vehicles
19 p3318 A69-35538

Active cooling systems for high performance reentry vehicles in thermal and shear stress environments
[AIAA PAPER 68-39016] 21 p3851 A69-39016

Line source technique for ablative heat shield materials thermal conductivity measurements, comparing vacuum and atmospheric test results
[AIAA PAPER 69-1013] 22 p3922 A69-40386

Low density polybenzimidazole composites as ablative heat shields, discussing arc-heated wind tunnel tests of linear and crosslinked structures
23 p4179 A69-41715

Atmospheric gas composition effects on shock layer radiative heat transfer and heat shield response in Venus entry simulated by earth reentry
[AIAA PAPER 68-1148] 24 p4394 A69-43248

Negative Poisson ratio of isotropic heat shield material pyrolytic graphite, noting thermodynamic validity
24 p4338 A69-43599

HEAT SINKS

Atmospheric heat sources and heat sinks distribution based on Cosmos satellite data
06 p0949 A69-17048

Space environment simulation for vacuum, solar radiation, heat sink and orbital motion, discussing oil contamination of optical surfaces
13 p2241 A69-28079

Transistor temperature and power limitations and thermal resistance calculation, discussing heat sink surface optimum design for power losses
16 p2760 A69-32047

HEAT SOURCES

Numerical analysis of temperature variation of spherical spinning satellite with and without radiatively coupled inner shell containing heat source
01 p0162 A69-10761

Axissymmetric model of unsteady convective cumulus cloud produced by time dependent heat source in unsteady atmosphere
02 p0274 A69-11436

DC arc plasma torch as heat source in plasma tunnel, discussing nonuniformity of plasma flame
02 p0291 A69-12424

Heat diffusion in cylinder with heat sources creating axisymmetric temperature distribution, using Gauss hypergeometric function and Meijer G-function
04 p0687 A69-15188

Atmospheric heat sources and heat sinks distribution based on Cosmos satellite data
06 p0949 A69-17048

One dimensional integral solution for cylindrical source generated transient temperature field and relation to thermal diffusivity of brain tissue
06 p0879 A69-17085

Constant thickness fin with arbitrarily distributed heat sources optimized using approximate physical model and closed form solution of field equation
[SAE PAPER 690198] 07 p1239 A69-18302

Temperature and displacement fields in unbounded elastic space due to instantaneous point heat source action
09 p1621 A69-21495

Heat sources in E region from electron temperature data analysis recorded by rockets during eclipses in July 1963
09 p1490 A69-21771

Unsteady free convection in incompressible viscous fluid having internal thermal source contained in bounded volume
09 p1621 A69-21792

Large scale heat sources influence on formation and dynamics of ultralong waves in atmosphere, using linear time dependent quasi-geostrophic model
09 p1491 A69-22164

Vacuum tube with cathode heated directly by external radioisotope source, noting heat pipe providing isothermal heat transfer
11 p1848 A69-24748

Ignition critical conditions based on reactions in condensed phase, discussing initiation from pulsed and continuous external heat sources, heat release by chemical reactions of ignition, etc
11 p2001 A69-25191

Unsteady heating of fuel mixture in vertical cylindrical container with Arrhenius heat source, discussing heat conduction equations and wall temperature effects
11 p2001 A69-25192

Acoustic frequency of longitudinal self oscillations during vibrational fuel combustion in afterburner, taking into account nonlinear properties of heat supply zone
11 p2002 A69-25339

Model, assuming electron thermal conductivity contribution, applied to studying solar plasma discharge characteristics in presence of three dimensional thermal sources in solar corona
12 p2149 A69-26680

Thermal stability of power transistor plates calculation using equivalent body with equivalent heat source at upper surface
12 p2042 A69-26881

Thermal stability of complex transistorized structures determined by extending method of single heat source equivalence to several interacting sources
12 p2042 A69-26882

Unsteady temperature distribution in solid sphere with variable internal heat source and surface subjected to variable heat flux
13 p2373 A69-27773

Temperature measurement associated with bubbles leaving heat source in subcooled pool boiling carbon tetrachloride analyzed, using high speed motion pictures by schlieren optical system
[ASME PAPER 68-HT-47] 13 p2374 A69-27779

Cellular convection suppression by parallel vertical thermally conducting walls inserted into bottom-heated fluid, analyzing effect on critical Rayleigh number
13 p2374 A69-27782

Stresses in infinite solid elastic circular cylinder due to rotating line source of heat
13 p2364 A69-28206

SNAP 13 generator designs to develop technology for isotope heated thermionic converters, describing tests, efficiencies, power outputs and life times
14 p2481 A69-29191

Heat pipes for heating emitters of thermionic converters at high temperatures, noting capillary optimization and thermal resistance values
14 p2539 A69-29208

Periodic radial heat flux in infinite cylinder with varying heat sources, assuming time variable heat exchange on surface
15 p2717 A69-30575

Thermoelastic stresses in isotropic circular cylinder with surface locally heated by external Newtonian heat source, considering various heat transfer conditions
15 p2714 A69-31178

Thermal conductivity of semiinfinite rod with insulated surface and constant internal heat source, considering finite heat propagation rate
15 p2719 A69-31181

Temperature field, strains and stresses induced in thin circular disk by unsteady heat source, noting time effect and resonant vibrations
17 p3054 A69-33021

Solar wind model for studying long wavelength turbulence as heat source for alpha particles and protons in solar plasma
18 p3186 A69-34299

Reflected shock front interaction with heated thin gaseous filament studied in shock tube by spark interferometric and schlieren technique
18 p3228 A69-34468

Asymptotic solution of supersonic linearized nonisotropic flow of viscous and heat conducting gas with internal heat sources past cylindrical shell, deriving surface pressure
18 p3089 A69-35460

Regenerative life support systems, discussing water reclamation, carbon dioxide removal, onboard oxygen generation and radio isotope thermal energy sources
19 p3262 A69-36318

Cascaded thermoelectric module for spacecraft power conversion via module integration with radio isotope heat source, bonding SiGe and PbTe stages
20 p3465 A69-37706

Circulation near turbopause effect on lower thermosphere composition changes, noting heat source for warmth over winter polar region
21 p3704 A69-38366

Thermal stress distribution induced in wedge by apex heat source analyzed using elasticity theory, considering lateral surface heat transfer
21 p3833 A69-38644

Co 60 kernel heat source for multikilowatt space power supplies, stressing design for maximum safety
23 p4187 A69-42257

ISOTEC thermoelectric generators for space power, describing design features, operation, power output and radioisotope heat source
23 p4189 A69-42270

Solid state chemical heat sources aboard unmanned planetary landing vehicles to maintain batteries and experiments operability during cold planetary nights
23 p4070 A69-42275

Brayton-B generator for 2-10 kwe production, describing design, heat source/rejection, efficiencies and preliminary test data analysis
23 p4071 A69-42278

HEAT STORAGE

Volatile liquid pressurization, discussing pressurants, heat sources and system design
[AIAA PAPER 68-630] 02 p0232 A69-12382

Molten salts thermal diffusivity measurement method at temperatures above melting point
[ASME PAPER 68-WA/ENER-5] 05 p0848 A69-16161

Heat storage cells for satellite solar power plants based on latent heat of fusion and single phase heat carrying agent
06 p0870 A69-17604

HEAT TESTS

U HIGH TEMPERATURE TESTS

HEAT TOLERANCE

Manual performance relationship to men exposed to cold, thermal neutral and hot environments, discussing finger dexterity and motor coordination tests
03 p0381 A69-14074

High temperature effects on physiological functions of man noting cardiovascular system and heart performance, body heat exchange and blood and urine composition
05 p0710 A69-16523

Mental and physical human performance characteristics under thermal loads noting admissible temperatures and endurance limits
08 p1263 A69-19940

Synergistic effects of prolonged heat exposure and whole body irradiation with ionizing radiation on survival time in hamsters
08 p1263 A69-20174

Brief intense thermal stresses effects on cardiovascular system of man, noting criticality of effective blood volume for circulatory competence
08 p1264 A69-20668

Skin temperature and cutaneous pain during warm water immersion, refuting subcutaneous thermal gradient hypothesis for stimulation of heat pain
08 p1267 A69-20683

Heat susceptibility and tolerance in astronauts obtained by plot of skin and oral temperatures for subject under thermal stress
10 p1644 A69-23376

Heat and humidity endurance limits in man
10 p1645 A69-23494

Artificial heat acclimatization effect on orthostatic tolerance in man exposed to stresses of heat, exercise and dehydration
16 p2746 A69-32810

High temperature effects on physiological functions of man noting cardiovascular system and heart performance, body heat exchange and blood and urine composition
18 p3096 A69-34742

Time required for acclimatization to work in high temperatures, noting rectal temperature and heart rate changes
21 p3654 A69-38905

Strenuous physical training effects on human tolerance for work in heat, measuring rectal and mean skin temperatures and heart rates
22 p3890 A69-40199

Severe heat stress effects on respiratory frequency, rectal temperature, blood gases and pH of conscious dog
23 p4081 A69-41432

Heat tolerance in case of SST aircraft air conditioning failure, discussing physiological and psychomotor reactions and time curves for metabolic activity levels
24 p4277 A69-43382

HEAT TRANSFER

NT AERODYNAMIC HEAT TRANSFER
NT CONDUCTIVE HEAT TRANSFER
NT CONVECTIVE HEAT TRANSFER
NT HYPERSONIC HEAT TRANSFER
NT LAMINAR HEAT TRANSFER
NT RADIATIVE HEAT TRANSFER
NT SUPERSONIC HEAT TRANSFER
NT TURBULENT HEAT TRANSFER

Heat transfer between arc column and discharge chamber wall of vortex linear plasmatron, using approximate similitude method
01 p0125 A69-10091

Heat exchange and hydraulic resistance in turbulent heat exchangers in longitudinal air flow calculated by criteria equations
01 p0173 A69-10092

Impulse and kinetic energy transfer in rarefied gases analyzed on basis of kinetic theory, considering surface curvature effect
01 p0173 A69-10093

Relationship between cooled surface temperature and pressure self oscillation frequency during heat transfer to turbulent fluid flow, showing temperature variations
01 p0173 A69-10094

Schlieren method for studying rotating sphere heat transfer during natural convection
01 p0174 A69-10095

Simple and shock waves in nonlinear unsteady heat and mass transfer, discussing conditions for transforming simple waves into shock waves
01 p0174 A69-10096

Mach-Zehnder interferometer for studying temperature distribution and heat transfer in turbulent jets, noting temperature dependence on jet thickness at different angles of attack
01 p0005 A69-10101

Linear partial differential equations for nonlinear intensive heat and mass transfer, discussing analogy between transfer processes and electromagnetic waves distribution
01 p0174 A69-10104

Thermographic phosphor technique to provide transient temperature measurements in impulse wind tunnel
01 p0078 A69-10152

Laser cone calorimeters calibration to determine heat capacity
01 p0079 A69-10220

Heat transfer situations in plasma flow indicates very high heat fluxes per unit area on surfaces with electric current
[ASME PAPER 68-HT-38] 01 p0175 A69-10314

Heat transfer principles analyzed in development of new quenchants for aluminum, noting properties of inversely water soluble polyalkylene glycols
01 p0087 A69-10900

Cryogenic expansion to pressures below triple point and resulting formation of solid-vapor mixtures, discussing flow and heat transfer characteristics in heated tubes
01 p0176 A69-11146

Flow nonuniformity measured in shock tubes by determining heat transfer rate to fine wire probes
01 p0062 A69-11219

Transformation laws for thermodynamic quantities confirming conventional formulation by mechanical model of heat
01 p0122 A69-11288

Heat transfer procedure and equipment during boiling under short term weightlessness
01 p0177 A69-11313

Time history of unsteady heat transfer in laminar boundary layer over semiinfinite flat plate due to step change in wall temperature or wall flow
01 p0177 A69-11401

Turbulent fluid transport properties predicted by simple model for fluid behavior, obtaining mass, momentum and energy diffusivities
01 p0177 A69-11402

Heat transfer between concentric cylinders at different temperatures measured for argon, neon and helium
01 p0177 A69-11403

Nonlinear diffusion of heat in semiinfinite wall having thermophysical characteristics dependent on temperature, showing dissymmetry between heating and cooling
01 p0177 A69-11404

Accommodation coefficient effect on linearized heat transfer in rarefied gas between parallel plates and concentric cylinders
01 p0177 A69-11405

Heat transfer dependence on direction of heat flow in stainless steel/aluminum interfaces, showing surface roughness and flatness influence
01 p0177 A69-11406

Frictional and heat transfer characteristics of laminar flow in porous tubes, using numerical solutions to flow and energy equations
01 p0177 A69-11408

Pressure to density ratio to analyze one dimensional high temperature gas flows with heat transfer, considering motion equations
02 p0350 A69-11576

Venus microwave phase effect analyzed assuming dry massive Venus atmospheric model, discussing heat transfer processes
02 p0319 A69-12108

Liquid nitrogen dispersed flow film boiling data accounting for droplet breakup by vapor acceleration, drag coefficient and heat transfer from wall
[ASME PAPER 68-HT-44] 02 p0351 A69-12203

Nucleate pool boiling heat transfer of liquid nitrogen from circular disks with different surface conditions including copper and nickel mirror finishes, roughness and coatings
02 p0352 A69-12207

Relativistic heat transfer formula and pressure definition in relativistic thermodynamics
02 p0352 A69-12253

Uniqueness and existence theorem concerning stability of solutions of mixed nonlinear boundary value problem, discussing generalized heat transfer phenomena
02 p0352 A69-12255

Electrically controlled heat transfer between flat parallel flow hydrocarbon diffusion flame and walls of combustion chamber
02 p0353 A69-12324

Heat transfer in pyrolytic graphite analyzed by hybrid computer simulation
02 p0353 A69-12387

Electric potential effects on heat transfer from plasma to solid wall, measuring heat input rates
02 p0290 A69-12423

Determining influence of blowing various gases into boundary layer on friction and heat and mass transfer when external flow velocity varies according to power law
02 p0234 A69-12581

Heat production rate equivalence to heat removal rate during ignition of ballistite powder by incandescent wires
02 p0354 A69-12668

Variational technique for determination of temperature fields due to nonuniform heat transfer over surface of heat producing body
03 p0531 A69-12864

Heat transfer in cooled portion of air gas flow area of high temperature gas turbines
03 p0495 A69-12957

Centrifugal force field influence on heat exchange between gas and blade cascade studied with noncooled blades at low temperatures
03 p0531 A69-12959

Diathermal regenerative cooling of combustion chambers and engine nozzles with supercritical heat transfer mode
03 p0495 A69-12970

Gas dynamic choking limitation on heat transfer capacity of heat pipe operating at low vapor pressures from comparison of theory and experiment
03 p0531 A69-12989

Heat transfer in crossed field MHD Couette flow for incompressible fluid, assuming linear wall temperature in flow direction
03 p0476 A69-13306

Heat input influence on hypersonic flows past sphere and circular cylinder
[DVL-844] 03 p0364 A69-13663

Heat transfer covering heat conduction, channel flow, boundary layer flow, separated flow, etc
04 p0684 A69-14354

Dynamic processes of heat and mass transfer in transpiration cooling of gas flow
04 p0684 A69-14355

Heat transfer through turbulent boundary layer on porous plate with blowing and suction, determining Stanton numbers
04 p0586 A69-14356

Average energy dissipation in MHD duct flow of arbitrary cross sectional shape, evaluating bulk temperature, net wall heat flux and pressure gradient
04 p0635 A69-14724

Mean temperature distribution through inner and outer regions of turbulent boundary layer with injection through heated porous wall
04 p0685 A69-14729

Heat transfer, suction and injection in plane Couette flow analyzed for Rivlin-Ericksen fluid, using perturbation method
04 p0589 A69-14970

Nondestructive testing of quality of electroexplosive devices based on determination of heat flow between bridge wire and surroundings
04 p0607 A69-14973

Magnetic field effects on heat transfer between Ar plasma flow and channel wall, noting effects of temperature and Reynolds number
04 p0636 A69-14989

Approximate hydrodynamic equations applied to analysis of heat transfer in real gas flow in tube, taking into account energy transfer by radiation
04 p0686 A69-14993

Heat release during boiling of downward flowing liquid oxygen film
04 p0687 A69-15161

Heat transfer between body and gas flow near stagnation point
04 p0544 A69-15412

Telemetry technique utilizing thermocouple sensors for base heating determinations on free flight blunt cone in shock tunnels, noting electrical noise reduction
[AIAA PAPER 68-407] 04 p0604 A69-15514

Turbulent flow transfers from applications point of view, noting example of cooling of heated wall
05 p0743 A69-15558

Partial differential equations solution using analog, digital and hybrid computers, discussing heat transfer in parallel flow exchanger
05 p0723 A69-15705

Flow and heat transfer on nonNewtonian fluid about disk rotating with time dependent velocity, using Runge-Kutta-Gill technique for numerical integration
05 p0745 A69-15793

Quantitative analysis of nonsteady temperature field in long cylinder for sudden heating of semiinfinite axisymmetric lateral surface
05 p0845 A69-15797

Tangential stress distribution and heat transfer in circular cylinder with attached wall jet
05 p0746 A69-16022

Heat transfer, temperature and velocity profiles in circular free jet can be described by heat conduction type equations
05 p0747 A69-16032

Pool boiling heat transfer from stainless steel coated with Teflon to produce nonwetted surfaces
[ASME PAPER 68-WA/HT-12] 05 p0847 A69-16119

Heat transfer in accelerated turbulent boundary layer between converging planes with varying wall temperature and decreasing Stanton number
[ASME PAPER 68-WA/HT-13] 05 p0847 A69-16120

Binary mixture condensation on cooled vertical plate, formulating predictive theory based on conservation laws and other physical principles
[ASME PAPER 68-WA/HT-21] 05 p0847 A69-16124

Uniform hot fluid injection effect on heat transfer in constant property turbulent boundary layer
[ASME PAPER 68-WA/HT-24] 05 p0847 A69-16126

Heat transfer characteristics of single lines of circular air jets impinging on concave cylindrical surfaces, discussing nozzle target spacing effect
[ASME PAPER 68-WA/GT-1] 05 p0848 A69-16137

Nuclear radiation influence on pool boiling heat transfer to liquid helium, using irradiated copper as boiling surface
[ASME PAPER 68-WA/PID-3] 05 p0791 A69-16164

Quasi-method of characteristics with application to fluid lines with frequency dependent wall shear and heat transfer
[ASME PAPER 68-WA/AUT-7] 05 p0750 A69-16181

Heat transfer performance of porous nozzle blade cascade represented by two dimensional mathematical model
05 p0812 A69-16400

Injection or suction at disk surface, noting effects on heat and mass transfer in laminar flow about rotating disk

06 p1029 A69-17002

Heat and mass transfer by catalytic effect at wall, noting interaction of laminar boundary layer on flat plate

06 p1030 A69-17115

Heat pipe for thermal control of terrestrial and aerospace energy conversion systems

06 p1030 A69-17189

Heat transfer and IC, discussing semiconductors thermal and electrical analogs and thermal properties

06 p0894 A69-17216

Heat transfer bibliography covering boundary layer, phase flow, conduction, liquid metals, low density, measurement techniques, natural convection, radiation, thermodynamic and transport properties, etc

06 p1033 A69-17558

Approximate expression for temperature distribution during heat transient in infinite solids of plane, cylindrical and spherical geometry

06 p1025 A69-17779

Blade to rotor heat transfer in turbines determined from temperature distribution of rod in medium with nonuniform temperature

06 p1034 A69-17870

Heat transfer from unseeded DC augmented propane air flame to water cooled probe placed beyond discharge zone

06 p1035 A69-17934

Fluid flow longitudinal temperature profiles for inclusion in heat transfer computer program [AIAA PAPER 69-30]

06 p1038 A69-18174

Computer program for predicting temperature distribution and heat transfer through coated and uncoated window systems of aerospace vehicles [AIAA PAPER 69-28]

06 p1038 A69-18178

Scaled models for spacecraft thermal control, considering radiation-conduction-convection heat transfer [SAE PAPER 690196]

07 p1116 A69-18304

Igniter design guidelines, types and characteristics of igniter materials [WSCIPAPER 68-32]

07 p1202 A69-18361

Heat transfer to wedge in nearly free-molecular hypersonic flow of strongly rarefied gas

07 p1050 A69-18707

Solid body surface temperature relation to heat flux during cooling by fluid flow solved on computer

07 p1241 A69-18923

Heat and mass transfer - Conference, Minsk, May 1968

07 p1243 A69-19732

Heat transfer in horizontal and vertical tubes with viscous gravity flow with boundary conditions

07 p1243 A69-19733

Turbulent flow effect on heat transfer in supersonic jet with plane infinite obstacle perpendicular to jet axis

07 p1243 A69-19738

Aluminum effect on ammonium percholate/polyformaldehyde mixtures combustion properties noting heat transfer decrease into k phase

08 p1375 A69-20338

Von Karman flow changes due to unsteady heat transfer from rotating disks impulsively changing temperatures, particularly steady state and response time

08 p1422 A69-20996

Heat transfer mechanism in solid body, deriving integrodifferential equation with classical equation and hyperbolic equation of heat propagation as special case

09 p1621 A69-21587

Homogeneous parabolic differential equation for heat transfer of two finite bodies in thermal contact solved by power series

09 p1532 A69-21628

Stagnation point heat transfer sensitivity to free stream turbulence attributed to external vorticity, noting correlation with Prandtl number

09 p1622 A69-21905

Transition of hypersonic boundary layers on conical body using shock tunnel, obtaining surface heat transfer distributions [AIAA PAPER 68-39]

09 p1482 A69-21943

Heat transfer effect on population inversion time variation in pulsed carbon dioxide laser and molecules excitation rates dependence on gas mixture composition

09 p1519 A69-22289

Thermal approach to pulsating combustion, determining temperature-time variation, frequency and pressure from mathematical model

09 p1625 A69-22694

Flame propagation normal velocity evaluated with heat transfer equation at flame front taking into account temperature, pressure and inert gas percentage

09 p1625 A69-22695

MHD flow and heat transfer between coaxial rotating disks under axial magnetic field, using powers expansion of Reynolds number

10 p1728 A69-23234

Equilibrium dissociating gas laminar flow in circular tube calculated for heat transfer and hydraulic resistance, using boundary layer equations

10 p1679 A69-23426

Heat and mass transfer between cryogenic fluid and superheated wall, analyzing experimental data

11 p1996 A69-24228

Heat transfer in single phase medium at near critical state parameters

11 p1997 A69-24230

Heat transfer in MHD parallel plate channel flow in entrance regions analyzed by Galerkin method, noting Hall current effect

11 p1923 A69-24290

Advances in heat transfer, Volume 5, covering Monte Carlo method, film and transition boiling, convective heat transfer, etc

11 p1997 A69-24456

Monte Carlo method application to heat transfer analysis including radiation, rarefied gas energy transfer and conduction

11 p1997 A69-24457

Film and transition boiling as functions of critical temperature, discussing role of heat transfer and vapor production

11 p1997 A69-24458

TWT heat pipe cooled depressed collector designed as compact heat transfer device and electrical insulator

11 p1847 A69-24746

Laminar Newtonian flow heat transfer to fluids with variable physical properties in vertical tubes with constant wall heat flux, considering viscosity and density

11 p2000 A69-25164

Ignition of condensed homogeneous combustible materials in presence of phase transition in heated layer, discussing temperature distribution and ignition delay time in ammonium perchlorate

11 p2000 A69-25189

Ignition critical conditions based on reactions in condensed phase, discussing initiation from pulsed and continuous external heat sources, heat release by chemical reactions of ignition, etc

11 p2001 A69-25191

Flame front propagation over solid fuel surface with hot igniting material injected into end-to-end cavity, discussing heat transfer by convection and radiation

11 p2001 A69-25193

Thermal conductivity of polycrystalline beryllium oxide as function of temperature and pressure in argon or helium atmosphere, discussing heat transfer mechanism

11 p1906 A69-25225

Differential catalytic thin film heat gage for measuring surface temperature variations and ionized flow heat transfer, noting insulating boundary layer thickness

11 p2002 A69-25231

Buoyancy effect on boundary layer flow over semi-infinite vertical plate heated to constant temperature in uniform free stream

11 p1874 A69-25352

Numerical integration of equations for three dimensional laminar boundary layer on sharp elliptical cones in supersonic flow of ideal gas, discussing heat exchange

11 p1821 A69-25477

Lumped element construction technique involving crossed coils to reduce ferrite produced heat in resonance isolators, using substituted YIG

11 p1856 A69-25632

Heat and mass transfer in laminar boundary layer on porous flat plate with variable suction or injection velocity and constant wall temperature

12 p2061 A69-25947

Unsteady temperature field and thermal stresses for anisotropic and orthotropic plates heated by heat sources and having Newton law heat transfer

12 p2177 A69-25992

Finite difference method for heat transfer for developing laminar flow at inlet of circular uniformly heated and isothermal tube, determining Nusselt number

12 p2062 A69-26242

Heat removal from laser ruby rod by Cu prism connected to cooling system, discussing limiting factors in heat transfer area size

12 p2108 A69-26592

Pressure and heating rate correlations for rocket exhausts impinging on flat plates and curved panels, generating axisymmetric real gas exhaust plumes

12 p2190 A69-26781

Internal flows of compressible fluids with heat transfer in accelerating nozzles and constant area ducts, simplifying equations by assuming one dimensional flow

12 p2012 A69-26790

X-15 research aircraft program piloting problems, ground facilities, heat transfer, space flight and steep reentry

12 p2014 A69-26872

Soviet book on liquid fuel rocket engines design covering gas expansion in nozzles, mixture formation, heat transfer, injectors and supply systems

12 p2148 A69-27078

Theoretical model describing electrodynamic plasma properties of HF flame discharge in air, heating discharge envelopes by heat diffusion from discharge channel surface

12 p2140 A69-27125

Thermographic phosphor coatings to obtain optical quantitative heat transfer distribution on wind tunnel models

12 p2099 A69-27150

Heat transfer between surfaces as secondary effect in gas bearing lubrication from analysis taking into account viscosity variation with temperature [ASME PAPER 68-LUBS-4]

13 p2267 A69-27286

Electric arc and hydrogen flow interaction at high pressure, showing radiation role in heat exchange

13 p2305 A69-27387

Velocity, enthalpy and mass flux radial distributions in laminar boundary layer from calorimetry of argon subsonic flow [ASME PAPER 68-HT-16]

13 p2374 A69-27776

Heat and mass transfer conditions in ablation of shear thinning and thickening fluids at stagnation point [ASME PAPER 67-HT-78]

13 p2374 A69-27778

Thermal emission from metal in contact with dielectric for cryogenic insulation applications

13 p2374 A69-27783

Heat transfer for incompressible inviscid fluid flow in cone, expressing solution in terms of dimensionless numbers

13 p2375 A69-27788

Transient heat transfer in formation of steady crossed fields MHD plane Couette flow for walls, giving momentum, induction and energy equations

13 p2375 A69-27791

Velocity and temperature profiles in gaseous turbulent boundary layer above liquid surface used to study liquid film cooling heat transfer

13 p2375 A69-27792

Collection of papers on heat transfer covering convective and radiative transfer, numerical methods, nucleate boiling, dropwise condensation, two phase flow, etc

13 p2375 A69-28138

Numerical methods for solving steady state and transient heat transfer problems suitable for high speed digital computer

13 p2376 A69-28141

Dropwise condensation, analyzing nucleation sites, growth, vapor capture, heat transfer rates and surface texture

13 p2376 A69-28143

Heat and mass transfer in two dimensional turbulent free shear flows including separated and reattached flows

13 p2377 A69-28145

Chemically reacting flow field and solid surfaces, formulating nonequilibrium laminar boundary layer equations for two dimensional and axisymmetric flows

13 p2377 A69-28147

Internal and external heat transfer instrumentation and equipment bioengineering, listing thermal conductivity and diffusivity of biological materials

13 p2213 A69-28150

Heat transfer involving particulate suspension, discussing characteristics of flowing suspension, inertia effects, impingement, deposition, radiation and electric charges

13 p2377 A69-28151

Heat flow resistance between solid bodies in contact in vacuum

13 p2378 A69-28338

Bibliography of books and periodicals concerning heat transfer classified under applications, boundary layer, channel flow, conduction, liquid metals, MHD, etc

13 p2379 A69-28341

Similarity theory similar to Nusselt and Stanton numbers obtained by triple analogy for heat, mass and momentum transfer

13 p2380 A69-28560

Finite thickness plate heat equation using Legendre polynomials

14 p2537 A69-28970

Coupled heat and mass transfer with zero order reactions in two phase systems consisting of drops, bubbles or solid particles

14 p2537 A69-29012

European heat pipe research emphasizing transportable heat quantities, heating rate and life duration

14 p2538 A69-29201

Corrosion mechanism in high temperature Nb-Zr/Li and Ta/Li heat pipes and heat transfer measurements, noting oxygen content of wall material

14 p2462 A69-29203

Multifoil thermal insulation using oxide particle layer separation, discussing insulation heat transfer characteristics as function of source temperature and oxide particle size

14 p2539 A69-29213

Heat transfer at gas flow stagnation point past blunt body under radiation from air layer in shock wave wake, using gray gas model

14 p2390 A69-29614

Bibliography of Soviet books and articles on heat and mass transfer covering thermodynamics, heat conduction, convection and radiation, etc

14 p2540 A69-29900

Magnetic field effect on heat and mass transfer in incompressible fluid MHD flow

14 p2500 A69-29901

Weak shock waves relaxation time and amplitude and acoustic velocity as functions of thermorelaxing media

15 p2590 A69-30103

Selectively pumped thermal vacuum test chamber for orbital heat transfer and environment simulation for flight vehicle performance prediction

15 p2587 A69-30392

Heat and mass transfer interaction at wall for laminar boundary layer on flat plate, considering catalytic effect of wall in atomic nitrogen recombination

15 p2716 A69-30415

Monograph on Prandtl number effect on heat transfer and pressure loss in artificially roughened channels

15 p2717 A69-30934

Injected gas flow nonisothermicity and transversity effects on friction, heat transfer and flow parameters at cylindrical tube inlet

15 p2592 A69-30986

Heat transfer - AICHE/ASME Conference, Philadelphia, August 1968

15 p2718 A69-31114

Heat and mass transfer in porous medium with bulk flow in thin adjacent channel, applying Green function analysis to hydrogen-oxygen fuel cell

15 p2552 A69-31115

Creeping flow model of Leidenfrost boiling with moving surface, discussing vaporization time for equivalent drop film boiling on stationary surface [AIChE PAPER 20]

15 p2718 A69-31116

Temperature distributions in layer with internal heat source and turbulent fluid flow cooling, deriving differential heat transfer equations

15 p2718 A69-31169

Wind tunnel investigation of turbulent gas flow heat transfer and hydrodynamic drag in variable pressure gradient field of divergent-convergent channel

15 p2548 A69-31173

Thermoelastic stresses in isotropic circular cylinder with surface locally heated by external Newtonian heat source, considering various heat transfer conditions

15 p2714 A69-31178

Plane Cauchy problem solution for differential equations in heat and mass transfer theory, applying contour integral method in matrix construction

15 p2719 A69-31262

Heat transfer in rarefied gas plane Couette flow determined by BGK model and moments method of half range distribution functions

16 p2876 A69-31688

Near free molecule heat transfer and density distribution between concentric spheres using BGK model equation and Knudsen iteration technique

16 p2877 A69-31921

Analytical expressions validity for skin friction in compressible turbulent boundary layer over wide range of Reynolds numbers and heat transfer conditions

16 p2771 A69-31926

Reacting gas ignition by sudden contact with heated noncatalytic surface, deriving heating time and transferred heat amount by Blasius perturbation method

16 p2878 A69-31955

Soviet bibliography of heat and mass transfer covering thermodynamics, aerohydrodynamics, MHD, transfer processes in various media, etc

16 p2878 A69-31960

Hybrid rockets combustion mechanism, discussing turbulent boundary layer with heat and mass transfer, chemical reactions, etc

16 p2879 A69-32002

Monograph on engineering calculations of momentum, heat and mass transfer through laminar boundaries having arbitrary pressure distribution and constant physical properties

16 p2879 A69-32203

Medium temperature fuel cells advantages including improved electrochemical reaction kinetics, water and heat removal

16 p2739 A69-32417

Injection film cooling effect on surface heat transfer downstream of flush nontangential injection holes and slots in turbine applications [AIAA PAPER 69-523]

16 p2843 A69-32703

Inlet thermal boundary layer thickness effect on conical nozzle heat transfer and boundary layer determined by operating nozzle with cooled/uncooled inlet [AIAA PAPER 69-474]

16 p2881 A69-32780

Linear heat flux in thin composite plate with internal point source, assuming no heat transfer at surface and neglectable temperature changes

17 p3068 A69-33126

Constant temperature heat pipe for thermal control of spacecraft components by direct coupling to external radiator [AIAA PAPER 69-632]

17 p3070 A69-33262

Optimal design for improving thermal performance of existing spacecraft thermally actuated louver system by increasing open-to-closed emittance ratio [AIAA PAPER 69-627]

17 p3071 A69-33269

Heat transfer suppression techniques in high temperature low density fiberglass insulation for flight vehicles [AIAA PAPER 69-606]

17 p3072 A69-33279

Shock layer properties, radiative and convective heat transfer about two hypersonic blunt bodies at zero angle of attack in assumed Martian atmosphere [AIAA PAPER 69-634]

17 p2891 A69-33281

Electron heat transfer and spherical probe characteristics in moving nonequilibrium plasma analyzed at stagnation region as function of solid surface potential [AIAA PAPER 69-699]

17 p3011 A69-33475

Transverse magnetic field effect on shear turbulence structure of magneto-fluid-mechanic pipe flow with and without heat transfer [AIAA PAPER 69-723]

17 p3012 A69-33497

Clear air turbulence uninfluenced by mesoscale disturbances or terrain, discussing relationship between density profile curvature and heat and momentum transfer

17 p2998 A69-33733

Heat transfer from cylindrical copper surface to liquid helium at 4 degrees K, discussing temperature fluctuations in nucleate boiling region

17 p3074 A69-33780

Terminal characteristics of composite superconductor, taking into account heat transfer to coolant, interface thermal contact resistance and superconductor size

17 p3007 A69-33792

Optimum ballast resistance of thin film heat transfer gage producing shock arrival time, thickness and structure data of low pressure shock tube

18 p3117 A69-34470

Heat transfer from molybdenum tube at high temperature to argon flow inside, using circulation principle

18 p3229 A69-34712

Transport processes effect in shock wave on hypersonic flow past blunt body in neighborhood of stagnant point, noting heat transfer

18 p3086 A69-34910

Thermal accommodation coefficients determination, comparing techniques based on free molecule flow heat flux data

18 p3230 A69-35071

Fluctuating heat transfer and flow measurements for circular cylinder in crossflow with simultaneously imposed transverse standing sound field

18 p3124 A69-35384

Calibration of inertial and surface temperature heat transfer transducers for hotshot and shock tube measurements developed and tested at ONERA [ONERA-TP-683]

19 p3305 A69-35726

Ferroelectric transducer for heat transfer rates and flow measurement in gaseous systems with autostabilized temperature, noting film coefficient

19 p3307 A69-35749

Supersonic transport aviation fuel thermal stability measurement data correlated with data deduced from heat transfer measurements

19 p3393 A69-36210

Applied mechanics - Conference, Waterloo, Ontario, Canada, May 1969

19 p3374 A69-36655

Heat transfer problem involving temperature determination of body and ambient medium, deriving existence and uniqueness theorems for boundary value problems in curvilinear regions

20 p3631 A69-36991

Unsteady heat transfer between gas flow and solid surface during melting

20 p3631 A69-37088

Reynolds analogy factor approximate calculation for turbulent boundary layer with pressure gradient

20 p3514 A69-37183

He and Ar arc-heated flows into reservoir and expansion in converging-diverging supersonic nozzles, considering flow equilibrium effect on heat transfer and enthalpy

20 p3631 A69-37198

Isotherms location in simple nonconstant area/diverging/ tube configuration investigated for heat transfer

20 p3632 A69-37219

Book on heat transfer from horizontal heating surfaces to stationary boiling liquids, heating surface roughness effect and bubble formation

20 p3633 A69-37917

Heat transfer to compressible laminar jet flowing along flat wall, obtaining distributions of temperature, wall shearing stress, heat transfer rates and jet thicknesses [ASME PAPER 69-FLCS-30]

20 p3516 A69-37979

Heat transfer in radial flow between two parallel plates, calculating Nusselt number for laminar and turbulent flows

20 p3633 A69-38176

Unsteady boundary layer flows of compressible fluid over semiinfinite flat plate, discussing heat transfer rate

20 p3518 A69-38318

Book on heat and mass transfer in recirculating flows, presenting elliptic differential equations and numerical solutions by computer

21 p3691 A69-38333

Heat transfer and hydrodynamic resistance for turbulent gas flow in longitudinal positive and negative pressure gradients analyzed using Reynolds number data

21 p3848 A69-38635

Thermal stress distribution induced in wedge by apex heat source analyzed using elasticity theory, considering lateral surface heat transfer

21 p3833 A69-38644

Heat loss from cylinders at low Reynolds numbers in N-He and N-Ne binary mixtures

21 p3848 A69-38706

Optimal boundary layer control ensuring minimum heat transfer to porous plate from incompressible flow of hot gas of cooling system

21 p3849 A69-38846

Gas heat transfer on turbine interblade channel surfaces and working blade end surfaces at operating Reynolds and Mach numbers

21 p3849 A69-38858

Heat transfer in curved channel as function of inlet configurations, obtaining Nusselt number equations for thermal and mixed convection and laminar flow

21 p3850 A69-38866

Velocity decay and heat transfer rates measurement in cylindrical wall jet formed by jet emerging through convergent nozzle

21 p3695 A69-38972

Transient heat transfer single blow temperature response functions characterized by first moment of downstream-upstream fluid temperature difference, showing curve matching applications

21 p3851 A69-39291

Instantaneous frozen layer thickness and temperature profile in solidified layer obtained by iteration technique

21 p3852 A69-39433

Heat pipes for isothermal and adaptable energy transfer for space applications, discussing temperature control by fluid choice

21 p3852 A69-39475

Time-optimal nuclear rocket propellant start-up with thermal stress constraints based on distributed parameter model, deriving algorithm for flow rate increase
21 p3768 A69-39632

Finite-difference grid procedure for predicting friction heat and mass transfer in two dimensional boundary layers
22 p3932 A69-40939

Heat transfer and surface thermal conduction characteristics of contact of two solid bodies, discussing pressure effect, measurement and analytical techniques
23 p4237 A69-41327

Sonic vapor flow heat transfer limitations in heat pipes for Na, K and Cs, showing strong influence of temperature and working fluid
23 p4239 A69-41719

Thermal isolation characteristics of low conductance interstitial materials determined, using test apparatus of axially loaded radiation shielded cylindrical column in vacuum
[AIAA PAPER 68-31] 23 p4239 A69-41889

Hypersonic turbulent flow heat transfer and pressure data for flat plate containing steps and cavities obtained in hypersonic wind tunnel
[AIAA PAPER 68-673] 23 p4060 A69-41902

Organic Rankine cycle system using heat absorption from turbine exhaust to provide increased electrical output and to power air conditioning
23 p4070 A69-42267

Prandtl number influence on heat transfer and pressure drop characteristics of roughened channels, determining friction factor
24 p4407 A69-42915

Graph analytical method for calculating heat transfer in diathermic exchangers during boiling together with critical thermal loads
24 p4408 A69-43080

Monte Carlo method applied to heat transfer in rarefied gas flow between parallel plates involving temperature jump in Knudsen layer
24 p4246 A69-43490

Heat exchange at stagnation point during interaction between underexpanded axisymmetric supersonic jet and flat obstruction, using method of characteristics
24 p4246 A69-43493

Intense heat exchange narrow zones on blunted semicone surfaces in hypersonic gas flows ascribed to large Reynolds numbers
24 p4246 A69-43494

Heat transfer to highly accelerated turbulent boundary layer with and without mass addition, presenting data in terms of Stanton number vs Reynolds number
[ASME PAPER 69-HT-53] 24 p4409 A69-43518

Heat and mass transfer in gas suspension, studying suspended particles effects on heat transfer by irreversible thermodynamics
[ASME PAPER 69-HT-34] 24 p4410 A69-43528

Heat transfer and fluid friction of hydrogen and helium gas flows undergoing turbulent to laminar flow transition in heated pipe
[ASME PAPER 69-HT-54] 24 p4303 A69-43539

Hydrodynamic inlet conditions effect on film boiling and near critical hydrogen heat transfer, using data from electrically heated various geometry test sections
[ASME PAPER 69-HT-27] 24 p4412 A69-43541

Heat transfer capability and startup behavior of sodium heat pipes, studying heat transfer limit due to vapor velocity at evaporator end
[ASME PAPER 69-HT-21] 24 p4412 A69-43547

Wick-limited heat pipe performance, discussing maximum, steady heat transfer rate and transient response
[ASME PAPER 69-HT-20] 24 p4413 A69-43549

Rotating wickless hollow shaft heat pipe utilizing centrifugal acceleration for return pumping of condensate and transferring high heat fluxes
[ASME PAPER 69-HT-19] 24 p4413 A69-43550

Luminescent turbulent boundary layer prediction using mixing length model modified for viscous sublayer structural changes near wall compared with heat transfer data
[ASME PAPER 69-HT-13] 24 p4303 A69-43556

Laminar, transition and turbulent boundary layer heat transfer measurements along wall in thermal entrance region of high temperature turbulent airflow through cooled tube
[ASME PAPER 69-HT-8] 24 p4414 A69-43560

Boundary layer equations with heat transfer for laminar and turbulent incompressible flows about two dimensional and axisymmetric flows, using finite difference method
[ASME PAPER 69-HT-7] 24 p4304 A69-43561

Taylor Goertler vortex formation effect on heat transfer through boundary layer on concave wall
[ASME PAPER 69-HT-3] 24 p4414 A69-43563

Heat finite propagation velocity effects on temperature distribution and heat flux for step temperature change at semiinfinite body surface
[ASME PAPER 69-HT-1] 24 p4414 A69-43564

Superimposed free vortex swirl effect on flow and heat transfer in three dimensional axisymmetric laminar boundary layer
24 p4304 A69-43584

Stagnation region heat transfer with nongray gas subjected to external radiation using two step continuum absorption coefficient model
24 p4415 A69-43590

Laminar sublayer thickness in compressible turbulent boundary layers with and without heat transfer
24 p4306 A69-43724

HEAT TRANSFER COEFFICIENTS

Polycrystalline corundum thermal conductivity coefficients determination, describing measuring procedures at low temperatures
01 p0101 A69-10108

Heat and mass transfer coefficients derived for reacting gas mixtures by applying variational principle
01 p0006 A69-10400

Alternating direction implicit (ADI) methods for solving parabolic heat conduction equation with variable coefficients in two and three space dimensions
01 p0106 A69-10987

Heat transfer coefficient for spherical protuberance on plate with turbulent boundary layer
[ASME PAPER 68-HT-2] 02 p0351 A69-12204

Heat transfer near stagnation point in axisymmetric turbulent jet impinging on circular disk
02 p0354 A69-12491

Minimum drag configurations with low heat transfer for hypersonic bodies of revolution, noting performance at supersonic speeds
02 p0191 A69-12578

Experimental apparatus for measuring heat transfer coefficients into boiling K in tubes, investigating vapor-liquid mixtures hydrodynamic and electrical properties
03 p0534 A69-14150

Cone tip blunting effect on cone local laminar heat transfer rate noting cone configuration, semivertex cone angle and Mach number
04 p0542 A69-14721

Forced convection heat transfer coefficient invariance to flow reversal in Stokes and potential streaming flows past isothermal particles of arbitrary shape
04 p0590 A69-15274

Hydrogen arc in axially parallel magnetic field produces higher plasma temperatures by reduced thermal conductivity coefficient
07 p1189 A69-18489

Heat convection coefficient for wires enclosed in cylindrical tubes filled with water or ethanol, showing dependence on inclination angle
07 p1242 A69-18926

Shear stress at wall, averaged velocity field and turbulent heat transfer coefficients in straight smooth non-circular channels used to compute temperature fields
07 p1243 A69-19734

Laminar heat transmission coefficients in combustion zone for particular oxygen and kerosene mixture
08 p1421 A69-20585

Convective heat exchange coefficients for human organism in aircraft surroundings under homogeneous temperature conditions, deriving acclimatization equations
[AGARDOGRAPH-111] 08 p1266 A69-20673

Monograph on heat transfer coefficients of polystyrene foams noting contribution of gas conduction, convection and radiation to total heat transfer
08 p1421 A69-20716

Zero sensitivity integrated RC filter circuits design, exploiting capacitors and resistors property of having same temperature coefficient
08 p1300 A69-21174

Temperature profiles and heat transfer coefficients in two phase liquid-liquid stratified laminar flow of variable immiscible film thickness with surface evaporation
09 p1622 A69-21904

Local heat transfer coefficients in oscillating turbulent boundary layer over flat plate
[ASME PAPER 69-GT-34] 09 p1623 A69-22490

Surface heat transfer coefficients under perforated plate of multiple square array round impinging air jets
[ASME PAPER 69-GT-4] 09 p1624 A69-22508

Heat transfer coefficients for free convection from single horizontal cylinder to fluids computed from empirical correlation
09 p1625 A69-22693

Flow and heat transfer measurements for heated air in subsonic flow through contraction section connecting tube to conical section
[JPL-TR-32-1348] 10 p1809 A69-23194

Heat transfer rates for water, acetone and alcohol droplets splattering from heated plate, noting effect of impact angle and velocity
10 p1809 A69-23196

Heat transfer at plate in hydrodynamically stabilized turbulent boundary layer region, obtaining formulas for calculating transfer coefficients
10 p1809 A69-23427

Temperature field calculation in infinite plate with heat transfer coefficient and ambient temperature arbitrary functions of time
10 p1809 A69-23430

Horizontal surface heat transfer coefficient under simultaneous free and forced convection calculated as function of temperature head, air flow velocity and area
10 p1810 A69-24085

LF measurements with positive or negative temperature coefficient resistors based on current-voltage characteristics
11 p1845 A69-24522

Temperature variation effects on heat transfer in laminar tube flow, taking into account constant wall temperature and heat flow density
12 p2189 A69-25762

Heat and mass transfer coefficients derived for reacting gas mixtures by applying variational principle
12 p2062 A69-26668

Heat transfer coefficients for carbon dioxide near thermodynamic critical point for flow through electrically heated duct, noting turbulent forced convection as mechanism
[ASME PAPER 68-HT-32] 13 p2373 A69-27769

Local film heat transfer coefficients variations effect on longitudinal constant area fin surface under turbulent flow
[ASME PAPER 68-HT-20] 13 p2373 A69-27770

Heat transfer coefficient deterioration between fluid and tube wall at supercritical pressure and high heat fluxes
[ASME PAPER 68-HT-39] 13 p2373 A69-27771

Combined conduction and radiation transfer equations solutions for absorbing-emitting gas, obtaining slip coefficient for diffusion solution correct boundary condition
13 p2374 A69-27784

Heat transfer coefficients for supersonic open cavity flow recompression steps noting influence of step and flow shapes
13 p2375 A69-27786

Triangular profile circular fins efficiency determined from differential equations solution governing temperature distribution
13 p2375 A69-27790

NOL hypervelocity launcher heat transfer and erosion analysis by experiment and computer simulation
[AIAA PAPER 69-336] 13 p2242 A69-28272

Heat and mass transfer coefficients in binary laminar boundary layer during natural convection, taking into account enthalpy and thermal diffusion effects
13 p2378 A69-28312

Turbulent heat exchange coefficient radiation absorption and diurnal vertical variations effects on temperature field in surface layer of sea and atmospheric boundary layer
14 p2472 A69-29462

Partially ionized multicomponent gas mixture kinetics in strong electromagnetic field, determining magnetic field, stress tensors and transfer coefficients
14 p2492 A69-29610

Thermal conductivity coefficients in solar corona and chromosphere computed and tabulated for H plasma
15 p2694 A69-30788

Ceramic heat transfer gage for supersonic wind tunnel investigation of blunt swept wing leading edges aerodynamic heating
15 p2613 A69-31272

Effective heat transfer coefficient lambda for microscopic Fe particles traversing rarefied air, oxygen and Ar target gases
16 p2769 A69-31870

Heat transfer in laminar separated flows with flat plate segment connections, indicating correlation between local heat transfer rates for successive regions
16 p2879 A69-32169

Internal heat transfer coefficients for impingement cooling of gas turbine airfoil leading edge
[AIAA PAPER 68-564] 17 p3022 A69-34021

Nonuniform heating rates during laminar boundary layer transition on slender cone at hypersonic speeds
18 p3085 A69-34435

Heat transfer coefficient approximation under thermal instability conditions complicated by radiant heat exchange at plate surface, noting aircraft design applications
18 p3230 A69-34984

Channel heat transfer determination based on thermal conductivity coefficients as functions of temperature gradients in channel wall materials
18 p3230 A69-34988

Seam welded U-type fin efficiency and effectiveness, studying effects of fin height, heat transfer coefficient and thermal resistance
19 p3452 A69-36371

Local heat transfer coefficients determined from temperature distribution on porous walls, deriving mathematical expressions for various surface geometries and transfer modes
20 p3630 A69-36977

Flat surfaces downstream of heated section and porous strip, determining film cooling effectiveness and heat flux from heat transfer coefficients ratios
20 p3631 A69-37096

Heat transfer coefficient and flow patterns of horizontal circular plate for various Rayleigh numbers, noting surface temperature
20 p3632 A69-37523

Heat and mass transfer coefficients in binary laminar boundary layer during natural convection obtained with integral equations and Karman-Polhausen method
21 p3848 A69-38633

Heat transfer coefficients, boundary layer thicknesses and temperature and velocity distributions in free convection boundary layer in closed axisymmetric volumes
21 p3848 A69-38634

Thermal conductivity coefficient of gas mixtures at low temperatures obtained using quantum diffusion model and Chapman-Enskog method for Boltzmann equation
21 p3848 A69-38638

Asymptotic method applied to nonlinear equations, determining thermal conductivity coefficient for temperature distribution in moving anisotropic media
21 p3848 A69-38642

Heat transfer coefficients evaluated from gas to rotating turbine blades in unsteady operation, using unsteady thermal conductivity and gradient methods
21 p3850 A69-38864

Heat transfer characteristics in evaporative, transpiration cooled porous systems
21 p3851 A69-39037

Constant surface heating of half space with temperature dependent thermal conductivity
21 p3851 A69-39292

Ablation effect on heat transfer coefficient of carbon, silica and ceramic cloths impregnated with phenolic resin subjected to torch testing and motor firing
21 p3753 A69-39800

Heat transfer from spheres in free finite width flow, determining heat transfer coefficient distribution as function of flow width and Reynolds number
21 p3855 A69-39849

Forced convection heat transfer coefficient for fully developed turbulent flow in circular tube with time-varying circumferential heat flux
22 p4051 A69-40921

Heat transfer coefficient of turbulent air flow found independent of temperature head during cooling
22 p4051 A69-41026

Thermal conductivity relationship to heat transport coefficients for gases and liquids with charged or uncharged particles
23 p4237 A69-41324

Rectangular fins arrangement on horizontal surfaces for optimum free convection heat transfer coefficient, considering fin weight, height and spacing effects
[ASME PAPER 69-HT-44] 24 p4409 A69-43517

Heat transfer during nitrogen tetroxide nucleate boiling at various pressures and heat fluxes
[ASME PAPER 69-HT-58] 24 p4411 A69-43536

Air flow laminarizing turbulent boundary layer, determining velocity, turbulence intensity, temperature profiles and local heat transfer coefficients
[ASME PAPER 69-HT-10] 24 p4413 A69-43558

Turbulent pipe flow with wall suction, calculating friction factor, pressure gradient, heat and mass transfer coefficients, velocity and temperature profiles
[ASME PAPER 69-HT-4] 24 p4414 A69-43562

HEAT TRANSMISSION

NT AERODYNAMIC HEAT TRANSFER

NT CONDUCTIVE HEAT TRANSFER

NT CONVECTIVE HEAT TRANSFER

NT HYPERSONIC HEAT TRANSFER

NT LAMINAR HEAT TRANSFER

NT RADIATIVE HEAT TRANSFER

NT SUPERSONIC HEAT TRANSFER

NT TURBULENT HEAT TRANSFER

Unsteady heat flow in finite composite hollow circular cylinder using inverse method of eigenfunction expansion / method of finite integral transformation/
01 p0175 A69-10230

Thermal stresses near spherical inclusion in elastic matrix with uniform heat flow
01 p0171 A69-11264

Heat flow measurement from moon interior planned for Apollo missions to determine temperature increase rate with depth during lunar year
[AAS PAPER 68-207] 02 p0313 A69-11482

Dynamics of moving gas bubble injected in quiescent liquid, considering velocity, heat flow and mass transfer
[ASME PAPER 67-WA/HT-30] 02 p0351 A69-12201

Sensible and latent heat meridional transport associated with standing eddies computed from climatic mean data
04 p0627 A69-15085

Water and heat removal unit for hydrogen/oxygen fuel cell systems, discussing temperature distribution, heat and liquid transport
05 p0704 A69-15676

Variational methods applied to unsteady heat flow, describing approximate method for unsteady temperature field in heat conducting body
05 p0845 A69-15794

Stress concentration at thermally insulated holes in elastic material created by disturbance of uniform heat flow at holes
06 p1021 A69-17184

Weightlessness effect on critical heat flow during forced motion of water in different kinds of channels
07 p1243 A69-19616

Vibrational relaxation effects on laminar boundary layer velocity profiles and temperature and on layer thicknesses and wall heat flow downstream of shock wave
08 p1303 A69-20269

Displacement effect due to subsonic reaction heat front behind shock wave in two dimensional supersonic flows
08 p1252 A69-20691

Electroconvective instability produced by uniform electric field in poorly conducting fluid under stabilizing vertical temperature gradient, noting heat flow increase
08 p1352 A69-20791

Thermal stress field under uniform heat flow due to elliptical elastic inclusion for anisotropic case
08 p1418 A69-21003

Transient heat flow in isotropic solids by electrical analog modeling in orthogonal curvilinear coordinate system
09 p1477 A69-22241

Steady laminar boundary layer flow calculations extended to temperature boundary layer for given heat flow or temperature distribution at wall
10 p1808 A69-22915

Heat propagation in discharge plasma heated by magnetosonic wave, constructing transverse temperature profile
10 p1741 A69-23896

Lunar radio emission constant component in presence of heat flow from interior, using stratified model of surface structure with two variants
11 p1956 A69-24398

Steady heat flow in cylindrical bodies with curvilinear rectangular cross sections, solving equation in form of Fourier series according to trigonometric functions
11 p2000 A69-24974

Shrinkage and heat release of polyglycol malinate binder during gamma radiation consolidation compared with thermochemical consolidation
12 p2117 A69-25991

Limiting heat power transported by sodium heat pipes dependent on capillary network geometry, inclination angle and operating temperature
14 p2538 A69-29205

Dimensionless approach to maximum flow in heat pipes and optimization of capillary structure
14 p2539 A69-29206

Liquid-vapor interaction in loop plates with different heat pipe capillary geometries using water as heat transporting medium
14 p2539 A69-29207

Thermal conductivity of semiinfinite rod with insulated surface and constant internal heat source, considering finite heat propagation rate
15 p2719 A69-31181

Second breakdown and other thermal instabilities analyzed by heat flow equation, obtaining stability criteria predicting reduced power dissipation for transistor at low currents
16 p2758 A69-31618

Relativistic exceptional wave propagating heat, computing speeds in direction orthogonal to heat vector
16 p2827 A69-32042

Earth surface heat flow pattern measurement and distribution techniques, considering relation to surface features and tectonic movements of crust
[AIAA PAPER 69-589] 17 p2961 A69-33284

Heat flow through ocean floor by measuring temperature gradient and thermal conductivity in ocean sediment
21 p3718 A69-39733

Heat flow in belt-type heat transport device allowing for conductive and mass transport effects, deriving expression for heat transfer capability
22 p4050 A69-40554

Thermal diffusivity measurement by nonsteady state methods, discussing time and temperature variables in heat flow differential equation
23 p4237 A69-41326

Lunar radio emission constant component in presence of heat flow from interior, using stratified model of surface structure with two variants
24 p4390 A69-43788

HEAT TREATMENT

NT ANNEALING

NT NITRIDING

NT PULSE HEATING

NT STRESS RELIEVING

NT TEMPERING

Beta titanium alloys mechanical properties improvement, discussing effects of alloying elements, heat treatment and high temperature deformation
01 p0093 A69-10213

Charge materials purity found to increase beta-Ti alloys properties
01 p0094 A69-10216

Chemical vapor deposited W and W-Re alloys investigated for deposition variables and heat treatment effects on mechanical properties
01 p0097 A69-10648

Maraging steels ductile and strength characteristics with increased Co and Mo as function of Ni content, tempering method and aging
01 p0098 A69-10731

Soviet book on structure of thin metal films covering electron microscopic and electronographic studies, crystallization and heat treatment effects
01 p0140 A69-11106

Light austenitic grain boundaries in heat treated Cr-Mo-W-V alloy steels
01 p0100 A69-11295

Steel selection for heat treated parts, discussing strength and hardness, service conditions, carbon content, quenching, cost, etc
01 p0101 A69-11397

Heat treatment and shot peening effects on Al alloy fatigue strength and fine crystallographic structure
04 p0614 A69-14576

Low temperature aging prior to higher temperature artificial aging increases Al alloys strength
04 p0614 A69-14634

Thermal strengthening effect in aluminum due to temperature fluctuations
04 p0615 A69-14638

Overheated maraging steel mechanical properties improvement by heat treatment
04 p0615 A69-14646

Alpha to gamma transformation kinetics in maraging steel during heating, studying alloying elements redistribution
04 p0616 A69-14648

Maraging steel with reduced Co, establishing optimal temperature range for short aging
04 p0616 A69-14650

Heat treatment effects on stress corrosion cracking resistance of Al-Zn-Mg alloys, using cantilever loading in aqueous solution
04 p0617 A69-14933

Hot working temperature effects on Rene 63 mechanical properties and microstructures, using tensile and stress rupture tests, electron microscopy and X ray diffraction analysis

05 p0781 A69-16446

Film processing effects on cryogenic mechanical properties of polyethylene terephthalate

05 p0785 A69-16490

Two stage thermal treatment inhibiting influence on swelling and porosity linked to Kirkendall effect during sintering of Fe-Ni powder mixtures

05 p0782 A69-16616

Electron microscopy of titanium alloys noting preparation, heat treatment of samples, crystallographic structure, etc

05 p0782 A69-16807

Electron microscopic and microdiffraction study of structure of quenched and annealed titanium alloy foils at high temperatures

05 p0783 A69-16810

Plastic deformation, aging, heat treatment and machining effect on structure of thin films of AMg11 alloy

05 p0783 A69-16814

Cadmium ionization energy in InAs using heat treatment in hydrogen to eliminate anomalies

06 p0979 A69-16998

Structure and critical superconductivity current of titanium niobium alloy as function of heat treatment and deformation

07 p1158 A69-18532

Nimonic alloys recovery analyzed by X rays and electrolytic phase separation, showing precipitated gamma phase effect

07 p1159 A69-18533

Ti alloys thermomechanical treatment effect on strength and plasticity characteristics, noting single and double phase alloys and rupture

07 p1161 A69-18766

Tin and zirconium addition effect on transformations of titanium alloys during heat treatment

07 p1162 A69-18775

Ti alloy beta phase variations in quantity, composition and dispersion during quenching, thermomechanical treatment and aging

07 p1163 A69-18777

Ductility as principal cause of postweld heat treated stress relaxation cracking in nickel based Waspaloy and alloy 718

08 p1318 A69-19964

Roll planishing and thermal treatments effects on gas tungsten arc welded Ti-6Al-4V alloy on residual stresses, tensile, formability and fracture toughness properties

08 p1319 A69-19966

Metallographic and X ray study of cellular decomposition and precipitation in superconducting niobium zirconium alloy, noting heat treatment effect on current carrying properties

08 p1331 A69-20192

Organic quenchant additive for distortion free heat treatment of dip-brazed aluminum parts

09 p1504 A69-22065

Titanium alloy castings fatigue behavior at room and elevated temperatures in annealed and heat treated conditions

09 p1619 A69-22497

Slow recombination centers parameters in CdSe single crystals during heat treatment in vacuum or hydrogen atmosphere

09 p1560 A69-22664

Heat treatments in inert gas atmosphere improve elastic foam polyurethane by reducing capability of toxic outgassing

10 p1716 A69-23503

Audio frequencies internal friction measurement of austenitic stainless steels subjected to heat treatment and corrosion, discussing time dependence and carbide precipitates morphology

10 p1713 A69-23819

Thermomechanical treatment effect on VT15 Ti alloy properties and welds after deformation, attaining high tensile strength and plastic properties

11 p1889 A69-24277

Aluminum alloy weld tensile strength increased by heat treatment, discussing weld porosity due to surface film of absorbed hydrogen

11 p1891 A69-24896

Heat treatment effect on Ti-Mn alloy microstructure, discussing fcc martensite transformation into alpha, beta and intermediate phases as function of aging

11 p1906 A69-25578

Residual stresses and strains in wound reinforced plastic fiber cylinders subjected to polymerization by heat treating

11 p1907 A69-25679

Yield to ultimate tensile strength ratio of titanium alloys subjected to thermomechanical treatment

11 p1906 A69-25683

Steels classification for welded construction according to heat treatment and metallurgical structures

12 p2111 A69-25826

Heat treatable low alloy steels weldability for lightweight ultrahigh strength pressure vessels, gear and shaft fabrication in aerospace applications

12 p2100 A69-25827

Ti-Nb alloy structure in heat treatment states analyzed by diffuse scattering of X ray lines and by electron microscope

12 p2112 A69-26036

Heat treatment effects on molybdenum-rhenium alloy field emission and surface structure in alpha and sigma phase regions

12 p2113 A69-26041

Eutectoid pearlite growth by pure iron-carbon specimen heat treatment

13 p2281 A69-28158

Aluminum alloys precipitation hardening types requiring solution heat treatment, quenching and artificial aging, noting advantages in strength and weldability

13 p2282 A69-28180

Induced stressing method for complex castings by controlled cooling during heat treatment applied to front frame of J-79 turbojet engine

13 p2269 A69-28184

Oil quench vacuum furnace with graphite cloth heating elements

14 p2456 A69-29894

Beta titanium alloys mechanical properties improvement, discussing effects of alloying elements heat treatment and high temperature deformation

15 p2637 A69-30269

Charge materials purity found to increase beta-Ti alloys properties

15 p2638 A69-30272

Heat treatment and shot peening effects on Al alloy fatigue strength and fine crystallographic structure

15 p2638 A69-30278

Discontinuous yielding characteristics of 2024 Al alloy determined for different conditions of solution, heat treatment and age hardening

15 p2639 A69-30598

Heat treatment effects on Te-doped GaAs, using photoluminescence and carrier concentration measurements to study defects formed

16 p2825 A69-31708

X ray diffractometer stress analysis of WC-Co cermets, discussing surface preparation and heat treatment

16 p2802 A69-32339

Microstructural factors role in metal fracture toughness, considering effects of deformation processing and heat treatment, grain size, structural refinement, fibering, etc

17 p2988 A69-33552

Heat treatment effect on stress corrosion cracking of ternary Al-Zn-Mg alloys noting aging strength, solution temperature, quenching rate and alloy content

17 p2990 A69-33676

Damping, fatigue and optimal heat treatment of Cr-Ni steel for compressor blades operating at temperatures up to 500 K

17 p2990 A69-33933

Forming and heat treatment process for stainless steel pressure containers using liquid N, discussing austenite-martensite transformation role

18 p3161 A69-34605

Al cryogenic quenching using liquid N for slow and uniform heat removal to eliminate distortion

18 p3150 A69-35419

Nickel maraging steel weld metal impact strength and fracture toughness improved by heat treatment

18 p3151 A69-35430

Heat treatment effects on mechanical properties of Ti-Fe and Ti-Fe-Al alloys

19 p3344 A69-36151

Pyrolyzed tetrathoxysilane for carburizing steels and Ti alloys at 850-1050 C

19 p3328 A69-36161

Heat treatment effect on superconducting properties of deformed Nb-Ta alloys, noting critical current density

19 p3345 A69-36303

Welding processes providing low hydrogen welds for high strength steels, discussing heat treatment, maraging steels, fracture toughness, fatigue and static strength

20 p3549 A69-37447

[SBAC PAPER 8]

Polycrystalline nickel foil microstructure after explosive shock loading and heat treatments, using transmission electron microscopy

20 p3563 A69-38126

Vacuum heat treating and joining process for various ferrous and nonferrous metals and alloys, discussing advantages, applications and economics

[ASM PAPER D8-22.3]

20 p3551 A69-38132

Ti-Al-V fasteners heat treated in beta field, showing superior mechanical properties to samples treated in alpha plus beta field

21 p3729 A69-38661

Creep resistance increase of Ni refractory alloy by thermovibrational treatment under stress relaxation conditions

21 p3744 A69-38869

Ti-Al-V forgings macro /prior beta/ grain size and in-process thermal treatment effects on fatigue life

[AIME PAPER S69-2]

21 p3732 A69-39470

Soviet book on heat treatment of Ti alloys emphasizing structural and phase composition changes

21 p3749 A69-39526

C and B influence on heat affected zone hot cracking and postweld heat treatment on Ni base superalloys

22 p3967 A69-39880

Composition and thermal treatment effects on weldability of precipitation hardened Ni base alloy, analyzing heat affected zone cracking sensitivity

22 p3968 A69-39885

Short period creep and relaxation in various heat resistant alloys under heat treatments and loads, determining temperature dependence of cyclic thermal instability

22 p3969 A69-40071

Multicomponent Nb alloy creep and rupture strength under loads after heat treatment, determining creep rates dependence on temperature

22 p3969 A69-40073

Heat treated Ti-Al-Fe alloys thermal, microstructural and X ray analyses of phase transformations in Ti-rich corner

22 p3969 A69-40074

Engineering alloys electrical resistivities measurement at various temperatures, noting temperature and heat treatment effects

[NAS-NRC PAPER D-5]

22 p3970 A69-40633

High temperature vacuum treatment of thick stainless steel sheets reducing hydrogen content and outgassing

23 p3958 A69-41217

Ingot dendrite arm spacing and thermomechanical treatment effects on fracture behavior and mechanical properties of Al alloy, finding ultimate and yield strengths

23 p4176 A69-41506

Plane strain fracture toughness of S-200 grade Be for 77-533 K temperature range, noting effects of loading, heat treatment and neutron irradiation

23 p4178 A69-42450

Single run reheated weld wrought steel H cracking tested by constant load rupture /static fatigue/ technique

24 p4320 A69-42943

HEATING

NT AERODYNAMIC HEATING

NT ARC HEATING

NT ATMOSPHERIC HEATING

NT BASE HEATING

NT GAS HEATING

NT INDUCTION HEATING

NT IONOSPHERIC HEATING

NT KINETIC HEATING

NT OHMIC DISSIPATION

NT PLASMA HEATING

NT PULSE HEATING

NT RADIANT HEATING

NT RADIO FREQUENCY HEATING

NT RESISTANCE HEATING

NT SHOCK HEATING

NT SOLAR HEATING

NT SUPERHEATING

NT TRANSIENT HEATING

Operational and integral heat balance method to obtain exact and approximate solution for monotonic heating of two layer unbounded plate

01 p0174 A69-10097

Vacuum heating and thermal cycling influence on mechanical and structural properties of aluminum sheets fabricated from sintered powder

02 p0266 A69-12126

Tubular light beam waveguide properties, studying changes related to heating and ionization of medium

02 p0258 A69-12644

Temperature distribution and vaporization rate boundary conditions on metal particle surface during preignition heating in oxygen containing medium
02 p0355 A69-12670

Thermodynamic cycle and optimum conditions of electric power source of MHD generator in combination with thermocompressor
09 p1435 A69-21592

Energy conversion with liquid metal working fluids in MHD generators, discussing single stage fully Car-notized process
13 p2372 A69-27482

Liquid metal multistage injection efficiency with sodium and potassium working fluids, noting preheating
13 p2372 A69-27483

Multirecompression heater for pure airflow tests of ballistic vehicles and hypersonic aircraft [AIAA PAPER 69-332]
13 p2242 A69-28268

Thermocompression joints strength measured using friction test, centrifuging and microtensile tests
15 p2573 A69-30081

HEATING EQUIPMENT

NT BOILERS

NT EVAPORATORS

NT FURNACES

NT SOLAR FURNACES

NT VACUUM FURNACES

NT VAPORIZERS

IR heating, discussing operation of IR emitters employing glass and quartz envelopes
03 p0411 A69-13548

Heating system providing symmetrical temperature field and specimen self centering for thermal resistance tests
10 p1696 A69-23845

Etching, spray etching and photo-resist methods for producing CrNi steel heating elements for propeller de-icing
12 p2102 A69-26370

Heat pipe boil-off control system for reducing cryogenic boil-off during long term space storage
12 p2191 A69-26793

Oil quench vacuum furnace with graphite cloth heating elements
14 p2456 A69-29894

Electrical failures in aircraft due to static electrification of electrically heated windscreens, noting materials for reducing surface resistivity
19 p3256 A69-36769

Autotransformer with static tap changer to provide varying power levels for controlled gradual heating of aircraft window to avoid thermal shock
22 p3869 A69-40414

Freon boiler designed for Rankine cycle heater fired on hydrocarbons with over 2000 F flame front temperature, considering radiant/convective heat transfer
23 p4068 A69-42239

HEAVY COSMIC RAY PRIMARIES

U PRIMARY COSMIC RAYS

HEAVY ELEMENTS

NT PLUTONIUM ISOTOPES

NT PLUTONIUM 238

Heavy xenon isotopic anomalies in carbonaceous chondrites, rejecting plutonium 244 spontaneous fission decay mechanism
05 p0819 A69-15625

Tungsten replacement by chromium or molybdenum in heavy metals shown possible for binding material of group 6A metals
05 p0780 A69-15991

Element synthesis in stars of galactic halo as possible explanation for heavy elements presence in supermassive objects
07 p1219 A69-19296

Nuclear particle plastic dielectric track detectors to record distribution of fissionable and heavy elements in nature and cosmic radiation
08 p1401 A69-20899

Temporal variation of metal content in galaxy, discussing stellar radiation pressure effects on heavy element abundance of interstellar gas
12 p2160 A69-26854

Heavy element abundances in peculiar A stars, investigating nucleosynthesis during massive stars evolution
14 p2527 A69-29945

Geochemistry of fission Xe component in chondrites, suggesting Xe derivation from superheavy elements with Z 112 to 119
15 p2681 A69-30325

HEAVY IONS

Spectrum and yield of emitted electrons resulting from passage of heavy ions through metal films
03 p0471 A69-13164

Heavy ion track thermal spike model to account for LET and temperature effects in radiation biology and chemistry
03 p0371 A69-13479

Accelerated helium and carbon ions effects on mutation-induction and nuclear inactivation in *Neurospora crassa* compared with X rays, discussing relative biological effectiveness/RBE/
03 p0373 A69-13490

Genetic effects in yeast induced by heavy ion radiation, studying lethality, mitotic segregation, allelic recombination and reverse mutation
03 p0373 A69-13491

Mammalian cell survival, chromosome abnormalities and recovery from heavy ion and X ray irradiation
03 p0373 A69-13492

Uranyl ions interaction with phospholipid and cholesterol monolayers, using surface pressure and potential measurements
11 p1832 A69-25641

Radiation damage in yeast cells irradiated by high energy C 12 ions evaluated from survival rate study
14 p2406 A69-28915

ELF and VLF wave propagation examined for heavy ions and lower ionospheric disturbance effects using numerical integration, noting standing wave field role for interpretation
18 p3125 A69-34254

Biological effects by cosmic ray heavy ions and solar flares, using direct correlation between damages caused and trajectories
23 p4089 A69-41831

HEAVY NUCLEI

Underground search for massive strongly interacting cosmic ray particles, using shower selecting extension array and interaction detecting telescope
02 p0310 A69-12831

Deuteron microbeam for simulating biological effects of ionization by heavy cosmic ray particles
03 p0373 A69-13493

Heavy cosmic ray particles effect in manned space flight, noting results of deuteron microbeam experiment
03 p0373 A69-13494

Mammalian radiobiological studies of effects of heavy particles, discussing therapeutically advantageous characteristics
03 p0374 A69-13499

Biological effects in man due to heavy particles emission during major solar cosmic ray events, noting protective effect of human body
03 p0374 A69-13500

Extraterrestrial background gamma radiation /0.3-2 Mev/ observations used to derive upper limits for cosmic ray protons and CNO nuclei in interstellar space
03 p0501 A69-13934

Heavy nuclei in cosmic rays analyzed in photographic emulsion tracks suggest supernova origin
04 p0649 A69-15422

Chemical composition of nuclear cosmic rays with Z greater than 22, noting etching techniques for utilizing meteoritic minerals as detectors
05 p0816 A69-16355

Energy spectrum and intensities of medium and very heavy nuclei in primary cosmic radiation
05 p0816 A69-16365

Heavy nuclei energy spectrum in primary cosmic rays explained by assuming two component charged nuclei
05 p0816 A69-16366

Interstellar flux of heavy and superheavy nuclei calculated, assuming nuclei injection with source spectrum similar to M nuclei
06 p0988 A69-17273

Heavy nuclei abundances and energy spectra in primary cosmic rays, using blob gap parameter as measure of primary ionization
06 p0988 A69-17274

Cellulose nitrate sheets applicability in detecting cosmic ray relativistic heavy nuclei, considering etchable tracks
06 p0924 A69-17286

Ablation rate of Saint-Severin amphoterite based on heavy primary cosmic ray track densities in surface samples
08 p1406 A69-20933

Satellite data on relative flux and group composition of heavy nuclei in primary cosmic rays
10 p1756 A69-22820

Heavy nuclei origin based on empirical abundance distribution, discussing stellar, galactic and cosmic events for nuclear genesis
17 p3009 A69-34190

Cosmic ray heavy nucleus ends flux by nuclear emulsions for balloon flights at various atmospheric depths
17 p3025 A69-34219

Energy spectrum of Fe group heavy nuclei from fossil track densities depth variation in hypersthene and oligoclase crystals from meteorite Saint-Severin, noting ablation
19 p3410 A69-36095

Densities and angular distributions of fossil tracks in meteorites produced by slowing down heavy primary cosmic ray nuclei
19 p3410 A69-36096

Cosmic protons and high energy heavy nuclei interaction with radiation in expanding universe, including estimates of light radiation influence on cosmic ray spectra
20 p3591 A69-38034

Trans-iron nuclei flux in primary cosmic radiation determined through high altitude balloon exposure of interleaved layers of nuclear photographic emulsion and plastic detectors
21 p3787 A69-38327

HEAVY WATER

Fine structure of vibrational spectra of molecular H and O, water and deuterium oxide, using molecular photoelectron spectrometer
01 p0023 A69-10141

Correlation effects in water and heavy water laser transitions based on cascade effects, discussing lines in resonator arms
09 p1515 A69-21349

Room temperature fatigue crack propagation rates for high strength aluminum alloy in heavy water environment compared with argon and distilled water
13 p2640 A69-30815

Laser harmonic frequency measurement application to absolute frequency determination of 84 micron heavy water laser
17 p2982 A69-33406

Molecular hydrogen, oxygen and deuterium additions effect on CW laser operation with ordinary and heavy water as active medium
21 p3738 A69-39131

HEIGHT

NT SCALE HEIGHT

Ionospheric irregularities height measurement using spaced receivers for recording satellite signals
01 p0064 A69-10428

Photoelectric measurement of chromospheric heights by method requiring neither high telescopic resolution nor best seeing, discussing trials during September 1967
08 p1385 A69-20070

Minimum height of monochromatic radiation ionization in atmosphere assuming spherical earth for space science applications
13 p2256 A69-28653

Tide dependent variations of critical frequencies of ionospheric layers minimal heights and maximum height of F 2 layer reflection
14 p2444 A69-29871

Lunar tidal oscillations in F 2 layer critical frequency and F region minimum virtual height at Huancayo during IGY/IGC to study solar cycle effects
16 p2784 A69-32613

Solar radio sources heights at 1424 and 696 MHz during near minimum solar activity
17 p3040 A69-33808

Absolute phase heights measurements in ionosphere for geometrical optics conditions, noting accuracy
17 p2927 A69-33859

Magnetic activity influence on polar auroras height
17 p2963 A69-33953

Emission intensity ratio change as function of polar auroral height compared to variation in atmospheric concentration ratio of oxygen to nitrogen
17 p2963 A69-33956

Postsunset apparent reflection height and electron density variability in equatorial F 2, discussing singularities of diurnal variation in November-January
17 p2967 A69-33984

Vortex wakes behind high lift wings, considering effects of height above ground and various tunnel heights and widths for STOL operations [AIAA PAPER 69-740]
18 p3083 A69-34405

Relative heights on western moon half computed and compared to values of Schmidt, U.S. Army Map Service and USAF Aeronautical Chart Information Center
18 p3196 A69-34693

Side-looking radar and IR line scanning as method for simultaneous stereo height mapping, using images produced from same vantage point

20 p3536 A69-36929

Ionosphere absolute phase height measurement methods independent of virtual height, using fixed frequency CW emission and pulsed sounding

20 p3520 A69-37032

Pilot balloon observation errors due to inaccurate balloon height determination, relating error determination to wind speed and direction errors

20 p3572 A69-37699

Physical exercise effect on adolescent males, comparing oxygen uptake, heart volume and height in training and nontraining groups

23 p4077 A69-41312

HEISENBERG THEORY

Heisenberg ferromagnet dynamics at low temperatures, calculating spectral weight function and other properties with low density expansion

01 p0135 A69-10016

Linear integrodifferential motion equations for turbulent flow within Heisenberg statistical turbulence theory

02 p0230 A69-11869

Anisotropic Heisenberg antiferromagnetism in spin wave approximation, calculating thermodynamic quantities in terms of elliptic integrals

12 p2144 A69-26500

Partially coherent radiation scattering determined using Heisenberg operator, noting radiation absorption dependence on interfrequency band coherence

16 p2797 A69-32050

HELICAL ANTENNAS

Helical log periodic and log periodic dipole arrays impedance and radiation patterns measurements have similar characteristics

02 p0219 A69-12337

Polarization stability improvement of helical beam antenna by increased turns, smaller pitch angle and decreased transverse electromagnetic mode amplitude

02 p0219 A69-12345

Electromagnetic field of infinite helical sheath, basing calculations on previous helical antenna studies

09 p1463 A69-21682

Helical and log conical helical antenna width reduction by loading of traveling wave antenna elements with isotropic material

11 p1852 A69-25315

Helix antennas for phased arrays for spacecraft, discussing performance and development

13 p2228 A69-27632

Seven helix antenna array components and operation mode at Berlin weather station, including biaxial rotor, preamplifier servoamplifier and VHF telemetry receiver

17 p2946 A69-33768

Antenna design, based on helical beam radiator data, providing checking facility giving automatic alarm

24 p4312 A69-42573

HELICAL FLOW

Inviscid incompressible fluid flow stability against helical disturbances in circular cylinder

06 p0910 A69-17332

Distribution of steady state solutions for equations of helical motion of body in infinite fluid, noting coaxial control surfaces

11 p1868 A69-24782

Helical motions of body bounded by multiply connected surface immersed in infinite ideal incompressible fluid, discussing congruence

11 p1868 A69-24790

Numerical solution to partial differential equations describing helical discharge in Ar with gas injection, discussing initial temperature distribution and radial distribution effects

12 p2141 A69-27131

HELICAL WINDINGS

Spiral trajectory winding rate of asymmetrical light beams in nonlinear media analyzed in geometric optics approximation, noting diffraction influence

13 p2298 A69-27662

Leaky waves propagation characteristics helix waveguide covered with slitted cylinder using transverse network representation, emphasizing small pitch angles, hybrid TE and TM modes, etc

14 p2422 A69-29752

HELICOPTER ATTITUDE INDICATORS

U ATTITUDE INDICATORS

U HELICOPTERS

HELICOPTER CONTROL

Flying qualities considerations in design and development of Huey Cobra for helicopter attack mis-

sion, describing stability and control augmentation systems

[AHS PAPER 217] 07 p1053 A69-18871

Helicopter stabilization systems design using optimal control theory to obtain multivariable feedback controller

12 p2014 A69-26764

Analog computer simulation of helicopter dynamics after main and tail rotor blades partial loss, showing banking and controllability

14 p2393 A69-29744

Integrated trajectory error display /ITED/ for flight path control of helicopters and VTOL, describing principles governing display synthesis

[AHS PAPER 314] 17 p3001 A69-33541

AH-56A helicopter manual and automatic terrain following and manual terrain avoidance systems, discussing nap-of-earth flight, design and simulation

[AHS PAPER 311] 17 p3002 A69-33544

Optimum automatic system for controlling helicopter formation flight, stressing transient response Q factor and transmission ratios

18 p3090 A69-34656

Higher harmonic pitch angle inputs to eliminate oscillatory helicopter blade root shear determined through teetering rotor model

18 p3089 A69-35233

Torsionally flexible blade controllable twist rotor with pitch horn and servoflap control, discussing optimum inputs, airloads and angles of attack contours

18 p3089 A69-35234

Positive pitch-flap coupling for controlling helicopter rotor blade motion stability involving blade in-plane deflections

20 p3463 A69-37808

Helicopter powering and positioning by CW microwave beam, describing antenna and sensor arrays, feasibility experiments, system applications, etc

23 p4063 A69-42534

Fluidic servoactuator controlled by hydraulic vortex valves using mechanical signals for helicopter stability augmentation system

24 p4255 A69-42800

Quadratic optimization applied to helicopter flight control design, assuming constant feedback gains and command step input with zero steady state error

24 p4253 A69-43279

HELICOPTER DESIGN

Elastomeric bearings for support of heavy loads and accommodation of oscillatory motions, considering molded type for helicopter tail rotor

01 p0085 A69-10406

Helicopter structures design for maximum practicable crashworthiness and survivability, comparing load factors and deformations with indicated human impacts tolerance

[AHS PAPER 225] 01 p0009 A69-10408

VTOL aircraft design for noise reduction, discussing localities tolerance, noise sources, operating cost, etc

01 p0009 A69-10421

Analytical design of SH-3 helicopter engine inlet ice deflector shield interior surfaces, defining potential flow pattern and moisture droplet trajectories

01 p0011 A69-11064

Composite main rotor blade for Sud-Aviation SA-330 helicopter consisting of steel spar/epoxy-glass envelope

[SAE PAPER 680693] 03 p0366 A69-13444

Helicopter rigid rotor system with blades of glass fiber reinforced plastic

04 p0548 A69-14817

Helicopter role, development and configurations, noting V/STOL competition impetus

05 p0700 A69-15547

BO-105 helicopter design, testing and characteristics noting four bladed rigid rotor

[AHS PAPER 200] 07 p1052 A69-18869

Flying qualities considerations in design and development of Huey Cobra for helicopter attack mission, describing stability and control augmentation systems

[AHS PAPER 217] 07 p1053 A69-18871

Coaxial multipurpose KA-26 helicopter design, discussing cruising speed, passenger capacity, range, flight ceiling, gross weight and piston engines

07 p1053 A69-18969

Fail-safe design principles and criteria for helicopter structures to prevent operational failure arising from undetected fatigue damage

[AIAA PAPER 69-213] 07 p1054 A69-19549

Sikorsky ABC /advancing blade concept/ helicopter program, discussing advantages and small scale wind tunnel experiments

[AIAA PAPER 69-217] 07 p1055 A69-19558

Compound rotary wing aircraft research, discussing XH-51A maneuverability program and UH-1 high Mach and high advance ratio program

[AIAA PAPER 69-218] 07 p1056 A69-19568

Fail-safe goals, design criteria, analytical methods and test procedures to achieve reliable damage tolerant dynamic rotating parts for V/STOL and helicopter transports

[AIAA PAPER 69-215] 07 p1237 A69-19569

TRAC variable diameter rotor design based on jackscrew mechanism applied to compound helicopter

[AIAA PAPER 69-221] 07 p1056 A69-19572

Helicopter seaworthiness, comparing full scale sea landing and flotation studies with model test results

08 p1255 A69-20653

Helicopters operation from small ships, describing underside harpoon mooring technique for Alouette 2 and 3

08 p1255 A69-20654

Manufacturer-supplier relationship in helicopter industry

09 p1502 A69-21388

Marchetti SV-20A and SV-20C twin turbine helicopters with two bladed rotors and fixed wings, discussing propeller on starboard engine rear of compound version

12 p2013 A69-26466

AH-56A Cheyenne armed compound helicopter designed to operate from unimproved bases with minimum support equipment, noting on-board fueling capacity

[AIAA PAPER 68-560] 12 p2017 A69-26770

Onboard magnetic anomaly detection system for Canadian helicopter, discussing magnetometer location, boom design and testing and equipment installation

[AIAA PAPER 68-487] 12 p2094 A69-26771

Helicopter design, discussing blade deicers, landing gear, vibration absorbers, cargo capacity, etc

13 p2202 A69-27836

High speed shafting design for helicopter power transmission systems, discussing shaft in OH-6A Cayuse light observation helicopter

[ASME PAPER 69-DE-5] 14 p2453 A69-28837

NASA flight test of hingeless rotor compound helicopter to determine lift sharing characteristics, showing rotor lift dependence on airspeed

14 p2393 A69-29702

Multiple shaker ground vibration test system for confidence in helicopter designs before flight testing and evaluation of force balancers

15 p2585 A69-30357

Rotary wing aircraft speed boundary widening without impairing low speed attributes, discussing structural design factors, airframe design and stability, etc

17 p2897 A69-33209

Critical review of paper on tail rotor structural design principles covering sizing, blade frequency and response and aeroelasticity

[AHS PAPER 342A] 17 p3059 A69-33503

OH-6A drive system design for lightweight, low cost high performance helicopter, discussing reliability from RVN combat data

[AHS PAPER 374] 17 p2900 A69-33514

Maximum helicopter level flight speed loads spectrum shape and severity related to rotor component fatigue design strength

[AHS PAPER 372] 17 p3059 A69-33516

Helicopter noise characteristics, discussing effects of noise reduction measures on design and operations

[AHS PAPER 352] 17 p2915 A69-33525

Helicopter power plant and drive and rotor systems influence on design, configuration, weight, payload and performance

[AHS PAPER 334] 17 p2901 A69-33528

Heavy lift helicopter design with 30 ton payload, considering fanjet drive hot cycle and shaft drive propulsion systems

[AHS PAPER 330] 17 p2901 A69-33532

VFW-H3 Sprinter prototype, discussing cost effectiveness, VFW-H2 test vehicle, hovering stability, dynamic takeoff characteristics, vibration level, noise level, reliability and maintenance

[AHS PAPER 303] 17 p2901 A69-33546

Tail rotor aerodynamics, discussing ambient conditions, maximum thrust, precession effects, fin interference, noise reduction, etc

[AHS PAPER 300] 17 p2895 A69-33549

Helicopter rotor vortex noise data analyzed for noise suppression, obtaining sound power equations

17 p2896 A69-34034

Army OH-6A helicopter light weight design, considering effects of WRAP /weight, radius, area, power/ factors on empty weight

[SAWE PAPER 781] 18 p3091 A69-34870

Crane helicopters for heavy lift transport mission, noting weight and size effect on productivity [SAWE PAPER 782] 18 p3091 A69-34905

Helicopter rotor blade construction and developments, discussing mass balance, fatigue life, fail-safe characteristics, cost and weight ceiling and plastic materials 19 p3329 A69-36768

French helicopter industry projected development for existing types, production models or final development and long range design programs 19 p3248 A69-36848

European cooperation in aircraft industry and application to Anglo-French helicopter program 19 p3456 A69-36849

B composite materials in helicopter development, including B and C filament production and B filament applications 22 p3971 A69-40899

Air mass mechanics, local lifting surface element aerodynamic response and aeroelastic blade response problems in lifting rotor technology 23 p4061 A69-41370

Compound helicopter transport for short haul transportation system for Northeast Corridor, discussing terminals near origin and destination, takeoff and landing patterns, etc [SAE PAPER 690419] 23 p4062 A69-41643

Twin engine five seater BO-105 military helicopter design and subsystems and shipboard compatibility evaluation 24 p4252 A69-42937

High speed compound helicopter rotor loads flight test program, discussing measured parametric effects [AIAA PAPER 68-980] 24 p4250 A69-43712

HELICOPTER ENGINES

T63 regenerative helicopter engine program, noting operational performance and engine-aircraft compatibility [AHS PAPER 212] 01 p0143 A69-10410

Turbine powered helicopter engine inlet air filtration system utilizing direct-connect S-bend duct 01 p0143 A69-11054

T-53 engine operation in U.S. Army helicopters noting design problems from compressor blade failure, sand and dust erosion and bearing and lubrication malfunctions [AHS PAPER 215] 07 p1203 A69-18867

Gas turbine propulsion engines for small single engine helicopters, discussing costs, performance and FAA tests [SAE PAPER 690310] 11 p1942 A69-24513

Marchetti SV-20A and SV-20C twin turbine helicopters with two bladed rotors and fixed wings, discussing propeller on starboard engine rear of compound version 12 p2013 A69-26466

American, French and Soviet medium weight helicopters tested in terms of main rotor blades construction, rotor performances and comparative power plant data 13 p2201 A69-27329

Helicopter power plant and drive and rotor systems influence on design, configuration, weight, payload and performance [AHS PAPER 334] 17 p2901 A69-33528

Helicopter engine dynamic analysis, discussing modeling techniques, rotor responses and turbine speed control simulations and transition from mathematical models to hardware components [AHS PAPER 332] 17 p2946 A69-33531

HELICOPTER PERFORMANCE

Navigation techniques for emergency helicopter services in medical evacuation and air/sea rescue missions, discussing displays and search patterns 02 p0279 A69-12363

Helicopter role, development and configurations, noting V/STOL competition impetus 05 p0700 A69-15547

Aerodynamic instrumentation to improve helicopter takeoff and landing piloting performance under high gross weight conditions 05 p0767 A69-16776

Characteristics, employment and tactics of Huey Cobra attack helicopter in Vietnam, discussing three primary weapon configurations 06 p0867 A69-17661

BO-105 helicopter design, testing and characteristics noting four bladed rigid rotor [AHS PAPER 200] 07 p1052 A69-18869

Coaxial multipurpose KA-26 helicopter design, discussing cruising speed, passenger capacity, range, flight ceiling, gross weight and piston engines 07 p1053 A69-18969

Helicopter flight safety as function of service duration, performance limitations and propulsion failure 07 p1054 A69-19313

Helicopter use in military activities noting role in overcoming combined enemy, weather and terrain conditions [AIAA PAPER 69-190] 07 p1244 A69-19547

Sikorsky ABC /advancing blade concept/ helicopter program, discussing advantages and small scale wind tunnel experiments [AIAA PAPER 69-217] 07 p1055 A69-19558

Engineering testing of aerodynamic efficiency of helicopter rotors during hovering with and without ground effect 08 p1254 A69-20169

Helicopter seaworthiness, comparing full scale sea landing and flotation studies with model test results 08 p1255 A69-20653

Multiengine helicopter scheduled passenger service operations in Europe 11 p2004 A69-24378

Helicopter rotors with rigid blades performance from viewpoint of controllability and load distribution 13 p2201 A69-27295

American, French and Soviet medium weight helicopters tested in terms of main rotor blades construction, rotor performances and comparative power plant data 13 p2201 A69-27329

Helicopter design, discussing blade deicers, landing gear, vibration absorbers, cargo capacity, etc 13 p2202 A69-27836

Helicopter airworthiness requirements, discussing need for international cooperation on safety regulations 13 p2202 A69-27837

Helicopter climatic testing, discussing component, systems and field tests and facilities 14 p2427 A69-29505

NASA flight test of hingeless rotor compound helicopter to determine lift sharing characteristics, showing rotor lift dependence on airspeed 14 p2393 A69-29702

Analog computer simulation of helicopter dynamics after main and tail rotor blades partial loss, showing banking and controllability 14 p2393 A69-29744

Rotary wing aircraft speed boundary widening without impairing low speed attributes, discussing structural design factors, airframe design and stability, etc 17 p2897 A69-33209

OH-6A drive system design for lightweight, low cost high performance helicopter, discussing reliability from RVN combat data [AHS PAPER 374] 17 p2900 A69-33514

Fatigue test loading spectra calculation methods, discussing helicopter rotating and nonrotating components tests [AHS PAPER 373] 17 p2945 A69-33515

Mission task performance oriented approach to winged helicopters flying and handling qualities, considering wings and horizontal stabilizers influence [AHS PAPER 360] 17 p2900 A69-33522

Rotary wing aircraft height-velocity testing, analyzing engine-out landing by combining flight tests with mathematical simulation model [AHS PAPER 353] 17 p2900 A69-33524

Vector airspeed measuring system /VAMS/ for helicopters and V/STOL aircraft utilizing gas discharge mass flowmeter to improve takeoff performance [AHS PAPER 350] 17 p2974 A69-33527

Crane helicopters for heavy lift transport mission, noting weight and size effect on productivity [SAWE PAPER 782] 18 p3091 A69-34905

Rotor airfoils design for helicopter performance optimization, noting hovering figure of merit and blade profile characteristics relationship 18 p3087 A69-35220

Combat fielded cargo-carrying CH-54A Flying Crane helicopter industry-government reliability/maintainability field test evaluation 19 p3247 A69-36017

Helicopter rotor blades instabilities during starting and stopping cycles, predicting aerodynamic loads by wind tunnel tests, determining negative/positive angles of attack 20 p3463 A69-37804

Dynamic stall characteristics of high speed symmetrical and cambered helicopter rotor blade airfoils from two dimensional wind tunnel determinations [AHS PAPER 206] 20 p3463 A69-37806

Passive helicopter rotor isolation for alleviating rotor induced vibration, using dynamic antiresonant vibration isolator 20 p3463 A69-37807

Helicopter main rotor noise from square tipped blades determined as function of tip speed, blade area and thrust 22 p3864 A69-40676

High speed compound helicopter rotor loads flight test program, discussing measured parametric effects [AIAA PAPER 68-980] 24 p4250 A69-43712

HELICOPTER PROPELLER DRIVE

High bypass ratio compound fan shaft engine design and performance for convertible rotary wing aircraft [ASME PAPER 69-GT-51] 09 p1572 A69-22511

OH-6A drive system design for lightweight, low cost high performance helicopter, discussing reliability from RVN combat data [AHS PAPER 374] 17 p2900 A69-33514

Helicopter power plant and drive and rotor systems influence on design, configuration, weight, payload and performance [AHS PAPER 334] 17 p2901 A69-33528

VFW-H3 Sprinter prototype, discussing cost effectiveness, VFW-H2 test vehicle, hovering stability, dynamic takeoff characteristics, vibration level, noise level, reliability and maintenance [AHS PAPER 303] 17 p2901 A69-33546

HELICOPTER ROTORS U ROTARY WINGS

HELICOPTER WAKES

Wake deformation for horizontal and vertical cylinders present in wake of hovering rotor, using flow visualization technique [AIAA PAPER 69-228] 07 p1051 A69-19551

Helicopter rotor wake distorted geometry prediction by analytical method, noting experimental results for rotor in forward flight [AIAA PAPER 69-196] 07 p1051 A69-19553

Helicopter hovering performance prediction from wake analysis by iteration, discussing wake interference significance and blade number influence [AHS PAPER 321] 17 p2895 A69-33538

Lifting line theory for hovering propellers deformed wakes based on continuous vortex sheet representation 18 p3087 A69-35217

Rotor static performance calculation with near wake interference effects on rotor inflow distribution, considering strip momentum theory 18 p3088 A69-35221

Helicopter rotors trailing vortices by flow visualization, comparing Euler and Runge-Kutta iterative solutions 23 p4150 A69-41376

HELICOPTERS

NT ALOUETTE HELICOPTERS

NT BO-105 HELICOPTER
NT CH-34 HELICOPTER
NT CH-46 HELICOPTER
NT CH-47 HELICOPTER
NT CH-54 HELICOPTER
NT H-56 HELICOPTER
NT MILITARY HELICOPTERS
NT OH-6 HELICOPTER
NT S-61 HELICOPTER
NT SA-330 HELICOPTER
NT SH-3 HELICOPTER
NT UH-1 HELICOPTER
NT XH-51 HELICOPTER

Soviet MI-8 and MI-4 passenger helicopters noise characteristics with turboprop and piston engines and during landing takeoff and horizontal flight 03 p0366 A69-13417

Helicopter, compounds and composite aircraft design trends 05 p0700 A69-15548

Statistical method to investigate time varying stresses in helicopter structures, considering service life evaluation 05 p0767 A69-16775

Boundary layer discontinuity on helicopter rotor blade in hovering using flow visualization [AIAA PAPER 69-197] 07 p1051 A69-19561

Helicopter rotor noise generation, propagation, reception and reduction, discussing design charts for rotational noise spectra as function of design and flight variables [AIAA PAPER 69-195] 07 p1055 A69-19563

Helicopter instability on ground with propulsion system operating and inoperative, discussing overturning, restoring moments and pilot training 09 p1433 A69-21385

Helicopter all-weather flight control system, using autostabilization and artificial horizon 09 p1435 A69-22778

Operational research applications to management problems, discussing specific airlines operations cases 11 p1822 A69-24377

Light aircraft and helicopter manufacturing methods, design concepts and materials, discussing aluminum airframes, riveting, fiberglass, UV curing, etc [SAE PAPER 690341] 11 p1822 A69-24498

Helicopter weight analysis in preliminary design and proposal field 15 p2550 A69-30463

Helicopter wind tunnel testing, discussing solutions in terms of test procedures and test bed equipment 16 p2735 A69-32075

Fatigue properties and test procedures for glass reinforced plastic rotor blades used in twin engine helicopter [AHS PAPER 370] 17 p3060 A69-33518

Multifunction helicopter rotor blade radar for navigation, IFR approach and fire control, including flight test results [AHS PAPER 315] 17 p2920 A69-33535

Onboard hybrid computer for helicopter fire control system, generating turret pointing angles and corrections 17 p2934 A69-34074

Helicopter rotor rotational and vortex noises prediction methods and trends 18 p3088 A69-35224

Flight surgeon observations of stress and fatigue effects on aircrew of first nonstop transatlantic helicopter flight, discussing fatigue ratings, sleep patterns, etc 19 p3262 A69-36450

Electrocardiographic and heart rate data recording of crew members during transatlantic helicopter flight and normal daily routine 19 p3263 A69-36451

Urinalysis of crew members of first transatlantic helicopter flight indicating interindividual endocrine-metabolic variability and circadian trends modification 19 p3263 A69-36452

Dornier R and D, discussing single and twin engined aircraft, utility aircraft, helicopter, VTOL transport, safety, etc 22 p3862 A69-39931

HELIO AIRCRAFT

Heligyro type takeoff and landing maneuvers, discussing M 211 takeoff jet thrust, pressure ratio, tip speed, etc 04 p0547 A69-14816

Solar sail structural design, discussing application as propulsion system for heligyro interplanetary spacecraft 06 p1015 A69-17591

HELIOCENTRIC ORBITS

U SOLAR ORBITS

HELIOGRAPHS

U SPECTROHELIOGRAPHS

HELIOGRAPHY

U SPECTROHELIOGRAPHS

HELIO-MAGNETISM

U SOLAR MAGNETIC FIELD

HELIO-METERS

Lunar libration constants determination based on Schlueter heliometer observations using Bessel-Wichmann method, allowing for limb irregularities 17 p3028 A69-32875

HELIO-METRY

U HELIO-METERS

HELIO-PORTS

Cost estimating relationships for vertiports and airports, comparing terminal costs per passenger for each facility [AIAA PAPER 69-208] 07 p1245 A69-19564

Federal, state and municipal jurisdictional aspects for heliport establishment, detailing regulations 13 p2381 A69-27433

HELITRONS

Regenerative amplification stability in nonretarded wave helitron and traveling wave mitron type devices 02 p0214 A69-11610

Regenerative amplification stability in nonretarded wave helitron and traveling wave mitron type devices 11 p1847 A69-24717

HELIUM

NT LIQUID HELIUM

Age and initial helium abundance of stars in M15 globular clusters estimated from stellar evolution lifetime ratio 01 p0149 A69-10135

Magnetron ionization gauge in helium for low pressure measurement, discussing striking characteristics and time lags 01 p0012 A69-10606

Solubility of helium in liquid fluorine increases with temperature exhibiting reverse order 01 p0142 A69-11258

Multiple velocity dispersion in normal hydrogen and normal hydrogen-helium mixtures at room temperature using ultrasonic interferometer 01 p0121 A69-11284

Nitrogen and helium as factors affecting human decompression stress severity, using urinary measurements reflecting various endocrine and metabolic changes 01 p0018 A69-11338

Mass spectrometer helium leak testing of cryogenic storage vessels, noting procedures and insulation and evacuation of jacket space 02 p0252 A69-11811

Viscosity and thermal conductivity of helium on basis of Lennard-Jones/6 to 9/ potential [ASME PAPER 67-WA/HT-1] 02 p0351 A69-12205

Elastic scattering cross section for low energy electrons on metastable He atoms, using polarized orbital method 03 p0469 A69-12922

He/Ne ratio effect on performance of He-Ne laser in annular cavity 04 p0612 A69-15176

Helium cryostat designed to operate under overload and vibrations and used for cooling onboard superconducting devices of Cosmos 140 satellite 04 p0585 A69-15407

He refrigerators, noting 4 K design for large scale fixed installations and 20 K small scale design for airborne applications 05 p0704 A69-15671

Corona and breakdown voltage in helium-oxygen atmospheres, analyzing conditions for manned space flight vehicles 05 p0730 A69-16241

Variable He star HZ29, noting unusually wide and shallow He I lines and possible mass and composition 06 p0998 A69-16931

First Born approximation cross sections for He excitation from ground state by proton impact calculated, using wave functions 06 p0960 A69-17027

Ionizing electron collisions with He, determining energies and angular correlation distributions of scattered and ejected electrons 06 p0962 A69-17191

Metastable helium abundance in interstellar and intergalactic space, inferring low energy cosmic ray concentration 06 p1010 A69-17973

Helium flux in lower thermosphere, using diffusion theory for multicomponent gas mixture to determine equation for equilibrium distribution 07 p1125 A69-18848

Atmospheric helium nonthermal escape mechanisms, noting ion loss from polar ionosphere 07 p1125 A69-18946

Tensile strength of alloys under high pressure of hydrogen and helium, discussing embrittlement [ASM PAPER D8-14.2] 07 p1169 A69-19667

Calculated profiles of He I 4471 and 4922 A and forbidden components star spectra, using quasi-static and impact approximations 07 p1224 A69-19713

He concentration measurement in transient He-air mixture by spectroscopic analysis of fluorescence excited by high energy electron beam 08 p1312 A69-19860

Population densities of UV bound resonance lines of neutral helium for 41-level model atom, discussing optical thickness and electron temperature and density 08 p1390 A69-20392

Helium production in Galaxy, assuming homogeneous evolution of some massive stars due to external factors 08 p1401 A69-20895

Radiogenic theory of origin of He in natural gas and absence of Ar from K 40 decay, discussing primordial earth atmosphere composition 08 p1311 A69-20947

Quadrupole mass filter for rocket-borne measurements of thermospheric helium content, discussing turbopause level and winter helium bulge 09 p1489 A69-21712

Helium-like ion resonance satellite lines in laboratory and solar plasmas, noting coincidence between satellite energy and energy level interval 09 p1598 A69-22158

High energy protons, helium and gamma rays observed by particle telescope on board OSO-C, obtaining integral rigidity spectra of proton and helium nuclei 09 p1579 A69-22172

Helium I line profiles including forbidden component, discussing electron and ion Stark broadening and thermal Doppler broadening 09 p1601 A69-22209

Primordial helium and horizontal branch star luminosity, obtaining luminosities in He burning phase for different He and metal abundances from models 09 p1601 A69-22211

Lyman alpha wing opacity effect on temperature scale and helium content in F and G subdwarf atospheres 09 p1607 A69-22431

Momentum transfer cross sections, recombination coefficients and ionization coefficients of working gases for MHD energy converter 10 p1733 A69-23446

Pulsed glow discharges in He and He-H mixtures for high current density, noting electric field and wall potential distributions 10 p1739 A69-23660

He I 10830 A line in beta Lyr shell observed by contact image converter tube, analyzing line structure and phase brightness 11 p1955 A69-24391

Laser light scattering in radiation driven breakdown waves in He, using high resolution streak photography to obtain diagnostic data 11 p1915 A69-24420

B star HD 191980 spectral variations from B-3 to B-8 noting helium to carbon line intensity ratio, interstellar D line strength and radial velocity measurements 11 p1958 A69-24594

Simultaneous photoexcitation and photoionization of He near threshold at 186 A, measuring probability 11 p1921 A69-24926

Gaseous He bubbles injection into liquid propellant launch vehicle fuel lines to reduce vehicle pogo oscillations by lowering feed system natural frequencies 11 p1967 A69-25498

Stellar evolution model for primeval He abundance in population II stars in globular clusters for big bang confirmation 12 p2156 A69-26228

Average ionization cross sections of atomic and molecular H and He beams ionized by plasma electrons with Maxwellian velocity distribution 12 p2138 A69-26542

Speech intelligibility in air at ground level and in helium-oxygen mixture at 18,000 ft 12 p2019 A69-26548

Hydrogen to He ratio effect on stellar atmospheric structure, considering flux relations, UVB color indices, H line profiles, electron and gas pressures 13 p2339 A69-27562

Electron density, temperature and dimensions of helium breakdown induced by Q switched ruby laser beam as function of space and time 14 p2492 A69-29636

B-type stellar spectra, discussing atmospheres and local thermal equilibrium from considerations of He I and P II lines relative strength 15 p2679 A69-30046

Helium gas shaft seal for spacecraft electrically driven LOX pump, noting advantages of floating carbon face seal type [ASLE FICFS PREPRINT 24] 15 p2621 A69-30498

Temperature and electron number density behind reflected shock in helium gas in T tube, noting Z pinch discharges 15 p2593 A69-31161

Photoionizing effect of hydrogen and helium UV glow in nighttime ionosphere compared with ground based IF ionosonde and sounding rocket observations 15 p2605 A69-31436

Cosmic helium origin, discussing evidence for big bang, galactic synthesis and stellar thermonuclear burning theories 16 p2853 A69-31598

Low temperature method for measuring breakdown threshold parameters of liquid and gaseous He by laser beam, observing stimulated Mandelstam-Brillouin scattering 16 p2796 A69-31799

He I/1.083 mu/ and O I/5577 A/ absolute brightness measured in sunlit aurora for various shadow heights of solar radiation, considering primary electron precipitation 16 p2780 A69-32311

Leak rate measurement accuracy of rate-of-rise technique for nitrogen, methane and He between millionth and thousandth torr 16 p2791 A69-32326

H alpha/D3 intensity ratio variations in peripheral regions of prominences may be due to dynamic conditions of material emitting radiations

17 p3029 A69-33051

Cross sections threshold behavior for Cs II resonance lines excitation due to Cs ion-He collision

17 p3008 A69-33388

Respiratory gas exchange in exercise during He-O breathing, analyzing effects on O consumption, carbon dioxide production and minute ventilation of human subjects

17 p2910 A69-33751

RF recombination lines measurement of helium for abundance in nebulas, comparing optical and radio values for H II regions

18 p3190 A69-34293

Temperature control below 5.2 K based on servoing He pressure above bath

18 p3136 A69-34641

He/Ne ratio effect on performance of He-Ne laser in annular cavity

18 p3152 A69-34718

HD 30353 He binary star invisible component suggested as KO type supergiant from IR photometric data

18 p3203 A69-35348

Energy dependence of elastic total collision cross section of identical He molecules, using velocity selected primary beams at low target temperature

19 p3378 A69-36186

Rate coefficients for chemiluminescent reactions of excited He with N, O, carbon monoxide and dioxide determined from spatial dependence of visible emission

20 p3483 A69-36936

Solar He abundance limits and discrepancies of CI 37 solar neutrino count experiment

20 p3592 A69-38068

Helium in atmosphere, aurora and solar wind, discussing geophysical problems, interplanetary neutral H, etc

21 p3710 A69-38509

Upper atmospheric H and He observations, showing Lyman alpha, H alpha measurements and H abundance values relative to Kockarts-Nicolet model

21 p3714 A69-38529

Spectroscopic analysis of nebula NGC 6302 for identification as highly excited gaseous nebula, noting He-H ratio

22 p4026 A69-40647

Electron and ion Stark broadening of allowed and forbidden, triplet and singlet transitions in neutral He at low electron densities, noting Doppler broadening

22 p3985 A69-40665

Solar He abundance determined from solar model photospheres line and continuum radiation

22 p4031 A69-40911

Globular cluster star age and initial He abundance from main sequence, horizontal branch and red giant tip models using radiative opacities

22 p4035 A69-41205

Galactic evolution using concept of stellar populations and correlation with metal and He abundances

23 p4218 A69-42323

Homogeneous axisymmetric anisotropic cosmological models, analyzing magnetic fields and initial anisotropies effect on 3K radiation and primordial He production

23 p4222 A69-42402

N or He additions effects on carbon dioxide laser design and power output

24 p4327 A69-42640

Primordial hydrogen and helium concentration in Pesyanoe meteorite measured by gas chromatography, indicating solar wind injection source

24 p4384 A69-43213

He I 10830 A line in beta Lyr shell observed by contact image converter tube, analyzing line structure and phase brightness

24 p4390 A69-43781

Positronium formation in positron-helium scattering, including polarizability in potentials appearing in final equations

24 p4353 A69-43815

Twilight helium emission observed by Fabry-Perot spectrometer, noting consistency with triplet He atom excitation by photoelectron collision with ground state atoms

[AFCL-69-0294]

14 p2440 A69-29124

Collisional equilibrium and nonuniform formation models for spatial gradient development of early afterglow of He plasma molecular excited state densities

16 p2782 A69-32465

Electron beam fluorescence probe and afterglow investigation for hypersonic He flow visualization, observing qualitative structure

19 p3291 A69-35722

HELIUM ATOMS

Metastable positive He molecules and He atoms decay in afterglow, taking into account simultaneous emission at 4650 angstroms during absorption studies

02 p0287 A69-11932

Atmospheric hydrogen and helium atoms emission in geomagnetic poles and winter hemisphere, comparing thermal dissipation and migration of light atoms

15 p2599 A69-31322

Steady state atomic He distribution according to solar atmosphere levels, involving formulation and solution of equilibrium equations for single and triplet levels

20 p3615 A69-38298

LTE departure calculated for He I in hot star model atmospheres for effects on populations of singlet and triplet states

21 p3801 A69-38761

H and He atoms escape from atmosphere under MHD waves action at exosphere boundary

23 p4156 A69-41847

Neutral He lines at 537 A and 584 A obtained by spectroheliometer on OSO 4, studying differences between quiet and active regions

23 p4222 A69-42405

HELIUM IONS

Alpha recombination coefficient of molecular helium ions measured in helium afterglow plasmas as function of electron density and gas temperature

02 p0283 A69-11834

Metastable positive He molecules and He atoms decay in afterglow, taking into account simultaneous emission at 4650 angstroms during absorption studies

02 p0287 A69-11932

Solar Lyman alpha, Lyman beta and Balmer alpha lines of He 2 for electron temperature and density and optical thickness of emitting layer

10 p1772 A69-22859

Hyperfine transition line of He 3 II for abundance in Messier 17 source by radio telescope

10 p1785 A69-24098

Simultaneous photoexcitation and photoionization of He near threshold at 186 A, measuring probability

11 p1921 A69-24926

Light ion abundance measurements of OGO satellites and field aligned diffusive equilibrium theory with temperature and concentration latitudinal variations

11 p1879 A69-25157

Spectrometric characteristics of He, H and molecular H ion recording counters as function of temperature

14 p2452 A69-29811

Transition probabilities of spectral lines in helium-like ions estimated from hydrogen magnetic dipole transitions, discussing single photon decay

15 p2695 A69-30892

Hydrogen and He ion distribution measurements, noting seasonal and local magnetic time variability

15 p2599 A69-31326

Plasmasphere hydrogen and He ion concentration models, using diffusive equilibrium theory for plasmasphere parameters

15 p2677 A69-31447

Two photon decay of metastable levels of hydrogenic and He-like ions in solar corona, depopulating via proton collisional excitation to 2p level

19 p3396 A69-36218

He I 1.083 micron resonance line in evening twilight airglow spectrum, discussing maxima, minima, decay patterns, etc

19 p3303 A69-36484

OGO 5 ion spectrometer for measuring oxygen, He and hydrogen ion concentration, noting functions as energetic particle analyzer and proton energy distribution measurement capability

19 p3314 A69-36679

Helium sequence ions spin forbidden transitions electric dipole oscillator strengths and transition probabilities evaluated by variational procedure

20 p3577 A69-38171

Explorer 34 observations of hydrogen and He ions in solar wind, noting number density variations and tentative association with geomagnetic storms

22 p4004 A69-40305

Off-diagonal matrix elements of Breit interaction between singlet-triplet transitions for helium isoelectronic sequences

22 p3986 A69-40783

Autoionized resonance transitions of He at 206.2-192.2 A using He continuum produced by capillary spark, also producing He II line spectra

23 p4191 A69-42149

Spectral distribution of two photon emission from metastable state of singly ionized He by broadband spectroscopic coincidence counting technique

23 p4220 A69-42378

HELIUM ISOTOPES

Helium isotopes escape mechanism from earth atmosphere related to polar wind ionospheric plasma flow from earth

01 p0077 A69-11240

Differential cross sections for elastic scattering of 600 Mev protons from He 3 between 19 and 45 degrees

03 p0472 A69-13464

Book on properties of liquid and solid helium 3 and 4 physical characteristics, phase behavior and experimental techniques

04 p0630 A69-14688

Experimental measurement of He and C isotope composition of cosmic radiation

05 p0817 A69-16709

Cosmic ray propagation model, considering determination of He interstellar spectrum and amount of matter traversed at low energies

06 p0988 A69-12720

Cosmic ray deuteron and He 3 secondary origin and determination of cosmic ray path length and residual interplanetary field modulation

08 p1378 A69-20066

Ionization and recombination processes in He 3 plasmas produced by neutron irradiation of H 3

10 p1738 A69-23488

Hyperfine transition line of He 3 II for abundance in Messier 17 source by radio telescope

10 p1785 A69-24098

Velocity dependence of temperature waves /second sound/ in liquid He II measured as function of relative velocity for normal and superfluid

13 p2297 A69-27460

He 3 production and loss in atmosphere, discussing precipitation of energetic magnetospheric particles, thermal escape, nonthermal processes, etc

14 p2435 A69-28965

He II excitation spectrum for interparticle potential using pair Hamiltonian with repulsive core and attractive well

17 p3008 A69-33118

Dilute solution of He 3 in He 4 near absolute zero measured for viscosity, showing temperature effect

21 p3772 A69-39582

Primordial He 3 and deuterium production from magnetic effects during nucleosynthesis epoch of big bang cosmologies

22 p4035 A69-41210

HELIUM PLASMA

LF radiation intensity oscillations of pulsed HF discharge in helium plasma, showing time dependence

01 p0128 A69-10347

Recombination reactions during postdischarge in helium plasma produced by laser beam, deriving equation for density evolution

01 p0128 A69-10394

Plasma decay at high pressure in helium and argon with cesium vapor admixture and pure cesium vapor, using Saha equation

03 p0480 A69-14052

Electron cyclotron instability and HF ionization in beam-plasma experiment using electron beam guided by magnetic field through He gas

05 p0798 A69-15612

Langmuir probe to determine helium plasma density effect on electron temperature from relation between spectral line intensities

05 p0804 A69-16376

Ion plasma oscillations harmonics in helium plasma produced by back diffusion source, relating harmonics amplitude to electron density

05 p0804 A69-16459

Velocity distribution of plasma electrons in electron beam generated He plasma using Boltzmann equation, neglecting electron-electron collisions

05 p0805 A69-16705

HELIUM AFTERGLOW

LF radiation intensity oscillations of pulsed HF discharge in helium plasma, showing time dependence

01 p0128 A69-10347

Metastable positive He molecules and He atoms decay in afterglow, taking into account simultaneous emission at 4650 angstroms during absorption studies

02 p0287 A69-11932

Time dependent behavior of atomic light emitted from pulsed helium afterglow, noting absorption measurements and spectrometric system

08 p1356 A69-20743

HELIXES

- Continuum emission and forbidden lines in helium plasma in linear Z-pinch tube, noting plasma electron density
08 p1369 A69-20887
- Shock heated helium plasma temperature measurements by spectroscopy compared to Rankine-Hugoniot calculations including ionization effect
09 p1548 A69-21963
- Ionization and recombination processes in He 3 plasmas produced by neutron irradiation of H 3
10 p1738 A69-23488
- Transport and balance coefficients in ionized neon and helium plasmas in homogeneous electric field, calculating electron mobility, diffusion coefficient, energy and collision parameters
10 p1740 A69-23722
- Ionization-recombination thermodynamic equilibrium upset causing spectral excitation in He arc plasma
10 p1742 A69-24077
- Diffusion and mass flow in steady state magnetically stabilized helium arc plasma effects on spectroscopic determinations of electron temperature, discussing degree of ionization
12 p2141 A69-27146
- Helium plasma electron temperature and concentration measured in arc in magnetic field by laser light scattering at electrons
14 p2496 A69-29780
- Collisional equilibrium and nonuniform formation models for spatial gradient development of early afterglow of He plasma molecular excited state densities
16 p2782 A69-32465
- Plasma decay at high pressure in helium and argon with cesium vapor admixture and pure cesium vapor, using Saha equation
18 p3181 A69-35045
- Laser radiation power and electron concentration in He-Ne plasma measured by microwave diagnostics
22 p3964 A69-40794
- Ionized He and Ar plasmas nonequilibrium nozzle flows, noting temperature difference between electron gas and atom-ion gas, calculating flow parameters
22 p3861 A69-41047
- HELIXES**
U CURVES [GEOMETRY]
- HELMETS**
EEG monitor helmet for aircraft or flight simulator programs, discussing sensing and transmitting system
12 p2023 A69-26553
- Quality assurance impact energy attenuation testing of U.S. Army flyer protective helmet, considering combined interaction of shell, foam liner and plastic pads
15 p2559 A69-30851
- Crash helmet impact protection capability, considering helmet construction
17 p2913 A69-33169
- Protective helmet design effectiveness against concussion and skull fracture as function of dimension, weight, load spreading, etc
17 p2913 A69-33177
- HELMHOLTZ EQUATIONS**
Phenomena satisfying inhomogeneous Helmholtz equation in cylindrical coordinates, inferring equivalent infinite series directly from integral-transform method
04 p0623 A69-14896
- Extension of Helmholtz classical problem of flows with discontinuous surfaces, considering two sources and transverse plane
14 p2433 A69-29683
- HELMHOLTZ VORTICITY EQUATION**
Finite element solution of Helmholtz equation and application to waveguides with complicated boundaries
03 p0404 A69-13598
- Hall effect destabilization influence in Kelvin-Helmholtz problem for ideal plasma, noting instability growth rate
03 p0478 A69-13804
- Ground influence on Helmholtz flow in presence of plate perpendicular to stream, reducing problem to mixed Volterra problem in complex half plane
04 p0590 A69-15221
- Kelvin-Helmholtz instability for interface between two uniform superposed fluids with constant densities and velocities in horizontal motion in oblique magnetic field
07 p1182 A69-19274
- HEMATOCRIT**
Hypoxia tolerances in nitrogen dilution chamber of chickens at sea level and high altitudes, discussing role of hematocrit and heart mass
22 p3874 A69-40214

- Aortic pressure effect on left ventricular function, emphasizing effect of heart rate hematocrit and oxygen consumption
23 p4092 A69-42061
- HEMATOCRIT RATIO**
Repeated blood sampling effect on plasma cholinesterase, acid phosphatase, alkaline phosphatase and hematocrit ratios in domestic chickens
10 p1644 A69-23158
- HEMATOLOGY**
Increased chronic acceleration physiological effects on chickens, comparing hematological observations with exercise capacity, survival and sexual development
10 p1641 A69-23041
- Repeated blood sampling effect on plasma cholinesterase, acid phosphatase, alkaline phosphatase and hematocrit ratios in domestic chickens
10 p1644 A69-23158
- Chronic acceleration effects on erythrocyte number, plasma volume, globulin fractions, erythrocyte size and plasma A/G ratio in chickens
11 p1828 A69-25458
- HEMISPHERE CYLINDER BODIES**
Axisymmetric vibration modes of cylindrical-hemispherical membrane tank partly filled with liquid [AIAA PAPER 67-75]
09 p1482 A69-21940
- HEMISPHERES**
Desinent cavitation on hemispherical nosed bodies in water at various temperatures and velocities, considering isothermal case for surface nuclei [ASME PAPER 69-FE-1]
20 p3516 A69-37986
- Stagnation point Mach number gradient, sonic point location and drag coefficient of hemisphere at zero angle of incidence
23 p4060 A69-41910
- HEMISPHERICAL SHELLS**
Closed form solution of convective heat transfer to yawed concave hemisphere in free molecule flow
02 p0354 A69-12529
- Axisymmetric oscillation modes and frequencies of hemispherical shell partially filled with liquid, using moment theory of shells
04 p0679 A69-14922
- Monopole antenna behavior over grounded metal hemisphere, noting application to spacecraft and broadcasting antennas erected on hill
08 p1282 A69-20040
- Elastoplastic response of intersecting hemispherical/cylindrical shell structures compared with plastic deformation predictions
09 p1615 A69-21922
- Axially symmetric vibrations of thin elastic spherical shell partially filled with liquid, considering shell as joined hemispheres with or without same thickness
16 p2873 A69-32129
- HEMOCYTES**
Human blood viscosity measurement over wide range of shear rates, obtaining rheological data, suggesting osmotic red cell crenation role
23 p4095 A69-42078
- HEMODYNAMIC RESPONSES**
Control mechanisms of hemodynamic shifts from dogs subjected to acceleration under anesthesia
02 p0198 A69-11503
- G suit inflation acute and prolonged effects on cardiovascular dynamics in recumbent and passively tilted individuals
06 p0883 A69-17843
- Cardiovascular responses of baboons and dogs subjected to anoxic near vacuum environment by rapid decompression
06 p0875 A69-17846
- Clinicomorphological changes in rabbit eyes vascular system by exposing transverse accelerations
08 p1262 A69-19832
- Bone marrow distribution in dogs as basis for study of compensatory reactions of hemopoietic organs in response to radiation damage
08 p1262 A69-19835
- Acceleration component in pelvis to head direction found influencing hyperemia of brain at various g forces
13 p2212 A69-28626
- Pubertal puppy and adult dog cardiovascular system during inhalation of various nitrogen-oxygen mixtures, comparing heart beat rates, minute blood volumes, etc
19 p3257 A69-36169
- Heart beat rate, arterial pressure, blood volume and peripheral blood pressure increase observed in dogs running 7 min at 10 km/hr
22 p3885 A69-40966

- Radioisotopic determination of haemodynamic and bioelectric disturbances of rat striated muscles subjected to acceleration and hypokinesia
24 p4268 A69-43409
- HEMODYNAMICS**
Intrarenal capillary hydrostatic pressure effect on hemodynamically induced changes in sodium excretion
07 p1063 A69-18625
- Hemodynamic characteristics of decortication in rabbits, noting upsets of compensatory and adaptive capabilities of cardiovascular system
22 p3888 A69-41271
- Pulsatile flow in coronary arteries simplified model compared with experiment in anesthetized dogs
23 p4098 A69-42105
- Cardiovascular autonomic effects dynamic characteristics under severe arterial hypoxia in unanesthetized rabbit
24 p4258 A69-42632
- HEMOGLOBIN**
NT OXYHEMOGLOBIN
Hemoglobin diffusion influence on oxygen uptake and release by red cells solved by calculus of finite differences
05 p0707 A69-15677
- Thyroid gland role in resistance and myoglobin content of skeletal muscles of flat land and high altitude acclimatized white rats
05 p0709 A69-16517
- Thyroid gland role in resistance and myoglobin content of skeletal muscles of flat land and high altitude acclimatized white rats
18 p3096 A69-34736
- Chronic hypoxic hypoxia on oxygen-hemoglobin dissociation curve and respiratory gas transport in man, considering altitude residents and heart and lung diseased patients
21 p3650 A69-38383
- Monomethylhydrazine absorption through canine skin noting metabolic aftereffects and methemoglobinemia
22 p3887 A69-41191
- Hemoglobin inhomogeneity in rats irradiated with lethal doses of X rays and fast neutrons, using fractions prepared by column chromatography
22 p3888 A69-41274
- Critical oxygen pressure dependence on buffer in diluted heart muscle sarcosome suspensions and effect of hemoglobin or myoglobin
23 p4080 A69-41427
- Oxygen steady state transfer across thin layers of centrifuged erythrocytes at 37 degrees C before and after hemoglobin saturation with CO
23 p4093 A69-42064
- O-hemoglobin dissociation curve shape effect on O affinity of hemoglobin
23 p4095 A69-42086
- Model for human hemoglobin dissociation into subunits taking into account molecular explanation of oxygen dissociation curves
23 p4097 A69-42096
- Hemoglobin O reaction model explaining molecular weight and oxygen dissociation curve dependence on hemoglobin concentration
23 p4097 A69-42097
- HEMOLYSIS**
Hyperoxia exposure and hemolysis in tocopherol deficient mice
06 p0874 A69-17837
- Renal pathology of acute methylhydrazine intoxication in dogs, noting hemolytic anemia and hemoglobinuric nephropathy
06 p0883 A69-17847
- In vivo hemolytic susceptibility to hyperoxia in mice deficient in tocopherol
07 p1066 A69-19422
- Hyperventilation induced hemolysis in dogs measured as function of exposure time, body temperature and blood pH
22 p3887 A69-41192
- Hemolysis rates in various blood flows, considering effects on energy dissipation
23 p4100 A69-42533
- HEMORRHAGES**
Ocular injuries during bailout from Vampire aircraft, noting hemorrhages
10 p1649 A69-23380
- Ultrasound-echo-encephalography in diagnosis of posttraumatic intercranial hemorrhage of skull and brain trauma, noting neuroradiological techniques
21 p3652 A69-38790

Rat dental pulp hemorrhages following acute hypoxia from exposure to decompression chambers, atmospheric pressure variations or high acceleration
21 p3661 A69-39276

Carbon dioxide inhalation and intravenous isoproterenol effects on hemorrhagic consolidation occurring after left pulmonary artery ligation in dogs
23 p4082 A69-41441

Receptor and adrenergic blockade effects on blood loss, tolerated period and metabolic sequelae of hypotension in dogs
23 p4098 A69-42102

HEOS A SATELLITE

Regulated high voltage DC to DC converter with output voltage programmable numerically, noting application on board HEOS A satellite
04 p0602 A69-15400

European highly eccentric orbit satellite /HEOS/ cislunar probe to explore interplanetary space for magnetic fields, cosmic radiation, solar wind and earth shock wave
17 p3050 A69-33397

International organization and project management procedures in design and construction of Heos 1 satellite for measuring charged particles energy distribution outside geomagnetic field
17 p3050 A69-33699

European Space Research Program report on HEOS-A satellite, noting planetary physics research particularly in magnetic fields, cosmic radiation and solar wind
18 p3207 A69-34628

HEOS SATELLITES

TD-1 astrophysical satellite and future ESRO projects, considering HEOS-0A2 and TD-2
17 p3051 A69-34217

HERCULES AIRCRAFT

U C-130 AIRCRAFT

HERCULES NOVA

Cyanogen molecules increase attributed to nova shell compression from analyzing absorption spectrum of DQ Herculis 1934 after brightness maximum
15 p2688 A69-30558

HERMETIC SEALS

Mathematical simulation of temperature and humidity changes in compartments of hermetically sealed space vehicle cabins
02 p0200 A69-11489

Sealed and unsealed relay coils temperature rise at simulated outer space air pressure levels
13 p2231 A69-28048

Aircraft secondary power sources reliability dependence on electric loads, charge control and maintenance, discussing hermetically sealed batteries features
17 p2905 A69-34113

HERMITIAN POLYNOMIAL

General predictor-corrector method for system of m ordinary first order differential equations proved stable if Hermitian forms with coefficients are positive definite
01 p0105 A69-10807

Lehmann-Machly procedure for lower and upper bounds to eigenvalues of Hermitian operators in Hilbert space
06 p1020 A69-17131

Wiener-Hermite expansion extended to include time dependent ideal random functions, discussing application to shear flow turbulence
15 p2644 A69-30201

Convolution property of Hermitian transform for odd integral values of n
15 p2645 A69-30863

Finite elements concept cast in topological framework, presenting generalizations of Lagrange and Hermite interpolation functions
15 p2711 A69-30874

Pulse compression using Hermitian functions, noting minimal rms error requirement in real system
16 p2755 A69-32585

Shock wave structure in single component monatomic gas by expanding Boltzmann equation distribution function in terms of Hermite polynomial
18 p3124 A69-35170

Spatially homogeneous Boltzmann equation containing initial distribution functions expandable into Hermitian polynomials analyzed via ordinary differential equations
19 p3373 A69-36202

HERTZSPRUNG-RUSSELL DIAGRAM

Position of binary stars in photometric diagrams at Geneva observatory, discussing sequence profile of HR diagram
03 p0517 A69-14094

Kinematic parameters of giant stars and stellar evolution, discussing variations as function of zone position in HR diagram
03 p0517 A69-14095

Rapid differential rotation effect on massive main sequence O and B stars, discussing bolometric magnitude deficiencies and shifted position in Hertzsprung-Russell diagram
07 p1220 A69-19390

Mass loss in Red Giant stage from statistical analysis of H-R diagrams of galactic clusters
08 p1396 A69-20642

Russell method application to combined data of both minima of eclipsing binary using electronic computers
08 p1408 A69-21136

Cepheid variable 1 Carinae position in H-R diagram suggested from microturbulent velocity role in pulsational instability
14 p2522 A69-29590

H-R diagrams of globular clusters, discussing evolution models with and without mass loss
14 p2527 A69-29943

Theoretical Hertzsprung-Russell diagram for star cluster NGC 1866, allowing stellar evolution study
17 p3038 A69-33720

Masses of visual binaries above main sequence with published orbits determined as function of position in H-R diagram, using spectroscopic parallaxes
18 p3195 A69-34429

HERZBERG BANDS

Herzberg bands synthetic spectra matched to various spectrograms to determine vibrational populations of molecular O state in nightglow
24 p4310 A69-43186

HETEROCYCLIC COMPOUNDS

NT ADENINES
NT ADENOSINE TRIPHOSPHATE [ATP]
NT ASCORBIC ACID
NT AZINES
NT AZOLES
NT INDOLES
NT PILOCARPINE
NT PYRIDOXINE
NT PYRROLES
NT RDX
NT TETRAZOLES
NT THIAMINE
NT TOCOPHEROL
NT TRYPTOPHAN
NT URIC ACID

Cl 35 nuclear quadrupole resonance spectra of 3,6-dichloropyridazine, tetrachloropyridazine, 2,6-dichloropyrazine and chloropyrazine
01 p0123 A69-10290

Mass spectra of quinoline and isquinoline N-oxides, discussing diagnostic values of fragmentation reactions for heteroaromatic N-oxide function presence
07 p1075 A69-19496

Gas-liquid and thin layer chromatography and nuclear magnetic resonance techniques to steric analysis of diketopiperazines
07 p1075 A69-19498

Electrical properties of tetracyanoquinodimethane /TCNQ/ complexes representing unit segments of non-conjugated and conjugated polymers
11 p1832 A69-25675

Heterocyclic-aromatic organic polymer adhesives used for high temperature structural purposes, discussing processing, testing, formulating and impact on basic research
14 p2469 A69-29346

Biochemical evolution role in porphyrin synthesis forming hemoproteids base, discussing assimilation of carbon dioxide in early earth atmosphere
23 p4088 A69-41814

HETERODYNING

NT OPTICAL HETERODYNING

Hologram heterodyne scanner for production from scanning coherent light beam of electrical signal corresponding to scanned hologram, noting camera tube application
03 p0431 A69-13827

Frequency conversion in microwave crystal mixer with EMF amplitude fluctuations in heterodyne
09 p1469 A69-22644

HETEROGENEITY

Structural microheterogeneities in monophase Ti alpha alloys, using complex phase analysis method
04 p0617 A69-14939

Combustion in heterogeneous systems, considering diffusion flames and fine droplets dispersed into gaseous oxidizer in fog form
06 p1032 A69-17421

Lunar interior chemical heterogeneity determined from model taking into account pressure, temperature and composition effects
19 p3425 A69-36421

HETEROTROPHS

Euglena gracilis grown heterotrophically, investigating respiratory physiology as function of glucose, acetate or ethanol growth supporting carbon source
10 p1647 A69-24186

HEURISTIC METHODS

Heuristic Dendral program to mechanize inductive inference in organic chemistry to determine isomers in chemical compounds
07 p1075 A69-19484

Heuristic methods to determine scientific activities planning emphasizing problem definition, purposes, possibilities of solution and difficulties
13 p2720 A69-30969

Computer-algorithm elements required for engineering design and invention problems including design requirements, selection of spaces for variables using computerized heuristics, etc
19 p3280 A69-36666

Heuristic process for constructing similarity parameters approximation solution of laminar and turbulent boundary layers equations
19 p3301 A69-36799

HEXAGONAL CELLS

Energy function invariants for cubic and hexagonal systems of anisotropic media with coupled stresses
01 p0169 A69-10811

Electronographic determination of ternary alloys of germanium antimony tellurides noting hexagonal laminarity with cell periods
02 p0298 A69-12046

Friction induced plastic deformation of Be-Co-Zn single crystals with HCP structure
02 p0254 A69-12627

Dislocation distributions in cold worked fcc, bcc and hcp metals, discussing dislocation structures in deformed single crystals and work hardening theories
05 p0778 A69-15754

Nodal precipitation and cellular solidification substructure in commercial purity nickel, discussing supercooling, NiO and eutectic composition
08 p1332 A69-20289

Pressure effects on hcp crystalline lattice alloys order-disorder transformations
11 p1937 A69-24704

Filamentary composites elastic constants calculation extended to hexagonal symmetry by long waves method
17 p3061 A69-33666

Hexagonal and nonhexagonal cell phenolic honeycomb design as energy dissipating material noting processing, composite constituents, cell configuration and usage environment
19 p3353 A69-35503

Numerical integration of atmospheric motion equations in global domain using hexagonal grid, including sphericity corrections and Coriolis term
19 p3364 A69-36509

HEXAHEDRITE

Dynamically deformed structures in chondrites and hexahedrites observed to discriminate among theories about origin of chondrules and meteorites
19 p3418 A69-36135

Shock histories of hexahedrites and Ga-Ge group III octahedrites based on metallographic and X ray diffraction analysis, noting meteorites shocked preterrestrially
19 p3418 A69-36136

HEXANITROSTILBENE /HNST/

Nuclear radiation damage vs thermal decomposition of diaminitrobenzene and hexanitrostilbene, analyzing unchanged residual compound
02 p0304 A69-12500

HIBERNATION

Specific antibody formation to influenza A virus vaccine /strain PR sub s/ in hibernating ground squirrels /Citellus tridecemlineatus/
08 p1263 A69-20173

Glucose, lactate, free fatty acids, hepatic glycogen and endocrine activity in fasting hibernating dormouse and rat in deep hypothermia
10 p1642 A69-23118

Hibernation seasonality, protein synthesis during periodic awakenings and importance of awakenings to maintenance and evolution of thyroid activity
10 p1642 A69-23120

Computer analysis of cortical and subcortical activity in yellow bellied marmot during sleep, hibernation and hypothermia
10 p1643 A69-23122

Radiation resistance of animals in hibernation and hypothermia, noting temperature dependence of protective effect

10 p1643 A69-23126

Mineral dynamics during hibernation and disuse atrophy in connection with organismal homeostasis and chronic-term manned space flight, noting skeletal effect of immobility

21 p3660 A69-39175

Body weight and organ sizes in hibernating cold and warmth adapted golden hamsters, discussing lungs, heart, kidney, pancreas and liver weight increases

23 p4084 A69-41462

HIERARCHIES

NT BBGKY HIERARCHY NT DICHOTOMIES

Higher dimensional Dirac Hamiltonians from L-matrix hierarchy using dimensional eigenvector

04 p0625 A69-15275

Buckling of long cylinders with homogeneous random axisymmetric geometric imperfections under axial compression, using truncated hierarchy technique

07 p1236 A69-19473

Compromise control in system with two hierarchy levels interrelated via lower level subsystems optimality criteria found by solving global criterion problem

08 p1297 A69-20415

Control signal interconnection of subsystems at different levels of hierarchical structure systems

12 p2050 A69-26089

Cybernetic approach to memory, proposing model characterized by hierarchical structural order and sequence to study physiological rhythms

23 p4110 A69-41983

HIGH ALTITUDE

Daytime sky radiation measurements by high altitude vehicles with spectrophotometer noting spectral radiance, luminance, polarization, albedo and near IR

08 p1317 A69-21071

Biological effects of cosmic ionizing radiation in supersonic commercial aircraft at high altitudes, showing spatial distribution based on balloon experiments

11 p1830 A69-24865

Topographic mapping by high altitude jet aircraft photography

18 p3134 A69-34339

HIGH ALTITUDE BALLOONS

Inner and outer meteorological balloon assembly for fast rising and high altitude sounding

01 p0010 A69-10541

Balloon flown High Altitude Particle Physics Experiments /HAPPE/ for research on high energy cosmic rays and particle interactions

03 p0499 A69-12943

Balloon-borne SPARMO detector SC 67 used for measuring radiation at high altitudes

05 p0762 A69-15823

Signal strength variations for balloon-borne VHF FM transmitter due to wave interference, noting application to balloon range estimation

06 p0886 A69-16925

High altitude plastic balloon platforms for atmospheric research noting increased capacities in altitude, payload and flight duration

06 p1010 A69-18067

Pressure-altitude transducers for atmospheric pressure measurements on balloon flights including diaphragm, thermoconductivity, radioactive density and hypsometer gauges

07 p1132 A69-18873

Stratospheric balloons launching and nacelles for measurement of cosmic rays, atmosphere high altitude characteristics, discussing French launching center

16 p2734 A69-31759

Stratospheric winds effect on instrument package suspended from high altitude balloon, discussing package displacements, yarn shapes and air drag characteristics

17 p2961 A69-33612

Trans-iron nuclei flux in primary cosmic radiation determined through high altitude balloon exposure of interleaved layers of nuclear photographic emulsion and plastic detectors

21 p3787 A69-38327

High altitude balloon stationkeeping system combining battery powered propeller and drag chute

22 p3866 A69-40941

Causes of ascent failures in high altitude balloons, discussing test methods and specifications revisions

24 p4251 A69-42714

Mathematical model for ascent and descent of high altitude tethered balloon, developing computer program and deriving differential equations of motion

24 p4254 A69-43722

HIGH ALTITUDE BREATHING

High altitude acclimatization effects on cardiovascular system, external respiration, blood composition, optical and vestibular analyzers in human subjected to various stresses

13 p2212 A69-28623

Bird respirator function at simulated high altitude, noting adequate support in case of rapid decompression

14 p2406 A69-29290

HIGH ALTITUDE ENVIRONMENTS

Renal effects of moderate hypoxia exposure in mice as reflected in urine volume and electrolyte excretion patterns during four days at simulated altitude

01 p0015 A69-10921

Blood volume in rats exposed to high altitude and deacclimated at ambient pressure, noting changes and control level restoration

01 p0015 A69-10922

RF voltage breakdown in solid state telemetry transmitters on sounding rocket, noting glow discharge initiated by energetic dissociated electrons

02 p0222 A69-12691

Visual feedback mechanisms in simulated high altitude conditions, discussing physiology of ocular homeostasis adaptation

06 p0882 A69-17647

Oxygen intake and body temperature of basal and sleeping Andean natives at high altitude

06 p0874 A69-17835

Neurological impairment in baboons exposed to prolonged decompression simulating high altitude aircraft cabin structural failure, noting neuropathological examination results

07 p1067 A69-19426

Prolonged hypokinesia effects on white rats resistance to convulsions induced by high altitude simulation

08 p1262 A69-19929

Stability of male cardiovascular, respiratory and motor systems functional conditions after physical activity in pure O medium at high altitude pressure

08 p1262 A69-19931

Monkey behavior in high atmosphere under weightless conditions, discussing problems connected with biological measurements, logic systems and vibration protection

09 p1447 A69-22722

Moisture losses of men wearing partial pressure suit with oxygen mask determined by changes in skin temperature and heat flow

10 p1647 A69-23591

Lubrication and operation of Hamilton Standard propellers in high altitude and low temperature environments

11 p1822 A69-24515

Accelerometer force balance used in measuring forces and moments acting on models in short duration rocket plume tests at simulated high altitude

13 p2264 A69-28285

High altitude environmental effects on adrenal glands and hypothalamic neurosecretion in rats

13 p2211 A69-28615

Glucose disappearance rate from dogs blood at simulated 27,000 ft altitude compared with tolerance at ground level, discussing chlorpromazine administration effect

14 p2408 A69-29305

Life in common by groups of four or five people isolated on high mountain under adverse conditions

21 p3661 A69-39267

Contact lenses hazards during high altitude aircraft piloting analyzed via bubble development

23 p4106 A69-41806

HIGH ALTITUDE PRESSURE

Blood coagulation in animals under acute hypoxia at exposures to pressure corresponding to 5000 m altitude, noting blood morphology

12 p2019 A69-26348

Test programs utilizing pitot probes to map exhaust plumes from liquid bipropellant engines in low ambient pressures conducted to verify calculations

16 p2869 A69-32746

HIGH ALTITUDE TESTS

Structure and mean molecular weight measurement of unknown atmosphere assessed from high altitude tests in earth atmosphere

03 p0512 A69-13699

X ray investigation of repeated simulated exposures to altitude and acceleration on healthy professional flyers

03 p0378 A69-14208

Ionosphere disturbances due to high altitude thermonuclear explosions, discussing experimental proof by Cosmos satellites short wave transmitter radio signal scintillation statistical evaluation

19 p3304 A69-36624

High altitude CAT regions length distribution determined from level flight path sampling data correlation

20 p3570 A69-37168

HIGH ASPECT RATIO

High aspect ratio submicroscopic whiskers of beta-SiC, investigating rheological properties of suspensions in various fluids

01 p0102 A69-11260

Slender wing theory extension to not-so-slender wings approached as singular perturbation problem, using matched asymptotic expansions method

04 p0544 A69-14891

HIGH ASPECT RATIO WINGS

U SLENDER WINGS

HIGH CURRENT

Inductively excited argon ion laser properties in high current regions

06 p0935 A69-17767

HIGH EFFICIENCY

U EFFICIENCY

HIGH ENERGY

U ENERGY

HIGH ENERGY ELECTRONS

Photometric measurement of atomic oxygen green line emissions and high energy electron flux using twilight sounding rocket

02 p0309 A69-12743

High latitude outer zone electrons boundary region during geomagnetically quiet periods

03 p0502 A69-14004

Energetic electron fluxes measured at 2000 km over auroral and polar regions and at 17 earth radii in magnetotail plasma sheet

03 p0503 A69-14013

Interplanetary relativistic electrons from solar flare events

04 p0650 A69-15528

Energetic electrons of terrestrial origin behind bow shock and upstream in solar wind

05 p0815 A69-16253

High resolution electron and proton energy measurements by sounding rockets indicating plasma sheet as source of energetic auroral electrons

05 p0756 A69-16273

Gamma ray production and high energy electrons in cosmic radiation

05 p0817 A69-16712

X ray astronomy use for probing hot regions of outer space and high energy electrons

06 p0991 A69-17307

Synchrotron radiation from trapped high energy electrons in Van Allen belt

06 p0992 A69-17324

Packet of finite amplitude VLF whistler waves, examining cyclotron resonance interaction with high energy electrons and development in magnetosphere

06 p0917 A69-17378

Electrostatic ionospheric waves excited around lower hybrid resonance frequency by high energy electrons

06 p0918 A69-17381

Radial diffusion of high energy electrons in outer radiation belts, determining statistically delay time between electron intensity variations

06 p0919 A69-17720

Cut-off boundary latitude and electron flux changes in midnight sector of outer radiation belt during magnetic bay periods from Injun 4 satellite data

07 p1204 A69-18836

Synchrotron radiation from relativistic electrons in magnetosphere, calculating variation with frequency and height of lines of force

08 p1306 A69-20182

Hydrogenic atoms ionization by high energy electrons, discussing cross sections for ejected electrons and total energy

08 p1356 A69-20738

Fast electron diffusion in stochastic magnetic field, obtaining diffusion coefficient as function of ratio of correlation time to Larmor period

08 p1368 A69-20807

Solar flare energetic electron access to polar zones from measurements made by nine channel magnetic spectrometer on polar orbiting vehicle

09 p1577 A69-21709

Hard X ray event spectrum representation by thermal bremsstrahlung spectrum emitted by energetic

electrons, determining various physical parameters of source

09 p1579 A69-22180

Energetic solar proton and electron event observed in July 1966 by Explorer 33 and OGO-C, noting association with invisible solar hemisphere flare

09 p1579 A69-22181

Relativistic solar electron detection in interplanetary space during July 7, 1966 proton flare event, noting energy spectrum and time history

10 p1767 A69-23766

Cosmic ray composition and nuclear interactions at very high energies, comparing results of Monte Carlo simulations with various experimental data

12 p2149 A69-26475

Plasmapause, plasma sheet and energetic trapped electrons in earth magnetosphere, considering slot, peak intensity and trapping boundary

12 p2151 A69-26953

ESRO 1 satellite measuring proton intensities and energy spectra of precipitated and magnetically trapped electrons

13 p2327 A69-27754

High energy electrons producing electromagnetic cascades in electron photon showers in lead measured by scintillation detectors

13 p2332 A69-28419

Charge sign ratio of primary cosmic ray electrons measured by balloon flown multistage spark chamber, studying east-west asymmetry

15 p2678 A69-31497

High energy electrons emission during alloy evaporation on hot metal filaments used for thin film deposition

16 p2827 A69-32016

Gamma ray flux from processes associated with high energy electrons from pulsar NP 0532, noting light polarization

20 p3588 A69-37410

Anisotropy of relativistic cosmic ray electrons, considering electron exposure time to synchrotron effects, energy loss from inverse Compton effect, etc

20 p3593 A69-38145

Monograph on whistler mode waves in plasma covering apparatus for studying gyroresonant interaction between whistler radiation and fast electrons

21 p3779 A69-39868

4 October 1965 type IV solar burst, studying acceleration mechanisms for fast electrons by comparing fine structure at various frequencies

22 p4001 A69-39983

Magnetospheric instabilities and whistler mode turbulence relationship to loss of high energy electrons from Van Allen belts

24 p4306 A69-42692

High energy nucleons and electrons accelerated in solar flares, considering interplanetary magnetic field effect on radiation properties near earth orbit

24 p4372 A69-43617

HIGH ENERGY INTERACTIONS

Cosmic ray air shower distribution from Crab Nebula, M87, M82, quasars, X ray sources and recent supernovae

02 p0308 A69-12597

Extensive air showers due to interaction of high energy particles with atmosphere, discussing astrophysics, cosmology and fundamental particle physics

03 p0498 A69-12938

Strong interactions at energies above 100 Gev, examining use of cosmic ray experiment for qualitative studies of interaction process

03 p0498 A69-12939

High energy strong interaction theory in cosmic ray physics, discussing Regge model, fireball production and quark problem

03 p0469 A69-12940

High energy interactions used to estimate energy of individual cosmic rays

03 p0498 A69-12941

High energy cosmic ray research facility at mountain altitudes, noting nucleon-proton interactions, particle identification and momentum analysis

03 p0499 A69-12942

Balloon flown High Altitude Particle Physics Experiments /HAPPE/ for research on high energy cosmic rays and particle interactions

03 p0499 A69-12943

High energy cosmic ray particles observed with SEZ-14 instrument aboard Proton 1 and 2 satellites

03 p0499 A69-12944

Ultrahigh energy interactions working model, suggesting interpretation of cosmic ray experimental data on basis of Aleph plus Pionization model

03 p0499 A69-12945

High energy interactions greater than 10 Gev from dosimetric point of view

03 p0371 A69-13477

Upper limit estimated for anomalous interaction between cosmic muons with greater than 100 Bev energy

06 p0986 A69-17246

Astrophysical aspects of primary energy spectrum deduced from shower size spectra and high energy interactions of extensive air showers

06 p0990 A69-17298

Extensive air showers characteristics based on models of high energy interactions of nucleons and pions with air nuclei

06 p0990 A69-17301

Muon component of extensive cosmic ray showers, discussing effect of multiplicity of secondary particles created by high energy nuclear interactions

07 p1207 A69-19325

Direct muon production, discussing range vs energy relation for favorable experiment and difficulties with observed muon flux isotropy

07 p1209 A69-19406

Compton scattering of microwave radiation on cosmic ray electrons proposed as mechanism generating 100 Mev cosmic gamma rays

09 p1580 A69-22295

Renormalizable weak interaction mechanism for generation of high energy muons from Tev cosmic rays in upper atmosphere

09 p1581 A69-22530

Weak interaction theory modifications needed for high energy cosmic ray muons to not violate conservation of probability

09 p1583 A69-22758

Superhigh energy cosmic ray interaction with neutrinos in universe, shape of cosmic ray spectrum and universe development

10 p1757 A69-22826

High energy cosmic radiation using Conversi detectors, noting design and internal efficiency

10 p1693 A69-23296

Line spectrum of flare gamma radiation due to atmosphere nuclei excitation by high energy proton acceleration

11 p1945 A69-24241

Poisson formula in double logarithmic approximation for photon emission cross section in analysis of bremsstrahlung involving high energy particles

11 p1922 A69-25758

Inelastic interactions between Tev cosmic particles and light element nuclei, describing design and operation of measuring apparatus and derivable data

12 p2093 A69-26583

High energy particle collisions, calculating inelastic interactions between cosmic nuclei

13 p2330 A69-28370

Nuclear emulsion high energy nucleon-nuclei interaction model accounting for two maxima track formation

13 p2303 A69-28371

Multiple particle production and resonance events during high energy particle collisions

13 p2303 A69-28372

High energy inelastic particle collisions observed at high altitude station, using Monte Carlo computations for nucleon-nucleon collision model

13 p2330 A69-28374

Four dimensional momenta transfer during high energy cosmic ray particle collisions, comparing various collision models

13 p2330 A69-28375

Gamma quanta produced during high energy nucleon-nuclei interaction of air atoms recorded with X ray film

13 p2303 A69-28376

High energy nuclear interactions in graphite block at high altitude, recording gamma quanta produced

13 p2330 A69-28377

Gamma quantum spectrum shape from high altitude X ray film and nuclear emulsion blackening, discussing high energy pion production

13 p2330 A69-28378

Fireball events, isobars and meson resonances in very high energy nuclear interactions, discussing dispersion and four momenta transfer methods

13 p2303 A69-28380

Pionization cross sections at 100 gev for interactions of cosmic ray neutrons and pions with C and Pb nuclei

13 p2330 A69-28382

Inelastic interaction cross sections of nuclear active particles at C and Fe in 70 to 1000 gev energy range

13 p2330 A69-28383

Inelastic interaction cross sections of nuclear active cosmic ray particles with atomic Fe and Pb in 100 to 1000 gev range

13 p2330 A69-28384

Mean free path of interaction of nuclear active particles in Fe with energies greater than 530 gev

13 p2303 A69-28385

Nuclear component energy flux absorption in Fe measured with ionization calorimeter

13 p2330 A69-28386

Nuclear interactions between high energy nuclear active particles and C nuclei, studying electron-photon component energy with nuclear photoemulsions

13 p2331 A69-28388

Asymmetrical showers in interaction of high energy nuclear active particles with atomic nuclei, estimating target particle mass

13 p2303 A69-28391

High energy nuclear active particles and muons studied with calorimeters, noting cascades muon origin and muon energy spectra

13 p2331 A69-28395

High energy scattering approximation valid from small to large angles, discussing errors and proton scattering by He

14 p2487 A69-29008

Nonlinear interactions of linearly polarized carbon dioxide laser signals in sulfur hexafluoride measured as function of angle between polarization planes

14 p2460 A69-29602

Three dimensional Monte Carlo calculations for hadronic component of extensive air showers using semiempirical model high energy nuclear interactions

15 p2678 A69-31482

High energy cosmic ray muon charge ratios at large zenith angles measured as function of momentum by using spectrometer

17 p3023 A69-33321

Photodisintegration of ultrahigh energy cosmic rays by universal radiation field, analyzing implications on origin and propagation time

18 p3188 A69-35006

Transverse momentum of fireball particles emitted in high energy inelastic collision related to emission angle and energy in accelerators

19 p3396 A69-36644

Cosmic protons and high energy heavy nuclei interaction with radiation in expanding universe, including estimates of light radiation influence on cosmic ray spectra

20 p3591 A69-38034

Matter and radiation interaction in hot model universe, investigating residual radiation spectrum deviation from Planck curve

21 p3797 A69-38536

Proton-antiproton high energy elastic scattering by bosons exchange, introducing vertex functions for non-local Lagrangian

21 p3775 A69-39467

Book on high energy astrophysics covering violent stellar phenomena, radio galaxies, quasars, pulsars, cosmic rays origin, mystery neutron stars, etc

22 p4008 A69-39900

Scattering of high energy Ar beams by room-temperature Ar, He and H molecules, deriving interaction energies at internuclear distances

22 p3988 A69-41187

Air showers muon threshold energies deep underground as function of zenith angle, discussing nucleon-air-nucleus collision parameters variation effect

23 p4207 A69-42497

High energy negative kappa meson-nucleon interactions with respect to multiplicity distribution of charged pions in nucleon-antinucleon annihilation, showing binomial distribution

24 p4351 A69-42791

HIGH ENERGY OXIDIZERS

Book on inorganic high energy oxidizers covering synthesis, structure and properties of fluoronitrogen, fluorine, fluorohalogen and oxygen compounds

12 p2146 A69-25824

HIGH ENERGY PROPELLANTS

High thrust fluorine engines and propellants

03 p0494 A69-12889

Material requirements for uncooled nozzles of solid propellant rocket motors burning aluminized propellants, discussing successful testing of pyrolytic graphite

06 p0946 A69-17530

HORA, flexible upper rocket stage, noting variable fuel tank capacity and high energy propulsion

08 p1409 A69-20094

Rocket engine high energy hybrid propellant performance optimization, discussing engine enlargement, oxidizer injection geometry, fuel additives, combustion gas vorticity, etc

11 p1943 A69-25428

Analytical model for liquid fluorine no-vent loading operations noting application to lightweight upper stage systems
[AIAA PAPER 69-579]

16 p2767 A69-32715

HIGH EXPLOSIVES

U EXPLOSIVES

HIGH FIELD MAGNETS

Cryogenic solenoids with pure Al conductor for production of strong magnetic fields, discussing softness and strain resistivity problems

12 p2016 A69-26497

NbN thin film production by refined reactive sputtering technique, discussing Pauli spin paramagnetism and spin orbit scattering in high field superconductivity

17 p3016 A69-33790

HIGH FREQUENCIES

Polarization rotation and phase delay effects as function of frequency for ionospherically propagated HF signals

02 p0208 A69-12331

Space charge limited square law diodes as HF mixers, noting low conversion loss of asymmetrical type

03 p0404 A69-13580

HF scattering of scalar plane wave by transparent sphere based on Watson transformation

07 p1181 A69-19033

HF breakdown of air using Boltzmann equation to determine net ionization frequency relation with electric field strength

08 p1357 A69-20810

Sporadic E region HF backscatter observed during IQSY, using PPI display

09 p1489 A69-21701

HF measurements by phase and amplification control of signal in impulse oscillography, noting accuracy in nanosecond range and signal distortion

11 p1880 A69-24541

Convective drift and flute instabilities of plasma stabilized by exerting HF forces on electrons, determining required HF field amplitudes

11 p1932 A69-25538

Transient behavior of transistor UHF oscillator, discussing network analysis for oscillation amplitude calculation by nonlinear transistor equivalent circuit diagram

11 p1854 A69-25613

Negative resistance effects computed for HF operation of SCL diodes, based on quantitative analysis of small signal response

12 p2038 A69-26349

Antenna suspension height variation effects on HF signals in ionospheric scattering lines

12 p2032 A69-26705

Shock pulse criterion limitations and HF transients technique for design and tests of structures and components

12 p2182 A69-26731

Multiple beam HF receiving antenna system for directivity, azimuthal coverage and noise limitation

13 p2228 A69-27631

Small signal, HF equivalent circuit for intrinsic metal oxide semiconductor field effect transistor, considering nonpinchoff and pinchoff modes

13 p2238 A69-28429

Disaccommodation component of magnetic aftereffect causing dynamic absorption of HF magnetic energy in ferrites

15 p2665 A69-30038

Atmospheric absorption calculations, noting direct D layer reflection effects on lower HF oblique propagation

16 p2752 A69-32389

Synchrotron radiation HF cut-off resulting from electrons with anisotropic pitch angle distribution for type IV solar radio bursts

22 p4006 A69-40577

Space simulation tests of satellite-borne quartz crystal oscillators for tracking based on Doppler effect

22 p3927 A69-40590

HF radio waves auroral absorption in ionosphere reviewed for first decade of riometry

22 p3902 A69-41218

HF receiver interference blanker, discussing limiter-blanker system, integration, effectiveness and squelch circuit

23 p4141 A69-42221

HIGH GAIN

High output laser amplifier consisting of glass and selenium oxychloride/Nd liquid lasers

23 p4173 A69-41565

HIGH GRAVITY ENVIRONMENTS

Sustained high deceleration load effects on quartz crystals during atmospheric entry studied by centrifuge test program on oscillator circuits

01 p0042 A69-10417

Electrodes for fuel cells with liquid electrolytes, discussing problems under weightless and high gravity situations

16 p2738 A69-32409

Environment effect on scientific and telecommunication equipment mounted on exploratory probe during Venus atmosphere entry for acceleration loading in design

19 p3431 A69-36037

HIGH LATITUDES

U POLAR REGIONS

HIGH LIFT DEVICES

U LIFT DEVICES

HIGH MELTING COMPOUNDS

U REFRACTORY MATERIALS

HIGH PASS FILTERS

Numerical filtering procedures for gust spectrum analyses compared for gain and phase lag frequency response characteristics, discussing gust acceleration spectra

01 p0084 A69-11052

Narrow bandpass filters based on ripple adjustment in response of low or high pass prototype

04 p0574 A69-14345

RLC filters transfer functions applied to development of high pass filter

08 p1300 A69-21176

High pass filters reflection group delay compared with low pass filters transmission group delay with Butterworth, Chebyshev and elliptic responses

21 p3686 A69-39139

Waveguide below cut-off high pass filters fabrication technique using slot cut into waveguide section

23 p4170 A69-42231

HIGH POLYMERS

Thermally stable polymers for high stress aerospace applications, noting chemical stability and structure of high polymers

12 p2117 A69-25853

Skin friction drag reducing high polymer solution injected into turbulent boundary layer to test effectiveness on marine vehicles

17 p2951 A69-33254

Craze formation and shear yielding considered for glassy polymers in terms of stress field requirements

17 p2993 A69-34169

Linear high polymer heat capacities by adding contributions from chain segments, deriving table of heat capacity contributions of polymer constituents

19 p3359 A69-36287

Heat conduction orientation anisotropy in linear amorphous high polymers due to uniaxial stretching, noting molecular weight distribution and temperature effects

19 p3359 A69-36443

Molecular engineering of high organic polymers, discussing molecular weight, crystallization, elastomers, fiber formers and building construction materials

20 p3566 A69-37598

HIGH PRESSURE

Ultrahigh pressure physics of materials, discussing apparatus, phase transitions and yield strength ductility relationships

02 p0260 A69-11803

High pressure rocket engine design, considering complete combustion, propellant feed system overall efficiency and thermodynamic gain

03 p0495 A69-12888

Graphite ablation in high pressure environments, extending existing analysis of thermochemical and thermomechanical behavior to include allotropic features
[AIAA PAPER 68-1153]

04 p0686 A69-14873

Viscosity of compressed nonreacting gas mixtures at high temperatures, discussing conditions for accurate calculation

05 p0845 A69-15895

Handbook of techniques in high pressure research and engineering, discussing construction materials, design and construction methods, measuring techniques, etc

07 p1137 A69-18412

Tensile strength of alloys under high pressure of hydrogen and helium, discussing embrittlement
[ASM PAPER D8-14.2]

07 p1169 A69-19667

Two way pyrotechnic high pressure gas valve for D2 satellite, noting resistance to leakage due to nearly monolithic construction

10 p1635 A69-23033

High pressure arc discharge diagnostics with spectroscopic method relating spectral profiles to central temperature, pressure and temperature distribution

12 p2094 A69-26968

High pressure AC arc heater system design criteria, discussing magnetic field, chamber gas flow, stabilizing elements, etc
[AIAA PAPER 69-348]

13 p2243 A69-28283

Elastohydrodynamic lubrication of square section high pressure face seals mounted on rigid housings, considering design charts for load and leakage
[ASLE FICFS PREPRINT 16]

15 p2621 A69-30493

High pressure combustion of ortho-barenes /carboranes/, determining formation heat and amounts of boric acid and carbon dioxide

21 p3670 A69-39625

Thomas-Fermi approximation applied to calculation of equations of state and thermodynamic functions at high pressure from differential equations of statistical atom model

22 p3984 A69-40186

Metals conductivity under high pressure, giving theories for electrons scattering cross sections on ions and for Debye temperature

22 p3980 A69-40187

HIGH PRESSURE OXYGEN

In vivo hyperbaric hyperoxia effect on erythrocytes unsaturated fatty acid composition alterations of tocopherol deficient mice

03 p0375 A69-14070

Induced high pressure HF discharge parameters computed for Ar, O and N by using electrical and thermal conductivity functions

15 p2662 A69-30976

Mice convulsions at varying hyperbaric oxygen pressures and carbon dioxide content correlated with decreasing brain alpha aminobutyric acid levels

19 p3257 A69-35972

Hyperbaric oxygen convulsions origin and site, studying pressure effect on brain electrical activity in rabbit by EEG

21 p3656 A69-38977

GABA shunt contribution to total metabolism of alpha ketoglutarate to succinate and high pressure O effect on system under in vitro conditions

22 p3877 A69-40776

HIGH Q

U Q FACTORS

HIGH RESOLUTION

Automatic heteroatomic plotting of high resolution mass spectral data, presenting relative intensity vs elemental composition in bar form

01 p0024 A69-10905

High range resolution by pulse to pulse frequency shifting, utilizing existing low resolution equipment by adding signal processing capability to receiver

03 p0388 A69-13181

High resolution magnetograph study of solar magnetic field, showing magnetic asymmetry and fluctuations

04 p0651 A69-14367

High resolution silver halide photoemulsions analyzed by holographic resolvometry using Ne-He laser to obtain interference patterns

15 p2606 A69-30052

Image intensifier and return beam sections of 4.5 inch high resolution vidicon and camera system for high definition signal readout

17 p2976 A69-34063

Multielement compound high resolution quick scan interferometer for rapidly changing solar burst observations at 3.75 GHz

18 p3118 A69-34968

Auroral spectroscopy for high resolution coverage at maximum wavelength range, discussing plane diffraction grating

21 p3707 A69-38486

HIGH SENSITIVITY

U SENSITIVITY

HIGH SPEED

High speed deformation of metals under pulse loading, noting role of maximum stress magnitude and deformation characteristics

12 p2113 A69-26043

Aerodynamic considerations of high speed hydrodynamics for underwater craft, noting rocket propulsion

13 p2245 A69-27418

HIGH SPEED CAMERAS
NT FRAMING CAMERAS

Ultrahigh speed holographic interferometry for studying plasmas produced by focused laser beam, noting electron density evolution in deuterium plasma

05 p0760 A69-15587

Electronically controlled spark gap system for HF optical frame separation based on Cranz-Schardin principle

05 p0763 A69-15985

High speed streak camera synchronization with shock tube process involving nonreacting gases or mixtures in pressure chamber

06 p0926 A69-17499

High speed photographic study of finely dispersed Al particles combustion and ignition in high temperature gas flows, noting dependence on oxidizers concentration

08 p1375 A69-20341

Book on photographic recording of high speed processes noting slit scanning, cinecameras, shutters, mirror rotation drive mechanisms, photographic materials, etc

08 p1317 A69-21033

Photography role in experimental research with applications to flight analysis and comparison with human visual accuracy

11 p1881 A69-24573

High speed photography - Conference, Stockholm, June 1968

12 p2080 A69-26135

Photoelectronic high speed image intensifier framing camera, showing single shot synchronized photography of electric spark in air

12 p2082 A69-26137

Shutter drive circuits for image converter camera noting focusing, deflection system, applications in plasma research, etc

12 p2082 A69-26138

Electron-optical image converter camera for wide time intervals, considering nanosecond electronic control and high voltage stabilized power supply

12 p2083 A69-26140

Nanosecond electron-optical image converter multiframe camera designed for reducing frame exposure time

12 p2083 A69-26141

Multiframe image converter registration of space-time ruby laser spot structure changes in Q switched regime prior to giant pulse formation

12 p2083 A69-26142

Image intensifier cascade tubes and slit type electronic cameras with high sensitivity multiple integral images, exemplifying projectile velocity measurements

12 p2083 A69-26143

Meshless shutter tube with nine images double deflection capability, using deflectron and semiconducting plates assembly

12 p2083 A69-26144

Diode type image shutter tube with proximity focusing for high speed photography

12 p2083 A69-26145

Ultrahigh speed photographic cameras with exposure times between 5 and 500 nsec, using image tube and high voltage pulse generator

12 p2083 A69-26146

Electronic image converter camera for observing rapidly evolving light phenomena consisting of high voltage pulse generator and biplanar tube image converter

12 p2084 A69-26147

RLC integrated low inductance circuit for magneto-optical high speed camera shutters, Q switched ruby laser and short light pulses in spark gap

12 p2084 A69-26149

Rotating mirror streak cameras in quantitative measurements of extreme compressions by shock waves, analyzing spatial and temporal resolving power

12 p2084 A69-26151

Practical time resolution of streak camera, discussing streak camera transfer function and measurement of resolution with pulsed laser diode emission

12 p2084 A69-26152

Continuously operating mirror scanning system for high speed photographic cameras, emphasizing maximum scanning speeds and framing rates

12 p2085 A69-26154

High speed streak camera for recording fast processes, noting changeability from optical to UV spectral range

12 p2085 A69-26155

Rotating mirror turbine with air cushion floating shaft for use in streak and framing cameras, noting framing rate

12 p2085 A69-26156

Rotating mirror framing camera with continuous access at f/18 aperture, discussing image transfer system, frame rate and capacity, etc

12 p2085 A69-26157

High speed continuous access framing camera design noting velocity doubler, parallax free aperture stop and polaroid film capability

12 p2085 A69-26158

Multiple lens high speed camera with mechanical shutter for investigating AC arc in circuit breaker during zero current, noting framing rate and capacity

12 p2085 A69-26159

Image intensifier for high speed spectrography of short duration faint radiation source, noting high speed shutter and resolution

12 p2085 A69-26160

Remote control spectrophotochronograph to study radiation of high speed high temperature processes, giving construction data and diagrams

12 p2085 A69-26161

Selective stroboscope with explosive bright light source and microsecond pulse duration for short flash period over large area, noting single frame separation method

12 p2086 A69-26162

Direct electron beam shadowgraph photographic /betagraphy/ technique for recording small high speed objects with 3 nanosecond exposure time

12 p2086 A69-26164

Shadow and schlieren photography, interferometry and quantitative data treatment obtainable by high speed multiframe photographic arrangement, using laser beam

12 p2086 A69-26165

Ultrahigh speed multiple framing photography system using sequentially modulated ruby laser and smear type camera applied to dynamic photoelasticity

12 p2086 A69-26166

Repetitive Q switched laser light source for interferometry, holography and high speed photography

12 p2087 A69-26170

Cine-holographic apparatus consisting of ruby laser and semitransparent mirror, noting capability of photographing within 10-100 nsec intervals

12 p2087 A69-26172

Q switched ruby laser application to high speed shadow photography and holography in study of gas flow around ballistic body

12 p2088 A69-26177

Schlieren high speed photography systems for ballistic projectile studies, discussing use of gas lasers as nanosecond light sources

12 p2088 A69-26182

Flow field over plain or complex bodies with pressure density changes, using high speed schlieren apparatus with color strip filter

12 p2088 A69-26183

Laser beam damage in glass blocks, noting high speed photographic study and absorption of light by inclusions

12 p2117 A69-26193

Fracture surfaces of thermally toughened glass plates using Cranz-Schardin spark camera, confirming internal front lead over front in surface layers

12 p2118 A69-26194

High speed photography of W strip fracture, considering electric current effects and electric circuit interruption by fracture

12 p2113 A69-26195

Ultrahigh speed cinematographic materials, discussing mirror turbines, streak and synchronized framing cameras

12 p2090 A69-26197

Streak camera for continuous photographing of dark and bright satellites up to 9 stellar magnitude

12 p2092 A69-26451

Flash radiography technique using tungsten wire explosion in vacuum to obtain ultrafast reproducible X ray pulse

12 p2092 A69-26480

High speed photographic study of plasma luminescence front and charged particle concentration front counter to electrodynamic force in crossed electric and magnetic fields

12 p2141 A69-27130

High speed photographs of plasma emission spectra in UV and soft X radiation spectrum regions, discussing theory, design and operation of facilities

14 p2496 A69-29784

High speed streak cameras applicability to low density theta pinch studies, describing image converters design, operation and block diagrams

14 p2496 A69-29787

High speed picture thermography in nondestructive testing, describing IR scanning frame rate and thermal image recording

15 p2618 A69-30316

High speed plate holder and shutter mechanisms for observing 20 May 1966 annular solar eclipse

15 p2686 A69-30534

KB-18A rotary prism moving film panoramic aerial strike camera

15 p2614 A69-31281

Kerr magneto-optic camera for 10 nsec exposures of dynamic magnetization configuration in magnetic thin film during high speed flux reversal

17 p2970 A69-32853

Nanosecond photography with superradiant light source, X rays or electrons using multipurpose electron accelerator, obtaining stop motion pictures

19 p3305 A69-35721

High speed photography using multiply pulsed ruby laser, Pockels cell modulation and smear camera for isochromatic and photoelastic pattern recording

19 p3306 A69-35731

High speed photography for hypervelocity aerobalistic ranges, using giant pulse ruby laser for front lighting

19 p3306 A69-35732

Dynamic Kerr observations of high speed flux reversal and relaxation process in permalloy thin films by magneto-optical camera with Q switched ruby laser

19 p3383 A69-36446

Holographic camera using Q switched laser for recording high speed interferograms in plasma diagnostics

19 p3315 A69-36726

Cranz-Schardin camera for high speed recording in dynamic photoelastic fringe pattern studies, discussing framing rates, fringe gradients and design

20 p3541 A69-37778

Photographic studies of explosive reactions with description of ultrahigh speed cameras

21 p3719 A69-38446

Pulse ruby laser-smear camera ultrahigh speed multiple frame recording system, describing applications to transmitted and scattered light photoelasticity

22 p3944 A69-40076

Photographic high speed recording system characteristics effects on dynamic photoelastic fringe patterns fidelity

22 p3945 A69-40077

HIGH STRENGTH

High modulus graphite/asbestos reinforced laminates, noting improved transverse strength and thermal properties

24 p4337 A69-43447

HIGH STRENGTH ALLOYS

NT MARAGING STEELS

Electron beam welding of beryllium, discussing procedures, weld quality and tensile strength efficiencies

02 p0252 A69-11863

Chromium bronze blanks compacted from granules for hardness and electrical conductivity, noting improved high strength characteristics over conventional production methods

02 p0266 A69-12127

Subcritical crack growth kinetics in high strength materials, suggesting growth rate control by reaction rate or diffusion

03 p0449 A69-13874

Low temperature aging prior to higher temperature artificial aging increases Al alloys strength

04 p0614 A69-14634

Columbium alloys properties, discussing creep strength, oxidation resistance, costs, production, etc

07 p1164 A69-18791

Elevated temperature mechanical properties data for commercially produced super-strength alloys supplemented by product description tables

08 p1328 A69-19913

Statistical techniques to develop nickel base superalloy with high temperature capabilities for jet engine turbine bucket applications

08 p1329 A69-20001

Fretting fatigue prevention in Al alloys, noting strength reduction due to fretting

09 p1526 A69-22148

Aluminum alloy weld tensile strength increased by heat treatment, discussing weld porosity due to surface film of absorbed hydrogen

11 p1891 A69-24896

- Preliminary natural aging effects on maximum strength properties obtained at various artificial aging temperatures for aluminum ternary alloy
11 p1905 A69-24921
- High strength alloys stress corrosion cracks, analyzing tensile ligament instability from plastic flow tests of bulk/compression/ specimens
13 p2277 A69-27404
- Fracture mechanics based on linear elasticity for evaluating crack propagation resistance, presenting plane strain fracture toughness test results for high strength alloys
[ASME PAPER 69-DE-10] 14 p2461 A69-28842
- Room temperature fatigue crack propagation rates for high strength aluminum alloy in heavy water environment compared with argon and distilled water
15 p2640 A69-30815
- Fracture processes in high strength materials, considering effect of stored elastic energy, component geometry, fracture toughness and environment
17 p2988 A69-33553
- Arrest mechanisms to halt crack before gross failure, involving material toughness exploitation and subduing stress by structural configuration
17 p3060 A69-33560
- Metallurgy, properties and applications of Co-Ni-Mo-Cr ultrahigh strength alloy, discussing corrosion
18 p3154 A69-34307
- Exposure tests of corrosion resistant claddings for high strength Al alloys protection, finding higher purity alloy cladding superiority
19 p3322 A69-35571
- High strength titanium alloys subcritical stress corrosion crack propagation, studying stress and environment effects on cleavage mode
19 p3343 A69-35922
- Fabrication effects on high strength Al alloy plate properties, comparing texture, plane strain fracture toughness, yield stress, ultimate tensile stress and elongation
19 p3346 A69-36437
- Alpha-beta Ti-Al-V-Mo-Zr alloy with high strength, fracture toughness and crack propagation resistance, low density and adequate ductility, discussing test results
[AIME PAPER S69-3] 21 p3747 A69-39472
- Optimal conditions for extrusion compacting of hard alloy mixtures plasticized with paraffin, determining plasticizer content, upsetting, pressure and temperature
22 p3956 A69-40635
- High strength austenitic Cr-Mn-Ni steel applicability to welded pressure vessels for cryogenic fluid storage, discussing operating temperature stability, weldability, etc
23 p4175 A69-41475
- Ingot dendrite arm spacing and thermomechanical treatment effects on fracture behavior and mechanical properties of Al alloy, finding ultimate and yield strengths
23 p4176 A69-41506
- HIGH STRENGTH STEELS**
NT MARAGING STEELS
- High temperature magnetic analysis of metallurgical structure of high strength steels and composites, including phase transformation and matrix grain structure
01 p0093 A69-10111
- Welding procedure for avoiding hydrogen cracking in high strength steels, stressing hydrogen escape from weld deposits
01 p0088 A69-11398
- High strength steel welding with physical properties equal to parent metal, discussing gas tungsten-arc, electron beam and plasma arc techniques
01 p0088 A69-11399
- Damping capacity and resistance to resonance fatigue of titanium and aluminum based steels and alloys
03 p0443 A69-13025
- Consumable electrode vacuum melted steels, discussing ausforming and stress corrosion cracking
04 p0604 A69-14528
- High strength martensitic aging steels alloying effects, phase transformation and aging
04 p0615 A69-14644
- Precipitation hardening stainless steels, discussing corrosion resistance, high strength, weldability, fabricability, heat treatment, etc
06 p0932 A69-17874
- Ultrahigh strength steel susceptibility to brittle failure, describing methods of testing rupture toughness and stress intensity factor
07 p1158 A69-18402

- Strength increase in steel components of aircraft, missiles and subsurfaces in relation to chronological application sequence, discussing ultimate strength
[ASM PAPER GG8-9.4] 07 p1169 A69-19675
- Retained austenite content control, strain aging and ausforming to improve toughness of high strength martensitic stainless steel without strength loss
08 p1330 A69-20010
- Constructional HY steels for high stress critical welded structures, discussing fracture mechanics stress intensity factor
08 p1333 A69-20405
- High strength steels welding processes effects on weld metal composition and microstructure, heat affected zone, etc
08 p1320 A69-20410
- Giant landing gear steel parts fabrication for Boeing 747 aircraft, discussing material and processing problems including Cr and Cd-Ti coatings application
09 p1434 A69-22064
- Cast and forged steel mechanical properties noting starting materials and production methods roles in cast steel improvement
11 p1904 A69-24644
- Heat treatable low alloy steels weldability for lightweight ultrahigh strength pressure vessels, gear and shaft fabrication in aerospace applications
12 p2100 A69-25827
- Covered electrode, submerged arc, electroslag, gas metal arc, gas tungsten arc and plasma arc welding processes application to high strength steels
12 p2100 A69-25828
- High strength steels, discussing ductility, austenite to martensite transformation for increased strain hardening rate and elongation and corrosion resistance
12 p2115 A69-26829
- Dynamic strain aging of Fe-Cr-C and Fe-Mo-C steels, analyzing strength, ductility and secondary hardening by using microprobes, foils diffraction and extraction replicas
13 p2276 A69-27403
- Bolt materials selection criteria in design of high strength lightweight joints, showing fatigue curves and temperature effects
13 p2268 A69-27758
- Tensile and creep deformation of fiber reinforced composites consisting of Mg-Li alloy matrix with high strength precipitation hardening stainless steel wire
17 p2986 A69-33073
- Plane strain fracture toughness of high strength steels and Ti alloy from precracked notched bend test method
19 p3346 A69-36436
- Crack growth in steel tested in hydrogenated condition, distilled water and in combination by acoustic emission, relating time intervals to hydrogen diffusion
19 p3350 A69-36893
- Welding processes providing low hydrogen welds for high strength steels, discussing heat treatment, maraging steels, fracture toughness, fatigue and static strength
[SBAC PAPER 8] 20 p3549 A69-37447
- Titanium strengthened high strength hot-rolled steels, discussing cooling rates leading to complete ferrite phase transformation
21 p3743 A69-38652
- High strength steel landing gear components corrosion protective finishes, discussing paint over bare steel, porous Cd plating and vacuum deposited Cd
21 p3743 A69-38730
- Metallurgy and properties of quenched and tempered high strength Ni-Co steels, discussing welding and aerospace applications
23 p4175 A69-41299
- Single run reheated weld wrought steel H cracking tested by constant load rupture /static fatigue/ technique
24 p4320 A69-42943
- HIGH TEMPERATURE**
- Electrothermal domains in semiconductors, examining domain velocity of motion under external potential
06 p0981 A69-17880
- Electrothermal domains in semiconductors, examining domain velocity of motion under external potential
14 p2503 A69-28789
- Corrosion mechanism in high temperature Nb-Zr/Li and Ta/Li heat pipes and heat transfer measurements, noting oxygen content of wall material
14 p2462 A69-29203
- Rate constants for recombination of atomic hydrogen with hydrogen molecules, hydrogen atoms and argon atoms at high temperatures behind shock waves
14 p2488 A69-29637

Intrinsic quantum-mechanical behavior of fully ionized gas at high temperature and low density, defining classical limit
14 p2502 A69-29992

HIGH TEMPERATURE AIR

- Very high temperature air flow laminar boundary layers on rotating bodies with unsteady chemical reactions, determining flow dynamic behavior
01 p0060 A69-10725
- Sikhote-Alin iron meteorite high temperature oxidation and ablation and simulation with Fe-Ni alloy, noting phase compositions and structure
01 p0025 A69-11373
- Zr-Be-Nb system oxidation resistance decrease at 650 degrees C ascribed to Be and Nb additions
02 p0262 A69-11844
- Air jet high temperature and low pressure influence on combustion stability in ramjet engine
03 p0531 A69-12968
- Large convective clouds in superheated air generated by static tests of Saturn 5 first stage
03 p0462 A69-14125
- Model for predicting characteristics of short duration intense microwave pulse propagating in heated high temperature air
04 p0634 A69-14453
- High temperature air plasma total radiant intensity measurements in shock tube
04 p0685 A69-14719
- Nickel structure alterations during interaction with high speed air flow at elevated temperatures
05 p0783 A69-16812
- Optical properties of hot air used to solve radiative transfer problems, including emissivities and absorption coefficients calculations
07 p1185 A69-19167
- Flow and heat transfer measurements for heated air in subsonic flow through contraction section connecting tube to conical section
[JPL-TR-32-1348] 10 p1809 A69-23194
- Energy transfer mechanisms between translational, rotational, vibrational, chemical and electronic degrees of freedom in hypersonic shock wave in high temperature air
12 p2063 A69-26969
- Air plasma electrical and thermal conductivity coefficients measured in wall stabilized DC arc at atmospheric pressure and high temperatures
15 p2663 A69-30979
- UV absorption coefficients of high temperature air measured in shock tube reflected region
18 p3230 A69-35073
- High temperature air spectral absorption indices determined at different pressures and temperatures
18 p3231 A69-35122
- Photoelectric measurements of UV absorption coefficients of high temperature air at specific temperature and wavelength ranges in pressure-driven shock tube
22 p4049 A69-40098
- Hot air balloon observational platform capabilities and advantages compared with helicopters, fixed wing aircraft and He balloons
22 p3865 A69-40810
- HIGH TEMPERATURE ALLOYS**
U HEAT RESISTANT ALLOYS
- HIGH TEMPERATURE ENVIRONMENTS**
- Cobalt base alloy for construction in high temperature corrosive environment, discussing mechanical properties, oxidation and corrosion resistance and phase stability
01 p0095 A69-10546
- BCS theory application to metallic modification of hydrogen for obtaining high temperature superconductor
04 p0642 A69-14680
- Mathematical model for estimating microbial survival in heat sterilization of spacecraft, including environmental and time cumulative effects
05 p0707 A69-15941
- High temperature effects on physiological functions of man noting cardiovascular system and heart performance, body heat exchange and blood and urine composition
05 p0710 A69-16523
- Rolling elements for high temperatures, discussing solid film lubricants, unlubricated rolling contact and materials and surface treatment
[IME PAPER 2] 07 p1138 A69-18566
- Instrumentation design problems connected with NERVA, considering high gamma and neutron radiations and temperature environments
[IEEE PAPER 2D-5] 07 p1134 A69-19189
- Glass/resin laminates behavior at high temperature
07 p1136 A69-19515

Arc jet generation and control noting application to hyperthermal aerospace environment studies, wind tunnels and materials heating and fabrication
08 p1371 A69-21128

Titanium-boron composites for gas turbines, mechanical properties and service life in high temperature environment
[ASME PAPER 69-GT-1] 09 p1527 A69-22510

Venus atmosphere origin, discussing high temperature effects and chemical composition via space probe and terrestrial observations
10 p1775 A69-23183

Space mission medical heat problems covering thermal characteristics and heat control, protection and resistance of space vehicle and astronaut adaptation
12 p2023 A69-26493

Ablation test specimen environment at high temperature, analyzing laboratory heating, pyrolysis gas diffusion, convective heating, critical stress and temperature profiles, etc
12 p2191 A69-26815

Tungsten disilicide coated Ta-W alloy oxidation mechanisms, comparing coatings protective properties at high temperatures
13 p2280 A69-28137

Barium vapor effect on converter materials, examining metals-ceramics compatibility at high temperatures
14 p2467 A69-29215

High temperature thermal resistance stability of multilayer cylindrical elements for thermionic converters determined by layer strain rate
14 p2539 A69-29218

Elastoplastic continua fire resistance at high temperatures, establishing plasticity condition and stress-strain relationships
14 p2536 A69-29598

Passive temperature indicators for maximum temperatures attained within rocket nozzle ablative materials
15 p2613 A69-31273

Strain gages to measure flight loads in high temperature environment, discussing selection, calibration techniques and performance characteristics
15 p2614 A69-31277

Airborne radomes reliability and high temperature environments, discussing missile nose cones, light weight ceramic techniques, circular polarization, etc
17 p2942 A69-34084

Polymer selection and plastics contribution to technologies, noting trend toward improved performance at elevated temperatures
18 p3161 A69-34610

High temperature effects on physiological functions of man noting cardiovascular system and heart performance, body heat exchange and blood and urine composition
18 p3096 A69-34742

Radiation effects produced by high temperatures of shock waves and nuclear explosion fireballs, air cooling, laser emission-matter interaction and optical phenomena
18 p3230 A69-34926

Barringerite as Fe-Ni phosphide occurring in meteorite Ollague pallastite, indicating troilite and schreibersite crystallization at high temperatures
18 p3205 A69-35433

Time required for acclimatization to work in high temperatures, noting rectal temperature and heart rate changes
21 p3654 A69-38905

Carbon monoxide dissociation at high temperatures observed spectroscopically, finding complex reaction chain with diatomic C as intermediate
23 p4113 A69-41692

Fastener materials selection for high temperature aircraft structures, considering various physical properties influence
24 p4325 A69-43441

HIGH TEMPERATURE FLUIDS

Chemical reactions activation energy at high temperature, noting cross section shape role for deducing activation energy from rate data
18 p3099 A69-34443

Level signaling device for high temperature conducting fluids, describing sensor construction and circuitry
20 p3536 A69-36980

HIGH TEMPERATURE GASES

Time dependent interaction of hot gas bubble with chemically reactive liquid stream, detailing thermal boundary layer theory
01 p0058 A69-10162

Collision integrals for high temperature gases calculated for high order potentials
01 p0124 A69-10929

Free bounded continuum processes effect in nonequilibrium gases of finite continuous opacity, noting curves of growth for finite plane parallel layer emission lines
01 p0121 A69-10959

Gases emissivity at high temperatures calculated for different gas layer thicknesses and atmospheric pressures, giving results in tabular form
02 p0285 A69-11567

Pressure to density ratio to analyze one dimensional high temperature gas flows with heat transfer, considering motion equations
02 p0350 A69-11576

Intermolecular interaction potentials for dissociating air components determined by calculating collision integrals for very high temperature gases
02 p0283 A69-11586

Integral spectral emissivity of gas arc plasmas at high temperatures and atmospheric pressure
02 p0291 A69-12484

Boundary layer local densities in high temperature gas flows obtained by measuring monochromatic soft X rays attenuation in layer
02 p0233 A69-12489

Photodissociation and photoionization of diatomic molecules at high temperatures with calculation of absorption cross sections
03 p0473 A69-14147

Constants in formulas describing temperature and pressure dependence of thermodynamic characteristics of high temperature monatomic ionized gases for positive ions
03 p0473 A69-14156

Motion of vapor derived from solid material vaporization and subsequent heating by nonequilibrium continuum radiation, noting continuity equations and energy transfer
04 p0686 A69-14985

Spectral line reversal method of measuring high temperatures of gases
05 p0761 A69-15763

Viscosity of compressed nonreacting gas mixtures at high temperatures, discussing conditions for accurate calculation
05 p0845 A69-15895

Emissivity of high temperature air and carbon dioxide-nitrogen mixtures in two diaphragm shock tube
06 p0911 A69-17348

Hot gas flows turbulence linear component intensity and frequency spectrum using optical measurement of pulse velocities
06 p0926 A69-17540

Gaseous film cooling at various hot gas acceleration rates and free stream turbulence levels
06 p1033 A69-17557

Fluidic vortex valve warm gas flow control for rocket application
[AIAA PAPER 69-118] 06 p0872 A69-18147

Static adhesion of metals in hot oxidizing gas environment, considering dry lubrication to prevent adhesion
[IME PAPER 4] 07 p1139 A69-18567

Hot gases optical properties based on real spectra, discussing radiative processes and cross sections calculation methods
07 p1185 A69-19166

Atomic and molecular excitation mechanisms in nonequilibrium gases up to 20000 K
08 p1354 A69-20146

Fortran 4 program for computation of equilibrium compositions of gas mixtures at high temperatures
08 p1278 A69-20154

High speed photographic study of finely dispersed Al particles combustion and ignition in high temperature gas flows, noting dependence on oxidizers concentration
08 p1375 A69-20341

Thermal and nonthermal radiation of hot gases using spectroscopic plasma diagnostics
08 p1363 A69-20463

Monograph on ignition, combustion and expansion in hypergolic liquid propellant mixtures at gas temperatures up to 3000 K for small rocket engines
08 p1375 A69-20723

High temperature regions cooling as applied to solar flares, considering energy losses due to heat conduction, bremsstrahlung, line emission and recombination radiation
09 p1588 A69-21362

Partially ionized Kr and Xe transport coefficients for various pressures and at high temperatures computed on basis of charged particle cross sections
09 p1548 A69-21935

Photometric methods for determination of H atom and hydroxyl radical concentrations in hot gases in convergent-divergent nozzles, noting Li/ lithium hydroxide absorption
09 p1496 A69-21952

Enthalpy distribution in plasma tube arc heater inlet flow region with hot and cold gas core boundary in presence of electric field
09 p1553 A69-22538

Hot gas ignition devices for solid propellant rocket motors, discussing ignition rod and microrockets
10 p1752 A69-23025

Intergalactic gas temperature and density reevaluated, considering neutral hydrogen distribution in galaxies peripheries and metagalactic background of ionizing UV radiation
11 p1946 A69-24589

Piston driven facilities for hot high pressure gas production including gas tunnels, heavy piston facilities, piston driven shock tunnels and high speed guns
11 p1862 A69-25012

Radiation studies of pressure driven shock tubes with atomic ionization at high temperatures, discussing thermal light sources, autoionization, etc
11 p1863 A69-25014

Planning, instrumentation and analysis of shock tube experiments in chemical kinetics, noting gas phase reaction rates at high temperatures
11 p1863 A69-25015

Electrostatic probe measurements in gas warmer than probe, demonstrating applicability of continuum theory for highly negative probe
11 p1930 A69-25274

Photometric and colorimetric characteristics of hot gas optically thin in continuous spectrum with optical thickness of several units in Balmer series lines
12 p2159 A69-26667

Blue continuum emission from hot carbon dioxide measured in shock tube, discussing applications to temperature measurement of gases containing carbon dioxide
14 p2427 A69-29014

Stellar Si burning at constant temperature studied for various initial abundance compositions, noting convergence toward pure Si relaxation
14 p2529 A69-29983

Induced high pressure HF discharge parameters computed for Ar, O and N by using electrical and thermal conductivity functions
15 p2662 A69-30976

Pressure, temperature, density and enthalpy of carbon dioxide behind primary and reflected shock waves determined by method suitable for computer
15 p2592 A69-31054

High gas stream temperature levels and distributions from transient and intermittent probe measurements
15 p2612 A69-31268

Microwave breakdown dependence on elevated gas temperature in electric arc shock tube, considering air, nitrogen and argon
16 p2749 A69-31693

Induction period of reactions behind incident shock waves traveling through undiluted high temperature CO and molecular oxygen mixtures, using CO flame spectra
16 p2877 A69-31768

High temperature radial turbine design for small gas turbine engines, discussing aerodynamic, structural and thermal analyses
[AIAA PAPER 69-524] 16 p2838 A69-32662

Fluidic vortex valve to modulate solid propellant generated hot gas flow
[AIAA PAPER 69-424] 16 p2844 A69-32723

Nongray equilibrium radiative heat transfer in viscous radiating shock layer around blunt body entering high temperature nonisothermal carbon dioxide-nitrogen atmosphere
[AIAA PAPER 69-636] 17 p3070 A69-33258

Radiative and conductive heat transfer in heated finite gaseous body with emphasis on collisional and radiative relaxation, noting cooling as two stage process
[AIAA PAPER 69-638] 17 p3073 A69-33311

Gladstone-Dale constants for dissociating high temperature oxygen determined for molecule and atom from density changes across shock
18 p3176 A69-34452

High temperature regions cooling as applied to solar flares, considering energy losses due to heat conduction, bremsstrahlung, line emission and recombination radiation
18 p3197 A69-34752

- High temperature combustion chamber as high velocity gas generator, noting application to MHD power generator research
18 p3184 A69-34931
- Time dependent equations for non-LTE occupation numbers of lower bound levels of hot gas or plasma outer layer atoms and ions
18 p3231 A69-35242
- Inelastic collisions and radiation effects on transport properties and shock structure in high temperature gases, obtaining density and temperature profiles
19 p3448 A69-36149
- Spectral absorption coefficients and emissivities of thermodynamic equilibrium mixture of various combustion products at high temperatures, based on graphs
19 p3266 A69-36840
- High gas stream temperatures determination from short exposure probe based on inferring temperature from transient response of sensor
20 p3536 A69-37005
- Modified model for vibration-dissociation relaxation coupling phenomena in nonequilibrium high temperature gas flow, discussing parameter U variation with kinetic temperature
20 p3514 A69-37208
- Electron band forces probable values of Meinel system positive N molecules and first positive system of nitrogen molecules at high temperatures
20 p3579 A69-37307
- Polytetrafluoroethylene ablation in high temperature argon, nitrogen, air and oxygen jets, discussing electric heater and heat flux measurement
20 p3632 A69-37522
- Destructive interaction of refractory carbides and graphite compositions with chemically active high temperature gas streams
21 p3751 A69-38640
- High temperature pneumatic systems for missile and space vehicle control, describing pressure regulators, flow controls, thrusters and analog valves
22 p3870 A69-41240
- Chemical reaction kinetics in high temperature gases in terms of collision theory, discussing gaseous statistics and Boltzmann equation
23 p4113 A69-41518
- Propellant ignition delay in contact of condensed fuel with hot reactive gas in shock tube, using graphical method and surface temperature fractional increase
23 p4199 A69-41897
- Hot gas flow through multilayer cylindrical shells, calculating temperature fields in walls
24 p4407 A69-42588
- HIGH TEMPERATURE LUBRICANTS**
- Two phase self lubricating composite materials for high temperature, detailing impact strength, friction and wear tests [IME PAPER 12]
07 p1137 A69-18560
- Rolling elements for high temperatures, discussing solid film lubricants, unlubricated rolling contact and materials and surface treatment [IME PAPER 2]
07 p1138 A69-18566
- Static adhesion of metals in hot oxidizing gas environment, considering dry lubrication to prevent adhesion [IME PAPER 4]
07 p1139 A69-18567
- Steel ball bearing high temperature fatigue life tested with synthetic paraffinic oil, fluorocarbon and polyphenyl ether [ASME PAPER 69-LUBS-18]
18 p3140 A69-34378
- Oil high temperature and oxidation conditions in aircraft piston engines, including physicochemical changes
24 p4321 A69-43141
- HIGH TEMPERATURE MATERIALS**
- U REFRACTORY MATERIALS**
- HIGH TEMPERATURE PLASMA**
- High temperature electron component of plasma produced by strong electron beam in adiabatic magnetic trap, deriving turbulent diffusion coefficient dependence
09 p1553 A69-22657
- Relativistic corrections to particle distribution functions for high temperature plasma in thermodynamic equilibrium by integrating Gibbs distribution
14 p2499 A69-29847
- High temperature ionized turbulent argon jet gasdynamics noting electron density
16 p2770 A69-31889
- Surface wave terms found in long wavelength limit during solution of initial value problem for semiinfinite hot plasma
24 p4356 A69-43364

HIGH TEMPERATURE PLASMAS

- Light scattering from plasmas embedded in homogeneous magnetic field, discussing solid state and high temperature gas plasmas
01 p0125 A69-10015
- Nonlinear hydromagnetic solitary wave propagation at angle to magnetic field in fully ionized quasi-neutral collisionless warm plasma, noting isotropic pressure effect
01 p0127 A69-10336
- High temperature, fully ionized plasma equation of state, using quantum statistical theory of low density electron-ion plasma in thermal equilibrium
01 p0128 A69-10346
- Double probe characteristics in flame with electronegative gas injection interpreted in terms of conduction of ions in ionized medium
01 p0176 A69-10385
- High temperature plasmas generated by exploding gold wires in vacuum, using time of flight technique for plasma densities and flow velocities
01 p0129 A69-10667
- Soviet book on high temperature plasma diagnostics methods covering measurement errors, holographic interferometers and light scattering
01 p0132 A69-11199
- High temperature measurement based on spectral line displacement and broadening due to Stark effect, noting diagrams for O, Na, Mg, Al and Si at various temperatures
03 p0481 A69-14146
- Electron emission from metal foils used to study lifetime, concentration and mean ion energy of hot plasma
03 p0481 A69-14211
- Continuous absorption of coefficient hydrogen-carbon plasma at 40,000 degrees K and 70 atm in 230-460 mm spectral range
04 p0639 A69-15371
- Plasma production by ultrashort pulse Q switched laser beam, discussing avoidance of initiation of breakdown wave
05 p0770 A69-15584
- Plasma instabilities produced by beam plasma discharge in mirror magnetic trap
05 p0803 A69-16212
- Hot plasma research at Polish Institute of Nuclear Research at Swierk
06 p0964 A69-17174
- Structure of plane shock wave of arbitrary force propagating across magnetic field in hot rarefied plasma
07 p1190 A69-18692
- Shot noise in dipole antenna immersed in hot plasma related to antenna input resistance, using Maxwellian velocity distribution
07 p1079 A69-18920
- Hot plasma containment by magnetic field, presenting results from stellarator for toroidal sheared magnetic field properties
07 p1190 A69-18929
- Thermonuclear neutron emission from high temperature deuterium plasma produced by focusing high power laser radiation on lithium deuteride surface [IEEE PAPER O-11]
07 p1153 A69-19072
- Collisionless shock waves in high beta plasmas and in cold plasmas
07 p1194 A69-19366
- Nuclear fusion reactor development, discussing magnetic field confinement of hot dense plasmas and electric power production economic possibilities
08 p1361 A69-20124
- High temperature high density theta-pinch plasma refraction measurements by interference refractometer with beam perpendicular to plasma axis
09 p1544 A69-21302
- Warm plasma addition to mirror confined hot plasma stabilizing convective loss cone mode
09 p1551 A69-22040
- Optical features of Sco-X-1, Tau-X-1 and Cyg-X-2 X ray sources, discussing optically thin hot plasma model for X ray emitter
10 p1682 A69-23327
- Power generating equipment operating with high temperature plasma as working medium requiring reactors with plasmized nuclear fuel coupled to MPD generators
10 p1738 A69-23489
- Gas film protection of quartz tube wall transparency loss due to hot plasma contact used to study UV emission during high power pulse discharges
11 p1926 A69-24616

Electrostatic probe measurements in gas warmer than probe, demonstrating applicability of continuum theory for highly negative probe
11 p1930 A69-25274

HF electrostatic waves propagation excited by electron beam in hot inhomogeneous plasma in magnetic field, studying wave transformation and absorption
11 p1931 A69-25364

High temperature plasma quasi-classical pseudopotential, binary function and free energy derived, using displacement and collective variable methods
11 p1934 A69-25701

Thermal conductivity of hydrogen plasma in transverse magnetic field at high temperatures
12 p2133 A69-25765

Joint probability distributions of electric microfield in hot ionized plasma consisting of noninteracting particles
12 p2139 A69-26871

UV radiation decreased transmittance through quartz exposed to plasma at high temperature and pressure, showing dependence on heated surface layer absorption
14 p2490 A69-29159

Millimeter and submillimeter microwave spectrometric studies of high temperature plasmas and noise emission, discussing instrumentation and absolute measurements
14 p2451 A69-29786

Scintillation counter to determine neutrons number and distribution in time in pulses generated in hot plasma
14 p2452 A69-29809

Thermodynamic Green function for Compton scatter cross section of photons by electrons in hot plasma
15 p2664 A69-31479

Continuous absorption of coefficient hydrogen-carbon plasma at 40,000 degrees K and 70 atm in 230-460 mm spectral range
16 p2822 A69-32118

Test apparatus for determining radiative properties of Ar plasma as function of high temperature and pressure [AIAA PAPER 69-601]
17 p3010 A69-33310

Plasma instabilities produced by beam plasma discharge in mirror magnetic trap
20 p3581 A69-37784

Mathematical model of nonlinear microwave breakdown for overdense and underdense plasma outside reentry vehicle, predicting nonlinear pulse transmission through high temperature plasma
20 p3495 A69-37853

High temperature equilibria from hydrocarbon plasma sources subjected to 3000 W RF electrodeless discharge
21 p3670 A69-39738

Equilibrium plasma configurations in magnetic field of two dimensional dipole analyzed under similar conditions to magnetospheric tail formation with neutral hot plasma layer
23 p4205 A69-41835

Soviet high temperature plasma physics research, discussing magnetic plasma containment by Tokamak traps
23 p4196 A69-42167

High temperature relatively dilute plasmas, discussing equations of motion, plasma oscillations, Landau damping, plasma confinement, etc
23 p4197 A69-42311

Guiding center Vlasov equation derived dielectric tensor of collisionless plasma, obtaining dispersion relation of Alfvén waves in warm plasma
23 p4197 A69-42416

High temperature plasma generation by high power laser beam irradiation on small solidified gas particle, detailing experimental equipment and procedures
24 p4354 A69-42645

Ionization equilibrium and radiative cooling of high temperature low density plasma, noting cosmic gas cooling curve of line emission from oxygen ion transitions
24 p4376 A69-42661

Error sources in magnetic field measurements using magnetic probes in high temperature plasmas, discussing detection, correction and elimination [AIAA PAPER 68-727]
24 p4316 A69-43571

Hot dense plasma used as driver gas producing plane stable current-free high Mach number shock fronts resembling plane blast waves
24 p4359 A69-43647

HIGH TEMPERATURE RESEARCH

- High temperature research on systems formed by zirconium dioxide with samarium and gadolinium sesquioxides near melting point
 - 01 p0101 A69-10044
- Zirconium corner in Zr-Nb-Cu phase diagram, plotting isothermal sections for high temperatures
 - 02 p0263 A69-11854
- Creep relaxation and kinking of aluminum-nickel whiskers at elevated temperature, noting permanent plastic deformation after heat treatment
 - 03 p0443 A69-13119
- Plasticity of metals under isothermal conditions at elevated temperatures
 - 04 p0671 A69-14454
- High temperature physical, mechanical and thermal properties of polycrystalline graphites, relating properties to manufacturing techniques and processing [AIAA PAPER 68-297]
 - 04 p0621 A69-15329
- Total and spectral emittance of cobalt surfaces conditioned by evaporating some cobalt from surface at high temperature in vacuo
 - 05 p0716 A69-16447
- Metal matrix composites highest potential for future use and development of filament-matrix compatibility in relation to high temperatures
 - 06 p0939 A69-16941
- Dynamic measurements of modulus of elasticity for polycrystalline nickel-tungsten alloys at elevated temperatures
 - 06 p0943 A69-17232
- Oxygen line absorption at elevated temperatures in Schumann-Runge system, estimating line widths
 - 06 p0962 A69-17803
- Static adhesion of metals in hot oxidizing gas environment, considering dry lubrication to prevent adhesion [IME PAPER 4]
 - 07 p1139 A69-18567
- Pressure-temperature dependence of nitrogen solubility in tungsten at 2400-3000 C
 - 07 p1168 A69-19602
- Consistency of high temperature equation of state of solids, considering Gruneisen parameter and lattice dynamics
 - 08 p1419 A69-19814
- Electron microscopy for continuous observation and recording of dynamic reactions in high temperature materials
 - 09 p1499 A69-22304
- Laser applications to high temperature, gas dynamical and plasma phenomena
 - 10 p1741 A69-23809
- Back stress role in strain rate equation for high temperature deformation and study of structure and applied stress effects
 - 11 p1987 A69-25388
- Pyrolytic zirconium carbide emissivity during initial heating compared with results for specimens prepared by powder metallurgy
 - 15 p2640 A69-30985
- H beta line for measuring radial temperature distribution in cylindrical hydrogen arc at one atm and to 150 A current in high temperature range
 - 15 p2671 A69-31101
- High temperature creep, discussing creep curves and activation energy
 - 17 p2986 A69-32911
- Machine for testing high temperature creep under variable tensile-compressive stress while maintaining specimen stability, noting discrepancy between creep strains in heat resistant alloy
 - 17 p3054 A69-33044
- High temperature electrochemical high performance batteries
 - 17 p2904 A69-33663
- High temperature and short duration flows - Conference, Freiburg University, West Germany, April 1967
 - 18 p3114 A69-34444
- Oxygen influence on low pressure ethylene decomposition on high temperature tungsten and Re ribbons surface
 - 19 p3266 A69-36732
- Book on high temperature materials covering creep phenomena, design considerations, load and temperature effects, various steels, superalloys, refractory metals, etc
 - 20 p3559 A69-37148
- High temperature pyrolysis of simple organic molecules in shock tube, considering diatomic C formation and decay rate
 - 23 p4113 A69-41693

HIGH TEMPERATURE TESTS

- Wires electrical explosion applications used to study equilibrium characteristics of metals and alloys at high temperatures
 - 02 p0280 A69-11581
- Zr-Be-Nb alloys mechanical tensile properties above room temperature for low concentrations of Be and Nb
 - 02 p0262 A69-11845
- Oxidation resistance of Zr-Nb-Mo alloys at high temperature in air or water
 - 02 p0264 A69-11857
- High temperature tensile strengths of uncoated boron filament and filament coated with silicon carbide
 - 02 p0270 A69-12731
- Gas turbine alloys composition role in high temperature corrosion resistance under high sulfur diesel fuel combustion
 - 03 p0444 A69-13309
- Shock tube equilibrium method for determining vapor pressure of platinum submicron particles by suspension in xenon-argon carrier gas at high temperatures
 - 03 p0532 A69-13319
- Li and Cs electrical conductivity measured from 300-1200 K, obtaining interpolation formulas by least squares method
 - 03 p0481 A69-14148
- Fluid stability, viscosity, compressibility, gas solubility and lubricating properties determination for high temperature hydraulic systems
 - 04 p0550 A69-14662
- High temperature eddy current crack detection technique for atomic reactor components under high thermal gradients
 - 04 p0607 A69-14972
- Structural stability of cobalt base superalloy at high temperature prolonged exposure under stress
 - 05 p0781 A69-16448
- Grain strain measurements use in studies of high temperature creep
 - 06 p0943 A69-17231
- Mechanical stability of pressed and forged Ti alloy gas turbine disks at high temperatures and rates of rotation
 - 06 p1026 A69-18018
- Polycrystalline W steady state creep rate at high temperatures noting effects of stress, grain size and sub-grain size
 - 07 p1158 A69-18241
- High temperature vacuum tensile test device for continuously direct recording various stress-strain diagram rates by interchangeable dynamometer scale
 - 07 p1117 A69-19319
- Thermal conductivity, electrical resistivity and degree of blackness of refractory metals at high temperatures measured by Bode and Eger-Disselhorst methods
 - 09 p1522 A69-21589
- Heat resistant nickel alloys static and dynamic properties at high temperature, creep-fatigue interaction, etc
 - 09 p1523 A69-21609
- Refractory compounds static strength temperature dependence at high temperatures measured in reference to melting temperature
 - 09 p1523 A69-21873
- Silica fabric reinforced phenolic composites mechanical properties at temperatures above cure level
 - 09 p1530 A69-22321
- High temperature magnetic testing and analysis of structure sensitive hysteresis properties
 - 09 p1512 A69-22375
- Titanium alloy castings fatigue behavior at room and elevated temperatures in annealed and heat treated conditions [ASME PAPER 69-GT-22]
 - 09 p1619 A69-22497
- Nickel alloy high temperature tests, noting coagulation of precipitated gamma prime phase, vacancies and creep rate increase
 - 09 p1528 A69-22733
- Superplasticity in W-Re alloys, noting tensile properties, grain size and strain rate sensitivity for various Re contents at high temperatures
 - 10 p1707 A69-22990
- Low cycle fatigue fracture behavior at high temperatures, noting fatigue crack behavior and crack density concept
 - 10 p1797 A69-23081
- Ultrasonics for automatic measurements of temperature and elastic moduli above 5000 F
 - 10 p1694 A69-23373

- Anharmonic lattice vibrations, specific heats and coefficient of linear expansion of solids at high temperatures, noting interatomic spacing
 - 10 p1809 A69-23653
- Brittle fracture at high temperatures in titanium alloys using scanning electron beam microanalysis, noting reaction diffusion with atmosphere and grain boundaries destruction
 - 10 p1713 A69-23823
- Refractory metals testing at high temperatures in vacuum, discussing equipment modifications, temperature measurement and residual gas problems
 - 10 p1714 A69-23848
- Bending creep vacuum testing device for brittle materials at high temperatures, noting load variation capability
 - 10 p1696 A69-23851
- Metal fatigue at elevated temperatures concerning viscosity, energy loss and stress, strain and temperature cycling
 - 10 p1803 A69-24043
- Zr-W high temperature phase relationships, noting Zr-zirconium tungstide eutectic temperature, zirconium tungstide peritectic temperature and Zr solubility in W
 - 11 p1903 A69-24578
- Reinforced metals properties and applications including fibers and lamination, notch sensitivity, brittle fracture, failure and heat resistance characteristics
 - 11 p1904 A69-24898
- Integral normal emissivity of electrically conducting materials heated to high temperatures by HF field of inductor, discussing measurement procedure and equipment
 - 11 p1888 A69-25230
- Heat resistant composites, discussing composition, properties and high temperature behavior, plastic materials, reinforcement filaments, whiskers and test methods
 - 12 p2117 A69-25855
- Stress corrosion cracking of titanium alloys in contact with high temperature fuel tank sealants
 - 12 p2112 A69-25945
- Beryllium oxide semiconductor thermistor for temperatures to 2500 K, discussing construction materials and test results
 - 12 p2092 A69-26478
- Furnace for automatic high temperature cycling in controlled oxidizing environment
 - 12 p2093 A69-26483
- Wing section of high lift/drag test vehicle for 2500 F reentry, describing design, manufacture and testing
 - 12 p2103 A69-26837
- Intermetallic compound precipitation effects on mechanical properties of Fe-Mo alloy at high temperatures
 - 12 p2116 A69-26925
- Friction and wear characteristics of ceramics and cermets as bearing materials, with tabulation of room temperature hardness and maximum service temperatures
 - 13 p2284 A69-27232
- Polycrystalline Re high temperature plastic deformation during tensile creep, including activation energy and substructure dislocation study
 - 13 p2280 A69-27767
- Actinium fueled thermionic generator design and characteristics, noting emitter temperature and material
 - 14 p2399 A69-29192
- Monograph on mechanical behavior of crystalline solids at elevated temperatures, discussing creep properties of metals, solid solutions and two phase alloys
 - 14 p2465 A69-29749
- Electrodeposits on molybdenum alloys in high temperature oxidizing environments, noting performance of Cr-Ni-Cr composite coating
 - 14 p2466 A69-29934
- Thermal diffusivity and conductivity of rolled plane parallel spectrally pure palladium preheated in vacuum and high temperatures
 - 15 p2636 A69-30045
- Tungsten vacuum-arc melted samples in deformed and recrystallized conditions, studying mechanical properties at temperatures near ductile to brittle transition
 - 15 p2637 A69-30267
- High temperature structural adhesives at temperatures of 350 F and higher including epoxies, polyimides, amide-imides and polybenzimidazoles
 - 15 p2642 A69-30329
- Vaporization rates of Ti, Zr, Hf, Nb and Ta carbides at high temperatures measured by Langmuir method
 - 15 p2640 A69-30983

Integral normal emissivity of Ta and Hf carbides at temperatures from 1300 to 3000 K measured by radiation method in vacuum

15 p2640 A69-30984

Water cooled split-flow probe measuring enthalpy of high temperature subsonic streams

15 p2614 A69-31275

High temperature capacitance strain gage development, discussing extensometer prototype systems

15 p2614 A69-31278

High temperature ultrasonic testing to measure and control solid materials early in processing

15 p2632 A69-31514

Creep rate and temperature effect on creep resistance shown in direct correlation with Al-Mg alloys strength by long term high temperature tests

16 p2801 A69-31782

Thermal EMF, electrical conductivity and Peltier effect in sintered refractory oxides at high temperature in air and in Ar

17 p3068 A69-32990

Fatigue crack growth rates in stainless steel at elevated temperature measured as function of oxygen pressure in resonant fatigue machine

17 p2987 A69-33074

Column method of measuring thermal conductivity of CO and oxygen in 350-1500 degrees K temperature range, discussing error sources and data reliability [AIAA PAPER 69-603]

17 p3073 A69-33298

Testing machine for in vacuo tensile testing of tubular metallic specimens at high temperatures and low pressures

18 p3117 A69-34604

Deformation studies of high melting point metals and alloys at high temperatures in vacuum, noting crack formation resistance and annealing time variations

18 p3155 A69-34651

Ti thermal diffusivity and conductivity at high temperatures measured from heat wave phase shift

18 p3156 A69-34699

Low cycle fatigue leading to failure on AISI 321 stainless steel as function of elevated temperature and straining frequency

18 p3219 A69-34834

Kinetics of titanium oxidation in transitional range at high temperatures, showing agreement with oxidation model

18 p3157 A69-35252

Annealed Cr structural changes during creep at 900 C in air, discussing crystalline disorientation X ray studies and stress

18 p3160 A69-35453

Nickel base superalloy high temperature fatigue properties, comparing crack initiation and propagation in directionally solidified and conventionally cast forms

19 p3342 A69-35919

Boron nitride and boron nitride composite under high temperatures in air and vacuum for various time periods, discussing thermal shock and oxidation resistance

19 p3359 A69-36208

Titanium alloys hot salt stress corrosion cracking, studying effects of chlorides and surface oxides

19 p3352 A69-36905

High temperature strain measurement based on strain gage with capacitance changes for structural analysis

20 p3537 A69-37006

Inorganic heat resistant coatings high temperature mechanical tests noting corrosion, safety factors and rigidity after heating and temperature gradients

20 p3538 A69-37360

Creep strain rate measurement at high temperatures by inductance strain gage to determine deformations from 0.2 microns

20 p3544 A69-37815

Refractory materials thermal conductivity high temperature measurement technique, discussing sample geometry, furnace design, temperature modulation and computerized simulation

21 p3742 A69-38422

External friction of refractory materials at high temperature in vacuum, discussing testing machine and methods including metallographic, X ray, spectral and electron diffraction analyses

21 p3690 A69-39154

Serrated yielding at high temperatures from dislocation theory viewpoint, considering critical strain relation to temperature and strain rate

21 p3749 A69-39710

Ablation effect on heat transfer coefficient of carbon, silica and ceramic cloths impregnated with phenolic resin subjected to torch testing and motor firing

21 p3753 A69-39800

High temperature electronic tensile testing device utilizing SCR to study strain rate effect on metals properties

21 p3727 A69-39811

Time-temperature method modified for combining stress relaxation data with stress or strain into single correlation curve, analyzing isothermal relaxation data

21 p3846 A69-39812

Mn, S and rare earth additions influence on Inconel alloy weld microfissuring including material, hot ductility and tensile strength data

22 p3967 A69-39883

Cu, Ni, Co, Cr and Ti effect on high temperature mechanical properties and stability after prolonged annealing of Al-Si alloy with added 1 percent Mg

22 p3968 A69-40063

Error correction of strain gage/cement combination reading relaxation under prolonged steady loading at elevated temperature

22 p4042 A69-40313

Thermal conductivity precision tests for refractory materials using ASTM method C 201-47, emphasizing sample preparation and calorimeter calibration

22 p3956 A69-40671

Spectral emissivity and radiation intensity spectral distribution measurements for heat-resistant materials at high temperature, using photographic method

23 p4238 A69-41330

Black body radiation at very high temperatures, discussing pion-nucleon interaction in pion gas in thermal equilibrium

23 p4238 A69-41358

Silicate glass impurity droplet formations on alumina single crystals polished surfaces analyzed by electron microprobe as function of high temperature

23 p4176 A69-41597

Dynamic hot corrosion rig test for operating environment and alloy composition effect on sulfidation attack during gas turbine fuel combustion

23 p4150 A69-42448

Thermochemical analysis of hot corrosion during sulfidation-oxidation of superalloy gas turbine engine components using Pourbaix method

23 p4178 A69-42449

Vacuum cured glass-reinforced polyimide laminate tests for use at elevated temperatures on F-111 aircraft

24 p4335 A69-42933

HIGH VACUUM ORBITAL SIMULATOR

Thermal vacuum simulator for testing manned Lunar Module Test Vehicle, using conformal skin heaters to control heating rates and skin temperature [AIAA PAPER 69-312]

09 p1479 A69-22386

HIGH VOLTAGES

High voltage controlled amplitude rectangular pulse generators having nanosecond buildup time

04 p0597 A69-14849

Controlled factorial experiments on high voltage vacuum breakdown, using Yates algorithm analysis on computer

05 p0731 A69-16244

HIGHWAYS

Ground access routes between business districts and airports compared for passenger transport modes [AIAA PAPER 68-1072]

12 p2059 A69-26773

HILBERT SPACE

NT BANACH SPACE

Unstable Volterra integral equation reduced to finding solutions for Fredholm integral equation by restricting solutions to closed ball in Hilbert space

01 p0103 A69-10004

Approximate solution convergence for linear operator equation in Hilbert space by least squares method

01 p0105 A69-10728

Bogoliubov transformations effect on quasi-free translationally invariant states of fermion fields, using Clifford algebra based on Hilbert space

03 p0455 A69-13364

First-kind operator equation solution by reduction to dual extremum problem, proving existence and convergence

04 p0622 A69-14622

Theorems concerning interspherical fractionally linear transformations of operators in Hilbert spaces formulated and proved, analyzing unit sphere during fractional linear transformation

05 p0787 A69-16423

Lehmann-Machly procedure for lower and upper bounds to eigenvalues of Hermitian operators in Hilbert space

06 p1020 A69-17131

Convergence of Bubnov-Galerkin method in complex separable Hilbert space, proving theorems for sufficient conditions

12 p2123 A69-26607

Variational formulation of nonlinear differential equations, treating vector fields in Hilbert spaces, finding relations useful in quantum mechanics

23 p4181 A69-41723

HILBERT TRANSFORMATION

Hilbert transform properties and application to random signals, analyzing analytic signal associated with general Gaussian random signal

08 p1271 A69-19915

Infinite strip plane elastic problem reduced to Hilbert problem by employing multiply connected region and biharmonic solutions

15 p2707 A69-30625

HILL DETERMINANT

Dynamic systems stability with periodically varying parameters analyzed by Hill type infinite determinant, exemplifying helicopter rotor aeroelastic stability in forward flight

11 p1990 A69-25510

Differential equations application to electrical circuit problems, solving voltage for series LCR networks and transforming Mathieu into Hill equation

12 p2052 A69-26351

HILL LUNAR THEORY

Five families of simple periodic symmetrical orbits in Hill limiting case of restricted three body problem, studying asymptotic forms

08 p1393 A69-20572

HILL METHOD

Hill stability in unbounded three body problem, analyzing motion in baricentric coordinate system, deriving equations for curves defining conditions for stability

04 p0652 A69-14543

Hill surfaces in triangular restricted four body problem, deriving equation of surface of zero relative velocity

04 p0660 A69-15038

Jacobi integral and Hill criterion for analyzing motion stability of natural satellites and large planets inside gravitational sphere

20 p3596 A69-37314

Hill method applied to motion theory for minor planet 11 Parthenope using computerized first order perturbations from principal planets

20 p3596 A69-37316

HILLER MILITARY AIRCRAFT

U MILITARY AIRCRAFT

HILSCH TUBES

Stationary velocity profile near jet driven vortex tube outer wall calculated by laminar boundary layer flow theory, neglecting wall curvature effects

05 p0798 A69-15610

Ranque vortex tube as cooling device in MA-3 ventilating garment

09 p1447 A69-22550

HINDRANCE

U CONSTRAINTS

HINGE MOMENTS

U TORQUE

HINGED ROTOR BLADES

U HINGES

U ROTARY WINGS

HINGELESS ROTORS

U RIGID ROTORS

HINGES

Life margin tests of oil lubricated oscillating caged needle roller bearings under service conditions duplicating helicopter rotor hinge pin locations [ASLE PAPER 68-LC-7]

15 p2622 A69-30609

Degrees of freedom requirements in hinge couplings of multibody satellites, examining main body attitude control

21 p3820 A69-39233

HIPPOCAMPUS

EEG electrode stimulated simian mental activity in problem solving during simulated space flight, discussing skull implantation and EEG recordings of hippocampus activity

17 p2910 A69-33749

Stimulation effects of reticular formation, hippocampus and septum on sensory responses of posterior hypothalamic neurones in cats

21 p3656 A69-38979

HISS

Simultaneous VLF hiss, auroral light and X rays observed during Norwegian balloon study

02 p0309 A69-12744

Auroral VLF emission bursts simultaneous with sharp ionospheric absorption dip and SC deflections in geomagnetic H, noting corpuscular ionization

24 p4308 A69-43001

HISTAMINES

- Dogs cardiovascular responses to histamine liberator /compound 48/80/, describing shock and acidosis with elevated histamine levels
22 p3873 A69-40206

HISTOGRAMS

- Histograms construction for azimuthal distribution of atmospherics from visual and photographic data obtained by CRT display goniometer
04 p0593 A69-15102
- Histogram approximation of plastic deformation of metals, analyzing tube under internal load and sandwiched layer compression
10 p1793 A69-22850
- Arbitrary circle distribution in plane transformed to corresponding distribution of spheres in space for size and shape distribution determination of disperse phase
20 p3627 A69-37764

HISTOLOGY

- Cosmic radiation genetic, cytological and histological changes, particularly of pathological nature, on ecological systems employed in long duration Soviet manned flights
01 p0016 A69-10948
- Physiological, cytochemical and histological effects on muscular activity, nervous system, adrenal and thyroid glands and liver of mice during 30 day hypokinesia
02 p0198 A69-11502
- Surgical radiolesion in human brain by high energy protons
03 p0374 A69-13501
- Histological investigation of internal organs of mice exposed to atmosphere with high oxygen content
05 p0709 A69-16513
- Immunological and histochemical methods for studying mice reactivity after long term exposure to hyperoxic atmosphere
07 p1065 A69-18975
- Structural and functional changes in cells as result of freezing of muscular tissue or suspension of erythrocytes
10 p1642 A69-23117
- Histochemical studies on nucleus basalis of Meynert of squirrel monkey
12 p2018 A69-25774
- Histochemical tests on enzymes distribution in rhesus and squirrel monkeys intrafusal and extrafusal muscle fibers
12 p2018 A69-25777
- Lactate dehydrogenase and monoamine oxidase distribution in medulla oblongata and cerebellum of squirrel monkey
12 p2018 A69-25778
- Pulmonary oxygen toxicity, analyzing reticulin and clastic tissue damage and hyaline membranes by histochemical techniques
14 p2407 A69-29298
- Histological changes in rat skin after 13 Mev proton irradiation, evaluating biopsies in tissue culture
14 p2407 A69-29299
- Histological investigation of internal organs of mice exposed to atmosphere with high oxygen content
18 p3096 A69-34732
- Immunological and histochemical methods for studying mice reactivity after long term exposure to hyperoxic atmosphere
20 p3479 A69-38223
- Albino guinea pigs respiration rates and ear skin histology after exposures to coherent ruby laser light
24 p4270 A69-42578
- Vascular interface histological and chemical responses to acute mechanical stress in dog aorta
24 p4257 A69-42625
- Fibrosis histological patterns of left ventricular papillary muscles from comparison of hearts with myocardial infarction, noting acute and healed mural lesions
24 p4261 A69-42724

HIVOS [SIMULATOR]

- U HIGH VACUUM ORBITAL SIMULATOR

HL-10 REENTRY VEHICLE

- Lifting Body Test Program at Edwards AFB compared with flight testing standards of high performance aircraft, discussing testing philosophy
06 p1017 A69-17671

HMX

- Slowly exploding wires for igniting self sustaining deflagrations in PETN, RDX, HMX and tetryl, comparing circuit parameters for detonation initiation
01 p0141 A69-10678

HO-6 HELICOPTER

- U OH-6 HELICOPTER

HODOGRAPHS

- Subsonic or transonic bidimensional flows around airfoils by hodograph method [ONERA-TP-645]
03 p0361 A69-12873
- Vehicle motion parameters in Newtonian central force field determined, using geometrical structures devised from properties of velocity hodograph
05 p0765 A69-16686
- Hodograph for lifting airfoil with subsonic velocity at infinity, using Chaplygin compressibility law for computation [ONERA-TP-631]
07 p1049 A69-18416
- Graphical method for plotting electrophysiological observations, showing hodographs application in biopotential studies of cortical reactions
11 p1829 A69-24540
- Kowalewski solution for motion of heavy body with fixed point, noting hodographs
11 p1917 A69-24776
- Construction of single headed spin detonation polar as confluence of shock and deflagration waves by two dimensional hodograph
19 p3451 A69-36368
- Compressible fluid two dimensional supersonic and one dimensional unsteady flows similarities shown graphically, discussing hodograph-speedgraph relationship
19 p3300 A69-36777
- Invariant transformations for hodograph matrix equations in gas dynamics
21 p3695 A69-39001
- Normalized hodographic mapping for constrained trajectory families, discussing mapping concepts, information content and applications [AIAA PAPER 69-924]
21 p3809 A69-39362
- HOHMANN TRAJECTORIES**
U ELLIPTICAL ORBITS
U TRANSFER ORBITS
- HOHMANN TRANSFER ORBITS**
U ELLIPTICAL ORBITS
U TRANSFER ORBITS
- HOLDERS**
NT FLAME HOLDERS
- Clamp type diode holders for obtaining CW coherent emission from gallium arsenide injection lasers
03 p0435 A69-12985

HOLE DISTRIBUTION

- Stress concentration near holes in three layer spherical shells, determining boundary conditions at hole perimeters for various loads
21 p3833 A69-38570

HOLE DISTRIBUTION [ELECTRONICS]

- Minority carrier density and diode current obtained as Laplace transforms from analyzing differential equations, describing charge carriers in semiconductor
01 p0049 A69-11361
- Photoluminescence measurement of distribution of majority carrier concentration in GaAs
03 p0489 A69-13893
- Electrical properties of crystals relation to variations of electron or hole distributions, discussing inhomogeneities
04 p0641 A69-14506
- Hole concentration at deep energy levels in p-type indium antimonide single crystals containing structural defects
07 p1199 A69-18687
- Photoconductivity of semiconductors with multivalley electron energy and isotropic hole spectra, discussing nonlinearity of field dependence
11 p1937 A69-24913
- Photoluminescence measurement of distribution of majority carrier concentration in GaAs
11 p1939 A69-25694
- Ultrahigh vacuum cleaved GaAs-Cs and GaAs-cesium monoxide photoemission acceptor densities, noting crystal parameters role
23 p4198 A69-41548

HOLE DISTRIBUTION [MECHANICS]

- Stress-strain state of isotropic elastic medium using equations with stress tensor, noting role of curvilinear hole
01 p0164 A69-10081
- Stress concentration near eccentric elliptical hole in spherical shell, using computer methods
01 p0165 A69-10089
- Three dimensional stress concentration around cylindrical hole in semiinfinite elastic body loaded at infinity, using Fredholm integral equation
01 p0172 A69-11332

- Unreinforced circular cutouts effects on buckling behavior of circular cylindrical shells under axial compression, using photoelastic plastic shells
03 p0523 A69-12988
- Successive approximations utilizing analytic stress functions used to obtain solution for infinite plate with arbitrary holes under biaxial stresses [ASME PAPER 68-PVP-1]
03 p0523 A69-12998
- Stress distribution near circular hole in elastic layer
04 p0667 A69-14266
- Stress concentration near arbitrary hole, assuming small deformations and physical nonlinearities
04 p0667 A69-14268
- Plane thermal stress distribution determined around holes under steady temperature distribution, using complex variable approach
05 p0836 A69-15877
- Plane problem of moment theory of elasticity for stress concentration near circular hole
05 p0842 A69-16502
- Stress concentration at thermally insulated holes in elastic material created by disturbance of uniform heat flow at holes
06 p1021 A69-17184
- Two dimensional stress distribution changes around rectangular hole with rounded corners for varying internal pressure and temperature
06 p1025 A69-17611
- Stress distribution in shallow spherical shell with smooth cornered rectangular hole or biperiodically arranged set of holes, using computer program
06 p1027 A69-18020
- Stress distribution around equal size holes at ends of crack for normal uniaxial tension, based on photoelastic and brittle lacquer technique
08 p1412 A69-20257
- Monograph on plane problem and bending problem for infinite elastic plate with doubly periodic set of circular holes
08 p1416 A69-20709
- Contour of axisymmetric holes in dimensional electron-beam machining calculated from density distribution of transmitted energy
08 p1321 A69-20727
- Stress concentration at circular hole in infinite plate for large strains and nonlinearity, analyzed by integral operator method
09 p1613 A69-21629
- Stress-strain state of infinite plate with elliptical eccentric reinforced hole, using quadrature method
09 p1613 A69-21630
- Asymptotic two dimensional moment theory of elasticity, analyzing stress concentration at curvilinear holes and fluctuating boundary loads
09 p1614 A69-21884
- Error estimates of stress concentration at free hole determined by two dimensional elasticity theory of thick plates
09 p1614 A69-21885
- Plastic strain intensity distribution in aluminum alloy specimen with central hole measured with marked orthogonal lattice
09 p1617 A69-22221
- Surface heat transfer coefficients under perforated plate of multiple square array round impinging air jets [ASME PAPER 69-GT-4]
09 p1624 A69-22508
- Numerical analysis for stresses in finite or infinite plate with arbitrary holes, considering boundary value problems
10 p1793 A69-22882
- Thickness and drilled holes effects on notch toughness of Charpy V notch bars over wide temperature range
10 p1798 A69-23087
- Couple-stresses and singular stress concentrations in elastic solids with locally unbounded deformations and stress reduction around hole
10 p1798 A69-23149
- Central circular hole effect on fundamental frequency of rectangular fixed edges plate, discussing hole size, square plates, etc [ASME PAPER 69-VIBR-62]
10 p1805 A69-24156
- Elastic unbounded isotropic plane weakened by doubly periodic system of identical holes, noting solution involving Cauchy type integral
11 p1972 A69-24652
- Stress distribution around holes in thin shells and plates during large elastic displacements, considering hole size, loading and shallow spherical shells
11 p1972 A69-24654
- Stress concentration in isotropic plates weakened by curvilinear holes subjected to loading at infinity, noting curvature at corner points of holes
11 p1972 A69-24655

Semibrittle material decompaction influence on stress distribution in infinite plate with edge loaded circular hole, noting stress-strain relation nonlinearities
11 p1972 A69-24656

Limiting equilibrium of plate weakened by curvilinear hole stress raiser with one or two cusps, obtaining stress-strain diagrams
11 p1973 A69-24658

Stress concentration at holes and cavities in thin elastic shells under static and dynamic loads, considering physical nonlinearities of material
11 p1974 A69-24665

Stress concentration around curvilinear holes in three layer spherical and cylindrical isotropic shells with hard and soft fillers under external loads
11 p1984 A69-25171

Boundary determination for separating elastic and plastic regions of infinite perforated sheet with triangular network of circular holes
11 p1996 A69-25736

Membrane and bending stresses around elliptic hole in thin circular cylindrical shell, considering axial tension
[NAL-TN-13] 13 p2362 A69-28123

Stress and displacement fields for uniaxially loaded infinite elastic continua with doubly periodic array of holes and inclusions, using finite element method
13 p2363 A69-28133

Stress concentration around holes in thin shells, including analysis of stress-strain state in cylindrical and spherical shells
14 p2532 A69-28977

Couple-stresses effect on stress concentration of plate containing infinite row of holes, solving linear elastic problem in isotropic Cosserat continua for plate
15 p2708 A69-30640

Thermal stresses in circular cylinder with regularly distributed cavities, establishing distribution laws for temperatures and stresses
15 p2714 A69-31196

Stresses in perforated ribbed cylindrical shell subjected to internal pressure using brittle coating, electrical strain gages, photoelasticity and micrometers
16 p2876 A69-32784

Iterative algorithm applied to shell theory boundary value problem of stress concentrations at shallow shell holes
19 p3436 A69-35847

Stress and strain concentration factors under initial stages of elastoplastic deformation for circular hole in infinite medium, using method of successive approximation
19 p3447 A69-36860

Thermal stress concentration near elliptical hole in thin walled liquid filled cylindrical shell in presence of temperature gradient across shell cross section
20 p3622 A69-37325

Enlargement of circular hole in disk with kinematic hardening and Tresca yield function compared with isotropic hardening
21 p3840 A69-39297

Infinite systems of algebraic equations in periodic problems for spherical shells with circular holes approximated by reduction method
23 p4227 A69-41706

Stress concentrations in circular plate with square hole subject to triaxial tension
23 p4227 A69-41712

Deflections of heated circular plates with or without concentric circular hole and with different boundary conditions and temperature distributions
23 p4234 A69-42412

HOLE MOBILITY

Electron-hole collisions effect on drift and electron and hole diffusion in semiconductors at high injection levels
01 p0137 A69-10257

Differential thermal EMF at room temperature in p-InSb as function of concentration for different electron and hole scattering mechanisms
06 p0981 A69-17881

Hole density/Zn concentration ratio in Zn doped solution grown p-type GaP, noting anomalous electrical properties
09 p1557 A69-21750

Electron-hole collisions effect on drift and electron and hole diffusion in semiconductors at high injection levels
09 p1559 A69-22650

Differential thermal EMF at room temperature in p-InSb as function of concentration for different electron and hole scattering mechanisms
14 p2503 A69-28790

Hole mobilities in InSb due to phonon and ionized impurities scattering on basis of strain potential constants
16 p2824 A69-31575

HOLES

Surface smoothness of laser beam holes, discussing possible damage and technology recommendations
04 p0606 A69-14607

HOLES [ELECTRON DEFICIENCIES]

Avalanche multiplication in abrupt silicon p-n junctions analyzed using ionization coefficient measurements for holes and electrons
01 p0135 A69-10038

P-n-p junctions photoconductivity decay observation, determining signal bulk minority carrier lifetime in thin n regions
01 p0136 A69-10242

Static problem of electric field intensity and space charge density distribution in semiconductor with hot electrons and holes
06 p0978 A69-16989

Microwave spectrum of n-InSb avalanche plasmas under magnetic field, considering dynamic current-voltage characteristics, hole wave instabilities and microwave emission processes
07 p1197 A69-18466

Hole density/Zn concentration ratio in Zn doped solution grown p-type GaP, noting anomalous electrical properties
09 p1557 A69-21750

Drawn n-p and p-n junctions obtained in Te and Zn doped GaSb single crystals prepared in pure He atmosphere by Czochralski method
10 p1745 A69-23329

LF noise mechanism for forward biased semiconductor p-n junction, noting charge carrier capture in electron traps of carrier depleted region
11 p1857 A69-25705

Electromagnetic wave propagation cut-off in slightly uncompensated electron hole plasma, discussing wave evanescence above critical magnetic field value
12 p2133 A69-25926

Photosimulation of electron hole and exciton mechanisms of NaI-Tl and KI-Tl single crystal scintillations
12 p2144 A69-26722

Magnetic and electric field effects on undamped electron-hole LF frequency plasma oscillations in spatially homogeneous nonpolar semiconductor
13 p2323 A69-28581

Periodicity of magnetothermal oscillations in pressure annealed pyrolytic graphite compared with hole carriers
14 p2504 A69-29005

Inhomogeneous distribution of nonequilibrium current carrier concentrations in semiconductors with electrons and holes of different lifetimes, noting instability
15 p2665 A69-30041

Photosimulation of electron hole and exciton mechanisms of NaI-Tl and KI-Tl single crystal scintillations
21 p3781 A69-39135

HOLLAND

U NETHERLANDS

HOLOGRAPHY

Ultrasonic holography applications in nondestructive testing, describing conversion of ultrasonic field into optical field
01 p0078 A69-10132

Three dimensional holography using scatter plates applicable to transilluminated objects in particular distribution of particles or phase disturbances
01 p0079 A69-10217

Hologram chromatic aberration compensation by two lens system
01 p0080 A69-10430

Multibeam recording technique producing speckle-free images in redundant holograms of transparencies
01 p0082 A69-10850

Holographic film sensitometric properties, plotting density vs log exposure and time vs gamma curve
01 p0082 A69-10851

Holographic measurement of sinusoidally vibrating Al sheet, verifying results with Twyman-Green interferometer
01 p0082 A69-10853

Holographic phase variation distribution recording by interference between reconstructed wave fronts from separate holograms
01 p0083 A69-10984

Holographic theory of visual memory behavior, discussing human tests in situation of prompted visual recall
01 p0083 A69-10985

Axisymmetric optical filter synthesis based on holographic technique for making Gabor zone plates, using scalar diffraction theory
02 p0249 A69-11927

Hyperstereoscopic and hypostereoscopic hologram images with doubled or halved interocular distance noting effect on image depth
02 p0249 A69-11931

Stroboscopic holography for repetitive scenes, using mode locked laser as source
02 p0250 A69-12411

Stroboscopic technique for obtaining interferential holograms of vibrating transparent and reflecting plates
02 p0251 A69-12561

Holographic laser type memory with bulk storage capacity and short readout time
03 p0428 A69-13116

Optical imaging systems achieving aperture synthesis by lensless Fourier transform holography, noting X ray astronomy, ultrasonic and space applications
03 p0430 A69-13324

Holographic and microwave technology relationship, noting side-looking radar photos and X band radiation
03 p0430 A69-13354

Hologram heterodyne scanner for production from scanning coherent light beam of electrical signal corresponding to scanned hologram, noting camera tube application
03 p0431 A69-13827

Hologram film nonlinearity effect in recording diffusely illuminated objects analyzed by means of amplitude transmittance
03 p0431 A69-13958

Lithium niobate single crystals for holographic storage, noting use for optical information storage, processing and display devices
03 p0432 A69-14184

Bleaching of absorption hologram diffraction gratings for improved light efficiency, discussing bleaching materials results
04 p0596 A69-14284

Submicron particles spatial location in three dimensional volume detected by Fraunhofer holography
04 p0596 A69-14292

Laser holography using colored KBr crystals subjected to hard gamma radiation as photosensitive material
04 p0598 A69-14855

Vibrational characteristics of sonar transducer analyzed by optical holographic interferometry
04 p0598 A69-14871

Holographic interferometer for isopachic stress analysis, utilizing photochromic recording for real time interference
04 p0599 A69-15013

Holography, discussing image formation, position, enlargement, aberration and application to stress analysis
04 p0601 A69-15186

Corollary of reciprocity theorem in holography
04 p0602 A69-15377

Ultrahigh speed holographic interferometry for studying plasmas produced by focused laser beam, noting electron density evolution in deuterium plasma
05 p0760 A69-15587

Plasma refractive index determination by holographic interferometry with double pulse ruby laser
05 p0761 A69-15620

Holograms applied to analysis of wave packets propagating in quasi-optical transmission lines
05 p0718 A69-15650

Holograms volume depth increased by reference beam splitting or by photographing holograms on same plate in sequence
05 p0761 A69-15651

Holography, discussing one beam recording, real time interferometry, pulsed laser, etc
05 p0761 A69-15774

Thermal self defocusing effect of laser beam in self focusing liquids, measuring refractivity changes by high speed double exposure holography
[IEEE PAPER J-7] 05 p0775 A69-16320

Antennas with any mean surface, prescribed feeder and radiation pattern synthesized by microwave holography
05 p0734 A69-16574

Stationary coherent /hologram/ radar and sonar using zone plate action to provide range information
05 p0721 A69-16578

- Strain releasing method for reduction of small local movements of recording holographic emulsions resulting in degradation of holographically reconstructed wavefronts
06 p0923 A69-16930
- Acoustic holograms, describing electronic method of reconstructing holographic image in order to avoid multiple image problem
06 p0923 A69-16933
- Time averaged optical holographic interferometry of standing longitudinal acoustic waves in square cross section duct
06 p0923 A69-17150
- Lippman-Bragg holograms production with high reconstruction efficiencies by suitable recording and processing techniques with commercially available photographic plates
06 p0926 A69-17481
- Holography for display devices, nondestructive testing, quality control, high speed, microscopy, acoustic testing, sonar, data storage, etc
06 p0928 A69-17873
- Optical Fourier transform applied to structural analysis of catalase crystalline media by gas laser
06 p0928 A69-17890
- Acoustical and microwave holography obviating need for real or simulated reference wave, using recording time for reference
06 p0928 A69-17902
- Laser displays for information transfer to provide improved computer driven read-out techniques, noting real image and holographic displays
06 p0928 A69-17924
- Ultrasonic holograms and optical reconstructions derived by scanning receiver or source
06 p0930 A69-18228
- Holographic interferometry, determining mechanical vibration amplitudes of compressor and turbine blades and airframe panel [SAE PAPER 690265]
07 p1130 A69-18313
- Fresnel pulse holograms of three dimensional diffuse objects by single mode ruby laser with or without Q switching
07 p1132 A69-18801
- Hologram form of forward scatter bistatic radar or sonar
07 p1078 A69-18866
- Hologram storing on photochromic film, obtaining equations for optimal exposure time [IEEE PAPER F-1]
07 p1133 A69-19053
- Holography principles to design high capacity high speed storage devices, using photochrome recording medium
07 p1133 A69-19158
- Microwave holographic reconstruction of metal objects inside purse by nonscanning method, visualizing microwave field by polaroid and liquid-crystal techniques
07 p1135 A69-19449
- Holography by scanning receiver, source, object or both source and receiver, discussing resolution, magnification, image position and aberrations
07 p1136 A69-19640
- Holography combined with laser interferometry for nondestructive testing in materials, components and assemblies
07 p1137 A69-19777
- Holographic developments, discussing interferometry, micro deflections, dynamic behavior of three dimensional structure, acoustical applications, etc
08 p1312 A69-19894
- Image degradation in holograms undersampled with respect to space-bandwidth product, noting signal to noise ratio and resolution
08 p1312 A69-20078
- High quality holography with illumination possessing low degree of spatial coherence by means of interferometric arrangement with amplitude division
08 p1312 A69-20081
- Back diffraction field behind hologram illuminated with laser beam, noting hologram image observation through beam cross section
08 p1312 A69-20086
- Reflection holograms with single mode pulsed ruby laser
08 p1313 A69-20164
- Holography applied to schlieren and phase contrast methods to enable visualization of minute phase change in light scattering object
08 p1313 A69-20176
- Stereoradiography using holographic techniques to examine internal structure of opaque objects
08 p1313 A69-20178
- Holography and similarity criterion for developing image recognition algorithm
08 p1314 A69-20417
- Holographic technique for measuring thin fluid film profiles using interference image reconstruction and helium-neon laser as coherent light source
08 p1317 A69-20873
- Helium-neon gas laser as coherent light source for holograms of vaporizing fuel films and for Michelson interferometer
08 p1327 A69-20874
- Formation and characteristics of flash produced in air by single pulse of Q switched ruby laser, using holographic interferograms
08 p1317 A69-21022
- Holographic displays using ultrasonic vibrations or laser outputs as optical sources, discussing recording materials, responses and computer applications
09 p1492 A69-21394
- Spatial size and velocity distributions for liquid or solid aerosols suspended in air flow using Q spoiled ruby laser and holography
09 p1492 A69-21418
- Borrmann effect and abnormal transmission and extinction observed by reconstruction of images of holograms recorded in three dimensional photosensitive medium
09 p1494 A69-21492
- Holographic image formation through turbulent medium simulated by shower glass, noting thickness variations and prismatic light deflection effects
09 p1494 A69-21559
- Holograms with unfiltered radiation obtained from superhigh pressure mercury lamp and incandescent lamp
09 p1495 A69-21671
- Time average holography for analysis of vibrations, overcoming fringe peak decrease with large amplitude and loss of phase information
09 p1495 A69-21749
- Holographic technique for reconstructing light wave front, developing algorithm for three dimensional images recognition
09 p1495 A69-21859
- Holographic technique application to radio and sound wave ranges, discussing incoherent holography development to overcome difficulties in image reconstruction of stationary objects
09 p1498 A69-22133
- Two dimensional signal analog correlation in noise background using optical spatial filtering Fraunhofer hologram and input as functions
09 p1499 A69-22276
- Holography, presenting state of art review, specifications of patents and extensive classified bibliography
09 p1502 A69-22773
- Light wave reconstruction including polarization, using single reference beam with depolarizing diffuser as source
10 p1690 A69-22951
- Shearing interferometry by simultaneous reconstruction of two wavefronts on single photographic plate
10 p1690 A69-22952
- Complex spatial filtering by holographic Fourier transform subtraction
10 p1690 A69-22953
- Modulated wave holography for detecting and reconstructing ultrasonic beam path, noting applicability to vibrating objects analysis
10 p1694 A69-23368
- Acoustical holography - Conference, Huntington Beach, California, December 1967, Volume 1
10 p1694 A69-23540
- Physical principles and practical methods in light and sound holography, comparing advantages and limitations
10 p1694 A69-23541
- Acoustic holographic measurement of surface deformation generated by sound waves impinging on gas-liquid interface, discussing acoustic amplitude components
10 p1695 A69-23542
- Imaging ultrasound by holography with reconstruction in light, comparing methods using scanned hologram and liquid surface
10 p1695 A69-23543
- Holographic techniques for acoustical imaging to obtain three dimensional images of opaque objects encountered in nondestructive testing
10 p1695 A69-23544
- Quantitative analysis of plane waves for weak interaction of two dimensional sound and light fields in acoustical imaging by diffracted light
10 p1695 A69-23545
- Digital reconstruction of images from optical holograms for acoustical data, discussing image degradations
10 p1695 A69-23547
- Qualitative analysis of recording phase only acoustic holograms of object wave instead of both phase and amplitude, considering fringe patterns and conjugate image
10 p1695 A69-23548
- Matrix method for acoustical holograms and optical reconstruction of virtual and conjugate images using laser light of 6328 Å wavelength
10 p1696 A69-23549
- Hologram obtained by recording interference pattern displayed by ultrasonic camera, discussing real time viewing
10 p1696 A69-23550
- Typographical spatial correlation filtering methods for reconstructing holographic images with ultrasonic waves, noting application to flaw recognition
10 p1696 A69-23551
- Alphabetical listing of references and abstracts of papers on acoustical holography
10 p1696 A69-23552
- Associative holographic memories, discussing recall systems, logic circuits, etc
10 p1697 A69-23868
- Computer generated holograms using binary transmittance for wave fronts and three dimensional images construction
10 p1697 A69-23869
- Holographic motion picture recorded using CW Q switched laser and conventional camera
10 p1697 A69-24002
- Magnetic reversible phase holograms on thin film Mn-Bi by Curie-point writing technique
10 p1706 A69-24007
- Holographic mode shapes used in conjunction with mechanical impedance approach for vibration analysis of turbine blades [ASME PAPER 69-VIBR-32]
10 p1806 A69-24174
- Double focus lens holography for diffusely reflecting surface deformation recording, discussing gas lasers, Polaroid photographic materials, etc
11 p1880 A69-24467
- Holograms on photochrome films by split beam He-Ne laser using special mirror system
11 p1881 A69-24631
- Holography - Conference, San Francisco, May 1968
11 p1881 A69-24675
- In-line, off-axis, incoherent light, computer generated and coded object beam holograms
11 p1882 A69-24676
- Fourier transform holography lensless recording using spherical wave as reference beam
11 p1882 A69-24677
- Fraunhofer hologram as interference pattern between Fraunhofer diffraction pattern and coherent background, noting role of distance in image deterioration
11 p1882 A69-24678
- Multicolor hologram recording and reconstruction gas lasers, discussing control of ghosts in three dimensional image
11 p1882 A69-24679
- Gas lasers coherence properties and availability for holography, discussing continuous power output of He-Ne, Ar and Kr ion lasers
11 p1895 A69-24680
- Holographic recording materials effect on optical reconstruction wave and hologram properties
11 p1882 A69-24681
- Pulsed laser holography advantages for recording small objects in motion and holographic interferometry advantages for complex surfaces and time-separated events
11 p1883 A69-24682
- Pulsed laser holography for recording interferograms of laser created plasma, discussing laser source properties, spatial and spectral coherence, double pulse mode, etc
11 p1895 A69-24683
- Holographic multiplexing for producing three dimensional reconstruction of nonlaboratory objects in horizontal direction, noting TV and X ray pictures applications
11 p1883 A69-24684
- Holography of moving diffuse object, noting bright unblurred image dependence on adaptation to velocity
11 p1883 A69-24685
- Coherent pulse laser holography for front and back lighted holograms of moving objects
11 p1895 A69-24686

Acoustic holography free surface and scanning methods, noting acoustical intensity role in phase stability

11 p1883 A69-24687

Holographic techniques application to optical systems for high resolution images of distant objects by overcoming atmospheric turbulence and light diffraction limitations

11 p1883 A69-24688

Single frequency Ar ion laser for deep field holography noting thermal compensation, servo stabilization, operating mode, high power and high coherence

11 p1895 A69-24689

Scenic holographic stereograms resolution and up/down scaling, discussing roles of projector lens and camera aperture

11 p1883 A69-24690

Holographic recording of three dimensional flow field velocities, applying theory of particle size assessment via Fraunhofer holography

11 p1884 A69-24691

Bias elimination in intensity pattern of incoherent holograms by introducing narrow band time modulation of light

11 p1885 A69-24846

Holographic scanning technique for laser beam deflection, noting two and three dimensional raster scanning

11 p1885 A69-24847

Ray tracing application to evaluating aberrations produced by Fresnel holograms for optimizing design of aplanatic lens holography system

11 p1885 A69-24848

Holographic reconstruction of spatial distribution of laser light field within and outside resonator, noting suitability for pulsed laser analysis

11 p1885 A69-24919

Large capacity holographic memory design based on page organization concept, considering lens parameters and hologram size

11 p1886 A69-25041

Holograms reconstructing images of points with diameters approximated by width of autocorrelation functions

11 p1886 A69-25058

Holography for temperature distribution measurement around heated wire, using He-Ne laser

11 p1887 A69-25197

Phototelegraphic transmission of holographs of objects in many shades through channel with limited number of signal levels

11 p1889 A69-25549

Light scattering materials for transparent objects holography, analyzing Christiansen filter and milk white and ground glass plates

11 p1889 A69-25550

Holographic in-focus projection of images on three dimensional focal planes of arbitrary shape, noting moire pattern strain analysis

11 p1889 A69-25653

Liquid crystals for photographically recording microwave holograms, noting impossibility of three dimensional image reconstruction with side-looking radar zone plates

12 p2079 A69-25917

Multiple information storage in sampled hologram in space division multiplexing holography, constructing hologram with sound waves and reconstructing images with laser light

12 p2079 A69-25921

Holography theory and applications including imaging, Fourier transforms and interferometry

12 p2086 A69-26169

Repetitive Q switched laser light source for interferometry, holography and high speed photography

12 p2087 A69-26170

Holography with pulsed lasers for high speed recording of amplitude and phase disturbances and rapid transient events, noting reconstruction evaluation problems

12 p2087 A69-26171

Cine-holographic apparatus consisting of ruby laser and semitransparent mirror, noting capability of photographing within 10-100 nsec intervals

12 p2087 A69-26172

Cinematic holography as continuous motion uninterrupted viewing system compared with standard cinematography, noting flicker-free shutterless reproduction

12 p2087 A69-26173

Holographic position and velocity measurement techniques for high speed objects from explosions

12 p2087 A69-26174

Deformation measurement by laser pulse holographic method, discussing laser source choice criteria

12 p2087 A69-26175

Holography for optical analysis of hypersonic aerodynamics in single shot firing tunnel

12 p2087 A69-26176

Q switched ruby laser application to high speed shadow photography and holography in study of gas flow around ballistic body

12 p2088 A69-26177

Holographic interference method for measuring film height in analyses of fluid film vaporization under blowing hot gas

12 p2088 A69-26178

Pulsed laser holography used in conjunction with schlieren three dimensional system for observing gas density gradients at different test positions

12 p2088 A69-26179

Fourier transform holograms by Fresnel zone-plate fringe interferometer, discussing source size and bandwidth

12 p2090 A69-26249

Atmospheric turbulence degradation of holographs resolution improved by geometrical optics and series-expansion methods, noting role of Gaussian and exponential refractive index structure

12 p2090 A69-26250

Twin image elimination in holography using single sideband object waves without offset reference wave introduction

12 p2090 A69-26253

Power spectrum of object flux transmittance using Fourier transform type holographic system compared to systems similar to correlator

12 p2090 A69-26254

Nonlinear holograms distortions analyzed by five point method utilizing relation between irradiance and amplitude transmittance of photographic emulsion

12 p2090 A69-26255

Holographic recording in spatially incoherent light, describing hologram reconstruction method

12 p2090 A69-26293

Coherent optical flaw detection and surface microstrain measurement techniques including holographic interferometry, optical correlation and diffraction

12 p2180 A69-26305

Mach-Zender interferometer to study discontinuities of transparent objects by holographic methods

12 p2091 A69-26369

Holographic plasma diagnostics covering phase, amplitude variations images, laser spark, theta pinch studies, etc

12 p2094 A69-26707

Lasers application to measurement techniques including alignment, direction, distance, elongation, interferometric, holographic, etc

12 p2094 A69-26903

Hologram recording on photosensitive material based on photoinduced polymerization showing good resolution and diffraction efficiencies

13 p2258 A69-27199

Hologram recording by offsetting reference beam temporal frequency instead of using reference beam spatial offset

13 p2258 A69-27201

Linear recording of object wave phase to produce acoustic holograms

13 p2259 A69-27243

Holographic storage of three dimensional measurement information using model formed by stacking plates

13 p2260 A69-27739

Single mode ruby laser for application to holography of ultrahigh speed three dimensional objects

13 p2262 A69-27980

Pulsed laser holographic interferometry of density field created by high speed projectile motion in air [AIAA PAPER 69-347]

13 p2263 A69-28282

Acoustic hologram recorded by laser flying spot scanner

13 p2265 A69-28662

Ultrasound holography for imaging opaque structures, noting distortion due to long wavelength of sound field and distortion reduction techniques

13 p2265 A69-28663

Image formation with arbitrary holographic surfaces achieved by reversing direction of propagation of diverging wave

14 p2450 A69-29582

High resolution silver halide photoemulsions analyzed by holographic resolmetry using Ne-He laser to obtain interference patterns

15 p2606 A69-30052

Laser holography using colored KBr crystals subjected to hard gamma radiation as photosensitive material

15 p2608 A69-30247

Stroboscopic technique for obtaining interferential holograms of vibrating transparent and reflecting plates

15 p2608 A69-30258

Interferometric technique for studying fracture specimens plastic zone using laser holography

15 p2609 A69-3068

Microwave hologram construction and image reconstruction by laser beam, analyzing results by matrix expression

15 p2610 A69-30802

Lasers and holography applications in astronomy including high resolution spectrographic diffraction gratings manufacture and astronomical objects photographic pictures evaluation

15 p2610 A69-3081

Book on principles of holography covering plane and volume holograms general theories, factors affecting image resolution, color holography, applications, etc

15 p2611 A69-3106

Stresses in fixed two dimensional photoelastic models analyzed by hologram interferometry, displaying isochromatic and isopachic interference patterns

15 p2611 A69-31110

Time average, multiple exposure and real time holographic interferometry based on image synthesis

15 p2611 A69-31146

Holographical interferometry with laser spark radiation containing fundamental and second harmonic wavelengths, confirming heavy particle densities decrease in plasma with time

16 p2789 A69-31771

Corollary of reciprocity theorem in holography

16 p2790 A69-32124

Holograms applied to analysis of wave packets propagating in quasi-optical transmission lines

16 p2754 A69-32507

Holograms volume depth increased by reference beam splitting or by photographing holograms on same plate in sequence

16 p2791 A69-32508

Multiple reference sources to improve field of view of lensless Fourier transform holography limitation due to modulation transfer function of film and turbulence

17 p2971 A69-32920

Holography of intensities, discussing recording of self luminous body by modulation of scattered radiation using optical Q switch

17 p2973 A69-33111

Holographic recording of temporal coherence pattern of wave train from pulsed radiation source, investigating single mode ruby laser

17 p2973 A69-33114

Point object image differential field during reconstruction by surface nonplanar holograms, determining image position and aberrations

17 p2981 A69-33115

Vibrating objects phase determined by time average and real time holographic interferometry

17 p2974 A69-33324

Holography application in gas turbine components stress and vibration analysis, discussing techniques and apparatus usable by nonspecialist and measurement accuracy

17 p2974 A69-33351

Tv transmission of two dimensional transparency hologram with reduced resolution requirements on camera tube, eliminating zero order terms

17 p2974 A69-33401

Microwave holography for antenna synthesis, radiation patterns and visible images reconstruction

17 p2976 A69-33891

Anamorphic holography, discussing optical and nonoptical wavelength processes and generation and reconstruction of holograms for radar applications

17 p2976 A69-34062

Multiple interference effect introduced by nonlinear characteristics of photographic material, measuring phase variations by holographic multiple beam interferometry

17 p2977 A69-34159

Electron microprobe to produce plane grating X ray hologram based on Lloyd mirror experiment principle

17 p2977 A69-34160

Liquid rocket combustion investigated by pulsed ruby laser holography at sea level rocket engine test stand, noting laminated glass acrylic window byproduct [AIAA PAPER 69-471]

17 p3075 A69-34200

Holographic cine-interferometry, using live fringe method with Q switched pulsed ruby lasers to obtain consecutive submicrosecond interferograms

18 p3133 A69-34265

Vibration measurement by hologram interferometry explaining interference fringes as linear combination of vibrating object classical modes

18 p3135 A69-34635

Strains in solids of any form, using moire method combined with holographic interferometry

18 p3139 A69-35280

Holographic interferometry for nondestructive testing of aircraft materials, discussing applications to quality control

19 p3322 A69-35576

Holographic method of a posteriori restoration of images formed by coherent and incoherent light by spatial frequency retrieval

19 p3304 A69-35603

Fraunhofer holography for measurement of three dimensional flowfield velocity components, investigating rectangular channel flow

19 p3305 A69-35729

Holographic velocimetry data reduction applicable to flow field holograms, using singlet interference pattern for spherical and plane wave illumination

19 p3305 A69-35730

Hologram imaging characteristics expression, deriving relations characterizing localization and dimensions of images

19 p3308 A69-35868

Weak displacements of opaque objects and optical distortion in solid state lasers analyzed by holographic interferometry

19 p3308 A69-35909

Plate material Poisson ratio determined by application of holographic interferometry to plate pure bending deformation contour lines

19 p3312 A69-36206

Holographic system to process signals received by pulse Doppler radar, noting real time operation with availability of instantaneous development image storage media

19 p3314 A69-36598

Holographic camera using Q switched laser for recording high speed interferograms in plasma diagnostics

19 p3315 A69-36726

Microwave holograms generated by spinning dipole field perturbation technique, showing zone plates and moire fringe resolution

19 p3315 A69-36824

Wide view angle holocamera to produce 360 degree hologram in strips for simultaneous image reconstruction from single laser beam

20 p3536 A69-36932

Scanned receiver acoustical holography for mapping or imaging sources of radiated acoustic energy on complex vibrator in water, noting application in air

20 p3576 A69-37323

Holographic wave front reconstruction emphasizing between-wave interference fringes, discussing application to microscopy, Thompson and Parrent disdrometer, interferometry, etc

20 p3540 A69-37637

Resolving power and field of view relations of holographic device for images recording through inhomogeneous atmosphere

20 p3540 A69-37728

Holographic image range contouring produced by multifrequency emission from resonant output reflector in pulsed ruby laser cavity

20 p3540 A69-37733

Sensitivity improvement for inertialess microwave signal scanning and readout by applying pulse compression concepts, discussing application to real time microwave imaging and holography

20 p3545 A69-37901

Vibrating surface relative phases visual observation by introducing small rotation between exposures of stroboscopic hologram

20 p3546 A69-38123

Holography application to three dimensional structure determination of weakly scattering semitransparent objects

20 p3546 A69-38198

Transverse and longitudinal laser modes in holography, noting Michelson interferometer interference pattern role

21 p3734 A69-38398

Image deblurring and aperture synthesis using a posteriori processing by Fourier transform holographic spatial filtering

21 p3722 A69-38793

Information processing with coherent light, discussing holographic interferometry, contour mapping, three dimensional pictures, holographic coding, etc

21 p3722 A69-38797

Fresnel pulse holograms of three dimensional diffuse objects by single mode ruby laser with or without Q switching

21 p3724 A69-38946

Holographic interferometry by single two wavelength laser pulse exposure, discussing variable sensitivity techniques

21 p3725 A69-39448

Holographic recording of focused images and reconstruction in white light, discussing optimal conditions, calculating ray paths

21 p3725 A69-39543

Optical properties of Gabor holograms with pure reference beam, discussing image reconstruction using He-Ne laser

21 p3726 A69-39624

Microholographic system for nonpseudoscopic stereoscopic image reconstruction of transparent and nontransparent microobjects

21 p3726 A69-39702

Randomly moving objects holography and reduction of stability requirement during exposure period due to automatic phase modulation

21 p3726 A69-39741

Small particle holography technique extended for dynamic properties of particle fields, determining velocity and density field, size distribution, flow structure and diffusion rate

21 p3726 A69-39776

Holograms capable of multiple imaging or reconstructing point images, using extended and correlated signal and reference sources in recording process

21 p3727 A69-39777

Resolution limitations in holographic images using single record, discussing lensless holography using plane reference waves

21 p3727 A69-39778

Flash holography using ruby laser, describing optical system arrangement

21 p3727 A69-39784

Holography applied to stress and vibration analysis of gas turbine blades, disks and small components

22 p4040 A69-39960

Wedge fringes visibility and localization in hologram interferometry during focusing on surface under examination for displacements

22 p3943 A69-40016

Extended source Fourier transform holography for single image synthesis of multiple identical images produced by multiple pinhole camera in X ray astronomy

22 p3943 A69-40019

Motion-distorted photograph deblurring method using extended range holographic Fourier transform division

22 p3944 A69-40020

Holographic photogrammetry compared with conventional holography in monocular and binocular parallax reconstruction and stationary stability of objects

22 p3944 A69-40044

Holography for engineering metrology, discussing interferometry, pattern interpretation, inspection techniques, etc

22 p3945 A69-40235

Holographic interferometry for surface strain and vibrations visualization, describing photographic recording techniques

22 p3945 A69-40244

Fresnel zone plate as converging and diverging lens in holographic image reconstruction, noting sine wave zone plate

22 p3947 A69-40864

Holographic technique of coherent light field transformation with desirable phase distribution from laser light beams of arbitrary wavefront characteristics

22 p3950 A69-41115

Holographic storage of electric signals in wideband pulsed carrier radar communications, noting Fourier transform in ultrasonic light modulator

23 p4164 A69-41626

Reconstruction properties of image plane holography for producing bright white light displays, using reference beams

23 p4164 A69-41627

Multiple index high contrast holographic contouring technique compared with analogous multiple frequency system

23 p4164 A69-41628

Hologram film nonlinearity effect on reconstructed image, discussing role of illumination type

23 p4165 A69-41636

Reconstruction of three dimensional holograms without reference beam, noting thick layered Lippmann emulsions and dyed alkali halide crystals

23 p4166 A69-41969

Acoustical holograms phase recording, combining external phase locked electronic reference beams

23 p4166 A69-42180

Optical imaging problems in ultrasonic holography including distortion, resolution and depth of field

23 p4166 A69-42181

Temporal reference acoustical holography with Sokolov ultrasound camera system using double pulsed ruby or scanning CW laser

23 p4166 A69-42182

Retroreflector and Scotchlite object images obtained in long range holography with Q switched ruby laser, noting atmospheric seeing conditions

23 p4167 A69-42184

Holographic interferometry for measuring small static displacements of diffusely reflecting surfaces

23 p4167 A69-42185

Phase and amplitude acoustical holography in opaque media, discussing medical diagnosis and underwater viewing

23 p4167 A69-42198

Acoustical holography principles and reconstruction techniques, noting advantages of liquid-surface and temporal reference holography over optical counterparts

23 p4167 A69-42199

Holography phototechnical and optical variants, discussing combination of conventional photography and wave front reconstruction

24 p4312 A69-42616

Linear motion blur compensation technique in photographic recordings by reconstruction of sharp image from hologram

24 p4314 A69-42972

Fraunhofer hologram of glass fiber by Be X rays reconstructed using He-Ne laser light

24 p4314 A69-42973

Holographic technique for reduction of image distortion during penetration through inhomogeneous medium

24 p4314 A69-42975

Microwave holography by two beam interference method, discussing operating principles, equipment, image reconstruction, etc

24 p4314 A69-42976

Holographic interferometry for determining total free electrons in plasma produced by irradiating solid hydrogen foils with giant pulse ruby laser

24 p4314 A69-42980

Image reconstruction by graphical method for equal wavelengths of recording and reconstructing radiation and equal scales of hologram

24 p4315 A69-43166

Hologram transmission by heterodyne scanning reference beam technique

24 p4283 A69-43333

Holo-diagram device for making and evaluating holograms for small deformations measurement in large machine tool parts

24 p4317 A69-43760

Hologram electronic transmission, obtaining required bandwidth reduction by differential recording of image and scene diffraction pattern

24 p4317 A69-43761

Microcrack detection by holographic interferometry, describing experimental apparatus and test procedure and results

24 p4317 A69-43763

Three dimensional shadowgraph-like images in single exposure holograms of diffusely illuminated flame explained as time average holographic interferograms

24 p4317 A69-43764

HOLOMORPHISM

U ANALYTIC FUNCTIONS

HOMEOSTASIS

Visual feedback mechanisms in simulated high altitude conditions, discussing physiology of ocular homeostasis adaptation

06 p0882 A69-17647

Head movements controlled for rapid vestibular adaptation in slow rotation room (SRR), preventing motion sickness

17 p2908 A69-33178

Aldosterone and hydrocortisone introduced into bladders of adrenalectomized dogs to restore sodium metabolism contributing to normal water-salt homeostasis

21 p3656 A69-38965

Mineral dynamics during hibernation and disuse atrophy in connection with organismal homeostasis and chronic-term manned space flight, noting skeletal effect of immobility

21 p3660 A69-39175

HOMEOTHERMS

High temperature acclimation, climates with heat dissipation problems and hibernation or torpor effects on metabolic depression in homeotherms

10 p1642 A69-23121

HOMING DEVICES

Random order linear homing systems analyzed by frequency methods employing method of proportional navigation, noting use of transfer functions
01 p0113 A69-10805

Virtual or projected miss distance for assessment of missile homing impairment effects, deriving expression based on kinematics
04 p0629 A69-15517

Strapped down phased array radar tracker mechanization with digital loop closure electronics for homing missiles, noting cost advantages
[AIAA PAPER 69-873] 21 p3763 A69-39399

Gliding cargo airdrop system including automatic homing and manual control
[AIAA PAPER 68-958] 24 p4254 A69-43723

HOMODYNE RECEPTION

Single band millimeter wave amplitude modulator for phase meters with homodyne frequency conversion
04 p0577 A69-14850

Homodyne frequency converter design using microwave oscillator with bitonal frequency modulation
14 p2451 A69-29801

Single band millimeter wave amplitude modulator for phase meters with homodyne frequency conversion
15 p2575 A69-30242

Homodyne detection of IR radiation from carbon dioxide laser scattered from moving diffuse target, noting applicability to IR radar, heterodyne spectroscopy, etc
17 p2971 A69-32913

HOMOGENEITY

Quality control of semiconductor materials, analyzing homogeneity by statistical distribution of nonequilibrium carriers based on photoconductivity measurement
04 p0642 A69-14856

Synthesizable automata with sequential homogeneous structure formed by standard fixed units combination
13 p2224 A69-27249

Air mass analysis, discussing homogeneity, quasi-barotropic fluids, noise elimination to arrive at smooth flow pattern, etc
15 p2647 A69-30193

Quality control of semiconductor materials, analyzing homogeneity by statistical distribution of nonequilibrium carriers based on photoconductivity measurement
15 p2667 A69-30248

Phase analysis of systems Mn-S, Mn-Se and MnS-MnSe by X ray diffraction techniques, revealing homogeneity ranges
20 p3485 A69-38286

HOMOGENEOUS TURBULENCE

Homogeneous turbulence, discussing turbulence decay, vorticity generation, Kolmogoroff theory and structure turbulence
05 p0745 A69-15772

Fluctuation velocity, apparent kinematic viscosity and turbulent shear stress in isothermal homogeneous free jets
06 p0909 A69-17169

Homogeneous turbulent gas flame front location as function of caloric value of mixture and flow velocity
08 p1420 A69-19998

Self consistent perturbation procedure for stationary homogeneous turbulence of incompressible fluid
10 p1680 A69-23648

Magnetic field and magnetic energy evolution in infinitely conducting homogeneous isotropic turbulent medium, applying results to galactic magnetic field model
10 p1783 A69-23793

Homogeneous turbulence in incompressible fluid, expanding field variable on ideal random basis
11 p1867 A69-24282

Atmospheric turbulent energy spectra in boundary surface layer, considering homogeneous axisymmetric model in presence of temperature and velocity gradients
12 p2067 A69-26355

Thermal shielding effectiveness of flat wall behind tangential blowing slit, considering case of quasi-isothermal homogeneous turbulent boundary layer
14 p2537 A69-28971

Radio wave propagation in homogeneous turbulent gyrotropic medium, presenting solution for fluctuations in direction of wave scattering by geometrical optics approximation
17 p2927 A69-33861

Homogeneous isotropic turbulence spectrum asymptotic behavior for various spectral energy transfer models
19 p3301 A69-36818

Final period of decay for viscoelastic fluid in homogeneous isotropic turbulence, deriving expressions for double correlation function and energy decay
22 p3928 A69-39891

HOMOLOGY

Homology within solar flare associated type 2 radio events from dynamic spectra
17 p3024 A69-33803

Solar hard and soft X rays time-intensity profiles showing homology with centimeter radio bursts, suggesting origin from same electrons
20 p3589 A69-37553

HONEYCOMB CORES

Bending method for unfolded honeycomb cores shaping for curvilinear sandwich structures
16 p2794 A69-32006

Lap-shear strengths of Mg-Al alloy bonded with nylon-epoxy adhesive, including anodized coating rolling schedule and honeycomb core fabrication
24 p4323 A69-43417

Damage repair techniques of polyimide honeycomb sandwich panels constructed with polyimide and Ti face sheets, using precured plugs, prepreg disks, sealants, etc
24 p4323 A69-43420

Corrosion resistant bonding materials, discussing metal-to-metal adhesive primers, Al honeycomb core and foil finish
24 p4334 A69-43421

HONEYCOMB STRUCTURES

Hypervelocity impact effect on structural honeycomb spacecraft wall configurations, stressing design and wall thickness parameters
[AIAA PAPER 68-314] 02 p0345 A69-12389

Shear strengths of polyimide and polybenzimidazole resin/fiberglass reinforced honeycomb materials compared to previous high temperature materials, noting lightweight sandwich aircraft structures
04 p0620 A69-14844

Jaguar combat trainer/tactical support aircraft to meet France and UK military requirement, noting supersonic performance and honeycomb construction
04 p0549 A69-15062

Nondestructive tests for determining braze bond quality of open face honeycomb seal rings, using low viscosity liquids with fluorescent additives
07 p1140 A69-18797

Paper-honeycomb sandwich radome structure for protecting monopulse UHF radar antennas used in BMEWS
07 p1111 A69-19537

Fabrication and processing techniques, tooling concepts and quality control for composite materials used in large aircraft, discussing honeycomb and sandwich structures
[ASM PAPER D8-25.4] 07 p1172 A69-19670

Diffusion bonded Ti honeycomb sandwich, demonstrating structural integrity, efficiency, low weight and cost effectiveness
12 p2115 A69-26828

Multiwall meteoroid protection design in Apollo program, discussing bumper, backup sheet and honeycomb cells insulation
[AIAA PAPER 69-372] 13 p2367 A69-28304

Hexagonal and nonhexagonal cell phenolic honeycomb design as energy dissipating material noting processing, composite constituents, cell configuration and usage environment
19 p3353 A69-35503

Salt bath brazing for honeycomb structures, describing brazing techniques for thoriated dispersed Ni and NiCr, Rene 41 and Ti honeycomb panels
19 p3320 A69-35557

Diffusion bonded Ti honeycomb sandwich, discussing production, structural efficiency, high strength/weight ratio, etc
19 p3320 A69-35558

Thermal control of Mars entry capsule with fiberglass honeycomb sandwich shell analyzed with and without aft thermal curtain, emphasizing cruise-flight phase
[AIAA PAPER 68-1082] 19 p3429 A69-35949

Ti honeycomb sandwich panels, comparing properties of Ti and Al based brazing alloys
21 p3730 A69-38665

Metallurgical and structural production of diffusion bonded titanium honeycomb sandwich panels for aerospace hardware weight saving
24 p4324 A69-43434

Al brazed Ti honeycomb sandwich structures brazed in vacuum and Ar, analyzing mechanical properties and corrosion resistance as functions of temperature and pressure
24 p4324 A69-43435

Structural airframe fasteners, reviewing systems for fatigue critical wing/fuselage structures, honeycomb panel attachments and data on fatigue life
24 p4325 A69-43437

Orthotropic fiberglass/epoxy faced honeycomb aircraft type sandwich structure elastic properties by edgewise compression test
24 p4403 A69-43443

Potting material reinforcing honeycomb structure for fastener installation prior to bonding face sheets to core, noting mechanical properties
24 p4326 A69-43466

Welded honeycomb sandwich structures of Ti, steel and similar materials for use in extreme thermal and acoustical environments
[AIAA PAPER 68-973] 24 p4326 A69-43716

HONING

Friction characteristics during diamond honing of different steel grades, determining lubricating and cooling liquids effect on friction coefficient
22 p3958 A69-41170

HOOKES LAW

Natural vibration properties of elastic free-free body obeying Hooke law analysis from equilibrium and motion equations, determining Green tensor
01 p0167 A69-10323

NonHookian behavior of stiff strong carbon fibers under stress
03 p0454 A69-13937

Plane stress theory for large elastic deformations of isotropic thin sheets, outlining successive substitutions method for neoHookean materials static and dynamic problems
13 p2359 A69-27320

Constitutive equations for living soft tissues freely deforming under negligible stresses with Hooke law as limit
14 p2535 A69-29366

Curvilinear planform plates natural oscillations, assuming small elastic bending strain obeying Hooke law
22 p4038 A69-39912

HORIZON

NT RADIO HORIZONS

Observable horizons in expanding universe, considering absorption of extragalactic radiation
04 p0648 A69-14566

IR horizon of earth from ionospheric IR emission spectra obtained by sounding capsule, discussing earth geometric horizon and particular spectral bands
[ONERA-TP-709] 15 p2601 A69-31370

Horizon definition for Apollo space navigation references from examining earth atmosphere visible and far IR spectrum
[AIAA PAPER 69-869] 21 p3763 A69-39395

HORIZON SCANNERS

Near field repeatable stimulator of infrared earth horizon sensors in variable environments and test levels, noting orbital conditions
[AIAA PAPER 69-322] 09 p1478 A69-22376

Instrument error analysis for spacecraft orientation and positioning near planet from planet disk observations
13 p2260 A69-27695

Star/horizon measurements for onboard spacecraft navigation without cloud cover obscuration, discussing sightings, data processing and evaluation
19 p3369 A69-35800

HORIZONTAL FINS

U FINS

HORIZONTAL FLIGHT

Optimal lift and thrust control programs to maximize range of missile in horizontal flight
09 p1610 A69-22086

Flight dynamics problems, determining extremum of functional by graph-analytical method and with aid of Pontryagin maximum principle
11 p1823 A69-25343

HORIZONTAL STABILIZERS

U STABILIZERS [FLUID DYNAMICS]

HORIZONTAL TAIL SURFACES

Unsteady aerodynamic forces on coplanar lifting surfaces in subsonic flow induced by wing/ horizontal tail interference
04 p0543 A69-14819

HORIZONTAL TAILS

U TAIL ASSEMBLIES

HORMONE METABOLISMS

- Hibernation seasonality, protein synthesis during periodic awakenings and importance of awakenings to maintenance and evolution of thyroid activity
10 p1642 A69-23120
- Urinary excretion of hormonal metabolites in intercontinentally flown test subjects, using gas chromatographic procedure for steroid identification
24 p4268 A69-43404

HORMONES

- NT ALDOSTERONE
NT CORTISONE
NT PITUITARY HORMONES
- Steroid hormones effect on nervous system and behavior from data on gonadectomized rats and monkeys treated with testosterone propionate
03 p0375 A69-13551
- Visceral afferent pathways influence on vasopressin secretion, ADH levels and urinary excretory patterns of dogs during surgical stress
05 p0708 A69-15970
- Identity between growth hormone degrading activity of pituitary gland and plasmin
06 p0873 A69-17105
- Decreased antidiuretic activity measured in blood of chronically centrifuged rats, noting role of antidiuretic hormone (ADH)
14 p2407 A69-29301
- Circadian rhythm phase shifts during ontogenesis produced by hormone concentration changes resulting from light variations
22 p3872 A69-40198
- Antidiuretic hormone (ADH) and bradykinin effects on human thermal and cholinergic sweating after subdermal injection in forearm, abdomen and leg
23 p4077 A69-41311

HORN ANTENNAS

- Far and near fringe radiation of asymmetrical mirror and horn antennas by method of boundary waves
02 p0214 A69-11601
- Symmetric and asymmetric metal flanges effects on radiation patterns of H plane sectoral horns, noting theoretical explanation and applications
02 p0216 A69-12027
- Asymmetric excitation of conducting flanges by primary aperture antenna and consequent radiation pattern
02 p0217 A69-12246
- Gain and radiation pattern of conical horn excited by conical waveguide, using geometric theory of diffraction
02 p0218 A69-12327
- Horn antenna far field radiation pattern distortion by isotropic plasma slab, noting attenuation variation with electron density
02 p0218 A69-12335
- Multimode direction tracking with polarization tracker used simultaneously, analyzing cross coupling and conical horn/reflector antenna
06 p0888 A69-17652
- Metal flanges position effect on radiation patterns of H-plane sectoral horn radiators
08 p1285 A69-20554
- Mode coefficients for geometrical optics field expansion at waveguide feed junction of sectoral horn
09 p1468 A69-22590
- Conducting flanges effects on H plane radiation patterns of E plane sectoral horns, noting improved beam width and gain and H plane beam tilting
10 p1665 A69-24063
- Far and near fringe radiation of asymmetrical mirror and horn antennas by method of boundary waves
11 p1846 A69-24708
- Power transmission efficiency between arbitrarily focused circular antennas with Gaussian amplitude illumination in Fresnel region for various phase illuminations and Fresnel numbers
11 p1851 A69-24991
- Conducting grill effect on E-plane radiation patterns of E-plane sectorial horns, giving data for various horns at different frequencies
11 p1836 A69-24992
- Horn exciter with fundamental and second mode in feeding waveguide of shallow paraboloid antennas
12 p2044 A69-27093
- Optical image diffraction method for analyzing radiation patterns of horn antenna sounding beams used in microwave measurement of expanding plasmoids
14 p2497 A69-29793
- Horn antenna with parabolic reflector for 30 cm wavelength, calculating field distribution, main and sidelobe radiation patterns and aperture efficiency
17 p2937 A69-33147

- Multifunction lightweight antenna system package for spin stabilized near synchronous satellite having axis normal to orbital plane
22 p3913 A69-40694

HOSPITALS

- Patient transportation and evacuation system at disposal of Paris hospital, using short and long haul aircraft, turbojets and helicopters
23 p4105 A69-41785
- Private one doctor one nurse clinic at Sydney airport, discussing history, operating conditions, medical record and statistics
23 p4105 A69-41786

HOT AIR

U HIGH TEMPERATURE AIR

HOT CATHODES

- Positive Ar ion energy distribution for beam extracted from nonmagnetic hot cathode gas discharge ion source under various source conditions
03 p0427 A69-13102
- Equivalent pressure concept verification for arc discharge with incandescent cathode in mercury vapor
03 p0478 A69-13843
- Relation between energy spectrum and potential drop in plasma expelled from hot cathode tube into vacuum derived by electrostatic analyzer
06 p0963 A69-16899
- Secondary emission and hollow cathode effects in low pressure hot cathode thyratron filled with hydrogen and with shield surrounded thermionic cathode
06 p0896 A69-17475
- Plasma flow from hot cathode discharge in magnetic field increases ion flux intensity and prevents flow divergence in vacuum
08 p1370 A69-21075
- Spectral lines emitted from low voltage discharge in cesium filled diode with hot cathode, giving current-voltage characteristics as function of pressure and temperature
14 p2491 A69-29260

HOT CYCLE PROPULSION SYSTEM

U TIP DRIVEN ROTORS

HOT ELECTRONS

- Temperature dependence of hot electron drift velocity in silicon at high electric fields, using space charge perturbation theory
01 p0135 A69-10120
- Transport phenomena in semiconductors in strong DC field, emphasizing electrical conductivity as function of crystallographic orientation
03 p0491 A69-14097
- Particles nonlinear motion in plasma in magnetic field with arbitrary electron velocity distribution, discussing wave discontinuity patterns
05 p0804 A69-16370
- Static problem of electric field intensity and space charge density distribution in semiconductor with hot electrons and holes
06 p0978 A69-16989
- Nitrogen, oxygen and air luminescence spectra excited by fast electrons at low gas pressures in IR spectral region compared with polar auroral spectra
10 p1687 A69-23916
- Electric drift instability in semiconductors with hot electrons, discussing diffusion, electron heat conduction, energy transfer, space charge density, etc
13 p2318 A69-27891
- Boltzmann equation for hot electron distribution functions in GaAs and threshold field in Gunn effect
15 p2665 A69-30025
- Hot electron plasma formation by injecting mega-electron volt ion beams followed by Lorentz trapping, noting advantages of DC operation
15 p2661 A69-30925
- Hot electron behavior in n-type InSb under magnetic fields at 4.2 and 1.7 K, plotting current-voltage and current-Hall voltage characteristics, etc
19 p3388 A69-36544
- Hot electrons effect on Fe-doped CdTe optical absorption by measuring optical transmission vs photon wavelength at liquid helium temperatures
19 p3389 A69-36551
- Kinetic equation describing dynamics of inhomogeneous cloud of fast electrons and ions trapped in earth magnetic field
20 p3520 A69-37029

HOT EXTRUDING

U EXTRUDING

HOT GAS SYSTEMS

U HIGH TEMPERATURE GASES

HOT GASES

U HIGH TEMPERATURE GASES

HOT JET EXHAUST

U HIGH TEMPERATURE GASES

U JET EXHAUST

HOT JETS

U JET FLOW

HOT MACHINING

- Titanium hot forming and sizing die fabrication concepts for aircraft structures [ASM PAPER D8-26.1]
07 p1143 A69-19671

HOT PLASMAS

U HIGH TEMPERATURE PLASMAS

HOT PRESSING

- Hot pressed boron nitride properties and fabrication, noting low moisture absorptivity and aerospace applications
02 p0270 A69-11802
- Compaction kinetics in continuous quasi-viscous medium having plastic flow material under applied load, discussing hot pressing of nichrome powders
04 p0618 A69-15389
- Nickel reinforced with mullite whiskers produced by hot pressing
05 p0782 A69-16794
- Solid lubricant compacts for ball bearing separator materials, describing fabrication, design and friction and wear properties in air and vacuum [ASLE PAPER 68-LC-16]
07 p1139 A69-18626
- Boron carbide body armor fabrication by hot pressing in graphite molds
08 p1320 A69-20411
- Photocells with p-n heterojunctions from sintered CdS, describing spectral sensitivity and temperature dependence of no-load photo EMF
08 p1374 A69-21084
- Bonded Al-B metal matrix composite materials hot press fabrication and design, discussing temperature pressure time cycles and honeycomb sandwich structures
09 p1510 A69-22351
- Hot pressed molybdenum disulphide-nickel composite film friction and wear tests in air and face seal configuration [ASLE FICFS PREPRINT 23]
15 p2620 A69-30491

HOT STARS

- NT A STARS
NT B STARS
NT O STARS
NT WHITE DWARF STARS

- Astronomical needs for atomic spectra, discussing emissions in Wolf-Rayet lines and Of stars and forbidden lines in absorption in sun and F-K stars
03 p0508 A69-13172
- Strong line profiles computed for models of hot expanding extended atmospheres of OB supergiants
07 p1223 A69-19637
- Space motions of bright F type stars from parallaxes obtained by photometry
08 p1386 A69-20074
- Wolf-Rayet star properties, model and mass loss
08 p1395 A69-20640
- General relativistic models of massive hot nonrotating stars with adiabatic temperature gradients consisting of ideal gas and radiation mixture
09 p1605 A69-22416
- Carbon rich star models with and without neutrinos, considering carbon burning, central stars of planetary nebulas and hot white dwarfs
09 p1606 A69-22419
- Structure and pulsational properties of massive stars with helium cores and thin hydrogen poor envelopes
09 p1606 A69-22421
- Far UV stellar astronomy, concerning very hot stars and interstellar gas composition studies
10 p1772 A69-22870
- Hot companion presence for RW Camelopardalis confirmed from UVB photometry
10 p1775 A69-23201
- Galactic nuclei congeneric and coexisting peculiarities, including hot star planar formations in spiral galaxies
12 p2164 A69-27027
- Azimuthal electric currents generation by Coriolis forces in hot stars with intensive radial flows in convective zones
13 p2350 A69-27862
- Spectrographic and photoelectric analyses of F type sharp line eclipsing binary HR 7484, tabulating masses, radii, color indices and absolute magnitudes
15 p2693 A69-30776
- Physical nature of HZ 22 short period hot subdwarf binary, noting arguments against normal B type binary hypothesis
17 p3044 A69-34181

Four color photometry data of late F type stars in general catalog tabulated with columns for HD and GC numbers, apparent visual magnitude, etc
18 p3195 A69-34430

Hydrostatic instability in high temperature stars in postNewtonian approximation
20 p3580 A69-37926

Hot star photogravitational acceleration determined from difference between apex and antiapex brightness, noting constant magnitude and direction of principal component of apex force
20 p3608 A69-38046

LTE departure calculated for He I in hot star model atmospheres for effects on populations of singlet and triplet states
21 p3801 A69-38761

Pion production rate for proton-proton interactions in hydrogen, discussing relevance to hot massive stars, charged pion decay probability and mu-neutrino production
21 p3792 A69-39615

Helium-carbon star BD plus 10 degrees 2179 re-analyzed by grid of constant flux models containing right amount of C
22 p4026 A69-40652

Wolf-Rayet stars formation, evolution, age, galactic distribution and relation with open star clusters
23 p4208 A69-41288

VV Cephei type binaries cool and hot primary stars light variations, discussing duration, orbital cycle correlation, mass loss, etc
24 p4386 A69-43346

HOT SURFACES

Heat transfer rates for water, acetone and alcohol droplets splattering from heated plate, noting effect of impact angle and velocity
10 p1809 A69-23196

Holography for temperature distribution measurement around heated wire, using He-Ne laser
11 p1887 A69-25197

Pressure waves interaction with solid fuel hot surface at HF based on linear theory of acoustic instability in condensed systems
13 p2371 A69-27383

Evaporation of liquid droplets from heating wall observed cinematographically, noting heat transfer by violent film boiling and conduction through thin vapor layer
15 p2718 A69-31117

HOT WATER ROCKET ENGINES

Explosive and pyrotechnical elements for Grillo 1, Grillo 2 and Trigone 1 hot water rockets, detailing nozzle closure and chemical reaction activation
10 p1753 A69-23028

HOT-WIRE ANEMOMETERS

Superlayer structure determination near turbulent boundary layer with zero pressure gradient, using constant temperature linearized hot-wire anemometers
01 p0061 A69-10759

Yaw parameter and curvature effects on accuracy of hot-wire anemometer, noting King law
03 p0426 A69-12845

Göttingen type wind tunnel, discussing stream characteristics and turbulence measurement by hot-wire anemometer
03 p0420 A69-14238

Inclined hot-wire and hot-film anemometers parameter dependent on length-to-diameter ratio used to describe deviations from cosine law
[ASME PAPER 68-WA/APM-16]
04 p0596 A69-14391

Incompressible turbulent boundary layers in channel flow using constant temperature hot-wire anemometer, emphasizing measurement in viscous sublayer
[ASME PAPER 68-FE-26]
05 p0747 A69-16066

Circular cylinder near wake in cross flow measured with hot-wire anemometry for various Reynolds numbers, noting data processing on digital computer
[ASME PAPER 68-FE-5]
05 p0747 A69-16068

Rotating hot wire and five hole pressure probes for determining complete velocity vector in subsonic flow
05 p0764 A69-16398

Hot-wire anemometer with no moving parts for measurement of three orthogonal components of wind velocity and wind direction
06 p0923 A69-16926

Linearizing circuit for low velocity hot-wire anemometry, using analysis of transistor circuit to generate desired function
06 p0927 A69-17701

Calibration curve for constant temperature hot-wire anemometer, taking into account high wire temperature and gas pressure effects
06 p0930 A69-18218

Superlayer structure in turbulent boundary layer without pressure gradient, using constant temperature linearized hot wire anemometers
07 p1118 A69-18299

Nonlinear control theory for constant temperature hot-wire anemometers with large velocity fluctuations, noting second harmonic generation
09 p1493 A69-21421

Tubulent flow problems, discussing hot-wire techniques, viscosity effect, compressibility surface curvature, turbulent boundary layers, heat transfer, etc
11 p1871 A69-25017

Hot wire and hot film anemometers for measuring turbulence in MHD flow noting applications in flowing mercury
11 p1886 A69-25087

Monograph on velocity distribution function in turbulent boundary layer, discussing hot wire anemometer for mean velocity, turbulence intensity and higher order moments determination
13 p2250 A69-28336

SNR improvement during low level turbulence measurements, examining correlation between hot-wire anemometers, including error analysis
14 p2446 A69-29018

Hot-wire anemometers calibration technique providing accurate and direct velocity measurements in slow moving liquids
17 p2971 A69-32901

Thermoanemometer filament frequency response measured by generator of velocity pulsations compared with conventional methods
19 p3308 A69-35856

Wall influence on thermoanemometer readings in incompressible air stream measured with wedge shaped film sensors
19 p3308 A69-35857

Liquid mercury flow turbulent intensity measured by quartz insulated Pt hot-film sensors, discussing calibration equation and measurement techniques
21 p3722 A69-38769

Monograph on hot wire anemometer measurements of velocity and temperature turbulence, discussing flow characteristics, calibration, etc
22 p3951 A69-41256

Constant temperature thermoanemometer design and subsystem operation applied to measurements of turbulent flow velocity and pulse characteristics
24 p4311 A69-42558

Hot-wire anemometer calibration technique for measuring velocity of very slowly moving liquids
[ASME PAPER 69-HT-A]
24 p4316 A69-43527

HOT-WIRE FLOWMETERS

Hot wire and hot film anemometers for measuring turbulence in MHD flow noting applications in flowing mercury
11 p1886 A69-25087

Hot wire sensitivity to velocity, temperature and density fluctuations of temperature varying flow field, discussing calibration curves and special cases
11 p1886 A69-25088

Turbulence measurement errors with inclined hot wires described by equations, assuming normal component cooling includes greater tangential cooling
18 p3134 A69-34442

HOT-WIRE TURBULENCE METERS

U TURBULENCE METERS

HOT WORKING

NT AUSFORMING

Ti alloy blanks production technology and quality control, noting rolling of sectional profiles
07 p1161 A69-18765

Creep and hot working strain-rates relationships, showing work hardening and dynamic recovery relative levels dependence on plot used
13 p2278 A69-27417

Hot extrusion process for steel and various metals in U.S. semifinished product industry, considering lubrication problems, research centers and development
15 p2618 A69-30228

In-process annealing and warm working temperature effects on long time creep rupture properties of Mo alloys tested in vacuum furnace
17 p2987 A69-33076

Polygonization and strengthening effects simultaneous action at grain boundaries increased thermal stability of thermomechanically treated Ni-Cr alloy
17 p2991 A69-33940

Plane strain forging of pure Al and Al-Cu alloy at low strain rates and elevated temperatures, in constant velocity compression test
17 p2979 A69-34137

Optimum conditions for producing Ti-V alloy sheet plated on one side with Nb by hot rolling
18 p3155 A69-34652

Polycrystalline ceramics chemical and microstructural control through thermomechanical and thermochemical hot forming techniques, discussing pressure sintering, hot extrusion, strain annealing, etc
24 p4321 A69-43338

HOTSHOT WIND TUNNELS

Roughness effects on boundary layer transition up to Mach 16 in hotshot wind tunnel
[AIAA PAPER 68-377]
13 p2242 A69-28213

Integrated double oblique shock scramjet for supersonic combustion tests and instrumentation development, discussing fuel injection through sonic orifices, combustion data, etc
[AIAA PAPER 69-827]
16 p2840 A69-32673

Calibration of inertial and surface temperature heat transfer transducers for hotshot and shock tube measurements developed and tested at ONERA
[ONERA-TP-683]
19 p3305 A69-35726

Double knife-edged double-crossing schlieren apparatus analyzed for operation principle and applied to measure hypersonic wake characteristics in hotshot tunnel
19 p3293 A69-35740

HOUSINGS

U RADOMES

HOVERCRAFT

U GROUND EFFECT MACHINES

HOVERCRAFT GROUND EFFECT MACHINES

Hovercraft range operating at constant speed as function of design efficiency, power apportionment, fuel consumption and initial specific resistance
03 p0367 A69-13909

Hovercraft and applications of air cushion principle, discussing large and small size vehicles, autostabilization, hybrids and ram wings
03 p0367 A69-14084

Semi amphibious Vosper VT 1 hovercraft for passengers and cars, discussing design, water contact propulsion, peripheral skirt, supercavitating propellers, structure, performance, etc
04 p0549 A69-15187

Airflow and power requirements of compressible hovercraft jet operating under equilibrium conditions
05 p0697 A69-15708

Hovercraft development by British Hovercraft Corporation, discussing technical contributions in design, control and propulsion, environmental tests, etc
12 p2014 A69-27140

Glass reinforced plastics for Hovermarine HM.2 sidewall hovercraft designed for ferry routes
13 p2201 A69-27542

Small hovercraft simple and bag skirts design characteristics, considering materials
13 p2202 A69-27545

Plenum chamber obstructions influence on hovercraft lift fan performance, discussing tests and losses due to flat plate at impeller outlet
13 p2202 A69-27546

HOVERING

Longitudinal dynamics of VTOL aircraft during hover-forward flight transition, using multiple time scale analysis
[AIAA PAPER 69-130]
06 p0869 A69-18157

Boundary layer discontinuity on helicopter rotor blade in hovering using flow visualization
[AIAA PAPER 69-197]
07 p1051 A69-19561

Human pilot adaptation in simulated multiloop VTOL hovering task with series loop closure model
10 p1650 A69-23878

Three dimensional potential surface flow past rotor blade in hover, accounting for compressibility and blade element theory limitations
[AHS PAPER 324]
17 p2895 A69-33537

Hover and forward speed aerodynamic characteristics of tracked air cushion vehicle (TACV) models, discussing wind tunnel tests
[AIAA PAPER 69-750]
18 p3084 A69-34410

Lifting line theory for hovering propellers deformed wakes based on continuous vortex sheet representation
18 p3087 A69-35217

HOVERING STABILITY

Water hover effects tested on tilt wing V/STOL seaplane model, noting effects of wind and waves on water passing through propellers
01 p0011 A69-11061

Advance indication based on extrapolation for aiding manual attitude control of VTOL aircraft in hovering flight, noting results on flight simulator
03 p0366 A69-13645

- Fixed point support properties of quasi-vertical peripheral jet hovercraft with two pressure stages
06 p0857 A69-16820
- Reaction forces for jet lift VTOL attitude control during hover and transition, considering hot gas and pitch ducting applications
[AIAA PAPER 69-545] 16 p2735 A69-32756
- Helicopter hovering performance prediction from wake analysis by iteration, discussing wake interference significance and blade number influence
[AHS PAPER 321] 17 p2895 A69-33538
- Slot height, position and trailing edge geometry effects on elliptically shaped rotors selected for hover efficiency, size, transitional gust insensitivity and rigidity
18 p3088 A69-35231
- HRB-1 HELICOPTER**
U CH-46 HELICOPTER
- HSS-2 HELICOPTER**
U SH-3 HELICOPTER
- HU-1 HELICOPTER**
U UH-1 HELICOPTER
- HUBS**
Bursts of high speed rotor occurring at diametric cross section and around hub as function of hub size
01 p0142 A69-10306
- Vortex lattice method correlation on rotor/wing configurations for aerodynamic characteristics, noting triangular and circular hub and blades
20 p3458 A69-37163
- HUGHES AIRCRAFT**
U OH-6 HELICOPTER
- HUGHES MILITARY AIRCRAFT**
U MILITARY AIRCRAFT
- HUGONIOT EQUATION OF STATE**
Stress-strain-time relations in magnesium alloy and aluminum plate impact load tests, discussing stress measurement, Hugoniot equation of state, yield point and dynamic response
08 p1330 A69-20102
- High pressure Hugoniot points made by hypervelocity gas gun, using laser beams to measure impact velocity and pressure transducer for impact stress
[AIAA PAPER 69-358] 13 p2264 A69-28291
- Finite control volume approach to shock Hugoniot in unidirectional fiber reinforced composite, computing shear force along matrix-fiber interface
[AIAA PAPER 69-359] 13 p2366 A69-28292
- High purity beryllium dynamic tests, determining Hugoniot equation of state, shock profile and spall threshold/onset of microcracking/for elastic pulses
[AIAA PAPER 69-360] 13 p2283 A69-28293
- Polydiethylene glycol-bis-allyl carbonate (PBAC)/Hugoniot equation of state, reporting shock data, discussing applications to propellant testing
16 p2879 A69-32179
- Hugoniot prediction for shock moving along longitudinal direction of unidirectional fiber reinforced composite
20 p3627 A69-37768
- Hugoniot equation of state of shock loaded W determined at room temperature and 950 C
20 p3564 A69-38127
- HUMAN BEHAVIOR**
Human behavior during stressed underground confinement, discussing adaptation processes
01 p0020 A69-10757
- Human visual systems ability to encode retinal images produced by different size objects
03 p0369 A69-13359
- Psychological aspects of crew members resistance to eject from aircraft in trouble
06 p0877 A69-16956
- Physiological or survival training emphasizing psychological approach
06 p0879 A69-16965
- Organization behavior models compared in theory of scientific and professional personnel management, noting compromise between excess restrictions and freedom
[AIAA PAPER 68-805] 08 p1422 A69-20196
- Organizational behavior of scientists noting working environments, effectiveness of work sections, research management and organizational development
08 p1423 A69-21124
- Human adaptation to various environments, emphasizing experimental space psychoneurology role in human behavior examinations during space missions
10 p1647 A69-23587
- Matrix computation operations devoid of sense and relevancy arising in interdisciplinary problems
11 p1910 A69-25522
- Human operators instrument-monitoring behavior noting optimal control, information processing, physical limitations, etc
12 p2022 A69-25929
- Human behavior simulation - NATO Conference, Paris, July 1967
12 p2024 A69-27079
- Man machine model for prediction of human control behavior, generating model from analysis of helicopter pilot tasks
12 p2025 A69-27082
- Model for temporal structure of human behavior from analysis of temporal information treatment in subjective synchronization task
12 p2025 A69-27084
- Models for cognitive behavior and psychomotor behavior for maintenance tasks
12 p2025 A69-27086
- Behavioral differences between engineers and scientists with reference to work environment
15 p2721 A69-31073
- Characteristics, incentive and promotional patterns and work adjustment of engineering technicians
15 p2723 A69-31242
- Guide for establishing harmonious relationships with design engineers within typical mechanical engineering department
17 p3077 A69-34198
- Mathematical basis for human operators purposeful behavior in complex systems control situation requiring decision reaching
19 p3260 A69-35895
- Environmental crowding effect on individual and group behavior in rat colony, using implanted passive resonant circuits for identification and passage information
19 p3257 A69-36243
- Organizational identification of scientists as professional employees, exploring degree of loyalty and perceived self prestige
21 p3855 A69-38765
- Life in common by groups of four or five people isolated on high mountain under adverse conditions
21 p3661 A69-39267
- Sensory and logic behavior model of sequence selection based on received information, considering perception, sense, desire, concept and criteria levels
23 p4109 A69-41976
- Learning model of motor behavior in brain cortex of higher animals and man, discussing M automaton, information reception, correlation, memory, emotions, desires and actions
23 p4109 A69-41977
- Group leadership attempting behavior dependence on situational and perceptual variables
23 p4110 A69-42015
- Group interaction finite Markov chain model, analyzing changes in interpersonal relationships based on balanced dyadic states
23 p4110 A69-42017
- HUMAN BEINGS**
Probability of biological development leading to human life on another planet
21 p3652 A69-38786
- Reticulocyte count comparison on trained and sedentary college male subjects before and after strenuous exercise, noting role in oxygen uptake
21 p3654 A69-38907
- Caucasian and Bantu males oxygen consumption at different work rates, gross body weight accounted for 70 percent of differences between individuals
21 p3655 A69-38911
- Atelectatic and direct toxic effects of oxygen on human subjects
22 p3873 A69-40208
- Linear models with self excitation for brightness and contrast perception studies in human visual system
22 p3881 A69-40862
- Pulmonary capillary blood flow pulse of healthy men in supine position recorded by nitrous oxide/plethysmograph and phonocardiogram
24 p4259 A69-42638
- HUMAN BODY**
Human body dynamic response to vibration combined with linear acceleration, noting changes in body mechanical impedance and resonance
01 p0022 A69-11335
- Acceleration, hypoxia and stress effects on humans and animals, noting latent functional disorders of organisms requiring special techniques for detection
02 p0197 A69-11488
- Data acquisition program for Apollo crew motion disturbances experiment consisting of ground simulations and orbital experiment establishing mathematical model of human body
02 p0201 A69-11759
- Mechanical model of human body used to study response to vibration, impact, blast and decompression loads
04 p0552 A69-14470
- Conduction equations for conduction cooling of human body solved by finite difference method
06 p0880 A69-17088
- Objective evaluation of metabolic reactivity of organism based on biophysical model compared with experimental individual
06 p0874 A69-17595
- Physiological functions of aged Japanese pilots, discussing height, weight, Rohrer index, obesity, vision deterioration and hearing disturbances
06 p0876 A69-18028
- Viscoelastic rod model of human spine subjected to accelerations
07 p1072 A69-19725
- Analog computer modeling of human systemic arterial tree, based on lump parameter circuit approximation
07 p1072 A69-19727
- Human body temperature regulating factors in low temperature environment, studying metabolism, lung ventilation and onset of shuddering
10 p1648 A69-23298
- Identifying human bodies torn apart or crushed in aircraft accidents, noting example of jet passenger plane crash
12 p2021 A69-25839
- High altitude acclimatization effects on cardiovascular system, external respiration, blood composition, optical and vestibular analyzers in human subjected to various stresses
13 p2212 A69-28623
- Body composition of USAF flying personnel, evaluating obesity by using radioactive potassium (K-40) method
14 p2409 A69-29295
- Glycolysis control by respiration in human leukocytes with and without Pasteur effect conditions
15 p2555 A69-30413
- Pulmonary ventilation and perfusion in normal supine subjects before and during exposure to lower body negative pressure measured using Xe-133
17 p2909 A69-33180
- Flow mechanics applications to medicine, discussing vascular and technical systems and measuring equipment adaptation to human organisms
17 p2915 A69-33771
- Ejection seat cushion dynamic characteristics influence on incidence of spinal injury during ejection, considering MIL specification dynamic model of human body
17 p2917 A69-34033
- Volume prediction of human body exposed to vacuum based on animal skin elasticity and anatomical features
19 p3258 A69-36456
- Human taste perception mechanism and taste system anatomy
21 p3652 A69-38783
- Control circuits in nature and sensory information data processing in human work, including servomechanism of brain-muscle system
21 p3652 A69-38784
- Carbon dioxide washout during square wave hyperventilation in man, postulating blood flow factor
22 p3885 A69-40975
- Oscillatory electric field disturbances monitored near human body concurrent with heart beat and respiration, showing signals unrelated to blood flow or streaming potentials
23 p4101 A69-41449
- Barometric pressure affecting convective heat transfer from human body in air, deriving empirical formula as function of air density, speed and temperature
24 p4267 A69-43384
- HUMAN CENTRIFUGES**
Physiological studies of centripetal and Coriolis accelerations effects on vestibular function of humans in rotating chamber
02 p0197 A69-11498
- Human acceleration tolerance dependence on age, profession and physical training from investigation of reactions to repeated centrifugal accelerations
07 p1065 A69-18980
- Human sensorimotor reactions during rotation in small radius apparatus at different speeds and torso inclinations
20 p3471 A69-37258

Human acceleration tolerance dependence on age, profession and physical training from investigation of reactions to repeated centrifugal accelerations
20 p3479 A69-38228

Human heart chronotropic reactions during centrifuge acceleration tests up to tolerance limit, establishing sinus tachycardia in various degrees
22 p3877 A69-40283

Jet pilot blood pressure response during positive acceleration in actual flight measured by telemetry compared with centrifuge test
23 p4089 A69-41822

Centrifugation for removal of bullet fragment floating freely in ventricular system of human brain to fixed life position in left lateral ventricle wall
24 p4265 A69-43372

Circulatory reactions of humans under g forces in centrifuge for various periods, with or without anti-g suit
24 p4267 A69-43385

HUMAN FACTORS ENGINEERING

Human factors in aviation - Conference, Los Angeles, June 1968
01 p0010 A69-10448

Human factors in aircraft systems, discussing personnel selection throughout design and manufacturing phases
01 p0019 A69-10449

Human engineering program plans for Phase 3 of SST Development Program in accordance with airframe and engine contracts
01 p0019 A69-10451

All-weather landing flight director systems and fault warning display simulator studies of Boeing 707-720B aircraft in Category 3-C environment
01 p0010 A69-10455

Modular three dimensional mockup technique for economizing and facilitating design of control and display equipment
02 p0202 A69-11953

Human factors evaluation of computer based information storage and retrieval system using questionnaire and interview techniques
02 p0204 A69-12220

Vertical contact analog display /VCAD/ design, emphasizing need for integrated and supplementary information to pilots in systematic way
03 p0379 A69-13361

Human inspection performance in quality control operations to assess visual inspection tasks accuracy
03 p0433 A69-13386

Airline operators economic oriented airframe maintenance problems, discussing cost accounting improvement
03 p0434 A69-13698

Visual factors of laser displays providing human factors recommendation for several visual variables
05 p0760 A69-15591

Medical fitness regulations for pilots, including federal and internal airline regulations
06 p1041 A69-16844

Professional activity of cosmonauts, considering training, mental and physical qualities and engineering background
[UN PAPER 68-95716] 06 p0879 A69-17036

Predictive scale of aircraft emergencies, analyzing human error rate under stress
06 p0880 A69-17208

Leisure time and recreation facilities during long duration space missions, discussing astronaut selection procedure, active recreation, passive enjoyment and exercise programs
06 p0880 A69-17209

Weightless simulators effectiveness for obtaining space systems maintainability criteria, using nonparametric experimental design for performance data
06 p0882 A69-17648

Flying safety and human factors relationships from job classification survey oriented toward social psychology
06 p0884 A69-18035

Management control systems, discussing malfunction, inefficiency and needs of human elements
07 p1244 A69-18963

Lunar shelter regenerative life support system performance and manned test
07 p1071 A69-19427

Occupational attrition estimation methods for determining personnel separation through marriage, death, retirement and transfer applied to engineering and nursing
07 p1245 A69-19728

Flight deck equipment guidelines in aircraft, discussing pilots natural senses, visual information, dis-

plays, logic and memory capable computers and ground controller
08 p1266 A69-20450

Aircraft head-up display systems emphasizing all-weather operations and equipment characteristics
08 p1315 A69-20451

Organizational behavior of scientists noting working environments, effectiveness of work sections, research management and organizational development
08 p1423 A69-21124

Improved suit for lunar wear, noting production and qualifying schedule and astronaut tests
08 p1267 A69-21146

Human engineering program at early design phase of SST aircraft to achieve maximum human efficiency and man machine compatibility
09 p1447 A69-22546

Neurological changes in men due to hypokinesia, analyzing tremor data, EEG recordings and stabilography fluctuations
10 p1647 A69-23585

Aircraft engine instrument displays evaluated by human factors, noting vertical scale design
[SAE PAPER 690328] 11 p1829 A69-24488

Business aircraft injury protection and impact survival design considerations, stressing upper torso restraint installations
[SAE PAPER 690335] 11 p1829 A69-24493

Target displacement and track coherence in pursuit tracking tasks experiments for human performance studies
11 p1829 A69-24737

Manned space stations for future space exploration, discussing earth-like environment, artificial gravity, human factors and time dependence
11 p1965 A69-25644

Man machine integration, detailing sensory input and motor /or output/ systems, control loop and social structure impact
11 p1831 A69-25656

FAA aircraft accident human factors investigation plan, discussing on-call pathologists, site organization and investigation, autopsy and result reporting
12 p2022 A69-25843

Alignment/test rig for head-up displays using laser light pencils
12 p2091 A69-26304

Complex piloting simulation including fatigue for optimizing man machine synergy, emphasizing human adaptability and computer precision and speed
12 p2025 A69-27083

Heart rate and respiratory response correlations in men during surface and underwater work, showing reasonable approximations of workload in surface-equivalent terms
14 p2406 A69-29293

Characteristics, incentive and promotional patterns and work adjustment of engineering technicians
15 p2723 A69-31242

Motivation and performance increase in R and D by incentive plans, discussing prestige, power, responsibility, recognition, work, salary, comfort, etc
17 p3075 A69-32963

Protective helmet design effectiveness against concussion and skull fracture as function of dimension, weight, load spreading, etc
17 p2913 A69-33177

Ergonomy and aviation medicine, discussing biotechnological aspects of information in man machine systems and observation tasks
17 p2915 A69-33770

Protective filter for inspiration valve of oxygen masks in high performance aircraft, reducing respiratory volume exchange with given pressure amplitude
17 p2916 A69-33773

Color coding effect on alphabetic filing names, comparing first and second letter codes and no color code condition
17 p2916 A69-34004

Minimum dimensions of circular nondetent knobs mounted on concentric shafts in case of nontolerable frequent inadvertent operation of adjacent coaxial knobs
17 p2916 A69-34005

Optimum knob crowding, measuring reach time, turning time, inadvertent touching and influence of knob spacing, diameter and configuration
17 p2916 A69-34006

Motion cues simulation system with seat of six differentially inflatable sections, discussing DYNASEAT
17 p2947 A69-34007

Human performance reliability, testing mathematical model application and implications of time to first error concept by vigilance task
18 p3097 A69-34478

Man-computer speech communication, discussing model and aspects of acoustics, phonetics, linguistics, language training, physiology, psychology, bionics, etc
18 p3107 A69-35099

Human ear frequency discrimination, discussing nonlinear functional modeling systems
18 p3097 A69-35440

Accelerate-stop criteria examined from human engineering standpoint, discussing flight simulator study of pilot reaction times for transition to rejected takeoff configuration
[AIAA PAPER 69-772] 19 p3244 A69-35650

Vertical vibrations effect on test subjects in supine position, noting human tolerances and mood changes
19 p3260 A69-35986

Reliability measurements based on maintenance records, considering human factor and life limiting and random chance design
19 p3327 A69-36013

Subsystem designs evaluated on basis of human reliability metric to select desirable design configurations
19 p3261 A69-36026

Impact mechanism in hip safety belt protection in vehicles, deriving motion for natural oscillations of upper part of human body model
20 p3482 A69-37595

Mathematical models of human vestibular system for dynamic space orientation, using control theory
21 p3662 A69-38728

Multiple cues in paired comparisons, discussing mathematical model of psychological process in information extraction and combination
21 p3664 A69-38970

Human radar operator effectiveness at night noting vigilance level lowering, discussing possible logic mechanism perturbation
21 p3666 A69-39268

Space cabin and suit pressures for decompression sickness avoidance and fire hazard alleviation
22 p3890 A69-40212

Representative data of actual forces and moments applicable to large spacecraft attitude control system for typical crew activities obtained through simulation programs
[AIAA PAPER 69-1006] 22 p3921 A69-40380

Cockpit displays for transport aircraft noting digital techniques and flight control-navigation integration
22 p3946 A69-40486

Flicker characteristics of eye color receptive systems by measuring modulation thresholds for sinusoidal flicker of color superimposed on complementary color background
22 p3880 A69-40851

Saccadic eye movements comparison during fixation and reading by contact lens optical lever technique
22 p3880 A69-40855

Human factors methods importance in nonmilitary flight simulation training, discussing cost factors and skills evaluation
22 p3894 A69-41138

Human angular acceleration sensitivity using rotation and oculogyril illusion perception as indicators, relating to spatial orientation and flight control task precision
23 p4101 A69-41674

SST flight crew operational requirements to achieve maximum human efficiency and man/machine compatibility, discussing pilot role, advanced flight instrumentation, etc
23 p4107 A69-41820

Human factors in air traffic control, considering personnel, equipment, environmental and social factors
23 p4108 A69-41828

Head-Up Display /HUD/ incorporated with autopilot for human participation in flight control for all-weather operation
23 p4109 A69-41871

Human sciences contribution to man-computer interaction based on review of relevant human factors literature
24 p4273 A69-43015

Man-computer interaction problems for human factors research, considering conversational languages development and evaluation, use patterns and interaction modeling
24 p4274 A69-43016

Display system design principles and procedures, discussing checklists, formal procedures and behavior theory
24 p4274 A69-43017

Manual vehicle control analysis based on feedback systems analysis and mathematical models for human operators engaged in control tasks
24 p4274 A69-43021

Ergonomic study of experimental tests design for comparing equipments efficiency with man
24 p4275 A69-43023

HUMAN FACTORS LABORATORIES

Relationship between human response to noise and physical parameter, discussing controlled laboratory investigation to determine duration effect on annoyance
18 p3097 A69-34324

Orbital biomedical laboratory for in-flight measurement to assure human safety and optimize astronaut performance in extended space mission
23 p4223 A69-41801

HUMAN PATHOLOGY

Surgical radiolesion in human brain by high energy protons
03 p0374 A69-13501

Corneal greyish opaque arc as warning of atheromatosis in flight crews
05 p0711 A69-16631

Cosmic radiation and hibernation physiopathology of human organism, noting beryl as radiation resisting agent in spacecraft design
06 p0874 A69-17645

Primates for space research, discussing selection, purchase, handling and use as controls in observations of disorders experienced by man
09 p1445 A69-22723

Pathology and aircraft accident causes noting environmental factors, injuries and preexisting diseases
12 p2021 A69-25838

Aviation pathology in aircraft accident investigation of accident survivability features and accident precipitation factors, noting cockpit structures and protective equipment
12 p2021 A69-25841

FAA aircraft accident human factors investigation plan, discussing on-call pathologists, site organization and investigation, autopsy and result reporting
12 p2022 A69-25843

Preventive medicine in handling airline pilots to avoid accidents attributable to disability and death from natural causes
12 p2024 A69-26559

Long microextensions on cultivated human liver cells, using scanning electron microscope
20 p3480 A69-38287

Chronic hypoxic hypoxia on oxygen-hemoglobin dissociation curve and respiratory gas transport in man, considering altitude residents and heart and lung diseased patients
21 p3650 A69-38383

Surface electromyography/EMG/ frequency analysis of normal and pathological muscle or nerve contraction as diagnostic tool for industrial physician
21 p3664 A69-38920

Airway distensibility effect on elastic behavior of human lungs, noting compliance and resistance at different breathing frequencies for diseased lungs
22 p3873 A69-40205

Serial ECG change from normal conduction to right bundle branch block in 59 patients without overt cardiac disease
23 p4085 A69-41677

Heart murmurs frequency analysis on patients to improve detection of aortic insufficiency in presence of mitral stenosis
24 p4279 A69-43800

HUMAN PERFORMANCE

NT ASTRONAUT PERFORMANCE

NT OPERATOR PERFORMANCE

NT PILOT PERFORMANCE

Holographic theory of visual memory behavior, discussing human tests in situation of prompted visual recall
01 p0083 A69-10985

Component total task relationships, analyzing simple and sequential practice effects with aid of Melton Complex Coordinator
02 p0203 A69-12214

Lunar gravity simulation effect on human performance, discussing fidelity requirements, self locomotion, metabolic rate and psychomotor task decrement
02 p0203 A69-12217

Human inspection performance in quality control operations to assess visual inspection tasks accuracy
03 p0433 A69-13386

Work and rest scheduling effect on working capacity and physiological state of male subjects in sealed chamber
03 p0381 A69-14201

Human auditory function during exposure to prolonged low barometric pressure unaffected with normal oxygen partial pressure
03 p0378 A69-14206

Cardiac function changes during orthostatic tests and problems in predicting reactions of cosmonauts in flight
03 p0381 A69-14229

Hypohydration effects on isometric muscular strength, noting decreasing trends in maximal strength
05 p0708 A69-15983

Vectorometric EKG analysis of cardiac activity during hypokinesia with and without exercise and medication
05 p0710 A69-16519

Ideal safety system for accident prevention, considering foreseeable and unforeseeable aspects to eliminate individual or collective human error
06 p1040 A69-16836

Finger dexterity in JMG-1 pressure gloves with regard to efficiency associated with fine adjustments
06 p0884 A69-18032

Auditory startle stimuli effect on human performance, noting decrease in mental and sensorimotor activity
07 p1066 A69-19421

Medical factors as probable cause of aircraft accidents, discussing psychological factors, CO poisoning, hypoxia, alcohol, etc
07 p1067 A69-19433

Mental and physical human performance characteristics under thermal loads noting admissible temperatures and endurance limits
08 p1263 A69-19940

Underwater experiment to determine man capability to perform scientific mission during 60 days isolation, noting task performance, social interaction and personal adjustment
08 p1300 A69-20113

Mild hypoxia effect on selective attention performance of human subjects at simulated 8000 ft altitude
09 p1445 A69-22553

Systolic murmurs and flight personnel evaluation, noting phonocardiographic definition and tracings of specific systolic murmurs
09 p1445 A69-22726

Stimuli human subjects can identify on unidimensional visual stimulus continuum, discussing apparatus and line length influence
10 p1641 A69-23039

Control operation time found dependent on gloves, physical characteristics of control and type of required operation
10 p1648 A69-23180

Glove characteristics effects on manipulability, finding operation time differences between gloved and barehanded operation dependent on type of required control operation
10 p1648 A69-23181

EEG, heart beat, respiration rates, body temperature, motor activity, physical and mental efficiency of man during anechoic chamber confinement
10 p1646 A69-23510

Moisture losses of men wearing partial pressure suit with oxygen mask determined by changes in skin temperature and heat flow
10 p1647 A69-23591

Human information processing rates during one and two axis compensatory tracking tasks with secondary auditory task
10 p1650 A69-23880

Target displacement and track coherence in pursuit tracking tasks experiments for human performance studies
11 p1829 A69-24737

Altitude climates effects on human performance, discussing oxygen consumption at moderate altitudes during vigorous physical activity
11 p1827 A69-24924

Polarity coincidence correlation method due to random processes state characterization applied to man machine systems
12 p0202 A69-25931

Aeronautical health service problems relating to efficiency of military and civil aviation personnel of all nations
12 p0203 A69-26490

Human vestibular reactions at various bodily rotation rates and planes, including counterrotation illusion and nystagmic reaction
12 p0200 A69-26564

Human operator as servo system element of subassemblies in tracking and equilibrium tasks, stressing results of electromyographic analysis
12 p0205 A69-27081

Mathematical models of human performance in man machine systems, discussing operations research, maintainability and real time computer simulation for command and control systems
12 p0205 A69-27085

Computer simulation models for prediction of individual and crew performance in man machine environments
12 p0206 A69-27087

Standardization requirement for laboratory and field research into vibration effects on humans, stressing subjective rating and performance measurements
13 p2213 A69-28091

Combined cueing and knowledge of results for transfer of training in visual monitoring
13 p2213 A69-28256

Astronaut selection and training in U.S. and U.S.S.R.
13 p2216 A69-28636

Noise measurement and scales in studying psychological and nonauditory physiological effects on human functioning
14 p2485 A69-29150

Fast visual task performance indoors found dependent on sound pressure level
15 p2550 A69-30305

Engineer performance related to organizational factors, discussing colleague contact, work diversity, number of subordinates and involvement in work
15 p2721 A69-31069

Telemetry techniques, based on pulse rate measurements, permitting continuous examination of humans under natural working conditions
15 p2559 A69-31228

Cardiovascular system, neuromuscular activity and mental fitness of subjects performing physical and mental assignments with prescribed work-rest schedule during confinement
17 p2906 A69-32936

Prolonged hypokinesia effect on human resistance to physical stress, noting prophylactic influence of physical exercises
17 p2907 A69-32939

Hand movements in water environment, weightlessness and normal gravity conditions, discussing inner coordinative structure and muscular efforts
17 p2915 A69-33385

Muscle motor performance under continuous practice conditions, analyzing individual differences, intrasubject variability and remoteness
17 p2911 A69-34003

Intermittent noise effects on human target detection to test neutral ratio dependence on noise intensity level, noting attention flexibility
17 p2911 A69-34008

Continuous and intermittent noise effects on audiovisual checking task performing subjects, considering omission errors
17 p2911 A69-34009

Mechanical vibration effects on human operation of various decimal input devices
17 p2916 A69-34010

Muscle power output relation to imposed load modified to accommodate inverse relationship between generated force and contraction speed for determining maximum strength
17 p2916 A69-34011

Psychophysical method of studying heart rate as indication of physiological fatigue
17 p2911 A69-34013

Guide for establishing harmonious relationships with design engineers within typical mechanical engineering department
17 p3077 A69-34198

Human performance reliability, testing mathematical model application and implications of time to first error concept by vigilance task
18 p3097 A69-34478

Vectorometric EKG analysis of cardiac activity during hypokinesia with and without exercise and medication
18 p3096 A69-34738

Factor analysis of complex perceptual-motor performance of man, measuring speed, flexibility, balance and strength
18 p3098 A69-35085

Flight and piloting influence on morbidity of civil aviation personnel, noting incidence of enteric, hemorrhoidal and respiratory diseases
18 p3098 A69-35303

Quiet military aircraft design factors, considering human hearing characteristics, noise suppression methods, propeller noise-performance relationships and jet engine noise nature
[AIAA PAPER 69-792] 19 p3243 A69-35637

Man machine modeling technique for establishing personnel performance requirements, discussing field tests 19 p3261 A69-36025

Controlled-variable prediction display based on Taylor series computation, describing acceleration system simulator and human operator performance 19 p3313 A69-36414

Recording instrument paper speed effect on pulse wave measurements precision, discussing multiple observer studies of left ventricular ejection time 19 p3258 A69-36449

Sensorimotor coordination of man performing graphic assignments in upright, reclining and prone position, discussing interaction of vestibular, visual and motor analysors 20 p3470 A69-37246

Motion sickness forms in human subjects subjected to induced rocking, noting impaired performance and sensorimotor reactions to visual stimuli 20 p3472 A69-37263

Human performance and adaptation to space flight effects under low calorie diet including optimal proportion of basic nutrients and amino acids 20 p3482 A69-37621

Human operator decision making in vehicle manual control, considering success likelihood and possible outcome costs based on signal detection model 20 p3482 A69-37720

Adaptive compensation to minimize human task in continuous manual control system using various models 20 p3482 A69-37721

Averaged cortical evoked response characteristics relationship to performance in traditional threshold procedures, discussing stimulus sensitivity and intensity control in central nervous system 21 p3653 A69-38897

Model for lateral inhibitory interaction in human retina, providing systematic account of simultaneous brightness contrast 21 p3653 A69-38898

Ear-hand coordination adaptability tested by exposure to auditory rearrangement entailing 30 degree rotation of interaural axis produced by electronic pseudophones 21 p3663 A69-38899

O uptake of middle aged men, comparing short and long term endurance running effects 21 p3654 A69-38904

Human performance assessed by pulse rate increment at onset of exercise on bicycle ergometer and decrement during recovery after fasting 21 p3655 A69-38910

Mathematical model of probability of errorless human performance for time continuous tasks for use in systems reliability analysis 21 p3664 A69-38971

Personality factors and job performance ratings relationship in radar controllers, computing Pearson correlation matrix based on age, education, motivational distortion, etc 21 p3665 A69-39169

Healthy, physically untrained students compared with trained athletes for differences in working capacity concerning orthostatic tolerance and blood pressure responses 22 p3889 A69-39940

Maximum voluntary isometric muscle strength relation to endurance time in static work during partial curarization 22 p3890 A69-40213

Exercise-temperature regulation in men under constant submaximal workload at various simulated altitudes, discussing exercise core temperature equilibrium level setting mechanisms 22 p3891 A69-40219

Prolonged wakefulness effect on human work capacity in isolated chamber, determining physical, intellectual and sensory capacities 22 p3877 A69-40280

Fixed interval human performance control under various histories of conditioning and response cost conditions, considering effects of postreinforcement pauses 23 p4100 A69-41437

Human observers visual monitoring of multiple meter display differentially controlled by concurrent signal scheduling 23 p4081 A69-41438

Human performance on button pressing task with fixed ratio fixed interval reinforcement schedules 23 p4081 A69-41439

Hand and thumb exercise effects on acquisition tracking task performance 23 p4101 A69-41453

Human mental performance impairment at simulated 8000 ft altitude indicated in increasingly difficult tests 23 p4102 A69-41680

Arterial oxygen partial pressures and heart beat rates measured in humans during acute hypoxia after altitude and ergometer training, noting sensorimotor performance 23 p4086 A69-41788

Healthy, physically untrained students compared with trained athletes for differences in working capacity concerning orthostatic tolerance and blood pressure responses 23 p4108 A69-41821

Point images reference groups identification by human operator with limited visual perception in background noise, comparing results with automatic system using selection algorithms 23 p4109 A69-41955

Mental patient performance in detecting and identifying visual signals under fixed interval schedule, noting nonuniform performance and comparing to normal subjects 23 p4091 A69-42014

Feedback effects and social facilitation of human vigilance performance, evaluating mere coaction vs potential evaluation 24 p4271 A69-42751

Visual and tactual interaction in judgments of vertical in dark room experiments, discussing effects of various reference systems 24 p4271 A69-42752

Personnel training and selection systems, applying information processing models to diagnostic testing in job classification for performance improvement 24 p4274 A69-43020

Adaptive manual control rapid variation determined by input, controlled element, task and programmed adaptation systems, discussing human strategy changes 24 p4274 A69-43022

Ergonomic study of experimental tests design for comparing equipments efficiency with man 24 p4275 A69-43023

Head movement affecting visual and kinesthetic localization accuracy, discussing free and fixed head conditions 24 p4275 A69-43118

Parameter identification algorithm identifying linear dynamic systems by digital computer used to identify human operator characteristics in closed loop control situation 24 p4276 A69-43320

HUMAN REACTIONS

Weak alternating electric field effects on human circadian rhythms 01 p0013 A69-10167

Noise and relations between environment and man, discussing sound perception, measurement and judgment of noise annoyance and harm 01 p0020 A69-10741

Soviet book on space physiology covering space flight and laboratory data on cerebral cortex function, digestive system, tissue changes, etc 01 p0014 A69-10743

Human psychological factors involved in genesis of contingent or conative negative variation using EEG activity measurements 01 p0015 A69-10904

Soviet book on human movements coordination during space flight covering space walks, lunar surface photographs, space docking, weightlessness, etc 01 p0018 A69-11180

Human endocrine-metabolic response to sequential decompression exposure during simulated orbital flight or extravehicular activity 01 p0022 A69-11337

Nitrogen and helium as factors affecting human decompression stress severity, using urinary measurements reflecting various endocrine and metabolic changes 01 p0018 A69-11338

Tinted ophthalmic media effect on detection and recognition of red signal lights in daylight, noting allowable coloration for aviation use 01 p0022 A69-11341

Ophthalmic 2 percent pilocarpine effect on normal ocular dynamics of various age groups, including visual acuity, accommodation and refraction 01 p0022 A69-11347

Hypokinesia and transverse accelerations combined effect on human cardiovascular system and regional blood circulation 02 p0197 A69-11495

Human nervous system and vestibular and auditory analysors functional changes under combined hypokinesia and radial accelerations effects 02 p0197 A69-11496

Weightlessness effects on organism in space flight along parabolic trajectories, discussing interaction between analysors 02 p0197 A69-11499

Differential and threshold sensitivity of acoustic analysors of humans under space flight factors 02 p0197 A69-11500

Hypokinesia and acceleration effects on human organism immunity and resistance to inflammatory diseases in 62 day test 02 p0198 A69-11513

Lateral acceleration effects on human kidney functions, noting increase in diuresis and erythrocytes in urine 02 p0198 A69-11514

Long term restriction of muscular activity noting effects on dynamics of cardiac contraction 02 p0198 A69-11515

External observer effect on human behavior during sensory deprivation tests conducted in isolation chambers as factor in estimating personality 02 p0200 A69-11516

Temporal pattern perception by human subjects required to integrate information presented in two modalities 02 p0200 A69-12724

Human reaction to aircraft engine noise, evaluating effective perceived noise level and constraints on engine design 02 p0204 A69-12766

Respiratory disturbances relationship to experience and attitudes toward gas anesthesia and response to different types of face mask 03 p0378 A69-12884

Stability and habituation of nonspecific galvanic skin responses during light and sound stimulation periods in medical students 03 p0380 A69-13462

Radiation effects in man, searching for dose relationships in prodromal syndrome 03 p0374 A69-13503

Manual performance relationship to men exposed to cold, thermal neutral and hot environments, discussing finger dexterity and motor coordination tests 03 p0381 A69-14074

Organic reaction and adaptation of rabbits and dogs to simulated weightlessness and acceleration compared with orbital flight data of human responses 03 p0376 A69-14192

Isolation effects on higher nervous activity, motor and vegetative reactions, muscular strength and emotional state 03 p0377 A69-14202

Human orienting reaction to sonic boom, determining degree of discomfort 03 p0378 A69-14210

Psychochemical research theory and methodology, relating biochemical phenomena to human brain function 04 p0553 A69-14976

Circadian rhythm effect between individuals of separate twin pairs, noting application to physiological research in medical genetics and human biometeorology 04 p0553 A69-15152

Rotational velocity estimates by observers during angular acceleration, noting vestibular function interpretation 04 p0554 A69-15332

Protein contained purine free basal and yeast ribonucleic acid diets effect on plasma and urinary uric acid production in male subjects 05 p0708 A69-15968

Psychophysical methods for determining perception threshold of angular acceleration in man during vertical rotation 05 p0708 A69-15969

Recorded vocal reactions of humans analyzed as characteristic of positive and negative emotions 05 p0709 A69-16518

Coriolis acceleration dosages applied in vestibulometric tests of male subjects inclined in rotating chair 05 p0710 A69-16521

Biochemical indicators of pilot reactions to flights complicated by unexpected autopilot failures, using postflight chemical analysis of blood and urine 05 p0710 A69-16525

Book on space clinical medicine covering hypoxia, ebullism, decompression, aerotitis, dehydration, hyperthermia, cabin atmosphere contamination, urinary calculus, etc
05 p0711 A69-16801

Physiological approach to tests and evaluation of aviation survival equipment, noting human reactions study under extreme conditions
06 p0877 A69-16953

Biological aspects of space exploration, analyzing human response to artificial environment in prolonged space missions
[UN PAPER 68-95715] 06 p0873 A69-17035

Human physiology advances in connection with space exploration, discussing internal medium adaptation to space environment
[UN PAPER 68-95729] 06 p0873 A69-17061

Sympathoadrenal activity during and after impact stress measured from urinary excretion of catecholamines and 17-hydroxycorticosteroids
06 p0875 A69-17839

Soviet cosmonauts physiological reactions during weightlessness, analyzing EKG, arterial pressure, heart and respiratory rates and motion coordination
07 p1060 A69-18570

Gravitational effects during physiological functions formation of human organism, noting myogenic tonus rearrangement as primary response
07 p1060 A69-18572

Human sensory reactions to short term weightlessness
07 p1060 A69-18574

Subjects sensory reactions to weightlessness during parabolic flight, studying coordination of writing, eating and drinking motions
07 p1060 A69-18575

Statistical study of heart beat, respiration rate and arterial pressure of man during intermittent accelerations and short term weightlessness
07 p1061 A69-18579

Sensory and physiological reactions experienced by cosmonauts during parabolic training flights, tabulating arterial pressure, heart beat and respiration rate
07 p1061 A69-18580

Human vestibular reactions during weightlessness preceded and followed by acceleration
07 p1061 A69-18581

Human and animal cardiovascular system reactions to weightlessness, noting vagus nerve role in adjusting organism
07 p1061 A69-18583

Pneumograms and EKG used to determine heart beat, respiration rates and systolic index of cosmonauts during Voskhod 2 flight
07 p1062 A69-18585

Human vestibular and sensory reactions to rotation and rocking, Coriolis acceleration and vestibular reaction inhibition on ground test stand for effects of temporary weightlessness
07 p1062 A69-18586

Vestibular-vegetative reactions during angular and Coriolis accelerations alternating with weightlessness, noting increased parasympathetic and sympathetic activity
07 p1062 A69-18587

Otolith and cupular apparatus interaction in human vestibular analyzer during gravitational changes
07 p1062 A69-18589

Decrease in bioelectric activity of skeletal muscles in animals and man during intermittent acceleration and weightlessness
07 p1062 A69-18591

Sensory and motor activity of human subjects exposed to reduced gravitation during aircraft motions along parabolic trajectories
07 p1062 A69-18592

Human postural muscle activity, motor reactions and dexterity during gravitational changes
07 p1063 A69-18593

Human motor reactions during weightlessness based on parabolic or orbital space flight observations, noting cosmonaut writing performance
07 p1063 A69-18595

Arbitrary human motions coordination in reorganization phases determined during weightlessness for cyclographic analysis of adjustment time
07 p1065 A69-18979

Human organism reaction to prolonged limitation of muscular activity during weightlessness simulated by bed rest, noting hypokinetic component of weightlessness
08 p1262 A69-19837

Work capacity and adaptation characteristics of humans confined in small chamber and experiencing effects of isolation and sensory deprivation
08 p1262 A69-19838

Stability of male cardiovascular, respiratory and motor systems functional conditions after physical activity in pure O medium at high altitude pressure
08 p1262 A69-19931

Hypokinesia muscular activity deficit in males confined to bed rest compensated for by physical exercise, noting orthostatic resistance, acceleration endurance, immunity, etc
08 p1263 A69-19932

Otolith apparatus response threshold under weightlessness conditions simulated by aircraft flight, measuring galvanic current threshold for banking
08 p1263 A69-19934

Social isolation and other sensory deprivations effects on human organism
08 p1263 A69-19937

Aircrew members skin temperature changes in response to intense diffuse thermal radiation, noting psychological response to exposure
[AGARDOGRAPH-111] 08 p1264 A69-20669

Thermoregulatory reactions of human body to sharp increase of ambient radiant temperature
[AGARDOGRAPH-111] 08 p1264 A69-20670

Human reactions to increasing heat exposure, noting thermoregulation and metabolic and evaporative heat loss
[AGARDOGRAPH-111] 08 p1265 A69-20675

Cold water immersion effects on man from physiological and physiopathological viewpoint, examining clothing effect
08 p1267 A69-20682

Long time physiological effects of rotating systems, surveying acceleration effects and rotation experiments on humans and rats
08 p1265 A69-21183

Physiologic and metabolic effects in humans undergoing therapeutic hypothermia
10 p1643 A69-23125

Psychological, physiological and biochemical responses to controlled diets, determining regional and total body sweat composition of men working in temperate environment
10 p1644 A69-23314

Hypokinesia effects on human neurology on extended space flights simulated by 72-day bed rest
10 p1646 A69-23506

Human physiology for exposure to acute hypoxia studied with variation pulsograms and indices of external respiration and pulmonary gas exchange
10 p1647 A69-23592

Biotelemetry of human physiological processes in space for assuring physiopsychological control and immediate intervention for emergencies, discussing application in Mercury and Gemini projects
12 p2023 A69-26491

Human nystagmic reaction variations due to simultaneous rotation of head and body, studying coriolis couple in horizontal semicircular canals
12 p2020 A69-26565

Book on earth atmosphere and outer space influence on human physiology for life support systems design
12 p2024 A69-27074

Standardization requirement for laboratory and field research into vibration effects on humans, stressing subjective rating and performance measurements
13 p2213 A69-28091

Physiopathological reactions of humans exposed to infrasonic vibrations applied via auricular canal, observing cardiac and circulatory hemodynamic troubles
13 p2215 A69-28590

Climatic environments development for physiological studies, considering ambient temperature, radiated heat and air velocity and movement
13 p2215 A69-28594

Closed life support systems tests, describing effects of long term /one year/ confinement of three human subjects
13 p2216 A69-28612

Prolonged dehydrated food diet effect on metabolism of humans, noting complete adaptation after three or four months
13 p2212 A69-28624

Combined hypoxic hypoxia and high ambient temperature found relieving strain on humans by increasing heat release by evaporation
13 p2212 A69-28628

Acoustical, psychological, sociological and political aspects of human reaction to SST sonic booms over populated areas, tabulating Boeing and Concorde boom intensities
14 p2408 A69-29151

Noise duration and spectral complexity effect on subjective rating of disturbance level
14 p2408 A69-29152

Auditory evoked response /AER/ as measure of narcosis induced at depth in diving personnel, discussing hyperbaric nitrogen and oxygen effects
14 p2407 A69-29302

Latent desynchronization, discussing life system and distortion, body rhythms coordination, circadian rhythms and adaptation to new system of time
15 p2557 A69-31457

Alternating electric field effects on circadian rhythms in men, discussing period shortening and internal desynchronization
15 p2557 A69-31461

Long distance air flights through different time zones, discussing circadian physiological cycles, light-dark ratio shifts effects and methods of lessening desynchronization effects
16 p2745 A69-32444

Phagocytic activity and carbohydrate metabolism in peripheral blood neutrophils of men exposed to atmosphere with increased O content, noting neutrophil energy exchange disorder role
17 p2907 A69-32942

Diphenidol and prochlorperazine effect on human semicircular canal function, noting failure of drug to alter vestibular responses
17 p2913 A69-33168

Urine excretion following water load in male subjects exposed to normal, hot/dry and comfortable/dry environment applied to airline crews
17 p2914 A69-33182

CH-46 helicopter flight simulation program for pilot response to large perturbation maneuvers, using six degrees of freedom mathematical models
[AHS PAPER 361] 17 p2946 A69-33521

Compensatory reactions to prolonged weightlessness in human and animal organisms emphasizing blood circulation, heart, metabolism, digestive and nervous systems
17 p2909 A69-33577

Relationship between human response to noise and physical parameter, discussing controlled laboratory investigation to determine duration effect on annoyance
18 p3097 A69-34324

Recorded vocal reactions of humans analyzed as characteristic of positive and negative emotions
18 p3096 A69-34737

Coriolis acceleration dosages applied in vestibulometric tests of male subjects inclined in rotating chair
18 p3096 A69-34740

Biochemical indicators of pilot reactions to flights complicated by unexpected autopilot failures, using postflight chemical analysis of blood and urine
18 p3096 A69-34744

Toxic effects of Freon R FE 1301 on animals and human beings at different concentrations, assessing judgement, alertness and neuromuscular skill
18 p3098 A69-35061

Tremographic studies of central nervous system during supersonic flight as engineering psychology application to man machine relations in aircraft-spacecraft industries
19 p3259 A69-35834

Space medicine to characterize nature and degree of changes in human functional capabilities due to space flight environment prolonged exposure
19 p3456 A69-36460

Visual and vestibular analysors interrelation in subjects receiving light pulses before and after rotation, noting role of cortical elements
20 p3470 A69-37249

Combined angular and centrifugal acceleration effects on human and animal eyes motion studied to explain weightlessness effects on humans
20 p3471 A69-37257

Human sensorimotor reactions during rotation in small radius apparatus at different speeds and torso inclinations
20 p3471 A69-37258

Coriolis acceleration effect on vestibulo-vegetative and vestibulo-somatic reflexes of humans subjected to forward tilting, noting pulse and respiration rates
20 p3472 A69-37259

Vestibular functions of humans subjected to Coriolis acceleration via prolonged rotation at different angular velocity rates
20 p3472 A69-37260

Human sleep during prolonged rotation, discussing electroencephalograms, acoustic signal frequency producing waking reaction, cutaneous galvanic reflex and deepness of sleep
20 p3472 A69-37261

Arbitrary human motions coordination in reorganization phases determined during weightlessness for cyclographic analysis of adjustment time
20 p3479 A69-38227

Male patients urine tests during sinusoidal vibration, noting catecholamine excretion as criterion of emotional stress under various environmental conditions
21 p3654 A69-38909

Physiological and psychological measurements of high pressure effects on man and animals, discussing decompression sickness, respiratory embarrassment, inert gas narcosis, helium tremble, etc
21 p3655 A69-38912

Carbon dioxide levels monitoring in spacesuit research including limits of physiological acceptability
21 p3665 A69-39170

Somatic radiation effects on human organism related to manned space flights
21 p3660 A69-39172

Desynchronization and resynchronization of human circadian rhythms of activity, body temperature and urine excretion during isolation in underground bunker in various conditions
21 p3660 A69-39173

Motion sickness susceptibility during parabolic flight, comparing weightlessness and hypergravity effects on normal and labyrinthine-defective subjects
21 p3660 A69-39176

Sleep habits of radar operators working in alternate crews in radar station on continuous watch
21 p3666 A69-39269

Radiotelemetric EEG recording variation possibility, examining dynamic behavior of human cerebral rhythms
22 p3889 A69-40158

Age and carbon dioxide tension effects on EEG of adolescents and adults, discussing end-tidal carbon dioxide during routine hyperventilation
22 p3872 A69-40162

Isometric tensions of detached lateral rectus muscles measured during strabismus surgery for mechanical components of human eye movements, giving muscle tone range
22 p3872 A69-40200

Circadian variations in human temperature regulation, measuring peripheral and rectal temperatures and peripheral heat and arterial blood flows in clothed resting males
22 p3872 A69-40201

Peripheral chemoreceptor carbon dioxide sensitivity, measuring human respiratory response to large carbon dioxide breath in oxygen at sea level and high altitude
22 p3890 A69-40207

Thermoregulatory responses to cooling in spinal man, discussing deep temperature sensitive structures and relationship between skin and central regulatory structures
22 p3873 A69-40209

Skin temperature change rate influence on sweating in male subjects, discussing role of central thermosensitive structures
22 p3874 A69-40210

Human metabolic response to hypothermia measured over wide range of work intensities and durations
22 p3891 A69-40215

Oxygen uptake and circulatory response in human male subjects during maximal treadmill and bicycle exercise
22 p3874 A69-40226

Human lung ventilation-perfusion scatter decreasing gas exchange efficiency during high altitude adaptation
22 p3875 A69-40227

Spatial distribution of amplitude and onset of pre-motion positivity, readiness and motor potential changes in human cerebral cortex preceding voluntary finger movements
22 p3875 A69-40261

Cortical responses by transient sensory stimulation of fingers EEG recorded, obtaining isomorphism between psychological and neurophysiological events
22 p3876 A69-40262

Zoellner illusion in human visual system measured as function of background pattern density consisting of intersect angles and background line spacing
22 p3879 A69-40841

Human visual response to moving spatially periodic patterns, analyzing critical frequencies, dependence on stimulus area and period, phase blindness and pattern reversal
22 p3880 A69-40850

Visual stimuli initiating horizontal eye vergence movement in human subjects, noting cerebral conditions for convergence
22 p3881 A69-40859

Subjective and objective thresholds of darkness adaptation in human subjects grouped from infancy to adulthood, using same variable intensity light source equipment
22 p3881 A69-40861

Retinal topography relation to blue arcs phenomenon, assessing disparity in photoreceptor location and associated neurones for analysis of critically sited plots
22 p3882 A69-40872

Angular velocity of visual stimulus effect on human torsional eye movements using sectorized disks
22 p3883 A69-40874

Spatial interactions and thresholds in identification and detection of compound visual stimuli
22 p3883 A69-40878

Response characteristics of human visual mechanisms sensitive to motion while varying adaptation stimulus contrast to control visual effectiveness
22 p3884 A69-40887

Human response to visual beat phenomena by combining intermittent stimuli, considering brightness estimation
22 p3884 A69-40889

Insensible water loss from human skin as function of ambient vapor concentration using IR gas analysis, applying results to water loss model revision
23 p4077 A69-41293

Antidiuretic hormone /ADH/ and bradykinin effects on human thermal and cholinergic sweating after subdermal injection in forearm, abdomen and leg
23 p4077 A69-41311

Physical exercise effect on adolescent males, comparing oxygen uptake, heart volume and height in training and nontraining groups
23 p4077 A69-41312

Heart rate measurements in ski jumpers with radio telemetric system revealing tachycardia during climbing and emotional stress
23 p4078 A69-41313

Fixed interval human performance control under various histories of conditioning and response cost conditions, considering effects of postreinforcement pauses
23 p4100 A69-41437

Telemetered heart rate response to progressively increased distance swimming competition compared with equidistance running events for change patterns, magnitude and recovery
23 p4100 A69-41444

Human sweat glands reflex responses to diverse skin cooling rates in hot room, discussing bath temperature step decrease effect on lower limb
23 p4082 A69-41446

Circadian rhythms characteristics of healthy human beings as reference standards for comparing investigation data from different continents
23 p4083 A69-41457

Frequency response transient vibration testing of standing man, discussing data analysis procedure, test stand, and Welch correction for instrument dynamics
23 p4101 A69-41494

Hypoxia acclimatization studied by subjecting groups to bicycle exercise at simulated high altitude and at ground level
23 p4086 A69-41678

Human physiological responses to angular acceleration during breath holding, Mi, Valsalva and Mueller respiratory maneuvers in hollow spherical simulator
23 p4102 A69-41679

Radio telemetry system for evaluating protective masks dynamic performance by remote simultaneous monitoring of respiration, acceleration and temperature data generated by human subjects
23 p4121 A69-41765

Hypoxia reaction elimination in human beings by repeated exposure to hypoxia, discussing nitrogen inhalation experiments and adaptive behavior of respiratory system
23 p4214 A69-41789

Space medicine to characterize nature and degree of changes in human functional capabilities due to space flight environment prolonged exposure
23 p4087 A69-41803

Klaxon hooter sudden sound used as auditory startle stimulus to determine hand sensorimotor activity and standing stability in pilot error causes
23 p4088 A69-41808

Alcoholic hangover effects on human balance system from flying demands viewpoint, discussing ocular-vestibular system disturbances
23 p4089 A69-41817

Subjects confined in caves for two to six months to note physiological rhythms time evolution and associated desynchronization and resynchronization
23 p4107 A69-41818

Subjective feeling of dampness correlation with relative humidity of air at zero and below zero C temperatures
23 p4109 A69-41870

EEG, ocular movements, gastric mobility and pH during human sleep from data transmitted by swallowed radio transmitter
23 p4093 A69-42063

Diurnal rhythms of heart rate and blood pressure reactions to posture changes on tilt table, finding orthostatic lability maxima
23 p4094 A69-42072

Human thermal regulatory mechanism using analog simulation compared with experimental results of resting subjects responses to climatic chamber
23 p4111 A69-42079

Human heart rate changes resulting from diving and breath holding exercises
23 p4095 A69-42083

Venous tone, peripheral venous pressure, skin and muscle blood flow, alterations of heart rate and respiration in men during leg exercise
23 p4096 A69-42090

Sound evoked DC changes on intact skull of adult humans using data from AgCl electrodes, investigating intensity function, analyzing data by computer
23 p4098 A69-42101

Blood flow, volume and venous pressure measurements in right hand at low and high altitudes in residents and newcomers
23 p4098 A69-42106

Psychological, psychophysiological and biochemical effects of prolonged sleep deprivation in human males, noting transient ego disruption
23 p4099 A69-42195

Human body responses to microwave irradiation, discussing thermal and nonthermal effects and damage to eyes and to information storage in living systems
23 p4111 A69-42216

Adrenosympathetic reaction in flight, studying contributions of physical and nervous stresses in physically trained and untrained persons
23 p4099 A69-42363

Psychological stress effect on human convergent and divergent thinking after presentation of disturbing or benign control films
24 p4269 A69-42555

Central circulatory responses of humans to rapid skin temperature changes during continuous exercises
24 p4258 A69-42633

Stewart-Hamilton theorems for total input-output analysis of body cholesterol in man
24 p4259 A69-42639

Electroretinogram and visually evoked cortical potential as response potentials in human visual system
24 p4271 A69-42644

Steady state model for human respiratory system analysis, discussing controlled and controlling parts
24 p4276 A69-43272

Brightness discrimination judgments for gray chips by humans, using psychophysical limits method and white, noncoherent red and He-Ne laser light sources
24 p4276 A69-43323

Urine sampling conditions for kidney function circadian rhythm during global flight, considering food and water intake, sampling intervals and body position
24 p4266 A69-43374

Human circulatory reactions to cumulative flight vegetative stimuli evaluated by cumulative stress simulation method
24 p4266 A69-43375

Circulatory reactions of humans under g forces in centrifuge for various periods, with or without anti-g suit
24 p4267 A69-43385

Circadian periodicity of human reaction times tested during normal diurnal cycles and 24 hour wakefulness, noting acoustic and visual stimuli effects on learning
24 p4267 A69-43387

HUMAN TOLERANCES

Helicopter structures design for maximum practicable crashworthiness and survivability, comparing load factors and deformations with indicated human impacts tolerance
[AHS PAPER 225] 01 p0009 A69-10408

Cardiovascular changes in male students during tilt and negative pressure tests with bed rest studied from heart rate, blood pressure and leg volume measurements
01 p0021 A69-11334

Prolonged decompression stress effects on humans in simulated orbital flight or extravehicular activity, investigating endocrine-metabolic disturbance by urinalysis

01 p0022 A69-11336

Basal metabolism in humans restricted to prolonged bed rest, noting decreased oxygen consumption rates

02 p0197 A69-11497

Biological effects in man due to heavy particles emission during major solar cosmic ray events, noting protective effect of human body

03 p0374 A69-13500

Physiological mechanisms of weightlessness on human organism, discussing adaptation to weightlessness

03 p0377 A69-14197

Daily sleep and wakefulness periodicity changes effect on heart rate, respiration and body temperature diurnal rhythms in human males under isolation conditions

03 p0377 A69-14203

Changes in blood circulation, external respiration and gas exchange rates in humans during prolonged hypodynamia

03 p0377 A69-14204

Human motor activity under hypodynamia and increased carbon dioxide, discussing positive effects of prescribed physical exercises

03 p0377 A69-14205

Impact/injury data used to estimate human tolerance to instantaneous accelerations

04 p0552 A69-14469

Mechanical model of human body used to study response to vibration, impact, blast and decompression loads

04 p0552 A69-14470

High temperature effects on physiological functions of man noting cardiovascular system and heart performance, body heat exchange and blood and urine composition

05 p0710 A69-16523

Cerebral circulation under longitudinal acceleration, discussing rheoplethysmographic measurements of heart rate

05 p0710 A69-16625

Professional activity of cosmonauts, considering training, mental and physical qualities and engineering background
[UN PAPER 68-95716]

06 p0879 A69-17036

Radiative, convective and evaporative heat losses and thermal comfort conditions for human beings, describing theoretically and empirically based equation

06 p0880 A69-17087

Cardiac arrhythmias during positive G sub x acceleration, treadmill exercise and tilt table testing

06 p0874 A69-17834

Human body cold tolerance and relation to BMR seasonal variation

06 p0876 A69-18024

Human acceleration tolerance dependence on age, profession and physical training from investigation of reactions to repeated centrifugal accelerations

07 p1065 A69-18980

Human acceleration tolerance under reduced pressures corresponding to various high altitudes, noting visual disorders

07 p1065 A69-18982

Human endurance during isolation in closed space with prescribed veloeometric exercises, noting impairment of functional capacity

08 p1263 A69-19933

Underwater experiment to determine man capability to perform scientific mission during 60 days isolation, noting task performance, social interaction and personal adjustment

08 p1300 A69-20113

Brief intense thermal stresses effects on cardiovascular system of man, noting criticality of effective blood volume for circulatory competence

08 p1264 A69-20668

Cold water immersion effects on man from physiological and physiopathological viewpoint, examining clothing effect

08 p1267 A69-20682

Skin temperature and cutaneous pain during warm water immersion, refuting subcutaneous thermal gradient hypothesis for stimulation of heat pain

08 p1267 A69-20683

Physiological effects of breathing cool dehumidified air in hot humid environment, tabulating tolerance time, heart rate, temperature changes and sweat loss

09 p1446 A69-22543

Heat and humidity endurance limits in man

10 p1645 A69-23494

Long term hypokinesia effect on cardiovascular system of athletes indicating human orthostatic resistance increase due to physical exercises

10 p1646 A69-23581

Prolonged bed rest effect on human myogenic tonus and proprioceptive reflexes, comparing test subjects with and without physical exercises

10 p1646 A69-23583

Combined effect of prolonged bed rest and acceleration exposure on human blood circulation, noting increased heart rate and arterial blood pressure

10 p1646 A69-23584

Human adaptation to various environments, emphasizing experimental space psychoneurology role in human behavior examinations during space missions

10 p1647 A69-23587

Limits of human tolerance to localized skin exposure to IR irradiation of various intensities from pain threshold observations, noting skin temperature role

10 p1647 A69-23589

EEG, EKG, respiratory motions and pulmonary ventilation recordings in study of carbon dioxide additions effect on human tolerance to hypoxic conditions

10 p1650 A69-23898

Human intolerance to bacteria as food, considering response to Hydrogenomonas eutropha and Aerobacter aerogenes

13 p2213 A69-27265

Human resistance to short duration high accelerations applied to aircraft ejection studies, noting bone damage, consciousness retention, etc

13 p2215 A69-28591

Autonomic nervous system role in controlling body functions after rapid decompression, increasing tolerance to pressure gradients by physical training

13 p2212 A69-28622

Human tolerance to SST sonic booms through scheduled community exposure, discussing physiological effects and acceptability level

14 p2541 A69-29153

Human noise tolerance laboratory and community studies, discussing proposed tone corrections for aircraft noise

15 p2719 A69-30374

Shield facility and Helmholtz coil system used to investigate chronic effects on man of zero magnetic field regulated to cancel geomagnetic field variations

15 p2586 A69-30382

Artificial heat acclimatization effect on orthostatic tolerance in man exposed to stresses of heat, exercise and dehydration

16 p2746 A69-32810

Aircraft noise acceptability tests based on listening in absence and presence of speech

18 p3097 A69-34325

High temperature effects on physiological functions of man noting cardiovascular system and heart performance, body heat exchange and blood and urine composition

18 p3096 A69-34742

Mechanical vibration effects on human body in industry and in terrestrial, aerial and nautical vehicles, discussing harmful frequencies and safety measures

19 p3259 A69-35605

Vertical vibrations effect on test subjects in supine position, noting human tolerances and mood changes

19 p3260 A69-35986

Test pilot vestibular training program to achieve higher tolerance of rotation, rocking and balancing and visual stimuli

20 p3472 A69-37266

Human acceleration tolerance dependence on age, profession and physical training from investigation of reactions to repeated centrifugal accelerations

20 p3479 A69-38228

Human acceleration tolerance under reduced pressures corresponding to various high altitudes noting visual disorders

20 p3480 A69-38230

Bicycle ergometer combined with induction clutch, investigating effect of eccentric dynamic work with arms and legs

21 p3663 A69-38902

Noise influence on heart rate and oxygen consumption of young male subjects under simultaneous physical stress

21 p3654 A69-38908

Human susceptibility to motion sickness under Coriolis acceleration during parabolic flight weightlessness

21 p3659 A69-39168

Strenuous physical training effects on human tolerance for work in heat, measuring rectal and mean skin temperatures and heart rates

22 p3890 A69-40199

Unilateral hypoventilation effect during bronchspirometry on human pulmonary blood flow

22 p3875 A69-40229

Heart rate responses and corresponding tolerance tests in trained athletes and nonathletes during simulated environmental extremes

23 p4102 A69-41683

High intensity and short duration acceleration effects on human beings, discussing mechanical resistance of spinal column and circulatory aspects

24 p4266 A69-43380

Heat tolerance in case of SST aircraft air conditioning failure, discussing physiological and psychomotor reactions and time curves for metabolic activity levels

24 p4277 A69-43382

Physical and physiological factors involved in determining aircraft passengers time of safe unconsciousness permissible after cabin decompression

24 p4278 A69-43398

Acoustic analyzer response of man during prolonged noise effect of varying pitch and intensity

24 p4278 A69-43408

HUMAN WASTES

NT FECES

NT SWEAT

NT URINE

Mineralized human wastes solutions utilization for Chlorella cultivation, noting growth rates

02 p0200 A69-11511

Physicochemical method for converting human urine and feces into carbohydrates in closed ecological systems

03 p0381 A69-14199

Biowaste propelled restojet control systems selection criteria based on NASA Manned Orbital Research Laboratory with six man crew

04 p0554 A69-15506

Physicochemical synthesis of monosaccharides from human waste products at atmospheric and elevated pressures, considering methane oxidation by nitrogen oxides and ozone

07 p1071 A69-18971

Reactors technical characteristics for high temperature mineralization of closed life systems biological wastes, deriving equations to estimate energy balance

10 p1649 A69-23504

Monosaccharide production from carbon dioxide from respiration or human waste incineration, evaluating toxicological effects of synthetic monosaccharides

15 p2557 A69-31471

Physicochemical synthesis of monosaccharides from human waste products at atmospheric and elevated pressures, considering methane oxidation by nitrogen oxides and ozone

20 p3483 A69-38219

Material recovery from metabolic and other wastes for long duration manned space missions, discussing carbon dioxide removal, bioregenerative food systems, etc

24 p4272 A69-42876

Urinary excretion of hormonal metabolites in intercontinentally flown test subjects, using gas chromatographic procedure for steroid identification

24 p4268 A69-43404

HUMIDITY

Meteorological PTU /pressure, temperature, humidity/ probe for lower atmospheric layers, discussing detectors and assembly qualities

04 p0601 A69-15229

Heat and humidity endurance limits in man

10 p1645 A69-23494

Wet steam injector power losses in nozzle as function of humidity, noting compensation of nozzle throat diameter and fluid flow rates

13 p2246 A69-27490

Water-air interface models unreliability in calculating atmospheric heat and humidity turbulent flow over ocean

14 p2443 A69-29839

Energy dissipation of solder-covered and solderless solar cells with TiAg contacts as function of storage time, temperature and humidity

19 p3253 A69-35706

Analog computer used to correct body plethysmographic chamber signal distortion due to inspired/expired air temperature and humidity differences

23 p4111 A69-42081

F-5 cockpit fogging during low flights and dive bombing in South Vietnam attributed to hot humid weather, recommending cockpit temperature control and pilot diet

24 p4277 A69-43376

HUMIDITY MEASUREMENT

HUMIDITY MEASUREMENT

Northern California humidity to 32 km utilizing alpha radiation hygrometer and associated balloon sounding equipment

03 p0461 A69-13345

Aspiration psychrometric probe for measurements of relative humidity of gas-vapor phase of gas flow containing liquid droplets

06 p0927 A69-17689

Solar radiation absorption measurements by balloon for atmospheric water vapor distribution

09 p1536 A69-21864

Dew /or frost/ point determination method for low temperature humidity measurement

09 p1502 A69-22691

Mean absolute relative humidity variations above earth surface over various time intervals during cloudless nights, obtaining spatial humidity differences and corresponding extinction coefficients

24 p4346 A69-43158

HUMMINGBIRD AIRCRAFT

U XV-4 AIRCRAFT

HUNTER F-2 AIRCRAFT

U F-2 AIRCRAFT

HURRICANES

Apollo 7 and weather satellite observation photographs of hurricane Gladys and typhoon Gloria

10 p1722 A69-22944

Fully developed whirls steady state structure, discussing tornadoes maximum azimuthal speed, hurricanes rotational speed, model for mature hurricane and numerical computation

[AIAA PAPER 69-671]

17 p2997 A69-33499

HUYGENS PRINCIPLE

Mathematical model of fields reradiated by Huygen sources in front of array for glide path site analysis

17 p3003 A69-34107

HYBRID COMPUTERS

Hybrid computers, discussing analog and digital devices combination and distinction between use of computer for general purpose computation and control purposes

02 p0212 A69-11997

Heat transfer in pyrolytic graphite analyzed by hybrid computer simulation

02 p0353 A69-12387

Functional optimization techniques for serial hybrid computer solution of partial differential equations, emphasizing algorithms handled on digital computer

04 p0566 A69-15344

Hybrid assumed mode solution of nonlinear partial differential equations /initial value problems/ in time-like independent variable

04 p0566 A69-15345

Hybrid computer algorithm for numerical integration of partial differential equations, using assumed sum separation of variables

04 p0566 A69-15346

Hybrid computational method for partial differential equations to reduce time of solution and error propagation

04 p0566 A69-15347

Iterative solution of continuous-time-discrete- space /CTDS/ equations as approach to hybrid computation of certain partial differential equations

04 p0567 A69-15348

Lockheed hybrid computer system, describing features implemented by modifying and augmenting digital batch processing system

04 p0567 A69-15349

Design and implementation of executive system for hybrid simulation, discussing requirements placed upon digital computer and operating software

04 p0567 A69-15350

Hybrid executive development based on digitally oriented software, explaining assembly language routing

04 p0567 A69-15351

Boeing/Vertol Hybrid Facility for solving engineering problems in V/STOL design and research

04 p0567 A69-15352

NASA-Ames hybrid simulation software systems, subsystems and implementation

04 p0567 A69-15353

Automatic preventive maintenance program for hybrid computer system by checking individual units

04 p0568 A69-15359

Diagnostic techniques development to test and perform preventive maintenance on hybrid system

04 p0568 A69-15360

Learning model of brain stem reticular formation based on nonlinear probabilistic hybrid computer concepts

05 p0711 A69-15802

Digital computer interface systems design for simulation, control, instrumentation and data processing, discussing hybrid computer linkages

05 p0723 A69-16195

Error analysis methods for inherent errors in analog, digital and linkage equipment of typical hybrid computer configuration

05 p0725 A69-16472

Medium scale integration for packaging hybrid electronic monolithic systems

05 p0735 A69-16752

Analog-hybrid computer configurations for average and rms values of signals with respect to time

06 p0891 A69-17220

Hybrid simulation of transport lag with variable time delay, noting dynamic range limitations due to digital computer processing and memory capacity

10 p1661 A69-23852

Asymptotic sampling error in closed loop hybrid systems, noting dependence on sampling period and execution time

12 p2053 A69-26508

Hybrid computer system for real time optimum feedback controller using iterative algorithms with rapid convergence, discussing simulation and performance

15 p2582 A69-30071

Automatic hybrid apparatus for solving linear equations, using Gauss-Seidel iterative method and stressing control arrangement, communication circuits, etc

15 p2572 A69-31089

Automated patching system design for analog and hybrid computers to reduce number of switches required

16 p2756 A69-32551

Onboard hybrid computer for helicopter fire control system, generating turret pointing angles and corrections

17 p2934 A69-34074

Automated analog scaling for in hybrid computer systems imposing magnitude and frequency constraints, using equations for amplifier input factors

18 p3105 A69-34617

Stability contours for sampling and delay effects analysis in analog/digital hybrid simulation loops, considering compensation quality over simulated system natural modes

21 p3680 A69-39609

Simulation of passively stabilized satellites using in-line hybrid computer

[AIAA PAPER 68-853]

21 p3680 A69-39758

Multispacecraft simultaneous simulation on hybrid computer using Encke perturbation method for translational motion and Hamilton quaternion method for inertial transformations

[AIAA PAPER 69-937]

22 p4036 A69-40320

Analog and digital computer elements combined in hybrid technique for aeronautic simulation

23 p4146 A69-41603

HYBRID PROPELLANT ROCKET ENGINES

Regression rate model for pressure sensitive hybrid combustion based on classical turbulent flame theory

[WSCI PAPER 68-22]

07 p1240 A69-18362

Rocket engine high energy hybrid propellant performance optimization, discussing engine enlargement, oxidizer injection geometry, fuel additives, combustion gas vorticity, etc

11 p1943 A69-25428

Hybrid chemical rocket theory and design noting radiation effects, regression and convective heat transfer

11 p1944 A69-25589

Hybrid motor in sounding rocket using amino plastic as fuel and nitric acid as oxidizer, discussing advantages in cost, handling, thrust, performance, etc

16 p2835 A69-31744

Hybrid rockets combustion mechanism, discussing turbulent boundary layer with heat and mass transfer, chemical reactions, etc

16 p2879 A69-32002

Regression rate of solid fuel in hybrid combustion determined as eigenvalue by Rayleigh flow model with evaporating boundary

16 p2879 A69-32013

Thrust magnitude and direction modulation of hybrid propellant engine, noting applications

17 p3019 A69-33337

Flame propagation mechanism on plastic fuel in oxygen-nitrogen atmospheres with variable pressures and at different initial fuel temperatures, discussing safety and ignition problems

17 p3074 A69-33662

Liquid, solid, hybrid propellant and nuclear, electric and air breathing rocket engines, discussing orbiting payload cost, controllability, operating environments, velocity, etc

19 p3395 A69-36321

High energy oxygen-free hybrid propulsion system using polyethylene propellant and F oxygen mixture as oxidizer

[DGLR-69-017]

23 p4202 A69-41930

Concentric or eccentric rotation effect on burning rate and geometry of small hybrid rocket motors using hydrogen peroxide-organic fuel

23 p4203 A69-41932

HYBRID PROPELLANTS

Deflagration of solid and hybrid propellants in steady state for missile and rocket propulsion applications

06 p0982 A69-17422

Hypergolic filling materials for solid fuels with hybrid propellant combinations, discussing ignition and combustion of ethylenimine derivatives

10 p1753 A69-24023

Polymethyl methacrylate burning rates in mixture with ammonium perchlorate or in hybrid systems when mixed with ammonium chloride

13 p2324 A69-28503

Low thrust reaction control for space missions, summarizing range and specific impulse characteristics for solid and hybrid systems

[AIAA PAPER 69-433]

16 p2834 A69-32745

Thermodynamics of propellant combination of Li hydride containing solid fuel with ethylenimine base, coupled with Cl trifluoride oxidizer and ammonium nitrate added

22 p3997 A69-39919

Combustion considerations in fuel rich solid and hybrid propellant systems in air breathing propulsion for comparison with metal ignition requirements

23 p4199 A69-41894

HYBRID PROPULSION

Hybrid chemical rocket theory and design noting radiation effects, regression and convective heat transfer

11 p1944 A69-25589

Hybrid propulsion chemical and technical problems, discussing solid fuel fragmentation and defining typical combustion modes

17 p3021 A69-33358

High energy oxygen-free hybrid propulsion system using polyethylene propellant and F oxygen mixture as oxidizer

[DGLR-69-017]

23 p4202 A69-41930

HYBRID ROCKET ENGINES

Burning rate of solid grains of hybrid rocket engine, using calculated diagrams for quick computations of engine

08 p1376 A69-20590

Boron combustion for air augmented rocket applications, discussing single boron particle ignition and combustion characteristics

16 p2828 A69-31737

HYDRATES

Gaseous hydrates formation in comet nuclei, discussing stability at given temperatures and pressures and solar radiation shielding by dust sheath

03 p0515 A69-14032

HYDRAULIC ACTUATORS

U ACTUATORS

HYDRAULIC ANALOGIES

Hydraulic analogy for shock and expansion waves arising in supersonic compressors due to three dimensionality of flow

[ONERA-TP-598]

02 p0187 A69-11621

Supersonic compressors for supersonic and subsonic air intakes, studying wave configuration at entry of circular cascade of blades with hydraulic analogy

[ONERA-TP-669]

05 p0699 A69-16340

Hydraulic analog for determining acoustic behavior of baffle cell used in liquid rocket engines, comparing ring and spoke type baffles

09 p1570 A69-22004

Fluidics /no moving part fluidics/, discussing diodes, capacitors, logic elements, temperature sensors, systems design, environmental factors, etc

17 p2904 A69-34067

HYDRAULIC CONTROL

Fluid mechanics of one stage momentum fluidic diode

02 p0195 A69-12071

Fluidic system controlling inlet guide vanes to high pressure compressor of two spool jet engine, using digital elements to drive hydraulic servosystem

02 p0305 A69-12090

- Fluidic numerical controls of linear or rotating motors, discussing pneumatic, hydraulic, hybrid logic components and amplifiers
04 p0550 A69-15082
- Electrohydraulic guidance of second stage of Diamant rocket used for orbiting satellites employing thrust vector orientation
04 p0551 A69-15183
- Electrohydraulic radar antenna telecontrol system, discussing pump assembly, hydraulic motor and pump control servojack
04 p0551 A69-15185
- Synthesis of simulated aircraft cabin pure fluidic temperature control system
[ASME PAPER 68-WA/FE-30]
05 p0705 A69-16103
- Electrohydraulic attitude servomechanism for controlling movements of pilot training cabin, describing hydraulic system and electric control circuit
06 p0906 A69-16966
- Hydraulic control valves for guidance of rockets by secondary liquid injection into nozzle skirt, discussing structure, single nozzle missile and mass gain
07 p1230 A69-19293
- Aircraft electrohydraulic primary control systems including electrical signal transmission, engine failure detection, signal structure and digital systems
08 p1347 A69-20872
- Collection of articles on fluid control components and systems design
08 p1256 A69-20948
- Fluidics in UK, discussing digital control elements and systems and transmission lines in alternating flow hydraulics
[AGARDOGRAPH-118]
08 p1257 A69-20952
- Peripheral fluidic devices for sequencing and monitoring machinery in hazardous areas, describing circuits
[AGARDOGRAPH-118]
08 p1257 A69-20954
- Fluidic control systems for angular rate and attitude stabilization flight-tested, noting good impact and acceleration resistance
[AGARDOGRAPH-118]
08 p1257 A69-20955
- Air powered fluid jet engine compressor bleed control stressing closing, reset and override operations
[ASME PAPER 69-GT-19]
09 p1571 A69-22498
- Vortex fluid devices in control systems, considering electrical, mechanical and hydraulic systems
09 p1443 A69-22740
- Active broadband vibration isolation of human subjects from severe vertical dynamic excitations experienced in low level high speed flight
[ASME PAPER 69-VIBR-65]
10 p1650 A69-24157
- Electrohydraulic vibration isolation systems with feedback, considering band and notch isolation, system stability and adjustable frequency response
[ASME PAPER 69-VIBR-40]
10 p1641 A69-24178
- Modular hydraulic power source systems for general aviation aircraft, discussing design selection, phase in and customer acceptance problems
[SAE PAPER 690329]
11 p1825 A69-24505
- Optimal parameters of hydraulic sensor of angular accelerations for given dynamic and geometrical requirements
13 p2259 A69-27432
- Fluidic control systems for industrial applications, discussing fluidic solutions to process problems
15 p2553 A69-31297
- Self contained remote sense remote control pressure regulator using pure fluid amplifiers, controlling large or small flow over wide pressure range
15 p2554 A69-31303
- Fluid controlled solid rocket motors design for Mars mission with acceleration level as parameter, discussing mission specifications, system design and component considerations
[AIAA PAPER 69-446]
16 p2841 A69-32687
- Fluidic thrust reversal control system for turbojet achieving cost and weight reduction, illustrating fluidic circuit and noting circuit reliability
17 p3018 A69-33329
- Brake system components automatic testing for pneumatic or hydraulic integrity essential to safe system performance
17 p2978 A69-33377
- Fluidic attitude control systems performance prediction from conventional control analysis emphasizing steady state positioning accuracy
17 p2904 A69-34069
- Pressure drop in control element of gas generator during readjustment of throttle in hydraulic supply line, noting assumptions
19 p3393 A69-35819
- Static and dynamic characteristics of pressure compensated oil-hydraulic flow control valves and relief valves with emphasis on linearized effects
19 p3256 A69-36713
- Fluid amplifiers for gas turbojet engines control, discussing hydraulic control and relationship between turbine rpm, fuel consumption and operating temperature
20 p3585 A69-36944
- Electrohydraulic servomechanism harmonic response showing nonlinear behavior, including jump resonance, analyzed by mathematical model and analog simulation
20 p3464 A69-36999
- Electrohydraulic servosystem to counteract atmospheric turbulence effects on B-52 global bombers, noting reduction in aircraft fatigue and structural damage
20 p3467 A69-38184
- Fluidic amplifiers development and logic applications, describing various elements and circuits
22 p3870 A69-41239
- Fluidic proportional level control and density control systems, discussing advantages of low initial and maintenance cost, long life and temperature, shock, radiation resistance, etc
22 p3870 A69-41241
- Miniature hydraulic controls with emphasis on four-way directional control valve for space and cost problems
22 p3870 A69-41243
- Fluidic servoactuator controlled by hydraulic vortex valves using mechanical signals for helicopter stability augmentation system
24 p4255 A69-42800
- Stability criteria for electrical interconnection in parallel operating valve controlled hydraulic servomotors applied to gimbaled system
24 p4256 A69-43310
- HYDRAULIC EQUIPMENT**
NT AIRCRAFT HYDRAULIC SYSTEMS
Ultrasonic quality control test methods for melt through welds in hydraulic line assemblies, noting equipment and surface roughness requirements
02 p0252 A69-11810
- Large hydraulic press forgings for light metals, discussing 50,000 ton machine used for Al alloys, tooling and die considerations
[ASM PAPER C7-5.1]
04 p0604 A69-14521
- Hydraulic press large closed die forging of various alloys and refractory materials, evaluating mechanical and metallurgical problems
[ASM PAPER C7-5.4]
04 p0604 A69-14522
- Fluid stability, viscosity, compressibility, gas solubility and lubricating properties determination for high temperature hydraulic systems
04 p0550 A69-14662
- Filtration and flow characteristics of wire cloths used in hydraulic systems described by expressions from measured properties
[ASME PAPER 68-WA/FE-39]
05 p0750 A69-16111
- Hydrostatic bearings, hydraulic drive system and hydraulic braking system for radio telescope with 2550 tons moving weight
[ASME PAPER 68-WA/PEM-2]
05 p0743 A69-16147
- Flow control valve for hydraulic motor speed regulation operated by remote pressure signal
11 p1827 A69-25646
- Hydraulic servo actuators load effect included in control loop actuator simulation
12 p2016 A69-26266
- Working fluids elastic characteristics variability effect on hydraulic actuator dynamics, studying adiabatic and isothermal conditions
14 p2405 A69-29423
- Hydraulic regenerative servoamplifier system for electrohydraulic actuator design, discussing specifications and test results
15 p2553 A69-31294
- Pressure in sealing groove and increase time due to pumping action of moving wall applied to force cylinder of translational motion, considering liquid in groove laminar
16 p2736 A69-32135
- Oscillation amplitude of rotor with hydraulic dampers on elastic supports by expanding forced vibration modes with friction in natural modes
16 p2837 A69-32136
- Turbopump weight minimization and low suction pressure requirements realized using high rotating speeds, hydraulic turbine driven upstream inducer and computer testing
[AIAA PAPER 69-552]
16 p2741 A69-32747
- Lubrication properties of mineral oils for power hydraulics using Stanhope-Shell four ball test machine
17 p2991 A69-32948
- Soviet book on hydraulic servo drive covering design and performance, static and dynamic characteristics and stability problems
18 p3093 A69-34356
- Transient performance of full flow hydraulic turbine driven two speed pump inducer system, formulating computer model
[AIAA PAPER 69-551]
18 p3140 A69-34415
- Discharge coefficient and opening time of pneumatic and hydraulic systems incorporating disks, nozzles and valves
18 p3094 A69-34981
- Forced pressure fluctuations in hydraulic systems of aircraft fuselages and engines, taking into account square law of losses at resistance points
18 p3094 A69-34991
- System engineering to select hydraulics subsystem for advanced fighter aircraft by cost effectiveness analysis, noting maintainability and reliability
19 p3254 A69-36012
- Hydraulic systems incipient failure detection, discussing destructive cavitation, component defects, human error, etc
19 p3255 A69-36018
- Hydraulic-powered self propelled six degree of freedom loading vehicle moving tests assembly to test chamber with high accuracy positioning
20 p3511 A69-38181
- Rotary actuator to create realistic control effects in hydraulic loading system of jet flight-training simulators
20 p3511 A69-38182
- Motion stability of hydraulic actuators with open loop control system in presence of nonlinear negative resistance damping
21 p3650 A69-39716
- Noise reduction research for hydraulic machines, examining piston pumps noise generating mechanism
22 p3870 A69-41238
- HYDRAULIC FLUIDS**
Hydraulic fluid cleanliness measured using microscopy, automatic particle counters and gravimetrics, discussing silting index and evaluator used by aerospace industry
19 p3256 A69-36715
- Soviet book on fluid contamination influence on aircraft hydraulic systems operational reliability covering friction, particle size, filtration, etc
21 p3649 A69-39530
- HYDRAULIC HEATING SOURCES**
U HEAT SOURCES
HYDRAULIC JETS
Water jet propulsion for air cushion vehicles, emphasizing inlet shape effect on performance and potential flow theory application to inlet design
08 p1254 A69-20115
- Mean drop size generated in vapor pressure regime of liquid water jet, noting effect of water temperature and orifice diameter
09 p1483 A69-21995
- Noncavitating and cavitating performance of low area ratio water jet pumps, analyzing efficiency, area ratio, throat length, nozzle spacing and diffuser geometry
18 p3095 A69-35176
- Water jets with greater than half sound speed created by shock wave impinging on cavity within liquid, discussing mechanism, maximum speed, shape, etc
19 p3301 A69-36815
- Forced and periodic motion of air or water jets impinging in double input vortex chamber described in terms of oscillator deriving energy from hydrodynamic instability
[ASME PAPER 69-FLCS-19]
20 p3465 A69-37981
- HYDRAULIC PUMPS**
U PUMPS
HYDRAULIC SHOCK
MHD channel mercury flow with hydraulic shock in transverse magnetic field, determining characteristic values distribution over range of principal parameters
13 p2307 A69-27499
- Liquid driver shock tubes dynamic and thermodynamic properties as functions of diaphragm pressure ratio and initial conditions
19 p3295 A69-36471
- HYDRAULIC TEST TUNNELS**
Hydraulic tank for visualizing flows around stationary models, noting absence of wall effects
[ONERA-TP-708]
17 p2956 A69-33588

HYDRAULIC VALVES

U VALVES

HYDRAULICS

Mechanical construction device for Carafoli profile in aerodynamics and hydraulics, establishing mechanism for tracing rounded and sharp trailing edges profiles

15 p2549 A69-31264

HYDRAZINE ENGINES

Fast heat-up electrothermal ammonia thruster role in development of hybrid resistojets in millipound thrust range

[AIAA PAPER 69-496] 16 p2838 A69-32649

Rocket motors using hydrazine as monopropellant, considering doping as means of using anhydrous hydrazine mixed with other products

17 p3019 A69-33340

Titian 3 transtage attitude control system hydrazine rocket engine design and performance, emphasizing problems associated with monopropellant

[AIAA PAPER 69-422] 19 p3394 A69-36300

Catalyst poisoning and hydrazine material compatibility during hydrazine propulsion systems sterilization and decontamination

21 p3786 A69-39768

Communication satellite systems using hydrazine engine thrust for trajectory correction, discussing trajectory deviations causes and ERNO engine design

[DGLR-69-013] 23 p4203 A69-42152

HYDRAZINES

NT CHLORPROMAZINE

NT METHYLHYDRAZINE

NT TETRAFLUROHYDRAZINE

Absorption coefficient of hydrazine and hydrogen peroxide determined with 2.5 angstrom bandwidth monochromator, giving results in graphical form

02 p0205 A69-11873

Hydrazine decomposition in glow discharge, analyzing emission spectra and threshold level of decomposition by gas chromatography

04 p0646 A69-14860

Liquid hydrazine ignition by nitrogen tetroxide gas based on stagnation flow principle, presenting threshold measurements

[WSCI PAPER 68-43] 06 p0983 A69-17792

Medical examinations of missile fuel handlers, noting some abnormal results in liver function tests and possible hydrazine toxicity

09 p1447 A69-22556

Vibration and absorption bands in IR spectra of diborene hydrazine stabilized by boiling in benzene

12 p2027 A69-26917

Reaction kinetics between hydrazine and esters in benzene solution at 55 C, using amides as catalytic agents

14 p2409 A69-29033

Isothiocyanates and phenyl isocyanate reaction with hydrazinoethanol and hydrazinoethyl hydrogen sulfate

16 p2747 A69-31808

Nonequilibrium initial condition combustion effects on propellant performance for hydrazine/chlorine pentafluoride and hydrogen/fluorine with equilibrium, kinetic and frozen nozzle flow

[AIAA PAPER 69-469] 16 p2832 A69-32659

Turbulent heat and mass diffusion in catalytic reactors for hydrazine decomposition, developing computer program to calculate temperature and reactant concentration distributions

[AIAA PAPER 69-421] 16 p2846 A69-32768

Aqueous hydrazine solution effect on Ti disulfide crystalline structure

23 p4112 A69-41426

Pressure effects in spontaneous ignition of interimpinging hydrazine and red fuming nitric acid (RFNA)/liquid streams in evacuated test chamber

24 p4415 A69-43667

Intermediate hydrazine-RFNA reaction product formed on injector nozzle and combustion chamber surfaces after fuel injection without ignition analyzed by various methods

24 p4365 A69-43669

HYDRIDES

NT BERYLLIUM HYDRIDES

NT BORANES

NT CARBORANES

NT CHLOROSILANES

NT DIBORANE

NT LITHIUM ALUMINUM HYDRIDES

NT LITHIUM HYDRIDES

NT METAL HYDRIDES

NT PHOSPHINES

NT SILANES

NT ZIRCONIUM HYDRIDES

Low temperature technique for preparing solid-solid diffusion sources for silicon device fabrication based on gaseous hydrides as reagents

07 p1198 A69-18619

Niobium hydride and tantalum hydride formation using metal powders, noting solid phases during dehydriding

09 p1448 A69-21599

Electrical resistivity decrease in niobium-hydrogen alloys during isothermal aging at low temperature attributed to hydride precipitation, noting reaction rate and activation energy

14 p2463 A69-29288

HYDROAEROMECHANICS

U. AERODYNAMICS

HYDROBAROPHONES

U. HYDROPHONES

HYDROBROMIC ACID

Thermal dissociation rate of HBr in Ar in 2100-4200 K temperature range by shock tube analysis, using IR emission and UV absorption

20 p3484 A69-37347

HYDROCARBON COMBUSTION

Sulfur organic compound formation effect on composition and structure of solid phase formed during hydrocarbon jet fuels oxidation

01 p0142 A69-11097

Olefins combustion studies, considering influence on hexane combustion at different oxidation stages leading to ignition

02 p0352 A69-12309

Temperature and pressure measurements in low temperature combustion of n pentane covering slow reaction and cool flame regions

02 p0353 A69-12321

Electrically controlled heat transfer between flat parallel flow hydrocarbon diffusion flame and walls of combustion chamber

02 p0353 A69-12324

Grey and very grey thermochemical tables for C-H and C-H-O species

[WSCI PAPER 68-38] 06 p0885 A69-17795

Ignition time of methane and acetylene, considering concentration and thermodynamic properties during reaction

[WSCI PAPER 68-41] 07 p1240 A69-18356

Flame front instability in air-propane mixtures established by motion picture study

08 p1421 A69-20344

UV, visible and near IR spectral characteristics of hydrocarbon-air flames with particulate Al, Mg and B, noting hot metal continuum and oxide emissions

11 p1940 A69-24483

Optical constants of soot applied to heat flux calculations, discussing soot particles concentration determination in hydrocarbon combustion products

[ASME PAPER 68-HT-13] 13 p2374 A69-27777

Transverse wave spacings for self sustaining detonations in oxygen and diluents mixtures with hydrogen, methane, acetylene or ethylene fuel, noting dilution

13 p2378 A69-28217

Steel cylinder wall materials effects on flame propagation at constant volume of propane-air mixtures

13 p2379 A69-28363

Burning velocity inhibitors effects on hydrocarbon-oxygen-nitrogen mixtures ignition temperature, reporting data on 20 additives at ambient temperature and pressure

[WSCI PAPER 69-14] 16 p2831 A69-32352

Kinetics of combustion promotion of hydrogen-hydrocarbon mixtures by active particles, free atoms and free radicals using differential equations

17 p3069 A69-33139

LF oscillations in simple combustion chamber using gaseous propane fuel, discussing association with progressive flame necking

18 p2320 A69-34837

Mono and bicyclic hydrocarbons effect on jet fuels combustion properties, considering burnup factor, deposit and smoke production levels

18 p3184 A69-35382

Perfluorocyclobutane-oxygen mixture combustion, measuring burning velocities and adiabatic equilibrium flame temperatures

21 p3852 A69-39594

Interferometric study of cool flame propagation in equimolar propane-oxygen mixtures, observing refractive index and temperature distribution changes

21 p3852 A69-39595

Laminar burning rate of premixed propane-air flames at one atmospheric pressure in DC electric fields, using cooled porous plug burned method

21 p3852 A69-39596

Major ions in chemi-ionization of hydrocarbon flames determined for heats of formation by photoionization mass spectrometer

22 p3896 A69-40727

HYDROCARBON FUELS

NT JET ENGINE FUELS

NT JP-4 JET FUEL

Hydrocarbon-air fuel cell producing electric power automatically for five days

01 p0013 A69-10965

Deposit formation in empty wing tanks due to autoxidative degradation of hydrocarbon fuel, noting results of environment simulation tests

[SAE PAPER 680733] 03 p0366 A69-13439

Electrochemical oxidation of n-octane based fuels containing aromatic, olefinic and naphthenic components

[ACS PAPER 93] 05 p0716 A69-16234

Long term electrochemical oxidation performance of n-octane based fuels containing aromatic, olefinic and naphthenic components

[ACS PAPER 94] 05 p0716 A69-16235

Combustion mixture composition dependence on electrical conductivity of products with potassium additive, discussing hydrocarbon fuels

06 p0870 A69-17908

Chemical kinetic model for hydrocarbon fuels combustion and application to multidimensional finite difference mixing analyses in hypersonic engines and nozzles

[AIAA PAPER 69-86] 06 p1037 A69-18119

Reaction kinetics package for pyrolysis and combustion of aliphatic hydrocarbon molecule, considering reaction rates definition

[WSCI PAPER 68-37] 07 p1073 A69-18353

Gas dynamics, thermodynamics, chemical properties, energy and products of hydrocarbon-air detonations in tubes under standard atmospheric conditions

[WSCI PAPER 68-26] 07 p1241 A69-18369

Flame burnout of atomized hydrocarbon fuel in gas turbine combustion chambers as function of ratio of time to total burnout time

08 p1420 A69-19999

Thin film metallic oxide catalysts for oxidation in low temperature cells using hydrogen and hydrocarbons and for oxygen reduction in acid electrolyte

16 p2738 A69-32408

Space storable regenerative cooling with FLOX/methane under conditions for small pump fed engine, describing injector and chamber design

[AIAA PAPER 69-509] 16 p2844 A69-32718

Packed bed catalytic reactors cooling capacity in promoting endothermic reactions of hydrocarbon fuels, using computerized temperature and composition profiles

[AIAA PAPER 69-588] 17 p3071 A69-33265

Benzene antidetonation properties improved by separating n-alkanes with synthetic zeolite

23 p4199 A69-42479

HYDROCARBONS

NT ACETYLENE

NT ALKANES

NT ALKENES

NT BENZENE

NT BUTADIENE

NT BUTANES

NT CHLOROBENZENES

NT CYCLIC HYDROCARBONS

NT ETHANE

NT ETHYLENE

NT MESITYLENE

NT METHANE

NT NAPHTHALENE

NT PARAFFINS

NT PENTANES

NT PROPANE

NT PROPYLENE

Hydrocarbon formation mechanisms under conditions resulting from graphite filament explosions in hydrogen atmospheres, emphasizing stepwise radical formation and methane role

01 p0120 A69-10675

Gas chromatographic determination of hydrocarbon quantity in methane in parts per billion range

03 p0382 A69-14115

Flame inhibition with electron attachment observed using halogenated hydrocarbons

06 p1034 A69-17926

Ignition of binary mixtures of hydrocarbons at high and minimum ignition temperatures of components

06 p1035 A69-17935

Adsorption kinetics of hydrocarbon oxidation on platinum electrode

08 p1268 A69-21052

Molecular ion C13H line found in zeta Oph at 4232.08 Å, measuring equivalent width and finding C12/C13 ratio
09 p1603 A69-22266

Test of Velikovsky theory for dense hydrocarbon clouds and dusts surrounding Venus, using IR reflection spectra
09 p1608 A69-22566

Temperature effects on phosphorescence lifetimes and intensities of aromatic hydrocarbons in polymethyl methacrylate, estimating activation energy for thermally activated nonradiative decay mode
10 p1652 A69-23523

Interstellar molecular hydrogen and CH photodissociation, discussing molecular formation rates in interstellar medium
10 p1781 A69-23672

Viscosity-temperature chart for hydrocarbons permitting linear extrapolations into low viscosity high temperature regions
10 p1753 A69-23975

Additions of dialkyl and diaryldithiophosphates of Ba, Ca, Zn, Pb and Ni as antioxidants and corrosion inhibitors for hydrocarbons
12 p2027 A69-27091

Electrochemical oxidation of hydrocarbons on platinum electrode, discussing adsorption kinetics
16 p2740 A69-32423

Gas phase arrest peak analogy with liquid phase oxygen cut-off during final stages of hydrocarbons gaseous oxidation reactions, noting active centers
21 p3669 A69-38805

High temperature equilibria from hydrocarbon plasma sources subjected to 3000 W RF electrodeless discharge
21 p3670 A69-39738

Aromatic and nonaromatic hydrocarbon fractions in terrestrial graphite, discussing classification and analysis by chromatography and mass spectrometry
22 p3934 A69-39890

Absorption coefficient measurement for hydrocarbon gases for He-Ne laser beam at 3.39 microns, tabulating coefficients, noting variations from spectroscopic data
23 p4174 A69-42192

HYDROCHLORIC ACID

Laser with molecular H and Cl mixture at HCl vibrational transitions
14 p2461 A69-29672

Passive Q switching of chemical laser operating on vibrational-rotational line of vibrational transition of HCl
16 p2796 A69-31840

HYDROCYANIC ACID

U HYDROGEN CYANIDES

HYDRODYNAMIC EQUATIONS

NT HELMHOLTZ VORTICITY EQUATION

Hydrodynamic analysis for determining steady flow region with closed separation area for Reynolds numbers to describe viscous mixing by Prandtl equations
02 p0190 A69-12570

Hydrodynamic theory of light scattering by dilute monatomic gases generalized by using linearized Burnett equations instead of Navier-Stokes equations
03 p0466 A69-13135

Short term weather forecasts by means of hydrodynamic equations in adiabatic approximation, noting atmospheric motions and processes, adiabatic invariants and meteorological fields
03 p0459 A69-13332

Exact solutions with helical symmetry for hydromagnetic dynamo problem steady state equations
03 p0476 A69-13380

Hydrodynamic model of atmospheric circulation in equatorial region, using group invariant method
03 p0462 A69-13931

MHD generator two dimensional analysis for studying edge effect, taking into account Hall effect
03 p0480 A69-14099

Approximate hydrodynamic equations applied to analysis of heat transfer in real gas flow in tube, taking into account energy transfer by radiation
04 p0686 A69-14993

Source and sink method application to direct axisymmetric problems of hydrodynamics
05 p0747 A69-16039

Viscous hydrodynamical equations for flow field exterior to obstacle moving with constant velocity, discussing force relationships, drag invariance and integral representations
07 p1121 A69-19298

Flapper valves in high pressure hydraulic aircraft systems, with hydrodynamic equations and charts for design and performance characteristics
09 p1435 A69-21296

Normal solutions of linearized Boltzmann equation for initial and boundary conditions in hydrodynamics solved by approximation
09 p1480 A69-21667

Hydrodynamic equations and Grad transport coefficients for nonequilibrium rarefied monatomic gases developed for molecular collisions
09 p1481 A69-21888

Navier-Stokes boundary value problem bifurcation solution analysis, determining stability ranges
10 p1677 A69-22901

Existence of motions of second type in explicit self similar strong shock solutions of Euler equations when velocity is linear function of coordinate
10 p1680 A69-23789

Hydrodynamic equations and conservation laws for nonviscous fluid in postNewtonian approximation of Brans-Dicke theory applied to gaseous mass dynamic instability
10 p1789 A69-24130

Two dimensional convective flow stability for arbitrary Rayleigh numbers in horizontal layer, assuming large Prandtl number and free boundary conditions
11 p2003 A69-25657

Electrohydrodynamic equations and transfer coefficients for multicomponent plasma with volumetric charge in electric field, discussing Ohm law and equations for plasma motion
12 p2135 A69-26399

Relativistic hydrodynamic equations for charged particles interacting in external scalar and gravitational fields, considering particle motion and scalar plasma dispersion
12 p2130 A69-26462

Two beam electron flux instability in crossed magnetic and inhomogeneous electric fields using linearized hydrodynamic and Lagrangian formalism approximation
12 p2133 A69-26714

Integral equations for classical elasticity boundary value problems, stressing analogous Stokes flow hydrodynamic equations
14 p2535 A69-29361

Ocean and atmospheric interactions analyzed by using hydrodynamic equations for boundary layers
14 p2442 A69-29838

External wind shear influence on isolated cumulus cloud evolution based on hydrodynamic and thermodynamic equations numerical integration
15 p2648 A69-30644

Hydrodynamic approximation to interplanetary gas motion influenced by solar flare caused perturbations
17 p3035 A69-33627

Drift waves parametric excitation in resistive plasma derived from fluid equations, assuming plane geometry with periodic boundary conditions in magnetic field and azimuthal directions
18 p3179 A69-34440

Hydrodynamic equations of laminar plane flow of incompressible viscous fluid in rectangular region, calculating velocity field by equivalent network and integration
19 p3297 A69-35853

Numerical program for gas dynamics of hydrodynamic flow and radiation transport in diffusion and grey body approximations
19 p3450 A69-36356

Linear hydrodynamic equations describing inviscid fluid flow past thin elastic cylindrical shells in circle with motions described by shallow shell equations
21 p3834 A69-38719

Hydrodynamic equations for radial solar wind expansion linearized and specialized to treat co-rotating perturbations
22 p4003 A69-40302

Hydrodynamic equations derived from Boltzmann equation, obtaining molecular expressions for transport coefficients
23 p4151 A69-41513

Boundary value problem of hydrodynamic equations discontinuous solution stability under random perturbations, analyzing combustion and detonation models
23 p4239 A69-41961

Instability theory of baroclinic vortices in incompressible and inviscid fluid, investigating symmetric meridional motions time evolution by numerical integration of hydrodynamic equations
23 p4153 A69-42346

Energetics of planetary boundary layer /Prandtl layer/ from system of hydrodynamic equations,

discussing flux divergence term importance in free-windless convection transition region
24 p4309 A69-43148

HYDRODYNAMIC STABILITY

U FLOW STABILITY

HYDRODYNAMIC TUNNELS

U PLASMA JET WIND TUNNELS

HYDRODYNAMICS

NT ELASTOHYDRODYNAMICS

NT ELECTROHYDRODYNAMICS

NT MAGNETOHYDRODYNAMICS

Gas combustion hydrodynamic stability using feedback equation and theorems for variations in mass and momentum vector
01 p0173 A69-10087

Weather forecasting, discussing atmospheric models and computer operations for long range forecasting based on hydrodynamic theory and statistics
01 p0108 A69-10398

Immersion depth influence on hydrofoil for flow of arbitrary depth with bottom consisting of free surface or solid wall
01 p0007 A69-11132

Hydrodynamics-electrodynamics analogies for electromagnetic light
01 p0121 A69-11134

Book on theoretical hydrodynamics covering Bernoulli equation, tensor and vector methods, two dimensional fluid motion, complex variables and conformal mapping
02 p0230 A69-11812

Boundary conditions for irrotational hydrodynamic field around sphere moving along axis of cylindrical tube containing incompressible fluid calculated by least squares method
03 p0415 A69-13362

Small oscillations of viscous incompressible fluid in container with free surface under action of potential force field
04 p0587 A69-14620

Cavitation stream calculation methods for ideal incompressible fluid with free boundaries, noting cavitation generators and Riabouchinsky problems
04 p0589 A69-14994

Stability of high speed rotors with sliding bearings
04 p0607 A69-15163

Velocities, accelerations and drag forces on spheres falling along center line in viscous fluid, considering different Reynolds numbers and Stokes approximation range
05 p0788 A69-15725

NonNewtonian hydrodynamics equations for non-linearly viscous and viscoelastic media, analyzing dependence on rheological model
05 p0745 A69-15786

Fifty years of N. E. Zhukovskii Central Aerohydrodynamic Institute in U.S.S.R.
06 p1043 A69-17390

Two dimensional boundary value problem for symmetrical entry of wedge into incompressible nonviscous fluid using complex variable theory
08 p1305 A69-20995

Characteristics of dynamic mechanical systems including solid state and hydrodynamic analogs of ideal incompressible fluids, based on statistical theory of turbulence
10 p1678 A69-23209

Stroboscopic generator of trains of high brightness light flashes for hydrodynamic and gas dynamic research, noting electronic control and thyratron circuits
11 p1879 A69-24235

Blasius-Chaplygin formula for generalizing Kutta-Joukowski theorem concerning jet profiles, calculating resultant of hydrodynamic forces
11 p1867 A69-24355

Hydrodynamic effects in flame spreading, ignitability and steady burning of liquid fuels, using analogy of films floating on water
11 p1999 A69-24484

Dynamics of turbulent motion of incompressible viscous fluid particles, using Lagrangian functions
11 p1867 A69-24536

Hydrodynamic calculation of 1.42 solar mass white dwarf supernova, considering instability and collapse initiation by electron capture
12 p2156 A69-26210

Aerodynamic considerations of high speed hydrodynamics for underwater craft, noting rocket propulsion
13 p2245 A69-27418

LF spectral analysis of flowing water pressure pulsations behind single bulge on hydrodynamic channel smooth wall at low disturbance level
13 p2246 A69-27535

LF spectrum analysis of hydrodynamic flow near-wall pressure pulsations over rough surfaced wall
13 p2246 A69-27537

Hydrodynamics of large scale atmospheric circulation, analyzing interactions between different scales and between atmosphere and underlying surface
13 p2253 A69-27849

Electric arc structure in hydrogen magnetic annular discharge computed using nonequilibrium hydrodynamics to analyze supersonic and subsonic processes
13 p2312 A69-28221

Nonlinear equations for motion of rigid body with cavity partially filled with ideally incompressible liquid
14 p2432 A69-29626

Hydrodynamic theory of climate and atmospheric circulation, emphasizing numerical experiments role in studying large scale processes
14 p2476 A69-29819

Convective heat and mass transfer coupling in laminar hydrodynamic duct flow, obtaining values for bulk and wall temperatures, transfer coefficients and rates, etc
15 p2716 A69-30004

Leakage in mechanical face seals with hydrodynamic films, noting misaligned seal theories for pumping with cavities and two fluids
[ASLE FICFS PREPRINT 19]
15 p2621 A69-30497

Nova outburst dynamics investigation by time dependent hydrodynamics computer program including energy transport by radiation and convection
15 p2692 A69-30769

Hydrogen oxygen rocket engine two phase liquid hydrogen pump capability and hydrodynamic design, analyzing constant-quality flow, acoustic effects, compressible flow and cavitation
[AIAA PAPER 69-549]
16 p2845 A69-32759

Planetary zonal flows hydrodynamic instability characteristics analysis, using quasi-geostrophic numerical model to study earth atmospheric cyclone wave role
17 p2960 A69-33149

Elastic circular cylindrical panel behavior in fluid with acoustic shock wave, allowing for propagation waviness of elastic stresses
18 p3216 A69-34579

Hydrodynamic noise as pseudosound field resulting from pressure variations in turbulent fluid flow, using Lighthill acoustic analogy
18 p3123 A69-34921

Ionization effects in hydrodynamic model of radiation driven breakdown wave propagation, obtaining wave velocity and absorbed laser flux density relationship
18 p3174 A69-35286

Hydrodynamic stability of incompressible fluid boundary layer flow during blowing or suction through porous surface, determining Reynolds number lower bounds
18 p3124 A69-35381

Hydrodynamic vertical or horizontal impact of sphere immersed in ideal heavy liquid of finite depth, considering container floor effect, surface pressure distribution, etc
19 p3299 A69-36393

Book on continuum mechanics and hydrodynamics covering elasticity, plasticity, thermodynamics, solid and structural mechanics, aerodynamics and gas dynamics
19 p3441 A69-36771

Group properties of adiabatic motion equations of medium in relativistic hydrodynamics, including solutions of subgroups applicable to multiple particle production
19 p3301 A69-36843

Plasma flow structure near frontal point in earth magnetosphere, using quasi-hydrodynamic two dimensional model to obtain power series solution
20 p3594 A69-37019

Hydrodynamics of turbulent gas flow through powder layer for vapor phase coating of particles, noting fluidized bed
20 p3548 A69-37363

Plasma oscillations of electrons of atomic system, using simple hydrodynamic model
20 p3580 A69-37818

Computation method of hydrodynamic blade cascade for compressible fluid and variable channel width by stream function
20 p3460 A69-37972

LF spectral analysis of flowing water pressure pulsations behind single bulge on hydrodynamic channel smooth wall at low disturbance level
20 p3518 A69-38202

LF spectrum analysis of hydrodynamic flow near-wall pressure pulsations over rough surfaced wall
20 p3518 A69-38203

Schlieren framing photography used for studying shock wave hydrodynamic structure and ignition dynamics during expansion into detonable gas region
21 p3849 A69-38803

Hydraulic resistance of pipes with flow vorticity produced by helical swirlers
21 p3695 A69-38862

Soviet book on hydrodynamic cascade theory covering mathematical methods and numerical solutions for ideal fluid flow problems
21 p3696 A69-39527

Soviet book on earth atmosphere fluctuations covering propagation of acoustic, gravity and gyroscopic waves using linearized equations of hydrodynamics
21 p3717 A69-39528

Hydrodynamic turbulence in statistical prediction for Burger equation, considering statistical inference problem for initial conditions and prediction criterion with estimable error
21 p3697 A69-39673

Book on porous bodies hydrodynamics covering motion equations for free, filtration, perfect and Newtonian fluids
23 p4150 A69-41501

Numerical integration of double integral with Cauchy type singularity for calculation of aerodynamic or hydrodynamic load on lifting body
23 p4182 A69-41913

HYDROELASTICITY

Hydrofoil vehicle flutter investigations including simple foils and struts, geometrical parameters, finite span, cavitation, etc
09 p1614 A69-21898

HYDROFLUORIC ACID

Hydrogen fluoride corrosive effects in cryogenic propellant, emphasizing contamination by particulate matter from corrosion products
21 p3783 A69-39486

Reaction zone following overdriven detonation wave propagating into mixtures of fluorine oxide and hydrogen molecules showing HF laser emission
22 p4052 A69-41188

Hydrogen fluoride chemical laser emission spectrum, studying rotational-vibrational transition of molecules triggered optically or electrically
23 p4172 A69-41493

HYDROFOIL CRAFT

Hydrofoil vehicle flutter investigations including simple foils and struts, geometrical parameters, finite span, cavitation, etc
09 p1614 A69-21898

HRV-1 navy research pusher amphibian aircraft, discussing hydrofoils and operational problems
10 p1633 A69-23223

Hydrofoils fully submerged in seawater at up to 140 knots and constant Froude number, discussing foils lift/drag ratios as function of speed and submergence
11 p1871 A69-25122

HYDROFOIL OSCILLATIONS

Hydrofoil vehicle flutter investigations including simple foils and struts, geometrical parameters, finite span, cavitation, etc
09 p1614 A69-21898

HYDROFOILS

Immersion depth influence on hydrofoil for flow of arbitrary depth with bottom consisting of free surface or solid wall
01 p0007 A69-11132

Hydrofoils fully submerged in seawater at up to 140 knots and constant Froude number, discussing foils lift/drag ratios as function of speed and submergence
11 p1871 A69-25122

Supercavitating flow past thin hydrofoils, determining flow velocity or acceleration potential near free surface
22 p3933 A69-41023

HYDROFORMING

Hydroextrusion effect on Mo structure and mechanical properties, noting improved ductility after high temperature annealing
02 p0267 A69-12189

HYDROGEN

NT DEUTERIUM
NT DEUTERIUM PLASMA
NT LIQUID HYDROGEN
NT ORTHO HYDROGEN
NT PARA HYDROGEN
NT TRITIUM

High pressure hydrogen environment on tensile properties of stainless steel with and without strain induced martensite
01 p0093 A69-10062

Fine structure of vibrational spectra of molecular H and O, water and deuterium oxide, using molecular photoelectron spectrometer
01 p0023 A69-10141

Neutral hydrogen content in directions of pulsars related to distance estimates
01 p0149 A69-10271

Pressure and temperature dependence of slow crack growth in hardened steel in gaseous hydrogen environment
01 p0096 A69-10612

Hydrocarbon formation mechanisms under conditions resulting from graphite filament explosions in hydrogen atmospheres, emphasizing stepwise radical formation and methane role
01 p0120 A69-10675

Gas content and impurities in aluminum melts, analyzing oxides and hydrogen interactions
01 p0098 A69-10958

Multiple velocity dispersion in normal hydrogen and normal hydrogen-helium mixtures at room temperature using ultrasonic interferometer
01 p0121 A69-11284

Welding procedure for avoiding hydrogen cracking in high strength steels, stressing hydrogen escape from weld deposits
01 p0088 A69-11398

Multiphoton ionization of molecular hydrogen and rare gases using Q switched Nd laser apparatus
02 p0283 A69-11701

Explosion limits in hydrogen-oxygen reaction measured in diffusion regime, giving rate constant of branching step
02 p0353 A69-12319

Reactions kinetics contribution to nonequilibrium recombination occurring in supersonic nozzle flow of combustion products of hydrogen in air
02 p0353 A69-12488

Combustion and flame stabilization in axisymmetric laminar or turbulent H flows, noting combustion rates and flame breakdown conditions
02 p0355 A69-12673

Hydrogen spectral line broadening under combined action of ions and electrons, tabulating values for calculation of absorption coefficient
04 p0651 A69-14373

Methods of protecting industrial steel against hydrogen corrosion at high temperatures and pressures including cladding, carbon additions, surface film coating, etc
04 p0613 A69-14432

BCS theory application to metallic modification of hydrogen for obtaining high temperature superconductor
04 p0642 A69-14680

Submillimeter water vapor laser power output for admixtures of H, N, carbon dioxide, methane, He and Ar, noting buffer effect of H
04 p0612 A69-15175

Hydrogen effect on interatomic bonds of Ti beta alloy and Young modulus, noting measurements at various temperatures
04 p0618 A69-15178

Diminished RF intensity of neutral hydrogen line near radio source W 49 due to diminished kinetic temperature of gas
04 p0662 A69-15253

Hydrogen adaptation effect on fluorescence of normal and Mn deficient algae, noting system II photosynthesis
04 p0554 A69-15325

Hydrogen molecular action in vacuum UV region during high current discharge
05 p0771 A69-15814

Explosive combustion of hydrogen at high pressures, showing attainment of constant value of hydrogen peroxide
05 p0849 A69-16615

Dissociation of hydrogen on tantalum using modulated molecular beam mass spectrometry
06 p0960 A69-17107

Natural orbital expansion coefficients of LCAO-MO-SCF-CI wave functions for ground state of H molecule
06 p0960 A69-17112

Chemisorption of H onto Nb (110) surface, measuring low energy electron diffraction and inelastic electron scattering from clean and H-covered surfaces
06 p0980 A69-17758

Absorption oscillator strengths for rotational lines in Lyman transition vibrational bands of molecular

hydrogen from equivalent widths measured photoelectrically 06 p0962 A69-17818

Angular dependence of low energy electron impact excitation cross section of lowest molecular hydrogen triplet states 06 p0962 A69-17820

Pulsar distance estimates based on evaluation of galactic H absorption of 21 cm radiation 06 p1012 A69-18225

Solar supergranules and hydrogen convection zone analysis based on polytropic atmosphere convection physics 07 p1211 A69-18408

Hydrogen molecule spectroscopy in vicinity of ionization limit, determining absorption and ionization cross sections and fluorescence 07 p1184 A69-18490

Hydride, cold, irreversible and reversible hydrogen brittleness in titanium and titanium alloys 07 p1162 A69-18772

Hydrogen absorption coefficients, giving number densities in hydrogen gas or plasma for wide range of temperature and pressure 07 p1184 A69-19165

Early phase of Stromgren sphere development in interstellar molecular hydrogen cloud, analyzing R-type dissociation-ionization fronts using quasi-steady flow 07 p1218 A69-19281

Cooling requirements for high speed polytetrafluorethylene lubricated ball bearings operating in cold hydrogen gas, developing minimum gas flow rate equation [ASLE PAPER 68-LC-2] 07 p1141 A69-19310

Depolarized Rayleigh line widths measured for carbon dioxide, nitrogen and hydrogen, using measurements to calculate reorientation cross sections [IEEE PAPER B-11] 07 p1157 A69-19485

Hydrogen concentration above earth surface during minimum solar activity from ionospheric rocket and satellite measurements 07 p1129 A69-19612

High pressure storage vessels for gaseous hydrogen, discussing failure, manufacturing controls and access for internal nondestructive inspection [ASM PAPER D8-14.1] 07 p1143 A69-19666

Tensile strength of alloys under high pressure of hydrogen and helium, discussing embrittlement [ASM PAPER D8-14.2] 07 p1169 A69-19667

Neutral hydrogen distribution and dynamics in galaxies, discussing observations by spectrographic transit telescope, data processing and profiles 07 p1224 A69-19711

Radiative cooling layer behind shock front from neutral interstellar hydrogen cloud collision at Mach 20, discussing molecular hydrogen abundance during cooling 08 p1381 A69-19796

Detonation wave propagation in H-O mixtures in supersonic flow, noting detonation front structure and velocity 08 p1420 A69-19882

Polarization of Lyman alpha radiation in hydrogen rare gas collisions calculated in Born and distortion approximations including rotational coupling 08 p1355 A69-20207

Hydrogen solubility in solid and liquid phases of nickel-molybdenum and nickel-tungsten alloys at high temperatures 08 p1333 A69-20448

Low latitudes observations of 21 cm line of H I in galactic center direction, giving contours maps of brightness temperature 08 p1392 A69-20562

Neutral hydrogen asymmetry in Galaxy M101 as evidence for tidal effects due to nearby companions, noting hydrogen emission spectra 08 p1394 A69-20625

Pulsar distance estimates, discussing effect of interstellar electron and H densities and temperature dependence of H density-electron density ratio within disk 08 p1397 A69-20698

Optical depth determination in absorption lines of interstellar neutral hydrogen clouds by spectral observation of variable intensity radio sources 08 p1398 A69-20774

Inelastic transport cross sections for Lyman alpha transitions in hydrogen 08 p1357 A69-20814

Carbon dioxide bending mode deactivation by orthohydrogen, parahydrogen and deuterium through rotational transitions 08 p1358 A69-21010

Segmented anode, carbon dioxide-hydrogen performance and hollow cathode erosion tests on low power MPD arc thruster, noting current measurements [AIAA PAPER 69-242] 09 p1563 A69-21236

Tables of effective electron cross sections and macroscopic coefficients, Volume 1, covering hydrogen and rare gas molecular and atomic interactions with electrons 09 p1541 A69-21579

Metals hydrogen embrittlement theory, discussing role of dynamic strain aging hypothesis in overcoming theory defects 09 p1523 A69-21849

Neutral hydrogen content and distribution of late type spiral galaxy NGC 6946 from 21 cm line measurements 09 p1598 A69-22187

Molecular hydrogen in Orion dark cloud from observed faint emission 09 p1599 A69-22191

High level hydrogen populations in gaseous nebulae, noting electron density range and temperature effect 09 p1604 A69-22406

Hydrogen diffusion flames stabilization by flame holders in supersonic flow at low stagnation temperature, measuring burning limits [DVL-815] 09 p1624 A69-22615

D type dissociation ionization front structure and associated shock fronts using quasi-steady flow approximation for Stromgren sphere development in interstellar molecular hydrogen cloud 10 p1772 A69-22858

Nb H alloys embrittlement, discussing hydride formation and resistance variation with temperature 10 p1707 A69-22989

Solid hydrogen mantle condensation accounting for lack of detectable alpha hydrogen in star clusters and OB associations 10 p1776 A69-23214

Solid hydrogen condensation on graphite grains for microwave background, discussing hydrogen grain promotion of galactic and stellar formation 10 p1776 A69-23216

Pulsed glow discharges in He and He-H mixtures for high current density, noting electric field and wall potential distributions 10 p1739 A69-23660

Interstellar molecular hydrogen and CH photodissociation, discussing molecular formation rates in interstellar medium 10 p1781 A69-23672

Magnetic fields in interstellar neutral hydrogen clouds in direction of radio source Cassiopeia A, noting field amplification 10 p1785 A69-24096

High velocity neutral hydrogen cloud formation by cold condensations in hot corona, ejection from galactic nucleus, extragalactic objects and supernova envelopes 11 p1954 A69-24364

Intergalactic gas temperature and density reevaluated, considering neutral hydrogen distribution in galaxies peripheries and metagalactic background of ionizing UV radiation 11 p1946 A69-24589

Hydrogen effect on temperature dependence of tensile strength and stress rupture strength of Ti alloys, considering annealing, quenching and aging 11 p1905 A69-24962

Hydrogen solubility in solid and liquid Ti close to melting point, showing no effect on welds and castings porosity 11 p1905 A69-24963

Molecular state of hydrogen gas in high density condensations in H II regions, discussing effects of nearby stars 11 p1963 A69-25258

Electrolytic hydrogen evolution reaction on Al covered by thin oxide in aqueous buffered acetate solutions 11 p1832 A69-25674

Hydrogen viscosity temperature dependence at constant density below room temperature 11 p2003 A69-25704

Correlation of stellar surface density distribution of young stars and neutral hydrogen gas in Small Magellanic Cloud 12 p2152 A69-25802

Pulsar distances estimated from neutral hydrogen absorption, using observations from 140 ft telescope 12 p2156 A69-26224

Nonmesonic to mesonic decay ratio estimated for delta hydrogen hyperfragments 12 p2133 A69-26298

Hydrogen embrittlement of stainless steel and effects on mechanical properties, discussing martensitic phase role 12 p2115 A69-26616

Velocity distribution and density of neutral hydrogen in southern portions of M 31 and Sc-type galaxy M 33 by 75 m radio telescope 12 p2166 A69-27038

Electric arc and hydrogen flow interaction at high pressure, showing radiation role in heat exchange 13 p2305 A69-27387

Linear oscillation modes of premain sequence star model of pure hydrogen composition with variable specific heats ratio, discussing dynamic instability of polytropes 13 p2336 A69-27449

Stellar atmosphere models of pure hydrogen in hydrostatic, radiative and statistical equilibrium, including Lyman-alpha and continua, discussing nonLTE deviations 13 p2338 A69-27560

Nuclear energized pulsational instability of stars based on linear quasi-adiabatic theory, including models with hydrogen burning shells 13 p2340 A69-27576

Hayashi effect modifications due to high opacity stellar atmosphere or presence of molecular hydrogen dissociation zone, discussing pressure dissociation role 13 p2342 A69-27594

Astronomical maps of integrated hydrogen density, dispersion and velocity of high galactic latitude neutral hydrogen concentration, discussing kinetic temperature 13 p2347 A69-27718

Neutral hydrogen cloud observed at high galactic latitude, discussing top intensity velocity, peak intensity dispersion, age, hydrogen mass and density 13 p2347 A69-27719

Charge transfer and vibrational excitations in hydrogen molecular ion-hydrogen gas collisions 13 p2302 A69-28196

Electric arc structure in hydrogen magnetic annular discharge computed using nonequilibrium hydrodynamics to analyze supersonic and subsonic processes 13 p2312 A69-28221

Air-hydrogen supersonic mixing and combustion, characterizing hot hydrogen jet discharging into supersonic concentric air stream at atmospheric pressure [AIAA PAPER 69-339] 13 p2378 A69-28275

Ionization of rare gases /H and N/ by nitrogen ions, determining cross sections of formation of slow ions and electrons 13 p2304 A69-28440

HNO role in hydrogen-NO reaction rate data reexamined by numerical integration of governing differential equations 13 p2218 A69-28457

Molecular hydrogen electron scattering, optical refractivity and molecular anisotropy used to construct model dipole spectrum consistent with oscillator strength rules 14 p2488 A69-29094

Emissivity of two photons decay from metastable 2s level of pure hydrogen gaseous nebula, noting radiative and collisional excitation 14 p2529 A69-29975

HO2 radical detection in rarefied H flame produced by HF discharges, recording high amplitude signals 15 p2716 A69-30054

Hydrogen Lyman alpha nightglow models, discussing solar photon scattering in geocorona and hydrogen vertical distribution 15 p2595 A69-30191

Hydrogen gas role in galaxy formation, estimating quantity needed to dissipate gas cloud contraction energy, discussing formation mechanics of molecular hydrogen 15 p2680 A69-30204

Diatomic hydrogen abundance evolution in uniform medium, discussing photodissociation effects and galactic evolution 15 p2680 A69-30205

Simulation of two phase hydrogen venting to space environment, discussing thrust effect measurements, flow instabilities and instrumentation 15 p2701 A69-30396

Spin temperature of interstellar neutral hydrogen calculated from 21 cm absorption spectra line profiles 15 p2681 A69-30411

Excited hydrogen radio lines observations, analyzing neutral and excited hydrogen distribution in galaxies 15 p2682 A69-30502

Nova thermal explosion, analyzing hydrogen combustion after penetration from white dwarf shell into degenerate core

15 p2682 A69-30507

Neutral hydrogen in dark dust clouds in 21 cm line, showing hydrogen excesses and deficiencies

15 p2691 A69-30763

Pure hydrogen stellar atmosphere nonLTE models, calculating surface temperature rise due to H alpha line effect on continuum energy balance

15 p2693 A69-30777

Molecular dissociation by line radiation absorption, applying results to hydrogen molecules in H I region dissociated by photons of mean interstellar UV radiation field

15 p2693 A69-30783

Neutral hydrogen high velocity clouds as possible extragalactic objects in Local Group not contracted to galactic dimensions or densities

15 p2694 A69-30785

Atomic H Lyman-alpha interstellar absorption line in theta Orionis spectrum, showing equivalent width relations to H column density and spin temperature

15 p2695 A69-30890

H beta line for measuring radial temperature distribution in cylindrical hydrogen arc at one atm and to 150 A current in high temperature range

15 p2671 A69-31101

Franck-Condon factors for band systems of molecular hydrogen, computing wave functions for vibrational levels using potential energy function, Part I

15 p2656 A69-31156

Franck-Condon factors for band systems of molecular hydrogen, computing wave functions for vibrational levels using potential energy function, Part II

15 p2656 A69-31157

Photoionizing effect of hydrogen and helium UV glow in nighttime ionosphere compared with ground based IF ionosonde and sounding rocket observations

15 p2605 A69-31436

Balmer alpha emission for abundance and distribution of hydrogen around earth, relating temporal variations to azimuth

15 p2700 A69-31437

Finite difference method for turbulent mixing and combustion of hydrogen injected parallel to supersonic air stream, considering vitiated and unvitiated air [AIAA PAPER 69-539]

16 p2877 A69-31844

Additives effect on flame propagation velocity and stability in N diluted hydrogen-chlorine propellants, noting entrained air role [WSCI PAPER 69-13]

16 p2831 A69-32353

Frequency distribution of star masses formed from solid H grains clouds, noting agreement with Salpeter initial mass function

16 p2862 A69-32372

Star formation in interstellar solid hydrogen clouds originating from cellular pressure created by hydrogen condensation onto interstellar grains

16 p2862 A69-32375

Prebreakdown currents measurement in H and N for deducing ionization coefficients via Townsend and Lucas equations respectively, noting validity by digital computer technique

16 p2815 A69-32574

Ozone concentration photochemistry between 30-35 km, determining parameters in Hampson theory /hydrogen-oxygen atmosphere/

16 p2787 A69-32636

Hydrogen effects on ELI Ti-Al-Sn alloy, conducting tensile, fretting and abrasion tests on stressed and thermal cycled specimens [AIAA PAPER 69-585]

16 p2803 A69-32760

Laboratory plasma produced by electromagnetically generated shock front propagation through unionized hydrogen [AIAA PAPER 69-693]

17 p2945 A69-33447

Radio wave absorption in interstellar H I regions, considering mean absorption coefficient dependence on height above galactic plane, evaluating planar electron density

17 p3034 A69-33608

Interstellar neutral hydrogen in mean galactic latitudes noting two different component types

17 p3039 A69-33766

Perturbation procedures applied to energy computation for ground and first excited state of hydrogen molecule at large separation

17 p3009 A69-34170

Quasars and intergalactic hydrogen density, using Schmidt law of increase in number density of quasars to construct plausible models

18 p3190 A69-34288

Zeeman effect measurement revealing magnetic fields in interstellar neutral H clouds

18 p3190 A69-34291

Submillimeter water vapor laser power output for admixtures of H, N, carbon dioxide, methane, He and Ar, noting buffer effect of H

18 p3152 A69-34717

Balmer alpha and Lyman beta intensities for multiple scattering calculated for hydrogen geocorona models by radiative transfer equations, discussing radiation transport through earth hydrogen atoms

18 p3128 A69-34943

N-type In-doped ZnSb with melt under H-gas preparation and properties

18 p3183 A69-35268

Hydrogen effect on embrittlement of Cr-Ni stainless steel from viewpoint of corrosion cracking, using reverse bending apparatus

19 p3358 A69-35774

Forbidden transitions in diatomic molecules with nonzero spin and zero orbital angular momentum, stressing application in outer planets and M stars hydrogen spectra

19 p3421 A69-36213

Spectral lines due to magnetic dipole transitions in fine structure levels in collisionally excited neutral H clouds, discussing theoretical difficulties in interpretation

19 p3379 A69-36225

Hydrogen jet structure ejected into vacuum from Laval nozzle at supersonic velocity, considering separation point from diffuser wall

19 p3240 A69-36601

Moisture and hydrogen role in hot chloride salt stress corrosion cracking of Ti alloys by radiotracer technique and mass spectrography

19 p3352 A69-36904

Thermal energy rate constants of ion-molecule reactions in gaseous hydrogen, deuterium and HD, using ion cyclotron resonance method

20 p3578 A69-36934

Reactivity of hydrogen with surface of Ti-Al-V alloy under fatigue cycling at ambient and cryogenic temperatures

20 p3557 A69-36960

Pulsar distance determined by electron content in line of sight to pulsar compared with neutral H amount integrated through galaxy in pulsar direction

20 p3597 A69-37409

Normal ionizing shock waves in H, analyzing shock velocities as function of drive magnetic field using Chapman-Jouguet hypothesis

21 p3691 A69-38332

Upper atmospheric H and He observations, showing Lyman alpha, H alpha measurements and H abundance values relative to Kockarts-Nicolet model

21 p3714 A69-38529

Inconel and aluminum tested in pressurized hydrogen at room temperature, using surface flawed fracture toughness specimens and preflawed pressure vessels

21 p3730 A69-38666

Franck-Condon factors for band systems of molecular hydrogen, computing wave functions for each electronic state by numerical solutions of radial Schroedinger equation

21 p3774 A69-38758

Hot salt stress corrosion of Ti alloy, discussing hydrogen generation during elevated temperature exposure and embrittlement as manifestation of strain rate

21 p3747 A69-39434

Galactic hydrogen distribution, discussing velocity field, spiral structure, symmetry, layer shape, ionization, spectra, etc

21 p3810 A69-39503

Hydrogen high level transition probabilities formula, giving two tables of oscillator strengths [AFRL-69-0301]

22 p3983 A69-40149

Absolute thermal conductivity measurements on fluid normal H and fluid parahydrogen, noting apparatus and data graphical presentation along isotherms, isochores and isobars [NAS-NRC PAPER D-1]

22 p3998 A69-40631

Cold neutral H cloud existence in Galaxy from measurements of 21 cm line spectra

22 p4025 A69-40644

Spectroscopic analysis of nebula NGC 6302 for identification as highly excited gaseous nebula, noting He-H ratio

22 p4026 A69-40647

Hydrogen-hydrogen excitation collisions by impact parameter treatment, investigating rotation coupling influence in four state cross sections approximation

22 p3987 A69-41007

Absorption features of 21 cm neutral hydrogen line in part of Cygnus X and of W 49, showing equal velocity contour diagrams from right ascension scans

22 p4034 A69-41200

Hydrogen permeability in Pd alpha phase measured, coupling with grain size measurements for grain boundary to bulk diffusivity ratio

23 p4175 A69-41502

Hydrogen-air reaction kinetics analyzed using standing wave normal shock noting wall effects, ignition delay and recombination [AIAA PAPER 67-479]

23 p4239 A69-41893

H concentration and pore formation in Ti fusion welds

24 p4319 A69-42885

Order-disorder transitions in solid hydrogen, discussing model to explain molecular rotation angular momentum operator fluctuations

24 p4350 A69-43119

Primordial hydrogen and helium concentration in Pesyanoe meteorite measured by gas chromatography, indicating solar wind injection source

24 p4384 A69-43213

Mixing spread of hydrogen plumes and air pollutants exhausted into open atmosphere, predicting subsonic free round jets air entrainment

24 p4300 A69-43257

Performance curves of cylindrical water heat pipe for performance map, observing free hydrogen accumulation [ASME PAPER 69-HT-15]

24 p4413 A69-43554

Low Reynolds number unsteady wake flows, using hydrogen bubble flow visualization in high concentration glycerine mixtures

24 p4298 A69-43691

Formation mechanism of positive ethyl ion and hydrogen molecule during interaction between positive methyl ion and methane molecule

24 p4280 A69-43814

HYDROGEN ATOMS

Resonance theory of thermomolecular recombination kinetics applied to hydrogen atoms

01 p0122 A69-10034

Ionization cross sections of excited states of hydrogen atoms and hydrogenoids calculated by Monte Carlo method

01 p0122 A69-10040

Partial maser effect in recombination lines of hydrogen atoms in nebular plasma due to overpopulation of energy levels at thermodynamic equilibrium

01 p0148 A69-10042

Shock front structure in radiative relaxation region in atomic H, calculating Lyman continuum effects

01 p0122 A69-10125

Statistical equilibrium equations solution for thermodynamic equilibrium variations of populations of very high energy levels in hydrogen and complex atoms

01 p0150 A69-10395

Electron impact excitation of Lyman alpha emission from 2p state of atomic H, noting discrepancy below 50 Mev

02 p0283 A69-12466

Excited atomic H state radiative mean life measurements using beam-foil excitation method

03 p0469 A69-12920

Free excited H atom Lyman alpha radiation intensity study using beam-foil excitation method

03 p0471 A69-13167

Solar hydrogen Lyman alpha line profile measurement by rocket-borne spectrograph, obtaining flux available for scattering by atomic hydrogen in geocorona

05 p0815 A69-16254

Two cavity large storage box atomic hydrogen maser, obtaining self excited oscillations coupled with high gain amplifier [IEEE PAPER C-8]

05 p0774 A69-16310

Electron impact ionization cross sections for second quantum level of atomic H, using Born exchange approximation and Vainshtein approximation

06 p0961 A69-17138

Diffusion coefficients of H atoms in mixtures of He and Ar with hydrogen by catalytic sink technique, discussing rigid sphere collision diameters

07 p1185 A69-19300

Perturbation methods for exchange and Coulomb energy of hydrogen molecule, calculating Hamiltonian by wave function

07 p1186 A69-19446

Dissociation-ionization fronts in interstellar molecular hydrogen clouds, analyzing effects of UV radiation from early stars

07 p1221 A69-19584

Monte Carlo method for calculating atomic hydrogen escape rate from carbon dioxide atmosphere, considering Mars and Venus atmospheres
08 p1386 A69-20076

Wing of solar line H-alpha for levels population of hydrogen atom in solar photosphere, discussing excitation temperature, absorption coefficient and thermodynamic equilibrium
08 p1390 A69-20394

Hydrogenic atoms ionization by high energy electrons, discussing cross sections for ejected electrons and total energy
08 p1356 A69-20738

Debye potential for effective interaction between electron and proton of hydrogen atom in partially ionized plasma
08 p1365 A69-20746

Oscillator forces and photoionization and photorecombination cross sections of electron transitions in hydrogen atom, considering approximation for total radiation probability
09 p1588 A69-21365

Steady state operation of atomic hydrogen maser by analogy with electronic circuits, calculating atomic magnetic susceptibility using density matrix and deriving equivalent circuits
09 p1517 A69-22093

Neutral atomic H content of small angular diameter galaxies, noting systematic radial velocities and total mass of galaxies
10 p1773 A69-22956

Primary processes leading to atomic and molecular hydrogen formation in hydrogen peroxide photolysis at 1236 Å, noting OH formation
10 p1652 A69-23527

Ionized gas flow from globule containing atomic H in interstellar space, noting surrounding H II region and radiation at ionization front
10 p1782 A69-23682

Direct Coulomb interaction matrix elements between hydrogen atoms in ground states calculated, presenting interaction potential
11 p1921 A69-24416

Equilibrium between H and OH radicals in turbulent H flames, noting component concentrations in H-O-N flames of different composition
11 p1999 A69-24487

D/H ratio in Venus exosphere, discussing isotopic fractionation mechanisms and Lyman alpha data from Mariner 5
11 p1962 A69-25145

Color excess and 21 cm line intensity of RR Lyrae stars at high latitudes, confirming correlation between dust and atomic hydrogen
12 p2063 A69-25808

Double focalization in atomic hydrogen maser by hexapolar magnets selecting hyperfine energy transitions
12 p2105 A69-26050

Average ionization cross sections of atomic and molecular H and He beams ionized by plasma electrons with Maxwellian velocity distribution
12 p2138 A69-26542

Spectral line formation in nonlinear multilevel atom line transfer problems, considering radiation transfer through plane parallel atmospheres of H and Mg atoms
12 p2133 A69-26967

Negative charge production by H atoms collisions with rare gases and hydrogen, noting smooth rise of cross section with energy for rare gases
13 p2302 A69-27459

Hydrogen atoms in interstellar grains as source of stellar flux absorption, noting crystal environment effect on atomic hydrogen Lyman alpha transition
13 p2337 A69-27518

Atomic hydrogen vertical profiles with increased high-low altitude ratio for interpreting observations of thermospheric and exospheric hydrogen abundance
14 p2440 A69-29130

Solar wind and solar breeze theories distinguished, discussing applications to geocoronal hydrogen emission and solar corona expansion
15 p2676 A69-30858

Resonances in elastic cross section for electron/hydrogen atom scattering noting wide structure
15 p2657 A69-31265

Atmospheric hydrogen and helium atoms emission in geomagnetic poles and winter hemisphere, comparing thermal dissipation and migration of light atoms
15 p2599 A69-31322

UV OGO observations of atomic hydrogen and oxygen in airglow, comparing results to exospheric models of hydrogen geocorona
15 p2603 A69-31400

Photoinduced shock processes involving metastable hydrogen atoms and molecules, discussing vibrational and rotational levels
16 p2813 A69-31754

Density ratios of H ions to H atoms in ground state calculated as function of quasi-neutral plasma electron density
16 p2820 A69-31770

Stripping and low-energy collisions of H atoms on O and N molecules, showing target ionization to projectile stripping ratio dependence on ionization potential
16 p2814 A69-31773

Sky brightness temperature spectra searched for neutral intergalactic atomic hydrogen radio emission, using horn-reflector antenna
18 p3190 A69-34285

Oscillator forces and photoionization and photorecombination cross sections of electron transitions in hydrogen atom, considering approximation for total radiation probability
18 p3197 A69-34755

Hydrogen bulge above springtime pole indicated by Lyman alpha radiation in earth geocorona, discussing hydrogen horizontal transport and hydrogen compounds dissociation as causes
18 p3129 A69-34956

Hydrogen atom excess charge creating universal repulsive force in analyzing cosmological gravitational contraction in terms of Newtonian mechanics
18 p3206 A69-35469

Atomic H ionization by proton impact analyzed to calculate ejected electrons angular and energy distributions by extending Rudge and Seaton theory
19 p3375 A69-35911

High velocity interstellar gas in H I and H II regions, emphasizing observations of neutral atomic hydrogen in and far from galactic plane
19 p3402 A69-35962

Photodissociation of diatomic hydrogen by solar radiation for Venus atmosphere investigation, considering H atoms production rate by Stecher-Williams process
20 p3609 A69-38102

Universal hydrogen distribution, discussing atomic hydrogen needed to close universe
20 p3610 A69-38140

Thermodynamic properties of hydrogen atoms, protons and electrons, using canonical group analysis to determine bound and free states
21 p3850 A69-38964

Primary H nuclei flux and spectrum near geomagnetic equator, discussing emulsion stack exposure
22 p4005 A69-40520

Projected surface density upper limit of neutral atomic H between M31 and M33 galaxies, noting brightness temperature between NGC 4631 and 4656
22 p4024 A69-40578

Quasars observation failure for red shifts beyond z suggested due to absorption of intergalactic neutral H
22 p4024 A69-40582

Impact parameter versions of two state and Born approximations to calculate single excitation cross sections of H atoms ground state collisions
22 p3987 A69-41006

Solar motions respecting high velocity atomic hydrogen clouds and local stellar group
22 p4035 A69-41209

Pt wire detector for flow regulation of atomic hydrogen beam, noting hydrogen maser application
22 p3950 A69-41232

H and He atoms escape from atmosphere under MHD waves action at exosphere boundary
23 p4156 A69-41847

Low energy galactic cosmic ray spectrum determined from ionization rate per hydrogen atom, correlating peak intensity with stellar particle emission high energy portion
24 p4365 A69-42608

HYDROGEN BONDS
Single run reheated weld wrought steel H cracking tested by constant load rupture /static fatigue/ technique
24 p4320 A69-42943

Polycrystalline ammonium cyanide IR absorption spectrum as function of temperature, discussing ammonium ion hydrogen bonding to C or N atoms
24 p4280 A69-43809

HYDROGEN CHLORIDE
U HYDROCHLORIC ACID

HYDROGEN COMPOUNDS
NT BERYLLIUM HYDRIDES
NT BORANES
NT CARBORANE
NT CHLOROSILANES
NT DEUTERIUM COMPOUNDS

NT DIBORANE
NT HEAVY WATER
NT HYDRIDES
NT LITHIUM ALUMINUM HYDRIDES
NT LITHIUM HYDRIDES
NT METAL HYDRIDES
NT PHOSPHINES
NT SILANES
NT ZIRCONIUM HYDRIDES

HI and DI reaction into HD and 2I, noting need for rotational or vibrational excitation in addition to translational energy of collision
01 p0123 A69-10686

Atmospheric ozone photochemistry, studying time dependence on hydrogen compounds, equilibrium concentration effects on reaction rates, latitude and season
06 p0916 A69-17004

SH above photosphere in solar atmosphere, discussing dissociation equilibrium of diatomic molecules and possible abundances
06 p1002 A69-17317

HYDROGEN CYANIDES
Sideband amplification via saturated gas resonance in 258 GHz reflection amplifier with hydrogen cyanide gas filled cylindrical cavity
07 p1145 A69-18479

Transition probabilities in repetitively Q modulated HCN maser radiation dependent on gas discharge current
09 p1516 A69-21626

Simultaneous HCN and HOH laser emission in pulsed discharge through mixture containing H, C, N and O
12 p2107 A69-26330

Pulsed HCN sealed laser long term operation, discussing behavior of 311 and 377 micron emissions
12 p2107 A69-26391

HCN laser line width measurement with high resolution spectrum analyzer indicating spectral widths caused by mechanical instability
17 p2979 A69-32850

HCN laser line gain measurements during continuous excitation as function of current and pressure for acetonitrile and water mixtures
19 p3339 A69-36695

Gas phase ion-molecule chemistry of HCN by ion-cyclotron resonance spectroscopy identifying individual reactions by double resonance
20 p3485 A69-38262

Frequency locking of HCN laser transition at 890 GHz to harmonic of crystal controlled oscillator
22 p3963 A69-40567

Short term frequency fluctuations of CW HCN masers reduced to 10 kHz by improving plasma stability
24 p4327 A69-42614

HYDROGEN DEUTERIUM OXIDE
U HEAVY WATER

HYDROGEN FLUORIDES
U HYDROFLUORIC ACID

HYDROGEN FUELS
Hydrogen-air supersonic combustion at low densities, discussing laboratory computer simulation based on boundary layer concepts and finite rate chemistry [WSCIPAPER 68-29]
07 p1240 A69-18358

Low temperature hydrogen fuel cells and basic electrolyte batteries design, discussing electrolyte concentration regulation by elimination of water formed
08 p1258 A69-21027

Kinetics of combustion promotion of hydrogen-hydrocarbon mixtures by active particles, free atoms and free radicals using differential equations
17 p3069 A69-33139

Temperature and concentration measurements of H radical in hydrogen flames
21 p3669 A69-38807

HYDROGEN IONS
Galactic H II regions morphology from high resolution radio observations, noting variation of electron density with region size
01 p0151 A69-10552

Elastic scattering of slow electrons by negative H and positive Li ions, calculating differential cross sections and phase shifts
03 p0469 A69-12924

Pulsed arc source using plasma jet to obtain intense hydrogen ion beam
03 p0412 A69-13842

Mass spectrometric technique applied to positive column of hydrogen glow discharge for plasma properties, including relative densities of various hydrogen ions
05 p0802 A69-15913

Molecular jets obtained by charge exchange of triatomic ion beams consisting of hydrogen, deuterium and nitrogen, noting formation, energy level, etc
05 p0797 A69-16339

Hydrogen ions collision-induced dissociation cross section angular dependence measured, showing qualitative agreement with theoretical predictions
05 p0798 A69-16698

Absolute isophotometry of hydrogen alpha photographs of bright galactic H II regions, attributing difference between theoretical and observed ratio to interstellar absorption
07 p1217 A69-19231

Southern Hemisphere galactic H II regions continuum thermal radiation at 6 cm, noting maps for 28 of 36 sources, peak temperatures and emission and half intensity widths
07 p1206 A69-19271

Dissociation equilibrium of negative H ions in solar type stellar atmospheres, noting H molecule vibrational and rotational levels and continuous thermal radiation
07 p1223 A69-19635

Radial distribution of H II regions in spiral galaxies, noting peak at 1/4 distance from center
08 p1384 A69-20052

Galactic H II regions and projected electron density or dispersion measures of pulsars, noting early stars
08 p1397 A69-20696

Charge exchange collisions in ground state and ionic hydrogen incident on cesium vapor, measuring beam components after passage through target
08 p1356 A69-20737

Electron impact ionization of negative H ions computed by wave expansion methods and compared with experiments
09 p1542 A69-21622

Contour maps of H II regions W12, Orion A, W43 and W51, listing flux densities and angular sizes of components
09 p1598 A69-22186

Radio spectra and structure of H II regions in emission nebula NGC 281 and unnamed nebula near NGC 2264
10 p1773 A69-22957

HI cloud densities near fronts of H II regions by gasdynamic calculations based on observational data for electron density, temperature and particle velocity
10 p1782 A69-23683

Radio brightness map at 22.25 MHz of galactic plane including H II regions IC 1805 and IC 1848, discussing LF absorption
10 p1787 A69-24115

Optical and radio measurements of electron temperature of H II regions obtained from brightness ratio of hydrogen line and continuum, considering isothermal model
11 p1950 A69-25110

Light ion abundance measurements of OGO satellites and field aligned diffusive equilibrium theory with temperature and concentration latitudinal variations
11 p1879 A69-25157

Molecular state of hydrogen gas in high density condensations in H II regions, discussing effects of nearby stars
11 p1963 A69-25258

Photographic studies of unsteady features of galaxies, discussing spectra, color, spiral arm instability and extragalactic H II regions
12 p2170 A69-27063

Steady state model envelopes of Bc stars, determining excitation and ionization states for hydrogen atoms
13 p2338 A69-27559

Galactic H II regions of high surface brightness in radio continuum surveyed at 1.95 cm wavelength with high resolution and positional accuracy
13 p2339 A69-27568

Isothermal H II region dynamics for moving central star, integrating equations numerically using holograph transformation and Riemann invariants
13 p2347 A69-27712

Ionized hydrogen regions in NGC 4449 from H alpha photography through narrow band interference filter, obtaining radial velocities
13 p2347 A69-27714

Messier 51 ionized hydrogen observations, discussing H II regions, radial velocities and galactic mass, rotation and noncircular nuclear motions
13 p2347 A69-27720

H II alpha and beta radio recombination lines strengths predicted, noting role of calculations of hydrogen energy levels non-LTE populations
14 p2517 A69-29088

Galactic anticenter region surveyed at 13.1 MHz, observing ionized hydrogen concentrations in galactic plane
14 p2519 A69-29370

Semiconductor materials and fabrication methods for surface barrier junction n-type and p-type silicon counters used in hydrogen ion flux recording
14 p2452 A69-29810

Spectrometric characteristics of He, H and molecular H ion recording counters as function of temperature
14 p2452 A69-29811

Hydrogen and He ion distribution measurements, noting seasonal and local magnetic time variability
15 p2599 A69-31326

Plasmasphere hydrogen and He ion concentration models, using diffusive equilibrium theory for plasmasphere parameters
15 p2677 A69-31447

Initial ionization processes in strong shock wave in hydrogen, determining ionization relaxation length and cross section of atom-atom excitation collisions
16 p2815 A69-31590

Magellanic-like galaxy NGC 4631 observed in H alpha light through narrow band interference filter, detecting and cataloging 88 H II regions
16 p2854 A69-31647

Density ratios of H ions to H atoms in ground state calculated as function of quasi-neutral plasma electron density
16 p2820 A69-31770

RF spectral line detection from ortho hydrogen ions in Omega Nebula and NML Cygnus
16 p2864 A69-32571

Pulsars distance determined using H II region data covering line of sight stars and Galaxy hydrogen distribution
17 p3026 A69-32858

H II regions distribution in nearby irregular I galaxies, attributing asymmetry to localized bursts of star formation
18 p3190 A69-34289

Depolarization of extragalactic radio sources at low Galactic latitudes attributed to ionized hydrogen produced by B2 star tunneling through interstellar hydrogen cloud
18 p3194 A69-34425

Atomic H ionization by proton impact analyzed to calculate ejected electrons angular and energy distributions by extending Rudge and Seaton theory
19 p3375 A69-35911

Dynamical effects in structure of H II equilibrium region left behind expanding ionization front, showing temperature as function of distance from star
19 p3403 A69-35966

Hydrogen molecular ion dissociation due to ion-molecule inelastic collisions, comparing measured and calculated velocity distributions of protons produced
19 p3375 A69-35985

Shock ionization by ion impact against triatomic H molecules gas target, showing positive ion production dependence on extraction voltage, collision chamber pressure, etc
19 p3378 A69-36188

Charge exchange cross sections and electron losses in hydrogen ion beam impacting on water vapor molecules
19 p3378 A69-36190

Two photon decay of metastable levels of hydrogenic and He-like ions in solar corona, depopulating via proton collisional excitation to 2p level
19 p3396 A69-36218

OGO 5 ion spectrometer for measuring oxygen, He and hydrogen ion concentration, noting functions as energetic particle analyzer and proton energy distribution measurement capability
19 p3314 A69-36679

Drift velocity and lateral diffusion of positive hydronium, hydrogen and K ions in hydrogen with zero field mobilities
20 p3580 A69-38026

Gas in H II regions and associated stars radial velocities correlation and systematic difference suggesting relationship between nebulae and stars
20 p3611 A69-38150

Photospheric radiation field role in temperature inversion of stellar chromospheres with dominant H ion opacity, postulating mechanical energy dissipation
20 p3613 A69-38173

Atlas of H II regions in 20 nearby galaxies
22 p4015 A69-40153

Explorer 34 observations of hydrogen and He ions in solar wind, noting number density variations and tentative association with geomagnetic storms
22 p4004 A69-40305

Possible star formation regions in Milky Way galaxy searched for compact H II regions, tabulating results
22 p4024 A69-40576

Radio recombination line data from H II regions interpreted in terms of single electron temperature, considering non-LTE / local thermodynamic equilibrium/ and clumping
22 p4025 A69-40645

Evolutionary dynamic model for H II region produced by massive stars within dense dust-laden clouds, discussing grain sputtering and time scales
22 p4025 A69-40646

Positively charged diatomic hydrogen molecules interstellar extinction and photodissociation cross section in terms of formation mechanisms
24 p4375 A69-42610

Proton ejection as hydrogen ion clusters by low energy electron bombardment of solid hydrogen
24 p4389 A69-43747

HYDROGEN ISOTOPES

NT DEUTERIUM

NT TRITIUM

Dissociation energy and vibrational terms of ground state hydrogen
05 p0796 A69-15908

Radiative cooling rates of bounded plasma of hydrogen isotopes, comparing dense deuterium plasma analytical results with brightness measurement
11 p1927 A69-25218

Lithium 6 and 7 fission following pion capture, searching for H 4 and 5
12 p2132 A69-26296

HYDROGEN OXYGEN ENGINES

NT M-1 ENGINE

NT RL-10-A-1 ENGINE

HM 4 rocket motor for second stage of Diogene booster, using LOX and hydrogen propellants
04 p0647 A69-15064

Fluidic secondary injection thrust vector control systems for solid propellant and hydrogen-oxygen rocket engines
10 p1753 A69-23561

Oxidizer injector face configuration for high power variable thrust rocket engine using hydrogen/oxygen propellant
16 p2835 A69-31749

Hydrogen oxygen rocket engine two phase liquid hydrogen pump capability and hydrodynamic design, analyzing constant-quality flow, acoustic effects, compressible flow and cavitation
16 p2845 A69-32759

Liquid oxygen and hydrogen rocket engine HM4 design and operation, discussing fuel, low temperatures and heat exchange
17 p3020 A69-33345

HYDROGEN OXYGEN FUEL CELLS

Water electrolysis, discussing oxygen generators for spacecraft prototype cells and testing
03 p0379 A69-12987

Oxygen supply inert diluent impurities effect on hydrogen-oxygen fuel cell performance
04 p0551 A69-15310

Water removal unit design for electrolyte reaction accumulation in hydrogen oxygen fuel cell systems
04 p0552 A69-15316

Water and heat removal unit for hydrogen/oxygen fuel cell systems, discussing temperature distribution, heat and liquid transport
05 p0704 A69-15676

Energy source for space environments based on compact cold hydrogen-oxygen fuel cell, discussing heat control and water elimination methods
08 p1260 A69-21041

Justi-Winsel extraction process by electrodialysis for removing product water from electrochemical reaction in H-O fuel cells
08 p1260 A69-21043

Hydrogen-oxygen fuel cells with conducting and nonconducting hydrophobic electrode matrices
08 p1261 A69-21055

Heat and mass transfer in porous medium with bulk flow in thin adjacent channel, applying Green function analysis to hydrogen-oxygen fuel cell
15 p2552 A69-31115

Hydrogen-oxygen low power space use fuel cell, noting geometrical and electrical characteristics of electrodes
16 p2738 A69-32412

Hydrogen-oxygen ion exchange membrane fuel cells for sounding balloons, discussing flight duration and power requirements, gas supply pressure effects, etc
16 p2738 A69-32413

Optimization of electrolytic extraction process of water from H-O fuel cells through choice of current density as function of electrolyte concentration
16 p2738 A69-32414

Hydrogen oxygen fuel batteries with hydrophobic porous film electrodes and alkaline electrolyte
16 p2740 A69-32426

Pseudosplitting/peroxide mechanism for O reduction at fuel cell cathodes, analyzing O molecule adsorption, H bonding and electron transfer at surface
16 p2748 A69-32809

High power density spacecraft hydrogen/oxygen fuel cells with open cycle heat and product-water removal subsystems and reactant tankage
23 p4076 A69-42309

HYDROGEN PEROXIDE

Absorption coefficient of hydrazine and hydrogen peroxide determined with 2.5 angstrom bandwidth monochromator, giving results in graphical form
02 p0205 A69-11873

Spacecraft sterilization by hydrogen peroxide solutions mixed with selected anion active detergents
05 p0713 A69-15943

Explosive combustion of hydrogen at high pressures, showing attainment of constant value of hydrogen peroxide
05 p0849 A69-16615

Primary processes leading to atomic and molecular hydrogen formation in hydrogen peroxide photolysis at 1236 Å, noting OH formation
10 p1652 A69-23527

Hydrogen peroxide electrode cathodic polarization studied for liquid oxidant use in methanol fuel cells
11 p1825 A69-24523

Highly concentrated hydrogen peroxide production, handling and storage, discussing crystallization process, equilibrium diagram, decomposition reduction and stabilizers
17 p3017 A69-33353

HYDROGEN PLASMA

NT DEUTERIUM PLASMA

High temperature, fully ionized plasma equation of state, using quantum statistical theory of low density electron-ion plasma in thermal equilibrium
01 p1128 A69-10346

Pressure rise and thermal conductivity in cylindrical hydrogen plasma column in axial magnetic field, assuming local thermal equilibrium
03 p0479 A69-13967

Double microwave interferometer for measuring hydrogen plasma decay
04 p0600 A69-15024

Hydrogen spectral line widening by plasma electrons emphasizing Lyman, Balmer and Paschen series
04 p0638 A69-15239

Continuous absorption of coefficient hydrogen- carbon plasma at 40,000 degrees K and 70 atm in 230-460 nm spectral range
04 p0639 A69-15371

Hydrogen plasma transport properties for semiclassical quantum potential calculated by Chapman-Enskog-Hilbert theory
05 p0799 A69-15735

Plasma flow in electromagnetic shock tube with various pressures and speeds, noting turbulence onset in shock layer
06 p0968 A69-17764

Relaxation theory of highly ionized hydrogen plasma noting applications to stimulated emission, radiation source development and electromagnetic radiation amplification
07 p1191 A69-18996

Hydrogen absorption coefficients, giving number densities in hydrogen gas or plasma for wide range of temperature and pressure
07 p1184 A69-19165

Spectroscopic analysis of hydrogen spark plasma discharge parameters at small PD values, discussing shock wave initiation accounting for transition to quasi-stable phases
08 p1360 A69-20100

Symmetric Alfven waves propagation in hydrogen plasma with nonuniform density distribution, deriving dispersion relations for fully ionized plasma
08 p1367 A69-20794

Impurity elimination from hydrogen plasma jets injected from coaxial source normal to octupole magnetic field
08 p1370 A69-21016

Electron multiplication during ionized H plasma exposure to annular electric field and magnetic field, including microwave diagnostics
09 p1543 A69-21299

Current instability in H plasma in electric field of large amplitude fast magnetosonic wave, noting plasma heating
09 p1552 A69-22526

Nonequilibrium distribution functions for neutral atoms excited states in optically thin low temperature singly ionized plasma containing ions, electrons and neutrals
10 p1731 A69-23437

Radiative cooling rates of bounded plasma of hydrogen isotopes, comparing dense deuterium plasma analytical results with brightness measurement
11 p1927 A69-25218

Free electron density upper limits in plasma attributed to negative ion formation, noting effect on ionization equilibrium calculations for stellar atmospheres
11 p1928 A69-25255

Thermal conductivity of hydrogen plasma in transverse magnetic field at high temperatures
12 p2133 A69-25765

LF wave propagation in DC discharge hydrogen plasma, noting self and artificial wave excitation
13 p2316 A69-28584

Hydrogen plasma heating by fast large amplitude magnetoacoustic wave, measuring resonance excitation and absorption of wave
14 p2493 A69-29643

Magnitude and type of wall losses from small opening in discharge tube for positive plasma column of low pressure glow discharge in hydrogen
14 p2493 A69-29691

Polychromator measurement of hydrogen plasma electron density produced by normal ionizing shock wave, using Stark broadening study of H beta line
14 p2494 A69-29767

Pulsed HF discharge analysis in hydrogen based on laser light scattering at plasma electrons, noting presence of satellites
14 p2451 A69-29781

Three component fast neutral beam for hydrogen plasma ion density and electron temperature determination, improving accuracy and reliability
14 p2452 A69-29812

Radial distribution functions for dense hydrogenous plasma near ionization temperature by solving Pereus-Yevick equations
14 p2502 A69-29998

Ambipolar to free diffusion transition in magnetized slab plasmas, discussing basic equations, iterative numerical procedure, characteristic parameters and H plasma
15 p2657 A69-30023

Thermal conductivity coefficients in solar corona and chromosphere computed and tabulated for H plasma
15 p2694 A69-30788

Hydrogen plasmas motions in multipole magnetic fields, discussing plasma polarization, double vortex flow patterns and field line configurations
15 p2661 A69-30924

Plasma experiments with TM-3 apparatus under stable discharge conditions in H, discussing energy loss mechanisms, transport coefficients, reciprocal lifetime, etc
16 p2820 A69-31795

Balmer line H alpha emission and absorption coefficients measured with hydrogen plasma generated in high current low voltage free burning arc
16 p2822 A69-32040

Continuous absorption of coefficient hydrogen- carbon plasma at 40,000 degrees K and 70 atm in 230-460 nm spectral range
16 p2822 A69-32118

Faraday effect and permittivity of hydrogen plasma measured simultaneously, determining electron density and collision frequency
17 p2919 A69-33394

Oblique hydromagnetic shock waves in magnetized hydrogen plasma enclosed in pyrex chamber by oscillatory zeta discharge, probing for front development and structure
17 p3013 A69-33823

Radiative energy transport quantities for hydrogen plasma including Plank and Rosseland mean absorption coefficients, discussing line and continuum radiation and optical limits
20 p3581 A69-37306

N and H plasmas and N-H plasma mixtures thermodynamic properties calculation, discussing numerical methods and corrections for electrostatic interactions
21 p3847 A69-38421

Ionized plasma motion under-stroke piston action by self similar solution of Navier-Stokes equations
22 p3991 A69-41021

Recombination and ionization coefficients for quasi-steady state homogenous H and hydrogenic ion plasmas based on collisional-radiative model
22 p3988 A69-41153

Collisional radiative recombination and ionization coefficients for weakly ionized H plasmas using rate equations
22 p3988 A69-41154

Classical path approximation in line broadening theory to derive impact and one-electron theories, with application to Stark broadening of Lyman series in hydrogen
23 p4193 A69-41379

Holographic interferometry for determining total free electrons in plasma produced by irradiating solid hydrogen foils with giant pulse ruby laser
24 p4314 A69-42980

Drift characteristics of hydrogen plasma partially captured by transverse magnetic field, finding drift rate dependence on magnetic field level
24 p4357 A69-43470

Hydrogen plasma-axisymmetric magnetic field interaction, studying plasmoid motions during exit from field
24 p4358 A69-43472

Hydrogen plasmoids in axisymmetric magnetic field with acute angle geometry produced by opposing coils, measuring induction current field and plasmoid density distribution
24 p4358 A69-43473

H plasmoid tail cut-off eliminating plasma impurities during injection across octupole magnetic field from coaxial source
24 p4358 A69-43474

Crossed inhomogeneous electric and magnetic fields effect on H plasma fluxes dynamic behavior, deriving plasma motion formula
24 p4358 A69-43475

Light scattering from ruby laser beam passing through collisionless shock produced by H plasma compression measured by photomultiplier
24 p4360 A69-43748

HYDROGEN RECOMBINATIONS

Resonance theory of thermomolecular recombination kinetics applied to hydrogen atoms
01 p0122 A69-10034

Partial maser effect in recombination lines of hydrogen atoms in nebular plasma due to overpopulation of energy levels at thermodynamic equilibrium
01 p0148 A69-10042

Absolute reddening curves derived for planetary nebulae by comparing radio continuum with hydrogen recombination lines
08 p1384 A69-20057

Radio recombination lines of galactic hydrogen as sensitive test for low energy cosmic ray existence in interstellar medium
09 p1580 A69-22273

Hydrogenic recombination decrements in gaseous nebulae, discussing effects of Lyman line leakage, Balmer line self absorption, internal dust, optical depth, etc
10 p1787 A69-24118

H II alpha and beta radio recombination lines strengths predicted, noting role of calculations of hydrogen energy levels non-LTE populations
14 p2517 A69-29088

Rate constants for recombination of atomic hydrogen with hydrogen molecules, hydrogen atoms and argon atoms at high temperatures behind shock waves
14 p2488 A69-29637

Unidentified cometary spectra line emission possible interpretations, examining atomic hydrogen abundance in cometary atmosphere and ionic hydrogen recombination
15 p2685 A69-30523

Hydrogen recombination in hot universe model, discussing emission of energetic quanta
15 p2690 A69-30734

Hydrogen laser operation time reduction attributed to hydrocarbon formation on inner surface of storage flask, promoting atomic hydrogen recombination
15 p2634 A69-30942

Recombination and ionization coefficients for quasi-steady state homogenous H and hydrogenic ion plasmas based on collisional-radiative model
22 p3988 A69-41153

Collisional radiative recombination and ionization coefficients for weakly ionized H plasmas using rate equations
22 p3988 A69-41154

HYDROGEN SULFIDE

Reaction between nickel-base alloy and hydrogen sulphide at high temperatures under atmospheric pressure, discussing activation energy 12 p2115 A69-26617

Germanium single crystals etching with water vapor and hydrogen sulfide in hydrogen flow system, studying concentration, pressure and temperature effects on surface reactions 22 p3970 A69-40737

HYDROGENATION

Hydrogen content effect on relaxation spectrum of alpha titanium, using nondestructive tests 01 p0096 A69-10614

Chemical vapor deposition of W-Mo-Re ternary alloys from hydrogen reduction of fluorides on Cu or Mo substrates 01 p0096 A69-10642

Solvent effect in catalytic hydrogenation reaction of Schiff bases of alpha-keto acids with optically active alpha-alkylbenzylamine 12 p2026 A69-25779

Optically active alanine synthesis from oxaloacetic acid by hydrogenolytic asymmetric transamination, noting role of decarboxylation 12 p2026 A69-25780

HYDROGENOMONAS

Hydrogenomonas eutropha as means of protein food source independent of conventional agriculture for animal feed supplement 10 p1644 A69-23306

Human intolerance to bacteria as food, considering response to Hydrogenomonas eutropha and Aerobacter aerogenes 13 p2213 A69-27265

NADH stimulation of ATP dependent carbon dioxide fixation in crude extracts of Hydrogenomonas facilis, considering allosteric regulation of phosphoribulokinase activity 15 p2554 A69-30036

Structural phospholipoprotein isolated from hydrogenomonas facilis and neurospora crassa 22 p3871 A69-40049

HYDROGRAPHY

IR measuring techniques for water surface temperature remote sensing 15 p2617 A69-31543

HYDROLOGY

Satellite automatic picture transmission application to meteorological and hydrological problems including wind estimates, atmospheric stability and cloud distributions [UN PAPER 68-95300] 01 p0108 A69-10462

Passive and active transmitters and receivers of electromagnetic radiation in earth orbital satellites to collect pictorial or numerical data to study hydrology [UN PAPER 68-95333] 01 p0064 A69-10487

Color and color IR aerial photography compared for estuarine and marshland research, considering detection of turbidity, pollution, salinity, etc 22 p3942 A69-40993

HYDROLYSIS

Enzymic decomposition of urea in urine, noting production of ammonia and effect of urea components on hydrolysis rate 08 p1265 A69-19834

Proline residue effects on hydrolysis of peptide bonds by thermolysin 15 p2561 A69-30083

Exonuclease function of DNA polymerase from Escherichia coli, discussing hydrolysis of polydeoxyribonucleotides and resistancy of oligonucleotides 22 p3898 A69-41073

HYDROMAGNETIC FLOW

U MAGNETOHYDRODYNAMIC FLOW

HYDROMAGNETIC STABILITY

U MAGNETOHYDRODYNAMIC STABILITY

HYDROMAGNETIC WAVES

U MAGNETOHYDRODYNAMIC WAVES

HYDROMAGNETICS

U MAGNETOHYDRODYNAMICS

HYDROMAGNETISM

U MAGNETOHYDRODYNAMICS

HYDROMECHANICS

U ELASTOHYDRODYNAMICS

U ELECTROHYDRODYNAMICS

U HYDRODYNAMICS

U HYDROSTATICS

U MAGNETOHYDRODYNAMICS

U MAGNETOHYDROSTATICS

HYDROMETEOROLOGY

Soviet book on automatic control and telemechanics in hydrometeorological measurements covering sensors, transducers, amplifiers, etc 01 p0111 A69-10997

Averaging procedures to represent highly time variable actual hydrometeorological fields by less variable equivalent fields 06 p0952 A69-17989

HYDRONIUM IONS

Drift velocity and lateral diffusion of positive hydronium, hydrogen and K ions in hydrogen with zero field mobilities 20 p3580 A69-38026

HYDROPHONES

Near field flow noise generated in boundary layer of water vehicle measured for rotating cylinder, ship and buoyant unit using hydrophone 17 p3004 A69-32953

HYDROPONICS

Sweet potatoes productivity and nutritive value as carbohydrates source in manned spaceflights 13 p2216 A69-28619

Cotton leaves reflectivity and transmittance measurements, discussing substrate salinity effects on internal structure of hydroponically grown plants 15 p2558 A69-30456

Carrot plants growing during 374 days in conveyor type aeroponic assembly, noting yield and morphological features 17 p2912 A69-32943

HYDROSPHERE [EARTH]

U EARTH HYDROSPHERE

HYDROSTATIC PRESSURE

Hydrostatic pressure effects on mechanical properties of hot pressed, extruded and rolled polycrystalline beryllium sheet 01 p0092 A69-10059

Buckling of electroformed thin conical shells under hydrostatic pressure, proving theory for cones of large taper ratio 02 p0347 A69-12515

Hydrostatic pressure effect on recombination emission in indium phosphide p-n junctions 04 p0639 A69-14428

Intrarenal capillary hydrostatic pressure effect on hemodynamically induced changes in sodium excretion 07 p1063 A69-18629

Grain-size refinement of beryllium castings and extrusions after compression in pressure chamber, determining effect on ductility 08 p1330 A69-20013

Incremental and corresponding total strain theories of plasticity used to analyze hydrostatic bulging of circular diaphragm 08 p1418 A69-20826

Complicated power metallurgical shapes fabricated by hydrostatic pressing, noting spheres, cones, rods, tubes and combinations 09 p1511 A69-22353

Radial hydrostatic bearing parameters calculated by pressure distribution diagram in bipolar coordinates, obtaining equations of motion 11 p1892 A69-25341

Hydrostatic pressure-cycling technique for controlled fatigue precracking of spin burst fracture toughness specimens, noting ultrasonic flaw detection 11 p1995 A69-25650

Axisymmetric plastic buckling of complete spherical shells subjected to external hydrostatic pressure 13 p2361 A69-27439

Dislocation pattern in thin Mo foils deformed by hydroextrusion observed by transmission electron microscope 14 p2463 A69-29311

Pressure losses in pipeline with venturi tube, calculating hydraulic resistance coefficient as function of structural parameters and pipeline length 15 p2612 A69-31180

Multipad externally pressurized spherical bearing fed with incompressible fluid for satellite attitude control systems tests 16 p2793 A69-31728

Hydroextrusion influence on mechanical properties of powder compacts of sintered Mo rods 16 p2803 A69-32491

Aerospace balancing system with hydrostatic spindle, describing component construction and functions [SAWE PAPER 737] 18 p3118 A69-34890

Theory for describing rotating fluid planets external geometry in state of hydrostatic equilibrium, noting role of equipotential surfaces 20 p3594 A69-37077

HYDROSTATICS

NT MAGNETOHYDROSTATICS

Hydrostatic journal gas bearings calculations for carrying capacity, gas consumption and optimal dimensions for maximum lifting capacity 03 p0432 A69-12960

Amplitude-frequency characteristics of rotor mounted on hydrostatic bearings calculated by equations of dynamic compliance method 03 p0432 A69-12961

Orifice compensated hydrostatic face seal under pressure and thermal loading for aircraft gas turbine [ASME PAPER 68-WA/LUB-6] 05 p0768 A69-16131

Hydrostatic tension test of brittle material using spherical specimen bonded into center of cube of matrix material 05 p0784 A69-16434

Book on fluid mechanics fundamentals and applications covering incompressibility and compressibility effects, viscosity, hydrostatics, aerostatics, one dimensional, potential, turbulent flow and boundary conditions 07 p1121 A69-19376

Nonlinear partial differential equations for solution of steady stratified flows, noting hydrostatic pressure distribution and horizontal and vertical scales 11 p1869 A69-24889

Liquids in zero g environment for controlling position of propellant within tank for restart of rocket engine, noting minimum energy principle applications 11 p1944 A69-25599

Plastic deformation effects by hydrostatic fluid extrusion on mechanical properties of Ni maraging steels 13 p2278 A69-27414

Hydrostatic tube extrusion, discussing equipment, techniques and commercial applications [SAE PAPER 690319] 15 p2617 A69-30093

Hydrostatic instability in high temperature stars in post-Newtonian approximation 20 p3580 A69-37926

Hydrostatic bearings analysis for high pressure cryogenic rocket engine turbopumps to predict steady state and time dependent performance, noting turbulence, inertia and compressibility 22 p3955 A69-40408

Total load factor static vertical component and lubricant flow rate square related to pocketed hydrostatic journal bearing revolutions 24 p4321 A69-43091

HYDROTHERMAL CRYSTAL GROWTH

Subsolidus equilibrium study in potassium tantalate K niobate system for dry and hydrothermal runs, using X ray powder diffraction and petrography 08 p1332 A69-20373

Percorait phase in nickel analog of clinochrysoile formed under hydrothermal conditions in Wolf Creek meteorite cracks 18 p3199 A69-34824

HYDROX ENGINES

U HYDROGEN OXYGEN ENGINES

HYDROXIDES

NT POTASSIUM HYDROXIDES

Interstellar gas masers account for properties of 18 cm emission lines from OH molecules 03 p0511 A69-13465

HYDROXYCORTICOSTEROID

U CORTISONE

HYDROXYL COMPOUNDS

NT ALCOHOLS

NT ETHYL ALCOHOL

NT GLYCOLS

NT METHYL ALCOHOLS

NT PHENOLS

Perhydroxyl radical electron spin resonance spectrum in solution of hydrogen peroxide and water at 77 K, noting g factor, hyperfine splitting and molecular structure 01 p0024 A69-10683

Reagent menthyl chloroformate use in optical analysis of asymmetric amino and hydroxyl compounds by gas chromatography 07 p1075 A69-19499

Wideband 1665 MHz OH emission source in Carina region of galaxy in weak continuous radiation region with low degree of polarization 08 p1397 A69-20772

RF spectral lines due to OH molecule detected in interstellar space in absorption of RF radiation from Casiopeia A source 09 p1586 A69-21295

OH emission source in constellation Canis Major discovered with interferometer in October 1968, noting nearby IR object 09 p1591 A69-21448

OH emission source in W24 during July 19, 1967 lunar occultation, obtaining better position for brighter OH emission feature

09 p1591 A69-21449

Collision broadening cross sections of OH UV transition at room temperature, using flash photolysis

09 p1543 A69-22252

Radio telescopic survey for OH emission at 1667 MHz in interstellar dust clouds for catalog compilation, tabulating results

09 p1603 A69-22267

Hydroxyl luminescence spectrographic observations at twilight in vibrational-rotational band from 10600 to 11200 Å

10 p1681 A69-22847

Position and polarization of 1720 MHz OH emission from W28, W44 and galactic center, considering unresolved concentrations of shell type nonthermal sources

10 p1776 A69-23220

Primary processes leading to atomic and molecular hydrogen formation in hydrogen peroxide photolysis at 1236 Å, noting OH formation

10 p1652 A69-23527

RF spectroscopy of OH molecule, RF absorption by galactic OH and radio emission from OH in dust clouds

10 p1781 A69-23671

Position of OH sources near seven galactic radio sources determined with two element variable-baseline interferometer, noting strong circular polarization

10 p1787 A69-24114

Condensation sources of maser radiation observed in W3 hydroxyl lines, discussing polarization and designation as protostars

11 p1954 A69-24379

Equilibrium between H and OH radicals in turbulent H flames, noting component concentrations in H-O-N flames of different composition

11 p1999 A69-24487

Hydroxyl microwave emission sources in Cygnus not connected with continuum emission

11 p1964 A69-25403

Lambda-doublet radiation from excited state of interstellar OH detected at 5 cm wavelength

13 p2335 A69-27312

Galactic OH emission sources time variations found in W49 and W75

14 p2517 A69-29085

Maser emission in interstellar OH ground state produced by IR pumping, noting population inversion mechanism

15 p2691 A69-30762

RF spectral lines due to OH molecule detected in interstellar space in absorption of RF radiation from Casiopeia A source

15 p2697 A69-31226

Hydroxyl band contamination of emission and background radiation from night sky

16 p2774 A69-31987

Intensity and rotational temperature seasonal variations of hydroxyl emission at different latitudes in upper atmosphere

16 p2775 A69-32081

Hydroxylamine complexes of inorganic salts preparation and characterization, including hygroscopic properties, chemical bonds, etc

17 p2917 A69-33657

Lambda doublet maser emission from excited OH rotational level, discussing conditions necessary for microwave radiation

18 p3185 A69-34292

Interstellar hydroxyl molecular clouds as radio wave sources, using very long baseline interferometry, suggesting natural masers in space for OH emissions

19 p3427 A69-36659

Satellite-anomalous OH radio emission sources, observing spatial distribution and Stokes parameters

20 p3610 A69-38146

Excitation temperatures and OH microwave line optical depths measured for dust clouds, discussing optical depths and LF radio absorption

20 p3611 A69-38147

Upper limits for OH microwave emissions from radio sources F transitions, discussing pumping mechanism role in emission detection

21 p3796 A69-38477

OH emission rise after sunset and decay at sunrise attributed to strong solar dissociation of ozone

21 p3712 A69-38520

Airflow and vertical eddy transport photochemical models, analyzing O green line and OH emission distribution

21 p3713 A69-38523

Upper atmosphere OH molecules vibrational temperature and total emission energy, measuring average seasonal variations

24 p4308 A69-43007

Condensation sources of maser radiation observed in W3 hydroxyl lines, discussing polarization and designation as protostars

24 p4389 A69-43769

HYDROXYLAMINE SULFATE

Hydroxylamine complexes of inorganic salts preparation and characterization, including hygroscopic properties, chemical bonds, etc

17 p2917 A69-33657

HYDROXYLAMMONIUM PERCHLORATES

Hydroxylamine complexes of inorganic salts preparation and characterization, including hygroscopic properties, chemical bonds, etc

17 p2917 A69-33657

HYGROMETERS

NT PSYCHROMETERS

Northern California humidity to 32 km utilizing alpha radiation hygrometer and associated balloon sounding equipment

03 p0461 A69-13345

HYGROSCOPICITY

Visibility improvement in warm fog by seeding with micron size hygroscopic particles, noting results for NaCl

01 p0111 A69-10696

Continental and maritime hygroscopic particles associated with increasing relative humidity, determining effect on backscattered power from laser beam using Mie scattering equations

17 p2981 A69-33160

HYPERBOLAS

Elastic two cavity revolving hyperboloid deformation by arbitrary forces solved by spherical functions

11 p1984 A69-25169

Multiple characteristics and Levi-Lax conditions for hyperbolicity to prove correctness of Cauchy problem

18 p3165 A69-35277

HYPERBOLIC COORDINATES

Partial difference methods from parabolic, elliptic and hyperbolic equations solved by splittings of locally one dimensional nature

21 p3754 A69-38745

HYPERBOLIC FUNCTIONS

Cauchy problem correctness for one dimensional hyperbolic equation of arbitrary order with data on degeneracy line

01 p0104 A69-10699

Boundary value problem of hyperbolic equation with discontinuous boundary conditions

04 p0622 A69-14617

Differential-difference equations and nonlinear initial boundary value problems for linear hyperbolic partial differential equations, noting procedure based on method of characteristics

04 p0623 A69-14949

Hyperbolic double waves found in compressible flow problems, presenting method of plotting all waves and determining geometrical characteristics

05 p0751 A69-16646

Kepler hyperbolic sine equation calculated for Arend-Roland comet for case of constant residues by false position method

06 p0997 A69-16821

General two dimensional second order hyperbolic differential equation analyzed by substitution method

06 p0948 A69-17786

Hyperbolic sine creep law, discussing limiting stresses for approximation by linear or exponential relationship

07 p1235 A69-19384

Mixed initial boundary problem for hyperbolic equations with given boundary outgoing variables, determining incoming data

08 p1342 A69-20347

Liapunov direct method in stability problems for semilinear and quasi-linear systems of hyperbolic partial differential equations with independent variables

09 p1534 A69-22799

Wave propagation in connected space-time for linear second order hyperbolic partial differential equation, describing unitary invariant theory

11 p1908 A69-24356

Existence theorems for hyperbolic genuinely nonlinear systems of conservation laws, studying Cauchy problem

11 p1909 A69-25163

Boundedness criteria for second order hyperbolic equation boundary value problem solution in Banach space

12 p2122 A69-26573

Boundary value problems for hyperbolic and mixed equations using model of wave, Lavrentiev- Bitsadze and Tricomi equations

12 p2123 A69-26727

Nonlinear hyperbolic partial differential equations with dissipation term for periodic solutions

12 p2124 A69-26929

Dirichlet problem for second order linear hyperbolic partial differential equations in cylindrical domain, deriving necessary and sufficient condition for solution uniqueness

12 p2124 A69-26932

Difference schemes for quasi-linear hyperbolic equations, with applications to three dimensional supersonic flow past bodies

14 p2430 A69-29475

Riemann problem with arbitrary jump data for extended hyperbolic systems of equations, showing conditions for unique solution

14 p2433 A69-29678

Asymptotic Krylov-Bogoliubov methods application to solving boundary value problems for hyperbolic quasi-linear equations with distributed parameters and retardation

15 p2653 A69-31192

Book on quasi-linear equations systems and application to gasdynamics, including problems involving systems of quasi-linear hyperbolic equations with two independent variables

16 p2771 A69-32113

Classical solution existence to mixed boundary value problems for second order hyperbolic operators obtained by Laplace transforms

18 p3165 A69-35313

Optimal generalized controls for systems under random forces described by hyperbolic partial differential equation system

23 p4144 A69-41957

Wrong boundary conditions influence decay in overdetermined difference approximations to hyperbolic partial differential equation

24 p4340 A69-43227

HYPERBOLIC NAVIGATION

NT DECCA NAVIGATION

NT LORAN

NT LORAN C

Hyperbolic marine and air navigation including TACAN, pulse modulation, rotating hyperbolic fields, sector beacons and all-weather landing aids

13 p2296 A69-27334

Maritime navigation hyperbolic charts for aircraft position determination

23 p4186 A69-42026

HYPERBOLIC REENTRY

Radiation self absorption effects on heating loads of blunt body during hyperbolic entry

21 p3644 A69-39040

HYPERBOLIC SYSTEMS

Software remechanization of conventional hyperbolic LORAN for totally passive closed loop one way direct range measurements to individual LORAN transmitters

17 p3002 A69-34079

Positive solutions of parabolic and hyperbolic partial differential equations arising as viscoelastic media equations of motion, noting maximum principle utilization

22 p3976 A69-41035

Iterative finite difference method for initial value problems applied to hyperbolic system representing one dimensional time dependent flow of compressible polytropic gas

24 p4340 A69-43226

HYPERBOLIC TRAJECTORIES

Spacecraft trajectory using microthrust and lunar gravitational attraction for acceleration into heliocentric orbit

09 p1593 A69-21620

Double galaxies consisting of components moving away from each other with hyperbolic velocities from statistical tests of hypotheses

10 p1775 A69-23203

Photographically observed meteor orbits 1937-1963, noting overestimation of hyperbolic orbits due to observation errors

15 p2697 A69-31253

Optimal rendezvous maneuver of pursuing vehicle with minimum fuel expenditure in approach stage on elliptic and hyperbolic orbits

15 p2701 A69-31548

HYPERCAPNIA

- Minimum fuel guidance from hyperbolic into specified circular orbit 19 p3367 A69-35663
- Optimal transfer between hyperbolic asymptotes about finite size planet, discussing twelve types of analytical solutions in terms of arrival, departure and escape velocities [AAS PAPER 69-242] 24 p4380 A69-42856

HYPERCAPNIA

- Dog adaptation to 60 or 90 mm Hg carbon dioxide in 260 mm Hg total pressure environment, noting arterial pH and bicarbonate level 03 p0375 A69-14071
- Irreversible blunted respiratory response to ventilation in high altitude natives, considering hypoxic and hypercapnic stimuli 12 p2018 A69-26130
- Ventilatory responses to hypercapnia and hypoxia in anesthetized and unanesthetized rabbits before and after bilateral cervical vagotomy 21 p3651 A69-38390
- Ventilatory response to hypoxia and hypercapnia in hypothermic anesthetized dogs, noting decreased sensitivity of central chemoreceptors to carbon dioxide 22 p3885 A69-40977

HYPERFINE STRUCTURE

- Fraunhofer lines hyperfine structure effect on solar abundances of V, Mn, Co, Cu and Ba, calculating equivalent line widths by ALGOL program 02 p0311 A69-11458
- Level crossing effect in stimulated emission and application to determination of hyperfine splitting in Xe 129 excited electronic state during laser transition 07 p1156 A69-19398
- Hyperfine transition line of He 3 II for abundance in Messier 17 source by radio telescope 10 p1785 A69-24098
- Double focalization in atomic hydrogen maser by hexapolar magnets selecting hyperfine energy transitions 12 p2105 A69-26050
- RF spectra for hyperfine structure of ortho-hydrogen molecular ion, calculating doubling constant for vibrational effects 15 p2693 A69-30784
- Hyperfine spectrum analysis of NaCl at low field using molecular beam electric resonance method, discussing Hamiltonian group representation 16 p2815 A69-32794

HYPERGEOMETRIC FUNCTIONS

- Asymptotic solutions for prolate spheroidal wave functions satisfying given differential equation, producing asymptotic expansions in terms of confluent hypergeometric functions 04 p0623 A69-14892
- Quasi-plane stress in rotating disks of unconventional profile emphasizing conical shaped disk analysis in terms of hypergeometric series 07 p1235 A69-19444
- Boundary value problem for elliptic-parabolic partial differential equations in theory of random processes, obtaining analytical solution in terms of hypergeometric functions 10 p1719 A69-23516
- Elliptic equation of degenerating order in neighborhood of degeneration hyperplane, discussing solution behavior 11 p1908 A69-24696
- Analytic continuation of Appell hypergeometric series into linear combination of four infinite series 12 p2123 A69-26605
- Series and integral expansions of Jacobi polynomials with positive kernel, noting ultraspherical polynomials 14 p2470 A69-28905
- Jacobi polynomial series analytical expansion, studying relationship to Taylor series singular points 21 p3757 A69-39537
- Approximation of linear unsteady dynamic systems at finite time interval expressed in Bessel or degenerate hypergeometric functions 22 p3917 A69-40616

HYPERGEOMETRY U HYPERSPACES

HYPERGLYCEMIA

- White rats hyperglycemia during blood sugar changes following single X ray dose, indicating increased sugar benefit in radiation damage treatment 21 p3658 A69-39057

HYPERGOLIC ROCKET PROPELLANTS

- Combustion response of hydrazine-nitrogen tetroxide hypergolic rocket propellants to transverse gas flows, noting coupled and uncoupled oscillations 01 p0175 A69-10112

- Liquid hydrazine ignition by nitrogen tetroxide gas based on stagnation flow principle, presenting threshold measurements [WSCIPAPER 68-43] 06 p0983 A69-17792

- Laboratory test stands for ignition, combustion and expansion processes experiments in hypergolic liquid fuels, noting minimal recombination gains 08 p1301 A69-20170

- Monograph on ignition, combustion and expansion in hypergolic liquid propellant mixtures at gas temperatures up to 3000 K for small rocket engines 08 p1375 A69-20723

- Qualitative and quantitative hazards analysis of potential accidents/incidents in Post Boost Propulsion System with hypergolic propellants, considering recovery 10 p1753 A69-22972

- Hypergolic filling materials for solid fuels with hybrid propellant combinations, discussing ignition and combustion of ethyleneimine derivatives 10 p1753 A69-24023

- Ignition delay of paraphenylenediamine associated with nitric acid, showing relation between grain diameter and hypergolic ignition mechanism, noting oxidizer concentration effects 15 p2561 A69-30185

- Fluorine injectors for main tank injection of space vehicle liquid hydrogen tank, including study of hypergolicity and reaction product freezing [AIAA PAPER 69-528] 16 p2767 A69-32717

- Continuous mode operation in hypergolic bipropellant low thrust rocket motors, discussing high temperatures reached by combustion chamber walls and cooling solutions 17 p3019 A69-33335

- Halon 1301 fire extinguisher for burning spilled hypergol on Apollo/Saturn LM adapter, discussing concentration requirements and exposure hazards 18 p3094 A69-35062

- Halon 1301/bromotrifluoromethane/ concentration for inerting Aerazine-50 spills or extinguishing fires, noting joint use of carbon dioxide and water 18 p3094 A69-35090

HYPERONS

- Particle physics and discovery of K mesons and hyperons emphasizing track recording, cloud and bubble chamber techniques 24 p4352 A69-43039

HYPEROXIA

- High oxygen tension effect on transport and incorporation of exogenous leucine and protein synthesis in *Pseudomonas saccharophila* cells 03 p0369 A69-13433
- In vivo hyperbaric hyperoxia effect on erythrocytes unsaturated fatty acid composition alterations of tocopherol deficient mice 03 p0375 A69-14070
- Histological investigation of internal organs of mice exposed to atmosphere with high oxygen content 05 p0709 A69-16513
- Electron microscopic changes in lungs of rats after repeated exposure to pure oxygen 05 p0709 A69-16514
- High oxygen concentration influence at normal pressure on evoked potential of cortical optic zone and subcortical zones 05 p0709 A69-16515
- Hyperoxia exposure and hemolysis in tocopherol deficient mice 06 p0874 A69-17837

- Immunological and histochemical methods for studying mice reactivity after long term exposure to hyperoxic atmosphere 07 p1065 A69-18975

- High oxygen concentration effect on conditioned reflex and associated EEG responses to light flash in rabbits occurs in well defined sequences 07 p1065 A69-18976

- In vivo hemolytic susceptibility to hyperoxia in mice deficient in tocopherol 07 p1066 A69-19422

- Prolonged exposure of rats to oxygen concentrations studied for effects on organisms 08 p1262 A69-19831

- Pathological changes in respiratory and cardiovascular systems of white rats due to various levels of hyperoxia 10 p1646 A69-23577

- Pulmonary oxygen toxicity, analyzing reticulin and elastic tissue damage and hyaline membranes by histochemical techniques 14 p2407 A69-29298

- Oxygen consumption and rectal temperature in male mice confined in nitrogen and helium diluted hyperoxic atmosphere at specific temperature and humidity ranges 17 p2906 A69-32932

- Phagocytic activity and carbohydrate metabolism in peripheral blood neutrophils of men exposed to atmosphere with increased O content, noting neutrophil energy exchange disorder role 17 p2907 A69-32942

- Histological investigation of internal organs of mice exposed to atmosphere with high oxygen content 18 p3096 A69-34732

- Electron microscopic changes in lungs of rats after repeated exposure to pure oxygen 18 p3096 A69-34733

- High oxygen concentration influence at normal pressure on evoked potential of cortical optic zone and subcortical zones 18 p3096 A69-34734

- Immunological and histochemical methods for studying mice reactivity after long term exposure to hyperoxic atmosphere 20 p3479 A69-38223

- High oxygen concentration effect conditioned reflex and associated EEG responses to light flash in rabbits occurring in well defined sequences 20 p3479 A69-38224

- Hyperoxia and pulmonary surfactant washout in pulmonary compliance measurements of rats subjected to 100 percent diatomic oxygen before asphyxial death 21 p3659 A69-39066

- Normobaric oxygen toxicity pathology in baboons and Macaca, irus and squirrel monkeys during 14 day exposure 21 p3660 A69-39179

- Air and saline P-V curves of rat lungs after hyperoxia, comparing hyperoxia effects to surfactant washout on pulmonary compliance 23 p4081 A69-41440

- Increased oxygen tension adaptation and effects on adrenocortical and sympatho-adreno-medullary activity in rats, indicating toxic conversion of epinephrine to indoles 23 p4087 A69-41791

- Coronary circulation response to hyperoxia after vagotomy and combined alpha and beta adrenergic receptors blockade in anesthetized intact dog 23 p4096 A69-42088

- Hyperoxia and hypoxia effects on mitotic activity in regenerating and normal rat liver exposed to environmental conditions 24 p4269 A69-43565

HYPERPLANES

- Function generator internal storage and dimensions diminished, approximating functions of several variables by hyperplane strip 14 p2425 A69-29142

- Image recognition algorithm for determination of hyperplane separating two finite sets of elements in Euclidean space 14 p2418 A69-29353

- Einstein equations solution for empty space without singularities containing metric, with closed homogeneous space type hypersurfaces expanding anisotropically 15 p2690 A69-30732

- D-stationary principle to determine optimum hypersurfaces in configuration space containing optimal motion trajectories 16 p2811 A69-31625

- Stability criteria for integral manifold formed by intersection of hypersurfaces in Euclidean n-dimensional space 21 p3770 A69-38850

HYPERSONIC AIRCRAFT

- Fluidic type temperature sensor for total temperature measurement for hypersonic aircraft in atmosphere 05 p0766 A69-16755

- Aircraft propelled at Mach 7, discussing low speed and transonic characteristics, stability, power plant integration and ONERA wind tunnel experiments [ONERA-TP-657] 07 p1052 A69-18414

- Turbojets, turbo-rockets and Ramjet turbines compared as propulsion systems for aircraft with speeds to Mach 7 08 p1376 A69-20656

- Coated refractory tantalum alloy as ductile, weldable material for application on hypersonic aircraft or reusable reentry vehicles at high temperatures 09 p1526 A69-22326

- Supersonic ramjet propelled air breathing booster for speeds up to Mach 12, discussing flight mechanics,

aerodynamics, propulsion, heating and air intake design

09 p1573 A69-22608

Aerodynamic problems posed by hypersonic flight from Mach 3 to 20, considering relationship to half cone with flat base

16 p2867 A69-31761

Integrated propulsion control system for ramjet Hypersonic Research Engine to operate at 3-8 Mach numbers

[AIAA PAPER 69-546]

16 p2845 A69-32744

Hypersonic aircraft induced changes in chemical and thermodynamic properties of air influencing aerodynamic forces on vehicle

17 p2895 A69-33576

Stream surface characteristics as criteria for hypersonic lifting bodies shapes for optimal aerodynamic and fuel performance

19 p3248 A69-36399

Drag influence on mission performance of hypersonic aircraft during climb and cruise, noting payload capacity

20 p3461 A69-37154

Aircraft propelled at Mach 7, discussing low speed and transonic characteristics, stability, power plant integration and ONERA wind tunnel experiments

21 p3644 A69-39164

Hypersonic wave riders lift and drag coefficients, lift drag ratio, shock profile and pressure distribution, discussing wind tunnel measurements of caret wings

21 p3645 A69-39802

HYPERSONIC BOUNDARY LAYER

Hypersonic boundary layer on flat plate with strong hypersonic viscous interaction and uniform surface blowing distribution

04 p0588 A69-14722

Interaction of laminar hypersonic boundary layer and supersonic corner expansion wave, discussing upstream influence, transverse pressure gradients and external flow

[AIAA PAPER 69-137]

06 p0913 A69-18078

Transition of hypersonic boundary layers on conical body using shock tunnel, obtaining surface heat transfer distributions

[AIAA PAPER 68-39]

09 p1482 A69-21943

Density and density fluctuations in hypersonic turbulent boundary layer on shock tunnel nozzle wall measured using electron beam probe

16 p2770 A69-31907

Density and velocity fluctuations in hypersonic turbulent boundary layer based on Wallace data

16 p2770 A69-31908

Critical review of paper on suction effect on hypersonic laminar boundary layer separation

16 p2771 A69-31928

Free stream disturbances influence on hypersonic boundary layer transition Reynolds number in heated and unheated flows

[AIAA PAPER 69-704]

17 p2953 A69-33453

Hypersonic boundary layer transition on blunt slender cones at M equal 10 obtained independent Reynolds number

[AIAA PAPER 69-705]

17 p2954 A69-33455

Three dimensional hypersonic laminar boundary layer subdivided into inner and outer regions, obtaining flow description by matching inner and outer solutions

[AIAA PAPER 69-710]

17 p2955 A69-33467

Compressible hypersonic turbulent boundary layers solution by finite difference method, relating mixing length to velocity profile shape factor

[AIAA PAPER 69-684]

17 p2955 A69-33474

Miniature probe with short time response for total temperature profile measurements in hypersonic turbulent boundary layer on wall of hypersonic tunnel nozzle

19 p3293 A69-35751

Free jet boundary layer in mixing zone of hypersonic gas flow past body

20 p3513 A69-37094

Hypersonic turbulent boundary layer separation over cone-cylinder flare configuration at zero angle of attack and high Reynolds number

22 p3930 A69-40557

Book on entropy gradient effect on laminar hypersonic boundary layers, covering external frictionless flow calculations based on momentum and energy integral theorems

22 p3930 A69-40618

Strong interaction between hypersonic boundary layer over flat plate and associated inviscid flow, discussing heating and vorticity effects, boundary layer edge, etc

22 p3860 A69-40896

Asymptotic description of laminar hypersonic boundary layer acceleration approaching sharp corner, assuming small interaction with outer inviscid flow

[AIAA PAPER 68-67]

23 p4059 A69-41883

Aerodynamic forces on hypersonic vehicle surfaces, deriving relations for weak interaction pressures induced in unsteady flow

24 p4306 A69-43676

HYPERSONIC COMBUSTION

Air intakes for fixed exhaust throat hypersonic ramjet engines, discussing configuration dependence on Mach number at beginning of combustion

[ONERA-TP-658]

07 p1203 A69-18418

HYPERSONIC FLIGHT

Air intakes for fixed exhaust throat hypersonic ramjet engines, discussing configuration dependence on Mach number at beginning of combustion

[ONERA-TP-658]

07 p1203 A69-18418

Supersonic combustion technology, noting air breathing propulsion systems for application to hypersonic flight

11 p2003 A69-25596

Aerodynamic problems posed by hypersonic flight from Mach 3 to 20, considering relationship to half cone with flat base

16 p2867 A69-31761

Shock layer properties, radiative and convective heat transfer about two hypersonic blunt bodies at zero angle of attack in assumed Martian atmosphere

[AIAA PAPER 69-634]

17 p2891 A69-33281

Nonequilibrium multicomponent ionization calculations for stagnation merged shock layer of hypersonic blunt body by successive accelerated replacement

[AIAA PAPER 69-655]

17 p2892 A69-33469

HYPERSONIC FLOW

Hypersonic flow of nonequilibrium diatomic gas on and near wedge, studying shock curvature variations

01 p0005 A69-10161

Pressure and shock shape determination for plane supersonic and low hypersonic flows past aerodynamic profiles

01 p0008 A69-11299

Hypersonic gas flow past blunt body problem solved by integral correlation method, taking into account radiation effects and gas dynamic parameter distribution in shock wave layer

02 p0188 A69-11651

Soviet book on hypersonic internal and external three dimensional viscous and nonviscous gas flow, emphasizing flow past slender blunt bodies

02 p0230 A69-11775

Hypersonic flow distribution and separation types over highly swept delta wings with trailing edge flaps at Mach 6

[AIAA PAPER 68-97]

02 p0189 A69-12522

Curved bodies substitution in unsteady hypersonic flow past slender sharp nosed bodies within framework of plane sections

02 p0191 A69-12576

Hypersonic flow past delta wings with attached shock wave, analysis leads to determination of closed flow pattern

02 p0191 A69-12577

Hypersonic perfect gas flow past delta wing with blunt edges at small angles of attack, noting constant drag coefficient

02 p0191 A69-12584

Soviet book on hypersonic flow past truncated cones at various angles of attack with allowance for physicochemical equilibrium transformations

03 p0362 A69-13633

Heat input influence on hypersonic flows past sphere and circular cylinder

[DVL-844]

03 p0364 A69-13663

One-dimensional self similar motion of relaxing gas, noting ODEs of process and gas dynamic parameters of flow field

04 p0588 A69-14623

Hypersonic turbulent boundary layer in adverse pressure gradients studied for transition, measuring static/pitot pressure, stagnation temperature and heat transfer rates

[AIAA PAPER 68-44]

04 p0588 A69-14716

Surface geometry of three dimensional inviscid hypersonic flows, developing tensor equations for geodesic, steepest descent and pressure approximations

04 p0542 A69-14718

Inviscid hypersonic flow of uniform equilibrium gas past axisymmetric blunt body

04 p0542 A69-14723

Stokes-like region around yawed needle in hypersonic strong interaction regime, discussing asymptotic analysis under Stewartson conditions

04 p0542 A69-14732

Shoulder pressure on slender cone/afterbody combinations in hypersonic inviscid flow of perfect gas

04 p0542 A69-14735

Blunt cone hypersonic roll damping derivative, using Mach number distribution and graphical integration

04 p0542 A69-14739

Rarefied hypersonic flow model for sharp flat plate in strong interaction regimes, discussing inviscid and viscous shock and merged layers subregions

04 p0589 A69-14747

Axisymmetric hypersonic flow of model gas over slender bodies with strong viscous interaction and shock wave extended to power law viscosity variation

05 p0744 A69-15720

Peculiarities of aerodynamic characteristics of flow past plate and pointed and blunt slender cones in viscous hypersonic thermodynamically ideal gas

05 p0699 A69-16673

Asymptotic theory concerning nonsimilar structure of blast wave with expanding interface applied to hypersonic perfect gas flow

06 p0860 A69-17636

Hypersonic body shaping for minimum drag and improved performance from view of flight regimes, discussing implications of pressure laws

[AIAA PAPER 69-181]

06 p0863 A69-18052

Autoration characteristics of various shapes in subsonic and hypersonic flows for mechanics of free flight reentry to earth impact

[AIAA PAPER 69-132]

06 p0863 A69-18062

Low temperature simulation of hypersonic melting ablation and wave patterns of gas-liquid interface

06 p0907 A69-18064

Experimental and numerical nonequilibrium shock layer around cones in hypersonic pure oxygen flows with simultaneous rotational, vibrational and dissociation relaxation

[AIAA PAPER 69-136]

06 p0864 A69-18141

Three dimensional hypersonic steady flow around blunt and pointed cones at nonzero angles of attack calculated by method of characteristics

[AIAA PAPER 69-187]

06 p0865 A69-18176

Drag coefficients for spheres and sharp cones in rarefied hypersonic air flow obtained in shock tunnel using free flight technique

[AIAA PAPER 69-140]

06 p0865 A69-18184

Flow near leading edge of sharp insulated and cooled flat plates, using Monte Carlo direct molecular simulation

[AIAA PAPER 69-141]

06 p0866 A69-18208

Hypersonic laminar boundary layers on compression corner model, studying flap lengths effects and mass transfer

[AIAA PAPER 69-36]

06 p0866 A69-18214

Heat transfer to wedge in nearly free-molecular hypersonic flow, of strongly rarefied gas

07 p1050 A69-18707

Approximation of Chaplygin plane motion equations of gas flow at high supersonic velocities

07 p1120 A69-18754

Hypersonic flow past blunt body near stagnation point, noting surface layer characterized by increased density and decreased entropy of gas

07 p1050 A69-18755

Laminar boundary layer flow on sphere in hypersonic flow of equilibrium dissociating air

07 p1050 A69-18756

Three dimensional optimum hypersonic wings construction for wave drag minimization for given lift

[AIAA PAPER 68-158]

09 p1430 A69-21944

Book on dynamics and thermodynamics of gas at hypersonic velocities and extremely high altitudes

09 p1483 A69-22400

Laminar boundary layer separation and heat transfer on zero incidence cone at hypersonic speed, noting wall temperature and Reynolds number effects

09 p1433 A69-22609

High enthalpy air flow in hypersonic conical nozzle, calculating chemical and thermodynamic nonequilibrium effects with computer program

09 p1433 A69-22610

Noninterfering instrumentation techniques to measure hypersonic flowfield parameters in wind tunnels, measuring flight time of pulsed laser generated spark for velocity

10 p1672 A69-23266

Axisymmetric bodies longitudinal contours for hypersonic flow minimum drag, considering Newtonian pressure distribution and skin friction

10 p1632 A69-23886

Angle of attack and Reynolds number effect on hypersonic flow past circular cone, obtaining shock wave shape
[ONERA-TP-692] 11 p1818 A69-24751

Kinetic theory for spherical expansion of hypersonic jet flow indicating translational freezing in hypersonic source expansion 11 p1870 A69-25006

Spherically blunted 15 degree semivertex angle cone flow field parameters at Mach 8.6, measuring pitot pressure and shock shape 11 p1818 A69-25143

Flat plate in two dimensional low density hypersonic flow wind tunnel tested for aerodynamic effects on spacecraft reentry 11 p1819 A69-25424

Aerodynamic characteristics of flat plate in viscous hypersonic flow incident at zero or small angle of attack, using numerical integration 11 p1820 A69-25471

Hypersonic viscous gas flow past thin bodies, deriving equations for interactions between boundary layer and external flow 11 p1820 A69-25472

Supersonic and hypersonic flow of rarefied gas around blunted cylinders at various angles of attack, noting pressure distribution on model surface 11 p1821 A69-25478

Aerodynamic measurements on Apollo CM model at hypersonic flow simulating earth orbital reentry trajectory 12 p2012 A69-26800

Laminar boundary layer studies by finite difference computer program for Mach numbers up to 15 13 p2248 A69-28173

Roughness effects on boundary layer transition up to Mach 16 in hotshot wind tunnel [AIAA PAPER 68-377] 13 p2242 A69-28213

Free flight sharp cone drag measurements in rarefied hypersonic flow 13 p2199 A69-28244

Longshot free piston gun tunnel for high Reynolds number hypersonic flow tests [AIAA PAPER 69-333] 13 p2249 A69-28269

Vitiated air contamination effects on combustion and hypersonic air breathing engine ground tests [AIAA PAPER 69-338] 13 p2325 A69-28274

Supersonic Preston tube correlations for Mach number and Reynolds number effects on hypersonic turbulent skin friction on adiabatic surfaces, simplifying correlation [AIAA PAPER 69-345] 13 p2249 A69-28280

Angle of attack and blunting effect on aerodynamic lift and drag coefficients of flat plates in hypersonic flow at low Reynolds number 13 p2200 A69-28358

Unsteady pressure on oscillating slender cone in hypersonic flow derived by expanding flow equations in powers of shock density parameter 14 p2389 A69-29020

Boundary layer physical and chemical processes effect on dynamic parameters of high temperature hypersonic gas flow past blunt bodies 14 p2391 A69-29620

Diffuser performance in hypersonic shock wind tunnel for nitrogen flow, discussing steady shock wave and separation zone formation time 14 p2391 A69-29622

Optimum surface for thick delta wing in hypersonic flow obtained by variational method, assuming closed leading and trailing edges 16 p2731 A69-31559

Wall pressure and heat flux distribution in hypersonic flow on delta wings at variable angle of attack for low Reynolds numbers 16 p2731 A69-31605

Subliming ablation effects on boundary layer transition for cones in hypersonic flow, discussing Reynolds numbers measured in wind tunnel tests [AIAA PAPER 68-40] 16 p2732 A69-31881

Streamline flow of ideal stable gas with constant ratio of specific heats around conical body with arbitrary taper, determining flow velocity components 16 p2732 A69-32126

Shock tunnel facility generating short duration high velocity high density air flow with equilibrium chemical simulation of free stream flight conditions [AIAA PAPER 68-17] 16 p2766 A69-32167

Monograph on solutions to equations for unsteady flow of ideal gases, with applications to hypersonic flows, based on three space coordinates and time 16 p2773 A69-32428

Aerodynamic characteristics of cone/cylinder and cone/cylinder/cone configurations with blunted cones in hypersonic flows at small angles of attack 17 p2889 A69-33122

Boundary layer trip geometry, size and location effect on position of transition at hypersonic speeds 17 p2950 A69-33249

Hypersonic slender cone zero angle of attack drag in rarefied continuum and noncontinuum flow in shock tunnel, indicating body dimension influence in transition regime [AIAA PAPER 69-711] 17 p2891 A69-33445

Exact similarity solutions of hypersonic small disturbance equations for steady flow, discussing equations of state and motion and dissociating gas flow [AIAA PAPER 69-707] 17 p2953 A69-33448

Eddy viscosity models adapting laminar boundary layer solution techniques to turbulent flows compared with measurements in hypersonic flows [AIAA PAPER 69-688] 17 p2954 A69-33454

Surface pressure and heat transfer over blunt conical body in hypersonic flow with uniform mass addition of various gases [AIAA PAPER 69-716] 17 p2891 A69-33463

Supersonic and hypersonic flow of inviscid ideal gas over conical delta wings using three dimensional method of characteristics [AIAA PAPER 69-646] 17 p2893 A69-33486

Flow field study of merging between bow shock and viscous layer upstream of highly cooled axisymmetric blunt body in rarefied hypersonic stream [AIAA PAPER 69-656] 17 p2893 A69-33498

Nonequilibrium, real gas and nose bluntness effects on hypersonic slender body flows, analyzing similitudes, free stream temperature, velocity and relaxation [AIAA PAPER 69-708] 17 p2894 A69-33501

Strong shock wave structural model, considering near molecular beam, upstream hypersonic and downstream subsonic flows and beam-continuum conversion by collision 18 p3120 A69-34457

Transport processes effect in shock wave on hypersonic flow past blunt body in neighborhood of stagnation point, noting heat transfer 18 p3086 A69-34910

Electron beam fluorescence probe and afterglow investigation for hypersonic He flow visualization, observing qualitative structure 19 p3291 A69-35722

Hypersonic rarefied gas flow past flat plate with sharp leading edge and past circular cylinder, noting wake structure similarity to viscous theory prediction 19 p3294 A69-35755

Aerodynamic characteristics of two dimensional nonexpandable flexible sail in hypersonic inviscid flow, discussing roles of sail length and chord and angle of attack 19 p3237 A69-35814

Nose bluntness effect on hypersonic flow for slender blunt bodies with arbitrarily shaped lateral surfaces at small attack angle 19 p3239 A69-36402

Wing tunnel and theoretical studies of hypersonic wall flow on cone, considering static pressure and convection heat flux density effects 19 p3241 A69-36759

Stagnation point heating in hypersonic gas flow past blunt bodies, considering radiative transfer effects on shock wave temperature and density distribution, wave separation, etc 20 p3457 A69-36981

Hypersonic gas flow past blunt bodies valid for any optical thickness of gas, allowing for absorption coefficients, dependence on temperature, pressure and frequency 20 p3457 A69-36993

Surface pressure, skin friction and heat transfer measurements on sharp flat plates and wedges in low density hypersonic flow, noting slip velocity 20 p3458 A69-37186

Free flight telemetered base pressure test data correlation for high Mach numbers, noting facilities and instrumentation 20 p3458 A69-37196

Conical delta wings in supersonic-moderate hypersonic flow, studying yaw effects on pressure distribution behind shock wave 20 p3459 A69-37593

Monte Carlo simulation for studying rarefied hypersonic gas flow about slender cones and flat plates 20 p3459 A69-37902

Monograph on forces exerted by air during yawing motion of sharp cones in supersonic and hypersonic flows by semilinear method 20 p3460 A69-37919

Three dimensional laminar boundary layer hypersonic flow about slender conical vehicles, analyzing 24 p4306 A69-43674

transverse surface curvature effect, studying Reynolds number, cone angle, etc [ASME PAPER 69-FE-23] 20 p3460 A69-37992

Gaseous injection effect on laminar boundary layer hypersonic flow around transpiration-cooled blunt bodies analyzed by integral method and Newtonian model 21 p3644 A69-39014

Optimum form for hypersonic profile with minimum drag for given bending strength solved by variational method 21 p3644 A69-39099

Axisymmetric and two dimensional flows over blunt bodies at high Mach numbers by integral relations method 21 p3645 A69-39790

Aerodynamic forces under space-like conditions measured by swing balance, using large scale molecular beams for rarefied hypersonic gas flow simulation [AIAA PAPER 69-1032] 22 p3924 A69-40400

Mach 8 flow field effects and forces on small delta tail surfaces mounted on body of revolution at various angles of attack [AIAA PAPER 68-891] 22 p3859 A69-40539

Hypersonic flow for low Reynolds number, including magnetic field and wall temperature effects on heat transfer and skin friction for blunt shapes 22 p3860 A69-40540

Shock wave detachment distance in front of spheres and cylinders in hypersonic flow, using magnetic shock tubes and Mach 5 and 18 wind tunnels 22 p3931 A69-40710

Piston motion influence on gaseous motion set up by constant energy explosion, applying to steady high Mach number flow past blunt nosed object 22 p3931 A69-40892

Frictionless supersonic and hypersonic flow of ideal gas of constant specific heat past cone with deformed axis at zero angle of attack 23 p4058 A69-41579

Radiative transfer effects in low Reynolds number or merged layer regime of hypersonic flow about axisymmetric blunt bodies, including thin shock layer theory 23 p4059 A69-41885

Mach 42 test measuring surface pressures, surface heat transfer rates and shock wave shapes in strong interaction regime for sharp and blunt plates [AIAA PAPER 68-720] 23 p4059 A69-41886

Hypersonic turbulent flow heat transfer and pressure data for flat plate containing steps and cavities obtained in hypersonic wind tunnel [AIAA PAPER 68-673] 23 p4060 A69-41902

Windward shock angle parameters on yawed cones correlated in single variable for hypersonic flow 23 p4060 A69-41918

Nonlifting blunt axisymmetric hypersonic shape determination to maximize pressure drag for given convective heat transfer, diameter and free-stream conditions 24 p4244 A69-42960

Underexpanded plane hypersonic gas jet injection into resting medium from straight nozzle, discussing shock wave formation 24 p4246 A69-43484

Intense heat exchange narrow zones on blunted semicone surfaces in hypersonic gas flows ascribed to large Reynolds numbers 24 p4246 A69-43494

Hypersonic viscous interaction, studying axisymmetric flow over slender sharp nose cones at zero angle of attack and three dimensional flow over sharp flat plate 24 p4248 A69-43579

Inviscid hypersonic flow over oscillating slender wedge, defining equivalent phase shift 24 p4248 A69-43582

Radiation equilibrium temperature measured downstream of transpiration cooled gas flow near slender cone vertex in continuous flow hypersonic tunnel 24 p4248 A69-43588

Perturbation equations for oscillating wedges and carot wings with attached bow shock in hypersonic and supersonic flows 24 p4249 A69-43659

Mass injection effects on viscous hypersonic low Reynolds number shock layer downstream and at stagnation point in blunt forebody region analyzed for non-reacting gas 24 p4249 A69-43663

Strong shock and Mach waves interaction generated downstream of thick wedge body shock in unsteady hypersonic and supersonic flows 24 p4306 A69-43674

Free flight telemetry base pressure measurements on slender cones and domed afterbodies in hypersonic laminar flow, using shock tunnel test facility [AIAA PAPER 68-698] 24 p4249 A69-43675

Cylindrical models in hypersonic rarefied flow, determining drag data by free flight technique 24 p4249 A69-43677

HYPERSONIC FORCES

Scaling laws for nose bluntness effects on hypersonic aerodynamics of bodies of revolution [AIAA PAPER 68-1158] 03 p0362 A69-13566

HYPERSONIC GLIDERS

Hypervelocity glide vehicle optimum maneuvers, finding lift optimal control law for maximization of final velocity or altitude 17 p3025 A69-32836

HYPERSONIC HEAT TRANSFER

Boundary layers and heat transfers at shock tube walls, establishing approximate solution of boundary layer equation for laminar and turbulent cases [ONERA-TP-647] 03 p0412 A69-12875

Heat transfer and drag of cylinders with cavities at hypersonic speeds measured by platinum film thermometer and strain gauge balance in gun tunnel [DVL-850] 04 p0543 A69-14822

Hypersonic laminar and transitional heat transfer rate distribution on spherically blunted cones 05 p0696 A69-15707

Laminar boundary layer separation and heat transfer on zero incidence cone at hypersonic speed, noting wall temperature and Reynolds number effects 09 p1433 A69-22609

Multirecompression heater for pure airflow tests of ballistic vehicles and hypersonic aircraft [AIAA PAPER 69-332] 13 p2242 A69-28268

Flow characteristics and wall heat transfer in separated flow region of annular cavity at free stream hypersonic speed and high gas temperature [AIAA PAPER 68-672] 20 p3458 A69-37185

Hypersonic flow for low Reynolds number, including magnetic field and wall temperature effects on heat transfer and skin friction for blunt shapes 22 p3860 A69-40540

Mach 42 test measuring surface pressures, surface heat transfer rates and shock wave shapes in strong interaction regime for sharp and blunt plates [AIAA PAPER 68-720] 23 p4059 A69-41886

HYPERSONIC INLETS

Shock wave-boundary layer interaction configurations for hypersonic propulsion device inlets under transitional and turbulent conditions, noting heat transfer rate 06 p0915 A69-18172

Collection of articles on ramjets including reaction propulsion, hypersonic inlets, combustion problems, Griffon aircraft, storable liquid fuels, etc 16 p2837 A69-32608

Turbulent boundary layer subject to sudden pressure variation due to rapid expansion or shock wave, noting application to hypersonic ramjet air intake [ICAS PAPER 68-42] 17 p2895 A69-33587

HYPERSONIC NOZZLES

Dense gas effects in free piston hypersonic wind tunnel, discussing Longshot facility, free piston cycle, reservoir conditions decay and hypersonic nozzle flow [AIAA PAPER 69-169] 06 p0907 A69-18188

High enthalpy air flow in hypersonic conical nozzle, calculating chemical and thermodynamic nonequilibrium effects with computer program 09 p1433 A69-22610

Laminar boundary layers in low density supersonic and hypersonic conical and axisymmetric nozzles, treating displacement, transverse curvature, velocity slip and temperature jump [AIAA PAPER 69-653] 17 p2954 A69-33458

HYPERSONIC REENTRY

Acoustic probe for measuring pressure fluctuations on hypersonic reentry vehicle, discussing flow characteristics and heat shield ablation effects on frequency response 01 p0008 A69-11278

Unsteady aerodynamics of ablating flared reentry body, noting complications due to blunted nose shear flow and entropy gradient effects 02 p0189 A69-12524

Flight tests in wide Mach number range of blunt nosed flare stabilized hypersonic reentry nose cone, deducing drag and stability coefficients [AIAA PAPER 68-1145] 03 p0521 A69-13668

Inert gas discontinuous injection into nonequilibrium laminar boundary layer 06 p0860 A69-17635

Transpiration cooling of reentry vehicle nosetips, noting two dimensional aspects of porous wall coolant flow and matrix-coolant energy exchange [AIAA PAPER 69-96] 06 p1039 A69-18212

Radiant heat transfer in hypersonic aerodynamic heating, discussing radiant flux and carbon dioxide concentration in reentry problems 11 p2002 A69-25233

Hypervelocity reentry simulation problems for slender and blunt bodies, defining significant parameters 15 p2681 A69-30376

Ion and electron distributions in chemical nonequilibrium boundary layer flow over hypersonic reentry vehicle, discussing plasma sheath and boundary layer thickness relations 16 p2769 A69-31874

Reentry flight test vehicle development for West German space program, using hypersonic model to determine controllability and aerodynamic stability 16 p2867 A69-31934

Radiative energy emission by blunt vehicle shock layer under severe entry conditions, discussing flow properties and radiative transfer coupling [AIAA PAPER 69-719] 18 p3084 A69-34416

Radiating gas flows during hypersonic planetary reentry, discussing atmospheric composition, shock layer characteristics, nonequilibrium flows, etc 20 p3513 A69-36982

Hypersonic parachute structural design using nylon ribbon, glass fiber heat shield and ablative coating construction [AIAA PAPER 68-963] 21 p3647 A69-39230

Reentry Vehicle Altitude-Velocity Sensor for continuously measuring hypersonic vehicles free stream density and velocity in atmosphere at low angle of attack [AIAA PAPER 69-866] 21 p3725 A69-39392

Spacecraft trajectory control algorithm for hypersonic reentry, describing onboard equipment role and simulation results 21 p3767 A69-39649

Hypersonic reentry spheres drag coefficients derived from radar measurements 23 p4059 A69-41898

Flight tests in wide Mach number range of blunt nosed flare stabilized hypersonic reentry nose cone, deducing drag and stability coefficients [AIAA PAPER 68-1145] 24 p4394 A69-43250

Near wake electron density distribution for reentry configuration models in shock tunnel with minimum flow interference [AIAA PAPER 68-161] 24 p4248 A69-43643

Image intensifier coupling to electron scanning image converter to increase time-resolving spectrograph sensitivity in simulated reentry studies 24 p4317 A69-43759

HYPERSONIC SHOCK

Shock tunnel hypersonic flow effect on critical Weber number for zirconium drop breakup in partially and fully molten states 12 p2063 A69-26802

Energy transfer mechanisms between translational, rotational, vibrational, chemical and electronic degrees of freedom in hypersonic shock wave in high temperature air 12 p2063 A69-26969

MGD hypersonic shock layer at spherically blunted body analyzed by utilizing induction equation including Hall effect [AIAA PAPER 69-722] 17 p3012 A69-33494

Electron concentration in hypersonic nonequilibrium shock layer flow by two wavelength laser interferometry, noting wavelength dependence of refractivity 19 p3306 A69-35742

Probe for spectral radiation from luminous gas-cap stagnation region to determine driver gas in test section of hypersonic shock tunnel 19 p3294 A69-35753

Conical delta wings in supersonic-moderate hypersonic flow, studying yaw effects on pressure distribution behind shock wave 20 p3459 A69-37593

HYPERSONIC SPEED

Lift drag ratio attainable by optimal transversal contour slender conical lifting body at hypersonic speeds 06 p0861 A69-17640

Leeward side of delta wing with sharp leading edges at hypersonic speeds, noting Prandtl-Meyer expansion [AIAA PAPER 68-675] 09 p1431 A69-21992

Hypersonic flight test data of Berenice missile compared to wind tunnel test data, discussing in-flight flow separation, Mach-Reynolds torque, etc 10 p1632 A69-23842

Nose bluntness effect on hypersonic unsteady aerodynamics of flared and conical bodies of revolution [AIAA PAPER 68-889] 12 p2012 A69-26794

Mach number, cone angle, bluntness and wall to recovery temperature ratio effects on slender cones boundary layer transition measurements at hypersonic speeds 17 p2890 A69-33250

Nonuniform heating rates during laminar boundary layer transition on slender cone at hypersonic speeds 18 p3085 A69-34435

Law of wall parameters for compressible turbulent boundary layer with air injection through wall determined by analyzing data for hypersonic speeds 21 p3692 A69-38685

Hypersonic lifting bodies with high lift-drag ratio, presenting flat-top wing-body combination aerodynamic characteristics 21 p3645 A69-39793

Newton formula and Ritz method to determine wing shape with blunt leading edge, considering minimum drag achievement at hypersonic velocities 24 p4247 A69-43497

HYPERSONIC TEST APPARATUS

Hypersonic surface measurements and flowfield properties about slender cones in hypersonic viscous interaction regime [AIAA PAPER 68-2] 02 p0189 A69-12520

Free flight static, dynamic stability and drag data for 10 degree semiangle cone obtained at 8-16 Mach numbers [AIAA PAPER 69-133] 06 p0862 A69-18050

Atmospheric entry testing in terms of velocity-altitude duplication, suggesting multistage rocket propelled aeroballistic range type testing [AIAA PAPER 69-166] 06 p0907 A69-18189

Hypersonic slipper bearing problem in rocket boosted sleds, discussing flow model consisting of laminar stagnation region and boundary layers [AIAA PAPER 68-756] 09 p1477 A69-22003

Hypersonic drag and shock wave characteristics of blunt bodies including cones, spherical nose and concave nose bodies 09 p1433 A69-22568

Hypersonic test equipment and programs at CEAT /France/, describing compressor, wind tunnels and several experiments 16 p2766 A69-32071

Kyoto University hypersonic gun tunnel equipment and performance data, discussing central control system, automatic operating system and double diaphragm device 22 p3927 A69-40587

HYPERSONIC VEHICLES

NT HL-10 REENTRY VEHICLE

Hypersonic lifting body configurations for maximum lift drag ratios and subject to volumetric efficiency, nose heating limit and skin friction constraints 02 p0189 A69-12378

Minimum drag configurations with low heat transfer for hypersonic bodies of revolution, noting performance at supersonic speeds 02 p0191 A69-12578

Hypersonic lifting body optimization under single and combined constraints of volumetric efficiency, heating and skin friction, using numerical search routine [AIAA PAPER 68-1157] 03 p0362 A69-13557

Limiting speed for target tracking hypersonic vehicle due to electrons formation through aerodynamic heating, calculating allowable flow conditions, maximum speeds and electron distribution 07 p1086 A69-19509

Ceramic radomes for hypervelocity aerospace vehicles, considering wide temperature environment effects on stability and properties 07 p1171 A69-19511

Hypersonic missile interceptor vibration characteristics in lower atmosphere, noting role of base pressure excitation 09 p1614 A69-21890

Hypersonic vehicles multivariable flight control systems, analyzing flight path in terms of equation of motion of longitudinal mode 12 p2128 A69-26066

Cone-conical-frustum configurations meeting center of gravity requirements for higher hypersonic lift-drag ratios in axisymmetric manned spacecraft 21 p3644 A69-39237

Aerodynamic forces on hypersonic vehicle surfaces, deriving relations for weak interaction pressures induced in unsteady flow 24 p4306 A69-43676

HYPERSONIC WAKES

Microwave and far IR molecular rotational absorption spectra investigated for measuring concentrations of reacting molecular and atomic species in hypersonic projectile wakes

01 p0006 A69-10961

Viscous interaction solution obtained for near wake of axisymmetric bodies by integral moment method and axisymmetric incompressible similar wake solutions

06 p0860 A69-17633

Laminar near wake flow field of two dimensional adiabatic circular cylinder with surface mass transfer

[AIAA PAPER 69-67] 06 p0862 A69-18044

Axisymmetric hypersonic near wake with base injection, discussing zero injection case, jet-plume interaction and mixing region

[AIAA PAPER 69-66] 06 p0914 A69-18115

Turbulent density fluctuations in near wake of hypersonic axisymmetric slender body measured photometrically with near UV absorption of sulfur dioxide in flow

[AIAA PAPER 69-70] 06 p0864 A69-18158

Electron density fluctuations in turbulent wakes of hypersonic projectiles in ballistic ranges, discussing use of cylindrical Langmuir probe for direct measurement

09 p1496 A69-21934

Analog simulation of cylinder wake potential for hypersonic motion in collisionless plasma

11 p1926 A69-24756

Nose bluntness and model scale effect on radial and axial variation of wake fluid and plasma properties by hypervelocity shock tunnel

[AIAA PAPER 69-330] 13 p2242 A69-28266

Laminar and turbulent hypersonic wakes trailing blunt bodies studied by finite difference method, taking into account pressure gradients and nonequilibrium chemical reactions effects

14 p2391 A69-29618

Hypersonic wakes interference effects induced by facility instrumentation, discussing results of wind/shock tunnel investigations

15 p2588 A69-30475

Steady state plasma wind tunnel for flow around ionospheric satellites, studying wakes of cylinders and spheres

[AIAA PAPER 69-673] 17 p2893 A69-33488

Laminar recompression behavior downstream of stagnation point behind hypersonic slender body, obtaining finite difference numerical solutions for near wake flow field

[AIAA PAPER 69-713] 18 p3085 A69-34417

Electrostatic probes calibration and use for hypersonic wakes behind projectiles in ballistic range

19 p3291 A69-35717

Ablating sphere viscous wake using image converter camera, computing luminance radial distribution by unit volume

19 p3306 A69-35739

Double knife-edged double-crossing schlieren apparatus analyzed for operation principle and applied to measure hypersonic wake characteristics in hotshot tunnel

19 p3293 A69-35740

Hypersonic rarefied gas flow past flat plate with sharp leading edge and past circular cylinder, noting wake structure similarity to viscous theory prediction

19 p3294 A69-35755

Mars entry capsule ionized wake producing circularly polarized antenna radiation null region, noting effect on communication blackout time

22 p3914 A69-40701

Bistatic radar scattering cross sections for reentry vehicle with ionized wake

23 p4116 A69-41593

Fluid mechanical structure of laminar hypersonic wake behind sharp circular cone, investigating flow field at zero angle of attack and adiabatic wall temperature

24 p4247 A69-43576

Near wake electron density distribution for reentry configuration models in shock tunnel with minimum flow interference

[AIAA PAPER 68-161] 24 p4248 A69-43643

HYPERSONIC WIND TUNNELS

U HYPERVELOCITY WIND TUNNELS

HYPERSONICS

Stimulating effects of space hypersonic experiments on technical and scientific progress, discussing steel degassing, welding, electroforming and geological applications

[UN PAPER 68-95459] 06 p0857 A69-17083

Holography for optical analysis of hypersonic aerodynamics in single shot firing tunnel

12 p2087 A69-26176

HYPERSPACES

Quantum geometrodynamics in superspace, noting dynamical evolution of geometry with no real mass energy sources

05 p0793 A69-15773

HYPERSPHERES

Einstein equations solution for empty space without singularities containing metric, with closed homogeneous space type hypersurfaces expanding anisotropically

15 p2690 A69-30732

HYPERTENSION

Essential hypertension in selection and evaluation of airline pilots, discussing use of thiazide therapy

06 p0875 A69-17850

Blood pressure measurements of pilots at rest during tests under stress on bicycle ergometer revealing transient hypertension

23 p4087 A69-41795

HYPERTHERMIA

Human metabolic response to hypothermia measured over wide range of work intensities and durations

22 p3891 A69-40215

HYPERTONIA

U OSMOSIS

HYPERTROPHY

U GROWTH

HYPERVELOCITY CRATERING

U PROJECTILE CRATERING

HYPERVELOCITY FLOW

Matched asymptotic expansions method applied to problem of hypervelocity atmospheric entry, noting solution division into outer Keplerian region and inner expansion region

09 p1430 A69-21964

Fluorescence stimulated by high energy electron and ion beams, determining vibrational temperature and concentration of molecular oxygen in high enthalpy wind tunnel flows

13 p2302 A69-28265

Nose bluntness and model scale effect on radial and axial variation of wake fluid and plasma properties by hypervelocity shock tunnel

[AIAA PAPER 69-330] 13 p2242 A69-28266

Isentropic compression tube with piston compressor for producing hypervelocity test flows, noting shock speeds

[AIAA PAPER 69-334] 13 p2249 A69-28270

Hypervelocity shock wave propagation in rarefied gas, observing anomalous wave attenuation

14 p2433 A69-29846

Pressure and temperature surveys of Mach 27-47 nozzle boundary layer at Ames M-50 He tunnel, determining velocity profiles, wall friction coefficient, etc

[AIAA PAPER 69-686] 17 p2953 A69-33441

Hypervelocity ionized gas flow analysis, allowing for finiteness of energy exchange duration between electrons and ions

19 p3379 A69-36383

Gaseous mixtures for hypervelocity applications, studying equilibrium conditions and thermodynamic properties for shock and constant volume heating processes

22 p4049 A69-40266

HYPERVELOCITY IMPACT

Hypervelocity impact effect on structural honeycomb spacecraft wall configurations, stressing design and wall thickness parameters

[AIAA PAPER 68-314] 02 p0345 A69-12389

Transient response of targets subjected to hypervelocity impacts and quantitative aspects of impact process, noting study of wax targets interiors

07 p1234 A69-19380

Hypersonic wind tunnel for erosion test of multiple particle impacts, considering dust on cork, carborazole and silicone rubber

[AIAA PAPER 69-341] 13 p2243 A69-28277

Computer program for compressible fluid flows with space and time dependent variables, discussing hypervelocity impact

[AIAA PAPER 69-353] 13 p2365 A69-28286

Characteristics method for stress waves from hypervelocity impact of circular cylinder on half space, discussing numerical diffusion effect on pressure and flow fields

[AIAA PAPER 69-355] 13 p2365 A69-28287

Numerical method for time dependent compressible Navier-Stokes equations applied to axisymmetric flow field produced by hypervelocity impact, examining viscous effects

[AIAA PAPER 69-354] 13 p2366 A69-28288

Projectile impacts into laminated targets consisting of plastic layers backed by Al substrates using SHAPE

code with hydrodynamic elastoplastic distortional model

[AIAA PAPER 69-356] 13 p2366 A69-28289

Hypervelocity impact of spheres on thin targets studied with numerical solutions utilizing STEEP code two dimensional technique based on hydrodynamic elastoplastic model

[AIAA PAPER 69-357] 13 p2366 A69-28290

High pressure Hugoniot points made by hypervelocity gas gun, using laser beams to measure impact velocity and pressure transducer for impact stress

[AIAA PAPER 69-358] 13 p2264 A69-28291

Experimental and predicted shock axial pressure variations for semiinfinite metallic targets during high velocity impact, using Al alloys and Cu

[AIAA PAPER 69-361] 13 p2366 A69-28294

Hypervelocity impact flash resolved into sub-microsecond continuum radiation pulse succeeded by slow rising long duration light pulse from neutral atomic line emission

[AIAA PAPER 69-364] 13 p2313 A69-28296

Impact crater cross section in fused silica, describing photomicrographic technique for distinguishing hypervelocity from low energy impacts

[AIAA PAPER 69-367] 13 p2366 A69-28299

Hypervelocity impact dynamics on copper cube targets imbedded with nickel wires, discussing terminal positions, Vickers hardness, flow fields, etc

[AIAA PAPER 69-368] 13 p2367 A69-28300

Fracture of bumper protected fuel tanks subjected to hypervelocity meteoroid impact, applying method of characteristics to stress wave propagation in tank walls

[AIAA PAPER 69-369] 13 p2367 A69-28301

Pyrex spheres accelerated to 15 km/sec by plasma rail gun to study hypervelocity impact in thin stainless steel and Al targets

[AIAA PAPER 69-378] 13 p2368 A69-28308

Bumper materials effect on two component hypervelocity impact shields performance, noting material density influence

[AIAA PAPER 69-379] 13 p2283 A69-28309

Two plate meteoroid shields effectiveness determined by analyzing debris cloud ejected behind front plate after hypervelocity impact

[AIAA PAPER 69-380] 13 p2368 A69-28310

Hypervelocity micrometeor impact sites identification on aluminized glass, using conchoidal pattern as criterion in analysis

18 p3199 A69-34952

HYPERVELOCITY LAUNCHERS

NOL hypervelocity launcher heat transfer and erosion analysis by experiment and computer simulation

[AIAA PAPER 69-336] 13 p2242 A69-28272

HYPERVELOCITY PROJECTILES

Microwave and far IR molecular rotational absorption spectra investigated for measuring concentrations of reacting molecular and atomic species in hypersonic projectile wakes

01 p0006 A69-10961

Recovery behavior of nickel strain hardened by impact loading by aluminum projectiles, showing microstructure correlation with stress levels

03 p0447 A69-13620

Ablation surface patterns and resulting roll torques and roll behavior of hypervelocity vehicles

[AIAA PAPER 69-180] 06 p1036 A69-18051

Schlieren high speed photography systems for ballistic projectile studies, discussing use of gas lasers as nanosecond light sources

12 p2088 A69-26182

Hypervelocity projectile size and density effect on ballistic limit of dual sheet spacecraft meteoroid protection structures, considering penetration of low and high density particles

[AIAA PAPER 69-376] 13 p2367 A69-28306

Pyrex spheres accelerated to 15 km/sec by plasma rail gun to study hypervelocity impact in thin stainless steel and Al targets

[AIAA PAPER 69-378] 13 p2368 A69-28308

Electrostatic probes calibration and use for hypersonic wakes behind projectiles in ballistic range

19 p3291 A69-35717

High speed photography for hypervelocity aeroballistic ranges, using giant pulse ruby laser for front lighting

19 p3306 A69-35732

Laser shadowgraph technique for visual observation of projectiles surface flying at hypersonic velocity along ballistic trajectory

22 p3963 A69-40601

HYPERVELOCITY WIND TUNNELS

NT CASCADE WIND TUNNELS

NT HOTSHOT WIND TUNNELS

NT PLASMA JET WIND TUNNELS

NT SHOCK TUNNELS

Intermittent traversing gear with stepping motor for small hypersonic helium wind tunnels

01 p0054 A69-10219

Blow-down facility for hypersonic testing of air breathing engines, describing test cell, air heating system, exhausters and data system

02 p0227 A69-11756

Ground simulation of reentry observables with ablation, studying ablation products interaction with flow-field of wave superheater hypersonic tunnel

02 p0229 A69-12502

Spatial distribution of three dimensional laminar boundary layer transition zone on sharp half angle cone from hypersonic wind tunnel tests [AIAA PAPER 69-12]

06 p0863 A69-18112

Dense gas effects in free piston hypersonic wind tunnel, discussing Longshot facility, free piston cycle, reservoir conditions decay and hypersonic nozzle flow [AIAA PAPER 69-169]

06 p0907 A69-18188

Free stream turbulence influence on stagnation zone heating in arc heated hypersonic facilities, obtaining stagnation point heating rates [AIAA PAPER 69-167]

06 p1039 A69-18198

Noninterfering instrumentation techniques to measure hypersonic flowfield parameters in wind tunnels, measuring flight time of pulsed laser generated spark for velocity

10 p1672 A69-23266

Hypersonic flight test data of Berenice missile compared to wind tunnel test data, discussing in-flight flow separation, Mach-Reynolds torque, etc

10 p1632 A69-23842

Time varying flow properties effects on hypersonic wind tunnel spectroscopic measurements, considering direct emission and electron beam techniques [AIAA PAPER 69-331]

13 p2242 A69-28267

Longshot free piston gun tunnel for high Reynolds number hypersonic flow tests [AIAA PAPER 69-333]

13 p2249 A69-28269

Axisymmetric hypersonic wind tunnel nozzle design by determining inviscid contour and correcting for turbulent boundary layer growth [AIAA PAPER 69-337]

13 p2200 A69-28273

Hypersonic wind tunnel for erosion test of multiple particle impacts, considering dust on cork, carborazole and silicone rubber [AIAA PAPER 69-341]

13 p2243 A69-28277

Multimegawatt arc heater for hypersonic continuous flow high enthalpy wind tunnel

15 p2586 A69-30378

Hypersonic test equipment and programs at CEAT /France/, describing compressor, wind tunnels and several experiments

16 p2766 A69-32071

Transient calibrations for Ge surface thermocouple heat flux sensors used in hypervelocity impulse tunnel

19 p3292 A69-35725

Miniature probe with short time response for total temperature profile measurements in hypersonic turbulent boundary layer on wall of hypersonic tunnel nozzle

19 p3293 A69-35751

Wing tunnel and theoretical studies of hypersonic wall flow on cone, considering static pressure and convection heat flux density effects

19 p3241 A69-36759

Hypersonic wave riders lift and drag coefficients, lift drag ratio, shock profile and pressure distribution, discussing wind tunnel measurements of caret wings

21 p3645 A69-39802

Kyoto University hypersonic gun tunnel equipment and performance data, discussing central control system, automatic operating system and double diaphragm device

22 p3927 A69-40587

Arc-heated hypersonic wind tunnel for simulated spacecraft reentry environment, aerodynamic heating characteristics and research applications

22 p3927 A69-40595

HYPERVENTILATION

Age and carbon dioxide tension effects on EEG of adolescents and adults, discussing end-tidal carbon dioxide during routine hyperventilation

22 p3872 A69-40162

Carbon dioxide washout during square wave hyperventilation in man, postulating blood flow factor

22 p3885 A69-40975

Hyperventilation induced hemolysis in dogs measured as function of exposure time, body temperature and blood pH

22 p3887 A69-41192

Hyperventilation effect on flight personnel, discussing oxygen and carbon dioxide partial pressures, symptoms and clinical signs

24 p4269 A69-43410

HYPNOSIS

EEG alpha activity relationship to laterality of reflective eye movements, indicating physiological correlates of hypnotizability

22 p3887 A69-41213

Hypnotic compounds properties influencing REM /rapid eye movements/ stage, discussing insomnia problems with jet flight crew and passengers

24 p4277 A69-43389

HYPODYNAMIA

Hypokinesia and nutrition deficiency effect on blood coagulation, noting combination with accelerations may lead to hypocoagulation

13 p2212 A69-28625

Prolonged hypokinesia effect on human resistance to physical stress, noting prophylactic influence of physical exercises

17 p2907 A69-32939

Muscular strength dynamometric measurements in subjects during prolonged inactivity with restricted caloric and protein intake, showing decrease in strength

21 p3653 A69-38901

Radioisotopic determination of haemodynamic and bioelectric disturbances of rat striated muscles subjected to acceleration and hypokinesia

24 p4268 A69-43409

HYPOLYCEMIA

Blood glucose measured before, during and after high performance aircraft flight for occurrence of fasting hypoglycemia

09 p1445 A69-22555

Metabolic relationship between hypoxia and hypoglycemia in Wistar rats, noting oxygen consumption, energy expenditure under insulin and hydrogen partial pressure decrease effect

09 p1445 A69-22727

Glider pilots fatigue attributed to nutritional habits

23 p4106 A69-41796

HYPOTENSION

Clinical spectrum of postural hypotension, treating vasodepressor syncope, orthostatic arterial anemia and idiopathic orthostatic hypotension

06 p0873 A69-17017

Responsiveness of cortex and visual pathway during transient hypotension induced by increased gravitational stress, discussing intraocular pressure of cat

22 p3878 A69-40779

Coronary vessel lumen changes under oligemic hypotension resulting from circulating blood volume decrease in anesthetized cats, discussing constrictory coronary vessel responses

23 p4084 A69-41470

Receptor and adrenergic blockade effects on blood loss, tolerated period and metabolic sequels of hypotension in dogs

23 p4098 A69-42102

HYPOTHALAMUS

Transverse acceleration effect on male rabbit frontal hypothalamus nuclei neurosecretory function, noting blood plasma antidiuretic activity

08 p1262 A69-19930

Hypothalamic motivational systems and stimulation, discussing behavior patterns and plasticity

09 p1444 A69-21310

High altitude environmental effects on adrenal glands and hypothalamic neurosecretion in rats

13 p2211 A69-28615

Hypoxic hypoxia effect on catecholamine content and cytochemical changes in hypothalamus of cat exposed to simulated altitude, using Euler method

14 p2407 A69-29297

Central adrenergic mechanisms role in neurosecretory function of hypothalamo-hypophyseal system of rabbits under transverse accelerations in centrifuge

15 p2554 A69-30055

Constant light/darkness effects on stress response rhythm of hypothalamic-pituitary-adrenocortical system in female rats

15 p2556 A69-31330

Electrode stimulated hypothalamic drinking in rats compared with drinking induced by water deprivation, noting difference in consumption

17 p2910 A69-33750

Lateral hypothalamic stimulation bound eating motivation in animals, comparing electrical stimulation and hunger elicited eating

17 p2910 A69-33752

Ventromedial hypothalamic /VMH/ lesions, body weight and food consumption changes in male and female rats, observing differential effects

17 p2910 A69-33756

Lateral and ventromedial hypothalamic areas functional interaction in rats, noting bilateral cuts producing hyperphagia

21 p3650 A69-38322

Stimulation effects of reticular formation, hippocampus and septum on sensory responses of posterior hypothalamic neurones in cats

21 p3656 A69-38979

Electrical stimulation effect on drive specificity in lateral hypothalamus area of sated rat, suggesting fallacy in previous conclusion concerning appetite

22 p3876 A69-40269

Aminazine and adrenaline effects on adrenocortical function in patients with diencephalic syndrome

22 p3888 A69-41272

Potent chemical factors released from anterior hypothalamus of rhesus monkeys in response to thermal stress during thermoregulation

23 p4084 A69-41472

Electrical self stimulation adaptability of hypothalamus or instrumental self reinforcing reaction in rats using skinner box technique

23 p4091 A69-42052

Positive pressure breathing effects on cerebral arterial and venous blood pressure, hypothalamus and adrenal glands catecholamine content and cerebrum histological changes in dogs

24 p4265 A69-43371

HYPOTHERMIA

White rat physiological processes while maintained on hypothermic cardiopulmonary bypass with small membrane type heart-lung machines

05 p0708 A69-15971

Glucose, lactate, free fatty acids, hepatic glycogen and endocrine activity in fasting hibernating dormouse and rat in deep hypothermia

10 p1642 A69-23118

Hypothermia induced alterations in biochemical processes studied with isolated rat liver perfused at low temperature

10 p1642 A69-23119

Computer analysis of cortical and subcortical activity in yellow bellied marmot during sleep, hibernation and hypothermia

10 p1643 A69-23122

Electrocardiograms of homeothermic animal, hibernator, warm and cool climate poikilothermic animals compared for hypothermia, considering metabolic changes contributing to EKG changes

10 p1643 A69-23123

Learned behavior performance failure in hypothermia as temperature dependent phenomenon using rat, guinea pig, chinchilla, mouse, gerbil and hamster

10 p1643 A69-23124

Physiologic and metabolic effects in humans undergoing therapeutic hypothermia

10 p1643 A69-23125

Radiation resistance of animals in hibernation and hypothermia, noting temperature dependence of protective effect

10 p1643 A69-23126

Altitude effects on body chilling rate in rats noting hypoxia role in inducing hypothermia

13 p2210 A69-28532

Vestibular reactions in rats under hypothermic conditions by measuring postrotatory nystagmus beats number and duration, respiration rates and rectal temperature

17 p2906 A69-32934

Ventilatory response to hypoxia and hypercapnia in hypothermic anesthetized dogs, noting decreased sensitivity of central chemoreceptors to carbon dioxide

22 p3885 A69-40977

HYPOTHESES

NT EXPECTANCY HYPOTHESIS

NT VORTICITY TRANSPORT HYPOTHESIS

Algorithm for hypothesis optimal tests by series during signal detection in presence of noise

13 p2222 A69-28509

Soviet book on cosmos and hypotheses covering origin and physical characteristics of earth, moon, Venus and Mars

20 p3596 A69-37234

HYPOTONIA

Decrease in bioelectric activity of skeletal muscles in animals and man during intermittent acceleration and weightlessness

07 p1062 A69-18591

Myocardial repolarization changes in healthy persons with restricted motor activity

07 p1066 A69-18984

Arterial tone and human muscular activity limitations, analyzing hypodynamic effects on aorta, arm and leg vessels constriction

10 p1647 A69-23586

Myocardial repolarization changes in healthy persons with restricted motor activity

20 p3480 A69-38232

HYPOVENTILATION

Unilateral hypoventilation effect during bronchspirometry on human pulmonary blood flow

22 p3875 A69-40229

HYPOVOLEMIA

Left ventricular function in intact anesthetized dogs analyzed during graded hypovolemia produced by lower body negative pressure

22 p3874 A69-40225

HYPOXEMIA

Human motor activity under hypodynamia and increased carbon dioxide, discussing positive effects of prescribed physical exercises

03 p0377 A69-14205

Neural integration of cardiorespiratory responses and suprabulbar control during arterial hypoxemia in rhinencephalic thalamic pontine rabbits

24 p4258 A69-42635

HYPOXIA

Renal effects of moderate hypoxia exposure in mice as reflected in urine volume and electrolyte excretion patterns during four days at simulated altitude

01 p0015 A69-10921

Hypoxia exposure effect on RNA synthesis in rat anterior pituitary cultured in vitro

01 p0015 A69-10923

Increasing hypoxia effects on rabbit EEG and light flash conditioned alimentary reflex for simulated altitude ascent, noting subcortical stimulation

02 p0197 A69-11492

Hypoxia effects on vestibular analyzer function of rats in pressure chambers at simulated altitudes from 11,000 to 12,000 m

02 p0198 A69-11506

Lactodehydrogenase activity and LDG isoenzymes ratio in various tissues of rats during exposure to prolonged hypoxia at simulated heights

02 p0199 A69-11982

Hypoxia effect on animal brain gamma-aminobutyric acid levels

04 p0552 A69-14482

High oxygen concentration influence on animal organisms noting respiration, pulmonary gas exchange, hypoxia, brain phosphorylation, immunological indices and morphological structure of rats and mice

05 p0709 A69-16512

Transient changes in oxygen consumption, carbon dioxide elimination and respiratory quotients during and after induced hypoxia to rabbits

06 p0876 A69-18026

Invertebrates resistance to explosive decompression and low end pressure, noting hypoxia and freezing as cause of death

07 p1059 A69-18537

Hypoxia warning system based on dry electrolyte oxygen sensor with millisecond response time

07 p1071 A69-19430

Sampled data regulator for maintenance of constant alveolar carbon dioxide during steady state and transient ventilatory responses to hypoxic stimulation

07 p1072 A69-19480

Mild hypoxia effect on selective attention performance of human subjects at simulated 8000 ft altitude

09 p1445 A69-22553

Acclimation to altitude hypoxia and duration of resistance to muscular effort in white Wistar rats on treadmill

09 p1445 A69-22725

Metabolic relationship between hypoxia and hypoglycemia in Wistar rats, noting oxygen consumption, energy expenditure under insulin and hydrogen partial pressure decrease effect

09 p1445 A69-22727

Glycolysis rate and lactic acid content in rats myocardium during adaptation to hypoxia, using pressure chamber

10 p1645 A69-23501

Human physiology for exposure to acute hypoxia studied with variation pulsograms and indices of external respiration and pulmonary gas exchange

10 p1647 A69-23592

EEG, EKG, respiratory motions and pulmonary ventilation recordings in study of carbon dioxide additions effect on human tolerance to hypoxic conditions

10 p1650 A69-23898

Irreversible blunted respiratory response to ventilation in high altitude natives, considering hypoxic and hypercapnic stimuli

12 p2018 A69-26130

Blood coagulation in animals under acute hypoxia at exposures to pressure corresponding to 5000 m altitude, noting blood morphology

12 p2019 A69-26348

Protective effect of hydrocortisone in rats observed during hypoxia

13 p2210 A69-27800

Altitude effects on body chilling rate in rats noting hypoxia role in inducing hypothermia

13 p2210 A69-28532

Combined hypoxic hypoxia and high ambient temperature found relieving strain on humans by increasing heat release by evaporation

13 p2212 A69-28628

Oxygen saturation in outflowing and inflowing renal blood in dogs under normal and hypoxic conditions, assessing cannula technique

14 p2406 A69-28916

Hypoxic hypoxia effect on catecholamine content and cytochemical changes in hypothalamus of cat exposed to simulated altitude, using Euler method

14 p2407 A69-29297

Antihypoxic preparations protective effect on white mice and rats subjected to gravitational accelerations

17 p2906 A69-32931

High oxygen concentration influence on animal organisms noting respiration, pulmonary gas exchange, hypoxia, brain phosphorylation, immunological indices and morphological structure of rats and mice

18 p3095 A69-34731

Pubertal puppy and adult dog cardiovascular system during inhalation of various nitrogen-oxygen mixtures, comparing heart beat rates, minute blood volumes, etc

19 p3257 A69-36169

Chronic hypoxic hypoxia on oxygen-hemoglobin dissociation curve and respiratory gas transport in man, considering altitude residents and heart and lung diseased patients

21 p3650 A69-38383

Ventilatory responses to hypercapnia and hypoxia in anesthetized and unanesthetized rabbits before and after bilateral cervical vagotomy

21 p3651 A69-38390

Heart muscle ultrastructure during general hypoxia in dogs, noting development of compensatory-adaptational and dystrophic changes in myocardial intracellular components

21 p3651 A69-38412

Rat dental pulp hemorrhages following acute hypoxia from exposure to decompression chambers, atmospheric pressure variations or high acceleration

21 p3661 A69-39276

Peripheral chemoreceptor carbon dioxide sensitivity, measuring human respiratory response to large carbon dioxide breath in oxygen at sea level and high altitude

22 p3890 A69-40207

Hypoxia tolerances in nitrogen dilution chamber of chickens at sea level and high altitudes, discussing role of hematocrit and heart mass

22 p3874 A69-40214

Ventilatory response to hypoxia and hypercapnia in hypothermic anesthetized dogs, noting decreased sensitivity of central chemoreceptors to carbon dioxide

22 p3885 A69-40977

Protein rates and RNA synthesis in cerebra of rats analyzed as factor of high altitude hypoxia adaptation

22 p3886 A69-41122

Effects of oxygen saturation variations of blood on rates of weight gain in isolated perfused canine lung, noting pulmonary edemogenesis

22 p3887 A69-41189

Anoxia effect on succinic dehydrogenase and lactic dehydrogenase activities in digestive glands and organs sensitive to oxygen tension changes

22 p3887 A69-41193

Cardiovascular effects of hypoxia in conscious and anesthetized dogs in environmental chamber, discussing artery pressure, tachycardia, stroke volume and cardiac output

23 p4078 A69-41314

Physical training effects under normal atmospheric pressure on high altitude hypoxia and acceleration resistance in rats, including survival times

23 p4079 A69-41383

Physiological response to steady state hypoxia from exposure to 12 percent oxygen atmosphere, noting minimal heart rate and blood pressure changes

23 p4085 A69-41673

Hypoxia acclimatization studied by subjecting groups to bicycle exercise at simulated high altitude and at ground level

23 p4086 A69-41678

Arterial oxygen partial pressures and heart beat rates measured in humans during acute hypoxia after altitude and ergometer training, noting sensorimotor performance

23 p4086 A69-41788

Hypoxia reaction elimination in human beings by repeated exposure to hypoxia, discussing nitrogen inhalation experiments and adaptive behavior of respiratory system

23 p4214 A69-41789

Flight altitude effects on pilot performance with comparison of sensory and mental functions, considering oxygen use and flight safety

23 p4106 A69-41794

Cardiovascular autonomic effects dynamic characteristics under severe arterial hypoxia in unanesthetized rabbit

24 p4258 A69-42632

Altered gaseous environments effect (parabiosis) on interferon production in mice injected with Newcastle disease virus, noting hypoxia role

24 p4262 A69-42888

Physical and physiological factors involved in determining aircraft passengers time of safe unconsciousness permissible after cabin decompression

24 p4278 A69-43398

Hyperoxia and hypoxia effects on mitotic activity in regenerating and normal rat liver exposed to environmental conditions

24 p4269 A69-43565

HYPSOMETERS

Hypsometric contour map of lunar surface from absolute altitude measurements of 1200 points on lunar surface

03 p0512 A69-13689

Lunar shape hypsometric peculiarities, analyzing heights and asymmetry in relation to lunar equator, central meridian and image plane

04 p0662 A69-15249

HYSTERESIS

Input transistor performance analysis in Schmitt trigger circuit, considering role of hysteresis

01 p0039 A69-10170

Hysteresis properties of membrane structures with soldered or rolled edges noting superiority of added elastic element in clamped area

01 p0087 A69-10828

Single degree of freedom structural damping estimations from viscous and hysteretic energy dissipation data

03 p0523 A69-12947

Forced flexural vibrations of elastic truss systems with allowance for hysteresis friction

03 p0432 A69-12953

Mathematical model for voltage step-down DC to DC converter with hysteretic bistable trigger circuit regulating output voltage

06 p0904 A69-17941

GaAs lasers radiation power hysteresis manifested in generating starts and stops at different injection current levels

07 p1157 A69-19593

High temperature magnetic testing and analysis of structure sensitive hysteresis properties

09 p1512 A69-22375

Bilinear hysteretic system undergoing random vibration, substantiating linearization analysis with analog computer simulation and comparing lifetime to linear system

[ASME PAPER 69-VIBR-25]

10 p1806 A69-24173

Energy dissipation in freely oscillating bodies under static stresses described by differential equation, assuming elliptical hysteresis loop

11 p1919 A69-25092

Hysteresis loop contour equation derivation based on energy dissipation dependence on stress amplitude in cyclically deformed vibrating system

11 p1985 A69-25176

Spool valve flow patterns within hysteresis region, discussing effects of valve geometry, Reynolds and cavitation numbers

11 p1827 A69-25645

Neutron irradiation and temperature effects on ferrite and Permalloy memory cores hysteresis loops

12 p2142 A69-26259

Hysteresis of on-off element with proportional feedback around element, noting autooscillations and results for electromagnetic relay

12 p2053 A69-26507

- Polycrystalline Fe-Ni, Fe-Ni-Co ferrites structure, magnetostriction, magnetization curves and hysteresis prior and after thermomagnetic treatment
13 p2319 A69-27992
- Dynamic stability of two degrees of freedom circulatory systems with bilinear hysteresis damping
13 p2363 A69-28127
- Ferrite core storages characteristics with rectangular hysteresis loop for digital control units, discussing optimal selection method
14 p2418 A69-29145
- Damping of gravity gradient stabilized satellites by hysteresis of materials, friction of viscous fluids, magnetic hysteresis and Foucault currents
17 p3047 A69-33230
- Gravity gradient satellite stabilization and magnetic hysteresis damping systems, outlining energy dissipation device involving torques
17 p3047 A69-33231
- Damping techniques using viscoelastic materials, discussing mechanical hysteresis
17 p2992 A69-33660
- Magnetic hysteresis dynamic model suitable for digital computer simulation of near-earth satellite attitude motions damping compared with experimentally generated loops
[AIAA PAPER 69-833] 21 p3821 A69-39364

I

I BEAMS

- Temperature distributions and thermal stresses in bimetallic I-beam structures with dissimilar materials for skins and webs and with kinetic heating inputs
06 p1024 A69-17610

IAPETUS

- Magnitude data for Saturn satellites compiled and analyzed, noting discrepancy for Iapetus
08 p1394 A69-20619

IBM 360 COMPUTER

- System/360 Continuous Modeling Program, detailing input language, user-defined functions and documentation
05 p0723 A69-16196
- Roseau onboard computer simulation by IBM 360, discussing use of assembly language and FORTRAN
20 p3502 A69-37396
- Real time operating system /RTOS/ 360 for spaceflight control, describing hardware, applications, task management and capacity, etc
21 p3679 A69-39602
- IBM 360-50 computer with I/O terminals to process PCM and analog data from Modular Auroral Probe series of sounding rockets on real time basis
23 p4133 A69-41764

ICARUS ASTEROID

- Icarus asteroid position measurements by astronomical photography, noting comparison for two South African observatories
01 p0150 A69-10373
- Icarus positions from photographic observations with astrophotograph
01 p0159 A69-11331
- Radar observation of Icarus at time of close approach, giving values of radius, rotation period and Doppler shift derived from spectrograms
02 p0323 A69-12300
- Project Icarus for reduction of threat of asteroid collision with earth by deflection or disintegration, noting guidance, control and communications for rocket
04 p0652 A69-14564
- Icarus observation by Triped-Metcalf method, tables show Icarus retreat and advance and velocities of eight asteroids neighboring earth
05 p0819 A69-15698
- Icarus radar and optical observations analyzed to verify general relativity predictions using Schwarzschild metrics and to estimate solar oblateness, Mercury mass, etc
13 p2350 A69-27823
- Icarus asteroid observed at Royal Observatory of Belgium with 40-cm double astrophotograph, tabulating acquired data
14 p2521 A69-29584
- TV-optical observations of asteroid Icarus, discussing installation, photographs and position
21 p3719 A69-38402

ICBM [MISSILES]

U INTERCONTINENTAL BALLISTIC MISSILES

ICE

- Critique of paper on water crystal existence on Venus, presenting arguments against existence of clouds of micron sized ice crystals
01 p0157 A69-11292
- Low temperature adhesive shear tests to measure force to break ice away from stainless steel surfaces coated with various bonded solid lubricants
19 p3323 A69-35581
- Gamma radiolysis of silver nitrate ice forming neutral Ag in magnetically distinct sites, discussing water dipoles rotation and electron paramagnetic resonance
22 p3992 A69-40574

ICE FORMATION

NT CLOUD GLACIATION

- Cloud instrumentation for measurement of icing conditions of airplane flight tests
01 p0055 A69-11044
- Vibrating rod automatic ice detection and control system for fixed and rotary wing aircraft
01 p0083 A69-11046
- Icing of airframes, discussing ice formation, deicing methods and protection of aircraft
02 p0192 A69-11889
- Supercooled water drop frozen and observed to undergo explosive shattering and ejection of ice splinters
02 p0275 A69-12693
- Ice nucleus formation in developing comet, discussing dissociation and vaporization characteristics of parent molecules as participants in process
06 p1004 A69-17537
- Anticing for all-weather operation of business jets, discussing atmospheric conditions, ice formations, prevention and removal systems
[SAE PAPER 690333] 11 p1822 A69-24500
- Variational statistics applied to hourly meteorological data for predicting airport runways icing conditions time and duration
12 p2127 A69-26900

- Vertical wind velocity profiles approximation accuracy determined by linear, exponential and logarithmic functions of altitude during ice and frost
13 p2293 A69-27846
- Dim astronomical sources observability from sunlit spacecraft, considering coma of micron sized ice crystals influence on scattering by condensation model
16 p2861 A69-32301
- Noctilucent clouds formation relation to ice sublimation, discussing rocket soundings
21 p3701 A69-38345
- EOLE constant level balloon flights in troposphere, discussing short lifetime due to overloading with ice in dense cirrus cloud
21 p3646 A69-38373

ICE NUCLEI

- Aircraft instrumentation system for cloud nucleation studies measures and records ice nucleus and aerosol concentration/distribution, temperature, etc
01 p0080 A69-10542
- Mathematical analysis for mechanism of spherical comet nucleus division as effect of nonuniform surface heating during rotation
04 p0659 A69-14997
- Ice nucleus formation in developing comet, discussing dissociation and vaporization characteristics of parent molecules as participants in process
06 p1004 A69-17537
- Comet Ikeya-Seki phenomena near perihelion interpreted from mean surface and ice nucleus internal layers temperatures
14 p2523 A69-29706
- Halley comet abrupt daily motion variation ascribed to solid particles ejection from ice nucleus stimulated by gas outflow
14 p2524 A69-29712

ICE PREVENTION

- Engine inlet thermal antiicing analysis, detailing computer programs to determine air flow velocity, water impingement and thermal requirements
01 p0055 A69-11045
- Vibrating rod automatic ice detection and control system for fixed and rotary wing aircraft
01 p0083 A69-11046
- Passive ice protection of aerodynamic surfaces by icephobic coating, measuring removal of ice under simulated conditions in tunnel tests
01 p0056 A69-11047
- Light aircraft all-weather flight feasibility, discussing storm and clear air turbulence detection and icing prevention
01 p0111 A69-11049

- Analytical design of SH-3 helicopter engine inlet ice deflector shield interior surfaces, defining potential flow pattern and moisture droplet trajectories
01 p0011 A69-11064
- Icing of airframes, discussing ice formation, deicing methods and protection of aircraft
02 p0192 A69-11889
- Anti-icing system for business jets, noting activation prior to encountering visible moisture
06 p0868 A69-17669
- Anticing for all-weather operation of business jets, discussing atmospheric conditions, ice formations, prevention and removal systems
[SAE PAPER 690333] 11 p1822 A69-24500

ICE REPORTING

- Radar backscatter analysis for Arctic ice identification, deriving ice surface roughness factors from Kirchhoff-Huygens principle
14 p2416 A69-29530

ICING

U ICE FORMATION

IDEAL FLUIDS

- Three dimensional sonic flow downstream from shock wave in nondissipative perfect fluid, introducing pseudorotating flow to obtain velocity field
03 p0362 A69-13363
- Hall effect destabilization influence in Kelvin-Helmholtz problem for ideal plasma, noting instability growth rate
03 p0478 A69-13804
- Ideal liquid small oscillations in vessel under close to weightlessness conditions, discussing surface tension, equilibrium conditions and solution by decomposing vector function space
03 p0418 A69-13811
- Primary frequency of oscillations of ideal liquid in cylindrical vessel with axially directed weak gravitational field
03 p0418 A69-13812
- Cavitation stream calculation methods for ideal incompressible fluid with free boundaries, noting cavitation generators and Riabouchinsky problems
04 p0589 A69-14994
- Equations of motion solved for solid body with ellipsoidal cavity containing ideal incompressible fluid in uniform eddy motion
06 p0957 A69-16823
- Ritz method for natural oscillations of ideal liquid in spherical vessel with various filling levels, considering vertical perturbing force
06 p0910 A69-17333
- Physical mechanism of stability loss in nonvortical flows of uniformly dense ideal fluids, discussing entropy production
06 p0911 A69-17498
- Thermodynamic and aerodynamic characteristics of organic Rankine cycle working fluids for ideal applicability to manufacturing
[SAE PAPER 690063] 07 p1057 A69-18308
- Natural modes and eigenfunctions of low amplitude oscillation determined by Ritz averaging method for ideal fluid with equilibrium surface in weak force field
07 p1119 A69-18746
- Theory of unsteady one dimensional motion of ideal compressible fluid, discussing equation of state
07 p1119 A69-18750
- Ideal fluid interaction with gravitational field, assuming internal energy as function of natural pressure and density
07 p1182 A69-19419
- Schwarzschild perfect fluid spheres stability to radial perturbations, noting fluid adiabatic index relation to critical value
07 p1221 A69-19585
- Arbitrary stationary foil in perfect incompressible fluid moving at constant velocity at infinity assuming plane, steady and irrotational flow
08 p1303 A69-20272
- Plane steady transonic flow of perfect fluid around airfoils with constant curvature using hodographic method, discussing various boundary conditions
09 p1429 A69-21605
- Surrounding fluid effects on free axisymmetric vibrations of thin elastic spherical shells, studying irrotational motions in compressible and incompressible ideal fluids
09 p1613 A69-21720
- Boundary value problem for gravity induced wave motion of ideal fluid in axisymmetric vessel with annular ribs, noting application to bodies of revolution
11 p1868 A69-24769

Optimum controller design for dynamic stability of ideal incompressible fluid in cavity of body constrained to horizontal rectilinear translational motions

11 p1966 A69-25330

Natural frequencies and forms of small vibrations of ideal liquid in spherical container with weak force field, considering surface tension forces

11 p1875 A69-25484

Axisymmetric detached flow past slender solid of revolution by ideal incompressible fluid at zero angle of attack and with small cavitation number

11 p1877 A69-25741

Ideal compressible fluid motion and heat transfer, noting convective heat transfer intensification with increased twisting velocity of flow

13 p2251 A69-28559

Ideal fluid unsteady rectilinear plane-parallel flow stability, calculating shear layers before breakdown by using modified Rayleigh method

14 p2431 A69-29606

Aerodynamic forces acting on harmonically oscillating thin profile in stalled plane parallel flow of ideal incompressible fluid

16 p2732 A69-32142

Flow rate of ideal fluid ejected from swirl injector taking into account radial component of flow velocity at nozzle exit

19 p3297 A69-35820

Hydrodynamic vertical or horizontal impact of sphere immersed in ideal heavy liquid of finite depth, considering container floor effect, surface pressure distribution, etc

19 p3299 A69-36393

Perturbed motion of solid body containing axisymmetric cavities partially filled with ideal incompressible fluid, solving boundary value problems of fluid oscillations

20 p3518 A69-38296

Optimal control of ideal noncompressible fluid vibrations partially filling rectangular container moving in horizontal direction

21 p3695 A69-38892

One dimensional flow of perfect compressible relativistic fluids, obtaining expression showing wave velocity dependence on relativistic speed of sound

22 p3931 A69-40711

MHD of ideal charged gravitating fluid by variational principle, considering Einstein general relativity theory

22 p3992 A69-41056

Dynamic behavior of gas bubble in ideal fluid plane flow, considering bubble shape, velocity field, gas pressure and stagnation point pressure determination

24 p4302 A69-43478

Unsteady axisymmetric potential flow of ideal incompressible fluid with free surfaces, deriving differential equations for gas bubble dynamics and surface geometry

24 p4302 A69-43500

IDEAL GAS

Difference methods in solution of incorrect Cauchy problem simulating ideal gas flow in nozzle

01 p0006 A69-10379

Continuum eigenfunction problem for hard sphere gas in spherically symmetric state, applying theory of singular integral equations

01 p0061 A69-10813

Thermodynamics of ideal multiatomic gases in local nonequilibrium, approximating real gas system by ergodic subsystems grouped by degrees of freedom

02 p0350 A69-11552

Hypersonic perfect gas flow past delta wing with blunt edges at small angles of attack, noting constant drag coefficient

02 p0191 A69-12584

Ideal gas spectra and density fluctuations correlations calculated during Markovian and nonMarkovian wandering of particles

03 p0477 A69-13414

Numerical computer results applied to supersonic flow of perfect gas past staggered cones

03 p0363 A69-13659

Ideal gas flow near stagnation line for blunt bodies, applying van Dyke series truncation method to numerical solution

03 p0364 A69-13660

Anisotropic nonlinear wave propagation in arbitrarily moving ideal gas, using singular surface/ray combined theories

04 p0630 A69-14532

Shoulder pressure on slender cone/afterbody combinations in hypersonic inviscid flow of perfect gas

04 p0542 A69-14735

Thermodynamic function tables for 30 gases under ideal gas conditions up to 6000 K

04 p0686 A69-15153

Second approximation to Boltzmann equation solved for rigid sphere gas by reducing integral equation to differential equation

04 p0633 A69-15434

Shock wave damping at large distances from body situated in ideal gas three dimensional flow

04 p0591 A69-15535

HF plane sound waves in ideal gases with internal dissipation, considering particular applications to dissociating diatomic and vibrational relaxing gases

05 p0792 A69-15723

Semiperfect gases with enthalpy dependent only on temperature, discussing validity of concept and Joule experiment on equivalence of heat and work

05 p0848 A69-16336

Peculiarities of aerodynamic characteristics of flow past plate and pointed and blunt slender cones in viscous hypersonic thermodynamically ideal gas

05 p0699 A69-16673

Nonisentropic simple waves in two dimensional steady flow of ideal gas

05 p0752 A69-16687

State variables of ideal gas in two phase region, discussing determination from equations of state and equation for internal energy and Maxwell criterion inapplicability

06 p1030 A69-17170

Hydromagnetic plasma stability in infinite electrical conductivity approximation applied to smooth closed systems, discussing ballooning instability mode

06 p0965 A69-17519

Asymptotic theory concerning nonsimilar structure of blast wave with expanding interface applied to hypersonic perfect gas flow

06 p0860 A69-17636

Bodies of revolution in sonic flow of ideal gas, showing same perturbational effect of source and dipole on flow before shock front

10 p1632 A69-23364

Invariant transformation of equations for ideal gas plane steady motions, noting application to gas flows with shock waves and eddies

10 p1680 A69-23709

Boltzmann equation for system of equations governing evolution of gas of identical particles with discrete velocity distribution, applying Chapman-Enskog method

11 p1921 A69-24325

Existence and completeness of eigenfunctions for boundary value problem arising in theory of small amplitude motions of stratified polytropic gas

11 p1868 A69-24884

Motion equations for ideal transonic gas flow, applying solutions to flow with incident shock waves of various profiles

11 p1820 A69-25468

Numerical integration of equations for three dimensional laminar boundary layer on sharp elliptical cones in supersonic flow of ideal gas, discussing heat exchange

11 p1821 A69-25477

Difference methods in solution of incorrect Cauchy problem simulating ideal gas flow in nozzle

12 p2012 A69-26671

Influence coefficients for compressible flow processes involving area, friction and total temperature changes

12 p2063 A69-26799

Transonic ideal gas flow past semiinfinite bodies, determining flow potentials from body perturbations and surface boundary conditions

14 p2390 A69-29476

Spatial supersonic ideal gas flows past blunt bodies analyzed by numerical finite difference methods, discussing flow fields and entropy

14 p2390 A69-29616

Thermal radiation effects on subsonic flow of ideal gray gas, calculating streamwise variations of flow properties

15 p2717 A69-30908

Book on three dimensional flow of ideal gases past smooth bodies, emphasizing utility of finite difference methods

16 p2771 A69-32003

Streamline flow of ideal stable gas with constant ratio of specific heats around conical body with arbitrary taper, determining flow velocity components

16 p2732 A69-32126

Monograph on solutions to equations for unsteady flow of ideal gases, with applications to hypersonic flows, based on three space coordinates and time

16 p2773 A69-32428

Shocks in gases, giving differential equation set for ideal gas behavior

17 p2948 A69-32845

Exhaust plume rarefaction from sonic orifice, considering continuum to transitional behavior for perfect gas [AIAA PAPER 69-657]

17 p2892 A69-33465

Supersonic and hypersonic flow of inviscid ideal gas over conical delta wings using three dimensional method of characteristics [AIAA PAPER 69-646]

17 p2893 A69-33486

Integral relation method analysis of supersonic gas flow past blunt body of revolution

18 p3086 A69-35051

Nonuniform supersonic flow of ideal inviscid gas impinging on plane obstacle, discussing flowfields and shock wave production in impact

19 p3239 A69-36397

Equilibrium Couette flow of ionized multicomponent ideal gas between moving catalytic plates, obtaining thermal flow formulas and thermal conductivity coefficient

19 p3240 A69-36403

Solar atmosphere radio emission generation by hydrodynamic shock wave interaction with coronal plasma, treating corona as ideal gas consisting of protons and electrons

22 p4009 A69-39984

Velocity and temperature boundary layers on plane wall developed by ideal shock tube flow for weak shock and expansion waves

22 p3932 A69-40894

Adiabatic plane ideal gas flow past airfoil, studying shock waves propagation effect on dynamic behavior

22 p3861 A69-41024

Transonic flows behind separated shock waves of ideal gases past bodies of various geometries

23 p4151 A69-41526

Frictionless supersonic and hypersonic flow of ideal gas of constant specific heat past cone with deformed axis at zero angle of attack

23 p4058 A69-41579

IDENTIFYING

Optical identifications for 17 Ohio survey sources with peaked or flat spectra

01 p0153 A69-10854

Optical identification of X ray source Cen XR-2 as variable star WX Cen, discussing colors and similarity to Sco X-1

01 p0145 A69-10857

Electrolytic marking process for aircraft component identification without use of stamping or engraving

02 p0253 A69-12065

Plant identification procedures by stepwise approximation and least squares methods

03 p0409 A69-13072

Channel identification coding for data compressors, deriving optimum code word length for bit compression ratio and overflow identification scheme

03 p0391 A69-13219

Nonlinear system on-line identification in presence of noise, using stochastic methods and analog equipment

03 p0401 A69-13764

Nonlinear system identification by learning model, assuming discrete on-line operation and Hammerstein form

05 p0737 A69-15805

Identification of finite memory, time discrete linear systems by Kiefer-Wolfowitz stochastic approximation procedures, presenting two algorithms for sequential identification

06 p0900 A69-17359

Linear regression and related procedures in identifying dynamic processes

06 p0901 A69-17360

Stochastic approximation algorithms for adaptive linear discrete time system identification using noisy input

06 p0904 A69-17940

Aircraft communications, navigation and identification, discussing role of satellites, common waveform modulation and electronics technology

07 p1085 A69-19178

Transponder design with planar triode for aircraft identification and air traffic control

09 p1462 A69-21411

Iterative identification method for nonlinear control systems with single element, based on criterial functional

14 p2426 A69-29306

Subcontractors documentation coordination system for Mississippi Test Facility, identifying end items for maintenance and spares provisioning

18 p3118 A69-35063

Robbins-Monro stochastic approximation method using algorithms for identifying finite memory time-discrete timestationary linear system from noisy input-output measurements

22 p3918 A69-41013

IDENTITIES

Matrix identity associated with linear digital filtering and recursive estimating determined using matrix projection operators and properties

22 p3975 A69-41014

IFR [RULES]

U INSTRUMENT FLIGHT RULES

IGNEOUS ROCKS

NT ANDESITE
NT BASALT
NT ENSTATITE
NT GRANITE
NT LAVA
NT MAGMA
NT MOLDAVITE
NT OLIVINE
NT PYROXENES

Partition coefficients between natural melts and plagioclase phenocrysts determined for rare earth elements and barium by mass spectrometry

08 p1310 A69-20944

Remanent magnetization properties in alkalic igneous complexes at Magnet Cove and Potash Suphur Spring, Ark., calculating paleomagnetic pole during Cretaceous

14 p2445 A69-29884

IGNIMBRITE

U LAVA

IGNITERS

NT DETONATORS
NT INITIATORS [EXPLOSIVES]
NT PRIMERS [EXPLOSIVES]

Electrical explosive devices for space applications including explosive bolts, primers and igniters

01 p0141 A69-10544

Igniter design guidelines, types and characteristics of igniter materials

[WSCI PAPER 68-32] 07 p1202 A69-18361

Igniter formulations characteristics, discussing desirable properties

10 p1750 A69-23009

Solid propellant rocket motors ignition and igniter performance, discussing ignition interior ballistics

16 p2829 A69-31997

IGNITION

NT ELECTRIC IGNITION
NT SOLID PROPELLANT IGNITION
NT SPARK IGNITION

Stabilized low temperature ignition of cyclohexane using vertical flow reactor

02 p0304 A69-12314

Fuel films ignition behind shock waves in air and oxygen

02 p0353 A69-12317

Heat production rate equivalence to heat removal rate during ignition of ballistite powder by incandescent wires

02 p0354 A69-12668

Photochemical ignition of low pressure fuel-oxidizer mixtures applied to unsensitized stoichiometric mixtures of methane-oxygen and hydrogen-oxygen

[WSCI PAPER 68-42] 06 p1034 A69-17791

Ignition of binary mixtures of hydrocarbons at high and minimum ignition temperatures of components

06 p1035 A69-17935

Sustained combustion initiation in subatmospheric gaseous fuel-oxidant mixtures by UV radiation at room temperature, measuring parameters as function of mixture pressure

[AIAA PAPER 69-88] 06 p0983 A69-18118

Gasdynamic flow shock wave phenomena during exploding wire dwell time inside metal vapor cylinder, noting effect on reignition

07 p1188 A69-18275

Adiabatic kinetic calculations of chemical additive effects on ignition delay of hydrogen-oxygen-argon gas mixtures

[WSCI PAPER 68-52] 07 p1239 A69-18316

Ignition time of methane and acetylene, considering concentration and thermodynamic properties during reaction

[WSCI PAPER 68-41] 07 p1240 A69-18356

Thermal explosion criterion used for explosion/ignition delay of exothermic material surrounding heated wires having good thermal conductivity

[WSCI PAPER 68-23] 07 p1240 A69-18359

High speed photographic study of finely dispersed Al particles combustion and ignition in high temperature

gas flows, noting dependence on oxidizers concentration

08 p1375 A69-20341

Monograph on ignition, combustion and expansion in hypergolic liquid propellant mixtures at gas temperatures up to 3000 K for small rocket engines

08 p1375 A69-20723

Hydrodynamic effects in flame spreading, ignitability and steady burning of liquid fuels, using analogy of films floating on water

11 p1999 A69-24484

Ignition dynamics of solid materials with differing kinetic and thermophysical parameters, emphasizing temperature growth during chemical reaction leading to ignition

11 p2000 A69-25188

Ignition of condensed homogeneous combustible materials in presence of phase transition in heated layer, discussing temperature distribution and ignition delay time in ammonium perchlorate

11 p2000 A69-25189

Equations for steady state combustion of fuel drops in oxidizing atmosphere integrated numerically, obtaining ignition and extinction conditions

13 p2379 A69-28456

Differential equations for ignited mode theory, considering ion and electron transport and energy flux

14 p2490 A69-29233

Preignition volt-ampere curves for thermionic cesium diodes exhibiting nonsaturation characteristics under low temperature and electron-rich emission conditions

14 p2403 A69-29253

Ignition delay of paraphenylenediamine associated with nitric acid, showing relation between grain diameter and hypergolic ignition mechanism, noting oxidizer concentration effects

15 p2561 A69-30185

Reacting gas ignition by sudden contact with heated noncatalytic surface, deriving heating time and transferred heat amount by Blasius perturbation method

16 p2878 A69-31955

Turbulent jet theory, thermal ignition theory and flameout characteristics of bluff body flame stabilizers

16 p2879 A69-32141

Gas phase ignition theory with feedback of homogeneous propellant exposed to stagnant gas after shock reflection

[AIAA PAPER 69-559] 16 p2880 A69-32740

Ignition hazards in electrical circuits contaminated by glycol fluids, describing hazard detection by RF methods, decontamination procedures, safety checks, etc

19 p3359 A69-36028

Schlieren framing photography used for studying shock wave hydrodynamic structure and ignition dynamics during expansion into detonable gas region

21 p3849 A69-38803

Thermal stability of reactive spherical shell, investigating spontaneous ignition of volatile fuel drop exposed to hot oxidizing environment

21 p3849 A69-38804

Hydrogen-air reaction kinetics analyzed using standing wave normal shock noting wall effects, ignition delay and recombination

[AIAA PAPER 67-479] 23 p4239 A69-41893

IGNITION LIMITS

Combustion chamber equation for liquid fuel rocket engine, considering time varying ignition lag

01 p0142 A69-10090

Temperature distribution and vaporization rate boundary conditions on metal particle surface during preignition heating in oxygen containing medium

02 p0355 A69-12670

Liquid hydrazine ignition by nitrogen tetroxide gas based on stagnation flow principle, presenting threshold measurements

[WSCI PAPER 68-43] 06 p0983 A69-17792

Low pressure deflagration limit dependence on strand size in terms of cross section dimensions for composite ammonium chlorate propellant

[AIAA PAPER 69-144] 06 p0983 A69-18162

Threshold criteria of gas phase thermal ignition for cellulose materials, considering heating by radiant energy

11 p1940 A69-24474

Steady propagation of flame front initiated by local ignitor /spark/ in gas mixture, discussing critical requirements, boundary conditions, etc

11 p2001 A69-25190

Ignition critical conditions based on reactions in condensed phase, discussing initiation from pulsed and continuous external heat sources, heat release by chemical reactions of ignition, etc

11 p2001 A69-25191

Diffusion flame stability at inlet of fuel stream into oxidizer, showing ignition coordinates dependence on fuel, oxidizer and ratio of burning/ flow rate

19 p3448 A69-35855

Discontinuity characteristics of trough-shaped flame stabilizers for combustion in wake of poorly streamlined body during period of ignition arrest

21 p3851 A69-39092

Propellant ignition delay in contact of condensed fuel with hot reactive gas in shock tube, using graphical method and surface temperature fractional increase

23 p4199 A69-41897

IGNITION SYSTEMS

Igniter design guidelines, types and characteristics of igniter materials

[WSCI PAPER 68-32] 07 p1202 A69-18361

Shock ignition procedure to keep pyrotechnic composition in optimum condition in space environment, describing test layouts and theory

10 p1749 A69-23007

Igniter formulations characteristics, discussing desirable properties

10 p1750 A69-23009

Electroexplosive devices protection by nonconducting composition against premature ignition by RFI in spacecraft environment, noting Apollo Standard Initiators

10 p1751 A69-23018

Electroexplosive devices design for extreme conditions, considering igniter, delay and functioning systems

10 p1751 A69-23020

Secondary explosives ignition by primers and other explosive wire devices on missiles, discussing circuitry and resistance to severe climatic and electrical environments

10 p1751 A69-23021

Hot gas ignition devices for solid propellant rocket motors, discussing ignition rod and microrockets

10 p1752 A69-23025

Soviet book on electric ignition systems for piston and jet engines and design aspects of different types of ignition systems

12 p2146 A69-26756

Solid rocket motor ignition system based on exothermic alloying of bimetallic wire constituents

[AIAA PAPER 69-425] 16 p2832 A69-32653

Initiation distance and time of detonation with weak ignition sources related to temperature, tube diameter, mixture composition and pressure

19 p3451 A69-36364

IGNITION TEMPERATURE

NT FLASH POINT

Analytical model for thrust-time curve during ignition transient of solid propellant rocket engines, discussing flame spreading

[WSCI PAPER 68-33] 07 p1203 A69-18365

Threshold criteria of gas phase thermal ignition for cellulose materials, considering heating by radiant energy

11 p1940 A69-24474

Cool flames nonisothermal two-stage ignition of neopentane-oxygen mixtures, discussing chain propagation due to isomerization

11 p1940 A69-24477

Thermal ignition of methane-oxygen mixture, observing flame propagation

13 p2380 A69-28459

Burning velocity inhibitors effects on hydrocarbon-oxygen-nitrogen mixtures ignition temperature, reporting data on 20 additives at ambient temperature and pressure

[WSCI PAPER 69-14] 16 p2831 A69-32352

Spontaneous reignition predictions for solid restartable rocket motors with solid propellant combustion terminated by liquid quenching

[AIAA PAPER 69-444] 16 p2842 A69-32695

Energy balance equation for two phase liquid-gas mixture ignition process, deriving formula for speed of combustion zone movement

18 p3231 A69-35123

Ignition of aircraft fluids leaked onto hot turbofan engine surfaces, considering cooling air direction, surface temperature, nacelle engine compartment ventilation, engine power, etc

[SAE PAPER 690436] 23 p4200 A69-41653

IGY [GEO PHYSICAL YEAR]

U INTERNATIONAL GEOPHYSICAL YEAR

ILLUMINANCE

Radiation pattern shaping from circular aperture antenna with constant illumination amplitude

[UN PAPER 68-95756] 01 p0029 A69-10524

Spacecraft illuminance by reflected solar radiation calculated by computer method

01 p0151 A69-10576

Direct light pressure effect on evolution of limited planetocentric orbits of small bodies, noting longitudes of ascending node and pericenter

05 p0823 A69-16043

Spacecraft illuminance by reflected solar radiation calculated by computer method

15 p2691 A69-30746

Direct light pressure effect on evolution of limited planetocentric orbits of small bodies, noting longitudes of ascending node and pericenter

20 p3606 A69-37952

ILLUMINATING

Aircraft instrument lighting color effects on posture, scotopic absolute and acuity threshold and legibility for reading of instruments

03 p0380 A69-14073

Laser ranging and illumination systems, discussing direction of pulsed monochromatic radiation to illuminate scene and utilization of reflected radiation for imaging

03 p0442 A69-14191

Aircraft instrument panel lighting color and intensity preference by pilots for taxiing, takeoff, cruising flight and landing

05 p0715 A69-16622

Aircraft instrument panel lighting, comparing red and white colors for general and peripheral vision

05 p0715 A69-16623

Incident integral light flux relations and visibility range equation derived for objects illuminated by narrow light beams in scattering media

10 p1725 A69-23971

Reversibility principle in transilluminated three dimensional photoelastic medium

14 p2535 A69-29359

Combined distribution density of elevations and slopes for illuminated areas of stable statistically homogeneous random surface exposed to parallel rays beam

15 p2569 A69-30948

Visual perception of three dimensional objects under simulated solar illumination in space considered in relation to manned spaceflight maneuvers

17 p2913 A69-33174

Incident integral light flux relations and visibility range equation derived for objects illuminated by narrow light beams in scattering media

21 p3772 A69-39657

Illumination effect on air navigation chart reading during flight, using questionnaire data

24 p4271 A69-42605

ILLUMINATION

Gold/polycrystalline cadmium selenide film contact found ohmic in darkness and barrier in light, noting potential distribution, electron concentration and energy gap

19 p3384 A69-36480

Constant illumination intensity effects fixed ratio lever pressing behavior for appetitive reinforcement with chimpanzee in temperature and humidity controlled environment

24 p4260 A69-42702

ILLUMINATORS

High repetition rate pulsed illuminator using electrodeless halogen discharge for rapid light extinction

04 p0599 A69-15021

Optoelectronic spectrum analyzer with raster illuminator for producing two dimensional Fourier transform to analyze two dimensional functions

10 p1725 A69-23301

Solar UV radiation measurements by balloon-borne monochromatic illuminator, using Cd-cathode photomultiplier detector

11 p1945 A69-24410

Portable electric lamp for work and photographic purposes in manned spacecraft, describing circuitry, construction and applications

[IES PREPRINT 30] 18 p3138 A69-35173

Briteye battlefield illumination flare configuration, candle power, burn duration and hot air balloon-type suspension system

20 p3461 A69-37166

ILLUSIONS

NT OCULOGRAPHIC ILLUSIONS

Apparent movement in peripheral vision induced by sequential flashing of spatially unresolved two dots, studying dynamics of illusion

16 p2746 A69-31556

Vestibulometric test program for flight surgeon appraisal of flying personnel, emphasizing singling out persons prone to illusory sensations

20 p3473 A69-37277

ILMENITE

Chemical analysis and paragenesis of manganian ilmenite from Sierran adamellite using electron microprobe

19 p3302 A69-35977

Ilmenite composition in equilibrated ordinary chondrites, analyzing Fe, Mg, Ti and Cr content

24 p4382 A69-42890

ILS (LANDING SYSTEMS)

U INSTRUMENT LANDING SYSTEMS

IMAGE CONTRAST

Photographic image degradation resulting from wave front distortion due to atmospheric refractive density gradients over long oblique optical path

01 p0107 A69-10223

Atmospheric influence on ground visibility reduction of airborne objects, using radiative transfer equation to calculate contrast transmission function

01 p0111 A69-11100

Imagery degradation by moisture condensation on thermal IR scanners optics during aircraft descent from higher to lower altitude

08 p1311 A69-19821

ATS satellite distorted photographs conversion into normal and Mercator projections, using computer programs

10 p1689 A69-22945

Visual observation of aerospacecraft, discussing object luminance, eye contrast sensitivity, atmospheric contrast transmission function and psychophysiological and atmospheric effects

10 p1649 A69-23872

Atmospheric turbulence degradation of holographs resolution improved by geometrical optics and series-expansion methods, noting role of Gaussian and exponential refractive index structure

12 p2090 A69-26250

Atmospheric turbulence effects on detection and resolution of incoherent objects, discussing error probabilities of threshold and maximum-likelihood systems

12 p2029 A69-26252

IR polarizing microscope with IR corrected objectives and eyepieces providing higher contrast, sharper focusing and less light scattering

12 p2093 A69-26595

Spotted scattered background contrast relation to scattering system geometry during laser scattering by suspended Lycopodium spores

13 p2273 A69-28550

Ultrasound holography for imaging opaque structures, noting distortion due to long wavelength of sound field and distortion reduction techniques

13 p2265 A69-28663

Panchromatic illumination in radar systems for image quality, tracking and detection problems, suggesting application to polypanchromatic radar

14 p2416 A69-29529

Linear mean square estimator for restoration of images degraded by system with bandlimited spread function

15 p2611 A69-31032

Finite resolution effect on solar granulation simulated by numerical experiments using two dimensional smeared pattern

17 p3029 A69-33046

Aerospace images information suppressing and enhancing methods to aid interpreter in making more accurate recognition and measurement of earth resources subjects

18 p3133 A69-34338

Visibility degree of noctilucent cloud determined from ratio of brightness contrast against sky to eye contrast threshold

19 p3362 A69-36410

Multispectral imaging system to increase contrast using optical mechanical scanner, multielement dispersing spectrometer and electronic signal processing equipment

20 p3540 A69-37737

Remote sensors discrimination and performance, discussing linear filter system, contrast ratio, tricolor systems and multispectral scanning system

20 p3493 A69-37743

Wedge fringes visibility and localization in hologram interferometry during focusing on surface under examination for displacements

22 p3943 A69-40016

Motion-distorted photograph deblurring method using extended range holographic Fourier transform division

22 p3944 A69-40020

Linear models with self excitation for brightness and contrast perception studies in human visual system

22 p3881 A69-40862

Human peripheral retina contrast sensitivity determined by measuring psychophysically for sinusoidal grating target describing luminance effects

22 p3882 A69-40870

Response characteristics of human visual mechanisms sensitive to motion while varying adaptation stimulus contrast to control visual effectiveness

22 p3884 A69-40887

Orthophotography as technique for eliminating distortions in vertical aerial photographs during conversion into uniform scale reproductions

22 p3949 A69-40998

Reconstruction properties of image plane holography for producing bright white light displays, using reference beams

23 p4164 A69-41627

Solar image selection device based on statistical analysis of photospheric contrast, noting use for electronic photography and location impaired observatory

23 p4213 A69-41697

IMAGE CONVERTERS

Lithium niobate based parametric image converter for IR to visible operation, discussing design factors performance calculations

[IEEE PAPER B-3] 07 p1150 A69-19048

Optical processing of planetary radar data for range Doppler image generation

08 p1270 A69-19816

Shutter drive circuits for image converter camera noting focusing, deflection system, applications in plasma research, etc

12 p2082 A69-26138

Photoelectric recorder with timebase image converter tube for investigating ultrashort light pulse transient response of laser

12 p2083 A69-26139

Electron-optical image converter camera for wide time intervals, considering nanosecond electronic control and high voltage stabilized power supply

12 p2083 A69-26140

Nanosecond electron-optical image converter multiframe camera designed for reducing frame exposure time

12 p2083 A69-26141

Multiframe image converter registration of space-time ruby laser spot structure changes in Q switched regime prior to giant pulse formation

12 p2083 A69-26142

Electronic image converter camera for observing rapidly evolving light phenomena consisting of high voltage pulse generator and biplanar tube image converter

12 p2084 A69-26147

High speed streak cameras applicability to low density theta pinch studies, describing image converters design, operation and block diagrams

14 p2496 A69-29787

Generalized quantum yield for sensitivity of photoelectric devices, considering multistage image converter and photomultiplier

14 p2496 A69-29788

Filamentary nebula IC 443 observation by Fabry-Perot etalon with image converter, determining radial, expansion velocities and H alpha line half width

15 p2686 A69-30538

Magnetically focused electronographic image converters in far UV photography and spectroscopy in space astronomy applications

17 p2972 A69-33084

X ray TV system with electronic-optical converter and X ray vidicon for industrial defectoscopy

18 p3138 A69-35113

Ablating sphere viscous wake using image converter camera, computing luminance radial distribution by unit volume

19 p3306 A69-35739

Image converter camera and astronomical telescope arrangement for photographing metal diaphragm openings in shock tube

20 p3538 A69-37227

Magnetically focused electronographic image converters for far UV photography and spectroscopy from sounding rockets, discussing stellar observations

20 p3543 A69-37801

Optical instruments as visual aids in scientific research including electron optical image converters detecting emissions invisible to human eye

22 p3943 A69-39974

Orthophotography as technique for eliminating distortions in vertical aerial photographs during conversion into uniform scale reproductions

22 p3949 A69-40998

IMAGE CORRELATORS

- Pseudorandom radar ranger /DIOMEDE/ using optical correlator and phase loop
03 p0393 A69-13254
- Holographic technique for reconstructing light wave front, developing algorithm for three dimensional images recognition
09 p1495 A69-21859

IMAGE DISSECTOR TUBES

- Image dissector meteorological cameras, discussing ATS-III and Nimbus systems, high resolution camera and multispectral cameras
18 p3137 A69-35101

IMAGE FILTERS

- Satellite digital video data analyzed by two dimensional filter computer technique, discussing biomedical applications
02 p0213 A69-12155
- Filter effectiveness in improving air to ground target identification performance on TV display
06 p0887 A69-17210
- Restoration of photographic images by optical spatial filtering with least mean square error filter in presence of random additive noise
15 p2611 A69-31033
- Glass filter systems for aerial color photography developed from spectral studies of sunlight, skylight and airlight in Rayleigh atmosphere
22 p3948 A69-40986
- Multispectral color aerial photography using broadband spectral filters for detecting and identifying small environmental features of earth surface
22 p3949 A69-40997

IMAGE INTENSIFIERS

- Fiber optic electrostatically focused image intensifier tube for recording star spectra with reduced exposure time [WERL-68-1C2-TAEC-P1]
04 p0603 A69-15444
- Image intensifier-vidicon closed circuit TV network for auroral cinematography at low light levels
06 p0925 A69-17382
- Auroral H beta intensities determined from photographs by image intensifier, describing equipment and data reduction method
10 p1684 A69-23824
- Electroluminescence and electroluminescent devices, considering semiconductor lasers, radiation sources and image amplifiers
11 p1899 A69-25198
- Crab Nebula pulsar detection by TV camera with image intensifier at focus of astronomical telescope, detailing instrumentation and observations
11 p1962 A69-25251
- Photoelectronic high speed image intensifier framing camera, showing single shot synchronized photography of electric spark in air
12 p2082 A69-26137
- Image intensifier cascade tubes and slit type electronic cameras with high sensitivity multiple integral images, exemplifying projectile velocity measurements
12 p2083 A69-26143
- Image intensifier for high speed spectrography of short duration faint radiation source, noting high speed shutter and resolution
12 p2085 A69-26160
- Pulsating and flaming auroral patches recorded by image intensifier vidicon camera, calculating upward field aligned speeds for luminosity enhancement
16 p2780 A69-32305
- Image intensifier and return beam sections of 4.5 inch high resolution vidicon and camera system for high definition signal readout
17 p2976 A69-34063
- Holographic method of a posteriori restoration of images formed by coherent and incoherent light by spatial frequency retrieval
19 p3304 A69-35603
- Quantitative photographs of low density flowfields during shock tunnel tests using electron beam excitation with image intensifier tube detector
19 p3292 A69-35723
- Low light level TV systems for military uses, describing design and operation of various image intensifier tubes
22 p3945 A69-40141

IMAGE ORTHICONS

- Ohz intensity variation in bright homogeneous auroras prior to and during breakup observed visually and with image orthicon TV systems
04 p0594 A69-15129

- Flaming auroras observations with auroral image orthicon TV systems, calculating electron release points on field line of station
05 p0758 A69-16413
- Image orthicon tube to detect low intensity pulsed light signals, formulating SNR in terms of resolvable image points
08 p1317 A69-21085
- Rocket trajectory determination by tracking on-board light source against star background with image orthicon TV system
12 p2033 A69-26965

IMAGE TUBES

- High dispersion IR image tube spectroscopy using telescope, discussing alpha Sco and alpha Boo spectral regions
07 p1074 A69-19203
- Silicon vidicon for near IR and visible radiation viewing describing spectral response, energy transfer characteristics, resolution and dark leakage currents
09 p1466 A69-22456
- Image tube storage target mesh electrode structure and transmission data for electron beams of various velocities, noting secondary electron redistribution control
11 p1848 A69-24749
- Image tube spectra observations of interstellar absorption band at 4430 A, noting emission band at 4400 A
11 p1965 A69-25658
- Image intensifier cascade tubes and slit type electronic cameras with high sensitivity multiple integral images, exemplifying projectile velocity measurements
12 p2083 A69-26143
- Meshless shutter tube with nine images double deflection capability, using deflectron and semiconducting plates assembly
12 p2083 A69-26144
- Diode type image shutter tube with proximity focusing for high speed photography
12 p2083 A69-26145
- Ultrahigh speed photographic cameras with exposure times between 5 and 500 nsec, using image tube and high voltage pulse generator
12 p2083 A69-26146

IMAGERY

- NT AERIAL PHOTOGRAPHY
NT ALL SKY PHOTOGRAPHY
NT ASTRONOMICAL PHOTOGRAPHY
NT AUTORADIOGRAPHY
NT CHRONOPHOTOGRAPHY
NT CINEMATOGRAPHY
NT CLOUD PHOTOGRAPHY
NT COLOR PHOTOGRAPHY
NT ELECTRO-OPTICAL PHOTOGRAPHY
NT ELECTRON PHOTOGRAPHY
NT HOLOGRAPHY
NT INFRARED PHOTOGRAPHY
NT KINOFORM
NT LUNAR PHOTOGRAPHY
NT PHOTOMICROGRAPHY
NT PHOTORECONNAISSANCE
NT RADAR PHOTOGRAPHY
NT RADIOGRAPHY
NT REPRODUCTION [COPYING]
NT ROCKET-BORNE PHOTOGRAPHY
NT SATELLITE-BORNE PHOTOGRAPHY
NT SCHLIENEN PHOTOGRAPHY
NT SHADOWGRAPH PHOTOGRAPHY
NT SPACEBORNE PHOTOGRAPHY
NT STEREOHELIOGRAPHS
NT SPECTROPHOTOGRAPHY
NT STEREOPHOTOGRAPHY
NT ULTRAVIOLET PHOTOMETRY
- Polarization effects of scattered coherent light on laser imagery, determining surface roughness and angle of incidence effects photographically on basis of Fung theory
11 p1896 A69-24849
- Solar telescope imaging quality measured as function of atmospheric turbulence and temperature above land level
14 p2453 A69-29973
- Multispectral scanner with multichannel spectrometer for earth observations, describing video image generation from detector elements output signals
19 p3310 A69-36066

IMAGES

- NT AFTERIMAGES
NT RETINAL IMAGES
- Coincidence error between star image and planet edge for entrance pupil and telescope magnification
08 p1314 A69-20383
- Image motion trajectory in rotating angular mirror having converging reflections from two surfaces, using precession theory of gyroscopes
11 p1881 A69-24562

- Spontaneous decomposition of image space into compact sets /images or classes/ using adaptive dispersion method to reduce system learning time
11 p1859 A69-24964
- Slow waves contribution to image radiation from array of line sources above ground plane, determining optimum height of lowest element of array
11 p1837 A69-25002
- Photodielectric tape camera with optical images stored on tape in form of charge pattern
16 p2792 A69-32558
- Solar image motion frequency spectra analysis via photoelectric equipment, showing influence on photographic pictures, spectra and modulation transfer functions for diffraction telescope
17 p3029 A69-33047
- Hologram imaging characteristics expression, deriving relations characterizing localization and dimensions of images
19 p3308 A69-35868
- After image measuring method of eccentric fixation during autokinetic light tracking
22 p3878 A69-40837
- Pilots body images determined by inkblot tests, considering effects of aircraft type, pilots experience, etc
23 p4112 A69-42364

IMAGING TECHNIQUES

- Digital computer system for storing, processing and displaying TV pictures
01 p0077 A69-10024
- Mirror photogrammetry geometric principles, studying photo pairs, mirror reflection and reduction methods
01 p0077 A69-10025
- Synchronous observations of satellites by photographic techniques from satellite stations, discussing reference stars plane coordinates and exposure time recording
01 p0027 A69-10224
- Multibeam recording technique producing speckle-free images in redundant holograms of transparencies
01 p0082 A69-10850
- Charge image detector for reading information as extended spatial charge distribution on dielectric layer surface, using vibrating conducting probe scanner
02 p0248 A69-11822
- Refractive index structure constant for different atmospheric turbulence conditions, discussing possibility of improved capabilities for imaging systems
02 p0275 A69-11930
- Hyperstereoscopic and hypostereoscopic hologram images with doubled or halved interocular distance, noting effect on image depth
02 p0249 A69-11931
- Monochrome pictorial encoding, discussing pulse code modulation, delta modulation and buffer storage techniques
02 p0213 A69-12154
- Stroboscopic holography for repetitive scenes, using mode locked laser as source
02 p0250 A69-12411
- Optical imaging systems achieving aperture synthesis by lensless Fourier transform holography, noting X ray astronomy, ultrasonic and space applications
03 p0430 A69-13324
- Aerospace sensor systems, discussing adaptive multimode sensors and multispectral sensing, electronic recognition of image components, laser radar and Raman scattering technique
03 p0431 A69-13851
- Laser ranging and illumination systems, discussing direction of pulsed monochromatic radiation to illuminate scene and utilization of reflected radiation for imaging
03 p0442 A69-14191
- Mars unmanned spacecraft mission profiles for surface imaging, noting influence of lighting requirements [SMPTE PAPER 104-21]
04 p0650 A69-14361
- Fourier coding method for coding images for digital transmission, achieving bandwidth reduction for televised images
04 p0556 A69-14429
- Holography, discussing image formation, position, enlargement, aberration and application to stress analysis
04 p0601 A69-15186
- Photographs of intensity of radio emission in millimeter band, using luminophor based on ZnS and CdS
04 p0560 A69-15272
- Temperature distribution over receiving layer of absorption edge image transformer, discussing thermal conduction influence on performance of thin film IR image receiver
04 p0631 A69-15280

Solar image or spectrum focal plane scanning technique with output beam displaced but undeviated relative to input beam for solar spectrophotometry
04 p0602 A69-15378

Algorithm generating same stereogram for two or more selected surfaces by extending random dot stereogram technique
04 p0603 A69-15445

Holograms volume depth increased by reference beam splitting or by photographing holograms on same plate in sequence
05 p0761 A69-15651

Acoustic holograms, describing electronic method of reconstructing holographic image in order to avoid multiple image problem
06 p0923 A69-16933

Blurred spaceborne photographic image reconstruction by spatial frequency filtration
[UN PAPER 68-95240] 06 p0923 A69-17080

Ranger pictures improvement by computer, eliminating image distortion due to electronic imaging systems
06 p0924 A69-17164

Map information display methods comparison for tactical image interpreters
06 p0924 A69-17212

Optical commutation to permit multifield monitoring and recording with one sensor by employing high resolution imaging fiber optics elements feeding common focusing lens
06 p0926 A69-17678

Specular reflection computer program utilizing virtual image technique to determine reflection characteristics of enclosed diffusely emitting surface
[AIAA PAPER 69-65] 06 p1040 A69-18215

Ultrasonic holograms and optical reconstructions derived by scanning receiver or source
06 p0930 A69-18228

Imaging systems for weld inspection, discussing physical factors and selection of radiation
07 p1139 A69-18796

Fourier transform algorithm introduction leading to image coding technique with image transformed by Hadamard matrix operator
07 p1078 A69-18859

Lithium niobate based parametric image converter for IR to visible operation, discussing design factors performance calculations
[IEEE PAPER B-3] 07 p1150 A69-19048

Three dimensional information pictures of chromospheric alpha H line using special camera attached to solar telescope diffraction grating spectrograph
07 p1217 A69-19241

Microwave holographic reconstruction of metal objects inside purse by nonscanning method, visualizing microwave field by polaroid and liquid-crystal techniques
07 p1135 A69-19449

Photoelectronic imaging systems in space exploration emphasizing acquisition time, storage capacity and transmission time
07 p1136 A69-19591

Holography by scanning receiver, source, object or both source and receiver, discussing resolution, magnification, image position and aberrations
07 p1136 A69-19640

Object restoration, discussing data processing method for single variable functions with small signal to noise ratios
07 p1137 A69-19721

Range-Doppler processing in pulsed radar applied to imaging of rigid rotating body with motion compensating resolution cells
08 p1270 A69-19861

Image degradation in holograms undersampled with respect to space-bandwidth product, noting signal to noise ratio and resolution
08 p1312 A69-20078

Holography and similarity criterion for developing image recognition algorithm
08 p1314 A69-20417

Quantitative spectroscopy and spectral photometry, discussing developed image properties and connection between exposure and image
08 p1315 A69-20467

Holographic technique for measuring thin fluid film profiles using interference image reconstruction and helium-neon laser as coherent light source
08 p1317 A69-20873

Galaxies classification using rectified images, noting pitch and inclination angles
08 p1408 A69-21135

Borrmann effect and abnormal transmission and extinction observed by reconstruction of images of holo-

grams recorded in three dimensional photosensitive medium
09 p1494 A69-21492

Holographic image formation through turbulent medium simulated by shower glass, noting thickness variations and prismatic light deflection effects
09 p1494 A69-21559

Holograms with unfiltered radiation obtained from superhigh pressure mercury lamp and incandescent lamp
09 p1495 A69-21671

Silicon diode array camera tube modified to permit X ray images to be displayed on TV monitor
09 p1463 A69-21845

Holographic technique for reconstructing light wave front, developing algorithm for three dimensional images recognition
09 p1495 A69-21859

Holographic technique application to radio and sound wave ranges, discussing incoherent holography development to overcome difficulties in image reconstruction of stationary objects
09 p1498 A69-22133

Laser spark image in air photographed in scattered laser radiation light, showing singularities and absence of beadlike structure
09 p1519 A69-22531

Multiple pinhole camera for X ray astronomy, suggesting cross correlation image recovery technique based on Fourier convolution theorem
09 p1502 A69-22768

Modulated wave holography for detecting and reconstructing ultrasonic beam path, noting applicability to vibrating objects analysis
10 p1694 A69-23368

Imaging ultrasound by holography with reconstruction in light, comparing methods using scanned hologram and liquid surface
10 p1695 A69-23543

Holographic techniques for acoustical imaging to obtain three dimensional images of opaque objects encountered in nondestructive testing
10 p1695 A69-23544

Quantitative analysis of plane waves for weak interaction of two dimensional sound and light fields in acoustical imaging by diffracted light
10 p1695 A69-23545

Acoustical transparencies illuminated by sound waves for optical imaging and ultrasonic diffraction, noting application to visualization of inhomogeneities in samples
10 p1695 A69-23546

Digital reconstruction of images from optical holograms for acoustical data, discussing image degradations
10 p1695 A69-23547

Qualitative analysis of recording phase only acoustic holograms of object wave instead of both phase and amplitude, considering fringe patterns and conjugate image
10 p1695 A69-23548

Matrix method for acoustical holograms and optical reconstruction of virtual and conjugate images using laser light of 6328 A wavelength
10 p1696 A69-23549

Hologram obtained by recording interference pattern displayed by ultrasonic camera, discussing real time viewing
10 p1696 A69-23550

Computer generated kinoform optical element operating on phase of incident waves and forming wave front reconstruction single image
10 p1697 A69-23867

Computer generated holograms using binary transmittance for wave fronts and three dimensional images construction
10 p1697 A69-23869

Electron beam addressed electrooptic light valve used as spatial filter, discussing electronic control and optical processing in real time
10 p1697 A69-23870

Statistical estimation theory giving angular resolution of imaging systems in terms of noise characteristics and modulation transfer function
10 p1725 A69-24048

Spectroheliograph technique, obtaining high resolution magnetic maps of solar magnetic fields directly in single image without photographic subtraction
11 p1880 A69-24432

Coherent optical target recognition through randomly turbulent medium for imaging system offsetting image degradation due to turbulence
11 p1894 A69-24470

Computer processed pictures including transformation of graphical material, picture generation from data or abstract rules, discussing procedures, instrumentation, color and applications
11 p1842 A69-24588

Holograms on photochrome films by split beam He-Ne laser using special mirror system
11 p1881 A69-24631

Multicolor hologram recording and reconstruction gas lasers, discussing control of ghosts in three dimensional image
11 p1882 A69-24679

Pulsed laser holography advantages for recording small objects in motion and holographic interferometry advantages for complex surfaces and time-separated events
11 p1883 A69-24682

Holographic multiplexing for producing three dimensional reconstruction of nonlaboratory objects in horizontal direction, noting TV and X ray pictures applications
11 p1883 A69-24684

Holography of moving diffuse object, noting bright unblurred image dependence on adaptation to velocity
11 p1883 A69-24685

Coherent pulse laser holography for front and back lighted holograms of moving objects
11 p1895 A69-24686

Acoustic holography free surface and scanning methods, noting acoustical intensity role in phase stability
11 p1883 A69-24687

Holographic techniques application to optical systems for high resolution images of distant objects by overcoming atmospheric turbulence and light diffraction limitations
11 p1883 A69-24688

Scenic holographic stereograms resolution and up/down scaling, discussing roles of projector lens and camera aperture
11 p1883 A69-24690

Imaging radar systems for employment on small spacecraft, fabricating small lightweight radar systems packages with integrated circuit techniques
11 p1835 A69-24695

Single and double mirror systems geometrical optical image aberrations noting focal number, angle of field, secondary magnification and mutual position tolerances
11 p1918 A69-24836

Ray tracing application to evaluating aberrations produced by Fresnel holograms for optimizing design of aplanatic lens holography system
11 p1885 A69-24848

Visible imaging of IR objects by conversion of IR frequency to visible with sum-frequency generation within nonlinear dielectric medium
11 p1897 A69-25037

Holograms reconstructing images of points with diameters approximated by width of autocorrelation functions
11 p1886 A69-25058

Solid state IR imaging using monolithic Ge mosaics of isolated sensor elements, discussing design, structure, fabrication, system readout and operation
11 p1938 A69-25307

Light scattering materials for transparent objects holography, analyzing Christiansen filter and milk white and ground glass plates
11 p1889 A69-25550

Holographic in-focus projection of images on three dimensional focal planes of arbitrary shape, noting moire pattern strain analysis
11 p1889 A69-25653

Planetary imaging systems design problems illustrated by Mars orbiter reconnaissance, discussing radiation effect on film, shielding, stereo method comparisons, color bands, etc
[SMPT PAPER 105-78] 12 p2078 A69-25770

Photoelectronic image devices, discussing detectors, electronography, Lallemand camera, spectracon and electron image multipliers
12 p2082 A69-26136

Multiple frame camera with image compensation as ballistic photodiode
12 p2084 A69-26153

Rotating mirror framing camera with continuous access at f/18 aperture, discussing image transfer system, frame rate and capacity, etc
12 p2085 A69-26157

Selective stroboscope with explosive bright light source and microsecond pulse duration for short flash period over large area, noting single frame separation method
12 p2086 A69-26162

Direct electron beam shadowgraph photographic (betagraphy) technique for recording small high speed objects with 3 nanosecond exposure time
12 p2086 A69-26164

Ultrahigh speed multiple framing photography system using sequentially modulated ruby laser and smear type camera applied to dynamic photoelasticity
12 p2086 A69-26166

Holography theory and applications including imaging, Fourier transforms and interferometry
12 p2086 A69-26169

Cinematic holography as continuous motion uninterrupted viewing system compared with standard cinematography, noting flicker-free shutterless reproduction
12 p2087 A69-26173

Pulsed laser holography used in conjunction with schlieren three dimensional system for observing gas density gradients at different test positions
12 p2088 A69-26179

Quantitative schlieren technique for one dimensional recording of light refraction in density gradients of high speed flow fields
12 p2088 A69-26181

HF interferometry for statistical-numerical oscillation analysis of unsteady plane transonic flow, constructing phase planes for study of wave surfaces propagation
12 p2089 A69-26188

Twin image elimination in holography using single sideband object waves without offset reference wave introduction
12 p2090 A69-26253

Power spectrum of object flux transmittance using Fourier transform type holographic system compared to systems similar to correlator
12 p2090 A69-26254

Active optics system for obtaining perfect mirror figure in orbiting astronomical telescope, using laser and white light sources, interferometers and data converter
12 p2092 A69-26423

Optical/mechanical IR line scanner imagery role in remote sensing
12 p2096 A69-26979

Radar imagery for agricultural land mapping, noting field and crop discrimination and parameters influencing radar return
12 p2097 A69-26986

Remote sensing and forest survey sampling designs, discussing nonstereo stratification, conventional photography and IR or radar imagery
12 p2097 A69-26991

Multispectral and calibrated Alaskan Arctic aerial survey of sea ice, thaw lakes and polygonal soils
12 p2075 A69-26996

Terrain photography applications and analysis including remote sensing of photographic systems and photointerpretation
12 p2098 A69-27006

Remote sensing of urban environments for metropolitan information systems noting photographic, thermal IR, radar and microwave applications
12 p2193 A69-27012

Linear recording of object wave phase to produce acoustic holograms
13 p2259 A69-27243

Ultrasonic images detection for nondestructive testing including surface-relief technique, Pohlman cell and scanning with piezoelectric transducers
13 p2269 A69-28661

Ultrasound holography for imaging opaque structures, noting distortion due to long wavelength of sound field and distortion reduction techniques
13 p2265 A69-28663

Image recognition algorithm for determination of hyperplane separating two finite sets of elements in Euclidean space
14 p2418 A69-29353

Panchromatic illumination in radar systems for image quality, tracking and detection problems, suggesting application to polypanchromatic radar
14 p2416 A69-29529

Remote sensor imaging techniques for simultaneous radar, IR and visible electromagnetic spectra of extensive land areas, presenting two clustering algorithms for multiple images
14 p2448 A69-29533

Image formation with arbitrary holographic surfaces achieved by reversing direction of propagation of diverging wave
14 p2450 A69-29582

Image quality of color disks in aerial photographs using panchromatic, color positive, color negative and false color films, measuring reflected sunlight
14 p2450 A69-29600

Image enhancement by coherent optical system without spatial filter, noting improved defocused transparencies
14 p2450 A69-29641

Optical image diffraction method for analyzing radiation patterns of horn antenna sounding beams used in microwave measurement of expanding plasmoids
14 p2497 A69-29793

Integrated landscape analysis with radar imagery for earth resources
15 p2608 A69-30454

Microwave hologram construction and image reconstruction by laser beam, analyzing results by matrix expression
15 p2610 A69-30802

Time average, multiple exposure and real time holographic interferometry based on image synthesis
15 p2611 A69-31146

Iris microphotometer with measurement and reference beams traversing plate in neighboring regions designed for stellar images measurement
16 p2790 A69-32225

Instrument for simultaneous observation of astronomical plate pairs for detection of stars with UV color excess
16 p2791 A69-32226

Holograms volume depth increased by reference beam splitting or by photographing holograms on same plate in sequence
16 p2791 A69-32508

Photographic system for astronaut training in Apollo Mission Simulator, using fixed camera and moving earth model coincident with strip color film past exposure slit
16 p2792 A69-32787

Multiple reference sources to improve field of view of lensless Fourier transform holography limitation due to modulation transfer function of film and turbulence
17 p2971 A69-32920

Mosaic mirror and lens camera system for multiple image high resolution photography
17 p2972 A69-33089

Point object image differential field during reconstruction by surface nonplanar holograms, determining image position and aberrations
17 p2981 A69-33115

Microwave holography for antenna synthesis, radiation patterns and visible images reconstruction
17 p2976 A69-33891

Anamorphic holography, discussing optical and nonoptical wavelength processes and generation and reconstruction of holograms for radar applications
17 p2976 A69-34062

Multispectral imaging remote sensors, analyzing energy sources affecting systems synthesis
17 p2977 A69-34064

Electron microprobe to produce plane grating X ray hologram based on Lloyd mirror experiment principle
17 p2977 A69-34160

Relative control data incorporation into sequential or simultaneous analytical triangulation systems, considering extraterrestrial photographs reduction
18 p3133 A69-34335

Aerospace images information suppressing and enhancing methods to aid interpreter in making more accurate recognition and measurement of earth resources subjects
18 p3133 A69-34338

Image dissector meteorological cameras, discussing ATS-III and Nimbus systems, high resolution camera and multispectral cameras
18 p3137 A69-35101

Optical imaging with partially coherent nonthermal light, discussing correlation function propagation, transfer functions, spatial Fourier analysis, weak visibility and matrix form
19 p3372 A69-35907

Optical imaging with partially coherent nonthermal light, discussing reconstruction of object from image and similarity between object and image, including detection
19 p3372 A69-35908

Thermal IR imaging devices for shape recognition and target position, emphasizing optical mechanical image or object plane scanners using point detectors
19 p3310 A69-36064

TV camera tubes with electron beam scanning adapted to IR imaging, emphasizing vidicon
19 p3311 A69-36069

Holographic system to process signals received by pulse Doppler radar, noting real time operation with availability of instantaneous development image storage media
19 p3314 A69-36598

Satellite IR hyperaltitude imagery for earth resources application, obtaining geological, meteorological and hydrological information
20 p3536 A69-36930

Scanned receiver acoustical holography for mapping or imaging sources of radiated acoustic energy on complex vibrator in water, noting application in air
20 p3576 A69-37323

Imaging radars - Conference, University of Michigan, July-August 1969
20 p3488 A69-37631

Imaging radar study based on optical imaging and electromagnetic wave processes, discussing Doppler signal processing, synthetic aperture radars and microwave holography
20 p3489 A69-37632

Holographic wave front reconstruction emphasizing between-wave interference fringes, discussing application to microscopy, Thompson and Parent disdrometer, interferometry, etc
20 p3540 A69-37637

Atmospheric phenomena effects on terrain imaging radar systems performance, discussing tropospheric turbulence and ionospheric irregularities
20 p3490 A69-37647

Imaging radar applications noting military surveillance, navigation assistance, iceberg detection, sea rescue operations, all-weather traffic surveys, terrain mapping, etc
20 p3491 A69-37649

Geological radar in regional and detail studies, discussing area side scanning imagery and lithology changes detection
20 p3491 A69-37652

Resolving power and field of view relations of holographic device for images recording through inhomogeneous atmosphere
20 p3540 A69-37728

Airborne imaging radar drawbacks and advantages, describing techniques to overcome defects
20 p3493 A69-37735

Multispectral imaging system to increase contrast using optical mechanical scanner, multielement dispersing spectrometer and electronic signal processing equipment
20 p3540 A69-37737

Thermal IR image forming devices, explaining principles of image and object plane scanning
20 p3540 A69-37738

Thermal scanner model block diagram presented including lens, filter, detector, CRT and camera, considering environmental factors affecting image character
20 p3541 A69-37740

Remote sensing by electromagnetic waves in microwave region, describing differences between microwave and optical sensing
20 p3493 A69-37741

Sensitivity improvement for inerteless microwave signal scanning and readout by applying pulse compression concepts, discussing application to real time microwave imaging and holography
20 p3545 A69-37901

Acoustic visualization for nondestructive testing, describing image formation by lenses, reflectors, holography, Bragg diffraction and phase contrast
20 p3512 A69-38269

Two channel TV Cassegrain telescope, describing color separation system for obtaining integral and monochromatic images of astronomical objects
20 p3547 A69-38309

Three dimensional X ray pictures of flaws shape and location in various materials
20 p3551 A69-38311

Orbital images for earth resources satellite mission planning using Mercury, Gemini and Apollo synoptic terrain photographs
21 p3721 A69-38632

Image deblurring and aperture synthesis using a posteriori processing by Fourier transform holographic spatial filtering
21 p3722 A69-38793

Holographic recording of focused images and reconstruction in white light, discussing optimal conditions, calculating ray paths
21 p3725 A69-39543

Optical properties of Gabor holograms with pure reference beam, discussing image reconstruction using He-Ne laser
21 p3726 A69-39624

Microholographic system for nonpseudoscopic stereoscopic image reconstruction of transparent and nontransparent microobjects
21 p3726 A69-39702

Randomly moving objects holography and reduction of stability requirement during exposure period due to automatic phase modulation

21 p3726 A69-39741

Holograms capable of multiple imaging or reconstructing point images, using extended and correlated signal and reference sources in recording process

21 p3727 A69-39777

Resolution limitations in holographic images using single record, discussing lensless holography using plane reference waves

21 p3727 A69-39778

Flash holography using ruby laser, describing optical system arrangement

21 p3727 A69-39784

Planetary nebulae imaging stratification effects on structural difference studies by slit and slitless spectrographs and narrow band photography

21 p3817 A69-39785

Extended source Fourier transform holography for single image synthesis of multiple identical images produced by multiple pinhole camera in X ray astronomy

22 p3943 A69-40019

Image disappearance or reappearance time controlled by inducing changes in alpha occurrence probability, executing on-line closed loop program detecting alpha rhythm

22 p3871 A69-40159

Stereoscopic shadow caster application to photographic stereoscopic projection for studying binocular stereopsis under kinetic viewing conditions in vision research

22 p3893 A69-40839

Fresnel zone plate as converging and diverging lens in holographic image reconstruction, noting sine wave zone plate

22 p3947 A69-40864

Color chemistry concept producing high quality color negatives and prints in existing black and white processing systems

22 p3948 A69-40990

Automatic discriminator design for identifying distorted image in noise based on ideal transmitter and use of split scanning beam

23 p4163 A69-41551

Mars landing site topography reconstructed via stereoscopic pictures returned by surface-based imaging systems

23 p4164 A69-41618

Hologram film nonlinearity effect on reconstructed image, discussing role of illumination type

23 p4165 A69-41636

Optical imaging problems in ultrasonic holography including distortion, resolution and depth of field

23 p4166 A69-42181

Temporal reference acoustical holography with Sokolov ultrasound camera system using double pulsed ruby or scanning CW laser

23 p4166 A69-42182

Retroreflector and Scotchlite object images obtained in long range holography with Q switched ruby laser, noting atmospheric seeing conditions

23 p4167 A69-42184

Phase and amplitude acoustical holography in opaque media, discussing medical diagnosis and underwater viewing

23 p4167 A69-42198

Acoustical holography principles and reconstruction techniques, noting advantages of liquid-surface and temporal reference holography over optical counterpart

23 p4167 A69-42199

Linear motion blur compensation technique in photographic recordings by reconstruction of sharp image from hologram

24 p4314 A69-42972

Holographic technique for reduction of image distortion during penetration through inhomogeneous medium

24 p4314 A69-42975

Microwave holography by two beam interference method, discussing operating principles, equipment, image reconstruction, etc

24 p4314 A69-42976

Image reconstruction by graphical method for equal wavelengths of recording and reconstructing radiation and equal scales of hologram

24 p4315 A69-43166

Three dimensional shadowgraph-like images in single exposure holograms of diffusely illuminated flame explained as time average holographic interferograms

24 p4317 A69-43764

Sobolev first embedding theorem providing relationship between global and local properties of functions in theory of differential equations

01 p1013 A69-10005

Computer aided circuit design by singular imbedding, beginning with prespecified topology and undetermined elements

07 p1115 A69-19148

Four dimensional space-time immersion in conformally flat six dimensional space or flat eight dimensional space, noting group of isometries of tangent spaces

10 p1774 A69-23162

One parameter operator imbedding to modify Newton method for solution of nonlinear equations

10 p1719 A69-23519

IMIDES

High temperature structural adhesives at temperatures of 350 F and higher including epoxies, polyimides, amide-imides and polybenzimidazoles

15 p2642 A69-30329

IMINES

Polymerization of monomers considered for direct synthesis of iminobenzylidene

10 p1651 A69-23308

Hypergolic filling materials for solid fuels with hybrid propellant combinations, discussing ignition and combustion of ethyleneimine derivatives

10 p1753 A69-24023

Propylene imine IR and Raman spectra, calculating thermodynamic functions based on rigid rotator harmonic oscillator model

14 p2410 A69-29922

Curing agents for carboxy and hydroxy functional prepolymers synthesis and evaluation including sulfonyl, acyl and ureido aziridines

16 p2747 A69-32777

IMMERSION

U SUBMERGING

IMMISCIBILITY

U SOLUBILITY

IMMITTANCE

U ELECTRICAL IMPEDANCE

IMMOBILIZATION

Physiological, cytochemical and histological effects on muscular activity, nervous system, adrenal and thyroid glands and liver of mice during 30 day hypokinesia

02 p0198 A69-11502

Hypokinesia and acceleration effects on human organism immunity and resistance to inflammatory diseases in 62 day test

02 p0198 A69-11513

Barbamyl effect with and without somatotrophic hormone injection in mice during prolonged isolation and hypokinesia, noting sleep duration

10 p1646 A69-23576

Long term hypokinesia effect on cardiovascular system of athletes indicating human orthostatic resistance increase due to physical exercises

10 p1646 A69-23581

Hypokinesia effects on transversostriated muscle fibers of mice, noting changes in myofibrillar apparatus, mitochondria and sarcoplasm

13 p2212 A69-28616

Immobilization effects on alpha rhythm, locomotor coordination and visual alimentary motor reflexes of cats

13 p2212 A69-28617

IMMUNITY

Hypokinesia and acceleration effects on human organism immunity and resistance to inflammatory diseases in 62 day test

02 p0198 A69-11513

IMMUNOLOGY

Immunological and histochemical methods for studying mice reactivity after long term exposure to hyperoxic atmosphere

07 p1065 A69-18975

Specific antibody formation to influenza A virus vaccine /strain PR sub s/ in hibernating ground squirrels /Citellus tridecemlineatus/

08 p1263 A69-20173

Sublethal ionizing radiation doses effect on hemolytic immunocompetent spleen cells in mice upon using chemical radiation protectors

13 p2210 A69-28334

Immunological and histochemical methods for studying mice reactivity after long term exposure to hyperoxic atmosphere

20 p3479 A69-38223

Local stress effect on immunocompetent cells differentiation in guinea pigs lymphatic ganglia, showing antibody producing cells number increase

22 p3877 A69-40277

Retarded immunological recovery in sublethally X-irradiated mice by additional thymic exposure reversal with injected marrow cells

22 p3887 A69-41194

IMP

NT EXPLORER 18 SATELLITE

Interplanetary magnetic field fluctuations obtained by IMP 2

05 p0824 A69-16264

IMP F and G solar cosmic ray spectrometer utilizing FET analog multiplier for onboard particle identification data processing

[IEEE PAPER 3C-3] 07 p1135 A69-19197

Cosmic ray detectors design for medium, low and very low energy events on IMP-1 spacecraft, noting PCM format

23 p4118 A69-41738

IMP-A

U EXPLORER 18 SATELLITE

IMP-D

U EXPLORER 33 SATELLITE

IMP-E

U IMP

IMPACT

NT ELECTRON IMPACT

NT HYPERVELOCITY IMPACT

NT ION IMPACT

NT POINT IMPACT

NT PROTON IMPACT

Trajectories of elastic bodies analyzed by Hertz theory of impact

02 p0349 A69-12829

Large signal model for analysis of RF output and efficiency of IMPATT diode oscillator, noting frequency tuning

05 p0733 A69-16555

Si IMPATT diode oscillator and amplifier for CW operation at 50 GHz noting fabrication, performance and phase locking properties

05 p0733 A69-16560

Explosive bonding technique, discussing choice of explosive and geometrical parameters to match material parameters

[ASME PAPER 69-DE-47] 14 p2454 A69-28849

IMPACT ACCELERATION

Dynamic analysis and development of response histories and tradeoff study charts for spherical impact limiters for protecting hard landing planetary payloads

04 p0683 A69-15508

Mathematical formula for estimating cost and efficiency of parachuting supplies, noting shock load reduction

07 p1053 A69-19140

Rats tolerance to impact accelerations from blood enzyme activity providing safety limits for living organisms

10 p1645 A69-23500

Plastic cylindrical shell buckling under axial impact, predicting velocity required to cause flexural waves

18 p3218 A69-34624

Impact mechanism in hip safety belt protection in vehicles, deriving motion for natural oscillations of upper part of human body model

20 p3482 A69-37595

Impact limiter system design for Mars landing vehicle noting balsa wood or phenolic honeycomb construction

[AIAA PAPER 68-161] 21 p3820 A69-39228

IMPACT DAMAGE

NT METEORITIC DAMAGE

NT RAIN IMPACT DAMAGE

Barrier penetration depth by meteorite particles at prethreshold impact velocities, taking into account energy dissipation on shock wave front

01 p0152 A69-10579

Trailing camera technique to photograph impact and projectile penetration into earth materials from above and behind test vehicle

02 p0227 A69-11760

Strain rate effect of large deflections of clamped circular viscoplastic plates subject to rigid mass impact

02 p0349 A69-12798

Asymptotic estimate derived for size distribution function of fragments resulting from brittle impact destruction of rigid object applied to meteorites and lunar craters

03 p0512 A69-13691

Structures response to explosive blast, discussing damage criterion in terms of blast wave impulse and critical time

04 p0671 A69-14476

Reaction vs time relations in accidental impact of large commercial aircraft against rigid surface, detailing stress analysis of nuclear power plants structures

09 p1613 A69-21677

IMBEDDINGS [MATHEMATICS]

NT INVARIANT IMBEDDINGS

Spacecraft sterilization requirements, evaluating viable organisms release probability from spacecraft as function of equipment fracturing

11 p1828 A69-25460

Microbial contamination release probability from solids fractured by impact, considering spacecraft sterilization requirements

11 p1828 A69-25461

Impact crater cross section in fused silica, describing photomicrographic technique for distinguishing hypervelocity from low energy impacts

[AIAA PAPER 69-367] 13 p2366 A69-28299

Hypervelocity impact dynamics on copper cube targets imbedded with nickel wires, discussing terminal positions, Vickers hardness, flow fields, etc

[AIAA PAPER 69-368] 13 p2367 A69-28300

Pyrex spheres accelerated to 15 km/sec by plasma rail gun to study hypervelocity impact in thin stainless steel and Al targets

[AIAA PAPER 69-378] 13 p2368 A69-28308

Barrier penetration depth by meteorite particles at prethreshold impact velocities, taking into account energy dissipation on shock wave front

15 p2709 A69-30749

Meteoroid penetration damage to spacecraft system, showing particle mass density distribution as protection criterion

21 p3805 A69-39229

Air pressure wave forces on missile from silo wall motion resulting from close nuclear blast, using acoustic wave equation for concentric cylinder flow

21 p3691 A69-39765

Meteorite impact hypothesis supported by autochthonous and mixed breccias, shattercones and microscopic shock deformation evidence in central uplift rocks at La Malbaie structure

22 p4021 A69-40410

Darwin and Macedon impact glasses related to Far Eastern tektites through age determination by fission track technique

23 p4210 A69-41344

IMPACT DECELERATION

U DECELERATION

IMPACT LOADS

Finite deformation mode stability for finite amplitude first diameter nonlinear plastic wave initiation and growth at impact face in long rods

02 p0342 A69-12279

Viscous effects on impact pressure measurements in free jet low density gas flows at high Mach numbers

02 p0234 A69-12633

Recovery behavior of nickel strain hardened by impact loading by aluminum projectiles, showing microstructure correlation with stress levels

03 p0447 A69-13620

Impulse buckling threshold for elastic-plastic cylinder with elastic core after development of unstable motion

04 p0671 A69-14414

Inelastic strain measurement in metals during cyclic loads by impact tester

04 p0674 A69-14539

Multidegree of freedom systems for modeling optimum design of cantilever and simply supported beams for sudden loading

04 p0674 A69-14590

Nonlinear boundary value problem of elastokinetics solved by step-by-step integration to study thin walled shells stability under axial impact

[DVL-853] 04 p0677 A69-14836

Impulse loaded elastic-plastic beam response approximate solutions based on uniqueness proof

[ASME PAPER 68-WA/APM-23] 05 p0840 A69-16188

Theoretical and experimental results on annealed tapered aluminum rods to assess one-dimensional rate independent theory of plastic wave propagation from longitudinal impact

06 p1022 A69-17365

Plastic deformation in bcc, fcc and hcp metals as function of initial impact load energy, noting strain hardening effects

07 p1166 A69-19144

Stress-strain-time relations in magnesium alloy and aluminum plate impact load tests, discussing stress measurement, Hugoniot equation of state, yield point and dynamic response

08 p1330 A69-20102

Hertz impact theory application to aircraft tire in operation, considering imperfectly elastic body with impact expressible by Newton recovery factor of about one

10 p1633 A69-22887

Dynamic plastic response of finite bar subject to axial impact load noting reflected waves, stress-strain-time histories and residual strain

11 p1991 A69-25512

Asymptotic solution of two dimensional problem of elastic impact of bars, showing longitudinal and surface waves decay with time

11 p1996 A69-25737

Transverse impact along flexible couplings, deriving motion equations in presence of elastoplastic deformation

12 p2178 A69-26034

High speed deformation of metals under pulse loading, noting role of maximum stress magnitude and deformation characteristics

12 p2113 A69-26043

Large plastic deformation of two metallic cylindrical flat ended missiles in mutual longitudinal impact

12 p2179 A69-26217

High velocity liquid lithium effect on structural materials for MHD power generators, discussing material loss

13 p2278 A69-27478

Structural stress under acceleration loading simulated by two dimensional photoelastic model noting improvement of fringe patterns quality

14 p2532 A69-28885

Axisymmetric impact of circular cylindrical plates, obtaining two dimensional dynamic stress distributions for materials of linear elastic compressibility and plastic behavior in shear

14 p2534 A69-29027

Clamped circular plates impulse load tests with sheet explosives, showing finite difference program for computing large deflection dynamic response

15 p2709 A69-30675

Annealed aluminum rods dynamically compressive impact loading used to study longitudinal plastic waves propagation velocity

15 p2709 A69-30677

Bird impact resistance of polyurethane foam filled tailplane

17 p2901 A69-33648

Circular cylindrical shell nonlinear response to uniform radial impulsive pressure, noting inextensibility constraint and equations of motion roles

[ASME PAPER 69-APM-26] 18 p3214 A69-34399

Periodic motions in single mass impact vibration system by point transformations method, noting complexity characteristics

18 p3172 A69-34565

Rod buckling under impact load, discussing compression strain wave front propagation

18 p3217 A69-34580

Viscous friction damping effect on impact vibrator stability, analyzing boundary region of multiply periodic single impact motion by point mapping

18 p3172 A69-34588

Stressed state analysis in dynamic brittle breakdown wave front of compression waves propagating in brittle rod under longitudinal impact

18 p3217 A69-34592

Thin walled cylindrical shells deflections under axial impact load, assuming deformations resembling cylindrical surface bending

18 p3217 A69-34599

Plastic cylindrical shell buckling under axial impact, predicting velocity required to cause flexural waves

18 p3218 A69-34624

Asynchronous gyrostat postimpact drift direction found orthogonal with respect to initial impulse by averaging method

19 p3311 A69-36192

Hydrodynamic vertical or horizontal impact of sphere immersed in ideal heavy liquid of finite depth, considering container floor effect, surface pressure distribution, etc

19 p3299 A69-36393

Monograph on beam impact force and bending stresses during transverse impact, noting Bernoulli and Hertz theories application

20 p3628 A69-37922

Impact pressures during two body collisions, correlating pressure with particle speed

21 p3836 A69-38943

Dynamic plasticity of nonsymmetrical free flight collision impact of crystalline solids, using linear temperature dependent stress-strain function and finite amplitude wave expansion

21 p3840 A69-39298

Impact effects on metallic materials deformation and wear, considering impact force, time and coefficients, penetration depth, deformation energy, etc

22 p3966 A69-39876

Reaction impulse during steel spheres impacts at lead surface in vacuum dependent on kinetic energy, velocity and spheres material

22 p4047 A69-41101

Central transverse impacts of sphere on free-free beams, investigating maximum strains variation with impact velocity by narrow band tuned circuit filter

23 p4235 A69-42455

Sphere set in motion at constant velocity by impulsive force submerged in incompressible fluid in half space

24 p4298 A69-42585

Dispersive pulse propagation in laminated composites compared with theoretical predictions for timing and amplitude of oscillations

[ASME PAPER 69-APMW-22] 24 p4401 A69-43097

Longitudinal elastic waves produced in truncated hollow Al cone due to steel spheres impact

[ASME PAPER 69-APMW-15] 24 p4401 A69-43101

IMPACT PREDICTION

Helicopter fire control systems evaluation by computer model for hit probability and impact point sensitivity to various parameters

[AHS PAPER 316] 17 p2933 A69-33540

IMPACT RESISTANCE

Force law determining impact processes of pyramidal and conical body penetration into smooth surface of rigid plastic metals

02 p0337 A69-11615

Explosives and propellants sensitivity to fragment impact, establishing threshold detonation velocity

04 p0645 A69-14473

Critical end-on impact velocities calculated for reentering solid and granular radioisotopic fuel rods with solid and granular earth materials

04 p0630 A69-14800

Remotely operated open-cup impact tester for studying impact initiation of reaction of various liquid fluorinating agents with metals and plastics

06 p0907 A69-17876

Fluidic control systems for angular rate and attitude stabilization flight-tested, noting good impact and acceleration resistance

[AGARDOGRAPH-118] 08 p1257 A69-20955

Bumper materials effect on two component hypervelocity impact shields performance, noting material density influence

[AIAA PAPER 69-379] 13 p2283 A69-28309

Bird impact resistance of polyurethane foam filled tailplane

17 p2901 A69-33648

IMPACT STRENGTH

Impact cyclic loading fatigue tests of smooth and notched duralumin, discussing increased impact strength resulting from initial underloading

07 p1167 A69-19317

Impact hardness of materials determined by Droz method of static hardness determination, noting tests on steel

10 p1801 A69-23850

Projectile impacts into laminated targets consisting of plastic layers backed by Al substrates using SHAPE code with hydrodynamic elastoplastic distortional model

[AIAA PAPER 69-356] 13 p2366 A69-28289

Nickel maraging steel weld metal impact strength and fracture toughness improved by heat treatment

18 p3151 A69-35430

Ni-Ti maraging steel hardness impact strength and thermal EMF changes during quenching

19 p3345 A69-36154

Boron fiber reinforced Al alloys spall failure and shock induced filament damage, using flyer plate technique

20 p3562 A69-37772

IMPACT TESTING MACHINES

Remotely operated open-cup impact tester for studying impact initiation of reaction of various liquid fluorinating agents with metals and plastics

06 p0907 A69-17876

Drop-weight tear tests dependence on specimen thickness and metallurgical properties

09 p1503 A69-21389

Impact testing machine with dropping load, noting provision for sample fastening to reduce reflected tensile wave effect

15 p2583 A69-30286

IMPACT TESTS

NT CHARPY IMPACT TEST

Perforation and penetration mechanisms of Styrofoam slabs, using impact tests with free falling and rifle powered projectiles

01 p0165 A69-10115

Free flight impact tests showing deformation curve for aluminum and copper single crystals representable as 1/4 power law

02 p0344 A69-12288

Free surface motion and stress measuring instrumentation, describing plate impact one dimensional strain configuration for determining mechanical properties under stress wave propagation

02 p0344 A69-12290

Hypervelocity impact effect on structural honeycomb spacecraft wall configurations, stressing design and wall thickness parameters

[AIAA PAPER 68-314] 02 p0345 A69-12389

FM/AM telemetry circuits with three axis piezoelectric accelerometer for measurements during impact tests of soft landing models

10 p1654 A69-23279

High pressure Hugoniot points made by hypervelocity gas gun, using laser beams to measure impact velocity and pressure transducer for impact stress

[AIAA PAPER 69-358] 13 p2264 A69-28291

Hypervelocity impact dynamics on copper cube targets imbedded with nickel wires, discussing terminal positions, Vickers hardness, flow fields, etc

[AIAA PAPER 69-368] 13 p2367 A69-28300

Penetration mechanics of multisheet structures based on discrete particle modeling of impact debris

[AIAA PAPER 69-371] 13 p2367 A69-28303

Aluminum double sheet target penetration resistance determined by studying high velocity pyrex glass impact effects on front/rear sheets and spacing

[AIAA PAPER 69-375] 13 p2367 A69-28305

Quality assurance impact energy attenuation testing of U.S. Army flyer protective helmet, considering combined interaction of shell, foam liner and plastic pads

15 p2559 A69-30851

Brittle toughness determination method compared with Robertson and notch impact tests, evaluating steel susceptibility to brittle failure propagation

16 p2795 A69-32796

Crash helmet impact protection capability, considering helmet construction

17 p2913 A69-33169

Cylindrically shaped projectiles low velocity impact upon horizontal surface of dry commercial Ottawa sand mass, estimating penetration for soft landing

21 p3839 A69-39231

Impact effects on metallic materials deformation and wear, considering impact force, time and coefficients, penetration depth, deformation energy, etc

22 p3966 A69-39876

Rain erosion process on aircraft surface, using single impact test apparatus with photographic recording and photoelastic study

23 p4227 A69-41872

Sand erosion behavior of metals and plastics in air blast rig under varying exposure time, angles of impact and tensile stress

24 p4363 A69-42787

Scale error correction technique for structural impact modeling using dissimilar materials, involving permanent deformation of spherical caps impacted into liquids

24 p4406 A69-43692

IMPACT TOLERANCES

Impact/injury data used to estimate human tolerance to instantaneous accelerations

04 p0552 A69-14469

Mechanical model of human body used to study response to vibration, impact, blast and decompression loads

04 p0552 A69-14470

Mars landers impactable power subsystems, considering thermoelectric generators, batteries, conversion equipment, Mars environment, etc

23 p4069 A69-42253

IMPEDANCE

NT ACOUSTIC IMPEDANCE
NT CONTACT RESISTANCE
NT ELECTRICAL IMPEDANCE
NT ELECTRICAL RESISTANCE
NT LC CIRCUITS
NT MECHANICAL IMPEDANCE
NT REACTANCE
NT RESPIRATORY IMPEDANCE

Impedance and gain approximation in transistor configurations, noting gyrator circuit

02 p0213 A69-11532

Impedance sheet approximation to plasma slab, considering plane wave propagation, plasma covered slot antenna and transmission loss

02 p0209 A69-12348

Emission of thin metallic antenna in randomly inhomogeneous medium, determining effective impedance

06 p0894 A69-17451

Cylindrical electromagnetic waves diffraction at impedance wedge in anisotropic cold plasma, using Maxwell equation and double contour integral

09 p1545 A69-21505

Emission of thin metallic antenna in randomly inhomogeneous medium, determining effective impedance

20 p3508 A69-37936

IMPEDANCE MATCHING

Variable impedance matching device employing lumped and homogeneous circuit elements and stub line technique

01 p0046 A69-10740

Mismatched errors associated with Y factor power ratio measurement effect on microwave noise-temperature calibrations

[JPL-TR-32-1345] 02 p0211 A69-12442

Lossy transmission line filters and wideband impedance matching

03 p0406 A69-13906

Impedance matching of volumetrically scanned waveguide arrays, stressing element spacing, surface wave impedance, etc

04 p0571 A69-14312

Impedance matching selection for phased array element, using element impedance data and equivalent circuit

04 p0572 A69-14323

Transistor scattering matrix parameters determination, emphasizing directional coupler errors and impedance mismatches

04 p0582 A69-15067

Thermal noise and other disturbances from mismatched two port isolator in low power microwave transmission antenna noise between generators and leads

07 p1108 A69-19486

Electric propulsion design, considering effects of weight, impedance matching, beam voltage regulation and operating point variations in formulating system mass and reliability

[AIAA PAPER 69-254] 09 p1569 A69-21879

Mismatch correction in microwave power measurements based on directional coupler techniques

12 p2038 A69-26055

Matched diodes in monolithic balanced mixer by diode array fabrication for noise suppression

13 p2233 A69-28071

Dispersion and coupling impedance of logarithmic spiral resting on anisotropic magnetodielectric layer for microwave devices design

13 p2235 A69-28512

360 degree varactor linear phase modulator, analyzing impedance matching, insertion loss, tuning design and serrodyne application

16 p2756 A69-31577

High resolution swept frequency reflectometer suitable for impedance matching in waveguides or coaxial lines

16 p2759 A69-31940

Coupling between electric dipoles in warm plasma, determining electron density and temperature from resonance peak of mutual impedance at electron plasma frequency

17 p2925 A69-33846

Interrelations among mutual coupling, element efficiency, active impedance and radiation patterns in linear arrays derived from infinite order difference equation

17 p2929 A69-33874

Active antenna impedance matching network constituting low noise device for electromagnetic interference measurements useful for automatic or manual scanning

17 p2943 A69-34131

Directional couplers design considerations for use in microwave power meters, analyzing directivity and mismatch effect on system error

19 p3282 A69-35826

Two loop resonant amplifiers design, considering mismatched, matched and optimally matched regimes

22 p3912 A69-40258

Small losses measurement in circulators and reciprocal quadrupoles, using scattering matrix to eliminate mismatch errors

22 p3875 A69-40259

Dispersion and coupling impedance calculation for symmetrical or helical slow wave structures employed in traveling and backward wave tubes

22 p3916 A69-40958

Equivalent circuit technique for dispersion equation and coupling impedance of slow wave structures of ring-rod systems, noting retardation

23 p4139 A69-41944

Double cellular surface geometry effect on dispersion and coupling impedance of two dimensional periodic resonator slow wave structure

23 p4140 A69-42048

IMPEDANCE MEASUREMENTS

Permittivity measurements by measuring impedance on thin cylinders in rectangular waveguide or in cavity formed by coaxial transmission line

02 p0222 A69-12756

Linear transistor models synthesis based on measured characteristics of four terminal admittance parameters

03 p0404 A69-13596

Admittance between terminals measured for stabilizing single loop negative feedback transistor amplifier

05 p0739 A69-16341

Large signal impedance measurements and dynamic characteristics explain Si avalanche diodes efficiency degradation at higher frequencies

06 p0893 A69-16938

Complex admittances and impedances of various networks determined by impedance bridge, describing frequency dependent limits of measurement parameters

09 p1501 A69-22578

RF measurement techniques and interpretation of bonding impedance characteristics through VHF region

12 p2040 A69-26472

Small signal quasi-stationary characteristics of pulse transistors including gain and input impedance calculations

13 p2227 A69-27423

Automatic device for impedances and complex transmission factors measurement at meter and decimeter wavelengths, noting reflection factor

13 p2235 A69-28520

Cardiac output determined simultaneously in adult male humans by thoracic impedance changes and radioisotope dilution

14 p2408 A69-29304

Input impedance measurement of radiating symmetrical HF and microwave antennas, using solid state oscillator for feeding

14 p2420 A69-29394

Transistors transfer admittances measured indirectly, evaluating mean square error for transfer parameters

14 p2420 A69-29396

Transistor scatter and admittance differential parameters measurements graphically correlated

14 p2420 A69-29397

Output impedance measurements for accurate calibration in UHF region, using mobile discontinuity and bolometer for linear or nonlinear systems

14 p2422 A69-29583

Complex load impedance determination by measuring maximum, minimum and load voltages in line, including error analysis

15 p2582 A69-30123

Junction diode field factor, comparing results of dynamic impedance and distortion measurement methods with deduced values of static characteristic

15 p2575 A69-30301

Linear array composed of dual mode elements radiating into parallel plate region, obtaining scan angle compensation of element impedance

17 p2929 A69-33875

Direct detection of ionospheric irregularity by device onboard San Marco satellite, utilizing antenna impedance fluctuations

21 p3715 A69-38562

IMPEDANCE PROBES

NT RADIO FREQUENCY IMPEDANCE PROBES

High speed compression waves, rarefaction waves and gas interface regions position and velocity measurement in shock tube by sensing electrical impedance

03 p0428 A69-13104

Three probe impedance meter with graphic arithmetical element designed to cover frequency range from 50-1000 MHz

[ONERA-TP-605] 05 p0764 A69-16590

IMPELLER BLADES

U ROTOR BLADES [TURBOMACHINERY]

IMPELLERS

NT PUMP IMPELLERS

Steady three dimensional flow through impeller of turbines with small number of blades and with edge cut hub, noting inefficiency of flow without impact

01 p0142 A69-10309

Flow in impellers of mixed and radial flow compressors for jet engines, turbochargers and automotive gas turbines, discussing velocity, load distribution, etc

[SAE PAPER 690033] 07 p1049 A69-18312

Unsteady relative flow in centrifugal impeller passage running at part capacity and zero flow observed by hydrogen bubble flow visualization method [ASME PAPER 69-GT-35] 09 p1432 A69-22489

Plenum chamber obstructions influence on hovercraft lift fan performance, discussing tests and losses due to flat plate at impeller outlet 13 p2202 A69-27546

Unsteady aerodynamic processes in centrifugal compressor stage with impeller, vaneless diffuser and annular receiver chamber 15 p2547 A69-30073

Centrifugal compressor impeller disk design, considering stress analysis for shielding portion profile determination to satisfy equal strength condition 17 p3057 A69-33193

Discrepancy between theoretical and experimental coefficients of friction losses on blades of centrifugal compressor impeller wheels, using lattice theory 23 p4058 A69-41727

IMPERFECTIONS
U DEFECTS

IMPERMEABILITY
U PERMEABILITY

IMPINGEMENT
NT JET IMPINGEMENT

Cumulative damage concept for rain erosion of solid materials, noting incubation period and similarity to microscopic damage in fatigue failure 12 p2187 A69-26848

Solid materials erosion rate as function of cumulative damage generated by liquid droplets impingement 16 p2794 A69-31904

Free flow field from underexpanded rocket motor nozzle and impingement effects of pressure and heat transfer to flat plate [AIAA PAPER 69-568] 16 p2842 A69-32693

Attitude control rocket exhaust plume impingement effect on electrical performance and mechanical damage of commercial silica covered silicon solar cells 19 p3252 A69-35700

Pressure effects in spontaneous ignition of interimpinging hydrazine and red fuming nitric acid /RF-NA/ liquid streams in evacuated test chamber 24 p4415 A69-43667

IMPLANTATION

MOSFET fabrication by ion implantation using gate metal as mask, noting source and drain alignment with gate and low feedback capacitance 05 p0734 A69-16563

Multichannel telemetry system for chronic implantation in animals to monitor physiological parameters 15 p2559 A69-31044

Single channel pressure telemetry unit with magnetic latching or RF switch for chronic implantation 23 p4100 A69-41295

IMPLEMENTATION
U PERFORMANCE

IMPLOSIONS

Nonuniform propagation of imploding shock waves by extending self similar solution to earlier times in implosion process when shock strength is finite 10 p1678 A69-22931

Mach reflection shock-shock locus in shock tube implosions generation by area change 16 p2766 A69-31919

Shock tube with cylindrical explosive to implode glass wall and produce high velocity glass particle jet, studying jet velocity and behavior and test gas pressure effects 18 p3116 A69-34460

IMPREGNATING

Tensile, bending and impact strengths of materials produced by metal porous blank impregnation with molten glass, noting metal density and sintering effects 15 p2643 A69-31188

IMPULSE GENERATORS

Dissipative fluid sphere motion due to impulsive point source calculated by finite difference scheme, assuming Voigt and Maxwell type internal friction mechanisms limitations 14 p2485 A69-29026

IMPULSE NOISE
U ELECTROMAGNETIC NOISE

IMPULSE TRANSFER ORBITS
U TRANSFER ORBITS

IMPULSES

Impulse bandwidth measurement error determination by trapezoidal numerical integration 03 p0398 A69-13902

Time varying linear system with input-output relation described by differential equation calculated for impulse response using Taylor series 09 p1459 A69-22580

Vignetting effect on impulse response of general coherent optical Fourier processor, noting time varying character and input position sensitivity 12 p2036 A69-25912

Backscattered impulse response waveforms of conducting circular cylinder for broadside incidence utilizing Fourier synthesis 17 p2917 A69-32918

Satellite motion orbital elements dependence on large short impulse arbitrarily directed in space, analyzing optimal orbits transfer and thrust control 21 p3818 A69-39821

IMPURITIES

Interstitial impurity effects on mechanical properties of molybdenum single crystals, considering temperature dependence of flow stress in bcc metals 01 p0095 A69-10609

Synthetic solid lubricants impurity detection by X ray diffraction and oxidation thermogravimetry 01 p0102 A69-10909

Impurity concentration in n-type indium antimonide semiconductors at liquid nitrogen temperatures estimated by current-voltage measurements 02 p0294 A69-11631

Thorium and La-compounds retained superconductivity to Pr and Tm concentrations due to crystal field splitting effect producing nonmagnetic singlet ground state 02 p0295 A69-11778

Intentional impurities effects on nitronium perchlorate thermal stability explained by change in cation and anion vacancies 02 p0304 A69-11899

GaAs injection lasers noting spectral function, I-V characteristics and relations among lasing wavelength, threshold current density and impurity concentration 02 p0256 A69-11993

Localized vibration modes of defects and IR absorption bands in compensated Si doped GaAs 02 p0299 A69-12402

Impurity concentration measurement for alloyed region of tunnel diode by determining Fermi level position 02 p0301 A69-12685

Impurity profiles and energy band diagram for cuprous sulfide-CdS heterojunction based on capacitance, Hall and electron microprobe measurements 03 p0368 A69-13075

Temperature dependence of elastic constants of highly and weakly doped n- and p-type GaAs 03 p0484 A69-13282

Josephson current dependence on nonmagnetic impurity concentration in pure and highly contaminated superconductor 03 p0484 A69-13284

Ground state energy for single magnetic impurity dissolved in nonmagnetic metal, applying cluster variation method to s-d interaction Hamiltonian 03 p0485 A69-13298

Impurities effect on defects in oxygen deficient niobium, tantalum and zirconium oxide scales at high oxygen pressures, noting relationship to metal oxidation 03 p0444 A69-13312

Si and iron impurities effects on duraluminum alloy structure and mechanical and plastic properties for fabrication from granules and rolling from ingots 03 p0452 A69-14120

Photoionization of donor impurities during absorption of IR radiation in n-type Te doped GaP at low temperatures 03 p0492 A69-14169

Diffusion in compounds of elements of groups III-V 04 p0641 A69-14502

Heterodiffusion of metallic impurities in body centered phases of doped zirconium and titanium, determining diffusion coefficients via radioactive isotopes 04 p0613 A69-14557

Spectral study of crystal lattice of gallium phosphides for influence of vacancies and impurities on band formation 04 p0643 A69-15258

P-type GaSb crystals with various impurity concentrations noting conductivity, transverse magnetoresistance, Hall effect and acceptor band width and conductivity 04 p0643 A69-15259

Electrical properties of n-type Cd tin arsenide single crystals with impurity concentrations at various temperatures 05 p0809 A69-16375

Recovery of carrier concentration and lifetime in n- and p-type Si during annealing after irradiation by 10 Mev electrons, noting impurities effects 06 p0974 A69-16865

Junction gate field effect transistor design covering geometries and impurity profiles 06 p0893 A69-17197

Titanium surface impurities effect on porosity in welds, proposing machining immediately before welding as solution 06 p0945 A69-17894

Oxide impurity effects causing potential shifts in Si covered by thick oxide layer studied with metal-oxide-Si electrical measurement and radiochemical analysis 07 p1072 A69-18272

Impurity atoms effects on Cu diffusion and solubility in GaAs, determining Hall coefficient temperature dependence and conductivity 07 p1199 A69-19009

Impurities effect on electron energy spectrum in semiconductors at zone boundary and arbitrary doping levels, using Green function 09 p1554 A69-21467

Temperature dependence of conductivity and Hall constant of GaAs single crystals with nickel impurity, noting diode structure and I-V curve shapes 09 p1555 A69-21475

Impurity concentrations in expansion tube flow, measuring radiation intensities [AIAA PAPER 68-371] 09 p1477 A69-21961

Specific heat dependence of beryllium at low temperatures on sample impurities, considering Debye temperature 09 p1527 A69-22399

Impurities effect on plastic flow stress and activation volume as functions of strain, strain rate and temperature in molybdenum crystals 10 p1710 A69-23089

Shallow impurity states in semiconductors, calculating bulk and surface energy eigenvalues in Si and Ge 10 p1745 A69-23361

Nitrogen impurities effect on electron energy balance in DC arc burning in inert gas 10 p1732 A69-23442

Interstellar diffuse absorption bands due to resonance lines of impurity atoms trapped in low temperature hydrocarbon matrices 10 p1781 A69-23677

Microimpurities in aluminum-yttrium garnets determined spectrographically by using gallium oxide as carrier and Teflon powder for fluorinator 10 p1747 A69-23843

Electrical conductivity of impurity semiconductors containing variable current carrier concentrations, discussing current-voltage characteristics 11 p1937 A69-24909

Equations for pn junction behavior valid at impurity concentrations beyond nondegenerate range, noting contact potential and carrier density 11 p1938 A69-25306

Metallic impurities effect on Ge surface charge and recombination properties, noting fast and slow electron density changes by forbidden band penetration 11 p1939 A69-25703

Photon loss coefficients in electron beam pumped GaAs laser showing dependence on doping type and impurity concentration, noting threshold current density measurement 13 p2271 A69-27467

Thermal accommodation coefficient and critical supersaturation for nucleation of mercury vapor on pyrex glass 13 p2321 A69-28005

Epitaxial layers impurity concentration and resistivity measurements by capacitive and three point probe methods 13 p2323 A69-28641

Temperature dependence of elastic constants of highly and weakly doped n- and p-type GaAs 14 p2508 A69-29655

Josephson current dependence on nonmagnetic impurity concentration in pure and highly contaminated superconductor 14 p2508 A69-29656

Electronic states of semiconductor acceptor centers at forbidden band deep levels, considering inner electron shell excitation in impurity ion 15 p2665 A69-30039

Impurities effect on electron energy spectrum in semiconductors at zone boundary and arbitrary doping levels, using Green function 15 p2669 A69-30712

Temperature dependence of conductivity and Hall constant of GaAs single crystals with nickel impurity, noting diode structure and I-V curve shapes 15 p2669 A69-30720

Multicomponent semiconductor compounds of non-stoichiometric composition, studying structure,

behavior and correlation between electrical properties and phase diagrams

15 p2670 A69-31243

Electrical conductivity of cesium iodide single crystals with anion and cation impurities noting temperature dependence

16 p2824 A69-31573

Hole mobilities in InSb due to phonon and ionized impurities scattering on basis of strain potential constants

16 p2824 A69-31575

Vibrational excess entropy in dilute solid solutions alloys calculated by changes in potential fields surrounding impurity atoms

16 p2798 A69-31706

Ammonium nitrate thermal decomposition activation by dyes and halides, noting endothermic and exothermic reactions, proposing models to study impurities role

17 p3016 A69-32830

Refractory metals fracture, discussing interstitial impurity addition effects in Group 5a and 6a metals

17 p2989 A69-33556

Gas ionization relaxation times from ion density profiles in shock tubes at low Mach numbers, discussing influence of impurities on ionization process

18 p3116 A69-34451

Impurity levels in semiconductors with multiconduction bands, noting impurities influence on photoluminescence, laser action and Gunn effect

19 p3385 A69-36514

InSb single crystals impurities incorporation and distribution, concluding electrical properties vary with homogeneity or heterogeneity of dopant microdistribution

19 p3389 A69-36547

Aircraft breathable LOX purity, water percentage and carbon dioxide and methane proportions, determining other contaminants after concentration by refrigeration

21 p3666 A69-39273

Impurities effect on corrosion of fluorine containing propellant oxidizer systems, noting aqueous and anhydrous hydrogen fluoride corrosion

21 p3784 A69-39487

Impurities effect on corrosivity of nitrogen tetroxide with tank construction metals, Al, stainless steel and Ti-Al-V alloy, noting temperature aging and concentration

21 p3748 A69-39488

Spin compensated state of localized magnetic impurity moment in space, calculating size range of magnetic impurity spin/conduction electron spin correlation function

22 p3983 A69-40061

Strong doping criterion for Si with deep level impurity centers based on electron spectra of fast surface traps

22 p3992 A69-40604

Silicate glass impurity droplet formations on alumina single crystals polished surfaces analyzed by electron microprobe as function of high temperature

23 p4176 A69-41597

Hafnium microstructure and impurity concentrations before and after electron beam melting

23 p4178 A69-42361

IMPURITY

U PURITY

IN-FLIGHT MONITORING

Space controlled microbiology, discussing telemetry control of waste material conversion in air and water pollution

[UN PAPER 68-95861] 01 p0014 A69-10456

Cardiac output during space flight based on rebreathing method for estimation of gas tension in mixed venous blood and Fick equation

[UN PAPER 68-95746] 01 p0151 A69-10527

Data analysis methods for integrated data processing system for onboard in-flight checkout for launch vehicle evaluation

[AIAA PAPER 67-911] 01 p0037 A69-11024

In-flight measurement of shock and vibration effects on aircraft and propulsion systems

01 p0084 A69-11051

In-flight and flight line checkout techniques for foreign object damage to jet engines

01 p0056 A69-11055

Man as main component of future spacecraft or planetary station closed ecological system, discussing spacecrew physiological monitoring for biological cycles optimization

01 p0020 A69-11076

Analytical techniques for in-flight monitoring of aerospace water supplies for potability, emphasizing rapidity, sensitivity and reproducibility

01 p0019 A69-11339

Satellite monitoring application to air traffic control in parallel track system, discussing lateral and longitudinal separation control

02 p0277 A69-11591

In-flight measurement of shear, bending moment and torque on lifting or control surfaces and loads on nose and main landing gear

04 p0677 A69-14842

Automatic processing of electrocardiograms recorded during space flight by computer

05 p0715 A69-16524

Telemetric system for in-flight measurements of jet pilot heart and circulatory system to determine flight stresses leading to pilot failure

05 p0715 A69-16707

Air Force Eastern Test Range data processing systems perform real time operations during in-flight phases of ballistic missiles and orbiting vehicles

05 p0727 A69-16772

Radiation protection plan for Apollo lunar mission based on real time monitoring of solar activity and radiation in spacecraft

[AIAA PAPER 69-19] 06 p0996 A69-18113

Solar flare in-flight radiation detection and warning system for Concorde SST, noting radiation hazards due to solar cosmic rays

07 p1131 A69-18551

Solar proton monitoring by particle detectors on-board rockets and IMP satellite

08 p1318 A69-21142

Symptom pattern observation technique for flight data analysis, discussing in-flight symptoms and SPOT chart in aircraft maintenance

10 p1669 A69-22982

Airborne integrated in-flight data system to record and evaluate various engine parameters of operating jet engines

10 p1660 A69-23262

Ruggedized ballistic range telemetry system survivability and in-flight stability after gun launching, presenting temperature, strain and stagnation point pressure measurements

10 p1654 A69-23281

Computer program for onboard medical checkups of spacecraft crews during extended space flights, discussing tests and intervals

10 p1649 A69-23505

Onboard test instrumentation for monitoring aircraft communication, navigation and identification systems, noting adaptive programming

11 p1866 A69-25080

Onboard checkout system concept, discussing philosophy, requirements, underlying considerations, system description, development and techniques of system selection

11 p1866 A69-25081

Monograph on physicochemical principles of takeoff monitoring systems for large aircraft covering taxiing, safety control systems design, analog simulation, etc

12 p2128 A69-26119

Blood pressure telemetry of pilot during flight including determination of psychophysical relations

15 p2559 A69-31229

EEG and pilots flight performance relations, discussing in-flight telemetric measurements from ground station

15 p2560 A69-31233

Fatigue life gage on operational aircraft providing in situ monitoring of fatigue damage prior to and during propagation of running fatigue cracks

15 p2613 A69-31271

Electromagnetic interference correction for airborne telemetry, illustrating actual and simulated data for interfering source signatures identification

16 p2754 A69-32575

Jet engine compressor stalls in-flight investigation up to Mach 2 on F-111A by pressure sensors, noting steady state distortion role

[AIAA PAPER 69-488] 16 p2843 A69-32706

Performance capabilities and handling quality characteristics of aircraft equipped for in-flight thrust reversing

[AIAA PAPER 68-880] 17 p2902 A69-34031

Automatic multichannel transient monitor for electrical transient detection and data processing, transmission and storage on aircraft

17 p2947 A69-34135

Automatic processing of electrocardiography recorded during space flight by computer

18 p3098 A69-34743

Strapdown inertial reference unit system for inflight reliability and maintainability, discussing design and components

19 p3370 A69-35803

Design concepts and principles of systems for monitoring of Concorde flight control actuators, considering servo control, control interconnections and control input system

20 p3467 A69-38190

In-flight test to determine variation effects in bank angle control parameters on cruise flight handling qualities, considering spiral stability

[AIAA PAPER 69-893] 21 p3648 A69-39425

Orbital biomedical laboratory for in-flight measurement to assure human safety and optimize astronauts performance in extended space mission

23 p4223 A69-41801

Monitoring devices and modular construction features of Rolls-Royce RB.211 three shaft turbofan engine, discussing maintainability

24 p4321 A69-43112

IN-FLIGHT THRUST MEASUREMENT

U THRUST MEASUREMENT

INACTIVATION

U DEACTIVATION

INCIDENCE

Incidence for three dimensional reentry trajectories preprogrammed as function of velocity, finding bank angle as function of inclination

03 p0504 A69-12858

Thermal dissociation of chlorine trifluoride behind incident shock waves at high temperature, discussing bimolecular reaction rate constant

[WSCI PAPER 68-40] 07 p1202 A69-18355

INCIDENT RADIATION

Normally incident linearly polarized electromagnetic wave reflection and transmission by semimfinite longitudinally drifting magnetoplasma in static magnetic field

01 p0134 A69-11290

Relation between color index over lunar surface and solar rays angle of incidence, noting supplementary emission attributed to surface luminescence

03 p0506 A69-13089

Angle of incidence influence on unpolarized and linear polarized light of solar cell short circuit current

04 p0551 A69-15312

Diffraction of plane electromagnetic waves obliquely incident on conducting rotated periodically tapered grating structure formed of infinite metal strips

05 p0723 A69-16788

Solid target output pulse magnitude and direction dependence on angle of incidence of intense laser beam

06 p0935 A69-17686

Solar absorptance and hemispherical emittance of metals at space conditions determined with cyclic incident radiation technique

[AIAA PAPER 69-60] 06 p0945 A69-18154

Ruby laser beam incident on steel surface in air or water measured for energies, determining reflected energy dependence on incident energy for self insulation effect

07 p1157 A69-19594

Resolving power increase in multibeam antenna, discussing signal demodulation through incident field breakdown

10 p1664 A69-23797

Computer generated kinoform optical element operating on phase of incident waves and forming wave front reconstruction single image

10 p1697 A69-23867

Incident integral light flux relations and visibility range equation derived for objects illuminated by narrow light beams in scattering media

10 p1725 A69-23971

Diffraction of plane electromagnetic wave incident on conducting sphere segment, deriving secondary electromagnetic field equations in geometrical optics approximation

11 p1846 A69-24613

Horizontally moving body wake scattering cross section calculated with allowance for sphericity of incident and scattered radio waves, using Bessel functions

12 p2031 A69-26699

Relation between color index over lunar surface and solar rays angle of incidence, noting supplementary emission attributed to surface luminescence

14 p2516 A69-28771

Inverse scattering technique for electromagnetic bistatic scattering by expressing field produced by incident plane wave as sum of incident field and Fourier transform

16 p2754 A69-32569

Complex index of refraction of naturally occurring rock and mineral as function of wavelength of incident radiation
17 p2973 A69-33093

Scattering of electromagnetic waves obliquely incident on inhomogeneous plasma column of parabolic radial density distribution, noting applications to ionospheric irregularities
18 p3102 A69-34963

Plane screen electrical shielding effectiveness calculation, using incident wave impedances associated with current loop and magnetic dipoles in transmission line equations
19 p3267 A69-35932

IR detectors defined as transducers producing electrical signal proportional to IR power incident on detector, classifying types
19 p3310 A69-36068

Lunar surface thermal radiation incident on unit area flat surface located at variable distance and orientation above moon, considering diffusion effects
21 p3803 A69-38973

Photographic and photometric study of absorption and reflection of ruby laser light incident on biological objects
21 p3665 A69-39060

Incident integral light flux relations and visibility range equation derived for objects illuminated by narrow light beams in scattering media
21 p3772 A69-39657

Diffuse reflection of electromagnetic longitudinal wave from magnetoactive plasma in oblique incidence
22 p3990 A69-40788

Gain modification from spectral splitting of optical transition by incident light wave on higher frequency coupled transition
22 p3965 A69-41125

Photomultiplier tubes performance enhancement by light incidence on photocathode at oblique angles explained by reflection
23 p4191 A69-42194

Electromagnetic waves incident upon anisotropic plasma, determining transmission and power reflection coefficients
24 p4282 A69-42978

INCLINATION

Satellite motion perturbations in vicinity of critical inclination, using Encke method of numerical integration
19 p3397 A69-35607

INCLUSIONS

Thermal stresses near spherical inclusion in elastic matrix with uniform heat flow
01 p0171 A69-11264

Grain boundary interaction energy with inclusion of second phase, describing equilibrium and boundary shape
03 p0449 A69-13880

Integral equations solved numerically for general nonhomogeneous elastic inclusion problem, using linear elasticity theory
03 p0530 A69-14064

Elastic equilibrium stress condition of anisotropic plates with circular isotropic inclusions
04 p0667 A69-14264

Axisymmetric stress field around spheroidal inclusions and cavities in transversely isotropic material [ASME PAPER 68-WA/APM-14]
04 p0669 A69-14400

Circular inclusion effect on stresses around line crack in sheet under tension based on elasticity theory
05 p0841 A69-16432

Thermal stress concentrations in vicinity of cylindrical elastic inclusions embedded in elastic matrix, using displacement functions and photothermoelasticity
07 p1171 A69-18726

Metal bath surface conditions for floating aluminum trioxide inclusions in pure iron and carbon steels
07 p1167 A69-19342

Thermal stress field under uniform heat flow due to elliptical elastic inclusion for anisotropic case
08 p1418 A69-21003

Black chondritic inclusions in Cumberland Falls meteorite, discussing inclusion chemical, mineralogical and electron probe data
19 p3416 A69-36127

Variational principle for Fredholm integral equations applied to inclusion and indentation problems in elasticity
19 p3440 A69-36589

Nonmetallic inclusions formation mechanism after reducing iron by Al, Zr and Ti, noting oxygen/reducing agent ratio role
22 p3969 A69-40069

Nonmetallic inclusions effect on steels cyclic strength dependence on inclusion composition and metallic matrix properties, derived from fatigue tests
22 p4047 A69-41064

Force maintaining rigid inclusion embedded in elastic plate with rigid boundaries
23 p4235 A69-42465

Overall elastic moduli evaluation for solid composite materials comprising matrix of homogeneous elastic materials embedded with cylindrical shape inclusions
24 p4396 A69-42731

Porosity and inclusions effects on Al arc weld fatigue properties at ambient and cryogenic temperatures
24 p4331 A69-42940

INCOHERENCE

Holograms with unfiltered radiation obtained from superhigh pressure mercury lamp and incandescent lamp
09 p1495 A69-21671

INCOHERENT SCATTERING

Radio waves incoherent scattering to measure electron concentration profiles at mean latitudes, allowing for collisions
01 p0065 A69-10575

High power radar for investigating ionosphere by incoherent scatter technique
03 p0398 A69-13768

Incoherent scatter power measurements, comparing square law signal detection, phase coherent receiver and parametric amplifier methods
07 p1085 A69-19222

Faraday rotation measurements using incoherent scatter to obtain ionospheric electron density profiles
07 p1085 A69-19223

Emission line formation in homogeneous chromosphere for noncoherent scattering, considering various chromosphere models
08 p1381 A69-19800

Incoherent wave scattering of particle orbits as nonlinear effect of LF instabilities
08 p1367 A69-20801

Incoherent scatter measurements of F region electron concentrations at solar activity minimum
10 p1684 A69-23825

Ionospheric measurements of electron density, electron and ion temperature profiles from strength of incoherent radio wave scattering
10 p1686 A69-23910

Two fluid continuum theory of incoherent scattering extended to include unequal electron and ion temperatures, considering backscatter power dependency on collision frequencies
14 p2510 A69-28946

Incoherent scatter observations of ionosphere, discussing radar equipment and measurement of electron density and temperature, ionic temperature and composition, etc
14 p2415 A69-29522

Radio waves incoherent scattering to measure electron concentration profiles at mean latitudes, allowing for collisions
15 p2597 A69-30745

Far IR radiation generation, considering incoherent sources, harmonic generators, electron tubes, relativistic electrons and quantum oscillators
22 p3982 A69-40669

Index of refraction turbulent fluctuations effect on beam traversing optically active medium, discussing far field diffraction pattern and incoherent scattering [AIAA PAPER 68-683]
24 p4304 A69-43578

INCOMPATIBILITY

Effective tensors of elastic moduli and yielding of composite materials, considering multiparticle interactions and use of equilibrium and incompatibility equations
13 p2360 A69-27382

INCOMPRESSIBILITY

Finite plane deformations theory extended to incompressible materials with logarithmic change of volume proportional to pressure
12 p2181 A69-26613

Variational principle based on assumed stress hybrid method suitable for finite element analysis of incompressible solids
13 p2368 A69-28348

INCOMPRESSIBLE FLOW

NT STOKES FLOW

Jet line in rotational incompressible plane flows around shrouded propeller blade, using electrical analog
01 p0058 A69-10037

Effect of steady flow of incompressible conducting fluid on magnetic dipole at center of sphere
01 p0128 A69-10363

INCOMPRESSIBLE FLOW

Stress field and force system within torsional flow of cylindrical mass of incompressible anisotropic fluid
02 p0229 A69-11558

Wing upper surface velocity distributions having peak near leading edge, considering incompressible flow at zero angle of attack [ONERA-TP-632]
02 p0187 A69-11618

Downstream pressure asymmetry effect on efflux angle and contraction coefficient of incompressible jet from two dimensional orifice
02 p0231 A69-12075

Exact solutions for Navier-Stokes equations for non-steady incompressible viscous flow near two dimensional or axisymmetrical stagnation point
02 p0233 A69-12527

Compressible and incompressible laminar boundary layer with constant wall shear stress, using initial profiles
02 p0233 A69-12535

Unsteady incompressible boundary layer flow over leading edge boundary layer calculated by three dimensional time dependent equations
02 p0233 A69-12543

Arbitrary phase shift vibrations of airfoil profiles in incompressible flow reduced to Fredholm equations, allowing for trailing vortices influence
02 p0190 A69-12574

Heat transfer in crossed field MHD Couette flow for incompressible fluid, assuming linear wall temperature in flow direction
03 p0476 A69-13306

Two dimensional flow of incompressible fluid near sharp leading edge of plate at zero incidence, discussing approximation error and friction stress
03 p0415 A69-13651

Analysis of solution of Navier-Stokes equations describing two dimensional flow of viscous incompressible fluid by finite difference techniques and introduction of curl
03 p0416 A69-13652

Incompressible turbulent boundary layer with near zero wall friction at circular cylinder situated longitudinally in flow
03 p0416 A69-13664

Steady flows of incompressible viscous fluid exterior or interior to circular cylinder
04 p0589 A69-14898

Unsteady hydromagnetic flow of viscous electrically conducting incompressible liquid over infinite conducting harmonically oscillating plate
04 p0638 A69-15093

Dynamic behavior of series and parallel flow thrust-balance systems for compressible and incompressible flow, using analog computer simulation
04 p0647 A69-15521

Equations of motion derived for incompressible and irrotational viscous fluids in special relativity
05 p0792 A69-15682

Incompressible jet flows, discussing two dimensional jet, axisymmetric laminar jet and turbulent free jet
05 p0746 A69-16008

Incompressible turbulent boundary layers in channel flow using constant temperature hot-wire anemometer, emphasizing measurement in viscous sublayer [ASME PAPER 68-FE-26]
05 p0747 A69-16066

Pressure distribution across short vortex chamber to exit radius with known inlet geometry based on incompressible flow model and visualization photographs [ASME PAPER 68-WA/FE-17]
05 p0748 A69-16093

Turbomachinery research, discussing two and three dimensional incompressible flow in cascades near end wall and in rotating machines
05 p0751 A69-16534

Incompressible two dimensional turbulent boundary layers calculated on phenomenological basis
06 p0908 A69-17133

Inviscid incompressible fluid flow stability against helical disturbances in circular cylinder
06 p0910 A69-17332

Incompressible laminar Falkner-Skan boundary layer suffering sudden acceleration by moving belt, noting boundary layer separation [AIAA PAPER 69-40]
06 p0912 A69-18049

Computer solution of incompressible two dimensional time dependent Navier-Stokes equations for oscillating body with rectangular boundaries [AIAA PAPER 69-185]
06 p0914 A69-18135

Turbulent incompressible MHD flow between two parallel smooth plates in transverse magnetic field, determining magnetic Reynolds number
07 p1195 A69-19736

Incompressible jets bounded by infinite auxiliary thin jets, discussing straight wall jets and establishing ex-

istence and uniqueness of boundary value problem solution
09 p1480 A69-21734

Krause numerical solution applied to normal injection in three dimensional incompressible laminar boundary layer
[DVL-902] 09 p1482 A69-21971

Incompressible two dimensional potential flow analysis with compressibility effects for thick highly cambered multibodies in cascade, noting slotted compressor blade performance
[ASME PAPER 69-GT-6] 09 p1432 A69-22507

Digital computer programs for aerodynamics of subsonic gas turbine combustion systems applicable to incompressible flow with specified flow boundaries, noting vortices distribution
09 p1573 A69-22621

Incompressible Newtonian flow between two parallel planes, noting marginal stability condition, mean velocity profile and turbulence
10 p1678 A69-22909

Incompressible axisymmetric flow in turbomachines, analyzing flow field and velocity distribution
10 p1631 A69-22910

Three dimensional laminar boundary layer of incompressible flow controlled by suction or injection, considering similarity flow solutions and role in satellite design
10 p1678 A69-22936

Vortex incompressible flow in thin cylindrical chamber, analyzing outer and inner region and interface tangential velocity, shear and static pressures
10 p1679 A69-23557

Asymptotic boundary curves for two dimensional and axisymmetric incompressible irrotational flows into throat of convergent duct
10 p1680 A69-23893

Numerical solutions for incompressible Newtonian flow around circular cylinder for various Reynolds numbers
11 p1867 A69-24279

Velocity profiles in unsteady laminar incompressible boundary layer over flat plate in shock tube by two parameter integral method
11 p1871 A69-25026

Turbulent wall jet growth in streaming two dimensional incompressible flow over plane smooth wall with pressure gradient
11 p1873 A69-25139

Similarity solutions for incompressible, steady hydrodynamic and thermal boundary layers on longitudinally curved walls, allowing for displacement and curvature effects
12 p2060 A69-25761

Viscous incompressible conducting fluid flow through porous coaxial nonconducting cylinders under radial magnetic field with pressure gradients functions of time
12 p2062 A69-26275

Different pressure and deflection measurements coherence in vortex flows verified assuming radial equilibrium conditions
12 p2012 A69-26362

Incompressible elastic-plastic solid flow through rough converging conical channel analyzed using Mises yield condition and Prandtl-Reuss equations
12 p2063 A69-27114

Incompressible uniform shear flows merging behind trailing edge of semiinfinite flat plate, using inner-outer expansion method based on Navier-Stokes equation
13 p2248 A69-28223

Boundary layer characteristics of incompressible flow in wind tunnel with asymmetric two dimensional contraction, discussing flow profiles
13 p2249 A69-28235

Relative variations of wall friction and thermal flux for laminar incompressible flow of constant volume mass
13 p2250 A69-28357

Laminar to turbulence transition in submerged and bounded jets, using schlieren visualization for compressible flow and birefringent visualization for incompressible flow
14 p2428 A69-28876

Flow stability of one dimensional Cartesian and cylindrical incompressible inviscid flows with no body forces and interfaces
14 p2429 A69-29013

Incompressible laminar jet bounded by two parallel walls or by three walls, using linearized analysis related to Oseen approximation
14 p2429 A69-29023

Boundary value problem in three dimensional boundary layer theory for incompressible flow near stagnation point
14 p2432 A69-29677

Three dimensional laminar boundary layer on semiinfinite permeable flat plate in viscous incompressible fluid flow, calculating velocity profiles and skin friction components
14 p2433 A69-29898

Incompressible two dimensional turbulent boundary layer equations with arbitrary pressure distribution solved by weighted residual method
[AIAA PAPER 69-397] 15 p2591 A69-30478

Incompressible attached wall jet /Coanda flow/ over circular cylinder with finite incompressible injection normal to surface
16 p2772 A69-32148

Incompressible turbulent boundary layer analysis by two region characterization for eddy viscosity, using Spalding generalized function and Prandtl free shear flow model
17 p2951 A69-33255

Conducting fluid incompressible flow in entrance of MHD channel by momentum integral method, permitting edge stress existence at boundary layer free stream interface
[AIAA PAPER 69-724] 17 p2952 A69-33436

Two dimensional incompressible flow past circular cylinder at moderate Reynolds number, reducing partial differential equations of motion by series truncation for flow field
17 p2896 A69-33600

Optimum pressure distribution and airfoil profiles for maximum lift without separation in incompressible flow determined by second order theory
[AIAA PAPER 69-739] 18 p3083 A69-34401

Three dimensional incompressible wake behind blunt obstacle at leading edge of flat plate compared with mathematical model by Oseen linearization
18 p3083 A69-34403

Low Reynolds number solutions for incompressible viscous flows resulting from finite disk steady rotation
18 p3121 A69-34784

Higher order boundary layer theory development from Prandtl simplification of Navier-Stokes equations to successive approximations for incompressible and compressible flows
18 p3123 A69-34923

Boundary layer equation for steady incompressible flow past flat plate with parabolic leading edge, obtaining series solution in inverse powers of Reynolds number
18 p3124 A69-35270

Viscous incompressible fluid flow around semiinfinite oscillating plate and skin friction on infinite cylinders oscillating parallel to length
19 p3237 A69-35620

Wall influence on thermoanemometer readings in incompressible air stream measured with wedge shaped film sensors
19 p3308 A69-35857

Predictability of deterministic fluid systems with many scales of motion using vorticity equation for two dimensional incompressible flow, noting application to earth atmosphere
19 p3303 A69-36404

Wall curvature effect on hydrodynamic stability of laminar incompressible boundary layer with respect to perturbing Tollmien-Schlichting waves
19 p3299 A69-36587

Transition in near wake, from study of base pressure on circular cylinders in incompressible flow
19 p3242 A69-36809

Initial phase of parachute inflation in incompressible flow
[AIAA PAPER 68-927] 20 p3461 A69-37165

Model predicting steady state input-output characteristics of vortex amplifiers operating in incompressible flow regime, correlating model with experimental data
[ASME PAPER 69-FLCS-20] 20 p3465 A69-37980

Unsteady laminar incompressible time dependent boundary layer flows with cylindrical symmetry, transverse boundaries and no swirl
[ASME PAPER 69-FE-47] 20 p3517 A69-37997

Three dimensional turbulent boundary layer over flat surface in incompressible flow calculated by finite difference method based on time averaged motion equations integration
21 p3693 A69-38767

Navier-stokes equation numerical integration for three dimensional incompressible flow, discussing annulus thermal convection and trigonometric transforms algorithm
21 p3694 A69-38770

Spectral equation for decaying isotropic turbulence of incompressible inviscid flow at large Reynolds number, using spectral cascading
21 p3694 A69-38835

Optimal boundary layer control ensuring minimum heat transfer to porous plate from incompressible flow of hot gas of cooling system
21 p3849 A69-38846

Aligned uniform magnetic field effect on hydromagnetic stability of two dimensional incompressible electrically conducting jet flow with large Reynolds number
22 p3931 A69-40687

Boundary layer calculation in incompressible turbulent flow with closed streamlines, avoiding von Mises equation
22 p3932 A69-40931

Airfoils and cascades design for incompressible flow by numerical methods
23 p4058 A69-41610

Numerical method for calculating unsteady two dimensional boundary layers in laminar incompressible flow
23 p4152 A69-42108

Rheoelectrical analog technique for low speed aerodynamic characteristics of finite wings in incompressible flow, using deep electrolytic tank for lifting surface calculations
23 p4061 A69-42351

Time dependent unsteady flow of incompressible and electrically conducting fluid between two infinite disks rotating in uniform axial magnetic field
23 p4153 A69-42410

Two dimensional incompressible inviscid fluid flow problems solution by conducting-paper analog with electrical equipotentials tracing, based on Laplace equation applicability
24 p4299 A69-43024

Design of vortex fluid amplifiers operating in incompressible flow regime, based on fluid properties and geometry effects on amplifier behavior
24 p4256 A69-43299

Symmetry properties of Cameron-Martin-Wiener kernels in isotropic velocity field, applied to one dimensional model of incompressible turbulent flow
24 p4301 A69-43358

Incompressible fluid flow inhomogeneities effect on oscillations of airfoils cascade, noting occurrence of parametric resonance in turbine engine blades
24 p4245 A69-43479

Boundary layer equations with heat transfer for laminar and turbulent incompressible flows about two dimensional and axisymmetric flows, using finite difference method
[ASME PAPER 69-HT-7] 24 p4304 A69-43561

INCOMPRESSIBLE FLUIDS

Small oscillations in solid body with arbitrary cavity partially filled with viscous incompressible fluid
01 p0165 A69-10084

Incompressible fluid steady motion in curved tube investigated by Fourier series, solving coupled nonlinear equations numerically
01 p0058 A69-10142

Boundary value problems for steady, three dimensional MHD flow of viscous incompressible conducting fluid past various bodies, proving existence of solutions
01 p0126 A69-10164

Vector potential used to express equations of incompressible fluid motion in form suitable for digital solution, discussing boundary conditions
01 p0058 A69-10228

Asymptotic forms of Navier-Stokes equations for laminar motions of incompressible viscous fluid, discussing validity and applications
[ONERA-TP-651] 01 p0059 A69-10383

Turbulent heat and mass transfer in rotating incompressible fluid flow analyzed by kinetic energy and shear stress equations
01 p0060 A69-10402

Mixed boundary value problem for system of Navier-Stokes equations for viscous incompressible fluid in stationary motion in vessel, noting rotating fluid
02 p0272 A69-12223

Accelerated plate motion effect on flow of electrically conducting viscous incompressible fluid past infinite flat plate in uniform magnetic field
02 p0289 A69-12237

Cylindrical jet stability of perfectly conducting, incompressible and inviscid fluid in presence of axial magnetic field
03 p0474 A69-13142

Boundary conditions for irrotational hydrodynamic field around sphere moving along axis of cylindrical tube containing incompressible fluid calculated by least squares method
03 p0415 A69-13362

- Finite difference solution of time dependent Navier-Stokes equation for incompressible fluids, using velocities and pressure as variables
03 p0415 A69-13369
- Difference schemes to solve Navier-Stokes equations for viscous incompressible fluid by substituting fourth order partial differential equation
03 p0415 A69-13650
- Motion and stability of solid body with cavity containing rotor and two incompressible nonmixing liquids with surface tension
03 p0418 A69-13814
- Laminar two dimensional free jet outflow of incompressible nonNewtonian pseudoplastic fluid from orifice into mass of same fluid
04 p0586 A69-14406
- Kinematic and dynamic relations determined for vortex flow of ideal incompressible fluid past circular cylinder, noting use for calibrating cylindrical adapters
04 p0541 A69-14484
- Rayleigh step journal bearings, considering pressure distribution, load capacity and attitude angle and optimal film thickness ratio for incompressible fluid lubrication
04 p0605 A69-14587
- Small oscillations of viscous incompressible fluid in container with free surface under action of potential force field
04 p0587 A69-14620
- Cavitation stream calculation methods for ideal incompressible fluid with free boundaries, noting cavitation generators and Riabouchinsky problems
04 p0589 A69-14994
- Ideal plane incompressible fluid flow past airfoil noting hydrodynamic effects, assuming presence of constant eddy
04 p0589 A69-14996
- Surface wave stability for horizontal layer of incompressible dielectric fluid in electric field, noting viscosity effect
04 p0638 A69-15193
- Boundary layer flow of viscous incompressible liquid past wedge embedded circular cylinder
04 p0590 A69-15276
- Differential rotation of sphere in viscous incompressible liquid, discussing pressure and skin friction drag between two hemispheres with different angular velocities
04 p0590 A69-15278
- Viscous incompressible fluid motion in two or more dimensions and with zero fluid velocity on domain boundary, determining lower bounds and uniqueness for solutions
04 p0626 A69-15311
- Solution to system of equations in boundary layer theory of steady incompressible fluid flow
05 p0751 A69-16454
- Equations of motion solved for solid body with ellipsoidal cavity containing ideal incompressible fluid in uniform eddy motion
06 p0957 A69-16823
- Secular equation for Couette flow stability in incompressible viscoelastic fluid
06 p0909 A69-17240
- Laminar source flow of viscous incompressible liquid between two parallel coaxial rotating porous disks
06 p0909 A69-17243
- Universal equations for three dimensional laminar boundary layer of incompressible fluid on walls of axisymmetric channel with vortical external flow
06 p0909 A69-17328
- Linear equations for three dimensional perturbations in boundary layer of viscous incompressible fluid flow on plane surface, discussing Tollmein-Schlichting waves
06 p0909 A69-17329
- Incompressible laminar boundary layer with normal suction or blowing, discussing approximate method for evaluating laminar friction on wing contour
06 p0911 A69-17781
- Unsteady flow of viscous incompressible conducting fluid in MHD generator channel, discussing external circuit inductance and flow velocity during start-up
06 p0969 A69-17915
- Motion of viscous incompressible fluid in interspace between rotating and parallel fixed permeable plane having supplementary fluid injection solved by Navier-Stokes equations
07 p1119 A69-18743
- Navier-Stokes equations for steady rotational motions of incompressible viscous fluid at small Reynolds numbers between rotational surfaces
07 p1119 A69-18748
- Stationary viscous incompressible fluid flow past rough surface, noting solution stability and friction stress determination for given pressure gradient
07 p1119 A69-18751
- Uniqueness theorem for laminar MHD duct flows
07 p1190 A69-18813
- Laminar and turbulent stresses in plane asymmetric incompressible flows analyzed based on Boussinesq formula for turbulent shear stresses
07 p1121 A69-19330
- Fluid motion and MHD disturbances in viscous incompressible fluid of finite electrical conductivity, studying axis of oscillating dipole perpendicular to exciting field
07 p1195 A69-19451
- Unsteady suction motion of viscous incompressible fluid under action of slowly rotating suction disk, noting fluid velocity variation
08 p1302 A69-19875
- Arbitrary stationary foil in perfect incompressible fluid moving at constant velocity at infinity assuming plane, steady and irrotational flow
08 p1303 A69-20272
- Integral of Navier-Stokes equations for steady three dimensional motion of incompressible viscous fluid, giving angular velocity vector projections
08 p1342 A69-20320
- Statistical dynamics of turbulent incompressible fluid, discussing harmonic function in Navier-Stokes equation
08 p1303 A69-20323
- Incompressible laminar thermal boundary layer unsteady development from state of rest in vicinity of wall of obstacle subjected to unsteady thermal field [ONERA-TP-680]
08 p1304 A69-20754
- Two dimensional boundary value problem for symmetrical entry of wedge into incompressible nonviscous fluid using complex variable theory
08 p1305 A69-20995
- Coaxial cylindrical shells oscillation frequencies with interspace filled with incompressible liquid determined as functions of liquid level and interspace width
09 p1612 A69-21483
- Three dimensional flow field of incompressible fluid with purely axial development in conical ducts and turbomachines
09 p1480 A69-21597
- Self gravitating incompressible fluid sphere free oscillations, deriving characteristic equations for arbitrary viscosities
09 p1481 A69-21790
- Unsteady free convection in incompressible viscous fluid having internal thermal source contained in bounded volume
09 p1621 A69-21792
- Incompressible fluid nonlinear oscillations in rectangular basin analyzed by Green function for mixed problem, calculating velocity potential and free surface approximations
09 p1483 A69-22711
- Incompressible fluid unsteady motion between journal and bearing solved in form of Reynolds number power series from stream functions
09 p1514 A69-22712
- Approximate solution method for Navier-Stokes equations for incompressible viscous fluids
10 p1718 A69-22861
- Incompressible fluid flow engine spiral casing, considering flow as potential flow
10 p1632 A69-22914
- Flow instability of incompressible nonconducting fluid in thin cylindrical conducting elastic pipe in constant uniform magnetic field
10 p1798 A69-23094
- Laminar flow heat transfer of viscous incompressible fluid in entrance region of circular tube, using nonlinear equations
10 p1809 A69-23195
- Characteristics of dynamic mechanical systems including solid state and hydrodynamic analogs of ideal incompressible fluids, based on statistical theory of turbulence
10 p1678 A69-23209
- Similarity solutions of laminar boundary layer equations for three dimensional flows of incompressible power law fluids
10 p1678 A69-23235
- Solid cylindrical body entrainment by viscous incompressible fluid flow in tube under constant pressure gradients and absence of gravitational force
10 p1678 A69-23366
- Self consistent perturbation procedure for stationary homogeneous turbulence of incompressible fluid
10 p1680 A69-23648
- Homogeneous turbulence in incompressible fluid, expanding field variable on ideal random basis
11 p1867 A69-24282
- Nonuniformity of magnetic field effect on steady flow of incompressible inviscid electrically conducting fluid in duct, considering Reynolds and Alfven numbers [JPL-TR-32-1376]
11 p1923 A69-24291
- Dynamics of turbulent motion of incompressible viscous fluid particles, using Lagrangian functions
11 p1867 A69-24536
- Formula in Prandtl-Batchelor theory describing motion of incompressible fluid in sphere interior verified experimentally
11 p1868 A69-24755
- Helical motions of body bounded by multiply connected surface immersed in infinite ideal incompressible fluid, discussing congruence
11 p1868 A69-24790
- Large amplitude symmetric and asymmetric irrotational motion of inviscid incompressible fluid with liquid-vapor interface in accelerating cylindrical container of revolution
11 p1871 A69-25124
- Second order effects on two dimensional laminar boundary layer flow of incompressible fluid
11 p1872 A69-25127
- Reverse transition in two dimensional accelerated incompressible turbulent boundary layer flow, noting skin friction coefficient and turbulent intensity profiles
11 p1872 A69-25129
- Steady incompressible fluids flow around stationary wings and through rotating blades cascades based on Prandtl airfoil theory of bound vortices
11 p1873 A69-25202
- Low Reynolds number stability of incompressible fluid half jet flow, investigating free laminar boundary layer instability
11 p1874 A69-25280
- Axisymmetric turbulent supersonic incompressible fluid jet, calculating momentum flow distribution and excess heat flow densities in basic segment
11 p1818 A69-25346
- Axisymmetric oscillations of two spherical shells with noncoinciding centers of curvature immersed in compressible or incompressible fluids
11 p1875 A69-25467
- Steady flow of viscous incompressible fluid studied with system of equations equivalent to Navier-Stokes equations and finite difference method
11 p1875 A69-25480
- Steady flow field for viscous incompressible fluid in rotating pipe with porous walls determined from Navier-Stokes equations
11 p1875 A69-25481
- Thin deformable body motion in disturbed potential flow of ideal incompressible fluid
11 p1876 A69-25488
- Free periods of oscillation of incompressible rotating fluid bounded by rigid concentric spheres, using Longuet-Higgins solution of Laplace tidal equation
11 p1876 A69-25558
- Axisymmetric detached flow past slender solid of revolution by ideal incompressible fluid at zero angle of attack and with small cavitation numbers
11 p1877 A69-25741
- Unsteady surface and internal waves diffraction induced by source in ideal incompressible fluid, obtaining solutions in form of convolution and transfer functions
12 p2061 A69-25953
- Inertia effect on incompressible fluid film pressure between two oscillating parallel plates, considering Reynolds number
12 p2102 A69-26241
- Iterative solutions of nonlinear integrodifferential dynamical equation for two point velocity correlation tensor in incompressible fluid turbulence studies
12 p2062 A69-26602
- Heat transfer for incompressible inviscid fluid flow in cone, expressing solution in terms of dimensionless numbers
13 p2375 A69-27788
- Monograph on return currents produced by confined jet of incompressible fluid with low initial ambient fluid velocity
13 p2250 A69-28335
- Three dimensional thermal laminar boundary layer around body moving with constant acceleration in incompressible fluid, considering wall temperature and Prandtl number
13 p2380 A69-28631

Viscous incompressible fluid self similar mixing problems, performing group analysis for complete boundary value problem

14 p2428 A69-28803

Nonlinear internal gravity waves in stratified atmosphere of unbounded inviscid incompressible fluid, noting wave amplitude inverse proportion to atmospheric density

14 p2441 A69-29574

Nonlinear equations for motion of rigid body with cavity partially filled with ideally incompressible liquid

14 p2432 A69-29626

Incompressible viscous fluid steady motion caused by rotating ellipsoid, determining drag moments for circular disk and sphere

14 p2432 A69-29627

Laser beam light pressure bending of incompressible liquid surface leading to beam self focusing in linear medium

14 p2461 A69-29674

Magnetic field effect on heat and mass transfer in incompressible fluid MHD flow

14 p2500 A69-29901

Circular curved foil steady oscillations near screen in semiinfinite space filled with incompressible fluid transformed into equivalent linearized problem

15 p2547 A69-30576

Steady rectilinear translational motion of circular disk-shaped slightly bent wings near solid wall in incompressible fluid medium in absence of vortices and external forces

15 p2547 A69-30583

Plane incompressible fluid interface stability in presence of transverse electric field, deriving equation of motion for perturbation amplitude

15 p2652 A69-30911

Drag and friction coefficients for laminar pulsating incompressible fluid flow in circular tubes obtained from Navier-Stokes equation

15 p2592 A69-30988

Eigenfrequency spectrum and stability of perfectly conducting inviscid incompressible fluids in cylindrical channels and twisted magnetic fields, noting flowfields and critical wavelengths

15 p2664 A69-31063

Numerical approximation of Taylor vortices in viscous incompressible fluid flow between concentric rotating cylinders, using truncated eigenexpansions

15 p2593 A69-31518

Three dimensional laminar jet mixing of incompressible viscous fluid from rectangular cross section nozzle into uniform stream

16 p2768 A69-31687

Multipad externally pressurized spherical bearing fed with incompressible fluid for satellite attitude control systems tests

16 p2793 A69-31728

Asymptotic behavior of one dimensional laminar flow of incompressible viscous fluid in infinite cylindrical tube, giving equations for boundary conditions and flow rate

16 p2769 A69-31831

Book on mechanics of deformable media covering fluid and solid mechanics and applications to irrotational flows of compressible and incompressible fluids

16 p2813 A69-32789

Monograph on ring airfoil theory with nonuniform incidence covering steady flow and shear flow transition into boundary value problem of potential theory

17 p2889 A69-32995

Statistical dynamics of turbulent incompressible fluid, discussing harmonic function in Navier-Stokes equation

17 p2952 A69-33313

Transformed Navier-Stokes equations for incompressible fluids flow, deriving forces acting on surface of bounded region

18 p3122 A69-34830

Buoyant plumes and thermals defined as vertical motions produced under gravity by density or temperature contrast between incompressible source fluid and environment

18 p3122 A69-34917

Laminar separation in incompressible fluid flowing past bluff body at high Reynolds number, investigating shock wave interaction with laminar boundary layers

18 p3122 A69-34918

Statistical dynamics and structure of turbulent shear flows in incompressible fluids of constant density, discussing Reynolds stress at critical layers

18 p3123 A69-34922

Hydrodynamic stability of incompressible fluid boundary layer flow during blowing or suction through

porous surface, determining Reynolds number lower bounds

18 p3124 A69-35381

Similarity solutions describing buoyancy effect on laminar and turbulent wakes of heated body in incompressible fluid vertically ascending flow

19 p3296 A69-35761

Hydrodynamic equations of laminar plane flow of incompressible viscous fluid in rectangular region, calculating velocity field by equivalent network and integration

19 p3297 A69-35853

Boundary conditions of incompressible viscous flow on semiinfinite plate edge defined using difference methods for Navier-Stokes equations

19 p3299 A69-36394

Incompressible fluid flow of given density and kinematic viscosity near trailing edge of flat plate

20 p3458 A69-37098

Axial velocity and static pressure for incompressible fluid flow through straight smooth porous tube [ASME PAPER 69-FE-44]

20 p3517 A69-38000

Statistical description of turbulence of viscous incompressible fluid at large Reynolds numbers, using velocity distribution probability

20 p3517 A69-38007

Incompressible electrically conducting fluid in presence of magnetic field and Coriolis forces, analyzing Rayleigh-Taylor instability by variational principles

20 p3577 A69-38195

Perturbed motion of solid body containing axisymmetric cavities partially filled with ideal incompressible fluid, solving boundary value problems of fluid oscillations

20 p3518 A69-38296

Second circle theorem for two dimensional irrotational flow of incompressible inviscid fluid in z plane

20 p3518 A69-38316

Viscous incompressible nonNewtonian fluids flow with treatment for steady rotational problems and oscillatory motion, considering primary and secondary motions

20 p3519 A69-38319

Momentum and energy equations for fluctuating flow of viscous incompressible conducting fluid past flat plate with time dependent suction under transverse magnetic field

21 p3691 A69-38445

Continuous cavitation model for incompressible fluid one dimensional unsteady motion

21 p3693 A69-38752

Incompressible viscous fluid flow past sphere at low Reynolds number, evaluating stream function and drag on sphere

21 p3694 A69-38771

Optimal control of ideal noncompressible fluid vibrations partially filling rectangular container moving in horizontal direction

21 p3695 A69-38892

Nonlinear incompressible potential flow with unbounded free surfaces, analyzing singularities in finite part of space

21 p3696 A69-39295

Spheres impulsive starting in incompressible viscous fluid, including Reynolds number and investigation time parameters in Navier-Stokes equation

21 p3696 A69-39296

Parallel shear flow equilibrium in inviscid nonheat-conducting incompressible fluid with density varying as function of vertical coordinate

21 p3697 A69-39743

Flow stability regions at surface of flight vehicle, considering boundary layer flow of incompressible fluid

21 p3645 A69-39827

Solid body filled with ideal incompressible liquid, analyzing stability of permanent rotations

21 p3773 A69-39837

Boundary layer development on body accelerating in viscous incompressible fluid, using straight lines approximation and asymptotic expansions

22 p3929 A69-40110

Oscillations of highly viscous incompressible fluid in partially filled cavity of body moving about fixed point, solving Navier-Stokes equations by asymptotic method

22 p3929 A69-40111

Finite element method application to minimum principle for incompressible lubrication problem, noting flow boundary conditions and squeeze film effects

22 p3955 A69-40406

Differential rotation of incompressible inviscid fluid of infinite electrical conductivity in spherical shell, noting toroidal magnetic field for sun

22 p4027 A69-40658

Integral equations of motion for plane steady flow of viscous incompressible electrically conducting fluid around flat plate

22 p3992 A69-41109

Velocity defect profile and skin friction law for incompressible equilibrium turbulent boundary layer using mixing length relation

22 p3934 A69-41180

Mixed boundary value problem for system of Navier-Stokes equations for viscous incompressible fluid in stationary motion in vessel, noting rotating fluid

23 p4183 A69-41974

Sphere set in motion at constant velocity by impulsive force submerged in incompressible fluid in half space

24 p4298 A69-42585

Parallel magnetic field effect on free boundary layer type flows stability of low Reynolds number between parallel streams of viscous incompressible conducting fluid

24 p4298 A69-42596

MHD flow of incompressible viscous fluid between rotating electrical insulator disks

24 p4354 A69-42599

Detachment in incompressible turbulent flows around thick body analyzed to predict base pressure, vortex volume, etc

24 p4299 A69-42674

INCONEL [TRADEMARK]

Microcracking susceptibility studies of Inconel 718 weld heat affected zones, noting hot ductility, weld circle patch and fillerless fusion welding tests

11 p1905 A69-24933

Weld cracking sensitivity of Inconel 713C investigated for determining aluminum content effect on weldability of nickel base heat resistant alloys

11 p1906 A69-25577

Oxygen environment influence on Inconel X-750 surface deformation and cracking during fatigue related to chemisorption and oxidation

20 p3558 A69-36966

Inconel and aluminum tested in pressurized hydrogen at room temperature, using surface flawed fracture toughness specimens and preflawed pressure vessels

21 p3730 A69-38666

Mn, S and rare earth additions influence on Inconel alloy weld microfissuring including material, hot ductility and tensile strength data

22 p3967 A69-39883

Titanium diboride electrodeposition on Inconel from molten salt electrolyte at high temperatures noting electrolyte metabolites and coating thickness range

22 p3970 A69-40735

Alloy Inconel 625 precipitation behavior and effect on short and long term properties, discussing tetragonal phase segregate and creep strength

22 p3971 A69-40802

INDENTATION

Electrode indentation in resistance spot welds related to weld strength for titanium, steel and aluminum alloy

01 p0086 A69-10538

Stress fields in Hertzian contact of parallel cylinders composed of anisotropic materials and transversely isotropic spherical bodies

08 p1414 A69-20524

Indentation of inhomogeneous rigid plastic solid by flat punch under plane strain conditions analyzed by perturbation method

11 p1986 A69-25244

Variational principle for Fredholm integral equations applied to inclusion and indentation problems in elasticity

19 p3440 A69-36589

Steady motion of frictionless indenters along surface of elastic layer in plane strain, using Fourier transform and Fredholm equations for numerical solution

21 p3837 A69-39155

INDEPENDENT VARIABLES

NT LATTICE PARAMETERS

Linear ordinary differential equations with exponential coefficients, giving solutions asymptotic behavior for large values of independent variable

01 p0103 A69-10231

Numerical digital computer determination of ultra subharmonic response for Duffing equation

01 p0104 A69-10235

Nonlinear time dependent parameters systems, analyzing governing differential equations in terms of elliptic functions

01 p0050 A69-10237

Darlington composite transistor hybrid parameters used to describe performance characteristics, noting load resistances and source
01 p0041 A69-10244

Asymptotic behavior of probabilities of large deviations of sums of independent random variables with moments of any order
01 p0104 A69-10264

Spacecraft motion parameters determination under controlled acceleration using information from inertial sensors
01 p0161 A69-10569

Satellite trajectories calculated in form of parameters derived from processing measured functions, considering optimum mathematical description selection
01 p0151 A69-10570

Wideband hybrid junctions synthesis from given parameters, suggesting matrix representation of ring circuits
01 p0043 A69-10593

Independent variables reduction in nonlinear partial differential equations, detailing group theory method
03 p0456 A69-13740

Bergman integral operator to solve second order differential equations with two independent variables
03 p0527 A69-13742

Inclined hot-wire and hot-film anemometers parameter dependent on length-to-diameter ratio used to describe deviations from cosine law
[ASME PAPER 68-WA/APM-16]
04 p0596 A69-14391

Algorithm for numerical solution of variational problems for functions of two independent variables and boundary value problems using local variations method
04 p0622 A69-14616

Finite element method for exact solution of more general problems with one independent variable and extension to many dependent variables
04 p0676 A69-14741

Electric quadrupole parameters, discussing relationship between voltages at terminals
04 p0579 A69-15228

Hybrid assumed mode solution of nonlinear partial differential equations /initial value problems/ in time-like independent variable
04 p0566 A69-15345

Finite differences for identifying partial differential equations and associated boundary conditions of distributed parameter system
[ASME PAPER 68-WA/AUT-1]
05 p0738 A69-16185

Microwave diodes on GaAs base, determining basic parameters and effects on crystal formation and device construction
05 p0730 A69-16222

Thermal management of integrated circuits design, noting dependence on circuit and component configurations and parameter variations
06 p0894 A69-17217

Optimal estimation of sampled stochastic process with finite state unknown parameters
06 p0901 A69-17362

Asymptotic solutions for nonlinear differential equations with gradually varying coefficients of great resistivity
06 p0947 A69-17392

Finite parameteric family of solutions to differential equations systems with deviating argument
06 p0948 A69-17500

Planetary distribution of ionospheric parameters analyzed, using geographic longitude and magnetic inclination as longitudinal and latitudinal coordinates
06 p0921 A69-17745

PCM bit synchronizer/signal conditioners performance characteristics and specification
07 p1106 A69-19120

Seal swell prediction methods extended to include three dimensional solubility parameter concept
[ASLE PAPER 68-LC-21]
07 p1171 A69-19306

Mathematical model of radar display, considering radar construction tube resolution, environment and eye perception parameters
07 p1136 A69-19504

Observability theory of dynamic objects application to composing measurements for space flights, solving parametric observability problem
07 p1087 A69-19605

Spacecraft tracking network for determining spacecraft motion parameters, noting application to coordinates and velocities determination for terrestrial observers
07 p1087 A69-19609

Components production process effect on reliability based on values and functional relations of internal parameters, noting influence on accelerated testing
08 p1319 A69-20346

Mixed initial boundary problem for hyperbolic equations with given boundary outgoing variables, determining incoming data
08 p1342 A69-20347

Control technique to make aircraft insensitive to parameter variations and to achieve desired response to control
08 p1255 A69-20719

Design parameters for optimum heavily loaded single rotation ducted fan characterized by ultimate wake vortex system
[AIAA PAPER 69-222]
08 p1253 A69-21030

Automated parameter search techniques applied to low thrust mission design, stressing trajectories and mission optimization
09 p1585 A69-21211

Two pulsars discovered during search with transit telescope at U.S. National Radio Astronomy Observatory, tabulating pulsar parameters
09 p1592 A69-21484

Efficiency of weather forecasts taking into account quality criteria and integrating index number, discussing optimization principle for new parameter
09 p1534 A69-21510

Power relations to fit radar meteorology parameters including rainfall, reflectivity function and attenuation rate
09 p1536 A69-21643

Diffusion bonding parameters for producing hollow Ti-Al compressor blades, discussing surface preparation, postbound heat treatment quality control and mechanical properties
[ASME PAPER 69-GT-46]
09 p1513 A69-22484

Data interpretation, discussing correlation describing effectiveness of independent variable and table giving values directly from sample size, t, z, F and chi square values
10 p1669 A69-23040

Flight data recorders history and regulations, discussing parameters and design of systems
10 p1691 A69-23247

Optimum control involving plants with intermediate position between lumped and distributed parameters
10 p1666 A69-23363

Geomagnetic micropulsations fluctuations during solar activity cycle showing changes in excitation frequency with change in corpuscular fluxes parameters
10 p1687 A69-23919

Equation derivation to determine optimal parameters of spacecraft orbital elements, considering constraints imposed on measured quantities
10 p1791 A69-24192

Optimization of autonomous system parameters, exemplifying by disturbed motion of gyroscope system
11 p1858 A69-24557

Output pulse parameters of short pulse thyristor generator as function of time constant, considering rise time of switch-on process
11 p1846 A69-24615

Oscillatory properties of solutions to second order nonlinear differential equations with delayed arguments
11 p1908 A69-24767

Approximate method for calculating linear multipoles antennas parameters in terms of power requirement, considering equidistant/non-equidistant element antennas
11 p1849 A69-24969

Damping accuracy sensitivity to circuit element tolerances in polynomial filters
11 p1850 A69-24970

Transfer function parameters identification by fault isolation technique using white noise stimulus and processor matrix of orthogonal filters
11 p1865 A69-25077

Computational method for quasi-optimal control with parameter sensitivity function, noting application to dynamical system model
11 p1859 A69-25165

Error analysis in conversion of two port scattering parameters used in microwave transistor characterization
11 p1852 A69-25200

Classification of second order quasi-linear partial differential equations with two independent variables in structural dynamics with emphasis on elastic structures
11 p1991 A69-25513

Tracking system for gain and time delay parameter measurements of compensatory control crossover model
12 p2022 A69-25930

Multivariable control systems - Conference, Duesseldorf, October 1968, Volume 2
12 p2045 A69-26058

Multivariable control systems - Conference, Duesseldorf, October 1968, Volume 1
12 p2046 A69-26069

Minimal representation in state variables for multivariable control system, discussing algorithms, identification methods and flow graph techniques
12 p2047 A69-26070

Higher root loci of polynomials for multivariable systems with coefficients polynomials of real parameter
12 p2048 A69-26073

Multivariable control system decoupling by appropriate choice of decoupling network structure and location in system
12 p2048 A69-26074

Multivariable automatic control system consisting of similar local subsystems studied by transforming system equations into equivalent diagonal form
12 p2048 A69-26076

Uncontrollable modes effect on transient/steady behavior and limit cycles characteristics of nonlinear multivariable control system
12 p2048 A69-26078

Linear closed loop control systems with periodically varying parameters analyzed by harmonics method using Fourier transforms
12 p2054 A69-26720

Dirichlet problem of linear degenerate second order differential elliptic systems with independent variables
12 p2123 A69-26729

Electrodeless plasmatron coupled with oscillator operating at 5-30 kHz, discussing parameters effect on operation mode and performance
12 p2140 A69-27123

Book on stress rupture parameters including least squares approach to Larson-Miller, Dorn, Manson-Haferd, Graham-Walles, Murry, Brozzo and Chitty-Duval
13 p2360 A69-27372

Analog simulation of nonlinear functions of single independent variable compared digital to analog representation principles
13 p2224 A69-27531

Critical parameters of isothermal quasi-degenerate white dwarfs calculated by energy method, allowing for relativity theory error and neutron irradiation effect
13 p2351 A69-27871

Parameter identification in linear dynamical systems with transport lags, discussing linear differential-difference equations and finite difference theory
13 p2289 A69-27945

Regional boundaries in control-parameter space constructed by computer algorithm, involving parameter vibration direction changes in parameter plane
13 p2225 A69-27967

Substituted lithium ferrites analyzed to obtain materials with small initial magnetic losses at different microwave ranges
13 p2320 A69-28000

Gas ring lasers, discussing optimal parameters, colliding waves interference, nonmutual effect and radiation polarization
13 p2272 A69-28175

Ionization fraction as independent variable in plasma transport correlation, noting role in pressure effect increase
13 p2313 A69-28241

Independent nature of variables in dimensional analysis, discussing temperature in kinetic and dimensional analyses
13 p2289 A69-28362

Wave parameters in coupled parallel surface wave transmission lines and dielectric waveguides, discussing phase velocities and spatial beat period
13 p2223 A69-28570

Varactor diode parameters measurements by microwave power reflection method
13 p2237 A69-28645

Parameters optimization in electronic equipment design, considering parameters and efficiency criteria as additive elements functions of dimensional chain
14 p2418 A69-28835

Root locus method for nonlinear systems analysis, determining existence, stability and parameters of periodic solutions
14 p2445 A69-28919

Searchless gradient self adaptive system for adjusting servosystem parameters to reference model characteristics, using auxiliary operator method
14 p2426 A69-29146

Transistor scatter and admittance differential parameters measurements graphically correlated
14 p2420 A69-29397

Electrokinetic converter of biochemical parameters for diagnosis and control of organism behavior, noting biomechanical utility
14 p2409 A69-29471

Monograph on Dirichlet problem for quasi-linear elliptic differential equations with many independent variables
14 p2471 A69-29599

Boundary layer physical and chemical processes effect on dynamic parameters of high temperature hypersonic gas flow past blunt bodies
14 p2391 A69-29620

Computer program for STV-F9 satellite communication parameters, using ELDO forecasting values as input data
14 p2530 A69-29689

Atmospheric dynamics parameters of Mercury, Venus, Mars and Jupiter, discussing generalized circulation theory
14 p2526 A69-29841

Multivariable linear time-variant systems noninteracting control problem, discussing realization by state variable feedback
15 p2582 A69-30024

Lumped and distributed parameter systems, discussing transfer matrix elements, connecting lines, etc
15 p2582 A69-30319

Three and n body problems solution by reduction of independent variables and maximum principle
15 p2652 A69-30448

Solid state and gas lasers operational parameters tabulation including pulse durations, powers, energy flux densities, electric and magnetic field strengths, etc
15 p2633 A69-30708

Spacecraft motion parameters determination under controlled acceleration using information from inertial sensors
15 p2702 A69-30739

Satellite trajectories calculated in form of parameters derived from processing measured functions, considering optimum mathematical description selection
15 p2691 A69-30740

Asymptotic Krylov-Bogoliubov methods application to solving boundary value problems for hyperbolic quasi-linear equations with distributed parameters and retardation
15 p2653 A69-31192

Statistical calculation of three dimensional frames of thin walled rods, using method of initial parameters in matrix form
15 p2714 A69-31199

Bilinear covariant of linear differential form involving 2n independent variables used for grouping to achieve symplectic and contact transformations
16 p2804 A69-31623

Asymptotic solutions to second order differential equations with slowly varying parameters and large resistance applied to mathematical pendulum damped swinging motion
16 p2804 A69-32253

System noise parameters derivation, using standard IRE definition as foundation and amplifier noise measurement as example for error analysis
16 p2755 A69-32800

He-Ne laser plasma behavior, establishing parameters for electron gas, cross sections of formation and annihilation and excited states lifetimes
17 p2982 A69-33390

Helicopter fire control systems evaluation by computer model for hit probability and impact point sensitivity to various parameters
[AHS PAPER 316]
17 p2933 A69-33540

Isonospheric parameter recording accuracy by vertical sounding, discussing errors in frequency-height curve
17 p2969 A69-34002

Asymptotic series expansion for solutions of differential equations containing parameter
18 p3163 A69-34328

Supported shafts natural vibration frequencies determination by averaging shaft parameters, noting suitability in HF ranges
18 p3147 A69-34546

State space structure of model reference adaptive control and parameter tracking systems subject to noise
18 p3111 A69-34686

Iteration process by difference scheme for numerical solution to Dirichlet problem of two dimensional Poisson equation
18 p3164 A69-34701

Parameter optimization of launch vehicle attitude control system of fixed structure for various computation techniques
18 p3210 A69-35092

Canonical transformations depending on small parameter, utilizing Lie series
19 p3397 A69-35608

Asymptotic behavior of probabilities of large deviations of sums of independent random variables with moments of any order
19 p3360 A69-36199

Digital frequency synthesizer design parameter selection, giving expressions for output frequency and division coefficient variations
19 p3284 A69-36594

State variables with delta functions for electrical network with discontinuously variable components, discussing application to parametron
19 p3287 A69-36763

Mach reflection limiting parameters of conical shock wave in Plexiglas cylinders, showing head wave curvature radius linear relationship to cylinder diameter
19 p3302 A69-36845

Eulerian correlation functions representation of wind variations in analytic form by three parameter function, noting field diagram
20 p3571 A69-37507

Orbital parameters of short-lived low altitude earth satellites assuming no atmospheric drag, no orbital precession and flat earth condition
21 p3798 A69-38626

Law of wall parameters for compressible turbulent boundary layer with air injection through wall determined by analyzing data for hypersonic speeds
21 p3692 A69-38685

Data transmission of variables in deterministic networks
21 p3673 A69-38775

Algebraic equations for determination of controller parameters, noting a priori fixed roots of characteristic equation
21 p3723 A69-38887

Space mission sensitivity to parameters of interest determined by Monte Carlo simulation samples
21 p3804 A69-39036

Unknown parameter experimental estimation based on signal direct observations with solution by stochastic approximations method
21 p3756 A69-39265

Parameter estimation using entropy of error as criterion function compared with mean square error analysis
21 p3757 A69-39664

Optimal explicit method for parameters estimation not restricted to linear Gaussian problem derived in canonical form
[AIAA PAPER 69-947]
22 p3975 A69-40330

Minimax sensitivity criteria used to synthesize filters for estimating state of first order plant subject to dynamic and/or statistical parameters uncertainties
22 p3918 A69-41016

Satellite orientation by determining rotation parameters about centers of mass with respect to certain coordinates
22 p4037 A69-41089

Book on systems stability with random parameters, considering linear and nonlinear control systems, with application to stochastic approximation
23 p4181 A69-41510

System asymptotic motion stability for given parameter values using algorithms with aid of R functions
23 p4191 A69-41704

Correcting deficiencies in parametric expressions for rate distortion function of Gaussian process under weighted square error criterion
24 p4281 A69-42722

Time independent interaction surface bounds to shells shakedown domain obtained for multiparameter loadings
24 p4396 A69-42732

Linear viscoelastic model parameters optimization for designing automobile lap seat belts, assuming abrupt impact stop
[ASME PAPER 69-APMW-25]
24 p4275 A69-43094

Slack variable to transform optimal control problem with scalar inequality constraint on state variables into unconstrained problem of higher dimension
24 p4291 A69-43270

Dynamic models for viscous fluid transmission lines using distributed parameter for accuracy and rational approximate form to avoid computational difficulty
24 p4301 A69-43289

Optimal deterministic inputs derived for estimating dynamic control system parameters from white observation noise
24 p4293 A69-43294

Distributed parameter systems stability as internal and input-output property, describing Liapunov functionals construction
24 p4293 A69-43307

Parameter identification algorithm identifying linear dynamic systems by digital computer used to identify human operator characteristics in closed loop control situation
24 p4276 A69-43320

Parametric influence on strength of brittle materials considering volume, surface, notch, strain rate, modulus variations and material variability effects
24 p4333 A69-43341

Physiological and psychological variables relationship in candidate pilots, noting age and educational level
24 p4268 A69-43406

Optimal control parameters for gyroscopic devices with constrained phase coordinates obtained on analog computer by introducing equivalent phase coordinates system
24 p4317 A69-43708

INDEXES [DOCUMENTATION]

NASA scientific and technical information program for building technical data and literature repository for scientists, engineers and technical managers, describing IAA and STAR
[UN PAPER 68-95317]
06 p1043 A69-17068

INDEXES [RATIOS]

Oxygen index test for precise flammability ratings of plastics on numerical basis, eliminating drawbacks of ignition, end point and nonequilibrium conditions operation
04 p0621 A69-14957

Oxygen index test for precise flammability ratings of plastics on numerical basis, eliminating drawbacks of ignition, end point and nonequilibrium conditions operation
08 p1335 A69-20114

Signal records from S 66 satellite with strong scintillations, noting fluctuation well described by Nakagami m-distribution and possibility of deriving relations between different indices
16 p2777 A69-32104

Scintillation index determination, discussing data reduction methods, standard test records, calibration at stations with modest equipment and simulation on digital computer
16 p2751 A69-32105

Circulation and temperature fields indices used for studying tropospheric-stratospheric interactions during stratospheric warming at constant pressure levels
22 p3977 A69-39929

INDIA

Satellite TV systems for India, alternatives and costs
[UN PAPER 68-95750]
01 p0028 A69-10495

Meteorological instrumentation in India for surface and upper air observation
02 p0248 A69-11817

Global solar radiation flux measurements over India during IQSY
02 p0307 A69-11819

Ozone vertical distribution variations over India observed by Brewer electrochemical ozonesonde, noting effects of dry and monsoon seasons
16 p2786 A69-32627

E region horizontal drift measurements at Ahmedabad from 1956 to 1966, noting solar activity and seasonal influences
17 p2962 A69-33678

Commercial satellite communication ground station at Arvi, India, discussing system design, operation and international standards
19 p3275 A69-36412

Nationwide TV system using synchronous communication satellite proposed for India, discussing antenna, modulation, multiplexed channels and educational aspects
19 p3275 A69-36413

INDIAN OCEAN

Cloud pattern characteristics in intertropical convergence zone above Indian and Pacific oceans from meteorological satellite photographs and cloud formation maps
14 p2473 A69-29728

INDICATING INSTRUMENTS

NT ANEMOMETERS
 NT APPROACH INDICATORS
 NT ATTITUDE INDICATORS
 NT CLOUD HEIGHT INDICATORS
 NT FLOW DIRECTION INDICATORS
 NT GYROCOMPASSES
 NT HOT-WIRE ANEMOMETERS
 NT MICROBALANCES
 NT PLAN POSITION INDICATORS
 NT POSITION INDICATORS
 NT SONIC ANEMOMETERS
 NT SPACECRAFT POSITION INDICATORS
 NT SPEED INDICATORS
 NT STRAIN GAGE BALANCES
 NT TACHOMETERS
 NT WEIGHT INDICATORS
 NT WIND VANES

Meteoroid penetration detector development program for spacecraft construction, discussing design, materials and environmental tests

02 p0338 A69-11749

Jet aircraft engines condition monitoring system for detecting malfunctions without engine disassembly [ASME PAPER 69-GT-66]

09 p1501 A69-22518

Aircraft engine instrument displays evaluated by human factors, noting vertical scale design [SAE PAPER 690328]

11 p1829 A69-24488

Constant velocity moving object influence on indications of vertical gyroscope having electromagnetic compensation with residual imbalance of sensor element

11 p1881 A69-24561

Soviet book on electroluminescent devices covering panels, indicator contrast levels, control, multicolor indicators, image conversion and storage and optoelectrical systems

11 p1850 A69-24976

Leak detection for aerospace hardware, discussing equipment, operations, checkout, etc

15 p2618 A69-30315

Passive temperature indicators for maximum temperatures attained within rocket nozzle ablative materials

15 p2613 A69-31273

INDICATORS

Takeoff indicator design based on solution of equilibrium equation for forces acting on aircraft along drag axis

24 p4253 A69-43085

INDIUM

Contact resistance of In or In-Ga on CdS single crystals

03 p0487 A69-13638

Indium abundances in chondritic and achondritic meteorites and terrestrial rocks determined by radiochemical neutron activation analysis

08 p1404 A69-20917

Light absorption of In and Ga thin films in various gaseous media, noting displacement of irregular absorption band

10 p1747 A69-23792

Indium, Rb and Cs abundances obtained from sunspot spectra by comparison with Zr and Ti lines

13 p2343 A69-27626

N-type In-doped ZnSb with melt under H-gas preparation and properties

18 p3183 A69-35268

INDIUM ALLOYS

Pressure and magnetostriction effects on magnetization curves of type 2 superconducting In-Tl alloy, noting Ginzburg-Landau parameter stress dependence

02 p0294 A69-11776

Contact resistance of In or In-Ga on CdS single crystals

03 p0487 A69-13638

INDIUM ANTIMONIDES

Intrinsic absorption temperature dependence in doped p-InSb, discussing forbidden transitions

01 p0136 A69-10255

Specific heats of Cu, GaAs, GaSb, InAs and InSb measured over low temperature ranges

01 p0140 A69-11252

Impurity concentration in n-type indium antimonide semiconductors at liquid nitrogen temperatures estimated by current-voltage measurements

02 p0294 A69-11631

Negative resistance behavior of InSb diodes at 77 K, extending double injection theory for insulators to extrinsic semiconductors

02 p0294 A69-11722

Numerical estimates for degenerate pinch in InSb, determining pinch parameters

02 p0300 A69-12638

Magnetoconductance of nonequilibrium plasmas in indium antimonides, noting anisotropy effect of electric and magnetic field orientation

03 p0486 A69-13463

InSb semiconductors electron scattering analysis at ionized impurities and optical and acoustical lattice vibrations with various polarizations

03 p0492 A69-14170

Transport phenomena analysis in n-InSb semiconductors during elastic/inelastic current carrier scattering

03 p0492 A69-14171

Temperature dependence of Hall coefficient, conductivity and carrier mobility in manganese doped indium antimonides

04 p0643 A69-15257

Longitudinal and transverse magnetoresistance in n-type InSb single crystals in magnetic fields, noting preparation effect on existence magnetophonon oscillations

04 p0643 A69-15262

Temperature dependence of n-InSb Hall coefficient and resistivity, noting increase in conductivity with degree of compensation associated with electrical breakdown

06 p0978 A69-16990

Quantum oscillations of Maggi-Righi-Leduc /MRL/ effect in n-InSb and n-InAs samples from single crystals at liquid helium temperature

06 p0979 A69-16992

Faraday effect at free carriers in indium antimonides and gallium arsenides, analyzing frequency dependence of rotation angle

06 p0979 A69-16996

Differential thermal EMF at room temperature in p-InSb as function of concentration for different electron and hole scattering mechanisms

06 p0981 A69-17881

Structural and electrical properties of indium antimonide and arsenide films, noting dependence of electron concentration and mobility on thickness

06 p0981 A69-17892

Microwave spectrum of n-InSb avalanche plasmas under magnetic field, considering dynamic current-voltage characteristics, hole wave instabilities and microwave emission processes

07 p1197 A69-18466

Nonisothermal wave propagation in n-type indium antimonide in orthogonal static and magnetic fields, considering instabilities and acoustic and polar optical phonon scattering

07 p1197 A69-18467

Dependence of microwave emission from n-InSb on crystalline orientations, noting anisotropy in case of rotation in perpendicular plane

07 p1198 A69-18647

Temperature dependence of conversion coefficients and sensitivity of n-type InSb detectors in millimeter and submillimeter ranges

07 p1199 A69-18683

Hole concentration at deep energy levels in p-type indium antimonide single crystals containing structural defects

07 p1199 A69-18687

Complex microwave incremental conductivity of InSb at 77 K in steady electric field using displaced Maxwellian distribution function

07 p1200 A69-19447

Selenium diffusion in indium antimonide, determining concentration gradients in junction space charge region by capacitance method

09 p1554 A69-21469

Electron states at deep levels in InSb by deriving equations for Bloch wave functions of conduction and valence bands

09 p1556 A69-21508

Strongly doped n-type indium antimonide, determining dependence of limiting electron concentration on dopant impurity nature

09 p1558 A69-21869

Intrinsic absorption temperature dependence in doped p-InSb, discussing forbidden transitions

09 p1559 A69-22648

Repeated stepwise annealing process to obtain homogenized InSb-GaSb alloys continuous solid solutions

10 p1745 A69-23331

Surface atomic structure effects on polar faces in InSb semiconductor crystal established from measurements of contact potential difference by dynamic capacitor

10 p1747 A69-23965

Dislocation mobility temperature dependence in n-type indium antimonide, noting role of covalent interatomic bonds

12 p2143 A69-26453

Electron cyclotron resonance measurement in n-type indium antimonide using far IR emission from HCN and water vapor lasers, noting magnetic field strength effects

13 p2270 A69-27200

Frenkel defects in light irradiated p-type InSb single crystals at subthreshold radiation energies

13 p2318 A69-27885

Electrical properties of p-type indium antimonide, noting effects of deep level compensation on ev values

13 p2318 A69-27895

N-type InSb single crystals with high dislocation density, investigating anisotropy of mobility, Hall effect and transverse and longitudinal magnetoresistance

14 p2503 A69-28734

Differential thermal EMF at room temperature in p-InSb as function of concentration for different electron and hole scattering mechanisms

14 p2503 A69-28790

Dislocations effect on carrier mobility and concentration in p-type and n-type InSb crystals

14 p2507 A69-29646

Absorption band edge position in p type indium antimonide thin films after heating, showing forbidden bandwidth function relationship to film thickness

15 p2666 A69-30044

Slow neutrons irradiation compensated high resistivity p-InSb current instability

15 p2666 A69-30058

Cyclotron resonance of minority carriers measured in p-type InSb, giving temperature dependences of absorption derivative and field ratio to line half width

15 p2667 A69-30068

Indium antimonide crystals polarity effect on photoeffect, analyzing quantum yields and energy spectrum

15 p2667 A69-30076

Selenium diffusion in indium antimonide, determining concentration gradients in junction space charge region by capacitance method

15 p2669 A69-30714

Nonuniform electrical resistivity distribution in InSb single crystals as function of growth direction

15 p2670 A69-31049

Negative resistance section of current-voltage curve for long diodes of p-type indium antimonide, noting magnetic field effects on electrical breakdown

15 p2581 A69-31149

Hole mobilities in InSb due to phonon and ionized impurities scattering on basis of strain potential constants

16 p2824 A69-31575

InSb thin films prepared by flash evaporation, discussing Hall measurements at various temperatures and electron mobility dependence on film thickness

18 p3182 A69-34348

Helicon wave dimensional resonance in n-InSb plasma waveguides at different wavelengths relative to wall thickness

19 p3383 A69-36479

Band structure and optical constants of InSb, InAs and GaSb, calculating linear momentum matrix elements and state density with spin-orbit effects included

19 p3385 A69-36515

Combined resonance transition in n-type InSb by IR radiation, plotting intensity against magnetic field for different carrier concentrations to infer band structure

19 p3385 A69-36520

Electroreflection study of inversion asymmetry and warping induced interband magneto-optical transitions in InSb, employing low temperature electric field modulation technique

19 p3386 A69-36521

Coherent emission from injection electron-hole plasma in indium antimonide without magnetic field, noting roles of crystal thickness and pinch effects

19 p3387 A69-36532

Hot electron behavior in n-type InSb under magnetic fields at 4.2 and 1.7 K, plotting current-voltage and current-Hall voltage characteristics, etc

19 p3388 A69-36544

Semiconductor plasma production effects and pinching and microwave radiation in InSb plasma, discussing impact ionization, two photon absorption and plasma lifetime

19 p3389 A69-36545

InSb instabilities and time dependence of transverse breakdown, performing Hall effect measurements on n-type InSb at 77 K

19 p3389 A69-36546

InSb single crystals impurities incorporation and distribution, concluding electrical properties vary with homogeneity or heterogeneity of dopant microdistribution

19 p3389 A69-36547

Temperature dependence of g-value in spin resonance in partially degenerate region in pure n-type InSb and InAs

19 p3389 A69-36549

Low temperature energy band gap in n-type single semiconductor crystals of In-Sb-Bi alloys analyzed by measuring Hall constant and optical absorption coefficient

19 p3390 A69-36552

Electron effective mass, density and mobility in /000/ and /111/ conduction band minima in Te-doped degenerate GaSb-InSb single crystals

19 p3390 A69-36555

Energy levels of multicharge acceptor centers and level splitting in InSb and GaAs deformed crystals, using multizone approximation

21 p3781 A69-39067

Frenkel defects in light irradiated p-type InSb single crystals at subthreshold radiation energies

21 p3782 A69-39144

Spectral dependence of optical absorption in InSb thin films under conditions of quantum dimensional effect, considering allowance for nonparabolic conduction zone

21 p3783 A69-39560

Negative surface potential effect on noise and photoconductivity in Ge doped p-type InSb single crystals at low temperature in vacuum

24 p4362 A69-43738

INDIUM ARSENIDES

Vacuum deposited n-type InAs films magnetoresistance coefficient dependences on length-to-width ratio, homogeneity moving carriers size and magnetic inductance

01 p0136 A69-10254

Solid solutions microstructure and electrical conductivity in InAs-CdS and InAs-CdS and InAs-CdSe systems

02 p0297 A69-11882

Dislocations effect on decomposition rates of solid solutions of InAs and Au, Ag or Cu

03 p0484 A69-13283

Temperature dependence of partial pressure of saturated As vapor over solid solutions of InAs-GaAs of different composition

04 p0642 A69-14938

Low temperature spectral distribution of impurity induced photoconductivity in p-type InSb crystals prepared by zone refining

04 p0644 A69-15270

Quantum oscillations of Maggi-Righi-Leduc (MRL) effect in n-InSb and n-InAs samples from single crystals at liquid helium temperature

06 p0979 A69-16992

Single crystal InAs wafers reflection spectra from specular surfaces, obtaining direct interzone transition values and fine structure

06 p0979 A69-16995

Charge carrier lifetime measured in intrinsic conductivity range of Cd doped InAs to define recombination mechanism, relating temperature dependence to surface impurities recombination

06 p0979 A69-16997

Cadmium ionization energy in InAs using heat treatment in hydrogen to eliminate anomalies

06 p0979 A69-16998

Structural and electrical properties of indium antimonide and arsenide films, noting dependence of electron concentration and mobility on thickness

06 p0981 A69-17892

InAs solid solutions reflection spectra with CdTe, CdS, CdSe and ZnTe compounds, determining conduction bands

07 p1198 A69-18511

Self modulated radiation modes of Te-doped n-type InAs injection lasers

07 p1148 A69-18685

Electrical resistance and Hall coefficient measurement in InAs-GaAs solid solutions system, giving temperature dependence of electron mobility

07 p1199 A69-18689

N type surface layer in p type sample noting effect on Hall constant and relationship to temperature

09 p1555 A69-21472

Vacuum deposited n-type InAs films magnetoresistance coefficient dependences on length-to-width ratio, homogeneity, moving carriers size and magnetic inductance

09 p1559 A69-22647

InAs thin film sensors using Hall effect to measure magnetic fields at cryogenic temperatures

10 p1696 A69-23717

InAs-InP solid solutions diffusion rate and lattice constant for various compositions

12 p2144 A69-26587

Indium arsenide electrical parameters analyzed by kinetic effects, considering conductivity, thermal and magnetothermal EMF and transverse Nerst-Ettingshausen effect

15 p2666 A69-30066

N type surface layer in p type sample noting effect on Hall constant and relationship to temperature

15 p2669 A69-30717

Solid solutions microstructure and electrical conductivity in InAs-CdS, InAs-CdS and InAs-CdSe systems

18 p3182 A69-35042

Band structure and optical constants of InSb, InAs and GaSb, calculating linear momentum matrix elements and state density with spin-orbit effects included

19 p3385 A69-36515

Indium arsenide injection laser observed for self modulation at LF modes, discussing nonMarkovian character of photon density relaxation

19 p3338 A69-36537

Anomalous phenomenon in resistance and magnetoresistance of cleaved InAs surface, plotting temperature and magnetic field variation effects, proposing explanation of anomaly

19 p3388 A69-36543

Temperature dependence of g-value in spin resonance in partially degenerate region in pure n-type InSb and InAs

19 p3389 A69-36549

INDIUM COMPOUNDS

Nonlinear voltage dependence on current in p-type indium selenide single crystals, detecting negative resistance under pulsed electric field

22 p3992 A69-40602

INDIUM PHOSPHIDES

Indium phosphide p-n junction current-voltage characteristics various temperatures, considering degree of doping effect

01 p0139 A69-10885

Electrical properties of p-n junctions of diffused Cd or Zn in indium phosphide

02 p0294 A69-11628

Thermal EMF in indium phosphide crystals as function of temperature, electron concentration and magnetic field strength, determining effective mass of electrons

03 p0489 A69-13889

Radiative recombination in p-n junctions in InP at various temperatures

03 p0492 A69-14166

Hydrostatic pressure effect on recombination emission in indium phosphide p-n junctions

04 p0639 A69-14428

Hall effect and magnetoresistance for compensated n-InP samples, discussing dependence on magnetic field

06 p0978 A69-16987

Magnetic susceptibility of InP-GaAs solid solutions at various temperatures and for varying GaP content

07 p1200 A69-19013

Gold diffusion and solubility in indium phosphide, analyzing temperature and vapor pressure effects

09 p1555 A69-21470

Thermal EMF in indium phosphide crystals as function of temperature, electron concentration and magnetic field strength, determining effective mass of electrons

11 p1939 A69-25690

Vapor phase epitaxial production of indium arsenic phosphide crystalline layers, discussing electron mobilities, electrical resistivities and doping

12 p2142 A69-25934

InAs-InP solid solutions diffusion rate and lattice constant for various compositions

12 p2144 A69-26587

Indium phosphide p-n junction current-voltage characteristics at various temperatures, considering degree of doping effect

12 p2144 A69-26649

Gold diffusion and solubility in indium phosphide, analyzing temperature and vapor pressure effects

15 p2669 A69-30715

Energy band gap variation as function of composition in In-Ga-P semiconductor crystals

19 p3390 A69-36553

Electric fields reducing recombination radiation intensity from bulk ionized GaAs and InP and shifting spectrum to lower energies, discussing self absorption

23 p4198 A69-41499

INDIUM SULFIDES

Field distribution and potential drop in semiconductor field emitter, noting nonlinear effects in indium trisulfide, electron mobility and multiplication factor

05 p0806 A69-15630

INDIUM TELLURIDES

InTe phase recrystallization in thin films composed of two InTe phase mixtures, showing random concentrations and distribution of centers growing as spherulites

24 p4361 A69-42993

InTe phase formation in thin film composed of two InTe phases, showing dependence on annealing in high vacuum and substrate temperature

24 p4361 A69-42994

Component proportion and diffraction spectrum of macroblock thin films of indium telluride phase of In-Te system, using X ray and microanalysis

24 p4361 A69-42995

INDOLES

NT TRYPTOPHAN

Mass spectra peaks of N-Acyl-2-indolinols fragmentation processes upon electron impact, noting compounds predominance in open chain tautomer gas phase

15 p2561 A69-30407

INDUCED FLUID FLOW

U FLUID FLOW

INDUCERS

U INTAKE SYSTEMS

INDUCTANCE

Inductive converters accuracy calculation by statistical method based on probability theory

13 p2259 A69-27424

Kinetic inductance measurements in linear circular and rectangular cylindrical superconductors, giving inductance temperature dependence for wires and both thick and thin films

17 p3016 A69-33783

INDUCTION

Perturbation method determination of gravitational induction for quasi-static axisymmetric systems

04 p0661 A69-15190

INDUCTION HEATING

Induction plasma device of continuous operation to simulate NASA designed gas core space propulsion reactor [AIAA PAPER 68-712]

22 p3979 A69-40548

INDUCTION SYSTEMS

U INTAKE SYSTEMS

INDUCTORS

Electromagnetic forming principles and applications describing large capacitor bank facility design for multipurpose research [ASTME PAPER MR68-418]

02 p0252 A69-11798

Maxwell equations solution for linear induction MHD machine coil area field components, allowing for finiteness of magnetic permeability of iron

07 p1059 A69-19028

Composite transistor simulation of circuit inductor effect for synthesizing frequency selective circuits

08 p1286 A69-20834

Io as unipolar inductor, analyzing interaction with Jupiter magnetosphere and decimetric synchrotron radiation

13 p2337 A69-27552

E shaped cores for miniaturized transformers and inductors from high permeability plastic bonded materials

13 p2237 A69-28586

Field equations for plane-parallel induction MHD machines with allowance for winding zone thickness and magnetic permeability of iron

14 p2405 A69-29914

Tubes faults monitoring in three phase Graetz converter bridges by measuring voltage across DC smoothing inductor

15 p2575 A69-30180

Coil under alternating current interacting with laminated conducting structure, giving recurrence formula for calculating deflector voltage

24 p4296 A69-42653

INDUSTRIAL PLANTS

Ammonium perchlorate grinding and blending facility, discussing process flow, machinery, etc [AIAA PAPER 69-516]

16 p2767 A69-32664

Monograph on laser communication system in IR for industrial environments

22 p3900 A69-40617

INDUSTRIAL SAFETY

Treatment procedure and preventive programs outlined for acute exposure to toxic rocket fuels or oxidizers

02 p0204 A69-12498

Industrial and workman safety concept evolution, discussing role in product design engineering [SAE PAPER 680676] 03 p0433 A69-13449

Explosive welding principles, applications, materials limitations and advantages, stressing safeness and low cost 18 p3151 A69-35479

INDUSTRIES

NT AEROSPACE INDUSTRY

NT AIRCRAFT INDUSTRY

NT DEFENSE INDUSTRY

Industrial loyalty and trade secrets, discussing preservation of forms of intellectual property posed by mobile employee and management policies 01 p0180 A69-10991

Estimate accuracy and project selection models in industrial research, examining company data for miscellaneous, technical and commercial failure 05 p0849 A69-15981

Data transmission techniques for aerospace and industrial applications, discussing radio link 08 p1271 A69-19906

Value engineering application to engineer recruiting phase of industrial relations 13 p2382 A69-28093

Value engineering proposal costs sustained by maintenance and overhaul industry in government contract negotiations, discussing reimbursement and proposed central agency 13 p2383 A69-28099

Value engineering ultimate objectives in industry, discussing engineering and procurement role in prorating goal to applicable departments 13 p2383 A69-28101

Behavioral differences between engineers and scientists with reference to work environment 15 p2721 A69-31073

Planning for safety of future supersonic air traffic including financing and coordination activity of government and industry 22 p4054 A69-41131

INELASTIC BODIES

U RIGID STRUCTURES

INELASTIC COLLISIONS

Elastic and inelastic collisions between deformable bodies, using Michelson interferometer with He-Ne laser as source 02 p0282 A69-12607

Inelastic collisions effect on electron energy distribution in low temperature diffusion dominated discharges 04 p0637 A69-15047

Free electron kinetic equation including inelastic electron-atom collisions derived for nonequilibrium low temperature plasma, showing interrelated electronic and atomic energy distribution 05 p0802 A69-15889

Physics of plasmas, Volume 2, Weakly ionized gas, covering inelastic collision, free electron scattering, intermediary plasmas, etc 06 p0963 A69-17165

Rotational inelastic transitions in atom-diatom collisions, discussing restricted distorted-wave approximation, transition probabilities, impact parameters, inelastic and glory quenching, etc 07 p1185 A69-19302

Cross sections for inelastic interactions of electrons with atoms and heavy impurity ions and processes of atomic excitation 07 p1195 A69-19652

Kinetic equations for polyatomic gases obtained by extending 13 moment approximation to solve inelastic Boltzmann equation, resulting in 17 moment approximation 08 p1357 A69-20784

Inelastic transport cross sections for Lyman alpha transitions in hydrogen 08 p1357 A69-20814

Rotational excitation and scattering cross sections for rigid diatomic molecules reduced to yield distorted wave approximation, resulting in inelastic transition probabilities 10 p1726 A69-23524

Inelastic interactions cross sections of slow electrons with adsorbed particles on W surface as function of temperature in surface bond vibrational region 12 p2132 A69-26114

Energy loss during inelastic collisions between electrons and ionospheric particles, determining ionospheric heating by UV radiation 13 p2252 A69-27614

Elastic and inelastic elementary particle collisions described by Feinman diagrams, discussing computer results for high energy particle interactions 13 p2303 A69-28369

High energy particle collisions, calculating inelastic interactions between cosmic nuclei 13 p2330 A69-28370

High energy inelastic particle collisions observed at high altitude station, using Monte Carlo computations for nucleon-nucleon collision model 13 p2330 A69-28374

Inelastic interaction cross sections of nuclear active particles at C and Fe in 70 to 1000 gev energy range 13 p2330 A69-28383

Soviet book on nuclear interactions in spacecraft shielding covering proton-Al nuclei inelastic interactions, secondary radiation, solar radiation effects, radiation belts, etc 14 p2481 A69-29817

Integrodifferential equation derived and solved for evolution of collisional model of asteroids and debris 14 p2526 A69-29879

Ionosphere D region low field conductivity in presence of high field disturbing signal, assuming inelastic electron-neutral particle collisions 16 p2850 A69-32190

Frequencies of charged secondaries numbers emitted from nucleon-nucleon and pion-nucleon inelastic collisions, observing multiplicity regularity 18 p3177 A69-35009

Hydrogen molecular ion dissociation due to ion-molecule inelastic collisions, comparing measured and calculated velocity distributions of protons produced 19 p3375 A69-35985

Inelastic collisions and radiation effects on transport properties and shock structure in high temperature gases, obtaining density and temperature profiles 19 p3448 A69-36149

Transverse momentum of fireball particles emitted in high energy inelastic collision related to emission angle and energy in accelerators 19 p3396 A69-36644

Inelastic collision cross sections for low energy interactions among electrons, ions, atoms and molecules determined as function of temperature, using approximate methods 23 p4194 A69-41520

Low energy electrons energy loss by inelastic collisions in moving through atmosphere, estimating cross sections and loss rates 24 p4351 A69-42763

INELASTIC SCATTERING

Angular correlation of inelastically scattered alpha particles and gamma rays emitted from 2-plus state of Sn 120 03 p0469 A69-13098

Angular correlation between inelastically scattered 42 Mev alpha particles and emitted gammas from 2-plus Ni 58 03 p0470 A69-13100

Transport phenomena analysis in n-InSb semiconductors during elastic/inelastic current carrier scattering 03 p0492 A69-14171

Cross section calculations for elastic and inelastic electron collisions with atoms, ions and molecules and ionization of atomic systems by electrons and photons 07 p1187 A69-19660

Quantum theory of line broadening and shift, relating adiabatic and diabatic collisions to elastic and inelastic scattering of perturbers 08 p1363 A69-20464

Optical potentials for rotational and vibrational transitions in inelastic molecular collisions, considering adiabatic and sudden approximations 08 p1358 A69-21008

Channel coupling effects in elastic electron-atom collisions involving electric dipole transitions, noting phase shifts and differential cross section 09 p1542 A69-21623

Inelastic interactions between Tev cosmic particles and light element nuclei, describing design and operation of measuring apparatus and derivable data 12 p2093 A69-26583

Inelastic interaction cross sections of nuclear active cosmic ray particles with atomic Fe and Pb in 100 to 1000 gev range 13 p2330 A69-28384

Inelastic scattering cross sections calculated, comparing results for various nuclear states expressed as Wood-Saxon radial and harmonic oscillator functions 14 p2504 A69-29006

Core polarization effects in inelastic scattering cross sections for several nuclei in 2s-1d shell, using Hartree-Fock wave functions and Born approximation 14 p2487 A69-29007

Inelastic proton scattering cross sections for target nuclei in 2s-1d shell calculated in distorted wave Born

approximation with projected Hartree-Fock wave functions 22 p3988 A69-41045

INELASTICITY

U ELASTIC PROPERTIES

INEQUALITIES

Rearrangement inequalities for positivity of nonquadratic transformations, discussing stability of nonlinear feedback loop described by difference equations 06 p0904 A69-17943

Control sets corresponding to desired stability behavior of controlled motion, giving theorem concerning differential inequality 11 p1910 A69-25412

Upper bounds for Bernstein-Kolmogoroff multidimensional inequalities, analyzing independent random vectors 11 p1910 A69-25698

Inequality theorems for multidimensional functional Volterra equations formulated and proved, deriving upper and lower solutions 13 p2290 A69-28684

Inequalities for coefficients of univalent functions 22 p3975 A69-40453

INERT ATMOSPHERE

Antifriction characteristics of hard lubricating coatings based on molybdenum disulfide and graphite in inert gas atmosphere and vacuum, determining thermal stability temperature ranges 13 p2269 A69-28053

Powder metallurgy all inert processing method for producing nickel base superalloys forgings, discussing microstructure, reproducibility, mechanical properties, etc [ASM PAPER GG-8-3-3] 21 p3745 A69-38929

INERT GASES

U RARE GASES

INERTIA

NT MACH INERTIA PRINCIPLE

Inertia effect of flow between eccentric cylinders with rotating outer cylinder, calculating pressure and shearing distribution and force on inner cylinder 01 p0059 A69-10307

Fatigue life, kinematics, dynamics, etc, of thrust loaded ball bearings, considering inertial effects of hollow balls 01 p0087 A69-10908

Axisymmetric form of stability loss of cylindrical shell under effect of axial load suddenly applied along generatrix, considering inertia forces and obtaining differential equations 06 p1021 A69-17181

Longitudinal and transverse vibrations of viscoelastic rods excited by inertia with aid of linear oscillator subjected to harmonic stress, using Kelvin-Voigt model 07 p1233 A69-19326

Inertia of electrically charged spherical body calculated on basis of relativistic stress energy 08 p1352 A69-20756

Inertia effect on incompressible fluid film pressure between two oscillating parallel plates, considering Reynolds number 12 p2102 A69-26241

Complex structures lumped weight and inertia parameters automatic computation based on finite weight element method, using SCOWL computer program 14 p2533 A69-29025

Inertial and gravitational mass equality reexamined, considering Galileo, Newton and Eotvos experiments 14 p2486 A69-29647

Oscillations and stability of cylindrical shell in gas flow taking into account inertia forces 16 p2875 A69-32287

Inertial characteristics determination error influence of solid body on damping system parameters 18 p3171 A69-34562

Spacecraft spherical motion about mass center under inertial force using Euler differential equations 21 p3830 A69-39838

Earth rotation rate variations connected to longitude variations of continentals time services, noting atmospheric circulation and inertial forces role 22 p4024 A69-40609

Inertial motions, equipotential surfaces and Coriolis forces on earth ellipsoid, discussing pendulum-like oscillations 24 p4346 A69-43156

INERTIA MOMENTS

U MOMENTS OF INERTIA

INERTIA PRINCIPLE

NT MACH INERTIA PRINCIPLE

- Secularly stable figures of equilibrium of rotating heterogeneous fluids of planetary size, noting dependence on laws of inertia and gravitation
03 p0513 A69-13780
- Inertial servomechanisms actuators, discussing dynamic characteristics, power, vibration damping, matching, couplers, etc
11 p1826 A69-25119
- INERTIA WHEELS**
U REACTION WHEELS
- INERTIAL ACCELEROMETERS**
U ACCELEROMETERS
- INERTIAL COORDINATES**
Inertial navigation systems trajectory parameters errors due to inaccurate initial coordinates input, deriving trigonometric functions for autonomous error determination
21 p3760 A69-38572
- Absolute atmospheric kinetic energy, comparing equations deduced from Euler equations with equations deduced from equations of motion for inertial system
24 p4345 A69-43151
- INERTIAL FORCES**
U INERTIA
- INERTIAL GUIDANCE**
NT STRAPDOWN INERTIAL GUIDANCE
Soviet book on inertial control of ballistic rockets covering rocket flight deviations measured by onboard sensors and computer
01 p0113 A69-10994
- Low visibility instrument landing of aircraft using ILAS and inertial guidance
01 p0114 A69-11012
- Inertial guidance system for ELDO launch vehicles
07 p1176 A69-18491
- Inertial guidance system synthesis for infantry missile with 1 n mile range against small hardened targets requiring 3 ft maximum miss distance
12 p2129 A69-26791
- Magnetic suspension device replacing mechanical bearings of inertial guidance systems gyro rotors, evaluating device strength and stability
14 p2479 A69-29492
- Europa 1 first stage attitude control system adaptation to Europa 2 requirements, discussing design modifications and improvements and inertial guidance system introduction
16 p2866 A69-31726
- Microminiature Elliott MCS 920 M digital computer for inertial guidance of CECLES-ELDO launcher, discussing construction, code, interrupt, guidance system and functions
20 p3501 A69-37391
- Spring restrained, momentum-wheel inertial orientation and stabilization system for exoatmospheric vehicles, noting mission constraints and hardware parameter variations allowances
21 p3819 A69-39214
- Reliability assessment of ballistic missile inertial guidance system, discussing objectives and requisites
22 p3953 A69-40028
- Programming and checkout of computer for Edo inertial guidance system, including flight simulation and autopilot tests
[AIAA PAPER 69-961] 22 p3978 A69-40342
- INERTIAL NAVIGATION**
NT GIMBALLESS INERTIAL NAVIGATION
Stabilized platform vibration in inertial navigation system with integral correction
01 p0112 A69-10086
- Schuler gyroscopic pendulum, noting magnitude requirement for gravitational field used in inertial navigation
02 p0248 A69-11593
- Soviet book on kinematics of inertial navigation systems covering systems classification, equations derivation and computer algorithms for error analyses
02 p0278 A69-11793
- Navigation system for American SST noting use of Doppler radar and inertial navigation
02 p0278 A69-12238
- Inertial navigation for commercial aircraft, discussing Sagem-Ferranti and Litton systems
02 p0278 A69-12239
- Error reduction in initial azimuth alignment and azimuth and level axis gyro drifts in long range air transport gyro accelerometer inertial systems
02 p0278 A69-12361
- Laser gyro in future inertial navigation systems for Category 1 landing without position updating
03 p0463 A69-13210

- Mathematical modeling of gyro drift rate in inertial navigation based on stationary and nonstationary time series analysis
03 p0463 A69-13213
- Equations for instability of stabilized platform of inertial navigation system with viscous friction in accelerometers
06 p0954 A69-16824
- SGN-10 inertial navigation system evaluation by Pan American World Airways
06 p0955 A69-17663
- Doppler radar inertial navigation, discussing developments in sensors and digital computers
06 p0956 A69-17859
- Maximum likelihood smoother using measurements containing correlated noise for application to continuous linear dynamic systems such as inertial navigation
06 p0956 A69-17938
- Hybrid OMEGA inertial system for following vehicle maneuver without lag developed by combining Schuler tuned inertial data and radio position data
07 p1177 A69-19209
- Aircraft position and velocity in directions normal to ILS reference path by correlation with inertial navigation system, noting minimal time controller
07 p1177 A69-19213
- Integrated inertial aircraft navigation with velocity and position aids, discussing in-flight calibration capabilities, performance under quick-reaction constraints and digital simulation results
08 p1349 A69-21196
- Optimum inertial/Doppler satellite navigation system, discussing position fixes application in resetting
08 p1349 A69-21199
- VOR/DME ground facilities accuracy improvement by complementing navigation computation with signals from inertial navigation system
[SAE PAPER 690338] 11 p1914 A69-24499
- Inertial navigation systems error analysis based on method of state variables
11 p1914 A69-25434
- Inertial navigation platform principles including acceleration and position of vehicle, single axis platforms and stabilized element coordination
12 p2078 A69-25872
- Pure inertial navigation system support by supplying additional or redundant navigational information, considering space flight applications and earth related problems
12 p2128 A69-25873
- Inertial navigation system sensors including one and two axis, laser, vibratory, gyroflex and free rotor gyros
12 p2078 A69-25874
- Deterministic linear observation systems and Kalman optimum linear filters application to performance improvement of inertial navigation systems
12 p2128 A69-26065
- Concorde SST equipment and systems noting microelectronics, automatic control, inertial navigation, head-up displays, linear instruments and hydraulic systems
12 p2091 A69-26360
- Litton LTN-51E inertial navigation system accuracy and reliability evaluated on basis of transpacific flights
[SAE PAPER 680299] 13 p2296 A69-28103
- Optimal linear space navigation policies including integrated nongravitational acceleration output from inertial measuring unit
14 p2479 A69-29487
- Ground testing method to evaluate inertial navigation systems dynamic errors by programmed platform drift rates, position output comparisons and error source identification
14 p2479 A69-29490
- Optimal navigation system for supersonic Concorde aircraft, discussing in-flight and terminal navigation methods
14 p2480 A69-29859
- Doppler and inertial self contained systems for long range navigation, considering air traffic control separation standards
15 p2651 A69-31544
- Inertial navigation system theory that uses increased numbers of newtonometers/force measuring devices/in place of gyroscopic sensitive elements
16 p2791 A69-32283
- Gyrocompassing precision problems related to gyro drift, input axis deviation and base motion compensation, describing inertial navigation platform alignment to true north
17 p2977 A69-34081
- Doppler inertial system with remote attitude capability, detailing sensor operation by airborne computers
17 p3002 A69-34097

- Observer theory application to hybrid inertial navigation systems, discussing error estimation and correction, real time mechanization, eigenvalues, etc
17 p3003 A69-34099
- Vibrations damping coefficient for asymptotic stability of inertial navigation system platform, determining stabilization errors
18 p3134 A69-34555
- Gyroscopic apparent rate meters generating steering moments in inertial navigation systems for determining moving object position and course
18 p3134 A69-34556
- Inertial aircraft navigation, describing instrument and error analyses with regard to simulation, error propagation and total system error
18 p3169 A69-34850
- Boeing 747 design and development, discussing aircraft characteristics, performance, inertial navigation system, production costs, etc
[SAWE PAPER 746] 18 p3091 A69-34907
- Kalman recursive filtering method applied to inertial navigation systems resetting
19 p3286 A69-36645
- Inertial navigation systems technology, discussing man machine dialog, alignment, etc
19 p3371 A69-36703
- Cost and maintenance calculations for inertial navigation system [INS/ based on three systems per aircraft, assuming 4000 hr/year aircraft utilization
19 p3371 A69-36734
- Inertial navigation systems trajectory parameters errors due to inaccurate initial coordinates input, deriving trigonometric functions for autonomous error determination
21 p3760 A69-38572
- Strapdown redundant experimental sensor inertial navigation package containing gyros and accelerometers, discussing signal real time processing by digital computer
[AIAA PAPER 69-851] 21 p3762 A69-39379
- Passively isolated and actively stabilized platform for inertial navigation components and systems tests
[AIAA PAPER 69-863] 21 p3690 A69-39423
- Guidance and navigation flight tests, demonstrating system performance improvements by onboard inertial system communicating with external navigation aid
[AIAA PAPER 69-842] 21 p3765 A69-39429
- Cumulative error in flight vehicle position determination by inertial navigation system, showing dependence on constant acceleration components
22 p3978 A69-40252
- Three channel inertial ship or aircraft navigator for determining gravity vector, using earth gravity field model
23 p4162 A69-41320
- Airline area navigation test programs involving use of VOR/DME signals and inertial navigation system within air traffic control system
23 p4185 A69-41662
- V/STOL aircraft radar inertial navigation system, describing approach and landing phase flight test results
[AAS PAPER 69-401] 24 p4252 A69-42831
- Geodetic and geophysical random uncertainties as fundamental limitations on terrestrial inertial navigation accuracy
[AIAA PAPER 68-847] 24 p4348 A69-43240
- INERTIAL PLATFORMS**
Soviet book on kinematics of inertial navigation systems covering systems classification, equations derivation and computer algorithms for error analyses
02 p0278 A69-11793
- Platform system of ELDO launch vehicle and necessary test and alignment equipment, discussing inertial platform system for future space projects
04 p0629 A69-14809
- Multiframe platform stabilization, analyzing dynamic coupling due to possible avoidance of adjusting moment and effect of coupling on attitude control
04 p0629 A69-14830
- Inertial navigation platform principles including acceleration and position of vehicle, single axis platforms and stabilized element coordination
12 p2078 A69-25872
- Fourth angle driving law for different four gimbal systems used for simulation display and inertial platform isolation
12 p2055 A69-26265
- Optimal linear space navigation policies including integrated nongravitational acceleration output from inertial measuring unit
14 p2479 A69-29487

Low cost inertial measurement unit /IMU/ for commercial and private aircraft, evaluating components and system [SAE PAPER 690337] 15 p2606 A69-30092

Gyrocompassing precision problems related to gyro drift, input axis deviation and base motion compensation, describing inertial navigation platform alignment to true north 17 p2977 A69-34081

Vibrations damping coefficient for asymptotic stability of inertial navigation system platform, determining stabilization errors 18 p3134 A69-34555

Mathematical basis for inertial vertical gyro development, considering Schuler conditions fulfillment with integral position correction 19 p3311 A69-36193

Miniature floated ball gimballess inertial platform construction, functions, readout, digital computer coupling, etc [AIAA PAPER 69-835] 21 p3761 A69-39366

Strapdown gimballess inertial measurement unit with general purpose computer, describing hardware, software and test results [AIAA PAPER 69-850] 21 p3765 A69-39426

INERTIAL REFERENCE SYSTEMS

Nonorthogonal multisensor strapdown inertial reference unit providing redundant capabilities and optimal performance 03 p0429 A69-13211

Optimizer for shaping control signal of hunting type system with plant in form of nonlinear inertialess element, examining inadequacy for system operation 07 p1115 A69-19757

Analytic platform or strapdown systems application, discussing closed and open loop leveling techniques 08 p1347 A69-19862

Rocket vehicle inertial attitude reference system, discussing flight control 09 p1609 A69-21618

Rigid space concept in gravitation theory, discussing reference systems with nonrigid and rigid background 14 p2484 A69-28863

Inertial systems in homogeneous isotropic expanding universe model, giving expression for line element accounting for Hubble effect 15 p2654 A69-31495

Time and fuel optimization of angular momentum alignment and nutation elimination of spin stabilized bodies with inertial reference direction 18 p3208 A69-34775

Attitude and heading reference devices for aircraft navigation, describing instruments, gyroscopes and gravity sensors 18 p3169 A69-34853

Strapdown inertial reference unit system for inflight reliability and maintainability, discussing design and components 19 p3370 A69-35803

Gyroscopic platforms automatic stability relative to inertial reference system, considering functional equations and error computation 21 p3760 A69-38734

Precision azimuth reference accuracy standards with confidence limits for gyrocompass evaluation, emphasizing astro and transfer angle repeatability [AIAA PAPER 69-859] 21 p3725 A69-39387

Motion analysis of symmetrical physical pendulum having mobile fulcrum for geocentric vertical indicator possibility 21 p3727 A69-39830

INERTIALESS STEERABLE ANTENNAS

Multiple beam electronically steerable retrodirective antenna array with automatic inertialess compensation for altitude or beacon location 02 p0212 A69-12816

Phased arrays applied to inertialess electronic steering of satellite antennas, discussing digitally steered, retrodirective and hybrid matrix arrays 17 p2942 A69-34083

Semiconductor phase shifting for inertialess antenna scanning at microwave to millimeter wavelengths, describing diode construction with emphasis on solving insertion loss [ONERA-TP-712] 23 p4143 A69-42519

INFARCTION

Experimental myocardial infarction in dogs, examining lysosomal enzymes activity changes in soluble and particle-bound fraction 24 p4259 A69-42636

Fibrosis histological patterns of left ventricular papillary muscles from comparison of hearts with myocardial infarction, noting acute and healed mural lesions 24 p4261 A69-42724

Supraventricular arrhythmias after acute myocardial infarction, noting benefit of early DC shock 24 p4262 A69-42729

INFECTIOUS

U INFECTIOUS DISEASES

INFECTIOUS DISEASES

NT INFLUENZA

Infectious diseases in space flight, considering environment role in infection transmission, occurrence and severity 20 p3479 A69-37973

Space cabin environment simulation effects on resistance to infection caused by pneumonia and influenza virus in rats 23 p4108 A69-41832

White mice survival rates and blood morphology and sedimentation rates in low ambient pressure confinement following infectious bacteria injection 24 p4267 A69-43397

INFINITY

Unlimited extrapolation into infinity to determine ranges of applicability of theories in relativistic cosmology noting paradoxes 14 p2516 A69-28867

INFLATABLE SPACECRAFT

U BEACON SATELLITES

U EXPLORER 22 SATELLITE

INFLATABLE STRUCTURES

NT BALLOONS

NT BEACON SATELLITES

NT EXPLORER 22 SATELLITE

NT HIGH ALTITUDE BALLOONS

NT METEOROLOGICAL BALLOONS

NT TETHERED BALLOONS

Inflatable solar shields for thermal protection of space vehicles utilizing cryogen propellants 06 p1017 A69-17609

Structural and aerodynamic developments in attached inflatable decelerators for deployment of payload at supersonic speeds [AIAA PAPER 68-929] 21 p3647 A69-39015

Recovery system for high altitude sounding rocket payloads, noting air inflated flotation device, payload separation and parachute deployment [AIAA PAPER 68-959] 21 p3820 A69-39227

Inflation effect on circular cylindrical cantilever beam subsequent response to bending loads, using theory of small deformations superimposed on large deformations 23 p4227 A69-41881

Large deflections of circular air mat plates consisting of inflatable structures of two membranes connected by inextensible cords network 24 p4405 A69-43688

INFLATING

Automatic inflators for life jackets and survival gear in emergencies activated after submersion in water 06 p0877 A69-16955

Canopy filling time for parachutes under infinite mass conditions, using continuity equation and parachute inflation concept [AIAA PAPER 68-12] 17 p2902 A69-34032

Initial phase of parachute inflation in incompressible flow [AIAA PAPER 68-927] 20 p3461 A69-37165

INFLUENCE COEFFICIENT

NT STRUCTURAL INFLUENCE COEFFICIENTS

Longitudinal stability derivatives prediction for rigid and elastic airplanes, using influence coefficient method [AIAA PAPER 69-131] 06 p0868 A69-18134

Influence function for vertical wind profile from pressure gradient field 09 p1536 A69-21867

Influence coefficients for compressible flow processes involving area, friction and total temperature changes 12 p2063 A69-26799

INFLUENZA

Resistance to bacterial pneumonia and influenza infection in space cabin environment tested on mice in simulation chamber 07 p1067 A69-19432

Specific antibody formation to influenza A virus vaccine /strain PR sub s/ in hibernating ground squirrels /Citellus tridecemlineatus/ 08 p1263 A69-20173

INFORMATION

U MATHEMATICAL TABLES

U TABLES [DATA]

INFORMATION PROCESSING

U DATA PROCESSING

INFORMATION RETRIEVAL

Charge image detector for reading information as extended spatial charge distribution on dielectric layer surface, using vibrating conducting probe scanner 02 p0248 A69-11822

Large scale information displays for group sharing in air traffic control, military operations and organization management 02 p0250 A69-12159

Scientific and technical information flow sources, showing DOD user need within defense industry and importance of local work environment 02 p0204 A69-12219

Human factors evaluation of computer based information storage and retrieval system using questionnaire and interview techniques 02 p0204 A69-12220

USAF accident information, reporting and retrieving, describing Directorate of Aerospace Safety structure and functioning 06 p1041 A69-16843

NASA scientific and technical information program for building technical data and literature repository for scientists, engineers and technical managers, describing IAA and STAR [UN PAPER 68-95317] 06 p1043 A69-17068

Chemical kinetic data evaluation, discussing compilation, production and publication programs, material content and arrangement and reliability estimates [WSCI PAPER 68-47] 07 p1073 A69-18320

Solid logic technology /SLT/ computer circuits, discussing IBM 360 computer reliability, failure analysis information retrieval, SLT module and failure rate 11 p1843 A69-24341

Soviet book on automated information retrieval systems covering computer languages, search in complex ordered codes, translation from Russian into computer language, etc 13 p2225 A69-27933

Saturn software configuration accounting and reporting system for document change and information retrieval 18 p3105 A69-34269

Dynamic Automated Reporting Technique /DART/ system for on-line conversational information storage and retrieval for use in large programs management 18 p3107 A69-35095

NASA current awareness service SCAN /selected current aerospace notices/, promoting selectivity in information transfer to abstract journals, accession lists and bibliographies 21 p3856 A69-39581

INFORMATION SYSTEMS

Saturn software configuration accounting and reporting system for document change and information retrieval 18 p3105 A69-34269

Operational system effectiveness information for reconnaissance drone system including test flights, discussing application to reliability and maintainability in project management 18 p3232 A69-34505

Aerospace technology application to commercial avionics system for cost effectiveness in functions expansion, phase-over, installation, maintenance and operation, discussing added information functions 18 p3108 A69-35069

Dynamic Automated Reporting Technique /DART/ system for on-line conversational information storage and retrieval for use in large programs management 18 p3107 A69-35095

Adaptive predicting filter mathematical model based on information probability, using adaptive systems latent memory 19 p3287 A69-36665

NASA current awareness service SCAN /selected current aerospace notices/, promoting selectivity in information transfer to abstract journals, accession lists and bibliographies 21 p3856 A69-39581

Loran C system for master station time and frequency dissemination, discussing application, coverage, timing accuracy and restrictions 23 p4116 A69-41601

Integrated adaptive data transmission system accepting analog inputs through information compressing sampler or digital inputs by sampling 23 p4121 A69-41760

Top-down initiating technique for forecasting future decade major systems requirements based on information progression [AAS PAPER 69-409] 24 p4417 A69-42803

INFORMATION THEORY

Book on probabilistic information theory-discrete and memoryless models covering information transmission, digitalized sources, generating functions, decoding error, systematic codes and sequential decoding
01 p0037 A69-11030

Multichannel digital data compression simulation, discussing algorithms, buffer queue control, identification coding and system performance measurements
02 p0213 A69-12814

Information theory application to study of biologically stimulating effects of low ionizing radiation doses, thermal energy and other environmental factors
03 p0369 A69-13434

Book on applications of information theory to dynamical systems with random initial conditions and cybernetic systems consisting of communication systems with feedback
04 p0580 A69-14520

Reliable information storage in memories designed from unreliable components
04 p0569 A69-15455

Reliable computation in computing systems designed from unreliable components, considering two models for component malfunctions
04 p0569 A69-15456

Topological codes and simplicial subclass information rates, minimum weights and word length
06 p0948 A69-17866

Informative properties of IR scanning equipment of meteorological satellites, discussing radiative flux measurements and thermal mapping
06 p0929 A69-17979

Subjective pilot ratings based on Cooper scale compared with aircraft handling criterion based on Shannon information theory, discussing pilot error and accident probability
08 p1254 A69-20458

Coherence theory of electromagnetic field from classical/wave/ or quantum/particle/ standpoint, stressing information theory
11 p1915 A69-24455

Entropy minimization in feature extraction by dimensionality reduction with linear transformation of pattern vectors, noting recognition time and storage space savings
11 p1909 A69-25291

Unknown channels classes epsilon capacity applied to estimating capacity of channels with additive noise, discussing models and upper and lower bounds
15 p2570 A69-31142

Communication channel information capacity determination through particle ensembles entropy analysis
19 p3334 A69-35885

Huffman minimum redundancy coding extension to run-length information based on Poisson distribution, including optimization and data compression applications
19 p3272 A69-36262

Information theory, circuit optimization and computer aided design in radio wave information transmission
19 p3286 A69-36432

Fourier transform techniques applications in optics, converting optical signal amplitude and phase information into electrical signal information
19 p3374 A69-36737

Information categories concept defined in relation to formulations of classical mechanics principles, considering theories of Newton, Gauss and Hertz
20 p3576 A69-37585

Data compression from standpoint of epsilon entropy theory, considering precise measure of channel capacity necessary to describe data source
23 p4134 A69-42526

Numerical computation of rate-distortion function $R(D)$ for certain memoryless message sources, discussing bounds, reduction to minimization problem and applications
24 p4284 A69-42719

Rocket IR astronomy in support of big bang hypothesis, considering photoelectric detectors and instrument system
10 p1772 A69-22868

Reddened M supergiant 119 Tauri IR spectra and IR absorption by CO and SiO molecules in stellar atmosphere and silicate mineral in interstellar grains
10 p1786 A69-24104

Double structure in IR near Trapezium region of M42 in Orion Nebula center
10 p1786 A69-24105

IR spectral distribution from region between stars of Trapezium in Orion Nebula
10 p1786 A69-24106

Coronal IR observations during solar eclipse revealing thermal emission zone at predicted interplanetary dust vaporization region
10 p1789 A69-24131

Collection of papers on IR astronomy covering lunar observations, stellar spectra, planetary atmospheres, galactic radio sources, etc
13 p2340 A69-27581

IR extragalactic radio sources including normal radio galaxies, quasars and Seyfert galaxies
13 p2342 A69-27597

IR emission from quasars, noting quasar 3C 273 B and synchrotron mechanism probability
13 p2342 A69-27598

Balloon-borne instrumentation for detection of far IR extended emission regions and bright point sources, describing results of initial flights
13 p2342 A69-27599

IR astronomy and cosmology, considering cosmic microwave background and isotropic radiation significance in distant IR
13 p2342 A69-27601

Instrumental investigation of submillimeter astronomy, noting advancements in semiconductor physics, quantum electronics and space astronomy
13 p2342 A69-27602

Millimeter and submillimeter astronomy, discussing lunar poleward darkening function, solar eclipse measurements, observations of Jupiter, Fourier transform and filter spectroscopy uses, etc
13 p2343 A69-27603

Submillimeter astronomy role for solar and atmospheric studies
13 p2343 A69-27604

Flux collectors and field imagers for IR astronomy, discussing design, construction and dimensions
13 p2239 A69-27605

IR astrophysics, discussing detection, instrumentation, IR stars and stellar evolution
14 p2516 A69-28868

Sunspot of 28 December 1967 studied by far IR scanning with interference and Reststrahlen filters defining bandpass, obtaining umbral temperature
17 p3029 A69-33050

Rocket-borne IR astronomical telescope high altitude observations compared with balloon observations
20 p3605 A69-37800

HgCdTe as IR satellite detector for terrestrial, atmospheric and ocean mapping, IR astronomy and optical communication
24 p4362 A69-43666

Seyfert galaxies IR radiation attributed to dust grains thermal emission of energy absorbed from galactic nucleus
24 p4374 A69-43741

INFRARED DETECTORS

IR optics for indicating dynamic mechanical component reliability via surface temperature variations
01 p0085 A69-10295

Aerial radiation temperature measurement, damping factor of atmosphere and determination of ground and water surface temperatures by radiometry
01 p0110 A69-10693

Temperature distribution over receiving layer of absorption edge image transformer, discussing thermal conduction influence on performance of thin film IR image receiver
04 p0631 A69-15280

Spectral response of fast GaAs point-contact diode in mm and submillimeter wavelength ranges
06 p0893 A69-16939

Onboard solid state neon cryostat for IR detector, noting resistance to missile vibration, acceleration and shock tests
06 p0906 A69-17103

IR scanning systems of meteorological satellites for detection of clouds and various underlying surfaces, determining detection probability and errors
06 p0952 A69-17986

IR evaluation of multilayer etched circuit boards, discussing testing of circuit distributive properties and individual layers
07 p1117 A69-19698

High responsivity high speed performance Ge bolometer detector for very far IR region, discussing performance theory and noise equivalent power
08 p1313 A69-20132

Evaporographic converter to test for striations/schlieren/ in materials used in IR
08 p1314 A69-20384

Eutectic anisotropic InSb-NiSb crystals applied to IR detection, noting sensitivity to carbon dioxide lasers
08 p1373 A69-20866

Rocket IR astronomy in support of big bang hypothesis, considering photoelectric detectors and instrument system
10 p1772 A69-22868

IR detection at sum or difference frequency by employing optically nonlinear crystal and laser in visible and photomultiplier
10 p1704 A69-23656

Aerobee rocket-borne liquid helium cooled telescope for IR night sky observations
11 p1885 A69-24852

Solid state IR imaging using monolithic Ge mosaics of isolated sensor elements, discussing design, structure, fabrication, system readout and operation
11 p1938 A69-25307

Up-converter IR detector noise characteristics for pulse and CW signal detection compared with photoconductive detector
12 p2029 A69-26329

Collision avoidance system for air traffic, discussing false signal discrimination via electronic measurement of light pulse duration from aircraft Xenon discharge beacon lamp
12 p2129 A69-26772

Earth resources remote sensing from spacecraft noting meteorology, oceanography, forestry, agriculture and IR detection of plant diseases and pollution
12 p2192 A69-26978

Airborne IR line scanning systems for latent forest fire detection, discussing discrimination module for automatic identification of hot targets
12 p2193 A69-26994

Airborne IR remote sensing techniques for fire detection, considering marginal and submarginal targets
12 p2098 A69-26995

Airborne scanning spectrometer for IR detection of clear air turbulence, presenting flight records
12 p2098 A69-26999

Airborne IR spectrometer for remote clear air turbulence detection, noting necessity for mirror stabilization in pitch axis
12 p2098 A69-27000

Airborne IR surveys in engineering studies of terrain, discussing instrumentation technology, data interpretability, economic feasibility, etc
12 p2098 A69-27007

Statistical properties of spatial radiance distribution of sky and forest backgrounds in IR, noting one dimensional Wiener spectra
12 p2131 A69-27072

IR radiation detection by photoconductor in microwave resonator noting electric field influence
13 p2223 A69-28639

IR astrophysics, discussing detection, instrumentation, IR stars and stellar evolution
14 p2516 A69-28868

Chopper modulated IR detection system error analysis through minimizing mean square error of approximating output function
14 p2450 A69-29639

IR radiation detection sensitivity emphasizing frequency up-conversion
17 p2969 A69-32839

IR radiometer to measure Jupiter atmospheric temperature by calculating certain constituents heat radiation levels through Planck formula assuming black body properties
17 p2974 A69-33425

Operational flight tests of IR atmospheric turbulence detection system
19 p3367 A69-35631

Differences concerning utilization of IR detectors, discussing nomenclature, fluctuations and definitions of detection, translation and readout
19 p3308 A69-35905

System components for spatial discrimination implementation scheme, discussing IR detector arrays and optical imagery processing
19 p3373 A69-36055

INFORMATION TRANSFER

U COMMUNICATING

INFORMATION TRANSMISSION

U DATA TRANSMISSION

INFRARED ASTRONOMY

Stellar spectra observed with 2.8-14 micron IR spectrometer, noting broad absorption feature near 5 and 8 microns
02 p0327 A69-12713

IR astronomy with ground based instruments noting Mars and Venus spectra, Jovian disk scans, solar radiometry, IR stars, quasars and galaxies
05 p0821 A69-15842

Object discrimination based on IR spectral differences, reviewing calibrated radiometers, relative spectrometers and imaging sensors
19 p3373 A69-36056

IR detector limiting noise voltage /photon noise/ due to photon arrival fluctuations at responsive element determined using Planck radiation law
19 p3309 A69-36059

Spectral parameters effect on IR instrument SNR, discussing range equations of point and extended sources and radiation-noise-limited detectors
19 p3310 A69-36061

IR detectors defined as transducers producing electrical signal proportional to IR power incident on detector, classifying types
19 p3310 A69-36068

IR measurements applications to meteorology, discussing IR radiation characteristics, atmospheric effects, thermal radiation detection and differences between real and black bodies
24 p4316 A69-43507

HgCdTe as IR satellite detector for terrestrial, atmospheric and ocean mapping, IR astronomy and optical communication
24 p4362 A69-43666

INFRARED FILTERS

Interference filter design for IR devices on Fresnel equation basis, analyzing plane electromagnetic wave propagation through stratified dielectric multilayer
19 p3373 A69-36053

Object discrimination based on IR spectral differences, reviewing calibrated radiometers, relative spectrometers and imaging sensors
19 p3373 A69-36056

INFRARED HORIZON SCANNERS
U HORIZON SCANNERS

INFRARED INSPECTION

Dynamic IR inspection to detect fatigue cracks in aircraft and missile structure from distance
11 p1861 A69-24262

IR techniques for nondestructive testing, discussing applications to heat injection and generation and IR test equipment capabilities
15 p2630 A69-31504

Automated IR fatigue crack detection in sonic test facility capable of subjecting large aircraft or missile structures to intense sound fields
15 p2631 A69-31505

Generalized parametric form of IR radiometric scan method applied to void detection problems, designing test techniques and establishing inspection procedure
15 p2631 A69-31506

IR inspection system for detecting interstitially caused alpha segregation in Ti alloy disks
24 p4318 A69-42757

INFRARED INSTRUMENTS

M-20 digital computer program designed for calculating statistical characteristics of signals from IR TV scanning system of Cosmos 122 meteorological satellite
06 p0929 A69-17980

IR polarizing microscope with IR corrected objectives and eyepieces providing higher contrast, sharper focusing and less light scattering
12 p2093 A69-26595

Balloon-borne instrumentation for detection of far IR extended emission regions and bright point sources, describing results of initial flights
13 p2342 A69-27599

IR techniques for nondestructive testing, discussing applications to heat injection and generation and IR test equipment capabilities
15 p2630 A69-31504

Interference filter design for IR devices on Fresnel equation basis, analyzing plane electromagnetic wave propagation through stratified dielectric multilayer
19 p3373 A69-36053

IR nonimage-forming instruments, stressing applications to communications, intrusion detection, ranging, etc
19 p3310 A69-36062

IR equipment to aid air navigation, discussing detection cells, temperature direction finding, mobile source tracking, etc
19 p3371 A69-36705

Monograph on low visibility landing in civil aviation, considering visibility determination methods and equipment and IR sighting devices
20 p3574 A69-38064

HF data transmission system unaffected by high energy electromagnetic fields using GaAs IR emitting diode, glass fiber optic light guide and photomultiplier tube
23 p4121 A69-41768

INFRARED LASERS

Negative Faraday effect and Doppler line width measurements for He-Ne IR gas laser tube by producing beat frequencies in ring laser system
01 p0088 A69-10028

Thin film thermocouple detector for molecular lasers operating in middle and far IR range
05 p0773 A69-16284

Pulsed water vapor laser with single Brewster window for operation between 20 and 120 microns, comparing performance with ordinary laser
05 p0776 A69-16334

Frequency and stability measurements in far IR laser region
07 p1146 A69-18482

He-Ne and He-Xe laser lines in IR tuned by axial magnetic field, observing Stark patterns of organic molecules
[IEEE PAPER C-5] 07 p1150 A69-19050

Iodine IR laser, discussing CW emission obtained at various wavelengths and attributed to electronic transitions in atom
[IEEE PAPER T-5] 07 p1154 A69-19082

Magneto-optic, acousto-optic, electro-optic and free carrier modulation of IR laser beams
07 p1158 A69-19743

Far IR radiation from water vapor laser, noting monochromaticity and strong linear polarization
10 p1702 A69-23160

IR He-Ne laser frequency response determined with inherently swept frequency modulator based on rotating corner reflector
10 p1702 A69-23347

Far IR lasing lines in hydrogen sulfide, sulfur dioxide and OCS, discussing output
10 p1706 A69-24008

Calorimeter for IR carbon-dioxide laser output power measurement, noting range calibration and accuracy
11 p1885 A69-24903

Far IR CW gas laser design for maximum output, discussing pulsed operation, wavelength measurement and radiation detection
11 p1898 A69-25051

Atmospheric boundary layer transparency to gas laser emissions in IR spectrum, determining attenuation factor dependence on humidity and visibility range
12 p2028 A69-25957

Pulsed IR laser optimal Q switching mode by using semiconductor mirror with nonparabolic dispersion law and changing mirror opening moment delay time
15 p2633 A69-30064

Optical IR yttrium-iron garnet rectifier increasing light intensity and system Q factor at low external magnetic field
17 p2981 A69-33117

Laser harmonic frequency measurement application to absolute frequency determination of 84 micron heavy water laser
17 p2982 A69-33406

Construction and components of laboratory water vapor laser emitting coherent radiation in far IR
21 p3738 A69-39446

Optical frequencies and polarizations of IR active phonons of tysonite lanthanide fluorides based on Kramers-Kronig reflectance spectra analysis
22 p3993 A69-40729

INFRARED PHOTOGRAPHY

Interpretation of IR cloud images transmitted by Nimbus 1 and Cosmos 122 satellites, using radiation temperature contrasts
06 p0952 A69-17984

IR camera determining surface temperatures, discussing construction and space applications
08 p1315 A69-20455

Large scale color and color IR aerial photography evaluation to determine interpretability for improving range resource inventories
11 p1880 A69-24265

TV IR cloud images interpretation transmitted by Cosmos 122, discussing specific features of cloud covers and underlying surfaces
11 p1912 A69-24826

Computer program for interpreting IR cloud pictures from Cosmos 122 satellite based on potential function method
11 p1884 A69-24833

Magellanic Clouds color composite photographs prepared from negatives taken in blue and IR light
12 p2152 A69-25801

Spectrum analysis of radio galaxy M82 nucleus, noting H alpha emission lines from analysis of IR photograph
13 p2335 A69-27310

IR TV cloud pictures from meteorological satellites used for sky condition diagnostics and forecasting through automatic interpretation by image brightness quantization
13 p2291 A69-27728

Color IR film improvement for high altitude remote sensor, using auxiliary minus-visual filters
15 p2609 A69-30457

Side-looking radar and thermal IR photography as mapping system, discussing resolution and distortion
15 p2612 A69-31162

Environmental studies using orbital photography, discussing color, color IR, black and white applications from Gemini and Apollo programs
18 p3132 A69-35275

HD 30353 He binary star invisible component suggested as KO type supergiant from IR photometric data
18 p3203 A69-35348

Satellite IR hyperaltitude imagery for earth resources application, obtaining geological, meteorological and hydrological information
20 p3536 A69-36930

M 82 direct photographs sequence observation in optical IR region, noting small nucleus and broadened inclined emission lines
21 p3799 A69-38649

Comparative photointerpretation from panchromatic, color and Ektachrome IR aerial photography
22 p3944 A69-40039

Color and color IR aerial photography compared for estuarine and marshland research, considering detection of turbidity, pollution, salinity, etc
22 p3942 A69-40993

INFRARED RADIATION
NT FAR INFRARED RADIATION
NT NEAR INFRARED RADIATION

IR emission in NGC 7027 spectrum and role of discrete line emissions, discussing magnetic dipole transitions, temperature and density
01 p0148 A69-10051

Reversed thermal conditions in mesopause, examining atomic oxygen IR radiation effect
01 p0062 A69-10129

Frequency mixing of IR signals with visible laser light in nonlinear crystals to detect IR signals
01 p0089 A69-10180

Jet stream cirrus radiative characteristics from airborne IR measurements, noting cirrus cloud emission and transmission and cirrus height and temperature estimates
01 p0110 A69-10694

Cirrus IR radiance model for explaining measured cloud radiance characteristics, considering thermal emission and irradiance scattering
01 p0111 A69-10848

Orbital spectroscopic and radiometric IR experiments, considering moon and Mars surface
[AAS PAPER 68-196] 02 p0312 A69-11474

Electric field induced IR absorption and Raman scattering by optical phonons in centrosymmetric crystals, discussing tensor coefficients
02 p0295 A69-11779

Solar continuum intensity determination in middle IR, obtaining solar disk center brightness temperature measurement by comparison with black body model
02 p0318 A69-12041

Linear absorption coefficient of seminsulating Cr doped GaAs for IR carbon dioxide laser radiation, discussing lattice absorption mechanism
02 p0258 A69-12619

Ferroelectric strontium barium niobate as sensitive detector of single pulse IR radiation, noting application to Q switched carbon dioxide laser output
02 p0300 A69-12623

Visible and IR nonequilibrium radiation from dilute gases of upper atmosphere, describing laboratory, ground, aircraft and rocket observations of reactions and interactions
02 p0247 A69-12810

Q switched laser based on light waves parametric interaction in nonlinear medium operating at wavelengths from UV to IR
03 p0439 A69-13054

IR heating, discussing operation of IR emitters employing glass and quartz envelopes
03 p0411 A69-13548

IR radiation of NML Cygnus with O/C ratio close to unity ascribed to circumstellar shell of graphite particles
03 p0513 A69-13775

Absorption and IR emission of nickel and cobalt doped alkali halides
03 p0490 A69-13941

Reflection indicatrices of aluminum oxide, MgO, Au and Pt surfaces for normal irradiation noting temperature and surface treatment effects
03 p0534 A69-14161

Carrier scattering mechanisms in n-type GaP, measuring IR radiation absorptivity in Te doped GaP
03 p0492 A69-14168

Photoionization of donor impurities during absorption of IR radiation in n-type Te doped GaP at low temperatures
03 p0492 A69-14169

IR absorption and reflection in doped n-GaSb, obtaining absorption coefficient for various impurity concentrations
03 p0492 A69-14174

Atmospheric refractive index for IR radiation in one to six micron region
04 p0591 A69-14300

Stratospheric aerosol investigation by IR and lidar, applying Mie theory to model aerosol size distribution
04 p0592 A69-14654

IR object discovered during T Tauri objects and diffuse nebulae study, discussing peculiarity
04 p0655 A69-14665

Lunar surface IR polarization measurements compared to visible and UV polarization
04 p0656 A69-14669

IR radiation heat transfer in polyatomic gases in limit of large path lengths
05 p0844 A69-15579

IR radiation in upper atmosphere, indicating sources of error in data
05 p0753 A69-16058

Dynamics of laser response in IR detection by means of optical mixing in He-Ne laser, noting bandwidth
05 p0776 A69-16331

IR radiation attenuation in transparency windows of atmosphere, using searchlights as radiation sources
05 p0760 A69-16695

Onset and development of typhoons observed by Cosmos satellites using TV type IR apparatus [UN PAPER 68-95774]
06 p0949 A69-17039

GaAs IR emitters efficiency due to semiconductor material band structure
06 p0894 A69-17248

IR radiative heat transfer in nongray gases for non-black bounding surfaces, considering diatomic gases with single vibration rotation band
06 p1033 A69-17559

Inverse problems in radiative transfer applied to remote measurements of IR radiation from planetary atmospheres, noting temperature and water vapor inversions
06 p0919 A69-17617

IR radiation at 10.6 micron from two point sources mixed with collimated ruby laser radiation in proustite, obtaining visible image
06 p0928 A69-17904

IR beam profiles of carbon dioxide laser permanently recorded on foamed polystyrene
07 p1156 A69-19305

Energy transfer in gases transmitting heat by interaction of thermal conduction and IR radiation
09 p1621 A69-21442

Relaxation times of carbon dioxide laser levels induced by radiation
09 p1515 A69-21488

High altitude radiant emittance of cirrus clouds and cloudless sky for IR transmissivity based on aircraft measurements
09 p1536 A69-21641

Bismuth bolometer as sensor recording IR radiation for thermal radiation fluctuations in atmosphere caused by temperature inhomogeneities
09 p1490 A69-21868

Outer solar coronal IR radiance measured by ground telescope and stratosphere balloon flight, noting interplanetary dust thermal emission
09 p1600 A69-22205

Bright celestial IR sources in Ursa Major detected in spectral region by rocket-borne telescope, discussing luminosities of quasi-stellar sources
09 p1603 A69-22230

IR excess from carbon-rich peculiar variable R Coronae Borealis and M7 variable associated with emission nebula R Aquarii attributed to circumstellar matter
09 p1603 A69-22263

IR nondestructive, in-process microweld evaluator, discussing energy correlations and tensile strength
09 p1510 A69-22347

IR emissivities of powdered silicates and cloudy atmosphere model of spectral emission for radiative transfer in condensed powder
10 p1778 A69-23414

IR radiation effects in cadmium sulfide crystals with green edge emission at low temperatures, discussing luminescence, photoconductivity and conductivity glow curves
10 p1746 A69-23565

Limits of human tolerance to localized skin exposure to IR irradiation of various intensities from pain threshold observations, noting skin temperature role
10 p1647 A69-23589

Spectrum of IR object NML Cygnus, discussing model based on circumstellar IR emission
10 p1785 A69-24101

Broadband photometry for circumstellar IR emission from cool stars, considering giant and carbon stars
10 p1786 A69-24102

Pulsed molecular nitrogen laser positive UV and IR systems interaction under varying gas pressure, applied voltage and tube diameters
11 p1893 A69-24346

Two dimensional autocorrelation functions of outgoing radiation fields usable as quantitative characteristics of cloud distribution structures
11 p1913 A69-24832

Rabbit corneal damage thresholds for Gaussian beams of carbon dioxide laser IR radiation at various exposure times
11 p1830 A69-24844

Visible imaging of IR objects by conversion of IR frequency to visible with sum-frequency generation within nonlinear dielectric medium
11 p1897 A69-25037

Wavelength dependence of polarization and UBVR photometry of highly polarized stars, correlating IR interstellar extinction with maximum polarization wavelength
12 p2153 A69-25809

Resonant vibrational energy transfer between specific mode of carbon dioxide and N molecules at high temperatures, monitoring IR emission
12 p2131 A69-25984

IR radiative temperature changes as function of latitude, season and height in region 30-110 km
12 p2064 A69-26008

NGC 4151 absolute intensities of wide emission of weak isolated and IR lines determined from photoelectric spectrophotometric measurements
12 p2164 A69-27023

Thermal and free-free emission from planetary nebulae based on graphite grain model, discussing IR fluxes
12 p2172 A69-27158

Residual interstellar gas from protostar formation detected as high luminosity IR object
13 p2327 A69-27593

Low resistance Bi thin film complex electrical impedance in IR range, stating methods and equivalent circuits for determining impedance
13 p2322 A69-28011

Atmospheric IR emission measured at high altitudes by interferometer spectrometers behind nitrogen cooled chopper
13 p2254 A69-28261

Incoming IR flux measurements at high altitude, noting flux increase due to water vapor condensation in troposphere
13 p2256 A69-28647

Intermediate band photometry of G, K and M stars in IR indicating continuous stellar radiation deviant from black bodies
14 p2520 A69-29375

Continuous IR parametric signal amplification in saturable absorber caused by carbon dioxide laser pumping
14 p2459 A69-29601

Electron temperature and concentration in plasma determined by measuring diamagnetic signal and IR radiation intensity, emphasizing usefulness in plasmoid head portion
14 p2496 A69-29785

Bidirectional reflectance of solar radiation and IR temperature data from Nimbus 2 satellite to differentiate clouds above snow surfaces
15 p2596 A69-30455

Global mean monthly charts for IR radiation temperature, based on Cosmos 144 satellite data
15 p2596 A69-30643

Maser emission in interstellar OH ground state produced by IR pumping, noting population inversion mechanism
15 p2691 A69-30762

Solar radiation actinometric and pyranometric observations during 20 May 1966 eclipse, examining IR component and spectral radiation energies
15 p2697 A69-31257

IR quenching of photocurrent under field effect in CdS crystal
16 p2827 A69-32044

Diurnal variations of IR atmospheric oxygen bands in airglow observed with filter photometer on balloon flights
16 p2776 A69-32091

Homodyne detection of IR radiation from carbon dioxide laser scattered from moving diffuse target, noting applicability to IR radar, heterodyne spectroscopy etc
17 p2971 A69-32913

Angular dependence of lunar nighttime IR radiation by invariant tensor techniques, noting surface roughness effect on radiation pattern [AIAA PAPER 69-597]
17 p3032 A69-33276

Directional characteristics of lunar IR radiation accounted for by crater model [AIAA PAPER 69-598]
17 p3033 A69-33285

Adiabatic and diabatic processes contributions to vertical atmospheric motions profile and IR cooling components comparison
17 p2962 A69-33689

Phenolic resin and silica cloth laminates transparency to IR radiation, noting experimental results
18 p3136 A69-34640

IR technology - Conference, Ann Arbor, June 1969
19 p3309 A69-36051

Temporal discrimination based on signal fluctuations emphasizing signal detection in presence of noise
19 p3373 A69-36057

Thermal IR imaging devices for shape recognition and target position, emphasizing optical mechanical image or object plane scanners using point detectors
19 p3310 A69-36064

IR absorption in n-type gallium phosphide doped with telluride or Si in 1.5-2.0 micron range, analyzing wavelength dependence
19 p3385 A69-36518

Combined resonance transition in n-type InSb by IR radiation, plotting intensity against magnetic field for different carrier concentrations to infer band structure
19 p3385 A69-36520

IR radiation in upper atmosphere, indicating sources of error in data
20 p3533 A69-37968

Correlating IR lunar nighttime temperature and bearing strength of lunar materials, using expressions of thermal conductivity and bearing strength of porous media in vacuo
20 p3613 A69-38248

Nongray greenhouse model of Venus atmosphere possessing IR opacity due to carbon dioxide, water and diatomic N compatible with Mariner 5 and Venera 4 results
20 p3615 A69-38259

Water vapor profiles in stratosphere from IR radiometric observations under cloudless conditions, indicating relation to tropospheric meteorological features
20 p3535 A69-38261

Galactic nucleus observations in 1.65-19.5 micron range with evidence for strong radiation at 10 and 20 microns, noting mechanisms for IR radiation
21 p3799 A69-38650

Total band absorbance of nonisothermal IR radiating gas, using wideband formulation of Curtis-Godson approximation and series expansion formulation
22 p3983 A69-40101

Carbon dioxide laser development, discussing gain, static amplifier and high pressure operations
22 p3962 A69-40474

Monograph on laser communication system in IR for industrial environments
22 p3900 A69-40617

Steady state distribution of visible and IR radiation in planetary atmosphere illuminated from outside, calculating atmospheric temperature profile
22 p4031 A69-40910

Heat resistant materials integral and spectral radiative properties in IR and visible regions determined by calorimetry and IR spectrometer
23 p4237 A69-41329

Fast neutron irradiation effect on IR absorption in single crystal GaAs for various fluences
23 p4198 A69-41540

Corrections for eliminating anomalous skin effect on IR emissivity for Ag, Cu, Au and Al
23 p4177 A69-42212

Mars thermal energy emission measurement by Mariner 1969 IR radiometer, indicating frozen carbon dioxide cap and minimum temperature
24 p4384 A69-43196

Thermal calculations of objects near lunar surface, considering IR emission directivity effects
24 p4385 A69-43254

IR measurements applications to meteorology, discussing IR radiation characteristics, atmospheric effects, thermal radiation detection and differences between real and black bodies
24 p4316 A69-43507

INFRARED REFLECTION

IR reflection and transmission properties of various semiconductor compounds, rubidium halides, strontium titanate, BN and Te
01 p0139 A69-10840

Reflection measurements in IR, investigating effect of angle of incidence and collimated beam on reflection spectra
01 p0120 A69-10891

IR absorption and reflection in doped n-GaSb, obtaining absorption coefficient for various impurity concentrations
03 p0492 A69-14174

Angular distribution measurements of visible and near IR radiation reflected from carbon dioxide cryodeposits formed on liquid nitrogen cooled surface in vacuum
[AIAA PAPER 69-63] 06 p0959 A69-18131

Diamond-like glassy semiconductor compound of cadmium germanium arsenide, determining optical lattice vibrations from IR reflection spectra
10 p1747 A69-23963

Germanium surface IR radiation absorption in vacuum at low temperatures, obtaining modulated interval reflection spectra
13 p2317 A69-27879

IR reflection spectra agreement for frost particles and Venus clouds, noting ice as clouds constituent
18 p3190 A69-34282

Ice clouds near IR spectral reflectivity dependence on particle size, noting application to planetary atmospheres
18 p3126 A69-34283

INFRARED SCANNERS

Informative properties of IR scanning equipment of meteorological satellites, discussing radiative flux measurements and thermal mapping
06 p0929 A69-17979

IR scanning systems of meteorological satellites for detection of clouds and various underlying surfaces, determining detection probability and errors
06 p0952 A69-17986

Imagery degradation by moisture condensation on thermal IR scanners optics during aircraft descent from higher to lower altitude
08 p1311 A69-19821

Near field repeatable stimulator of infrared earth horizon sensors in variable environments and test levels, noting orbital conditions
[AIAA PAPER 69-322] 09 p1478 A69-22376

Optical/mechanical IR line scanner imagery role in remote sensing
12 p2096 A69-26979

Tenuous cirrus cloud influence on 6.4-6.9 micron Nimbus 2 water observations, discussing equivalent black body temperatures correspondence to cloud and clear areas
12 p2075 A69-27003

Airborne and satellite IR survey over active effusive eruption at Surtsey, Iceland, comparing thermal energy yield and radiant emission to ground measurements
12 p2076 A69-27011

Sky mapping in IR, using IR photometer on TD1 ESRO satellite
13 p2260 A69-27606

High speed picture thermography in nondestructive testing, describing IR scanning frame rate and thermal image recording
15 p2618 A69-30316

European geostationary satellite orbit inclination and eccentricity modification for maximum observation time of Northern Hemisphere by high resolution IR radiometer
15 p2650 A69-31389

IR measuring techniques for water surface temperature remote sensing
15 p2617 A69-31543

Sunspot of 28 December 1967 studied by far IR scanning with interference and Restrahlens filters defining bandpass, obtaining umbral temperature
17 p3029 A69-33050

Ocean and water surface temperature measurement by IR remote sensing from aircraft and satellites, discussing accuracy and data correction
[AIAA PAPER 69-590] 17 p2973 A69-33286

Lunar surface brightness temperatures from IR observations, determining thermal emission directional characteristics to infer surface temperatures from Surveyor data
[AIAA PAPER 69-593] 17 p3033 A69-33302

TV camera tubes with electron beam scanning adapted to IR imaging, emphasizing vidicon
19 p3311 A69-36069

Side-looking radar and IR line scanning as method for simultaneous stereo height mapping, using images produced from same vantage point
20 p3536 A69-36929

Thermal IR image forming devices, explaining principles of image and object plane scanning
20 p3540 A69-37738

Thermal scanner model block diagram presented including lens, filter, detector, CRT and camera, considering environmental factors affecting image character
20 p3541 A69-37740

Effusive volcanic eruptions recorded by high thermal sensitivity satellite-borne IR systems
21 p3721 A69-38631

INFRARED SPECTRA

IR and Raman spectra of solid and matrix isolated methylamine and deuterium derivatives, locating amine twisting vibration in solid phase IR spectra
01 p0023 A69-10287

Methane IR absorption band centered near structure
01 p0023 A69-10289

Low temperature grinding technique for IR spectra of propellants and binders in potassium bromide disks
01 p0082 A69-10892

Statistical band model and line by line calculations of transmittance for IR bands in absorption spectra of ozone and water vapor
[AFCRL-68-0505] 01 p0124 A69-10919

Very far IR techniques applications in molecular and solid state spectroscopy and relationship with impurity band conduction
02 p0296 A69-11791

Spectral measurements for matrix isolated lithium fluoride extended into far IR to obtain evidence for linear lithium fluoride dimer
02 p0205 A69-12465

IR and violet sulfur lines for Seyfert galaxies, noting substantial reddening in nuclei
02 p0325 A69-12593

Induced combinational scattering /ICS/ on IR active transitions, deriving equations with allowance for population variation
02 p0282 A69-12636

Far IR and Raman spectra of ethylene carbonate, gamma butyrolactone and cyclopentanone, noting consistency with hindered pseudorotation
02 p0206 A69-12723

Night airglow spectrum between four and four microns, noting sequence of hydroxyl bands
03 p0426 A69-14251

Stellar spectra taken with rapid scanning Michelson interferometer, noting IR excess due to radiation from clouds surrounding stars
04 p0655 A69-14667

IR astronomy with ground based instruments noting Mars and Venus spectra, Jovian disk scans, solar radiometry, IR stars, quasars and galaxies
05 p0821 A69-15842

Parameters and relative errors tabulated from IR spectral emittance of Mo, Nb, Zr and Ta near 1400 K
05 p0846 A69-15903

Water and carbon dioxide IR spectra compared with laboratory measurements
05 p0759 A69-16638

Atmospheric IR spectral transparency measurement, describing optical system, recording devices and data processing
05 p0759 A69-16639

Communications of Lunar and Planetary Laboratory, Volume 7, covering IR solar spectrum atlas reports and solar spectrometer for airborne IR observations
06 p1008 A69-17807

Arizona-NASA atlas of IR solar spectrum, reproducing photometric tracings obtained from CV-990 aircraft flights
06 p1008 A69-17808

IR solar spectrum tables and graphs covering 10,657-12,857 A
06 p1008 A69-17809

NASA atlas of IR solar spectrum, reporting B and 4 meter spectrometer recordings over band containing methane telluric absorptions
06 p1008 A69-17810

Shock tube study of ammonia oxidation at high temperature, detecting molecular species in reaction zone by IR emission
06 p0885 A69-17936

IR absorptance of CO below room temperature, determining strength and half widths of lines in R branch of fundamental band
07 p1183 A69-19644

IR zero one band of molecular O observed in day airglow with ground based scanning grating spectrometer
08 p1306 A69-20096

Near IR transparent aluminocalcium glasses with improved spectral properties
08 p1336 A69-20386

Polymers and organic optical cements transparent in 1 to 13 micron IR region, noting organosilicon resin
08 p1336 A69-20387

IR photoconductivity spectra at surface of gold doped silicon, establishing monopolarity
08 p1373 A69-21073

Absolute spectrophotometry of IR lines in planetary nebulae spectra determined by diffraction spectrograph
09 p1590 A69-21380

Luminescence spectra of molecular gases excited by fast electrons in infrared spectral region, noting H alpha line
09 p1590 A69-21382

IR spectrum of NML Cygnus star with Michelson interferometer, noting CO bands and IR excess
09 p1602 A69-22229

Nonadiabatic collision broadening theory for IR spectral lines applied to carbon dioxide-carbon dioxide and carbon dioxide-nitrogen collisions, estimating rotational line widths
09 p1543 A69-22250

Photoelectric spectrum scanning and IR photometric observations of Scorpius XR-1 X ray source
09 p1604 A69-22401

Test of Velikovsky theory for dense hydrocarbon clouds and dusts surrounding Venus, using IR reflection spectra
09 p1608 A69-22566

IR emissivities of powdered silicates and cloudy atmosphere model of spectral emission for radiative transfer in condensed powder
10 p1778 A69-23414

IR and Raman spectra of gas and liquid phase methylhydrazine and deuterated methylhydrazines, discussing vibrational motions, H bonding and thermodynamic functions
10 p1752 A69-23528

Nitrogen, oxygen and air luminescence spectra excited by fast electrons at low gas pressures in IR spectral region compared with polar auroral spectra
10 p1687 A69-23916

Far IR laser lines in hydrogen sulfide, sulfur dioxide and OCS, discussing output
10 p1706 A69-24008

IR spectral distribution from region between stars of Trapezium in Orion Nebula
10 p1786 A69-24106

Brightness temperatures and spectra of Venus, Mars, Jupiter and moon measured from 8 to 14 microns by reflector and prismatic spectrometer
11 p1956 A69-24395

Real time Fourier spectroscopic system for synthesis of spectrum of interferogram, noting polystyrene IR transmission spectra
11 p1884 A69-24837

Carbon dioxide temperature distribution, absorption and concentration as functions of molecular dissociation behind shock wave determined by measuring IR bands intensity
11 p1873 A69-25226

Balloon-borne IR spectrometry to study atmospheric nitric acid vapor compared with absorption by ozone and methane
11 p1879 A69-25407

Calcite IR absorption dependence on pressure, discussing calcite-aragonite transformation
12 p2141 A69-25783

IR absorption spectrum of Br-doped n-CdTe specimen, considering donor level transfer mechanism
12 p2142 A69-25979

Limits for Martian surface materials established by comparing visible and IR spectra with laboratory spectra
12 p2156 A69-26225

INFRARED SPECTROMETERS

Vibration and absorption bands in IR spectra of diborene hydrazine stabilized by boiling in benzene 12 p2027 A69-26917

Lunar thermal anomalies in various craters observed during lunar night by IR methods, with data suggesting hot and cold regions 12 p2171 A69-27092

IR objective-prism survey along southern Milky Way for identifying high luminosity stars 13 p2335 A69-27314

IR observations of ETA Carinae to 20 microns, noting continued increase in flux density into IR 13 p2335 A69-27316

IR spectroscopic observations of moon to interpret molecular vibration spectra in terms of molecular composition, discussing rock surface roughness effects 13 p2341 A69-27582

IR day and night airglow of upper atmosphere utilized for atmospheric energy content and reactions analysis 13 p2252 A69-27585

IR airglow spectra measured by two beam interferometer on balloon, noting carbon dioxide and OH emission bands 13 p2252 A69-27586

Atmosphere effects on solar IR spectra, discussing role of absorbing molecule distribution in transmittance calculations 13 p2341 A69-27589

Expected IR line spectra of gaseous nebulae based on physical conditions, listing line intensities 13 p2342 A69-27595

Atmospheric ozone vertical distribution and total amount determined by radiative transfer and perturbation theory, presenting error analysis 13 p2255 A69-28493

Water and carbon dioxide IR spectra compared with laboratory measurements 14 p2433 A69-28794

Atmospheric IR spectral transparency measurement, describing optical system, recording devices and data processing 14 p2433 A69-28795

IR spectral transmittance and physicochemical properties of tellurite glasses with vanadium and cerium oxides, showing polymer chains in structure 14 p2468 A69-29329

Propylene imine IR and Raman spectra, calculating thermodynamic functions based on rigid rotator harmonic oscillator model 14 p2410 A69-29922

Source functions of IR Fraunhofer lines obtained using solar disk equivalent width method, noting LTE role 14 p2528 A69-29961

Synthesis of N-/trimethylsilylalkyl/ diamines and N-/trimethylsilylalkyl/-N-/2-mercaptoethyl/ diamines, determining structure by IR spectra 15 p2561 A69-30414

Atmospheric transmission functions dependences on absorbing material, pressure and temperature in 15 micron band of carbon dioxide, introducing corrections 15 p2597 A69-30653

IR horizon of earth from ionospheric IR emission spectra obtained by sounding capsule, discussing earth geometric horizon and particular spectral bands [ONERA-TP-709] 15 p2601 A69-31370

Atmospheric IR spectra determination from transmission functions overlapping effects of atmospheric gases 16 p2814 A69-31792

Spectral variations of red variable stars analyzed by objective-prism spectra in near IR 16 p2860 A69-32235

Two channel IR radiometer for 1969 Mariner mission measuring equivalent black body surface temperature 17 p2972 A69-33085

IR reflection spectra agreement for frost particles and Venus clouds, noting ice as clouds constituent 18 p3190 A69-34282

Ice clouds near IR spectral reflectivity dependence on particle size, noting application to planetary atmospheres 18 p3126 A69-34283

Vertical tropospheric humidity distribution estimation from IR spectra obtained by TIROS satellites 18 p3126 A69-34284

IR and optical measurement of Crab pulsar NP 0532, analyzing energy density per pulse and smoothness of visual data 18 p3191 A69-34318

Absolute spectrophotometry of IR lines in planetary nebulae spectra determined by diffraction spectrograph 18 p3198 A69-34768

Luminescence spectra of molecular gases excited by fast electrons in IR spectral region, noting H alpha line 18 p3176 A69-34770

Spectroheliograms interpretation obtained in line cores of neutral oxygen IR multiplets 18 p3204 A69-35388

Atmospheric slant path molecular absorption and emission from band model methods, discussing computer program prediction capabilities 19 p3375 A69-36052

Object discrimination based on IR spectral differences, reviewing calibrated radiometers, relative spectrometers and imaging sensors 19 p3373 A69-36056

Electromagnetic field signatures in optical IR spectrum of satellite-borne sensors, analyzing spectral, spatial and temporal distributions, polarization and phase 19 p3309 A69-36060

Forbidden lines of O I, O II, S II, N II and A III in red and near IR spectra of NGC 1976, IC 418 and II 4997 19 p3422 A69-36222

IR spectra of Eta Carinae, confirming nitrogen and sulfur abundance 19 p3423 A69-36229

Free electrons influence on reflection coefficient of semiconductor in IR spectra, showing selective modulation with change in carrier concentration 20 p3583 A69-37610

TiO bands identified in Mira variables IR region, discussing rotational structure and band strength-temperature relation 20 p3611 A69-38158

IR spectrum of NML Cygnus star using rapid scanning Michelson interferometer, estimating temperature from CO bands 21 p3800 A69-38678

Papers of Lunar and Planetary Laboratory, Volume 9, covering IR solar spectrum 21 p3800 A69-38681

Solar spectrum data covering wavelength intervals from 13138-14707 and 12187-17731 A and 1.4 micron water band 21 p3800 A69-38682

Solar IR spectrum recorded by LPL B spectrometer on NASA CV-990 aircraft using one micron grating, noting resolution 21 p3800 A69-38683

Emission band intensities of carbonyl fluoride in 2.0-6.0 micron region with scanning spectrometer, comparing results for room and shock temperature with theoretical data 21 p3669 A69-38759

Horizon definition for Apollo space navigation references from examining earth atmosphere visible and far IR spectrum [AIAA PAPER 69-869] 21 p3763 A69-39395

Visible and IR spectral reflectivity of Apollo lunar landing sites, attributing reflectivity differences to compositional and/or mineralogical differences 21 p3815 A69-39586

Lunar surface IR emissivity comparison spectra including proposed Apollo landing sites, indicating Si-O ratio difference for Plato crater 21 p3815 A69-39587

Relative IR spectral reflectivity of selected lunar surface areas measured using double beam photoelectric filter photometer 21 p3815 A69-39588

IR molecular radiation spectra of upper atmosphere in 3-8 micron range investigated by rockets and satellites, discussing radiation energy density during magnetic storms 21 p3792 A69-39772

Jupiter spectrum observations in 2.8-14 micron range, describing absorption strength and brightness temperature, basing analysis on ammonia, methane and hydrogen absorption 22 p4028 A69-40662

Dielectric constant and IR spectra of Ba titanate single crystals doped with hydroxyl, showing dependence on temperature and crystal thickness 22 p3995 A69-41157

Defect structure of ceramic Ba titanate doped with Cr ions, evaluating visible, IR and EPR spectra 22 p3996 A69-41160

IR directional and hemispherical emittance of spacecraft thermal control coatings, comparing values determined by various measurement techniques 23 p4164 A69-41633

IR excess of R CrB type variable star RY Sgr, noting visual brightness and radiation in 2.0-3.4 micron range 23 p4220 A69-42377

Equivalent width measurements of Arcturus IR line spectra using Fourier transform spectroscopy, tabulating results 23 p4222 A69-42453

IR lattice spectra of rare earth Al, Ga and Fe garnets, discussing oxygen anion, translational rare earth cation and crystal lattice external motions 24 p4360 A69-42974

Brightness temperatures and spectra of Venus, Mars, Jupiter and moon measured from 8 to 14 microns by reflector and prismatic spectrometer 24 p4390 A69-43785

INFRARED SPECTROMETERS

Atmospheric temperature and airglow spectra from IR measurements noting OH bands, atmospheric structure between 10 and 200 km at midlatitude and atmospheric absorption [UN PAPER 68-95471] 01 p0108 A69-10464

Stellar spectra observed with 2.8-14 micron IR spectrometer, noting broad absorption feature near 5 and 8 microns 02 p0327 A69-12713

IR spectrometer for Nimbus meteorological satellite for terrestrial spectral radiance data for atmospheric temperature profiles 06 p0926 A69-17621

Life raft thermal protection against exposure of aircrews to cold, noting chemically fueled heaters and IR reflective liners 06 p0883 A69-17841

Detection of micron Ne emission line from planetary nebula IC 418 using IR spectrometer 09 p1591 A69-21452

Airborne scanning spectrometer for IR detection of clear air turbulence, presenting flight records 12 p2098 A69-26999

Airborne IR spectrometer for remote clear air turbulence detection, noting necessity for mirror stabilization in pitch axis 12 p2098 A69-27000

Atmospheric IR emission measured at high altitudes by interferometer spectrometers behind nitrogen cooled chopper 13 p2254 A69-28261

Static temperature measurement in arc-tunnel tests producing high velocity air streams by duplex scanning IR spectrometer 19 p3294 A69-35752

Modular Michelson interferometer used as IR spectrometer for absorption and dispersion studies, describing instrument construction, range and accuracy 20 p3538 A69-37297

Grating spectrometer for far IR, discussing light source, reflection gratings, filters, etc 21 p3726 A69-39682

INFRARED SPECTROPHOTOMETERS

Paschen series line contours for hydrogen in solar spectrum plotted from IR spectrophotometric data 01 p0148 A69-10126

Lunar surface IR polarization measurements compared to visible and UV polarization 04 p0656 A69-14669

Multiband photoelectric photometer for near IR observations, tabulating magnitudes, colors, spectral irradiance, radii and effective temperatures of late type stars 13 p2342 A69-27592

INFRARED SPECTROSCOPY

Rapid scan spectroscopy, reviewing dispersion optical and interferometric systems and electronic image converters 01 p0082 A69-10836

High dispersion IR image tube spectroscopy using telescope, discussing alpha Sco and alpha Boo spectral regions 07 p1074 A69-19203

Mars and Earth atmospheric carbon dioxide simulation and spectroscopic measurement for developing planetary surface pressure estimating procedures from IR transmission measurements 08 p1354 A69-20151

Glass fibers size, finish and surface treatment identification by pyrolysis attenuated total reflectance IR spectroscopy 09 p1448 A69-22315

Water content of tektites, impactites and artificial glass of tektite composition using IR absorption measurements 10 p1778 A69-23413

- IR spectrometric analysis of flames of composite rocket propellants, maintaining diffusion flames between surfaces of decomposing ammonium perchlorate and fuel source
[WSCIPAPER 69-10] 16 p2831 A69-32350
- Antimony trisulfide natural light reflection and transmission in and near IR region, noting spectral temperature and time dependence peculiarities
19 p3384 A69-36481
- Continuous IR radiation source using electrically heated Mo ribbon, comparing emission from V shape and flat portions
19 p3313 A69-36491
- Satellite determination of underlying surface temperature by IR spectroscopy, measuring emitted radiation in atmospheric windows
21 p3759 A69-39114
- Stellar IR spectroscopy, describing absorption and emission lines of various atoms and molecules, atmospheric composition, problems with variable stars, etc
21 p3811 A69-39510
- Polycrystalline ammonium cyanide IR absorption spectrum as function of temperature, discussing ammonium ion hydrogen bonding to C or N atoms
24 p4280 A69-43809

INFRARED TRACKING

- Encoding and decoding in IR tracking system, analyzing chopping rotating FM reticle pattern
19 p3268 A69-36058

INFRASONIC FREQUENCIES

- Infrasonic waves recordings from Saturn 5 vehicle, observing signal reversal occurrence
03 p0509 A69-13358
- Acoustic and electromagnetic energy propagation in lower ionosphere and atmosphere for energy pulse generation by chemical explosion
07 p1078 A69-18844
- Auroral infrasonic waves morphology related to temporal and spatial distributions of supersonic auroral motions during polar magnetic storms
11 p1878 A69-25152
- Physiopathological reactions of humans exposed to infrasonic vibrations applied via auricular canal, observing cardiac and circulatory hemodynamic troubles
13 p2215 A69-28590
- Infrasonic waves identified with supersonic auroral electrojets crossing zenith from northwest during substorm activity
16 p2780 A69-32303
- Saturn F-1 rocket engine as generator of infrasonic waves and magnetic fluctuations, noting ignition and cut-off signal characteristics
24 p4365 A69-43415

INGESTION [BIOLOGY]

- NT DRINKING
- NT EATING
- Electrical stimulation effect on drive specificity in lateral hypothalamus area of sated rat, suggesting fallacy in previous conclusion concerning appetite
22 p3876 A69-40269

INGESTION [ENGINES]

- Steam ingestion tests on carrier aircraft gas turbine engines, analyzing inlet pressure and temperature distortion in steam-air environment
01 p0143 A69-11062
- Real time real temperature exhaust gas reingestion and structural heating test facility for jet lift V/STOL configurations
[AIAA PAPER 69-310] 09 p1479 A69-22388
- Ingestion and flow field characteristics of interaction of two heated parallel air jets, discussing VTOL exhaust ingestion tests
[AIAA PAPER 68-79] 12 p2012 A69-26761

INGOTS

- Optimal processing parameters for producing ingots and semifinished products from corrosion resistant Ti alloys with added Mo
11 p1902 A69-24273
- Acicular crystals growth and dendrites orientation in Mo ingots prepared by electron beam and arc melting analyzed by X rays
11 p1903 A69-24538
- Macrostructure of steel, zinc and aluminum ingots using electromagnetic vibrations during crystallization, for stress relieving of welded structures
14 p2456 A69-29916

INHABITANTS

U MOUNTAIN INHABITANTS

INHALATION

U RESPIRATION

INHIBITION [PSYCHOLOGY]

- Paradoxical inhibition negative feedback principle in oscillatory systems, using mathematical model of nerve membrane
23 p4112 A69-42444

INHIBITORS

- NT WEAR INHIBITORS
- Glycolysis rate role in regulation of substrate inhibition of dehydrogenases
01 p0015 A69-10931
- Aluminum corrosion and inhibition mechanisms in ethylene glycol/water solutions, using controlled powder immersion tests
02 p0265 A69-11895
- Flame inhibition with electron attachment observed using halogenated hydrocarbons
06 p1034 A69-17926
- Amino acid biosynthesis control in microorganisms by end product /feedback/ inhibition of enzyme action
06 p0876 A69-18238
- Burning velocity inhibitors effects on hydrocarbon-oxygen-nitrogen mixtures ignition temperature, reporting data on 20 additives at ambient temperature and pressure
[WSCIPAPER 69-14] 16 p2831 A69-32352

INHOMOGENEITY

- Basic equations for optimum inhomogeneity in pressure vessels of maximum rigidity derived, using thick walled spherical shell
01 p0167 A69-10326
- Spherical shell pressure vessels investigated for optimum inhomogeneity and rigidity using Lagrange polynomials
01 p0167 A69-10327
- Surface charge distribution in silicon p-n junctions noting luminescence of microplasmas and inhomogeneous properties
02 p0294 A69-11629
- Nonlinear mode interactions in spatially inhomogeneous laser, analyzing suppression, phase locking and linear coupling among cavity modes
02 p0258 A69-12632
- Plastically twisted prismatic bars with transverse discontinuous inhomogeneity, using sand hill analogy to determine stress field and limiting torque
03 p0524 A69-13021
- Book on continuum theory of inhomogeneities in simple bodies
05 p0833 A69-15727
- Inhomogeneities in materially uniform simple bodies described in terms of third order tensor field, treating contorted anisotropy
05 p0833 A69-15728
- Cauchy equation derived, giving rise to definite differential equation for materially uniform elastic bodies with inhomogeneities
05 p0834 A69-15730
- Nonuniform distribution and concentration of doping materials in semiconductors determined by measuring optical reflection coefficient
05 p0764 A69-16664
- Homogeneous linear systems conditions for asymptotic growth of solutions of nonhomogeneous linear differential equations system
08 p1342 A69-20348
- Inhomogeneity distribution of carrier concentration and electrovoltaic effect in GaAs devices analyzed by scanning electron microscope
09 p1557 A69-21746
- Mass spectrometric analysis of silicon carbide for inhomogeneity in sample, noting metallic impurities
09 p1448 A69-22313
- Bolometric luminosity-red shift relations of Friedmann dust universes corrected for inhomogeneities, using locally inhomogeneous Swiss cheese models
09 p1605 A69-22411
- Elasticity theory upper and lower bounds for two and three dimensional inhomogeneous problems and applications to plates
10 p1794 A69-22889
- Radio astronomical investigations of small scale inhomogeneity motion and dimensions in interplanetary plasma, using observations of 3C 48 scintillations in 1967
10 p1782 A69-23711
- Antiplane strain model for describing cracks and dislocation arrays within circular cylindrical inhomogeneity surrounded by elastic material
10 p1803 A69-24031
- Electrical conductivity of impurity semiconductors containing variable current carrier concentrations, discussing current-voltage characteristics
11 p1937 A69-24909

Thermodynamic properties of materials in critical region, discussing inhomogeneity

- 11 p2003 A69-25440
- Inhomogeneous permittivity and boundary effects influence on electric fields of laser with open cavity containing inhomogeneous active medium
12 p2110 A69-26908
- Mixed state of type 2 superconductors, stressing alloying elements effects in solid solution and structural inhomogeneities
12 p2145 A69-27119
- Elastic-plastic bending of rectangular plates with asymmetrically inhomogeneous material in plastic range, using modified Ritz method
14 p2533 A69-28984
- Drift of F 2 layer inhomogeneities compared for IGY and IQSY
14 p2443 A69-29866
- Similarity and correlation methods for drift of ionospheric inhomogeneities in Antarctica
14 p2444 A69-29867
- Ionospheric sporadic E layer inhomogeneities drift, discussing altitude dependence of velocity and direction
14 p2444 A69-29869
- Inhomogeneity effects on elastic waves generated by impulsive loading of surface using asymptotic method, discussing high stress intensification regions
16 p2873 A69-32157
- Dyadic Green function technique extended to problems of electromagnetic scattering in inhomogeneous media with spherical symmetry
17 p2924 A69-33837
- E layer inhomogeneities analysis concerning drift, chaotic processes, statistical parameters and reliability of data processing
17 p2962 A69-33896
- Laser emission divergence reduced by compensating optical inhomogeneity of active elements with prismatic reflector in resonator
17 p2983 A69-33970
- Chromospheric inhomogeneities rapid changing properties observable in H and K lines above sunspot umbrae
18 p3204 A69-35389
- Laser emission during disturbed quasi-equilibrium, considering emission spatial inhomogeneity due to arbitrary radiative transitions
19 p3333 A69-35876
- Book on antennas in inhomogeneous media, discussing impedances for dielectric loading, reentry, ionosphere and buried environment, wire antennas in free space, etc
19 p3268 A69-36150
- Twisting of spherical shell of nonhomogeneous isotropic material with variable shear modulus and inner surface assumed to be stress free
20 p3619 A69-36911
- Semiinverse method for elastic nonhomogeneity problems, considering case of seismic wave propagation
20 p3624 A69-37589
- Ground station equipment for studying motions and structure of ionospheric inhomogeneities by combined space-frequency diversity reception, noting altitude dependence of ionospheric parameters
20 p3510 A69-37693
- Resolving power and field of view relations of holographic device for images recording through inhomogeneous atmosphere
20 p3540 A69-37728
- Layer model of random discrete inhomogeneities used to derive harmonic wave one dimensional scattering field and mean square of field
21 p3673 A69-38993
- Harrison primordial inhomogeneity postulate concerning baryon numbers distribution in universe, precluding possibility of considering cosmic rays bulk as universal
21 p3810 A69-39469
- Amplification saturation in spatially inhomogeneous laser field, relating power to active medium and resonator parameters
21 p3740 A69-39549
- Inhomogeneities effect on thermoelectric power and thermal efficiency of semiconductor thermocouple with constant forbidden band width
22 p3994 A69-40933
- Rectangular waveguide with inhomogeneity represented by half space dielectric filling with boundary causing polarization, obtaining reflection elimination or minimization reflection
23 p4125 A69-42047

- Holographic technique for reduction of image distortion during penetration through inhomogeneous medium 24 p4314 A69-42975
- Stress wave propagation in nonhomogeneous elastic media, considering curvilinear characteristics transformation into equal slope straight lines by change of independent variable 24 p4403 A69-43574

INITIAL VALUE PROBLEMS

U BOUNDARY VALUE PROBLEMS

INITIATION

- Microcracking susceptibility studies of Inconel 718 weld heat affected zones, noting hot ductibility, weld circle patch and fillerless fusion welding tests 11 p1905 A69-24933

INITIATORS [EXPLOSIVES]

NT DETONATORS

NT PRIMERS [EXPLOSIVES]

- Capacitance-voltage relationships for PETN initiation by various diameter gold exploding bridgewires, noting optimum capacitance dependence on energy transfer efficiency 01 p0141 A69-10679

- Nondestructive testing of quality of electroexplosive devices based on determination of heat flow between bridge wire and surroundings 04 p0607 A69-14973

- Insensitive explosive trigger or initiator consisting of metal/metal oxide powder with low shock sensitivity and high thermal stability 04 p0646 A69-15300

- Igniferous materials for electrical initiation of explosive in extreme conditions, considering nitrophenol salts and pyrotechnics 10 p1750 A69-23015

- Initiation of priming explosives by electrons, photons, electrical discharges and laser radiation 10 p1751 A69-23017

- Electroexplosive devices protection by nonconducting composition against premature ignition by RFI in spacecraft environment, noting Apollo Standard Initiators 10 p1751 A69-23018

- Safety requirements of test ranges, considering RF hazards to electroexplosive devices 10 p1751 A69-23019

- Electroexplosive devices design for extreme conditions, considering igniter, delay and functioning systems 10 p1751 A69-23020

- Electroexplosive element design for safe reliable devices in liftoff and space environment, considering stray electric currents, RF fields and electrostatic discharges 10 p1752 A69-23022

- ELDO Europa 1 Fairings Jettisoning System and explosive devices, discussing heat shield structure and safety regulations 10 p1635 A69-23027

- Exploding bridgewire /EBW/ systems compared to hot-wire initiators for Mars space probe 17 p2905 A69-34108

INJECTION

- NT CARRIER INJECTION
- NT FLUID INJECTION
- NT FUEL INJECTION
- NT GAS INJECTION
- NT ION INJECTION
- NT LIQUID INJECTION
- NT SECONDARY INJECTION
- NT WATER INJECTION

- Injection or suction at disk surface, noting effects on heat and mass transfer in laminar flow about rotating disk 06 p1029 A69-17002

- Unsteady boundary layer with distributed injection or suction on porous plate, determining acceleration and flow parameter functions from velocity profiles 21 p3692 A69-38609

INJECTION CARBURATORS

U FUEL INJECTION

INJECTION GUIDANCE

- Apollo translunar injection burn simulation, analyzing polynomial solutions of optimum geometry and characteristic velocity [AAS PAPER 68-150] 21 p3820 A69-39225

- Parking orbit optimal orientation for minimal impulsive maneuvers total velocity increment in three dimensional capture-escape mission [AIAA PAPER 69-918] 21 p3808 A69-39347

- Rendezvous, intercept and injection optimal control laws derived from inhomogeneous linear differential equations with quadratic performance index 23 p4224 A69-41921

- Atlas/Centaur/Surveyor flights guidance accuracy, discussing postflight analysis of injection errors due to hardware, software and propulsion system [AIAA PAPER 68-842] 24 p4348 A69-43239

INJECTION LASERS

- Maximum power efficiency of pulsed injection laser with Fabry-Perot cavity expressed in terms of two dimensionless geometric variables 01 p0089 A69-10119

- P-n junction cut-off current density and ohmic losses effect on injection laser efficiency determined by using quality parameter 01 p0091 A69-10883

- Continuous wave GaAs injection lasers operation at high temperatures shown possible by using available threshold current densities with suitable heat sink materials 02 p0255 A69-11710

- Injection laser emission from gallium arsenide base films grown epitaxially from gas phase in moist hydrogen atmosphere 02 p0255 A69-11879

- GaAs injection lasers noting spectral function, I-V characteristics and relations among lasing wavelength, threshold current density and impurity concentration 02 p0256 A69-11993

- GaAs injection laser transmission losses and threshold current density under influence of external optical coupling with spherical mirror 02 p0260 A69-12687

- Clamp type diode holders for obtaining CW coherent emission from gallium arsenide injection lasers 03 p0435 A69-12985

- Uniaxial pressure applied to p-n junction of GaAs injection laser, discussing effects on threshold current and wavelength 03 p0441 A69-13848

- Gallium arsenide injection lasers properties, analyzing band structure, optical transitions, recombination lifetimes, conduction band states, optical gain, etc 05 p0772 A69-16228

- GaAs injection diode laser cooled by closed cycle gas refrigeration system, noting time required to reach laser operating temperature 05 p0777 A69-16793

- Memory effect in injection lasers output characteristics, noting anomalous increases in pulsed emission intensity with increasing current-pulse repetition rate 07 p1147 A69-18542

- Self modulated radiation modes of Te-doped n-type InAs injection lasers 07 p1148 A69-18685

- Gradual output degradation mechanism in GaAs injection lasers, attributing internal radiative quantum efficiency reduction to nonradiative recombination centers formation 07 p1148 A69-18857

- Dynamics of injection lasers, discussing picosecond pulse generation [IEEE PAPER O-1] 07 p1153 A69-19071

- GaAs lasers radiation power hysteresis manifested in generating starts and stops at different injection current levels 07 p1157 A69-19593

- Semiconductor laser with isolated diodes in cavity, noting watt-ampere characteristics during nonuniform excitation and threshold curves 08 p1326 A69-20539

- Microwave modulation of GaAs injection laser radiation, using Zaleskii recording method and liquid nitrogen to cool laser diode 12 p2105 A69-26031

- P-n junction cut-off current density and ohmic losses effect on injection laser efficiency determined by using quality parameter 12 p2109 A69-26647

- Close confinement GaAs p-n junction lasers with reduced optical loss at room temperature 14 p2457 A69-28893

- Gallium arsenide injection laser for communication systems with pulse frequency modulation, noting power output dependence on crystal quality 14 p2459 A69-29349

- Efficient extinction in optically coupled GaAs injection lasers achieved by selecting quenching radiation frequency close to operating frequency 15 p2633 A69-30059

- Injection semiconductor lasers emission characteristics, discussing gallium arsenide diodes, nonlinear losses in pulsed mode, laser interactions, etc 16 p2796 A69-31949

- GaAs dual diode laser structure used to give electrical control of laser threshold and permit study of optical flux and current density role 17 p2980 A69-32959

- Monograph on GaAs injection laser electrical and optical properties during crystallization out of solution covering principle, p-n junction fabrication, I-V characteristics, doping effect, etc 17 p2982 A69-33571

- Amplitude and output spectra of optical quantum amplifier based on GaAs injection laser, noting values in traveling wave and regeneration mode 19 p3336 A69-36348

- Injection lasers threshold characteristics, studying temperature and doping level effects on current density and radiation energy 19 p3337 A69-36527

- Injection lasers external quantum efficiency, stimulated and spontaneous emission and photoluminescence measurements 19 p3337 A69-36528

- Magnetic field effects on emission line shift, threshold current and power output of GaAs injection laser, discussing spontaneous radiation in magnetic field 19 p3387 A69-36529

- GaAs p-n injection laser output at 4.2 K in strong transverse magnetic field, deducing effective mass and g-factor from stimulated emission peak shift 19 p3387 A69-36530

- Coherent emission from injection electron-hole plasma in indium antimonide without magnetic field, noting roles of crystal thickness and pinch effects 19 p3387 A69-36532

- Radiation dynamics of GaAs injection semiconductor laser, plotting spike period dependence on resonator length 19 p3337 A69-36535

- GaAs-P injection laser time delay measured from start of current flow in p-n junction diode, studying effects of memory, temperature and reverse bias 19 p3387 A69-36536

- Indium arsenide injection laser observed for self modulation at LF modes, discussing nonMarkovian character of photon density relaxation 19 p3338 A69-36537

- Stimulated emission at current pulse end ascribed to external resonator turn-on time delay effects with GaAs injection lasers at room temperature 21 p3734 A69-38408

- Memory effect in injection lasers output characteristics, noting anomalous increases in pulsed emission intensity with increasing current-pulse repetition rate 21 p3735 A69-38694

- GaAs injection laser properties calculation with doping levels for exponential band tails formation, deriving threshold currents, lasing frequencies, I-V characteristics, etc 22 p3959 A69-40012

- Emission dynamics and fine pulse structure in GaAs injection lasers, determining pulse duration and amplitude dependence on current and resonator length 22 p3963 A69-40603

- Amplification coefficient, luminescence power and spacing between Fermi quasi-levels in GaAs diode injection lasers, using spectral absorption dependence 22 p3965 A69-40801

- Intensity of optical pulses from CW GaAs injection lasers observed with fast sampling techniques 23 p4173 A69-41500

- Oscillographic recording of GaAs laser ultrashort radiation pulses, using isolated injection regions and semiconductor photodiode as photoelectric converter 24 p4329 A69-43740

INJECTORS

NT VORTEX INJECTORS

- Condensing injector cycles internal efficiency for high velocity liquid metal flows in closed cycle MHD power plants 02 p0194 A69-11582

- Injector vaporizer performance in liquid metal MHD system, using model for total and static pressure distribution 06 p0871 A69-17918

- Injector design based on MHD injector components performance, establishing minimum diffuser nozzle area 06 p0872 A69-17920

- Liquid metal MHD systems efficiency when operating with pressure jump in diffuser nozzle 06 p0872 A69-17921

- Wet steam injector power losses in nozzle as function of humidity, noting compensation of nozzle throat diameter and fluid flow rates 13 p2246 A69-27490

- Oxidizer injector face configuration for high power variable thrust rocket engine using hydrogen/oxygen propellant 16 p2835 A69-31749

Oxygen difluoride-diborane propellant injector and chamber design criteria applied to unmanned spacecraft rocket engine development
[AIAA PAPER 69-508] 16 p2839 A69-32671

Fluorine injectors for main tank injection of space vehicle liquid hydrogen tank, including study of hypergolicity and reaction product freezing
[AIAA PAPER 69-528] 16 p2767 A69-32717

Electroforming methods in design and fabrication of liquid propellant rocket motor injectors and composite thrust chambers
[AIAA PAPER 69-583] 16 p2794 A69-32757

Space storable hydrocarbon fuel blended FLOX propellant performance with coaxial injector including characteristic velocity, chamber geometry, pressure and heat flux distribution
[AIAA PAPER 69-507] 16 p2835 A69-32772

Rocket performance optimization by extending injector design technology to high performance injectors for space storable FLOX/LPG propellants
[AIAA PAPER 69-506] 16 p2846 A69-32778

Liquid propellant rocket injectors response to HF chamber pressure oscillations using one dimensional model
21 p3786 A69-39235

INJUN SATELLITES

Injun 5 satellite VLF electric and magnetic field observations, discussing antenna operation, Poynting flux and noise band measurements
22 p3938 A69-40503

INJUN 5 SATELLITE U EXPLORER 40 SATELLITE

INJURIES

NT BACK INJURIES
NT BAROTRAUMA
NT BRAIN DAMAGE
NT BURNS [INJURIES]
NT CRASH INJURIES
NT EJECTION INJURIES
NT LESIONS
NT NOISE INJURIES
NT PULMONARY LESIONS
NT RADIATION INJURIES

Head injuries evaluation in aircrew, noting motor cycle accidents
10 p1649 A69-23378

Injury stress vs acceleration specification as valid criterion for pilots subjected to high acceleration, introducing models and illustrating with ejection example
17 p2913 A69-33008

Acceleration injury noting water immersion effect on cat lung due to intense body vibration, suggesting restraint as practical solution
17 p2913 A69-33009

Air evacuation of maxilla-facially wounded persons from place of accident, noting helicopter use
24 p4270 A69-42603

INLET FLOW

Energy dissipation at rounded pipe entrance in viscous fluid, showing relation between entrance loss and radius of roundness
01 p0059 A69-10308

Engine inlet thermal antiicing analysis, detailing computer programs to determine air flow velocity, water impingement and thermal requirements
01 p0055 A69-11045

Vitiated inlet air effects on J60-P-6 turbojet engine performance at sea level for various simulated flight Mach numbers
01 p0143 A69-11063

Confined jet mixing region at entrance of tubular reactor, discussing mass and momentum transfer, chemical conversion and effect of Reynolds number
[AICHE PAPER 25A] 04 p0586 A69-14508

Coaxial flow jet chamber flow patterns dependence on inlet gas velocity, density and length/diameter ratio
[AICHE PAPER 25B] 04 p0587 A69-14509

Entry region flow and convective heat transfer prediction in cooled vertical pipe open at both ends, considering wall temperature
05 p0845 A69-15717

Circulation, geometry and viscosity effects on speed of surge in bathtub vortex
05 p0744 A69-15718

Suction effect on incompressible flow through step expansion in circular pipe through sudden enlargement, considering inlet flow with thin boundary layer
[ASME PAPER 68-FE-11] 05 p0748 A69-16074

Inlet velocity profiles distortion effects on flow regimes and performance in two dimensional diffusers with turbulent boundary layers
[ASME PAPER 68-WA/FE-25] 05 p0698 A69-16100

Inlet conditions influence on two annular diffusers performance, using low speed tests
[ASME PAPER 68-WA/FE-38] 05 p0698 A69-16110

Conical diffuser/exit duct performance and model for estimating energy losses, discussing inlet flow and Reynolds number
[ASME PAPER 68-WA/FE-45] 05 p0698 A69-16112

Oblique shock wave propagation through two dimensional steady nonuniform incoming flow, discussing higher order theory via irrotational or rotational disturbances of arbitrary amplitude
[AIAA PAPER 69-39] 06 p0913 A69-18103

Shockload on axial intake fan leading edge of radial flow compressor, calculating flow field
08 p1251 A69-20604

Lift engine model compressor response to inlet pressure distortion to determine nature and extent of critical area of spoiling for axial flow compressors
[ASME PAPER 69-GT-29] 09 p1571 A69-22493

Incident flow in variable cross section tubes using analytic asymptotic calculation
10 p1677 A69-22897

Laminar flow heat transfer of viscous incompressible fluid in entrance region of circular tube, using nonlinear equations
10 p1809 A69-23195

Duct entrance region flow, analyzing eigenvalue problem and nonlinear transformation simplification
11 p1874 A69-25285

Ejector-diffuser performance improvement by reduction of backflow with orifice plate installed at inlet of straight diffuser duct
11 p1819 A69-25382

Finite difference method for heat transfer for developing laminar flow at inlet of circular uniformly heated and isothermal tube, determining Nusselt number
12 p2062 A69-26242

Steady state flow of viscous conducting liquid in inlet of channel with or without transverse magnetic field, emphasizing approach to Hartmann-Poiseuille patterns downstream
12 p2138 A69-26626

Exhaust gas reingestion and inlet flow distortion in V/STOL lift engines, discussing static and wind tunnel testing using fighter configuration models
[AIAA PAPER 68-78] 12 p2012 A69-26762

Aerodynamic effects of lift jet and lift fan inlets in transition flight, analyzing inlet momentum lift, inlet lip lift and drag
[AIAA PAPER 68-637] 12 p2014 A69-26767

Navier-Stokes equations of slow viscous fluid laminar flow near pipe inlet and exit with negligible mass forces, discussing velocity and pressure distribution
13 p2244 A69-27258

Diffuser inlet geometry, studying effects of straight section length on flow pattern and diffuser resistance
14 p2391 A69-29899

Inlet shape and Reynolds number effects on entrance flow development, using laser flowmeter based on Doppler effect to obtain laminar velocity profiles
15 p2589 A69-30001

Aerodynamic losses and stage efficiency in partial admission turbines, using flat bladed rotor experiments and rotors of different blade pitch
15 p2547 A69-30290

Injected gas flow nonisothermicity and transversity effects on friction, heat transfer and flow parameters at cylindrical tube inlet
15 p2592 A69-30986

Compressor surge effect on mixed compression inlet flow from numerical solution of one dimensional unsteady inviscid flow equations in variable area duct
[AIAA PAPER 69-484] 16 p2841 A69-32682

Inlet thermal boundary layer thickness effect on conical nozzle heat transfer and boundary layer determined by operating nozzle with cooled/uncooled inlet
[AIAA PAPER 69-474] 16 p2881 A69-32780

Conducting fluid incompressible flow in entrance of MHD channel by momentum integral method, permitting edge stress existence at boundary layer free stream interface
[AIAA PAPER 69-724] 17 p2952 A69-33436

Statistical analysis in inlet air flow dynamics, discussing inlet duct design and pressure variations
[AIAA PAPER 68-649] 17 p2896 A69-34020

Fueling process in internal combustion engines having fuel admission systems with different flow cross sections
19 p3393 A69-35824

Diffusion flame stability at inlet of fuel stream into oxidizer, showing ignition coordinates dependence on fuel, oxidizer and ratio of burning/flow rate
19 p3448 A69-35855

Diffuser for high performance centrifugal compressors based on discrete pipe drillings
[ASME PAPER 68-GT-38] 19 p3240 A69-36420

NonNewtonian power law fluids flow behavior in circular pipe entry region, taking into account energy loss due to viscous dissipation in boundary layer
19 p3240 A69-36472

NACA submerged intake performance at M 2.5, considering total pressure and mass flow ratios, drag coefficient and boundary layer thickness effects
19 p3242 A69-36819

Potential flow interaction effects between blade rows in axial flow compressor stage, emphasizing inlet guide vane-rotor interaction
21 p3643 A69-38439

Heat transfer in curved channel as function of inlet configurations, obtaining Nusselt number equations for thermal and mixed convection and laminar flow
21 p3850 A69-38866

Subsonic compressible flow at two dimensional inlets, analyzing field representation, boundaries, surface configuration and optimal wedge
23 p4060 A69-41915

Spanwise velocity profiles through cascades and axial flow turbomachines, analyzing loading, secondary losses and inlet conditions interacting on downstream profile
23 p4061 A69-42110

Turbulent boundary layer at inlet section of gas blown tube based on solutions of energy and momentum equations, deriving relations for inlet section length
24 p4300 A69-43079

Hydrodynamic inlet conditions effect on film boiling and near critical hydrogen heat transfer, using data from electrically heated various geometry test sections
[ASME PAPER 69-HT-27] 24 p4412 A69-43541

INLET NOZZLES

Sonic nozzle optimal profile determination with and without cylindrical throats, noting sonic line curvature importance on discharge coefficient
02 p0188 A69-12037

Pressure recovery of straight channel divergence diffusers at high inlet Mach numbers
[ASME PAPER 68-WA/FE-19] 05 p0698 A69-16095

Turbomachinery multiple pure tone noise associated with acoustic resonance of inlet cavities examined by narrow band filter tracking integer multiples of rotative speed
[ASME PAPER 69-GT-2] 09 p1572 A69-22509

Large scale axisymmetric inlet systems performance capabilities, reviewing theoretical and experimental programs
[AIAA PAPER 68-580] 17 p3022 A69-34018

INLET PRESSURE

Lift engine inlet development for XV-4B aircraft, discussing tests, pressure distortion and recovery during simulated hover and transitional flight
[AIAA PAPER 68-636] 20 p3585 A69-37150

INLETS [DEVICES]

U INTAKE SYSTEMS

INNER RADIATION BELT

Inner Van Allen belt proton dose rate and spectral charged particle environment profiles correlated, noting agreement with theoretical values
01 p0145 A69-11081

Electron flux intensities and energy spectra in inner radiation zone, noting decay constants
01 p0147 A69-11235

Cosmos satellites monitoring electrons distribution in inner radiation belt suggest intensity stability for solar activity cycle
01 p0147 A69-11309

Nonadiabatic particle losses effect on integral proton flux in inner radiation belt, discussing proton energy spectrum
06 p0921 A69-17742

Bimodal diffusion mechanism for acceleration of trapped electrons and protons in earth radiation belts, noting particle intensity profiles and energy spectra
09 p1576 A69-21708

Inner radiation zone including data on electrons, protons and heavier particles and results from high altitude nuclear tests
12 p2152 A69-27144

Low altitude trapped protons in inner radiation belt during solar minimum period, using emulsion detectors on polar-orbiting satellite
18 p3187 A69-34944

- RF synchrotron emission from electrons trapped in earth magnetic field observed by satellite, using magnetospheric environment model
18 p3128 A69-34948
- Cosmic ray albedo neutron decay /CRAND/ source for trapped protons, showing disagreement with intensities in inner zone measured on OV1 2 spacecraft
22 p4005 A69-40512
- Cosmos 137 proton spectra data obtained in inner radiation belt agreeing with Relay 1 data
22 p4007 A69-41093

INOCULUM

- Inoculum dose effect on complement-fixing antigen production, heat lability and separation from BHK-21 cells infected with lymphocytic choriomeningitis virus
24 p4263 A69-43336

INORGANIC COATINGS

- NT ANODIC COATINGS
NT CERAMIC COATINGS
- Cleaning, deoxidizing and chromating process effects on chromate coated Al, using salt spray corrosion tests
19 p3321 A69-35570
- Inorganic heat resistant coatings high temperature mechanical tests noting corrosion, safety factors and rigidity after heating and temperature gradients
20 p3538 A69-37360
- Zr and Nb carbide coatings on Nb, Ta Mo and W, investigating methods for coating and base metal combinations
20 p3560 A69-37362

INORGANIC COMPOUNDS

- NT AMMONIA
NT LIQUID AMMONIA
- Refractory metal oxidation protection by inorganic compounds at high temperatures, discussing protective mechanisms
09 p1526 A69-22322
- Book on inorganic high energy oxidizers covering synthesis, structure and properties of fluoronitrogen, fluorine, fluorohalogen and oxygen compounds
12 p2146 A69-25824
- Life origin and organic-inorganic systems, emphasizing protein colloids-mineral salts interactions at protocell stage
14 p2408 A69-29632
- Radiation effect on inorganic solids isothermal decomposition induction period, deriving equations for conditions representing various kinetics combinations during irradiation [WSCIPAPER 69-21]
16 p2832 A69-32359
- Hydroxylamine complexes of inorganic salts preparation and characterization, including hygroscopic properties, chemical bonds, etc
17 p2917 A69-33657
- Liquid filter cells design with emphasis on filters usable for inorganic and organic liquids
21 p3770 A69-38679

INORGANIC NITRATES

- U AMMONIUM NITRATES
U SILVER NITRATES

INORGANIC PEROXIDES

- U HYDROGEN PEROXIDE

INORGANIC SULFIDES

- U CADMIUM SULFIDES
U COPPER SULFIDES
U HYDROGEN SULFIDE
U INDIUM SULFIDES
U LEAD SULFIDES
U MOLYBDENUM DISULFIDES
U MOLYBDENUM SULFIDES
U WURTZITE
U ZINC SULFIDES

INPUT

- Input transistor performance analysis in Schmitt trigger circuit, considering role of hysteresis
01 p0039 A69-10170
- End correction for input admittance of electrically thick monopole antenna with arbitrary radius driven from coaxial line
02 p0219 A69-12346
- Input signal piecewise linear approximation for investigating response of dynamic automatic control systems to nonstandard input signal
14 p2426 A69-29143

INPUT/OUTPUT ROUTINES

- Aerodynamic research for rotary wing and V/STOL aircraft, suggesting analytical techniques with software packages designed around standard input/output formats
23 p4146 A69-41373
- Telological systems behavior modeling based on input, output, goals, operation duration, etc
23 p4134 A69-42059

- Stewart-Hamilton theorems for total input-output analysis of body cholesterol in man
24 p4259 A69-42639

INSECTICIDES

- U DICHLORODIPHENYLTRICHLOROETHANE
U URETHANES

INSECTS

- NT BEETLES
NT DROSOPHILA
NT PUPA

- Drosophila melanogaster flies reproductive behavior and Tradescantia paludosa chromosome patterns after weightlessness onboard Vostok 3 and 4
07 p1063 A69-18597

- Radar application to meteorology, entomology and ornithology, discussing clear air turbulence detection and flight tracking of birds and insects
12 p2034 A69-27004

- Depolarization degree of angel echo signals measured by radar station, indicating insects and other foreign particles in atmosphere as reflection sources
16 p2779 A69-32274

- Angel sources rate of motion observed at automatic tracking coherent pulse station, obtaining coincidence with wind and insect velocities
16 p2779 A69-32276

- Insects mutational responses to space flight and associated radiation on biosatellite 2 compared with ground based controls
20 p3476 A69-37618

- Nervous system relations to insect flight musculature of lift and thrust mechanism
21 p3651 A69-38780

- Virulike particles in fat body cells and oenocytes of Drosophila melanogaster imagoes, in glial cells of cephalic ganglionic center of flies and in gamma radiated cells
23 p4091 A69-42021

INSENSITIVITY

- U SENSITIVITY

INSERTION

- Low thrust guidance for multirevolution trajectory required for earth parking orbit transfer to parabolic orbit insertion, noting advantages over high thrust scheme [AAS PAPER 69-403]
24 p4379 A69-42832

INSERTION LOSS

- Radome material insertion loss measurement by radiometric method noting error analysis
02 p0251 A69-12434
- Reciprocal latching ferrite phase shifters application to lightweight scanned phased arrays, noting quasi-circularly polarized modes with lowest insertion loss
04 p0572 A69-14320

- Peak acoustic attenuation frequency shifts and peak power insertion losses in air flow ducts related to air specific weight changes
07 p1117 A69-19700

- 360 degree varactor linear phase modulator, analyzing impedance matching, insertion loss, tuning design and serrodyne application
16 p2756 A69-31577

- Dual channel waveguide insertion loss test set for calibrations at 90 GHz in radio astronomy and communication systems, using sprayed thermistor mount
16 p2760 A69-31945

- Channel dropping filter for millimeter wave in low loss circular waveguide for overland telecommunications in bandwidth over 10 GHz
17 p2936 A69-33032

- Semiconductor phase shifting for inertialess antenna scanning at microwave to millimeter wavelengths, describing diode construction with emphasis on solving insertion loss [ONERA-TP-712]
23 p4143 A69-42519

INSERTS

- NT NOZZLE INSERTS

- Stresses due to nucleus of thermoelastic strain in infinite elastic solid with two rigid circular inserts
16 p2872 A69-31906

INSOLATION

- Daily insolation observations at Blue Hill, Massachusetts, correlated by month with observations of temperature, snow cover, winds, sunshine, sky cover, pressure and precipitation
01 p0066 A69-10862
- Earth surface temperature change quantitative determination due to Milankovitch insolation variations
03 p0426 A69-14232

INSPECTION

- NT INFRARED INSPECTION
NT X RAY INSPECTION

- Imaging systems for weld inspection, discussing physical factors and selection of radiation
07 p1139 A69-18794

- High pressure storage vessels for gaseous hydrogen: discussing failure, manufacturing controls and access for internal nondestructive inspection [ASM PAPER D8-14.1]
07 p1143 A69-19664

- Passenger aircraft flight readiness verification: discussing flaw and corrosion detection and rivet joint inspection methods
11 p1822 A69-24524

- Remote disassembly and inspection methods for evaluating NRX-AG reactor components performance [AIAA PAPER 69-511]
16 p2810 A69-32744

- Radioactive Kr as gaseous penetrant for nondestructive test inspections, noting high sensitivity
19 p3322 A69-35574

- Holography for engineering metrology, discussing interferometry, pattern interpretation, inspection techniques, etc
22 p3945 A69-40233

INSTABILITY

- U STABILITY

INSTALLATION

- U INSTALLING

INSTALLING

- Aerodynamic characteristics of power plant installation, discussing nacelle design from viewpoint of aircraft performance and economic efficiency
17 p2898 A69-33215

- Clamping and sealing fastener for single direction installation consisting of pin, collar and sealing collar with insert
22 p3957 A69-40831

INSTITUTIONS

- U BUREAU [ORGANIZATIONS]

INSTRUCTIONS

- U EDUCATION

INSTRUCTORS

- Witkin Rod and Frame Testing of pilots and engineers requiring greater field independence in pilots: discussing applications to pilot instructor selection
12 p2023 A69-26556

INSTRUMENT APPROACH

- Multifunction helicopter rotor blade radar for navigation, IFR approach and fire control, including flight test results [AHS PAPER 315]
17 p2920 A69-33535
- All-weather landing in civil air operations, discussing ground/air systems in tracking, visual reference and aircraft performance required for safe landing capability
20 p3574 A69-38119

INSTRUMENT COMPENSATION

- NT TEMPERATURE COMPENSATION

- Automatic control systems correction by compensation for nonlinear statistical dynamic characteristics with aid of nonlinear devices
01 p0053 A69-10801

- Solar X ray flare absolute flux correction, taking into account geometric obliquity factor variation with angles between satellite spin axis and satellite-sun line
01 p0147 A69-11242

- Compensation method for measurement of mismatched noise source effective temperature independent of reflection coefficient, noting error analysis
02 p0210 A69-12441

- Multiple beam electronically steerable retrodirective antenna array with automatic inertialess compensation for altitude or beacon location
02 p0212 A69-12816

- Optical pumping distortion compensation in glass laser rod by changing coolant temperature, obtaining mode locked laser pulses
04 p0609 A69-14286

- Optimal compensating loop in stabilization circuit of uniaxial gyrostabilizer
04 p0597 A69-14604

- Dry friction stabilizing effect on motion of astatic gyroscope with quasi-elastic compensation
04 p0597 A69-14605

- Radiation compensating thermocouple for gas temperature measurement, noting advantage over single thermocouples
04 p0598 A69-14916

- Satellite-borne auroral particle spectrometer calibration to minimize uncertainty in measuring absolute particle flux of electrons and protons
04 p0599 A69-15022

- Low DC current measurement on board satellite, noting absence of elaborate compensation
04 p0602 A69-15399

Automatic compensation of unwanted signal level fluctuation in measuring setups including microwave generators and detectors

06 p0903 A69-17489

Calibration curve for constant temperature hot-wire anemometer, taking into account high wire temperature and gas pressure effects

06 p0930 A69-18218

Sky background light automatic compensation in stellar photography, using single or double channel photometer

08 p1313 A69-20247

Linearization unit for compensating hyperbolic characteristic of capacitive displacement sensor used for contactless displacement measurement

08 p1317 A69-20879

Specifying electrical isolation and error signals suppression due to presence of common mode voltage in passive signal handling and conditioning equipment

10 p1654 A69-23272

Optimum calibration interval program for determining test equipment calibration frequencies on basis of mean time between failures and acceptable reliability levels

10 p1699 A69-23288

Spectral baseline instability correction for time of flight mass spectrometer operating at source pressures up to one torr

10 p1693 A69-23345

Constant velocity moving object influence on indications of vertical gyroscope having electromagnetic compensation with residual imbalance of sensor element

11 p1881 A69-24561

Multiple frame camera with image compensation as ballistic phototheodolite

12 p2084 A69-26153

Comparative calibration characteristics determination, discussing absolute measurements method for thermal conductivity parameters

12 p2091 A69-26363

Bandwidth potential increase of parametric amplifier obtained by adding active filter elements to signal circuit, noting satellite communication band

12 p2039 A69-26380

Solar spectroscopic techniques, discussing instrumentation problems affecting photosphere line spectra, SNR in absorption spectra and near IR spectra

13 p2341 A69-27588

Electrical properties of p-type indium antimonide, noting effects of deep level compensation on ϵ_v values

13 p2318 A69-27895

Ballistic deviations limits for aircraft vertical gyroscope taking into account aircraft vertical movements, using compensation in system

14 p2445 A69-28899

Direct phase measuring and measured phase compensating microwave devices designed for plasma diagnostics applications

14 p2452 A69-29804

Laser emission divergence reduced by compensating optical inhomogeneity of active elements with prismatic reflector in resonator

17 p2983 A69-33970

Buffer shift register with feedback control during tape recorder playback to obtain variable delay to compensate for recorder time base error

19 p3312 A69-36284

Airborne imaging radar motion compensation and sensing problems concerning perturbed signal correction, discussing spatial sensitivity measures and constraints

20 p3490 A69-37645

Light sources with uniform variable luminance field designed for calibrating cameras used in space exploration

21 p3726 A69-39580

Isoclinic angle errors effects on photoelastic fringe order measurements accuracy

22 p3945 A69-40082

Calcium K line strengths in A stars measured by narrow band spectrometer compensated for seeing and transparency variations

22 p4015 A69-40154

Screw-nut feeder and adjustor systems with compensation for clearance and wear of cutting tools, determining efficiency for conversion of rotary to translational motion

23 p4168 A69-41414

Accelerated motion influence on onboard vertical gyro with design based on free astatic gyro with electromagnetic compensation

23 p4163 A69-41553

Wideband telemetry recording error compensator for reducing flutter and interchannel time-base error in magnetic tape instrumentation

23 p4137 A69-41775

Surface accuracy of large diameter radio telescopes maintained by uncoupling reflector surface from backup structure, using active compensation

23 p4149 A69-42136

RMS surface error compensation in radome-housed Cassegrain parabolic antenna including weight analysis

23 p4150 A69-42137

Linear motion blur compensation technique in photographic recordings by reconstruction of sharp image from hologram

24 p4314 A69-42972

INSTRUMENT ERRORS

Micrometeorites acoustic recordings on Cosmos 135, investigating data reliability influenced by appearance of thermal noise

01 p0152 A69-10578

Phase ionosonde cost, possibilities and errors

01 p0071 A69-11163

Solid body automatic orientation, discussing data units for angular error and angular velocity

-01 p0122 A69-11302

Geomagnetic field H and Z components measured by proton magnetometer, applying supplementary field method for error correction

02 p0238 A69-11675

Rubidium self oscillating magnetometer long term stability, noting changes affecting accuracy and sensitivity

02 p0250 A69-12394

Mismatched errors associated with Y factor power ratio measurement effect on microwave noise-temperature calibrations

02 p0211 A69-12442

VOR path course errors, emphasizing effects of propagation and receiver processing

03 p0392 A69-13245

Instrument and rounding-off errors of aircraft computers as function of digital network dimensions

04 p0563 A69-14491

Radiation compensating thermocouple for gas temperature measurement, noting advantage over single thermocouples

04 p0598 A69-14916

Evaluation tests of fixed frequency variable tension vibroscope for filaments and wires, noting instrument errors and corrections

04 p0599 A69-15018

Errors in amplitudes and phases recorded by earth tide recording equipment determined, using special multiflex galvanometer

04 p0601 A69-15305

Strapdown gyros in back to back connection for reduction of component cross coupling errors

04 p0603 A69-15473

Tensiometric aerodynamic balances in great velocity ranges, discussing measurements, elastic elements and tensiometric balance construction and measuring errors nature

05 p0762 A69-15922

Expressions for calculating filtering errors resulting from insufficient information about useful signal and noise characteristics

05 p0740 A69-16668

Error origin and control in high gain operational amplifier in time differentiation of voltage signal used for photoemission studies

06 p0897 A69-17700

Upper wind observation and computation accuracy, comparing radar and slide rule instrument errors

06 p0950 A69-17788

Automatic remotely operated sodium D line reversal temperature measuring apparatus, analyzing systematic errors

06 p1035 A69-17932

Nonstationary aerodynamic load for harmonically oscillating body in fluid flow with constant mean velocity measured, determining errors as functions of system parameters

07 p1050 A69-18752

Root mean square time delay error with respect to playback time and autocorrelation function of tape recorded sine wave for studying jitter spectra

07 p1132 A69-18827

Boresight error in missile radome-antenna combination due to reflection and surface wave effects

07 p1111 A69-19536

Noise-signal receiver amplitude-limitation effect on noise measurement in presence of pulsed interference

07 p1088 A69-19754

Phase error and amplitude and phase modulation in aircraft VOR omni receiver in vicinity of reflecting objects, noting asymmetrical filter effect

08 p1271 A69-19863

Pointing calibration of Haystack parabolic antenna by using radiometric measurements of cosmic ray sources

08 p1281 A69-20032

Coincidence error between star image and planet edge for entrance pupil and telescope magnification

08 p1314 A69-20383

Radio interferometer antenna array spatial characteristics obtained as function of geographical coordinates of site for reducing observation errors

08 p1314 A69-20434

Error analysis of high resolution balloon-borne temperature sensor and comparison of temperature data with simultaneous rawinsonde measurements

09 p1494 A69-21642

Microwave interferometer circuits errors, considering interferometers with phase detector, logic counting circuits, frequency conversion and amplitude modulation

09 p1496 A69-22029

Refraction errors in plasma density measurement by microwave interferometry

09 p1496 A69-22031

Operational errors of floating gyroscopes with hydrostatic unloading of bearings, establishing eccentricity tolerances, axes misalignment and temperature field nonuniformity

09 p1497 A69-22103

Kinematics of vertical gyroscope mounted in additional servo frame, determining kinematic errors due to rotor axis deviation

09 p1498 A69-22108

Gyroscope error due to axial play of inner gimbal of Cardan mounting during base circular vibrations, noting axial clearance reduction

09 p1498 A69-22110

Calibration for instrument systems including strain gages, piezoelectric, thermoelectric and thermoresistive transducers

10 p1691 A69-23229

Noise in instrumentation systems, considering coupling and current noise source and reduction by isolation and filtering

10 p1691 A69-23231

Photogrammetry for three dimensional geodesy, discussing satellite triangular methods, refraction anomalies, error corrections, etc

10 p1682 A69-23390

Algorithm for determining readings dispersion during cosmic ray recording, considering cosmic rays variability, statistical nature and instrument errors

10 p1770 A69-23906

Satellite mounted radiometers for determining albedo variations, using Fredholm equation with allowance for instrument errors

10 p1689 A69-23969

Nonpolar latitude variations due to observation errors, discussing instrumental, computational and meteorological influence, particularly refraction resulting from climatic conditions

11 p1952 A69-24257

HF measurements by phase and amplification control of signal in impulse oscillography, noting accuracy in nanosecond range and signal distortion

11 p1880 A69-24541

Inertial navigation systems error analysis based on method of state variables

11 p1914 A69-25434

Optimal scale factor selection to ensure minimum error variance in signal detection against random noise background for input limited range of measuring instrument

12 p2079 A69-25966

Multielectrode plasma probe with potential negative with respect to plasma, noting effect of microoptical features of probe on accuracy of I-V measurements

12 p2138 A69-26538

Instrument error analysis for spacecraft orientation and positioning near planet from planet disk observations

13 p2260 A69-27695

Refraction error in measurements with simple and radar interferometers, considering atmospheric effect

13 p2221 A69-27961

Ferrite parameters measurement in alternating fields based on continuous analysis of magnetic, magnetizing and measuring circuits for assessing errors

13 p2320 A69-27996

Plasma microwave interferometry error due to refraction and beam displacement at receiving antenna aperture
13 p2312 A69-28113

Ionization calorimeter energy measurement systematic errors
13 p2331 A69-28394

Geomagnetic field H and Z components measured by proton magnetometer, applying supplementary field method for error correction
13 p2257 A69-28706

Directional gyroscope with interframe correlation, discussing errors during object pitching and banking
14 p2446 A69-28923

Electrolytic vertical indicators response errors, discussing nonlinear properties of transducer steady state characteristics
14 p2446 A69-28925

Atmospheric multifrequency probing accuracy limitation imposed by irregularities based on scatter theory
14 p2449 A69-29535

Dynamic instrumental errors of quasi-steady state mechanical meters approximated by graph analytical method
14 p2451 A69-29747

Instrumental accuracy of discrete filter during measurement of initial phase of signal dependent on phase structure
15 p2574 A69-30139

Calibration of interference measuring instruments, stressing input impedance calibration of field intensity meters
15 p2577 A69-30375

Micrometeorites acoustic recordings on Cosmos 135, investigating data reliability influences by appearance of thermal noise
15 p2691 A69-30748

Barometric altimeters development, discussing servo and three pointer types, accuracy, Central Air Data Computer repeater function and future trends
15 p2610 A69-30859

Reflecting or reradiating obstacle proximity as cause of siting errors in azimuth radio measurements, discussing omnidirectional obstacles effect
15 p2651 A69-31090

Thermocouple probe measurement error evaluation by parallel plate analytical model
16 p2789 A69-31903

Piloting errors due to false instrument readings during turbulent atmosphere flight
16 p2734 A69-32007

Azimuth error from observations of circumpolar stars at greatest elongation using transit instrument
17 p3028 A69-32878

Differences in latitude readings obtained with two zenith telescopes, showing Pearson distribution of type VII and influence of observation conditions
17 p2959 A69-32879

Photomicroscope film plane inclination adjusted to improve circle readings measurement, noting instrument errors role in star declinations errors
17 p2970 A69-32881

Contact thermocouples to measure temperature of wall exposed to radiation, evaluating errors
17 p2975 A69-33596

Gyrocompassing precision problems related to gyro drift, input axis deviation and base motion compensation, describing inertial navigation platform alignment to true north
17 p2977 A69-34081

Measurement errors and geometry effects on navigational accuracy, determining maximum allowable error for measuring devices employed
17 p3002 A69-34098

Turbulence measurement errors with inclined hot wires described by equations, assuming normal component cooling includes greater tangential cooling
18 p3134 A69-34442

Casing bearings dry friction force moment effect on double rotor gyrocompass sensor motion, showing diminished device accuracy at high latitudes
18 p3135 A69-34560

Inertial aircraft navigation, describing instruments and error analyses with regard to simulation, error propagation and total system error
18 p3169 A69-34850

Automatic celestial navigation, discussing star trackers design, mathematics of celestial fix and relationship to errors and physical and environmental constraints
18 p3169 A69-34852

Dynamic performance accuracy of astatic gyroscope with three degrees of freedom improved by inner gimbal mass increase
19 p3308 A69-35825

Directional couplers design considerations for use in microwave power meters, analyzing directivity and mismatch effect on system error
19 p3282 A69-35826

Wall influence on thermoanemometer readings in incompressible air stream measured with wedge shaped film sensors
19 p3308 A69-35857

Meteorological corrections of meson megatelescope data based on hourly ground-level pressures and temperatures, considering vector and regression analyses
19 p3308 A69-35991

Errors in sighting and identifying geodetic contour points on aerial photographs, considering stereocomparators parallaxes effect
21 p3719 A69-38404

Gyroscopic platforms automatic stability relative to inertial reference system, considering functional equations and error computation
21 p3760 A69-38734

Precision autocollimating solar sensor design for attitude alignment changes, including detector calibration and sounding rocket flight test results [AIAA PAPER 69-858]
21 p3762 A69-39386

Satellite mounted radiometers for determining albedo variations, using Fredholm equation with allowance for instrument errors
21 p3717 A69-39655

Temperature control instrumentation accuracy in terms of static errors and dynamic errors minimizing costs
22 p3954 A69-40037

Standardizing strain gage with long time stability characteristics, analyzing statistically strain calibration results
22 p3945 A69-40078

Maximum errors of telemetering systems under interchannel transient distortions in multistage amplifier of video signals
22 p3899 A69-40250

Probability characteristics of total error in vertical gyroscope evaluated from component errors along suspension axes
22 p3946 A69-40251

Resistance thermometer for measuring rapidly varying gas temperatures, optimizing length to eliminate heat transfer to mounting
23 p4163 A69-41557

Distortion processes in ear, discussing sound pressure level (SPL) measurements in rigid-walled couplers
23 p4085 A69-41573

Analyzing conditions for variable magnetic and electric noise occurrence at input of nuclear precession magnetometer used in field strengths measurements
23 p4165 A69-41852

Antenna pointing and tracking accuracy by identifying error sources in servo, structural, mechanical and alignment factors
23 p4125 A69-42126

RMS surface error compensation in radome-housed Cassegrain parabolic antenna including weight analysis
23 p4150 A69-42137

Radial velocity errors in high dispersion astronomical spectrographs in terms of variable spectral shifts along plate produced by mirror surface irregularities
23 p4167 A69-42189

Pb isotopic analysis using double spike mass spectrometric method to achieve reproducibility and accuracy, discussing principles and performance
24 p4280 A69-42733

Extragalactic radio sources flux densities at 5009 MHz tabulated, ascribing accuracy variations to uncertainty in receiver gain and dish efficiency
24 p4382 A69-42922

Empirical determination of equivalent frequency characteristics of nonlinear system in random noise, assessing measurement errors
24 p4289 A69-42950

Scattered light meter accuracy as function of aerosol particles atmospheric distribution according to size, analyzing measurement errors
24 p4343 A69-42966

Astatic gyro motion with horizontal rotor axis, defining suspension error with allowance for external force moments
24 p4317 A69-43707

INSTRUMENT FLIGHT RULES

Rotary wing handling qualities, discussing analytical tools, design and IFR capabilities for higher speed range
05 p0701 A69-15550

Multifunction helicopter rotor blade radar for navigation, IFR approach and fire control, including flight test results [AHS PAPER 315]
17 p2920 A69-33539

Air traffic control, discussing objectives, government responsibilities and airspace organization, including U.S. system
18 p3170 A69-34859

INSTRUMENT LANDING SYSTEMS
NT AUTOMATIC LANDING CONTROL

All-weather landing factors for aircraft and pilots, describing instrument landing system, runway and visibility, pilot and crew procedures, etc
01 p0112 A69-10445

Low visibility instrument landing of aircraft using ILAS and inertial guidance
01 p0114 A69-11012

Air traffic control at Los Angeles International Airport, discussing simultaneous parallel ILS approaches and departures and STOL problems
01 p0057 A69-11356

Low visibility landing, discussing problems of radioguidance geometry, visibility measurement, aircraft dynamics, pilot psychology, regulation and politics
01 p0114 A69-11391

Flight inspection positioning system, discussing microwave interferometer angle calibration for instrument landing
03 p0430 A69-13680

Low visibility aircraft landing, discussing total system approach, modern electronic developments, collision avoidance, safety and air traffic control
03 p0465 A69-13853

V/STOL operations in intercity and intracity service, discussing technical feasibility and need for steep approach instrument landing system
05 p0703 A69-16723

Aircraft position and velocity in directions normal to ILS reference path by correlation with inertial navigation system, noting minimal time controller
07 p1177 A69-19213

Scanning beam landing systems for VTOL aircraft
07 p1178 A69-19631

STOL aircraft intercity test flights emphasizing curved ILS approach, using onboard computer for altitude and distance data
08 p1347 A69-20601

Airborne ILS marker beacon receivers and secondary surveillance radar transponder using microelectronic equipment, noting thermal dissipation problems [AGARDOGRAPH-114]
08 p1292 A69-20991

All-weather landing including zero-zero, discussing planning in Europe and U.S.A.
10 p1722 A69-23698

Manual control displays for instrument landing approach of large subsonic jet transport, evaluating closed loop system performance and scanning workload
10 p1650 A69-23877

Microwave scanning beam landing guidance system for Swedish tactical aircraft Saab 37 Viggen, reviewing ground station and onboard equipment
16 p2735 A69-32057

Direction defining radio beacons performance, discussing signal amplitude and phase comparison systems and Doppler techniques
17 p2918 A69-33028

Vertical path guidance computer, noting applications to feeder airlines and airtaxi services operating from airports with VOR/TACAN only
17 p3003 A69-34104

On-course monitoring for instrument landing system glide path operating with far field samples
17 p3003 A69-34105

Multisensor data processing technique for fail operational landing commands, using real time error analysis inherent in Kalman filter
17 p3003 A69-34106

TAPIR automatic pilot, describing components and automatic landing
19 p3371 A69-36704

Correlation protected ILS implementing conventional ILS with no operational restrictions on air traffic control, taking into account changing terminal conditions
22 p3978 A69-39963

Steep descent landing systems developmental phases for VTOL aircraft, discussing noise abatement, approach angle and descent rates
22 p3978 A69-40674

Low visibility VSTOL instrument landing system and associated electronic structures, discussing instrument to visual flight transition
22 p3979 A69-40675

Localizer acquisition system quasi-optimization technique based on time optimal control theory, with application to SST ILS problem
24 p4348 A69-43312

INSTRUMENT ORIENTATION

Solar X ray flare absolute flux correction, taking into account geometric obliquity factor variation with angle between satellite spin axis and satellite-sun line
01 p0147 A69-11242

Rocket released probe orientation determination from polarization measurements on telemetry signal
02 p0207 A69-11813

Astronomical alignment accuracy by rocket Cassiopeia system, discussing scientific payload rotation and orientation by celestial bodies
03 p0462 A69-12850

Error analysis of orientation methods for extraterrestrial stereophotogrammetric mapping [JPL-TR-32-1344]
03 p0429 A69-13299

Optical sighting method for determining orientation of rocket on launch pad by laser collimator, noting lining up of Cassiopeia system
06 p0930 A69-17104

Separable payload control for three axis orientation of sounding rocket instruments, discussing error sensors and pointing accuracies
06 p1014 A69-17583

Analytic platform or strapdown systems application, discussing closed and open loop leveling techniques
08 p1347 A69-19862

Spectral study of Stokes vector for light scattered by natural objects, recommending phase and optical axis inclination angles for aircraft measurements
09 p1588 A69-21367

Stabilized gyroscope platform internal dynamics analysis, outlining optimal orientation for full compensation of cross couplings
09 p1499 A69-22240

Large steerable mm wave radio telescope of Simeiz observatory in U.S.S.R. noting computer aided pointing system
10 p1674 A69-23805

Gyroscopes orientation influence on dynamic drift of triaxial power gyrostabilizer on rocking platform, noting optimum orientations
11 p1881 A69-24560

Spectral study of Stokes vector for light scattered by natural objects, recommending phase and optical axis inclination angles for aircraft measurements
18 p3198 A69-34756

Computerized prediction of RF instrumentation system signal margins for missile flight tests based on trajectory and range balance equation
18 p3103 A69-35097

Quartz compasses designed for orientation of electronic devices with respect to magnetic meridians at low horizontal component values
23 p4166 A69-41869

Portable He-Ne laser design featuring positional adjustment for use in aligning optical systems
24 p4327 A69-42924

INSTRUMENT PACKAGES

NT APOLLO LUNAR SURFACE EXPERIMENTS PACKAGE

Magnetometer experiment for Apollo project to measure lunar surface magnetic field, describing mission requirements and instrumentation [AAS PAPER 68-206]
02 p0312 A69-11481

Buoyant station with science package designed for long duration missions with horizontal mobility in Venus atmosphere
02 p0333 A69-11745

Manned spacecraft systems design optimization for extended space missions replacement modules
05 p0830 A69-16380

Surveyor lunar scientific payload and results, discussing TV camera, soil mechanics and surface sampler, alpha scattering instrument, small magnets and surface analysis
06 p1001 A69-17162

Attitude control system for maintaining orientation of experimental package relative to space stabilized platform, noting transient response and steady state accuracy
06 p0955 A69-17587

Small Scientific Satellite program, discussing payload for investigating magnetosphere and near interplanetary space [IEEE PAPER 3C-1]
07 p1230 A69-19195

Vela 4 satellite energetic particle experiment, describing instruments design and operation [IEEE PAPER 3C-2]
07 p1134 A69-19196

Pyrotechnic activated calorimeter for reentry package design of vehicles entering earth atmosphere at lunar return velocities
10 p1669 A69-23026

Transpondersondes for atmospheric measurements, considering ground tracking, radiosondes, rocket-sondes and flight results
10 p1692 A69-23257

Flight instrument package for change of energy absorption and energy radiation of vehicle surfaces during various phases of space vehicle mission
15 p2613 A69-31269

Stratospheric winds effect on instrument package suspended from high altitude balloon, discussing package displacements, yarn shapes and air drag characteristics
17 p2961 A69-33612

Atmospheric wind shear velocity snapping effect on yarn suspending instrument package from balloon gondola during parachute recovery
17 p2975 A69-33613

Duplex servoactuator package sized for stabilator channel of F-4 aircraft providing compact integrated control surface positioning [AIAA PAPER 69-788]
19 p3249 A69-35640

Strapdown redundant experimental sensor inertial navigation package containing gyros and accelerometers, discussing signal real time processing by digital computer [AIAA PAPER 69-851]
21 p3762 A69-39379

Gyro test package, dynamic test facility and real time attitude algorithm to investigate operational capabilities of strapdown inertial attitude package [AIAA PAPER 69-849]
21 p3765 A69-39424

Dornier ASTRID attitude stabilization system design for spinning rocket nose cone with instrument payload, using first stage biaxial inertial platform and second stage star tracker
21 p3826 A69-39639

Thermal design of missile mounted S band telemetry transmitter package based on temperature control system, using heat-of-fusion characteristics of wax material
22 p3909 A69-39945

INSTRUMENTAL ANALYSIS

U AUTOMATION

INSTRUMENTATION

U INSTRUMENTS

INSTRUMENTS

Digital data processing equipment for space flight PCM telemetry
03 p0393 A69-13290

Aerospace instrumentation - Conference, Cranfield, Beds., England, March 1968
05 p0765 A69-16747

Radiation effects on NERVA out-of-core instrumentation, discussing cryogenic temperature measurements and transducer measuring pressure at gamma heating rates
06 p0956 A69-16882

Fundamentals of aerospace instrumentation - ISA Conference, Boston, June 1968, Volume I
10 p1690 A69-23224

Instrumentation in the aerospace industry - Conference, Boston, June 1968, Volume I4
10 p1670 A69-23245

Noninterfering instrumentation techniques to measure hypersonic flowfield parameters in wind tunnels, measuring flight time of pulsed laser generated spark for velocity
10 p1672 A69-23266

Second order system equations to approximate transfer function of homogeneous pneumatic instrumentation line terminated with pressure transducer
10 p1692 A69-23267

Instrumentation - ISA Conference, New York, October 1968
15 p2615 A69-31286

Instrumentation - ISA Conference, New York, October 1968
15 p2553 A69-31293

Instrumentation in aerospace simulation facilities - Conference, Farmingdale, New York, May 1969
19 p3289 A69-35714

INSULATED STRUCTURES

Silicon dioxide dielectric isolation for high speed low power circuits, noting saturation resistance and transient characteristics
02 p0221 A69-12470

Gas breakdown model for analyzing breakdown of Ce vapor filled crack in thermionic trilayer insulator
09 p1441 A69-21840

Super insulation blankets comprised of dacron sailcloth, silk net or aluminized mylar, describing crinkling, cutting, sewing and hole drilling techniques
09 p1507 A69-22330

Multiwall meteoroid protection design in Apollo program, discussing bumper, backup sheet and honeycomb cells insulation [AIAA PAPER 69-372]
13 p2367 A69-28304

INSULATION

U ELECTRICAL INSULATION

U MULTILAYER INSULATION

U THERMAL INSULATION

INSULATORS

Electric field control of growth rates of insulating organic crystals from vapor phase
01 p0135 A69-10140

Negative resistance behavior of InSb diodes at 77 K, extending double injection theory for insulators to extrinsic semiconductors
02 p0294 A69-11722

Metal-insulator transition, observability and transition in ionic lattices and polar liquids
03 p0489 A69-13922

Solid insulator performance in vacuum, analyzing breakdown factors
05 p0731 A69-16243

Gamma radiation effects on gate threshold voltages in modified oxide insulators in MOS structures
06 p0976 A69-16876

Dielectric relaxation for analysis of defect structure, microstructure, surface behavior, structural changes kinetics and environmental effects in insulators and semiconductors
09 p1559 A69-22307

INTAKE SYSTEMS

NT AIR INTAKES

NT ENGINE INLETS

NT HYPERSONIC INLETS

NT SUPERSONIC INLETS

Ram recovery of flush intake for air cushion vehicles noting influence of intake geometry, placement and incidence angle
01 p0005 A69-10026

Water jet propulsion for air cushion vehicles, emphasizing inlet shape effect on performance and potential flow theory application to inlet design
08 p1254 A69-20115

M 3.5 two dimensional mixed compression inlet system with self restart using flexible variable ramp system [AIAA PAPER 69-447]
16 p2845 A69-32732

Turbopump weight minimization and low suction pressure requirements realized using high rotating speeds, hydraulic turbine driven upstream inducer and computer testing [AIAA PAPER 69-552]
16 p2741 A69-32747

Transient performance of full flow hydraulic turbine driven two speed pump inducer system, formulating computer model [AIAA PAPER 69-551]
18 p3140 A69-34415

INTEGERS

Integer programming method for optimizing constrained reliability problems with several system failure modes
20 p3504 A69-37069

INTEGRAL CALCULUS

Numerical evaluation of curvilinear integrals and areas, using digital computer
01 p0106 A69-10867

Integrals of nonlinear equations of evolution and solitary waves, discussing double wave solutions of Korteweg-de Vries equation
03 p0468 A69-13825

Analytical expressions for integrals involving Euler and Bernoulli numbers
04 p0624 A69-14969

Random processes study by special integral calculus containing deltas and theorems, with application to stationary processes
05 p0718 A69-15881

Convergence of improper integral evaluated along solution of differential equation, noting use in asymptotic control theory
05 p0788 A69-16481

Characteristic coefficients in method of integral relations calculated by Lagrange interpolation, noting application to numerical solution of differential equations
06 p0857 A69-17102

Torsion theory for modules over integral domain, giving definition of injective sums
13 p2287 A69-27339

Integration formulas involving integrand derivatives simplified by decreasing integrating power in terms of polynomials

18 p3164 A69-34615

Algorithm for definite integrals evaluation, using Clenshaw-Curtis and Romberg quadratures combination in each subinterval

20 p3498 A69-36947

Soviet book on integral methods of calculations in theory of turbulent jets and wakes, covering turbulent boundary layers, laminar mixing, etc

20 p3518 A69-38211

Criterion for class of differential equations ensuring absence of nontrivial periodic solutions

22 p3974 A69-39897

Navier-Stokes equations numerical integration based on biharmonic operator inversion by alternating direction method of Douglas-Rachford type

22 p3932 A69-40928

Surface integration technique used in conjunction with wedge diffraction theory to analyze TEM radiation patterns of parallel plate waveguides

23 p4136 A69-41581

Table of definite and indefinite integrals of products of exponential integrals with elementary or transcendental functions

24 p4341 A69-43324

INTEGRAL EQUATIONS

NT FREDHOLM EQUATIONS

NT SINGULAR INTEGRAL EQUATIONS

NT VOLTERRA EQUATIONS

NT WIENER HOPF EQUATIONS

Bounds from asymptotic behavior of solutions of nonlinear integrodifferential equation arising from nonlinear oscillators in acoustics

01 p0103 A69-10001

Simultaneous partial integro-differential equations governing natural vibrations of arbitrary cross section cylindrical tubes, suggesting Fourier series solution

01 p0164 A69-10065

Unsteady heat flow in finite composite hollow circular cylinder using inverse method of eigenfunction expansion/method of finite integral transformation/

01 p0175 A69-10230

Distribution of moment of first passage through positive level for homogeneous process with independent increments and exponential characteristic function, constructing integral equation

01 p0104 A69-10265

Eigenproblem for displacement integral equations with finite cosine transform kernels, extending Roark-Wing numerical method for eigenvalues to kernels

01 p0106 A69-10986

Integral operators on space of Borel measurable functions bounded considering weight function, giving condition for infinite complex matrices, mapping analytic sequence spaces

01 p0107 A69-11244

Stress transfer from loaded matrix to single fiber in composite materials determined by series and step formulations

01 p0172 A69-11271

Atmospheric temperature profiles by regularizing algorithm, discussing influence of random errors in measured radiation and kernel of integral equation on interpretation accuracy

02 p0274 A69-11448

Cosmic ray propagation in interplanetary space taking into account reverse effect on solar wind, deriving integrodifferential equation

02 p0306 A69-11657

Linear integrodifferential motion equations for turbulent flow within Heisenberg statistical turbulence theory

02 p0230 A69-11869

Convergence of Muthopp collocation method for numerical solution of linear singular integrodifferential equation, noting use in airfoil, propeller and elasticity theory

02 p0271 A69-12056

Infinite system of first order integral equations derived from Prandtl boundary layer equation and continuity equation

02 p0231 A69-12059

Electromagnetic wave propagation problems, using asymptotic solutions of differential and integral equations in domains containing transition points

02 p0208 A69-12130

Nonlinear integrodifferential equations of parabolic type with delayed argument, discussing boundary value problems with caloric and hereditary operators

02 p0273 A69-12249

Integral prediction method for arbitrary continuous function on right hand side of nonhomogeneous linear differential equation with constant coefficients

03 p0455 A69-13022

Compatibility equations in plane micropolar thermoelasticity theory obtained by associated matrix method

03 p0525 A69-13607

Integral equation solution for plate with internal support

03 p0528 A69-13799

Uniform asymptotic expansion series for saddle point integrals applied to probability distribution in noise interference problems

03 p0398 A69-13832

Integral equations solved numerically for general nonhomogeneous elastic inclusion problem, using linear elasticity theory

03 p0530 A69-14064

Infinite phased dipole array, discussing integral equation, current distributions and active admittances

04 p0571 A69-14316

Generalized Riemann-Liouville fractional integrodifferential operator and application to representation of analytic and harmonic functions inside circle

04 p0622 A69-14512

Optimal control theory applied to systems described by partial differential/integral equations

04 p0581 A69-14571

Mathematical modeling of Gaussian and nonGaussian processes obtained by linear and nonlinear transformations of white Gaussian noise, noting Markov processes

04 p0623 A69-14694

Equilibrium and compatibility equations for axisymmetric stress distribution in finite length anisotropic elastic cylinder reduced to single integrodifferential equation

04 p0676 A69-14709

Phenomena satisfying inhomogeneous Helmholtz equation in cylindrical coordinates, inferring equivalent infinite series directly from integral-transform method

04 p0623 A69-14896

Book on linear boundary value problems of mathematical physics based on Green function covering Hilbert spaces, integral equations and spectral theory of differential operators

04 p0625 A69-15232

Linear integral equations for brightness coefficients and auxiliary functions in semiinfinite atmosphere, expressing atmospheric albedo using moments and Chandrasekhar function

04 p0662 A69-15237

Modified Karman-Pohlhausen pulse integral equation for calculating boundary layers is more accurate when seeking flow separation point

04 p0591 A69-15408

Second approximation to Boltzmann equation solved for rigid sphere gas by reducing integral equation to differential equation

04 p0633 A69-15434

Engineering solution for integrodifferential equations of physical systems with electronic circuits

05 p0724 A69-16468

Stress-strain state of infinite plate with two holes of different diameter solved, using integral equation derived for two dimensional problem in elasticity theory for anisotropic medium

05 p0843 A69-16680

Stress-strain state of shell having one end clamped and other under concentrated bending moments and concentrated force acting along generatrix solved by integral equation

05 p0843 A69-16681

Riemann problem in regions, showing integral operators become bounded if closed rectifiable Jordan curve without cusps becomes curve of bounded rotation

06 p0947 A69-16893

Residue contributions to integrals associated with admittance of plasma or dielectric covered circular aperture antenna used to calculate surface wave contribution to waveguides

06 p0896 A69-17477

Iterative solution of integral equation and uniform convergence conditions of function sequence approximating incremental stress distribution in elastic-plastic structures

06 p1024 A69-17510

Integrodifferential equation for plasma oscillations solved for effect of ion Larmor radius size and intrinsic electric field on flute instability of axially symmetric plasma

06 p0966 A69-17520

Integral equation solution with Mellin inversion formulas for light scattering problems

06 p0949 A69-17887

Soviet collection of papers on boundary value problems and integral equations

07 p1172 A69-18499

Differential equations with singular problem solutions analyzed by reducing problem to solution of integro-differential equation

07 p1174 A69-19004

Viscous hydrodynamical equations for flow field exterior to obstacle moving with constant velocity, discussing force relationships, drag invariance and integral representations

07 p1121 A69-19298

Fundamental problems of plane elastostatics with stress couples reduced to solution of integral equations, noting uniqueness theorem in plate bending theory

07 p1233 A69-19328

Diffuse reflection and transmission of parallel rays by homogeneous two layer slab, solving simultaneous integro-differential equations governing auxiliary functions

08 p1350 A69-19799

Wolf and generalized Parseval theorems applied to transformation of integral equation to S-plane in systems analysis

08 p1271 A69-19865

Partially translatable one parameter continuous transformation group for complete system of integrals in celestial mechanics, discussing Wintner nonisolating integral and Poincare theorem

08 p1382 A69-19872

Viscoelastic problem solutions for hereditary media, using Laplace transforms or solutions of integral equations for inaccurately approximated kernels

08 p1412 A69-20329

Stability theorem for nonlinear mixed integral equations in boundary value problems

08 p1343 A69-20355

Heat transfer mechanism in solid body, deriving integrodifferential equation with classical equation and hyperbolic equation of heat propagation as special case

09 p1621 A69-21587

Integrodifferential equations describing longitudinal oscillation properties in nonlinear region of electron Maxwellian plasma waves and two cold electron beams

09 p1550 A69-22026

Diffraction problem on cylindrical bodies of arbitrary shape reduced to integral equations by using Green functions for free spaces

09 p1459 A69-22634

Singular integral equation for velocity in linearized Rayleigh problem in rarefied gas flow field solved by applying Luke weight coefficients

10 p1679 A69-23596

Integral equation and related optimal regularization problems, finding operator in class of operators defined on set of functions

10 p1721 A69-23882

Equivalence of initial boundary value problem and integral equations obtained by regularization using potential theory

10 p1721 A69-23959

Integral representation for velocity and pressure fields produced by horizontal motion of two dimensional bodies below or on free surface of viscous liquid

11 p1866 A69-24278

Asymptotic methods for integral equations of plane mixed problems of elasticity theory for nonclassical regions

11 p1971 A69-24647

Mixed boundary value problem in theory of axisymmetric potential of three dimensional boundary layer reduced to solution of linear integral equation

11 p1918 A69-24787

Transition density function of randomly excited diffusion process and confinement probability at fixed spatial point satisfying integrodifferential equation involving functional derivatives

11 p1860 A69-25451

Excitation coefficients of waves subjected to sudden expansion in radiating waveguide using integral relations, noting convergence

11 p1855 A69-25621

Vibration eigenfrequencies of helicopter blades, discussing equation integration problems

11 p1995 A69-25673

Theorem for integral expansion applied to boundary value problems of mathematical physics and elasticity theory for single sheet hyperboloids of revolution

11 p1910 A69-25731

Bending of half strip rigidly fastened along short edge, constructing integral equation for normal stress at clamping, investigating corners singularities

11 p1996 A69-25734

Pitch angle distribution function of thermal protons in magnetosphere taking into account earth gravitational field

12 p2067 A69-26354

General theorems derived for Noether operator applied to integral equation with automorphic kernel

12 p2122 A69-26574

Cylinder buckling and other boundary value problems, applying inverse differential operators to solution of integrodifferential equations

12 p2186 A69-26841

Integral equation solved by successive approximation procedure for determining mass distribution in galaxies on radial velocity basis, applying to NGC 7331

13 p2353 A69-28325

Energy transfer by simultaneous conduction and radiation between two media in intimate contact, detailing numerical solution method for resulting coupled nonlinear integrodifferential equations

13 p2378 A69-28340

Cosmic ray propagation in interplanetary space taking into account reverse effect on solar wind, deriving integrodifferential equation

13 p2333 A69-28688

Contact problem for half plane with elastic stiffener reduced to Prandtl integrodifferential equation, determining contact stresses

14 p2531 A69-28804

Completeness theorem for integrodifferential operator to establish Schwarzschild criterion for stability of gaseous masses

14 p2470 A69-28902

Series and integral expansions of Jacobi polynomials with positive kernel, noting ultraspherical polynomials

14 p2470 A69-28905

Contact problem between elastic cylinder and rigid punch analyzed using integral equation, singularity isolation and series expansion

14 p2532 A69-28972

Integral equations for classical elasticity boundary value problems, stressing analogous Stokes flow hydrodynamic equations

14 p2535 A69-29361

Integrodifferential equation derived and solved for evolution of collisional model of asteroids and debris

14 p2526 A69-29879

Integral formulation of scattering theory extended to Coulomb interactions by expanding Green function and treating kernel singularities

14 p2489 A69-29995

Book on Bessel functions with physical applications covering solution of Bessel and associated equations, integral representations, Fourier-Bessel series, Hankel transforms, etc

15 p2643 A69-30037

Green function construction for boundary value problems of heat conduction on rectilinear segment with dynamic boundaries, using integral equations

15 p2716 A69-30075

Energy budget equations applicable to limited atmospheric region using available potential energy concept, discussing relation to global energy

15 p2648 A69-30221

Plane contact problems in elasticity theory allowing for cohesive forces solved by integral and differential equations

15 p2706 A69-30578

Optimization of control system described by linear parabolic integrodifferential equation, using dynamic programming approach

15 p2645 A69-31024

Starting weight increments in aircraft designs having various structural features and dimensions

16 p2735 A69-32144

Monograph on Navier-Stokes equations with integral relations approximate solution and application to flow around flat plate of finite length

17 p2949 A69-32993

Simultaneous integral equations numerical solution for open optical resonator mode analysis, using kernel function and Fresnel approximation

17 p2983 A69-33883

Local radiation characteristics calculation method, consisting of reducing integral equations to linear algebraic equations, applied to solve radiative heat exchange problems

18 p3229 A69-34713

Integral scalar equation describing signal attenuation by acoustically soft disk for mirror-shadow method of ultrasonic flaw detection

18 p3137 A69-35109

Radiant heat transfer integral equations solutions accuracy determined from differences between geometric and resolving angular emission factors

18 p3230 A69-35119

Regular integral equations solvability for boundary value problems in shallow shell theory, using method of potential representations and Green matrices

18 p3224 A69-35309

Thin walled shell temperature and strain fields described by integrodifferential equations based on Kirchhoff hypothesis and coupled thermoelasticity reciprocity equations

18 p3225 A69-35368

Rarefied gas flow between parallel plates using linearized Boltzmann transport equation, deriving integral equation for mass flow velocity

19 p3296 A69-35621

Krein solution method for linear integral equations of first kind and related differential equations

19 p3360 A69-35780

Engineering equations for elastic thin plate oscillations of materials with properties described by linear integral Volterra-Boltzmann operators

19 p3437 A69-35989

Distribution of moment of first passage through positive level for homogeneous process with independent increments and exponential characteristic function, constructing integral equation

19 p3360 A69-36200

Function theoretic solution of dual integral equations applied to boundary value problem of supersonic flow over infinite span thin wing

19 p3239 A69-36311

Similarity method applied to linear integrodifferential equations of neutron transport in homogeneous space

19 p3361 A69-36774

Elastic shell theory to regularize singular integrodifferential equation, investigating load transfer from reinforcing ribs to circular cylindrical shell and numerical solution correlation

19 p3443 A69-36792

Drag minimization as extremization of products integrals powers, noting application to optimum wings and fuselages

19 p3242 A69-36800

Combined heat transfer by radiation and conduction in disperse media /thermal insulation/ described by system of nonlinear integrodifferential equations

20 p3631 A69-37097

Linear nonstationary system with singular point analyzed for stability necessary and sufficient conditions using Riemann-Mellin conversion integrals and Laplace transforms

21 p3685 A69-38451

Boundary layer flow past permeable surface, generalizing integral equations for case with suction

21 p3691 A69-38573

Heat and mass transfer coefficients in binary laminar boundary layer during natural convection obtained with integral equations and Karman-Polhausen method

21 p3848 A69-38633

Natural oscillations of free surface liquid and elastic bottom of cylindrical cavity determined by integrodifferential equations based on liquid level

21 p3693 A69-38720

Radiation field several wavelengths from dipole above plane earth, simplifying rigorous integral expression for Hertz vector by method of operators

21 p3770 A69-38748

Control function ensuring minimal response time of controlled plant with motion described by integral equations system, using method of distributed moments

21 p3685 A69-38847

Saint Venant torsion problem using rederivation of integral equation by transferring external geometrical problem into internal static problem

21 p3836 A69-39003

Equivalence of initial boundary value problem and integral equations obtained by regularization using potential theory

21 p3756 A69-39150

Optimal generalized random controls using stochastic integral equation in deterministic problem

21 p3756 A69-39266

Integrals of motion for minimum fuel rocket trajectories in inverse square field calculated for constant power and constant exhaust rockets

[AIAA PAPER 69-904] 21 p3806 A69-39336

Asymptotic solution, existence and uniqueness of integral equations occurring in elasticity theory and mathematical physics

21 p3772 A69-39618

Integral relations method applied to air jet flow along cylinder with boundary layer control by suction or blowing

21 p3698 A69-39845

Nonresonant Green functions of auxiliary boundary value problems for deriving integral equations for Dirichlet and Neumann diffractions at open screens

22 p3901 A69-40949

Fredholm integral equation for source function of Greenhouse effect and finite atmospheres solved by computational algorithm

23 p4239 A69-41607

Bogoliubov method of partial averaging for nonlinear integral equations, noting application to automatic gain control theory

23 p4181 A69-41731

Nonlinear loaded integrodifferential equation analytical and formal solutions, noting role of characteristic number relation to unity

24 p4339 A69-42595

INTEGRAL FUNCTIONS

U ENTIRE FUNCTIONS

INTEGRAL TRANSFORMATIONS

NT CONVOLUTION INTEGRALS

NT FOURIER TRANSFORMATION

NT HILBERT TRANSFORMATION

NT LAPLACE TRANSFORMATION

Shock waves collision with supersonically moving axisymmetric slender bodies analyzed by integral transform method, noting application to shock-shock interaction

03 p0413 A69-13010

Operator methods in engineering sciences, discussing integral transformations, Riesz method application to Cauchy problem, etc

03 p0457 A69-13744

Generalized Riemann-Liouville fractional integrodifferential operator and application to representation of analytic and harmonic functions inside circle

04 p0622 A69-14512

One to one mappings of Fourier series of analytic almost periodic functions and Dirichlet series, discussing satisfaction of functional equation

05 p0786 A69-15882

Thermal stresses for mixed boundary conditions calculated from combined use of integral transforms and variational techniques, reducing computational labor

10 p1801 A69-23429

Integral transform solutions for Griffith cracks in brittle fracture theory, discussing disk and penny shaped cracks in cylinders and thick plates

10 p1801 A69-23688

Integral transforms in composite one dimensional space and application to boundary value problems of physics

11 p1910 A69-25574

General theorems derived for Noether operator applied to integral equation with automorphic kernel

12 p2122 A69-26574

Nonuniform flowfield from supersonic penetration of plane shock by three dimensional pointed planar wing, using integral transform method to study field perturbation pressure

13 p2199 A69-27323

Finite integral transform determination for solving circular plates forced vibrations with time dependent conditions

15 p2704 A69-30306

Galerkin-Kantorovich-Dorodnitsyn/GKD/ multimoment integral method improved reversed flow formulation for lower branch similar flows

17 p2958 A69-34054

Intensity integral inversion for Doppler core of strong solar absorption lines to obtain line source function for solar atmosphere

21 p3796 A69-38478

Integral transformation applicability to inverse problems concerning interaction potential energy between particle pairs in n-dimensional Euclidean space

23 p4182 A69-41960

INTEGRATED CIRCUITS

Microwave applications of monolithic and hybrid semiconductor circuit technologies, considering cost and performance

01 p0039 A69-10188

X band mixer with reactively terminated image, using gallium arsenide barrier diodes and microwave integrated circuit techniques

01 p0039 A69-10189

Microwave amplifier design with hybrid integrated circuits of thin film lumped elements, noting gain and efficiency of transistor circuits

01 p0039 A69-10190

Performance characteristics of microstrip ferrite devices for hybrid microwave integrated circuit systems, including meander line phasers and YIG elements

01 p0040 A69-10191

Thin ferrite use in microwave integrated circuits including phase shifters, latching circulators, isolators and phase and amplitude modulators
01 p0040 A69-10192

Hybrid integrated parametric amplifier design considerations for fabrication in microstrip transmission line
01 p0040 A69-10193

Diode structure optimization for monolithic integrated circuit for Ku-band reflective phase shifter
01 p0040 A69-10195

Gallium arsenide single crystal epitaxy with doping/concentrations into semiinsulating microwave circuits
01 p0040 A69-10196

Microstrip transmission line integrated circuits on semiinsulating GaAs substrates, showing feasibility at millimeter wave frequencies
01 p0040 A69-10197

Hybrid microstrip integrated microwave circuits, discussing substrate and conductor materials and fabrication processes
01 p0040 A69-10199

Small signal characteristics and frequency response of diode-stabilized integrated linear circuits, discussing feedback, impedance, bias-diode, etc
01 p0041 A69-10204

Integrated circuit manufacturing status, discussing raw materials, crystal imperfections, surface damage, epitaxy and diffusion techniques
01 p0045 A69-10650

Phased array radar cost improvement based on solid state devices and microwave integrated circuits application
01 p0048 A69-11039

Linear integrated circuit communication systems based on subsystem approach, showing example of IF strip and audio AGC/squelch amplifier
01 p0035 A69-11389

Integrated circuit piezoelectric systems limitations and advantages
01 p0049 A69-11413

Planar technology application to germanium electronic components and integrated circuits
02 p0214 A69-11597

Integrated circuits technology, discussing thin film, monolithic compatible and hybrid circuit techniques
02 p0216 A69-12050

Traveling high electric field domains in bulk semiconductors use in high speed integrated electronics, noting domain properties of GaAs and CdS
02 p0216 A69-12144

Large scale integration /LSI/ arrays, discussing high yield manufacturing methods based on fixed nondiscretionary connections among components
02 p0254 A69-12467

Air gap isolated microcircuit beam-lead devices fabrication, operation, electrical performance and radiation resistance
02 p0221 A69-12469

P-i-n structure isolation method for fabricating monolithic integrated circuits
02 p0222 A69-12471

Wafer chip assembling technique for high density interconnection of silicon devices in large monolithic electronic systems, noting application to MOS shift register
02 p0222 A69-12472

Circulator power splitting and isolating function in integrated microwave network
02 p0222 A69-12475

Breadboard chip for use in computer aided design and analysis of integrated circuits, describing components and application to differential amplifiers
03 p0402 A69-13008

Noise susceptibility of integrated circuits in digital systems, discussing sources and specifications
03 p0410 A69-13579

High speed modular multiplier and digital filter for LSI development
04 p0567 A69-15354

Large scale integration and batch-fabricated processing of logic and storage elements for fourth generation computer, discussing partitioning design
04 p0567 A69-15355

Device and logic/system designers and design aids interaction, emphasizing engineering trends in large scale integration area using MOS arrays
04 p0568 A69-15356

Insulated junction integrated circuit transistor operation with various terminal connections corresponding to diode switching of transistor
05 p0730 A69-16217

Medium scale integration for packaging hybrid electronic monolithic systems
05 p0735 A69-16752

Ionizing radiation effects in microcircuits, using lumped model technique to derive mathematical model from electronic characteristics and boundary values of each semiconductor
06 p0977 A69-16886

Integrated circuit interconnection patterns computerized design, discussing automatic laser mask-making control
06 p0931 A69-17199

Metal oxide semiconductor random-access memories, discussing large scale integration and static and dynamic circuits chip size
06 p0894 A69-17203

Heat transfer and IC, discussing semiconductors thermal and electrical analogs and thermal properties
06 p0894 A69-17216

Thermal management of integrated circuits design, noting dependence on circuit and component configurations and parameter variations
06 p0894 A69-17217

IC selection for minimum thermal effects, discussing speed, power dissipation, maximum operating frequency and noise threshold
06 p0894 A69-17219

Electronic controller with integrated circuits and inexpensive SCR as coupler or interface between card reader and frequency synthesizer designed for untended operation
06 p0897 A69-17704

Computer model for n-p-n transistor in integrated circuit using substrate p-n junction isolation
07 p1114 A69-18246

Balanced diode shunt bridges with electronically tunable carrier selection high-Q N-path filter from 0 to 200 kHz, using single integrated module
07 p1089 A69-18249

Large scale integration of monolithic integrated circuits as interconnected circuits on semiconductor
07 p1090 A69-18372

Ferrite microstrips substrates role in integrated circuits, noting application of hybrid technology
07 p1090 A69-18399

Integration forms suitable for fabrication of hybrid and monolithic microwave integrated circuits
07 p1096 A69-18441

MOS technique applied to fabrication of integrated monolithic miniature circuits
07 p1099 A69-18494

Substrates containing silicon regions separated by silicon dioxide or ceramic dielectrics, prepared by lamination in hot press, noting applications to integrated circuits
07 p1100 A69-18617

Dielectrics refill and decal air isolation for silicon integrated circuit components
07 p1100 A69-18618

Alternative balancing technique utilizing linear combination of two equal and opposite drift characteristics to minimize drift in integrated differential amplifiers
07 p1102 A69-18874

Precision monolithic circuits fabrication techniques, describing differential amplifier design incorporating emitter feedback and direct DC errors compensation
07 p1102 A69-18875

Monolithic operational amplifier design combining junction FET with n-p-n transistor
07 p1103 A69-18876

Multistage amplifier design with frequency compensation by eliminating stages in HF region
07 p1103 A69-18877

Monolithic planar process to fabricate DC coupled amplifiers having less than nanosecond risetime
07 p1103 A69-18878

Analog multiplier using differential transistor pairs, discussing FM/AM detection, suppressed carrier modulation and TV chroma demodulation
07 p1103 A69-18880

All-diffused process to build monolithic high power series voltage regulator with separately optimized DC and AC characteristics
07 p1103 A69-18881

Temperature sensitivity of frequency of integrated oscillators, giving design method for achieving temperature compensation
07 p1103 A69-18882

Monolithic HF circuits stability in TV and HF devices noting need for appropriate amplifiers
07 p1103 A69-18883

Integrated four transistor bridge network used for self neutralized active element in tuned RLC amplifier design
07 p1103 A69-18884

Direct coupled monolithic IF amplifier with active gain control, analyzing large signal response, stability and available gain and noise behavior
07 p1104 A69-18885

Integrated frequency selective amplifier design for radio frequencies based on feedback configurations with positive real zero in loop transmission function
07 p1104 A69-18886

Control system utilizing digital and linear integrated circuits for low power testing of Pewee I reactor core Rover program [IEEE PAPER 2B-6]
07 p1179 A69-19188

Radiation effects on integrated circuits, stressing components design for maximum tolerance
07 p1113 A69-19779

Microelectronics technology and economics, discussing semiconductor integrated, discrete component and thin film hybrid circuits and MOSFET devices [AGARDOGRAPH-114]
08 p1291 A69-20983

Microcircuits, integrated circuits and other monolithic solid state circuits failure mechanisms examined and applied to reliability methodology [AGARDOGRAPH-114]
08 p1292 A69-20987

Microelectronic equipment for aerospace application and integrated circuit production in UK [AGARDOGRAPH-114]
08 p1292 A69-20992

Integrated circuit production, development and research in Germany [AGARDOGRAPH-114]
08 p1292 A69-20994

Catastrophic failures in logic circuit and system design, considering thermal effects, complexity, statistical methods and computer use
08 p1299 A69-21107

Integrated semiconductor circuits reliability in electronics and microelectronics, discussing hybrid and monolithic circuits in thin/thick film design and on Si monocrystals
08 p1294 A69-21118

Zero sensitivity integrated RC filter circuits design, exploiting capacitors and resistors property of having same temperature coefficient
08 p1300 A69-21174

Wire, lead frame, direct bonding and beam lead techniques for interconnecting active elements into hybrid circuits
09 p1508 A69-22338

Electronic systems partitioning in preparation for MOS large scale integration for system performance and cost improvement
09 p1466 A69-22451

Optimum microcircuit analog to digital converter for aerospace environment by combining monolithic circuits and thin film resistors
10 p1636 A69-23282

High speed ten-bit analog to digital converter with medium scale integration /MSI/ elements, considering conversion accuracy and time
11 p1845 A69-24520

Large scale integration applications to avionics including self testing, self repair, cost factors, etc
11 p1845 A69-24530

Integrated tunnel diode amplifiers, discussing low noise, bandwidth, reliability, miniaturization and applications
11 p1854 A69-25611

Thin film lumped passive elements for microwave power amplifier integrated circuits, discussing distributed reactances, element size and fabrication, etc
11 p1856 A69-25654

Circuit designs using differential amplifier devices or operational amplifier integrated circuits
11 p1857 A69-25664

Operational amplifier integrated circuits applications, discussing simple and transducer amplifiers, operational circuits, wave shapers and generators and power supplies
11 p1857 A69-25665

Large scale integrated circuit accumulator chip as control element for design of digital system by design automated techniques
12 p2037 A69-25942

Integrated circuits, discussing development from transistors and vacuum tubes, operation, fabrication and applications
12 p2038 A69-26331

Tactical air navigation system redesign with integrated circuits, obtaining weight reduction and improved performance and reliability
13 p2227 A69-27389

Thin film cermet resistors for integrated circuits produced by thermal vapor deposition in vacuum, cathodic sputtering and explosive vapor deposition
13 p2268 A69-27466

Pulse frequency integral estimate devices with integrating chemotron tetraodes for automatic systems metering applications
13 p2227 A69-27522

Microwave propagation in coupled pairs of microstrip transmission lines for integrated circuit design, discussing dielectric Green function
13 p2229 A69-27672

Microstrip circulator size reduction attained by tight inductive ferrite coupling for incorporation with microwave integrated circuits
13 p2230 A69-27679

Book on integrated circuits covering fabrication techniques, basic semiconductor theory, thin film, monolithic, compatible circuits, packaging, etc
14 p2419 A69-29002

Doppler radar clearance hole packaging method for ruggedized dual in-line integrated circuits with conventional etching, tooling and double-sided printed wiring techniques
14 p2419 A69-29102

Engineering problems in IC microminiaturization, dividing devices according to suitability for microminiaturization
15 p2576 A69-30352

Linear metal oxide semiconductor integrated circuits, discussing advantages, disadvantages and use of current source load device to improve voltage gain and swing
15 p2577 A69-30594

Integrated circuit failure analysis in military and space applications utilizing type-test programs
15 p2624 A69-30820

Large scale integration /LSI/ and medium scale integration /MSI/ circuits evolution and requirements, noting onboard computers and space applications
15 p2625 A69-30825

Reliability of integrated circuits with emphasis on errors
15 p2626 A69-30831

Third generation computer reliability including preparation and test of integrated logic circuits
15 p2626 A69-30832

Production line requirements for MOS and IC, considering high reliability at minimum cost for space applications
15 p2627 A69-30841

Transistors and IC reliability for memory control evaluated by Concerto subprograms
15 p2627 A69-30842

Reliability of high resolution accelerometer composed of semiconductor integrated circuits
15 p2627 A69-30843

Disturbances simulation in instrumentation utilizing digital integrated circuits for reliability computation in complex circuits
15 p2628 A69-30848

Electron beam exposure system to photoetch integrated circuit patterns without photomasks, using electronic computer for automatic pattern generation and registration
15 p2579 A69-31039

Glass ceramic coated and bonded silicon semiconductor material in integrated circuits devices fabrication, noting matched thermal expansion
15 p2669 A69-31040

Stripline microwave integrated circuits in terms of building blocks and components, discussing hybrids, backward wave coupler, balanced modulators and mixers, etc
15 p2579 A69-31075

Approximate solution for coupled microstrip transmission lines in integrated circuits, discussing impedance, capacitance and testing
15 p2580 A69-31078

Similarity between semiconductor discrete devices and integrated circuits, considering materials, processing and failure modes
15 p2580 A69-31128

Integrated circuits screens, developing sequence of life and environmental tests to remove units of potential reliability hazards
15 p2580 A69-31130

Large scale integrated MOS devices tests for space applications, establishing quality specifications
15 p2580 A69-31131

Integrated circuits failure analysis in space program applications, describing electrical analog for notification, fact gathering, part analysis and corrective action functions
15 p2580 A69-31132

Counter for decimal counting and numeric display applications using integrated fluid logic elements
15 p2616 A69-31295

Metal oxide semiconductor integrated circuits, showing failure rates and degradation causes
16 p2759 A69-31851

Integrated circuits effect on electronic equipment design and production technology
16 p2762 A69-32578

Large scale integrated circuits reliability with emphasis on multilayer metalization, designing test vehicles for failure mechanisms
17 p2935 A69-32887

Scanning electron mirror microscope advantages over electron mirror and scanning electron microscopes for examining integrated circuits
17 p2971 A69-32891

Al interconnections discontinuities at integrated circuit contact windows observed by scanning electron microscope, noting catastrophic failure and Si presence
17 p2936 A69-32893

Test structure model for studying semiconductor-insulator interface related failure mechanisms in large scale integrated circuitry
17 p2936 A69-32894

Digital IC radiosonde system, discussing sampling, pulse width modulation, time multiplexing, follow-on subsystems, etc
17 p2937 A69-33675

NDC-1070 solid state computer design featuring TTL, MSI and hybrid circuits, offering memory capacity flexibility and rapid maintainability
17 p2933 A69-34060

Integrated nonvolatile read-write memory with addressing using variable threshold field effect transistor including cell operation, channel shielding and circuit
17 p2942 A69-34120

Integrated circuit ultrahigh speed analog to digital converter, considering interactions at high digital rates and video bandwidths
17 p2943 A69-34125

Beam lead sealed junction transistor and integrated circuits reliability, describing test conditions and failure mechanisms
18 p3145 A69-34497

Book on digital electronics for scientists covering digital circuits and instruments for measurement, control or computation
18 p3112 A69-34915

Epoxy molding compounds performance on DIP integrated circuits, determining comparative moisture protection provided by encapsulants
19 p3280 A69-35546

Integrated circuits failure analysis techniques utilizing pin-to-pin curve tracer tests and thermal measurements
19 p3282 A69-35786

Failure mechanisms and analyses of large scale integrated circuits based on bipolar and MOS transistors, describing measurement and probing techniques
19 p3282 A69-35787

Microelectronics and IC process and quality control check list including conductor screening, resistor abradings and discrete part attachment
19 p3283 A69-36020

Oscillator without reactive components for integrated circuit biotelemetry, noting transmission in AM broadcast band
19 p3261 A69-36244

Phase locked loop design of desensitized monolithic integrated circuits for FM multiplex signal filtering and demodulation, describing external tuning
19 p3273 A69-36274

Current mode gates and flip-flops with subnanosecond propagation delay for integrated logic circuits, discussing memories dimensions, LSI arrays, etc
20 p3505 A69-37342

Integrated logic circuits assembly for digital computers, considering high density, mechanical environment, reliability, accessibility and costs
20 p3505 A69-37401

Electrical properties of passive line elements of hybrid integrated circuits on insulating substrates for radio systems
21 p3684 A69-39563

Lasers as tools for integrated circuits fabrication, noting roles of various laser operating parameters
21 p3742 A69-39705

Spacecraft integration electronics modular packaging, discussing slice housing concept and design criteria including environmental resistance, reliability, performance, etc
22 p3910 A69-39949

Failure analysis on semiconductor devices and integrated circuits, discussing procedure for factual information representing present condition of device
22 p3953 A69-40032

Hybrid microwave IC assembly techniques, discussing active devices connection to substrate with thick or thin film metallizations
22 p3912 A69-40068

MSI 12 bit digital to analog converter in integrated circuit form using MOS switching circuit [AIAA PAPER 69-968]
22 p3906 A69-40349

Electromagnetic interference /EMI/ characteristics of various digital logic ICs
23 p4141 A69-42219

Active Ni centers properties in Si with emphasis on increasing and reducing minority carrier lifetime in silicon integrated circuits, discussing energy levels
24 p4360 A69-42759

Boron tribromide-oxygen reaction kinetics effects on IC base diffusion uniformity, correlating uniformity with electrical properties
24 p4360 A69-42760

Si integrated circuits single and composite layered metallization systems, comparing characteristics of various refractory and noble metals
24 p4286 A69-42761

Hybrid and monolithic integrated microcircuits application to electronic digital computer structures
24 p4284 A69-42907

Thin film field effect transistors and integrated microcircuits, investigating active and passive elements fabrication
24 p4419 A69-42908

Microwave integrated circuit applications to reflective and transmissive phased arrays, discussing radar system elements
24 p4286 A69-43109

Integrated TTL flip-flop circuits, describing functional principles of circuits with DC and capacitive coupling
24 p4287 A69-43130

INTEGRATION [REAL VARIABLES]
U MEASURE AND INTEGRATION

INTEGRATORS
NT DIGITAL INTEGRATORS

Time dependent functions integration by glow discharge tube and oscillator, discussing device for voltage measurement and applications in meteorology and geophysics
02 p0251 A69-12773

Difference schemes for heat conduction analog simulation on electric integrators
03 p0410 A69-13300

Solid state sampling circuit for low pulse repetition frequencies to improve signal to noise ratio, noting ratio of holding to learning time
11 p1849 A69-24900

Dynamic multistable analog integrator capable of prolonged retention of integration, giving differential equation of device
13 p2224 A69-27427

Analog correlator performance interpreted as output SNR dependence on input signals and integrating system characteristics, covering filters and finite time integrators
14 p2413 A69-29485

Plasma diagnostics FM phase meter circuits tests, considering raster phase indicators, phase detectors and frequency integrators
14 p2497 A69-29797

Mean drift rates of single and two rotor gyroscopic linear acceleration integrators mounted on irregularly rocking base
18 p3135 A69-34586

Mathematical modeling techniques applied to thermoelastic cooling for plate without clamping and mechanical loads, examining integrator schematic diagram
21 p3680 A69-39851

HF vibrations effect on motion of gyroscopic linear acceleration integrator, showing additional error in flight vehicle acceleration measurements
22 p3946 A69-40253

INTEGRODIFFERENTIAL EQUATIONS
U DIFFERENTIAL EQUATIONS
U INTEGRAL EQUATIONS

INTELLIGENCE
U ARTIFICIAL INTELLIGENCE

INTELLIGIBILITY
U SPEECH RECOGNITION

INTELSAT SATELLITES

Fucino earth station operation with Early Bird and Intelsat 2-F3 satellites receiving equipment and transmission system [UN PAPER 68-95455] 01 p0028 A69-10493

Communication satellites systems, discussing Intelsat satellite specifications and modulation methods for multiple access 03 p0383 A69-12870

Time division multiple access system for INTELSAT satellite, analyzing burst preamble and selection of frame period 03 p0388 A69-13179

Design evolution of mechanically despun antenna systems from ATS to INTELSAT, discussing RF and control systems 03 p0403 A69-13239

Intelsat application satellites, considering economy and global telecommunication 03 p0535 A69-13592

Earth station system for ground based communications with Intelsats 2 and 3 noting antennas, receivers, transmitters and power supplies 05 p0741 A69-15667

Mechanically and electronically despun spacecraft antennas, comparing designs and projected performances for spin stabilized Intelsat 3 satellite 06 p0897 A69-17590

Space communication, discussing global network of Intelsat satellites ground facilities, regional switching, RF channels, etc 06 p0890 A69-17860

Power traveling wave tubes in ground stations for INTELSAT 3 direction finding system 07 p1094 A69-18426

Economic planning of satellite earth station equipment in relation to expected traffic demand, emphasizing specifications for communication via Intelsat 2 and 3 satellites 07 p1117 A69-19347

Intelsat 2 satellite structural design for Apollo communications 08 p1408 A69-19907

INTELSAT for design, construction, launching and maintenance of global communication satellites, noting transponders 09 p1457 A69-22466

Waveguide feeder for Goonhilly Downs satellite communication antenna reducing feeder loss for use with low elevation Intelsat 3 satellite 17 p2935 A69-32849

INTELSAT program, discussing U.S. proposals regarding domestic services, separate satellite programs, etc 20 p3637 A69-37121

INTELSAT 1964 agreements consistency with multilateral international agreements, including UN General Assembly and International Telecommunication Union 20 p3638 A69-37122

Frequency assignment methods for Intelsat 2 and 3 communication satellites [AIAA PAPER 68-454] 21 p3674 A69-39226

More earth station equipment and design for satellite communication in INTELSAT network including antenna, feed and tracking, interconnect system, etc 22 p3900 A69-40679

Intelsat 3 communications satellite mechanically despun high gain directive antenna, discussing system, control electronics, design and performance 22 p3913 A69-40691

Solar cells arrays degradation in Intelsat spacecraft at synchronous altitude, noting shielding gaps and low energy proton influence 23 p4072 A69-42287

INTENSIFICATION
U AMPLIFICATION

INTENSIFIER TUBES
U IMAGE INTENSIFIERS

INTENSIFIERS
U IMAGE INTENSIFIERS
U IMAGE ORTHICONS

INTERACTIONS
Slot type jet interaction flow tests at free stream Mach 4 and 5, describing equipment, procedure and results 24 p4249 A69-43686

INTERATOMIC FORCES
Adiabatic elastic constants of molybdenum-rich rhenium alloys, studying concentration effects on bulk modulus, Debye temperatures and interatomic forces 04 p0613 A69-14455

Unperturbed Hamiltonian transformation applied to existing perturbation theories for exchange forces between atoms to obtain correct long range behavior 07 p1184 A69-18288

Relaxation method for configurations and energies of atoms and stress induced crack opening displacements in crystalline solids 10 p1796 A69-23067

Born-Mayer parameters simplifying computation of interatomic potential, tabulating numerical values for 104 mononuclear pairs of neutral ground state atoms 13 p2301 A69-27453

Interatomic potential between alkali ions and rare gas atoms, using model accounting for repulsive and attractive exchange forces 16 p2815 A69-32464

He II excitation spectrum for interparticle potential using pair Hamiltonian with repulsive core and attractive well 17 p3008 A69-33118

INTERCEPTION

Virtual or projected miss distance for assessment of missile homing impairment effects, deriving expression based on kinematics 04 p0629 A69-15517

Digital computer motion pictures generation for ground controlled intercept simulation 06 p0906 A69-17397

Flight times compared for intercept and pure pursuit missile trajectories 20 p3618 A69-37716

Computer program /TACTICS/ for simulating three vehicles simultaneous motion in space, considering interceptor-target guidance and intercept trajectories [AIAA PAPER 69-890] 21 p3678 A69-39415

Automated programmed instruction /API/ for training backup interceptor control personnel to conduct air defense operations [AIAA PAPER 69-956] 22 p3905 A69-40338

Rendezvous, intercept and injection optimal control laws derived from inhomogeneous linear differential equations with quadratic performance index 23 p4224 A69-41921

INTERCEPTOR AIRCRAFT

U FIGHTER AIRCRAFT

INTERCEPTORS

Quasi-optimum proportional navigation for interceptor missiles, discussing feedback guidance law and attack geometry 24 p4348 A69-43292

INTERCONNECTION

U JOINING

INTERCONTINENTAL BALLISTIC MISSILES

NT MINUTEMAN ICBM

U.S.S.R. manned bomber role in air strategy, discussing mutual effects of U.S.-U.S.S.R. military posture developments and ICBM 14 p2392 A69-29431

INTERFACE STABILITY

Metal/alumina interfaces strength, examining correlation with wetting and bonding and martensitic transformations 03 p0447 A69-13612

Shape and stability of interface between liquids subjected to surface tension and mass force field in vessel 03 p0417 A69-13809

Fiber-matrix interfacial bond function and bond strength role in fiber composites mechanical behavior 03 p0450 A69-13881

Moving and stationary interphase boundaries segregation during phase transformation, discussing embrittlement 03 p0450 A69-13883

Kelvin-Helmholtz instability for interface between two uniform superposed fluids with constant densities and velocities in horizontal motion in oblique magnetic field 07 p1182 A69-19274

Rayleigh-Taylor instability for interface between two uniform superposed fluids under combined effect of horizontal and vertical magnetic fields 07 p1182 A69-19275

Radio signal spectrum scattered at oscillating interface calculated in Kirchhoff approximation, determining scattering factors 08 p1275 A69-20432

Interfacial charge relaxation oversteability in tangential electrical field, discussing electromechanical polarization surface waves propagation and dielectrophoretic orientation of liquids in zero gravity space 08 p1353 A69-20792

Ion Landau damping and finite Larmor radius effects on dispersion relation of Kelvin-Helmholtz instability due to shear in ion fluid velocity 08 p1367 A69-20799

Microlayer thickness in nucleate boiling, studying liquid-vapor interface motion of growing bubble near heated surface 13 p2375 A69-27789

Shock development in electrothermal shock tube with performance simulation of mechanical shock tube with hot driver but turbulent or unstable driver-shock interface 14 p2427 A69-29768

Interlaminar shear strength development for utilization of unidirectional strength and stiffness of graphite fibers, discussing epoxy resin-fiber interface improvement 15 p2642 A69-30312

Normal modes stability analysis of fluid layer adjacent to flat plate submerged in liquid, considering effects of interfacial surface tension and buoyant forces [AIAA PAPER 69-386] 15 p2590 A69-30476

Turbulent viscoelastic gas ingestion and fluid inertia analysis using stability of dynamic gas-liquid interface between rotating cylinders [ASLE FICFS PREPRINT 31] 15 p2621 A69-30496

Plane incompressible fluid interface stability in presence of transverse electric field, deriving equation of motion for perturbation amplitude 15 p2652 A69-30911

Small amplitude motions of plane interface between fluids stressed by initially perpendicular electric field, modeling fluids as ohmic conductors 16 p2811 A69-31667

Hydrostatic stability and damping characteristics of perforated plates and screens for passive propellant control schemes from drop tower tests [AIAA PAPER 69-531] 16 p2833 A69-32691

Orbital refueling techniques, discussing vapor-liquid interface stability, pressurant requirements, transfer line chilldown, propellant transfer dynamics, dielectrophoresis, suction speed estimating and system tradeoffs [AIAA PAPER 69-564] 16 p2869 A69-32733

Hele-Shaw and porous medium fuel tank systems behavior in simulated low gravity environment, studying sloshing, wetting, funneling and fuel-driver gas interface stability [AIAA PAPER 69-678] 17 p3021 A69-33444

Cylindrical bubbles stability in vertical pipes from photographs, describing wake, spacing, pressure pulsations and convection cells effects [ASME PAPER 69-HT-28] 24 p4411 A69-43540

Plasma-dynamic forces used to suppress fuel-propellant interface turbulence in coaxial jet gas core reactors 24 p4349 A69-43679

INTERFACES

NT FLUID BOUNDARIES

NT GAS-SOLID INTERFACES

NT JET BOUNDARIES

NT LIQUID-LIQUID INTERFACES

NT LIQUID-SOLID INTERFACES

NT LIQUID-VAPOR INTERFACES

NT SOLID-SOLID INTERFACES

Design of interface between Mariner Mars spacecraft and Mars planetary entry/landing capsule [AIAA PAPER 68-1162] 03 p0521 A69-13671

Physical and mechanical properties of surfaces and interfaces - Conference, Raquette Lake, New York, August 1967 03 p0448 A69-13867

Surface and interface phenomena in engineering technology, determining mechanical or electronic properties 03 p0434 A69-13868

Interfaces role in Ni-base superalloy, discussing grain boundaries and coherent/incoherent phase boundaries 03 p0449 A69-13878

Dynamic shear stresses at interface of embedded thin elastic filament and elastic matrix after subjecting filament to concentrated longitudinal line load 05 p0831 A69-15577

Interface states effects on characteristics of p-channel MOS transistors 06 p0979 A69-17117

Electronic structure of clean metallic interfaces, considering electron, ion and surface interactions for metal-vacuum interface 13 p2321 A69-28008

Energetics in solid film lubricants vacuum deposition methods, showing dependence on interfacial and film characteristics 14 p2454 A69-29001

Eccentric face seal with tangentially varying film thickness, analyzing leakage flow proportional to eccentricity and surface waviness
[ASLE FICFS PREPRINT 15B]

15 p2620 A69-30484

Attenuation of small perturbations in shape of plane shock wave propagating into uniform medium in presence of rigid or interfacial boundaries

15 p2592 A69-31145

Moving load at plane interface between two elastic media in space related to direct trirectangular trihedron with vertically descending Oz axis

16 p2870 A69-31829

Electrohydrodynamics of fluids having uniform electrical properties, emphasizing shear effects for interfacially confined electromechanical coupling

18 p3123 A69-34919

Thermal contact conductance of thermally thick specimens with thermocouples not located at interface

20 p3632 A69-37521

Dynamic equilibrium of making and breaking adhesion bonds between polymer segments and dissimilar surfaces through water, allowing thermal stresses relaxation

24 p4326 A69-43458

INTERFACIAL ENERGY

Friction coefficient dependence on interfacial potential between solids

12 p2129 A69-25982

Coating deposition theory on high temperature materials, discussing interfacial energy and wetting properties of molten metal drop on solid base material surface

20 p3560 A69-37358

Scalar waves propagation in bounded randomly fluctuating media, emphasizing interface effects on coherent wave motion

21 p3675 A69-39283

INTERFACIAL TENSION

Composite material mechanical failure due to detachment of microfiber ends from elastic matrix while under tension

01 p0171 A69-11259

Shape and stability of interface between liquids subjected to surface tension and mass force field in vessel

03 p0417 A69-13809

Equilibrium problem for fluid subjected to gravitational forces and surface tension, proposing algorithm for numerical solution

03 p0417 A69-13810

Ideal liquid small oscillations in vessel under close to weightlessness conditions, discussing surface tension, equilibrium conditions and solution by decomposing vector function space

03 p0418 A69-13811

Motion and stability of solid body with cavity containing rotor and two incompressible nonmixing liquids with surface tension

03 p0418 A69-13814

Small oscillations of viscous incompressible fluid in container with free surface under action of potential force field

04 p0587 A69-14620

Fluid support by capillary forces, fluid support by pressure with surface tension stabilization and capillary gas barriers for long life missions
[AIAA PAPER 68-465]

04 p0646 A69-15505

Physicotechnical problems of weightlessness, considering cohesive forces, surface tension and mechanical behavior of fluids and weightlessness simulation techniques

07 p1070 A69-18568

Rotating incompressible liquid drop held together by surface tension noting spheroidal and toroidal shapes, energies and case of surrounding denser medium

07 p1120 A69-19267

Stability of rotating liquid mass held together by surface tension

07 p1121 A69-19268

Sliding friction technique to determine contact area and surface microtopography between abraded metals and polymers

08 p1319 A69-19994

Inhomogeneous half planes equilibrium bonded by elastic layer, noting tangential stresses at interfaces

09 p1611 A69-21482

Mass transfer during interfacial turbulence induced by Marangoni effect in physical model

09 p1621 A69-21903

Correlation between interfacial tension in binary and ternary systems and reciprocal solubility of bulk phases, assuming concentration as function of thickness

09 p1448 A69-21909

Interfacial stress between thermally grown silicon dioxide and single crystal silicon correlated with oxide compressive strength

10 p1744 A69-23177

Interfacial pressure distribution during slip damping in clamped rectangular beams subjected to vibration

10 p1800 A69-23350

Surface-active additives effect on crystallization kinetics of silicate glasses, discussing surface tension

11 p1907 A69-25032

Natural frequencies and forms of small vibrations of ideal liquid in spherical container with weak force field, considering surface tension forces

11 p1875 A69-25484

Normal modes stability analysis of fluid layer adjacent to flat plate submerged in liquid, considering effects of interfacial surface tension and buoyant forces
[AIAA PAPER 69-386]

15 p2590 A69-30476

Surface tension gradients caused thermocapillary convection solved for spherical fluid film under weightlessness conditions

19 p3452 A69-36392

Surface tension of simple liquids consisting of interacting spherical particles, considering density variation in liquid-vapor phase transition zone

19 p3452 A69-36725

Pulmonary surfactant identification on modified Wilhelmy balances, by measurement of areas corresponding to minimum surface tension, using tracheal lavage from dogs and rats

21 p3651 A69-38387

Vacuum apparatus for measuring uniaxially loaded metal surfaces interfacial adhesion, showing surface oxide removal effectiveness influence in adhesion strength

21 p3689 A69-38594

INTERFERENCE

Two polarization light interference scattered by moving and fixed atoms, obtaining forward scattered light intensity

17 p3005 A69-33109

INTERFERENCE DRAG

Aerodynamic interference effects arising from jet efflux of V-STOL aircraft, developing vortex sheet theory for jet interference

05 p0696 A69-15566

Critical flutter behavior of variable geometry aircraft with wing of 70 degree leading edge sweep, noting wing-tail interference

11 p1991 A69-25517

Exhaust nozzle/airframe interference test evaluation for twin engine supersonic fighter
[AIAA PAPER 69-430]

16 p2733 A69-32730

Power plant installation on swept winged transport aircraft, discussing interference drag sources, high lift problems, unorthodox installations, nacelle effects, etc

17 p2898 A69-33214

INTERFERENCE GRATING

Moire fringe interpolation and multiplication by shifting master interference grating, noting increased measurement sensitivity

03 p0524 A69-13063

Electron bombardment effects on performance characteristics of UV gratings

08 p1318 A69-21097

Moire fringes, discussing fringe multiplication by filtering to obtain small strain measurement sensitivity and engraving technique for wave front reconstruction

12 p2099 A69-27164

Electromagnetic wave diffraction in vacuum by equidistant conducting grating, deriving integrodifferential equations for calculating amplitudes

17 p2930 A69-33886

Multiple interference effect introduced by nonlinear characteristics of photographic material, measuring phase variations by holographic multiple beam interferometry

17 p2977 A69-34159

Electron microprobe to produce plane grating X ray hologram based on Lloyd mirror experiment principle

17 p2977 A69-34160

Coupled Fabry-Perot interferometer for microwave spectra with improved selectivity of interference filter

22 p3947 A69-40800

INTERFERENCE LIFT

Wind tunnel wall interference effects in wind tunnel testing of STOL aircraft by inducing interference velocities
[AIAA PAPER 68-399]

17 p2947 A69-34022

INTERFERENCE MONOCHROMATIZATION

U DIFFRACTION

U MONOCHROMATIZATION

INTERFEROGRAMS

U INTERFEROMETRY

INTERFEROMETERS

NT FABRY-PEROT INTERFEROMETERS
NT MACH-ZEHNDER INTERFEROMETERS
NT MICHELSON INTERFEROMETERS
NT MICROWAVE INTERFEROMETERS
NT RADIO INTERFEROMETERS

Short baseline radiating satellite interferometer concept for reducing satellite navigation systematic errors for aircraft and ships

03 p0463 A69-13208

Acoustical thermometer-interferometer to measure air temperature between 20 and 50 km

03 p0429 A69-13269

Laser interferometer gauges for machine tool accuracy, discussing operation, application, manufacture, cost and closed loop numerical control systems

04 p0606 A69-14880

Coupled cavity carbon dioxide laser interferometer with feedback for measurement of transient plasma density in theta pinch, noting sensitivity

06 p0935 A69-17706

Focused electromagnetic beam interferometers and antenna parameters for measuring electron density in plasma diagnostics

07 p1132 A69-18865

Navigation satellites system designed for ATC without requirement for onboard transmitter, discussing spectrum occupancy, satellite power, lane ambiguities and computational procedures

07 p1177 A69-19212

High quality holography with illumination possessing low degree of spatial coherence by means of interferometric arrangement with amplitude division

08 p1312 A69-20081

Optical resonator as Q meter, discussing error capability and construction

08 p1312 A69-20106

Distance measurements of several hundred feet to resolution of three millionth of inch by applying He-Ne laser interferometer

09 p1519 A69-22475

Laser frequency drift effect on operation of three mirror interferometer, noting wave reflection by two compounded mirrors

11 p1895 A69-24720

Fourier transform holograms by Fresnel zone-plate fringe interferometer, discussing source size and bandwidth

12 p2090 A69-26249

Precision optical systems tests, using two beam interferometer and CW gas laser to examine reflected or transmitted wavefront contours

12 p2092 A69-26421

Stellar diameter interferometric measurements, discussing double slit arrangement and illumination in focal plane

13 p2334 A69-27305

Acoustical thermometer-interferometer to measure air temperature between 20 and 50 km

14 p2445 A69-28777

Multifrequency interferometer for inhomogeneous plasma density soundings

14 p2497 A69-29795

Interferometer for measuring electric fields spatial correlation function at camera aperture, describing laser light coherence measurements after propagation through turbulent atmosphere

15 p2653 A69-31164

Observations of 123 southern radio sources made with two clement variable spacing interferometer, tabulating and graphing results

15 p2696 A69-31166

Interferometric displacement transducer for measuring linear displacements up to one and one-half inches

15 p2614 A69-31280

Three antenna interferometer angle measurement accuracy dependent on antenna spacing, deriving optimal spacing value

16 p2758 A69-31730

Holographic cine-interferometry, using live fringe method with Q switched pulsed ruby lasers to obtain consecutive submicrosecond interferograms

18 p3133 A69-34265

Cylindrical concave surface quality control by contactless comparison with reference surface, using interferometer with Twyman system and continuous laser

19 p3311 A69-36196

Observation time influence on interferometers resolution limits due to radio wave phase fluctuations

21 p3682 A69-39122

Fiber optics interferometers, analyzing light propagation along dielectric light pipes and wave interference

24 p4315 A69-43162

Tilted etalons to obtain tunable single mode emission from gas lasers noting fabrication simplicity, vibration insensitivity and low insertion loss resulting in high efficiency
24 p4329 A69-43752

INTERFEROMETRY NT DIFFERENTIAL INTERFEROMETRY

Streak interferometry method for measuring transient deformation data on metallic solid surfaces
01 p0078 A69-10117

Holographic phase variation distribution recording by interference between reconstructed wave fronts from separate holograms
01 p0083 A69-10984

Radio telescope for Owens Valley Radio Observatory, noting interferometer array of steerable antennas and signal wavelength influence on telescope reflector accuracy
02 p0229 A69-11974

Interferometric laser beam scanner using hollow cathode mercury ion laser output
04 p0609 A69-14288

Holographic interferometer for isopachic stress analysis, utilizing photochromic recording for real time interference
04 p0599 A69-15013

Line profile and optical interferometry in astronomy and geophysics
05 p0760 A69-15590

Plasma refractive index determination by holographic interferometry with double pulse ruby laser
05 p0761 A69-15620

Holography, discussing one beam recording, real time interferometry, pulsed laser, etc
05 p0761 A69-15774

Time averaged optical holographic interferometry of standing longitudinal acoustic waves in square cross section duct
06 p0923 A69-17150

Holographic interferometry, determining mechanical vibration amplitudes of compressor and turbine blades and airframe panel [SAE PAPER 690265]
07 p1130 A69-18313

Holography combined with laser interferometry for nondestructive testing in materials, components and assemblies
07 p1137 A69-19777

Monograph on interferometric studies of unsteady shock waves in theta pinch driven shock tube, discussing flow characteristics in helium and hydrogen
08 p1304 A69-20710

Reflection interferometry for visual evidence of surface deformation of rock and metal samples using two beam Fizeau fringe system
09 p1496 A69-22012

Laser resonator loss factor and axial mode frequency calculation by interferometry
09 p1520 A69-22679

Shearing interferometry by simultaneous reconstruction of two wavefronts on single photographic plate
10 p1690 A69-22952

Resonator interferometry of pulsed submillimeter wave lasers, analyzing mode structure, pulse shapes and molecular mechanism of laser emission
10 p1705 A69-23810

Intensity interferometry by two photon excitation of fluorescence trace for three mode laser under phase locking, free running and FM-like conditions
10 p1705 A69-23811

Conventional interferometry advances due to gas laser development, discussing basic concepts and methods of interferometers
11 p1881 A69-24599

Pulsed laser holography advantages for recording small objects in motion and holographic interferometry advantages for complex surfaces and time-separated events
11 p1883 A69-24682

Pulsed laser holography for recording interferograms of laser created plasma, discussing laser source properties, spatial and spectral coherence, double pulse mode, etc
11 p1895 A69-24683

Real time Fourier spectroscopic system for synthesis of spectrum of interferogram, noting polystyrene IR transmission spectra
11 p1884 A69-24837

Distance vs time and velocity vs time measurements for high speed model missiles by means of laser interferometry and optical Doppler shift method
11 p1886 A69-25042

Brightness temperature distributions from intensity interferometric measurements reconstructed by computation
11 p1888 A69-25256

Shadow and schlieren photography, interferometry and quantitative data treatment obtainable by high speed multiframe photographic arrangement, using laser beam
12 p2086 A69-26165

Holography theory and applications including imaging, Fourier transforms and interferometry
12 p2086 A69-26169

Repetitive Q switched laser light source for interferometry, holography and high speed photography
12 p2087 A69-26170

Quantitative interferometric analysis of shock induced wavelength variations in glass and polished steel plates using Q switched ruby laser light source
12 p2089 A69-26185

HF interferometry for statistical-numerical oscillation analysis of unsteady plane transonic flow, constructing phase planes for study of wave surfaces propagation
12 p2089 A69-26188

Coherent optical flow detection and surface microstrain measurement techniques including holographic interferometry, optical correlation and diffraction
12 p2180 A69-26305

Laser interferometer determining spatial distribution of neon metastable state in He-Ne active discharge, discussing lens effects
12 p2108 A69-26636

Lasers application to measurement techniques including alignment, direction, distance, elongation, interferometric, holographic, etc
12 p2094 A69-26903

Shadow, schlieren and interferometric methods for study of transonic, supersonic and hypersonic fields of aerodynamics, using refractivity variations in heterogeneous medium
12 p2060 A69-26934

Natural unbroken tektite surface examination by interferometry, discussing fringe patterns for pit shapes and sizes
12 p2173 A69-27175

Multichannel optical interference fluid manometer, using laser light source for fringe pattern photographic record
13 p2263 A69-28190

Pulsed laser holographic interferometry of density field created by high speed projectile motion in air [AIAA PAPER 69-347]
13 p2263 A69-28282

Optical refraction effects from refractive index gradients in stressed models as limitation on moire interferometry usefulness in Boussinesq problem and expanding pulse studies
14 p2531 A69-28883

Interferometric technique for studying fracture specimens plastic zone using laser holography
15 p2609 A69-30681

Stresses in fixed two dimensional photoelastic models analyzed by hologram interferometry, displaying isochromatic and isopachic interference patterns
15 p2611 A69-31110

Time average, multiple exposure and real time holographic interferometry based on image synthesis
15 p2611 A69-31146

Holographical interferometry with laser spark radiation containing fundamental and second harmonic wavelengths, confirming heavy particle densities decrease in plasma with time
16 p2789 A69-31771

Electron density measurement method in plasma or vacuum based on refraction index in optical frequency range using laser interferometer mismatch as criterion
16 p2798 A69-32583

Interferometric observations of radio source VRO 42 22 01 listed with antenna separations in wavelengths and with resolution direction
17 p3026 A69-32861

Multiple interference effect introduced by nonlinear characteristics of photographic material, measuring phase variations by holographic multiple beam interferometry
17 p2977 A69-34159

Shock heated argon thermal conductivity studied by optical interferograms, deriving equation for measured mean value
18 p3228 A69-34459

Vibration measurement by hologram interferometry, explaining interference fringes as linear combination of vibrating object classical modes
18 p3135 A69-34635

Thermal coefficient of optical glasses refractive index determined by interferometry, noting relation to glass chemical composition
18 p3172 A69-35013

Strains in solids of any form, using moire method combined with holographic interferometry
18 p3139 A69-35280

Holographic interferometry for nondestructive testing of aircraft materials, discussing applications to quality control
19 p3322 A69-35576

Solid state laser emission frequency control and retuning using dispersive resonators, analyzing interference methods for wavelength measurement
19 p3331 A69-35865

Plate material Poisson ratio determined by application of holographic interferometry to plate pure bending deformation contour lines
19 p3312 A69-36206

Holographic camera using Q switched laser for recording high speed interferograms in plasma diagnostics
19 p3315 A69-36726

Frequency controlled unmodulated laser for long path interferometry, noting servoloop correction of frequency relative to Lamb dip
20 p3553 A69-37303

Intensity interferometer applications comparison with Michelson interferometer, discussing sensitivities, radio and optical wavelength astronomy, space plane waves, etc
21 p3722 A69-38794

Holographic interferometry by single two wavelength laser pulse exposure, discussing variable sensitivity techniques
21 p3725 A69-39448

Wedge fringes visibility and localization in hologram interferometry during focusing on surface under examination for displacements
22 p3943 A69-40016

Spatial coherence of He-Ne laser beam studied in Young interference experiment, noting multimode light percentage attributed to weak transverse modes
22 p3960 A69-40018

Strain measurement by interferometer with gas laser source emphasizing long period measurement problem
22 p3960 A69-40189

Holography for engineering metrology, discussing interferometry, pattern interpretation, inspection techniques, etc
22 p3945 A69-40235

Laser interferometric length measurement by fringe counting, considering mechanical and optical systems limitations and design tolerances
22 p3960 A69-40238

Holographic interferometry for surface strain and vibrations visualization, describing photographic recording techniques
22 p3945 A69-40244

Holographic interferometry for measuring small static displacements of diffusely reflecting surfaces
23 p4167 A69-42185

Holographic interferometry for determining total free electrons in plasma produced by irradiating solid hydrogen foils with giant pulse ruby laser
24 p3414 A69-42980

Microcrack detection by holographic interferometry, describing experimental apparatus and test procedure and results
24 p3417 A69-43763

Three dimensional shadowgraph-like images in single exposure holograms of diffusely illuminated flame explained as time average holographic interferograms
24 p3417 A69-43764

INTERGALACTIC MEDIA

Submillimeter wavelength astronomy noting instruments, prestellar matter, interstellar and intergalactic matter state and composition, IR stars, planetary atmospheres, etc
05 p0821 A69-15843

Metastable helium abundance in interstellar and intergalactic space, inferring low energy cosmic ray concentration
06 p1010 A69-17973

Galactic and intergalactic ionic fine structure transitions effect on background microwave radiation intensity
09 p1590 A69-21445

Supplemented data to analyze intergalactic gas diffuse X ray background radiation
10 p1792 A69-24209

Thermal balance of intergalactic gas, discussing plasma energy losses due to He emission and reverse Compton electron scattering and rapid cooling effect
11 p1954 A69-24381

Nonthermal intergalactic bremsstrahlung model as isotropic X ray background due to subcosmic electron interactions with thermal ionized gas in expanding universe
11 p1947 A69-24595

Intergalactic matter capture by NGC 1614 nucleus, stellar ejection from galaxies, explosive separation of close binary and other unsteady phenomena in galaxies 12 p2169 A69-27061

Doppler effect significance in radio astronomy including galaxies relative motion and information concerning isolated hydrogen clouds between galaxies 16 p2853 A69-31565

Sky brightness temperature spectra searched for neutral intergalactic atomic hydrogen radio emission, using horn-reflector antenna 18 p3190 A69-34285

Microwave background anisotropy induced by gravitational effects interpreted using spatially flat Friedmann model for substratum 18 p3190 A69-34286

Quasars and intergalactic hydrogen density, using Schmidt law of increase in number density of quasars to construct plausible models 18 p3190 A69-34288

Thermal balance of intergalactic gas, discussing plasma energy losses due to He emission and reverse Compton electron scattering and rapid cooling effect 24 p4389 A69-43771

INTERGRANULAR CORROSION

Failure mechanism for intergranular stress corrosion cracking of vacuum annealed unalloyed Ti in alcohol iodine solutions 16 p2798 A69-31717

Precipitation hardening, microstructure and dislocation influence on intergranular stress corrosion cracking /SCC/ of high strength Al alloys examined by transmission electron microscopy 19 p3351 A69-36898

INTERIOR BALLISTICS

Solid fuel rocket engine thrust and chamber pressure development curves from charge and engine geometry, heat of explosion and kinetic characteristics 16 p2836 A69-31994

Solid propellant rocket motors ignition and igniter performance, discussing ignition interior ballistics 16 p2829 A69-31997

INTERLAYERS

NT MULTILAYER INSULATION

Interlayer slip in layered wood beams with nail joints analyzed in terms of small deflection theory 01 p0169 A69-10638

Seasonal variations in thickness of ionospheric E-F interlayer region during daylight and maximum integral ionization values 02 p0239 A69-11682

Seasonal variations in thickness of ionospheric E-F interlayer region during daylight and maximum integral ionization values 13 p2257 A69-28713

Longitudinal modulus of interlaminar slip during creep of fiberglass reinforced plastic determined by bending tests of beams under concentrated force 18 p3163 A69-35365

INTERLOCKING

U LOCKING

INTERMEDIATE FREQUENCY AMPLIFIERS

Linear integrated circuit communication systems based on subsystem approach, showing example of IF strip and audio AGC/squelch amplifier 01 p0035 A69-11389

Direct coupled monolithic IF amplifier with active gain control, analyzing large signal response, stability, available gain and noise behavior 07 p1104 A69-18885

Clutter residues of coherent MTI radar receiver, emphasizing IF stages saturation nonlinearity affecting cancelling circuits performance 13 p2220 A69-27941

Noise stability of FM receiver with automatic control of IF amplifier resonance frequency in presence of weak noise 15 p2564 A69-30144

Bandwidth requirement of single channel monopulse limiter, discussing signals conversion to IF 16 p2761 A69-32471

INTERMEDIATE RANGE BALLISTIC MISSILES

U POLARIS MISSILES

INTERMETALLICS

Irradiation influence on yield stress of Ni-Al intermetallics noting temperature dependence and electron dosage 01 p0095 A69-10608

Diffusion data in binary compound semiconductors, tabulating impurities, electrical behavior, temperature variations and diffusion coefficients 02 p0296 A69-11809

Ferromagnetic ordering effect on gadolinium dialuminide thermoelectric power, measuring temperature dependence of power and electrical resistivity 03 p0485 A69-13322

Diffusion in compounds of elements of groups III-V 04 p0641 A69-14502

Radiation effects on III-V compounds, considering damage in solar cells and luminescence, light emitting and Esaki diodes 04 p0641 A69-14504

Ti-Zr-Sn alloys phase equilibria and interaction between titanium stannide and solid solution of Ti and Zr 07 p1162 A69-18770

Microstructure relationship to tensile strength and creep resistance in Zn-Ni-Ti alloy extrusions, discussing role of finely dispersed intermetallic particles 08 p1329 A69-20002

Fatigue characteristics of unidirectionally solidified Al-intermetallic aluminum nickel eutectic alloy consisting of discontinuous Al-Ni intermetallic whiskers in Al matrix 08 p1329 A69-20006

Temperature dependence of single crystal elastic constants of nickel aluminide determined by ultrasonic wave propagation measurement 08 p1332 A69-20288

V phase structure and V and E phase lattice constants for ternary systems /Ti, Zr, Nb or Ta/-/Ni, Co or Fe/-/Si or Ge/ 10 p1708 A69-22992

Intermediate Ni-Nb intermetallic formation as decomposition product from supersaturated Ni rich Ni-Nb solid solution aged above room temperature 10 p1708 A69-22993

Unidirectionally solidified eutectic composite of Al and Cu-Al intermetallic, noting tensile properties at room and high temperatures 10 p1708 A69-22995

Electron fractography of aluminum alloy fatigue for intermetallic particles and inclusions effects on crack growth 10 p1795 A69-23065

Magnetic reversible phase holograms on thin film Mn-Bi by Curie-point writing technique 10 p1706 A69-24007

Gadolinium-cobalt system investigation by X ray diffraction thermoanalysis and metallography for intermetallic compounds, noting structure transformation and homogeneity 11 p1903 A69-24574

Intermetallic compound precipitation effects on mechanical properties of Fe-Mo alloy at high temperatures 12 p2116 A69-26925

Composition, gamma structure and mechanical properties of three unidirectionally solidified eutectics within Ni-Al-Cb, Ni-Al-Zr and Ni-Al-Ti systems 13 p2277 A69-27407

Controllable process for forming Ti-Ni intermetallic wear resistant coating on Ti alloys, discussing techniques, weight saving advantage, gear tests, etc 19 p3323 A69-35582

Ti sub 3, Rh sub 5 and Hf sub 3, Rh sub 5 existence and isomorphism confirmed by crystallographic and X ray methods 19 p3343 A69-35920

Stoichiometric NiAl slip line and dislocation structures during creep at high temperatures, considering possible creep mechanisms 19 p3343 A69-35923

Diffusion processes, composition and structure of vapor deposited Ni coatings on Nb substrate, plotting intermetallic compounds growth against temperature 20 p3560 A69-37366

INTERMODULATION

Intermodulation and cross modulation distortions in double balanced modulator 04 p0573 A69-14341

Cross modulation of amplitude modulated wave propagating in nonlinear dispersive plasma, obtaining electric vector 07 p1086 A69-19228

Spectral distribution of intermodulation noise of AM and FM transmission systems calculated by probability theory 08 p1271 A69-19916

Noise power ratio at output of wideband amplifier with angle modulated multicarrier input, obtaining intermodulation products from Bessel functions expansion 08 p1285 A69-20595

Intermodulation noise distorting arbitrary frequency-modulated multicarrier microwave signal in satellite transponder, emphasizing nonlinear energy dissipation and AM-FM conversion 11 p1841 A69-25634

Receivers EMC, discussing single parameter to evaluate susceptibility to desensitization, cross modulation and intermodulation 23 p4142 A69-42232

INTERMOLECULAR FORCES

Intermolecular interaction potentials for dissociating air components determined by calculating collision integrals for very high temperature gases 02 p0283 A69-11586

Numerical solution for excitation of oscillations in diatomic molecules during atom-molecule collisions at high temperatures, determining intermolecular interaction forces 02 p0284 A69-12485

Depolarized Rayleigh line widths measured for carbon dioxide, nitrogen and hydrogen, using measurements to calculate reorientation cross sections [IEEE PAPER B-11] 07 p1157 A69-19485

Near resonant transfer of vibrational energy from carbon dioxide nu 3 mode to N 14 and N 15 molecules in collisions 08 p1358 A69-21011

Intermolecular potential function relation to individual macroscopic properties extended to simultaneous fit of all possible pair combinations 10 p1652 A69-23391

Crack propagation through layer of viscous fibers joining orthotropic elastic half planes 10 p1803 A69-24029

London-van der Waals interaction energy of symmetric molecular pair calculated in perturbation theory second order as infinite series in negative powers of separation 12 p2131 A69-26606

Molecular beam scattering analysis by four parameter B-C intermolecular potential, plotting expansion coefficients against reduced curvature 13 p2301 A69-27206

Gas-gas interactions second virial coefficients measured at various temperatures, comparing experimental data with results calculated by Kihara potential 14 p2488 A69-29927

Valence force constants for nitric acid evaluated from fundamental mode vibration spectra by matrix method 15 p2561 A69-30467

Temperature dependence of intermolecular interaction averaged potentials with respect to vibrational states 15 p2655 A69-30982

Heated supersonic beam study of He-Ar intermolecular potential, determining total elastic collision cross section as function of velocity in scattering chamber 19 p3377 A69-36183

INTERNAL COMBUSTION ENGINES

NT BRISTOL-SIDDELEY OLYMPUS 593 ENGINE

NT DUCTED FAN ENGINES

NT GAS TURBINE ENGINES

NT HELICOPTER ENGINES

NT J-79 ENGINE

NT J-85 ENGINE

NT JET ENGINES

NT PULSEJET ENGINES

NT RAMJET ENGINES

NT SUPERSONIC COMBUSTION RAMJET ENGINES

NT T-53 ENGINE

NT TURBOFAN ENGINES

NT TURBOJET ENGINES

NT TURBOPROP ENGINES

NT WANKEL ENGINES

Rotary engines, discussing scissor, eccentric rotor, multiple rotor and revolving block types 07 p1203 A69-18910

Book on Wankel RC engine design and performance covering sealing, timing, life, lubrication, etc 11 p1942 A69-25237

Fueling process in internal combustion engines having fuel admission systems with different flow cross sections 19 p3393 A69-35824

INTERNAL ENERGY

Ideal fluid interaction with gravitational field, assuming internal energy as function of natural pressure and density 07 p1182 A69-19419

Atmospheric energy budget of latent and sensible heat and potential energy between equator and 60 degree N
12 p2066 A69-26132

Linear thermal anomaly on western margin of Mare Humorum, rejecting internal heating origin
21 p3797 A69-38535

Variational method using Hamilton principle and calculus of variations to determine elastic curve and internal forces in static or dynamic loaded beam
22 p4043 A69-40459

INTERNAL FRICTION

Internal friction measurement apparatus for non-metallic solids, noting variations of Young modulus in extremely low loss materials
03 p0428 A69-13108

Temperature dependence of internal friction in molybdenum wire in moderate and high temperatures
03 p0446 A69-13576

Relaxation mechanism of low temperature internal friction peaks in niobium quenched to room temperature
03 p0447 A69-13617

Internal friction temperature effects on amplitude dependence in niobium and molybdenum
04 p0614 A69-14635

Complex form internal friction maximum composed of interstitial atoms in molybdenum solid solution
04 p0615 A69-14640

Amplitude dependent internal friction of materials under inhomogeneous strain, giving values for torsional, free longitudinal and transverse vibration modes
08 p1331 A69-20175

Stress graphitizing and boron codposition effect on dynamic mechanical properties of pyrolytic carbon, noting increase in internal friction and dynamic modulus
10 p1716 A69-23036

Audio frequencies internal friction measurement of austenitic stainless steels subjected to heat treatment and corrosion, discussing time dependence and carbide precipitates morphology
10 p1713 A69-23819

Stability of high speed single mass rotor with internal friction on damped anisotropic supports, considering support stiffness
[ASME PAPER 69-VIBR-2]
10 p1805 A69-24160

Dissipative fluid sphere motion due to impulsive point source calculated by finite difference scheme, assuming Voigt and Maxwell type internal friction mechanisms limitations
14 p2485 A69-29026

Love wave amplitude data satisfying earth model with intrinsic internal friction at depths assumed due to single thermally activated relaxation
15 p2596 A69-30624

Clevis design for reduced friction errors associated with round hole clevis in plane strain fracture toughness measurements
15 p2612 A69-31150

Plastic expansion in metals due to alternating torsional and static tensile loading
16 p2875 A69-32291

Free-free transverse vibration damping phenomena, calculating strain amplitude dependence of internal friction at various frequencies
17 p3051 A69-32961

Forced harmonic oscillations of one dimensional mechanical girder systems allowing for nonlinear resisting forces calculated by boundary value problem reduction to Cauchy problem
17 p3064 A69-33917

Surface layer role in strengthening of iron determined from examining temperature dependence of internal friction during thermomechanical treatments
17 p2991 A69-33939

Annealing temperature effect on Ni-Ti alloys internal friction, noting peak connected with solid solution grain boundaries
18 p3158 A69-35443

High temperature anelastic effect in Mo single crystals ascribed to internal friction peak due to electronic interactions between dislocations and C interstitials
24 p4332 A69-43031

INTERNAL PRESSURE

Mixed boundary value problem of elastostatics for isotropic elastic cylinder containing strip crack opened by internal pressure, using auxiliary functions
01 p0167 A69-10317

Ductile creep rupture of thin walled membrane shell of revolution subjected to time dependent internal pressure and strain hardening
[ASME PAPER 68-WA/MET-15]
05 p0838 A69-16153

Circumferential buckling of ellipsoid of revolution due to internal pressure, assuming linear deflection and uniform thin shell
[ASME PAPER 68-WA/PVP-12]
05 p0840 A69-16190

Stress calculation for internal pressure in moment-less shell of revolution
05 p0843 A69-16690

Fatigue crack propagation in cylindrical shells under fluctuating internal pressure, considering stress intensity factor
10 p1795 A69-23066

Deformations and stresses in pressure vessel with elliptical cross section under uniform internal pressure, noting radial deflection and membrane, bending and skin stress
11 p1983 A69-25023

Orthotropic cylindrical shell stability under uniform axial compression and internal pressure, taking into account subcritical state duration
14 p2532 A69-28981

Creep strain rate and stress distribution of thick walled cylinders under internal pressure at elevated temperature, using variational principle
15 p2703 A69-30070

Heated cylindrical shell with braces subjected to given compression and internal pressure, having elastic beams along edges, analyzing local deformations effect on shell strength and stability
16 p2873 A69-32131

Plastic failure under internal pressure of aluminum spherical shells with single radial or oblique nozzle based on limit analysis theory
17 p3052 A69-32983

Longitudinal crack in cylindrical shell under internal pressure, calculating normal and bending stress singularity strengths against curvature/cracklength parameter
18 p3212 A69-34346

Plastic inhomogeneity effects on yield stress of isotropic spherical shell and long cylindrical tube under internal pressure
24 p4405 A69-43672

INTERNAL STRESS

U RESIDUAL STRESS

INTERNATIONAL COOPERATION

International experimentation with U.S. communications satellites, noting design variations with participants and restraintless information exchange
[UN PAPER 68-95421]
01 p0108 A69-10474

Legal problems in space navigation and solution through international law including air and outer space limits, regulating authority and damage liability
[UN PAPER 68-95475]
01 p0179 A69-10511

Meteorological satellite observations value to Southern Hemisphere
[UN PAPER 68-95213]
01 p0109 A69-10513

NASA programs and opportunities for international cooperation in space
[UN PAPER 68-95367]
01 p0179 A69-10516

San Marco project, discussing Italian Space Commission and NASA cooperation, equatorial range concept and development
[UN PAPER 68-95862]
01 p0180 A69-10518

International liability for damage caused by launching of objects into outer space
[UN PAPER 68-95337]
01 p0180 A69-10525

Book on Demeter-earth resources satellite system covering design, instrumentation, cost estimates, economic benefits and political considerations
01 p0163 A69-11333

Collection of papers on French space effort covering space sciences and applications, vehicles and boosters, launch sites, tracking, international cooperation, etc
02 p0315 A69-11901

Book on international law and uses of outer space covering effects of UN General Assembly Resolutions and Outer Space Treaty
02 p0356 A69-12676

International satellite system for commercial aircraft communications and air traffic control
03 p0464 A69-13238

European space research program, discussing government, science and industry in developing satellites and sounding rockets
03 p0520 A69-13584

U.S.-European cooperation in space activities, discussing implementation by COSPAR and jointly owned industrial corporations
03 p0535 A69-13586

Cooperation in developing space programs between Western Europe and U.S.
03 p0535 A69-13588

Cooperation between U.S. and Europe in space programs, discussing contracts and conditions
03 p0535 A69-13590

Cooperation between U.S. and Europe in communication satellite programs
03 p0535 A69-13591

Topics and objectives of Third Eurospace U.S.-European Conference, Munich, June 1968
03 p0535 A69-13594

U.S.-European cooperation, stressing unsatisfactory role of European industry and governments in space projects
03 p0536 A69-13595

Aerial navigation regulation and international law discussing 1944 Chicago convention for international cooperation
05 p0849 A69-15681

German Air Force Center of Aeronautical Medicine discussing organization, work projects and proposed mutual cooperation with French counterpart
05 p0850 A69-16629

French and German cooperative program Project T Symphonie to develop telecommunications satellite for radio and TV broadcasting
05 p0830 A69-16817

International problems of air traffic control, discussing legal and political basis for organization and ATC liability
06 p1042 A69-16846

German-American interplanetary vehicle to investigate interplanetary space and solar characteristics
06 p1012 A69-16970

Legal and technical aspects of international cooperation in spacecraft crew rescue operations signed by UN General Assembly
06 p1042 A69-17033

International cooperation results in field of optical tracking of satellites for solving problems of atmospheric physics, geophysics and geodesy
06 p1042 A69-17050

U.S.S.R. international cooperation in outer space exploration for peaceful purposes, stressing space meteorology, communications, biology and medicine
[UN PAPER 68-95669]
06 p1043 A69-17054

International 28-station global instrumentation ground support network for space tracking and data acquisition
[UN PAPER 68-95912]
06 p1043 A69-17059

Interamerican Experimental Network of Meteorological Investigation with Rockets/EXAMET-NET/, discussing atmospheric parameters measurement at high altitude
[UN PAPER 68-95903]
06 p0950 A69-17062

Satellite telecommunications, discussing Australian experience, ground stations location, national network and international cooperation
[UN PAPER 68-95286]
06 p0886 A69-17066

Soviet and French coordinated geophysical studies at magnetically conjugate points in northern U.S.S.R. and Indian Ocean
06 p0918 A69-17391

Concorde supersonic transport and Jaguar Military Strike/Trainer programs, discussing management and international cooperation
06 p1043 A69-17831

World satellite telecommunications network, discussing recommendations with reference to signal transmission, acoustic echoes, etc
07 p1079 A69-18942

PCM telemetry system for sounding rocket payloads flown in polar light zone within German-American project AZUR
07 p1081 A69-19099

Satellite communications history covering passive and active satellites and Communication Satellite Act, impact
07 p1085 A69-19182

Legal problems in space navigation and solution via international law including air and outer space limits, regulating authority and damage liability
07 p1244 A69-19233

Regulatory content of international agreements concerning communication satellites problems
08 p1422 A69-20584

Reliability terms for electrical apparatus, equipment and systems, indicating need for international standardization
08 p1292 A69-21108

Communication satellite systems role in world telecommunication network, discussing traffic type, volume and routing, earth stations location and capacities and orbit selection
09 p1449 A69-21271

International air traffic regulations for reciprocity and conventions between contracting states
09 p1626 A69-22092

Auroral French rocket probe in Norway, studying low energy particles, relations between electron showers and high altitude electric fields, etc
09 p1498 A69-22160

Yearbook of air and space law /1966/ covering documents on legal doctrines, treaties, regional arrangements, national bibliographies, Warsaw Convention, Hague Protocol, etc
10 p1811 A69-23986

Meteorological rocket probes in Spain for wind and temperature measurements, including stratospheric circulation data
11 p1877 A69-24519

European space research program, discussing government, science and industry in developing satellites and sounding rockets
11 p1966 A69-25102

Concorde SST industrial project in international cooperation and stage in transport history including supersonic boom, weight, fuel consumption rates and aerodynamic heating
12 p2013 A69-26356

European Space Research Organization projects including satellites and sounding rocket launchings for various missions
12 p2175 A69-26922

International space law definitions, technology, regulations, role of industry and government, etc
13 p2381 A69-27529

Airline ticket as international commodity, discussing regulations and agreements concerning appearance, loss, transferability, etc
13 p2381 A69-27530

International law governing aerospace activities /1966 to 2066/
13 p2382 A69-27829

European earth resource satellite systems technology, applications and costs
13 p2356 A69-27833

Application satellites effects on European economy
13 p2382 A69-27834

Helicopter airworthiness requirements, discussing need for international cooperation on safety regulations
13 p2202 A69-27837

Internationalized defense marketing, suggesting formation of international consortia of industrial companies to design and produce defense systems
14 p2540 A69-28933

Comets considered as natural interplanetary space probes, stressing need for international cooperation on solar system studies
15 p2679 A69-30011

Communications mission of Symphonie project and satellite communications subsystem design
15 p2562 A69-30084

Outer space law principle sources including divine law, UN and NASA contractors regulations
15 p2720 A69-31052

Mass supersonic air transport physiological problems, reporting findings of FAUSST committee concerning ozone toxicity, pressure drops, sonic booms, time zone physiology, etc
15 p2556 A69-31225

Australian space research including space flight programs in cooperation with NASA
15 p2724 A69-31450

Electrophysiological /electrosplanchnogram/ medical data transmission via satellite from France to U.S. for real time computer processing
16 p2746 A69-32070

Franco-British aeronautical cooperation and Concorde development agreement of 29 November 1962
17 p3075 A69-32840

UFOs from sociological viewpoint, stressing need for international cooperation in exobiological research
17 p3076 A69-32974

International organization and project management procedures in design and construction of Heos 1 satellite for measuring charged particles energy distribution outside geomagnetic field
17 p3050 A69-33699

German research satellite Azur design and production management
17 p3050 A69-33700

Franco-Soviet rocket probe launchings for measuring daytime/nighttime ions and neutrons
18 p3210 A69-35282

Article 8 /I/ of Carriage by Air Act, 1932 compared to Warsaw Convention Article 8 /I/, noting definition of legal liability of carrier
19 p3455 A69-36331

Airworthiness certification of civil aircraft, discussing international cooperation on inspection, accident investigation, etc
19 p3456 A69-36688

ITU space communication projects, discussing frequency registration, progress reports from member countries and committees, UN resolutions, communication satellites, etc
19 p3456 A69-36821

European cooperation in aircraft industry and application to Anglo-French helicopter program
19 p3456 A69-36849

Treaty on Outer Space interpretation regarding establishment of international space agency with sufficient authority
20 p3635 A69-37103

1967 Space Treaty Article 11, discussing provisions concerning private exploitation and supernational body authority
20 p3635 A69-37107

ESRO and legal liability in damage suits concerning satellite protection and environmental control
20 p3635 A69-37108

Space law legal liability definitions for damage caused by space objects, discussing juridical principle and procedure
20 p3636 A69-37110

1967 Space Treaty legal aspects of consultation, suggesting international permanent body setup for resolving technical and political matters
20 p3636 A69-37111

Agreement on Rescue and Return of Astronauts and Return of Objects Launched into Outer Space, discussing unintended landing
20 p3636 A69-37113

Agreement on Rescue and Return of Astronauts and Return of Objects Launched into Outer Space, noting humanitarian considerations and indemnity for services rendered
20 p3636 A69-37114

UN agreement provisions on international cooperation for rescuing astronauts and objects in case of accident, distress, emergency or unintended landing
20 p3637 A69-37116

Space vehicles registration within Treaty on Outer Space to provide protection for vehicle and third parties in cases of damage
20 p3637 A69-37117

Satellite telecommunication systems coordination, discussing transformation feasibility of consortium or international organ into international organization
20 p3637 A69-37120

INTELSAT program, discussing U.S. proposals regarding domestic services, separate satellite programs, etc
20 p3637 A69-37121

INTELSAT 1964 agreements consistency with multilateral international agreements, including UN General Assembly and International Telecommunication Union
20 p3638 A69-37122

International cooperation regarding space telecommunication systems, discussing INTELSAT and INTERSPUTNIK roles in achieving international coordination and equality
20 p3638 A69-37125

Space law history, discussing Space Treaty and UN Declaration of Legal Principles
20 p3638 A69-37128

Multiple use doctrines in space law for resource utilization, discussing formation of planning commissions and licensing agencies
20 p3639 A69-37133

Planetary resources control and use from legal and policy standpoints, discussing space treaty effects on international law
20 p3639 A69-37134

International organizations and planning for earth observation satellite program involving exploitation in communications, meteorology and aircraft
21 p3855 A69-38622

Communication satellites with regard to international arrangements for fruitful exploitation noting COSMAT, INTELSAT, European and international developments
22 p4052 A69-40276

INTERNATIONAL GEOPHYSICAL YEAR

Meridional flow, angular momentum and energy flux in atmosphere calculated from IGY data
08 p1346 A69-20312

Solar radio emission data during IGY covering solar terrestrial disturbances, broadband bursts, solar indices, etc
14 p2513 A69-29321

Sudden enhancement of atmospherics recorded during IGY, noting time lag between flare and SEA maximum
16 p2778 A69-32192

High latitude geomagnetic field quiet solar diurnal variations during magnetically quiet IGY winter days, relating type and amplitude at low and midlatitudes
17 p2964 A69-33960

Physical model for IGY radio aurora data correlated with Brice magnetospheric convection model
18 p3125 A69-34231

**INTERNATIONAL LAW
NT SPACE LAW**

Aerial navigation regulation and international law, discussing 1944 Chicago convention for international cooperation
05 p0849 A69-15681

International problems of air traffic control, discussing legal and political basis for organization and ATC liability
06 p1042 A69-16846

Legal and technical aspects of international cooperation in spacecraft crew rescue operations signed by UN General Assembly
06 p1042 A69-17033

Interpretation of term peaceful in Space Treaty and use of outer space including celestial bodies
07 p1244 A69-19234

Regulatory content of international agreements concerning communication satellites problems
08 p1422 A69-20584

International air traffic regulations for reciprocity and conventions between contracting states
09 p1626 A69-22092

Air carrier liability for nuclear weapons damage, discussing international agreements
11 p2003 A69-24260

Aircraft hijacking prevention through technical and legal means, discussing national and international air piracy laws
13 p2381 A69-27528

Airline ticket as international commodity, discussing regulations and agreements concerning appearance, loss, transferability, etc
13 p2381 A69-27530

Air piracy legal aspects as determined by Swiss law and Treaty of Tokyo
19 p3454 A69-35979

Legal liability in civil aviation, proposing international treaty
19 p3454 A69-35980

Article 8 /I/ of Carriage by Air Act, 1932 compared to Warsaw Convention Article 8 /I/, noting definition of legal liability of carrier
19 p3455 A69-36331

Space law legal liability definitions for damage caused by space objects, discussing juridical principle and procedure
20 p3636 A69-37110

1967 Space Treaty legal aspects of consultation, suggesting international permanent body setup for resolving technical and political matters
20 p3636 A69-37111

1967 Space Treaty peaceful activities definition, suggesting explicit provisions regarding treaty province, enforcement machinery and implementation
20 p3636 A69-37112

Amendments considered for international law regarding earth and space rescue services as result of contemporary U.S. manned space flight programs
20 p3637 A69-37115

Juridical norms defined by Madrid, Belgrade and Washington conferences regulating exploration and utilization of extraterrestrial bodies and space, considering satellite communications networks
20 p3638 A69-37123

Legal principles observed for international telecommunication systems establishment by means of artificial satellites regarding states interests and rights
20 p3638 A69-37124

International legal liability for personal injury or property damage caused by space activities
20 p3638 A69-37127

International space law basic ideas and future trends, considering freedom of exploration, UN proposals, space demilitarization, etc
20 p3639 A69-37131

Domestic and international law compared in connection with space program, considering legal aspects of

using satellites in discovering and exploiting earth resources

20 p3639 A69-37132

Custody, jurisdictional conflict and prosecution problems of in-flight crimes, discussing federal judicial jurisdiction and Tokyo Convention ratification

22 p4053 A69-40708

Book on law making in International Civil Aviation Organization covering membership problems, air navigation and transport safety, settling of disputes, etc

23 p4240 A69-41297

INTERNATIONAL PRACTICAL TEMPERATURE U TEMPERATURE SCALES

INTERNATIONAL QUIET SUN YEAR

Global solar radiation flux measurements over India during IQSY

02 p0307 A69-11819

Book containing 1960-1965 /including IQSY/ chronological tables of solar and geophysical events, discussing solar activity, geomagnetic, ionospheric, auroral and cosmic ray research

02 p0321 A69-12165

Ionospheric current systems for various selected very quiet and slightly disturbed international quiet days based on Northern Hemisphere observatories data

03 p0423 A69-13518

Sporadic E region HF backscatter observed during IQSY, using PPI display

09 p1489 A69-21701

Collection of articles on proton flare project /July 1966 event/ during IQSY, covering solar magnetic field, chromosphere, photosphere, solar activity, etc

10 p1760 A69-23725

Visual, photographic and spectral observations of comets during IQSY, discussing comets Tomita-herber-Honda 1964c and Ikeya-Seki 1965f

14 p2525 A69-29716

Solar activity history and morphology /1964-1965/

15 p2679 A69-30006

Cosmic ray observations on synoptic scale, discussing equipment and programs of IQSY world array of monitor stations

15 p2673 A69-30012

IQSY low energy galactic and solar cosmic ray observations made by various satellites and space probes, including hydrogen and helium energy spectra

15 p2673 A69-30014

IQSY night airglow photometric observations, summarizing zenith intensity and north/south intensity ratio data

15 p2594 A69-30019

Book on cosmic ray variations and solar activity during IQSY covering energy spectrum, outer space radiation, magnetosphere, etc

16 p2849 A69-32052

Solar radio emission during quiet sun years 1964-1965 mapped using Stanford spectroheliograph, attributing slowly varying component to electron density enhancement

18 p3188 A69-35395

Daily solar radio noise intensity at 10.7 cm with slowly varying components and quiet sun emission, revealing rise only and absorption bursts

19 p3401 A69-35758

Auroral arcs orientation curves for IQSY evaluated from all sky camera data, comparing results with IGY curves

24 p4308 A69-43009

INTERNATIONAL SATS FOR IONOSPHERIC STUDY U ISIS SATELLITES

INTERPLANETARY COMMUNICATION

Communication systems in interplanetary space covering telemetry, remote control, Doppler and distance measurements, coherent PCM/PSK/PM, demodulation, deep space network, etc

12 p2027 A69-25875

Deep space telemetry bit errors increased by reference signal phase noises and partial RF signal suppression, calculating equivalent signal to noise ratio degradation

13 p2223 A69-28609

INTERPLANETARY DUST NT ZODIACAL DUST

Micrometeorite and meteoric dust data obtained in Soviet space flights

01 p0155 A69-10939

Gaseous hydrates formation in comet nuclei, discussing stability at given temperatures and pressures and solar radiation shielding by dust sheath

03 p0515 A69-14032

Lunar libration clouds, discussing visual observation at small phase angles for estimation of dominant cloud particle size

05 p0827 A69-16527

Doppler shift in zodiacal light spectrum, noting variation of dust concentration and possible orbits

06 p1012 A69-18227

Micron and submicron particle cumulative flux upper limits in satellite micrometeoroid environment of Gemini 12

07 p1215 A69-18845

Photoelectric ejection of grain electrons by solar quanta balance with solar wind electron capture by grain for interplanetary grain equilibrium potential

09 p1593 A69-21655

Outer solar coronal IR radiance measured by ground telescope and stratosphere balloon flight, noting interplanetary dust thermal emission

09 p1600 A69-22205

Test of Velikovsky theory for dense hydrocarbon clouds and dusts surrounding Venus, using IR reflection spectra

09 p1608 A69-22566

Coronal IR observations during solar eclipse revealing thermal emission zone at predicted interplanetary dust vaporization region

10 p1789 A69-24131

Solar radiation pressure on interplanetary dust particles calculated as function of radius and density, noting asteroidal origin of dielectric and absorbing particles

11 p1956 A69-24397

Interplanetary dust and distribution study by micrometeorite analyzer and by zodiacal light observations using solar probe

15 p2694 A69-30879

Meteor showers contribution to interplanetary dust flux based on relative number of particles of various size

15 p2697 A69-31308

Cumulative flux of interplanetary and cislunar space dust particles by Mariner 4 and OGO 3 spacecraft, noting particle impact rate

15 p2699 A69-31394

Zodiacal light brightness and polarization measurements from space probes approximated by Mie scattering of interplanetary dust particles

16 p2857 A69-32092

Interplanetary dust sources investigation based on physical and orbital parameters, noting derivation from asteroids and meteorites

19 p3415 A69-36119

Zodiacal light confirmed as caused predominantly by flattened circumsolar dust cloud

20 p3597 A69-37336

Moon possible origin, discussing spin off from earth, accretion from same dust cloud or formed elsewhere and captured

20 p3603 A69-37559

Solar radiation pressure on interplanetary dust particles calculated as function of radius and density, noting asteroidal origin of dielectric and absorbing particles

24 p4390 A69-43787

INTERPLANETARY EXPLORER U EXPLORER 18 SATELLITE

INTERPLANETARY FLIGHT

Shock layer gas radiation influence on deep space missile shape, noting evaluation by flow equations

01 p0007 A69-11070

Clinical problems during interplanetary flights, stressing need for diagnostic algorithms and automated medical equipment

02 p0202 A69-12121

Voyage to planets - Conference, Washington, D.C., March 1967

02 p0323 A69-12301

Benefits accruing from swingby operation, considering space flights past Jupiter, Saturn and other planets

02 p0326 A69-12663

Space rendezvous problem as applicable to interplanetary missions, discussing steps in rendezvous maneuvers to permit final docking

03 p0511 A69-13401

Interplanetary transportation network involving numerous spacecraft on various planetary flyby trajectories, discussing integration of gravity thrust, braking and scramjet concept

03 p0511 A69-13402

Space flight launches, interplanetary transfer orbits, flyby orbits and capture orbits for solar probe with 0.3 AU perihelion and Jupiter satellite probe

04 p0657 A69-14826

NERVA rocket engine with 200,000-250,000 lb thrust to replace Saturn 5 upper stage for manned interplanetary flights, discussing Mars flight

08 p1410 A69-21029

Interplanetary low thrust mission analysis model, discussing major elements interactions

09 p1585 A69-21206

Maximum capacity estimation for one way transportation systems to moon and Mars, analyzing technical and economic aspects

09 p1586 A69-21297

Monograph on requirements for high speed interplanetary flights with nuclear engines and refueling at destination

09 p1586 A69-21298

Power requirements for tracking, telecommand and telemetry of spacecraft over interplanetary distances, considering transmission problems, equipment weight and reliability

10 p1652 A69-22984

Third phase dynamics of planetary approach of earth-Mars journey, computing approach trajectory on two body spacecraft-Mars assumption

11 p1968 A69-25725

Hardware limitations on communications, instrumentation and data handling for manned deep space missions

13 p2219 A69-27666

Thermal stresses in rotating cylindrical interplanetary body heated by solar radiation

16 p2871 A69-31901

Mission windows for single and multiple planet swingbys past Jupiter to outer planets

[AAS PAPER 68-115] 19 p3402 A69-35936

Approach navigation accuracy for planetary atmosphere braking to orbit about Mars and Venus

[AAS PAPER 68-122] 19 p3402 A69-35937

Evaluation method for straddown spacecraft guidance systems on automated interplanetary missions, using cost and system performance efficiency probability model

[AIAA PAPER 68-828] 19 p3370 A69-35953

Communications, instrumentation and data handling for manned planetary missions, discussing data rate limitations

21 p3674 A69-39018

Spacecraft guidance analysis of multiple outer planet mission utilizing gravity assist swingbys to achieve planetary flybys with single spacecraft

[AAS PAPER 68-109] 21 p3761 A69-39205

Triple planet ballistic flybys, discussing mission opportunities and launch windows

[AAS PAPER 68-114] 21 p3805 A69-39206

CircumJovian powered and free return trajectories, analyzing round trip missions and departure opportunities

[AAS PAPER 68-117] 21 p3805 A69-39207

Direct flight and Jupiter swingby heliocentric trajectory modes of elliptic capture orbits compared for unmanned missions to outer planets

[AAS PAPER 68-105] 21 p3805 A69-39221

Exploration capabilities provided by Jupiter gravity assisted trajectories compared to direct ballistic flight trajectories

[AAS PAPER 68-116] 21 p3805 A69-39224

Interplanetary periodic orbits and flyby dates for multiple Earth-Venus swingby missions, describing various iterative solutions for trajectory

[AIAA PAPER 69-931] 21 p3809 A69-39359

Targeting technique for Atlas/Centaur Mariner Mars 1969 mission, noting suitability to flyby, orbiter or landing interplanetary missions

[AIAA PAPER 69-881] 21 p3764 A69-39407

Evaluation technique for astronautics subsystems in automated spacecraft designed for interplanetary missions, considering operation times, navigation updating and midcourse correction

[AIAA PAPER 69-882] 21 p3764 A69-39408

Interplanetary midcourse velocity correction schedules optimization, discussing timing equations modifications, mission simulation and role of earth based radar

21 p3766 A69-39646

Reconnaissance missions for outer planets exploration, discussing spacecraft design constraints, multiple planet fly-by, planetary orbiter, etc

[AAS PAPER 69-291] 24 p4381 A69-42864

Meteoroid shower model for interplanetary flight hazard evaluation, suggesting shower zone defining on ecliptic plane

24 p4385 A69-43258

Interplanetary space travel medical problems during long duration missions, noting earth diagnostic and therapeutic methods adaptation, drugs selection, astronaut medical training, etc

24 p4278 A69-43396

INTERPLANETARY GAS

Formation mechanism for heterogeneous structure of interplanetary plasma based on plasma instability from temperature anisotropy

02 p0314 A69-11638

Continuity and momentum equations for cosmic ray gas particles in interplanetary region
06 p0992 A69-17379

Interplanetary plasma flow simulation around earth magnetosphere and planets not considering initial conditions influence
09 p1577 A69-21768

Compressible gas flow problem in point body gravitational field solved with reference to sun and interstellar gas
09 p1577 A69-21769

Cosmic protons interaction with interplanetary plasma, analyzing beam energy loss due to excitation of longitudinal electrostatic oscillations
10 p1760 A69-23617

Radio astronomical investigations of small scale inhomogeneity motion and dimensions in interplanetary plasma, using observations of 3C 48 scintillations in 1967
10 p1782 A69-23711

Interplanetary plasma subsequent to July 7, 1966 flare monitored by detectors on Pioneer 6 and Explorer 33
10 p1783 A69-23775

Interplanetary plasma flow directional velocity distribution from solar atmosphere active regions found inhomogeneous
12 p2149 A69-26698

Magnetic field fluctuations of interplanetary plasma, considering anisotropic temperature instabilities
14 p2517 A69-29064

Photoionizing effect of hydrogen and helium UV glow in nighttime ionosphere compared with ground based IF ionosonde and sounding rocket observations
15 p2605 A69-31436

Langmuir probe to determine space vehicle orientation in ionospheric or interplanetary plasma, discussing apparatus, accuracy and application
17 p3001 A69-33222

Hydrodynamic approximation to interplanetary gas motion influenced by solar flare caused perturbations
17 p3035 A69-33627

Comet tails orientation determination for solar wind and interplanetary plasma investigation, considering geometrical difficulties and suggesting computation procedure
20 p3599 A69-37467

Antimatter motion in solar system and earth atmosphere, discussing vaporization and annihilation energy in collisions with interplanetary gas atoms
22 p4034 A69-41100

INTERPLANETARY MAGNETIC FIELDS

Magnetometric equipment on board Luna 10 and Venera 4 space stations for studying magnetic field in interplanetary space, describing circuit and metrological characteristics
01 p0080 A69-10582

Stable fluxgate magnetometer sensor for exploration of space magnetic fields, discussing equipment specifications and performance tests
[IEEE PAPER 10.2] 01 p0081 A69-10715

Interplanetary magnetic field measurements in lunar wake, noting magnetic perturbations pattern and absence of shocks
01 p0157 A69-11228

Geomagnetic response asymmetry related to solar direction of polarity in interplanetary magnetic field
01 p0077 A69-11236

Solar cosmic rays diffusion relationship to interplanetary magnetic field power spectrum from high energy proton and electron observations
01 p0147 A69-11243

Dipole models of geomagnetism at earth surface used to calculate magnetic field in outer space
02 p0238 A69-11673

Geomagnetic and interplanetary field variation measurements from Mariners 2, 4 and 5, noting correlation between solar phenomena and geomagnetic storms
02 p0241 A69-11737

Galactic cosmic ray modulation by interplanetary magnetic fields, discussing compatibility of several models with experimental data
03 p0498 A69-12933

Cosmic ray and solar wind properties, discussing solar wind measurements, interplanetary magnetic field and solar wind sounding by cosmic rays
03 p0500 A69-13355

Charged particle dynamics in spiral interplanetary magnetic field model, discussing electric drift velocity, point of origin and distribution
03 p0503 A69-14015

Atmospheric, geomagnetic and interplanetary effects on cosmic ray flow, noting anisotropy and diurnal variation phase and amplitude averages
04 p0649 A69-14683

Interplanetary magnetic field intensities, solar and stellar fields measured by Zeeman effect, discussing fields of Jupiter, Mars, Venus and moon
04 p0657 A69-14810

Adiabatic motion of hydromagnetic fluid behind spherical fast shock wave for Parker solar wind model
04 p0660 A69-15126

Large scale pattern in solar magnetic field correlated with interplanetary magnetic field
04 p0665 A69-15532

Coronal structure predicted for September 22, 1968 solar eclipse by model constructed for large structure of coronal and interplanetary magnetic fields
05 p0818 A69-15602

Solar and interplanetary magnetic fields and plasmas, noting in situ observations by satellites and space probes of sector patterns, solar cosmic rays and wind
05 p0821 A69-15841

Interplanetary magnetic field fluctuations obtained by IMP 2
05 p0824 A69-16264

Anisotropies in Forbush decreases in March 1966, noting dependence on interplanetary magnetic field structure
06 p0990 A69-17290

Cosmic ray daily variations relationship to geomagnetic activity, sector structure of interplanetary magnetic field and sunspot activity
06 p0990 A69-17291

Lunar core electrical conductivity determination based on induced magnetic field arising from time varying interplanetary magnetic field associated with solar wind plasma
07 p1215 A69-18832

Proton flare activity dependence on Bartel active longitudes and sector structure boundaries of interplanetary magnetic field
07 p1205 A69-19248

Cosmic ray deuteron and He 3 secondary origin and determination of cosmic ray path length and residual interplanetary field modulation
08 p1378 A69-20066

Mariner 2 data on large scale variations in magnetic field, solar wind density and temperature in interplanetary plasma
09 p1592 A69-21540

Sudden commencement associated discontinuities in interplanetary magnetic field observed by IMP 3 satellite, stressing shocks and tangential and rotational discontinuities
09 p1598 A69-22183

Diffusion coefficient and cosmic ray motion in solar system, using satellite data of interplanetary magnetic field
10 p1757 A69-22822

Interplanetary magnetic fields characteristics and magnetic inhomogeneities spectra from cosmic ray variation studies used to obtain scattering mean free path
10 p1757 A69-22824

Cosmic ray anisotropy and diurnal density variation, analyzing influence of interplanetary magnetic field and subsonic solar wind
10 p1757 A69-22828

Cosmic ray anisotropy relation to scattering and sectorial structure of interplanetary magnetic field using neutron monitor data
10 p1758 A69-22834

Simultaneous interplanetary magnetic field measurements by geocentric satellites Explorer 33 and IMP 3 of MHD shock wave associated with July 8, 1966 sudden storm commencement
10 p1783 A69-23773

Interplanetary magnetic field sectoral structure effect on diurnal cosmic ray intensity and geomagnetic field, noting field direction influence
10 p1769 A69-23905

Microscale fluctuations in interplanetary magnetic field, considering proton thermal energy and magnetic field energy densities
10 p1785 A69-24100

Stochastic and ergodic aspects of magnetic lines of force, discussing cosmic ray diffusion in interplanetary magnetic field
10 p1770 A69-24111

Interplanetary magnetic field near Venus, analyzing data by magnetometer onboard Venera 4
10 p1791 A69-24199

Green function solution to Maxwell equations for interplanetary and coronal magnetic fields above photosphere, considering field at source surface
11 p1958 A69-24429

Dipole models of geomagnetism at earth surface used to calculate magnetic field in outer space
13 p2257 A69-28704

Geomagnetic variability relations to interplanetary magnetic field transverse fluctuations, discussing data from Mariner flights
14 p2510 A69-28948

Correlation coefficients between radial components of interplanetary magnetic field and solar wind velocity from Mariner 5 data due to Alfvén waves
14 p2510 A69-28949

Interplanetary sector structure during rising portion of 1966-1967 sunspot cycle, giving recurrence period of interplanetary field
14 p2517 A69-28957

Cosmic ray intensity preceding Forbush effects as function of chromospheric flares solar longitude and solar wind velocity
14 p2512 A69-29044

Relativistic solar proton propagation fluctuation effects in interplanetary magnetic field during cosmic ray intensity increase
14 p2512 A69-29045

Cosmic ray angular distribution spectrum and interplanetary magnetic field properties determined from semidiurnal cosmic ray variations data
14 p2512 A69-29046

Magnetic field fluctuations of interplanetary plasma, considering anisotropic temperature instabilities
14 p2517 A69-29064

Solar cosmic rays diffusion enclosure in interplanetary space magnetic boundary suggested from balloon, satellite and ground observations of solar flare neutron component
14 p2513 A69-29067

Pc 2-4 geomagnetic pulsations abrupt disappearance on global scale ascribed to magnetosphere boundary stabilization, noting interplanetary magnetic field role
14 p2438 A69-29080

Magnetospheric plasma motion associated with Alfvén mode time fluctuations of magnetic field in solar wind
14 p2521 A69-29382

Magnetic field variations in magnetosphere and interplanetary space correlated with polar magnetic disturbances from dynamic morphology data
14 p2441 A69-29387

Solar activity and large scale magnetic field distribution in discrete latitude zones, including interplanetary magnetic field above ecliptic
14 p2528 A69-29966

Discontinuities in interplanetary magnetic field direction presented on mesoscale from Pioneer 6 observation, emphasizing distribution in time
14 p2528 A69-29970

Solar wind existence verified by direct measurements of interplanetary magnetic field and plasma, reviewing solar corona studies by satellites and space probes
15 p2679 A69-30010

Cosmic ray intensity underground measurements, discussing solar modulation processes, sidereal day variations and interplanetary magnetic field influence
15 p2673 A69-30013

Solar corpuscular radiation component from satellite and interplanetary space probe geophysical data, discussing interplanetary magnetic field geometry and corpuscular fluxes
15 p2684 A69-30516

Magnetometric equipment on board Luna 10 and Venera 4 space stations for studying magnetic field in interplanetary space, describing circuit and metrological characteristics
15 p2610 A69-30752

Lunar dynamic response to discontinuities in interplanetary magnetic field to determine electrical conductivity and internal temperature
15 p2700 A69-31442

Neutral point theory applied to solar wind and magnetospheric physics, discussing magnetic field reconstructions
16 p2846 A69-31596

Interplanetary magnetic field radial dependence from Mariner 4 measurements between earth and Mars, indicating fluctuations produced by dynamic processes in solar wind
16 p2856 A69-31964

Interplanetary magnetic fields from Explorer 33 magnetometer relationship to surface geomagnetic variations emphasizing unified view
16 p2862 A69-32309

Interplanetary medium parameters strong variations during low solar activity derived from Mariner 2 data
16 p2851 A69-32517

Mariner 2 data on large scale variations in magnetic field, solar wind density and temperature in interplanetary plasma
16 p2864 A69-32535

European highly eccentric orbit satellite /HEOS/ cislunar probe to explore interplanetary space for magnetic fields, cosmic radiation, solar wind and earth shock wave

17 p3050 A69-33397

Geomagnetic storms and Forbush decreases accounted for by interplanetary solar corpuscular streams effects described by interplanetary magnetic field structure, noting independence of flares

18 p3187 A69-34937

Stream structure in interplanetary magnetic field during 1966, analyzing geomagnetic activity and solar particles and Forbush decrease anisotropy

18 p3199 A69-34938

Earth bow shock waves in far upstream interplanetary medium observed from magnetic data of Explorer 34 satellite

18 p3199 A69-34941

Interplanetary and photospheric magnetic fields polarities observed by Mariner 4 and with solar magnetograph, noting noncorrelated data along latitudinal strip

18 p3205 A69-35399

Solar cosmic ray anisotropies in terms of model with particles propagating along interplanetary magnetic field undergoing pitch-angle scattering

18 p3189 A69-35400

Power spectra of interplanetary magnetic field fluctuations determined from Pioneer 6 satellite data, relating results to galactic cosmic rays modulation

20 p3603 A69-37554

Topology of interplanetary field lines in magnetotail, using solar electrons as tracers with moon as absorber

20 p3609 A69-38078

Solar wind plasma effects on lunar wake umbral and penumbral interplanetary magnetic field anomalies, evaluating roles of electrons and ions

20 p3609 A69-38095

Venus magnetosphere induced by piling up magnetic field from solar wind due to ionospheric conductivity and collisions with planetary atmospheric particles

21 p3794 A69-38381

Homogeneous conducting moon-solar wind interactions, describing time dependent lunar magnetic and electric fields induced by interplanetary magnetic field variations

22 p4023 A69-40518

Cosmic ray flux intensity increases, discussing effects of solar wind, corpuscular flux velocity and interplanetary magnetic field

23 p4205 A69-41838

Interplanetary magnetic field role in interaction between terrestrial magnetosphere, solar plasma and solar flux energy transfer

23 p4214 A69-41865

Day-to-day changes of cosmic ray diurnal variation measured on meson and neutron components, showing relationship with interplanetary magnetic field

23 p4206 A69-42012

Critique of magnetic response model for interaction of moon and interplanetary plasma magnetic field proposed by Blank and Sill

24 p4384 A69-43190

High energy nucleons and electrons accelerated in solar flares, considering interplanetary magnetic field effect on radiation properties near earth orbit

24 p4372 A69-43617

Solar wind disturbances associated with flares

24 p4373 A69-43620

INTERPLANETARY MEDIUM NT ZODIACAL DUST

Interplanetary magnetic field measurements in lunar wake, noting magnetic perturbations pattern and absence of shocks

01 p0157 A69-11228

Solar and interplanetary magnetic fields and plasmas, noting in situ observations by satellites and space probes of sector patterns, solar cosmic rays and wind

05 p0821 A69-15841

Solar wind electron component detection by plasma experiment on Pioneer 6, particularly class 2B flare and quiet period

05 p0816 A69-16275

Cosmic dust concentration in interplanetary space near earth, noting suitability of satellite observation

06 p0999 A69-16971

Interplanetary medium parameters strong variations during low solar activity derived from Mariner 2 data

09 p1575 A69-21522

Mach number values and propagation rates of wear disturbances in interplanetary medium obtained from Mariner 2 data during low solar activity

09 p1575 A69-21523

Mariner 2 data on large scale variations in magnetic field, solar wind density and temperature in interplanetary plasma

09 p1592 A69-21540

Charged particle acceleration in interplanetary medium, discussing protons and plasma oscillations interactions

09 p1575 A69-21541

Cosmic ray particle behavior in interplanetary medium, solving model equation for cosmic ray diffusion in cloud of outgoing scattering centers

09 p1575 A69-21598

Interplanetary scintillation of radio sources to determine size and motion of plasma irregularities in solar wind for fine structure

09 p1594 A69-21658

Electron content of earth-Venus interplanetary medium measured by observing relative propagation time of radar pulses to Venus

09 p1594 A69-21697

Low energy proton flux in neighborhood of Moon measured by Luna 12 satellite indicating magnetized plasma region effect on burst

09 p1577 A69-21773

Solar flare relation to interplanetary scintillation indices and power spectra

09 p1582 A69-22751

Cosmic ray variations as means of studying solar wind characteristics and interplanetary medium

10 p1755 A69-22811

Starlight extinction by interplanetary medium evidenced from confirming correlation between star brightness on ecliptic and elongation

10 p1775 A69-23198

Mariner 2 measurements of geomagnetic field and interplanetary plasma parameters for analyzing interaction between interplanetary medium and magnetosphere during decreased solar activity

10 p1769 A69-23900

Discontinuities in interplanetary magnetic field direction presented on mesoscale from Pioneer 6 observation, emphasizing distribution in time

14 p2528 A69-29970

Solar wind existence verified by direct measurements of interplanetary magnetic field and plasma, reviewing solar corona studies by satellites and space probes

15 p2679 A69-30010

Low energy solar protons and alpha particles from 28 May 1967 solar flare used as probes of interplanetary medium

16 p2847 A69-31965

Interplanetary medium parameters strong variations during low solar activity derived from Mariner 2 data

16 p2851 A69-32517

Mach number values and propagation rates of weak disturbances in interplanetary medium obtained from Mariner 2 data during low solar activity

16 p2851 A69-32518

Mariner 2 data on large scale variations in magnetic field, solar wind density and temperature in interplanetary plasma

16 p2864 A69-32535

Charged particle acceleration in interplanetary medium, discussing protons and plasma oscillations interactions

16 p2851 A69-32536

Interplanetary proton and alpha particle radial gradients determined from Mariner data, considering Forbush decrease, particle solar origin, galactic cosmic radiation, etc

20 p3592 A69-38096

Charged particle acceleration in interplanetary plasma from analysis of cosmic ray intensity increases accompanied by SC magnetic storms and Forbush effects

21 p3788 A69-38587

Solar magnetic field measurements for fine structure of magnetic asymmetry at different heights and within sunspots, discussing asymmetry for corona and interplanetary space

22 p4010 A69-39990

Laboratory experiments applicability to interplanetary plasma physics, describing simulations of solar wind interactions, magnetosphere, collisionless shock waves, etc

22 p4028 A69-40689

Interplanetary shock waves structure and evolution, discussing propagation in collision free media by wave-particle interactions

23 p4222 A69-42394

INTERPLANETARY MONITORING PLATFORM U IMP

INTERPLANETARY NAVIGATION

Planetary navigation using spacecraft measurements and Doppler data from earth-based radio tracking, determining accuracy for earth-Mars trajectory

19 p3368 A69-35791

Navigational accuracy of two way Doppler tracking of interplanetary spacecraft during heliocentric and planetary encounter trajectory phases [AIAA PAPER 69-899]

21 p3761 A69-39334

INTERPLANETARY PROPULSION U ROCKET ENGINES

INTERPLANETARY SPACE

Chemical composition of upper atmosphere and interplanetary space measured by Soviet sounding balloons and rockets, discussing flask sampling technique

01 p0025 A69-10940

Parameters of solar wind responsible for geomagnetic activity, relating magnetic storm features to physical structure of interplanetary space and solar wind bubbles

02 p0240 A69-11725

Automatic bioprobe life support system for long duration interplanetary space flight, discussing blood leech as suitable research animal

02 p0199 A69-11828

Galactic cosmic rays energy modulation spectrum in interplanetary space, showing influence of solar wind velocity and diffusion coefficient dependence

03 p0501 A69-13527

Magnetopause, magnetosheath, bow shock and adjoining interplanetary domain study by IMP-1 satellite, discussing macroscopic plasma variables and fluid model for solar wind

07 p1129 A69-19374

Zodiacal dust density in interplanetary space

08 p1407 A69-20938

Cosmic ray intensity temperature dependence in stratosphere and anisotropy in interplanetary space determined from measurements over Arctic and Antarctic regions

09 p1575 A69-21542

Reflected particle acceleration at magnetospheric bow shock front attributed to interplanetary electric field

09 p1577 A69-21714

Short term variability of solar proton flux in interplanetary space during solar flare activity, using data from cosmic ray detector on Pioneer 7

09 p1582 A69-22754

Satellite data on galactic cosmic ray variations near magnetosphere and in interplanetary space, discussing Forbush decreases

10 p1756 A69-22819

Galactic and solar cosmic ray modulation in interplanetary space during different phases of 11 year solar activity cycle

10 p1758 A69-22833

Solar activity effect on interplanetary electromagnetic field according to cosmic ray modulation data, noting ineffective correlation and solar wind effects

10 p1759 A69-22841

Soviet collection of articles on cosmic physics, Number 3, Comets, sun and interplanetary space

14 p2522 A69-29703

Comet scintillations and tail characteristics studied to obtain information on interplanetary flux field, magnetic fields and planetary structures

14 p2523 A69-29704

Comets considered as natural interplanetary space probes, stressing need for international cooperation on solar system studies

15 p2679 A69-30011

Cosmic ray intensity temperature dependence in stratosphere and anisotropy in interplanetary space determined from measurements over Arctic and Antarctic regions

16 p2851 A69-32537

Optimum solar cell cover glass systems selected by studying interplanetary space environment effects of proton impact, temperature and concurrent illumination on radiation damage

19 p3253 A69-35702

Outer anisotropic galactic cosmic particle flux distortion in interplanetary space, analyzing scattering in solar wind by isotropic diffusion equations

23 p4205 A69-41837

IMP 4 satellite measurements of cosmic ray electrons in interplanetary space compared to predictions of electron intensity from interstellar proton-electron collisions

24 p4365 A69-42667

INTERPLANETARY SPACECRAFT NT EXPLORER 18 SATELLITE NT MARINER SPACE PROBES NT MARINER SPACECRAFT

NT MARINER 1 SPACE PROBE
 NT MARINER 2 SPACE PROBE
 NT MARINER 4 SPACE PROBE
 NT MARINER 5 SPACE PROBE
 NT MARINER 6 SPACE PROBE
 NT MARINER 7 SPACE PROBE
 NT MARINER-MERCURY 1973
 NT MARS PROBES
 NT PIONEER SPACE PROBES
 NT PIONEER 6 SPACE PROBE
 NT PIONEER 7 SPACE PROBE
 NT PIONEER 8 SPACE PROBE
 NT PIONEER 9 SPACE PROBE
 NT VENUS PROBES
 NT VIKING LANDER SPACECRAFT
 NT ZOND SPACE PROBES
 NT ZOND 5 SPACE PROBE
 NT ZOND 6 SPACE PROBE

Space simulation tests in TFS /Technological Feasibility Spacecraft/ program, discussing two interplanetary cruise modes and deorbit mode selected for simulation

02 p0227 A69-11757

Product assurance role in spacecraft sterilization to maintain planetary biological environments integrity in space programs for extraterrestrial life determination

03 p0379 A69-13400

Interplanetary transportation network involving numerous spacecraft on various planetary flyby trajectories, discussing integration of gravity thrust, braking and scramjet concept

03 p0511 A69-13402

Interplanetary orbits for probe launched from earth to reencounter earth, noting relationship to three body problem

03 p0514 A69-13782

German-American interplanetary vehicle to investigate interplanetary space and solar characteristics

06 p1012 A69-16970

Solar sail structural design, discussing application as propulsion system for heliogyro interplanetary spacecraft

06 p1015 A69-17591

Multimission interplanetary probe using solar electric propulsion

06 p0984 A69-17593

Interplanetary Pioneer spacecraft development and systems engineering aspects

06 p1017 A69-17605

Radio channel circuit outlined for tracking interplanetary spacecraft and probes with signal delay time prediction

06 p0888 A69-17623

Multiple impulse orbital departure window for manned interplanetary spacecraft, discussing launch delay, space assembly, refueling and checkout, etc [AIAA PAPER 69-126]

06 p1010 A69-18065

Analytical technique for unmanned spacecraft sizing for planetary missions, considering scientific objectives, characteristics and requirements [AIAA PAPER 69-125]

06 p1018 A69-18076

Transonic dynamic stability of free flight half angle cones in wind tunnel for high drag planetary entry vehicles, discussing Mars entry trajectories [AIAA PAPER 69-105]

06 p1019 A69-18209

Pre-design and mission analysis software capability for sizing, design, fabrication and developmental testing of flight hardware for electrically propelled interplanetary spacecraft

09 p1585 A69-21210

Advanced reconnaissance electric planetary spacecraft /AREPS/ concept for repeated coverage of Mars or Venus surface, using solar-photovoltaic system [AIAA PAPER 69-253]

09 p1585 A69-21244

Solar electric propulsion mission simplification by staging concept, discussing thrust combination, weight tradeoffs, design and Jupiter flyby probe [AIAA PAPER 69-251]

09 p1586 A69-21245

Flight control system for automatic interplanetary stations /AIS/, comparing Venera series orientation and correction system to Mariner systems

10 p1792 A69-24198

Spacecraft sterilization requirements, evaluating viable organisms release probability from spacecraft as function of equipment fracturing

11 p1828 A69-25460

Deep space data return, discussing system function, design, operational interfaces and interplanetary spacecraft data compression methods

14 p2517 A69-29096

Integrated structural and dynamic testing plans for proposed large interplanetary spacecraft, discussing acoustic testing, testing environments and flight environment transformation into laboratory

15 p2588 A69-30399

Nuclear solid core rocket engine performance for interplanetary orbital launch of spacecraft by multibit injection [AIAA PAPER 69-535]

16 p2810 A69-32660

Minimal electric propulsion systems for interplanetary spacecraft, discussing payload, reduced trip time and low thrust systems for Jupiter flyby [AIAA PAPER 69-499]

16 p2844 A69-32714

Passive attitude stabilization of interplanetary probe, using conically shaped sails elastically connected to payload

17 p3047 A69-33225

Scientific findings from interplanetary spacecraft radio propagation experiments, particularly Mariner 5 data

19 p3267 A69-35940

Propulsion system performance relationship to manned planetary mission capability, discussing anticipated performance of advanced propulsion concepts

20 p3586 A69-38118

Mission and planetary vehicles characteristics affecting design of solid propellant motors and thrust vector control systems in planetary orbiters and landers [AIAA PAPER 68-815]

21 p3819 A69-39031

Navigational accuracy of two way Doppler tracking of interplanetary spacecraft during heliocentric and planetary encounter trajectory phases [AIAA PAPER 69-899]

21 p3761 A69-39334

Mathematical model for determining thrust interplanetary spacecraft orbit, considering time history of position, velocity and thrust acceleration [AIAA PAPER 69-901]

21 p3806 A69-39335

Analytical technique for unmanned spacecraft sizing for planetary missions, considering scientific objectives, characteristics and requirements [AIAA PAPER 69-125]

21 p3828 A69-39770

High efficiency boost regulator design and tests for planetary spacecraft, considering input and output voltages

23 p4075 A69-42302

INTERPLANETARY TRAJECTORIES

Planetary swingby theory mechanics and applications for optimization of interplanetary trajectories

02 p0331 A69-12818

Vehicle trajectory motion in transition region of three body problem, noting equations of motion, first order solutions, etc

03 p0505 A69-13001

Orbital trajectories about Mars or Venus, considering reentry to earth, planet perturbation effect, total mission time and orbital distance from planet

05 p0823 A69-16042

Minimum fuel control of spacecraft orbital elements for transfers between elliptical orbits by low variable thrust propulsion, noting interplanetary trajectory optimization

06 p0955 A69-17579

Low thrust interplanetary trajectories optimization, discussing hardware design considerations

09 p1585 A69-21209

Midcourse maneuvers in interplanetary guidance, considering spin stabilized spacecraft flyby for Jupiter mission

13 p2354 A69-28504

Interplanetary swingby trajectory correcting maneuvers for space vehicles return to earth after planet orbiting with emphasis on singular points

19 p3427 A69-36613

Trajectory optimization of space vehicle with continuous thrust based on regularized equations, comparing perturbation method for earth-Jupiter rendezvous transfer [AAS PAPER 68-099]

20 p3595 A69-37173

Orbital trajectories about Mars or Venus, considering reentry to earth, planet perturbation effect, total mission time and orbital distance from planet

20 p3606 A69-37951

Periodic orbits for interplanetary flight, using patched conic analysis for determining inclined elliptic free fall trajectory shuttling between earth and Venus [AAS PAPER 68-102]

21 p3804 A69-39203

Trajectory analysis of multiplanet Grand Tour mission to four large outer planets on single flight, discussing mission planning [AIAA PAPER 68-1055]

22 p4023 A69-40544

Recurrent Lagrange multipliers for optimal low thrust earth-Jupiter transfers, using three dimensional solar system model

23 p4215 A69-41896

Earth-Mars and earth-Venus economical transfers derived for optimal conditions with respect to characteristic velocity, obtaining exact numerical solution [AAS PAPER 69-241]

24 p4380 A69-42855

INTERPLANETARY TRANSFER ORBITS

Book on planetocentric, lunar and interplanetary transfer techniques covering communications and coordinate system selection, minimum fuel and time transfer and rendezvous, etc

04 p0652 A69-14458

Optimum low thrust interplanetary transfers involving swingby trajectory past intermediate planet analyzed, assuming impulsive velocity change at planet

06 p1006 A69-17572

Direct flight and Jupiter swingby heliocentric trajectory modes of elliptic capture orbits compared for unmanned missions to outer planets [AAS PAPER 68-105]

21 p3805 A69-39221

INTERPOLATION

Interpolation of deflections of vertical from horizontal gravity gradients, discussing potential applications to photogrammetry

02 p0243 A69-12012

Invariant imbedding and sequential interpolating filters for nonlinear processes [ASME PAPER 68-WA/AUT-3]

05 p0738 A69-16183

Interpolation filters with restricted transmission zeros in transmission function capable of reconstructing continuous function from equidistant sample values

05 p0735 A69-16617

Presampling filtering, discussing effects on rms interpolation error for sampled data systems

07 p1083 A69-19129

Optimal control approximate synthesis partial differential equation solution in form of interpolation polynomial for functions of many variables

08 p1299 A69-21068

Extrapolation and interpolation for data compression including polynomial concept

12 p2027 A69-25877

Parabolic interpolation method for values of function given for certain values of argument and of first derivative, including numerical examples

12 p2121 A69-26434

Subsatellite point velocity determination by interpolation method using observation data without knowledge of orbital elements

12 p2158 A69-26435

Finite elements concept cast in topological framework, presenting generalizations of Lagrange and Hermite interpolation functions

15 p2711 A69-30874

Optimal control approximate synthesis partial differential equation solution in form of interpolation polynomial for functions of many variables

16 p2765 A69-32483

Qualitative interpolation formula for phonon frequency spectrum of mass disordered alloys three dimensional systems at high concentrations

20 p3583 A69-37279

Antennas aperture radiation patterns optimal interpolation synthesis permitting confident control of main lobe shape

22 p3916 A69-40953

Optical interpolation for GZ-1 orthoprojector in storage mode, noting electronic contour plotter

22 p3951 A69-41247

Integro-interpolation difference schemes for gas dynamic equations system satisfying laws of mass, momentum, energy conservation and energy balance

23 p4151 A69-41527

Osculatory interpolation explicit method demonstration with error terms determination

24 p4341 A69-43230

INTERPOLATORS

U REPEATERS

INTERPRETATION

1967 Space Treaty peaceful activities definition, suggesting explicit provisions regarding treaty province, enforcement machinery and implementation

20 p3636 A69-37112

INTERROGATION

Centralized control with variable step interrogation of control points

08 p1298 A69-20422

INTERRUPTION

Plasma physics of electric arc transition from conducting plasma to insulating gas in electric circuit interruption, noting interrupter interaction with power system

12 p2133 A69-25905

INTERSTELLAR COMMUNICATION

Interstellar communication in search for extraterrestrial intelligence, discussing radio objects, OH emission regions and pulsating stars

17 p3028 A69-32971

INTERSTELLAR GAS

UV and X ray radiations of stars and interstellar gas of Milky Way and remote galaxies

02 p0316 A69-11906

Interstellar gas field dynamic instability, discussing enhanced ambipolar diffusion in twisted field

02 p0326 A69-12707

Spectrophotometric studies of planetary NGC 6543 gaseous nebula, measuring emission line intensities, electron density and temperature [ARL-68-0200]

02 p0327 A69-12708

Cosmic MHD, discussing mechanisms responsible for solar phenomena and dynamics of interstellar medium

02 p0293 A69-12789

Rotation and orientation of cosmic dust particles due to collisions with interstellar gas particles

03 p0511 A69-13420

Interstellar gas masers account for properties of 18 cm emission lines from OH molecules

03 p0511 A69-13465

Ammonia gas molecules in interstellar medium, discussing detection in direction of galactic center by means of microwave emission

03 p0518 A69-14258

Diminished RF intensity of neutral hydrogen line near radio source W 49 due to diminished kinetic temperature of gas

04 p0662 A69-15253

Gas accretion on neutron star surface as energy source for X ray radiation

05 p0814 A69-15847

Energy flux into earth thermosphere due to fast corpuscular neutrals arising from charge transfer collisions between solar protons and neutral interstellar H

05 p0817 A69-16654

Pulsar distance estimates based on evaluation of galactic H absorption of 21 cm radiation

06 p1012 A69-18225

Helium closed cycle cooled very low noise high gain parametric amplifier for investigating interstellar atomic hydrogen radiation

07 p1098 A69-18461

Dissociation-ionization fronts in interstellar molecular hydrogen clouds, analyzing effects of UV radiation from early stars

07 p1221 A69-19584

Astronomical unit determined by measuring Doppler shift of spectral features of galactic hydrogen

07 p1222 A69-19590

Stellar galactic orbit perturbation by irregularities in distribution of gas cloud for motion inclined to galactic plane

07 p1223 A69-19634

Gas remnant of large scale explosive event in galactic plane at 60 degree longitude, discussing resultant extension on line profile

07 p1225 A69-19717

Radiative cooling layer behind shock front from neutral interstellar hydrogen cloud collision at Mach 20, discussing molecular hydrogen abundance during cooling

08 p1381 A69-19796

Optical depth determination in absorption lines of interstellar neutral hydrogen clouds by spectral observation of variable intensity radio sources

08 p1398 A69-20774

Motion and dispersion of peculiar velocities of stars in gravitational condensing interstellar gas

09 p1589 A69-21371

Radio wavelength range observations of NO molecule lines in interstellar space

09 p1590 A69-21377

Neutral hydrogen content and distribution of late type spiral galaxy NGC 6946 from 21 cm line measurements

09 p1598 A69-22187

Steady axisymmetric gas flow from galactic center, determining supersonic to subsonic transition by equations of motion

09 p1599 A69-22189

Attractive and disruptive forces in conversion of interstellar gas into stars, discussing self gravitation, galactic magnetic field and cosmic ray pressure

09 p1599 A69-22190

Molecular hydrogen in Orion dark cloud from observed faint emission

09 p1599 A69-22191

Radio recombination lines of galactic hydrogen as sensitive test for low energy cosmic ray existence in interstellar medium

09 p1580 A69-22273

High level hydrogen populations in gaseous nebulae, noting electron density range and temperature effect

09 p1604 A69-22406

D type dissociation ionization front structure and associated shock fronts using quasi-steady flow approximation for Stromgren sphere development in interstellar molecular hydrogen cloud

10 p1772 A69-22858

Far UV stellar astronomy, concerning very hot stars and interstellar gas composition studies

10 p1772 A69-22870

Phase equilibrium and dynamics of gas volume heated by cosmic rays and cooled by radiation

10 p1760 A69-23136

Solid hydrogen mantle condensation accounting for lack of detectable alpha hydrogen in star clusters and OB associations

10 p1776 A69-23214

Mass and velocity distribution of interstellar clouds from Oort model simulated by Monte Carlo method on computer, predicting rogue cloud existence

10 p1779 A69-23608

RF spectroscopy of OH molecule, RF absorption by galactic OH and radio emission from OH in dust clouds

10 p1781 A69-23671

Interstellar molecular hydrogen and CH photodissociation, discussing molecular formation rates in interstellar medium

10 p1781 A69-23672

Ionized gas flow from globule containing atomic H in interstellar space, noting surrounding H II region and radiation at ionization front

10 p1782 A69-23682

HI cloud densities near fronts of H II regions by gasdynamic calculations based on observational data for electron density, temperature and particle velocity

10 p1782 A69-23683

Interstellar gas model based on calculations of heating by low energy cosmic rays, noting gravitational compression to form clouds

10 p1770 A69-24095

Magnetic fields in interstellar neutral hydrogen clouds in direction of radio source Cassiopeia A, noting field amplification

10 p1785 A69-24096

Radio brightness map at 22.25 MHz of galactic plane including H II regions IC 1805 and IC 1848, discussing LF absorption

10 p1787 A69-24115

Nebular abundances allowing for temperature variations in nebula along line of sight, correcting changes in electron temperature along path of observation

10 p1787 A69-24116

Hydrogenic recombination decrements in gaseous nebulae, discussing effects of Lyman line leakage, Balmer line self absorption, internal dust, optical depth, etc

10 p1787 A69-24118

Virial theorem extended to investigate star condensations in large interstellar gas clouds

10 p1787 A69-24119

High velocity neutral hydrogen cloud formation by cold condensations in hot corona, ejection from galactic nucleus, extragalactic objects and supernova envelopes

11 p1954 A69-24364

Low energy cosmic rays and plasma turbulence in heating and ionizing interstellar gas, discussing acceleration and galactic sources

11 p1945 A69-24380

Intergalactic gas temperature and density reevaluated, considering neutral hydrogen distribution in galaxies peripheries and metagalactic background of ionizing UV radiation

11 p1946 A69-24589

Optical and radio measurements of electron temperature of H II regions obtained from brightness ratio of hydrogen line and continuum, considering isothermal model

11 p1950 A69-25110

Gravitational stability of spheroidal expansions of rotating gas masses in astronomy, noting mechanism for fragmentation in cosmology

11 p1962 A69-25112

Molecular state of hydrogen gas in high density condensations in H II regions, discussing effects of nearby stars

11 p1963 A69-25258

Theoretical models corresponding to initial phases in thermal-gravitational collapse of spherical clouds from interstellar gas for stellar formation

11 p1963 A69-25261

Correlation of stellar surface density distribution of young stars and neutral hydrogen gas in Small Magellanic Cloud

12 p2152 A69-25802

Planetary nebulae radial velocities in large and small Magellanic Clouds compared with young objects rotational pattern and interstellar gas densities and velocities

12 p2155 A69-25898

M 31 galaxy ionized gas region high resolution spectroscopy, emphasizing radial velocities in O II lines at various distances from nucleus

12 p2163 A69-27027

Successive explosions produced two gas systems observed in six Seyfert galaxy nuclei by spectrophotometry, using diffraction spectrographs

12 p2164 A69-27022

Rotation curve peculiarities of Sc type galaxy NGC 3432 ascribed to noncircular gas motions

12 p2164 A69-27031

Residual interstellar gas from protostar formation detected as high luminosity IR object

13 p2327 A69-27593

Expected IR line spectra of gaseous nebulae based on physical conditions, listing line intensities

13 p2342 A69-27595

Isothermal H II region dynamics for moving central star, integrating equations numerically using holograph transformation and Riemann invariants

13 p2347 A69-27712

Ionized hydrogen regions in NGC 4449 from H alpha photography through narrow band interference filter, obtaining radial velocities

13 p2347 A69-27714

Astronomical maps of integrated hydrogen density, dispersion and velocity of high galactic latitude neutral hydrogen concentration, discussing kinetic temperature

13 p2347 A69-27718

Neutral hydrogen cloud observed at high galactic latitude, discussing top intensity velocity, peak intensity dispersion, age, hydrogen mass and density

13 p2347 A69-27719

Radio emitting clouds properties as function of distance to parent galaxy nucleus

13 p2352 A69-27874

Rocket observations of Lyman alpha anisotropic galactic radiation, noting distribution of neutral interstellar hydrogen near sun

14 p2516 A69-28952

Interstellar gas radio and optical spectral lines of neutral H compared with Ca and neutral Na, discussing critically low velocity gas distribution

14 p2519 A69-29135

Spin temperature of interstellar neutral hydrogen calculated from 21 cm absorption spectra line profiles

15 p2681 A69-30411

Free electron concentrations and dispersion in H I regions noting ionized interstellar gas components role

15 p2681 A69-30420

Distribution model for ionized interstellar gas over galactic disk for explaining radio emission absorption and depolarization from discrete sources

15 p2695 A69-30935

Interstellar particle penetration into solar system, discussing impact ionization of earth ionosphere by interstellar neutral hydrogen and helium

15 p2699 A69-31390

Star formation in interstellar solid hydrogen clouds originating from cellular pressure created by hydrogen condensation onto interstellar grains

16 p2862 A69-32375

Origin of galactic gamma rays, discussing evidence in support of interstellar gas in galactic disk and production of neutral pions and bremsstrahlung

16 p2852 A69-32806

Pulsars distance determined using H II region data covering line of sight stars and Galaxy hydrogen distribution

17 p3026 A69-32858

Galactic X ray sources density nearly proportional to interstellar gas density squared, discussing X ray intensities estimation, galactic age, etc

17 p3030 A69-33069

Radio wave absorption in interstellar H I regions, considering mean absorption coefficient dependence on height above galactic plane, evaluating planar electron density

17 p3034 A69-33608

Interstellar H I regions and clouds heating and ionization by low energy cosmic rays from quantitative models, noting pressure equilibrium role

17 p3038 A69-33726

Interstellar neutral hydrogen in mean galactic latitudes noting two different component types

17 p3039 A69-33766

Zeeman effect measurement revealing magnetic fields in interstellar neutral H clouds

18 p3190 A69-34291

Optically thin gas surrounding X ray source, plotting electron temperature and ionization equilibrium of hydrogen, He, carbon, nitrogen, oxygen and neon
18 p3186 A69-34295

Depolarization of extragalactic radio sources at low Galactic latitudes attributed to ionized hydrogen produced by B2 star tunneling through interstellar hydrogen cloud
18 p3194 A69-34425

Motion and dispersion of peculiar velocities of stars in gravitational condensing interstellar gas
18 p3198 A69-34760

Radio wavelength range observations of NO molecule lines in interstellar space
18 p3198 A69-34765

High velocity interstellar gas in H I and H II regions, emphasizing observations of neutral atomic hydrogen in and far from galactic plane
19 p3402 A69-35962

Dynamic effects in structure of H II equilibrium region left behind expanding ionization front, showing temperature as function of distance from star
19 p3403 A69-35966

Forbidden emission lines used to study interstellar gas, discussing gas ionization, neutral hydrogen, calcium lines, etc
19 p3424 A69-36235

Interstellar hydroxyl molecular clouds as radio wave sources, using very long baseline interferometry, suggesting natural masers in space for OH emissions
19 p3427 A69-36659

Radio wave diffraction by inhomogeneities arising from ionized gas clouds in interstellar medium
19 p3428 A69-36882

NonJeans gravitational instability of stars and interstellar gas in Galaxy due to wave interaction with stars having velocity near wave phase velocity
20 p3607 A69-38037

Gas in H II regions and associated stars radial velocities correlation and systematic difference suggesting relationship between nebulae and stars
20 p3611 A69-38150

Ammonia inversion radiation in Sgr B2 region, observing distribution of density, velocity and rotational excitation
21 p3799 A69-38647

Interstellar absorption of 10 A X rays from sources in Scorpio-Sagittarius region, noting gas density between earth and Crab Nebula
21 p3788 A69-38648

Galactic gaseous disk dynamics, considering interstellar gas behavior and cosmic ray-magnetic field instability
21 p3802 A69-38824

Atlas of H II regions in 20 nearby galaxies
22 p4015 A69-40153

Possible star formation regions in Milky Way galaxy searched for compact H II regions, tabulating results
22 p4024 A69-40576

Cold neutral H cloud existence in Galaxy from measurements of 21 cm line spectra
22 p4025 A69-40644

Solar motions respecting high velocity atomic hydrogen clouds and local stellar group
22 p4035 A69-41209

Complex phenomena in theoretical astronomy including neutrino pair emission in stellar interiors, molecular H in interstellar gas, neutron stars, etc
23 p4217 A69-42316

IC 3258 emission line spectrum observations, discussing blueshift, extragalactic location, possible nature, etc
23 p4219 A69-42374

Carbon isotopes compared in interstellar formaldehyde transition for galactic nucleosynthesis, discussing spectrum analysis of radio astronomical telescope observations
23 p4220 A69-42376

High radial velocity gas cloud near Seyfert type galaxy NGC 4939 nucleus investigated spectroscopically
24 p4375 A69-42609

Positively charged diatomic hydrogen molecules in interstellar extinction and photodissociation cross section in terms of formation mechanisms
24 p4375 A69-42610

Circular arm with elliptical cross section used as magnetohydrodynamical model of helical magnetic field in spiral arms to demonstrate interstellar gas flow path
24 p4388 A69-43640

Low energy cosmic rays and plasma turbulence in heating and ionizing interstellar gas, discussing acceleration and galactic sources
24 p4375 A69-43770

INTERSTELLAR MAGNETIC FIELDS

Interstellar gas field dynamic instability, discussing enhanced ambipolar diffusion in twisted field
02 p0326 A69-12707

Numerical calculation of trajectories of high energy cosmic rays in galactic disk, using quasi-longitudinal model of magnetic field
03 p0501 A69-13960

Ionization fronts stability, taking into account ionizing photons absorption effect in H II region and interstellar magnetic field
04 p0650 A69-14363

Galactic magnetic field estimation obtained from cosmic ray electron spectrum and radio data
05 p0828 A69-16612

Cosmic ray electron energy spectrum compared with galactic radio noise for estimating galactic magnetic field
06 p0992 A69-17377

Polarization and intensity distribution of extended supernova remnant in Centaurus, discussing remnant effect on galactic magnetic field
09 p1598 A69-22184

Solar wind and galactic magnetic field buffer layer, analyzing cosmic rays effect and space-time distribution
10 p1757 A69-22825

Cosmic ray modulation by solar wind, discussing anisotropic diffusion during propagation through interstellar magnetic field
10 p1759 A69-22842

Mean distance between magnetic clouds in space determined from measuring anisotropy coefficient of high energy radiation
10 p1760 A69-23293

Polarization to extinction ratio criterion to choose interstellar cloud model, discussing magnetic field strength requirements
10 p1781 A69-23673

Magnetic field and magnetic energy evolution in infinitely conducting homogeneous isotropic turbulent medium, applying results to galactic magnetic field model
10 p1783 A69-23793

Magnetic fields in interstellar neutral hydrogen clouds in direction of radio source Cassiopeia A, noting field amplification
10 p1785 A69-24096

Density wave theory of galactic spirals, discussing hydrogen distribution, young star distribution, stellar migration, magnetic field structure, density waves in stellar formation, etc
10 p1786 A69-24109

Stochastic model of interstellar magnetic field to account for observed cosmic ray mean life
10 p1771 A69-24112

Galactic magnetic field along Orion arm from dispersion and rotation measures of linearly polarized radiation from pulsar psr 0833-45
13 p2335 A69-27311

Shield facility and Helmholtz coil system used to investigate chronic effects on man of zero magnetic field regulated to cancel geomagnetic field variations
15 p2586 A69-30382

Galactic magnetic field structure and strength, considering cosmic ray flux, continuum radio emission, starlight polarization, star formation, etc
15 p2694 A69-30857

Interstellar cloud models, considering gas pressure, cosmic ray flux, magnetic field values, etc
16 p2853 A69-31599

Viscous and thermal generators applicability to production of spin generated galactic magnetic fields in primordial fireball
16 p2866 A69-32812

Zecman effect measurement revealing magnetic fields in interstellar neutral H clouds
18 p3190 A69-34291

Interstellar matter, considering objects size, solar wind structure, galactic parameters, magnetic fields and cosmic ray heating
21 p3802 A69-38819

Galactic radio emission and magnetic field strength and structure, using radio surveys to obtain information on cosmic rays
21 p3790 A69-38820

Galactic gaseous disk dynamics, considering interstellar gas behavior and cosmic ray-magnetic field instability
21 p3802 A69-38824

Galactic field augmentation by dynamo action from highly condensed objects, considering Crab Nebula field production by central body
22 p4035 A69-41207

Galactic magnetic field existence arguments, discussing general and optical evidences, radio emissions, Faraday rotation from extragalactic sources and from pulsars, etc
23 p4217 A69-42321

Galactic magnetic field origin from galactic turbulence, calculating individual Fourier components in random turbulent velocity
24 p4375 A69-42658

Circular arm with elliptical cross section used as magnetohydrodynamical model of helical magnetic field in spiral arms to demonstrate interstellar gas flow path
24 p4388 A69-43640

INTERSTELLAR MATTER

Neutral hydrogen content in directions of pulsars related to distance estimates
01 p0149 A69-10271

Various reaction mechanisms proposed for interstellar medium, discussing formation and destruction of interstellar molecules
04 p0653 A69-14613

Stellar spectra taken with rapid scanning Michelson interferometer, noting IR excess due to radiation from clouds surrounding stars
04 p0655 A69-14667

Comet Arend-Roland orbit, deducing interstellar origin from nongravitational orbital energy increase
04 p0660 A69-15036

Submillimeter wavelength astronomy noting instruments, prestellar matter, interstellar and intergalactic matter state and composition, IR stars, planetary atmospheres, etc
05 p0821 A69-15843

Pulsar amplitude variations due to scintillation effects arising from irregular plasma refraction by general interstellar medium between source and solar system
05 p0825 A69-16354

Cosmic ray propagation, discussing interstellar matter effect on composition and diffusion effect necessary to study radiation models
05 p0816 A69-16361

Neutral interstellar matter particle fluxes and densities for earth, noting effects on upper atmosphere gas densities
05 p0828 A69-16653

Frequency structure of pulse energy or pulsar intensity, emphasizing total energy density received per pulse
05 p0828 A69-16660

Diamond dust as major component of interstellar dust to explain observed properties
05 p0828 A69-16662

Book on diffuse matter in space covering observations of interstellar gas, grains, particle interaction and star formation
06 p0997 A69-16833

Cosmic ray propagation model, considering determination of He interstellar spectrum and amount of matter traversed at low energies
06 p0988 A69-17270

Interstellar flux of heavy and superheavy nuclei calculated, assuming nuclei injection with source spectrum similar to M nuclei
06 p0988 A69-17273

Metastable helium abundance in interstellar and intergalactic space, inferring low energy cosmic ray concentration
06 p1010 A69-17973

Time variation of velocity spheroid dispersion, axis ratio and vertex deviation in Galaxy due to star-cloud encounters
07 p1215 A69-18668

Local interstellar electron spectrum limits from measurements of cosmic ray electrons, nonthermal galactic radio emission and solar modulation effects
07 p1206 A69-19269

Early phase of Stromgren sphere development in interstellar molecular hydrogen cloud, analyzing R-type dissociation-ionization fronts using quasi-steady flow
07 p1218 A69-19281

Atomic collision processes in astrophysics noting stellar continuum spectra, Ca ion and He lines, solar corona, heat balance in H I regions and planetary nebulae
07 p1224 A69-19653

Milky Way local spiral arm 10 MHz absorption, noting interstellar absorption effect and evidence for cool electron gas
08 p1383 A69-19900

Spatial distribution of stars and obscuring matter in Milky Way field in Kapteyn Selected Area 195 in Circinus, cataloging UVB photometry of stars
08 p1389 A69-20246

Cosmic ray negatron and positron spectra using balloon-borne magnetic spectrometer, obtaining absolute solar modulation of positron flux
08 p1380 A69-20728

Chemical composition of diffuse Orion Nebula and stars compared for lighter elements, considering solar system formation from interstellar medium
08 p1402 A69-20908

Molecular line intensity requirement in line of sight for detecting interstellar water vapor cloud, assuming transparent atmosphere and ideal radio telescope
09 p1591 A69-21446

Further microwave emission lines and ammonia clouds in Sagittarius region, tabulating relevant transitions in ammonia and water
09 p1597 A69-22150

Contour maps of H II regions W12, Orion A, W43 and W51, listing flux densities and angular sizes of components
09 p1598 A69-22186

Far IR source in galactic center detected at 100 microns, noting thermal emission of interstellar dust grains as possible mechanism
09 p1603 A69-22264

Radio telescopic survey for OH emission at 1667 MHz in interstellar dust clouds for catalog compilation, tabulating results
09 p1603 A69-22267

Interstellar reddening material distribution within 2500 parsecs of sun, noting concentration in galactic plane, spiral arms and cloud complexes
10 p1773 A69-22961

Polarization to extinction ratio criterion to choose interstellar cloud model, discussing magnetic field strength requirements
10 p1781 A69-23673

Interstellar grain model consisting of elongated dielectric particles represented by infinite circular cylinders reproducing interstellar extinction in IF far UV spectra
10 p1781 A69-23674

Interstellar dust alignment mechanisms investigated by Monte Carlo model, discussing grain velocity maintenance by radiation pressure and effects of magnetic constraint on charged grain trajectory
10 p1781 A69-23675

Interstellar diffuse absorption bands due to resonance lines of impurity atoms trapped in low temperature hydrocarbon matrices
10 p1781 A69-23677

Interstellar extinction models of classical Mie particles and quantum mechanical polycyclic aromatic molecules
10 p1781 A69-23679

Diffuse galactic radiation reinterpretation by solving same transfer problem exactly for properties of interstellar particles
10 p1782 A69-23680

Interstellar dust distribution ideas to explain observed variability in starlight polarization and similar phenomena
10 p1785 A69-24050

Reddened M supergiant 119 Tauri IR spectra and IR absorption by CO and SiO molecules in stellar atmosphere and silicate mineral in interstellar grains
10 p1786 A69-24104

Interstellar formaldehyde detection in absorption against galactic and extragalactic radio sources, discussing chemical evolution
10 p1786 A69-24108

Flare stars observational and known aggregate characteristics in Coal Sack region
10 p1790 A69-24141

Photoelectric and photographic observations in UVB system of open star clusters, analyzing dispersion in two color diagrams, noting absorbing material structure
11 p1951 A69-24247

Interstellar medium density distribution as function of stellar action spherical coordinates applied to determining stellar motion forces and B stars brightness difference
11 p1955 A69-24386

Pulsar distances estimated from neutral hydrogen absorption, using observations from 140 ft telescope
12 p2156 A69-26224

Optical constants of bulk diamonds compared with interstellar extinction, calculating extinction curves for diamond particles from Mie theory
12 p2157 A69-26230

Interstellar gas and dust clouds inclination to plane of M31 galaxy spiral arms
12 p2159 A69-26664

Interacting galaxies theories, characteristics and terminology, discussing galactic radio sources and properties of matter
12 p2169 A69-27055

Interacting NGC 4485 and 4490 galaxies instability, establishing early stage of evolution from morphological and spectroscopic results of photographic observations
12 p2169 A69-27056

Lambda-doublet radiation from excited state of interstellar OH detected at 5 cm wavelength
13 p2335 A69-27312

Hydrogen atoms in interstellar grains as source of stellar flux absorption, noting crystal environment effect on atomic hydrogen Lyman alpha transition
13 p2337 A69-27518

Dielectronic recombination influence on radio recombination lines of carbon under typical nebular conditions
13 p2346 A69-27703

Cosmic rays suggested as origin of interstellar grain alignment, discussing galactic central radiation, gas collisions and isotropic bombardment
13 p2333 A69-28469

Monograph on interstellar extinction computations covering theoretical curves for spherical metal and graphite particles, albedo, optical constants, normalization, temperature dependence, etc
14 p2516 A69-28901

Extinction efficiency of graphite core interstellar grains with solid hydrogen and ice mantles, using theoretical models
14 p2486 A69-29587

Amplitude and scale of microscopic fluctuations of electron density within M8 from brightness ratios of O II lines, using multiple shell model
14 p2514 A69-29949

Emission of two photons decay from metastable 2s level of pure hydrogen gaseous nebula, noting radiative and collisional excitation
14 p2529 A69-29975

Excited hydrogen radio lines observations, analyzing neutral and excited hydrogen distribution in galaxies
15 p2682 A69-30502

Interstellar absorption and spatial distribution in northern Aquila with absence of early O-B2 stars, including luminosity function
15 p2683 A69-30513

Milky Way structure, discussing dust bridge and density of absorbing matter between spiral arms of Sagittarius and Carina Cygnus
15 p2683 A69-30514

Interstellar radio absorption influence on spatial distribution of cosmic radio emission observations with fixed multiple dipole antenna arrays
15 p2687 A69-30545

Maser emission in interstellar OH ground state produced by IR pumping, noting population inversion mechanism
15 p2691 A69-30762

Optimization techniques for stellar kinetic theory problems, discussing kinematics distribution function, cosmic gas dynamics, interstellar matter, etc
15 p2695 A69-31004

Matter traversal of high energy primary galactic cosmic ray protons from antiproton flux and energy measurements
15 p2678 A69-31491

Interstellar cloud models, considering gas pressure, cosmic ray flux, magnetic field values, etc
16 p2853 A69-31599

Pulsars properties, nature and utilization for interstellar medium study including radiation mechanisms, white dwarf stars and neutron star development
16 p2855 A69-31762

MHD of interstellar gas-dust medium, analyzing gas-dust flow and gas-dust shock waves in magnetic fields
16 p2823 A69-32590

Photoelectric method to measure galactic reflection nebulae brightness, color and polarization used to explore interstellar grains physical nature
17 p3032 A69-33104

Pulsars properties and distribution in galactic coordinates, deriving interstellar medium properties and physical nature of objects based on neutron star rotation
17 p3040 A69-33800

H II regions distribution in nearby irregular I galaxies, attributing asymmetry to localized bursts of star formation
18 p3190 A69-34289

Search for diffuse galactic light component between 2100-2800 A by rocket measurements of night sky brightness, showing low albedo of interstellar dust
18 p3202 A69-35210

Solid para hydrogen coated graphite particles expulsion into interstellar medium from star formation regions, considering mantles stability and particles extinction efficiency, albedo and phase function
20 p3601 A69-37499

Cepheus light attenuation curve explained by applying polymodal particle size distribution, obtaining interstellar dust density
20 p3608 A69-38041

Spectra of peculiar S zero galaxy NGC 7625 with irregular dust distribution, discussing central spheroidal rotation and mass
20 p3610 A69-38140

Galaxy NGC 3593 with large amounts of interstellar dust, calculating galactic mass and central density
20 p3610 A69-38142

Irregular galaxy NGC 3077 with interstellar dust measuring velocity field by spectroscopy
20 p3610 A69-38144

Interferometric photoelectric scans of interstellar Na D-lines in stellar spectra using Pepsios spectrometer
20 p3611 A69-38148

Interstellar grains formation and composition, suggesting mixture of graphite particles in carbon stars and silicates in oxygen-rich giants
20 p3615 A69-38260

Soft x ray extragalactic background flux measurements, considering correction for absorption by interstellar medium
21 p3788 A69-38541

X ray sources and diffuse background radiation observed in gamma and X ray spectral regions, considering electromagnetic waves attenuation by interstellar matter
21 p3789 A69-38817

Interstellar matter, considering objects size, solar wind structure, galactic parameters, magnetic fields and cosmic ray heating
21 p3802 A69-38819

Spectrophotometric analysis of interstellar absorption in direction of IC 1805 cluster, noting anomalies
21 p3814 A69-39576

Soviet collection of papers on nebulas and interstellar medium covering computer simulation, photometric observation results, etc
21 p3816 A69-39721

Pleiades cluster and ambient interstellar medium structure analyzed for spectral distribution based on plane-parallel scattering model
21 p3817 A69-39727

Neutrons, protons and alpha particles abundance resulting from nuclear evolution of nondegenerate matter exploding at very high temperatures
22 p3980 A69-40148

Bok globules in Orion nebula, deriving temperature and density data
22 p4022 A69-40465

Molecular collision pumping mechanism for anomalous microwave absorption by formaldehyde rotational transition in Galaxy dust cloud
22 p4029 A69-40768

High radial velocity matter of bright region near Trapezium in Orion Nebula, determining electron density lower limit and mean velocity
22 p4029 A69-40769

Polarization fluctuations of starlight indicating turbulent structure of interstellar medium, noting pulsar signal dispersion and Faraday rotation
22 p4030 A69-40771

Strong IR millimeter wave emission from galactic center due to interstellar dust grains resembling semiconductor structure
23 p4215 A69-42115

Extragalactic universe major constituents and physical properties of normal, radial and compact galaxies, discussing missing matter existence
23 p4217 A69-42317

Stellar evolutionary ages and gravitational theory relations based on initial abundance ratio U 235/U 238 and present interstellar medium heavy element content
23 p4219 A69-42329

Spiral and irregular galaxies integral properties and relations, discussing optical and 21-cm observations, hydrogen masses, statistical corrections, hydrogen line optical depths, etc
23 p4220 A69-42383

Equal velocity contour diagrams for interstellar matter emission and absorption study in Cassiopeia-Perseus region
24 p4384 A69-43050

Interstellar medium density distribution as function of stellar action spherical coordinates applied to determining stellar motion forces and B stars brightness difference
24 p4390 A69-43776

INTERSTELLAR MICROWAVE SPECTRA
U MICROWAVE SPECTRA

INTERSTELLAR RADIATION

- Ammonia gas molecules in interstellar medium, discussing detection in direction of galactic center by means of microwave emission
03 p0518 A69-14258
- Radio spectra of supernova remnants Cygnus Loop and IC443, noting possible radiation from shell source
06 p1003 A69-17322
- Interstellar light absorption in Milky Way region of Cepheus analyzed by excess color technique
07 p1216 A69-18855
- Cosmic ray astrophysics, discussing chemical composition, energy spectrum and galactic sources
07 p1205 A69-18909
- Diffuse interstellar absorption bands and doublet line, noting large intensities of forbidden transitions
08 p1395 A69-20639
- RF spectral lines due to OH molecule detected in interstellar space in absorption of RF radiation from Casiopeia A source
09 p1586 A69-21295
- Contour maps of supernova remnants HB 9, Simeis 147 and IC 443, noting spectra showing radiation nonthermal
09 p1604 A69-22408
- Mean distance between magnetic clouds in space determined from measuring anisotropy coefficient of high energy radiation
10 p1760 A69-23293
- Asymmetrical profiles of 4430 A interstellar absorption band, discussing stellar and electronographic spectra
10 p1781 A69-23676
- Image tube spectra observations of interstellar absorption band at 4430 A, noting emission band at 4400 A
11 p1965 A69-25658
- Molecular dissociation by line radiation absorption, applying results to hydrogen molecules in H I region dissociated by photons of mean interstellar UV radiation field
15 p2693 A69-30783
- Interstellar hydromagnetic waves due to streaming cosmic rays indicated by pulsar scintillations studies
15 p2676 A69-30889
- Atomic H Lyman-alpha interstellar absorption line in theta Orionis spectrum, showing equivalent width relations to H column density and spin temperature
15 p2695 A69-30890
- RF spectral lines due to OH molecule detected in interstellar space in absorption of RF radiation from Casiopeia A source
15 p2697 A69-31226
- Supernovae spectra observation suggesting tracing as broad band interstellar absorption rather than emission features on continuum
15 p2701 A69-31534
- BCD classification for cepheids, discussing /sigma/ surface definition, locus of normal stars of population I and interstellar reddening
17 p3038 A69-33725
- Sodium D line profiles in interstellar clouds, determining absorbers velocity distributions
20 p3611 A69-38149
- Invalidity of Pagel method for intrinsic and interstellar reddening for peculiar objects, discussing excitation mechanism for forbidden lines of ionized Fe for Eta Carinae
21 p3815 A69-39616
- Soviet collection of papers on nebulae and interstellar medium covering computer simulation, photometric observation results, etc
21 p3816 A69-39721
- Catalog of reflection nebulae with known dimensions and flux characteristics noting spectrum characteristics
21 p3816 A69-39722
- Interstellar extinction in UV from zeta and epsilon Persei spectra obtained with scanner attached to telescope mounted in pointed Aerobee rocket
22 p4030 A69-40772

INTERSTELLAR SPACE

- Cosmic radiation propagation in interstellar space, discussing differential kinetic energy spectra of protons, He, C and O nuclei and Fe
06 p0988 A69-17269
- Physical conditions of intergalactic space in Local Group using virial theorem and assuming energy equipartition, discussing temperature, ionized hydrogen density, turbulent motions, etc
08 p1381 A69-19795
- Water in interstellar regions detected by microwave emission from 6 sub 16 to 5 sub 23 rotational transition
08 p1383 A69-19896

Spacecraft motion parameters and physical characteristics of space determined from statistical analysis of measurement data

09 p1495 A69-21764

Galactic discontinuity near longitude 140 degrees attributed to stars deficiency in anticenter quadrant or interstellar cloud obscuration

10 p1776 A69-23215

Mean distance between magnetic clouds in space determined from measuring anisotropy coefficient of high energy radiation

10 p1760 A69-23293

Pulsars distance determined using H II region data covering line of sight stars and Galaxy hydrogen distribution

17 p3026 A69-32858

Grains with high defect concentration in circumstellar and interstellar space from energetic particles and photons bombardment, discussing lifetime and optical properties

22 p4023 A69-40472

INTERSTELLAR TRAVEL

Bibliography of interstellar travel and communication

03 p0510 A69-13397

Advanced propulsion systems propulsive capabilities in connection with interstellar flights, considering rocket and ramjet propulsion, energy requirements and stellar plasma

06 p0984 A69-17631

Interstellar minimum fuel and time optimal trajectories for acceleration limited rockets determined by applying Pontryagin maximum principle to relativistic rocket equations of motion

20 p3602 A69-37530

Reduced flight time interstellar round trip propulsion system with relativistic velocity capabilities, discussing vehicle with solar sail and magnetic course reversal [AAS PAPER 69-388]

24 p4363 A69-42829

INTERSTITIALS

Interstitial impurity effects on mechanical properties of molybdenum single crystals, considering temperature dependence of flow stress in bcc metals

01 p0095 A69-10609

Vacancies and interstitials in metals - Conference, Julich, West Germany, September 1968

02 p0267 A69-12185

Elastic constants of point defects for bcc and fcc crystals with vacancies and interstitials calculated by Born-Huang method for nonprimitive lattices

02 p0267 A69-12186

Complex form internal friction maximum composed of interstitial atoms in molybdenum solid solution

04 p0615 A69-14640

Work hardening characteristics of Ta and Ta-base alloy single crystals as function of temperature and interstitial concentration

05 p0778 A69-15758

Whiskerized graphite fiber in resin matrix composites, analyzing interstitial growth characteristics, resin infiltration, layup and compaction

09 p1511 A69-22360

Order-disorder in alloys with several phase transition temperatures, discussing crystal lattices, interstitial alloys, atomic and magnetic ordering

11 p1936 A69-24702

Transition metal interstitial compounds thin film preparation and superconducting properties, emphasizing high critical temperature, rock salt structure and NbN base

13 p2321 A69-28009

Internal friction, Young modulus and resistivity measurements for stage I interstitials in electron irradiated tungsten

13 p2284 A69-28682

Strain aging of polycrystalline Nb containing interstitial impurities as function of temperature, discussing interstitial role in recovery substages

15 p2636 A69-30194

Refractory metals fracture, discussing interstitial impurity addition effects in Group 5a and 6a metals

17 p2989 A69-33556

Thermal isolation characteristics of low conductance interstitial materials determined, using test apparatus of axially loaded radiation shielded cylindrical column in vacuum [AIAA PAPER 68-31]

23 p4239 A69-41889

INTESTINES

NT RECTUM

Rats on casein, soybean and Chlorella diets for protein source noting soybean diet produced no appreciable changes in intestinal flora

02 p0197 A69-11490

Protein free diets effects on rat intestinal microflora, noting decrease in lactic acid bacteria and increase in spore forming bacteria

05 p0709 A69-16516

Protein free diets effects on rat intestinal microflora, noting decrease in lactic acid bacteria and increase in spore forming bacteria

18 p3096 A69-34735

Fire hazard in closed chamber associated with interstitial hydrogen and methane formed by space diets, comparing Gemini-type and bland diets

20 p3482 A69-37622

INTOXICATION

Alcoholic hangover effects on human balance system from flying demands viewpoint, discussing ocular-vestibular system disturbances

23 p4089 A69-41817

INTRACRANIAL PRESSURE

Blood circulation in brain during acceleration analyzed by tensometric sensors and electroplethysmography, noting intracranial sensitivity to gravitational changes

06 p0874 A69-17646

INTRAMOLECULAR STRUCTURES

Rotational spectrum of ethylene episulfide to determine molecular structure, particularly orientation of C sub 2 S ring

08 p1268 A69-20535

INTRAOCULAR PRESSURE

Glaucoma in commercial airline pilots noting value and safety of routine tonometry

03 p0376 A69-14078

Responsiveness of cortex and visual pathway during transient hypotension induced by increased gravitational stress, discussing intraocular pressure of cat

22 p3878 A69-40779

Indentation tonometry for occult pathology and glaucoma in commercial pilots

23 p4088 A69-41805

INTRUDER AIRCRAFT

U A-6 AIRCRAFT

INVALIDITY

U ERRORS

INVARIANCE

NT GAUGE INVARIANCE

Group invariant solutions of differential equation systems applied to quasi-linear partial differential equations of motion of air masses

02 p0274 A69-11444

Lorentz invariant theories of gravitation compared with Einstein general relativity tests with respect to one body motion observations

02 p0318 A69-12094

Invariance principle application in gyroscopical systems, noting effect of external disturbances and system noise

04 p0597 A69-14603

Invariant subspaces, controllability and observability of linear dynamic systems

05 p0740 A69-16597

Analysis and synthesis of optimal linear time invariant systems with uncertain or unknown parameters, considering mean square error

06 p0902 A69-17405

Linear noisy two port preceded by nonreciprocal lossless network analyzed, showing existence of associated quantity invariant under lossless transformation

07 p1104 A69-18891

Mathematical formulas for rigidity distribution of inhomogeneous multilayer shells, discussing invariance property

07 p1232 A69-19011

Plane symmetric perfect fluid cosmological model derived from class I considerations, evaluating scalar invariants for line element

07 p1222 A69-19586

Maxwellian field and second order invariant system in vacuum in three dimensional Riemannian space with positive-definite metric, discussing Lorentz invariant equations

09 p1541 A69-22392

Functional equations of physical systems in strong coupling solved by quantum theory model of anharmonic oscillator, discussing relativistic invariant field theories

09 p1541 A69-22393

Variational method for necessary and sufficient conditions of terminal state invariance of dynamic control system

10 p1718 A69-23206

Canonical invariance of Hamiltonians noting nature of solutions of differential equations, existence of

- periodic solutions and application to three body problem
10 p1721 A69-23987
- Degree of knottedness of tangled vortex lines, discussing vorticity distribution for inviscid flow and MHD invariants
11 p1872 A69-25126
- Multidimensional self adjusting systems design by achieving parametric invariance, using sensitivity theory
11 p1861 A69-25711
- Newtonian invariant mechanics, giving inertial interpretation of gravitation and Hubble expansion of universe
15 p2654 A69-31214
- Time dependent collimated light diffuse reflection and transmission by finite inhomogeneous atmosphere, using principle of invariance
18 p3132 A69-35345
- Second rank Dirac spinors with invariant components relative to Lorentz group transformations
19 p3361 A69-36817
- Variational method for necessary and sufficient conditions of terminal state invariance of dynamic control system
21 p3756 A69-39147
- Invariance theory in automatic dynamic systems
23 p4145 A69-42368
- Absolute invariance of perturbations affecting dynamic plant achievable by inertial measurement of highest derivatives
23 p4145 A69-42369
- Invariance conditions for steady and unsteady systems by differential method compared to variational approach
23 p4145 A69-42371
- Absolute invariance conditions for closed isolated subsystem of nonlinear differential equations of Cauchy normal form
23 p4183 A69-42372
- ### INVARIANT IMBEDDINGS
- Initial value method applied to Fredholm integral equation for radiative transfer, neutron transport and multiple scattering, verifying invariant imbedding method
01 p0103 A69-10002
- Invariant imbedding and sequential interpolating filters for nonlinear processes
[ASME PAPER 68-WA/AUT-3]
05 p0738 A69-16183
- Invariant imbedding and multipoint boundary value problems in control theory and identification of systems
05 p0787 A69-16478
- Iterative methods for composite layer slabs transport models, using invariant imbedding approach to transport theory
08 p1343 A69-20353
- Cauchy problem of invariant imbedding satisfying nonlinear boundary value problem, discussing optimal control and radiative transfer applications
09 p1531 A69-21413
- Dynamic programming determining optimal feedback control policies for optimal trajectories based on invariant imbedding
11 p1910 A69-25410
- Invariants method and applications in classical and relativistic physics emphasizing theory of relativity, physical and mathematical theories relations and group theory applications
14 p2484 A69-28860
- Suboptimal closed loop control of nonlinear systems subject to quadratic performance indices by invariant imbedding concepts and maximum principle
18 p3111 A69-34678
- ### INVENTIONS
- Untutilized ideas in university laboratories, showing generation and implementation enhancement by marketing experience and product development background
15 p2720 A69-30596
- ### INVENTORY CONTROLS
- Stationary inventory problems analysis, discussing inventory policy, recursive and or limiting procedures, stationary point processes, stock delivery time instants, etc
12 p2192 A69-26750
- Remote sensing technology application to improving range resource inventories, discussing aerial photography, descent, IR and radar scanning, etc
12 p2098 A69-26992
- ### INVERSIONS
- NT CENTRIFUGING STRESS
NT INTERFACIAL TENSION
- NT POPULATION INVERSION
NT STRUCTURAL STRAIN
NT TEMPERATURE INVERSIONS
NT VOLUMETRIC STRAIN
- Oblique matrix pseudoinverse concept extended, discussing elementary properties and applications
01 p0104 A69-10315
- Continued fraction inversion to rational fraction of two polynomials based on state space formulation and Routh algorithm
16 p2805 A69-32470
- Second harmonic generation in laser with center of inversion following deformation by media beam or static pressure
19 p3332 A69-35872
- ### INVERTEBRATES
- NT BEETLES
NT CRABS
NT DROSOPHILA
NT FLAGELLATA
NT FLATWORMS
NT INSECTS
NT MICROSPORES
NT PARAMECIA
NT PROTOZOA
NT PUPA
NT SPORES
NT WORMS
- Pyridine nucleotide-linked D-lactate dehydrogenase stereospecificity in various species of invertebrates
01 p0018 A69-11198
- Invertebrates resistance to explosive decompression and low end pressure, noting hypoxia and freezing as cause of death
07 p1059 A69-18537
- Invertebrate endoskeletal cartilage and cartilage-like tissues occurrence and nature, discussing cellular tissues and origin
15 p2555 A69-30412
- ### INVERTERS
- NT STATIC INVERTERS
- Wideband inverter operational amplifier frequency response, open and closed loop transfer functions, beta, settling time and slew rate limits, discussing HF performance prediction
11 p1857 A69-25666
- Electromagnetic processes analysis in autonomous inverters simplified by linear graph method to derive characteristic equation
24 p4255 A69-42571
- ### INVESTIGATION
- U ACCIDENT INVESTIGATION
U AIRCRAFT ACCIDENT INVESTIGATION
- ### INVESTMENT CASTING
- Heat resistant nickel alloys for castings, tabulating chemical composition, mechanical properties, heat treatment, weldability, etc
09 p1522 A69-21608
- Cast high temperature alloys for gas turbine components, discussing production, temperature capability, composition, oxidation, hot corrosion and weldability
[IME PAPER 10]
12 p2147 A69-25795
- Nondestructive thermal method of measuring wall thickness and channel blockage in investment castings used in aircraft parts production
24 p4312 A69-42754
- Ti and Ti alloys investment castings mechanical properties, dimensional control and corrosion resistance in aircraft and aerospace structural application
24 p4324 A69-43433
- ### INVISCID FLOW
- NT STAGNATION FLOW
- Potential flow of stream interaction with two dimensional thin jet, discussing jet penetration depth
01 p0007 A69-11019
- Nonlinear weak shock wave diffraction around convex angled corners in polytropic inviscid thermally nonconducting gas
03 p0412 A69-12848
- Cylindrical jet stability of perfectly conducting, incompressible and inviscid fluid in presence of axial magnetic field
03 p0474 A69-13142
- Inviscid cavity and wake flows behind submerged bodies, analyzing mathematical and theoretical models
04 p0587 A69-14608
- Surface geometry of three dimensional inviscid hypersonic flows, developing tensor equations for geodesic, steepest descent and pressure approximations
04 p0542 A69-14718
- Inviscid hypersonic flow of uniform equilibrium gas past axisymmetric blunt body
04 p0542 A69-14723
- Irrotational almost uniform plane flow of two immiscible inviscid liquids on horizontal bottom in channel noting permanent gravity waves
04 p0590 A69-15099
- Two dimensional unsteady flow of inviscid polytropic gas using analysis of similarity solutions in homogeneous flow
04 p0590 A69-15154
- Flow pattern induced by oscillatory point source in rotating inviscid liquid
04 p0591 A69-15277
- Inviscid incompressible fluid flow stability against helical disturbances in circular cylinder
06 p0910 A69-17333
- Stream function approximation for plane axisymmetric vortex free transonic inviscid gas flow
06 p0910 A69-17333
- Pressure distribution determined from laminar viscous-inviscid interactions in supersonic flow, including flows with heat transfer
[AIAA PAPER 69-7]
06 p0913 A69-18099
- Large amplitude waves in inviscid flows of stably stratified fluids over barriers with constant density upstream constructed from vortex pairs and doublets
08 p1346 A69-20313
- One strip method of integral relations applied to inviscid supersonic blunt body problem
09 p1430 A69-21972
- Mach wave and anisentropic supersonic flow interaction, considering constant entropy along streamlines and layer of entropy discontinuities/interfaces
10 p1631 A69-22906
- Large amplitude symmetric and asymmetric irrotational motion of inviscid incompressible fluid with liquid-vapor interface in accelerating cylindrical container of revolution
11 p1871 A69-25124
- Hamilton principle for inviscid compressible fluid in Euler coordinates, analyzing shortcomings found in variational principles and model in Lagrangian coordinates
11 p1875 A69-25483
- Inviscid reacting flow free of molecular transport analyzed locally near stagnation point, using Lighthill-Freeman gas model
11 p1876 A69-25560
- Diffusion-stabilized difference schemes for inviscid compressible flow equations in conservation form for arbitrary number of space dimensions
12 p2062 A69-26624
- Heat transfer for incompressible inviscid fluid flow in cone, expressing solution in terms of dimensionless numbers
13 p2375 A69-27788
- Inviscid supersonic flow in right angle corner of varied angular intersecting wedges with bow waves and remaining planar up to intersection line
13 p2200 A69-28251
- Flow stability of one dimensional Cartesian and cylindrical incompressible inviscid flows with no body forces and interfaces
14 p2429 A69-29013
- Spoiler effect on aerodynamic characteristics of airfoil with hinged flap in inviscid fluid plane flow
15 p2549 A69-31223
- Cylindrical viscous jet transition points from stable to unstable modes of oscillation found same as for inviscid jet
16 p2773 A69-32570
- Supersonic and hypersonic flow of inviscid ideal gas over conical delta wings using three dimensional method of characteristics
[AIAA PAPER 69-646]
17 p2893 A69-33486
- Conservation theorems for energy and mean circulation in inviscid rotating fluid, noting inertial wave spectrum continuity
18 p3121 A69-34550
- Aerodynamic characteristics of two dimensional nonexpandable flexible sail in hypersonic inviscid flow, discussing roles of sail length and chord and angle of attack
19 p3237 A69-35814
- Nonuniform supersonic flow of ideal inviscid gas impinging on plane obstacle, discussing flowfields and shock wave production in impact
19 p3239 A69-36397
- Stratified fluid flow past obstacle, considering steady inviscid flow with nonlinear convection and vertical acceleration
19 p3240 A69-36474
- Supersonic inviscid flow past wing-body configuration, determining pressure distribution
20 p3458 A69-37099

Second circle theorem for two dimensional irrotational flow of incompressible inviscid fluid in z plane
20 p3518 A69-38316

Linear hydrodynamic equations describing inviscid fluid flow past thin elastic cylindrical shells in circle with motions described by shallow shell equations
21 p3834 A69-38719

Spectral equation for decaying isotropic turbulence of incompressible inviscid flow at large Reynolds number, using spectral cascading
21 p3694 A69-38835

Differential rotation of incompressible inviscid fluid of infinite electrical conductivity in spherical shell, noting toroidal magnetic field for sun
22 p4027 A69-40658

Strong interaction between hypersonic boundary layer over flat plate and associated inviscid flow, discussing heating and vorticity effects, boundary layer edge, etc
22 p3860 A69-40896

Semianalytic solution for axisymmetrical supersonic inviscid flow near stagnation region of spherically blunted body with detached shock waves
22 p3861 A69-41178

Boundary value problem solution for inviscid fluid flow past compliant body with analytical behavior of flow discontinued at points
23 p4151 A69-41525

Airfoils and cascades design for incompressible flow by numerical methods
23 p4058 A69-41610

Numerical methods for radiation transport for inviscid stagnation flows, detailing spectral nature of radiation emission and absorption
[AIAA PAPER 68-664] 23 p4059 A69-41890

Inviscid transonic flow past circular arc bodies of revolution, applying Hosokawa technique to pressure distribution solution
23 p4059 A69-41899

Two dimensional incompressible inviscid fluid flow problems solution by conducting-paper analog with electrical equipotentials tracing, based on Laplace equation applicability
24 p4299 A69-43024

Inviscid hypersonic flow over oscillating slender wedge, defining equivalent phase shift
24 p4248 A69-43582

Electron temperature and density of inviscid free molecular nozzle flow of shock tunnel measured with thin wire Langmuir probes
24 p4317 A69-43648

Similarity solutions to massive blowing problem, discussing inviscid flow model compatible with no-slip condition
24 p4305 A69-43658

INVISIBILITY
U VISIBILITY

INVOLUNTARINESS
U INVOLUNTARY ACTIONS

INVOLUNTARY ACTIONS
Eye movement control mechanisms during binocular fixation used to determine corrective roles of flicks and drifts
22 p3883 A69-40876

Human response to visual beat phenomena by combining intermittent stimuli, considering brightness estimation
22 p3884 A69-40889

IODIDES
NT CESIUM IODIDES
NT SILVER IODIDES

HI and DI reaction into HD and $2I$, noting need for rotational or vibrational excitation in addition to translational energy of collision
01 p0123 A69-10686

Phase diagram of BiTeI degenerate semiconductor crystals synthesized by heat treatment, discussing crystallization methods and physical properties
02 p0294 A69-11540

Photolysis of t -butyl iodide at low temperatures as source of t -butyl peroxy radicals for synthesis of peroxides
07 p1073 A69-18375

IODINE
Steel corrosion by iodine noting effects of water and oxygen
03 p0444 A69-13310

Iodine IR laser, discussing CW emission obtained at various wavelengths and attributed to electronic transitions in atom
[IEEE PAPER T-5] 07 p1154 A69-19082

Iodine fluorescence spectra excited by krypton ion laser, analyzing spectral series and vibrational rotational levels
07 p1156 A69-19304

Failure mechanism for intergranular stress corrosion cracking of vacuum annealed unalloyed Ti in alcohol iodine solutions
16 p2798 A69-31717

Pure quadrupole resonance spectrum of iodine-127 in solid stannic iodide measured in specific temperature range at atmospheric pressure
22 p3986 A69-40726

IODINE COMPOUNDS
NT CESIUM IODIDES
NT IODIDES
NT SILVER IODIDES

Laser action from atomic bromine produced by flash photolysis of gaseous iodine monobromide, discussing pulsed output, optical gain, chemical reversibility and atomic excitation
19 p3337 A69-36444

IODINE ISOTOPES
Iodine 123 decay via gamma ray emission, noting energies of several transitions
03 p0470 A69-13099

ION ATOM INTERACTIONS
Spectroscopy of fast atoms resulting from fast ion impact with gas targets and electron capture into excited state
03 p0471 A69-13162

Frictional forces and collision frequencies for ions moving in neutral gases
03 p0421 A69-13328

Parametric or impact parameter treatment for describing ion-atom collision at low or high impact velocities, reexamining approximate treatments
05 p0797 A69-16697

Atomic excitation and ionization involving inner shell electrons during collisions between atoms and ions, examining photoabsorption by inner shell electrons
07 p1187 A69-19659

Atomic and electronic collisions experimental study techniques, noting three data logging systems
07 p1187 A69-19662

Forward scattering of metastable and ground state argon atoms after argon ion-atom charge transferring collisions, discussing excitation resonances
08 p1354 A69-19809

Drift measurements of rate constants for charge transfer in ion-molecule processes
08 p1355 A69-20210

Li atoms and O interactions with electron radiation produced defects in Si studied by IR spectroscopy
09 p1554 A69-21337

Interatomic potential between alkali ions and rare gas atoms, using model accounting for repulsive and attractive exchange forces
16 p2815 A69-32464

ION BEAMS
High current electron bombardment ion source for production of low energy ion beams without metastable contamination
03 p0428 A69-13106

Beam-foil spectroscopy problems noting light collection, spectrograph design, broadening of spectral lines by Doppler effect and other complications
03 p0470 A69-13161

Beam-foil spectroscopy above 5.5 Mev for multiply ionized atoms, noting use of Tandem accelerator, spectral resolution, beam intensity and Doppler effect
03 p0471 A69-13163

Intensity of visible and UV light from beam of positive deuterium molecular ions excited by passage through thin C foil
03 p0471 A69-13166

Crossed beam studies of ion-molecule reaction mechanisms, crossing approximately monoenergetic ion beam with thermal molecular beam
03 p0382 A69-13460

Pulsed arc source using plasma jet to obtain intense hydrogen ion beam
03 p0412 A69-13842

Ion beam interaction with plasma in presence of charge exchange and zero external magnetic field, studying stability of system
03 p0481 A69-14200

Mean life measurement of excited ions electronic levels using beam foil light source, emphasizing beam particle monitoring and theoretical equations
04 p0595 A69-14278

Static beam deflection in beam foil spectroscopy for determining parent ionization stage of emitting ions
04 p0595 A69-14279

RF sputter etching of microcircuits and components
04 p0606 A69-14874

Charge transfer cross sections for slow ion production in nitrogen molecular ion beams incident on hydrogen and deuterium
05 p0796 A69-15914

Molecular jets obtained by charge exchange of triatomic ion beams consisting of hydrogen, deuterium and nitrogen, noting formation, energy level, etc
05 p0797 A69-16339

Ion accelerators design for Kaufman thrusters in terms of beam optics and grid lifetime, using digital computer and electrolytic tank analog
[AIAA PAPER 69-261] 09 p1567 A69-21261

Equilibration potentials between dense thrust beam and dilute space plasma measured in wind tunnel
[AIAA PAPER 69-263] 09 p1568 A69-21728

Crossed beam apparatus with mass selected variable energy primary beam for study of angular and velocity spectra of ion-molecule reactions
12 p2092 A69-26477

Plasma ion oscillations excited in plasma consisting of ion beam and thermal electrons produced by back diffusion sources
13 p2304 A69-27301

Beam-foil technique for measuring radiative lifetimes of excited electronic states in ionic species of O, including transition probabilities
13 p2301 A69-27452

Plasma lens device for focusing ion or plasma beams with closed electron drift
13 p2307 A69-27658

Synthesized plasma from neutralized mercury ion beam ejected from electron bombardment source, analyzing temperature, plasma sheath and stability
14 p2502 A69-29956

Charge transfer cross section between mercury ion and Cs assessed, considering ion engine positive ion beam neutralization
16 p2835 A69-31895

Oscillations excitation between ion cyclotron and electron plasma frequency in He ion beam generated plasma
17 p3014 A69-33830

Beam foil technique to measure energy transition levels radiative lifetime for nitrogen ions
17 p3009 A69-34154

Lunar based optical workshop and repair facility, using ion beam technique to polish and repair optical element surfaces
18 p3113 A69-34243

Ion beam sputtering, evaporation and electrical degradation of Al contacted Si solar cells observed in high temperature cyclic tests
19 p3250 A69-35686

Charge exchange cross sections and electron losses in hydrogen ion beam impacting on water vapor molecules
19 p3378 A69-36190

Excited states lifetime of carbon dioxide and nitrous oxide ions deduced from spontaneous radiative deexcitation in vacuum after passage through gaseous target
22 p3985 A69-40715

Bipolar HF p -type Si transistors preparation by B and P ion beams and planar technology masking technique, obtaining p - n - p structure
22 p3916 A69-40960

Crossed beam apparatus /evatron/ for studying energy spectra of crossed positive ethylene ion beams and neutral ethylene molecule beams
24 p4280 A69-43813

ION CHAMBERS
U IONIZATION CHAMBERS

ION CHARGE
Charge and degree of ionization of nickel alloyed with molybdenum analyzed by electrolytic ion migration method
07 p1159 A69-18535

Instability in pyrolytic silicon dioxide films on Ge substrate under bias at room temperature consisting of positively charged ion motion
07 p1200 A69-19010

Unsuccessful attempt to observe high charge ion lines generated by dielectronic recombination in solar corona at 5-cm wavelength
15 p2689 A69-30568

Thermal diffusion coefficient for fully ionized plasma containing mixture of arbitrary charge ions in topside ionosphere
16 p2775 A69-32084

ION CONCENTRATION
Field strength, electron temperature and ion concentration fluctuations in axial direction determined from

measurements between homogeneous and stratified plasma columns
05 p0800 A69-15736

Nondegenerate dense plasma thermodynamic stability by nonclassical methods, discussing atomic concentration dependence on ionic concentration
05 p0802 A69-15892

Negative ion-molecule reactions in nitrous oxide using mass spectrometer, noting negative ion concentration pressure dependence
06 p0960 A69-17106

Positive ion concentration in subsonic high velocity laminar flames determined by interpreting kinetic and diffusion factors of adding cesium to flame
13 p2380 A69-28463

OGO 5 spectrometric studies of topside ionospheric ion concentrations, noting difference between nighttime and sunlit pass
15 p2599 A69-31345

Plasmasphere hydrogen and He ion concentration models, using diffusive equilibrium theory for plasmasphere parameters
15 p2677 A69-31447

Ion collecting cylindrical electrostatic probes as flow field tracing instruments in low density slightly ionized flows
19 p3291 A69-35718

OGO 5 ion spectrometer for measuring oxygen, He and hydrogen ion concentration, noting functions as energetic particle analyzer and proton energy distribution measurement capability
19 p3314 A69-36679

Plasma ion and electron concentration perturbations in wake of body moving at high velocity in collisionless plasma under steady magnetic field
20 p3459 A69-37659

Fuel cells ionic concentration changes across porous matrix during operation, measuring voltage losses due to pH changes and liquid junction potentials
[ECS PAPER 335] 20 p3466 A69-38069

Fluorescence properties of nucleotides, polynucleotides and phosphorylated derivatives as function of temperature, pH and ionic strength
22 p3898 A69-41078

ION CURRENTS

Noiseproof ionization manometer with ion current dual modulation for ultrahigh vacuum measurement in magnetic field with extraneous charged particles interference
03 p0429 A69-13263

Plasma rotation in current layer of pulsed inductive accelerator
[AIAA PAPER 68-86] 04 p0635 A69-14702

Ion and electron contaminating currents removal in vacuum evaporating devices, using biased field plates
04 p0577 A69-14875

Cesium contact ion microthruster experiment on-board ATS 4, measuring emission currents and spacecraft potentials
[AIAA PAPER 69-297] 09 p1561 A69-21218

Side wall currents in unignited hardware type thermionic energy converters, discussing work function and heat choke
09 p1439 A69-21822

Predicting electrode geometry effect on saturation ion currents in diode exposed to ionizable vapor in equilibrium with liquid Ce
09 p1440 A69-21832

Tangential drag measurements at electrodes of arc in plasma accelerator, ion current partitioning at cathode and electrode damage
[AIAA PAPER 67-657] 13 p2312 A69-28219

Surface type airborne electrostatic probes in ambipolar diffusion flux, measuring ion saturation current, discussing electrode contamination and temperature and ablation tests
[AIAA PAPER 69-700] 17 p2974 A69-33443

Cesium contact ion microthruster experiment on-board ATS 4, measuring emission currents and spacecraft potentials
[AIAA PAPER 69-297] 24 p4365 A69-43238

ION CYCLOTRON RADIATION

Ion cyclotron drift loss cone instability for cases of steep particle density gradients, magnetic field gradients and finite plasma dimensions
02 p0288 A69-12169

Ion cyclotron wave generation in RF self sustained mode improved by installing grid structures in plasma near magnetic mirrors
03 p0474 A69-13113

Wave fields and coupling of RF power to ion cyclotron waves in finite length thermal collisional plasma column
03 p0474 A69-13114

Harmonic ion cyclotron waves shown to possess stop and passband characteristics, supporting quasi-static ion cyclotron mode theory
06 p0970 A69-17953

Electrons resonant heating in beam plasma discharge, discussing ion cyclotron wave excitation in hot electron plasma produced by electron beam
09 p1549 A69-22016

Plasma ions turbulent heating during electron-acoustic instability in field of circularly polarized electromagnetic wave at ion cyclotron frequency
10 p1728 A69-23137

Ion-molecule reaction kinetics in nitrogen-hydrogen mixtures using ion cyclotron resonance
12 p2131 A69-25985

Oscillations excitation between ion cyclotron and electron plasma frequency in He ion beam generated plasma
17 p3014 A69-33830

Acetonitrile ion-molecule chemistry using ion cyclotron resonance, discussing reaction of vibrationally excited methyl ions from electron impact
19 p3265 A69-36290

Propagation, damping, power coupling and plasma heating characteristics of harmonic ion cyclotron waves, noting temperature effects
21 p3777 A69-39455

ION DENSITY [CONCENTRATION]

NT IONOSPHERIC ION DENSITY

NT MAGNETOSPHERIC PROTON DENSITY

NT PROTON DENSITY [CONCENTRATION]

Exosphere diurnal and latitudinal variations in electron and proton content, ion composition, and electron, proton and positive O ion densities
01 p0063 A69-10422

Ion concentrations and temperature measurements by magnetic trap on Cosmos 5 between 1000-1200 km
02 p0306 A69-11656

Solar coronal ion abundance analyses from extreme UV emission lines
02 p0327 A69-12719

Electron and positive ion density measurements during nighttime auroral absorption event
03 p0421 A69-13327

Discontinuities in plasma situated in magnetic field, noting drift of quasi-neutral inhomogeneities of electron and ion density
04 p0634 A69-14431

Theoretical analysis of fixed stratification, taking into account nonlinear effects and variation in charged particle concentration along plasma column
04 p0636 A69-14783

Potential gradient, small ion density and space charge density measurements for atmosphere on Atlantic Ocean during 1965
04 p0594 A69-15159

Mars lower ionosphere ionization from spectroscopic and Mariner 4 occultation data, discussing various ionization sources
07 p1213 A69-18607

Nitrogen ion number density time dependence by mass spectrometric probing of decaying nitrogen plasmas, noting molecular ion production by colliding metastable nitrogen molecules
07 p1184 A69-19141

Ion number densities time dependence in pink afterglow of N measured with quadrupole mass spectrometer
08 p1308 A69-20292

Emissive probes for measuring plasma potentials over different ion density ranges on SERT spacecraft, detailing calibration and mechanical and electronic configurations
[AIAA PAPER 69-272] 09 p1492 A69-21217

Surface ion behavior on planar semiconductor devices determined by measuring effect of time, humidity, temperature, voltage and previous testing history
10 p1743 A69-23173

Two dimensional flow of unipolar medium in electrodynamic power generation channel, discussing stationary model, electric field and ion density distributions
10 p1638 A69-23486

Monograph on method and results of measurements of mobilities spectrum ion density and conductivity in upper troposphere and stratosphere
11 p1877 A69-24636

Light ion abundance measurements of OGO satellites and field aligned diffusive equilibrium theory with temperature and concentration latitudinal variations
11 p1879 A69-25157

Free electron density upper limits in plasma attributed to negative ion formation, noting effect on

ionization equilibrium calculations for stellar atmospheres
11 p1928 A69-25255

Ion-acoustic wave experiments for disturbance travels in plasma sheath, obtaining ion number density
11 p1929 A69-25272

Nonlinear algebraic equation system describing populations of excited atoms of low pressure nonequilibrium cesium plasma, determining ionization coefficient and molecular ion concentration
11 p1934 A69-25567

Population densities, pumping rates, lifetimes, etc., of singly ionized krypton ion laser
12 p2109 A69-26638

NGC 4151 bright lines intensity, electron density, temperature and ions quantity evaluation from spectrograms with 140 A/mm dispersion
12 p2164 A69-27021

Ion concentrations and temperature measurements by magnetic trap on Cosmos 5 between 1000-1200 km
13 p2333 A69-28687

Time and altitude induced variations in daytime NO and molecular and atomic oxygen ions
14 p2435 A69-29050

Ionization mechanisms in ignited mode cesium thermionic converter, discussing positive ions production for electron space charge neutralization and ion density calculations
14 p2404 A69-29258

Three component fast neutral beam for hydrogen plasma ion density and electron temperature determination, improving accuracy and reliability
14 p2452 A69-29812

Electron and ion density distributions in propagating current sheet in Z pinch discharge in argon obtained by microwave reflection interferometer
16 p2816 A69-31639

Temperature gradients effect on ion flute mode in low beta plasma having density gradients in x direction, obtaining instability condition
16 p2819 A69-31689

Atmospheric ion concentration increment by electrostatic lens to facilitate electrical properties measurements of charged particles in submicroscopic range
17 p2971 A69-32928

Ion energy distribution function and density profile in strong implosion wave generated by theta pinch discharge, investigating compression wave in deuterium
17 p3013 A69-33821

Gas ionization relaxation times from ion density profiles in shock tubes at low Mach numbers, discussing influence of impurities on ionization process
18 p3116 A69-34451

Atmospheric aerosols influence on ion density profile in stratosphere obtained from numerical solution of equilibrium ionization equation
18 p3129 A69-34962

Ion density, electrical conductivity and weighted mean mobility deduced from Gardien capacitor I-V characteristics used in balloon sounding of stratosphere
18 p3130 A69-34970

Ion and electron fluxes and drag force dependence on electrostatic charge and velocity of interstellar dust particle
19 p3425 A69-36562

Ion density, electric field and electron temperature responses to gas density perturbation calculated for acoustic wave propagation in gas discharge using hydrodynamic equations
20 p3578 A69-38243

Negative ion concentrations in plasma by flash photodissociation, using Q switched laser for irradiation
21 p3778 A69-39574

Ionization formula linking nitrogen ion charge density ratio to plasma temperature
22 p3990 A69-40714

Mass spectrometric analysis of lunar material from soil vaporization products ion component by electron beam
22 p4034 A69-41107

Air electrical conductivity reduction in fog ascribed to small ions concentration, increase in droplets capture efficiency and particle concentration
24 p4347 A69-43509

ION DISTRIBUTION

Nighttime sporadic E layer occurrence due to ionization redistribution established, noting concurrent F region electron concentration decrease
03 p0423 A69-13536

Charge carrier concentration determination by double probe in plasma with Druyvesteyn distribution of incident electron flow
05 p0800 A69-15737

Dominant ionic species in cesium plasma through mass spectrometer analysis, measuring total ion and electron currents

09 p1544 A69-21335

Earth thermal plasmasphere contraction subsequent to solar flare obtained from ion mass spectrometers on OGO satellites

10 p1683 A69-23777

Ionospheric molecular ion concentration vertical profile analysis for verifying neutral gas temperature maxima in connection with two ion production maxima

10 p1688 A69-23930

Models for emission line region of 3C 273, considering ionization distributions for estimation of relative abundances

10 p1790 A69-24137

Nighttime distribution of nitrogen ion and lambda 5755 emission in ionosphere with incidence of aurora

12 p2066 A69-26110

Ionized gas height scale changes in polar ionosphere obtained, assuming Chapman type ionization distribution

14 p2436 A69-29052

Hydrogen and He ion distribution measurements, noting seasonal and local magnetic time variability

15 p2599 A69-31326

E region ionization redistribution by neutral winds, comparing calculated vertical drift velocities to observed electron density profiles

15 p2677 A69-31395

Ion and electron distributions in chemical nonequilibrium boundary layer flow over hypersonic reentry vehicle, discussing plasma sheath and boundary layer thickness relations

16 p2769 A69-31874

Ion, electron and neutral temperatures from ion composition distribution, assuming no change in vertical distribution within horizontal distance between upleg and downleg measurements

16 p2849 A69-31990

Relationship between sporadic E and 5577 A nightglow emission attributable to ionization redistribution in E region due to dynamic processes

16 p2788 A69-32782

Geomagnetic control of geographic distribution of F 2 layer midday ionization based on data from ionospheric vertical sounding stations

17 p2966 A69-33982

Ionization stratification and chemical abundances in planetary nebula NGC 7662, discussing density fluctuations effect on N II and O II lines

18 p3191 A69-34294

Franco-Soviet rocket probe launchings for measuring daytime/nighttime ions and neutrons

18 p3210 A69-35282

Steady state vertical distribution of small ions in ground layer assuming atmospheric dynamic and thermal sublayers, calculating air resistance and electric field potential

21 p3715 A69-38836

ION EMISSION

Spacecraft attitude ion sensor using charged thermal ions of earth atmosphere as reference, stressing reliability, economy and response

01 p0079 A69-10293

Spherical and cylindrical probes emitting electrons and ions in unbounded plasma, deriving I-V characteristics equations

02 p0247 A69-11569

Static beam deflection in beam foil spectroscopy for determining parent ionization stage of emitting ions

04 p0595 A69-14279

Emission continuum intensity of negative nitrogen ion in nitrogen and air plasmas

04 p0639 A69-15370

Ion formation and ion secondary emission during sputtering, discussing Saha-Langmuir equation, probability theory, simultaneous processes, mass spectroscopic analyses, etc

08 p1355 A69-20616

Cesium contact ion microthruster experiment on-board ATS 4, measuring emission currents and spacecraft potentials

09 p1561 A69-21218

Longitudinal inhomogeneities in plasma of Q machines caused by ion emission from hot plate at different radial positions

14 p2502 A69-29959

Emission continuum intensity of negative nitrogen ion in nitrogen and air plasmas

16 p2822 A69-32117

Ion production in K/diatom Br system by high energy K beam, obtaining total ionization cross section as function of energy

19 p3378 A69-36187

Ruby laser-ultrahigh vacuum device for studying electron and ion emissions and light absorption of materials, noting influence of adsorbed gas layers

20 p3553 A69-37406

Oxygen pressure effect on oxide layer composition on W surface by secondary ion-ion emission

21 p3746 A69-39071

Cesium contact ion microthruster experiment on-board ATS 4, measuring emission currents and spacecraft potentials

[AIAA PAPER 69-297] 24 p4365 A69-43238

Proton ejection as hydrogen ion clusters by low energy electron bombardment of solid hydrogen

24 p4389 A69-43747

ION ENGINES

NT CESIUM ENGINES

Mercury ion thrusters and facilities automatic controls durability testing, discussing vacuum chamber systems, unattended operation and control

[AIAA PAPER 68-576] 02 p0229 A69-12385

Alkali metal ion sources noting cesium ion engine development for space propulsion

[ECS PAPER 170B] 03 p0478 A69-13859

Telemetered data obtained by lantar 1 automatic ionospheric laboratory, detailing argon-ion plasma engine performance

05 p0830 A69-16056

High voltage mercury electron bombardment ion thruster power efficiency

[ECS PAPER 170D] 05 p0812 A69-16233

Multimission interplanetary probe using solar electric propulsion

06 p0984 A69-17593

Electric propulsion research in Japan, considering cesium ion thruster, plasma acceleration and thrust by electric explosion of fine wires

06 p0984 A69-17629

Electron bombardment mercury ion thruster plasma properties and performance, computing ion beam current, discharge losses and propellant utilization efficiency

[AIAA PAPER 69-256] 09 p1560 A69-21214

Cesium contact ion microthruster experiment on-board ATS 4, measuring emission currents and spacecraft potentials

[AIAA PAPER 69-297] 09 p1561 A69-21218

Space charge sheath electric thruster principles, construction and performance using laboratory test model

[AIAA PAPER 69-282] 09 p1563 A69-21235

Extraction and acceleration mechanism in RF ion motors, fixing plasma potential with extraction anode

[AIAA PAPER 69-284] 09 p1564 A69-21237

Digital computer simulation and analysis of control loops for ion thruster control

[AIAA PAPER 69-239] 09 p1564 A69-21240

RF ion thrusters using self sustaining electrodeless discharge

[AIAA PAPER 69-285] 09 p1565 A69-21247

West German activity in field of electrostatic propulsion, discussing ion thrusters, colloid thruster development and mission analysis

[AIAA PAPER 69-288] 09 p1565 A69-21248

Ion thrusters and various microthrusters/electron bombardment ion and pulsed plasma/ for proposed European missions

[AIAA PAPER 69-274] 09 p1565 A69-21250

30 cm diameter mercury bombardment low impulse thruster development for potential space applications, discussing performance and control

[AIAA PAPER 69-238] 09 p1566 A69-21256

Research and development program in annular slit colloid thruster technology, proving thruster feasibility by performance tests

[AIAA PAPER 69-287] 09 p1566 A69-21257

Ion accelerators design for Kaufman thrusters in terms of beam optics and grid lifetime, using digital computer and electrolytic tank analog

[AIAA PAPER 69-261] 09 p1567 A69-21261

Electrostatic electron bombardment ion thruster with magneto-electrostatically contained plasma

[AIAA PAPER 69-260] 09 p1567 A69-21262

Electrostatic thrusters using RF ion sources to optimize payload ratios, terminal velocities, propellants, life span and efficiencies

09 p1568 A69-21489

Electron bombardment thrusters for low specific impulse operation, discussing electrode structures fabrication by bonding alumina disk to metal electrode

[AIAA PAPER 69-301] 09 p1568 A69-21730

Thermionic space power reactor design, detailing Critical Experiment problems

09 p1441 A69-21835

Out-of-core thermionic reactor power increase by using central heat pipe in coaxial cavity

09 p1441 A69-21836

Stability analysis including delayed collector and structure coefficients, showing thermionic reactor instability with all negative reactivity coefficients

09 p1442 A69-21841

Liquid mercury cathode electron bombardment thrusters applicability to electric propulsion missions

[AIAA PAPER 69-302] 09 p1569 A69-21876

Kaufman thruster with predominant radial field, noting electron mobility across ion extraction screen and advantages of uniform plasma distribution

[AIAA PAPER 69-259] 09 p1569 A69-21877

Thrust vectoring system using accelerator displacement to reduce alignment errors in multiaperture electron bombardment ion engines

[AIAA PAPER 68-543] 09 p1570 A69-21985

Porous structures, using spherical tungsten powders, discussing metallurgy, sintering, temperature effects and performance characteristics in ion engines

10 p1710 A69-23166

Causes and magnitudes of thrust misalignment of Kaufman type electron bombardment ion thruster

[AIAA PAPER 69-303] 10 p1753 A69-23362

Ionic propulsion application to geostationary satellite attitude correction

10 p1753 A69-23841

Nuclear type cylindrical thermionic converter with porous adsorbent structure and liquid cesium tank

14 p2397 A69-29174

Fast and thermal thermionic reactor systems characteristics including fissile material, components mass, power output and flattening and design features

14 p2480 A69-29182

Thermionic reactor systems, discussing hybrid nuclear rocket/nuclear electric Mars mission, design features, performance and electric power characteristics

14 p2480 A69-29183

Thermionic reactor design for electric propulsion with emphasis on reactor power and fuel energy and fast neutron flux

14 p2509 A69-29184

Thermionic converter with external fuel surrounding inner emitter annulus for use in in-core reactors

14 p2480 A69-29185

Out-of-core thermionic reactor concept for space power supply using lithium heat pipes in crossed layers

14 p2480 A69-29187

In-core thermionic reactor space power plants stability and control criteria, comparing linear and nonlinear models

14 p2481 A69-29189

Deposition and interdiffusion of W layers on Mo emitter of in-core thermionic reactor, investigating microstructure of transition zone

14 p2462 A69-29210

Thermionic reactors U.S.S.R. space and other programs, considering power output, heat exchange and losses, neutron physics and design parameters

14 p2404 A69-29277

Nuclear energy systems, discussing U.S. reactor concepts with emphasis on thermionic systems and space applications

14 p2404 A69-29278

Charge transfer cross section between mercury ion and Cs assessed, considering ion engine positive ion beam neutralization

16 p2835 A69-31895

Electric propulsion, discussing plasma research, MPD thruster and arcs, ion thruster research and spacecraft integration

[AIAA PAPER 69-497] 16 p2838 A69-32655

Discharge chamber plasma processes in electron bombardment ion thrusters, considering factors affecting thruster performance

[AIAA PAPER 69-494] 16 p2845 A69-32735

RF ion thrusters using electrodeless self sustaining mercury discharge, describing basic theory, component design, performance optimization and test results

17 p3018 A69-33326

Hall ion thruster prime propulsion system, considering low and high voltage mode in plasma source I-V characteristics

17 p3019 A69-33338

Development and applications of ion propulsion covering electrostatic acceleration of particles, Cs contact and electron bombardment ion thrusters, space missions, etc

17 p3020 A69-33354

Kaufman ion thruster ESKA 18 operation principles and design compared to RIT 10 and SERT 2, discussing discharge and focusing characteristics and propulsion parameters

17 p3022 A69-33605

Electric propulsion systems for manned planetary exploration flights, discussing arc jet, ion and plasma engines 18 p3185 A69-35108

Telemetered data obtained by Iantar 1 automatic ionospheric laboratory, detailing argon-ion plasma engine performance 20 p3618 A69-37966

Laboratory prototype of RF ion engines for space test, discussing components optimization 22 p3998 A69-39904

HF ion engine RIT 10, Kaufman ion engine ESKA, Hall effect ion engine HIT and MPD engine compared for state of development [DGLR-69-021] 23 p4202 A69-41928

Optimization of RF ion thruster cluster engines for ascending trajectory, discussing unfolding mechanism of solar cell panels [DGLR-69-022] 23 p4203 A69-41933

Kaufman ionic thruster /ESKA 18/ principles, design, electrical circuit, working and experimental characteristics, compared with RIT 10 and SERT II 23 p4203 A69-41934

Thermionic reactor concepts and development in U.S., comparing strengths and weaknesses 23 p4186 A69-42245

Thermionic reactors for auxiliary space power and electric propulsion applications, discussing converter development regarding nuclear fuel elements 23 p4186 A69-42246

West German research in thermionic diodes and reactors, describing terrestrial version of thermal in-core thermionic reactor project 23 p4188 A69-42258

Power conditioner for use with SERT II mercury ion thruster, describing electrical and mechanical design and operation 23 p4075 A69-42301

Cesium contact ion microthruster experiment on-board ATS 4, measuring emission currents and spacecraft potentials [AIAA PAPER 69-297] 24 p4365 A69-43238

ION EXCHANGE MEMBRANE ELECTROLYTES

ABEPAC fuel cell with ion exchange membrane electrolyte impregnated with sulfuric acid solution, describing electrodes and bipolar collectors 08 p1259 A69-21040

Ion exchange fuel cells for emitter-receiver on atmospheric constant ceiling balloon, stressing pressure effect on operation and fuel storage 08 p1260 A69-21042

Manned spacecraft fuel cell selection and design, discussing Gemini ion exchange membrane and Apollo Bacon cell systems 16 p2737 A69-32406

Power source with electrolyte consisting of ion exchange membrane in aqueous solution of sulfuric acid 16 p2738 A69-32411

Fuel cells with solid membranes with ion conductivity, discussing proton electrolyte 16 p2740 A69-32424

ION EXCHANGE RESINS

Activated carbons and ion exchange resins bactericidal action as function of silver coating techniques 13 p2216 A69-28621

Sequence preparation of protected peptide polymer bond with anion exchange resin using solid phase transesterification 24 p4279 A69-42713

Transesterification of amino acid peptide alkyl and fatty acid esters by treatment with anion-exchange resin 24 p4280 A69-43513

ION EXCHANGING

Electron temperature and concentration and solar UV absorption data from sounding rockets, estimating ion exchange rate, recombination coefficient and heat flux 03 p0422 A69-13508

X ray study of scandium containing ferrites, establishing lattice stresses due to ion replacement in octahedral interstices 03 p0491 A69-14053

Purines, pyrimidines and nucleosides absorption by Li-, Na-, Mg- and Ca-montmorillonite in aqueous solutions over range pH 2-12 by cation exchange 05 p0716 A69-15973

Absorption of nucleosides, purine and pyrimidine derivatives by Co-, Cu- and Ni-montmorillonite taking place by cation exchange process 05 p0716 A69-15974

Effective cross section of resonant cesium ions charge exchange determined by retarding field method, considering dependence on ion velocity 06 p0959 A69-16908

Potassium ion resonant charge exchange, determining relation between effective cross section and ion velocity, using retarding field method 06 p0959 A69-16909

Hydrogen-oxygen ion exchange membrane fuel cells for sounding balloons, discussing flight duration and power requirements, gas supply pressure effects, etc 16 p2738 A69-32413

Free lysine and dinitrophenyl /DNP/ derivatives determined quantitatively by ion exchange chromatography 17 p2917 A69-33651

X ray study of scandium containing ferrites, establishing lattice stresses due to ion replacement in octahedral interstices 18 p3182 A69-35046

ION EXTRACTION

Wall space charge layer effect on ion extraction from weakly ionized plasma, using quadrupole mass spectrometer 07 p1188 A69-18276

Kaufman thruster performance dependence on transmission of ion extraction optics and magnetic field shape [AIAA PAPER 69-257] 09 p1569 A69-21878

Shock ionization by ion impact against triatomic H molecules gas target, showing positive ion production dependence on extraction voltage, collision chamber pressure, etc 19 p3378 A69-36188

Electrodialysis method for depleting positive Na, K, Ca and Mg ions from Anabaena flos-aquae A-37, noting algae survival rate 23 p4079 A69-41387

ION GAGES

U IONIZATION GAGES

ION-GAS INTERACTIONS

U GAS-ION INTERACTIONS

ION IMPACT

Spectroscopy of fast atoms resulting from fast ion impact with gas targets and electron capture into excited state 03 p0471 A69-13162

Impact ionization and tunneling effect during electroluminescence of zinc sulfides 06 p0980 A69-17261

Plasma spectral line shifting and broadening under ion and electron impact 07 p1187 A69-19720

Electron emission of probe caused by impinging ions and photons, discussing model for low plasma densities 08 p1361 A69-20232

Si planar IMPATT diodes anomalous mode continuous wave UHF oscillations, noting DC density and DC/RF power conversion efficiency 17 p2934 A69-32846

Shock ionization by ion impact against triatomic H molecules gas target, showing positive ion production dependence on extraction voltage, collision chamber pressure, etc 19 p3378 A69-36188

Charge exchange cross sections and electron losses in hydrogen ion beam impacting on water vapor molecules 19 p3378 A69-36190

Townsend discharge formation time determination, taking into account impact ionization in positive ion cloud moving from anode to cathode 19 p3381 A69-36603

Spectral line broadening and shift due to electron and ion shocks in impact theory 20 p3580 A69-37828

ION INJECTION

Nonmagnetic plasma deceleration in quasi-stationary magnetic field with coaxial injector and barrier field 03 p0481 A69-14212

MOSFET fabrication by ion implantation using gate metal as mask, noting source and drain alignment with gate and low feedback capacitance 05 p0734 A69-16563

Properties of ion implanted GaAs diodes fabricated at room temperature, analyzing light emission, resistance and breakdown voltage [ECS PAPER 172] 08 p1284 A69-20369

Fast Ba ion filament cloud injection into ionosphere using explosive shaped charge technique, noting application to ionospheric electric field measurement 09 p1539 A69-21752

Hot electron plasma formation by injecting megaelectron volt ion beams followed by Lorentz trapping, noting advantages of DC operation 15 p2661 A69-30929

ION IRRADIATION

NT DEUTERON IRRADIATION
NT PROTON IRRADIATION

Numerical solution method for equation of electric field affected by permanent flux of ionic currents 01 p0128 A69-10364

Inactivation by heavy ions of esterase activity of dried trypsin as function of temperature during irradiation 03 p0372 A69-13488

Free radicals produced in ribonuclease, lysozyme and trypsin during exposure in vacuum and various temperatures to electron and heavy ion irradiation 03 p0372 A69-13484

Genetic effects in yeast induced by heavy ion radiation, studying lethality, mitotic segregation, allelic recombination and reverse mutation 03 p0373 A69-13491

Mammalian cell survival, chromosome abnormalities and recovery from heavy ion and X ray irradiation 03 p0373 A69-13492

Angular distribution of particles sputtered from GaAs and GaP single crystals, bombarding faces with Ar ions at low energy 04 p0640 A69-14452

P-n junctions and device structures formed by ion implantation, using Hall effect and channeling techniques to evaluate implanted layer nature 06 p0974 A69-16862

Kinetics of homogeneous and heterogeneous growth of centers of new phase of semiconductor during ion bombardment as function of radiation dose 06 p0978 A69-16985

Metal atom production by bombarding metal with positive ions from microwave discharge, obtaining isolation in inert gas matrix and UV spectra 06 p0957 A69-17113

Gaussian summation for ion implantation profile control in semiconductors, describing computer program selecting optimum energies to fit predetermined profiles 11 p1857 A69-24546

Excited levels in Li I produced by Li 7 ion passage through carbon foil, measuring excitation mean lives by beam foil technique 13 p2301 A69-27454

Radiation damage in yeast cells irradiated by high energy C 12 ions evaluated from survival rate study 14 p2406 A69-28915

Activation energy of annealing of lattice defects in Au films deposited under irradiation with Au ions 18 p3182 A69-34349

Plasma electron beam for welding, deriving beam current from secondary emission by ion bombardment, discussing gas pressure, equipment and applications 19 p3320 A69-35555

ION MICROSCOPES

Field ion microscope study of imaging solute atoms of dilute Pt-based W, Pd, Co, Ni and Au alloys 01 p0092 A69-10055

Metals study using field ion microscope for detecting dislocations, crystal boundaries and growth surfaces and surface diffusion energies 06 p0943 A69-17376

Grain boundaries structure in tungsten wire using auto ion microscope, showing misorientation corresponds to high density coincidence site lattices 08 p1329 A69-19943

ION MOTION

HF plasma ionic composition dependence on discharge conditions and ions translational energy 01 p0129 A69-10682

Ion-ion velocity space instability due to difference between ion temperatures perpendicular and parallel to magnetic field 03 p0475 A69-13154

Gas segregation in positive column of DC discharge due to axial ion motion analyzed using conservation equation 08 p1361 A69-20145

Diffusion coefficient, velocity distribution function and velocity averages for gaseous ions moving in strong electric fields, considering ion-gas molecule charge transfer collisions 08 p1355 A69-20209

Magnetospheric gusts of streaming positive ions in equatorial plane detected by ATS 1 synchronous satellite 09 p1574 A69-21309

Linear ion accelerators noting particle motion, RF cavity design, RF power sources, injection and applications
09 p1553 A69-22697

Surface ion behavior on planar semiconductor devices determined by measuring effect of time, humidity, temperature, voltage and previous testing history
10 p1743 A69-23173

Early disturbances in active migration of potassium 42 ions in irradiated erythrocytes in rats, showing relation between influx and energy exchange in cells
10 p1647 A69-23966

Finite ion Larmor radius effect on gravitational instability of two superposed fluids in uniform rotation, analyzing interchange perturbations and vortex sheet
12 p2062 A69-26461

Vertical ionization drift in F region as function of electron density, ionization coefficient and recombination coefficient
12 p2070 A69-26584

Ion cloud ambipolar diffusion and motion dependence on initial configuration and close magnetic field alignment above 95 km, discussing observations of meteor trains
12 p2074 A69-26961

MHD generator analysis, formulating boundary value problem for ion diffusion and Fourier series solution for end effect of electrodes pair
13 p2208 A69-27613

Electron and ion mobility in multiple cusp magnetic fields related to Polytron experiment
14 p2499 A69-29852

Structural formula of slowly cooled Mg and Al-Mg microwave ferrites, noting ion mobility during cooling
15 p2670 A69-31184

Ion-neutral air motion in F region under time dependent electric and constant magnetic field effect, using partial differential equations
16 p2777 A69-32181

Pressure gradients and moving ions driven neutral-air winds in F region, using asymmetric pressure model
16 p2779 A69-32302

Kinesonde radio sounding system for three dimensional ground observations of E region microstructure and vertical motion of neutral air and ions
18 p3125 A69-34250

Electric field variations in vicinity of auroral forms from motions of Ba vapor clouds released from Nike-Tomahawk rockets
18 p3128 A69-34935

Townsend discharge formation time determination, taking into account impact ionization in positive ion cloud moving from anode to cathode
19 p3381 A69-36603

Wind velocity components calculation at F-sphere maximum level, taking into account electrodynamic drift of ionospheric plasma and ion motion
20 p3519 A69-36972

Kinetic equation describing dynamics of inhomogeneous cloud of fast electrons and ions trapped in earth magnetic field
20 p3520 A69-37029

Plasma microinstabilities due to ion and electron anisotropic velocity distributions, considering frequencies near harmonics of ion cyclotron frequency
24 p4355 A69-42686

ION OSCILLATION
U PLASMA OSCILLATIONS

ION PROBES

Positive ion beam probe for approximate static electric field distribution in low pressure RF discharges, analyzing deflection data for potential distributions
02 p0287 A69-11838

Expansion anisotropy in angular distribution of laser produced plasmas in terms of drifting and expanding sphere model, discussing particle velocities, currents and time integrated counts
05 p0804 A69-16460

D region ionizable constituent density /presumably nitric oxide/ measured, using blunt probe to detect changes in conductivity produced by Lyman alpha ionizing radiation
15 p2598 A69-31316

Multiple electrode probe characteristics in rarefied plasma flow created by ion source, noting electrode potential role
19 p3314 A69-36622

Molecular ion concentrations determined using flat probe collector trap on Cosmos 5 satellite at 200-300 km
20 p3519 A69-37021

Langmuir plate and spherical ion probe experiments aboard Explorer 31, measuring concentrations and temperatures of thermal electrons and ions
20 p3545 A69-37881

Spacecraft pitch and yaw angles measurement using environmental positive ion probes, discussing Gemini flight tests and attitude control systems
24 p4315 A69-43241

ION PRODUCTION RATES

Ion formation rate in F 2 layer in southern polar cap, noting effect of season, latitude and solar activity
02 p0238 A69-11679

Pulsed arc source using plasma jet to obtain intense hydrogen ion beam
03 p0412 A69-13842

Charge multiplication in crystals, analyzing ionization rate, avalanche breakdown in p-n junctions, pair production and impact of impurities
04 p0641 A69-14503

Charge transfer cross sections for slow ion production in nitrogen molecular ion beams incident on hydrogen and deuterium
05 p0796 A69-15914

Photoelectric absorption studies on molecular nitrogen indicate predissociation contributing to atomic nitrogen production in upper atmosphere
05 p0756 A69-16282

Ion current output vs gas component partial pressure determined to measure ion source efficiency employing electron impact ionization
06 p0960 A69-16919

Nitrogen ion number density time dependence by mass spectrometric probing of decaying nitrogen plasmas, noting molecular ion production by colliding metastable nitrogen molecules
07 p1184 A69-19141

Ion formation and ion secondary emission during sputtering, discussing Saha-Langmuir equation, probability theory, simultaneous processes, mass spectroscopic analyses, etc
08 p1355 A69-20616

Ionospheric molecular ion concentration vertical profile analysis for verifying neutral gas temperature maxima in connection with two ion production maxima
10 p1688 A69-23930

Oxygen and NO ions yields produced by dissociative attachment of electrons to nitrogen dioxide as function of electron energy, considering electron affinities lower limits
13 p2301 A69-27363

Ion formation rate in F 2 layer in southern polar cap noting effect of season, latitude and solar activity
13 p2257 A69-28710

Metastable ions formation and detection in double focusing mass spectrometer, calculating location of decomposition in electrostatic analyzer and doubly charged ions transition
15 p2561 A69-30021

Lyman alpha radiation ionization rate in lower ionosphere, noting various charged particle concentration parameters
15 p2605 A69-31438

Nocturnal D region conductivity enhancement relation to X radiation from Scorpius XR-1 and other sources, calculating ion production rate
17 p3024 A69-33378

Effective rate coefficients of ion-molecular processes, dissipative recombination and ion production in F 2 layer at midlatitudes
17 p2966 A69-33979

Shock ionization by ion impact against triatomic H molecules gas target, showing positive ion production dependence on extraction voltage, collision chamber pressure, etc
19 p3378 A69-36188

Ion production rates vertical distribution and temporal changes at midlatitudes during solar activity minimum and maximum above F 2 layer
20 p3525 A69-37656

Attachment coefficients for negative oxygen ion formation in low energy electron swarms over various voltage/pressure ratios
21 p3774 A69-39238

Low energy galactic cosmic ray spectrum determined from ionization rate per hydrogen atom, correlating peak intensity with stellar particle emission high energy portion
24 p4365 A69-42608

ION PROPULSION

Electromagnetic ion acceleration in steady electric and magnetic fields chosen to match fields of Alkali Plasma Hall Accelerator /ALPHA/
[AIAA PAPER 69-111] 06 p0985 A69-18175

MPD plasma acceleration in West Germany, discussing Hall acceleration, electrodeless plasma acceleration by electromagnetic waves and space charge neutralized Hall ion thruster
[AIAA PAPER 69-279] 09 p1564 A69-21238

Ion spacecraft propulsion systems, discussing components and characteristics of reaction type rocket engines and electrical thrust devices
11 p1944 A69-25593

Electric and chemical rocket propulsion systems
13 p2325 A69-28255

Ion propulsion applied to geostationary satellites attitude control, discussing thrust levels, cesium ionization, colloidal propulsion, etc
16 p2837 A69-32068

RF ion thrusters using electrodeless self sustaining mercury discharge, describing basic theory, component design, performance optimization and test results
17 p3018 A69-33326

Kaufman ion thruster ESKA 18 operation principles and design compared to RIT 10 and SERT 2, discussing discharge and focusing characteristics and propulsion parameters
17 p3022 A69-33605

Cs contact ion microthruster system design, fabrication and flight qualification, noting control logic/power conditioning unit and electronic packaging
[AIAA PAPER 68-552] 21 p3785 A69-39212

Asteroid exploration by solar photovoltaic powered ion propelled probe, discussing spacecraft design, mission and 1975 Mariner utilization
[AAS PAPER 69-322] 24 p4381 A69-42868

ION PUMPS

Ultrahigh vacuum electron microscope using differential sputter ion pumps to obtain low contamination environment
04 p0599 A69-15016

Differential ion pumping for vacuum deposition of thin films
06 p0907 A69-17709

Tritium contamination reduction in small ion accelerators for neutron production, discussing pumping problems and vacuum systems
12 p2059 A69-26499

MHD mercury flow in rotating torus with little friction investigated for Reynolds numbers, considering induction pump forces and magnetic field influences
14 p2500 A69-29907

ION RECOMBINATION

Alpha recombination coefficient of molecular helium ions measured in helium afterglow plasmas as function of electron density and gas temperature
02 p0283 A69-11834

Low density limit to three body ionic recombination coefficients in various gases
04 p0632 A69-14679

Combination rate constants for H-F-O reactions, discussing expressions and relative efficiencies with Argon as third body
04 p0646 A69-14743

Effective gradient method modification for analyzing three body ionic recombination compared with diffusion method
05 p0795 A69-15661

Atomic flux from Cs and K ion recombination on hot end plates of Q machine measured, noting contribution to total plasma end loss rate
08 p1358 A69-19810

Three body ionic recombination coefficient for moderate and high gas densities, taking into account variability in mean free path and trapping radii
09 p1542 A69-21624

Unidentified cometary spectra line emission possible interpretations, examining atomic hydrogen abundance in cometary atmosphere and ionic hydrogen recombination
15 p2685 A69-30523

Lower auroral ionosphere rocket measurements of electrons, positive ions and energy particles, deriving height variation of ion pair production and ion-ion recombination
16 p2778 A69-32187

Preferential ion recombination in gases under high pressure, noting no dependence of recombination on average energy
17 p2949 A69-32999

Effective rate coefficients of ion-molecular processes, dissipative recombination and ion production in F 2 layer at midlatitudes
17 p2966 A69-33979

Radiative recombination of atomic oxygen ions in nighttime F region UV radiation detected by polar-orbiting OGO 4 satellite
18 p3129 A69-34957

Dielectric recombination in plasma, considering role in populating highly excited levels
20 p3580 A69-38016

Ionic excited states statistical equilibrium populations calculated for various electron densities and temperatures including effects of dielectronic, radiative and three body recombinations
22 p3985 A69-40666

ION SCATTERING

Electron detachment cross sections for negative atomic and molecular O ions with incident energies between 3 and 100 ev
09 p1542 A69-21625

Exospheric temperature variations by Thomson scattering related to solar and geomagnetic activity, discussing seasonal effect on thermospheric variables
15 p2604 A69-31409

Alpha-scattering experiments by Surveyor missions, studying hypothesis regarding lunar origin of eucrites and howardites
20 p3597 A69-37341

Elastic differential Li ion scattering cross sections on helium, nitrogen and oxygen
24 p4354 A69-43817

ION SHEATHS

Space charge sheath electric thruster principles, construction and performance using laboratory test model [AIAA PAPER 69-282]
09 p1563 A69-21235

Dynamic growth of positive ion sheath on plane electrode in mercury plasma, measuring sheath thickness and current
12 p2134 A69-26099

ION SOURCES

NT DUOPLASMATRONS
NT PLASMATRONS

Electrode geometry for mass spectrometer ion source to measure electron ionization cross section of low vapor pressure materials
01 p0080 A69-10605

Ion formation rate in F 2 layer in southern polar cap, noting effect of season, latitude and solar activity
02 p0238 A69-11679

Positive Ar ion energy distribution for beam extracted from nonmagnetic hot cathode gas discharge ion source under various source conditions
03 p0427 A69-13102

High current electron bombardment ion source for production of low energy ion beams without metastable contamination
03 p0428 A69-13106

Alkali metal ion sources noting cesium ion engine development for space propulsion [ECS PAPER 170B]
03 p0478 A69-13859

Ion velocity distribution for high vacuum ion source, noting factors influencing dispersion
06 p0959 A69-16916

Ion current output vs gas component partial pressure determined to measure ion source efficiency employing electron impact ionization
06 p0960 A69-16919

Ion formation rate in F 2 layer in southern polar cap noting effect of season, latitude and solar activity
13 p2257 A69-28710

Semiautomatic recording device to determine gas discharge ion and electron sources operation modes optimum parameters
15 p2658 A69-30237

Plasma three electrode source ion-optical characteristics, noting beam angular divergence dependence on spacing between discharge cavity and intermediate electrode
15 p2658 A69-30240

Electron impact field ionization source for mass measurement of molecular ions, noting organic geochemistry applications
15 p2608 A69-30428

ION TEMPERATURE

Excitation heating energy pumping mechanism for explaining dynamic equilibrium in C rich arc plasmas with high ion temperature/electron temperature ratio
01 p0126 A69-10276

Spacecraft ionospheric probe for simultaneous measurement of electron temperature and density, plasma space potential, ion composition, etc
01 p0081 A69-10760

Neutral gas temperature variations effect on electron ion temperature height profile in tidally generated sporadic E layer with wind shear of gravity wave origin
01 p0073 A69-11176

Ion concentrations and temperature measurements by magnetic trap on Cosmos 5 between 1000-1200 km
02 p0306 A69-11656

Ion-ion velocity space instability due to difference between ion temperatures perpendicular and parallel to magnetic field
03 p0475 A69-13154

Electron, ion and neutral particle temperatures of upper atmosphere
04 p0592 A69-14975

Particles nonlinear motion in plasma in magnetic field with arbitrary electron velocity distribution, discussing wave discontinuity patterns
05 p0804 A69-16370

Ion temperature diurnal variations at 250-475 km obtained from Thomson scatter spectra
05 p0757 A69-16407

Ion composition and charged particle temperatures at 300-600 km from sounding rocket and topside sounder Alouette 2 measurements
07 p1124 A69-18839

Plasma mixed ion heating by small scale HF turbulent electron sound pulsations
09 p1548 A69-21673

Nonlinear longitudinal oscillations in nonisothermal electron plasma with Maxwellian distribution in velocity space and different temperatures of electrons and ions
09 p1550 A69-22025

Ionospheric measurements of electron density, electron and ion temperature profiles from strength of incoherent radio wave scattering
10 p1686 A69-23910

Electron-ion temperature relaxation near interface of two semiinfinite nonmagnetized different temperature plasmas brought into thermal contact
11 p1923 A69-24296

Ion and electron temperature and density measurement by Thomson scattering with low resolution monochromator for Salpeter parameter near unity
11 p1925 A69-24310

Reversible ion heating by atmospheric tides, noting radar Thomson scatter observations of E region ion temperature height profiles
11 p1879 A69-25159

Wave damping in plasma, developing Boltzmann analysis of electron mode dispersion relations involving momentum transfer and relaxations of electron-ion temperature and anisotropy
13 p2305 A69-27377

Global coverage of positive ion composition and temperature, and electron density and temperature measurements during AURORA mission of ESRO 1 satellite
13 p2253 A69-27753

Ion concentrations and temperature measurements by magnetic trap on Cosmos 5 between 1000-1200 km
13 p2333 A69-28687

Ionospheric electron and ion temperatures correlated with electron concentration profile as measured by rockets and satellites
14 p2510 A69-28942

Two fluid continuum theory of incoherent scattering extended to include unequal electron and ion temperatures, considering backscatter power dependency on collision frequencies
14 p2510 A69-28946

Electron and ion temperatures height variations in sporadic E layers, noting effects of neutral gas temperature changes
14 p2440 A69-29127

Plasma ion temperature measurement based on integral neutron yield, noting density determination
14 p2498 A69-29808

Turbulent diffusion and ion heating in plasmas in presence of current instability
15 p2662 A69-30959

Magnetic field lines curvature effect on plasma instabilities due to ion temperature gradient, noting frictional gravitation field simulation
16 p2816 A69-31636

Ion, electron and neutral temperatures from ion composition distribution, assuming no change in vertical distribution within horizontal distance between upleg and downleg measurements
16 p2849 A69-31990

Intensity and rotational temperature seasonal variations of hydroxyl emission at different latitudes in upper atmosphere
16 p2775 A69-32081

Ionization density, velocity and temperatures oscillations revealed by Thomson scatter observations of gravity waves in F regions
16 p2779 A69-32198

Ion energy distribution function and density profile in strong implosion wave generated by theta pinch

discharge, investigating compression wave in deuterium
17 p3013 A69-33821

Lower ionosphere electron concentration confirmed as function of electron and ion temperature by satellite and probe data
17 p2966 A69-33981

Solar wind temperature, using distribution function, for solar wind ions in anisotropic Maxwell distribution form
19 p3396 A69-36631

Rarefied nonmagnetic plasma in wake of body moving at higher than electron and ion thermal velocities
20 p3525 A69-37661

Ionospheric parameters of ion and electron density and temperature and ionic species compared by direct measurement probes on Explorer 31 satellite
20 p3531 A69-37882

Ionospheric electron and ion concentration and temperature by Langmuir plate and spherical ion probe on Explorer 31 and ionosonde on Alouette 2
20 p3531 A69-37883

Ionic composition determined by combining Alouette topside sounder electron density profiles with electron and ion temperatures measured by ground based Thomson scatter sounder
20 p3532 A69-37898

Homogeneous magnetoactive plasma longitudinal oscillations stability with fast monoenergetic ions addition, noting ion temperature increase stabilizing effect
22 p3990 A69-40789

Ion temperature measurement in rarefied multicomponent plasma by temperature relation to ion beam divergence rate, comparing results to pyrometric measurements
23 p4196 A69-41839

ION TRAPS (INSTRUMENTATION)

Ion concentrations and temperature measurements by magnetic trap on Cosmos 5 between 1000-1200 km
02 p0306 A69-11656

Deep trapping levels caused by ion implantation doping, discussing level effects on electrical characteristics of zinc implanted GaAs diodes
05 p0808 A69-16287

Rotating plasma behavior in magnetic mirror trap, using radial electric field
10 p1740 A69-23716

Ion concentrations and temperature measurements by magnetic trap on Cosmos 5 between 1000-1200 km
13 p2333 A69-28687

Electron trap behavior on charged spacecraft, obtaining expressions for current to aperture and internal retarding electrodes for all apertures and spacecraft potentials
16 p2849 A69-31976

Planar thermal ion and electron trap experiments on Explorer 31 satellite, measuring ion and electron density and temperature and ionic composition
20 p3544 A69-37878

Solar wind sample collection, describing experiment to determine ion flux capture efficiency for various metal foils
23 p4205 A69-41539

IONIC COLLISIONS

Spectrum and yield of emitted electrons resulting from passage of heavy ions through metal films
03 p0471 A69-13161

Low collision energy charge transfer and dissociative charge transfer between rare gas ions and molecular nitrogen, measuring nitrogen ion kinetic energy distributions
05 p0796 A69-15909

Ion-molecule collisions of Ar-Co and N-No pairs, discussing charge exchange reaction rates and spiraling nature
05 p0797 A69-16428

ELF radio waves reflection coefficients calculated from two layer ionospheric model, noting ion collision frequency effect in Schumann resonance frequency band
07 p1124 A69-18820

Electron collisional excitation cross section calculations for atoms and ions using modified Born approximation taking into account three physical effects
07 p1187 A69-19658

Electron-ion collisions during forbidden lines excitation in gaseous nebulae, using Hartree-Fock functions and variational principles
08 p1391 A69-20530

Charge exchange collisions in ground state and ionic hydrogen incident on cesium vapor, measuring beam components after passage through target
08 p1356 A69-20737

Vibrational excitation in He, H and N ion- molecule collisions on nitrogen first negative system, studying relative band intensities
08 p1356 A69-20739

Electron detachment cross sections for negative atomic and molecular O ions with incident energies between 3 and 100 ev
09 p1542 A69-21625

Quantum mechanical description of ionizing reactions of highly charged positive ions in solar corona, obtaining approximate sum and selection rules
09 p1596 A69-22054

Ionization instability in low temperature magnetized plasma, analyzing electron concentration perturbation caused by Joule heating during electron-ion collisions
10 p1741 A69-23962

Crossed beam apparatus with mass selected variable energy primary beam for study of angular and velocity spectra of ion-molecule reactions
12 p2092 A69-26477

Slow charged products of charge exchange collisions by ions in molecular gases, comparing kinetic energies during various reactions
13 p2301 A69-27455

Charge transfer and vibrational excitations in hydrogen molecular ion-hydrogen gas collisions
13 p2302 A69-28196

Ion drag effects on acoustic gravity waves propagation in isothermal F region, discussing indicated wave damping
14 p2434 A69-28944

Conductivity tensor of collisional plasma in magnetic field, basing method on iterative procedure
14 p2503 A69-29999

Electrical conductivity tensor of many component collisional relativistic plasma in magnetic field and near equilibrium, expressing collisional part as momentum integral
14 p2503 A69-30000

Mode-mode coupling calculation for finite amplitude collisional drift waves demonstrating inherently nonlinear phenomena
15 p2660 A69-30916

Magnetic field lines curvature effect on plasma instabilities due to ion temperature gradient, noting frictional gravitation field simulation
16 p2816 A69-31636

Spatial ion wave echoes emphasizing echo line shape analysis and effects of ion-neutral and ion-ion collisions
16 p2818 A69-31676

Electrostatic probes in nonequilibrium collision dominated ionized gas flow ballistic ranges
19 p3291 A69-35716

Ion cyclotron double resonance technique to identify collision-induced ion fragmentation pathways illustrated with p-chloroethylbenzene
19 p3265 A69-36292

Parameters of DC discharge between concentric cylinders calculated for plasma probes by pressure theory, noting ion neutral collisions and magnetic field effects
21 p3776 A69-38712

Collision processes in gaseous nitrogen leading to production of positive triatomic, diatomic and monatomic nitrogen ions
22 p3986 A69-40722

Recombination and ionization coefficients for quasi-steady state homogenous H and hydrogenic ion plasmas based on collisional-radiative model
22 p3988 A69-41153

Atoms and ions collision strengths and photoionization cross sections for nitrogen, oxygen and neon fitted to interpolation formulas for temperature and frequency effects
22 p3988 A69-41244

Computer made movies and time history plots for ion-dipole collisions involving polar molecules /CO, HCL and acetonitrile/
24 p4352 A69-43124

ION CONDUCTIVITY
U ION CURRENTS

ION CRYSTALS
Multiphonon orbit-lattice relaxation of excited states of rare earth ions in crystals, measuring fluorescence lifetimes, quantum efficiencies and transition rates
01 p0134 A69-10011

Proton energy distributions for passage through NaCl, KCl, KBr, Si and Ge single crystals at various angles relative to /100/ and /110/ crystallographic planes
01 p0140 A69-11109

Raman effect in potassium dichromate single crystal, discussing symmetrical and antisymmetrical internal vibrations of free ions
12 p2105 A69-26285

Ba titanate modifiers, classifying cations replacing Ti and Ba ions
22 p3996 A69-41161

IR lattice spectra of rare earth Al, Ga and Fe garnets, discussing oxygen anion, translational rare earth cation and crystal lattice external motions
24 p4360 A69-42974

IONIC DIFFUSION
Plasma wave conversion into electromagnetic waves in strong magnetic field, studying nonlinear coalescence and scattering on thermal and epithermal ions
11 p1922 A69-24245

Light ion abundance measurements of OGO satellites and field aligned diffusive equilibrium theory with temperature and concentration latitudinal variations
11 p1879 A69-25157

Diffusion of ion-electron pairs produced by photoionization upstream of strong shock waves to shock tube walls based on particle flux and Poisson equations
11 p1866 A69-25275

Ionic diffusion in topside ionosphere analyzed using multiple gas mixture diffusion formula, noting Coulomb ionic collision role
14 p2441 A69-29381

Applicability and limitations of diffusive equilibrium in topside ionosphere, noting plasma density distribution along magnetic field line
20 p3531 A69-37887

Drift velocity and lateral diffusion of positive hydronium, hydrogen and K ions in hydrogen with zero field mobilities
20 p3580 A69-38026

Cerebral and retinal capillary permeability to ions in rats analyzed by electron microscope using Prussian blue reaction
23 p4081 A69-41433

IONIC MOBILITY
Oxygen ions motion in oxygen, measuring drift velocities in glow discharge
05 p0795 A69-15662

Charge and degree of ionization of nickel alloyed with molybdenum analyzed by electrolytic ion migration method
07 p1159 A69-18535

Magnetoactive plasma containing fast monoenergetic ions noting stability at drift frequencies and in terms of Alfvén wave buildup
09 p1546 A69-21566

Cs and K ions drift velocity calculations in vapors of own atoms under various electric field strengths effect
11 p1922 A69-24226

Monograph on method and results of measurements of mobilities spectrum ion density and conductivity in upper troposphere and stratosphere
11 p1877 A69-24636

Drift velocity and longitudinal and transverse diffusion coefficient for low energy N ions in N gas in mass spectrometer at room temperature
13 p2302 A69-27458

Maximum likelihood methods applied to device performing ion swarm experiments, measuring positive ion mobility in hydrogen
16 p2788 A69-31670

IONIC PROPELLANTS
U ION ENGINES

IONIC REACTIONS
Enhanced 6300 angstrom emission from F region auroral latitudes in terms of reaction between oxygen ions and atoms
01 p0062 A69-10137

Ion reactions with neutral molecules, discussing analogies with conventional chemical systems
01 p0124 A69-10859

Metal ionic reactions with weak chemical bond breaking and three body reactions forming molecular ions without bond breaking, discussing sporadic E deionization
01 p0071 A69-11168

Carbon monoxide ion dynamics in envelopes of comets exhibiting fountain behavior, discussing electron-collisional ionization within envelopes as main plasma production mechanism
02 p0310 A69-11423

Crossed beam studies of ion-molecule reaction mechanisms, crossing approximately monoenergetic ion beam with thermal molecular beam
03 p0382 A69-13460

Negative ion-molecule reactions in nitrous oxide using mass spectrometer, noting negative ion concentration pressure dependence
06 p0960 A69-17106

Reaction rates coefficients of oxygen ions with molecular oxygen and nitrogen in nighttime F region over Moscow based on loss coefficient estimate
06 p0919 A69-17724

Two body rate coefficients for charge transfer reactions of nitrogen, oxygen and NO positive ions to Na atoms measured using flowing afterglow system
07 p1185 A69-19303

Ion-molecule reactions constants studied directly in ionosphere, using air injection from geophysical probe and airborne RF mass spectrometer
08 p1311 A69-21159

Ionic and biradical mechanisms in thermal and photo cis-trans isomerizations elucidated by planar and twisted configurations of polyenes
13 p2216 A69-27618

Vapor phase reaction sequence to explain water cluster ions in D region
14 p2434 A69-28940

Escherichia coli B/r cells plasmolyzed in sucrose observed under phase contrast, noting plasmolysis reduction in ions presence
19 p3257 A69-35973

Ion structure of keto and enol and McLafferty rearrangements determined by ion cyclotron resonance spectroscopy
19 p3265 A69-36288

Acetonitrile ion-molecule chemistry using ion cyclotron resonance, discussing reaction of vibrationally excited methyl ions from electron impact
19 p3265 A69-36290

Reactions determining ion composition in E region, discussing neutral composition variations from day to night and during solar activity cycles
20 p3520 A69-37031

Absorption and fluorescent spectra, relaxation times and quantum efficiencies measured for glasses doped with trivalent erbium, reviewing spectroscopic parameters involved with laser effect
22 p3962 A69-40476

Formation mechanism of positive ethyl ion and hydrogen molecule during interaction between positive methyl ion and methane molecule
24 p4280 A69-43814

IONIC WAVES
Asymptotic method for analyzing small long wave perturbations in plasma, showing instability with respect to perturbations propagating at angles to ion-acoustic wave
01 p0131 A69-10788

Ion acoustic wave dispersion in highly ionized Ar plasma in longitudinal magnetic field, noting effects of several phenomena
01 p0133 A69-11216

Plasma ion oscillation suppression by intensified electron plasma oscillations
02 p0287 A69-11934

Standing ion-acoustic wave excitation in weakly ionized plasma, noting isothermal compression of electron gas
02 p0292 A69-12555

Electron fluid compression coefficient from simultaneous measurement and correlation of absolute magnitudes of ion acoustic wave potential and accompanying plasma density perturbation
03 p0475 A69-13148

Decay stability of large amplitude neutral wave into two ion acoustic waves in weakly ionized plasma
03 p0475 A69-13158

Electron plasma oscillations diffusion due to scattering by large amplitude ion wave background, noting electron wave spectrum evolution
03 p0483 A69-14256

Two fluid MHD equations in form of nonlinear ion waves with magnetic vector
04 p0662 A69-15244

Similarity/law for ionization waves noting relations for frequency, wavelengths, amplification, propagation velocities and phase shifts
05 p0799 A69-15633

Equations describing chemical kinetics and conservation law derived for ionization relaxation processes behind shock wave front in air
05 p0746 A69-15891

Longitudinal acoustic waves propagation in partially ionized gas in external electric field, taking into account ionic collisions with electrons and neutral particles
06 p0963 A69-17079

Ion-acoustic wave excitation in plasma layer affected by incident p-polarized magnetic wave, deriving expressions for reflection, transmission and energy absorption coefficients
08 p1370 A69-21025

Plasma oscillation intensities at combination frequencies under assumption of plasma wave and ion acoustic wave propagating along z axis
09 p1550 A69-22024

Asymptotic method for analyzing small long wave perturbations in plasma, showing instability with respect to perturbations propagating at angles to ion-acoustic wave
10 p1653 A69-23107

Combination backscattering on ionic sound waves assumed responsible for unexpected features of radio signals reflected from sun
10 p1776 A69-23219

Ion-acoustic wave experiments for disturbance travel in plasma sheath, obtaining ion number density
11 p1929 A69-25272

Unstable ion sound wave propagation across magnetic field in collisionless shock waves, noting drift instability
11 p1930 A69-25273

Electrical DC conductivity of turbulent plasma decreased in presence of ion waves
13 p2305 A69-27302

Moving striations relations to ion acoustic waves in DC discharge in neon at various pressures, discharge currents and measurement excitation modes
14 p2494 A69-29695

Standing ion-acoustic wave excitation in weakly ionized plasma, noting isothermal compression of electron gas
15 p2658 A69-30252

Steady oscillations of active nonlinear system of nonisothermal plasma and charged particle flux, noting steady ion-acoustic waves
15 p2662 A69-30947

Spatial ion wave echoes emphasizing echo line shape analysis and effects of ion-neutral and ion-ion collisions
16 p2818 A69-31676

Nonlinear mixing of Ar plasma ion wave and externally applied electromagnetic wave
16 p2820 A69-31769

Solar corona heating ascribed to Landau damping of ionacoustic waves generated in motion of photospheric granules
17 p3030 A69-33060

Signal wave scattering and transmission by ionized medium disturbed by high power pumping wave, studying wave interactions with Born approximation for bounded medium
17 p2928 A69-33871

VLF wave propagation phase velocity prediction for airborne Omega computer, using scatter model based on abnormal ionosphere
17 p3002 A69-34077

Atmospheric whistlers and ion acoustic waves interaction in nonisothermal plasma, determining damping frequencies, decrements and wave polarization
18 p3180 A69-35024

Waves in auroral ionosphere due to particle precipitation, indicating ionospheric plasma instabilities
18 p3130 A69-35187

Asymptotic method for analyzing small long wave perturbations in plasma, showing instability with respect to perturbations propagating at angles to ion-acoustic wave
20 p3582 A69-38005

Parametric excitation theory involving Langmuir and ion-acoustic waves for homogeneous plasma slab with specular particle reflection at slab walls
20 p3582 A69-38245

Collisionless damping of large amplitude ion acoustic waves excited externally in thermally ionized Cs plasma
22 p3991 A69-41008

Acoustic wave propagation in plasma, analyzing ionic and electron sound caused by oscillation and relaxation processes using Landau and Vlasov kinetic equations
23 p4196 A69-41726

Tubular light beam waveguide properties, studying changes related to heating and ionization of medium
02 p0258 A69-12644

Similarity law for ionization waves noting relations for frequency, wavelengths, amplification, propagation velocities and phase shifts
05 p0799 A69-15633

Gas velocity variations in ionizing shock wave propagating along magnetic field applied to conducting piston motion
05 p0801 A69-15787

Large signal model for analysis of RF output and efficiency of IMPATT diode oscillator, noting frequency tuning
05 p0733 A69-16555

Atomic excitation and ionization involving inner shell electrons during collisions between atoms and ions, examining photoabsorption by inner shell electrons
07 p1187 A69-19659

Atomic collision theory, discussing cross section calculations by Gryzinski classical method, variational methods and Faddeev equations for three particles
07 p1187 A69-19661

Electron collision excitation of positive ions, calculating collision cross sections for transitions between levels of P term
07 p1187 A69-19714

Quantum mechanical description of ionizing reactions of highly charged positive ions in solar corona, obtaining approximate sum and selection rules
09 p1596 A69-22054

O, Ne, Si and Fe ionization equilibria in low density plasma, including dielectronic recombination and autoionization processes in calculations
09 p1543 A69-22404

Plasma ionization instability linear growth problem analyzed in bounded region
10 p1735 A69-23461

Radar and photographic studies of meteors from Leonid and Perseid showers, presenting velocities, luminescence and ionization
10 p1783 A69-23895

Ionization equilibrium for ions of solar abundant elements between C and Ni calculated as function of electron temperature
11 p1928 A69-25262

Current-voltage characteristics and ionization equilibrium of low voltage arc plasma in narrow gap of thermionic converter at high current density
11 p1933 A69-25554

Ionization instability in plasma enclosed by two infinitely segmented and ideally emitting electrode walls and two insulator walls
12 p2134 A69-26095

Electromagnetic wave phase characteristics after free space passage through statistical medium with wave disturbance producing density and ionization fluctuations
14 p2435 A69-29049

Ionization and recombination in low temperature plasmas, noting fast electron distribution function deviation from Maxwellian form and calculation for Cs plasma
15 p2658 A69-30256

Unsteady nonadiabatic shock waves in stellar gas dynamics, analyzing energy losses due to ionization at shock fronts by extended Chiznell-Wisem method
15 p2682 A69-30508

Fuel cell oxygen electrode problems, noting oxygen ionization reaction and disk electrodes role
16 p2739 A69-32416

Gas velocity variations in ionizing shock wave propagating along magnetic field applied to conducting piston motion
18 p3181 A69-35038

Forbidden lines in solar corona, discussing ionization equilibrium and excitation of levels in highly ionized atoms
19 p3422 A69-36216

Shock wave interaction and bow shock wave establishment near sphere in presence of ionization relaxation, using time resolved schlieren photography
19 p3450 A69-36361

Shock wave effect on ionization of detonation waves in propane-O mixtures producing stable high velocity plasma, measured by double probe method
21 p3853 A69-39745

IONIZATION CHAMBERS

NT BUBBLE CHAMBERS
NT CLOUD CHAMBERS
NT GEIGER COUNTERS
NT PROPORTIONAL COUNTERS
NT SPARK CHAMBERS

Nuclear active cosmic ray component particle energy spectrum and nuclear cascade avalanches curves, using ionization calorimeter with Pb absorber
13 p2303 A69-28399

High energy mu-mesons component of atmospheric cosmic ray showers by particle impact penetration using multiple underground ionization chambers
13 p2332 A69-28409

Electron and proton components contribution to reverse current production after particle shower through upper Cu wall of ionization chamber with lower Pb wall
13 p2304 A69-28417

IONIZATION COEFFICIENTS

Avalanche multiplication in abrupt silicon p-n junctions analyzed using ionization coefficient measurements for holes and electrons
01 p0135 A69-10038

Initial ionization rates and collision cross sections in shock heated argon in low pressure shock tube, using double electrostatic probes
01 p0132 A69-11206

Drift and diffusion of electron pulse advancing through gas, providing physical basis for Townsend ionization coefficient
04 p0633 A69-15443

Cloud chamber for measuring specific ionization in relativistic region by muons in gases, using drop counting method
06 p0925 A69-17303

Ionization index, electron formation and effective recombination coefficient in E 2 layer, noting solar activity effect
06 p0920 A69-17725

Two fluid approximation of one dimensional steady state flow of inviscid plasma with thermal gradients, considering ionization and recombination processes
07 p1189 A69-18691

Collisional excitation and ionization rates comparison in statistical equilibrium model atmosphere calculations
08 p1385 A69-20065

Ionization and attachment coefficients in oxygen at low pressures, noting Paschen curves near minimum sparking potential and secondary ionization coefficient
08 p1354 A69-20099

Rational approximation for coefficients used in calculating hydrogenic photoionization Gaunt factors
08 p1354 A69-20153

Nonlinear algebraic equation system describing populations of excited atoms of low pressure nonequilibrium cesium plasma, determining ionization coefficient and molecular ion concentration
11 p1934 A69-25567

Prebreakdown currents measurement in H and N for deducing ionization coefficients via Townsend and Lucas equations respectively, noting validity by digital computer technique
16 p2815 A69-32574

Effective rate coefficients of ion-molecular processes, dissipative recombination and ion production in F 2 layer at midlatitudes
17 p2966 A69-33979

Recombination and ionization coefficients for quasi-steady state homogeneous H and hydrogenic ion plasmas based on collisional-radiative model
22 p3988 A69-41153

Collisional radiative recombination and ionization coefficients for weakly ionized H plasmas using rate equations
22 p3988 A69-41154

IONIZATION COUNTERS

U RADIATION COUNTERS

IONIZATION CROSS SECTIONS

Ionization cross sections of excited states of hydrogen atoms and hydrogenoids calculated by Monte Carlo method
01 p0122 A69-10040

Electron impact ionization cross section in cesium vapor measured with Tate-Smith apparatus
01 p0137 A69-10285

Electrode geometry for mass spectrometer ion source to measure electron ionization cross section of low vapor pressure materials
01 p0080 A69-10605

Electron impact ionization cross sections and rate coefficients from ground state given for free atoms and ions from hydrogen to calcium
01 p0125 A69-10992

Multiphoton ionization cross section of atom via perturbed Green function, considering light wave electromagnetic field perturbing effects on atomic levels
02 p0283 A69-11539

Multiphoton ionization of molecular hydrogen and rare gases using Q switched Nd laser apparatus 02 p0283 A69-11701

Slow proton irradiation of ribonucleic thin layers, determining differential inactivation cross section for various proton energies 03 p0371 A69-13482

Collisional ionization cross section for Fe ions evaluated to estimate solar corona temperature 04 p0651 A69-14365

Emission continuum intensity of negative nitrogen ion in nitrogen and air plasmas 04 p0639 A69-15370

Emission cross sections of first negative band system of nitrogen under electron impact excitation 05 p0795 A69-15617

Three energy dependent quantities examined for gases, describing relation between ionization yields, cross section and loss functions 05 p0795 A69-15660

Atomic Li photoionization cross sections calculated with Brueckner-Goldstone many body perturbation theory 06 p0961 A69-17134

Electron impact excitation cross sections for emission from first negative bands of positive N molecule ion 06 p0961 A69-17135

Electron impact ionization cross sections for second quantum level of atomic H, using Born exchange approximation and Vainshtein approximation 06 p0961 A69-17138

Hydrogen molecule spectroscopy in vicinity of ionization limit, determining absorption and ionization cross sections and fluorescence 07 p1184 A69-18490

Photoionization cross section measurements for sodium line by analyzing electron-ion recombination radiation from sodium seeded plasma, determining electron temperatures and concentrations 07 p1184 A69-19164

Cross section calculations for elastic and inelastic electron collisions with atoms, ions and molecules and ionization of atomic systems by electrons and photons 07 p1187 A69-19660

Highly ionized low density plasmas production by strong UV radiation 08 p1360 A69-20080

Cross sections computed for excitation and ionization of atoms and ions by electrons, using peaking approximation to evaluate Coulomb-Born matrix approximation 08 p1355 A69-20206

Hydrogenic atoms ionization by high energy electrons, discussing cross sections for ejected electrons and total energy 08 p1356 A69-20738

Total ionization cross section for symmetric collisions measured as function of energy by using neutral atomic beams of neon and krypton 08 p1356 A69-20740

Electron impact cross sections for diatomic molecule ionization and excitation from modified Gryzinski theory, discussing results from molecular models 09 p1542 A69-22249

Complex trajectory method for describing tunnel effect during atom ionization in strong light wave field, using quasi-classical approximation 09 p1543 A69-22658

Polarized Hartree-Fock model computing photoionization cross sections for Li isoelectronic sequence, listing phase shifts for partial waves of scattered electrons 11 p1922 A69-25260

Cross section for ionization of atoms by positive ion bombardment near threshold 11 p1922 A69-25322

Optical cross section measurements for electron excitation from ground state of nitrogen 12 p2132 A69-26246

Average ionization cross sections of atomic and molecular H and He beams ionized by plasma electrons with Maxwellian velocity distribution 12 p2138 A69-26542

Ionization of rare gases /H and N/ by nitrogen ions, determining cross sections of formation of slow ions and electrons 13 p2304 A69-28440

Efficiency parameter beta for ion and electron production by meteoric processes, noting importance to nighttime sporadic E ionization 14 p2520 A69-29372

Binary encounter model for ionization by charged particle impact modified to evaluate cross section for ionization of positive ions by electron impact 14 p2489 A69-29996

Ionization within intersecting alkali atomic and slow electron beams, observing ionization cross sections increment near ionization threshold 15 p2655 A69-30726

Elementary processes cross sections in charged states changes during proton-hydrogen molecule interactions 15 p2655 A69-30963

Initial ionization processes in strong shock wave in hydrogen, determining ionization relaxation length and cross section of atom-atom excitation collisions 16 p2815 A69-31590

Emission continuum intensity of negative nitrogen ion in nitrogen and air plasmas 16 p2822 A69-32117

Energy spectrum of secondary electrons and fluorescent efficiency in 3914 Å band, obtaining ionization cross section 16 p2850 A69-32315

Cross sections threshold behavior for Cs II resonance lines excitation due to Cs ion-He collision 17 p3008 A69-33388

Differential cross sections for secondary electron production in atomic ionization by charged particle impact, using classical binary encounter approximation 17 p3009 A69-34189

Chemical reactions activation energy at high temperature, noting cross section shape role for deducing activation energy from rate data 18 p3099 A69-34443

Atomic excitation and ionization by thermal electrons, using Monte Carlo trajectories to determine adiabatic collisions effects on energy transfer near dissociation limit 18 p3176 A69-34790

Ground and metastable state photoionization cross sections of BaI to explain artificial Ba clouds, using many channel quantum defect method 18 p3177 A69-35238

Ion production in K/diatomic Br system by high energy K beam, obtaining total ionization cross section as function of energy 19 p3378 A69-36187

Atom-atom collisional excitation cross sections obtained from ionization cross sections, noting Thomson classical theory 20 p3580 A69-37500

Atoms and ions collision strengths and photoionization cross sections for nitrogen, oxygen and neon fitted to interpolation formulas for temperature and frequency effects 22 p3988 A69-41244

Cs ionization by bromine, measuring relative cross section velocity dependence by crossed molecular beam technique 23 p4194 A69-42208

Lyman alpha radiation from electron collisions with simple H-containing molecules, finding dissociative excitation cross section role 24 p4351 A69-43033

Ionization and light emission cross sections for collisions of protons and hydrogen atoms with atmospheric nitrogen used to analyze auroral events 24 p4368 A69-43177

IONIZATION FREQUENCIES

Electron impact ionization cross sections and rate coefficients from ground state given for free atoms and ions from hydrogen to calcium 01 p0125 A69-10992

Fast type r moving striations in plasmas and dependence of ionization frequency on electron mean energy 03 p0477 A69-13801

Nonequilibrium ionization rate in arc discharge, studying perturbations effect in near cathode Langmuir layer 04 p0635 A69-14763

Numerical decile value maps of sporadic E layer ionization critical frequency for each month of solar cycle minimum and maximum year 10 p1682 A69-23418

High latitude ionization spikes observed by POGO spacecraft, noting frequency correlation with magnetic disturbances and development by high energy electron injections 14 p2511 A69-28950

Photoionization rates temperature dependence in upper atmosphere for O atoms and molecules and N molecules from computer calculations, allowing for earth sphericity 23 p4157 A69-41857

IONIZATION GAGES

NT BAYARD-ALPERT IONIZATION GAGES

Magnetron ionization gauge in helium for low pressure measurement, discussing striking characteristics and time lags 01 p0012 A69-10606

Noiseproof ionization manometer with ion current dual modulation for ultrahigh vacuum measurement in magnetic field with extraneous charged particles interference 03 p0429 A69-13263

Nonmagnetic quadrupole ionization gauge, discussing systems design and electron oscillations 13 p2262 A69-28020

Ionization sensors and detectors classification and dynamic calibration for pressure measurement 13 p2262 A69-28083

Nonmagnetic ionization gage consisting of quadrupole lens systems excited at HF, discussing electron focusing during operation 13 p2263 A69-28084

Atmospheric density measurements by triaxial accelerometer system, ionization gauges and orbital decay of OV1-15 satellite 15 p2602 A69-31384

Buried collector ionization gage for measurements in 100 billion torr pressure range using shielded collector to lower X ray current 16 p2791 A69-32324

Bent beam ionization gage linearity from calibrated nude Modulated Bayard-Alpert /MBA/ gage, discussing buried collector and tabulated magnetron gages 22 p3950 A69-41216

IONIZATION POTENTIALS

Ionization losses of Ge 72 atoms stopping in Ge, noting no cut-off indicative of energy gap effects 01 p0140 A69-11245

Electrons relaxation caused by ionization and recombination in nonequilibrium plasma, using Kerrenbrock model 03 p0477 A69-13609

Cadmium ionization energy in InAs using heat treatment in hydrogen to eliminate anomalies 06 p0979 A69-16998

Plasma ionization enhancement by laser line radiation matched to specific atomic transitions [AIAA PAPER 69-47] 06 p0972 A69-18186

Partial reflections from ionosphere, analyzing electron number densities, noting relation between D region ionization increases and small solar proton events 07 p1205 A69-18956

Ion-molecule reactions constants studied directly in ionosphere, using air injection from geophysical probe and airborne RF mass spectrometer 08 p1311 A69-21159

Nighttime electric fields and vertical ionospheric drifts near magnetic equator concurrent measurements 09 p1489 A69-21705

Thermodynamic stability of dense plasma consisting of electrons and charged ions, plotting ionization potential as function of electron density and temperature 11 p1922 A69-24232

Chain mechanism of arc discharge development in crossed electric and magnetic fields explained by direct ionization of neutral particles by ions 11 p1932 A69-25540

Ionization fraction as independent variable in plasma transport correlation, noting role in pressure effect increase 13 p2313 A69-28241

High energy ionization bursts in cosmic ray showers electron photon component, obtaining bursts power spectrum and component energy dependence 13 p2332 A69-28404

Cesium ions decay time in thermionic converter operating in gas kinetic mode by pulse ionization, noting dependence on interelectrode potential distribution 14 p2403 A69-29252

MHD channel flow calculations by quasi one dimensional approximation, considering potential drops at electrodes 14 p2500 A69-29904

Approximate ionization potentials for high ionization stages of elements with atomic numbers 31 to 92 obtained by binding energy calculations 14 p2488 A69-29923

Ion nitride hardening of Mo-Ti alloy at 1300 degrees C in cathode glow discharge tube 15 p2637 A69-30212

Microwave induced ionization wave propagation in rare gases, noting rapid electron density increase at wave front and subsequent slow plasma decay
16 p2818 A69-31671

Stripping and low-energy collisions of H atoms on O and N molecules, showing target ionization to projectile stripping ratio dependence on ionization potential
16 p2814 A69-31773

MH-alpha 328-116 /V 1016 Cyg/ star spectrum, indicating object evolution toward higher ionization states
19 p3424 A69-36234

Absorption spectrum of NO molecule, analyzing f complexes electron structure, ionization potential and quadrupole moment
22 p3984 A69-40477

Dissociation energy and ionization potential measured for gaseous SiO and GeO
22 p3896 A69-40725

Ionization wavefronts nonlinear analysis including energy effects and ionization wave structure, discussing Joule heating due to transverse electric field
22 p3990 A69-40758

Ionization rate limiting processes behind strong shock waves in pure N, plotting electron density profile diagrams
24 p4302 A69-43367

IONIZED GASES

NT CATIONS
NT CESIUM PLASMA
NT CHARGED PARTICLES
NT COLD PLASMAS
NT COLLISIONLESS PLASMAS
NT COSMIC PLASMA
NT ELECTRON PLASMA
NT PLASMA CLOUDS
NT PLASMA JETS
NT PLASMA LAYERS
NT PLASMA SHEATHS
NT PLASMA SLABS
NT RELATIVISTIC PLASMAS
NT ROTATING PLASMAS
NT SOLAR WIND
NT STELLAR WINDS
NT THERMAL PLASMAS
NT TOROIDAL PLASMAS

High temperature, fully ionized plasma equation of state, using quantum statistical theory of low density electron-ion plasma in thermal equilibrium
01 p0128 A69-10346

Double probe characteristics in flame with electronegative gas injection interpreted in terms of conduction of ions in ionized medium
01 p0176 A69-10385

Faraday rotation of plane polarized microwave beam for measuring precursor ionization from exploding wire discharge in various gases
01 p0129 A69-10663

Statistical analysis of polarization of two component nonisothermal electron-ion Coulomb gas plasma containing microfluctuations
02 p0286 A69-11707

Scaling laws for RF discharge experiments in ionized environments, considering proper limit variables for simulation of electron density
02 p0283 A69-12241

Free fluid hydrodynamics equations applied to weakly ionized plasma stability, considering drift oscillations excitation
02 p0291 A69-12553

Automatic recording of neutral atom temperature and free electron density of partially ionized gas by Fabry-Perot interferometer
03 p0428 A69-13111

Decay stability of large amplitude neutral wave into two ion acoustic waves in weakly ionized plasma
03 p0475 A69-13158

Frictional forces and collision frequencies for ions moving in neutral gases
03 p0421 A69-13328

Tradeoffs among beam divergence, power output and mirror alignment tolerances of high power argon ion lasers operating in various low order transverse modes
03 p0440 A69-13549

Constants in formulas describing temperature and pressure dependence of thermodynamic characteristics of high temperature monatomic ionized gases for positive ions
03 p0473 A69-14156

Ionization fronts stability, taking into account ionizing photons absorption effect in H II region and interstellar magnetic field
04 p0650 A69-14363

Ionized medium effect on polarization of synchrotron radiation from monoenergetic distribution of electrons
04 p0648 A69-14420

Nonlinear and second order thermal diffusion of electrons in ionized gas
04 p0636 A69-14878

Partially ionized hydrogen transport coefficients, using expressions containing collision integrals for charged particles
04 p0637 A69-15051

Boltzmann equation for weakly ionized gas electron component, solved by transformation to integral equation, applied to Lorentz gas in alternating electric field
05 p0795 A69-15619

Continuous UV noble gas ion lasers, noting small signal gain and power output limit at various current densities for strong lines
05 p0775 A69-16321

Collision induced instability of partially ionized gases having large Ramsauer effect in external magnetic field, analyzing nonlinear characteristics
05 p0804 A69-16441

Electron distribution function for homogeneous weakly ionized gas in presence of alternating electric field, discussing solution of Boltzmann equations
05 p0797 A69-16604

Spatial and temporal characteristics of two component electron-ion nonisothermal plasma and penetration of external LF electric field into plasma
05 p0806 A69-16745

Longitudinal acoustic waves propagation in partially ionized gas in external electric field, taking into account ionic collisions with electrons and neutral particles
06 p0963 A69-17079

Stagnation point electrostatic probe measurements of flowing partially ionized high density monatomic gases
06 p0964 A69-17196

Ionized plasma electrical conductivity in magnetic field calculated by supplementing BGK collision terms with Vlasov equation
06 p0965 A69-17482

Weakly ionized wakes study in free quasi-molecular regime of supersonic flow, using Langmuir probe in wind tunnels, discussing ion density distribution
06 p0966 A69-17639

Weakly ionized gas flow past discontinuous wall potential used to study edge effects and interaction problems for single and multiple flush electrostatic probes
06 p0972 A69-18191

High efficiency ion lasers without additional axial magnetic field
06 p0938 A69-18221

Wall space charge layer effect on ion extraction from weakly ionized plasma, using quadrupole mass spectrometer
07 p1188 A69-18276

Stabilized frequency single mode ionized argon laser, discussing intensity of electric field in cavity and mode selector
07 p1145 A69-18475

Highly ionized plasma acceleration by intrinsic radiation achieved by deep cooling of free electrons
07 p1195 A69-19595

Electron collisional excitation cross sections for upper states in Ar ion lasers
07 p1157 A69-19656

Vacuum UV perturbation spectroscopy compatibility with resonance transitions in Ar ion laser
08 p1324 A69-20161

High Q capacitance loaded coaxial cavity resonator for study of electric susceptibility of ionized gas
08 p1313 A69-20214

Ambipolar diffusion in electron concentration inhomogeneities of weakly ionized plasma in magnetic field analyzed by linearized quasi-hydrodynamic equations
08 p1362 A69-20426

Collisional theory of longitudinal wave propagation for two fluid viscous ionized plasmas formulated from coupled Maxwell and Boltzmann equations
08 p1367 A69-20796

Partially ionized argon plasma stagnation flow past blunt body using multifluid theory, obtaining flow profiles
08 p1369 A69-20817

Partially ionized plasma oscillations in crossed magnetic and electric fields, noting role of LF particle collisions
08 p1370 A69-21079

Electrical conductivity of partially ionized plasma, noting nonapplicability of Enskog-Chapman method and use of Lorentzian gas model
09 p1546 A69-21584

High time resolution electrical conductivity measurement of ionized plasma gas flow, using changes in Q of circuit
09 p1546 A69-21588

Partially ionized Kr and Xe transport coefficients for various pressures and at high temperatures computed on basis of charged particle cross sections
09 p1548 A69-21935

Conductivity probe design for tenuous plasmas and ionized gases, discussing experimental confirmation of theoretical behavior
09 p1496 A69-21936

Temperature stability of slightly ionized gas for arbitrary collision cross sections, discussing electron temperature variation as function of electric field strength
09 p1551 A69-22039

Gas lasers, discussing amplification, resonance, internal and external mirror lasers, outputs, and He-Ne, carbon dioxide and ion lasers
09 p1517 A69-22121

Weak discontinuities in wave propagation, studying ionized gas nonsteady flow having electrical conductivity in magnetic field
10 p1727 A69-22916

Effect of degree of expansion of ionized gas in nozzle on specific power of MHD generator
10 p1636 A69-23103

Noble gas additives for triggering stability of pulsed argon ion lasers, discussing repetition rate and power loss
10 p1702 A69-23341

Unstabilizing effect of inhomogeneities on magnetoacoustic waves in slightly ionized gases with current perpendicular to magnetic field
10 p1734 A69-23459

Effective Ohm law for inhomogeneous weakly ionized gas and Hartmann flow analysis, noting electron density fluctuation effect on conductivity
10 p1735 A69-23462

Pulse and CW breakdown criteria for plasmas subject to spatially nonuniform electric fields, using variational formulation
10 p1739 A69-23650

Ionized gas flow from globule containing atomic H in interstellar space, noting surrounding H II region and radiation at ionization front
10 p1782 A69-23682

Neon discharges, discussing similarities in type p plasma ionization waves generated by pulsing
10 p1740 A69-23721

Transport and balance coefficients in ionized neon and helium plasmas in homogeneous electric field, calculating electron mobility, diffusion coefficient, energy and collision parameters
10 p1740 A69-23722

High temperature gas mixture plasmas thermodynamical properties, emphasizing Debye electrostatic interactions and electron states
10 p1810 A69-23794

Single mode generation and Lamb dip in argon ion gas laser obtained by thin quartz plate inserted near plane mirror of resonator
10 p1706 A69-24080

Electrical conductivity of partially ionized noble gases Ar, He, Xe and Kr, considering electron temperature and electron-electron interactions
11 p1923 A69-24295

Explosive and reversible onset of helical instability in weakly ionized discharge plasmas, noting ambient noise level role
11 p1924 A69-24299

Electron number density LF oscillations for ionized gas identified with periodic solutions to neutral and charged particle plasma continuity equations
11 p1925 A69-24315

Weakly ionized gas in crossed electromagnetic fields, formulating Ohm law from Ginzburg equations
11 p1925 A69-24319

Single frequency Ar ion laser for deep field holography noting thermal compensation, servo stabilization, operating mode, high power and high coherence
11 p1895 A69-24685

Low order transverse modes in Ar ion lasers, analyzing beam divergence, output, mirror alignment and cavity configurations
11 p1896 A69-24841

Nonlinear HF conductivity of fully ionized plasma considering applied electromagnetic field frequency close to electron plasma frequency
11 p1929 A69-25271

Ionosphere temperature profiles, discussing heating and cooling of electron gas and ion gases and thermal balance

12 p2063 A69-25903

Acoustic wave generation in neutral particle component of weakly ionized gas by variation of electron temperature with low power RF signal

12 p2134 A69-26096

Boundary layer parameters behind shock wave front in ionized gas calculated with allowance for charged particle diffusion

12 p2139 A69-26713

Joint probability distributions of electric microfield in hot ionized plasma consisting of noninteracting particles

12 p2139 A69-26871

M 31 galaxy ionized gas region high resolution spectroscopy, emphasizing radial velocities in O II lines at various distances from nucleus

12 p2163 A69-27020

Ionized gas cloud eruption from galactic nucleus deduced from observed hydrogen line at 5.1 cm

12 p2171 A69-27068

Soviet monograph on plasma diagnostics by lasers, describing interferometry, optical field visualization, schlieren and shadow photography

12 p2139 A69-27075

Infinitely long journal bearing using ionized gas lubricant with magnetic field applied axially and electric field applied transversely to fluid film [ASME PAPER 68-LUBS-30]

13 p2267 A69-27287

Plasma ion oscillations excited in plasma consisting of ion beam and thermal electrons produced by back diffusion sources

13 p2304 A69-27301

Transport equation describing drift, diffusion and reaction of iron swarm influenced by electric field in gas

13 p2306 A69-27457

Refractory ceramic materials thermal stability in high temperature subsonic ionized gas flow products, emphasizing zirconia and magnesia

13 p2285 A69-27472

Optical maser induced electrical breakdown interaction with superhigh pressure ionized gases, using optical interferometry and holography

13 p2273 A69-28464

Time and altitude induced variations in daytime NO and molecular and atomic oxygen ions

14 p2435 A69-29050

Ionized gas height scale changes in polar ionosphere obtained, assuming Chapman type ionization distribution

14 p2436 A69-29052

Partially ionized multicomponent gas mixture kinetics in strong electromagnetic field, determining magnetic field, stress tensors and transfer coefficients

14 p2492 A69-29610

Time averaged stress tensor for ionized plasma in HF electromagnetic field, considering collisions

14 p2493 A69-29649

Electrical conductivity ratio of weakly ionized turbulent gas to quiescent gas as function of electron temperature

14 p2502 A69-29991

Intrinsic quantum-mechanical behavior of fully ionized gas at high temperature and low density, defining classical limit

14 p2502 A69-29992

Free fluid hydrodynamics equations applied to weakly ionized plasma stability, considering drift oscillations excitation

15 p2658 A69-30250

Free electron concentrations and dispersion in H I regions noting ionized interstellar gas components role

15 p2681 A69-30420

Flush electrostatic probe edge effect, considering Couette flow of weakly ionized compressible gas past discontinuous wall potential

15 p2653 A69-30912

Distribution model for ionized interstellar gas over galactic disk for explaining radio emission absorption and depolarization from discrete sources

15 p2695 A69-30935

Ion-acoustic oscillations effect on weakly ionized plasma electrical conductivity, using BGK collision integral model

15 p2662 A69-30970

Mode competition of 5861 and 6470 A lines in ionized Kr laser attributed to electronic level excitation processes

15 p2635 A69-31106

Weakly ionized plasma electron heating by interaction with HF electromagnetic field calculated using Boltzmann transport equation

15 p2665 A69-31480

Disturbance currents from penetration of acoustic waves in weakly ionized gas, analyzing wave interaction with DC glow discharge

15 p2665 A69-31547

Electron concentration and mass density behind reflected shock in ionizing argon, using time resolved two wavelength interferometry

16 p2771 A69-31918

Boltzmann kinetic equation describing rarefied neutral or weakly ionized gas state evolution, showing solution existence, uniqueness and successive approximation convergence

16 p2814 A69-31958

Thermal diffusion coefficient for fully ionized plasma containing mixture of arbitrary charge ions in topside ionosphere

16 p2775 A69-32084

Ion momentum transfer through charge exchange in mixture of ion gases and parent neutral gases under thermal nonequilibrium, noting role of Boltzmann equation

16 p2822 A69-32108

Flow field of highly ionized arc heated supersonic free jet, using continuous flow test facility [AIAA PAPER 68-135]

16 p2772 A69-32153

Nonequilibrium ionized gas flow past insulated wall with corners under magnetic field, discussing flow characteristics

17 p3010 A69-32865

Preferential ion recombination in gases under high pressure, noting no dependence of recombination on average energy

17 p2949 A69-32999

Interferometric study of electron concentration and mass density profiles through ionized argon thermal end-wall layer formed in shock tube [AIAA PAPER 69-694]

17 p3074 A69-33477

Current distribution and scattering cross section of missile with plume/ionized trail/of tapered conductivity due to plane wave electromagnetic excitation

17 p2921 A69-33671

HF electromagnetic waves penetration into slightly ionized plasma analyzed by Maxwell and kinetic equations, giving penetrating electric field by WKB formula

17 p2932 A69-34220

Lorentz gas approximation to Boltzmann collision operator generalized for heavy molecule nonMaxwellian gas distribution function, obtaining equilibrium distribution applicable to ionized gas

18 p3179 A69-34438

Positive ion concentration in D region, using spherical stationary electrostatic probe in weakly ionized collision dominated gas

18 p3128 A69-34804

Ion collecting cylindrical electrostatic probes as flow field tracing instruments in low density slightly ionized flows

19 p3291 A69-35718

Plasma density and potential distributions along circular cylinder surface in weakly ionized high speed low pressure gas flow, noting boundary layer separation point

19 p3380 A69-35839

Forbidden lines emitted by gaseous nebulae, emphasizing relative intensities of O II and O III lines

19 p3422 A69-36220

Hypervelocity ionized gas flow analysis, allowing for finiteness of energy exchange duration between electrons and ions

19 p3379 A69-36383

Equilibrium Couette flow of ionized multicomponent ideal gas between moving catalytic plates, obtaining thermal flow formulas and thermal conductivity coefficient

19 p3240 A69-36403

Radio wave diffraction by inhomogeneities arising from ionized gas clouds in interstellar medium

19 p3428 A69-36882

Similarity rule in hydrodynamically transcritical regime in ionized multifluid gas

20 p3515 A69-37594

Electron-ion gas ambipolar diffusion effect on F 2 layer electron density vertical distribution variations

20 p3525 A69-37655

Low energy plasma escape flow from polar region (polar wind), examining H, He and O ions participation in expansion

21 p3713 A69-38528

Negative ion influence on electrical conductivity of partially ionized multicomponent gas mixtures, basing analysis on thermodynamic calculations of composition

21 p3774 A69-38867

Self similar solution to one dimensional isothermal ionized gas outflow from ionization front in half space filled with neutral gas exposed to quanta flux

21 p3771 A69-38997

Electron temperature profile across shock wave in weakly ionized nonequilibrium argon by numerical integration of energy conservation equation, noting three body recombination

21 p3698 A69-39791

Boltzmann equation analysis used to study near surface electron temperature for weakly ionized plasmas, showing nonequilibrium absorption layer governing electron temperature profile

22 p3989 A69-40528

Atmospheric small gaseous ions nature and properties, discussing solid elastic and composite interaction, complex, cluster, intermediate and Langevin ions, etc

22 p3940 A69-40538

Mars upper atmosphere ionized carbon dioxide and CO emission spectra in 1900-4300 A region measured by Mariner 6, observing atomic hydrogen and oxygen lines

22 p4023 A69-40568

Ionized plasma motion under plane piston action by self similar solution of Navier-Stokes equations

22 p3991 A69-41021

Electron transport coefficients determined for weakly and fully ionized gases under various conditions

23 p4195 A69-41517

Moving striations as plasma oscillations arising from transit time delays of neutral and charged particles moving through ionized gas, using continuity equation

24 p4356 A69-43122

Convective thermal flux at stagnation point in multicomponent partially ionized gas injected flow past body, considering effective ambipolar diffusion coefficient

24 p4246 A69-43485

IONIZED PLASMAS

U PLASMAS (PHYSICS)

IONIZING RADIATION

NT ALPHA PARTICLES

NT BETA PARTICLES

NT COSMIC RAY SHOWERS

NT COSMIC RAYS

NT FAR ULTRAVIOLET RADIATION

NT GAMMA RAY BEAMS

NT GAMMA RAYS

NT LYMAN ALPHA RADIATION

NT LYMAN BETA RADIATION

NT NEAR ULTRAVIOLET RADIATION

NT PRIMARY COSMIC RAYS

NT SECONDARY COSMIC RAYS

NT SOLAR COSMIC RAYS

NT SOLAR X-RAYS

NT ULTRAVIOLET RADIATION

NT X RAYS

Meteorological rocket measurement of ionizing radiation flux in upper atmosphere, noting flux decrease with increasing electron energy

01 p0144 A69-10586

Gas chromatography technique for separation and purification of chemical compounds for ionizing radiation detectors

02 p0249 A69-12011

Information theory application to study of biologically stimulating effects of low ionizing radiation doses, thermal energy and other environmental factors

03 p0369 A69-13434

Accelerated helium and carbon ions effects on mutation-induction and nuclear inactivation in Neurospora crassa compared with X rays, discussing relative biological effectiveness (RBE)

03 p0373 A69-13490

Ionizing action of radiation due to heating substance in laser beam focus, discussing highly ionized plasma production

03 p0479 A69-13998

Radiation processed wood-plastic materials produced by impregnating natural wood with liquid monomer followed by ionizing radiation induced polymerization

04 p0605 A69-14582

Solar X ray source identification using D layer ionization behavior during eclipse

04 p0650 A69-15533

Microorganisms and viruses susceptibility to sterilization by ionizing radiation, heat and combination of radiation and heat, considering space materials damage elimination

05 p0713 A69-15947

Space flight factors, ionizing radiation and combined effects on vitamin C content in onion bulbs
05 p0708 A69-16510

Large area X ray collector, matrix detector for ionizing radiation and inflatable gas counter, considering application to X ray optics and astronomy
05 p0794 A69-16587

Prediction technique for surface effect causing Si bipolar transistors gain degradation under ionizing radiation
06 p0976 A69-16879

Ionizing radiation effects in microcircuits, using lumped model technique to derive mathematical model from electronic characteristics and boundary values of each semiconductor
06 p0977 A69-16886

Ionizing radiation-initiated degradation of deoxyribonucleic acid in bacteria, noting role of defective prophage
07 p1068 A69-19494

Linville model for describing elementary phenomena of electronic equipment in terms of physical data applied to irradiated semiconductor diode and transistor
08 p1280 A69-19974

Synergistic effects of prolonged heat exposure and whole body irradiation with ionizing radiation on survival time in hamsters
08 p1263 A69-20174

Ionizing radiation effects on space charge of MOS devices, showing electron-hole pairs within oxide and electron injection from cathode
08 p1373 A69-20864

Corpuscular radiation contributions to D layer ionization determined from intensity measurements
09 p1577 A69-21770

Space electric fields research by artificial clouds of vaporized barium launched by rockets, noting neutral atmosphere and ionospheric results
09 p1492 A69-22800

Chemical and biological means of safeguarding body of astronaut against ionizing radiation and vibration
10 p1648 A69-23297

Ionospheric disturbances after July 7, 1966 proton flare noting flare ionizing radiation, high energy solar proton effects and low energy solar plasma
10 p1684 A69-23784

Drift and tunnel effect of MOS transistors under ionizing electron and X ray irradiation, considering fabrication, electrical characteristics and D-2 satellite tests
11 p1848 A69-24873

Planar transistor gain degradation under weak ionizing radiation, considering operating voltage and temperature conditions
11 p1848 A69-24874

Ionizing radiation effects on combustion of ammonium perchlorate compacts with and without fuel addition, considering X ray, electron and plasma radiation
11 p1941 A69-25194

Soviet book on quality control of materials and machine parts by ionizing radiation covering radiation hazards and protection
13 p2268 A69-27935

Sublethal ionizing radiation doses effect on hemolytic immunocompetent spleen cells in mice upon using chemical radiation protectors
13 p2210 A69-28334

Solar ionizing radiation sources, discussing activity at sunspot minimum, temperature, density and solar wind effects, X ray and UV spectra, etc
15 p2673 A69-30007

Meteorological rocket measurement of ionizing radiation flux in upper atmosphere, noting flux decrease with increasing electron energy
15 p2675 A69-30756

Planar bipolar transistors degradation under thermal and ionizing radiation stresses, analyzing surface recombination currents of silica films and silica-silicon interfaces
15 p2625 A69-30826

Passive components reliability subjected to ionizing radiation for families, types, batches and individuals
15 p2627 A69-30838

Diurnal variations in radiation sensitivity of mice and rats to irradiation with median lethal doses, noting sine curve survival function
15 p2557 A69-31458

Myocardial changes in rabbits after general chronic ionizing irradiation attributed to lower cardiac activity, hypertrophy and dystrophy
17 p2906 A69-32929

Cosmic ionizing radiation effects on electronic elements operation based on radiation and matter interaction principles
17 p2937 A69-33583

Auroral absorption bays from 1963 to 1964, noting effect of ionization agent intensity changes on absorption diurnal variations
17 p2965 A69-33965

X ray absorption in surrounding gas sphere as function of continuous absorption, electron scattering and diffuse ionizing radiation, using radiative transfer theory
18 p3186 A69-34296

Space flight factors, ionizing radiation and combined effects on vitamin C content in onion bulbs
18 p3095 A69-34729

Biological effects of radioactivity and X rays irradiation of whole body and cells, considering DNA degradation
19 p3257 A69-35978

Solar ionizing radiation increase during flares of 21 and 23 May 1967 determined from ionospheric electron density concentrations
20 p3590 A69-37558

Collection of papers on mechanisms of biological action of ionizing radiation covering radiation sickness dynamics, radiation damage, X ray effects, etc
21 p3656 A69-39049

Nervous system reactions and resistance to ionizing radiation noting role of functional, morphological and physicochemical changes in nerve tissues
21 p3659 A69-39061

Ionizing radiation histological and neurohistological effects in rabbits esophagus, stomach and ileocecal region intramural plexes
21 p3659 A69-39063

S-4 human blood experiment during Gemini 2 flight, studying spaceflight ionizing radiation interaction effects on single and multiple break chromosome aberrations
23 p4085 A69-41600

IONOGRAMS

Ducted echoes on topside ionograms and whistler diffuseness at midlatitudes, noting common occurrence of phenomena
01 p0029 A69-10551

Ionospheric perturbations involving stratifications at various heights move toward LF and HF sections of ionograms
03 p0423 A69-13538

Criticism of overlay analysis method for F 1 region ionograms
05 p0757 A69-16403

Ray tracing of Z-mode in tilted layer ionosphere to explain Z-mode echoes in ionograms
05 p0758 A69-16412

Sporadic E layers compared with model of electron concentration profile, using rocket measured profile data for computing ionogram
06 p0922 A69-17750

Formulas for ray paths in ionized layers with application to oblique ionograms and duct modes
07 p1078 A69-18913

Single polynomial analysis of ionograms, determining electron density profiles from small number of measured heights
07 p1125 A69-18915

Synthesis of oblique incidence ionograms for quasi-linear ionospheric model with spherical earth-ionosphere geometry neglecting geomagnetic field
08 p1274 A69-20044

Electron density profile from oblique ionogram calculated by iteration, assuming concentric spherically stratified ionosphere
10 p1684 A69-23826

E region radio waves triple splitting observed in probe ionograms, analyzing diurnal and seasonal variations in Z component reflections occurrence
12 p2031 A69-26686

Ionograms in vertical depletion duct in horizontally stratified isotropically refractive plasma, considering vertical propagation and ray paths traces dependence on electron concentration
14 p2434 A69-28945

Ionograms for nonmonotonic vertical distribution of electron concentration in ionosphere from rocket and ground sounding
14 p2437 A69-29071

ISIS A satellite fixed and sweep frequency ionograms indicating electron density variations, ionospheric resonances and Cerenkov radiation
15 p2604 A69-31416

High latitude stations vertical ionograms in absence of ionospheric reflections due to low solar activity periods, discussing interpretation methods
20 p3529 A69-37690

Ionogram processing procedure, discussing presence of vertically moving ionospheric disturbances
20 p3529 A69-37691

Data acquisition and processing ionograms from Alouette satellites telemetered sweep frequency topside sounding data
20 p3503 A69-37866

Receiving and display telemetry system for obtaining direct ionospheric topside ionograms from Alouette satellite, discussing video data tape recording cost
20 p3507 A69-37868

Real time pulse frequency modulation telemetry receiving system for direct readout of ionograms from topside sounders, using off-shelf components
20 p3508 A69-37866

Alouette 1 and 2 topside sounder ionograms analyzed with emphasis on low electron density, spread F and field aligned propagation
20 p3529 A69-37866

Electron density profiles from topside ionogram compared to ground based sounding results, discussing error corrections
20 p3495 A69-37866

Computer aided data interpretation system converting ionograms to vertical electron density profiles
20 p3504 A69-37866

Alouette 2 ionograms secondary resonances data indicating day-night effect in relative frequency of occurrence
20 p3496 A69-37889

Two-hop signals observed on high latitude Alouette 2 topside ionograms found propagating in field aligned cylindrical ionospheric ducts
20 p3531 A69-37896

Sideband structure of transmitted frequency spectrum exhibited by plasma wave features on topside ionograms, noting harmonic resonances
20 p3496 A69-37899

Propagation characteristic model study of kinked Z trace observed on topside ionograms and explained by magnetoionic theory
20 p3531 A69-37899

Alouette topside ionograms of ionospheric storms at midlatitudes indicating critical frequencies difference between F 1 and F 2 layers
20 p3532 A69-37899

Proton cyclotron echoes on ionograms obtained from topside ionosphere by Alouette 2 satellite
24 p4310 A69-43181

IONOSONDES

Phase ionosonde cost, possibilities and errors
01 p0071 A69-11161

Graphs of ionospheric measurements by vertical incidence sounding during Antarctic expedition, describing instrumentation and sounding techniques
10 p1681 A69-23311

Ionospheric data acquisition and utilization for improved radio communications, considering contact between engineers and physicists, ionosondes, data reliability for prediction, etc
17 p2961 A69-33401

Ionosonde electric circuit modified to permit radio wave absorption measurements over wide frequency range, calculating electron collision frequencies in ionosphere
17 p2968 A69-33999

Kinesonde radio sounding system for three dimensional ground observations of E region microstructure and vertical motion of neutral air and ions
18 p3125 A69-34250

IONOSPHERE

NT D REGION
NT E-2 LAYER
NT E REGION
NT F REGION
NT F 1 REGION
NT F 2 REGION
NT LOWER IONOSPHERE
NT SPORADIC E LAYER
NT UPPER IONOSPHERE

Ionospheric plasma electrostatic resonances from Alouette satellite signal observations
01 p0067 A69-10989

Midlatitude ionospheric wind profiles noting seasonal and time differences in circulation patterns, speed, shear, wavelength, energy content and dissipation
01 p0072 A69-11171

Electrostatic plasma wave instabilities in ionosphere along auroral field lines, noting critical electron flux and subsequent acceleration of electrons
01 p0075 A69-11222

Free atmospheric turbulence theory extended to include ionosphere, deriving equations for horizontal ionospheric wind together with turbulence coefficient
02 p0274 A69-11671

- Charged particle motion caused by ELF electromagnetic waves in presence of constant magnetic field, noting earth ionosphere application
02 p0240 A69-11712
- Mariner 4 Martian ionospheric data interpreted in terms of E, F1 and F2 regions
02 p0320 A69-12113
- Mariner 4 ionospheric densities to deduce Martian atmospheric modes, discussing validity of using ionospheric properties to discriminate between models
02 p0320 A69-12114
- Gain from communications operation at maximum usable frequency estimated on basis of long range ionospheric prediction technique adapted to computer
03 p0421 A69-13377
- Earth ionosphere resonator natural frequencies, considering diurnal variation and geomagnetic field eccentricity
03 p0422 A69-13512
- Portable amplitude and frequency recording system for studying ionosphere by radio signals from artificial satellites
04 p0597 A69-14748
- Ionosphere structure, properties and research techniques
04 p0594 A69-15166
- Curvilinear plasma motions in ionosphere same as cyclones and anticyclones in troposphere, solving ionospheric unstable wind as function of pressure gradients
06 p0919 A69-17722
- Planetary distribution of ionospheric parameters analyzed, using geographic longitude and magnetic inclination as longitudinal and latitudinal coordinates
06 p0921 A69-17745
- Synthesis of oblique incidence ionograms for quasi-linear ionospheric model with spherical earth-ionosphere geometry neglecting geomagnetic field
08 p1274 A69-20044
- Ion-molecule reactions constants studied directly in ionosphere, using air injection from geophysical probe and airborne RF mass spectrometer
08 p1311 A69-21159
- Solar quiet day variations studied by annual amplitude dependence on number of sunspots, considering E layer ionization
09 p1575 A69-21550
- Daily observational results of solar phenomena, cosmic rays, geomagnetic variations, ionosphere, radio wave propagation and airglow arranged according to solar rotation number
10 p1771 A69-22808
- Weakly attenuated components of VLF mode spectrum associated with propagation below anisotropic ionospheres as function of frequency and azimuth
10 p1655 A69-23417
- Low energy particles during solar proton flare and effects on magnetosphere, cosmic ray intensity, ionosphere and geomagnetic activity
10 p1768 A69-23786
- Reflection coefficient of electromagnetic wave reflected from thin ionization layer, using frequency dependence of amplitude to estimate ionospheric layer thickness
10 p1686 A69-23912
- Electron flux parameters determination from ionograms and reflected signal amplitudes between 120-130 km, considering electron collision frequencies
10 p1688 A69-23931
- Ionosphere temperature profiles, discussing heating and cooling of electron gas and ion gases and thermal balance
12 p2063 A69-25903
- Production source of ionization due to low energy electron influx and inclusion in ionospheric continuity equation, noting quiet ionosphere
12 p2066 A69-26112
- Nightglow intensity variations at sunspot minimum from measurements in South West Africa, considering relationship to ionospheric vertical movements and density variations
12 p2066 A69-26133
- Sea tides and ionospheric effects on lunar variation of geomagnetic field vertical component
12 p2161 A69-26957
- Free atmospheric turbulence theory extended to include ionosphere, deriving equations for horizontal ionospheric wind and turbulence coefficient
13 p2295 A69-28709
- Gain from communications operation at maximum usable frequency estimated on basis of long range ionospheric prediction technique adapted to computer
14 p2433 A69-28827
- I-V characteristics of electron emitting satellite in ionosphere, analyzing spherical Langmuir probe in collisionless plasma in magnetic field
14 p2511 A69-28956
- Suprathermal electrons energy distributions as function of magnetic latitude in polar ionosphere obtained by Explorer 31 satellite observation
14 p2512 A69-28963
- Correlation function of auroral reflection radio signals with allowance for polar ionospheric scattering and pulse signal transmission and reception
14 p2436 A69-29055
- Electron flux-atmosphere interaction solved by numerical integration on computer, discussing auroral ionosphere
14 p2513 A69-29069
- Ion chemistry of D and E regions to be studied during years of solar maximum in framework of IQSY/IUCSTP
14 p2439 A69-29111
- Daytime ionospheric screening effect on low latitude geomagnetic micropulsations estimated using ionosphere model
14 p2441 A69-29380
- Soviet collection of papers on ionosphere covering polarization state of reflected radio waves, ionospheric models, inhomogeneities
14 p2443 A69-29861
- Ion-molecular reactions measurements in ionosphere by VV type device and RF mass spectrometer
15 p2603 A69-31407
- Radar Thomson scatter from nonthermal steady state level of plasma waves in ionosphere measured, studying role of angle between wave vector and magnetic field
16 p2818 A69-31678
- Atmospheric density at 130-160 km measured from satellite 1968-59B orbit, noting agreement with CIRA 1965
16 p2776 A69-32095
- Solar quiet day variations studied by annual amplitude dependence on number of sunspots, considering E layer ionization
16 p2851 A69-32545
- Earth core conductivity effects on ionospheric shielding against geomagnetic changes from external sources, noting earth-ionosphere coupling
17 p2959 A69-32925
- Geomagnetic field effects on microwave noise spectrum in earth-ionosphere resonator, calculating field energy spectrum near resonance maximum, discussing excitation by lightning
17 p2918 A69-33034
- Langmuir probe to determine space vehicle orientation in ionospheric or interplanetary plasma, discussing apparatus, accuracy and application
17 p3001 A69-33222
- Steady state plasma wind tunnel for flow around ionospheric satellites, studying wakes of cylinders and spheres
17 p2893 A69-33488
- [AIAA PAPER 69-673]
Ionospheric studies - Conference, Alma-Ata, U.S.S.R., September 1965
17 p2965 A69-33977
- Soviet book on ionospheric processes summarizing published studies covering neutral atmosphere structure, ionizing solar radiation component composition and intensity, etc
18 p3126 A69-34358
- Near and antipodal fields in earth-ionosphere waveguide using mode theory, ray theory, zonal harmonics series and method of images to derive field representations
19 p3283 A69-35931
- Radio wave sphericity influence on scattering at moving body wake in ionosphere, determining scattering cross section principal maximum
20 p3486 A69-37024
- Cold plasma approximation of whistler excitation of lower hybrid resonance at wake of body moving through ionosphere, comparing results with Alouette satellite observations
20 p3519 A69-37025
- Earth ionosphere and magnetosphere electrodynamics state analyzed as function of neutral gas small scale motions, considering magnetic disturbances and ionospheric discontinuities
20 p3519 A69-37026
- Solar activity effect on short term meteorological processes and dynamic state of mesosphere and ionosphere, emphasizing relationship to entire atmosphere dynamics
20 p3590 A69-37684
- Retarding potential analyzers determining ionospheric structure, noting linearization of analysis
22 p3940 A69-40523
- LF hydromagnetic waves propagation along geomagnetic field lines in gyrotropic ionosphere model taking Hall effect into account
23 p4157 A69-41864
- IONOSPHERE EXPLORER A**
U EXPLORER 20 SATELLITE
IONOSPHERIC ABSORPTION
U ELECTROMAGNETIC ABSORPTION
IONOSPHERIC BLACKOUT
U BLACKOUT [PROPAGATION]
IONOSPHERIC COMPOSITION
D region composition at and shortly after sunrise, noting negative ion factor changes, ionization source and quasi-equilibrium conditions
01 p0066 A69-10597
- Ionic composition and temperature of nighttime topside ionosphere from analysis of incoherent backscatter spectra, discussing solar activity effects
01 p0076 A69-11233
- Rocket sounding for studying positive ions nighttime composition in E layer after magnetic storm at midlatitudes
02 p0239 A69-11686
- Algorithm for N/h ionospheric profiles calculations using both x and o magnetoionic components, taking into account interlayer and underlying ionization influence
02 p0239 A69-11687
- Plasmapause and relation to ion composition in topside ionosphere, using Bohm coefficient for turbulent diffusion
02 p0246 A69-12741
- Dissociative velocity rates of oxygen and ozone in ionosphere obtained by exponential approximation for molecular concentration distribution
02 p0246 A69-12769
- High power radar for investigating ionosphere by incoherent scatter technique
03 p0398 A69-13768
- Ion cut-off whistlers observed during VLF experiment aboard OGO 2 and OGO 4, noting possible application to relative ionospheric proton concentration determination
03 p0426 A69-14029
- Total ionospheric electron content determination from measurement of phase differences of satellite transmission, discussing data processing and differential Doppler effect measurements
04 p0592 A69-14766
- Ionosphere structure, properties and research techniques
04 p0594 A69-15166
- Ionospheric plasma flute instability considered as possible cause of occurrence of elongated small scale inhomogeneities in F2 layer
08 p1309 A69-20425
- Radio waves polarization scattered at ionospheric discontinuities analyzed for vertical incidence, determining modulus distributions and polarization factor argument
09 p1453 A69-21527
- Ions and electrons in ionosphere diffusion tensor components and ambipolar diffusion coefficient expressions derived for nonisothermal plasma
12 p2071 A69-26700
- Horizontal gradients below satellite orbit effect on reduced and minimum difference in Doppler frequency shifts of coherent radio waves from satellite in inhomogeneous ionosphere
13 p2219 A69-27701
- Rocket sounding for studying positive ions nighttime composition in E layer after magnetic storm at midlatitudes
13 p2258 A69-28717
- Algorithm for N/h ionospheric profiles calculations using both x and o magnetoionic components, taking into account interlayer and underlying ionization influence
13 p2258 A69-28718
- OGO 5 spectrometric studies of topside ionospheric ion concentrations, noting difference between nighttime and sunlit pass
15 p2599 A69-31345
- Diurnal variations of atmospheric ion composition at 100-200 km from rocket experiments
15 p2603 A69-31401
- Ionospheric ion composition at 130-155 km during meteor shower Orionides activity from geophysical rocket-borne RF mass spectrometer data
15 p2603 A69-31406
- Nighttime, twilight and daytime rocket experiments for ion composition of polar ionosphere at 100-180 km
15 p2604 A69-31414

Simultaneous solution of continuity and heat conduction equations for ionospheric plasma consisting of electrons, atomic O ions and neutral gas species, discussing varying solar flux effects
16 p2849 A69-32082

Simultaneous solution of continuity and heat conduction equations for ionospheric electrons, ions and neutral species for studying F region magnetic storm behavior
16 p2775 A69-32083

Radio waves polarization scattered at ionospheric discontinuities analyzed for vertical incidence, determining modulus distributions and polarization factor argument
16 p2754 A69-32522

Vertical ionospheric perturbations shown responsible for Z component in F region
17 p2969 A69-34000

Simultaneous ionospheric ion and electron measurements by various radiophysical methods, relating results to period of flight of vertical space probe
20 p3486 A69-37028

Reactions determining ion composition in E region, discussing neutral composition variations from day to night and during solar activity cycles
20 p3520 A69-37031

Soviet collection of papers on ionospheric studies covering ionospheric composition, propagation, disturbances, sounding, etc
20 p3523 A69-37654

High latitude ionosphere data from Alouette-ISIS program, describing various F, E and D regions parameters
20 p3530 A69-37868

Ionospheric parameters of ion and electron density and temperature and ionic species compared by direct measurement probes on Explorer 31 satellite
20 p3531 A69-37882

Ionic composition determined by combining Alouette topside sounder electron density profiles with electron and ion temperatures measured by ground based Thomson scatter sounder
20 p3532 A69-37898

F region vertical density profiles for positive ions and neutral molecules of various gases determined from rocket-borne mass spectrometer data
21 p3702 A69-38354

Ionosphere characteristics in terms of airglow, describing daytime F/D layers formation model provided by photoionization, loss processes and ambipolar diffusion
21 p3712 A69-38517

Daytime electron and ion composition model for height range from 150 to 1500 km at moderate latitudes and minimum solar activity
21 p3714 A69-38555

Nighttime F region nonlinear recombination and variable drift effects, suggesting empirical model
21 p3715 A69-38559

Rocket measurements of diurnal variations of F region concentrations and temperature of molecular N and O, showing disagreement with satellite drag data
22 p3939 A69-40515

Nighttime F region time-altitude variations in aeronomic parameters calculated under conditions close to solar activity maximum
23 p4156 A69-41844

RF impedance probe used for ionospheric composition measurements, describing antenna operation in ion-electron cyclotron frequency range
24 p4308 A69-43008

IONOSPHERIC CONDUCTIVITY

Solar eclipse effects on ionospheric conductivity and geomagnetic field at and near dip equator observed at Huancayo, Peru
02 p0241 A69-11728

Diurnal variation in horizontal magnetic component of South American stations close to electrojet during IGY
02 p0246 A69-12771

Conductivity and permittivity for ion and electron resonance region of ionospheric plasma model calculated in quasi-hydrodynamic approximation
10 p1686 A69-23908

Geomagnetic field directed hydromagnetic waves propagation in lower ionosphere, noting inhomogeneous conductivity, Hall effect and lines of forces role
10 p1687 A69-23926

D region ionizable constituent density/presumably nitric oxide/ measured, using blunt probe to detect changes in conductivity produced by Lyman alpha ionizing radiation
15 p2598 A69-31316

Ionosphere D region low field conductivity in presence of high field disturbing signal, assuming inelastic electron-neutral particle collisions
16 p2850 A69-32190

Faraday rotation measurements in ionosphere by geostationary satellite ATS-3 as evidence of considerable nighttime electron transport
17 p2959 A69-32926

Nocturnal D region conductivity enhancement relation to X radiation from Scorpius XR-1 and other sources, calculating ion production rate
17 p3024 A69-33378

Venus magnetosphere induced by piling up magnetic field from solar wind due to ionospheric conductivity and collisions with planetary atmospheric particles
21 p3794 A69-38381

Sharply bounded homogeneous ionospheric model to solve modal equation, discussing lower ionospheric conductivity from VLF transmission sudden enhancements of strength /SES/
21 p3714 A69-38554

IONOSPHERIC CROSS MODULATION

Ground based partial reflection and cross modulation or wave interaction techniques compared for studying D region electron densities
15 p2606 A69-31537

IONOSPHERIC CURRENTS

NT AURORAL ELECTROJETS

NT EQUATORIAL ELECTROJET

Magnetic field data fromOGO-2 spacecraft and surface magnetic observatories, noting magnetic storm occurrence and magnetosphere inflation and detection of polar ionospheric currents
01 p0069 A69-11125

Ionospheric current systems for various selected very quiet and slightly disturbed international quiet days based on Northern Hemisphere observatories data
03 p0423 A69-13518

Geomagnetic field quiet day solar variations current system calculated, using 2000 LT as zero level basis
03 p0424 A69-13541

Nighttime E layer mean variations noting critical frequencies, electron density and seasonal and solar activity effects at sunset, midnight and sunrise
03 p0398 A69-13899

Field aligned Birkeland currents generation at auroral latitudes
05 p0755 A69-16266

Energy transfer through ionospheric electrons, discussing degradation of fast electrons and role of neutral gas motion in ionospheric currents
07 p1128 A69-19369

Average geomagnetic storm ranges as function of latitude, noting disturbances caused by ring and ionospheric currents
09 p1489 A69-21715

Ionospheric movements from sampling radio diffraction pattern at 89 points and conversion into visible pattern
09 p1492 A69-22756

Toroidal magnetic fields in ionosphere associated with solar quiet daily variations producing electric current and equatorial auroral electrojets
10 p1681 A69-22805

Dynamo action produced magnetospheric currents in ionosphere computable without knowing real horizontal ionospheric current system
10 p1685 A69-23836

Electrical phenomena in upper atmosphere and solar wind may control geomagnetic disturbances and aurorae
10 p1686 A69-23903

Rocket sounding data on ionospheric currents at mid and low latitudes, showing absence in D and above E region
10 p1686 A69-23909

Solar quiet currents in three dimensional ionosphere, considering ionospheric conductivity and horizontal layer equations
12 p2074 A69-26955

Computer program for worldwide analysis of mean hourly values of field components into constituent fields and associated ionospheric current systems
12 p2074 A69-26958

Tangential solar wind discontinuity observed by Vela 2A satellite, producing ground magnetic disturbances conjunctively with magnetospheric, ground and ionospheric currents
14 p2512 A69-29041

Surface impedance of spherical earth isolated by nonconducting atmosphere from ionospheric currents producing alternating electromagnetic field
14 p2438 A69-29082

Strong vertical wind in low ionosphere due to short period reflected gravity waves, obtaining standing wave system
15 p2606 A69-31444

Wind effects on ionospheric electric currents, using equivalent circuits to study tidal modes and current patterns
16 p2775 A69-32083

U shaped polar auroras development, examining relation with magnetic activity and current system configuration in lower ionosphere
17 p2963 A69-33923

Electric field variations in vicinity of auroral form from motions of Ba vapor clouds released from Nike Tomahawk rockets
18 p3128 A69-34923

Ionospheric electric current systems dynamics in polar latitude in relation to 1966 geomagnetic storms
18 p3130 A69-35188

Rocket-released magnetometer probe for upper atmospheric measurements, discussing construction, flight, sensitivity and ionosphere current detection
19 p3309 A69-35992

Lower ionosphere electric fields and currents vertical profiles above geomagnetic equator under quiet geomagnetic conditions from rocket data
20 p3521 A69-37053

High latitude magnetospheric convection patterns determined from ionospheric current distribution using magnetic disturbance plots
21 p3709 A69-38503

Field-aligned currents effect on ionosphere and precipitation of auroral primary particles, analyzing with mathematical model of ionospheric density height distribution
21 p3710 A69-38506

Ionospheric currents geophysical DC electric fields measurement from sounding rockets, indicating anticorrelation with auroral luminosity
21 p3710 A69-38508

Ionospheric perturbations generation by time variable alternating electrical currents at polar latitudes, constructing radiation patterns for gravitational waves
23 p4155 A69-41842

IONOSPHERIC DISTURBANCES

NT SUDDEN IONOSPHERIC DISTURBANCES

Ionospheric irregularities height measurement using spaced receivers for recording satellite signals
01 p0064 A69-10428

Sporadic E layer boundary frequencies disturbances at midlatitudes, noting solar activity effects, diurnal variations and effect of meteor fluxes
01 p0066 A69-10600

Linearized perturbation treatment developed for photochemical and dynamical effects in gravity wave production of E-region ionospheric irregularities, including ion convergence
01 p0073 A69-11175

Cross field plasma instability resulting in charge density irregularities shown to meet requirements for ionospheric irregularities model
01 p0073 A69-11178

Equatorial and auroral electrojets, discussing origin theories and ionospheric irregularities
02 p0236 A69-11433

Space diversity reception as applied to radio astronomical investigation of large scale ionospheric inhomogeneities
02 p0237 A69-11665

Effective temperature values of ozone used to determine onset time and disturbance height in ionosphere
02 p0238 A69-11670

Anomalous radio wave absorption in polar aurora region ionosphere, discussing disturbance characteristics
02 p0207 A69-11688

F layer disturbance showing pronounced difference in corpuscular flux effect on day and nighttime ionosphere
03 p0512 A69-13517

Ionospheric perturbations involving stratifications at various heights move toward LF and HF sections of ionograms
03 p0423 A69-13538

Sporadic E irregularities in producing amplitude variations in radio star observations and satellite transmission
04 p0594 A69-15125

Antarctic spread F irregularities, examining models and performing ray tracing
04 p0595 A69-15439

Sudden VHF phase anomalies produced by solar flare induced ionospheric disturbances during July 1968
05 p0719 A69-15980

Lower ionospheric diurnal variations in electron density observed by beacon satellite, noting effect on high power VHF forward scatter circuits
05 p0757 A69-16405

Satellite scintillation at high latitudes and possible relation to soft particle precipitation
05 p0757 A69-16406

Ionospheric irregularities movement theories
05 p1125 A69-16416

Spatial distribution of vertically moving ionized formations in ionosphere suggests acoustic gravity waves excited in polar regions as cause
06 p0922 A69-17749

Coherent frequencies method for irregular component of satellite signal phase lead due to ionospheric inhomogeneities between satellite and ground station
06 p0890 A69-17799

Period fluctuations in ionospheric plasma resonance amplitude, proposing hypothesis in terms of quasi-electrostatic surface waves guided by antenna wire
07 p1125 A69-18847

Magnetospheric and high latitude ionospheric disturbances, bulk motion /convective/ flow pattern and electric field distribution
07 p1128 A69-19370

Ionospheric and tropospheric effects on microwave propagation including Faraday rotation, atmospheric refraction, attenuation and noise
08 p1272 A69-19958

Ionospheric plasma flute instability considered as possible cause of occurrence of elongated small scale inhomogeneities in F 2 layer
08 p1309 A69-20425

Lower ionosphere effect on LF electromagnetic disturbances, comparing propagation and damping of clockwise and counterclockwise polarized waves
09 p1487 A69-21637

Model of auroral backscatter from E region including ionospheric refraction, comparing computations to experimental HF auroral backscatter data for aspect sensitivity
09 p1488 A69-21700

Regular disturbance in topside ionosphere on summer nights from continuous records of ionospheric electron content, discussing magnetic activity and sunspot number effects
09 p1489 A69-21703

Irregular regions in Antarctic ionosphere from Polar Ionosphere Beacon Satellite S-66 recordings, obtaining irregularities density from nulls clarity
09 p1490 A69-21716

Ionospheric disturbances after July 7, 1966 proton flare noting flare ionizing radiation, high energy solar proton effects and low energy solar plasma
10 p1684 A69-23784

Subauroral traveling ionospheric disturbances and fading due to diffraction observed by geostationary satellites
10 p1685 A69-23831

Ionospheric discontinuities drift velocities from diversity reception data indicating no dependence on solar activity
10 p1686 A69-23911

Hourly N/h/ profiles of F region calculated from nomograms by normal integral method during magnetic disturbance, measuring region temperature
10 p1687 A69-23928

Diurnal variations in sporadic E layer and wind in ionosphere during equinox and solstice periods, noting wind shear mechanism and ambient electron density
10 p1688 A69-23932

Midlatitude ionospheric disturbances accompanied by auroral type radio absorption observed by radio astronomy and probes during May 26, 1967 storm
10 p1688 A69-23935

Acoustic waves in ionosphere relation to electron content fluctuations detected from beacon satellite BE-B signals
[AFCR-69-0291] 12 p2065 A69-26104

Space diversity reception as applied to radio astronomical investigation of large scale ionospheric inhomogeneities
13 p2257 A69-28696

Effective temperature values of ozone used to determine onset time and disturbance height in ionosphere
13 p2257 A69-28701

Anomalous radio wave absorption in polar aurora region ionosphere, discussing disturbance characteristics
13 p2224 A69-28719

Large scale ionospheric inhomogeneities anisotropy, dimensions and drift velocities from simultaneously measured irregular refraction
14 p2436 A69-29053

Radio astronomical observations of shape and drift velocity of focusing ionospheric discontinuities
14 p2436 A69-29054

Radio waves propagation along polar auroras region, obtaining ionospheric parameters for magnetic disturbances based on penetration probability
14 p2436 A69-29058

Oscillations intervals with diminishing period observed during magnetic storms, noting relationship to midlatitude disturbances in F region
14 p2436 A69-29060

Linearized perturbation for photochemical and dynamical effects in internal atmospheric gravity wave production of E region ionospheric irregularities
14 p2440 A69-29128

Multiple ground based geophysical sensors for detecting ionospheric phenomena, discussing continuous magnetic tape data recording, common time base and station operation
14 p2448 A69-29526

Zonal drift influence on morning ionization anomaly in F region, noting shifts to West with increasing height and electron production rate
14 p2442 A69-29732

Inhomogeneities effect on polarization of radio waves reflected from ionosphere, based on permittivity tensor
14 p2417 A69-29862

Ionospheric inhomogeneity model for motion of infinite elliptical cylinder of cold plasma in neutral particle flow and ambient electrostatic and magnetostatic fields
14 p2500 A69-29864

Ionospheric inhomogeneities models for plasma motions, considering electron-ion collisions
14 p2443 A69-29865

Radio equipment for studying ionospheric inhomogeneities using space diversity reception, presenting vertical component of drift velocities of small scale inhomogeneities
14 p2453 A69-29876

Fresnel irregularities calculated from radio wave partial reflection from lower ionosphere measured by rocket probes
15 p2604 A69-31420

Faraday rotation measurements of signals from Explorer 22 analyzed to determine scintillation boundary in auroral ionosphere
15 p2605 A69-31443

Charge density irregularities of midlatitude ionospheric E region related to cross field plasma instability noting turbulence
16 p2773 A69-31972

Ionization troughs below F 2 layer maximum due to ionospheric disturbances detected by Antarctica ionograms direction of arrival data
16 p2775 A69-32080

Satellite radio signal scintillation variations association with sporadic E and spread F and dependence on magnetic activity in Southern Hemisphere during sunspot minimum
16 p2780 A69-32307

Ionospheric winter anomaly duration in height range of mesopause region based on zenith angle dependence of absorption at LF
16 p2782 A69-32456

Synoptic observations of F 2 region in magnetically conjugate regions of Kerguelen and Archangel, comparing critical frequencies during magnetic and ionospheric disturbances
16 p2784 A69-32612

Horizontal drifts and anisotropy of irregularities in ionospheric F 2 region by pulse fading drift records
17 p2960 A69-33164

Ionosphere depression influence on VLF signals phase and amplitude calculated by mode theory and integral equations system representing aperture fields
17 p2920 A69-33418

Daytime magnetoionospheric disturbances in auroral zone, discussing time lag of perturbations for absorption and geomagnetic field bays
17 p2964 A69-33962

Traveling ionospheric disturbances in form of large scale electron concentration discontinuities created by propagating internal gravitational waves
17 p2966 A69-33980

Ionospheric electron concentration variation during positive perturbation based on N/h/ profiles
17 p2967 A69-33986

Vertical ionization displacements in F region as trace distortions on ionograms observed at low, mid and high altitudes during daytime
17 p2969 A69-33998

Vertical ionospheric perturbations shown responsible for Z component in F region
17 p2969 A69-34000

Radio echo from south showing origin from irregularities in F but not E region, discussing propagation modes for particular record
18 p3125 A69-34252

ELF and VLF wave propagation examined for heavy ions and lower ionospheric disturbance effects using numerical integration, noting standing wave field role for interpretation
18 p3125 A69-34254

Scattering of electromagnetic waves obliquely incident on inhomogeneous plasma column of parabolic radial density distribution, noting applications to ionospheric irregularities
18 p3102 A69-34963

Ionospheric radio propagation, considering D and F region theory and ionospheric disturbances
19 p3303 A69-36428

Nighttime F 2 region temperature distribution under geomagnetically calm and disturbed conditions calculated from Alouette 1 satellite data
19 p3304 A69-36623

Ionosphere disturbances due to high altitude thermonuclear explosions, discussing experimental proof by Cosmos satellites short wave transmitter radio signal scintillation statistical evaluation
19 p3304 A69-36624

Earth ionosphere and magnetosphere electrodynamic state analyzed as function of neutral gas small scale motions, considering magnetic disturbances and ionospheric discontinuities
20 p3519 A69-37026

Perturbed ionospheric regions acting as radio wave focusing lens, discussing frequency, power and pattern selection
20 p3486 A69-37048

Positive and negative correlations in F 2 layer perturbations observed by network of paired conjugate ionospheric stations at low latitude
20 p3521 A69-37050

Atmospheric phenomena effects on terrain imaging radar systems performance, discussing tropospheric turbulence and ionospheric irregularities
20 p3490 A69-37647

F zero layer occurrence relation to solar, magnetic and ionospheric activity levels variations from Ashkhabad observations /1958- 1964/
20 p3527 A69-37671

Ionospheric and magnetic disturbances at midlatitudes related, noting individual and simultaneous disturbances
20 p3527 A69-37673

F 2 layer midlatitude positive disturbances observed during IGY on quiet and disturbed days, noting positive to negative transition latitudes
20 p3527 A69-37674

Small scale inhomogeneities motions in E and sporadic E layers, processing data with method of full correlation analysis and statistical method
20 p3528 A69-37683

Vertically moving disturbances relationship to behavior of E and F layers over Tiflis, noting sporadic E layers formation
20 p3528 A69-37685

Vertically moving ionospheric disturbances altitude estimated from geomagnetic pulsations in earth electromagnetic field
20 p3528 A69-37686

Correlation analysis accuracy using Fischer transformation in processing recorded data of small scale ionospheric inhomogeneities
20 p3503 A69-37688

Ionogram processing procedure, discussing presence of vertically moving ionospheric disturbances
20 p3529 A69-37691

Ground station equipment for studying motions and structure of ionospheric inhomogeneities by combined space-frequency diversity reception, noting altitude dependence of ionospheric parameters
20 p3510 A69-37693

Topside equatorial ionosphere structure and behavior, describing anomaly development and decay
20 p3530 A69-37869

Ionospheric electron density irregularities observed by topside sounders showing shape, dimensions across magnetic field and variation percent, discussing resulting radio echoes
20 p3530 A69-37870

Doppler observations of ionospheric motions associated with magnetic micropulsations, noting hydromagnetic and neutral gas waves
20 p3535 A69-38194

Particle trapping and plasma oscillations in satellite disturbed ionosphere observed from Ariel and Alouette

measurements, discussing frequency and wavelength relation 21 p3787 A69-38357

Simulation and display for radar ground-backscatter signatures by computer ray tracing, using model ionosphere containing realistic traveling disturbances 21 p3717 A69-39280

Latitude variation of radio satellite scintillation related to small scale ionospheric irregularities 22 p3899 A69-39972

Fluctuations of polarization induced fading periods in short wave transmissions of Soviet earth satellites, showing relation to ionospheric inhomogeneities 22 p3942 A69-41095

Thermonuclear explosion Operation Starfish effect on ionospheric state from recording in Central Kazakhstan, studying frequency characteristics 22 p3942 A69-41097

Ionospheric perturbations generation by time variable alternating electrical currents at polar latitudes, constructing radiation patterns for gravitational waves 23 p4155 A69-41842

Ionization irregularities in equatorial E region observed in various scale sized by rocket-borne Langmuir and plasma-noise probes 23 p4160 A69-42430

Ionospheric irregularities effect on accurate satellite position determination in near real time 23 p4132 A69-42549

Solar X-ray spectrum as function of sunspot group type based on Solrad satellites flux data, discussing relationship to lower ionosphere characteristics variations 24 p4372 A69-43615

IONOSPHERIC DRIFT

North-south ionospheric drift velocities near magnetic equator, noting marked seasonal characteristics and diurnal variations 01 p0062 A69-10138

Electrostatic polarization field formation by acoustic wave propagation through ionosphere, calculating effect on ionization drift velocity 01 p0068 A69-11110

Phase path variations at three closely spaced points, measuring horizontal drifts at E region level, investigating time shift variability in spaced fading records 03 p0421 A69-13329

Horizontal drifts at E region level measured in India by spaced phase path technique 03 p0421 A69-13330

Plasma drift global distribution due to neutral gas motion in F 2 region, noting effect on electron concentration distributions 03 p0422 A69-13513

Nighttime variations of F region electron density profiles at Puerto Rico, discussing seasonal and solar cycle variations in temperature and vertical drift velocity 03 p0503 A69-14017

Drift periodic echoes in outer zone electron flux due to magnetospheric disturbance 05 p0815 A69-16259

Ionospheric drift measurements made on adjacent antenna arrays during IQSY 05 p0757 A69-16409

Solar cycle influence on winds in lower ionosphere 05 p0759 A69-16421

Day and night reversals in NmF2 north-south asymmetry related to neutral wind direction 06 p0918 A69-17384

Energy transfer through ionospheric electrons, discussing degradation of fast electrons and role of neutral gas motion in ionospheric currents 07 p1128 A69-19369

Nighttime electric fields and vertical ionospheric drifts near magnetic equator concurrent measurements 09 p1489 A69-21705

Nonequilibrium ionization in central regions of low temperature plasma, describing charged particle drift by using diffusion time concept 10 p1732 A69-23440

F 2 layer drift relation to current systems of dynamo region confirmed at middle and high latitudes 10 p1682 A69-23611

Ionospheric discontinuities drift velocities from diversity reception data indicating no dependence on solar activity 10 p1686 A69-23911

Ionospheric irregularities drift and anisotropy parameters variation with true reflection height during magnetically disturbed conditions 10 p1659 A69-24062

Vertical ionization drift in F region as function of electron density, ionization coefficient and recombination coefficient 12 p2070 A69-26584

Diurnal and seasonal variations in drift velocity vector of small scale inhomogeneities in F 2 region 12 p2070 A69-26688

Vertical drift velocity of ionospheric F region during eclipse and on control day based on chemical reaction coefficients models, discussing electron density distribution 12 p2077 A69-27109

Position stability of ionospheric sporadic E layer 14 p2435 A69-29038

Large scale ionospheric inhomogeneities anisotropy, dimensions and drift velocities from simultaneously measured irregular refraction 14 p2436 A69-29053

Radio astronomical observations of shape and drift velocity of focusing ionospheric discontinuities 14 p2436 A69-29054

Zonal drift influence on morning ionization anomaly in F region, noting shifts to West with increasing height and electron production rate 14 p2442 A69-29732

Drift of F 2 layer inhomogeneities compared for IGY and IQSY 14 p2443 A69-29866

Similarity and correlation methods for drift of ionospheric inhomogeneities in Antarctica 14 p2444 A69-29867

F 2 region small scale inhomogeneities drift observations showing seasonal and diurnal velocity and direction changes 14 p2444 A69-29868

Ionospheric sporadic E layer inhomogeneities drift, discussing altitude dependence of velocity and direction 14 p2444 A69-29869

Random motions velocity of ionospheric inhomogeneities by extreme lines delineation of diffraction pattern during amplitude recording of reflected signal 14 p2444 A69-29872

Frequency diversity reception system for drift of small scale ionospheric inhomogeneities, noting circuit diagrams 14 p2452 A69-29875

E region ionization redistribution by neutral winds, comparing calculated vertical drift velocities to observed electron density profiles 15 p2677 A69-31395

Correlation between F region electrons vertical motion velocity variations and E region electrons horizontal motions in equatorial ionosphere 16 p2779 A69-32193

Combined midlatitude neutral air wind and equatorial electrodynamic drift effect on F 2 layer diurnal variations 16 p2781 A69-32316

Horizontal drifts and anisotropy of irregularities in ionospheric F 2 region by pulse fading drift records 17 p2960 A69-33164

E region horizontal drift measurements at Ahmedabad from 1956 to 1966, noting solar activity and seasonal influences 17 p2962 A69-33678

E layer inhomogeneities analysis concerning drift, chaotic processes, statistical parameters and reliability of data processing 17 p2962 A69-33896

Vertical distribution of ionospheric drift velocity in auroral zone, evaluating role and intensity of electric field formed in dynamo region 17 p2964 A69-33964

Magnetic declination effect on F 2 layer critical frequency diurnal variations attributed to vertical ionospheric drift due to neutral air winds 18 p3126 A69-34256

Wind velocity components calculation at F-sphere maximum level, taking into account electrodynamic drift of ionospheric plasma and ion motion 20 p3519 A69-36972

Upper ionosphere Thomson scatter, electron number density measurements and topside sounding results during geomagnetic storms using electrodynamic drift theory 20 p3530 A69-37872

Causal and semiphenomenological theories concerning equatorial F 2 region, discussing electrodynamic drift theory and transequatorial winds 20 p3531 A69-37888

Ionosphere drift measurements in LF range, noting relationship between correlation and similar-fade analyses for velocity data 21 p3714 A69-38557

Nighttime F region nonlinear recombination and variable drift effects, suggesting empirical model 21 p3715 A69-38559

Magnetic activity effects on horizontal drifts, anisotropy and random change characteristics of E region ionization irregularities 21 p3715 A69-38561

Daytime drift velocities and signal fading characteristics of equatorial and blanketing sporadic E layer irregularities, noting independence of electrojet intensity 23 p4160 A69-42429

IONOSPHERIC ELECTRON DENSITY

Night ionosphere electron content changes in Southern Hemisphere, discussing diffusion from exosphere and corpuscular radiation as sources of ionization 01 p0063 A69-10423

Electron production rate and density created by galactic and solar cosmic rays in lower D region, considering ionization for PCA 01 p0063 A69-10426

Topside ionosphere average height distributions of electron density and geomagnetic field intensity from Alouette 2 data over Japan, noting ionic composition 01 p0065 A69-10548

Electron density and temperature, ion density, composition and temperature and plasma space potential relative to space vehicle potential measured by spherical probe assembly 01 p0065 A69-10549

Radio waves incoherent scattering to measure electron concentration profiles at mean latitudes, allowing for collisions 01 p0065 A69-10575

Ionization, neutralization and charge exchange processes in ionosphere, detailing dependence of photodissociation and collision detachment of negative ions 01 p0066 A69-10598

Spacecraft ionospheric probe for simultaneous measurement of electron temperature and density, plasma space potential, ion composition, etc 01 p0081 A69-10760

Soviet studies of ionospheric electron densities by means of geophysical rockets and satellites 01 p0067 A69-10944

Amplitude scintillations of satellite radio signals during sunrise due to ionospheric turbulence induced electron content variations 01 p0067 A69-10980

Nighttime sporadic E rocket measurements, discussing descending layer thickness and electron density and lower boundary 01 p0071 A69-11165

Vertical wind profiles and electron density profiles in E region, determining time dependence and ionization drift velocity 01 p0072 A69-11172

Electron concentration in ionospheric outer regions determined from coherent frequencies recorded on-board OGO-A 01 p0147 A69-11323

Ionospheric electron content, slab thickness and scintillation occurrence measurements at low latitude stations 02 p0235 A69-11427

Ionospheric electron density determined from Faraday effect, using ATS-3 radio signals 02 p0237 A69-11660

Seasonal variations in thickness of ionospheric E-F interlayer region during daylight and maximum integral ionization values 02 p0239 A69-11682

E region electron concentration measurements during large solar zenith angles, noting anomalous behavior during low solar activity periods 02 p0239 A69-11683

Ionosphere studies in France noting lower ionosphere dynamics, ionospheric winds, plasma electron densities, electron and ion temperature and ion-neutron collision frequency 02 p0242 A69-11903

Middle ionosphere temperature diurnal variations analyzed on basis of rocket experiments and electron density asymmetry 02 p0246 A69-12768

Electron and positive ion density measurements during nighttime auroral absorption event 03 p0421 A69-13327

Plasma drift global distribution due to neutral gas motion in F 2 region, noting effect on electron concentration distributions

03 p0422 A69-13513

Electron concentration profile change in ionospheric F region in auroral zone during negative magnetic bay disturbances

03 p0423 A69-13530

Electron concentration in lower ionosphere based on measurement of Faraday rotation of polarization plane of radio waves scattered by meteor trail

03 p0423 A69-13535

Nocturnal electron concentrations and temperature at Manitoba measured by rocket-borne Langmuir probe, compared with F 1 region

03 p0502 A69-14008

Nighttime variations of F region electron density profiles at Puerto Rico, discussing seasonal and solar cycle variations in temperature and vertical drift velocity

03 p0503 A69-14017

Midlatitude nighttime total ionospheric electron content during magnetically disturbed periods from geostationary satellites Canary Bird and ATS 3

03 p0426 A69-14030

Total ionospheric electron content determination from measurement of phase differences of satellite transmission, discussing data processing and differential Doppler effect measurements

04 p0592 A69-14766

Bearing deviation in model HF transionospheric propagation with three dimensional electron density variation and no magnetic field

04 p0559 A69-15209

Mechanism for noon electron concentration maximum in F region at midlatitudes found to be recombination process

05 p0753 A69-16031

Error introduced into total electron content data by changes in ionospheric layer height

05 p0816 A69-16281

Lunar tide effect on height distribution and velocity of ionospheric electron density daily variations near magnetic equator

05 p0756 A69-16401

Internal atmospheric gravity waves in F region observed with electron density profiles deduced from vertical incidence ionograms, obtaining phase velocities

05 p0756 A69-16402

Lower ionospheric diurnal variations in electron density observed by beacon satellite, noting effect on high power VHF forward scatter circuits

05 p0757 A69-16405

Simultaneous rocket measurements of D region temperatures and electron densities on anomalous winter day

05 p0758 A69-16411

Ionospheric electron content and slab thickness changes during magnetic storm in June 1965 using Faraday rotation and critical frequencies

05 p0759 A69-16420

Electron formation in lower ionosphere due to cosmic ray-atmosphere interaction, analyzing ionization of subrelativistic and relativistic solar and galactic cosmic rays

06 p0920 A69-17726

Ionospheric D layer electron concentration profile from radio wave absorption frequency dependence

06 p0920 A69-17729

Sporadic E layers compared with model of electron concentration profile, using rocket measured profile data for computing ionogram

06 p0922 A69-17750

Formation dynamics of thin sporadic layers of E region, determining maximum ionization and electron concentration and electron-neutral atoms collision frequency

06 p0922 A69-17751

Electron density distribution stationary with respect to sun determined by Alouette 1 measurements over winter pole, noting relation to high density plasma

06 p0922 A69-18224

Approximation formulas of Appleton-Hartree equations for nighttime medium wave frequency absorption in E region of ionosphere, discussing electron density

07 p1122 A69-18295

Solar eclipse variations of E layer critical frequency explained by quasi-equilibrium between electron density and ionizing soft X ray radiation

07 p1204 A69-18823

Single polynomial analysis of ionograms, determining electron density profiles from small number of measured heights

07 p1125 A69-18915

Partial reflections from ionosphere, analyzing electron number densities, noting relation between D region ionization increases and small solar proton events

07 p1205 A69-18956

Faraday rotation measurements using incoherent scatter to obtain ionospheric electron density profiles

07 p1085 A69-19223

D region electron density vertical profiles measured using partially reflected echoes from lower ionosphere

08 p1307 A69-20189

D region electron concentrations and collision frequencies obtained from high power wave interactions experiment, presenting average winter collision frequency model

09 p1489 A69-21702

Regular disturbance in topside ionosphere on summer nights from continuous records of ionospheric electron content, discussing magnetic activity and sunspot number effects

09 p1489 A69-21703

Diurnal variation of D region electron production rates, discussing Lyman alpha ionization of nitric oxide

09 p1577 A69-21717

Electron production rates variations in lower ionosphere cosmic layer related to meteorological, geomagnetic and cosmic conditions

10 p1759 A69-22839

Cosmic ray absorption and modulation in lower ionosphere at midlatitudes, considering 11 year variations, Forbush effects and solar radiation on electron concentration

10 p1759 A69-22840

Ionospheric conditions following solar proton flare observed with topside sounders of Alouette satellites, showing electron density depletion and hydromagnetic wave relationship

10 p1684 A69-23781

Incoherent scatter measurements of F region electron concentrations at solar activity minimum

10 p1684 A69-23825

Electron density profile from oblique ionogram calculated by iteration, assuming concentric spherically stratified ionosphere

10 p1684 A69-23826

Nonlinear charge exchange and dissociative recombination effects on night F region decay compared with linear theory

10 p1685 A69-23832

Topside ionospheric electron density profiles compared for magnetically quiet and disturbed periods surrounding December 17, 1962 magnetic storm

10 p1685 A69-23835

Ionospheric measurements of electron density, electron and ion temperature profiles from strength of incoherent radio wave scattering

10 p1686 A69-23910

Ionospheric slopes and range frequency characteristics obtained from oblique incidence sounding of horizontally nonuniform ionosphere

10 p1686 A69-23914

Hourly N/h profiles of F region calculated from nomograms by normal integral method during magnetic disturbance, measuring region temperature

10 p1687 A69-23928

Molecular reaction rates and ion/electron vertical profile and concentrations in equatorial ionosphere, applying computer simulation to numerical solution of continuity equations

10 p1688 A69-23929

Diurnal variations in sporadic E layer and wind in ionosphere during equinox and solstice periods, noting wind shear mechanism and ambient electron density

10 p1688 A69-23932

Ionospheric electron content gradients from Faraday rotation observations of radio beacon satellites for direction finding of HF radio waves

11 p1837 A69-25004

Nighttime maxima anomaly in electron concentration of ionospheric F layer at midlatitudes, considering diffusion and recombination

12 p2064 A69-26007

Acoustic waves in ionosphere relation to electron content fluctuations detected from beacon satellite BE-B signals

[AFCLR-69-0291]

12 p2065 A69-26104

Vertical ionization drift in F region as function of electron density, ionization coefficient and recombination coefficient

12 p2070 A69-26584

Electron concentration fluctuation in ionospheric inhomogeneities estimated from Cassiopeia A radio emission

12 p2070 A69-26687

Electron concentration in polar ionosphere measured by coherent scattering method

12 p2071 A69-26703

Lower ionosphere electron densities measured during solar eclipse by Nike-Apache rockets

12 p2073 A69-26861

Vertical drift velocity of ionospheric F region during eclipse and on control day based on chemical reaction coefficients models, discussing electron density distribution

12 p2077 A69-27109

Global coverage of positive ion composition and temperature, and electron density and temperature measurements during AURORAE mission of ESRO 1 satellite

13 p2253 A69-27753

Ionospheric electron density determined from Faraday effect, using ATS-3 radio signals

13 p2256 A69-28691

Seasonal variations in thickness of ionospheric E-F interlayer region during daylight and maximum integral ionization values

13 p2257 A69-28713

E region electron concentration measurements during large solar zenith angles, noting anomalous behavior during low solar activity periods

13 p2258 A69-28714

Magnetic storm time variations of electron concentrations in upper ionosphere near north geomagnetic pole, discussing magnetic time, altitude and latitude dependence

14 p2510 A69-28939

Ionospheric electron and ion temperatures correlated with electron concentration profile as measured by rockets and satellites

14 p2510 A69-28942

Ionograms in vertical depletion duct in horizontally stratified isotropically refractive plasma, considering vertical propagation and ray paths traces dependence on electron concentration

14 p2434 A69-28945

Ionospheric horizontal discontinuities of electron density distribution parameters effect on penetration frequency, skip distances and arrival angles

14 p2436 A69-29057

Ionograms for nonmonotonic vertical distribution of electron concentration in ionosphere from rocket and ground sounding

14 p2437 A69-29071

Radio wave absorption coefficient in lower ionosphere related to total radiation absorption and electron concentration profile

14 p2411 A69-29075

Electron density profiles in outer ionosphere and integral of electron density measured with coherent radio waves emitted from Electron satellite

14 p2438 A69-29106

Seasonal variations of electron density profiles in lower ionosphere measured by differential absorption using partial reflections

14 p2438 A69-29109

Noon electron densities between 65-90 km from measurements of differential absorption of partial reflections, discussing seasonal variations at midlatitudes

14 p2439 A69-29110

British and Soviet D region electron density distributions from same VLF and LF propagation data

14 p2439 A69-29112

Rocket sounding measurements of ionospheric D region electron density profile during 20 May 1966 solar eclipse, discussing D region ionization source

14 p2439 A69-29116

Rocket measured electron densities of nighttime auroral E region over Canada at different magnetic activity levels, noting frequency and plasma density relations

14 p2439 A69-29117

Polar cap absorption riometer recorded during 2-6 September 1966 event compared to satellite measurements of solar protons, discussing diurnal variations and oxygen role in associative detachment reactions

14 p2440 A69-29126

Radio wave reflections from edge of large scale depressions of ionospheric electron density observed by topside sounding satellites, discussing ionogram recordings

14 p2415 A69-29521

Sporadic E layer frequency characteristics dependence on reflected signal fading, showing fine structure influence and maximum value of mean electron concentration

14 p2442 A69-29733

Radio signals F region scattering related to electron density fluctuations in ionosphere

14 p2444 A69-29870

Radio waves incoherent scattering to measure electron concentration profiles at mean latitudes, allowing for collisions

15 p2597 A69-30745

Sporadic E layer nighttime electron density profiles obtained by Langmuir probe equipped sounding rockets

15 p2603 A69-31398

Electron temperature observation in daytime ionosphere, considering energy loss to ions and neutral particles

15 p2603 A69-31402

Morning, daytime and nighttime rocket measurements of electron flux in upper atmosphere at 80-165 km altitudes, noting energy flux

15 p2677 A69-31413

ISIS A satellite fixed and sweep frequency ionograms indicating electron density variations, ionospheric resonances and Cerenkov radiation

15 p2604 A69-31416

Simultaneous middle and low latitude Thomson scatter measurements, comparing electron density, temperature and exospheric temperature data on quiet and disturbed days

15 p2604 A69-31418

Gyroplasma probe data from rocket observations, determining winter ionospheric electron density profiles, electron temperature and electrostatic cyclotron waves effect

15 p2606 A69-31446

Ground based partial reflection and cross modulation or wave interaction techniques compared for studying D region electron densities

15 p2606 A69-31537

Rocket measurements of upper F region electron temperature and density profiles, for particle and energy balance of ionosphere topside, noting diffusive equilibrium

16 p2848 A69-31975

Polar Ionosphere Beacon Satellite S-66 signals measured for large scale horizontal gradients in total electron content of Antarctic ionosphere at sunspot minimum and maximum

16 p2774 A69-31989

Lunar tidal variations of electron concentration in F 2 region near magnetic equator showing large latitudinal dependence

16 p2776 A69-32090

Nighttime decreases in F 2 layer heights at near conjugate stations in low latitudes, using electron density profiles

16 p2778 A69-32186

LF ground based absorption results compared with rocket measured D region electron density profiles

16 p2778 A69-32188

F 2 critical frequency data at Hawaii for clarifying total electron content data obtained by geostationary satellite measurement of Faraday signal rotation

16 p2779 A69-32196

Decameter waves Doppler shift shown inversely proportional to wave frequency from electron density variation caused by acoustic wave propagation in ionosphere

16 p2755 A69-32610

First order Doppler shift in ionosphere and horizontal gradients influence, discussing total electron content determination method made from geodetic satellites using two coherent frequencies

16 p2755 A69-32614

Doppler shift measurements at two coherent frequencies from Diadem satellites to determine ionospheric electron content, discussing accuracy and parameters defining satellite passage

16 p2785 A69-32615

Electron production rate in low ionosphere, discussing parameters of ionizing solar cosmic rays and earth environment

17 p3022 A69-33035

Rocket-borne AM radio receiver for Faraday rotation experiments to measure lower ionosphere electron density, giving circuit diagrams

17 p2936 A69-33062

Spectrum and cross section of radio wave scattering in two temperature plasma, relating differential backscattering cross section to ionospheric electron density fluctuations

17 p2930 A69-33895

High latitude geomagnetic disturbances, incoming electron fluxes and riometric absorption relationship in lower ionosphere studied by X ray bremsstrahlung with sounding balloons

17 p2964 A69-33961

Unsteady model taking into account photoionization, neutralization and diffusion, describing electron concentration diurnal and seasonal variations in ionosphere F 2 region at midlatitudes

17 p2966 A69-33978

Traveling ionospheric disturbances in form of large scale electron concentration discontinuities created by propagating internal gravitational waves

17 p2966 A69-33980

Lower ionosphere electron concentration confirmed as function of electron and ion temperature by satellite and probe data

17 p2966 A69-33981

Postsunset apparent reflection height and electron density variability in equatorial F 2, discussing singularities of diurnal variation in November-January

17 p2967 A69-33984

Ionospheric electron concentration variation during positive perturbation based on N/h profiles

17 p2967 A69-33986

Planetary ionospheric effect of 15 July 1959 sudden commencement magnetic storm based on N/h profiles of earth day and night sides

17 p2967 A69-33987

Solar flares with subcosmic radiation in proton active region of May 1967, discussing X ray emission effects, calculating D region recombination coefficient and electron concentration

17 p3025 A69-34226

Ionospheric absorption and virtual heights relationships for electron density distribution in lower ionosphere, computing model profiles

18 p3125 A69-34248

Irregularities distribution in antarctic ionosphere from polarization angle fluctuations of satellite S-66 radio signals, discussing diurnal magnetic and solar cycle effects

18 p3125 A69-34249

Reexamination of polar F region electron density diurnal variation data contradicting King-Kohl theory of rotating neutral winds role

18 p3125 A69-34255

Anomaly of F region electron content vs polar geographic latitude and local mean time

18 p3126 A69-34257

Lower ionospheric electron concentration and collision frequency measurements by Nike-Apache rockets, suggesting geomagnetic anomaly in D region

18 p3127 A69-34798

D region electron densities from multifrequency absorption measurements by proton spectra analysis, noting cubic approximation

18 p3127 A69-34799

Equatorial electrojet current distribution determined using equivalent circuit method and magnetic force model, noting electron density profile influence on current density

18 p3130 A69-35186

Ionospheric data of local and integral electron concentration obtained by measuring phase shift of satellite emitted coherent radio waves

20 p3519 A69-37022

Ionospheric electron content and concentration variations analysis based on data of radio waves propagating from satellite, considering Doppler shift and Faraday effect

20 p3486 A69-37027

Simultaneous ionospheric ion and electron measurements by various radiophysical methods, relating results to period of flight of vertical space probe

20 p3486 A69-37028

F region electron and ion concentration vertical distribution, discussing various ionization reactions

20 p3520 A69-37030

Solar ionizing radiation increase during flares of 21 and 23 May 1967 determined from ionospheric electron density concentrations

20 p3590 A69-37558

Predawn F 2 layer critical frequency enhancement at Johannesburg, discussing electron density hump from corpuscular ionization increase

20 p3523 A69-37576

Electron-ion gas ambipolar diffusion effect on F 2 layer electron density vertical distribution variations

20 p3525 A69-37655

Temperature effect on electron concentration steady distribution in F 2 layer

20 p3525 A69-37657

Altitude variations at and near maximum electron concentration in quiet F 2 layer during solar activity maximum from sounding at southern geomagnetic pole

20 p3526 A69-37662

Electron density distribution in northern and southern polar regions ionosphere based on 1958 and 1959 observations at high geomagnetic relatively low geographic latitudes

20 p3526 A69-37664

Occurrence, development and disappearance of diffused reflections, relating dynamic behavior to ionospheric electron concentration

20 p3529 A69-37687

RF impedance probe digital system for ionospheric measurements based on antenna resonance phenomena

20 p3542 A69-37791

Doppler technique for ionospheric electron density measurement by VLF ground based radio transmitter noting HF method

20 p3542 A69-37792

Topside ionogram reduction for ionospheric electron density determination, using geomagnetic strength at all heights, iteration and change of variables

20 p3529 A69-37864

Electron density profiles from topside ionograms compared to ground based sounding results, discussing error corrections

20 p3495 A69-37865

Global electron density distribution morphology in topside ionosphere during sunspot minimum from Alouette 1 and 2 ionograms

20 p3530 A69-37867

Ionospheric electron density irregularities observed by topside sounders showing shape, dimensions across magnetic field and variation percent, discussing resulting radio echoes

20 p3530 A69-37870

Upper ionosphere Thomson scatter, electron number density measurements and topside sounding results during geomagnetic storms using electrodynamic drift theory

20 p3530 A69-37872

Cylindrical electrostatic probes on Alouette 2 and Explorer 31 satellites used in intersatellite comparison of directly measured ionospheric electron temperature and density

20 p3544 A69-37876

Explorer 31 ion mass spectrometer calibrated in flight and compared with Alouette 2 topside electron concentration data

20 p3545 A69-37879

Ionospheric parameters of ion and electron density and temperature and ionic species compared by direct measurement probes on Explorer 31 satellite

20 p3531 A69-37882

Ionospheric electron and ion concentration and temperature by Langmuir plate and spherical ion probe on Explorer 31 and ionosonde on Alouette 2

20 p3531 A69-37883

Auroral midlatitude red arcs ground and satellite data, noting field aligned electron density depression, plasma temperature increase and O plus-H plus transition altitude

20 p3532 A69-37897

Ionic composition determined by combining Alouette topside sounder electron density profiles with electron and ion temperatures measured by ground based Thomson scatter sounder

20 p3532 A69-37898

Rocket observation of ionospheric electron and positive ion densities and dayglow emission intensities in twilight conditions

21 p3702 A69-38355

Nocturnal electron/ion density balance in F region ionosphere from examining 6300 A emission

21 p3712 A69-38518

Daytime electron and ion composition model for height range from 150 to 1500 km at moderate latitudes and minimum solar activity

21 p3714 A69-38555

Ionospheric electron density and collision frequency profiles examined for changes during December 1967 to January 1968 stratospheric warming

21 p3714 A69-38556

Direct detection of ionospheric irregularity by device onboard San Marco satellite, utilizing antenna impedance fluctuations

21 p3715 A69-38562

Ariel 3 satellite observations, including topside ionospheric variations with time and solar activity, electron density, temperature measurements, etc

21 p3716 A69-39257

Explorer 22 observations of ionosphere electron content, describing measuring equipment and data evaluation

22 p3935 A69-39977

Ionospheric vertical columnar electron content at midlatitudes near solar cycle minimum based on Faraday rotation data from Explorer 22

22 p3939 A69-40505

Faraday effect measurements by polar orbiting satellites for vertical distribution of ionospheric electron density

22 p3941 A69-40718

Ionospheric electron content satellite measurements during 20 May 1966 annular solar eclipse

22 p4007 A69-40916

- Midlatitude F region continuity equation solutions, including eastward electric field effects on electron density
22 p3941 A69-40917
- Midlatitude ionospheric electron density rocket data survey, including nighttime and daytime N/h profiles for specific solar activities
23 p4155 A69-41563
- Electron concentration vertical profile in ionosphere in presence of horizontal wind shifts determined using E layer charged particle redistribution approximation
23 p4155 A69-41840
- Magnetic activity effect on electron density in topside ionospheres determined from Alouette 1 data statistical analysis
23 p4156 A69-41856
- Ionospheric F region equatorial anomaly in electron density showing high correlation with equatorial electrojet range and poor correlation with Fugene range
23 p4160 A69-42432
- Faraday rotation diurnal variation plotted by analyzing radio transmissions from Canary Bird geostationary satellite, considering ionospheric electron density peak
23 p4160 A69-42433
- Ionospheric electron content measurement from Faraday fading on satellite BE-B, using computer program for data reduction as function of latitude
23 p4160 A69-42434
- Ionospheric electron content measurements at low latitudes close spaced frequency and differential Doppler shift technique, using BE-B and BE-C satellite transmission
23 p4161 A69-42435
- Topside ionosphere response to magnetic storms, using Explorer 22 satellite electron concentration and temperature measurements
23 p4161 A69-42438
- Ionospheric range difference errors after correction for position fixing from satellite, considering elevation angle, latitude, day time, spatial and time electron content correlation
23 p4128 A69-42505
- Ionospheric electron content and distribution at low altitudes from satellite S 66 data, describing seasonal variations of equatorial anomaly peak
24 p4367 A69-43010
- ### IONOSPHERIC F-SCATTER PROPAGATION
- Statistical characteristics of magnetoionic components of obliquely incident waves, obtaining envelope distribution of signal reflected from F 2 layer
02 p0314 A69-11691
- E layer fine scale structure, F 1 reactions and F 2 reflected signals analysis during 20 May 1966 solar eclipse
13 p2255 A69-28541
- Statistical characteristics of magnetoionic components of obliquely incidence waves, obtaining envelope distribution of signal reflected from F 2 layer
13 p2355 A69-28722
- Radio signals F region scattering related to electron density fluctuations in ionosphere
14 p2444 A69-29870
- Cosmic radio emission absorption during IQSY at 24.6 MHz, relating diurnal variation of absorption and geomagnetic index F scatter occurrence
17 p2968 A69-33992
- Supercritical frequencies horizontal gradient ducting effects on backscatter sounding of F region magnetic field aligned irregularities
22 p3941 A69-40913
- Radio wave scattering cross section in wake of body moving in ionosphere, using simplified procedure with asymptotic expressions
22 p3901 A69-41094
- ### IONOSPHERIC HEATING
- Polar ionosphere heating by spill-over electron energy during strong geomagnetic disturbances, giving mathematical representation
02 p0237 A69-11664
- Oxygen electron cooling effect on ionospheric electron temperatures, noting discrepancy removal throughout day at all altitudes
02 p0245 A69-12739
- Reversible ion heating by atmospheric tides, noting radar Thomson scatter observations of E region ion temperature height profiles
11 p1879 A69-25159
- Joule heating role in generating internal gravity wave energy in auroral electrojet region, using linear model
12 p2064 A69-26010
- Energy loss during inelastic collisions between electrons and ionospheric particles, determining ionospheric heating by UV radiation
13 p2252 A69-27614
- Polar ionosphere heating by spill-over electron energy during strong geomagnetic disturbances, giving mathematical representation
13 p2257 A69-28695
- Ionospheric heating and velocity dependence of collision cross sections on transversely propagated equatorial hydromagnetic waves, discussing ordinary and extraordinary modes
23 p4161 A69-42437
- ### IONOSPHERIC ION DENSITY
- Ionospheric negative ion coefficient variations, analyzing formation microprocesses
01 p0066 A69-10599
- Spacecraft ionospheric probe for simultaneous measurement of electron temperature and density, plasma space potential, ion composition, etc
01 p0081 A69-10760
- Rocket sounding for studying positive ions nighttime composition in E layer after magnetic storm at midlatitudes
02 p0239 A69-11686
- Topside ionosphere composition data by energy spectrometer on satellite Ariel 1, discussing positive ions and diurnal, seasonal and secular variations
03 p0424 A69-13806
- Solar X ray source identification using D layer ionization behavior during eclipse
04 p0650 A69-15533
- Rocket measured profiles of electron density and ion abundances in E region, discussing role of minor atmospheric constituents
05 p0757 A69-16408
- Atmospheric helium normal thermal escape mechanisms, noting ion loss from polar ionosphere
07 p1125 A69-18946
- Nighttime Venus ionosphere models compared with Mariner 5 observations, discussing implications with regard to He and H abundance consequences and nightglow
09 p1594 A69-21695
- Hourly N/h profiles of F region calculated from nomograms by normal integral method during magnetic disturbance, measuring region temperature
10 p1687 A69-23928
- Molecular reaction rates and ion/electron vertical profile and concentrations in equatorial ionosphere, applying computer simulation to numerical solution of continuity equations
10 p1688 A69-23929
- Ionospheric molecular ion concentration vertical profile analysis for verifying neutral gas temperature maxima in connection with two ion production maxima
10 p1688 A69-23930
- Nighttime distribution of nitrogen ion and lambda 5755 emission in ionosphere with incidence of aurora
12 p2066 A69-26110
- F 1 layer formation relationship to height variations in ionic concentrations, determining different ion concentration combinations
12 p2071 A69-26702
- Rocket sounding for studying positive ions nighttime composition in E layer after magnetic storm at midlatitudes
13 p2258 A69-28717
- Ionized gas height scale changes in polar ionosphere obtained, assuming Chapman type ionization distribution
14 p2436 A69-29052
- Horizontal electric fields relations to charged particle fluxes in polar auroral ionosphere
14 p2437 A69-29070
- Vertical motion of ionized formations in ionospheric F region related to sporadic E layer
14 p2437 A69-29074
- Diurnal variations of atmospheric ion composition at 100-200 km from rocket experiments
15 p2603 A69-31401
- Ion whistlers recorded by Alouette 2 VLF receiver providing information on ion composition of terrestrial ionosphere, showing variation with latitude and relationship to solar cycle
15 p2604 A69-31410
- Nighttime, twilight and daytime rocket experiments for ion composition of polar ionosphere at 100-180 km
15 p2604 A69-31414
- Lyman alpha radiation ionization rate in lower ionosphere, noting various charged particle concentration parameters
15 p2605 A69-31438
- Spectrometric rocket measurements of ion concentrations between 200 and 630 km
16 p2774 A69-31974
- Rocket measurements of upper F region electron temperature and density profiles, for particle and energy balance of ionosphere topside, noting diffusive equilibrium
16 p2848 A69-31975
- Ionization troughs below F 2 layer maximum due to ionospheric disturbances detected by Antarctica ionograms direction of arrival data
16 p2775 A69-32080
- Ionization density, velocity and temperatures oscillations revealed by Thomson scatter observations of gravity waves in F regions
16 p2779 A69-32198
- Sporadic E ionization by rocket sounding, comparing positive ion density measurements with separate wind shear observations
16 p2780 A69-32310
- Relationship between sporadic E and 5577 A nightglow emission attributable to ionization redistribution in E region due to dynamic processes
16 p2788 A69-32782
- Geomagnetic control of geographic distribution of F 2 layer midday ionization based on data from ionospheric vertical sounding stations
17 p2966 A69-33982
- Reflection and ionization heights diurnal variations in F region, obtaining data for sporadic E formation
17 p2968 A69-33995
- Vertical ionization displacements in F region as trace distortions on ionograms observed at low, mid and high altitudes during daytime
17 p2969 A69-33998
- Positive ion concentration in D region, using spherical stationary electrostatic probe in weakly ionized collision dominated gas
18 p3128 A69-34804
- Ion depletion in high latitude exosphere, considering OGO 2 simultaneous observations of positive ion concentration, VLF signal propagation and whistlers
18 p3187 A69-34939
- Field aligned ionospheric F layer ion density irregularities, using simultaneous hourly radar echo and spread F data and detailed ray path calculations
18 p3129 A69-34958
- Solar flares less than 10 A X rays effect on ionospheric ionization between 60 and 100 km
19 p3397 A69-36754
- Molecular ion concentrations determined using flat probe collector trap on Cosmos 5 satellite at 200-300 km
20 p3519 A69-37021
- Simultaneous ionospheric ion and electron measurements by various radiophysical methods, relating results to period of flight of vertical space probe
20 p3486 A69-37028
- F region electron and ion concentration vertical distribution, discussing various ionization reactions
20 p3520 A69-37030
- Inhomogeneities time buildup in lower ionosphere weakly ionized plasma during charged particle concentration perturbations and source temperature variations
20 p3525 A69-37658
- F 2 critical frequency meridional cross sections latitude profiles based on global network ionospheric stations observations, confirming daytime Northern Hemisphere ionization maximum
20 p3526 A69-37661
- Solar activity effect on F 2 layer geometrical parameters, plotting prognostic maps using nomographic methods
20 p3526 A69-37663
- Diurnal, seasonal and cyclic altitude and maximum ionization median value variations of undisturbed ionosphere from vertical sounding data obtained at Yakutsk, Siberia
20 p3527 A69-37668
- Cosmic radio emission absorption in D, E region and in F 2 layer above and below electron concentration maximum from vertical ionospheric sounding 1959 over Moscow
20 p3590 A69-37676
- Alouette satellite VLF observations data of ionosphere ion composition determined from ion whistlers and noise bands with LF cut-off
20 p3530 A69-37873
- Explorer 31 ion mass spectrometer calibrated in flight and compared with Alouette 2 topside electron concentration data
20 p3545 A69-37879
- Ionospheric parameters of ion and electron density and temperature and ionic species compared by direct measurement probes on Explorer 31 satellite
20 p3531 A69-37882

Ionospheric electron and ion concentration and temperature by Langmuir probe and spherical ion probe on Explorer 31 and ionosonde on Alouette 2
20 p3531 A69-37883

Plasma temperature and ion concentration profiles determined from simultaneous measurements by Alouette 2 and Explorer 31 satellites of electron density, temperature and ion abundance
20 p3532 A69-37896

Auroral midlatitude red arcs ground and satellite data, noting field aligned electron density depression, plasma temperature increase and O plus-H plus transition altitude
20 p3532 A69-37897

Diurnal and seasonal variations of primary atmospheric ions in topside ionosphere correlated with solar zenith angle, using ion mass spectrometer on Explorer 32
20 p3534 A69-38087

Ion layer separation in temperate-zone sporadic E, obtaining layer shape by superimposition of density distributions
20 p3535 A69-38106

F region vertical density profiles for positive ions and neutral molecules of various gases determined from rocket-borne mass spectrometer data
21 p3702 A69-38354

Rocket observation of ionospheric electron and positive ion densities and dayglow emission intensities in twilight conditions
21 p3702 A69-38355

Distributions, seasonal variations and ionospheric implications of mesospheric nitric oxide concentration
21 p3703 A69-38364

Lower thermosphere ion and neutral minor constituent concentrations in nighttime auroral zone, considering ionization due to electron precipitation and bremsstrahlung
21 p3704 A69-38365

Nocturnal electron/ion density balance in F region ionosphere from examining 6300 Å emission
21 p3712 A69-38518

Daytime electron and ion composition model for height range from 150 to 1500 km at moderate latitudes and minimum solar activity
21 p3714 A69-38555

Magnetic activity effects on horizontal drifts, anisotropy and random change characteristics of E region ionization irregularities
21 p3715 A69-38561

Solar L alpha and X ray emission contribution to lower ionosphere ion production, discussing altitudinal, latitudinal and temporal variations
22 p4008 A69-41096

Ionization irregularities in equatorial E region observed in various scale sized by rocket-borne Langmuir and plasma-noise probes
23 p4160 A69-42430

IONOSPHERIC NOISE NT WHISTLERS

Large amplitude Pc 1 events at College, Alaska, noting more ionospheric cosmic noise absorption accompanying large events
[AFRL-69-0059] 02 p0244 A69-12397

Ionospheric LF radio noise cut-off near proton gyrofrequency, discussing satellite ELF and VLF observations
03 p0399 A69-14021

Continuous and triggered audio frequency noise bands associated with ionospheric lower hybrid resonance frequency observed on OGO 2
05 p0754 A69-16257

Ionospheric background noise levels and sources determined from Alouette data
20 p3495 A69-37874

Ionospheric lower hybrid resonance (LHR) noise discovered by Alouette 1, describing possible mechanisms for origin
21 p3702 A69-38358

VLF and LF emission characteristic features and origin mechanism in auroral regions of ionosphere, discussing satellite observation of noise spectrum in space
21 p3708 A69-38495

Ionospheric VLF electrostatic noise observed by sounding rocket, noting proton gyrofrequency harmonics effects within emission attenuation bands
21 p3714 A69-38550

IONOSPHERIC PROPAGATION

Radio wave abnormal absorption in auroral zone of ionosphere, investigating index of frequency dependence in absorption vs frequency relation
01 p0063 A69-10425

Ionospheric inhomogeneities vertical and latitudinal distributions and diurnal variations, measuring Explorer 22 signals Faraday fading with space diversity reception
01 p0064 A69-10446

Signal absorption in negative ionospheric ions effect on maximal frequency for space radio communication [UN PAPER 68-95272]
01 p0029 A69-10529

Ducted echoes on topside ionograms and whistler diffuseness at midlatitudes, noting common occurrence of phenomena
01 p0029 A69-10551

Coherence ratio of ionospherically propagated radio waves measured for phase difference between pairs of antennas
01 p0032 A69-10967

Specular component of ionospherically reflected radio waves between antenna array elements measured for statistical variations
01 p0032 A69-10968

Hydromagnetic wave propagation in current carrying regions of ionosphere and magnetosphere using macroscopic equations, deriving dispersion relation
01 p0067 A69-10972

Electrostatic polarization field formation by acoustic wave propagation through ionosphere, calculating effect on ionization drift velocity
01 p0068 A69-11110

Optical path variations and angle of emergence calculation in dynamic ionosphere
01 p0068 A69-11111

Numerical maps of sporadic E critical frequency for solar cycle maximum and minimum to estimate propagation
01 p0070 A69-11160

Sudden magnetic field increase associated with July 8, 1966 sudden commencement observed by OGO 3 satellite in magnetotail
01 p0075 A69-11226

LF continuous wave rocket propagation in D region presented in terms of electron density profiles
01 p0076 A69-11232

Ionosphere formed waveguide electromagnetic field determined by expression, accounting for radio wave absorption during communications via artificial satellites
02 p0206 A69-11661

Sudden cosmic noise absorption in ionosphere confirms relationship with solar chromospheric flares
02 p0306 A69-11667

Terrain roughness effect on ionospheric radio wave absorption measurement data compared with theoretical results
02 p0207 A69-11669

Ionospheric sporadic E layer reflection duration during solar activity cycle analyzed as function of critical frequency
02 p0207 A69-11684

Anomalous radio wave absorption in polar aurora region ionosphere, discussing disturbance characteristics
02 p0207 A69-11688

Lower ionosphere vertical motions found responsible for nighttime variation of radio waves total field strength
02 p0207 A69-11689

Ionosphere studies in France noting lower ionosphere dynamics, ionospheric winds, plasma electron densities, electron and ion temperature and ion-neutron collision frequency
02 p0242 A69-11903

Polarization rotation and phase delay effects as function of frequency for ionospherically propagated HF signals
02 p0208 A69-12331

Ionospheric radio signal reflection measurements based on ground to rocket pulse propagation
02 p0245 A69-12736

Ionospheric absorption measurements using beacon satellite emission compared to Kazantsev results
02 p0246 A69-12742

Sunrise effects in lower D region by solar eclipse, discussing anomaly in ionospheric absorption due to negative ion factor or recombination coefficient
02 p0246 A69-12767

Narrowing of ionospheric absorption anomaly in D region during solar eclipses in long and medium wave ranges due to recombination equation variability
02 p0246 A69-12770

Decameter wideband directional antenna system for investigation of ionosphere by retrodiffusion method
03 p0402 A69-12860

ELF radio wave propagation characteristics using two layered ionospheric model, noting deeper penetration than VLF
03 p0421 A69-13326

Polarization diversity analysis to avoid fading in microwave scatter links in D and E layers
03 p0394 A69-13378

Stationary and nonstationary weak discontinuity surfaces propagation for ideal and viscous compressible conductive atmosphere with regard to heat flux, using Hadamard method
03 p0422 A69-13511

Ionospheric midday radio wave absorption as function of geomagnetic latitude, season and solar activity from pulsed vertical radar sounding data
03 p0394 A69-13521

Absorption as factor influencing correlation between solar activity, sporadic E layer probability of occurrence and reflection stability
03 p0423 A69-13537

Radio wave absorption in ionosphere at five fixed frequencies for determining correlation with changes in sporadic E layer parameters
03 p0423 A69-13539

Ionospheric beam deflection maximum and minimum levels, deriving equations for maximum usable frequency at given ionization conditions and radiation angles
03 p0424 A69-13540

Horizon focusing gain for radio waves reflected obliquely from ionosphere, noting effects of transmitter location and ionosphere geometry
03 p0395 A69-13627

Propagation of long electromagnetic waves in ionosphere and exosphere, discussing thunderstorm noise spectrum
03 p0396 A69-13702

Statistical characteristics of multibeam signals reflected obliquely from ionosphere
03 p0396 A69-13708

LF hydromagnetic waves propagation in ionospheric waveguide duct resulting from minimum in Alfvén speed near F 2 ionization peak
03 p0399 A69-14023

Correlation of received signals with diversified angles of arrival due to scattering by turbulently excited ionosphere
03 p0399 A69-14129

Bearing deviation in model HF transionospheric propagation with three dimensional electron density variation and no magnetic field
04 p0559 A69-15209

Equivalent hop and equivalent ionospheric parameters for short wave long distance radio links in ionospheric radio propagation
04 p0560 A69-15402

VLF phase measurements for apparent and equivalent diurnal height variation for lower ionosphere waveguide
05 p0752 A69-15666

Sudden VHF phase anomalies produced by solar flare induced ionospheric disturbances during July 1968
05 p0719 A69-15980

Ionospheric models for studying nature of difference in relationships between HF radio waves Doppler shifts and changing ionosphere
05 p0755 A69-16269

Bandwidth effect on wave recordings cross spectra interpretation from spatially separated sites, deriving relationship between propagation velocity and velocity bandwidth
05 p0756 A69-16272

Internal atmospheric gravity waves in F region observed with electron density profiles deduced from vertical incidence ionograms, obtaining phase velocities
05 p0756 A69-16402

Ray tracing of Z-mode in tilted layer ionosphere to explain Z-mode echoes in ionograms
05 p0758 A69-16412

Whistler mode propagation in homogeneous electron plasma situated in longitudinal electrostatic field, using Fokker-Planck model
05 p0758 A69-16417

Electrostatic ionospheric waves excited around lower hybrid resonance frequency by high energy electrons
06 p0918 A69-17381

Cosmic radio noise absorption in ionosphere, discussing diurnal, seasonal and longer variations of integral absorption
06 p1008 A69-17727

Numerical methods for VLF electromagnetic wave propagation in earth-ionosphere waveguide, discussing boundary conditions assignment effect at ionosphere on eigenvalues
06 p0920 A69-17732

- Multichannel HF resolution spectral analyzer of pulses reflected from ionosphere applied to dependence of cross correlation coefficient on frequency separation
06 p0897 A69-17740
- Long wave radio stations field intensity spectral analysis data evaluated to determine vertical ionospheric displacements at sunset and sunrise
06 p0922 A69-17752
- Meridional radio communication between radio station at South Geomagnetic Pole and amateur SSB radio stations in U.S.S.R.
06 p0889 A69-17753
- Coherent frequencies method for irregular component of satellite signal phase lead due to ionospheric inhomogeneities between satellite and ground station
06 p0890 A69-17799
- Induced and combination scattering of high HF radio waves in ionosphere and magnetosphere
07 p1076 A69-18521
- ELF radio waves reflection coefficients calculated from two layer ionospheric model, noting ion collision frequency effect in Schumann resonance frequency band
07 p1124 A69-18820
- Plasma frequency resonances observed by topside sounders interpreted as slowly propagating waves suffering oblique reflection, noting effects of nonhorizontal magnetic field
07 p1124 A69-18837
- Formulas for ray paths in ionized layers with application to oblique ionograms and duct modes
07 p1078 A69-18913
- Polarization of ionospherically propagated HF radio waves for various times, frequencies and path azimuths applied to distortion in radio communication
07 p1078 A69-18916
- Earth dipole magnetic field effect on bearing deviation in HF transionospheric propagation analyzed by computer ray tracing
07 p1086 A69-19224
- Reflected radio wave amplitude distributions related to distributions of curvature at reflector
07 p1086 A69-19225
- Nonlinear modulation distortions of high power radio waves propagating in ionosphere, noting electron temperature increase from radio wave
07 p1088 A69-19746
- Reflection and transmission scattering coefficients for step type transition between two uniform waveguides with surface impedance boundaries, discussing coupled differential equations
08 p1272 A69-20020
- Lower ionosphere and earth-ionosphere waveguide effects on polarization characteristics of transmitted radio whistlers
08 p1306 A69-20181
- Long range HF propagation in equatorial zone observed with San Marco 2 satellite, discussing overall conditions of ionosphere
08 p1276 A69-20593
- Forward and backscattering of radio waves at electron concentration discontinuity near reflecting ionospheric layer with vertical nonuniformity
09 p1453 A69-21525
- Ionospheric scattered radio wave field amplitude and phase variations assessed for diffraction at regular phase screen
09 p1453 A69-21526
- Radio waves polarization scattered at ionospheric discontinuities analyzed for vertical incidence, determining modulus distributions and polarization factor argument
09 p1453 A69-21527
- Lower ionosphere effect on LF electromagnetic disturbances, comparing propagation and damping of clockwise and counterclockwise polarized waves
09 p1487 A69-21637
- HF ionospheric radar ground scatter map showing separated land-sea backscattered radio waves by Doppler technique
09 p1454 A69-21681
- Doppler effect in ionospheric acoustic perturbations caused by strong ground explosion, noting accord with nonlinear acoustic wave propagation theory
09 p1488 A69-21694
- VHF satellite signal scintillation by ionospheric irregularities with sharp boundary /such as sporadic E/, noting diffraction pattern dependence on phase shift
09 p1489 A69-21713
- VLF electromagnetic wave propagation in earth-ionosphere waveguide with reflections from ionosphere, noting TE and TM mode coupling and mode conversion
09 p1460 A69-22699
- Transequatorial propagation mode for waves in VHF band twice scattered by field aligned irregularities in electron density
10 p1653 A69-23192
- Magnetoionic formulas similarity in ionospheric radio propagation and atmospheric acoustic gravity wave propagation above electron gyrofrequency
10 p1655 A69-23419
- One way measurement of dual inband frequency diversity improvement on HF ionospheric path with frequency division multiplexed FSK modulation
10 p1656 A69-23536
- Low energy particle effects on midlatitude lower ionosphere conditions after July 7, 1966 proton flare, using ground based measurement
10 p1684 A69-23782
- Phase fluctuations measurements of obliquely incident signal reflected from ionosphere performed over distance of 1300 km, showing amplitude dependence
10 p1657 A69-23913
- Geomagnetic field directed hydromagnetic waves propagation in lower ionosphere, noting inhomogeneous conductivity, Hall effect and lines of forces role
10 p1687 A69-23926
- Vertical probe observations of short radio waves propagation through sporadic E at various frequencies and path lengths
10 p1657 A69-23933
- Radio signals and concentrated noise amplitudes probability distributions reflected from ionosphere and scattered in troposphere calculated for Rayleigh and log-normal fading
11 p1833 A69-24440
- Propagated ray paths plotted as functions of frequency and launch angle to predict signal dispersions
11 p1837 A69-25003
- Iono-index about hard emission of solar active regions, analyzing field fluctuations and SID in D region under daytime conditions
12 p2148 A69-26107
- Pulsed radio waves for measuring phase height in E region, showing short period fluctuations
12 p2066 A69-26111
- Ionospheric plasma density vertical profile by measuring reflected radio waves phase frequency characteristics
12 p2070 A69-26685
- Refractive index and attenuation factor of ionosphere
12 p2070 A69-26689
- Antenna suspension height variation effects on HF signals in ionospheric scattering lines
12 p2032 A69-26705
- Differential absorption by measurement of phase difference of ionospherically propagated incoherent radio wave signals under quasi-longitudinal conditions
12 p2032 A69-26857
- VLF wave propagation along mixed path in curved earth-ionosphere waveguide, considering reflection and transmission coefficients of modes
12 p2032 A69-26858
- Auroral and polar zone ionosphere effects on propagation in HF through low VHF spectrum, considering nongreat circle mode, sporadic E ionization, etc
12 p2032 A69-26859
- Pi 2 micropulsations at African low latitude stations, considering damping effect on ionospheric micropulsation transmission signal dispersion and SNR
12 p2074 A69-26959
- Electromagnetic step-function plane waves propagation in ionosphere using Fourier transform and Bessel functions
12 p2034 A69-27132
- Errors in Appleton-Bayton equation for skip distance of radio waves in ionosphere
13 p2218 A69-27214
- Numerical integration for coupling between two modes of propagation /electron and proton whistlers/
13 p2254 A69-27981
- F cosine i theorem validity for VLF radio wave absorption in ionosphere tested using exponential electron density models, noting Brewster angle influence on reflection coefficient
13 p2222 A69-28473
- Long range ionospheric propagation of ultrashort radio waves, obtaining diurnal and seasonal characteristics of reflected signals amplitude and duration
13 p2255 A69-28543
- Ionosphere formed waveguide electromagnetic field determined by expression, accounting for radio wave absorption during communications via artificial satellites
13 p2224 A69-28692
- Sudden cosmic noise absorption in ionosphere confirming relationship with solar chromosphere flares
13 p2334 A69-28698
- Terrain roughness effect on ionospheric radio wave absorption measurement data compared with theoretical results
13 p2224 A69-28700
- Ionospheric sporadic E layer reflection duration during solar activity cycle analyzed as function of critical frequency
13 p2224 A69-28715
- Anomalous radio wave absorption in polar aurora region ionosphere, discussing disturbance characteristics
13 p2224 A69-28719
- Lower ionosphere vertical motions found responsible for nighttime variation of radio waves total field strength
13 p2224 A69-28720
- Polarization diversity analysis to avoid fading in microwave scatter links in D and E layers
14 p2410 A69-28829
- Ion drag effects on acoustic gravity waves propagation in isothermal F region, discussing indicated wave damping
14 p2434 A69-28944
- Latitudinal cut-off of manmade VLF signals in short path through ionosphere to OGO 2 satellite, noting strong noise following signal cut-off
14 p2434 A69-28958
- Forward and backscatter soundings compared to verify focusing mechanism of HF sky waves
14 p2435 A69-28967
- Ionospheric horizontal discontinuities of electron density distribution parameters effect on penetration frequency, skip distances and arrival angles
14 p2436 A69-29057
- Radio waves propagation along polar auroras region, obtaining ionospheric parameters for magnetic disturbances based on penetration probability
14 p2436 A69-29058
- Seasonal variation in ionospheric radiation absorption related to time variation between sunrise and constant angle attainment of sun
14 p2437 A69-29072
- Radio wave absorption coefficient in lower ionosphere related to total radiation absorption and electron concentration profile
14 p2411 A69-29075
- Noon ionospheric absorption data for Freiburg on different frequencies for lunar variation of ionospheric absorption of radio waves
14 p2438 A69-29104
- Satellite 40 mc signal scintillations near sunspot minimum, noting scintillation index dependence on angle between radio ray and magnetic field
14 p2439 A69-29114
- Fourier analysis of ionospheric wave reflection pulses for frequency contents and relative phase angles
14 p2440 A69-29351
- Ionospheric radio wave absorption at midlatitude, noting mesospheric zonal wind inversion
14 p2441 A69-29418
- Bearing errors reduction in vertical loop HF direction finders for ionospherically propagated signals in dual channel system
14 p2413 A69-29493
- Radio wave reflections from edge of large scale depressions of ionospheric electron density observed by topside sounding satellites, discussing ionogram recordings
14 p2415 A69-29521
- Inhomogeneities effect on polarization of radio waves reflected from ionosphere, based on permittivity tensor
14 p2417 A69-29862
- Tide dependent variations of critical frequencies of ionospheric layers minimal heights and maximum height of F 2 layer reflection
14 p2444 A69-29871
- Random motions velocity of ionospheric inhomogeneities by extreme lines delineation of diffraction pattern during amplitude recording of reflected signal
14 p2444 A69-29872
- Recording installation of ionospheric reflected radio signal fluctuations and amplitudes of resulting signals simultaneously at three points, discussing antenna commutator circuit
14 p2452 A69-29874
- Solar X rays intensity and spectrum effects on E layer critical frequency and D region ionospheric absorption
15 p2677 A69-31346
- Doppler geodetical measurements, emphasizing relative orientation between station and orbit influence on

coordinates determination accuracy, presenting electromagnetic wave propagation theory
15 p2601 A69-31375

Fresnel irregularities calculated from radio wave partial reflection from lower ionosphere measured by rocket probes
15 p2604 A69-31420

Ground based partial reflection and cross modulation or wave interaction techniques compared for studying D region electron densities
15 p2606 A69-31537

Auroral absorption influence on ionospheric wave propagation calculated for distances over 4000 km
16 p2749 A69-31603

Book on ionospheric radio waves covering geomagnetism and sun, whistler propagation, oblique propagation, satellite sounding, etc
16 p2749 A69-31715

Earth ionosphere cavity model for atmospheric waveform shape, considering ELF pulse distortion after propagation through antipode
16 p2750 A69-31978

VLF radio wave propagation in waveguide channel formed by earth and inhomogeneous anisotropic ionosphere
16 p2751 A69-32032

Partial reflections method of Gardner and Pawsey for determining vertical profile of electron collision frequencies in lower ionosphere and upper D layer
16 p2775 A69-32034

Second order correction to first order Faraday rotation equation for quasi-transverse propagation of ionospheric radio waves obtained from Appleton-Hartree equation
16 p2777 A69-32101

Atmospheric absorption calculations, noting direct D layer reflection effects on lower HF oblique propagation
16 p2752 A69-32389

Numerical method based on thin film optics to determine ionospheric electromagnetic transmission and reflection coefficients for vertical incidence
16 p2752 A69-32392

Thin film optical method generalization accounting for intermode coupling and oblique incidence in plane stratified magnetoionic medium applied to ionospheric LF and hydromagnetic propagation
16 p2753 A69-32393

Forward and backscattering of radio waves at electron concentration discontinuity near reflecting ionospheric layer with vertical nonuniformity
16 p2754 A69-32520

Ionospheric scattered radio wave field amplitude and phase variations assessed for diffraction at regular phase screen
16 p2754 A69-32521

Radio waves polarization scattered at ionospheric discontinuities analyzed for vertical incidence, determining modulus distributions and polarization factor argument
16 p2754 A69-32522

Decameter waves Doppler shift shown inversely proportional to wave frequency from electron density variation caused by acoustic wave propagation in ionosphere
16 p2755 A69-32610

Radio waves ionospheric absorption dependence on equivalent frequency, showing marked difference for summer and winter conditions
17 p2918 A69-32927

Sudden phase anomalies on radio paths compared with calculated results for satellite observed solar X ray flux intensities to explain sudden ionospheric disturbances
17 p2959 A69-33006

Ionosphere depression influence on VLF signals phase and amplitude calculated by mode theory and integral equations system representing aperture fields
17 p2920 A69-33418

Ray methods application to partial differential equations for electromagnetic wave propagation in ionosphere, discussing strongly and weakly anisotropic inhomogeneous plasma
17 p2925 A69-33840

Scattered ionospheric reflection distribution at evening/morning periods showing deviation, using coherent method
17 p2927 A69-33860

Radio wave propagation in homogeneous turbulent gyrotropic medium, presenting solution for fluctuations in direction of wave scattering by geometrical optics approximation
17 p2927 A69-33861

Horizontally stratified ionosphere radio wave reflection and transmission properties, calculating full wave by differential equations
17 p2927 A69-33862

Complex refractive index profiles and wave polarizations calculated for electromagnetic waves transmission through ionosphere at micropulsation frequencies
17 p2927 A69-33864

Earth-ionosphere waveguide excitation by lightning discharges and geomagnetic field influence on ELF noise spectrum
17 p2928 A69-33865

LF radio waves propagation in ionosphere by combining ray tracing in complex space with geometrical theory of diffraction, including diffraction by earth
17 p2928 A69-33866

High latitude geomagnetic disturbances, incoming electron fluxes and riometric absorption relationship in lower ionosphere studied by X ray bremsstrahlung with sounding balloons
17 p2964 A69-33961

Ionospheric radio wave absorption measurements by A1 method at 2.2 MHz, showing height estimates of absorption region and winter anomaly
17 p2968 A69-33993

Reflection and ionization heights diurnal variations in F region, obtaining data for sporadic E formation
17 p2968 A69-33995

Time dependent diffuse reflections related to solar activity, showing diffusion intensity variations with sporadic E layer height and electron concentration
17 p2968 A69-33997

VLF wave propagation phase velocity prediction for airborne Omega computer, using scatter model based on abnormal ionosphere
17 p3002 A69-34077

Ionospheric absorption and virtual heights relationships for electron density distribution in lower ionosphere, computing model profiles
18 p3125 A69-34248

ELF and VLF wave propagation examined for heavy ions and lower ionospheric disturbance effects using numerical integration, noting standing wave field role for interpretation
18 p3125 A69-34254

Anisotropic ionospheric model for VLF TM and TE modes excitation, noting nighttime phase velocity variations
18 p3101 A69-34797

ELF wave propagation in earth-ionosphere waveguide, considering ionospheric vertical inhomogeneity and models for ambient and disturbed /PCA/ conditions
18 p3101 A69-34949

Antarctic VLF emissions observations at 12 kHz, showing dependence on geomagnetic disturbances, auroras and radio absorption in ionosphere
18 p3102 A69-34964

Ion and temperature effects on lower ionosphere refractive index for VLF radio wave propagation
18 p3102 A69-34971

Whistler vertical propagation downwards through inhomogeneous ionosphere in vertical magnetic field, deriving wave equation, calculating transmission and reflection coefficients
18 p3130 A69-34972

Ionospheric radio propagation, considering D and F region theory and ionospheric disturbances
19 p3303 A69-36428

Scattering cross sections of radio waves at wake of vertically moving body near reflecting ionospheric layer, noting wave sphericity influence
20 p3486 A69-37023

Electromagnetic field of horizontal LF electric dipole formed by thin ionosphere layer between anisotropic planes
20 p3521 A69-37047

Perturbed ionospheric regions acting as radio wave focusing lens, discussing frequency, power and pattern selection
20 p3486 A69-37048

Recording technique for measuring short period variations of radio signal reflections altitudes from ionosphere applicable to fast ionospheric processes
20 p3521 A69-37054

ELF radio wave propagation characteristics analyzed by two layer ionosphere model
20 p3488 A69-37285

Soviet collection of papers on ionospheric studies covering ionospheric composition, propagation, disturbances, sounding, etc
20 p3523 A69-37654

Lower ionosphere radiation absorption at 4.01 MHz determined using A-3 method in measuring radio wave field between radio transmitters
20 p3528 A69-37675

Ionospheric radio wave absorption seasonal and diurnal variations over Tiflis from pulsed ionospheric sounding at 2.2 MHz
20 p3491 A69-37677

Residual nighttime radio wave absorption in ionosphere, noting absorption-magnetic activity relation existence
20 p3528 A69-37678

Frequency dependence of radio wave absorption in ionosphere at 2.2-4 MHz by impulse method, noting effect of sporadic layer
20 p3491 A69-37680

Short radio wave damping of earth satellite transmitter due to ionospheric diffraction resulting from increasing satellite-ground station distance
20 p3491 A69-37689

High latitude stations vertical ionograms in absence of ionospheric reflections due to low solar activity periods, discussing interpretation methods
20 p3529 A69-37690

F layer penetration frequencies predictions compared with Alouette topside data
20 p3530 A69-37871

Ionospheric topside plasma resonances observed by fixed and swept frequency satellite-borne sounders
20 p3531 A69-37884

Topside ionospheric magnetic field aligned irregularities using satellite observations of nonvertical electromagnetic wave propagation and delayed echo generation
20 p3495 A69-37885

Ionospheric resonances due to plasma nonlinearities near spacecraft, noting effects on radio signal propagation
20 p3495 A69-37886

Two-hop signals observed on high latitude Alouette 2 topside ionograms found propagating in field aligned cylindrical ionospheric ducts
20 p3531 A69-37890

Propagation characteristic model study of kinked Z trace observed on topside ionograms and explained by magnetoionic theory
20 p3531 A69-37893

Sudden frequency deviations of HF radio waves propagated through ionosphere correlated with solar microwave bursts and optical flare events
20 p3592 A69-38101

Rocket observations of VLF ionospheric resonances, noting artificial stimulation of detectable amplitude noise with cut-off at low hybrid resonance frequency
21 p3671 A69-38356

Auroras and VLF emissions observations at ground stations to correlate emissions with auroral displays, noting low ionospheric absorption role
21 p3708 A69-38494

Phase amplitude recording of radio waves reflected from D and F regions of ionosphere, reversing smoothing process by Fourier methods
21 p3672 A69-38558

Electron collisions effect on polarization of waves reflected from ionosphere
22 p3941 A69-40922

Nighttime atmospherics shape analysis created by lightning and propagating in earth lower ionosphere waveguide
22 p3941 A69-40961

HF radio waves auroral absorption in ionosphere reviewed for first decade of riometry
22 p3902 A69-41218

Circular or linear polarization diversity reception for VHF earth-station-satellite communications through turbulent ionosphere, assuming Rayleigh distribution fading
23 p4115 A69-41585

MHD waves attenuation in ionosphere due to gyrorelaxation, reducing analysis to determination of anomalous absorption of acoustic waves
23 p4155 A69-41841

Cosmic radio emission anomalous absorption measurements during PCA following July, August, September 1966 proton flares
23 p4156 A69-41845

Ionosphere reflected radio waves field strength measurements, obtaining formula for ground wave discrimination
23 p4123 A69-41861

Approximate expressions derived from Appleton-Hartree magnetoionics formula tested for validity in computation of radio wave absorption in model ionospheric layers
23 p4126 A69-42354

Ionospheric radio waves constant absorption term obtained from sunrise and sunset data

23 p4127 A69-42424

Ionospheric nondeviative radio wave absorption, noting roles of collisional and working frequencies and solar zenith angle

23 p4127 A69-42425

Ionospheric range difference errors after correction for position fixing from satellite, considering elevation angle, latitude, day time, spatial and time electron content correlation

23 p4128 A69-42505

Ionospheric absorption relationship to major stratospheric sudden warmings, considering regional coincidence and interaction mechanism

24 p4306 A69-42680

Auroral VLF emission bursts simultaneous with sharp ionospheric absorption dip and SC deflections in geomagnetic H, noting corpuscular ionization

24 p4308 A69-43001

Proton cyclotron echoes on ionograms obtained from topside ionosphere by Alouette 2 satellite

24 p4310 A69-43189

Polar cap ionospheric response to solar cosmic ray events observed by Mariners 2 and 4 solar proton measurements used to test magnetosphere models

24 p4373 A69-43621

IONOSPHERIC SOUNDING

Artificial visible plasma clouds in space interacting with electric and magnetic fields around earth

01 p0151 A69-10533

Inner and outer meteorological balloon assembly for fast rising and high altitude sounding

01 p0010 A69-10541

Scattered solar Lyman alpha radiation measurement by Vertical Space Probe station in upper atmosphere including UV radiation

01 p0152 A69-10577

Spacecraft ionospheric probe for simultaneous measurement of electron temperature and density, plasma space potential, ion composition, etc

01 p0081 A69-10760

Methodological problems in studying ionosphere by phase measurements without taking into account geomagnetic field, noting value of main results

02 p0237 A69-11668

Ion formation rate in F 2 layer in southern polar cap, noting effect of season, latitude and solar activity

02 p0238 A69-11679

Ionosphere studies in France noting lower ionosphere dynamics, ionospheric winds, plasma electron densities, electron and ion temperature and ion-neutron collision frequency

02 p0242 A69-11903

Ionosphere structure, properties and research techniques

04 p0594 A69-15166

Multielectrode analyzers for measuring properties of ionospheric charged particles

05 p0761 A69-15702

Nonvertical propagation effects on high altitude topside ionosphere sounder data reduction, using ray tracing

07 p1124 A69-18838

Ion composition and charged particle temperatures at 300-600 km from sounding rocket and topside sounder Alouette 2 measurements

07 p1124 A69-18839

Hydrogen concentration above earth surface during minimum solar activity from ionospheric rocket and satellite measurements

07 p1129 A69-19612

F2 layer diffusion and sporadic E layer characteristics from equatorial ionosphere soundings on Zaria schooner

09 p1486 A69-21548

Vertical ionospheric motions near magnetic equator measured by Doppler shifts of incoherent scatter frequency spectra

09 p1489 A69-21704

Fast Ba ion filament cloud injection into ionosphere using explosive shaped charge technique, noting application to ionospheric electric field measurement

09 p1539 A69-21752

Ionospheric movements from sampling radio diffraction pattern at 89 points and conversion into visible pattern

09 p1492 A69-22756

Upper hybrid and modified plasma resonance on basis of rocket-borne gyroplasma probe data

10 p1726 A69-22807

Graphs of ionospheric measurements by vertical incidence sounding during Antarctic expedition, describing instrumentation and sounding techniques

10 p1681 A69-23315

Ionospheric conditions following solar proton flare observed with topside sounders of Alouette satellites, showing electron density depletion and hydromagnetic wave relationship

10 p1684 A69-23781

Ionospheric slopes and range frequency characteristics obtained from oblique incidence sounding of horizontally nonuniform ionosphere

10 p1686 A69-23914

Polar cap sporadic E investigation with backscatter at 28 MHz, noting geographic distribution, annual and diurnal variations

12 p2069 A69-26464

Soviet rocket and satellite studies of upper atmosphere and ionosphere

13 p2251 A69-27347

Soviet satellite-borne radio waves studies of ionosphere, considering wave amplitudes, Doppler frequency shifts and outer ionosphere properties

13 p2252 A69-27349

Automatic recording and data processing for ionospheric radiosonde observations from ground stations, giving block diagrams and subsystems

13 p2225 A69-27610

Trapped aerosols below temperature inversions causing lidar echoes in troposphere layers, discussing simultaneous balloon refractometer, thermometer and ground based lidar soundings

13 p2254 A69-28475

Methodological problems in studying ionosphere by phase measurements without taking into account geomagnetic field, noting value of main results

13 p2257 A69-28699

Ion formation rate in F 2 layer in southern polar cap noting effect of season, latitude and solar activity

13 p2257 A69-28710

Ionospheric electron and ion temperatures correlated with electron concentration profile as measured by rockets and satellites

14 p2510 A69-28942

Ionograms for nonmonotonic vertical distribution of electron concentration in ionosphere from rocket and ground sounding

14 p2437 A69-29071

Rocket and satellites topside sounding of earth ionosphere, determining magnetoplasma structure and resonance

14 p2438 A69-29101

Radio pulse sounding of ionospheric structure and motions, discussing digital ionosonde, data analysis methods, etc

14 p2415 A69-29519

High resolution azimuth and elevation arrays sensing remote ionosphere and sea surface characteristics, discussing backscatter data for ionosphere and sea scatter

14 p2448 A69-29520

Radio wave reflections from edge of large scale depressions of ionospheric electron density observed by topside sounding satellites, discussing ionogram recordings

14 p2415 A69-29521

Incoherent scatter observations of ionosphere, discussing radar equipment and measurement of electron density and temperature, ionic temperature and composition, etc

14 p2415 A69-29522

Multiple ground based geophysical sensors for detecting ionospheric phenomena, discussing continuous magnetic tape data recording, common time base and station operation

14 p2448 A69-29526

Reference oscillator frequency instability effect on radio signals phase shift in ionosphere measurements, evaluating errors

14 p2444 A69-29873

Satellite radio observation for ionospheric parameters, utilizing Doppler and Faraday phenomena, signals fluctuations and sporadic phenomena

15 p2594 A69-30028

Scattered solar Lyman alpha radiation measurement by Vertical Space Probe station in upper atmosphere including UV radiation

15 p2691 A69-30747

ESRO 1/Aurora scientific satellite for ionospheric phenomena observation, discussing management structure and development process

15 p2702 A69-31080

ESRO 1/Aurora satellite for Arctic ionosphere and aurora observation, discussing electrons and protons measurements and auroral photometry

15 p2702 A69-31081

D region ionizable constituent density /presumably nitric oxide/ measured, using blunt probe to detect

changes in conductivity produced by Lyman alpha ionizing radiation

15 p2598 A69-31316

Diurnal variations of wind velocity, temperature and density at high altitude measured by Skylark rockets

15 p2598 A69-31319

IR horizon of earth from ionospheric IR emission spectra obtained by sounding capsule, discussing earth geometric horizon and particular spectral bands [ONERA-TP-709]

15 p2601 A69-31370

Ionospheric VLF emission and particle measurements, discussing energy, distribution and flux of protons and electrons

15 p2605 A69-31425

Gyroplasma probe data from rocket observations, determining winter ionospheric electron density profiles, electron temperature and electrostatic cyclotron waves effect

15 p2606 A69-31446

Vertical incidence pulse dispersion with application to Alouette 1, discussing echo width, sounder system bandwidth and frequency gradient of ionospheric virtual height

16 p2750 A69-31977

Low latitude sporadic E layer associated with geomagnetic activity studied in Hong Kong using proton precession magnetometer and standard ionosonde

16 p2779 A69-32195

Electronic collision frequency measurement at F layer peak near ground sunrise time

16 p2779 A69-32197

Sporadic E ionization by rocket sounding, comparing positive ion density measurements with separate wind shear observations

16 p2780 A69-32310

F 2 layer diffusion and sporadic E layer characteristics from equatorial ionosphere soundings on Zaria schooner

16 p2784 A69-32543

First order Doppler shift in ionosphere and horizontal gradients influence, discussing total electron content determination method made from geodetic satellites using two coherent frequencies

16 p2755 A69-32614

Doppler shift measurements at two coherent frequencies from Diadem satellites to determine ionospheric electron content, discussing accuracy and parameters defining satellite passage

16 p2785 A69-32615

NonMaxwellian electron velocity distribution influence on ionospheric measurements by Thompson scattering, explaining disagreement between scattering and probe measurements of electron temperature

16 p2788 A69-32647

Ionospheric data acquisition and utilization for improved radio communications, considering contact between engineers and physicists, ionosondes, data reliability for prediction, etc

17 p2961 A69-33402

Absolute phase heights measurements in ionosphere for geometrical optics conditions, noting accuracy

17 p2927 A69-33859

Polar ionosphere investigation based on vertical sounding and riometric observations, earth electromagnetic field and polar auroras spectrum intensity variations

17 p2963 A69-33950

Latitude variations of day and night ionospheric critical frequencies, inhomogeneity and ionization, discussing generation of r type sporadic E layer in auroral zone

17 p2964 A69-33963

Geomagnetic control of geographic distribution of F 2 layer midday ionization based on data from ionospheric vertical sounding stations

17 p2966 A69-33982

Ionospheric parameter recording accuracy by vertical sounding, discussing errors in frequency-height curve

17 p2969 A69-34002

Midday aurora oval and polar cap region airborne observation, noting relation to sporadic E layer

18 p3126 A69-34258

Earth albedo effect on ionospheric D layer determined from aircraft sounding of E layer echo amplitude above reflecting cloud cover

18 p3127 A69-34800

Franco-Soviet rocket probe launches for measuring daytime/nighttime ions and neutrals

18 p3210 A69-35282

Gas dynamics of interactions of tenuous ionosphere with moving satellites and diagnostic probes, using collision-free plasma kinetics methods

18 p3132 A69-35409

OGO-F electric and electromagnetic fields measurement for ionosphere using dipole antenna, emphasizing broadband observation covering whistler mode waves
19 p3284 A69-36677

Molecular ion concentrations determined using flat probe collector trap on Cosmos 5 satellite at 200-300 km
20 p3519 A69-37021

Ionosphere absolute phase height measurement methods independent of virtual height, using fixed frequency CW emission and pulsed sounding
20 p3520 A69-37032

Positive and negative correlations in F 2 layer perturbations observed by network of paired conjugate ionospheric stations at low latitude
20 p3521 A69-37050

Soviet collection of papers on ionospheric studies covering ionospheric composition, propagation, disturbances, sounding, etc
20 p3523 A69-37654

F 2 layer seasonal anomaly, discussing global distribution observed by network of ionospheric stations
20 p3526 A69-37666

Diurnal, seasonal and cyclic altitude and maximum ionization median value variations of undisturbed ionosphere from vertical sounding data obtained at Yakutsk, Siberia
20 p3527 A69-37668

Sporadic E layer structure and behavior during solar cycle from vertical sounding, discussing semiopaque region, reflection multiplicity, active height, wind effects, etc
20 p3528 A69-37681

Sporadic E layer large scale irregularities direction and velocity determined by inclined backscatter method, using plan position indicator
20 p3528 A69-37682

Data acquisition amount estimation technique for vertical panoramic sounding of ionosphere
20 p3492 A69-37692

RF impedance probe digital system for ionospheric measurements based on antenna resonance phenomena
20 p3542 A69-37791

Ionospheric satellites objectives and development resulting from topside sounder and ISIS programs
20 p3529 A69-37855

Ionospheric satellite series Alouette-ISIS, discussing successive engineering and management constraints leading to ISIS-C design
20 p3618 A69-37856

Explorer 20 satellite for obtaining fixed frequency pulse soundings of ionospheric topside, discussing transceiver-dipole antenna instrumentation and payload
20 p3618 A69-37857

Sweep frequency ionospheric topside sounder design for Alouette and ISIS satellites, discussing influence of experiment requirements and spacecraft limitation and environments
20 p3507 A69-37859

Real time pulse frequency modulation telemetry receiving system for direct readout of ionograms from topside sounders, using off-shelf components
20 p3508 A69-37862

Alouette 1 and 2 topside sounder ionograms analyzed with emphasis on low electron density, spread F and field aligned propagation
20 p3529 A69-37863

Ionospheric electron density irregularities observed by topside sounders showing shape, dimensions across magnetic field and variation percent, discussing resulting radio echoes
20 p3530 A69-37870

Cylindrical electrostatic probes on Alouette 2 and Explorer 31 satellites used in intersatellite comparison of directly measured ionospheric electron temperature and density
20 p3544 A69-37876

Plasma temperature and ion concentration profiles determined from simultaneous measurements by Alouette 2 and Explorer 31 satellites of electron density, temperature and ion abundance
20 p3532 A69-37896

Ionic composition determined by combining Alouette topside sounder electron density profiles with electron and ion temperatures measured by ground based Thomson scatter sounder
20 p3532 A69-37898

Corpuscular radiation indicated as ionization source in lower ionosphere from rocket sounding data, noting role in D region formation
21 p3787 A69-38352

Lower ionosphere over geomagnetic equator during evening twilight characterized by solar disturbances, using rocket-borne Langmuir and plasma noise probes
21 p3702 A69-38353

Diurnal intensity variations in OI 5577 A line emission connected with vertical movements in 90 km level of atmosphere
21 p3713 A69-38525

Ionosphere drift measurements in LF range, noting relationship between correlation and similar-fade analyses for velocity data
21 p3714 A69-38557

Radio FM pulse compression for vertical ionosphere sounding
21 p3674 A69-39082

Antenna reactance from sounding rocket in ionosphere, showing variations relationship to rocket spin period
22 p3934 A69-39964

Ground antenna array for ionospheric physics experiments, consisting of wire dipoles connected to receive circular or linear polarization
24 p4286 A69-42607

Atmospheric density above 158 km altitude measured near equator with cold cathode magnetron pressure gage on satellite OV1-15
24 p4310 A69-43179

IONOSPHERIC STORMS

NT SUDDEN IONOSPHERIC DISTURBANCES

Latitudinal variations in auroral and subauroral region F layer diurnal and magnetic storm pattern shown by scintillation measurements
01 p0069 A69-11127

F region response to solar proton flare characterized by two phase ionospheric storm as measured at ground base stations
10 p1684 A69-23783

Initial phases of ionospheric and magnetic storms compared from data, noting good correlation due to ionospheric fields influence
17 p2967 A69-33988

F region during earth passage through solar corpuscular stream, analyzing critical frequencies, virtual height, magnetogram H component and ionospheric storm effects attributed to downward drift
17 p2967 A69-33989

Upper ionosphere Thomson scatter, electron number density measurements and topside sounding results during geomagnetic storms using electrodynamic drift theory
20 p3530 A69-37872

Alouette topside ionograms of ionospheric storms at midlatitudes indicating critical frequencies difference between F 1 and F 2 layers
20 p3532 A69-37894

IONOSPHERIC TEMPERATURE

Neutral gas temperature variations effect on electron-ion temperature height profile in tidally generated sporadic E layer with wind shear of gravity wave origin
01 p0073 A69-11176

Ionic composition and temperature of nighttime topside ionosphere from analysis of incoherent backscatter spectra, discussing solar activity effects
01 p0076 A69-11233

Oxygen electron cooling effect on ionospheric electron temperatures, noting discrepancy removal throughout day at all altitudes
02 p0245 A69-12739

Middle ionosphere temperature diurnal variations analyzed on basis of rocket experiments and electron density asymmetry
02 p0246 A69-12768

Ionospheric electron temperature probe analysis based on Japanese Kappa rocket data
05 p0761 A69-15701

Gravity waves observed by ionospheric temperature measurements in F region
05 p0754 A69-16262

Diurnal variations of neutral and charged particle temperatures in equatorial F region
05 p0755 A69-16270

Langmuir probe experiment measurement of upper region electron temperature on Explorer 32 conflict with Jicamarca Radar Observatory measurements
05 p0756 A69-16283

Ion temperature diurnal variations at 250-475 km obtained from Thomson scatter spectra
05 p0757 A69-16407

Simultaneous rocket measurements of D region temperatures and electron densities on anomalous winter day
05 p0758 A69-16411

Maximum ionization altitude, thickness, electron density profile and temperature mean variations in summer of IGY and IQSY at Moscow station
09 p1486 A69-21544

Electron gas heating at E region altitudes as function of ionization of atmospheric gases, noting rocket experiments during solar eclipse
09 p1490 A69-21772

Ionospheric molecular ion concentration vertical profile analysis for verifying neutral gas temperature maxima in connection with two ion production maxima
10 p1688 A69-23930

Radar backscatter and rocket profiles of ionospheric electron temperature, noting agreement in daytime flight measurements
11 p1951 A69-25162

Global coverage of positive ion composition and temperature, and electron density and temperature measurements during AURORAE mission of ESRO 11 satellite
13 p2253 A69-27753

Electron temperature observation in daytime ionosphere, considering energy loss to ions and neutral particles
15 p2603 A69-31402

Simultaneous solution of continuity and heat conduction equations for ionospheric plasma consisting of electrons, atomic O ions and neutral gas species, discussing varying solar flux effects
16 p2849 A69-32082

Maximum ionization altitude, thickness, electron density profile and temperature mean variations in summer of IGY and IQSY at Moscow station
16 p2783 A69-32539

Nighttime F 2 region temperature distribution under geomagnetically calm and disturbed conditions calculated from Alouette 1 satellite data
19 p3304 A69-36623

Topside ionospheric structure from Alouette 2 data, discussing thermopause temperature, plasma temperature, electron density profiles, satellite plasma frequency, etc
20 p3532 A69-37895

Auroral midlatitude red arcs ground and satellite data, noting field aligned electron density depression, plasma temperature increase and O plus-H plus transition altitude
20 p3532 A69-37897

Ionospheric electron temperature profiles for midday equinoctial conditions noting protonospheric and conjugate heating effects
22 p3939 A69-40506

Rocket measurements of diurnal variations of F region concentrations and temperature of molecular N and O, showing disagreement with satellite drag data
22 p3939 A69-40515

Conjugate regions 6300 A airglow enhancement during predawn, noting photoelectrons role in heating dark ionosphere region by producing fast electron flux
24 p4308 A69-43011

IONOSPHERICS

NT DAWN CHORUS

NT HISS

Aeronomic parameters effect on ionospheric effect of SC magnetic storm, calculating maximum ionization levels, F layer ionization and vertical ionization profile parameters
09 p1486 A69-21546

Proposed index for measuring ionospheric scintillations, describing simplified scaling method
16 p2752 A69-32106

Aeronomic parameter effect on ionospheric effect of SC magnetic storm, calculating maximum ionization levels, F layer ionization and vertical ionization profile parameters
16 p2783 A69-32541

Phase modulation in pseudo-noise ionospheric communication system for reducing F region CW signal fading
18 p3104 A69-35308

Lower ionosphere over geomagnetic equator during evening twilight characterized by solar disturbances, using rocket-borne Langmuir and plasma noise probes
21 p3702 A69-38353

IONS

NT ANIONS

NT ANTIPROTONS

NT CATIONS

NT CESIUM ION

NT DEUTERONS

NT FERRIC ION

NT HEAVY IONS

NT HYDROGEN IONS

NT HYDRONIUM IONS

NT METAL IONS

NT MOLECULAR IONS

- NT NITROGEN IONS
NT PROTONS
NT SOLAR PROTONS
NT TRIVALENT IONS
- C III 2p super 2 presuper 1 D level mean life measurement using beam-foil technique, noting corresponding Einstein A coefficient
07 p1184 A69-18643
- Stigmatic profiles of solar C II doublet resonance lines obtained by rocket-borne echelle spectrograph
09 p1592 A69-21456
- Major ions in chemi-ionization of hydrocarbon flames determined for heats of formation by photoionization mass spectrometer
22 p3896 A69-40727
- [IMPACT PREDICTION]**
U COMPUTERIZED SIMULATION
QSY [INTERNATIONAL QUIET]
U INTERNATIONAL QUIET SUN YEAR
- RASERS**
U INFRARED LASERS
IRIDIUM
- Chemical vapor deposition of iridium coatings on graphites for high temperature oxidation protection, discussing parameters for iridium compounds and optimum depositing conditions
01 p0097 A69-10643
- Gold and iridium concentrations in meteoritic and terrestrial materials by neutron activation, discussing chondrules, meteoritic troilite and metallic spherules
08 p1404 A69-20918
- RISES [MECHANICAL APERTURES]**
- Reflection coefficient of double discontinuity consisting of two closely spaced inductive irises in rectangular waveguide
09 p1453 A69-21444
- Iris beam waveguide transmission loss as function of irises alignment, iris frame width and guide axis curvature
13 p2233 A69-28070
- Wave propagation in open periodic two dimensional iris waveguide and beam reconstruction by diffraction, considering existence and character of modal fields
16 p2753 A69-32394
- RON**
- Dynamic tensile stress-strain curves for annealed Al, Cu and Fe at constant strain rates, describing experimental method
03 p0524 A69-13065
- Galvanostatic transients of iron passive in 2N sulfuric acid, noting space charge effects and zero field current variation
[ECS PAPER 84] 03 p0382 A69-13858
- Solar Fe abundance from photospheric permitted Fe and forbidden Fe II lines, noting equivalent widths of two Fe II lines
03 p0515 A69-14036
- Si and iron impurities effects on duraluminum alloy structure and mechanical and plastic properties for fabrication from granules and rolling from ingots
03 p0452 A69-14120
- Collisional ionization cross section for Fe ions evaluated to estimate solar corona temperature
04 p0651 A69-13465
- Residual gas effect on fatigue behavior of pure iron subjected to alternating bending load in ultrahigh vacuum
04 p0616 A69-14846
- Fe doped Ga-as p-i-n structure electrical conductivity, Hall effect, thermally induced currents, space charge bounded currents and current instability
04 p0643 A69-15263
- Trivalent iron doped andalusite crystals dielectric and maser properties, investigating spin-lattice relaxation, cross relaxation times and inversion ratio
[IEEE PAPER C-2] 07 p1150 A69-19049
- Mean square radii for assigned terms of Fe I energy diagram for Van der Waals line broadening
08 p1392 A69-20559
- Iron line absence in emission spectrum of thermal X ray sources, constraining proposed thermal models
09 p1580 A69-22231
- O, Ne, Si and Fe ionization equilibria in low density plasma, including dielectronic recombination and autoionization processes in calculations
09 p1543 A69-22404
- Neutrino loss effects on evolution of pure iron stars, considering white dwarf, presupernova models and iron-helium transition
09 p1606 A69-22420
- Spatial distribution of residual nuclei produced in thick Fe targets by one and three GeV protons, noting total production and longitudinal variation of production
10 p1760 A69-23411
- Transport equation describing drift, diffusion and reaction of iron swarm influenced by electric field in gas
13 p2306 A69-27457
- Oscillator strengths and wavelengths of X ray and EUV transitions in highly ionized iron line spectra
13 p2326 A69-27554
- Fe III line profiles and equivalent widths from spectrograms of zeta Cas and gamma Peg for Fe abundance, using model atmospheres
13 p2347 A69-27715
- Gallium arsenide Fe-doped diodes efficiency as high speed switches from measured current-voltage characteristics at various temperatures
13 p2319 A69-27898
- Mean free path of interaction of nuclear active particles in Fe with energies greater than 530 gev
13 p2303 A69-28385
- Nuclear component energy flux absorption in Fe measured with ionization calorimeter
13 p2330 A69-28386
- Ni alloys phase precipitation and Fe substitution effects on heat resistant alloys
13 p2283 A69-28488
- Field equations for plane-parallel induction MHD machines with allowance for winding zone thickness and magnetic permeability of iron
14 p2405 A69-29914
- Temperature effects on magnetomechanical damping in Fe, Ni and mumetal, noting behavior difference due to domain structures
15 p2639 A69-30586
- Fe II forbidden lines profiles and equivalent widths prediction for solar photospheric spectrum, deducing photospheric Fe abundance
16 p2854 A69-31652
- Coronal Fe ionization lines X, XIII and XIV photographed by UV coronagraph
16 p2847 A69-31661
- Effective heat transfer coefficient lambda for microscopic Fe particles traversing rarefied air, oxygen and Ar target gases
16 p2769 A69-31870
- MH alpha 328116 /Cygnum/ spectrum noting three Fe IV lines
16 p2866 A69-32815
- Absolute gf values for Fe I and Fe II lines between 3190 and 3315 A measured by spectral absorption through shock heated gas containing Fe
18 p3175 A69-34304
- Solar Fe II lines theoretical equivalent widths calculations, estimating influence of photosphere model on iron abundance data
18 p3191 A69-34305
- Molten iron plane melt flow duration and mass in bimetallic castings production determined using nomogram
18 p3149 A69-35289
- High field susceptibility in Fe and Ni and high field Mossbauer study in Fe relating results to band structure and models of ferromagnetism
19 p3383 A69-36050
- Iron distribution inconsistency indicated in Group H and L chondrites through Ni and Co analysis of fractionated samples, plotting atomic ratios on Prior diagram
19 p3407 A69-36078
- Mossbauer spectra of Fe minerals in unequilibrated ordinary chondrites, noting ratios of olivine to pyroxene iron
19 p3408 A69-36082
- Intensity ratios effect of forbidden Fe and Ca transitions in solar corona on Fe/Ca ratio, noting cascading configurations
19 p3422 A69-36219
- Mass dependence of self diffusion in Fe by serial sectioning in alpha, gamma and delta phases, determining isotope effect with Fe radioactive isotopes
19 p3346 A69-36440
- Mercury internal constitution and chemical composition, discussing models with iron cores and iron admixtures in mantle
20 p3597 A69-37331
- Solar corona Fe XII emission spectral lines relative intensity analyzed as function of temperature electron density
20 p3603 A69-37548
- C content and microstructure effect on electrochemical parameters of Fe and steels in dilute sulfuric acid, discussing Tafel constants and current density
20 p3563 A69-38002
- Revised solar iron abundance by photospheric Fe I lines analysis using Garz and Kock f values, noting influence on solar photospheric model
21 p3796 A69-38475
- Fe whiskers formation and cross section determination by Fe dichloride reduction
22 p3919 A69-40233
- King furnace absorption source used with spectrometer in relative oscillator strength measurement, with experiments on lines of Fe I
22 p4022 A69-40466
- Photoionization model of Seyfert galaxy extended to calculate temperatures, luminosities and sizes of zones emitting forbidden Fe X /6374 A/ and Fe XIV /5303 A/
22 p4024 A69-40581
- Ferredoxin from thermophilic and mesophilic Clostridia, noting difference in heat stability due to iron and sulfide environments
22 p3897 A69-41068
- Fe abundance in sun and carbonaceous chondrites, noting agreement between solar and meteorite abundances of Ni, Mg, Si and Li
24 p4385 A69-43223
- IRON ALLOYS**
- NT AUSTENITIC STAINLESS STEELS
NT BAINITIC STEEL
NT CARBON STEELS
NT CHROMIUM STEELS
NT HIGH STRENGTH STEELS
NT MARAGING STEELS
NT MARTENSITIC STAINLESS STEELS
NT NICKEL STEELS
NT STAINLESS STEELS
NT STEELS
- Deformation in aged Fe-Cr alloy studied for rate-controlling solid solution mechanism as function of stress
01 p0095 A69-10601
- Lattice parameters of austenitic Fe-Ni alloys as function of titanium content, using Debye-Scherrer camera
03 p0443 A69-13123
- Low carbon maraging steel, studying age hardening behavior of iron-manganese-nickel alloys with titanium additions
05 p0781 A69-16541
- Sintered W-Ni-Fe alloys strength and precipitation hardening characteristics for various compositions and cooling conditions
05 p0782 A69-16798
- Electron microscopic study of structural changes occurring during aging of martensite in Fe-Ni Ti alloy
05 p0783 A69-16813
- Grain size dependence of yield, flow and fracture stresses of Fe-Co-V alloy for 77-298 K
07 p1166 A69-19264
- Czechoslovakian heat resistant iron-carbon-aluminum alloy Pyroferal, properties and applications
07 p1168 A69-19345
- Dislocation damping measurements made on Fe-18Cr-Ni alloys, noting damping relation to nickel content and stacking fault
08 p1334 A69-20576
- Alloying elements effects on structure, mechanical properties, aging and composition of precipitation hardening intermetallic phases in Ni and Fe based alloys
09 p1525 A69-22143
- Supersaturation of dissolved B in splat quenched Fe-Ni-B alloys, noting interstitial and substitutional B in martensitic and austenitic phases
10 p1707 A69-22987
- Composition and sintering temperature cooling effects on fracture properties of W-Ni-Fe alloys, using electron microscope fractography
10 p1711 A69-23333
- Initial aging stage in Fe-Ni-Ti alloys using diffuse X ray scattering with electron microscopy of thin foils
10 p1712 A69-23720
- Fe-Fe interactions influence on increase in thermoelectric power with applied magnetic field at low temperatures for dilute alloys of Fe in Au
10 p1639 A69-23861
- Meteorite fragment from Arizona Meteor Crater, establishing probable history from shock loading experiments on iron alloys
12 p2158 A69-26344
- Intermetallic compound precipitation effects on mechanical properties of Fe-Mo alloy at high temperatures
12 p2116 A69-26925
- Structural features of Fe-Ni massive martensite observed by light, electron and hot stage microscopies showing parallel block packet
13 p2276 A69-27401
- Precipitation influence on martensite formation kinetics and structure of Fe-Ni Ti alloys
13 p2279 A69-27765

Metallographic study of microstructure recrystallization of 50 Ni-50 Fe alloy during annealing using special etchants and methods

13 p2281 A69-28155

Nital etchant and sodium bisulfite stain for morphology of quenched dilute alloy Fe-Ni martensite

13 p2282 A69-28166

Martensite transformation with fcc lattice in Ti alloys containing 5.9 percent Fe analyzed as function of cooling rate using X ray analysis

15 p2636 A69-30105

Heat resistant Fe and Cu alloys creep index affected by temperature, testing time and specimen grain size

15 p2639 A69-30569

Dispersoids and temperature effect on coercive force of 19 Co base and 10 Fe plus 27 percent Co base

15 p2669 A69-30689

Surface layer role in strengthening of iron determined from examining temperature dependence of internal friction during thermomechanical treatments

17 p2991 A69-33939

TiNi compound alloying with Al and Fe, considering effect on hot hardness at various temperatures

18 p3157 A69-35249

Phase shape deformation and austenite stabilization in Fe-Ni and Fe-Ni-Ti alloys following secondary alpha phase of reversed martensite-austenite transformation

18 p3159 A69-35448

Isothermal and thermal martensite transformations on polished surfaces of Fe-Ni-Mo alloys

19 p3344 A69-35983

Autodiographic methods for diffusion and phase transformation in Fe-Cr alloys by application of photographic emulsion with tracer element on metal surface

20 p3561 A69-37416

Crystallographic relations between mother gamma phase and bulk martensitic structure of Fe-Ni alloys with less than 20 percent Ni, using radioisotopes

20 p3562 A69-37781

Smooth and notched tensile properties of Fe-Ni alloys in liquid Hg, discussing ductility and toughness

20 p3563 A69-38025

Plastic deformation combined effect with aging on mechanical properties of phase-hardened austenitic Fe-Ni-Ti alloys

21 p3746 A69-38956

Nonmetallic inclusions formation mechanism after reducing iron by Al, Zr and Ti, noting oxygen/ reducing agent ratio role

22 p3969 A69-40069

Alloy softening in bcc Fe-N and Fe-Ni, discussing causes of thermal stress component reduction in interstitial and substitutional alloys

22 p3969 A69-40164

Equilibrium vapor compositions and activities over Fe-Cr-Ni alloys at 1600 C determined by collecting effusate from thorium Knudsen cells

23 p4175 A69-41503

Ternary diffusion at high temperature in Fe-Co-Ni alloy system covering entire ternary phase diagram, including computed interdiffusion coefficients

23 p4176 A69-41505

Coherent matrix precipitates observation in Fe-Ni-Cr alloy by transmission electron microscopy, discussing yield strength and elongation dependence on aging conditions

23 p4176 A69-41508

IRON CHLORIDES

Relative oscillator strengths of 3500-5600 A Fe I lines in omission of arc burning in Ar with iron chloride admixture

20 p3581 A69-37823

IRON COMPOUNDS

NT CHROMITES
NT COHENITE
NT CORDIERITE
NT FAYALITE
NT FERRITES
NT ILMENITE
NT MAGNETITE
NT SCHREIBERSITE
NT TROILITE

Cr-S and Cr-Fe-S systems phase relations, using silica tube and collapsible tube experiments, correlating formation conditions of meteoritic sulfide assemblages

19 p3359 A69-36123

Charge transport in n and p type samples of beta phase semiconducting iron disilicide, noting effect of room temperature doping

19 p3390 A69-36556

IRON ISOTOPES

Mass dependence of self diffusion in Fe by serial sectioning in alpha, gamma and delta phases, determining isotope effect with Fe radioactive isotopes

19 p3346 A69-36440

IRON METEORITES

NT SIKHOTE-ALIN METEORITE

Shock loading history effect on solid state response of iron meteorites to annealing at moderate temperatures permits deductions about thermal history

01 p0149 A69-10134

Meteorite structure and origin, discussing cosmic dust analysis and collection, Tungusk silicate-magnetite spherules, asteroid collisions and meteorite ages

01 p0159 A69-11367

Sikhote-Alin iron meteorite high temperature oxidation and ablation and simulation with Fe-Ni alloy, noting phase compositions and structure

01 p0025 A69-11373

Uranium content in fragments from iron meteorites determined by fission fragment track recording

01 p0026 A69-11377

Chinghe iron meteorite discovery site, noting no crater or impact traces

01 p0160 A69-11380

South African octahedrite containing inclusions of troilite and graphite veined with kamacite

03 p0507 A69-13097

Iron meteorites and possible utilization by primitive man, noting long resistance to decay

03 p0515 A69-14033

Mossbauer spectra of shocked and unshocked iron meteorite and fayalite

03 p0517 A69-14231

Lunar mascons size and depth calculated in terms of mare formed by low velocity iron meteorites impact

04 p0654 A69-14629

Electron microprobe analysis of potassium feldspar in Weekeroo Station meteorite

04 p0659 A69-14979

Widmanstatten angles relation to orientation of plane of section in iron meteorites

07 p1217 A69-19235

Trace element distribution in metal phase of chondrites and iron meteorites, using neutron activation analysis with radiochemical separation

08 p1404 A69-20921

Trace elements distribution in Smithonia iron meteorite by spark source mass spectrometry, noting terrestrial weathering effects

08 p1404 A69-20922

Chlorine as indicator of terrestrial contamination in iron meteorites, using neutron activation analysis and metallographic observation

08 p1405 A69-20923

Radiation ages of silicate inclusions in iron meteorites based on Sr evolution diagrams

08 p1405 A69-20927

Kodaikanal iron meteorite measurements for cosmogenic rare gases and K-Ar isotopes ages for glass inclusions

09 p1596 A69-22047

Structure transitions in iron meteorites from Widmanstatten to granular pattern to study Barringer crater and Canon diablo meteorites formation

09 p1597 A69-22154

Tritium and argon 39 measurements of stone and iron meteorites, discussing decay and production rates and cosmic ray intensity

09 p1604 A69-22398

Meteorite fragment from Arizona Meteor Crater, establishing probable history from shock loading experiments on iron alloys

12 p2158 A69-26344

Freshly fallen meteorites from Portugal and Mexico, determining exposure age and classifying into iron meteorite and carbonaceous chondrite types

12 p2160 A69-26935

Tishomingo iron meteorite metallography, noting nickel content and martensitic microstructure evolution

13 p2353 A69-28159

Metallography of iron meteorites emphasizing Canyon Diablo anomaly

13 p2353 A69-28169

Iron and stone meteorites ablation using electrodeless plasmatron and filmed onto IR films

15 p2697 A69-31252

Silicon in iron meteorites and earth core determined by activation analysis on octahedrites, hexahedrites and ataxites

16 p2865 A69-32807

Structure of meteorite Gibeon section containing taenite grains and annealing twins indicating plastic deformation of taenite followed by recrystallization and grain growth

17 p3034 A69-33586

Boron, Li and Cl contents in iron and stone meteorites by fluorometric, thermal-neutron activation

and pyrohydrolytic separation methods, tabulating results

19 p3408 A69-36003

Cosmic-ray-produced stable and long-lived nuclides in iron meteorites, considering shielding effect on spaliation production

19 p3411 A69-36009

Ar 39 and Cl 36 production rates and ratios in stony and stony-iron meteorites metal phases, discussing terrestrial age calculation

19 p3411 A69-36101

Cosmic ray produced Be 10 in iron meteorites (terrestrial age determination, considering Cl 36 and rare gas analysis

19 p3412 A69-36101

K and Ar 40 determination in iron meteorites by neutron activation for K/Ar dating

19 p3412 A69-36101

Isotopic age determinations on iron and stony meteorites, discussing Rb-Sr and K-Ar results, internal isochrones, Kodaikanal data and planetary formation

19 p3413 A69-36101

Magnetic properties of stone, stony-iron and iron meteorites, discussing natural remanent magnetization origin in parent bodies and magnetic susceptibility

19 p3415 A69-36122

Iron meteorites genetic classification based on parent body cooling rate and Ga-Ge trace element content

19 p3416 A69-36122

Iron meteorites analysis for Ni, Co, P, C, S and Cu elements by milling technique, noting superiority degree based on Co-Ni correlation

19 p3417 A69-36130

Kamacite analysis for P and Ni in chondrites, pallasite and iron meteorites, considering cooling rate and rhabdite

19 p3417 A69-36130

Fe-Ni-P phase diagram studies applied to schreibersite and rhabdite formation in iron meteorites

19 p3417 A69-36133

Morphologies and mechanical properties for identification of phosphides/schreibersite/ and carbides/cohenite/ in iron meteorites, noting nucleation and growth

19 p3417 A69-36133

Iron meteorites microscopic and macroscopic features due to preterrestrial mechanical deformation, stressing local displacements encountered in normal octahedral kamacites

19 p3418 A69-36134

Spallogenic rare gas concentrations and isotopic ratios in taenite of iron meteorites measured mass spectrometrically and compared with kamacite values

19 p3419 A69-36135

Trapped rare gases in Fe phase and silicate inclusions of Campo del Cielo Meteorite, El Taco

19 p3419 A69-36140

Stony meteorite barium isotopes and iron meteorite and terrestrial silicate inclusions analyzed using double spike method for laboratory fractionation correction

19 p3425 A69-36422

Neutron activation method for Mn 53 in meteorites by X ray and gamma counters, noting extraction of Mn 54 free reference source

20 p3601 A69-37504

Meteorites Ni-Fe metal structures analysis as part of petrology study of mesosiderites

20 p3602 A69-37536

Chemical classification of iron meteorites with Ge concentrations between 80 and 200 ppm, reporting concentrations of Ge, Ni, Ga and Ir

20 p3602 A69-37537

Hoba meteorite surface radioactive isotope composition measured, finding terrestrial age from Ni-59 activity

22 p4021 A69-40411

Bogou iron meteorite Ni-Cu-Zn contents determined by radiochemical methods

23 p4209 A69-41321

IRON OXIDES

NT CHROMITES
NT ILMENITE
NT MAGNETITE

Emissivity and other radiative characteristics of stainless steel oxides heated to various temperatures in air

03 p0453 A69-14157

IROQUOIS HELICOPTER U UH-1 HELICOPTER

IRRADIANCE

NT ILLUMINANCE
NT SOLAR CONSTANT

Atmospheric optical data recorded by instrumented aircraft near Crater Lake, discussing surface spectral irradiance data

01 p0111 A69-10846

Nonlinear holograms distortions analyzed by five point method utilizing relation between irradiance and amplitude transmittance of photographic emulsion

12 p2090 A69-26255

Solar spectral irradiance measured by airborne instruments, discussing construction, calibration, etc., of photoelectric filter radiometer and Leiss monochromator

16 p2861 A69-32261

IRRADIATION

NT AURORAL IRRADIATION
NT DEUTERON IRRADIATION
NT ELECTRON IRRADIATION
NT ION IRRADIATION
NT NEUTRON IRRADIATION
NT PROTON IRRADIATION
NT X RAY IRRADIATION

Cutaneous receptor response to microwave irradiation, measuring warmth sensory effects in human forehead with radiometer
[AGARDOGRAPH-111] 08 p1266 A69-20677

Electric vector transformation for three dimensional photoelastic medium irradiated by light in reverse direction, noting optical systems of birefringent plates and rotators

12 p2180 A69-26339

Luminescence effects on apparent size and shape of foveally fixated targets of various forms

19 p3259 A69-36458

IRREGULARITIES

Irregular pressure profiles and pressure-time histories when using octofluorocyclobutane and sulfur hexafluoride in explosive driven shock tube
[AIAA PAPER 68-730] 24 p4297 A69-43577

IRREVERSIBLE PROCESSES

Thermodynamic foundations of permanent deformation theory, noting parallel to viscoelastic material theory

02 p0350 A69-11714

Onsager reciprocity relations applied to thermodynamics of nonlinearity and noise in diodes

04 p0574 A69-14435

Variational methods for nonequilibrium thermodynamic processes noting fluctuation theory introduction

04 p0551 A69-15314

Thermodynamics of fluid materials and characterization of thermodynamics of irreversible processes, using constitutive equations

06 p0959 A69-18222

Hydrodynamic stability and entropy decrease in flow in three dimensional space, using irreversible thermodynamics principles

10 p1808 A69-22892

Book on thermodynamics of irreversible processes covering chemical reactions, relaxation phenomena, permeation, osmosis, electroosmosis, thermosmosis, electric conduction, diffusion, etc

11 p1999 A69-24533

Thermal efficiencies of liquid-metal MHD generator cycles, analyzing optimum parameters, working fluid and partial irreversibilities

13 p2205 A69-27484

Classical plasticity theory modified to include finite elastic and plastic strain components by considering thermoelasticity and plastic work irreversible processes

13 p2362 A69-28119

Linear irreversible thermodynamics theory as applied with conservation principles and Maxwell relations to charged particle motion in electromagnetic field, noting Onsager coefficients role

17 p3075 A69-34142

Irreversibility resulting from composition changes in operating fuel cell anode and cathode chambers and cell geometry influence

18 p3093 A69-34781

Entropy definition for nonequilibrium states, using mathematical theory of stability of motion applied to kinetic equations of irreversible processes

23 p4238 A69-41366

Heat and mass transfer in gas suspension, studying suspended particles effects on heat transfer by irreversible thermodynamics

[ASME PAPER 69-HT-34] 24 p4410 A69-43528

IRRIGATION

Plant and soil thermal behavior for various conditions of crop species, plant spacing, tillage, irrigation and aerial thermal scanner imagery

12 p2075 A69-26989

IRRITATION

U TOXICITY AND SAFETY HAZARD

IRROTATIONAL FLOW U POTENTIAL FLOW

ISENTROPIC PROCESSES

Approximate methods for integration of equations of plane isentropic motion of gas at supersonic velocities

05 p0699 A69-16674

Isentropic compression tube with piston compressor for producing hypervelocity test flows, noting shock speeds

[AIAA PAPER 69-334] 13 p2249 A69-28270

Simple waves in compressible isentropic flows of inviscid nonheat-conducting gas free of shock waves

18 p3121 A69-34534

Flow discharge characteristics of nozzle during swirling gas flow ejection, considering isentropic and isothermal limiting cases

24 p4247 A69-43499

ISING MODEL

U FERROMAGNETISM
U MATHEMATICAL MODELS

ISIS-A

NT ALOUETTE 1 SATELLITE

ISIS A satellite fixed and sweep frequency ionograms indicating electron density variations, ionospheric resonances and Cerenkov radiation

15 p2604 A69-31416

Antenna systems design for ISIS-A scientific satellite, discussing antenna array of 13 radiators for telemetry, command, beacon and experimental purposes

17 p2918 A69-33030

ISIS SATELLITES

NT ALOUETTE 1 SATELLITE
NT ALOUETTE 2 SATELLITE
NT ISIS-A

Ionospheric satellites objectives and development resulting from topside sounder and ISIS programs

20 p3529 A69-37855

Ionospheric satellite series Alouette-ISIS, discussing successive engineering and management constraints leading to ISIS-C design

20 p3618 A69-37856

Sweep frequency ionospheric topside sounder design for Alouette and ISIS satellites, discussing influence of experiment requirements and spacecraft limitation and environments

20 p3507 A69-37859

ISLANDS

U GREAT BRITAIN
U JAPAN

ISOBARS (PRESSURE)

Temperatures and geopotentials of isobaric surfaces in Northern and Southern Hemispheres compared for summer and winter seasons

14 p2473 A69-29724

Turbulence coefficient in layers between main isobaric surfaces based on wind and temperature fields analysis

15 p2648 A69-30646

Error sources in forecasts for heights of isobaric surfaces obtained by numerical integration of prognostic equations of equivalent barotropic models

19 p3361 A69-35770

ISOBUTANE

U BUTANES

ISOCHORIC PROCESSES

Heat capacity at constant volume determined for nitromethane, trinitrotoluene and difluoromethane alkanes

[WSCI PAPER 68-39] 07 p1202 A69-18368

Specific isochoric heat capacity of pure fluids, considering thermal equation of state, vapor pressure and boundary conditions at critical point

11 p2001 A69-25201

ISOCROMATICS

High speed photography using multiply pulsed ruby laser, Pockels cell modulation and smear camera for isochromatic and photoelastic pattern recording

19 p3306 A69-35731

ISOCYANATES

Isothiocyanates and phenyl isocyanate reaction with hydrazinoethanol and hydrazinoethyl hydrogen sulfate

16 p2747 A69-31808

ISOENERGETIC PROCESSES

Conduction band anisotropy in n-type cadmium tin arsenides, analyzing galvanomagnetic tensor and distribution of isoenergetic surfaces for electrons

03 p0488 A69-13888

Turbulent free shear layers in isoenergetic flow, correlating theory and experiment
[ASME PAPER 68-FE-9] 05 p0748 A69-16077

Conduction band anisotropy in n-type cadmium tin arsenides, analyzing galvanomagnetic tensor and distribution of isoenergetic surfaces for electrons

11 p1939 A69-25689

ISOLATION

NT SOCIAL ISOLATION

Work capacity and adaptation characteristics of humans confined in small chamber and experiencing effects of isolation and sensory deprivation

08 p1262 A69-19838

EEG, heart beat, respiration rates, body temperature, motor activity, physical and mental efficiency of man during anechoic chamber confinement

10 p1646 A69-23510

Optical carrier single channel telemetry system providing complete electrical isolation between shock tube data acquisition and data recording instrumentation

14 p2449 A69-29561

Life in common by groups of four or five people isolated on high mountain under adverse conditions

21 p3661 A69-39267

Internal interactions of continua and concept of thermal isolation, discussing second law of thermodynamics

22 p4050 A69-40450

ISOLATORS

NT VIBRATION ISOLATORS

Circulator power splitting and isolating function in integrated microwave network

02 p0222 A69-12475

Substrates containing silicon regions separated by silicon dioxide or ceramic dielectrics, prepared by lamination in hot press, noting applications to integrated circuits

07 p1100 A69-18617

Dielectrics refill and decal air isolation for silicon integrated circuit components

07 p1100 A69-18618

ISOMERIZATION

Cool flames nonisothermal two-stage ignition of neopentane-oxygen mixtures, discussing chain propagation due to isomerization

11 p1940 A69-24477

Ionic and biradical mechanisms in thermal and photo cis-trans isomerizations elucidated by planar and twisted configurations of polyenes

13 p2216 A69-27618

ISOMERS

Temperature dependent isomer shift and anharmonic binding of Sn 119 in niobium stannide, measuring Mossbauer recoil free fraction

01 p0134 A69-10009

Heuristic Dendral program to mechanize inductive inference in organic chemistry to determine isomers in chemical compounds

07 p1075 A69-19484

Isoprenoids and isomeric alkanes identification in carbonaceous chondrites by gas-chromatographic mass-spectrometric analyses, including results from trillite nodules

19 p3414 A69-36113

Ion structure of keto and enol and McLafferty rearrangements determined by ion cyclotron resonance spectroscopy

19 p3265 A69-36288

DENDRAL program used to construct all possible acyclic structural isomers of C, H, N and O

23 p4114 A69-42214

ISOMORPHISM

Ti sub 3, Rh sub 5 and Hf sub 3, Rh sub 5 existence and isomorphism confirmed by crystallographic and X ray methods

19 p3343 A69-35920

ISOPHOTES

Zodiacal light isophotes and near-earth component from relationship between brightness at various geomagnetic latitudes and position of moon

03 p0512 A69-13693

Isophotal wavelengths of U, B, V and R bright star systems for replacing spectrophotometry with broad-band multicolor data

08 p1408 A69-21134

Isophot system characterizing photometric structure of elongated celestial objects constructed by equidensitometric method based on Sabatier photographic phenomenon

11 p1952 A69-24255

Polarimetric and photometric observations of comet Ikeya-Seki 1965f, plotting isophotes of head and polarized light distribution in tail

15 p2685 A69-30525

Photographic photometry of comet Ikeya-Seki during passage near sun, plotting isophotes of coma and tail and brightness distribution diagrams

15 p2685 A69-30527

ISOPLETHS

Orion nebula isophotal contours optical observation for three continuum colors /blue, yellow and IR/ and H alpha
22 p4031 A69-40942

ISOPLETHS

U NOMOGRAPHS

ISOPYCNIC PROCESSES

Diffusive flow with isopycnic lateral boundaries in porous medium and density distribution of diffusive motion, noting exact solution equivalence to previous solution
11 p1869 A69-24887

ISOSTASY

Lunar gravitational anomalies from internal density variation viewpoint, discussing isostasy in maria
04 p0654 A69-14631

Lunar mascons and maria isostasy, discussing time requirements
20 p3604 A69-37564

Book on gravimetry covering gravity measurement on land and in ocean, gravity anomalies, isostasy, geodetic applications, Eotvosian measurements and terrestrial tides
21 p3715 A69-39000

ISOSTERIC PROCESSES

U ISOPYCNIC PROCESSES

ISOTHERMAL FLOW

Fluctuation velocity, apparent kinematic viscosity and turbulent shear stress in isothermal homogeneous free jets
06 p0909 A69-17169

MHD generator plasma anisotropic instability caused by amplified magnetosonic waves propagating normal to current
11 p1922 A69-24227

Radial electric field effect on pressure drop in isothermal laminar flow of dielectric liquid through stainless steel tube, considering ion drag
12 p2136 A69-26401

Self similar solution to one dimensional isothermal ionized gas outflow from ionization front in half space filled with neutral gas exposed to quanta flux
21 p3771 A69-38997

Heat pipes for isothermal and adaptable energy transfer for space applications, discussing temperature control by fluid choice
21 p3852 A69-39475

ISOTHERMAL LAYERS

Nb-Zr-Cr alloys solidus surface and isothermal sections, using optical pyrometry, microstructural and X ray analyses
08 p1333 A69-20440

Solar atmosphere five minute oscillations observed by Frazier divided into two harmonic atmospheric model for studying oscillation region height and mean temperature
13 p2343 A69-27627

Shock waves from accelerated, decelerated and stationary axisymmetric bodies flying at supersonic velocities in stratified isothermal atmosphere
15 p2551 A69-31171

Earth based microwave data revealed isothermal layer in extrapolating Venus atmospheric profile below region probed by Mariner 5 and Venera 4
16 p2852 A69-31553

Shock wave propagation in isothermal atmosphere, discussing radiation and ionization effects on thermal jump
16 p2858 A69-32207

Radiant heat transfer predictions between isothermal plates based on diffuse plus specular directional property model
[AIAA PAPER 69-624] 17 p3070 A69-33259

Thermal wind instability by numerical integration of equations of motion, noting convective cells tilt
17 p2998 A69-33734

Desinent cavitation on hemispherical nosed bodies in water at various temperatures and velocities, considering isothermal case for surface nuclei
[ASME PAPER 69-FE-1] 20 p3516 A69-37986

Lower boundary approximation for theory of thermal laminar steady state boundary layer on isothermal immersed plate
23 p4150 A69-41334

ISOTHERMAL PROCESSES

Radiation from isothermal sphere in vacuum having spherical scattering indicatrix solved by Bubnov-Galerkin method with allowance for scattering
01 p0174 A69-10106

Chemical composition effect on duraluminum supersaturated solid solution stability, presenting time vs temperature C curves of isothermal decomposition
01 p0094 A69-10396

Menabrea theorem for nonisothermal transformations of anisotropic elastic body with internal incompressibility constraint and initial stress
02 p0341 A69-12197

Heat conduction with change of phase in three dimensional melting and solidification problem under isotherm conditions and balanced energy at interface
02 p0354 A69-12548

Condensation-enhanced vaporization rates in nonisothermal systems, noting fume nucleation augmentation of rates into cooler environments
03 p0532 A69-13122

Plasticity of metals under isothermal conditions at elevated temperatures
04 p0671 A69-14454

Isothermal diode as study basis for internal complex controlling thermionic energy conversion
09 p1439 A69-21827

Audio frequencies internal friction measurement of austenitic stainless steels subjected to heat treatment and corrosion, discussing time dependence and carbide precipitates morphology
10 p1713 A69-23819

Isothermal theory of cool flames, discussing oscillations-fuel consumption relations, kinetics, etc
11 p1970 A69-24476

Sublimation in ammonium perchlorate propellants combustion, discussing low temperature isothermal processes, linear regression rates measurements and low ambient pressure
11 p1940 A69-24481

Ions and electrons in ionosphere diffusion tensor components and ambipolar diffusion coefficient expressions derived for nonisothermal plasma
12 p2071 A69-26700

Critical parameters of isothermal quasi-degenerate white dwarfs calculated by energy method, allowing for relativity theory error and neutron irradiation effect
13 p2351 A69-27871

Isothermal deformations in linear viscoelastic material under uniaxial stress, determining optimum strain rate history for maximum work lower bound
15 p2707 A69-30637

Radiative heat transfer in nonisothermal scattering media of plane, spherical and cylindrical geometries separated by particle cloud
16 p2878 A69-31925

Radiation effect on inorganic solids isothermal decomposition induction period, deriving equations for conditions representing various kinetics combinations during irradiation
[WSCI PAPER 69-21] 16 p2832 A69-32359

Acoustic gravity waves generated in isothermal atmosphere by ground energy source calculated using stationary phase method and kinematic theory
18 p3129 A69-34953

Isothermal and thermal martensite transformations on polished surfaces of Fe-Ni-Mo alloys
19 p3344 A69-35983

Total band absorbance of nonisothermal IR radiating gas, using wideband formulation of Curtis-Godson approximation and series expansion formulation
22 p3983 A69-40101

Flow discharge characteristics of nozzle during swirling gas flow ejection, considering isentropic and isothermal limiting cases
24 p4247 A69-43499

ISOTHERMS

Isothermal sections construction of zirconium corner of ternary phase diagram of Zr-Mo-V system from microstructure of cast and quenched alloy specimens
02 p0262 A69-11846

Isothermal sections construction of Zr-V-Ni system phase diagram from study of alloys at 1000, 700 and 500 C
02 p0263 A69-11848

Heat conduction in medium with phase transitions, solving one dimensional nonlinear problem by calculation of isotherms and reduction to Cauchy problem
19 p3453 A69-36838

Isotherms location in simple nonconstant area /diverging/ tube configuration investigated for heat transfer
20 p3632 A69-37219

Heated body cooling off study via temperature field isothermal lines visualization on TV screen
20 p3539 A69-37437

Free convection flows about inclined infinite cylinders with isothermal surfaces
24 p4416 A69-43687

ISOTOPE EFFECT

Temperature dependence of isotope thermotransport in liquid K and Rb using steel capillary cells
03 p0533 A69-13970

Saturated absorption by Ne inside 6328 A He-Ne laser, discussing selection of Ne isotopes in gain and loss tubes
07 p1149 A69-18892

Isotope shifts in 4416 A cadmium laser, showing change of double peaked to single peaked profile with doubled active tube length
10 p1705 A69-23819

Mass dependence of self diffusion in Fe by serial sectioning in alpha, gamma and delta phases, determining isotope effect with Fe radioactive isotopes
19 p3346 A69-36444

ISOTOPE SEPARATION

Thermal neutron capture cross section at high temperature irradiations determined for W 184, describing radiochemical separation and flux counting techniques
24 p4315 A69-43199

ISOTOPES

NT ALUMINUM 26
NT ARGON ISOTOPES
NT BERYLLIUM 7
NT BERYLLIUM 10
NT BERYLLIUM ISOTOPES
NT BORON ISOTOPES
NT BORON 10
NT CADMIUM ISOTOPES
NT CALCIUM ISOTOPES
NT CARBON ISOTOPES
NT CARBON 12
NT CARBON 13
NT CARBON 14
NT CESIUM 133
NT CHROMIUM ISOTOPES
NT COBALT ISOTOPES
NT COBALT 60
NT DEUTERIUM
NT HELIUM ISOTOPES
NT HYDROGEN ISOTOPES
NT IODINE ISOTOPES
NT IRON ISOTOPES
NT KRYPTON ISOTOPES
NT KRYPTON 85
NT LANTHANUM ISOTOPES
NT LEAD ISOTOPES
NT LITHIUM ISOTOPES
NT MAGNESIUM ISOTOPES
NT MANGANESE ISOTOPES
NT NEON ISOTOPES
NT NITROGEN 16
NT OXYGEN ISOTOPES
NT OXYGEN 18
NT PHOSPHORUS 32
NT PLUTONIUM ISOTOPES
NT PLUTONIUM 238
NT POLONIUM ISOTOPES
NT POTASSIUM ISOTOPES
NT POTASSIUM 40
NT RADIOACTIVE ISOTOPES
NT RADIUM 226
NT RUBIDIUM ISOTOPES
NT RUBIDIUM 86
NT SCANDIUM ISOTOPES
NT SODIUM ISOTOPES
NT SODIUM 22
NT STRONTIUM ISOTOPES
NT STRONTIUM 90
NT TELLURIUM
NT THORIUM ISOTOPES
NT THULIUM ISOTOPES
NT TRITIUM
NT URANIUM ISOTOPES
NT URANIUM 235
NT VANADIUM ISOTOPES
NT XENON ISOTOPES
NT XENON 129
NT XENON 133
NT ZIRCONIUM ISOTOPES
NT ZIRCONIUM 95

Orientation of diamagnetic ground state Pb 207 atoms with nonzero orbital angular momentum by means of optical pumping and determination of nuclear moment
07 p1156 A69-19399

S-process nucleosynthesis and temperature averaged neutron capture cross sections studied in relation to solar system, considering elemental and specific isotopic abundances
08 p1357 A69-20899

Lead isotopes nucleosynthesis by three mechanisms and contribution of mechanisms to abundances, noting chronology in nucleosynthesis
08 p1357 A69-20899

Formation ratios of light isotopes in spallation reactions compared to observed stellar and solar abundances of lithium, beryllium and boron, discussing astrophysical implications
08 p1401 A69-20900

Relative intensities of lines in vibration and rotation bands of isotopic carbon dioxide in planet Venus, tabulating partition functions
15 p2656 A69-31154

Stony meteorite barium isotopes and iron meteorite and terrestrial silicate inclusions analyzed using double spike method for laboratory fractionation correction
19 p3425 A69-36422

ISOTOPIC LABELING

Tyrosine transaminase activity estimation by radioactive isotopic assay method, discussing application to rat liver and other organs
01 p0014 A69-10902

Tryptic digestion of C terminal tritiated peptides analyzed with Scenedesmus ferrodoxin, noting use for protein structural study
10 p1648 A69-24190

Calcium isotopes tracer migration in caged rats in metabolism study
13 p2212 A69-28618

Z-micron sections removed from metal specimens by microtome for radiotracer study of mass dependence of self diffusion
19 p3313 A69-36490

Sympathetic nerve liberated noradrenaline increasing melatonin synthesis, using C 14 tracer for monitoring
22 p3871 A69-40051

Compartmental models for radioactive tracer experiments with known tracer material amount, using generalized Spearman simultaneous estimation procedure
24 p4339 A69-42765

ISOTROPIC MEDIA

Stress-strain state of isotropic elastic medium using equations with stress tensor, noting role of curvilinear hole
01 p0164 A69-10081

Microwave signal nonlinear interaction in isotropic positive column
01 p0127 A69-10282

Energy transport in atmosphere studied by considering sphere in isotropic fluid in infinite field without gravity, using first law of thermodynamics
01 p0667 A69-11032

Linear stationary thermoelasticity equations for Cosserat continua, discussing static and kinematic conditions, anisotropy and centrosymmetric isotropy equations
02 p0336 A69-11557

Glan-Thompson and Rochon prisms modified by replacing one of two calcite halves of cemented oriented birefringent crystals with glass
02 p0280 A69-11924

General solutions of three dimensional elasticity theory applied to isotropic disks and plates, emphasizing homogeneous solutions
03 p0526 A69-13738

Elastic equilibrium stress condition of anisotropic plates with circular isotropic inclusions
04 p0667 A69-14264

Axisymmetric stress field around spheroidal inclusions and cavities in transversely isotropic material [ASME PAPER 68-WA/APM-14]
04 p0669 A69-14400

Electromagnetic wave propagation in moving isotropic refractive media, giving Maxwell-Minkowski and EM wave equations
04 p0557 A69-14760

Electromagnetic wave propagation in spherically stratified isotropic media, presenting generalized refractive index profiles for electric type fields
04 p0563 A69-15492

Theory of inhomogeneous simple bodies applied for universal solutions for incompressible laminated bodies
05 p0834 A69-15732

Real and imaginary parts of homogeneous isotropic electron plasma complex refractive index, noting application to plane electromagnetic wave propagation
07 p1193 A69-19183

Cylindrical antenna input impedance in isotropic plasma, assuming weak three dimensional plasma diffusion
08 p1285 A69-20428

Families of eigenfunctions concept for stress and strain tensors of proper motions in continuous isotropic medium, considering vortices and gradients
08 p1417 A69-20752

Compatibility theorem extension to three dimensional rigid plastic bodies with stress and velocity discontinuities, noting isotropic bodies with convex yield surface
08 p1418 A69-20845

Differential equations for normal propagation of plane electromagnetic waves in isotropic stratified inhomogeneous gyration medium, discussing boundary conditions and reflection properties
08 p1353 A69-21000

Simply supported isotropic cylindrical panel stability under axial compression, obtaining asymptotic series expansion for upper critical stress
08 p1419 A69-21182

Transient heat flow in isotropic solids by electrical analog modeling in orthogonal curvilinear coordinate system
09 p1477 A69-22241

Reciprocity theorems of coupled and uncoupled thermoelasticity for macroisotropic and microisotropic simple homogeneous solids with microstructure
09 p1618 A69-22259

Longitudinal and transverse wave propagation in compressible isotropic turbulent plasma, noting mode coupling effect [AFCLR-69-0289]
10 p1729 A69-23424

Lame problem for elastic isotropic medium having free energy dependent on medium deformation and deformation gradients, estimating minimum surface curvature
11 p1970 A69-24632

Stress concentration in isotropic plates weakened by curvilinear holes subjected to loading at infinity, noting curvature at corner points of holes
11 p1972 A69-24655

Three dimensional bending problem for thick isotropic plate with curvilinear hole and normal and tangential stress applied to edge of hole
11 p1973 A69-24657

Optimum cooling of homogeneous isotropic cylindrical body with constraints on magnitude of thermoelastic stresses
11 p1976 A69-24772

Three dimensional problem of elasticity for transversely isotropic medium with cylindrical anisotropy, using partial differential equations for unknown functions
11 p1983 A69-25091

Nonlinear DC magnetic fields for nonhomogeneous isotropic current free regions in presence of ferromagnetic materials, discussing analytic solutions of boundary value problems
11 p1888 A69-25311

Helical and log conical helical antenna width reduction by loading of traveling wave antenna elements with isotropic material
11 p1852 A69-25315

Propagation of intensity modulated light rays in semiinfinite isotropic dispersive medium, discussing phase shift and modulation depth
12 p2029 A69-26026

Representation formula for response function of elastic materials having given isotropy group
12 p2188 A69-26926

Controllable motions of compressible homogeneous isotropic solids, anisotropic solids and fluids with memory under constant body force
12 p2189 A69-27118

Frequency equation for thickness effects on axisymmetric radial and rotatory vibrations of empty or fluid filled isotropic spherical shell
13 p2363 A69-28185

Microstresses and distortions in quasi-isotropic solid bodies under strain evaluated by correlation functions
14 p2531 A69-28806

Spectral distribution of fluctuations in stable plasma in absence of external fields, emphasizing electric field fluctuations, quasi-steady states, isotropic plasmas and thermodynamic equilibrium
14 p2490 A69-29103

Torsion of composite prismatic rod consisting of three different isotropic materials with two interfaces converging on cross section contour corner point
15 p2707 A69-30579

Stress concentration near circular nonreinforced hole at bending of transversely isotropic rectangular plate analyzed in terms of transverse shear theory
15 p2707 A69-30580

Cylindrical wave propagation in thermoelastic incompressible isotropic solids, considering cases of zero and nonzero coefficient of thermic dilation
15 p2707 A69-30626

Couple-stresses effect on stress concentration of plate containing infinite row of holes, solving linear elastic problem in isotropic Cosserat continua for plate
15 p2708 A69-30640

Nonlinear boundary value problems for isotropic plasma with known magnetic field, examining electromagnetic waves scattering at magnetic fluctuations
15 p2569 A69-30938

Bending theory for two layer plate made of isotropic material under sinusoidal load obtained by elasticity and classical theory based methods
15 p2714 A69-31198

Natural vibration of isotropic plates in temperature field with nonuniform distribution over plate
16 p2871 A69-31891

Somigliana dislocations effects on displacement field in linear isotropic elastic medium represented by integral with respect to line delineating surface
17 p3053 A69-33020

Initial thermostructural stresses in homogeneous quasi-isotropic two component medium, solving statistical boundary value problem thermoelastically
17 p3058 A69-33316

Infinite isotropic elastic plate vibration under vertical harmonic load, deriving vertical displacement at center of loaded area
17 p3058 A69-33408

Self channeling of light in nonlinear isotropic medium using exact solutions of nonlinear Maxwell equations for two dimensional case
17 p3007 A69-33975

Linear isotropic elastic continuum dislocations distribution, deriving transport equations by statistical methods, noting analogy between energy/momentum and MHD equations
18 p3212 A69-34352

Transverse shear deformation and rotatory inertia effects on large amplitude lateral free vibrations of transversely isotropic plates [ASME PAPER 69-APM-10]
18 p3213 A69-34386

Plane light wave propagation in homogeneous isotropic medium with fluctuating dielectric constant using perturbation theory and integrating energy conservation law
18 p3173 A69-35127

Isotropic plate critical strength measurements, evaluating role of material shear modulus
18 p3225 A69-35361

Refractive index profiles yielding wave functions expressed in terms of standard transcendental functions for electric fields in spherically stratified isotropic media
19 p3372 A69-35618

Natural frequencies of thin oblique angled isotropic plates, discussing closed form solution to differential equations
19 p3438 A69-36312

Plane elastic deformation in isotropic homogeneous medium using displacement vector, discussing finite difference equations and application to rectangular boundary
19 p3441 A69-36719

Homogeneous heat flux effect on limit load of isotropic plate with rectilinear through crack, noting conditions for crack propagation
19 p3441 A69-36744

Twisting of spherical shell of nonhomogeneous isotropic material with variable shear modulus and inner surface assumed to be stress free
20 p3619 A69-36911

Mathematical relations for ring laser beams polarization conditions, using slanted isotropic plate and phase circulator to separate polarization plane
20 p3553 A69-37606

Transverse vibrations of isotropic solid rectangular beam with secondary effects of rotary inertia and shear deformation retained
21 p3832 A69-38447

Plate bending theory modified for applying successive linear conjugates method to partially clamped isotropic plate and plate with circular hole
21 p3834 A69-38721

Stress-strain state in thin isotropic plate with circular hole under lateral bending and torsional moments
21 p3835 A69-38725

Model of isotropic polycrystal generalized to composite materials including mechanical mixtures, calculating macroscopic constants in heat conduction, diffusion and elasticity
21 p3752 A69-39193

Isotropic ideal bidimensional filter in interpretation of anomalous gravity fields, especially for separating local and regional effects
21 p3724 A69-39246

Antenna noise spectrum in collisionless isotropic plasma, considering plasma fluctuation theory and reciprocity theorem
21 p3683 A69-39284

Linear elastic isotropic materials for model tests, describing properties of material composed of Araldite B and air
21 p3844 A69-39319

ISOTROPIC TURBULENCE

Quantitative analysis of light intensity dependent changes in optical rotation angle of isotropic media caused by laser beam

22 p3959 A69-40017

Prolate spheroidal antennas operation in isotropic plasmas, studying effects of collision frequency, electron temperature and antenna length on admittance, radiation and current distribution

22 p3914 A69-40702

Kinetic beam instability development in homogeneous dust/gas cylinder rotating in hot invariable medium under arbitrary perturbations

22 p4032 A69-41017

Reflection and transmission coefficients for harmonic electromagnetic wave incident at parabolic layer of stratified isotropic plasma

22 p3901 A69-41020

Large elastic deformations of isotropic materials by deflection of composite parallelepiped composed of elastic incompressible materials, applying Rivlin solutions

22 p4048 A69-41277

Deformation tractions in undeformed and curved cuboid flexure and inverse flexure determined by stress-strain relations for homogeneous isotropic compressible materials

23 p4226 A69-41521

Radiative heat transfer in nonisothermal absorbing and emitting media without scattering and with anisotropic and isotropic scattering

23 p4239 A69-41632

Vector properties of isotropic strain hardenable materials in stress vector space applied to tubular brass subject to biaxial tension and complex loading

23 p4227 A69-41714

ISOTROPIC TURBULENCE

Diffusion of suspended particles in isotropic turbulence field of dispersed medium

02 p0234 A69-12579

Electrodynamics of turbulent conducting media based on nonrelativistic MHD

03 p0479 A69-13972

Rays associated Fokker-Planck relation for isotropic turbulence diffusion equation, discussing logarithmic refractive index, moments and path length

08 p1272 A69-20021

Magnetic field and magnetic energy evolution in infinitely conducting homogeneous isotropic turbulent medium, applying results to galactic magnetic field model

10 p1783 A69-23793

Sound field generation by isotropic turbulence through finite strength shock, estimating acoustic energy flux from supersonic jet containing shock waves

11 p1872 A69-25130

Time variability of horizontal wind as function of time provided by Kolmogoroff structure functions for components of isotropic turbulence

18 p3167 A69-34829

Homogeneous isotropic turbulence spectrum asymptotic behavior for various spectral energy transfer models

19 p3301 A69-36818

Approximate formula for energy spectrum of isotropic turbulence at large wave numbers, showing agreement with Gaussian exponential form

21 p3694 A69-38834

Spectral equation for decaying isotropic turbulence of incompressible inviscid flow at large Reynolds number, using spectral cascading

21 p3694 A69-38835

Final period of decay for viscoelastic fluid in homogeneous isotropic turbulence, deriving expressions for double correlation function and energy decay

22 p3928 A69-39891

Model for statistically isotropic homogeneous turbulence in incompressible fluid, representing turbulence as superposition of individual vortex sheets

22 p3930 A69-40525

Transverse spectra and structural functions of fluctuations for plane waves of different frequencies propagating in isotropic turbulent medium

23 p4117 A69-41728

Symmetry properties of Cameron-Martin-Wiener kernels in isotropic velocity field, applied to one dimensional model of incompressible turbulent flow

24 p4301 A69-43358

ISOTROPY

NT ISOTROPIC MEDIA

Green function applied to isotropic scattering of radiation in three dimensional homogeneous space

07 p1241 A69-18808

Transverse waves instability in relativistic plasma, noting condition of isotropy and existence of electromagnetic waves

07 p1193 A69-19032

Reduced modulus of elasticity dependence on form of plane stressed state, assuming initially anisotropic body with transversely isotropic elastic properties

11 p1986 A69-25182

ITALY

Fucino earth station operation with Early Bird and Intelsat 2-F3 satellites receiving equipment and transmission system

[UN PAPER 68-95455] 01 p0028 A69-10493

CENFAM radar receiving system for meteoric and upper atmospheric data on amplitude, range and direction of meteor echoes through interferometer pairs

13 p2354 A69-28649

Meteorological problems in Italy analyzed by digital computer program through numerical integration of atmospheric models to provide weather forecasts

13 p2295 A69-28651

Richardson number in vertical tropospheric region of maximum wind computed from data on jet streams observed in winter over radiosonde stations in Italy

13 p2295 A69-28656

Italian space research report to COSPAR covering international cooperation, extrasolar X rays, electron density measurements with San Marco 2 satellite, etc

15 p2725 A69-31465

Monte Cardiga telemetry station associated with sounding rocket range at Salto di Quirra, Sardinia, describing equipment, telemetry system capabilities and flexibility

20 p3512 A69-38280

ITERATION

NT ITERATIVE SOLUTION

Patch panel programmed DDA computer having MHz iteration rate and 35 bit usable word length, discussing system design and demonstration model

17 p2934 A69-34073

Alternating direction iteration method for nonlinear systems of equations applied to steady state heat conduction problem with nonlinear boundary conditions

18 p3163 A69-34329

Nonlinear estimation with noisy data, considering least squares fit, sequential /Kalman/ estimate and iterated sequential scheme

21 p3686 A69-39370

ITERATIVE SOLUTION

Convergence theorems for perturbed Newton methods for solution of nonlinear equation systems, suggesting algorithm holding Jacobian matrix elements constant during iterations

01 p0106 A69-10988

Iterative process for determining periodic solutions of nonlinear nonautonomous periodic differential equations without weak nonlinearity hypothesis applied to nonlinear synchronization

02 p0271 A69-11550

Modal substitution method for free vibration analysis of large discrete undamped dynamic systems

02 p0338 A69-11747

Optimal control problems for Markov chains solved by iterative method, using nonlinear finite difference equations to approximate degenerate elliptic functions

02 p0224 A69-11963

Iterative transfer of boundary values to fictitious contour in numerical solution of partial differential equations

[ONERA-TP-646] 03 p0454 A69-12874

Optimum overrelaxation factor in diagnostic and forecast calculations

03 p0458 A69-13033

Iterative method of determining orthogonalized bases for representation of sampled data signals

03 p0391 A69-13231

Iterative method to solve large sets of algebraic equations in approximate solution of multidimensional partial differential equations by implicit numerical techniques

03 p0456 A69-13554

P-n junction under arbitrary transient conditions, solving one dimensional, two carrier transport equations by numerical iterative method

03 p0487 A69-13639

Trajectory optimization, obtaining sequence of control functions by iterative application of maximum principle /min H/ to nonoptimal functions

04 p0548 A69-14827

Numerical solution of elliptic equations by iteration result in convergence prevention and solution of Laplace and Poisson equations with singular Laplace operator

04 p0625 A69-15133

Iterative solution of continuous-time-discrete-space /CTDS/ equations as approach to hybrid computational of certain partial differential equations

04 p0567 A69-15348

Iterative guidance mode /IGM/ applied to effective gravity vector prediction, acceleration measurement of noise sensitivity and energy limitations

[AIAA PAPER 67-620] 04 p0629 A69-15500

Iteration method for determination of critical buckling load for straight rods

05 p0832 A69-15600

Bairstow-Hitchcock iterative method analog computer simulation by steepest descent

05 p0723 A69-15930

Difference iteration method for solving three dimensional Dirichlet problem presented as system of planar Dirichlet problems

05 p0787 A69-16450

Identification of finite memory, time discrete linear systems by Kiefer-Wolfowitz stochastic approximation procedures, presenting two algorithms for sequential identification

06 p0900 A69-17350

Iterative solution of integral equation and uniform convergence conditions of function sequence approximating incremental stress distribution in elastic-plastic structures

06 p1024 A69-17510

Successive approximation for iterative construction of near optimum guidance

06 p0954 A69-17577

Radiative transfer iteration for gray medium between concentric spheres and for constant heat generating spherical region imbedded in gray medium

08 p1420 A69-20153

Structural iterative design convergence to minimum weight proved by dual linear programming, discussing global convergence and convergence rate

08 p1413 A69-20350

Iterative methods for composite layer slabs transport models, using invariant imbedding approach to transport theory

08 p1343 A69-20350

Iterative method for least square polynomial curve fitting with abscissas and ordinates subject to error

08 p1343 A69-20827

Algorithm with iterative technique for nonlinear minimax approximations

08 p1344 A69-20829

Iterative Chebyshev approximation for computerized network design by linearizing original nonlinear programming

08 p1299 A69-21170

Optimal linear quick response problem solving by fast convergence iterative procedure

09 p1473 A69-21791

Five parameter class of linear iterative methods for solution of linear equations systems in application to elliptic boundary value problems

10 p1718 A69-22870

Nonlinear Lagrange equations and iterative solutions for studying strain state of mechanical structures on basis of very small displacements

10 p1793 A69-22880

Iterative processes for solution of linear algebraic equations for n dimensional vectors in given space

10 p1718 A69-23208

Factorization procedure for iterative solution of systems of algebraic equations from discretization of elliptic boundary value problems

10 p1719 A69-23520

Iterative method for numerical solution of linear algebraic equations for stationary probability distributions in queueing and reliability theory

10 p1721 A69-23691

Least squares iterative program, deriving orbits for binaries HD 93403 and HD 135240

11 p1963 A69-25257

Iterated logarithm law proved for class of stationary series extended to systems of dependent random variables with complete couplings

11 p1910 A69-25699

Iterative algorithm to determine transition probability final distribution in Markov extremal systems

11 p1861 A69-25712

Time optimal controls for multivariable linear systems by computer programming of iterative calculations /Neustadt and fast convergence methods/

12 p2050 A69-26090

Inverse iteration method insensitive to small eigenvalue errors for finding eigenvectors

12 p2121 A69-26510

Iterative solutions of nonlinear integrodifferential dynamical equation for two point velocity correlation tensor in incompressible fluid turbulence studies
12 p2062 A69-26602

Higher order difference method for equilibrium and eigenvalue problems of two dimensional structures using iterative solution
13 p2365 A69-28239

Iterative solution of linear systems for computation of global stiffness matrix reciprocal
13 p2365 A69-28249

Iterative identification method for nonlinear control systems with single element, based on criterial functional
14 p2426 A69-29306

Iterative solution for difference equations approximating displacement vector determination problem in theory of elasticity, investigating algorithm convergence
14 p2536 A69-29479

Finite element and iteration method for large deflection of rectangular plate, considering stiffness matrix for bending
15 p2706 A69-30435

Cantilever beam profile optimization methods using iterative analog computation to achieve minimum deflection, showing application of Pontryagin maximum principle
15 p2709 A69-30671

Automatic hybrid apparatus for solving linear equations, using Gauss-Seidel iterative method and stressing control arrangement, communication circuits, etc
15 p2572 A69-31089

Boundary layer over impulsively started flat plate, describing flow transition from unsteady /Rayleigh/ to steady /Blasius/ state by iterative methods
16 p2769 A69-31812

Gradient iterative methods for finite element eigenvalue problem associated with stability and vibrations of elastic systems based on Rayleigh quotient
16 p2871 A69-31898

Starting weight increments in aircraft designs having various structural features and dimensions
16 p2735 A69-32144

Optimum overestimate to obtain bound permitting use as convergence criterion for iterative process in orbital glider reentry trajectory optimization
[ONERA-TP-628] 16 p2805 A69-32332

Soviet monograph on projective-iterative methods of solving operator equations in generalized metric and structurally normalized spaces
16 p2805 A69-32366

Adaptive random search algorithm utilizing boundary cost-function hypersurfaces measurement to implement Pontryagin maximum principle, discussing hybrid computer use, iterative solution and convergence properties
17 p2933 A69-33745

Laser eigenmodes determined iteratively from eigenvalue equation including spatial inversion inhomogeneities, atomic density and local loss
17 p2984 A69-34046

Iteration process by difference scheme for numerical solution to Dirichlet problem of two dimensional Poisson equation
18 p3164 A69-34701

Convergence of methods of tangential parabolas and hyperbolas used in nonlinear equation solution with nondifferentiable operators
18 p3164 A69-34707

Linear boundary value problem solution using iterative method
18 p3165 A69-35050

Orbits computation by Picard successive approximations method, discussing iterative numerical perturbation techniques
19 p3398 A69-35615

Computer iteration accelerator based on modified Aitken process, noting application to vectors
20 p3498 A69-36950

Periodic orbits in nonlinear dynamical system constructed with iterative method based on modification of generalized Newton-Raphson technique
[AAS PAPER 68-085] 20 p3595 A69-37171

Literal solution to equations of motion applied to lunar theory using electronic computer with series convergence
21 p3796 A69-38474

Coupled gyroscopic systems two parameter stabilization problem analyzed for steady state characteristics by iterative method
21 p3723 A69-38829

Ludwig method generalized for iterative solution of nonlinear equations systems
21 p3755 A69-39002

Iterative processes for solution of linear algebraic equations for n dimensional vectors in given space
21 p3756 A69-39149

Molodenskii boundary value problem exact solution by successive approximations for determination of earth figure, noting quasi-geoid surface
21 p3716 A69-39248

Instantaneous frozen layer thickness and temperature profile in solidified layer obtained by iteration technique
21 p3852 A69-39433

Iterative method for reducing filters required for optimal Kalman filter design maintaining parameter estimation accuracy
21 p3687 A69-39463

Numerical calculations for boundary layer flows allowing similar solutions, using iterative numerical integration of integral equation
22 p3929 A69-39925

Iterative and vectoral methods for correcting computed direction cosine matrix errors
23 p4134 A69-42543

Iterative integration method of numerical quadrature over finite interval for analytic function, taking into account simple nonanalytic singularities in integrand
24 p4341 A69-43229

I
IZSAK ELLIPSOID
U ELLIPSOIDS
U GEODESY

J

J-79 ENGINE

Induced stressing method for complex castings by controlled cooling during heat treatment applied to front frame of J-79 turbojet engine
13 p2269 A69-28184

J-85 ENGINE

Inlet produced dynamic distortion and effects on stall margin of J-85 turbojet engine from supersonic wind tunnel tests
[AIAA PAPER 69-487] 16 p2840 A69-32676

JACKS [ELECTRICAL]

U ELECTRIC CONNECTORS

JACOBI INTEGRAL

Jacobi integral and Hill criterion for analyzing motion stability of natural satellites and large planets inside gravitational sphere
20 p3596 A69-37314

JACOBI MATRIX METHOD

Reduction of partitioned submatrices functions for expediting calculations of hypercirculant and hyperhyper Jacobi analytic functions
18 p3163 A69-34330

Eigenvalue conversion of second variation test for algebraic and differential constraints to Jacobi accessory minimum problem by introducing norm in coordinate perturbation space
19 p3400 A69-35672

JACOBI POLYNOMIALS

U HYPERGEOMETRIC FUNCTIONS

JAGUAR AIRCRAFT

Jaguar combat trainer/tactical support aircraft to meet France and UK military requirement, noting supersonic performance and honeycomb construction
04 p0549 A69-15062

Jaguar aircraft equipment conformity to maximum standardization with equipment for other programs
04 p0550 A69-15063

Automatic navigation and sighting system for French specified Jaguar combat aircraft development
16 p2809 A69-31760

Jaguar aircraft design and operational characteristics, noting supersonic performance at high altitudes and during maneuvers
20 p3463 A69-37928

JAMMING

Soviet book on electronic countermeasures and intelligence covering jamming methods for automatic systems
03 p0385 A69-12927

Radar or ECM/ECM system simulation by digital computer, using signal and jamming spectral inputs
03 p0400 A69-13200

Jamming susceptibility, noting corrections for multiple noise sources and sidelobe level for antenna pattern
14 p2414 A69-29501

Tactical Satellite Communications /Tacsat/ cost reduction, discussing jamming avoidance and mitigation

tion, communications security, capacity increase and spectrum conservation

20 p3497 A69-38315

JAPAN

Japanese space research organizations, sounding rockets, meteorology, satellite communications, geodesy, etc
[UN PAPER 68-95563] 01 p0151 A69-10501

Ship and aircraft traffic conditions in Japan and neighboring areas and requirements for navigation satellite system
[UN PAPER 68-95226] 01 p0113 A69-10520

Scientific satellite 1 solar cell panels power output dependence on temperature and spin calculated and compared with results for outdoor sunlight
15 p2552 A69-30072

Atmospheric observations in Japan during last 40 years, discussing relation to meteorology, statistical characteristics, whistlers, noise phenomena, periodic variations, solar effects and ray theory
15 p2595 A69-30418

Japan space research covering sounding rockets, balloons, satellites and facilities
15 p2725 A69-31466

Low level jet stream near meso-low on stationary front in Japanese rainy season analyzed from radar echoes, noting appearance of vertical current
16 p2809 A69-32601

JR 100 F lift jet engines for Japanese national aerospace laboratory produced as part of VTOL developing program
21 p3785 A69-38608

JARRING

U MECHANICAL SHOCK

JC-130 AIRCRAFT

U C-130 AIRCRAFT

JEANS THEORY

Finite Larmor radius, finite conductivity, rotation and Hall current effects on Jeans criterion for gravitational instability of plasma
10 p1729 A69-23408

JEES

U AUTOMOBILES

JET AIRCRAFT

NT A- 300 AIRCRAFT
NT A- 6 AIRCRAFT
NT A- 7 AIRCRAFT
NT AN-24 AIRCRAFT
NT B- 52 AIRCRAFT
NT B- 70 AIRCRAFT
NT BAC 111 AIRCRAFT
NT BOEING 2707 AIRCRAFT
NT BOEING 707 AIRCRAFT
NT BOEING 747 AIRCRAFT
NT BUCCANEER AIRCRAFT
NT C- 5 AIRCRAFT
NT C-130 AIRCRAFT
NT C-141 AIRCRAFT
NT CL- 84 AIRCRAFT
NT CONCORDE AIRCRAFT
NT CV-990 AIRCRAFT
NT DC 8 AIRCRAFT
NT DC 10 AIRCRAFT
NT DH 121 AIRCRAFT
NT DO- 31 AIRCRAFT
NT E-2 AIRCRAFT
NT F- 2 AIRCRAFT
NT F- 4 AIRCRAFT
NT F- 5 AIRCRAFT
NT F- 104 AIRCRAFT
NT F- 106 AIRCRAFT
NT F- 111 AIRCRAFT
NT G- 91 AIRCRAFT
NT L-1011 AIRCRAFT
NT OV-10 AIRCRAFT
NT P-1127 AIRCRAFT
NT SAAB 37 AIRCRAFT
NT SE- 210 AIRCRAFT
NT TU-104 AIRCRAFT
NT TU-134 AIRCRAFT
NT TU-144 AIRCRAFT
NT TURBOFAN AIRCRAFT
NT TURBOPROP AIRCRAFT
NT VC-10 AIRCRAFT
NT XC-142 AIRCRAFT
NT XV- 4 AIRCRAFT

Piloting aspects of jet V/STOL aircraft for poor weather operations without complicated ground aids, discussing deceleration transition, forward speed and final approach angle
01 p0010 A69-10868

Reliability and maintenance economics for jet transport operations of 1980s, discussing Aircraft Integrated Data System /AIDS/ sensors design
[AIAA PAPER 68-207] 01 p0011 A69-11022

Aircraft and engine parameters for maximum theoretical range of turbojet for given cruising speed
03 p0366 A69-12950

Business jet aircraft use for air transport pilot training instead of simulating devices, noting pilot cabins
03 p0366 A69-13643

Design parameters optimization for V/STOL jet aircraft with lift engines mounted in wing pod, discussing wing loading and aspect ratio, power plant, etc
04 p0547 A69-14812

Anti-icing system for business jets, noting activation prior to encountering visible moisture
06 p0868 A69-17669

Commercial jet safety, analyzing aircraft accidents and accident rates
06 p0868 A69-17829

V/STOL commercial intercity jet aircraft design concept for high density short haul travel featuring low noise, high economy, reliability and tandem wing configuration
[AIAA PAPER 69-200] 07 p1056 A69-19571

Monograph on length requirements for takeoff and landing of jet transports covering airport classification, roll distance formulas and long range transport performance nomograms
08 p1301 A69-20717

Onboard gas turbine auxiliary power units for executive jet transport aircraft
[SAE PAPER 690332] 11 p1824 A69-24501

Thrust reversers for business jet aircraft, discussing federal aircraft regulation requirements for ground and in-flight qualification
[SAE PAPER 690311] 11 p1941 A69-24512

Jumbo jet instrument landing difficulties, suggesting specific improvements in aircraft and airport equipment
15 p2549 A69-30189

Dassault Mercure short haul jumbo jet, discussing production costs and market potential
15 p2550 A69-30317

Dassault Mercure high speed twin turbojet aircraft, discussing capacity, range, propulsion, profitability threshold, etc
15 p2550 A69-30318

German VFW 614 short haul commercial jet aircraft design, marketing, etc
16 p2734 A69-31805

Medium range Tu-154 three jet transport aircraft, detailing fuselage, airfoil, tail unit, landing gear, propulsion unit and circuitry
16 p2735 A69-32073

Jet aircraft runway friction due to mud and water noting relation to takeoff length
17 p2903 A69-34216

Wind shear effects on jet aircraft approach, discussing airspeed and glide path position maintenance requirements
[AIAA PAPER 69-796] 19 p3367 A69-35634

Jumbo jet audio entertainment and service systems, describing digital pulse multiplexing technique
19 p3285 A69-35806

Runway grade relation to jet aircraft takeoff length
19 p3296 A69-36874

Jumbo jet passenger loading devices including overwing bridges, transporters and terminal integration
20 p3511 A69-37916

Jet aircraft quasi-level flight above flat earth, deriving equation of path minimizing linear combination of fuel consumption and flight time
21 p3647 A69-39006

Statistics of jet aircraft accidents including worldwide data and safety trends
22 p4054 A69-41128

Jet transport operation and accidents statistics, analyzing world data, accident causes and safety gap
22 p4054 A69-41130

Safety implications of technological developments in aviation, discussing standards and statistical data for supersonic transports and jumbo jets
22 p3867 A69-41134

Third generation jet aircraft safety, discussing accident prevention and survival
22 p4054 A69-41142

Commercial jet aircraft thrust reversers and noise suppressors developed by Rolls-Royce, discussing compatibility, reliability and applications
[SAE PAPER 690410] 23 p4200 A69-41638

Refused takeoff as critical maneuver in ground operations during jet transport accident investigation, emphasizing pilot anticipation of conditions and preplanning actions
[SAE PAPER 690378] 23 p4062 A69-41654

Jet runway design, construction and operation, discussing surface texture, lightning, grooving, etc
[SAE PAPER 690377] 23 p4147 A69-41670

Jumbo jet role in air transportation, discussing future traffic growth, pilot problems and aircraft size limitations
23 p4063 A69-41819

Short haul transport aircraft development, discussing twin jet Mercure aircraft with low operation cost and Category III weather conditions landing
24 p4250 A69-42565

V/STOL commercial intercity jet aircraft design concept for high density short haul travel featuring low noise, high economy, reliability and tandem wing configuration
[AIAA PAPER 69-220] 24 p4251 A69-42648

Aero L-39 low wing cantilever monoplane jet trainer developed in Czechoslovakia
24 p4251 A69-42797

JET AIRCRAFT NOISE

Sonic bang intensities in stratified atmosphere obtained by geometrical acoustics and linear theory modifications to take account of nonlinear effects
01 p0008 A69-10056

Aircraft noise suppression, discussing community aspects of jet and fan noise and physical mechanisms of jet noise
01 p0009 A69-10349

Skin panel stresses for random acoustic loading, determining aircraft structure responses
03 p0530 A69-14092

Jet engine inlet noise control by modification of inlet guide vanes
05 p0811 A69-15622

Fan compressor noise reduction indicating effects of design, number of blades, vane/blade ratio, aerodynamic parameters and blade spacing
[ASME PAPER 69-GT-9] 09 p1571 A69-22505

Turbomachinery multiple pure tone noise associated with acoustic resonance of inlet cavities examined by narrow band filter tracking integer multiples of rotative speed
[ASME PAPER 69-GT-2] 09 p1572 A69-22509

Jet airliners noise characteristics, calculating spectral content and duration of perceived noise level and total noise level
09 p1435 A69-22637

Jet noise causes and suppression, discussing nozzle exit area geometry
15 p2671 A69-30372

Jet and compressor noise, discussing noise suppression techniques and engineering applications
[AIAA PAPER 68-550] 17 p3022 A69-34019

Jet noise effect on real estate value, discussing market survey, insulation and navigation easement costs and litigation damages
[AIAA PAPER 69-802] 19 p3288 A69-35594

Technology trends in airbreathing propulsion, discussing noise control for subsonic jet transports, turbine blade cooling, etc
[AIAA PAPER 69-774] 19 p3244 A69-35648

Cold subsonic coaxial jets observed for relationship between noise output and flow characteristics, showing effect of relative annular and central jet velocities
20 p3513 A69-37063

Acoustic field due to jet aircraft in motion, describing convection parameter modification in generalized sound pressure equation
20 p3462 A69-37757

Dornier Do 31 VTOL jet aircraft noise alleviation in far field, discussing shielding, interference, ground attenuation and reflection
22 p3862 A69-39932

Jet engine noise technology evaluation, noting effects on airport neighbor
[RAES PAPER 13] 22 p3999 A69-40492

Building block approach to turbofan engine design, discussing fuel consumption, noise and component research
[RAES PAPER 14] 22 p3999 A69-40493

Quadrupole self and cross correlations of directional jet noise patterns, including frequency spectra and corrections
22 p3931 A69-40891

JET AMPLIFIERS

Pressure gain estimates in analog jet amplifier based on total pressure measurements in main jet interaction region
02 p0195 A69-12076

Jet fluidic differential amplifier transfer function determination, describing interconnection dynamics
11 p1824 A69-24350

Gas jets collision flowing from parallel wall channels: applying solution to calculating geometrical characteristics of fluid jet amplifiers
12 p2016 A69-25877

Analog jet elements of pneumatics operating on direct interaction between streams, calculating statistical characteristics for analog jet amplifying element
14 p2393 A69-28744

Fluidic direct impact modulator design, studying effects of pressure levels and nozzle geometries
[ASME PAPER 69-FLCS-38] 20 p3465 A69-37978

Proportional fluid jet amplifier with flat saturation characteristics, describing gain, differential output pressures and noise levels
[ASME PAPER 69-FLCS-21] 20 p3466 A69-37981

JET AUGMENTED WING FLAPS

U WING FLAPS

JET BLAST EFFECTS

Real time real temperature exhaust gas reingestion and structural heating test facility for jet lift V/STOL configurations
[AIAA PAPER 69-310] 09 p1479 A69-22388

Jet influence and aerodynamic force changes on V/STOL aircraft in transitional and high speed flight investigated in wind tunnel tests for fighter aircraft
16 p2734 A69-31937

Ground jet suppression fences for VTOL aircraft: prepared pads, investigating erosion reduction and particle entrainment
[AIAA PAPER 68-639] 17 p2902 A69-34028

Blast angle effect on fanjet gas dynamics in crosswind, using equations for free lateral flow trajectories and reverse flow regions
21 p3850 A69-38863

JET BOUNDARIES

Jet line in rotational incompressible plane flows around shrouded propeller blade, using electrical analog
01 p0058 A69-10037

Incompressible laminar jet bounded by two parallel walls or by three walls, using linearized analysis related to Oseen approximation
14 p2429 A69-29023

Free jet boundary layer in mixing zone of hypersonic gas flow past body
20 p3513 A69-37094

JET CONDENSERS

Jet condenser at very low pressure in organic Rankine cycle power conversion system noting role in power efficiency
23 p4068 A69-42238

JET CONTROL

Fluid amplifiers, discussing digital and proportional jet-interaction devices and circuits
05 p0704 A69-16004

Direction changing of large solid propellant motors by changing jets angle or gas injection
07 p1230 A69-19291

Aerodynamic characteristics of elliptical airfoils with jet circulation control for VTOL rotors including dual jets and cyclic results
[AIAA PAPER 69-741] 18 p3084 A69-34406

Spacecraft control systems with computer command redundant jets for linear and angular pulses, relating configuration design to level-of-redundancy and task dimension
[AIAA PAPER 69-845] 21 p3822 A69-39375

JET DAMPING

U DAMPING

U SPIN REDUCTION

JET ENGINE FUELS

NT JP-4 JET FUEL

Jet fuel lubricity evaluation by ball-on-cylinder device
[ASLE PREPRINT 68AM 4A-2] 01 p0083 A69-10914

Permissible JP-5 fuel sulfur content effect on hot corrosion of protective coated Ni-base superalloys in marine environment, noting atmospheric sea salt role
01 p0141 A69-11059

Sulfur organic compound formation effect on composition and structure of solid phase formed during hydrocarbon jet fuels oxidation
01 p0142 A69-11097

Disulfide effects on jet fuel operating characteristics and demercaptanization influence on thermal stability, corrosive action and sedimentation
01 p0142 A69-11098

Corrosive characteristics of jet fuels near condensing water studied by weight loss method, using copper alloy plates
01 p0142 A69-11099

Combustion products temperature and composition in chamber or at nozzle exit calculated for fuels containing excess oxidizer ratios greater than unity
04 p0684 A69-14486

Aluminum corrosion by fungi isolated from jet fuel system with predominance of *Cladosporium resinae*, noting protective coatings
04 p0616 A69-14765

Aluminum corrosion by fungus culture isolated from jet fuel system
06 p0941 A69-17123

Turbine and jet engines kerosene fuels tests in small and medium size laboratory combustion chambers
13 p2240 A69-27932

Jet fuel quality improvement by adding isopropylolactadecylamine and other substances because of surface-active and sorptive qualities
16 p2828 A69-31562

Mono and bicyclic hydrocarbons effect on jet fuels combustion properties, considering burnup factor, deposit and smoke production levels
18 p3184 A69-35382

Supersonic transport aviation fuel thermal stability measurement data correlated with data deduced from heat transfer measurements
19 p3393 A69-36210

Open cell ester-base polyurethane foam effect on fuel-utilizing microorganisms growth in jet fuel-water systems
24 p4271 A69-42700

JET ENGINES

NT BRISTOL-SIDDELEY OLYMPUS 593 ENGINE
NT DUCTED FAN ENGINES
NT J-79 ENGINE
NT J-85 ENGINE
NT PULSEJET ENGINES
NT RAMJET ENGINES
NT SUPERSONIC COMBUSTION RAMJET ENGINES
NT T-53 ENGINE
NT TURBOFAN ENGINES
NT TURBOJET ENGINES
NT TURBOPROP ENGINES

In-flight and flight line checkout techniques for foreign object damage to jet engines
01 p0056 A69-11055

Coaxial jet mixing regimes in jet engines, determining requirements for compatibility by applying aerodynamic theory of ejectors
[ONERA-TP-599] 02 p0187 A69-11619

Pressure oscillation production in wind tunnel by hinged plates in test section walls to test jet engine inlets under controlled conditions
02 p0229 A69-12537

Electrochemical grinding application to metal cutting of refractory alloys in aircraft jet engine overhaul
[SAE PAPER 680662] 03 p0433 A69-13453

Combustion in high power jet engine combustion chamber in case of continuous and intermittent liquid fuel injection
08 p1421 A69-20762

Jet engine gas flow, temperature, velocity and pressure measurements by analog and digital systems
08 p1316 A69-20869

Jet mixing applications to aircraft engines, discussing one dimensional calculation of coaxial streams mixing inside conduit
09 p1429 A69-21305

Air powered fluid jet engine compressor bleed control stressing closing, reset and override operations
[ASME PAPER 69-GT-19] 09 p1571 A69-22498

Effective cost improvement of product and profit planning activity in jet engines production stressing J47 and J79 engines
[ASME PAPER 69-GT-61] 09 p1513 A69-22516

Jet aircraft engines condition monitoring system for detecting malfunctions without engine disassembly
[ASME PAPER 69-GT-66] 09 p1501 A69-22518

Airborne integrated in-flight data system to record and evaluate various engine parameters of operating jet engines
10 p1660 A69-23262

Howell engine hot section analyzer /HSA/ developed to improve maintenance, flight safety and costs of jet aircraft engines
10 p1671 A69-23263

Fluidic compressor bleed control unit for TF-30 jet engine to prevent stall at low rpm operation
10 p1753 A69-23559

Soviet book on electric ignition systems for piston and jet engines and design aspects of different types of ignition systems
12 p2146 A69-26756

Concorde jet engine silencer concept and characteristics
[AIAA PAPER 67-391] 12 p2148 A69-26759

Shorter combustors for high temperature jet engines of high speed aircraft, considering lifetime, shroud scoops, overheating, warpage, etc
14 p2509 A69-29433

Face seals for jet engine mainshaft bearing compartments, emphasizing oil film and gas film seals
[ASLE FICFS PREPRINT 28] 15 p2620 A69-30487

Jet engine intershaft bearing oil feed design, discussing use of nonrotating feed link and improvement of oil scavenging at high altitudes
15 p2671 A69-30702

Monograph on dynamic behavior of jet engines especially during perturbations based on linear theory
15 p2671 A69-30931

Thermocouples precision used for measuring metal temperatures of cooled jet engine turbine buckets
15 p2613 A69-31274

Jet engine compressor stalls in-flight investigation up to Mach 2 on F-111A by pressure sensors, noting steady state distortion role
[AIAA PAPER 69-488] 16 p2843 A69-32706

Temperature and flow measurements in jet engine combustion chamber, discussing design and calibration of gasdynamic thermometer, double thermocouple and flow probe
17 p2945 A69-32947

Aerodynamic characteristics of plane inviscid fluid jets expanding over curvilinear surface, deriving force equations for surfaces in jet and rocket engines
19 p3296 A69-35815

Jet engine compressors and fans, combustors, turbines and composite materials in evaluating thrust-weight ratio, engine size, weight and life, etc
19 p3395 A69-36322

Jet engine risetime effect on spacecraft orientation control system performance, assuming monotonic or external thrust mode
19 p3370 A69-36619

JR 100 F lift jet engines for Japanese national aerospace laboratory produced as part of VTOL developing program
21 p3785 A69-38608

Jet engine noise technology evaluation, noting effects on airport neighbor
[RAES PAPER 13] 22 p3999 A69-40492

DC-10 aircraft CF6 engine thrust reverser and spoiler design features impacting operational characteristics, maintainability, noise reduction, structural concept, control and actuation system
[SAE PAPER 690411] 23 p4200 A69-41639

Jet engine combustion temperature measurements by thermocouples or gas analysis noting errors involved
23 p4165 A69-41650

JT9D engine fuel and vane control systems for Boeing 747, noting computing system positioning of throttle valve for fuel flow control
[SAE PAPER 690405] 23 p4201 A69-41658

Sonic diagnostic engine analyzer for detecting jet engine malfunctions prior to failure
24 p4312 A69-42758

JET EXHAUST

Jet engine exhaust composition and methods for reducing smoke emission through burner design changes, noting primary zone fuel and airflow pattern
[SAE PAPER 680348] 03 p0495 A69-13350

Aircraft test setup design and techniques to simultaneously measure engine thrust and engine thrust minus drag, noting nozzle configurations variations effect
[AIAA PAPER 68-395] 12 p2059 A69-26769

Circular jet flow exhausting at right angles from plane wall into uniform cross flow, considering application to V/STOL aircraft
17 p2896 A69-34036

JET FLAMES
U FLAMES

JET FLAPS

Thin jet-flapped airfoil flow analysis in ground proximity at small angle of incidence, assuming inviscid incompressible flow
09 p1431 A69-22275

Numerical solutions of thick cambered jet flap in ground effect for flat plate and diamond shaped airfoil
[AIAA PAPER 69-738] 18 p3083 A69-34404

Circulation controlled rotor aerodynamics with tangentially ejected air from surface slots of lifting body, noting performance at advance ratios and thrust coefficients
18 p3089 A69-35232

Jet flap as alternative to rigid diffuser for momentum propulsion, discussing thrust augmentation
[AIAA PAPER 69-777] 19 p3393 A69-35645

Monograph on interaction between primary and jet flapped secondary airfoils covering line-vortex use for lift augmentation, aerodynamic characteristics, etc
19 p3242 A69-36820

Thin jet flapped airfoil analysis with wake fully developed from leading edge and jet flow reflected from ground
22 p3861 A69-41184

JET FLOW

NT AIR JETS
NT PERIPHERAL JET FLOW
NT SUPERSONIC JET FLOW

Thermal radiation effects on two dimensional steady MHD jet of conducting ionized gas confined by magnetic field
02 p0287 A69-11831

Performance cost functions for reaction jet controlled system during on-off limit cycle for stable and unstable plant
02 p0278 A69-11965

Three dimensional wakes and jets, discussing center-line velocity, half width growth and velocity irregularities
02 p0190 A69-12549

Flame stabilization by jet flame holders for case of different composition of jets and incident flow
03 p0531 A69-12956

Laminar two dimensional free jet outflow of incompressible nonNewtonian pseudoplastic fluid from orifice into mass of same fluid
04 p0586 A69-14406

Coaxial flow jet chamber flow patterns dependence on inlet gas velocity, density and length/diameter ratio
[AIChE PAPER 25B] 04 p0587 A69-14509

Fast response thin skinned calorimeters for high heat flux profiles of arc jet flows
04 p0602 A69-15427

Stationary velocity profile near jet driven vortex tube outer wall calculated by laminar boundary layer flow theory, neglecting wall curvature effects
05 p0798 A69-15610

Airflow and power requirements of compressible hovercraft jet operating under equilibrium conditions
05 p0697 A69-15708

Incompressible jet flows, discussing two dimensional jet, axisymmetric laminar jet and turbulent free jet
05 p0746 A69-16008

Flow characteristics about curved lateral jet, discussing effect of pitot tube nozzle shape and turbulence
05 p0746 A69-16017

Plane supersonic flows separated by thin film shaped jet, deriving pressure as function of deviation
05 p0746 A69-16020

Heat transfer, temperature and velocity profiles in circular free jet can be described by heat conduction type equations
05 p0747 A69-16032

Flow field for single or multiple jets firing forward into oncoming supersonic free stream, noting effect of forward extending cylindrical body
[AIAA PAPER 69-69] 06 p0864 A69-18164

Stream function for plane free sonic gas jet flowing past profile
07 p1050 A69-18740

Navier-Stokes equations solved for viscous incompressible fluid flow due to laminar jet flow into channel in presence of magnetic field
07 p1120 A69-18997

Laminar conducting wall jet injected in transverse magnetic field, analyzing partial differential equations obtained
07 p1192 A69-19020

Analytical model of spoiler generated sound in jet pipe, presenting data on level, spectrum and directivity of sound
07 p1183 A69-19462

Jet flow and wakes in external stream and tailored pressure gradients, deriving similarity solutions for boundary layer equations
08 p1252 A69-20782

Incompressible jets bounded by infinite auxiliary thin jets, discussing straight wall jets and establishing existence and uniqueness of boundary value problem solution
09 p1480 A69-21734

Closed form solution for boundary shape of undeexpanded axisymmetric jet in still air
09 p1482 A69-21968

Thin jet-flapped airfoil flow analysis in ground proximity at small angle of incidence, assuming inviscid incompressible flow

09 p1431 A69-22275

Blasius-Chaplygin formula for generalizing Kutta-Joukowski theorem concerning jet profiles, calculating resultant of hydrodynamic forces

11 p1867 A69-24355

Kinetic theory for spherical expansion of hypersonic jet flow indicating translational freezing in hypersonic source expansion

11 p1870 A69-25006

Low Reynolds number stability of incompressible fluid half jet flow, investigating free laminar boundary layer instability

11 p1874 A69-25280

Spacecraft attitude control with minimum energy control logic for small constant disturbance torques, considering reaction jet torques and fuel consumption

11 p1966 A69-25446

Sodium liquid-metal jet MHD generators tested under constant and rising magnetic fields and off and on loads

13 p2208 A69-27511

Resonance tube excitation from energy depletion in central part of subsonic jet supplying tube

13 p2247 A69-27738

Reduction of noise from underexpanded axisymmetric jet flows using radial jet flow impingement [AIAA PAPER 68-81]

13 p2248 A69-28212

Monograph on return currents produced by confined jet of incompressible fluid with low initial ambient fluid velocity

13 p2250 A69-28335

Oscillation in resonance tubes excited by subsonic jet, analyzing pressure and frequency for small Mach numbers by using wave diagram

13 p2370 A69-28630

Laminar to turbulence transition in submerged and bounded jets, using schlieren visualization for compressible flow and birefringent visualization for incompressible flow

14 p2428 A69-28876

Attachment and separation of free jet from wall, discussing model equations for wall attachment fluid amplifier

14 p2428 A69-28877

Incompressible laminar jet bounded by two parallel walls or by three walls, using linearized analysis related to Oseen approximation

14 p2429 A69-29023

Unsteady jet viscous fluid flow under pulse variations based on Prandtl equations, showing turbulent motion analogy

14 p2432 A69-29608

One dimensional approximation for free jet nozzle flow in perpendicular magnetic field, calculating velocity distributions

14 p2501 A69-29910

Numerical analysis for spreading of free turbulent gas jets with arbitrary uneven initial distribution of momentum and heat and mass fluxes

15 p2590 A69-30157

Monograph on static pressure and turbulence in free jets and jet flames covering radial velocity oscillations with and without chemical reactions, confined jets turbulence, etc

15 p2719 A69-31190

Trails arising in wake of fan type jets in transverse gas flow during uniform fuel-air mixture combustion

16 p2879 A69-32140

Linearized motion equations for conducting gas in magnetic and electric field solved for coaxial channel and free jet, assuming small Reynolds number and parallel flow

17 p3010 A69-33016

Mach disk and Riemann wave location, size and strength in underexpanded jet flows, proposing model for conservation equation satisfaction [AIAA PAPER 69-665]

17 p2954 A69-33460

Circular jet flow exhausting at right angles from plane wall into uniform cross flow, considering application to V/STOL aircraft

17 p2896 A69-34036

Rarefied gas dynamics for continuous medium and discrete molecules assemblage, discussing flow over blunt model and free jet flow from sonic orifice

18 p3122 A69-34812

Rarefied gas dynamics of blunt and sharp-pointed slender bodies in supersonic stream and free jet sonic expansion into high vacuum

18 p3123 A69-34924

Aerodynamic characteristics of plane inviscid fluid jets expanding over curvilinear surface, deriving force equations for surfaces in jet and rocket engines

19 p3296 A69-35815

Force on circular plate near screen due to incident potential incompressible jet flow

19 p3297 A69-35816

Solid surface roughness influence on reflection of thermal energy molecular jets, showing shock determined by incidence angle

19 p3377 A69-36180

Jet and Mach disk density measured by fluorescence electron beam technique, calculating Mach disk thickness from density profiles

19 p3239 A69-36396

Boundary layer formed in miniature nozzle studied for effect on jet spreading discharged into space at high Mach numbers

19 p3395 A69-36760

Rocket nozzle control by side forces produced by secondary gas stream injection observed for relationship with inclination angle to nozzle axis

20 p3457 A69-37065

Shock structure in two dimensional or axisymmetric jet flows under transverse impingement by low energy jets [ASME PAPER 69-FLCS-41]

20 p3515 A69-37975

Heat transfer to compressible laminar jet flowing along flat wall, obtaining distributions of temperature, wall shearing stress, heat transfer rates and jet thicknesses [ASME PAPER 69-FLCS-30]

20 p3516 A69-37979

LF switching in wall attachment type digital wall amplifiers, studying visual and quantitative values for switch pressure and flow as function of geometric variables [ASME PAPER 69-FLCS-31]

21 p3649 A69-38604

Velocity decay and heat transfer rates measurement in cylindrical wall jet formed by jet emerging through convergent nozzle

21 p3695 A69-38972

Pulsed performance of saturated steam reaction jet, comparing steam performance to nine gases for equal temperatures and thrust levels

21 p3785 A69-39021

Simultaneous passage of two unmixed gas flows through joint two circuit turbojet nozzle into ambient medium

21 p3785 A69-39094

Jet deflection in drifting subsonic gas flow

21 p3644 A69-39096

Concentration distribution of admixture in semibounded jet propagating along nonheat conducting plate, obtaining concentration profiles for various thermal and diffusion Prandtl numbers

21 p3854 A69-39844

Integral relations method applied to air jet flow along cylinder with boundary layer control by suction or blowing

21 p3698 A69-39845

Thermal boundary layer formed during laminar jet flow over flat porous plate, discussing temperature distribution and mass transfer at plate surface

21 p3854 A69-39846

Coaxial turbulent compressible gas jets propagation, discussing mass buildup data in coaxial jets

21 p3645 A69-39847

Aligned uniform magnetic field effect on hydromagnetic stability of two dimensional incompressible electrically conducting jet flow with large Reynolds number

22 p3931 A69-40687

Pitching characteristics of three dimensional peripheral jet ground effect machines with compartment partition along pitch axis, considering longitudinal static stability and dynamic pitching motion

22 p3866 A69-40818

Aerodynamics of twisted jet propagating in same fluid by asymptotic expansion, analyzing twist influence on heat transfer

24 p4244 A69-43057

JET IMPINGEMENT

Potential flow of stream interaction with two dimensional thin jet, discussing jet penetration depth

01 p0007 A69-11019

Heat transfer near stagnation point in axisymmetric turbulent jet impinging on circular disk

02 p0354 A69-12491

Supersonic gas jet impingement on inclined plane barrier, calculating parameters by approximation

03 p0413 A69-12958

Heat transfer characteristics of single lines of circular air jets impinging on concave cylindrical surfaces, discussing nozzle target spacing effect [ASME PAPER 68-WA/GT-1]

05 p0848 A69-16137

Impinging jet flames on furnace hearth, analyzing thermal boundary layer characteristics and convective heat transfer rates

06 p1035 A69-17933

Axisymmetric jet impingement against solid plane from tube at finite distance, using nonlinear partial differential equation in finite difference form [AICHE PAPER 31F]

08 p1302 A69-19847

Supersonic jet impingement on flat plate, showing shock wave profiles and slipstream surface at stations parallel to nozzle axis

08 p1252 A69-20841

Surface heat transfer coefficients under perforated plate of multiple square array round impinging air jets [ASME PAPER 69-GT-4]

09 p1624 A69-22508

Cavity formation on water and wet cement surfaces by impingement of axisymmetric air jet noting cavity shape, depth and diameter

11 p1869 A69-24888

Pressure and heating rate correlations for rocket exhausts impinging on flat plates and curved panels, generating axisymmetric real gas exhaust plumes

12 p2190 A69-26781

Reduction of noise from underexpanded axisymmetric jet flows using radial jet flow impingement [AIAA PAPER 68-81]

13 p2248 A69-28212

Impingement pressure analysis associated with two phase cryogenic propellant venting to space environment

16 p2869 A69-32753

Internal heat transfer coefficients for impingement cooling of gas turbine airfoil leading edge [AIAA PAPER 68-564]

17 p3022 A69-34021

Water jets with greater than half sound speed created by shock wave impinging on cavity within liquid, discussing mechanism, maximum speed, shape, etc

19 p3301 A69-36815

Shock structure in two dimensional or axisymmetric jet flows under transverse impingement by low energy jets [ASME PAPER 69-FLCS-41]

20 p3515 A69-37975

Forced and periodic motion of air or water jets impinging in double input vortex chamber described in terms of oscillator deriving energy from hydrodynamic instability [ASME PAPER 69-FLCS-19]

20 p3465 A69-37981

Circular liquid jet oblique impingement on flat surface, noting dry zone occurrence at small angles due to lateral flow deflection

21 p3691 A69-38551

Supersonic fan-shaped jet formation by identical colliding underexpanded jets, calculating subsonic flow between interaction plane and curvilinear shock wave

21 p3643 A69-38643

Polymer films damage due to supersonic plasma jets, comparing fracture relief of oriented and unoriented polymers

21 p3752 A69-39081

Free and dividing streamlines shapes for two dimensional jet from parallel walls penetrating into counterstream, discussing finite cavities

22 p3859 A69-40143

Jet dynamic characteristics injected into supersonic air slipstream incident on flat body, calculating configuration, shock wave geometry and parameters distribution in flow field

24 p4250 A69-43710

JET LIFT

Temperature stresses analysis for jet lift VTOL aircraft structure during takeoff and landing, discussing fire hazard in lift pod

04 p0548 A69-14841

Engines for V/STOL application, discussing aerodynamics of thrust lift and lift jet engines

05 p0811 A69-15553

Aerodynamic effects of lift jet and lift fan inlets in transition flight, analyzing inlet momentum lift, inlet lip lift and drag [AIAA PAPER 68-637]

12 p2014 A69-26767

Reaction forces for jet lift VTOL attitude control during hover and transition, considering hot gas and pitch ducting applications [AIAA PAPER 69-545]

16 p2735 A69-32756

Ground simulations data of jet lift V/STOL compared with visual flight results, studying hover, lateral quick start and stop maneuver [AHS PAPER 362]

17 p2946 A69-33519

JET MIXING FLOW

- Plane MHD jets with variable conductivity, showing effective mixing length as function of distance
01 p0130 A69-10773
- Meksyn method application to problems of jet mixing and jet reattachment
02 p0233 A69-12530
- Confined jet mixing region at entrance of tubular reactor, discussing mass and momentum transfer, chemical conversion and effect of Reynolds number [AICHE PAPER 25A]
04 p0586 A69-14508
- Axial deviation of gas flow resulting from mixing turbulent gas jets
04 p0591 A69-15411
- Jet perpendicular penetration prediction from holes or tubes, discussing resultant gas stream mixing and temperature profiles [ASME PAPER 68-WA/GT-8]
05 p0750 A69-16143
- Mixing and combustion of gaseous and particle laden jets in air stream, analyzing turbulent, coaxial and jet mixing flows [AIAA PAPER 69-33]
06 p1038 A69-18146
- Fuel mixing mechanism in diffusion type supersonic combustion, noting influence of combustor configuration and fuel density [AIAA PAPER 69-32]
07 p1242 A69-19266
- Jet mixing applications to aircraft engines, discussing one dimensional calculation of coaxial streams mixing inside conduit
09 p1429 A69-21305
- Excess velocity and temperature decay laws in axisymmetric jet in transverse flow obtained via jet momentum and heat conservation equations
10 p1679 A69-23568
- Mixing zone of plane jet in rectangular nozzle mounted at end of controlled velocity wind tunnel
12 p2062 A69-26287
- Discontinuity coefficient on boundaries of mixing zone of plane jet, observing homogeneity of thermal and kinematic structures
13 p2247 A69-27978
- Air-hydrogen supersonic mixing and combustion, characterizing hot hydrogen jet discharging into supersonic concentric air stream at atmospheric pressure [AIAA PAPER 69-339]
13 p2378 A69-28275
- Fluctuating turbulent stress measurements in mixing layer of two dimensional jets including intensity, spatial correlation and wave-number fluctuating stress frequency spectra
14 p2431 A69-29577
- Three dimensional laminar jet mixing of incompressible viscous fluid from rectangular cross section nozzle into uniform stream
16 p2768 A69-31687
- Combustion effects on mixing of axisymmetric supersonic and turbulent free jets to obtain species concentrations, pitot pressures and temperatures [AIAA PAPER 69-538]
16 p2843 A69-32705
- Vortex motion enhancement of jet penetration and spreading in supersonic fuel injection into large diameter combustors [AIAA PAPER 69-664]
17 p2953 A69-33437
- Jet injection into free circular cross section cross wind using curvilinear dynamic model, assuming negligible Archimedean forces effect
18 p3124 A69-35149
- Cold subsonic coaxial jets observed for relationship between noise output and flow characteristics, showing effect of relative annular and central jet velocities
20 p3513 A69-37063
- Laminar jet mixing of incompressible viscous fluid issuing from rectangular nozzle into uniform stream, considering various boundary conditions [ASME PAPER 69-FLCS-22]
20 p3516 A69-37976
- Flow separation and reattachment points and line of zero velocity jet mixing determined by injecting smoke [ASME PAPER 69-FE-29]
20 p3517 A69-37994
- Supersonic fan-shaped jet formation by identical colliding underexpanded jets, calculating subsonic flow between interaction plane and curvilinear shock wave
21 p3643 A69-38643
- Turbulent gas jet mixing in chamber with four inlet nozzles
21 p3785 A69-39102
- Free and dividing streamlines shapes for two dimensional jet from parallel walls penetrating into counterstream, discussing finite cavities
22 p3859 A69-40143

JET NOZZLES

- Interactions between outer and inner jets behind maximum cross section of jet engine nozzle [ONERA-TP-600]
02 p0187 A69-11620

Diathermal regenerative cooling of combustion chambers and engine nozzles with supercritical heat transfer mode
03 p0495 A69-12970

Noise intensity measurements in far field of circular nozzle for jet noise composition
17 p2957 A69-33602

Soviet monograph on turbines and jet nozzles for two phase flows covering gas-particle velocity and temperature differences, turbine design, etc
20 p3586 A69-38209

JET PILOTS

U AIRCRAFT PILOTS

JET PLUMES

U PLUMES

JET PROPULSION

Biowaste propelled resistojet control systems selection criteria based on NASA Manned Orbital Research Laboratory with six man crew [AIAA PAPER 68-121]
04 p0554 A69-15506

Isotopic propulsion engine development problems, emphasizing single channel thermal power engine with hydrogen working fluid
05 p0811 A69-15596

Water jet propulsion for air cushion vehicles, emphasizing inlet shape effect on performance and potential flow theory application to inlet design
08 p1254 A69-20115

Book on theory and design of jet, rocket, nuclear, ion and electric propulsion systems noting combustion, detonation, fluid injection and space mission applications
11 p1943 A69-25582

Optimum adaptation of propulsion gas generators to power jet driven rotors with blown flap control, considering jet engine, fanjet and engine driven compressor
17 p3020 A69-33344

Jet flap as alternative to rigid diffuser for momentum propulsion, discussing thrust augmentation [AIAA PAPER 69-777]
19 p3393 A69-35645

JET PUMPS

Jet pump head rise deterioration parameter for prediction of cavitation
05 p0745 A69-15791

Bleed air environmental system utilizing air to air jet pumps as flow multipliers for cabin pressurization air supply in commercial turboprop aircraft [SAE PAPER 690331]
11 p1941 A69-24494

Jet pump actuation of intermittently operating variable density closed circuit subsonic wind tunnels, measuring wind tunnel power factor
11 p1892 A69-25371

Noncavitating and cavitating performance of low area ratio water jet pumps, analyzing efficiency, area ratio, throat length, nozzle spacing and diffuser geometry
18 p3095 A69-35176

JET STREAMS [METEOROLOGY]

Objective layer of maximum wind /LRMW/ analysis technique for Northern Hemisphere jet stream, noting generation of initial guess fields
01 p0110 A69-10689

Jet stream cirrus radiative characteristics from airborne IR measurements, noting cirrus cloud emission and transmission and cirrus height and temperature estimates
01 p0110 A69-10694

Barotropic instability analyses by method of jet stream like fields and energy transport from zonal current to wave disturbances based on vorticity equation
02 p0276 A69-12758

Aircraft reports of clear air turbulence over North Atlantic, discussing jet stream proximity and large amplitude ridge associated with occlusion point
08 p1345 A69-19885

Jet flows instabilities with vertical and horizontal velocity drifts from numerical integration of atmospheric motion equations linearized with respect to small perturbations
12 p2125 A69-25950

Jet stream winds direction correlated with direction of LF pressure disturbances crossing microbarograph array
12 p2125 A69-26015

Richardson number in vertical tropospheric region of maximum wind computed from data on jet streams observed in winter over radiosonde stations in Italy
13 p2295 A69-28656

Equatorial jet stream excitation of longitudinal waves, analyzing plasma beam instability and spectrum of short wave inhomogeneities by quasi-hydrodynamic equations
14 p2437 A69-29073

Jet stream vertical wind shear chart construction for aircraft with gas turbine propulsion
14 p2473 A69-29730

Jet streams as indicators of atmospheric circulation, considering all altitude observance and dynamics-energetics aspects
14 p2477 A69-29831

Self maintenance of absolute angular momentum in atmosphere as explanation of subtropical jet stream origin
15 p2647 A69-30192

Low level jet stream near meso-low on stationary front in Japanese rainy season analyzed from radar echoes, noting appearance of vertical current
16 p2809 A69-32601

Jet stream blocking process simulation using geostrophic system of equations, considering effects of orography and contrast heating due to land-sea distribution
16 p2809 A69-32602

Asteroidal jet streams from Hirayama family Flora, difficult to reconcile with exploded planet view
17 p3030 A69-33070

Papers on experimental and theoretical research on atmospheric circulations, jetstream and cyclonic disturbances
17 p2999 A69-33757

Planetary jetstream and general circulation energy transformations, applying circulation model results to specific weather situations
17 p3000 A69-33758

Lateral mixing of air masses in jet stream by water fluid model experiments, discussing steady and non-steady state turbulent momentum exchange
17 p3000 A69-33759

Cyclonic vortices production by horizontal convergence in rotating water bowl as function of bottom surface inclination, modeling cyclogenesis in jet stream entropy field
17 p3000 A69-33760

Satellite photograph analysis to investigate interaction between subtropical and polar front jet streams
18 p3166 A69-34827

Cirrus clouds occurrence, position and wind velocities on jetstream axes based on statistical analysis of aerological data and satellite TV pictures
19 p3366 A69-36669

Synoptic and mesoscale cloud patterns near low level jet from Tiros 7 and 8 photographs, noting status formation and dissipation
20 p3570 A69-37404

JET THRUST

Performance cost functions for reaction jet controlled system during on-off limit cycle for stable and unstable plant
02 p0278 A69-11965

Engines for V/STOL application, discussing aerodynamics of thrust lift and lift jet engines
05 p0811 A69-15553

Spacecraft attitude control with minimum energy control logic for small constant disturbance torques, considering reaction jet torquers and fuel consumption
11 p1966 A69-25446

Thrust balance for scale model of powered nacelle fan jet engine from drag analysis in wind tunnel, deriving fan nozzle velocity coefficient
13 p2199 A69-27446

Minimum time single axis capture of satellite spinning about pitch axis by low thrust jets, considering gravity gradient phenomenon
17 p3048 A69-33237

Jet engine risetime effect on spacecraft orientation control system performance, assuming monotonic or extremal thrust mode
19 p3370 A69-36619

Pulsed performance of saturated steam reaction jet, comparing steam performance to nine gases for equal temperatures and thrust levels
21 p3785 A69-39021

Controllers design for reaction jet controlled aerospace vehicles, studying second order pitch-plane representation with actuator modeled as pure delay [AIAA PAPER 69-854]
21 p3822 A69-39382

Turbofan engine influence on civil transport aircraft design as function of thrust, discussing engine ratings, number of engines, APU and thrust engine
22 p3862 A69-39961

Nonlinear adaptive reaction jet attitude control for long life space vehicles, providing optimal performance over bias acceleration disturbances [AIAA PAPER 69-945]
22 p4036 A69-40328

JET VANES

- Fluidic system controlling inlet guide vanes to high pressure compressor of two spool jet engine, using digital elements to drive hydraulic servosystem
02 p0305 A69-12090
- Compressor inlet Mach number choice to control high performance variable stator compressors geometry
[ASME PAPER 69-GT-14] 09 p1571 A69-22502
- JT9D engine fuel and vane control systems for Boeing 747, noting computing system positioning of throttle valve for fuel flow control
[SAE PAPER 690405] 23 p4201 A69-41658

JETAVATORS

U GUIDE VANES

JETS

- V/STOL air intakes and jets simulation in wind tunnel tests, noting thrust simulation possibilities
11 p1866 A69-25431
- Shock tube with cylindrical explosive to implode glass wall and produce high velocity glass particle jet, studying jet velocity and behavior and test gas pressure effects
18 p3116 A69-34460

JETTISON SYSTEMS

- Small column insulated delay /SCID/ aircraft seat ejection systems, illustrating weight saving
06 p0877 A69-16957
- ELDO Europa 1 Fairings Jettisoning System and explosive devices, discussing heat shield structure and safety regulations
10 p1635 A69-23027
- Test facility for qualification of satellite fairings jettisoning system, describing accelerating tower and recording and control instrumentation
16 p2765 A69-31739

JETTISONING

- Full scale and transonic wind tunnel store separation characteristics, outlining uses of heavy and light scaling methods
17 p2896 A69-34035

JITTER

U VIBRATION

JODRELL BANK OBSERVATORY

- Jodrell Bank RF digital autocorrelation spectrometer based on time delay related to signal power spectrum through Fourier transform
17 p2970 A69-32856

JOINING

NT EXPLOSIVE WELDING

- Oxide ceramics finishing processes, discussing leaching, machining, surface finishing, strengthening by compressive surface layers and joining
09 p1510 A69-22350
- Silicated alumina attachment for high temperature radomes and leading surface heat shields, discussing stress concentration and load transfer
09 p1477 A69-22370
- Vacuum heat treating and joining process for various ferrous and nonferrous metals and alloys, discussing advantages, applications and economics
[ASM PAPER D8-22.3] 20 p3551 A69-38132

JOINTS (JUNCTIONS)

- NT BUTT JOINTS
- NT LAP JOINTS
- NT METAL JOINTS
- NT RIVETED JOINTS
- NT SEAMS (JOINTS)
- NT SOLDERED JOINTS
- NT SPOT WELDS
- NT WELDED JOINTS
- Structural analysis by direct moment distribution, Volume 1, covering statistically indeterminate structures formed of prismatic members
01 p0165 A69-10156
- Spar attachments of aircraft wings analyzed with respect to weight and applied loads, determining optimum bolt diameter ratio to lug width
04 p0673 A69-14496
- Shim joints design for composite material structural members reinforcement in joint region, considering weight factor
[AIAA PAPER 68-341] 11 p1987 A69-25369
- Bolt materials selection criteria in design of high strength lightweight joints, showing fatigue curves and temperature effects
13 p2268 A69-27758
- Composite airframe structural joint design and weight considerations for boron and glass fiber reinforced plastic materials
[ASM PAPER W9-23.1] 14 p2535 A69-29448
- Thermocompression joints strength measured using friction test, centrifuging and microtensile tests
15 p2573 A69-30081

Wire-wrap solderless joints production technology in electronic equipment

- 16 p2763 A69-32579
- Reliable structural joints and attachments design for components fabricated from nonmetallic refractory brittle materials, discussing departures from conventional practices
17 p3061 A69-33569
- Torque calculations about joints of rigidly chain-like arranged clusters of flying bodies
18 p3208 A69-34776
- Rigidity of rotors with pin joints, calculating moments of inertia at connected sections of turbine shaft disks utilizing similarity concept
19 p3324 A69-35832

Adhesives and adhesive resin bonding, describing internal stresses in joints, joints design for bonding, strength, bonding processes and testing

- 21 p3752 A69-38932
- Intersection plane stresses in internally pressurized cylindrical shells joined over elliptic face
22 p4040 A69-39978
- Plane-truss joints displacements determined by graph-analytic method, discussing representation of fictitious forces and moments
23 p4225 A69-41420
- Traction stresses distribution over contact surfaces using photoelastic frozen stress model
23 p4235 A69-42461
- Adhesive joints design with uniform shear stress for prestressing wood beams
24 p4323 A69-43425
- Composite-to-metal joints design and fabrication, using carbon yarn in epoxy matrix for missile interstage application
24 p4323 A69-43426
- Adhesive bonded joints for glass resin composite sandwich helicopter structures, describing aircraft applications
24 p4403 A69-43462

JORDAN FORM

- Riemann problem in regions, showing integral operators become bounded if closed rectifiable Jordan curve without cusps becomes curve of bounded rotation
06 p0947 A69-16893
- Rational transfer function matrix realization into irreducible Jordan canonical form state equation by nonsingular transformations
12 p2122 A69-26511

JOSEPHSON JUNCTIONS

- Electromagnetic waves parametric interactions during unsteady Josephson effect as function of wavelength ratio, magnetic field penetration and contact dimensions
02 p0293 A69-11464
- Josephson voltage-frequency relation independence of superconductor nature, noting e/h value and importance to voltage standards and quantum electrodynamics
02 p0299 A69-12599
- Josephson current dependence on nonmagnetic impurity concentration in pure and highly contaminated superconductor
03 p0484 A69-13284
- Superconductor tunnel junction with noise, calculating frequency pulling, radiation linewidth and voltage power spectrum in AC Josephson effect
03 p0486 A69-13387
- Magnetic field dependences of Josephson critical current in high and low current Josephson junctions, discussing influence of induced self field
04 p0640 A69-14437
- Electromagnetic properties associated with presence of overlapping bands in pure superconductors, discussing temperature dependence
05 p0810 A69-16802
- Temperature dependence of Josephson critical current in superconductor model having anisotropic energy gap
05 p0810 A69-16803
- Experiments on Josephson tunneling junctions and superconducting contacts to demonstrate quantum electronic properties of superconductors
[IEEE PAPER D-7] 07 p1200 A69-19052
- Stationary Josephson effect used to determine fluctuations influence on superconducting tunneling
09 p1556 A69-21669
- Josephson effects in superconductivity and superfluidity including electron tunneling DC and AC effects, basic and double junctions
11 p1938 A69-25240
- Josephson current dependence on nonmagnetic impurity concentration in pure and highly contaminated superconductor
14 p2508 A69-29656

Josephson current density distribution in thin film superconductors, determining relation between tunneling current density and magnetic field for films with/without current

- 15 p2667 A69-30196
- Regenerative Josephson effect detector with feedback-narrowed far IR response as tunable millimeter and submillimeter wave radiation detector
19 p3313 A69-36417
- Josephson frequency-voltage relation at microwave and far IR frequencies compared, using radiation induced steps
20 p3583 A69-37418
- Josephson currents interaction with LF surface plasmons in superposed thin dielectric and superconducting metal films, noting I-V characteristics
22 p3992 A69-40420

JOUKOWSKI TRANSFORMATION

- Pressure distribution in two dimensional incompressible potential flow on Joukowski airfoils with normal upper surface spoilers, emphasizing potential flow theory
[AIAA PAPER 69-737] 18 p3083 A69-34402

Joule HEATING

U OHMIC DISSIPATION
U RESISTANCE HEATING

JOURNAL BEARINGS

- Gas flow analysis for externally pressurized porous journal gas bearing, considering circumferential flow in bearing clearance and porous bushing
01 p0085 A69-10312
- Whirl instability of externally pressurized gas journal bearing with peripheral feeding holes, discussing analytical natural frequency of shaft bearing systems
02 p0254 A69-12426
- Hydrostatic journal gas bearings calculations for carrying capacity, gas consumption and optimal dimensions for maximum lifting capacity
03 p0432 A69-12960
- Rayleigh step journal bearings, considering pressure distribution, load capacity and attitude angle and optimal film thickness ratio for incompressible fluid lubrication
04 p0605 A69-14587
- Pressurized fluid journal bearing with fluid fed into space between shaft and shell from plenum chamber in bearing housing through circumferential slots
06 p0931 A69-17529
- Optimum geometrical design of multipad externally pressurized journal bearings
07 p1141 A69-19439
- Rotors linear vibrations due to unbalanced shaft rotating on lubricated bearings taking into account lubricant damping
07 p1235 A69-19441
- Incompressible fluid unsteady motion between journal and bearing solved in form of Reynolds number power series from stream functions
09 p1514 A69-22712
- Analytic solution for whirl in finite journal bearing with continuous lubricating film using Fedor approach
[ASME PAPER 69-VIBR-55] 10 p1700 A69-24147
- Herringbone grooved gas lubricated journal bearing static and dynamic characteristics analyzed approximately, noting pressure distribution and vibration amplitudes
[ASME PAPER 68-LUBS-7] 13 p2265 A69-27269
- Matched asymptotic expansions to obtain slider bearing load carrying capacity
[ASME PAPER 68-LUBS-18] 13 p2266 A69-27270
- Herringbone grooved gas lubricated journal bearing stability, testing effects of geometries and clearances on onset speed for half frequency whirl
[ASME PAPER 68-LUBS-25] 13 p2266 A69-27271
- Load carrying capacity and friction calculated for pivoted pad journal bearings for machine design use
[ASME PAPER 68-LUBS-27] 13 p2266 A69-27275
- Linearized theory for stability of self acting gas journal bearings with noncircular members and elements of flexibility and damping, noting three lobed rotor
[ASME PAPER 68-LUBS-45] 13 p2266 A69-27277
- Externally pressurized gas lubricated journal and thrust bearings designs, citing reference literature
[ASME PAPER 68-LUBS-8] 13 p2267 A69-27282
- Gas lubricated hybrid journal bearings with external pressure, noting load capacity and stability in steady state and dynamic analyses
[ASME PAPER 68-LUBS-21] 13 p2267 A69-27284

- Infinitely long journal bearing using ionized gas lubricant with magnetic field applied axially and electric field applied transversely to fluid film [ASME PAPER 68-LUBS-30] 13 p2267 A69-27287
- Spiral grooved turbulent screw seal/viscoseal/analysis, combining results of spiral grooved journal bearing study with turbulent fluid film theory [ASLE FICFS PREPRINT 32] 15 p2619 A69-30482
- Pressure distribution in self acting hydrodynamic journal bearings without end leakage, presenting closed form solution for nonhomogeneous Reynolds equation with turbulence considerations 18 p3139 A69-34270
- Load capacities of graphite lined journal bearings, discussing factors affecting wear rates [SAWE PAPER 68-LC-9] 18 p3148 A69-35002
- Pressure increment due to inertia of rotating fluid film at journal bearing periphery theoretically estimated and measured 20 p3548 A69-37085
- Total load factor static vertical component and lubricant flow rate square related to pocketed hydrostatic journal bearing revolutions 24 p4321 A69-43091
- JOURNALS [SHAFTS]**
U SHAFTS [MACHINE ELEMENTS]
JP-4 JET FUEL
 JP-4 fuel emulsions properties, handling characteristics and safety performance, noting satisfactory shelf life and thermal stability [ASME PAPER 68-GT-24] 06 p0982 A69-17190
- Fuel control systems using emulsified fuel, noting exposure effects and temperature and pressure characteristics [ASME PAPER 69-GT-40] 09 p1571 A69-22486
- JUDGMENTS**
 Noise level perception and subjective judgments for broadband noise with single, modulated and multiple tones, considering tone correction procedures 11 p1830 A69-24796
- JUNCTION DIODES**
 Capacitance variation in junction varactors with linear graded, abrupt and hyperabrupt junctions, storage switching diodes and storage varactors 01 p0038 A69-10168
- GaP p-n structures creation for diode sources of green and red radiation, comparing diffusion and epitaxial methods 01 p0137 A69-10259
- Negative resistance behavior of InSb diodes at 77 K, extending double injection theory for insulators to extrinsic semiconductors 02 p0294 A69-11722
- Punch-through microwave negative resistance diode explained and contrasted with similar Read and Shockley structures 02 p0215 A69-11938
- Cavity excitation and support of limited space-charge accumulation mode oscillations in n-GaAs epitaxial diode 02 p0297 A69-11940
- GaAs Gunn diode oscillators operating at Q band frequencies 02 p0297 A69-11944
- Parametric frequency divider using reverse biased hyperabrupt junction diodes to provide nonlinear capacitance 02 p0217 A69-12152
- Beam-lead fabrication on dual Schottky barrier diodes for low noise integrated microwave mixers 02 p0222 A69-12474
- Magnetic field effect on amplitude, frequency and form of LF oscillations in Gunn diodes 02 p0222 A69-12684
- Anisotropic pressure influence on silicon diodes parameters 02 p0223 A69-12839
- Space charge limited square law diodes as HF mixers, noting low conversion loss of asymmetrical type 03 p0404 A69-13580
- Plane reflector with variable reflection coefficient for electromagnetic centimeter waves, consisting of plane grating of semiconductor diodes mounted in waveguide 03 p0406 A69-13938
- Small transverse dimensions effect and domain formation criterion for surface oriented Gunn diodes prepared on thin epitaxial GaAs layers 04 p0639 A69-14335
- Hybrid Gunn domain and LSA mode operation in oversized bulk and epitaxially grown GaAs, noting large signal impedance data 04 p0639 A69-14339
- Radiation effects on III-V compounds, considering damage in solar cells and luminescence, light emitting and Esaki diodes 04 p0641 A69-14504
- Diffusion capacitance of p-n junctions, short base semiconductor diodes and p-n-p transistor, discussing systematic error in quasi-steady state calculation 04 p0580 A69-15489
- Emitter base lateral diode carrier injection effect on current gain properties of small area double diffused planar transistors 05 p0728 A69-15808
- Spectral output time variation of GaAs diode laser operating in Fabry-Perot modes 05 p0772 A69-15961
- Recombination radiation of tellurium and zinc doped GaAs alloy type diodes, discussing luminescence spectra, current-voltage characteristics and temperature effects 05 p0729 A69-16210
- Deep trapping levels caused by ion implantation doping, discussing level effects on electrical characteristics of zinc implanted GaAs diodes 05 p0808 A69-16287
- Microwave absorption and series resistance of silicon mesa parametric amplifier diodes, discussing p-n junction and dielectric loss mechanism 05 p0732 A69-16347
- Statistical studies of current-voltage characteristics of zinc-doped silicon diodes 05 p0732 A69-16425
- P-n planar avalanche photodiode without guard ring noting electrical properties, uniform multiplication and fabrication 05 p0733 A69-16559
- Threshold failure levels of semiconductor diodes and transistors due to pulse voltages 06 p0977 A69-16883
- Gallium arsenide double injection diode using vacuum deposited film electrode on single crystal substrate, noting current controlled negative resistance 06 p0893 A69-17156
- Solid state diodes made by pulsed laser irradiation of polished silicon surfaces, discussing application to integrated circuit design 06 p0893 A69-17157
- Broadband hybrid junction of parallel transmission lines application to four diode star mixer/modulator 06 p0896 A69-17485
- Silicon double injection diode, discussing HF noise measurement, Nyquist noise equivalent circuit for double injection process and source of LF noise 06 p0898 A69-17762
- Potential barrier curvature influence in aluminum trioxide tunnel junctions, noting ionic space-charge effect on shape 07 p1196 A69-18243
- Oversized GaAs Gunn effect diodes operated in L and S bands at harmonics of fundamental transit time frequency with high power and efficiency 07 p1196 A69-18444
- Computer model of Gunn diode, discussing operations under pulse bias voltage and in resonator 07 p1097 A69-18449
- Conditions for existence of stationary high field domain in Gunn diode 07 p1097 A69-18450
- Mechanically and electronically tunable resonator for driving IMPATT and Gunn diodes 07 p1097 A69-18455
- Barrier capacitance of semiconductor diodes for exact temperature measurement, discussing application to temperature to frequency converters 07 p1100 A69-18556
- Relaxation oscillations in Si p-n junction diode reverse-biased into avalanche calculated by computer program 07 p1101 A69-18651
- Forward transient response characteristics of high resistivity, long base, low lifetime p-n silicon diodes doped with Au, noting voltage oscillations 07 p1101 A69-18652
- Observation of photocurrents generated in Schottky barrier diodes on barium titanate, suggesting practical utility of photon-to-electron conversion efficiencies 07 p1104 A69-18905
- Semiconductor diode noise experimental measurements indicating fluctuation-dissipation theorem/FDT/inapplicability to all quasi-equilibrium systems 07 p1113 A69-19596
- Silicon on sapphire semiconductor technology for diode arrays used as read-only memories, discussing capacitance, resistance and pattern encoding by laser 07 p1113 A69-19767
- Gunn effect memory loop in pulse diodes consisting of two Gunn diodes connected in series 08 p1279 A69-19912
- Optimal electroluminescent efficiencies for vapor grown gallium arsenide phosphide diodes, analyzing current spreading, absorption, impurity and composition effects [ECS PAPER 103] 08 p1284 A69-20366
- Properties of ion implanted GaAs diodes fabricated at room temperature, analyzing light emission, resistance and breakdown voltage [ECS PAPER 172] 08 p1284 A69-20369
- Noise properties of junction diodes and bipolar transistors as basis for low noise amplifiers design 08 p1286 A69-20839
- Destructive breakdown in Schottky barrier diodes by evaporating contact metal through mask onto silicon, showing local heating by thin wax layer 08 p1286 A69-20860
- Richardson constant for thermionic emission in Schottky barrier diodes, noting effect of surface shadows 08 p1286 A69-20865
- Response time of semiconductor diode from dependence of equivalent capacitance on direct displacement current 08 p1287 A69-20889
- Internal electric field effect of diode with inhomogeneously doped base on lifetime of strong reverse current generated during instantaneous switching 08 p1287 A69-20890
- Failure mechanism in high-voltage semiconductor diodes explained by effect of reverse voltage pulses, considering design reliability 08 p1294 A69-21116
- Radiative tunneling shifting peak spectra in abrupt asymmetrically doped GaAs junctions 09 p1544 A69-21336
- Anomalous mode avalanche diodes for pulse power generation noting output, efficiency, mode of operation, microwave oscillations and IMPATT diodes 09 p1466 A69-22455
- Gunn diode operating to VHF range with coaxial line to generate rectangular waves and to function as memory element 09 p1467 A69-22587
- GaP p-n structures creation for diode sources of green and red radiation, comparing diffusion and epitaxial methods 09 p1559 A69-22652
- High performance silicon carbide backward diode, discussing device design and operational characteristics 09 p1470 A69-22787
- Gunn diode reliability improvement by using device structures preventing high field domains from reaching anode 09 p1470 A69-22788
- Gunn diode field distribution with distributed capacitance electrode analyzed with one dimensional computer simulation 09 p1470 A69-22789
- Voltage dependence of red and green electroluminescence in GaP diodes prepared by growing n-type liquid epitaxial layer on p-type solution grown substrate 10 p1663 A69-23664
- Quenched one dimensional bulk GaAs oscillators with linearly increasing and decreasing concave and convex doping gradients, showing profiles 10 p1663 A69-23667
- Forward and reverse current-voltage characteristics and reverse biased capacitance for nZnSe-pGe emitter base diodes of heterojunction transistors 11 p1851 A69-25114
- Emission and diffusion theories of metal-semiconductor contacts for describing current characteristics of abrupt isotype nGe-nGaAs heterojunction 11 p1938 A69-25115
- Solar cell equation series resistance and junction recombination parameters determination, considering I-V characteristics 11 p1826 A69-25395
- Frequency noises suppression in Gunn diode oscillators by frequency stabilization, using high Q external cavity 11 p1853 A69-25608
- Resonant load impedance effects on Gunn diode oscillators output fluctuations, noting maximum power conditions 11 p1853 A69-25609
- Fabrication procedure for microwave epitaxial GaAs diodes applicable for switching purposes 12 p2035 A69-25831

Probability distributions of characteristics of mass produced semiconductor rectifier diodes
12 p2035 A69-25832

Solar cells physical properties and functions, considering band structure of semiconductors, p-n junction diodes and photovoltaic effect, efficiency calculations and radiation damage
12 p2015 A69-25864

Microstripline circuit for stabilizing oscillating frequency of Gunn diodes prepared with GaAs slices
12 p2036 A69-25924

Laser emission noise and voltage noise cross correlation coefficient for CW GaAs laser diodes at 77 K, noting strong dependence on bias current
12 p2038 A69-26328

Negative resistance effects computed for HF operation of SCL diodes, based on quantitative analysis of small signal response
12 p2038 A69-26349

Laser diode output efficiency increased in presence of transverse magnetic field suppressing higher order TE and TM modes
12 p2039 A69-26353

Differential capacitance, diffusion voltage and exponent alpha of hyperabrupt junction varactor
12 p2039 A69-26375

Gallium arsenide thermometer calibration in 1 to 100 K range using interpolation formula derived from p-n junction diode equation
12 p2093 A69-26484

Bismuth doped lead tin telluride diode lasers with low threshold currents at cryogenic temperatures, discussing doping effect
12 p2109 A69-26641

Direct modulation characteristics of semiconductor junction laser, analyzing resonance phenomenon, bias current, admittance, modulation frequency limit and emission lifetime
12 p2110 A69-27069

Negative resistance formation in impurity compensated semiconductor diodes ascribed to injected carrier drift path increment with increasing current, deriving I-V characteristics
13 p2230 A69-27877

Photoelectric characteristics of thin film CdS-CdTe heterojunction diodes, considering I-V illuminance, spectral characteristics and conduction band continuity
13 p2230 A69-27882

Electroluminescence of p-GaAs diodes analyzed over temperature range of linear dependence of lasing on injection current
13 p2230 A69-27887

Gallium arsenide diode nonequilibrium carriers absorption of He-Ne laser radiation under emission conditions
13 p2272 A69-27893

Capture centers effect on current-voltage characteristic of p-i-n diodes during injection, noting negative resistance appearance
13 p2236 A69-28525

Current-voltage characteristics of p-n-p diodes, discussing collector voltage effect on current carrier concentration distribution in diode base
13 p2236 A69-28531

Forward current decrease in Si mesa diodes under fast neutron irradiation ascribed to increase in base resistance
13 p2236 A69-28549

Square wave generator for junction laser power supply
13 p2274 A69-28643

Small signal transient characteristics of semiconductor diodes analyzed by charge method, studying processes during p-n junction diode switching at low currents
14 p2419 A69-28918

SiC and GaP diodes used as low power light sources, studying electroluminescence in p-n region under pulsed excitation
14 p2419 A69-29325

Strain sensor using p-n heterojunction diode fabricated by vacuum evaporation onto flexible substrate
14 p2422 A69-29555

Solar conversion efficiencies of p-n and n-p diodes calculated for specified semiconductor heterojunctions using Anderson diffusion model
15 p2552 A69-30034

Current effects on quantum efficiency of gallium phosphide junction diodes emitting red light
15 p2575 A69-30174

Transit time effects in silicon space charge limited diodes, studying frequency characteristics of small signal equivalent circuit
15 p2575 A69-30181

Junction diode field factor, comparing results of dynamic impedance and distortion measurement methods with deduced values of static characteristic
15 p2575 A69-30301

Negative resistance section of current-voltage curve for long diodes of p-type indium antimonide, noting magnetic field effects on electrical breakdown
15 p2581 A69-31149

Gallium phosphide Schottky barrier diodes, discussing construction and metals used, barrier height relationships to impurity concentration and temperature, rectifying characteristics and internal quantum efficiency
16 p2757 A69-31613

Carrier lifetime in p-nu-n diodes, discussing error of forward pulsed diode method by Wilson and alternative model
16 p2757 A69-31615

Uniaxial stress effect in Schottky barrier diodes measured by beam balance noting higher sensitivity
16 p2758 A69-31619

Optimum metal contact stripe width for CW operation of GaAs junction lasers bonded on copper heat sink
16 p2796 A69-31698

Nanosecond pulse generator circuits based on four layer Si diodes designed for semiconductor laser excitation
18 p3153 A69-35257

Junction lasers current-voltage characteristics, discussing coherence-pinch effect as explanation of threshold behavior
19 p3337 A69-36531

Metal-semiconductor contact current-voltage characteristic derived from modified diode theory taking into account electron distribution function
19 p3391 A69-36608

Gunn effect applied to digital electronics, discussing diode characteristics, microwave amplifier design, pattern recognition, analog- numerical conversion, etc.
19 p3285 A69-36708

Recombination radiation of tellurium and zinc doped GaAs alloy type diodes, discussing luminescence spectra, current-voltage characteristics and temperature effects
20 p3506 A69-37783

Near constant phase variable attenuator for RF signal containing Doppler information, centering design around p-i-n diode as control element
21 p3681 A69-38410

Book on physics of microwave semiconductor diodes covering p-n junction theory and device characteristics and applications
21 p3682 A69-38990

Electroluminescence of p-GaAs diodes, analyzing temperature range of linear dependence of lasing on injection current
21 p3682 A69-39145

Digital computer determination of stimulated emission time delay, Q switching temperature and current region and impurity profile effect across junction in junction lasers
22 p3962 A69-40561

Lasing properties of Ni-doped GaAs diodes evaluated by plotting resonance, mode amplitudes and frequencies for various bias currents and external capacitance
22 p3912 A69-40606

Lasing properties of spontaneous emission hemispherical semiconductor diode with AlAs-GaAs junctions measured by calibrated silicon photocell
22 p3964 A69-40608

JUNCTION TRANSISTORS

Circuit for linear voltage amplitude to pulse width conversion using controlled unijunction monostable multivibrator
02 p0217 A69-12151

Gradual capture in p-n junctions and p-n-p transistors at AC voltage, noting diffusion capacitance and resistance
03 p0491 A69-14051

Plane of symmetry determination for generalized junction gate field effect transistors extended to include impurity profiles and bias voltage conditions
04 p0574 A69-14344

Diffusion capacitance of p-n junctions, short base semiconductor diodes and p-n-p transistor, discussing systematic error in quasi-steady state calculation
04 p0580 A69-15489

Insulated junction integrated circuit transistor operation with various terminal connections corresponding to diode switching of transistor
05 p0730 A69-16217

Double diffused planar Ge p-n-p and p-n-p transistors with high switching speed, noting fabrication and performance
05 p0809 A69-16557

Recovery and long term reliability of Si p-n-p transistors subject to gamma radiation, using military specifications for failure
06 p0976 A69-16878

Junction gate field effect transistor design covering geometries and impurity profiles
06 p0893 A69-17197

Computer model for n-p-n transistor in integrated circuit using substrate p-n junction isolation
07 p1114 A69-18246

Second breakdown in semiconductors, studying thermal feedback connected with temperature time dependence of junction electrical properties
08 p1294 A69-21115

Time delay in temperature controlled transistorized time delay circuit determined by transistor unsteady thermal processes
12 p2043 A69-26883

MOS and junction transistors damage due to radiation, noting decrease in collector current under fast neutron dose
13 p2227 A69-27514

One dimensional analysis of static collector emitter saturation voltage of epitaxial and triple diffused devices, considering transistor with lightly doped collector
14 p2421 A69-29545

Double diffused transistor with Gaussian impurity distribution analyzed by power series for carrier density distribution and frequency response
16 p2758 A69-31616

Beam lead sealed junction transistor and integrated circuits reliability, describing test conditions and failure mechanisms
18 p3145 A69-34497

Book on field effect and bipolar junction transistors and microcircuits, covering ideal and practical amplifiers, circuit characteristics, etc.
20 p3505 A69-37147

Generation-recombination noise due to trapped charge fluctuation at impurity centers in Si junction gate field effect transistors transition regions, using lumped equivalent circuit
22 p3911 A69-40009

Two dimensional analysis of junction transistor electrical behavior, analyzing DC and AC crowding effects, conduction and impedance of base and collector
22 p3911 A69-40011

JUNCTIONS

Wideband hybrid junctions synthesis from given parameters, suggesting matrix representation of ring circuits
01 p0043 A69-10593

JUPITER (PLANET)

Jupiter outer satellites orbits determination with computer program based on modified Cowell/Moulton methods for adjusting initial conditions
01 p0158 A69-11330

Brightness temperature maps for Jovian thermal radiation obtained through 8-14 micron window of atmosphere
02 p0309 A69-12715

Jupiter, Venus and Mars 8.6 mm radio emission, obtaining average disk brightness temperatures
02 p0327 A69-12716

Jupiter radio physics, discussing prebiological phase, low IR and microwave radio temperature and magnetic field
02 p0330 A69-12805

Photovoltaic properties of CdS thin film solar cells and silicon cells at Jupiter temperature and solar intensity
03 p0368 A69-13076

Symmetric baroclinic instability role in Jupiter equatorial acceleration
03 p0508 A69-13347

Changes in bands of Jupiter /1962-1965/ from astronomical synoptic mapping program, tabulating overall and chromatic intensities and longitudinal velocities
03 p0512 A69-13696

Polarized radio emission from Jupiter, giving hypothesis of radiation belts deformation by solar wind
03 p0512 A69-13703

Surface temperatures for Galilean satellites of Jupiter calculated through corresponding lunations, assuming synchronous orbits with respect to Jupiter
03 p0513 A69-13776

Space flight launches, interplanetary transfer orbits, flyby orbits and capture orbits for solar probe with 0.3 AU perihelion and Jupiter satellite probe
04 p0657 A69-14826

Non-Io controlled fifth source of Jupiter decametric radiation from/near visible planetary disk
05 p0813 A69-15604

Europa control of decametric emission from Jupiter
05 p0813 A69-15605

Jupiter microwave radiation flux density at 81 MHz, noting spectrum of microwave emission
05 p0827 A69-16506

Jupiter unmanned flyby probes trajectory and mission analysis, considering planetary gravitational field role for trajectory shaping and flight times
06 p1007 A69-17598

Groups of drifting lanes of emission in fine structure of dynamic spectra of Jupiter decasecond decametric radiation bursts
06 p1008 A69-17958

Particle flux and dose rates in Jupiter Van Allen belts based on assumed synchrotron radiation from trapped electrons in dipole magnetic field
[AIAA PAPER 69-18]
06 p0997 A69-18129

Orbiter and rotator models of pulsating radio sources, considering relationship between lack of Faraday rotation and similar polarization in decametric radiation from Jupiter
08 p1397 A69-20688

Chemical abundances in planetary atmospheres based on spectroscopic determinations, considering terrestrial and Jovian planets
08 p1406 A69-20934

Venus and Jupiter observations by earth paraboloid antenna, discussing average brightness temperatures and upper limit for Venus water vapor abundance
09 p1600 A69-22206

Thermal models for Jupiter and Saturn corresponding to completely convective structure, using De Marcus state equations
09 p1607 A69-22428

Orbits of asteroids surrounding commensurabilities with Jupiter, discussing theory for origin of Kirkwood gaps
10 p1778 A69-23604

Venus and Jupiter low resolution UV spectra obtained with servocontrolled star tracking telescope in Aerobee rocket, noting Lyman alpha radiation characteristics
[JHU-TR-15]
10 p1788 A69-24121

Venus and Jupiter brightness temperature and radio emission at 2.25 and 8 mm wavelengths observed with radio telescope
11 p1956 A69-24396

Jupiter red spot visibility, establishing partial dependence on solar activity
11 p1964 A69-25404

Io as unipolar inductor, analyzing interaction with Jupiter magnetosphere and decimetric synchrotron radiation
13 p2337 A69-27552

Jupiter decametric radio emission periodicity attributed to undiscovered satellite in unstable orbit, discussing application to satellite discovery
13 p2343 A69-27622

Linear polarization measurements at 6 cm, determining rotation period associated with Jupiter cm radiation
13 p2343 A69-27623

Photographic observations of fifth satellite and disk of Jupiter against stars background for mean motion and regression of nodes
13 p2345 A69-27653

Midcourse maneuvers in interplanetary guidance, considering spin stabilized spacecraft flyby for Jupiter mission
13 p2354 A69-28504

Electron plasma oscillations and electron whistler of solar wind near Jupiter orbit
14 p2513 A69-29115

Zonal harmonics of Legendre polynomial series of Jupiter attractive force function effects on motion of fifth satellite
14 p2521 A69-29463

Instrumental observations of Jupiter opposition in 1967 and 1968
16 p2858 A69-32205

Mass of Jupiter system from motion of Doris, using variational equations for initial rectangular coordinates and velocities with respect to mass of Jupiter
16 p2863 A69-32403

Jupiter photochemistry above 1000 A, noting methane and ammonia photolysis zones, atmospheric pressures and hydrogen recombinations
17 p3032 A69-33165

Heliosphere boundary location significance for Jovian magnetosphere configuration, considering inverse correlation between sunspot number and Jovian decametric radio emission
17 p3033 A69-33379

IR radiometer to measure Jupiter atmospheric temperature by calculating certain constituents heat radiation levels through Planck formula assuming black body properties
17 p2974 A69-33425

Jupiter red spot prominence correlation with Zurich sunspot number
17 p3045 A69-34185

Jovian radio sources intermittency, recording difficulties, longitudinal drift and theories concerning origin
18 p3196 A69-34690

Polar flattening influence of Jupiter on artificial satellite motion around Callisto noting orbital perturbations
18 p3199 A69-34913

Jupiter decametric radio source analysis suggesting two component model of rotation at both constant and variable rotational periods
18 p3202 A69-35212

Jupiter observations /1966-1967/, discussing variations in size and position of polar caps and tropical belts
18 p3203 A69-35337

Jupiter swingby flight mode application to probe missions requiring solar polar regions overflight at close perihelion distances
19 p3401 A69-35915

Crab Nebula radio brightness at 2.16 and 8.2 mm measured and compared to Jupiter flux density
19 p3428 A69-36875

Jupiter tenth satellite reobserved, discussing calculations and computer techniques for determining orbit
[AAS PAPER 68-140]
20 p3595 A69-37194

H alpha auroral activity on Jupiter isolated by using Fabry-Perot etalons, showing photograph reproductions
20 p3598 A69-37414

Hansen method applied to Jupiter tenth satellite orbit correction and perturbations, describing computer program and formulas used
20 p3602 A69-37529

Polarization ellipse orientation at source from Faraday fringes on Jupiter decametric radio bursts swept frequency records
20 p3594 A69-38169

Jupiter mass determined by applying Cowell numerical integration to equations of motion for ninth satellite
21 p3795 A69-38468

CircumJovian powered and free return trajectories, analyzing round trip missions and departure opportunity
[AAS PAPER 68-117]
21 p3805 A69-39207

Exploration capabilities provided by Jupiter gravity assisted trajectories compared to direct ballistic flight trajectories
[AAS PAPER 68-116]
21 p3805 A69-39224

Perturbative effects of Jupiter moons on spacecraft flyby and postencounter heliocentric trajectories, noting precision targeting
[AIAA PAPER 69-932]
21 p3809 A69-39361

Jupiter mass determined from observations of four minor planets perturbations
22 p4013 A69-40121

Rocket UV spectra indicating Venus atmosphere weak absorption and low ozone abundance and possible Jupiter surface depressions
22 p4028 A69-40661

Jupiter spectrum observations in 2.8-14 micron range, describing absorption strength and brightness temperature, basing analysis on ammonia, methane and hydrogen absorption
22 p4028 A69-40662

Galilean satellites perturbing effect on motion of fifth Jupiter satellite
23 p4214 A69-41730

Recurrent Lagrange multipliers for optimal low thrust earth-Jupiter transfers, using three dimensional solar system model
23 p4215 A69-41896

Pioneer F/G mission to Jupiter by NASA for exploring interplanetary medium, asteroid belt, planet and environment
[AAS PAPER 69-290]
24 p4381 A69-42863

Venus and Jupiter brightness temperature and radio emission at 2.25 and 8 mm wavelengths observed with radio telescope
24 p4390 A69-43786

JUPITER ATMOSPHERE

Jovian atmospheric rotational temperature from rotational lines in methane band
01 p0153 A69-10856

Galactic Jupiter Probes investigating Jupiter atmosphere and emissions and deep space cosmic radiation
02 p0324 A69-12303

Blunt and conical body optimum heat shield shapes for Jupiter atmospheric entry, noting shallow flight path
[AIAA PAPER 68-1150]
03 p0520 A69-13565

Changes in bands of Jupiter /1962-1965/ from astronomical synoptic mapping program, tabulating overall and chromatic intensities and longitudinal velocities
03 p0512 A69-13696

Dark equatorial belt of Jupiter atmosphere in 1962 and 1963, noting photometric contrasts, molecular absorption and possible structure
04 p0658 A69-14961

Jupiter Red Spot visual observations in 1966 and 1967 noting changes in size, color and planetographic coordinates and variation of apparent intensity
04 p0659 A69-14963

Shock tube measurements of radiation from simulated Jupiter atmosphere related to thermodynamic conditions encountered by entry probe
[AIAA PAPER 69-184]
06 p0908 A69-18207

Jupiter Red Spot vorticity at perimeter indicated by interaction with dark spots circulating along south equatorial belt
07 p1213 A69-18606

Jovian limb H alpha line due to auroral emission obtained from high dispersion spectra with long light path through upper atmosphere
07 p1214 A69-18614

Methane absorption distribution in 6190 A band over Jupiter disk based on spectrograms, noting center to limb variations
11 p1960 A69-24730

Spectrum analysis of Jupiter atmospheric composition, obtaining abundances of minor constituents
12 p2155 A69-26205

Jupiter polarization wavelength dependence noted in observations of 5 seconds diameter regions near poles and equator related to Rayleigh-Chandrasekhar molecular scattering theory
13 p2348 A69-27805

Atmospheric motions on Jupiter, considering highly symmetric flow, baroclinic waves and red spot
15 p2694 A69-30856

Dark equatorial belt of Jupiter atmosphere in 1962 and 1963, noting photometric contrasts, molecular absorption and possible structure
18 p3197 A69-34724

Jupiter Red Spot visual observations in 1966 and 1967 noting changes in size, color and planetographic coordinates and variation of apparent intensity
18 p3197 A69-34726

Cloud layer multiple scattering in Jovian atmosphere, discussing influence on Lorentzian contour of planetary absorption lines
18 p3203 A69-35332

Jupiter observations /1966-1967/, discussing variations in size and position of polar caps and tropical belts
18 p3203 A69-35337

Methane abundance and rotational temperature of Jupiter, considering effects of line saturation
20 p3613 A69-38174

Venus, Mars and Jupiter lower atmospheric motions, considering atmospheres thermal and chemical composition
21 p3811 A69-39511

Jupiter magnetospheric radio emissions, discussing magnetic field and plasma-magnetic interactions
21 p3812 A69-39517

Methane rotational temperature in Jovian atmosphere deduced from equivalent widths of lines at 1.1 micron band
22 p4028 A69-40663

Jupiter Red Spot semiregular oscillations from photographic measurements, determining mean period and amplitude
24 p4383 A69-43002

JUPITER RED SPOT

Jupiter Great Red Spot in terms of homogeneous fluid rapid rotation, Rossby number, stagnant region, Taylor column and stratification

20 p3609 A69-38060

Jupiter Red Spot semiregular oscillations from photographic measurements, determining mean period and amplitude

24 p4383 A69-43002

K

K BAND

U EXTREMELY HIGH FREQUENCIES

K LINES

Equivalent widths of K line of single ionized calcium and central depths of unidentified broad absorption in O and B stars spectra

08 p1389 A69-20250

K alpha lines in solar soft X ray spectra noting instrumental effect

09 p1580 A69-22232

Chromospheric heating and polarization in late stars, considering association with Ca II K line emission cores

13 p2340 A69-27579

Ca 2 resonance line profiles in large disk flares and in surrounding plage, discussing H and K line behavior

17 p3023 A69-33054

Chromospheric inhomogeneities rapid changing properties observable in H and K lines above sunspot umbrae

18 p3204 A69-35389

Balmer and Ca II K/line profiles computed by program based on model atmospheres, comparing computed and observed data for F stars

19 p3426 A69-36578

Ti emission and absorption K spectra in Ti-Al intermetallics, suggesting hypothesis concerning long wave and fundamental subbands origin

21 p3749 A69-39787

Core profiles of H alpha, H beta, H and K from spectrograms of plages

22 p4010 A69-39993

Calcium K line strengths in A stars measured by narrow band spectrometer compensated for seeing and transparency variations

22 p4015 A69-40154

Hartree-Fock calculations for wavelengths of K alpha X ray transitions, tabulating configuration and term energies, dipole integrals and relative multiplet strengths

22 p3984 A69-40156

K-alpha band characteristics of N spectra stimulated in nitrides of transition metals by X rays

22 p3974 A69-41118

K-MESONS

K meson-light nucleus scattering lengths calculated using multiple scattering theory with Kim zero range

15 p2655 A69-30309

Particle physics and discovery of K mesons and hyperons emphasizing track recording, cloud and bubble chamber techniques

24 p4352 A69-43039

KA BAND

U EXTREMELY HIGH FREQUENCIES

KALMAN-SCHMIDT FILTERING

Kalman optimal filter for linear distributed parameter systems with Gaussian disturbances and measurement noise

01 p0034 A69-11143

Structure oriented parallel algorithms for matrix operations, noting applicability to real time calculations for discrete Kalman filter and control problems

02 p0224 A69-11743

Planetary atmosphere determination error analysis using Kalman filter, noting results of simulated Martian atmosphere entry

02 p0331 A69-12806

Optimal filter design for estimating state of linear dynamical system in presence of high measurement noise

04 p0582 A69-14877

Limited memory optimal filter theory, output and standard filter divergence due to errors

06 p0905 A69-17946

Orthogonal projection derived equation to optimally estimate state of nonstationary linear discrete systems with time delay, developing Kalman type filter

09 p1473 A69-22437

Kalman filter with delayed states as observables, discussing extra computer effort and modeling technique

09 p1473 A69-22438

Kalman equations of optimal recursive filter for linear discrete system extended to continuous system through limiting procedure

11 p1859 A69-25408

Modeling errors in linear discrete stochastic system effects on Kalman filter state estimates

11 p1860 A69-25448

Kalman sequential estimation adaptation to target maneuvers without sacrificing tracking accuracy in nonmaneuvering portions of trajectory

11 p1861 A69-25455

Adaptive filtering to prevent divergence observed in application of Kalman filter to orbit determination

12 p2045 A69-26059

Deterministic linear observation systems and Kalman optimum linear filters application to performance improvement of inertial navigation systems

12 p2128 A69-26065

Modeling nonstationary random processes using linear time-invariant difference equation, with applications to Kalman filtering and gyro drift

14 p2479 A69-29486

Optimal filtering of linear distributed parameter systems corrupted by boundary and/or volume stochastic disturbances

15 p2565 A69-30183

Initial-convergence examination of Kalman filter for various autonomous navigation modes [AIAA PAPER 67-623]

16 p2809 A69-31875

Multisensor data processing technique for fail operational landing commands, using real time error analysis inherent in Kalman filter

17 p3003 A69-34106

Filtering and optimal control problems for discrete stochastic dynamical systems, describing various feedback controls and midcourse guidance optimization

18 p3109 A69-34660

Parameter sensitivity analysis of discrete suboptimal filters from optimal rmse estimate of actual system performance measure

18 p3110 A69-34675

Adaptive filter for estimating system noise inputs from actual residuals developed to control Kalman filter in satellite orbit estimation

18 p3110 A69-34676

Kalman filter based on calculus of variations, evaluating object trajectory during vertical atmospheric descent

19 p3307 A69-35794

Kalman recursive filtering method applied to inertial navigation systems resetting

19 p3286 A69-36645

Weighting coefficients calculations by recursive algorithm for designing optimal discrete adaptive Kalman filter

20 p3509 A69-37142

Discrete filters for optimal processing of downlinked satellite data, considering inverse filter development by Kalman filtering techniques

21 p3677 A69-39462

Iterative method for reducing filters required for optimal Kalman filter design maintaining parameter estimation accuracy

21 p3687 A69-39463

Kalman filter simulation for estimating aircraft position and velocity from airborne digital computer data in zero-zero landing system [AIAA PAPER 69-944]

22 p3978 A69-40327

Adaptive filtering to prevent divergence observed in application of Kalman filter to orbit determination

23 p4146 A69-42446

Kalman-Bucy filtering technique for estimation of initial conditions and smoothing in linear dynamic systems, noting rectilinear motion of randomly accelerated spacecraft

23 p4132 A69-42546

Optimal deterministic estimation and feedback control for linear nonstationary process and measurement systems defined by Riccati equations, including Kalman-Bucy filter

24 p4291 A69-43276

KAMACITE

Kamacite analysis for P and Ni in chondrites, palasite and iron meteorites, considering cooling rate and rhadbit

19 p3417 A69-36131

Iron meteorites microscopic and macroscopic features due to preterrestrial mechanical deformation, stressing local displacements encountered in normal or acicular kamacites

19 p3418 A69-36134

Morphological, chemical and X ray analysis of urelite meteorite, identifying diamonds with kamacite and troilite admixtures from carbonaceous material

21 p3816 A69-396260

KAMAN MILITARY HELICOPTERS

U MILITARY HELICOPTERS

KAONS

Cosmic ray muons angular distribution measuring device for determining pion/kaon ratio

13 p2332 A69-28421

KAPOETA ACHONDRITE

Distribution and origin of primordial He, Ne and Ar in Fayetteville and Kapoeta meteorites extracted and analyzed by laser-microprobe mass spectrometer

19 p3419 A69-36142

KAPPA ROCKET VEHICLES

Ionospheric electron temperature probe analysis based on Japanese Kappa rocket data

05 p0761 A69-15701

KARHUNEN-LOEVE EXPANSION

Pattern recognition method dependent on preselection of good variables, discussing SELFIC and relationship to Karhunen-Loeve expansion and factor analysis

07 p1088 A69-18386

Pattern recognition as part of statistical communication theory, using Karhunen-Loeve expansion to minimize root-mean-square errors, showing application to handwritten numerals

09 p1461 A69-22292

KARMAN VORTEX STREET

Standing twin vortices in wake behind thin flat plate normal to flow visualized by Al dust, noting Karman vortex street

18 p3086 A69-35167

Karman vortex street formation indicated by smoke visualization method study of laminar wake behind single cylinder

21 p3644 A69-38687

KC-130 AIRCRAFT

U C-130 AIRCRAFT

KELVIN TEMPERATURE SCALE

U TEMPERATURE SCALES

KEPLER LAWS

Matrizants construction for Keplerian motions, discussing Hamiltonian character of variational equations for planar two body problem

03 p0513 A69-13779

Kepler third law application to radar determinations of astronomical unit of length in general relativity

04 p0657 A69-14698

Regularization of perturbed Keplerian motion in three dimensional space by means of Levi-Civita transformation generalized to three dimensions

05 p0827 A69-16602

Kepler hyperbolic sine equation calculated for Arend-Roland comet for case of constant residues by false position method

06 p0997 A69-16821

Table of computerized three place E-M solutions for Kepler equation, noting revision of Astrand table

10 p1777 A69-23395

Gauss method for Kepler equation ephemeris computation in nearly parabolic orbits, using expansions suitable for high speed computers

12 p2171 A69-27154

Optimum orbital transfer of material point subjected to reactive force with minimum mass loss, discussing Kepler motion kinematics

13 p2346 A69-27698

Discrepancy between Kepler first two laws and corresponding Newton propositions, noting necessary substitution of ovals for elliptical orbits

15 p2695 A69-31011

Relativistic generalization for polar Sommerfeld rosette of Fourier series expansions by Lagrange and Bessel for particle motion in Keplerian field

16 p2811 A69-31607

Simplified method for derivation of universal gravitation law from Kepler law of planetary orbits

16 p2813 A69-32481

Cowell equations modified for exact integration of pure Keplerian orbits, considering secular effects

18 p3165 A69-34842

Optimal transfers between Keplerian orbits for time free case, considering hyperbolas, ellipses external to and intersecting attracting planet

19 p3399 A69-35669

Minimum impulse transfer of vehicle between noncoplanar Kepler orbits, applying optimal control principles to formulation

23 p4214 A69-41878

KERNEL FUNCTIONS

- Kernel function applied to compressible fluid flow computation for linear procedure to determine subsonic flow patterns
01 p0058 A69-10225
- Eigenproblem for displacement integral equations with finite cosine transform kernels, extending Roark-Wing numerical method for eigenvalues to kernels
01 p0106 A69-10986
- Approximation for discretization error of discrete analog of Bergman harmonic kernel, discussing discretization error in Dirichlet and Neumann problems for Laplace equation
03 p0456 A69-13555
- Integral equation solution with Mellin inversion formulas for light scattering problems
06 p0949 A69-17887
- Viscoelastic problem solutions for hereditary media, using Laplace transforms or solutions of integral equations for inaccurately approximated kernels
08 p1412 A69-20329
- Stability and bending of flexible plates and shallow shells obeying hereditary relations solved by singular kernel functions
08 p1413 A69-20335
- Numerical and kernel expansion procedures for laser mode, discussing Gaussian quadrature numerical integration for conversion to matrix equation
08 p1328 A69-21091
- General theorems derived for Noether operator applied to integral equation with automorphic kernel
12 p2122 A69-26574
- Collision integral kernels of kinetic equation for single component gas density matrix derived by Bogolubov-Gubov method
14 p2458 A69-29169
- Semidefinite Peano kernels of stable forms
15 p2644 A69-30450
- Substitute kernel approximation for acoustic waves radiative transfer equations for nongray gas near equilibrium
15 p2717 A69-30791
- Diffraction of modal field by semiinfinite waveguide, integral representation for Wiener Hopf kernel factorization and applications to open resonators
17 p2930 A69-33888
- Orthogonal polynomials in three dimensional contact problems without friction, discussing construction of kernels over finite and semiinfinite intervals
22 p4041 A69-40113
- Symmetry properties of Cameron-Martin-Wiener kernels in isotropic velocity field, applied to one dimensional model of incompressible turbulent flow
24 p4301 A69-43358
- KEROSENE**
- Kerosene droplets combustion stability studied by motion pictures, discussing pressure, temperature and O concentrations effects in turbulent carbon dioxide flow
08 p1421 A69-20345
- Turbine and jet engines kerosene fuels tests in small and medium size laboratory combustion chambers
13 p2240 A69-27932
- KERR CELLS**
- Kerr effect apparatus for measurements of pure liquids and solutions involving comparison of two luminous fluxes with aid of photomultiplier
01 p0078 A69-10039
- Copper exploding wire Kerr-cell time-resolved absorption spectra analysis, considering copper atom transition
01 p0118 A69-10665
- High speed photodetector frequency characteristics using multimode gas laser and Kerr cell
10 p1707 A69-24211
- Kerr constant verification device to study electrooptic liquids properties
12 p2084 A69-26148
- KERR ELECTROOPTICAL EFFECT**
- Kerr effect apparatus for measurements of pure liquids and solutions involving comparison of two luminous fluxes with aid of photomultiplier
01 p0078 A69-10039
- Kerr effect and electrostriction during self focusing of high power laser beam in gases and liquids
04 p0611 A69-14792
- Kerr constant verification device to study electrooptic liquids properties
12 p2084 A69-26148

KERR MAGNETOOPTICAL EFFECT

- Quasi-static Kerr magneto-optic observation and procedure to predict results of dynamic flux reversal in thin Ni-Fe films
[IEEE PAPER 11.7] 01 p0138 A69-10716
- Quantum theory of electrical birefringence of noninteracting diamagnetic molecules /Kerr effect/ subjected to static electric field and polarized plane wave
02 p0279 A69-11538
- Kerr magneto-optic camera for 10 nsec exposures of dynamic magnetization configuration in magnetic thin film during high speed flux reversal
17 p2970 A69-32853
- Dynamic Kerr observations of high speed flux reversal and relaxation process in permalloy thin films by magnetooptical camera with Q switched ruby laser
19 p3383 A69-36446
- KESTREL AIRCRAFT**
U P-1127 AIRCRAFT
- KETONES**
NT ACETONE
- Ion structure of keto and enol and McLafferty rearrangements determined by ion cyclotron resonance spectroscopy
19 p3265 A69-36288

KEYING

- U FREQUENCY SHIFT KEYING
U PHASE SHIFT KEYING
- KIDNEY DISEASES**
U NEPHRITIS
- KIDNEYS**
- Lateral acceleration effects on human kidney functions, noting increase in diuresis and erythrocytes in urine
02 p0198 A69-11514
- Rapid global transportation effect on circadian rhythmic patterns in human body functions, discussing kidney excretion and pituitary adrenal cortical system
09 p1444 A69-22545
- Renal vascular circulation in carotid occlusion pressor reflex by vasoconstriction in absence of renal autoregulation
22 p3887 A69-41190
- Urine sampling conditions for kidney function circadian rhythm during global flight, considering food and water intake, sampling intervals and body position
24 p4266 A69-43374

KINEMATIC EQUATIONS

- Soviet book on kinematics of inertial navigation systems covering systems classification, equations derivation and computer algorithms for error analyses
02 p0278 A69-11793
- Dynamic equations for offset unsymmetric gyroscope with obliquely placed rotor, using dual transformation matrices
[ASME PAPER 68-WA/DE-5] 05 p0764 A69-16170
- Kinematics of vertical gyroscope mounted in additional servo frame, determining kinematic errors due to rotor axis deviation
09 p1498 A69-22108
- Drift rate of gyroscopic devices in space based on kinematic theorem, stressing free gyroscope subjected to harmonically varying moment
09 p1498 A69-22111
- Thermodynamics of strain rate sensitive elastoviscoplastic solids, considering kinematic description of plastic deformation and choice of state variables
11 p1994 A69-25601
- Airframe stability of VAK 191 examined by displacement method, using matrix calculations within Automatic System of Kinematic Analysis
20 p3462 A69-37515
- Kinematic dynamo waves, discussing excitation and maintenance of magnetic field by assumed motion of uniformly conducting fluid using small parameter and numerical methods
22 p3989 A69-40195

KINEMATICS

- NT BODY KINEMATICS
- Equations of motion for kinematics of complex mechanisms, noting methods and relations
01 p0115 A69-10165
- Sun motion with respect to extragalactic universe, discussing local supercluster kinematics
03 p0513 A69-13769
- Kinematic parameters for elastic slender body aid in description of motion of body
04 p0668 A69-14271
- Planar linkages kinematic synthesis and design, using Newton-Raphson iteration technique to solve nonlinear equations
04 p0604 A69-14517

Solar motion in distant objects kinematics, suggesting simultaneous solutions of local motion and galactic rotation parameters

- 04 p0654 A69-14627
- General kinematic yield mechanism and associated kinematically adequate multiplier formulated for structural elements characterized by plane deformation state
05 p0831 A69-15684
- Kinematics of electrochemical machining defined as quasi-steady process
[ASME PAPER 68-WA/PROD-22] 05 p0769 A69-16194
- Stellar samples with various luminosity and A star kinematic properties, discussing influence on application of hydrodynamics equations to evolution problems
07 p1224 A69-19712
- Relativistic kinematics analog model for deformable continua, introducing deformation gradient and tensors
08 p1416 A69-20693
- Four gimbal Cardan suspension gyroscope kinematics for nonperpendicular arrangement
09 p1502 A69-22705
- Kinematic equations of motion of body about fixed point, considering Steklov solution
11 p1918 A69-24791
- Single mirror scanning geometry and kinematics, analyzing spatial motion of objects plane mirror image
12 p2091 A69-26367
- Spiral galaxies rotation curve fluctuations attributed to kinematic properties of galactic matter and gas components
12 p2170 A69-27062
- Relativistic kinematics of continuum motion by invariant derivatives of deformation measures, discussing rigid body motion in Born sense
12 p2189 A69-27116
- Solar cycle kinematical model based on field amplification by solar differential rotation including fluctuations in eruption rate
13 p2337 A69-27548
- Power gyrostabilizer kinematic structure synthesis, applying matrix methods to design variables
14 p2446 A69-28924
- Nonlinear programming for calculating static and kinematic failure of one dimensional structures by extending results from linear programming
14 p2418 A69-29597
- Noctilucent clouds morphological and kinematic characteristics based on photographs
18 p3132 A69-35335
- MHD dynamo construction with emphasis on fluid motion effect on magnetic field, considering spatially periodic dynamo derivation from kinematic considerations
22 p3989 A69-40196
- Pressure loads and balancing force determination in kinematic pairs of link gear of landing mechanism
23 p4062 A69-41415
- Dynamic uniaxial tensile stress-strain data obtained at high rates by measuring kinematics of symmetrically expanding thin ring specimens
24 p4330 A69-42735
- KINESCOPES**
U PICTURE TUBES
- KINETIC ENERGY**
- Impulse and kinetic energy transfer in rarefied gases analyzed on basis of kinetic theory, considering surface curvature effect
01 p0173 A69-10093
- Radiation problem in general theory of relativity investigated by momentum energy tensor, formulating criterion for gravitational radiation
01 p0116 A69-10435
- Motion, field momentum and field kinetic energy equations of concentrated dislocations based on Zorski field theory of defects
02 p0336 A69-11556
- Thermalization of kinetic energy of plasma flow by shock phenomena produced by magnetic mirror field
02 p0289 A69-12176
- Plasma radiation, including atomic processes and radiation by variation of constituent kinetic energy
03 p0483 A69-14237
- Alkali metals thermoelectric power and energy dependence of Heine-Abarenkov pseudopotential, taking into account anisotropy effects
05 p0809 A69-16507
- Cosmic radiation propagation in interstellar space, discussing differential kinetic energy spectra of protons, He, C and O nuclei and Fe
06 p0988 A69-17269
- Lithium, Be, B and fluorine nuclei in cosmic radiation, discussing nature of spectra
06 p0988 A69-17271

Atmospheric circulation intensity measurement, using potential energy conversion to kinetic or kinetic energy dissipation by friction

07 p1175 A69-18947

Tropospheric energy cycle interannual variability and quasi-biennial oscillation from geostrophic computations of eddy kinetic energy, energy transfer and internal redistribution

07 p1129 A69-19628

Transmission line analogs and kinetic power theorems for space charge waves amplification in semiconductors, considering internal effect and wave excitation

10 p1748 A69-24052

Energy release in quasars through nonmassive gravitational collapse compared with local objects, noting cosmological luminosities

10 p1785 A69-24091

Mean and eddy motions in atmosphere described by mathematical expressions for total and mean kinetic energies

11 p1911 A69-24323

Slow charged products of charge exchange collisions by ions in molecular gases, comparing kinetic energies during various reactions

13 p2301 A69-27455

Variable fluid and field velocity HF induction generator, determining interaction between fluid dynamic forces and magnetic field and kinetic energy

13 p2207 A69-27502

Conditions governing application of reduced Nielsen equations to anholonomic systems dynamics, discussing kinetic energy function

13 p2288 A69-27924

Optimal control for minimization of heating and acceleration forces to reduce kinetic energy of reentry vehicle in space missions

13 p2352 A69-27960

MHD generator design using shock wave kinetic energy produced by explosion in shock tube with superconducting magnetic system

14 p2393 A69-28911

Energetics in solid film lubricants vacuum deposition methods, showing dependence on interfacial and film characteristics

14 p2454 A69-29001

Convective instability by active stress, discussing composition dependent stress fields in continuous and mechanically isolated material and chemical to kinetic energy conversion

14 p2540 A69-29634

Atmospheric circulation integral characteristics, calculating kinetic energy in Northern Hemisphere

14 p2476 A69-29824

Kinetic energy conversion into heat in moving viscous media, formulating equations as volume integrals of spherical harmonics products

14 p2487 A69-29980

Kinetic energy balance equation of mean zonal flow in symmetrical polar cap derived from basic concepts of mechanics, discussing relative coordinate system rotation

15 p2595 A69-30219

Equations for gradually changing motion by differentiating momentum and energy equations with respect to abscissa noting wall resistance, viscosity, turbulence and Coriolis coefficients

15 p2593 A69-31489

Potential and kinetic energy of cylindrical thin shell with cutout approximated by two dimensional finite difference methods, obtaining eigenvalue problem

16 p2874 A69-32158

Zonal flow intensity, velocity and kinetic energy of standing and traveling waves compared for Northern and Southern Hemispheres

17 p2997 A69-33392

Stars kinetic energy and escape rates from isolated cluster with arbitrary stellar mass distributions, assuming spherical symmetry and velocity distribution isotropy

17 p3038 A69-33721

Kinetic inductance measurements in linear circular and rectangular cylindrical superconductors, giving inductance temperature dependence for wires and both thick and thin films

17 p3016 A69-33783

Gas-surface energy transfer experiment on OGO-F satellite, measuring upper atmosphere kinetic energy flux to determine accommodation and drag coefficients, density, etc

19 p3255 A69-36680

Meridional circulations in kinetic energy budget of Northern Hemisphere troposphere based on winter and summer climatic mean data, noting Hadley circulation

20 p3523 A69-37505

Kinetic energy of sunspot rotational motion transferred to electromagnetic energy in filamentary currents, noting time variations in solar atmosphere preconditioning for flare

20 p3589 A69-37550

Temperature potentials in cylinder of known radius, investigating optimal heating regime and thermal kinetic factor effect on maximum potential magnitude

21 p3837 A69-39089

Solar wind kinetic energy density using geomagnetic field horizontal component daily variation, treating earth as plasma probe

24 p4308 A69-42968

Horizontal wind speeds kinetic energy spectrum near surface, discussing diurnal variations

24 p4343 A69-43063

Absolute atmospheric kinetic energy, comparing equations deduced from Euler equations with equations deduced from equations of motion for inertial system

24 p4345 A69-43151

KINETIC EQUATIONS

NT HELMHOLTZ VORTICITY EQUATION

NT HYDRODYNAMIC EQUATIONS

NT KINEMATIC EQUATIONS

Krook kinetic relaxation equation generalized to include approximate kinetic equations with velocity independent collision frequency

02 p0234 A69-12582

Second dielectric virial coefficient of rare gases derived by cluster method

04 p0632 A69-14865

Kinetic model equation for electron plasma incorporating collision terms for model scattering

04 p0636 A69-15042

Model kinetic integral equation for describing flow in transition region at leading edge of tapered body in rarefied gas

05 p0697 A69-16040

Kinetic equation for plasma in external inhomogeneous nonstationary electromagnetic field, noting perturbation theory and Vlasov approximation

05 p0805 A69-16700

Chemical kinetic numerical integration techniques applied to equations for chemical relaxation

07 p1073 A69-18315

Kinetic description of inhomogeneous plasma in ring approximation, discussing Vlasov equation and velocity distribution function

07 p1193 A69-19034

Interaction between atom and plane monochromatic traveling wave taking into account pressure effect occurring in strong collision model

08 p1354 A69-19954

Exact solution to kinetic equation for resonant three wave coupling in weakly turbulent plasmas, assuming only single triplet of modes interaction

08 p1360 A69-19989

Modified truncation for BBGKY hierarchy for plasma, obtaining kinetic equation identical with Balescu-Lenard equation

08 p1360 A69-19990

Quantum paramagnetic amplifier saturating power dependence on input pulses length and frequency determined by kinetic equations solution

08 p1325 A69-20436

Kinetic equations for polyatomic gases obtained by extending 13 moment approximation to solve inelastic Boltzmann equation, resulting in 17 moment approximation

08 p1357 A69-20784

Plasma kinetic equation obtained by method similar to Chapman-Enskog method

08 p1369 A69-20816

Thermogravimetric plastics analysis data applied as constants to degradation kinetics equations used in charring-ablator digital computer programs

09 p1529 A69-22312

Performance analysis of combustion chambers with continuous air admission along flame tube, deriving governing equation from reaction kinetics

09 p1624 A69-22618

Condensation kinetics in clouds, determining cloud spectrum evolution taking stochastic processes into account

10 p1722 A69-23972

Nonlinear integrodifferential kinetic equation for weak turbulence of resonant four wave processes, considering spectral energy density

11 p1921 A69-24294

Local potential method extended to study plasma oscillations inhomogeneous kinetic equations in presence of linear or nonlinear collision operators

11 p1925 A69-24316

Resonance radiation output effect on electron distribution according to energies and concentration in low temperature plasma, solving relevant kinetic equations

11 p1935 A69-25797

Solution for kinetic energy equation for organic semiconductors with narrow conduction band situated in strong electric field

12 p2144 A69-26674

Oscillations and decomposition of diatomic gas molecules at high temperatures during atom/molecule collisions, deriving kinetic equations for energy level changes

13 p2302 A69-27797

Near electrode layer calculation in low temperature plasma, solving kinetic ion equation for quasi-neutral and Poisson equation for space charge regions

13 p2312 A69-28111

Correlation functions of fluctuations in electronic characteristics of nonequilibrium electron gas during scattering, determining spectral densities and populations by kinetic equation Green function

13 p2314 A69-28444

Collision integral kernels of kinetic equation for simple component gas density matrix derived by Bogoliubov-Gubov method

14 p2458 A69-29166

Kinetic energy balance equation of mean zonal flow in symmetrical polar cap derived from basic concepts of mechanics, discussing relative coordinate system rotation

15 p2595 A69-30219

N precipitation kinetics in deformed Nb, finding constant in rate equation dependent on temperature and correlated to precipitates nature

15 p2639 A69-30583

Coupled kinetic equations for inhomogeneous systems treated as simultaneous equations in time, obtaining solutions by successive approximation

15 p2660 A69-30913

Linearized kinetic equation for perturbed electron distribution function, detailing plasma oscillations along magnetic field by Landau collision term

16 p2818 A69-31674

Radiation effect on inorganic solids isothermal decomposition induction period, deriving equations for conditions representing various kinetics combinations during irradiation

16 p2832 A69-32359

Klein theorem kinetic energy corrections taking into account breakdown of equipartition theorem

16 p2823 A69-32469

Turbulent kinetic energy equation for determining turbulent flow fields applied to free mixing problem of constant density streams

17 p2956 A69-33492

Transformed kinetic equation used to study relaxation of quantum oscillator to thermodynamic equilibrium state

18 p3152 A69-35126

Stratified cloud transport and evolution, solving kinetic equations by numerical method

21 p3759 A69-39119

Condensation kinetics in clouds, determining cloud spectrum evolution taking stochastic processes into account

21 p3760 A69-39658

Numerical analysis of plane Couette flow of rarefied binary gas mixture using relaxation type kinetic model equations, discussing slip velocity, friction coefficient, etc

22 p3931 A69-40778

Entropy definition for nonequilibrium states, using mathematical theory of stability of motion applied to kinetic equations of irreversible processes

23 p4238 A69-41366

Kinetic equations for fully ionized plasmas and approximate derivation method for generalized Fokker-Planck equation including nonadiabatic effect

23 p4195 A69-41515

Two stream plasma instability in equatorial electrojet extended to nonlinear domain by nonlinear treatment of ion kinetic equation

24 p4310 A69-43182

KINETIC FRICTION

NT SLIDING FRICTION

Three term formula for describing vertical wind velocity distribution in upper boundary layer of atmosphere, taking into account friction and orography effects

02 p0240 A69-11708

KINETIC HEATING

NT AERODYNAMIC HEATING

NT OHMIC DISSIPATION

NT SHOCK HEATING

Heavy ion track thermal spike model to account for LET and temperature effects in radiation biology and chemistry

03 p0371 A69-13479

Temperature rise of micron sized silver particles on carbon film due to electron beam heating, setting up heat balance equation

04 p0640 A69-14449

Concorde design problems due to kinetic heating, aerodynamic characteristics, structure, equipment, modified delta wing planform, etc

12 p2012 A69-26358

KINETIC THEORY

NT CHAPMAN-ENSKOG THEORY

NT EYRING THEORY

NT MIXING LENGTH FLOW THEORY

NT TRANSPORT THEORY

Impulse and kinetic energy transfer in rarefied gases analyzed on basis of kinetic theory, considering surface curvature effect

01 p0173 A69-10093

Inhomogeneous magnetically confined plasma stability, examining dissipative effects on spectra of drift oscillations with kinetic theory

01 p0126 A69-10187

Kinetic features of martensitic transformation of nickel steels dependent on plastic deformation degree at 525 C

02 p0267 A69-12190

Kinetic theory of fracture initiation, discussing changes in relative orientation distribution of network chains

02 p0345 A69-12401

Kinetic theory model of plasma sheath transition, analyzing sheath structure in unignited mode of thermionic converter

03 p0368 A69-13125

Kinetic theory of sound propagation in rarefied gas using generalized orthogonal polynomial expansion, evaluating adequacy of nonequilibrium distribution postulated by Mintzer

03 p0466 A69-13156

Electromagnetic properties of bounded isotropic plasma in kinetic approximation

03 p0477 A69-13712

Kinetic theory to determine wave increments propagating across magnetic field in system of relativistic electrons in cold plasma

04 p0635 A69-14555

Distribution functions for fast electrons near anode calculated by kinetic theory, assuming weakly ionized plasma with smaller Debye length than collision mean free path

04 p0635 A69-14764

Nonlinear and second order thermal diffusion of electrons in ionized gas

04 p0636 A69-14878

Nonequilibrium statistical physics for kinetic theory of gases and statistical mechanics, noting irreversibility and entropy

05 p0793 A69-15769

Kinetic model construction of maximum number of Boltzmann collision integral properties

05 p0797 A69-16679

Kinetics of homogeneous and heterogeneous growth of centers of new phase of semiconductor during ion bombardment as function of radiation dose

06 p0978 A69-16985

Kinetic boundary value problem of gas flow over plane wall with constant mass-velocity gradient

06 p0910 A69-17346

Kinetic theory of sharp leading edge parallel to supersonic flow using Boltzmann equation, determining flow field

06 p0861 A69-17637

Ratios of gas kinetic electron-atom collision integrals of Ramsauer for Ar

06 p0963 A69-17822

Chemical kinetic model for hydrocarbon fuels combustion and application to multidimensional finite difference mixing analyses in hypersonic engines and nozzles

[AIAA PAPER 69-86]

06 p1037 A69-18119

Finite kinetics calculations by computer programs to generate reactions among prescribed reactants

[WSCI PAPER 68-54]

07 p1072 A69-18314

Book on theory of kinetic equations covering classical mechanics, Liouville equation and distribution functions, kinetic equations relation to fluid dynamics, KBG equations, etc

07 p1180 A69-18411

Initial stage of motion in Rayleigh problem, calculating time variable velocity of tangential stress on and velocity of gas near plate

07 p1118 A69-18701

Kinetic theory development of equations for multicomponent gaseous mixtures symmetric diffusion coefficients

07 p1186 A69-19395

Electromagnetic wave reflection from moving plasma characterized by conductivity for slow waves, calculating reflection and absorption factors

07 p1196 A69-19748

Kinetic theory for plasma, considering electric field fluctuations time evolution simultaneously with one particle distribution time evolution and Landau damping in wave equation

08 p1360 A69-19991

Gas kinetics application to various flow problems by solving Boltzmann equation for monoatomic single component gas

08 p1351 A69-20708

Kinetic theory for weak shock generation by impulsive piston, using Fourier and Laplace transforms to solve BGK equation

08 p1304 A69-20783

Kinetic theory model of plasma sheath transition applied to sheath structure in unignited mode of thermionic converter

09 p1440 A69-21828

Enskog method for Boltzmann equation, analyzing asymptotic nature of integral kinetic equation for molecular mean free paths and Laplace probabilities

09 p1481 A69-21889

Kinetic theory of electromagnetic wave passage through magnetoactive plasma, discussing dispersion and specular and diffuse reflection

09 p1550 A69-22022

Kinetic theory of electromagnetic wave propagation in infinite laminated plasma with different dielectrics, determining attenuation

09 p1550 A69-22023

Galaxies and galactic clusters regarded as particles in kinetic theory of cosmology, discussing distribution function choice and red shift

09 p1605 A69-22410

Boltzmann H function for moderately dense gas of identical particles with discrete velocity distribution in cases of nonisotropic binary and ternary collisions

10 p1725 A69-23790

Plane wave solutions for acoustic propagation in polyatomic gas by using Sirovich-Thurber method for polyatomic kinetic models

11 p1920 A69-24287

Boltzmann equation with BGK model as governing equation for sharp leading edge problem in supersonic flow

11 p1817 A69-24288

Boltzmann equation for system of equations governing evolution of gas of identical particles with discrete velocity distribution, applying Chapman-Enskog method

11 p1921 A69-24325

Slip flow problem for general specular-diffuse boundary condition in kinetic theory of gases, noting molecular distribution function

11 p1869 A69-24893

Kinetic theory for examining transition regime of rarefied gas dynamics, discussing Boltzmann equations and models with related boundary value problems

11 p1870 A69-25005

Kinetic theory for spherical expansion of hypersonic jet flow indicating translational freezing in hypersonic source expansion

11 p1870 A69-25006

Kinetic theories applied to shock wave structure study of monatomic gas

11 p1870 A69-25007

Tonks-Dattner resonances in plasma column, using linearized Vlasov equation for coupling to plasma waves of time varying electric fields

11 p1929 A69-25266

Independent nature of variables in dimensional analysis, discussing temperature in kinetic and dimensional analyses

13 p2289 A69-28362

Knudsen arcs kinetic theory with cesium/inert gas mixtures in narrow gap between parallel plate electrodes, discussing fast particle beams and electron scattering

14 p2491 A69-29245

Kinetic theory of fluctuations in turbulent plasmas based on construction of many particle distribution functions

14 p2502 A69-29989

Kinetic theory of gases collision cross section definition compared to usual definition, discussing time reversed collisions

14 p2488 A69-29993

Coupled kinetic equations for inhomogeneous systems treated as simultaneous equations in time, obtaining solutions by successive approximation

15 p2660 A69-30913

Metal particles evaporation kinetics in plasma arc, determining total and unsteady evaporation time by spectroscopy and absorption radiography

15 p2663 A69-30990

Optimization techniques for stellar kinetic theory problems, discussing kinematics distribution function, cosmic gas dynamics, interstellar matter, etc

15 p2695 A69-31004

Magnetic field lines curvature effect on plasma instabilities due to ion temperature gradient, noting frictional gravitation field simulation

16 p2816 A69-31636

Book on mathematical methods in kinetic theory covering boundary value problems associated with Boltzmann equation, model equations, rarefied gas dynamics, etc

16 p2811 A69-31721

Linearized Boltzmann equation in kinetic theory for weakly ionized plasma electrons under alternating electric and circularly polarized magnetic field, noting higher harmonics generation

16 p2820 A69-31752

Kinetic theory and gas-surface interactions for upper atmospheric density measurements by mass spectrometers, pressure gages and satellite drag, detailing adsorption effect

16 p2776 A69-32089

Metal oxide particle growth processes in rocket chambers and nozzles, using generalized kinetic-coagulation equation

[AIAA PAPER 69-541]

16 p2844 A69-32724

Supersonic leading edge problem using nonlinear Boltzmann equation with ellipsoidal model, calculating molecular distribution functions for flow field

[AIAA PAPER 69-652]

17 p2892 A69-33464

Kinetic theory of stationary laser emission under quasi-equilibrium conditions, analyzing emission modes

19 p3332 A69-35874

Laser multimode emission kinetic theory, discussing quasi-equilibrium disturbance effects and nature of inhomogeneity

19 p3333 A69-35875

Finite elements general theory applied to wave propagation, gas kinetics, nonlinear partial differential equations, continuum mechanics and fluid dynamics

20 p3567 A69-36948

Rice-Ramsperger-Kassel kinetic theory applied to sulfur hexafluoride injection into boundary layer of high speed reentry vehicle

20 p3514 A69-37226

Necessary and sufficient conditions of kinetic processes involving two systems of point masses

21 p3771 A69-39087

Quantum-mechanical theory of unimolecular kinetics and predissociation developed from generalized Fano theory of resonant scattering

22 p3986 A69-40724

Kinetic theory for macroscopic transport phenomena in N-component polyatomic gas mixtures with internal degrees of freedom under nonlocal thermodynamic equilibrium

23 p4238 A69-41435

Acoustic wave propagation in plasma, analyzing ionic and electron sound caused by oscillation and relaxation processes using Landau and Vlasov kinetic equations

23 p4196 A69-41726

KINETICS

NT ELECTROKINETICS

NT KINETIC ENERGY

NT NEWTON THEORY

NT REACTION KINETICS

NT VARIABLE MASS SYSTEMS

Kinetics of vaporization of metals with surface subjected to incident radiation flux noting pulse duration

02 p0350 A69-11577

Lithium aluminum hydride thermal decomposition using isothermal kinetics and differential thermal and thermogravimetric analyses, noting decomposition in four stages

02 p0304 A69-11898

Thermodynamic and kinetic interactions of high melting point metal oxides reduction by carbon

03 p0445 A69-13568

Q switched Ruby laser metastable state population kinetics and resonator losses, discussing internal energy redistribution with subsequent absorption spectrum changes

04 p0610 A69-14381

Cylindrical thermionic diode with rhenium emitter for diode kinetic experiments, presenting test data from prototype diode with thimble water cooled
09 p1438 A69-21818

Longitudinal electric field penetration into semibounded plasma using kinetic approximation, assuming diffusive plasma particles reflection from plasma boundary
12 p2138 A69-26711

Composition dependence of carbon activity and carbon diffusivity in austenite
13 p2279 A69-27763

Q switched ruby laser metastable state population kinetics and resonator losses, discussing internal energy redistribution with subsequent absorption spectrum changes
14 p2456 A69-28754

System kinetics synthesis for nonlinear multiple lumped parameter system having responses in boundary region of phase-time space
16 p2812 A69-32247

Device quantity failure kinetics or time dependence effect on time-to-failure distribution resulting from given device degradation coefficients distribution
17 p2936 A69-32895

Monograph on motion of solid body with cavities containing viscous liquid, covering kinetics involving completely or partly filled fluids
20 p3578 A69-38200

Emission kinetics of passive Q switched laser without constraints on relaxation time and switching characteristics of absorption centers and medium
21 p3740 A69-39550

KINFOFORM

Computer generated kinoform optical element operating on phase of incident waves and forming wave front reconstruction single image
10 p1697 A69-23867

KIRCHHOFF-HELMHOLTZ FLOW

U PIPE FLOW

KIRCHHOFF-HUYGENS PRINCIPLE

U DIFFRACTION

U WAVE PROPAGATION

KIRCHHOFF LAW OF NETWORKS

Kirchhoff equations for synthesis of passive dipole arrays, obtaining best approximation to radiation patterns
23 p4138 A69-41935

KIRCHHOFF LAW OF RADIATION

Longitudinal thermoelastic wave propagation in infinite plate, proving generalized Kirchhoff theorem
03 p0528 A69-13924

KIRKENDALL EFFECT

Two stage thermal treatment inhibiting influence on swelling and porosity linked to Kirkendall effect during sintering of Fe-Ni powder mixtures
05 p0782 A69-16616

KITE BALLOONS

U TETHERED BALLOONS

KLEIN-GORDON EQUATION

Space-time diffraction for asymptotic solution of Klein-Gordon equation, studying one dimensional dispersive medium
05 p0802 A69-15930

KLYSTRONS

Microwave selective filter using resonant cavity with single coupling component in feedback circuit of amplifier traveling wave tube or klystron
01 p0042 A69-10384

Permanent magnets used in conjunction with magnetrons, crossed-field amplifiers, klystrons, traveling wave tubes and microwave ferrite devices [IEEE PAPER 2.3]
01 p0045 A69-10713

Klystron bunching analysis, adding electron overtaking formulation to existing nonlinear space-charge wave theory
02 p0215 A69-11939

Stabilization system for klystron automatic frequency control, noting use in voice communication microwave generators and resonance spectroscopy
02 p0216 A69-12096

CW klystron amplifiers design limitations at Ku and Ka bands, discussing operation characteristics
03 p0405 A69-13724

High power transmitting tubes for INTELSAT satellite communication earth stations, including multicavity klystrons and wideband TWT
05 p0728 A69-15668

Frequency vs power absorption characteristics of deactivated klystrons, noting resonance frequencies and perturbation effect of electron beam loading
05 p0729 A69-15978

Design of coupled cavity extended interaction output resonators for klystron amplifiers
07 p1095 A69-18431

Double gap catchers for klystron amplifiers and oscillators
07 p1095 A69-18432

High power microwave interactions in pulsed electron beam plasma klystron
07 p1095 A69-18433

UHF high power klystron for DESY synchrotron, discussing design, short circuited load operation, phase variations and optimum RF outputs
07 p1096 A69-18434

FM noise in two and three chamber klystron oscillators, discussing tubes to reduce noise and relative merits of active or passive stabilization circuits
07 p1096 A69-18438

Van der Pol nonlinear oscillation theory adapted to microwave reflex klystrons, explaining locked and unlocked monotonic operational modes
09 p1466 A69-22444

DC to RF energy conversion in ungridded klystron gaps, calculating efficiency and optimum load conductance as function of gap dimensions
12 p2041 A69-26629

Current harmonics in triode klystron for frequency multipliers, noting modulation voltage
13 p2234 A69-28510

FM homodyne phase meter with klystron oscillator for measuring plasma electron concentration, giving block diagrams of meter, detector and oscillator
14 p2451 A69-29800

Small signal analysis of processes in klystron resonators involving beam-field interaction
15 p2573 A69-30117

Space charge effects on trigger current and reflector voltages of reflex klystron
15 p2574 A69-30131

Beat frequency measurements in far IR due to harmonic mixing of klystrons, discussing noise role
17 p3006 A69-33674

Electrostatically focused klystron /EFSK/ small signal gain calculations based on lens cell space charge wave analysis
18 p3109 A69-35294

Axially symmetric magnetic fields for constant radius annular electron beams reflection, applying results to design of reflex klystron millimeter oscillator
19 p3267 A69-35930

Telemetry by reflex klystron accelerometer and seismometer with on air or coaxial cable signal transmission
19 p3272 A69-36255

Reflex klystron with closed electron flux in crossed electric and magnetic fields permitting inertialess frequency returning
21 p3682 A69-39128

Mush cathode fabrication and characteristics for high power klystrons, comparing efficiency to oxide cathodes
23 p4144 A69-42532

KNOBS

Minimum dimensions of circular nondetent knobs mounted on concentric shafts in case of nontolerable frequent inadvertent operation of adjacent coaxial knobs
17 p2916 A69-34005

Optimum knob crowding, measuring reach time, turning time, inadvertent touching and influence of knob spacing, diameter and configuration
17 p2916 A69-34006

Control knob optimum diameter for minimum operation time, noting frictional resistance
21 p3664 A69-38969

KNOWLEDGE

U PARADOXES

U PHILOSOPHY

KNUDSEN FLOW

Low voltage Knudsen arc in cesium argon mixture using tungsten electrodes, analyzing current voltage characteristics
06 p0963 A69-16920

Monte Carlo method to calculate distributions describing particle behavior in Knudsen cell, clarifying relationship between gaseous collisions and Knudsen number
06 p0908 A69-17111

Monte Carlo solution of linearized Boltzmann equation in rarefied gas dynamics, noting Knudsen layer and Couette flow applications
06 p0910 A69-17345

Collimated nozzle beam for probing low density gas flows, discussing transition from free molecular to isentropic flow and Knudsen numbers
07 p1136 A69-19467

Response times for entire Knudsen number range in straight round pressure pipes, using digital computer in final integration
10 p1677 A69-22900

One dimensional unsteady monotonic Maxwellian gas flow at small Knudsen numbers using Hilbert method, noting validity for shear flows
14 p2432 A69-29611

Coanda effect of separated jets reattachment to wall at high Knudsen number in pneumatic fluidic devices discussing Reynolds and Mach numbers effect [ASME PAPER 69-FLCS-37]
21 p3692 A69-38602

Rarefaction onset along streamline from rocket nozzle with small Knudsen number at exit plane
23 p4152 A69-41920

Monte Carlo method applied to heat transfer in rarefied gas flow between parallel plates involving temperature jump in Knudsen layer
24 p4246 A69-43490

KNUDSEN GAGES

Monte Carlo method to calculate distributions describing particle behavior in Knudsen cell, clarifying relationship between gaseous collisions and Knudsen number
06 p0908 A69-17111

Zirconium niobium alloys thermodynamic properties measured by Knudsen effusion method using zirconium
07 p1165 A69-18940

Equilibrium vapor compositions and activities over Fe-Cr-Ni alloys at 1600 C determined by collecting effusate from thoria Knudsen cells
23 p4175 A69-41503

KOLMOGOROFF THEORY

Statistical model of turbulent flow confirms Kolmogoroff hypothesis of equilibrium zone at large Reynolds numbers
03 p0413 A69-12949

Upper bounds for Bernstein-Kolmogoroff multidimensional inequalities, analyzing independent random vectors
11 p1910 A69-25698

Time variability of horizontal wind as function of time provided by Kolmogoroff structure functions for components of isotropic turbulence
18 p3167 A69-34829

KRONECKER PRODUCT

U ORTHOGONALITY

KROOK EQUATION

Krook kinetic relaxation equation generalized to include approximate kinetic equations with velocity independent collision frequency
02 p0234 A69-12582

Boltzmann equation with BGK model as governing equation for sharp leading edge problem in supersonic flow
11 p1817 A69-24288

Bhatnagar-Gross-Krook model for plane shock structure, considering moment and least squares methods and shock density gradient error analysis
12 p2063 A69-27112

Plane shock layer structure in pseudo-Maxwellian monatomic gas, integrating Krook equation for gas molecule velocity
14 p2432 A69-29613

KRYPTON

Total ionization cross section for symmetric collisions measured as function of energy by using neutral atomic beams of neon and krypton
08 p1356 A69-20740

Partially ionized Kr and Xe transport coefficients for various pressures and at high temperatures computed on basis of charged particle cross sections
09 p1548 A69-21935

Population densities, pumping rates, lifetimes, etc, of singly ionized krypton ion laser
12 p2109 A69-26638

Mode competition of 5861 and 6470 A lines in ionized Kr laser attributed to electronic level excitation processes
15 p2635 A69-31106

Radiation cooling behind strong shock in Kr as function of plasma luminosity near end of relaxation zone
18 p3171 A69-34450

Ar-Kr integral collision cross sections based on density measurements of Ar beam passed through liquid nitrogen cooled Kr filled scattering chamber
19 p3378 A69-36185

KRYPTON ISOTOPES

Spontaneous symmetric fission of superheavy elements near doubly magic nucleus as explanation for Xe and Kr isotopic composition anomalies in meteorites
20 p3601 A69-37503

KRYPTON 85

Radioactive Kr as gaseous penetrant for nondestructive test inspections, noting high sensitivity
19 p3322 A69-35575

KU BAND

U SUPERHIGH FREQUENCIES

KUTTA-JOUKOWSKI CONDITION

Blasius-Chaplygin formula for generalizing Kutta-Joukowski theorem concerning jet profiles, calculating resultant of hydrodynamic forces
11 p1867 A69-24355

Shape, position and velocity of vortex wakes shed in unsteady multienergy flows near trailing edge, applying Kutta condition
[ASME PAPER 69-APMW-19]
24 p4245 A69-43099

L

L BAND

U ULTRAHIGH FREQUENCIES

L-1011 AIRCRAFT

L-1011 Tri-Star aircraft systems and safety provisions, discussing automatic flight control system, propulsion, noise reduction, galley, coat storage and cabin window shades
[AIAA PAPER 69-828]
19 p3243 A69-35598

Design and economic concepts of Lockheed L-1011 wide body trijets, discussing airport and airways congestion alleviation, passenger appeal, etc
[RAES PAPER 15]
22 p3863 A69-40494

L-1011 fail operative automatic landing system design, operational characteristics and test programs
[SAE PAPER 690407]
23 p4185 A69-41657

LABELING [MARKING]

U MARKING

LABOR

Occupational attrition estimation methods for determining personnel separation through marriage, death, retirement and transfer applied to engineering and nursing
07 p1245 A69-19728

Efficient allocation of maintenance resources in USAF, analyzing B-52 costs and substitution of capital for labor
13 p2382 A69-28041

LABORATORIES

NT ENGINE TESTING LABORATORIES
NT ENVIRONMENTAL LABORATORIES
NT HUMAN FACTORS LABORATORIES
NT LUNAR MOBILE LABORATORIES
NT LUNAR RECEIVING LABORATORY
NT MANNED ORBITAL LABORATORIES
NT MANNED ORBITAL RESEARCH LABORATORIES
NT SPACE LABORATORIES

Independent testing laboratory management, outlining requirements specialized to fit continued growth conditions
15 p2720 A69-30402

Unutilized ideas in university laboratories, showing generation and implementation enhancement by marketing experience and product development background
15 p2720 A69-30596

Air cushion vehicle research and development laboratory testing, plans, support equipment, monitoring by TV, etc
15 p2589 A69-30865

Measurable and strategic characteristics of Army laboratories management, considering papers published, inventions and laboratory performance
15 p2721 A69-31070

Experiments integrated into single automated laboratory to detect extraterrestrial life through measuring metabolism and growth in planetary surface material
17 p2912 A69-32969

Technical communication patterns in R and D laboratories, discussing effects of work structure, social relations, etc
20 p3640 A69-38019

Laboratory experiments applicability to interplanetary plasma physics, describing simulations of solar

wind interactions, magnetosphere, collisionless shock waves, etc
22 p4028 A69-40689

LABORATORY EQUIPMENT

Equipment for minimum cost laboratory for thin and thick film hybrid circuits
04 p0559 A69-15198

High temperature vacuum tensile test device for continuously direct recording various stress-strain diagram rates by interchangeable dynamometer scale
07 p1117 A69-19319

Solid state ozone generator for preparing ozone in known concentrations to 1000 ppm in air for laboratory studies
10 p1693 A69-23346

Laboratory device for investigating thermionic energy converters and measuring current-voltage characteristics by static/dynamic methods
18 p3136 A69-34700

LABYRINTH

NT COCHLEA

NT VESTIBULES

Labyrinth polarization effect on stimulation and neuron activity in visual cortex of cats, using electroencephalograph
20 p3469 A69-37244

Vestibular neurons activity in decerebrized cats under ipsilateral and contralateral labyrinth polarization combined with acoustic and caloric stimulation
20 p3471 A69-37254

Cats vestibular neurons reactions to labyrinths mon- and binaural polarization and caloric stimulation
20 p3471 A69-37255

LACTATES

Pyridine nucleotide-linked D-lactate dehydrogenase stereospecificity in various species of invertebrates
01 p0018 A69-11198

Catalytic, physical and chemical properties of enzyme lactate dehydrogenase isolated from lobster tail muscle
22 p3897 A69-41069

LACTIC ACID

Glycolysis rate and lactic acid content in rats myocardium during adaptation to hypoxia, using pressure chamber
10 p1645 A69-23501

LAG [DELAY]

U TIME LAG

LAGRANGE COORDINATES

Resonant long period orbits around Lagrange equilibrium points, discussing formal expansions method for three body problem
07 p1225 A69-19719

Hamilton principle for inviscid compressible fluid in Euler coordinates, analyzing shortcomings found in variational principles and model in Lagrangian coordinates
11 p1875 A69-25483

Density perturbation mode in Lifshitz relativistic theory for expanding universe gravitational instability, adopting Lagrangian coordinate condition to eliminate physically meaningless solution
15 p2652 A69-30203

First approximation stability of triangular Lagrange solutions of restricted elliptical three body problem, formulating power series for orbital eccentricity
20 p3575 A69-37318

Renormalization of second order self energy part of photon and lowest order corrections to single photon vertex using Lagrange vector meson density
21 p3775 A69-39468

LAGRANGE EQUATIONS OF MOTION

U EULER-LAGRANGE EQUATION

LAGRANGE MULTIPLIERS

Dynamic programming and indeterminate Lagrange multipliers to formulate optimal control for discrete systems
05 p0737 A69-15886

Lagrange multipliers of variational problem of point motion and isochronal derivatives in field of attraction of axisymmetric planet
05 p0823 A69-16015

Coasting arc determination in rocket trajectory problems by Lagrange multipliers
09 p1595 A69-21969

Ordinary and inverse variational methods for stress-strain state of solid body, using Lagrange multipliers to reduce variational problem
10 p1793 A69-22885

Optimal control of one dimensional fluid flows with characteristic velocity passing through zero, showing

Lagrange multipliers continuous and bounded in optimal solution
11 p1934 A69-25728

Coplanar impulsive transfers and second variation test, using maximum principle and Lagrangian multiplier technique for propellant expenditure minimization
19 p3400 A69-35676

Recurrent Lagrange multipliers for optimal low thrust earth-Jupiter transfers, using three dimensional solar system model
23 p4215 A69-41896

LALLEMAND CAMERAS

Photoelectronic image devices, discussing detectors, electronography, Lallemand camera, spectracon and electron image multipliers
12 p2082 A69-26136

Lallemand electronic camera application for spectroscopic observations of unsteady phenomena in galactic nuclei at 4000 A, noting radial velocities
12 p2163 A69-27017

LAMB WAVES

Self locking of three laser modes in He-Ne laser on basis of Lamb theory
05 p0773 A69-16290

FM Lamb wave system for flaws and defects detection in thin metal sheets
10 p1699 A69-23048

Monochromatic waves propagation in infinite micropolar elastic plate, treating Lamb and Love waves
11 p1995 A69-25605

Axisymmetric Lamb wave propagation in semi-infinite micropolar elastic solid, considering time varying load on half space boundary
24 p4406 A69-43730

LAMBERT LAW

U BOUGUER LAW

LAMBERT SURFACE

Lambert problem of fitting conic to two position vectors with specified time interval solved numerically by Newton-Raphson iteration
03 p0518 A69-14250

Horizontal Situation Display /HSD/ map computer mechanization transforming earth location to X, Y coordinates for Lambert conformal projection
[AIAA PAPER 69-987]
22 p3908 A69-40367

LAME FUNCTIONS

Natural vibrations of cylindrical panels analyzed on basis of Lame parameters, shell equations and energy method
04 p0674 A69-14592

Geopotential represented in ellipsoidal harmonics, discussing Lame functions generation and rectangular-ellipsoidal coordinates relation and orbital elements perturbations
15 p2599 A69-31333

LAME WAVE EQUATIONS

Lame problem for elastic isotropic medium having free energy dependent on medium deformation and deformation gradients, estimating minimum surface curvature
11 p1970 A69-24632

LAMINAR BOUNDARY LAYER

Turbulent to laminar boundary layer reversal by applying negative pressure gradient
01 p0058 A69-10066

Unsteady laminar boundary layer near thermally insulated rotating disk, establishing solutions describing motion
01 p0059 A69-10361

Soviet monograph on laminar boundary layer in presence of suction covering incompressible flow through porous surface, drag reduction and optimal suction at high velocities
01 p0060 A69-10615

Very high temperature air flow laminar boundary layers on rotating bodies with unsteady chemical reactions, determining flow dynamic behavior
01 p0060 A69-10725

Time history of unsteady heat transfer in laminar boundary layer over semiinfinite flat plate due to step change in wall temperature or wall flow
01 p0177 A69-11401

Unsteady laminar boundary layer flow at curved surfaces, analyzing frequency and curvature parameter influence on basis of small disturbances method
[DVL-863]
02 p0231 A69-12053

Asymptotic laminar boundary layer in compressible gas in presence of normal and tangential velocity components at body surface
02 p0231 A69-12138

Transient laminar boundary layer development on flat plate following impulsive start of surrounding fluid

motion, obtaining temperature and velocity distribution relationship [ASME PAPER 68-HT-10] 02 p0232 A69-12208

Stability of laminar flow along flexible boundary using broken linear velocity profile 02 p0232 A69-12353

Compressible and incompressible laminar boundary layer with constant wall shear stress, using initial profiles 02 p0233 A69-12535

Boundary layers and heat transfers at shock tube walls, establishing approximate solution of boundary layer equation for laminar and turbulent cases [ONERA-TP-647] 03 p0412 A69-12875

Turbulent laminar boundary layer reversion to laminar state associated with departures from inner layer velocity distribution in presence of favorable pressure gradients 03 p0414 A69-13016

Unsteady compressible laminar boundary layer flow over insulated or isothermal flat plate moving with arbitrary time variant velocity in viscous fluid 04 p0588 A69-14715

Laminar compressible viscous boundary layer with arbitrary external pressure distribution, using implicit multiple difference method 04 p0591 A69-15294

Stationary velocity profile near jet driven vortex tube outer wall calculated by laminar boundary layer flow theory, neglecting wall curvature effects 05 p0798 A69-15610

Stability of laminar natural convection boundary layer flow, discussing thermal capacity coupling between fluid and wall and Prandtl number 05 p0744 A69-15719

Laminar boundary layer equations, discussing generalized similar solutions based on parametric approximation 05 p0746 A69-16019

Time dependent two dimensional incompressible laminar boundary layers analysis, discussing application to transient flow over semiinfinite flat plate [ASME PAPER 68-FE-10] 05 p0748 A69-16076

Two dimensional incompressible laminar boundary layer on curved wall for potential velocity inversely proportional to distance along origin [ASME PAPER 68-WA/FE-20] 05 p0749 A69-16096

Similar solutions for laminar boundary layer formed by convective and compressible flows 05 p0751 A69-16463

Heat and mass transfer by catalytic effect at wall, noting interaction of laminar boundary layer on flat plate 06 p1030 A69-17115

Universal equations for three dimensional laminar boundary layer of incompressible fluid on walls of axisymmetric channel with vortical external flow 06 p0909 A69-17328

Wall temperature and Mach number effect on heat flux distribution at spreading line of flow for supersonic gas on ellipsoid of revolution 06 p0858 A69-17331

Laminar boundary layer separation and reattachment near concave corner on cooled reentry body in supersonic flow 06 p0911 A69-17592

Inert gas discontinuous injection into nonequilibrium laminar boundary layer 06 p0860 A69-17635

Pressure distribution, heat transfer rates and shear stresses in laminar boundary layer of supersonic viscous flow incident on corner point of body 06 p0861 A69-17641

Incompressible laminar boundary layer with normal suction or blowing, discussing approximate method for evaluating laminar friction on wing contour 06 p0911 A69-17781

Incompressible laminar Falkner-Skan boundary layer suffering sudden acceleration by moving belt, noting boundary layer separation [AIAA PAPER 69-40] 06 p0912 A69-18049

Interaction of laminar hypersonic boundary layer and supersonic corner expansion wave, discussing upstream influence, transverse pressure gradients and external flow [AIAA PAPER 69-137] 06 p0913 A69-18078

Radiation profiles in ablating flat plate air-Teflon laminar boundary layer, discussing visible, UV and IR wavelengths [AIAA PAPER 69-99] 06 p1037 A69-18086

Nonsimilar laminar boundary layer solutions with negative pressure gradient compared to experimental boundary layer velocity profiles, momentum and displacement thicknesses [AIAA PAPER 69-35] 06 p0913 A69-18094

Spatial distribution of three dimensional laminar boundary layer transition zone on sharp half angle cone from hypersonic wind tunnel tests [AIAA PAPER 69-12] 06 p0863 A69-18112

Stability theory application to laminar boundary layer transition prediction on two dimensional and axisymmetric flows having pressure distributions in incompressible flow 06 p0914 A69-18127

Hypersonic laminar boundary layers on compression corner model, studying flap lengths effects and mass transfer [AIAA PAPER 69-36] 06 p0866 A69-18214

Laminar boundary layer on axisymmetric blunt body in dissociated air taking into account nonequilibrium homogeneous chemical reactions 07 p1050 A69-18734

Chemical reactions in boundary layer on porous plate in oxygen stream, discussing similar solution of laminar boundary layer equations with flame front 07 p1119 A69-18735

Laminar boundary layer flow on sphere in hypersonic flow of equilibrium dissociating air 07 p1050 A69-18756

Solution velocity and turbulence effects on solvent cleaning of corrosion resistant steel tubing, discussing fluidity forces and cleaning formulation 08 p1318 A69-19807

Laminar boundary layer behavior in neighborhood of separation, discussing regressive influence beyond separation in Prandtl equations [ONERA-TP-677] 08 p1303 A69-19878

Vibrational relaxation effects on laminar boundary layer velocity profiles and temperature and on layer thicknesses and wall heat flow downstream of shock wave 08 p1303 A69-20269

Wall temperature influence on intensity of transverse flow of three dimensional laminar boundary layer resulting from transverse pressure gradient 08 p1251 A69-20274

Incompressible laminar thermal boundary layer unsteady development from state of rest in vicinity of wall of obstacle subjected to unsteady thermal field [ONERA-TP-680] 08 p1304 A69-20754

Transient free convection laminar boundary layer equations for heat transfer from vertical semiinfinite flat plate 08 p1305 A69-20842

Heat flux effect on laminar boundary layer separation in supersonic flow stressing free interaction zone 09 p1429 A69-21690

Numerical integration of equations of three dimensional laminar boundary layer in conical flow, using integral relation method 09 p1430 A69-21789

Two dimensional supersonic flow along adiabatic curved ramp noting separation, attached flow and laminar boundary layer interaction with external stream [AIAA PAPER 68-109] 09 p1430 A69-21949

Krause numerical solution applied to normal injection in three dimensional incompressible laminar boundary layer [DVL-902] 09 p1482 A69-21971

Laminar boundary layer separation and heat transfer on zero incidence cone at hypersonic speed, noting wall temperature and Reynolds number effects 09 p1433 A69-22609

Steady laminar boundary layer flow calculations extended to temperature boundary layer for given heat flow or temperature distribution at wall 10 p1808 A69-22915

Three dimensional laminar boundary layer of incompressible flow controlled by suction or injection, considering similarity flow solutions and role in satellite design 10 p1678 A69-22936

Similarity solutions of laminar boundary layer equations for three dimensional flows of incompressible power law fluids 10 p1678 A69-23235

Laminar boundary steady two dimensional constant velocity flow over curved surface equation derived from Navier-Stokes equation 11 p1867 A69-24375

Velocity profiles in unsteady laminar incompressible boundary layer over flat plate in shock tube by two parameter integral method 11 p1871 A69-25026

Low Reynolds number stability of incompressible fluid half jet flow, investigating free laminar boundary layer instability 11 p1874 A69-25280

Three dimensional laminar boundary layer near windward generator of cone subjected to uniform mass transfer by suction or injection 11 p1874 A69-25281

Numerical integration of equations for three dimensional laminar boundary layer on sharp elliptical cone in supersonic flow of ideal gas, discussing heat exchange 11 p1821 A69-25477

Universal laminar boundary layer equations, analyzing form of Prandtl equations not containing external flow velocity 11 p1876 A69-25490

Diffusion coefficients for laminar multicomponent dissociating boundary layer at surfaces of thermally decomposing protective coatings 12 p2190 A69-25890

Heat and mass transfer in laminar boundary layer on porous flat plate with variable suction or injection velocity and constant wall temperature 12 p2061 A69-25947

Laminar compressible subsonic boundary layer flow on symmetrical cylinder bounded by circular arcs noting zero/nonzero angle of attack 12 p2062 A69-26272

Tolerable surface roughness for transition stability in incompressible laminar boundary layer, including analysis of two and three dimensional roughness shape effects 12 p2063 A69-26774

Thermal radiation effects on laminar free convection boundary layer of vertical flat plate, studying absorbing and nonabsorbing gases [ASME PAPER 68-HT-43] 13 p2373 A69-27772

Velocity, enthalpy and mass flux radial distributions in laminar boundary layer from calorimetry of argon subsonic flow [ASME PAPER 68-HT-16] 13 p2374 A69-27776

Laminar MGD electrode boundary layer of thermal nonequilibrium plasma from collisionless Langmuir sheath and continuum theories 13 p2310 A69-28031

Chemically reacting flow field and solid surfaces, formulating nonequilibrium laminar boundary layer equations for two dimensional and axisymmetric flows 13 p2377 A69-28147

Laminar boundary layer studies by finite difference computer program for Mach numbers up to 15 13 p2248 A69-28173

Unique solution proven for laminar boundary layer equations of flow of revolution in unsteady state 13 p2248 A69-28195

Loitsianski method of parametric approximation extended to include flat plate with constant surface suction and flow past circular cylinder 13 p2249 A69-28247

Heat and mass transfer coefficients in binary laminar boundary layer during natural convection, taking into account enthalpy and thermal diffusion effects 13 p2378 A69-28312

Relative variations of wall friction and thermal flux for laminar incompressible flow of constant volume mass 13 p2250 A69-28357

Three dimensional thermal laminar boundary layer around body moving with constant acceleration in incompressible fluid, considering wall temperature and Prandtl number 13 p2380 A69-2863

Temperature disturbance amplification in laminar natural convection boundary layer formed on vertical flat surface measured with hot-wire anemometers 14 p2430 A69-29575

Three dimensional laminar boundary layer on semiinfinite permeable flat plate in viscous incompressible fluid flow, calculating velocity profiles and skin friction components 14 p2433 A69-29898

Heat and mass transfer interaction at wall for laminar boundary layer on flat plate, considering catalytic effect of wall in atomic nitrogen recombination 15 p2716 A69-30415

Laminar boundary layer control by combined blowing and suction, analyzing surface roughness influence concerned with underwater vehicle skin friction reduction [AIAA PAPER 69-387] 15 p2591 A69-30477

Similarity solutions for laminar compressible boundary layer with reverse flow, considering various wall/stagnation temperature ratios 15 p2591 A69-30907

Laminar boundary layer equation solution representing velocity profile by fourth degree polynomial 15 p2593 A69-31263

Temperature profiles in laminar boundary layer with endothermal reaction investigated using nitrogen plasma jet in rarefied gas wind tunnel

16 p2821 A69-31833

Supersonic laminar boundary layer separation calculated by integral method using free parameters for velocity and enthalpy profiles, considering boundary layer-external flow interaction

16 p2731 A69-31834

Laminar boundary layer on rotating blades and yawed infinite wings, solving partial differential equations numerically by implicit finite difference scheme on computer

16 p2732 A69-31885

Turbulent boundary layer laminarization in conical nozzle flow, measuring velocity profiles and friction coefficient

[JPL-TR-32-1407] 16 p2732 A69-31894

Critical review of paper on suction effect on hyper-sonic laminar boundary layer separation

16 p2771 A69-31928

Compressible laminar boundary layer equations solutions for nonunit Prandtl number by direct numerical integration

16 p2772 A69-32173

Monograph on engineering calculations of momentum, heat and mass transfer through laminar boundaries having arbitrary pressure distribution and constant physical properties

16 p2879 A69-32203

Amplified boundary layer oscillations and transition at swept flat nosed wing attachment line with/without boundary layer suction analyzed by wind tunnel tests

17 p2890 A69-33251

Electron temperature and number density measured at atmospheric pressure in plasma thermal laminar boundary layer adjacent to cooled wall

[AIAA PAPER 69-692] 17 p3011 A69-33446

Eddy viscosity models adapting laminar boundary layer solution techniques to turbulent flows compared with measurements in hypersonic flows

[AIAA PAPER 69-688] 17 p2954 A69-33454

Laminar boundary layers in low density supersonic and hypersonic conical and axisymmetric nozzles, treating displacement, transverse curvature, velocity slip and temperature jump

[AIAA PAPER 69-653] 17 p2954 A69-33458

Three dimensional hypersonic laminar boundary layer subdivided into inner and outer regions, obtaining flow description by matching inner and outer solutions

[AIAA PAPER 69-710] 17 p2955 A69-33467

Laminar boundary layer control on two dimensional body by combined blowing and suction in presence of roughness, noting skin friction reduction

[AIAA PAPER 68-641] 17 p2957 A69-34015

Nonuniform heating rates during laminar boundary layer transition on slender cone at hypersonic speeds

18 p3085 A69-34435

Nonequilibrium laminar boundary layer of dissociating air on axisymmetric body determined using concentration profiles of oxygen and nitrogen components

19 p3239 A69-36395

Wall curvature effect on hydrodynamic stability of laminar incompressible boundary layer with respect to perturbing Tollmien-Schlichting waves

19 p3299 A69-36587

Three dimensional laminar boundary layer on conical body of revolution in low Reynolds number compressible fluid flow

19 p3241 A69-36762

Heuristic process for constructing similarity parameters approximation solution of laminar and turbulent boundary layers equations

19 p3301 A69-36799

Heat and mass transfer on vertical surface under combined free and forced convection, solving laminar boundary layer equations by stream function

19 p3453 A69-36844

Unsteady laminar incompressible time dependent boundary layer flows with cylindrical symmetry, transverse boundaries and no swirl

[ASME PAPER 69-FE-47] 20 p3517 A69-37997

Laminar boundary layer on funnel wall, considering internal vortical and radial flow

21 p3692 A69-38611

Heat and mass transfer coefficients in binary laminar boundary layer during natural convection obtained with integral equations and Karman-Polhausen method

21 p3848 A69-38633

Gaseous injection effect on laminar boundary layer hypersonic flow around transpiration-cooled blunt bodies analyzed by integral method and Newtonian model

21 p3644 A69-39014

Laminar corner boundary layer flow with suction, discussing Navier-Stokes equations and steady state heat conduction problems

21 p3696 A69-39578

Laminar free convection from horizontal infinite strip with downward facing thermally insulated vertical walls at edges, noting boundary layer thickness and flow pattern

21 p3853 A69-39672

Effective thermal conductivity parallel to laminations and total conductance for combined parallel and normal heat flow in multilayer insulation

[AIAA PAPER 68-765] 21 p3853 A69-39763

Temperature-vorticity analogy for viscous two dimensional fluid flow extended to compressible flows, noting enthalpy and shear stress analogy

22 p3929 A69-39892

Numerical calculations for boundary layer flows allowing similar solutions, using iterative numerical integration of integral equation

22 p3929 A69-39925

Book on entropy gradient effect on laminar hypersonic boundary layers, covering external frictionless flow calculations based on momentum and energy integral theorems

22 p3930 A69-40618

Linear normal mode instability of three dimensional laminar and turbulent shear layers, analyzing relations between velocity profile, eddy viscosity and oscillations

22 p3932 A69-40893

Lower boundary approximation for theory of thermal laminar steady state boundary layer on isothermal immersed plate

23 p4150 A69-41334

Initial pressure rise and consequent laminar boundary layer separation during interaction with shock wave

23 p4151 A69-41691

Gas concentration measurement during injection into laminar boundary layer streaming along porous plate, using quadrupole resonance mass spectrometer

23 p4058 A69-41695

Laminar boundary layer in steady compressible gas flow past plane wing profile, studying surface temperature and suction effects

23 p4058 A69-41709

Pressure measurement modifications of quasi-steady flow model for interaction between reflected shock wave and laminar boundary layer in shock tube

23 p4152 A69-41903

Laminar boundary layers on slender paraboloids, analyzing skin friction formula and extension for transverse curvature ranges

23 p4152 A69-41904

Numerical method for calculating unsteady two dimensional boundary layers in laminar incompressible flow

23 p4152 A69-42108

Steady constant density two dimensional flow in laminar boundary layer over permeable curved surfaces, showing effects of suction or blowing

23 p4153 A69-42399

Boundary layer separation zones in laminar, transition and turbulent fluid flows past conical bodies with widening skirts

24 p4245 A69-43481

Laminar boundary layer separation in supersonic flow, constructing method for flow distribution functions, perturbed flow region dimensions and pressure perturbation amplitude

24 p4246 A69-43482

Heat transfer data for laminar, transition and turbulent natural convection boundary layers from water experiment on constant heat flux vertical plate

[ASME PAPER 69-HT-D] 24 p4410 A69-43525

Luminescent turbulent boundary layer prediction using mixing length model modified for viscous sublayer structural changes near wall compared with heat transfer data

[ASME PAPER 69-HT-13] 24 p4303 A69-43556

Van Driest-Bradshaw model for calculating sublayer function for self preserving luminescent boundary layers, discussing porous surface suction or acceleration effects

[ASME PAPER 69-HT-12] 24 p4304 A69-43557

Air flow laminarizing turbulent boundary layer, determining velocity, turbulence intensity, temperature profiles and local heat transfer coefficients

[ASME PAPER 69-HT-10] 24 p4413 A69-43558

Laminar, transition and turbulent boundary layer heat transfer measurements along wall in thermal entrance region of high temperature turbulent airflow through cooled tube

[ASME PAPER 69-HT-8] 24 p4414 A69-43560

Superimposed free vortex swirl effect on flow and heat transfer in three dimensional axisymmetric laminar boundary layer

24 p4304 A69-43584

Physical flows characteristics with self similar laminar boundary layers, performing inverse transformation of Falkner-Skan equation

24 p4304 A69-43586

Compressible laminar boundary layer behind shock or thin expansion wave past moving flat plate solved by transforming governing equations into Blasius equation

24 p4305 A69-43596

Quasi-steady laminar flat plate boundary layer in shock tube determined by reducing boundary layer equations to linear differential equations

24 p4305 A69-43632

High enthalpy shock tube and nozzle gas flows for incident shock Mach numbers analyzed for laminar boundary layers and boundary layer transitions

24 p4305 A69-43664

Laminar sublayer thickness in compressible turbulent boundary layers with and without heat transfer

24 p4306 A69-43724

LAMINAR BOUNDARY LAYER SEPARATION

U BOUNDARY LAYER SEPARATION

LAMINAR FLAMES

U FLAMES

LAMINAR FLOW

NT BLASIUS FLOW

NT HARTMANN FLOW

NT STRATIFIED FLOW

Tangential velocity profile growth in laminar axial flow through concentric annulus with rotating inner cylinder, using Navier-Stokes equations for prediction

01 p0058 A69-10143

Linear stability of steady and time dependent plane Poiseuille flow

01 p0175 A69-10333

Asymptotic forms of Navier-Stokes equations for laminar motions of incompressible viscous fluid, discussing validity and applications

[ONERA-TP-651] 01 p0059 A69-10383

Potential flow of stream interaction with two dimensional thin jet, discussing jet penetration depth

01 p0007 A69-11019

Linear stability of parallel flow in concentric annulus for infinitesimal axisymmetric disturbances

01 p0061 A69-11201

Two dimensional compressible inviscid laminar gas flows unsteady processes studied by extending method of characteristics

01 p0008 A69-11360

Laminar natural convection of electrically conducting fluid under magnetic field, noting temperature profiles

01 p0134 A69-11407

Frictional and heat transfer characteristics of laminar flow in porous tubes, using numerical solutions to flow and energy equations

01 p0177 A69-11408

Natural convection boundary layer stability on heated isothermal vertical plane wall, discussing Grashof number as laminar to turbulent flow transition criterion

02 p0188 A69-12038

Laminar flow of anisotropic Ericksen fluid near wall at large Reynolds numbers, discussing Newtonian behavior, viscosity coefficient and particle orientation

02 p0231 A69-12141

Plate temperature oscillation effects on forced convection laminar viscous incompressible MHD boundary layer flow from semiinfinite flat plate

02 p0288 A69-12143

Stability of laminar flow along flexible boundary using broken linear velocity profile

02 p0232 A69-12353

Algorithm for Orr-Sommerfeld equation applied to stability of laminar flow, noting profile resembling mean velocity profile of turbulent flow in flat tube

02 p0233 A69-12573

Supersonic flow past blunt body with convex corner calculated to establish sonic point on body

03 p0362 A69-13406

Eigenvalues for Orr-Sommerfeld equation by difference technique for Reynolds number range 5780-729000, determining Poiseuille flow stability in plane channel

03 p0416 A69-13654

Laminar flow of viscous fluid along wall with fixed leading edge and moving surface, discussing conditions of boundary layer formation and dynamic similarity

03 p0417 A69-13792

Steady laminar flow in two dimensional channel with different permeability porous walls and large injection at both walls

03 p0417 A69-13795

Instability and disturbance amplification in external laminar natural convection boundary layer over vertical flat surface with uniform heat flux

03 p0533 A69-13951

Laminar accelerating flow of thin film falling along vertical wall, emphasizing growth and decrease of boundary layer and film thickness

[ASME PAPER 68-APM/Z] 04 p0586 A69-14388

Laminar two dimensional free jet outflow of incompressible nonNewtonian pseudoplastic fluid from orifice into mass of same fluid

04 p0586 A69-14406

Relaminarization of turbulent flow, studying velocity profiles at various axial cross sections in porous wall tube with fluid injection

04 p0586 A69-14409

Thermal explosion in Poiseuille flow of reacting viscous fluid in infinite circular cylindrical channel or between two rotating infinite cylinders

04 p0686 A69-14986

Perfect magnetofluid model to study laminar flow stability along magnetic field, considering time dependences and rigid and free boundaries

04 p0637 A69-15045

Laminar heat transfer in circular pipes in low Peclet number flow case with laminar velocity profile, discussing Hagen-Poiseuille flows

04 p0687 A69-15397

Three dimensional boundary layers, extending Prandtl independence principle to laminar compressible flow over convex body

05 p0743 A69-15556

Laminar flow on swept low drag suction wings at high Reynolds numbers

05 p0696 A69-15557

Velocity profiles for laminar flow of homogeneous liquid in pipe inlet at small and moderate Reynolds numbers

05 p0743 A69-15578

Laminar flow of isotropic binary gas mixture in circular cylindrical tube with porous walls, determining concentration, field variation with wall suction Reynolds number

05 p0744 A69-15618

Laminar flow of nonNewtonian fluids described via rheological three parameter model

05 p0744 A69-15678

Laminar flow of stably stratified fluid with uniform upstream velocity and density gradient past thin flat plate, discussing upstream wake and boundary layer

05 p0745 A69-15724

Incompressible jet flows, discussing two dimensional jet, axisymmetric laminar jet and turbulent free jet

05 p0746 A69-16008

Forced laminar flow convection in horizontal tube with variable viscosity and free convection effects

[ASME PAPER 68-WA/HT-20] 05 p0847 A69-16123

Laminar flow stability parameter presenting coupling ratio between angular momentum change and loss rate by frictional drag

05 p0750 A69-16187

Injection or suction at disk surface, noting effects on heat and mass transfer in laminar flow about rotating disk

06 p1029 A69-17002

Laminar flow stability along flexible boundary, using broken linear velocity profile instead of boundary layer profile

06 p0909 A69-17207

Laminar source flow of viscous incompressible liquid between two parallel coaxial rotating porous disks

06 p0909 A69-17243

Turbulence hypothesis for velocity of laminar fluid flow at dividing line, considering basic pressure and adiabatic mixing zones

06 p0910 A69-17330

Laminar near wake flow field of two dimensional adiabatic circular cylinder with surface mass transfer

[AIAA PAPER 69-67] 06 p0862 A69-18044

Xenon flash lamps with electrolytic capacitors designed for photographic studies of laminar flows of viscous fluids

07 p1116 A69-18259

Similarity functions defined for laminar or turbulent separation in nonuniform supersonic flow

[ONERA-TP-659F] 07 p1050 A69-18417

Pressure distribution on star-shaped bodies in wind tunnel at Mach 4 and Reynolds number .000006

07 p1050 A69-18703

Boundary layer approximation for steady laminar flow of viscous incompressible fluid past paraboloid of revolution, obtaining vorticity distribution

07 p1120 A69-18812

Navier-Stokes equations solved for viscous incompressible fluid flow due to laminar jet flow into channel in presence of magnetic field

07 p1120 A69-18997

Laminar conducting wall jet injected in transverse magnetic field, analyzing partial differential equations obtained

07 p1192 A69-19020

Laminar flow of viscous conducting fluid between parallel walls in traveling magnetic field, using Hartmann number expansion

07 p1192 A69-19023

Compressibility parameters role in pressure distribution derived for radial laminar compressible fluid flow between two disks

07 p1121 A69-19321

Laminar and turbulent stresses in plane asymmetric incompressible flows analyzed based on Boussinesq formula for turbulent shear stresses

07 p1121 A69-19330

Corrected stability limit for Poiseuille flow in pipes, annuli and channels, discussing flow between cylinders

07 p1121 A69-19475

Suction effect on temperature distribution and heat transfer in plane Couette flow and laminar flow in circular pipe

08 p1303 A69-20371

Transformation of laminar stationary incompressible boundary layer equations for body of revolution in incident flow, using difference method

08 p1252 A69-20703

Bounds on mass and momentum transport by turbulent flow between parallel plates derived for Couette and Poiseuille flows

08 p1305 A69-20840

Flow visualization tracer for quantitative measurements for laminar and turbulent flow, discussing mean velocity and shear stress

09 p1495 A69-21911

Permanent flow of solenoidal vector line rotation in steady nondegenerate rotational flow having complex lamellar unit normal to streamline

10 p1727 A69-22862

Laminar flow heat transfer of viscous incompressible fluid in entrance region of circular tube, using nonlinear equations

10 p1809 A69-23195

Hydromagnetic laminar natural convection flow and heat transfer of nonNewtonian fluid between parallel electrically conducting walls

10 p1728 A69-23237

Equilibrium dissociating gas laminar flow in circular tube calculated for heat transfer and hydraulic resistance, using boundary layer equations

10 p1679 A69-23426

MHD boundary layer nonlinear instability, treating laminar to turbulent flow transition as reversible process

10 p1734 A69-23452

MHD flows in MHD generator channel under magnetic field, analyzing steady laminar flow during entry and Hall effect on conductivity temperature dependence

10 p1734 A69-23455

Laminar elasticoviscous flow of liquid with short memory in two dimensional channel with porous walls

10 p1680 A69-23668

Differential equation for laminar flow of nonNewtonian fluid in annulus with porous walls of nonuniform permeability, considering inelastic and suction Reynolds numbers

10 p1680 A69-23690

Base drag effects on maximum lift drag ratio airfoils determined for moderate supersonic laminar and turbulent flows

10 p1633 A69-24060

Laminar flow stream containing periodic fluctuation of mass fraction of chemical species over flat plate with reactive surface

11 p1813 A69-24284

Dynamics of conducting fluid stream coupled to elastic medium by transverse electric or parallel magnetic field, considering stability of system

11 p1923 A69-24289

Convection heat transfer and flow in rotating bodies, discussing laminar, turbulent and mixed flow in cones and disks, spheres and cylinders

11 p1998 A69-24459

Second order effects on two dimensional laminar boundary layer flow of incompressible fluid

11 p1872 A69-25127

Criteria for reversion of turbulent to laminar flow / reverse transition/ as special cases of Reynolds number criterion, noting boundary layer properties role

11 p1873 A69-25133

Laminar Newtonian flow heat transfer to fluids with variable physical properties in vertical tubes with constant wall heat flux, considering viscosity and density

11 p2000 A69-25163

Self similar axisymmetric and plane laminar viscous gas channel flows noting exponential or hyperbolic law of decrease in static pressure along channel

11 p1875 A69-25488

Boundary layer calculation during laminar MHD channel flow under crossed magnetic and electric fields using successive approximation method

11 p1932 A69-25490

Finite difference method for heat transfer field developing laminar flow at inlet of circular uniform heated and isothermal tube, determining Nusselt number

12 p2062 A69-26242

Heat flux in two dimensional laminar separation zone in supersonic flow, measuring convection coefficient and wall pressure

12 p2011 A69-26289

Radial electric field effect on pressure drop in isothermal laminar flow of dielectric liquid through stainless steel tube, considering ion drag

12 p2136 A69-26400

Imaging for flowfield of nonuniform parallel streamlines with thin airfoil represented by vorticity distribution, noting change of lift and moment

12 p2012 A69-26775

Navier-Stokes equations of slow viscous fluid laminar flow near pipe inlet and exit with negligible mass forces, discussing velocity and pressure distribution

13 p2244 A69-27258

Piston-like laminar liquid metal flow in MHD generator to increase thermodynamic efficiency of cycle and to generate electricity by synchronous principle

13 p2206 A69-27491

Laminar-turbulent transition in MHD channel in transverse and longitudinal magnetic fields, discussing Reynolds equation for large Hartmann numbers

13 p2307 A69-27500

Supersonic wake flow visualization, obtaining direct photographs of various smoke streamlines

13 p2200 A69-28281

Kolmogorov-Prandtl turbulence energy hypothesis extended from turbulent region of one dimensional flow to laminar sublayer, obtaining numerical solutions for Couette flow

13 p2250 A69-28339

Temperature factor effect on transition from laminar to turbulent flow in boundary layer of plate

13 p2251 A69-28558

Incompressible laminar jet bounded by two parallel walls or by three walls, using linearized analysis related to Oseen approximation

14 p2429 A69-29023

Displacement of liquid by insoluble liquid from horizontal circular tube during laminar flow, analyzing flow characteristics

14 p2431 A69-29607

Radiating gray gas laminar jet in thermodynamic equilibrium ejected from plane nozzle into wake analyzed using boundary layer, divergence and transfer equations

14 p2432 A69-29612

Pressure drop fluctuations amplitude and frequency effect on channel resistance and magnetic field effect on fluctuations intensity in laminar conducting fluid flow

14 p2501 A69-29909

Convective heat and mass transfer coupling in laminar hydrodynamic duct flow, obtaining values for bulk and wall temperatures, transfer coefficients and rates, etc

15 p2716 A69-30004

Gas visco seals performance analyzed for continuum flow regime, noting coefficient agreement with laminar flow analysis

[ASLE FICFS PREPRINT 34] 15 p2621 A69-30494

Steady incompressible MHD laminar flow between parallel porous disks solved for large Reynolds and Hartmann numbers

15 p2662 A69-30968

Drag and friction coefficients for laminar pulsating incompressible fluid flow in circular tubes obtained from Navier-Stokes equation

15 p2592 A69-30988

Two dimensional laminar convection cells asymptotic behavior for high Rayleigh number, discussing Robinson and Pillow models for fluid between horizontal plates heated from below

16 p2767 A69-31588

Self excited vibrating laminar diffusion flames, discussing coupling, jet spacing radial heat transfer and boundary layer interaction

16 p2876 A69-31711

Asymptotic behavior of one dimensional laminar flow of incompressible viscous fluid in infinite cylindrical tube, giving equations for boundary conditions and flow rate

16 p2769 A69-31831

Laminar-turbulent transition in boundary layer on thermally decomposing surface, discussing gasification rate, Reynolds number effects, heat transfer and turbulence onset mechanism

16 p2878 A69-31951

Forced laminar flow convection in horizontal tube with variable viscosity and free convection effects [ASME PAPER 68-WA/HT-20]

17 p3068 A69-32902

Two term expansion for Nusselt number for laminar natural convection about isothermal horizontal cylinder in fluid with vanishingly small Prandtl number

17 p3068 A69-33014

Separated flow patterns in base flow at body recesses, emphasizing shock wave boundary layer interaction, laminar flow and flow in front of recess

17 p2949 A69-33124

Adiabatic compressible turbulent equilibrium boundary layer integral method analysis extended to study nonequilibrium laminar flows, deriving dissipation integrals, presenting numerical solutions [AIAA PAPER 69-689]

17 p2955 A69-33481

Transformation of two dimensional boundary value equations for laminar power law nonNewtonian fluid flow to yield similar solutions

17 p2957 A69-34016

Laminar separation in incompressible fluid flowing past bluff body at high Reynolds number, investigating shock wave interaction with laminar boundary layers

18 p3122 A69-34918

Boundary layer transition from laminar to turbulent flow on flat plate, considering supersonic and hypersonic flow, pressure gradients, surface curvature and roughness, etc

18 p3123 A69-34920

Asymptotic solution of supersonic linearized nonisotropic flow of viscous and heat conducting gas with internal heat sources past cylindrical shell, deriving surface pressure

18 p3089 A69-35460

Laminar flow of viscous compressible fluid with density dependent on temperature, calculating steady state Navier-Stokes equations using vector function

19 p3297 A69-35852

Hydrodynamic equations of laminar plane flow of incompressible viscous fluid in rectangular region, calculating velocity field by equivalent network and integration

19 p3297 A69-35853

Coupling conditions by distinct equations for two laminar flow regions, studying near wake and considering Euler, Navier-Stokes and Prandtl correlations [ONERA-TP-738]

19 p3299 A69-36649

Unsteady laminar MHD flow of electrically conducting viscous fluid between porous coaxial circular cylinders under radial magnetic field

20 p3581 A69-36912

Energy losses due to drag in unstable laminar fluid flow in tube

20 p3513 A69-36973

Rotta analysis for linear flow transformation into turbulent flow, discussing Reynolds numbers

20 p3513 A69-37086

Laminar flow of compressible viscous gas in channels of variable cross section

20 p3457 A69-37089

Electron density distribution in laminar air boundary layer on sharp wedges and cones predicted by reducing chemical kinetic model to ordinary differential equations [AIAA PAPER 68-733]

20 p3458 A69-37181

Stability theory formulation for evaluation of boundary layer transition from laminar to turbulent states [AIAA PAPER 68-669]

20 p3514 A69-37184

Flow characteristics and wall heat transfer in separated flow region of annular cavity at free stream hypersonic speed and high gas temperature [AIAA PAPER 68-672]

20 p3458 A69-37185

External natural convection flows, studying laminar instability, transition and turbulence in boundary layer flow

20 p3633 A69-37718

Heat transfer to compressible laminar jet flowing along flat wall, obtaining distributions of temperature, wall shearing stress, heat transfer rates and jet thicknesses [ASME PAPER 69-FLCS-30]

20 p3516 A69-37979

Slip ratios in annular two phase flow for case of laminar flow in film and no entrainment of liquid in vapor [ASME PAPER 69-FE-43]

20 p3517 A69-37995

Heat transfer in radial flow between two parallel plates, calculating Nusselt number for laminar and turbulent flows

20 p3633 A69-38176

Naimark theorem extended to class of nonself-adjoint eigenvalue problems in hydrodynamic stability, considering Orr-Sommerfeld equation and Taylor stability problem

21 p3754 A69-38426

Computational method for nonlinear two and three dimensional disturbances in plane parallel flows applied to transverse disturbances in plane Poiseuille flow

21 p3691 A69-38464

Propagation characteristics of steady adiabatic one dimensional laminar flames in premixed gases, considering activation energy and Lewis number

21 p3849 A69-38802

Ammonia addition effect on laminar flame speeds of propane-air mixtures

21 p3849 A69-38809

Heat transfer in curved channel as function of inlet configurations, obtaining Nusselt number equations for thermal and mixed convection and laminar flow

21 p3850 A69-38866

Membrane vibration problems for combined free and forced laminar convection through vertical ducts, obtaining expressions for velocity, temperature and Nusselt numbers

21 p3851 A69-38974

Laminar corner boundary layer flow with suction, discussing Navier-Stokes equations and steady state heat conduction problems

21 p3696 A69-39578

Laminar burning rate of premixed propane-air flames at one atmospheric pressure in DC electric fields, using cooled porous plug burned method

21 p3852 A69-39596

Channel flows energy stability, discussing Couette and plane Poiseuille flows, velocity profiles, vorticity maxima, etc

21 p3697 A69-39675

Thermal boundary layer formed during laminar jet flow over flat porous plate, discussing temperature distribution and mass transfer at plate surface

21 p3854 A69-39846

Free and dividing streamlines shapes for two dimensional jet from parallel walls penetrating into counterstream, discussing finite cavities

22 p3859 A69-40143

Laminar MHD flow in porous walled channel in transverse magnetic field, determining velocity distributions, induced fields and current over channel cross section

22 p3989 A69-40256

Laminar viscous flow and skin friction near trailing edge of flat plate analyzed by modified Oseen approximation, noting accuracy for high Reynolds numbers

22 p3930 A69-40683

Free viscous layers structure at large Reynolds numbers, using matched asymptotic expansions for two dimensional compressible flow

22 p3932 A69-40927

Boundary layer calculation in incompressible turbulent flow with closed streamlines, avoiding von Mises equation

22 p3932 A69-40931

Asymptotic description of laminar hypersonic boundary layer acceleration approaching sharp corner, assuming small interaction with outer inviscid flow [AIAA PAPER 68-67]

23 p4059 A69-41883

Limit-cycle oscillations of unstable plane Poiseuille flow analyzed by nonlinear Navier-Stokes equations

24 p4298 A69-42600

Laminar flow in porous circular pipe with constant suction or injection applied at wall

24 p4298 A69-42618

Mass injection by strong blowing across Couette-Poiseuille shear flow

24 p4301 A69-43354

Laminar flow swirling motion in circular duct, studying separation and reversal

24 p4301 A69-43355

Solution stability and secondary solutions growth beyond critical points investigation for Burgers equations for laminar-turbulent transition

24 p4302 A69-43360

Laminar flow in horizontal circular tubes with uniform heat flux, analyzing combined free and forced convection effects on secondary flow

24 p4409 A69-43519

Numerical program solving partial differential equations parabolic system for internal turbulent gas flow extended to flows undergoing circular tube laminarization by heating [ASME PAPER 69-HT-52]

24 p4409 A69-43520

Transverse curvature effect on laminar free convection heat transfer from vertical isothermal cylinders [ASME PAPER 69-HT-G]

24 p4410 A69-43522

Inverse transition from turbulent to laminar flow in radial diffusers, noting nonagreement of transition point prediction methods [ASME PAPER 69-HT-33]

24 p4247 A69-43530

Natural convection flow, discussing initial instability of laminar flow, disturbance amplification and transition to turbulent flow [ASME PAPER 69-HT-29]

24 p4411 A69-43531

Plane Poiseuille flow with nonlinear temperature distribution, studying vortex type secondary flow onset due to buoyant forces [ASME PAPER 69-HT-37]

24 p4411 A69-43533

Turbulent flow in circular porous tube laminarized by uniform mass injection through tube wall, measuring velocity and turbulence intensity by impact probe [ASME PAPER 69-HT-57]

24 p4303 A69-43537

Heat transfer and fluid friction of hydrogen and helium gas flows undergoing turbulent to laminar flow transition in heated pipe [ASME PAPER 69-HT-54]

24 p4303 A69-43539

Boundary layer equations with heat transfer for laminar and turbulent incompressible flows about two dimensional and axisymmetric flows, using finite difference method [ASME PAPER 69-HT-7]

24 p4304 A69-43561

Free flight telemetry base pressure measurements on slender cones and domed afterbodies in hypersonic laminar flow, using shock tunnel test facility [AIAA PAPER 68-698]

24 p4249 A69-43675

LAMINAR FLOW AIRFOILS

Design and fabrication of plane and trapezoidal fiberglass wings with laminar plastic profiles for aerodynamic tests, including wing rigging and slotted wing

19 p3324 A69-35831

LAMINAR FLOW CONTROL

U BOUNDARY LAYER CONTROL

LAMINAR HEAT TRANSFER

Transverse pressure gradient and streamwise derivatives effect on free convection laminar heat transfer on isothermal vertical plate at low Prandtl numbers

01 p0177 A69-11409

Transverse curvature effect on skin friction and heat transfer in laminar flows past slender circular cylinders

02 p0232 A69-12210

Heat transfer of steady laminar flow of incompressible, viscous and electrically conducting fluid between parallel porous plates

02 p0289 A69-12235

Cone tip blunting effect on cone local laminar heat transfer rate noting cone configuration, semivertex cone angle and Mach number

04 p0542 A69-14721

Laminar heat transfer in circular pipes in low Peclet number flow case with laminar velocity profile, discussing Hagen-Poiseuille flows

04 p0687 A69-15397

Hypersonic laminar and transitional heat transfer rate distribution on spherically blunted cones

05 p0696 A69-15707

Step function factor for laminar heat transfer from rotating disk with surface temperature changing stepwise in uniform forced stream

06 p1029 A69-17003

Laminar heat transfer in electrically conducting fluids flowing in parallel plate channels [JPL-TR-32-1335]

06 p1033 A69-17555

Pressure distribution, heat transfer rates and shear stresses in laminar boundary layer of supersonic viscous flow incident on corner point of body

06 p0861 A69-17641

Laminar heat transmission coefficients in combustion zone for particular oxygen and kerosene mixture

08 p1421 A69-20585

- Hot air open circuit wind tunnel for testing vaporized fuel films heat and mass transfer over flat plates
08 p1302 A69-20878
- Laminar flow heat transfer of viscous incompressible fluid in entrance region of circular tube, using nonlinear equations
10 p1809 A69-23195
- Temperature variation effects on heat transfer in laminar tube flow, taking into account constant wall temperature and heat flow density
12 p2189 A69-25762
- Heat transfer in laminar separated flows with flat plate segment connections, indicating correlation between local heat transfer rates for successive regions
16 p2879 A69-32169
- Nonequilibrium laminar heat transfer in viscous flow of chemically unstable gases past blunt body and plate
20 p3513 A69-37087
- Natural convection local heat transfer on constant heat flux inclined surfaces for water and air in laminar, transition and turbulent regimes
[ASME PAPER 69-HT-C] 24 p4410 A69-43526
- Boundary layer and heat transfer measurements for turbulent boundary layer laminarizing in conical nozzle flow with wall cooling
[ASME PAPER 69-HT-56] 24 p4303 A69-43538
- LAMINAR JETS**
U JET FLOW
- LAMINAR MIXING**
- Nonequilibrium dissociation effects on constant pressure laminar mixing for diatomic molecules and atoms, analyzing concentration and temperature of free shear layer
04 p0588 A69-14733
- Laminar mixing of two semiinfinite parallel streams, deriving equations and boundary conditions by applying perturbation technique
05 p0744 A69-15714
- Thin wall flow of circular jets in bounded transverse flow, showing hydrodynamic parameter of mixture effect on jets dimensionless path
10 p1679 A69-23567
- Three dimensional laminar jet mixing of incompressible viscous fluid from rectangular cross section nozzle into uniform stream
16 p2768 A69-31687
- Laminar jet mixing of incompressible viscous fluid issuing from rectangular nozzle into uniform stream, considering various boundary conditions
[ASME PAPER 69-FLCS-22] 20 p3516 A69-37976
- Soviet book on integral methods of calculations in theory of turbulent jets and wakes, covering turbulent boundary layers, laminar mixing, etc
20 p3518 A69-38211
- LAMINAR WAKES**
- Laminar two dimensional viscous wake behind finite flat plate, investigating upstream and downstream flow field of trailing edge region for high Reynolds numbers
[ASME PAPER 68-WA/APM-20] 04 p0541 A69-14387
- Laminar and turbulent hypersonic wakes trailing blunt bodies studied by finite difference method, taking into account pressure gradients and nonequilibrium chemical reactions effects
14 p2391 A69-29618
- Flow measurements about high Mach number low Reynolds number laminar wake behind spherically blunted cones, including surface and wake flow field data, radial wake profiles, etc
[AIAA PAPER 69-714] 17 p2894 A69-33500
- Laminar recompression behavior downstream of stagnation point behind hypersonic slender body, obtaining finite difference numerical solutions for near wake flow field
[AIAA PAPER 69-713] 18 p3085 A69-34417
- Similarity solutions describing buoyancy effect on laminar and turbulent wakes of heated body in incompressible fluid vertically ascending flow
19 p3296 A69-35761
- Axisymmetric laminar and turbulent wakes of body in flow with streamwise pressure gradient, discussing velocity defects and profiles
19 p3296 A69-35762
- Karman vortex street formation indicated by smoke visualization method study of laminar wake behind single cylinder
21 p3644 A69-38687
- Nonlinear finite-amplitude instability of two dimensional compressible laminar wake flows, using Fourier expansion and Landau equation
24 p4245 A69-43557
- Fluid mechanical structure of laminar hypersonic wake behind sharp circular cone, investigating flow

field at zero angle of attack and adiabatic wall temperature
24 p4247 A69-43576

LAMINATED MATERIALS U LAMINATES LAMINATES NT MULTILAYER INSULATION

- Balsa wood laminates as aircraft structural material noting thermal properties, fire and fatigue resistance, weight savings, etc
01 p0101 A69-10595
- Interlayer slip in layered wood beams with nail joints analyzed in terms of small deflection theory
01 p0169 A69-10638
- Stress distribution in composite cantilever beams of three layers with end loading solved by closed form elasticity method
01 p0172 A69-11266
- Thermal protection by ablation calculated, emphasizing blocking phenomenon and effectiveness of laminated and reinforced resins
02 p0351 A69-11890
- Fiberglass reinforced plastic laminates failure under biaxial compression due to layer separation with strain energy as endurance criterion
02 p0270 A69-12142
- Fracture process in composite films of stressed tetrafluoroethylene and fluorinated ethylene propylene
02 p0270 A69-12368
- Multilayered shells equivalence to single layer shells for stress analysis, vibrations and stability
02 p0346 A69-12509
- Sandwich panel construction, examining design with respect to panel size, thickness and weight limit
03 p0524 A69-13124
- Heat removal in multilayer superconducting devices, determining optimum number of layers
03 p0493 A69-14225
- Thickness twist and face shear vibrations of laminated layer, determining frequencies from stress equations of motion, constitutive equations and boundary conditions
[ASME PAPER 68-WA/APM-10] 04 p0668 A69-14392
- Time harmonic vibrations and wave propagation in laminated plate, using elasticity theory equations and continuum theory for layered medium
04 p0675 A69-14685
- Laminated plates vibrational characteristics calculations by transition matrices, relating stresses and displacements under load
04 p0679 A69-14907
- Attenuation calibration of optical resonator using transparent plate coated by thin metal layer
04 p0613 A69-15415
- Three dimensional photoelastic analysis based on optical theory of multilayer reflection technique
04 p0683 A69-15496
- Theory of inhomogeneous simple bodies applied for universal solutions for incompressible laminated bodies
05 p0834 A69-15732
- Bending equations for shallow elastic three layer asymmetric shell with different isotropic layers and transversely isotropic rigid filler at various temperatures
05 p0840 A69-16197
- Critical axisymmetric loads for instability in orthotropic multilayer conical shells obeying Hooke law under axial compression or external pressure
05 p0840 A69-16198
- Cryogenic flexibility of thin polymeric film plies for use as spacecraft positive expulsion bladders
05 p0769 A69-16486
- Stability of three layer cylindrical shell in gas stream, analyzing oscillation mode and critical flutter dependence on filler resistance to transverse shear
05 p0843 A69-16683
- Delamination effects on strength degradation of filament wound composites
06 p0946 A69-17126
- Free vibration of thin laminated orthotropic cylindrical shells
06 p1020 A69-17145
- Stress-strain relations for laminar anisotropic medium from known mechanical properties of layers for application to fiber reinforced plastics
06 p1021 A69-17176
- Glow discharge technique for dielectric layer deposition between metal interconnection patterns in multilayer integrated circuits, noting adhesion and feedthrough problems
06 p0931 A69-17201

- Optimal computer calculation procedure for medium thickness anisotropic laminar plates with shear applied to rectangular and hinged plates
06 p1026 A69-18015
- Ferrite microstrips substrates role in integrated circuits, noting application of hybrid technology
07 p1090 A69-18399
- Substrates containing silicon regions separated by silicon dioxide or ceramic dielectrics, prepared by lamination in hot press, noting applications to integrated circuits
07 p1100 A69-18617
- Dielectrics reflow and decal air isolation for silicon integrated circuit components
07 p1100 A69-18618
- Stress-strain response up to ultimate failure and ultimate strength of laminated composite with nonlinear orthotropic lamina
07 p1170 A69-18710
- Antisymmetric cross ply and angle ply laminated plates deflection under transverse loading with coupling between bending and middle-plane extension
07 p1231 A69-18711
- Laminated composite fracture statistical theory with stress enhancements in elements next to primary fracture, comparing elastic and plastic matrices
07 p1170 A69-18712
- Unsymmetrically laminated simply supported plates approximate solutions, considering potential energy and reduced stiffness matrix
07 p1232 A69-18725
- Mathematical formulas for rigidity distribution of inhomogeneous multilayer shells, discussing invariance property
07 p1232 A69-19011
- Glass/resin laminates behavior at high temperature
07 p1136 A69-19515
- High temperature polyimide laminates for radomes and other supersonic aircraft components, discussing index flexural strength, dielectric constant and dissipation factor
07 p1171 A69-19545
- Translunar cracks in laminated graphite filament composites, noting effect of thermal stresses due to cooling
08 p1337 A69-20483
- Multidirectional boron-epoxy laminates shear strengths and elastic moduli, calculating in-plane tension and compression
08 p1337 A69-20484
- Laminates and filament wound structures using carbon fibers with silicon carbide whiskerized surfaces, noting compositing and laminating techniques
08 p1339 A69-20501
- Fire retardant thermally stable electrical grade thermoset resins tested for flexural and dielectric strength and weight loss
08 p1340 A69-20506
- Fiber composite design, discussing contribution of filament diameter, number, content and properties, ply parameters and void content to structural response
08 p1341 A69-20512
- Multilayer orthotropic cylindrical shells stability under distributed external load and off-center compression, analyzing subcritical deformation on critical load
09 p1613 A69-21685
- Complete solution for punching smooth interface double layer Tresca material in plane deformation, including Coulomb material
09 p1617 A69-22048
- Multilayer pressure vessel load carrying capacity calculated, using Huber-Mises yield condition to estimate axial force influence
09 p1618 A69-22257
- Failure modes in fiberglass reinforced epoxy laminates subjected to compression loadings, discussing cracks formation and delamination at glass-resin interface
09 p1529 A69-22305
- Fracture toughness of laminated adhesive bonded structures and monolithic aluminum, considering fracture stresses and ductile and brittle failure
09 p1526 A69-22318
- Fiber glass reinforced plastic backing phase of composite armor, noting test method for evaluation of performance
09 p1507 A69-22319
- Super insulation blankets comprised of dacron sailcloth, silk net or aluminized mylar, describing crinkling, cutting, sewing and hole drilling techniques
09 p1507 A69-22330

Polyimide materials, discussing lamination and applications in electronic circuitry such as interconnection cables and multilayer interconnection boards
09 p1511 A69-22354

Glass reinforced polyimide laminate fabrication, discussing metal foil laminates
09 p1530 A69-22363

Thermoplastic resins as matrices for glass reinforced plastics and aerospace structural and nonstructural adhesives
09 p1530 A69-22365

Polyimide glass fabric laminates with nonflammable characteristics for high O concentration spacecraft environments applications
09 p1531 A69-22366

Interfacial pressure distribution during slip damping in clamped rectangular beams subjected to vibration
10 p1800 A69-23350

Natural frequencies and associated composite loss factor for laminated plate with alternate elastic and viscoelastic layers, deriving partial differential equations [ASME PAPER 69-VIBR-68]
10 p1805 A69-24158

Reinforced metals properties and applications including fibers and lamination, notch sensitivity, brittle fracture, failure and heat resistance characteristics
11 p1904 A69-24898

Bending theory for truncated multilayer anisotropic conical shells, defining relations between displacements and external forces
11 p1984 A69-25141

Two dimensional elastic stress wave propagation in thick multilayered cylindrical shells for nonuniform external pressure distribution
11 p1991 A69-25511

Book on design procedures for modern fibrous composites emphasizing stiffness properties and calculations, covering laminates orthotropic lamina, etc
12 p2179 A69-26238

Fatigue life of Al alloy thin laminated sheets, considering cyclic frequency and temperature effects
12 p2180 A69-26359

Laminated plates vibrational characteristics calculations by transition matrices, relating stresses and displacements under load
12 p2182 A69-26660

Mathematical bending theory for three layer elastic plates containing light or rigid fillers
12 p2182 A69-26678

Simply supported laminated anisotropic rectangular plate with coupling occurring between bending and in-plane extension, discussing stiffness analysis by Fourier series method
12 p2184 A69-26808

Finite deflection discrete element analysis of sandwich plates and cylindrical shells with unbalanced laminated faces
12 p2185 A69-26821

Temperature effects on mechanical properties and fracture behavior of lamellar Ni-nickel titanide intermetallic eutectic alloy showing dependence on intermetallic constituent
13 p2277 A69-27406

Projectile impacts into laminated targets consisting of plastic layers backed by Al substrates using SHAPE code with hydrodynamic elastoplastic distortional model [AIAA PAPER 69-356]
13 p2366 A69-28289

Penetration mechanics of multisheet structures based on discrete particle modeling of impact debris [AIAA PAPER 69-371]
13 p2367 A69-28303

Current-voltage characteristics of p-n-p-n diodes, discussing collector voltage effect on current carrier concentration distribution in diode base
13 p2236 A69-28531

Uniaxial compressive stability of rectangular boron-epoxy laminated plates clamped on loaded edges, determining buckling loads by Southwell plots
13 p2287 A69-28669

End loaded two layer laminated elastic strip stress concentration and self equilibrating traction distribution analyzed by eigenvalue equation
13 p2370 A69-28672

Free vibrations of laminated anisotropic rectangular plates with clamped edges analyzed by Rayleigh-Ritz energy method
13 p2371 A69-28673

Woven roving construction and fill/warp ratio effects on flexural strengths of four ply laminates
14 p2469 A69-29414

Pyrolyzed refractory laminates for high temperature applications, analyzing mechanical and thermal properties
15 p2618 A69-30313

Stress waves analysis in laminates design, assuming one dimensional linear elastic response to plane stress pulse on flat laminated plate surface
16 p2872 A69-31923

Laminated critical rate dampers consisting of ring shaped thin corrugated steel plates inserted between bearing and rotor, showing dependence on static load
17 p3066 A69-33945

Laminated anisotropic plate equations from thin plate theory including nonlinear terms, inertia and thermal stresses [ASME PAPER 69-APM-15]
18 p3213 A69-34390

Phenolic resin and silica cloth laminates transparency to IR radiation, noting experimental results
18 p3136 A69-34640

Creep calculation with temperature considerations for multilayer cylinder under nonisothermal load, comparing stress-strain state of viscoelastic and elastic cylinders
18 p3225 A69-35358

Polyimide resin system for glass reinforced laminates, noting processing characteristics and curing
19 p3353 A69-35505

Syntactic foam prepreg for low density laminate construction, presenting design and mechanical test data
19 p3353 A69-35512

Glass overlaid B filament laminates interleaved with C and silica fabrics, evaluating ablative properties in solid rocket motor tests
19 p3354 A69-35515

High modulus graphite epoxy composite material laminates fabricated and tested, correlating filament strength variation effect with composite tensile strength
19 p3354 A69-35518

Flexible-rigid hybrid polyimide-epoxy glass multilayer board to fill gap between all flexible and all rigid circuit boards
19 p3319 A69-35545

Strength analysis of three layer rectangular plates under complex load and support distributions
19 p3434 A69-35827

Glass fiber laminates based on epoxy organosilicon resins, discussing various hardeners effects on strength, etc
19 p3358 A69-35903

Vibration response approximation of three layer sandwich beam with nonlinear viscoelastic material core during flexural vibrations
20 p3619 A69-36910

Composite laminates in cylindrical bending, discussing classical laminated plate theory limitations by comparing boundary value problems to corresponding theory of elasticity solutions
20 p3626 A69-37760

Unbalanced cross-plyed elliptic laminated plates with bending membrane coupling, analyzing membrane boundary conditions with clamping assumed
20 p3626 A69-37762

Storage and loss moduli measurement for laminated glass fiber reinforced epoxy composite beams, discussing moduli prediction
20 p3627 A69-37763

Transverse shear deformation effect on bending of laminated rectangular plates, obtaining solutions for bending deflections, flexural vibration frequencies and buckling loads
20 p3627 A69-37770

Laminated composites ultimate strength prediction based on consecutive yield procedure with step-wise reduction of strength or load-carrying capacity used as design criterion
20 p3627 A69-37773

Axially symmetric distribution of residual strain in multilayered filament wound ring analyzed and compared with experimental results
20 p3628 A69-37774

Multilayer sandwich panels containing unequal facings with distinct orthotropic cores, calculating dynamic load and stability of triangular panels
21 p3832 A69-38418

Experimental facility for studying heat conductivity of multicontact metallic and nonmetallic materials /plates/ in vacuum at low temperatures under various loads
21 p3721 A69-38639

Collection of papers on composite engineering laminates covering mechanics, fiber reinforced plastics, sandwich construction, metal-clad products and flame sprayed coatings
21 p3752 A69-38930

Aluminum alloy laminates composed of two metallurgically bonded Al alloys of different composition
21 p3745 A69-38936

Approximate solution of unsteady thermal conductivity for plate with unlimited number of layers
21 p3851 A69-39083

Effective thermal conductivity parallel to laminations and total conductance for combined parallel and normal heat flow in multilayer insulation [AIAA PAPER 68-765]
21 p3853 A69-39763

Ultrasonic method for detecting strength defects in filament wound materials
21 p3733 A69-39798

Laminated random media stochastic displacement, using perturbation procedure to derive mean wave propagation deterministic equations
22 p4040 A69-39979

Hot gas flow through multilayer cylindrical shells, calculating temperature fields in walls
24 p4407 A69-42588

Coil under alternating current interacting with laminated conducting structure, giving recurrence formula for calculating deflector voltage
24 p4296 A69-42653

Vacuum cured glass-reinforced polyimide laminate tests for use at elevated temperatures on F-111 aircraft
24 p4335 A69-42933

Interlaminar shear stresses in cross-plyed three ply symmetric laminated composite plate, analyzing interlaminar stress distribution under simple tension
24 p4399 A69-43052

Dispersive pulse propagation in laminated composites compared with theoretical predictions for timing and amplitude of oscillations [ASME PAPER 69-APMW-22]
24 p4401 A69-43097

Geometric dispersion of transient stress waves in linearly elastic laminated composite based on sinusoidal modes [ASME PAPER 69-APMW-20]
24 p4401 A69-43098

Carbon fiber reinforced plastic components aerospace applications, discussing honeycomb sandwich satellite structure for investigating lamination methods, shapes, bonding and machining
24 p4336 A69-43209

Materials problems in microelectronic circuits, discussing multilayer interconnection arrays production by thick film or print-and-fire process
24 p4333 A69-43212

High performance void free carbon fiber laminates preparation using polyimide resins, describing flexural strengths, moduli and interlaminar shear strengths
24 p4325 A69-43445

High modulus graphite/asbestos reinforced laminates, noting improved transverse strength and thermal properties
24 p4337 A69-43447

LAMINATIONS
U LAMINATES

LAND
Multispectral orbital photography used to obtain urban land-use data [AAS PAPER 69-483]
24 p4307 A69-42837

LANDAU DAMPING
Landau damping in plasma, noting competing effects of nonlinearities and collisions on formation of plateau in spatially homogeneous distribution function
01 p0133 A69-11215

MHD waves, Landau damping and magnetosonic waves in homogeneous relativistic Vlasov plasma
04 p0636 A69-15043

Nonlinear interactions of positive and negative energy electrostatic modes of plasma immersed in magnetic field, discussing instability criterion and Landau damping [IAEA PAPER CN-24/E-13]
07 p1196 A69-19768

Landau damping of long wavelength ion acoustic waves in collision-free one dimensional plasma with gravity field
08 p1359 A69-19983

Ion Landau damping and finite Larmor radius effects on dispersion relation of Kelvin-Helmholtz instability due to shear in ion fluid velocity
08 p1367 A69-20799

Particle-wave interactions in weakly turbulent collisionless plasma, discussing ensemble average distribution function, diffusion, nonlinear Landau damping and nonlinear instabilities
08 p1368 A69-20803

Landau type interaction between electron beam and whistler/helicon/ wave electric field within semiconductor /InSb/
10 p1742 A69-24107

Landau dispersion relation solutions, noting higher order Landau poles and coupling of spatial Landau modes and least damped wave

11 p1929 A69-25265

High order plasma wave echoes formulation and relation to initial perturbations based on Landau solution of initial value problem for Vlasov equation

15 p2861 A69-30926

Stationary phase method of integration for growth and decay of resonant plasma oscillations excited by small pulsed dipole, noting Landau damping

16 p2817 A69-31641

Linearized kinetic equation for perturbed electron distribution function, detailing plasma oscillations along magnetic field by Landau collision term

16 p2818 A69-31674

Temporal damping rate for small amplitude linearly polarized TEM mode in plasma, using Landau equation

16 p2818 A69-31675

Noise emission and Landau damping of plasma resonances related by network theory including Nyquist formula, discussing noise temperature in free fall region

16 p2822 A69-32038

Solar corona heating ascribed to Landau damping of ionacoustic waves generated in motion of photospheric granules

17 p3030 A69-33060

Damping of plane sinusoidal wave in cold collisionless plasma, studying supercritical amplitude oscillatory process

18 p3180 A69-34703

Landau damping and echo in plasma, discussing theory, Van Kampen waves, finite amplitude wave attenuation, spin, cyclotron and plasma wave echoes

20 p3582 A69-38012

Relativistic solution by Landau procedure of initial value problem for one dimensional electron plasma wave coexisting with charged immobile background

21 p3778 A69-39579

Collisionless damping of large amplitude ion acoustic waves excited externally in thermally ionized Cs plasma

22 p3991 A69-41008

LANDING

U AIRCRAFT LANDING

U BLIND LANDING

U CRASH LANDING

U DITCHING [LANDING]

U GLIDE LANDINGS

U LUNAR LANDING

U PLANETARY LANDING

U SKID LANDINGS

U SOFT LANDING

U SPACECRAFT LANDING

U VERTICAL LANDING

U WATER LANDING

LANDING AIDS

NT APPROACH INDICATORS

NT ARRESTING GEAR

NT AUTOMATIC LANDING CONTROL

NT INSTRUMENT LANDING SYSTEMS

NT RUNWAY LIGHTS

Terminal area navigation and landing guidance systems for V/STOL intercity transport aircraft, considering radio guidance, aircraft control and system interaction

17 p2897 A69-33210

Fog removal by high power carbon dioxide lasers, evaluating possibility of clearing airport runways [AIAA PAPER 69-670]

17 p2945 A69-33449

Aircraft carrier landing system performance, variations in pilot experience, aircraft types and environment, emphasizing night carrier recovery

17 p2916 A69-34012

Landing guidance devices under difficult weather, discussing landing mechanics for land and carrier based aircraft

18 p3170 A69-34857

Lockheed C-130 Hercules modified as STOL aircraft studied in laboratory by computerized simulation and graphics techniques for pilot view during landing

18 p3092 A69-35466

Sensory physiology of pilot landing guided by runway lighting, stressing visibility influence

19 p3260 A69-35987

Wave-off Decision Device to define potential aircraft carrier-ramp-strike wave-off criteria for aircraft approach

20 p3573 A69-37161

Ground based guidance for land-landing manned spacecraft with low velocity descent systems, discussing high and low altitude glide path intercept and spiral

[AIAA PAPER 69-864] 21 p3762 A69-39390

Kalman filter simulation for estimating aircraft position and velocity from airborne digital computer data in zero-zero landing system

[AIAA PAPER 69-944] 22 p3978 A69-40327

LANDING GEAR

Air cushion landing gear in civil air transport, discussing system concept, advantages and LA 4 aircraft experimental application

02 p0193 A69-12690

In-flight measurement of shear, bending moment and torque on lifting or control surfaces and loads on nose and main landing gear

04 p0677 A69-14842

Landing gear requirements for aircraft design, discussing tire pressure, wheel arrangement, brakes for loading and aircraft weight

08 p1255 A69-21161

Giant landing gear steel parts fabrication for Boeing 747 aircraft, discussing material and processing problems including Cr and Cd-Ti coatings application

09 p1434 A69-22064

Boron filaments reinforced epoxy aircraft landing gear structure prototype, discussing development, fabrication, and testing

09 p1508 A69-22340

V/STOL undercarriage design, considering influence of aircraft operation, engine installation, rough/soft ground capability, etc

09 p1435 A69-22781

Foam carpet and airport equipment to prevent fires and explosions from retracted gear landings

10 p1674 A69-23708

Optimum and suboptimum shock and vibration isolators, discussing three criteria and tradeoff between relative motion and accelerative force

[ASME PAPER 69-VIBR-45] 10 p1808 A69-24183

HF brake excited vibration damping in aircraft landing gear, obtaining closed form solution

[AIAA PAPER 68-312] 11 p1823 A69-25370

Landing shock attenuation system for Surveyor spacecraft, describing hydraulic cylinder and piston arrangement for damping, computerized shock absorber design and landing process simulation

[ASME PAPER 69-DE-54] 14 p2530 A69-28848

Tire test machine for tire parameter determination in aircraft landing gear shimmy stability studies

[AIAA PAPER 68-311] 17 p2902 A69-34029

Aircraft landing gear cylinder reinforcement rings design for minimum weight, using optimization iteration method for planar frames with elastic supports

[AIAA PAPER 68-328] 17 p3066 A69-34030

Steerable landing gear system consisting of freely castoring corotating wheel nose gear, tiltable axle and main gear skids for lifting body spacecraft

[AIAA PAPER 69-790] 19 p3243 A69-35639

C-5A transport landing gear assembly design, illustrating air turbine kneeling-drive module

20 p3466 A69-38179

Hydraulic power pack for automatically raising or lowering landing gear in small aircraft

20 p3467 A69-38183

High strength steel landing gear components corrosion protective finishes, discussing paint over bare steel, porous Cd plating and vacuum deposited Cd

21 p3743 A69-38730

Pressure loads and balancing force determination in kinematic pairs of link gear of landing mechanism

23 p4062 A69-41415

LANDING INSTRUMENTS

NT APPROACH INDICATORS

C-141 Category IIIB all weather landing system, discussing system concept, components, operations and performance

14 p2479 A69-29701

Jumbo jet instrument landing difficulties, suggesting specific improvements in aircraft and airport equipment

15 p2549 A69-30189

Multisensor data processing technique for fail operational landing commands, using real time error analysis inherent in Kalman filter

17 p3003 A69-34106

Self monitored subsystems in automatic flight control of Concorde, describing operation mode and landing display

17 p3003 A69-34196

Monograph on low visibility landing in civil aviation, considering visibility determination methods and equipment and IR sighting devices

20 p3574 A69-38064

LANDING MODULES

NT LUNAR LANDING MODULES

NT LUNAR MODULE

NT MARS EXCURSION MODULE

Apollo LM and CSM tracking systems boresight shift reducible by decreasing modulation indices or scaling factor alpha

10 p1672 A69-23277

Mars lander thermal control system design parameters including environment, power duty cycle and lander size and weight

[AIAA PAPER 69-610] 17 p3072 A69-33274

Planetary lander model thermal design, analysis and testing, emphasizing lightweight multilayer insulation, discussing thermal/vacuum testing

[AIAA PAPER 69-612] 17 p3049 A69-33296

Daily communication link geometry between spacecraft in elliptical orbit and landed capsule, establishing spacecraft visibility contours for landing site latitude

[AAS PAPER 68-110] 21 p3805 A69-39223

LANDING SIMULATION

All-weather landing flight director systems and fault warning display simulator studies of Boeing 707-720B aircraft in Category 3-C environment

01 p0010 A69-10455

Planetary landing vehicle design optimization, considering effects of trajectory, guidance and environmental parameters under uncertainty

[AIAA PAPER 69-128] 06 p1018 A69-18107

Rotary wing aircraft height-velocity testing, analyzing engine-out landing by combining flight tests with mathematical simulation model

[AHS PAPER 353] 17 p2900 A69-33524

Takeoff and landing analysis digital computer program (TOLA) developed by Air Force Flight Dynamics Laboratory for quantitative performance analysis

[AIAA PAPER 69-810] 19 p3289 A69-35630

Aircraft characteristics influence on longitudinal handling qualities during carrier approach from visual landings on moving base simulator

[AIAA PAPER 69-894] 21 p3648 A69-39418

Longitudinal flying qualities evaluation by pilots in carrier approach flight simulation, describing experiment apparatus, procedures and results

[AIAA PAPER 69-895] 21 p3648 A69-39419

Aircraft flying qualities research program, discussing Navy test pilot evaluations and longitudinal handling characteristics for simulated carrier landing task

[AIAA PAPER 69-897] 21 p3648 A69-39421

LANDING SITES

NT LUNAR LANDING SITES

Longitudinal range dispersion of unmanned Mars landers using VM-8 and VM-9 atmospheric models, discussing Syrtis Major as possible landing site

02 p0324 A69-12390

Search theory application to planetary exploration overall strategy for improving landing site decisions

09 p1595 A69-21994

Mars landing site topography reconstructed via stereoscopic pictures returned by surface-based imaging systems

23 p4164 A69-41618

Bulk, selective particulate and hard rock samplers for landed extraterrestrial geological and biological instruments performing on-site analysis

23 p4146 A69-41620

LANDING SPEED

Stopping barriers for jet aircraft landing design and operation

11 p1862 A69-24354

LANDMARKS

Apollo landmark sighting by astronaut using Apollo onboard navigation system, simulating cloud cover effects with Monte Carlo technique

01 p0110 A69-10692

LANDSCAPE

U TERRAIN

U TOPOGRAPHY

LANGEVIN FORMULA

Langevin equation for interacting molecule system derived by Fourier transformation of Hamiltonian, noting physical correspondence to equation for shear viscosity in monatomic liquids

16 p2815 A69-32370

LANGMUIR PROBES

U ELECTROSTATIC PROBES

LANGUAGE PROGRAMMING

Space oriented programming languages and compilers for translating languages, discussing software generating tools under development for space missions

04 p0564 A69-15297

Research center for investigating man/computer interaction, discussing display systems, computers, languages and data entities

04 p0566 A69-15342

System/360 Continuous Modeling Program, detailing input language, user-defined functions and documentation
05 p0723 A69-16196

Computer programming language for three dimensional geometry at symbolic level, noting use for placement problems
05 p0724 A69-16382

Remote terminal computer for rotary-wing vehicles design, discussing programming language, engineer-computer interface and applications
07 p1052 A69-18868

Universal test equipment compiler /UTEC/ built for use with languages designed to control automatic test equipment
11 p1842 A69-25066

Soviet book on automated information retrieval systems covering computer languages, search in complex ordered codes, translation from Russian into computer language, etc
13 p2225 A69-27933

Coding of morphological evolution in time of auroral displays as generalization of existing IUGG code
13 p2256 A69-28655

Block structures and indirect addressing, discussing SNOBOL modifications and naming constraints
19 p3280 A69-36207

Onboard satellite computer design and programming language criteria, considering cost, reliability, weight, volume and energy requirements
20 p3499 A69-37379

Algorithm for programming language grammars conversion into pushdown store automata translators
21 p3679 A69-39607

Coding aspects of computers use in civil engineering, discussing language selection, program partitioning and storage use
22 p3903 A69-40139

NASA computer language CLASP coordinated with evolution of SPL /Space Programming Language/ for aeronautics and space programming
[AIAA PAPER 69-957] 22 p3905 A69-40339

Machine independent telemetry oriented language /MITOL/ to develop computer programs for real time and postflight telemetry data processing
22 p3905 A69-40340

Computer memory reduction through Fortran higher level language, discussing tradeoff between costs saved and additional logic hardware
[AIAA PAPER 69-963] 22 p3905 A69-40344

LANGUAGES
U ALGOL
U FORTRAN
U HANDWRITING
U MACHINE ORIENTED LANGUAGES

LANTHANIDE SERIES METALS
U RARE EARTH ELEMENTS

LANTHANUM
Lanthanum and hafnium effect on transition and recrystallization temperatures of tungsten and tungsten base alloys
05 p0782 A69-16797

La-Rh system study by powder X ray diffraction, metallographic and differential thermal analysis, constructing equilibrium diagram and determining crystal structure data
21 p3744 A69-38739

LANTHANUM COMPOUNDS
Thorium and La-compounds retained superconductivity to Pr and Tm concentrations due to crystal field splitting effect producing nonmagnetic singlet ground state
02 p0295 A69-11778

Lanthanum hexaboride single crystal field emitters for vacuum devices, describing construction and performance
09 p1468 A69-22601

Semiconducting properties of lanthanum-cobalt oxide measured, using Seebeck coefficient for analysis as function of resistivity
21 p3780 A69-38612

LANTHANUM FLUORIDES
Stimulated emission of water cooled CW Nd doped lanthanum fluoride at room temperature
08 p1323 A69-19945

Optical frequencies and polarizations of IR active phonons of tysonite lanthanide fluorides based on Kramers-Kronig reflectance spectra analysis
22 p3993 A69-40729

LANTHANUM ISOTOPES
Lanthanum isotopes beta decay, analyzing excitation of near spherical daughter nuclei of barium isotopes
01 p0122 A69-10100

LAP JOINTS

Adhesive bonded lap joint strength dependence on adherend mechanical properties under conditions of homogeneous adherend and cohesive failure
09 p1530 A69-22317

Polyethylene stainless steel lap joints and polyethylene samples yield strengths measurements at high temperature, suggesting yield mechanism based on dislocation loops
16 p2794 A69-32573

Outdoor aging effects on unstressed Al-Al lap shear joints bonded by various polymeric adhesives
19 p3320 A69-35562

Outdoor aging effects on unstressed adhesive-bonded Al to Al lap shear joints
24 p4319 A69-42932

LAPLACE EQUATION

Generalized alternating-direction implicit method involving extra parameter for solving Laplace equation used for 3d model problem
01 p0107 A69-11366

Finite difference methods to solve Cauchy problem for three dimensional Laplace equation
03 p0424 A69-13661

Digital computer solution of Laplace equation using dynamic relaxation method to introduce dynamic terms into basic equation
05 p0697 A69-15713

Solvability of third boundary value problem for Laplace operator in three dimensional domains bounded by irregular surfaces
07 p1173 A69-18497

Dynamic programming approach to numerical solution of elliptic boundary value problems, using Laplace equations
11 p1910 A69-25411

Network method for Dirichlet problem of Laplace equation in regions with rounded corners, noting polar and composite errors
12 p2123 A69-26730

Elliptic second order equation showing nonequivalent regularity conditions for Laplace and continuous coefficient equations
13 p2288 A69-27743

Green functions for Laplace, Poisson and transient heat diffusion equations solved by matrix multiplication
15 p2710 A69-30870

Series expansion for exponent of singularity of Laplace equation for flow near apex of plane delta wing
19 p3240 A69-36590

LAPLACE TRANSFORMATION

MHD boundary layer equations in Blasius problem reduced to differential equations and solved by Laplace transform
01 p0127 A69-10337

Eigenvalue problem for Laplace operator for two dimensional region with boundary composed of piecewise-analytical simple closed curves solved by finite difference method
02 p0271 A69-11650

Inverse Laplace transform determination method for periodic functions applied to rectangular pulse train and rectified sine wave
02 p0271 A69-11983

Variational theorems on eigenvalues of Laplace finite difference operator with first order boundary conditions
03 p0457 A69-14230

Digital filter transfer functions design by sampled data transformation, noting role of analog filters
04 p0584 A69-15461

Probability theory and Laplace functions used to determine pulse coincidence probability of two random independent pulse streams in given time
05 p0719 A69-16224

Delta functions use in extending domain of Laplacian operator in quantum mechanics
07 p1174 A69-19495

Wolf and generalized Parseval theorems applied to transformation of integral equation to S-plane in systems analysis
08 p1271 A69-19865

Viscoelastic problem solutions for hereditary media, using Laplace transforms or solutions of integral equations for inaccurately approximated kernels
08 p1412 A69-20329

Kinetic theory for weak shock generation by impulsive piston, using Fourier and Laplace transforms to solve BGK equation
08 p1304 A69-20783

Laplace transform applied to linear array analysis and synthesis, discussing transform singularity correspondence to array structure
09 p1532 A69-21600

Circuit function determination from Laplace transforms without calculating transient state matrix, using numerical method
09 p1472 A69-21785

Linear two dimensional partial differential equations solved by Laplace transforms on analog computer
12 p2123 A69-26717

Book on control theory covering automatic and remote position control, diagrams, transfer functions, operators, Laplace transform use with differential equations
13 p2238 A69-28345

Asymptotic behavior of function in Cauchy problem solution for heat conduction, basing method on Laplace transform inversion formula
13 p2380 A69-28685

Localization and convergence of Fourier series for fundamental systems of functions of Laplace operator, including eigenfunctions and trigonometric systems
15 p2644 A69-30287

Transient vibration linear analysis using Duhamel integral and Fourier and Laplace transformations, deriving receptances and application to aeroelastic systems
18 p3211 A69-34326

Classical solution existence to mixed boundary value problems for second order hyperbolic operators obtained by Laplace transforms
18 p3165 A69-35313

Finite difference analogs with increasing error terms applied to simple differential Laplace operator for accuracy determination
19 p3365 A69-36510

Linear nonstationary system with singular point analyzed for stability necessary and sufficient conditions using Riemann-Mellin conversion integrals and Laplace transforms
21 p3685 A69-38451

Boundary layer equations solved for MHD version of Falkner-Skan problem, using Laplace transform and steepest descent technique
21 p3693 A69-38750

Laplace transforms in heat conduction theory in three dimensional infinite homogeneous body
21 p3851 A69-39011

LARGE SCALE INTEGRATION
Large scale integration /LSI/ and medium scale integration /MSI/ circuits evolution and requirements, noting onboard computers and space applications
15 p2625 A69-30825

Large scale integrated circuits reliability with emphasis on multilayer metalization, designing test vehicles for failure mechanisms
17 p2935 A69-32887

Test structure model for studying semiconductor-insulator interface-related failure mechanisms in large scale integrated circuitry
17 p2936 A69-32894

Computer aided design of machines with custom LSI arrays, describing error detection procedures and MOS logic circuits
17 p2942 A69-34121

Threshold logic for LSI to realize broad range of functions noting signal control, gate characteristics, weighting, etc
17 p2943 A69-34122

Failure mechanisms and analyses of large scale integrated circuits based on bipolar and MOS transistors, describing measurement and probing techniques
19 p3282 A69-35787

Computer organization design employing distributed processor to provide general purpose computing while taking advantage of large scale integration
21 p3856 A69-39133

LSI oriented cellular array implementation of complex arithmetic functions for aerospace computers, describing techniques of automatic switching-in of spare modules for failures
[AIAA PAPER 69-964] 22 p3906 A69-40345

LARMOR PRECESSION
Integrodifferential equation for plasma oscillations solved for effect of ion Larmor radius size and intrinsic electric field on flute instability of axially symmetric plasma
06 p0966 A69-17520

Ion Landau damping and finite Larmor radius effects on dispersion relation of Kelvin-Helmholtz instability due to shear in ion fluid velocity
08 p1367 A69-20799

Finite Larmor radius, finite conductivity, rotation and Hall current effects on Jeans criterion for gravitational instability of plasma
10 p1729 A69-23408

Finite ion Larmor radius effect on gravitational instability of two superposed fluids in uniform rotation, analyzing interchange perturbations and vortex sheet
12 p2062 A69-26461

Finite Larmor radius effects on gravitational instability of rotating anisotropic plasma for transverse wave propagation mode
13 p2346 A69-27704

LASER COMMUNICATION U OPTICAL COMMUNICATION

LASER MODES

Saturation peak half widths on Ne energy level population inside single frequency Michelson-type He-Ne laser by tuned differential spectrometry, observing power broadening
01 p0089 A69-10182

Carbon dioxide laser stabilization using laser profile and three mirror system
01 p0089 A69-10183

Optically bistable operation of continuous wave GaAs p-n junction laser at 20 K
01 p0090 A69-10565

Carbon dioxide laser pulsed mode for generating giant pulses, noting applications and electron impact role
01 p0090 A69-10787

Pulses generated by mode locked Nd glass laser, analyzing compression by gratings
01 p0091 A69-10817

Laser wavelength selection device for parallel wavelength separation or recombination of laser beams external to laser cavities
01 p0091 A69-10841

Time correlation of photons emitted by krypton gas discharge tube and helium-neon multimode laser
02 p0255 A69-11611

Transverse mode selection effects on wave front of long pulsed ruby laser beam
02 p0257 A69-12409

Ruby laser modifications for pulse transmission mode operation and cavity dumping, noting peak power output
02 p0257 A69-12410

Stroboscopic holography for repetitive scenes, using mode locked laser as source
02 p0250 A69-12411

Frequency difference of traveling waves in accelerated rotating ring laser
02 p0257 A69-12417

Radiation damage in CdS irradiated by normal mode or Q-switched ruby laser, discussing stimulated Brillouin scattering
02 p0257 A69-12614

Laser transition and photon energy of lightly doped GaAs, showing many body electron-hole-lattice interactions
02 p0257 A69-12615

Nonlinear mode interactions in spatially inhomogeneous laser, analyzing suppression, phase locking and linear coupling among cavity modes
02 p0258 A69-12632

Laser pulse parameters generated in stationary locked mode regime with resonance modulation of losses
02 p0258 A69-12641

Transverse radiation field distribution in CW laser found by geometrical optics approximation, assuming active two level medium and mode close to threshold
02 p0258 A69-12642

Mode locking and ultrashort pulses in giant pulses in giant pulse ruby laser with heated nitrobenzene or alpha-chloronaphthalene in resonator
02 p0259 A69-12655

Dynamic mode locking of CW He-Ne laser by external regenerative feedback using RF beats between axial modes
02 p0260 A69-12657

Ring lasers emission modes, studying nonlinearity effects on radiation field spatial-temporal distribution
03 p0437 A69-13040

Parametric light generation in resonator with nonlinear medium, discussing continuous pumping with laser modes matched with pumping frequency
03 p0437 A69-13044

Ruby laser emission spectral line narrowing due to lasing modes reduction
03 p0439 A69-13059

Laser longitudinal oscillation modes beat frequencies measurement by grouping photoelectron velocities by HF field containing photomultiplier cathode
03 p0440 A69-13265

Single oscillation mode gas laser theory, calculating nonlinear susceptibility, gain profile, power tuning characteristics and oscillation frequency with Bloch equations
03 p0440 A69-13296

Selection of transverse oscillations of unstable Nd laser resonator modes with system of two mirrors and two variable focal length convex lenses
03 p0440 A69-13426

Tradeoffs among beam divergence, power output and mirror alignment tolerances of high power argon ion lasers operating in various low order transverse modes
03 p0440 A69-13549

Light pulse narrowing in laser in linear mode operation with inertialess bleachable filter
03 p0440 A69-13716

Technique to obtain desirable longitudinal oscillation mode for radiation of Ne-He laser
03 p0441 A69-13844

Bistable operating mode of GaAs semiconductor laser involving light emission shifts
03 p0441 A69-14175

Single picosecond mode locked optical pulse selection from train of pulses of Q switched Nd-glass laser using optics external to oscillator cavity
03 p0441 A69-14185

Simultaneous phase locking of longitudinal and transverse laser modes in He-Ne laser
03 p0441 A69-14188

Optical pumping distortion compensation in glass laser rod by changing coolant temperature, obtaining mode locked laser pulses
04 p0609 A69-14286

Single transverse electromagnetic mode power output for laser radar transmitter, using near hemispherical mirror resonator
04 p0609 A69-14287

Oscillation mode selection in gas lasers by thin film absorber in resonator, using standing wave electric fields periodicity
04 p0610 A69-14384

Traveling waves interaction effects on emission modes of gas laser with circular resonator
04 p0611 A69-14545

Laser interferometer gauges for machine tool accuracy, discussing operation, application, manufacture, cost and closed loop numerical control systems
04 p0606 A69-14880

Carbon dioxide laser noting output for added gases, efficiency, energy levels, excitation mechanism and tuning to single line and mode
04 p0612 A69-15173

High power single mode ruby laser, using multiple-mirror rods with plane-parallel end surfaces for generating longitudinal and transverse mode
05 p0770 A69-15700

Gas laser frequency stabilization, considering electromechanical control systems
05 p0773 A69-16230

Buildup modes of He-Ne laser in presence of other strongly oscillating modes, noting gain interaction effects
05 p0773 A69-16289

Self locking of three laser modes in He-Ne laser on basis of Lamb theory
05 p0773 A69-16290

High power stable modes of operation of argon laser, observing stable output spectra
05 p0773 A69-16292

Mode locked laser as stroboscopic light source potential by investigating expansion of laser produced plasma by schlieren photography
05 p0774 A69-16315

Fast digitalized scan laser using Nd-YAG as active medium and containing crossed array of lithium niobate electro-optic switches for mode selection
05 p0775 A69-16326

Mode suppression by mixed polarization in Michelson interferometer type of optical resonator
05 p0776 A69-16330

Ruby laser characteristics at 78 K, discussing emission threshold, optimum feedback, modes, etc
05 p0777 A69-16546

Radiation of laser active element with random inhomogeneities of refractive index, discussing beam divergence, operation modes and Q switched operation
05 p0777 A69-16550

Active element inverse population distribution effects on laser radiation angular divergence during lower and higher oscillation modes
06 p0932 A69-16913

Optical breakdown in air by mode synchronization operation of ultrashort pulses from neodymium laser
06 p0934 A69-17546

Light pulse duration and other parameters for ruby and Nd-glass lasers operating in synchronized mode regime determined by Armstrong method
06 p0934 A69-17549

CW laser mode steady excitation and narrow bandwidth obtainable by highly stable pumping and stable temperature of active element
06 p0934 A69-17681

Mode locked Nd glass laser to pump organic dye laser, obtaining continuously tunable picosecond pulses
06 p0935 A69-17759

Q switching and mode locking of neodymium selenium oxygen chlorine liquid laser, discussing power output and nature of pulses
06 p0935 A69-17776

Laser resonators, noting relation of light path between mirrors to half wavelength and line equivalence of lenses and resonators
06 p0937 A69-18005

Instrument profile of grating spectrograph determined by applying He-Ne laser mode separated in Fabry-Perot interferometer
07 p1131 A69-18405

Stabilized frequency single mode ionized argon laser, discussing intensity of electric field in cavity and mode selector
07 p1145 A69-18475

Emission frequency stabilizing effect in concentric sapphire-coated ruby laser, noting frequency independence from temperature fluctuations and thermal stresses
07 p1147 A69-18543

Self modulated radiation modes of Te-doped n-type InAs injection lasers
07 p1148 A69-18685

Fresnel pulse holograms of three dimensional diffuse objects by single mode ruby laser with or without Q switching
07 p1132 A69-18801

Measurement of helium-neon laser radiation divergence emitted in TEM sub nm modes
07 p1148 A69-18804

Single mode output power from 6328 A He-Ne laser through mode coupling induced by added absorption cell containing excited Ne
07 p1149 A69-18901

Organic dye lasers characteristics, describing broad continua produced for nanosecond absorption spectroscopy
07 p1150 A69-19047

Single mode single frequency carbon dioxide laser operating on single rotational-vibrational transition
07 p1151 A69-19058

He-Ne laser self locking of modes and spectrum weeding out at small absorption
07 p1151 A69-19059

Beam distortion in low order Gaussian-Laguerre modes propagating through saturable laser amplifier, noting uniform and Bessel small signal gain distributions
07 p1152 A69-19065

Dynamics of injection lasers, discussing picosecond pulse generation
07 p1153 A69-19071

Single mode carbon dioxide laser Lamb dip and vibration rotation lines absorption coefficients
07 p1153 A69-19075

Phase locking phenomenon of multitransverse longitudinal modes in He-Ne lasers, discussing mechanism of self locking phenomenon
07 p1153 A69-19076

Mode power spectra observations for ring and normal He-Ne lasers at 6328 A
07 p1155 A69-19087

Output and beat frequency of carbon dioxide laser with various resonator configurations realizing single mode operation
07 p1156 A69-19157

Induced emission cross section of neodymium glass laser in quasi-steady mode measured as function of rod section, mirror reflectivity and output
07 p1156 A69-19161

Optical heterodyning with single mode carbon dioxide laser and triglycine sulfate pyroelectric detector, noting detector sensitivity threshold
07 p1156 A69-19332

Helium-Ne laser beat frequencies between neighboring axial modes shifting linearly with inserted cavity loss
07 p1156 A69-19412

Lamb theory of mode self locking in gas lasers approximated to provide criteria for self locking
07 p1156 A69-19413

Single mode intensity measured for 0.6328 micron He-Ne laser as function of cavity Q, using Lamb semiclassical theory
07 p1157 A69-19414

Stable limiting cycles of laser resulting from mutual synchronization of phase shifted oscillation modes
07 p1158 A69-19752

Frequency doubling of laser light with variable Q switched resonator
07 p1158 A69-19753

Amplification curve change of active substance due to saturation by self field of He-Ar laser, discussing axial operation modes instability
08 p1323 A69-19942

Gas laser modes strong coupling and single moding induced by saturable absorbing medium within cavity resonator
08 p1324 A69-20166

Mutual influence of two laser modes, showing reduced transition rates due to perturbation of lower level
08 p1325 A69-20283

Mutual influence of two different laser modes corresponding to two transitions with same ground level, using He-Ne DC laser
08 p1325 A69-20284

Normal multimode laser action with and without phase locking, using exact steady state solution of Fokker-Planck equation
08 p1325 A69-20291

Quantum paramagnetic amplifier saturating power dependence on input pulses length and frequency determined by kinetic equations solution
08 p1325 A69-20436

Q switched single mode ruby laser pulse passage through traveling wave amplifier decreases beam divergence
08 p1326 A69-20542

Laser operation through semiclassical dispersion theory, presenting dipole moment and population density equations derived from quantum theory
08 p1326 A69-20571

Argon laser frequency spectrum instability caused by competing axial oscillations
08 p1327 A69-21023

Lasing characteristics of Nd-glass laser when cavity radiation varies with time, discussing rapid damping of relaxation oscillations of laser intensity
08 p1327 A69-21024

Carbon dioxide laser with two gas absorption cells in cavity for emission wavelength control and HF pulsed mode of operation
08 p1327 A69-21088

Gas laser frequency stabilization by coupled oppositely circularly polarized components of single cavity mode in axial magnetic field
08 p1327 A69-21090

Numerical and kernel expansion procedures for laser mode, discussing Gaussian quadrature numerical integration for conversion to matrix equation
08 p1328 A69-21091

Mode locking via nonlinear polarizations in multimode solid state lasers
09 p1514 A69-21344

Free carrier magnetoplasma effect used for far IR phase matched difference frequency generation in semiconductors, discussing carbon dioxide laser transitions
09 p1556 A69-21578

Mode locked He-Ne laser pulses compression by multiple reflections from interferometer after application of linear electro-optic frequency sweep
09 p1516 A69-21745

Solid state lasers, noting normal, continuous and single mode oscillations, Q switching, power output limitations, mode locking and liquid lasers
09 p1517 A69-22120

Gas lasers, discussing amplification, resonance, internal and external mirror lasers, outputs, and He-Ne, carbon dioxide and ion lasers
09 p1517 A69-22121

Mode locked laser operation, noting output and applications to optical communication, high speed photography, nonlinear optics and frequency standards
09 p1518 A69-22123

Periodic model variations in ruby and neodymium lasers with tilted mirrors, discussing factors in resonator misalignment
09 p1520 A69-22663

Laser resonator loss factor and axial mode frequencies calculation by interferometry
09 p1520 A69-22679

Intensity distribution in principal mode of TEM oscillations at various gain amplification levels, plotting intensity distribution generated by argon ion CW laser
09 p1520 A69-22685

Simultaneous action of RF perturbation between Zeeman sublevels of atomic transition sustaining gas laser oscillations, discussing single pi mode laser operation
10 p1704 A69-23808

Intensity interferometry by two photon excitation of fluorescence trace for three mode laser under phase locking, free running and FM-like conditions
10 p1705 A69-23811

Mode locked ruby laser for short duration pulse production, noting relation to reciprocal linewidth
10 p1705 A69-23813

Resonator field inhomogeneities effect on transient processes in quantum oscillator, considering two active crystals in cavity
10 p1705 A69-23948

Traveling wave passive Q switched laser with bleachable absorber filter, analyzing unsteady processes without expanding field along natural resonator modes
10 p1705 A69-23949

Mode interactions in argon lasers between two spectral lines noting effect on output
10 p1705 A69-24003

Single mode generation and Lamb dip in argon ion gas laser obtained by thin quartz plate inserted near plane mirror of resonator
10 p1706 A69-24080

High speed photodetector frequency characteristics using multimode gas laser and Kerr cell
10 p1707 A69-24211

Monograph on laser stroscopy in megahertz range covering spark photography comparison, concept of modes, resonators, applications, etc
11 p1893 A69-24368

Pulsed solid state Nd doped calcium tungstate fundamental longitudinal modes selection by insertion of Fabry-Perot interferometers, lenses and diaphragms into resonator
11 p1894 A69-24471

Ruby laser unsteady modes with ruby filter, discussing conditions for pulsed, monopulse and steady mode transitions, with formulas for steady emission
11 p1894 A69-24619

Giant pulse buildup time in Nd-glass laser with passive shutter determined by comparing Q factor and peak power ratios of different modes
11 p1894 A69-24621

Perturbation theory applied to emitting density matrix in nonlinear polarization of resonance media, considering gas laser in coaxial magnetic field
11 p1895 A69-24630

Time correlation of photons emitted by krypton gas discharge tube and helium-neon multimode laser
11 p1895 A69-24718

Laser frequency drift effect on operation of three mirror interferometer, noting wave reflection by two compounded mirrors
11 p1895 A69-24720

Low order transverse modes in Ar ion lasers, analyzing beam divergence, output, mirror alignment and cavity configurations
11 p1896 A69-24841

Singly resonant optical parametric oscillator, noting single mode and multimode oscillation for various pump powers, pump wave depletion and mode competition
11 p1897 A69-25038

Coherence phenomena for gas laser transitions coupled by common level, noting coherent superposition
11 p1898 A69-25045

He-Ne laser output phase fluctuations between adjacent modes during unlocked and self locked condition, noting cavity optical length short term fluctuations influence
11 p1898 A69-25048

Ideal mode conversion and transmission by circular aperture of cylindrically symmetric cavity
11 p1899 A69-25056

Free emission spectrum analysis of ruby laser with external mirrors and elimination of axial mode discrimination
11 p1900 A69-25547

Ruby laser performance with perturbing effect of standing wave field on homogeneity of deexcitation of level populations eliminated by HF modulation
11 p1900 A69-25569

Organic cyanine dye solution laser pumped by Q switched ruby and another dye laser, discussing spectral distribution and modes
11 p1900 A69-25580

Frequency stabilization of He-Ne laser, using external Ne absorption tube in variable magnetic field as frequency standard
11 p1900 A69-25678

Two transverse modes locking with multiple longitudinal modes in He-Ne laser, noting separate locking and alternate quenching
12 p2104 A69-25923

Transverse mode dependence of spiking behavior for ruby laser pumped by pulsed argon ion laser
12 p2104 A69-25928

Resonant vibrational energy transfer between specific mode of carbon dioxide and N molecules at high temperatures, monitoring IR emission
12 p2131 A69-25984

Absorption characteristics of thin metallic films in standing light wave for mode selection and conversion in lasers
12 p2104 A69-26024

Frequency stability of He-Xe laser with nonresonant feedback, noting spectral line width dependence on number of interacting modes
12 p2105 A69-26049

Mode locked lasers for measuring fast radiative decay in fluorescent systems
12 p2105 A69-26310

Single mode laser oscillations buildup for 0.633 micron transition of He-Ne laser at levels above threshold using fast intracavity chopper
12 p2105 A69-26318

Off axial mode selection in circular cross section solid state lasers due to nonuniformity of excitation by focusing of pump power
12 p2106 A69-26320

Nonlinear crystal generated second harmonic power measured for multimode He-Ne 0.63 micron self locked laser
12 p2106 A69-26321

Mode interaction in lasers with homogeneous line broadening, analyzing rate equations for radiation fields of operating modes for asymptotic values of mode intensities
12 p2106 A69-26323

Laser gain medium dispersion expressions applied to multimode ring laser operation with mode spacing less than pressure broadened atomic linewidth
12 p2106 A69-26324

Transverse passive mode locking by dye technique for neodymium glass laser with confocal cavity
12 p2107 A69-26327

Laser diode output efficiency increased in presence of transverse magnetic field suppressing higher order TE and TM modes
12 p2039 A69-26353

Standing wave theory for steady state performance of Raman laser oscillator extended for time variation of exciting laser pulse
12 p2108 A69-26634

Gallium arsenide junction laser resonant modes from theoretical model, calculating frequency separation
12 p2108 A69-26637

Standing waves and single mode room temperature laser emission from electron beam pumped cadmium sulfide thin crystal, discussing emission at 77 K
12 p2109 A69-26639

Atmospheric effects on laser beam width, using Born approximation and Gaussian model to obtain TEM mode scattered power expressions
12 p2111 A69-27166

Analytic expressions for predicted widths of AM and FM mode locked pulses in homogeneous lasers
13 p2270 A69-27191

Breakdown in air produced by picosecond mode locked laser pulses showing evidence for self focusing
13 p2270 A69-27196

Spectral criterion for distinguishing mode locked and nonmode locked laser signals
13 p2270 A69-27197

Anomalous interaction of argon and krypton ion laser lines, considering connecting radiative transitions and cross modulation
13 p2270 A69-27204

Ultrasonic vibrations effect on emission of ruby laser with externally mounted mirrors
13 p2271 A69-27534

Ruby and neodymium glass traveling wave laser free generation spectra kinetics, noting mode transitions as function of pumping levels
13 p2271 A69-27655

LASER MODES

Single mode ruby laser for application to holography of ultrahigh speed three dimensional objects
13 p2262 A69-27980

Spectral width of emission of laser resonator in nonstationary mode in presence of active medium, noting time dependence
14 p2456 A69-28736

Oscillation mode selection in gas lasers by thin film absorber in resonator, using standing wave electric fields periodicity
14 p2456 A69-28757

Carbon dioxide laser inversion kinetics, combining pulse pumping with Q switching to observe rise, life and decay times
14 p2457 A69-28926

Pulsed lasers with pure carbon dioxide and mixture with N and He, discussing inversion mechanism, peak emission power and gas temperature effects in different modes
14 p2458 A69-29162

Ruby laser filled with single emission mode of oscillation using uniform pumping
14 p2458 A69-29164

Laser beam light pressure bending of incompressible liquid surface leading to beam self focusing in linear medium
14 p2461 A69-29674

Gas laser secondary modes emission and beat frequency spectrum widths, using results of Lamb lasers theory
15 p2633 A69-30121

Ruby laser lasing modes spectral time dependence attributed to population inversion inertia responsible for mode competition
15 p2633 A69-30725

Q switched ruby laser giant pulses during pumping by another Q switched laser exhibit simple shape and low duration
15 p2634 A69-30727

Characteristics of neodymium-glass laser with unstable resonator noting transverse modes and radiation angular distribution
15 p2634 A69-30730

Power coupling among modes in semiconductor lasers in presence of spontaneous or forced microwave modulation of population inversion
15 p2634 A69-30875

Spatial and energy characteristics of laser with nonuniform transmittance across resonator mirrors, analyzing transverse modes interaction
15 p2634 A69-30962

Mode competition of 5861 and 6470 A lines in ionized Kr laser attributed to electronic level excitation processes
15 p2635 A69-31106

Frequency selector for gas laser, considering monochromatic emission and multimode oscillation
16 p2795 A69-31608

OgaAs platelet laser modes time behavior, discussing control by electron-hole pair density
16 p2796 A69-31704

Passive mode locking of pulsed Nd-YAG laser using saturable absorber, noting two photon fluorescence contrast ratio
16 p2797 A69-32019

Cavity linear phase anisotropy and axial magnetic field effect on single mode Zeeman gas laser
16 p2798 A69-32606

Time behavior of output intensity and polarization of single cavity mode internal mirror Zeeman laser in axial magnetic field
16 p2798 A69-32607

Multiple mode phase locking of He-Ne laser with fixed cavity length and laser tube fixed position in cavity, generating high speed optical pulses
17 p2980 A69-32957

Optical heterodyne communication system with single mode and frequency carbon dioxide laser, noting coherent photon noise limit
17 p2919 A69-33086

Mode patterns and far field distribution for gas lasers operated in lowest order Gaussian transverse mode
17 p2981 A69-33090

FM detecting resolution using free running multimode uniphase Ar laser with Doppler broadened bandwidth
17 p2981 A69-33091

Single frequency lasers using thin metal film mode selection filters, discussing film properties and experiments with Ar ion and Nd-YAG lasers
17 p2982 A69-33399

GaAs diode laser pulse train emission during pumping near threshold
17 p2982 A69-33421

Wave interaction in gas ring laser, delineating single mode emission zones as function of pumping, emission frequency position and Q factor differences
17 p2982 A69-33632

Laser action and spontaneous emission at atomic oxygen transition, discussing pulsed emission mode in argon-oxygen laser
17 p2982 A69-33633

Laser pulse development dynamics taking into account phase relations between field and active medium polarization
17 p2983 A69-33695

Simultaneous integral equations numerical solution for open optical resonator mode analysis, using kernel function and Fresnel approximation
17 p2983 A69-33883

Laser eigenmodes determined iteratively from eigenvalue equation including spatial inversion inhomogeneities, atomic density and local loss
17 p2984 A69-34046

Statistical model for coherent functions obtained from laser equation, showing amplitude and frequency coupling of radiation fluctuations
18 p3152 A69-34820

Neodymium laser emission temporal structure in mode self locking regime with Q switching by saturable filter
18 p3152 A69-35016

Spectral inhomogeneity effect on spectrum of modes emitted by semiconductor *p-n* junction/laser
18 p3152 A69-35023

Semiconductor optical quantum amplifiers in pulse mode operation, describing arrangement for studying performance including pulse duration and current controls
18 p3153 A69-35258

Radiation dynamics of semiconductor GaAs injection laser with pulsed and continuous modes operation of diodes
18 p3154 A69-35495

Self mode locking of carbon dioxide laser with high order transverse mode oscillations in vibrational-rotational transitions of P branch
19 p3330 A69-35602

He-Ne laser light noises due to discharge current fluctuations and random mode beat
19 p3330 A69-35760

Kinetic theory of stationary laser emission under quasi-equilibrium conditions, analyzing emission modes
19 p3332 A69-35874

Laser multimode emission kinetic theory, discussing quasi-equilibrium disturbance effects and nature of inhomogeneity
19 p3333 A69-35875

Laser emission in system of four level centers, determining nonuniform emission line broadening due to disturbed quasi-equilibrium distribution of electron subsystem elementary excitations
19 p3333 A69-35877

Single and two mode laser emission dependence on pumping power distribution between four level active centers of different types
19 p3333 A69-35878

Relation between angular divergence, spectral characteristics and kinetic behavior of laser operating in various pulsed modes
19 p3333 A69-35879

Mode coupling effects in CW gas ring lasers, considering excitation density pulsations, traveling waves dispersion, polarization, etc
19 p3334 A69-36046

Mathematical model of CW ring laser mode coupling in limits of low excitation
19 p3334 A69-36047

Lamb theory of Doppler broadened gas laser extended to arbitrary intensities for single mode operation, calculating detuning curves and inversion densities
19 p3335 A69-36048

Internal modulation of HeNe laser in asynchronous regime, evaluating range and efficiency with regard to external modulation
19 p3335 A69-36341

Amplitude and output spectra of optical quantum amplifier based on GaAs injection laser, noting values in traveling wave and regeneration mode
19 p3336 A69-36348

Gas laser oscillation mode selection and self synchronization based on separation in two mirror cavity with nonlinear absorption
19 p3336 A69-36350

Continuous explosion laser study of stationary detonation waves to determine conditions leading to

partial population inversion and critical population density
19 p3336 A69-36360

Indium arsenide injection laser observed for self modulation at LF modes, discussing nonMarkovian character of photon density relaxation
19 p3338 A69-36537

Gallium arsenide junction lasers operating above threshold, showing resonant modes dependence of steady state gain function and frequency dependence of spatial gain distribution
19 p3338 A69-36691

Spectrum of axial modes of laser with inhomogeneous longitudinal pumping, dividing parameter space into steady emission regions
19 p3339 A69-36880

Stable mode generation in ruby laser with ability for modulation, using convex resonator and uniform illumination
20 p3553 A69-37607

Neodymium glass laser emission spatial characteristics, investigating higher laser modes excitation
20 p3554 A69-37725

Single mode He-Ne laser frequency stabilization by Zeeman effect
20 p3554 A69-37729

Simultaneous mode locking of Nd YAG laser and intracavity second harmonic generation in high temperature Li niobate or BaNa niobate
20 p3555 A69-37731

Carbon dioxide laser pulsed mode for generating giant pulses, noting applications and electron impact role
20 p3555 A69-38004

Ultrasonic vibrations effect on emission of ruby laser with externally mounted mirrors
20 p3556 A69-38201

Transverse and longitudinal laser modes in holography, noting Michelson interferometer interference pattern role
21 p3734 A69-38398

Interaction between modes of radiation field and active medium in laser with nonresonant feedback, discussing amplitude stabilization of total radiation
21 p3735 A69-38581

Emission frequency stabilizing effect in concentric sapphire-coated ruby laser, noting frequency independence from temperature fluctuations and thermal stresses
21 p3735 A69-38695

Coherent radiation short pulses from mode locked laser permitting schlieren photography of plasma growth
21 p3736 A69-38795

Fresnel pulse holograms of three dimensional diffuse objects by single mode ruby laser with or without Q switching
21 p3724 A69-38946

Measurement of helium-neon laser radiation divergence emitted in TEM sub nm modes
21 p3736 A69-38949

Spectral characteristics of Q switched single frequency ruby laser with tunable emission frequency in giant pulse mode
21 p3737 A69-38991

Quantum theory for single mode laser radiation, considering photon distribution function and mean field damping decrement by phase quantum fluctuations
21 p3737 A69-38996

Frequency stabilization in He-Ne three mode laser by stabilizing LF oscillations via automatic adjustment of laser resonator length
21 p3738 A69-39078

Multimode He-Ne laser radiation polarization modulation as function of magnetic field, cavity anisotropy and frequency, using Macaluso-Corbino effect
21 p3739 A69-39447

Mode locking of organic dye laser by pumping laser with mode locked pulse train from Nd-glass laser, obtaining spectral bandwidth
21 p3740 A69-39545

Annular gas laser cavity designs with additional mirrors for longitudinal oscillation mode selection, noting positive results for He-Ne laser
21 p3740 A69-39553

Spectral, angular and temporal characteristics of traveling wave mode ruby laser emission, noting high transverse divergence effect on mode operation
21 p3741 A69-39554

Eigenmodes of asymmetric cylindrical confocal laser resonator with single output coupling aperture, obtaining diffraction loss factors and mirror field distributions
21 p3741 A69-39564

Pulse width increase in mode locked laser caused by phase deviations, noting optical elements with quadratic dispersion of refractive index
21 p3741 A69-39683

Mode locked laser output intensity, studying effect of random phase variations on pulses
21 p3741 A69-39684

Laser modulation theoretical analysis based on high speed laser oscillators, discussing high energy physics research applications
22 p3959 A69-39975

Spatial coherence of He-Ne laser beam studied in Young interference experiment, noting multimode light percentage attributed to weak transverse modes
22 p3960 A69-40018

Transverse mode selection in rotating mirror neodymium doped calcium tungstate laser by inserting slit and edge into resonator
22 p3961 A69-40316

Cavity Q dependence of intensity of single mode He-Ne laser above threshold for quantum and semiclassical theories
22 p3961 A69-40415

Single mode high power He-Ne laser with Michelson interferometer in cavity, describing performance determination method
22 p3962 A69-40473

Frequency locking of HCN laser transition at 890 GHz to harmonic of crystal controlled oscillator
22 p3963 A69-40567

Lasing properties of Ni-doped GaAs diodes evaluated by plotting resonance, mode amplitudes and frequencies for various bias currents and external capacitance
22 p3912 A69-40606

Spectrum characteristics of plasma generated by pulses of solid state laser radiation on metals and alloys in regular and quasi-stable regimes of emission
22 p3964 A69-40793

Axial mode frequencies, loss coefficients and optimal parameters of three and four mirror resonators of gas lasers, including designs with maximum selectivity
22 p3964 A69-40796

Frequency discrimination in optical harmonic generators, discussing spectral width of wideband laser for supershort pulses and spectral device, using frequency dependence of mode locking direction
22 p3965 A69-40964

Longitudinal modes locking and ultrashort light pulse generation in laser cavity resonator with nonlinear refractive index
23 p4171 A69-41389

Electron excitation and collisional energy transfer processes in laser level of pure carbon dioxide fill and carbon dioxide-water vapor mixture
23 p4171 A69-41390

Mode locked ruby laser with picosecond pulses using rooftop prism cavity with helical flashtube for pumping
23 p4172 A69-41395

Low energy ultrafast flashtube systems as optical pumps for lasers using fast decaying fluorescent materials/organic dyes/
23 p4174 A69-42187

Laser quantum theory compared to stationary atoms semiclassical theory, emphasizing role of cavity mode spatial structure
24 p4327 A69-42789

Laser cavity modes phase equality demonstrated by oscilloscope trace in two photon fluorescent method
24 p4327 A69-42981

Emission spectrum of nonself locked He-Ne ring laser, deriving phase relations for LF intermode oscillations
24 p4328 A69-43159

Beam divergence and multimode laser visible emission influence on power and angular structure of second optical harmonic generated in KDP crystals
24 p4328 A69-43161

Ruby laser second harmonic generation statistical characteristics with dielectric surface scatterer, showing variety of modes and high cross sectional stability
24 p4328 A69-43164

Transitions competition in He-Ne laser pulse operating in single mode with nonuniform gain saturation
24 p4328 A69-43165

Tilted etalons to obtain tunable single mode emission from gas lasers noting fabrication simplicity, vibration insensitivity and low insertion loss resulting in high efficiency
24 p4329 A69-43752

Isolation technique using exploding mirror shutter in multistage high gain laser system to overcome amplified target feedback during pulse lasing of reflective targets
24 p4330 A69-43762

LASER OUTPUTS

Emission and frequency shift angles of antiStokes radiation from trapped filaments of laser light in liquids
01 p0114 A69-10012

Continuous wave laser absolute power measurement by calorimeter consisting of wire wound in shape of cone
01 p0078 A69-10029

Maximum power efficiency of pulsed injection laser with Fabry-Perot cavity expressed in terms of two dimensionless geometric variables
01 p0089 A69-10119

Laser CRT with beam pumped aluminumized CdS crystals, discussing single spot low duty operation
01 p0039 A69-10175

Frequency mixing of IR signals with visible laser light in nonlinear crystals to detect IR signals
01 p0089 A69-10180

Optimum coupling for intracavity second harmonic generation in multilevel lasers
01 p0089 A69-10181

Electro-optic Q switch using lithium niobate as electro-optic material, comparing performance to conventional device using potassium di-deuterium phosphate
01 p0089 A69-10184

Laser cone calorimeters calibration to determine heat capacity
01 p0079 A69-10220

Target production device for deuterium plasma clouds in vacuum with Q switched neodymium laser
01 p0090 A69-10222

Light emission and transmission generated from laser interaction with lithium hydride in vacuum, noting laser energy variations effects
01 p0127 A69-10281

Laser Doppler velocity profile measurement at localized points in flow stream without disturbing flow
01 p0090 A69-10298

Recombination reactions during postdischarge in helium plasma produced by laser beam, deriving equation for density evolution
01 p0128 A69-10394

Photographic film blackening under high intensity laser radiation indicating two photon mechanism as responsible
01 p0080 A69-10429

Exploding wire heating technique using combination of focused laser beam electric field intensity and pulsed power electric current
01 p0090 A69-10666

Ultrashort light pulses in lasers with nonlinear absorber, evaluating random intensity peak probability created by intensity fluctuations and axial modes buildup
01 p0090 A69-10791

Active medium high gain during giant pulse generation shown to lead to radiation fluctuations
01 p0091 A69-10792

Continuous nonresonant visible radiation from Ar ion laser by utilization of wide bore, wall stabilized gas discharges, noting long time frequency stability
01 p0091 A69-10815

Drilling and welding with sealed-off continuous carbon dioxide gas laser with outcoming beam collimated by Ge lens
01 p0086 A69-10821

Continuous laser beam power output meter based on wire resistance thermometry method
01 p0081 A69-10822

Ruby laser crystals optical inhomogeneity and residual mechanical stresses effects on laser beam angle of divergence
01 p0139 A69-10831

Laser wavelength selection device for parallel wavelength separation or recombination of laser beams external to laser cavities
01 p0091 A69-10841

Pulsed nitrogen laser design involving gas discharge tube fed by low impedance parallel plate transmission line
01 p0091 A69-10842

Laser beam spectra for modulation by electrooptic Doppler shift, considering sawtooth and triangular functions for applied electric field
01 p0091 A69-10843

Carbon dioxide spectral line broadening and self broadening coefficients, using carbon dioxide laser radiant energy
01 p0091 A69-10844

Laser beam phase fluctuations for propagation through turbulent atmosphere, noting interferometer for simultaneous measurements for pairs of rays
01 p0091 A69-10845

One dimensional expansion of laser beam, using pairs of prisms with continuous wave output
01 p0091 A69-10852

P-n junction cut-off current density and ohmic losses effect on injection laser efficiency determined by using quality parameter
01 p0091 A69-10883

Amplification equations for calculating unsteady lasing in Q switched ruby laser, considering changes in populations and fields along cavity
01 p0092 A69-10888

Intense laser emission interaction with current carriers in semiconductors, analyzing dependence of thermoelectric field produced by light absorption on intensity, frequency and temperature
01 p0139 A69-10895

Intracavity laser diffraction gratings for single wavelength output
01 p0092 A69-10897

Liquid lasers compound range of organic type, circulating system of inorganic type and power peaks
01 p0092 A69-11194

Hydrodynamic model of laser produced solid particle plasma, giving distributions of pressure, density, temperature and velocity
01 p0132 A69-11210

Sparks from laser induced arc breakdown due to focusing of laser beam, noting evidence for initiation by self focusing
01 p0092 A69-11246

Time compression system with ultrasonic diffraction cell allows coherent light optical spectrum analyzer to function at audiofrequencies
01 p0035 A69-11283

Q switched laser excitation flash spectroscopic analysis of naphthalene, describing equipment arrangement and experimental results
02 p0254 A69-11544

Transmission of coherent ruby laser radiation through traveling wave amplifier noting spatial field structure changes
02 p0255 A69-11608

Induced discharge laser wave propagation in medium with active and absorbing admixtures, determining stationary wave shape and velocity range
02 p0206 A69-11609

Carbon dioxide ionization by Q switched laser beam, using proportional counter
02 p0255 A69-11702

Preionization of gases by laser beam using theory based on molecular equilibrium concentration and collision excitation
02 p0283 A69-11703

Continuous wave GaAs injection lasers operation at high temperatures shown possible by using available threshold current densities with suitable heat sink materials
02 p0255 A69-11710

Laser applications in metal working including dissimilar metal welding, hole drilling, material removal and dynamic balancing
[ASTME PAPER MR68-406]
02 p0252 A69-11796

Soviet book on spectral, spatial and time characteristics of lasers covering luminescence and resonator theories, electromagnetic field structure and radiation dispersion
02 p0255 A69-11800

Bragg reflection of electrons by standing light waves of giant pulse laser
02 p0255 A69-11833

Injection laser emission from gallium arsenide base films grown epitaxially from gas phase in moist hydrogen atmosphere
02 p0255 A69-11879

Polarized low temperature laser excited Raman spectra of thulium gallium garnet
02 p0256 A69-11925

Plasma production by laser irradiation of solid, calculating numerically time variations of temperature distribution, laser intensity and evaporated layer depth
02 p0256 A69-11935

Polymethyl methacrylate irradiated by laser in vacuum to study mechanism responsible for gas formation
02 p0270 A69-11980

Energy characteristics of laser with passive Q switch, taking into account internal reflections
02 p0256 A69-11999

Ruby laser limiting gain, stimulated emission loss, noise loss and spectral distribution determined by radiation intensity, pumping power and mirror reflection
02 p0256 A69-12000

Mechanical thermal stresses effects during laser flash illumination of GaAs, discussing temperature dependence of radiative recombination

02 p0256 A69-12245

Ruby laser output energy degradation due to pump light absorption by color centers of ruby rod

02 p0256 A69-12358

Transverse mode selection effects on wave front of long pulsed ruby laser beam

02 p0257 A69-12409

Ruby laser modifications for pulse transmission mode operation and cavity dumping, noting peak power output

02 p0257 A69-12410

Critical values of laser formed solid angle determined in plasma diagnostics of scattering spectrum density distribution

02 p0251 A69-12416

Laser radiation hazards due to direct or reflected viewing determined by evaluating output characteristics and environmental factors effects

02 p0204 A69-12497

Short laser radiation pulses spectral characteristics determination with device converting laser emission frequency by nonlinear electro-optical crystals

02 p0257 A69-12560

Frequency and time dependent gains of dye solution lasers for pumping by lasers and flashlamps

02 p0257 A69-12616

Organic dye laser frequency variation with temperature, noting absorption and fluorescence spectra

02 p0258 A69-12617

Linear absorption coefficient of seminsulating Cr doped GaAs for IR carbon dioxide laser radiation, discussing lattice absorption mechanism

02 p0258 A69-12619

Dye solution laser wavelength shift and simultaneous oscillations at different wavelength ranges for pumping by another dye laser

02 p0258 A69-12620

Laser pulse parameters generated in stationary locked mode regime with resonance modulation of losses

02 p0258 A69-12641

Transverse radiation field distribution in CW laser found by geometrical optics approximation, assuming active two level medium and mode close to threshold

02 p0258 A69-12642

Chain and branched halogen-hydrogen reactions kinetic analysis for developing chemical laser with radiation energy weakly dependent on pumping energy

02 p0259 A69-12645

High power output CW laser oscillation measured at 4416 Å laser transition in Cd 2 using single isotope of Cd 114

02 p0259 A69-12653

Two photon fluorescence technique for display of picosecond laser pulses, discussing mode locking and ruby laser contrast ratios

02 p0259 A69-12654

Oscilloscope display of sample of subnanosecond light pulse, using optical analog of electronic sampling oscilloscope

02 p0259 A69-12656

Dynamic mode locking of CW He-Ne laser by external regenerative feedback using RF beats between axial modes

02 p0260 A69-12657

Laser oscillation frequency shift dependence on discharge current in 6328 Å He-Ne laser

02 p0260 A69-12658

Laser produced sparks in 200 kG magnetic field in air, butane and helium at atmospheric pressure

02 p0260 A69-12659

Tunable optical parametric oscillator using argon laser CW output as pump and lithium niobate as nonlinear crystal

02 p0260 A69-12701

Transverse magnetic field influence on power and polarization of helium-neon laser emission

02 p0260 A69-12844

Giant pulse generation by Q switched water cooled CW ruby laser in narrow spectral range, discussing laser design and operation principles

03 p0435 A69-12982

Electro-optical device using KDP crystal for laser beam deflection at temperatures near Curie point

03 p0435 A69-12984

Clamp type diode holders for obtaining CW coherent emission from gallium arsenide injection lasers

03 p0435 A69-12985

Radiation absorption variations in KC-19 CdSe glass during ruby laser radiation, noting microcrystals and nonlinear effects role in determining optical properties

03 p0436 A69-13036

Light wave propagation in gyrotropic crystals, examining laser frequency shift circularly polarized by modulating field

03 p0436 A69-13037

Ruby laser radiation nonlinear absorption coefficient measurement in CdS, ZnS and SiC semiconductor crystals, noting light limiting effects

03 p0436 A69-13038

Efficient conversion of Q switched neodymium-glass laser output into second harmonic obtained for low output levels at fundamental frequency

03 p0437 A69-13046

Q switched lasers powerful outputs obtainable at sum frequency, discussing frequency mixing in nonlinear dispersive media

03 p0438 A69-13047

Q switched neodymium-glass laser output conversion into second optical harmonic by passing beam through double Galilean telescope with adjustable focus

03 p0438 A69-13048

Pyroelectric crystals transparent at laser output wavelength used for recording transmitted radiation, noting response of triglycine sulfate crystal

03 p0438 A69-13050

Ruby laser light beam self focusing in sodium chloride and potassium bromide crystals

03 p0438 A69-13051

Two photon absorption and stimulated emission mechanism of CdS-CdSe mixed crystals investigated by ruby laser output

03 p0438 A69-13052

Q switched ruby laser nonlinear absorption in optically transparent organic liquids attributed to two quantum process with large cross section

03 p0439 A69-13055

Second optical harmonic generation in uniaxial negative potassium dihydrogen phosphate, noting influence of generating process on angular structure and output power

03 p0439 A69-13057

Ruby laser emission spectral line narrowing due to lasing modes reduction

03 p0439 A69-13059

Holographic laser type memory with bulk storage capacity and short readout time

03 p0428 A69-13116

Laser gyro in future inertial navigation systems for Category I landing without position updating

03 p0463 A69-13210

Time dependent photoelectron multiplier with low noise for recording long wave laser light pulses

03 p0440 A69-13264

Laser longitudinal oscillation modes beat frequencies measurement by grouping photoelectron velocities by HF field containing photomultiplier cathode

03 p0440 A69-13265

Holographic and microwave technology relationship, noting side-looking radar photos and X band radiation

03 p0430 A69-13354

Solid state laser Q switched by rotating prism emitting giant pulse before two mirrors in parallel

03 p0440 A69-13365

Raman effect in liquid glycerol obtained with 4880 Å ionized argon laser, determining valence vibrational frequencies

03 p0440 A69-13366

Tradeoffs among beam divergence, power output and mirror alignment tolerances of high power argon ion lasers operating in various low order transverse modes

03 p0440 A69-13549

Beam laser as frequency standard, considering wavelength and molecular transfer constraints imposed by technology limitations and frequency stability requirements

03 p0440 A69-13715

Light pulse narrowing in laser in linear mode operation with inertialess bleachable filter

03 p0440 A69-13716

Pulse compression by optical correlation techniques, discussing laser beam control by diffraction grating in ultrasonic delay line

03 p0397 A69-13732

Technique to obtain desirable longitudinal oscillation mode for radiation of Ne-He laser

03 p0441 A69-13844

Temperature dependence of He-Ne laser output at various wavelengths over low temperature range

03 p0441 A69-13845

Reduction of optical breakdown threshold in laser focus by superimposed microwave field

03 p0441 A69-13996

Ionizing action of radiation due to heating substance in laser beam focus, discussing highly ionized plasma production

03 p0479 A69-13996

Breakdown plasmoids produced by lasers

03 p0480 A69-14058

Arc and HF discharges in Ne-He lasers, comparing output power, spectral line intensities and reduced electric field vs reduced tube radius plots

03 p0441 A69-14132

Thermionic emission and dispersion of plasma created by monopulse of laser radiation focused on solid target, discussing plasma temperature determination methods

03 p0441 A69-14144

Cavity arrangement to obtain pulse durations of 0.5 to 10 microseconds with ruby laser

03 p0441 A69-14142

Single picosecond mode locked optical pulse selection from train of pulses of Q switched Nd-glass laser using optics external to oscillator cavity

03 p0441 A69-14183

Sinusoidal phase modulation role in spectral line broadening observed in trapped filaments of laser and Raman light

03 p0442 A69-14189

Laser ranging and illumination systems, discussing direction of pulsed monochromatic radiation to illuminate scene and utilization of reflected radiation for imaging

03 p0442 A69-14191

Threshold conditions for laser pumping with emission of perfect black body

03 p0442 A69-14220

Metal surface degradation by constant density laser radiation, computing screening effect

03 p0442 A69-14221

Single transverse electromagnetic mode power output for laser radar transmitter, using near hemispherical mirror resonator

04 p0609 A69-14287

Interferometric laser beam scanner using hollow cathode mercury ion laser output

04 p0609 A69-14288

High power output from submillimeter continuous wave gas laser

04 p0609 A69-14289

Mic total and differential backscattering cross sections at laser wavelengths for Junge size distribution aerosol models

04 p0609 A69-14290

Gases optical pumping by self radiation laser action, discussing high intensity oscillatory transitional wide bands of molecular gases

04 p0610 A69-14382

Interatomic collisions effect on multimode He-Ne lasers output power and spectral composition

04 p0610 A69-14383

Maximum inversion density and output power of Ne-He laser, given optimal discharge in hollow cathode

04 p0610 A69-14422

Power and time characteristics of He-Ne laser pumped by microwave pulses

04 p0610 A69-14423

Frequency mixing of organic dye solution laser radiation with ruby laser radiation, showing broader UV spectrum

04 p0610 A69-14424

Emission amplification coefficients of gas laser using pure carbon dioxide, carbon dioxide/air mixtures and carbon dioxide/air/helium mixtures

04 p0611 A69-14426

Resonant interaction of radiation from liquid nitrogen cooled ruby laser with ruby crystal in temperature range 4.2-100 K

04 p0611 A69-14439

Gas laser generation frequency control by emission absorption saturation effect, inserting neon filled emission absorbing cell into resonator

04 p0611 A69-14550

Surface smoothness of laser beam holes, discussing possible damage and technology recommendations

04 p0606 A69-14607

Pumping light filtration conditions effect on transition frequency of rubidium atoms

04 p0611 A69-14779

Kerr effect and electrostriction during self focusing of high power laser beam in gases and liquids

04 p0611 A69-14792

Helium-neon gas laser cavity beam for automatic high speed particle sizing

04 p0611 A69-15023

Homopolar generator as energy store for large laser pumping

04 p0612 A69-15151

Carbon dioxide laser noting output for added gases, efficiency, energy levels, excitation mechanism and tuning to single line and mode

04 p0612 A69-15173

Submillimeter water vapor laser power output for admixtures of H, N, carbon dioxide, methane, He and Ar, noting buffer effect of H

04 p0612 A69-15175

He/Ne ratio effect on performance of He-Ne laser in annular cavity

04 p0612 A69-15176

Output characteristics of slowly Q switched neodymium in calcium tungstate laser

04 p0612 A69-15206

Laser radiation influence on effectiveness of frequency doubling in KDP crystal

04 p0612 A69-15375

Optimal modulation shape for light emission flux as function of photoresistance detector and resonance amplifier pulse characteristics

04 p0560 A69-15376

Standard Leningrad-2 photoexposure meter applied to measurement of power of laser continuously operating in visual spectral range

04 p0602 A69-15405

Laser power increase noting influence of Mandelstam-Brillouin induced backscattering

04 p0612 A69-15414

Deuterium plasma heating by means of high power focused pulsed laser beam, noting initial energy of laser and pulse duration

05 p0769 A69-15583

Plasma production by ultrashort pulse Q switched laser beam, discussing avoidance of initiation of breakdown wave

05 p0770 A69-15584

Magnetic field confinement of plasma produced by focusing Q switched laser output on solid deuterium pellet

05 p0798 A69-15585

Laser light scattering by plasma using theory of ionospheric scattering of radar signals, determining scattered spectrum

05 p0798 A69-15586

Visual factors of laser displays providing human factors recommendation for several visual variables

05 p0760 A69-15591

Photon number and amplitude fluctuations of laser radiation in case of inhomogeneously broadened atomic line and for steady state condition

05 p0770 A69-15631

Rb 87 vapor laser short term frequency stability independent of vapor concentration, noting use as frequency standard

05 p0770 A69-15656

Time dependence of laser output in C and N atoms following dissociative excitation transfer explained in terms of measured populations of excited states

05 p0795 A69-15663

Relaxation rates of water vapor laser lines obtained with split discharge laser

05 p0771 A69-15810

Phase grating formation in giant pulse laser Q switching liquid by reflecting light beam from Lippman plate at Bragg angle

05 p0771 A69-15811

Thermionic electron emission from Mo and W targets irradiated by CW carbon dioxide laser beam

05 p0771 A69-15812

Gas laser pulse induced attenuated and nonattenuated plasma radiation recording, determining absorption coefficients

05 p0762 A69-15900

Spectroscopy of potassium vapor using laser induced fluorescence, noting laser line coincides with several molecular transitions

05 p0771 A69-15907

Spectral output time variation of GaAs diode laser operating in Fabry-Perot modes

05 p0772 A69-15961

Laser photolysis and spectroscopy for photographic recording of absorption spectra of transient intermediates in nanosecond reactions

05 p0772 A69-16025

Thin film thermocouple detector for molecular lasers operating in middle and far IR range

05 p0773 A69-16284

Visible laser frequency stabilization scheme and simultaneous determination of frequency in terms of time standard

05 p0773 A69-16291

Gallium arsenide electro-optic switch measuring signal time response to radiation step of homogeneously broadened carbon dioxide, He and nitrogen laser amplifier

05 p0773 A69-16293

Critical population inversion for xanthene dye solution laser, analyzing optical loss due to triplet state concentration [IEEE PAPER A-2]

05 p0773 A69-16307

Thermal self actions of CW laser beams in solids and liquids with wind or convection flow, discussing self focusing and defocusing [IEEE PAPER E-12]

05 p0774 A69-16311

Thermal self defocusing effect of laser beam in self focusing liquids, measuring refractive changes by high speed double exposure holography [IEEE PAPER J-7]

05 p0775 A69-16320

Brewster angle window degradation of high power ionized argon gas lasers [IEEE PAPER L-4]

05 p0775 A69-16322

Finite cross relaxation rate effect on spectral distribution in CW laser oscillator output with inhomogeneous broadening, noting population inversion distribution [IEEE PAPER T-2]

05 p0776 A69-16327

Mode suppression by mixed polarization in Michelson interferometer type of optical resonator

05 p0776 A69-16330

Stabilization method for composite cavity single frequency laser, noting insensitivity to oscillation power level variations

05 p0776 A69-16333

Pulsed water vapor laser with single Brewster window for operation between 20 and 120 microns, comparing performance with ordinary laser

05 p0776 A69-16334

Selective resonators for laser emission spectral structure control, proposing dispersion power increase by inserting telescopic system

05 p0777 A69-16371

Conversion of emission from pulse tube using neodymium laser with luminophor solution filled active element, discussing pumping nonlinear absorption kinetics

05 p0777 A69-16373

Semiconductor laser generation efficiency increased by using external resonator and by signal amplification

05 p0777 A69-16378

Laser scatter measurements in mesosphere and above for optical radar system parameters

05 p0758 A69-16414

Expansion anisotropy in angular distribution of laser produced plasmas in terms of drifting and expanding sphere model, discussing particle velocities, currents and time integrated counts

05 p0804 A69-16460

Pulsed ruby laser threshold and output energy for different relative orientations of rectangular prism and ruby crystal main crystallographic axis

05 p0777 A69-16526

Ruby laser characteristics at 78 K, discussing emission threshold, optimum feedback, modes, etc

05 p0777 A69-16546

Radiation of laser active element with random inhomogeneities of refractive index, discussing beam divergence, operation modes and Q switched operation

05 p0777 A69-16550

Laser beam scattering by acoustic waves of ionized crystal, reconsidering stimulated Brillouin emission theory for ultrasonic yield

05 p0777 A69-16610

Optical simulation of microwave antennas with variable profile reflectors, investigating radiation patterns by photometric scanning of photographs obtained with He-Ne laser

05 p0736 A69-16781

Electron concentration in pulsed plasma measured with Fabry-Perot interferometer and laser radiation source

06 p0963 A69-16911

Zeeman effect in He-Ne lasers during simultaneous emissions at various gas pressures and currents in magnetic fields

06 p0932 A69-16912

Active element inverse population distribution effects on laser radiation angular divergence during lower and higher oscillation modes

06 p0932 A69-16913

Laser based on xanthene series dyes and excited by neodymium laser second harmonic radiation, noting radiation spectra

06 p0932 A69-16914

Mass spectrometric studies of plasmas produced by laser beam interaction with solid materials

06 p0932 A69-16921

Continuous and pulsed lasing characteristics during discharge in pure oxygen noting ozone formation and removal at tube walls

06 p0932 A69-16923

GaAs laser excited by fast electrons exhibiting high efficiency and output power at room and liquid nitrogen temperatures

06 p0933 A69-16994

Carbon dioxide Q switched laser nonlinear amplification characteristics in vibrational-rotational bands

06 p0933 A69-17118

Solid state diodes made by pulsed laser irradiation of polished silicon surfaces, discussing application to integrated circuit design

06 p0893 A69-17157

Laser measurement techniques for plasma diagnostics, spectroscopy, angular rotation rate, distance, velocity and alignment of tools and assemblies [ASME PAPER 68-DE-21]

06 p0933 A69-17167

Lasing threshold and spectral characteristics of organic dye solutions, using excitation of second harmonic of monopulse ruby laser

06 p0933 A69-17255

Pulsed laser emission of atomic N in mixture of molecular N and He, noting effects of pressure and frequency and duration of excitation pulses

06 p0933 A69-17258

Gas laser operating on pure O-He-Ne-Ar mixture at liquid N temperatures, noting atomic O transitions, pulsed operation and energy level populations

06 p0933 A69-17259

He-Ne laser gain dependence on temperature noting influence of pumping conditions, discharge tube filling and geometry

06 p0934 A69-17260

CW room temperature laser using lanthanum sodium molybdate crystals with positive trivalent Nd ion impurity

06 p0934 A69-17262

Spectrum and amplitude fluctuations of laser light propagating through liquid helium, obtaining spatial correlation function of refractive index fluctuations

06 p0957 A69-17267

Metastable level population measurement in laser crystal based on luminescence changes under influence of stimulated emission

06 p0934 A69-17457

Electro-optical effect in Cr-doped GaAs single crystals at room temperature, discussing carbon dioxide laser radiation modulation by GaAs

06 p0934 A69-17466

Alternated magnetic field effects on lasing in ionized Ar

06 p0934 A69-17467

X rays detection from laser produced deuterium plasma through calibrated absorbers, presenting electron temperatures

06 p0964 A69-17479

Lippman-Brugg holograms production with high reconstruction efficiencies by suitable recording and processing techniques with commercially available photographic plates

06 p0926 A69-17481

Optical breakdown in air by mode synchronization operation of ultrashort pulses from neodymium laser

06 p0934 A69-17546

Light pulse duration and other parameters for ruby and Nd-glass lasers operating in synchronized mode regime determined by Armstrong method

06 p0934 A69-17549

Stimulated radiative recombination process for ramjet propulsion, investigating delay chamber required for vibration-to-translation conversion

06 p0984 A69-17630

Gas laser operation at high pressures, examining threshold pumping and power output dependence on pressure to optimize parameters

06 p0934 A69-17680

Ion laser emission cessation with increasing pressure, magnetic field and current strength due to lower transition level lifetime increase

06 p0934 A69-17682

He-Ne laser with small spark gap optimum parameters dependent on active medium and resonator field structure

06 p0935 A69-17683

Solid target output pulse magnitude and direction dependence on angle of incidence of intense laser beam

06 p0935 A69-17686

Mode locked Nd glass laser to pump organic dye laser, obtaining continuously tunable picosecond pulses

06 p0935 A69-17759

Inductively excited argon ion laser properties in high current regions

06 p0935 A69-17767

Semiconductors reflectivity enhancement by irradiating with Q switched ruby laser output

06 p0935 A69-17768

Ultrashort light pulse generation and measurement of half width, using saturable dye to mode lock Nd-glass laser

06 p0935 A69-17769

Mechanism for laser surface damage of glasses working through optical absorption, fluorescence, chemical reaction by quenching and breakdown

06 p0935 A69-17771

Q switching and mode locking of neodymium selenium oxygen chlorine liquid laser, discussing power output and nature of pulses

06 p0935 A69-17776

Temperature dependence of laser induced damage in plastic Q switch made of polyethylmethacrylate and vanadyl phthalocyanine for ruby laser

06 p0936 A69-17777

Laser emission of neodymium salt dissolved in polonium-chlorine, discussing fluorescence intensity

06 p0936 A69-17778

High power noble gas CW UV ion laser with W disk structure, showing continuous UV output limitation by optical degradation effects

06 p0936 A69-17900

IR radiation at 10.6 micron from two point sources mixed with collimated ruby laser radiation in proustite, obtaining visible image

06 p0928 A69-17904

Laser applications to situations requiring highly bunched high power density light beams

06 p0938 A69-18012

Ammonium perchlorate high temperature decomposition by using carbon dioxide laser pyrolysis/mass spectrometry

[AIAA PAPER 69-143]

06 p0885 A69-18111

Plasma ionization enhancement by laser line radiation matched to specific atomic transitions

[AIAA PAPER 69-47]

06 p0972 A69-18186

High efficiency ion lasers without additional axial magnetic field

06 p0938 A69-18221

Subpicosecond structure in output spikes of Nd-glass laser observed by employing two photon fluorescence displays inside laser cavity

06 p0938 A69-18231

Sixth order correlations of laser beam fluctuations near threshold from delayed coincidence measurements with three photodetectors, noting time constants

07 p1144 A69-18252

Laser excited vibrational fluorescence for determining vibrational energy transfer rates in HCl-carbon dioxide, HCL-HI and HI-carbon dioxide

07 p1144 A69-18289

Halide salts, semiconductors and nonoxide glasses as materials for high power laser windows

07 p1144 A69-18401

Quantum electronics trends, discussing output power, mode control, stability and lifetime of CW and Q switched lasers and parametric interactions in nonlinear optics

07 p1144 A69-18468

Streaming gas effect on carbon dioxide-nitrogen-helium laser power, discussing gas renewal phenomenon and evacuation rate

07 p1145 A69-18476

Rate equation analysis for internally optically pumped millimeter wave maser operating in laser crystal

07 p1146 A69-18480

Helium-neon laser for optical correction and guide beam techniques

07 p1146 A69-18484

Plasma diagnostics using scattering of laser electromagnetic radiation by plasma density function, discussing plasma species collision effect on line profiles

07 p1131 A69-18485

Giant pulse generation by switched laser rapid pumping of neodymium doped glass laser

07 p1146 A69-18486

Tandem amplifier system of glass and selenium-oxychloride liquid lasers, discussing input power/output pulse relation and population inversion density measurement

07 p1147 A69-18487

Synchronizing ruby and Nd-glass laser pulses by means of passive bleachable dye solution liquid Q switch

07 p1147 A69-18530

Time stabilization method for lasing in electro-optically Q switched ruby laser with saturable absorber in cavity

07 p1147 A69-18531

Helium-neon laser output power dependence on spark-gap cross section geometry, analyzing diffusion equation and population inversion

07 p1147 A69-18541

Memory effect in injection lasers output characteristics, noting anomalous increases in pulsed emission intensity with increasing current-pulse repetition rate

07 p1147 A69-18542

Output polarization rotation sensitivity to axial magnetic field varied by variable angle quartz flat inside He-Ne laser resonator

07 p1198 A69-18646

Circuit producing electrical and optical oscillations simultaneously constructed by combining semiconductor laser diode with photodiode

07 p1148 A69-18688

Photoconductivity induced by laser pulses in semiconductor with parabolic dispersion law, linear transition and nonequilibrium carrier concentration higher than equilibrium carrier concentration

07 p1148 A69-18690

Standing waves effect on spectral and power characteristics of laser with plane mirrors, determining dependence on pumping power

07 p1148 A69-18800

Fabry-Perot laser operation having third mirror inserted on optical axis, analyzing equations solution stability according to Liapunov

07 p1148 A69-18802

Helium-neon laser radiation of given spectral compositions, noting relation between spatial coherence and controlled number of frequencies

07 p1148 A69-18803

Measurement of helium-neon laser radiation divergence emitted in TEM sub nm modes

07 p1148 A69-18804

Picosecond laser pulses application to nonlinear optics, atomic and molecular systems transient response, optically generated plasmas, spectroscopy, high speed photography, etc

07 p1148 A69-18856

Gradual output degradation mechanism in GaAs injection lasers, attributing internal radiative quantum efficiency reduction to nonradiative recombination centers formation

07 p1148 A69-18857

Brewster angle lenses for low cost low loss laser beam transmission system

07 p1148 A69-18863

Q switched laser quasi-periodic short pulse emission pattern evolution from broadband noise source, using fluctuating dipole model

07 p1149 A69-18897

Saturated absorption by Ne isotope 6328 A He-Ne laser, discussing selection of Ne isotopes in gain and loss tubes

07 p1149 A69-18898

Laser beam absorption induced index changes associated with thermal blooming observed in iodine doped carbon tetrachloride, using Mach-Zehnder interferometer

07 p1149 A69-18899

Laser light scattering with orientation saturation of microsystems by electric field, noting application to optical anisotropy of macromolecules and colloidal particles

07 p1149 A69-18900

Single mode output power from 6328 A He-Ne laser through mode coupling induced by added absorption cell containing excited Ne

07 p1149 A69-18901

Radiation pressure effects on laser produced carbon plasma in vacuum, discussing target surface superheating, plume boundary, plume density precursor and electron and ion temperature merging

07 p1190 A69-18902

Pulse broadening in MHD copper vapor laser

07 p1149 A69-18904

Boundary value problem of temperature field and heat conduction in transparent media heated by laser

radiation producing thermoelastic stresses leading to breakdown

07 p1149 A69-18922

Pumping power effect on He-Ne laser amplification factor dependence on temperature and discharge currents

07 p1149 A69-18933

Nonpolarized single frequency gas laser radiation produced by interferential effects in complex resonator

07 p1149 A69-18936

Temperature profile and power density distribution in metastable level of ruby laser rod during pumping in air

07 p1150 A69-18937

Atmospheric extinction coefficient and backscattering function determined by laser radar using differential equation

07 p1126 A69-18966

Organic dye lasers characteristics, describing broad continuous production for nanosecond absorption spectroscopy

[IEEE PAPER A-3]

07 p1150 A69-19047

Pulses from Q switched carbon dioxide laser for studying Q switching techniques

[IEEE PAPER G-2]

07 p1150 A69-19054

Laser small signal step response measured, deducing medium bandwidth

[IEEE PAPER G-9]

07 p1151 A69-19056

Radiative lifetime for nitrous oxide 001-100 transition, laser level absolute population densities and saturation parameter measured in nitrous oxide-nitrogen-He laser

[IEEE PAPER G-10]

07 p1151 A69-19057

Single mode single frequency carbon dioxide laser operating on single rotational-vibrational transition

[IEEE PAPER G-11]

07 p1151 A69-19058

Nonsaturated gain of laser radiation in gas discharge in carbon dioxide with N and He

07 p1151 A69-19060

Spontaneous and stimulated Raman emission in liquids, obtaining picosecond pulse duration and laser light linewidth

[IEEE PAPER H-6]

07 p1152 A69-19063

Continuous wave and pulsed IR signals amplification on carbon dioxide laser amplifiers, discussing design, construction and performance of transmitter

[IEEE PAPER J-1]

07 p1152 A69-19064

Time resolved spectrum of high current pulsed argon laser discharge, noting primary laser output and afterglow

[IEEE PAPER L-12]

07 p1152 A69-19068

Output properties of Nd-selenium oxychloride liquid laser, detailing cell construction and output dependence on cell geometry and optical feedback

[IEEE PAPER M-8]

07 p1153 A69-19070

Dynamics of injection lasers, discussing picosecond pulse generation

[IEEE PAPER O-1]

07 p1153 A69-19071

Thermonuclear neutron emission from high temperature deuterium plasma produced by focusing high power laser radiation on lithium deuteride surface

[IEEE PAPER O-11]

07 p1153 A69-19072

Frequency reproducibility of He-Ne laser, using absorption dependence on frequency in strong field standing wave limit to provide stabilization

[IEEE PAPER P-4]

07 p1153 A69-19073

Stimulated Compton scattering for laser action, noting voltage tunability and gain at far IR wavelengths

[IEEE PAPER S-9]

07 p1154 A69-19081

Iodine IR laser, discussing CW emission obtained at various wavelengths and attributed to electronic transitions in atom

[IEEE PAPER T-5]

07 p1154 A69-19082

Collision broadened spectral line shape obtained in impact approximation using Anderson formulation compared to output of gas lasers

[IEEE PAPER T-6]

07 p1154 A69-19083

Laser induced gas breakdown by focusing nanosecond pulses in air and deuterium

[IEEE PAPER U-3]

07 p1155 A69-19085

Phase matched optical harmonic generation by anomalous dispersion in liquid media, using dye fuchsin red

[IEEE PAPER V-9]

07 p1155 A69-19086

Gain enhancement effect of CO on carbon dioxide CW laser performance by accelerating relaxation of bending mode

07 p1155 A69-19088

Scaled carbon dioxide lasers life and power outputs with Xe and H additives

07 p1155 A69-19091

Output and beat frequency of carbon dioxide laser with various resonator configurations realizing single mode operation

07 p1156 A69-19157

Induced emission cross section of neodymium glass laser in quasi-steady mode measured as function of rod section, mirror reflectivity and output

07 p1156 A69-19161

Velocity measurement by combination of Doppler principle and schlieren method involving reflection, refraction or diffraction of laser beam

07 p1135 A69-19259

Iodine fluorescence spectra excited by krypton ion laser, analyzing spectral series and vibrational rotational levels

07 p1156 A69-19304

IR beam profiles of carbon dioxide laser permanently recorded on foamed polystyrene

07 p1156 A69-19305

Giant pulse production of Nd-glass laser with aid of coherent pumping by second harmonic of Q switched laser, noting pulse duration

07 p1156 A69-19333

Single mode intensity measured for 0.6328 micron He-Ne laser as function of cavity Q, using Lamb semiclassical theory

07 p1157 A69-19414

Spectrum of light scattered by particles suspended in turbulent fluid

07 p1157 A69-19417

Pilot protection against laser hazards, discussing protective eyeglasses, fireproof clothing and materials

07 p1072 A69-19436

GaAs lasers radiation power hysteresis manifested in generating starts and stops at different injection current levels

07 p1157 A69-19593

Ruby laser beam incident on steel surface in air or water measured for energies, determining reflected energy dependence on incident energy for self insulation effect

07 p1157 A69-19594

Proportionality between log-amplitude variance and 7/6 power of wavenumber for horizontal propagation from spherical wave transmitter to point detector

07 p1157 A69-19641

Laser color TV projection-display system using moving mirrors and dual polarization scanner

07 p1137 A69-19740

Laser modulation at optical and near IR frequencies, discussing beam characteristics changes and information transmission

07 p1158 A69-19742

Magneto-optic, acousto-optic, electro-optic and free carrier modulation of IR laser beams

07 p1158 A69-19743

Holography combined with laser interferometry for nondestructive testing in materials, components and assemblies

07 p1137 A69-19777

Carbon dioxide laser excitation by fast proton beams, noting generation power increase

08 p1323 A69-19802

Carbon dioxide laser radiation frequency controlled by varying boron trichloride pressure in cell inserted in resonator

08 p1323 A69-19804

Flow diagnostics for high enthalpy nonequilibrium gas flows in shock tubes using long pulse ionized Ar gas laser

08 p1323 A69-19879

Li niobate crystal emission excited by Ar laser beam, deriving laser action formulas

08 p1323 A69-19941

Stimulated emission of laser employing crystal and glass lasers doped with neodymium ions, using high temperature spectroscopy

08 p1323 A69-19944

Stimulated emission of water cooled CW Nd doped lanthanum fluoride at room temperature

08 p1323 A69-19945

Nonlinear amplification of powerful light pulses in Nd glass

08 p1323 A69-19946

Transparent dielectrics destruction by laser radiation noting stress development in medium

08 p1324 A69-19947

Micromachining with laser beam, choosing mirrors and lenses of optical system to provide uniform energy distribution for microwelding or hole boring

08 p1324 A69-19980

Laser beams self focussing interpreted as photon contraction due to equivalent gravitational attraction

with gravitational constant proportional to nonlinear refractive index

08 p1324 A69-20085

Back diffraction field behind hologram illuminated with laser beam, noting hologram image observation through beam cross section

08 p1312 A69-20086

Small signal pulsed gas laser amplification limits, discussing time dependency, temperature effects, relaxation rates and energy transfer

08 p1324 A69-20098

Flowing CO-N-He laser with power enhancement and high efficiency, noting role of gases

08 p1324 A69-20163

Picosecond light pulse measurement by two photon excitation of photographic film

08 p1313 A69-20165

Gas laser modes strong coupling and single moding induced by saturable absorbing medium within cavity resonator

08 p1324 A69-20166

Laser welding in nonconventional applications and tiny components

08 p1319 A69-20203

Quantum theory of laser, discussing stationary photon distribution and correlation function for intensity fluctuations

08 p1324 A69-20221

Collision cross sections between monatomic gas impurities and metastable atoms in He-Ne laser from output curve and impurity partial pressure

08 p1325 A69-20278

Normal multimode laser action with and without phase locking, using exact steady state solution of Fokker-Planck equation

08 p1325 A69-20291

Molecular beam gas laser operating at transitions between ground state and resonance excited state of inert gas atom, obtaining population inversion

08 p1325 A69-20325

Natural intensity fluctuations spectrum of He-Ne laser, determining modulation coefficient dependence on output

08 p1325 A69-20431

Light intensity dispersion logarithm calculated along axis of laser beam propagating in atmosphere

08 p1351 A69-20437

Plasma diagnostics by use of lasers, discussing Thomson scattering and problems arising from light scattering applications

08 p1326 A69-20471

Laser beam diffraction method for measurement of apparent filament diameters, emphasizing high modulus carbon filaments

08 p1316 A69-20499

Inhomogeneous laser beams self focusing effects in organic liquids recorded on bases of induced stimulated scattering

08 p1326 A69-20538

Gas laser emission natural frequency fluctuations spectral density measured by auxiliary heterodyne laser

08 p1326 A69-20540

Q switched single mode ruby laser pulse passage through traveling wave amplifier decreases beam divergence

08 p1326 A69-20542

GaAs laser employing external resonator with thin film active substance, noting output power and emission thresholds during electron beam excitation

08 p1326 A69-20543

Emission spectrum of laser employing electron-vibrational transitions in samarium doped calcium difluoride crystal, noting spectrum shift with increasing crystal temperature

08 p1326 A69-20544

Picosecond light pulse generation by solid state laser interpreted by fluctuating intensity spikes arising from random emission interference in out-of-phase modes

08 p1326 A69-20548

Laser operation through semiclassical dispersion theory, presenting dipole moment and population density equations derived from quantum theory

08 p1326 A69-20571

Kine films of gas flows within highly luminous transient arc taken by laser schlieren technique

08 p1316 A69-20615

Biological effects of laser radiation on mammalian retina, noting thermal injury [AGARDOGRAPH-111]

08 p1266 A69-20676

Nonlinear optical effects in He-Ne and ruby lasers noting laser gain, frequency splitting, frequency differences in coupled lasers and frequency band narrowing

08 p1327 A69-20768

Design of ruby laser for stability, lifetime, maintenance and safety requirements of commercial users, discussing power, pulse duration and beam divergence

08 p1327 A69-20881

Book on laser communication system design covering modulation and detection methods

08 p1277 A69-20884

Luminous discharge at nonabsorbing surface when exposed to single pulse ruby laser beam, suggesting photoionization in surface layer

08 p1327 A69-21021

Formation and characteristics of flash produced in air by single pulse of Q switched ruby laser, using holographic interferograms

08 p1317 A69-21022

Laser rubies emission characteristics operating at different temperatures in common resonator, studying kinetics for pumping powers

08 p1327 A69-21076

Atmospheric effects on laser beam attenuation, noting application to optical visibility measurement by ruby laser

08 p1327 A69-21089

Laser beam propagation in scattering media, noting attenuation coefficients for coherent and incoherent radiation

08 p1328 A69-21092

Laser stimulated gamma-optical transitions illustrated by gamma-optical absorption detection in dysprosium ethyl sulfate

08 p1328 A69-21185

Alkali halide crystals destruction by laser radiation for estimating optical strength, discussing impact ionization hypothesis

08 p1328 A69-21188

Solid state laser radiation damage in polymers during tensile and compression loads using microstructural analysis

08 p1328 A69-21190

Laser produced blast wave expansion measured by microwave technique, obtaining surface temperature and electron density

09 p1514 A69-21324

Dispersion corrected three wavelength laser heterodyne system for plasma electron density and neutral density measurements

09 p1544 A69-21331

Second harmonic generation conversion efficiencies at 5300 A with KDP and lithium niobate crystals, using Nd-glass laser of high radiance and narrow bandwidth

09 p1514 A69-21333

Pulse velocity in self locked He-Ne laser, noting air turbulence effects prevention

09 p1514 A69-21347

Holographic displays using ultrasonic vibrations or laser outputs as optical sources, discussing recording materials, responses and computer applications

09 p1492 A69-21394

Motion measurement using Doppler shift of scattered laser light, noting high resolution

09 p1492 A69-21398

Spatial size and velocity distributions for liquid or solid aerosols suspended in air flow using Q spoiled ruby laser and holography

09 p1492 A69-21418

Electro-optical shutter for Nd-glass laser with high peak power pulses, discussing switching time, contrast ratio and synchronization

09 p1493 A69-21422

Far IR laser pulse shape and duration

09 p1515 A69-21424

Laser triggered spark gap and Pockels cells producing consistently repeatable controlled duration pulses

09 p1515 A69-21427

Highly turbulent boundary layers on walls in channels using laser light sources

09 p1515 A69-21434

Coherent light fluxes detection, noting correlation characteristics of output signals of photomultiplier illuminated by multimode He-Ne laser

09 p1515 A69-21438

Emission intensity and beam divergence of p-n junction GaAs laser with nonlinear passive element in resonator

09 p1515 A69-21474

Relaxation times of carbon dioxide laser levels induced by radiation

09 p1515 A69-21488

Optimal conditions for gas discharge in tubes with hollow cathodes in He-Ne mixture for obtaining lasing at Ne line wavelength

09 p1516 A69-21507

Three dimensional laser Doppler velocity instrument for mean velocity and turbulence measurements in subsonic jet shear layer
[SAE PAPER 690266] 09 p1494 A69-21555

Stimulated Mandelstam-Brillouin scattering in compressed N and H as function of pressure, using ruby laser pulses 09 p1516 A69-21562

Carbon dioxide-nitrogen-helium laser with RF excitation of discharge plasma, noting high power per unit length 09 p1516 A69-21678

Light polarization from stimulated Brillouin effect in compressed gaseous nitrogen, presenting depolarization variations as function of gas density and laser power 09 p1516 A69-21691

Picosecond structure of low power laser signals using calcite beam splitter and potassium diphosphate second harmonic generator 09 p1516 A69-21742

Optical parametric noise in water by ruby laser beam for phase matched four photon process 09 p1539 A69-21751

Gain, output power and radiation directivity of He-Ne traveling wave laser with nonresonant feedback 09 p1517 A69-21796

Fabry-Perot fringes maxima in frequency response of laser interferometer, describing passive technique using eight wave plate 09 p1517 A69-21915

Laser induced breakdown spark ignition of detonable and nondetonable chemically reactive gas mixtures, noting blast waves [AIAA PAPER 68-146] 09 p1622 A69-21951

Laser beam optical scintillation under atmospheric turbulence conditions, showing log amplitude variance saturation and decrease 09 p1517 A69-22079

Laser beam scintillation at night over long atmospheric horizontal paths, showing log amplitude covariance observation in agreement with theoretical prediction 09 p1517 A69-22080

Lasers, reviewing output properties, control and modulation characteristics, and applications to communications, plasma generation, measurement, high temperature metallurgy, etc 09 p1517 A69-22118

Laser oscillations, discussing oscillation frequency, oscillation time, noise and spectrum width, pumping and lasing materials, line broadening and giant pulse generation 09 p1517 A69-22119

Solid state lasers, noting normal, continuous and single mode oscillations, Q switching, power output limitations, mode locking and liquid lasers 09 p1517 A69-22120

Gas lasers, discussing amplification, resonance, internal and external mirror lasers, outputs, and He-Ne, carbon dioxide and ion lasers 09 p1517 A69-22121

Semiconductor lasers, discussing materials, oscillation wavelengths, excitation methods, operating principles, fabrication, GaAs p-n junction laser and applications 09 p1518 A69-22122

Mode locked laser operation, noting output and applications to optical communication, high speed photography, nonlinear optics and frequency standards 09 p1518 A69-22123

Fabry-Perot resonator and beam waveguide systems for laser beams, noting mode coupling and separation in laser optical systems 09 p1518 A69-22125

Phototubes, photodiodes, photoconductors, quantum detectors, nonlinear optical detectors and heterodyne receiving systems for photodetection of laser outputs 09 p1518 A69-22126

Passive electromagnetic circuit elements for laser light control such as circulators, isolators and phase shifters, discussing coherent light and polarization 09 p1518 A69-22127

Laser beam modulation and deflection methods involving control of amplitude, phase, frequency and direction, noting use of semiconductor p-n junctions 09 p1518 A69-22128

Atmospheric propagation properties of laser light, discussing particle absorption, gaseous absorption and refractive index disturbance effects 09 p1518 A69-22129

Optical communications applications with emphasis on large capacity transmission 09 p1456 A69-22131

Pulsed laser radar and applications to upper atmosphere observation equipment and distance measuring devices 09 p1456 A69-22132

Laser control of French rocket head guidance system, discussing gyroscopic master, stellar or solar detectors, etc 09 p1518 A69-22162

Laser radiation produced by continuous glow discharge within Al hollow cathode, determining laser power in terms of He-Ne mixture pressures 09 p1519 A69-22245

Pulsed ruby laser of small output for hole drilling, studying correlation of vaporization, hole diameter and depth with laser output 09 p1504 A69-22247

Laser induced line narrowing in coupled Doppler broadened transitions, noting mode crossing and spontaneous emission 09 p1519 A69-22282

Metallic systems microbonding and joining reliability, noting electron and laser beam welding and deposited film connections 09 p1510 A69-22348

Optical motor system to efficiently convert laser energy into mechanical rotational energy, giving equations for controlling motor speed 09 p1442 A69-22457

Distance measurements of several hundred feet to resolution of three millionth of inch by applying He-Ne laser interferometer 09 p1519 A69-22475

Laser evaporation vapors from refractory materials to produce surface temperature for carrying out reactions in gaseous phase and thin film preparation 09 p1519 A69-22476

Laser spark image in air photographed in scattered laser radiation light, showing singularities and absence of beadlike structure 09 p1519 A69-22531

Coherent radiation brightness increased from liquid N Raman laser, using off-axial pumping 09 p1520 A69-22533

Rubidium vapor laser pumping induced frequency shifts eliminated by detuning resonator without decreasing output power 09 p1520 A69-22636

Temperature effect on pulsed laser action on electron transitions in diatomic molecules for rotational relaxation, discussing excitation mechanisms 09 p1520 A69-22654

Ruby laser emission absorption in transparent dielectrics, noting crack formation and propagation producing opacity 09 p1520 A69-22655

Pulsed plasma production when focusing Q switched laser on solid target surface, noting high temperature effects and optical diagnostics methods 09 p1520 A69-22656

Frequency effects in laser with nonlinearly absorbing gas cell inserted in resonator, noting self stabilization of generation frequency 09 p1520 A69-22661

Laser resonator loss factor and axial mode frequencies calculation by interferometry 09 p1520 A69-22679

Two mirror resonators, discussing curvatures formation and stability conditions to derive natural frequencies 09 p1520 A69-22680

Gas laser output increase by nonconstricted discharge in aluminum tube cathode with mirror resonator 09 p1520 A69-22681

Liquid laser gain measurement via luminescence intensity, noting optical pumping thermal effect 09 p1520 A69-22683

Stimulated Mandelstam-Brillouin scattering at second harmonic of ruby laser and neodymium glass laser 09 p1520 A69-22684

First Stokes component of stimulated Mandelstam-Brillouin scattering and line defects caused by self focusing of single pulse laser beam 09 p1521 A69-22686

Lasers industrial manufacturing applications, discussing processing operations and measurement and inspection techniques 09 p1521 A69-22783

Carbon dioxide laser beam deflection and thermal defocusing due to wind in absorbing medium 10 p1701 A69-22949

Carbon dioxide laser combining gas flow with fluid mixing to achieve high gain 10 p1701 A69-22954

Laser applications to production line metal working, discussing economics, welding, drilling, automation, thermal and atmospheric effects, etc 10 p1698 A69-22983

Trivalent rare earth ions Stark structure based on spectroscopic observations of stimulated transitions in lasers 10 p1701 A69-23129

Amplitude fluctuations and line width of traveling wave and standing wave He-Ne laser, considering saturation effects 10 p1701 A69-23135

Far IR radiation from water vapor laser, noting monochromaticity and strong linear polarization 10 p1702 A69-23161

Optical frequency standards, discussing lasers VHF stability, RF and optical ranges, long and short term effects, etc 10 p1702 A69-23299

Ceramic substrate cutting with carbon dioxide laser by scribing perforation pattern, 10 p1699 A69-23302

Gaussian laser beam reflection and refraction at curved interface between media of different refractive indices, considering tilted ellipsoidal interfaces 10 p1725 A69-23309

Thermal diffusion and free thermal convection in fluids by diffraction interferometer, using laser for light source 10 p1702 A69-23431

Excitation of ultrathin Cd/SeS/ platelets with mode locked He-Ne laser for excitons formation, discussing time delay 10 p1703 A69-23512

Laser pulse picosecond substructure measurements, using pulse compression and second harmonic generation techniques 10 p1703 A69-23514

Matrix method for acoustical holograms and optical reconstruction of virtual and conjugate images using laser light of 6328 A wavelength 10 p1696 A69-23549

Peaked electron emission from nickel surface with large work function under laser radiation, discussing emission pulses, electron currents and surface temperature time variations 10 p1703 A69-23572

Stimulated emission of trivalent Nd ions in glass base, explaining connection between efficiency and emission polarization by interaction of laser modes with ions 10 p1703 A69-23618

Q switching combined with pulsed pumping of carbon dioxide laser for observing optimal Q switching instant, noting pulse energy increase 10 p1703 A69-23619

Stress effect on laser damage crack orientation in transparent organic dielectrics, estimating gas pressure in cracks 10 p1703 A69-23621

Nonlinear susceptibility tensor components and refractive index variations of liquids and glasses in high intensity ruby laser field, using interference methods 10 p1703 A69-23622

Dynamics of external loss modulation and Q switching methods of generating ultrashort pulses in mode locking laser 10 p1703 A69-23623

Gas laser with nonlinear absorbing cell in resonator, discussing effective gain dependence on squared field amplitude, hysteresis phenomena and output power 10 p1704 A69-23625

Low voltage He-Ne laser, noting outputs for various pressures and grid anode separations 10 p1704 A69-23652

Nd glass laser for emission of high radiance diffraction limited pulses, noting long path air breakdown and second harmonic generation 10 p1704 A69-23654

IR detection at sum or difference frequency by employing optically nonlinear crystal and laser in visible and photomultiplier 10 p1704 A69-23656

Laser emission lines produced by pulsed electrical discharge through ammonia 10 p1704 A69-23666

Quantum phase noise in He-Ne laser, considering amplitude fluctuation, spontaneous emission and oscillator linewidth 10 p1704 A69-23669

Coherent detection spectroscopy with laser oscillator, emphasizing high resolution and applications in astronomical spectroscopy and IR 10 p1696 A69-23684

Resonator interferometry of pulsed submillimeter wave lasers, analyzing mode structure, pulse shapes and molecular mechanism of laser emission
10 p1705 A69-23810

Isotope shifts in 4416 A cadmium laser, showing change of double peaked to single peaked profile with doubled active tube length
10 p1705 A69-23812

Mode locked ruby laser for short duration pulse production, noting relation to reciprocal linewidth
10 p1705 A69-23813

Neodymium doped YAG laser efficiency dependence on pump power level and spectral filtering of pump light
10 p1705 A69-23814

Mode interactions in argon lasers between two spectral lines noting effect on output
10 p1705 A69-24003

Sulfur dioxide-helium laser pulsed and CW submillimeter outputs
10 p1706 A69-24005

Far IR lasing lines in hydrogen sulfide, sulfur dioxide and OCS, discussing output
10 p1706 A69-24008

Self focusing of CW argon laser beam due to absorptive heating in crown glass, emphasizing time dependence of beam diameter as function of distance
10 p1706 A69-24009

Q switching techniques for solid state lasers at room temperature for high peak power, discussing mechanical systems, electro-optic and magneto-optic shutters
10 p1706 A69-24018

Electron concentration and temperature dependence on gas temperature as factor determining He-Ne laser output at 6328 A
10 p1706 A69-24078

Damping of solid state laser relaxation oscillations in power output due to diffusion of excitation
10 p1706 A69-24079

Laser radiation induced stress waves in transparent media using dynamic photoelastic technique
10 p1707 A69-24213

Laser radiation backscatter along oblique paths in atmosphere, calculating transmission over horizontal and oblique paths
10 p1659 A69-24220

Laser radiation spectrum scattered by low temperature plasma electrons at atmospheric pressure
11 p1922 A69-24233

Nonlinear confining and deconfining forces of laser light interaction with inhomogeneous plasma, analyzing macroscopic motion based on ponderomotive force description
11 p1923 A69-24297

Conventional and dual beam laser Doppler methods for velocity measurement of solids, liquids and gases
11 p1893 A69-24333

Pulsed tunable lasers, emphasizing dye lasers for visible and near visible light in specialized spectroscopy
11 p1893 A69-24343

Dye lasers CW operation feasibility, showing sufficient quenching of rhodamine 6G triplet state by oxygen dissolved in methanol
11 p1893 A69-24344

Pulsed molecular nitrogen laser positive UV and IR systems interaction under varying gas pressure, applied voltage and tube diameters
11 p1893 A69-24346

Laser light scattering in radiation driven breakdown waves in He, using high resolution streak photography to obtain diagnostic data
11 p1915 A69-24420

Laser beam for determining instrumental profile of high resolution double pass solar spectrograph, noting influence of slits width
11 p1893 A69-24431

Population inversion distribution and wave processes in optical amplifier, showing beam transformation of constant section and dependence on crystal characteristics
11 p1893 A69-24447

He-Ne laser light coherence distortion by atmospheric turbulence
11 p1894 A69-24452

Q switched carbon dioxide laser power increased by placing bleachable /boron tetrachloride/ filter in resonator
11 p1894 A69-24454

Collection of papers on electron beam and laser beam technology covering cold electron emitters, space charge flow, gas lasers, microelectronics, thin polycrystalline films
11 p1846 A69-24596

Laser application to welding, drilling and other processes involving material removal for microelectronic circuits and components fabrication
11 p1846 A69-24600

Output power losses in lasers with inhomogeneous active rods, deriving formulas for losses in ruby and Nd-glass laser rods
11 p1926 A69-24603

Statistical characteristics of photocurrent pulse amplitudes during cathode exposure to gas laser outputs
11 p1834 A69-24611

Specific level role in emission of optical radiation by ruby laser stimulated calcium fluoride crystals doped with divalent Dy ions
11 p1894 A69-24618

Power output and radiation spectra of trivalent Nd doped liquid lasers based on phosphoryl chloride with tin and titanium chlorides
11 p1894 A69-24620

Giant pulse buildup time in Nd-glass laser with passive shutter determined by comparing Q factor and peak power ratios of different modes
11 p1894 A69-24621

Molecular carbon dioxide laser radiation emission in tube containing low pressure atmospheric air, using C cathode and Al cold cathode
11 p1895 A69-24625

Holograms on photochrome films by split beam He-Ne laser using special mirror system
11 p1881 A69-24631

Gas lasers coherence properties and availability for holography, discussing continuous power output of He-Ne, Ar and Kr ion lasers
11 p1895 A69-24680

Coherent pulse laser holography for front and back lighted holograms of moving objects
11 p1895 A69-24686

Ruby laser crystals optical inhomogeneity and residual mechanical stresses effects on laser beam angle of divergence
11 p1936 A69-24698

Transmission of coherent ruby laser radiation through traveling wave amplifier noting spatial field structure changes
11 p1895 A69-24715

Induced discharge laser wave propagation in medium with active and absorbing admixtures, determining stationary shape and velocity range
11 p1895 A69-24716

Laser beam welding effectiveness for TWT with coaxial input and output lines
11 p1896 A69-24741

Gas laser materials, fabrication and performance, analyzing gas cleanup, cathode degradation, bore erosion and optical surface contamination effects
11 p1896 A69-24743

Equal inclination interference fringes effects on laser beam reflection from plane parallel glass plates, evaluating angular distance between adjacent fringes
11 p1896 A69-24840

Low order transverse modes in Ar ion lasers, analyzing beam divergence, output, mirror alignment and cavity configurations
11 p1896 A69-24841

Turbulence induced depolarization of linearly polarized He-Ne laser beam at 6328 A traversing atmosphere near ground level
11 p1896 A69-24842

Probability of ocular damage for illumination by pulsed laser beam transmitted through atmosphere, developing safety nomograph for eye hazard analysis
11 p1830 A69-24843

Rabbit corneal damage thresholds for Gaussian beams of carbon dioxide laser IR radiation at various exposure times
11 p1830 A69-24844

Laser radar eye hazard for fixed and variable transmitter intensities, considering eye damage magnitude and successful detection magnitude of transmitter intensity
11 p1830 A69-24845

Polarization effects of scattered coherent light on laser imagery, determining surface roughness and angle of incidence effects photographically on basis of Fung theory
11 p1896 A69-24849

Lasers applied to simulation of effects of X ray or gamma ray bursts on semiconductor devices
11 p1896 A69-24877

Calorimeter for IR carbon-dioxide laser output power measurement, noting range calibration and accuracy
11 p1885 A69-24903

Holographic reconstruction of spatial distribution of laser light field within and outside resonator, noting suitability for pulsed laser analysis
11 p1885 A69-24919

High power short duration diffraction limited laser pulse generation with optically swept laser glass slab forming amplifier chain
11 p1897 A69-25036

Singly resonant optical parametric oscillator, noting single mode and multimode oscillation for various pump powers, pump wave depletion and mode competition
11 p1897 A69-25038

Electro-optic broadband laser light modulator designs and modulation characteristics, computing curve set for evaluation of various materials
11 p1897 A69-25039

Atmospheric scattering behavior under reduced visibility conditions for laser wavelengths of 0.69 and 1.06 micron
11 p1837 A69-25040

Distance vs time and velocity vs time measurements for high speed model missiles by means of laser interferometry and optical Doppler shift method
11 p1886 A69-25042

Glass lasers with trivalent rare earth ions noting properties, characteristics and recent developments
11 p1898 A69-25043

Coherence phenomena for gas laser transitions coupled by common level, noting coherent superposition
11 p1898 A69-25045

Gas laser transitions and power broadening, analyzing saturation and gain profiles of He-Ne laser by light probe
11 p1898 A69-25046

He-Ne laser output phase fluctuations between adjacent modes during unlocked and self locked condition, noting cavity optical length short term fluctuations influence
11 p1898 A69-25048

Stimulated emission cross section measurement of Nd ions in calcium tungstate using Edwards method
11 p1938 A69-25049

High power CW carbon dioxide laser saturation and discharge conditions analyzed by rate equation
11 p1898 A69-25050

Far IR CW gas laser design for maximum output, discussing pulsed operation, wavelength measurement and radiation detection
11 p1898 A69-25051

Electro-optically Q switched Nd doped calcium tungstate laser for producing two controlled pulses, noting application to other solid state lasers
11 p1899 A69-25052

Carbon dioxide laser for production of high peak power pulse, discussing mw peak power design and oscillation problem in high gain amplifiers
11 p1899 A69-25053

Photoelectric, calorimetric and photon-momentum methods for measuring laser output energy and power emphasizing liquid, wire and pyroelectric calorimeters
11 p1899 A69-25196

Temperature and electron concentration in plasma spark obtained in air by focusing Q switched laser radiation
11 p1928 A69-25235

Microwave analysis of plasmas produced by laser beam on aluminum spheres, noting expansion velocity and electron density
11 p1930 A69-25287

Ruby laser light scattered at 90 degrees by dense plasma focus, analyzing signal detection
11 p1899 A69-25324

Fractures in refractory metals surface layers due to Q switched laser pulses
11 p1899 A69-25402

Laser pulse deflection by acoustooptical system consisting of ultrasonic cell and oscillator
11 p1840 A69-25423

Calcite crystals stability anisotropy to ruby laser radiation, studying threshold power as function of beam polarization
11 p1900 A69-25553

Fluctuations in angle of arrival of laser and thermal radiation beams over near ground path
11 p1840 A69-25570

Optical satellite tracking system using multicoincidence method of photon signal counting by Q switched laser
11 p1841 A69-25579

Laser radiation transmission in atmosphere examined for information transmission applications
11 p1841 A69-25638

Laser radiation in vacuum effects on metals and alloys 11 p1906 A69-25684

Intensity fluctuations of single frequency gas laser at 3.39 microns, discussing fluctuation minimization methods 11 p1900 A69-25750

Transformation of Q switched neodymium laser radiation into Stokes component during stimulated combination scattering in liquid nitrogen 11 p1900 A69-25751

Gas ionization by UV radiation emitted by pellet, target or portion of gas in laser beam focus, using polished metallic mirrors 11 p1901 A69-25754

Nonuniform standing wave fields spatial distribution in active rod of ruby laser effects on laser radiation dynamic parameters, discussing radiation spectrum width 11 p1901 A69-25756

Airborne Q switched ruby laser for studying upper atmosphere meteoric formations optical characteristics and kinetics against background of underlying surface 12 p2125 A69-25955

Atmospheric boundary layer transparency to gas laser emissions in IR spectrum, determining attenuation factor dependence on humidity and visibility range 12 p2028 A69-25957

Pulsed laser emission from carbon dioxide collisionally pumped by vibrationally excited DF produced by reacting fluorine oxide with deuterium 12 p2104 A69-25986

Second harmonic conversion of giant pulse Nd laser emission related to beam divergence and space-time distribution of radiation, noting energy relationship 12 p2104 A69-26022

Power output of He-Ne laser as function of transverse magnetic field strength 12 p2104 A69-26023

Spectrum analysis of aluminum plasma excited by giant pulse ruby laser radiation, discussing temperature and density 12 p2134 A69-26027

Reabsorption effect of emitted quantum on lifetime of excited levels in gas laser, determining capture factor 12 p2104 A69-26028

Emission spectrum of ruby laser as function of relative orientation of resonator and active crystal axes, noting spectrum width 12 p2104 A69-26029

Microwave modulation of GaAs injection laser radiation, using Zaleskii recording method and liquid nitrogen to cool laser diode 12 p2105 A69-26031

Shadow and schlieren photography, interferometry and quantitative data treatment obtainable by high speed multiframe photographic arrangement, using laser beam 12 p2086 A69-26165

Deformation measurement by laser pulse holographic method, discussing laser source choice criteria 12 p2087 A69-26175

Schlieren high speed photography systems for ballistic projectile studies, discussing use of gas lasers as nanosecond light sources 12 p2088 A69-26182

Regulated pulse lasers under free oscillation for photographing distant objects by illumination with shortened light pulses 12 p2089 A69-26190

Laser beam damage in glass blocks, noting high speed photographic study and absorption of light by inclusions 12 p2117 A69-26193

Alignment/test rig for head-up displays using laser light pencils 12 p2091 A69-26304

Mode locked lasers for measuring fast radiative decay in fluorescent systems 12 p2105 A69-26310

Spontaneous emission of carbon dioxide lasers, studying emission in Second Positive System of nitrogen as function of discharge current and laser output power 12 p2105 A69-26316

Disaligning and velocity changing collisions influence on laser light induced saturation peaks or holes in velocity distribution of Ne atoms 12 p2105 A69-26317

Ruby crystal optical homogeneity and relation to main laser emission characteristics, discussing optical and structural surface properties [IEEE PAPER U-7] 12 p2106 A69-26322

Laser emission noise and voltage noise cross correlation coefficient for CW GaAs laser diodes at 77 K, noting strong dependence on bias current 12 p2038 A69-26328

Simultaneous HCN and HOH laser emission in pulsed discharge through mixture containing H, C, N and O 12 p2107 A69-26330

Laser diode output efficiency increased in presence of transverse magnetic field suppressing higher order TE and TM modes 12 p2039 A69-26353

Pulsed HCN sealed laser long term operation, discussing behavior of 311 and 377 micron emissions 12 p2107 A69-26391

Laser output power amplitude fluctuations effect on beat frequency stability for traveling waves in annular laser with broadened Doppler emission line 12 p2107 A69-26541

Laser Doppler flowmeter for heterodyne detection of laser light scattered from moving fluid applied to fluid velocity and velocity distribution measurements 12 p2093 A69-26546

Q switched ruby laser with rotating prism, considering single pulse operation by increasing switching rate 12 p2107 A69-26588

Optical alignment for lasers with electro-optical Q switching and mutually misaligned ruby rod, KDP crystal and polarizing prism 12 p2107 A69-26589

Giant pulses from laser with electro-optical quartz shutter, noting advantageous optical and mechanical properties of quartz 12 p2108 A69-26591

Heat removal from laser ruby rod by Cu prism connected to cooling system, discussing limiting factors in heat transfer area size 12 p2108 A69-26592

Contrast interference patterns obtained in Michelson interferometer at various path differences, using He-Ne laser as light source 12 p2108 A69-26593

Phase pulsations between normal frequencies and combination tones in CW gas laser output, analyzing observations by scanning interferometer 12 p2108 A69-26635

P-n junction cut-off current density and ohmic losses effect on injection laser efficiency determined by using quality parameter 12 p2109 A69-26647

Holographic plasma diagnostics covering phase, amplitude variations images, laser spark, theta pinch studies, etc 12 p2094 A69-26707

Pulsed or continuous radiation generated in laser having active element of neodymium glass fragments 12 p2109 A69-26715

Incandescent cathode temperature effect on He-Ne laser output, ascertaining mixture parameters, cathode voltage and power dependence on discharge current 12 p2109 A69-26716

Gas lasers, including stimulated emission in monochromatic field of traveling and standing plane waves, spontaneous emission with stimulated transitions, etc 12 p2109 A69-26906

Standard phenomenological laser rate equations for population inversion and light intensity generalized by considering intensity dependent losses and Einstein coefficients 12 p2110 A69-27014

Direct modulation characteristics of semiconductor junction laser, analyzing resonance phenomenon, bias current, admittance, modulation frequency limit and emission lifetime 12 p2110 A69-27069

Soviet monograph on plasma diagnostics by lasers, describing interferometry, optical field visualization, schlieren and shadow photography 12 p2139 A69-27075

Atmospheric effects on laser beam width, using Born approximation and Gaussian model to obtain TEM mode scattered power expressions 12 p2111 A69-27166

YAG-Nd laser continuous operation using incoherent injection luminescent pumping by gallium arsenide phosphide light emitting diodes at liquid nitrogen temperature 13 p2270 A69-27192

Spectral criterion for distinguishing mode locked and nonmode locked laser signals 13 p2270 A69-27197

Intense ultrashort pulse widths determination by two photon fluorescence patterns, using model of partial laser mode locking 13 p2270 A69-27198

Shift of certain Hg spectral line by high power pulse from Nd laser through perturbation of atomic energy levels 13 p2270 A69-27202

Temperature effects on polarization degree, threshold current and delay of radiation from GaAs laser diodes with diffused Zn 13 p2227 A69-27328

Signal strength of two beam interferometers with laser illumination, considering modulation depth of interference pattern 13 p2259 A69-27450

Photographic layers darkening process, using widely spaced or single giant pulses of ruby laser 13 p2260 A69-27612

Laser light scattered from arc discharge, observing enhanced plasma oscillations 13 p2307 A69-27629

Potassium vapor radiative perturbation by ruby laser radiation in glass cell with end windows, studying emission line structure 13 p2271 A69-27656

Neodymium laser emission of organic molecules in UV region noting molecular absorptivity and fluorescence 13 p2271 A69-27657

Carrier dragging in CdS single crystals under Q switched ruby laser light due to photon stream 13 p2271 A69-27661

Gallium arsenide diode nonequilibrium carriers absorption of He-Ne laser radiation under emission conditions 13 p2272 A69-27893

Cadmium telluride laser characteristics including emission wavelength and electron beam threshold current density 13 p2272 A69-27896

Single frequency ruby laser emission spectrum coincidence with interacting laser radiation at instant of Q switching 13 p2272 A69-27911

FM laser pulse formation time characteristics noting modulated resonator losses 13 p2272 A69-28114

He-Ne laser transition line shape and gain curve through width, considering spectral frequency characteristics, output power and gas temperature and concentration 13 p2272 A69-28115

Quasi CW solid state doped lasers excited by pyrotechnic pump sources with potassium perchlorate oxidant and zirconium fuel, noting power to weight ratio 13 p2272 A69-28116

Multichannel optical interference fluid manometer, using laser light source for fringe pattern photographic record 13 p2263 A69-28190

Collective scattering of light from ruby laser by cold dense deuterium plasma produced by electrical discharge, deducing density and electron temperature 13 p2273 A69-28366

Ruby and neodymium glass lasers applicability to metal working, investigating factors affecting integral pulse power stability 13 p2273 A69-28431

Gas laser modulation steady state characteristics with KDP crystal in cavity, noting output power dependence on applied electric field 13 p2273 A69-28432

Laser radiation absorption in xenon plasma, noting dependence on intensity due to atoms ionization 13 p2314 A69-28442

Optical maser induced electrical breakdown interaction with superhigh pressure ionized gases, using optical interferometry and holography 13 p2273 A69-28464

Power output of ruby laser stimulated by strong pinch discharge plasma flux at 4000-7000 A in He 13 p2273 A69-28530

Spotted scattered background contrast relation to scattering system geometry during laser scattering by suspended Lycopodium spores 13 p2273 A69-28550

Square wave generator for junction laser power supply 13 p2274 A69-28643

Spectral width of emission of laser resonator in nonstationary mode in presence of active medium, noting time dependence 14 p2456 A69-28736

Gases optical pumping by self radiation laser action, discussing high intensity oscillatory transitional wide bands of molecular gases

14 p2456 A69-28755

Interatomic collisions effect on multimode He-Ne lasers output power and spectral composition

14 p2456 A69-28756

Submillimeter wave generated in ZnTe by difference frequency mixing of Q switched ruby laser, discussing beat power

14 p2457 A69-28927

Frequency shifts of Lamb dip minimum in helium-neon laser, considering effects of discharge tube parameters and gas pressure

14 p2457 A69-28929

Optically swept glass slab laser design, discussing pulse length and peak power

14 p2457 A69-28930

Polarization dependent gain saturation and nonlinearity induced anisotropy in He-Ne laser amplifier

14 p2457 A69-28931

Ruby laser beam effects on CdS crystals optical properties, measuring absorption spectrum and light dispersion in crystal

14 p2457 A69-28999

Laser emission field effect on discharge current in pure carbon dioxide and mixtures with molecular N and He

14 p2458 A69-29161

Pulsed lasers with pure carbon dioxide and mixture with N and He, discussing inversion mechanism, peak emission power and gas temperature effects in different modes

14 p2458 A69-29162

Composite ruby laser optical inhomogeneity effect on spectral, temporal and angular emission characteristics

14 p2458 A69-29163

He-Ne laser traveling wave output power, obtaining end mirror reflection coefficient optimal value

14 p2458 A69-29165

Passive Q switch laser single pulse formation time and spectral width using balance equations

14 p2458 A69-29166

CdS crystals emission spectrum during two photon excitation by ruby laser, noting dependence on pump power

14 p2458 A69-29167

Optical rectification effect in lithium metaniobate crystals under neodymium laser radiation, comparing results with data for potassium dihydrophosphate crystals

14 p2458 A69-29168

Fluorite crystal laser activated by divalent samarium, discussing characteristics in pulsed operation mode

14 p2458 A69-29328

Single crystals garnets Raman spectra using laser radiation, separating phonon spectra of host lattices from electronic Raman effect

14 p2507 A69-29334

Gallium arsenide injection laser for communication systems with pulse frequency modulation, noting power output dependence on crystal quality

14 p2459 A69-29349

Laser beam discrete deflection method using Wollaston prism and electro-optical switch for changing polarization plane

14 p2459 A69-29391

Ruby laser reflected and transmitted light intensity following radiation focusing on cuvette containing cyclohexane, noting dependence on incident pulse power

14 p2459 A69-29392

He-Ne lasers operation at 6328 Å, discussing optimum design parameters for power, life and stability

14 p2459 A69-29429

Linear polarization achieved in He-Ne laser by applying external transverse magnetic field to plasma discharge

14 p2459 A69-29569

Nonlinear interactions of linearly polarized carbon dioxide laser signals in sulfur hexafluoride measured as function of angle between polarization planes

14 p2460 A69-29602

Enhanced plasma heating in absorption zone of laser-induced gas breakdown at spherical blast wave shock front

14 p2460 A69-29604

Electron density, temperature and dimensions of helium breakdown induced by Q switched ruby laser beam as function of space and time

14 p2492 A69-29636

Log amplitude fluctuations of laser beam in turbulent atmosphere, obtaining asymptotic expressions for near field of transmitter aperture

14 p2460 A69-29638

Self resonant energy transfer mechanisms in active media for lasers investigated by two methods

14 p2460 A69-29644

Stimulated emission of cerium trifluoride-positive trivalent Nd ion laser noting absorption, luminescence, excitation, emission spectra and metastable state lifetime

14 p2460 A69-29645

Laser radiation conversion during induced combination scattering, discussing stabilization of emission mode of first Stokes component

14 p2460 A69-29648

Three level He-Ne laser, showing nonlinear interference effects on gain line shape and use in magnetic field and frequency stabilization

14 p2460 A69-29671

Laser with molecular H and Cl mixture at HCl vibrational transitions

14 p2461 A69-29672

Pulsed HF discharge analysis in hydrogen based on laser light scattering at plasma electrons, noting presence of satellites

14 p2451 A69-29781

Bibliography on laser applications in plasma physics covering plasma diagnostics and production

14 p2498 A69-29842

Undulation in output waveforms of pulsed water vapor laser observed with In-doped Ge detector

14 p2461 A69-29887

Plasma temperature measurement by resonant laser radiation absorption, assuming Saha-Boltzmann relation

14 p2501 A69-29954

Laser-nonlinear crystal dynamical interactions, studying saturation and coherence properties of second harmonic wave generated inside laser cavity

15 p2632 A69-30026

Efficient extinction in optically coupled GaAs injection lasers achieved by selecting quenching radiation frequency close to operating frequency

15 p2633 A69-30059

Gas lasers output power calculation based on operating transition with mixed contour due to natural and Doppler broadenings

15 p2633 A69-30079

Pulsed ruby lasers for welding fine wires for electrical interconnections, considering laser energy and pulse duration effects

15 p2617 A69-30097

Continuous butt welding with CW carbon dioxide laser, noting heat affected area, remelt zone and weld efficiency

15 p2617 A69-30099

Automatic frequency control of laser and regenerative amplifier, considering frequency stability

15 p2633 A69-30238

Short laser radiation pulses spectral characteristics determination with device converting laser emission frequency by nonlinear electro-optical crystals

15 p2633 A69-30257

Calorimeter for CW laser output power absolute measurement, discussing operation principles, structural features, circuit and accuracy

15 p2608 A69-30320

Solid state and gas lasers operational parameters tabulation including pulse durations, powers, energy flux densities, electric and magnetic field strengths, etc

15 p2633 A69-30708

Emission intensity and beam divergence of p-n junction GaAs laser with nonlinear passive element in resonator

15 p2633 A69-30719

Lasing kinetics, emission spectrum and directivity of ruby laser with spatially homogeneous population inversion

15 p2634 A69-30729

Characteristics of neodymium-glass laser with unstable resonator noting transverse modes and radiation angular distribution

15 p2634 A69-30730

Two photon absorption excitation of luminescence in ruby crystals by neodymium laser radiation, determining luminous intensity dependence on pumping intensity

15 p2634 A69-30731

Electron scattering due to Kapitza-Dirac effect in laser standing wave field

15 p2634 A69-30736

Microwave hologram construction and image reconstruction by laser beam, analyzing results by matrix expression

15 p2610 A69-30802

Lenses spherical aberration role in studying laser induced breakdown of gases, considering intense ionization collinear regions multiplicity along optic axis

15 p2634 A69-30878

Lasers and holography applications in astronomy including high resolution spectrographic diffraction gratings manufacture and astronomical objects photographic pictures evaluation

15 p2610 A69-30880

Molecular beam behavior in constant electric and magnetic fields, applying laser frequency dependence on magnetic field orientation to resonator

15 p2655 A69-30943

Statistical characteristics of Q switched He-Ne laser emission gain fluctuations during transient process from subthreshold to superthreshold value

15 p2634 A69-30960

Unsaturation frequency discriminator influence in semiconductor laser feedback loop on laser emission spectrum

15 p2635 A69-30967

Scintillation magnitude related to range and turbulence strength in near earth optical propagation, using pulsed and helium-neon laser

15 p2570 A69-31030

Gas laser cutting of thin carbon films on thick pyrex glass and ceramic substrates

15 p2635 A69-31037

Pumping energy absorbed by active element of neodymium glass during laser emission related to activator concentration

15 p2635 A69-31104

Optimal parameters of cuvette for use with helium-neon laser as excitation source to record combination light scattering spectra of powdery materials

15 p2635 A69-31105

Mode competition of 5861 and 6470 Å lines in ionized Kr laser attributed to electronic level excitation processes

15 p2635 A69-31106

Quantum mechanics method for obtaining photocount distribution from optical maser photoelectron counting statistics

15 p2635 A69-31238

Atomic coherence and inhomogeneous broadening effects on laser amplifier ultrashort electromagnetic high peak power pulses

15 p2635 A69-31239

Laser Doppler heterodyning for monitoring motion noting solid surfaces vibration, liquid and solid surfaces linear velocity and turbulence in liquids and gases

15 p2614 A69-31276

Fluid flow velocity measurements by Doppler shift of laser light scattered from moving fluid, determining beat frequencies

15 p2616 A69-31291

Laser flowmeter for pulse flow of highly corrosive rocket fuels and oxidizers with measured rise times less than 10 msec

15 p2616 A69-31292

Scintillation of ground based spherical wave laser source viewed from space analyzed from Geos 2 satellite laser tracking, noting stellar scintillation correspondence

15 p2570 A69-31309

Photography of laser echoes on satellites, tabulating results

15 p2570 A69-31311

Space direction by compensation method of cosmic triangulation network, using laser and optical observations of artificial satellites

15 p2699 A69-31377

Ellipsometric dimensions calculations with aid of laser radiation, stressing formulas for compensator and polarizer assemblies

15 p2636 A69-31474

Mechanical testing of high temperature materials subjected to thermal cycling by high power pulsed laser beam

15 p2636 A69-31512

Frequency selector for gas laser, considering monochromatic emission and multimode oscillation

16 p2795 A69-31608

Laser measurements of earth-moon distance applied to determinations of earth axis motion and lunar shape, relief, dimensions and motion

16 p2788 A69-31624

Laser radiation absorption by inhomogeneous overdense plasma, discussing effects of plasma expansion on energy coupling efficiency

16 p2818 A69-31679

Ruby laser output energy degradation due to pump light absorption by color centers, discussing roles of defects and impurities in center formation

16 p2795 A69-31697

Q switched laser produced blast waves in low pressure Ar, discussing gas density and time dependence roles

16 p2796 A69-31705

Holographical interferometry with laser spark radiation containing fundamental and second harmonic wavelengths, confirming heavy particle densities decrease in plasma with time

16 p2789 A69-31771

Lasing influence on electron energy distribution in gas discharge measured with Langmuir probe, showing electron-electron interaction insufficient to maintain equilibrium

16 p2796 A69-31772

Low temperature method for measuring breakdown threshold parameters of liquid and gaseous He by laser beam, observing stimulated Mandelstam-Brillouin scattering

16 p2796 A69-31799

Laser cavity optimization for producing minimum short light pulse width in fast Q switching of optical maser

16 p2796 A69-31802

Gas laser application to magnetospectroscopy of graphite, Bi, As and pyrolytic graphite single crystals

16 p2796 A69-31822

Injection semiconductor lasers emission characteristics, discussing gallium arsenide diodes, nonlinear losses in pulsed mode, laser interactions, etc

16 p2796 A69-31949

Monomode giant pulse generation from neodymium glass laser by coherent pumping

16 p2797 A69-32018

Plasma magnetic field and electron density measured by Faraday rotation using resonant gas laser radiation

16 p2822 A69-32041

Laser amplifier nonlinear losses effect on light beam propagation, studying arbitrary waveform development into asymptotic steady state pulse (SSP)

16 p2797 A69-32043

Laser radiation influence on effectiveness of frequency doubling in KDP crystal

16 p2797 A69-32122

Optimal modulation shape for light emission flux as function of photoresistance detector and resonance amplifier pulse characteristics

16 p2752 A69-32123

Increase or decrease in light absorption by plasma particles found dependent on laser intensity level

16 p2797 A69-32382

Atmospheric gas constituents number densities determined as function of altitude by correlating laser beam scattering and absorption data

16 p2781 A69-32387

Semiclassical theory of quantum generators, examining laser system response to effect of monochromatic standing wave based on kinetic equation for density matrix

16 p2798 A69-32480

Rb 87 vapor laser short term frequency stability independent of vapor concentration, noting use as frequency standard

16 p2798 A69-32513

Wave front resistivity in laser produced plasma interacting with magnetic field enhanced by two stream instability

16 p2823 A69-32564

Electron density measurement method in plasma or vacuum based on refraction index in optical frequency range using laser interferometer mismatch as criterion

16 p2798 A69-32583

Tunable far IR radiation generated from difference frequency between two Q switched ruby lasers using lithium niobate and quartz as mixing crystals

16 p2798 A69-32603

Time behavior of output intensity and polarization of single cavity mode internal mirror Zeeman laser in axial magnetic field

16 p2798 A69-32607

Dielectric breakdown thresholds and cavitation in organic liquids observed during Q switched and pulsed ruby radiation

17 p2979 A69-32826

Laser effect in neodymium glass, estimating efficiency of light energy output vs electric energy input

17 p2984 A69-32828

HCN laser line width measurement with high resolution spectrum analyzer indicating spectral widths caused by mechanical instability

17 p2979 A69-32850

Self Q switching of pumped neodymium-doped YAG and ruby lasers obtained by static misalignment of mirror and pumped laser filament

17 p2979 A69-32916

Line width and intensity correlation of laser radiation noting damping constant

17 p2980 A69-33012

Laser induced gas breakdown covering breakdown mechanism and plasma expansion and decay, with bibliography

17 p2980 A69-33026

Angular structure of second optical harmonic for cylindrical lens focusing of ND laser beam into negative KDP crystal

17 p2981 A69-33110

Laser emission spatial structure transformation determined from ratio between focused spot radius and distance between lens and output mirror

17 p2981 A69-33111

Broadband intracavity SHF modulation of He-Ne laser emission in 10 cm band, showing agreement with calculations

17 p2981 A69-33112

Spontaneous gas laser emission from level coupled by spontaneous transition with emitting level, obtaining atoms interaction with laser field velocity distribution and spectral line width

17 p2981 A69-33116

Continental and maritime hygroscopic particles associated with increasing relative humidity, determining effect on backscattered power from laser beam using Mie scattering equations

17 p2981 A69-33160

Molecular beam gas laser operating at transitions between ground state and resonance excited state of inert gas atom, obtaining population inversion

17 p2981 A69-33315

Long path difference vacuum Michelson interferometer application to far IR and IR laser wavelength measurements compared with 6328 Å He-Ne wavelength

17 p3006 A69-33405

Laser harmonic frequency measurement application to absolute frequency determination of 84 micron heavy water laser

17 p2982 A69-33406

Fog removal by high power carbon dioxide lasers, evaluating possibility of clearing airport runways [AIAA PAPER 69-670]

17 p2945 A69-33449

Laser technology and effects on materials fracture

17 p2989 A69-33557

Rb 87 vapor laser output power dependence on magnetic field strength and resonator detuning, discussing laser and atomic transition frequency tuning

17 p2983 A69-33694

Phase fluctuation measurements of laser beam propagating through turbulent atmosphere

17 p2927 A69-33855

Laser beam propagation through turbulent medium, investigating statistical distribution of phase shift fluctuations

17 p2976 A69-33857

Physical mechanisms for nonlinearities in electromagnetic wave propagation, analyzing plane wave instability, self focused beams propagation and laser oscillations

17 p2928 A69-33867

Laser emission divergence reduced by compensating optical inhomogeneity of active elements with prismatic reflector in resonator

17 p2983 A69-33970

Gas laser power dip in presence of elastic collisions, using equilibrium equations for particles velocity distribution function

17 p2983 A69-33972

Molecular gas absorption coefficient dependence on laser emission energy density, considering disturbed equilibrium distribution of molecules

17 p2983 A69-33973

Polarized emission from Nd activated glass, establishing S and P polarization component energy dependence on pumping energy

17 p2984 A69-33974

Laser action in quantum system, analyzing absorption constant relation to spontaneous/stimulated emission constants, energy level population inversion, pumping, etc

17 p2984 A69-34150

Optical parametric oscillator output/signal/frequency locked to absorbing atomic transition, discussing effective linewidth

18 p3133 A69-34263

Carbon dioxide flowing gas laser pumped by thermally excited nitrogen, discussing power gain and absence of chemical and charged particle effects

18 p3151 A69-34264

Damage thresholds to ocular tissues from laser radiation, presenting comparative theoretical curves and recommended safe working levels

18 p3097 A69-34312

Submillimeter water vapor laser power output for admixtures of H₂, N₂, carbon dioxide, methane, He and Ar, noting buffer effect of H

18 p3152 A69-34717

He/Ne ratio effect on performance of He-Ne laser in annular cavity

18 p3152 A69-34718

Wavelength dependence of total and depolarized backscattered laser light cross section for rough metallic surfaces

18 p3172 A69-35011

Neodymium laser emission temporal structure in mode self locking regime with Q switching by saturable filter

18 p3152 A69-35016

Ruby laser stimulated emission spatial, temporal, energetic and spectral characteristics during disruption in spherical cavity containing strongly scattering medium

18 p3152 A69-35026

Electron current flow from metal target in gas due to laser radiation, showing increased dependence on gas pressure

18 p3152 A69-35124

Laser stimulated gamma-optical transitions illustrated by gamma-optical absorption detection in dysprosium ethyl sulfate

18 p3152 A69-35154

Alkali halide crystals destruction by laser radiation for estimating optical strength, discussing impact ionization hypothesis

18 p3152 A69-35157

Solid state laser radiation damage in polymers during tensile and compression loads using microstructural analysis

18 p3152 A69-35159

Optical distance measurement using laser and atmospheric dispersion method through average refractive index determination over path

18 p3152 A69-35198

Intensity changes in visible sidelight emission from carbon dioxide laser switched on and off, calculating vibrational temperatures

18 p3153 A69-35243

Luminophors for carbon dioxide laser radiation visualization noting controlled sensitivity, quick response and resolution

18 p3153 A69-35259

Ionization effects in hydrodynamic model of radiation driven breakdown wave propagation, obtaining wave velocity and absorbed laser flux density relationship

18 p3174 A69-35286

Stimulated reflection experiment for correlation between coherent photon beams from independent lasers

18 p3153 A69-35292

Gas and solid state lasers optical resonance and radiation generation, frequency properties, frequency shift, spectra and Zeeman effect

18 p3154 A69-35408

Radiation dynamics of semiconductor GaAs injection laser with pulsed and continuous modes operation of diodes

18 p3154 A69-35495

Time variation of laser flare plasma temperature related to pulse parameters, using soft X radiation from plasma

18 p3154 A69-35496

High power pulsed laser welding system for structural alloys and parts, discussing pulse length, repetition rate, shielding and applicability

19 p3320 A69-35556

Focused Gaussian laser beam expansion due to thermal changes in refractive index of air, noting focused spot area increase with pulse energy

19 p3330 A69-35601

Nonlinear analog of conical refraction in biaxial crystals, considering birefringence in piezoelectric uniaxial crystals and laser beam propagation

19 p3330 A69-35604

High speed photography for hypervelocity aeroballistic ranges, using giant pulse ruby laser for front lighting

19 p3306 A69-35732

Electron concentration in hypersonic nonequilibrium shock layer flow by two wavelength laser interferometry, noting wavelength dependence of refractivity

19 p3306 A69-35742

Shock wave propagation through collisionless magnetized plasma, using gun driven, laser and cesium plasma flow methods

19 p3379 A69-35759

He-Ne laser light noises due to discharge current fluctuations and random mode beat

19 p3330 A69-35760

Ruby laser resonator losses resulting from changes in mirror transmittance or inclination, or introduction of bleachable absorbers

19 p3331 A69-35863

Solid state CW laser frequency control during operation, discussing emission properties and laser applications

19 p3331 A69-35864

Solid state laser emission frequency control and retuning using dispersive resonators, analyzing interference methods for wavelength measurement

19 p3331 A69-35865

ZnS-CdS crystals luminescence during varied forbidden bandwidth, discussing two photon and ruby laser excitation and temperature dependence

19 p3331 A69-35866

Stimulated emission characteristics of CdS-CdSe mixed crystals subjected to two photon excitation, studying pulse energy at 77 K as function of pumping power

19 p3332 A69-35867

Nonlinear Maxwell equations applied to non-monochromatic emission for nonlinear crystal situated in resonator, examining generation of second optical harmonic

19 p3332 A69-35869

Laser emission theory for indirect band-band transitions, considering light absorption by free carriers in semiconductors with polar and unpolar scattering

19 p3332 A69-35873

Kinetic theory of stationary laser emission under quasi-equilibrium conditions, analyzing emission modes

19 p3332 A69-35874

Laser multimode emission kinetic theory, discussing quasi-equilibrium disturbance effects and nature of inhomogeneity

19 p3333 A69-35875

Laser emission during disturbed quasi-equilibrium, considering emission spatial inhomogeneity due to arbitrary radiative transitions

19 p3333 A69-35876

Laser emission in system of four level centers, determining nonuniform emission line broadening due to disturbed quasi-equilibrium distribution of electron subsystem elementary excitations

19 p3333 A69-35877

Laser radiation modulation at EHF by linear electro-optical effect of KDP and ADP crystals

19 p3334 A69-35884

Multilayer lead oxide and cryolite dielectric coatings stability to ruby laser radiation, noting breakdown coherent radiation power densities

19 p3334 A69-35886

Coherent radiation generation using gas lasers, analyzing interaction between EM radiation and matter

19 p3335 A69-36067

Coherent radiation detection using laser optical sine waves, considering detection by heterodyning, laser preamplifier and parametric amplification

19 p3335 A69-36070

Multiphoton luminescence and photocurrent excitation by ruby and neodymium laser beams of KCl-Eu single crystals, noting brightness dependence on laser beam power

19 p3335 A69-36165

Cylindrical concave surface quality control by contactless comparison with reference surface, using interferometer with Twyman system and continuous laser

19 p3311 A69-36196

Memory matrices sensitivity to laser beams with various emission power densities, considering matrices of thin metal layers on transparent base

19 p3335 A69-36198

Internal modulation of HeNe laser in asynchronous regime, evaluating range and efficiency with regard to external modulation

19 p3335 A69-36341

Rb 87 vapor laser pumping, output, spectral line width and emission frequency approximated in three level system

19 p3335 A69-36342

Rb 87 vapor laser output power and spectral line width dependence on optical pumping intensity and atom density in resonator

19 p3336 A69-36343

Light induced shift of Rb 87 vapor laser emission frequency during modulated optical pumping, discussing elimination by filter temperature and tuning

19 p3336 A69-36344

Pulse ruby lasers with mercury lamps for pumping noting improved efficiency, power and temperature regime due to reduced IR radiation

19 p3336 A69-36347

Amplitude and output spectra of optical quantum amplifier based on GaAs injection laser, noting values in traveling wave and regeneration mode

19 p3336 A69-36348

Water vapor laser submillimeter emission spectra, considering rotational and vibrational lasing transitions due to electron impact and molecular interactions

19 p3336 A69-36349

Pulsed water vapor laser high power operation and strongest component wavelength measurement

19 p3337 A69-36416

Laser action from atomic bromine produced by flash photolysis of gaseous iodine monobromide, discussing pulsed output, optical gain, chemical reversibility and atomic excitation

19 p3337 A69-36444

Injection lasers threshold characteristics, studying temperature and doping level effects on current density and radiation energy

19 p3337 A69-36527

Magnetic field effects on emission line shift, threshold current and power output of GaAs injection laser, discussing spontaneous radiation in magnetic field

19 p3387 A69-36529

GaSb p-n injection laser output at 4.2 K in strong transverse magnetic field, deducing effective mass and g-factor from stimulated emission peak shift

19 p3387 A69-36530

Coherent emission from injection electron-hole plasma in indium antimonide without magnetic field, noting roles of crystal thickness and pinch effects

19 p3387 A69-36532

Temperature effects on threshold current density, emission wavelength and polarization of PbSe diode lasers

19 p3337 A69-36533

GaAs lasers emission dynamics, considering threshold amplification, spontaneous noise, nonlinear operation, etc

19 p3337 A69-36534

Radiation dynamics of GaAs injection semiconductor laser, plotting spike period dependence on resonator length

19 p3337 A69-36535

GaAs-P injection laser time delay measured from start of current flow in p-n junction diode, studying effects of memory, temperature and reverse bias

19 p3387 A69-36536

Power, efficiency and temperature dependence of emission spectra and threshold current density in electron beam pumped GaAs laser, noting doping concentration

19 p3338 A69-36538

He-Ne laser discharges noise and oscillations classified, investigating interaction between intrinsic oscillations

19 p3338 A69-36605

HCN laser line gain measurements during continuous excitation as function of current and pressure for acetonitrile and water mixtures

19 p3339 A69-36695

Carbon dioxide lasers near IR spontaneous emission spectra

19 p3339 A69-36697

Flat wire grid calorimeter used as radiation sensor in measuring pulsed ruby laser

19 p3339 A69-36755

He-Ne laser communication feasibility experiments, discussing modulation, detection, operating parameters, etc

19 p3279 A69-36756

Spectrum measurement of He-Ne laser by Fabry-Perot interferometer, determining mirrors flatness

20 p3536 A69-36945

Wavelength-surface temperature relationship of ruby laser, discussing thermal control of emission wavelength

20 p3552 A69-36967

Gas mixtures CW gain characteristics at 337 mu as function of pressure, current, mixture and flow rate, considering HCN laser systems

20 p3552 A69-36995

Laser Doppler velocimeter (LDV) for fluid velocity measurements, noting advantages

20 p3552 A69-37004

Frequency controlled unmodulated laser for long path interferometry, noting servolop correction of frequency relative to Lamb dip

20 p3553 A69-37303

Vibrational displacement phase measurement by Michelson interferometer with laser source

20 p3538 A69-37320

He-Ne laser temperature condition optimization based on calculation and experiment

20 p3553 A69-37356

He-Ne laser output intensity saturations in presence of axial magnetic field, noting moving and fixed minima

20 p3553 A69-37433

Threshold power, gain, output power and radiation energy during optical pumping of Q switched molecular laser by black body radiation

20 p3554 A69-37722

Resonant parametric oscillator stable and random phases, considering smooth frequency tuning and two quantum luminescence laser construction

20 p3554 A69-37723

Neodymium glass laser emission spatial characteristics, investigating higher laser modes excitation

20 p3554 A69-37725

Differential equations for field amplitude and level populations applicable to solid state lasers output power pulsations

20 p3554 A69-37726

Nonmonochromatic laser emission frequency characteristics, studying second harmonic generation in nonlinear KDP crystal

20 p3554 A69-37727

He-Ne laser emission tuning with thin absorbing metallic film situated near reflecting mirror

20 p3555 A69-37730

Holographic image range contouring produced by multifrequency emission from resonant output reflector in pulsed ruby laser cavity

20 p3540 A69-37733

Metastable level population measurement in laser crystal based on luminescence changes under influence of stimulated emission

20 p3555 A69-37940

Electro-optical effect in Cr-doped GaAs single crystals at room temperature, discussing carbon dioxide laser radiation modulation by GaAs

20 p3555 A69-37949

Alternated magnetic field effects on lasing in ionized Ar

20 p3555 A69-37950

Electro-optical tuning effect on frequency of parametric laser with KDP crystal, noting Curie point

20 p3555 A69-38003

Ultrashort light pulses in lasers with nonlinear absorber, evaluating random intensity peak probability created by intensity fluctuations and axial modes buildup

20 p3555 A69-38009

Active medium high gain during giant pulse generation shown to lead to radiation fluctuations

20 p3555 A69-38010

Output power spectra of Pb-Sn-Te diode laser above threshold of oscillation, demonstrating inverse dependence of line width on laser power

21 p3734 A69-38326

Ruby laser goniometric and telemetric echoes by photographing Geos satellites

21 p3671 A69-38335

Temperature dependence of stimulated light power from GaAs junction lasers operated at constant bias current above threshold

21 p3734 A69-38437

Solid state traveling medium laser pulsed emission characteristics and nonlinear intensity distribution

21 p3735 A69-38438

Interaction between modes of radiation field and active medium in laser with nonresonant feedback, discussing amplitude stabilization of total radiation

21 p3735 A69-38581

Gas molecule collision influence on photon echo intensity produced by two linearly polarized laser pulses incident on sulfur hexafluoride

21 p3774 A69-38589

Vacuum restoration by laser evaporation of active media /getters/ and vapor condensation on cold substrate applicable to nonmetallic active media /titanium-magnesium oxide/

21 p3735 A69-38590

Continuously operating multipurpose wind tunnel for laser light scattering experiments in supersonic two phase flow

21 p3689 A69-38596

Helium-neon laser output power dependence on spark-gap cross section geometry, analyzing diffusion equation and population inversion

21 p3735 A69-38693

LASER OUTPUTS

Memory effect in injection lasers output characteristics, noting anomalous increases in pulsed emission intensity with increasing current-pulse repetition rate
21 p3735 A69-38694

Q switched laser pulse propagation in nonlinear laser amplifier using bitemporal relativity theory, deriving five dimensional wave equation revealing superlight signal existence
21 p3770 A69-38839

Giant Q switched laser pulse interaction with C target in background gas showing complex luminous shock structure near target as function of time
21 p3736 A69-38942

Standing waves effect on spectral and power characteristics of laser with plane mirrors, determining dependence on pumping power
21 p3736 A69-38945

Fabry-Perot laser operation having third mirror inserted on optical axis, analyzing equations solution stability according to Liapunov
21 p3736 A69-38947

Helium-neon laser radiation of given spectral compositions, noting relation between spatial coherence and controlled number of frequencies
21 p3736 A69-38948

Measurement of helium-neon laser radiation divergence emitted in TEM sub nm modes
21 p3736 A69-38949

Laser radiation increased absorption in opaque solid body attributed to vaporization, analyzing factors determining thermodynamic equilibrium between condensed and gaseous phases
21 p3736 A69-38962

Deposited beta active thallium isotope materials angular distribution after vaporization by Q switched laser beam determined by target fragment recoil
21 p3737 A69-38992

Quantum theory for single mode laser radiation, considering photon distribution function and mean field damping decrement by phase quantum fluctuations
21 p3737 A69-38996

Current carrier concentration and magnetic field as factors influencing laser frequency resonance mixing in semiconductors with narrow forbidden bands
21 p3737 A69-38998

Electron beam pumped semiconductor laser light beam amplitude and phase distribution, studying effects of inhomogeneous excitation by model
21 p3737 A69-39041

Photographic and photometric study of absorption and reflection of ruby laser light incident on biological objects
21 p3665 A69-39060

He-Ne laser emission attenuation coefficient relation to water content of artificial fogs for 0.63, 1.15 and 3.39 microns
21 p3738 A69-39118

Argon ion laser single frequency output spectrum characteristics
21 p3738 A69-39140

Laser induced multiphoton ionization and cascade breakdown in high pressure gases, considering roles of refractive index, laser nonideal output and beam self focusing
21 p3738 A69-39445

Construction and components of laboratory water vapor laser emitting coherent radiation in far IR
21 p3738 A69-39446

Holographic interferometry by single two wavelength laser pulse exposure, discussing variable sensitivity techniques
21 p3725 A69-39448

Distance measuring method limitations for modulated CW laser determined by laser transmitter receiver in conjunction with retroreflector target fixed position
21 p3739 A69-39457

Laser profilometer to measure sea wave profiles from airborne platform, describing transmitter, receiver and signal processor
21 p3739 A69-39461

Laser design for smooth emission frequency retuning, discussing equations for laser field oscillations, two photon resonance, tensor analysis, quantum emission, etc
21 p3739 A69-39539

Emission from polymethine dye solution during optical pumping with pulses from Q switched Nd glass laser, discussing emission spectral, temporal and energy characteristics
21 p3739 A69-39542

Time characteristics and second harmonic of radiation of Nd laser containing lens systems, producing second harmonic in KDP crystal
21 p3740 A69-39544

Pumping and excitation spectra of solid solutions of cryptocyanine in glycerine irradiated by ruby laser, discussing population inversion and scattering and vibrational transitions
21 p3740 A69-39546

Amplification saturation in spatially inhomogeneous laser field, relating power to active medium and resonator parameters
21 p3740 A69-39549

Emission kinetics of passive Q switched laser without constraints on relaxation time and switching characteristics of absorption centers and medium
21 p3740 A69-39550

Gas dynamic processes during vaporization of solid material under Nd laser emission, using high speed photography
21 p3740 A69-39551

Shadow photography study of electrical discharge set off by laser spark
21 p3740 A69-39552

Spectral, angular and temporal characteristics of traveling wave mode ruby laser emission, noting high transverse divergence effect on mode operation
21 p3741 A69-39554

Negative ion concentrations in plasma by flash photodissociation, using Q switched laser for irradiation
21 p3778 A69-39574

Focal plane observation of granulation phenomena on scattering surface illuminated by coherent light from gas laser
21 p3741 A69-39575

Laser applications in combustion research, discussing interferometric, schlieren and deflection mapping, holography, velocity measurement, scattering, laser spectroscopy, ignition by laser beams, etc
21 p3741 A69-39589

Analogy between Cerenkov and quasi-Cerenkov radiation in nonlinear crystal by intense laser light used to determine conditions for quasi-Cerenkov radiation
21 p3741 A69-39669

Pulse width increase in mode locked laser caused by phase deviations, noting optical elements with quadratic dispersion of refractive index
21 p3741 A69-39683

Mode locked laser output intensity, studying effect of random phase variations on pulses
21 p3741 A69-39684

Absorption spectra from excited metastable states in tunable dye laser pumped atomic Ca, using fast flashlamp continuum
21 p3775 A69-39740

Peak power ranges of Q switched CO-air-He molecular laser, noting recovery time and CO vibrational temperature
21 p3742 A69-39742

Power density and time history of pulsed molecular nitrogen laser, discussing dependence on fill pressure and electric circuit parameters
21 p3742 A69-39779

Normal frequencies, force constants and moment of inertia of carbon dioxide isotope molecules from spectroscopic data, calculating atmospheric transmission of carbon dioxide laser radiation
21 p3742 A69-39780

Asymmetry method for precision alignment of rectilinear systems, using laser light diffraction behind misaligned target
21 p3742 A69-39781

Structural changes in Mo single crystal under action of laser radiation of various power densities
21 p3750 A69-39842

Laser application to distance measurement in air for determining atmospheric influence, using two wavelengths
22 p3959 A69-39901

Output power of CW lasers employing HCN and water vapor active medium
22 p3959 A69-39958

Laser modulation theoretical analysis based on high speed laser oscillators, discussing high energy physics research applications
22 p3959 A69-39975

GaAs injection laser properties calculation with doping levels for exponential band tails formation, deriving threshold currents, lasing frequencies, I-V characteristics, etc
22 p3959 A69-40012

Quantitative analysis of light intensity dependent changes in optical rotation angle of isotropic media caused by laser beam
22 p3959 A69-40017

Spatial coherence of He-Ne laser beam studied in Young interference experiment, noting multimode light percentage attributed to weak transverse modes
22 p3960 A69-40018

Laser range measurement from earth to lunar retroreflector to study earth tipping and gravitational constant secular decrease
22 p3960 A69-40190

He-Ne laser system for micromachining thin film photolithographic masks, describing computer controlled coordinate table and product quality
22 p3954 A69-40236

Gas laser-Doppler radar system for moving materials velocity and length measurements in industrial processes
22 p3955 A69-40237

Laser interferometric length measurement by fringe counting, considering mechanical and optical systems limitations and design tolerances
22 p3960 A69-40238

Photoelectric methods for pulsed and CW lasers output power and energy measurements
22 p3961 A69-40239

Laser safety factors in open air applications, discussing pulse length, energy spatial distribution, atmospheric attenuation, human eye sensitivity, etc
22 p3892 A69-40241

Calorimeters for laser energy measurement, discussing radiation damage avoidance and modifications for various modes
22 p3961 A69-40243

Device measuring light pressure and pulse energy of laser emission by converting kinetic energy into potential energy of twisted elastic suspension thread
22 p3961 A69-40246

Cavity Q dependence of intensity of single mode He-Ne laser above threshold for quantum and semiclassical theories
22 p3961 A69-40415

Laser beam self focusing in plasma in terms of ponderomotive acceleration due to light intensity gradient
22 p3961 A69-40417

Carbon dioxide laser development, discussing gain, static amplifier and high pressure operations
22 p3962 A69-40474

Absorption and fluorescent spectra, relaxation times and quantum efficiencies measured for glasses doped with trivalent erbium, reviewing spectroscopic parameters involved with laser effect
22 p3962 A69-40476

Density, ion temperature, electron temperature and ion drifts in Ba or Ba doped plasmas determined by resonance fluorescence and optical pumping
22 p3962 A69-40532

Ruby laser resonator mirror mechanical vibrations effects on emission temporal behavior, spectral output and far field pattern, describing conditions for spiking
22 p3962 A69-40562

Spiking behavior detection in Q switched light output from GaAs pulsed junction laser, noting width at high pumping levels
22 p3963 A69-40563

Carbon dioxide and carbon dioxide mixture mirror Q switched laser peak power generation, using pulsed excitation
22 p3963 A69-40564

Electron beam pumped dislocation free GaAs lasers filamentary and nonuniform emission characteristics from X ray topographs before and after bombardment
22 p3963 A69-40565

Q switched pulsed discharge carbon dioxide laser, determining peak power dependence on delay between pulse excitation and Q switching
22 p3963 A69-40566

Laser shadowgraph technique for visual observation of projectiles surface flying at hypersonic velocity along ballistic trajectory
22 p3963 A69-40601

Lasing properties of spontaneous emission hemispherical semiconductor diode with AlAs-GaAs junctions measured by calibrated silicon photocell
22 p3964 A69-40608

Laser produced Sb and Te vaporization near critical point, using time of flight mass spectrometer
22 p3993 A69-40719

Photographic study of epoxy resin breakdown kinetics under pulsed laser beams, showing crack area as function of time
22 p3973 A69-40743

Laser radiation power and electron concentration in He-Ne plasma measured by microwave diagnostics
22 p3964 A69-40794

Population and excitation rates of working levels of carbon dioxide laser calculated on basis of emission

power, amplification coefficient and spontaneous emission intensity

22 p3964 A69-40795

Neodymium activated glass laser efficiency as function of absorption of pumping and emission energy by glass

22 p3964 A69-40797

Mach-Zehnder laser interferometer for measurements of electron density in transient Hg vapor plasma, noting agreement with microwave measurements

22 p3965 A69-40924

Argon laser lower operating level decay probabilities, using spectrum analysis to study role of radiative decay

22 p3965 A69-40965

Holographic technique of coherent light field transformation with desirable phase distribution from laser light beams of arbitrary wavefront characteristics

22 p3950 A69-41115

Electron-positron pair formation in electromagnetic field created by coherent laser light focused into vacuum with ideal lens

22 p3965 A69-41116

Chemical high pressure laser action produced by stimulated phototransition of electrons at contact moment between pair of reacting nonexcited gas molecules

22 p3965 A69-41117

Quantum mechanical multimode correlation functions derivation and applications to laser theory

22 p3965 A69-41152

Reaction zone following overdriven detonation wave propagating into mixtures of fluorine oxide and hydrogen molecules showing HF laser emission

22 p4052 A69-41188

Mirror mount for shock tube laser cavity with alignment capability, noting seal against internal pressures

22 p3951 A69-41233

Pumping model for analyzing stimulated and enhanced potassium multiphoton emission primed by ruby laser-stimulated Raman electronic radiation

23 p4171 A69-41391

Gaseous absorption cell variable attenuator for carbon dioxide laser radiation at specific wavelength, using forced convection to eliminate thermal defocusing effects

23 p4172 A69-41396

Far IR gas laser with linearly polarized radiation output obtained by using echelette reflection grating in place of end mirror

23 p4172 A69-41400

Slow combustion laser spark at intensity below optical breakdown obtained by focusing radiation pulse of Nd glass laser in discharge gap

23 p4172 A69-41492

Hydrogen fluoride chemical laser emission spectrum, studying rotational-vibrational transition of molecules triggered optically or electrically

23 p4172 A69-41493

Nitrogen-carbon dioxide-helium lasers CW operation at various pressures and N flow rates

23 p4173 A69-41496

Closed cycle gas cooling techniques for self contained CW kilowatt carbon dioxide laser, relating output power to flow velocity and input power

23 p4173 A69-41497

Intensity of optical pulses from CW GaAs injection lasers observed with fast sampling techniques

23 p4173 A69-41500

High output laser amplifier consisting of glass and selenium oxychloride/Nd liquid lasers

23 p4173 A69-41565

Output power dependence of repetitively Q switched carbon dioxide laser on repetition time measured with thermopile, noting decrease in mirror system

23 p4173 A69-41566

Photochromic film behavior under high power argon ion laser excitation studied for display and computer memory applications, using excitation model

23 p4173 A69-41629

Pure water vapor and water vapor-air mixture continuum absorption of carbon dioxide laser radiation measured to determine atmospheric attenuation

23 p4173 A69-41631

Sweep tuning gas laser and output power vs frequency characteristics, demonstrating tuning ability within entire Doppler bandwidth

23 p4174 A69-41635

Temporal reference acoustical holography with Sokolov ultrasound camera system using double pulsed ruby or scanning CW laser

23 p4166 A69-42182

Retroreflector and Scotchlite object images obtained in long range holography with Q switched ruby laser, noting atmospheric seeing conditions

23 p4167 A69-42184

Absorption coefficient measurement for hydrocarbon gases for He-Ne laser beam at 3.39 microns, tabulating coefficients, noting variations from spectroscopic data

23 p4174 A69-42192

Ground to satellite laser ranging experiments for daylight satellite range measurements

23 p4174 A69-42193

Neodymium laser radiation effect on electrical and histomorphological properties of liver in rats and hamsters

23 p4111 A69-42344

Laser hazard probability assessment in various applications, discussing power characteristics, attenuation by absorption and scattering and radiant energy spatial distribution

24 p4327 A69-42576

Albino guinea pigs respiration rates and ear skin histology after exposures to coherent ruby laser light

24 p4270 A69-42578

Photosynthesis enhancement in seaweed after alternate exposure to gas laser and tungsten lamp white light passed through IR narrow band filter

24 p4270 A69-42580

N or He additions effects on carbon dioxide laser design and power output

24 p4327 A69-42640

High temperature plasma generation by high power laser beam irradiation on small solidified gas particle, detailing experimental equipment and procedures

24 p4354 A69-42645

Blast wave energy determination of laser-induced gas breakdown in hydrogen, nitrogen, helium, argon and xenon in pressure chamber

24 p4299 A69-42651

Ruby laser crystal energy emission related to crystal rate of motion

24 p4327 A69-42652

Laser granularity effects on brightness discrimination [AAS PAPER 69-464]

24 p4272 A69-42843

Log amplitude mean value for Gaussian or laser-like optical beam propagating horizontally in turbulent atmosphere

24 p4282 A69-42970

Fraunhofer hologram of glass fiber by Be X rays reconstructed using He-Ne laser light

24 p4314 A69-42973

Amplified radiation of laser used for coherent optical pumping in two level low pressure gas laser

24 p4327 A69-43067

Ultrashort laser light pulses self focusing and determination of focal points coordinates

24 p4328 A69-43068

Emission spectrum of nonself locked He-Ne ring laser, deriving phase relations for LF intermode oscillations

24 p4328 A69-43159

Polarization characteristics of He-Ne ring laser emission with circularly anisotropic resonator, analyzing ellipticity as function of half wave cavity plate

24 p4328 A69-43160

Beam divergence and multimode laser visible emission influence on power and angular structure of second optical harmonic generated in KDP crystals

24 p4328 A69-43161

High power ruby laser pulse generation by diffraction modulator, employing modulated ultrasonic traveling waves at minimum resonator transmission losses

24 p4328 A69-43163

Transitions competition in He-Ne laser pulse operating in single mode with nonuniform gain saturation

24 p4328 A69-43165

Teflon dielectric properties evaluated during fast laser beam heating, noting presence of C by microwave measurement

24 p4336 A69-43266

Oscillographic recording of GaAs laser ultrashort radiation pulses, using isolated injection regions and semiconductor photodiode as photoelectric converter

24 p4329 A69-43740

Diffraction coupling of power from carbon dioxide laser, computing angular distribution of output light

24 p4329 A69-43753

Thermal turbulence effects on phase fluctuations of laser beams, studying temporal decay of mean square refractive index fluctuation with fringe pattern displacements

24 p4329 A69-43754

Dielectric and semiconductor films vacuum deposition by CW carbon dioxide laser, discussing optical properties

24 p4329 A69-43755

Scanning Fabry-Perot interferometer interaction with laser source, calculating laser intensity and oscillation frequency changes for weak mode coupling

24 p4329 A69-43756

GaAs laser diodes differential external quantum efficiency and gain per unit length dependence on laser reflectivity, taking into account optical losses

24 p4330 A69-43766

GaAs laser diodes differential external quantum efficiency and gain per unit length dependence on laser resonator length, taking into account optical losses

24 p4330 A69-43767

GaAs junction laser total stimulated light power dependence on resonator length taking into account optical losses

24 p4330 A69-43768

LASER RADAR

U OPTICAL RADAR

LASERS

NT ARGON LASERS
NT CARBON DIOXIDE LASERS
NT CHEMICAL LASERS
NT GALLIUM ARSENIDE LASERS
NT GAS LASERS
NT INFRARED LASERS
NT INJECTION LASERS
NT LIQUID LASERS
NT ORGANIC LASERS
NT PULSED LASERS
NT Q SWITCHED LASERS
NT RING LASERS
NT RUBY LASERS
NT SEMICONDUCTOR LASERS
NT SOLID STATE LASERS

Laser gyro applications including guidance, navigation and control problems

02 p0248 A69-11741

Laser applications in metal working including dissimilar metal welding, hole drilling, material removal and dynamic balancing

[ASTME PAPER MR68-406]

02 p0252 A69-11796

Laser application to machine tool accuracy and alignment

[ASTME PAPER MR68-407]

02 p0252 A69-11797

Glass pleats and cold cathodes in laser discharging tube, discussing angular displacements

03 p0435 A69-12981

Pumping beam width influence on optical range resonator excited coupled oscillations, deriving approximate equations

03 p0437 A69-13043

Parametric light generation employing KDP nonlinear crystals with mechanically tuned frequency

03 p0437 A69-13045

Cathode sputtering and thermal evaporation in vacuum used for preparing thin dielectric coatings on mirrors of optical resonators containing nonlinear crystals

03 p0438 A69-13049

Laser display technology, discussing experimental systems, light sources, modulation and scanning

03 p0431 A69-13850

Neodymium glass properties degradation during laser operation due to short wave pumping radiation and stimulated emission

03 p0442 A69-14219

Optical performance of coupled Fabry-Perot resonators with additional mirrors, determining frequency separation parameters due to third mirror

04 p0612 A69-15372

Papers on gas, glass and injection lasers, nonlinear optics and frequency stabilization of gas lasers

05 p0772 A69-16225

Laser displays for information transfer to provide improved computer driven read-out techniques, noting real image and holographic displays

06 p0928 A69-17924

Collection of papers on lasers noting solid state, gas and semiconductor types, basic principles and applications

06 p0936 A69-18002

Lasers, reviewing phenomenology, physical and theoretical fundamentals, quantized energy levels, population of energy levels and laser components

06 p0936 A69-18003

Atomic physics of lasers and active materials, noting multiplet spectra of atoms, molecular spectroscopy, energy level population distribution and amplification

06 p0937 A69-18004

Laser resonators, noting relation of light path between mirrors to half wavelength and line equivalence of lenses and resonators
06 p0937 A69-18005

Laser amplifiers and oscillators, discussing conversion of active atom excitation energy into light energy
06 p0937 A69-18006

External and internal modulation methods in lasers noting phase, amplitude and frequency modulation, birefringence, electrooptics and Stark and Zeeman effects
06 p0937 A69-18010

Fluctuation phenomena in electromagnetic field in optical spectral region and coherence characteristics of optical fields, analyzing quantum noise
06 p0937 A69-18011

Microwave and optical generation and amplification - Conference, Hamburg, September 1968
07 p1090 A69-18420

Difference frequency generation by multiple quantum transition from laser medium considered as resonant optical frequency mixing device
07 p1144 A69-18470

Traveling wave microwave and optical resonators synthesis, determining design conditions for resonant frequencies
07 p1145 A69-18477

Desired laser characteristics for space communications compared to existing lasers
07 p1146 A69-18483

Automatic laser tracker system for close-up photographic coverage of rocket test [SMPT PREPRINT 101-91]
07 p1116 A69-18949

Optical resonator as Q meter, discussing error capability and construction
08 p1312 A69-20106

Ion laser construction, detailing water cooled quartz tubes, electrodes, adjustable mirrors, etc
09 p1515 A69-21487

Lasers, reviewing output properties, control and modulation characteristics, and applications to communications, plasma generation, measurement, high temperature metallurgy, etc
09 p1517 A69-22118

Nonlinear optics, discussing materials, polarization, harmonic generation, light mixing, parametric amplification and oscillation, stimulated scattering, absorption, reflection, refractivity and self focusing
09 p1518 A69-22124

Fabry-Perot resonator and beam waveguide systems for laser beams, noting mode coupling and separation in laser optical systems
09 p1518 A69-22125

Light wave reconstruction including polarization, using single reference beam with depolarizing diffuser as source
10 p1690 A69-22951

Laser theory and operations including types and applications
10 p1702 A69-23384

Laser applications to high temperature, gas dynamical and plasma phenomena
10 p1741 A69-23809

Resonator field inhomogeneities effect on transient processes in quantum oscillator, considering two active crystals in cavity
10 p1705 A69-23948

Lasers and opto-electronics - Conference, University of Southampton, England, March 1969
11 p1897 A69-25034

Active scanning Fabry-Perot interferometer interaction with mode matched laser resonator, analyzing phase and intensity of reflected wave of active three mirror resonator
11 p1886 A69-25047

Dielectric loss tangents measurements combining coherent optical resonator with microwave techniques, noting application at mm wavelengths
12 p2080 A69-26057

Lasers application to measurement techniques including alignment, direction, distance, elongation, interferometric, holographic, etc
12 p2094 A69-26903

Soviet collection of papers on nonlinear optics, discussing lasers, electromagnetic interactions, Q switching, dynamics, etc
12 p2109 A69-26905

Laser active media polarization in strong electromagnetic fields, solving boundary value problems
12 p2110 A69-26907

Inhomogeneous permittivity and boundary effects influence on electric fields of laser with open cavity containing inhomogeneous active medium
12 p2110 A69-26908

Two photon and resonance parametric lasers nonlinear polarization theory, deriving equations for electromagnetic field oscillations
12 p2110 A69-26910

Zeeman laser with one end mirror exhibiting x-y-type loss anisotropy, considering resonance condition for round trip pass and self consistent field equations
13 p2271 A69-27398

Laser based on carbon dioxide molecules formed chemically in electrical discharge studied for designing special carbon electrode laser
13 p2274 A69-28585

Acoustic hologram recorded by laser flying spot scanner
13 p2265 A69-28662

Quasi-distribution function differential equation for laser field with nonMarkoffian character derived from density matrix master equation
14 p2486 A69-29633

Laser spark plasma initial development phase showing high electron temperature and concentration, continuous spectrum emission, line broadening and shock wave formation
14 p2461 A69-29779

Helium plasma electron temperature and concentration measured in arc in magnetic field by laser light scattering at electrons
14 p2496 A69-29780

Negative dispersion of light in neodymium activated calcium tungstate single crystal using neodymium glass laser source, analyzing interference bands in spectral diagrams
15 p2632 A69-30051

Energy exchange between active centers in silicate and phosphate glass, comparing luminescent and lasing properties
15 p2632 A69-30053

Wave reflection in laser resonators with ferrite end faces, determining oscillation spectra and wave amplitudes
15 p2579 A69-30954

NASA laser systems for satellite tracking, determining ranging accuracy by comparing laser and computed reference orbital data
15 p2571 A69-31312

Lasers for satellite range measurements, discussing power output, mount, accuracy and data
15 p2571 A69-31337

Optical performance of coupled Fabry-Perot resonators with additional mirrors, determining frequency separation parameters due to third mirror
16 p2797 A69-32119

Quantum electronics, Volume 2, Maser amplifiers and oscillators
17 p2982 A69-33687

Simultaneous integral equations numerical solution for open optical resonator mode analysis, using kernel function and Fresnel approximation
17 p2983 A69-33883

Polarization, frequency and energy characteristics of lasers with resonators containing polarization transforming elements
17 p2983 A69-33967

Laser technology applications stressing engineering, control, communications, medicine, space sciences, holography, computers, etc
17 p2984 A69-34163

Book on laser operation and applications, discussing radiation characteristics, monochromatic properties, coherence, directionality, polarization, power, excited state kinetics, optical transitions, etc
18 p3151 A69-34357

Wave equation of electromagnetic field of optical resonator with arbitrary mirrors, utilizing Schroedinger equation and equivalent mechanical system
19 p3333 A69-35880

Apollo 11 moon reflector-laser beam experiment, discussing range changes produced by axial rotation and orbital motion and use for earth-moon dynamics
19 p3339 A69-36766

Nonlinear optics, properties, light waves interaction, forced scattering and application in laser technology
20 p3555 A69-38014

Vortex flow air cooling system for lasers using vortex effect of gas separation, resulting in minimum weight and dimensions and high cooling efficiency
21 p3734 A69-38399

Ring laser bias in angular rotation measurement using optical phase shifters
21 p3735 A69-38651

Laser research from theoretical stage to present, discussing applications
21 p3736 A69-38781

Lasers as tools for integrated circuits fabrication, noting roles of various laser operating parameters
21 p3742 A69-39705

Lasers and mechanical engineering - Conference, London, November 1968
22 p3960 A69-40234

Intersatellite microwave laser communication system for ATS-F and ATS-G, discussing experiment, functional design and parameters
23 p4120 A69-41758

Portable He-Ne laser design featuring positional adjustment for use in aligning optical systems
24 p4327 A69-42924

RF and microwave signal variable delay and processing using laser-acoustic interactions, photodetector and electrical-to-acoustical transducer
24 p4283 A69-43027

Lunar laser beam retroreflection observations, showing agreement with predicted ephemeris and signal strength
24 p4384 A69-43197

Laser beam circuitry miniaturization facilitating laser circuit assembly isolation from thermal, mechanical and ambient changes
24 p4328 A69-43327

LASV U F-111 AIRCRAFT

LATCHES

Microminiature latching relay design and manufacturing cost
13 p2232 A69-28049

LATENCY U REACTION TIME

LATERAL CONTROL

Missile control during propulsion period, emphasizing vane deflection required for lateral wind compensation
01 p0163 A69-11297

Semipassive attitude control system providing one degree pointing accuracies in all axes
07 p1226 A69-18326

Thrust, bank angle and angle of attack of aircraft minimum fuel lateral turns at constant altitude and specified velocities
13 p2203 A69-28245

Lifting rotor dynamics and undesirable characteristics reduction, discussing feedback control systems for pitch and roll [AHS PAPER 340A]
17 p2899 A69-33509

VSTOL aircraft aerodynamic roll motion control requirements at low speeds
20 p3574 A69-37514

LATERAL OSCILLATION

Longitudinal structural vibration and lateral bending response mass and spring coupling in Saturn AS-502 during boost with longitudinal excitation by pogo effect [AIAA PAPER 69-58]
06 p1019 A69-18204

Stability analysis of missile lateral supersonic flutter based on Lagrange equations, considering conservative thrust, control deviation and aerodynamic forces
17 p3045 A69-32946

Vibrating circular plate standing wave lateral displacements visualization by photographically recorded moire patterns
20 p3537 A69-37067

LATERAL STABILITY

Equations of motion of point restricted tethered parafoil for investigating longitudinal and lateral dynamic stability
01 p0009 A69-10415

Supersonic interference on lateral stability of planar configurations analyzed using wind tunnel data [AIAA PAPER 68-21]
02 p0189 A69-12377

Root locus method applied to longitudinal and lateral stability of aircraft with flexible fuselage and wing
04 p0677 A69-14835

Lateral stability of glider towed by cable in steady rectilinear horizontal flight, deriving motion equations as ordinary differential equations
09 p1433 A69-21498

Attitude control system effect on roll resonance in rocket boosted projectile
09 p1610 A69-22001

Satellite three axis attitude control analysis showing rolling and longitudinal stabilization possibility by flywheel, with validity tested by analog simulation
17 p3048 A69-33240

Stress-strain state in thin isotropic plate with circular hole under lateral bending and torsional moments
21 p3835 A69-38725

LATERALITY U LATERAL STABILITY

LATERALIZATION U LATERAL CONTROL

LATITUDE NT GEOMAGNETIC LATITUDE

Time and latitude variations of blanketing sporadic E of different intensities

01 p0070 A69-11159

Latitude dependence of earth spectral radiation intensities, discussing satellite observations in equatorial and subtropical regions

03 p0422 A69-13507

Sunrise modal interference patterns for VLF propagation, analyzing variations with latitude

03 p0396 A69-13628

Mean tropospheric wind vectors periods compared to annual variations of earth rotation and pole latitude

08 p1309 A69-20854

Solar activity influence on cosmic ray intensity 11 year variation, taking into account heliostitudinal movement of sunspot regions in solar cycle as evidence of density gradient

10 p1754 A69-22802

Nonpolar LF latitude variations based on spectroscopic and harmonic analysis of zenith telescope and prismatic astrolabe observations

11 p1956 A69-24401

Seasonal and latitudinal models of atmospheric wind and temperature structure between 30 and 120 km altitude

15 p2600 A69-31367

Latitude variations of day and night ionospheric critical frequencies, inhomogeneity and ionization, discussing generation of r type sporadic E layer in auroral zone

17 p2964 A69-33963

Latitudinal variations in conditions for F 1 layer occurrence probability and stability during solar activity minimum period

20 p3527 A69-37669

Satellite observations of auroral particle precipitations indicating latitude dependence of auroral electrons averaged pitch angle and energy spectral distributions

22 p3938 A69-40502

Nonpolar LF latitude variations based on spectroscopic and harmonic analysis of zenith telescope and prismatic astrolabe observations

24 p4391 A69-43791

LATITUDE MEASUREMENT

Royal Belgian Observatory studies on time, meridian, seismological and gravimetric services, latitude variation due to polar motion, terrestrial tides and geodetic satellites

08 p1306 A69-19992

Latitude measurements for features on Saturn, discussing means and standard deviations

08 p1394 A69-20618

Nonpolar latitude variations due to observation errors, discussing instrumental, computational and meteorological influence, particularly refraction resulting from climatic conditions

11 p1952 A69-24257

Nutation period of 18.6 years using data from International Latitude Service

17 p3027 A69-32868

Earth polar coordinates determined from latitude observations, discussing weighting functions for determining polar motion

17 p2959 A69-32869

Nighttime latitude variations in Danjon astrolabe observations at Poltava, noting decrease from early evening to midnight

17 p2959 A69-32870

Differences in latitude readings obtained with two zenith telescopes, showing Pearson distribution of type VII and influence of observation conditions

17 p2959 A69-32879

LATTICE IMPERFECTIONS

U CRYSTAL DEFECTS

LATTICE PARAMETERS

Lattice deformation relationship to dislocation density in vanadium carbide powders

02 p0265 A69-12001

Temperature dependence of A and C periods of Y crystal lattice at 77 to 300 K, discussing preparation of Y films and anomalous thermal expansion

02 p0298 A69-12047

Lattice parameters of austenitic Fe-Ni-Ti alloys as function of titanium content, using Debye-Scherrer camera

03 p0443 A69-13123

X ray study of scandium containing ferrites, establishing lattice stresses due to ion replacement in octahedral interstices

03 p0491 A69-14053

Young modulus of sintered nonporous titanium, zirconium and chromium nitrides, computing charac-

teristic temperature and root mean square atomic displacements in lattices

06 p0938 A69-16830

Lattice strains in matrix phase of aluminum-boron and copper-tungsten composites measured by X ray diffraction

06 p0939 A69-16944

Oxygen diffusion parameters in beta-titanium measured by successive layer removal, noting lattice constant dependence on temperature

07 p1163 A69-18783

Lattice location of dopant elements implanted into Ge determined by carbon ion backscattering, noting substitutional concentrations above thermal equilibrium solubilities

07 p1199 A69-18903

Relative heats of formation and reduced melting temperatures of lanthanide compounds correlated to lanthanide contraction

07 p1168 A69-19597

InAs-InP solid solutions diffusion rate and lattice constant for various compositions

12 p2144 A69-26587

Characteristic temperature, Young modulus and rms atomic displacement in metal borides of various porosities, using dynamic method based on ultrasonic oscillations measurement

12 p2115 A69-26615

Mu phase lattice constants and cell volume in Nb-Zn system

15 p2636 A69-30086

Nb and Ti carbides investigated for lattice parameters, microhardness and resistivity in homogeneity domain

15 p2638 A69-30282

GaAs zinc gallium selenide solid solutions properties, analyzing lattice constant, microhardness, forbidden zone and concentration relationships

15 p2670 A69-31050

Phase equilibria in ternary systems Nb-Fe-B and Nb-Co-B, determining structural types and lattice constants by using X ray and microstructural analysis

15 p2641 A69-31246

Titanium alloy martensites crystallography by electron microscope, discussing lattice parameters and spontaneous transformation

18 p3154 A69-34245

X ray study of scandium containing ferrites, establishing lattice stresses due to ion replacement in octahedral interstices

18 p3182 A69-35046

Critical transition temperature of vanadium oxide semiconductors as function of doping element content and lattice constant, using X ray diffraction

23 p4198 A69-41564

Spin-phonon systems thermal noise, based on combined lattice and spin lattice Hamiltonian densities, applied to acoustic noise field measurements

24 p4350 A69-43061

LATTICE VIBRATIONS

Carbon dioxide laser for observing nonlinear effects related to electron interaction with lattice vibration within semiconductors

03 p0437 A69-13041

InSb semiconductors electron scattering analysis at ionized impurities and optical and acoustical lattice vibrations with various polarizations

03 p0492 A69-14170

Displacement correlations and frequency spectra for mass disordered lattices, deriving cluster expansion for phonon Green function

03 p0493 A69-14241

Hydrodynamic and lattice vibrations equations for coupled waves in ion semiconductors in external electric and magnetic fields, observing sound amplification

06 p0978 A69-16897

Finite amplitude longitudinal wave propagation in lattices analyzed by study of compressive wave in chain of mass points with nearest neighbor interaction

06 p1022 A69-17367

Consistency of high temperature equation of state of solids, considering Gruneisen parameter and lattice dynamics

08 p1419 A69-19814

Time average holography for analysis of vibrations, overcoming fringe peak decrease with large amplitude and loss of phase information

09 p1495 A69-21749

Anharmonic lattice vibrations, specific heats and coefficient of linear expansion of solids at high temperatures, noting interatomic spacing

10 p1809 A69-23653

Diamond-like glassy semiconductor compound of cadmium germanium arsenide, determining optical lattice vibrations from IR reflection spectra

10 p1747 A69-23963

Raman effect in potassium dichromate single crystal, discussing symmetrical and antisymmetrical internal vibrations of free ions

12 p2105 A69-26285

Solid state physics applications to fracture problems and structure of solids, considering crystallography, lattice vibrations, defects, electron bands, alloys and surface physics

13 p2316 A69-27221

Bound excitons spectra in Cu doped gallium arsenide crystals, analyzing line oscillation structure and uniaxial compression effect

16 p2824 A69-31571

Lattice vibration theory of solid state diffusion for Cu including anharmonic effects formulated using equilibrium statistical mechanics, considering interacting phonon events

17 p3015 A69-32822

Raman spectrum of solid alpha-nitrogen at low temperatures, calculating scattering intensities and Raman active librational lattice vibrations

23 p4194 A69-42204

IR lattice spectra of rare earth Al, Ga and Fe garnets, discussing oxygen anion, translational rare earth cation and crystal lattice external motions

24 p4360 A69-42974

LATTICES

Foldable tubular connection application to expandable lattice structure, analyzing cross sectional distortions

06 p1024 A69-17608

LATTICES [MATHEMATICS]

NT BOOLEAN ALGEBRA

NT BOOLEAN FUNCTIONS

Serial BCD binary coder design, using Karnaugh diagrams to minimize synchronous and asynchronous counter stages

09 p1467 A69-22579

LAUNCH COMPLEXES

U LAUNCHING BASES

LAUNCH DATES

Europe 1 carrier rocket prelaunch wind load calculations as base for launch or delay decision

01 p0160 A69-10032

Launch opportunity and window constraints, considering injection energy and precision, reference body occultation, communications range, etc

20 p3617 A69-37287

LAUNCH VEHICLE CONFIGURATIONS

Turquoise satellite booster, using stages of SSBS and MSBS ballistic missiles

02 p0334 A69-12232

Cryogenic core concept for flexible and economical delivery system [AIAA PAPER 68-812]

21 p3827 A69-39753

LAUNCH VEHICLES

NT ATLAS CENTAUR LAUNCH VEHICLE
NT ATLAS SLV-3 LAUNCH VEHICLE
NT CENTAUR LAUNCH VEHICLE
NT DIAMANT LAUNCH VEHICLE
NT ELDO LAUNCH VEHICLE
NT EUROPA LAUNCH VEHICLES
NT EUROPA 1 LAUNCH VEHICLE
NT EUROPA 2 LAUNCH VEHICLE
NT EUROPA 3 LAUNCH VEHICLE
NT RECOVERABLE LAUNCH VEHICLES
NT SATURN LAUNCH VEHICLES
NT SATURN 5 LAUNCH VEHICLES
NT SCOUT LAUNCH VEHICLE
NT TITAN LAUNCH VEHICLES
NT TITAN 3 LAUNCH VEHICLE

Data analysis methods for integrated data processing system for onboard in-flight checkout for launch vehicle evaluation [AIAA PAPER 67-911]

01 p0037 A69-11024

Soviet rocketry origin, technology, launch vehicles, boosters and orbital assembly concept

01 p0162 A69-11066

Systematic approach to standard launch vehicle based on governmental expenditure minimization while attaining mission goals

01 p0162 A69-11096

Low profile bulkheads for launch vehicles and spacecraft compartments to obtain structural weight reduction [AIAA PAPER 68-355]

02 p0334 A69-12370

Liquid propellant space launch vehicles longitudinal modes natural frequency, discussing coupled engine-propellant supply system stability [AIAA PAPER 68-289]

02 p0335 A69-12393

LAUNCH WINDOWS

Future space programs as governed by cost limitations, suggesting development of economical launch vehicle for shuttling between earth and orbital space stations

02 p0326 A69-12680

Angular motion during first stage cut-off of Europa 1 launch vehicle from flight tests compared with theoretical predictions

03 p0519 A69-12856

HM 4 rocket motor for second stage of Diogene booster, using LOX and hydrogen propellants

04 p0647 A69-15064

Spacecraft launching facilities and payload capabilities in next decade, discussing orbits, spacecraft size and volume, attitude stabilization and positional accuracy

06 p1012 A69-16857

Dynamics of carrier rockets and space vehicles having complex three dimensional thin walled constructions with cavities containing liquids

[UN PAPER 68-95622] 06 p1013 A69-17051

Optimum attitude program for multistage satellite launch vehicle with impact restrictions

07 p1229 A69-18492

Space boosters, performance of launch vehicles and requirements for future U.S. space launch capability from USAF vantage point

08 p1410 A69-20882

Future launch vehicle programs for automated space missions, discussing higher launch velocities and economics

[AIAA PAPER 68-447] 09 p1610 A69-21983

Computer design for booster/satellite control, discussing systems reliability, low power and tradeoffs

11 p1843 A69-25320

Materials rating method in pressure vessel applications, considering impact on design of minimum cost space launch vehicle

12 p2175 A69-26844

Soviet space program, discussing launch sites, series of launch vehicles and mission identification

13 p2381 A69-27303

Boosters and space vehicles including earth satellites, lunar probes and interplanetary spacecraft

13 p2356 A69-27914

Market analysis program to evaluate relationship between launch vehicle jettison weight and total cost based on all projected missions

[SAWE PAPER 776] 18 p3208 A69-34872

Rocket launch system cost role in space operations, discussing low cost expendable drop tank and Triamese reusable launch vehicle/spacecraft concepts

18 p3210 A69-35087

Parameter optimization of launch vehicle attitude control system of fixed structure for various computation techniques

18 p3210 A69-35092

Earth orbital space program mission effectiveness increased through utilization of standby launch vehicles, spacecraft and space station systems

19 p3430 A69-36010

Reliability study of launch support equipment, presenting failure data for mechanical and electromechanical components

19 p3295 A69-36023

Attitude control system for launch vehicles, providing commanded thrust vector angle proportional to desired angular displacement of acceleration vector

21 p3819 A69-39032

Launch vehicle cost reduction by minimizing software, fabricating in commercial shops and avoiding sophistication, parts and acts of man

21 p3857 A69-39688

Cost reduction steps in reusable launch vehicle design, discussing aircraft design and development experience application

21 p3826 A69-39689

Launch systems evolution, cost reduction breakthrough approach and application to future space transportation

21 p3857 A69-39692

Vehicle designs and cost analyses for launch vehicle selection to minimize costs of 40,000-150,000 pound payload placement into orbit

21 p3827 A69-39694

Support software costs reduction for launch vehicle systems by implementing computer techniques to provide requisite data

[AIAA PAPER 69-978] 22 p4052 A69-40358

Adaptive cost equations in computer programs supporting launch vehicle long range planning, based on launch vehicle anticipated usage

[AAS PAPER 69-164] 24 p4392 A69-42815

Launch vehicle upper stage requirements in space missions, discussing space engine for lunar, planetary and interplanetary exploration

[AAS PAPER 69-359] 24 p4418 A69-42828

Cost analysis in low cost launch vehicle studies emphasizing sustaining engineering and plant economics

24 p4393 A69-43120

Attitude control system with rate of change limiter to minimize launch vehicle drift during first stage ascent through atmosphere

24 p4394 A69-43277

Launch vehicle control system synthesis based on mode control theory state variable formulations

24 p4394 A69-43278

LAUNCH WINDOWS

Mission capability differences between direct and orbital Mars missions as to launch period selection, targeting capability and error analysis

02 p0331 A69-12821

Release windows for auxiliary body ejection from satellite in eccentric orbit, discussing visibility, celestial body interference, etc

03 p0505 A69-13003

Solar radiation protection of radiometers and spectrometers on reentry vehicle by launching times and solar view field selection

04 p0666 A69-15511

Multiple impulse orbital departure window for manned interplanetary spacecraft, discussing launch delay, space assembly, refueling and checkout, etc

[AIAA PAPER 69-126] 06 p1010 A69-18065

Mission windows for single and multiple planet swingbys past Jupiter to outer planets

[AAS PAPER 68-115] 19 p3402 A69-35936

Launch opportunity and window constraints, considering injection energy and precision, reference body occultation, communications range, etc

20 p3617 A69-37287

Optimum midcourse impulses effects on heliocentric launch window, comparing two and three impulse delta 5 performance for two and three dimensional solar system models

[AAS PAPER 68-095] 21 p3804 A69-39201

Triple planet ballistic flybys, discussing mission opportunities and launch windows

[AAS PAPER 68-114] 21 p3805 A69-39206

Mission analysis for 1972 Venus launch opportunity, discussing launch period selection and trajectory constraints for Atlas/Centaur vehicle

[AAS PAPER 68-135] 21 p3805 A69-39208

Synchronous communications satellite launch constraints for fixed time or node, noting application to IDCSP/A mission and sun angle, occultation and transfer orbit

[AIAA PAPER 68-445] 22 p4036 A69-40543

LAUNCHERS

NT AIRCRAFT LAUNCHING DEVICES

NT CATAPULTS

NT GUN LAUNCHERS

NT HYPERVELOCITY LAUNCHERS

NT MOBILE MISSILE LAUNCHERS

NT ROCKET LAUNCHERS

High enthalpy, Mach and Reynolds number flight studies on ballistic ranges, describing launchers, flight simulation, measuring and recording techniques

06 p0860 A69-17632

Cape Kennedy Space Center mobile launchers and auxiliary equipment for Saturn vehicles, discussing functions, design and systems

24 p4297 A69-43036

LAUNCHING

NT AIR LAUNCHING

NT LUNAR LAUNCH

NT ORBITAL LAUNCHING

NT ROCKET LAUNCHING

NT SPACECRAFT LAUNCHING

International liability for damage caused by launching of objects into outer space

[UN PAPER 68-95337] 01 p0180 A69-10525

LAUNCHING BASES

NT CAPE KENNEDY LAUNCH COMPLEX

French space center in Guiana, discussing geographic location advantages for payload, rocket launching, space rendezvous, etc

02 p0228 A69-11920

General purpose space vehicle ground support equipment adapted from special purpose systems, discussing checkout, launch control and data monitoring requirements

[AIAA PAPER 69-308] 09 p1479 A69-22385

Centro Ricerche Aerospaziali objectives, equipment and activities in aerospace research, including space

flight simulation facilities and scientific satellite launching range

15 p2724 A69-31456

Stratospheric balloons launching and nacelles for measurement of cosmic rays, atmosphere high altitude characteristics, discussing French launching center

16 p2734 A69-31759

General purpose space vehicle ground support equipment adapted from special purpose systems, discussing checkout, launch control and data monitoring requirements

[AIAA PAPER 69-308] 22 p3927 A69-40552

LAUNCHING DEVICES

U LAUNCHERS

LAUNCHING SITES

Temporary launching sites for rocket probes, discussing CNES activity, Dragon and Titus programs and mobile launching units

02 p0228 A69-11921

Spacecraft launching facilities and payload capabilities in next decade, discussing orbits, spacecraft size and volume, attitude stabilization and positional accuracy

06 p1012 A69-16857

Belier rocket launching facilities in Guiana, describing pads, tracking system, telecommunications network, etc

09 p1477 A69-22161

Soviet space program, discussing launch sites, series of launch vehicles and mission identification

13 p2381 A69-27303

Microbiology quality assurance program for planetary mission, considering spacecraft sterilization during fabrication, test and launch site activities

15 p2559 A69-31124

Failure data role in management of launch operations reliability program

19 p3294 A69-36022

LAVA

Volcanic gas from lava lake, noting carbon and sulfur gases depletion during cooling and solidification

02 p0236 A69-11466

Magnetic analysis by successive double heat treatment of miocene lava cooled during geomagnetic polarity reversal for determining field intensity

16 p2788 A69-32646

LAW

Aircraft noise alleviation through flight procedures improvement, home building modification and noise standards legislation

14 p2392 A69-29154

LAW [JURISPRUDENCE]

NT INTERNATIONAL LAW

NT LEGAL LIABILITY

NT PENALTIES

NT SPACE LAW

Industrial loyalty and trade secrets, discussing preservation of forms of intellectual property posed by mobile employee and management policies

01 p0180 A69-10991

Legal problems in hovercraft classification, discussing problems in adapting existing transport legislation to hovercraft operation

04 p0689 A69-14942

Federal government contracting, discussing legality of NASA service contracts

05 p0850 A69-15987

Air safety, emphasizing misunderstandings or unresolved problems in accident prevention connected with law/safety interface

06 p1040 A69-16837

Book on law of airspace covering property rights, legal aspects of airspace utilization, airspace transactions, courts role, damage suits, etc

07 p1244 A69-18709

Federal, state and municipal jurisdictional aspects for heliport establishment, detailing regulations

13 p2381 A69-27433

FAA jurisdictional procedures for law infringement, discussing civil codes, delegation of enforcement authority and routine violations including low flying, weather, etc

16 p2882 A69-32335

Telemetric control of urban transportation systems and law enforcement, considering automobiles as prime vehicle

19 p3272 A69-36256

Air cushion vehicle legal status and cargo and passenger liability

19 p3455 A69-36330

Custody, jurisdictional conflict and prosecution problems of in-flight crimes, discussing federal jurisdiction and Tokyo Convention ratification

22 p4053 A69-40708

LAWS

- U CLOSURE LAW
- U CONSERVATION LAWS
- U HOOKES LAW
- U KEPLER LAWS
- U KIRCHHOFF LAW OF RADIATION
- U NEWTON PRESSURE LAW
- U RADIATION LAWS
- U SCALING LAWS
- U SIMILITUDE LAW

LC CIRCUITS

Broadband LC filters having prescribed amplitude response and constant group delay, emphasizing IF filters for radio relays

05 p0732 A69-16343

Delta functions spectrum in reciprocal time domain for LC and RC structures due to impulse response in distributed parameters

09 p1471 A69-21327

Narrow band LC 70 MHz IF filter design method

12 p2036 A69-25915

Autooscillatory process in n-circuit tunnel diode LC oscillators acted upon by external sinusoidal voltages

16 p2764 A69-32256

Networks of ideal inductors, capacitors and periodically operated switches with no energy loss, deriving frequency-power formulas from response functions

18 p3111 A69-34682

LCRE REACTOR

- U LITHIUM COOLED REACTOR EXPERIMENT

LEAD [METAL]

Lead isotope composition and concentrations of U, Th, Ra, total Pb and Pb 210 in recent volcanic rocks, noting disequilibrium due to chemical fractionations

04 p0593 A69-15011

Orientation of diamagnetic ground state Pb 207 atoms with nonzero orbital angular momentum by means of optical pumping and determination of nuclear moment

07 p1156 A69-19399

Lead isotopes nucleosynthesis by three mechanisms and contribution of mechanisms to abundances; noting chronology in nucleosynthesis

08 p1357 A69-20897

Tensile tests on time dependent Pb and cellulose nitrate, including stress-strain curve prediction from creep test data

19 p3445 A69-36829

LEAD ACETATES

Equatorial mounted solar energy concentrator efficiency compared to unconcentrated sunlight and artificial UV-visible light source in reducing Pb tetraacetate solution in acetic acid

16 p2736 A69-31814

LEAD ALLOYS

Superconducting flux-flow resistivity minimum in Pb-Tl alloy, discussing thermal dissipation associated with temperature gradients across moving fluxoid

07 p1198 A69-18642

Creep long term deformation characteristics of plate and tube lead alloy model material predicted from short term room temperature creep deformation

21 p3844 A69-39320

LEAD COMPOUNDS

Plateau effect in burning of platonized propellants due to lead compound additives

03 p0494 A69-12881

Soviet book on methods of investigating semiconductors as applied to lead chalcogenides PbTe, PbSe and PbS covering physical and physicochemical properties

12 p2145 A69-26851

LEAD ISOTOPES

Pb isotopic analysis using double spike mass spectrometric method to achieve reproducibility and accuracy, discussing principles and performance

24 p4280 A69-42733

LEAD OXIDES

Multilayer lead oxide and cryolite dielectric coatings stability to ruby laser radiation, noting breakdown coherent radiation power densities

19 p3334 A69-35886

LEAD SELENIDES

Temperature effects on threshold current density, emission wavelength and polarization of PbSe diode lasers

19 p3337 A69-36533

LEAD SULFIDES

Lead sulfide single crystals and polycrystalline films growth studied by electron microscopy during vacuum deposition on NaCl and other substrates

10 p1743 A69-23002

Nonequilibrium conductivity and radiation of CdS, GaAs and PbS single crystals in waveguide cell under electron beam

13 p2318 A69-27886

LEAD TELLURIDES

Chemical compatibility estimation of lead and tin tellurides thermoelectric materials with metallic alloys

04 p0551 A69-15315

PbTe single crystal films growth on KCl studied by electron microscope, observing vapor crystal mechanism without coalescence of contacting crystals

10 p1745 A69-23323

Sb addition effect on electrical conductivity and Hall effect in PbTe single crystals over temperature range

11 p1939 A69-23706

Substructural patterns of epitaxial PbTe films obtained by condensation of vaporized PbTe on NaCl crystal surfaces, discussing formation kinetics and morphology

12 p2144 A69-26675

Thin PbTe semiconductor films electrical properties measured in air and vacuum, showing dependence on thickness and conditions of preparation

21 p3782 A69-39242

Thermoelectric generators using hot junction pressure contacted lead telluride technique, presenting model for long term performance characteristics

23 p4188 A69-42262

LEAD TITANATES

Phase diagram, dielectric and magnetic properties of Bi manganate/Pb titanate solid solutions of perovskite structure, showing dependence on composition and temperature

22 p3996 A69-41163

LEADERSHIP

Group leadership attempting behavior dependence on situational and perceptual variables

23 p4110 A69-42015

LEADING EDGE SLATS

Leading edge flap angle and planform effects on low speed vortex patterns of flat plate double delta wings, measuring aerodynamic forces

17 p2890 A69-33246

LEADING EDGE SWEEP

Critical flutter behavior of variable geometry aircraft with wing of 70 degree leading edge sweep, noting wing-tail interference

11 p1991 A69-25517

LEADING EDGES

NT SHARP LEADING EDGES

Unsteady incompressible boundary layer flow over leading edge boundary layer calculated by three dimensional time dependent equations

02 p0233 A69-12543

Laminar flow of viscous fluid along wall with fixed leading edge and moving surface, discussing conditions of boundary layer formation and dynamic similarity

03 p0417 A69-13792

Test of similarity theory of leading edge vortices above slender wings in subsonic conical flow

04 p0543 A69-14820

Model kinetic integral equation for describing flow in transition region at leading edge of tapered body in rarefied gas

05 p0697 A69-16040

Delta wing head wave at zero angle of attack in steady supersonic flow during transition from subsonic to supersonic leading edges

[DVL-871] 06 p0858 A69-17242

Discontinuity effect on Ekman layer development at leading edge of flat plate

07 p1120 A69-19044

Shockload on axial intake fan leading edge of radial flow compressor, calculating flow field

08 p1251 A69-20604

Transonic flow around airfoils with constant curvature in uniform asymptotic stream, studying leading edges in exact form

09 p1429 A69-21606

Leading edge conditions of obstacle exuding fuel into oxidizer stream, using Oseen equations in parabolic coordinate system

11 p1997 A69-24307

Delta wing in three dimensional supersonic flow analyzed by method of characteristics, discussing leading edge problems

11 p1820 A69-25425

Analytical model for free convection heat transfer from vertical plates with nonhorizontal leading edges, discussing flow field

13 p2379 A69-28342

Conical flow past cruciform wing-body and tail-body systems, considering various positions of leading edges with respect to Mach cone

15 p2548 A69-31002

Optimum surface for thick delta wing in hypersonic flow obtained by variational method, assuming closed leading and trailing edges

16 p2731 A69-31559

Supersonic leading edge problem using nonlinear Boltzmann equation with ellipsoidal model, calculating molecular distribution functions for flow field

[AIAA PAPER 69-652] 17 p2892 A69-33464

Leading edge vortices and shock detachment flow over delta wings, discussing drag reduction due to lift

17 p2896 A69-34025

Boundary layer equation for steady incompressible flow past flat plate with parabolic leading edge, obtaining series solution in inverse powers of Reynolds number

18 p3124 A69-35270

Supersonic flow past antisymmetrical thin delta wing by flow separation from subsonic leading edges, noting wing surface pressures

19 p3241 A69-36779

Thin jet flapped airfoil analysis with wake fully developed from leading edge and jet flow reflected from ground

22 p3861 A69-41184

Newton formula and Ritz method to determine wing shape with blunt leading edge, considering minimum drag achievement at hypersonic velocities

24 p4247 A69-43497

LEAKAGE

Leak flow rates of nitrogen and helium at various pressure gradients measured by gas chromatography and mass spectroscopy

01 p0079 A69-10297

Liquid hydrogen circulation pump design emphasizing liquid leaks

01 p0087 A69-11148

Mass spectrometer helium leak testing of cryogenic storage vessels, noting procedures and insulation and evacuation of jacket space

02 p0252 A69-11811

Mass spectrometer leak testing by calibrated enclosure method for quantification of gaseous leaks in large complex systems

04 p0598 A69-14974

Leak testing of welded pressure and vacuum vessels, considering nature of flow of gases through small restrictions

07 p1140 A69-18799

Circularly polarized waveguide mode simulation for multislotted leaky waveguide harmonic content measurement

07 p1105 A69-19046

Bubble leak testing of components to understand effects of gas and liquid viscosity, surface tension, pressure differential and temperature

09 p1503 A69-21391

Y-circulators specified, measured and calculated values correlated as function of leakage matrix elements and terminating dipoles reflection

09 p1473 A69-22114

Leaky helix and solid metal waveguides propagation losses measured by shuttle pulse method in SHF

13 p2233 A69-28063

Graphical method for plotting contours of Rice distribution function as rocket-borne radar reflection data, determining leakage factor

14 p2416 A69-29536

Leak detection for aerospace hardware, discussing equipment, operations, checkout, etc

15 p2618 A69-30315

Back pressure control system for heat leak evaluation tests of cryogenic containers, discussing component selection and error analysis

15 p2702 A69-30397

Misalignment and eccentricity effect on face seal, discussing leakage dependence on phase angle

[ASLE FICFS PREPRINT 15A] 15 p2620 A69-30483

Eccentric face seal with tangentially varying film thickness, analyzing leakage flow proportional to eccentricity and surface waviness

[ASLE FICFS PREPRINT 15B] 15 p2620 A69-30484

Noncontacting minimum leakage dynamic seal requiring liquid-vapor interface with leakage tolerance

[ASLE FICFS PREPRINT 40] 15 p2620 A69-30485

Lubrication and leakage control mechanics of face seals, considering liquid to vapor boundary within interface

[ASLE FICFS PREPRINT 22]

- 15 p2620 A69-30486
Sealing mechanism theory with face seal applications, taking into account load carrying capacity and no leakage pressure gradient
[ASLE FICFS PREPRINT 18]
- 15 p2620 A69-30489
Elastohydrodynamic lubrication of square section high pressure face seals mounted on rigid housings, considering design charts for load and leakage
[ASLE FICFS PREPRINT 16]
- 15 p2621 A69-30493
Leakage in mechanical face seals with hydrodynamic films, noting misaligned seal theories for pumping with cavities and two fluids
[ASLE FICFS PREPRINT 19]
- 15 p2621 A69-30497
Leakage prediction through mechanical seal by theoretical equation developed from basic fluid mechanics
[ASLE FICFS PREPRINT 17]
- 15 p2621 A69-30499
Load support and leakage from microasperity lubricated face seals, developing hydrodynamic lubricant films
[ASLE FICFS PREPRINT 21]
- 15 p2622 A69-30500
Semiconductor devices leak testing methods including liquids, helium mass spectrometer, Radflo and hermetic seal tests
- 16 p2758 A69-31712
Leak rate measurement accuracy of rate-of-rise technique for nitrogen, methane and He between millionth and thousandth torr
- 16 p2791 A69-32326
Leak tests for sealed electronic circuits using helium mass spectrometer
- 18 p3138 A69-35271
Density field surrounding leaking circular hatch of spacecraft treated as free molecular flow from annulus, superposing far field of effusive orifice flow
- 21 p3695 A69-39035
Seals leak testing for complex manned spacecraft structures
[AIAA PAPER 69-1030]
- 22 p3924 A69-40399
Leak detection techniques efficiency determined for airtight atmospheric air sampling devices used at low pressure and concentration
- 24 p4296 A69-42656
- LEARNING**
NT ASYMPTOTIC METHODS
NT CONDITIONING [LEARNING]
NT ITERATIVE SOLUTION
NT PROBLEM SOLVING
NT THEOREM PROVING
NT TRANSFER OF TRAINING
- Cost prediction equations used in perturbed environment of learning curves subjected to design change in industry
- 01 p0180 A69-10652
Muscle motor performance under continuous practice conditions, analyzing individual differences, intraindividual variability and remoteness
- 17 p2911 A69-34003
Circadian periodicity of human reaction times tested during normal diurnal cycles and 24 hour wakefulness, noting acoustic and visual stimuli effects on learning
- 24 p4267 A69-43387
- LEARNING MACHINES**
Mathematically stylized simple systems representing systems with functional law varying as function of acquired experience
- 01 p0050 A69-10377
Artificial intelligence application to design of off-line and on-line learning control systems for controlling spacecraft attitudes
- 04 p0581 A69-14568
Limited speech recognition system /LISPER/ simplifies recognition by computer designed as research vehicle and pattern recognition system
- 04 p0565 A69-15338
Learning model of brain stem reticular formation based on nonlinear probabilistic hybrid computer concepts
- 05 p0711 A69-15802
Markov extremum drift dual compensation in optimal systems with learning experiments
- 05 p0741 A69-16671
On-line optimization of stochastic control systems based on learning controller model, discussing computer simulation results
- 06 p0900 A69-17354
Learning control system design, using a priori information in subgoal selection, control situation grid extensions and controller initialization
- 06 p0900 A69-17355

Self organizing and learning control systems, adaptive systems theory and defining self organizing control systems

07 p1114 A69-18382

Cybernetic structural model for learning and mentalization comprehending symbol systems, languages, homeostatic mechanisms, etc

07 p1070 A69-18385

Learning matrices applied to mathematical relationship establishment during adaptation stage between input and output of adaptive systems

07 p1088 A69-18387

Adaptive threshold detection, using stochastic approximation techniques to derive receiver structures capable of learning optimum threshold setting during actual operation

11 p1839 A69-25297

Mathematically stylized simple systems representing systems with functional law varying as function of acquired experience

12 p2054 A69-26670

Self adaptive system for recognition of dynamic shapes, discussing self structuring by learning, incomplete pattern recognition, logic element network, etc

12 p2054 A69-27080

Learning control systems research and applications noting trainable controllers, reinforcement control, Bayesian estimation and stochastic approximation

18 p3112 A69-35093

Brain and machine model of pattern recognition, pattern synthesis, memory, learning and speech, using concept of similarity, context and signal analysis

24 p4273 A69-42909

LEARNING THEORY

NT REINFORCEMENT [PSYCHOLOGY]
NT TRANSFER OF TRAINING

Spatiotemporal patterns learning among sensory and motor organs with linearly ordered components by nonlinear networks in terms of embedding fields theory

22 p3887 A69-41196

Learning model of motor behavior in brain cortex of higher animals and man, discussing M automaton, information reception, correlation, memory, emotions, desires and actions

23 p4109 A69-41977

LEAST SQUARES METHOD

Approximate solution convergence for linear operator equation in Hilbert space by least squares method

01 p0105 A69-10728

Plant identification procedures by stepwise approximation and least squares methods

03 p0409 A69-13072

Damping factor automatic determination by use of second derivatives of residuals for damped least squares method of optical design

04 p0630 A69-14295

Deterministic pattern classification algorithms, discussing abstraction problem, stochastic algorithms, minimum error scheme and modified least squares scheme

06 p0892 A69-17395

Iterative method for least square polynomial curve fitting with abscissas and ordinates subject to error

08 p1343 A69-20827

Least squares local smoothing by polynomials of noisy data in n dimensions

08 p1344 A69-20830

Smoothing data stability by least squares method, noting applicability to computer processing at random sequences

09 p1532 A69-21754

Algorithm for calculating Bayes estimates for unsteady Gaussian signals separation in presence of unsteady Gaussian noise by least squares method

11 p1833 A69-24443

Least squares iterative program, deriving orbits for O binaries HD 93403 and HD 135240

11 p1963 A69-25257

Photogrammetric networks equalization by method of least squares, using external orientation elements of aerial photographs

12 p2079 A69-26032

Book on stress rupture parameters including least squares approach to Larson-Miller, Dorn, Manson-Haferd, Graham-Waltes, Murry, Brozzo and Chitty-Duval

13 p2360 A69-27372

Solar eclipses phases and elements calculation by Fortran language computer, using least squares method

13 p2336 A69-27447

Stress in elastic cylinder under thermal expansion with one end clamped expressed by series expansion of biharmonic function using least squares method

14 p2534 A69-29284

Polynomial and nonlinear equations of state for solids and liquids analyzed using uncommon statistical and least squares methods

14 p2486 A69-29470

Satellite triangulation by least squares method based on conditions relating to observing stations coordinates, concerning synchronous observations in directions and distances

15 p2594 A69-30030

Nonlinear least squares optimization program applied to atmospheric temperature sounding, solving for temperatures at various altitudes from simulated carbon dioxide intensity measurements

17 p2960 A69-33156

Least squares method of smoothing curves or surfaces involving orthogonal base functions, discussing matrices conditioning and structure eigenmodes

18 p3218 A69-34643

Geodetic satellite measurements employing curve fitting approach using least squares analysis to resolve atmospheric refraction and shimmer problem

18 p3104 A69-35202

Polynomial approximations in perturbational navigation and guidance schemes including Chebyshev and least square approximations

19 p3368 A69-35664

Least squares method application to boundary value problem approximate solution for plane, axisymmetric, creeping and incompressible irrotational flows

19 p3299 A69-36475

Optimal timing of measurements to minimize dispersion of navigational observation parameters by least squares method with application to Keplerian orbit elements

19 p3370 A69-36614

Synthetic aperture terrain imaging radar system optimal design, considering noise-free and random noise conditions using least squares method and signal to noise ratios

20 p3489 A69-37639

Least square or least mean square approximation methods in abstract pattern recognition, noting unknown probability density function

20 p3504 A69-38285

Relation between smoothed and filtered linear least squares estimates of signal process in white noise from deriving resolvent identity of covariance function

21 p3754 A69-38432

Unitary matrix representing generalized inverses, proving weak method of steepest descent for least squares solution of equations

21 p3755 A69-38926

Earth-pole wobble /1951-1966/ by spectral analysis using least square fit method

21 p3716 A69-39244

Nonlinear estimation with noisy data, considering least squares fit, sequential /Kalman/ estimate and iterated sequential scheme

21 p3686 A69-39370

General linear state estimation from algebraic viewpoint without probability theory concepts, establishing least squares parameter estimation

23 p4182 A69-41880

Satellite attitude estimation from onboard telescope celestial sightings using iterative least squares method, considering measurement error noise and axes wobble

24 p4348 A69-43244

Iterative weighted least squares method for reconstructing time history of coupled rotation and flexural oscillations of Radio Astronomy Explorer satellite

24 p4394 A69-43291

LEAVES

Cotton leaves reflectivity and transmittance measurements, discussing substrate salinity effects on internal structure of hydroponically grown plants

15 p2558 A69-30456

Temperatures of radiantly heated sun and shade leaves of white oak measured in low speed wind tunnel, considering differences in convective heat dissipation

18 p3095 A69-34540

LEE WAVES

Finite difference method for calculating lee waves incident on obstacle with arbitrary vertical distribution of main flow horizontal velocity and temperature

10 p1722 A69-23967

Statistical analysis of lee wave clouds from satellite TV pictures, determining lengths and air flow direction

11 p1912 A69-24828

Motion of slender axisymmetric bodies in rotating fluid, relating Long hypotheses to flow reversal and dipole distribution effects on lee waves

13 p2248 A69-28170

Turbulence origin and structure in stably stratified media for finite disturbance instability in sloping flows experimentally observed with visualization techniques

17 p2999 A69-33735

Lee waves and orographic wind phenomena in Rocky Mountains near Boulder, noting stratospheric standing gravity waves and turbulence sampled by HI-CAT U-2
17 p2999 A69-33738

Finite difference method for calculating Lee waves incident on obstacle with arbitrary vertical distribution of main flow horizontal velocity and temperature
21 p3759 A69-39653

LEG [ANATOMY]

Leg volume changes in response to lower body negative pressure due to blood redistribution
17 p2908 A69-33171

White mice gastrocnemius muscle wet mass, dry mass and noncollagen-nitrogen (NCN)/content, noting (NCN)/content dependence on body mass
23 p4080 A69-41406

LEGAL LIABILITY

Legal problems in space navigation and solution through international law including air and outer space limits, regulating authority and damage liability [UN PAPER 68-95475]
01 p0179 A69-10511

International liability for damage caused by launching of objects into outer space [UN PAPER 68-95337]
01 p0180 A69-10525

Manufacturer and assembler liability for injuries caused by design defects resulting from engineering errors in aircraft products
01 p0180 A69-11392

Litigation for aircraft accidents, discussing legal and fiscal aspects and deterrent effect contributing to aviation safety
01 p0181 A69-11393

Aviation insurance function in providing risk capital in expanding aviation enterprises at fair and equitable rates, discussing air safety
06 p1041 A69-16845

International problems of air traffic control, discussing legal and political basis for organization and ATC liability
06 p1042 A69-16846

Air carrier legal responsibility for commercial air safety as compared to liability in other transportation modes
06 p1042 A69-16847

Federal government legal liability for commercial air safety in aircraft accident suits
06 p1042 A69-16848

Aircraft parts manufacturer liability in air accidents, discussing litigation and warranties
06 p1042 A69-16849

Tort system of U.S. law effect on air safety promotion, discussing liability influence on government, manufacturers and airlines
06 p1042 A69-16850

Aviation industry passenger liability, discussing negligence litigation, compensation standards and roles of government, manufacturers and courts
06 p1042 A69-16851

Legal consequences of discrepancies between freight rates for airline tickets and bills of lading and actual invoices, discussing liability areas and regulated tariff
07 p1244 A69-19232

Legal problems in space navigation and solution via international law including air and outer space limits, regulating authority and damage liability
07 p1244 A69-19233

Air carrier liability for nuclear weapons damage, discussing international agreements
11 p2003 A69-24260

Sonic boom damage legal claims, discussing causal relationship validity and claims processing
14 p2541 A69-29155

Legal, social and physical effects of supersonic flight, discussing damage claims validity and recovery resulting from breaking of sound barrier
17 p3075 A69-32841

Jet noise effect on real estate value, discussing market survey, insulation and navigation easement costs and litigation damages [AIAA PAPER 69-802]
19 p3288 A69-35594

Air piracy legal aspects as determined by Swiss law and Treaty of Tokyo
19 p3454 A69-35979

Legal liability in civil aviation, proposing international treaty
19 p3454 A69-35980

Air cushion vehicle legal status and cargo and passenger liability
19 p3455 A69-36330

Article 8 // of Carriage by Air Act, 1932 compared to Warsaw Convention Article 8 //, noting definition of legal liability of carrier
19 p3455 A69-36331

ESRO and legal liability in damage suits concerning satellite protection and environmental control
20 p3635 A69-37108

Outer Space Treaty of 1967, discussing Article 4 and arms control
20 p3636 A69-37109

Space law legal liability definitions for damage caused by space objects, discussing juridical principle and procedure
20 p3636 A69-37110

International lawyers proposal for compulsory registration of space activities in connection with astronauts rescue and damages liability
20 p3637 A69-37118

Legal principles observed for international telecommunication systems establishment by means of artificial satellites regarding states interests and rights
20 p3638 A69-37124

International legal liability for personal injury or property damage caused by space activities
20 p3638 A69-37127

Liability for personal and property damage due to space activities [AAS PAPER 69-042]
24 p4418 A69-42826

LEGENDRE CODE
U COMPUTER PROGRAMMING
U NEUTRON SCATTERING

LEGENDRE FUNCTIONS

Summation of Legendre series by transformation into integrals and use of recurrence relations
01 p0171 A69-11072

Legendre polynomial description of radiation pattern of group of radiators, discussing design of linear radiators
02 p0209 A69-12341

Optimum addition of abscissas in quadrature formulas by expansion of abscissas equation in Legendre polynomials
03 p0455 A69-13372

Unsteady atmospheric motions on planetary scale using Legendre polynomials
08 p1311 A69-21158

Brightness coefficients for isotropic scattering of homogeneous plane layer in turbid medium, using Legendre polynomials
11 p1960 A69-24733

Nonrelativistic theory of rotating configurations in terms of gravitational potential, center mass density and variable angular velocity
12 p2159 A69-26662

Finite thickness plate heat equation using Legendre polynomials
14 p2537 A69-28970

Boltzmann equation for Lorentzian plasma in elliptic magnetic field solved by expanding distribution function in Legendre polynomials
17 p3009 A69-32827

LEIDENFROST PHENOMENON

Creeping flow model of Leidenfrost boiling with moving surface, discussing vaporization time for equivalent drop film boiling on stationary surface [AIChE PAPER 20]
15 p2718 A69-31116

LEM [LUNAR MODULE]
U LUNAR MODULE

LENGTH

Characteristic length constant in open cosmological model of large scale properties of real space-time, noting relation to other constants
09 p1608 A69-22528

Gas laser-Doppler radar system for moving materials velocity and length measurements in industrial processes
22 p3955 A69-40237

Laser interferometric length measurement by fringe counting, considering mechanical and optical systems limitations and design tolerances
22 p3960 A69-40238

LENNARD-JONES GAS

Viscosity and thermal conductivity of helium on basis of Lennard-Jones (6 to 9) potential [ASME PAPER 67-WA/HT-1]
02 p0351 A69-12205

Prigogine-Nicolis-Misguich transport theory tested with inert gas liquids and compared with Rice-Allnatt theory, based on modified Lennard-Jones potential model
04 p0589 A69-14863

LENS ANTENNAS

Geodesic lens radar antennas, discussing air filled devices operated in TEM mode, inclusive Luneberg lenses, double layer pillboxes and parabolic lenses
03 p0402 A69-13184

Radio wave field distortions by dielectric prisms in lens waveguides, discussing beam transformation, noting both geometrical optics effects and diffraction role
11 p1833 A69-24436

LENS DESIGN

Hologram chromatic aberration compensation by two lens system
01 p0080 A69-10430

Tinted ophthalmic media effect on detection and recognition of red signal lights in daylight, noting allowable coloration for aviation use
01 p0022 A69-11341

Plastic virtual infinity lens system for large aperture cathode ray tube direct view simulator displays
05 p0760 A69-15592

Collimator lens design for transforming axisymmetric primary field into prescribed secondary field
06 p0895 A69-17454

Double focus lens holography for diffusely reflecting surface deformation recording, discussing gas lasers, Polaroid photographic materials, etc
11 p1880 A69-24467

Ray tracing application to evaluating aberrations produced by Fresnel holograms for optimizing design of aplanatic lens holography system
11 p1885 A69-24848

Focusing power of hyperbolic gas lens for light beam waveguides, noting temperature distribution measurements and pole separation
12 p2107 A69-26392

Electromagnetic field in idealized medium of uniformly curved gas lens for light beam waveguide, describing lens radius effects on incident beam spot
13 p2270 A69-27181

Nonmagnetic ionization gage consisting of quadrupole lens systems excited at HF, discussing electron focusing during operation
13 p2263 A69-28084

Simulated gravitational lens made of Plexiglass for demonstrating stellar gravitational lens phenomena, presenting partial cross section
15 p2653 A69-31163

Atmospheric ion concentration increment by electrostatic lens to facilitate electrical properties measurements of charged particles in submicroscopic range
17 p2971 A69-32928

Optical computerized design procedure for Ritchey-Chretien corrector, combining ray deviation error function and third order aberration design techniques
17 p2972 A69-33087

Mosaic mirror and lens camera system for multiple image high resolution photography
17 p2972 A69-33089

Collimator lens design for transforming axisymmetric primary field into prescribed secondary field
20 p3508 A69-37939

Gas lens system for periodic light beam waveguide, describing gas enclosed in circular cylinder and heated by specific temperature distribution
24 p4350 A69-43332

LENSES

NT CONTACT LENSES
NT WIDE ANGLE LENSES

Gas lens distortion of Gaussian light beam in sequence of lenses with same aberration, using shuttle pulse technique
01 p0120 A69-10849

Brewster angle lenses for low cost low loss laser beam transmission system
07 p1148 A69-18863

Equivalent network representation of feedthrough lens array taking into account mutual coupling between elements to predict performance characteristics
08 p1280 A69-20014

Flare or stray light measured in long focus photographic objectives by photometric sphere and spherical segments without collimator
12 p2093 A69-26590

Lenses spherical aberration role in studying laser induced breakdown of gases, considering intense ionization collinear regions multiplicity along optic axis
15 p2634 A69-30878

Objective lens of AVR-2 refractor at Poltava Observatory measured for spherical aberration, astigmatism, field curvature, coma and distortion
17 p2970 A69-32883

Angular structure of second optical harmonic for cylindrical lens focusing of ND laser beam into negative KDP crystal
17 p2981 A69-33110

Laser emission spatial structure transformation determined from ratio between focused spot radius and distance between lens and output mirror
17 p2981 A69-33111

Electrostatically focused klystron /EFSK/ small signal gain calculations based on lens cell space charge wave analysis

18 p3109 A69-35294

Fresnel zone plate as converging and diverging lens in holographic image reconstruction, noting sine wave zone plate

22 p3947 A69-40864

Viscoelastic properties of lenses extracted from cats and dogs analyzed as function of displacement using computer simulation

22 p3883 A69-40875

Camera lenses and techniques for aerial color photography, discussing atmospheric influences, filters, films and exposure times

22 p3950 A69-40999

LENTICULAR BODIES

Supercritical elastic states in convex shells produced by load in presence of thermal flux, noting no flux effect on states

09 p1617 A69-22078

Supercritical elastic states in convex shells produced by load in presence of thermal flux, noting no flux effect on states

23 p4228 A69-41970

LEONID METEORIDS

Meteor spectrum from 1966 Leonid shower considered to be closer to comet nucleus spectra than previous spectra

04 p0655 A69-14664

Radar and photographic studies of meteors from Leonid and Perseid showers, presenting velocities, luminescence and ionization

10 p1783 A69-23895

Micrometeoroid showers proximity to epsilon Leonid showers in earth orbit, analyzing Helfenzreider comet role from satellite data

14 p2522 A69-29588

17 November 1966 Leonids return, tabulating data from previous returns starting with October 899

14 p2525 A69-29715

Leonid meteoroids mass distribution law exponent evaluation based on unstable meteoric radio echo durations integral distribution

18 p3203 A69-35334

LEPTONS

NT ANTINEUTRINOS

Leptonic quarks with various charges in cosmic rays, determining upper limit of flux in underground measurements

02 p0306 A69-11547

Lepton nonconservation implications for experiments involving solar neutrinos, showing effect on capture rate at earth for pep neutrinos

23 p4194 A69-41596

LES

U LINCOLN EXPERIMENTAL SATELLITES

LESA [LUNAR EXPLORATION SYSTEM]

U LUNAR EXPLORATION SYSTEM FOR APOLLO

LESIONS

NT PULMONARY LESIONS

Visceral lesions observed in mice and rats exposed to ultrashort waves indicating no pathological modification of physiology of reproduction [AGARDOGRAPH-111]

08 p1266 A69-20679

Rabbit corneal damage thresholds for Gaussian beams of carbon dioxide laser IR radiation at various exposure times

11 p1830 A69-24844

Ventromedial hypothalamic /VMH/ lesions, body weight and food consumption changes in male and female rats, observing differential effects

17 p2910 A69-33756

Olfactory bulb removal effects on uptake decline of telencephalic norepinephrine, noting use for mapping adrenergic pathways

22 p3871 A69-40055

LETHALITY

Microorganisms death by exposure to high intensity visible and UV light, discussing effect of endogenous photosensitized oxidation on caratoid-containing Rhodotorula glutinis

20 p3475 A69-37613

LETTERS [SYMBOLS]

U SYMBOLS

LEUCINE

High oxygen tension effect on transport and incorporation of exogenous leucine and protein synthesis in *Pseudomonas saccharophila* cells

03 p0369 A69-13433

Anoxia effects on leucine-super 3 H incorporation by submandibular gland cells of neonatal rats, discussing cytoplasmic proteins synthesis impairment-

22 p3887 A69-41195

LEUKOCYTES

NT EOSINOPHILS

NT LYMPHOCYTES

Glycolysis control by respiration in human leukocytes with and without Pasteur effect conditions

15 p2555 A69-30413

Phagocytic activity and carbohydrate metabolism in peripheral blood neutrophils of men exposed to atmosphere with increased O content, noting neutrophil energy exchange disorder role

17 p2907 A69-32942

Pre and postflight leukocyte chromosome aberration analyses of Gemini astronauts

17 p2908 A69-33173

Radioprotective effects of 5-azacytidine on bone marrow and blood leukocytes of X ray irradiated AKR mice

23 p4080 A69-41429

Radiation effects on population kinetics of granulocyte system forming bone marrow, discussing radiosensitivity and radiation-induced granulocytopenia

23 p4090 A69-41965

LEVEL [HORIZONTAL]

Bamberg zenith telescope investigation, noting level constant dependence on level tube bubble length

17 p2970 A69-32882

LEVEL [QUANTITY]

NT ATOMIC ENERGY LEVELS

NT ELECTRON STATES

NT ENERGY LEVELS

NT GROUND STATE

NT INTERMOLECULAR FORCES

NT MOLECULAR ENERGY LEVELS

Automatic level measuring system, consisting of decade control oscillator, digital level generator and selective level meter for 200Hz-2MHz range

09 p1501 A69-22577

LEVELING

Analytic platform or strapdown systems application, discussing closed and open loop leveling techniques

08 p1347 A69-19862

LEVERS

Lever support systems for telescopes noting tilt compensation, acceleration balance and problems of friction, pivot viscosity, thermal effects and weight

12 p2057 A69-26410

LEVITATION

Manned relativistic space flight limitations dependence on biomagnetic levitation of human body in inhomogeneous magnetic field to compensate inertial forces during acceleration

22 p3889 A69-39906

LEWIS BASE

Lewis acidity of alanes, discussing interactions of trimethylalane with amines, ethers and phosphines

07 p1074 A69-18630

LEWIS NUMBERS

Adiabatic model deflagration limits for steady linear monopropellant burning at Lewis number of unity and one step gas phase reaction

24 p4415 A69-43670

LIABILITIES

U LEGAL LIABILITY

LIAPUNOV FUNCTIONS

LCL /Liapunov, Cetaev and LaSalle/ functions for autonomous systems of second order extended to more general differential equation systems

01 p0103 A69-10007

Multivariable PFM control system stability analysis using Liapunov function as Hermitian quadratic form

01 p0050 A69-10207

Stochastic Lurie type systems stability using Liapunov method

01 p0050 A69-10240

Stability properties of discrete-continuous feedback control systems with signal dependent sampling

02 p0226 A69-12733

Conditions for solution existence for n differential equations and Liapunov functions

05 p0787 A69-16451

Stability of differential systems with random parameters, developing Liapunov function approach and application to Ito equation

05 p0788 A69-16484

Pulsed control systems stability with frequency pulse modulation analyzed by Liapunov direct method

05 p0740 A69-16670

Soviet achievements in space research, comparing satellites with U.S. counterparts

06 p1005 A69-175616

Transient stability of AC generator analyzed by Liapunov direct method, considering effects of flux decay, speed governor and voltage regulator

07 p1058 A69-18644

Fabry-Perot laser operation having third mirror inserted on optical axis, analyzing equations solution stability according to Liapunov

07 p1148 A69-18802

Liapunov functions construction for linear and nonlinear differential equations, including nth degree systems with multiple nonlinearities

07 p1181 A69-19001

Periodic solutions of autonomous system oscillations with many degrees of freedom based on Poincare method applied to Liapunov systems

07 p1183 A69-19680

Almost periodic systems stability criteria derived from differential inequalities and Liapunov function, considering existence and uniqueness

09 p1532 A69-21612

Solutions boundedness in autonomous nonlinear systems with single nonlinearity, using Lure type Liapunov functions to prove theorems

09 p1533 A69-22449

Liapunov direct method in stability problems for semilinear and quasi-linear systems of hyperbolic partial differential equations with independent variables

09 p1534 A69-22799

Liapunov functions generation for deterministic ordinary differential equations, discussing integral methods, quadratic forms, partial differential equations, canonical forms, etc

11 p1908 A69-24317

Liapunov functions applied to stability analysis of nonlinear multivariable direct and indirect control systems with time lags

12 p2048 A69-26079

Stability conditions for control systems consisting of linear multivariable stationary neutral plant and multivariable pulse frequency modulator, using Liapunov direct method

12 p2049 A69-26080

Liapunov matrix equation solution, discussing restriction removal

12 p2121 A69-26377

Liapunov function construction with numerical algorithm, considering systems described by $dx/dt = f(x,y)$ and $dy/dt = g(x,y)$

12 p2122 A69-26520

Energy metric algorithm for Liapunov functions generation, discussing stability conditions in Wall and Moc work

12 p2122 A69-26521

Asymptotic stability inferred by examining higher order derivatives of Liapunov function, noting application to learning and adaptive control

12 p2122 A69-26522

Boundary value problems of thermoelasticity, discussing existence and uniqueness theorems, ellipticity, thermoelastopotentials, Liapunov-Tauber theorem, Fredholm theorems, etc

12 p2182 A69-26726

Multivariable PFM control system stability analysis using Liapunov function as Hermitian quadratic form

14 p2424 A69-28741

Periodic solution to equations describing nonlinear autonomous time lag system close to Liapunov systems

14 p2482 A69-28799

Control systems synthesis for nonlinear plants with known Liapunov functions and constraints, considering stability

14 p2424 A69-28819

Sufficient conditions for asymptotic stability of motion in finite and whole of nonlinear systems by Liapunov second method

15 p2652 A69-30660

Cetaev /A, lambda/ estimates of approximate integrations of system of ordinary differential equations, analyzing stability with aid of Liapunov functions

15 p2644 A69-30664

Asymptotic Liapunov stability of perturbed solutions to weakly coupled multifrequency systems

15 p2654 A69-31258

Stability and asymptotic stability theorems related to Liapunov second method, considering linear differential equations zero solution

15 p2654 A69-31259

Nonlinear nonconservative systems asymptotic stability analysis, emphasizing Zubov construction procedure for Liapunov functions

16 p2873 A69-32059

Stability determination for nonlinear automatic control systems, describing mathematical methods based on Liapunov functions
16 p2804 A69-32242

Absolute stability, stability in whole and engineering stability in reference to Liapunov stability applicability
16 p2874 A69-32244

Liapunov functions applications in motion stability theory problems, considering dynamic systems, periodic orbits, optimum damping and control
16 p2804 A69-32248

Stability conditions for time lag differential equation systems over finite interval employing Liapunov functions, noting similarity with systems having continuously acting disturbances
17 p2995 A69-33616

Exponential boundedness of system motion for Lure type forced systems, using quadratic Liapunov functions
18 p3164 A69-34674

Instability criterion for motion differing from criteria of Liapunov and Chetaev
18 p3174 A69-35317

Conservation laws and Liapunov stability of free rotation of rigid body about principal axes derived from kinetic energy and angular momentum
19 p3397 A69-35612

Quadratic Liapunov function existence for exponentially stable linear system with varying coefficients described by vector differential equations
19 p3359 A69-35617

Liapunov first stability theorem generalized for differential equations in Banach space
19 p3360 A69-35860

Liapunov method applied to stability evaluation of multiparameter self adaptive nonsearch gradient servosystems
19 p3286 A69-35891

Liapunov stability theory for motion of spacecraft with flexible and moving parts in force free space [AAS PAPER 68-125]
20 p3617 A69-37180

Fabry-Perot laser operation having third mirror inserted on optical axis, analyzing equations solution stability according to Liapunov
21 p3736 A69-38947

Asymptotic stability of differential equations solutions in linear normalized spaces via Liapunov theorems extension
21 p3755 A69-39105

Stability of two differential equations in critical case, obtaining Liapunov stability and instability
21 p3755 A69-39107

Frequency domain and Liapunov instability criteria for attitude control system design of large booster, noting nonlinear feedback [AIAA PAPER 69-853]
21 p3687 A69-39381

Extension of Liapunov systems to time lag systems with small periodic parameter
22 p3980 A69-40107

Liapunov stochastic stability direct method analog used for estimating reliability of redundant systems with constant recovery time
23 p4144 A69-41953

Dynamic characteristics of nonlinear discrete systems by motion division method, using discontinuous Liapunov function for stability criteria
23 p4144 A69-41956

Distributed parameter systems stability as internal and input-output property, describing Liapunov functionals construction
24 p4293 A69-43303

Liapunov functionals for time delay systems by path integrals in state space, using convolution equations involving distributions with compact support
24 p4295 A69-43317

LIBRARIES

Three leveled computer program library compiled for numerical analysis
01 p0036 A69-10709

LIBRATION

Optical ranging technique for studying lunar physical libration by measuring distance between earth observatory and two fixed points on lunar surface
01 p0158 A69-11311

Photographic investigation of gegenschein and cloud satellites at L sub 5 earth-moon libration point, noting gegenschein intensity peak
07 p1212 A69-18602

Ideal resonance problem with single critical term for case of libration solved by modified Poincare method, considering 24-hr satellite
12 p2152 A69-25800

Autonomous two degrees of freedom Hamiltonian system triangular libration points found stable for all mass ratios in circular restricted three body problem
12 p2155 A69-25883

Libroelastic wave propagation and dispersion characteristics /solid carbon dioxide/ evaluated by using Raman scattering measurements
13 p2286 A69-28668

Lunar libration constants determination based on Schlueter heliometer observations using Bessel-Wichmann method, allowing for limb irregularities
17 p3028 A69-32875

Lunar libration point L4 photographs taken during 6 October 1968 eclipse showing no discrete objects or clouds
20 p3613 A69-38249

LIBRATIONAL MOTION

Raman spectra and temperature dependent nuclear quadrupole resonance frequencies of p-dichlorobenzene and p-dichlorobenzene-D, calculating librational amplitudes
01 p0122 A69-10286

Three body problem, discussing impossibility of libration points of gravitating ellipsoid
01 p0155 A69-10957

Stability characteristics of small and moderately sized short period Trojan librations in sun-Jupiter restricted three body problem
01 p0158 A69-11329

Attitude control system for gravity gradient stabilized satellite in synchronous and near synchronous equatorial orbits, discussing libration damping methods
03 p0504 A69-12857

Lunar libration clouds, discussing visual observation at small phase angles for estimation of dominant cloud particle size
05 p0827 A69-16527

Magnetic sample-and-hold damping using geomagnetic field for libration damping of gravity gradient stabilized satellite in near synchronous equatorial orbit
07 p1227 A69-18337

Long life gravity gradient stabilization system using Vee configured control moment gyros to semipassively damp vehicle librations
07 p1228 A69-18345

Rotational dynamics equations in linearized matrix form applied to satellite librations in circular orbit and gyroscope motion
11 p1970 A69-24608

Libration point relay satellites for continuous communication link between earth and lunar far side, discussing trajectories and halo orbit stationkeeping
15 p2680 A69-30188

Mimas-Tethys commensurability of motions and inclinations, calculating libration amplitude variation by numerical integration
16 p2861 A69-32241

Stability of motions about triangular libration points in elliptic restricted three body problem [AAS PAPER 68-090]
20 p3595 A69-37175

Rotational motion bounds of satellites exhibiting parametric resonance under small librations in orbital plane
20 p3617 A69-37191

Closed form solution to stability of coupled libration motion of slender axisymmetric satellite in circular orbit limited to small amplitude vibrations
22 p4008 A69-39936

Periodic solutions for gravity-gradient stabilized satellite librating in orbital plane, using elliptic sine function and harmonic balance method
23 p4224 A69-41876

Stability analysis of periodic solutions associated with planar librations of gravity oriented satellite using linear perturbation analysis
24 p4388 A69-43649

LICHENS

Cladonia rangiferina resistance to stresses, considering suitable indices for stress response
18 p3095 A69-34539

Norwegian lichen species chemical investigation for aromatic compounds, hydroxy fatty acids, amino acids, soluble and bound sugars
23 p4080 A69-41428

LIDAR

U OPTICAL RADAR

LIE GROUPS

NT SPINOR GROUPS

Lie groups for equations of motion in quantum mechanics or field theory determined by operator analysis
02 p0282 A69-12840

Lie algebra of second order linear differential equations
02 p0273 A69-12841

Stored energy function of hyperelastic material by Lie group extension of Truesdell theorem on symmetry groups
04 p0680 A69-14945

Group classification of solutions to Hopf equation according to type of viscosity coefficient
07 p1118 A69-18700

Canonical transformations depending on small parameter, utilizing Lie series
19 p3397 A69-35608

Grobner method of Lie series applied to numerical integration of spacecraft trajectories and n-body problems
23 p4223 A69-42476

LIENARD POTENTIAL

Necessary and sufficient conditions for solution boundedness for Lienard equation with forcing function
02 p0272 A69-12132

LIFE [DURABILITY]

NT FATIGUE LIFE

NT HALF LIFE

NT PLASMA LIFETIME

NT SATELLITE LIFETIME

NT SERVICE LIFE

NT STORAGE STABILITY

Direct reading device for minority carriers lifetimes measurement in semiconductor single crystals
01 p0078 A69-10073

P-n-p junctions photoconductivity decay observation, determining signal bulk minority carrier lifetime in thin n regions
01 p0136 A69-10242

Radiative lifetimes for four N II excited states emitting UV during transition to lower level
02 p0280 A69-11928

Minority carriers lifetime measurement in degenerate GaAs, showing dependence on current density and operating temperature
03 p0483 A69-12917

Planar transistor reliability test results noting failure rate, stability and effect of temperature
03 p0402 A69-13006

EUV emission line radiative lifetime measurement by foil-excitation technique, noting correction for cascading, He II and transition probabilities for N II and O III
03 p0471 A69-13165

Mean life measurement of excited ions electronic levels using beam foil light source, emphasizing beam particle monitoring and theoretical equations
04 p0595 A69-14278

Cumulative damage theories application to fatigue data for high strength materials, discussing stress levels
04 p0668 A69-14379

Laws of wear and average life, noting application to electric connector reliability
04 p0579 A69-15320

High temperature effects on gallium arsenide crystals current carriers lifetime, discussing recombination characteristics and impurity photoconductivity
05 p0809 A69-16551

Growth induced dislocation effect on lifetime of minority charge carriers in silicon single crystals
06 p0980 A69-17551

He-Ne laser capillary end contamination with consideration of life lengthening, discussing thermal properties of argon ion laser with pyrolytic graphite
07 p1145 A69-18474

Film thickness effect on wear life of resin bonded solid lubricant film compared for various load test conditions [ASLE PREPRINT 68AM 7C-4]
07 p1139 A69-18624

C III 2p super 2 presuper 1 D level mean life measurement using beam-foil technique, noting corresponding Einstein A coefficient
07 p1184 A69-18643

Sealed carbon dioxide lasers life and power outputs with Xe and H additives
07 p1155 A69-19091

Internal electric field effect of diode with inhomogeneously doped base on lifetime of strong reverse current generated during instantaneous switching
08 p1287 A69-20890

SERT 2 thruster hollow cathode durability tested in bell jar [AIAA PAPER 69-304]
09 p1562 A69-21224

Lifetime of highly soluble isolated dense spherical solute particle in solvent, taking into account molecular diffusion, kinetic limitations, etc
10 p1651 A69-22939

Excited levels in Li I produced by Li 7 ion passage through carbon foil, measuring excitation mean lives by beam foil technique
13 p2301 A69-27454

Lifetime of vibrational levels of carbon dioxide molecules as function of discharge current and power dissipation, noting gas heating
13 p2273 A69-28579

Nonlinear homogeneous uniaxial ferromagnetic resonance, analyzing stationary regime lifetime and vibrational spectrum
14 p2503 A69-28989

Pulsar dispersion-removing technique, discussing pulsar mean flux density decrease with age
14 p2517 A69-29091

Sirene 302 thermionic converter lifetime during irradiation in Triton immersion pile, considering effects on conversion efficiency
14 p2481 A69-29198

Self lubricating bearings lifetime calculated as function of lubricant in pores and consumption rate, noting temperature effects
15 p2618 A69-30281

Rate gyro life and reliability, discussing gas bearings separating rotor from stator by thin gas film with conventional oil film characteristics
15 p2608 A69-30410

Load, speed and coating thickness effect on wear life of resin bonded solid lubricant, using oscillating motion and low pressure blocks
[ASLE PREPRINT 69AM 5C-3]
15 p2619 A69-30474

Mass-produced silicon transistors reliability, presenting tables and curves of lifetime tests
15 p2626 A69-30833

Lifetime of structural plastics under vibration loading, considering polystyrene and polyformaldehyde samples under tension
15 p2643 A69-30972

Electron excitation and phase shift method for radiative lifetimes of Ar II UV transitions
15 p2656 A69-31034

Semiconductor rectifiers economic life testing with synthetic circuits utilizing thyristor switch
15 p2579 A69-31041

Integrated circuits screens, developing sequence of life and environmental tests to remove units of potential reliability hazards
15 p2580 A69-31130

Electronic component life test sampling plans based on lognormal distribution and instantaneous failure rate or hazard rate criterion
15 p2630 A69-31137

Equipment life cycle costs computer simulation for design and changes evaluation, including maintenance analysis example
15 p2723 A69-31138

Microwave power loss and semiconductor conductivity relationship measured for carrier lifetime and mobility, noting nonlinearity and accuracy
16 p2825 A69-31617

Lifetime of ground state oxygen molecular ions in sunlight from photodetachment rate by free electron production measurement from ions in buffer gas
16 p2848 A69-31973

Automatic nonrepairable control elements reliability evaluated statistically with differentiable lifetime distribution function
16 p2764 A69-32199

Elastomer hardness criteria ensuring maximum life and performance of rotary shaft seals
16 p2794 A69-32432

Semiconductor life potential evaluation based on electrical parameters measurements at various voltages over wide temperature range
18 p3144 A69-34489

Mean lives of upper decay levels of lithium isotopes accelerated by electromagnetic isotope separator and directed through thin carbon foil
18 p3177 A69-35012

Plasma electron beam for welding, deriving beam current from secondary emission by ion bombardment, discussing gas pressure, equipment and applications
19 p3320 A69-35555

Injection level effects on minority carrier lifetimes in lithium-doped devices and solar cells irradiated by electrons and reactor neutrons
19 p3252 A69-35698

Bayesian confidence limits for systems reliability, considering exponential and unspecified life distribution subsystems
19 p3328 A69-36041

Electrical slippings assembly development with low dynamic resistance and long lifetime for space simulation testing, noting wear rate of rings and brushes
[AIAA PAPER 69-1035]
22 p3925 A69-40402

Mean adsorption lifetimes and activation energies of Ag and Au on polycrystalline tungsten substrate in ultrahigh vacuum system free of hydrocarbon contamination
23 p4198 A69-41542

Pulsars turn off time compared to Galaxy age, discussing physical theory and pulsar models
24 p4389 A69-43745

LIFE DETECTORS

Extraterrestrial life detection methods based on soil or atmospheric sampling, discussing enzyme activity, DNA determination, microbial growth, etc
01 p0021 A69-11093

Wolf Trap life detector design to sample and culture Martian surface dirt for microorganism growth
02 p0201 A69-11769

Mars biological exploration, discussing life detection, chemical and biological experimental strategy
[AIAA PAPER 68-1122]
03 p0375 A69-13700

Integrated device to detect biological growth and catabolic and anabolic activity in extraterrestrial exploration
15 p2556 A69-31306

Life detection for space missions based on detecting optical asymmetry in biogenic molecules by gas chromatography involving diastereomeric esters synthesis
15 p2556 A69-31315

Experiments integrated into single automated laboratory to detect extraterrestrial life through measuring metabolism and growth in planetary surface material
17 p2912 A69-32969

Extraterrestrial life detection experiments integrated into single multipurpose space laboratory, including chemical analyses, metabolism identification, observation for molecular and/or cellular growth and replication
17 p2912 A69-32970

Life on Mars, past and future missions, possibilities of metabolic system and analysis methods
23 p4212 A69-41612

Spaceborne planetary UV spectroscopic search for atoms and molecules basic to life, specifically molecular N and water vapor photodissociation products
23 p4113 A69-41616

Sequential analyses of planetary surface sample for extraterrestrial life detection, discussing chemistry, morphology, growth and metabolism for life attributes
23 p4213 A69-41623

LIFE RAFTS

Survival of aircrew after successful ejection over water and boarding life raft
06 p0878 A69-16958

Life raft thermal protection against exposure of aircrews to cold, noting chemically fueled heaters and IR reflective liners
06 p0883 A69-17841

Insulated one man life raft for sea survival in arctic or subarctic conditions, evaluating thermal protection with endurance time and rectal temperature
12 p2020 A69-26550

LIFE SCIENCES

Life sciences and space research - COSPAR Conference, London, July 1967
01 p0016 A69-11073

Superconductors and living matter behavior, studying conditional parallelism via microstructure, cryogenic and electronic fundamentals
04 p0644 A69-15321

Experimental research concerned with origin of life, studying synthesis of precursor polymers and self assembly into protocells
10 p1641 A69-23035

Origin of life in terms of polymers synthesis under thermodynamic and geological conditions
12 p2017 A69-25764

Origin of life data, discussing self ordered polymers, propagative cell-like systems, protozooids, cellular evolution, etc
12 p2018 A69-25781

Gravity independence of life processes in terrestrial organisms concluded from zero gravity experiments with algae, hatched larvae, etc
18 p3095 A69-34692

Life sciences and space research on biological effects of radiation in space - COSPAR Conference, Tokyo May 1968
20 p3474 A69-37612

Evolution of life as creation of order from chaos, noting molecules self ordering capability
21 p3651 A69-38577

Thermal energy effects on life processes, discussing living cell metabolism, biochemical reactions, enzymatic action and protein catalytic functions, etc
21 p3652 A69-38783

Life on Mars, past and future missions, possibilities of metabolic system and analysis methods
23 p4212 A69-41612

LIFE SPAN

Mortality kinetics of Drosophila melanogaster, comparing effects of gamma radiation-induced life shortening and natural aging
15 p2555 A69-30444

LIFE SUPPORT SYSTEMS

NT CLOSED ECOLOGICAL SYSTEMS

NT EMERGENCY LIFE SUSTAINING SYSTEMS

Biological problems in prolonged space voyages including oxygen replacement, water supply and food regeneration
01 p0020 A69-11075

Chlorella and Scenedesmus unicellular algae mixture tested for biological protein value in humans for possible food source
01 p0021 A69-11079

Automatic life support system tried on leeches for space applications
01 p0021 A69-11080

Mathematical models of energy and mass transfer processes in closed loop multicomponent life support systems
01 p0021 A69-11316

Allelopathy, discussing application to gas liberating activity of edible plants as ingredients of space flight life support systems
02 p0198 A69-11509

Automatic bioprobe life support system for long duration interplanetary space flight, discussing blood leech as suitable research animal
02 p0199 A69-11828

Water electrolysis, discussing oxygen generators for spacecraft prototype cells and testing
03 p0379 A69-12987

Parametric analysis of life support systems developing scaling laws adapted to computer solutions, discussing manned orbital missions
[SAE PAPER 680746]
03 p0379 A69-13438

Wet oxidation process for management of organic waste products in closed ecologies of long term multimanned space missions
[SAE PAPER 680714]
03 p0380 A69-13443

Chemical nitrogen fixation methods for life support systems, discussing organometallic chlorides and bromides
03 p0382 A69-14198

Portable astronaut life support systems for extravehicular activities
[AICHE PAPER 42C]
04 p0554 A69-14511

Efficient life support systems for prolonged space missions, discussing scientific and experimental research
[UN PAPER 68-95778]
06 p0879 A69-17040

Astronaut extravehicular protection systems, discussing space suit, life support and thermal control subsystems and micrometeoroid protection
06 p0882 A69-17643

Lunar shelter regenerative life support system performance and manned test
07 p1071 A69-19427

Book on earth atmosphere and outer space influence on human physiology for life support systems design
12 p2024 A69-27074

Lithium peroxide utilization feasibility for oxygen supply and carbon dioxide control in extravehicular portable life support systems
[AIAA PAPER 69-620]
17 p2914 A69-33303

Parametric thermal control weight and power requirements for spacecraft life support systems, considering number of cabins, crew activity, heating, cooling and regeneration
[AIAA PAPER 69-621]
17 p2914 A69-33305

Artificial life support systems for sealed environments with application to specific missions, noting cryogenics use
17 p2915 A69-33682

Medical and biological laboratory ground experiments role in development of life support systems and

- suitable environments for prolonged manned space flights
18 p3098 A69-35165
- Regenerative life support systems, discussing water reclamation, carbon dioxide removal, onboard oxygen generation and radio isotope thermal energy sources
19 p3262 A69-36318
- Soviet book on cosmos and microorganism utilization for creating regenerative life support in spacecraft
20 p3467 A69-37230
- Regenerative life support system development, considering synthesized organic compounds and microorganisms as foods for long duration space missions
20 p3477 A69-37623
- Life support system sterilization maintenance problem for biosatellite experiment over one year
20 p3477 A69-37624
- Oxygen supply and carbon dioxide absorption in long term life support systems, noting energy balances comparison of ecological systems
20 p3477 A69-37625
- Mathematical model of optimal partially closed life support system consisting of man, recycling unit, storage unit and waste disposal outlet
22 p3892 A69-40272
- Radioisotope thermal energy (RITE) source for integrated life support systems for two man 180 day space station mission, determining optimum material selection and design details
23 p4189 A69-42268
- Dynamic power and life support systems electrical/thermal integration for manned spacecraft using low temperature Rankine cycle generator
23 p4189 A69-42269
- Unstabilized astronaut, hand-held and integrated life support EVA maneuvering units tested in gimbaled six degree of freedom servo driven moving base simulator [AAS PAPER 69-516]
24 p4272 A69-42850
- Material recovery from metabolic and other wastes for long duration manned space missions, discussing carbon dioxide removal, bioregenerative food systems, etc [AAS PAPER 69-143]
24 p4272 A69-42876
- LIFETIME (DURABILITY)**
U LIFE (DURABILITY)
- LIFT**
NT INTERFERENCE LIFT
NT JET LIFT
NT ROTOR LIFT
- Lifting wing profiles in uniform transonic compressible fluid flow calculated by analog method, noting hodograph method simplification
02 p0187 A69-11536
- Lift from unsteady flow past cascade of slender profiles with stagger angle reduced to solution of Fredholm integral equation
02 p0190 A69-12575
- Aerodynamics of flap balanced swivel airfoils, discussing lift curve slope, incidence change response and application of control forces and movements
03 p0364 A69-13908
- Lift and drag parameters of axisymmetric bodies in Newtonian flow at random incidence by summation of appropriate portions
04 p0542 A69-14745
- Zhukovskii lifting force theorem application to slender wing profile and airfoil lattice in linearized supersonic flow
05 p0697 A69-16023
- Lift fluctuation on airfoil due to transverse and chordwise gusts applied to rotating fan and compressor blade design [ASME PAPER 68-FE-28]
05 p0697 A69-16070
- Rotating turbomachinery design to minimize fluctuating lift on isolated airfoils, presenting cascade geometry by quasi-steady analysis [ASME PAPER 68-WA-FE-12]
05 p0698 A69-16092
- Lifting force and moments acting on slender wing of finite span and arbitrary planform moving at constant mean velocity in unsteady flow
06 p0858 A69-17338
- Three dimensional atmospheric entry trajectories equations for satellite with aerodynamic lift, examining aerodynamic factors and bank angle effects
07 p1230 A69-19608
- Optimal lift and thrust control programs to maximize range of missile in horizontal flight
09 p1610 A69-22086
- Computerized design of optimal direct lift controller for aircraft and aerodynamic surfaces, using Kalman linear state regulator theory
12 p2014 A69-26765
- Spacecraft horizontal maneuvers in homogeneous gravitational field to achieve soft landing on planetary surface, including optimal liftoff and orbital transfer
13 p2356 A69-27685
- Aerodynamic lift and moment fluctuations of sphere at supercritical Reynolds numbers measured by hot-wire anemometers, noting dependence on time
14 p2390 A69-29573
- Stabilizing methods for supersonic aircraft, noting effect of aircraft characteristic parameters on magnitude of balancing coefficients of lifting force
16 p2735 A69-32127
- Lift and drag determination for moving rectangular coils over infinite plane sheet for magnetic suspension and guidance for rocket sleds
17 p2946 A69-33789
- Direct lift controller design for aircraft approach and landing by computer program based on Kalman linear state regulator theory
17 p2902 A69-34027
- Optimum pressure distribution and airfoil profiles for maximum lift without separation in incompressible flow determined by second order theory [AIAA PAPER 69-739]
18 p3083 A69-34401
- Vortex wakes behind high lift wings, considering effects of height above ground and various tunnel heights and widths for STOL operations [AIAA PAPER 69-740]
18 p3083 A69-34405
- Wind tunnel tests of swept wing fighter aircraft for transonic buffet onset lift coefficient resulting from camber and leading and trailing edge deflection [AIAA PAPER 69-793]
19 p3238 A69-36297
- Rotating turbomachinery design to minimize fluctuating lift on isolated airfoils, presenting cascade geometry by quasi-steady analysis [ASME PAPER 68-WA-FE-12]
19 p3240 A69-36419
- Lift engine inlet development for XV-4B aircraft, discussing tests, pressure distortion and recovery during simulated hover and transitional flight [AIAA PAPER 68-636]
20 p3585 A69-37150
- Potential flow theory applied to determination of airfoil separated vortex flow and maximum lift and Reynolds number dependence
20 p3459 A69-37421
- Schweikhard method for measuring changes in lift, drag and pitching moment of fixed wing aircraft as function of distance from ground
20 p3462 A69-37423
- Engine powered lift civil aircraft certification factors taking into account traffic growth, accident rates, learning rate and acceptable safety level
22 p3862 A69-39962
- Lift coefficients of idealized tunnel type ram wing consisting of truncated semiconical shell computed by lifting surface theory
22 p3860 A69-40819
- Optimum climb trajectories at constant lift coefficient, using variational methods with final altitude and final flight path angle as end point constraints
24 p4254 A69-43727
- LIFT AUGMENTATION**
Lift augmentation by lateral blowing over lifting surface, discussing wind tunnel pressure tests on wings, flaps and stabilizers [AIAA PAPER 69-193]
07 p1051 A69-19554
- Gas turbine engine shaft face seal with self acting lift augmentation preventing rubbing contact, noting disadvantages of labyrinth and conventional seals [ASLE FICFS PREPRINT 27]
15 p2621 A69-30492
- Monograph on interaction between primary and jet flapped secondary airfoils covering line-vortex use for lift augmentation, aerodynamic characteristics, etc
19 p3242 A69-36820
- Flight control and stability of STOL transport aircraft with powered-lift boundary layer control system augmented lift
20 p3462 A69-37513
- LIFT COEFFICIENTS**
U AERODYNAMIC COEFFICIENTS
- LIFT DEVICES**
Subsonic lifting surface analysis accuracy tested by planar circular wing theory
04 p0543 A69-14818
- Unsteady aerodynamic forces on coplanar lifting surfaces in subsonic flow induced by wing/horizontal tail interference
04 p0543 A69-14819
- Design of high lift devices in relation to fixed wing subsonic transport aircraft, considering lift, drag, stability and control
05 p0695 A69-15544
- Flight evaluation of direct lift control on DC-8 super 63 jet transport
06 p0867 A69-17666
- Numerical method for attacking-lifting problems of general three dimensional wing executing arbitrary motion in potential flow [AIAA PAPER 69-23]
06 p0862 A69-18040
- Subsonic lifting surface theory including leading edge, discussing singularities in solution of integral equation for determination of aerodynamic properties [AIAA PAPER 69-37]
06 p0865 A69-18167
- Lifting pressure distributions on oscillating surfaces in subsonic flows using doublet lattice method for various surface geometries [AIAA PAPER 68-73]
09 p1430 A69-21946
- Lifting surface theory for cascade of blades in subsonic shear flow, determining blade surface pressure distribution, distinguishing shear and uniform flow compressibility effects
16 p2731 A69-31592
- Weight estimation of structures and systems unique to VTOL aircraft, considering remote fan and high bypass engine lift propulsion concepts [SAWE PAPER 784]
18 p3090 A69-34868
- Monograph on weight and performance tradeoff methodology for selection of high lift devices [SAWE PAPER 761]
18 p3091 A69-34906
- JR 100 F lift jet engines for Japanese national aerospace laboratory produced as part of VTOL developing program
21 p3785 A69-38608
- Book on optimal aerodynamic shapes by means of variational method, covering conventional and triangular thick wing lift systems in supersonic flow
21 p3644 A69-39667
- LIFT DISTRIBUTION**
U FORCE DISTRIBUTION
- LIFT DRAG RATIO**
Hypersonic lifting body configurations for maximum lift drag ratios and subject to volumetric efficiency, nose heating limit and skin friction constraints
02 p0189 A69-12378
- Lift efficiency of and stabilization by square flare on high speed missile, comparing wind tunnel measurements with circular conical flare
02 p0190 A69-12544
- Variable geometry features applied to lifting spacecraft to overcome inherent incompatibility and provide low speed and tangential landing capabilities [AIAA PAPER 68-1164]
03 p0520 A69-13562
- Space vehicle flight automatic optimization for maximum L/D reentry, considering perturbations causing trajectory inclination changes during roller coaster reentry
05 p0830 A69-16045
- Lift drag ratio for conical sector with V-shaped wing at zero incidence
06 p0858 A69-17340
- Lift drag ratio attainable by optimal transversal contour slender conical lifting body at hypersonic speeds
06 p0861 A69-17640
- Approximation formula for calculating descent speed and lift-drag ratio
10 p1633 A69-22873
- Base drag effects on maximum lift drag ratio airfoils determined for moderate supersonic laminar and turbulent flows
10 p1633 A69-24060
- Hydrofoils fully submerged in seaway at up to 140 knots and constant Froude number, discussing foils lift/drag ratios as function of speed and submergence
11 p1871 A69-25122
- Linear and second order theory for maximum lift to drag ratio airfoils at moderate supersonic speed, considering length, thickness and area
13 p2199 A69-28214
- Space vehicle flight automatic optimization for maximum L/d reentry, considering perturbations causing trajectory inclination changes during roller coaster reentry
20 p3618 A69-37954
- Cone-conical-frustum configurations meeting center of gravity requirements for higher hypersonic lift-drag ratios in axisymmetric manned spacecraft
21 p3644 A69-39237
- Hypersonic lifting bodies with high lift-drag ratio, presenting flat-top wing-body combination aerodynamic characteristics
21 p3645 A69-39793
- Wingtip mounted propellers effect on wing lift and induced drag, varying lift to drag ratio by changing in-flight aspect ratio
24 p4250 A69-43713

Wind tunnel model one component magnetic support and balance system for sphere drag investigation at subsonic Mach numbers
[AIAA PAPER 68-401] 24 p4298 A69-43714

LIFT FANS

Tip turbine driven flush thin profile wing or platform lift fan design and operating considerations
05 p0696 A69-15554

Hovering fan powered V/STOL aircraft effects on objects on ground, discussing related dust and debris problems
05 p0701 A69-15565

Aerodynamic effects of lift jet and lift fan inlets in transition flight, analyzing inlet momentum lift, inlet lip lift and drag
[AIAA PAPER 68-637] 12 p2014 A69-26767

Integrated lift, propulsion and control in Aeromobile air cushion vehicle, considering ram wing and gimbal fan plenum chamber vehicles
13 p2201 A69-27543

Plenum chamber obstructions influence on hovercraft lift fan performance, discussing tests and losses due to flat plate at impeller outlet
13 p2202 A69-27546

Turbofan V/STOL with separate lift units for takeoff and landing, discussing commercial and military applications, cost effectiveness and operational characteristics
13 p2203 A69-28354

Self contained lift fan concept and circulation controlled rotor aircraft power plants for high speed VTOL transports
17 p2897 A69-33208

VTOL aircraft lift systems, propulsion, airframes, dynamic and aerodynamic characteristics, control systems, missions, safety, configurations and environment
[AIAA PAPER 68-977] 20 p3461 A69-37149

RB 202 self contained lift fan engine design for high speed interurban civil VTOL operations, considering weight, cost, noise and fuel consumption
22 p3862 A69-39933

LIFTING BODIES

NT HL-10 REENTRY VEHICLE

NT M-2 LIFTING BODY

NT M-2F2 LIFTING BODY

NT RESEARCH AIRCRAFT

NT X-24 AIRCRAFT

Polygonal wing planform pressure distribution in incompressible flow calculated on basis of lifting surface theory
01 p0008 A69-11298

Hypersonic lifting body configurations for maximum lift drag ratios and subject to volumetric efficiency, nose heating limit and skin friction constraints
02 p0189 A69-12378

Hypersonic lifting body optimization under single and combined constraints of volumetric efficiency, heating and skin friction, using numerical search routine
[AIAA PAPER 68-1157] 03 p0362 A69-13557

In-flight measurement of shear, bending moment and torque on lifting or control surfaces and loads on nose and main landing gear
04 p0677 A69-14842

Plane subcritical flow past lifting aerofoil analyzed using conformal mapping and difference scheme on annular mesh inside circle
06 p0859 A69-17470

Lift drag ratio attainable by optimal transversal contour slender conical lifting body at hypersonic speeds
06 p0861 A69-17640

Subsonic lifting surface theory including leading edge, discussing singularities in solution of integral equation for determination of aerodynamic properties
[AIAA PAPER 69-37] 06 p0865 A69-18167

Hodograph for lifting airfoil with subsonic velocity at infinity, using Chaplygin compressibility law for computation
[ONERA-TP-631] 07 p1049 A69-18416

Lift augmentation by lateral blowing over lifting surface, discussing wind tunnel pressure tests on wings, flaps and stabilizers
[AIAA PAPER 69-193] 07 p1051 A69-19554

Aeroelastic divergence and stability range for cantilevered and end supported structures computed as function of forward resistance and lift caused by wind
16 p2870 A69-31557

Hypervelocity glide vehicle optimum maneuvers, finding lift optimal control law for maximization of final velocity or altitude
17 p3025 A69-32836

Circulation controlled rotor aerodynamics with tangentially ejected air from surface slots of lifting body,

noting performance at advance ratios and thrust coefficients
18 p3089 A69-35232

Second order theory for steady or unsteady subsonic flow past slender lifting bodies of finite thickness
[AIAA PAPER 68-75] 20 p3458 A69-37182

Lifting body stability augmentation systems design, development, ground tests and flight data including frequency response, limit cycle and structural resonance
[AIAA PAPER 69-887] 21 p3647 A69-39413

Lift coefficients of idealized tunnel type ram wing consisting of truncated semiconical shell computed by lifting surface theory
22 p3860 A69-40819

Numerical integration of double integral with Cauchy type singularity for calculation of aerodynamic or hydrodynamic load on lifting body
23 p4182 A69-41913

Nonlinear longitudinal dynamics of lifting orbital vehicle in near circular orbit, considering translational motion components effecting orbital decay or dilatation
[AAS PAPER 69-244] 24 p4392 A69-42857

LIFTING REENTRY VEHICLES

NT HL-10 REENTRY VEHICLE

Lifting body type M2-F1 and M2-F2 aircraft enabling astronauts to make own landings at choice airport
03 p0366 A69-13367

Porous ceramic heat shields for lifting reentry vehicles, noting crack propagation resistance and load redistribution
[SAE PAPER 680643] 03 p0453 A69-13457

Variable geometry features applied to lifting spacecraft to overcome inherent incompatibility and provide low speed and tangential landing capabilities
[AIAA PAPER 68-1164] 03 p0520 A69-13562

Boundary layer transition to turbulence shown to have influence on magnitude of lifting reentry body heating rate
[AIAA PAPER 68-1155] 03 p0416 A69-13674

Lifting body entry vehicles in low speed flight test program for determining handling qualities, discussing M2-F2 glide flights
05 p0702 A69-15571

Lifting reentry spacecraft performance examined in context of realistic aerodynamic characteristics at low flight Reynolds numbers
06 p0860 A69-17634

Lifting reentry dynamic stability of flare stabilizers and flap controls
[AIAA PAPER 69-182] 06 p1017 A69-18053

Angle of attack and bank angle for orbiting reentry glider, determining optimal trajectory for ground landing at given point
[ICAS PAPER 68-41] 11 p1966 A69-24750

Intermittent flow facilities for ballistic and lifting reentry flight simulation including shock tubes, ballistic ranges and shock and gun tunnels
11 p1863 A69-25016

Lifting entry concepts for return from earth orbit, discussing deceleration, heating and heat protection
11 p1968 A69-25720

Thermostructural simulation of lifting vehicle panel design, considering safety and trajectory shaping of flying laboratory
12 p2060 A69-26836

Steerable landing gear system consisting of freely casting corotating wheel nose gear, tiltable axle and main gear skids for lifting body spacecraft
[AIAA PAPER 69-790] 19 p3243 A69-35639

Steepest ascent convergence improved in orbital glider reentry trajectories optimization problems, discussing bang-bang and cosine control-variable changes
19 p3398 A69-35666

Aerodynamic performance tests of autotative unpowered rotor entry vehicle model at various Mach numbers and angles of attack
[AIAA PAPER 68-950] 20 p3458 A69-37155

Subsonic glide landing approach guidance for unpowered lifting vehicles, using perturbation feedback and approximation of heading and position coordinates
[AIAA PAPER 69-865] 21 p3763 A69-39391

Hypersonic lifting bodies with high lift-drag ratio, presenting flat-top wing-body combination aerodynamic characteristics
21 p3645 A69-39793

Boundary layer transition to turbulence shown to have influence on magnitude of lifting reentry body heating rate
[CIAA PAPER 68-1155] 24 p4300 A69-43251

Adaptive control function technique to design lateral stability augmentation system for hypothetical manned, lifting body entry vehicle
24 p4394 A69-43301

LIFTING ROTORS

Tip turbine driven flush thin profile wing or platform lift fan design and operating considerations
05 p0696 A69-15554

Small and full scale model tests for feasibility of retracted rotor aircraft for high speed flight
[AIAA PAPER 69-219] 07 p1055 A69-19550

Wake deformation for horizontal and vertical cylinders present in wake of hovering rotor, using flow visualization technique
[AIAA PAPER 69-228] 07 p1051 A69-19551

Helicopter rotor wake distorted geometry prediction by analytical method, noting experimental results for rotor in forward flight
[AIAA PAPER 69-196] 07 p1051 A69-19553

Lifting rotor blades flapping response to atmospheric turbulence, discussing time averaging and perturbation schemes
[AIAA PAPER 69-206] 07 p1057 A69-19577

Lifting rotor dynamics and undesirable characteristics reduction, discussing feedback control systems for pitch and roll
[AHS PAPER 340A] 17 p2899 A69-33509

Lifting rotors with thrust or tilting moment feedback control, deriving blade equations of motion
[AHS PAPER 340] 17 p2899 A69-33510

Discrete sound radiation theory considering rotational noise as dominant rotor noise and stressing fluctuating forces as typical of helicopter rotor
18 p3090 A69-34323

Air mass mechanics, local lifting surface element aerodynamic response and aeroelastic blade response problems in lifting rotor technology
23 p4061 A69-41370

LIFTING SURFACES

U LIFT DEVICES

U SURFACES

LIGHT [VISIBLE RADIATION]

NT AIRGLOW

NT COHERENT LIGHT

NT DAYGLOW

NT GEGENSCHIEIN

NT GEORONAL EMISSIONS

NT NIGHTGLOW

NT SKY RADIATION

NT SUNLIGHT

NT TWILIGHT GLOW

NT ZODIACAL LIGHT

Frequency mixing of IR signals with visible laser light in nonlinear crystals to detect IR signals
01 p0089 A69-10180

Continuous nonresonant visible radiation from Ar ion laser by utilization of wide bore, wall stabilized gas discharges, noting long time frequency stability
01 p0091 A69-10815

Photoinhibition of cell division and growth in Euglenoid flagellates by fluorescent and incandescent visible light
01 p0014 A69-10903

UV and visible light interaction effect on biological activity of Paramecia unicellular infusoria, noting cell division rates and cell deaths
01 p0017 A69-11085

Test method to compare grazing incidence X ray telescope performance in visible light and in X rays
02 p0248 A69-11736

Absorption oscillator strengths of Ba 2 lines in UV and visible spectral regions, using cascade arc in argon with barium vapor
02 p0242 A69-11872

Unsteady phenomena during light pulses interaction in media with polarization, considering group delay, dispersion spreading and space-time analogy
02 p0259 A69-12646

High power output CW laser oscillation measured at 4416 A laser transition in Cd 2 using single isotope of Cd 114
02 p0259 A69-12653

Optical radiation from galaxies, discussing starlight, nonthermal flux and radiation from hot gas
02 p0326 A69-12706

Parametric light generation employing KDP nonlinear crystals with mechanically tuned frequency
03 p0437 A69-13045

Q switched lasers powerful outputs obtainable at sum frequency, discussing frequency mixing in nonlinear dispersive media
03 p0438 A69-13047

Aperture effects in nonlinear optical processes associated with second harmonic and parametric generation of light
03 p0439 A69-13056

Intensity of visible and UV light from beam of positive deuterium molecular ions excited by passage through thin C foil
03 p0471 A69-13166

Visible light extinction properties of continental and maritime air, probing urban, desert and oceanic atmospheres with stable photodiode radiometer
04 p0596 A69-14280

Continuous radiation production in positive plasma column of inert gas considered as manifestation of plasma electrons bremsstrahlung from interaction with gas atoms
05 p0800 A69-15741

Light valving techniques applied to large screen display of computer generated video information, noting electron beam control mechanism for transmitted light
06 p0928 A69-17922

Angular distribution measurements of visible and near IR radiation reflected from carbon dioxide cryodeposits formed on liquid nitrogen cooled surface in vacuum
[AIAA PAPER 69-63] 06 p0959 A69-18131

Visible radiation scattering around Venus spherical atmosphere computed on basis of Venus 4 and Mariner 5 data
07 p1213 A69-18609

Picosecond light pulse measurement by two photon excitation of photographic film
08 p1313 A69-20165

Spherical wave generalization for plane light wave propagating in turbulent medium, describing circular objective averaging effect on intensity fluctuations
08 p1351 A69-20438

Image orthicon tube to detect low intensity pulsed light signals, formulating SNR in terms of resolvable image points
08 p1317 A69-21085

Optical parametric noise in water by ruby laser beam for phase matched four photon process
09 p1539 A69-21751

Light waves refractive index distribution from balloon sounding data found to decrease with height in winter regardless of time of day
09 p1536 A69-21917

Chromium concentrations induced line shift in ruby single crystals spectra, determining principal lines position
10 p1744 A69-23321

Total solar eclipse of September 22, 1968 in Siberia, discussing instrumentation and solar light radiation, corona, prominences, spicules, etc
10 p1782 A69-23696

Light absorption of In and Ga thin films in various gaseous media, noting displacement of irregular absorption band
10 p1747 A69-23792

Pulsed tunable lasers, emphasizing dye lasers for visible and near visible light in specialized spectroscopy
11 p1893 A69-24343

Visible imaging of IR objects by conversion of IR frequency to visible with sum-frequency generation within nonlinear dielectric medium
11 p1897 A69-25037

Absorption characteristics of thin metallic films in standing light wave for mode selection and conversion in lasers
12 p2104 A69-26024

High speed streak camera for recording fast processes, noting changeability from optical to UV spectral range
12 p2085 A69-26155

Holographic recording in spatially incoherent light, describing hologram reconstruction method
12 p2090 A69-26293

Electric vector transformation for three dimensional photoelastic medium irradiated by light in reverse direction, noting optical systems of birefringent plates and rotators
12 p2180 A69-26339

Light interaction with stacked leaves and plant canopy, determining reflectance and transmittance
12 p2097 A69-26985

Law of optical radiation and photometric characteristics of quasars, noting photometric effect of strong emission lines and color dependence on red shift
12 p2168 A69-27052

Light curve shape as function of color, changing period and polarization angle of Crab Nebula optical pulsar
12 p2172 A69-27170

Vela pulsar investigated for optical pulsations, noting negative result for expected brightness
12 p2173 A69-27173

Temporal correlations in light field from laser at threshold of oscillation, measuring He-Ne CW gas laser by photoelectron count
13 p2271 A69-27399

Extragalactic radio sources parameters analyzed for distinguishing quasars from dominant luminous radio galaxies by radio spectra
13 p2348 A69-27801

Frenkel defects in light irradiated p-type InSb single crystals at subthreshold radiation energies
13 p2318 A69-27885

Hypervelocity impact flash resolved into submicrosecond continuum radiation pulse succeeded by slow rising long duration light pulse from neutral atomic line emission
[AIAA PAPER 69-364] 13 p2313 A69-28296

Electrical conductivity and optical spectra changes of strontium titanate single crystals under constant electric field action
15 p2666 A69-30043

Light intensity during coherent scattering based on complex refraction index of medium, noting scattering by clouds and diffraction by semitransparent hole
15 p2635 A69-31108

Light effects on circadian rhythms in monkeys, describing changes in deep body temperature and locomotor activity phase relationships
15 p2556 A69-31336

Spectrum of clipped noise in optical spectroscopy, considering double clipping at zero photon number
15 p2571 A69-31486

Photoelectric observations of W Ursae systems, including observed and computed times of minimum light and period change
16 p2863 A69-32399

Metagalactic light measurements by lunar based night sky photography
18 p3189 A69-34242

UBV photoelectric investigation on southern globular clusters NGC 2808 and 1851, presenting star magnitudes and colors in tabular form and estimating reddening
18 p3190 A69-34290

Night sky Cerenkov light detectors observations of pulsars CP 1133, NP 0532 and NP 0527, noting instrumental limitation in detecting ultrashort light pulses
18 p3200 A69-34994

Intensity changes in visible sidelight emission from carbon dioxide laser switched on and off, calculating vibrational temperatures
18 p3153 A69-35243

Photomechanical and electromechanical effects in semiconductors, considering indentation microhardness decrease caused by light irradiation or electric field
19 p3386 A69-36526

Photographic photometry investigation of Light distribution in spiral galaxies NGC 681, 972 and 1084, discussing mass distribution
20 p3599 A69-37476

Microorganisms death by exposure to high intensity visible and UV light, discussing effect of endogenous photosensitized oxidation on caratoid- containing Rhodotorula glutinus
20 p3475 A69-37613

Eye elemental response to individual frequency jumps in oscillations of light, noting transient effect polarity
21 p3650 A69-38320

Diurnal entrainment deviations and atmospheric turbulence effects on flash photographs from Geos 1
21 p3793 A69-38339

Frenkel defects in light irradiated p-type InSb single crystals at subthreshold radiation energies
21 p3782 A69-39144

Horizon definition for Apollo space navigation references from examining earth atmosphere visible and far IR spectrum
[AIAA PAPER 69-869] 21 p3763 A69-39395

Luminance additivity for human visual system in terms of photometric methods based on direct brightness matching, incremental threshold, etc
22 p3880 A69-40849

Luminance threshold for compound stimulus detection measured as function of two components relative luminance
22 p3880 A69-40852

Emission lines in optical spectra of radio galaxy nuclei, considering time dependent energy release nature
22 p4034 A69-41174

Flashlamp-excited organic dye lasers capable of tunable emission throughout most of visible spectrum
22 p3966 A69-41219

Heat resistant materials integral and spectral radiative properties in IR and visible regions determined by calorimetry and IR spectrometer
23 p4237 A69-41329

Optical ultrashort pulse compression with paired diffraction gratings in terms of phase shift frequency dependence and Fresnel diffraction analogy
23 p4171 A69-41392

Extragalactic universe major constituents and physical properties of normal, radio and compact galaxies, discussing missing matter existence
23 p4217 A69-42317

Law of optical radiation and photometric characteristics of quasars, noting photometric effect of strong emission lines and color dependence on red shift
24 p4375 A69-42552

Photosynthesis enhancement in seaweed after alternate exposure to gas laser and tungsten lamp white light passed through IR narrow band filter
24 p4270 A69-42580

Rotating mirrors used for light signal Doppler frequency shifting
24 p4351 A69-43806

LIGHT ABSORPTION
U ELECTROMAGNETIC ABSORPTION
LIGHT ADAPTATION

High oxygen concentration influence at normal pressure on evoked potential of cortical optic zone and subcortical zones
05 p0709 A69-16515

Darkness adaptation, observing relationship between left and right eye
16 p2745 A69-32448

High intensity light adaptation effects on visibility of raster scan, TV type and avionic displays for symbol luminance needs
16 p2746 A69-32788

High oxygen concentration influence at normal pressure on evoked potential of cortical optic zone and subcortical zones
18 p3096 A69-34734

Pigeon visual adaptation to flickering light, attributing ERG b-wave postadaptation rebound to retina bipolar cells inhibition
23 p4084 A69-41463

Rabbits long term reversible retinal function changes due to short high intensity light flashes, noting ERG suppression
23 p4084 A69-41468

Mathematical model construction to simulate light adaptation in human vision based on Maxwell disk experimental results
23 p4110 A69-41985

LIGHT AIRCRAFT
NT G- 91 AIRCRAFT
NT OH- 6 HELICOPTER
NT SC- 7 AIRCRAFT

Light aircraft all-weather flight feasibility, discussing storm and clear air turbulence detection and icing prevention
01 p0111 A69-11049

Fiat G.91Y subsonic light tactical fighter, discussing fixed armaments and weapons facilities
02 p0193 A69-12679

Light passenger aircraft of glass fiber reinforced plastic, using hose construction technique
03 p0454 A69-13822

Light aircraft hazards due to trailing vortex generated by heavy transport aircraft, suggesting specific procedures for takeoff, landing and flight phase
[SAE PAPER 680220] 04 p0549 A69-14930

LFU 205 light aircraft design and construction with fiberglass reinforced plastic
08 p1321 A69-20867

Human survivability in severe light plane slow speed accidents due to stalling, turning, takeoff or approach, discussing crash load vectors and magnitude
[SAE PAPER 690336] 11 p1822 A69-24492

Light aircraft and helicopter manufacturing methods, design concepts and materials, discussing aluminum airframes, riveting, fiberglass, UV curing, etc
[SAE PAPER 690341] 11 p1822 A69-24498

On-off multiple tank fuel systems for single and twin engine light aircraft, noting fail-safe design
[SAE PAPER 690334] 11 p1825 A69-24502

Gas turbine propulsion engines for small single engine helicopters, discussing costs, performance and FAA tests
[SAE PAPER 690310] 11 p1942 A69-24513

Performance correction and nonstandard day performance prediction for analyzing turbocharged reciprocating aircraft engines in light aircraft applications
[SAE PAPER 690309] 11 p1942 A69-24514

Short range passenger aircraft, considering payloads, weights and economical classification
13 p2201 A69-27294

FAA additional airworthiness standards for small aircraft in air taxi and commercial operations, noting safety levels
[SAE PAPER 690320] 15 p2549 A69-30090

Light aircraft emergency downed position indicators installation program, discussing transmitter minimum performance standards, listening watch insurance, etc
17 p2931 A69-34102

Light rigid civil aircraft response to continuous atmospheric turbulence estimated using two rigid body degrees of freedom method for vertical and lateral gusts
[AIAA PAPER 69-766] 19 p3433 A69-35657

All-plastic light passenger aircraft with inflated tube construction for shell, discussing design and performance
21 p3728 A69-38461

Automated design system producing wire format data for cabling avionics subsystems of light attack aircraft
[AIAA PAPER 69-976] 22 p3912 A69-40356

Cockpit noise intensity during normal cruising operations at various altitudes for 15 different single engine general aviation light aircraft
23 p4102 A69-41676

LIGHT AMPLIFIERS

Gas laser amplifier nonlinear behavior in axial magnetic fields and operating with two polarized light signals of strong or weak intensities
01 p0088 A69-10010

Reflection elimination for single dielectric film on solid laser material substrate, calculating reflectance as function of frequency
02 p0256 A69-11926

Bleaching of absorption hologram diffraction gratings for improved light efficiency, discussing bleaching materials results
04 p0596 A69-14284

Electron radiation temperature measurement in carbon dioxide laser with N and He additions by microwave technique, noting average electron energy and optical gain
04 p0611 A69-14445

Nonstationary nonlinear wave phenomena in ultrashort high intensity light pulse formation, discussing nonstationary stimulated Raman scattering and picosecond pump reduction of Raman amplification
[IEEE PAPER H-5] 05 p0774 A69-16316

Laser amplifiers and oscillators, discussing conversion of active atom excitation energy into light energy
06 p0937 A69-18006

Tandem amplifier system of glass and selenium-oxychloride liquid lasers, discussing input power/output pulse relation and population inversion density measurement
07 p1147 A69-18487

Beam distortion in low order Gaussian-Laguerre modes propagating through saturable laser amplifier, noting uniform and Bessel small signal gain distributions
[IEEE PAPER J-3] 07 p1152 A69-19065

Parametric light interactions application to optics stressing nonlinear spectrograph and cavity and traveling wave oscillator
[IEEE PAPER K-5] 07 p1152 A69-19066

Nonlinear amplification of powerful light pulses in Nd glass
08 p1323 A69-19946

Small signal pulsed gas laser amplification limits, discussing time dependency, temperature effects, relaxation rates and energy transfer
08 p1324 A69-20098

Carbon dioxide laser combining gas flow with fluid mixing to achieve high gain
10 p1701 A69-22954

Ultrashort light pulses nonlinear amplification in medium with finite transverse relaxation time and linear radiation losses
10 p1702 A69-23139

Amplification factor of He-Ne traveling wave light amplifier, discussing frequency stability and telescopic wave front broadening for uniform radiation distribution
11 p1894 A69-24623

Carbon dioxide-N-He laser amplifier, noting gain time dependence and thermal relaxation rate after gas heating
11 p1899 A69-25054

Gain decrease due to saturation during amplification of pulses from Q switched carbon dioxide laser oscillator, noting rotational sublevels relaxation rate
11 p1899 A69-25055

Single frequency sealed off carbon dioxide amplifier, giving saturated gain
12 p2109 A69-26640

Optical IR yttrium-iron garnet rectifier increasing light intensity and system Q factor at low external magnetic field
17 p2981 A69-33117

LIGHT BEAMS

Continuous laser beam power output meter based on wire resistance thermometry method
01 p0081 A69-10822

Laser beam phase fluctuations for propagation through turbulent atmosphere, noting interferometer for simultaneous measurements for pairs of rays
01 p0091 A69-10845

Gas lens distortion of Gaussian light beam in sequence of lenses with same aberration, using shuttle pulse technique
01 p0120 A69-10849

One dimensional expansion of laser beam, using pairs of prisms with continuous wave output
01 p0091 A69-10852

Light field inside deep layers of turbid medium illuminated by narrow beam, discussing beam deviations inside medium, deviation dispersions and correlation coefficient
02 p0274 A69-11449

Bragg reflection of electrons by standing light waves of giant pulse laser
02 p0255 A69-11833

Mean square amplitude and phase fluctuations for propagation of light beam with Gaussian amplitude distribution through medium with randomly varying refractivity
02 p0208 A69-12308

Tubular light beam waveguide properties, studying changes related to heating and ionization of medium
02 p0258 A69-12644

Pumping beam width influence on optical range resonator excited coupled oscillations, deriving approximate equations
03 p0437 A69-13043

Ruby laser light beam self focusing in sodium chloride and potassium bromide crystals
03 p0438 A69-13051

Coordinates interpretation in Schwarzschild problem, projecting space of events by light beams onto Galilean system at infinity
03 p0506 A69-13090

Ionizing action of radiation due to heating substance in laser beam focus, discussing highly ionized plasma production
03 p0479 A69-13998

Kerr effect and electrostriction during self focusing of high power laser beam in gases and liquids
04 p0611 A69-14792

Scanned laser beam display techniques based on cathode ray tube technology, noting flying spot scanner and beam deflection
04 p0600 A69-15028

Thermal self actions of CW laser beams in solids and liquids with wind or convection flow, discussing self focusing and defocusing
[IEEE PAPER E-12] 05 p0774 A69-16311

Atmospheric vertical density and pressure profiles determined from satellite measurements of light beam phase shift and refraction angle
05 p0760 A69-16694

Electric and magnetic fields of narrow coherent polarized light beam in free space, noting longitudinal field components due to beam narrowness
05 p0777 A69-16789

Laser resonators, noting relation of light path between mirrors to half wavelength and line equivalence of lenses and resonators
06 p0937 A69-18005

Laser applications to situations requiring highly bunched high power density light beams
06 p0938 A69-18012

Electromagnetic field strength of narrow polarized monochromatic light beam, noting spatial curvature and twisting in beam current line
07 p1147 A69-18524

Velocity measurement by combination of Doppler principle and schlieren method involving reflection, refraction or diffraction of laser beam
07 p1135 A69-19259

IR beam profiles of carbon dioxide laser permanently recorded on foamed polystyrene
07 p1156 A69-19305

Micromachining with laser beam, choosing mirrors and lenses of optical system to provide uniform energy distribution for microwelding or hole boring
08 p1324 A69-19980

Self modulation, self steepening and spectral development of light in small scale trapped filaments, noting influence of relaxation time
08 p1352 A69-20745

Vaporization of mist of small droplets by intense light beam for droplet extinction rate proportional to absorbed radiant energy
09 p1539 A69-21346

Emission intensity and beam divergence of p-n junction GaAs laser with nonlinear passive element in resonator
09 p1515 A69-21474

Low current arc discharge plasma diagnostics by light probe, analyzing deviation of resonance level population from equilibrium described by Saha equation
09 p1546 A69-21586

Laser beam optical scintillation under atmospheric turbulence conditions, showing log amplitude variance saturation and decrease
09 p1517 A69-22079

Laser beam scintillation at night over long atmospheric horizontal paths, showing log amplitude covariance observation in agreement with theoretical prediction
09 p1517 A69-22080

Fabry-Perot resonator and beam waveguide systems for laser beams, noting mode coupling and separation in laser optical systems
09 p1518 A69-22125

Passive electromagnetic circuit elements for laser light control such as circulators, isolators and phase shifters, discussing coherent light and polarization
09 p1518 A69-22127

Laser beam modulation and deflection methods involving control of amplitude, phase, frequency and direction, noting use of semiconductor p-n junctions
09 p1518 A69-22128

Gaussian laser beam reflection and refraction at curved interface between media of different refractive indices, considering tilted ellipsoidal interfaces
10 p1725 A69-23309

Imaging ultrasound by holography with reconstruction in light, comparing methods using scanned hologram and liquid surface
10 p1695 A69-23543

Sinusoidally modulated light beam propagation in turbid media, studying phase velocity and attenuation coefficient as function of modulation frequency
10 p1658 A69-23951

Incident integral light flux relations and visibility range equation derived for objects illuminated by narrow light beams in scattering media
10 p1725 A69-23971

Conventional and dual beam laser Doppler methods for velocity measurement of solids, liquids and gases
11 p1893 A69-24333

Laser beam for determining instrumental profile of high resolution double pass solar spectrograph, noting influence of slits width
11 p1893 A69-24431

Population inversion distribution and wave processes in optical amplifier, showing beam transformation of constant section and dependence on crystal characteristics
11 p1893 A69-24447

Holographic scanning technique for laser beam deflection, noting two and three dimensional raster scanning
11 p1885 A69-24847

Fluctuations in angle of arrival of laser and thermal radiation beams over near ground path
11 p1840 A69-25570

Three dimensional log amplitude and phase fluctuation distributions of collimated and focused Gaussian beams propagated through random inhomogeneous medium, evaluating mean-square values
12 p2130 A69-26393

Atmospheric effects on laser beam width, using Born approximation and Gaussian model to obtain TEM mode scattered power expressions
12 p2111 A69-27166

Optical detection signals optimization in optical pumping, discussing light beam propagation direction, spectral composition and polarization characteristics 12 p2111 A69-27180

Spiral trajectory winding rate of asymmetrical light beams in nonlinear media analyzed in geometric optics approximation, noting diffraction influence 13 p2298 A69-27662

Vertical refraction effect on gas laser beam propagation near earth surface under various meteorological conditions, comparing index for diffuse light 13 p2220 A69-27827

Weakly divergent intense light beam propagation in laminar optically inhomogeneous medium with self focusing possibility analyzed by perturbation theory 13 p2223 A69-28568

Coordinates interpretation in Schwarzschild problem, projecting space of events by light beams onto Galilean system at infinity 14 p2516 A69-28772

Log amplitude fluctuations of laser beam in turbulent atmosphere, obtaining asymptotic expressions for near field of transmitter aperture 14 p2460 A69-29638

Plasma temperature measurement by resonant laser radiation absorption, assuming Saha-Boltzmann relation 14 p2501 A69-29954

Emission intensity and beam divergence of p-n junction GaAs laser with nonlinear passive element in resonator 15 p2633 A69-30719

Combined distribution density of elevations and slopes for illuminated areas of stable statistically homogeneous random surface exposed to parallel rays beam 15 p2569 A69-30948

Laser amplifier nonlinear losses effect on light beam propagation, studying arbitrary waveform development into asymptotic steady state pulse /SSP/ 16 p2797 A69-32043

Multibeam transmission in optical beam waveguides by simulation, discussing intensity profiles phase fronts and cross scattering 17 p2974 A69-33400

Electron beam pumped semiconductor laser light beam amplitude and phase distribution, studying effects of inhomogeneous excitation by model 21 p3737 A69-39041

Optical properties of Gabor holograms with pure reference beam, discussing image reconstruction using He-Ne laser 21 p3726 A69-39624

Incident integral light flux relations and visibility range equation derived for objects illuminated by narrow light beams in scattering media 21 p3772 A69-39657

Steady state mathematical modeling of light field structure for narrow collimated light beams propagating in artificial dispersive media 22 p3981 A69-40245

Algorithm for numerical modeling by Monte Carlo method of diffusion bounded light beams in dispersive media, applying to light pulse in cloudlike medium 22 p3981 A69-40248

Holographic technique of coherent light field transformation with desirable phase distribution from laser light beams of arbitrary wavefront characteristics 22 p3950 A69-41115

Light field long term behavior in dispersive medium with finite optical thickness by asymptotic solution of unsteady transport equation 22 p3983 A69-41267

Reconstruction of three dimensional holograms without reference beam, noting thick layered Lippmann emulsions and dyed alkali halide crystals 23 p4166 A69-41969

Log amplitude mean value for Gaussian or laser-like optical beam propagating horizontally in turbulent atmosphere 24 p4282 A69-42970

Beam divergence and multimode laser visible emission influence on power and angular structure of second optical harmonic generated in KDP crystals 24 p4328 A69-43161

Gas lens system for periodic light beam waveguide, describing gas enclosed in circular cylinder and heated by specific temperature distribution 24 p4350 A69-43332

Angular distribution of He-Ne laser beam scattered by artificial fog from data by light detection devices at various angles 24 p4328 A69-43503

LIGHT DURATION

U FLASH
U PULSE DURATION
LIGHT ELEMENTS

Large hydraulic press forgings for light metals, discussing 50,000 ton machine used for Al alloys, tooling and die considerations [ASM PAPER C7-5.1] 04 p6004 A69-14521

Cosmic ray Li, Be and B nuclei measurements, analyzing differential energy spectra, L-M ratio, atmospheric and solar modulation 08 p1380 A69-20638

Model for nucleosynthesis of Li, Be and B in solar system from mass spectrometric measurements of high energy proton production of light elements 08 p1401 A69-20901

Stellar abundances of lithium, deuterium, beryllium and boron indicating nonthermal atmospheric origin 08 p1403 A69-20912

Inelastic interactions between Tev cosmic particles and light element nuclei, describing design and operation of measuring apparatus and derivable data 12 p2093 A69-26583

Photoelectric and visual minima tabulated for eclipsing binaries, calculating light elements 12 p2160 A69-26853

Solar system light elements investigated assuming Li, Be and B abundance as nuclear reaction products of high energy particles accelerated in early sun formation 13 p2354 A69-28495

Stellar light element abundances, discussing evolution models for various star types 16 p2866 A69-32816

Intermediate energy protons elastic and quasi-elastic scattering from light nuclei, correlating p-D, p-He-3, p-p and p-He-4 data with various scattering models 24 p4352 A69-43123

Differential cross section and polarization measurements for elastic scattering of high energy protons from light nuclei 24 p4352 A69-43125

LIGHT EMISSION

NT BIOLUMINESCENCE
NT CHEMILUMINESCENCE
NT ELECTROLUMINESCENCE
NT FLUORESCENCE
NT LUMINESCENCE
NT LUNAR LUMINESCENCE
NT OPTICAL RESONANCE
NT PHOSPHORESCENCE
NT PHOTOLUMINESCENCE
NT SHOCK WAVE LUMINESCENCE
NT THERMOLUMINESCENCE
NT X RAY FLUORESCENCE

Light emission and transmission generated from laser interaction with lithium hydride in vacuum, noting laser energy variations effects 01 p0127 A69-10281

Continuous and time-resolved absorption and emission spectra studies produced by exploding wires in gases, discussing effects of environment, pressure and electrical energy 01 p0118 A69-10664

Auroral emission rates and heating effects as function of altitudes 02 p0235 A69-11426

Short laser radiation pulses spectral characteristics determination with device converting laser emission frequency by nonlinear electro-optical crystals 02 p0257 A69-12560

Emitted light and excited state populations resulting from two electron collisional radiative recombination related to free electron density 03 p0469 A69-12923

Diurnal, magnetic and solar cycle dependences of auroral emission variations and auroral occurrence 03 p0420 A69-13325

UV induced excited-state properties of DNA using optical emission and electron spin resonance methods 03 p0372 A69-13488

Bistable operating mode of GaAs semiconductor laser involving light emission shifts 03 p0441 A69-14175

Optimal modulation shape for light emission flux as function of photoresistance detector and resonance amplifier pulse characteristics 04 p0560 A69-15376

Quasar and radio galaxy evolution, discussing energy release rate and particle acceleration effects on radio and optical emissions 05 p0822 A69-15852

Ratio of volume emission rate of 5577 A photons to volume emission rate of one band of positive nitrogen molecule first negative system in aurora 05 p0756 A69-16360

Conversion of emission from pulse tube using neodymium laser with luminophor solution filled active element, discussing pumping nonlinear absorption kinetics 05 p0777 A69-16373

Flaming auroras observations with auroral image orthicon TV systems, calculating electron release points on field line of station 05 p0758 A69-16413

Red light emitting p-n junctions in GaP fabricated by epitaxial growth 06 p0979 A69-16999

Electron impact excitation cross sections for emission from first negative bands of positive N molecule ion 06 p0961 A69-17135

GaAs IR emitters efficiency due to semiconductor material band structure 06 p0894 A69-17248

Light generation by laser organic dye liquid solution with negative absorption on activator molecules and induced combination scattering for solvent molecules 06 p0933 A69-17256

Frequency doubling of laser light with variable Q switched resonator 07 p1158 A69-19753

Energy dissipation of solar particles in atmosphere for 3914 and 5577 A bands, computing light emissions associated with PCA 08 p1378 A69-20186

Properties of ion implanted GaAs diodes fabricated at room temperature, analyzing light emission, resistance and breakdown voltage [ECS PAPER 172] 08 p1284 A69-20369

Time dependent behavior of atomic light emitted from pulsed helium afterglow, noting absorption measurements and spectrometric system 08 p1356 A69-20743

Formation and characteristics of flash produced in air by single pulse of Q switched ruby laser, using holographic interferograms 08 p1317 A69-21022

Ratio of volume emission rates of 5577 A and band of positive N molecular ion first negative system for use in auroral observations 09 p1491 A69-22607

Optical flashes recorded from Crab Nebula M1 close to central double star with periodicity equal to radio pulses discovered earlier 11 p1962 A69-25250

Poisson formula in double logarithmic approximation for photon emission cross section in analysis of bremsstrahlung involving high energy particles 11 p1922 A69-25758

Photochemical attitude control rocket adaptable to self contained command signal or remote signal transmission, discussing light irradiation of propellant for thrust control 12 p2148 A69-26801

Optical radiation detection from pulsar PSR 0833-45 associated with supernova remnant in Vela, noting UV excess from plates using U and B filters 13 p2337 A69-27516

Auroral luminosity determination by two photometers on ESRO 1 satellite 13 p2253 A69-27752

Photon emission from highly relativistic stars, using computed differential light delays to calculate blurring of spherically symmetrical emission pulses 13 p2350 A69-27825

Light emission intensity correlation functions associated with LF oscillations in beam plasma discharge 14 p2498 A69-29814

Aurora electron and proton excitation patterns determined spectroscopically, discussing ground based observations of emission geomagnetic latitude-time distribution 15 p2593 A69-30017

Current effects on quantum efficiency of gallium phosphide junction diodes emitting red light 15 p2575 A69-30174

Short laser radiation pulses spectral characteristics determination with device converting laser emission frequency by nonlinear electro-optical crystals 15 p2633 A69-30257

Sco X-1 fluctuating optical and X ray emission observed simultaneously, determining total energy flux and plasma radius and density 15 p2676 A69-30885

Close binary system components approximated by two nonsimilar ellipsoids, obtaining interpretation of light curves 15 p2695 A69-30957

LIGHT COMMUNICATION

U OPTICAL COMMUNICATION

Optimal modulation shape for light emission flux as function of photoresistance detector and resonance amplifier pulse characteristics
16 p2752 A69-32123

Pulsating and flaming auroral patches recorded by image intensifier vidicon camera, calculating upward field aligned speeds for luminosity enhancement
16 p2870 A69-32305

Prebreakdown and breakdown electrical properties and light emission during destructive breakdown in thin film capacitors
16 p2761 A69-32323

Electromagnetic /ULF, VLF/ and light emissions development during magnetic substorms, discussing varied pulsations present in development phases
16 p2788 A69-32648

Nanosecond optical pulses from Crab pulsar NP 0532 detection indicating negative observations
16 p2865 A69-32801

Emission intensity ratio change as function of polar auroral height compared to variation in atmospheric concentration ratio of oxygen to nitrogen
17 p2963 A69-33956

Ionospheric processes associated with changes in polar aurora height, noting glow in E layer and soft electron emission into earth atmosphere
17 p2964 A69-33957

Light curve of pulsar NP 0532 represented with oblique rotator hypothesis, assuming concentrated emission at opposite spots on star
18 p3192 A69-34321

White light solar corona brightness distribution observations /1964-1967/, considering solar radio flux relationship and equatorial electron densities
18 p3205 A69-35394

Parametric conversion kinetics of monochromatic light waves in nonlinear crystals, using quantized electromagnetic field to study amplification and generation
19 p3332 A69-35870

Light emitting diodes /LED/, discussing operating voltage vs color, diode materials and applications
20 p3505 A69-37702

Ionospheric currents geophysical DC electric fields measurement from sounding rockets, indicating anticorrelation with auroral luminosity
21 p3710 A69-38508

Coherent light emission by molecules excited by laser pulses having duration comparable to active medium polarization relaxation time
21 p3737 A69-38999

Quantitative criteria imposed on balloon measurements of auroral emissions from Kiruna, considering times of sunrise and sunset at different altitudes
21 p3716 A69-39250

Nonlinear intensity transitions involving order of magnitude increases in visible luminosity of RF generated plasmas, noting inductive field and electron density influence
23 p4196 A69-41546

Auroral short period pulsations in 6300 A O I, discussing percentage modulation, quenching rate, etc
24 p4309 A69-43171

Ionization and light emission cross sections for collisions of protons and hydrogen atoms with atmospheric nitrogen used to analyze auroral events
24 p4368 A69-43177

LIGHT GAS GUNS

Variable resistance strain gages for study of light gas guns operating characteristics, including chamber pressure and piston velocity
19 p3306 A69-35736

LIGHT INTENSITY

U LUMINOUS INTENSITY

LIGHT MODULATION

NT ULTRASONIC LIGHT MODULATION

Laser beam spectra for modulation by electrooptic Doppler shift, considering sawtooth and triangular functions for applied electric field
01 p0091 A69-10843

Optical modulation near intrinsic edge in n-type bulk GaAs due to Franz-Keldysh effect, noting carrier production by photon initiated excitation
02 p0300 A69-12650

Laser display technology, discussing experimental systems, light sources, modulation and scanning
03 p0431 A69-13850

Transverse electro-optical effect in piezoelectric crystals, using light modulation
04 p0639 A69-14427

Optimal modulation shape for light emission flux as function of photoresistance detector and resonance amplifier pulse characteristics
04 p0560 A69-15376

Wideband multichannel optical signals nonlinear distortions during transmission by electrooptical modulators using Pockels effect
05 p0718 A69-15655

Electron beam modulation of germanium reflectance
05 p0807 A69-15816

Wideband microwave KDP light modulator for amplitude and phase modulation, using ring-plane traveling wave circuit
05 p0732 A69-16553

Electro-optical effect in Cr-doped GaAs single crystals at room temperature, discussing carbon dioxide laser radiation modulation by GaAs
06 p0934 A69-17466

Optical breakdown in air by mode synchronization operation of ultrashort pulses from neodymium laser
06 p0934 A69-17546

Automatic closed loop distortionless control of magnetic field modulation using light sensitive resistor as one leg of attenuator
06 p0897 A69-17708

External and internal modulation methods in lasers noting phase, amplitude and frequency modulation, birefringence, electrooptics and Stark and Zeeman effects
06 p0937 A69-18010

Absorption edge broadening by electric field in Gunn domain of N-GaAs crystals
07 p1197 A69-18454

Signal conversion by multiple modulation in optical communication system, discussing electrooptic modulators and modulation spectrum
07 p1075 A69-18472

Self modulated radiation modes of Te-doped n-type InAs injection lasers
07 p1148 A69-18685

Laser modulation at optical and near IR frequencies, discussing beam characteristics changes and information transmission
07 p1158 A69-19742

Magneto-optic, acousto-optic, electro-optic and free carrier modulation of IR laser beams
07 p1158 A69-19743

Natural intensity fluctuations spectrum of He-Ne laser, determining modulation coefficient dependence on output
08 p1325 A69-20431

Self modulation, self steepening and spectral development of light in small scale trapped filaments, noting influence of relaxation time
08 p1352 A69-20745

Book on laser communication system design covering modulation and detection methods
08 p1277 A69-20884

Laser beam modulation and deflection methods involving control of amplitude, phase, frequency and direction, noting use of semiconductor p-n junctions
09 p1518 A69-22128

Sinusoidally modulated light beam propagation in turbid media, studying phase velocity and attenuation coefficient as function of modulation frequency
10 p1658 A69-23951

Bias elimination in intensity pattern of incoherent holograms by introducing narrow band time modulation of light
11 p1885 A69-24846

Electro-optic broadband laser light modulator designs and modulation characteristics, computing curve set for evaluation of various materials
11 p1897 A69-25039

Propagation of intensity modulated light rays in semiinfinite isotropic dispersive medium, discussing phase shift and modulation depth
12 p2029 A69-26026

Microwave modulation of GaAs injection laser radiation, using Zaleskii recording method and liquid nitrogen to cool laser diode
12 p2105 A69-26031

Direct modulation characteristics of semiconductor junction laser, analyzing resonance phenomenon, bias current, admittance, modulation frequency limit and emission lifetime
12 p2110 A69-27069

Optimal modulation shape for light emission flux as function of photoresistance detector and resonance amplifier pulse characteristics
16 p2752 A69-32123

Wideband multichannel optical signals nonlinear distortions during transmission by electro-optical modulators using Pockels effect
16 p2754 A69-32512

Electro-optical crystals resonance modulator for coherent light beams and microwave frequencies,

describing application to multichannel TV transmission system
19 p3266 A69-35763

Laser radiation modulation at EHF by linear electro-optical effect of KDP and ADP crystals
19 p3334 A69-35884

Internal modulation of HeNe laser in asynchronous regime, evaluating range and efficiency with regard to external modulation
19 p3335 A69-36341

Light induced shift of Rb 87 vapor laser emission frequency during modulated optical pumping, discussing elimination by filter temperature and tuning
19 p3336 A69-36344

Indium arsenide injection laser observed for self modulation at LF modes, discussing nonMarkovian character of photon density relaxation
19 p3338 A69-36537

Stable mode generation in ruby laser with ability for modulation, using convex resonator and uniform illumination
20 p3553 A69-37607

Electro-optical effect in Cr-doped GaAs single crystals at room temperature, discussing carbon dioxide laser radiation modulation by GaAs
20 p3555 A69-37949

Alford and Gold light modulation effect expanded to include one frequency spectrum with Doppler shift, discussing applications to optical radar for range and velocity measurements
21 p3672 A69-38409

Multimode He-Ne laser radiation polarization modulation as function of magnetic field, cavity anisotropy and frequency, using Macaluso-Corbino effect
21 p3739 A69-39447

Distance measuring method limitations for modulated CW laser determined by laser transmitter receiver in conjunction with retroreflector target fixed position
21 p3739 A69-39457

Optical rectification in crystals by excitation of nonlinear /time constant and space variable/ polarization
23 p4174 A69-41874

LIGHT PRESSURE

U ILLUMINANCE

LIGHT SCATTERING

NT HALOS

Light scattering from plasmas embedded in homogeneous magnetic field, discussing solid state and high temperature gas plasmas
01 p0125 A69-10015

Three dimensional holography using scatter plates applicable to transilluminated objects in particular distribution of particles or phase disturbances
01 p0079 A69-10217

Multiple light scattering and reflection elimination from observed light brightness indicatrix to obtain true light scattering indicatrix, discussing error analysis
01 p0074 A69-11184

Atmospheric optical properties stability determination for various optical densities, assuming horizontally homogeneous medium with properties constant during observation
01 p0074 A69-11186

Turbulence characteristics from light wave fluctuation measurements, discussing applications to small scale inhomogeneities in atmospheric temperature distribution
02 p0274 A69-11437

Multiple light scattering in planetary atmospheres, discussing diffuse reflection and transmission by atmosphere of particles with anisotropic scattering pattern
02 p0319 A69-12105

Light-light interaction in homogenous media ascribed to multilevel atomic system simultaneous excitation by both fields
02 p0258 A69-12637

Light wave propagation in gyrotropic crystals, examining laser frequency shift circularly polarized by modulating field
03 p0436 A69-13037

Resonance light pulse propagation in one dimensional medium containing n and m quantum emitters located in Fabry-Perot resonator
03 p0437 A69-13039

Ruby laser to study stimulated Mandelstam-Brillouin scattering in liquids and in various crystals in UV
03 p0438 A69-13053

Particle size distribution determination by measuring light beam extinction in turbid medium with photometer
03 p0428 A69-13110

Hydrodynamic theory of light scattering by dilute monatomic gases generalized by using linearized Burnett equations instead of Navier-Stokes equations
03 p0466 A69-13135

Polarization of laser radiation scattered forward and back in artificial fog and smoke
03 p0393 A69-13275

Ring laser field space-time pattern from light waves scattered at discontinuities, discussing equations of motion of solid state laser
03 p0441 A69-14140

Linear integral equations for brightness coefficients and auxiliary functions in semiinfinite atmosphere, expressing atmospheric albedo using moments and Chandrasekhar function
04 p0662 A69-15237

Light polarization of night sky components scattered by troposphere
04 p0595 A69-15247

Laser light scattering by plasma using theory of ionospheric scattering of radar signals, determining scattered spectrum
05 p0798 A69-15586

Passive Q switching of solid state lasers based on stimulated Mandelstam-Brillouin light scattering
05 p0770 A69-15699

Differential cross section frequency dependence for resonant scattering of monochromatic light by dilute gas atoms
[IEEE PAPER T-8]
05 p0776 A69-16328

Laser scatter measurements in mesosphere and above for optical radar system parameters
05 p0758 A69-16414

Laser beam scattering by acoustic waves of ionized crystal, reconsidering stimulated Brillouin emission theory for ultrasonic yield
05 p0777 A69-16610

Multiple light scattering in spherical planetary atmosphere based on geometrical model, calculating twilight glow brightness
05 p0828 A69-16632

Nonscattered, singly and multiply scattered light of beam from point source analyzed at boundary layer of turbid medium
05 p0789 A69-16640

Attitude stabilized balloon telescope for measuring interplanetary scattered light and nightglow
06 p0999 A69-16972

Directly backscattered light /echoes/ from dielectric plane surface with roughness and volume scattering, comparing indicatrices with moon echo
06 p0887 A69-17173

Rayleigh scattering cross sections for He, C, N and O compared with corresponding absorption coefficients, noting opacity of H deficient stars
06 p1002 A69-17319

Integral equation solution with Mellin inversion formulas for light scattering problems
06 p0949 A69-17887

Water droplet simulation by glass spheres used in study of light scattering at cloud particles
06 p0953 A69-17992

Photoelectric equipment for nephelometric simulation studies of light scattering by cloud particles
06 p0953 A69-17993

Theta pinch plasma electron density and temperature distributions measured using Thompson scattering of laser light and plasma bremsstrahlung
06 p0972 A69-18220

Visible radiation scattering around Venus spherical atmosphere computed on basis of Venus 4 and Mariner 5 data
07 p1213 A69-18609

Laser light scattering with orientation saturation of microsystems by electric field, noting application to optical anisotropy of macromolecules and colloidal particles
07 p1149 A69-18900

Velocity measurement by combination of Doppler principle and schlieren method involving reflection, refraction or diffraction of laser beam
07 p1135 A69-19259

Spectrum of light scattered by particles suspended in turbulent fluid
07 p1157 A69-19417

Quantum mechanical, dipole approximation, nonresonance light scattering cross sections expressed in terms of oscillator strengths and refractive indices
07 p1183 A69-19645

Vector equation of transfer for planetary atmosphere describing light scattering by anisotropic particles and analysis of resonance line scattering
08 p1385 A69-20063

Holography applied to schlieren and phase contrast methods to enable visualization of minute phase change in light scattering object
08 p1313 A69-20176

Collective interactions of electromagnetic waves in plasma, discussing light scattering from electron fluctuations, stimulated emission and anomalous absorption
08 p1361 A69-20220

Scattered light reduction in sunspot photometry, noting eliminating effect when observing spectral lines or narrow spectral regions
08 p1389 A69-20251

Atmospheric turbidity and visibility measuring instrument /videograph/ using light backscattering, noting shipboard, coast guard service, large cities and weather stations applications
08 p1314 A69-20376

Fraunhofer line distortion on scattering from zodiacal dust cloud for various particle density and size distributions, discussing Keplerian orbits
08 p1308 A69-20391

Plasma diagnostics by use of lasers, discussing Thomson scattering and problems arising from light scattering applications
08 p1326 A69-20471

Inhomogeneous laser beams self focusing effects in organic liquids recorded on bases of induced stimulated scattering
08 p1326 A69-20538

Laser operation through semiclassical dispersion theory, presenting dipole moment and population density equations derived from quantum theory
08 p1326 A69-20571

Laser beam propagation in scattering media, noting attenuation coefficients for coherent and incoherent radiation
08 p1328 A69-21092

Spectral study of Stokes vector for light scattered by natural objects, recommending phase and optical axis inclination angles for aircraft measurements
09 p1588 A69-21367

Spatial distribution of velocity, spatial correlation and ergodicity of turbulent flow, using spectrum of intensity fluctuations of scattered laser light
09 p1493 A69-21491

Stimulated Mandelstam-Brillouin scattering in compressed N and H as function of pressure, using ruby laser pulses
09 p1516 A69-21562

Automatic counter for concentration of cloud condensation nuclei in thermal diffusion chamber, measuring light scattering coefficient of cloud
09 p1494 A69-21640

Spacecraft debris atmosphere effects on observations, discussing contamination of exposed optical surfaces and light scattering by ice particles from cabin water vapor leakage
09 p1487 A69-21654

Optical transfer function in single scattering approximation for light scattering media consisting of large particles
09 p1536 A69-21865

Laser spark image in air photographed in scattered laser radiation light, showing singularities and absence of beadlike structure
09 p1519 A69-22531

Stimulated Mandelstam-Brillouin scattering at second harmonic of ruby laser and neodymium glass laser
09 p1520 A69-22684

First Stokes component of stimulated Mandelstam-Brillouin scattering and line defects caused by self focusing of single pulse laser beam
09 p1521 A69-22686

Scattered light mean intensity determination in twilight aerosol atmosphere from satellite observations, formulating boundary value problem
10 p1689 A69-23970

Incident integral light flux relations and visibility range equation derived for objects illuminated by narrow light beams in scattering media
10 p1725 A69-23971

Laser radiation backscatter along oblique paths in atmosphere, calculating transmission over horizontal and oblique paths
10 p1659 A69-24220

Laser radiation spectrum scattered by low temperature plasma electrons at atmospheric pressure
11 p1922 A69-24233

Spectral broadening measurements of ruby laser light scattered by density fluctuations in theta pinch plasma
11 p1924 A69-24304

Ion and electron temperature and density measurement by Thomson scattering with low resolution monochromator for Salpeter parameter near unity
11 p1925 A69-24310

Laser light scattering in radiation driven breakdown waves in He, using high resolution streak photography to obtain diagnostic data
11 p1915 A69-24420

Integral time characteristics for unsteady light scattering by using solution to corresponding steady state problem of light pulse scattering in medium
11 p1915 A69-24604

Polarization effects of scattered coherent light on laser imagery, determining surface roughness and angle of incidence effects photographically on basis of Fung theory
11 p1896 A69-24849

Atmospheric scattering behavior under reduced visibility conditions for laser wavelengths of 0.69 and 1.06 micron
11 p1837 A69-25040

Single and clad glass fibers radii and refractive indices measurements on basis of laser light scattering
11 p1918 A69-25044

Ruby laser light scattered at 90 degrees by dense plasma focus, analyzing signal detection
11 p1899 A69-25324

Light scattering materials for transparent objects holography, analyzing Christiansen filter and milk white and ground glass plates
11 p1889 A69-25550

Unicellular microorganisms size and concentration estimates based on light scattering measurements of suspensions in spectrophotometer cuvette compartment
11 p1829 A69-25643

Propagation of intensity modulated light rays in semiinfinite isotropic dispersive medium, discussing phase shift and modulation depth
12 p2029 A69-26026

Fiber optics application to fiberscopes and fused fiber optic plates, noting surface coating for light scattering prevention
12 p2084 A69-26150

Flare or stray light measured in long focus photographic objectives by photometric sphere and spherical segments without collimator
12 p2093 A69-26590

IR polarizing microscope with IR corrected objectives and eyepieces providing higher contrast, sharper focusing and less light scattering
12 p2093 A69-26595

Spectroscopy application to spontaneous combination scattering of light
12 p2108 A69-26618

Laser light scattered from arc discharge, observing enhanced plasma oscillations
13 p2307 A69-27629

Lunar surface light scattering data cataloged for various phase angles from photometric observations of lunar features brightness
13 p2344 A69-27648

Light scattering from high reflectivity dielectric mirrors, measuring angular power distribution from beam axis by scanning with narrow slit
13 p2298 A69-27663

Collective scattering of light from ruby laser by cold dense deuterium plasma produced by electrical discharge, deducing density and electron temperature
13 p2273 A69-28366

Spotted scattered background contrast relation to scattering system geometry during laser scattering by suspended Lycopodium spores
13 p2273 A69-28550

Microstructure of light scattering media consisting of large size spherical particles
14 p2481 A69-28737

Double light scattering near critical point, examining angular distribution
14 p2482 A69-28738

Polarization of laser radiation scattered forward and back in artificial fog and smoke
14 p2410 A69-28783

Nonscattered, singly and multiply scattered light of beam from point source analyzed at boundary layer of turbid medium
14 p2482 A69-28796

Light scattering in single component systems near critical point analyzed by critical phenomena classical theory and Rayleigh theory
14 p2485 A69-28995

Light diffusive reflection from rough surface measured as function of angle of incidence in presence of specular component by goniospectrophotometer
14 p2485 A69-29171

Laser radiation conversion during induced combination scattering, discussing stabilization of emission mode of first Stokes component

14 p2460 A69-29648

Transfer equation and Bouguer-Lambert-Beer equation application to multiple light scattering in plane medium

14 p2487 A69-29663

Sunspot equivalent line widths calculated using sunspot models, considering influence of light scatter correction

14 p2525 A69-29721

Helium plasma electron temperature and concentration measured in arc in magnetic field by laser light scattering at electrons

14 p2496 A69-29780

Pulsed HF discharge analysis in hydrogen based on laser light scattering at plasma electrons, noting presence of satellites

14 p2451 A69-29781

Negative dispersion of light in neodymium activated calcium tungstate single crystal using neodymium glass laser source, analyzing interferential bands in spectral diagrams

15 p2632 A69-30051

Polarization and angular distribution of 6328 A He-Ne laser light scattered by latex-sphere hydrosols, comparing coherent and incoherent scattering patterns

15 p2595 A69-30223

Remote polarized light source photometric observation on background of polarized light scattered horizontally, considering atmosphere optical state effect on laser communications

15 p2649 A69-30655

Recording arrangement aperture effect on plasma scattering spectrum during plasma parameter determination by light scattering technique

15 p2664 A69-30996

Optimal parameters of cuvette for use with helium-neon laser as excitation source to record combination light scattering spectra of powdery materials

15 p2635 A69-31105

Light intensity during coherent scattering based on complex refraction index of medium, noting scattering by clouds and diffraction by semitransparent hole

15 p2635 A69-31108

Thermodynamic Green function for Compton scatter cross section of photons by electrons in hot plasma

15 p2664 A69-31479

Wavelength dependence of linear polarization of sunlight scattered by Venus, noting temporal variations in UV

16 p2860 A69-32236

Wavelength dependence of polarization of sunlight scattered by Venus atmosphere, including Rayleigh and Mie scattering mechanisms

16 p2860 A69-32237

Dim astronomical sources observability from sunlight spacecraft, considering coma of micron sized ice crystals influence on scattering by condensation model

16 p2861 A69-32301

Atmospheric gas constituents number densities determined as function of altitude by correlating laser beam scattering and absorption data

16 p2781 A69-32387

Spontaneous and stimulated aspects of light scattering by absorbing media, relating refraction index to temperature variations and external stresses

16 p2798 A69-32449

Polychromatic scattering of light in medium with three energy level atoms

16 p2813 A69-32589

Time dependent radiation diffusion in inhomogeneous stationary medium applied to diffuse reflection of light

16 p2813 A69-32591

Zenith sky Umkehr observed with Dobson spectrophotometer at twilight, discussing light scattering by aerosols in lower stratosphere

16 p2786 A69-32634

Homodyne detection of IR radiation from carbon dioxide laser scattered from moving diffuse target, noting applicability to IR radar, heterodyne spectroscopy, etc

17 p2971 A69-32913

Two polarization light interference scattered by moving and fixed atoms, obtaining forward scattered light intensity

17 p3005 A69-33109

Multiple light scattering solutions accuracy by diffraction peak omission from cloud and haze analytic phase functions compared for optically thick and thin planetary atmospheres

17 p3032 A69-33159

Spectral study of Stokes vector for light scattered by natural objects, recommending phase and optical axis inclination angles for aircraft measurements

18 p3198 A69-34756

Optical constants changes in germanium determined by modulation method of measuring light reflected at different angles

18 p3173 A69-35014

Plane light wave propagation in homogeneous isotropic medium with fluctuating dielectric constant using perturbation theory and integrating energy conservation law

18 p3173 A69-35127

Coherent light scattering from rough surface, studying effects of target tilt, translation and rotation on speckle patterns produced

18 p3174 A69-35281

Holography application to three dimensional structure determination of weakly scattering semitransparent objects

20 p3546 A69-38198

Continuously operating multipurpose wind tunnel for laser light scattering experiments in supersonic two phase flow

21 p3689 A69-38596

Ozone measurement from satellite by direct beam and scattered light methods employing UV sunlight attenuation

21 p3721 A69-38625

Forced recombination scattering of light on Rayleigh polarization waves in isotropic solid body with small elastooptical constants

21 p3770 A69-38963

Rotation effect of secondary principal axes in scattered light photoelasticity by dual observation method, deriving light intensity

21 p3844 A69-39317

Focal plane observation of granulation phenomena on scattering surface illuminated by coherent light from gas laser

21 p3741 A69-39575

Scattered light mean intensity determination in twilight aerosol atmosphere from satellite observations, formulating boundary value problem

21 p3717 A69-39656

Incident integral light flux relations and visibility range equation derived for objects illuminated by narrow light beams in scattering media

21 p3772 A69-39657

IC 2118 nebula luminosity study by polarimetry and photometry, showing role of light scattering and color properties

21 p3817 A69-39726

Scattered light photoelasticity dual observation method, describing automatic data collecting and interpreting system

22 p3945 A69-40079

Light field long term behavior in dispersive medium with finite optical thickness by asymptotic solution of unsteady transport equation

22 p3983 A69-41267

Radiative transfer theory applied to layer cloud with normal liquid moisture content, discussing volume extinction, scattering and absorption coefficients, etc

23 p4184 A69-42177

Stimulated Brillouin scattering application to measurement of hypersonic velocities and absorption in gigahertz frequency range, laser frequency shifting and Q switching, etc

23 p4167 A69-42183

Distribution function for thermalization distances derived for infinite atmosphere with plane source in noncoherent light scattering

23 p4192 A69-42403

Scattered light methods inaccuracies for nondestructive analysis of generally stressed photoelastic models, noting modified Mini-max method

24 p4396 A69-42737

Instrumentation and data interpretation method for particle size determination by low-angle light scattering

24 p4313 A69-42764

Angular distribution of He-Ne laser beam scattered by artificial fog from data by light detection devices at various angles

24 p4328 A69-43503

Light scattering from ruby laser beam passing through collisionless shock produced by H plasma compression measured by photomultiplier

24 p4360 A69-43748

LIGHT SCATTERING METERS

Multiple light scattering and reflection elimination from observed light brightness indicatrix to obtain true light scattering indicatrix, discussing error analysis

01 p0074 A69-11184

Shipboard standard visibility measurements by means of AEG-FFM scattered light recorder aboard Meteor in Atlantic Ocean during 1965

04 p0628 A69-15158

Scattered light meter accuracy as function of aerosol particles atmospheric distribution according to size, analyzing measurement errors

24 p4343 A69-42966

LIGHT SOURCES

NT ILLUMINATORS

Exploding wires as light source for quantitative spectroscopy, noting optically thin plasma clouds with radial symmetry

01 p0117 A69-10658

Retinal burns from intense light sources using rabbit eyes as function of irradiation rate, exposure time and image size

02 p0204 A69-12496

Mean life measurement of excited ions electronic levels using beam foil light source, emphasizing beam particle monitoring and theoretical equations

04 p0595 A69-14278

Mode locked laser as stroboscopic light source potential by investigating expansion of laser produced plasma by schlieren photography

05 p0774 A69-16315

Detection time to light point source noting response to dark, star field and glare source backgrounds

06 p0881 A69-17215

Strong light flashes detected from fast pulsar NP 0532 in Crab Nebula, discussing time-averaged optical flux

08 p1394 A69-20622

Strong light flashes from pulsar NP 0532 in Crab Nebula, noting UVB photometric analysis of nebular brightness

08 p1394 A69-20623

Rotating and oscillating magnetic neutron stars causing pulsars radio and optical signals, stressing UV line emissions theory

08 p1394 A69-20624

Helium-neon gas laser as coherent light source for holograms of vaporizing fuel films and for Michelson interferometer

08 p1327 A69-20874

Holograms with unfiltered radiation obtained from superhigh pressure mercury lamp and incandescent lamp

09 p1495 A69-21671

Thermal diffusion and free thermal convection in fluids by diffraction interferometer, using laser for light source

10 p1702 A69-23431

Stroboscopic generator of trains of high brightness light flashes for hydrodynamic and gas dynamic research, noting electronic control and thyatron circuits

11 p1879 A69-24235

Tilting filter photometer for faint light source spectrophotometry, discussing digital approach used with photomultipliers

11 p1884 A69-24834

Vacuum spark light source for extreme UV noting mechanical trigger, compatibility with clean vacuum system and magnetic confinement of ions

11 p1885 A69-24839

Radioactive light sources in photoelectric photometry, analyzing characteristics, brightness and stability of light flux and energy spectrum

11 p1951 A69-25421

Astronomical wide field cameras of large aperture ratio to detect extended near UV light sources outside atmosphere

12 p2080 A69-26127

Selective microscope with explosive bright light source and microsecond pulse duration for short flash period over large area, noting single frame separation method

12 p2086 A69-26162

Repetitive Q switched laser light source for interferometry, holography and high speed photography

12 p2087 A69-26170

Schlieren high speed photography systems for ballistic projectile studies, discussing use of gas lasers as nanosecond light sources

12 p2088 A69-26182

SiC and GaP diodes used as low power light sources, studying electroluminescence in p-n region under pulsed excitation

14 p2419 A69-29325

Fabry-Perot interferometer for studying spatial distribution of plasma electron concentration, discussing resolution using solid state gas laser light source

14 p2451 A69-29777

Remote polarized light source photometric observation on background of polarized light scattered horizontally, considering atmosphere optical state effect on laser communications

15 p2649 A69-30655

Nanosecond photography with superradiant light source, X rays or electrons using multipurpose electron accelerator, obtaining stop motion pictures

19 p3305 A69-35721

Dual beam white or nearly monochromatic light source providing programmed repetitive sample illumination with variable intensity, pulse duration and sequence for photosynthesis research

19 p3312 A69-36378

Aircraft measurements of scintillation of ground based light source, calculating autocorrelation functions and intensity fluctuations spectra

19 p3279 A69-36881

Hg injection lamp with high power and variable spectral energy distribution as light source for testing solar radiation effects

20 p3510 A69-37630

Space contamination due to manned vehicles and debris atmosphere effects on dim light source observations

21 p3793 A69-38341

Electron paramagnetic resonance line splitting between two nondegenerate Zeeman levels, using ruby laser as pumping source

21 p3735 A69-38582

Breakdown mechanism in GaAs, Si and CdSe semiconductors under intense light pulses ascribed to thermal impact

21 p3737 A69-39042

Light sources with uniform variable luminance field designed for calibrating cameras used in space exploration

21 p3726 A69-39580

Xenon plasma continuous illumination sources design and operation for night and color aerial photography covering photogrammetric resource surveys, ground traffic, flight paths, etc

22 p3950 A69-41000

Rod signals elicited by flashes in human eye measured, deriving relation between nerve signal size in rods and flashes energy

23 p4099 A69-42119

Light sources in 0.15-20 micron spectral range from published literature, unpublished reports, light source manufacturers and individuals

23 p4191 A69-42190

Brightness discrimination judgments for gray chips by humans, using psychophysical limits method and white, noncoherent red and He-Ne laser light sources

24 p4276 A69-43323

LIGHT SPEED

Constant acceleration relativistic rocket flight from inertial rocket and terrestrial point of view compared, examining light flash transmission and arrival time

09 p1609 A69-21959

Local creation of mass in steady state universe as source of static field energy propagating away at speed of light

09 p1601 A69-22212

Crab Nebula pulsar observations confirming wavelength independence of light velocity in space

12 p2157 A69-26233

Einstein second postulate concerning invariability of light vector in vacuum experimented for validity, using earth and moon as light rays launching and reflecting media

13 p2354 A69-28650

Particle and light motions in Schwarzschild field, discussing acceleration beyond speed of light in reference /S/ frame of time independent coordinate systems

17 p3006 A69-33741

Shock wave structure dissipation in gaseous medium with microscopic particle velocities asymptotically approaching light velocity

17 p2958 A69-34145

Optimal information selection for determining spacecraft trajectory, considering atmosphere, light speed and series expansion coefficients of planetary gravitational potentials

19 p3427 A69-36627

Negative time interval implications for meta particle at superluminal velocity with respect to two reference frames, noting causality paradoxes

20 p3598 A69-37412

Superluminal group velocities in relation to causality axion, considering sound propagation in ultradense matter and particles of imaginary mass (tachyons)

21 p3769 A69-38543

Q switched laser pulse propagation in nonlinear laser amplifier using bitemporal relativity theory, deriving five dimensional wave equation revealing superlight signal existence

21 p3770 A69-38839

LIGHT TRANSMISSION

Optical absorption coefficients for triphenylmethylarsonium tetracyanoquinodimethan complex single crystal, evaluating reflectance

01 p0140 A69-10934

Atmospheric influence on ground visibility reduction of airborne objects, using radiative transfer equation to calculate contrast transmission function

01 p0111 A69-11100

Earth atmosphere transmission coefficients determination by relation between transparency and daytime sky brightness, noting limits of applicability

01 p0074 A69-11185

Atmospheric transmission factor and optical stability determination by photometer, estimating error due to solar aureole

01 p0075 A69-11193

Tinted ophthalmic media effect on detection and recognition of red signal lights in daylight, noting allowable coloration for aviation use

01 p0022 A69-11341

Light field inside deep layers of turbid medium illuminated by narrow beam, discussing beam deviations inside medium, deviation dispersions and correlation coefficient

02 p0274 A69-11449

Transmission of coherent ruby laser radiation through traveling wave amplifier noting spatial field structure changes

02 p0255 A69-11608

Electron plasmas near plane metallic surfaces, determining transmittance and reflectance of incident light waves and surface waves dispersion characteristics

02 p0286 A69-11788

Multiple light scattering in planetary atmospheres, discussing diffuse reflection and transmission by atmosphere of particles with anisotropic scattering pattern

02 p0319 A69-12105

Mean square amplitude and phase fluctuations for propagation of light beam with Gaussian amplitude distribution through medium with randomly varying refractivity

02 p0208 A69-12308

Transparency decrease in plexiglass during interaction with dense plasma, noting absorption independence of plasma pressure and dependence on wavelength

03 p0482 A69-14222

Optical waveguide with optimum refractive index distribution for equalizing group velocities of different modes and minimizing waveform distortion

04 p0575 A69-14749

IR radiation attenuation in transparency windows of atmosphere, using searchlights as radiation sources

05 p0760 A69-16695

Spectrum and amplitude fluctuations of laser light propagating through liquid helium, obtaining spatial correlation function of refractive index fluctuations

06 p0957 A69-17267

Light transmission through body wall of living colorable desert iguanas measured by spectrophotometry, discussing skin pigment effects

07 p1059 A69-18373

Instrument for measuring light transmission in atmosphere to determine runway visual range

07 p1132 A69-18673

Brewster angle lenses for low cost low loss laser beam transmission system

07 p1148 A69-18863

Statistical properties of intensity fluctuations of light fields consisting of incoherent Gaussian component heterodyned with single frequency coherent beam

07 p1182 A69-19416

Optical absorption index for molten beryllium oxide based on measurements of small beryllium/ solid propellant rocket motor exhaust plumes

08 p1351 A69-20149

Self modulation, self steepening and spectral development of light in small scale trapped filaments, noting influence of relaxation time

08 p1352 A69-20745

Laser beam propagation in scattering media, noting attenuation coefficients for coherent and incoherent radiation

08 p1328 A69-21092

Borrmann effect and abnormal transmission and extinction observed by reconstruction of images of holo-

grams recorded in three dimensional photosensitive medium

09 p1494 A69-21492

Constant acceleration relativistic rocket flight from inertial rocket and terrestrial point of view compared, examining light flash transmission and arrival time

09 p1609 A69-21959

Laser beam scintillation at night over long atmospheric horizontal paths, showing log amplitude covariance observation in agreement with theoretical prediction

09 p1517 A69-22080

Mass displacement in light path due to interaction with gravitational wave accompanying light pulse, discussing general relativity tests for time delay and starlight bending

09 p1540 A69-22081

Atmospheric propagation properties of laser light, discussing particle absorption, gaseous absorption and refractive index disturbance effects

09 p1518 A69-22129

Light waves transmission and beam guidance, analyzing solid lens type guide and automatic light path stabilizer

09 p1518 A69-22130

Carbon dioxide laser beam deflection and thermal defocusing due to wind in absorbing medium

10 p1701 A69-22949

Light flux intensity fluctuation dispersion and averaging effect for passage through circular receiving aperture

10 p1658 A69-23950

Sinusoidally modulated light beam propagation in turbid media, studying phase velocity and attenuation coefficient as function of modulation frequency

10 p1658 A69-23951

Transmission of coherent ruby laser radiation through traveling wave amplifier noting spatial field structure changes

11 p1895 A69-24715

Turbulence induced depolarization of linearly polarized He-Ne laser beam at 6328 A traversing atmosphere near ground level

11 p1896 A69-24842

Atmospheric interference effects on optical PCM signal, analyzing absorption, beam bending, scintillation and correlation with visibility and weather

11 p1888 A69-25308

Laser radiation transmission in atmosphere examined for information transmission applications

11 p1841 A69-25638

Propagation of intensity modulated light rays in semifinite isotropic dispersive medium, discussing phase shift and modulation depth

12 p2029 A69-26026

Fiber optics application to fiberoptics and fused fiber optic plates, noting surface coating for light scattering prevention

12 p2084 A69-26150

Regulated pulse lasers under free oscillation for photographing distant objects by illumination with shortened light pulses

12 p2089 A69-26190

Distortionless propagation of light through optical two level atoms medium, considering relation to Poynting theorem, hyperbolic secant solution and pendulum analogy

12 p2130 A69-26313

Three dimensional log amplitude and phase fluctuation distributions of collimated and focused Gaussian beams propagated through random inhomogeneous medium, evaluating mean-square values

12 p2130 A69-26393

Electromagnetic field in idealized medium of uniformly curved gas lens for light beam waveguide, describing lens radius effects on incident beam spot

13 p2270 A69-27181

Optical surface wave propagation on thin dielectric film waveguides, noting applications to integrated optical data processors

13 p2229 A69-27676

Independently fluctuating Poisson light signals detected by receiver with inertialess photodetector, developing algorithm for estimating amplitude of useful signals

13 p2223 A69-28552

Weakly divergent intense light beam propagation in laminar optically inhomogeneous medium with self focusing possibility analyzed by perturbation theory

13 p2223 A69-28568

Reversibility principle in transilluminated three dimensional photoelastic medium

14 p2535 A69-29359

LIGHTHILL GAS MODEL

Ruby laser reflected and transmitted light intensity following radiation focusing on cuvette containing cyclohexane, noting dependence on incident pulse power 14 p2459 A69-29392

Log amplitude fluctuations of laser beam in turbulent atmosphere, obtaining asymptotic expressions for near field of transmitter aperture 14 p2460 A69-29638

Two photon interaction between ultrashort light pulse and medium, showing pulse propagation through medium without absorption 15 p2634 A69-30966

Pressure and wavelength dependence of molecular O absorption coefficient near 1215 Å, utilizing UV emission from crossed beam atomic collision 15 p2656 A69-31031

Flexible glass fiber optics, discussing total internal reflection, light and image transmission, digit display and waveguide for laser communication 16 p2789 A69-31933

Laser amplifier nonlinear losses effect on light beam propagation, studying arbitrary waveform development into asymptotic steady state pulse /SSP/ 16 p2797 A69-32043

Incident energy transfer to particles due to nonlinear interactions during passage of intense light beam through plasma, considering decay into plasma waves 16 p2822 A69-32046

Phase fluctuation measurements of laser beam propagating through turbulent atmosphere 17 p2927 A69-33855

Laser beam propagation through turbulent medium, investigating statistical distribution of phase shift fluctuations 17 p2976 A69-33857

Self channeling of light in nonlinear isotropic medium using exact solutions of nonlinear Maxwell equations for two dimensional case 17 p3007 A69-33975

Reflection reduction properties of symmetrical, light transmitting three layer coating consisting of zinc sulfide-magnesium fluoride-zinc sulfide films 18 p3173 A69-35147

Monochromatic undulating light vertical refraction path curvature radii calculation based on refractive index 18 p3174 A69-35201

Time dependent collimated light diffuse reflection and transmission by finite inhomogeneous atmosphere, using principle of invariance 18 p3132 A69-35345

Reflection and transmission measurements on as grown surfaces of tetracyanoquinodimethane, obtaining optical constants by Kramer-Kronig method 18 p3183 A69-35477

Nonlinear analog of conical refraction in biaxial crystals, considering birefringence in piezoelectric uniaxial crystals and laser beam propagation 19 p3330 A69-35604

Solar cell integral covers optical losses in vacuum as function of degradation by UV exposure, noting accelerated testing for time-cost reduction 19 p3253 A69-35703

Optical imaging with partially coherent nonthermal light, discussing correlation function propagation, transfer functions, spatial Fourier analysis, weak visibility and matrix form 19 p3372 A69-35907

Hot electrons effect on Fe-doped CdTe optical absorption by measuring optical transmission vs photon wavelength at liquid helium temperatures 19 p3389 A69-36551

Light refraction in Venusian atmosphere from Venera 4 probe measured data, noting horizontal rays traversing planet along circumference at 8.3 km height 19 p3427 A69-36625

Optical and thermal attenuation of current induced by low energy electron bombardment in CdS crystal 19 p3392 A69-36727

Trajectory of light ray propagating through atmosphere based on known refractive index defined by function of special Cartesian coordinates 21 p3675 A69-39245

Spectral dependence of optical absorption in InSb thin films under conditions of quantum dimensional effect, considering allowance for nonparabolic conduction zone 21 p3783 A69-39560

Superwide angle camera with aerial photogrammetric lens system, discussing light distribution, rotary disk shutter, etc 22 p3944 A69-40047

Coherent light propagation through turbulent atmosphere observed by applying He-Ne lasers to simultaneous measurements of scintillation effects over homogeneous optical paths 24 p3434 A69-43114

Fiber optics interferometers, analyzing light propagation along dielectric light pipes and wave interference 24 p3415 A69-43162

Light transmission through curved dielectric rectangular rod, studying optical waveguides of various cross sectional dimensions and radii of curvature 24 p2487 A69-43329

LIGHTHILL GAS MODEL
Inviscid reacting flow free of molecular transport analyzed locally near stagnation point, using Lighthill-Freeman gas model 11 p1876 A69-25560

LIGHTHILL METHOD
Lighthill method based expressions derived for discontinuity shape formed during shock wave diffraction near small angle 02 p0234 A69-12588

Sound radiation from vibrating bodies, noting errors in Lighthill conclusion 02 p0282 A69-12800

LIGHTING
U ILLUMINATING
LIGHTING EQUIPMENT
NT ARC LAMPS
NT FLASH LAMPS
NT ILLUMINATORS
NT MERCURY LAMPS
NT QUARTZ LAMPS
NT RUNWAY LIGHTS
NT XENON LAMPS

Aircraft instrument lighting color effects on posture, scotopic absolute and acuity threshold and legibility for reading of instruments 03 p0380 A69-14073

LIGHTNING
Lightning strikes to aircraft, discussing corona discharge, electric fields and meteorological measurements during thunderstorm in cumulonimbus 03 p0458 A69-13031

Aircraft radomes lightning protection, discussing evaluation by experimental methods and simulation 07 p1142 A69-19535

Susceptibility of high modulus graphite and boron fiber epoxy composites to lightning damage, noting degradation by pulse current 08 p1338 A69-20486

Electromagnetic energy spectra of lightning expressed as function of electric field spectral density of atmospheric 14 p2437 A69-29076

Electromagnetic noise radiation structure during lightning flash by measuring time duration distribution between pulses 14 p2445 A69-29885

Earth-ionosphere waveguide excitation by lightning discharges and geomagnetic field influence on ELF noise spectrum 17 p2928 A69-33865

Terrestrial radio noise from lightning discharges measured by Ariel 3 satellite to deduce sources distribution 21 p3759 A69-39259

Ball lightning as positively charged region of electroluminescent air maintained in dynamic structure and molecular composition by atmospheric electric field 22 p3940 A69-40536

Nighttime atmospherics shape analysis created by lightning and propagating in earth lower ionosphere waveguide 22 p3941 A69-40961

ELF atmospherics excitation, discussing cloud to ground and intracloud lightning discharges Fourier integration and current moment spectrum 23 p4115 A69-41562

Aircraft fuel vent line sensitivity to lightning hazards, using flame propagation and arrester experiments with high voltage and high current facilities [SAE PAPER 690434] 23 p4062 A69-41651

Peak field strengths of atmospheric radio noise bursts from lightning flashes at VHF and flash distance estimates at tropical latitudes 23 p4126 A69-42355

LIGNIN
Lignin presence in New Zealand moss gametophytes observed for characteristic color reaction and UV spectra, noting contrast with north temperate species 17 p2912 A69-34176

LIMBS

Limb darkening nonlinearity effects on solutions for brightness curves of eclipsing binaries 09 p1588 A69-21364

Electronic device utilizing scanning beam to evaluate limb photographs, reducing errors by introducing second generator with frequency proportional to deflecting potential variation 17 p2970 A69-32884

Limb darkening on earth night side observed by Aerobee rocket, with explanation based on atmospheric opacity in water vapor and carbon dioxide bands 17 p2960 A69-33167

Limb darkening nonlinearity effects on solutions for brightness curves of eclipsing binaries 18 p3197 A69-34754

Limb effect of solar Fraunhofer lines determined by telescope equipped with autocollimated type diffraction spectrograph 20 p3607 A69-38044

Photoelectric spectrometer observations of 1966 total solar eclipse, discussing limb darkening curves for regions of continuum 1.5 Å wide around 5728 and 6404 Å 22 p4027 A69-40659

LIMBS [ANATOMY]
NT FOREARM
NT HAND [ANATOMY]
NT LEG [ANATOMY]

Gilson cuvette densitometer used for blood flow measurement in canine forelimb and human forearm and hand during constant intrabrachial arterial dye infusion 23 p4077 A69-41294

LIME
U CALCIUM OXIDES
LIMITATIONS
U CONSTRAINTS
LIMITER AMPLIFIERS

Zero memory frequency independent nonlinearities response to modulated input noting FM limiter, band-pass limiter and AC carrier control systems 01 p0034 A69-11142

Bandwidth requirement of single channel monopulse limiter, discussing signals conversion to IF 16 p2761 A69-32471

LIMITER CIRCUITS
Smooth limiter effect on output of SNR for unbalanced and balanced FM discriminators, noting role of error function 07 p1106 A69-19127

Hard limiting effect on sum of three or four sinusoidal signals noting output amplitudes, signal suppression and negative suppression effect 09 p1451 A69-21311

Limiting incoherent or coherent interference signals at frequency of biphasic or quadriphase digital signal 14 p2413 A69-29483

Performance of oscillating limiter driven by noise corrupted FM signals covering frequency deviations, carrier to noise ratio, etc 14 p2413 A69-29497

Time function multiplex system for simultaneous communication via satellite between number of stations, considering transmission capacity decrease due to hard limiting amplifier 17 p2919 A69-33320

Filtering optimization prior to limiting digital signals in strong noise, detailing bandwidth choice of single pole low pass filter 21 p3676 A69-39450

HF receiver interference blanker, discussing limiter-blanker system, integration, effectiveness and squelch circuit 23 p4141 A69-42221

Cascaded limiter and phase detector, analyzing SNR transfer characteristics for specific PM signals 23 p4131 A69-42525

LIMITS [MATHEMATICS]
Boundedness theorem for all solutions of class of nonlinear second order differential equations 02 p0271 A69-11549

Parametric vibrations of self excited elastic and aeroelastic systems with traveling waves, determining stable vibration boundaries 02 p0337 A69-11561

Limit load analysis of three dimensional rigid perfectly plastic continua by approximate variational method 02 p0338 A69-11721

Geometric optics inverse scattering method for smooth conducting convex bodies of revolution, demonstrating bounds on size and shape 02 p0280 A69-11929

Elasticity theory upper and lower bounds for two and three dimensional inhomogeneous problems and applications to plates

10 p1794 A69-22889

Turbulent transport processes mathematical model, determining upper and lower bounds

10 p1677 A69-22895

Rate estimates of convergence of multidimensional central limit theorem for sequence of identically distributed independent random variables with third order finite moments

10 p1719 A69-23400

Linear differential equations solutions boundedness and unboundedness criteria, determining quantitative relations

12 p2120 A69-26035

Approximate solution of boundary value problems for Fokker-Planck equation to determine probability of exceeding limits in nonlinear automatic control systems

12 p2054 A69-26653

Thermodynamic equivalence of limit theorems for canonical and grand canonical ensembles, discussing Massieu-Planck function analog relation by Legendre transformation

12 p2191 A69-27148

Second order differential equations eigenvalues with Sturm boundary conditions analyzed by difference method

13 p2288 A69-27922

Boundedness in mean square of solutions derived for linear differential equations forced oscillations with nonwhite Gaussian random functions parameters

16 p2873 A69-32058

Simultaneous unbounded solutions existence to homogeneous linear differential equations with continuous positive elastic and dissipative coefficients

16 p2804 A69-32251

Maximum rms error comparison of redundancy reduction techniques, emphasizing limiting slope technique and worst case interpolation error

19 p3273 A69-36264

Existence theorem for limits of minimizing sequences in optimal control problems, applying results to systems governed by partial differential equations

19 p3287 A69-36724

Generalized limit theorem for reliability replacing Drenick exponential theorem

20 p3547 A69-37068

Polya concept of maximum and minimum densities of series applied to entire functions of finite order with positive zeros

20 p3568 A69-37442

Variational problem for nonlinear functionals connected with finite plasticity, extending existence and uniqueness theorems to limit analysis

21 p3837 A69-39157

Homogeneous Markovian sum of sequence of random quantities series, deriving limiting theorem for sum density

21 p3757 A69-39538

Upper and lower bounds for growth or decay rate of solutions of parabolic differential equations for indefinitely increasing time

21 p3757 A69-39565

Upper and lower bounds for certain classes of partial differential equations associated with variational problems in theory of deterministic control processes

22 p3976 A69-41034

Numerical computation of rate-distortion function R/D/ for certain memoryless message sources, discussing bounds, reduction to minimization problem and applications

24 p4284 A69-42719

Bellman equation analyzed for higher derivatives, suggesting bounded partial derivatives of optimal feedback control function

24 p4341 A69-43234

Composite media elastic moduli upper and lower bounds determination using variational principles to characterize displacement and stress in time harmonic deformation

24 p4406 A69-43701

LINCOLN EXPERIMENTAL SATELLITES

Lincoln experimental satellites, discussing transition to UHF bands and orbital launching

07 p1087 A69-19630

Pulsed plasma microthruster propulsion system for synchronous orbit LES 6 satellite

[AIAA PAPER 69-298] 09 p1562 A69-21227

Solar cells volt-ampere characteristics calibrated at various solar incidence angles on LES-6 satellite in synchronous orbit

19 p3254 A69-35712

Solar cell degradation experiments on LES 4 and 5 satellites, discussing decay values and times for Si and CdTe cells with different cover thicknesses

19 p3254 A69-35713

Orbital results for Automatic Orbit Control System of Lincoln Experimental Satellite LES 6, using pulsed plasma microthrusters and self contained orbit measurement and control methods

[AIAA PAPER 69-934] 21 p3824 A69-39428

Electromagnetic attitude control system for Lincoln Experimental Satellite 5 in near-synchronous equatorial orbit, noting onboard error detection in closed control loop

21 p3827 A69-39755

LINE CURRENT

Closed analytic expressions for vector potential and magnetic field generated by axisymmetric multipole line currents

06 p0965 A69-17518

Magnetohydrostatic cavity formed round magnetic field of line dipole-line current combination by infinitely conducting plasma at uniform pressure

08 p1369 A69-20998

Plasma cavity shape formed by magnetic field effect due to several parallel line currents

[ISAS-433] 09 p1553 A69-22569

Electric field vertical and radial components for time harmonic electric line sources with piecewise sinusoidal current distribution

11 p1836 A69-24995

LINE SHAPE

Free bounded continuum processes effect in nonequilibrium gases of finite continuous opacity, noting curves of growth for finite plane parallel layer emission lines

01 p0121 A69-10959

Spectral line shapes broadened by electron impacts, taking into account contribution of radiation produced by perturbing electrons

06 p0961 A69-17136

Emission line profiles in spherical atmosphere expanding with constant radial velocity computed by Monte Carlo methods

06 p1009 A69-17965

Satellite components of lines formed in stellar type differentially rotating disk

07 p1219 A69-19336

Green function method for atomic line broadening in plasma radiation, including electron correlations and quantum effects

08 p1361 A69-20147

Line shape for dynamic Stark effect during optical resonance field irradiation calculated as function of relaxation constants and beam intensity

08 p1325 A69-20282

Far IR laser pulse shape and duration

09 p1515 A69-21424

Stigmatic profiles of solar C II doublet resonance lines obtained by rocket-borne echelle spectrograph

09 p1592 A69-21456

Laser induced line narrowing in coupled Doppler broadened transitions, noting mode crossing and spontaneous emission

09 p1519 A69-22282

High pressure arc discharge diagnostics with spectroscopic method relating spectral profiles to central temperature, pressure and temperature distribution

12 p2094 A69-26968

NGC 4151 absolute intensities of wide emission of weak isolated and IR lines determined from photoelectric spectrophotometric measurements

12 p2164 A69-27023

Luminosity changes in quasar 3C 273, describing corrections introduced into luminosity curve obtained by iris photometer

12 p2167 A69-27044

He-Ne laser transition line shape and gain curve through width, considering spectral frequency characteristics, output power and gas temperature and concentration

13 p2272 A69-28115

Light saturation development of line profile component of normal Zeeman triplet in sunspot umbrae

14 p2528 A69-29964

Spatial ion wave echoes emphasizing echo line shape analysis and effects of ion-neutral and ion-ion collisions

16 p2818 A69-31676

Spectral characteristics of B stars group, reviewing causes of spectral line profile deformation

16 p2855 A69-31828

Balmer and Ca II/K line profiles computed by program based on model atmospheres, comparing computed and observed data for F stars

19 p3426 A69-36578

GaAs laser used as optical sweep generator for display of Cs 133 spectral line shape, studying fluorescence and radiation lifetime

19 p3339 A69-36696

Sodium D line profiles in interstellar clouds, determining absorbers velocity distributions

20 p3611 A69-38149

Neutral titanium Fraunhofer lines 4534, 4562, 5210 and 5238 A, investigating profiles and asymmetries using spectrophotoelectrical methods

21 p3795 A69-38467

LINE SPECTRA

NT BALMER SERIES

NT D LINES

NT ELECTRONIC SPECTRA

NT FRAUNHOFER LINES

NT H ALPHA LINE

NT H BETA LINE

NT H GAMMA LINE

NT H LINES

NT K LINES

NT LYMAN SPECTRA

NT PASCHEN SERIES

NT RYDBERG SERIES

NT TELLURIC LINES

Red shift pattern in quasar emission spectra consistent with fractional screening charges on emitting atom nuclei

01 p0153 A69-10855

Jovian atmospheric rotational temperature from rotational lines in methane band

01 p0153 A69-10856

Ionized calcium lines in spectra of light bridges of sunspots, observed by diffraction spectroscopy, indicating similarity to chromospheric flares

01 p0154 A69-10894

Statistical band model and line by line calculations of transmittance for IR bands in absorption spectra of ozone and water vapor

[AFCL-68-0505] 01 p0124 A69-10919

Spectral lines source functions for formation in multilevel atom and radiative transfer in atmosphere of three level Na atoms and four level O atoms

01 p0124 A69-10962

Polarization of nightglow, line vs continuum

02 p0235 A69-11428

Ionized metals emission lines intensity in chromosphere observed with coronagraph, determining hydrogen concentration

02 p0314 A69-11635

Solar growth curves constructed for solar disk center using various metal lines

02 p0314 A69-11637

Line reversal and excitation temperatures in low pressure flames

02 p0350 A69-11709

Spectrophotometric studies of planetary NGC 6543 gaseous nebula, measuring emission line intensities, electron density and temperature

[ARL-68-0200] 02 p0327 A69-12708

Photometric measurement of atomic oxygen green line emissions and high energy electron flux using twilight sounding rocket

02 p0309 A69-12743

Weighting functions for finite optically thick atmospheres, discussing emission line formation

02 p0328 A69-12755

Plasmas in galaxies, spiral structures and radio galaxies, discussing quasar line and continuum spectra

02 p0329 A69-12790

Line identification methods in solar extreme UV and X ray regions

03 p0507 A69-13171

Spectral line identification in quasars, noting emission lines characteristic of emission nebulas and absorption lines of stellar atmospheres

03 p0508 A69-13173

F values for Ti II, Cr II and Fe II by empirical astrophysical line strength analysis, discussing f value determination from stellar growth curve

03 p0508 A69-13175

Absorption oscillator strengths of S I and S II lines between 1100 and 2000 A, using arc burning light source

03 p0479 A69-13968

Solar emission line absorption by oxygen and nitrogen atomic lines, discussing effect on upper atmosphere composition measurements

03 p0425 A69-14019

Arc and HF discharges in Ne-He lasers, comparing output power, spectral line intensities and reduced electric field vs reduced tube radius plots

03 p0441 A69-14139

High temperature measurement based on spectral line displacement and broadening due to Stark effect,

noting diagrams for O, Na, Mg, Al and Si at various temperatures

03 p0481 A69-14146

Beam foil spectroscopy for measuring wavelengths and spectral line intensities

04 p0595 A69-14276

Superradiant and laser spectroscopy in second positive system of molecular nitrogen

04 p0609 A69-14285

Time variations of chromospheric network of bright points covering solar disk in spectrograms, noting contrast and interspaces variation with 11-year solar cycle

04 p0651 A69-14372

Hydrogen spectral line broadening under combined action of ions and electrons, tabulating values for calculation of absorption coefficient

04 p0651 A69-14373

Far IR observations of atmospheric molecular lines, using high altitude aircraft platforms

04 p0628 A69-15146

Emission lines structure in quasar spectra, analyzing problem of weak absorption lines identification

04 p0662 A69-15236

Hydrogen spectral line widening by plasma electrons emphasizing Lyman, Balmer and Paschen series

04 p0638 A69-15239

Diminished RF intensity of neutral hydrogen line near radio source W 49 due to diminished kinetic temperature of gas

04 p0662 A69-15253

Spectral study of crystal lattice of gallium phosphides for influence of vacancies and impurities on band formation

04 p0643 A69-15258

Line profile and optical interferometry in astronomy and geophysics

05 p0760 A69-15590

Spectral line reversal method of measuring high temperatures of gases

05 p0761 A69-15763

Lithium abundance determination difficulties for undisturbed solar photosphere, noting Li I resonance line identification and model choice

05 p0821 A69-15849

Red, blue and no bias light effects on spectral response of copper sulfide-cadmium sulfide cell, using model incorporating photoconductive layer

05 p0808 A69-16358

Oxygen absorption coefficients for atomic silicon in spectral range of Schumann-Runge bands

06 p0960 A69-17090

Identification of emission lines from 3200 to 7000 Å in Eta Carinae spectrum, noting P Cygni-like absorption lines

06 p1002 A69-17263

Mass motions in solar flares using line profiles and filtergrams

06 p0993 A69-17427

Solar moustaches H alpha profiles spectroscopic studies indicating near symmetry

06 p0994 A69-17435

Oxygen line absorption at elevated temperatures in Schumann-Runge system, estimating line widths

06 p0962 A69-17803

Non-equilibrium low temperature plasma theory for ionization and particle distribution based on discrete and continuous spectra states, discussing electron distribution function

06 p0969 A69-17906

Lunar occultations of galactic center region observed at 1667 MHz indicating OH absorption origin in uniform rotating cloud

06 p1009 A69-17961

Planetary nebulae NGC 7662 and IC 418 forbidden line spectra compared with computer model predictions, noting evidence for dynamical effects and filamentary structure

06 p1009 A69-17963

Radio recombination lines in populations of highly excited states of hydrogen, discussing collisional transition effects

06 p1010 A69-17970

Velocities of neutral and ionic species in MPD flow determined from Doppler shift of selected spectral lines

[AIAA PAPER 69-109] 06 p0971 A69-18116

Doppler shift measurements of axial and rotational velocities in MPD arc, using reference lines from iron arc

[AIAA PAPER 69-110] 06 p0972 A69-18171

Spectral line profiles of 3 Centauri A during microdisturbance, showing turbulent velocity and metal element abundances

07 p1211 A69-18407

Jovian limb H alpha line due to auroral emission obtained from high dispersion spectra with long light path through upper atmosphere

07 p1214 A69-18614

Evening twilight nitric oxide density profile in gamma bands deduced from rocket measurements

07 p1125 A69-18842

Water vapor absorption line for nitrogen and oxygen mixtures with frequency measurements at various pressures and temperatures, discussing attenuation and line breadth

07 p1184 A69-18911

He-Ne and He-Xe laser lines in IR tuned by axial magnetic field, observing Stark patterns of organic molecules

[IEEE PAPER C-5] 07 p1150 A69-19050

Time resolved spectrum of high current pulsed argon laser discharge, noting primary laser output and afterglow

[IEEE PAPER L-12] 07 p1152 A69-19068

Collision broadened spectral line shape obtained in impact approximation using Anderson formulation compared to output of gas lasers

[IEEE PAPER T-6] 07 p1154 A69-19083

Franck-Condon factors for high rotational levels of nitrogen calculated in Morse potential approximation for application to plasma diagnostics

07 p1185 A69-19169

Stokes phenomenon, considering continuity solution of differential equations across Stokes lines

07 p1174 A69-19220

Forbidden S I lines due to transitions within ground configuration identified in Fraunhofer spectrum of sun, noting photospheric abundance of S

07 p1217 A69-19237

Solar spectral line profiles for photosphere disturbed by short period acoustic waves

07 p1217 A69-19239

Fe II lines relative intensities in eta Carinae spectrum, discussing possible intrinsic reddening of object and representation of visible and near IR continuum

07 p1217 A69-19253

Iodine fluorescence spectra excited by krypton ion laser, analyzing spectral series and vibrational rotational levels

07 p1156 A69-19304

Spectrum data of Nova Vulpeculae /1968/ summarized concerning dispersion figures

07 p1220 A69-19337

Lines displacement in binary star spectrum due to blending, presenting graphs displaying magnitude of effect under various conditions

07 p1223 A69-19624

Strong line profiles computed for models of hot expanding extended atmospheres of OB supergiants

07 p1223 A69-19637

IR absorbance of CO below room temperature, determining strength and half widths of lines in R branch of fundamental band

07 p1183 A69-19644

Planetary nebula IC 4642 spectral line intensities measured by photographic spectrophotometry compared to previous measurements, noting no evidence for changes

08 p1383 A69-19898

Paschen line intensity measured as function of position across Orion Nebula

08 p1384 A69-20058

Hartree-Fock calculations of coronal forbidden transition lines in Ar I isoelectric sequence, obtaining wavelengths, magnetic dipole and electric quadrupole transition probabilities

08 p1385 A69-20071

Radiative transfer equation solution for spectral line formed in two dimensionally varying atmosphere extended to continuum radiation in inhomogeneous atmospheres

08 p1386 A69-20077

Spectra of envelope star HD 217050, analyzing metallic lines as function of central depths

08 p1387 A69-20121

Absolute excitation cross sections for emission of second positive bands of nitrogen under electron impact

08 p1355 A69-20208

Nine spectra of recurrent Nova T Pyxidis during fifth /1966/ outburst compared to previous outbursts

08 p1391 A69-20396

Electron-ion collisions during forbidden lines excitation in gaseous nebulae, using Hartree-Fock functions and variational principles

08 p1391 A69-20530

Forbidden resonance line of Ca II in Arcturus from spectrograms at widely different times of year

08 p1392 A69-20558

Mean square radii for assigned terms of Fe I energy level diagram for Van der Waals line broadening

08 p1392 A69-20559

Low latitudes observations of 21 cm line of H I in galactic center direction, giving contours maps of brightness temperature

08 p1392 A69-20562

Electron temperatures and internal turbulence in H II regions of Sagittarius arm measured by high resolution interference method

08 p1392 A69-20566

Mass loss observed in Of, Wolf-Rayet and OB supergiant stars from P-Cygni profiles in far UV resonance lines

08 p1395 A69-20641

Spectroscopic residual intensities variation of metallic and hydrogen lines of eclipsing system R Canis Majoris with phase, discussing surrounding gaseous matter

08 p1396 A69-20646

Emission line galaxy NGC 5253, discussing radial velocity, line width and excitation and similarity to Seyfert galaxies

08 p1407 A69-21132

RF spectral lines due to OH molecule detected in interstellar space in absorption of RF radiation from Cassiopeia A source

09 p1586 A69-21295

Water molecules radio spectral lines from microwave emission sources in Galaxy studied for variability, size and polarization

09 p1587 A69-21307

Absolute spectrophotometry of IR lines in planetary nebulae spectra determined by diffraction spectrograph

09 p1590 A69-21380

Molecular line intensity requirement in line of sight for detecting interstellar water vapor cloud, assuming transparent atmosphere and ideal radio telescope

09 p1591 A69-21446

Detection of micron Ne emission line from planetary nebula IC 418 using IR spectrometer

09 p1591 A69-21452

Stigmatic profiles of solar C II doublet resonance lines obtained by rocket-borne echelle spectrograph

09 p1592 A69-21456

Cosmos 92 satellite observation of night airglow flare, discussing NO bands emission and origin

09 p1485 A69-21533

Physical conditions in nuclei of various Seyfert galaxies deduced from line intensities, noting permitted and forbidden lines formation in different regions

09 p1596 A69-22056

Helium-like ion resonance satellite lines in laboratory and solar plasmas, noting coincidence between solar satellite energy and energy level interval

09 p1598 A69-22158

Subdwarf HD 25329 studied with model atmosphere approach, using H alpha, Na I and Mg I profiles for effective temperature

09 p1600 A69-22199

Green and red coronal line polarization observed during solar eclipses, discussing nonpolarization of red line and observation instrument error

09 p1600 A69-22204

Rotational Raman scattering in planetary atmospheres, analyzing spectra of deep solar Fraunhofer lines

09 p1601 A69-22207

Red autoionizing lines relative gf values for calcium measured by shock tube experiment

09 p1601 A69-22208

Helium I line profiles including forbidden component, discussing electron and ion Stark broadening and thermal Doppler broadening

09 p1601 A69-22209

Boltzmann plots derived from spatially integrated spectral line intensities emitted from nonuniform gaseous plasmas, discussing Boltzmann temperature

09 p1552 A69-22251

Radio recombination lines of galactic hydrogen as sensitive test for low energy cosmic ray existence in interstellar medium

09 p1580 A69-22273

Line blanketing for two level atom with spectral line formed in pure absorption and noncoherent scattering, studying wavelength and depth dependence

09 p1606 A69-22424

Atomic line spectrum computation for F-K supergiant or cepheid, using observational data on standard star spectrum

10 p1771 A69-22854

Auroral spectrum observations for absolute brightness of nitrogen Meinel and ING systems, con-

- sidering background night airglow and atmospheric extinction
10 p1681 A69-23161
- Chromium concentrations induced line shift in ruby single crystals spectra, determining principal lines position
10 p1744 A69-23321
- Laser emission lines produced by pulsed electrical discharge through ammonia
10 p1704 A69-23666
- Coronal line intensity distribution for period of proton flare
10 p1763 A69-23732
- Active prominence during solar flare with loop-like shape of spectral line profiles, discussing turbulent velocities and limb flares
10 p1764 A69-23739
- Isotope shifts in 4416 Å cadmium laser, showing change of double peaked to single peaked profile with doubled active tube length
10 p1705 A69-23812
- Mode interactions in argon lasers between two spectral lines noting effect on output
10 p1705 A69-24003
- Spectral lines relative intensities for bright medium excitation gaseous planetary nebula IC 3568, using photoelectric spectrum scanner and spectrophotometry technique
10 p1787 A69-24117
- Spectral measurement of luminous trails produced by injecting high velocity submicron diameter iron particles into gaseous targets compared with meteor spectra
10 p1790 A69-24142
- Tunable Fabry-Perot interferometer for photoelectric measurements of absorption and emission line contours and line center particle concentrations
10 p1698 A69-24212
- Line spectrum of flare gamma radiation due to atmosphere nuclei excitation by high energy proton acceleration
11 p1945 A69-24241
- He I 10830 Å line in beta Lyr shell observed by contact image converter tube, analyzing line structure and phase brightness
11 p1955 A69-24391
- B star HD 191980 spectral variations from B-3 to B-8 noting helium to carbon line intensity ratio, interstellar D line strength and radial velocity measurements
11 p1958 A69-24594
- Magnetic fields, green corona emission and filaments relationship at high solar latitudes using synoptic charts
11 p1964 A69-25416
- IR absorbance data for atmospheres of ammonia and ammonia nitrogen mixtures at various wavelengths indicating absorption in strong line region for gas pressures used
12 p2132 A69-26247
- Forbidden solar corona lines transition probability in vacuum UV region
12 p2157 A69-26334
- Spectral line formation in nonlinear multilevel atom line transfer problems, considering radiation transfer through plane parallel atmospheres of H and Mg atoms
12 p2133 A69-26967
- Resonance line radiation transfer in finite homogeneous cylinders of various shapes and optical thicknesses using Monte Carlo method
12 p2191 A69-26970
- NGC 4151 absolute intensities of wide emission of weak isolated and IR lines determined from photoelectric spectrophotometric measurements
12 p2164 A69-27023
- Red shift determinations and line identifications for quasars, using spectrograph with electro-optical converter
12 p2168 A69-27048
- Ionized gas cloud eruption from galactic nucleus deduced from observed hydrogen line at 5.1 cm
12 p2171 A69-27068
- Spectrum of abnormal B-type star HR 3817, noting Balmer line profiles and instrumentation
12 p2172 A69-27160
- Shift of certain Hg spectral line by high power pulse from Nd laser through perturbation of atomic energy levels
13 p2270 A69-27202
- Statistical tests for cosmological hypothesis for origin of absorption lines in spectra of quasars, considering red shifts
13 p2234 A69-27307
- Scorpius XR-1 X ray emission spectra, discussing Fe emission line near 7 keV plasma models, supernova mass and cosmic abundance
13 p2325 A69-27313
- Relative intensities of selected Si two multiplets calculated and compared with solar spectrum and plasma source ZETA values
13 p2326 A69-27551
- NGC 4194 galaxy emission line spectrum analysis showing presence of highly excited gas in nucleus and in bright central region similar to NGC 7714
13 p2339 A69-27571
- Line absorption effect on opacity and main sequence model stars noting luminosity, radius and mass of convective core
13 p2340 A69-27578
- Expected IR line spectra of gaseous nebulae based on physical conditions, listing line intensities
13 p2342 A69-27595
- Potassium vapor radiative perturbation by ruby laser radiation in glass cell with end windows, studying emission line structure
13 p2271 A69-27656
- Dielectronic recombination influence on radio recombination lines of carbon under typical nebular conditions
13 p2346 A69-27703
- Astronomical unit determined by measuring radial velocity of radio wavelength spectral line source
13 p2350 A69-27822
- Magnetic A star HD 152107 anomalous intensification of Balmer series H lines observed by spectrograms
13 p2352 A69-27873
- He-Ne laser transition line shape and gain curve through width, considering spectral frequency characteristics, output power and gas temperature and concentration
13 p2272 A69-28115
- Excited hydrogen RF spectral lines from nebula NGC 6618, calculating frequency for transitions by Balmer formula
13 p2353 A69-28433
- Interstellar gas radio and optical spectral lines of neutral H compared with Ca and neutral Na, discussing critically low velocity gas distribution
14 p2519 A69-29135
- Spectral lines emitted from low voltage discharge in cesium filled diode with hot cathode, giving current-voltage characteristics as function of pressure and temperature
14 p2491 A69-29260
- Forbidden transition probabilities of solar corona lines in vacuum UV range
14 p2519 A69-29355
- Emission line fluxes of southern planetary nebulae in Magellanic Clouds and Galaxy measured photoelectrically, giving upper limit to H beta emission of Magellanic planetary
14 p2520 A69-29376
- X ray investigation of niobium, aluminum and niobium-aluminum systems to obtain K-spectra and L-spectra
14 p2508 A69-29664
- Fe and Ti line growth in 12 July 1961 solar flare spectrum, finding ionized titanium, neutral and ionized iron excitation temperatures
14 p2514 A69-29720
- Electron densities measurement in plasmas in magnetic fields from profiles of spectral lines, noting Stark and Zeeman effect
15 p2657 A69-30027
- Spin temperature of interstellar neutral hydrogen calculated from 21 cm absorption spectra line profiles
15 p2681 A69-30411
- Spectral emission of active prominences, showing looplike lines during quiet phases and differences in turbulent velocities magnitude
15 p2674 A69-30510
- Lasing kinetics, emission spectrum and directivity of ruby laser with spatially homogeneous population inversion
15 p2634 A69-30729
- Canum Venaticorum variable A star spectrum, listing all lines observed between 5000 and 6650 Å
15 p2692 A69-30773
- Solar Mg b and Na D line spectra, computing profiles for Doppler cores of lines for multilevel model atoms and selected chromospheric parameter ranges
15 p2693 A69-30779
- Coronal limb enhancement photometric study by spectroheliograms, comparing maximum brightness profiles in lines of different temperature in extreme UV
15 p2693 A69-30781
- Spectral Pt II lines in Ap stars of Hg class observed during analysis of double lined spectroscopic binary HR 4072
15 p2695 A69-30891
- Transition probabilities of spectral lines in helium-like ions estimated from hydrogen magnetic dipole transitions, discussing single photon decay
15 p2695 A69-30892
- Electron excitation and phase shift method for radiative lifetimes of Ar II UV transitions
15 p2656 A69-31034
- Relative intensities of lines in vibration and rotation bands of isotopic carbon dioxide in planet Venus, tabulating partition functions
15 p2656 A69-31154
- RF spectral lines due to OH molecule detected in interstellar space in absorption of RF radiation from Casiopeia A source
15 p2697 A69-31226
- Quasi-stellar and related objects emission and absorption red shifts tabulation suggesting absorption lines origin
15 p2701 A69-31532
- Bound excitons spectra in Cu doped gallium arsenide crystals, analyzing line oscillation structure and uniaxial compression effect
16 p2824 A69-31571
- Spectral characteristics of B stars group, reviewing causes of spectral line profile deformation
16 p2855 A69-31828
- Thermosphere neutral wind speed measured from observing Doppler shift in O I 6300 night airglow line with Fabry-perot interferometer
16 p2776 A69-32093
- Green line suppression in type B aurorae based on negative ion-electron chemistry below O transition region
16 p2778 A69-32191
- Radial velocity and spectral line variations of HD 124224, suggesting main sequence star of B6 to B9 spectral type
16 p2859 A69-32223
- Chromospheric spectrum outside of eclipse, wave lengths 3040 to 9266 Å, listing emission lines taken at McMath solar telescope
16 p2861 A69-32257
- Transition probability for 5577 Å auroral green line determined from measuring number density of O atoms in oxygen-helium discharge and emitted line intensity
16 p2781 A69-32319
- Error analysis of one bit autocorrelation method of spectral estimation, noting decrease in spectral variance with increased sampling rate
16 p2752 A69-32390
- Electron impact broadening of isolated spectral lines emitted by neutral atoms in plasma
16 p2823 A69-32468
- Cosmos 92 satellite observation of night airglow flare, discussing NO bands emission and origin
16 p2783 A69-32528
- RF spectral line detection from ortho hydrogen ions in Omega Nebula and NML Cygnus
16 p2864 A69-32571
- Asymptotic formulas for X and Y functions for resonance radiation scattering in layer, analyzing Doppler absorption and line profiles
16 p2813 A69-32588
- Hydrogen line profiles, equivalent widths and electron densities for peculiar alpha 2 CVn and gamma Lyr stars
16 p2864 A69-32594
- Spectroscopic study of P Cygni showing ionization temperature, Balmer decrement agreement with calculated value and chemical composition
16 p2864 A69-32595
- MH alpha 328116 /Cygnus/ spectrum noting three Fe IV lines
16 p2866 A69-32815
- Wolf 359 flare spectra obtained with Palomar telescope, noting hydrogen and He line enhancement, broadening and violet shifting
16 p2852 A69-32817
- Cloud scattering corrections added to synthetic spectrum analysis of carbon dioxide bands and water vapor line in Venus spectrum
17 p3032 A69-33161
- Cross sections threshold behavior for Cs II resonance lines excitation due to Cs ion-He collision
17 p3008 A69-33388
- Spectral lines radial velocities and profiles observed on 48 Librae from 1950-1962
17 p3038 A69-33722
- Red shift table for six galaxies near Coma Cluster from spectrograms of absorption lines
17 p3044 A69-34182

Ionization stratification and chemical abundances in planetary nebula NGC 7662, discussing density fluctuations effect on N II and O II lines
18 p3191 A69-34294

Absolute gf values for Fe I and Fe II lines between 3190 and 3315 Å measured by spectral absorption through shock heated gas containing Fe
18 p3175 A69-34304

Absolute spectrophotometry of IR lines in planetary nebulae spectra determined by diffraction spectrograph
18 p3198 A69-34768

Electronic levels excitation in S I and II by beam foil method
18 p3177 A69-35015

Quiet aurora atomic O red and green lines intensity ratio measured from rocket
18 p3201 A69-35192

Computer program to predict spectra from electronic transitions of diatomic molecules and atoms, noting line intensity distribution by Voigt profile
18 p3177 A69-35239

Cloud layer multiple scattering in Jovian atmosphere, discussing influence on Lorentzian contour of planetary absorption lines
18 p3203 A69-35332

Atomic and molecular absorption lines and width measurement in spectrum of WZ Cassiopeiae carbon star in visual and IR region
18 p3204 A69-35350

Spectroheliograms interpretation obtained in line cores of neutral oxygen IR multiplets
18 p3204 A69-35388

Emission line spectrum for ionization and excitation in solar coronal structures, tabulating intensities from ground based eclipses observations
19 p3422 A69-36217

Forbidden lines emitted by gaseous nebulae, emphasizing relative intensities of O II and O III lines
19 p3422 A69-36220

Forbidden lines of O I, O II, S II, N II and A III in red and near IR spectra of NGC 1976, IC 418 and II 4997
19 p3422 A69-36222

Spectral lines due to magnetic dipole transitions in fine structure levels in collisionally excited neutral H clouds, discussing theoretical difficulties in interpretation
19 p3379 A69-36225

Forbidden lines in slow nova RR Tel spectrum, comparing ionization rate with RR Pic
19 p3423 A69-36230

Intensity variations of Eta Carinae emission lines
19 p3423 A69-36231

Forbidden transitions in emission line spectra of variables near minimum light, finding origin in hot chromosphere
19 p3424 A69-36232

MH alpha 328-116 spectral characteristics noting weak continuum, emission lines from forbidden transitions and absence of absorption
19 p3424 A69-36233

MH-alpha 328-116 / V 1016 Cyg/ star spectrum, indicating object evolution toward higher ionization states
19 p3424 A69-36234

Forbidden emission lines used to study interstellar gas, discussing gas ionization, neutral hydrogen, calcium lines, etc
19 p3424 A69-36235

Forbidden emission lines in spectra of normal, radio and Seyfert galaxies and quasars, giving information about quasi-stellar mean densities, temperatures, ionization, etc
19 p3424 A69-36236

He I 1.083 micron resonance line in evening twilight airglow spectrum, discussing maxima, minima, decay patterns, etc
19 p3303 A69-36484

Solar atmosphere line source function showing frequency dependence as consequence of spectral line disappearance at solar limb
20 p3588 A69-37540

Solar corona Fe XII emission spectral lines relative intensity analyzed as function of temperature electron density
20 p3603 A69-37548

Relative oscillator strengths of 3500-5600 Å Fe I lines in emission of arc burning in Ar with iron chloride admixture
20 p3581 A69-37823

Giant stars UVB reddening line slopes determined from photometric data
20 p3608 A69-38047

Effective thinness approximation for spectral line formation from photon degradation processes and random walk of scattered photons, discussing optical thickness
20 p3612 A69-38159

Autoionization lines effect on stellar structure by computing contributions to Rosseland mean opacity
20 p3612 A69-38165

Ce II line reversal from absorption to emission in solar spectrum, noting reversal position dependence on wavelength and line source function scattering term
20 p3613 A69-38168

Absorption spectrum of diatomic oxygen excited by AC silent discharge photographed with vacuum spectrograph, associating lines with Schumann-Runge band
20 p3581 A69-38276

Magnetic ordering in dysprosium phosphate observed by high resolution spectral line intensity measurements, finding Neel temperature
21 p3773 A69-38331

Intensity integral inversion for Doppler core of strong solar absorption lines to obtain line source function for solar atmosphere
21 p3796 A69-38478

Diurnal intensity variations in OI 5577 Å line emission connected with vertical movements in 90 km level of atmosphere
21 p3713 A69-38525

Electron paramagnetic resonance line splitting between two nondegenerate Zeeman levels, using ruby laser as pumping source
21 p3735 A69-38582

Line statistics for representation of line absorption coefficient distribution for solar type stars
21 p3801 A69-38762

Tabulation of solar UV spectrum features between 3650 and 3000 Å from intercomparison of photoelectric records and Second Revised Rowland, indicating wavelength relocations
22 p4014 A69-40146

Fourier spectrum analysis of solar line oscillation sequences, discussing power spectra and lifetime of oscillation phase
22 p4019 A69-40286

P Cygni spectroscopy indicating existence and atmospheric structure of accelerating envelope about star, computing line profiles
22 p4023 A69-40471

Radiative energy transport in moving gaseous media in local thermodynamic equilibrium, assuming spectral line shifts by temperature and pressure variations
22 p3982 A69-41018

Emission lines in optical spectra of radio galaxy nuclei, considering time dependent energy release nature
22 p4034 A69-41174

Xenon laser CW operation on unclassified spectral lines of high ionization states, using laser induced spectroscopy
23 p4172 A69-41399

Interferometrically measured wavelengths tabulated for Th lines in 2747-4572 Å range, using liquid nitrogen cooled hollow cathode lamp and Fabry-Perot interferometer
23 p4191 A69-42150

Carbon monoxide presence in Martian atmosphere from Mars line spectra, giving content, surface pressure and concentration
23 p4220 A69-42379

Daylight observations of Comet Ikeya-Seki 1965-f at perihelion passage, discussing resulting emission line spectra within comet head
23 p4221 A69-42386

Carroll Fourier transform method applied to stellar spectra lines to determine small rotational velocities
23 p4222 A69-42404

Neutral He lines at 537 Å and 584 Å obtained by spectroheliometer on OSO 4, studying differences between quiet and active regions
23 p4222 A69-42405

Red shift determinations and line identifications for quasars, using spectrograph with electro-optical converter
24 p4375 A69-42551

Photoelectric measurements of emission line intensities for low density planetary nebula with moderate excitation located near north galactic pole, deriving abundances
24 p4376 A69-42662

Tabulation of photographic and photoelectric spectrophotometrically obtained relative spectral line intensities for planetary nebula IC 5217, discussing interstellar absorption
24 p4376 A69-42663

Model atmosphere analysis of line identifications and equivalent width data for relatively cool Ap star HD 204411, discussing atmospheric composition
24 p4376 A69-42664

Absorption lines in stellar spectra and significance in cosmogony, discussing ionized Ca K line detection during delta Orionis study, K and H lines components, etc
24 p4383 A69-42999

Multichannel spectral line receiver for 210 ft Australian radio telescope with front ends covering wide frequency range
24 p4283 A69-43115

Free Na atoms production for spectral line reversal procedure, facilitating procedure by replacing NaCl and chromium carbonyl by sodium azide
24 p4297 A69-43589

He I 10830 Å line in beta Lyr shell observed by contact image converter tube, analyzing line structure and phase brightness
24 p4390 A69-43781

P Cygni characteristics and spectrum analysis, describing absorption lines, line widths, atmospheric composition, light variations, etc
24 p4391 A69-43803

LINEAR ACCELERATORS

H resonator for charged particle beams combination at output of double beam linear accelerator
05 p0727 A69-15639

Linear ion accelerators noting particle motion, RF cavity design, RF power sources, injection and applications
09 p1553 A69-22697

H resonator for charged particle beams combination at output of double beam linear accelerator
16 p2762 A69-32497

LINEAR ARRAYS

NT ENDFIRE ARRAYS NT YAGI ANTENNAS

Planar arrays of linear antennas above stratified medium, showing antenna impedance and current distribution expressed in terms for free space environment
01 p0042 A69-10343

Phased array radar antennas emphasizing beam steering of transmitting linear array with number of phase shifters
01 p0049 A69-11390

Green function for linear antennas in warm plasma fed by coaxial air filled transmission line, computing current distribution and input admittance
02 p0215 A69-11942

Dual band shunt slot linear array for S and X band radiation patterns generated from single aperture
02 p0219 A69-12344

Triangular lattice arrays radiation characteristics similarity to linear tapered arrays, noting sidelobe level
04 p0570 A69-14308

Planar array multiple beam generation and position determination using N-port Butler matrices
04 p0570 A69-14309

Asymptotic decay of coupling for infinite phased arrays proved valid for infinite parallel linear plate array immersed in magnetized cold plasma
04 p0571 A69-14314

Mutual coupling and element efficiency for infinite linear arrays of dipoles
04 p0571 A69-14317

Electronic scanning antenna system consisting of ceramic rod linear array, power distributor, electronic ferrite phase shift feed and driver
04 p0572 A69-14327

Random phase errors in end-fed linear antenna arrays
04 p0578 A69-15211

Propagation constant and radiation of center fed linear antenna with feed points displaced transverse to antenna axis and immersed in warm compressible plasma
06 p0896 A69-17476

Synthesis of symmetrical linear array space factors in main beam and grating lobes by spacing distributions and element excitation adjustment
07 p1108 A69-19466

Coupling between array antennas shown to reduce reflecting properties of Van Atta reflector consisting of linear half wave dipoles
08 p1282 A69-20037

Self focusing linear array for communication satellites, evaluating reradiated field taking into account mutual coupling between elements
08 p1289 A69-20970

Converging solutions for imaginary admittance and current distribution in linear cylindrical antennas
08 p1295 A69-21165

Laplace transform applied to linear array analysis and synthesis, discussing transform singularity correspondence to array structure

09 p1532 A69-21600

Velocity, lifting force, pressure moment and circulation around linear array of thin foils with direction normal to profile chords calculated by Birnbaum-Glauret method

11 p1817 A69-24348

Atmospheric turbulence effect on linear antenna gain in direction of radiation pattern maximum determined together with antenna dimensions

11 p1844 A69-24435

Approximate method for calculating linear multipole antennas parameters in terms of power requirement, considering equidistant/nonequidistant element antennas

11 p1849 A69-24969

Passive magnetic elements array calculation for radiation pattern, discussing emitter position

13 p2235 A69-28513

Current distribution along linear antenna array taking into account interaction between neighboring elements and effect on antenna radiation characteristics

13 p2236 A69-28572

Spatial frequency distribution of linear array with randomly located elements from probabilistic analysis

17 p2929 A69-33873

Interrelations among mutual coupling, element efficiency, active impedance and radiation patterns in linear arrays derived from infinite order difference equation

17 p2929 A69-33874

Linear array composed of dual mode elements radiating into parallel plate region, obtaining scan angle compensation of element impedance

17 p2929 A69-33875

Cramer-Rao and split-beam tracker techniques compared for optimum bearing error attainable with linear passive sonar array in spatially incoherent noise environment

20 p3576 A69-37322

Scattered field of linear array of center loaded cylindrical elements illuminated by plane electromagnetic wave

20 p3494 A69-37838

LINEAR CIRCUITS

Small signal characteristics and frequency response of diode-stabilized integrated linear circuits, discussing feedback, impedance, bias- diode, etc

01 p0041 A69-10204

Wide range linear delay circuit with compensated bootstrap circuit generating linear ramp waveform and regenerative Schmitt trigger comparator

01 p0041 A69-10241

Computer analysis of linear active nontime varying circuits by two graph topological approach based on Binet-Cauchy theorem

01 p0037 A69-11349

Linear integrated circuit communication systems based on subsystem approach, showing example of IF strip and audio AGC/squelch amplifier

01 p0035 A69-11389

Stability of linear passive time variable circuits, discussing validity of circuit elements replacement by gyrator equivalents

05 p0739 A69-16348

Noise description of linear n ports obtainable from spot noise parameters of two ports formed from n port

05 p0741 A69-16732

Transversal equalizer circuit consisting of delay line and variable sampler and reinsertion coupler for microwave frequencies

07 p1102 A69-18671

Linear noisy two port preceded by nonreciprocal lossless network analyzed, showing existence of associated quantity invariant under lossless transformation

07 p1104 A69-18891

Control system utilizing digital and linear integrated circuits for low power testing of Pewee 1 reactor of Rover program [IEEE PAPER 2B-6]

07 p1179 A69-19188

Linear electronic circuit canonical synthesis by computer, using algorithm based on linear and nonlinear programming

09 p1472 A69-21781

Linearized radio circuits frequency characteristics calculations using digital computers, noting system nodes number influence on computer rate

09 p1472 A69-21783

Computer programs for linear systems fault isolation, discussing technique theory and limitations

12 p2040 A69-26568

LINEAR EQUATIONS

Linear partial differential equations for nonlinear intensive heat and mass transfer, discussing analogy between transfer processes and electromagnetic waves distribution

01 p0174 A69-10104

Linear ordinary differential equations with exponential coefficients, giving solutions asymptotic behavior for large values of independent variable

01 p0103 A69-10231

Second order systems of linear differential equations eliminating all nonessential difficulties associated with initial value problem

01 p0104 A69-10316

Approximate solution for Dirichlet problem for linear Karman differential equation used in thin plate deflections obtained by Bubnov- Galerkin method

01 p0105 A69-10700

Exchange rule to solve system of linear matrix equations in sense of Chebyshev, giving various algorithms

01 p0105 A69-10705

A priori and a posteriori estimates of direct methods accuracy in solving linear algebraic equations

01 p0105 A69-10727

Approximate solution convergence for linear operator equation in Hilbert space by least squares method

01 p0105 A69-10728

Difference schemes stability for solving linearized gasdynamic equations obtained by representing transition matrices in form of two matrix sum

01 p0060 A69-10729

Reduction principle for study of linear differential equations stability

01 p0106 A69-10956

Soviet book on linear differential equations in Banach space covering equations with unrestricted operators, continuous semigroups, partial differential equations and asymptotic methods

01 p0106 A69-10996

Linear stationary thermoelasticity equations for Cosserat continua, discussing static and kinematic conditions, anisotropy and centrosymmetric isotropy equations

02 p0336 A69-11557

Linear integrodifferential motion equations for turbulent flow within Heisenberg statistical turbulence theory

02 p0230 A69-11869

Integration for equations governing linearized thermoelastic transformations of incompressible solids

02 p0340 A69-12033

Approximate solution of linear functional, singular integral and integrodifferential equations by general theory of approximate methods

02 p0272 A69-12163

First boundary value problem for linear second order parabolic equation with unbounded lowest order discontinuous coefficients and free terms, discussing solvability

02 p0272 A69-12222

Soviet book on linear and quasi-linear second order elliptic equations, emphasizing boundary value problems in various functional spaces

02 p0273 A69-12566

Lic algebra of second order linear differential equations

02 p0273 A69-12841

Integral prediction method for arbitrary continuous function on right hand side of nonhomogeneous linear differential equation with constant coefficients

03 p0455 A69-13022

Zero solution asymptotic stability for linear differential equations with continuous functions

03 p0465 A69-13129

Finite difference method for symmetric positive linear differential equations, discussing methods to solve finite difference equations generated

03 p0455 A69-13370

Linearized time dependent equation for photovoltaic distribution in nonuniformly illuminated p-n junction

03 p0486 A69-13636

Linear differential equation theory corresponding to metric theory of dynamic systems, proving theorems with results of qualitative theory of differential equations

04 p0621 A69-14358

Comparison and oscillation theory of linear differential equations, discussing zeros of solutions and Sturm type theorems

04 p0622 A69-14598

Green matrix of periodic boundary value problem for system of linear differential equations

04 p0624 A69-15098

Doubly infinite sets of simultaneous linear equations used in electromagnetic boundary value problems solved by Asymptotic Anticipation Method

04 p0560 A69-15214

Linear integral equations for brightness coefficients and auxiliary functions in semiinfinite atmosphere, expressing atmospheric albedo using moments and Chandrasekhar function

04 p0662 A69-15237

Ascent algorithm for Chebyshev solution of inconsistent linear equations, noting use for linear programming

04 p0626 A69-15318

Approximate method to determine nonstationary thermal fields in solid bodies with thermal capacity and thermoconductivity coefficient depending linearly on temperature

04 p0688 A69-15409

First order linear differential equations having complementary solutions of exponential type to determine effective initial and boundary conditions

05 p0786 A69-15926

Phase error mean square value in phase lock loop determined from linear differential equations to determine output SNR and noise threshold

05 p0720 A69-16342

Linear differential equations with sinusoidal coefficients analyzed with aid of trinomial recursions

05 p0787 A69-16464

Existence of minimal solutions of doubly infinite trinomial linear recursions of Poincare-Perron type

05 p0787 A69-16465

Analog simulation of water hammer type phenomena governed by linear constant coefficient partial differential equations

05 p0751 A69-16475

Optimal control of system governed by linear parabolic equation with white noise inputs, using mathematical model to generate distributed system analog

05 p0740 A69-16599

Linear equations for three dimensional perturbations in boundary layer of viscous incompressible fluid flow on plane surface, discussing Tollmein-Schlichting waves

06 p0909 A69-17329

Second order half linear differential equation solutions compared with linear equation, investigating differences

07 p1172 A69-18262

Hyperbolic sine creep law, discussing limiting stresses for approximation by linear or exponential relationship

07 p1235 A69-19384

Galerkin method of moments applied to stochastic bounded linear operator equation, discussing statistically homogeneous operator case and electric field in dielectric

07 p1174 A69-19472

Unstable regions prediction for reciprocal system governed by linear equations with periodic coefficients, noting application to rotating shaft and helicopter rotor

08 p1413 A69-20401

Plane H polarized electromagnetic wave diffraction incident on array of rectangular rods described by linear algebraic equations

08 p1275 A69-20433

Singular perturbation problem for elliptic linear partial differential equation, studying asymptotic expansion of solution in vicinity of singular points in nonconvex domain

08 p1352 A69-20751

Duality between effect and influence problems in linear elastoplasticity, obtaining rules for influence functions plotting

09 p1612 A69-21604

Normal solutions of linearized Boltzmann equation for initial and boundary conditions in hydrodynamics solved by approximation

09 p1480 A69-21667

Linear elliptic partial differential equations, deriving sufficient conditions on coefficients for equations to be oscillatory in certain unbounded domains

09 p1533 A69-22771

Five parameter class of linear iterative methods for solution of linear equations systems in application to elliptic boundary value problems

10 p1718 A69-22878

Iterative processes for solution of linear algebraic equations for n dimensional vectors in given space

10 p1718 A69-23208

Probable spectrum stability criterion and reducibility derived for linear differential equation having recursion or almost periodic coefficients

10 p1720 A69-23562

LINEAR FILTERS

Correction of linear functional differential equations with time delay showing error due to incorrect interchange of order of integration involving Stieltjes integral

10 p1721 A69-23642

Iterative method for numerical solution of linear algebraic equations for stationary probability distributions in queueing and reliability theory

10 p1721 A69-23691

Uniqueness and nonuniqueness of solutions of initial value problems for second order semilinear parabolic equations

10 p1722 A69-24069

Wave propagation in connected space-time for linear second order hyperbolic partial differential equation, describing unitary invariant theory

11 p1908 A69-24356

Mixed boundary value problem in theory of axisymmetric potential of three dimensional boundary layer reduced to solution of linear integral equation

11 p1918 A69-24787

Linear thin shell theory in complex dependent variable form for determining fourth order partial differential equations, considering elastic shells with edge loads

11 p1978 A69-24811

Green tensor construction for systems of linear differential equations with constant coefficients

11 p1996 A69-25730

Observation process optimization in system described by linear differential equations of motion reduceable to optimal control problem

12 p2027 A69-25882

Linear differential equations solutions boundedness and unboundedness criteria, determining quantitative relations

12 p2120 A69-26035

Nonlinear multivariable control systems synthesis, considering synthesis expressibility in known linear formulation

12 p2048 A69-26077

Cauchy problem solution for linear/nonlinear differential equations with analytic right hand sought in form of power series

12 p2120 A69-26199

Periodic solution to boundary value problem for quasi-linear parabolic equation with nonlinear boundary conditions obtainable by Rothe method

12 p2121 A69-26282

Linear two dimensional partial differential equations solved by Laplace transforms on analog computer

12 p2123 A69-26717

Dirichlet problem of linear degenerate second order differential elliptic systems with independent variables

12 p2123 A69-26729

Enclosures for large eigenvalues of ordinary second and fourth order differential equations based on asymptotic solutions of linear homogeneous second order differential equations

12 p2124 A69-26892

Linear difference equations with exponential coefficients for numerical methods of integrating differential equations

13 p2288 A69-27526

Nonnegative solutions of second order linear divergence structure parabolic differential equations, discussing Cauchy problem solution, Green function, etc

13 p2290 A69-28539

Functional analysis methods to solve Cauchy problem for linear nonhomogeneous differential equations with delayed argument

15 p2643 A69-30101

Book on solution of linear ordinary differential equations and simultaneous systems using bar statics-equivalent beam method

15 p2711 A69-30929

Optimization of control system described by linear parabolic integrodifferential equation, using dynamic programming approach

15 p2645 A69-31024

Automatic hybrid apparatus for solving linear equations, using Gauss-Seidel iterative method and stressing control arrangement, communication circuits, etc

15 p2572 A69-31089

Bilinear covariant of linear differential form involving $2n$ independent variables used for grouping to achieve symplectic and contact transformations

16 p2804 A69-31623

Boundedness in mean square of solutions derived for linear differential equations forced oscillations with nonwhite Gaussian random functions parameters

16 p2873 A69-32058

Book on quasi-linear equations systems and application to gasdynamics, including problems involving systems of quasi-linear hyperbolic equations with two independent variables

16 p2771 A69-32113

Simultaneous unbounded solutions existence to homogeneous linear differential equations with continuous positive elastic and dissipative coefficients

16 p2804 A69-32251

Generalized finite difference approximations of linear partial differential operators in space based on functional approximations

16 p2756 A69-32552

Optimal linear mean square filtering for piecewise linear correlation functions

17 p2933 A69-33621

Wave propagation in two dimensional anisotropic media with several perturbation speeds, using Lundquist linear equations ensuring lacunas presence

17 p2925 A69-33841

Local radiation characteristics calculation method, consisting of reducing integral equations to linear algebraic equations, applied to solve radiative heat exchange problems

18 p3229 A69-34713

Linear boundary value problem solution using iterative method

18 p3165 A69-35050

Simplification of linear equation of first kind with Tikhonov smoothing functionals

18 p3165 A69-35052

Elastic stability of sandwich materials in microvolume under compressive force analyzed using three dimensional linearized equations for small subcritical strains

18 p3226 A69-35374

Krein solution method for linear integral equations of first kind and related differential equations

19 p3360 A69-35780

Structural analysis of thin walled conical shell with variable external loading and Winkler-base elastic filler, using linear differential equation with variable coefficients

19 p3436 A69-35846

Linearization of equations of motion for three body problem, emphasizing linear far side libration point as related to possible landing

19 p3402 A69-35961

Engineering equations for elastic thin plate oscillations of materials with properties described by linear integral Volterra-Boltzmann operators

19 p3437 A69-35989

Atmospheric temperature and moisture fields obtained by linear equations and objectively analyzed, considering underlying sea surface energy and cumulus cloud distribution

20 p3523 A69-37351

Continuous optimal control problems, proving direct solutions existence for case of differential equations system linearity in control and state variables

21 p3684 A69-38431

Linearized dispersion equation for isotropic electron plasma without external fields solved by harmonic function model

21 p3775 A69-38564

Iterative processes for solution of linear algebraic equations for n dimensional vectors in given space

21 p3756 A69-39149

Operational calculus for n -variable functions analogous to Mikusinski method for single variable functions, giving applications to linear partial differential equations with constant coefficients

21 p3756 A69-39500

Asymptotic methods for differential equations containing parameter, discussing reduction to integral equations system

22 p3976 A69-41124

First boundary value problem for linear second order parabolic equation with unbounded lowest order discontinuous coefficients and free terms, discussing solvability

23 p4182 A69-41973

Positive cyclic systems of linear differential equations, proving existence and projective uniqueness of solution having positive n components for all t

24 p4340 A69-43131

P-Q norms generalized inverse concept of matrix derived from extension of Penrose best approximate solution of linear equations

24 p4342 A69-43703

LINEAR FILTERS

Optimum linear filters for signal detection against background noise using Hodges-Lehmann method

02 p0223 A69-11565

Linear filter performance degradation due to modeling error in estimate of state vector of stochastic linear dynamic systems

02 p0225 A69-11971

Proper digital filters devoid of transient response analyzed as extension of time invariant filters

02 p0213 A69-12815

Linear processing effect on digital communications systems performance by channel impulse response and input-output relationship as distributional convolution equation

03 p0391 A69-13226

Linear and nonlinear filtering, discussing models for signal process, linear white noise problem, optimal estimates, colored noise and finite dimensional approximation

04 p0581 A69-14696

Spectral density of response of linear discrete filter with multiple input and output periods to random signal

04 p0584 A69-15419

Limited memory optimal filter theory, output and standard filter divergence due to errors

06 p0905 A69-17946

Differential equations for minimum variance linear filter separating signals from additive correlated noise, using discrete time optimum formulas

06 p0905 A69-18121

Design and construction of linear digital filters for signal processing, discussing digital filtering of various signals for space research

08 p1297 A69-20303

Kalman filter with delayed states as observables, discussing extra computer effort and modeling technique

09 p1473 A69-22438

Discrete Fourier transforms, discrete linear filters and spectrum weighting for purpose of sidelobe reductions

10 p1666 A69-23888

Linear active adjustable VLF filters for polynomial transfer functions

11 p1859 A69-25392

Adaptive filtering to prevent divergence observed in application of Kalman filter to orbit determination

12 p2045 A69-26059

Deterministic linear observation systems and Kalman optimum linear filters application to performance improvement of inertial navigation systems

12 p2128 A69-26065

Smoothing problem for linear discrete time system, converting problem to special case of standard linear filtering problem

12 p2122 A69-26525

Optimal filtering of linear distributed parameter systems corrupted by boundary and/or volume stochastic disturbances

15 p2565 A69-30183

Linear mean square estimator for restoration of images degraded by system with bandlimited spread function

15 p2611 A69-31032

Microwave bandpass linear phase filters design and synthesis for simultaneous flat amplitude and delay response

16 p2759 A69-31941

Optimal linear mean square filtering for piecewise linear correlation functions

17 p2933 A69-33621

Continuously powered deep space vehicle orbit determination, discussing state estimation accuracy and use of continuous data filtering

19 p3402 A69-35939

Temporal position of pulse signal on noise background determined by measuring signal passage time through linear filter zero point

19 p3278 A69-36596

Book on linear digital filtering and discrete spectrum analysis, emphasizing frequency domain description of signals and systems

20 p3487 A69-37146

Remote sensors discrimination and performance, discussing linear filter system, contrast ratio, tricolor systems and multispectral scanning system

20 p3493 A69-37743

Sequential filter equations for nonlinear system dynamics and observational model with linear estimator, comparing difference between white and colored noise filter results

21 p3686 A69-39371

Stable linear system /shaping filter/ synthesis transforming stationary white noise into random process having given covariance function

21 p3688 A69-39661

- Minimax sensitivity criteria used to synthesize filters for estimating state of first order plant subject to dynamic and/or statistical parameters uncertainties 22 p3918 A69-41016
- Linear filtering effects in channel with binary direct sequence antipodal biphase modulation in presence of white noise and sinusoidal interference, noting variance 23 p4122 A69-41774
- Adaptive filtering to prevent divergence observed in application of Kalman filter to orbit determination 23 p4146 A69-42446

LINEAR PREDICTION

- Linear random processes including law of large numbers, covariance estimation and linear to normal process relationship 01 p0029 A69-10555
- Algorithms for error analysis, optimum filtering sensitivity and fixed interval smoothing solutions to linear estimation problems 02 p0224 A69-11961
- Optimal filter design for estimating state of linear dynamical system in presence of high measurement noise 04 p0582 A69-14877
- Nonlinear programming computational algorithm for recursive optimal estimates of constrained states of linear system 06 p0902 A69-17403
- General linear state estimation from algebraic viewpoint without probability theory concepts, establishing least squares parameter estimation 23 p4182 A69-41880

LINEAR PROGRAMMING

- Book on advanced linear programming computing techniques covering algebraic theory and construction of computer programs 01 p0035 A69-10701
- Incorrect variational and linear programming problems in optimal control theory, emphasizing regularization technique by Tikhonov 03 p0409 A69-13067
- Optimum structural design based on linear, nonlinear and dynamic programming [SAE PAPER 680752] 03 p0525 A69-13437
- Levinson duality theorem for linear programs in complex space proved on basis of duality theorem for linear programming in real space 04 p0623 A69-14947
- Ascent algorithm for Chebyshev solution of inconsistent linear equations, noting use for linear programming 04 p0626 A69-15318
- Iterative Chebyshev approximation for computerized network design by linearizing original nonlinear programming 08 p1299 A69-21170
- Linear electronic circuit canonical synthesis by computer, using algorithm based on linear and nonlinear programming 09 p1472 A69-21781
- Processing of data obtained in continuous tracking of space objects using computer algorithms 10 p1791 A69-24193
- Linear programming algorithms for optimal structural weight design 12 p2181 A69-26566
- Information collection by remote sensing and related economic principles, presenting mathematical formulation of linear programming model 12 p2193 A69-26988
- Incorrect variational and linear programming problems in optimal control theory, emphasizing regularization technique by Tikhonov 14 p2424 A69-28749
- Tolerance limits for uncertain requirements vector in linear programming with random variation, introducing nonparametric statistics with sensitivity analysis [AAS PAPER 69-079] 24 p4340 A69-42821

LINEAR SYSTEMS

- Multiple transmission principles, examining linear systems, synchronous and asynchronous codes and channel interference 01 p0026 A69-10068
- Optimal control of discrete and continuous stochastic linear dynamical systems, discussing algorithms for instantaneous weighted minimum mean square error performance 01 p0051 A69-10439
- Controllability of dynamic systems obtained by studying vector function increments along system trajectories 01 p0051 A69-10698

- Algorithms for linear system of first order differential equations, emphasizing equations associated with computer oriented circuit design 01 p0036 A69-10708
- Random order linear homing systems analyzed by frequency methods employing method of proportional navigation, noting use of transfer functions 01 p0113 A69-10805
- Single frequency oscillations in stochastic quasi-linear differential equations with delay 01 p0170 A69-10825
- Kalman optimal filter for linear distributed parameter systems with Gaussian disturbances and measurement noise 01 p0034 A69-11143
- Two parameter dynamic system of fourth order optimization based on gradient method modified for discrete optimization 02 p0224 A69-11594
- Asymptotic stability conditions for delayed quasi-linear nonautonomous systems periodic solutions derived by Shimanov method 02 p0280 A69-11705
- Optimal adaptive control of discrete linear systems with unknown gain, considering Gaussian distribution functions and random disturbances 02 p0224 A69-11962
- Computational algorithm for determining piecewise-constant feedback gains for linear system optimal control 02 p0224 A69-11964
- Optimal control problem for linear regulators with constant external disturbance 02 p0225 A69-11970
- Pulse transfer function estimation for single input and output linear stationary discrete systems using iterative algorithm and quasi-linearization method 02 p0225 A69-11972
- Correlation of overshoot with gain crossover frequency, phase crossover frequency, phase margin and velocity error constant for linear feedback control systems 02 p0225 A69-12026
- Circuit for linear voltage amplitude to pulse width conversion using controlled unijunction monostable multivibrator 02 p0217 A69-12151
- Book on dynamics of linear and nonlinear systems covering mathematical methods for control system design 02 p0225 A69-12228
- Book on stability criteria for linear mechanical engineering systems covering response characteristics, encirclement theorem, Routh and Hurwitz criterions, root loci, D partition, etc 02 p0281 A69-12276
- Thermal noise from passive linear multiports, noting influence of temperature and absorption coefficients 02 p0211 A69-12443
- Matrix representation of linear active two port noise figures and charts in terms of power wave variables 02 p0211 A69-12444
- Linear differential equations zero solution stabilization by control formed as linear combination of measured coordinates of object 03 p0408 A69-12972
- Linear pulse control systems monotone stabilization, estimating required number of controls 03 p0409 A69-12975
- Passive linear FM pulse compression radar systems detection capability compared with matched filter performance 03 p0390 A69-13218
- Role of second order internal resonance in problem of stability of equilibrium of system neutral in linear approximation 03 p0466 A69-13404
- Necessary conditions for stability of trivial solutions of parabolic systems of partial differential equations 03 p0456 A69-13405
- Linear transistor models synthesis based on measured characteristics of four terminal admittance parameters 03 p0404 A69-13596
- Synthesis of optimal second order systems with linear control 03 p0410 A69-13864
- Book on qualitative theory of sampled data systems 04 p0630 A69-14563
- Optimal control of linear stochastic systems using noise measurement data mathematical model 04 p0581 A69-14569

- Optimal linear controller synthesis with minimized trajectory sensitivity achieved by using quadratic cost function 04 p0582 A69-14941
- Linear mechanical systems idealized by single degree of freedom system with viscous damping subjected to combined deterministic and random excitation 04 p0680 A69-14968
- Nonsteady coordinates of linear delay system determined from observable linear combination of phase coordinates 04 p0583 A69-15094
- Periodic cycles in linear closed loop integral pulse FM systems, discussing existence conditions, periodic formulae and stability criterion 05 p0737 A69-15865
- Stability theorems for discrete linear circulatory systems with N degrees of freedom for static and dynamic loss of stability in presence of velocity dependent forces 05 p0836 A69-15875
- Solution regularity for class of quasi-linear second order elliptic systems, applying results to regularity of extremals of particular integral 05 p0786 A69-15927
- Linear optimal control problems with quadratic performance indices, developing system equivalence for matrix Riccati equation [ASME PAPER 68-WA/AUT-17] 05 p0738 A69-16175
- Sensitivity matrix in multivariable feedback control systems, discussing loop gain matrix design to achieve desired insensitivity to system error sources [ASME PAPER 68-WA/AUT-9] 05 p0738 A69-16179
- Analytical measure of quality of controllability for linear dynamic system and computational procedure for maximizing adjustable structural parameters [ASME PAPER 68-WA/AUT-4] 05 p0738 A69-16182
- Autocorrelation function distortion determined for Barker signal passing through linear system and RC filter, noting passband influence on function shape 05 p0720 A69-16443
- Explicit solubility of asymptotically periodic linear systems of differential equations 05 p0788 A69-16483
- Root sensitivity of linear feedback control systems calculated with signal flow graph and transforming circle 05 p0740 A69-16588
- Invariant subspaces, controllability and observability of linear dynamic systems 05 p0740 A69-16597
- Synthesis of linear controlled systems with variable parameters, reducing parameter determination problem to Chobyshev approximation of relations between linear components 06 p0899 A69-16829
- Linear theory of equilibrium and nonequilibrium gas flows applied to steady two dimensional nonequilibrium flow of inviscid nonheat-conducting gas 06 p0909 A69-17327
- Linear distributed parameter system identification by stochastic approximation, obtaining constant parameters sequentially 06 p0900 A69-17358
- Identification of finite memory, time discrete linear systems by Kiefer-Wolfowitz stochastic approximation procedures, presenting two algorithms for sequential identification 06 p0900 A69-17359
- Finite amplitude longitudinal wave propagation in lattices analyzed by study of compressive wave in chain of mass points with nearest neighbor interaction 06 p1022 A69-17367
- Analysis and synthesis of optimal linear time invariant systems with uncertain or unknown parameters, considering mean square error 06 p0902 A69-17405
- Optimal control of linear systems with state variables generated by linear feedback from output variables, considering time variance 06 p0903 A69-17406
- Linear network analysis by topological formulas for derivation of k-tree terms without generation of k-trees of graph 06 p0903 A69-17409
- Linear antenna synthesis for optimal separation of plane waves providing maximum SNR with allowance for statistical phase distribution of field 06 p0895 A69-17460
- Digital simulation design for linear dynamic systems, noting role of digital transfer function 06 p0906 A69-17491

Synthesis of optimum linear antenna using algorithm
06 p0897 A69-17543

Optimization procedure developed and applied to minimum fuel midcourse guidance of spacecraft, discussing optimal closed loop control of linear stochastic systems
06 p0955 A69-17576

Linear recurring sequences over finite fields, discussing application to error correcting codes
06 p0948 A69-17863

Maximum likelihood smoother using measurements containing correlated noise for application to continuous linear dynamic systems such as inertial navigation
06 p0956 A69-17938

Stochastic approximation algorithms for adaptive linear discrete time system identification using noisy input
06 p0904 A69-17940

Optimization of control independent cost functions in multidimensional system with linear controllers
06 p0905 A69-17945

Linear state variable feedback to obtain asymptotic stabilization of linear dynamic systems
06 p0905 A69-17947

Linear closed loop control system poorly damped response to deterministic inputs improved by stability constraint for minimization of mean squared error
06 p0905 A69-17950

Nonautonomous linear systems stability, with coefficient varying with bounded time function and bounded derivative
08 p1296 A69-19922

Homogeneous linear systems conditions for asymptotic growth of solutions of nonhomogeneous linear differential equations system
08 p1342 A69-20348

Multiplication of solutions of homogeneous linear differential systems
08 p1342 A69-20349

Bandwidth restriction effect on performance of linear codes for digital communication with space vehicles, noting bit and word error probabilities
08 p1276 A69-20597

Command inputs handling by linear optimal control theory, investigating Riccati matrix differential equation convergence
08 p1298 A69-20856

Book on analysis and synthesis of linear active networks covering filter design, negative resistance, network theorems and stability, amplifier role, etc.
08 p1298 A69-20885

Optimal control synthesis for linear plant operating in noise environment, applying dual control theory
08 p1299 A69-21070

Linear shift register synthesis algorithm found to coincide with Berlekamp iterative algorithm for decoding BCH codes
09 p1470 A69-21317

Optimum gathering of information for linear automatic control system with distributed parameters in presence of random input disturbance
09 p1471 A69-21437

Decoupling by state variable feedback and determination of inverse extended to linear time varying multivariable system
09 p1472 A69-21680

Continuous signal over finite time intervals represented by impulse functions of linear channel
09 p1454 A69-21723

Linear systems analysis by generalized numbers method, discussing algorithms for manual or computer analysis
09 p1472 A69-21778

Equations adaptable to computer for RLC circuits containing linear and nonlinear n-terminal networks derived by nodal method
09 p1472 A69-21779

Optimal controls for linear systems with matrix elements and vector components discrete functions of time
09 p1473 A69-21787

Optimal linear quick response problem solving by fast convergence iterative procedure
09 p1473 A69-21791

Orthogonal projection derived equation to optimally estimate state of nonstationary linear discrete systems with time delay, developing Kalman type filter
09 p1473 A69-22437

Optimal closed loop control system for linear time varying system with two independent parameters, noting trajectory sensitivity in large launch booster
09 p1473 A69-22439

Adaptive control algorithm operating on-line to make discrete time adjustments in controller parameters of continuous time control system
09 p1474 A69-22441

Stationary controller design for linear time varying control systems with state variables not always accessible for feedback
09 p1474 A69-22443

Correlation between responses of linear systems for transient input as performance criterion for servomechanisms
09 p1475 A69-22536

Nonlinear one element control system design based on correlation between responses of linear systems
09 p1475 A69-22537

Time varying linear system with input-output relation described by differential equation calculated for impulse response using Taylor series
09 p1459 A69-22580

Optimal control of discrete processes with bounded phase coordinates, proving optimality conditions
09 p1475 A69-22668

Control system controllability under discontinuous control constraints, presenting optimal response rate linear system synthesis with continuous restriction on control function
09 p1475 A69-22670

Liapunov direct method in stability problems for semilinear and quasi-linear systems of hyperbolic partial differential equations with independent variables
09 p1534 A69-22799

Time optimal controlled linear systems with optimally chosen parameters, considering arbitrary second order oscillator controllability
10 p1666 A69-22922

Root sensitivity of characteristic equation of linear automatic control system to system parameter changes applied to aircraft angular stabilization
10 p1666 A69-23610

Optimal control of time invariant uncontrollable linear systems, noting asymptotic stability
10 p1666 A69-23887

Optimal controls for differential system nonlinear in state function and linear in control function
10 p1667 A69-24057

Time varying linear optimal control system sensitivity obtained by comparing closed loop with open loop sensitivity to parameter variations
10 p1667 A69-24058

Differential games solution value function constructible from solutions to associated one player optimal control problems
10 p1667 A69-24059

Magnitude limited random excitation effect on linear system response, using single degrees of freedom model representing idealized mechanical structure [ASME PAPER 69-VIBR-41]
10 p1807 A69-24179

Multiparameter optimum damping for harmonically excited linear stable strictly dissipative n degrees of freedom system, locating multivariable saddle points [ASME PAPER 69-VIBR-42]
10 p1807 A69-24180

Displacement and acceleration criterion for synthesizing optimum linear vibration isolator systems subject to random input [ASME PAPER 69-VIBR-44]
10 p1807 A69-24182

Conjugated gradient components of optimization criterion in automatic control determined by applying sensitivity method to computation
11 p1857 A69-24367

Drift elimination in linear system identification using binary m-sequences by crosscorrelating over two periods of output
11 p1834 A69-24547

Order of finite order linear continuous completely controllable completely observable system, using impulse response matrix and order of corresponding differential equations
11 p1858 A69-24567

Steady state and dynamic characteristics of linear plant with constant lag element based on correlation function moments
11 p1859 A69-24965

Kalman equations of optimal recursive filter for linear discrete system extended to continuous system through limiting procedure
11 p1859 A69-25408

Open loop suboptimal control for linear time dependent tradeoff between energy expenditure and probability of target set entry
11 p1860 A69-25443

Modeling errors in linear discrete stochastic system effects on Kalman filter state estimates
11 p1860 A69-25448

Asymptotic stability of discrete homogeneous linear minimum-variance estimation formulas
11 p1860 A69-25449

Stability of linear time-varying systems via examples, comparing various techniques
11 p1861 A69-25452

Optimal multivariable linear control system design, based on Pontryagin principle using Laplace transform method, providing good approximation to finite interval controllers
11 p1861 A69-25663

Transient response of linear time invariant system from state transition matrix, eliminating evaluation of eigenvalues
12 p2120 A69-25913

Feedback design for monotonically stabilized linear sampled data control system
12 p2045 A69-25961

Linear bridge circuits design having proportional output signal to first or second derivative of input signal envelope
12 p2037 A69-25962

Terminal optimal control problem for linear system having control criterion not dependent on all phase coordinates
12 p2045 A69-25965

Linear automatic control system floating response to harmonic effects achieved by coinciding open loop system transfer function poles with disturbance pattern poles
12 p2045 A69-25967

Linear vibrational systems natural frequencies and damping characteristics determined from system reaction to pulse effect
12 p2178 A69-26004

Digital control algorithm based on self adaptive linear model of multivariable processes used for feed-forward control of output signals
12 p2046 A69-26063

Deterministic linear observation systems and Kalman optimum linear filters application to performance improvement of inertial navigation systems
12 p2128 A69-26065

Group theory application to multidimensional symmetrical linear dynamic control systems optimization, considering natural vibrations of three material points
12 p2129 A69-26071

Matrix transfer functions factorization to obtain irreducible representations of multivariable control systems used for studying invariant linear multidimensional processes
12 p2047 A69-26072

Canonical forms for observable and controllable linear time invariant systems by simultaneous transformations of system state and input and output vectors
12 p2048 A69-26075

Stability conditions for control systems consisting of linear multivariable stationary neutral plant and multivariable pulse frequency modulator, using Liapunov direct method
12 p2049 A69-26080

Optimal control trajectories computation for bilinear regulator problems including neutron kinetics of nuclear reactor
12 p2049 A69-26083

Third order multivariable control systems calculation with linear differential equations describing plant for design and digital optimization
12 p2049 A69-26085

Controllability of linear multivariable time invariant optimal systems with additive parameters using Kalman controllability definition, noting role of Pontryagin principle
12 p2050 A69-26086

Sampled data time optimal control of linear multivariable system based on determination of system state variables control time and minimum sampling intervals
12 p2050 A69-26088

Time optimal controls for multivariable linear systems by computer programming of iterative calculations /Neustadt and fast convergence methods/
12 p2050 A69-26090

Discrete linear optimal control system with quadratic performance index synthesized by dynamic programming method, obtaining matrix equations
12 p2050 A69-26091

Dynamic properties and reliability of linear time invariant multivariable control systems
12 p2051 A69-26093

Equivalent subsystems for designing multivariable linear automatic control system

12 p2052 A69-26280

Integral representation for continuous linear stochastic processes with independent pieces, assuming convergence in probability for sequence of random variables

12 p2121 A69-26365

Optimal control of discrete time linear system with random parameters, noting case of additive noise in measurements

12 p2052 A69-26501

Feedback control of linear systems subject to sudden changes in parameter values

12 p2052 A69-26502

Near optimum regulator design technique for high order linear systems, using singular perturbation method to reduce system order

12 p2052 A69-26503

Nondeterministic differential games with imperfect state information, emphasizing linear system with quadratic cost functional and additive white Gaussian noise

12 p2053 A69-26505

Complete observability in linear time invariant systems decoupled via state-variable feedback, deriving sufficient conditions

12 p2053 A69-26514

Asymptotic controllability of linear system, giving stabilization procedures based on solutions to limiting differential equations

12 p2053 A69-26515

Feedback controller compensator for invariant linear systems having unstable modes

12 p2054 A69-26517

Controllability of stationary linear multivariable systems using frequency domain criterion with application to optimal control laws for minimum fuel and time control problems

12 p2054 A69-26519

Lumped linear system state estimation with optimal linear smoothing instead of filtering, noting smoothing lag and variance

12 p2122 A69-26524

Smoothing problem for linear discrete time system, converting problem to special case of standard linear filtering problem

12 p2122 A69-26525

Linear closed loop control systems with periodically varying parameters analyzed by harmonics method using Fourier transforms

12 p2054 A69-26720

Asymptotically stable discrete time closed loop linear systems synthesis, presenting feedback matrix as illustration

13 p2287 A69-27238

Eigenvalue approximation for first order systems by introducing artificial periodicity through successive impulse functions of alternate sign

13 p2287 A69-27242

Stability test for linear unit feedback control system with second order lag and dead time compensated by PIO controller

13 p2238 A69-27395

Optimal controller design and transfer functions in linear stabilization systems subjected to unknown disturbances determined by variational calculus

13 p2259 A69-27425

Soviet monograph on design and theory of linear induction pumps for liquid metals covering electromagnetic phenomena, optimized dimensions, etc

13 p2209 A69-27926

Parameter identification in linear dynamical systems with transport lags, discussing linear differential-difference equations and finite difference theory

13 p2289 A69-27945

Iterative solution of linear systems for computation of global stiffness matrix reciprocal

13 p2365 A69-28249

Linear automatic control optimization by modified Newton method for determining real function zero value of real argument

13 p2239 A69-28436

Set of states for control system described by linear differential equation with constant coefficients and brought to zero phase coordinates

13 p2239 A69-28437

Quasi-L-analytic functions for ordinary linear operator L

13 p2290 A69-28484

Energy separability method for linear systems in transient evolution using two new identities

13 p2370 A69-28634

Optimal linear control systems with time limits on transient processes synthesized by reducing optimization to algebraic equations solution

14 p2425 A69-28820

Linear control design to synthesize system with prescribed spectrum, deriving formula yielding control coefficients as function of eigenvalues

14 p2425 A69-28821

Compensating /feedback/ loops determination method for linear two dimensional control system, achieving self regulation

14 p2425 A69-28908

Input signal piecewise linear approximation for investigating response of dynamic automatic control systems to nonstandard input signal

14 p2426 A69-29143

Linear dynamic stability of spinning satellite in elliptic orbit, applying perturbation method to determine Floquet solutions

14 p2534 A69-29318

Multivariable linear time-variant systems noninteracting control problem, discussing realization by state variable feedback

15 p2582 A69-30024

Optimal filtering of linear distributed parameter systems corrupted by boundary and/or volume stochastic disturbances

15 p2565 A69-30183

Stochastic saturating systems optimal control computation, considering attitude control and tracking system design by elliptical differential equation of dynamic programming

15 p2582 A69-30601

Power spectral density response of uniform beams to random pressures, evaluating joint acceptance of systems with pressure field

15 p2713 A69-31143

[ASA PAPER SVT2]

Equilibrium cracks propagation in linear hereditary elastic media using Volterra principle

15 p2715 A69-31201

Linear fluid amplifier with beam-deflection proportional active element, discussing optimum maximally flat frequency response

15 p2553 A69-31299

Linear high resolution gate function in blocking out analog signals or reproducing signal amplitudes at output, noting semiconductor elements utilization

15 p2581 A69-31523

Singular and sliding modes /unique extremals/ in calculus of variations for optimal control problems with nonlinear equations and linear control

16 p2764 A69-31629

Book on correlation theory of statistically optimal systems covering linear continuous, discrete, nearly optimal, nonlinear, decision element and adaptive systems

16 p2764 A69-32114

Autocorrelation function distortion determined for Barker signal passing through linear system and RC filter, noting passband influence on function shape

16 p2753 A69-32475

Optimal control synthesis for linear plant operating in noise environment, applying dual control theory

16 p2765 A69-32485

Linear feedback additive noise communication systems formulated in terms of arbitrary operations at transmitting and receiving points

17 p2944 A69-33626

Linear computer-controlled closed loop systems sensitivity analysis, deriving estimation error incremental covariance to demonstrate quality deterioration under perturbed initial conditions, parameters, etc

17 p2944 A69-33742

Observer theory application to hybrid inertial navigation systems, discussing error estimation and correction, real time mechanization, eigenvalues, etc

17 p3003 A69-34099

Network Analysis for Systems Application Program development for batch and on-line solution of circuit problems

18 p3111 A69-34680

Algorithm for minimizing expected value of quadratic performance index in closed loop optimal control of linear time varying systems

18 p3111 A69-34688

Random vibrations in linear systems during spectral and correlation analysis, noting nonlinear systems

18 p3227 A69-35491

Quadratic Liapunov function existence for exponentially stable linear system with varying coefficients described by vector differential equations

19 p3359 A69-35617

Linear optimal control problem for system with variable terminals, proving maximum principle and transversality conditions under minimum constraints

19 p3285 A69-35859

Stability of interrelated linear dynamic control systems with distributed parameters evaluated by using differential equations

19 p3286 A69-35892

Algorithms for equivalence equation to approximate transient processes in higher order linear system by transient processes of lower order linear models

19 p3286 A69-36191

Linear-elastic fracture mechanics applied to environment enhanced crack growth /stress corrosion cracking/

19 p3349 A69-36888

Optimal linear recursive estimators for uncertain observation, considering false alarm probability

20 p3485 A69-36922

Invertibility of linear time invariant dynamical control systems, discussing L-inverses, sequential circuits, inherent integration, reproducibility, pointwise and functional inverses

20 p3509 A69-37138

Linear time varying processes minimal time control by maximum principle to construct extremal control as explicit time function

20 p3509 A69-37139

Trajectory sensitive vector introduction into closed loop linear optimal control, considering linear or nonlinear formulations

20 p3509 A69-37141

Book on stochastic optimal linear estimation and control, discussing probability theory, models and continuous and discrete time linear systems

20 p3509 A69-37143

Continuous signal over finite time intervals represented by impulse functions of linear channel

20 p3488 A69-37459

Damped linear system asymptotic stability inferred from dynamical equation structure, considering matrix eigenvalues and Thomson-Tait-Chetaev stability theorem

20 p3623 A69-37531

Linear radar system theory including Fourier transforms, linear superposition and input/output ratio for deterministic and random signals, discussing filter and sampling theory

20 p3489 A69-37633

Difference method for initial value problems in quasi-linear hyperbolic first order approximations extended to wider quasi-linear problems, assessing convergence

20 p3568 A69-37833

Monograph on frequency response characteristics of mechanical oscillator chains, calculating forced vibrations in linear systems

20 p3577 A69-37920

Linear antenna synthesis for optimal separation of plane waves providing maximum SNR with allowance for statistical phase distribution of field

20 p3508 A69-37943

Linear nonstationary system with singular point analyzed for stability necessary and sufficient conditions using Riemann-Mellin conversion integrals and Laplace transforms

21 p3685 A69-38451

Self excited oscillations in systems with one linearity symmetrical with origin determined by harmonic balance method

21 p3685 A69-38463

Large parameter variations effect on linear feedback control systems performance, optimal or suboptimal

21 p3685 A69-38726

Random variable used as model for unknown parameter in linear system, describing orthonormal expansion for evaluating mean-integral-squared error

21 p3685 A69-38727

Dynamic stability of linear systems with periodic coefficients based on iterative formulas, evaluating transition matrix

21 p3685 A69-38779

Control system generating compensating reactions for correcting trajectory deviations due to uncontrollable random factors, discussing linear automatic control system optimization

21 p3770 A69-38853

Model performance index /PI/ providing criterion for approximating one dynamic flight control system by another based on geometrical representation of linear autonomous systems

21 p3764 A69-39410

[AIAA PAPER 89-885]

LINEAR TRANSFORMATIONS

Linear multichannel spatial motion control systems for vehicles orbiting in earth atmosphere at supersonic velocities

21 p3766 A69-39645

Existence theorem for linear stochastic systems optimal control described by differential equation with random coefficients, providing rms stabilization

22 p3917 A69-40116

Controllability and linear closed-loop controls in linear periodic systems

22 p3917 A69-40572

Linear flight control system synthesis by using optimal control theory associated with quadratic performance index

22 p3864 A69-40588

Approximation of linear unsteady dynamic systems at finite time interval expressed in Bessel or degenerate hypergeometric functions

22 p3917 A69-40616

Suboptimal linear regulators design method yielding feedback controller for multivariable linear systems subject to parameter variations

22 p3918 A69-41012

Robbins-Monro stochastic approximation method using algorithms for identifying finite memory time-discrete time-stationary linear system from noisy input-output measurements

22 p3918 A69-41013

Cauchy problem for partial differential equations linear parabolic system with coefficients depending on unknown functions

23 p4181 A69-41410

Bounded input-output stability for lumped distributed systems by poles examination in S plane, considering transient response of linear time invariant systems

23 p4144 A69-41568

Linear system propagation time measurement independent of input or output time functions

23 p4165 A69-41700

Optimal control problems, discussing properties of signal producing response signals with transient functions at independent outlets of linear dynamic system

23 p4145 A69-41958

Absolute invariance of perturbations affecting dynamic plant achievable by inertial measurement of highest derivatives

23 p4145 A69-42369

Matrix method for free and forced oscillations of complex linear damping system with known linear vectors

23 p4236 A69-42484

Kalman-Bucy filtering technique for estimation of initial conditions and smoothing in linear dynamic systems, noting rectilinear motion of randomly accelerated spacecraft

23 p4132 A69-42546

Electromagnetic processes analysis in autonomous inverters simplified by linear graph method to derive characteristic equation

24 p4255 A69-42571

Pattern classification and iterative methods of linear/nonlinear dynamic plants identification, introducing phi machine as universal plants model

24 p4284 A69-42672

Weighting function of linear dynamic plant with steady random sampling determined with iterative method similar to stochastic approximation

24 p4289 A69-42951

Optimal deterministic estimation and feedback control for linear nonstationary process and measurement systems defined by Riccati equations, including Kalman-Bucy filter

24 p4291 A69-43276

Suboptimal closed loop controller for linear time varying process subject to additive random disturbances and measurement noises

24 p4292 A69-43285

Feedback controller for linear stationary differential systems with time lag and fixed unknown parameters, noting closed loop transfer function role

24 p4293 A69-43293

Minimal time closed loop controller design for linear systems with bounded control amplitudes and rates

24 p4293 A69-43304

Frequency domain stability criteria for open and closed loop distributed parameter linear time invariant systems

24 p4294 A69-43309

Time-invariant multivariable linear systems, discussing structure theorem for controllable systems and application to decoupling problem

24 p4294 A69-43314

State variable feedback design of m-input, m-output time invariant linear systems requiring noninteraction and exact transfer functions, considering coupled core nuclear reactor

24 p4294 A69-43315

Stability of linear systems with convolution operator in forward loop and time-varying gain in feedback loop analyzed for frequency- and time- domain conditions

24 p4295 A69-43316

Parameter identification algorithm identifying linear dynamic systems by digital computer used to identify human operator characteristics in closed loop control situation

24 p4276 A69-43320

LINEAR TRANSFORMATIONS

Quasi-linear approximation for spectrum analysis of LF plasma wave oscillations in steady electric field

14 p2492 A69-29468

Numerical absolute stability test for nonlinear discrete systems using bilinear transformation

17 p2994 A69-32848

Statistical characteristics of linear transformations of gravity field anomalies by linear operators, noting computation of covariance function

21 p3716 A69-39247

LINEAR VIBRATION

Normal modes and natural frequencies of combined linear elastic structures resting on immovable base

04 p0678 A69-14870

Limiting amplitude of output shaft vibrations of servodrive operated in linear region as function of frequency

04 p0584 A69-15417

Rotors linear vibrations due to unbalanced shaft rotating on lubricated bearings taking into account lubricant damping

07 p1235 A69-19441

Hydropendulum bearing linear horizontal vibration effect on vertex vibration, analyzing zero initial phase using precession theory

10 p1697 A69-24086

Linear and torsional vibration parameters measuring methods, discussing transducer characteristics

22 p3943 A69-39926

LINEARITY

NT COLLINEARITY

Book on nonlinear boundary value problems for ordinary second order differential equations, illustrating difference between linear and nonlinear problems concerning existence and uniqueness

04 p0622 A69-14600

Articles on automatic control systems stability, discussing relation between method of Lure and Popov criteria

05 p0740 A69-16667

Linearity range of viscoelastic properties of fiberglass reinforced plastics, calculating stress-strain state

18 p3163 A69-35364

Ordinary differential equations in linear topological space extended from Fattorini investigation, emphasizing use of linear operator

19 p3360 A69-36599

LINEARIZATION

Pulse transfer function estimation for single input and output linear stationary discrete systems using iterative algorithm and quasi- linearization method

02 p0225 A69-11972

Nonlinear boundary value problems direct generalized solutions based on linearization of Bubnov-Galerkin and Ritz method

02 p0272 A69-12136

Method of particular solutions for use with quasi-linearization in solving nonlinear boundary value problems

02 p0273 A69-12550

Statistical linearization of nonlinear memory type elements with stationary Gaussian input, applying Wiener method to one class of problems

03 p0409 A69-13005

Statistical linearization coefficients for arbitrary nonlinearities in automatic control systems via techniques applying characteristic functions

03 p0409 A69-13071

Dynamic programming application to function generation, determining breakpoints for best linear approximation of one dimensional function

03 p0401 A69-13765

Nonlinear constitutive equations for mixture of two elastic solids linearized, assuming small displacements and subsequent temperature changes

03 p0529 A69-14063

Random motion of particle with nonlinear damping, obtaining velocity spectrum by solving associated nonstationary Fokker-Planck equation and using equivalent linearization technique

04 p0561 A69-15454

Linearizing circuit for low velocity hot-wire anemometry, using analysis of transistor circuit to generate desired function

06 p0927 A69-17701

Linearization unit for compensating hyperbolic characteristic of capacitive displacement sensor used for contactless displacement measurement

08 p1317 A69-20879

Bilinear hysteretic system undergoing random vibration, substantiating linearization analysis with analog computer simulation and comparing lifetime to linear system [ASME PAPER 69-VIBR-25]

10 p1806 A69-24173

Statistical linearization coefficients for arbitrary nonlinearities in automatic control systems via techniques applying characteristic functions

14 p2424 A69-28753

Statistical linearization of strong nonlinearity in series with random-gain amplifier element, deriving formulas for statistical gain parameters

14 p2425 A69-28920

Distribution function, harmonic and statistical linearization methods applied to study forced oscillations in nonlinear oscillatory system

16 p2813 A69-32284

Quasi-linearization algorithm for solution of boundary value problems for ordinary differential equations, formulating representation and convergence theorems

17 p2994 A69-32835

Linearization of relationship between stress concentration factor and reciprocal of strain hardening exponent enabling shakedown to pressure vessels formulated by mathematical model

20 p3620 A69-37002

Quasi-linearization to overcome dynamic programming dimensionality difficulties, reducing computer memory requirement and computation time

21 p3754 A69-38751

Retarding potential analyzers determining ionospheric structure, noting linearization of analysis

22 p3940 A69-40523

Digital signal processing electronic device for linearizing signals from sensors with nonlinear frequency output by modifying time signal frequency

22 p3915 A69-40935

LINERS

U LININGS

LINES

Early type stars spectrophotometric parameters, discussing hydrogen beta, gamma and delta line widths, magnitude, etc

10 p1777 A69-23387

LINES [GEOMETRY]

NT CHORDS [GEOMETRY]

Visual backward masking experiment for studying overlapping and nonoverlapping contours of target and masking stimuli straight line

22 p3879 A69-40843

Visual succession threshold for sides of square contour affected by presenting single line on parallel contour sides

22 p3882 A69-40868

LINES OF FORCE

Free access of low energy galactic particles to solar wind lines of force due to stochastic nature of lines

01 p0147 A69-11238

F 2 layer cut-off frequency predawn increase caused by sunrise, resulting in photoelectrons transfer along force lines at magnetically conjugate point

02 p0238 A69-11681

Characteristic time on motion of magnetic lines of force in medium with Hall effect

02 p0290 A69-12399

Graphical representation of stress distributions and forces on dislocations

03 p0529 A69-13973

Magnetic lines curvature behind pseudostationary hydromagnetic shock determined, assuming parallel magnetic field and velocity vectors

04 p0638 A69-15092

Neutral sheet structure and orientation in geomagnetic tail, computing field lines on basis of Explorer 14 magnetic field measurements

05 p0753 A69-16256

Oscillating electric dipole in cold plasma with ideal conductivity along lines of force of external magnetic field

06 p0921 A69-17743

- Computational techniques for determining magnetic field geometry for backscatter reflections
07 p1125 A69-18850
- Magnetic lines of force penetration into magnetosphere accompanied by plasma insertion generating ring current responsible for main phase of magnetic storm
10 p1687 A69-23923
- Geomagnetic field directed hydromagnetic waves propagation in lower ionosphere, noting inhomogeneous conductivity, Hall effect and lines of forces role
10 p1687 A69-23926
- Stochastic and ergodic aspects of magnetic lines of force, discussing cosmic ray diffusion in interplanetary magnetic field
10 p1770 A69-24111
- F 2 layer cut-off frequency predawn increase caused by sunrise, resulting in photoelectrons transfer along force lines magnetically conjugate point
13 p2257 A69-28712
- Hydromagnetic waves propagation in finitely conducting fluid mass immersed in nonuniform magnetic field, using curvilinear coordinates based on lines of force
14 p2491 A69-29336
- Magnetic field lines curvature effect on plasma instabilities due to ion temperature gradient, noting frictional gravitation field simulation
16 p2816 A69-31636
- Horizontal magnetic variation peak at eight degree dip latitude, noting F region contribution to magnetic tubes of force integrated transverse conductance
16 p2778 A69-32189
- Geomagnetic field lines coordinates calculation based on coefficients obtained in spherical harmonic analysis
20 p3522 A69-37060
- High latitude limit of closed geomagnetic field lines indicated by high latitude electron boundary in outer radiation zone during Alouette satellite energy particle experiment
20 p3531 A69-37875
- Topology of interplanetary field lines in magnetotail, using solar electrons as tracers with moon as absorber
20 p3609 A69-38078
- LF hydromagnetic waves propagation along geomagnetic field lines in gyrotronic ionosphere model taking Hall effect into account
23 p4157 A69-41864
- LING-TEMCO-VOUGHT AIRCRAFT**
U A-7 AIRCRAFT
U XC-142 AIRCRAFT
- LING-TEMCO-VOUGHT MILITARY AIRCRAFT**
U MILITARY AIRCRAFT
- LINGUISTICS**
U MACHINE TRANSLATION
U SEMANTICS
- LININGS**
NT ROCKET LININGS
Dielectric properties of high loss nonmagnetic microwave materials used for waveguide absorbers and anechoic chamber linings
12 p2079 A69-26047
- LINKAGES**
Planar linkages kinematic synthesis and design, using Newton-Raphson iteration technique to solve nonlinear equations
04 p0604 A69-14517
- Daily communication link geometry between spacecraft in elliptical orbit and landed capsule, establishing spacecraft visibility contours for landing site latitude
[AAS PAPER 68-110] 21 p3805 A69-39223
- LINKING**
U JOINING
- LILOUVILLE EQUATIONS**
Liouville and Poisson equations solutions for locally ellipsoid stellar velocity distributions with constant coefficients
02 p0310 A69-11455
- Final motions of Hamiltonian conservative systems, analyzing Liouville type, homogeneous and similar systems
09 p1540 A69-21882
- General solution of Liouville equation for collisionless system of gravitationally interacting particles, with distribution function locally isotropic in momentum space
09 p1605 A69-22412
- Time dependent evolution of probability pressure distribution maximum obtained from Liouville equation
14 p2472 A69-29406
- Fokker-Planck plasma collision equation derived from Boltzmann equation, Markov process and Liouville equation
23 p4195 A69-41516
- LIPID METABOLISM**
Acetate carbon 14 utilization in centrifuged rats, analyzing metabolism by measuring plasma glucose, FFA and lipids synthesis
07 p1067 A69-19429
- Hypothermia induced alterations in biochemical processes studied with isolated rat liver perfused at low temperature
10 p1642 A69-23119
- LIPIDS**
NT LIPOPROTEINS
Uranyl ions interaction with phospholipid and cholesterol monolayers, using surface pressure and potential measurements
11 p1832 A69-25641
- Physical and psychic stress effects on phosphatidyl glycerol and related phospholipids concentration in human and rat blood plasma
23 p4088 A69-41815
- LIPOPROTEINS**
Structural phospholipoprotein isolated from hydrogenomonas facilis and neurospora crassa
22 p3871 A69-40049
- LIPSCHITZ CONDITION**
Boundary value problems for second order differential equation with continuous f satisfying local Lipschitz condition
07 p1173 A69-18730
- Existence and uniqueness for nonlinear boundary value problems satisfying Lipschitz condition
10 p1721 A69-23640
- Synthesis for nonlinear second order differential equations with terms satisfying Lipschitz condition, using two person games optimal strategy
11 p1910 A69-25602
- LIQUEFIED GASES**
NT LIQUID AMMONIA
NT LIQUID HELIUM
NT LIQUID HYDROGEN
NT LIQUID NITROGEN
NT LIQUID OXYGEN
Liquefied propane fog dispersal at Medford-Jackson airport, Oregon
04 p0585 A69-14918
- Thermal design and test for liquefied gas vessels under unsteady insulation cooling conditions
04 p0687 A69-15162
- Simple fluids viscosity dependence on density analyzed by molecular theory, exemplifying with liquid argon
13 p2299 A69-28036
- Cooldown of vacuum insulated transfer lines using liquid N and H, discussing flow characteristics reproduction by digital computer program
[NAS-NRC PAPER I-1] 22 p4050 A69-40625
- LIQUID AMMONIA**
Reaction rate and mechanism for low temperature reaction between lithium hydride and liquid ammonia, noting chemisorbed ammonia dissociation at interface
01 p0025 A69-11285
- Electrochemical oxidation of fuels in liquid ammonia, evaluating electrode surfaces as catalysts
[ECS PAPER 212] 03 p0382 A69-13857
- ATS 3 spacecraft ammonia-fueled resistojet engine test performance
[AIAA PAPER 68-553] 21 p3786 A69-39754
- LIQUID ATOMIZATION**
Mean drop size generated in vapor pressure regime of liquid water jet, noting effect of water temperature and orifice diameter
09 p1483 A69-21995
- Fuel jet shape in air stream/mechanical atomization calculated as function of stream and fuel injection parameters
11 p2002 A69-25336
- Thermodynamic atomization in MHD energy conversion through convergent-divergent nozzles, noting nozzle efficiency and droplet size
13 p2245 A69-27477
- Quantitative analysis of interaction between spray and ambient atmosphere, discussing atomization of flat sheet and drop behavior relationship to operating conditions
15 p2717 A69-30465
- LIQUID COOLED REACTORS**
NT LITHIUM COOLED REACTOR EXPERIMENT
NT NRX REACTORS
NT PLUM BROOK REACTOR
- Liquid metals as coolants in breeder and space vehicle reactors for stable two phase flows
05 p0803 A69-15998
- LIQUID COOLING**
NT FILM COOLING
Water cooling jackets of plastic textile reinforced film for high inside temperature reduction in protective clothing
06 p0883 A69-18027
- Liquid fuel rocket engine design for cooling by propellant counter flows
08 p1376 A69-20588
- Personal cooling in inadequately air conditioned cockpits, considering dry air, air ventilated suits and liquid circulated tubes near skin
[AGARDOGRAPH-111] 08 p1267 A69-20684
- Argon ion laser with water cooled mercury pool cathode shielded by U-bent section trap, considering advantages as compared to oxide cathodes
12 p2107 A69-26326
- Spray oil cooling to reduce aircraft generator weight, enhance reliability and lengthen overhaul intervals
15 p2552 A69-30326
- Temperature distributions in layer with internal heat source and turbulent fluid flow cooling, deriving differential heat transfer equations
15 p2718 A69-31169
- Heat transfer characteristics in evaporative, transpiration cooled porous systems
21 p3851 A69-39037
- Instantaneous frozen layer thickness and temperature profile in solidified layer obtained by iteration technique
21 p3852 A69-39433
- LIQUID CRYSTALS**
Cholesteric liquid crystals application to trace contamination detection, describing color response measurement
06 p0885 A69-17842
- Liquid crystals for photographically recording microwave holograms, noting impossibility of three dimensional image reconstruction with side-looking radar zone plates
12 p2079 A69-25917
- Skin friction measurement in aerodynamic tests using thin liquid crystal coatings with changes in maximum light scattering wavelength in response to shearing forces
14 p2427 A69-29029
- Cholesteric liquid crystal film application to test surfaces for thermal mapping, giving technique for flaw pattern determination
15 p2631 A69-31507
- LIQUID DROPS**
U DROPS [LIQUIDS]
- LIQUID DYNAMICS**
U FLUID DYNAMICS
- LIQUID FILLED SHELLS**
Soviet book on vibrations of elastic shell partly filled with fluid covering different stages in procedure for shells of axisymmetric configuration
02 p0346 A69-12480
- Finite difference schemes for axisymmetric oscillations of shells of revolution filled with liquid
03 p0523 A69-12951
- Soviet collection of articles on dynamics of fluid-containing bodies under weightlessness conditions
03 p0417 A69-13808
- Primary frequency of oscillations of ideal liquid in cylindrical vessel with axially directed weak gravitational field
03 p0418 A69-13812
- Bubble motion inside liquid in spherical cavity, allowing for bubble surface deformation
03 p0418 A69-13813
- Motion and stability of solid body with cavity containing rotor and two incompressible nonmixing liquids with surface tension
03 p0418 A69-13814
- Stability of steady motion of body with cavity containing one or several nonmixing liquids as problem of bounded oscillations about motion
03 p0418 A69-13815
- Magnetoelastic vibrations of fluid filled cylindrical cavity in infinite solid medium in presence of uniform axial magnetic field
03 p0528 A69-13927
- Approximate method for finding solution of weak free convection in partially filled vessel in gravitational field
04 p0685 A69-14619
- Axisymmetric oscillation modes and frequencies of hemispherical shell partially filled with liquid, using moment theory of shells
04 p0679 A69-14922

Temperature distribution and thermal stresses in liquid filled cylindrical shell 04 p0682 A69-15413

Liquid rise in partially filled circular cylinder with free surface accelerated from rest to constant angular velocity [ASME PAPER 68-FE-13] 05 p0747 A69-16065

Whirl dynamics of partially liquid filled spinning rotor mounted on elastic shaft, noting synchronous critical speed and asynchronous whirl speed [ASME PAPER 68-WA/APM-25] 05 p0768 A69-16189

Equations of motion solved for solid body with ellipsoidal cavity containing ideal incompressible fluid in uniform eddy motion 06 p0957 A69-16823

Dynamics of carrier rockets and space vehicles having complex three dimensional thin walled constructions with cavities containing liquids [UN PAPER 68-95622] 06 p1013 A69-17051

Oscillations of cylindrical orthotropic three layer shell having ideal fluid flow at variable rate, establishing parametric resonance and determining limits of shell motion instability regions 06 p1022 A69-17186

Ritz method for natural oscillations of ideal liquid in spherical vessel with various filling levels, considering vertical perturbing force 06 p0910 A69-17333

Liquid filled cylindrical container motion with longitudinal forces applied to base, obtaining stability conditions for natural oscillations 08 p1419 A69-21181

Coaxial cylindrical shells oscillation frequencies with interspace filled with incompressible liquid determined as functions of liquid level and interspace width 09 p1612 A69-21483

Axisymmetric vibration modes of cylindrical-hemispherical membrane tank partly filled with liquid [AIAA PAPER 67-75] 09 p1482 A69-21940

Vibration characteristics of circular cylindrical shells containing water under axial excitation, investigating bubble formation and shell-liquid interaction [ASME PAPER 69-VIBR-4] 10 p1805 A69-24162

Natural frequencies and mode shapes for longitudinal oscillations of liquid filled elastic circular cylindrical tank with flexible inverted conical bulkhead [ASME PAPER 69-VIBR-11] 10 p1806 A69-24165

Formula in Prandtl-Batchelor theory describing motion of incompressible fluid in sphere interior verified experimentally 11 p1868 A69-24755

Boundary value problem for gravity induced wave motion of ideal fluid in axisymmetric vessel with annular ribs, noting application to bodies of revolution 11 p1868 A69-24769

Motion of body with cavity containing liquid based on Kharlamov solution, noting gyrostatic moment and liquid sloshing effect 11 p1868 A69-24775

Kharlamov method for influence of turbulent motion of liquid in cavity on inertial motion of body containing cavity 11 p1868 A69-24788

Liquid filled elastic shells natural frequencies and oscillation modes, deriving eigenfunction system from liquid velocity potential boundary conditions to determine dynamic load 11 p1870 A69-24951

Large amplitude symmetric and asymmetric irrotational motion of inviscid incompressible fluid with liquid-vapor interface in accelerating cylindrical container of revolution 11 p1871 A69-25124

Cylindrical propellant tanks dynamic stability and parametric resonance, analyzing axial preload, liquid depth, top impedance and ullage pressure by Donnell theory 11 p1899 A69-25499

Solid body motions containing cavity filled with viscous fluid under influence of gravity, formulating motion equations for fluid and body 12 p2061 A69-25884

Blood vessel model in form of cylindrical shell filled with liquid for studying cardiovascular system dynamic and static problems 12 p2018 A69-25989

Frequency equation for thickness effects on axisymmetric radial and rotatory vibrations of empty or fluid filled isotropic spherical shell 13 p2363 A69-28185

Nonlinear equations for motion of rigid body with cavity partially filled with ideally incompressible liquid 14 p2432 A69-29626

Soviet book on partially liquid filled solid body dynamics from viewpoint of space and aircraft applications 14 p2530 A69-29815

Axially symmetric vibrations of thin elastic spherical shell partially filled with liquid, considering shell as joined hemispheres with or without same thickness 16 p2873 A69-32129

Plane oscillations of liquid in rectangular elastic vessel determined to obtain frequencies and mode shapes of natural oscillations from velocity potential boundary conditions 17 p2950 A69-33200

Stable motions determination of solid bodies with liquid filled cavities and satellites motions stability in central Newtonian force field 17 p3005 A69-33228

Stationary liquid under pressure effect on energy dissipation of rectilinear pipelines under pure bending 17 p2904 A69-33930

Rotary motion stability of axisymmetric solid body or gyroscope suspended on string and containing ellipsoidal cavity filled with liquid 18 p3135 A69-34558

Liquid filled rigid bodies motion stability defined and solved for system with infinite number of degrees of freedom 19 p3301 A69-36810

Thermal stress concentration near elliptical hole in thin walled liquid filled cylindrical shell in presence of temperature gradient across shell cross section 20 p3622 A69-37325

Perturbed motion of solid body containing axisymmetric cavities partially filled with ideal incompressible fluid, solving boundary value problems of fluid oscillations 20 p3518 A69-38296

Fluid motion in free falling partially filled cylindrical vessel due to sudden vertical velocity change, considering free surface disturbances 21 p3692 A69-38684

Asymmetrical oscillations of cylindrical shell with elastic bottom containing liquid, discussing liquid level influence on natural oscillation frequencies 21 p3834 A69-38718

Natural oscillations of free surface liquid and elastic bottom of cylindrical cavity determined by integrodifferential equations based on liquid level 21 p3693 A69-38720

Rotating stratified fluid in thermally insulated cylinder, studying angular velocity abrupt change effects under stable temperature distribution 21 p3694 A69-38768

Optimal control of vibrations of liquid in cylindrical container with vertical generatrix and flat bottom, using dynamic programming 21 p3694 A69-38849

Optimal control of liquid vibrations in rectangular container moving in horizontal direction, deriving algebraic equations system for optimal functional 21 p3694 A69-38854

Optimal control of ideal noncompressible fluid vibrations partially filling rectangular container moving in horizontal direction 21 p3695 A69-38892

Motion of body with cavity completely filled with viscous fluid about center of mass in potential mass-force field, applying small parameter method 22 p3980 A69-40109

Oscillations of highly viscous incompressible fluid in partially filled cavity of body moving about fixed point, solving Navier-Stokes equations by asymptotic method 22 p3929 A69-40111

Spherical vessel partially liquid-filled and supported by equatorial ring, studying axisymmetric oscillations under external forces 24 p4300 A69-43069

Energy dissipation in oscillating sphere filled with viscous fluid, giving fluid response by solving Navier-Stokes equation 24 p4305 A69-43587

Pressure wave transmission in liquid filled tubes, determining attenuation and phase shift for hemodynamics applications 24 p4279 A69-43798

LIQUID FLOW NT OPEN CHANNEL FLOW NT WATER FLOW

Time dependent interaction of hot gas bubble with chemically reactive liquid stream, detailing thermal boundary layer theory 01 p0058 A69-10162

Pressure pulses propagation in nonsteady fluid flow through expansible tubes, noting computer solution 02 p0232 A69-12477

Irrotational almost uniform plane flow of two immiscible inviscid liquids on horizontal bottom in channel, noting permanent gravity waves 04 p0590 A69-15055

Velocity profiles for laminar flow of homogeneous liquid in pipe inlet at small and moderate Reynolds numbers 05 p0743 A69-15578

Liquid rise in partially filled circular cylinder with free surface accelerated from rest to constant angular velocity [ASME PAPER 68-FE-13] 05 p0747 A69-16065

Liquid flow systems dynamic response to periodic disturbances of system structural supports 05 p0747 A69-16073

Viscous electrically conducting liquid flow through insulating porous medium in presence of transverse magnetic field in region of validity of Darcy law 05 p0805 A69-16603

Cauchy problem for nonstationary linearized Navier-Stokes equations for fixed container partially filled with liquid 06 p0959 A69-17888

Liquid flow field about oscillating flat plate, comparing visualization results with numerical solution of Navier-Stokes equations [AIAA PAPER 69-226] 07 p1121 A69-19565

Electrodes behavior for fuel cells with liquid electrolyte under high-g and weightlessness conditions, discussing spontaneous liquid motion 08 p1259 A69-21038

Kharlamov method for influence of turbulent motion of liquid in cavity on inertial motion of body containing cavity 11 p1868 A69-24788

Parallel flow of viscous liquid film with free surface down inclined plane, noting growth of initially infinitesimal amplitude waves and finite amplitude wave stability 11 p1869 A69-24891

Forced discontinuous vibrations of liquid in conduit experimentally analyzed, discussing test devices and procedures 11 p1875 A69-25485

Radial electric field effect on pressure drop in isothermal laminar flow of dielectric liquid through stainless steel tube, considering ion drag 12 p2136 A69-26401

Liquid flow MHD alternating current generator design, considering induced current in rotor and resulting magnetic field in pole gap 13 p2206 A69-27495

Liquid metal MHD power plant system tested under open and closed loop conditions for liquid circulation 13 p2208 A69-27510

Displacement of liquid by insoluble liquid from horizontal circular tube during laminar flow, analyzing flow characteristics 14 p2431 A69-29607

Water vapor recondensation effect on structure of liquid particle flow into vacuum 16 p2769 A69-31869

Pressure in sealing groove and increase time due to pumping action of moving wall applied to force cylinder of translational motion, considering liquid in groove laminar 16 p2736 A69-32135

Liquid draining motion from transversely moving cylindrical tank in time varying gravity field with outlet pipe at bottom, discussing flow rate and free surface [AIAA PAPER 69-679] 17 p2953 A69-33440

Fluidic sensor for measuring gas and liquid velocities, describing design and principles of operation 18 p3133 A69-34308

Micropolar liquid basic flows, considering case with coupling constant relating microstructure to macroscopic flow greater than viscosity coefficient 18 p3121 A69-34786

Temperature distributions and heat transfer in thermal entrance region for Hartmann liquid flows under constant pressure gradient between parallel electrically conducting walls at rest 21 p3847 A69-38442

Nonlinear differential equations for flow of viscous liquid thin sheet on horizontal plane, solving initial value problems for zero slope bed 21 p3697 A69-39680

Forced convection liquid flow past heated flat plate with variable viscosity and thermal conductivity, analyzing velocity and temperature distribution in boundary layer 22 p4051 A69-40685

Pressure activated superfluid valve design and operation for liquid He transfer from reservoir to cold finger 22 p3870 A69-41237

Hot-wire anemometer calibration technique for measuring velocity of very slowly moving liquids
[ASME PAPER 69-HT-A] 24 p4316 A69-43527

LIQUID-GAS MIXTURES

NT AEROSOLS
NT FOG

Experimental apparatus for measuring heat transfer coefficients into boiling K in tubes, investigating vapor-liquid mixtures hydrodynamic and electrical properties
03 p0534 A69-14150

Combustion in heterogeneous systems, considering diffusion flames and fine droplets dispersed into gaseous oxidizer in fog form
06 p1032 A69-17421

High velocity gas stream induced shattering of liquid drops, disintegration rate and breakup time
[AIAA PAPER 68-83] 09 p1482 A69-21947

Spark ignition of liquid fuel droplets atomized in air analyzed by spark discharge visualization for two phase mixture
09 p1623 A69-22220

Two phase MHD generator with gas in liquid metal emulsions, discussing loops efficiency
13 p2306 A69-27479

Sound effects on turbulent flame in gasoline-air mixture jet in Toepfer device with pulsed light source, measuring ionization in combustion zone
17 p3069 A69-33141

Energy balance equation for two phase liquid-gas mixture ignition process, deriving formula for speed of combustion zone movement
18 p3231 A69-35123

Automatic ultrasonic method for determining dissolved gases content in liquid sample, using increasing acoustic oscillations amplitude for bubble development
19 p3308 A69-35822

LIQUID HELIUM

Liquid helium cooled broadband parametric amplifier, discussing circuits and noise performance
02 p0221 A69-12458

Book on properties of liquid and solid helium 3 and 4 physical characteristics, phase behavior and experimental techniques
04 p0630 A69-14688

Nuclear radiation influence on pool boiling heat transfer to liquid helium, using irradiated copper as boiling surface
[ASME PAPER 68-WA/PID-3] 05 p0791 A69-16164

Velocity of 1 MHz sound waves in He 4 along isotherms just above critical temperature, noting specific heat ratio for 4.5 and 5 K isotherms
06 p0957 A69-17142

Spectrum and amplitude fluctuations of laser light propagating through liquid helium, obtaining spatial correlation function of refractive index fluctuations
06 p0957 A69-17267

Helium cooled low noise high gain parametric preamplifier for satellite communication by stagger tuning stages
07 p1098 A69-18460

Helium closed cycle cooled very low noise high gain parametric amplifier for investigating interstellar atomic hydrogen radiation
07 p1098 A69-18461

Helium cooled low noise high gain wideband parametric amplifier for spacecraft communication
07 p1099 A69-18462

Liquid helium vented and nonvented storage container design and handling techniques
10 p1810 A69-24016

Aerobee rocket-borne liquid helium cooled telescope for IR night sky observations
11 p1885 A69-24852

Dielectric constant of liquid hydrogen and hydrogen-helium mixtures measured with resonance method
14 p2487 A69-29668

Heat transfer from cylindrical copper surface to liquid helium at 4 degrees K, discussing temperature fluctuations in nucleate boiling region
17 p3074 A69-33780

Steady state performance of multistrand superconducting compound conductors in current sharing state, using heat measurement from metal surface to He bath
17 p3016 A69-33786

Transition temperature depression in rotating liquid He based on increased inertial density of excitations
23 p4192 A69-42335

LIQUID HYDROGEN

Ball bearings lubrication and wear in cryogenic hydrogen turbopumps by transfer films provided from self lubricating cage
01 p0084 A69-10109

High pressure transfer system to deliver liquid hydrogen to testing equipment and liquid hydrogen/liquid oxygen engines
01 p0013 A69-11145

Liquid hydrogen circulation pump design emphasizing heat leaks
01 p0087 A69-11148

Gaseous and liquid H refractive index variations with pressure and density below room temperature, noting Lorentz-Lorentz function variations
02 p0281 A69-12180

Current mode amplifier circuit used with carbon resistors for measuring low flow rates of liquid hydrogen from small containers
04 p0577 A69-15025

Radioisotopic propulsion stage design with liquid hydrogen working fluid, stressing tank insulation and hydrostatic flight behavior
05 p0811 A69-15595

Natural convection heat transfer for incipient vapor formation in liquid H and N and for nucleate boiling of liquid H
[ASME PAPER 68-WA/PID-4] 05 p0848 A69-16165

Whirling liquid hydrogen layer thermal and hydrodynamical conditions, noting application to cold neutrons source in high flux beam reactor
05 p0849 A69-16818

Fluid and thermodynamic modeling for ground test simulation of nuclear rocket vehicle liquid hydrogen propellant behavior
[SAE PAPER 690201] 07 p1178 A69-18306

Dielectric constant of liquid hydrogen and hydrogen-helium mixtures measured with resonance method
14 p2487 A69-29668

Neutron and photon transport properties in liquid hydrogen obtained from measuring radiation environment in propellant tank mockup suspended above NERVA reactor
[AIAA PAPER 69-475] 16 p2810 A69-32716

Fluorine injectors for main tank injection of space vehicle liquid hydrogen tank, including study of hypergolicity and reaction product freezing
[AIAA PAPER 69-528] 16 p2767 A69-32717

Pressurant gas requirements for pressurized discharge of liquid hydrogen from propellant tanks for optimum pressurization system designs
[AIAA PAPER 69-526] 16 p2845 A69-32737

Hydrogen check valve with low cracking pressure and flow pressure drop for hydrogen vent system at Saturn launch pad
[AIAA PAPER 69-578] 16 p2845 A69-32738

Hydrogen oxygen rocket engine two phase liquid hydrogen pump capability and hydrodynamic design, analyzing constant-quality flow, acoustic effects, compressible flow and cavitation
[AIAA PAPER 69-549] 16 p2845 A69-32759

Slush hydrogen for spacecraft propulsion, discussing fabrication, conservation and storage
17 p3017 A69-33339

Twin spool hydrogen turbopump performance at zero net positive suction pressure (NPSP) saturated fluid in propellant tank, including steady state and simulated transient engine tests
[AIAA PAPER 69-550] 18 p3140 A69-34414

Liquid hydrogen pumping for Phoebus reactor, discussing feed systems, nozzles, configurations, design, testing, etc
[AIAA PAPER 67-478] 21 p3769 A69-39751

Payload optimization factors for orbital storage of liquid hydrogen, considering payload cost of agitation, tank pressure, pressurant weight, etc
[AIAA PAPER 69-1007] 22 p4021 A69-40381

Liquid solid mixtures of parahydrogen flow characteristics in pipe, globe valve, orifices and venturi, determining pressure loss
[NAS-NRC PAPER F-5] 22 p3998 A69-40626

Slush H and N gels preparation and characteristics, including measurements of weight bearing capacity of gel as function of percent mass silica gelant
22 p3998 A69-40632

Optimal design and materials for cryogenic storage of O and H on lunar surface
[AAS PAPER 69-051] 24 p4296 A69-42882

Hydrodynamic inlet conditions effect on film boiling and near critical hydrogen heat transfer, using data from electrically heated various geometry test sections
[ASME PAPER 69-HT-27] 24 p4412 A69-43541

LIQUID INJECTION
NT WATER INJECTION

Nosetip cooling system based on discrete subsonic forward liquid injection through ablative nosetip opening of blunted reentry vehicle
[AIAA PAPER 68-1141] 03 p0532 A69-13559

Electric components encapsulation by combining liquid resin techniques and transfer molding
04 p0607 A69-14955

Hydraulic control valves for guidance of rockets by secondary liquid injection into nozzle skirt, discussing structure, single nozzle missile and mass gain
07 p1230 A69-19293

Combustion in high power jet engine combustion chamber in case of continuous and intermittent liquid fuel injection
08 p1421 A69-20762

Lateral spreading of liquids injected into supersonic flow, discussing dependence on Mach number and scattered light and schlieren photographs of spray structure
09 p1482 A69-21966

Stationary radial source flow of liquid particles into vacuum, discussing boundary value problem equations, parameters effects on flow structure and flow field characteristics
13 p2248 A69-28210

LIQUID LASERS
Solid state liquid and semiconductor lasers, detailing conditions for producing stimulated emission and applications
01 p0092 A69-11068

Liquid lasers compound range of organic type, circulating system of inorganic type and power peaks
01 p0092 A69-11194

Organic dye laser frequency variation with temperature, noting absorption and fluorescence spectra
02 p0258 A69-12617

Dye solution laser wavelength shift and simultaneous oscillations at different wavelength ranges for pumping by another dye laser
02 p0258 A69-12620

Frequency mixing of organic dye solution laser radiation with ruby laser radiation, showing broader UV spectrum
04 p0610 A69-14424

Laser based on xanthene series dyes and excited by neodymium laser second harmonic radiation, noting radiation spectra
06 p0932 A69-16914

Lasing threshold and spectral characteristics of organic dye solutions, using excitation of second harmonic of monopulse ruby laser
06 p0933 A69-17255

Light generation by lasing organic dye liquid solution with negative absorption on activator molecules and induced combination scattering for solvent molecules
06 p0933 A69-17256

Q switching and mode locking of neodymium selenium oxygen chlorine liquid laser, discussing power output and nature of pulses
06 p0935 A69-17776

Tandem amplifier system of glass and selenium-oxochloride liquid lasers, discussing input power/output pulse relation and population inversion density measurement
07 p1147 A69-18487

Spontaneous and stimulated Raman emission in liquids, obtaining picosecond pulse duration and laser light linewidth
[IEEE PAPER H-6] 07 p1152 A69-19063

Circulating liquid laser system using neodymium in selenium oxochloride, discussing cooling advantages and components
[IEEE PAPER M-70] 07 p1153 A69-19069

Output properties of Nd-selenium oxochloride liquid laser, detailing cell construction and output dependence on cell geometry and optical feedback
[IEEE PAPER M-8] 07 p1153 A69-19070

Correlation effects in water and heavy water laser transitions based on cascade effects, discussing lines in resonator arms
09 p1515 A69-21349

Liquid laser gain measurement via luminescence intensity, noting optical pumping thermal effect
09 p1520 A69-22683

Dye lasers CW operation feasibility, showing sufficient quenching of rhodamine 6G triplet state by oxygen dissolved in methanol
11 p1893 A69-24344

Liquid lasers properties and composition including organic complex compounds, organic dyes, rare earth elements in polyphosphoric acid, etc
11 p1893 A69-24353

Power output and radiation spectra of trivalent Nd doped liquid lasers based on phosphoryl chloride with tin and titanium chlorides
11 p1894 A69-24620

LIQUID LEVELS

Passive Q switching of chemical laser operating on vibrational-rotational line of vibrational transition of HCl

16 p2796 A69-31840

Frequency and time dependent gain characteristics of dye lasers, using computer program for rate equations for populations

17 p2980 A69-33025

Mode locking of organic dye laser by pumping laser with mode locked pulse train from Nd-glass laser, obtaining spectral bandwidth

21 p3740 A69-39545

High output laser amplifier consisting of glass and selenium oxychloride/Nd liquid lasers

23 p4173 A69-41565

LIQUID LEVELS

Ritz method for natural oscillations of ideal liquid in spherical vessel with various filling levels, considering vertical perturbing force

06 p0910 A69-17333

Level signaling device for high temperature conducting fluids, describing sensor construction and circuitry

20 p3536 A69-36980

Natural oscillations of free surface liquid and elastic bottom of cylindrical cavity determined by integrodifferential equations based on liquid level

21 p3693 A69-38720

Circular baffle mounted above flat-bottomed cylindrical tank outlet, discussing effect on remaining tank fluid volume and flow behavior under low gravity conditions

21 p3696 A69-39232

LIQUID-LIQUID INTERFACES

Shape and stability of interface between liquids subjected to surface tension and mass force field in vessel

03 p0417 A69-13809

Motion and stability of solid body with cavity containing rotor and two incompressible nonmixing liquids with surface tension

03 p0418 A69-13814

Temperature profiles and heat transfer coefficients in two phase liquid-liquid stratified laminar flow of variable immiscible film thickness with surface evaporation

09 p1622 A69-21904

Displacement of liquid by insoluble liquid from horizontal circular tube during laminar flow, analyzing flow characteristics

14 p2431 A69-29607

Normal modes stability analysis of fluid layer adjacent to flat plate submerged in liquid, considering effects of interfacial surface tension and buoyant forces [AIAA PAPER 69-386]

15 p2590 A69-30476

Plane incompressible fluid interface stability in presence of transverse electric field, deriving equation of motion for perturbation amplitude

15 p2652 A69-30911

LIQUID MERCURY

U MERCURY [METAL]

LIQUID METAL COOLED REACTORS

U LITHIUM COOLED REACTOR EXPERIMENT

LIQUID METALS

NT MERCURY [METAL]

NT MERCURY VAPOR

Vaporization waves in metals, discussing thermodynamic function of carrying liquid metal through successive states on liquidus line in two phase region

01 p0117 A69-10655

Liquid copper electrical conductivity temperature dependence at very high temperatures from magnetic diffusion and flux penetration measurements, noting exploding wires role

01 p0119 A69-10673

Condensing injector cycles internal efficiency for high velocity liquid metal flows in closed cycle MHD power plants

02 p0194 A69-11582

Metallic dismountable thermionic converter enclosed in mica sealed vacuum chamber, giving I-V characteristics, optimal temperature of liquid cesium phase and output power

02 p0194 A69-11587

Thermodynamic study of carburization of liquid titanium and zirconium, examining effects of atmosphere, graphite porosity and alloying elements

03 p0446 A69-13572

Alloy elements effect on spreading of liquid titanium and zirconium alloys on graphite

03 p0446 A69-13573

Liquid metal adsorption induced embrittlement, noting bond strength reduction and grain boundaries penetration

03 p0448 A69-13872

Stability of ductility and fatigue strength of stainless steel under longtime static loads in vacuum and in liquid lithium

03 p0450 A69-13912

Temperature dependence of isotope thermotransport in liquid K and Rb using steel capillary cells

03 p0533 A69-13970

Electromotive force along magnetic field induced by liquid metal flow /alpha effect/, giving foundation for self excitation of electromagnetic field

04 p0635 A69-14547

Liquid metals as coolants in breeder and space vehicle reactors for stable two phase flows

05 p0803 A69-15998

Nitrogen solubility measured in liquid Fe-Cr-Ni-Al alloys, noting solubility increase with increasing Al content

06 p0942 A69-17228

Nitrogen solubility in liquid Fe-Cr-Ni alloys increases with increased Cr concentration between 1550-1700 C and at one atm N pressure

06 p0942 A69-17229

Alloying elements effect on nitrogen solubility in liquid Fe-Cr-Ni alloys, defining quantitatively changes in solubility

06 p0943 A69-17234

Liquid metal MHD systems efficiency when operating with pressure jump in diffuser nozzle

06 p0872 A69-17921

Dielectric constant of liquid metals emphasizing Green function techniques for Wick theorem, Feynman diagrams, Dyson equation and diagrams in impulse space

07 p1196 A69-18298

Thermodynamic properties of binary and ternary liquid metal systems, noting electromotive force and vapor pressure measurements

07 p1165 A69-18939

Metal bath surface conditions for floating aluminum trioxide inclusions in pure iron and carbon steels

07 p1167 A69-19342

Safety problems associated with transient boiling of liquid metals in fast nuclear reactors, emphasizing behavioral differences between liquid metals and water

08 p1420 A69-20101

Momentum and energy transfers analogy in turbulent convection fluid flow emphasizing difficulties in case of liquid metals

09 p1480 A69-21687

Nitrogen solubility in molten niobium and molybdenum at high temperatures in argon flow

10 p1710 A69-23213

Hydrogen solubility in solid and liquid Ti close to melting point, showing no effect on welds and castings porosity

11 p1905 A69-24963

Wetting and sessile drop contact angles between liquid binary Al alloys and solid Be, boron carbide and graphite under vacuum and in He [ACS PAPER 15-C-68F]

12 p2114 A69-26301

Shock tunnel hypersonic flow effect on critical Weber number for zirconium drop breakup in partially and fully molten states

12 p2063 A69-26802

Speed of sound and shock waves in two phase flows of liquid metal MHD generators, considering droplets uniformly dispersed in gaseous phase

13 p2245 A69-27475

Laser Doppler method for measuring local particle velocities in two phase flows of liquid-metal MHD generators

13 p2260 A69-27476

Two phase MHD generator with gas in liquid metal emulsions, discussing loops efficiency

13 p2306 A69-27479

Energy conversion with liquid metal working fluids in MHD generators, discussing single stage fully Carnotized process

13 p2372 A69-27482

Liquid metal multistage injection efficiency with sodium and potassium working fluids, noting preheating

13 p2372 A69-27483

Thermal efficiencies of liquid-metal MHD generator cycles, analyzing optimum parameters, working fluid and partial irreversibilities

13 p2205 A69-27484

Liquid metal two phase flow MHD generators efficiency prediction, discussing end losses and flow velocity

13 p2205 A69-27485

Optimal cycle parameters for liquid metal single component MHD cycle, employing condensing ejector in front of generator

13 p2205 A69-27488

Liquid metal MHD generator cycles thermodynamic analysis, considering multicycle operation improvement with heat regeneration

13 p2372 A69-27489

Piston-like laminar liquid metal flow in MHD generator to increase thermodynamic efficiency of cycle and to generate electricity by synchronous principle

13 p2206 A69-27491

Liquid-metal MHD space power generation system using intermittent vaporization slugs shooting at 2700 R peak temperature

13 p2206 A69-27492

Liquid metal MHD induction generators design and performance, considering effect of geometry, operating conditions, fluid properties and power level on efficiency

13 p2207 A69-27503

Single wavelength design with compensation compared to multiwavelength design without compensation for liquid metal MHD induction converter, discussing optimization

13 p2207 A69-27504

Transient response in liquid-metal conduction MHD generators, analyzing constant magnetic field using differential equation

13 p2207 A69-27506

Optimal mean radius and half height of channel of liquid metal coaxial linear induction MHD generator with unilateral and bilateral excitation

13 p2207 A69-27507

Rayleigh-Taylor instability in synchronous liquid metal MHD generators, showing stabilization by channel positioning and threshold power rating

13 p2307 A69-27508

Liquid metal induction MHD generator I-V characteristics at no load permitting self excitation with capacitors

13 p2208 A69-27509

Liquid metal MHD power plant system tested under open and closed loop conditions for liquid circulation

13 p2208 A69-27510

Induction, helical and straight through liquid metal MHD generators tested under independent and self excitation conditions

13 p2208 A69-27512

Three phase high temperature liquid metal induction MHD generator performance, noting velocity profile nonuniformity influence

13 p2208 A69-27513

Heats of solution of Ag and Cu in dilute Ag-Cu-Sn alloys at 720 K, using liquid metal-solution calorimeter

13 p2279 A69-27759

Soviet monograph on design and theory of linear induction pumps for liquid metals covering electromagnetic phenomena, optimized dimensions, etc

13 p2209 A69-27926

Luminous spherical fog layer surrounding burning zirconium droplet during free fall through oxygen containing atmosphere, noting effect on mass and heat transfer processes

13 p2380 A69-28462

Sessile drops contact angles of alkali liquid metals on Re, W, Mo, Ta and Nb substrates related to substrate surface bare work function

14 p2506 A69-29270

Nuclear energy conversion for long space missions, comparing dynamic Brayton, liquid metal MHD gas, dynamic Rankine and LMMHD Rankine cycles

16 p2810 A69-31748

Heats of solution of Au and Cu in dilute Au-Cu-Sn alloys determined using liquid metal solution calorimeter, calculating self interaction coefficients

17 p2987 A69-33077

Silicon and boron carbides wettability with liquid metals during contact reactions at various temperatures, discussing wetting mechanism

18 p3156 A69-35153

Liquid metal sprayer design including calculation of nozzles for subsonic and supersonic gas outflow

21 p3728 A69-38613

MHD losses in liquid metal converters due to nonideal magnetic field profile and to flow hydraulics

21 p3649 A69-39483

LIQUID NITROGEN

Liquid nitrogen dispersed flow film boiling data accounting for droplet breakup by vapor acceleration, drag coefficient and heat transfer from wall [ASME PAPER 68-HT-44]

02 p0351 A69-12203

Nucleate pool boiling heat transfer of liquid nitrogen from circular disks with different surface conditions including copper and nickel mirror finishes, roughness and coatings

02 p0352 A69-12207

Bistable operating mode of GaAs semiconductor laser involving light emission shifts

03 p0441 A69-14175

Gamma irradiated silver carbonate EPR at liquid nitrogen temperatures

05 p0716 A69-15915

Natural convection heat transfer for incipient vapor formation in liquid H and N and for nucleate boiling of liquid H
[ASME PAPER 68-WA/PID-4]

05 p0848 A69-16165

Inception of nucleate boiling with liquid nitrogen, noting surface finish effects
[ASME PAPER 68-WA/PID-10]

05 p0848 A69-16167

Liquid nitrogen inertant for continuous suppression of pressurized fuel tank explosion

05 p0703 A69-16505

Spontaneous Raman band shapes and depolarization ratios in liquid nitrogen and oxygen measured and compared to gas, discussing time dependence of rotational motion

06 p0962 A69-17817

Axisymmetric liquid nitrogen turbulent jet propagating under supercritical pressure in gaseous nitrogen medium

07 p1049 A69-18398

Film boiling of subcooled liquid nitrogen in turbulent flow tubes, using one dimensional mathematical model of rod-flow regime

07 p1243 A69-19737

Coherent radiation brightness increased from liquid N Raman laser, using off-axial pumping

09 p1520 A69-22533

Transformation of Q switched neodymium laser radiation into Stokes component during stimulated combination scattering in liquid nitrogen

11 p1900 A69-25751

Noise sources in S band parametric amplifier with GaAs varactor diode measured at liquid nitrogen temperature, considering noise reduction

15 p2578 A69-30636

Al cryogenic quenching using liquid N for slow and uniform heat removal to eliminate distortion

18 p3150 A69-35419

Slush H and N gels preparation and characteristics, including measurements of weight bearing capacity of gel as function of percent mass silica gelant

22 p3998 A69-40632

Film-nucleate boiling transition for liquid nitrogen in vertical forced flow in electrically heated tube, discussing conduction model and agreement with visual experiment
[ASME PAPER 69-HT-26]

24 p4412 A69-43542

LIQUID OXIDIZERS

Pressure effects in spontaneous ignition of interimpinging hydrazine and red fuming nitric acid (RFNA)/ liquid streams in evacuated test chamber

24 p4415 A69-43667

LIQUID OXYGEN

Soviet papers on apparatus and machines of oxygen and cryogenic installations covering film boiling, gas vessel, thermal design, etc

04 p0686 A69-15160

Heat release during boiling of downward flowing liquid oxygen film

04 p0687 A69-15161

LOX prevalue accumulator system with He pressurant for prevention of Pogo effect on Saturn 5

04 p0666 A69-15298

Liquid oxygen shear viscosity dependence on temperature and pressure obtained by measuring electrical characteristics of immersed torsional vibrating crystal

05 p0846 A69-15916

Vulcanizable elastomers suitable for contact with liquid oxygen, discussing preparation, mechanical properties, transition temperature and structure

05 p0717 A69-16497

Fluorinated polyurethanes synthesis for liquid oxygen environments and cryogenic structural utility, noting structural effects on LOX compatibility

05 p0717 A69-16498

Spontaneous Raman band shapes and depolarization ratios in liquid nitrogen and oxygen measured and compared to gas, discussing time dependence of rotational motion

06 p0962 A69-17817

Specific heats of oxygen at coexistence from triple point to critical point and corresponding values for liquid phase

10 p1808 A69-23187

Tabulating experimental constant volume specific heats of fluid oxygen from triple point to 300 K at pressures to 350 atm

10 p1808 A69-23188

LOX thermodynamic properties from triple point to 250K and pressures to 350 atm, tabulating at uniform densities and temperatures

10 p1808 A69-23189

Oxygen boiling point studied via calibration of capsule type platinum resistance thermometers

14 p2540 A69-29888

Helium gas shaft seal for spacecraft electrically driven LOX pump, noting advantages of floating carbon face seal type
[ASLE FICFS PREPRINT 24]

15 p2621 A69-30498

Aircraft breathable LOX purity, water percentage and carbon dioxide and methane proportions, determining other contaminants after concentration by refrigeration

21 p3666 A69-39273

Saturated liquid oxygen dielectric constant measurements to calculate polarizability
[NAS-NRC PAPER D-3]

22 p3998 A69-40620

Optimal design and materials for cryogenic storage of O and H on lunar surface
[AAS PAPER 69-051]

24 p4296 A69-42882

Raman scattering during external and internal motion of oxygen molecules condensed phases, observing gamma and liquid phase bandwidths during stretching vibrations

24 p4353 A69-43808

LIQUID PHASES

Lattice gas model liquid-vapor phase properties calculated with allowance for thermal expansion

06 p1029 A69-16896

Liquid phase radical oxidation with intermediate and end products in same phase, discussing products, hydroperoxidation and liquid systems explosiveness

06 p1032 A69-17425

Liquid and vapor phase microscale panel cokers applied to screening synthetic lubricants for aircraft turbine engines
[ASLE PAPER 68-LC-22]

07 p1140 A69-19309

Thermodynamic consequences of Lindemann mechanism for fusion of pure body, discussing application to isolated equilibrium system of solid and liquid phases

07 p1242 A69-19322

Microstructural changes during liquid phase sintering of alloys, considering temperature effect on carbide grain growth and activation energies

07 p1168 A69-19599

Specific heats of oxygen at coexistence from triple point to critical point and corresponding values for liquid phase

10 p1808 A69-23187

Materials and products fluid state processing in space, discussing g, zero-g and induced forces effect on fluid matter and process, cost and operational effectiveness

19 p3324 A69-35588

Hall coefficient and conductivity measured as function of temperature for liquid Au, Cu and Ag tellurides and liquid alloy systems Bi-Te and Ti-Te

20 p3584 A69-38024

Gas phase arrest peak analogy with liquid phase oxygen cut-off during final stages of hydrocarbons gaseous oxidation reactions, noting active centers

21 p3669 A69-38805

Electrical conductivity of rare earth metals La, Ce, Pr and Nd in solid and liquid states by rotating magnetic field method

21 p3781 A69-39070

Soviet book on liquid binary systems covering physicochemical analysis and quantitative methods

21 p3670 A69-39529

Vapor pressure measurements on liquid fluorine from triple to critical point at one degree K intervals
[NAS-NRC PAPER H-2]

22 p3998 A69-40624

Carbon trioxide formation during ozone photolysis in liquid carbon dioxide and sulfur hexafluoride, noting ozone disappearance quantum yield independence of oxygen/ozone ratio

23 p4112 A69-41338

LIQUID POTASSIUM

Experimental apparatus for measuring heat transfer coefficients into boiling K in tubes, investigating vapor-liquid mixtures hydrodynamic and electrical properties

03 p0534 A69-14150

Oxygen effects in Type 316 stainless steel, Nb-Zr alloy liquid potassium system, discussing thermal convection and forced circulation loops and corrosion rates

12 p2112 A69-25943

Effective electrical conductivity of two phase vapor-potassium flow in flat duct at flow temperature 800 C, showing dependence on volumetric vapor content

13 p2306 A69-27480

LIQUID PROPELLANT ROCKET ENGINES

NT F-1 ROCKET ENGINE

NT HYDRAZINE ENGINES

NT HYDROGEN OXYGEN ENGINES

NT M-1 ENGINE

NT RL-10-A-1 ENGINE

Combustion chamber equation for liquid fuel rocket engine, considering time varying ignition lag

01 p0142 A69-10090

Nondestructive testing of brazed liquid propellant rocket engine components and assemblies, describing radiographic, ultrasonic, thermographic, and leak test methods

01 p0085 A69-10534

Solid, liquid and advanced propulsion techniques in France, discussing Diamant program and Europa booster

02 p0334 A69-11919

Pressurization system for liquid rockets, analyzing inert weight and complexity reduction using Saturn 5 S-4B stage

02 p0305 A69-12386

Liquid propellant space launch vehicles longitudinal modes natural frequency, discussing coupled engine-propellant supply system stability
[AIAA PAPER 68-289]

02 p0335 A69-12393

Combustion oscillations in liquid and solid propellant engines, noting destructive effect of LF vibrations and acoustic instability

02 p0305 A69-12494

High pressure rocket engine design, considering complete combustion, propellant feed system overall efficiency and thermodynamic gain

03 p0495 A69-12888

Liquid fuel rocket engine design for cooling by propellant counter flows

08 p1376 A69-20588

Performance analysis for electrothermal thruster using lithium propellant with supersonic heat addition
[AIAA PAPER 69-286]

09 p1567 A69-21267

Space storable propulsion system comparison, discussing liquid propellants performance and thermodynamic analysis
[AIAA PAPER 68-614]

09 p1570 A69-21981

Radiographic, ultrasonic, thermographic and leak test quality control for brazed liquid propellant rocket engine components

10 p1699 A69-23054

Simplified model of ignition tests with liquid propellant rocket engines under high vacuum conditions, giving possible parameter for evaluation of simulation of real conditions
[DVL-831]

10 p1754 A69-24022

Gaseous He bubbles injection into liquid propellant launch vehicle fuel lines to reduce vehicle pogo oscillations by lowering feed system natural frequencies

11 p1967 A69-25498

Combustion instability problems in rocket motors, emphasizing strongly coupled pressure oscillations in combustion chambers

11 p2003 A69-25597

Liquids in zero g environment for controlling position of propellant within tank for restart of rocket engine, noting minimum energy principle applications

11 p1944 A69-25599

Electron beam welding of Lunar Module Descent Engine, emphasizing variable area injector element and manifold assembly problems and techniques

12 p2102 A69-26621

Helmholtz resonance in rocket injectors as function of frequency response of interaction between chamber pressure and dissolved gas-fuel injection flow rate

12 p2148 A69-26806

Galerkin method applied to axial, transverse and three dimensional linear combustion instability problems in liquid propellant rocket motors

14 p2538 A69-29021

Mixture ratio distribution, injector/chamber performance and nozzle effects on specific impulse of liquid propellant rocket engine using hydrazine and oxygen

16 p2828 A69-31724

Combustion in liquid propellant rockets, discussing acrothermochemical steady state and nonsteady behavior analysis and experiments

16 p2835 A69-31732

Feed-system-coupled combustion instability linearized mathematical models for liquid fuel rocket engines, discussing nonrigid injector and method for instability elimination

16 p2836 A69-32001

Vaporization interaction liquid rocket performance model, discussing performance loss evaluation and test data
[AIAA PAPER 69-470]

16 p2838 A69-32663

- Droplet vaporization model representing combustion processes of longitudinal oscillations in liquid rocket combustor [AIAA PAPER 69-483] 16 p2841 A69-32689
- Test programs utilizing pitot probes to map exhaust plumes from liquid bipropellant engines in low ambient pressures conducted to verify calculations [AIAA PAPER 69-575] 16 p2869 A69-32746
- Electroforming methods in design and fabrication of liquid propellant rocket motor injectors and composite thrust chambers [AIAA PAPER 69-583] 16 p2794 A69-32757
- Cost optimization of mixture ratio control systems for liquid propellant launch vehicles, considering open and closed loop systems [AIAA PAPER 69-441] 16 p2870 A69-32775
- Interagency Chemical Rocket Propulsion Group method of treating measurement error for liquid rocket engine performance parameters, using uncertainty model [AIAA PAPER 69-734] 16 p2846 A69-32781
- Rocket engine with turbopump supplied liquid propellant, describing ejector, pump assembly, gas generator and control devices 17 p3019 A69-33341
- Soviet monograph on liquid rocket as controlled plant covering rocket bodies, liquids motion stabilization and gyrosystem positioning 18 p3206 A69-34333
- Liquid, solid, hybrid propellant and nuclear, electric and air breathing rocket engines, discussing orbiting payload cost, controllability, operating environments, velocity, etc 19 p3395 A69-36321
- Nonlinear periodic oscillations in liquid rocket combustion chambers for different chamber models and burning rate response formulations 19 p3449 A69-36352
- Loaded bipropellant liquid propulsion system sterilization studies on structural and nonmetallic materials suitability for use in oxidizer [AIAA PAPER 68-631] 21 p3785 A69-39025
- Liquid propellant rocket injectors response to HF chamber pressure oscillations using one dimensional model 21 p3786 A69-39235
- Liquid fuel propulsion systems for geostationary satellites, discussing transfer orbits, payload increase and required thrust for various satellite trajectories [DGLR-69-014] 23 p4202 A69-41929
- LIQUID ROCKET PROPELLANTS**
- NT AEROZINE
- NT CRYOGENIC ROCKET PROPELLANTS
- NT GELLED ROCKET PROPELLANTS
- NT HYPERGOLIC ROCKET PROPELLANTS
- NT MONOPROPELLANTS
- Solubility of helium in liquid fluorine increases with temperature exhibiting reverse order 01 p0142 A69-11258
- Rocket propellant safety, discussing thermal, mechanical and impact sensitivity tests of solid and liquid propellants 02 p0302 A69-11525
- Dry heat sterilization and ethylene oxide decontamination test equipment for bipropellant liquid propulsion system 02 p0228 A69-11764
- Pressure and flow transients in liquid rocket engine feed systems predicted by method of characteristics 03 p0495 A69-12991
- Characteristics of liquid propellant explosions, analyzing detonation, shock wave formation and deflagration 04 p0645 A69-14474
- Saturn fireball thermal environment associated with liquid propellant explosions, using analytical model 04 p0645 A69-14475
- Yield and combustion physics of liquid propellant explosions determined from analytic charts 04 p0646 A69-14477
- Mixing function vs time relationship for liquid propellant explosion hazards prediction, noting thermocouple grid for maximum information 04 p0646 A69-14478
- Wedge shaped charge technique for evaluation of detonation hazards of liquid explosives 04 p0646 A69-14479
- Liquid explosive testing from point of view of liquid mobility 04 p0646 A69-14481
- Method for solving propellant sloshing in rotationally symmetric rocket tanks with arbitrary internal boundaries 04 p0665 A69-14840

- Optimal length conditions of liquid rocket combustion chambers, considering propellants, injection conditions, etc, noting graphs and differential equations solutions 08 p1376 A69-20606
- Hydrodynamic effects in flame spreading, ignitability and steady burning of liquid fuels, using analogy of films floating on water 11 p1999 A69-24484
- Liquid rocket propellants chemical reactions identification during kinetic expansion [WSCIP PAPER 68-7] 11 p1942 A69-24906
- Soviet book on liquid fuel rocket engines design covering gas expansion in nozzles, mixture formation, heat transfer, injectors and supply systems 12 p2148 A69-27078
- Propellant pressurization system for British Black Arrow composite vehicle, describing valve design and performance 14 p2509 A69-29629
- Advanced liquid fuels and oxidizers development from rocket propulsion reaction principle 16 p2828 A69-31747
- Liquid propellant injector design for rocket thrust chambers, discussing mass and mixture ratio regulation 16 p2836 A69-31999
- Liquid expulsion by direct pressurization of propellant tank in spinning missile system, demonstrating feasibility with subscale hardware [AIAA PAPER 69-527] 16 p2838 A69-32651
- ICRPG liquid propellant thrust chamber performance evaluation methodology, reviewing imperfections and limitations [AIAA PAPER 69-468] 16 p2838 A69-32657
- Analytical model for liquid fluorine no-vent loading operations noting application to flightweight upper stage systems [AIAA PAPER 69-579] 16 p2767 A69-32715
- Contaminants formation during pulse mode operation of liquid bipropellant attitude control rocket engine, discussing exhaust plume effects [AIAA PAPER 69-574] 16 p2870 A69-32774
- Rocket performance optimization by extending injector design technology to high performance injectors for space storable FLOX/LPG propellants [AIAA PAPER 69-506] 16 p2846 A69-32778
- Modified liquid fueled pulsating combustion chamber operating as Helmholtz cavity resonator, measuring chamber pressure as function of time 17 p3074 A69-33410
- Physical and physiological hazards of cryogenic liquids, emphasizing fire and explosion problems associated with storage and handling 17 p3017 A69-33684
- Liquid rocket combustion investigated by pulsed ruby laser holography at sea level rocket engine test stand, noting laminated glass acrylic window byproduct [AIAA PAPER 69-471] 17 p3075 A69-34200
- Temperature, applied stress and pressurization effects on materials corrosion by liquid F and F containing oxidizers 21 p3748 A69-39485
- Multiple outlets for reducing stratification-induced liquid propellant supply temperature rise, preventing cavitation problems in supply pumps [AAS PAPER 69-395] 24 p4363 A69-42830
- LIQUID ROTATION**
- U ROTATING LIQUIDS**
- LIQUID SLOSHING**
- Spherical false bottom influence on propellant sloshing in circular tank [DVL-843] 03 p0416 A69-13665
- Method for solving propellant sloshing in rotationally symmetric rocket tanks with arbitrary internal boundaries 04 p0665 A69-14840
- Electric field influence on fluid oscillation modes for Korteweg-Helmholtz force density on incompressible dielectric liquid immersed in electric field 04 p0591 A69-15504
- Axisymmetric vortex free motion of ideal fluid in conical container with spherical bottom under axial acceleration 06 p0910 A69-17335
- Hydraulic analog for determining acoustic behavior of baffle cell used in liquid rocket engines, comparing ring and spoke type baffles 09 p1570 A69-22004
- Incompressible fluid nonlinear oscillations in rectangular basin analyzed by Green function for mixed problem, calculating velocity potential and free surface approximations 09 p1483 A69-22711

- Motion of body with cavity containing liquid based on Kharlamov solution, noting gyrostatic moment and liquid sloshing effect 11 p1868 A69-24775
- Liquid filled elastic shells natural frequencies and oscillation modes, deriving eigenfunction system from liquid velocity potential boundary conditions to determine dynamic load 11 p1870 A69-24951
- Wave propagation on heavy fluid surface forming splashes in container with vertical walls 13 p2247 A69-27746
- Liquid sloshing in vessel of complex geometry reduced to boundary value problem 14 p2428 A69-28969
- Nonlinear equations for motion of rigid body with cavity partially filled with ideally incompressible liquid 14 p2432 A69-29626
- Liquid free surface response to mass force variation during space flight near zero-g, discussing effects on ignition 16 p2866 A69-31735
- Plane oscillations of liquid in rectangular elastic vessel determined to obtain frequencies and mode shapes of natural oscillations from velocity potential boundary conditions 17 p2950 A69-33200
- Satellites and space vehicles attitude control mathematical model accounting for nonrigidity, sloshing and energy dissipation in vehicle interior 17 p3048 A69-33239
- Hele-Shaw and porous medium fuel tank systems behavior in simulated low gravity environment, studying sloshing, wetting, funnelling and fuel-driver gas interface stability [AIAA PAPER 69-678] 17 p3021 A69-33444
- Soviet monograph on liquid rocket as controlled plant covering rocket bodies, liquids motion stabilization and gyrosystem positioning 18 p3206 A69-34333
- Tank configurations allowing for sloshing in liquid fuel reaction control system in spinning satellite 18 p3219 A69-34796
- Acoustic pumping system for propellant control at zero gravity, describing system operation by hydraulic analogy for liquid sloshing prevention 20 p3548 A69-37294
- Rocket body elastic vibrations, liquid fuel supply oscillations and engine thrust vibrations effects on system stability 20 p3617 A69-37604
- Fluid motion in free falling partially filled cylindrical vessel due to sudden vertical velocity change, considering free surface disturbances 21 p3692 A69-38684
- Optimal control of liquid vibrations in rectangular container moving in horizontal direction, deriving algebraic equations system for optimal functional 21 p3694 A69-38854
- Optimal control of ideal noncompressible fluid vibrations partially filling rectangular container moving in horizontal direction 21 p3695 A69-38892
- Simulated low gravity propellant sloshing in spherical, ellipsoidal and cylindrical tanks, discussing Bond number simulation and tank geometry effects [AIAA PAPER 69-1004] 22 p3921 A69-40378
- LIQUID SODIUM**
- Standing Alfvén wave resonances in liquid sodium 01 p0131 A69-10820
- Heat transfer rates from high temperature spheres into subcooled liquid sodium during forced convection, noting surface vapor formation [ASME PAPER 67-WA/HT-32] 02 p0351 A69-12202
- Liquid sodium corrosive action on vanadium, niobium, titanium and zirconium involving oxygen exchange from liquid to solid metal phase and energy of formation 10 p1713 A69-23821
- Thermodynamic efficiency of MHD cycles for liquid Na with multistage injection and injection condensation 13 p2205 A69-27487
- Sodium liquid-metal jet MHD generators tested under constant and rising magnetic fields and off and on loads 13 p2208 A69-27511
- Limiting heat power transported by sodium heat pipes dependent on capillary network geometry, inclination angle and operating temperature 14 p2538 A69-29205
- Liquid sodium penetration into stainless steel grain boundaries, using laser microprobe 18 p3154 A69-35473

LIQUID-SOLID INTERFACES

Liquid oxides wetting and spreading capabilities on refractory metal surfaces, noting chemical reaction oxide reducing effect
02 p0265 A69-11884

Heat conduction with change of phase in three dimensional melting and solidification problem under isothermal conditions and balanced energy at interface
02 p0354 A69-12548

Thermodynamic study of carburization of liquid titanium and zirconium, examining effects of atmosphere, graphite porosity and alloying elements
03 p0446 A69-13572

Dynamic and interfacial fluid effects in mechanical face seals, discussing hydrodynamic pressure generation
04 p0606 A69-14798

Microscopic time lapse movies in solid/liquid interface profile during melting and freezing of materials for spacecraft thermal control as reversible heat sink [AIAA PAPER 69-95]
06 p1038 A69-18126

Liquid surface active media /kerosene, water, castor oil/ effect on strength of V notched polymethyl methacrylate specimens
09 p1528 A69-21852

Vibration characteristics of circular cylindrical shells containing water under axial excitation, investigating bubble formation and shell-fluid interaction [ASME PAPER 69-VIBR-4]
10 p1805 A69-24162

Thin liquid film equilibrium on rotating sphere, determining conditions for detachment as function of angular velocity
12 p2061 A69-25886

Wetting and sessile drop contact angles between liquid binary Al alloys and solid Be, boron carbide and graphite under vacuum and in He [ACS PAPER 15-C-68F]
12 p2114 A69-26301

Electrical end losses in liquid-metal MHD generators with variable conductivity, noting working fluids and aspect ratios
13 p2206 A69-27493

Sessile drops contact angles of alkali liquid metals on Re, W, Mo, Ta and Nb substrates related to substrate surface bare work function
14 p2506 A69-29270

Seal selection criteria based on maintaining fluid film between faces, discussing facial heat generation and dissipation, speed and size effects, etc [ASLE FICFS PREPRINT 25]
15 p2620 A69-30488

Evaporation of liquid droplets from heating wall observed cinematographically, noting heat transfer by violent film boiling and conduction through thin vapor layer
15 p2718 A69-31117

Self ignition of solid/fluid particles suspended in gas flow, discussing heat transfer coefficient, critical temperatures, etc
17 p3070 A69-33142

Liquid oxides wetting and spreading capabilities on refractory metal surfaces, noting chemical reaction oxide reducing effect
18 p3156 A69-35044

Electron reactivity of one equivalent oxidizing agents at ZnO surface by electrochemical reduction
19 p3392 A69-36731

Stress corrosion cracking mechanisms in liquid-solid metal combinations and solvent exposed plastics, discussing adsorption processes and cathodic polarization inhibition
19 p3349 A69-36887

Book on heat transfer from horizontal heating surfaces to stationary boiling liquids, heating surface roughness effect and bubble formation
20 p3633 A69-37917

Liquid solid mixtures of parahydrogen flow characteristics in pipe, globe valve, orifices and venturi, determining pressure loss [NAS-NRC PAPER F-5]
22 p3998 A69-40626

LIQUID SURFACES

Parametric instability of horizontal surface of ideally conducting or very high dielectric constant liquid in varying perpendicular electric field
06 p0957 A69-17542

Free surface of electrically conducting liquid in gradually varied supercritical regime in horizontal rectangular channel
08 p1362 A69-20273

Interfacial charge relaxation overstability in tangential electrical field, discussing electromechanical polarization surface waves propagation and dielectrophoretic orientation of liquids in zero gravity space
08 p1353 A69-20792

Draining liquid surface dip formation in tanks of arbitrary shapes and drain hole positions
09 p1483 A69-21999

Imaging ultrasound by holography with reconstruction in light, comparing methods using scanned hologram and liquid surface
10 p1695 A69-23543

Integral representation for velocity and pressure fields produced by horizontal motion of two dimensional bodies below or on free surface of viscous liquid
11 p1866 A69-24278

Characteristic frequencies approximation formula for gas bubbles in liquids compared with exact solutions
11 p1915 A69-24582

Cavity formation on water and wet cement surfaces by impingement of axisymmetric air jet noting cavity shape, depth and diameter
11 p1869 A69-24888

Wave propagation on heavy fluid surface forming splashes in container with vertical walls
13 p2247 A69-27746

Gas chromatography based on sampling gas-vapor phase at liquid surface for determining volatile oxygen containing compounds in biological media
13 p2216 A69-28627

Laser beam light pressure bending of incompressible liquid surface leading to beam self focusing in linear medium
14 p2461 A69-29674

Liquid free surface response to mass force variation during space flight near zero-g, discussing effects on ignition
16 p2866 A69-31735

Nonlinear free surface effects in low gravity tank draining, finding domains of validity for linearized and nonlinear analyses [AIAA PAPER 69-680]
17 p2953 A69-33450

Surface tension gradients caused thermocapillary convection solved for spherical fluid film under weightlessness conditions
19 p3452 A69-36392

LIQUID-VAPOR EQUILIBRIUM

Lattice gas model liquid-vapor phase properties calculated with allowance for thermal expansion
06 p1029 A69-16896

Gravitational effects on thermodynamic variable equilibrium composition of liquid-vapor binary mixtures near critical point, discussing changes in phase with altitude
11 p1999 A69-24914

Vapor-liquid transition in inert gases based on Monte Carlo method, including comparison with van der Waal equation and plasma ionization equilibrium
15 p2655 A69-30981

Surface tension of simple liquids consisting of interacting spherical particles, considering density variation in liquid-vapor phase transition zone
19 p3452 A69-36725

Einstein development of theory of fluctuations applied to homogeneous nucleation, calculating activation energy, liquid drop-vapor system equilibrium state peculiarity, etc
22 p3938 A69-40448

LIQUID-VAPOR INTERFACES

Liquid nitrogen dispersed flow film boiling data accounting for droplet breakup by vapor acceleration, drag coefficient and heat transfer from wall [ASME PAPER 68-HT-44]
02 p0351 A69-12203

Pressure induced variations in stability constant characterizing bubble structure in two phase boundary layer of several liquids during boiling with natural convection
03 p0534 A69-14149

Hot inert gas bubble thermal stability in cool reactive liquid
11 p1998 A69-24475

Large amplitude symmetric and asymmetric irrotational motion of inviscid incompressible fluid with liquid-vapor interface in accelerating cylindrical container of revolution
11 p1871 A69-25124

Effective electrical conductivity of two phase vapor-potassium flow in flat duct at flow temperature 800 C, showing dependence on volumetric vapor content
13 p2306 A69-27480

Air-water and steam-water flows in two phase Laval nozzles, measuring flow rates and temperature and pressure variation
13 p2245 A69-27481

Steam-water convergent condensing injector with supersonic inlet vapor, discussing axial pressure profiles and discharge pressure
13 p2372 A69-27486

Microlayer thickness in nucleate boiling, studying liquid-vapor interface motion of growing bubble near heated surface
13 p2375 A69-27789

Gas-liquid chromatography of natural protein amino acids in biological substances, noting separation characteristics
13 p2217 A69-28258

Liquid-vapor interaction in loop plates with different heat pipe capillary geometries using water as heat transporting medium
14 p2539 A69-29207

Water-air interface models unreliability in calculating atmospheric heat and humidity turbulent flow over ocean
14 p2443 A69-29839

Noncontacting minimum leakage dynamic seal requiring liquid-vapor interface with leakage tolerance [ASLE FICFS PREPRINT 40]
15 p2620 A69-30485

Lubrication and leakage control mechanics of face seals, considering liquid to vapor boundary within interface [ASLE FICFS PREPRINT 22]
15 p2620 A69-30486

Froude number for scaling wind stress at air-water interface, verifying logarithmic wind profile and relating shear velocity to surface roughness
17 p2996 A69-33152

Surface tension of simple liquids consisting of interacting spherical particles, considering density variation in liquid-vapor phase transition zone
19 p3452 A69-36725

Vapor pressure equation for oxygen and nitrogen derived by adding nonanalytic term, correlating equation with observed data [NAS-NRC PAPER H-1]
22 p4051 A69-40628

Cylindrical bubbles stability in vertical pipes from photographs, describing wake, spacing, pressure pulsations and convection cells effects [ASME PAPER 69-HT-28]
24 p4411 A69-43540

LIQUIDS

NT AEROZINE

NT CRYOGENIC ROCKET PROPELLANTS

NT GELLED ROCKET PROPELLANTS

NT HYDRAULIC FLUIDS

NT HYPERGOLIC ROCKET PROPELLANTS

NT LIQUEFIED GASES

NT LIQUID AMMONIA

NT LIQUID HELIUM

NT LIQUID HYDROGEN

NT LIQUID METALS

NT LIQUID NITROGEN

NT LIQUID OXIDIZERS

NT LIQUID OXYGEN

NT LIQUID POTASSIUM

NT LIQUID ROCKET PROPELLANTS

NT LIQUID SODIUM

NT MERCURY [METAL]

NT MONOPROPELLANTS

NT ORGANIC LIQUIDS

NT ROTATING LIQUIDS

Standing wave methods for measuring permittivities of liquids having attenuation coefficients over considerable range
04 p0599 A69-15015

Heat capacity at constant volume determined for nitromethane, trinitrotoluene and difluoramine alitanes [WSCJ PAPER 68-39]
07 p1202 A69-18368

Thermal diffusion and free thermal convection in fluids by diffraction interferometer, using laser for light source
10 p1702 A69-23431

Nonlinear susceptibility tensor components and refractive index variations of liquids and glasses in high intensity ruby laser field, using interference methods
10 p1703 A69-23622

Modulus of elasticity changes and stress relaxation spectra of viscoelastic liquids measured by acoustic methods
11 p1887 A69-25206

Polyurethane corrosion resistance in various liquids determined from changes in sample hardness, weight, volume and deformation
18 p3162 A69-35360

Gupta stability solution extended to liquid anisotropic viscoelastic films, analyzing surface and shear wave perturbations in material structures
22 p3929 A69-39893

Thermal conductivity relationship to heat transport coefficients for gases and liquids with charged or uncharged particles
23 p4237 A69-41324

- Thermal conductivity and specific heat of groups of liquid substances as functions of temperature, giving curves, tables and conversion factors
23 p4238 A69-41336
- Centrifugal forces effect on stability of inviscid liquid film over rotating cylinder away from stagnation region, noting film thickness stabilization effect
24 p4305 A69-43597
- LITERATURE**
U DOCUMENTATION
- LITHERGOLIC PROPELLANTS**
U HYBRID PROPELLANTS
- LITHIUM**
- Elastic scattering of slow electrons by negative H and positive Li ions, calculating differential cross sections and phase shifts
03 p0469 A69-12924
- Potential energy functions based on electronegativities instead of spectroscopic parameters for Li and K molecules
03 p0472 A69-13805
- Li and Cs electrical conductivity measured from 300-1200 K, obtaining interpolation formulas by least squares method
03 p0481 A69-14148
- Secondary cells with liquid lithium anodes and immobilized fused salt electrolytes
04 p0552 A69-15330
- Lithium metal spray structural cooling system for refractory materials
[AIAA PAPER 68-358] 04 p0688 A69-15509
- Lithium abundance determination difficulties for undisturbed solar photosphere, noting Li I resonance line identification and model choice
05 p0821 A69-15849
- Lithium abundance in sunspots and undisturbed solar atmosphere from measurements of solar atmosphere and spot spectra
05 p0821 A69-15850
- Microchemical analysis for diffusion measurement of laser produced lithium plasma in uniform magnetic field
05 p0762 A69-15960
- Atomic Li photoionization cross sections calculated with Brueckner-Goldstone many body perturbation theory
06 p0961 A69-17134
- Performance analysis for electrothermal thruster using lithium propellant with supersonic heat addition
[AIAA PAPER 69-286] 09 p1567 A69-21267
- Li atoms and O interactions with electron radiation produced defects in Si studied by IR spectroscopy
09 p1554 A69-21337
- Cepheid variable and F and G stars observed for neutral lithium line, searching for resonance lines of ionized beryllium in similar stars
09 p1604 A69-22402
- High velocity liquid lithium effect on structural materials for MHD power generators, discussing material loss
13 p2278 A69-27478
- Lithium depletion in main sequence stars of one solar mass, suggesting c-folding time scale indicated by Coma Cluster data
14 p2517 A69-29089
- Corrosion mechanism in high temperature Nb-Zr/Li and Ta/Li heat pipes and heat transfer measurements, noting oxygen content of wall material
14 p2462 A69-29203
- Saturated Li vapor pressure measured by static equilibrium technique based on use of null membrane, tabulating pressures for various temperatures
15 p2656 A69-30997
- Nonaqueous lithium anode high energy density electrochemical primary generators, considering energy factors and electrolytic couples
16 p2740 A69-32427
- Li variation effects on solar cell properties indicating cell performance control by amount introduced near p-n junction
19 p3252 A69-35695
- Boron, Li and Cl contents in iron and stone meteorites by fluorometric, thermal-neutron activation and pyrohydrolytic separation methods, tabulating results
19 p3408 A69-36085
- Stellar lithium and beryllium, discussing production and destruction processes in stellar atmospheres and abundance in various stars
21 p3810 A69-39505
- Vacuum distillation determination of O in Li, evaluating accuracy through O additions and recoveries, method blank and residue identification
22 p3897 A69-40932

- Elastic differential Li ion scattering cross sections on helium, nitrogen and oxygen
24 p4354 A69-43817
- LITHIUM ALLOYS**
- Noncollinear single cavity optical parametric oscillation with specified energy conversion using ruby laser-pumped lithium niobate, discussing tuning
14 p2460 A69-29605
- LITHIUM ALUMINUM HYDRIDES**
- Lithium aluminum hydride thermal decomposition using isothermal kinetics and differential thermal and thermogravimetric analyses, noting decomposition in four stages
02 p0304 A69-11898
- LITHIUM COMPOUNDS**
- Ferroelectric domain structure to explain microcracks nucleated at twinband intersections in mechanically deformed lithium niobate
03 p0486 A69-13618
- Lithium niobate crystals thermal properties measured at various temperatures
03 p0487 A69-13730
- Lithium niobate single crystals for holographic storage, noting use for optical information storage, processing and display devices
03 p0432 A69-14184
- Li niobate crystal emission excited by Ar laser beam, deriving laser action formulas
08 p1323 A69-19941
- Second harmonic generation conversion efficiencies at 5300 Å with KDP and lithium niobate crystals, using Nd-glass laser of high radiance and narrow bandwidth
09 p1514 A69-21333
- Ferroelectric Li niobate single crystals internal magnetic field analysis by acoustic EPR, establishing field induced hypersound resonance absorption in spin systems
09 p1556 A69-21563
- Microwave frequency room temperature acoustic surface wave propagation losses in lithium niobate measured by laser light deflection, discussing propagation and insertion losses
10 p1703 A69-23511
- Substituted lithium ferrites analyzed to obtain materials with small initial magnetic losses at different microwave ranges
13 p2320 A69-28000
- Optical rectification effect in lithium metaniobate crystals under neodymium laser radiation, comparing results with data for potassium dihydrophosphate crystals
14 p2458 A69-29168
- Elastic microwaves propagation attenuation along lithium niobate crystals trigonal axis at various temperatures
15 p2665 A69-30040
- Ruby laser Q switching with electro-optical shutter based on Li metaniobate crystals by applying static, single pulse or periodic potential to Pockels cell
19 p3336 A69-36346
- LITHIUM COOLED REACTOR EXPERIMENT**
- Systems analysis of Rankine cycle nuclear-electric potassium space power system using Li cooled fast reactor and high temperature turbine inlet
23 p4189 A69-42266
- LITHIUM FLUORIDES**
- Mechanical properties of lithium fluoride single crystals, taking into account equilibrium lattice defect structures
01 p0138 A69-10602
- Spectral measurements for matrix isolated lithium fluoride extended into far IR to obtain evidence for linear lithium fluoride dimer
02 p0205 A69-12465
- Thermogravimetric study of oxidation protection of refractory metals by fused LiF coating, noting oxidation retardation of Ta, Nb and W
19 p3341 A69-35573
- Integrated reflection coefficient with unpolarized incident X radiation for mosaic and perfect LiF crystals, presenting coefficient as function of wavelength
20 p3582 A69-37137
- LITHIUM HYDRIDES**
- Light emission and transmission generated from laser interaction with lithium hydride in vacuum, noting laser energy variations effects
01 p0127 A69-10281
- Reaction rate and mechanism for low temperature reaction between lithium hydride and liquid ammonia, noting chemisorbed ammonia dissociation at interface
01 p0025 A69-11285
- Lithium hydride microplasma expansion in vacuum using charge collectors, time of flight detectors and spectroscopy of light emission
02 p0286 A69-11704

- Thermodynamics of propellant combination of Li hydride containing solid fuel with ethyleneimine base, coupled with Cl trifluoride oxidizer and ammonium nitrate added
22 p3997 A69-39919
- Self consistent field molecular orbital method in LCAO/linear combination of atomic orbitals/ approximation applied to LiH ground state for potential energy curve
22 p3985 A69-40721
- Compton profile from single crystal of LiH measured with X ray scattering, noting valence-electron momentum distribution role
22 p3993 A69-40730
- LITHIUM ISOTOPES**
- Early F stars Li/Be abundance ratios estimation from change in solar Be abundance, discussing stellar Li isotopes ratios
10 p1785 A69-24099
- Lithium 6 and 7 fission following pion capture, searching for H 4 and 5
12 p2132 A69-26296
- Negative pion from 600 MeV synchrocyclotron stopped in thin Li 6 target in search for excited states of triton
12 p2132 A69-26297
- Excited levels in Li I produced by Li 7 ion passage through carbon foil, measuring excitation mean lives by beam foil technique
13 p2301 A69-27454
- Formation cross sections of Li, Be and B isotopes produced from oxygen 16 spallation via high energy protons related to astrophysics and cosmic ray physics
14 p2512 A69-28968
- Mean lives of upper decay levels of lithium isotopes accelerated by electromagnetic isotope separator and directed through thin carbon foil
18 p3177 A69-35012
- Meteorite Li isotopic composition variations to determine neutron role in nucleosynthesis of solar system light elements
19 p3408 A69-36084
- Solar neutrinos capture rate estimation by using Li 7 as detector
20 p3588 A69-37420
- LITHIUM OXIDES**
- Lithium peroxide utilization feasibility for oxygen supply and carbon dioxide control in extravehicular portable life support systems
[AIAA PAPER 69-620] 17 p2914 A69-33303
- LITHOGRAPHY**
- Computer tape controlled pulsed externally excited gas laser mask making machine with micropositioning coordinate table for integrated circuit fabrication
06 p0931 A69-17200
- He-Ne laser system for micromachining thin film photolithographic masks, describing computer controlled coordinate table and product quality
22 p3954 A69-40236
- LITHOLOGY**
- Side-looking airborne radars (SLAR)/ application to geological exploration of remote unmapped areas
12 p2099 A69-27009
- Fractionation of abundant lithophile element ratios of Si, Mg, Ca, Al and Ti in carbonaceous, common and enstatite chondrites
19 p3409 A69-36087
- LITHOSPHERE**
U EARTH PLANETARY STRUCTURE
- LIVER**
- Xenon, krypton, nitrogen and nitrous oxide effect on respiration rate of rat liver slices at various oxygen partial pressures
03 p0375 A69-14069
- Brain norepinephrine effect on daily rhythmic changes in activity of tyrosine transaminase in livers of starved adrenalectomized rats
05 p0707 A69-15582
- Medical examinations of missile fuel handlers, noting some abnormal results in liver function tests and possible hydrazine toxicity
09 p1447 A69-22556
- Microvillar bleb formation in proton irradiated primate hepatocytes with electron microscope, noting sinusoidal lumen
10 p1641 A69-23045
- Hypothermia induced alterations in biochemical processes studied with isolated rat liver perfused at low temperature
10 p1642 A69-23119
- Hepatic tyrosine transaminase rhythm in rats under various conditions of lighting, food consumption and dietary protein content
17 p2910 A69-33755

Acetate-2-C 14 conversion to C 14 carbon dioxide and C 14 fatty acids in rats with 2/3 of liver removed
19 p3257 A69-35976

Long microextensions on cultivated human liver cells, using scanning electron microscope
20 p3480 A69-38287

Successive X ray doses effect on oxidative phosphorylation of vitamin B 1 in white rats liver tissue ultrastructure during and after irradiation, establishing thiamine biosynthesis suppression
21 p3658 A69-39056

Mitochondrion-endoplasmic reticulum connection in hepatocytes, discussing possible protein molecule transfer
23 p4083 A69-41455

Neodymium laser radiation effect on electrical and histomorphological properties of liver in rats and hamsters
23 p4111 A69-42344

Hyperoxia and hypoxia effects on mitotic activity in regenerating and normal rat liver exposed to environmental conditions
24 p4269 A69-43565

LIZARDS

Light transmission through body wall of living colorable desert iguanas measured by spectrophotometry, discussing skin pigment effects
07 p1059 A69-18373

LOAD DISTRIBUTION [FORCES]

Thin cylindrical shell deformation and stress under concentrated radial loading, analyzing singularity at load point
01 p0166 A69-10301

Yield surface after prestraining under radial loading, analyzing formation of yield corner
01 p0166 A69-10303

Hollow finite cylinder stress-strain analysis under normal loads on end faces solved by four partial differential equations
01 p0168 A69-10359

Galerkin method for solving dimensionless Reissner equation for symmetrically loaded thin nonshallow shells of revolution
01 p0168 A69-10380

Helicopter structures design for maximum practicable crashworthiness and survivability, comparing load factors and deformations with indicated human impacts tolerance
[AHS PAPER 225] 01 p0009 A69-10408

Plastic zone generation by slots cut in tensile test specimens before and during loading, discussing redistribution
01 p0098 A69-10762

Deflection of orthotropic sandwich plates with unequal facing thickness with edges subjected to uniform and concentrated loading
01 p0172 A69-11270

Uniqueness formulation of concentrated load problem in linear theory of couple-stress elasticity
02 p0338 A69-11720

Bending of freely supported plates of polygonal planforms under transverse load with aid of R functions
02 p0341 A69-12140

Elastic analogue in creep stress analysis under time dependent boundary conditions and strain hardening theory
02 p0345 A69-12418

Matrix displacement method for nonlinear elastic analysis of shells of revolution under symmetrical and axisymmetrical loadings
02 p0346 A69-12511

Internal elastoplastic stress distribution within reinforced plastics subjected to force normal to internal filaments direction
02 p0347 A69-12513

Point load subjected deflections of cantilevers and circular rings found using electronic analog computers
03 p0522 A69-12865

Equilibrium stability of elastic circular arch constrained in rigid cavity and subjected to uniformly distributed parallel loading
03 p0524 A69-13066

Integral equation solution for plate with internal support
03 p0528 A69-13799

Load diffusion from transverse tension bar into semiinfinite elastic sheet, considering line and area contact methods of stringer attachment
[ASME PAPER 68-WA/APM-15] 04 p0669 A69-14396

Large finite deflections of clamped thin elastic circular plate subject to transverse concentrated load at center solved by power series
04 p0675 A69-14596

Annular plate clamped at inner and outer boundaries and subject to point load, computing deflection
04 p0676 A69-14725

Kirchhoff-Love hypothesis error dependence on stressed state variability index in theory of elasticity for closed spherical shell under uniform surface load
04 p0680 A69-14927

Symmetrical bending of laterally loaded circular micropolar plates
04 p0682 A69-15291

Plane shear pressure wave propagation in elastic-plastic half space for various combined normal and shearing loadings
05 p0835 A69-15798

Plastic moments calculation of continuous steel beams under various loading patterns
05 p0837 A69-16035

Three dimensional deformation and buckling of circular ring, discussing in-plane and out of plane deformations and loads
[ASME PAPER 68-WA/DE-4] 05 p0839 A69-16169

Creep properties of EP-376 steel under slowly varying loads
05 p0782 A69-16692

Post-wrinkling nonlinear behavior of conical shell of revolution subjected to bending loads
[AIAA PAPER 69-90] 06 p1027 A69-18074

Spherical caps axisymmetric static and dynamic buckling under load, using axisymmetric nonlinear elastic shell theory approximation and finite difference equations
[AIAA PAPER 69-89] 06 p1028 A69-18133

Current load distribution for optimizing MHD generator efficiency determined by variational method, noting dependence on relative length
07 p1058 A69-19012

Flexible rotor blade dynamic response to radially moving force, emphasizing helicopter rotor vibration characteristics associated with tip-vortex impingement
[AIAA PAPER 69-203] 07 p1054 A69-19546

Plasticity theories for nonisothermal loading, considering plastic strain
07 p1237 A69-19681

Stability of cylindrical shells under concentrated annular loads using finite difference method, discussing critical loads, moments and errors
07 p1238 A69-19688

Differential equation reduction for vibrational motion of rectangular plates subjected to variable tangential forces, discussing dynamic stability
08 p1415 A69-20666

Plastic yielding of tensile V-notched aluminum alloys elements with intermediate thickness and various shoulder ratios, studying thickness effect on yield load
09 p1612 A69-21499

Governing equations for bending of fixed isotropic circular sandwich plate subjected to eccentric concentrated load
09 p1615 A69-21926

Uniform gravity load effect on buckling of beam continuously supported by soft foundation and subjected to uniform lateral load
09 p1615 A69-21927

Fatigue life evaluation by programmed fatigue strength tests, using frequency distribution of load set amplitudes
09 p1620 A69-22573

Gyrorotor center axial displacements due to axial load, noting equal load distribution between bearings with resilient cover plates
09 p1502 A69-22703

Plates stability and corner stress-strain state under variable loads calculated by method analogous to structural mechanics
10 p1792 A69-22849

Concentrated loads in elastic Cosserat continuum involving body moments and small deformations
10 p1799 A69-23151

Superimposed tool vibration function in deep drawing, ironing and cold forging, discussing equipment instrumentation, emphasizing dynamic force measurement
[ASME PAPER 69-VIBR-8] 10 p1700 A69-24164

Strength analysis of revolving shallow shell with jumpwise thickness variations under axisymmetric distributed load, considering rigidity and plastic deformation
11 p1968 A69-24318

Statistical parameters of critical load distribution in buckling of imperfectly sensitive elastic structures, noting probability of failure
11 p1969 A69-24415

Elastic isotropic half plane weakened by circular hole with concentrated force applied along hole contour, considering stress distribution
11 p1972 A69-24653

Strain energy for two and three dimensional crack systems subjected to varying loads, detailing loading and crack geometry effects on fracture criterion
11 p1974 A69-24669

Differential equations for effect of sinusoidal force with slowly varying frequency on dynamic behavior of nonlinear vibrator, using phase surface technique
11 p1916 A69-24760

Vibration problem of supported beam elastically restrained against rotation at both ends solved by Hermitian and linear differential operators
11 p1976 A69-24794

Optimum design of shells loaded by concentrated forces, discussing thickness relation to middle surface, loading point and manufacturing considerations
11 p1979 A69-24812

Finite deformation equations for flat annular membranes deduced from equations for thin shells of revolution, discussing displacement equations and fixed edge forces
11 p1979 A69-24813

Symmetrically loaded weak moment shells of revolution made of materials with different moduli of elasticity
11 p1980 A69-24819

Time scales for creep stress redistribution in structures subject to step loading
11 p1980 A69-24879

Thin conical elastic shell stress-strain state calculated by computer for arbitrary thicknesses and loading conditions, considering temperature and edge forces effects
11 p1981 A69-24943

Gas turbine disk calculation and plastic flow theory, considering loading conditions and elastoplastic strains due to centrifugal forces and nonuniform heating
11 p1982 A69-24945

Limit loads for circular and annular plates of smoothly varying profile under uniformly distributed transverse loads
11 p1982 A69-24946

Stress analysis of reinforced cylindrical shells under external loading, using Vlasov semimomentless theory
11 p1982 A69-24949

Bent plates elastoplastic stress-strain state determination by elastic solution and finite differences, considering linear strengthening under uniform distribution of load
11 p1985 A69-25175

Rectangular aluminum alloy rods carrying capacity under compression loads applied eccentrically to rod ends
11 p1986 A69-25326

Nonlinear equations solvability for elastic cylindrical shells found existing for arbitrary load and clamping conditions
12 p2177 A69-25881

Warping rigidity effect on stability of cantilever bar under eccentric follower end load, discussing bending torsional flutter and buckling
12 p2179 A69-26212

Clamped edge anisotropic elliptical plate bending under varying loads, assuming torsional rigidity bearing constant ratio to geometric mean of bending rigidities
12 p2180 A69-26269

Optimal additional loading at zero moment stress-strain state in simply connected shell of complex design under external loads, using successive approximation
12 p2181 A69-26610

Axisymmetric deformation of thin orthotropic laminar spherical shells under internal loads calculated on computer using Legendre polynomials
12 p2181 A69-26611

Galerkin method for solving dimensionless Reissner equation for symmetrically loaded thin nonshallow shells of revolution
12 p2182 A69-26679

Nonlinear structure undergoing arbitrary load history including temperature variations solved by computerized force and subordinated step procedure
12 p2185 A69-26823

Orthotropic properties and stress fields for configurations of fiber or whisker reinforced composite materials subjected to nonaxial loading, considering infinite elastic matrix
12 p2186 A69-26824

Load deflection equation solution based on row operations, involving three passes of coefficient matrix, using wavefront processing and modified Gauss algorithm
13 p2358 A69-27208

Matched asymptotic expansions to obtain slider bearing load carrying capacity
[ASME PAPER 68-LUBS-18]

13 p2266 A69-27270

Helicopter rotors with rigid blades performance from viewpoint of controllability and load distribution

13 p2201 A69-27295

Three dimensional deformation and buckling of circular ring, discussing in-plane and out of plane deformations and loads
[ASME PAPER 68-WA/DE-4]

13 p2360 A69-27420

Variational method used to determine accuracy of approximation technique for dielectric slab on sidewall of rectangular waveguide

13 p2233 A69-28072

Discrete element plastic analysis of long prismatic bars under transverse loading in longitudinal direction, based on matrix displacement method

13 p2365 A69-28237

Donnell small displacement equations for arbitrary open noncircular cylindrical shells under arbitrary normal pressure loadings

13 p2365 A69-28248

Stress intensity for Griffith crack with asymmetric distribution of surface tractions

13 p2369 A69-28352

Autonomous and nonautonomous transient processes in conservative and nonconservative nonlinear systems, deriving equations describing perturbations under loads, solving by asymptotic method

13 p2300 A69-28529

Infinite cylindrical shell stability under circular load solved by linearization about bending moment stress state and Galerkin method

14 p2531 A69-28808

Plasticity theory approximation variants for complex loading, analyzing strain trajectories using Prandtl-Reiss theory

14 p2532 A69-28978

Book on fatigue strength in construction covering structural strength and stability, load design, metal physical properties, elasticity and plasticity theories, stress concentration, strain buildup, etc

14 p2534 A69-29333

Bending of elastic triangular plates with free and supported corners under uniformly distributed transverse load determined using Ritz method

14 p2535 A69-29410

Strains determination for laterally edge loaded rectangular plate and sagittas determination of perpendicularly loaded plate proved analogous

15 p2704 A69-30295

Structural fatigue-inducing random load spectrum analyzed and computed for laboratory simulation

15 p2705 A69-30363

Bending theory of orthotropic plates with variable elastic modulus under transverse loads, utilizing stress-strain relations and Kirchhoff-Love hypothesis

15 p2708 A69-30661

Surface displacements at end of elastic semiinfinite circular cylinders due to annular axisymmetric loading, employing Boussinesq solution

15 p2711 A69-30872

Panel flutter under loads along profile, evaluating constraints dynamic characteristics by Hamilton principle

15 p2712 A69-31001

Cylindrical shell bending subjected to internal pressure and force uniformly distributed on round section solved by numerical integration of differential equations

15 p2653 A69-31195

Rotatory cylindrical shells supported at corners under symmetric load, determining deformation in arbitrary locations by moire method

15 p2715 A69-31546

Linear static deformation and buckling of shallow spherical shells under asymmetric load by solving two dimensional finite difference equations

16 p2871 A69-31897

Buckling load of cylindrical shell with inclined stiffeners, using method for stability of thin walled cylinder under transverse end load at free end

16 p2872 A69-31912

Stress and deformation in cross section of beam during complex loading using steepest-descent method

16 p2873 A69-32132

Parabolic and cardioid plates bending under uniform load by using point matching technique

16 p2874 A69-32166

Load carrying capacity of circular plates under axisymmetric load

16 p2875 A69-32289

Local buckling of infinite continuous plane elastic membrane under longitudinal load in form of concentrated forces

16 p2875 A69-32293

Aircraft and missile dynamic characteristics for heavy loads and large heat flux, noting small harmonic vibrations of heated structures in plastic domain
[ICAS PAPER 68-38]

17 p3061 A69-33589

Thin circular ring stability under uniform external transverse loading at various angles, discussing transverse shear deformation effects and buckling

17 p3061 A69-33707

Carrying cables shape optimization for suspended structures under load, using minimum weight criterion

18 p3212 A69-34354

Cylindrical and conical panels dynamic responses to time varying load distributions, using trigonometric series coupled with finite difference methods
[ASME PAPER 69-APM-22]

18 p3214 A69-34396

Load analysis for elastoplastic bodies by Prandtl-Reuss theory and Mises yield condition, considering avoidance of difficulties associated with nonlinear partial differential equation solution

18 p3216 A69-34571

Toroidal, spherical and conical shells limiting equilibrium under various loading and support conditions

18 p3216 A69-34572

Ponderable annular region under symmetrically applied concentrated forces, obtaining solution for stress state by successive approximations

18 p3216 A69-34577

Longitudinal oscillations of homogeneous elastic rod under nonconservative force at one end, deriving equations of motion and stability conditions

18 p3216 A69-34578

Lightweight structural design problem of stress concentration associated with load diffusion in rectangular panels with constant stress flanges

18 p3219 A69-34785

Stress-strain state of shells under concentrated loading, emphasizing positive Gaussian curvature

18 p3219 A69-34832

Spherical shells axisymmetric equilibrium properties under uniformly distributed external compression

18 p3224 A69-35318

Phenomenological creep theory for woven fiberglass reinforced plastic under moderate loads

18 p3226 A69-35373

Strength analysis of three layer rectangular plates under complex load and support distributions

19 p3434 A69-35827

Residual deformation of elastoplastically bent thin circular plate after perfect unloading from large deflection, considering equilibrium and compatibility conditions

19 p3438 A69-36306

Elastic shell theory to regularize singular integrodifferential equation, investigating load transfer from reinforcing ribs to circular cylindrical shell and numerical solution correlation

19 p3443 A69-36792

Bending of normally loaded simply supported rectangular plates in large deflection range solved by nonlinear differential equations and minimum potential energy principle

19 p3445 A69-36828

Elastic stiffness, kinematically equivalent loads and initial loads due to initial strains of FUGA 6 element, describing program for matrices generation

19 p3447 A69-36852

Optimal plastic design of circular sandwich ring assuming symmetric loading, minimum plastic resistance and cost justification of stronger cross section

20 p3625 A69-37590

Torsional-flexural buckling of thin walled open sections under eccentric load, emphasizing singly symmetric sections loaded in plane of symmetry

20 p3625 A69-37653

Energy formulation extended for plane anisotropic rectangular plates, handling nonuniform properties and loadings

20 p3627 A69-37766

Load carrying capacity of orthotropic circular cylindrical shell under uniformly distributed normal load, considering edge support conditions

20 p3629 A69-38075

Solution procedure for torus with given surface loads or displacements, using series expansion of generalized analytical functions, discussing stress concentration near toroidal cavity

21 p3839 A69-39192

Plasticity of tubular steel annealed in vacuum furnace and subjected to complex tension and torsion along deformation trajectories containing salient point

21 p3839 A69-39197

Cylindrical shell stability during loading by uniform external pressure represented by Fourier series, determining critical pressure by solving nonlinear equations

21 p3846 A69-39715

Postbuckling of filled circular cylindrical shell using Ritz energy method for load deformation relation, discussing stabilizing effect of core

22 p4038 A69-39895

Load transfer to sheet metal plate from bonded strip axially loaded by single force, assuming linear viscoelastic adhesive layer

22 p4038 A69-39896

Cosserat theory on couple stresses applied to stress distribution in semiinfinite plate, using Fourier transform method

22 p4038 A69-39902

Strain anisotropy matrix construction for various strain anisotropies from elastic properties of expression relating stress and elastic strain deviators

22 p4039 A69-39915

Momentless orthotropic spherical shell of variable thickness stress analyzed, assuming large deformations under uniform axisymmetric load distribution

22 p4039 A69-39916

Elastoplastic analysis of thin plates deformation, discussing loading conditions effects

22 p4041 A69-40064

Stress analysis fundamental equation for variable thickness plate under concentrated load, using two dimensional Dirac delta function

22 p4041 A69-40144

Stress distribution on surface of stator vane loaded statically as cantilever derived by brittle coatings, strain gages and three dimensional photoelasticity

22 p4042 A69-40310

Dynamic stability of circular isotropic plate with central hole subjected to torsional moment uniformly distributed over both edges by equilibrium equation

22 p4043 A69-40455

Solid viscosities effects on dynamic load factors of hollow sphere subjected to uniformly distributed impulsive loads, using three element model

22 p4044 A69-40598

Wrinkling of pressurized cylindrical and conical fixed free membrane column under lateral load, considering membrane sheets elastic properties

22 p4045 A69-40814

Photoelastic technique of stress-freezing and slicing to determine bending stresses in transversely loaded plate supported at corners

22 p4045 A69-40900

Meridional crack problem for cylindrical and spherical shells solved for uniform membrane load and bending moment, obtaining stress intensity components

22 p4046 A69-41041

Elastically symmetric thin plate stress-strain state under uniformly distributed load applied to edges

22 p4046 A69-41061

Pressure loads and balancing force determination in kinematic pairs of link gear of landing mechanism

23 p4062 A69-41415

External load distribution in bracket between bolts and joint, verifying Reshetov mounting bolt formulas

23 p4168 A69-41417

Statics of axisymmetric deformation of cylindrical and conical shells of revolution of moderate thickness under uniformly and nonuniformly distributed loads

23 p4226 A69-41705

Stress analysis of cylindrical tubes under torsional and transverse static loads based on vibrational theory, applied to rectangular cantilever tube

23 p4228 A69-41916

Plates and shells under concentrated loads, analyzing stress-strain state

23 p4228 A69-41986

Rib cross sections distribution for cylindrical shell under concentrated longitudinal forces obtainable by designing for minimum strain energy

23 p4228 A69-41988

Tilttable conventional radio telescopes possibilities of passing gravitational limit for diameter and shortest wavelength, discussing dead load

23 p4231 A69-42138

Field transfer matrices for simultaneous treatment of free and forced vibrations and buckling through axially loaded Timoshenko beam

23 p4234 A69-42400

Plane problem of infinite strip weakened by crack, determining crack form under uniformly distributed tensile loads applied to edges

24 p4395 A69-42592

Local stress distribution in cylindrical shells at concentrated load area solved by shallow shell theory
24 p4395 A69-42593

Structural materials deformation response to loading conditions and stress or strain cycle analysis to predict failure, including creep and stress relaxation
24 p4398 A69-42771

Single series solution for rectangular plate deflection under arbitrarily located concentrated load, considering monolithic slab beam connection case
24 p4404 A69-43593

Crack propagation in plate with stiffening ribs /riveted stringers/ under concentrated and tensile loads, determining rivet points displacements
24 p4406 A69-43709

LOAD FACTORS

U LOADS [FORCES]

LOAD TESTING MACHINES

Low speed four-ball lubricating oil testing machine eliminating thermal effects associated with frictional heating for load carrying capacities of thin lubricant films
07 p1140 A69-18968

Analytical method for designing pressure circular bearings verified by experiments concerning loading capacity
16 p2792 A69-31560

Tension-torsion-compression load testing machine of technological possibilities and accuracy [ONERA-TP-596]
17 p2945 A69-33065

LOAD TESTS

Europe 1 carrier rocket prelaunch wind load calculations as base for launch or delay decision
01 p0160 A69-10032

Off-axis test for hard orthotropic composite materials, discussing fixture design to reduce shear coupling effect
01 p0103 A69-11273

Harmonic oscillations in tunnel diode circuits for three intersection points of loadline with characteristic curve, discussing larger total positive circuit resistance case
06 p0898 A69-17801

Static endurance of aircraft structural elements under single and multiple loading, based on real alloys and crystalline materials theories
07 p1231 A69-18554

Yield points compared for axial and biaxial tensile loading of aluminum alloy sheets
10 p1801 A69-23849

Compact device for low temperature neutron irradiation of deformed specimens under tensile stress, emphasizing specimen carrier
11 p1862 A69-24901

Rod load capacity changes due to random overloads constituting upper limit of stress probability distribution density function used in programmed fatigue tests
11 p1985 A69-25180

Trident 2E and 3B structural design and fail- safe tests, noting difference in fuselage length
13 p2202 A69-27972

Design and test criteria for dynamically loaded structures from various viewpoints, discussing statistical variations, load strength and limitations
15 p2618 A69-30368

Saturn 5 boost phase environment simulation on Apollo stages, discussing fixtures, load devices, instrumentation and ground test
15 p2588 A69-30405

Sealing mechanism theory with face seal applications, taking into account load carrying capacity and no leakage pressure gradient [ASLE FICFS PREPRINT 18]
15 p2620 A69-30489

Clamped circular plates impulse load tests with sheet explosives, showing finite difference program for computing large deflection dynamic response
15 p2709 A69-30675

Aluminum models of single cell simply supported folded plates to study instability phenomena possibly occurring in actual structure
15 p2709 A69-30679

Fatigue life estimation for irregularly varying loads with emphasis on ground-air-ground stress cycles in aircraft
17 p3052 A69-32977

Moire reflection technique applied to study of stress-strain state of partially clamped rectangular cantilever plates under various loads
17 p3058 A69-33203

Fatigue test loading spectra calculation methods, discussing helicopter rotating and nonrotating components tests [AHS PAPER 373]
17 p2945 A69-33515

Load capacities of graphite lined journal bearings, discussing factors affecting wear rates [SAWE PAPER 68-LC-9]
18 p3148 A69-35002

WC-Co alloys structural changes under loads near yield limit, noting formation of slip bands
18 p3158 A69-35261

Structural design optimization based on reliability analysis stressing proof-load test and weight savings consideration under cost constraint
19 p3437 A69-36033

Simply supported rectangular plates experiments showing prediction on buckling load
19 p3447 A69-36854

Anisotropy coefficients obtained during annealed Al sheet tests based on stress-strain characteristics, noting fading memory effects
19 p3447 A69-36857

Cage and roller slip in high speed roller bearings over steady radial loads by measurement and theory
20 p3547 A69-37066

Vestibulometric tests for flight surgeon appraisal of applicants in flying profession, comparing Coriolis forces cumulative load tests with conventional tests
20 p3481 A69-37278

Experimental facility for studying heat conductivity of multicontact metallic and nonmetallic materials /plates/ in vacuum at low temperatures under various loads
21 p3721 A69-38639

Estimation of program fatigue life curves from equivalent load program using Miner law
21 p3846 A69-39810

LOADING

Helical and log conical helical antenna width reduction by loading of traveling wave antenna elements with isotropic material
11 p1852 A69-25315

LOADING FORCES

U LOADS [FORCES]

LOADING MOMENTS

Concentrated loads in elastic Cosserat continuum involving body moments and small deformations
10 p1799 A69-23151

Weak moment shells made from materials with different elastic moduli, developing theory based on undeformable normals
18 p3225 A69-35367

Complex representation of strain and displacement state in spherical shell using membrane theory, deriving shear forces resulting from single moment loading
21 p3831 A69-38416

LOADING OPERATIONS

Order-disorder transformations in nickel alloys under loading operations
11 p1904 A69-24706

Airport planning for large aircraft loading of passengers, baggage and cargo containers
17 p2948 A69-34208

Aircraft design determined by airport environment and facilities defined as pavement strength, passenger and baggage loading and aircraft handling, noting noise abatement
17 p2948 A69-34209

Technical problems in converting long service civil aircraft to obtain more volume, easier loading access or greater flexibility
20 p3461 A69-36919

Jumbo jet passenger loading devices including overwing bridges, transporters and terminal integration
20 p3511 A69-37916

Hydraulic-powered self propelled six degree of freedom loading vehicle moving tests assembly to test chamber with high accuracy positioning
20 p3511 A69-38181

LOADING RATE

Fatigue endurance of structural elements determined from stress rupture strength under high and low loading rates
04 p0673 A69-14536

Plastic deformation in bcc, fcc and hcp metals as function of initial impact load energy, noting strain hardening effects
07 p1166 A69-19144

Loading rate effects on fracture energy in carboxy terminated liquid Hycar toughened cantilever cleaved epoxy resin
08 p1338 A69-20491

Reliability of individual components of multicomponent systems under variable loads, using asymptotic distribution of minimal values
08 p1322 A69-21103

Heat release in combustion chambers of propulsion and lift engines considering various parameters of materials and design problems
09 p1625 A69-22619

Progressive accelerated fatigue testing for reliability in determining fatigue limits
10 p1800 A69-23349

Deformation rates effect on failure of cast aluminum alloys under various loading rates for tension and compression
21 p3746 A69-38958

Loading rate effects on fracture characteristics of unidirectional fiber reinforced materials, discussing fiber-resin interface strength
22 p3974 A69-41212

Plane strain fracture toughness of S-200 grade Be for 77-533 K temperature range, noting effects of loading, heat treatment and neutron irradiation
23 p4178 A69-42450

LOADING WAVES

U ELASTIC WAVES

U LOADS [FORCES]

LOADS [FORCES]

NT AERODYNAMIC LOADS

NT AXIAL COMPRESSION LOADS

NT AXIAL LOADS

NT BLAST LOADS

NT COMPRESSION LOADS

NT CRITICAL LOADING

NT CYCLIC LOADS

NT DYNAMIC LOADS

NT EDGE LOADING

NT GUST LOADS

NT IMPACT LOADS

NT RANDOM LOADS

NT ROLLING CONTACT LOADS

NT SHOCK LOADS

NT STATIC LOADS

NT THRUST LOADS

NT TRANSIENT LOADS

NT VIBRATORY LOADS

NT WING LOADING

Hollow rolling elements for reducing centrifugal load on high performance bearings, discussing production, fatigue life, etc
01 p0085 A69-10294

Crack growth in ceramics from velocity measurements on glass and sapphire as function of applied force, temperature and moisture environment
01 p0101 A69-10767

Handbook on fatigue properties for product design covering metals stress conditions, machine parts load and stress determination, cyclic stress, etc
01 p0170 A69-10918

Uniqueness formulation of concentrated load problem in linear theory of couple-stress elasticity
02 p0338 A69-11720

Limit load analysis of three dimensional rigid perfectly plastic continua by approximate variational method
02 p0338 A69-11721

Ti for high temperature use in supersonic aircraft, noting compressibility limit on maneuvering load factor and cooling by H
02 p0192 A69-11891

Dispersion equation for two dimensional periodic slow wave structure formed by periodically sequential loading
03 p0407 A69-13981

Photoelastic analysis of HF stress waves propagating in bars and plates subjected to damped sinusoidal loading [ASME PAPER 68-WA/APM-27]
04 p0669 A69-14397

Two point boundary value problems for determining buckling behavior of two hinged circular arches [ASME PAPER 68-WA/APM-18]
04 p0669 A69-14399

Thin cantilevered plate theory extended to large in-extensional deflections to account for geometry changes in bending moments [ASME PAPER 68-APM/BB]
04 p0670 A69-14401

Plates yield point loads limit determination formulated as mathematical programming problem, using finite element representations for velocity and moment fields [ASME PAPER 68-WA/APM-21]
04 p0670 A69-14405

Legendre transformation application to plane elastoplastic loading waves, examining shock front formation in interaction region
04 p0673 A69-14495

Prolonged loading effect on mechanical properties of 18Kh2N4VA steel at low temperature, discussing notched and unnotched specimens

04 p0614 A69-14573

Turbine blade loading in terms of surface diffusion and loading factors, discussing tandem and jet flap blades and vortex generators
[ASME PAPER 68-WA/GT-11]

05 p0812 A69-16136

Transistorized frequency detector for sensing system load changes affects speeds of control valves of prime movers

06 p0896 A69-17478

Dynamic stability of systems with distributed parameters subjected to parametric loading, considering parametrically excited systems with infinite degrees of freedom

07 p1231 A69-18502

Accuracy of deformation theory in case of simple loading, analyzing external forces under conditions not satisfying loading theorem

07 p1237 A69-19684

Minimum weight analysis of Michell trusses transmitting given load to bars within allowable range of axial stress

08 p1410 A69-19893

Optimization of plane smooth rectangular panels of constant cross section subjected to loading and heating conditions

08 p1417 A69-20821

Solid state laser radiation damage in polymers during tensile and compression loads using microstructural analysis

08 p1328 A69-21190

Holonomous and sclerononomous dynamic systems steady state motion stability under effect of generalized forces derived on basis of Liapunov theory

10 p1724 A69-22929

Deformation of thermoplastics under tensile loading, discussing types of loading

10 p1716 A69-22942

Stress concentration in isotropic plates weakened by curvilinear holes subjected to loading at infinity, noting curvature at corner points of holes

11 p1972 A69-24655

Plastic analysis of shallow spherical rigid plastic shell, using shell deflection equations to establish load-deflection relationship

11 p1980 A69-24823

Elastic two cavity revolving hyperboloid deformation by arbitrary forces solved by spherical functions

11 p1984 A69-25169

Electric analogy technique for torsion and flexure functions of uniform beams with terminal loads, considering Neumann boundary value problem

11 p1995 A69-25649

Hydraulic servo actuators load effect included in control loop actuator simulation

12 p2016 A69-26266

Dynamic response of imperfect circular cylinder to constant velocity load, noting applicability of Hoff nonlinear equation for dynamic buckling of columns

13 p2359 A69-27260

Load carrying capacity and friction calculated for pivoted pad journal bearings for machine design use
[ASME PAPER 68-LUBS-27]

13 p2266 A69-27275

Thermal and mechanical stability of fused silica lightweight mirror structures, examining impact and shear strengths of fused joints

13 p2261 A69-27954

Load factor role in nonequilibrium ionization process in Faraday-type generator, determining relationship with conductivity

13 p2314 A69-28361

MOS unitoron switching circuit operation subjected to nonlinear load, using analytic approximations of current-voltage characteristics

13 p2234 A69-28507

Prolonged loading effect on mechanical properties of 18Kh2N4VA steel at low temperature, discussing notched and unnotched specimens

15 p2638 A69-30274

Expression derived for arbitrary system subjected to external loading, using Cauchy equations for relationship between external plane forces and internal stresses

15 p2713 A69-31018

Bending theory for two layer plate made of isotropic material under sinusoidal load obtained by elasticity and classical theory based methods

15 p2714 A69-31198

Full stress design feasibility as function of load conditions, indeterminacy order and structure topology

16 p2872 A69-31915

Loading path criterion for total strain /deformation/ plasticity theory based on Sanders loading function, discussing case of thermally loaded bar

17 p3062 A69-33711

Muscle power output relation to imposed load modified to accommodate inverse relationship between generated force and contraction speed for determining maximum strength

17 p2916 A69-34011

Flexure functions of triangular sections under terminal loads, using electric analogy to study function effect on section shape and material Poisson ratio

17 p3066 A69-34050

Nonlinear partial differential equations solutions in theory of thin elastic spherical shells subjected to temperature fields and external loading

17 p3067 A69-34147

Growth rate of stability loss intrinsic modes in elastic shells under severe load, discussing stress distribution during buckling

18 p3217 A69-34598

Positive Gaussian curvature shell under concentrated forces, analyzing stresses and strains relation to load distance using Thompson and Legendre functions

18 p3218 A69-34601

Plastics behavior under loading and performance prediction, considering engineering design applications

18 p3161 A69-34609

Solid state laser radiation damage in polymers during tensile and compression loads using microstructural analysis

18 p3152 A69-35159

Transient processes of strain wave propagation in elastic shells and plates under time varying loads

18 p3224 A69-35321

Limiting equilibrium stress state of unbounded brittle body with elliptical crack under monotonically increasing tensile or compression load, noting influence of crack curvature

19 p3441 A69-36745

Equations of deformation for elastoviscoplastic bodies with different properties under loading and unloading conditions

19 p3445 A69-36812

Turbine rotors load dependent unstable motions, considering exciting forces origins, external and internal damping, etc

20 p3628 A69-37918

Cutting tools measured as function of cutting rate and cutting tool geometry during boring of Cr-Ni steel pipe blanks

21 p3731 A69-38878

Spring mass nonlinear systems under constant force excitation, studying step function responses of systems with various restoring force characteristics

21 p3836 A69-38985

Strain rate-load relations in elastoplastic shells reaching yield point, discussing variational method applicability

21 p3838 A69-39189

Automatic structural analysis by matrix force method, giving diagrams of load paths, equilibrium sequence and flow chart

21 p3843 A69-39311

Film thickness and normal load effect in thin films solid friction, noting dependence on deformation at contact

22 p3955 A69-40407

Strain gage and mechanical types of load-determining bolts selected on basis of application requirements and installation costs

22 p3957 A69-40829

Elasticity boundary value problems solution based on equilibrating method and differential equation

22 p4046 A69-40967

Pairs existence of symmetrical equilibrium forms in nonlinear shallow shell under load made applicable to nonshallow shells equilibrium

22 p4047 A69-41062

Time averaged and fluctuating wind load effects on large radio telescope structures, discussing wind shear and turbulence influence on steady and unsteady loading

23 p4230 A69-42125

Stressed state of thin plate with circular hole under normal and breaking force applied over hole perimeter

23 p4233 A69-42341

Stress concentration in shallow spherical perforated shell under loads, reducing boundary value problem to infinite algebraic equations solution

23 p4233 A69-42342

Time independent interaction surface bounds to shells shakedown domain obtained for multiparameter loadings

24 p4396 A69-42732

LOCALIZATION

U POSITION [LOCATION]

LOCATION

U POSITION [LOCATION]

LOCI

Control system analysis and synthesis by means of generalized root-locus method on digital computer

07 p1114 A69-18291

Time optimal control of soft spring showing switching locus changes

24 p4289 A69-42955

LOCKHEED AIRCRAFT

NT C-5 AIRCRAFT

NT C-130 AIRCRAFT

NT C-141 AIRCRAFT

NT F-104 AIRCRAFT

NT L-1011 AIRCRAFT

NT XH-51 HELICOPTER

NT XV-4 AIRCRAFT

Lockheed 1011 Tristar with three turbofan engines for large capacity medium range service, noting configuration, aerodynamics, structure and cutaway drawings

08 p1255 A69-21143

YF-12A interceptor aircraft development and testing, discussing titanium alloys application, aerodynamics and thermodynamics, escape systems for high speed and altitude tests

[AIAA PAPER 69-757] 19 p3245 A69-35652

Lockheed 1011 propulsion system design relating to system and component maintainability, reliability, performance and noise

[SAE PAPER 690390] 23 p4201 A69-41665

LOCKHEED CL-595 HELICOPTER

U XH-51 HELICOPTER

LOCKHEED MILITARY AIRCRAFT

U MILITARY AIRCRAFT

LOCKHEED XV-4A AIRCRAFT

U XV-4 AIRCRAFT

LOCKHEED 186 HELICOPTER

U XH-51 HELICOPTER

LOCKING

Lock-on characteristics of automatic tracking systems evaluated for case of variable vector signal, calculating transient response

11 p1861 A69-25716

LOCOMOTION

NT ASTRONAUT LOCOMOTION

NT WALKING

Light effects on circadian rhythms in monkeys, describing changes in deep body temperature and locomotor activity phase relationships

15 p2556 A69-31336

Rats locomotion in centrifugally generated gravity fields determined for in-space behavioral studies of earth organisms gravity requirements

19 p3263 A69-36457

Cell interactions and motions correlation for animal locomotion

21 p3662 A69-39708

LOG PERIODIC ANTENNAS

Helical log periodic and log periodic dipole arrays impedance and radiation patterns measurements have similar characteristics

02 p0219 A69-12337

Extensive air shower radio pulse polarization, using log periodic EW- and NS-arm antennas

04 p0595 A69-15425

Log-periodic circuits for application to microwave amplifiers in antenna design, noting bandwidth

05 p0739 A69-16554

Phasing of active region of log-periodic array antennas by modulated impedance feeders, discussing monopole and slot arrays

08 p1281 A69-20015

Log periodic antenna with vertically polarized omnidirectional radiation constant over bandwidth

08 p1281 A69-20033

Backfire log periodic cavity-backed slot array, giving H plane power patterns with near field plots along array

08 p1281 A69-20035

Space frequency filter antennas, using multiple terminals for signal processing as function of frequency and angle

08 p1290 A69-20977

Radiation field of log periodic dipole array calculated as function of observation point and dipole currents

10 p1664 A69-23802

Log periodic dipole array antennas simulated with simple RLC circuit loading uniform transmission line

11 p1850 A69-24977

Vertically polarized log periodic antenna consisting of unipole vertical radiators with side radiators for achieving minimum size
16 p2763 A69-32580

Deployable cross log periodic dipole /LPD/ array on conducting cone as potential application to spacecraft or missile requiring frequency independence in VHF-UHF band
22 p3913 A69-40693

LOG SPIRAL ANTENNAS

Electromagnetic multipole left- and right-hand circularly polarized modal fields for multiarm log spiral antennas, discussing current distributions, multipole coefficients and field patterns
08 p1281 A69-20018

Dispersion and coupling impedance of logarithmic spiral resting on anisotropic magnetodielectric layer for microwave devices design
13 p2235 A69-28512

Monograph on radiation zones and phase center of two arm conical logarithmic spiral antenna covering wideband design, near field measurements and far field integration
17 p2937 A69-33572

Asymmetric surface waves in radial spiral structures above conducting plane, analyzing spiral thickness and plane influence on dispersion and energy characteristics
22 p3916 A69-40951

LOGARITHMIC RECEIVERS

Reflected radar signal random fluctuations suppressed by using antenna, receiving channels and logarithmic amplifiers
04 p0556 A69-14490

Logarithmic amplifiers amplitude characteristics accuracy obtained by gain variations or successive summation of voltages, plotting curves illustrating error variations vs gain
15 p2574 A69-30128

Noise parameters at output of logarithmic detector separating two AM signals with overlapping spectra
15 p2564 A69-30148

LOGARITHMS

Iterated logarithm law proved for class of stationary series extended to systems of dependent random variables with complete couplings
11 p1910 A69-25699

LOGIC

Majority logic decoding of Euclidean or projective geometry codes in two steps
06 p0891 A69-17867

Sensory and logic behavior model of sequence selection based on received information, considering perception, sense, desire, concept and criteria levels
23 p4109 A69-41976

LOGIC CIRCUITS

NT THRESHOLD GATES

Monolithic sense amplifier for laminated-ferrite memories including provision for strobing, detecting, pulse forming and internal inversion logic using thermal feedback control
01 p0039 A69-10174

Gunn effect application in fast logic circuit devices including comparators, adder and shift register circuits
01 p0042 A69-10438

Universal NOR element design with resistors, determining permissible combinations for static mode of operation by computer method
01 p0037 A69-10746

Magnetic core logic circuit system for bidirectional stepping motor drive voltage power supply control in proper phase and time sequence
01 p0047 A69-11000

Full multiplier design based on stable iterative array cells interconnected to provide logical functions, noting capabilities for binary numbers
01 p0048 A69-11138

Fluid logic circuits miniaturization for flow in straight and curved channels of various cross sections
02 p0196 A69-12084

Variable time delay achievement in fluid logic circuits based on Coanda effect devices
02 p0196 A69-12085

Noise susceptibility of integrated circuits in digital systems, discussing sources and specifications
03 p0410 A69-13579

CASSANDRE programming language for digital systems, noting application to logic systems
03 p0401 A69-14179

Comparison of electric, electronic and fluidic logic circuits
04 p0583 A69-15083

Transistor-transistor logic switching circuits design for use in frequency dividers with variable division ratios in frequency processing systems
05 p0729 A69-15963

Requirements for analysis and synthesis of diagnostic tests for detecting faults in combinational logic circuit
06 p0892 A69-17408

Closed loop time optimal control achieved by exploiting generalization properties of threshold logic networks
[AIAA PAPER 69-77] 06 p0905 A69-18092

Gunn effect diodes application to ultrafast pulse electronic circuitry for computer logic
07 p1089 A69-18244

Self organizing trainable logical networks /TLN/ as stable controllers in multiaxis vehicle control problem, reviewing TLN concepts and training theory
07 p1070 A69-18388

Gunn effect pulse devices with resistive loading, discussing logic, circuits and low power consumption
07 p1097 A69-18453

Two signal four quadrant multiplier design having subnanosecond response
07 p1103 A69-18879

Logic circuit for semiconductor current gain sensing switch
07 p1113 A69-19744

MOS technology developments for higher speeds in logic circuits
07 p1113 A69-19765

Gunn effect memory loop in pulse diodes consisting of two Gunn diodes connected in series
08 p1279 A69-19912

Computer aided design methods for electronics and logic systems, noting linear circuits and one dimensional transistors
08 p1278 A69-19970

MOS transistor logic circuit performance optimization through component geometry and feed voltage
08 p1280 A69-19977

Nonlinear feedback shift register circuit design by logical sequences
08 p1298 A69-20835

Pure fluid amplifying logic and energy converting elements, discussing parameters, characteristics and working principles
[AGARDOGRAPH-118] 08 p1257 A69-20951

Peripheral fluidic devices for sequencing and monitoring machinery in hazardous areas, describing circuits
[AGARDOGRAPH-118] 08 p1257 A69-20954

Ultrahigh speed systems and logic circuits specifications implementation into electrical design, discussing circuit selection, line propagation delays, noise margins and temperature effects
[AGARDOGRAPH-114] 08 p1298 A69-20985

Catastrophic failures in logic circuit and system design, considering thermal effects, complexity, statistical methods and computer use
08 p1299 A69-21107

Cesium microthruster system using beam deflection for satellite control, describing ion engine subsystem and control logic/power conditioner subsystem
[AIAA PAPER 69-292] 09 p1569 A69-21875

Engine usage indicator to cumulate small gas turbine engine exposure to certain deterioration, presenting circuit logic block diagram
[ASME PAPER 69-GT-69] 09 p1572 A69-22519

Analog multiplier with controlled current splitting devices and feedback technique for stabilization of transfer characteristics, noting implementation in bipolar transistor
09 p1475 A69-22584

Suboptimum decision feedback communications systems incorporating simple digital processing compared with optimum Wald scheme
10 p1656 A69-23534

Wall attachment phenomenon /Coanda effect/ basis for jet elements in digital and/or pulse-mode systems
10 p1638 A69-23553

Associative holographic memories, discussing recall systems, logic circuits, etc
10 p1697 A69-23868

Solid logic technology /SLT/ computer circuits, discussing IBM 360 computer reliability, failure analysis information retrieval, SLT module and failure rate
11 p1843 A69-24341

Digital logic techniques for high speed satellite communications, noting general purpose logic cards
12 p2040 A69-26465

Lower bound for time required for group multiplication by logic circuits, using modified Winograd method for Abelian group
12 p2034 A69-26752

Logic family with low power consumption subjected to 1 Mev electrons analyzed within telemetry circuit concept for space application
15 p2625 A69-30830

Third generation computer reliability including preparation and test of integrated logic circuits
15 p2626 A69-30832

Arbitrary single gate failures diagnosis in combinational logic circuits not requiring fault table construction
15 p2583 A69-31112

Logic circuits abstract synthesis for detecting signals against noise background using known conditional quantized signal distributions
16 p2749 A69-31627

Computer aided design of machines with custom LSI arrays, describing error detection procedures and MOS logic circuits
17 p2942 A69-34121

Analytical, graphical and graph-analytical methods for synthesis of passive circuits ensuring air removal from chambers of pneumatic logic control and servomechanisms
18 p3093 A69-34831

Pneumatic control circuits design based on logic functions and truth tables, noting fluid logic application
19 p3256 A69-36714

Book on digital magnetic logic, considering digital magnetic core circuits consisting of magnetic components and interconnecting conductors
20 p3498 A69-37144

Photon actuated switch consisting of 10 input binary logic gate and solid state relay to reduce aerospace vehicles self generated noise
20 p3505 A69-37289

Current mode gates and flip-flops with subnanosecond propagation delay for integrated logic circuits, discussing memories dimensions, LSI arrays, etc
20 p3505 A69-37342

Integrated logic circuits assembly for digital computers, considering high density, mechanical environment, reliability, accessibility and costs
20 p3505 A69-37401

Multistable logic circuitry with 10 stability levels based on phased pulse principle, noting efficiency and complexity in man machine interface
21 p3686 A69-39065

Electromagnetic interference /EMI/ characteristics of various digital logic ICs
23 p4141 A69-42219

Logic networks of Boolean analogs analyzed by algebraic signal flow theory, introducing variational derivative for test detection in combinational and sequential networks
[AAS PAPER 69-236] 24 p4288 A69-42811

Hybrid techniques to produce thin and thick film microcircuits and logic system parameters
24 p4286 A69-42906

Integrated TTL flip-flop circuits, describing functional principles of circuits with DC and capacitive coupling
24 p4287 A69-43130

LOGIC DESIGN

Book on error detecting logic for digital computers covering error detection codes, logic circuits, checkers in data paths, etc
02 p0212 A69-11453

Comparison of electric, electronic and fluidic logic circuits
04 p0583 A69-15083

Device and logic/system designers and design aids interaction, emphasizing engineering trends in large scale integration area using MOS arrays
04 p0568 A69-15356

Digital nth order phase locked loop for FM demodulation
04 p0561 A69-15452

Predictive logic control of on-off system with one position sensor
[ASME PAPER 68-WA/AUT-14] 05 p0830 A69-16134

Digital controller weighting function sectionalization to simplify logic in developing adaptive control system
05 p0739 A69-16386

Computer aided design methods for electronics and logic systems, noting linear circuits and one dimensional transistors
08 p1278 A69-19970

Multistable logic circuitry with 10 stability levels based on phased pulse principle, noting efficiency and complexity in man machine interface
21 p3686 A69-39065

Computer organization design employing distributed processor to provide general purpose computing while taking advantage of large scale integration
21 p3856 A69-39133

Computer memory reduction through Fortran higher level language, discussing tradeoff between costs saved and additional logic hardware
[AIAA PAPER 69-963] 22 p3905 A69-40344

Digital data systems fault detection and isolation, describing diagnostic programs and hardware
[AIAA PAPER 69-967] 22 p3906 A69-40348

CRT display system coupling interface with magnetic storage determined from algorithms and time diagrams, describing character storage and system logic design
22 p3908 A69-40936

Fluidic amplifiers development and logic applications, describing various elements and circuits
22 p3870 A69-41239

Fluid logic feedback control circuit synthesis using synthesis table, describing procedure to assign memory valves and switching signals
24 p4292 A69-43290

LOGICAL ELEMENTS

Universal NOR element design with resistors, determining permissible combinations for static mode of operation by computer method
01 p0037 A69-10746

Pneumatic elements, discussing development from process control via modules systems to logic elements and fluid sensors
02 p0197 A69-12795

Large scale integration and batch-fabricated processing of logic and storage elements for fourth generation computer, discussing partitioning design
04 p0567 A69-15355

Chronological development and future trends in high speed logic and memory hardware technology and implementation
04 p0569 A69-15366

Pure fluid amplifying logic and energy converting elements, discussing parameters, characteristics and working principles
[AGARDOGRAPH-118] 08 p1257 A69-20951

Large scale integrated circuit accumulator chip as control element for design of digital system by design automated techniques
12 p2037 A69-25942

Self adaptive system for recognition of dynamic shapes, discussing self structuring by learning, incomplete pattern recognition, logic element network, etc
12 p2054 A69-27080

Microwave interferometer with digital-logic elements for phase shift measurements in pulsed plasmas without frequency range limitations
14 p2452 A69-29802

Counter for decimal counting and numeric display applications using integrated fluid logic elements
15 p2616 A69-31295

Fluidic logic elements using suction to influence main jet, outlining operation principles
16 p2736 A69-31835

Aircraft solid state electric system logic level tested functionally by built-in test equipment (BITE) operated on ground during preflight tests
17 p2977 A69-34110

Tristable fluid amplifiers, analyzing J functions of staticized variable, ternary logical characteristics, input equations, flow stability and switching measurements
24 p4255 A69-43298

LOGISTICS

NT LUNAR LOGISTICS

NT SPACE LOGISTICS

Helicopters and fixed wing STOL and VTOL aircraft for intertheater military logistics transportation, discussing C-5A role in 1970s
07 p1053 A69-19177

Simulation to correlate integrated logistic support recommendations for dynamic analysis of planned logistic network
10 p1668 A69-22975

Model simulation in program planning for space station with emphasis on accommodation of logistics
10 p1669 A69-22976

On job training of logistic publications engineers, emphasizing technical publications and system engineering and development for Minuteman program
10 p1811 A69-22977

Integrated Logistics Support (ILS) cost effectiveness, discussing management of systems elements in addition to prime equipment including computer programs, training, maintenance, etc
15 p2722 A69-31126

Development, manufacturing and logistic costs of reliability improvement in electronic equipment design
18 p3231 A69-34485

Ballistic missile and aircraft operational effectiveness, discussing data collection, reliability, availability and capability surveillance by computer
18 p3145 A69-34500

Maintainability and maintenance analysis in managing integrated logistic support (ILS) system
19 p3455 A69-36035

C-5 air force logistic transport, discussing structural design, configuration, payload, aerodynamics and flight testing
[AIAA PAPER 69-758] 19 p3248 A69-36295

Logistics management developed for Apollo Applications Program of NASA Manned Spacecraft Center [AAS PAPER 69-204] 24 p4417 A69-42812

LOH HELICOPTER

U OH-6 HELICOPTER

LONG RANGE NAVIGATION

U LORAN

LONG RANGE WEATHER FORECASTING

Satellites role in observing and forecasting global atmospheric behavior, discussing World Weather Watch and Global Atmospheric Research Program
06 p0916 A69-16854

Eole program to further data acquisition for climatology and weather forecasting
[UN PAPER 68-95831] 06 p0950 A69-17073

Long range prediction of zonal westerlies based on lunar cycles or quasi-biennial oscillations, considering aliasing problem
07 p1175 A69-18945

Long range weather forecasts attempt from relation between northern Atlantic Ocean water temperature anomaly and monthly satellite cloud data changes
20 p3569 A69-36987

Weather prediction, considering mathematical and empirical procedures, computer applications, atmospheric instability, etc
21 p3757 A69-38324

Soviet book on synoptic climatological and heliogeophysical long term weather forecasts, discussing monthly and seasonal anomalies, sun-earth interrelations, solar corpuscular elements, etc
21 p3759 A69-39523

LONG TERM EFFECTS

Atmospheric model development relating temperature, density, moisture and energy measurements from satellite observations for long term weather forecasting
[UN PAPER 68-95397] 01 p0108 A69-10463

Secular change examination in cislunar geomagnetic tail field gradient during summers of 1966 and 1967, using Explorer 33 and 35 results
01 p0077 A69-11237

Secular perturbations produced by comet belt beyond Neptune on orbits of periodic comets of large aphelion
01 p0158 A69-11327

Long term creep characteristics of metal structures from short duration relaxation tests, summarizing data on rheologically stable materials
[ONERA-TP-639] 02 p0337 A69-11626

Automatic bioprobe life support system for long duration interplanetary space flight, discussing blood leech as suitable research animal
02 p0199 A69-11828

Quasi-biennial oscillation in tropical stratosphere as result of long period gravity waves interaction with zonal wind
03 p0461 A69-13342

Cylindrical wave approximation modified to include axial effects, discussing time histories of deflection and applicability range
04 p0671 A69-14410

Long term electrochemical oxidation performance of n-octane based fuels containing aromatic, olefinic and naphthenic components
[ACS PAPER 94] 05 p0716 A69-16235

Permissible radiation doses for extended space missions, discussing clinical tests on dogs
05 p0708 A69-16508

Orthostatic intolerance, with assessment of circulatory problem of weightlessness in prolonged space flight
06 p0873 A69-17016

Leisure time and recreation facilities during long duration space missions, discussing astronaut selection procedure, active recreation, passive enjoyment and exercise programs
06 p0880 A69-17209

Dogs blood coagulation system functional state after 22 day space flight onboard Cosmos 110
08 p1262 A69-19830

Long term modulation of cosmic rays by solar activity explained by Parker solar wind model, noting confirmation by direct satellite measurements
08 p1379 A69-20533

Long time physiological effects of rotating systems, surveying acceleration effects and rotation experiments on humans and rats
08 p1265 A69-21183

Geomagnetic secular variations calculated by comparison of satellite, oceanic and aeromagnetic surveys
09 p1485 A69-21534

Total planet interaction energy of comets passing through solar system, showing non-Gaussian shape of distribution
10 p1774 A69-22970

Barbamy effect with and without somatotrophic hormone injection in mice during prolonged isolation and hypokinesia, noting sleep duration
10 p1646 A69-23576

Secular perturbations of remote satellites within lunar gravitation field, comparing observations and analytical data
10 p1779 A69-23614

Deimos and Phobos mutual secular perturbations from calculated masses and orbital elements, using canonical systems of equations
10 p1780 A69-23615

Various glacial periods mechanism ascribed to combination of long term solar activity cycle and polar migration
11 p1877 A69-24409

Drift velocity of earth magnetic field based on spherical harmonic analysis of geomagnetic secular variation
12 p0777 A69-27111

Nickel base superalloys long time carbide and intermetallic phases stability at high temperatures
13 p2277 A69-27405

Earth mantle and core friction interaction suggested as cause of secular change in orbital motion obliquity
13 p2253 A69-27821

Secular instability of steadily rotating stars, analyzing meridional motions in radiation zones by linear perturbation theory
13 p2354 A69-28566

Closed life support systems tests, describing effects of long term /one year/ confinement of three human subjects
13 p2216 A69-28612

Pharmacology for long term manned space flights
13 p2211 A69-28613

Geomagnetic field secular variations relation to variations of magnetic field of optimum dipoles, noting earth core role
14 p2436 A69-29061

Lacerta OB 1 B spectroscopic binaries periods and orbital elements, noting limits for secular variation
14 p2519 A69-29137

Secular terms for parallel component of electric current parallel to permanent magnetic field in toroidal MHD oscillations
14 p2492 A69-29369

First order secular and aperiodic perturbations in Keplerian orbital elements of synchronous satellite due to earth gravitational field eccentricity
14 p2521 A69-29466

Secular fluctuations of atmospheric circulation over Northern Hemisphere analyzed using isobaric and composite-kinematic surface maps, discussing analogies with Southern Hemisphere
14 p2478 A69-29836

Secular decline in absolute brightness of comet Encke from photometric curves obtained during past and present century
15 p2684 A69-30518

Transient and long lasting space environment stresses, discussing accelerations, vibrations, shocks, rapid descent in vacuum, temperature variations, gravity, etc
15 p2625 A69-30824

Aluminum alloys high temperature creep effects distinguished from effects of long period at high temperature, discussing tensile test data and deformation-time curves
16 p2800 A69-31781

Geomagnetic secular variations calculated by comparison of satellite, oceanic and aeromagnetic surveys
16 p2783 A69-32529

Cosmic ray electron spectrum data obtained by balloon flights, showing electron flux reduction above 500 Mev with increasing solar activity
16 p2851 A69-32566

Long range perturbations of satellites and asteroids with arbitrary inclination and eccentricity, illustrating motion around moon, oblate and spherical planets using energy integral
17 p3031 A69-33098

Vacuum and thermal environment long term influence on thermal resistance for Mg to aluminum and Mg to Mg bolted joints
[AIAA PAPER 69-628] 17 p3073 A69-33309

Permissible radiation doses for extended space missions, discussing clinical tests on dogs
18 p3095 A69-34727

Cowell equations modified for exact integration of pure Keplerian orbits, considering secular effects
18 p3165 A69-34842

Upper limit of solar oblateness determined from secular stability of differential rotation during evolution
18 p3202 A69-35214

Long term stability of orthotropic cylindrical shells under transverse shear stresses, calculating critical stress using Kirchhoff-Love model
18 p3225 A69-35357

Long term creep rupture data based on short term tests in form of Larson-Miller time-temperature curves
18 p3150 A69-35422

Materials evaluation for devices with long term underground exposure, including field tests at tropical locations
19 p3321 A69-35568

Modified Monte Carlo model applied to computerized meteorite orbit evolution, simulating secular perturbations by imposing sinusoidal variation on orbital elements
19 p3414 A69-36117

Geomagnetic field total vector modulus secular variations from airborne measurements
20 p3522 A69-37061

Oxygen supply and carbon dioxide absorption in long term life support systems, noting energy balances comparison of ecological systems
20 p3477 A69-37625

Gravitational constant secular change from considering relativistic cosmology and galactic structure, deriving equations of Newtonian cosmology
22 p4017 A69-40173

Strain measurement by interferometer with gas laser source emphasizing long period measurement problem
22 p3960 A69-40189

Laser range measurement from earth to lunar retroreflector to study earth tipping and gravitational constant secular decrease
22 p3960 A69-40190

Light pressure induced secular effect contributing to planetary satellites and lunar orbits evolution calculated by numerical integration
22 p4033 A69-41084

Anomalies of isotropic cosmic ray secular variations at high latitudes based on supermonitor neutron data
23 p4206 A69-41854

High reliability of solenoid and pressure regulating valves under long duration space missions, considering design, tests and controls
[AAS PAPER 69-238] 24 p4319 A69-42854

Acoustic analyzer response of man during prolonged noise effect of varying pitch and intensity
24 p4278 A69-43408

LONG WAVE RADIATION

Long wave radiative heat flux in boundary layers of cloud during solid overcast, discussing dependence on various cloud and atmospheric parameters
03 p0458 A69-13271

Propagation of long electromagnetic waves in ionosphere and exosphere, discussing thunderstorm noise spectrum
03 p0396 A69-13702

Long wave radio stations field intensity spectral analysis data evaluated to determine vertical ionospheric displacements at sunset and sunrise
06 p0922 A69-17752

Calibrating long wave actinometric instruments designed for Soviet meteorological satellites
06 p0929 A69-17978

Vertical distribution of ascending long wave radiation, employing actinometric radio sondes
06 p0953 A69-17990

Long wave radiative water vapor cooling in troposphere determined by numerical prediction model, including vertical distribution of cloud and moisture effects
07 p1175 A69-18896

Long wave propagation at 164 kHz in India during 1966 and 1967, determining D region recombination coefficient and long wave absorption diurnal variation
10 p1659 A69-24065

Long wave radiation fields calculations based on radiation transport equations, identifying differences between associated transmission functions
12 p2125 A69-25951

Long wave radiative heat flux in boundary layers of cloud during solid overcast, discussing dependence on various cloud and atmospheric parameters
14 p2471 A69-28779

Extraatmospheric long and short wave radio astronomy since first artificial satellite, including device carriers effectiveness of earth satellites, lunar orbiters, rockets and balloons
15 p2682 A69-30504

Filamentary composites elastic constants calculation extended to hexagonal symmetry by long waves method
17 p3061 A69-33666

Saturn emission peak and flux density at 408 MHz determined by cross telescope, discussing mechanism for enhanced radiation at long wavelengths
17 p3041 A69-33813

Long wave radiation influx toward atmospheric layers generated naturally by clouds, discussing radiation cooling of atmosphere in cloudy and clear weather
21 p3758 A69-39112

LONGITUDE

U SOLAR LONGITUDE

LONGITUDE MEASUREMENT

Simultaneous observations of altitudes of stars and moon for determination of longitude without time by navigators
14 p2479 A69-29855

LONGITUDINAL CONTROL

Semipassive attitude control system providing one degree pointing accuracies in all axes
07 p1226 A69-18326

Hypersonic vehicles multivariable flight control systems, analyzing flight path in terms of equation of motion of longitudinal mode
12 p2128 A69-26066

Spacecraft longitudinal control during reentry of lunar orbiter into atmosphere, analyzing final range prediction, trajectory tracking and accelerometers performance
13 p2355 A69-27681

Lifting rotor dynamics and undesirable characteristics reduction, discussing feedback control systems for pitch and roll
[AHS PAPER 340A] 17 p2899 A69-33509

Fighter aircraft higher order control system dynamics effects on longitudinal handling qualities evaluated by in-flight simulator for role of pilot induced oscillations tendencies
19 p3245 A69-35655

Aircraft characteristics influence on longitudinal handling qualities during carrier approach from visual landings on moving base simulator
[AIAA PAPER 69-768] 19 p3245 A69-35655

Aircraft characteristics influence on longitudinal handling qualities during carrier approach from visual landings on moving base simulator
[AIAA PAPER 69-894] 21 p3648 A69-39418

Longitudinal flying qualities evaluation by pilots in carrier approach flight simulation, describing experiment apparatus, procedures and results
[AIAA PAPER 69-895] 21 p3648 A69-39419

Aircraft flying qualities research program, discussing Navy test pilot evaluations and longitudinal handling characteristics for simulated carrier landing task
[AIAA PAPER 69-897] 21 p3648 A69-39421

Longitudinal flying qualities of aircraft, comparing attitude and altitude control data
[AIAA PAPER 69-898] 21 p3648 A69-39422

LONGITUDINAL STABILITY

Equations of motion of point restricted tethered parafoil for investigating longitudinal and lateral dynamic stability
01 p0009 A69-10415

Liquid propellant space launch vehicles longitudinal modes natural frequency, discussing coupled engine-propellant supply system stability
[AIAA PAPER 68-289] 02 p0335 A69-12393

Longitudinal short wave stability in conducting quasi-one dimensional gas flow, considering regions of high thermal emission
02 p0233 A69-12487

Aircraft stability during sideslip, discussing influence of fuselage/wing interference
04 p0548 A69-14824

Root locus method applied to longitudinal and lateral stability of aircraft with flexible fuselage and wing
04 p0677 A69-14835

Longitudinal dynamics of VTOL aircraft during hover-forward flight transition, using multiple time scale analysis
[AIAA PAPER 69-130] 06 p0869 A69-18157

Longitudinal stability of V/STOL aircraft at low speeds, discussing three tilt wings and quad ducted propeller configurations
[AIAA PAPER 69-194] 07 p1055 A69-19566

Longitudinal stability of unsteady motion of flight vehicle along ballistic trajectory, using linear differential equations
07 p1230 A69-19701

Saturn 5 unstable longitudinal oscillation due to coupling of structure and LOX line frequencies solved by helium injection
11 p1967 A69-25497

Gaseous He bubbles injection into liquid propellant launch vehicle fuel lines to reduce vehicle pogo oscillations by lowering feed system natural frequencies
11 p1967 A69-25498

Electrically driven thin fluid jet stability in longitudinal field between two plate electrodes, discussing role of Ohm law in calculating jet potential
12 p2136 A69-26402

Aircraft neutral stability empirical and mathematical aspects, considering control stabilization, damping and phugoid motion
15 p2551 A69-31012

Saturn 5 longitudinal instability /POGO/ precluded by lowering S-IC stage propulsion system resonance below structural frequency
[AIAA PAPER 69-548] 16 p2868 A69-32658

Droplet vaporization model representing combustion processes of longitudinal oscillations in liquid rocket combustor
[AIAA PAPER 69-483] 16 p2841 A69-32689

Close coupled accumulators for suppressing missile longitudinal oscillations /POGO/ developed for Gemini and Titan 3, including pump interaction
[AIAA PAPER 69-547] 16 p2869 A69-32729

Stability criteria for longitudinal combustion instability tested for generality using data from various solid propellant formulations
[AIAA PAPER 69-480] 16 p2834 A69-32736

Satellite three axis attitude control analysis showing rolling and longitudinal stabilization possibility by flywheel, with validity tested by analog simulation
17 p3048 A69-33240

Wing flaps and blow-off and suction effect on longitudinal balance of landing TU-104 aircraft, noting air suction at wing leading edge
19 p3247 A69-35818

Homogeneous magnetoactive plasma longitudinal oscillations stability with fast monoenergetic ions addition, noting ion temperature increase stabilizing effect
22 p3990 A69-40789

Pitching characteristics of three dimensional peripheral jet ground effect machines with compartment partition along pitch axis, considering longitudinal static stability and dynamic pitching motion
22 p3866 A69-40818

Nonlinear longitudinal dynamics of lifting orbital vehicle in near circular orbit, considering translational motion components effecting orbital decay or dilatation
[AAS PAPER 69-244] 24 p4392 A69-42857

LONGITUDINAL WAVES

NT COMPRESSION WAVES

NT PLANE WAVES

Electric field in plasma half space determined by longitudinal wave normal mode analysis, using BKG particle conserving collision model
01 p0134 A69-11287

Instability of longitudinal plasma waves propagating across magnetic field in plasma with electrons and ions drifting with different velocities across field
02 p0286 A69-11830

Planetary long waves behavior in atmospheric models, explaining unsteady components by means of filtered equations
03 p0459 A69-13274

Nonlinear interaction between waves in relativistic plasma, determining probability between transverse and longitudinal waves with different phase velocities
03 p0397 A69-13710

Technique to obtain desirable longitudinal oscillation mode for radiation of He-Ne laser
03 p0441 A69-13844

Longitudinal thermoelastic wave propagation in infinite body, proving generalized Kirchhoff theorem
03 p0528 A69-13924

Propagation of longitudinal transverse loading and unloading waves /with cylindrical symmetry/ in non-homogeneous elastic/viscoplastic medium, accounting for plastic dilatational strains
03 p0528 A69-13929

Longitudinal and transverse elastic waves propagation in medium with random inhomogeneities, deriving scattering coefficients in Born approximation for Fraunhofer region
04 p0667 A69-14262

Longitudinal stress pulse propagation in finite length free-free bar with variable cross section, noting stresses in projectile impacting plane target
04 p0671 A69-14412

Higher modes of longitudinal wave propagation in dispersive thin elastic rod, noting response to laser pulse
04 p0678 A69-14869

Torsional or longitudinal vibrations of nonuniform bar with elastic end constraints, developing frequency and mode form equations suitable for computer
04 p0681 A69-15196

Longitudinal acoustic waves propagation in partially ionized gas in external electric field, taking into account ionic collisions with electrons and neutral particles
06 p0963 A69-17079

Time averaged optical holographic interferometry of standing longitudinal acoustic waves in square cross section duct
06 p0923 A69-17150

Finite amplitude longitudinal wave propagation in lattices analyzed by study of compressive wave in chain of mass points with nearest neighbor interaction
06 p1022 A69-17367

Large amplitude longitudinal wave propagation in elastic rod solved by method of characteristics, prescribing end velocity as step function of time
07 p1233 A69-19176

Longitudinal and transverse vibrations of viscoelastic rods excited by inertia with aid of linear oscillator subjected to harmonic stress, using Kelvin-Voigt model
07 p1233 A69-19326

Longitudinal electrostatic oscillations in plasma with Fermi distribution of energies, noting oscillation frequency dependence on electron density
08 p1359 A69-19985

Collisional theory of longitudinal wave propagation for two fluid viscous ionized plasmas formulated from coupled Maxwell and Boltzmann equations
08 p1367 A69-20796

Beam-plasma dispersion relations, obtaining dispersion equation for plasma waves and dispersion curves for longitudinal waves
11 p1925 A69-24366

Elastic waves propagation in micropolar cylinder, treating longitudinal and torsional monochromatic waves in Cosserat medium
11 p1995 A69-25606

Transformation of longitudinal plasma wave into electromagnetic wave during collision with dielectric in plasma
11 p1934 A69-25708

Asymptotic solution of two dimensional problem of elastic impact of bars, showing longitudinal and surface waves decay with time
11 p1996 A69-25737

Viscoelastic models for solving longitudinal oscillations of one degree of freedom system under dynamic load, taking into account energy dissipation
12 p2177 A69-25995

Planetary long waves behavior in atmospheric models, explaining unsteady components by means of filtered equations
14 p2472 A69-28782

Equatorial jet stream excitation of longitudinal waves, analyzing plasma beam instability and spectrum of short wave inhomogeneities by quasi-hydrodynamic equations
14 p2437 A69-29073

Acoustic bulk-surface wave transducer for shear or longitudinal wave transformation in nonpiezoelectric material at HF
15 p2607 A69-30167

Collisional emission and absorption of longitudinal waves due to particle encounters in numerical experiments on one dimensional one species plasma
15 p2661 A69-30921

Maser amplification of 9.5 GHz longitudinal elastic waves in divalent nickel impurity ions doped sapphire by stimulated emission from inverted spin population
16 p2795 A69-31554

Electronic-ultrasonic amplifiers with external electron stream and longitudinal or surface wave studied for damping influence, deriving dispersion equation
16 p2761 A69-32061

Elastoplastic boundaries of wave propagation of combined longitudinal and torsional stresses at tube end
[ASME PAPER 69-APM-13]

Longitudinal plasma waves collision damping calculations using Rostoker test particle method
18 p3213 A69-34389

18 p3179 A69-34439

Longitudinal and transverse wave propagation in homogeneously deformed isotropic elastic solids, considering Hadamard and Green materials
19 p3440 A69-36588

Longitudinal waves propagation in unbounded thermoelastic medium expressed as surface integrals generalizing Kirchhoff theorem
19 p3444 A69-36804

Longitudinal elastic waves produced in truncated hollow Al cone due to steel spheres impact
[ASME PAPER 69-APMW-15]
24 p4401 A69-43101

LOOK ANGLES

U AZIMUTH
U ELEVATION ANGLE

LOOP ANTENNAS

Low polarization error HF loop antenna array direction finder performance tests, comparing measured bearings with polarimeter and conventional crossed loops data
01 p0048 A69-11006

Electromagnetic scattering from thin wire loops under various impedance loadings, considering positive and negative resistors effect combined with reactive networks
11 p1837 A69-25000

Radiation field produced by parasitic loop counterpoise antenna, obtaining far field from geometrical diffraction theory
20 p3507 A69-37840

Microwave breakdown characteristics predictable for circular loop antennas from near electric field analysis
21 p3683 A69-39281

LOOPS

Hybrid loop properties determination using quadrupole algebra, noting frequency dependence of input impedance and voltage transmission
04 p0582 A69-15072

Data transition tracking in digital communication systems by decision directed phase tracking loops
07 p1082 A69-19108

Frequency feed forward open loop technique for lowering threshold and linearity of FM demodulators
07 p1106 A69-19128

LORAN

Long distance VLF multirange navigation fix errors as function of angles of cut of position lines and range errors, presenting error isograms
14 p2478 A69-29484

Doppler and inertial self contained systems for long range navigation, considering air traffic control separation standards
15 p2651 A69-31544

Software remechanization of conventional hyperbolic LORAN for totally passive closed loop one way direct range measurements to individual LORAN transmitters
17 p3002 A69-34079

Navigation equations, discussing earth geometry, coordinates, gravity, dead reckoning and radio computations with regard to LORAN
18 p3169 A69-34845

Geographical position coordinates of radio operator determined by distance difference measurement using Loran and digital computer methods
23 p4186 A69-42027

LORAN C

Visual receiving equipment for consistency determination of Loran-C sky wave signals apparent arrival times
12 p2029 A69-26052

Atomic and astronomical time and frequency measurement via Loran C and VLF/Omega phase tracking receivers
15 p2615 A69-31285

Loran C system for master station time and frequency dissemination, discussing application, coverage, timing accuracy and restrictions
23 p4116 A69-41601

LORENTZ FORCE

Lorentz force sustained energy discharge, discussing cesium added argon flow across magnetic field in disk channel
06 p0969 A69-17910

Turbulence formation in conducting liquid at increasing Reynolds numbers, discussing cause of spontaneous magnetic field appearance
11 p1955 A69-24392

Hall type electromagnetic plasma accelerator, with thrust affected only by Lorentz forces in external magnetic field, compared to pure Hall accelerator
11 p1866 A69-25214

MHD Stokes flow for rotating disk in parallel magnetic field, showing Lorentz force inhibiting effect on fluid motion
13 p2305 A69-27325

Rayleigh-Taylor instabilities in two fluid hydraulic model, noting perturbation direction and Lorentz forces effects on instabilities growth time
13 p2310 A69-28033

Plasma rotation by Lorentz force in homopolar gas discharge device, considering centrifugal forces effect on flow pattern
13 p2315 A69-28556

Hot electron plasma formation by injecting megaelectron volt ion beams followed by Lorentz trapping, noting advantages of DC operation
15 p2661 A69-30925

Electrically charged earth satellite motion under action of Lorentz force produced by geomagnetic field interaction, relating field trajectories to acceleration
19 p3431 A69-36615

Turbulence formation in conducting liquid at increasing Reynolds numbers, discussing cause of spontaneous magnetic field appearance
24 p4390 A69-43782

LORENTZ GAS

Electron distribution function of isotropic homogeneous Lorentzian plasma subjected to frequency modulated electric field calculated by successive approximation method
02 p0285 A69-11543

Weighting functions effect in calculating average scalar electrical conductivity in Lorentzian gas
04 p0638 A69-15317

Boltzmann equation for weakly ionized gas electron component, solved by transformation to integral equation, applied to Lorentz gas in alternating electric field
05 p0795 A69-15619

Equations for frequency portions of electron-velocity distribution function in Lorentz plasma under influence of time periodic electromagnetic fields with two fundamental frequencies
05 p0800 A69-15743

Electrical conductivity of partially ionized plasma, noting nonapplicability of Enskog-Chapman method and use of Lorentzian gas model
09 p1546 A69-21584

Transport coefficients for almost Lorentzian mixture, computed as perturbation to coefficients for true Lorentzian mixture, compared to Chapman-Enskog method results
11 p1997 A69-24286

Elastic collision operator for relativistic Lorentz gas converted to differential form using Fokker-Planck limit for anisotropy segments
16 p2817 A69-31668

Boltzmann equation for Lorentzian plasma in elliptic magnetic field solved by expanding distribution function in Legendre polynomials
17 p3009 A69-32827

Lorentz gas approximation to Boltzmann collision operator generalized for heavy molecule nonMaxwellian gas distribution function, obtaining equilibrium distribution applicable to ionized gas
18 p3179 A69-34438

Nonlinear electron conductivity of Lorentz plasma subjected to frequency modulated electric field
21 p3778 A69-39573

Time dependent diffusion of light particles of Lorentz fluid approximated by Boltzmann equation leading to microscopic telegrapher equation
22 p3984 A69-40530

Boltzmann equation for electron distribution function of Lorentzian plasma traversed by transverse traveling wave, showing existence and uniqueness of solution
24 p4354 A69-42675

LORENTZ TRANSFORMATIONS

Lorentz invariant theories of gravitation compared with Einstein general relativity tests with respect to one body motion observations
02 p0318 A69-12094

Electromagnetic fields in vacuum extended to fields in presence of matter, deriving field equations covariant under Lorentz proper and improper transformations
02 p0281 A69-12196

Validity of Lorentz invariance, discussing nuclear magnetic resonance test on torque for spin of electrons, muons and neutrons
18 p3176 A69-35007

Second rank Dirac spinors with invariant components relative to Lorentz group transformations
19 p3361 A69-36817

Planck-Einstein equation derivation in special theory of relativity, discussing relativistic measurement of thermodynamic values in terms of Lorentz transformations 24 p4349 A69-42748

LOSSES

Reynolds and Mach numbers influence on loss coefficient magnitude at straight airfoil lattice 03 p0364 A69-13788

Loss factors effects on substrate choice in production of microwave printed circuit components 04 p0578 A69-15199

Active region doping effect on laser diode threshold current, noting current dependence on loss coefficient in interband transition model without selection rule 06 p0933 A69-17257

Aerodynamic losses and stage efficiency in partial admission turbines, using flat bladed rotor experiments and rotors of different blade pitch 15 p2547 A69-30290

LOSSLESS EQUIPMENT

Linear noisy two port preceded by nonreciprocal lossless network analyzed, showing existence of associated quantity invariant under lossless transformation 07 p1104 A69-18891

Networks of ideal inductors, capacitors and periodically operated switches with no energy loss, deriving frequency-power formulas from response functions 18 p3111 A69-34682

LOST WAX PROCESS

U INVESTMENT CASTING

LOUVERS

Thermal considerations of spacecraft external panel effects on specular louver systems, discussing heat dissipation and computer program [AIAA PAPER 69-26] 06 p1037 A69-18097

Optimal design for improving thermal performance of existing spacecraft thermally actuated louver system by increasing open-to-closed emittance ratio [AIAA PAPER 69-627] 17 p3071 A69-33269

LOVE WAVES

Monochromatic waves propagation in infinite micropolar elastic plate, treating Lamb and Love waves 11 p1995 A69-25605

Love-wave propagation at UHF observed by thin film surface wave transducers 13 p2218 A69-27203

Love stress function derivation from equilibrium equations 13 p2364 A69-28233

Love wave amplitude data satisfying earth model with intrinsic internal friction at depths assumed due to single thermally activated relaxation 15 p2596 A69-30624

Generalized Love functions in axisymmetric micropolar elasticity, deriving stress functions expressing all static components 19 p3440 A69-36585

LOW ALTITUDE

Monograph on flight mechanics and control technology of low flight vehicles at high flight velocities, discussing altitude control design, power spectra, etc 11 p1823 A69-24638

Navigation and guidance systems for low altitude aircraft flight safety noting position determination, cockpit environment and fail-safe operation 17 p3002 A69-34080

Low altitude trapped protons in inner radiation belt during solar minimum period, using emulsion detectors on polar-orbiting satellite 18 p3187 A69-34944

LOW ALTITUDE SUPERSONIC VEHICLES

U F-111 AIRCRAFT

LOW ASPECT RATIO

Vortex breakdown effect on aerodynamic coefficients of small aspect ratio delta wings during yawing 04 p0543 A69-14821

Slender wing theory extension to not-so-slender wings approached as singular perturbation problem, using matched asymptotic expansions method 04 p0544 A69-14891

LOW ASPECT RATIO WINGS

NT DELTA WINGS

NT TRAPEZOIDAL WINGS

Theoretical nonlinear method for calculating aerodynamic forces on low aspect ratio wings at high angles of attack and wide range of Mach numbers 21 p3644 A69-39084

LOW DENSITY FLOW

Ion collecting cylindrical electrostatic probes as flow field tracing instruments in low density slightly ionized flows 19 p3291 A69-35718

Quantitative photographs of low density flowfields during shock tunnel tests using electron beam excitation with image intensifier tube detector 19 p3292 A69-35723

Surface pressure, skin friction and heat transfer measurements on sharp flat plates and wedges in low density hypersonic flow, noting slip velocity 20 p3458 A69-37186

Carbon dioxide free jet expanding from conical nozzle into low density atmosphere, using freeze up method 22 p4000 A69-40594

LOW DENSITY GASES

U RAREFIED GASES

LOW DENSITY MATERIALS

Low density polybenzimidazole composites as ablative heat shields, discussing arc-heated wind tunnel tests of linear and crosslinked structures 23 p4179 A69-41715

Shear load, cohesion and internal friction measurements of low bulk density particulate silicates of complex shape, noting significance for lunar comparison 24 p4383 A69-43040

LOW DENSITY RESEARCH

High speed streak cameras applicability to low density theta pinch studies, describing image converters design, operation and block diagrams 14 p2496 A69-29787

LOW DENSITY WIND TUNNELS

Diagnostic techniques for high speed low density DVL plasma wind tunnel noting problems of pressure, temperature, hot-wire and calorimetric measurements [DVL-849] 04 p0584 A69-14823

Plasma parameters, except ion temperature, obtained from current-voltage characteristics of flowing plasma measured by electrostatic probes in low density wind tunnel 16 p2816 A69-31637

Laminar boundary layers in low density supersonic and hypersonic conical and axisymmetric nozzles, treating displacement, transverse curvature, velocity slip and temperature jump [AIAA PAPER 69-653] 17 p2954 A69-33458

LOW FINENESS RATIO

U FINENESS RATIO

LOW FREQUENCIES

Transistorized LF generator, discussing tradeoff due to frequency range, harmonic distortion and output stability 04 p0579 A69-15225

Electron number density LF oscillations for ionized gas identified with periodic solutions to neutral and charged particle plasma continuity equations 11 p1925 A69-24315

Nonpolar LF latitude variations based on spectroscopic and harmonic analysis of zenith telescope and prismatic astrolabe observations 11 p1956 A69-24401

LF measurements with positive or negative temperature coefficient resistors based on current-voltage characteristics 11 p1845 A69-24522

LF negative resistance of X band Gunn diodes with lumped components, using coaxial circuit 12 p2039 A69-26387

LF wave propagation and emission in magnetosphere, discussing steady noise and discrete emissions 12 p2072 A69-26745

High efficiency LF oscillations in avalanche diodes, noting evidence for parametric generation and condition for high efficiency 13 p2227 A69-27239

Extragalactic radio sources, observing nonlinear LF spectra for quasars and linear LF spectra for radio galaxies 13 p2351 A69-27867

Soft damping system required by LF vibrational loads 18 p3171 A69-34563

Hearing at LF, comparing noise and tone thresholds 21 p3664 A69-38986

Near field effects on accuracy of LF shielded enclosure measurements compared to open field environment 23 p4141 A69-42226

LF instability in plasmas and hydromagnetic fluids, discussing MHD equations, Rayleigh-Taylor instability, interchange mode, Kelvin-Helmholtz instability, etc 24 p4355 A69-42683

Nonpolar LF latitude variations based on spectroscopic and harmonic analysis of zenith telescope and prismatic astrolabe observations 24 p4391 A69-43791

LOW FREQUENCY BANDS

NT VERY LOW FREQUENCIES

LF ground based absorption results compared with rocket measured D region electron density profiles 16 p2778 A69-32188

LOW GRAVITY

U REDUCED GRAVITY

LOW LATITUDES

U TROPICAL REGIONS

LOW LEVEL TURBULENCE

Low altitude atmospheric turbulence model evaluated from analysis of A-6A aircraft gust load data, comparing model estimates with aircraft response characteristics 01 p0056 A69-11053

SNR improvement during low level turbulence measurements, examining correlation between hot-wire anemometers, including error analysis 14 p2446 A69-29018

LOW MASS

U MASS

LOW NOISE

Noise generation and propagation in linear N cascaded mismatched two port networks, noting application to microwave measurements in low noise technology 02 p0211 A69-12445

Dual reflector antenna design methods for obtaining necessary phase and amplitude illumination across secondary aperture in low noise applications 11 p1852 A69-25316

Multimode tracking /SYMMTRAC I and II/ feeds for low noise antennas, noting feed performance 11 p1852 A69-25317

LOW PASS FILTERS

Filter uncertainty for time or frequency resolution in analysis of waveform, decomposing characteristic functions and determining least uncertain realizable filter 02 p0226 A69-12306

Generalized digital low pass filter synthesis by recursion technique, noting coefficient sensitivity simplification 03 p0403 A69-13227

Narrow bandpass filters based on ripple adjustment in response of low or high pass prototype 04 p0574 A69-14345

Active RC low pass filters sensitivity to component changes, discussing effect of below minimum limit value 04 p0578 A69-15070

Digital filter design with complex coefficients for analytic signals and complex envelopes 04 p0579 A69-15460

Digital spectra analysis by Fourier transform and comb filter for determination of voltage and power spectra 05 p0722 A69-16762

Presampling filtering, discussing effects on rms interpolation error for sampled data systems 07 p1083 A69-19129

Surface effects at interface between linear and nonlinear media representing transmission lines of low pass filter type 07 p1088 A69-19755

Error probability for discriminator detection of wide-band PCM/FM, considering IF bandwidth/bit duration product and low pass filtering effect 08 p1271 A69-19864

Transfer function of low pass filters with Chebyshev attenuation characteristic in stopband and predetermined phase or delay time realized by ladder network 08 p1300 A69-21171

Digital sampled data spectra conditioning, deriving linear functions for low pass, bandpass and band rejection numerical filters and spectrum shaping 10 p1654 A69-23292

Low pass filters synthesis based on Chebyshev polynomials properties noting requirements of critical frequency, frequency response decline rate and tolerance range 11 p1887 A69-25210

Ultra lowpass filter circuit with two point contact Ge diodes and capacitor 12 p2039 A69-26379

Low pass quasi-optical waveguide filters, using metal strips in dielectric material to obtain broad stopband and low dissipation loss

13 p2229 A69-27675

Chebyshev polynomial of even order used in synthesis of equally terminated low pass lumped and distributed filters of even order

13 p2233 A69-28068

Mathematical optimization to achieve near equal-ripple response in passband for coaxial low pass filters having unequal line lengths

16 p2757 A69-31583

High pass filters reflection group delay compared with low pass filters transmission group delay with Butterworth, Chebyshev and elliptic responses

21 p3686 A69-39139

Filtering optimization prior to limiting digital signals in strong noise, detailing bandwidth choice of single pole low pass filter

21 p3676 A69-39450

LOW PRESSURE

NT HIGH ALTITUDE PRESSURE

Qualitative mechanisms to explain Langmuir paradox, discussing wall mechanism for Maxwellian distribution formation in low pressure discharges

06 p0960 A69-16922

Low pressure measurement by electron scattering using Born approximation

07 p1181 A69-19218

HF instability of low pressure discharge in magnetic field, discussing plasma diffusion and oscillations

11 p1927 A69-24912

Magnitude and type of wall losses from small opening in discharge tube for positive plasma column of low pressure glow discharge in hydrogen

14 p2493 A69-29691

Monograph on large scale cloud distribution in extratropical low pressure regions, using classical meteorological observations and Tiros weather satellites data

15 p2650 A69-31212

Inflight spontaneous pneumothorax case of civilian pilot lung collapse experience during exposure to reduced ambient pressure, discussing etiology, incidence, treatment and disposition

17 p2909 A69-33183

Bayard-Alpert type ionization gage for low pressures with and without modulation, discussing role of electron oscillations

20 p3464 A69-37407

Portable multiunit low pressure chamber with locks, permitting water replenishment, feeding of animals under continuous pressure and gas mixtures

22 p3891 A69-40217

White mice survival rates and blood morphology and sedimentation rates in low ambient pressure confinement following infectious bacteria injection

24 p4267 A69-43397

LOW PRESSURE CHAMBERS

U VACUUM CHAMBERS

LOW SPEED

Vortex motion of separated flow from slender wings and rotor loading, discussing computer role in low speed aerodynamic research

05 p0696 A69-15562

LOW SPEED HANDLING

U CONTROLLABILITY

LOW SPEED STABILITY

Test facilities and techniques for low speed flight problems of aircraft handling qualities, stability, control and performance

05 p0741 A69-15575

Longitudinal stability of V/STOL aircraft at low speeds, discussing three tilt wings and quad ducted propeller configurations

[AIAA PAPER 69-194] 07 p1055 A69-19566

LOW SPEED WIND TUNNELS

NT SUBSONIC WIND TUNNELS

Diffusion characteristics of turbulent flow produced by square mesh grid in low speed wind tunnel

13 p2250 A69-28496

LOW TEMPERATURE

Thermoelectric and thermomagnetic properties of bismuth at low temperatures, assuming thermal EMF due to phonon capture of carriers

03 p0488 A69-13885

Audio frequency noise in p channel MOST at cryogenic temperatures, noting trap contribution

06 p0979 A69-17151

Pyroelectric thermometry for measurements at low temperatures with emphasis on calorimetry, discussing pyroelectric coefficients, dielectric constants and resistivities

09 p1493 A69-21423

Thermoelectric and thermomagnetic properties of bismuth at low temperatures, assuming thermal EMF due to phonon capture of carriers

11 p1938 A69-25686

Low temperature specific heat of praseodymium magnesium nitrate

12 p2026 A69-25784

LOW TEMPERATURE BRAZING

Low temperature low cost dip brazing technique for light weight magnesium alloy electronic packaging structures, noting distortion

09 p1509 A69-22346

LOW TEMPERATURE ENVIRONMENTS

Solar absorptance, total hemispherical emittance and absorptance/emittance ratio for metals at cryogenic temperatures measured simultaneously with sinusoidally perturbed incident radiation

01 p0176 A69-10847

Low temperature effects on calf thymus deoxynucleoprotein, crystalline egg albumin and fibrillar actin, noting molecular weight and viscosity changes

01 p0018 A69-11089

Silica glass hardness relationship to pressure induced densification at low temperatures

03 p0453 A69-13616

MOST devices characteristics at cryogenic temperatures, studying variation in gain over audio frequency range

03 p0405 A69-13642

Free electron kinetic equation including inelastic electron-atom collisions derived for nonequilibrium low temperature plasma, showing interrelated electronic and atomic energy distribution

05 p0802 A69-15889

Cryogenic behavior of adhesive materials used in fabrication of liquid hydrogen/liquid oxygen powered Saturn S-4B stage

05 p0784 A69-16487

Film processing effects on cryogenic mechanical properties of polyethylene terephthalate

05 p0785 A69-16490

Cryogenic mechanical properties of epoxy resins and glass/epoxy composites

05 p0785 A69-16491

Mechanical behavior of polyethylene terephthalate at cryogenic temperatures

05 p0785 A69-16494

Molecular motion in polytetrafluoroethylene crystals at cryogenic temperatures, noting crystal defect permitting angular displacements of chain segments

05 p0797 A69-16495

Vulcanizable elastomers suitable for contact with liquid oxygen, discussing preparation, mechanical properties, transition temperature and structure

05 p0717 A69-16497

Fluorinated polyurethanes synthesis for liquid oxygen environments and cryogenic structural utility, noting structural effects on LOX compatibility

05 p0717 A69-16498

Bearing lubrication at low temperature, examining safety limits, working fluid in liquid or gaseous state

[IME PAPER 9] 07 p1138 A69-18565

Human body temperature regulating factors in low temperature environment, studying metabolism, lung ventilation and onset of shuddering

10 p1648 A69-23298

Cryogenic conductive heat transfer in solids, low temperature insulation and liquid-vapor interfaces, discussing boiling heat transfer, injection cooling and frost formation

11 p1998 A69-24461

Lubrication and operation of Hamilton Standard propellers in high altitude and low temperature environments

[SAE PAPER 690323] 11 p1822 A69-24515

Model for shock propagation from point energy source into cold atmosphere with exponential density variation

11 p1871 A69-25123

Germanium surface IR radiation absorption in vacuum at low temperatures, obtaining modulated interval reflection spectra

13 p2317 A69-27879

Deep freezing of nuclear precession magnetometer elements for improving instrument characteristics

14 p2446 A69-29083

Alloying elements effects on low temperature metal fracture, considering changes in ductile-brittle transition flow due to solute

17 p2988 A69-33551

Supereconducting cavities for resolving optically induced changes in dielectric constant of CdS at 4.2 K

17 p3016 A69-33782

Adaptor for Debye-Scherrer powder camera to take high quality photographs even at liquid N temperature

19 p3313 A69-36493

Stress corrosion cracking of alpha Ti in liquid nitrogen tetroxide and various methanol environments, considering failure mechanisms

19 p3352 A69-36906

Solid state chemical heat sources aboard unmanned planetary landing vehicles to maintain batteries and experiments operability during cold planetary nights

23 p4070 A69-42275

Adhesive bonding of optical components, discussing material types, test methods, problem of operation at cryogenic temperature, etc

24 p4326 A69-43465

LOW TEMPERATURE PHYSICS

Heisenberg ferromagnet dynamics at low temperatures, calculating spectral weight function and other properties with low density expansion

01 p0135 A69-10016

Specific heats of Cu, GaAs, GaSb, InAs and InSb measured over low temperature ranges

01 p0140 A69-11252

Microscopic theory of superconductivity, considering quantitative physical properties of low temperature electric current flow

02 p0293 A69-11432

Graphite specific heat temperature dependence at low temperatures, noting Wigner effect for neutron irradiation

02 p0269 A69-11782

Fluorescence and phosphorescence from tryptophan powders stimulated at low temperatures with UV, vacuum UV, fast electrons and X rays

03 p0372 A69-13487

Low temperature conductance peaks observed in tunneling measurements on aluminum-phosphosilicate glass-degenerate silicon sandwich structures

03 p0493 A69-14183

Transitions in glasses at low temperatures, noting molecular relaxation dependence on copolymer composition

04 p0621 A69-15308

Self Q switching of ruby lasers at 77 K, noting saturable absorber giant pulse process obtained by shielding part of laser rod from pump

05 p0776 A69-16332

Fermi surface topology effects on Nernst-Ettingshausen coefficient from measurements in magnetic fields to 3.3 tesla and 1.2-4.2 K temperatures in metallic tin

05 p0808 A69-16357

Cryogenic behavior of adhesive materials used in fabrication of liquid hydrogen/liquid oxygen powered Saturn S-4B stage

05 p0784 A69-16487

Mechanical relaxation of poly 4 methyl pentene 1 at cryogenic temperatures, discussing temperature dispersion curve and secondary absorption associated with thermal motion of side chains

05 p0785 A69-16492

Polymer glasses low temperature transitions, relating structure and transition temperature

05 p0717 A69-16493

Molecular motion in polytetrafluoroethylene crystals at cryogenic temperatures, noting crystal defect permitting angular displacements of chain segments

05 p0797 A69-16495

Magnetoresistance of tellurium single crystals with various current carrier concentration at liquid helium temperatures

06 p0978 A69-16986

Quantum oscillations of Maggi-Righi-Leduc (MRL) effect in n-InSb and n-InAs samples from single crystals at liquid helium temperature

06 p0979 A69-16992

Electron irradiation annealing and modification of 35 and 65 K defects in n-type Ge induced by 1 Mev electrons at low temperature

06 p0980 A69-17757

IR absorptance of CO below room temperature, determining strength and half widths of lines in R branch of fundamental band

07 p1183 A69-19644

Thermal expansion of polymers at cryogenic temperatures

07 p1172 A69-19730

Very low temperature dependence of thin single crystal Al plates electrical resistance, noting Umklapp processes contribution

10 p1711 A69-23620

Composition and thermodynamic properties of gaseous system reacting at low temperatures with con-

densified phase formation, discussing iterative process convergence in approximation

11 p2001 A69-25223

Temperature effects on noise levels in field effect transistors, discussing Lorentz spectrum

11 p1853 A69-25391

Hydrogen viscosity temperature dependence at constant density below room temperature

11 p2003 A69-25704

Low temperature method for measuring breakdown threshold parameters of liquid and gaseous He by laser beam, observing stimulated Mandelstam-Brillouin scattering

16 p2796 A69-31799

Low temperature creep mechanisms, discussing thermal activation of dislocation slip in perfect crystals

17 p2985 A69-32909

Radiative and conductive heat transport mechanisms at cryogenic temperature applicable to thermal energy transport minimizing technique in containment system

17 p3074 A69-33680

Thermal conductivity coefficient of gas mixtures at low temperatures obtained using quantum diffusion model and Chapman-Enskog method for Boltzmann equation

21 p3848 A69-38638

Nernst effect in pyrolytic graphite at low temperatures including thermal EMF, electrical conductivity, thermal conductivity and magnetoresistance coefficients

21 p3753 A69-39562

LOW TEMPERATURE TESTS

Mechanical properties of AZ5G-Zr-Cr alloy welded sheet subjected to biaxial stress at low temperature

01 p0088 A69-11152

Relaxation mechanism of low temperature internal friction peaks in niobium quenched to room temperature

03 p0447 A69-13617

Prolonged loading effect on mechanical properties of 18Kh2N4VA steel at low temperature, discussing notched and unnotched specimens

04 p0614 A69-14573

Mechanical properties and stress concentration sensitivity of structural alloys at low temperature

04 p0614 A69-14574

Mechanical and physical properties and cryogenic wear tests performed on composite materials, considering NERVA cryogenic turbopump bearing retainer development

[ASME PAPER 68-WA/LUB-10]

05 p0768 A69-16133

Cryogenic mechanical properties of epoxy resins and glass/epoxy composites

05 p0785 A69-16491

Cooling requirements for high speed polytetrafluorethylene lubricated ball bearings operating in cold hydrogen gas, developing minimum gas flow rate equation

07 p1141 A69-19310

Compact device for low temperature neutron irradiation of deformed specimens under tensile stress, emphasizing specimen carrier

11 p1862 A69-24901

Thermal expansion coefficients of Nb-Zr-Ti alloy and plexiglass at 10-300 K from dilatometric measurements

11 p1905 A69-24917

Peltier measurements below 4 K capable of measuring low Seebeck coefficient on high resistivity alloys and in presence of magnetic field

14 p2449 A69-29563

Prolonged loading effect on mechanical properties of 18Kh2N4VA steel at low temperature, discussing notched and unnotched specimens

15 p2638 A69-30274

Mechanical properties and stress concentration sensitivity of structural alloys at low temperature

15 p2638 A69-30275

Temperature effects on fracture of various alloys, presenting strength and toughness values tested at cryogenic temperatures

17 p2990 A69-33567

Alpha Ti-Al and Ti alloys plastic deformation at low temperatures, noting slip and twin mechanisms role

18 p3158 A69-35444

Fuel resistant elastomers evaluated for seal compounds for low temperature capability, noting epichlorohydrin-ethylene oxide as promising sealant

19 p3356 A69-35534

Low temperature bond failures of room temperature vulcanizing methyl-phenyl adhesive bonds attributed to thermal stress cracking of primer, presenting in-process tests

19 p3321 A69-35563

Solar cell characteristics at low temperatures, noting efficiency increase with decreasing temperature

19 p3251 A69-35691

High speed brittle fracture of polycarbonate resin subjected to static bending in liquid nitrogen determined from crack propagation speed of surface coating

19 p3358 A69-35776

Voltage and temperature dependence of zero-bias anomaly in GaAs p-n junction at 0.40-60 K, investigating voltage dependence of differential resistance

19 p3388 A69-36542

InSb instabilities and time dependence of transverse breakdown, performing Hall effect measurements on n-type InSb at 77 K

19 p3389 A69-36546

Optical pumping in pure Si at 77 K, noting dichroism conditions for dipolar electric transitions in cubic crystal

19 p3389 A69-36548

High resistivity gallium arsenide single crystal LF current oscillations at low temperature, investigating electron heating effect and mechanisms

19 p3391 A69-36609

Protective coatings for high melting point metals, discussing prevention of low temperature coating breakdown due to oxidation

20 p3561 A69-37375

Experimental facility for studying heat conductivity of multicontact metallic and nonmetallic materials /plates/ in vacuum at low temperatures under various loads

21 p3721 A69-38639

Al alloys sheet, plate and weldments crack behavior and fracture toughness at cryogenic temperatures, using notched and surface flawed plane strain specimens

[ASM PAPER W9-19.3]

21 p3743 A69-38669

Rat survival rate after prolonged gradually decreased body temperature without motion restraint or kept in fixed position

22 p3877 A69-40278

Tensile cryostat for low temperature strain measurement, discussing design, insulation and vacuum sealed environment for heat leak reduction

[NAS-NRC PAPER J-3]

22 p3947 A69-40627

Mechanical properties of welded joints in Kh 18N9T steel at very low temperatures using austenitic-ferritic and austenitic welds

22 p3958 A69-41204

Low temperature mechanical properties of structural materials for high energy propulsion systems, using low boiling point propellants as liquid hydrogen, fluorine and oxygen

23 p4177 A69-42159

LOW THRUST

NT MICROTHRUST

Satellites trajectories under influence of earth oblateness and low radial thrust acceleration by nonlinear mechanics asymptotic method, discussing osculating orbits

16 p2856 A69-32009

Numerical integration of plane orbital transfers with multiple powered arcs, minimizing propellant expenditure of small thrust chemical rocket

19 p3400 A69-35673

LOW THRUST PROPULSION

NT ELECTROMAGNETIC PROPULSION

NT ELECTROSTATIC PROPULSION

NT ION PROPULSION

NT PLASMA PROPULSION

NT SOLAR PROPULSION

Optimum control determination for low thrust spacecraft to minimize time for passing through radiation belt

01 p0113 A69-10571

Low thrust spacecraft motion continuous correction by dynamic programming, assuming continuous information on system state including fuel consumption

01 p0113 A69-10572

Spacecraft orbital maneuvers by means of low thrust, discussing optimization and several orbital transfer examples

03 p0522 A69-14086

Power requirements of low thrust space engine for maneuvers and optimum overlappings theory for selection of power plant

04 p0666 A69-14920

Low thrust nuclear engine using hydrogen suitable for transfer missions

05 p0791 A69-15598

Minimum fuel consumption for low thrust jet engine propelled space vehicles maneuvering in circular trajectories

05 p0829 A69-15879

Optimum low thrust interplanetary transfers involving swingby trajectory past intermediate planet analyzed, assuming impulsive velocity change at planet

06 p1006 A69-17572

Spacecraft optimum low thrust trajectory analyzed by Hamilton-Jacobi perturbation theory, obtaining canonic constants of motion

06 p1007 A69-17574

Spacecraft electric propulsion parameters and launching vehicle characteristics in low thrust mission simulation, discussing spacecraft path

09 p1584 A69-21202

Low thrust mission simulation dependence on hardware definition, discussing power plant characteristics, jet velocity and thruster efficiency

09 p1584 A69-21204

Interplanetary low thrust mission analysis model, discussing major elements interactions

09 p1585 A69-21206

Low thrust mission analysis techniques and computer programs, discussing electric propulsion

09 p1585 A69-21208

Low thrust interplanetary trajectories optimization, discussing hardware design considerations

09 p1585 A69-21209

Automated parameter search techniques applied to low thrust mission design, stressing trajectories and mission optimization

09 p1585 A69-21211

Pulsed plasma microthruster propulsion system for synchronous orbit LES 6 satellite

[AIAA PAPER 69-298]

09 p1562 A69-21227

30 cm diameter mercury bombardment low impulse thruster development for potential space applications, discussing performance and control

[AIAA PAPER 69-238]

09 p1566 A69-21256

Electron bombardment thrusters for low specific impulse operation, discussing electrode structures fabrication by bonding alumina disk to metal electrode

[AIAA PAPER 69-301]

09 p1568 A69-21730

Hollow cathode mercury electron bombardment thruster design, emphasizing low specific impulse operation and discharge chamber improvements

[AIAA PAPER 69-300]

09 p1569 A69-21880

Low thrust space probe mission to Halley comet, utilizing nuclear electric propulsion

10 p1772 A69-22864

Low thrust propulsion devices high response impulse testing, describing limitations imposed by solenoid valve time response

10 p1672 A69-23278

Optimum control determination for low thrust spacecraft to minimize time for passing through radiation belt

15 p2651 A69-30741

Low thrust spacecraft action continuous correction by dynamic programming, assuming continuous information on system state including fuel consumption

15 p2651 A69-30742

Low thrust trajectories for minimum time rendezvous between continuous thrust interceptor and passive target vehicle, comparing calculus of variations and steepest ascent analyses

16 p2857 A69-32177

Minimal electric propulsion systems for interplanetary spacecraft, discussing payload, reduced trip time and low thrust systems for Jupiter flyby

[AIAA PAPER 69-499]

16 p2844 A69-32714

Low thrust reaction control for space missions, summarizing range and specific impulse characteristics for solid and hybrid systems

[AIAA PAPER 69-433]

16 p2834 A69-32745

Continuous mode operation in hypergolic bipropellant low thrust rocket motors, discussing high temperatures reached by combustion chamber walls and cooling solutions

17 p3019 A69-33335

Optimal overlapping theory to select nonthrottled low thrust spacecraft engines power, noting spacecraft mass invariability

18 p3184 A69-34583

Feasibility of automatic stationkeeping for synchronous satellites by using solar sailing techniques and low thrust systems

[AAS PAPER 68-151]

19 p3429 A69-35950

Halley Comet rendezvous mission, comparing low thrust mode with ballistic Jupiter or Saturn swingby mode

[AIAA PAPER 69-933]

21 p3809 A69-39360

Low thrust guidance for multirevolution trajectory required for earth parking orbit transfer to parabolic orbit insertion, noting advantages over high thrust scheme

[AAS PAPER 69-403]

24 p4379 A69-42832

LOW VISIBILITY

- Low visibility instrument landing of aircraft using ILAS and inertial guidance
01 p0114 A69-11012
- Low visibility landing, discussing problems of radio guidance geometry, visibility measurement, aircraft dynamics, pilot psychology, regulation and politics
01 p0114 A69-11391
- Optical measurements through retrorocket plumes of landing spacecraft, investigating reduced landing site visibility and modulation transfer function
02 p0248 A69-11765
- Low visibility aircraft landing, discussing total system approach, modern electronic developments, collision avoidance, safety and air traffic control
03 p0465 A69-13853
- Atmospheric scattering behavior under reduced visibility conditions for laser wavelengths of 0.69 and 1.06 micron
11 p1837 A69-25040
- Monograph on low visibility landing in civil aviation, considering visibility determination methods and equipment and IR sighting devices
20 p3574 A69-38064
- Low visibility VSTOL instrument landing system and associated electronic structures, discussing instrument to visual flight transition
22 p3979 A69-40675

LOW VOLTAGE

- Low voltage He-Ne laser, noting outputs for various pressures and grid anode separations
10 p1704 A69-23652
- Low voltage Knudsen arc in cesium-argon mixture for thermal emission converters
14 p2403 A69-29248

LOW WING AIRCRAFT

- Safety measures for aircraft ditching at sea, discussing low wing configuration advantages and life rafts
14 p2392 A69-29697

LOWER ATMOSPHERE

- NT OZONOSPHERE
NT STRATOSPHERE
NT TROPOPAUSE
NT TROPOSPHERE
- Venus lower atmosphere noting graphically wide variation of surface pressure estimates
02 p0319 A69-12103
- Mars lower atmospheric pressure, temperature and composition, noting consistency between photometric, spectroscopic and occultation techniques
02 p0319 A69-12104
- Molecular O 0.7620 micron absorption band in pure O and air, noting rotational lines mean half width and lower atmosphere transmission function
03 p0458 A69-13272
- Meteorological PTU/pressure, temperature, humidity/probe for lower atmospheric layers, discussing detectors and assembly qualities
04 p0601 A69-15229
- Lower atmosphere pressure field determination based on meteorological satellite observations of amount and types of clouds and upper boundary altitude
06 p0952 A69-17987
- Acoustic and electromagnetic energy propagation in lower ionosphere and atmosphere for energy pulse generation by chemical explosion
07 p1078 A69-18844
- Meteorological observation problems from satellites, considering lower atmosphere measurements and accuracies
09 p1537 A69-22690
- Cosmic ray electrons and gamma quanta at lower atmosphere recorded with balloon equipment, plotting vertical profiles of electron energy spectra
10 p1758 A69-22830
- Fluctuations in angle of arrival of laser and thermal radiation beams over near ground path
11 p1840 A69-25570
- Radiation attenuation in hazy lower atmosphere, calculating attenuation coefficients and using spherical model of haze particles and empirical formula for haze spectra
11 p1913 A69-25571
- Statistical turbulence theory applied to turbulent flow transport properties in lower atmosphere
12 p2125 A69-25894
- Turbulent boundary layer in lower atmosphere downwind of abrupt change of surface roughness, determining surface shear stress and roughness height
12 p2125 A69-26014

- Optical radar studies of lower atmosphere, giving Mie theory calculations of clear atmosphere volume backscattering cross sections for four laser wavelengths
12 p2033 A69-27001
- Molecular O 0.7620 micron absorption band in pure O and air, noting rotational lines mean half width and lower atmosphere transmission function
14 p2487 A69-28780
- Remote sensing of lower atmosphere refractive structure, using Rake tropospheric scatter channel-sounding technique
14 p2448 A69-29525
- Atmospheric circulation by energy concepts, giving quantitative analysis of interaction between upper and lower atmosphere
14 p2477 A69-29825
- Earth based microwave data revealed isothermal layer in extrapolating Venus atmosphere profile below region probed by Mariner 5 and Venera 4
16 p2852 A69-31553
- Soviet collection of papers on physics of atmospheric boundary layer covering wind profile, turbulent energy balance, etc
20 p3571 A69-37694
- Wind velocity below 100 meters from Laikhtman atmospheric boundary layer model, solving equations for horizontally homogeneous, stationary and nonadvective air flow
20 p3571 A69-37695
- Components of turbulent energy balance at 1 and 4 meter heights, discussing average motion energy transformation into turbulent energy
20 p3571 A69-37696
- Planetary boundary layer top formation, considering particle velocity, earth surface roughness role, geostrophic wind, etc
21 p3715 A69-38566
- Venus, Mars and Jupiter lower atmospheric motions, considering atmospheres thermal and chemical composition
21 p3811 A69-39511
- Lower atmospheric temperature continuous radio measurement as function of altitude, calculating temperature gradient
24 p4342 A69-42677
- Simultaneous lower atmosphere clear air turbulence analysis by multiwavelength radar, jet aircraft and special rawinsondes
24 p4342 A69-42894

LOWER IONOSPHERE
NT D REGION

- Ionosphere studies in France noting lower ionosphere dynamics, ionospheric winds, plasma electron densities, electron and ion temperature and ion-neutron collision frequency
02 p0242 A69-11903
- VLF phase measurements for apparent and equivalent diurnal height variation for lower ionosphere waveguide
05 p0752 A69-15666
- Solar cycle influence on winds in lower ionosphere
05 p0759 A69-16421
- Mars lower ionosphere ionization from spectroscopic and Mariner 4 occultation data, discussing various ionization sources
07 p1213 A69-18607
- Acoustic and electromagnetic energy propagation in lower ionosphere and atmosphere for energy pulse generation by chemical explosion
07 p1078 A69-18844
- Lower ionosphere and earth-ionosphere waveguide effects on polarization characteristics of transmitted radio whistlers
08 p1306 A69-20181
- D region electron density vertical profiles measured using partially reflected echoes from lower ionosphere
08 p1307 A69-20189
- Lower ionosphere effect on LF electromagnetic disturbances, comparing propagation and damping of clockwise and counterclockwise polarized waves
09 p1487 A69-21637
- Ionization in lower ionosphere over polar cap under solar corpuscular fluxes measured by radio wave absorption
10 p1759 A69-22838
- Electron production rates variations in lower ionosphere cosmic layer related to meteorological, geomagnetic and cosmic conditions
10 p1759 A69-22839
- Cosmic ray absorption and modulation in lower ionosphere at midlatitudes, considering 11 year variations, Forbush effects and solar radiation on electron concentration
10 p1759 A69-22840

- Low energy particle effects on midlatitude lower ionosphere conditions after July 7, 1966 proton flare, using ground based measurement
10 p1684 A69-23782
- Geomagnetic field directed hydromagnetic waves propagation in lower ionosphere, noting inhomogeneous conductivity, Hall effect and lines of forces role
10 p1687 A69-23926
- Lower ionosphere electron densities measured during solar eclipse by Nike-Apache rockets
12 p2073 A69-26861
- Nonuniform two dimensional hydromagnetic waves incident on idealized lower ionosphere, discussing validity of various models
12 p2074 A69-26960
- Neutral gas ionization in lower ionosphere, discussing physicochemical reactions, recombination coefficients, equilibrium processes, etc
13 p2255 A69-28540
- Lower ionospheric homonuclear O combinations nonequilibrium processes by simplified balance equations, determining height distributions and ozone concentration
13 p2255 A69-28542
- Ion pair annihilation average rate by single aerosol particle action in lower ionosphere noctilucent clouds
14 p2434 A69-28941
- Nighttime molecular O densities between 100-130 km determined from Schumann-Runge absorption data for successive far UV spectra of hot star
14 p2435 A69-28959
- Effective recombination coefficient in lower ionosphere determined from charged particle spectra obtained by rocket sounding in Canada
14 p2511 A69-28960
- Radio wave absorption coefficient in lower ionosphere related to total radiation absorption and electron concentration profile
14 p2411 A69-29075
- Seasonal variations of electron density profiles in lower ionosphere measured by differential absorption using partial reflections
14 p2438 A69-29109
- Polar cap absorption riometer recorded during 2-6 September 1966 event compared to satellite measurements of solar protons, discussing diurnal variations and oxygen role in associative detachment reactions
14 p2440 A69-29126
- Waveguide mode propagation theory for determining earth-ionosphere spherical waveguide upper boundary height diurnal variation for VLF waves
15 p2595 A69-30224
- Corpuscular radiation intensity during geomagnetic disturbances measured during rocket flights at 50-100 km, discussing effects on lower ionospheric radio absorption
15 p2677 A69-31327
- Fresnel irregularities calculated from radio wave partial reflection from lower ionosphere measured by rocket probes
15 p2604 A69-31420
- Lyman alpha radiation ionization rate in lower ionosphere, noting various charged particle concentration parameters
15 p2605 A69-31438
- Strong vertical wind in low ionosphere due to short period reflected gravity waves, obtaining standing wave system
15 p2606 A69-31449
- Partial reflections method of Gardner and Pawsey for determining vertical profile of electron collision frequencies in lower ionosphere and upper D layer
16 p2775 A69-32034
- Electron production rate in low ionosphere, discussing parameters of ionizing solar cosmic rays and earth environment
17 p3022 A69-33035
- Rocket-borne AM radio receiver for Faraday rotation experiments to measure lower ionosphere electron density, giving circuit diagrams
17 p2936 A69-33062
- U shaped polar auroras development, examining relation with magnetic activity and current system configuration in lower ionosphere
17 p2963 A69-33952
- High latitude geomagnetic disturbances, incoming electron fluxes and riometric absorption relationship in lower ionosphere studied by X ray bremsstrahlung with sounding balloons
17 p2964 A69-33961
- Lower ionosphere electron concentration confirmed as function of electron and ion temperature by satellite and probe data
17 p2966 A69-33981

Ionospheric absorption and virtual heights relationships for electron density distribution in lower ionosphere, computing model profiles

18 p3125 A69-34248

ELF and VLF wave propagation examined for heavy ions and lower ionospheric disturbance effects using numerical integration, noting standing wave field role for interpretation

18 p3125 A69-34254

Ion and temperature effects on lower ionosphere refractive index for VLF radio wave propagation

18 p3102 A69-34971

Physical process providing EMF for maintaining electrical structure of stratosphere and mesosphere shown to center in lower ionospheric thermally driven tidal motions

18 p3130 A69-35103

Lower ionosphere electric fields and currents vertical profiles above geomagnetic equator under quiet geomagnetic conditions from rocket data

20 p3521 A69-37053

Lower ionosphere geomagnetic field local gradients determination by partial reflection method

20 p3522 A69-37055

Inhomogeneities time buildup in lower ionosphere weakly ionized plasma during charged particle concentration perturbations and source temperature variations

20 p3525 A69-37658

Lower ionosphere radiation absorption at 4.01 MHz determined using A-3 method in measuring radio wave field between radio transmitters

20 p3528 A69-37675

Lower ionospheric effective electron collision number from cosmic noise recordings and radio wave absorption data obtained by vertical sounding rocket

20 p3528 A69-37679

Corpuscular radiation indicated as ionization source in lower ionosphere from rocket sounding data, noting role in D region formation

21 p3787 A69-38352

Lower ionosphere over geomagnetic equator during evening twilight characterized by solar disturbances, using rocket-borne Langmuir and plasma noise probes

21 p3702 A69-38353

Turbulent field structure between 90-120 km estimated from sodium clouds diameters variation ejected from rockets

21 p3713 A69-38524

Sharply bounded homogeneous ionospheric model to solve modal equation, discussing lower ionospheric conductivity from VLF transmission sudden enhancements of strength /SES/

21 p3714 A69-38554

Ionosphere drift measurements in LF range, noting relationship between correlation and similar-fade analyses for velocity data

21 p3714 A69-38557

Nighttime atmospherics shape analysis created by lightning and propagating in earth lower ionosphere waveguide

22 p3941 A69-40961

Solar L alpha and X ray emission contribution to lower ionosphere ion production, discussing altitudinal, latitudinal and temporal variations

22 p4008 A69-41096

Lower ionosphere vertical wind velocity profiles determined from rocket-released grenade glow cloud photographs, developing cloud buoyancy effect empirical model

23 p4154 A69-41305

WE and SN wind components models from 60 to 130 km for different months and latitudes, discussing meridional and interhemispheric circulations

23 p4154 A69-41306

Thermotidal energy transfer from lower neutral atmosphere to and above lower ionosphere, considering tidal wave transmission mechanism

23 p4155 A69-41561

Earth sphericity and earth-ionosphere waveguide effects on terrestrial atmospherics, deriving form by computer

23 p4157 A69-41860

Ionospheric electron content and distribution at low altitudes from satellite S 66 data, describing seasonal variations of equatorial anomaly peak

24 p4367 A69-43010

Lower ionosphere atmospheric density, temperature and pressure profiles diurnal variations from data of radio meteor echoes

24 p4311 A69-43504

LOX [OXYGEN]

U LIQUID OXYGEN

LOX-HYDROGEN ENGINES

U HYDROGEN OXYGEN ENGINES

LRC CIRCUITS

U RLC CIRCUITS

LRV [VEHICLE]

U LUNAR ROVING VEHICLES

LSI

U LARGE SCALE INTEGRATION

LUBRICANT TESTS

Sulfide addition agents for diester lubricating grease and organic resin solid film lubricants, noting formulation and tests for steel and molybdenum

01 p0102 A69-10907

Low speed four-ball lubricating oil testing machine eliminating thermal effects associated with frictional heating for load carrying capacities of thin lubricant films

07 p1140 A69-18968

Bearing deposition test for evaluating degradation characteristics of aircraft gas turbine engine lubricants

10 p1700 A69-24070

Dry lubricant films of soft metals, self lubricating plastics and crystalline powders, noting design and tests

15 p2642 A69-30328

Test methods for lubricants vapor pressure and flash point determination

[ASLE PAPER 68-LC-23] 15 p2642 A69-30607

Lubrication properties of mineral oils for power hydraulics using Stanhope-Shell four ball test machine

17 p2991 A69-32948

Steel ball bearing high temperature fatigue life tested with synthetic paraffinic oil, fluorocarbon and polyphenyl ether

[ASME PAPER 69-LUBS-18] 18 p3140 A69-34378

Oxygen concentration effects on oxidation of synthetic paraffinic and type II ester lubricants determined from ball bearing tests at 400 and 450 degrees F

18 p3149 A69-35177

Aircraft gas turbine engine lubricant evaluation and systems design from standpoint of effective oil life and lubricant stability requirements

[SAE PAPER 690424] 23 p4200 A69-41648

LUBRICANTS

NT GAS LUBRICANTS

NT HIGH TEMPERATURE LUBRICANTS

NT LUBRICATING OILS

NT SOLID LUBRICANTS

Friction and wear behavior of mechanical face seals, considering techniques and lubricants for increasing product of pressure and sliding velocity

02 p0253 A69-12160

Idealized slider bearings with Maxwell liquid as lubricant, analyzing elasticity effects on pressure, load capacity and friction

02 p0253 A69-12413

Sodium nitrite and sodium stearate as grease additives for lubrication of ball bearings running in helium

[IME PAPER 1] 07 p1137 A69-18559

Bearing lubrication at low temperature, examining safety limits, working fluid in liquid or gaseous state

[IME PAPER 9] 07 p1138 A69-18565

Liquid and vapor phase microscale panel cokers applied to screening synthetic lubricants for aircraft turbine engines

[ASLE PAPER 68-LC-22] 07 p1140 A69-19309

Pressure properties of fluorides and silicofluorides as cutting and grinding lubricants for titanium

[ASLE PAPER 68-LC-20] 07 p1141 A69-19311

Angular inertia of lubricant in MHD hydrostatic thrust bearings, obtaining critical angular speed of rotor

09 p1503 A69-21443

Load support and leakage from microasperity lubricated face seals, developing hydrodynamic lubricant films

[ASLE FICFS PREPRINT 21] 15 p2622 A69-30500

Test methods for lubricants vapor pressure and flash point determination

[ASLE PAPER 68-LC-23] 15 p2642 A69-30607

Synthetic lubricants characteristics and aircraft applications, describing common products and properties

18 p3163 A69-35481

Wear resistance of briquetted lubricants from fluoroplast and molybdenum disulfide under pressure

21 p3733 A69-39805

LUBRICATING OILS

Erosion damage of bearing alloy lining in thin lubricating oil film, considering Cu-Pb alloy and tin base white metal

01 p0094 A69-10313

Mechanical properties of free rolling contact surfaces subject to high loads, discussing effect of oil film separation and fatigue crack initiation

02 p0339 A69-11989

Thin film lubricant effect on machine dynamic performance, proposing inclusion with machine structure for reducing vibration effect

03 p0435 A69-13948

Quantitative amounts of contaminants oil from piston engine and life of oil lubricant in engine

04 p0604 A69-14500

Oil lubricant vapors under frictional working conditions in vacuum analyzed by mass spectrometer and gas-liquid chromatography concerning molecular weight and composition

[IME PAPER 11] 07 p1137 A69-18558

Analytic solution for whirl in finite journal bearing with continuous lubricating film using Fedor approach [ASME PAPER 69-VIBR-55]

10 p1700 A69-24147

Spectrometric oil analysis procedure /SOAP/ for predicting failure of oil wetted parts in small turboprop aircraft engines

[SAE PAPER 690325] 11 p1941 A69-24508

Load capacity, stiffness and flow requirement of capillary and orifice compensated oil lubricated externally pressurized rectangular thrust bearings

12 p2102 A69-26239

Physicochemical and operational properties of trimethylol propane esters as lubricating oils under static and dynamic conditions

12 p2103 A69-27090

Life margin tests of oil lubricated oscillating caged needle roller bearings under service conditions duplicating helicopter rotor hinge pin locations

[ASLE PAPER 68-LC-7] 15 p2622 A69-30609

Jet engine intershaft bearing oil feed design, discussing use of nonrotating feed link and improvement of oil scavenging at high altitudes

15 p2671 A69-30702

Hydrodynamic conical and spherical spiral grooved grease bearings replacement of gyro ball bearings for extended space missions

[AIAA PAPER 69-836] 21 p3732 A69-39367

Engine oil analysis applied to commercial airline operations, ensuring lubricating qualities retention and detecting oil-wetted component failures

[SAE PAPER 690423] 23 p4169 A69-41647

Aircraft gas turbine engine lubricant evaluation and systems design from standpoint of effective oil life and lubricant stability requirements

[SAE PAPER 690424] 23 p4200 A69-41648

Oil high temperature and oxidation conditions in aircraft piston engines, including physicochemical changes

24 p4321 A69-43141

LUBRICATION

NT BOUNDARY LUBRICATION

NT SELF LUBRICATION

NT SPACECRAFT LUBRICATION

Ball bearings lubrication and wear in cryogenic hydrogen turbopumps by transfer films provided from self lubricating cage

01 p0084 A69-10109

Radial face seals lubricating mechanism noting surface waviness effect on film thickness fluctuations

01 p0087 A69-10910

Jet fuel lubricity evaluation by ball-on-cylinder device

[ASLE PREPRINT 68AM 4A-2] 01 p0083 A69-10914

Elastohydrodynamic lubrication, discussing film thickness and dependence on fluid hydrodynamics and contact zone deformation

01 p0088 A69-11324

Rayleigh step journal bearings, considering pressure distribution, load capacity and attitude angle and optimal film thickness ratio for incompressible fluid lubrication

04 p0605 A69-14587

Dynamic and interfacial fluid effects in mechanical face seals, discussing hydrodynamic pressure generation

04 p0606 A69-14798

Transverse magnetic field effect on three dimensional nonisothermal lubrication layer of conducting gas at small magnetic Reynolds number

04 p0607 A69-14990

Miniature ball and jewel bearings and gear lubrication in ultrahigh vacuum tests for space environment operation

[IME PAPER 6] 07 p1138 A69-18562

Rotors linear vibrations due to unbalanced shaft rotating on lubricated bearings taking into account lubricant damping

07 p1235 A69-19441

Lubrication and operation of Hamilton Standard propellers in high altitude and low temperature environments

[SAE PAPER 690323] 11 p1822 A69-24515

- Elastohydrodynamic lubrication of square section high pressure face seals mounted on rigid housings, considering design charts for load and leakage [ASLE FICFS PREPRINT 16] 15 p2621 A69-30493
- Lubrication - Conference, Atlantic City, October 1968 15 p2622 A69-30604
- Lubrication and lubrication systems literature including compressible and incompressible fluid films, automotive, bearing, gear, friction, wear and boundary lubrication, seals and sealing systems 15 p2628 A69-30900
- Contact conformity effects on spinning torque and friction coefficient in angular contact ball bearings from lubricated and unlubricated tests [ASME PAPER 68-LUB-10] 15 p2628 A69-30901
- Elastohydrodynamic lubrication film thickness in finite elliptical contact determined by two dimensional Reynolds equation in inlet region, using finite difference approximation [ASME PAPER 69-LUBS-17] 18 p3120 A69-34379
- Ball bearing lubrication simulation by rolling disk apparatus, emphasizing surface slip and related thermal effects alterable by geometric expansion [ASME PAPER 69-LUBS-16] 18 p3140 A69-34380
- Elastohydrodynamic solution for ball torque spinning without rolling in nonconforming groove, showing increase in torque with stress and spinning and decreasing conformity [ASME PAPER 69-LUBS-11] 18 p3140 A69-34381
- Elastohydrodynamic theory of spherical bodies in normal approach contact, discussing lubrication and elasticity equations [ASME PAPER 69-LUBS-3] 18 p3213 A69-34384
- Finite element method application to minimum principle for incompressible lubrication problem, noting flow boundary conditions and squeeze film effects 22 p3955 A69-40406
- Pressure distribution in gas lubrication layer of infinite radial sliding bearings, approximating differential equation by simple formulas 23 p4168 A69-41412
- High speed radially resistant ball bearing, analyzing effect of lubrication film on axial rigidity 23 p4169 A69-41555
- Elastohydrodynamic lubrication of cylindrical rubber surface sliding over glass plate, using optical interference technique 23 p4171 A69-42531
- LUBRICATION SYSTEMS**
- Space lubrication system for Orbiting Solar Observatory program, discussing theoretical high vacuum principles and flight performance and environmental test data 02 p0252 A69-11766
- Optimum geometrical design of multipad externally pressurized journal bearings 07 p1141 A69-19439
- Lubrication systems for high speed machinery, discussing wet and dry sump arrangements, gearbox heat rejection, oil flow requirements, X-22A aircraft, etc [ASME PAPER 69-DE-65] 14 p2454 A69-28845
- Face seals for jet engine mainshaft bearing compartments, emphasizing oil film and gas film seals [ASLE FICFS PREPRINT 28] 15 p2620 A69-30487
- Lubrication and lubrication systems literature including compressible and incompressible fluid films, automotive, bearing, gear, friction, wear and boundary lubrication, seals and sealing systems 15 p2628 A69-30900
- Electromagnetic field pumping effects in electrically conductive gas lubricants, producing gas film between surfaces without external pressurization 15 p2629 A69-31003
- Aircraft engine lubrication system design, discussing bearings reduction, oil compartment scavenging, scaling, cooling, pressurization, etc 18 p3185 A69-35244
- Aircraft engine lubrication system design, discussing bearings reduction, oil compartment scavenging, scaling, cooling, pressurization, etc 24 p4363 A69-42780
- Total load factor static vertical component and lubricant flow rate square related to pocketed hydrostatic journal bearing revolutions 24 p4321 A69-43091
- LUCITE [TRADEMARK]**
U POLYMETHYL METHACRYLATE

- LUDER BANDS**
U PLASTIC DEFORMATION
U YIELD POINT
- LUMENS**
Coronary vessel lumen changes under oligemic hypotension resulting from circulating blood volume decrease in anesthetized cats, discussing constrictory coronary vessel responses 23 p4084 A69-41470
- LUMINAIRES**
U ARC LAMPS
U FLASH LAMPS
U MERCURY LAMPS
U QUARTZ LAMPS
U RUNWAY LIGHTS
U XENON LAMPS
- LUMINANCE**
Surface recombination rate effect on lux-ampere characteristic of photomagnetic effect in CdS single crystals of low and high photosensitivity 05 p0809 A69-16377
- High altitude observations of luminous wake behind Black Brant 2 rockets by mounted dual wavelength spatially scanning photometer 06 p0918 A69-17511
- Foveal luminances for chromatic and absolute thresholds for hue identification in case of small targets 07 p1183 A69-19649
- Ablating sphere viscous wake using image converter camera, computing luminance radial distribution by unit volume 19 p3306 A69-35739
- Luminance additivity for human visual system in terms of photometric methods based on direct brightness matching, incremental threshold, etc 22 p3880 A69-40849
- Luminance threshold for compound stimulus detection measured as function of two components relative luminance 22 p3880 A69-40852
- Human peripheral retina contrast sensitivity determined by measuring psychophysically for sinusoidal grating target describing luminance effects 22 p3882 A69-40870
- Comparative study of differential luminance threshold and spatial summation exponent for solid and annular objects with equal surfaces 22 p3883 A69-40877
- Retinal mechanisms determining visual band movement thresholds obtained by manipulation of retinal locus, luminance, arc length and spectral distribution of moving stimulus 22 p3883 A69-40879
- Blue cone mechanism contribution to mesopic function in producing Purkinje shift with luminance decrease, measuring sensitivity by flicker technique 22 p3883 A69-40880
- Radiation scattering by thick planetary atmosphere according to Rayleigh law, considering luminance variation and absorption ray polarization 23 p4213 A69-41698
- LUMINESCENCE**
NT BIOLUMINESCENCE
NT CHEMILUMINESCENCE
NT ELECTROLUMINESCENCE
NT FLUORESCENCE
NT LUNAR LUMINESCENCE
NT OPTICAL RESONANCE
NT PHOSPHORESCENCE
NT PHOTOLUMINESCENCE
NT SHOCK WAVE LUMINESCENCE
NT THERMOLUMINESCENCE
NT X RAY FLUORESCENCE
- Surface charge distribution in silicon p-n junctions noting luminescence of microplasmas and inhomogeneous properties 02 p0294 A69-11629
- Ionized metals emission lines intensity in chromosphere observed with coronagraph, determining hydrogen concentration 02 p0314 A69-11635
- Coronagraphic determination of hydrogen concentration in luminescence regions of ionized metals in lower chromosphere 03 p0420 A69-13086
- Gallium phosphide luminescence near indirect transition during multiphoton excitation by Q switched ruby and Nd laser beams 03 p0489 A69-13892
- Luminescence spectra due to radiative recombination of optically injected carriers in Co 60 gamma ray and neutron irradiated Si at low temperature 03 p0494 A69-14243

- Moment method used to determine pulsed radiation instability propagating in luminescent scattering medium 04 p0610 A69-14425
- Recombination radiation of tellurium and zinc doped GaAs alloy type diodes, discussing luminescence spectra, current-voltage characteristics and temperature effects 05 p0729 A69-16210
- Metastable level population measurement in laser crystal based on luminescence changes under influence of stimulated emission 06 p0934 A69-17457
- Quantum mechanical perturbation treatment of optical parametric luminescence in nonlinear lithium niobate crystals, noting applications to nonlinear phase matching problems [IEEE PAPER K-8] 07 p1152 A69-19067
- Absorption and emission spectra of ruthenium 2 complexes dissolved in rigid glasses, discussing crystal field theory and luminescence 07 p1200 A69-19219
- Spectral distribution and energy of luminous radiation emitted during theta pinch in Ar plasma, noting energy maximum as function of pressure 08 p1362 A69-20280
- Luminescence spectra of molecular gases excited by fast electrons in infrared spectral region, noting H alpha line 09 p1590 A69-21382
- Hydroxyl luminescence spectrographic observations at twilight in vibrational-rotational band from 10600 to 11200 Å 10 p1681 A69-22847
- Luminescence quantum yield in neodymium glass, noting independence to stimulating light frequency 10 p1702 A69-23211
- Nitrogen, oxygen and air luminescence spectra excited by fast electrons at low gas pressures in IR spectral region compared with polar auroral spectra 10 p1687 A69-23916
- Gallium phosphide luminescence near indirect transition during multiphoton excitation by Q switched ruby and Nd laser beams 11 p1939 A69-25693
- Ga phosphide p-n junctions formation from GaP-Ga solution, discussing electrical and luminescence properties 13 p2323 A69-28642
- Coronagraphic determination of hydrogen concentration in luminescence regions of ionized metals in lower chromosphere 14 p2433 A69-28768
- Effects of cold electron and light emission centers from dispersed Au films in electric field, as universal qualities characterizing dispersed metal films 14 p2504 A69-28992
- Energy exchange of rare earth ions in uranyl phosphate liquids and glasses, studying sensitized luminescence origin 14 p2485 A69-29034
- Energy exchange between active centers in silicate and phosphate glass, comparing luminescent and lasing properties 15 p2632 A69-30053
- Slowly varying component of solar radio emission, evaluating resolution of radio telescopes in sunspot studies and localized areas luminescence 15 p2674 A69-30503
- Two photon absorption excitation of luminescence in ruby crystals by neodymium laser radiation, determining luminous intensity dependence on pumping intensity 15 p2634 A69-30731
- Radiative luminescence of gas discharge plasmas in channel with substantial radial heat transfer determined from energy balance measurement 15 p2662 A69-30978
- Luminescence spectra of aromatic polymers, monomers and dimers under high energy electron excitation using molecular resonance model 16 p2828 A69-32792
- Luminescence spectra of molecular gases excited by fast electrons in IR spectral region, noting H alpha line 18 p3176 A69-34770
- ZnS-CdS crystals luminescence during varied forbidden bandwidth, discussing two photon and ruby laser excitation and temperature dependence 19 p3331 A69-35866
- Two photon excitation of luminescence in complex uranyl compound single crystals using Q switched ruby laser 19 p3334 A69-35982

- Tau-luminescence in thin gamma-colored and uncolored ruby crystals containing Cr ions measured, discussing ions absorption spectrum changes
19 p3335 A69-36166
- Photocurrents and recombination luminescence in n-type diamonds subjected to UV, Ti 204 and X ray irradiation indicating local electron centers formation
19 p3383 A69-36167
- Luminescence effects on apparent size and shape of focally fixated targets of various forms
19 p3259 A69-36458
- Active center chemical bond alteration influences on luminescence characteristics of phosphate glasses, noting quick energy transfer via ions
20 p3552 A69-37017
- Resonant parametric oscillator stable and random phases, considering smooth frequency tuning and two quantum luminescence laser construction
20 p3554 A69-37723
- Recombination radiation of tellurium and zinc doped GaAs alloy type diodes, discussing luminescence spectra, current-voltage characteristics and temperature effects
20 p3506 A69-37783
- Metastable level population measurement in laser crystal based on luminescence changes under influence of stimulated emission
20 p3555 A69-37940
- Transparency and luminescence yield of plastic scintillators prepared from polymethyl methacrylate, comparing naphthalene and benzene compound additions with polystyrene
21 p3724 A69-39073
- LUMINESCENT INTENSITY**
U LUMINOUS INTENSITY
- LUMINOSITY**
NT STELLAR LUMINOSITY
- Mechanism responsible for luminosity of long duration meteor trains, discussing color changes, band emission and train spectra as function of height and duration
01 p0154 A69-10874
- Shock waves luminescence temperature dependence measured by UV and visible radiation, noting dependence on front glow duration
03 p0415 A69-13411
- Conversion of emission from pulse tube using neodymium laser with luminophor solution filled active element, discussing pumping nonlinear absorption kinetics
05 p0777 A69-16373
- Coherent radiation brightness increased from liquid N Raman laser, using off-axial pumping
09 p1520 A69-22533
- Pulsating and flaming auroral patches recorded by image intensifier vidicon camera, calculating upward field aligned speeds for luminosity enhancement
16 p2780 A69-32305
- Laser ignited Zr droplet free fall combustion in oxygen, analyzing metal conservation and luminosity correlation assuming reflux action from fog layer [WSCIPAPER 69-1]
16 p2830 A69-32342
- Luminous tenuous collimated electron beam from plume of MPD arc in fiberglass vacuum tank, examining beam trajectory in geomagnetic fields
20 p3582 A69-38236
- Upper atmosphere particles, luminosity and electron concentration measurements documented in input, storage and energy radiation classes, determining recombination coefficients
21 p3707 A69-38491
- LUMINOUS INTENSITY**
NT ILLUMINANCE
NT LUMINANCE
- Kerr effect apparatus for measurements of pure liquids and solutions involving comparison of two luminous fluxes with aid of photomultiplier
01 p0078 A69-10039
- LF radiation intensity oscillations of pulsed HF discharge in helium plasma, showing time dependence
01 p0128 A69-10347
- Intense laser emission interaction with current carriers in semiconductors, analyzing dependence of thermoelectric field produced by light absorption on intensity, frequency and temperature
01 p0139 A69-10895
- Thermoluminescence intensity of dolomite specimens from Kaali meteorite craters, discussing meteorite impact thermomechanical effect and crystal lattice defects
01 p0159 A69-11371
- Mean annual intensity distribution of 5303 angstrom coronal line on solar limb determined for 11-year solar activity cycle
03 p0506 A69-13084
- Particle size distribution determination by measuring light beam extinction in turbid medium with photometer
03 p0428 A69-13110
- Intensity of visible and UV light from beam of positive deuterium molecular ions excited by passage through thin C foil
03 p0471 A69-13166
- Zodiacal light isophotes and near-earth component from relationship between brightness at various geomagnetic latitudes and position of moon
03 p0512 A69-13693
- Q switches transparency as function of incident light intensity
04 p0610 A69-14385
- Optical generation in organic luminophor solutions in 400-650 nm range
04 p0612 A69-15374
- Aircraft instrument panel lighting color and intensity preference by pilots for taxiing, takeoff, cruising flight and landing
05 p0715 A69-16622
- Flare star AD Leo observations by continuous photoelectric monitoring, noting light curves properties
06 p1008 A69-17697
- Laser applications to situations requiring highly bunched high power density light beams
06 p0938 A69-18012
- Photographic investigation of gegenschein and cloud satellites at L sub 5 earth-moon libration point, noting gegenschein intensity peak
07 p1212 A69-18602
- Nightglow intensities correlated with atmospheric ozone concentration and stratospheric temperatures
07 p1123 A69-18675
- Solar eclipse variations of E layer critical frequency explained by quasi-equilibrium between electron density and ionizing soft X ray radiation
07 p1204 A69-18823
- Laboratory measurement data of low light level TV performance converted to anticipated real world performance data
07 p1132 A69-18948
- Minimal angle of resolution /MAR/ between point and extended circular source and between point source and simulated horizon, studying irradiation effects on manual navigation
07 p1177 A69-19208
- Luminosity distance, distance by apparent size, number counts, background radiation and apparent angular motion of sources in homogeneous anisotropic model universe
07 p1218 A69-19282
- Simultaneous photographic and radar observations of meteors, determining absolute stellar magnitude of meteor as function of parameters
08 p1390 A69-20337
- Natural intensity fluctuations spectrum of He-Nc laser, determining modulation coefficient dependence on output
08 p1325 A69-20431
- Light intensity dispersion logarithm calculated along axis of laser beam propagating in atmosphere
08 p1351 A69-20437
- Picosecond light pulse generation by solid state laser interpreted by fluctuating intensity spikes arising from random emission interference in out-of-phase modes
08 p1326 A69-20548
- Kine films of gas flows within highly luminous transient arc taken by laser schlieren technique
08 p1316 A69-20615
- Solar phenomena correlation with brightness variations of comet Alcock 1963b, noting sunspot maximum followed by maximum in absolute magnitude of comet
08 p1394 A69-20620
- Strong light flashes from pulsar NP 0532 in Crab Nebula, noting UVB photometric analysis of nebular brightness
08 p1394 A69-20623
- Luminous discharge at nonabsorbing surface when exposed to single pulse ruby laser beam, suggesting photoionization in surface layer
08 p1327 A69-21021
- Whipple and Douglas-Hamilton systematic corrections for periodic comets, considering constant coma brightness of P/Tempel 2 since 1874-1904 observations
08 p1408 A69-21137
- Differential brightness of night airglow spectrum, obtaining rotational temperature by comparison with synthetic spectra
09 p1488 A69-21656
- Bright celestial IR sources in Ursa Major detected in spectral region by rocket-borne telescope, discussing luminosities of quasi-stellar sources
09 p1603 A69-22230
- Gamma ray luminosity of typical type I supernovae remnant computed by assuming Ni 56 radioactive decay energy origin of optical luminosity
09 p1581 A69-22409
- Bolometric luminosity-red shift relations of Friedmann dust universes corrected for inhomogeneities, using locally inhomogeneous Swiss cheese models
09 p1605 A69-22411
- Liquid laser gain measurement via luminescence intensity, noting optical pumping thermal effect
09 p1520 A69-22683
- Radiometric observations of Venus brightness temperature variation used to determine phase effect at 8.6 mm wavelength
10 p1773 A69-22959
- Maximum indicative absolute magnitudes of 33 supernovae, discussing usefulness as distance indicators
10 p1774 A69-22967
- Magnetograph in Italian observatory for weak solar magnetic field longitudinal components avoiding differential amplifier by electronic compensation
10 p1693 A69-23311
- Dark adaptation mechanisms studied from light intensity recovery after experimental flash, using electroretinography methods
10 p1647 A69-23588
- Intensity interferometry by two photon excitation of fluorescence trace for three mode laser under phase locking, free running and FM-like conditions
10 p1705 A69-23811
- Moving striations in plasmas, presenting measurements of relative phases of electron temperature, plasma potential and luminous intensity near Pupp current limit
10 p1741 A69-23859
- Radar and photographic studies of meteors from Leonid and Perseid showers, presenting velocities, luminescence and ionization
10 p1783 A69-23895
- Light flux intensity fluctuation dispersion and averaging effect for passage through circular receiving aperture
10 p1658 A69-23950
- Scattered light mean intensity determination in twilight aerosol atmosphere from satellite observations, formulating boundary value problem
10 p1689 A69-23970
- Center to limb variations of sunspot-photosphere brightness ratio, considering umbra darkening and radiative equilibrium
11 p1946 A69-24426
- Photoelectric measurements of nightglow intensities during sunspot minima by zenith photometer, considering background continuum
11 p1877 A69-24584
- Transistorized electrophotometer for polarimetric and photometric analysis of weak light fluxes, noting pulse amplifying and shaping circuits
11 p1884 A69-24735
- Tilting filter photometer for faint light source spectrophotometry, discussing digital approach used with photomultipliers
11 p1884 A69-24834
- Model for radiative transfer in atmosphere-ocean system by Monte Carlo method, considering Rayleigh and Mie scattering
11 p1877 A69-24851
- Evolutionary stages of visual binary components based on magnitudes and color indices
11 p1962 A69-25111
- Pulsars and ancient chinese records of supernova explosions, relating luminous intensities, radio sources and evolution
11 p1963 A69-25253
- Radioactive light sources in photoelectric photometry, analyzing characteristics, brightness and stability of light flux and energy spectrum
11 p1951 A69-25421
- Photoelectric polarimeter to record sky light intensity in form of polarized components, detailing construction and operation
12 p2078 A69-25892
- Nightglow intensity variations at sunspot minimum from measurements in South West Africa, considering relationship to ionospheric vertical movements and density variations
12 p2066 A69-26133
- Standard phenomenological laser rate equations for population inversion and light intensity generalized by

considering intensity dependent losses and Einstein coefficients

12 p2110 A69-27014

Spiral galaxy nuclei, relating nuclei luminosity to galactic luminosity

12 p2165 A69-27028

Photographic magnitudes of galactic nuclei, presenting plots for stellar magnitude distribution of galactic nuclei

12 p2165 A69-27029

Radio galaxy identification and luminosity measurement, noting limitations of red shift observation methods

12 p2165 A69-27032

Absolute radio luminosity relation to surface brightness of extragalactic radio sources, finding volume radiation coefficient of spiral and radio galaxies

12 p2166 A69-27035

Luminosity changes in quasar 3C 273, describing corrections introduced into luminosity curve obtained by iris photometer

12 p2167 A69-27044

Quasar properties from cosmological nature, discussing red shift, luminosity, radiation intensity, absorption features, distribution, chemical composition, etc

12 p2168 A69-27049

Galaxies NGC 4402 and NGC 4438 structure, luminosity and color from two color photometric study of Virgo cluster center

12 p2169 A69-27058

Photoelectric observation of RR Lyrae stars in globular clusters to estimate reddening near galactic poles, considering color indices

12 p2172 A69-27157

Recently discovered comets including Comet Thomas, discussing magnitudes and perihelions

12 p2172 A69-27161

Light curve shape as function of color, changing period and polarization angle of Crab Nebula optical pulsar

12 p2172 A69-27170

Optical identification of radio source 3C 230, suggesting removal from quasar list

12 p2173 A69-27171

Star twinkling absence for lunar observation laboratory, noting star distance measurement and laser action in stellar atmospheres

12 p2173 A69-27172

Relative intensities of selected Si two multiplets calculated and compared with solar spectrum and plasma source ZETA values

13 p2326 A69-27551

Galactic H II regions of high surface brightness in radio continuum surveyed at 1.95 cm wavelength with high resolution and positional accuracy

13 p2339 A69-27568

Optical wavelength backscattering functions for nebulae in Pleiades cluster, noting color differences and surface brightness

13 p2340 A69-27577

Auroral luminosity determination by two photometers from ESO 1 satellite

13 p2253 A69-27752

Photometric data and law of rotation in symmetry plane for constructing mathematical model of mass and luminosity distribution in M 31

13 p2351 A69-27870

Q switches transparency as function of incident light intensity

14 p2456 A69-28758

Mean annual intensity distribution of 5303 A coronal line on solar limb determined for 11-year solar activity cycle

14 p2515 A69-28766

Photoelectric observations of NGC 1275, noting increase in nucleus brightness

14 p2517 A69-29086

Emission line fluxes of southern planetary nebulae in Magellanic Clouds and Galaxy measured photoelectrically, giving upper limit to H beta emission of Magellanic planetary

14 p2520 A69-29376

Ruby laser reflected and transmitted light intensity following radiation focusing on cuvette containing cyclohexane, noting dependence on incident pulse power

14 p2459 A69-29392

Photoelectric observation of passage of stars through meridian, detailing error sources and corrective technique

14 p2521 A69-29507

Luminescent material density distribution in comet Arend-Roland 1956h head determined from observed brightness variation with distance

14 p2524 A69-29711

Plasma electron temperature determination by line intensity ratio of beryllium-like ions, noting excitation functions

14 p2496 A69-29789

Light emission intensity correlation functions associated with LF oscillations in beam plasma discharge

14 p2498 A69-29814

Amplitude and scale of microscopic fluctuations of electron density within M8 from brightness ratios of O II lines, using multiple shell model

14 p2514 A69-29949

IQSY night airglow photometric observations, summarizing zenith intensity and north/south intensity ratio data

15 p2594 A69-30019

Measured atmospheric refraction of bright astronomical objects less than calculated data for large zenith distances

15 p2679 A69-30161

Secular decline in absolute brightness of comet Encke from photometric curves obtained during past and present century

15 p2684 A69-30518

Surface brightness distribution in comet Arend-Roland tail from diffusion model and photometric investigation of photographs obtained by 40-cm astrograph

15 p2684 A69-30519

Seyfert galaxy NGC 4151 electrophotometric investigation in UVB, confirming nucleus optical variability observed in visible and IR

15 p2686 A69-30536

Radial brightness and color variation curves for Seyfert galaxies plotted from measurements with concentric diaphragm in UVB

15 p2686 A69-30537

Crab Nebula lunar occultation observed by Cassegrain array of deep space communication facility, finding radio brightness distribution similar to optical

15 p2687 A69-30539

Planet Mars stellar magnitude found dependent on processes occurring in atmosphere and at surface

15 p2689 A69-30566

Cometary tails maximum lengths compared with orbit parameters and absolute magnitudes, proposing classification scheme

15 p2689 A69-30566

Earth reflected solar radiation spatial, angular and spectral distributions measured by telephotometers onboard Cosmos 149

15 p2596 A69-30650

Rotation curve, mass and M/L ratio of Sc galaxy NGC 6574, discussing nucleus and systemic velocity

15 p2691 A69-30764

Scintillation magnitude related to range and turbulence strength in near earth optical propagation, using pulsed and helium-neon laser

15 p2570 A69-31030

Light intensity during coherent scattering based on complex refraction index of medium, noting scattering by clouds and diffraction by semitransparent hole

15 p2635 A69-31108

Spectrum of clipped noise in optical spectroscopy, considering double clipping at zero photon number

15 p2571 A69-31486

Optical generation in organic luminophor solutions in 400-650 nm range

16 p2797 A69-32121

Sudden enhancement of atmospheric recorded during IGY, noting time lag between flare and SEA maximum

16 p2778 A69-32192

Spectroscopic observations of HD 4174 star by superimposition of emission and M1-I absorption spectra, revealing intensity and radial velocity variations

16 p2858 A69-32214

Four color photoelectric photometry of bright galaxies in Virgo Cluster, analyzing properties in nuclear regions

16 p2860 A69-32230

Transition probability for 5577 A auroral green line determined from measuring number density of O atoms in oxygen-helium discharge and emitted line intensity

16 p2781 A69-32319

Increase or decrease in light absorption by plasma particles found dependent on laser intensity level

16 p2797 A69-32382

High intensity light adaptation effects on visibility of raster scan, TV type and avionic displays for symbol luminance needs

16 p2746 A69-32788

Time variation of optical intensity of Sco X-1 X ray source, evaluating photometric data by power spectral analysis

16 p2852 A69-32805

Line width and intensity correlation of laser radiation noting damping constant

17 p2980 A69-33012

Holography of intensities, discussing recording of self luminous body by modulation of scattered radiation using optical Q switch

17 p2973 A69-33113

Lunar surface brightness temperatures from IR observations, determining thermal emission directional characteristics to infer surface temperatures from Surveyor data

[AIAA PAPER 69-593]

17 p3033 A69-33302

Br molecular dissociation rate in argon excess determined, considering visible emission intensity behind shock front

18 p3176 A69-34465

Eyewitness data concerning bright bolide observed over Dzhaus /Uzbek SSR/, tabulating estimations for occurrence time, light duration, color, sound and trajectory azimuths

18 p3196 A69-34536

Intensity changes in visible sidelight emission from carbon dioxide laser switched on and off, calculating vibrational temperatures

18 p3153 A69-35243

Emission line spectrum for ionization and excitation in solar coronal structures, tabulating intensities from ground based eclipses observations

19 p3422 A69-36217

Intensity ratios effect of forbidden Fe and Ca transitions in solar corona on Fe/Ca ratio, noting cascading configurations

19 p3422 A69-36219

Collisional excitation of forbidden lines in planetary nebulae from 5537/5517 intensity ratio measurements, noting density and intensity relationship

19 p3422 A69-36221

Intensity variations of Eta Carinae emission lines

19 p3423 A69-36231

Spiral galaxy linear diameter relation to luminosity applied to Virgo galactic clusters, noting effect on distance modulus and Hubble constant

19 p3427 A69-36652

He-Ne laser output intensity saturations in presence of axial magnetic field, noting moving and fixed minima

20 p3553 A69-37433

Spectroscopic and photographic observations of compact galaxies, discussing distances, absolute magnitudes, linear dimensions, Hubble diagram position and correlations with objects showing similar characteristics

20 p3600 A69-37483

Lunar brightness variations during eclipse on 13 April 1968 measured photoelectrically, suggesting nonuniform diurnal distribution of atmospheric scatterers for observed asymmetry

20 p3601 A69-37510

Dynamic cathode ray tube spot size measurement by two slit technique, noting relationship to beam current and luminance

21 p3719 A69-38329

Rocket observation of ionospheric electron and positive ion densities and dayglow emission intensities in twilight conditions

21 p3702 A69-38355

Rocket photometer observations of midnight atomic oxygen glow at 6300 A during ascending and descending flights

21 p3703 A69-38360

Spectrum, latitude dependence and diurnal variation of night airglow emission, noting space and time correlation and magnetic activity relationship to luminous intensity

21 p3711 A69-38514

Luminous efficiency for electron induced molecular nitrogen bands, discussing thick- and thin-target measurements of fluorescent efficiencies

21 p3774 A69-38521

Optical observations of pulsar NP 0532, comparing light curves in IR and UV, noting polarization

21 p3799 A69-38645

Emission band intensities of carbonyl fluoride in 2.0-6.0 micron region with scanning spectrometer, comparing results for room and shock temperature with theoretical data

21 p3669 A69-38759

Arend-Roland comet head luminescence intensity, considering radiation scattering by dust component

21 p3804 A69-39080

Rotation effect of secondary principal axes in scattered light photoelasticity by dual observation method, deriving light intensity
21 p3844 A69-39317

Light sources with uniform variable luminance field designed for calibrating cameras used in space exploration
21 p3726 A69-39580

Scattered light mean intensity determination in twilight aerosol atmosphere from satellite observations, formulating boundary value problem
21 p3717 A69-39656

Mode locked laser output intensity, studying effect of random phase variations on pulses
21 p3741 A69-39684

Quantitative analysis of light intensity dependent changes in optical rotation angle of isotropic media caused by laser beam
22 p3959 A69-40017

Low light level TV systems for military uses, describing design and operation of various image intensifier tubes
22 p3945 A69-40141

Cavity Q dependence of intensity of single mode He-Ne laser above threshold for quantum and semiclassical theories
22 p3961 A69-40415

Radio observations of elliptical and spiral noncluster galaxies, noting correlation between magnitude and radio emission in elliptical galaxies
22 p4025 A69-40639

Amplification coefficient, luminescence power and spacing between Fermi quasi-levels in GaAs diode injection lasers, using spectral absorption dependence
22 p3965 A69-40801

Local electroretinogram responses produced in cats by light intensity incremental changes
22 p3878 A69-40835

High intensity flash effects on local electroretinogram, late receptor and slow potentials and ganglion cell activity in area centralis of cat retina
22 p3883 A69-40882

Light field long term behavior in dispersive medium with finite optical thickness by asymptotic solution of unsteady transport equation
22 p3983 A69-41267

Nonlinear intensity transitions involving order of magnitude increases in visible luminosity of RF generated plasmas, noting inductive field and electron density influence
23 p4196 A69-41546

Autonomous circadian rhythm in man under complete isolation and light-dark cycles and illumination intensity changes
23 p4094 A69-42071

Rod signals elicited by flashes in human eye measured, deriving relation between nerve signal size in rods and flashes energy
23 p4099 A69-42119

IR excess of R CrB type variable star RY Sgr, noting visual brightness and radiation in 2.0-3.4 micron range
23 p4220 A69-42377

Physiological circadian rhythms in isolated and nonisolated Macaca Nemestrina living under varied light intensities, noting telemetered deep body temperature, urine volume and sodium, etc
24 p4261 A69-42707

Instrumentation and data interpretation method for particle size determination by low-angle light scattering
24 p4313 A69-42764

Laser granularity effects on brightness discrimination [AAS PAPER 69-464]
24 p4272 A69-42843

LUNAR ATMOSPHERES

Lunar surface gas adsorption mechanism for lunar atmosphere absence
05 p0824 A69-16062

Lunar atmosphere molecule and atom concentration from isotropic and uniform surface evaporation due to micrometeorite impact
10 p1783 A69-23921

Lunar surface gas adsorption mechanism for lunar atmosphere absence
15 p2680 A69-30261

Gas particle concentrations on moon due to solar wind, surface emissions and atmospheric contamination by lunar operations and rocket motor products
18 p3189 A69-34236

LUNAR BASES

Lunar surface power plants, considering weight constraint for various systems using nuclear power, solar cell/fuel cells and H₂O reactant regeneration
01 p0013 A69-11396

Stellar photometry during occultations by earth, discussing feasibility of lunar based observations
13 p2345 A69-27651

Lunar colony development, detailing construction of permanent lunar bases taking into account oxygen, food, water, power and transportation
13 p2240 A69-27906

Lunar soil as building material and extraction of water, oxygen and rocket propellants from lunar materials for lunar colony needs
13 p2352 A69-27907

Lunar based physics and chemistry, discussing exploration of and survival in lunar environment
18 p3112 A69-34235

Lunar laboratory physical and chemical experiments including scattering phenomena, molecular and atomic beams and gas cloud photochemistry
18 p3113 A69-34237

Metagalactic light measurements by lunar based night sky photography
18 p3189 A69-34242

Lunar based optical workshop and repair facility, using ion beam technique to polish and repair optical element surfaces
18 p3113 A69-34243

Manned lunar bases from legal viewpoint, discussing national jurisdiction, personnel policies, mineral rights, etc
20 p3637 A69-37119

Apollo 11 mission and future space exploration prospects including moon base, manned space station, reusable shuttle vehicles, etc
23 p4211 A69-41477

Design, fabrication and evaluation of lunar base solar array power modules, emphasizing structural/dynamic, thermal vacuum and acoustic tests
23 p4072 A69-42288

Electrical power system synthesis for manned lunar base for surface explorations of increasing energy requirements and duration, discussing thermal control, reliability, etc
23 p4076 A69-42541

Manned facilities design, construction and maintenance on extraterrestrial bodies, discussing astrophysical and lunar surface data requirements [AAS PAPER 69-208]
24 p4296 A69-42875

Optimal design and materials for cryogenic storage of O and H on lunar surface [AAS PAPER 69-051]
24 p4296 A69-42882

LUNAR COMMUNICATION

Radio wave scattering characteristics of lunar surface in 3 cm wavelength by Luna 8 and Luna 9 automatic stations and Surveyor spacecraft
15 p2571 A69-31359

LUNAR COMPOSITION

Lunar composition analysis by measuring atomic and nuclear radiation emission from orbiter [AAS PAPER 68-197]
02 p0312 A69-11475

Surveyor 6 magnet experiment following lunar landing, noting presence of magnetic material in Sinus Medii indicating basaltic composition
02 p0317 A69-12015

Surveyor 5 alpha particle backscattering instrument measurement, TV pictures of lunar surface elemental composition and magnetic and mechanical measurements
02 p0317 A69-12023

Surveyor 5 Mare Tranquillitatis landing site similarity to Oceanus Procellarum sites, discussing surface material elemental composition and lunar structure
02 p0321 A69-12224

Large scale lunar surface photographs for estimating conical formations identified with terrestrial stratovolcanoes
03 p0507 A69-13093

Lunar surface composition, hardness, porosity, microstructure and transparency based on polarization of reflected light
04 p0658 A69-14958

Possible evolution of earth continents and ocean basin, considering ultrabasic, basic, and intermediate to acidic lunar highlands chemical composition
06 p1000 A69-17006

Lunar rock composition monitored by Luna 9 and 13 soft landed lunar probes [UN PAPER 68-95769]
06 p1000 A69-17041

Origin of moon indicating pristine structure on basis of mascons, alpha scattering and crater formation
06 p1001 A69-17160

Cosmic ray induced radioactivity in lunar surface and meteorites calculated together with cosmic ray intensity variations
10 p1756 A69-22817

Lunar surface chemical composition using RF mass spectrometer
10 p1698 A69-24207

Densor material beneath lunar maria revealed by precise tracking of lunar orbiting spacecraft, discussing geology and evolution
11 p1953 A69-24339

Lunar surface pore water/or ice/ detection by active orbital or surface electromagnetic experiments, noting water effect on reflection coefficient
11 p1958 A69-24693

Moon internal structure, discussing aggregation origin of Moon parallel to earth and three layer model of nife core, sima mantle and porous sheath
12 p2160 A69-26896

Large scale lunar surface photographs for estimating conical formations identified with terrestrial stratovolcanoes
14 p2516 A69-28775

Spectral reflectivity differences /color differences/ on lunar surface in visible region, indicating compositional difference origins
17 p3037 A69-33653

Gas chromatograph-mass spectrometer combination for in situ analysis of lunar organic matter, describing instrument design and operation
18 p3113 A69-34238

Lunar surface composition, hardness, porosity, microstructure and transparency based on polarization of reflected light
18 p3196 A69-34721

Lunar interior chemical heterogeneity determined from model taking into account pressure, temperature and composition effects
19 p3425 A69-36421

Mare Tranquillitatis surface chemical composition data from Surveyor 5, comparing element abundances with meteorites and terrestrial rocks
20 p3601 A69-37517

Moon composition and similarities to Mars explained by silicates in solar system raw material
20 p3604 A69-37563

Visible and IR spectral reflectivity of Apollo lunar landing sites, attributing reflectivity differences to compositional and/or mineralogical differences
21 p3815 A69-39586

Lunar rocks types determination by mass spectrometry, describing results of terrestrial rocks tests
22 p4034 A69-41106

Model of moon accumulated at low temperatures, discussing lunar surface layer characteristics
24 p4383 A69-42936

LUNAR CRATERS

NT TYCHO CRATER

Crater Copernicus photograph, discussing misinterpretation of Orbiter 2 lunar surface photograph on basis of effective temperature contours analysis
01 p0154 A69-10898

Lunar rays nature from terrestrial observations and surface photographs by lunar probes, noting high crater concentration structure
02 p0236 A69-11642

Lunar crater formation studied to explain distortion in large craters or maria, discussing mass concentrations indicated by positive residuals of gravimetric map
04 p0654 A69-14632

IR observations of lunar crater and maria enhanced thermal emission during eclipse, constructing model of cratered surface to analyze thermal behavior
04 p0654 A69-14656

Lunar craters compared with underground explosion craters on earth, determining criteria for identifying explosion craters on moon
04 p0656 A69-14670

Lunar intermare crater density variations data tabulation, presenting quantitative and qualitative estimates
04 p0656 A69-14671

Lunar crater count observations of mare surface and ejecta blanket in Orientale basin
04 p0656 A69-14672

Lunar premare and postmare craters distributions, discussing latitude independence and sources of impacting bodies
04 p0656 A69-14673

Lunar crater densities inside Tycho, Aristarchus and Copernicus
04 p0656 A69-14674

Statistics of central peaks in lunar craters drawn from catalog
04 p0656 A69-14675

Mountain structures surrounding lunar craters, discussing possible origin by impacting planetesimals shock waves
04 p0661 A69-15142

Mare Orientale basin satellite photographs suggest asteroid impact formation

04 p0664 A69-15421

Collapse theory of dimple craters, analogies with terrestrial sink holes and dimple craters as channels for gas escape from interior

05 p0818 A69-15589

Origin of moon indicating pristine structure on basis of mascons, alpha scattering and crater formation

06 p1001 A69-17160

Nature and origin of lunar far side Tsiolkovsky crater

06 p1003 A69-17386

Elastic limit of lunar outer layer determined from analysis of lunar crater dimensions variations as functions of diameter

07 p1212 A69-18600

Regolith thickness distribution at Lunar Orbiter sites, correlating thickness directly with cratering density

07 p1213 A69-18604

Meteor explosion theory of origin of lunar craters and round maria, suggesting endogenic origin

10 p1784 A69-23960

Volcanic origin of lunar crater Dawes based on photogeological evidence obtained from Lunar Orbiter 5 photographs

11 p1952 A69-24264

Lunar far side craters profile and structure determined from Zond 3 photographs using photometric method

11 p1959 A69-24725

Lunar far side craters vertical profiles plotted from photometric cross sections of Zond 3 photographs

11 p1959 A69-24726

Lunar surface layer structure by statistical analysis of data concerning craters and stones distribution as shown by lunar orbiter photographs

12 p2154 A69-25816

Lunar thermal anomalies in various craters observed during lunar night by IR methods, with data suggesting hot and cold regions

12 p2171 A69-27092

Lunar craters circularity measurements relation to age, discussing fracture system and stress history associated with mare formation

13 p2344 A69-27645

Lunar surface evolution, discussing relationship between craters erosional stage and areal density

14 p2528 A69-29947

Lunar relief mechanism based on experimental cratering by pasty projectiles, proposing terrestrial magma genesis

15 p2698 A69-31373

Orientation in proximity of moon and on moon surface utilizing maria, craters, etc

16 p2855 A69-31929

Giant lunar craters, discussing lunar age and defining surface steady state

16 p2863 A69-32404

Lunar rotation elements determined from distances between Moesting A and limb craters, using Iakovkin position angle method

17 p3028 A69-32876

Directional characteristics of lunar IR radiation accounted for by crater model [AIAA PAPER 69-598]

17 p3033 A69-33285

Temperature distribution in shadowed lunar craters formulated in Fredholm integral equations, showing constant temperature and correction for soil thermal inertia

17 p3033 A69-33291

Far and near side lunar crater chains regularities in distribution and size

18 p3202 A69-35329

Lunar rivers as coalesced chain craters resulting from gas emission along fracture beneath lunar regolith

18 p3205 A69-35436

Standing waves on moon, discussing annular and radial structures of lunar craters and global tectonic patterns

20 p3604 A69-37565

Crater distribution and population curves for Surveyor 1 vicinity, discussing Flamsteed P ring floor characteristics

21 p3800 A69-38675

Lunar near side crater overlap, considering formation of Tycho Association

21 p3800 A69-38676

Ephemeris calculations and lunar craters and reference stars coordinates measured from photographic plates, using digital computers

22 p4024 A69-40610

Module landing effects on lunar surface, deriving erosion law from Surveyor 5 engine firing test and vacuum test data

23 p4211 A69-41388

LUNAR CRUST

Lunar surface mechanical properties at Surveyor 5 site

02 p0321 A69-12225

Thermal conditions of upper blanket of lunar surface during eclipse, using data to calculate lunar radio emission

03 p0506 A69-13088

Penetration type soil analyzer used by Luna 13 automatic lunar station for mechanical strength of lunar surface

03 p0430 A69-13424

Lunar surface layer density measured radiometrically with scattered gamma rays by Luna 13

03 p0430 A69-13425

Lunar surface formation, emphasizing density variations and mass concentrations

04 p0654 A69-14633

Lunar surface material chemical composition in lunar mare and on Tycho crater north rim, noting Surveyors 5, 6, and 7 alpha analyses

04 p0655 A69-14658

Mathematical density-depth model proposed for lunar outermost layer compared to Matveev model, noting Surveyor estimates

04 p0655 A69-14659

Lunar surface composition, hardness, porosity, microstructure and transparency based on polarization of reflected light

04 p0658 A69-14958

Sinuuous rill and water distribution on lunar surface from Orbiter 4 high resolution photographs

05 p0818 A69-15606

Lunar surface gas adsorption mechanism for lunar atmosphere absence

05 p0824 A69-16062

Lunar history reexamination including added mantle convection and recent rocket data

05 p0825 A69-16303

Elastic limit of lunar outer layer determined from analysis of lunar crater dimensions variations as functions of diameter

07 p1212 A69-18600

Regolith thickness distribution at Lunar Orbiter sites, correlating thickness directly with cratering density

07 p1213 A69-18604

Hypotheses concerning mechanism of lunar maria formation, discussing molten rock layer below lunar crust

10 p1782 A69-23710

Lunar surface layer structure by statistical analysis of data concerning craters and stones distribution as shown by lunar orbiter photographs

12 p2154 A69-25816

Martian diagonal and longitudinal-meridional canals mapped into grid systems, noting differences between Martian and lunar crusts tectonic activity

13 p2337 A69-27533

Thermal conditions of upper blanket of lunar surface during eclipse, using data to calculate lunar radio emission

14 p2515 A69-28770

Lunar surface gas adsorption mechanism for lunar atmosphere absence

15 p2680 A69-30261

Lunar mascon origin from collisions of large masses with lunar surface

15 p2698 A69-31328

Lunar surface composition, hardness, porosity, microstructure and transparency based on polarization of reflected light

18 p3196 A69-34721

Chemical analysis of lunar surface by devices exploiting alpha particle backscattering and proton production by alphas placed by Surveyor 5, 6 and 7

22 p4012 A69-40088

Electrical conductivity of uppermost lunar surface layers, indicating dry powdered rocks with frequency independent dielectric loss tangent

22 p4023 A69-40570

Undulating dunelike deposits of surface debris similar to base-surge deposits in maar volcanoes and tuff rings, discussing underground ice existence

23 p4216 A69-42203

Model of moon accumulated at low temperatures, discussing lunar surface layer characteristics

24 p4383 A69-42936

LUNAR DUST

Cumulative flux of interplanetary and cislunar space dust particles by Mariner 4 and OGO 3 spacecraft, noting particle impact rate

15 p2699 A69-31394

Picogram dust particle flux in selenocentric space measurement by Lunar Explorer 35, showing enhancement during meteor showers

15 p2699 A69-31396

Geocentric orbital elements determination of lunar particles expelled into space by meteorite impact, using spheres of influence method

18 p3202 A69-35330

Lunar morphology evolution by dust transport on surface, discussing possibility of fluidization

23 p4221 A69-42392

LUNAR ECHOES

Directly backscattered light /echoes/ from dielectric plane surface with roughness and volume scattering, comparing indicatrices with moon echo

06 p0887 A69-17173

Lunar surface pore water /or ice/ detection by active orbital or surface electromagnetic experiments, noting water effect on reflection coefficient

11 p1958 A69-24693

Apollo 11 moon reflector-laser beam experiment, discussing range changes produced by axial rotation and orbital motion and use for earth-moon dynamics

19 p3339 A69-36766

Lunar laser beam retroreflection observations, showing agreement with predicted ephemeris and signal strength

24 p4384 A69-43197

LUNAR ECLIPSES

Thermal conditions of upper blanket of lunar surface during eclipse, using data to calculate lunar radio emission

03 p0506 A69-13088

Lunar transient luminous events and eclipse anomalies, proposing solid surface and gas luminescence as explanation

04 p0653 A69-14615

Radiometric observations of moon during total lunar eclipse at 3.33 mm, noting decrease in equivalent black body disk temperature

10 p1789 A69-24132

Thermal conditions of upper blanket of lunar surface during eclipse, using data to calculate lunar radio emission

14 p2515 A69-28770

Lunar brightness variations during eclipse on 13 April 1968 measured photoelectrically, suggesting nonuniform diurnal distribution of atmospheric scatterers for observed asymmetry

20 p3601 A69-37510

Radiometric measurement of lunar areas during eclipse of 18 October 1967 at mm wavelengths, considering temperature changes and cooling rates

20 p3613 A69-38247

Lunar libration point L4 photographs taken during 6 October 1968 eclipse showing no discrete objects or clouds

20 p3613 A69-38249

LUNAR EFFECTS

Interplanetary magnetic field measurements in lunar wake, noting magnetic perturbations pattern and absence of shocks

01 p0157 A69-11228

Lunar wake in solar wind at large distances, noting no satellite evidence of lunar magnetic field and evidence for lunar generated turbulence

03 p0514 A69-14007

Lunar laser ranging for testing Einstein and Brans-Dicke gravitational theories, discussing pulse transit time and dominant nonNewtonian correction

05 p0825 A69-16362

Lunar tide effect on height distribution and velocity of ionospheric electron density daily variations near magnetic equator

05 p0756 A69-16401

Lunar daily geomagnetic periodicities by periodogram or spectral analysis, comparing amplitudes obtained by spectral analysis to those by harmonic analysis

07 p1123 A69-18817

Lunar diurnal variation parameters at Irkutsk determined from IGY data concerning geomagnetic field components

10 p1687 A69-23918

Sea tides and ionospheric effects on lunar variation of geomagnetic field vertical component

12 p2161 A69-26957

Noon ionospheric absorption data for Freiburg on different frequencies for lunar variation of ionospheric absorption of radio waves

14 p2438 A69-29104

Literal algebra /SPASM/ computer program critical verification of Kozai short period lunar perturbations, discussing errors

15 p2699 A69-31381

Micropulsation records for full moon effect on hydromagnetic emission activity of magnetosphere, noting W and Kp indices

16 p2774 A69-31979

Sun and moon effects on earth satellite orbit

22 p4030 A69-40901

LUNAR ENVIRONMENT

Lunar surface vehicle mathematical models, discussing design influence of low gravity, atmosphere absence, temperature extremes and surface roughness

05 p0741 A69-15673

Lunar environment simulation, discussing space suit encumbrances on astronaut performance, gravity effects, surface texture, illumination, confinement and isolation

06 p0906 A69-17388

Apollo lunar TV camera for real time pictures during all phases of Apollo lunar landing mission, describing camera tube, circuitry and optics

07 p1133 A69-19137

Surveyor electronic engineering design for lunar environment, discussing vacuum and temperature effects

11 p1958 A69-24633

Lunar visual environment effects on astronaut control manipulation task performance, discussing solar illumination simulation facility

12 p2059 A69-26554

Lunar surface environmental factors including molecular gas behavior under weak gravity and low atmospheric density, radiation and temperature effects, meteorite bombardment, etc

13 p2352 A69-27904

Moon environment for scientific experiments, emphasizing lunar surface properties, lack of man-made electromagnetic waves, vacuum and weak gravity force

13 p2240 A69-27910

Orientation in proximity of moon and on moon surface utilizing maria, craters, etc

16 p2855 A69-31929

Solar system physical environments surveyed from exobiological viewpoint

17 p2907 A69-32968

Lunar based physics and chemistry, discussing exploration of and survival in lunar environment

18 p3112 A69-34235

Molecular beam experiments on moon, noting lunar environmental advantages for studies of beam-beam scattering, beam-surface interactions, beam-field deflection, etc

18 p3113 A69-34240

Lunar conditions differing from simulations in laboratories, examining surface, physicochemical properties and friction

18 p3113 A69-34241

Lunar origin, geological composition and water existence controversies from data gathered by various lunar probes

18 p3196 A69-34631

Manned testing of EVA equipment in thermal-vacuum environment for qualification of Apollo extravehicular mobility unit, using lunar surface thermal simulator

[AIAA PAPER 69-992] 22 p3893 A69-40370

Human habitation conditions on moon from viewpoint of solar and lunar radiation, vacuum and gravitation effects including solar energy utilization

23 p4111 A69-42213

LUNAR EVOLUTION

Lunar surface formation, emphasizing density variations and mass concentrations

04 p0654 A69-14633

Origin of moon indicating pristine structure on basis of mascons, alpha scattering and crater formation

06 p1001 A69-17160

Lunar mass concentrations /mascons/ origin and nature, postulating primordial lunar atmosphere and hydrosphere and carbon derived from primordial organic compounds

08 p1397 A69-20697

Meteor explosion theory of origin of lunar craters and round maria, suggesting endogenic origin

10 p1784 A69-23960

Moon internal structure, discussing aggregation origin of Moon parallel to earth and three layer model of nife core, sima mantle and porous sheath

12 p2160 A69-26896

Moon-earth system origin emphasizing mass distribution

13 p2352 A69-27902

Lunar geophysical features origin, noting mascons influence and surface rigidity

13 p2352 A69-27903

Chemical composition of earth, Venus, Mars, Mercury and moon calculated from mathematical models, constructing approximate equations of state at high pressure

14 p2526 A69-29878

Lunar origin theories, considering moon/earth mass ratio, earth-moon system angular momentum deficiency and differential volatilization in earth

14 p2527 A69-29882

Lunar surface evolution, discussing relationship between craters erosional stage and areal density

14 p2528 A69-29947

Lunar relief mechanism based on experimental cratering by pasty projectiles, proposing terrestrial magma genesis

15 p2698 A69-31373

Moon density and nucleation of planets, explaining low density and absence of heavy core by late aggregation from nonmetallic particles

16 p2865 A69-32808

Lunar origin, geological composition and water existence controversies from data gathered by various lunar probes

18 p3196 A69-34631

Catastrophic and noncatastrophic alternatives for earth capture of moon, discussing tidal action and spin-orbit resonance

18 p3198 A69-34823

Planetary cosmogony problems involving protoplanetary cloud origin, matter condensation, planets formation and moon origin, noting iron content in chondrites

18 p3205 A69-35437

Moon possible origin, discussing spin off from earth, accretion from same dust cloud or formed elsewhere and captured

20 p3603 A69-37559

Lunar Orbiter data for existence of unequal mass distributions in lunar interior confirmed by manned Apollo 8 and 10 flights, discussing origin

20 p3606 A69-37933

Lunar maria structure and evolution as homologous transient gravity wave systems from impact craters on crust

21 p3803 A69-38982

Lunar morphology evolution by dust transport on surface, discussing possibility of fluidization

23 p4221 A69-42392

Model of moon accumulated at low temperatures, discussing lunar surface layer characteristics

24 p4383 A69-42936

LUNAR EXPLORATION

Heat flow measurement from moon interior planned for Apollo missions to determine temperature increase rate with depth during lunar year

[AAS PAPER 68-207] 02 p0313 A69-11482

U.S. space program projections, discussing earth orbit operations, lunar and planetary explorations, costs and timetable

02 p0355 A69-11744

Lunar geoscience role in lunar mission planning, discussing costs, reduced gravity effects, sample mass limits and seismology

03 p0510 A69-13391

Lunar surface vehicle mathematical models, discussing design influence of low gravity, atmosphere absence, temperature extremes and surface roughness

05 p0741 A69-15673

Lunar studies and moon exploration noting moon motion, lunar rotation dependence on orbital motion, lunar figure and topography and mass distribution

05 p0820 A69-15835

Soviet explorations of moon, Venus, Mars and interplanetary space, noting objectives of future lunar explorations

[UN PAPER 68-95719] 06 p1000 A69-17055

Post-telescopic lunar exploration, discussing Apollo program and development of selenology

[JPL-TR-52-1399] 06 p1001 A69-17159

Lunar exploration sites selection based on telescopic studies and geological maps

06 p1001 A69-17161

Surveyor lunar scientific payload and results, discussing TV camera, soil mechanics and surface sampler, alpha scattering instrument, small magnets and surface analysis

06 p1001 A69-17162

Human expansion in space, discussing moon landing and exploitation

13 p2352 A69-27901

Lunar astronauts psychological problems, discussing isolation from outside world, gravitational and extreme light effects, protective space suits, etc

13 p2210 A69-27905

Lunar colony development, detailing construction of permanent lunar bases taking into account oxygen, food, water, power and transportation

13 p2240 A69-27906

Lunar soil as building material and extraction of water, oxygen and rocket propellants from lunar materials for lunar colony needs

13 p2352 A69-27907

Vehicles for lunar surface exploration and transportation including flying machines and wheeled vehicles

13 p2352 A69-27908

Space travel and lunar exploration medical problems

13 p2210 A69-27909

Lunar physics and chemistry - IAA Conference, Belgrade, September 1967

18 p3112 A69-34234

Lunar based physics and chemistry, discussing exploration of and survival in lunar environment

18 p3112 A69-34235

Spacecraft lunar observations, especially data from Surveyor landings

18 p3205 A69-35410

Hopping transporter vehicle designs for lunar exploration providing low fuel consumption at high average speed

[AIAA PAPER 68-1139] 22 p3927 A69-40547

Apollo Extravehicular Communication Telemetry System for monitoring astronaut portable life support system, space suit performance and body functions on lunar surface

23 p4121 A69-41767

Manned lunar exploration programs and site evaluation concerning volcanic processes, chemical and mineralogical differentiation, atmosphere and protobiological materials

23 p4216 A69-42200

Planning lunar surface experiments in nets or at selected sites for optimum scientific return

[AAS PAPER 69-207] 24 p4381 A69-42874

LUNAR EXPLORATION SYSTEM FOR APOLLO

Medium temperature fuel cells, noting reliability and high efficiency leading to selection for lunar exploration vehicle of Apollo project

08 p1260 A69-21046

LUNAR FAR SIDE

Communications system considerations for lunar libration point relay satellite to support Apollo lunar far side mission

03 p0388 A69-13180

Selenographic technique for tying in lunar far side space photographs based on earth disk position measurements with respect to moon limb

05 p0763 A69-16055

Nature and origin of lunar far side Tsiolkovsky crater

06 p1003 A69-17386

Lunar far side craters profile and structure determined from Zond 3 photographs using photometric method

11 p1959 A69-24725

Lunar far side craters vertical profiles plotted from photometric cross sections of Zond 3 photographs

11 p1959 A69-24726

Lunar far side surface spectral inhomogeneities in UV from Zond 3 measurements

12 p2154 A69-25817

Libration point relay satellites for continuous communication link between earth and lunar far side, discussing trajectories and halo orbit stationkeeping

15 p2680 A69-30188

Surface structure asymmetry of near and far sides of moon, considering earth radiation and gravity pull

18 p3206 A69-35439

Linearization of equations of motion for three body problem, emphasizing lunar far side libration point as related to possible landing

19 p3402 A69-35961

Selenographic technique for tying in lunar far side space photographs based on earth disk position measurements with respect to moon limb

20 p3545 A69-37965

Cartographic tying-in of Zond 3 lunar surface photographs to verify maps of moon far side
20 p3608 A69-38051

LUNAR FLIGHT

Maximum capacity estimation for one way transportation systems to moon and Mars, analyzing technical and economic aspects
09 p1586 A69-21297

Aeronomic phenomena observed near Altair and theta Aquila ascribed to Apollo 8 lunar flight
11 p1957 A69-24411

Saturn 5 translunar payload capability enhancement by fuel biasing, propellant utilization systems, trajectory shaping and programmed mixture ratio scheme [AIAA PAPER 69-451]
16 p2839 A69-32669

Navigation state vector update effect on lunar mission completion capability for Saturn 5, emphasizing hardware and scheme errors and accelerometer failure [AIAA PAPER 69-883]
21 p3764 A69-39409

Quasi-optimum control law for minimum-time bounded acceleration rendezvous in central force field using Friedland technique, with application to lunar flight
24 p4349 A69-43313

LUNAR GEOLOGY

Lunar surface early geologic evolution noting bearing on earth geologic history [AAS PAPER 68-202]
02 p0312 A69-11478

Lunar seismic velocity distribution data indicates broad low velocity zone together with possible extensive melting at depth [AAS PAPER 68-205]
02 p0312 A69-11480

Heat flow measurement from moon interior planned for Apollo missions to determine temperature increase rate with depth during lunar year [AAS PAPER 68-207]
02 p0313 A69-11482

Lunar geoscience role in lunar mission planning, discussing costs, reduced gravity effects, sample mass limits and seismology
03 p0510 A69-13391

Communications of lunar and planetary laboratory, Volume 7, covering lunar radiation, lunar craters, Vesta rotation, etc
04 p0655 A69-14668

Lunar crater densities inside Tycho, Aristarchus and Copernicus
04 p0656 A69-14674

Mountain structures surrounding lunar craters, discussing possible origin by impacting planetesimals shock waves
04 p0661 A69-15142

Lunar high density mass concentrations effect on Lunar Orbiters accelerations, discussing lunar gravity field determination
04 p0661 A69-15145

Lunar rock composition monitored by Luna 9 and 13 soft landed lunar probes [UN PAPER 68-95769]
06 p1000 A69-17041

Lunar exploration sites selection based on telescopic studies and geological maps
06 p1001 A69-17161

Lunar geology information obtained by Ranger space missions
06 p1001 A69-17163

Fine structure and geology of lunar surface from Luna, Ranger, Surveyor and Orbiter data
07 p1212 A69-18547

Lunar mass concentrations /mascons/ origin and nature, postulating primordial lunar atmosphere and hydrosphere and carbon derived from primordial organic compounds
08 p1397 A69-20697

Lunar radio emission constant component in presence of heat flow from interior, using stratified model of surface structure with two variants
11 p1956 A69-24398

Lunar craters circularity measurements relation to age, discussing fracture system and stress history associated with mare formation
13 p2344 A69-27645

Lunar geophysical features origin, noting mascons influence and surface rigidity
13 p2352 A69-27903

Lunar surface features as observed by orbiting and landing craft, discussing particle layer, rocks, craters, effects of erosion, meteorite impact, etc
15 p2698 A69-31356

Faint lunar craters, discussing lunar age and defining surface steady state
16 p2863 A69-32404

Seismic regions location prediction on visible lunar side based on transient events, hot spots and gravity anomalies
18 p3193 A69-34363

Lunar origin, geological composition and water existence controversies from data gathered by various lunar probes
18 p3196 A69-34631

Lunar volcanism origin of tektite and pearlite, noting no cosmic ray effects
20 p3597 A69-37338

Alpha-scattering experiments by Surveyor missions, studying hypothesis regarding lunar origin of eucrites and howardites
20 p3597 A69-37341

Volcano-Tectonic origin of lunar mare terrain from Apollo 8 photograph showing faulting pattern identical with uppermost Pleistocene-Holocene faulting
20 p3604 A69-37570

Organic geochemical investigations of lunar rock samples based on analysis methods for carbonaceous meteorites and early Precambrian sedimentary rocks
20 p3476 A69-37616

Lunar Orbiter data for existence of unequal mass distributions in lunar interior confirmed by manned Apollo 8 and 10 flights, discussing origin
20 p3606 A69-37933

Data on mass distribution of terrestrial fragmented rocks to interpret lunar rock samples, noting origin of asteroids and meteorites
20 p3613 A69-38250

NASA lunar receiving laboratory for lunar rock samples examination by gamma ray spectrometry for induced radioactive nuclides and naturally occurring isotopes
20 p3512 A69-38271

Papers of Lunar and Planetary Laboratory, Volume 8, covering lunar craters, rock fragmentation, stellar photometry, etc
21 p3799 A69-38674

Lunar near side crater overlap, considering formation of Tycho Association
21 p3800 A69-38676

Tektite origin theories, discussing Surveyor experiments effects on lunar geology and Tektite origin
22 p4012 A69-40086

Apollo lunar sample collection and analysis, discussing astronauts activity and equipment, sample types, laboratories for radioactive counting and gas analysis, etc
22 p3919 A69-40191

Jadeite /high pressure sodium aluminum pyroxene/ shock-induced phase assemblage from oligoclase, noting relevance to lunar rock samples investigation
22 p3941 A69-40569

Physicomachanical properties of tuff rock based on similarity to lunar surface rock, determining natural density, porosity and compression strength
22 p4034 A69-41105

Lunar rocks types determination by mass spectrometry, describing results of terrestrial rocks tests
22 p4034 A69-41106

Apollo 11 observations of lunar surface glazing, considering radiation heating due to solar outbursts, rocket exhaust effects, shock heating or volcanism, erosion, etc
23 p4216 A69-42202

Lunar rocks and fines samples physical, chemical, mineralogical and biological preliminary analysis at Lunar Receiving Laboratory
24 p4382 A69-42935

Lunar radio emission constant component in presence of heat flow from interior, using stratified model of surface structure with two variants
24 p4390 A69-43788

LUNAR GRAVITATION

Lunar mascons, interpreting lunar gravitational field anomalies over maria in terms of near-surface slab-like model for maria structure
04 p0654 A69-14630

Lunar gravitational anomalies from internal density variation viewpoint, discussing isostasy in maria
04 p0654 A69-14631

Lunar gravitational field and figure, discussing astronomical observations based on trajectory measurements of Luna 10 lunar orbiter
09 p1589 A69-21375

Doppler tracking data from Lunar Orbiter missions for studying lunar gravity anomalies, plotting acceleration on lunar surface Mercator projection
15 p2697 A69-31313

Lunar mass and gravitational field determined from lunar satellite dynamics, using potential function in terms of spherical harmonics
15 p2699 A69-31405

Lunar localized subsurface mass concentration association with circular maria, noting two large mascon basins from gravity data and orbital photography
16 p2864 A69-32446

Lunar gravimetric data reprocessed to present in usable and readable form, plotting acceleration on Mercator projection of lunar surface
18 p3194 A69-34413

Lunar gravitational field and figure, discussing astronomical observations based on trajectory measurements of Luna 10 lunar orbiter
18 p3198 A69-34763

Lunar gravitational potential and lunar surface radius vector binomial series coefficients determination from Luna 10 data used for lunar surface shape calculations
20 p3596 A69-37308

Moments of inertia and gravity field of moon, noting application to earth tides
22 p4030 A69-40902

Lunar gravitational field data from Lunar Orbiter spacecraft reprocessed, discussing mascon effects on moon structure and evolution theories
24 p3379 A69-42785

LUNAR GRAVITATIONAL EFFECTS

Lunar gravity simulation effect on human performance, discussing fidelity requirements, self locomotion, metabolic rate and psychomotor task decrement
02 p0203 A69-12217

Lunar influences on meteoroid influx to earth, tabulating binomial distributions and probabilities of meteorite falls according to different lunar angles
04 p0655 A69-14663

Lunar high density mass concentrations effect on Lunar Orbiters accelerations, discussing lunar gravity field determination
04 p0661 A69-15145

Lunar environment simulation, discussing space suit encumbrances on astronaut performance, gravity effects, surface texture, illumination, confinement and isolation
06 p0906 A69-17388

Spacecraft trajectory using microthrust and lunar gravitational attraction for acceleration into heliocentric orbit
09 p1593 A69-21620

Secular perturbations of remote satellites within lunar gravitation field, comparing observations and analytical data
10 p1779 A69-23614

Circumpolar satellite orbits under lunar and solar perturbations based on two fixed centers problem, considering large amplitude disturbances
10 p1780 A69-23616

Solar and lunar effects on motions of polar orbiting satellites, discussing variable intermediate orbits
14 p2521 A69-29460

Lunar simulator for metabolic studies, using BPMU for assessing O consumption of test subjects at rest and various speeds of ambulation
17 p2914 A69-33187

Seismic regions location prediction on visible lunar side based on transient events, hot spots and gravity anomalies
18 p3193 A69-34363

Residuals from earth based coherent two way radio Doppler data from Lunar Orbiter three orders of magnitude larger than observations from spacecraft [AAS PAPER 68-131]
21 p3828 A69-39766

LUNAR GRAVITY SIMULATOR

Lunar simulator for metabolic studies, using BPMU for assessing O consumption of test subjects at rest and various speeds of ambulation
17 p2914 A69-33187

LUNAR LANDING

Optimal landing of spacecraft on moon surface from low circular orbit, analyzing rocket thrust, altitude and landing site distance effect on spacecraft mass
19 p3431 A69-36616

Module landing effects on lunar surface, deriving erosion law from Surveyor 5 engine firing test and vacuum test data
23 p4211 A69-41388

Lunar landing decision, analyzing American space policy making process with aid of Huntington model [AAS PAPER 69-500]
24 p4418 A69-42853

LUNAR LANDING MODULES

Electrical, thermal and mechanical requirements in design of Landing Radar Electronic Assembly for Apollo Lunar Module
10 p1663 A69-23537

Lunar surface temperature distribution measured by IR pyrometer, predicting temperature rise due to Lunar Excursion Module landing
13 p2341 A69-27583

Lunar colony development, detailing construction of permanent lunar bases taking into account oxygen, food, water, power and transportation

13 p2240 A69-27906

Apollo 10 lunar landing module, detailing weight, shape, electronic system and rendezvous radar

18 p3207 A69-34629

LASSO /modified S-4B/IU/ vehicle mission to place in orbit two unmanned Lunar Modules for landing of radio and optical telescopes on lunar surface

18 p3136 A69-34813

Apollo lunar module landing radar, discussing descent phases, operating modes, assemblies and Surveyor radar

19 p3267 A69-35797

Apollo 11 guidance and navigation systems involved in lunar landing, describing command and service modules design

24 p4295 A69-42550

LUNAR LANDING SITES

PostApollo lunar passive seismic experiments, discussing probable results of present program, exploration sites and additional network stations and instruments

[AAS PAPER 68-204] 02 p0312 A69-11479

Surveyor 5 Mare Tranquillitatis landing site similarity to Oceanus Procellarum sites, discussing surface material elemental composition and lunar structure

02 p0321 A69-12224

Lunar surface mechanical properties at Surveyor 5 site

02 p0321 A69-12225

Gray tone differences between undisturbed lunar surface and darker ejecta observed around Surveyor 1 footpads, discussing possible albedo differences

04 p0660 A69-15124

Photographic results of Lunar Orbiter program noting possible Apollo sites

05 p0822 A69-15858

Lunar exploration sites selection based on telescopic studies and geological maps

06 p1001 A69-17161

Regolith thickness distribution at Lunar Orbiter sites, correlating thickness directly with cratering density

07 p1213 A69-18604

Surveyor lunar landing procedures and results including instrumentation, lunar topography, selenology, chemical and physical properties, solar corona and earth laser output observations

15 p2681 A69-30324

NASA lunar survey and mapping for generating Apollo satellite landing navigation control, using analytic photogrammetry, camera position and altitude data of lunar topography

20 p3536 A69-36931

Spectral reflectivity and emissivity observations of proposed Apollo landing sites compared with other lunar localities and unmanned lunar probe data

21 p3815 A69-39585

Visible and IR spectral reflectivity of Apollo lunar landing sites, attributing reflectivity differences to compositional and/or mineralogical differences

21 p3815 A69-39586

Lunar surface IR emissivity comparison spectra including proposed Apollo landing sites, indicating Si-O ratio difference for Plato crater

21 p3815 A69-39587

Manned lunar exploration programs and site evaluation concerning volcanic processes, chemical and mineralogical differentiation, atmosphere and protobiological materials

23 p4216 A69-42200

Planning lunar surface experiments in nets or at selected sites for optimum scientific return

[AAS PAPER 69-207] 24 p4381 A69-42874

LUNAR LAUNCH

Apollo/Saturn 5 base at Kennedy Space Center and facilities and equipment supporting manned lunar mission, discussing site location choice and launch complex design concept

16 p2767 A69-32429

LUNAR LIMB

Tropospheric inhomogeneities properties and wind conditions in relation to lunar limb image deformations

01 p0156 A69-11182

Solar wind interaction with moon, discussing core/surface layer conductivity and lunar limb shock wave formation

03 p0502 A69-14006

Lunar libration constants determination based on Schluter heliometer observations using Bessel-Wichmann method, allowing for limb irregularities

17 p3028 A69-32875

Lunar rotation elements determined from distances between Moesting A and limb craters, using Iakovkin position angle method

17 p3028 A69-32876

Lunar libration point L4 photographs taken during 6 October 1968 eclipse showing no discrete objects or clouds

20 p3613 A69-38249

Bright lunar limb zenith distances measured by equal altitudes method, deriving Ephemeris- Atomic Time A3 and Ephemeris-TU2 time relations

23 p4208 A69-41289

LUNAR LOGISTICS

PostApollo lunar passive seismic experiments, discussing probable results of present program, exploration sites and additional network stations and instruments

[AAS PAPER 68-204] 02 p0312 A69-11479

LUNAR LUMINESCENCE

Relation between color index over lunar surface and solar rays angle of incidence, noting supplementary emission attributed to surface luminescence

03 p0506 A69-13089

Lunar transient luminous events and eclipse anomalies, proposing solid surface and gas luminescence as explanation

04 p0653 A69-14615

Lunar surface light scattering data cataloged for various phase angles from photometric observations of lunar features brightness

13 p2344 A69-27648

Relation between color index over lunar surface and solar rays angle of incidence, noting supplementary emission attributed to surface luminescence

14 p2516 A69-28771

Lunar surface characteristics, discussing light polarization, lunar radiation, solar radiation and meteorite impact effects, etc

16 p2856 A69-32069

Solar proton bombardment of lunar surface, discussing luminescence and chemical effects

22 p4012 A69-40089

LUNAR MAGNETIC FIELDS

Earth and lunar magnetic field studies in U.S.S.R., discussing Soviet earth satellite and lunar probe data

01 p0066 A69-10943

Interplanetary magnetic field measurements in lunar wake, noting magnetic perturbations pattern and absence of shocks

01 p0157 A69-11228

Secular change examination in cislunar geomagnetic tail field gradient during summers of 1966 and 1967, using Explorer 33 and 35 results

01 p0077 A69-11237

Lunar electrical parameters range determination using models

[AAS PAPER 68-199] 02 p0312 A69-11477

Magnetometer experiment for Apollo project to measure lunar surface magnetic field, describing mission requirements and instrumentation

[AAS PAPER 68-206] 02 p0312 A69-11481

Lunar magnetic moment and surface field, discussing Explorer 35 field measurements

03 p0514 A69-14005

Soviet astronomical radio-astronomical probe and orbiter lunar studies including surface photography, gravitational and magnetic measurements and soft landed probes

13 p2336 A69-27353

Time dependent magnetic field induced inside rotating spherical conductor by external sources applied to moon

14 p2518 A69-29121

Lunar magnetic field measurements by Mariner 4 near sun-moon line extension, discussing search for lunar wake

16 p2856 A69-31986

Equations of transformation for hourly data harmonic terms used in computation and representation of solar and lunar daily magnetic variations

16 p2782 A69-32457

Lunar components in mean values of geomagnetic field daily variations, discussing lunar phase during selected quiet days

16 p2782 A69-32458

Solar wind plasma effects on lunar wake umbral and penumbral interplanetary magnetic field anomalies, evaluating roles of electrons and ions

20 p3609 A69-38095

Lunar Explorer 35 measurements of lunar surface electromagnetic properties, magnetic fields and solar wind-moon interactions

21 p3794 A69-38379

Homogeneous conducting moon-solar wind interactions, describing time dependent lunar magnetic and electric fields induced by interplanetary magnetic field variations

22 p4023 A69-40518

Critique of magnetic response model for interaction of moon and interplanetary plasma magnetic field proposed by Blank and Sill

24 p4384 A69-43190

Auroral activity and lunar phases correlation from IMP-1 measurements of lunar magnetic field

24 p4311 A69-43502

LUNAR MAPS

Geological-morphological mapping of moon interpretation and lunar surface structural peculiarities

03 p0505 A69-12898

Tectonic map compiled for visible and far sides of moon, noting correlations between earth and moon tectogenesis

03 p0505 A69-12899

Hypsometric contour map of lunar surface from absolute altitude measurements of 1200 points on lunar surface

03 p0512 A69-13689

Lunar shape hypsometric peculiarities, analyzing heights and asymmetry in relation to lunar equator, central meridian and image plane

04 p0662 A69-15249

Unified lunar control photogrammetric network produced by mapping satellite in 28 day polar orbit, using recurrent partitioning

05 p0819 A69-15628

Lunar exploration sites selection based on telescopic studies and geological maps

06 p1001 A69-17161

Lunar coordinate corrections from solar ring coronagraphic observations of 20 May 1966 annular solar eclipse

15 p2686 A69-30532

Relative heights on western moon half computed and compared to values of Schmidt, U.S. Army Map Service and USAF Aeronautical Chart Information Center

18 p3196 A69-34693

Cartographic tying-in of Zond 3 lunar surface photographs to verify maps of moon far side

20 p3608 A69-38051

Lunar surface photographic mapping by Ranger, Surveyor and Lunar Orbiter projects, emphasizing image resolution and coverage

21 p3719 A69-38325

LUNAR MARIA

Surveyor 5 Mare Tranquillitatis landing site similarity to Oceanus Procellarum sites, discussing surface material elemental composition and lunar structure

02 p0321 A69-12224

Magnetic experiment on Surveyor 5 revealing magnetic material presence in Mare Tranquillitatis, discussing analogy to powdered basalt

02 p0321 A69-12226

Lunar mascons size and depth calculated in terms of mare formed by low velocity iron meteorites impact

04 p0654 A69-14629

Lunar mascons, interpreting lunar gravitational field anomalies over maria in terms of near-surface slab-like model for maria structure

04 p0654 A69-14630

Lunar gravitational anomalies from internal density variation viewpoint, discussing isostasy in maria

04 p0654 A69-14631

Lunar crater formation studied to explain distortion in large craters or maria, discussing mass concentrations indicated by positive residuals of gravimetric map

04 p0654 A69-14632

Lunar intermare crater density variations data tabulation, presenting quantitative and qualitative estimates

04 p0656 A69-14671

Lunar crater count observations of mare surface and ejecta blanket in Orientale basin

04 p0656 A69-14672

Lunar premare and postmare craters distributions, discussing latitude independence and sources of impacting bodies

04 p0656 A69-14673

Mare Orientale basin satellite photographs suggest asteroid impact formation

04 p0664 A69-15421

Nondimensional Jeffreys number as ratio of Reynolds to Froude number for gravitational motion of viscous masses, with application to lunar maria and plastic ice

07 p1218 A69-19262

Lunar mass concentrations /mascons/ origin and nature, postulating primordial lunar atmosphere and

- hydrosphere and carbon derived from primordial organic compounds
08 p1397 A69-20697
- Primitive elemental abundances in solar system, discussing composition of sun, meteorites and lunar maria
08 p1403 A69-20914
- Hypotheses concerning mechanism of lunar maria formation, discussing molten rock layer below lunar crust
10 p1782 A69-23710
- Meteor explosion theory of origin of lunar craters and round maria, suggesting endogenic origin
10 p1784 A69-23960
- Denser material beneath lunar maria revealed by precise tracking of lunar orbiting spacecraft, discussing geology and evolution
11 p1953 A69-24339
- Modified Diggelen photometric method in lunar topography, analyzing surface brightness and inclinations in mare regions and Korolev thalassoid
11 p1959 A69-24724
- Lunar craters circularity measurements relation to age, discussing fracture system and stress history associated with mare formation
13 p2344 A69-27645
- Lunar surface and earth early satellite system, discussing maria distribution, satellite impacts and close passage collisions
13 p2345 A69-27654
- Lunar surface gamma radiation observed by Luna 10 spectrometer, suggesting basalt-like minerals composition of lunar maria
13 p2333 A69-28635
- Orientation in proximity of moon and on moon surface utilizing maria, craters, etc
16 p2855 A69-31929
- Lunar localized subsurface mass concentration association with circular maria, noting two large mascon basins from gravity data and orbital photometry
16 p2864 A69-32446
- Mare Tranquillitatis surface chemical composition data from Surveyor 5, comparing element abundances with meteorites and terrestrial rocks
20 p3601 A69-37517
- Convection within moon as explanation of maria on near side, presence of mascons, etc
20 p3603 A69-37561
- Lunar mascons and maria isostasy, discussing time requirements
20 p3604 A69-37564
- Volcano-Tectonic origin of lunar mare terrain from Apollo 8 photograph showing faulting pattern identical with uppermost Pleistocene-Holocene faulting
20 p3604 A69-37570
- Linear thermal anomaly on western margin of Mare Humorum, rejecting internal heating origin
21 p3797 A69-38535
- Lunar maria structure and evolution as homologous transient gravity wave systems from impact craters on crust
21 p3803 A69-38982
- Lunar regolith from Surveyor Program pictorial data of lunar maria
22 p4012 A69-40087
- LUNAR MOBILE LABORATORIES**
- Moon environment for scientific experiments, emphasizing lunar surface properties, lack of man-made electromagnetic waves, vacuum and weak gravity force
13 p2240 A69-27910
- LUNAR MODULE**
- Aerothermal-structural reentry safety evaluation for SNAP-27 radioisotope Graphite Lunar Module Fuel Cask at orbital and superorbital velocities
[AIAA PAPER 68-1166] 03 p0465 A69-13561
- System designs for manned spacecraft gravity gradient stabilization of Saturn S-4B stage at 400 km and lunar module at synchronous altitude
07 p1228 A69-18338
- Thermal vacuum simulator for testing manned Lunar Module Test Vehicle, using conformal skin heaters to control heating rates and skin temperature
[AIAA PAPER 69-312] 09 p1479 A69-22386
- Electron beam welding of Lunar Module Descent Engine, emphasizing variable area injector element and manifold assembly problems and techniques
12 p2102 A69-26621
- Thermal vacuum /TV/ manned test operations related to Apollo lunar module in simulated space environment
15 p2558 A69-30394

- Lunar module multilayer radiation insulation for thermal control, testing aluminum coated Mylar and Kapton sheets
[AIAA PAPER 69-609] 17 p3073 A69-33304
- Apollo Lunar Module Environmental Control System /LM/ECS/ steady state performance simulation techniques, discussing vacuum chamber data of LTA-8/LM-3
[AIAA PAPER 69-616] 17 p2903 A69-33307
- Halon 1301 fire extinguisher for burning spilled hypergol on Apollo/Saturn LM adapter, discussing concentration requirements and exposure hazards
18 p3094 A69-35062
- Apollo navigation, guidance and control systems in command module and lunar module, discussing inertial, optical and computer hardware operation
19 p3369 A69-35799
- Lunar module motion during optimal ascent from moon surface into circular orbit of command module, noting descent maneuver similarity
19 p3431 A69-36617
- Manual attitude control for Lunar Module employing directional stability, coordinated turn and attitude command
[AIAA PAPER 69-892] 21 p3824 A69-39417
- Encapsulation effects on piece parts in high density package, considering unexpected part failures elimination in Lunar Module Signal Conditioning Electronic Assembly
22 p3910 A69-39953
- Mission simulation testing in thermal vacuum environment for Apollo Lunar Module, noting conformal skin heaters
[AIAA PAPER 69-991] 22 p3920 A69-40369
- LM descent engine behavior upon contact with lunar surface simulated, basing test condition on statistical trajectory analysis indicating fire until touchdown possibility
[AIAA PAPER 69-1020] 22 p3923 A69-40391
- Aerothermal-structural reentry safety evaluation for SNAP-27 radioisotope Graphite Lunar Module Fuel Cask at orbital and superorbital velocities
[AIAA PAPER 68-1166] 22 p3979 A69-40551
- Module landing effects on lunar surface, deriving erosion law from Surveyor 5 engine firing test and vacuum test data
23 p4211 A69-41388
- LUNAR OBSERVATORIES**
- Communications of lunar and planetary laboratory, Volume 7, covering lunar radiation, lunar craters, Vesta rotation, etc
04 p0655 A69-14668
- Lunar spherical astronomy, discussing coordinate transformations, precessional and nutational motions, etc
21 p3798 A69-38605
- LUNAR OCCULTATION**
- NT SOLAR ECLIPSES**
- Lunar occultations of radio source Sagittarius A observed at various frequencies between 230 and 2400 MHz, obtaining diameter, position and decimeter band flux densities
06 p1009 A69-17960
- Lunar occultations of galactic center region observed at 1667 MHz indicating OH absorption origin in uniform rotating cloud
06 p1009 A69-17961
- OH emission source in W24 during July 19, 1967 lunar occultation, obtaining better position for brighter OH emission feature
09 p1591 A69-21449
- Stellar occultations by moon observed with ear and eye method, not taking into account corrections to radio time signals
10 p1776 A69-23205
- Antenna for lunar occultation observations at 81.5 MHz, detailing experimental procedure and data reduction
10 p1779 A69-23606
- Sagittarius A occultation by moon, determining peak brightness and flux density of radio source
11 p1958 A69-24592
- Spectroscopic and eclipsing binaries in zodiac tabulated for photometric studies at lunar occultations
12 p2171 A69-27152
- Crab Nebula lunar occultation observed by Cassegrain array of deep space communication facility, finding radio brightness distribution similar to optical
15 p2687 A69-30539
- Lunar occultations analyzed to determine Moon position and ephemeris time, confirming adopted values of node and perigee motions
20 p3601 A69-37494

LUNAR ORBITER

- Lunar composition analysis by measuring atomic and nuclear radiation emission from orbiter
[AAS PAPER 68-197] 02 p0312 A69-11475
- Lunar Orbiter mission objectives and orbit design
[AIAA PAPER 68-47] 04 p0664 A69-15503
- Sinusoid rill and water distribution on lunar surface from Orbiter 4 high resolution photographs
05 p0818 A69-15606
- Photographic system in Lunar Orbiter spacecraft
05 p0829 A69-15857
- Photographic results of Lunar Orbiter program noting possible Apollo sites
05 p0822 A69-15858
- Spacecraft longitudinal control during reentry of lunar orbiter into atmosphere, analyzing final range prediction, trajectory tracking and accelerometers performance
13 p2355 A69-27681
- Meteoroid flux measured by Explorer 16 and Lunar Orbiter, analyzing penetration rate, average velocity and consistency with photographic meteors
13 p2349 A69-27820
- Doppler tracking data from Lunar Orbiter missions for studying lunar gravity anomalies, plotting acceleration on lunar surface Mercator projection
15 p2697 A69-31313
- Scientific space research program /1968-1978/ outlining advanced lunar orbiter and Mars, Venus and Mercury probes
18 p3193 A69-34360
- Lunar Orbiter Parts Program for selection and control of electronic and electrical parts, discussing reliability and flight failures
18 p3207 A69-34520
- Orbit parameters identification method based on given tracking data span applied to lunar orbiter tracking using Fourier analysis
19 p3401 A69-35916
- Lunar Orbiter data for existence of unequal mass distributions in lunar interior confirmed by manned Apollo 8 and 10 flights, discussing origin
20 p3606 A69-37933
- Lunar surface erosion processes revealed by Lunar Orbiter photographs of boulder concentrations
21 p3794 A69-38378
- Lunar Orbiter missions pre- and postflight error analyses compared to estimate dispersions from reference trajectory
[AAS PAPER 68-108] 21 p3805 A69-39220
- Residuals from earth based coherent two way radio Doppler data from Lunar Orbiter three orders of magnitude larger than observations from spacecraft
[AAS PAPER 68-131] 21 p3828 A69-39766
- Telecommunications performance of two lunar relay satellite system /LRSS/, determining operation capabilities with Apollo communications system
23 p4129 A69-42508
- LUNAR ORBITS**
- Optical ranging technique for studying lunar physical libration by measuring distance between earth observatory and two fixed points on lunar surface
01 p0158 A69-11311
- Lunar high density mass concentrations effect on Lunar Orbiters accelerations, discussing lunar gravity field determination
04 p0661 A69-15145
- Asymptotic solutions of restricted three body problem for one parameter periodic orbits in earth-moon synodic system, determining motion near moon
04 p0663 A69-15382
- Explorer 35 measurements of low energy plasma in lunar orbit made by planar multigrad sensor programmed as retarding potential analyzer
05 p0825 A69-16278
- Reentry trajectories from lunar surface and orbit obtained by computer with allowance for initial data spread
09 p1594 A69-21756
- Earth-moon and moon-earth trajectory parameters related to lunar orbit conditions for synthesizing lunar orbit trajectory
18 p3196 A69-34704
- Catastrophic and noncatastrophic alternatives for earth capture of moon, discussing tidal action and spin-orbit resonance
18 p3198 A69-34823
- Lunar occultations analyzed to determine Moon position and ephemeris time, confirming adopted values of node and perigee motions
20 p3601 A69-37494

Literal solution to equations of motion applied to lunar theory using electronic computer with series convergence

21 p3796 A69-38474

Real time targeting for Apollo lunar orbit insertion maneuver burn, discussing impulsive maneuvers for flight control
[AIAA PAPER 68-848]

21 p3828 A69-39760

Light pressure induced secular effect contributing to planetary satellites and lunar orbits evolution calculated by numerical integration

22 p4033 A69-41084

LUNAR PHASES

Lunar thermal radiation measurements at 8.6 and 3.2 mm wavelengths, noting brightness temperature-time relationship in curves and as Fourier components

02 p0327 A69-12717

Lunar surface spectral reflectivity variations with time, noting phase angle effects on color contrast

13 p2349 A69-27819

Lunar components in mean values of geomagnetic field daily variations, discussing lunar phase during selected quiet days

16 p2782 A69-32458

Auroral activity and lunar phases correlation from IMP-1 measurements of lunar magnetic field

24 p4311 A69-43502

LUNAR PHOTOGRAPHS

Crater Copernicus photograph, discussing misinterpretation of Orbiter 2 lunar surface photograph on basis of effective temperature contours analysis

01 p0154 A69-10898

Lunar rays nature from terrestrial observations and surface photographs by lunar probes, noting high crater concentration structure

02 p0236 A69-11642

Geological-morphological mapping of moon interpretation and lunar surface structural peculiarities

03 p0505 A69-12898

Large scale lunar surface photographs for estimating conical formations identified with terrestrial stratovolcanoes

03 p0507 A69-13093

Lunar crater count observations of mare surface and ejecta blanket in Orientale basin

04 p0656 A69-14672

Selenographic technique for tying in lunar far side space photographs based on earth disk position measurements with respect to moon limb

05 p0763 A69-16055

Lunar geology information obtained by Ranger space missions

06 p1001 A69-17163

Ranger pictures improvement by computer, eliminating image distortion due to electronic imaging systems

06 p0924 A69-17164

Relative lunar altitudes determination from shadow measures on earth based lunar photographs by direction-cosine method

07 p1225 A69-19770

Comparator measures for relative lunar altitudes on Yerkes lunar photographs, estimating selenographic positions from grids of orthographic atlas of moon

07 p1225 A69-19771

Selenodetic measurements on Yerkes lunar star trailed photographs, considering limb and star trail

07 p1225 A69-19772

Yerkes star trailed lunar photographs with ephemeris values of moon libration for selenodetic coordinates of secondary points, discussing errors and altitudes

07 p1225 A69-19773

Tucson selenodetic triangulation for coordinated points, considering measures on Yerkes star trailed plates

07 p1225 A69-19774

Lunar far side craters profile and structure determined from Zond 3 photographs using photometric method

11 p1959 A69-24725

Lunar far side craters vertical profiles plotted from photometric cross sections of Zond 3 photographs

11 p1959 A69-24726

Large scale lunar surface photographs for estimating conical formations identified with terrestrial stratovolcanoes

14 p2516 A69-28775

Moon pictures from Apollo 8 spacecraft including full moon, crater Tsiolkovsky and unidentified area showing volcanism

14 p2527 A69-29889

Apollo 8 photooptics, considering TV camera and broadcasts, photographic equipment and visual observation

15 p2609 A69-30469

Geometric shape of lunar profile from annular phase of 20 May 1966 annular solar eclipse coronagraph plates, applying Fourier series and Pascal limaçon approximation

15 p2686 A69-30531

NASA photogrammetric lunar activities, discussing imagery and control data by Lunar Orbiter and photogrammetric data reduction for preparing manned lunar landing

18 p3133 A69-34336

Volcano-Tectonic origin of lunar mare terrain from Apollo 8 photograph showing faulting pattern identical with uppermost Pleistocene-Holocene faulting

20 p3604 A69-37570

Selenographic technique for tying in lunar far side space photographs bases on earth disk position measurements with respect to moon limb

20 p3545 A69-37965

Cartographic tying-in of Zond 3 lunar surface photographs to verify maps of moon far side

20 p3608 A69-38051

Lunar libration point L4 photographs taken during 6 October 1968 eclipse showing no discrete objects or clouds

20 p3613 A69-38249

Lunar surface photographic mapping by Ranger, Surveyor and Lunar Orbiter projects, emphasizing image resolution and coverage

21 p3719 A69-38325

Surveyor spacecraft instrumentation, describing TV camera design and operation, photographic requirements and techniques, lunar surface characteristics, etc

22 p4011 A69-40043

LUNAR PHOTOGRAPHY

Lunar Orbiter mission objectives and orbit design
[AIAA PAPER 68-47]

04 p0664 A69-15503

Sinuuous rill and water distribution on lunar surface from Orbiter 4 high resolution photographs

05 p0818 A69-15606

Photographic system in Lunar Orbiter spacecraft

05 p0829 A69-15857

Photographic results of Lunar Orbiter program noting possible Apollo sites

05 p0822 A69-15858

Absolute coordinates of 906 lunar features derived and tabulated, eliminating errors due to atmospheric turbulence by using 120 lunar negatives

07 p1213 A69-18612

Volcanic origin of lunar crater Dawes based on photogeological evidence obtained from Lunar Orbiter 5 photographs

11 p1952 A69-24264

Surveyor 7 TV system in photon integration mode, analyzing slow scan vidicon storage characteristics and dark current limitations

12 p2078 A69-25772

Soviet lunar probe Zond 6 achievements in controlled Earth landing and lunar surface photography

13 p2355 A69-27342

Soviet astronomical radio-astronomical probe and orbiter lunar studies including surface photography, gravitational and magnetic measurements and soft landed probes

13 p2336 A69-27353

Lunar surface light scattering data cataloged for various phase angles from photometric observations of lunar features brightness

13 p2344 A69-27648

Photogrammetric calibration of Surveyor 7 stereo mirror based on vector analysis

13 p2263 A69-28199

Extraterrestrial imagery, discussing earth based telescopes, IR imagery, moon mapping, lunar and planetary probes, Lunar Orbiter photos interpretation and sensors for detecting life

15 p2690 A69-30711

Lunar localized subsurface mass concentration association with circular maria, noting two large mascon basins from gravity data and orbital photography

16 p2864 A69-32446

Lunar rotation parameters determined from photographs and visual observations independent of moon profile

17 p3027 A69-32874

NASA lunar survey and mapping for generating Apollo satellite landing navigation control, using analytic photogrammetry, camera position and altitude data of lunar topography

20 p3536 A69-36931

NASA Lunar Orbiter Program of lunar photography from orbiting spacecraft

21 p3794 A69-38377

Lunar surface erosion processes revealed by Lunar Orbiter photographs of boulder concentrations

21 p3794 A69-38378

Photogrammetric camera system developed from NASA requirements to document lunar surface environment during manned space flight exploration

22 p3948 A69-40989

Lunar photometric function near zero phase from Apollo 8 closeup photography, noting higher reflected brightness than at 1.5 degree phase angle

23 p4220 A69-42380

LUNAR PROBES

NT LUNIK LUNAR PROBES

NT LUNIK 9 LUNAR PROBE

NT LUNIK 10 LUNAR PROBE

NT LUNIK 12 LUNAR PROBE

NT LUNIK 13 LUNAR PROBE

NT RANGER LUNAR PROBES

NT SURVEYOR LUNAR PROBES

NT SURVEYOR 1 LUNAR PROBE

NT SURVEYOR 5 LUNAR PROBE

NT SURVEYOR 6 LUNAR PROBE

NT SURVEYOR 7 LUNAR PROBE

Earth and lunar magnetic field studies in U.S.S.R., discussing Soviet earth satellite and lunar probe data

01 p0066 A69-10943

Lunar rays nature from terrestrial observations and surface photographs by lunar probes, noting high crater concentration structure

02 p0236 A69-11642

Direct analysis of lunar surface chemical composition, considering soft landing probe and X ray isotope fluorescence method

11 p1832 A69-24629

Lunar orbital mission plans intended to optimize spacecraft procurement, flight schedules, science objectives and available funds

18 p3193 A69-34362

Spectral reflectivity and emissivity observations of proposed Apollo landing sites compared with other lunar localities and unmanned lunar probe data

21 p3815 A69-39585

LUNAR PROGRAMS

NT APOLLO PROJECT

NT SURVEYOR PROJECT

National space program management, discussing NACA and NASA, lunar mission planning, procedures and program flexibility and responsibility

01 p0178 A69-10468

Improved suit for lunar wear, noting production and qualifying schedule and astronaut tests

08 p1267 A69-21146

Manned lunar exploration programs and site evaluation concerning volcanic processes, chemical and mineralogical differentiation, atmosphere and protobiological materials

23 p4216 A69-42200

Technology flow for future manned earth orbit and lunar operations and planetary exploration

24 p4380 A69-42840

Planning lunar surface experiments in nets or at selected sites for optimum scientific return

24 p4381 A69-42874

LUNAR RADAR ECHOES

Specific effective scattering area on lunar surface using Luna 13 signals from Oceanus Procellarum measured with radar employing antenna with narrow radiation pattern

01 p0158 A69-11312

Millimeter wave lunar radar system component specifications and design with paraboloidal antenna, emphasizing reflectivity of moon

03 p0397 A69-13725

LUNAR RADIATION

Lunar thermal radiation measurements at 8.6 and 3.2 mm wavelengths, noting brightness temperature-time relationship in curves and as Fourier components

02 p0327 A69-12717

Thermal conditions of upper blanket of lunar surface during eclipse, using data to calculate lunar radio emission

03 p0506 A69-13088

Lunar surface IR polarization measurements compared to visible and UV polarization

04 p0656 A69-14669

Gray tone differences between undisturbed lunar surface and darker ejecta observed around Surveyor 1 footpads, discussing possible albedo differences

04 p0660 A69-15124

LUNAR RAYS

Lunar radio emission polarization characteristics, considering knife-edge type radiation pattern effect of antenna array
08 p1391 A69-20423

Microwaves from celestial objects noting radio emission from sun, moon and Jupiter, cosmic fireball and pulsars
08 p1407 A69-21125

Lunar photon leakage spectrum due to photons from capture and inelastic scattering of neutrons by galactic cosmic rays
09 p1597 A69-22088

Radiometric observations of moon during total lunar eclipse at 3.33 mm, noting decrease in equivalent black body disk temperature
10 p1789 A69-24132

Lunar radio emission constant component in presence of heat flow from interior, using stratified model of surface structure with two variants
11 p1956 A69-24398

IR spectroscopic observations of moon to interpret molecular vibration spectra in terms of molecular composition, discussing rock surface roughness effects
13 p2341 A69-27582

Lunar surface gamma radiation observed by Luna 10 spectrometer, suggesting basalt-like minerals composition of lunar maria
13 p2333 A69-28635

Thermal conditions of upper blanket of lunar surface during eclipse, using data to calculate lunar radio emission
14 p2515 A69-28770

Angular dependence of lunar nighttime IR radiation by invariant tensor techniques, noting surface roughness effect on radiation pattern
[AIAA PAPER 69-597] 17 p3032 A69-33276

Directional characteristics of lunar IR radiation accounted for by crater model
[AIAA PAPER 69-598] 17 p3033 A69-33285

Radio emission measurements of moon at 3.2 cm by artificial moon method, calculating radio temperature and phase amplitudes
20 p3608 A69-38052

Automatic planetary electrophotometer designed for earth atmosphere and lunar photometry, noting operational data
20 p3547 A69-38310

Lunar surface thermal radiation incident on unit area flat surface located at variable distance and orientation above moon, considering diffusion effects
21 p3803 A69-38973

Thermal calculations of objects near lunar surface, considering IR emission directivity effects
24 p4385 A69-43254

Lunar radio emission constant component in presence of heat flow from interior, using stratified model of surface structure with two variants
24 p4390 A69-43788

LUNAR RAYS

Lunar rays nature from terrestrial observations and surface photographs by lunar probes, noting high crater concentration structure
02 p0236 A69-11642

Lunar radio emission linear polarization radial dependence at 0.8-cm wavelength using radio telescope, determining dielectric constant of emitting layer
15 p2697 A69-31251

LUNAR RECEIVING LABORATORY

NASA lunar receiving laboratory for lunar rock samples examination by gamma ray spectrometry for induced radioactive nuclides and naturally occurring isotopes
20 p3512 A69-38271

NASA Lunar Receiving Laboratory functional areas and physical, chemical, biological and quarantine activities for crew and lunar samples
21 p3690 A69-38896

Lunar rocks and fines samples physical, chemical, mineralogical and biological preliminary analysis at Lunar Receiving Laboratory
24 p4382 A69-42935

LUNAR ROVING VEHICLES

Predictive display technique for remote manual control of roving lunar and planetary surface vehicles
06 p0928 A69-17925

LUNAR SATELLITES

NT EXPLORER 18 SATELLITE
NT IMP

Artificial lunar satellite orbital motion calculated by numerical integration, including solar and lunar electromagnetic radiation pressure effects
04 p0662 A69-15251

Lunar mass and gravitational field determined from lunar satellite dynamics, using potential function in terms of spherical harmonics
15 p2699 A69-31405

Hill method for satellite motion with reference to rectangular rotating axes system with origin at moon center of gravity, obtaining intermediate orbits
16 p2855 A69-31656

Short term motion of lunar satellite, discussing third body disturbing functions and perturbation solution of nonsingular orbit elements
19 p3402 A69-35934

Research satellite, commercial satellite, lunar spacecraft and military satellite missions, discussing Intelsat, Comsat, Early Bird, MOL and ESRO space program
19 p3432 A69-36750

**LUNAR SCATTERING
U DIFFUSE RADIATION**

LUNAR SEISMOGRAPHS

PostApollo lunar passive seismic experiments, discussing probable results of present program, exploration sites and additional network stations and instruments
[AAS PAPER 68-204] 02 p0312 A69-11479

Lunar seismic velocity distribution data indicates broad low velocity zone together with possible extensive melting at depth
[AAS PAPER 68-205] 02 p0312 A69-11480

Lunar seismology, discussing Apollo 11 instrumentation and experiments, moonquakes and travel times measurements and lunar tides
19 p3315 A69-36765

Apollo 11 passive seismic experiment design and objectives, describing seismometer characteristics and lunar interior
20 p3539 A69-37516

Miniaturized seismic refraction system for manned lunar landings consisting of geophones, three channel amplifier, calibrator and logarithmic compressor
23 p4162 A69-41533

LUNAR SHADOW

Moon effect on intensity and angular distribution of energetic electron and proton shadowing as observed by Explorer satellites
05 p0824 A69-16252

Lunar umbra interception by Titus rockets during solar eclipse, measuring UV and IR flux
06 p0986 A69-17101

LUNAR SHELTERS

Lunar shelter regenerative life support system performance and manned test
07 p1071 A69-19427

LUNAR SOIL

Penetration type soil analyzer used by Luna 13 automatic lunar station for mechanical strength of lunar surface
03 p0430 A69-13424

Lunar surface layer density measured radiometrically with scattered gamma rays by Luna 13
03 p0430 A69-13425

Lunar surface material chemical composition in lunar mare and on Tycho crater north rim, noting Surveyors 5, 6, and 7 alpha analyses
04 p0655 A69-14658

Lunar surface composition, hardness, porosity, microstructure and transparency based on polarization of reflected light
04 p0658 A69-14958

Gray tone differences between undisturbed lunar surface and darker ejecta observed around Surveyor 1 footpads, discussing possible albedo differences
04 p0660 A69-15124

Surveyor lunar scientific payload and results, discussing TV camera, soil mechanics and surface sampler, alpha scattering instrument, small magnets and surface analysis
06 p1001 A69-17162

Lunar surface chemical composition using RF mass spectrometer
10 p1698 A69-24207

Direct analysis of lunar surface chemical composition, considering soft landing probe and X ray isotope fluorescence method
11 p1832 A69-24629

Moon environment for scientific experiments, emphasizing lunar surface properties, lack of man-made electromagnetic waves, vacuum and weak gravity force
13 p2240 A69-27910

Temperature distribution in shadowed lunar craters formulated in Fredholm integral equations, showing

constant temperature and correction for soil thermal inertia
[AIAA PAPER 69-595] 17 p3033 A69-33291

Lunar surface uppermost layer physical and mechanical properties investigated by soilmeter-penetrometer and radiation densimeter on Luna 13
18 p3113 A69-34239

Particulate thermophysical lunar soil model for measuring lunation nighttime and eclipse cooling, noting applicability to IR surface brightness temperature of Mercury hot pole
18 p3191 A69-34303

Lunar surface bulk density determined from laboratory and spacecraft measurements of static bearing capacity as functions of depth and solids percentage
18 p3193 A69-34366

Lunar surface composition, hardness, porosity, microstructure and transparency based on polarization of reflected light
18 p3196 A69-34721

Correlating IR lunar nighttime temperature and bearing strength of lunar materials, using expressions of thermal conductivity and bearing strength of porous media in vacuo
20 p3613 A69-38248

Electrical conductivity of uppermost lunar surface layers, indicating dry powdered rocks with frequency independent dielectric loss tangent
22 p4023 A69-40570

Mass spectrometric analysis of lunar material from soil vaporization products ion component by electron beam
22 p4034 A69-41107

Module landing effects on lunar surface, deriving erosion law from Surveyor 5 engine firing test and vacuum test data
23 p4211 A69-41388

Lunar rocks and fines samples physical, chemical, mineralogical and biological preliminary analysis at Lunar Receiving Laboratory
24 p4382 A69-42935

Lunar surface material mechanical properties from Surveyor observations, analyzing grain size, rock density, internal friction, cohesion and bulk density compared to Luna observations
24 p4383 A69-42962

Shear load, cohesion and internal friction measurements of low bulk density particulate silicates of complex shape, noting significance for lunar comparison
24 p4383 A69-43040

LUNAR SPACECRAFT

NT APOLLO SPACECRAFT
NT EXPLORER 18 SATELLITE
NT IMP
NT LUNIK LUNAR PROBES
NT LUNIK 9 LUNAR PROBE
NT LUNIK 10 LUNAR PROBE
NT LUNIK 12 LUNAR PROBE
NT LUNIK 13 LUNAR PROBE
NT RANGER LUNAR PROBES
NT SURVEYOR LUNAR PROBES
NT SURVEYOR 1 LUNAR PROBE
NT SURVEYOR 5 LUNAR PROBE
NT SURVEYOR 6 LUNAR PROBE
NT SURVEYOR 7 LUNAR PROBE

Lunar surface features as observed by orbiting and landing craft, discussing particle layer, rocks, craters, effects of erosion, meteorite impact, etc
15 p2698 A69-31356

LUNAR SURFACE VEHICLES

Flight test evaluation of small one man lunar flying device /POGO/, discussing vehicle control, pressure suit factors and piloting differences
[AIAA PAPER 68-240] 02 p0229 A69-12379

Lunar surface vehicle mathematical models, discussing design influence of low gravity, atmosphere absence, temperature extremes and surface roughness
05 p0741 A69-15673

Vehicles for lunar surface exploration and transportation including flying machines and wheeled vehicles
13 p2352 A69-27908

Hopping transporter vehicle designs for lunar exploration providing low fuel consumption at high average speed
[AIAA PAPER 68-1139] 22 p3927 A69-40547

LUNAR TEMPERATURE

Lunar surface temperatures and thermal characteristics from Surveyor 5 thermal engineering data gathered during lunar days, eclipse and nights
02 p0321 A69-12227

IR observations of lunar crater and maria enhanced thermal emission during eclipse, constructing model of cratered surface to analyze thermal behavior
04 p0654 A69-14656

Radiometric observations of moon during total lunar eclipse at 3.33 mm, noting decrease in equivalent black body disk temperature

10 p1789 A69-24132

Lunar thermal anomalies in various craters observed during lunar night by IR methods, with data suggesting hot and cold regions

12 p2171 A69-27092

Lunar surface temperature distribution measured by IR pyrometer, predicting temperature rise due to Lunar Excursion Module landing

13 p2341 A69-27583

Lunar dynamic response to discontinuities in interplanetary magnetic field to determine electrical conductivity and internal temperature

15 p2700 A69-31442

Lunar surface thermal characteristics revised from analysis of error sources in daytime lunar surface temperatures derived from Surveyor 5 compartment data [AIAA PAPER 69-594]

17 p3033 A69-33287

Lunar temperature prediction with emphasis on variable property models, noting assumptions about physical properties appearing in heat conduction equations

18 p3194 A69-34374

Book on thermal processes of earth and moon covering heat generation and transfer, internal temperatures, gravitational energy, etc

19 p3401 A69-35887

Convection within moon as explanation of maria on near side, presence of mascons, etc

20 p3603 A69-37561

Radiometric measurement of lunar areas during eclipse of 18 October 1967 at mm wavelengths, considering temperature changes and cooling rates

20 p3613 A69-38247

Correlating IR lunar nighttime temperature and bearing strength of lunar materials, using expressions of thermal conductivity and bearing strength of porous media in vacuo

20 p3613 A69-38248

Linear thermal anomaly on western margin of Mare Humorum, rejecting internal heating origin

21 p3797 A69-38535

LUNAR TIDES

Lunar tidal effects on F 2 critical frequency and height maximum, evaluating variations with altitude

01 p0063 A69-10424

Lunar tide effect on height distribution and velocity of ionospheric electron density daily variations near magnetic equator

05 p0756 A69-16401

Long range prediction of zonal westerlies based on lunar cycles or quasi-biennial oscillations, considering aliasing problem

07 p1175 A69-18945

Luni-solar tide interpretation in F2 critical frequency based on sum and difference frequencies production by nonlinear atmospheric response to forces

10 p1685 A69-23829

Cometary, lunar and solar effects on precipitation, considering joint influence of meteoric streams and moon

11 p1965 A69-25420

Ocean circulation as climate regulator, discussing role in redistributing climate-changing energy input from solar radiation or lunar tidal friction into atmosphere

12 p2067 A69-26333

Cyclic vector amplitude error from noisy data corrected for calculating geophysical lunar tidal effects

12 p2033 A69-26956

Semimonthly lunar variation in D region absorption, discussing phase reversal of lunar tides between equatorial and high latitudes

14 p2439 A69-29113

Tide dependent variations of critical frequencies of ionospheric layers minimal heights and maximum height of F 2 layer reflection

14 p2444 A69-29871

Lunar tidal variations of electron concentration in F 2 region near magnetic equator showing large latitudinal dependence

16 p2776 A69-32090

Lunar tidal oscillations in F 2 layer critical frequency and F region minimum virtual height at Huancayo during IGY/IGC to study solar cycle effects

16 p2784 A69-32613

Lunar seismology, discussing Apollo 11 instrumentation and experiments, moonquakes and travel times measurements and lunar tides

19 p3315 A69-36765

Lunar semimonthly variations in noon values of D region absorption at Singapore, noting opposite phases of lunar tides in D and F regions

22 p4035 A69-41211

Solar quiet and lunar electric current systems deduced from geomagnetic data, discussing electrical conductivities and wind models in dynamo region

23 p4160 A69-42427

LUNAR TOPOGRAPHY

Analytic photogrammetric determination of lunar control coordinates from Ranger photography

01 p0147 A69-10022

Lunar surface early geologic evolution noting bearing on earth geologic history [AAS PAPER 68-202]

02 p0312 A69-11478

Magnetometer experiment for Apollo project to measure lunar surface magnetic field, describing mission requirements and instrumentation [AAS PAPER 68-206]

02 p0312 A69-11481

Selenodetic data results and calculations of moon visible physical surface do not agree

02 p0314 A69-11643

Lunar surface temperatures and thermal characteristics from Surveyor 5 thermal engineering data gathered during lunar days, eclipse and nights

02 p0321 A69-12227

Particle size frequency distributions and lunar surface materials, showing impossibility of distinguishing between impact fragmentation of surface and pyroclastic rock deposition

02 p0325 A69-12567

Geological-morphological mapping of moon interpretation and lunar surface structural peculiarities

03 p0505 A69-12898

Tectonic map compiled for visible and far sides of moon, noting correlations between earth and moon tectogenesis

03 p0505 A69-12899

Relation between color index over lunar surface and solar rays angle of incidence, noting supplementary emission attributed to surface luminescence

03 p0506 A69-13089

Large scale lunar surface photographs for estimating conical formations identified with terrestrial stratovolcanoes

03 p0507 A69-13093

Electron beam meter application as lunar surface electric field detector, discussing breadboard model and performance characteristics

03 p0429 A69-13221

Lunar surface layer density measured radiometrically with scattered gamma rays by Luna 13

03 p0430 A69-13425

Hypsometric contour map of lunar surface from absolute altitude measurements of 1200 points on lunar surface

03 p0512 A69-13689

Moon figure from meridional measurements of visible diameters at different angles of libration, deriving equation for polar and equatorial compression of lunar ellipsoid

03 p0512 A69-13690

IR observations of lunar crater and maria enhanced thermal emission during eclipse, constructing model of cratered surface to analyze thermal behavior

04 p0654 A69-14656

Quasi-specular bistatic radar measurements of oblique scattering properties of lunar surface using telemetry carrier from Explorer 35 as lunar orbiting radar beacon

04 p0655 A69-14657

Lunar glowing spots near Aristarchus considered volcanic eruptions of molten material

04 p0657 A69-14676

Lunar and Martian annular formations and structures, discussing classification, morphological characteristics, incidence frequencies and area sizes

04 p0658 A69-14959

Mountain structures surrounding lunar craters, discussing possible origin by impacting planetesimals shock waves

04 p0661 A69-15142

Lunar shape hypsometric peculiarities, analyzing heights and asymmetry in relation to lunar equator, central meridian and image plane

04 p0662 A69-15249

Mare Orientale basin satellite photographs suggest asteroid impact formation

04 p0664 A69-15421

Sinuuous rill and water distribution on lunar surface from Orbiter 4 high resolution photographs

05 p0818 A69-15606

Large mass concentrations /mascons/ effect on moon dynamical figure, considering production of asymmetries

05 p0820 A69-15762

Lunar studies and moon exploration noting moon motion, lunar rotation dependence on orbital motion, lunar figure and topography and mass distribution

05 p0820 A69-15835

Photographic results of Lunar Orbiter program noting possible Apollo sites

05 p0822 A69-15858

Polarization-albedo relationship for selected lunar maria, highlands and mountains in five passbands suggesting optical path length function of effective refractive index and particle size

05 p0829 A69-16663

Possible evolution of earth continents and ocean basin, considering ultrabasic, basic, and intermediate to acidic lunar highlands chemical composition

06 p1000 A69-17006

Lunar exploration sites selection based on telescopic studies and geological maps

06 p1001 A69-17161

Lunar geology information obtained by Ranger space missions

06 p1001 A69-17163

Fine structure and geology of lunar surface from Luna, Ranger, Surveyor and Orbiter data

07 p1212 A69-18547

Absolute coordinates of 906 lunar features derived and tabulated, eliminating errors due to atmospheric turbulence by using 120 lunar negatives

07 p1213 A69-18612

Lunar scattering of meter radio waves emitted by Luna 11 and 12 satellites, relating glide angle scattering coefficients to satellite altitude

07 p1087 A69-19615

Quantitative radar determinations of radio wave scattering cross section of lunar surface layer

07 p1087 A69-19621

Relative lunar altitudes determination from shadow measures on earth based lunar photographs by direction-cosine method

07 p1225 A69-19770

Comparator measures for relative lunar altitudes on Yerkes lunar photographs, estimating selenographic positions from grids of orthographic atlas of moon

07 p1225 A69-19771

Selenodetic measurements on Yerkes lunar star trailed photographs, considering limb and star trail

07 p1225 A69-19772

Lunar gravitational field and figure, discussing astronomical observations based on trajectory measurements of Luna 10 lunar orbiter

09 p1589 A69-21375

Relative heights on moon, tabulating lunar topography and comparing micrometric measurements and map data

10 p1782 A69-23697

Lunar atmosphere molecule and atom concentration from isotropic and uniform surface evaporation due to micrometeorite impact

10 p1783 A69-23921

Lunar radio emission constant component in presence of heat flow from interior, using stratified model of surface structure with two variants

11 p1956 A69-24398

Modified Diggelen photometric method in lunar topography, analyzing surface brightness and inclinations in mare regions and Korolev thalassoid

11 p1959 A69-24724

Lunar far side craters profile and structure determined from Zond 3 photographs using photometric method

11 p1959 A69-24725

Lunar surface layer structure by statistical analysis of data concerning craters and stones distribution as shown by lunar orbiter photographs

12 p2154 A69-25816

Lunar surface layer temperature field dynamics obtained from stable periodic solution to parabolic differential equation with nonlinear nonautonomous boundary conditions

12 p2157 A69-26281

Gaussian particle size distribution with porosity and surface irregularity corrections used to determine mean particle size of lunar surface material at Surveyor sites

12 p2158 A69-26371

Lunar thermal anomalies in various craters observed during lunar night by IR methods, with data suggesting hot and cold regions

12 p2171 A69-27092

Soviet astronomical radio-astronomical probe and orbiter lunar studies including surface topography, gravitational and magnetic measurements and soft landed probes

13 p2336 A69-27353

Lunar surface temperature distribution measured by IR pyrometer, predicting temperature rise due to Lunar Excursion Module landing 13 p2341 A69-27583

Lunar topography harmonic analysis, noting sample point density and evenness variations effects on estimated coefficients 13 p2344 A69-27647

Lunar surface light scattering data cataloged for various phase angles from photometric observations of lunar features brightness 13 p2344 A69-27648

Lunar surface and earth early satellite system, discussing maria distribution, satellite impacts and close passage collisions 13 p2345 A69-27654

Lunar surface spectral reflectivity variations with time, noting phase angle effects on color contrast 13 p2349 A69-27819

Lunar geophysical features origin, noting mascons influence and surface rigidity 13 p2352 A69-27903

Lunar surface environmental factors including molecular gas behavior under weak gravity and low atmospheric density, radiation and temperature effects, meteorite bombardment, etc 13 p2352 A69-27904

Vehicles for lunar surface exploration and transportation including flying machines and wheeled vehicles 13 p2352 A69-27908

Moon environment for scientific experiments, emphasizing lunar surface properties, lack of man-made electromagnetic waves, vacuum and weak gravity force 13 p2240 A69-27910

Lunar surface gamma radiation observed by Luna 10 spectrometer, suggesting basalt-like minerals composition of lunar maria 13 p2333 A69-28635

Relation between color index over lunar surface and solar rays angle of incidence, noting supplementary emission attributed to surface luminescence 14 p2516 A69-28771

Large scale lunar surface photographs for estimating conical formations identified with terrestrial stratovolcanoes 14 p2516 A69-28775

Vacuum chamber model for sinuous rilles on lunar surface produced by aqueous erosion under ice blanket 14 p2485 A69-28873

Visual orientation near moon and at surface, considering terrestrial and lunar objects reflectivity and light reflection at various angles of incidence 14 p2525 A69-29750

Lunar surface evolution, discussing relationship between craters erosional stage and areal density 14 p2528 A69-29947

Surveyor lunar landing procedures and results including instrumentation, lunar topography, selenology, chemical and physical properties, solar corona and earth laser output observations 15 p2681 A69-30324

Lunar surface features as observed by orbiting and landing craft, discussing particle layer, rocks, craters, effects of erosion, meteorite impact, etc 15 p2698 A69-31356

Radio wave scattering characteristics of lunar surface in 3 cm wavelength by Luna 8 and Luna 9 automatic stations and Surveyor spacecraft 15 p2571 A69-31359

Lunar relief mechanism based on experimental cratering by pasty projectiles, proposing terrestrial magma genesis 15 p2698 A69-31373

Laser measurements of earth-moon distance applied to determinations of earth axis motion and lunar shape, relief, dimensions and motion 16 p2788 A69-31624

Orientation in proximity of moon and on moon surface utilizing maria, craters, etc 16 p2855 A69-31929

Lunar surface characteristics, discussing light polarization, lunar radiation, solar radiation and meteorite impact effects, etc 16 p2856 A69-32069

Giant lunar craters, discussing lunar age and defining surface steady state 16 p2863 A69-32404

Directional characteristics of lunar IR radiation accounted for by crater model [AIAA PAPER 69-598] 17 p3033 A69-33285

Lunar surface brightness temperatures from IR observations, determining thermal emission directional

characteristics to infer surface temperatures from Surveyor data [AIAA PAPER 69-593] 17 p3033 A69-33302

Lunar photometric function determined using modified Hapke surface model and corrected Lommel-Seeliger law for surface roughness and crater distribution [AIAA PAPER 69-596] 17 p3033 A69-33308

Spectral reflectivity differences /color differences/ on lunar surface in visible region, indicating compositional difference origins 17 p3037 A69-33653

Lunar gravimetric data reprocessed to present in usable and readable form, plotting acceleration on Mercator projection of lunar surface 18 p3194 A69-34413

Relative heights on western moon half computed and compared to values of Schmidt, U.S. Army Map Service and USAF Aeronautical Chart Information Center 18 p3196 A69-34693

Lunar and Martian annular formations and structures, discussing classification, morphological characteristics, incidence frequencies and area sizes 18 p3197 A69-34722

Lunar gravitational field and figure, discussing astronomical observations based on trajectory measurements of Luna 10 lunar orbiter 18 p3198 A69-34763

Lunar rivers as coalesced chain craters resulting from gas emission along fracture beneath lunar regolith 18 p3205 A69-35436

Surface structure asymmetry of near and far sides of moon, considering earth radiation and gravity pull 18 p3206 A69-35439

Depth distribution of primary cosmic radiation fluxes and secondary nuclear-active particles in stone meteorites and surface layer of planets, moon and asteroids 19 p3410 A69-36092

Rivers on moon, discussing possibilities of water existence on lunar surface in view of temperature, gravity and atmospheric conditions 19 p3419 A69-36145

NASA lunar survey and mapping for generating Apollo satellite landing navigation control, using analytic photogrammetry, camera position and altitude data of lunar topography 20 p3536 A69-36931

Lunar gravitational potential and lunar surface radius vector binomial series coefficients determination from Luna 10 data used for lunar surface shape calculations 20 p3596 A69-37308

Volcano-Tectonic origin of lunar mare terrain from Apollo 8 photograph showing faulting pattern identical with uppermost Pleistocene-Holocene faulting 20 p3604 A69-37570

Lunar surface scattering properties at 2.5 cm wavelength determined using computerized backscattering diagram and equations for obtaining scattering data 20 p3606 A69-37971

Cartographic tying-in of Zond 3 lunar surface photographs to verify maps of moon far side 20 p3608 A69-38051

Steady state sunlit lunar surface electrostatic charge and potential distributions, noting electrons photoemission and solar wind particles collection 20 p3609 A69-38077

Radiometric measurement of lunar areas during eclipse of 18 October 1967 at mm wavelengths, considering temperature changes and cooling rates 20 p3613 A69-38247

Lunar surface photographic mapping by Ranger, Surveyor and Lunar Orbiter projects, emphasizing image resolution and coverage 21 p3719 A69-38325

Lunar surface erosion processes revealed by Lunar Orbiter photographs of boulder concentrations 21 p3794 A69-38378

Figure and inhomogeneities relationship for moon, Mercury, Venus, Mars and earth, discussing circular basins and mascons 21 p3803 A69-38980

Lunar maria structure and evolution as homologous transient gravity wave systems from impact craters on crust 21 p3803 A69-38982

Lunar surface structure and formation, discussing impact craters, interplanetary collisions, volcanic traces, lunar soil, etc 21 p3811 A69-39514

Lunar surface IR emissivity comparison spectra including proposed Apollo landing sites, indicating Si-O ratio difference for Plato crater 21 p3815 A69-39587

Relative IR spectral reflectivity of selected lunar surface areas measured using double beam photoelectric filter photometer 21 p3815 A69-39588

Surveyor spacecraft instrumentation, describing TV camera design and operation, photographic requirements and techniques, lunar surface characteristics, etc 22 p4011 A69-40043

Lunar regolith from Surveyor Program pictorial data of lunar maria 22 p4012 A69-40087

Solar proton bombardment of lunar surface, discussing luminescence and chemical effects 22 p4012 A69-40089

Random processes correlation functions determined by stochastic differential equations applied to lunar surface statistical characteristics determination 22 p4033 A69-41092

Physicomechanical properties of tuff rock based on similarity to lunar surface rock, determining natural density, porosity and compression strength 22 p4034 A69-41105

Lunar morphology evolution by dust transport on surface, discussing possibility of fluidization 23 p4221 A69-42392

Lunar radio emission constant component in presence of heat flow from interior, using stratified model of surface structure with two variants 24 p4390 A69-43788

LUNAR TRAJECTORIES

NT CIRCULUNAR TRAJECTORIES

NT EARTH-MOON TRAJECTORIES

NT MOON-EARTH TRAJECTORIES

Vehicle trajectory motion in transition region of three body problem, noting equations of motion, first order solutions, etc 03 p0505 A69-13001

Book on planetocentric, lunar and interplanetary transfer techniques covering communications and coordinate system selection, minimum fuel and time transfer and rendezvous, etc 04 p0652 A69-14458

Lunar Orbiter missions pre- and postflight error analyses compared to estimate dispersions from reference trajectory [AAS PAPER 68-108] 21 p3805 A69-39220

LUNATION

U MONTH

LUNEBERG LENSES

U RADAR CORNER REFLECTORS

LUNG MORPHOLOGY

Sheet geometry of lung blood vessel system, discussing histological evidence and fluid dynamic consequences of sheet flow 19 p3263 A69-36656

Air and saline P-V curves of rat lungs after hyperoxia, comparing hyperoxia effects to surfactant washout on pulmonary compliance 23 p4081 A69-41440

LUNGS

Electron microscopic changes in lungs of rats after repeated exposure to pure oxygen 05 p0709 A69-16514

Electron microscopic changes in lungs of rats after repeated exposure to pure oxygen 18 p3096 A69-34733

Pulmonary arterial pressure for perfusion of excised dog lungs after inflation not due to shunt channels through atelectasis areas 21 p3651 A69-38386

Ventilation-perfusion inequality increase effects on lung overall gas exchange, using digital model 21 p3662 A69-38388

Airway distensibility effect on elastic behavior of human lungs, noting compliance and resistance at different breathing frequencies for diseased lungs 22 p3873 A69-40205

Atelectatic and direct toxic effects of oxygen on human subjects 22 p3873 A69-40208

Lower body negative pressure /LBNP/ effects on ventilation and lung volumes, presenting lung model for pulmonary gas exchange changes 22 p3891 A69-40222

Carbon monoxide effect on dog lung volume, mechanical properties and diffusing capacity 22 p3874 A69-40224

Diffusion in biological systems by random walks with emphasis on gaseous diffusion in lung, noting probabilistic tree model

22 p3885 A69-40978

Effects of oxygen saturation variations of blood on rates of weight gain in isolated perfused canine lung, noting pulmonary edemogenesis

22 p3887 A69-41189

Pulmonary emphysema effect on expiratory flow limitation from static pressure-volume and flow volume curves during natural and forced deflation of hamster lungs

23 p4082 A69-41442

Sequential lung emptying at varying expiratory flow rates at increasing acceleration levels using expired nitrogen analysis

23 p4083 A69-41448

LUNIK LUNAR PROBES

Soviet lunar and planetary probes, reviewing payload characteristics, principal mission features and photographs associated with Luna, Mars, Venera and Zond series

01 p0162 A69-10938

Penetration type soil analyzer used by Luna 13 automatic lunar station for mechanical strength of lunar surface

03 p0430 A69-13424

Unannounced propellant weight and thrust of Soviet Luna spacecraft based on Luna 12 lunar orbit injection maneuver

08 p1409 A69-19969

Soviet lunar effort in Luna probe series, outlining characteristics, performance and missions

09 p1609 A69-21583

LUNIK 9 LUNAR PROBE

Luna 9 automatic station flight control complex, detailing communication, orientation and stabilization systems operation after separation from acceleration module

10 p1792 A69-24197

LUNIK 10 LUNAR PROBE

Magnetometric equipment on board Luna 10 and Venera 4 space stations for studying magnetic field in interplanetary space, describing circuit and metrological characteristics

01 p0080 A69-10582

Magnetometric equipment on board Luna 10 and Venera 4 space stations for studying magnetic field in interplanetary space, describing circuit and metrological characteristics

15 p2610 A69-30752

LUNIK 12 LUNAR PROBE

Low energy proton flux in neighborhood of Moon measured by Luna 12 satellite indicating magnetized plasma region effect on burst

09 p1577 A69-21773

LUNIK 13 LUNAR PROBE

Lunar surface uppermost layer physical and mechanical properties investigated by soilmeter-penetrator and radiation densimeter on Luna 13

18 p3113 A69-34239

LYAPUNOV FUNCTIONS

U LYAPUNOV FUNCTIONS

LYMAN ALPHA RADIATION

Scattered solar Lyman alpha radiation measurement by Vertical Space Probe station in upper atmosphere including UV radiation

01 p0152 A69-10577

Absorption coefficients of molecular oxygen at Lyman alpha line and vicinity measured by vacuum spectroscopy

01 p0076 A69-11230

Mariner 5 Venus Lyman alpha emission observations, noting atomic hydrogen and oxygen resonance radiation measurements and apparent presence of molecular hydrogen or deuterium

[AAS PAPER 68-220] 02 p0313 A69-11486

Electron impact excitation of Lyman alpha emission from 2p state of atomic H, noting discrepancy below 50 Mcv

02 p0283 A69-12466

Excited atomic H state radiative mean life measurements using beam-foil excitation method

03 p0469 A69-12920

Free excited H atom Lyman alpha radiation intensity study using beam-foil excitation method

03 p0471 A69-13167

Chromosphere fine structure in Lyman alpha intensity, compiling isophote map

03 p0515 A69-14039

Temperature dependence of O VIII Lyman alpha/Lyman beta radiation ratio in solar corona, noting coronal temperature

03 p0516 A69-14042

Solar hydrogen Lyman alpha line profile measurement by rocket-borne spectrophotometer, obtaining flux available for scattering by atomic hydrogen in geocorona

05 p0815 A69-16254

Lyman-alpha observations of Venus by Mariner 5 analyzed, assuming resonance scattering of flux by hydrogen or deuterium atoms in Venus atmosphere

05 p0815 A69-16255

Polarization of Lyman alpha radiation in hydrogen rare gas collisions calculated in Born and distortion approximations including rotational coupling

08 p1355 A69-20207

Inelastic transport cross sections for Lyman alpha transitions in hydrogen

08 p1357 A69-20814

Deuterium escape in Venus upper atmosphere to explain anomalous Lyman-alpha glow observed by Mariner 5

[SRCC-91] 09 p1594 A69-21696

Diurnal variation of D region electron production rates, discussing Lyman alpha ionization of nitric oxide

09 p1577 A69-21717

Radiation fields of Lyman alpha to Lyman 10 calculated for model planetary nebulas with constant and exponential density distributions in spherical symmetry

09 p1604 A69-22407

Lyman alpha wing opacity effect on temperature scale and helium content in F and G subdwarf atmospheres

09 p1607 A69-22431

Solar Lyman alpha radiation scattering into antisolar geocorona, noting inaccessibility of region to solar wind

09 p1583 A69-22760

Solar Lyman alpha, Lyman beta and Balmer alpha lines of He 2 for electron temperature and density and optical thickness of emitting layer

10 p1772 A69-22859

Venus and Jupiter low resolution UV spectra obtained with servocontrolled star tracking telescope in Aerobee rocket, noting Lyman alpha radiation characteristics

[JHU-TR-15] 10 p1788 A69-24121

D/H ratio in Venus exosphere, discussing isotopic fractionation mechanisms and Lyman alpha data from Mariner 5

11 p1962 A69-25145

Stellar atmosphere models of pure hydrogen in hydrostatic, radiative and statistical equilibrium, including Lyman-alpha and continua, discussing nonLTE deviations

13 p2338 A69-27560

Rocket observations of Lyman alpha anisotropic galactic radiation, noting distribution of neutral interstellar hydrogen near sun

14 p2516 A69-28952

Hydrogen Lyman alpha nightglow models, discussing solar photon scattering in geocorona and hydrogen vertical distribution

15 p2595 A69-30191

Scattered solar Lyman alpha radiation measurement by Vertical Space Probe station in upper atmosphere including UV radiation

15 p2691 A69-30747

Atomic H Lyman-alpha interstellar absorption line in theta Orionis spectrum, showing equivalent width relations to H column density and spin temperature

15 p2695 A69-30890

Pressure and wavelength dependence of molecular O absorption coefficient near 1215 A, utilizing UV emission from crossed beam atomic collision

15 p2656 A69-31031

D region ionizable constituent density /presumably nitric oxide/ measured, using blunt probe to detect changes in conductivity produced by Lyman alpha ionizing radiation

15 p2598 A69-31316

Geocoronal Lyman alpha short term and 27-day variations observed byOGO 4 spacecraft attributed to flux variability at solar emission line center

15 p2699 A69-31404

OGO 5 satellite measurements of intensity and width of Lyman alpha line scattered by hydrogen geocorona

15 p2699 A69-31412

Lyman alpha radiation ionization rate in lower ionosphere, noting various charged particle concentration parameters

15 p2605 A69-31438

Hydrogen bulge above springtime pole indicated by Lyman alpha radiation in earth geocorona, discussing hydrogen horizontal transport and hydrogen compounds dissociation as causes

18 p3129 A69-34956

Statistical relation between expansion velocities and radii of planetary nebulas due to Lyman-c and diffuse Lyman-alpha radiation

19 p3426 A69-36575

Upper atmospheric H and He observations, showing Lyman alpha, H alpha measurements and H abundance values relative to Kockarts-Nicolet model

21 p3714 A69-38529

Solar L alpha and X ray emission contribution to lower ionosphere ion production, discussing altitudinal, latitudinal and temporal variations

22 p4008 A69-41096

Lyman alpha radiation from electron collisions with simple H-containing molecules, finding dissociative excitation cross section role

24 p4351 A69-43033

LYMAN BETA RADIATION

Excited atomic H state radiative mean life measurements using beam-foil excitation method

03 p0469 A69-12920

Temperature dependence of O VIII Lyman alpha/Lyman beta radiation ratio in solar corona, noting coronal temperature

03 p0516 A69-14042

Solar Lyman alpha, Lyman beta and Balmer alpha lines of He 2 for electron temperature and density and optical thickness of emitting layer

10 p1772 A69-22859

Balmer alpha and Lyman beta intensities for multiple scattering calculated for hydrogen geocorona models by radiative transfer equations, discussing radiation transport through earth hydrogen atoms

18 p3128 A69-34943

LYMAN SPECTRA

Shock front structure in radiative relaxation region in atomic H, calculating Lyman continuum effects

01 p0122 A69-10125

Absorption oscillator strengths for rotational lines in Lyman transition vibrational bands of molecular hydrogen from equivalent widths measured photoelectrically

06 p0962 A69-17818

Radiation fields of Lyman alpha to Lyman 10 calculated for model planetary nebulas with constant and exponential density distributions in spherical symmetry

09 p1604 A69-22407

Rocket spectrographic observations of Alpha Virginis noting hydrogen Lyman absorption lines

13 p2338 A69-27555

Photodestruction rate of H molecules by absorption of Lyman or Weber band radiation in interstellar space calculated at various distances from early stars

18 p3204 A69-35351

Classical path approximation in line broadening theory to derive impact and one-electron theories, with application to Stark broadening of Lyman series in hydrogen

23 p4193 A69-41379

LYMPH

NT LYMPHOCYTES

Chronic congestive heart failure in dogs compared to pulmonary system, discussing effect on cardiac lymphatics

23 p4078 A69-41364

Enzymatic processes of glucose metabolism in immature rats lymphatic tissues during exercise-induced elevated corticosteroid secretion

23 p4080 A69-41405

LYMPHOCYTES

Macromolecular ring shaped components corresponding to hemagglutinin studied in Limulus polyphemus hemolymph by electron microscopy

16 p2742 A69-31864

Local stress effect on immunocompetent cells differentiation in guinea pigs lymphatic ganglia, showing antibody producing cells number increase

22 p3877 A69-40277

Inoculum dose effect on complement-fixing antigen production, heat lability and separation from BHK-21 cells infected with lymphocytic choriomeningitis virus

24 p4263 A69-43336

LYOPHILS

U COLLOIDS

LYRAE CONSTELLATION

He I 10830 A line in beta Lyr shell observed by contact image converter tube, analyzing line structure and phase brightness

11 p1955 A69-24391

Color excess and 21 cm line intensity of RR Lyrae stars at high latitudes, confirming correlation between dust and atomic hydrogen

12 p2063 A69-25808

Photoelectric observation of RR Lyrae stars in globular clusters to estimate reddening near galactic poles, considering color indices

12 p2172 A69-27157

RR Lyrae gap stellar model atmospheres including radiation spectra, temperature radiation and convection, etc

13 p2338 A69-27561

Solar UV radiation reflected from Echo satellites measured and compared with UV fluxes from Lyrae

14 p2447 A69-29408

Variability of period of RR Lyrae type stars in globular cluster M3, deriving seasonal moments of stellar maxima and light curve elements

15 p2683 A69-30511

Absolute spectrophotometric gradients determined from energy distribution in UV beta Lyr spectrum, confirming gradual variations in light curve shape and spectral characteristics

15 p2688 A69-30557

Monograph on proper motions of RR Lyrae variables, discussing data acquisition analysis

15 p2700 A69-31493

Hydrogen line profiles, equivalent widths and electron densities for peculiar alpha 2 CVn and gamma Lyr stars

16 p2864 A69-32594

Photometric and spectroscopic data for southern RR Lyrae variables, deriving period, light curves in three colors, mean radial velocity and spectral types

21 p3801 A69-38764

Photometric data for variable stars in Lyra and Cygnus including eclipsing variables

23 p4215 A69-42009

He I 10830 A line in beta Lyr shell observed by contact image converter tube, analyzing line structure and phase brightness

24 p4390 A69-43781

LYSINE

Time of heating effect on thermal polymerization of L-lysine free base

13 p2218 A69-28439

Free lysine and dinitrophenyl /DNP/ derivatives determined quantitatively by ion exchange chromatography

17 p2917 A69-33651

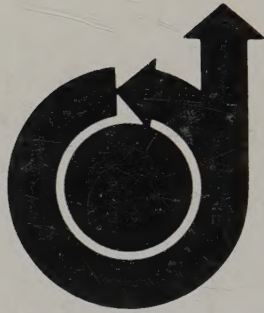
Pyrimidine polyribonucleotides or purine polyribonucleotides binding to lysine- or arginine-rich proteinoids considered for abiogenesis

23 p4113 A69-41509

LYSOZYME

Long lived radicals produced in crystalline ribonuclease and lysozyme by 120-Mev protons studied by ESR spectroscopy

03 p0372 A69-13485



AIAA TECHNICAL INFORMATION SERVICE

750 THIRD AVENUE

NEW YORK, N. Y. 10017

R